TRANSACTIONS

OF THE

AMERICAN INSTITUTE

OF

ELECTRICAL ENGINEERS

VOLUME 66

1947

PUBLISHED BY THE
AMERICAN INSTITUTE OF ELECTRICAL ENGINEERS
33 WEST 39TH STREET
NEW YORK 18, N. Y., U. S. A.

M621.305
AM4

COPYRIGHT 1947
BY THE
AMERICAN INSTITUTE OF ELECTRICAL ENGINEERS

Printed in the United States of America by
The Mack Printing Company, Easton, Pa.

Index

1. Technical-Subject Index

A Self-Balancing Capacitance Bridge. Foley..797–801
Acceleration With a Vacuum Tube, The Measurement of. Ramberg.....735–40
Accuracy of Temperature Measurements on Coil Surfaces. Beede, Cain.....586–90; disc. 590
Adjustable Frequency Control of High-Speed Induction Motors. Heumann.....719–25
Adjustable-Speed A-C Brush-Shifting Motor, Impedance Relationships of the. Baumann.....1460–2
Advancements in the Design of Long-Scale Indicating Instruments. Rowell, Millar.....155–60
Aging Tests on Class A Insulation, Preliminary Report on Laboratory. (Committee Report).....879–81; disc. 881
Aids for Electromechanical System Development, Laboratory. Newton, White....315–19; disc. 319
AIEE Officers and Committees for 1947–48....1724–37
AIEE Publication Policy Becomes Effective in January 1947, New.....1721–3
Air Circuit Breakers, Selective Tripping of Low-Voltage. Deans.....971–6; disc. 976
Air, Determination of Corona Starting Voltages for Nonuniform Fields in. Hutton..1674–9; disc. 1680
Air Gap Reactance of Polyphase Machines, The. Alger, West.....1331–43
Air Switches for Line Sectionalizing and Load Transfer, Automatic Control of. Rich, Kirwen.....293–9; disc. 299
(Air Transportation) Electric Equipment Required in a Modern 6-Component Wind Tunnel Model Suspension System. Cox.....1258–66
(Air Transportation) The Calibration of Ignition Crest Voltmeters. Davis, Warren....99–104; disc. 104
Airborne Magnetometers for Search and Survey. Felch, Means, Slonczewski, Parratt, Rumbaugh, Tickner.....640–50
Airborne Radar to Increase Airline Safety, Using. Ayer.....1387–95
Aircraft, A Capacitance-Type Fuel-Measurement System for. Pearson.....1363–8
Aircraft Alternators Using Electronic Frequency Changers, Parallel Operation of. Bowlus, Nims.....31–8
Aircraft D-C Generators, An Integrated Control System for. McClinton.....94–8
Aircraft, Electric Drive for. Crom.....1359–62
Aircraft Electric Power Protective Systems. Austin.....1375–82
Aircraft Generator Power Center, D-C. Bottemiller.....1267–70
Aircraft, Ground Power Supply for Modern. Owen, Murray, Rosenstein.....1296–1303
Aircraft Window Deicing, Control and Power Systems for. Mershon.....1400–05
Airline Safety, Using Airborne Radar to Increase. Ayer.....1387–95
Airplanes, Automatic Temperature Control for Transport. Hedges.....1197
Airport Runway and Approach Lighting. Kevern.....1396–9
Alloy, Hiperco—A Magnetic. Stanley, Yensen..714–8
A-C Brush-Shifting Motor, Impedance Relationships of the Adjustable-Speed. Baumann.....1460–2
A-C Crane Motors, A Thrustor Lowering Control System for. Schwarz-Kast.....139–44; disc. 144
A-C Power Transmission, Economics of Long-Distance. Crary, Johnson.....1092–9; disc. 1099
A-C Stator Windings, The Application of Surge Comparison Testing Equipment to Fractional Horsepower. Buchanan.....1356–8
A-C Turbine Generators, Liquid Cooling of. Fechheimer.....553–61; disc. 561
Alternators Using Electronic Frequency Changers, Parallel Operation of Aircraft. Bowlus, Nims..31–8
Altitude Flashover and Corona Correction on Small Ceramic Bushings. Pendleton.....1324–30
Aluminum Anodes, Cathodic Protection of Steel Water Tanks Using. Sudrabin, Mears.....197–200
Ampere-Demand Meter, A Polyphase Thermal. Petzinger.....167–74
Amplifier, Direct Coupled Oscillograph. Christian.....1383–6
Amplifier, Some Fundamentals of a Theory of the Transductor or Magnetic. Lamm.....1078–85
Amplifier Using Biased Saturable Core Reactors, A Balanced. Kirschbaum, Harder.....273–8
Analogy, Dimensionless Analysis of Servomechanisms by Electrical. Part I. McCann, Herwald..111–18
Analogy, Solution of the General Voltage Regulator Problem by Electrical. Harder..815–25; disc. 825
Analysis, An Extension of Impact Speed-Drop. Crever.....191–6
Analysis and an Optimum Synthesis of Linear Servomechanisms, The. Herr, Gerst.....959–70
Analysis and Equivalent Circuit of a Variable-Ratio Frequency Changer, Tensorial. Kron...1503–06
Analysis of Motor Selection for Brass-Slab Rolling-Mill Service, An. Berkeley.....185–9; disc. 189
Analysis of Servomechanisms by Electrical Analogy, Dimensionless. Part I. McCann, Herwald..11–18
Analysis of Speed Regulators Under Impact Loads, General. McCann, Osbon, Kirschbaum..1243–52
Analysis to Automatic Control Systems, The Application of Lead Networks and Sinusoidal. Schwartz.....69–76; disc. 76
Anodes, Cathodic Protection of Steel Water Tanks Using Aluminum. Sudrabin, Mears.....197–200
Anodizing Applications, Automatically Controlled Copper-Oxide Rectifiers for Electroplating and. Buckley.....181–4
Apparatus, Gaseous Insulation for High-Voltage. Camilli, Chapman.....1463–9; disc. 1469
Application of Complex Logarithmic and Geometric Mean Distances, Theory and. Higgins.....12–16
Application of Heterodyne Modulation to Wide-Banded Frequency-Modulated Television Relays, The. Boothroyd.....1126–30
Application of Lead Networks and Sinusoidal Analysis to Automatic Control Systems, The. Schwartz.....69–76; disc. 76
Application of Rural Carrier Telephone System. Bartlink, Cook, Cowan, Messmer....511–18; disc. 517
Application of Storage Batteries to the Control of Switchgear, The. Hoxie.....1561–9; disc. 1569
Application of Supersonic Flaw Detectors, Design and. Erdman.....1271–6
Application of Surge Comparison Testing Equipment to Fractional Horsepower A-C Stator Windings, The. Buchanan.....1356–8
Application of Synchronous and Induction Motors to Chippers, The. Baker, Lory.....1070–7
Application of Western Union Multiplex to Navy Radio, The. Hoover.....1478–82
Applications, Automatically Controlled Copper-Oxide Rectifiers for Electroplating and Anodizing. Buckley.....181–4
Applications, Frequency Shift Telegraphy—Radio and Wire. Davey, Matte.....479–93; disc. 493
Applications of the Electrodynamic Instrument Mechanism. Corson, Millar.....1131–6
Approach Lighting, Airport Runway and. Kevern.....1396–9
Approach to Speed and Tie Line Control, Theoretical. Brandt.....24–9; disc. 29
Arc-Back Testing of Graphite. Pakala, Cuculiu..439–42
Arrester Discharges, Field Research on Lightning. McCann, Beck.....625–9; disc. 629
Arresters—Tidd 500-Kv Test Lines, Transformers and Lightning. Lane, Hodnette, Bellaschi, Beck.....1613–18; disc. 1618
Asymmetrical Stator and Rotor, Equivalent Circuit of the Primitive Rotating Machine With. Kron.....17–23; disc. 23
Automatic Circuit Recloser, An Improved. Wallace.....255–8; disc. 259
Automatic Control of Air Switches for Line Sectionalizing and Load Transfer. Rich, Kirwen.....293–9; disc. 299
Automatic Control of Hydroelectric Generating Stations. Brown, Derr.....343–55; disc. 355
Automatic Control Systems, The Application of Lead Networks and Sinusoidal Analysis to. Schwartz.....69–76; disc. 76
Automatic Operation of Electric Boilers. Eaton.....1061–8; disc. 1068
Automatic Switching Schemes for Capacitors. Cuttino.....311–14
Automatic Switching, The Economics of Using Capacitors in Amounts to Require. Butler.....322–7; disc. 327
Automatic Temperature Control for Transport Airplanes. Hedges.....1197
Automatically Controlled Copper-Oxide Rectifiers for Electroplating and Anodizing Applications. Buckley.....181–4
Auxiliary-Power Equipment, Modern Railway Passenger-Car. MacLeod, Hause.....930–8

B

Balanced Amplifier Using Biased Saturable Core Reactors, A. Kirschbaum, Harder.....273–8
Balancing Capacitance Bridge, A Self-. Foley..797–801
Band-Width Characteristics of Pulse Modulation, Distortion and. Kraus, Ordung.....984–8
Basic for Distance Relaying on 3-Phase Systems, Fundamental. Lewis, Tippett.....694–708; disc. 708
(Basic Sciences) Determination of Corona Starting Voltages for Nonuniform Fields in Air. Hutton.....1674–9; disc. 1680
(Basic Sciences) Diffusion of Electric Current into Rods, Tubes, and Flat Surfaces. Miller.....1496–1502
(Basic Sciences) Eddy Currents in Disks: Driving and Damping Forces and Torques. Moore.....1–10; disc. 10
(Basic Sciences) Effective Resistance of Isolated Nonmagnetic Rectangular Conductors. Dwight.....549–52
(Basic Sciences) Machine Computation of Power Network Performance. Dunstan....610–20; disc. 621
(Basic Sciences) The Physics of Electronic Semiconductors. Pearson.....209–14
(Basic Sciences) The Probable Breakdown Voltage of Paper Dielectric Capacitors. Brooks.....1137–44; disc. 1144
(Basic Sciences) Theory and Application of Complex Logarithmic and Geometric Mean Distances. Higgins.....12–16
Basic Servomechanism Types, A Comparison of Two. Harris.....83–92; disc. 92
Basis for Generator Reserve, Outage Expectancy as a. Seelye.....1483–8
Batteries to the Control of Switchgear, The Application of Storage. Hoxie.....1561–9; disc. 1569
Bearing Deviation Indicator for Sonar. Schuck, Stedman, Hathaway, Butz.....1285–95
Bearing Practice for Vertical Water Wheel Generators, Modern. Laffoon, Baudry.....363–9; disc. 369
Bearings at the Bonneville Plant of the Corps of Engineers, War Department, The Design and Performance of the Vertical Generator Thrust. Lewis, Gordon.....1231–7; disc. 1237
Board of Directors, Report of the.....1698–1720
Boilers, Automatic Operation of Electric. Eaton.....1061–8; disc. 1068
Bonneville Plant of the Corps of Engineers, War Department, The Design and Performance of the Vertical Generator Thrust Bearings at the. Lewis, Gordon.....1231–7; disc. 1237
Brakes and Drum Brakes for PCC Cars, Recent Developments in Track. Vouch.....302–04
Braking by Self-Excitation of Squirrel-Cage Motor, Dynamic. Srinivasan, Thomas.....145–8
Braking of a Single D-C Series Motor, Dynamic. Leitch.....149–54
Braking of Two D-C Series Motors, Dynamic. Leitch.....787–91
Braking Resistors and Control for Diesel-Electric Locomotives. Weiser.....229–32
Braking, The Design of New York Subway Motors for Dynamic. Widell.....808–10
Brass-Slab Rolling-Mill Service, An Analysis of Motor Selection for. Berkley.....185–9; disc. 189
Breakdown Voltage of Paper Dielectric Capacitors, The Probable. Brooks.....1137–44; disc. 1144
Breaker Current Measurements During Reignitions and Recovery, Circuit-. Lewis....1253–7; disc. 1257
Breakers, An Improved Overcurrent Tripping Device for Low-Voltage Circuit. Rawlins, Sandin.....1149–53; disc. 1153
Breakers, Selective Tripping of Low-Voltage Air Circuit. Deans.....971–6; disc. 976
Bridge, A Self-Balancing Capacitance. Foley..797–801
Bridges, Electronic Null Detectors for Use With Impedance. Lamson.....535–40
Broadcast Stations, Television Equipment for. Lawrence.....443–52
Broken Conductor Effect on Sags in Suspension Spans. Bisiri, Landau.....1181–8
Brush Characteristics by the Dynamotor Method, Dynamic. Herman.....759–63

Brush-Shifting Commutator Motor (Schrage Type), The Circle Diagram of the Polyphase. Franklin.....1667–72; disc. 1672
Brush-Shifting Motor, Impedance Relationships of the Adjustable-Speed A-C. Baumann.....1460–2
Burning of Wood Structures by Leakage Currents. Rus.....279–84; disc. 285
But Where No Overhead Facilities Exist, Can the Trolley Coach Compete Economically With the Gas or Diesel. Gaus.....264–8; disc. 268
Bushings, High Altitude Flashover and Corona Correction on Small Ceramic. Pendleton.....1324–30

C

Cable Carrier System, An Improved. Black, Brooks, Wier, Wilson.....741–46; disc. 746
Cable Carrier, Systems, New Test Equipment and Testing Methods for. Tidd, Rosen, Wenk..726–30
Cable Network, Frequency Division Techniques for a Coaxial. Crane, Dixon, Huber.....1451–5
Cable Switching, Resistors for 138-Kv. Sadler, Blakeslee.....39–46; disc. 46
Cable Telegraphy, Some Modern Techniques in Ocean. Cramer.....494–500; disc. 500
Cables, Gas Pressure for Telephone. Giese.....471–8
Cables, Internal Corona Discharges in Insulated. Greenfield.....591–600; disc. 600
Cage Motor, Dynamic Braking by Self-Excitation of Squirrel-. Srinivasan, Thomas.....145–8
Cage Rotor, The "Cooperspun" Squirrel. Anderson.....1312–14
Calculating Probability of Generating Capacity Outages. Lyman.....1471–7; disc. 1477
Calculating Stability, The Transient-Energy Method of Magnuson.....747–55; disc. 755
Calculation of Leakage Reactance of Induction Motors, Some Phases of. Liwschitz, Formhals.....1409–12; disc. 1412
Calculation of Slot Constants. Puchstein.....1315–22; disc. 1322
Calculations for Single-Phase Magneto, Shading Coil. Evans.....134–7; disc. 137
Calculations, Ignitor Characteristic and Circuit. Marshall.....1519–24
Calculations on Shaded Pole Motors, Performance. Trickey.....1431–8; disc. 1438
Calibration of Ignition Crest Voltmeters, The. Davis, Warren.....99–104; disc. 104
Canada, Electric Furnace Practice in. Balleny..917–24
Capacitance Bridge, A Self-Balancing. Foley..797–801
Capacitance Fuel Gauges. Clark, Adolphe.....1189–96; disc. 1196
Capacitance-Type Fuel-Measurement System for Aircraft, A. Pearson.....1363–8
Capacitor Motor, The Equivalent Circuit of the. Chang.....631–40
Capacitor Motors, A Design Method for. Lloyd, Chang.....651–7; disc. 657
Capacitor Start Motors, A Design Method for. Chang.....1369–74
Capacitors, Automatic Switching Schemes for. Cuttino.....311–14
Capacitors in Amounts to Require Automatic Switching, The Economics of Using. Butler..322–7; disc. 327
Capacitors, The Probable Breakdown Voltage of Paper Dielectric. Brooks.....1137–44; disc. 1144
Capacity Determined by the Probability Method, Generating Reserve. Calabrese.....1439–50
Capacity Outages, Calculating Probability of Generating. Lyman.....1471–7; disc. 1477
Capacity Problems of a Combined Hydro and Steam System, Probability Methods Applied to Generating. Loane, Watchorn.....1645–54; disc. 1654
Car Equipment for New York City's Subway System, Modern. Cordts.....247–9; disc. 250
Car, Some Recent Developments in the PCC. Cooper.....288–92; disc. 292
Carrier Channels, Operation of Power Line. Lenner.....888–93; disc. 893
Carrier System, An Improved Cable. Black, Brooks, Wier, Wilson.....741–6; disc. 746
Carrier System for Power Lines, A New Single-Side-Band. Lenehan.....826–30; disc. 830
Carrier Systems, New Test Equipment and Testing Methods for Cable. Tidd, Rosen, Wenk...726–30
Carrier Telephone System, Application of Rural. Bartelink, Cook, Cowan, Mesmer..511–17; disc. 517
Carrier Telephone System for Rural Service, A. Barstow.....501–07
Cars, Motor Control for Latest New York Transit System Subway. Riley.....900–03
Cars, Recent Developments in Track Brakes and Drum Brakes for PCC. Vouch.....302–04
Cathode-Ray Oscilloscope, Quantitative Determination of Magnetic Properties by Use of. Zamsky..783–7
Cathode-Ray Sensing Element, A Magnetic Compass With. Kliever, Syrdal.....529–34
Cathode-Ray Spectrograph, The. Feldt, Berkley.....105–10
Cathodic Protection of Steel Water Tanks Using Aluminum Anodes. Sudrabin, Mears.....197–200
Cavities at 10,000 Megacycles, Measurement of High Q. Lange.....161–6
Cell, Electrical Characteristics of the Junction in a Simplified Selenium Rectifier. Angello...175–80
Cellulose Insulation Impregnated With Semi-conducting Liquids, The Dielectric Properties of. Clark.....55–62; disc. 62
Center, D-C Aircraft Generator Power. Bottemiller.....1267–70
Ceramic Bushings, High Altitude Flashover and Corona Correction on Small. Pendleton.....1324–30
Changer, Suddenly Applied Loads on a Variable-Ratio Frequency. Carter, Maginniss, Rothe....1489–95
Changer, Tensorial Analysis and Equivalent Circuit of a Variable-Ratio Frequency. Kron.....1503–06
Changers, Parallel Operation of Aircraft Alternators Using Electronic Frequency. Bowlus, Nims..31–8
Channels, Operation of Power Line Carrier. Lenner.....888–93; disc. 893
Characteristic and Circuit Calculations, Ignitor. Marshall.....1519–24
Characteristics by the Dynamotor Method, Dynamic Brush. Herman.....759–63
Characteristics of Current Transformers During Faults, Part II. Rothe, Concordia.....731–4
Characteristics of Pulse Modulation, Distortion and Band-Width. Krauss, Ordung.....984–8
Characteristics of Resistance Welding Tools, Electrical. Callender.....393–404
Characteristics of the Junction in a Simplified Selenium Rectifier Cell, Electrical. Angello.....175–80
Charging Current at High Voltage, The Interruption of. Leeds, Van Sickle.....373–80; disc. 381
Cheyenne Wells, Colo., Rural Radiotelephone Experiment at. Moore, Seyler, Wright.....525–8
Chippers, The Application of Synchronous and Induction Motors to. Baker, Lory.....1070–7
Chopped Waves on Transformers, A Study of the Relative Severity of Steep Front Waves and. Vogel.....64–6; disc. 66
Circle Diagram of the Polyphase Brush-Shifting Commutator Motor (Schrage Type), The. Franklin.....1667–72; disc. 1672
Circuit-Breaker Current Measurements During Reignitions and Recovery. Lewis..1255–7; disc. 1257
Circuit Breakers, An Improved Overcurrent Tripping Device for Low-Voltage. Rawlins, Sandin.....1149–53; disc. 1153
Circuit Breakers, Selective Tripping of Low-Voltage Air. Deans.....971–6; disc. 976
Circuit Calculations, Ignitor Characteristic and. Marshall.....1519–24
Circuit Feed Regulator, A New Grinding. Jones.....1240–2
Circuit of a Variable-Ratio Frequency Changer, Tensorial Analysis and Equivalent. Kron....1503–06
Circuit of the Capacitor Motor, The Equivalent. Chang.....631–40
Circuit of the Induction Motor, Leakage Reactance of the Squirrel Cage Rotor With Respect to the Stator Harmonics and the Equivalent. Liwschitz.....1407–08
Circuit of the Primitive Rotating Machine With Asymmetrical Stator and Rotor, Equivalent. Kron....17–23; disc. 23
Circuit Recloser, An Improved Automatic. Wallace.....255–8; disc. 259
Circuits, Grounding of Instrument Transformer Secondary. (Committee Report).....419–20
Circuits, Sectionalizing and Internal Transformer Fusing on Rural Power. Watkins..383–8; disc. 388
City Transportation, Trolley Coaches and PCC Street Cars Provide Successful. Clardy.....925–9
Class A Insulation, Preliminary Report on Laboratory Aging Tests on. (Committee Report).....879–81; disc. 881
Coaxial Cable Network, Frequency Division Techniques for a. Crane, Dixon, Huber.....1451–9
Code Modulation, Pulse. Black, Edson.....895–9
Coil Calculations for Single-Phase Magnets, Shading. Evans.....134–7; disc. 137
Coil Surfaces, Accuracy of Temperature Measurements on. Beede, Cain.....586–90; disc. 590
Coils, Data on the High-Frequency Resistance of Coils. Wittig.....764–9
Collectors for High-Speed Service, Developments in Current. Langer.....51–4
Colorado, Rural Radiotelephone Experiment at Cheyenne Wells. Moore, Seyler, Wright.....525–8
(Committee Report) Grounding of Instrument Transformer Secondary Circuits.....419–20
(Committee Report) Preliminary Report on Laboratory Aging Tests on Class A Insulation..879–81; disc. 881
(Committee Report) Present-Day Grounding Practices on Power Systems. (Committee Report).....1525–48; disc. 1548
(Committee Report) Progress in Power Generation—1940–46.....1681–97
(Committee Report) Relay Protection of Power Transformers.....911–15; disc. 915
Committees for 1947–48, AIEE Officers and....1724–37
(Communication) A Carrier Telephone System for Rural Service. Barstow.....501–07
(Communication) A Frequency Modulation Telegraph Terminal Without Relays. Cusack, Michon.....1165–70; disc. 1170
(Communication) A New Microwave Television System. Wentz, Smith.....465–70
(Communication) A 60-Cycle Hysteresis Loop Tracer for Small Samples of Low-Permeability Material. Wiegand, Hansen.....119–31; disc. 131
(Communication) Air-Borne Magnetometers for Search and Survey. Felch, Means, Slonczewski, Parratt, Rumbaugh, Tickner.....640–50
(Communication) An Electronic Regenerative Repeater for Teletypewriter Signals. Hearn..904–11
(Communication) An Improved Cable Carrier System. Black, Brooks, Wier, Wilson....741–6; disc. 746
(Communication) Applications of Rural Carrier Telephone System. Bartelink, Cook, Cowan, Mesmer.....511–17; disc. 517
(Communication) Bearing Deviation Indicator for Sonar. Schuck, Stedman, Hathaway, Butz.....1285–95
(Communication) Distortion and Band-Width Characteristics of Pulse Modulation. Krauss, Ordung.....984–8
(Communication) Distortion in a Pulse Count Modulation System. Clavier, Panter, Grieg.....989–1005; disc. 1005
(Communication) Frequency Division Techniques for a Coaxial Cable Network. Crane, Dixon, Huber.....1451–9
(Communication) Frequency Shift Telegraphy—Radio Radio and Wire Applications. Davey, Matte.....479–93; disc. 493
(Communication) Gas Pressure for Telephone Cables. Giese.....471–8
(Communication) Joint Use of Pole Lines for Rural Power and Telephone Services. Campbell, Hill, Moore, Schola.....519–24; disc. 524
Communication, Modulation in. Cowan.....792–6
(Communication) New Test Equipment and Testing Methods for Cable Carrier Systems. Tidd, Rosen, Wenk.....726–30
(Communication) Postwar Television Receiver Design. Pugsley.....453–8
(Communication) Pulse Code Modulation. Black, Edson.....895–9
(Communication) Pulse Echo Measurements on Telephone and Television Facilities. Abraham, Lebert, Maggio, Schott.....541–8; disc. 548
(Communication) Radio-Noise Influence of 230-Kv Lines. Norden.....677–81; disc. 682
(Communication) Rural Radiotelephone Experiment at Cheyenne Wells, Colo. Moore, Seyler, Wright.....525–8
(Communication) Some Modern Techniques in Ocean Cable Telegraphy. Cramer....494–500; disc. 500
(Communication) Submarine Detection by Sonar. Keller.....1217–30
Communication System, TVA Co-ordinated. Talmage.....1022–34; disc. 1034
(Communication) Television Equipment for Broadcast Stations. Lawrence.....443–52
(Communication) Television Network Facilities. Abraham, Rommes.....459–64
(Communication) The Application of Heterodyne Modulation to Wide-Band Frequency-Modulated Television Relays. Boothroyd.....1126–30
(Communication) The Application of Western Union Multiplex to Navy Radio. Hoover.....1478–82
(Communication) The Stromberg-Carlson XY Dial Telephone System. Reed.....432–8
Commutator Motor (Schrage Type), The Circle Diagram of the Polyphase Brush-Shifting. Franklin.....1667–72; disc. 1672
Comparison of Two Basic Servomechanism Types, A. Harris.....83–92; disc. 92
Comparison Testing Equipment to Fractional Horsepower A-C Stator Windings, The Application of Surge. Buchanan.....1356–8
Compass With Cathode-Ray Sensing Element, A Magnetic. Kliever, Syrdal.....529–34
Compensators, Metering With Transformer-Loss. Schleicher.....851–61; disc. 861
Complex Logarithmic and Geometric Mean Distances, Theory and Application of. Higgins.....12–16
Computation of Power Network Performance, Machine. Dunstan.....610–20; disc. 621
Computing Thermal Transients, Simplified Graphical Method of. Narbutovskih.....78–81; disc. 82
Conductor Effect on Sags in Suspension Spans, Broken. Bisiri, Landau.....1181–8
Conductors and a Method for Studying Them, Galloping. Tornquist, Becker.....1154–61; disc. 1161
Conductors, Effective Resistance of Isolated Nonmagnetic Rectangular. Dwight.....549–52

Considerations on High-Voltage Lines and Design Features of Tidd 500-Kv Test Lines, Corona. Wagner, Wagner, Peterson, Gross ..... 1583–90; disc. 1590
Constant-Current Motor Systems, Electronic. Livingston ..... 425–30; disc. 430
Constant-Frequency Generator, A Variable-Speed. Roys, Nader, Spotts ..... 1414–17; disc. 1417
Constants, Calculation of Sko. Puchstein ..... 1315–22; disc. 1322
Control and Power Systems for Aircraft Window Deicing. Mershon 1400–05
Control for Diesel-Electric Locomotives, Braking Resistors and. Weiser 229–32
Control for Latest New York Transit System Subway Cars, Motor. Riley 900–03
Control for Transport Airplanes, Automatic Temperature. Hedges 1197
Control, Functionalized Resistance Welding. Stadum, Large, Hartwig 414–18
Control of Air Switches for Line Sectionalizing and Load Transfer, Automatic. Rich, Kirwen ..... 293–9; disc. 299
Control of High-Speed Induction Motors, Adjustable Frequency. Heumann 719–25
Control of Hydroelectric Generating Stations, Automatic. Brown, Derr ..... 343–55; disc. 355
Control of Slip-Ring Motors by Means of Unbalanced Primary Voltages. Schmitz ..... 1103–1112; disc. 1112
Control of Switchgear, The Application of Storage Batteries to the. Hoxie ..... 1561–9; disc. 1569
Control of Thyratron Rectifiers, The Shunt Tube. Potter 421–4
Control, Radar Technique in an Industrial. Cockrell 269–72
Control System for A-C Crane Hoists, A Thrustor Lowering. Schwarz-Kast ..... 139–44; disc. 144
Control System for Aircraft D-C Generators, An Integrated. McClinton 94–8
Control System for Wind Tunnel Drives, A. Heidenreich ..... 1637–43; disc. 1643
Control Systems, Developments in Diesel-Electric Traction-Generator Excitation. Brancke, Adams ..... 223–8; disc. 228
Control Systems for Diesel-Electric Locomotives. Developments in. Henshaw 233–41
Control Systems, The Application of Lead Networks and Sinusoidal Analysis to Automatic. Schwartz ..... 69–76; disc. 76
Control, Theoretical Approach to Speed and Tie Line. Brandt ..... 24–9; disc. 29
Controlled Copper-Oxide Rectifiers for Electroplating and Anodizing Applications, Automatically. Buckley 181–4
Cooling of A-C Turbine Generators, Liquid. Pechheimer ..... 553–61; disc. 561
Co-ordinated Communication System, TVA. Talmage ..... 1022–34; disc. 1034
Copper-Oxide Rectifiers for Electroplating and Anodizing Applications, Automatically Controlled. Buckley 181–4
Copper-Oxide Rectifiers, Higher Voltage. Smith 220–2
"Copperspun" Squirrel Cage Rotor, The. Anderson 1312–14
Core Reactors, A Balanced Amplifier Using Biased Saturable. Kirachbaum, Harder 273–8
Cores, Interlaminar Eddy Current Loss in Laminated. Beiler, Schmidt ..... 872–7; disc. 877
Corona Considerations on High-Voltage Lines and Design Features of Tidd 500-Kv Test Lines. Wagner, Wagner, Peterson, Gross ..... 1583–90; disc. 1590
Corona Correction on Small Ceramic Bushings, High Altitude Flashover and. Pendleton 1324–30
Corona Discharges in Insulated Cables, Internal. Greenfield ..... 591–600; disc. 600
Corona Starting Voltages for Nonuniform Fields in Air, Determination of. Hutton ..... 1674–9; disc. 1680
Corps of Engineers, War Department, The Design and Performance of the Vertical Generator Thrust Bearings at the Bonneville Plant of the. Lewis, Gordon ..... 1231–7; disc. 1237
Correction on Small Ceramic Bushings, High Altitude Flashover and Corona. Pendleton 1324–30
Cotton Industry in the South, Electrification of the. Bobe ..... 201–08; disc. 208
Coupled Oscillograph Amplifier, Direct. Christian 1383–6
Coupling Method, A Simplified Double-Film Kydonograph With an Improved. Waghorne ..... 1114–16; disc. 1116
Crane Hoists, A Thrustor Lowering Control System for A-C. Schwarz-Kast ..... 139–44; disc. 144
Crest Voltmeters, The Calibration of Ignition. Davis, Warren ..... 99–104; disc. 104
Criteria of D-C Interrupters, Performance. Boehne, Jang ..... 1172–80; disc. 1180
Current at High Voltage, The Interruption of Charging. Leeds, Van Sickle ..... 373–80; disc. 381
Current Collectors for High-Speed Service, Developments in. Langer 51–4
Current into Rods, Tubes, and Flat Surfaces, Diffusion of Electric. Miller 1496–1502
Current Loss in Laminated Cores, Interlaminar Eddy. Beiler, Schmidt ..... 872–7; disc. 877
Current Measurements During Reignitions and Recovery, Circuit-Breaker. Lewis ..... 1253–7; disc. 1257
Current Motor Systems, Electronic Constant-. Livingston ..... 425–30; disc. 430
Current Transformers During Fault, Transient Characteristics of. Part II, Rothe, Concordia 731–4
Current, Transient Voltage Rise in Transformers Due to Interruption of Exciting. Srinivasan, Vogel 1632–6
Currents, Burning of Wood Structures by Leakage. Ross ..... 279–84; disc. 285
Currents in Disks, Driving and Damping Forces and Torques, Eddy. Moore ..... 1–10; disc. 10

D

Damping Forces and Torques, Eddy Currents in Disks: Driving and. Moore ..... 1–10; disc. 10
Data on the High-Frequency Resistance of Coils. Witzig 764–9
Deicing, Control and Power Systems for Aircraft Window. Mershon 1400–05
Demand Meter, A Polyphase Thermal Ampere-. Petringer 167–74
Design and Application of Supersonic Flaw Detectors. Erdman 1271–6
Design and Performance of the Vertical Generator Thrust Bearings at the Bonneville Plant of the Corps of Engineers, War Department, The. Lewis, Gordon ..... 1231–7; disc. 1237
Design, High-Voltage Power-Transformer. Part II. Mallett ..... 1086–91; disc. 1091
Design Method for Capacitor Motors, A. Lloyd, Chang ..... 651–7; disc. 657
Design Method for Capacitor Start Motors, A. Chang 1369–74
Design of Long-Scale Indicating Instruments, Advancements in the. Rowell, Millar 155–60
Design of New York Subway Motors for Dynamic Braking, The. Widell 808–10
Design, Postwar Television Receiver. Pugsley 453–8
Detection by Sonar, Submarine. Keller 1217–30
Detector Relay Protection, Typical Transformer Faults and Gas. Madill ..... 1052–8; disc. 1058
Detectors, Design and Application of Supersonic Flaw. Erdman 1271–6
Detectors for Use With Impedance Bridges, Electronic Null. Lamson 535–40
Determination of Corona Starting Voltages for Nonuniform Fields in Air. Hutton ..... 1674–9; disc. 1680
Determination of Magnetic Properties by Use of Cathode-Ray Oscilloscope, Quantitative. Zamsky 783–7
Development in Quebec, Hydroelectric Power. Lawton 1006–21
Development, Laboratory Aids for Electromechanical System. Newton, White ..... 315–19; disc. 319
Developments in Connection With Hot-Line Insulator Washing, Tests and. Hill 1203–16
Developments in Control Systems for Diesel-Electric Locomotives. Henshaw 233–41
Developments in Current Collectors for High-Speed Service. Langer 51–4
Developments in the PCC Car, Some Recent. Cooper ..... 288–92; disc. 292
Developments in Track Brakes and Drum Brakes for PCC Cars, Recent. Vouch 302–04
Deviation Indicator for Sonar, Bearing. Schuck, Stedman, Rathaway, Butz 1285–95
Device for Low-Voltage Circuit Breakers, An Improved Overcurrent Tripping. Kawlins, Sandin ..... 1149–53; disc. 1153
Diagram of the Polyphase Brush-Shifting Commutator Motor (Schrage Type), The Circle. Franklin ..... 1667–72; disc. 1672
Dial Telephone System, The Stromberg-Carlson XY. Reed 432–8
Dielectric Capacitors, The Probable Breakdown Voltage of Paper. Brooks ..... 1137–44; disc. 1144
Dielectric Heating—The Measurement of Loss Under Rising Temperature. Whitehead 947–9
Dielectric Properties of Cellulose Insulation Impregnated With Semiconducting Liquids, The. Clark ..... 55–62; disc. 62
Diesel Bus Where No Overhead Facilities Exist?, Can the Trolley Coach Compete Economically With the Gas or. Gaus ..... 264–8; disc. 268
Diesel-Electric Locomotive for the Seaboard Air Line Railway, A 3,000 Horsepower. Staples, Weybrew, Atwell 215–19
Diesel-Electric Locomotives, A Power Plant Regulating System for. Lewis ..... 242–6; disc. 246
Diesel-Electric Locomotives, Braking Resistors and Control for. Weiser 229–32
Diesel-Electric Locomotives, Developments in Control Systems for. Henshaw 233–41
Diesel-Electric Traction-Generator Excitation Control Systems, Developments in. Brancke, Adams ..... 223–8; disc. 228
Diffusion of Electric Current into Rods, Tubes, and Flat Surfaces. Miller 1496–1502
Dimensionless Analysis of Servomechanisms by Electrical Analogy. McCann, Herwald. Part I 111–18
Direct Coupled Oscillograph Amplifier. Christian 1383–6
D-C Aircraft Generator Power Center. Bottemiller 1267–70
D-C Generators, An Integrated Control System for Aircraft. McClinton 94–8
D-C Interrupters, Performance Criteria of. Boehne, Jang ..... 1172–80; disc. 1180
D-C Series Motor, Dynamic Braking of a Single. Leitch 149–54
Discharges, Field Research on Lightning Arrester. McCann, Beck ..... 625–9; disc. 629
Discharges in Insulated Cables, Internal Corona. Greenfield ..... 591–600; disc. 600
Disks: Driving and Damping Forces and Torques, Eddy Currents in. Moore ..... 1–10; disc. 10
Distance Relaying on 3-Phase Systems, Fundamental Basis for. Lewis, Tippett ..... 694–708; disc. 708
Distances, Theory and Application of Complex Logarithmic and Geometric Mean. Higgins 12–16
Distortion and Band-Width Characteristics of Pulse Modulation. Kraus, Ordung 984–8
Distortion in a Pulse Count Modulation System. Clavier, Panter, Grief ..... 989–1005; disc. 1005
(Distribution) Galloping Conductors and a Method for Studying Them. Tornquist, Becker ..... 1154–61; disc. 1161
Distribution in Textile Plants, Power. McConnell 659–62
(Distribution) Internal Corona Discharges in Insulated Cables. Greenfield ..... 591–600; disc. 600
(Distribution) Photographic Study of Lightning. Hagenguth ..... 577–83; disc. 583
(Distribution) Resistors for 138-Kv Cable Switching. Sadler, Blakeslee ..... 39–46; disc. 46
Division Techniques for a Coaxial Cable Network, Frequency. Crane, Dixon, Huber 1451–9
Double-Film Kydonograph With an Improved Coupling Method, A Simplified. Waghorne ..... 1114–16; disc. 1116
Drive for Aircraft, Electric. Crom 1359–62
Drives, A Control System for Wind Tunnel. Heidenreich ..... 1637–43; disc. 1643
Drives for Textile Finishing Ranges, Electric. Moore, Uhl 684–94
Drives, Rotating Stability Regulators for Synchronous Motor. Schaelchlin ..... 884–7; disc. 887
Driving and Damping Forces and Torques, Eddy Currents in Disks:. Moore ..... 1–10; disc. 10
Drop in the Welder Throat Loaded With Ferromagnetic Materials, The Voltage. Stein 356–62
Drum Brakes for PCC Cars, Recent Developments in Track Brakes and. Vouch 302–04
Dynamic Braking by Self-Excitation of Squirrel-Cage Motor. Srinivasan, Thomas 145–8
Dynamic Braking of a Single D-C Series Motor. Leitch 149–54
Dynamic Braking, The Design of New York Subway Motors for. Widell 808–10
Dynamic Brush Characteristics by the Dynamotor Method. Herman 759–63
Dynamometer for Small Motor Measurements, A High Precision. Duff ..... 1344–8; disc. 1348
Dynamotor Method, Dynamic Brush Characteristics by the. Herman 759–63

E

Echo Measurements on Telephone and Television Facilities, Pulse. Abraham, Lebert, Maggio, Schott ..... 541–8; disc. 548
Economic Supply of Energy in Hydroelectric Systems Factors in the. Frampton, Floyd ..... 1117–24; disc. 1124
Economical Fractional Horsepower Ratings, The Hysteresis Motor—Advances Which Permit. Roters ..... 1419–30; disc. 1430
Economically With the Gas or Diesel Bus Where No Overhead Facilities Exist?, Can the Trolley Coach Compete. Gaus ..... 264–8; disc. 268
Economics of Long-Distance A-C Power Transmission. Crary, Johnson ..... 1092–9; disc. 1099
Economies of Using Capacitors in Amounts to Require Automatic Switching, the. Butler ..... 322–7; disc. 327
Eddy Current Loss in Laminated Cores, Interlaminar. Beiler, Schmidt ..... 872–7; disc. 877
Eddy Currents in Disks: Driving and Damping Forces and Torques. Moore ..... 1–10; disc. 10
Effective Resistance of Isolated Nonmagnetic Rectangular Conductors. Dwight 549–52

Electric Boilers, Automatic Operation of. Eaton ..... 1061–8; disc. 1068
Electric Current into Rods, Tubes, and Flat Surfaces, Diffusion of. Miller 1496–1502
Electric Drive for Aircraft. Cron 1359–62
Electric Drives for Textile Finishing Ranges. Moore, Uhl 684–94
Electric Equipment for 2-for-1 Twister. Gwaltney, Burnham 811–14
Electric Equipment Required in a Modern 6-Component Wind-Tunnel Model Suspension System. Cox 1258–66
Electric Furnace Practice in Canada. Bailey 917–24
Electric Locomotives, A Power Plant Regulating System for Diesel-. Lewis ..... 242–6; disc. 246
(Electric Machinery) A Design Method for Capacitor Motors. Lloyd, Chang ..... 651–7; disc. 657
(Electric Machinery) A High Precision Dynamometer for Small Motor Measurements. Duff ..... 1344–8; disc. 1348
(Electric Machinery) A Study of the Relative Severity of Steep Front Waves and Chopped Waves on Transformers. Vogel ..... 64–6; disc. 66
(Electric Machinery) A Variable-Speed Constant-Frequency Generator. Roys, Nader, Spotts ..... 1414–17; disc. 1417
(Electric Machinery) Accuracy of Temperature Measurements on Coil Surfaces. Beede, Cain ..... 586–90; disc. 590
(Electric Machinery) Dynamic Brush Characteristics by the Dynamotor Method. Herman 759–63
(Electric Machinery) Equivalent Circuit of the Primitive Rotating Machine With Asymmetrical Stator and Rotor. Kron ..... 17–23; disc. 23
(Electric Machinery) High-Voltage Power-Transformer Design. Part II. Mallett ..... 1086–91; disc. 1091
(Electric Machinery) Hiperco—A Magnetic Alloy. Stanley, Yensen 714–18
(Electric Machinery) Interlaminar Eddy Current Loss in Laminated Cores. Beiler, Schmidt ..... 873–7; disc. 877
(Electric Machinery) Liquid Cooling of A-C Turbine Generators. Fechheimer ..... 553–61; disc. 561
(Electric Machinery) New NEMA Fractional-Horsepower Motor Standards; Their Effect on Refrigeration and Pump Applications. Potter 508–10
(Electric Machinery) Preliminary Report on Laboratory Aging Tests on Class A Insulation (Committee Report) ..... 879–81; disc. 881
(Electric Machinery) Short-Circuit Requirements for Transformers. Garin 710–13
(Electric Machinery) Silicone Insulation as Applied to Naval Electric Power Equipment. Walker ..... 977–80; disc. 980
(Electric Machinery) Simplified Graphical Method of Computing Thermal Transients. Narbutovskih ..... 78–81; disc. 82
(Electric Machinery) The "Copperspun" Squirrel Cage Rotor. Anderson 1312–14
(Electric Machinery) The Design and Performance of the Vertical Generator Thrust Bearings at the Bonneville Plant of the Corps of Engineers, War Department. Lewis, Gordon ..... 1231–7; disc. 1237
(Electric Machinery) The Dielectric Properties of Cellulose Insulation Impregnated With Semiconducting Liquids. Clark ..... 55–62; disc. 62
(Electric Machinery) The Equivalent Circuit of the Capacitor Motor. Chang 631–40
(Electric Machinery) The Horsepower Output of Polyphase Motors. Robinson 770–5
(Electric Machinery) The Hysteresis Motor—Advances Which Permit Economical Fractional Horsepower Ratings. Roters ..... 1419–30; disc. 1430
(Electric Machinery) The Magnetomotive Force of 2-Layer Windings of Rotating Machines. Stein 756–8
(Electric Machinery) The Multistage Rotoroll. Liwschitz 564–8
(Electric Machinery) The Transient-Energy Method of Calculating Stability. Magnusson ..... 747–55; disc. 755
(Electric Machinery) Typical Transformer Faults and Gas Detector Relay Protection. Madill ..... 1052–8; disc. 1058
Electric Power at Extra High Voltages, Transmission of. Sporn, Monteith ..... 1571–7; disc. 1577
Electric Power Equipment, Silicone Insulation as Applied to Naval. Walker ..... 977–80; disc. 980
Electric Power Protective Systems, Aircraft. Austin 1375–82
Electric Power Systems With Improved Instruments, Testing Governor Performance on. Allen, Hess ..... 329–39; disc. 339
(Electric Welding) Electrical Characteristics of Resistance Welding Tools. Callender 393–404
(Electric Welding) Functionalized Resistance Welding Control. Stadum, Large, Hartwig 414–18
(Electric Welding) The Voltage Drop in the Welder Throat Loaded With Ferromagnetic Materials. Stein 356–62
(Electric Welding) Voltage Changes Caused by Resistance Welding Loads. Johnson, Peterson, Rhoades ..... 664–73; disc. 674
Electrical Analogy, Dimensionless Analysis of Servomechanisms by. McCann, Herwald. Part I 111–18
Electrical Analogy, Solution of the General Voltage Regulator Problem by. Harder ..... 815–24; disc. 825
Electrical Characteristics of Resistance Welding Tools. Callender 393–404
Electrical Characteristics of the Junction in a Simplified Selenium Rectifier Cell. Angello 175–80
Electrical Utility Industry During World War II, The German. Noest ..... 1037–47; disc. 1047
Electricity in Hospital Operating Rooms, Hazards of Static. Williams ..... 1146–7; disc. 1147
Electrification of the Cotton Industry in the South. Bobe ..... 201–08; disc. 208
(Electrochemistry) Automatically Controlled Copper-Oxide Rectifiers for Electroplating and Anodizing Applications. Buckley 181–4
(Electrochemistry) Cathodic Protection of Steel Water Tanks Using Aluminum Anodes. Sudrabin, Mears 197–200
(Electrochemistry) Electrical Characteristics of the Junction in a Simplified Selenium Rectifier Cell. Angello 175–80
(Electrochemistry) Higher Voltage Copper-Oxide Rectifiers. Smith 220–2
Electrodynamic Instrument Mechanism, Applications of the. Corson, Millar 1131–6
Electromechanical System Development, Laboratory Aids for. Newton, White ..... 315–19; disc. 319
(Electrometallurgy) Cathodic Protection of Steel Water Tanks Using Aluminum Anodes. Sudrabin, Mears 197–200
(Electrometallurgy) Electrical Characteristics of the Junction in a Simplified Selenium Rectifier Cell. Angello 175–80
Electronic Constant-Current Motor Systems. Livingston ..... 425–30; disc. 430
Electronic Frequency Changers, Parallel Operation of Aircraft Alternators Using. Bowlus, Nims 31–8
Electronic Null Detectors for Use With Impedance Bridges. Lamson 535–40
Electronic Regenerative Repeater for Teletypewriter Signals, An. Hearn 904–11
Electronic Semiconductors, The Physics of. Pearson 209–14
Electronic Stabilizer for Power Transmission. Alexanderson, Prince ..... 950–3; disc. 953
Electronic Telemetering System. Foster, Kiefer 802–7
(Electronics) A Magnetic Compass With Cathode-Ray Sensing Element. Kliever, Syrdal 529–34
(Electronics) Air-Borne Magnetometers for Search and Survey. Felch, Means, Slonczewski, Parratt, Rumbaugh, Tickner 640–50
(Electronics) Arc-Back Testing of Graphite. Fakala, Cucullu 439–42
(Electronics) Ignitor Characteristics and Circuit Calculations. Marshall 1519–24
(Electronics) The Measurement of Acceleration With a Vacuum Tube. Ramberg 735–40
(Electronics) The Shunt Tube Control of Thyratron Rectifiers. Fowler 421–4
Electroplating and Anodizing Applications, Automatically Controlled Copper-Oxide Rectifiers for. Buckley 181–4
Element, A Magnetic Compass With Cathode-Ray Sensing. Kliever, Syrdal 529–34
Energy in Hydroelectric Systems, Factors in the Economic Supply of. Frampton, Floyd ..... 1117–24; disc. 1124
Energy Method of Calculating Stability, The Transient-. Magnusson ..... 747–55; disc. 755
Energy Regulating Systems, Two-Stage Rotoroll for Low-. Kimball 1507–11
Engineers, War Department, The Design and Performance of the Vertical Generator Thrust Bearings at the Bonneville Plant of the Corps of. Lewis, Gordon ..... 1231–7; disc. 1237
Equipment and Testing Methods for Cable Carrier Systems, New Test. Tidd, Rosen, Wenk 726–30
Equipment for Broadcast Stations, Television. Lawrence 443–52
Equipment for Tidd High-Voltage Test Lines, Switchgear. Lane, Wyman ..... 1619–21; disc. 1621
Equipment for 2-for-1 Twister, Electric. Gwaltney, Burnham 811–14
Equipment for New York City's Subway System, Modern Car. Cordts ..... 247–9; disc. 250
Equipment, Modern Railway Passenger-Car Auxiliary-Power. MacLeod, Hause 930–8
Equipment Required in a Modern 6-Component Wind-Tunnel Model Suspension System, Electric. Cox 1258–66
Equipment, Silicone Insulation as Applied to Naval Electric Power. Walker ..... 977–80; disc. 980
Equipment to Fractional Horsepower A-C Stator Windings, The Application of Surge Comparison Testing. Buchanan 1356–8
Equivalent Circuit of a Variable-Ratio Frequency Changer, Tensorial Analysis and. Kron 1503–06
Equivalent Circuit of the Capacitor Motor, The. Chang 631–40
Equivalent Circuit of the Primitive Rotating Machine With Asymmetrical Stator and Rotor. Kron ..... 17–23; disc. 23
Excitation Control Systems, Developments in Diesel-Electric Traction-Generator. Brancke, Adams ..... 223–8; disc. 228
Excitation of Squirrel-Cage Motor, Dynamic Braking by Self-. Srinivasan, Thomas 145–8
Excitation Problems in Hydroelectric Generators Supplying Long Transmission Lines. Killgore ..... 1277–82; disc. 1282
Exciting Current, Transient Voltage Rise in Transformers Due to Interruption of. Srinivasan, Vogel 1632–6
Expectancy as a Basis for Generator Reserve, Outage. Seelye 1483–8
Experience With Single-Pole Relaying and Reclosing on a Large 132-Kv System. Trainor, Parks ..... 405–11; disc. 411
Experiment at Cheyenne Wells, Colo., Rural Radiotelephone. Moore, Seyler, Wright 525–8
Extension of Impact Speed-Drop Analysis, An. Outage. Seelye 191–6

F

Facilities, Television Network. Abraham, Romnes 459–64
Factors in the Economic Supply of Energy in Hydroelectric Systems. Frampton, Floyd ..... 1117–24; disc. 1124
Faults and Gas Detector Relay Protection, Typical Transformer. Madill ..... 1052–8; disc. 1058
Faults, Transient Characteristics of Current Transformers During. Part II. Rothe, Concordia 731–4
Feed Regulator, A New Grinding Circuit. Jones 1240–2
Ferromagnetic Materials, The Voltage Drop in the Welder Throat Loaded With. Stein 356–62
Field Investigation of Lightning Surges at Substations. Gross, McCann ..... 569–74; disc. 574
Field Research on Lightning Arrester Discharges. McCann, Beck ..... 625–9; disc. 629
Fields in Air, Determination of Corona Starting Voltages for Nonuniform. Hutton ..... 1674–9; disc. 1680
Film Klydonograph With an Improved Coupling Method, A Simplified Double-. Waghorne ..... 1114–16; disc. 1116
Finishing Ranges, Electric Drives for Textile. Moore, Uhl 684–94
Flashover and Corona Correction on Small Ceramic Bushings, High Altitude. Pendleton 1324–30
Flaw Detectors, Design and Application of Supersonic. Erdman 1271–6
Force of 2-Layer Windings of Rotating Machines, The Magnetomotive. Stein 756–8
Forces and Torques, Eddy Currents in Disks: Driving and Damping. Moore ..... 1–10; disc. 10
Fractional-Horsepower Motor Standards; Their Effect on Refrigeration and Pump Applications, New NEMA. Potter 508–10
Fractional Horsepower Ratings, The Hysteresis Motor—Advances Which Permit Economical. Roters ..... 1419–30; disc. 1430
Frequency Changer, Suddenly Applied Loads on a Variable-Ratio. Carter, Maginnis, Rothe 1489–95
Frequency Changer, Tensorial Analysis and Equivalent Circuit of a Variable-Ratio. Kron 1503–06
Frequency Changers, Parallel Operation of Aircraft Alternators Using Electronic. Bowlus, Nims 31–8
Frequency Control of High-Speed Induction Motors, Adjustable. Heumann 719–25
Frequency Division Techniques for a Coaxial Cable Network. Crane, Dixon, Huber 1451–9
Frequency Generator, A Variable-Speed Constant-. Roys, Nader, Spotts ..... 1414–17; disc. 1417
Frequency-Modulated Television Relays, The Application of Heterodyne Modulation to Wide-Band. Boothroyd 1126–30
Frequency Modulation Telegraph Terminal Without Relays, A. Cusack, Michon ..... 1165–70; disc. 1170
Frequency Resistance of Coils, Data on the High-. Witzig 764–9
Frequency Shift Telegraphy—Radio and Wire Applications. Davey, Matte ..... 479–93; disc. 493
Fuel Gauges, Capacitance. Clark, Adolphe ..... 1189–96; disc. 1196
Fuel-Measurement System System for Aircraft, A Capacitance-Type. Pearson 1363–8
Functionalized Resistance Welding Control. Stadum, Large, Hartwig 414–18
Fundamental Basis for Distance Relaying on 3-Phase Systems. Lewis, Tippett ..... 694–708; disc. 708

Fundamentals of a Theory of the Transductor or Magnetic Amplifier, Some. Lamm.....1078–85
Furnace Practice in Canada, Electric. Balfour..917–24
Fusing on Rural Power Circuits, Sectionalizing and Internal Transformer. Watkins..383–8; disc. 388

G

Galloping Conductors and a Method for Studying Them. Tornquist, Becker.....1154–61; disc. 1161
Gap Reactance of Polyphase Machines, The Air. Alger, West.....1331–43
Gas Detector Relay Protection, Typical Transformer Faults and. Madill.....1052–8; disc. 1058
Gas or Diesel Bus Where No Overhead Facilities Exist?, Can the Trolley Coach Compete Economically With the. Gauss.....264–8; disc. 268
Gas Pressure for Telephone Cables. Giese.....471–8
Gaseous Insulation for High-Voltage Apparatus. Camilli, Chapman.....1463–9; disc. 1469
Gauges, Capacitance Fuel. Clark, Adolphe.....1189–96; disc. 1194
General Analysis of Speed Regulators Under Impact Loads. McCann, Osbon, Kirschbaum...1243–52
General Mobile Telephone System. Romines, O'Connor.....1658–66
Generating Capacity Outages, Calculating Probability of. Lyman.....1471–7; disc. 1477
Generating Capacity Problems of a Combined Hydro and Steam System, Probability Methods Applied to. Loane, Watchorn.....1645–54; disc. 1654
Generating Reserve Capacity Determined by the Probability Method. Calabrese.....1439–50
Generating Stations, Automatic Control of Hydroelectric. Brown, Derr.....343–55; disc. 355
Generating Units, The Maintenance of Hydroelectric. Robertson, Standing.....776–82
(Generation) Hydroelectric Power Development in Quebec. Lawton.....1006–21
Generation, Progress in Power—1940–46. (Committee Report).....1681–97
Generator, A Variable-Speed Constant-Frequency. Roys, Nader, Spotts.....1414–17; disc. 1417
Generator Excitation Control Systems, Developments in Diesel-Electric Traction-. Brancke, Adams.....223–8; disc. 228
Generator Power Center, D-C Aircraft. Bottemiller.....1267–70
Generator Reserve, Outage Expectancy as a Basis for. Seelye.....1483–8
Generator Thrust Bearings at the Bonneville Plant of the Corps of Engineers, War Department, The Design and Performance of the Vertical. Lewis, Gordon.....1231–7; disc. 1237
Generators, An Integrated Control System for Aircraft D-C. McClinton.....94–8
Generators, Liquid Cooling of A-C Turbine. Fechheimer.....553–61; disc. 561
Generators, Modern Bearing Practice for Vertical Water Wheel. Laffoon, Baudry.....363–9; disc. 369
Generators, Resynchronizing of. Concordia, Temnikobelskii.....1512–18
Generators Supplying Long Transmission Lines, Excitation Problems in Hydroelectric. Killgore.....1277–82; disc. 1282
Geometric Mean Distances, Theory and Application of Complex Logarithmic and. Higgins.....12–16
German Electrical Utility Industry During World War II, The. Noest.....1037–47; disc. 1047
Governor Performance on Electric Power Systems With Improved Instruments, Testing. Allen, Hess.....329–39; disc. 339
Graphical Method of Computing Thermal Transients, Simplified. Narbutovskih.....78–81; disc. 82
Graphite, Arc-Back Testing of. Pakala, Cucullu.....439–42
Grinding Circuit Feed Regulator, A New. Jones.....1240–2
Ground Power Supply for Modern Aircraft. Owen, Murray, Rosenstein.....1296–1303
Grounding of Instrument Transformer Secondary Circuits. (Committee Report).....419–20
Grounding Practices on Power Systems, Present-Day. (Committee Report).....1525–48; disc. 1548

H

Hardware for Tidd 500-Kv Test Lines, Insulators and Line. Gross, McCoy, Sheadel.....1592–1602; disc. 1602
Harmonics and the Equivalent Circuit of the Induction Motor, Leakage Reactance of the Squirrel Cage Rotor With Respect to the Stator. Liwschitz.....1407–08
Hazards of Static Electricity in Hospital Operating Rooms. Williams.....1146–7; disc. 1147
Heating—The Measurement of Loss Under Rising Temperature, Dielectric. Whitehead.....947–9
Heterodyne Modulation to Wide-Band Frequency-Modulated Television Relays, The Application of. Brothroyd.....1126–30
High Altitude Flashover and Corona Correction on Small Ceramic Bushings. Pendleton.....1324–30
High-Frequency Resistance of Coils, Data on the. Wittig.....764–9
High Q Cavities at 10,000 Megacycles, Measurement of Lange.....161–6
High Precision Dynamometer for Small Motor Measurements, A. Duff.....1344–8; disc. 1348
High-Speed Induction Motors, Adjustable Frequency Control of. Heumann.....719–25
High-Speed Service, Developments in Current Collectors for. Langer.....51–4
High-Temperature Railway Motor, Investigation of Silicone Insulation on. Grant, Kauppi, Moses.....305–10; disc. 310
High-Voltage Apparatus, Gaseous Insulation for. Camilli, Chapman.....1463–9; disc. 1469
High-Voltage Lines and Design Features of Tidd 500-Kv Test Lines, Corona Considerations on. Wagner, Wagner, Peterson, Gross..1583–90; disc. 1590
High-Voltage Power Transformer Design, Part II. Mallett.....1086–91; disc. 1091
High-Voltage Test Lines, Switchgear Equipment for. Lane, Wyman.....1619–21; disc. 1621
High Voltage, The Interruption of Charging Current at. Leeds, Van Sickle.....373–80; disc. 381
High-Voltage Transmission Lines, Switching. Johnson, Wilson.....1552–60; disc. 1560
High Voltages, A Simple and Inexpensive Method for Accurately Measuring Steady-State and Transient. Levinton.....1304–10; disc. 1310
High Voltages, Transmission of Electric Power at Extra. Sporn, Monteith.....1571–7; disc. 1577
Higher Voltage Copper-Oxide Rectifiers. Smith.....220–2
Hiperco—A Magnetic Alloy. Stanley, Yensen...714–8
Hoists, A Thrustor Lowering Control System for A-C Crane. Schwarz-Kast.....139–44; disc. 144
Horsepower A-C Stator Windings, The Application of Surge Comparison Testing Equipment to Fractional. Buchanan.....1356–8
Horsepower Diesel-Electric Locomotive for the Seaboard Air Line Railway, A 3,000. Staples, Waybrew, Atwell.....215–19
Horsepower Motor Standards; Their Effect on Refrigeration and Pump Applications, New NEMA Fractional-. Potter.....508–10
Horsepower Output of Polyphase Induction Motors, The. Robinson.....770–5
Horsepower Ratings, The Hysteresis Motor—Advances Which Permit Economical Fractional. Roters.....1419–30; disc. 1430
Hospital Operating Rooms, Hazards of Static Electricity in. Williams.....1146–7; disc. 1147
Hot-Line Insulator Washing, Tests and Developments in Connection With. Hill.....1203–16
Hydro and Steam System, Probability Methods Applied to Generating Capacity Problems of a Combined. Loane, Watchorn.....1645–54; disc. 1654
Hydroelectric Generating Stations, Automatic Control of. Brown, Derr.....343–55; disc. 355
Hydroelectric Generating Units, The Maintenance of. Robertson, Standing.....776–82
Hydroelectric Generators Supplying Long Transmission Lines, Excitation Problems in. Killgore.....1277–82; disc. 1282
(Hydroelectric) Modern Bearing Practice for Vertical Water Wheel Generators. Laffoon, Baudry.....363–9; disc. 369
Hydroelectric Power Development in Quebec. Lawton.....1006–21
Hydroelectric Systems, Factors in the Economic Supply of Energy in the. Frampton, Floyd.....1117–24; disc. 1124
Hysteresis Loop Tracer for Small Samples of Low-Permeability Material, A 60-Cycle. Wiegand, Hansen.....119–31; disc. 131
Hysteresis Motor—Advances Which Permit Economical Fractional Horsepower Ratings, The. Roters.....1419–30; disc. 1430

I

Ignition Crest Voltmeters, The Calibration of. Davis, Warren.....99–104; disc. 104
Ignitor Characteristic and Circuit Calculations. Marshall.....1519–24
Impact Loads, General Analysis of Speed Regulators Under. McCann, Osbon, Kirschbaum...1243–52
Impact Speed-Drop Analysis, An Extension of. Crever.....191–6
Impedance Bridges, Electronic Null Detectors for Use With. Lamson.....535–40
Impedance Relationships of the Adjustable-Speed A-C Brush-Shifting Motor. Baumann.....1460–2
Impregnated With Semiconducting Liquids, The Dielectric Properties of Cellulose Insulation. Clark.....59–62; disc. 62
Improved Automatic Circuit Recloser, An. Wallace.....255–8; disc. 259
Improved Cable Carrier, System, An. Black, Brooks, Wier, Wilson.....741–6; disc. 746
Improved Overcurrent Tripping Device for Low-Voltage Circuit Breakers, An. Rawlins, Sandin.....1149–53; disc. 1153
Indicating Instruments, Advancements in the Design of Long-Scale. Rowell, Millar.....155–60
Indicator for Sonar, Bearing Deviation. Schuck, Steedman, Hathaway, Butt.....1285–95
Induction Motor, Leakage Reactance of the Squirrel Cage Rotor With Respect to the Stator Harmonic and the Equivalent Circuit of the. Liwschitz.....1407–08
Induction Motors, Adjustable Frequency Control of High-Speed. Heumann.....719–25
Induction Motors, Reactances of Squirrel-Cage. Lloyd, Giusti, Chang.....1349–55
Induction Motors, Some Phases of Calculation of Leakage Reactance of. Liwschitz, Formhals.....1409–12; disc. 1412
Induction Motors, The Horsepower Output of Polyphase. Robinson.....770–5
Induction Motors to Chippers, The Application of Synchronous and. Baker, Lory.....1070–7
(Industrial Control) A Control System for Wind Tunnel Drives. Heidenreich.....1637–43; disc. 1643
(Industrial Control Devices) A Balanced Amplifier Using Biased Saturable Core Reactors. Kirschbaum, Harder.....273–8
(Industrial Control Devices) Adjustable Frequency Control of High-Speed Induction Motors. Heumann.....719–25
(Industrial Control Devices) Control of Slip-Ring Motors by Means of Unbalanced Primary Voltages. Schmitz.....1103–1112; disc. 1112
(Industrial Control Devices) Dynamic Braking of Two D-C Series Motors. Leitch.....787–91
(Industrial Control Devices) Rotating Stability Regulators for Synchronous Motor Drives. Schaelchlin.....884–7; disc. 887
(Industrial Control Devices) Some Fundamentals of a Theory of the Transductor or Magnetic Amplifier. Lamm.....1078–85
(Industrial Control Devices) A Thrustor Lowering Control System for A-C Crane Hoists. Schwarz-Kast.....139–44; disc. 144
(Industrial Control Devices) Dynamic Braking by Self-Excitation of Squirrel-Cage Motor. Srinivasan, Thomas.....145–8
(Industrial Control Devices) Dynamic Braking of a Single D-C Series Motor. Leitch.....149–54
(Industrial Control Devices) Shading Coil Calculations for Single-Phase Magnets. Evans..134–7; disc. 137
Industrial Control, Radar Technique in an. Cockrell.....269–72
(Industrial Power Applications) An Analysis of Motor Selection for Brass-Slab Rolling-Mill Service. Berkley.....185–9; disc. 189
(Industrial Power Applications) An Extension of Impact Speed-Drop Analysis. Crever.....191–6
(Industrial Power Applications) Electrification of the Cotton Industry in the South. Bobo.....201–08; disc. 208
(Industrial Power Applications) Power Distribution in Textile Plants. McConnell.....659–62
Industry During World War II, The German Electrical Utility. Noest.....1037–47; disc. 1047
Industry in the South, Electrification of the Cotton. Bobo.....201–08; disc. 208
Inexpensive Method for Accurately Measuring Steady-State and Transient High Voltages, A Simple and. Levinton.....1304–10; disc. 1310
Influence of 230-Kv Lines, Radio-Noise. Rorden.....677–81; disc. 682
Instrument Mechanism, Applications of the Electrodynamic. Corson, Millar.....1131–6
Instrument Transformer Secondary Circuits, Grounding of. (Committee Report).....419–20
Instrumentation and Measurement—Tidd 500-Kv Test Lines. Tremaine, Lippert....1624–30; disc. 1630
(Instruments) A Comparison of Two Basic Servomechanism Types. Harris.....83–92; disc. 92
(Instruments) A Polyphase Thermal Ampere-Demand Meter. Petzinger.....167–74
(Instruments) A Self-Balancing Capacitance Bridge. Foley.....797–801
(Instruments) A Simplified Double-Film Klydonograph With an Improved Coupling Method. Waghorne.....1114–16; disc. 1116
Instruments, Advancements in the Design of Long-Scale Indicating. Rowell, Millar.....155–60
(Instruments) Air-Borne Magnetometers for Search and Survey. Felch, Means, Slonczewski, Parratt, Rumbaugh, Tickner.....640–50
(Instruments) Capacitance Fuel Gauges. Clark, Adolphe.....1189–96; disc. 1196
(Instruments) Design and Application of Supersonic Flaw Detectors. Erdman.....1271–6

(Instruments) Direct Coupled Oscillograph Amplifier. Christian 1383–6
(Instruments, Electronic) Electronic Null Detectors for Use With Impedance Bridges. Larnson 535–40
(Instruments) Electronic Telemetering System. Foster, Kiefer 802–07
(Instruments) Metering With Transformer-Loss Compensators. Schleicher ..... 851–61; disc. 861
(Instruments) Quantitative Determination of Magnetic Properties by Use of Cathode-Ray Oscilloscope. Zamsky 783–7
Instruments, Testing Governor Performance on Electric Power Systems With Improved. Allen, Hess ..... 329–39; disc. 339
(Instruments) The Application of Lead Networks and Sinusoidal Analysis to Automatic Control Systems. Schwartz ..... 69–76; disc. 76
(Instruments) The Calibration of Ignition Crest Voltmeters. Davis, Warren ..... 99–104; disc. 104
(Instruments) The Cathode-Ray Spectrograph. Feldt, Berkley 105–10
Insulated Cables, Internal Corona Discharges in. Greenfield ..... 591–600; disc. 600
Insulation as Applied to Naval Electric Power Equipment, Silicone. Walker ..... 977–80; disc. 980
Insulation for High-Voltage Apparatus, Gaseous. Camilli, Chapman ..... 1463–9; disc. 1469
Insulation Impregnated With Semiconducting Liquids, The Dielectric Properties of Cellulose. Clark ..... 55–62; disc. 62
Insulation, Lightning and 60-Cycle Power Tests on Wood-Pole Line. Bellaschi ..... 838–47; disc. 847
Insulation on High-Temperature Railway Motor, Investigation of Silicone. Grant, Kauppi, Moses ..... 305–10; disc. 310
Insulation, Preliminary Report on Laboratory Aging Tests on Class A. (Committee Report) ..... 879–81; disc. 881
Insulator Washing, Tests and Developments in Connection With Hot-Line. Hill 1203–16
Insulators and Line Hardware for Tidd 500-Kv Test Lines. Gross, McCoy, Sheadel ..... 1592–1602; disc. 1602
Integrated Control System for Aircraft D-C Generators, An. McClinton 94–8
Interlaminar Eddy Current Loss in Laminated Cores. Beiler, Schmidt ..... 872–7; disc. 877
Internal Corona Discharges in Insulated Cables. Greenfield ..... 591–600; disc. 600
Internal Transformer Fusing on Rural Power Circuits, Sectionalizing and. Watkins ..... 383–8; disc. 388
Interrupters, Performance Criteria of D-C. Boehne, Jang ..... 1172–80; disc. 1180
Interruptions of Charging Current at High Voltage, The. Leeds, Van Sickle ..... 373–80; disc. 381
Investigation of Lightning Surges at Substations, Field. Gross, McCann ..... 569–74; disc. 574
Investigation of Silicone Insulation on High-Temperature Railway Motor. Grant, Kauppi, Moses ..... 305–10; disc. 310
Investigation on the 25-Kv System of the West Penn Power Company, Lightning. Bowen, Beck ..... 831–6; disc. 836
Isolated Nonmagnetic Rectangular Conductors, Effective Resistance of. Dwight 549–52

J

Joint Use of Pole Lines for Rural Power and Telephone Services. Campbell, Hill, Moore, Scholz ..... 519–24; disc. 524
Junction in a Simplified Selenium Rectifier Cell, Electrical Characteristics of the. Angello 175–80

K

Klydonograph With an Improved Coupling Method, A Simplified Double-Film. Waghorne ..... 1114–16; disc. 1116

L

Laboratory Aging Tests on Class A Insulation, Preliminary Report on. (Committee Report) ..... 879–81; disc. 881
Laboratory Aids for Electromechanical System Development. Newton, White ..... 315–19; disc. 319
Laminated Cores, Interlaminar Eddy Current Loss in. Beiler, Schmidt ..... 872–7; disc. 877
(Land Transportation) A Power Plant Regulating System for Diesel-Electric Locomotives. Lewis ..... 242–6; disc. 246
(Land Transportation) Modern Railway Passenger-Car Auxiliary-Power Equipment. MacLeod, Hause 930–8
(Land Transportation) Motor Control for Latest New York Transit System Subway Cars. Riley 900–03
(Land Transportation) Proposed Rapid Transit System for Toronto. Duncan 939–46
(Land Transportation) Special 10-Car Train for the New York City Transit System. Sinclair ..... 251–4; disc. 254
(Land Transportation) The Design of New York Subway Motors for Dynamic Braking. Widell 808–10
(Land Transportation) Trolley Coaches and PCC Street Cars Provide Successful City Transportation. Clardy 925–9
Layer Windings of Rotating Machines, The Magnetomotive Force of 2-. Stein 756–8
Lead Networks and Sinusoidal Analysis to Automatic Control Systems, The Application of. Schwartz ..... 69–76; disc. 76
Leakage Currents, Burning of Wood Structures by. Ross ..... 279–84; disc. 285
Leakage Reactance of Induction Motors, Some Phases of Calculation of. Liwschitz, Formhals ..... 1409–12; disc. 1412
Leakage Reactance of the Squirrel Cage Rotor With Respect to the Stator Harmonics and the Equivalent Circuit of the Induction Motor. Liwschitz 1407–08
Lighting, Airport Runway and Approach. Kevern 1396–9
Lightning and 60-Cycle Power Tests on Wood-Pole Line. Bellaschi ..... 838–47; disc. 847
Lightning Arrester Discharges, Field Research on. McCann, Beck ..... 625–9; disc. 629
Lightning Arresters—Tidd 500-Kv Test Lines, Transformers and. Lane, Hodnette, Bellaschi, Beck ..... 1613–18; disc. 1618
Lightning Investigation on the 25-Kv System of the West Penn Power Company. Bowen, Beck ..... 831–6; disc. 836
Lightning, Photographic Study of. Hagenguth ..... 577–83; disc. 583
Lightning Surges at Substations, Field Investigation of. Gross, McCann ..... 569–74; disc. 574
Line Carrier Channels, Operation of Power. Lenzner ..... 888–93; disc. 893
Line Conductors—Tidd 500-Kv Test Lines. Peterson, Simmons, Hickernell, Noyes ..... 1603–11; disc. 1611
Line Hardware for Tidd 500-Kv Test Lines, Insulators and. Gross, McCoy, Sheade. 1592–1602; disc. 1602
Line Insulation, Lightning and 60-Cycle Power Tests on Wood-Pole. Bellaschi ..... 838–47; disc. 847
Line Insulator Washing, Tests and Developments in Connection With Hot-. Hill 1203–16
Line Sectionalizing and Load Transfer, Automatic Control of Air Switches for. Rich, Kirwen ..... 293–9; disc. 299
Linear Servomechanisms, The Analysis and an Optimum Synthesis of. Herr, Gerst 959–70
Lines, A New Single-Side-Band Carrier System for Power. Lenehan ..... 826–30; disc. 830
Lines and Design Features of Tidd 500-Kv Test Lines, Corona Considerations on High-Voltage. Wagner, Wagner, Peterson, Gross ..... 1583–90; disc. 1590
Lines, Excitation Problems in Hydroelectric Generators Supplying Long Transmission. Kilgore ..... 1277–82; disc. 1282
Lines for Rural Power and Telephone Services, Joint Use of Pole. Campbell, Hill, Moore, Scholz ..... 519–24; disc. 424
Lines, Instrumentation and Measurement—Tidd 500-Kv Test. Tremaine, Lippert ..... 1624–30; disc. 1630
Lines, Insulators and Line Hardware for Tidd 500-Kv Test. Gross, McCoy, Sheadel ..... 1592–1602; disc. 1602
Lines, Performance of 161-Kv and 115-Kv Transmission. Hapgood, Almon ..... 863–9; disc. 869
Lines, Radio-Noise Influence of 230-Kv. Rorden ..... 677–81; disc. 682
Lines, Switchgear Equipment for Tidd High-Voltage Test. Lane, Wyman ..... 1619–21; disc. 1621
Lines, Switching High-Voltage Transmission. Johnson, Wilson ..... 1552–60; disc. 1560
Lines, Transformers and Lightning Arresters—Tidd 500-Kv Test. Lane, Hodnette, Bellaschi, Beck ..... 1613–18; disc. 1618
Liquid Cooling of A-C Turbine Generators. Fechheimer ..... 553–61; disc. 561
Liquids, The Dielectric Properties of Cellulose Insulation Impregnated With Semiconducting. Clark ..... 55–62; disc. 62
Load Transfer, Automatic Control of Air Switches for Line Sectionalizing and. Rich, Kirwen ..... 293–9; disc. 299
Loaded With Ferromagnetic Materials, The Voltage Drop in the Welder Throat. Stein 356–62
Loads, General Analysis of Speed Regulators Under Impact. McCann, Osborn, Kirschbaum 1243–52
Loads on a Variable-Ratio Frequency Changer, Suddenly Applied. Carter, Maginniss, Rothe 1489–95
Loads, Voltage Changes Caused by Resistance Welding. Johnson, Peterson, Rhoades ..... 664–73; disc. 674
Locomotive for the Seaboard Air Line Railway, A 3,000 Horsepower Diesel-Electric. Staples, Weybrew, Atwell 815–19
Locomotive, A Power Plant Regulating System for Diesel-Electric. Lewis ..... 242–6; disc. 246
Locomotives, Braking Resistors and Control for Diesel Electric. Weiser 229–32
Locomotives, Developments in Control Systems for Diesel-Electric. Henshaw 235–41
Logarithmic and Geometric Mean Distances, Theory and Application of. Higgins 12–16
Long-Distance A-C Power Transmission, Economics of. Crary, Johnson ..... 1092–9; disc. 1099
Long-Scale Indicating Instruments, Advancements in the Design of. Rowell, Millar 155–60
Loop Tracer for Small Samples of Low-Permeability Material, A 60-Cycle Hysteresis. Wiegand, Hansen ..... 119–31; disc. 131
Loss Compensators, Metering With Transformer-. Schleicher ..... 851–61; disc. 861
Loss in Laminated Cores, Interlaminar Eddy Current. Beiler, Schmidt ..... 872–7; disc. 877
Loss Under Rising Temperature, Dielectric Heating—The Measurement of. Whitehead 947–9
Low-Energy Regulating Systems, Two-Stage Rotorol for. Kimball 1507–11
Lowering Control System for A-C Crane Hoists, A Thrustor. Schwarz-Kast ..... 139–44; disc. 144
Low-Permeability Material, A 60-Cycle Hysteresis Loop Tracer for Small Samples of. Wiegand, Hansen ..... 119–31; disc. 131
Low-Voltage Air Circuit Breakers, Selective Tripping of. Deans ..... 971–6; disc. 976
Low-Voltage Circuit Breakers, An Improved Overcurrent Tripping Device for. Rawlins, Sandin ..... 1149–53; disc. 1153

M

Machine Computation of Power Network Performance. Dunstan ..... 610–20; disc. 621
(Machine Tools) The Application of Synchronous and Induction Motors to Chippers. Baker, Lory 1070–7
Machine With Asymmetrical Stator and Rotor, Equivalent Circuit of the Primitive Rotating. Kron ..... 17–25; disc. 23
Machines, The Air Gap Reactance of Polyphase. Alger, West 1331–45
Machines, The Magnetomotive Force of 2-Layer Windings of Rotating. Stein 756–8
Magnetic Alloy, Hiperco—A. Stanley, Yensen 714–18
Magnetic Amplifier, Some Fundamentals of a Theory of the Transductor or. Lamm 1078–85
Magnetic Compass With Cathode-Ray Sensing Element, A. Kliever, Syrdal 529–34
Magnetic Properties by Use of Cathode-Ray Oscilloscope, Quantitative Determination of. Zamsky 783–7
Magnetometers for Search and Survey, Air-Borne. Felch, Means, Slonczewski, Parratt, Rumbaugh, Tickner 640–50
Magnetomotive Force of 2-Layer Windings of Rotating Machines, The. Stein 756–8
Magnets, Shading Coil Calculations for Single-Phase. Evans ..... 134–7; disc. 137
Maintenance of Hydroelectric Generating Units, The. Robertson, Standing 776–82
Material, A 60-Cycle Hysteresis Loop Tracer for Small Samples of Low-Permeability. Wiegand, Hansen ..... 119–31; disc. 131
Materials, The Voltage Drop in the Welder Throat Loaded With Ferromagnetic. Stein 356–62
Mean Distances, Theory and Application of Complex Logarithmic and Geometric. Higgins 12–16
Measuring Steady-State and Transient High Voltages, A Simple and Inexpensive Method for Accurately. Levinton ..... 1304–10; disc. 1310
Measurement of Acceleration With a Vacuum Tube, The. Ramberg 735–40
Measurement of High Q Cavities at 10,000 Megacycles. Lange 161–6
Measurement of Loss Under Rising Temperature, Dielectric Heating—. Whitehead 947–9
Measurement System for Aircraft, A Capacitance-Type Fuel-. Pearson 1363–8
Measurement—Tidd 500-Kv Test Lines, Instrumentation and. Tremaine, Lippert ..... 1624–30; disc. 1630
Measurements, A High Precision Dynamometer for Small Motor. Duff ..... 1344–8; disc. 1348
(Measurements) A Polyphase Thermal Ampere-Demand Meter. Petzinger 167–74
Measurements During Reignition and Recovery, Circuit-Breaker Current. Lewis ..... 1253–7; disc. 1257
(Measurements) Metering With Transformer-Loss Compensators. Schleicher ..... 851–61; disc. 861
Measurements on Coil Surfaces, Accuracy of Temperature. Beeds, Cain ..... 586–90; disc. 590
Measurements on Telephone and Television Facilities, Pulse Echo. Abraham, Lebert, Maggio, Schott ..... 541–8; disc. 548
Mechanism, Applications of the Electrodynamic Instrument. Corson, Millar 1131–6
Megacycles, Measurement of High Q Cavities at 10,000. Lange 161–6

Meter, A Polyphase Thermal Ampere-Demand. Petzinger 167–74
Metering With Transformer-Loss Compensators. Schlecher ..... 851–61; disc. 861
Method, A Simplified Double-Film Klydonograph With an Improved Coupling. Waghorne ..... 1114–16; disc. 1116
Method, Dynamic Brush Characteristics by the Dynamotor. Hermaa 759–63
Method for Accurately Measuring Steady-State and Transient High Voltages, A Simple and Inexpensive. Levinton ..... 1304–10; disc. 1310
Method for Capacitor Start Motors, A Design. Chang 1369–74
Method for Studying Them, Galloping Conductors and a. Tornquist, Becker ..... 1154–61; disc. 1161
Method, Generating Reserve Capacity Determined by the Probability. Calabrese 1439–50
Method of Calculating Stability, The Transient-Energy. Magnuson ..... 747–55; disc. 755
Method of Computing Thermal Transients, Simplified Graphical. Narbutovskih ..... 78–81; disc. 82
Methods Applied to Generating Capacity Problems of a Combined Hydro and Steam System, Probability. Loane, Watchorn ..... 1645–54; disc. 1654
Methods for Cable Carrier Systems, New Test Equipment and Testing. Tidd, Rosen, Wenk 726–30
Microwave Television System, A New. Wentz, Smith 465–70
(Mining) A New Grinding Circuit Feed Regulator. Jones 1240–2
Mobile Telephone System, General. Romors, O'Connor 1658–66
Model Suspension System, Electric Equipment Required in a Modern 6-Component Wind-Tunnel. Cox 1258–66
Modern Aircraft, Ground Power Supply for. Owen, Murray, Rosenstein 1296–1303
Modern Bearing Practice for Vertical Water Wheel Generators. Laffoon, Baudry ..... 363–9; disc. 369
Modern Car Equipment for New York City's Subway System. Cordts ..... 247–9; disc. 250
Modern Railway Passenger-Car Auxiliary-Power Equipment. MacLeod, Hause 930–8
Modern Techniques in Ocean Cable Telegraphy, Some. Cramer ..... 494–500; disc. 500
Modulation, Distortion and Band-Width Characteristics of Pulse. Krauss, Ordung 984–8
Modulation in Communication. Cowan 792–6
Modulation, Pulse Code. Black, Edson 895–9
Modulation System, Distortion in a Pulse Count. Clavier, Panter, Grieg ..... 989–1005; disc. 1005
Modulation Telegraph Terminal Without Relays, A Frequency. Cusack, Michon ..... 1165–70; disc. 1170
Modulation to Wide-Band Frequency Modulated Television Relays, The Application of Heterodyne. Boothroyd 1126–30
Motor—Advances Which Permit Economical Fractional Horsepower Ratings, The Hysteresis. Roters ..... 1419–30; disc. 1430
Motor Control for Latest New York Transit System Subway Cars. Riley 900–03
Motor Drives, Rotating Stability Regulators for Synchronous. Schaelchlin ..... 884–7; disc. 887
Motor, Dynamic Braking by Self-Excitation of Squirrel-Cage. Srinivasan, Thomas 145–8
Motor, Dynamic Braking of a Single D-C Series. Leitch 149–54
Motor, Impedance Relationships of the Adjustable-Speed A-C Brush-Shifting. Baumann 1460–2
Motor, Investigation of Silicone Insulation on High-Temperature Railway. Grant, Kauppi, Moses ..... 305–10; disc. 310
Motor, Leakage Reactance of the Squirrel Cage Rotor With Respect to the Stator Harmonics and the Equivalent Circuit of the Induction. Liwschitz 1407–08
Motor Measurements, A High Precision Dynamometer for Small. Duff ..... 1344–8; disc. 1348
Motor, (Schrage Type), The Circle Diagram of the Polyphase Brush-Shifting Commutator. Franklin ..... 1667–72; disc. 1672
Motor Selection for Brass-Slab Rolling-Mill Service, An Analysis of. Berkley ..... 185–9; disc. 189
Motor Standards; Their Effect on Refrigeration and Pump Applications, New NEMA Fractional-Horsepower. Potter 508–10
Motor Systems, Electronic Constant-Current. Livingston ..... 425–30; disc. 430
Motor, The Equivalent Circuit of the Capacitor, Chang 631–40
Motors, A Design Method for Capacitor. Lloyd, Chang ..... 651–7; disc. 657
Motors, A Design Method for Capacitor Start. Chang 1369–74
Motors, Adjustable Frequency Control of High-Speed Induction. Heumann 719–25
Motors by Means of Unbalanced Primary Voltages, Control of Slip-Ring. Schmitz ..... 1103–1112; disc. 1112
Motors, Dynamic Braking of Two D-C Series. Leitch 787–91
Motors for Dynamic Braking, The Design of New York Subway. Widell 808–10
Motors, Performance Calculations on Shaded Pole. Trickey ..... 1431–8; disc. 1438
Motors, Reactances of Squirrel-Cage Induction. Lloyd, Giusti, Chang 1349–55
Motors, Some Phases of Calculation of Leakage Reactance of Induction. Liwschitz, Formhals ..... 1409–12; disc. 1412
Motors, The Horsepower Output of Polyphase Induction. Robinson 770–5
Motors to Chippers, The Application of Synchronous and Induction. Baker, Lory 1070–7
Multiplex to Navy Radio, The Application of Western Union. Hoover 1478–82
Multistage Rototrol, The. Liwschitz 564–8

N

Naval Electric Power Equipment, Silicone Insulation as Applied to. Walker ..... 977–80; disc. 980
Navy Radio, The Application of Western Union Multiplex to. Hoover 1478–82
NEMA Fractional-Horsepower Motor Standards; Their Effect on Refrigeration and Pump Applications, New. Potter 508–10
Network Facilities, Television. Abraham, Romnes 459–64
Network, Frequency Division Techniques for a Coaxial Cable. Crane, Dixon, Huber 1451–9
Network Performance, Machine Computation of Power. Dunstan ..... 610–20; disc. 621
Networks and Sinusoidal Analysis to Automatic Control Systems, The Application of Lead. Schwartz ..... 69–76; disc. 76
New York City Transit System, Special 10-Car Train for the. Sinclair ..... 251–4; disc. 254
New York City's Subway System, Modern Car Equipment for. Cordts ..... 247–9; disc. 250
New York Subway Motors for Dynamic Braking, The Design of. Widell 808–10
New York Transit System Subway Cars, Motor Control for Latest. Riley 900–03
Noise Influence of 230-Kv Lines, Radio. Rordes ..... 677–81; disc. 682
Nonmagnetic Rectangular Conductors, Effective Resistance of Isolated. Dwight 549–52
Null Detectors for Use With Impedance Bridges, Electronic. Lamson 535–40

O

Ocean Cable Telegraphy, Some Modern Techniques in. Cramer ..... 494–500; disc. 500
Officers and Committees for 1947–48, AIEE 1724–37
132-Kv System, Experience With Single-Pole Relaying and Reclosing on a Large. Trainor, Parks ..... 405–11; disc. 411
Operating Rooms, Hazards of Static Electricity in Hospital. Williams ..... 1146–7; disc. 1147
Operation of Aircraft Alternators Using Electronic Frequency Changers, Parallel. Bowlus, Nims 31–8
Operation of Electric Boilers, Automatic. Eaton ..... 1061–8; disc. 1068
Operation of Power Line Carrier Channels. Lenner ..... 888–93; disc. 893
Optimum Synthesis of Linear Servomechanisms, The Analysis and an. Herr, Gerst 959–70
Oscillograph Amplifier, Direct Coupled. Christian 1383–6
Oscilloscope, Quantitative Determination of Magnetic Properties by Use of Cathode-Ray. Zamsky 783–7
Outage Expectancy as a Basis for Generator Reserve. Seelye 1483–8
Outages, Calculating Probability of Generating Capacity. Lyman ..... 1471–7; disc. 1477
Output of Polyphase Induction Motors, The Horsepower. Robinson 770–5
Overcurrent Tripping Device for Low-Voltage Circuit Breakers, An Improved. Rawlins, Sandin ..... 1149–53; disc. 1153
Overhead Facilities Exist?, Can the Trolley Coach Compete Economically With the Gas or Diesel Bus Where No. Gauss ..... 264–8; disc. 268
Oxide Rectifiers for Electroplating and Anodizing Applications, Automatically Controlled Copper-. Buckley 181–4

P

Paper Dielectric Capacitors, The Probable Breakdown Voltage of. Brooks ..... 1137–44; disc. 1144
(Paper) Preliminary Report on Laboratory Aging Tests on Class A Insulation. (Committee Report) ..... 879–81; disc. 881
Parallel Operation of Aircraft Alternators Using Electronic Frequency Changers. Bowlus, Nims 31–8
Passenger-Car Auxiliary-Power Equipment, Modern Railway. MacLeod, Hause 930–8
PCC Car, Some Recent Developments in the. Cooper ..... 288–92; disc. 292
PCC Cars, Recent Developments in Track Brakes and Drum Brakes for. Vouch 302–04
PCC Street Cars Provide Successful City Transportation, Trolley Coaches and. Clardy 925–9
Performance Calculations on Shaded Pole Motors. Trickey ..... 1431–8; disc. 1438
Performance Criteria of D-C Interrupters. Boehne, Jang ..... 1172–80; disc. 1180
Performance, Machine Computation of Power Network. Dunstan ..... 610–20; disc. 621
Performance of 161-Kv and 115-Kv Transmission Lines. Hapgood, Almon ..... 863–9; disc. 869
Performance of the Vertical Generator Thrust Bearings at the Bonneville Plant of the Corps of Engineers, War Department, The Design and. Lewis, Gordon ..... 1231–7; disc. 1237
Performance on Electric Power Systems With Improved Instruments, Testing Governor. Allen, Hess ..... 329–39; disc. 339
Permeability Material, A 60-Cycle Hysteresis Loop Tracer for Small Samples of Low-. Wiegand, Hansen ..... 119–31; disc. 131
Phases of Calculation of Leakage Reactance of Induction Motors, Some. Liwschitz, Formhals ..... 1409–12; disc. 1412
Photographic Study of Lightning. Hagenguth ..... 577–83; disc. 583
Physics of Electronic Semiconductors, The. Pearson 209–14
Plant Regulating System for Diesel-Electric Locomotives, A Power. Lewis ..... 242–6; disc. 246
Pole Lines for Rural Power and Telephone Services, Joint Use of. Campbell, Hill, Moore, Scholz ..... 519–24; disc. 424
Pole Motors, Performance Calculations on Shaded. Trickey ..... 1431–8; disc. 1438
Pole Relaying and Reclosing on a Large 132-Kv System, Experience With Single-. Trainor, Parks ..... 405–11; disc. 411
Policy Becomes Effective in January 1947, New AIEE Publication 1721–3
Polyphase Brush-Shifting Commutator Motor, (Schrage Type), The Circle Diagram of the. Franklin ..... 1667–72; disc. 1672
Polyphase Induction Motors, The Horsepower Output of. Robinson 770–5
Polyphase Machines, The Air Gap Reactance of. Alger, West 1331–43
Polyphase Thermal Ampere-Demand Meter, A. Petzinger 167–74
Postwar Television Receiver Design. Pugsley 453–8
Power and Telephone Services, Joint Use of Pole Lines for Rural. Campbell, Hill, Moore, Scholz ..... 519–24; disc. 524
(Power Applications) Data on the High-Frequency Resistance of Coils. Witzig 764–9
(Power Applications) Electric Drives for Textile Finishing Ranges. Moore, Uhl 684–94
(Power Applications, Industrial) An Analysis of Motor Selection for Brass-Slab Rolling-Mill Service. Berkley ..... 185–9; disc. 189
(Power Applications, Industrial) An Extension of Impact Speed-Drop Analysis. Crever 191–6
(Power Applications, Industrial) Automatic Operation of Electric Boilers. Eaton ..... 1061–8; disc. 1068
(Power Applications, Industrial) Dielectric Heating—The Measurement of Loss Under Rising Temperature. Whitehead 947–9
(Power Applications, Industrial) Electric Equipment for 2-for-1 Twister. Gwaltney, Burnham 811–4
(Power Applications, Industrial) Electric Furnace Practice in Canada 917–24
(Power Applications, Industrial) Electrification of the Cotton Industry in the South. Bobe ..... 201–08; disc. 208
Power at Extra High Voltages, Transmission of Electric. Sporn, Monteith ..... 1571–7; disc. 1577
Power Center, D-C Aircraft Generator. Bottemiller 1267–70
Power Circuits, Sectionalizing and Internal Transformer Fusing on Rural. Watkins ..... 383–8; disc. 388
Power Development in Quebec, Hydroelectric. Lawton 1006–21
Power Distribution in Textile Plants. McConnell 659–62
Power Equipment, Modern Railway Passenger-Car Auxiliary-. MacLeod, Hause 930–8
Power Equipment, Silicone Insulation as Applied to Naval Electric. Walker ..... 977–80; disc. 980
(Power Generation) Automatic Control of Hydroelectric Generating Stations. Brown, Derr ..... 343–55; disc. 355
(Power Generation) Calculating Probability of Generating Capacity Outages. Lyman ..... 1471–7; disc. 1477
(Power Generation) Excitation Problems in Hydroelectric Generators Supplying Long Transmission Lines. Killgore ..... 1277–82; disc. 1282

(Power Generation) Factors in the Economic Supply of Energy to Hydroelectric Systems. Frampton, Floyd....1117–24; disc. 1124
(Power Generation) Generating Reserve Capacity Determined by the Probability Method. Calabrese....1439–50
(Power Generation) Modern Bearing Practice for Vertical Water Wheel Generators. Laffoon, Baudry....363–9; disc. 369
Power Generation—1940–46, Progress in. (Committee Report)....1681–97
(Power Generation) Outage Expectancy as a Basis for Generator Reserve. Seelye....1483–8
(Power Generation) Probability Methods Applied to Generating Capacity Problems of a Combined Hydro and Steam System. Loane, Watchorn....1645–54; disc. 1654
(Power Generation) Resynchronizing of Generators. Concordia, Temoshok....1512–18
(Power Generation) Suddenly Applied Loads on a Variable-Ratio Frequency Changer. Carter, Maginnis, Rothe....1489–95
(Power Generation) Tensorial Analysis and Equivalent Circuit of a Variable-Ratio Frequency Changer. Kron....1503–06
(Power Generation) Testing Governor Performance on Electric Power Systems With Improved Instruments. Allen, Hess....329–39; disc. 339
(Power Generation) The Design and Performance of the Vertical Generator Thrust Bearings at the Bonneville Plant of the Corps of Engineers, War Department. Lewis, Gordon....1231–7; disc. 1237
(Power Generation) The German Electrical Utility Industry During World War II. Noest....1037–47; disc. 1047
(Power Generation) The Maintenance of Hydroelectric Generating Units....776–82
(Power Generation) The Transient-Energy Method of Calculating Stability. Magnusson....747–55; disc. 755
(Power Generation) Theoretical Approach to Speed and Tie Line Control. Brandt....24–9; disc. 29
Power Line Carrier Channels, Operation of. Lessner....888–93; disc. 893
Power Lines, A New Single-Side-Band Carrier System for. Lenehan....826–30; disc. 830
Power Network Performance, Machine Computation of. Dunstan....610–20; disc. 621
Power Plant Regulating System for Diesel-Electric Locomotives, A. Lewis....242–6; disc. 246
Power Protective Systems, Aircraft Electric. Austin....1375–82
Power Supply for Modern Aircraft, Ground. Owen, Murray, Rosenstein....1296–1303
(Power System Applications) Operation of Power Line Carrier Channels. Lessner....889–93; disc. 893
(Power System Application) TVA Co-ordinated Communication System. Talmage....1022–34; disc. 1034
Power Systems for Aircraft Window Deicing, Control and. Mershon....1400–05
Power Systems, Present-Day Grounding Practices on. (Committee Report)....1525–48; disc. 1548
Power Systems With Improved Instruments, Testing Governor Performance on Electric. Allen, Hess....329–39; disc. 339
Power Tests on Wood-Pole Line Insulation, Lightning and 60-Cycle. Bellaschi....838–47; disc. 847
Power-Transformer Design, High-Voltage. Part II. Mallett....1086–91; disc. 1091
Power Transformers, Relay Protection of. (Committee Report)....911–15; disc. 915
Power Transmission, Economics of Long-Distance A-C. Crary, Johnson....1092–9; disc. 1099
Power Transmission, Electronic Stabilizer for. Alexanderson, Prince....950–3; disc. 953
Practices on Power Systems, Present-Day Grounding. (Committee Report)....1525–48; disc. 1548
Precision Dynamometer for Small Motor Measurements. A High. Duff....1344–8; disc. 1348
Preliminary Report on Laboratory Aging Tests on Class A Insulation. (Committee Report)....879–81; disc. 881
Present-Day Grounding Practices on Power Systems. (Committee Report)....1525–48; disc. 1548
Pressure for Telephone Cables, Gas. Giese....471–8
Primary Voltages, Control of Slip-Ring Motors by Means of Unbalanced. Schmitz....1103–1112; disc. 1112
Primitive Rotating Machine With Asymmetrical Stator and Rotor, Equivalent Circuit of the. Kron....17–23; disc. 23
Probability Method, Generating Reserve Capacity Determined by the. Calabrese....1439–50
Probability Methods Applied to Generating Capacity Problems of a Combined Hydro and Steam System. Loane, Watchorn....1645–54; disc. 1654
Probable Breakdown Voltage of Paper Dielectric Capacitors, The. Brooks....1137–44; disc. 1144
Problems in Hydroelectric Generators Supplying Long Transmission Lines, Excitation. Kilgore....1277–82; disc. 1282
Problems of a Combined Hydro and Steam System, Probability Methods Applied to Generating Capacity. Loane, Watchorn....1645–54; disc. 1654
(Proceedings) New AIEE Publication Policy Becomes Effective in January 1947....172)–3
Progress in Power Generation—1940–46. (Committee Report)....1681–97
Properties by Use of Cathode-Ray Oscilloscope, Quantitative Determination of Magnetic. Zamsky....783–7
Properties of Cellulose Insulation Impregnated With Semiconducting Liquids, The Dielectric. Clark....55–62; disc. 62
Proposed Rapid Transit System for Toronto. Duncan....939–46
Protection of Power Transformers, Relay. (Committee Report)....911–15; disc. 915
Protection of Steel Water Tanks Using Aluminum Anodes, Cathodic. Sudrabin, Mears....197–200
Protection, Typical Transformer Faults and Gas Detector Relay. Madill....1052–8; disc. 1058
(Protective Devices) An Improved Automatic Circuit Recloser. Wallace....255–8; disc. 259
(Protective Devices) An Improved Overcurrent Tripping Device for Low-Voltage Circuit Breakers. Rawlins, Sandin....1149–53; disc. 1153
(Protective Devices) Circuit-Breaker Current Measurements During Reignitions and Recovery. Lewis....1253–7; disc. 1257
(Protective Devices) Field Investigation of Lightning Surges at Substations. Gross, McCann....569–74; disc. 574
(Protective Devices) Field Research on Lightning Arrester Discharges. McCann, Beck....625–9; disc. 629
(Protective Devices) Grounding of Instrument Transformer Secondary Circuits. (Committee Report)....419–20
(Protective Devices) Lightning Investigation on the 25-Kv System of the West Penn Power Company. Bowen, Beck....831–6; disc. 836
(Protective Devices) Performance Criteria of D-C Interrupters. Bodine, Jang....1172–80; disc. 1180
(Protective Devices) Present-Day Grounding Practices on Power Systems. (Committee Report)....1525–48; disc. 1548
(Protective Devices) Resistors for 138-Kv Cable Switching. Sadler, Blakeslee....39–46; disc. 46
(Protective Devices) Sectionalizing and Internal Transformer Fusing on Rural Power Circuits. Watkins....383–8; disc. 388
(Protective Devices) Selective Tripping of Low-Voltage Air Circuit Breakers. Deans....971–6; disc. 976
(Protective Devices) The Interruption of Charging Current at High Voltage. Leeds, Van Sickle....373–80; disc. 381
(Protective Devices) Transient Characteristics of Current Transformers During Faults. Part II. Rothe, Concordia....731–4
Protective Systems, Aircraft Electric Power. Austin....1375–82
Publication Policy Becomes Effective in January 1947, New AIEE....1721–3
Pulse Code Modulation. Black, Edson....895–9
Pulse Count Modulation System, Distortion in a. Clavier, Panter, Grieg....989–1005; disc. 1005
Pulse Echo Measurements on Telephone and Television Facilities. Abraham, Lebert, Maggio, Schott....541–8; disc. 548
Pulse Modulation, Distortion and Band-Width Characteristics of. Krauss, Ordung....984–8
Pump Applications, New NEMA Fractional-Horsepower Motor Standards; Their Effect on Refrigeration and. Potter....508–10

Q

Q-Cavities at 10,000 Megacycles, Measurement of High. Lange....161–6
Quantitative Determination of Magnetic Properties by Use of Cathode-Ray Oscilloscope. Zamsky....783–7
Quebec, Hydroelectric Power Development in. Lawton....1006–21

R

Radar Technique in an Industrial Control. Cockrell....269–72
Radar to Increase Airline Safety, Using Airborne. Ayer....1387–95
Radio and Wire Applications, Frequency Shift Telegraphy—. Davey, Matte....479–93; disc. 493
Radio-Noise Influence of 230-Kv Lines. Rorden....677–81; disc. 682
Radiotelephone Experiment at Cheyenne Wells, Colo., Rural. Moore, Seyler, Wright....525–8
Radio, The Application of Western Union Multiplex to Navy. Hoover....1478–82
Railway, A 3,000 Horsepower Diesel-Electric Locomotive for the Seaboard Air Line. Staples, Weybrew, Atwell....215–19
Railway Motor, Investigation of Silicone Insulation on High-Temperature. Grant, Kauppi, Moses....305–10; disc. 310
Railway Passenger-Car Auxiliary-Power Equipment, Modern. MacLeod, Hause....930–8
Ranges, Electric Drives for Textile Finishing. Moore, Uhl....684–94
Rapid Transit System for Toronto, Proposed. Duncan....939–46
Ratings, The Hermetic Motor—Advances Which Permit Economical Fractional Horsepower. Roters....1419–30; disc. 1430
Ratio Frequency Changer, Suddenly Applied Loads on a Variable-. Carter, Maginnis, Rothe....1489–95
Ratio Frequency Changer, Tensorial Analysis and Equivalent Circuit of a Variable-. Kron....1503–06
Ray Spectrograph, The Cathode-. Feldt, Berkley....105–10
Reactance of Induction Motors, Some Phases of Calculation of Leakage. Liwschitz, Formhals....1409–12; disc. 1412
Reactance of Polyphase Machines, The Air Gap. Alger, West....1331–43
Reactance of the Squirrel Cage Rotor With Respect to the Stator Harmonics and the Equivalent Circuit of the Induction Motor, Leakage. Liwschitz....1407–08
Reactances of Squirrel-Cage Induction Motors. Lloyd, Giusti, Chang....1349–55
Reactors, A Balanced Amplifier Using Biased Saturable Core. Kirschbaum, Harder....273–8
Receiver Design, Postwar Television. Pugsley....453–8
Recent Developments in the PCC Car, Some. Cooper....288–92; disc. 292
Recent Developments in Track Brakes and Drum Brakes for PCC Cars. Vouch....302–04
Recloser, An Improved Automatic Circuit. Wallace....255–8; disc. 259
Reclosing on a Large 132-Kv System, Experience With Single-Pole Relaying and. Trainor, Parks....405–11; disc. 411
Recovery, Circuit-Breaker Current Measurements During Reignitions and. Lewis....1253–7; disc. 1257
Rectangular Conductors, Effective Resistance of Isolated Nonmagnetic. Dwight....549–52
Rectifier Cell, Electrical Characteristics of the Junction in a Simplified Selenium. Angello....175–80
Rectifiers for Electroplating and Anodizing Applications, Automatically Controlled Copper-Oxide. Buckley....181–4
Rectifiers, Higher Voltage Copper-Oxide. Smith....220–2
Rectifiers, The Shunt Tube Control of Thyratron. Potter....421–4
Refrigeration and Pump Applications, New NEMA Fractional-Horsepower Motor Standards; Their Effect on. Potter....508–10
Regulating System for Diesel-Electric Locomotives, A Power Plant. Lewis....242–6; disc. 246
Regulating Systems, Two-Stage Rototrol for Low-Energy. Kimball....1507–11
Regulator, A New Grinding Circuit Feed. Jones....1240–2
Regulator Problem by Electrical Analogy, Solution of the General Voltage. Harder....815–25; disc. 825
Regulators for Synchronous Motor Drives, Rotating Stability. Schaelchlin....884–7; disc. 887
Regulators Under Impact Loads, General Analysis of Speed. McCann, Osbon, Kirchbaum....1243–52
Reignitions and Recovery, Circuit-Breaker Current Measurements During. Lewis....1253–7; disc. 1257
Relative Severity of Steep Front Waves and Chopped Waves on Transformers, A Study of the. Vogel....64–6; disc. 66
Relationships of the Adjustable-Speed A-C. Brush Shifting Motor, Impedance. Baumann....1460–2
Relay Protection of Power Transformers. (Committee Report)....911–15; disc. 915
Relay Protection, Typical Transformer Faults and Gas Detector. Madill....1052–8; disc. 1058
Relaying and Reclosing on a Large 132-Kv System, Experience With Single-Pole. Trainor, Parks....405–11; disc. 411
Relaying on 3-Phase Systems, Fundamental Basis for Distance. Lewis, Tippett....694–708; disc. 708
Relays, A Frequency Modulation Telegraph Terminal Without. Cusack, Michon....1165–70; disc. 1170
Relays, The Application of Heterodyne Modulation to Wide-Band Frequency-Modulated Television. Bowthroyd....1126–30
Repeater for Teletypewriter Signals, An Electronic Regenerative. Hearn....904–11
Report of the Board of Directors....1698–1720
Report on Laboratory Aging Tests on Class A Insulation, Preliminary. (Committee Report)....879–81; disc. 881
Requirements for Transformers, Short-Circuit. Garin....710–13
Research on Lightning Arrester Discharges, Field. McCann, Beck....625–9; disc. 629
Reserve Capacity Determined by the Probability Method, Generating. Calabrese....1439–50
Reserve, Outage Expectancy as a Basis for Generator. Seelye....1483–8

Resistance of Coils, Data on the High-Frequency. Wissig 764–7
Resistance of Isolated Nonmagnetic Rectangular Conductors, Effective. Dwight 549–52
Resistance Welding Control, Functionalized. Stadum, Large, Hartwig 414–18
Resistance Welding Loads, Voltage Changes Caused by. Johnson, Peterson, Rhoades ..... 664–73; disc. 674
Resistance Welding Tools, Electrical Characteristics of. Callender 393–404
Resistors and Control for Diesel-Electric Locomotives, Braking. Weiser 229–32
Resistors for 138-Kv Cable Switching. Sadler, Blakeslee ..... 39–47; disc. 46
Resynchronizing of Generators. Concordia, Temobok 1512–18
Rise in Transformers Due to Interruption of Exciting Current, Transient Voltage. Srinivasan, Vogel 1632–6
Rods, Tubes, and Flat Surfaces, Diffusion of Electric Current into. Miller 1496–1502
Rolling-Mill Service, An Analysis of Motor Selection for Brass-Slab. Berkley ..... 185–9; disc. 189
Rotating Machine With Asymmetrical Stator and Rotor, Equivalent Circuit of the Primitive. Kron ..... 17–23; disc. 23
(Rotating Machinery) A Design Method for Capacitor Start Motors. Chang 1369–74
(Rotating Machinery) Calculation of Slot Constants. Puchstein ..... 1315–22; disc. 1322
(Rotating Machinery) Impedance Relationships of the Adjustable-Speed A-C Brush-Shifting Motor. Baumann 1460–2
(Rotating Machinery) Leakage Reactance of the Squirrel Cage Rotor With Respect to the Stator Harmonics and the Equivalent Circuit of the Induction Motor. Liwschitz 1407–18
(Rotating Machinery) Performance Calculations on Shaded Pole Motors. Trickey ..... 1431–8; disc. 1438
(Rotating Machinery) Reactances of Squirrel-Cage Induction Motors. Lloyd, Giusti, Chang 1349–55
(Rotating Machinery) Some Phases of Calculation of Leakage Reactance of Induction Motors. Liwschitz, Formhals ..... 1409–12; disc. 1412
(Rotating Machinery) The Air Gap Reactance of Polyphase Machines. Alger, West 1331–43
(Rotating Machinery) The Application of Surge Comparison Testing Equipment to Fractional Horsepower A-C Stator Windings. Buchanan 1356–8
(Rotating Machinery) The Circle Diagram of the Polyphase Brush-Shifting Commutator Motor (Schrage Type). Franklin ..... 1667–72; disc. 1672
(Rotating Machinery) Two-Stage Rototrol for Low-Energy Regulating Systems. Kimball 1507–11
Rotating Machines, The Magnetomotive Force of 2-Layer Windings of. Stein 756–8
Rotating Stability Regulators for Synchronous Motor Drives. Schaelchlin ..... 884–7; disc. 887
Rotor, Equivalent Circuit of the Primitive Rotating Machine With Asymmetrical Stator and. Kron ..... 17–23; disc. 23
Rotor, The "Copperspun" Squirrel Cage. Anderson 1312–14
Rotor With Respect to the Stator Harmonics and the Equivalent Circuit of the Induction Motor, Leakage Reactance of the Squirrel Cage. Liwschitz 1407–08
Rototrol for Low-Energy Regulating Systems, Two-Stage. Kimball 1507–11
Rototrol, The Multistage. Liwschitz 564–8
Runway and Approach Lighting, Airport. Kevern 1396–9
Rural Carrier Telephone System, Application of. Bartelink, Cook, Cowan, Messmer ..511–17; disc. 517
Rural Power Circuits, Sectionalizing and Internal Transformer Fusing on. Watkins ..383–8; disc. 388
Rural Power and Telephone Services, Joint Use of Pole Lines for. Campbell, Hill, Moore, Schola ..... 519–24; disc. 524
Rural Radiotelephone Experiment at Cheyenne Wells, Colo. Moore, Seyler, Wright 525–8
Rural Service, A Carrier Telephone System for. Barstow 501–07

S

(Safety) Hazards of Static Electricity in Hospital Operating Rooms. Williams ..... 1146–7; disc. 1147
Safety, Using Airborne Radar to Increase Airline. Ayer 1387–95
Sags in Suspension Spans, Broken Conductor Effect on. Bussi, Landau 1181–8
Samples of Low-Permeability Material, A 60-Cycle Hysteresis Loop Tracer for Small. Wiegand, Hansen ..... 119–31; disc. 131
Saturable Core Reactors, A Balanced Amplifier Using Biased. Kirschbaum, Harder 273–8
Scale Indicating Instruments, Advancements in the Design of Long-. Rowell, Millar 155–60
(Schrage Type) The Circle Diagram of the Polyphase Brush-Shifting Commutator Motor. Franklin ..... 1667–72; disc. 1672
Seaboard Air Line Railway, A 3,000 Horsepower Diesel-Electric Locomotive for the. Staples, Weybrew, Atwell 215–19
Search and Survey, Air-Borne Magnetometers for. Folch, Means, Slonczewski, Parratt, Rumbaugh, Tickner 640–50
Secondary Circuits, Grounding of Instrument Transformer. (Committee Report) 419–20
Sectionalizing and Internal Transformer Fusing on Rural Power Circuits. Watkins ..... 383–8; disc. 388
Sectionalizing and Load Transfer, Automatic Control of Air Switches for Line. Rich, Kirwen ..... 293–9; disc. 299
Selection for Brass-Slab Rolling-Mill Service, An Analysis of Motor. Berkley ..... 185–9; disc. 189
Selective Tripping of Low-Voltage Air Circuit Breakers. Deans ..... 971–6; disc. 976
Selenium Rectifier Cell, Electrical Characteristics of the Junction in a Simplified. Angello 175–80
Self-Excitation of Squirrel-Cage Motor, Dynamic Braking by. Srinivasan, Thomas 145–8
Semiconducting Liquids, The Dielectric Properties of Cellulose Insulation Impregnated With. Clark ..... 55–62; disc. 62
Semiconductors, The Physics of Electronic. Pearson 209–14
Sensing Element, A Magnetic Compass With Cathode-Ray. Kliever, Syrdal 529–34
Series Motors, Dynamic Braking of Two D-C. Leitch 787–91
Series Motor, Dynamic Braking of a Single D-C. Leitch 149–54
Service, An Analysis of Motor Selection for Brass-Slab Rolling-Mill. Berkley ..... 185–9; disc. 189
Service, Developments in Current Collectors for High-Speed. Langer 51–4
Servomechanism Types, A Comparison of Two Basic. Harris ..... 83–92; disc. 92
Servomechanisms by Electrical Analogy, Dimensionless Analysis of. Part I. McCann, Herwald ..111–18
(Servomechanisms) General Analysis of Speed Regulators Under Impact Loads. McCann, Osbon, Kirschbaum 1243–52
(Servomechanisms) Laboratory Aids for Electromechanical System Development. Newton, White ..... 315–19; disc. 319
(Servomechanisms) Solution of the General Voltage Regulator Problem by Electrical Analogy. Harder ..... 815–25; disc. 825
Servomechanisms, The Analysis and an Optimum Synthesis of Linear. Herr, Gerst 959–70
(Servomechanisms) The Application of Lead Networks and Sinusoidal Analysis to Automatic Control Systems. Schwartz ..... 69–76; disc. 76
Severity of Steep Front Waves and Chopped Waves on Transformers, A Study of the Relative. Vogel ..... 64–6; disc. 66
Shaded Pole Motors, Performance Calculations on. Trickey ..... 1431–8; disc. 1438
Shading Coil Calculations for Single-Phase Magnets. Evans ..... 134–7; disc. 137
Shift Telegraphy—Radio and Wire Applications. Frequency. Davey, Matte ..... 479–93; disc. 493
Short-Circuit Requirements for Transformers. Garin 710–13
Shunt Tube Control of Thyratron Rectifiers, The. Potter 421–4
Side-Band Carrier System for Power Lines, A New Single-. Lenehan ..... 826–30; disc. 830
Signals, An Electronic Regenerative Repeater for Teletypewriter. Hearn 904–11
Silicone Insulation as Applied to Naval Electric Power Equipment. Walker ..... 977–80; disc. 980
Silicone Insulation on High-Temperature Railway Motor, Investigation of. Grant, Kauppi, Moses ..... 305–10; disc. 310
Simple and Inexpensive Method for Accurately Measuring Steady-State and Transient High Voltages, A. Levinton ..... 1304–10; disc. 1310
Simplified Double-Film Klydonograph With an Improved Coupling Method, A. Waghorne ..... 1114–16; disc. 1116
Simplified Graphical Method of Computing Thermal Transients. Narbutovskih ..... 78–81; disc. 82
Simplified Selenium Rectifier Cell, Electrical Characteristics of the Junction in a. Angello 175–80
Single D-C Series Motor, Dynamic Braking of a. Leitch 149–54
Single-Phase Magnets, Shading Coil Calculations for. Evans ..... 134–7; disc. 137
Single-Pole Relaying and Reclosing on a Large 132-Kv System, Experience With. Trainor, Parks ..... 405–11; disc. 411
Single-Side-Bank Carrier System for Power Lines, A New. Lenehan ..... 826–30; disc. 830
Sinusoidal Analysis to Automatic Control Systems, The Application of Lead Networks and. Schwartz ..... 69–76; disc. 76
Six-Component Wind-Tunnel Model Suspension System, Electric Equipment Required in 4. Cox 1258–66
60-Cycle Hysteresis Loop Tracer for Small Samples of Low-Permeability Material, A. Wiegand, Hansen ..... 119–31; disc. 131
Sixty-Cycle Power Tests on Wood-Pole Line Insulation, Lightning and. Bellaschi ..... 838–47; disc. 847
Slip-Ring Motors by Means of Unbalanced Primary Voltages, Control of. Schmitz1 ..... 103–1112; disc. 1112
Slot Constants, Calculation of. Puchstein ..... 1315–22; disc. 1322
Solution of the General Voltage Regulator Problem by Electrical Analogy. Harder ..... 815–25; disc. 825
Some Phases of Calculation of Leakage Reactance of Induction Motors. Liwschitz, Formhals ..... 1409–12; disc. 1412
Sonar, Bearing Deviation Indicator for. Schuck, Stedman, Hathaway, Buts 1285–95
Sonar, Submarine Detection by. Keller 1217–50
South, Electrification of the Cotton Industry in the. Bobe ..... 201–08; disc. 2–8
Spans, Broken Conductor Effect on Sags in Suspension. Bissiri, Landau 1181–8
Special 10-Car Train for the New York City Transit System. Sinclair ..... 251–4; disc. 254
Spectrograph, The Cathode-Ray. Feldt, Berkley 1107–110
Speed A-C Brush-Shifting Motor, Impedance Relationships of the Adjustable-. Baumann 1460–2
Speed and Tie Line Control, Theoretical Approach to. Brandt ..... 24–9; disc. 29
Speed Constant-Frequency Generator, A Variable-. Roys, Nader, Spotts ..... 1414–17; disc. 1417
Speed-Drop Analysis, An Extension of Impact 191–6
Speed Regulators Under Impact Loads, General Analysis of. McCann, Osbon, Kirschbaum 1243–52
Squirrel-Cage Induction Motors, Reactances of. Lloyd, Giusti, Chang 1349–55
Squirrel-Cage Motor, Dynamic Braking by Self-Excitation of. Srinivasan, Thomas 145–8
Squirrel Cage Rotor, The "Copperspun." Anderson 1312–14
Squirrel Cage Rotor With Respect to the Stator Harmonics and the Equivalent Circuit of the Induction Motor, Leakage Reactance of the. Liwschitz 1407–08
Stability Regulators for Synchronous Motor Drives, Rotating. Schaelchlin ..... 884–7; disc. 887
Stability, The Transient-Energy Method of Calculating. Magnuson ..... 747–55; disc. 755
Stabilizer for Power Transmission, Electronic. Alexanderson, Prince ..... 950–3; disc. 953
Standards: Their Effect on Refrigeration and Pump Applications, New NEMA Fractional-Horsepower Motor. Potter 508–10
Starting Voltages for Nonuniform Fields in Air, Determination of Corona. Hutton ..1674–9; disc. 1680
Static Electricity in Hospital Operating Rooms, Hazards of. Williams ..... 1146–7; disc. 1147
Stations, Automatic Control of Hydroelectric Generating. Brown, Derr ..... 343–55; disc. 355
Stations, Television Equipment for Broadcast. Lawrence 443–52
Stator and Rotor, Equivalent Circuit of the Primitive Rotating Machine With Asymmetrical. Kron ..... 17–23; disc. 23
Stator Harmonics and the Equivalent Circuit of the Induction Motor, Leakage Reactance of the Squirrel Cage Rotor With Respect to the. Liwschitz 1407–08
Stator Windings, The Application of Surge Comparison Testing Equipment to Fractional Horsepower A-C. Buchanan 1356–8
Steady-State and Transient High Voltages, A Simple and Inexpensive Method for Accurately Measuring. Levinton ..... 1304–10; disc. 1310
Steam System, Probability Methods Applied to Generating Capacity Problems of a Combined Hydro and. Loane, Watchorn ..... 1645–54; disc. 1654
Steel Water Tanks Using Aluminum Anodes, Cathodic Protection of. Sudrabin, Mears 197–200
Steep Front Waves and Chopped Waves on Transformers, A Study of the Relative Severity of. Vogel ..... 64–6; disc. 66
Storage Batteries to the Control of Switchgear, The Application of. Hoxie ..... 1561–9; disc. 1569
Street Cars Provide Successful City Transportation, Trolley Coaches and PCC. Clardy 925–9
Stromberg-Carlson XY Dial Telephone System, The. Reed 432–8
Study of Lightning, Photographic. Hagenguth ..... 577–83; disc. 583
Study of the Relative Severity of Steep Front Waves and Chopped Waves on Transformers, A. Vogel ..... 64–6; disc. 66
Submarine Detection by Sonar. Keller 1217–50
Substations, Field Investigation of Lightning Surges at Gross, McCann ..... 569–74; disc. 574
Subway Cars, Motor Control for Latest New York Transit System. Riley 900–03

Subway Motors for Dynamic Braking, The Design of New York. Widell.....806–18
(Subway) Special 10-Car Train for the New York City Transit System. Sinclair....251–4; disc. 254
Subway System, Modern Car Equipment for New York City's. Cordts.....247–9; disc. 250
Suddenly Applied Loads on a Variable-Ratio Frequency Changer. Carter, Maginnis, Rothe....1489–95
Supersonic Flaw Detectors, Design and Application of. Erdman.....1271–6
Supply for Modern Aircraft, Ground Power. Owen, Murray, Rosenstein.....1296–1303
Supply of Energy in Hydroelectric Systems, Factors in the Economic. Frampton, Floyd.....1117–24; disc. 1124
Surfaces, Accuracy of Temperature Measurements on Coil. Beede, Cain.....586–90; disc. 590
Surfaces, Diffusion of Electric Current into Rods, Tubes, and Flat. Miller.....1496–1502
Surge Comparison Testing Equivalent to Fractional Horsepower A-C Stator Windings, The Application of. Buchanan.....1356–8
Surges at Substations, Field Investigation of Lightning. Gross, McCann.....569–74; disc. 574
Survey, Air-Borne Magnetometers for Search and. Felch, Means, Slonczewski, Parratt, Rumbaugh, Tickner.....640–50
Suspension Spans, Broken Conductor Effect on Sags In. Bisiiri, Landau.....1181–8
Suspension System, Electric Equipment Required in a Modern 6-Component Wind-Tunnel Model. Cox.....1258–66
Switches for Line Sectionalizing and Load Transfer, Automatic Control of Air. Rich, Kirwen.....293–9; disc. 299
Switchgear Equipment for Tidd High-Voltage Test Lines. Lane, Wyman.....1619–21; disc. 1621
(Switchgear) Gaseous Insulation for High-Voltage Apparatus. Camilli, Chapman....1463–9; disc. 1469
Switchgear, The Application of Storage Batteries to the Control of. Hoole.....1561–9; disc. 1569
Switching High-Voltage Transmission Lines. Johnson, Wilson.....1552–60; disc. 1560
Switching, Resistors for 138-Kv Cable. Sadler, Blakeslee.....39–46; disc. 46
Switching Schemes for Capacitors, Automatic. Cuttino.....311–14
Switching, The Economies of Using Capacitors in Amounts to Require Automatic. Butler.....322–7; disc. 327
Synchronous and Induction Motors to Chippers, The Application of. Baker, Lory.....1070–7
Synchronous Motor Drives, Rotating Stability Regulators for. Schaechlin.....884–7; disc. 887
Synthesis of Linear Servomechanisms, The Analysis and an Optimum. Herr, Gerst.....959–70
System, An Improved Cable Carrier. Black, Brooks, Wier, Wilson.....741–6; disc. 746
System, Application of Rural Carrier Telephone. Bartelink, Cook, Cowan, Messmer..541–18; disc. 517
System, Distortion in a Pulse Count Modulation. Clavier, Panter, Grieg.....989–1005; disc. 1005
System, Electronic Telemetering. Foster, Kiefer..802–07
System for Aircraft, A Capacitance-Type Fuel-Measurement. Pearson.....1363–8
System for Aircraft D-C Generators, An Integrated Control. McClinton.....94–8
System for A-C Crane Hoists, A Thrustor Lower Control. Schwarz-Kast.....139–44; disc. 144
System for Diesel-Electric Locomotives, A Power Plant Regulating. Lewis.....242–6; disc. 246
System for Rural Service, A Carrier Telephone. Barstow.....501–07
System for Toronto, Proposed Rapid Transit. Duncan.....939–46
System for Wind Tunnel Drives, A Control. Heidenreich.....1637–43; disc. 1643
System, General Mobile Telephone. Romnes, O'Connor.....1658–66
System, Probability Methods Applied to Generating Capacity Problems of a Combined Hydro and. Loane, Watchorn.....1645–54; disc. 1654
Systems, Aircraft Electric Power Protective. Austin.....1375–82
Systems for Aircraft Window Deicing, Control and Power. Mershon.....1400–05
Systems, New Test Equipment and Testing Methods for Cable Carrier. Tidd, Rosen, Wenk.....726–30
Systems, Present-Day Grounding Practices on Power. (Committee Report).....1525–48; disc. 1548
Systems, Two-Stage Rototrol for Low-Energy Regulating. Kimball.....1507–11

T

Tanks Using Aluminum Anodes, Cathodic Protection of Steel Water. Sudrabin, Mears.....197–200
Technique in an Industrial Control, Radar. Cockrell.....269–72
Techniques for a Coaxial Cable Network, Frequency Division. Crane, Dixon, Huber.....1451–9
Techniques in Ocean Cable Telegraphy, Some Modern. Cramer.....494–500; disc. 500
Telegraph Terminal Without Relays, A Frequency Modulation. Cusack, Michon..1165–70; disc. 1170
Telegraphy—Radio and Wire Applications, Frequency Shift. Davey, Matte.....479–93; disc. 493
Telegraphy, Some Modern Techniques in Ocean Cable. Cramer.....494–500; disc. 500
Telemetering System, Electronic. Foster, Kiefer..802–07
Telephone and Television Facilities, Pulse Echo Measurements on. Abraham, Lebert, Maggio, Schott.....541–8; disc. 548
Telephone Cables, Gas Pressure for. Giese.....471–8
Telephone Services, Joint Use of Pole Lines for Rural Power and. Campbell, Hill, Moore, Scholz.....519–24; disc. 524
Telephone System, Application of Rural Carrier. Bartelink, Cook, Cowan, Messmer..511–17; disc. 517
Telephone System for Rural Service, A Carrier. Barstow.....501–07
Telephone System, General Mobile. Romnes, O'Connor.....1658–66
Telephone System, The Stromberg-Carlson XY Dial. Reed.....432–8
Teletypewriter Signals, An Electronic Regenerative Repeater for. Hearn.....904–11
Television Equipment for Broadcast Stations. Lawrence.....443–52
Television Facilities, Pulse Echo Measurements on Telephone and. Abraham, Lebert, Maggio, Schott.....541–8; disc. 548
Television Network Facilities. Abraham, Romnes.....459–64
Television Receiver Design, Postwar. Pugsley....453–8
Television Relays, The Application of Heterodyne Modulation to Wide-Band Frequency-Modulated. Boothroyd.....1126–30
Television System, A New Microwave. Wentz, Smith.....465–70
Temperature Control for Transport Airplanes, Automatic. Hedges.....1197
Temperature, Dielectric Heating—The Measurement of Loss Under Rising. Whitehead.....947–9
Temperature Measurements on Coil Surfaces, Accuracy of. Beede, Cain.....586–90; disc. 590
Temperature Railway Motor, Investigation of Silicone Insulation on High-. Grant, Kauppi, Moses.....305–10; disc. 310
TVA Co-ordinated Communication System. Talmage.....1022–34; disc. 1034
Tensorial Analysis and Equivalent Circuit of a Variable-Ratio Frequency Changer. Kron.....1503–06
Terminal Without Relays, A Frequency Modulation Telegraph. Cusack, Michon..1165–70; disc. 1170
Test Equipment and Testing Methods for Cable Carrier Systems, New. Tidd, Rosen, Wenk.....726–30
Test Lines, Corona Considerations on High-Voltage Lines, and Design Features of Tidd 500-Kv. Wagner, Wagner, Peterson, Gross..1583–90; disc. 1590
Test Lines, Instrumentation and Measurement—Tidd 500-Kv. Tremaine, Lippert..1624–30; disc. 1630
Test Lines, Insulators and Line Hardware for Tidd 500-Kv. Gross, McCoy, Sheadel..1592–1602; disc. 1602
Test Lines, Line Conductors—Tidd 500-Kv. Peterson, Simmons, Hickernell, Noyes..1603–11; disc. 1611
Test Lines, Switchgear Equipment for Tidd High-Voltage. Lane, Wyman.....1619–21; disc. 1621
Test Lines, Transformers and Lighting Arresters—Tidd 500-Kv. Lane, Hodnette, Bellachi, Beck.....1613–18; disc. 1618
Testing Equipment to Fractional Horsepower A-C Stator Windings, The Application of Surge Comparison. Buchanan.....1356–8
Testing Governor Performance on Electric Power Systems With Improved Instruments. Allen, Hess.....329–39; disc. 339
Testing of Graphite, Arc-Back. Pakala, Cucullu.....439–42
Tests and Developments in Connection With Hot-Line Insulator Washing. Hill.....1203–16
Tests on Class A Insulation, Preliminary Report on Laboratory Aging. (Committee Report).....879–81; disc. 881
Tests on Wood-Pole Line Insulation, Lightning and 60-Cycle Power. Bellaschi.....838–47; disc. 847
Textile Finishing Ranges, Electric Drives for. Moore, Uhl.....684–94
Textile Plants, Power Distribution in. McConnell.....659–62
Theoretical Approach to Speed and Tie Line Control. Brandt.....24–9; disc. 29
Theory and Application of Complex Logarithmic and Geometric Mean Distances. Higgins.....12–16
Theory of the Transductor or Magnetic Amplifier, Some Fundamentals of a. Lamm.....1078–85
Thermal Ampere-Demand Meter, A Polyphase. Petzingen.....167–74
Thermal Transients, Simplified Graphical Method of Computing. Narbutovskih.....78–81; disc. 82
3-Phase Systems, Fundamental Basis for Distance Relaying on. Lewis, Tippett..694–708; disc. 708
3,000 Horsepower Diesel-Electric Locomotive for the Seaboard Air Line Railway, A. Staples, Weybrew, Atwell.....215–19
Throat Loaded With Ferromagnetic Materials, The Voltage Drop in the Welder. Stein.....356–62
Thrust Bearings at the Bonneville Plant of the Corps of Engineers, War Department, The Design and Performance of the Vertical Generator. Lewis, Gordon.....1231–7; disc. 1237
Thrustor Lowering Control System for A-C Crane Hoists, A. Schwarz-Kast.....139–44; disc. 144
Thyratron Rectifiers, The Shunt Tube Control of. Potter.....421–4
Tidd 500-Kv Test Lines, Corona Considerations on High-Voltage Lines and Design Features of. Wagner, Wagner, Peterson, Gross.....1583–90; disc. 1590
Tidd 500-Kv Test Lines, Instrumentation and Measurement—. Tremaine, Lippert..1624–30; disc. 1630
Tidd 500-Kv Test Lines, Insulators and Line Hardware for. Gross, McCoy, Sheadel..1592–1602; disc. 1602
Tidd 500-Kv Test Lines, Line Conductors—. Peterson Simmons, Hickernell, Noyes..1603–11; disc. 1611
Tidd 500-Kv Test Lines, Transformers and Lightning Arresters—. Lane, Hodnette, Bellaschi, Beck.....1613–18; disc. 1618
Tidd High-Voltage Test Lines, Switchgear Equipment for. Lane, Wyman.....1619–21; disc. 1621
Tie Line Control, Theoretical Approach to Speed and. Brandt.....24–9; disc. 29
Tools, Electrical Characteristics of Resistance Welding-. Callender.....393–404
Toronto, Proposed Rapid Transit System for. Duncan.....939–46
Torques, Eddy Currents in Disks: Driving and Damping Forces and. Moore.....1–10; disc. 10
Tracer for Small Samples of Low-Permeability Material, A 60-Cycle Hysteresis Loop. Wiegand, Hansen.....119–31; disc. 131
Track Brakes and Drum Brakes for PCC Cars, Recent Developments in. Vouch.....302–04
Traction-Generator Excitation Control Systems, Developments in Diesel-Electric. Brancke, Adams.....223–8; disc. 228
Train for the New York City Transit System, Special 10-Car. Sinclair.....251–4; disc. 254
Transductor or Magnetic Amplifier, Some Fundamentals of a Theory of the. Lamm.....1078–85
Transfer, Automatic Control of Air Switches for Line Sectionalizing and Load. Rich, Kirwen.....293–9; disc. 299
Transformer Design, High-Voltage Power-. Part II. Mallett.....1086–91; disc. 1091
Transformer Faults and Gas Detector Relay Protection, Typical. Madill.....1052–8; disc. 1058
Transformer Fusing on Rural Power Circuits, Sectionalizing and Internal. Watkins..383–8; disc. 388
Transformer-Loss Compensators, Metering With. Schleicher.....851–61; disc. 861
Transformer Secondary Circuits, Grounding of Instrument. (Committee Report).....419–20
Transformers, A Study of the Relative Severity of Steep Front Waves and Chopped Waves on. Vogel.....64–6; disc. 66
Transformers and Lightning Arresters—Tidd 500-Kv Test Lines. Lane, Hodnette, Bellaschi, Beck.....1613–18; disc. 1618
Transformers Due to Interruption of Exciting Current, Transient Voltage Rise in. Srinivasan, Vogel.....1632–6
Transformers During Faults, Transient Characteristics of Current. Part II. Rothe, Concordia....731–4
(Transformers) Preliminary Report on Laboratory Aging Tests on Class A Insulation. (Committee Report).....879–81; disc. 881
Transformers, Relay Protection of Power. (Committee Report).....911–15; disc. 915
Transformers, Short-Circuit Requirements for. Garin.....710–13
Transient Characteristics of Current Transformers During Faults. Part II. Rothe, Concordia..731–4
Transient-Energy Method of Calculating Stability, The. Magnuson.....747–55; disc. 755
Transient High Voltages, A Simple and Inexpensive Method for Accurately Measuring Steady-State and. Levinton.....1304–10; disc. 1310
Transient Voltage Rise in Transformers Due to Interruption of Exciting Current. Srinivasan, Vogel.....1632–6
Transients, Simplified Graphical Method of Computing Thermal. Narbutovskih.....78–81; disc. 82
Transit System for Toronto, Proposed Rapid. Duncan.....939–46
Transit System, Special 10-Car Train for the New York City. Sinclair.....251–4; disc. 254

Transit System Subway Cars, Motor Control for Latest New York. Riley.....900–03
(Transmission) Broken Conductor Effect on Sags in Suspension Spans. Bissri, Landau.....1181–8
(Transmission) Burning of Wood Structures by Leakage Currents. Ross.....279–84; disc. 285
(Transmission) Corona Considerations on High-Voltage Lines and Design Features of Tidd 500-Kv Test Lines. Wagner, Wagner, Peterson, Gross.....1583–90; disc. 1590
Transmission, Economics of Long-Distance A-C Power. Crary, Johnson.....1092–9; disc. 1099
Transmission, Electronic Stabilizer for Power. Alexanderson, Prince.....950–3; disc. 953
(Transmission) Experience With Single-Pole Relaying and Reclosing on a Large 132-Kv System. Trainor, Parks.....405–11; disc. 411
(Transmission) Field Investigation of Lightning Surges at Substations. Gross, McCann.. 569–74; disc. 574
(Transmission) Galloping Conductors and a Method for Studying Them. Tornquist, Becker.....1154–61; disc. 1161
(Transmission) Instrumentation and Measurement—Tidd 500-Kv Test Lines. Tremaine, Lippert.....1624–30; disc. 1630
(Transmission) Insulators and Line Hardware for Tidd 500-Kv Test Lines. Gross, McCoy, Shenfel.....1592–1602; disc. 1602
(Transmission) Internal Corona Discharges in Insulated Cables. Greenfield.....591–600; disc. 600
(Transmission) Lightning and 60-Cycle Power Tests on Wood-Pole Line Insulation. Bellaschi.....838–47; disc. 847
(Transmission) Lightning Investigation on the 25-Kv System of the West Penn Power Company. Bowen, Beck.....831–6; disc. 836
(Transmission) Line Conductors—Tidd 500-Kv Test Lines. Peterson, Simmons, Hickernell, Noyes.....1603–11; disc. 1611
Transmission Lines, Excitation Problems in Hydroelectric Generators Supplying Long. Killgore.....1277–82; disc. 1282
Transmission Lines, Performance of 161-Kv and 115-Kv. Hapgood, Almon.....863–9; disc. 869
Transmission Lines, Switching High-Voltage. Johnson, Wilson.....1552–60; disc. 1560
Transmission of Electric Power at Extra High Voltages. Sporn, Monteith.....1571–7; disc. 1577
(Transmission) Photographic Study of Lightning. Hagenguth.....577–83; disc. 583
(Transmission) Radio-Noise Influence of 230-Kv Lines. Korden.....677–81; disc. 682
(Transmission) Switchgear Equipment for Tidd High-Voltage Test Lines. Lane, Wyman.....1619–21; disc. 1621
(Transmission) Tests and Developments in Connection With Hot-Line Insulator Washing. Hill..1203–16
(Transmission) The Interruption of Charging Current at High Voltage. Leeds, Van Sickle.....373–80; disc. 381
(Transmission) The Probable Breakdown Voltage of Paper Dielectric Capacitors. Brooks.....1137–44; disc. 1144
(Transmission) Transformers and Lightning Arresters—Tidd 500-Kv Test Lines. Lane, Hodnette, Bellaschi, Beck.....1613–18; disc. 1618
Transport Airplanes, Automatic Temperature Control for. Hedges.....1197
(Transportation, Air) A Capacitance-Type Fuel-Measurement System for Aircraft. Pearson.....1363–8
(Transportation, Air) Aircraft Electric Power Protective Systems. Austin.....1375–82
(Transportation, Air) Airport Runway and Approach Lighting. Kevern.....1396–9
(Transportation, Air) An Integrated Control System for Aircraft D-C Generators. McClinton.....94–8
(Transportation, Air) Automatic Temperature Control for Transport Airplanes. Hedges.....1197
(Transportation, Air) Control and Power Systems for Aircraft Window Deicing. Mershon.....1400–05
(Transportation, Air) D-C Aircraft Generator Power Center. Bottemiller.....1267–70
(Transportation, Air) Electric Drive for Aircraft. Crom.....1359–62
(Transportation, Air) Electric Equipment Required in a Modern 6-Component Wind Tunnel Model Suspension System. Cox.....1258–66
(Transportation, Air) Ground Power Supply for Modern Aircraft. Owen, Murray, Rosenstein...1296–1303
(Transportation, Air) Parallel Operation of Aircraft Alternators Using Electronic Frequency Changers. Bowlus, Nims.....31–8
(Transportation, Air) The Calibration of Ignition Crest Voltmeters. Davis, Warren.....99–104; disc. 104
(Transportation, Air) Using Airborne Radar to Increase Airline Safety. Ayer.....1387–95
(Transportation Land) A Power Plant Regulating System for Diesel-Electric Locomotives. Lewis.....242–6; disc. 246
(Transportation, Land) A 3,000 Horsepower Diesel-Electric Locomotive for the Seaboard Air Line Railway. Staples, Weybrew, Atwell.....215–19
(Transportation, Land) Braking Resistors and Control for Diesel-Electric Locomotives. Weiser..229–32
(Transportation, Land) Can the Trolley Coach Compete Economically With the Gas or Diesel Bus Where No Overhead Facilities Exist? Gauss.....264–8; disc. 268
(Transportation, Land) Developments in Control Systems for Diesel-Electric Locomotives. Henshaw.....233–41
(Transportation, Land) Developments in Current Collectors for High-Speed Service. Langer.....51–4
(Transportation, Land) Developments in Diesel-Electric Traction-Generator Excitation Control Systems. Brancke, Adams.....223–8; disc. 228
(Transportation, Land) Investigation of Silicone Insulation on High-Temperature Railway Motor. Grant, Kauppi, Moses.....305–10; disc. 310
(Transportation, Land) Modern Car Equipment for New York City's Subway System. Cordts.....247–9; disc. 250
(Transportation, Land) Modern Railway Passenger-Car Auxiliary-Power Equipment. MacLeod, Hause.....930–8
(Transportation, Land) Motor Control for Latest New York Transit System Subway Cars. Riley..900–03
(Transportation, Land) Proposed Rapid Transit System for Toronto. Duncan.....939–46
(Transportation, Land) Recent Developments in Track Brakes and Drum Brakes for PCC Cars. Vouch.....302–04
(Transportation, Land) Some Recent Developments in the PCC Car. Cooper.....288–92; disc. 292
(Transportation, Land) Special 10-Car Train for the New York City Transit System. Sinclair.....251–4; disc. 254
(Transportation, Land) The Design of New York Subway Motors for Dynamic Braking. Widell.808–10
Transportation, Trolley Coaches and PCC Street Cars Provide Successful City. Clardy.....925–9
Tripping Devices for Low-Voltage Circuit Breakers, An Improved Overcurrent. Rawlins, Sandin.....1149–53; disc. 1153
Tripping of Low-Voltage Air Circuit Breakers, Selective. Deans.....971–6; disc. 976
Trolley Coach Compete Economically With the Gas or Diesel Bus Where No Overhead Facilities Exist?, Can the. Gauss.....264–8; disc. 268
Trolley Coaches and PCC Street Cars Provide Successful City Transportation. Clardy.....925–9
Tube Control of Thyratron Rectifiers, The Shunt. Potter.....421–4
Tube, The Measurement of Acceleration With a Vacuum. Ramberg.....735–40
Tubes, and Flat Surfaces, Diffusion of Electric Current into Rods. Miller.....1496–1502
Tunnel Drives, A Control System for Wind. Heidenreich.....1637–43; disc. 1643
Tunnel Model Suspension System, Electric Equipment Required in a Modern 6-Component Wind-. Cox.....1258–66
Turbine Generators, Liquid Cooling of A-C. Fechheimer.....553–61
25-Kv System of the West Penn Power Company, Lightning Investigation on the. Bowen, Beck.....831–6; disc. 836
Twister, Electric Equipment for 2-for-1. Gwaltney, Burnham.....811–14
Two Basic Servomechanism Types, A Comparison of. Harris.....83–92; disc. 92
2-for-1 Twister, Electric Equipment for. Gwaltney, Burnham.....811–14
2-Layer Windings of Rotating Machines, The Magnetomotive Force of. Stein.....756–8
Two-Stage Rototrol for Low-Energy Regulating Systems. Kimball.....1507–11
230-Kv Lines, Radio-Noise Influence of. Korden.....677–81; disc. 682
Typical Transformer Faults and Gas Detector Relay Protection. Madill.....1052–8; disc. 1058

U

Units, The Maintenance of Hydroelectric Generating. Robertson, Standing.....776–82
Utility Industry During World War II, The German Electrical. Noest.....1037–47; disc. 1047

V

Vacuum Tube, The Measurement of Acceleration With a. Ramberg.....735–40
Variable-Ratio Frequency Changer, Suddenly Applied Loads on a. Carter, Maginnis, Rothe...1489–95
Variable-Ratio Frequency Changer, Tensorial Analysis and Equivalent Circuit of a. Kron.....1503–06
Variable-Speed Constant-Frequency Generator, A. Roys, Nader, Spotts.....1414–17; disc. 1417
Vertical Generator Thrust Bearings at the Bonneville Plant of the Corps of Engineers, War Department, The Design and Performance of the. Lewis, Gordon.....1231–7; disc. 1237
Vertical Water Wheel Generators, Modern Bearing Practice for. Laffoon, Baudry.....363–9; disc. 369
Voltage Changes Caused by Resistance Welding Loads. Johnson, Peterson, Rhoades.....664–73; disc. 674
Voltage Copper-Oxide Rectifiers, Higher. Smith..220–2
Voltage Drop in the Welder Throat Loaded With Ferromagnetic Materials, The. Stein.....356–62
Voltage Lines and Design Features of Tidd 500-Kv Test Lines, Corona Considerations on High. Wagner, Wagner, Peterson, Gross.....1583–90; disc. 1590
Voltage of Paper Dielectric Capacitors, The Probable Breakdown. Brooks.....1137–44; disc. 1144
Voltage Regulator Problem by Electrical Analogy. Solution of the General. Harder..815–25; disc. 825
Voltage Rise in Transformers Due to Interruption of Exciting Current, Transient. Srinivasan, Vogel.....1632–6
Voltage Transmission Lines, Switching High-. Johnson, Wilson.....1552–60; disc. 1560
Voltages, A Simple and Inexpensive Method for Accurately Measuring Steady-State and Transient High. Levinton.....1304–10; disc. 1310
Voltages, Control of Slip-Ring Motors by Means of Unbalanced Primary. Schmitz.....1103–1112; disc. 1112
Voltages for Nonuniform Fields in Air, Determination of Corona Starting. Hutton..1674–9; disc. 1680
Voltages, Transmission of Electric Power at Extra High-. Sporn, Monteith.....1571–7; disc. 1577
Voltmeters, The Calibration of Ignition Crest. Davis, Warren.....99–104; disc. 104

W

War II, The German Electrical Utility Industry During World. Noest.....1037–47; disc. 1047
Washing, Tests and Developments in Connection With Hot-Line Insulator. Hill.....1203–16
Water Tanks Using Aluminum Anodes, Cathodic Protection of Steel. Sudrabin, Mears.....197–200
Water Wheel Generators, Modern Bearing Practice for Vertical. Laffoon, Baudry.....363–9; disc. 369
Waves and Chopped Waves on Transformers, A Study of the Relative Severity of Steep Front. Vogel.....64–6; disc. 66
Welder Throat Loaded With Ferromagnetic Materials, The Voltage Drop in the. Stein.....356–62
Welding Control, Functionalized Resistance. Stadum, Large, Hartwig.....414–18
Welding Loads, Voltage Changes Caused by Resistance. Johnson, Peterson, Rhoades.....664–73; disc. 674
Welding Tools, Electrical Characteristics of Resistance. Callender.....393–404
West Penn Power Company, Lightning Investigation on the 25-Kv System of the. Bowen, Beck.....831–6; disc. 836
Western Union Multiplex to Navy Radio, The Application of. Hoover.....1478–82
Wide-Band Frequency-Modulated Television Relays, The Application of Heterodyne Modulation to. Boothroyd.....1126–30
Wind Tunnel Drives, A Control System for. Heidenreich.....1637–43; disc. 1643
Wind-Tunnel Model Suspension System, Electric Equipment Required in a Modern 6-Component. Cox.....1258–66
Windings of Rotating Machines, The Magnetomotive Force of 2-Layer. Stein.....756–8
Windings, The Application of Surge Comparison Testing Equipment to Fractional Horsepower A-C Stator. Buchanan.....1356–8
Window Deicing, Control and Power Systems for Aircraft. Mershon.....1400–05
Wire Applications, Frequency Shift Telegraphy—Radio and. Davey, Matte.....479–93; disc. 493
Wood-Pole Line Insulation, Lightning and 60-Cycle Power Tests on. Bellaschi.....838–47; disc. 847
Wood Structures by Leakage Currents, Burning of. Ross.....279–84; disc. 285
World War II, The German Electrical Utility Industry During. Noest.....1037–47; disc. 1047

X

XY Dial Telephone System, The Stromberg-Carlson. Reed.....432–8

2. Author Index

Abraham, L. G.; A. W. Lebert, J. B. Maggio, J. T. Schott. Pulse Echo Measurements on Telephone and Television Facilities....541–8; disc. 548
Abraham, L. G.; H. I. Romnes. Television Network Facilities....459–64
Adams, G. M.; C. A. Brancke. Developments in Diesel-Electric Traction-Generator Excitation Control Systems....223–8
Adler, H. A. Disc....1656
Adolphe, M. H.; N. C. Clark. Capacitance Fuel Gauges....1189–96
Alexanderson, Ernst F. W.; D. C. Prince. Electronic Stabilizer for Power Transmission..950–3; disc. 958
Alger, P. L.; H. R. West. The Air Gap Reactance of Polyphase Machines....1331–43
Allen, J. E.; W. B. Hess. Testing Governor Performance on Electric Power Systems With Improved Instruments....329–39; disc. 342
Almon, C. P., Jr.; K. E. Hapgood. Performance of 161-Kv and 115-Kv Transmission Lines....863–9; disc. 871
Alspaugh, R. M. Disc....355
Anderson, A. E. Disc....1569
Anderson, G. R. The "Copperpun" Squirrel Cage Rotor....1312–14
Andres, F. E.; R. W. Caswell. Disc....285, 848
Angello, Stephen James. Electrical Characteristics of the Junction in a Simplified Selenium Rectifier Cell....175–80
Antine, L. T.; R. L. Ashley. Disc....1654
Appleman, Glen. Disc....836
Asbury, C. E. Disc....259, 390
Ashley, R. L.; L. T. Antine. Disc....1654
Atkinson, R. W. Disc....603, 1630
Atwell, C. A.; D. R. Staples; T. L. Weybrew. A 3,000 Horsepower Diesel-Electric Locomotive for the Seaboard Air Line Railway....215–19
Austin, B. O. Aircraft Electric Power Protective Systems....1375–82
Avery, C. L. Disc....340
Aydelott, John C. Disc....292
Ayer, R. W. Using Airbone Radar to Increase Airline Safety....1387–95

B

Bachelor, A. T. Disc....208
Baker, R. R.; M. R. Lory. The Application of Synchronous Induction Motors to Chippers....1070–7
Ballard, B. G. Disc....548
Balleny, J. L. Electric Furnace Practice in Canada....917–24
Barkle, J. R., Jr. Disc....1283
Barnes, E. C. Disc....1412
Barstow, J. M. A Carrier Telephone System for Rural Service....501–07
Bartelink, E. H. B.; L. E. Cook, F. A. Cowan, G. R. Messmer. Application of Rural Carrier Telephone System....511–18; disc. 518
Bartlett, S. C. Disc....517
Baudry, R. A.; C. M. Laffoon. Modern Bearing Practice for Vertical Water Wheel Generators....363–9; disc. 371
Baumann, Fred. Impedance Relationships of the Adjustable-Speed A-C Brush-Shifting Motor....1460–2
Beck, Edward; W. C. Bowen. Lightning Investigation on the 25-Kv System of the West Penn Power Company....831–6; disc. 836
Beck, Edward; F. A. Lane, J. K. Hodnette, P. L. Bellaschi. Transformers and Lightning Arresters—Tidd 500-Kv Test Lines....1613–18; disc. 1618
Beck, Edward; G. D. McCann. Field Research on Lightning Arrester Discharges....625–9; disc. 630
Becker, C.; E. L. Tornquist. Galloping Conductors and a Method for Studying Them....1154–61; disc. 1163
Beede, H. Martin; Bernard M. Cain. Accuracy of Temperature Measurements on Coil Surfaces....586–90
Beiler, A. C.; P. L. Schmidt. Interlaminar Eddy Current Loss in Laminated Cores....872–7; disc. 877
Bellaschi, P. L. Lightning and 60-Cycle Power Tests on Wood-Pole Line Insulation....838–47; disc. 847
Bellaschi, P. L. Disc....574, 882, 1560, 1581
Bellaschi, P. L.; F. A. Lane, J. K. Hodnette, Edward Beck. Transformers and Lightning Arresters—Tidd 500-Kv Test Lines....1613–18; disc. 1618
Berkley, Carl; Rudolph Feldt. The Cathode-Ray Spectrograph....105–10
Berkley, L. H. An Analysis of Motor Selection for Brass-Slab Rolling-Mill Service....185–9; disc. 190
Bills, Glenn W. Disc....622
Birch, L. W. Disc....268
Bisiri, Alfio; Maurice Landau. Broken Conductor Effect on Sags in Suspension Spans....1181–8
Black, H. S.; F. A. Brooks, A. J. Wier, I. G. Wilson. An Improved Cable Carrier System....741–6; disc. 746
Black, H. S.; J. O. Edson. Pulse Code Modulation....895–9
Blakeslee, T. M. Disc....382
Blakeslee, T. M.; E. K. Sadler. Resistors for 138-Kv Cable Switching....39–46; disc. 49
Blankmeyer, W. H. Disc....1034
Bobe, S. A. Electrification of the Cotton Industry in the South....201–08
Bodine, R. B. Disc....1282
Boehne, E. W. Disc....47, 381
Boehne, E. W.; M. J. Jang. Performance Criteria of D-C Interrupters....1172–80
Boothroyd, Wilson P. The Application of Heterodyne Modulation to Wide-Band Frequency-Modulated Television Relays....1126–30
Bottemiller, E. L. D-C Aircraft Generator Power Center....1267–70
Bowen, William C.; E. Beck. Lightning Investigation on the 25-Kv System of the West Penn Power Company....831–6; disc. 836
Bower, James, Jr. Disc....605
Bowlus, Cyl. T.; T. T. Nine. Parallel Operation of Air-Craft Alternators Using Electronic Frequency Changers....31–8
Bramhall, F. B. Disc....493
Brancke, C. A.; G. M. Adams. Developments in Diesel-Electric Traction-Generator Excitation Control Systems....223–8
Brandt, Robert. Theoretical Approach to Speed and Tie Line Control....24–9; disc. 30
Brooks, F. A.; A. J. Wier, I. G. Wilson, H. S. Black. An Improved Cable Carrier System....741–6; disc. 746
Brooks, Hamilton. The Probable Breakdown Voltage of Power Dielectric Capacitors....1137–44
Brown, M. J.; W. A. Derr. Automatic Control of Hydroelectric Generating Stations....343–55
Brownlee, W. R. Disc....326, 517, 916, 1060, 1101
Brownlee, W. R.; J. A. Elzi. Disc....1548
Buchanan, Lloyd W. The Application of Surge Comparison Testing Equipment to Fractional Horsepower A-C Stator Windings....1356–8
Buchanan, W. B. Disc....1116, 1161
Buckley, Joseph J. Automatically Controlled Copper-Oxide Rectifiers for Electroplating and Anodizing Applications....181–4
Burnham, H. J.; E. C. Gwaltney. Electric Equipment for 2-for-1 Twister....811–14
Butler, J. W. The Economics of Using Capacitors in Amounts to Require Automatic Switching....322–7; disc. 328
Butz, A. N., Jr., C. K. Stedman, O. H. Schuck, J. L. Hathaway. Bearing Deviation Indicator for Sonar....1285–95

C

Cahen, Francois. Disc....1581
Cain, Bernard M.; H. Martin Beede. Accuracy of Temperature Measurements on Coil Surfaces....586–90
Calabrese, Giuseppe. Generating Reserve Capacity Determined by the Probability Method....1439–50
Callender, E. M. Electrical Characteristics of Resistance Welding Tools....393–404
Calvert, J. F.; J. A. M. Lyon. Disc....10
Camilli, G.; J. J. Chapman. Gaseous Insulation for High-Voltage Apparatus....1463–9
Campbell, J. W.; L. W. Hill; L. M. Moore; H. J. Scholz. Joint Use of Pole Lines for Rural Power and Telephone Services....519–24
Carter, C. K.; F. J. Maginnis, F. S. Rothe. Suddenly Applied Load on a Variable-Ratio Frequency Changer....1489–95
Caswell, R. W.; F. E. Andrews. Disc....285, 848
Chang, Sheldon S. L. A Design Method for Capacitor Start Motors....1369–74
Chang, Sheldon S. L. The Equivalent Circuit of the Capacitor Motor....631–40
Chang, Sheldon S. L.; T. C. Lloyd. A Design Method for Capacitor Motors....652–7; disc. 658
Chang, S. S. L.; T. C. Lloyd, V. F. Giusti. Reactances of Squirrel-Cage Induction Motors....1349–55
Chapman, J. J.; G. Camilli. Gaseous Insulation for High-Voltage Apparatus....1463–9
Charles, Mario C. Disc....1035
Chestnut, H. Disc....92
Christian, Dean R. Direct Coupled Oscillograph Amplifier....1383–6
Cisna, V. J. Disc....1549
Clardy, W. J. Trolley Coaches and PCC Street Cars Provide Successful City Transportation....925–9
Clark, F. M. The Dielectric Properties of Cellulose Insulation Impregnated With Semiconducting Liquids....55–62; disc. 63
Clark, N. C.; M. H. Adolphe. Capacitance Fuel Gauges....1189–96
Clarke, J. G.; A. G. Conrad, F. Zweig. Disc....1672
Clavier, A. G.; P. F. Panter, D. D. Grieg. Distortion in a Pulse Count Modulation System....989–1005; disc. 1005
Cockrell, W. D. Radar Technique in an Industrial Control....269–72
Cole, Guerney H. Disc....877
Cole, Harold. Disc....675
(Committee Reports) See "Committee Reports" and other entries in Technical Subject Index
Concordia, C. Disc....825
Concordia, C.; F. S. Rothe. Transient Characteristics of Current Transformers During Faults. Part II....731–4
Concordia, C.; M. Temoshok. Resynchronizing of Generators....1512–18
Conrad, A. G.; F. Zweig, J. G. Clarke. Disc....1672
Cook, L. E.; F. A. Cowan, G. R. Messmer, E. H. B. Bartelink. Application of Rural Carrier Telephone System....511–18; disc. 518
Cooper, S. B. Some Recent Developments in the PCC Car....288–92; disc. 292
Cordis, B. F. Modern Car Equipment for New York City's Subway System....247–9
Corson, A. J.; N. P. Millar. Applications of the Electrodynamic Instrument Mechanism....1131–6
Cowan, F. A. Modulation in Communication....792–6
Cowan, F. A.; E. H. B. Bartelink; L. E. Cook; G. R. Messmer. Application of Rural Carrier Telephone System....511–17
Cox, H. Orville. Electric Equipment Required in a Modern 6-Component Wind-Tunnel Model Suspension System....1258–66
Cramer, C. H. Some Modern Techniques in Ocean Cable Telegraphy....494–500
Crane, R. E.; J. T. Dixon, G. H. Huber. Frequency Division Techniques for a Coaxial Cable Network....1451–9
Crary, S. B. Disc....870, 956, 1550
Crary, S. B.; I. B. Johnson. Economics of Long-Distance A-C Power Transmission....1092–9; disc. 1099
Crever, F. E. An Extension of Impact Speed-Drop Analysis....191–6
Crom, George C. Electric Drive for Aircraft....1359–62
Cronin, L. D. Disc....285
Crouse, C. H. Disc....1430
Cuculin, C. J.; Wm. E. Pakala. Arc-Back Testing of Graphite....439–42
Cusack, P. H.; A. E. Michon. A Frequency Modulation Telegraph Terminal Without Relays....1165–70; disc. 1171
Cutting, W. H. Automatic Switching Schemes for Capacitors....311–14

D

Dakin, T. W. Disc....62
Davey, J. R.; A. L. Matte. Frequency Shift Telegraphy—Radio and Wire Applications....479–93
Davis, W. L.; C. E. Warren. The Calibration of Ignition Crest Voltmeters....99–104
Davison, A. E. Disc....681
Deans, William. Selective Tripping of Low-Voltage Air Circuit Breakers....971–6; disc. 976
DeForest, C. W. Disc....1049
Del Mar, W. A. Disc....602, 882, 981
Derr, W. A.; M. J. Brown. Automatic Control of Hydroelectric Generating Stations. Brown, Derr....343–55
Derr, W. A. Disc....411
Dewey, C. G. Disc....708
Dixon, J. T.; R. E. Crane, G. H. Huber. Frequency Division Techniques for a Coaxial Cable Network....1451–9
Doggett, L. A. Disc....138, 1322
Douglas, John F. H. Disc....1112, 1323
Dovjikov, Alexander. Disc....954
Doyle, A. M. Disc....915
Duff, C. K. Disc....1124
Duff, J. E. A High Precision Dynamometer for Small Motor Measurements....1344–8; disc. 1348
Duncan, W. E. P. Proposed Rapid Transit System for Toronto....939–46
Duncan, W. E. Disc....893
Dunham, J. M. Disc....517
Dunstan, L. A. Machine Computation of Power Network Performance....610–20; disc. 623
Dwight, Herbert B. Effective Resistance of Isolated Nonmagnetic Rectangular Conductors....549–52

E

Eaton, M. Automatic Operation of Electric Boilers....1061–8; disc. 1069
Edson, J. O.; H. S. Black. Pulse Code Modulation....895–9

Edwards, R. S. Disc. 320
Ekvall, H. N. Disc. 849
Elzi, J. A.; W.R. Brownlee. Disc. 1548
Enos, H. A. Disc. 524
Erdman, Donald C. Design and Application of Supersonic Flaw Detectors 1271–6
Espenschied, Lloyd. Disc. 493
Evans, C. T. Shading Coil Calculations for Single-Phase Magnets 134–7; disc. 138
Evans, E. A. Disc. 583

F

Falk, Benjamin. Disc. 1430
Farrell, William J.; J. L. Solomon. Disc. 674
Fechheimer, Carl J.; Liquid Cooling of A-C Turbine Generators 553–61; disc. 563
Fechheimer, Carl J. Disc. 1113
Felch, E. P.; W. J. Means; T. Slonczewski; L. G. Parratt; L. H. Rumbaugh; A. J. Tickner. Air-Borne Magnetometers for Search and Survey 640–50
Feldt, Rudolph; Carl Berkley. The Cathode-Ray Spectrograph 105–10
Finzi, L. A. Disc. 82, 389
Fleming, D. B. Disc. 1058
Floyd, G. D. Disc. 871, 1091, 1655
Floyd, G. D.; A. H. Frampton. Factors in the Economic Supply of Energy in Hydroelectric Systems 1117–24; disc. 1125
Foley, A. H. A Self-Balancing Capacitance Bridge 797–801
Formhals, W. H.; M. M. Liwachitz. Some Phases of Calculation of Leakage Reactance of Induction Motors 1409–13; disc. 1412
Foster, George E.; W. M. Kiefer. Electronic Telemetering System 802–7
Frampton, A. H.; G. D. Floyd. Factors in the Economic Supply of Energy in Hydroelectric Systems 1117–24; disc. 1125
Franklin, Paul W. The Circle Diagram of the Polyphase Brush-Shifting Commutator Motor (Schrage Type) 1667–72; disc. 1672
Franklin, R. F. Disc. 877
Fuller, John L. Disc. 590

G

Garbarini, Robert F. Disc. 319
Garin, A. N. Short-Circuit Requirements for Transformers 710–13
Gault, J. S. Disc. 190
Gaus, J. H. Can the Trolley Coach Compete Economically With the Gas or Diesel Bus Where No Overhead Facilities Exist? 264–8
George, E. E. Disc. 30, 916
George, E. E.; R. E. Pierce. Disc. 1100
Gerst, Irving; Donald Herr. The Analysis and an Optimum Synthesis of Linear Servomechanisms 959–70
Giese, R. C. Gas Pressure for Telephone Cables 471–8
Gilbert, J. J. Disc. 500
Giusti, Victor F.; T. C. Lloyd, S. S. L. Chang. Reactances of Squirrel-Cage Induction Motors 1349–55
Glasnow, F. A. Disc. 1405
Gooding, F. H. Disc. 601
Gordon, T. W. Disc. 371
Gordon, T. W.; F. M. Lewis. The Design and Performance of the Vertical Generator Thrust Bearings at the Bonneville Plant of the Corps of Engineers, War Department 1231–7; disc. 1239
Grant, George. Disc. 980
Grant, George, III; T. A. Kauppi; Graham Lee Moses. Investigation of Silicone Insulation on High-Temperature Railway Motor 305–10
Greene, N. J. Disc. 310
Greenfield, E. W. Internal Corona Discharges in Insulated Cables 591–600; disc. 606
Greer, Lanier. Disc. 228
Grieg, D. D.; A. G. Clavier. P. F. Panter. Distortion in a Pulse Count Modulation System 989–1005; disc. 1005
Gross, Eric T. B. Disc. 411, 916, 1050, 1059, 1550
Gross, I. W.; G. D. McCann. Field Investigation of Lightning Surges at Substations 569–74; disc. 576
Gross, I. W.; R. L. McCoy; J. M. Sheadel. Insulators and Line Hardware for Tidd 500-Kv Test Lines 1592–1602; disc. 1602
Gross, I. W.; G. F. Wagner, Anthony Wagner, E. L. Peterson. Corona Considerations on High-Voltage Lines and Design Features of Tidd 500-Kv Test Lines 1583–90
Grosser, Jr., E. H. Disc. 682
Gwalney, E. C.; H. J. Burnham. Electric Equipment for 2-for-1 Twister 811–14

H

Hagenguth, J. H. Photographic Study of Lightning 577–83; disc. 585
Hagenguth, J. H. Disc. 66, 574
Halperin, Herman. Disc. 63, 600, 881
Hanna, M. R. Disc. 310
Hansen, W. W.; D. E. Wiegand. A 60-Cycle Hysteresis Loop Tracer for Small Samples of Low-Permeability Material 119–31; disc. 132
Hapgood, K. E.; C. P. Almon, Jr. Performance of 161-Kv and 115-Kv Transmission Lines 863–9; disc. 871
Harder, E. L. Solution of the General Voltage Regulator Problem by Electrical Analogy 815–25; disc. 825
Harder, E. L. Disc. 708, 915
Harder, E. L.; H. S. Kirschbaum. A Balanced Amplifier Using Biased Saturable Core Reactors 273–8
Harper, J. D. Disc. 870
Harris, Herbert. A Comparison of Two Basic Servomechanism Types 83–92; disc. 93
Hartwig, E. C.; C. B. Stadum; W. E. Large. Functionalized Resistance Welding Control 414–18
Hartzell, H. W. Disc. 836
Hathaway, J. L.; G. H. Schuck, C. K. Stedman, A. N. Butz, Jr. Bearing Deviation Indicator for Sonar 1285–95
Hause, Jack; D. R. MacLeod. Modern Railway Passenger-Car Auxiliary-Power Equipment 930–8
Hearn, R. B. An Electronic Regenerative Repeater for Teletypewriter Signals 904–11
Heberlein, G. E. Disc. 209
Hedges, R. E. Automatic Temperature Control for Transport Airplanes 1197
Heidenreich, Allan H. A Control System for Wind Tunnel Drives 1637–43; disc. 1643
Henry, R. T. Disc. 1579
Henshaw, M. D. Developments in Control Systems for Diesel-Electric Locomotives 23–41
Herman, C. J. Dynamic Brush Characteristics by the Dynamotor Method 759–63
Herr, Donald L. Disc. 320
Herr, Donald; Irving Gerst. The Analysis and an Optimum Synthesis of Linear Servomechanisms 959–70
Herzog, Eugene. Disc. 1643
Hess, W. B.; J. E. Allen. Testing Governor Performance on Electric Power Systems With Improved Instruments 329–39; disc. 342
Herwald, S. W.; G. D. McCann. Dimensionless Analysis of Servomechanisms by Electrical Analogy. Part I 111–18
Heilmann, G. W. Adjustable Frequency Control of High-Speed Induction Motors 719–25
Heumann, G. W. Disc. 144
Hickernell, L. F.; E. L. Peterson, D. M. Simmons, M. E. Noyes. Line Conductors—Tidd 500-Kv Test Lines 1603–11; disc. 1611
Hicks, Ben C. Disc. 915, 1060
Higgins, Thomas James. Theory and Application of Complex Logarithmic and Geometric Mean Distances 12–16
Hill, G. Leslie. Tests and Developments in Connection With Hot-Line Insulator Winding 1203–16
Hill, L. W.; J. W. Campbell; L. M. Moore; H. J. Scholz. Joint Use of Pole Lines for Rural Power and Telephone Services 519–24
Hoard, R. V. Disc. 1284
Hobbs, M. H. Disc. 1621
Hodnette, J. K.; F. A. Lane, P. L. Bellaschi, Edward Beck. Transformers and Lightning Arresters—Tidd 500-Kv Test Lines 1613–18; disc. 1618
Hoffman, C. H. Disc. 621
Holm, J. G. Disc. 411, 755, 1580, 1611
Holm, J. G.; A. M. Taylor. Disc. 955
Hoover, Ray. The Application of Western Union Multiplex to Navy Radio 1478–82
Hoover, W. G. Disc. 1257
Howard, S. B. Disc. 629
Howe, W. M.; H. E. Trekell. Disc. 861
Hoxie, E. A. The Application of Storage Batteries to the Control of Switchgear 1561–9; disc. 1569
Huber, G. H.; R. E. Crane, J. T. Dixon. Frequency Division Techniques for a Coaxial Cable Network 1451–9
Huntly, E. D. Disc. 562
Hutton, John G. Determination of Corona Starting Voltages for Nonuniform Fields in Air 1674–9; disc. 1680

J

Jang, M. J.; E. W. Boehne. Performance Criteria of D-C Interrupters 1172–80
Jeanne, P. A. Disc. 517
Jeffrey, Fraser. Disc. 189
Jessel, Joseph J. A. Disc. 622
Johnson, A. A. Disc. 1551
Johnson, I. B.; S. B. Crary. Economics of Long-Distance A-C Power Transmission 1092–9; disc. 1099
Johnson, I. B.; H. A. Peterson; C. M. Rhoades, Jr. Voltage Changes Caused by Resistance Loads 664–73; disc. 675
Johnson, I. B.; J. R. Wilson. Switching High-Voltage Transmission Lines 1552–60; disc. 1560
Johnson, I. B. Disc. 381
Johnson, Walter C. Disc. 623
Jones, D. M. Disc. 1578
Jones, J. N. A New Grinding Circuit Feed Regulator 1240–2
Jore, B. Disc. 606

K

Kaspar, F. P. Disc. 1162
Kauppi, T. A.; George Grant, III; Graham Lee Moses. Investigation of Silicone Insulation on High-Temperature Railway Motor 305–10
Keller, A. C. Submarine Detection by Sonar 1217–30
Kenefake, E. W. Disc. 830, 1034
Kevern, G. M. Airport Runway and Approach Lighting 1396–9
Kiefer, William M.; G. E. Foster. Electronic Telemetering System 802–07
Killgore, C. L. Excitation Problems in Hydroelectric Generators Supplying Long Transmission Lines 1277–82
Killgore, C. L. Disc. 1238
Killian, S. C.; M. Stene. Disc. 300
Kimball, A. W. Two-State Rotorol for Low-Energy Regulating Systems 1507–11
Kimbark, Edward W. Disc. 709, 755
King, Robert E. Disc. 76
Kinghorn, J. H.; Philip Sporn. Disc. 412
Kirschbaum, H. S.; E. L. Harder. A Balanced Amplifier Using Biased Saturable Core Reactors 273–8
Kirschbaum, H. S.; G. D. McCann, W. O. Osborn. General Analysis of Speed Regulators Under Impact Loads 1243–52
Kirwen, M. S.; F. W. Rich. Automatic Control of Air Switches for Line Sectionalizing and Load Transfer 293–9; disc. 301
Kliever, Waldo H.; Richard R. Syrdal. A Magnetic Compass With Cathode-Ray Sensing Element 529–34
Knapp, E. W. Disc. 869, 1069
Krauer, O. Disc. 1417
Krauss, H. L.; P. F. Ordung. Distortion and Bandwidth Characteristics of Pulse Modulation 984–8
Kron, Gabriel. Equivalent Circuit of the Primitive Rotating Machine With Asymmetrical Stator and Rotor 17–23
Kron, Gabriel. Tensorial Analysis and Equivalent Circuit of a Variable-Ratio Frequency Changer 1503–06

L

Laffoon, C. M.; R. A. Baudry. Modern Bearing Practice for Vertical Water Wheel Generators 363–9; disc. 371
Lakey, A. B. Disc. 1238
Lamm, A. Uno. Some Fundamentals of a Theory of the Transductor or Magnetic Amplifier 1078–85
Lamm, A. Uno. Disc. 887, 956
Lamson, Horatio W. Electronic Null Detectors for Use With Impedance Bridges 535–40
Landau, Maurice; Alfio Bisiri. Broken Conductor Effect on Sags in Suspension Spans 1181–8
Lane, F. A. Disc. 1569
Lane, F. A.; J. K. Hodnette, P. L. Bellaschi, Edward Beck. Transformers and Lightning Arresters—Tidd 500-Kv Test Lines 1613–18; disc. 1618
Lane, F. A.; B. W. Wyman. Switchgear Equipment for Tidd High-Voltage Test Lines 1619–21; disc. 1621
Lange, R. W. Measurement of High Q Cavities at 10,000 Megacycles 161–6
Langer, B. F. Developments in Current Collectors for High-Speed Service 51–4
Large, W. E.; C. B. Stadum; E. C. Hartwig. Functionalized Resistance Welding Control 414–18
Lawrence, Walter L. Television Equipment for Broadcast Stations 443–52
Lawton, F. L. Hydroelectric Power Development in Quebec 1006–21
Lawton, F. L. Disc. 916, 1059, 1069, 1091, 1124
Lebert, A. W.; J. B. Maggio, J. T. Schott, L. G. Abraham. Pulse Echo Measurements on Telephone and Television Facilities 541–8; disc. 548
Leeds, W. M.; R. C. Van Sickle. The Interruption of Charging Current at High Voltage 373–80; disc. 382

Leitch, John D. Dynamic Braking of a Single D-C Series Motor 149–54
Leitch, John D. Dynamic Braking of Two D-C Series Motors 787–91
Leitch, John D. Disc. 1113
Lenehan, B. E. A New Single-Side-Band Carrier System for Power Lines ..... 826–30; disc. 830
Lenehan, B. E. Disc. 10, 1430
Lenner, H. W. Operation of Power Line Carrier Channels ..... 888–93; disc. 894
LaVisconte, Lester. Disc. 622
Levinton, H. L. A Simple and Inexpensive Method for Accurately Measuring Steady-State and Transient High Voltages ..... 1304–10; disc. 1311
Lewis, C. B. A Power Plant Regulating System for Diesel-Electric Locomotives 242–6
Lewis, F. M.; T. W. Gordon. The Design and Performance of the Vertical Generator Thrust Bearings at the Bonneville Plant of the Corps of Engineers, War Department ..... 1231–7; disc. 1239
Lewis, Laurel, J. Circuit-Breaker Current Measurements During Reignitions and Recovery 1253–7
Lewis, W. A.; L. S. Tippett. Fundamental Basis for Distance Relaying on 3-Phase Systems 694–708
Lewis, W. A. Disc. 1577
Lewis, W. W. Disc. 1550
Lincks, G. Fred. Disc. 259, 388
Lippert, G. D.; R. L. Tremaine. Instrumentation and Measurement—Tidd 500 Kv Test Lines ..... 1624–30; disc. 1630
Livingston, O. W. Electronic Constant-Current Motor Systems ..... 425–30; disc. 431
Liwschitz, M. K. Leakage Reactance of the Squirrel Cage Rotor With Respect to the Stator Harmonics and the Equivalent Circuit of the Induction Motor 1407–08
Liwschitz, M. M.; W. H. Formhals. Some Phases of Calculation of Leakage Reactance of Induction Motors ..... 1409–13; disc. 1412
Liwschitz, M. M. Multistage Rototrol, The 564–8
Lloyd, T. C.; Sheldon S. L. Chang. A Design Method for Capacitor Motors 652–8
Lloyd, T. C.; V. F. Giusti, S. S. L. Chang. Reactances of Squirrel-Cage Induction Motors 1349–55
Loane, E. S.; C. W. Watchorn. Probability Methods Applied to Generating Capacity Problems of a Combined Hydro and Steam System ..... 1645–54; disc. 1657
Loane, E. S.; C. W. Watchorn. Disc. 1477
Loomis, R. O. Disc. 391
Lorraine, R. G. Disc. 981
Lory, M. R.; R. R. Baker. The Application of Synchronous Induction Motors to Chippers 1070–7
Lunge, G. S. Disc. 29
Lusignan, J. T. Disc. 849
Lyman, W. J. Calculating Probability of Generating Capacity Outages ..... 1471–7; disc. 1477
Lyon, J. A. M.; J. F. Calvert. Disc. 10

M

Maclachlin, Wills. Disc. 1147
MacLeod, D. R.; Jack Hause. Modern Railway Passenger-Car Auxiliary-Power Equipment 930–8
Madill, J. T. Typical Transformer Faults and Gas Detector Relay Protection ..... 1052–8; disc. 1060
Madill, J. T. Disc. 916, 1091, 1124
Maggio, J. B.; J. T. Schott, L. G. Abraham, A. W. Lebert. Pulse Echo Measurements on Telephone and Television Facilities ..... 541–8; disc. 548
Maginniss, F. J.; G. K. Carter, F. S. Rothe. Suddenly Applied Loads on a Variable-Ratio Frequency Changer 1489–95
Magnusson, P. C. The Transient-Energy Method of Calculating Stability ..... 747–55; disc. 755
Mallett, M. B. High-Voltage Power-Transformer Design. Part II ..... 1086–91; disc. 1091
Maney, W. L. Disc. 1124
Manning, M. L. Disc. 982
Marcy, H. Tyler. Disc. 93
Marsden, D. J. Disc. 48
Marshall, D. E. Ignitor Characteristic and Circuit Calculations 1519–24
Matte, A. L.; J. R. Davey. Frequency Shift Telegraphy—Radio and Wire Applications 479–93
Mayer, Robert W. Disc. 76
Mayott, G. W. Disc. 1047
McCann, G. D.; Edward Beck. Field Research on Lightning Arrester Discharges ..... 625–29; disc. 630
McCann, G. D.; I. W. Gross. Field Investigation of Lightning Surges at Substations ..... 569–74; disc. 576
McCann, G. D.; S. W. Herwald. Dimensionless Analysis of Servomechanisms by Electrical Analogy. Part I 111–18
McCann, G. D.; W. O. Osbon, H. S. Kirschbaum. General Analysis of Speed Regulators Under Impact Loads 1243–52
McClinton, A. T. An Integrated Control System for Aircraft D-C Generators 94–8
McClure, J. B. Disc. 1048
McConnell, J. D. Power Distribution in Textile Plants 660–5
McCoy, R. L.; I. W. Gross, J. M. Sheadel. Insulators and Line Hardware for Tidd 500-Kv Test Lines ..... 1592–1602; disc. 1602
McCreary, H. J. Disc. 131
Meador, J. R. Disc. 67
Meahl, Harry R. Disc. 548
Means, W. J.; E. P. Felch; T. Slonczewski; L. G. Parratt; L. H. Rumbaugh; A. J. Tickner. Air-Borne Magnetometers for Search and Survey 640–50
Mears, R. B.; L. P. Sudrabin. Cathodic Protection of Steel Water Tanks Using Aluminum Anodes 197–200
Melvin, H. L. Disc. 849
Merrell, Edwin J. Disc. 603
Mershon, C. L. Control and Power Systems for Aircraft Window Deicing 1400–05
Messmer, G. R.; E. H. B. Bartelink, L. E. Cook, F. A. Cowan. Application of Rural Carrier Telephone System ..... 511–18; disc. 518
Metcalf, C. N. Disc. 29
Michon, A. E.; F. H. Cussack. A Frequency Modulation Telegraph Terminal Without Relays ..... 1165–70; disc. 1171
Millar, N. P.; A. J. Corson. Applications of the Electrodynamic Instrument Mechanism 1131–6
Millar, N. P.; R. M. Rowell. Advancements in the Design of Long-Scale Indicating Instruments 155–60
Miller, K. W. Diffusion of Electric Current into Rods, Tubes, and Flat Surfaces 1496–1502
Moore, A. D. Eddy Currents in Disks: Driving and Damping Forces and Torques 1–10
Moore, J. Harold; Paul K. Seyler, S. B. Wright. Rural Radiotelephone Experiment at Cheyenne Wells, Colo. 525–8
Moore, L. M.; H. J. Scholz, J. W. Campbell, L. W. Hill. Joint Use of Pole Lines for Rural Power and Telephone Services 519–24
Moore, Myron M. Disc. 623
Moore, R. B.; H. C. Uhl. Electric Drives for Textile Finishing Ranges 684–94
Mortensen, S. H. Disc. 561
Moses, Graham Lee. Disc. 981
Moses, Graham Lee; George Grant, III, T. A. Kauppi. Investigation of Silicone Insulation on High-Temperature Railway Motor ..... 305–10; disc. 310
Monteith, A. C.; Philip Sporn. Transmission of Electric Power at Extra High Voltages ..... 1571–7; disc. 1582
Montsinger, V. M. (Closure of Committee Report) Preliminary Report on Laboratory Aging Tests on Class A Insulation ..... 879–81; disc. 882
Mott, G., Jr. Disc. 1348
Murphy, T. H. Disc. 246
Murray, J. A.; T. B. Owen, A. Rosenstein. Ground Power Supply for Modern Aircraft 1296–1303

N

Nader, Joseph; C. S. Roys, M. Spotts. A Variable-Speed Constant-Frequency Generator ..... 1414–17; disc. 1417
Narbutovskih, Paul: Simplified Graphical Method of Computing Thermal Transients ..... 78–81; disc. 82
Needs, S. J. Disc. 1237
Newton, George C., Jr.; W. T. White. Laboratory Aids for Electromechanical System Development 315–19
Nichols, B. R. Disc. 340
Nims, P. T.; O. E. Bowlus. Parallel Operation of Aircraft Alternators Using Electronic Frequency Changers 31–8
Noest, John G. The German Electrical Utility Industry During World War II ..... 1037–47; disc. 1050
Nonken, G. C. Disc. 1469
Noyes, M. E.; E. L. Peterson, D. M. Simmons, L. F. Hickernell ..... 1603–11; disc. 1611

O

Obrecht, R. G. Disc. 1035
O'Connor, R. R.; H. I. Romnes. General Mobile Telephone System 1658–66
Oldacre, M. S. Disc. 286
Olmstead, E. G. Disc. 1282
Olmsted, Leonard M. Disc. 260
Oppenheimer, F. Disc. 341
Ordung, P. F.; H. L. Krauss. Distortion and Band-Width Characteristics of Pulse Modulation 984–8
Osbon, W. O.; G. D. McCann, H. S. Kirschbaum. General Analysis of Speed Regulators Under Impact Loads 1243–52
Owen, T. B.; J. A. Murray, A. Rosenstein. Ground Power Supply for Modern Aircraft 1296–1303

P

Pakala, Wm. E.; C. J. Cuculla. Arc-Back Testing of Graphite 439–42
Panter, P. F.; A. G. Clavier, D. D. Grieg. Distortion in a Pulse Count Modulation System ..... 989–1005; disc. 1005
Parks, C. E.; J. J. Trainor. Experience With Single-Pole Relaying and Reclosing on a Large 132-Kv System ..... 405–11; disc. 412
Parratt, L. G.; E. P. Felch; W. J. Means; T. Slonczewski, L. H. Rumbaugh, A. J. Tickner. Air-Borne Magnetometers for Search and Survey 640–50
Pearson, D. B. A Capacitance-Type Fuel-Measurement System for Aircraft 1363–8
Pearson, D. B. Disc. 1196
Pearson, G. L. The Physics of Electronic Semiconductors 209–14
Pearson, Thomas J., Jr. Disc. 861
Peirce, Roger M.; Victor Siegfried. Disc. 601
Pendleton, W. W. High Altitude Flashover and Corona Correction on Small Ceramic Bushings 1324–30
Peters, H. P.; R. B. Squires. Disc. 621
Peterson, E. L.; D. M. Simmons, L. F. Hickernell, M. E. Noyes. Line Conductors—Tidd 500-Kv Test Lines ..... 1603–11; disc. 1611
Peterson, E. L.; C. F. Wagner, A. Wagner, I. W. Gross. Corona Considerations on High-Voltage Lines and Design Features of Tidd 500-Kv Test Lines 1583–90
Peterson, E. N. Disc. 1656
Peterson, H. A.; C. M. Rhoades, Jr., I. B. Johnson. Voltage Changes Caused by Resistance Welding Loads ..... 664–73; disc. 675
Peterson, T. F. Disc. 1631
Peterson, William S. Disc. 1579, 1590, 1602
Pettee, A. D. Disc. 603
Pettinger, A. J. A Polyphase Thermal Ampere-Demand Meter 167–74
Phillips, H. W. Disc. 1655
Pierce, R. R.; E. E. George. Disc. 1100
Pollard, E. I. Disc. 369
Potter, C. P. New NEMA Fractional-Horsepowers Motor Standards; Their Effect on Refrigeration and Pump Applications 508–10
Potter, C. P. Disc. 590
Potter, J. A. The Shunt Tube Control of Thyratron Rectifiers 421–4
Prince, David C. Disc. 1101
Prince, D. C.; E. F. W. Alexanderson. Electronic Stabilizer for Power Transmission ..... 950–3; disc. 958
Puchlowski, K. P. Disc. 430
Puchstein, A. F. Calculation of Slot Constants ..... 1315–22; disc. 1322
Pugsley, D. W. Postwar Television Receiver Design 453–8

Q

Quinn, R. F. Disc. 261

R

Ramberg, Walter. The Measurement of Acceleration With a Vacuum Tube 735–40
Rankin, A. W. Disc. 23
Ratz, E. G. Disc. 1059
Rawlins, H. L. Disc. 976
Rawlins, H. L.; Jerome Sandin. An Improved Overcurrent Tripping Device for Low-Voltage Circuit Breakers ..... 1149–53; disc. 1153
Reardon, K. N. Disc. 301
Reed, H. R. The Stromberg-Carlson XY Dial Telephone System 432–8
Reed, R. B. Disc. 836
Reid, C. R. Disc. 1069
Rhea, T. R. Disc. 246
Rhoades, C. M., Jr.; I. B. Johnson; H. A. Peterson. Voltage Changes Caused by Resistance Welding Loads ..... 664–73; disc. 675
Rich, F. W.; M. S. Kirwen. Automatic Control of Air Switches for Line Sectionalizing and Load Transfer ..... 293–9; disc. 301
Rietz, Earl B. Disc. 47
Riley, L. G. Motor Control for Latest New York Transit System Subway Cars 900–03
Riley, L. G. Disc. 250
Robertson, A. S.; R. O. Standing. The Maintenance of Hydroelectric Generating Units 776–82

Robinson, R. C. The Horsepower Output of Polyphase Induction Motors.....770–5
Romnes, H. I.; L. G. Abraham. Television Network Facilities.....459–64
Romnes, H. I.; R. R. O'Connor. General Mobile Telephone System.....1658–66
Rorden, H. L. Radio-Noise Influence of 230-Kv Lines.....677–81; disc. 682
Rothe, F. S.; G. K. Carter, F. J. Maginnis. Suddenly Applied Loads on a Variable-Ratio Frequency Changer.....1489–95
Rosen, S.; H. A. Wenk; W. H. Tidd. New Test Equipment and Testing Methods for Cable Carrier Systems.....726–30
Rosenstein, Allen; T. B. Owen, J. A. Murray. Ground Power Supply for Modern Aircraft.....1296–1303
Ross, M. D. Disc.....561
Ross, Paul M. Burning of Wood Structures by Leakage Currents.....279–84; disc. 286
Ross, Paul M. Disc.....849
Rotors, Herbert C. The Hysteresis Motor—Advances Which Permit Economical Fractional Horsepower Ratings.....1419–30; disc. 1430
Rothe, F. S. Disc.....621
Rothe, F. S.; C. Concordia. Transient Characteristics of Current Transformers During Faults. Part II.....731–4
Rothpletz, Max W. Disc.....361, 390
Rowell, R. M.; N. P. Millar. Advancements in the Design of Long-Scale Indicating Instruments.....155–60
Roys, Carl S.; J. Nadar, M. Spotts. A Variable-Speed Constant-Frequency Generator..1414–17; disc. 1417
Rudge, W. J. Disc.....261
Rumbaugh, L. H.; E. P. Felch, W. J. Means, T. Slonczewski, L. G. Parratt, A. J. Tickner. Air-Borne Magnetometers for Search and Survey.....640–50
Runciman, A. S. Disc.....1162
Ryan, J. E. Disc.....137

S

Sadler, E. K.; T. M. Blakeslee. Resistors for 138-Kv Cable Switching.....39–46; disc. 49
St. Clair, H. P.; Philip Sporn. Disc.....381
Samuels, M. K. Disc.....1579
Samuels, M. M. Disc.....391, 1549
Sandin, Jerome; H. L. Rawlins. An Improved Overcurrent Tripping Device for Low-Voltage Circuit Breakers.....1149–53; disc. 1153
Schaelchlin, W. Rotating Stability Regulators for Synchronous Motor Drives.....884–7; disc. 887
Schleicher, G. B. Metering With Transformer-Loss Compensators.....851–61; disc. 862
Schmidt, P. L.; A. C. Beiler. Interlaminar Eddy Current Loss in Laminated Cores.....872–7; disc. 877
Schmitz, N. L. Control of Slip-Ring Motors by Means of Unbalanced Primary Voltages.....1103–1112; disc. 1113
Schols, H. J.; J. W. Campbell, L. W. Hill, L. M. Moore. Joint Use of Pole Lines for Rural Power and Telephone Services.....519–24
Schott, J. T.; L. G. Abraham, A. W. Lebert, J. B. Maggio. Pulse Echo Measurements on Telephone and Television Facilities.....541–8; disc. 548
Schroeder, T. W. Disc.....327
Schuck, O. H.; C. K. Stedman, J. L. Hathaway, A. N. Butz, Jr. Bearing Deviation Indicator for Sonar.....1285–95
Schwartz, George J. The Application of Lead Networks and Sinusoidal Analysis to Automatic Control Systems.....69–76; disc. 77
Schwarz-Kast, E. L. A Thruster Lowering Control System for A-C Crane Hoists.....139–44; disc. 144
Seelye, Howard P. Outage Expectancy as a Basis for Generator Reserve.....1483–8
Seyler, Paul K.; J. Harold Moore; S. B. Wright. Rural Radiotelephone Experiment at Cheyenne Wells, Colorado.....525–8
Shanck, R. B. Disc.....1170
Sheadel, J. M.; I. W. Gross, R. L. McCoy. Insulators and Line Hardware for Tidd 500-Kv Test Lines.....1592–1602; disc. 1602
Shepley, J. M.; C. B. Walton. Disc.....623
Sheppard, R. Disc.....339
Siegfried, Victor, Roger M. Peirce. Disc.....601
Simmons, D. M.; E. L. Peterson, L. F. Hickernell, M. E. Noyes. Line Conductors—Tidd 500-Kv Test Lines.....1603–11; disc. 1611
Sinclair, J. J. Special 10-Car Train for the New York City Transit System.....251–4
Skeats, W. F. Disc.....46
Slemon, Gordon R. Disc.....1591
Slonczewski, T.; E. P. Felch, W. J. Means, L. G. Parratt, L. H. Rumbaugh, A. J. Tickner. Air-Borne Magnetometers for Search and Survey.....640–50
Smith, B. M. Disc.....132
Smith, Frank V. Disc.....412
Smith, I. R. Higher Voltage Copper-Oxide Rectifiers.....220–2
Smith, K. D.; J. F. Wentz. A New Microwave Television System.....465–70
Smith, Robert W. Disc.....976, 1153
Smith, Roy M. Disc.....261
Smithley, R. S. Disc.....300
Smythe, William R. Disc.....11
Snell, D. S. Disc.....562
Sohon, Harry. Disc.....1180
Solomon, J. L.; William J. Farrell. Disc.....674
Spease, J. F. Disc.....1238
Sporn, Philip. Disc.....575
Sporn, Philip; J. H. Kinghorn. Disc.....412
Sporn, Philip; A. C. Monteith. Transmission of Electric Power at Extra High Voltages.....1571–7; disc. 1582
Sporn, Philip; H. P. St. Clair. Disc.....381
Spotts, Melvin; C. S. Roys, J. Nader. A Variable-Speed Constant-Frequency Governor.....1414–17; disc. 1417
Squires, R. B.; H. P. Peters. Disc.....621
Srinivasan, A.; M. A. Thomas. Dynamic Braking by Self-Excitation of Squirrel-Cage Motor.....145–8
Srinivasan, A.; F. J. Vogel. Transient Voltage Rise in Transformers Due to Interruption of Exciting Current.....1632–6
Stacey, J. D. Disc.....1144
Stadum, C. B.; W. E. Large; E. C. Hartwig. Functionalized Resistance Welding Control.....414–18
Standing, R. O. Disc.....370
Standing, R. O.; A. S. Robertson. The Maintenance of Hydroelectric Generating Units.....776–82
Stanley, J. K.; T. D. Yensen. Hiperco—A Magnetic Alloy.....714–18
Staples, D. R.; T. L. Weybrew, C. A. Atwell. A 3,000 Horsepower Diesel-Electric Locomotive for the Seaboard Air Line Railway.....215–19
Starr, E. C. Disc.....381, 575, 600, 682, 847, 953, 1099, 1577, 1590
Stauder, L. F. Disc.....1112
Stedman, C. K.; O. H. Schuck, J. L. Hathaway, A. N. Butz, Jr. Bearing Deviation Indicator for Sonar.....1285–95
Steele, R. B. Disc.....1170
Stein, G. M. The Voltage Drop in the Welder Throat Loaded With Ferromagnetic Materials.....356–62
Stein, J. M. The Magnetomotive Force of 2-Layer Windings of Rotating Machines.....756–8
Steiner, H. C. Disc.....957
Stene, M.; S. C. Killian. Disc.....300
Stewart, A. L. Disc.....1068
Stickley, G. W. Disc.....1162
Stone, H. B. Disc.....1438
Sudrabin, L. P.; R. B. Mears. Cathodic Protection of Steel Water Tanks Using Aluminum Anodes.....197–200
Sumner, W. A. Disc.....389
Syrdal, Richard R.; Waldo H. Kliever. A Magnetic Compass With Cathode-Ray Sensing Element.....529–34

T

Talmage, T. DeWitt. TVA Co-ordinated Communication System.....1022–34; disc. 1034
Tatum, George M. Disc.....1047
Taylor, H. D. Disc.....561
Tebo, Gordon B. Disc.....1161
Temoshok M.; C. Concordia. Resynchronising of Generators.....1512–18
Thomas, M. A.; A. Srinivasan. Dynamic Braking by Self-Excitation of Squirrel-Cage Motor.....145–8
Thurber, J. P. Disc.....746
Tickner, A. J.; E. P. Felch, W. J. Means, T. Slonczewski, L. G. Parratt, L. H. Rumbaugh. Air-Borne Magnetometers for Search and Survey.....640–50
Tidd, W. H.; S. Rosen, H. A. Wenk. New Test Equipment and Testing Methods for Cable Carrier Systems.....726–30
Tilles, Abe. Disc.....1602, 1611, 1622, 1631
Tippett, L. S.; W. A. Lewis. Fundamental Basis for Distance Relaying on 3-Phase Systems.....694–708
Tirk, C. J. Disc.....1310
Tornquist, E. L.; C. Becker. Galloping Conductors and a Method for Studying Them.....1154–61; disc. 1163
Trainor, J. J.; C. E. Parks. Experience With Single-Pole Relaying and Reclosing on a Large 132-Kv System.....405–11; disc. 412
Treat, Robert. Disc.....1048
Trekell, H. E.; W. M. Howe. Disc.....861
Tremaine, R. L.; G. D. Lippert. Instrumentation and Measurement—Tidd 500-Kv Test Lines.....1624–30; disc. 1630
Trickey, P. H. Performance Calculations on Shaded Pole Motors.....1431–8; disc. 1438
Trickey, P. H. Disc.....657

U

Uhl, H. C.; R. B. Moore. Electric Drives for Textile Finishing Ranges.....684–94
Umansky, L. A. Disc.....190, 1643

V

Van Ness, B., Jr. Disc.....370
Van Ryan, A. Disc.....261
Van Sickle, R. C. Disc.....48
Van Sickle, R. C.; W. M. Leeds. The Interruption of Charging Current at High Voltage.....373–80; disc. 382
Vencill, G. J. Disc.....339
Vivian, J. H. Disc.....1283
Vogel, F. J. A Study of the Relative Severity of Steep Front Waves and Chopped Waves on Transformers.....64–6; disc. 67
Vogel, F. J. Disc.....1618, 1680
Vogel, F. J.; A. Srinivasan. Transient Voltage Rise in Transformers Due to Interruption of Exciting Current.....1632–6
Vouch, S. J. Recent Developments in Track Brakes and Drum Brakes for PCC Cars.....302–04

W

Waghorne, J. H. A Simplified Double-Film Klydonograph With an Improved Coupling Method.....1114–16
Wagner, Anthony; C. F. Wagner, E. L. Peterson, I. W. Gross. Corona Considerations on High-Voltage Lines and Design Features of Tidd 500-Kv Test Lines.....1583–90
Wagner, C. F.; A. Wagner, E. L. Peterson, I. W. Gross. Corona Considerations on High-Voltage Lines and Design Features of Tidd 500-Kv Test Lines.1583–90
Wagner, W. C. Disc.....1147
Walker, H. P. Silicone Insulation as Applied to Naval Electric Power Equipment.....977–80; disc. 980
Wallace, J. M. An Improved Automatic Circuit Reclosser.....255–8; disc. 262
Wallace, J. M. Disc.....390
Walton, A. W. Disc.....894
Walton, C. B.; J. M. Shepley. Disc.....623
Ward, J. B. Disc.....622
Warren, C. E.; W. L. Davis. The Calibration of Ignition Crest Voltmeters.....99–104
Watchorn, C. W.; E. S. Loane. Probability Methods Applied to Generating Capacity Problems of a Combined Hydro and Steam System.....1645–54; disc. 1657
Watkins, Bruce O. Sectionalizing and Internal Transformer Fusing on Rural Power Circuits.....383–8; disc. 391
Weaver, H. E. Disc.....285
Webb, R. L. Disc.....981
Weiner, E. F. Braking Resistors and Control for Diesel-Electric Locomotives.....229–32
Wenk, H. A.; W. H. Tidd, H. A. Wenk. New Test Equipment and Testing Methods for Cable Carrier Systems.....726–30
Wentz, J. F.; K. D. Smith. A New Microwave Television System.....465–70
West, H. R.; P. L. Alger. The Air Gap Reactance o Polyphase Machines.....1331–43
Weybrew, T. L.; D. R. Staples, C. A. Atwell. A 3,000 Horsepower Diesel-Electric Locomotive for the Seaboard Air Line Railway.....215–19
White, W. T.; George C. Newton, Jr. Laboratory Aids for Electromechanical System Development.....315–19
Whitehead, J. B. Dielectric Heating—The Measurement of Loss Under Rising Temperature.....947–9
Whitehead, J. B. Disc.....1145
Wickham, W. H. Disc.....285
Widell, B. A. The Design of New York Subway Motors for Dynamic Braking.....808–10
Widmer, A. E. Disc.....606
Wiegand, D. E.; W. W. Hansen. A 60-Cycle Hysteresis Loop Tracer for Small Samples of Low-Permeability Material.....119–31; disc. 132
Wier, A. J.; I. G. Wilson, H. S. Black, F. A. Brooks. An Improved Cable Carrier System.....741–6; disc. 746
Williams, Horatio B. Hazards of Static Electricity in Hospital Operating Rooms.....1146–7
Willis, C. H. Disc.....954
Wilson, I. G.; H. S. Black, F. A. Brooks, A. J. Wier. An Improved Cable Carrier System.....741–6; disc. 746

Wilson, J. R.; I. B. Johnson. Switching High-Voltage Transmission Lines.....1552–60; disc. 1560
Wittig, W. F. Data on the High-Frequency Resistance of Coils.....764–9
Woods, G. M. Disc.....250, 254
Wright, S. B.; J. Harold Moore, Paul K. Seyler. Rural Radiotelephone Experiment at Cheyenne Wells, Colo.....525–8
Wyman, R. W.; F. A. Lane. Switchgear Equipment for Tidd High-Voltage Test Lines.....1619–21; disc. 1621

Y

Yensen, T. D.; J. K. Stanley. Hiperco—A Magnetic Alloy.....714–18

Z

Zamsky, J. Quantitative Determination of Magnetic Properties by Use of Cathode-Ray Oscilloscope.....783–7
Zimmerman, S. W. Disc.....104
Zweig, F.; A. G. Conrad, J. G. Clarke. Disc.....1672

Preface

This 66th volume of the TRANSACTIONS of the American Institute of Electrical Engineers contains all approved technical program papers and related discussions presented at general meetings and District meetings during the calendar year, in accordance with the improved publication policy adopted by the board of directors at its May 1946 meeting.

The technical papers and discussions in the volume were presented at these meetings:

1. 1947 winter general meeting, New York, N. Y., January 27–31, 1947.
2. North Eastern District Meeting, Worcester, Mass., April 23–25, 1947.
3. Summer general meeting, Montreal, Que., Can., June 9–13, 1947.
4. Pacific general meeting, San Diego, Calif., August 26–29, 1947.
5. Middle Eastern District meeting, Dayton, O., September 23–25, 1947.
6. Midwest general meeting, Chicago, Ill., November 3–7, 1947.

In addition this volume contains:

1. 1947 annual report of the board of directors.
2. A complete listing of AIEE officers and committees for 1947–48.
3. New AIEE Publication Policy—Effective in January 1947.

Full correlation of all material in this volume has been accomplished by means of the multientry index beginning on page 1738. Reference to any of the several subject entries for a technical paper will lead directly to the paper and to any published discussion on that paper.

Statements and opinions given in papers and discussions published in TRANSACTIONS are the expressions of contributors for which the American Institute of Electrical Engineers assumes no responsibility.

Errata

1. Page 1363. Add the following footnote: "The double triode circuit was originated by William Brauner, now research engineer, The Franklin Institute Laboratories for Research and Development, Philadelphia, Pa."

Eddy Currents in Disks: Driving and Damping Forces and Torques

A. D. MOORE
FELLOW AIEE

Synopsis: When two a-c fluxes, in quadrature, pass through a disk, driving forces and torques are produced. Theory is developed herein, and formulas and procedures are presented whereby the force or torque can be solved for, even when the fluxes are irregular as to area and distribution. As an example, the driving torque of a watthour meter is solved for. A chart for greatly facilitating the work is described.

When a constant flux (or fluxes) passes through a rotating disk, a damping or braking torque is produced. With the aid of what may be a new concept, theory, formulas, and procedures are presented whereby the torque may be found, even though the flux (or fluxes) has an irregular area. To illustrate, the damping torque of a watthour meter is computed. The method can deal also with fluxes of nonuniform density. A chart is described which greatly reduces the work.

When a disk with constant flux through it is moved translationally, damping forces occur. Curves covering a wide range are presented, by which those designing the damping for accelerometers and other instruments may design easily in direct fashion rather than by trial-and-error. For their benefit, this part of the paper is written so that it is complete in itself.

For both driving and damping torques, reciprocity laws are proved; when needed, these laws greatly reduce the time required for a solution.

It is often true that apparently complex devices can be analyzed with relative simplicity, whereas a simple-appearing device may require complex analysis. Eddy-current devices, structurally, are the simplest of electric mechanisms. Yet, because the eddy currents are not confined to easily identifiable paths, analysis has yielded scanty returns, and engineering design has limped along as best it could. This is true, even though some devices have been known for half a century or more; and speedometers and watthours, to name only two devices, are numbered in the millions. The literature of a basic character is notable for its paucity.

Lack of progress probably stems directly from an old difficulty, the usual tendency of analysts to proceed in terms of straightforward mathematics. The truth is that such methods simply cannot solve disk eddy-current problems in general. Irregular flux areas and densities can be handled practicably only by approximate methods such as are developed herein.

Conditions

As to a-c driving fluxes, this paper is limited to those cases in which disk resistance effect is large compared to disk reactance effect. As to damping fluxes, the paper is limited to cases in which the disk is thin enough, or velocity low enough, (or both) so that the eddy currents are not strong enough to have much effect in redistributing the flux. Meters and instruments usually meet these conditions.

The a-c driving flux treatment deals only with fluxes in quadrature. If actual fluxes are not in quadrature, only the quadrature components are effective in producing a net force.

A-C Driving Torques

A large thin metal disk, as in Figure 1, is pierced by fluxes Φ_J and Φ_K. These are the rms values of a-c fluxes, in quadrature. Such fluxes will be called a flux pair. Each is a uniform flux within a circle. The distance between circle centers J and K is S centimeters. The fluxes have a sine wave variation at frequency f. The circles do not overlap.

The variation of Φ_K sets up concentric eddies in quadrature with Φ_K. Eddy current maximum occurs when Φ_J is maximum. Φ_K eddies act on Φ_J to produce a sine squared wave of force. It will be shown that the average force, F_{KJ} in dynes, acting along JK or S, is

$$F_{KJ} = G/S \tag{1}$$

where G is developed further along.

The force F_{KJ} is actually a resultant force made up of an infinitude of forces, each due to an element of current reacting with the flux in the J-circle. The problem of finding the resultant can be avoided by resorting to a familiar analogous situation.

In the analogy, the two circles become sections of long parallel conductors normal to the paper. Conductor currents, I_J and I_K, are distributed uniformly. I_K sets up a concentric magnetic field. It long since has been shown

(*a*). That outside its conductor, the field due to I_K is the same as if I_K were centered (concentrated in a wire of infinitesimal section at K).

(*b*). That the force due to the distributed I_J reacting with the flux of I_K is the same as it would be if I_J were centered at J.

(*c*). The force per unit length for such a combination is proportional to $(I_J I_K)/S$.

From the analogy, it is clear that in our disk case, Φ_K can be centered at K, becoming a pencil of flux; Φ_J can be centered at J; and

$$F_{KJ} \propto \Phi_J \Phi_K / S \tag{2}$$

Development of G

In Figure 2, Φ_K has been centered, thereby becoming a flux pencil. In centering Φ_J, we have the privilege of moving it into the infinitesimal square, ds by ds, at J. The force originating in this square is F_{KJ}, and it now can be developed fully.

The effective voltage E developed by

Paper 47-1, recommended by the AIEE committee on basic sciences for presentation at the AIEE winter meeting, New York, N. Y., January 27-31, 1947. Manuscript submitted July 9, 1946; made available for printing October 1, 1946.

A. D. Moore is professor of electrical engineering at the University of Michigan, Ann Arbor, Mich.

Φ_K in the disk (turns=1) and acting around the current ring of ds width is given by the familiar equation

$$E=2\pi f\Phi_K\times10^{-8} \tag{3}$$

To find R, the resistance of the current ring,

ρ = disk resistivity, ohm per centimeter
b = disk thickness, centimeters
$2\pi S$ = path length
bds = path section

$$R=\frac{\rho 2\pi S}{bds} \tag{4}$$

To find the rms current of the ds by ds square

$$I=\frac{E}{R}$$
$$=2\pi f\Phi_K\times10^{-8}\div\left(\frac{\rho 2\pi S}{bds}\right)$$
$$=\frac{fb\Phi_K\times10^{-8}}{\rho S}ds \tag{5}$$

The dynes force is given by the familiar form, $BIL/10$. In the ds by ds square, $B=\Phi_J/(ds)(ds)$, I is given by equation 5, and L is equal to ds. The force is then

$$F_{KJ}=\left[\frac{\Phi_J}{(ds)(ds)}\right]\left[\frac{fb\Phi_K10^{-8}}{\rho S}ds\right]\left[ds\right]\frac{1}{10}$$
$$=\frac{fb\Phi_J\Phi_K\times10^{-9}}{\rho S} \tag{6}$$

Let

$$G=\frac{fb\Phi_J\Phi_K\times10^{-9}}{\rho} \tag{7}$$

$$F_{KJ}=\frac{G}{S}\text{ dynes} \tag{1}$$

Because this force is the product of two effective values, and because the current and flux concerned are in phase, the force F_{KJ} is the time average of the actual force.

Torque

The torque T_{KJ} (see Figure 1) due to force F_{KJ} acting at lever arm D about some point O, in dyne-centimeters, is

$$T_{KJ}=F_{KJ}D$$
$$=G\frac{D}{S} \tag{8}$$

Reciprocity Law and Torque of a Flux Pair

It is obvious that in addition to F_{KJ}, there is an equal force F_{JK}, due to J-eddies acting on Φ_K. Thus there is a reciprocity law as to forces. The total force is the sum of the two. Thus, for a flux pair (either in nonoverlapping circles or as pencils) the total, F_p, is

$$F_p=2\frac{G}{S} \tag{9}$$

As to torque, both forces act with lever arm D. Thus there is a torque reciprocity law. Then the total torque T_p for a flux pair is

$$T_p=2G\frac{D}{S} \tag{10}$$

Circular Disk

If an a-c flux pencil at K, Figure 3, pierces a circular disk of radius A centimeters, the eddy currents occur in eccentric circles. Morton[1] gives the equation for the eccentricity. It is not included here, because a simplification used herein consists of avoiding the problem of dealing with eccentric current paths. The image concept is resorted to.

On a very large plate or disk, Figure 3, lay out the disk circle as shown. Extend OK. The image of the K-pencil of flux can be located at K', by theory long since developed. If $OK=R$,

$$KK'=(A^2-R^2)/R$$
$$OK'=KK'+R$$
$$=\frac{A^2-R^2}{R}+R$$
$$=\frac{A^2}{R} \tag{11}$$

The image or K'-pencil is equal to the K-pencil but is opposite in sign. Acting together, this pencil pair will set up the double eccentric eddy pattern; and within the disk circle, the eddies are identical with what the K-pencil alone would set up in the real disk.

Passing to Figure 4, we avoid eccentricity troubles by dealing with the flux pencils individually. In the large disk, the K-pencil sets up component concentric eddies about itself; and likewise, for the K'-pencil. (Note that this pair within itself creates no net force; the eddies of each are in quadrature with the flux of the other.)

The foregoing is applied in Figure 5, where a disk is acted on by a flux pair. The flux Φ_K can be centered first at K. The K-pencil image at K' is located next. The flux pair creates a total force as expressed in equation 9 and a total torque as given by equation 10. Similarly, the flux pair Φ_J and $\Phi_{K'}$ yield another (smaller) force and torque, the force acting along S' at lever arm D'. Since the image flux is opposite to the K-pencil, the image torque opposes the direct torque; and the net torque is

$$T_p=2G\left(\frac{D}{S}-\frac{D'}{S'}\right) \tag{12}$$

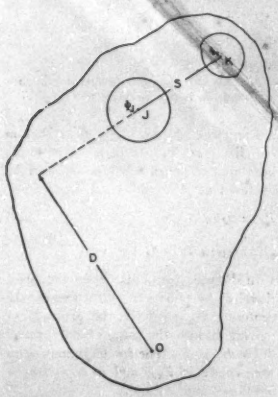

Figure 1. Large disk and flux pair

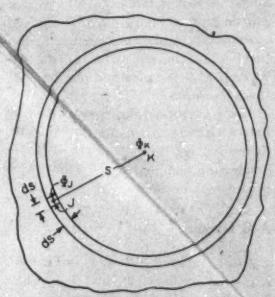

Figure 2. Force, centered fluxes

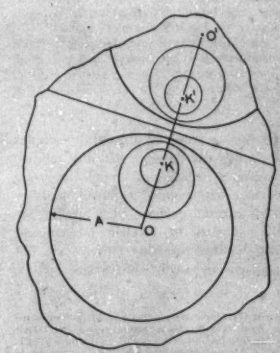

Figure 3. Flux pencil, image, and eccentric eddy-current pattern

General Torque Expression: Circular Disk and a Flux Pair

To develop a general torque expression, we will use the additional constructions given in Figure 5. Instead of lever arms D and D', lever arm $C=OJ$ will be used. This calls for the use, not of the whole forces along S and S', but of their horizontal components (taking C as vertical). The components are H/S and H'/S', respectively, times the two forces. The total torque can be written then

$$T_p=2G\left(\frac{C}{S}\frac{H}{S}-\frac{C}{S'}\frac{H'}{S'}\right)$$

$$=2GC\left(\frac{H}{S^2}-\frac{H'}{S'^2}\right) \tag{13}$$

In equation 13, H, H', S^2, and S'^2 can be replaced as follows: if θ is the angle between C and R

$$H=R\sin\theta$$

$$H'=\frac{A^2}{R}\sin\theta$$

Using the cosine law of triangles

$$S^2=C^2+R^2-2CR\cos\theta$$

and

$$S'^2=C^2+(A^2/R)^2-2C(A^2/R)\cos\theta$$

$$T_p=2GC\left[\frac{R\sin\theta}{C^2+R^2-2CR\cos\theta}-\frac{(A^2/R)\sin\theta}{C^2+(A^2/R)^2-2C(A^2/R)\cos\theta}\right] \tag{14}$$

$$=2G\left[\frac{\sin\theta}{(C/R)+(R/C)-2\cos\theta}-\frac{\sin\theta}{(CR/A^2)+(A^2/CR)-2\cos\theta}\right] \tag{15}$$

$$=G\left[\frac{\sin\theta}{\frac{1}{2}\left(\frac{C}{R}+\frac{R}{C}\right)-\cos\theta}-\frac{\sin\theta}{\frac{1}{2}\left(\frac{CR}{A^2}+\frac{A^2}{CR}\right)-\cos\theta}\right] \tag{16}$$

If J and K are equidistant from O, $C=R$, and the torque reduces to

$$T_p=G\left[\frac{\sin\theta}{1-\cos\theta}-\frac{\sin\theta}{\frac{1}{2}\left(\frac{C}{A}\right)^2+\frac{1}{2}\left(\frac{A}{C}\right)^2-\cos\theta}\right] \tag{17}$$

Variation of Disk Torque With Flux Pair Radius

Let the a-c driving fluxes of a circular disk consist of a flux pair at the same radius ($C=R$). Either circle may be of any size. However, the circles may not overlap, nor may they fall partly outside the disk, if the equations are to hold. If θ is taken constant at 30 degrees, for example, a curve of torque versus C for a disk of fixed A can be worked out. This curve, for $G=1$ (for example, when $f=60$, $b=0.0915$, $\Phi_J=\Phi_K=22.7$ maxwells, and $\rho=2.83\ (10)^{-6}$, G is unity) is shown in Figure 6 in terms of T_p versus C/A. The trends of this curve are interesting.

As C approaches A, the images move in closer to the disk circle and have an increasing negative torque effect.

As the flux pair is made to retreat from the disk edge, the images move out and diminish in effect, and the net torque increases. But as C is reduced further, one is tempted to conclude that since low C means low lever arm, the torque would fall off again. But it must be remembered that under the conditions, S is proportional to C, and that eddy current strength, for example, caused by Φ_K through J, is inversely proportional to S. Therefore, torque will not fall off. Inspection of equation 17 shows that as C/A approaches zero, T_p approaches a constant value. The achievement of greatest torque at least possible radius may be somewhat surprising.

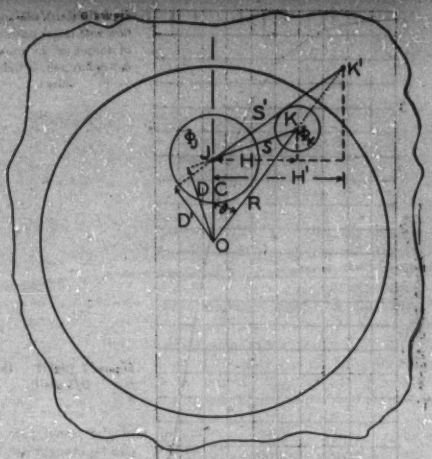

Figure 5. Torque of a flux pair

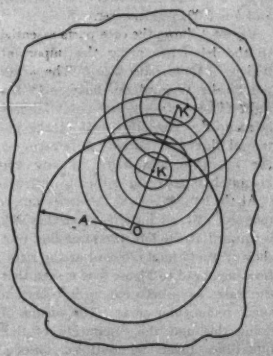

Figure 4. Concentric eddy currents caused by individual flux pencils

Disk Torque Due to Irregular Fluxes

Disk driving torque can arise due to two fluxes in quadrature, neither flux being contained within a circular area and both having irregular density distribution. Moreover, the fluxes may overlap greatly. The watthour meter presents just such a problem. A feasible method for finding the torque will be developed now.

The area where a flux pierces the disk can be divided into a number of rectangular areas, each containing a known amount of flux. The other flux is treated likewise. In each little area, the flux of that area is centered arbitrarily; it becomes a flux pencil located somewhere within the area. Any error thus introduced will be treated later. If the two fluxes are Φ_J and Φ_K, every J-pencil's eddies must be allowed to react with every K-pencil; also (for the images) every J'-pencil must be allowed to react with every K-pencil; and a summation must be arrived at somehow. The amount of work involved in the solution could be great, if carried out in terms of equation 14 or equation 15.

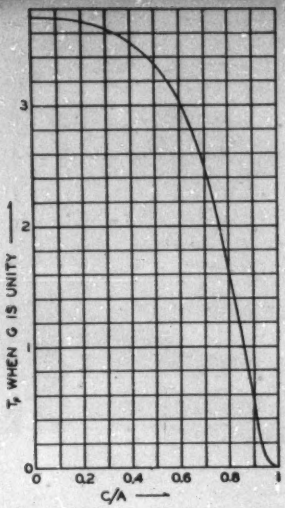

Figure 6 (left). Variation with radial position of torque of an equal-radius flux pair, G being unity

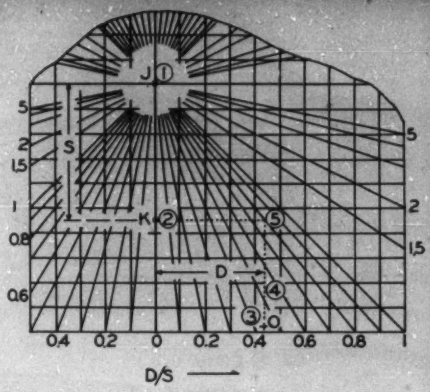

Figure 7 (right). The D/S chart

Instead of using these general forms, it is much faster to retreat to the form of the torque as given in equation 10. The case can be drawn to scale, D, S, D', and S' values can be measured directly, and the computing can be done by using a slide rule. Even so, the fairly accurate treatment of a watthour meter would call for many measurements and a good deal of slide rule work. The writer therefore devised a labor-saving chart.

The D/S Chart

Figure 7 shows a limited portion of a D/S chart. It is of very simple construction, composed of a centimeter grid and radial lines, the location of which will be obvious after a little study. The chart is put on tracing cloth.

In use, a pencil J is to react with another pencil K to produce a component torque about O. (Steps are shown on the chart by circled numbers.)

Step 1. The chart is placed on the drawing with apex over J.

Step 2. The chart axis is made to pass through K.

Step 3. Note where the disk center O is.

Step 4. Move parallel to the axis from O until opposite K.

Step 5. Read the D/S value of the slant line through the last point found, or interpolate as may be necessary.

After determining the G-value pertaining to the particular flux strengths of the two pencils, equation 10 will give the torque of the pencil pair. Further procedures can be brought out best in the watthourmeter study.

Driving Torque of a Watthour Meter

The theory and methods presented have been given a thorough trial by the writer's application of them to a Duncan watthour meter rated 5 ampere, 115 volt, single-phase, 60 cycle, type MF-A. The processes and results will be given here in condensed form. The meter chosen is the one so ably described by Green.[2] For more complete data than can be given here, see his paper. Green gives the nominal torque as 46 gram-millimeters at 575 watts. But this was for a 5-spoked disk. Later, a solid disk was adopted which, according to information obtained from the company, raised the nominal torque to 51. For the aluminum disk, A is 4.45 centimeters (3.5 inches), and b is 0.0915 centimeter.

Figure 8 shows the core parts essential to the job of mapping the important regions of the driving fluxes. The writer graphically mapped the fluxes. At the right (Figure 8) half the potential flux is mapped. The other half of the potential flux (not shown) duplicates on the left the right half. At any one instant, both halves are either up or down.

At the left (Figure 8) the series flux is mapped. At an instant when this flux is upward at the left, the same flux (not shown) would be downward at the right. Looking ahead to Figure 9, it is seen that the fluxes have been cut up into certain small rectangular areas. The means of doing this and the computing of flux quantities must be outlined briefly. For field mapping techniques, one may refer to Moore.[3]

Potential Flux

Consider the flux in a path in the map of Figure 8, such that the path is defined by any curvilinear square and an axial dimension (into the paper) of one inch. It can be shown that the reluctance in air is such that one ampere-turn acting on the reluctance will set up 3.19 maxwells of flux.

The potential coil furnishes 162 rms ampere-turns. The core's axial dimension is 0.60 inch. A tube, as mapped, has two curvilinear volumes in series. The flux per tube is then $(3.19\times162\times0.60)/2=155$ maxwells. Counting from the center at t to as far as x, the span tx takes in 4.4 tubes. Weak flux beyond x was omitted. The points u, v, and w were spotted in then so that the spans tu, uv, vw, and wx each contains 1.1 tubes, or $(1.1\times155)=170$ maxwells. In Figure 9, the axial dimension was divided into four equal parts. We thus have divided the right potential flux into 16 parts, each containing $(170\div4)$ or 42.5 maxwells.

These fluxes must be centered, and this must be done with care. The only problem is in the centering locations in the tx direction. In Figure 8, the points marked *1*, *2*, *3*, and *4* were spotted in by reading the map in order to place these not halfway along tu, uv, and so forth but at mid-flux positions.

There are also 16 similar potential flux areas to the left (Figure 9).

Series Flux

There are 60 rms ampere-turns on each gap, setting up the series flux. Flux per tube is then $(3.19\times60\times0.6)/2$, or 57.5 maxwells. The series flux included in this study (left, Figure 8) reaches

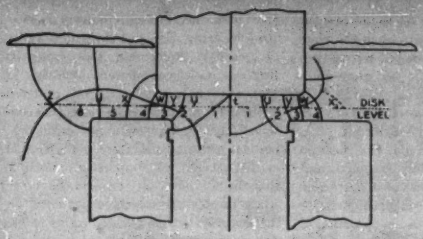

Figure 8. Watthour-meter flux map

from t to z, taking in 6.1 tubes. Weak flux beyond z was omitted.

If we now divide the series flux so as to cut it into rectangles of equal flux amounts, this advantage is gained: G will be the same for any pair. But there is a worse disadvantage. Some potential rectangles will overlap partially some series rectangles, and special problems will be created. An alternative was adopted. The potential pattern of rectangles was laid over the series map (t, u, v, w, left) and the differing amounts of series flux in each span were read from the series map. The remaining series flux falls in the spans xy and yz, and two more series flux values were read off there. These two were centered at *5* and *6*.

By this scheme, the potential and series rectangles fall into two classes: (1) they are separated or, at closest, merely touch; (2) or, where they overlap they completely coincide and drop out of consideration.

The series flux is divided thus into six unequal tube fractions, these being 0.65, 0.95, 1.2, 1.4, 0.9, and 1.0, reading from t to z. At 57.5 maxwells per tube, these amount to 37.3, 54.6, 69.0, 80.5, 51.7, and 57.5 maxwells. After dividing the 0.6 inch dimension into four equal parts as before, the series rectangles have fluxes (same order) equal to 9.33, 13.65, 17.25, 20.1, 12.91, 14.38.

Values of G

All potential fluxes are alike, 42.5 maxwells. But there are six series flux values. Using them, and $f=60$, $b=0.915$, $\rho=2.83\ (10)^{-6}$ for aluminum at 20 degrees centigrade, the six G-values obtained are 0.767, 1.12, 1.416, 1.651, 1.06, and 1.18.

Organization

The areas in Figure 9 have been identified in terms of lettered rows (A, B, C, D) and numbered columns (1, 2, 3, 4, 5, 6). Any area with any letter and any number from 1–4 contains 42.5 maxwells of potential flux. As to series flux, in either half, $A1$ and $C1$, as examples, contain 9.33 maxwells; whereas, $D6$ has 14.38 maxwells.

Images

After centering the fluxes, the left potential pencils were imaged, and the images identified by primes (Figure 9).

It was not necessary to use series flux pencil images, because the reciprocity law takes care of their effects in the equations already written for torque.

Routine

Suppose the right potential $A1$ pencil is allowed to react with all the left series pencils, one by one. The apex of the D/S chart is placed over the $A1$ pencil and held there by a needle point. The chart then is swung about easily. The axis is moved over a left series pencil. The routine described quickly leads to recording a D/S value. The work of multiplying each value by $2G$ is saved by organizing properly the tables for recording D/S. Only the sum of appropriate D/S values need be multiplied by its proper $2G$. The results of four sets of operations must be set down here.

Torques as Found

Left potential fluxes acting on right series fluxes gave a torque of 1,513 dyne-centimeters, which includes reciprocity. However, an equal torque comes from right potentials acting on left series. The total is then 3,026.

Left potential images with right series gave 450. This is doubled also, yielding a total of 900, which acts negatively. Summing up so far, the net torque is 3,026−900, or 2,126.

It is usual to explain the driving torque of the watthour meter in terms of the actions of fluxes that are separated distinctly. The torque found so far comes from such fluxes. But this meter has a torque of 51 gram-millimeters; and the torque found above, 2,126, amounts only to $(2{,}126\times10)/981=21.7$ gram-millimeters. This is less than half the needed amount.

But more torque can be found, and from sources perhaps heretofore neglected. In considering left potential and left series flux, it has been invitingly easy to

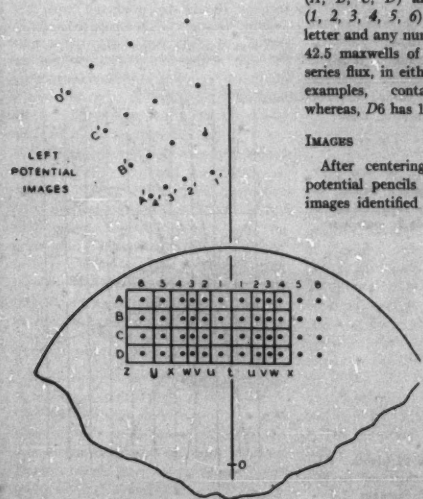

Figure 9. Watthour-meter flux rectangles, centerings, and potential images

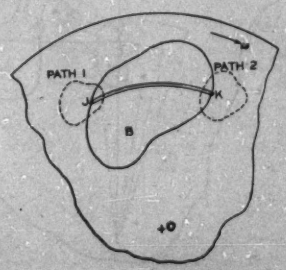

Figure 10. Flux band and pencil pair

jump to the conclusion that because these two fluxes are approximately alike and roughly superimposed, they can produce little torque, if any; likewise, for right potential and right series. But the facts are surprising. There is a fair amount of cancellation where the two areas of a pair are identical in position; and there is a good deal of negative torque where a pair teams up to act the wrong way. In spite of all that, left potential with left series yields a torque of 1,152 which, doubled, gives a total of 2,304. Left potential images with left series give 145 which, doubled, gives a total negative of 290. The net torque thus additionally found is 2,304−290=2,014, which is just about equal to the 2,126 already found. Two fluxes "approximately alike and roughly superimposed" had better not be neglected!

The total then is 2,126+2,014=4,140 dyne-centimeters, or 42.2 gram-millimeters.

Predicted Versus Actual Torque

The Duncan meter has an overload plate made of laminations. It partly surrounds the tops of the series poles. Its purpose is to correct the inherent overload droop in the accuracy curve, caused by series flux damping effect. The construction and theory of the plate do not concern us here. However, the plate somewhat changes the amounts and distributions of the driving fluxes and, according to Green, serves to increase the torque by seven per cent when the plate is introduced. Our predicted torque then becomes 1.07×42.2, or 45 gram-millimeters.

The predicted torque of 45 is 12 per cent below the 51 nominal torque.

An exact check would not be too meaningful unless a very complete and careful study were made of a particular meter. This in part is true because of variations of meters in production caused by allowable variations of air gaps, characteristics of iron, and so on. It is not necessary for meters to be exceedingly close duplicates as to driving torque, because there is a good range of adjustment of damping flux for securing accuracy in the calibration process. Other reasons for failing to check exactly will be taken up now in discussing sources of errors.

Errors in the Method

There are three sources of error in the foregoing procedure.

Centering Noncircular Flux. In a flux pair, uniform flux in a circle is centered without error. But error results when uniform rectangular flux is centered. For parallel rectangles, Dwight[4] conveniently furnishes the correction under another guise, forces between parallel strap conductors. In the meter, the worst error occurs for the adjacent areas $A2$ and $A3$, $B2$ and $B3$, and so forth. The uncorrected force found by centering is about 25 per cent high. But most of the other adjacent flux pairs have a much smaller error. For example, for adjacent squares, force found by centering is only two per cent high. It is the writer's opinion that the total predicted torque is only two or three per cent high, attributable to centering error.

Nonuniform Density. The centering error was concerned with uniform density. Another error arises due to nonuniformity of density. Remember that potential flux was mid-flux centered; but that in rectangles 1–4, series flux was centered arbitrarily at these same potential centers. This is convenient but erroneous, because the two fields are not identical in distribution. The writer's opinion is that the nonuniformity error in the meter study is only two or three per cent, on the low side. Thus the two errors so far discussed may nearly nullify.

2-Dimensional Treatment. The map of Figure 8 is a 2-dimensional map, drawn as if the axial dimension were great. Actually, this dimension is only 0.60 inch. Since the shortest gap is nominally 0.125 inch, it is certain that there is a good deal of useful fringing flux both inside (radially) and outside of the limits shown in Figure 9. The actual distribution would give weaker fluxes than those allowed to the A and D levels but also additional flux outside the A-level and inside the D-level.

The error due to using the 2-dimensional map and omitting fringing (and also omitting weak fluxes beyond x and z) easily could account for all of the difference between predicted and actual torques.

Possibilities

In a device, if the flux distributions were determined actually by measurement and were used in a study no more detailed than that used for the meter, forces or torques should be predicted with an over-all error of no more than five per cent.

A less detailed study, using only a few

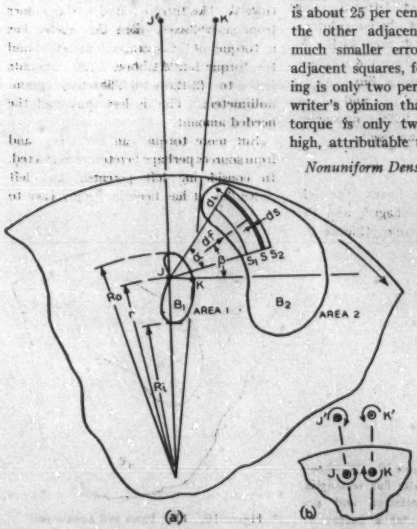

Figure 11 (left). J-pencil acting on part of area 2, polarities

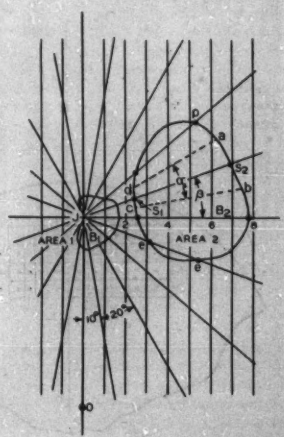

Figure 12 (right). Alpha chart for $\alpha=20$ degrees

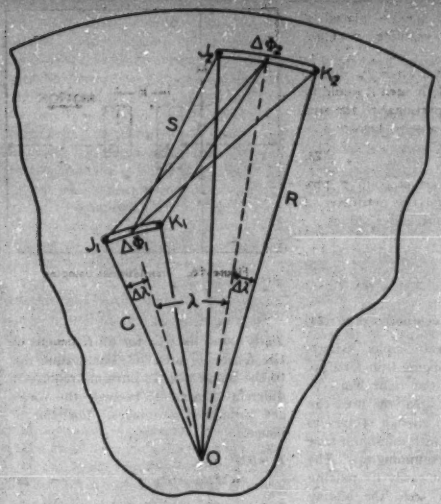

Figure 13. Damping reciprocity law

rectangles and capable of solution in a relative short time, will yield reasonably good values of torque.

In the meter study, the work with the chart, the summing up, and the computing of torque requires about eight hours. This does not include time for drawing and flux mapping.

Damping Forces and Torques

An electromagnet or a permanent magnet puts a flux, uniformly distributed and of density B, through a circular rotating disk, within the area shown in Figure 10. The area has any size and shape. There may be more than one area, each with its own density.

The description of the Foucault currents caused by rotation, and the finding of resulting forces and torques heretofore have not been attacked successfully for such general cases. Solutions can be achieved by means of what is believed to be a new concept, by the use of some of the a-c developments already described and of some developments yet to be mentioned.

Flux Band and Pencil-Pair Concept

The flux can be divided into bands, each of constant radius and narrow width, such as band JK in Figure 10. Radial elements of metal sweep through the flux of the band and set up a constant electromotive force around any such paths as path 1 and path 2

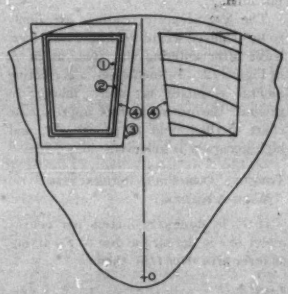

Figure 14. Watt-hour meter damping

The concept referred to above is this: the same electromotive force can be set up around such paths in a *fixed* disk by means of pencils of flux piercing the disk at J and K, these being opposite flux pencils, and both increasing or decreasing at the same rate. Adoption of this concept makes it possible to define the currents set up by the JK flux band and by all other such bands. The concept of fixed-disk-and-pencil-pair is used only to to define the currents. The currents are allowed then to react with the actual flux in order to find forces and torques.

The adoption of the changing pencil pair makes it possible to adopt the image and concentric current ideas already fully outlined in the a-c developments.

Force Due to a Pencil, and Flux in an Angle

In Figure 11, there are two flux areas, area 1 and area 2, with densities B_1 and B_2. A narrow flux band JK at radius r in area 1 is replaced for current effects by flux pencils J and K changing through a fixed disk. As in previous developments, J has its (opposite) image pencil J', and K has its (opposite) image pencil K'. We then have four flux pencils through a large disk, each setting up concentric eddies about itself. The resultant of these four current patterns would be identical within the disk circle, with the actual current set up in the rotating disk by the JK flux band. Such of these concentric currents as pass through the areas will react with B_1 and B_2 to produce forces.

Throughout, we may think either of the flux pencils as all constantly increasing or as decreasing. Herein, they will be treated as decreasing. With rotation as shown in Figure 11, and with downward B_1 flux, the electromotive force due to flux band JK would be outward. Then the four pencils would have signs as shown in Figure 11*b*, and they would set up currents as shown. These currents are such as would tend to prevent the (decreasing) change of the flux pencils.

The flux band electromotive force due to rotation, in volts per radial centimeter, is

$$E = \omega r B_1 \times 10^{-8} \tag{18}$$

ω is angular velocity in radians per second.

Ascribing this electromotive force to flux pencils in a fixed disk, we now find the current element di of width ds, flowing concentrically about J at radius S from J. The resistance R offered to di is given by equation 4. Then

$$di = \frac{E}{R}$$
$$= \frac{bEds}{\rho 2\pi S}$$

Consider the resultant dynes force df

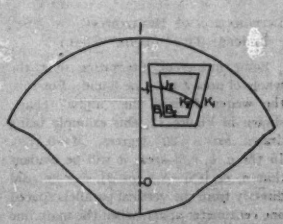

Figure 15. Nonuniform flux

caused by the di current arc within the angle α (see Figure 11). It is shown easily that the force due to the current arc is the same as if the current flowed along the chord. By symmetry, the force acts through J.

$$\text{Chord} = 2S \sin \frac{\alpha}{2}$$

$$F = (BIL)/10 \text{ dynes, in general}$$

$$df = 0.1 B_2 2S \sin \frac{\alpha}{2} \cdot di$$

$$= \left(0.2 B_2 \sin \frac{\alpha}{2}\right) S \frac{bEd}{\rho 2\pi S}$$

$$= \left(0.1 B_2 \sin \frac{\alpha}{2}\right) \frac{bE}{\pi\rho} ds \qquad (19)$$

Let F_a in dynes per centimeter of r designate the forces due to J-currents acting on B_2 flux contained within the area bounded by arcs of radius S_1 and S_2, and angle α.

$$F_a = \int_{s_1}^{s_2} df$$

$$= \left(0.1 B_2 \sin \frac{\alpha}{2}\right) \frac{bE}{\pi\rho} \int_{s_1}^{s_2} ds$$

$$= \left(0.1 B_2 \sin \frac{\alpha}{2}\right) \frac{bE}{\pi\rho} (S_2 - S_1) \qquad (20)$$

If OJ (equal to radius r) is taken vertically, we need the horizontal component of F_a which, acting through J on lever arm r or OJ, produces torque about O. The horizontal component, F_{aH}, is

$$F_{aH} = \cos \beta \cdot F_a$$

$$= \left(\sin \frac{\alpha}{2}\right) \left[(S_2 - S_1) \cos \beta\right] 0.1 \frac{bB_2E}{\pi\rho}$$

$$= \left(\sin \frac{\alpha}{2}\right) \left[(S_2 - S_1) \cos \beta\right] 0.1 \frac{bB_2}{\pi\rho} \omega r B_1 \times 10^{-8}$$

$$= \left(\sin \frac{\alpha}{2}\right) \left[(S_2 - S_1) \cos \beta\right] \frac{\omega r b B_1 B_2 \times 10^{-9}}{\pi\rho} \qquad (21)$$

To abbreviate, let $M = \sin \alpha/2$, $n = [(S_2 - S_1) \cos \beta]$, w' = the fraction.

$$F_{aH} = Mnw' \qquad (22)$$

Integration of Horizontal Forces: The "Alpha" Chart

Some means of integrating over the whole of area 2 must be found. For this, the writer devised the "alpha" chart, shown in Figure 12, this example being drawn for $\alpha = 20$ degrees, $M = 0.1736$. In the a, b, c, d area, it will be evident that n, or $[(S_2 - S_1) \cos \beta]$, can be read directly from the vertical parallels spaced one centimeter apart, when the main line of the chart is lined up through disk center O and chart apex is placed at pencil J. In this example, $n = 6.9 - 2.4 = 4.5$.

The total horizontal force F_H due to J-currents through Φ_2 in area 2 would be (approximately) proportional to the sum of the several F_{aH} values. Let

$$N = \Sigma n \qquad (23)$$

In the example, start at point p, proceed clockwise around the perimeter of area 2, and read off successive values.

$$N = (5.2 + 6.9 + 7.7 + 5.3) - (3.1 + 2.5 + 2.4 + 2.5)$$

In general

$$F_H = MNw' \text{ dynes per centimeter of } r \qquad (24)$$

In practice, several "alpha" charts are needed, with α ranging from small to large. By selecting the right chart to use on a near or far area, the area can be sliced always into enough sectors to insure high accuracy with minimum time spent at reading and summing up. The summing is done most easily by putting the readings directly onto the adding machine.

The less accurate readings are likely to be achieved where the radial lines soon leave after entering the area, as at ee in Figure 12. In such cases, a correcting mental estimate is easily made. In general, the errors of this approximate chart method tend to cancel out, and high accuracy is achieved.

Torque: One Flux Interacting With Another

If T_r in dyne-centimeters per centimeter of r is the torque due to F_H acting at lever arm r (or OJ), then

$$T_r = F_H r$$

$$= MNw'r$$

$$= MN \frac{\omega b B_1 B_2 \times 10^{-9}}{\pi\rho} r^2 \qquad (25)$$

Let

$$W = \frac{\omega b B_1 B_2 \times 10^{-9}}{\pi\rho}$$

$$T_r = MNWr^2 \qquad (26)$$

Appropriately select several different radii from inner radius R_i to outer radius R_o, and find MNr^2 for each. This work is routinized and carried out in tabular form with the aid of "alpha" charts. W is common throughout and should be omitted until the tabulations are added up.

Plot a curve of MNr^2 versus r. Find the mean ordinate and call it T_A. Then, if Ij in dyne-centimeters is the torque due to all J-pencils on the J-side of area 1,

$$T_J = T_A(R_o - R_i)W \qquad (27)$$

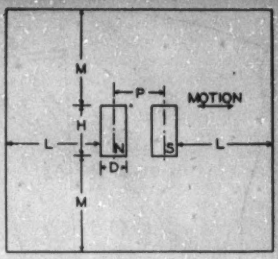

Figure 16. Translational damping

T_K is found likewise for all K-pencils on the K-side of area 1. The torque due to the image-pencil's currents requires a different treatment, because the forces act through the images. For the J' image,

$$T_r = (OJ')F_H$$

$$= MNw'(OJ') \qquad (28)$$

N is found by now centering the "alpha" chart apex at J'. As previously shown in equation 11, $OJ' = A^2/r$. Then

$$T_r = MN \frac{\omega r b B_1 B_2 \times 10^{-9}}{\pi\rho} \frac{A^2}{r}$$

$$= MN \frac{\omega b B_1 B_2 \times 10^{-9}}{\pi\rho} A^2$$

$$= MNWA^2 \qquad (29)$$

For the same several radii from R_i to R_o as used before, MNA^2 is found and plotted. T_A is obtained, and

$$T_J' = T_A(R_o - R_i)W \qquad (30)$$

T_K' is found likewise.

All four torques are combined then to get the net torque T_{12}, expressed positively as a braking torque; thus

$$T_{12} = T_K - T_J - T_K' + T_J' \qquad (31)$$

The routine above was presented in order to make the analysis easily understood. However, it requires plotting four curves. This can be avoided by combining, in the tabulation of data, the MNr^2 and MNA^2 values (four in all for each r used) and then plotting only one curve and finding only one T_A from it.

T_{12} is the torque due to all currents originated by area 1, acting on the flux of area 2.

Reciprocity Law

It will be shown next that here again a reciprocity law holds. As far as the writer knows, this law has not been proved heretofore. In Figure 13, let flux bands J_1K_1 and J_2K_2 each subtend

the small angle $2\Delta\lambda$ and each be Δr radially. Their centers, where $\Delta\Phi_1$ and $\Delta\Phi_2$ can be centered for force purposes, subtend the angle λ. Current due to pencils J_1 and K_1 act on $\Delta\Phi_2$ to give two forces; J_2 and K_2 act on $\Delta\Phi_1$, giving two more forces. Four forces and torques are involved. Force $J_1\Delta\Phi_2$ is proportional to $\Delta\Phi_1\Delta\Phi_2$. Force $K_2\Delta\Phi_1$ is proportional to $\Delta\Phi_2\Delta\Phi_1$. These flux products correspond to G of equation 16 which, aside from constants, is a flux product. The bracket of equation 16 takes care of the geometry (including images) to find the torque of a flux pair. The value of the bracket will be the same for both forces, since C and R are common, and θ is $\lambda+\Delta\lambda$ for each. Therefore, torque $J_1\Delta\Phi_2$ equals torque $K_2\Delta\Phi_1$. Likewise, torques $J_2\Delta\Phi_1$ and $K_1\Delta\Phi_2$ are equal, θ now being $\lambda-\Delta\lambda$ for each. A reciprocity law therefore obtains for the flux bands, and if the incremental values are taken as infinitesimals the proof is rigidly correct. Next, any area 1 or area 2 can be built up of such bands. That which is true for the parts will be true for the wholes. Then the total torque due to two flux areas is (except for self-torques)

$$T=2T_{12} \tag{32}$$

Self-Torque

Each area of course also produces torque on a self basis, its own eddies acting on its own flux. The same general procedure holds for finding it. With chart apex at J, for instance, the chart is read around the boundary of area 1.

When there are two flux areas, the self-torques are in general larger, and often much larger, than the interaction torque.

Torque Due to One Circular Area of Flux

Smythe[5] gives an accurate equation for torque due to disk rotation through a single circular area of flux. A case was selected as follows:

$A=13$ centimeters
Flux circle radius $=2.5$ centimeters
$C=10$ centimeters
$\omega=1$
$b=0.1$ centimeter
$B=1{,}000$
$\rho=2.83\ (10)^{-6}$

For this case, the accurate torque (Smythe equation) is 27,000 dyne-centimeters. By the methods presented here, and using only five radii aside from R_1 and R_n, we get 27,200. The use of "alpha" charts involves graphical methods, and so the difference is even smaller than might be expected.

Watthour-Meter Damping Torque

The methods were given a full trial by predicting the damping torque of a Duncan watthour meter. The alnico magnet poles are below the disk; the armature is above. In Figure 14, 1 is the perimeter of a pole face. Flux as measured by ballistic galvanometer and search coil 2 was 2,400 maxwells. Flux measured through search coil 3 was 3,000 maxwells. For computing torque, the arbitrary area 4 was adopted, along with the assumption that it carries 3,000 maxwells at uniform density. At the right, in Figure 14, the area 4 is shown, and the arcs show the radii of flux bands used in the solution. The images are not shown. The time required for the solution, including making the drawing, locating the pencils, using the "alpha" charts, tabulating and adding data, and finding T_A and T, was about five hours.

The damping torque was computed for these conditions,

$\omega=3.02$ (being for 575 watts, 28.75 rpm)
$b=0.0915$
$\rho=2.83\ (10)^{-6}$
Predicted torque $=48.5$ gram-millimeters
Meter's nominal torque $=51$

In view of the arbitrary treatment given the flux, and the neglect of flux outside of area 3, the close agreement must be considered somewhat fortuitous.

Nonuniform Flux Distribution

These methods can be extended to handle flux areas having any flux distribution. Contour lines would be drawn within the area, and between successive contour lines the density would be considered constant. As a simple example, Figure 15 shows a case having only two contour lines. The easiest treatment is secured by letting B_1 cover the entire area, whereupon the inner area has the additional component (B_2-B_1). Pencils J_1 and K_1 are then caused by B_1. Pencils J_2 and K_2 are attributable to (B_2-B_1). J_1 and K_1, via the "alpha" chart, act on the entire area of B_1 density and also on the inner area of (B_2-B_1) density. Pencils J_2 and K_2 likewise react on both areas. Most damping fluxes come from permanent magnets. In nearly all such cases, the flux distribution will not be known with enough certainty to warrant more than a 2-contour treatment, if that.

Translational Damping

Accelerometers and other instruments often are damped by means of a disk-and-magnet combination, the relative movement being translational. The problem involves forces only, not torques. Otherwise, the "alpha" charts and the routines already described are applied readily. A reciprocity law obtains, but the proof is omitted; anyone able to follow the proof for the rotational reciprocity law can prove easily the translational law.

Many of those concerned with instrumentation heretofore have had to meet their damping needs by rather blind trial-and-error work. The writer therefore has worked out a series of cases, leading to a family of curves. These curves enable intelligent design to be carried out in a very simple fashion.

In Figure 16, two opposite fluxes pierce the disk in parallel rectangles. The motion is horizontal. Using the dimensions (centimeters) as indicated, first find the dimensionless ratios X and Y, where $X=P/D$ and $Y=H/D$. Take these to the curves of Figure 17 and find F'. Next compute W. If

$V=$ velocity, centimeters per second
$b=$ disk thickness, centimeters
$\rho=$ disk resistivity, ohm per centimeter (for aluminum at 20 degrees centigrade, $2.83\ (10)^{-6}$)
$B=$ gausses (maxwells per square centimeter)

$$W=\frac{VbB^2\times10^{-9}}{\pi\rho}$$

Then

$$F=WD^2F' \tag{33}$$

To derive the curves the writer computed for Y-values of one, two and four,

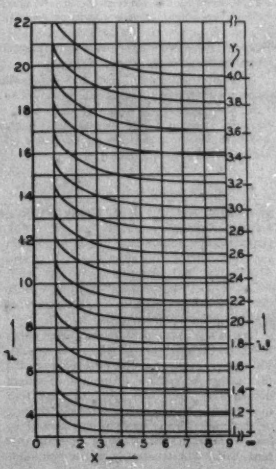

Figure 17. F' curves for translational damping

and several values of X. The curves for Y of one, two, and four are correct, it is believed, to within two per cent or better. As originally plotted on logarithm paper, it was possible to interpolate for intermediate curves with good accuracy. Any intermediate curve should be correct to within five per cent or better.

The curves have a broader utility than is indicated by equation 33 alone. First note in Figure 17 that as the rectangles approach each other (at X of unity they are adjacent) any one curve rises because of mutual effect. Conversely, when separated by as much as $X=9$ the curve is nearly horizontal; nearly all the force then is caused by the eddy currents of each flux acting on itself. F_∞' has been computed and shown on the chart; these are F' values when $X=\infty$. Two additional uses for the curves then can be made.

First, a single isolated rectangle of flux yields a force (dynes)

$$F=\left(\frac{1}{2}\right)WD^2F_\infty' \tag{34}$$

Second, two flux rectangles as in Figure 16, but containing like fluxes, give a force due to an F' as much less than F_∞' as the direct reading from the chart is above F_∞'. Restated, if F' is as read directly, the force is

$$F=WD^2(2F_\infty'-F') \tag{35}$$

Translational: Size and Shape of Disk

The curves are based on a disk with edges remote, in any direction from either rectangle. However, the writer feels safe in saying that if the disk edge is no closer to the rectangle, anywhere, than twice the length of the rectangle's diagonal, the force will be no more than four per cent below the predicted value. But there undoubtedly will be cases in which an even smaller disk must be used.

The M dimensions in Figure 16 can be reduced, even to zero if necessary, and the only effect is to reduce the force. At $M/H=1/2$, the force still might be 70 per cent of predicted force.

Reduction of L below $L/H=1$ will begin to affect appreciably the linearity of damping. How much would depend also on relative displacement. As a guess, if $L/H=1/2$ and displacement is $L/4$, the force for a given velocity might vary as much as three per cent from average.

A-C Flux Damping

The damping of disks moving through an a-c flux is subject to the same analyses and procedures as were presented for nonvarying flux. The average force or torque will be found by using the rms values of flux or density.

References

1. Torque in a Bipolar Induction Meter, **Ralph M. Morton.** AIEE Transactions, volume 55, 1936, April section, pages 354–8.

2. A New Watt-Hour Meter, **Stanley Green.** AIEE Transactions, volume 54, 1935, October section, pages 1073–84.

3. Fundamentals of Electrical Design (book). **A. D. Moore.** McGraw-Hill Book Company. New York, N. Y., 1927.

4. Electrical Coils and Conductors (book). **H. B. Dwight.** McGraw-Hill Book Company, New York, N. Y., 1945.

5. On Eddy Currents in a Rotating Disk, **W. R. Smythe.** AIEE Transactions, volume 61, 1942, September section, pages 681–4.

Discussion

B. E. Lenehan (Westinghouse Electric Corporation, Newark, N. J.): Problems which are basically magnetic field problems are nearly always more difficult than circuit problems, mainly because they are in three dimensions. Their solution generally becomes possible only if they can be reduced to two dimensions; then the field can be plotted and an approximate solution obtained.

This necessary approximation limits the accuracy and usefulness of such a method. Heretofore, it generally has been considered simpler and more accurate to construct samples to investigate the effects of the various factors, rather than to depend on a lengthy and involved mathematical solution.

The method in this paper uses analogy to a field problem which has been solved and applies the superposition idea to obtain results by a relatively simple method. The time required compares favorably with that of constructing and testing samples. We plan to investigate the method and check its practicability.

Some conclusions in the paper seem to be contrary to experience, but this is evidently the result of assuming constant fluxes in instead of constant flux densities. The latter is a more logical assumption. When two fluxes assumed constant are brought toward the center, the area occupied must decrease with the radius. When constant flux density is assumed, the fluxes decrease in this manner, so the torque factor is multiplied by C^2/A^2. This leads to another possibility of integrating the torque in polar co-ordinates by equation 16. If Figure 6 of the paper is replotted with T_pC^2/A^2 as ordinate, which corresponds to constant flux density, the curve yields a broad maximum around $C/A=0.7$, which agrees with experience. This is shown in Figure 1 of this discussion.

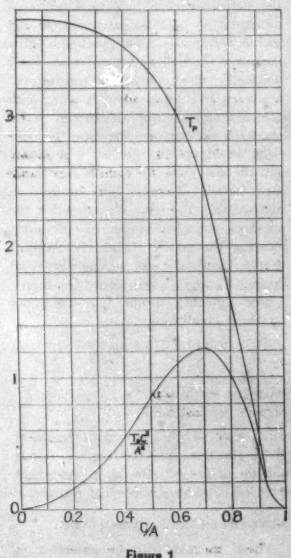

Figure 1

Our procedure in cases of this kind has been to map the flux pattern and estimate the current stream lines set up by the voltage field and compute the torque by electrodynamic formulas against the current flux, essentially the same procedure as used in the cross-field theory of the induction motor. This permits an estimate of the effects of disk reactance, which is of importance on frequencies above 60 cycles.

The procedure outlined by Professor Moore is interesting and should prove to be valuable, particularly when used as a preliminary step to a full investigation using test samples with the several variables involved.

J. A. M. Lyon and **J. F. Calvert** (Northwestern University, Evanston, Ill.): This paper is very stimulating from the point of view of engineering analysis. Professor Moore has had the courage to set aside classical mathematical procedures and to develop his own analysis for eddy currents and torques in circular disks.

One of the impressive points of this paper has been the clarity of the author in making his theory apply for the edge effects of a disk using the method of images. Some of us probably have been prone to think that in order to provide either sufficient driving or damping torque, pole pieces should be located near the periphery of an eddy current disk. The treatment of the boundary conditions by the image method, which

gives rise to an interpretation including negative torques, certainly aids in obtaining a clear physical picture of the dependence of net torque on the positions of the bundles of magnetic flux piercing the disk.

It may be of interest to note in connection with this paper the similarity in form of the following general relations

$$\int H \cdot dl = \int\int i \cdot dS \tag{1}$$

$$\int E \cdot dl = \int\int = \frac{dB}{dt} \cdot dS$$
$$= -\frac{d\phi}{dt}$$
$$= \int \rho i \cdot dl \tag{2}$$

where in rationalized MKS units

H = magnetic field intensity
B = magnetic flux density
S = area
l = length of path
E = electric field intensity
ϕ = magnetic flux
i = current density
ρ = resistivity in the disk

Whereas we normally think of a current in electric machines as linked by the flux, we find here that it is convenient to think of the flux linked by a current. Equation 2 may be used to map a 2-dimensional current field in the disk both outside and inside the changing flux. If this is done (in a manner analogous to that normally employed in mapping 2-dimensional magnetic fields using equation 1) by the use of equation 2, tubes of equal current are drawn everywhere over the disk, and these are intersected by a family of lines at right angles to the directions of the current flow. These would be arranged to result in curvilinear squares outside the pencil of changing flux and curvilinear rectangles on the disk inside the pencil of changing flux. On the disk the I^2R or heat loss is the same in each curvilinear square which lies outside the region of changing flux and is less in each curvilinear rectangle which lies within the region of changing flux by the ratio of length to width of the rectangle. Here length is taken in the direction of the current flow in the disk.

Refer now to the electrical analogue in Professor Moore's paper where the flux pencil has been replaced by a current and where the edge effect of the disk has been replaced by imaged conductors. Instead of imaged conductors a current sheet of appropriate densities might be assumed at the line representing the edge of the disk. For details see reference 1. This procedure is not limited to disk boundaries which permit imaging. Possibly a similar procedure might be used in accordance with equation 2 using a sheet of flux at the line representing the edge of the disk.

The charts which Professor Moore has presented as aids to actual computation of torques are a good example of how he vigorously has pushed his analytical theories to a successful conclusion by actually providing the tools to use for the solution of a variety of problems.

REFERENCE

1. FORCES IN TURBINE GENERATOR STATOR WINDINGS, J. F. Calvert. AIEE TRANSACTIONS, volume 50, 1931, pages 178–94.

William R. Smythe (California Institute of Technology, Pasadena, Calif.): The replacement of a flux band by a pencil pair greatly reduces the labor of calculating the eddy current damping torque on a rotating disk and may be justified as follows:

Consider the narrow flux band of Figure 10 of the paper with width δr across which the ohmic voltage drop is negligible compared with the uniform potential difference $V_+ - V_-$ maintained between its boundaries by the electromotive force, equation 18, generated inside. Outside the boundary where there are no sources nor sinks of current the divergence of the area current density i must be zero and by Ohm's law i equals the product of the area conductivity b/ρ by the negative potential gradient. Writing the relations symbolically gives

$$\nabla \cdot i = -\nabla \cdot (b/\rho) \nabla V$$
$$= -(b/\rho) \nabla^2 V$$
$$= 0 \tag{1}$$

Thus the differential equation and boundary conditions satisfied by V are

$$\nabla^2 V = 0$$
$$V_+ - V_- = \omega r B \, \delta r \times 10^{-8} \tag{2}$$

Now let two infinite parallel wires carrying currents I and $-I$ pierce the current shell normally at opposite ends of the flux band which coincides with a section of the magnetic shell that joins them. The differential equation and boundary conditions satisfied by the scalar magnetic potential Ω of this shell are then

$$\nabla^2 \Omega = 0$$
$$\Omega_+ - \Omega_- = I \tag{3}$$

Evidently the solutions of equations 2 and 3 are mathematically identical provided we identify $\omega r B \delta r \times 10^{-8}$ with I, V with Ω, and i with bH/ρ.

The law of Biot and Savart shows that at any point P the value of $-\nabla \Omega$ or H that satisfies equation 3 is determined by the radius vectors drawn from the two wires to P. Similarly i must be determined by vectors drawn from the ends J and K of the flux band. The component of H resulting from the K-wire is $2I/S_k$ so that of i resulting from K is

$$i_k = \frac{2\omega b r B \delta r}{\rho S_k} \times 10^{-8} \tag{4}$$

and is normal to S_k. Now from equation 5 we may write the current density caused by a flux pencil in the form

$$i_k = \frac{I}{ds} = \frac{b}{\rho S_k} \frac{d\phi_k}{dt} \times 10^{-8} \tag{5}$$

Therefore, the flux band may be replaced by two equal and opposite flux pencils, one at each end, whose strengths are

$$\phi_{k,J} = \pm 2\omega B r \delta r t \tag{6}$$

Theory and Application of Complex Logarithmic and Geometric Mean Distances

THOMAS JAMES HIGGINS
MEMBER AIEE

THE geometric mean distance D_1 between a point and a plane geometric part (a line segment, curve segment, closed curve, or area lying in a plane containing the point) is defined by

$$\log D_1 = (1/S_1) \int_{S_1} \log d \, dS \qquad (1)$$

wherein d is the distance between the given point and an arbitrary point in the second geometric part, and S_1 is the length or area of this part.

The geometric mean distance D_{12} between two coplanar geometric parts S_1 and S_2 is

$$\log D_{12} = (1/S_1S_2) \int_{S_2} \int_{S_1} \log d \, dS_1 \, dS_2 \qquad (2)$$

wherein d is the distance between arbitrary points in the given geometric parts, and S_1 and S_2 are the respective lengths or areas of these parts. If S_1 and S_2 are identical in shape and position, D_{11} is termed the self geometric mean distance of $S_1 \equiv S_2$ to itself. If S_1 and S_2 are nonidentical, D_{12} is termed the mutual geometric mean distance between S_1 and S_2.

The logarithm of a geometric mean distance is termed a logarithmic mean distance. Equations 1 and 2 evidence the general definition of the logarithmic mean distance between two geometric parts as the average value of the summation of the logarithms of the distances between all possible pairs of points comprising the two geometric parts, the two points of a pair being chosen from different geometric parts.

Obviously, knowledge of the logarithmic mean distance furnishes knowledge of the corresponding geometric mean distance and conversely. Accordingly, in developing general theory it is only necessary to speak of one of the two. In textbooks, which maintain the tradition established in Maxwell's text,[1] the geometric mean distance is dealt with. Inasmuch, however, as the logarithmic mean distance rather than the geometric mean distance is utilized in actual practice [for example, the d-c or low-frequency a-c inductance of a transmission line or an industrial bus comprised of two nonmagnetic parallel cylindrical conductors of cross sections S_1 and S_2 is

$$L = 2 \log (D_{12}^2/D_{11}D_{22})$$
$$= 4 \log D_{12} - 2 \log D_{11} - 2 \log D_{22}$$

abhenrys per centimeter of line or bus length] it would seem preferable to work in terms of the logarithmic mean distance, as is done in the remainder of this paper.

As indicated by equations 1 and 2, evaluation of the logarithmic mean distance between two specified geometric parts requires a one- (for a point and a line or curve segment) to four-fold (for two plane areas) integration, of difficulty depending on the shape and relative location of the specified geometric parts. In general, if the given configuration is other than one of the several simple cases which long have been evaluated, the mathematical difficulties associated with integrating equations 1 and 2 are very considerable (see, for example, the analysis encompassed in obtaining the logarithmic mean distance for the not very complicated geometrical arrangement of two arbitrarily located parallel-sided rectangles treated in reference 2).

Recently, however, the writer has evolved a method for determining logarithmic mean distances in which the just mentioned mathematical difficulties are largely obviated. This method hinges on the use of complex variable theory rather than the real variable theory utilized by Maxwell[1,3] (originator of the theory of logarithmic mean distance), Gray,[4] Guye,[5,6] Sumec,[7] Orlich,[8,9,10] Rosa,[11,12,13] Grover,[10,13,14] and all others[17] who to date have calculated logarithmic mean distances. In essence, the method involves expressing the right-hand member of equations 1 or 2 as the real or imaginary part of an integral which is a function of the complex variable $z = x + iy$. This complex integral, unlike the real integrals of equations 1 and 2, is evaluated easily. Moreover, the resulting complex expression, hereafter termed the complex logarithmic distance, yields yet another advantage.

The formulas for the logarithmic mean distances of the geometric configurations encountered in practice comprise algebraic summation of a number of logarithmic, arctangentic, and algebraic terms. Because of the many transcendental terms, numerical computation with these formulas is most laborious. In consequence, it is most desirable to know the equivalent rapidly converging series which is especially suited to computation. The series equivalent of a given formula commonly has been obtained, to date, by replacing each component term by its power series, and summing corresponding powers of the variable. Obtaining the equivalent series of a specified logarithmic mean distance in this fashion requires, however, a considerable amount of labor. Contrari-

Paper 47-2, recommended by the AIEE committee on basic sciences for presentation at the AIEE, winter meeting, New York, N. Y., January 27–31, 1947. Manuscript submitted July 29, 1946; made available for printing October 11, 1946.

THOMAS JAMES HIGGINS is associate professor of electrical engineering, Illinois Institute of Technology, Chicago, Ill.

wise, the equivalent series of the complex logarithmic mean distance can be derived with little labor, and from this series can be obtained by inspection the real or imaginary part which is the desired series for the logarithmic mean distance.

It appears, therefore, that use of the complex variable rather than the real variable largely eliminates the mathematical difficulties encountered in working out specific formulas for logarithmic mean distances and in obtaining their equivalent series.

Now much of the theory pertinent both to the design and to the calculation of the resulting electrical and mechanical performance of power[18] and communication[19] transmission lines, industrial distribution busses[17,20,21] transformer windings,[22,23] coils and solenoids for induction heating units and various other purposes,[16,23] and of yet other current-carrying apparatus is couched in terms of logarithmic mean distances. In consequence, it is obviously most desirable that the above mentioned advantages stemming from use of complex logarithmic mean distances be generally available.

The requisite theory is developed under the heading "General Theory." Application of this theory and substantiation of the very considerable advantages accruing to use of it are afforded by solution of typical problems given under "Illustrative Examples."

General Theory

Given the real integral

$$G(X,Y) = \int_{S_1} E(X,Y)dS \qquad (3)$$

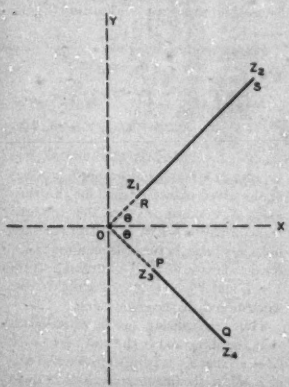

Figure 1. Relative location of two line segments

let $Z = \Psi(W)$ be a conformal transformation[24] which maps the line or curve segment S_1 of the $Z = X + iY$ plane on a line segment U_1 in the right-hand half of the $W = U + iV$ plane. In virtue of the specified transformation X, Y and $dS = |dZ/dW|dU$ are known functions of U and V. Substituting accordingly in equation 3 yields

$$G[X(U,V),\ Y(U,V)] = \int_{U_1} E[X(U,V),\ Y(U,V)]|dZ/dW|dU \qquad (4)$$

or equivalently

$$H(U,V) = \int_{U_1} F(U,V)dU \qquad (5)$$

whereof

$$H(U,V) = G(X,Y)$$

and

$$F(U,V) = E(X,Y)|dZ/dW|$$

Let $F(U,V) = f_1(U,V)$ be the real part of an analytic function $f(W) = f_1(U,V) + if_2(U,V)$. Consider the complex integral

$$\begin{aligned} h(W) &= \int_{U_1} f(W)dW \\ &= \int_{U_1}(f_1+if_2)\ d(U+iV) \\ &= \int_{U_1}(f_1\ dU - f_2\ dV) + \\ &\qquad i\int_{U_1}(f_2\ dU + f_1\ dV) \end{aligned} \qquad (6)$$

Over the path of integration $U = U_1$ we have $dU = dU$ and $dV = 0$.
Thus

$$\begin{aligned} h(W) &= \int_{U_1} f_1\ dU + i\int_{U_1} f_2\ dU \\ &= \int_{U_1} F(U,V)\ dU + i\int_{U_1} f_2 dU \end{aligned} \qquad (7)$$

The right-hand member of equation 5 is the real part of the right-hand member of equation 7; whence $H(U,V)$ must be the real part of $h(W)$. Similarly, if $F(U,V)$ is taken as the imaginary part of $f(W)$, $H(U,V)$ will be the imaginary part of $h(W)$.

The foregoing analysis is to be epitomized as follows:

Theorem I. Let $Z = \Psi(W)$ be a conformal transformation which maps the linear segment S_1 of the Z plane on the line segment U_1 in the right-hand half of the W plane. If under this transformation the real function $E(X,Y)\ dS$ goes over into the real part or the imaginary part of the complex function $f(W)dW$, the real integral $\int_{S_1} E(X,Y)dS$ is, respectively, the real part or the imaginary part of the complex integral $\int_{U_1} f(W)dW$.

In a precisely similar fashion the following can be established:

Theorem II. Let $Z = \Psi(W)$ be a conformal transformation which maps the linear segment S_1 of the Z plane on the line segment V_1 in the upper half of the W plane. If under this transformation the real function $E(X,Y)dS$ goes over into the real part or the imaginary part of the complex function $f(W)dW$, the real integral $\int_{S_1} E(X,Y)dS$ is, respectively, the imaginary part or the negative of the real part of the complex integral $\int_{V_1} f(W)dW$.

With reference to logarithmic mean distance theory the importance of the analysis indicated in theorems I and II is as follows. Determination of a logarithmic mean distance necessitates evaluation of a multiple integral whereof the successive integrals are of the type of equation 3. Commonly, evaluation in terms of real variables hinges on transforming the integral in question into an integral of the form of equation 5 through appropriate change in the variable of integration. Successful determination of the change to be made depends heavily on the skill and experience of the calculator; further, the transformed integral, though simpler than the original integral, usually is yet difficult to integrate. These difficulties increase with successive integrals. If these obstacles are surmounted, the resulting formula for the logarithmic mean distance is complicated in form, contains numerous transcendental terms, and requires considerable analytic manipulation before the equivalent series, or formulas pertinent to special cases of the general geometric configuration, can be derived from the formula for the general case.

Such analytic difficulties do not ensue when the complex variable approach sketched previously is utilized. The conformal transformation to be used is more

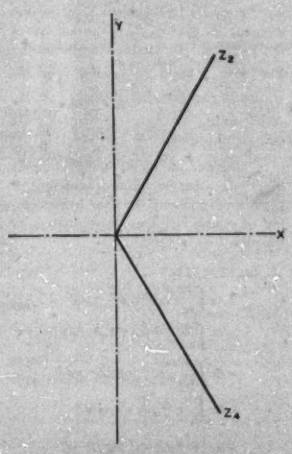

Figure 2. Two identical line segments of length a and 120-degree included angle

or less obvious. Application of this transformation to the given integral in accordance with Theorem I or II automatically effects the desired change of variable; usually, the associated complex integral is so simple that it can be integrated by inspection. Successive integrals are handled as easily. The resulting formula for the complex logarithmic mean distance is simple in form, contains few terms, and is manipulated readily to yield the equivalent series or formulas pertinent to special cases of the given geometrical configuration. Selection of the real or imaginary part yielding the real logarithmic mean distance is a matter of inspection.

In substantiation of these remarks and in illustration of the analytic detail encompassed in use of the complex variable analysis consider the following examples.

Illustrative Examples

Example 1. The problem is to calculate the logarithmic mean distance between two arbitrarily located line segments (Figure 1).

From equation 2 we have

$$\log D_{12} = (1/S_1S_2)\int_{S_2}\int_{S_1}\log\left[(X-x)^2+(Y-y)^2\right]^{1/2}dS_1\,dS_2$$
$$= (1/S_1S_2)\int_{S_2}\int_{S_1}\log|Z_1-z_1|dS_1\,dS_2 \tag{8}$$

wherein (X, Y) are the co-ordinates of an arbitrary point in S_1 and (x, y) those of an arbitrary point in S_2.

The conformal transformation $W = Ze^{-i\theta}$ maps the line segment S_1 on the line segment $|Z_1| \leq U_1 \leq |Z_2|$ of the real axis of the W plane. Under the transformation we obtain

$$\int_{S_1}\log|Z-z|dS_1 = \int_{|Z_1|}^{|Z_2|}\log|We^{i\theta}-z|\times|e^{i\theta}|dU$$
$$= \int_{|Z_1|}^{|Z_2|}\log|We^{i\theta}-z|dU \tag{9}$$

In virtue of the identity, log (complex function) = log (modulus of function) + i (phase of function), the right-hand member of equation 9 can be evaluated by theorem I as follows:

$$\int_{S_1}\log|Z-z|dS_1$$
$$= Re\int_{|Z_1|}^{|Z_2|}\log(We^{i\theta}-z)dW$$
$$= Re\int_{|Z_1|}^{|Z_2|}e^{-i\theta}\log(We^{i\theta}-z)dW\,e^{+i\theta}$$
$$= Re\int_{|Z_1|e^{i\theta}}^{|Z_2|e^{i\theta}}e^{-i\theta}\log(Z-z)dZ$$
$$= Re\int_{Z_1}^{Z_2}e^{-i\theta}\log(Z-z)dZ$$
$$= Re\left\{e^{-i\theta}\left[(Z-z)\log(Z-z)-(Z-z)\right]_{Z_1}^{Z_2}\right\} \tag{10}$$

wherein Re indicates the real part of the complex expression.

The conformal transformation $W = ze^{i\theta}$ maps the line segment S_2 on the line segment $|Z_3| \leq U_2 \leq |Z_4|$ of the real axis of the W plane. Under this transformation we obtain in the fashion

$$\int_{S_2}\left(\int_{S_1}\log|Z-z|dS_1\right)dS_2$$
$$= \int_{S_2}Re\left\{e^{-i\theta}\left[(Z-z)\log(Z-z)-(Z-z)\right]_{Z_1}^{Z_2}\right\}dS_2$$
$$= \int_{|Z_3|}^{|Z_4|}Re\left\{e^{-i\theta}\left[(Z-We^{-i\theta})\times\log(Z-We^{-i\theta})-(Z-We^{-i\theta})\right]_{Z_1}^{Z_2}\right\}\times|e^{-i\theta}|dU$$
$$= Re\int_{Z_3}^{|Z_4|}e^{-i\theta}\left[(Z-We^{-i\theta})\times\log(Z-We^{-i\theta})-(Z-We^{-i\theta})\right]_{Z_1}^{Z_2}dW$$
$$= Re\int_{|Z_3|_e-i\theta}^{|Z_4|_e-i\theta}e^{-i\theta}e^{i\theta}\left[(Z-We^{-i\theta})\times\log(Z-We^{-i\theta})-(Z-We^{-i\theta})\right]_{Z_1}^{Z_2}\times dW\,e^{-i\theta}$$
$$= Re\int_{|Z_3|_e-i\theta}^{|Z_4|_e-i\theta}\left[(Z-We^{-i\theta})\times\log(Z-We^{-i\theta})-(Z-We^{-i\theta})\right]_{Z_1}^{Z_2}\times dW\,e^{-i\theta}$$
$$= Re\int_{Z_3}^{Z_4}\left[(Z-z)\log(Z-z)-(Z-z)\right]_{Z_1}^{Z_2}dz$$
$$= Re\left\{\left(\left[-\frac{1}{2}(Z-z)^2\log(Z-z)+\frac{3}{4}(Z-z)^2\right]_{Z_1}^{Z_2}\right)_{Z_3}^{Z_4}\right\} \tag{11}$$

Substituting from equation 11 in equation 2 yields the desired logarithmic mean distance

$$\log D_{12} = -(1/S_1S_2)Re\left\{\left[\left[\frac{1}{2}(Z-z)^2\times\log(Z-z)-\frac{3}{4}(Z-z)^2\right]_{Z_1}^{Z_2}\right]_{Z_3}^{Z_4}\right\} \tag{12}$$

For the general configuration of Figure 1, $Z_1 = OR\,e^{i\theta}$, $Z_2 = OS\,e^{i\theta}$, $Z_3 = OP\,e^{-i\theta}$ $Z_4 = OQ\,e^{-i\theta}$ and $2\theta = \phi$. Substituting in the right-hand member of equation 12 and effecting the indicated analysis as detailed in Appendix I yields

$$2RS\,PQ\log D_{12} = [2OR\,OP-(OR^2+OP^2)\times\cos\phi]\log RP+[2OS\,OQ-(OS^2+OQ^2)\cos\phi]\log SQ-[2OS\,OP-(OS^2+OP^2)\cos\phi]\log SP-[2OR\,OQ-(OR^2+OQ^2)\cos\phi]\times\log RQ-[OP^2\,\overline{SPR}-OQ^2\,\overline{SQR}+OR^2\,\overline{PRQ}-OS^2\,\overline{PSQ}]\sin\phi-3RS\,PQ \tag{13}$$

wherein, for example, $\overline{SPR}$ indicates the radian measurement of the angle SPR.

Confirmatively, equation 13 is identical with the known formula derived by Maxwell.[1,3] The very considerable simplicity of the derivation given here is appreciated best by comparing it with the analysis involved in direct integration of equation 8 as effected in Maxwell's[1] original derivation.

Example 2. The problem is to derive the geometric mean distance between two identical line segments of length a, relatively located as in Figure 2.

For this particular case of the general configuration of Figure 1, $Z_1 = Z_3 = 0$, $Z_2 = Z_4 = ae^{i\pi/3}$. Substituting in equation 12 and performing the indicated arithmetic as detailed in Appendix II yields

$$\log D_{12} = \log a+\frac{3}{4}\log 3+\frac{\sqrt{3}\pi}{12}-\frac{3}{2} \tag{14}$$

Confirmatively, the same value is yielded by equation 13. But in deriving equation 14 from equation 13 considerable manipulation is required. Thus, inasmuch as $OP = OR = RP = 0$, L'Hospital's Theorem[25] must be utilized to determine the values of the indeterminate term $[2OR\,OP-(OR^2+OP^2)\cos\phi]\log RP$; the limiting values of $\overline{SPR}$ and $\overline{PRQ}$ must be discerned; the proper quadrantal algebraic signs must be assigned to the trigonometric functions—a fact not clear from Maxwell's statement of the formula of equation 13. Contrariwise, obtaining equation 14 from equation 12 requires only routine calculation with complex numbers.

Example 3. The problem is to determine the logarithmic mean distance between two parallel-sided rectangular areas of arbitrary relative location (Figure 3).

From equation 2 we have

$$RSrs\log D_{12} = \int_0^s\int_0^r\int_{P+s}^{P+S+s}\int_{D+r}^{D+R+r}\log\left[(X-x)^2+(Y-y)^2\right]^{1/2}dX\,dY\,dx\,dy \tag{15}$$

Each of the differential elements dX, dY, dx, and dy is parallel to a co-ordinate axis of the given plane. Hence for the variables X, Y taken in turn the required transformation is $Z = W$ and for the variables x, y taken in turn the required transformation is $z = W$. Accordingly $X = x = U$ and $Y = y = V$, indicating that we work directly in the given plane.

Thus, recognizing (as in equation 8) that the integrand is the real part of log $(Z-z)$, that dX is parallel to the real axis of Z, dY to the imaginary axis of Z, dx to the real axis of $z(\equiv Z)$ and dY to the imaginary axis of z we obtain by succes-

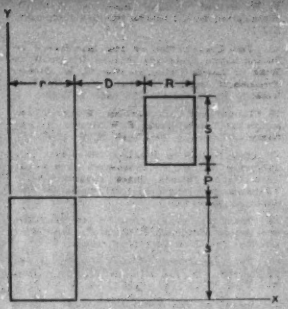

Figure 3. Relative location of two parallel-sided rectangles

sive application of theorems I and II

$$RSrs \log D_{11} = \int_0^r \int_0^s \int_{P+s}^{P+S+s} \left[Re \times \int_{(D+r)+iY}^{(D+R+r)+iY} \log (Z-z) dZ \right] dY\, dx\, dy$$

$$= \int_0^r \int_0^s \int_{P+s}^{P+S+s} Re \left\{ [(Z-z) \times \log (Z-z) - (Z-z) \Big]_{(D+r)+iY}^{(D+R+r)+iY} \right\} \times dY\, dx\, dy$$

$$= \int_0^r \int_0^s \int_{P+s}^{P+S+s} \left\{ Re[(Z-z) \times \log (Z-z) - (Z-z) \Big]_{D+r}^{D+R+r} dY\, dx\, dy \right.$$

$$= \int_0^r \int_0^s \left[\left[Im \left\{ \frac{1}{2}(Z-z)^2 \log(Z-z) - \frac{3}{4}(Z-z)^2 \right\} \right]_{D+r}^{D+R+r} \right]_{P+s}^{P+S+s} dx\, dy$$

$$= \int \left[\left[\left[Im \left\{ \frac{1}{6}(Z-z)^3 \log (Z-z) - \frac{11}{36}(Z-z)^3 \right\} \right]_{D+r}^{D+R+r} \right]_{P+s}^{P+S+s} \right]_0^s dy$$

$$= -\frac{1}{24} \left[\left[\left[Re \left\{ (Z-z)^6 \log(Z-z) - \frac{25}{12}(Z-z)^4 \right\} \right]_{D+r}^{D+R+r} \right]_{P+s}^{P+S+s} \right]_0^s \quad (16)$$

Recalling the identity

$$\log (Z-z) = \log [(X-x)^2 + (Y-y)^2]^{1/2} + i \tan^{-1}[(Y-y)/(X-x)] \quad (17)$$

wherein the arc tangent takes on the proper quadrantal value in accordance with use of the principal branch of the logarithmic function $[-\pi < \text{phase } (Z-z) \equiv \tan^{-1} (Y-y)/(X-x) \leq \pi]$, we obtain from equation 16

$$RSrs \log D_{11} = -\frac{25}{12} RSrs - \frac{1}{24} \sum_{i=1}^{4} \sum_{j=1}^{4} (-1)^{i+j} K(A_i, B_j) \quad (18)$$

wherein

$$K(A_i, B_j) = (A_i^6 - 6A_i^4 B_j^2 + B_j^6) \log (A_i^2 + B_j^2)^{1/2} - 6A_i^5 B_j \tan^{-1}(B_j/A_i) + 4A_i B_j^5 \tan^{-1} (B_j/A_i) \quad (19)$$

and

$$A_1 = |D+R+r|;\ A_2 = |D+R|;\ A_3 = |D|;\ A_4 = |D+r| \quad (20)$$

$$B_1 = |P+S+s|;\ B_2 = |P+S|;\ B_3 = |P|;\ B_4 = |P+s| \quad (21)$$

The ease with which equation 18 is obtained is appreciated readily if the present derivation be compared with the original derivation[2] of this formula, effected by direct integration of equation 15.

Example 4. The problem is to determine the series equivalent of the formula for the self geometric mean distance of a rectangular area having sides r and s.

The configuration of this example is a special case of Figure 3; the rectangles are identical and coincident. Hence $R = r$, $S = s$, $D = -r$, $P = -s$, whence equations 20 and 21 yield $A_1 = A_3 = r$, $A_2 = A_4 = 0$, $B_1 = B_3 = s$, and $B_2 = B_4 = 0$. Substituting appropriately in equations 18 and 19 yields

$$\log D_{11} = -\frac{25}{12} - \left(\frac{1}{6} r^2 s^2\right) [(r^4 - 6r^2 s^2 + s^4) \log (r^2+s^2)^{1/2} - 4r^2 s \tan^{-1} s/r + 4rs^2 \tan^{-1} s/r - r^4 \log r - s^4 \log s] \quad (22)$$

In virtue of the relationship of equations 16, 17, and 18 it is obvious that the algebraic sum of the first three terms in the bracketed quantity in the right-hand member of equation 22 is $Re[(r + is) \times \log (r+is)]$. This noted, it is evident that the bracketed quantity can be written in the form, $Re[r^4(1 + t)^4 \log(1 + t)] - 6r^2 s^2 \log r$, wherein t is the complex number (ir/s). Accordingly equation 22 can be written

$$\log D_{11} = -\frac{25}{12} + \log r - \frac{1}{6}(r/s)^2 \times Re[(1+t)^4 \log (1+t)] \quad (23)$$

Now $(1+T) \log(1+T)$, wherein T is a complex variable, can be expanded in a power series about the point $T = 0$. This power series represents the function for all values of T such that $|T| < 1$. At $T = -1$, whereof $|T| = 1$, the function has a singularity—a branch point; whence in general the function is not represented by its power series at points such that $|T| \geq 1$. Applying Taylor's theorem yields

$$(1+T)^4 \log (1+T) = T + \frac{7}{2}T^2 + \frac{13}{3}T^3 + \frac{25}{12}T^4 + \ldots \quad (24)$$

wherein $|T| < 1$.

In our particular case we are interested in the real part of the series corresponding to the special value, $T = t = (ir/s)$. Substituting in equation 24 and selecting the real part yields

$$Re[(1+t)^4 \log (1+t)] = -\frac{7}{2}(r/s)^2 + \frac{25}{12}(r/s)^4 - \ldots \quad (25)$$

valid for $(r/s) < 1$. Substituting from equation 25 into equation 23 yields the desired equivalent series

$$\log D_{11} = \log r - \frac{25}{12} + \frac{7}{12}(r/s)^4 - \frac{25}{72}(r/s)^6 + \ldots \quad (26)$$

This series is identical with the known formula. The ease with which it is derived is appreciated readily by one who proceeds to derive it directly from equation 22 by expanding the component terms in power series and summing corresponding powers of (r/s). Yet equation 22 is the simplest of the formulas for logarithmic mean distances between rectangular areas which are utilized in, say, the design of industrial distribution busses.

Appendix I

From equation 12 we have

$$2RS\,PQ \log D_{12} = Re\{ -[(Z_3 - Z_4)^2 \times \log (Z_3 - Z_4) - 3(Z_3 - Z_4)^2/2] + [(Z_3 - Z_4)^2 \log (Z_3 - Z_4) - 3(Z_3 - Z_4)^2 + 2] + [(Z_1 - Z_4)^2 \log (Z_1 - Z_4) - 3(Z_1 - Z_4)^2/2] - [(Z_1 - Z_4)^2 \times \log (Z_1 - Z_4) - 3(Z_1 - Z_4)^2/2]\} \quad (27)$$

Typically

$$(Z_3 - Z_4) = |Z_3| (\cos \theta + i \sin \theta) - |Z_4| \times (\cos \theta - i \sin \theta) = (|Z_3| - |Z_4|) \cos \theta + i(|Z_3| + |Z_4|) \times \sin \theta \quad (28)$$

whence by recalling simple trigonometric transformations for $2\theta = \phi$ yields

$$(Z_3 - Z_4)^2 = (|Z_3|^2 + |Z_4|^2) \cos \phi - 2|Z_3||Z_4| + i(|Z_3|^2 - |Z_4|^2) \sin \phi = (OS^2 + OQ^2) \cos \phi - 2OS\,OQ + i(OS^2 - OQ^2) \sin \phi \quad (29)$$

Next

$$\log (Z_3 - Z_4) = \log |Z_3 - Z_4| + i \text{ phase } (Z_3 - Z_4) = \log QS + i(\theta + \overline{OSQ}) \quad (30)$$

Accordingly

$$Re\{ -[(Z_3 - Z_4)^2 \log (Z_3 - Z_4) - 3(Z_3 - Z_4)^2/2]\} = [2OS\,OQ - (OS^2 + OQ^2) \cos \phi] \times \log QS + (\theta + \overline{OSQ})(OS^2 - OQ^2) \times \sin \phi - 3[(OS^2 + OQ^2) \cos \phi - 2OS\,OQ]/2 \quad (31)$$

The real parts of the other three terms in the right-hand member of equation 27 can be written down by analogy. Adding these four real parts, cancelling like terms, and transforming the four terms typified by $[OS^3(\overline{OSQ}-\overline{OSP})\sin\phi]$ into the form typified by $[OS^3\,\overline{PSQ}\sin\phi]$ yields equation 13.

Appendix II

From Figure 2 we have $Z_1=Z_2=0$, $Z_3=ae^{i\pi/3}$, $Z_4=\overline{Z}_3=ae^{-i\pi/3}$, $RS=PQ=a$. Substituting in equation 27 yields

$$\begin{aligned}2a^3\log D_{12} &= Re\{-[(Z_3-\overline{Z}_3)^3\log(Z_3-\overline{Z}_3)-\\ &\quad 3(Z_3-\overline{Z}_3)^3/2]+[Z_3^3\log Z_3-\\ &\quad 3Z_3^3/2]+[\overline{Z}_3^3\log(-\overline{Z}_3)-3\overline{Z}_3^3/2]\}\\ &= Re[-(Z_3-\overline{Z}_3)^3\log(Z_3-\overline{Z}_3)+\\ &\quad Z_3^3\log Z_3+\overline{Z}_3^3\log(-\overline{Z}_3)-3Z_3\overline{Z}_3]\end{aligned} \tag{32}$$

Substituting as indicated in equation 32, performing the indicated simple complex arithmetic in which $\log(-\overline{Z}_3)=\log ae^{i2\pi/3}$ inasmuch as we are working on the principal branch $-\pi <$ phase $Z \leq \pi$), and collecting like terms yields equation 14.

References

1. A Treatise on Electricity and Magnetism (third edition). J. C. Maxwell. Clarendon Press, Oxford, England, volume 2, 1892, pages 324–8.

2. Formulas for the Geometric Mean Distance of Rectangular Areas and of Line Segments. T. J. Higgins. *Journal of Applied Physics*, New York, N. Y., volume 14, 1943, pages 188–95.

3. On the Geometrical Mean Distance of Two Figures in a Plane. J. C. Maxwell. *Transactions*, Edinburgh Royal Society (Edinburgh, Scotland), volume 26, 1872, pages 729–33.

4. Theory and Practice of Absolute Measurements in Electricity and Magnetism (second edition). A. Gray. Macmillan and Company (London, England), volume 2, part 1, 1921, pages 475–87.

5. Coefficient Self-Induction des Fils Parallèles Égaux et Equidistants, Dont les Sections Sont Reparties sur une Circonférence. C. E. Guye. *Comptes Rendus* (Paris, France), volume 119, 1894, pages 219–21.

6. Sur la Moyenne Distance Géometrique des Éléments d'un Ensemble de Surfaces et Son Application au Calcul des Coefficients D'Induction. C. E. Guye. *Comptes Rendus* (Paris, France), volume 118, 1894, pages 1329–32.

7. Berechnung der Selbstinduktion Gerader Leiter und Rechteckiger Spulen. J. K. Sumec. *Electrotechnische Zeitschrift* (Berlin, Germany), volume 27, 1906, pages 1175–9.

8. Über Starkstrom Widerstände mit Kleiner Selbstinduktion. E. Orlich. *Zeitschrift für Instrumentenkunde* (Berlin, Germany), volume 29, 1909, pages 241–56.

9. Über Die Induktionswirkungen Paralleler Gestreckter Leiter. E. Orlich. *Elektrotechnische Zeitschrift* (Berlin, Germany), volume 29, 1908, pages 310–13.

10. Kapazität und Induktivität: Ihre Begriffe Bestimmung Berechnung, und Messung (book). E. Orlich. Brunswick, Germany, 1909.

11. On the Geometrical Mean Distances of Rectangular Areas and the Calculation of Self-Inductance. E. B. Rosa. *Bulletin*, Bureau of Standards, Washington, D. C., volume 3, 1907, pages 1–41.

12. The Self- and Mutual Inductances of Linear Conductors. E. B. Rosa. *Bulletin*, Bureau of Standards, Washington, D. C., volume 4, 1907–1908, pages 301–44.

13. Formulas and Tables for the Calculation of Mutual and Self-Inductance. E. B. Rosa, L. Cohen. *Bulletin*, Bureau of Standards, Washington, D. C., volume 5, 1908–1909, pages 1–132.

14. Additions to the Formulas for the Calculation of Mutual and Self-Inductance. F. W. Grover. *Bulletin*, Bureau of Standards Washington, D. C., volume 14, 1918–1919, pages 537–70.

15. The Calculation of the Inductance of Single-Layer Coils and Spirals Wound With Wire of Large Cross Section. F. W. Grover. *Proceedings*, Institute of Radio Engineers, New York, N. Y., volume 17, 1929, pages 2053–63.

16. Inductance Calculations: Working Formulas and Tables (book). F. W. Grover. D. Van Nostrand Company, New York, N. Y., 1946.

17. The Design of Bus-Bar Industrial Distribution Systems: An Epitomization of Available Data. Thomas James Higgins. AIEE Transactions, volume 64, 1945, pages 385–400; discussion, pages 486–8.

18. Principles of Electric Power Transmission (second edition). L. F. Woodruff. John Wiley and Sons, Inc., New York, N. Y., chapter 2.

19. Electromagnetic Waves (book). S. A. Schelkunoff. D. Van Nostrand Company, Inc., New York, N. Y., 1943, pages 176–9.

20. Formulas for the Calculation of the Inductance of Linear Conductors of Structural Shape. Thomas James Higgins. AIEE Transactions, volume 62, 1943, February section, pages 53–7.

21. Formulas for Calculating Short-Circuit Forces Between Conductors of Structural Shape. Thomas James Higgins. AIEE Transactions, volume 62, 1943, October section, pages 659–63.

22. Weitere Entwicklung der Allgemeinen Methode zur Berechnung der Streuung von Transformatoren. G. Petrow. *Elektrotechnik und Maschinenbau* (Vienna, Austria), volume 52, 1934, pages 396–400.

23. Electrical Coils and Conductors; Their Electrical Characteristics and Theory (book). H. B. Dwight. McGraw-Hill Book Company, Inc., New York, N. Y., 1945.

24. Mapping of Fields. E. Weber. Electrical Engineering, volume 53, December 1934, pages 1563–70.

25. Elements of the Differential and Integral Calculus (book). W. A. Granville, P. F. Smith, W. A. Longley. Ginn and Company, New York, N. Y., 1934, pages 174–6.

No Discussion

Equivalent Circuit of the Primitive Rotating Machine With Asymmetrical Stator and Rotor

GABRIEL KRON
MEMBER AIEE

Synopsis: The equations and equivalent circuits of all standard types of rotating electric machinery operating under arbitrary conditions may be derived as special cases of a single generalized rotating machine, the so-called primitive machine. This paper derives the steady-state equivalent circuit of the primitive machine having unbalanced rotor as well as stator. That is, the load or transmission line connected to a salient-pole synchronous machine is assumed to be unbalanced (due to faults, short circuits, and so forth), or the load connected to the slip rings of an induction motor is assumed to be unbalanced. The single-phase alternator, instrument Selsyns, and also sudden short-circuit studies are cases that require an infinite series of time harmonics in the stator and rotor windings in addition to the fundamental. It is assumed that these time harmonics are due to space waves with fundamental pairs of poles rotating at different speeds. The effect of the harmonic space waves is not considered. A paper by A. W. Rankin[1] shows network analyzer studies made of the harmonic currents and torques of a single-phase alternator.

The Balanced Primitive Machine

THE equivalent circuit of the primitive machine in which either the stator or the rotor is balanced has been given in reference 2 and is reproduced in Figure 1. There are two stator and two rotor windings assumed with one member having salient poles. As was shown, the inductances represent the underlying magnetic circuit in which the fluxes flow, and the position of the resistance represents the arrangement of the coils on the magnetic circuit.

While the reactances are calculated at unit frequency, the fundamental frequency of currents along the stationary reference axes is assumed to be f, a fraction of unity. The numbers $f + v$, and so forth, by which the resistances and impressed voltages are divided, show the actual frequencies of the currents in the particular coils. In commutator machines where the ratio of the generated to induced voltages due to a flux line is not unity but k, the rotor speed v should be replaced by kv. The resultant flux linking each coil is the voltage E while the torque due to the coil is the power E^*i.

The Unbalanced Primitive Machine

When both the stator and rotor winding are unbalanced (still assuming saliency on one member only), in the stator (or field) flow not only a current of frequency f, but also even harmonics of the rotor speed v, namely $f \pm 2v$, $f \pm 4v$, and so forth. In the rotor (or armature) flow in addition to f odd harmonics of v, namely $f \pm v$, $f \pm 3v$, $f \pm 5v$, and so forth.

For each frequency of stator and rotor currents there exists in the equivalent circuit a set of forward and backward meshes (Figure 2) that are coupled together by the unbalanced rotor (armature) impedances. The stator and rotor circuits are staggered and are coupled together through the air gap reactances. Again the numbers by which the resistances and impressed voltages are divided show the actual frequency of currents in the coil, such as $f - 2v$ or $f + 3v$. While the two stator reference axes are denoted by d and q, the two rotor reference axes, along which the resistances and reactances are known, are denoted by a and b. For an induction motor a and b are the slip-ring axes, while for a synchronous machine they are the armature axes.

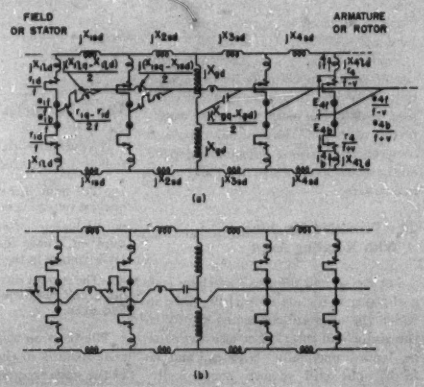

Figure 1. Two different forms of the equivalent circuit of the primitive rotating machine

Paper 47-3, recommended by the AIEE committee on electric machinery for presentation at the AIEE winter meeting, New York, N. Y., January 27-31, 1947. Manuscript submitted May 31, 1946; made available for printing October 22, 1946.

GABRIEL KRON is a consulting engineer, General Electric Company, Schenectady, N. Y.

Table I. Calculation of Torques

Constant Torques

$E_{-y}{}^*i^{f-y}=W_1+jQ_1$	$E_{b-z}{}^*i^{b-z}=W_4+jQ_4$
$E_{xf}{}^*i^{fx}=W_2+jQ_2$	$E_{bz}{}^*i^{\ z}=W_5+jC_5$
$E_{yf}{}^*i^{fy}=W_3+jC_3$	$E_{bz}{}^*i^{zb}=W_6+jC_6$
	$T=W_1+\ldots W_6$

Second Harmonic Torques

$E_{-y}{}^*i^{2f}=W_1+jQ_1$	$E_{-2z}{}^*i^{2z}=W_4+jQ_4$
$E_{xf}{}^*i^{2f}=W_2+jQ_2$	$E_{zb}{}^*i^{2z}=W_5+jQ_5$
$E_{yf}{}^*i^{2f}=W_3+jQ_3$	$E_{2b}{}^*i^{2b}=W_6+jQ_6$
$E_{-y}{}^*i^{-4f}=W_7+jQ_7$	$E_{-2b}{}^*i^{-4b}=W_{10}+jQ_{10}$
$E_{xf}{}^*i^{-4f}=W_8+jQ_8$	$E_{zb}{}^*i^{-2b}=W_{11}+jC_{11}$
$E_{yf}{}^*i^{2f}=W_9+jC_9$	$E_{2b}{}^*i^{2b}=W_{12}+jQ_{12}$
$T=\sqrt{(W_1+\ldots W_{12})^2+[(Q_1+\ldots Q_6)-(Q_7+\ldots Q_{12})]^2}$	

Analogous formulas apply to higher harmonic torques.

The Frequency of Torques

The torques still are measured as cross products of E^*i. The frequency of the latter is determined easily simply by matching the frequencies of E and i as manifested by the resistances in the respective coils. For instance, the actual frequency of E_{xf} is $f+v$ and of i^{-2f} is $f-3v$. Hence, the frequency of the torque due to them is $T=E^*i=-f-v+f-3v=-4v$. Table I gives the torques of various frequencies.

Special Cases

The various types of machines, synchronous and induction, differ from the primitive machine by having certain meshes open. For commutator machines the meshes are not only open but are interconnected in the same manner as the actual machine windings are. When certain windings in a machine are short-circuited permanently the analogous meshes in the equivalent circuit may be removed, but all open-circuit reactances must be replaced by short-circuit (transient and subtransient) reactances.

Figures 3 and 4 give the equivalent circuits of the unbalanced slip-ring induction motor and the single-phase alternator. It should be noted that in the single-phase alternator the mutual couplings between the various harmonics depend on the asymmetry of the direct and quadrature axes.

The Primitive Machine With Rotating Axes

Let the second primitive machine (say a slip-ring induction motor) be given in which the axes are connected rigidly to the stator and rotor. Let also the rotor be loaded unequally, ($r_{ra}\neq r_{rb}$, and so forth), but still smooth magnetically. Because the equation of voltage is

$$e=R\cdot i+p(L\cdot i) \tag{1}$$

the transient impedance tensor is $Z=R+pL$

$$Z=\begin{array}{c|c|c|c|c|}
 & d_s & q_s & a & b \\
\hline
d_s & r_{ds}+L_{ds}p & & M_dp\cos\theta & -M_dp\sin\theta \\
\hline
q_s & & r_{qs}+L_{qs}p & M_qp\sin\theta & M_qp\cos\theta \\
\hline
a & M_dp\cos\theta & M_qp\sin\theta & r_a+L_{Sa}p+L_Dp\cos 2\theta & -L_Dp\sin 2\theta \\
\hline
b & -M_dp\cos\theta & M_qp\cos\theta & -L_Dp\sin 2\theta & r_b+L_{Sb}p-L_Dp\cos 2\theta \\
\hline
\end{array} \tag{2}$$

$$\left.\begin{aligned}
L_D&=\frac{M_d-M_q}{2}\\
L_S&=\frac{M_d+M_q}{2}\\
L_{Sa}&=l_{ra}+\frac{M_d+M_q}{2}\\
L_{Sb}&=l_{rb}+\frac{M_d+M}{2}
\end{aligned}\right\} \tag{3}$$

where l_{ra} and l_{rb} represent the leakage inductances of the rotor and any inductive load.

For an alternator θ is replaced by $-\theta$.

The equation of torque is

$$f=\frac{1}{2}i\cdot\frac{\partial L}{\partial\theta}\cdot i \tag{4}$$

The Frequencies of Currents

If a current with frequency f is assumed to flow in the stator, then (if $\theta=v\omega t$)

1. The term d_sa shows that an $f\pm v$ frequency voltage is induced in the rotor.
2. Assuming an $f\pm v$ current in the rotor, the term ad_s shows that the latter induces an $f\pm 2v$ voltage in the stator.
3. The current due to the latter in turn induces an $f\pm 3v$ frequency voltage in the rotor and so on.

The term aa shows that any rotor current induces in the rotor itself voltages of the same frequency or larger (smaller) by $2v$. Similarly, the term d_sd_s shows that a stator current induces in the stator only voltages of the same frequency.

Summarizing the frequencies of the currents,

1. In the stator flow $f, f\pm 2v, f\pm 4v, f\pm 6v\ldots$ (even harmonics of v)
2. In the rotor flow $f\pm v,\ f\pm 3v,\ f\pm 5v$ (odd harmonics of v)

Time Harmonics

The question now arises, how these various frequencies of voltages may arise. Let sinusoidal windings be assumed on stator and rotor, that is, windings in which only a flux with the fundamental number of pairs of poles can induce a voltage. (This assumption neglects space harmonics, hence excludes squirrel cages.) In that case, higher time harmonics may be induced only by fluxes that rotate faster than the impressed flux. In particular, these fluxes must rotate faster by $\pm 2v$, $\pm 4v$, $\pm 6v$, and so forth as the fundamental flux when viewed from the stator (or faster by $\pm v$, $\pm 3v$, $\pm 5v$, when viewed from the rotor).

Hence, if an infinite set of reference frames is introduced rotating by $\pm 2v$, $\pm 4v$, $\pm 6v$, with respect to a set of reference frames stationary on both stator and rotor, then along these rotating reference frames the time harmonics under consideration must appear as fundamental frequency quantities.

The fact will be ignored that each rotating flux induces not only a voltage that rotates with the same speed as the flux but also other voltages rotating at other speeds. That is, harmonic terms (sine and cosine expressions) in the Z tensor of all reference frames will be neglected and only the constant term kept. This assumption is equivalent to ignoring the second order effects due to the time harmonics. (The time harmonic itself is a second order effect of the fundamental.)

In other words, each of the above reference frames originates another infinite set of reference frames rotating with $\pm 2v$, $\pm 4v$ . . . with respect to itself. Each of the latter in turn starts still an additional infinite set of frames. As a consequence along each frame rotating

with $=2\theta$, $=4\theta$, and so forth, not one current exists, but an infinite set of currents. All of these, but one, will be neglected.

The Primitive Machine With Stationary Axes

As a starting point it is possible to use the rotating axes a, b, or the stationary axes d and q, or the spin axes f, b of the equivalent circuits (that is, symmetrical components on d and q.) In the following the case of stationary axes d and q only will be considered.

Along the d and q axes, using

$$C = \begin{array}{c|cccc} & d_s & q_s & d_r & q_r \\ \hline d_s & 1 & & & \\ q_s & & 1 & & \\ d_r & & & \cos\theta & \sin\theta \\ q_r & & & -\sin\theta & \cos\theta \end{array} \qquad (5)$$

Z becomes (if p also refers to L)

$$Z' = C_t \cdot Z \cdot C + C_t \cdot L \cdot pC + C_t \cdot pL \cdot C \qquad (6)$$

When $r_a = r_b$ and $L_{sa} = L_{sb}$, then these matrices reduce to the usual form since

$$L_{sa} + L_D = L_{rd}$$
$$L_{sa} - L_D = L_{rq}$$

The Equations of Voltage and Torque

In terms of G' and L' the equation of voltage is now

$$e' = R' \cdot i' + L' \cdot pi' + (pL') \cdot i' + G' p\theta \cdot i'$$

But, since $pL' = \dfrac{\partial L'}{\partial \theta}\dfrac{d\theta}{dt} = \dfrac{\partial L'}{\partial \theta} p\theta$, the equation of voltage is

$$e' = R' \cdot i' + L' \cdot pi' + \frac{\partial L'}{\partial \theta} p\theta \cdot i' + G' p\theta \cdot i' \qquad (10)$$

The equation of torque is

$$f' = i' \cdot G' \cdot i' + \frac{1}{2} i' \cdot \frac{\partial L'}{\partial \theta} \cdot i' \qquad (11)$$

(See page 211, equation 27.17, and page 212, equation 27.21 of reference 3 where $\partial L'/\partial\theta$ was assumed to be zero)

The extra terms represent the Christoffel symbol

$$[\alpha\beta, \gamma] = \frac{\partial L_{\beta\gamma}}{\partial x^\alpha} - \frac{1}{2}\frac{\partial L_{\alpha\beta}}{\partial x^\gamma}$$

so that

$$[\alpha\beta, \gamma] i^\alpha i^\beta = \left(\frac{\partial L_{\beta\gamma}}{\partial x^\alpha} - \frac{1}{2}\frac{\partial L_{\alpha\beta}}{\partial x^\gamma}\right) i^\alpha i^\beta \qquad (12)$$

the first term giving the extra harmonic generated-voltages $\dfrac{\partial L'}{\partial \theta} p\theta \cdot i'$ and the second term the extra harmonic torque $1/2 i' \cdot \dfrac{\partial L'}{\partial \theta} \cdot i'$. The equation of motion of a machine with unbalanced rotor and stator is then (if $S_{\alpha\beta\gamma}$ is the torsion tensor)

$$e_\alpha = R_{\alpha\beta} i^\beta + L_{\alpha\beta} p i^\beta + [\beta\gamma, \alpha] i^\beta i^\gamma + 2S_{\beta\alpha\gamma} i^\beta i^\gamma \qquad (13)$$

The interesting fact follows that the effect of the asymmetry in both members is to introduce the Christoffel symbol in the dynamical equation of motion, even though the reference axes are all stationary.

$$\begin{array}{c|cccc} & d_s & q_s & d_r & q_r \\ \hline d_s & L_{ss}p & & M_d p & \\ q_s & & r_{ss} + L_{ss}p & & M_q p \\ d_r & M_d p & M_d p\theta & \begin{array}{c} \dfrac{r_a + r_b}{2} + \dfrac{r_a - r_b}{2}\cos 2\theta \\ + \left[\left(\dfrac{L_{sa} + L_{sb}}{2}\right) + L_D + \left(\dfrac{L_{sa} - L_{sb}}{2}\right)\cos 2\theta\right] p \\ - \left(\dfrac{L_{sa} - L_{sb}}{2}\right)\sin 2\theta\, p\theta \end{array} & \begin{array}{c} \dfrac{(r_a - r_b)}{2}\sin 2\theta \\ + \left(\dfrac{L_{sa} - L_{sb}}{2}\right)\sin 2\theta p - \\ - \left[L_D - \left(\dfrac{L_{sa} + L_{sb}}{2}\right) - \left(\dfrac{L_{sa} - L_{sb}}{2}\right)\cos 2\theta\right] p\theta \end{array} \\ q_r & -M_d p\theta & M_q p & \begin{array}{c} \left(\dfrac{r_a - r_b}{2}\right)\sin 2\theta \\ + \left(\dfrac{L_{sa} - L_{sb}}{2}\right)\sin 2\theta\, p \\ - \left[L_D + \left(\dfrac{L_{sa} + L_{sb}}{2}\right) - \left(\dfrac{L_{sa} - L_{sb}}{2}\right)\cos 2\theta\right] p\theta \end{array} & \begin{array}{c} \dfrac{r_a + r_b}{2} - \dfrac{r_a - r_b}{2}\cos 2\theta \\ + \left[\left(\dfrac{L_{sa} + L_{sb}}{2}\right) - L_D - \left(\dfrac{L_{sa} - L_{sb}}{2}\right)\cos 2\theta\right] p \\ + \left(\dfrac{L_{sa} - L_{sb}}{2}\right)\sin 2\theta\, p\theta \end{array} \end{array} \qquad (7)$$

where p now does not refer to L'.

It should be noted that because of the unbalanced rotor now R', L', and G' are all functions of θ. Also

$$G' = C_t \cdot G \cdot C \qquad (8)$$

$$G' = \begin{array}{c|cccc} & d_s & q_s & d_r & q_r \\ \hline d_s & & & & \\ q_s & & & & \\ d_r & & M_q & \left(\dfrac{L_{sa} - L_{sb}}{2}\right)\sin 2\theta & \left(\dfrac{L_{sa} + L_{sb}}{2}\right) - L_D - \left(\dfrac{L_{sa} - L_{sb}}{2}\right)\cos 2\theta \\ q_r & -M_q & & -\left(\dfrac{L_{sa} + L_{sb}}{2}\right) - L_D - \left(\dfrac{L_{sa} - L_{sb}}{2}\right)\cos 2\theta & -\left(\dfrac{L_{sa} - L_{sb}}{2}\right)\sin 2\theta \end{array} \qquad (9)$$

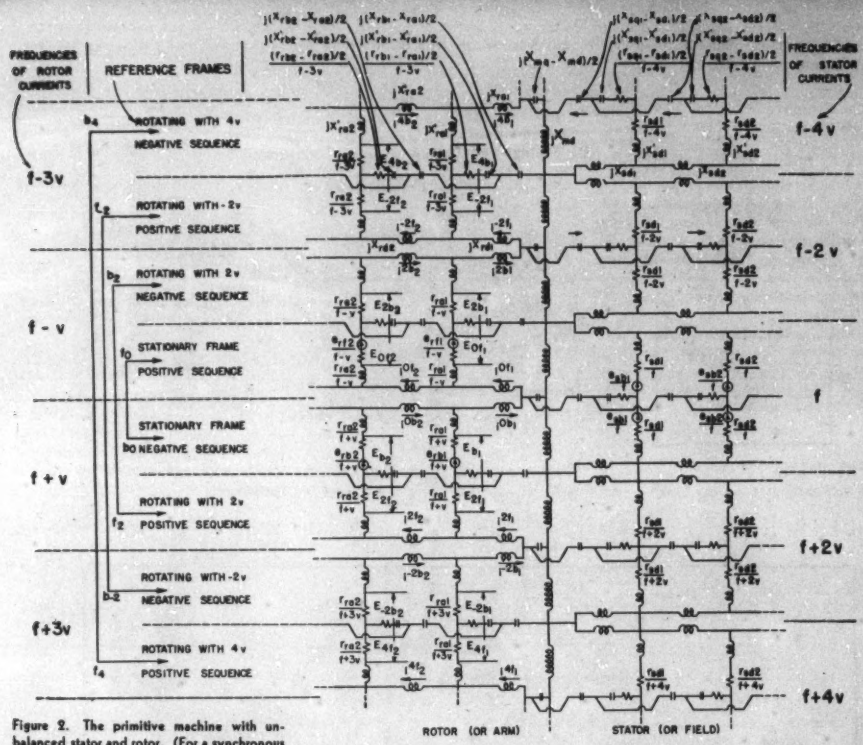

Figure 2. The primitive machine with unbalanced stator and rotor. (For a synchronous machine v and i (or E) have opposite sign)

The Successive Steps of Transformations

Let the following four sets of reference frames be introduced, each frame consisting of two perpendicular stator and two perpendicular rotor axes,

1. A stationary frame. This is the standard frame.
2. A frame rotating with an instantaneous velocity $2p\theta = 2v$ clockwise (in the same direction as the rotor v).
3. A frame rotating with $2p\theta$ counterclockwise.
4. A frame rotating with $4v$ clockwise. Only the rotor frame will be considered.

There are also additional frames rotating with $-4v$, $\pm 6v$, and so forth, but they are not considered in the analysis, only in the equivalent circuit. Their effect follows automatically from those of the $\pm 2v$ and $\pm 4v$ frames.

Three successive transformations will be performed.

1. Starting with the stationary d_r, q_r rotor axes, the corresponding C is given in (14).

$$C = \begin{array}{c|cccccccccccccc|}
 & d_{s0} & q_{s0} & d_{r0} & q_{r0} & d_{r1} & q_{r1} & d_{s1} & q_{s1} & d_{s-1} & q_{s-1} & d_{r-1} & q_{r-1} & d_{r4} & q_{r4} \\
\hline
d_s & 1 & & & & & & \cos 2\theta & -\sin 2\theta & \cos 2\theta & \sin 2\theta & & & & \\
q_s & & 1 & & & & & \sin 2\theta & \cos 2\theta & -\sin 2\theta & \cos 2\theta & & & & \\
d_r & & & 1 & & \cos 2\theta & -\sin 2\theta & & & & & \cos 2\theta & \sin 2\theta & \cos 4\theta & -\sin 4\theta \\
q_r & & & & 1 & \sin 2\theta & \cos 2\theta & & & & & -\sin 2\theta & \cos 2\theta & \sin 4\theta & \cos 4\theta \\
\hline
\end{array} \tag{14}$$

$$C = \begin{array}{c|cccccccccc|}
 & o_s & o_r & 2_r & 2_s & -2_s & -2_r & 4_r & 4_s & -4_s & -4_r \\
\hline
s & 1 & & & C_2 & C_{-2} & & & C_4 & C_{-4} & \\
r & & 1 & C_2 & & & C_{-2} & C_4 & & & C_{-4} \\
\hline
\end{array} \qquad C = \begin{array}{c|cc|}
 & & \\
\hline
s & C_{2n} & \\
r & & C_{2n} \\
\hline
\end{array}$$

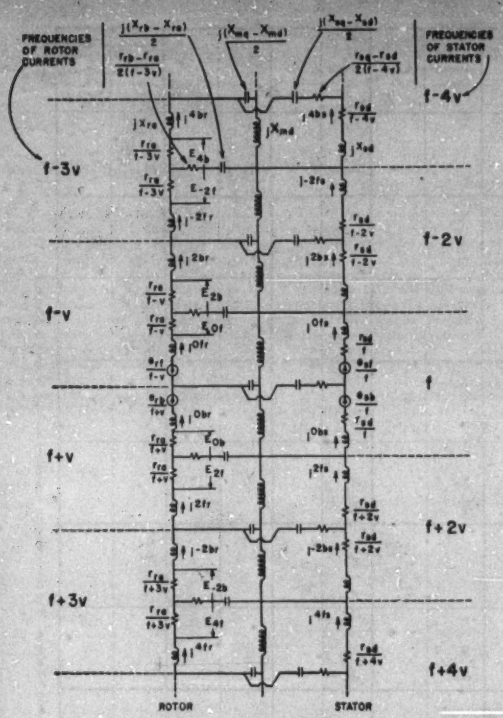

Figure 3. Slip-ring induction motor with unbalanced load

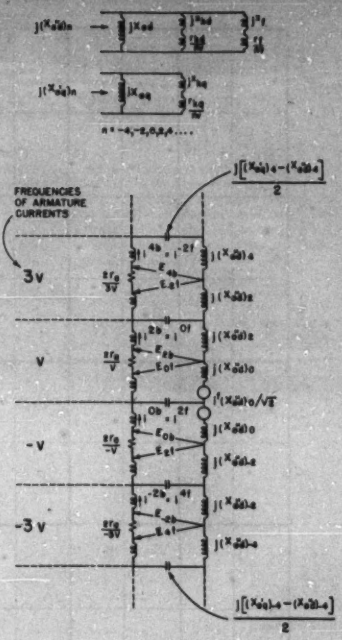

Figure 4. Single-phase alternator

where $n = \pm$ integer

2. Symmetrical components are introduced by

$$C_s = \frac{1}{\sqrt{2}}\begin{array}{c|cc} & f_{-n} & b_{-n} \\ \hline d_{-n} & 1 & 1 \\ q_{-n} & -j & j \end{array}$$

$$C_s' = \frac{1}{\sqrt{2}}\begin{array}{c|cc} & b_n & f_n \\ \hline d_n & 1 & 1 \\ q_n & j & -j \end{array} \qquad (15)$$

It must be remembered that along the backward rotating frames (including the stationary frame) the order in C_s is f, b, while along the forward rotating frames the order in C_s is b, f (C_s' will be denoted then by C_s). Hence

$$C' = \begin{array}{c|ccccccc} & 0_s & 0_r & 2_r & 2_s & -2_s & -2_r & 4_r \\ \hline 0_s & C_s & & & & & & \\ 0_r & & C_s & & & & & \\ 2_r & & & C_s' & & & & \\ 2_s & & & & C_s' & & & \\ -2_s & & & & & C_s & & \\ -2_r & & & & & & C_s & \\ 4_r & & & & & & & C_s' \end{array} \qquad (16)$$

3. p is replaced by $jf\omega$, Z' replaced by $n^{-1}\cdot Z'$, and e by $n^{-1}\cdot e$ where n is the "frequency tensor" whose diagonal terms are given by the array

f_{s0}	b_{s0}	f_{r0}	b_{r0}	f_{r2}	b_{r2}	f_{s2}	b_{s2}	f_{s-2}	b_{s-2}	f_{r-2}	b_{r-2}	f_{r4}	b_{r4}
f	f	$f-v$	$f+v$	$f-v$	$f+v$	$f-2v$	$f+2v$	$f-2v$	$f+2v$	$f-3v$	$f+3v$	$f-3v$	$f+3v$

(17)

	$\bar{f}_{so}$	$\bar{b}_{so}$	$\bar{f}_{ro}$	$\bar{b}_{ro}$	$\bar{b}_{r2}$	$\bar{f}_{r2}$	$\bar{b}_{s2}$	$\bar{f}_{s2}$	$\bar{f}_{s-2}$	$\bar{b}_{s-2}$	$\bar{f}_{r-2}$	$\bar{b}_{r-2}$	$\bar{b}_{r4}$	$\bar{f}_{r4}$
$\bar{f}_{so}$	$\frac{r_{ds}+r_{qs}}{f}+j(X_{ds}+X_{qs})$	$\frac{r_{ds}-r_{qs}}{f}+j(X_{ds}-X_{qs})$	$2jX_S$	$2jX_D$										
$\bar{b}_{so}$	$\frac{r_{ds}-r_{qs}}{f}+j(X_{ds}-X_{qs})$	$\frac{r_{ds}+r_{qs}}{f}+j(X_{ds}+X_{qs})$	$2jX_D$	$2jX_S$										
$\bar{f}_{ro}$	$2jX_S$	$2jX_D$	$\frac{r_a+r_b}{f-v}+j(X_{Sa}+X_{Sb})$	$2jX_D$	$\frac{r_a-r_b}{f-v}+j(X_{Sa}-X_{Sb})$									
$\bar{b}_{ro}$	$2jX_D$	$2jX_S$	$2jX_D$	$\frac{r_a+r_b}{f+v}+j(X_{Sa}+X_{Sb})$		$\frac{r_a-r_b}{f+v}+j(X_{Sa}-X_{Sb})$								
$\bar{b}_{r2}$			$\frac{r_a-r_b}{f-v}+j(X_{Sa}-X_{Sb})$		$\frac{r_a+r_b}{f-v}+j(X_{Sa}+X_{Sb})$		$2jX_S$		$2jX_D$		$2jX_D$			
$\bar{f}_{r2}$				$\frac{r_a-r_b}{f+v}+j(X_{Sa}-X_{Sb})$		$\frac{r_a+r_b}{f+v}+j(X_{Sa}+X_{Sb})$		$2jX_S$		$2jX_D$		$2jX_D$		
$\bar{b}_{s2}$					$2jX_S$		$\frac{r_{ds}+r_{qs}}{f-2v}+j(X_{ds}+X_{qs})$		$\frac{r_{ds}-r_{qs}}{f-2v}+j(X_{ds}+X_{qs})$		$2jX_D$			
$\bar{f}_{s2}$						$2jX_S$		$\frac{r_{ds}+r_{qs}}{f+2v}+j(X_{ds}+X_{qs})$		$\frac{r_{ds}-r_{qs}}{f+2v}$		$2jX_D$		
$\bar{f}_{s-2}$					$2jX_D$		$\frac{r_{ds}-r_{qs}}{f-2v}+j(X_{ds}-X_{qs})$		$\frac{r_{ds}+r_{qs}}{f-2v}+j(X_{ds}+X_{qs})$		$2jX_S$			
$\bar{b}_{s-2}$						$2jX_D$		$\frac{r_{ds}-r_{qs}}{f+2v}+j(X_{ds}-X_{qs})$		$\frac{r_{ds}+r_{qs}}{f+2v}+j(X_{ds}+X_{qs})$		$2jX_S$		
$\bar{f}_{r-2}$					$2jX_D$		$2jX_D$		$2jX_S$		$\frac{r_a+r_b}{f-3v}+j(X_{Sa}+X_{Sb})$		$\frac{r_a-r_b}{f-3v}+j(X_{Sa}-X_{Sb})$	
$\bar{b}_{r-2}$						$2jX_D$		$2jX_D$		$2jX_S$		$\frac{r_a+r_b}{f+3v}+j(X_{Sa}-X_{Sb})$		$\frac{r_a-r_b}{f+3v}+j(X_{Sa}-X_{Sb})$
$\bar{b}_{r4}$											$\frac{r_a-r_b}{f-3v}+j(X_{Sa}-X_{Sb})$		$\frac{r_a+r_b}{f-3v}+j(X_{Sa}+X_{Sb})$	
$\bar{f}_{r4}$												$\frac{r_a-r_b}{f+3v}+j(X_{Sa}-X_{Sb})$		$\frac{r_a+r_b}{f+3v}+j(X_{Sa}+X_{Sb})$

Figure 5. The final Z'' is given in equation 18 above. The corresponding equivalent network is given in Figure 2.

References

1. Asynchronous and Single-Phase Operation of Synchronous Machines, A. W. Rankin. AIEE Transactions, volume 65, 1946, pages 1092–1102.

2. Equivalent Circuit of the Primitive Machine, Gabriel Kron. *General Electric Review*, Schenectady, N. Y., March 1946, pages 43–9.

3. A Short Course in Tensor Analysis for Electrical Engineers (book), Gabriel Kron. John Wiley and Sons, Inc., New York, N. Y., 1942.

4. Overvoltages Caused by Unbalanced Short Circuits—Effect of Amortisseur Windings, Edith Clarke, C. R. Weygandt, and C. Concordia. AIEE Transactions, volume 57, 1938, August section, pages 453–66.

Discussion

A. W. Rankin (General Electric Company, Schenectady, N. Y.): Quantitative data on synchronous machine operating characteristics as calculated from the equivalent circuits developed by Gabriel Kron are given in a related paper by this discusser.[1] This paper contains calculated data illustrating the torque–slip and current–slip curves of a synchronous machine during asynchronous operation, and calculated data of the damper-bar currents during both asynchronous and single-phase operation. The calculated data of single-phase operation were obtained from the equivalent circuits developed by Kron in the paper now under discussion, and the calculated data of asynchronous operation were obtained from equivalent circuits developed by Kron in a previous article.[2]

Parts *C* and *D* of this paper[1] present calculated data of single-phase operation for both purely reactive and purely resistive loading. This study is of value as it shows the magnitude of the currents in the leading and trailing damper bars, and in addition gives quantitative information on the harmonic torques.

Parts *A* and *B* of the paper[1] are devoted to the study of constant-speed asynchronous operation. Quantitative data are given of the torque–slip characteristics and of the current distribution in the leading and trailing bars of the damper windings.

This reference to the paper[1] is made at this point in order to indicate the location of the quantitative data which complement the circuit developments in the paper by Kron.

References

1. Asynchronous and Single-Phase Operation of Synchronous Machines, A. W. Rankin. AIEE Transactions, volume 65, 1946, pages 1092–1102.

2. Equivalent Circuit of the Salient-Pole Synchronous Machine, Gabriel Kron, *General Electric Review* (Schenectady, N. Y.), volume 44, 1941, pages 679–83.

Theoretical Approach to Speed and Tie Line Control

ROBERT BRANDT
ASSOCIATE AIEE

Synopsis: Frequency error is an indicator of the amount of excess or deficiency of generation on a whole interconnection, and a frequency–generation line may be established for the whole or for any section which is separated from all others by tie lines over which control may be desired. Automatic equipment is available using these fundamentals under the name of load biased frequency control, which will make the required adjustments to generation to restore normal speed and tie line loadings with a minimum of false moves and by means of which each section will handle, in normal operation, only its own load changes, regardless of the speed of response of its prime movers to correcting impulses. Methods of automatic control by the selective frequency blocking system and the master flat frequency station method are examined and found wanting. The use of uncontrolled speed-sensitive governors with small droop is shown to be disadvantageous if operated in parallel with automatic bias equipment. Consideration is given to practical matters of operation, including an improvement in handling manual generation shifts, action of controller in time of trouble, effect of errors in determining the frequency–generation line, and desirable characteristics of governors.

Characteristics of a Single System

ON any isolated 60-cycle system a speed of just 60 cycles represents an exact balance between the amount of generation and the amount of load. Any speed other than 60 cycles indicates either an excess or a deficiency of generation. There is a definite relation between speed and generation which may be plotted, as shown in Figure 1, as a straight line of a certain slope. (Investigations at various locations indicate a complex relation between load, frequency, and voltage. This discussion uses frequency as the tangible variable to be measured, avoiding the question of whether the underlying cause of the variation is more or less caused by speed alone or associated changes in voltage.) The actual amount of this slope depends on the characteristics of the system load. Perhaps it is not exactly a straight line, but a straight line seems to represent it fairly well in the range which concerns us. In words, slope is an expression of the number of kilowatts to be added to or subtracted from the generation to change the frequency by a definite amount. It follows that as the total load gets larger, the number of kilowatts required to change the frequency by a set amount also must grow, assuming that the load characteristics remain about the same. Thus, also, from day to night, when the load levels vary as much as three to one or even more, the slope of the speed–generation line must change. To calculate the slope of this line from theoretical consideration is difficult, if not impossible, because it would require a detailed analysis of the characteristics of each item of connected apparatus on the system, both customer's and power company's. A more practical approach is the experimental one. That is, find out how many kilowatts must be added to affect the speed, say 1/20 cycle. The result obtained by a test of this sort will not be the theoretical slope, but will be a more useful figure because it reflects exact operating characteristics, not merely of the customers' loads, but also all of the prime movers whose governors have not been definitely blocked. If a deliberate effort is made at a given plant to raise the system speed, some governors, being on the edge of their dead bands, will come into action to oppose the change and thus the apparent slope, if measurement is being made at one location, will be larger in terms of kilowatts per unit speed change than the theoretical slope. Incidentally, this characteristic suggests that the true operating slope of any system is not a straight line, but one which curves in the general manner of the dotted line of Figure 1. That is, if the effort is made to move the speed further from 60 cycles more governors will reach the edge of their dead bands to oppose the change, and, in theory, it should become impossible (with limited kilowatts at the regulating plant) to raise the speed beyond some point not very far from 60 cycles because the manual change at the measuring plant will be nullified completely by unblocked governors at other locations. To relate this condition to practice, we must remember that on most systems it is quite possible for the speed to ride as much as one-tenth cycle above or below standard for minutes on end, even though 90 per cent of the capacity on the system is under the control of governors, theoretically set to maintain 60 cycles. In the discussion following we refer to the resultant slope produced by loads plus random governor effects, and assume it to be a straight line.

Two Systems With Tie Line Between

Consider now the situation when two previously isolated systems are connected by a single or by a group of tie lines. First, the two systems may be considered over-all as one, and for the pair all the foregoing statements still hold. There is a definite over-all slope for the generation–frequency line and any deviation from 60 cycles becomes a measure of either the excess or deficiency of genera-

Paper 47-4, recommended by the AIEE committee on power generation for presentation at the AIEE winter meeting, New York, N. Y., January 27–31, 1947. Manuscript submitted January 28, 1946; made available for printing October 23, 1946.

ROBERT BRANDT is with the New England Power Company, Boston, Mass.

tion. We cannot tell how much of the error is lodged on either side of the tie line. It is possible, however, by considering at the same time both the speed and the amount by which the tie line is over or under schedule to identify at once not only the system responsible for the error, but also the magnitude of that error. This may be explained by a consideration of Figures 2 and 3. Figure 2 represents the purchasing system. Essentially the diagram is the same as that which would be drawn for the system if it were isolated, except that the kilowatt scale reads in terms of deviation from schedule rather than kilowatt error in generation. That this diagram may be drawn properly in this manner follows from the thought that with a system isolated and generating say 10,000 kw more than would be required for 60 cycles, its frequency would rise a known amount, say for instance 1/20 cycle. Suppose the tie line were feeding into the system 10,000 kw above the desired schedule. This excess on the tie acts the same as though generation in one of the local plants were raised by a similar amount, and the effect on the frequency is the same. Figure 3, which represents the selling company, is exactly the same except that the slope of the line has been reversed. This is done merely for convenience and has no particular significance. It could be drawn the other way with appropriate changes in the captions and quadrants. Note that for each system, the slope to be drawn represents the proper slope of that system when isolated. The number of interconnections has no bearing on it. If it were desired to draw for the whole interconnection a single diagram of the type of Figure 1, then the over-all slope line as shown in Figure 4 would be the sum of the individual slopes of all systems involved. To take a concrete example, assume that the selling company has a load of 1,000,000 kw and a generation–frequency slope of 30,000 kw per one-tenth cycle. Assume that the buying company is smaller with a load of 500,000 kw and a slope of 10,000 kw per one-tenth cycle. These, incidentally, are the slopes plotted in Figures 2 and 3. (These examples are illustrative only. The kilowatts per unit speed change, in relation to the total load, is probably larger than the actual figure for most systems.) Figure 4 for the pair of systems must have a slope of 40,000 kw per one-tenth cycle. The justice of this reasoning easily is seen. Suppose the systems were of equal size and with similar load characteristics. When tied together it would require twice as many kilowatts to change both of them by a tenth of a cycle as it would to change either one by the same amount. However, suppose one of the systems was very small compared to the other, with a slope say of 1,000 kw per one-tenth cycle, while the larger system remained the same as our example in Figure 3. The large system then completely overshadows the small one and only 31,000 kw would be needed to change the speed on the combination by one-tenth cycle.

Suppose now that on the 1,000,000 kw–500,000 kw interconnection there appears a speed error of plus 1/20 cycle. It follows from Figure 4 that somewhere at a location as yet unknown there is excess generation of 20,000 kw. Suppose further that the buying company finds itself with 5,000 kw "above schedule coming in" and the selling company, therefore, with a similar amount "over schedule out." This is the condition of point 1 on Figures 2 and 3. It is possible now to locate the generation error entirely on the selling system, since the purchasing company is exactly on its own speed–generation line. Both the tie line and the speed will be restored to normal without any effort on the buying company's part, if the seller will reduce his generation by 20,000 kw. Suppose a second case marked as point 2 on Figures 2 and 3. The speed is 1/20 cycle high, but the tie line is exactly on schedule. In this case each system is responsible for as much of the error as is necessary to change its own speed if isolated by just 1/20 cycle. For the small system this is 5,000 kw, and for the large system 15,000 kw; they add to give the 20,000-kw error of Figure 4.

Consider now one more situation marked as point 3. The speed error is unchanged from the two previous cases, but the tie is now 10,000 kw over schedule toward the purchasing company. Obviously the selling company should reduce its generation. Just as truly, but not so obviously without an examination of Figure 2, the buying company should increase its generation in spite of the high frequency. The decrease should be 25,000 kw, the increase should be 5,000 kw, and the net change will be just the amount required to restore the interconnection speed as well as schedule to normal. Here we see the usefulness of the lines which have been drawn parallel to the main slope line in Figures 2 and 3, and marked drop or raise so many thousand kilowatts. It is thus possible for either system, by noting merely the speed error and the tie line error, to determine at once how many kilowatts and in what direction it should change generation on its own system so that it may be doing its share in restoring the combination to normal and accomplishing the desired result of handling its own load swings on its own plants.

It might appear that satisfactory control, following the foregoing principles, could be accomplished without automatic equipment by having a dispatcher with a tie line telemeter, a frequency indicator, and a chart (similar to those shown in Figures 2 or 3) analyze the situation and order appropriate generation adjustments. Such is not the case

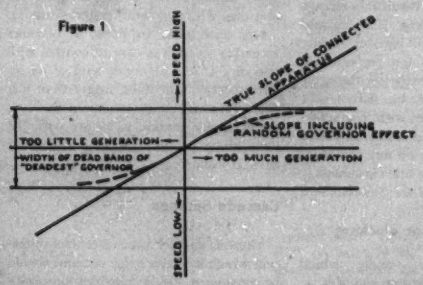

Figure 1

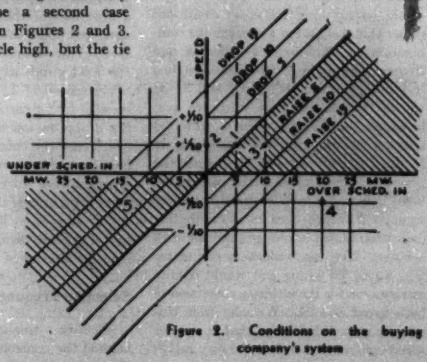

Figure 2. Conditions on the buying company's system

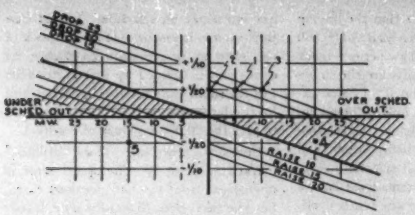

Figure 3. Conditions on the selling company's system (simultaneously with Figure 2)

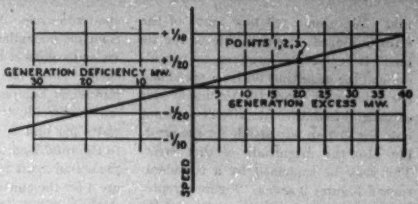

Figure 4. Conditions on the combined interconnection of Figures 2 and 3

The time consumed and the undivided attention required both eliminate definitely any such "manual" approach. The ordinary biased automatic tie line load controller accomplishes exactly the desired result in theory, at least, and approximates it in practice if the bias has been selected properly and all the rest of the control mechanism responds properly. At this point it may be well to repeat the statement previously made by others that the term "bias" as currently used is somewhat misleading and represents nothing other than a measure of the amount of generation change required for a given speed change on a particular system, if isolated. In other words, it is nothing but our generation–frequency line.

It appears that the systems shown in Figures 2 and 3 with their interconnecting tie line and control equipment, operating along the slope lines as indicated, should be able to control both the speed and the scheduled interchange without any station anywhere on the interconnection acting as a master frequency control station. Not only is this true, but the addition of a master frequency control station would be definitely to the disadvantage of smooth operation. Such a station, which is responsive only to speed, will do the wrong thing and upset conditions rather than help them whenever the combination of conditions of schedule and frequency error lie in the cross-hatched segments shown in Figures 2 and 3. It will be remembered that when we analyzed the conditions at point 3, we found that on the buying company shown in Figure 2 it was necessary to increase the generation even though the speed was high. No master frequency control equipment, which does not have tie line indication biased into it, could make such a move. Yet, any reduction of generation would be wrong and would require extra moves for the ultimate correction of both speed and tie. We may from this reasoning say definitely that a master speed control station is a liability rather than an asset when operated in parallel with biased automatic tie line equipment.

From the same reasoning, it follows that what operating men for many years have spoken of as the free help that comes from uncontrolled governors is not in all cases a help. That is, those governors which happen to be on the edge of their dead bands and which therefore are prodded into activity by a very slight change in speed will be a help only when the tie and frequency errors do not produce a point in the cross-hatched segments. The unintentional error caused by this situation is less on big systems and more on small systems, because on a small system the slope of the speed–generation line is more nearly vertical and thus the cross-hatched segment is larger. When it comes to making a decision as to whether it is more advantageous to do nothing than to do something that is wrong a fraction of the time, it seems as though the "do nothing" theory would be just about as satisfactory. This brings us to the conclusion that all governors which are not to receive their instructions from master equipment which is sensitive to both speed and tie line schedule error had better be rendered insensitive to small changes either by operating hard up against a load limit stop or preferably by a fairly steep droop characteristic. It is suggested that such a droop might well be of the order of five per cent. On such a governor, if the dead band could be narrowed down to the vanishing point, a speed error of one-tenth of a cycle on a 100,000-kw unit would result in a change of generation of 3,300 kw. There would seem to be no particular harm in having the droop as much as ten per cent, in which case the contribution for the same frequency error would be halved. A supersensitive governor with characteristics approaching the isochronous should not be allowed at large on any combination of systems using tie line bias unless it is under control of the bias mechanism.

Selective Frequency or Blocking

Selective frequency, under which method the controller at one end of a tie always is blocked and at the other end active, is illustrated in Figure 5. It represents an attempt to identify the source of error by mechanical means, much as an operator would by noting the directions of speed and tie errors, and to force the correction to originate from the proper end. The feature of this type of control is that it is qualitative only and takes no account of amount; thus the units under its control are inactive whenever there is, for instance, a combination of high frequency and "over schedule in." The implication is that whenever this situation occurs, the trouble lies on the far side of the tie line and the other party should make all the correction. Such a situation is the truth only when the operating point lies on the speed–generation line. To expand this line to fill a whole quadrant is oversimplification. Thus selective frequency operation is at best a partial answer. It avoids the errors which an uncontrolled governor would make with conditions inside the cross-hatched segment, but it fails to make the moves which are required from a consideration of the situation illustrated in Figures 2 and 3.

Complex Interconnections

All of the foregoing principles derived apply equally well to complex interconnections where several systems are involved with many tie lines. It becomes necessary in such a case to control with reference to the algebraic sum of all interconnection schedules, rather than just one. The bias characteristic of the controller should remain as before with the same slope as the system itself would have, if isolated.

Cascade Settings

There is another type of control operation which has seen some use and should be considered. It is called for simplicity

"cascade setting." Tie line bias is used, but instead of allowing each system to set for its own natural slope the intermediate systems of a sprawling interconnected string are set for the sum of the slopes of all systems on one side or the other. Measurement of the ties is confined to one direction only instead of measuring all ties and operating on the net. This feature provides about the only advantage of the method because the multiple metering required on a large system with many connections becomes complicated and expensive. To illustrate, assume a simple case of three systems in a row—*A*, *B*, and *C*—with ties in each direction from *B*. The natural slopes are respectively 20,000, 15,000, and 5,000 kw per one-tenth cycle. Assume initially a balanced conditions with loads on each system of 100,000 kw generation equal to the load, and zero schedule on each tie.

Under the cascade system the controller at *A* would be set at 20,000 kw per one-tenth cycle and at *C* for 5,000 kw per one-tenth cycle (the systems on the ends are on ordinary tie line bias; the cascade applies only to intermediate systems). System *B*, if it measures and controls only the tie toward *A*, would be set at 20,000 kw per one-tenth cycle (the sum of its own and system *C*'s natural bias); or if it measures and controls the tie toward *C*, it would be set at 35,000 kw per one-tenth cycle. Assume this latter case and assume a sudden new load of 20,000 kw appears on system *A*. The deficiency of generation is now 20,000 kw which is enough to reduce the speed of the whole group by half of one-tenth cycle. System *C* at this reduced speed has an excess generation of 2,500 kw which flows toward *B*. Its controller correctly makes no move. System *A* also at the reduced speed has a deficiency of 10,000 kw which it pulls over the tie from *B*. Its own controller, however, will call for an increase of 20,000 kw, which is proper. System *B*, with its large bias (see Figure 6) and noting only the tie in the direction of *C*, will call for an increase of 20,000 kw on its own generators (point 6), even though it is in no way responsible for the disturbance, and would do nothing if normal bias were used with net metering (point 7). Theoretically *A* will make the proper correction and restore equilibrium without the generators on system *B* ever making the full adjustment. However, some contribution will be made both on *A* and on *B* which will call for further corrective moves later. Speed of response to controller demands is important. In effect, the cascade system makes every intermediate system underwrite and guarantee the correction not only of its own load but of every load on the far side of the tie which is controlled. The system therefore is bad and cannot fail to upset smooth operation. Only where the more remote systems are insignificantly small and the metering complicated can it be justified.

Miscellaneous Operational Considerations

Speed of Response

Automatic operation with a tie line bias, such as has been discussed, and with no station anywhere on the interconnection acting as master frequency controller, has the operational advantage that it eliminates completely all the difficulties previously experienced with varying speeds of response. In the past it has been felt, and probably with justice, that some controllers, being more sensitive than others, make corrections which should be made elsewhere and thus do extra work and require later readjustments. By operating along a generation-frequency line, the time element disappears since each system will stop its correcting as soon as it reaches its own line with no reference to whether or not any other system has completed that part of the adjustment which falls to its share.

Effect of Operating on Wrong Generation–Frequency Line

Because at any instant it is difficult to determine the exact slope of the generation–frequency line, it may be expected in practice that many cases will occur when the bias controller is set improperly. It is worth while to consider what happens in such an instance. Figure 7 illustrates one example. The same buying and selling systems are represented but each of their controllers is set with a slope which is twice the true value in kilowatts per unit speed change. Conditions at point *A* are the same as those used previously in point 3. The analysis is simple because the buying system in the first instance believes itself to be on a proper slope and, therefore, does nothing. The selling system imagines it should drop 40,000 kw instead of the proper figure of 25,000 kw. (Note that the controllers on the combined systems believe that the excess generation is 40,000 kw instead of the true figure of 20,000 kw. The seller assumes the whole error to be on his end of the tie line.) Luckily, all the correction is not made at once, and if, for instance, the first correction amounts to 10,000 kw, conditions will reach point *B* as the actual response will be in accordance with the true (but unknown as far

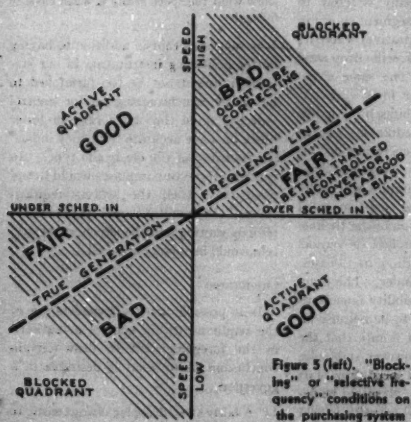

Figure 5 (left). "Blocking" or "selective frequency" conditions on the purchasing system

Figure 6 (right). Cascade setting conditions on system *B* after added load comes on system *A*

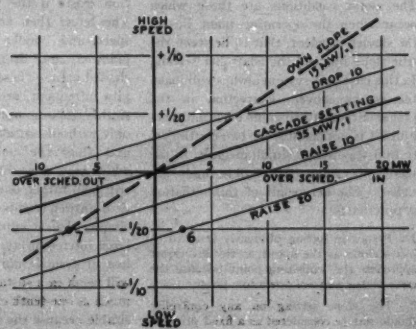

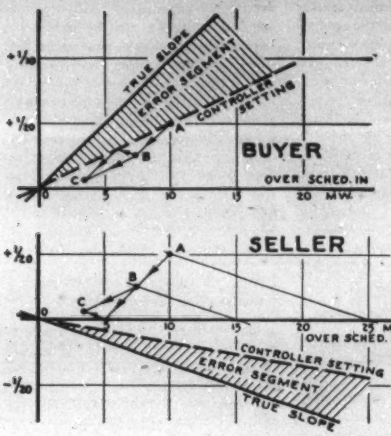

Figure 7. Conditions existing when controllers are set for wrong amount of bias. First two steps only are shown, subsequent steps will spiral in toward point 0

as the controller is concerned) slope. At this point the selling system still feels that more correction is necessary and the buyer also has been jolted into activity. From here on, the condition, as a result of any given correcting impulse, becomes a matter of chance; that is, it depends on which controller gets its work in first. However, one point is clear, and that is that gradually the combination will trend (probably in a spiral) toward a proper correction at the point where the true and the controller setting slopes cross; that is, at proper speed and schedule. The process may be long and may require extra moves to compensate for some that are made in the wrong direction.

As a special case of a controller with an erroneous setting, we may list either flat frequency or flat tie line control. In the case of Figure 7, the errors in setting caused no particular inconvenience. The worst conditions are those which occur when the operating point lies in the shaded segment, that is, between the true slope line and the controller setting. In this case, one system always will make the wrong move. Correction in the proper direction will come eventually because it is not possible for two controllers to find themselves simultaneously in the shaded sector but errors will be made, initially. The net result of this situation in practice is

1. **Errors in setting obviously tend to be less serious as the speed or tie line errors approach the vanishing point because the error sector narrows down to a point.**

2. **The slope setting on any controller should not be considered as a fixed proposition to be established and forgotten, but should be subject to prompt adjustment under the direction of the system dispatcher who will determine largely from experience and trial and error the value which produces the best results at a given time.**

Action in Time of Trouble

When an emergency occurs in which a substantial block of generation is suddenly lost, power flow will readjust itself faster than any automatic equipment can hope to keep up with it. We need consider only what happens shortly afterward when the control has had a chance to come into action. If the buying company loses capacity and the speed drops, the condition will result in "over schedule in." The selling company is likely to find itself in the shaded segment shown in Figure 3 (point 4 is illustrative) where its automatic control also will drop and make matters worse. The same situation exists if the seller loses capacity. The buyer then finds himself with low speed and "under schedule in," as at point 5, and drops generation in his shaded area. These two situations, happily infrequent, are examples where desirable response would be based on speed only without consideration of the tie line, and thus the uncontrolled governors which may come into action, in all cases, will help rather than hinder. The practical answer to this possibility is perhaps simpler than it appears to be because on large interconnections it is rare that the loss of a single unit, however suddenly, will result in a sustained speed drop of as much as one-tenth cycle. It might be desirable because the speed actually is held within fairly narrow limits to have all automatic control cut out when speed errors as large as say 0.15 cycle exist. Such a remedy should be approached cautiously if it is usual to run the tie line with a schedule nearly up to its limit, because the invitation to overload which is implied when tie indication is cut off from the controllers may cause the line to trip and thus cease all usefulness.

Manual Adjustments of Generation

At times when the load is changing rapidly and occasionally at other times, it is necessary to make generation adjustments on units which are not under automatic control. It generally is believed that these adjustments are a major cause of tie line irregularities as well as speed errors. There is a common standing rule which says that no adjustments of generation ever shall be made in a direction which increases an existing speed error. This rule should produce good results unless the system in question finds itself in one of the cross-hatched segments shown in Figures 2 and 3. A more accurate operating rule would be never to drop generation below the frequency–generation line or raise it in cases above the line, but this is not practical unless tie line indication can in some manner be made available to all stations. There are two reasons why the present rule is not fully successful.

1. **With the best good will in the world, an operator who has been ordered to raise a generator 10,000 kw will not take the time always to do it properly if the speed shows slight rising tendencies.**

2. **Most station frequency indicating instruments are not sufficiently accurate to show what the speed really is when close to 60 cycles.**

It is suggested that in addition to having better indicating instruments in our stations, it might not be too farfetched to have the synchronizing motor control switches wired through a raise or lower block on some accurate frequency indicator (possibly of the electronic type). In this way correcting impulses would be applied only when the system required them. The operator would be relieved of tedious waiting and the effect on the system would be much improved.

Governors

It is possible after a consideration of the requirements for control as outlined in the foregoing text to draw certain conclusions as to what is desirable in a governor.

1. **A fairly steep drooping characteristic to**

prevent wandering and unwanted assistance based on speed indications alone.

2. If the governor could come into action quickly on errors above 0.10 or 0.15 cycles, it would help to sustain the system in time of trouble. Therefore, there is some argument for a droop characteristic which would be steep when close to 60 cycles and quite flat as the error gets larger.

3. The dead band certainly should be held to a minimum.

4. There should be a quick and positive response to whatever means is provided for moving the droop characteristic parallel to itself as is done with the synchronizing motor. Studies made on various systems around the country have demonstrated that the synchronizing motor is far from perfect for this purpose since its response is neither definite nor uniform under all conditions.

Conclusions

1. The slope of the speed–generation line measures the power required to produce a definite variation in system speed.

2. The line may be used in conjunction with the deviation from schedule of a tie line to indicate the magnitude, direction, and location of the corrective effort needed to restore both speed and tie to schedule.

3. The method is applicable to complex as well as simple interconnections.

4. The method lends itself readily to the use of automatic equipment under the name tie line bias.

5. Tie line and speed control by this method, being definite, eliminates the disturbing feature of different control systems having different speeds of response.

6. The slope of the generation–frequency line for any particular system is not constant, but variable with load conditions.

7. A flat frequency master controller is a liability on an interconnection where biased tie line controllers are in operation.

8. Prime mover governors, sensitive to speed only, and free to act, are not conducive to steady speed and tie line conditions. They are troublesome in proportion as they are more nearly isochronous.

9. Automatic control of tie lines by selective frequency is not as effective as by tie line bias.

10. Tie line bias with cascade settings is generally unsatisfactory.

11. In time of system trouble caused by sudden loss of capacity, controllers sensitive to frequency only would be helpful were it not for the danger of overloading and tripping out of interconnecting tie lines.

12. A blocking relay is suggested to prevent manual generation changes from being made in such direction as to increase a frequency error.

13. Under normal conditions, governors not under the control of automatic tie line equipment should be relatively insensitive.

14. Governors under the control of automatic tie line equipment should respond definitely, quickly, and uniformly, over full gate range.

Discussion

C. N. Metcalf (Consolidated Edison Company of New York, Inc., New York, N. Y.): These comments are to suggest a simple method of determining the frequency–generation line described by Robert Brandt in his paper. In this method, the approximate frequency–generation line for any system can be determined without isolating that system from the rest of the interconnection.

The Consolidated Edison Company of New York, Inc., is using Leeds and Northrup load-frequency control equipment to control the load on its ties to the Northeast Interconnection (Consolidated Edison, Niagara Hudson, and New England Power Companies). For the most part, tie line bias control is used.

The Leeds and Northrup load-frequency control equipment records frequency and the deviation of tie line load from a scheduled setting. By a detailed inspection and matching of these two charts, a number of points of coincident and abrupt changes in tie line load and frequency were selected which reasonably could be assumed to have been caused external to the Consolidated Edison System.

By Brandt's terms, Consolidated Edison was the "selling company" with scheduled tie line load out for the points selected. Thus an abrupt decrease in tie line load (out) and a coincident increase in frequency would be caused by excess generation external to the Consolidated Edison System. The amount of load rejected by the tie line has the same effect as adding this amount of generation to the Consolidated Edison System and would result in the same increase in frequency.

Similarly, an abrupt increase in tie line load and a coincident decrease in frequency would be caused by a deficiency of generation external to the Consolidated Edison System. The amount of increase in tie line load (out) would have the same effect as dropping this amount of generation by the Consolidated Edison System and would result in the same decrease in frequency.

This method of determination is based on careful selection of the points of coincident changes so that load and generation changes, for the system being studied, will be negligible. The selected points were within the frequency band of 59.85 and 60.15 cycles in which there would be little if any governor action. Also frequency changes of less than 0.05 cycle could not be used with any reliability.

As the points of coincident changes selected were at different hours of the day and for different days over a 2-month period, the total system generated load at these times varied considerably. Therefore, the measured changes in the tie line load were adjusted to a common base of 1,500 megawatts total generation for plotting purposes.

The average line drawn through the points of adjusted tie line load change plotted against corresponding frequency change, indicates a frequency–generation line of 30 megawatts per 0.1 cycle for 1,500 megawatts load on the Consolidated Edison System. This may be high, as previous papers have indicated a value of about one per cent of system load per 0.1 cycle as compared to two per cent determined by this method with the limited number of cases to date. However, the grouping of the plotted points is such as to indicate that this approximate determination is fairly close for the Consolidated Edison System.

The optimum bias setting for tie line load bias for any system depends on a number of factors such as fluctuating railroad load, system and tie line capacities, speed of response of the governors and servo mechanisms to load-frequency control impulses. The optimum setting undoubtedly will be determined after trial operation at various values. However, an approximate determination of the frequency–generation line should be very helpful in deciding on the optimum bias setting.

G. S. Lunge (General Electric Company, Schenectady, N. Y.): This paper is one of the most complete analytical treatments of this subject that has appeared in the English language and, despite its modest title, contains many practical suggestions that undoubtedly are based on actual operating experience.

The author suggests that even at generating stations not containing any automatic load-frequency control equipment, blocking relay equipment (possibly of electronic type) would be very helpful in preventing injudicious manual adjustment of generator output by the operator.

Such equipment is already available commercially and can be arranged readily to block "raise" impulses to the governor synchronizing motor from the control switch (or switches), if the system is operating above the desired frequency/net kilowatt interchange characteristic line by a definite amount, and to block "lower" impulses to the governor synchronizing motor, if the system is operating below this characteristic line. This relay equipment consists essentially of a ratio type milliammeter actuating (without use of actual contacts) two electronic relays controlling interposing relays in the governor synchronizing motor control circuits. One winding in the ratio type milliammeter is supplied with a direct current proportional to the frequency as measured by a photoelectric recorder, and the other winding is supplied with a direct current proportional to the totalized tie line load, as totalized at the area load dispatcher's office.

The least expensive arrangement using this blocking relay equipment is to install it only at the area load dispatcher's office, and transmit, as required, "block raise" and "block lower" signals to the manually controlled generating stations. Where dis

tances are large, this can be accomplished conveniently by a frequency-shift carrier-current load control channel, which is capable of sending either of two types of signals (or neither signal), as required.

At a later date, if an automatic frequency controller is substituted at any station for manual control of its output, these same blocking impulses can be used in a similar manner to selective frequency control, to prevent undesirable action on the part of the controller, but without the disadvantages of the usual selective frequency control to which the author calls attention.

Such an arrangement is less expensive than providing a tie line load biased frequency control equipment at each generating station, biased by the area net tie line load interchange as telemetered to each station from the area load dispatcher's office. It also will be recognized that it is applicable to any type of frequency control equipment that operates via the governor synchronizing motor of the prime mover. This system also provides fully centralized automatic control in the hands of the area load dispatcher, thereby relieving the individual generating station operators from having to readjust the bias settings in their individual generating stations in accordance with telephoned instructions from the dispatcher.

E. E. George (Ebasco Services, Inc., New York, N. Y.): This paper, in spite of the first word in its title, presents a very practical analysis of many controversial features of interconnected system operation. Many of the present-day conflicting opinions result from overemphasis of only one side of the argument. The conclusions in this paper may need further comment.

Conclusions 3 and 4 might be combined in the statement that net bias load control is always highly advantageous and on complicated systems is almost essential to satisfactory operation.

Conclusion 6 is a further argument for net control because variable bias with load conditions is hardly practical unless the bias setting for each system is independent of other systems.

Conclusions 7 and 8 well might be qualified by emphasis on the fact that they are based on normal operating conditions. In emergencies flat frequency controllers and speed sensitive governors have important advantages. In the case of systems with weak tie lines or poor manual handling of block changes, emergencies are more or less routine, and proper operation of governors is almost indispensable.

A few further conclusions appear desirable to bring out the results of the analyses in the paper.

1. Most of the small continuous swinging of load on tie lines is caused by differences in governors as to dead band, slope, and speed setting.

2. Most of the sudden load changes on tie lines are caused by block load changes made manually to keep automatic regulating units within range.

3. Many of the large drifts in load on tie lines are caused by either insufficient maneuvering range on regulating plants or poorly co-ordinated block changes, or both.

4. A governor with large slope will operate the overspeed shutdown device if all load is lost, delaying service restoration.

5. Base load control would be helpful in keeping governors normally off of straight speed control and yet permit them to act promptly when the frequency goes outside of predetermined limits. Safe emergency performance cannot be obtained by blocking governors, crowding limit springs, or using gate limits. Such things tend to make emergencies more serious than necessary.

6. The most effective means of general improvement of tie line operation is to place more units in each plant under automatic tie line control and to place more plants on each system on automatic tie line control. This not only increases speed of response and range of response but also reduces block changes and leaves fewer governors on straight speed control.

7. The characteristics of system load may be determined by blocking all governors and opening a loaded tie line. Similar tests may be made with some of the governors in service, and by subtraction the effective regulation of the governors can be approximated.

Robert Brandt: In various discussions of the method of tie line bias the idea frequently is brought out that it permits, or even more definitely that it provides, a "contribution" to a neighbor who may be in trouble. There is an implication that something extra is done to provide support in such a condition. This statement should be clarified. The support is there but the extra is not. An examination of Figure 3 will show that a selling company will go "over schedule out" during conditions of low frequency while it is still operating on its own speed-generation line; that is, when the speed is low the selling company satisfied to supply to its neighbors on a net basis more power than had been scheduled. Such a situation comes about quite naturally and not from any altruism inherent in the control equipment. When the speed on the interconnection is low the amount of generation which would be sufficient to carry the load of the selling system at 60 cycles becomes more than enough at a figure less than 60 cycles, and the difference is the amount which goes out over the ties, and has given rise to the "contribution" idea. Similarly, a buying company operating on its speed-generation line, with its controller making no corrective move, is satisfied when it is taking less than its desired schedule, if the speed be low.

Parallel Operation of Aircraft Alternators Using Electronic Frequency Changers

O. E. BOWLUS
MEMBER AIEE

P. T. NIMS
ASSOCIATE AIEE

Synopsis: This paper reports initial work on an electronic method for operating several main aircraft engine driven alternators in parallel to supply the electrical loads of an airplane. This would make unnecessary any mechanical constant speed drive for each generator. An electronic frequency changer is associated with each alternator and the outputs of the changers paralleled at the load bus. Synchronization, load division, and provision for reactive power are discussed, and test data obtained from two 4-kva units are presented.

As a result of the considerable increase in the size of military aircraft and the subsequent necessity for larger power driven equipment, great changes were made in recent years in the requirements for electric power in large airplanes. It soon became apparent that the 24-volt d-c systems were not adequate because of the considerable weight penalty imposed by the size of the conductors required to carry the power loads. This led to the consideration of higher voltage systems and also the use of alternating current.

These considerations have been examined and reported in several papers.[1,2] As shown in another paper,[3] the power system for large military aircraft was standardized upon as 400-cycle alternating current, three phase, 208 volts line to line. An initial move has been the development of a 40-kva alternator unit to replace the d-c generators previously used.[4] However, as several alternators must be used to provide the necessary electric power on large military aircraft, the parallel operation of these alternators presented new problems which had to be solved before the new a-c generators could be brought into full use.

Among the requirements to be fulfilled were the following:

1. Parallel operation of alternators into a common load bus.
2. Automatic division of load between alternators.
3. Provision for cutting out a defective unit without disturbing the others.

The first requirement can be met easily provided the alternators are driven at the same speed. However, as it was desirable that, in the case of large military aircraft, the generators be driven by the main engines, this introduced a serious problem. Because of the variations in the rotating speed of the airplane engines, parallel operation of the generators was impossible unless some means were introduced to either

1. Provide a variable speed mechanical drive between the engine and alternator, with a governor to maintain constant alternator speed; or,
2. Drive the alternators at variable engine speed and change the variable frequency output from each alternator to a constant frequency for paralleling.

As no satisfactory variable speed drive was available at the time, and since a frequency changing unit, in addition to permitting synchronization of the alternators, also could be designed to meet requirements 2 and 3, such a unit appeared to offer desirable features for the parallel operation of the alternators.

Description of Frequency Changer

The electronic frequency changer is in essence an electronic commutator which accomplishes the conversion of power with a wide range of input frequencies to a constant output frequency.

Functionally, the device has two distinct circuits, a power circuit and a control circuit. The power circuit accomplishes the actual frequency conversion and has associated with it the voltage regulating circuit, the load division circuit, overload protection, and the necessary control circuits for starting the device and applying load. The control circuit establishes the output frequency, provides the necessary phase displacement of control signals to the power circuit to establish a 3-phase output, and incorporates the necessary circuits for synchronizing two frequency changers.

Regulation of average line output voltage is accomplished by controlling the excitation of the alternator supplying input power. This excitation control is accomplished by a carbon pile regulator. Since the output frequencies of units operating in parallel are maintained exactly in step by interconnection of the oscillators which determine the output frequency, circulation of reactive current between units is not a problem and load division is accomplished by controlling the relative excitations of the alternators supplying the units. This function is performed by a load equalizer network which is energized when the units are operated in parallel.

For an airplane installation, the units would be connected as shown schemati-

Paper 47-5, recommended by the AIEE committee on air transportation for presentation at the AIEE winter meeting, New York, N. Y., January 27-31, 1947. Manuscript submitted May 1, 1946; made available for printing October 23, 1946.

O. E. Bowlus is in the electrophysical laboratory and P. T. Nims is in the research department of the Chrysler Corporation, Detroit, Mich.

The work described in this paper was performed under a contract with the Air Technical Service Command. The authors are indebted to the Air Technical Service Command and Chrysler Corporation for permission to publish this paper.

cally in Figure 1. The generator may be mounted directly on the engine if an adequate pad is available and vibration not too severe, or driven by a power take-off shaft; the frequency changer would be in the nacelle and would be connected to the main power lines running through the wing to the fuselage. Other wires would be connected to the necessary meters and control switches at the flight engineer's station.

Electronic frequency changers have been used on public utilities systems for a nonsynchronous tie[5] but for aircraft applications some differences in the control system and the number of power tubes used are desirable. These differences permit operation of any one changer alone and without rotating equipment floating on the line.

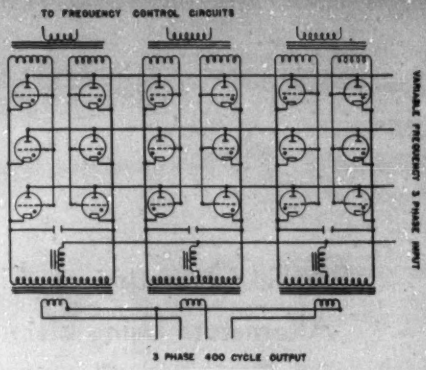

Figure 2. Power circuit 1 suitable for supplying either 3-phase or single-phase constant - frequency power from a 3-phase variable - frequency source

Description of Test Unit

At the request of Army Air Forces, experimental work on a pair of 4-kva units of this type was undertaken. The 4-kva size was chosen as representing the largest unit which could be built at reasonable cost with commercially available tubes.

For laboratory purposes two 30-volt 11-kva alternators were used because of their availability and a 3-phase step-up transformer was used to supply the necessary voltage to the tubes. For convenience, the control circuit and power tube filaments were supplied from a 115-volt 60-cycle source.

Two different power circuits were built and tested. The first one, Figure 2, has relatively simple current paths and current flows through only one tube in series. It is in essence three independent single-phase frequency changers and is of especial interest if only single-phase output is needed. The circuit is of the parallel inverter type.[6]

Less favorable characteristics of the circuit for this purpose are as follows:

1. High values of direct current through the input neutral introduce I^2R losses in the step-up transformer (or in the alternator if the step-up transformer is eliminated).

2. A low power factor is presented to the step-up transformer and alternator.

3. Requires an output transformer as well as inductive reactors.

The net result is increased weight and lower efficiency as compared to power circuit 2.

When capacitors are connected in series with the output lines, the circuit performs about as well as circuit 2. The tube peak inverse voltage is higher and some difficulty was experienced from this standpoint when operating at heavy load and when applying or removing heavy loads. Tube service is not as severe with power circuit 2.

Power circuit 2, the one finally adopted, is shown in Figure 3. This specific circuit embodies suggestions by J. Boyer of the Westinghouse Electric Corporation. This circuit uses three center-tapped reactors to replace the output transformers and commutating reactors. Its operation is discussed in the appendix. The necessary capacitors and the voltage regulator circuit also are shown. Figures 4 and 5 show the interior of this unit.

Voltage Regulation

A 30-volt d-c type carbon pile regulator was used with a 3-phase step-down transformer and a 3-phase selenium rectifier.

When used with aircraft d-c generators, the tendency for the carbon pile regulator to flutter at low values of field current can be eliminated by careful adjustment of the stack pressure. For this application, the flutter could not be adjusted out. An antiflutter circuit consisting of a small transformer, an electrolytic capacitor, and a resistor was designed to produce a magnetic pull on the regulator armature out of phase with the pull tending to produce flutter. Little difficulty with flutter was experienced thereafter.

Overload Relays

Instantaneous relays connected directly in each of the three input lines from the step-up transformer were used to protect against serious faults but not against sustained overload. Although an additional thermal delay relay could be used to protect against sustained overload, none was used in these experimental units, the d-c ammeter being sufficient to warn

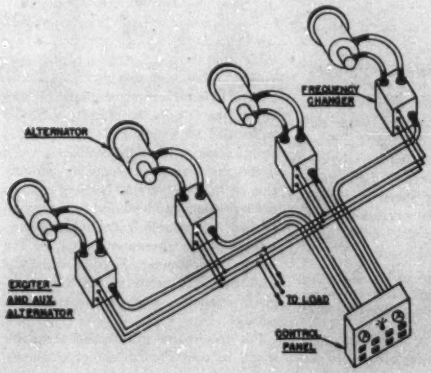

Figure 1. Four electronic frequency changers connected to provide parallel operation from four alternators each driven from one of the main aircraft engines

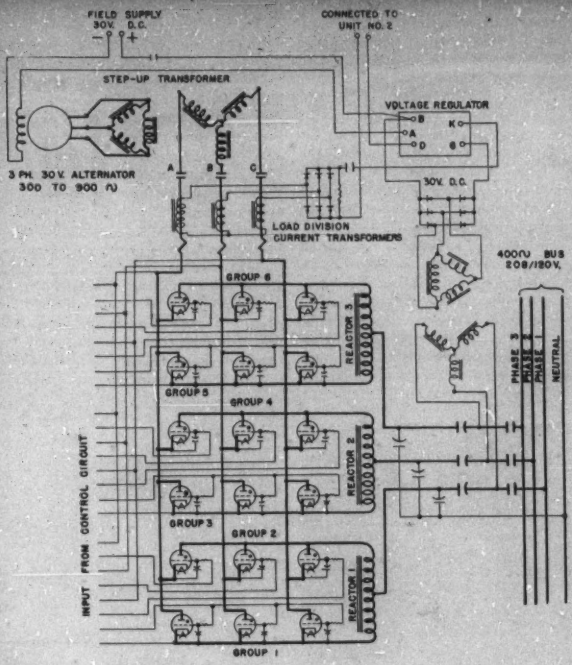

Figure 3. Power circuit 2 suitable for supplying 3-phase constant-frequency power from a 3-phase variable-frequency source

This circuit does not require a neutral connection in the step-up transformer secondary (or in the alternator if the step-up transformer is eliminated)

the operator when he is overloading the tubes.

Control Circuit

Although a number of circuit variations were tried, the same general outline was followed throughout the development. The biggest improvement came with the substitution of vacuum tubes for gas tubes wherever possible. Vacuum tubes have proved to be inherently more stable for this application. The control circuits as built up for experimental purposes are shown in Figures 6 and 7.

The 400-cycle output frequency is determined by a single-tube *884* saw-tooth oscillator operating at 2,400 pulses per second. Output from this tube controls a 3-tube *6J5* switching or counting circuit in such a manner that the three tubes fire in sequence, each 800 times per second. This is the method used to obtain 120 degrees displacement between phases of the output frequency. Each of the three *6J5* tubes controls a pair of *6V6GT* tubes in a flip-flop circuit wherein each tube passes plate current one half of the time. When one tube is "on" the other is "off." The "on"-"off" relation reverses with each pulse from the *6J5*. The period between reversals represents one-half cycle of the output frequency.

The square wave output voltages from the flip-flop circuits are transmitted through transformers to the grids of the *FG-67* power tubes. A square wave input to the grids is desirable because each of the power tubes must be able to start passing plate current at any point during a half cycle. To insure that the tube will be ready to pass current when the plate becomes positive with respect to cathode, the grid must be held in conducting position for the full half-cycle. On the next half-cycle, the same grids must be held sufficiently negative to prevent flow of plate current for the full half-cycle.

Transformer coupling must be used between control circuit and power circuit because the cathodes of the various power tubes cannot remain at the same potential. Some difficulty was experienced in keeping transient voltages set up by the opening of contactors from getting back into the control circuit, causing the two control circuits to drop out of synchronism. Placing small capacitors across the contactor hold-up coils eliminated this trouble. Any change in load on the control circuit such as turning the power circuit on or off or failure of power tubes to commutate has an effect upon the stability of the flip-flop circuit. This effect was minimized by placing a resistance load across the primary of each transformer in the flip-flop circuit such that a change in driving power to the grids of the power tubes represents a small change in total load on the flip-flop circuit.

Synchronization

Three separate components of the control circuit must be synchronized with corresponding components in the second control circuit.

Figure 4. A 4-kva electronic frequency changer

Front view with outer panels removed

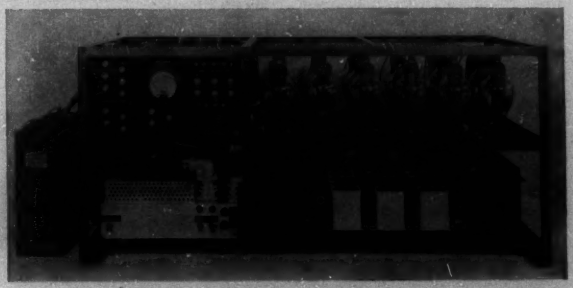

Figure 5. A 4-kva electronic frequency changer

Top view with outer panels removed

1. First the *884* oscillators must be synchronized. A portion of the plate saw-tooth signal is fed from each tube to the grid of the opposite tube. The resulting frequency will be equal to that of the fastest circuit rather than an average of the two. These connections are permanent except when it is desired to operate one unit entirely separate from the other. A dummy connector plug then is used in place of the synchronizing cable.

2. Next, the 3-tube *6J5* counting circuits must be synchronized. By means of an auxiliary tube, a signal is fed from the plate of a *6J5* tube in one circuit to the grid of the corresponding tube in the other circuit. A switch momentarily is closed to obtain synchronization.

3. Finally, the 6-tube *6V6GT* flip-flop circuits must be synchronized. The six tubes in each circuit are maintained in proper firing sequence by two small capacitors connected between screen of one pair and grid of another pair. There still remains the possibility of the six tubes in one circuit being 180 degrees out of phase with the other circuit. A small capacitor between a plate in one circuit and a grid in the other brings them in phase by closing a momentary-contact switch.

A single double-pole momentary-contact switch performs synchronizing operations 2 and 3 simultaneously. No synchronizing lamps are necessary—merely flip the momentary contact switch when in doubt.

Parallel and Series Capacitors

By parallel capacitors are meant the capacitors which are connected either line to line or line to neutral across the output of the frequency changer. These may be connected either on the tube side or the load side of the three series capacitors one of which is connected in series with each output line.

The purpose of both the parallel and the series capacitors is to assist in the commutation of current between the power tubes. The grid of a thyratron tube can be used to prevent or control the instant of start of plate current flow, but once the plate current is flowing, other means must be provided to turn off the current. The capacitors provide this means by causing the plate to go negative at the instant the grid is made negative and remain negative for a time sufficient to deionize the tube. After this delay of a few microseconds, the grid again regains control. More detailed explanation is given in the appendix.

Figure 6. Control unit for 4-kva electronic frequency changer

The capacitance is determined by the operating requirements. Parallel capacitors are desirable for light loads while series capacitors are more effective for heavy loads. Since the load current flows through the series capacitors, the capacitive volt-amperes supplied by them increases with load, whereas the capacitive volt-amperes supplied by the parallel capacitors remain essentially constant. At no-load open circuit, the series capacitors have no effect on the operation and the capacitive volt-amperes must be supplied by parallel capacitors. By reducing sufficiently the microfarad rating of the series capacitors, the changer can be made to function normally with the output terminals short-circuited together. In view of the fact that the voltage regulation within the changer suffers from a large reactive drop in the output lines, it is desirable to make the series capacitance as high as is consistent with starting heavy loads. In this aircraft application, the largest induction motor determines the size of the series capacitor.

For parallel operation of two changers, it was found desirable to connect the parallel capacitors on the tube side of the series capacitors and to keep the micro-

Figure 7. Circuit diagram of one control unit

Synchronizing connections are indicated for parallel operation with a second unit. Output connections are shown for operation with the power circuit in Figure 3

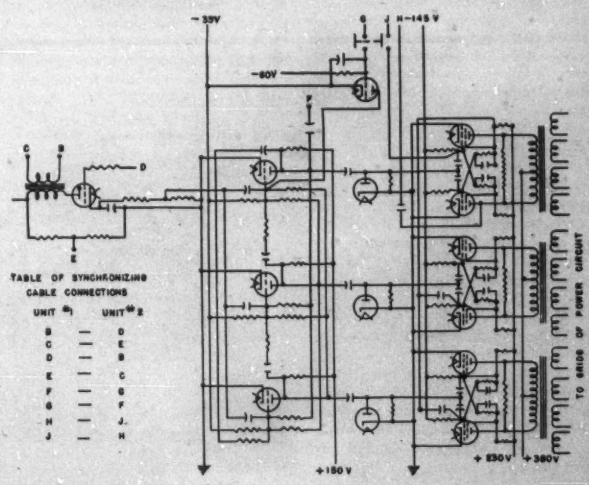

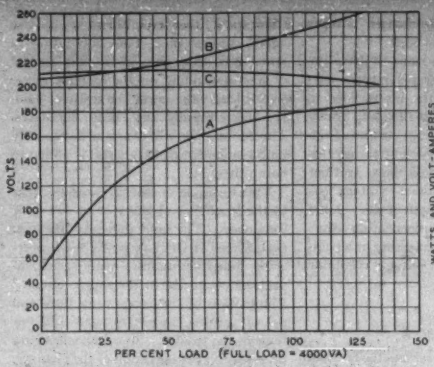

Figure 9A. Curves showing how the input voltage varies with applied load

A—Step-up transformer secondary line to line voltage

B—Output line to line voltage ahead of the series capacitors

C—Output line to line voltage

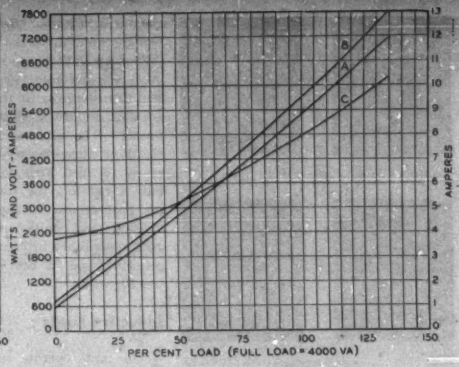

Figure 9B. Curves showing input power and tube current

A—Input watts supplied by step-up transformer secondary winding

B—Input volt-amperes supplied by step-up transformer secondary winding

C—Tube current (sum of three tubes in one group)

farad capacitance of the series capacitors as high as possible. This will be discussed under parallel operation.

Contrary to expectations, the capacitors need be neither large in physical size nor heavy. Standard oil-filled 60-cycle capacitors of normal voltage rating appear to stand up on 400 cycles without excessive heating. However, no extended life test was made. To provide maximum cooling surface per microfarad of capacitance (in the case of the parallel capacitors), a number of small units were connected in parallel to make up the total desired capacitance. With forced air cooling, the size and weight no doubt could be reduced further. It is estimated that the weight could be reduced to approximately one-fifth the total active weight of the changer.

To increase the efficiency of the changer at light loads, a portion of the parallel capacitance can be connected permanently across some of the individual heavy loads.

Parallel Operation and Load Division

Parallel operation is accomplished by synchronizing the two control circuits so that the output signal of one is exactly in phase with the other. When this is accomplished, the output contactors may be closed onto the 400-cycle bus. Synchronization of the control circuits is accomplished by the flip of a momentary-contact switch.

The test units as built must be paralleled at no-load or when the load on each is approximately the same, because of the action of the series capacitors. When the load is identical on both, the output terminal voltages are exactly in phase. When one is unloaded and the other loaded, the terminal voltages are no longer in phase. The power tubes are fired in phase but the load current through the series capacitor on the loaded unit causes the terminal voltage on this unit to lead the terminal voltage on the unloaded unit. The greater the differences in load, the greater will be the change in phase. When the load on the one unit becomes greater than approximately 2,500 volt-amperes, they cannot be paralleled successfully. This is another reason why the capacitance of the series capacitors should be made as high as possible.

In connection with the foregoing, it was found desirable to connect the parallel capacitors on the tube side of the series capacitors. With them on the load side the drop across the series capacitor is increased further, interfering that much more with parallel operation.

For motor loads it might be possible to place part of the series capacitance between the output terminals and the motor where it would not interfere with parallel operation. A combination of series and parallel capacitance might be chosen such that the motor would operate at its rated voltage.

The first attempt at load division was to place a current transformer in each of the output lines. A voltage proportional to load, obtained from the drop across a resistor in one of the secondaries, was applied across a resistor in series with the corresponding phase of the primary of the voltage regulator step-down transformer. All three phases were so connected, the resistors being inserted at the neutral of

Figure 8. Efficiency curves

A—$\frac{\text{Output watts}}{\text{Step-up transformer output watts}}$

B—$\frac{\text{Output watts}}{\text{Step-up transformer output watts} + \text{filament watts} + \text{control circuit watts}}$

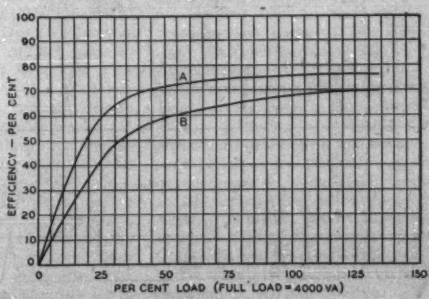

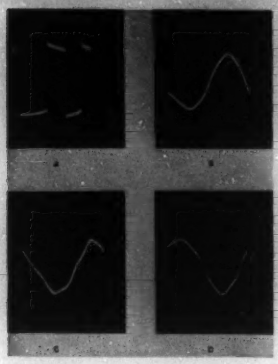

Figure 10. Oscillograms of output wave form

A—Square-wave output voltage from control unit. This voltage is applied to the grids of the power tubes

B—400-cycle output voltage at no load

C—400-cycle output voltage, full load unity power factor

D—400-cycle output voltage, three-horsepower motor load, plus 3,000 watts resistive load. Three 4-microfarad capacitors are connected line to line to correct partially for the inductive reactance of the motor

the Y-connected primary. Wires were connected from the step-down transformer in one changer to the step-down transformer in the other changer to obtain cross-compensation. This system worked well at heavy loads but was not satisfactory at light loads. One changer would tend to drive the other.

The tendency for one unit to drive the other was overcome by placing the current transformers in the input lines to the changer just after the step-up transformer. The alternating current from the three single-phase current transformers is rectified with a 3-phase rectifier into a resistor, the direct voltage being proportional to input load. Load division and cross-compensation then are accomplished by connecting to a compensating coil in the voltage regulator (see Figure 3).

Inductive Loads

The units operate satisfactorily with static inductive load providing there is sufficient capacitance in the circuit to insure commutation of the tubes. Conceivably, enough capacitance could be connected permanently into the units to take care of any inductive load, no matter how large. However, to reduce circulating reactive current and obtain reasonably good efficiency at light and medium loads, it is desirable to provide only enough capacitance within the unit to handle medium loads.

Motor Loads

Motors, from the standpoint of being an inductive load, present no special problem. Capacitors, when needed, can be connected across the motor for power factor correction.

Motor operation was found to be unstable and erratic. The motor will come up to normal speed, then immediately drop to a low speed, then rapidly rise again, and so on. This fluctuation in speed goes through a cycle in a second or less, depending on the amount of resistive load—the lower the resistive load, the more rapidly the speed fluctuates. The fluctuations will continue indefinitely unless sufficient resistive load is added to damp them out.

This unstable operation is not peculiar to the frequency changer or to 400-cycle frequency. The same difficulty has been experienced on 60-cycle power when operating induction motors with series capacitors connected in the supply circuit.[7] Elimination of the series capacitors and use of parallel capacitors alone will not remedy the trouble. Since capacitors are necessary to the operation of the changer, the only means of eliminating the unstable condition appears to be to damp it out. Resistive load being small in comparison to induction motor load on aircraft makes it necessary to achieve damping with a minimum of resistance to prevent undue waste of electric energy.

A 3-horsepower motor requires approximately 2,400 watts resistive load when operated from one frequency changer, and approximately 4,800 watts resistive load when operated from two changers in parallel. This load, of course, can be lamp load or some other useful load in the airplane.

Neutral for 4-Wire System

An artificial neutral must be provided to obtain a 4-wire, 3-phase system. Either Y-connected inductive reactors or capacitors may be used for this purpose, but capacitors were found to be more desirable. Inductors, if used, present an inductive load to the changer thereby requiring additional capacitance. Zigzag connection of the inductors was found desirable to stabilize the neutral. By connecting the parallel capacitors line–neutral rather than line–line, no additional capacitors are required for power factor correction. The capacitors, in addition to providing the same degree of stability of the neutral, do not carry a weight penalty.

At best, the artificial neutral will handle only a small single-phase load without unbalancing both line–line and line–neutral voltages.

Weight

Because these units were intended for laboratory test only, no attempt was made to make them with minimum possible weight. Each unit weighs 245

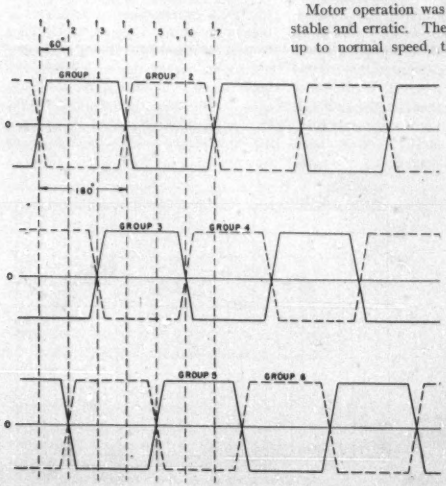

Figure 11. Showing phase relationship of the square-wave voltages applied to the control grids of the power tubes in Figure 3

Table I

Step-Up Transformer Output				Tube Amp, Sum of 3 Tubes		Output							
Watts	Amp	Volts	Va	D-C	A-C	Line-Line Volts Ahead of Series Cap	Volts Across Series Cap	Line-Line Volts Load	Line-Neutral Volts Load	Amp	Watts	Va	Power Factor
Resistive Load													
560	8.4	50	728	3.75	6.05	207	0	211	121	0	0	0	
3,312	13.2	159	3,640	5.72	9.6	224	38.5	213	127	6.64	2,432	2,445	
6,160	21.0	183	6,670	9.0	15.3	253	76	206	117	13.1	4,720	4,678	
Inductive Load, 1,250 Va													
960	4.67	128	1,035	2.15	3.7	171	21	207	118	3.67	624	1,316	47.3
3,152	11.1	180	3,460	4.93	7.8	193	43	209	124	7.66	2,464	2,775	88.8
5,840	19.1	188	6,225	8.17	13.9	227	72	221	120	13.0	4,592	4,760	96.5

pounds. With forced air cooling and lightweight design, it is estimated the weight could be reduced to approximately 70 pounds. It also has been estimated that a 40-kva unit might weigh 300 pounds.

Test Results

Two units were built and operated satisfactorily in parallel. Each unit has its individual control circuit and the control circuits were synchronized for parallel operation by pushing a button. Load division was accomplished very easily.

Heavy resistive loads could be handled under all conditions. Inductive loads larger than approximately 1,250 volt-amperes per unit required power factor correction for satisfactory operation. Power factor correction can be accomplished by adding small capacitors across the inductive load.

A single unit or both in parallel would start and operate a 3-horsepower induction motor, provided a large resistive load was already on the line or applied with the motor. One-quarter-horsepower motors operated satisfactorily without additional resistive load and without power factor correction. Large motors required power factor correction and the presence of sufficient resistive load to stabilize operation.

While the test circuit had only one-tenth the volt-ampere capacity that probably could be used in an airplane, some of the test results are of interest in indicating the trend of the performance. One such test was variation of alternator speed; input frequency was varied from 300 cycles to 900 cycles with negligible effects on output frequency, voltage, and watts. Load division data were taken with one unit operating at a 450-cycle input frequency and the other unit at 300, 500, 700, and 900 cycles successively. Frequency of incoming power seemed to have no noticeable reflection on the ability of the units to share load; however, the load division did display a tendency to drift at times as the voltage regulators heated up.

When the input frequency becomes equal to the output frequency, only 12 of the 18 power tubes transmit power. This means that the tube size has to be chosen with this in mind or else the generator drive ratio chosen with respect to the operating speed range of the engine to minimize operation at these input frequencies. At other speeds, the division of load between tubes is good and substantially independent of individual tube characteristics. In fact, any one power tube can be removed from the circuit bodily with only minor effects on the output. This argues well for the reliability of the circuit.

As the experimental unit used a step-up transformer to raise the alternator voltage to the necessary value, and also as the filament and control power were supplied from a separate source, the most useful efficiency figure is the ratio (output watts)/(transformer output watts+filament watts+control circuit watts). This figure most nearly reflects actual operating conditions. This efficiency is shown in Figure 8 for power circuit 2 with resistive load. Loads of lower power factor seem to make only small changes in these values. This is probably caused by the effect of the large fixed loss—410 watts for filaments, and 210 watts for control—or a total of 15 per cent of the rated output.

A summary of the voltages, current, and powers in various parts of power circuit 2 is given in Figure 9. It is interesting to note that the voltage regulator markedly increases the input voltage to the changer, with increase in load, in order to hold the output voltage substantially constant, and that this increase is more than enough to compensate for the drop in the series capacitors. Table I gives some similar data for an inductive load as well as a resistive load.

Wave form of the output varies slightly with load. Figure 10 shows the wave form of one phase of the 400-cycle output under three operating conditions and also the voltage applied to the grid of one of the tubes.

Possible Future Development

The test circuit was built as a scaled-down model of a 40-kva unit. A full size frequency changer presumably would be operated directly from an alternator designed for the purpose, and no step-up transformer would be required. Also, an auxiliary alternator probably would be used to supply filament heating power and the various voltages required for the control circuit. Further savings in tube size and weight of some components might be achieved by using a higher voltage (and hence reduced current) in the power tube circuits. This would be more convenient using power circuit number one as it has provision for stepping down the output voltage to the standard 208 volts.

For some commercial aircraft with large single-phase loads, such as lighting, radio, and cooking, it might be advantageous to consider a complete single-phase system using capacitor type motors. For use with an electronic frequency changer, this would give a relatively high power factor load suited to a 6-tube changer of the type of circuit 1. In view of the simplicity of the power and control circuits, this is an attractive possibility. While single-phase loading of a conventional generator is not desirable, the interposition of a frequency changer distributes this single phase load equally among the three phases of the generator, reducing the weight penalty to be expected for a single-phase system. There is also some saving in cable weight caused by the lesser amount of insulation in a single wire ground return system.

Appendix. Principle of Operation of Power Circuit 2

For convenience, the 18 power tubes of Figure 3 may be divided into six groups of three each. Two such groups may be associated with each phase of the constant frequency output. In each phase, one group has the three anodes connected together to one end of a center-tapped reactor; the other group has the three cathodes connected together to the other end of the reactor. For each output phase group, each line of the variable frequency input is connected to one of three cathodes of one tube group and to one of three anodes of the other group. In each phase, a voltage is fed to the control grids of the two groups of three so that they are 180 degrees out of phase with respect to each other. This voltage is supplied in the form of a square wave with the result that in each phase the grids of one group of three tubes are held positive with respect to the cathodes while the grids of the other group of three tubes are held negative. The square wave being supplied at 400 cycles, each group of three tubes is made to pass current for a half cycle of the output frequency and to block passage of current the succeeding half cycle. All three phases receive identical control voltages except that the square wave to each phase is displaced 120 degrees from the other two phases.

Referring now to Figure 11, at instant t_1

(a). Tubes in group 2 rendered nonconducting.
(b). Tubes in group 1 rendered conducting.
(c). Tubes in group 5 are conducting.
(d). Tubes in group 4 are conducting.
(e). Tubes in group 3 are nonconducting.
(f). Tubes in group 6 are nonconducting.

Between instant t_1 and t_2

(a). Passage of current is from input lines A, B, and C through groups 1 and 5, left half of reactors 1 and 3, phase 1 and 3 of load, phase 2 of load, right half of reactor 2, group 4, and return to lines A, B, and C.

At instant t_2

(a). Tubes in group 5 rendered nonconducting.
(b). Tubes in group 6 rendered conducting.
(c). Tubes in group 1 are conducting.
(d). Tubes in group 4 are conducting.
(e). Tubes in group 2 are nonconducting.
(f). Tubes in group 3 are nonconducting.

Between instant t_2 and t_3

(a). Passage of current is from input lines A, B, and C, through group 1, left half of reactor, phase 1 of load, phases 4 and 6 of load, right half of reactors 4 and 6, groups 4 and 6, and return to lines A, B, and C.

This process likewise may be traced through for instants t_3, t_4, t_5, and t_6. Instant t_7 is identical to t_1, and the cycle repeats.

It may be observed that while group 1 is conducting, current will pass through the tube connected to the input line which is most positive. As the voltage on this line falls below that of another line, the current automatically changes over to the tube connected to that line. The three tubes act as rectifiers of the input voltage to supply unidirectional current to the left end of reactor 1 during every other half cycle of the output frequency. Obviously, the input frequency is not dependent in any way upon the output frequency and vice versa.

The capacitors shown connected line to line across the output assist the center-tapped reactors in commutating the current from one group of three tubes to the group of three tubes connected to the other end of the common reactor. Referring again to phase 1 involving groups 1 and 2, the left end of reactor 1 is negative with respect to the center tap an instant before the grids of group 1 change from negative to positive At the instant the grids of group 1 are made positive (and the grids of group 2 are made negative) the tube of group 1 having the most positive potential between plate and cathode, fires bringing, instantaneously, the potential of the left end of the reactor to a positive voltage with respect to the center tap by virtue of the low tube drop which exists when a tube is passing current. This sudden change of the left end of the reactor from a negative to a positive potential is transmitted by transformer action to the right end such that it changes the right end from a positive potential to a negative potential. This sudden drop in potential causes the plates of the tubes in group 2 to go negative with respect to the cathodes. The tubes of group 2 will be extinguished and the grids regain control providing there is sufficient capacity between output lines to enable the plates to remain negative with respect to cathodes long enough for the tubes to deionize. Lack of sufficient capacity between lines will give poor commutation, erratic operation, and will damage the tubes if the condition is allowed to persist.

Capacitors also are placed in series with the output lines to assist in commutating the tubes under application of heavy loads. A low capacitance is more effective in helping commutation than high capacitance. However, the capacitance must be made as high as possible, consistent with good commutation, in order to hold to a minimum the reactive drop in the output lines.

References

1. Applications of Electric Power in Aircraft, T. B. Holliday. Electrical Engineering, volume 60, May 1941, pages 218–25.

2. Basic Considerations in Selection of Electric Systems for Large Aircraft, W. K. Boice, L. G. Levoy, Jr. AIEE Transactions, volume 63, 1944, June section, pages 279–87.

3. Why Tomorrow's Planes Will Have A-C Electric Systems, T. B. Holliday. *Electrical Manufacturing*, New York, N. Y., volume 32, July 1943, page 88.

4. A 40-Kva 400 Cycle Aircraft Alternator, H. E. Kenaipp, C. G. Veinott. AIEE Transactions, volume 63, 1944, November section, pages 816–21.

5. The Electronic Converter for Exchange of Power, F. W. Cramer, L. W. Morton, A. G. Darling. AIEE Transactions, volume 63, 1944, pages 1059–66.

6. Parallel Inverter With Resistance Load, C. F. Wagner, AIEE Transactions, volume 54, 1935, November section, pages 1227–35.

7. Self-Excitation of Induction Motors With Series Capacitors, C. F. Wagner. AIEE Transactions, volume 60, 1941, pages 1241–7.

No Discussion

Resistors for 138-Kv Cable Switching

E. K. SADLER
MEMBER AIEE

T. M. BLAKESLEE
MEMBER AIEE

DISCUSSIONS of overvoltages that are produced by closing and opening capacitor circuits have appeared in several articles.[1-4] All the authors conclude that such overvoltages can be reduced by momentarily inserting resistors in series with the circuit as the circuit breaker opens to interrupt the charging current. Installations of 138-kv underground cable by the Department of Water and Power in 1943 provided an excellent field laboratory for capacitive-current switching. This paper describes and presents results of an investigation of problems incident to interrupting 138-kv cable charging current.

Tests were performed on the Toluca-Fairfax West circuit which is one of two 138-kv links between receiving station D and receiving station E. This circuit consists of five miles of 138-kv underground cable and seven miles of overhead line. Details of the underground cable may be obtained from reference 5. The charging current of this circuit is 80 amperes per phase at normal voltage.

The investigation was well under way when on August 26, 1943, a lightning arrester failed from overvoltage produced by de-energizing the Toluca-Fairfax East circuit from the receiving station E terminal. The arrestors are located at the junction between overhead and underground sections of the circuit and a voltage in the order of three times normal is required for breakdown.

The circuit breakers installed on this circuit are tank type, solenoid-operated and function on the dethermalizing arc-quencher principle described in reference 6. Switching tests without and with resistors in the circuit breakers are described in this paper and the final design of a step-type 800–2,000-ohm resistor is presented. A theoretical discussion of the effect of resistors in circuit breakers handling charging current is given in the appendix.

Conclusions

1. Transient overvoltages caused by arc restriking when switching capacitive circuits can be limited by resistors across the main contacts of circuit breakers.

2. A definite limitation is imposed upon overvoltages produced at the point of circuit interruption by the use of resistors (Figure 8). The limitation depends upon the ratio of the ohmic value of resistance used in the circuit breaker to the ohmic value of capacitive reactance of the circuit being interrupted (R/X_c).

3. Transient overvoltages which occur at the point of circuit interruption may produce higher overvoltages at other points on the power system as a result of amplification of the transient frequencies through system circuits.

4. Restriking on contacts interrupting resistor current does not cause overvoltages with ratios of R/X_c as low as 0.6 and probably does not cause overvoltages with ratios considerably below this value.

5. Increasing the speed of contact separation reduces restriking in the circuit breaker. It is doubtful if increased speed is justified from this standpoint alone as resistors definitely limit the voltage and the restrikes

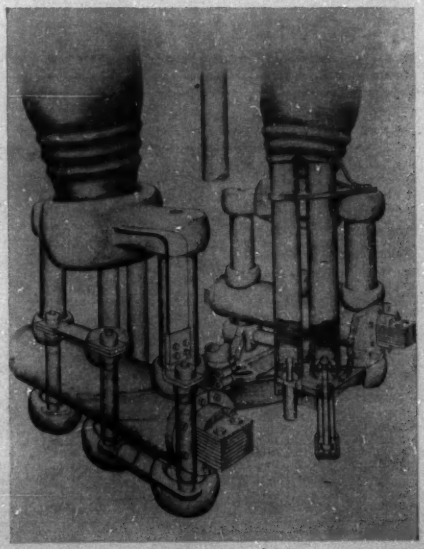

Figure 1. Arrangement of resistors and auxiliary contacts in 138-kv circuit breaker

Paper 47-6, recommended by the AIEE committees on protective devices and power transmission and distribution for presentation at the AIEE winter meeting, New York, N. Y., January 27–31, 1947. Manuscript submitted July 15, 1946; made available for printing October 24, 1946.

E. K. SADLER is chief engineer, Kelman Electric and Manufacturing Company, Los Angeles, Calif., and T. M. BLAKESLEE is superintendent of testing laboratories, Department of Water and Power, Los Angeles, Calif.

The work of Jesse L. Thompson in designing resistors and resistor contacts, and the oscillographic test work of G. A. Stockwell are gratefully acknowledged.

do not put any undue stress on the circuit breaker.

6. A step-type resistor of 800–2,000 ohms can be added to existing circuit breakers on the cable circuits of the Department of Water and Power without replacing the existing arc quenchers, linkages, or operating mechanisms.

Resistor and Auxiliary Contact Design

The final design for installation in the circuit breakers on the cable circuits consists of an 800–2,000-ohm step-type resistor which, with the 1,000-ohm capacitive reactance of a 5-mile 138-kv cable, results in an R/X_c ratio of 0.8. The curves developed in the appendix and presented in Figure 8 show that this value of the ratio limits overvoltages to 1.5 times normal at the point of circuit interruption. Figure 1 shows the arrangement of the resistors and the necessary auxiliary contacts in the circuit breaker, and Figure 2 presents a schematic diagram of the electric circuit.

The step-type resistor requires two sets of auxiliary contacts for interrupting resistor current. The moving members of these contacts consist of bayonets attached to the circuit breaker crosshead. The bayonets slide into stationary contacts having spring pressure members at the bottom of the resistor tubes. The final or second auxiliary contact which interrupts the 2,000-ohm resistor current incorporates a built-in quick-break spring mechanism. The head on the bayonet tip catches on the spring contact as the crosshead falls in the opening stroke of the circuit breaker, thereby arresting motion of the bayonet and compressing the built-in spring. When the spring is fully compressed, the bayonet head is pulled through the contact, releasing the spring which gives a quick break to the bayonet contact. This quick break improves the performance of this contact in effecting final interruption of the circuit. It should be pointed out, however, that the quick-break action is not necessary from the standpoint of the production of overvoltages (see conclusion 4).

The rate of energy dissipation in the resistor is less during capacitor switching than it is during short-circuit switching, making the latter condition the necessary

Table I. Times-Normal Voltages From De-energization of Toluca-Fairfax West Circuit, Circuit Breakers Without Resistors

Oscillogram Number	Bus Voltage at Switching Station				Bus Voltage at Remote Station			Circuit Voltage	
	A-Φ*	A-Φ	B-Φ	C-Φ	A-Φ	B-Φ	C-Φ	At Switching Station A-Φ*	At Remote Station A-Φ*
Switching from receiving station *D*									
3,475		1.55	1.48	1.11					
3,476		1.82	1.20	1.44					
3,477		1.27	1.57	1.57					
3,555	1.24	1.15	1.16	1.18	1.09	1.15	1.09	1.00	1.00
3,556	1.10	1.07	1.16	1.23	1.04	1.04	1.14	1.00	1.00
3,557	1.12	1.11	1.34	1.18	1.09	1.17	1.11	1.00	1.03
3,558	1.42				1.06	1.04	1.14	1.06	1.06
3,559					1.41	1.13	1.36		1.15
3,560					1.15	1.23	1.20		1.00
3,561	1.25				1.23	1.46	1.09	1.22	1.26
3,580	1.17	1.16	1.07	1.29	1.10	1.10	1.30	1.15	1.21
3,581	1.58	1.50	1.41	1.11	1.25	1.30	1.09	1.53	1.49
3,582	1.55	1.45	1.29	1.12	1.25	1.20	1.09	1.03	1.15
3,583	1.55	1.50	1.38	1.41	1.33	1.25	1.30	1.00	1.00
3,584	1.43	1.41	1.50	1.30	1.25	1.30	1.25	1.13	1.26
3,585	1.02	1.01	1.32	1.14	1.00	1.13	1.07	1.00	1.00
3,586	1.29	1.26	1.52	1.39	1.15	1.31	1.28	1.37	
3,587	1.63	1.32	1.14	1.27	1.32	1.06	1.14	1.06	
3,588	1.25	1.12	1.16	1.21	1.09	1.09	1.20	1.03	
3,589	1.17	1.15	1.43	1.25	1.06	1.27	1.20	1.00	
3,590	1.48	1.39	1.07	1.17	1.27	1.09	1.17	1.35	
3,591	1.21	1.21	1.29	1.29	1.12	1.13	1.20	1.00	
3,784	1.64	1.44	1.31	1.26	1.30	1.16	1.12	1.21	1.15
3,785	1.54	1.45	1.43	1.21	1.26	1.27	1.15	1.58	1.56
3,786	1.42	1.40	1.10	1.49	1.12	1.04	1.32	1.53	1.53
3,787	1.17	1.15	1.48	1.46	1.05	1.40	1.33	1.03	1.15
3,788	1.66	1.58	1.38	1.31	1.30	1.26	1.21	1.25	1.26
3,789	1.28	1.26	1.58	1.07	1.19	1.37	1.11	1.22	1.28
3,790	1.23	1.16	1.29	1.22	1.08	1.23	1.17	1.08	1.14
3,791	1.20	1.19	1.31	1.57	1.10	1.23	1.31	1.07	1.09
3,792	1.31	1.34	1.36	1.38	1.19	1.27	1.34	1.33	1.22
Switching from receiving station *E*									
3,490		1.25	1.07	1.29					
3,491		1.28	1.09	1.29					
3,492		1.17	1.18	1.22					
3,616	1.04	1.08	1.07	1.17	1.11	1.16	1.67	1.06	1.00
3,617	1.10	1.11	1.07	1.06	1.19	1.07	1.24	1.10	1.06
3,618	1.33	1.38	1.13	1.09	1.84	1.35	1.33	2.11	2.19
3,619	1.06	1.02	1.06	1.13	1.10	1.16	1.65	1.11	1.08
3,620	1.31	1.25	1.05	1.08	1.61	1.12	1.30	1.28	1.31
3,621	1.10	1.09	1.18	1.16	1.17	1.75	1.72	1.11	1.03
3,622	1.09	1.09	1.02	1.04	1.17	1.13	1.30	1.14	1.15
3,623	1.08	1.10	1.10	1.17	1.21	1.51	1.51	1.13	1.09
3,630	1.03	1.02	1.16	1.13				1.27	
3,631	1.10	1.06	1.23	1.20				1.11	
3,632	1.08	1.05	1.06	1.14				1.10	
3,633	1.10	1.07	1.20	1.15				1.13	
3,634	1.01	1.02	1.04	1.10					
3,635	1.09	1.04	1.10	1.09					
3,636	1.18	1.12	1.27	1.04				1.37	

* Voltage from capacitance potential divider.

criterion for design. The parameters for this situation are system voltage and value of resistance. For any given system voltage the energy dissipated in the resistor rises rapidly as the value of resistance is decreased. An 800-ohm resistor on a 138-kv system must be designed to handle 8 megawatts for the time it is required to be in the circuit.

This important factor of time that the resistor is in the circuit should include the time the resistor must carry current during both closing and opening strokes. Speed–time characteristics of circuit breakers generally are such that resistors are in the circuit an appreciably shorter time during closing than opening. This is fortunate, for if the circuit breaker is used for synchronizing, a closure between systems that are over 60 degrees out of phase increases the resistor current over the short-circuit values.

The resistors used on this project incorporate a factor of safety against burnout of from 2.5 to 3. The resistors are made up of Nichrome V wire, wound in helix, on grooved bakelite tubes, and the factors of safety were determined by actual performance of short sections of resistor helix observed under oil.

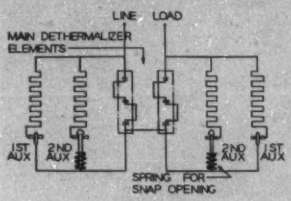

Figure 2 (above). Schematic diagram of 800–2,000-ohm step-type resistor circuit in 138-kv circuit breaker

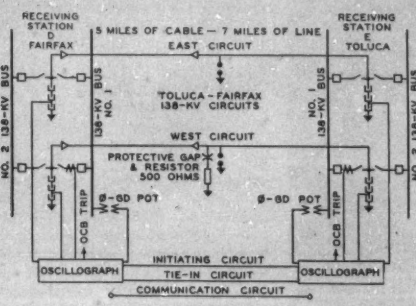

Figure 3. One-line diagram of 138-kv and measuring circuits for switching tests

Description of Test Setup

A 1-line diagram showing the 138-kv circuits and the measuring circuits is given in Figure 3. Oscillographs were located at the terminal stations and arranged to be initiated simultaneously from either point. The experience with the failure of a lightning arrestor at Nichols Canyon junction between overhead and underground sections prompted installation of 500-ohm resistors and protective gaps set to break down at two times the normal voltage. Voltage measurements on the 138-kv buses were obtained through star-connected potential transformers at the terminal stations. *A*-phase-to-ground voltages on both ends of the circuit being switched were obtained through capacitance potential dividers made from the coupling capacitor potential devices that are installed permanently on the circuit. The capacitor stack of these devices consists of two 0.0033-microfarad capacitors in series. A 25-microfarad capacitor was substituted for the potential device and the voltage across this capacitor was used for the oscillograph. Because the ohmic value of the oscillograph circuit is in the order of 50 times that of the 25-microfarad capacitor at 60 cycles per second, such a

Table II. Times-Normal Voltages From De-energization of Toluca-Fairfax West Circuit, Circuit Breakers With Resistors

Oscillogram Number	Bus Voltage at Switching Station A–Φ*	Bus Voltage at Switching Station A–Φ	Bus Voltage at Switching Station B–Φ	Bus Voltage at Switching Station C–Φ	Bus Voltage at Remote Station A–Φ	Bus Voltage at Remote Station B–Φ	Bus Voltage at Remote Station C–Φ	Circuit Voltage At Switching Station A–Φ*	Circuit Voltage At Remote Station A–Φ*
Switching from receiving station *D* with 2,000-ohm resistors									
3,567	1.27	1.20	1.05	1.13	1.09	1.00	1.09	1.35	1.29
3,568	1.40	1.32	1.13	1.14				1.32	
3,569	1.21	1.18	1.07	1.07	1.06	1.06	1.09	1.26	1.00
3,570	1.05	1.03	1.04	1.06	1.02	1.00	1.02	1.03	1.00
3,571	1.25	1.20	1.03	1.09				1.32	
3,572	1.26	1.21	1.36	1.27	1.11	1.21	1.20	1.22	
3,573	1.29	1.27	1.03	1.06	1.15	1.02	1.07	1.35	
3,575					1.21	1.04	1.22		1.15
3,577					1.21	1.04	1.20		1.00
3,579					1.06	1.09	1.03		1.03
Switching from receiving station *E* with 720–2,000-ohm resistors									
3,751	1.00	1.00	1.02	1.07	1.03	1.06	1.24	1.00	1.00
3,752	1.02	1.04	1.07	1.11	1.06	1.11	1.33	1.00	1.00
3,753	1.11	1.08	1.14	1.02	1.36	1.19	1.05	1.11	1.02
3,754	1.11	1.10	1.09	1.10	1.30	1.17	1.00	1.09	1.00
3,757					1.09	1.17	1.00		
Switching from receiving station *E* with 600–2,000-ohm resistors									
3,761	1.08	1.06	1.06	1.05	1.14	1.12	1.23	1.05	1.00
3,762	1.11	1.07	1.06	1.02	1.11	1.15	1.03	1.09	1.13
3,763	1.05	1.04	1.06	1.04	1.06	1.16	1.09	1.03	1.15
3,764		1.06	1.10	1.05	1.05	1.25	1.11		1.00
3,765		1.04	1.10	1.05	1.07	1.07	1.10		1.10
3,766	1.11	1.13	1.08	1.08	1.18	1.25	1.11	1.09	1.05
3,767		1.06	1.08	1.10	1.12	1.25	1.18		1.09
3,768		1.04	1.01	1.05	1.05	1.08	1.15		1.04
3,771					1.23	1.08	1.03		1.12
3,772					1.18	1.22	1.15		1.05

* Voltage from capacitance potential divider

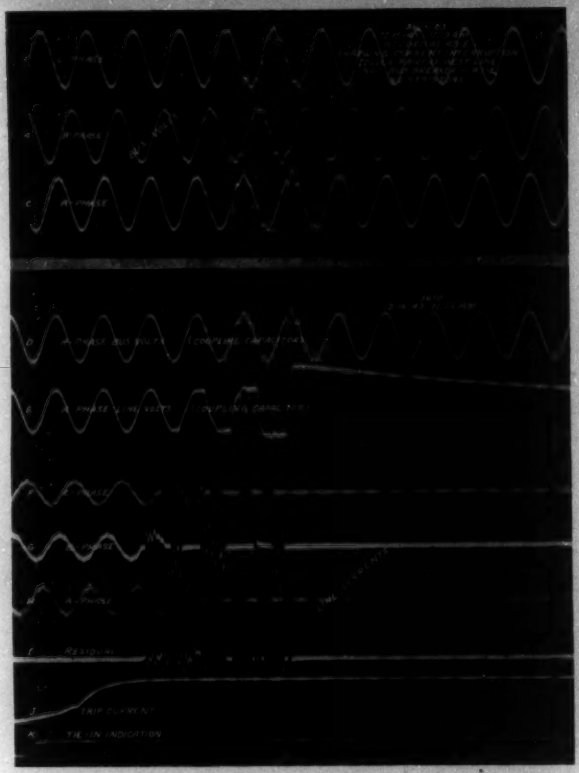

(A)

A—Oscillograms 3,618-03 and 3,618 from receiving station *E*, the switching point

B—Oscillogram 2C18L-W2 from receiving station *D*, the remote end of the circuit

(B)

capacitance divider gives faithful reproduction of the 138-kv circuit voltage. By using capacitance potential dividers available on the line not being switched, comparison of *A*-phase system voltage as recorded by potential transformer and by capacitance divider was obtained. Comparison of these records shows that the potential transformer is satisfactory for recording system voltages at the frequencies encountered in these tests. Circuit currents were obtained from bushing current transformers in the circuit breakers used for switching.

Control of the circuit breaker under test was given the oscillograph and simultaneous operation of the oscillograph at the remote end was accomplished over an initiating circuit set up through communication cable between the two stations. Current in a tie-in circuit was recorded by both oscillographs so records from the two instruments could be identified in time.

Circuit Switching Tests Without Resistors

Thirty-one tests were made in which the Toluca-Fairfax West circuit was de-energized from receiving station *D*. Six of these tests were made with the 7-mile overhead line disconnected at Nichols Canyon. So far as could be determined, however there was no difference in performance with or without this 7-mile line section. The maximum overvoltage recorded on these tests was 1.82 times normal. This occurred on *A*-phase-to-ground system voltage in one of the early tests in which no measurements were made of voltage appearing on the circuit being dropped. In the 19 tests in which measurements of circuit voltage (*A*-phase only) were made, the maximum was 1.58 times normal. Complete data are presented in Table I.

Twenty-one tests were made in which the Toluca-Fairfax West circuit was de-energized from receiving station *E*. The maximum overvoltage recorded in these tests was 2.19 times normal. This occurred on the circuit voltage at the remote end; the corresponding circuit voltage at the end being switched was 2.11 times normal. The maximum system overvoltage recorded on these tests was 1.84 times normal and this occurred on the bus voltage at receiving station *D*; the corresponding bus voltage at receiving sta-

Figure 4. Typical oscillograms showing circuit de-energization from receiving station *E*

Circuit breaker without resistors

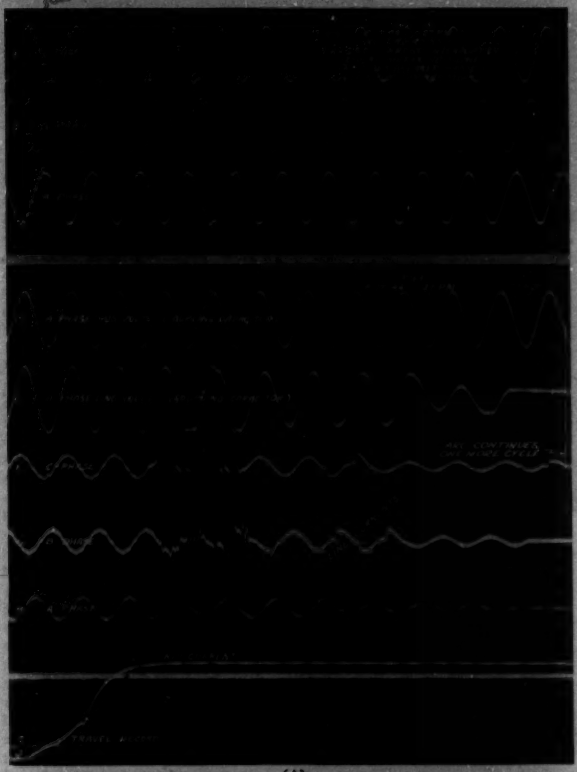

(A)

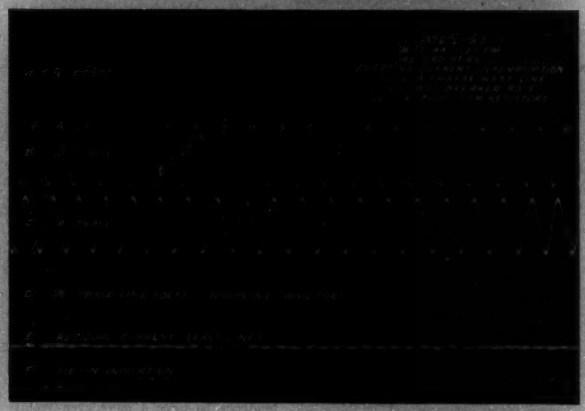

(B)

tion E, the point of origin of the transient, was 1.38 times normal. The higher voltage at the remote station is the result of rise caused by cable-charging current at transient frequency being drawn through the reactance of the 7-mile line (see conclusion 3). Figure 4 presents typical records obtained by de-energization from the receiving station E end. Complete data are presented in Table I.

These tests show that overvoltages from restriking are materially less when the circuit is de-energized from the receiving station D terminal. This arises because of the effect of the capacitance of the other cable circuit which remains connected to the receiving station D bus. The reason for the beneficial effect of capacitance on the system side of the circuit breaker is explained in reference 2.

Circuit Switching Tests With Resistors

The first tests were conducted using a single resistance of 2,000 ohms across the circuit breaker contacts. This gives an R/X_c ratio of 2 on a 5-mile cable and limits the overvoltages produced at the point of circuit interruption to 2.3 times normal in accordance with Figure 8. Amplification of transient overvoltages through system circuits makes a lower value of R/X_c desirable. The step-type resistor was developed next and tests were made using 720–2,000- and 600–2,000-ohm combinations.

The step-type resistor tests were made from the receiving station E terminal. They included four complete circuit de-energizations using the 720–2,000-ohm combination and ten interruptions with the 600–2,000-ohm resistor. The first auxiliary contacts which effect a change from the low to high value of resistance parted two cycles after the main circuit breaker contacts. The second auxiliary contacts which effect final interruption of the circuit parted five cycles later.

The maximum overvoltage recorded in these step-type resistor tests was 1.36 times normal. This occurred with the 720–2,000-ohm resistor and appeared on the bus at the remote station again emphasizing the importance of conclusion 3.

Figure 5. Typical oscillograms showing circuit de-energization from receiving station E

Circuit breaker with 600–2,000-ohm resistors

A. Oscillograms 3,761–03 and 3,761 from receiving station E, the switching point

B. Oscillogram 3,761L-W2 from receiving station D, the remote end of the circuit

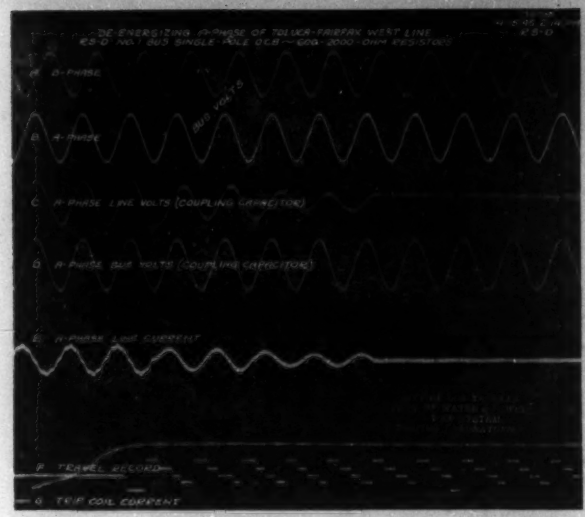

Figure 6. Oscillogram showing interruption of 80-ampere charging current by single-pole circuit breaker with 600–2,000-ohm resistors

Test producing no restrikes

The maximum appearing on the system at the point of circuit interruption was 1.13 times normal and the maximum on the circuit being interrupted was 1.15 times normal. Complete data appear in Table II.

Figure 5 presents typical oscillograms showing interruption of charging current with the circuit breaker equipped with 600–2,000-ohm resistors. These oscillograms show restriking on the main contacts with the attendant disturbance to voltage. They show restriking on the first auxiliary contacts which switch the circuit from 600 to 2,000 ohms, although this restriking produces no disturbance to system voltage. Some restriking occurs on the high-speed 2,000-ohm resistor contacts, but again this has no effect upon system voltage. Comparison of these oscillograms with Figure 4 brings out the beneficial effect of the step-type resistor.

The fact that no overvoltages resulted from restrikes on the contact interrupting the 2,000-ohm resistor current prompted tests to determine if the 2,000-ohm step could be eliminated. Tests were conducted on both the plain-break bayonet and the high-speed bayonet auxiliary contacts. Restriking occurred on both types of contacts and the arcing period was too long to be tolerated in normal operation of the circuit breaker. It was concluded that the step-type resistor is essential for satisfactory performance.

The tests showed that in spite of copious restriking on the contacts interrupting the 600-ohm resistor current, no overvoltage results from this restriking. The 600-ohm resistance gives an R/X_c ratio of 0.6 for a 5-mile cable circuit. It is quite likely, judging from these tests, that a considerably lower ratio of R/X_c must be reached before overvoltages will appear as a result of direct interruption of the resistor current (see conclusion 4).

Single-Phase Switching Tests

The normal speed of the crosshead in the circuit breakers on the Toluca-Fairfax circuits is 2.37 feet per second. To get an increased speed for test purposes, the full kicker-spring action was applied to one pole by disconnecting the remaining two poles from the circuit breaker control mechanism. This increased the crosshead speed to 5.3 feet per second.

Tests were conducted at receiving station D and the 600–2,000-ohm resistors were used. Single-pole operation enabled tests switching charging currents of 80, 160, and 240 amperes by using one phase of the cable circuit, then two and three phases, respectively, in parallel.

Six oscillograms covering the interruption of 80 amperes were taken, and restriking on the main circuit breaker contacts occurred on only two tests. Figures 6 and 7 show conditions with no restrikes and with restrikes respectively. Comparison of Figure 7 with Figure 5 shows the improvement gained by high contact speed.

Five oscillograms were taken interrupting 160-amperes charging current or the equivalent of ten miles of 138-kv cable circuit. With the 600-ohm resistor this is an R/X_c ratio of 1.2. A single restrike on the main contacts occurred on each of the five tests. Restriking occurred on all four tests made interrupting 240 amperes, which represents an R/X_c ratio of 1.8 or the equivalent of 15 miles of cable.

The tests with the single-pole circuit breaker demonstrate the improvement obtained by increasing contact speed. It is doubtful, however, if any great increase in speed is justified purely from a charging-current interruption standpoint as resistors, which have to be installed anyway because of the randomness of restriking, put a definite limit to the value of overvoltage produced.

This series of tests with the three values of charging current gives an empirical demonstration of the increase in overvoltages with increase in value of the ratio R/X_c. The maximum overvoltages obtained in the three cases were 1.04 times normal for 80 amperes ($R/X_c = 0.6$), 1.16 times normal for 160 amperes ($R/X_c = 1.2$), and 1.67 times normal for 240 amperes ($R/X_c = 1.8$). These actual values are appreciably lower than the theoretical values shown in Figure 8 partly because of the beneficial effect of the other cable circuit connected to the bus.

Short-Circuit Performance

This section of the paper discusses and reports the short-circuit performance of resistor-equipped circuit breakers. The application of resistors to a circuit breaker does not delay clearing system faults. It is true that the resistor delays actual disconnection of the circuit by several cycles, but the system is relieved of the fault just as quickly with the resistor-equipped circuit breaker as it is without resistors. The short-circuit performance of the main interrupting elements of the circuit breaker is in no way adversely affected by the use of the type of resistors described in this paper. However, outside of a tendency to force a more even voltage distribution over the interrupting ele-

ments of the circuit breaker, resistors have little beneficial effect on the interruption of fault currents.

Consider, for example, a short circuit on a 138-kv system involving a current of 8,000 amperes to be interrupted with a circuit breaker equipped with 800–2,000-ohm step-type resistors. The opening of the main circuit breaker contacts inserts the 800-ohm resistor in the circuit, and this resistor limits the current to 80,000/800 or 100 amperes. The resistor current is in phase with the voltage whereas the short-circuit current is lagging, making the difference current which the main contacts are required to interrupt still 8,000 amperes for all practical purposes. The duty on the main contacts, therefore, is unaffected by the presence of the resistor. Furthermore, the drain from the system is reduced from 8,000 to 100 amperes so the short-circuit disturbance is removed effectively from the power system by the operation of the main circuit breaker contacts. Final disconnection of the circuit does not take place until the 2,000-ohm resistor current of 40 amperes is interrupted by the second auxiliary contacts about four cycles later.

One pole of a circuit breaker equipped with 600–2,000-ohm resistors was subjected to actual short-circuit tests to demonstrate ability of the resistor to sustain this duty. The short-circuit tests consisted of five opening operations and four closing-opening operations. Oscillograms of the short-circuit tests showed satisfactory performance of the auxiliary contacts, and the resistor upon inspection gave no indication of excessive heat or deterioration.

Appendix. Protection Against Overvoltages Afforded By Resistors on Capacitor Switching

The insertion of resistance in series with the circuit as the main contacts of the circuit breaker part provides a path for discharge of the capacitor permitting decay of its voltage. Capacitor voltage thus tends to follow system voltage to an extent dependent upon the value of resistance, thereby reducing the value of the voltage across the circuit breaker contacts. This not only reduces the probability of restriking but reduces the value of overvoltages produced by restrikes when they do occur.

The protection afforded by resistors across circuit breaker contacts can be determined by an analysis of the circuit characteristics. This treatment of the situation uses the following symbols:

E_{m_s} = maximum instantaneous value of system voltage

e_s = instantaneous value of system voltage

R = ohmic value of resistance across circuit breaker contacts

C = farad value of line, cable, or capacitor

X_c = ohmic value of line, cable, or capacitive reactance

$\varphi = \tan^{-1} X_c/R$

E_{m_c} = maximum instantaneous value of voltage across X_c

e_c = instantaneous value of voltage across X_c

e_R = instantaneous value of voltage across R

$\epsilon = 2.71828$, the base of natural logarithms

t = time in seconds from instant R is effectively inserted in the circuit

E_{t1} = value of transient voltage on first restrike

E_{t2} = value of transient voltage on second restrike

E_{tc} = value of transient voltage on closing

The problem may be handled by expressing conditions of the circuit as the circuit breaker main contacts part to insert resistance in series with the line or cable X_c. Tests show that regardless of the point on the voltage cycle at which the high-voltage circuit-breaker contacts part, no significant change in current flow takes place until a zero value in the current cycle is reached. This makes it convenient to express system voltage by

$$e_s = E_{m_s} \cos \omega t \qquad (1)$$

as this expression has a value E_{m_s} when $t = 0$, the time at which the circuit change takes place.

At this time the instantaneous value of voltage across the capacitor must also be E_{m_s} but it immediately begins to change to a final value which may be expressed by

$$e_c = E_{m_c} \sin (\omega t + \varphi) \qquad (2)$$

In going from the one value to the other it passes through a transient state as the capacitor, which finds itself with more than enough voltage to satisfy the new steady-state conditions, begins to discharge through the resistance. The time constant of this transient discharge is determined by C and R. The complete expression for e_c is

$$e_c = E_{m_c} \sin (\omega t + \varphi) + (E_{m_s} - E_{m_c} \sin \varphi) \times \epsilon^{-t/RC} \qquad (3)$$

Equation 3 was demonstrated correct by oscillographic tests on miniature circuits in the laboratory.

The voltage which appears across the open contacts of the circuit breaker is the difference between e_s and e_c.

$$e_R = E_{m_s} \cos \omega t - E_{m_c} \sin (\omega t + \varphi) - (E_{m_s} - E_{m_c} \sin \varphi) \epsilon^{-t/RC} \qquad (4)$$

For the first restrike that might occur, the theoretical value reached by the transient voltage is the sum of the instantaneous value of system voltage and the voltage across the circuit breaker.[8]

$$E_{t1} = 2E_{m_s} \cos \omega t - E_{m_c} \sin (\omega t + \varphi) - (E_{m_s} - E_{m_c} \sin \varphi) \epsilon^{-t/RC} \qquad (5)$$

This expression may be simplified and brought to unit voltage basis by making $E_{m_s} = 1$ and expressing E_{m_s} in terms of E_{m_s} and the angle φ.

$$E_{t1} = 2 \cos \omega t - \sin \varphi \sin (\omega t + \varphi) - (\cos^2 \varphi) \epsilon^{-t/RC} \qquad (6)$$

Figure 7. Oscillogram showing interruption of 80-ampere charging current by single-pole circuit breaker with 600–2,000-ohm resistors

Test producing restrikes

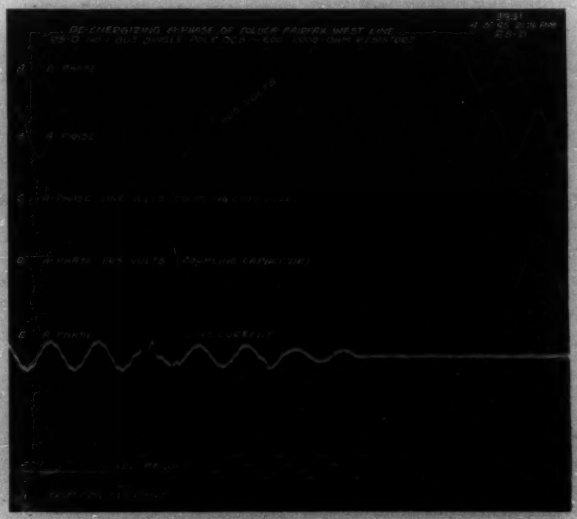

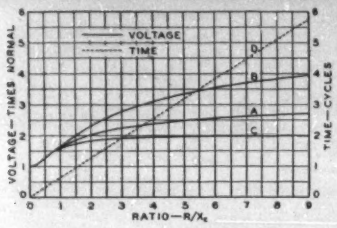

Figure 8. Overvoltage protection obtained by resistors on capacitive switching

A—Overvoltage resulting from first restrike

B—Overvoltage resulting from second restrike

C—Overvoltage resulting from energization

D—Time that resistor should be in circuit on energization

The value of t for zero value of the differential of this equation establishes the maximum value of the transient overvoltage that occurs from a first restrike. Theoretically it can be argued that the most likely time for the restrike to occur is when the voltage across the circuit breaker contacts E_R is a maximum, but practically the "randomness" of the restriking performance may allow a restrike at some other time. It is believed, therefore, that the most pessimistic view should be taken for a design basis and the maximum E_{t1} should be determined irrespective of the voltage across the circuit breaker contacts. Actually for values of $R/X_c=2$ and above, the maximum value of E_{t1} occurs practically simultaneous with the maxium value of e_R but as the value of R/X_c de creases below 2 this is not the case. Field experience with a ratio of $R/X_c=0.6$ gave overvoltages, whereas no overvoltages should occur with this ratio under the premise that the circuit breaker does not restrike after e_R reaches its maximum. In this discussion, therefore, the pessimistic view is taken.

The differential of equation 6 is difficult to solve for t so the maximum values of E_{t1} were determined graphically for various values of φ. For this work it is convenient to express RC of equation 6 in terms of φ.

$$E_{t1}=2\cos\omega t-\sin\varphi\sin(\omega t+\varphi)-(\cos^2\varphi)\epsilon^{-2\pi\theta t\tan\varphi} \quad (7)$$

From the graphical determination of E_{t1} for various values of φ, the curve A of Figure 8 was plotted. This curve shows the theoretical maximum overvoltages that can occur as a result of one restrike for various values of R/X_c.

Curve B of Figure 8 shows the theoretical maximum overvoltages that can result from a second restrike. The curve is based, of course, upon the pessimistic point of view that the first restrike occurs at a time that gives maximum E_{t1} and further that the restriking arc is interrupted at the first current zero of this transient.

Curve B is based upon equation 8 which was developed by a process similar to that used to obtain equation 7.

$$E_{t2}=2\cos(\omega t+\theta)-\sin\varphi\sin(\omega t+\varphi+\theta)-[E_{t1}-\sin\varphi\sin(\varphi+\theta)]\epsilon^{-2\pi\theta t\tan\varphi} \quad (8)$$

The angle θ in this expression is $(180-\omega t)$ where t has the value which gave maximum overvoltage E_{t1} on the first restrike. It is determined graphically from equation 7.

The protection from overvoltages afforded by the resistor when energizing a capacitive circuit is of interest as a theoretical maximum of two times normal is possible without resistors. In order that minimum overvoltage be assured on energization the resistance must be in the circuit for a sufficient time to allow the energizing transient to die down to an insignificant value before the main contacts of the circuit breaker close.

The conventional time constant of a circuit represents the time required for the transient to decrease to 0.368 of its initial value. This is the value of ϵ^{-1} and is too high for the case at hand, so ϵ^{-4} was selected arbitrarily. This gives a factor of 0.02 for the initial transient which is negligible.

In the case of the capacitor-resistor circuit, the transient term is $\epsilon^{-t/RC}$ and the time t for the transient to decrease to 0.02 of its initial value may be obtained for any particular values of R and C by equating $-t/RC=4$. If t is expressed in cycles on a 60-cycle-per-second basis then

$$t=0.637R/X_c \text{ cycles} \quad (9)$$

Curve D of Figure 8 was plotted from this expression and shows the time in cycles that the resistance must be in the circuit on the closing operation if the overvoltages incident to closing the main circuit breaker contacts are to be limited to the values shown by curve C of the same figure.

Curve C was obtained from equation 6 after eliminating the transient term.

$$E_{t_c}=2\cos\omega t-\sin\varphi\sin(\omega t+\varphi) \quad (10)$$

This expression may be expanded and differented with respect to t.

$$E_{t_c}=2\cos\omega t-\sin\varphi\cos\varphi\sin\omega t-\sin^3\omega\cos\omega t$$

$$\frac{dE_{t_c}}{dt}=-2\sin\omega t-\sin\varphi\cos\varphi\times\cos\omega t+\sin^3\varphi\sin\omega t \quad (11)$$

The value of t at which E_{t_c} is a maximum is found by equating this differential to zero

$$\frac{\cos\omega t}{\sin\omega t}=\frac{\sin^3\varphi-2}{\sin\varphi\cos\varphi}$$

$$\cot\omega t=\frac{\sin^3\varphi}{\sin\varphi\cos\varphi}-\frac{2}{\frac{1}{2}\sin 2\varphi}$$

$$=\frac{\sin\varphi}{\cos\varphi}-\frac{4}{\sin 2\varphi}$$

$$\omega t=\cot^{-1}\left(\tan\varphi-\frac{4}{\sin 2\varphi}\right) \quad (12)$$

Equation 12 gives the values of t to substitute in equation 10 to obtain maximum values of E_{t_c} for various values of φ and as the angle φ is determined by R and C, this procedure gives data for curve C of Figure 8.

The curves of Figure 8 are convenient as they enable a quick determination of the theoretical limits to the maximum overvoltages obtained by using resistors in any particular application.

References

1. Switching Overvoltage Hazard Eliminated in High-Voltage Oil Circuit Breakers, **Lloyd F. Hunt, E. W. Boehne, H. A. Peterson.** AIEE Transactions, volume 62, 1943, February section, pages 98–106.

2. The Cause and Control of Some Types of Switching Surges, **T. W. Schroeder.** AIEE Transactions, volume 62, 1943, November section, pages 696–700.

3. Tests and Analysis of Circuit-Breaker Performance When Switching Large Capacitor Banks, **T. W. Schroeder, E. W. Boehne, J. W. Butler.** AIEE Transactions, volume 61, 1942, November section, pages 821–31.

4. Effect of Restriking on Recovery Voltage, **C. Concordia, W. F. Skeats.** AIEE Transactions, volume 58, 1939, August section, pages 371–5.

5. New 138-kv Cable Lines in Los Angeles, **Carroll G. Mansfield.** AIEE Transactions, volume 63, 1944, pages 1240–9.

6. Dethermalizing Arc Quenchers, **Lloyd F. Hunt, Fred H. Cole.** AIEE Transactions, volume 62, 1943, November section, pages 720–4.

Discussion

W. F. Skeats (General Electric Company, Philadelphia, Pa.): In view of the advantages obtained by the use of resistors in circuit breakers particularly for the interruption of charging currents, when no single value of resistance gives the desired control, one naturally may consider a 2-step resistor. The authors of this paper have used such a resistor and have arranged to operate simultaneously two oscillographs a number of miles apart so as to get an indication of voltages at a point on the system other than that at which the breaker operation takes place.

These measurements have revealed the interesting fact that voltages at remote locations may be higher under some circumstances than at the point at which switching takes place. More surprising is the fact, not commented on by the authors, that these remote voltages were higher with both combinations of 2-step resistors than with the

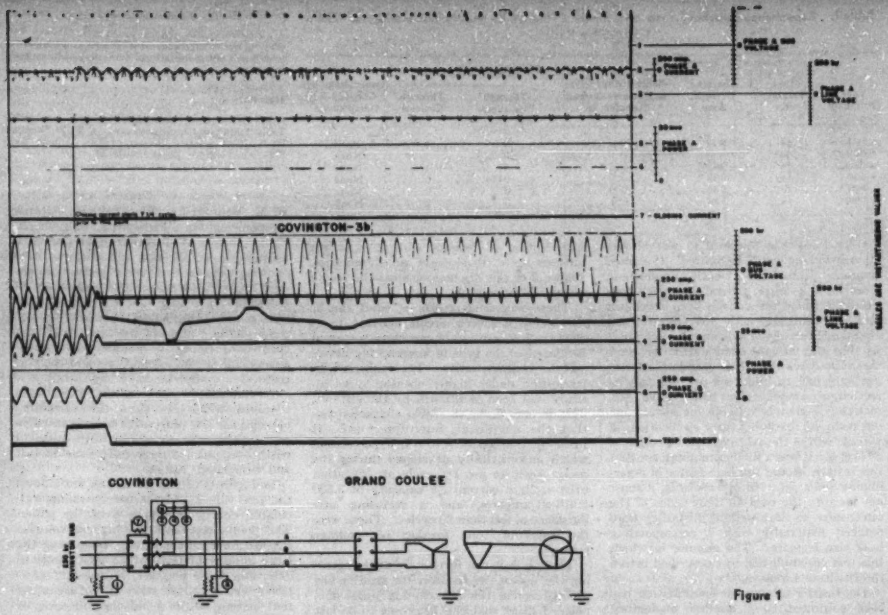

Figure 1

ingle 2,000-ohm resistor. According to Table I, the maximum value for remote voltage was 1.22 with the single 2,000-ohm resistor against 1.36 and 1.25 with the 2-step resistors. It would be very interesting to know whether any explanation of this fact has occurred to the authors.

In attempting to analyze these tests, it also would be helpful to know what the connections were to the rest of the system.

E. W. Boehne (General Electric Company, Philadelphia, Pa.): The authors have presented an interesting paper on the art of interrupting leading current at high voltage. Field tests of the type presented are invaluable in evaluating the effectiveness of the various artifices of interruption. Their paper presents for the first time, data obtained on circuits whose capacitance consisted, in part, of cables. The oscillograms show that the high frequency current following a restrike has little tendency to interrupt following the first loop of high frequency current. This tendency is unusual from the writer's experience and prompts the question as to whether, in the opinion of the authors, this phenomenon is a characteristic of the cable circuits interrupted or a characteristic of the interrupter employed? In any event, it undoubtedly contributed to the low magnitude of surges obtained.

On the basis of lightning surges, arresters are initiated in the neighborhood of three times normal line to neutral crest. However, when the long flat-top voltages accompanying capacitor switching are encountered the lightning arrester initiates at a lower voltage which probably does not exceed 2.3 to 2.5 times normal. This trend is important to the protection engineer and further emphasizes the desirability of keeping high energy switching surges below twice normal voltage crest.

The characteristic of any interrupter unquestionably plays a part in the final determination of the means of accomplishing this goal. The authors are to be congratulated in achieving this result and presenting it in such an able manner. The low values of resistance used to accomplish their result are compatible with the exceedingly low opening speeds given in the paper. In other words, low opening speeds naturally require lower ohmic values of resistance to hold the voltage gradient to a safe level across the opening gap. It follows that much higher opening speeds will allow resistors of much larger ohmic value to produce the same voltage gradient across the opening break. The nominal tested ratio of ohms per pole to capacitive ohms to neutral of two is based upon an opening speed of from 6 to 7 feet per second on contact parting. It is reasonable to expect that this ratio will drop from 2 to 0.6 or 0.8 when the contact opening speed is between 2 and 3 feet per second.

These and other variations between various types of interrupters suggest that a satisfactory result, established by test, be sought for each style of interrupter and that no attempt be made to standardize upon a specific ohmic value of resistance for all field conditions. There is little doubt, however, that for a specific interrupter with a definite opening speed, that the true criterion of the resistance per pole is the capacitive ohms to neutral of the circuit.

Earl B. Rietz (General Electric Company, Philadelphia, Pa.): I believe that the authors should have restated in their introduction the obvious conclusion that the requirements for resistors arise only when there is restriking during capacitance current interruption. I mention this because there is a well-known type of oil breaker which from all the evidence available does not restrike and where one does not have to worry about overvoltages or resistor designs. This is the low oil content impulse breaker and 138-kv breakers of this type are operated by the Department of Water and Power of Los Angeles. Some of these breakers have been in service since 1934 and their excellent performance on capacitance current interruption is unquestioned. Figure 1 of this discussion shows a normal interruption of 200 miles of 230-kv line using the same type of breaker, and attention is called to the positive current clearing trace.

But, there were economic reasons which prevented the universal application of this type of breaker and it has been necessary to devise a means of limiting overvoltages on line switching for the tank type breaker designs. This problem came to a head in 1941 on the 230-kv Boulder Dam breakers and a description of the solution is included in the authors' references. A similar solution has been worked out for the 115- to 161-kv breakers. Therefore, for the past several years all General Electric breakers, 115 to

Table I. Capacitance Switching Tests on a Single 115–161-Kv Multibreak Interrupter With a 1,350-Ohm Resistor

Test Number	Test Voltage, Kv	Charging Current, Amp	Contact Separation at Resistor Current Transfer, In.	Number Restrikes: Through Interrupter	Number Restrikes: Through Resistor	Overvoltage by Cathode-Ray Oscilloscope
991	44	142	0.1	0	0	None
992	44	138	0.3	0	1	None
993	44	132	0.3	0	1	None
994	44	132	0.0	0	0	None
995	44	132	0.0	0	0	None
996	44	138	0.1	0	2	None

230 kv, have been equipped so overvoltages from switching would be limited. It seemed impractical to study each application. Therefore, a more general approach was necessary and a resistor has been developed and co-ordinated with the interrupting characteristics of the multibreak interrupter so that the integral combination will give the desired results. This standard resistor not only had to limit the overvoltages on capacitance switching but had to have thermal characteristics suitable for instantaneous reclosing involving three applications of voltage within the relatively short period of 20 cycles. It was a further requirement that this resistor should not be a factor in determining tank size. In other words, it must not increase the over-all dimensions of the interrupter so that striking distances were reduced materially with a corresponding tank size increase. The manner in which this was accomplished was described before the Institute a year ago.[1]

The resistor-interrupter combination has been subjected to a number of factory switching tests. Cathode-ray oscillographs were used to measure the transient voltage conditions as it is considered that these give a much more accurate picture than the slower acting magnetic oscillographs.

Table I is a tabulation of tests made with 44 kv across a single interrupter equivalent to one-half of leg voltage at 154 kv. They are of interest because from a voltage and capacity standpoint, they represent a more severe condition than described by the authors where the charging current was only 80 amperes against the 130 amperes on these tests. There was no restriking recorded in the initial circuit interruption within the interrupter. Therefore, there were no overvoltages. Current transfer almost at the time of main contact separation illustrates the inherent ability of multibreak interrupters to interrupt light currents and avoid restriking. On one of these tests, there are two restrikes recorded before the interruption of resistor current. As the authors state, these have no significance. Figure 2 of this discussion shows the record of this operation.

These successful results on what can be considered a severe circuit indicate to us that the interruption of capacitance current is related to the type of interrupting device and its characteristics. The improved interruption under higher opening speed already had been mentioned by the authors. This is one of the desirable characteristics that the multibreak interrupter has. It works at a speed of 7 to 8 feet per second which automatically developed during the design tests to get $1^1/_2$-cycle arc duration even at light currents, a capacity of 3,500 millivolt-amperes, and a reclosing performance of less than 20 cycles. Those were the goals of "one breaker per voltage rating".

There is just one further thought regarding the use of the resistors for grading the voltage across the interrupting units of a pole. I think that this has come to be just as important a use for them as the one described in this paper. Minimum interrupting times demand that each interrupter be used to its fullest efficiency so that the voltage to be interrupted is shared equally. Why take longer times because of unequal distribution? Graded interrupters also seem to present the logical approach to supervoltages and superratings. Each unit can be tested more easily to capacity and when connected in series will give reasonable assurance of meeting rating.

Summarizing,

1. The oil impulse breaker has not evidenced any restriking on capacitance current interruption and therefore would represent the best answer for capacitance switching.

2. All General Electric high-voltage tank-type oil breakers are now furnished with interrupters and built-in resistors to avoid restriking.

3. The excellent performance of these modern breakers on line switching results from proper co-ordination of the interrupter and resistor designs.

4. Resistors also reduce interrupting times by grading the voltage across the interrupting elements which will aid materially in extending voltage and interrupting limits.

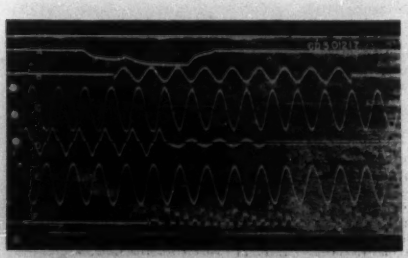

Figure 2

REFERENCE

1. A NEW LINE OF HIGH-VOLTAGE OUTDOOR TANK-TYPE OIL CIRCUIT BREAKERS, W. F. Skeats, E. B. Rietz. AIEE TRANSACTIONS, volume 65, 1946, April section, pages 224–31.

R. C. Van Sickle (Westinghouse Electric Corporation, East Pittsburgh, Pa.): E. K. Sadler and T. M. Blakeslee have presented an important collection and study of data showing the effects of using resistors in circuit breakers to reduce the magnitude of transient switching overvoltages. Such data made during actual switching on systems, can be compared with calculated and theoretical values to validate the assumptions made in the calculations and the correctness or completeness of the theory.

As mentioned by the authors, the voltages obtained were less than the calculated maximums, the differences being caused in part by the presence of a parallel cable. I wish to emphasize these differences in test and calculated values.

In Figure 3 of this discussion are plotted the test values and the corresponding calculated curves of Figure 8 of the paper. The points represent the highest voltages reached for each condition. Because of the large number of tests which were made to determine these voltages, we have an additional strong confirmation of the argument that because of the modifying influences of breaker characteristics and circuit damping, the actual voltages reached while switching capacitive currents are much lower than predicted by calculations.

D. J. Marsden (Westinghouse Electric Corporation, San Francisco, Calif.): E. K. Sadler and T. M. Blakeslee are to be complimented for the paper just presented. The field test data relative to potential phenomena substantiates, at least qualitatively, the theoretical aspects of the problem, and are most interesting from the fundamental viewpoint. Inasmuch as electric circuits of this nature are difficult if not impossible to duplicate on a full scale basis in manufacturer's laboratories, it becomes essential to the industry that field tests such as these be made. This applies particularly in regard to tests such as those covered by this paper, as well as problems involved in switching long unfaulted high voltage transmission lines.

Resistors for voltage control have been applied to power circuit breakers for many years. The work covered by the paper just presented appears to be the first American application of the step type resistance principle to power circuit breakers of this rating.

In work of this character it should be kept in mind that the electrical and mechanical design of the resistor assembly must be considered very carefully in order to prevent the insertion into an otherwise fundamentally good design of a hazard even greater than that resulting from switching surges. This remark applies particularly in regard to shielding, increase in space requirements

and the associated reduction of electrical clearances, the mechanical complication of auxiliary "snap-action" contacts, and the relative location of the two resistor assemblies required in the step type design. Specifically in regard to the latter, following interruption of the current through the 600-ohm resistor, the bottom of this resistor assumes the same potential as the top, so that full potential appears between the bottom of the two parallel resistors, which appear from Figure 1 to be located quite close together. Furthermore, because of space requirements, it may prove quite difficult to apply this step type resistor to breakers included in the general design trend toward reduction of oil content of tank type oil circuit breakers.

Considering the 49 cable switching operations that were made without employing interrupter shunting resistors in which only one test indicated transient voltages more than two times normal and that equal to approximately 2.2 times normal, it becomes difficult to justify the increase in cost and complication of the step type resistor as compared with a single resistor unit of moderate ohmic value. Perhaps the authors would comment further on this point.

Complete information is not available in regard to the influence of low ohmic value resistors employed in circuit breakers applied to high speed reclosing duty. In asmuch as the mechanical problems relative to high speed breaker reclosing are being solved gradually, the speed at which the reclosing cycle may be adjusted is limited only by the deionization time of the temporary fault. Furthermore as the relay operating times and breaker interrupting times have been decreased to values of the order of 3 to 5 cycles, adding a deionization time of about 8 cycles of 138-kv service makes possible successful reclosing within only 12 cycles after the initial tripping impulse. However, if complete opening of the circuit is delayed several cycles by the use of resistors, the minimum reclosing time thereby is affected adversely.

In view of the excellent progress that has been made by design engineers in recent months toward improvement in the interrupting and charging current performance of oil circuit breakers it appears to me that we should guard against halting this development work by prematurely accepting the low ohmic value resistor as a total and complete solution to the charging current interrupting problem as contrasted with developments in design which offer comparably low switching surge overvoltages. Perhaps the low ohmic value resistors should be applied only in those instances where, either because of interrupter design or special circuit conditions, transient voltages as high as three times normal are likely to occur.

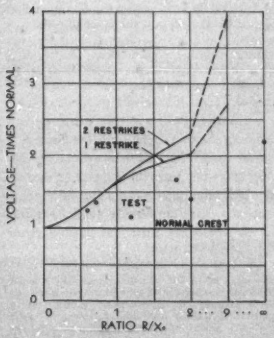

Figure 3

Figure 4. System connections for cable switching tests

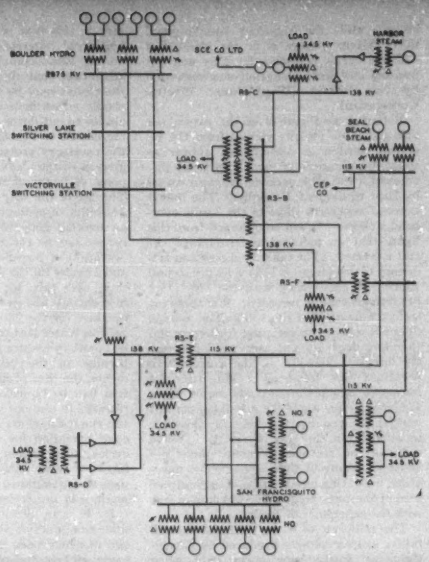

E. K. Sadler and **T. M. Blakeslee:** In response to the suggestion of W. F. Skeats, Figure 4 is presented with this closing discussion to show the main connections for these cable-switching tests. In addition to the generating units shown there are a few small generating sources, both hydro and steam, which tie in to the receiving station 34.5-kv load networks. The number of generating units connected at the various times the tests were made was subject, of course, to the demands of the system at the time. The rated capacities of the synchronous units shown on the diagram are Boulder, 495 megavolt-amperes; San Francisquito plants, 129 megavolt-amperes; Seal Beach, 81 megavolt-amperes; Harbor, 81 megavolt-amperes; frequency changer at *RS-C*, 60 megavolt-amperes; synchronous condensers at *RS-B* and *RS-E*, 60 megavolt-amperes each; and synchronous condenser at *RS-A*, 30 megavolt-amperes.

The Boulder 287.5-kv transmission line sections are each approximately 90 miles in length. The 115-kv San Francisquito circuits are about 33 miles long, and the Seal-Beach 115-kv circuits are 24 miles long. The 115-kv lines between *RS-E* and *RS-A* are 11 miles long and those between *RS-A* and *RS-F* are 4.5 miles long. The 138-kv connections between *RS-E* and *RS-D* are described in the paper; the 138-kv lines between *RS-F* and *RS-B* are 8 miles long, those between *RS-B* and *RS-C* are 11 miles long, and the 138-kv cable connecting Harbor Steam with *RS-C* is 2.4 miles long.

Skeats points out that the maximum value of the voltage at the remote station was greater in the case of the step-type resistor than it was with the single 2,000-ohm resistor and he quotes values from Table II of the paper. This is explained by the fact that the single 2,000-ohm resistor switching tests were made at the receiving station *D* terminal of the circuit. When switching from this end there was no amplification of the transient system voltages. Indeed, the voltages at receiving station *E*, the remote station, were less than the corresponding system voltages at the point of circuit interruption. Furthermore, the magnitude of overvoltages produced by restrikes was limited by the presence of the other cable connected directly to the receiving station *D* bus. Switching from receiving station *E*, however, produced higher system voltages at receiving station *D*, the remote station, because, as stated in the paper, of a rise resulting from cable charging current at transient frequency being drawn through the reactance of the 7-mile line.

E. W. Boehne's question about the failure of the restriking current to interrupt at first current zero is an interesting point. It is primarily a characteristic of the cable circuits interrupted rather than of the interrupter. It will be observed from a study of Figure 4 of the paper, which shows an interruption from the receiving station *E* terminal, that the frequency of the restriking current is in the order of 740 cycles per

second, while the frequency superimposed upon system voltage is in the vicinity of 400–500 cycles per second. This was felt unusual and its explanation was suggested by Ray Witzke (Westinghouse Electric Corporation).

Referring to Figure 3 of the paper, the line and cable circuits viewed from the receiving station E 138-kv bus appear as shown by Figure 5 (presented with this discussion) if the cable sections are represented by their equivalent T circuits. The inductances L represent those of the 7-mile overhead sections. It will be observed from this figure that an inductance–capacitance circuit is formed. The calculated resonant frequency of this circuit is 715 cycles per second which is a good check with the 740 cycles per second actually recorded. It is apparent from the figure that the 138-kv bus voltage does not reflect this resonant frequency and therefore does not put zero voltage across the breaker contacts at the current-zero points of this frequency. This resonant frequency is superimposed, of course, upon the basic frequency of the restriking current which basic frequency is essentially the same as appears on the system voltage. While some of the restriking current pulses are extended, many of them are of short duration, indicating interruption at first current zero of the basic frequency, which is in line with the experience of Boehne.

The criticism of Earl B. Reitz is well taken, as overvoltages produced by capacitor-circuit interruption occur only when there is restriking. The impulse type of circuit breaker mentioned by Rietz was tested on the cable charging current and gave an excellent account of itself. The arc was cleared at first current zero following contact parting and no restrikes occurred. It is, however, obvious that a resistor-equipped breaker limits any overvoltages that may result from circuit energization, although resistors probably could not be justified on this count alone.

D. J. Marsden points out the necessity for careful design in any resistor installation having in mind such factors as shielding, reduction of electrical clearances, and the mechanical complication of auxiliary resistor contacts. There is no question that all of these factors must be considered carefully. In the particular case covered in the paper, shielding of the resistor tubes was not necessary because of the oversize tanks of the breakers involved. Generally speaking, however, shielding of the resistors is worthwhile in order to allow use of minimum tank diameter.

The auxiliary contacts used were necessary in this type of breaker because of the horizontal interrupting elements. While adding some complication they have the advantage that the time the resistor is in the circuit may be controlled easily by the simple adjustment of these contacts. The ability to cut down the time resistors are in the circuit to the minimum required to get the necessary protection from overvoltages gives a distinct advantage from the standpoint of factor of safety against burn-out. The use of the snap-action contact and the flexibility of contact adjustment resulted in an over-all time (dead-time basis) the resistors are in the circuit on a close-open operation of 3 cycles for the 800-ohm step and 5 cycles for the 2,000-ohm step. In contrast with this, for example, is the recent installation of resistors in the circuit breakers for the 230-kv lines of the Metropolitan Water District at Boulder. Although no auxiliary resistor contacts were necessary because of the vertical interrupting elements, the time of normal cross-head operation had to be accepted for switching the resistors in and out of the circuit. As a result the resistors are in the circuit on a close-open operation for an over-all time of 16 cycles. This means that either there is less factor of safety against burn-out or higher values of resistance must be used with a sacrifice in protection against over-voltages.

R. C. Van Sickle's discussion indicates some compunction about the use of resistors and Marsden finds it difficult to justify the increased cost and complication of resistors on the basis of the 49 tests made without resistors wherein only one test resulted in 2.2 times normal voltage. Of these 49 tests, 31 were de-energizations of the circuit from the receiving station D terminal, where the presence of the other cable limits the theoretical voltage build-up to 2 times normal instead of 3 times normal for one restrike. Switching from receiving station E is the most serious situation and the maximum of 2.2 was obtained out of 18 tests switching the circuit from this end. Also it will be recalled from the paper that a lightning arrester failed from overvoltage produced by switching out one of these circuits in normal operation. The failure of arresters is something that could not be tolerated. The manufacturer of the arresters stated that they could be expected to fail under these conditions, so it was apparent that something had to be done. As resistors offered a satisfactory solution, their installation certainly was justified.

As a further comment along this line, papers on switching charging currents have mentioned what has come to be known as

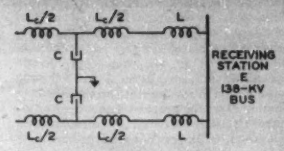

Figure 5. Equivalent diagram of line and cable circuits

"randomness of the restriking phenomena." The test work on the 138-kv cables definitely showed that restriking is a random thing. In addition to this, tests on a self-extinction principle circuit breaker without resistors at Boulder, interrupting charging current at 287.5-kv resulted in the discharge operation of a line lightning arrester once out of 21 tests. Subsequent records of normal operation of this line have disclosed another arrester discharge out of 21 line interruptions. An arrester discharge requires a voltage between 2.2 and 3 times normal and such discharges are likely to be damaging to the arresters.

Automatic reclosing is not in the situation covered by the paper. As Marsden points out, resistors delay the complete opening of the circuit by several cycles and therefore may adversely affect minimum reclosing time. In this connection the ability, previously mentioned in this discussion, of being able to adjust resistor time would offer considerable advantage. Where resistors have an adverse effect in fast reclosing applications, breakers that do not restrike on charging currents must be applied. The discussion by Rietz, however, indicates successful use of resistors in breakers for reclosing service.

As pointed out in the appendix of the paper, the application of resistors not only limits the overvoltages but also reduces the probability of the occurence of restrikes. Data presented in the paper indicate the advantages of high speed. The results of six tests by Rietz gave no restrikes, this performance being attributed to high speed and the use of resistors. Do these six tests guarantee that restrikes will never occur? Because resistors have to be used, it would seem prudent, in view of the random nature of restriking in a self-extinction principle circuit breaker, to use the value of resistance which establishes the desired limit to overvoltage, should restrikes occur. A guarantee of a definite overvoltage limit thus is obtained in any particular application.

Developments in Current Collectors for High-Speed Service

B. F. LANGER
NONMEMBER AIEE

THE CURRENT COLLECTORS used on most electrified railroads with overhead trolleys consist of diamond-shaped pantograph frames which support channel-shaped collectors, or shoes. Figure 1 shows a typical pantograph of the type used in high-speed main line service. The pantograph opens and closes to accommodate major changes in the height of the wire such as occur at bridges and tunnels. It is held up by means of springs. Special cams or linkages in the operating mechanism give the shoe a constant pressure against the wire for a range in height of several feet. Pantographs used in high-speed service also have secondary springs between the frame and the shoe in order to cushion the blows produced by sudden periodic or incidental irregularities, such as hard spots in the catenary. The pantograph of Figure 1 uses two shoes, each of which is supported by a pair of shoe levers, which are held up by spring action. The action of the shoe levers constitutes the secondary springing. The shoes are pivoted freely to the extremities of the shoe levers and thus can rotate about a horizontal axis perpendicular to the direction of motion.

A good current collector must not damage the trolley wire through heavy blows, excessive fatigue stresses, or excessive wear, and must have long shoe life. In order to have these qualities, the shoe must follow the wire smoothly at all speeds. The pantograph frames now in use have been found to operate satisfactorily at all operating speeds as far as following the major variations in wire height are concerned. At speeds above about 70 miles per hour, however, considerable difficulty has been encountered with the behavior of the shoes themselves and their secondary springs. Following are a few of the phenomena which have been observed:

1. At high speeds it is quite common to see a shoe flutter violently against the wire, which results in excessive arcing. Close examination of this flutter has shown that it is not a vibration of the shoe on its secondary springs, but a rotation about a horizontal axis perpendicular to the trolley wire.

2. It is difficult to obtain equal pressures on the two shoes of a double-shoe pantograph. In some of the mechanisms used, such as that of Figure 1, the wind force and wire friction tend to lift the leading shoe and depress the trailing shoe because of the arrangement of the supporting levers.

3. Secondary-spring systems which use pins and links have a tendency to bind and thus nullify the secondary springing.

The present paper describes some studies recently made by the Westinghouse Electric Corporation which have disclosed some of the causes of erratic operation and have resulted in a shoe and shoe mounting which give extremely smooth operation at the highest operating speeds. The engineers who co-operated in this development were H. C. Werner, formerly of the Westinghouse Research Laboratories; J. M. Robinson, section engineer in charge of pantographs and railway gearing; R. O. Heinemann, who designed the apparatus and conducted most of the tests; and the author.

Paper 47-8, recommended by the AIEE committee on land transportation for presentation at the AIEE winter meeting, New York, N. Y., January 27-31, 1947. Manuscript submitted April 1, 1946; made available for printing October 29, 1946.

B. F. LANGER is with the Westinghouse Electric Corporation, East Pittsburgh, Pa.

The Collector Shoe as a Cam-Follower

The problem of making a correct collector follow irregularities in a wire at high speeds immediately suggests the similar problem of the cam follower. Suppose (see Figure 2) a follower of mass M is pressed against a cam by a spring of stiffness K with an average force P_0.

Let the shape of the cam be represented by the function

$$y = y_0 \cos \frac{2\pi x}{l}$$

The relative horizontal velocity between the cam and its follower is

$$V = x/t$$

If

$$\omega = (2\pi V)/l$$

the required motion of the follower is

$$y = y_0 \cos \omega t$$

The acceleration of the follower at any instant is

$$\frac{d^2y}{dt^2} = -y_0\omega^2 \cos \omega t$$

The spring force at any instant is

$$P_0 - y_0 K \cos \omega t$$

The pressure of the follower against the cam is

$$P_0 - y_0(K - M\omega^2) \cos \omega t$$

and this can be kept continuously positive by making P_0 sufficiently large. This means that the follower can be kept in continuous contact with the cam by making the spring setup force sufficiently large, no matter how soft the spring is. A soft spring is better than a stiff spring because it results in less fluctuation of contact pressure. A light follower is also advantageous. Damping in the spring is detrimental because part of the spring force must be used to overcome the damping force.

The essential difference between the

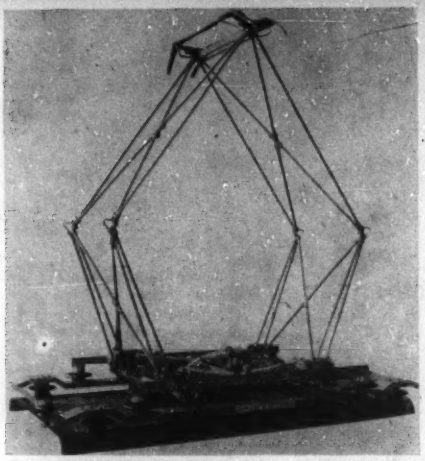

Figure 1. Typical pantograph for high-speed service

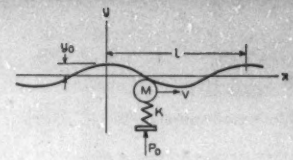

Figure 2. Cam-follower

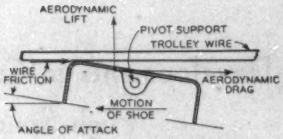

Figure 3. Forces on collector shoe

cam follower and the pantograph shoe is that the pantograph shoe does not follow a fixed path. It pushes the trolley wire up between its supports and thus the amplitude of the oscillation is a function of the magnitude of the wire pressure. The exact solution of such a system involves considerable mathematical difficulty and has not been found necessary.

One phenomenon connected with this system which can be investigated easily, however, is the possibility of the collector shoe attaining a resonant velocity at which the lifting of the wire between supports would become excessively large. This velocity occurs when the speed of the collector equals the speed of propagation of a wave along the wire, and is

$$V = \sqrt{\frac{Tg}{w}}$$

where

V = speed in feet per second
T = wire tension in pounds
g = acceleration of gravity (32.2 feet per second^2)
w = weight of wire in pounds per foot

For a 0000 bronze wire under 4,000 pounds tension (the usual tension at 60 degrees Fahrenheit) this speed is 312 miles per hour. Thus the tension would have to be reduced to about one-tenth normal value to bring the resonant speed to 100 miles per hour.

The Collector Shoe as an Airfoil

When a collector shoe is carried along at high speed it is subjected to considerable wind force. In the conventional construction, a channel-shaped shoe is pivoted about a point below the wire (see Figure 3) and wind forces give it appreciable lift and drag. Because of wire friction, the shoe is tilted to an angle of attack between 0 and 10 degrees, which makes the lift larger than it would be if the contact surface remained horizontal. Wind tunnel tests were made on a conventional channel-shaped shoe with the results shown in Figure 4, curve *A*. The magnitude of the lift force was found to be sufficient to increase the wire pressure by over 100 per cent under operating conditions. This results in increased shoe and wire wear.

Various modifications of the shoe were tried, and the best practical construction was found to be a channel with a slot cut along the top and holes in the flanges. The lift coefficient for this shoe is shown in curve *B* of Figure 4. This shows a worth-while reduction in lift, but the wind tunnel tests disclosed another more important advantage which was entirely unexpected. The solid shoe had a strong tendency to flutter about its pivot support when held in the neighborhood of plus 5-degree angle of attack, whereas the shoe with the slots and holes was quite stable. The flutter observed in the wind tunnel was identical with the type of oscillation which has been observed in high-speed operation.

The flutter which occurs in channel-shaped shoes is an example of a self-induced oscillation. Its causes can be

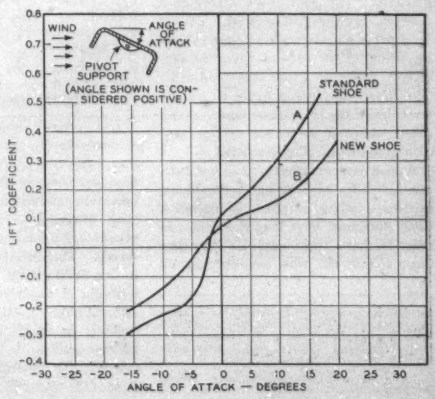

Figure 4. Lift coefficients of standard (solid) shoe section and new section with cutouts

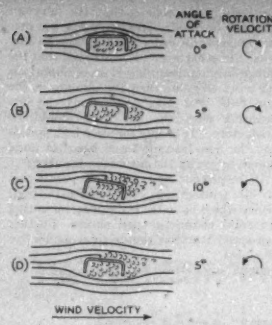

Figure 5. Air flow around collector shoe at various angles of attack

understood by reference to Figure 5. This shows the channel section in the wind stream at various points of the oscillation between 0 and 10 degrees angle of attack. In Figure 5*A* the shoe is horizontal but has started to rotate in a clockwise direction. In Figure 5*B*, it has rotated to an angle of 5 degrees. The flow follows the top surface of the channel because of the rounded corner. Like an airfoil with a positive angle of attack, the shoe has a lift force and an aerodynamic moment. The moment on the shoe is clockwise about the pivot support and aids the rotational velocity. In Figure 5*C*, the angle has increased to 10 degrees, at which point the flow can no longer follow the upper surface of the shoe. This results in a decrease of aerodynamic moment. At this point also, the wire pressure has built up to a sufficient value on the leading edge of the shoe to stop its clockwise rotation and start it back in the second half cycle of the oscillation. In Figure 5*D*, the shoe is passing again through the 5-degree angle, but in the opposite direction. If held in this position for any time, the flow over the top surface would re-establish itself as in Figure 5*B*, but this cannot happen instantaneously. Thus the aerodynamic moment (which now opposes the rotation) is smaller for the condition shown in Figure 5*D* than it was in Figure 5*B*. Therefore, over a complete cycle of the oscillation the aerodynamic moment has put energy into the oscillation because the moment which aids the oscillation is larger than the moment which opposes the oscillation. This results in net energy input and instability.

It can be shown that if the pivot support of the shoe is below the trolley wire, the wire friction also produces instability. The wire friction produces a clockwise moment about the pivot all through the complete cycle. Because of the different flow patterns, however, the aerodynamic lift is greater in Figure 5*B* than in Figure 5*D*. Therefore, the wire friction and the moment which it produces are greater during the half cycle when the moment aids rotation than they are during the half cycle when the moment opposes rotation. If the effective center of rotation of the shoe were above the trolley wire, the direction of the friction moment would be reversed, and the net result of friction would be to damp the oscillation.

The wind tunnel tests showed that the shoe with the slots and holes has not only a smaller lift coefficient than the solid section but also is aerodynamically stable. It is a poor airfoil but a good current collector.

Figure 6. Leaf-spring shoe mounting

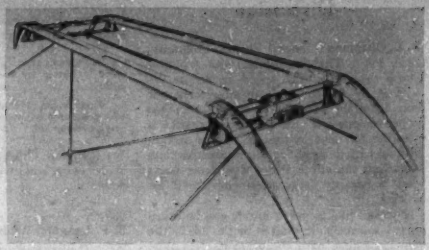

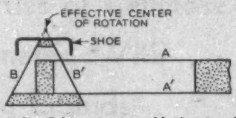

Figure 7. Schematic view of leaf-spring shoe mounting

The Leaf-Spring Shoe Mounting

As a result of the foregoing studies, the shoe and shoe-mounting shown in Figure 6 were designed and built. The shoes contain the slots and holes which gave the lowest lift coefficient and the best stability in the wind tunnel tests. The secondary spring system contains no pins or levers, but is made up entirely of leaf springs. Figure 7 shows this spring system schematically, and Figure 6 in perspective view. Its action is based on the well-known principle that a body supported on two flat springs has an effective center of rotation at the point of intersection of the springs. The horizontal springs *A* and *A′* are parallel to each other and therefore give a vertical flexibility to the shoe without allowing any rotation. Therefore, wire friction and wind resistance do not lift the leading shoe and depress the trailing shoe, as occurs in the conventional shoe-lever mounting.

Rotational flexibility is obtained with the inclined springs *B* and *B′*. The extensions of the center lines of these springs intersect at a point above the wire. Therefore the center of rotation of the shoe is above the point of contact with the trolley wire, and the wire friction force results in stable instead of unstable motion, as previously explained.

Thus the design shown in Figure 6 has the following advantages over conventional constructions:

1. The shoes contain cutouts which give them low lift coefficient and aerodynamic stability.
2. The cutouts in the shoe allow the use of thicker material for equal weight, and thus give greater wearing depth and longer life.
3. The vertical flexibility is obtained with horizontal springs which act as parallel-motion devices. Therefore wire friction and wind resistance do not lift the leading shoe and depress the trailing shoe, as occurs in some double-shoe pantographs.
4. Elastic pivots have been used in place of the usual pin connections to the shoes. These improve the stability by placing the effective center of rotation above the trolley wire.
5. The new mounting contains no sliding surfaces so that all wear is eliminated except at the point of contact with the wire.
6. The springs are practically frictionless so that the full spring force is available for maintaining contact between the shoe and the wire.

A pantograph of the type shown in Figure 6 has been built and tried out in service. Observation at all speeds up to the highest commonly used showed that it justified all expectations. There was no evidence of shoe flutter at any speed, the only arcing being at switches and crossovers. In fact, the operation appeared to be affected only by the condition of the wire, and not at all by the speed. Further service experience is required to prove its mechanical adequacy, but it is believed that this model already has proved the correctness of the principles on which its design is based.

Discussion

R. L. Chapman (General Electric Company, Erie, Pa.): The developments of a pantograph design for high-speed service as described by Langer is quite interesting not only from the point of view that a needed improvement in existing equipment is possible but also in that it can be accomplished with a simplification in construction, including the elimination of wearing parts that previously have been considered essential.

I would like to ask if arcing can be minimized or largely eliminated by the use of the new type shoe with the otherwise old type of pivoted support; or, stated differently, can this development be divided into the following two parts?

1. Improvement in existing pantographs with respect to flutter, by the use of the new type shoe only.
2. Further improvement in over-all performance with decreased maintenance by use of the complete new development.

I feel that Langer and his associates are to be congratulated on a needed job well done.

B. F. Langer: We have not made sufficient tests to answer R. L. Chapman's question positively. We believe that the development can be divided into two parts, but prefer to reverse the order which Chapman suggests. In other words, it is believed that the change in shoe mounting is more important and more effective than the cutouts in the shoe itself. For most applications, the new mounting with the old shoe should be satisfactory. It is only for very high speeds that the aerodynamic force becomes large enough to justify the cutouts in the shoes.

At the present time, we are in production on 30 pantographs for moderate-speed service which have the leaf-spring mounting and solid channel-shaped shoes. Further high-speed tests on the original model are scheduled.

The Dielectric Properties of Cellulose Insulation Impregnated With Semiconducting Liquids

F. M. CLARK
ASSOCIATE AIEE

THE ideal and classical conception of a dielectric material includes the property of zero loss. Such an ideal material has not been realized but its conception has been the motivating influence which has prompted the continued search for dielectrics of the lowest possible loss characteristic. Conversely, it frequently is concluded that liquids of highly conducting characteristics are poorly suited for dielectric application.

Added emphasis is given to the arguments against the use of highly conducting liquids as impregnants of cellulosic electrical insulation by the dictates of experience. When an impregnated insulation fails under conditions of normal commercial usage, the failure invariably is proceeded by the chemical and dielectric deterioration of the insulation. This deterioration most frequently can be traced to changes in the liquid impregnant which are manifested inevitably in a lowered resistivity and increased dielectric loss. But this type of dielectric deterioration in an insulating liquid which is normally of low loss must not be accepted as indicative that all liquids having high loss properties are, ipso facto, of equal hazard. The factors which are involved in the chemical changes leading to higher loss in a liquid normally characterized by low loss usually present a hazard to continued dielectric use for reasons entirely aside from the loss characteristic itself. Mineral oil, for example, may deteriorate in commercial use and lose its initially low loss quality. The complete dielectric failure of the composite paper–oil insulation, however, is more likely caused by the loss of dielectric strength and the consequent formation of destructive corona at the normal voltage rating of the apparatus than to the increased conduction in the dielectric itself up to the point of accumulated heating. Deterioration products in oil which are responsible for this loss in dielectric strength and drop in corona formation voltage include the formation of gases, water, and low molecular weight acids.

The Normal Loss Level

Liquids suitable for the impregnation of cellulosic insulation have a "normal level" of resistivity or dielectric loss to which, in commercial use, they tend to revert from the more highly "refined" value obtained in the laboratory or factory. This "normal level" value varies widely with the chemical type of the liquid, being higher for the hydrocarbon compositions and lower for liquids composed of hydrocarbon substituents, such as the halogenated, nitrated, or esterified compounds. At its normal level of resistivity or dielectric loss, however, the dielectric strength of each class of liquids is high. In fact, because of a more equitable stress distribution, liquids of the lower resistivity or higher loss classification may possess even higher breakdown value than those of the lower loss hydrocarbon group. It is only when a liquid changes from its normal level of loss classification to one of higher loss that serious dielectric hazard is introduced. This hazard is usually traceable to the presence of contamination or products of deterioration which are reflected in an increased dielectric loss, but which to a greater degree affect the chemical stability of the insulation and lead to decreased ionization value and dielectric strength. The increase in dielectric loss, per se, is generally only of secondary importance. The case of mineral oil already referred to is an illustration of this type of hazard.

The object of the present paper is to illustrate the abnormalities which are met when cellulosic insulation is impregnated

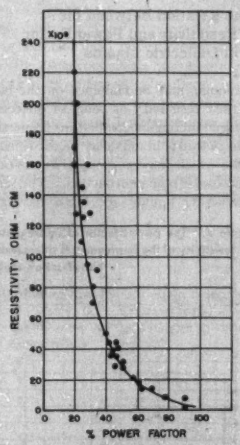

Figure 1. The relation between the resistivity and 60-cycle power factor of a typical dielectric liquid

A 60-cycle power factor measured at 30 volts per mil
Resistivity measured at 500 volts direct current after one minute of electrification

Paper 47-9, recommended by the AIEE committee on electric machinery for presentation at the AIEE winter meeting, New York, N. Y., January 27–31, 1947. Manuscript submitted September 10, 1946; made available for printing October 31, 1946.

F. M. CLARK is technical consultant on insulation and staff assistant to the manager of engineering, apparatus department, General Electric Company, Pittsfield, Mass.

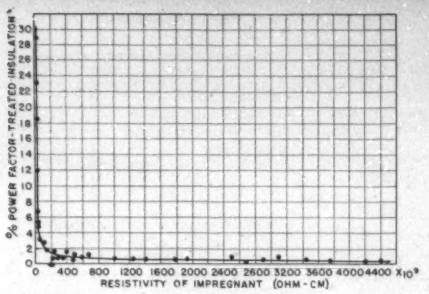

Figure 2. The relation between the resistivity of the impregnating liquid and the power factor of the impregnated cellulose sheet

Cellulose sheet—0.0004-inch kraft capacitor paper
Power factor measured at 60 cycles
Resistivity measured at 500 volts direct current after one minute of electrification

with high-loss liquids. These abnormalities are seized upon in the development of a new type of capacitor which is characterized by a high ratio of electrical capacitance per unit of physical volume. Such a capacitor offers promise of engineering application at voltages above those at which electrolytic capacitors can be used continuously with safety and below those at which the usual paper-spaced oil or askarel-treated capacitor can be used with economy. Such voltages include continuous alternating voltage application at 110 or 220 volts or intermittent voltage application up to and including 440 or 550 volts.

The Relation Between the Resistivity and Power Factor in Dielectric Liquids

Liquids may be classified on the basis of their resistivity as being of dielectric, semiconducting or conducting properties. The dielectric liquids may be classified as those which possess a resistivity greater than 1×10^9 ohm-centimeters. The semiconducting liquids are those having a resistivity lower than 1×10^9 but higher than 1×10^6 ohm-centimeters. Liquids having a resistivity lower than 1×10^6 ohm-centimeters are classed as conducting. The present paper deals primarily with the semiconducting liquids.

The resistivity or specific resistance of a dielectric liquid is the resistance in ohms of a quantity of the liquid one centimeter long and having a cross section of one square centimeter. The power factor is the cosine of the vectorial angle existing between the current and voltage applied to the insulation. It represents the ratio of the dissipated to the apparent power input in a circuit (watts/volt-amperes). In a circuit containing only resistance, the power factor is unity. In a dielectric, the power factor represents the total losses and varies with voltage, temperature, and frequency.

In Figure 1 is represented the normal relation between the 60-cycle power factor and the resistivity of a typical dielectric liquid.

In Figure 2 is illustrated the normally expected relation between the resistivity of the impregnating liquid and the power factor of the treated paper sheet.

The data of Figure 2 are confined to liquid resistivity values contained in the classification of "dielectric." It is this type of relationship which has warned investigators away from the consideration of liquids of even lower resistivity values (the semiconductors).

The Power Factor of Insulation as Related to the Resistivity of the Impregnant in the Semiconducting Range

Kraft paper, when impregnated with a semiconducting liquid having a resistivity in the range from 1×10^6 to 1×10^9 ohm-centimeters, shows marked abnormality in its dielectric power factor. From an extremely high power factor which is characteristic of kraft paper impregnated with a dielectric liquid having a resistivity of about 1×10^9 ohm-centimeters, the power factor of the treated insulation drops with the continued decrease in the impregnant resistivity below 1×10^9 ohm-centimeters. A minimum power factor of about three per cent is obtained when the kraft paper is impregnated with a liquid having a resistivity of about 0.01×10^9 ohm-centimeters (10×10^6). Further decrease in resistivity results in a rapid increase in the power factor of the treated insulation, a power factor of about 80 to 100 per cent being obtained when the impregnant resistivity is 0.001×10^9 (1×10^6) ohm-centimeters or lower.

Figure 3 illustrated the relation between the power factor of the impregnated kraft paper and the resistivity of the liquid impregnant in the semiconducting range (1×10^9 to 1×10^6 ohm-centimeters).

Figure 4 illustrates the power factor of kraft paper as a function of the resistivity of the liquid impregnant over the total

Figure 3. The power factor of impregnated kraft paper decreases as the resistivity of the impregnant is decreased through the semiconductor - classification range

Kraft paper used—0.0004-inch capacitor tissue
Power factor measured at 60 cycles
Resistivity measured at 500 volts direct current after one minute of electrification

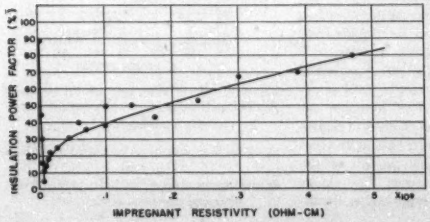

Figure 4. Showing the 60-cycle power factor of 0.0004-inch impregnated kraft capacitor paper as a function of the resistivity of the impregnating compound over the range from 10×10^{13} to 1×10^6 ohm-centimeters

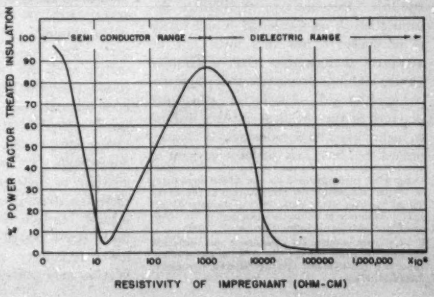

range of dielectric and semiconducting classification. The abnormal power factor behavior in the semiconducting range of impregnant resistivity is illustrated clearly. It is this abnormality which is the subject of further analysis in subsequent paragraphs.

The Test Assembly for Cellulose Sheets Impregnated With Highly Conducting Liquids

Kraft paper impregnated with mineral oil or askarel is widely used as the solid dielectric in high voltage engineering practice. Treated with mineral oil, it is used as the insulation for high voltage cables. It is the most widely used spacer employed in capacitor manufacture. In this application it is commonly treated with askarel, the synthetic noninflammable type of impregnant.

In order to illustrate the dielectric behavior of kraft paper when impregnated with a liquid, it is most convenient to test the treated kraft paper in the form of a capacitor. For this purpose, typical capacitor windings were prepared. The dielectric consisted of two or three sheets of 0.0004-inch kraft paper which were wound between 0.0003-inch aluminum foil armatures. The capacitor windings were of sufficient length to give about $2^1/_2$ microfarads capacity when treated with mineral oil. The rolls were assembled in a standard terne plate capacitor case, the cover with its bushings was soldered in place, and the capacitor dried and impregnated through two holes arranged in the side near the top and bottom. After drying and impregnation these treating holes were soldered to give an hermetically-sealed container conveniently suitable for the detailed testing to which the dielectric was to be submitted. Figure 5 illustrates a typical test assembly.

Tricresyl Phosphate Compositions

Tricresyl phosphate is a liquid which lends itself satisfactorily to the study of the highly conducting liquids of the semiconducting classification. It possesses the following average properties:

Specific gravity (15.5 degrees centigrade compared with water at 15.5 degrees centigrade)	1.182
Saybolt universal viscosity (37.8 degrees centigrade)	107 seconds
Refractive index (25 degrees centigrade)	1.5550

Tricresyl phosphate is characterized by a normal level of resistivity of about 1×10^9 ohm-centimeters at 100 degrees centigrade. This classifies the liquid in the lower dielectric range or the upper range of the semiconducting grouping.

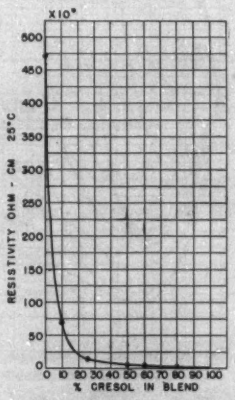

Figure 6. The resistivity of tricresyl phosphate–cresol compositions

When tricresyl phosphate is heated at temperatures above 100 degrees centigrade, it is pyrogenically decomposed with the formation of cresol or cresylic compounds. Such heat-treated compositions have reduced resistivities. Values as low as 1×10^8 ohm-centimeters are obtained when tricresyl phosphate is pyrogenically decomposed at 150 degrees centigrade. It is necessary in order to obtain resistivity values as low as 1×10^8 ohm-centimeters that the tricresyl phosphate be blended with a semiconducting liquid such as cresol. The resistivity of such blends is indicated in Figure 6.

The Power Factor of Kraft Paper Impregnated With Tricresyl Phosphate Compositions

The resistivity change illustrated in Figure 6 produced by the addition of the semiconducting cresol to tricresyl phosphate is reflected in an abnormality in the power factor of treated kraft paper. The power factor of the capacitor assembly described falls rapidly to a minimum of about 3.5 per cent when impregnated with a blend consisting of 20 to 30 per cent cresol in 80 to 70 per cent tricresyl phosphate. This is illustrated in Figure 7. The relationship between the resulting resistivity of the treating composition and the power factor of the treated paper is shown in Figure 8.

The minimum value observed in the power factor of kraft paper impregnated with the semiconducting compositions consisting of tricresyl phosphate and cresol is not peculiar to the cresol component. Using tricresyl phosphate as the solvent, the addition of a wide variety semiconducting solutes in order to decrease the resistivity of the impregnant produces similarly low power factor in the

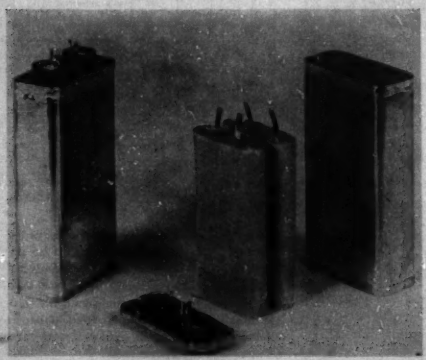

Figure 5 (left)

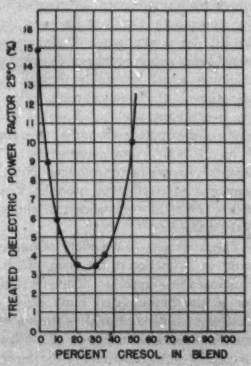

Figure 7 (right). Showing the 60-cycle power factor of 0.0004-inch kraft capacitor paper as a function of the cresol content of the tricresyl phosphate impregnating composition

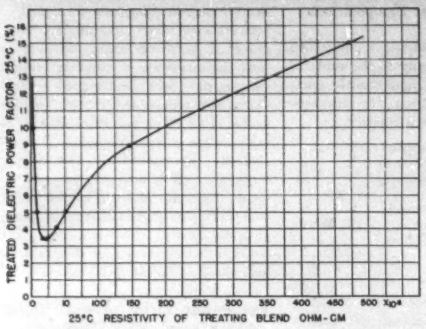

Figure 8. The 60-cycle power factor of capacitor kraft paper when impregnated with tricresyl phosphate compositions decreases to a minimum as the resistivity of the impregnant is decreased by the addition of cresol

treated kraft paper. Such semiconducting solutes comprise the phenols, the amines, the organic acids, and nitro compounds. However, the addition of water and alcohol compounds (glycerine, glycols, and so forth) or compounds having dielectric properties produces little decrease in the power factor of the impregnated kraft paper. The power factor of kraft paper impregnated with these compound blends is illustrated by the data of Figure 9. The relation existing between the power factor of the kraft paper and the resistivity of the impregnating composition is illustrated in Figure 10.

The Power Factor of Kraft Paper Impregnated With Compositions Not Including Tricresyl Phosphate

The decrease in the power factor of kraft paper impregnated with semiconducting liquids is independent of the use of tricresyl phosphate. The important factor producing this desirable result is the resistivity of the impregnating composition. As the resistivity of the semiconducting impregnant decreases from the upper limit 1×10^9 to its lower limit 1×10^6, the power factor of the impregnated kraft paper decreases steadily to a minimum which invariably, despite wide variations in the chemical composition of the impregnant, is obtained with a resistivity of the impregnant in the range from 1 to 20×10^6 ohm-centimeters. The minimum power factor obtained with the impregnated kraft paper, however, varies widely with the composition of the impregnant used.

The resistivity of a variety of impregnants as a function of the composition is illustrated in Figure 11. The power factor of the impregnated kraft paper as affected by the composition of the impregnant is illustrated in Figure 12. Figure 13 correlates the resistivity of the impregnating composition and the power factor of the treated kraft paper dielectric. The composition of the impregnants used and the impregnant resistivity corresponding to the lowest power factor obtained for the treated kraft paper in each case is summarized in Table I.

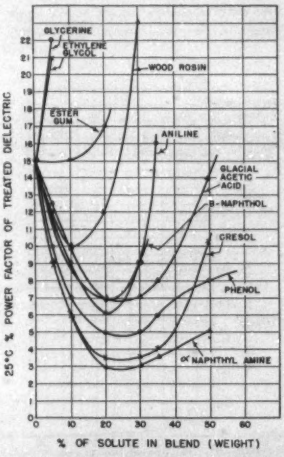

Figure 9. The power factor of the impregnated kraft paper is decreased by the addition of various types of semiconducting compounds to tricresyl phosphate used for the impregnation of the paper

Table I

Impregnant and Per-Cent Composition	Minimum Kraft Paper Power Factor, Per Cent	Resistivity of Impregnant at Lowest Kraft Paper Power Factor, Ohm-Centimeters
Cresol (47)–dibutyl phthalate (53)	4.7	4×10^6
Dibutyl tartrate (85)–dibutyl phthalate (15)	7.2	15×10^6
Cresol (11)–dibutyl tartrate (89)	4.5	20×10^6
Nitrobenzene (80)–cable oil (20)	5.1	2×10^6

The Effect of the Paper Spacer

The power factor characteristics described in the foregoing paragraphs for kraft paper impregnated with a semiconducting liquid are not characteristic of all insulations so treated but are markedly affected by the type of cellulosic sheet which is studied. Within the type classification of kraft paper, wide variations in the power factor of the treated sheet are produced as the result of physical changes in the sheet itself. In Figure 14 is illustrated the change in the power factor of the impregnated kraft paper which is associated with change in the density of the paper sheet.

More remarkable, however, is the effect produced by change in the chemical nature of the dielectric cellulosic sheet. Each type of paper, although subject to variation in power factor as the result of changes in the sheet itself (density and air resistance) has nevertheless a minimum power factor value which is characteristic of the paper used. As illustrated in Table II, among all of the sheet insulations tested, kraft paper sheets are characterized by the lowest power factor values.

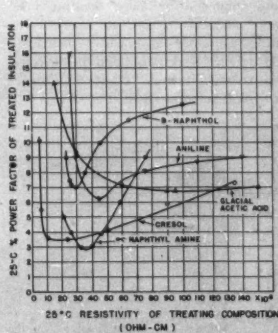

Figure 10. Although the power factor of the impregnated kraft paper is decreased by the addition of a wide variety of semiconductor compounds to the tricresyl phosphate used for the impregnation, the minimum power factor obtained for the impregnated paper is affected by the type of semiconductor compound used

Equally interesting is the effect produced when a "mixed" dielectric pad is impregnated with a semiconducting liquid. Using a cresol tricresyl phosphate blend having a resistivity of 15×10^8 ohm-centimeters, capacitors containing alternate sheets of kraft paper and cotton or linen paper were prepared. By varying the number and thickness of the various sheets, the percentage of kraft paper has been varied over a wide range of dielectric composition. As the percentage of kraft paper present in the dielectric pad is increased in this manner, the high power-factor characteristic of the linen and cotton paper when used alone is reduced radically. Figure 15 illustrates the relation established. With dielectric pads consisting of 50 per cent or more of kraft paper, the power factor relation to the decreasing concentration of the second sheet is not affected by the chemical nature of the latter (cotton or linen).

The Capacitance Effect

It is an axiom that to obtain the lowest dielectric loss (power factor) in a heterogeneous dielectric such as an impregnated paper, a dielectric liquid of relatively low dielectric constant must be used. This results in part from purely electrical factors involving the molecular effects which accompany increase in the dielectric constant; but from a practical standpoint this results largely because of the greater solvent action increasingly possessed by liquids having dielectric constants of the higher magnitudes. Small increments in solvent contamination may seriously affect the initially high liquid resistivity with resultant increase in the power factor of the treated dielectric.

The high microfarad capacitance values obtained with cellulosic insulations impregnated with the semiconducting liquids belie the low dielectric constant characteristic of the individual component or components of the composite dielectric. Cellulose is attributed a dielectric constant value in the range from 5 to 7. Tricresyl phosphate has a dielectric constant of 7. The dielectric constant of ortho- and paracresol is about 6. Yet as the resistance of the liquid impregnant of kraft paper is decreased from 1×10^9 ohm-centimeters which is characteristic of tricresyl phosphate to a value in the range from 10 to 50×10^6, the capacitance increases to abnormally high values. The relation between the microfarad capacitance of such a capacitor and the resistance of the liquid impregnant (tricresyl phosphate-cresol blends) is illustrated in Figure 16. Figure 17 illustrates the increase in the capacitance of this same type of capacitor when the tricresyl phosphate "solvent" liquid is modified by the use of a wide variety of chemical types of semiconducting solutes. In similar manner the capacitance of dielectrics consisting of linen, cotton, or other cellulosic sheet materials is changed by the use of semiconducting impregnants.

An explanation of this abnormal capacitance behavior is obtained from a study of the effect produced when the clamping pressure applied to the dielectric is changed within wide limits, thereby changing the relative amounts of liquid and solid present in the dielectric pad, as well as changing the total distance between the electrode armatures. As is well known, in a truly dielectric pad, variations of this type are expected to be reflected in a changing electrical capacity of the dielectric assembly. When the cellulose sheet is impregnated with a semiconducting liquid having a resistivity in the range from 10 to 20×10^6 ohm-centimeters, substantially no change in the electrical capacity of the dielectric is observed. This is illustrated in Table III and in the data of Figure 18.

It is apparent that the physical changes introduced in the modifications of the dielectric described in Table III and in Figure 18 cannot involve any change in the dielectric constant of the assembly which would be of sufficient magnitude to explain the results obtained. The answer lies in the peculiarities of the semiconducting liquid. The true capacitance is determined solely by the thickness of the kraft paper dielectric used which is in all cases 0.0004 inch. Modifications in the total

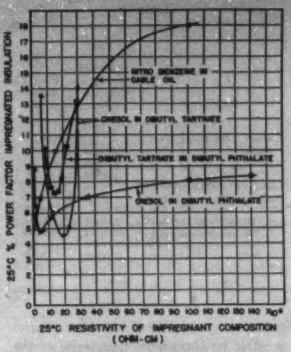

Figure 13. Showing the power factor of impregnated kraft paper as a function of the type and resistivity of the impregnating composition

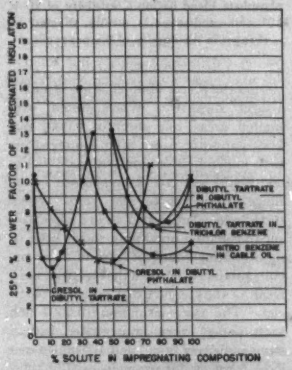

Figure 12. Showing the 60-cycle power factor of the impregnated kraft paper as affected by the composition of the semiconductor impregnant

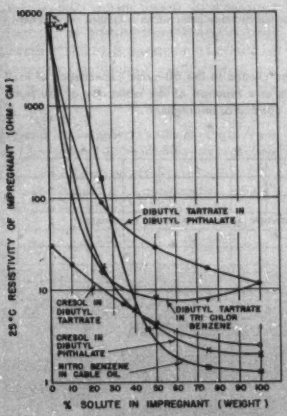

Figure 11. Showing the resistivity of semiconductor liquid blends as a function of their composition

Table II

Consistency of Impregnated Sheet	Range of Minimum Power Factor After Impregnation With Semiconducting Liquid, Per Cent
Linen paper	28–40
Cellate paper	16–23
Cotton	50–60
Cellophane	30–40
Creped kraft	25–35
Kraft	3–6

Table III

Dielectric	Total Dielectric Thickness Between Electrodes, In.	Electrical Capacity, μf
1 sheet 0.0004-inch kraft paper	0.0004	1.0
	0.00044	1.0
	0.0008	1.0
1 sheet of 0.0004-inch kraft paper in series with 1 sheet of:		
0.004-inch cheese cloth	0.0044	1.02
0.005-inch cheese cloth	0.0054	1.04
0.007-inch cheese cloth	0.0074	1.00
0.0075-inch cheese cloth	0.0079	0.98

distance between the electrode armatures is offset by the high conductivity of the liquid impregnant which in effect serves as a high-resistant conductor, thereby effectively bringing the electrode surfaces in close contact with the surface of the dielectric kraft paper sheet. Thus, although the apparent dielectric constant of the assembly is increased greatly by the modifications listed, the real dielectric constant remains unchanged, the abnormal capacitance increase being brought about by the introduction of a liquid electrode.

The Dielectric Strength

It has long been the desire of electrical manufacturers of low-voltage equipment to use a thin 1-sheet dielectric. This has been especially true in the manufacture of low-voltage capacitors rated for operation at voltages not exceeding 110 or 220 volts. The presence of conducting metal or carbon particles in the paper has prevented the practical application of such a 1-sheet dielectric. When tested over limited areas, one sheet of 0.0004-inch kraft capacitor paper after impregnation with mineral oil or similarly good dielectric liquid will give a breakdown in the range from 200 to 400 volts. When tested over a larger area, as in a capacitor, such insulation invariably shows little or no insulating value, because of short circuits produced between the electrodes as a result of the presence of conducting particles. The same insulation (0.0004-inch kraft paper) when impregnated with a semiconducting liquid and assembled in a loose form, as for example, with a total distance between the electrodes about 50 to 100 per cent greater than the paper thickness itself will show the dielectric strength characteristic of the small area tests as normally carried out in the laboratory examination of oil or Pyranol*-treated paper. This is illustrated in the data of Figure 19. At room temperature (25 degrees centigrade), the dielectric

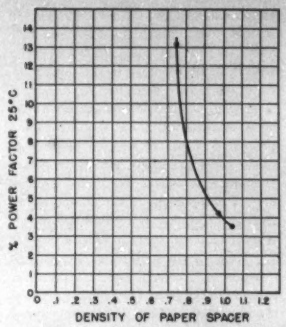

Figure 14. The power factor of kraft paper when impregnated with a cresol–tricresyl phosphate blend having a resistivity of 20 × 10^6 ohm-centimeters is greatly affected by changes in the density of the paper sheet

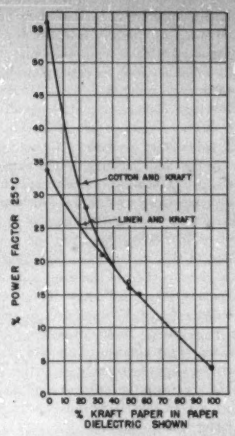

Figure 15. The power factor of the impregnated cellulosic insulating pad impregnated with a semiconductor composition is a function of the amount of kraft paper contained in its assembly

Semiconductor impregnant—cresol–tricresyl phosphate composition having a resistivity of 15 × 10^6 ohm-centimeters

* Pyranol is the General Electric Company copyrighted trade name which is applied to designate a dielectric liquid of the asparel type.

Figure 16. Showing the increase in the 60-cycle electrical capacity of a kraft paper spaced capacitor which accompanies the decreasing resistivity of the liquid impregnant throughout the semiconductor classification range

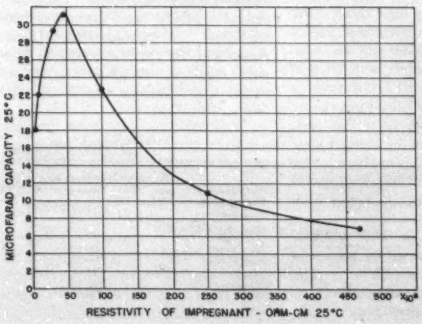

Figure 17. Showing the change in the 60-cycle capacitance of kraft paper spaced capacitors as a function of the resistivity of the semiconductor impregnant

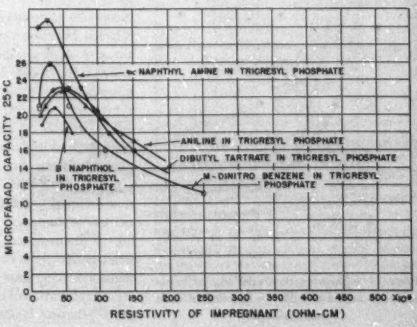

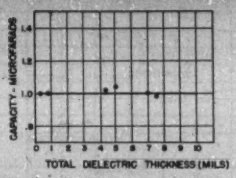

Figure 18. A change in the total distance between the electrodes of a kraft paper capacitor impregnated with a semiconducting liquid is not reflected in the 60-cycle electrical capacitance as long as the kraft paper sheet is not altered

Kraft paper dielectric—one sheet 0.0004-inch capacitor paper

Distance between electrodes obtained by variations in the clamping pressure and by the use of a porous cheesecloth spacer

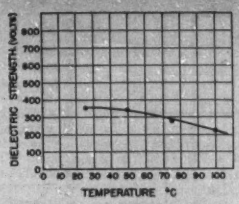

Figure 19. Showing the 60-cycle dielectric strength–temperature relation for a kraft paper capacitor impregnated with a tricresyl–phosphate–cresol blend having a resistivity of 10 to 20 × 10^6 ohm-centimeters

Dielectric—1-sheet 0.0004-inch kraft capacitor paper

Assembly of capacitor—loosely clamped to give a "liquid film" at least equal in thickness to the kraft paper sheet

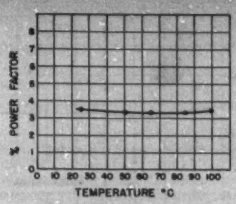

Figure 22. Showing the 60-cycle power-factor–temperature relation for the Permalytic capacitor

Dielectric—0.0004-inch kraft capacitor paper

Impregnant—Cresol–tricresyl phosphate semiconductor blend

strength of the 0.0004-inch kraft paper therein illustrated is 360 volts (900 volts per mil). This ability of the one sheet of 0.0004-inch kraft paper dielectric to resist breakdown when impregnated with a semiconducting liquid is associated with the ability of the liquid to act as a liquid conductor while at the same time manifesting a dielectric strength of about 150 to 200 volts per mil under the usual test conditions. The effect of the conducting particles in the paper sheet thereby is masked effectively.

The Permalytic Capacitor

In the industrial application of capacitors, two requirements are inevitably imposed. The capacitor dielectric must be electrically stable and the capacitor must occupy the smallest possible physical space per microfarad of capacitance. Dielectric stability is paramount because of the severe conditions of electric stress and temperature to which the capacitor may be exposed in normal service.

In the manufacture of capacitors, Pyranol and similar impregnants of the askarel type possess advantage. The dielectric constant of these impregnants is about five. Their use gives the smallest physical capacitor volume per microfarad of any liquid impregnant heretofore used commercially in the manufacture of paper-spaced capacitors. However, even the application of this type of capacitor at voltages in the range of 110 to 220 volts gives relatively large physical volume per microfarad. The physical volumes per microfarad for typical capacitors of this type are given in the following tabulation

2,400-v rating	41.3 cubic in. per kva
360-v rating	58.4 cubic in. per kva
230-v rating	117.0 cubic in. per kva

The large physical volume per kilovolt-ampere of electrical capacity is caused principally by the limitations imposed by the paper spacer. It has been found on the basis of experience that the use of a laminated dielectric composed of less than three sheets of capacitor paper introduces a manufacturing hazard because of the presence of conducting particles in the paper sheet which greatly affect the dielectric strength. Nevertheless, even a 2-sheet dielectric of the thinnest type gives a capacitor of large bulk. A capacitor containing two sheets of 0.0003-inch capacitor paper when operated at 230 volts, operates at a stress of 383 volts per mil. Such a capacitor occupies a physical volume of 45.5 cubic inches per kilovolt-ampere. When operating at 110 volts the dielectric stress is only 183 volts per mil. At 110 volts, such a capacitor occupies a space of 182 cubic inches per kilovolt-ampere. Such applications are uneconomical and are usually objectionable because of space limitations. The Permalytic capacitor, based on the behavior described for the semiconducting impregnated paper spacer, presents an economical solution to the problem presented. The Permalytic capacitor is defined as a kraft paper spaced capacitor of the usual type, the impregnant of which consists of a semiconducting liquid.

The Permalytic capacitor is characterized by a physical volume equal to about 40 per cent of that of the askarel type of capacitor and about 30 per cent of the

Figure 20. Comparative size of various types of 20-microfarad 110-volt 60-cycle capacitors

A—Mineral oil, 42.8 cubic inches
B—Pyranol, 27.0 cubic inches
C—Permalytic, 11.5 cubic inches

(A) (B) (C)

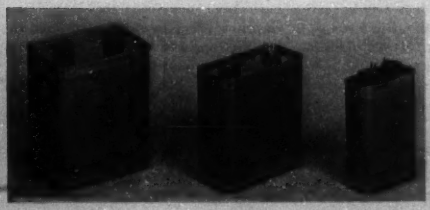

Figure 21. Comparative size of various types of 115-volt 1-kva capacitors

A—Permalytic, 270 cubic inches
B—Pyranol, 620 cubic inches
C—Mineral oil, 847 cubic inches

(A) (B) (C)

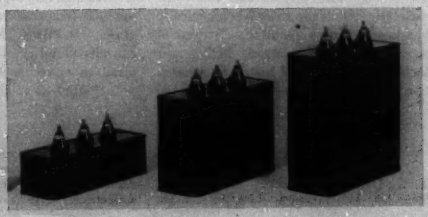

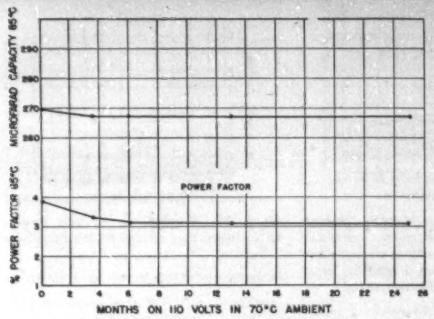

Figure 23. Showing the dielectric stability of a 1-kva 110-volt Permalytic capacitor

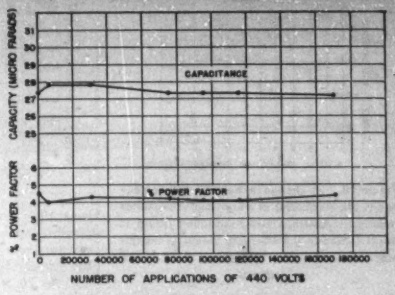

Figure 25. Showing the dielectric stability of the Permalytic capacitor on 440-volt a-c intermittent duty

Voltage application—$1^1/_2$ seconds on, $58^1/_2$ seconds off during each minute

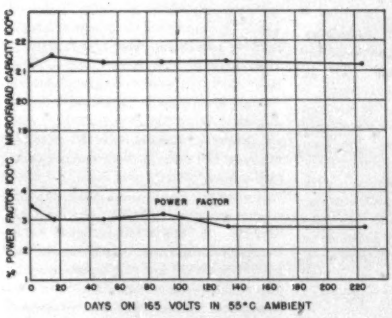

Figure 24. Showing the dielectric stability of the 165-volt motor type Permalytic capacitor

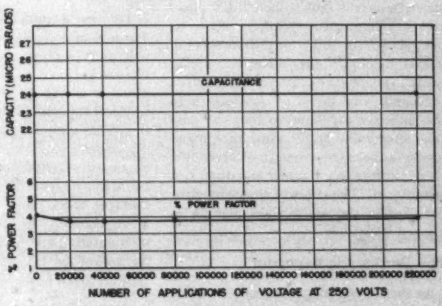

Figure 26. Showing the dielectric stability of the Permalytic capacitor on 250-volt a-c intermittent duty

Voltage application—$1^1/_2$ seconds on, $58^1/_2$ seconds off during each minute

physical volume of the oil or wax impregnated capacitor per kilovolt-ampere. Figures 20 and 21 illustrate the relative sizes of typical low voltage mineral-oil Pyranol and Permalytic types of capacitors.

The Permalytic capacitor operates with a power factor of about three per cent. It is adapted technically and economically for use at continuous voltages up to approximately 220 volts and for intermittently applied voltages as high as 440 or 550 volts, applications where the dielectric type of capacitor is economically handicapped in its operation. Because of its small size and relatively high power factor, the problems of heat dissipation in operation react against the use of the Permalytic capacitor on continuous voltages higher than about 220 volts.

The power factor of the Permalytic capacitor is substantially constant over the usual temperature range from 25 to 75 degrees centigrade. This is illustrated in the data of Figure 22. The 25-degree-centigrade power factor of 3.5 per cent is not exceeded by increase in temperature up to 100 degrees centigrade.

The electrical characteristics of the Permalytic capacitor are stable during operation on continuously applied voltages. This is illustrated in the data of Figure 23 which describes the behavior of a 1-kva 110-volt capacitor operating in an ambient temperature of 70 degrees centigrade. In Figure 24 the power factor and capacity stability of a 165-volt 20-microfarad capacitor is illustrated.

In Figure 25 is illustrated the capacitance and power factor stability of the Permalytic capacitor rated at 440 volts on intermittent voltage duty, 440 volts being applied $1^1/_2$ seconds in each minute. Figure 26 illustrates the dielectric stability of the Permalytic capacitor rated at 250 volts, the voltage being applied for $1^1/_2$ seconds in each minute.

In view of the characteristics which have been described, the Permalytic capacitor offers interesting possibilities for those applications where a small dependable low-cost low-voltage capacitor is required.

Discussion

T. W. Dakin (nonmember; Westinghouse Research Laboratories, East Pittsburgh, Pa.): F. M. Clark's paper has demonstrated experimentally a very interesting phenomenon that may occur in heterogeneous dielectrics. The power factor maximum shown in Figure 4 of the paper, which results when the resistivity of an impregnant is decreased, has been observed before. An analysis of an equivalent circuit for the

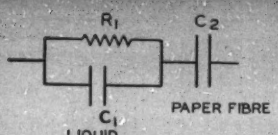

Figure 1A

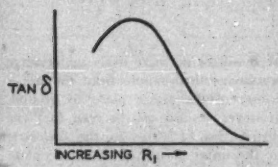

Figure 1B

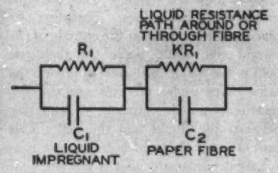

Figure 2A

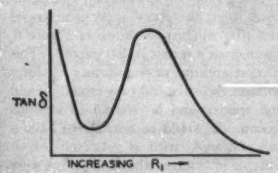

Figure 2B

system, where an essentially loss-free capacitance is placed in series with a second capacitance which is in parallel with a resistance, as in Figure 1A of this discussion, will show that the dissipation factor of such a combination will increase and pass over a maximum as the resistance is decreased, as in Figure 1B. The analogy of this circuit with the impregnated paper is obvious. The capacitance C_1 and resistance R_1 represent the impregnant, and the capacitance C_2, the solid paper fiber, the power factor of which is neglected.

Clark's data show that a minimum occurs as the resistance is decreased still further. This could occur if there is a resistance leakage path around the paper fibers. This resistance, therefore, should be much higher than the equivalent resistance of the impregnant R_1 shown in Figure 1A of this discussion, but should be proportional to it. Let it be designated as KR_1, where K is a proportionality constant greater than unity. This resistance would appear in parallel with the paper fiber capacitance C_2, Figure 1A of this discussion. Our new equivalent circuit then is as shown in Figure 2A. An analysis of this circuit shows that its dissipation factor has both a maximum and a minimum as in Figure 2B like those demonstrated experimentally by Clark. The expression for the dissipation factor of equivalent circuit in Figure 2A is

$$\frac{(1+K)+W^2R_1^2K(C_1^2+KC_2^2)}{WR_1(C_1+K^2C_2+W^2R_1^2K^2(C_1C_2^2+C_2C_1^2))}=\tan\delta$$

where

$W=2\pi f$

Sample calculations using reasonable values for C_1 and C_2 have shown that the proportionality constant K should be about 50 to 100 to get the proper separation of minimum from maximum shown by Clark's data. It is assumed that C_1 and C_2 are of the same order of magnitude, and, for purposes of calculation, they are taken equal to the dielectric constant times the capacitance of a centimeter cube in vacuum. This is consistent with resistance in ohm-centimeters. This calculation shows that the minimum occurs at a resistivity of impregnant of about 10^9 ohm-centimeters, which is in reasonably close agreement with Clark's data considering the crudeness of the assumptions made in the calculation.

A more careful examination of the analogy between the equivalent circuit and the actual dielectric situation may lead to a still better agreement with the experimental results. No account was taken in these calculations of the distribution of space in the over-all dielectric between the paper fiber and the impregnant; it merely being assumed that there was an equal and uniform mixture of liquid impregnant and solid paper fiber.

This equivalent circuit analogy gives an explanation of why Clark obtained a surprisingly low power factor with a rather low resistivity liquid impregnant in paper. The equivalent circuit analogy for the explanation of the behavior of composite insulation was used by H. H. Race,[1] and the present discussion extends the analogy to the special conditions existing in Clark's experiments.

Reference

1. Capacitance and Loss Variations with Frequency and Temperature in Composite Insulation, Hubert H. Race. AIEE Transactions, volume 52, 1933, pages 682–92.

Herman Halperin (Commonwealth Edison Company, Chicago, Ill.): The author is to be commended for doing the unexpected in developing a suitable dielectric using semiconducting liquids. It would be of interest to know the specific inductive capacity for these capacitors.

According to the paper, the capacitors consist of only one layer of paper but the clamping is so loose that the liquid film layer is at least equal to the paper thickness. By this method, it is indicated that the breakdown of weak spots in the paper is avoided. This raises the question as to whether the liquid film separation can be maintained indefinitely, especially in curved portions of the wrappings.

F. M. Clark: T. W. Dakin's analysis is of interest. In accordance with this analysis, leakage measurements over the surface of the various types of paper fibers may lead to an explanation of the power factor values obtained as the composition of the spacer is changed. Although not clearly indicated in the paper, semiconductor impregnants which attack the spacer fiber (pulp) invariably give high power factor for the impregnated sheet. Furthermore, improperly dried cellulose spacers yield higher than the normally expected power factor. These facts appear to be in accord with Dakin's analysis.

The specific inductive capacity of the various semiconducting liquids varies widely with their composition. Tricresyl phosphate has a specific inductive capacity of about 7. Most of the compound blends have a specific inductive capacity in the range from 6 to 14. Despite this wide range of the specific inductive capacity of the liquid, the final capacitance of the capacitor for a given condition can be predicted merely from calculations based on the characteristic of the treated paper without reference to the thickness of the liquid film (tightness of clamping).

Experience has shown that the effect of weak spots in the paper layer are eliminated effectively by insuring the presence of a thick layer of the semiconducting liquid as is obtained by having a loosely clamped structure or its equivalent. Dielectric failure on life test rarely, if ever, has been traced to the presence of conducting particles in the paper sheet.

A Study of the Relative Severity of Steep Front Waves and Chopped Waves on Transformers

F. J. VOGEL
MEMBER AIEE

THE USE of reinforced turn-to-turn insulation on the line coils of transformers is nearly as old as the art. The amount used was a matter of individual belief and custom on the part of the designer. The same is essentially true of the insulation between coils. In the effort to remove empirical practices and place design work on a sounder basis, it was found necessary to find means of evaluating the dielectric strength of line coil assemblies as well as to find the actual voltage stresses which existed. It usually is thought that the dielectric strength of assemblies under oil is purely a question of the separation and the materials. One direct result of this latter reasoning is the belief that if a given voltage stress is obtained between the line coils of a transformer, it is immaterial whether it is the result of a sudden voltage rise as from a steep front wave, or the sudden voltage drop obtained by a gap flashover.

It is the purpose of this paper to show why the actual strength between coils cannot be estimated so easily, and why the strength between coils is not the same with voltage rise or fall.

More specifically, a typical arrangement of transformer winding is studied to determine its dielectric strength near the line terminals under impulse conditions. It is then apparent that it is difficult to estimate the strength of such assemblies and that an approximate method for estimating the strength is required. The shape of the dielectric field for both steep rise and steep collapse of voltage is shown, and the relative stress in both cases is estimated. These show that the steep rise is generally much more to be feared and that special precautions, shielding, or special winding arrangements are necessary.

Paper 47-16, recommended by the AIEE committee on electric machinery for presentation at the AIEE winter meeting, New York, N. Y., January 27-31, 1947. Manuscript submitted October 11, 1946; made available for printing November 13, 1946.

F. J. VOGEL is a professor in the department of electrical engineering, Illinois Institute of Technology, Chicago, Ill.

General Voltage Stress Considerations

A representative transformer is shown on Figure 1. The dielectric field between the line and second coil is to be studied, and Figure 2 shows a section of these coils, taken from the area outlined by dotted lines in Figure 1. Let us first assume that the winding is uniformly spaced. The voltage distribution of such a winding is shown on Figure 3 for a steep front wave. Figure 4 shows the dielectric field which would be obtained with the coil arrangement in Figure 2, but with an applied 60-cycle test to the whole winding. Figure 5 shows the dielectric field obtained with the voltage distribution shown in Figure 3.

Figure 5 shows clearly that the dielectric strength between the two first coils is affected by the presence of the whole dielectric field. The highest stresses are at the points A and B. If the insulation at both places is the same or in proportion to the stresses immediately at the corners, failure along the columns of coils starting at B will be no more likely under surge conditions than failure from the upper corner of the static plate to ground. However, it also will be seen that the distribution of stress in the dielectric at the upper corner of the static plate to ground may be different in the cases of Figures 4 and 5. This in turn means that the dielectric strength is not the same under both conditions. Shielding, by placing line potential at the outside of the second coil, could make the dielectric field in the major insulation approach the same shape under 60-cycle and impulse conditions, at the expense of insulating between the shield and the coil. This case is not considered here because it is not used universally and is not the general case.

When a transformer has had a surge applied to it, the surge appears to travel along its winding as shown in Figure 6, taken from a recent AIEE paper.[1] This is representative of transformer windings without excessive end turn insulation and coil spacing and is referred to for this reason. It would be possible to have a gap flashover with a relatively steep collapse of voltage, when coils 1 to 4 were at about the same potential. Figure 7 shows how different the field conditions are when the voltage and dielectric field collapse than when it is applied. The maximum voltage stress is at C instead of A and is of lower magnitude even though the stress between coils is the same, because the voltage to ground is so much less.

Comparison of Stresses, Initial Distribution of Entering Wave, or Chopped Waves

In a previous paper, the effect of the entering wave, provided it is of steep front, was discussed.[2] A typical insulation arrangement was shown similar to Figure 2 in this paper and Figure 4 in the previous paper. For this condition a specific example, that of a 138-kv transformer, was taken and it was shown that it could have a full wave surge strength

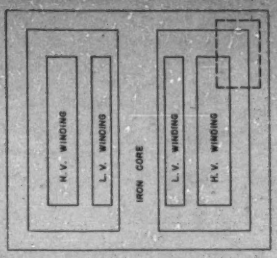

Figure 1. Typical arrangement of core and coils in circular coil transformer

of 760 kv based on a 275-kv 60-cycle test with a major stress at A or B. However, if the voltage surge were to collapse suddenly, it is seen that the maximum stress would be no longer at A or B but at C. From Figure 7, it is also seen that conditions are much better than they previously were because the gradient at C is much less after flashover than it was initially at B, as shown in Figure 5. B is now at ground potential and C only at 50 per cent of the surge voltage at the line at the time it was chopped. If C were equally as well-insulated as B, and the proportions were as shown in Figure 8 of this paper and Figure 6 of the former paper, the total voltage at C could be 63

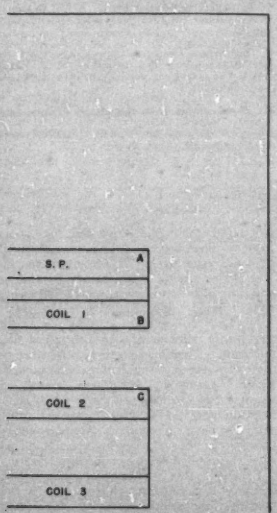

Figure 2. Section of line coils and static plate in dotted section of Figure 1

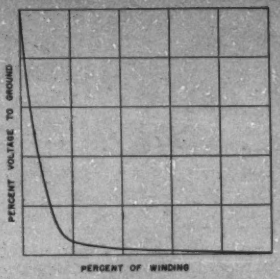

Figure 3. Typical voltage distribution of steep front surge α = 14, 40 coils, with no voltage penetration

This is case where there is a large number of turns in the line coils

per cent of that originally from A to G. If the original surge strength at A was 820 kv, the dielectric strength from C to B should then be 518 kv. If because of distribution, the voltage at C is only 50 per cent of the original surge, it would be only 380 kv or less. Without going into further detail, it is seen that the conditions are vastly different. In fact I believe that because of distribution of stress, many transformers have been built with point C insulated for about two-thirds of the strength of B, and have withstood both impulse tests of the American Standards Association type and steep fronts in the order of those stated in the previous paper.[9] Another way of saying this is to state that the voltage stress at C for the chopped wave, as compared to that at B on initial distribution, is only about 65 per cent. In a recent discussion,[8] kilovolt values of 412 for chopped waves and 347 for steep front waves were quoted for stresses between coils with 2-per-cent turns. If the 412 kv were derated on the aforementioned basis of severity, it would become equivalent to 412×0.65 or 267 kv as compared to 347 kv for the steep front, although this is still not quite a true picture of the actual comparative strengths because time factors are not considered.

Besides the coil edges, the flat area between the coils and the turn-to-turn insulation is stressed. The field between flat coil surfaces is obviously less concentrated than at the coil corners, and failure at the corners would be expected unless faulty oil impregnation or material were obtained. Likewise, core type transformers seldom have more than 50 volts per turn based on their normal 60-cycle rating. If so, a similar transformer to the one just discussed would have not over 2,760 total turns. Two per cent would be 55 turns. If the turn-to-turn stress were distributed fairly evenly, we

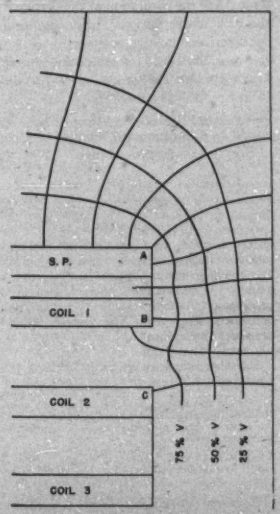

Figure 4. Approximate field plot of dielectric field adjacent to section shown in Figure 2 during 60-cycle test

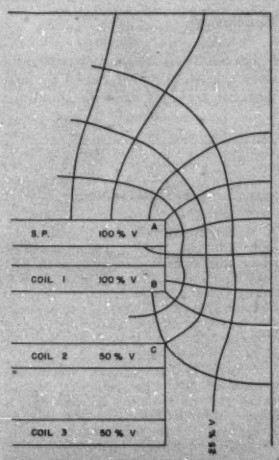

Figure 5. Approximate field plot of dielectric field under impulse conditions as shown in Figure 3

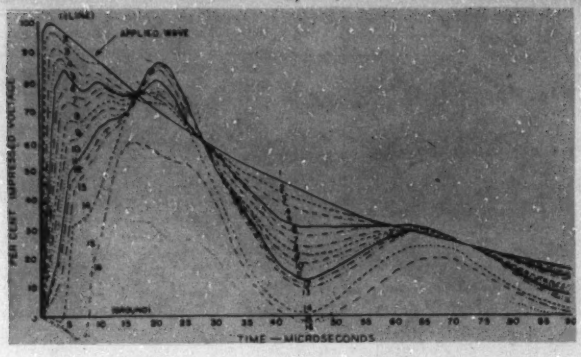

Figure 6. Variation of stresses in core type transformer with time, taken from Figure 4 of reference 1

It is seen that a large part of the line coils are at the same voltage after 18 microseconds

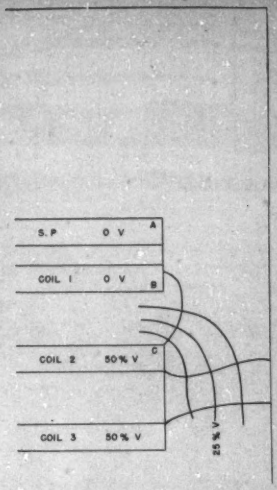

Figure 7. Approximate field plot of dielectric field under impulse conditions at time of chopping surge

would have 412/55 or less than 8 kv per turn. Very little turn-to-turn insulation would be required to stand that stress, indicating clearly that the use of excessive turn-to-turn insulation is not warranted, as the dangerous stress is at the coil corners. Even with considerably less turns and allowing for some variation from uniform stress, the turn-to-turn stresses are low and not a likely cause of failure for this type of transformer. Even today many engineers believe that extra turn-to-turn insulation on the line coils is desirable, and text books state that it is required seemingly on an empirical basis. Actually, its use is undesirable in many cases.

Conclusion

The results of this study show that the steep change in voltage caused by surge flashover does not stress the insulation between coils in a core type transformer in the same manner, nor nearly as severely as a steep front surge. The important parts of the line coil insulation are the corners of the inner and outer diameters of the coils, and not the flat area nor the turn-to-turn insulation in most cases. The value of methods of evaluating the strength of the insulation at the corners of the coils under various stress conditions as described in the previous paper[2] is shown. The need of supplying special insulation at these corners, or of shielding is apparent. If steep front waves are obtained in practice, the use of such waves would be recommended for test in place of the present chopped waves

References

1. Dielectric Strength and Protection of Modern Dry-Type Air-Cooled Transformers. P. L. Bellaschi, Edward Beck. AIEE Transactions, volume 64, 1945, November section, pages 759–62.

2. Standards and Insulation Characteristics of Oil-Insulated Transformers. F. J. Vogel. AIEE Transactions, volume 64, 1945, April section, pages 167–71.

3. Discussion by J. H. Hagenguth of Standards and Insulation Characteristics of Oil-Insulated Transformers. AIEE Transactions, 1945, volume 64, pages 431–3.

Discussion

J. H. Hagenguth (General Electric Company, Pittsfield, Mass.): The meat of Professor Vogel's paper seems to be in the first paragraph under "Comparison of Stresses, Initial Distribution of Entering Wave, or Chopped Waves." Unfortunately however, the use of numerical values for several different coil stacks is confusing and the proof of his statements cannot be verified.

It is possible that Professor Vogel intends to point out that for the steep-front chopped waves, the relative stress between coils is greater than for the standard chopped waves because of the simultaneous existence of high coil-to-coil and high coil-to-ground stresses. (Figure 5 of paper). The coil-to-ground stresses then may initiate a breakdown of the insulation to ground at B, which, in turn, might result in a coil-to-coil failure from B to C because of the high stresses existing between these two points. For chopped waves (Figure 7 of paper) the situation is considerably more favorable in his opinion, because at the time of high coil-to-coil stress from B to C, point B is at ground potential and the failure cannot be initiated at that point.

However, such an analysis neglects the facts that

1. Coil-to-coil stresses may be higher than those obtained by the initial distribution of Figure 3 of the paper at times other than those accounting for the initial distribution.

2. Stresses to ground are produced at points B and C by the chopped wave previous to the chopping.

Professor Vogel, in reference 2 of his paper, assumes a ratio of crest voltage of a steep-front wave chopped at 1 μs to a chopped wave chopped at 3 μs of 1.25. This implies that the strength of the insulation to ground at B is then equivalent for a steep front chopped wave and for a wave chopped at 3 μs, respectively. Therefore, if the insulation to ground is insufficient for one, it will fail also on application of the other type of wave.

Highest coil-to-coil stresses are not necessarily coincident with the initial distribution. They may occur either before or after the crest of the applied wave is reached. Figure 1 shows how coil-to-coil stresses on the front of the chopped wave reach their maximum peak before crest is reached, while after the chop, maximum stress of opposite polarity is obtained approximately 0.3 μs after the applied wave has decayed to zero.

I believe the fundamental difficulty in arriving at definite conclusions lies in the fact that the relative severity of the two types of waves varies greatly with different types of transformers and depends principally on the following factors: natural

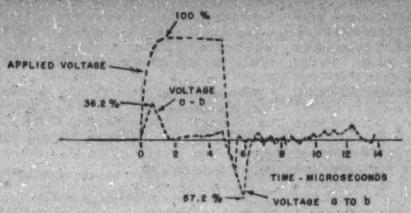

Figure 1. Voltage transient between coils in a transformer winding when a 1.5x40μs wave chopped at 5μs is applied

Tap *a*—3.8 per cent from line end of winding

Tap *b*—7.4 per cent from line end of winding

frequency of oscillation, turn density per inch length of winding, degree of shielding, shape of the applied wave and the volt-time curve of the insulation and electrode assembly.

In general, the relative severity will vary from one transformer to another, and it is impossible to promulgate general conclusions as Professor Vogel attempts to do.

Several papers[1,2,3] have been written in the past few years which show that the bus voltages in stations protected by lightning arresters are held well below the full wave test levels of the transformers in the stations investigated. Judging from the data collected in such field investigations, and based on service experience and service requirements, a thorough study of the insulation test levels might prove valuable.

REFERENCES

1. LIGHTNING INVESTIGATION ON 132-KV TRANSMISSION SYSTEM OF THE AMERICAN GAS AND ELECTRIC COMPANY, I. W. Gross, G. D. Lippert. AIEE TRANSACTIONS, volume 61, 1942, April section, pages 178–84.

2. COMBINED LIGHT AND POWER SYSTEMS FOR INDUSTRIAL PLANTS, D. L. Beeman. AIEE TRANSACTIONS, volume 65, 1946, February section, pages 76–83.

3. FIELD INVESTIGATION OF LIGHTNING SURGES AT SUBSTATIONS, I. W. Gross, G. D. McCann. AIEE TRANSACTIONS, volume 66, 1947.

J. R. Meador (General Electric Company, Pittsfield, Mass.): F. J. Vogel has presented an interesting discussion of the dielectric field at the line end of a small unshielded core-type transformer. It is obvious, as pointed out by Vogel, that the dielectric field at the edge of a coil depends not only on the voltage to the adjacent coil but also on the location of ground. Numerical values are used to illustrate the method of attacking the problem. The values used, however, appear to be taken from such unrelated sources that the general conclusions are questionable.

The original assumptions are that the winding is uniformly spaced (that is, turns per coil and coil ducts are the same in the body of the winding as at the ends) and has the proportions shown in Figure 2 of the paper. For such a winding the impulse voltage distribution in Figure 3 and the field plots in Figure 4 and Figure 5 are undoubtedly correct. The field plots show the spacing between coils to be one-half the spacing to ground. Surely this is not representative of a 138-kv winding. Such a space factor does not appear to be practical, even for a high voltage unshielded winding. If the proportions are not representative, then the conclusions regarding the voltage stresses at the coil edges have limited validity. Also, there is no reason to believe that the voltages across two per cent of winding given in reference 3 were from a transformer whose proportions were similar to those in the field plots.

The rather broad conclusions concerning turn insulation also appear to be drawn from meager data. Taking Vogel's assumptions and applying them to a large transformer, some radically different conclusions can be drawn. Assume a Y-connected, unshielded 132-kv transformer with 200 volts per turn rather than 50, and 60 coils instead of 40. With winding uniformly spaced, the turns per coil is between six and seven.

In an unshielded winding of this sort the static plate has little effect on the impulse voltage distribution, except across the line coil. The voltage distribution is, however, sensitive to rate of change of voltage. In fact, for very steep waves, the turn to turn voltages near the line end are, in a rough way, proportional to the rate of change of voltage. On the American Standards Association chopped wave the voltage drops from 750 kv to essentially zero in 0.05 to 0.2 microsecond. Taking an average value of 0.1 microsecond, the average rate of change of voltage is 7500 kv per microsecond. Contrast this with the usual steep wave test which rises at 1000 kv per microsecond. The turn to turn voltages on the chopped tail actually will not be 7.5 times as much as on the steep front. However, a ratio of two or three to one would be expected. The coil to coil voltages also would be higher on the chopped tail but not necessarily in the same ratio.

With regard to actual turn stresses, the first few coils will have turn to turn voltages approximating what is obtained by assuming a 7500-kv-per-microsecond front penetrating the winding in traveling-wave fashion. If the developed length of a turn is, say, 14 feet, the turn voltage will approximate $14/1{,}000 \times 7{,}500 \approx 105$ kv (where 1,000 feet per microsecond is the assumed rate of propagation). Some 10 per cent to 20 per cent from line end tests on coils of this type have shown the turn voltages are one-half or less of those near the line end. The coil to coil voltages have a similar ratio.

My conclusions for the large transformer are

1. That the turn to turn voltages at the line end are not negligible by any means.

2. That the turn to turn voltages at the line end are at least twice as great as in the main body of the winding.

3. That the turn to turn voltages at the line end on the chopped wave tail are at least twice as great as on the steep wave front.

Of course, it should be pointed out that the effect of the rapid voltage decay on the tail of the steep wave is similar to that of the chopped wave. However, Vogel's conclusions are based entirely on the front of the steep wave and the tail of the chopped wave.

This discussion is not an argument for or against steep waves or chopped waves but merely an attempt to show that the author's conclusions are too broad to be drawn from the evidence presented.

F. J. Vogel: I was very much interested in J. H. Hagenguth's discussion, because in previous discussions he brought out the opinion that chopped waves led to high coil to coil voltages and therefore were about as dangerous as stresses on the front of the wave which actually resulted in slightly higher coil to coil voltages. This was as much of a generalization as any I have attempted, and one I do not believe to be true on the basis of this paper.

In presenting my paper, I stated that there had been many statements made which were not generally true, and that in this paper one particular case was presented and analyzed, and logical conclusions for this one case drawn. If this point of view is adhered to, I do not believe that there is too much difficulty in following the first paragraph under "Comparison of Stresses, Initial Distribution of Entering Wave, or Chopped Waves."

However, Hagenguth truly did understand the point made regarding the severity of the stresses between coils as indicated in the second paragraph of his discussion. In the case shown in Figure 6 of my paper, the coil to coil stresses between the line coils are clearly higher in the initial distribution than at any time later. However, as Hagenguth states and later shows, they may be higher provided the line turns are heavily reinforced and oscillated with the main body of the transformer winding. This is not a desirable construction in my opinion; all design engineers may not desire to follow it, and those that do not should not be forced to use unnecessary reinforcing for empirical or other reasons. Thus, fact number one does not apply to the conditions given.

The second fact cited is true, that stresses to ground are produced at edge *C* by chopped waves before chopping, or by full waves also. However, the stress at *B* is lower the higher the actual potential is at *C*, so what of it? In spite of what might appear to be the general tenor of these remarks, I believe that the first steps to agreement have been taken in recognizing the fact that what may be true for one design practice may not be for another. Also, it is not desirable to burden one practice with the requirements of another provided a serviceable design that can be proven is obtained. The latter part of Hagenguth's discussion leads in this direction, and to this I can subscribe completely.

I think J. R. Meador's discussion, too, assumes some statements that were not made. I did not state that the field plots shown were exactly the same as those encountered in a 138-kv design, but I can assure him that the proportions and voltages between coils are in the same order as many that have been designed and tested. How they were obtained can not be de-

scribed in detail because I do not feel that I am free to do it, but his statement as to space factor is his assumption and is not true. Meador is entirely correct in one respect, however. In the case of a very large transformer, few turns per coil may require more turn insulation than in the transformer I described. However, 50 volts per turn could correspond to about 15,000 kva for a 3-phase core-type transformer, which is reasonably large. Because the kilovolt-amperes vary about as the volts per turn squared, 200 volts per turn would be used for a whopper, but Meador did not give figures for the size that he assumed using his design procedure.

I was very much interested in Meador's statements regarding penetration of voltage into the line coils. The methods used are questionable and not entirely sound, but even so I can agree partly to his conclusions and still not seriously invalidate my own reasoning. For example, if we had 50 per cent of the voltage on the chopped wave across two coils, we would have 750 kv divided by 24 between turns, or about 30 kv between turns instead of 105 kv. In this case, the copper would be quite heavy, and the space required by the turn insulation not great in proportion to Meador's use of 1,000 feet per microsecond as a rate of wave penetration is far too small, the surge actually being transmitted much faster because of the capacity between the static plate and the adjacent turns as well as the capacity between turns. The turn-to-turn insulation should be in proportion to the requirements for extemely large units, just the same as the coil-to-coil insulation should be in proportion to the requirements. Incidentally this type of winding might not be used, because parallel paths or windings could reduce the stresses and improve the winding. If Meador's conclusion read that the "turn-to-turn stresses at the line end for extremely large units or heavy currents are not always negligible," it would not conflict violently with the conclusion that turn-to-turn insulation is not the limiting feature "in most cases."

With respect to Meador's third conclusion, it might be noted that a steep front wave has both a front and tail, as he states, and the coil-to-coil insulation still may be stressed more severely on the front of the wave than on the tail.

Again, I wish to give my belief that there is not a complete difference of opinion between these discussions and the content of my paper, but a difference in the extent to which the conclusions can be applied. I think that the study for the revision of dielectric tests for transformers is helped by the discussion. I hope that in this closure I have answered satisfactorily most of the important objections raised.

The Application of Lead Networks and Sinusoidal Analysis to Automatic Control Systems

GEORGE J. SCHWARTZ
ASSOCIATE AIEE

Synopsis: Design considerations relating to the construction of a high performance servomechanism are discussed here. In particular, the improvement in performance that may be achieved through the use of lead networks* and the valuable guides to system synthesis afforded by sinusoidal analysis[1-4] are demonstrated. Direct reference to an armature-controlled d-c motor system** designed by the author is made and its dynamic characteristics are considered in detail in order to show the correlation between theory and practice as applied to a servomechanism design.

ARMATURE-CONTROLLED d-c motor servomechanisms have been built in great quantities during the past five years. In such systems a two stage d-c generator often serves as the primary power source controlling the servomotor. The motor, in turn, is driven by the generator output voltage which is roughly proportional to the error in the closed-cycle system. The simple automatic controller thus formed suffers the inherent limitation of a tendency toward instability for any reasonable degree of static stiffness. Stabilized operation can be attained, however, through the introduction of high-pass degenerative output feedback, often referred to as antihunt control. A servomechanism of this type is indicated in Figure 1. Such systems provide high positioning and following accuracy and it is possible to obtain ratios of input velocity to positional error or lag, commonly called the velocity-error constant, greater than 600 radians per second per radian of error. When still higher accuracy is necessary it may be provided by cascade circuits in the electronic amplifier, which produce additional error compensation or integral control.†

The use of an anticipatory or lead network in conjunction with the output feedback can increase the natural frequency greatly and hence the transient performance of a system. The increased natural frequency of the system often can make possible such an increase in steady-state accuracy that integral control or other error-compensation means are unnecessary.

A detailed consideration of the synthesis and design processes involved in predicting the optimum type and amount of control effects to introduce into a high performance control system is beyond the scope of this paper. This subject already has been treated at length in the literature.[6-9]

The prescribed aim of this paper is to demonstrate, with the aid of transfer loci, the improvement in a d-c motor control system that may be achieved through the use of output feedback and one type of anticipatory network. Only the mathematical preliminaries to the synthesis or analysis of a control system will be considered.

The system to be considered is indicated in Figure 2. The considerations presented in this paper, however, are not peculiar to this type of servomechanism but may be applied to many control systems. The approach offered is particularly applicable to those systems employing dynamoelectric amplification of the Ward Leonard or amplidyne variety.

Although the mathematical analysis presented presupposes a linear system, the same families of transfer loci and resonance curves may be constructed, through physical measurements, for nonlinear systems. Useful guides to nonlinear system design may be obtained by applying the same stability and performance criteria to these experimentally derived curves.

The D-C Motor Servomechanism

The lags resulting from energy storage in the electromagnetic elements and the inertial effect of the power motor and controller output member are the principle factors limiting the transient performance of the simple servo systems represented by Figure 1. These basic systems also display limited response speed and often large transient errors because of the relatively large time constant unavoidably associated with the feed-back and error correction circuits. The system accuracy under sinusoidal and random input conditions improves as the output feed-back time constant is reduced. However, the oscillatory tendencies of the system also are enhanced by shortening this time constant. The accuracy of such systems under transient conditions therefore is determined to a great extent by the degree of stability required.

The delays inherent in the amplifier-generator and the antihunt control associated with it may be compensated

* A lead network is defined as one which introduces a positive phase angle which increases with frequency in the frequency range over which the servo system operates.

** The servo system described in this paper was developed while the author was associated with the servomechanisms laboratory of the Massachusetts Institute of Technology, Cambridge, Mass.

† Integral control may be defined as a control effect whose magnitude is proportional to the integrated effect of all previous errors.

Paper 47-7, recommended by the AIEE committee on instruments and measurements for presentation at the AIEE winter meeting, New York, N. Y., January 27-31, 1947. Manuscript submitted August 16, 1946; made available for printing October 28, 1946.

GEORGE J. SCHWARTZ is with the Arma Corporation, Brooklyn, N. Y.

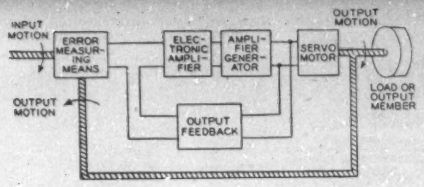

Figure 1. Armature-controlled d-c motor servomechanism

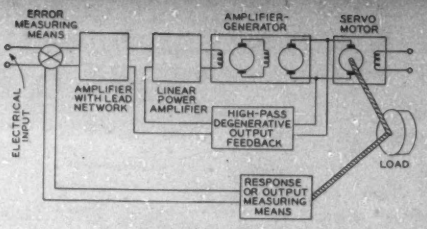

Figure 2. D-c motor servomechanism with output feedback and cascade lead network

partially through the introduction of anticipation, or derivative action, into the amplifier controlling the fields of the amplifier-generator. The use of either output feedback or lead networks alone may produce tolerable results, but the combined action of both effects in proper proportion can produce excellent operation for a properly adjusted system.

Mathematical Analysis

A mathematical analysis is valuable in predetermining quantitatively a controller design and in explaining various phenomena which appear in the response of the completed system. For more complicated control systems, of which most servomechanisms are typical, the use of the sinusoidal analysis yields a solution which is handled easily and from which results are obtained readily. The transfer functions* provided by the sinusoidal approach are particularly potent in the consideration of servo systems with compensating feedback and lead networks.

The transfer function permits a detailed study of the dynamic characteristics of the various elements of a control system and the product of all the component transfer functions yields the transfer function for the over-all system.

The tranfer function for a physical system will be, in general, of the form

$$\frac{\theta_o(j\omega)}{\epsilon(j\omega)} = F(j\omega) = \frac{K(1+a_1 j\omega)(1+a_2 j\omega)(1+a_3 j\omega)\ldots}{j\omega(1+b_1 j\omega)(1+b_2 j\omega)(1+b_3 j\omega)\ldots} \quad (1)$$

where K, a_1, b_1, and so forth are physical constants of the system, $\theta_o(j\omega)$ is the servo output or response function, and $\epsilon(j\omega)$ is the error function of the complex frequency vector $j\omega$. $\theta_o(j\omega)$ and $\epsilon(j\omega)$ are related to the input or driving function $\theta_i(j\omega)$ by the relationship

$$\epsilon(j\omega) = \theta_i(j\omega) - \theta_o(j\omega) \quad (2)$$

* A transfer function is the vector ratio of the output to input of any physical system specifying the performance of that system as a function of the frequency of its input.

The magnitude of many of the physical constants determining the factors in this expression are at the discretion of the servo designer, and it is possible to modify certain of these factors and to introduce others so as to produce a more desirable transfer function. In regard to the d-c motor systems already described, both the magnitude and time constant of the anticipation and output feedback as well as the amplifier-generator gain, in general, may be varied at will in order to produce optimum performance.

Sinusoidal analysis is especially valuable because the transfer locus, or complex vector plot of the transfer function, clearly depicts the changes in system performance accomplished through the introduction of a wide range of control effects and the variation of certain of the physical constants involved.

Formulation of System Transfer Function

The first step in the analysis of an existing or proposed servomechanism is the formulation of its basic transfer function. The transfer function for the system under consideration will now be derived.

(*a*). The control preamplifier contains a linear voltage amplifier and a compensating or lead network as shown in Figure 3. If the voltage amplifier is assumed to be ideal—constant amplitude and zero phase shift response—the compensated preamplifier can be shown to have a response characterized by the equation

$$\frac{\text{Output voltage}}{\text{Input voltage}} = \frac{E_L}{\epsilon} = K_1 \frac{R_2}{R_1+R_2} \frac{1+R_1C_1 j\omega}{1+\frac{R_1R_2}{R_1+R_2}C_1 j\omega} \quad (3)$$

where K_1 is the constant d-c gain of the voltage amplifier. Other constants are designated in Figure 3.

This expression is simply the transfer function for a linear amplifier with anticipation or derivative control added. If the following quantities are defined:

T_L = lead network time constant

$$= \frac{R_1R_2}{R_1+R_2}C_1$$

A_L = lead network attenuation $= \dfrac{R_1+R_2}{R_2}$

the preamplifier transfer function becomes

$$\frac{E_L}{\epsilon} = \frac{K_2}{A_L}\frac{1+A_L T_L j\omega}{1+T_L j\omega} \quad (4)$$

(*b*). The transfer function for the output feed-back circuit is easily found to be

$$\frac{E_{OF}}{E_O} = \frac{R_3C_3 j\omega}{1+R_3C_3 j\omega} K_3 \quad (5)$$

where K_3 is the percentage of amplifier-generator output voltage fed back.

If the output feed-back time constant is defined as

$$T_{OF} = R_3C_3 \quad (6)$$

then

$$\frac{E_{OF}}{E_O} = \frac{K_3 T_{OF} j\omega}{1+T_{OF} j\omega} \quad (7)$$

(*c*). The transfer function for the amplifier-generator is merely the ratio of armature open-circuit output voltage to control field current. If the generator first-stage control fields are driven from high resistance pentodes the resulting control field time constant is negligible. The only important time delay in the amplifier-generator, therefore, is that effecting the build-up of flux in the fields of the second stage. If, as was done in the system under consideration, the amplifier-generator is compensated completely for cross-magnetization and armature reaction effects, the amplifier-generator-time constant T_A is simply the ratio of armature inductance to resistance. The transfer function for the simplified amplifier-generator becomes

$$\frac{E_O}{I_F} = \frac{K_4}{1+T_A j\omega} \quad (8)$$

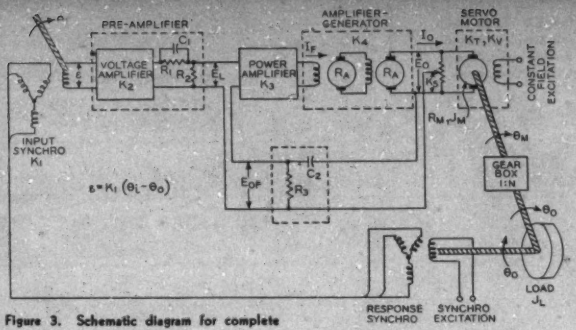

Figure 3. Schematic diagram for complete servo system

where

E_O = amplifier-generator open-circuit output voltage

I_F = control field current

K_4 = amplifier-generator gain in volts per ampere

$T_A = L_A/R_A$

(*d*). The derivation of the servomotor transfer function is simplified if the inductance of the motor armature circuit is neglected. In many practical applications this assumption is valid. The following voltage and torque relationships yield the motor transfer function or ratio of shaft angular position to applied armature voltage.

Amplifier-generator generated voltage $= E_O$

$$= K_V \frac{d\theta_M}{dt} + (R_A + R_M) I_o \tag{9}$$

Motor torque =

$$= (J_M + N^2 J_L) \frac{d^2\theta_M}{dt^2} \tag{10}$$

where K_T is the motor torque per unit current, K_V is the motor back electromotive force per unit speed, and $N^2 J_L$ is the effective load inertia reflected to the motor shaft.

From equations 9 and 10

$$E_O = K_V \frac{d\theta_M}{dt} + \frac{(R_A + R_M)(J_M + N^2 J_L)}{K_T} \times \frac{d^2\theta_M}{dt^2} \tag{11}$$

For the case of the sinusoidal functions to be considered here, we may let $j\omega$ represent differentiation with respect to time, hence

$$\frac{d}{dt} = j\omega, \frac{d^2}{dt^2} = -\omega^2, \ldots\ldots$$

Equation 11 may be reduced to

$$\frac{\theta_M}{E_O} = \frac{1/K_V}{j\omega\left[1 + \frac{(R_A + R_M)(J_M + N^2 J_L)}{K_T K_V} j\omega\right]} \tag{12}$$

If we define the output time constant

$$T_o = \frac{(R_A + R_M)(J_M + N^2 J_L)}{K_T K_V} \tag{13}$$

then

$$\frac{\theta_M}{E_O} = \frac{1/K_V}{j\omega(1 + T_o j\omega)} \tag{14}$$

and because

$$\theta_o = N\theta_M \tag{15}$$

$$\frac{\theta_o}{E_O} = \frac{N/K_V}{j\omega(1 + T_o j\omega)} \tag{16}$$

In the special case of an unloaded motor ($J_L = 0$) driven from a zero impedance source ($R_A = 0$) this output time constant simplifies to the basic motor time constant

$$T_M = \frac{R_M J_M}{K_T K_V} \tag{17}$$

(*e*). If the individual control elements of Figure 3, namely, amplifier, feed-back circuit, amplifier-generator, and servomotor, are considered now in their proper physical relationship, the following expression results:

$$I_F = \left[\frac{K_2}{A_L} \frac{1 + A_L T_L j\omega}{1 + T_L j\omega} \epsilon - K_3 \frac{T_{OF} j\omega E_O}{1 + T_{OF} j\omega}\right] K_4 \tag{18}$$

Combining the expression for servo error, $\epsilon = K_1(\theta_i - \theta_o)$, with equations 8, 16, and 18, the complete system transfer function results

$$\frac{\theta_o}{\epsilon}(j\omega) = \frac{NK_1K_2K_3K_4(1/K_V)(1/A_L)}{j\omega(1 + T_o j\omega)\left(\frac{K_3K_4K_5T_{OF}j\omega}{1 + T_{OF}j\omega} + 1 + T_A j\omega\right)} \frac{1 + A_L T_L j\omega}{1 + T_L j\omega} \tag{19}$$

Value of Transfer Function

It should be stressed that the servo-analysis thus far has considered only the system transfer function or ratio of servo output to servo error. No mention has been made yet of what would appear to be the servo designer's primary concern, namely the ratio of servo output to servo input. The emphasis on error rather than input was intentional and is based on the following points:

1. Stability, the fundamental requirement of a servo, depends solely on output as a function of error not of input.

2. The sinusoidal analysis of a servomechanism is based on properties of its system transfer function.

3. If the transfer function of a system is known, the response or output-input vector ratio easily can be derived both graphically and analytically. Consider for example the servo represented in Figure 4*A*. If this system is characterized by a transfer function $\theta_o(j\omega)/\epsilon(j\omega) = F(j\omega)$, then the response function $\theta_o(j\omega)/\theta_i(j\omega)$ is related to the transfer function by the expression

$$\frac{\theta_o}{\theta_i}(j\omega) = F'(j\omega) = \frac{F(j\omega)}{1 + F(j\omega)} \tag{20}$$

A similar relationship exists for a feed-back amplifier having a direct gain or transfer function μ and a feed-back factor $-\beta$. Under these conditions the over-all response or amplification for the amplifier is expressed by

$$\frac{\text{Output voltage}}{\text{Input voltage}} = \frac{\mu}{1 + \mu\beta}$$

The servomechanism is a special case of the feed-back amplifier in which $\beta = 1$.

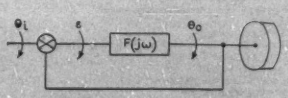

Figure 4A. Servo block diagram

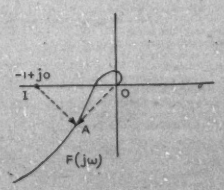

Figure 4B. Typical servo transfer locus

Consider now the typical transfer locus sketched in Figure 4*B*. The vector *OA* is seen to represent the value of the transfer function $F(j\omega_1)$ while the vector *IA* represents $1 + F(j\omega_1)$ at the angular frequency ω_1. The system response to that frequency therefore is represented by equation 20 and is equal to the ratio of the vector *OA* to the vector *IA*.

Physical Characteristics of Servo System

Having derived the transfer function for the servomechanism, the physical constants of the system should be evaluated next by calculation or measurement. The system under discussion was typical of many power drives in the 1-horsepower class built for military application. The servomotor employed was rated at $^1/_2$ horsepower at a speed of 3,000 rpm and was geared to its output or load member through a reduction of 432 to 1. The inertia of the load was 20,000 pound-feet-squared. A synchro data transmission system operating at 36 times the speed of the load was used to measure error in the system and supply appropriate electrical signals to the electronic control amplifier.

The time constant for the 500-watt amplifier-generator employed was calculated to be approximately 0.02 second. The output voltage was directly proportional to control field current up to 75 per cent of rated output voltage, thus indicating no excessive magnetic saturation in the iron. The generator gain over the linear range was approximately 45 volts per milliampere. The amplifier-generator well represented an ideal generator in displaying an internal resistance of only 20 ohms.

On the basis of the expression previously derived, the servomotor time constant $T_M = R_M J_M / K_T K_V$ was calculated to be 0.024 second. This figure, of course, has no practical significance because the motor as employed in a servo system is coupled to a large inertial load and driven from a generator of finite impedance. The actual output time constant

$$T_o = \frac{(R_M + R_A)(J_M + N^2 J_L)}{K_T K_V} \tag{13}$$

was 0.24 second. The load inertia almost quadrupled the original time constant and the amplifier-generator armature resistance of only nine ohms served almost to triple this figure. The desirability of low load inertia and the importance of designing for low armature resistance are apparent.

The output torque of the servomotor was proportional to motor armature amperes up to one-half of rated current; motor torque sensitivity K_T over this range was approximately 0.47 pound-foot per ampere.

Figure 5. Transfer loci for complete control systems and their individual components

$$F_a(j\omega) = \frac{N}{K_V} \frac{1}{j\omega(1+T_o j\omega)}$$

$$F_b(j\omega) = \frac{K_3 K_4}{1+T_A j\omega}$$

$$F_c(j\omega) = \frac{K_5 T_{OF} j\omega}{1+T_{OF} j\omega}$$

$$F_d(j\omega) = \frac{1+A_L T_L j\omega}{1+T_L j\omega}$$

$$F_e(j\omega) = \frac{1}{\dfrac{K_3 K_4 K_5 T_{OF} j\omega}{1+T_{OF} j\omega} + 1 + T_A j\omega}$$

$$F_A(j\omega) = \frac{N K_1 K_2 K_3 K_4 (1/K_V)(1/A_L)}{j\omega(1+T_o j\omega)(1+T_A j\omega)}$$

$$F_B(j\omega) = \frac{N K_1 K_2 K_3 K_4 (1/K_V)(1/A_L)}{j\omega(1+T_o j\omega)\left(\dfrac{K_3 K_4 K_5 T_{OF} j\omega}{1+T_{OF} j\omega} + 1 + T_A j\omega\right)}$$

$$F_C(j\omega) = \frac{\dfrac{N K_1 K_3 K_3 K_4}{K_V A_L} \quad \dfrac{1+A_L T_L j\omega}{1+T_L j\omega}}{j\omega(1+T_o j\omega)\left(\dfrac{K_3 K_4 K_5 T_{OF} j\omega}{1+T_{OF} j\omega} + 1 + T_A j\omega\right)}$$

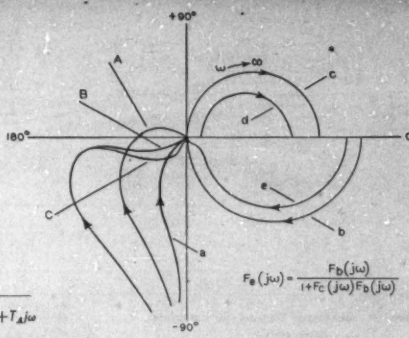

The values of pertinent amplifier-generator and control circuit constants are tabulated in Table I.

Sinusoidal Analysis

Having derived the transfer function for the system and determined the values of the unalterable parameters involved, the function should be plotted with the ultimate aim of detecting the effect of the individual components and control effects on the over-all system response.

The manner in which the transfer functions for the individual components combine to produce the complete system locus is indicated graphically in Figure 5. Curves *a*, *b*, *c*, and *d* are plots of the transfer functions for the output members (equation 16), the amplifier-generator (equation 8), the output feedback (equation 7), and the lead network (equation 4), respectively. These curves indicate the general shape of the functions but are not plotted to scale. The arrowheads on the curves indicate the direction of increasing frequency.

Curve *e* is derived from curves *b* and *c* and represents the amplifier-generator lag factor as modified by the re-entrant output feed-back loop. This factor appears in the denominator of the complete system transfer function (equation 19). The mathematical relationship between curves *b*, *c*, and *e* is indicated also in Figure 5.

The elimination of both output feedback and anticipation from our complete control simplifies the system and modifies the transfer function to the basic form

$$\frac{\theta_o}{\epsilon}(j\omega) = \frac{N K_1 K_2 K_3 K_4 (1/K_V)(1/A_L)}{j\omega(1+T_o j\omega)(1+T_A j\omega)} \tag{21}$$

The locus for this function is formed

Table I. Amplifier-Generator and Control Circuit Constants

Motor to load gear ratio	$N = 1/432$
Synchro sensitivity (for 36 speed synchro system)	$K_1 = 2{,}060$ volts per radian
Voltage amplifier gain	$K_2 = 7.1$ (21.3 for curve *C* of Figure 9)
Power amplifier gain	$K_3 = 0.002$ ampere per volt
Amplifier-generator gain	$K_4 = 45{,}000$ volts per ampere
Feed-back factor	$K_5 = 0.5$
Motor torque sensitivity	$K_T = 0.47$ pound-foot per ampere
Motor voltage sensitivity	$K_V = 0.64$ volt per radian per second
Lead network attenuation	$A_L = 11$
Lead network time constant	$T_L = 0.009$ second
Output feed-back time constant	$T_{OF} = 0.50$ second (4.0 seconds for curve *D* of Figures 8 and 9)
Amplifier-generator time constant	$T_A = 0.021$ second
Load inertia	$J_L = 20{,}000$ pound-feet^2
Motor inertia	$J_M = 0.048$ pound-foot^2
Motor armature resistance	$R_M = 5.75$ ohms
Amplifier-generator armature resistance	$R_A = 9.0$ ohms

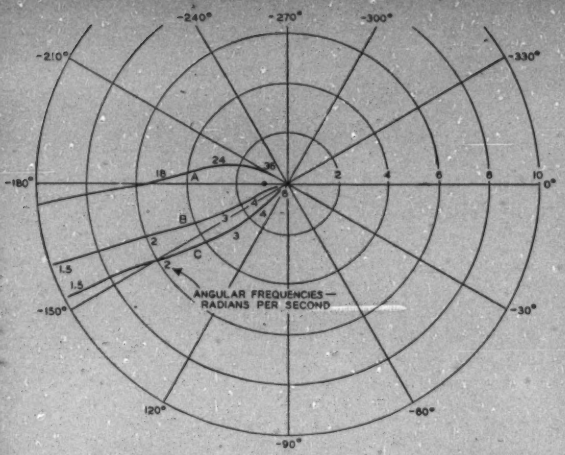

Figure 6. Transfer loci for d-c motor servomechanism demonstrating effect of output feedback and lead network

A—Basic d-c motor system

$$\frac{\theta_o}{\epsilon}(j\omega) = \frac{432}{j\omega(1+0.24j\omega)(1+0.021j\omega)}$$

B—System with output feedback $T_{OF} = 0.5$ second

$$\frac{\theta_o}{\epsilon}(j\omega) = \frac{432}{j\omega(1+0.24j\omega)\left(\frac{22.5j\omega}{1+0.5j\omega}+1+0.021j\omega\right)}$$

C—System with lead network and output feedback

$T_{OF} = 0.5$ second

$T_L = 0.009$ second

$$\frac{\theta_o}{\epsilon}(j\omega) = \frac{432(1+0.1j\omega)/(1+0.009j\omega)}{j\omega(1+0.24j\omega)\left(\frac{22.5j\omega}{1+0.5j\omega}+1+0.021j\omega\right)}$$

from curves *a* and *b* of Figure 5 and is plotted as curve *A*.

The addition of output feedback to the basic system modifies the transfer function to the form

$$\frac{\theta_o}{\epsilon}(j\omega) = \frac{NK_1K_2K_3K_4(1/K_V)(1/A_L)}{j\omega(1+T_a j\omega)\left(\frac{K_3K_4K_5T_{OF}j\omega}{1+T_{OF}j\omega}+1+T_A j\omega\right)} \tag{22}$$

The locus for this function is the product of curves *a* and *e* and is plotted in Figure 5 as curve *B*.

The complete system function (equation 19) likewise is determined from the vector product of curves *a*, *e*, and *d* and is sketched in Figure 5 as curve *C*. Transfer loci for the complete power drive (equation 19) and its two modifications, (equations 21 and 22), are plotted to scale in Figure 6.

Equations 21 and 22 show that the effect of adding output feedback to the uncompensated system is to change the amplifier-generator lag factor from $(1 + T_A j\omega)$ to

$$1+T_A j\omega+\frac{K_3K_4K_5T_{OF}j\omega}{1+jT_{OF}\omega}$$

The tendency of the output feedback to increase, at low frequencies, the lag introduced in the system by the amplifier-generator may not be completely apparent from these expressions; the transfer loci for this system, however, show this effect with considerable clarity.

Further analysis of the transfer loci can be guided by a few fundamental properties of servomechanisms, feed-back amplifiers, and any closed-loop system. For example, a system is unstable if its transfer function, when plotted from negative to positive infinite frequency, embraces the point $(-1 + j0)$. It also follows that the oscillatory tendencies of a system are indicated by the proximity of its transfer function to the $(-1 + j0)$ point at any frequency. The characteristic of prime importance for a fast servomechanism is that the portion of the transfer locus which most closely approaches this point in the complex plane be of high frequency and that this portion be sufficiently remote from the $(-1 + j0)$ point so that a preset condition of stability is not exceeded.

With these properties of the transfer function in mind, the curves of Figure 6 clearly display the improvement in system performance made possible through the combined action of output feedback and a lead network.

Curve *A* shows the basic uncompensated servo system to be violently unstable unless the system gain or static stiffness is reduced to a small fraction of the value permitted by a well-stabilized system. For any practical purpose this system is useless. Adding the output feedback has a tremendous stabilizing effect and produces a very practical system as indicated by curve *B*. The additional degree of stability and increased resonant frequency required for a high performance system are afforded through the use of the anticipation network. The transfer function for a d-c motor system modified by both output feedback and a lead network is plotted as curve *C*. This transfer locus represents the complete system already described.

These loci are plotted to a logarithmic amplitude scale in Figure 7 in order to describe the transfer functions over a more complete frequency spectrum. The pronounced effect of the output feedback, particularly at low frequencies where it tends to introduce an additional 90-degree lag in the system, is more obvious from these curves. The effect of the lead network is also shown to be concentrated in the relatively narrow band of frequencies about resonance (for normal "fast" systems this band is from $\omega = 10$ to $\omega = 100$).

Curves *B* and *C* are replotted to an expanded scale in Figure 8 to emphasize further the effect of the lead network in the middle or resonant frequency region. Curve *D* of Figure 8 represents a system with output feedback whose time constant T_{OF} has been increased from 0.5 second to 4.0 seconds. As demonstrated by curves *B* and *D*, increasing T_{OF} improves the stability of the system by moving the transfer locus away from the point $(-1 + j0)$. This stabilizing effect may only be continued within narrow limits, however, because an increase in T_{OF} increases the transient errors in the system, and a very large value for T_{OF} introduces other undesirable effects into the system.

A system with long output feed-back time constant ($T_{OF} = 4.0$ seconds) was explored in the course of development of the finally adopted system which had a relatively short output feed-back time constant ($T_{OF} = 0.5$ second) and a lead network. Response curves for these two

systems are plotted as curves C and D of Figure 9.* The use of the lead network permits a much shorter output feed-back time constant and hence a much faster system with no important reduction in stability. These response curves are derived from the algebraic manipulation of equation C of Figure 6, equation D of Figure 8, and equation 20.

Also plotted in Figure 9 as curves C' and D' are measured response curves for the actual systems built in the laboratory in accordance with the design considerations already discussed. The correlation between the theoretically predicted and actually achieved results is indicated.

Another Approach Afforded by Sinusoidal Analysis

It is interesting and instructive to consider in more detail the effect of the various control elements on over-all response. In particular, to consider the contribution of each element to the net amplitude and phase response at any given frequency—this is another approach afforded by sinusoidal analysis.

The transfer function for the simplified system without output feedback or anticipation already has been expressed in equation 21. The phase characteristics of this function are plotted as a function of the driving frequency in Figure 10.

Phase characteristics of the d-c motor system with output feedback are plotted also in Figure 10. This system is represented by the transfer function of equation 22. The effects of the output feedback are demonstrated by these plots.

* The value of the preamplifier gain K_1 employed in the derivation of curve C has been increased to three times the value employed in curve D and in Figures 6, 7, and 8.

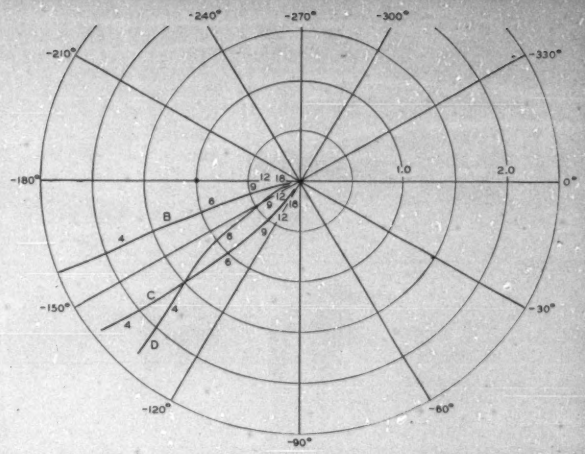

Figure 8. Transfer loci of Figure 6 plotted to expanded scale to accentuate characteristics of transfer loci in vicinity of resonance

B and C—See Figure 6
D—System with output feedback
$T_{OF} = 4.0$ seconds

$$\frac{\theta_{ie}}{\epsilon}(j\omega) = \frac{432}{j\omega\left(1+0.24j\omega\right)\left(\frac{180j\omega}{1+4.0j\omega}+1+0.021j\omega\right)}$$

At zero and very low frequencies, the effect of the output feedback is negligible and the entire system displays the low frequency properties of the motor and amplifier-generator alone. As the frequency is increased the feed-back term begins to introduce an increasing negative angle into the transfer locus for the servomechanism and rotating it in a clockwise direction toward the negative real axis (see Figure 7). The action of the output feedback at low frequencies is not unlike that of a cascade integral controller.

At higher frequencies in the vicinity of resonance, the phase characteristic, in the absence of output feedback, introduces an increasing negative phase angle. This effect shifts the transfer locus toward the $(-1 + j0)$ point in the very range of frequencies in which resonance should occur and such phase shift should be avoided. In this range of frequencies, the output feedback rapidly and very effectively decreases the negative phase angle associated with the transfer function. The feedback also permits the use of increased gain in the system in this frequency range. Stability is maintained in the presence of increased gain in the middle frequency range only because of the very material reduction in negative phase shift.

As frequency is increased further into the high frequency range, the output feedback has a progressively diminishing effect; the response of the system once again is determined solely by the amplifier-generator and motor characteristics.

Considering the effects of the individual parameters of the system, a decrease in the output feedback gain K_8 increases the magnitude of the transfer function in the middle range of frequencies and thus changes the scale of the transfer locus at these frequencies. Decreasing feed-back

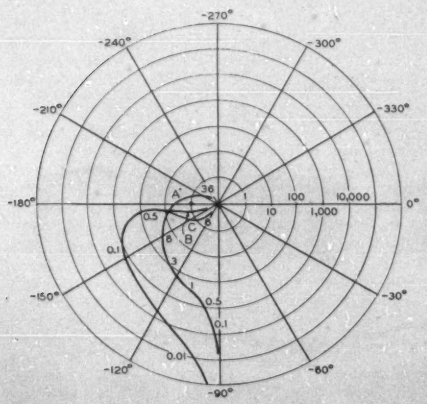

Figure 7. Transfer loci plotted to logarithmic scale to display low frequency region

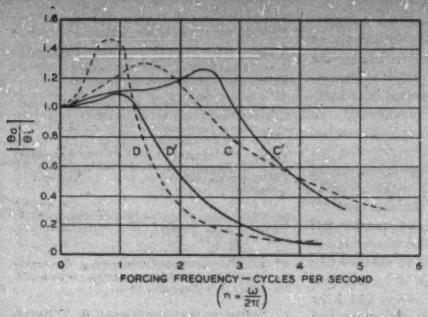

Figure 9. Theoretical and experimental response curves

C and *D*—Calculated response curves corresponding to transfer loci of curves *C* and *D* of Figure 8

C' and *D'*—Experimental response curves derived from measurements on actual equipment

C'—System with output feedback and lead network ($T_{OF} = 0.5$ second)

D'—System with output feedback alone ($T_{OF} = 4.0$ seconds)

gain also narrows the middle frequency band and alters the position of this band in the frequency spectrum.

A change in the output feed-back time constant T_{OF} also serves to shift the position of the middle range of frequencies but has little effect on the amplitude of the transfer function within this band. By adjusting K_4 and T_{OF}, this middle range of frequencies may be moved until the resonant point lies within its bounds.

An increase in the amplifier-generator gain K_4 improves the frequency response by widening the middle frequency range.

The results of the introduction of anticipation through the use of lead networks is shown also in the curves of Figure 10. It may be seen that the lead network has the effect both of widening the middle frequency range and of introducing large positive angles throughout this entire range. The lead network has the beneficial effect of rotating the transfer locus in the middle range of frequencies farther away from the negative real axis, so that the frequency at which the locus most closely approaches the $(-1 + j0)$ point is of considerably higher frequency than it would be in the absence of this correction. To achieve maximum corrective effect in the vicinity of resonance, the lead network time constant T_L and the attenuation A_L should be adjusted so that maximum positive lead angle is introduced in this region. In the system under consideration, T_L was approximately 0.009 second and A_L was set equal to 11. These constants produce a maximum phase rotation of 58 degrees at a frequency of 4.8 cycles per second.

In the improved system the actual

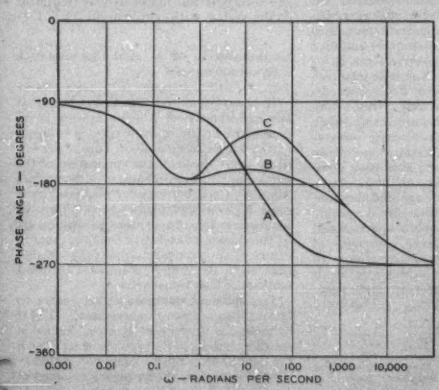

Figure 10. Servomechanism phase characteristics

A, *B*, and *C*—Plots of argument of transfer function as a function of frequency for systems indicated in Figure 6

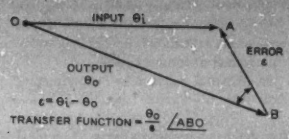

Figure 11. Servomechanism vector diagram

amplifier-generator time constant T_A was small enough so that a reasonable increase in its magnitude would not have affected the transfer function appreciably. T_A, under these conditions, becomes important only at frequencies considerably higher than those encountered by a servomechanism.

The Experimental Approach

Experimental verification of theoretical curves is both desirable for evaluation of the theoretical synthesis and design and necessary as a guide to recognizing defects and indicating the course of redesign.

Derivation of the transfer locus involves the measurement of the servo output, the system error, and the phase angle between them; the solution of the triangle *ABO* of Figure 11 is therefore necessary. From an experimental standpoint, the triangle *ABO* is solved most easily through the measurement of θ_i, ϵ, and θ_o. The angle *ABO* between θ_o and ϵ, or the argument of the transfer function, may be calculated then by the law of cosines. Unless very precise measurements are made, however, this method is highly inaccurate because at low frequencies ϵ is very small compared to θ_i and θ_o.

The direct measurement of θ_o, ϵ, and the angle *ABO* is more accurate but requires special measuring equipment. These measurements may be made most directly with the aid of a 2-element recording oscillograph giving a simultaneous plot of θ_o and ϵ and the possibility of scaling the phase shift between them.

Experimental derivation of the response, or $|\theta_o/\theta_i|$, curve however is readily obtainable. The only measuring equipment necessary is a stop watch for determining frequency and an oscillograph or other amplitude measuring device. The construction of the response curve simply entails the determination of the amplitude of θ_o and θ_i for a series of frequencies over the desired range. As the quantity ultimately desired is the ratio θ_o/θ_i at each frequency, the determination of the absolute value of either quantity alone is not necessary.

The required sinusoidal inputs may be derived mechanically by a simple scotch yoke or electrically by driving a rotatable transformer at constant speed.

In general, sufficient experimental data may be derived from the response curve so that recourse to an experimental transfer locus is unnecessary. A typical servo development often is based on a design dictated by the theoretical study of transfer loci and enhanced and verified by experimentally derived response curves.

Conclusions

Sinusoidal analysis has been applied to an armature-controlled d-c motor servomechanism in order to suggest a method of analyzing such systems and to demonstrate the very material improvement in system performance which may be achieved through the introduction of lead networks in conjunction with degenerative output velocity feedback. The transfer loci and resonance curves presented evidence this improvement.

Of the several methods of analyzing control systems, the sinusoidal approach offered here is considered one of the most straightforward and expeditious means of predicting the performance of a system and of indicating methods for improvement. Stability considerations based on Routh's criteria[10] often fail to indicate the direction and degree to which system redesign should be concentrated in order to obtain a higher degree of stability. In addition, methods of analysis concerned with the transient or indicial response of a system, notably the classical application of Heaviside operational calculus,[11] often prove much more cumbersome and laborious. In regard to the transfer loci of Figure 9, a high degree of correlation is not necessary in order to substantiate theoretical predictions in a control system design. Saturation effects and other nonlinearities neglected or overlooked generally serve to distort the transfer function and reduce calculated resonant peaks. Of far more importance and a sufficient justification for the analysis however, is a condition as was achieved in this paper, in which both theoretical and experimental curves demonstrate essentially the same effect caused by variation of a particular physical parameter.

References

1. Dynamic Behavior and Design of Servomechanisms, G. S. Brown, A. C. Hall. *Transactions*, American Society of Mechanical Engineers, New York, N. Y., volume 68, July 1946, pages 503–24.

2. Fundamental Theory of Servomechanisms (book), L. A. MacColl. D. Van Nostrand Company, New York, N. Y., 1945.

3. Parallel Circuits in Servomechanisms, H. Tyler Marcy. AIEE Transactions, volume 65 1946, August–September section, pages 521–9.

4. The Frequency Response of Automatic Control Systems, Herbert Harris, Jr. AIEE Transactions, volume 65, 1946, August–September section, pages 539–46.

5. Transients in Linear Systems (book), M. F. Gardner, J. L. Barnes. John Wiley and Sons, New York, N. Y., 1942.

6. Control Problems, N. Minorsky. *Journal of the Franklin Institute*, Philadelphia, Pa., volume 232, November 1941, December 1941.

7. Theory of Servomechanisms, H. L. Hazen. *Journal of the Franklin Institute*, Philadelphia, Pa., volume 218, September 1934.

8. Design Factors Controlling the Dynamic Performance of Instruments, C. S. Draper, G. P. Bentley. *Transactions*, American Society of Mechanical Engineers, New York, N. Y., volume 62, July 1940, pages 421–32.

9. Optimum Settings for Automatic Controllers, J. G. Ziegler, N. B. Nichols. *Transactions*, American Society of Mechanical Engineers, New York, N. Y., volume 64, November 1942, pages 759–68.

10. Dynamics of a System of Rigid Bodies, Part II, (book), E. J. Routh. MacMillan and Company, (London, England), 1930.

11. Heaviside's Operational Calculus (book), E. J. Berg. McGraw-Hill Book Company, New York, N. Y., 1936.

Discussion

Robert E. King (Arma Corporation, Brooklyn, N. Y.): The author's paper describes the successful solution of an exacting problem in servomechanism design. However, one of the conclusions stated by the author when applied to servomechanisms generally seems to minimize more than is warranted the effect of ever present nonlinearities.

It is clear that in the case described such nonlinearities as were present were not important because they did not manifest themselves in unwanted resonance peaks. However, this implies that considerable care was taken to obtain gear trains with small back-lash, that coulomb friction was small, that the amplidyne selected showed linear output over its normal operating range, and that the electronic amplifiers likewise were linear over their operating ranges. The resulting assemblage of linear components then performed in accordance with the author's discussion of the pertinent theory. It should be noted that the lack of agreement in the theoretical and experimental response curves shown in Figure 9 of the paper may in part result from nonlinearities.

In many cases the components used in servomechanisms possess linearity for small operating ranges or even none at all. The problem of obtaining specified performance under these conditions may become extremely difficult because the behavior of the servomechanism is so divergent from that expected on the basis of linear theory. It appears, therefore, that all reasonable means of eliminating or minimizing nonlinearities should be employed in the development of a servomechanism in order that the predicted performance based on linear theory may be obtained. Moreover, as the requirements are made more stringent nonlinearities tend to become relatively more important, and they may become the limiting factors in performance.

In the analysis of linear servomechanisms, as in the present case, the advantages of sinusoidal over transient analysis are recognized generally. When, however, the servomechanism has marked nonlinearities the only analytical approach to the stability and performance requirements seems to be through study of the differential equation representing the behavior of the system. In the limited number of cases where any analysis is practicable it is sometimes possible to apply usefully Routh's criteria for stability. Theoretical studies of a few highly nonlinear servomechanisms have been given in the literature.

Finally, because the design and development of a servomechanism for a specific application is a problem of economics as well as engineering, the relative economics of solutions obtained by combinations of analytical studies and experiment probably represents the most important single problem for the designer.

References

1. Periodic Processes in Free Pseudo-Linear Oscillatory Systems, H. Bulgakov. *Journal* of the Franklin Institute, (Philadelphia, Pa.), June 1943, page 591.

2. On the Method of Van der Pol and Its Applications to Nonlinear Control Problems, H. Bulgakov. *Journal* of the Franklin Institute, January 1946, page 30.

Robert W. Mayer (General Electric Company Schenectady, N. Y.): There are two points in this paper which I should like to discuss. The first point relates to the requirements stated for a high performance system, and the second is the mathematical treatment of the system with output feedback.

Requirements of a High Performance Servomechanism

In many instances it has been stated that the performance of a servo system is increased by extending its frequency response to the higher frequencies. This is not entirely true. Instead, the application of the particular servomechanism determines whether or not its frequency response represents high or low performance. That is, the performance of a servomechanism should be based upon its ability to meet the requirements of its particular application, rather than upon its ability to respond to input motions at high frequencies.

Two different applications may serve as illustrations. First, if a servomechanism is to be used as a portion of the error channel of another servo loop, the problem of stabilizing the over-all loop can be simplified considerably by extending the frequency response of

the component servomechanism beyond that of the other components of the over-all loop. This many times requires a frequency response having cutoff at high frequencies. On the other hand, for applications in which the error signal contains a large amount of noise and smooth operation with low errors is of importance, it is usually desirable to cutoff the frequency response at as low a frequency as possible. Thus, for the latter application a high performance servomechanism would be one which maintained a minimum of error at the lower operating frequency and whose frequency response cutoff as rapidly as possible thereafter in order to minimize the effects of noise. In this case, a servomechanism having a high frequency response would not be considered a high performance servomechanism.

Analysis of Output Feedback

In this paper the analysis indicates that the amplifier-generator open-circuit voltage E_O is applied to the feed-back filter. Such a condition can result only if the armature resistance R_M of the motor is high compared to the internal impedance R_A of the generator; that is, if the motor does not load the generator. This is not the case in this servomechanism. A more accurate solution may be realized, therefore, by considering the effect of this loading on the generator.

Equation 7 of the paper shows

$$\frac{E_{OF}}{E_O}=\frac{K_sT_{OF}j\omega}{1+T_{OF}j\omega}$$

Instead, this should be written as

$$\frac{E_{OF}}{E_{OL}}=\frac{K_sT_{OF}j\omega}{1+T_{OF}j\omega} \tag{1}$$

Where E_{OL} is now the output of the generator modified by the effect of motor loading.

The expression for E_{OL} may be found as follows:

Referring to Figure 3 of the paper and using $j\omega=d/dt$, the amplifier-generator output voltage under load will be

$$E_{OL}=K_Yj\omega\theta_M+R_MI_o \tag{2}$$

But from equation 10 of the paper

$$I_o=\frac{J_M+N^2J_L}{K_T}(j\omega)^2\theta_M \tag{3}$$

And from equation 11 of the paper

$$(j\omega)^2\theta_M=\frac{K_T}{(R_M+R_A)(J_M+N^2J_L)}\times[E_O-K_Yj\omega\theta_M] \tag{4}$$

From equation 14 of the paper

$$K_Yj\omega\theta_M=\frac{1}{1+T_aj\omega}E_O \tag{5}$$

Substituting equation 5 of this discussion into equation 4, and the result into equation 3 and then into equation 2 gives

$$E_{OL}=\frac{1}{1+T_aj\omega}E_O+\frac{R_M}{R_A+R_M}\times\left[1-\frac{1}{1+T_aj\omega}\right]E_O \tag{6}$$

which may be written as

$$\frac{E_{OL}}{E_O}=\frac{1+\left(\frac{R_M}{R_A+R_M}\right)T_aj\omega}{1+T_aj\omega} \tag{7}$$

Substituting this into equation 1 of this discussion gives the proper result for equation 7 of the paper under load, that is,

$$\frac{E_{OF}}{E_O}=\frac{K_sT_{OF}j\omega}{1+T_{OF}j\omega}\cdot\frac{1+\left(\frac{R_M}{R_A+R_M}\right)T_aj\omega}{1+T_aj\omega} \tag{8}$$

The effect of equation 8 is to considerably modify the transfer function in the critical regions about the point $(-1+j0)$. The net result is a corresponding change in the calculated frequency response curves. For the case with output feedback alone and $T_{OF}=4$ sec (curve D) the calculated curve now gives a resonant peak of

$M=1.15$

at frequency

$f=1.11$ cycles per second

This curve agrees quite closely with the experimental result of Figure 9. It also represents for most applications an improvement in performance over the original curve D in as much as the value of M is considerably lower.

For the case with output feedback and a lead network and with K_s three times the value employed in curve D, the calculated curve for Curve C now gives a resonant peak of

$M=1.06$

at frequency

$f=0.8$ cycle per second

The lower value of M, again represents a calculated improvement in performance. However, the calculated results are in error with the experimental results as far as the resonant frequency is concerned. Further examination of the transfer function with the aid of an attenuation phase diagram[1] shows that the experimental curve could not cut off as rapidly as it does in the region following resonance unless additional time constants becomeing effective in that region of higher frequencies were present. Such time constants would, on the other hand, cause very little change in the results of curve D since its resonant frequency is much lower. This leads to the conclusion that possibly there were other smaller time-constants present in the amplifier or motor which should have been included in the analysis to gain more accurate results at higher frequencies.

Reference

1. Fundamental Theory of Servomechanisms (book), L. A. MacColl. D. Van Nostrand Company, New York, N. Y., 1945.

G. J. Schwartz: R. W. Mayer's definition of a high performance servomechanism introduces a consideration of practical importance that is too often neglected in theoretical study. It is indeed advantageous and often necessary for a servomechanism to reproduce faithfully the low frequency components of its input and yet attenuate or smooth the higher frequency components and random noise. This problem generally requires special design consideration and the application of different criteria for high performance. For the system discussed in the paper, however, the more common performance specifications existed so that a servomechanism with high natural frequency and reasonably low amplification was desirable; high performance in this general case implied accurate response at high frequencies.

I am indebted to R. W. Mayer for his more complete treatment of output feedback from the amplifier-generator armature terminals. Mayer's discussion supplements my approximate or simplified treatment because, as he clearly points out, the analysis presented in the paper is only valid in applications in which the motor armature resistance is large compared to the resistance of the amplifier-generator armature. In the example cited, R_A is in fact larger than R_M so that the loading of the generator by the motor must be considered if an accurate representation of the system is to be obtained.

In the development of a high performance servomechanism every effort should be exerted to produce linear components, particularly if the system is to be adaptable to exact mathematical description and analysis. R. E. King's concern over nonlinearities is accordingly well-founded. As indicated in King's references, reasonable linear approximations to pseudo-linear systems may be made. In general, however, Routh's criteria and continuous transient analysis, as well as the sinusoidal approach, break down when applied to highly nonlinear systems and discontinuous servomechanisms of the relay or contactor type, and recourse must be had to the step by step transient solution.

King's remarks on the economic aspects of system development are particularly pertinent, because the economies to be derived from a well-organized combination of analytical and experimental study cannot be overlooked.

Simplified Graphical Method of Computing Thermal Transients

PAUL NARBUTOVSKIH
MEMBER AIEE

DURING RECENT YEARS the operators of electric equipment—power transformers in particular—became increasingly aware of the inherent overload capacity which their equipment has on transient overloads. This capacity is caused by a reservoir for storing up heat generated by the power losses, and this reservoir is always present in the form of conductor copper, iron, and the structural and insulating materials. Although the operation of equipment making use of the transient overload capacity can be done by actually keeping track of the equipment temperature, or by the use of protective relays geared in some way to the copper temperature[1], or both, any planning of the system's loading ahead of time requires a method, and preferably a simple method, of estimating the available overload capacity of the individual pieces of equipment.

A number of simplified methods for computing thermal transients have been offered in the past, both graphical and semigraphical, based on more or less complex charts and possessing different degrees of generality.[2,3,9] Thus, the method described in this paper is not a venture in a new direction. It is believed, however, that the method described herein possesses a degree of simplicity and generality which makes it worthy of offering in addition to the previously suggested procedures.

Late in 1944 the essential feature of this method was suggested by the author to the AIEE transformer subcommittee, and was included in a recently published paper.[4] This publication, however, did not cover the details of the method, nor was the author fully aware at that time of its convenience and possibilities.

Paper 47-10, recommended by the AIEE committee on electric machinery for presentation at the AIEE winter meeting, New York, N. Y., January 27–31, 1947. Manuscript submitted August 2, 1946; made available for printing November 4, 1946.

PAUL NARBUTOVSKIH is an engineer, transformer engineering department, Westinghouse Electric Corporation, Sharon, Pa.

Fundamentals of Thermal Transients

The method described in this paper, as well as any other method, is based on the acceptance of a certain specific law of the transient temperature variation under a fixed load. Generally, although it is not quite accurate, the exponential law, representing theoretical solution for thermal transients under the condition of simple proportionality between the rate of heat dissipation by a hot surface and its temperature rise over the ambient temperature, is accepted because of its convenience. Expressed as a formula for a system consisting of a single thermal reservoir, this law is

$$\theta_t = \theta_i + (\theta_u - \theta_i)(1 - \epsilon^{-t/T}) \qquad (1)$$

where

θ_t = the transient temperature rise above ambient temperature at time t

θ_i = the initial temperature rise at time $t = 0$, caused by a continuous power loss of W_i watts

θ_u = the ultimate temperature rise at time $t = \infty$, if the given loss W_u were allowed for an indefinitely long time

T = the time constant of the apparatus expressed in the same units of time (minutes or hours) as time t, so that the ratio t/T is dimensionless

ϵ = the base of natural logarithms

Equation 1 applies to both heating and cooling transients, depending on whether $\theta_u > \theta_i$, or $\theta_u < \theta_i$, respectively. In the case of an oil-insulated transformer the equation approximately represents either the oil or the windings temperature rise transients taken separately.[5]

Although details of the theory of thermal transients are outside of the scope of this paper, and the reader is referred for information to other publications[6,7,8] a few remarks about computation of θ_i, θ_u, and T from the basic data on the equipment are considered in order to complete the picture.

If not otherwise known, quantities θ_i and θ_u may be computed from the test or design value of the temperature rise at continuous normal rated load θ_0 using equations 2 and 3, the second form of which applies specifically to transformers

$$\theta_i = \theta_0\left(\frac{W_i}{W_0}\right)^n = \theta_0\left(\frac{1+kP_i^2}{1+k}\right)^n \qquad (2)$$

$$\theta_u = \theta_0\left(\frac{W_u}{W_0}\right)^n = \theta_0\left(\frac{1+kP_u^2}{1+k}\right)^n \qquad (3)$$

where

θ_0, θ_i, θ_u = the ultimate temperature rises, corresponding to the continuous losses of W_0, W_i, and W_u watts, respectively

P_i, P_u = the corresponding per-unit-kilovolt-ampere loads

k = the ratio of copper loss to iron loss at rated load

n = the exponent whose value, with a fair degree of accuracy, may be taken as 0.8 for self-cooled and as 1.0 for forced-cooled equipment.

A convenient chart for computing θ_i and θ_u according to equations 2 and 3 was given previously in the technical literature.[3]

The time constant is a composite effect of the heat storage capacity of the equipment, losses, and the ultimate tempera-

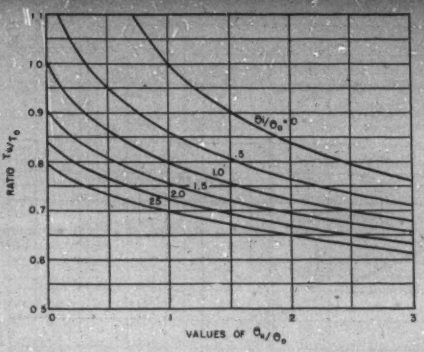

Figure 1. Variation of time constant with load conditions as represented by equation 4

ture rise produced by these losses. Equations for computing the time constant for transformers have been given and are conservative.[2,3,5]

In connection with the time constant, it may be mentioned that for self-cooled apparatus the actual thermal transient deviates from that described by equation 1 because of a nonlinear relation between the losses and the temperature rise of a hot surface. It is always possible, however, to find a value of the time constant for any load condition, which, when used with equation 1, will make the approximate exponential temperature curve match the initial slope and the ultimate temperature rise of the actual nonexponential transient temperature curve. If the time constant satisfying this condition is known for some reference load value starting with zero temperature rise, then, for any other load, and starting at any other temperature rise (θ_i), it may be shown (see the appendix) that the time constant will be given by the expression

$$T_u = T_0 \times \frac{\dfrac{\theta_u}{\theta_0} - \dfrac{\theta_i}{\theta_0}}{\dfrac{W_u}{W_0} - \dfrac{W_i}{W_0}} \qquad (4)$$

where

T_u = the corrected value of the time constant for applied loss of W_u watts, causing an ultimate temperature rise of θ_u

T_0 = the reference known value of the time constant obtained with a loss of W_0 watts applied to a cold unit (most conveniently defined for 100-per-cent load starting cold)

θ_u, θ_i, θ_0 = the final temperature rises corresponding to continuous losses of W_u, W_i, and W_0 watts, of which θ_i is the starting temperature for the transient under consideration

An idea of the variation of the time constant with load condition as defined by equation 4 for the value of exponent $n = 0.8$ may be gained by inspection of Figure 1. This graph may be used for determining the time constant from a reference value in the absence of more direct information.

The use of equation 4 complicates the computations of thermal transients. For the practical operating range of overloads and temperature rises, however, the error introduced by using the same value of the time constant is not great. The graphical method of computations described herein is given primarily for this case. With some obvious modifications it will apply equally well to the case when a correction in the time constant is used.

The Graphical Method

The substance of the graphical method described in this paper is in the use of a special co-ordinate paper, on which any exponential transient given by equation 1 plots as a straight line. To accomplish this, the time co-ordinate of this paper is marked with the values of dimensionless function $u = t/T$ to satisfy the following equation of the scale

$$x = l(1 - \epsilon^{-u}) \qquad (5)$$

where

x = distance in inches from the left-hand end of the scale up to the point marked with the value of u

l = total length of the scale in inches up to the value of $u = \infty$

Thus, the time co-ordinate is given in terms of the ratio t/T. This requires a simple multiplication of u by the time constant T in order to obtain the actual values of time, T being known. However, at the same time it makes the paper universally applicable to representing any exponential transient, whether thermal or electrical (RC or RL circuits), as a straight line. The plot will be a straight line regardless of whether the temperature rise above ambient temperature or the actual total temperature including the ambient temperature is represented on the graph.

For a complete representation of a simple transient it is sufficient to know any two points on the time–temperature curve. These points, when plotted on the transient co-ordinate paper and connected by a straight line, will represent a com-

Figure 2. Representation of simple heating and cooling transients on the transient co-ordinate paper

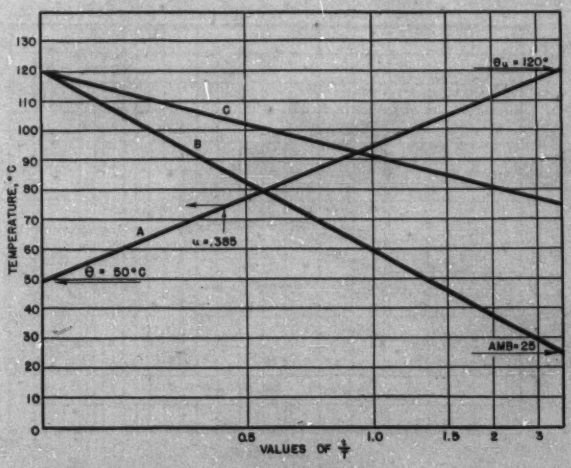

plete thermal transient from the beginning and to the end of time. Thus, starting with a given initial temperature θ_i and computing the ultimate temperature θ_u by the use of equation 3, one may conveniently obtain the required two points. Referring to Figure 2, curve A, let $\theta_i = 50$ degrees centigrade be the starting temperature and $\theta_u = 120$ degrees centigrade be the ultimate temperature at $t = \infty$. A straight line connecting these two points will be a plot of the complete transient. To obtain the temperature at any instant, say, $t = 2^1/_2$ hours, for a transformer whose time constant is 6.5 hours, it is sufficient to compute the ratio $u = t/T = 2.5/6.5 = 0.385$, and read the value of the temperature directly from the graph, $\theta = 72^1/_2$ degrees centigrade.

An inverse problem can be readily solved. Thus, to determine how long the same load can be maintained without exceeding a temperature of 90 degrees centigrade, obtain from the graph $t/T = 0.85$, giving $t = (0.85)(6.5) = 5^1/_2$ hours.

To visualize more systematically what problems may be solved by the use of the simple graph, such as curve A, Figure 2, one must remember that equation 1, which the graph represents, contains five variables—θ_t, θ_i, θ_u, t, and T. If any four of these are known in some way, the fifth one may be found from the graph. No other method can do more.

The same co-ordinate paper, which we may call the "exponential transient co-ordinate paper," will represent cooling curves as straight lines as well. Thus curve B, Figure 2, represents a cooling transient with all load discontinued after reaching a 120-degree-centigrade temperature. The ultimate temperature in this case is the 25-degree-centigrade ambient temperature. Curve C is a cooling curve when the load was reduced to a value leading to 75 degrees centigrade ultimate temperature after reaching 120 degrees centigrade.

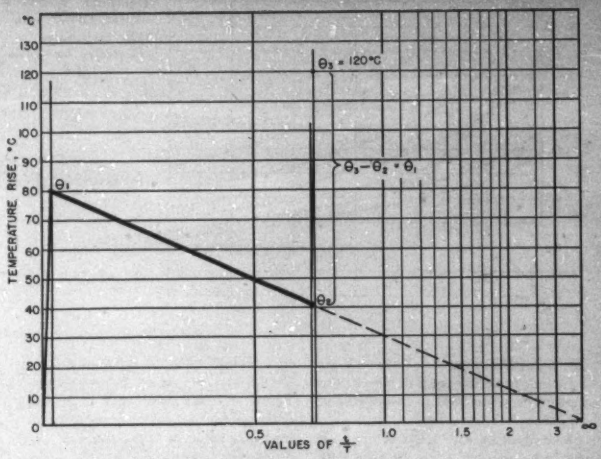

Figure 4. Application of the transient co-ordinate paper to the determination of temperature rise θ_1 which occurs after the first application of load in a load cycle consisting of two applications of the same load, with a cooling period in between

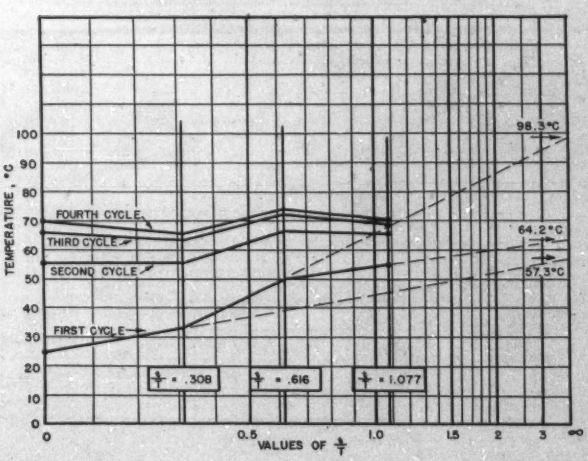

Figure 3. Thermal transient caused by a repeated load cycle, represented on the transient co-ordinate paper

Application to Recurrent Load Cycles

The use of the same co-ordinate paper may be extended to more complex problems with which either the operator or the designer of equipment may be concerned. One such case is the computation of transient transformer temperature under a complex load cycle. To illustrate the method as applied to a somewhat hypothetical case, consider Figure 3. It represents a thermal oil transient under a repeated application of load cycle given in Table I, in a power transformer whose oil rise at rated load is 45 degrees centigrade, time constant is $6^1/_2$ hours and the copper-to-iron loss ratio is 2.5 at rated load, operated at 25-degree-centigrade ambient temperature. The first step in plotting the graph of the composite thermal transient is to compute the ultimate temperature rises corresponding to each load, and the values of ratio t/T for values of time at which the load changes. These computations are accomplished using equations 2 and 3 and the results are tabulated in Table I.

The values of $u = 0.308$, $u = 0.615$, and $u = 1.077$ represent the turning points on the graph at which the loads and slopes of the curves change. It will be noted that it is not necessary to draw the transient curve for each load beginning at $t = 0$. It

Table 1

Per Cent Load	Hours Operated	Ultimate Temp Rise, C	Ultimate Temp	Total at End of Period: Time (t), Hours	$u=t/T$
75	2	32.3	57.3	2	0.308
150	2	73.3	98.3	4	0.615
90	3	39.2	64.2	7	1.077

is, rather, possible and convenient to draw the transient curve as one continuous curve for a complete load cycle, each following load period picking up at the point where the previous load period left off. When the load cycle is repeated, the terminal temperature value of the previous cycle is taken as the starting point of the new cycle.

After the preliminary computations of the ultimate temperatures and the turning points are completed, and the data located on the transient co-ordinate paper, the actual plotting of the thermal transient is so simple that any number of successive load cycles may be plotted without taking the pencil off the paper. When the load cycle is long it may have to be subdivided into shorter periods, because the accuracy of the graph is not good for values of $t/T>3$.

Application to More Complex Problems

An example of thermal problem in which a designer of equipment may be interested, and which can be handled by the same method, is illustrated in Figure 4. In this case the problem consists in designing a piece of equipment for the following load cycle:

Full load	$1^1/_2$ minutes
Cooling with all power disconnected	1 hour
Full load	$1^1/_2$ minutes

At the end of this load cycle the hot-spot temperature rise is not to exceed 120 degrees centigrade.

The equipment can be designed properly if the temperature rise during the first period of load application θ_1 is found. The result obviously will depend on the time constant of the equipment, which must be either computed or estimated and is, for the purpose of illustration, $1^1/_2$ hours.

Although the problem of determining θ_1 may be solved analytically, the graphical method is simpler. It consists of merely locating the turning-point values of the ratio t/T on the transient co-ordinate paper, and adjusting the slope of the cooling curve $(\theta_1-\theta_2-0)$ so as to make $\theta_2-\theta_2=\theta_1$ (which is a justifiable approximation, as the load period is very short compared to the time constant). The answer $\theta_1=79^1/_2$ degrees centigrade may now be read.

Some Practical Drawbacks

Although the method of handling computations of transient temperatures described in this paper is simple and flexible and adopts itself to the solution of fairly complex problems, it has one drawback. It requires the use of a special co-ordinate paper which, being new, is not available on the market. It may be recalled, however, that at one time the engineering profession did not have the assistance of the logarithmic co-ordinate paper. The author's experience with the transient co-ordinate paper in printed form has been so gratifying that, in his opinion, the printing of this paper for general distribution would be entirely justifiable.

Appendix. Derivation of Equation 4

The premises on which this formula is based are as follows:

1. The initial rate of temperature change during the transient computed by the exponential equation 1 should be the same as the actual.

2. The initial and the final temperature rises, as obtained from equation 1, should be the same as the actual.

3. The intermediate values of the transient temperature rise are permitted to deviate from the actual.

To use condition 1 just mentioned, the initial rate of temperature change may be obtained from equation 1 and equated to that obtained from the fundamental equation.

The fundamental equation is

$$W_u=W_s+C\frac{d\theta}{dt} \tag{6}$$

where

W_u = the total heating power
W_s = power dissipated by the external surfaces—a variable function of time
C = thermal capacity

From equation 6 the initial rate of temperature rise is

$$\left(\frac{d\theta}{dt}\right)_{t=0}=\frac{1}{C}(W_u-W_i) \tag{7}$$

where

W_i = the power loss which, when supplied continuously, caused the initial temperature rise θ_i, with which the thermal transient started

The initial rate of increase in temperature rise from equation 1 is

$$\left(\frac{d\theta}{dt}\right)_{t=0}=\frac{\theta_u-\theta_i}{T_u} \tag{8}$$

Equating equations 8 and 7, and solving for T_u

$$T_u=C\frac{\theta_u-\theta_i}{W_u-W_i} \tag{9}$$

Eliminating C, from Equation 9 using the value of a reference time constant T_0

$$T_0=C\times\frac{\theta_0}{W_0}$$

The final relation is obtained

$$T_u=T_0\frac{\left(\frac{\theta_u}{\theta_0}-\frac{\theta_i}{\theta_0}\right)}{\left(\frac{W_u}{W_0}-\frac{W_i}{W_0}\right)}$$

It may be noticed that as far as the premises are concerned this expression does not depend on any assumed law of variation of the heat dissipated by a hot surface with its temperature rise.

References

1. Loading Transformers by Copper Temperature, H. V. Putnam, W. M. Dann. AIEE Transactions, volume 58, 1939, October section, pages 504–9.

2. Quick Determination of Safe Transformer Overloads, R. C. Cheek. *Westinghouse Engineer*, East Pittsburgh, Pa., February 1943, pages 11–15.

3. Temperatures Produced by Overloading Oil-Immersed Transformers, E. W. Tipton. *Electrical Engineering*, volume 63, September 1944, pages 335–7.

4. Guides for Operation of Transformers, Regulators, and Reactors. AIEE Transformer Subcommittee. AIEE Transactions, volume 64, 1945, November section, pages 797–805.

5. Predetermination of Self-Cooled Oil-Immersed Transformer Temperatures Before Conditions Are Constant, W. H. Cooney. AIEE Transactions, volume 44, 1925, pages 611–18.

6. Effect of Load Factor on Operation of Power Transformers by Temperature, V. M. Montsinger. AIEE Transactions, volume 59, 1940, November section, pages 632–6.

7. Hot-Spot Winding Temperatures in Self-Cooled Oil-Insulated Transformers, P. J. Vogel, Paul Narbutovskih. AIEE Transactions, volume 61, 1942, March section, pages 133–6.

8. Emergency Overloading of Air-Cooled Oil-Immersed Power Transformers by Hot-Spot Temperatures, V. M. Montsinger, P. M. Ketchum. AIEE Transactions, volume 61, 1942, pages 906–16.

9. Effect of Overloads on Transformer Life, L. C. Nickols. AIEE Transactions, volume 53, 1934, December section, pages 1616–21.

Discussion

L. A. Finzi (Carnegie Institute of Technology, Pittsburgh, Pa.): It may be mentioned that the problem of thermal transients in a homogeneous body with infinite internal conductivity has been solved by Newton. During the last 40 years an enormous number of papers have been published in the United States and abroad offering simple graphical methods of computation; hence, it is very difficult to add anything new on the subject. Perhaps engineers could not withstand the temptation to work out such procedures just for the sake of their inherent elegance. I have sinned myself along the same line; in a paper published some 15 years ago, while advocating the introduction of two separate time constants for the transformer as a whole and for the windings only, I developed also a kind of nomogram which I seldom have used since. As a matter of fact, the expressions to be computed are not so complicated as to require all this; one may use the slide rule to advantage or simply may refer to a table of exponential functions. If one prefers graphical methods, ordinary semilogarithmic paper may be good enough.

Yet the very abundance of such publications may indicate something else. It may indicate that some need is felt over and over again to make the operator in the field more conversant with the meaning and practical importance of the thermal transient. From this point of view we should congratulate Paul Narbutovskih for his contribution; his special paper has simplicity, and even the most unskilled person should be able to master its mechanism quite rapidly.

However, there may be other difficulties irking the man in the field in addition to those of plain arithmetic; it is possible that he may feel uncertain about the value of the time constant of his transformer. Of course, there are numerous publications giving instructions for its experimental determination, such as the "American Standards for Transformers, Regulators, and Reactors," 1945, but it would be much simpler if the manufacturers made a practice of giving this information along with the other customary specifications; the manufacturers are best qualified for the job because they have design data, test floor facilities, and engineers who are more accustomed to work with these concepts.

The thermal capacity of a piece of apparatus may have considerable practical importance when handling variable loads; in fact, it may become a deciding factor when one has to choose among transformers of different design, which otherwise equally meet the electrical specifications. A good practical knowledge of its meaning may easily result in noticeable savings.

Reference

1. Overloading Oil Immersed Transformers, L. A. Finzi. *Elektrotechnik und Maschinenbau* (Vienna, Austria), 1932, number 46.

P. Narbutovskih: It is the writer's pleasure to acknowledge that, unbeknown to him at the time of submitting his paper for publication, a co-ordinate paper which would plot a thermal transient as a straight line was suggested by L. C. Nichols in 1934, reference 9 of the paper. In his paper Nichols suggests three different co-ordinate papers: one for heating transient in transformer oil; one for cooling transient in transformer oil; and one for either heating or cooling transient in the winding gradient. The first of these papers fits a theoretical thermal transient for a specific case of zero initial temperature rise. The second paper fits a specific case of cooling down to a zero ultimate temperature rise, both papers based on the assumption that the rate of heat dissipation from a hot surface is proportional to the 0.8 power of its temperature rise. The third variety of the co-ordinate paper suggested by Nichols is based on the exponential solution and is identical with that proposed by the writer.

With due regard for the excellent treatment of the subject by L. C. Nichols, the use of several co-ordinate papers appears practically unjustifiable for several reasons.

First, it may be shown that the general case of either heating or cooling transient, when the temperature rise is not proportional to the first power of the heat loss, cannot be represented exactly as a straight line on the co-ordinate paper of this type. The form suggested by Nichols applies exactly only to the case in which the initial temperature rise is zero. When this condition is not satisfied a change of the time scale will be required.

Other reasons against the use of several co-ordinate papers are

1. It unnecessarily complicates the method which is otherwise very simple.
2. It does not lend itself conveniently to handling thermal transients on cyclic loads.
3. It does not apply to forced-cooled transformers.
4. It is not adaptable to more complex problems involving transient temperatures.

In order to compare the relative accuracy of the different methods, Table I was compiled. Each column represents a transient temperature rise at the same instant of time computed by different methods, different columns for different initial and ultimate temperature conditions, as indicated. The methods referred to by letter in the first column are as follows:

A. Exact solution. Because it does not seem possible to obtain this in terms of elementary functions for the general case when the heat loss is not proportional to the first power of temperature rise, this exact solution is obtained here in the following form of an infinite series.

For a heating transient

$$\frac{t}{T_0}=\left(\frac{\theta_u}{\theta_0}\right)^{1-n}\left[\left(\frac{\theta}{\theta_u}\right)+\frac{\left(\frac{\theta}{\theta_u}\right)^{n+1}}{n+1}+\frac{\left(\frac{\theta}{\theta_u}\right)^{2n+1}}{2n+1}+\dots\right]_{\theta_i}^{\theta}$$

$$=\left(\frac{\theta_u}{\theta_0}\right)^{1-n}\sum_{k=0}^{k=\infty}\frac{1}{kn+1}\times\left[\left(\frac{\theta}{\theta_u}\right)^{kn+1}-\left(\frac{\theta_i}{\theta_u}\right)^{kn+1}\right] \quad (1)$$

or a cooling transient

$$\frac{t}{T_0}=\left(\frac{\theta_u}{\theta_0}\right)^{1-n}\sum_{k=0}^{k=\infty}\frac{1}{kn-1}\times\left[\left(\frac{\theta_u}{\theta}\right)^{kn-1}-\left(\frac{\theta_u}{\theta_i}\right)^{kn-1}\right] \quad (2)$$

In the foregoing

t—Time to reach a variable temperature θ

T_0—Time constant for zero initial temperature rise and θ_0 as the final temperature rise (presumably for 100 per cent load, starting cold)

θ_u—Ultimate temperature at $t=\infty$

θ_i—Initial temperature rise at $t=0$

n—Exponent in the relation between the heat loss and the ultimate temperature rise $\frac{W_u}{W_0}=\left(\frac{\theta_u}{\theta_0}\right)^n$. In this case $n=1.25$.

Equations 1 and 2 require no correction in the time constant. Outside of this virtue, needless to say, they are extremely cumbersome to use. Besides, the series converge very slowly except for small values of time.

Other methods used in Table I are

B. Exponential solution, assuming that the temperature rise varies as the first power of loss. No correction in the time constant.

C. Same as *B*, except the time constant is corrected as per Figure 1 in the article.

D. Co-ordinate paper proposed by Nichols for heating transients. No correction in time constant.

E. Same as *D*, except the time constant is corrected as per Figure 1 in the article (which, incidentally, is the same as that suggested in a different form by Nichols).

In Table I of this closure, a temperature rise of 50 degrees centigrade at rated load is assumed.

An interesting conclusion from Table I is that all methods give results that are not too widely different. The use of methods *B* and *D* leads to the least accurate result and, under high overload conditions, may lead to a serious error. Method *E* is precise so long as the initial rise is zero. For all practical purposes, methods *C* and *E* are about equally accurate, giving results very close to those obtained by the exact solution and erring on opposite sides.

L. A. Finzi made a very valid point when he said that the accuracy of computed results depends not only on the method of computation, but on the basic data with which one starts. In regard to the thermal

Table I. Comparison of Oil Temperature in Self-Cooled Transformer, as Computed by Different Methods, in Degrees Centigrade

Method of Computation	Final Rise = 50 C		Final Rise = 100 C	
	Initial Rise = 0 C	Initial Rise = 25 C	Initial Rise = 0 C	Initial Rise = 50 C
A. Exact	25	37½	50	75
B. Exponential, not corrected	23½	36	41½	69
C. Exponential, corrected	23½	37	46½	74
D. Co-ordinate paper for heating transient, not corrected	25	38½	44	70½
E. Same as *D*, corrected	25	38	50	76

transients in transformers, these data include the following: the top oil temperature rise, the winding hot-spot gradient, both at rated load, the time constant, and the loss ratio.

These four quantities, with the exception of one (namely, the hot-spot winding gradient to the top oil) may be determined with reasonable accuracy either by direct measurement or by computation. There is, however, no satisfactory and accepted method of determining the hot-spot winding gradient. The usual test procedure by manufactures does not yield this quantity. The AIEE Standards provide an arbitrary hot spot allowance of 10 degrees centigrade over the average winding temperature, measured by resistance. Yet a relatively small error in this quantity may cause a large error in the computed winding hot-spot temperature on high overloads.

In view of these and other uncertainties, the use of the exponential solution for thermal transients appears to be entirely satisfactory. Of course, for actual computations one may prefer to use the available formulas directly. I do not believe in constructing elaborate charts and graphs, to avoid making a simple multiplication or division, a procedure in which many have indulged in the past. But if much labor required in handling exponential functions can be replaced by just a few simple preliminary calculations and a few straight lines drawn on a special co-ordinate paper, such a simplification should be welcomed.

A Comparison of Two Basic Servomechanism Types

HERBERT HARRIS
ASSOCIATE AIEE

IN THE DESIGN of electric servomechanisms for data transmission or for torque amplification applications, a choice must be made for the best means to stabilize the system and for minimizing static and dynamic errors. In this paper, two methods of stabilization which have common application will be compared. Both of these servomechanisms have been analyzed by others,[1-4,6] but not on a comparative basis and not with the introduction of limitations imposed by response delays.

A block diagram of the first type is shown in Figure 1. The servomotor and its load is characterized by an inertia J and a coulomb or dry friction load F. The torque of the servomotor is assumed to be proportional to the amplifier signal but it is delayed by some electromagnetic storage with a time constant T_M.

Motor torque delays may be caused by inductance in the control field of a d-c motor or by a resonant circuit in the control of an a-c motor. Such delays are of the single exponential type in that a sudden change in amplifier signal will produce a change in torque proportional to

$$(1-e^{-t/T_M})$$

The operational transfer function for this type of delay is

$$1/(1+T_M p)$$

In order to stabilize the control loop a lead network with a transfer function

$$\frac{1+T_A p}{1+T_B p}$$

is introduced to transform the error signal. Such a transfer function may be obtained by the RC network shown or by other means. This method of stabilization has evolved from the concept of using an error derivative, but a true derivative cannot be obtained by a network without a delay, as represented by the denominator $(1+T_B p)$.

The second servomechanism system to be discussed is shown in Figure 2. It evolved from the principle of feeding back a signal proportional to the servomotor speed as a means for stabilization. This simple type has the disadvantage that following a constant speed input necessitates a steady-state error or speed lag, as the speed generator will then feed back a constant signal. Introducing the RC network prevents the passage of such a constant signal, but allows the higher frequency stabilizing signals to pass.

Performance Criteria

Prior to undertaking a design analysis of a servomechanism it is well to state specifically what parameters are of interest and to set up criteria of good performance. In the following discussion some statements will be made which are not immediately evident but will be proved later.

In design, the static sensitivity of the system is often of primary importance. If a load torque F is placed on the output shaft it must be balanced by a motor torque proportional to a so-called static or positional error. The gain of the control loop may be expressed in terms of a sensitivity constant K_s which is defined as the motor torque per unit error. Therefore the error required to balance the load F is F/K_s, and usually is specified to be less than a given value. Analysis will show that there is a limit to the value of K_s which depends on the motor inertia J and the delay time T_M. This limit is of vital interest in determining whether a given motor is suitable for a particular application. A parameter τ_s with the dimensions of time is used to relate J to K_s for convenience in expression, but it has little physical meaning.

$$\tau_s^2 = J/K_s \qquad (1)$$

If the input is given a constant acceleration, the error will attain a constant value proportional to the acceleration after transients have died out. This acceleration lag is a good measure of the dynamic errors of these servomechanisms because many common input motions vary with sufficient smoothness that the error will be approximately equal to the sum of the static and acceleration errors. As a measure of the acceleration error, a second parameter τ_a with the dimensions of time is introduced by the relation

$$\text{Acceleration error} = \tau_a^2 \times \text{acceleration} \qquad (2)$$

Analysis will show that the reduction of τ_a^2 also is limited by the motor response delay T_M.

The delay limits the reduction of the parameters τ_s and τ_a because if T_M is relatively too large, either the servomechanism will be unstable or the oscillations introduced during a transient disturbance will damp too slowly. Therefore, another criterion for good performance is the specification of a certain maximum number of cycles required for an oscillatory "mode to" decay. Alternatively it is satisfactory to specify a maximum value for the resonance peak which measures the amplitude of the output steady-state oscillations for a unit sinusoidal input, at any frequency. As the sinusoidal analysis is the basis for this discussion, it is de-

Paper 47-F2, recommended by the AIEE committee on instruments and measurements for presentation at the AIEE winter meeting, New York, N. Y., January 27-31, 1947. Manuscript submitted August 19, 1946; made available for printing November 7, 1946.

HERBERT HARRIS is in the research laboratories of Sperry Gyroscope Company, Inc., Great Neck, N. Y.

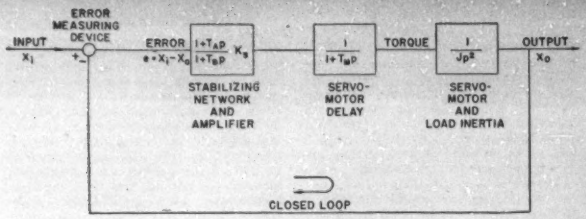

TYPICAL LEAD NETWORK

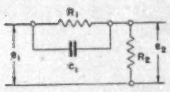

$$\frac{e_2}{e_1} = \frac{R_2}{R_1+R_2}\,\frac{1+R_1C_1p}{1+R_1C_1\frac{R_2}{R_1+R_2}p} = \frac{T_B}{T_A}\,\frac{1+T_Ap}{1+T_Bp}$$

Figure 1. Servomechanism stabilized by lead network

sirable to introduce this concept and its use more carefully.

The characterizing feature of a closed cycle servomechanism is that an error signal e, which is the difference between the input (or desired output) x_i and the actual output x_o, is used for controlling motor torque. Thus

$$e = x_i - x_o \tag{3}$$

and

$$\frac{x_i}{x_o} = \frac{e}{x_o} + 1 \tag{4}$$

If the input motion x_i is an oscillation of fixed frequency and amplitude for a sufficient time to allow transients to die out, both x_o and e will be oscillations of the same frequency but with different amplitudes and phases. Under these circumstances x_i/x_o and e/x_o may be considered as complex numbers or vectors of magnitude equal to the ratio of the two amplitudes of oscillation, and of an angle with respect to the real axis which is equal to the phase difference between the two oscillations. These two ratios are inverse transfer functions because they represent the ratio of input to output rather than the usual output to input ratio. The use of inverse functions is principally a matter of convenience.[4,5]

At very low frequencies the output will follow the input quite well and the ratio of the two amplitudes will be near unity. At very high frequencies the output will be unable to follow the input so that the magnitude of the transfer function x_o/x_i will approach zero while $|x_i/x_o|$ approaches infinity. At some intermediate frequency range a resonant peak is likely to occur at which the output amplitude is greater than the input amplitude. Thus $|x_o/x_i| > 1$ and $|x_i/x_o| < 1$. If this resonant peak is too high then after any transient disturbance the output will tend to oscillate at a frequency near resonance and damp very slowly. The choice of an allowable value for the resonant peak is partly a matter of experience and partly a matter of correlation between the transient method of analysis and the frequency response method.

For this paper a maximum value for $|x_o/x_i|$ of 1.25 or a minimum value for $|x_i/x_o|$ of 0.8 has been chosen as a performance criterion. This value, of course, is somewhat arbitrary, but the justification is presented that if higher values are chosen, any accidental variation of design parameters will produce a rapid deterioration of performance, while 1.25 still allows appreciable tolerances.

Because e/x_o may be interpreted as a complex number or vector it may be plotted as a point, for one frequency, on the complex plane as shown in Figure 3. Then in accordance with equation 4, the vector x_i/x_o may be interpreted as the vector to this point from the point $(-1+j0)$. As the criterion for satisfactory damping is to be that the magnitude of x_i/x_o should never be less than 0.8 at any frequency, it is necessary that the vectored point should not fall inside the circle of radius 0.8. The procedure for analysis shall be to draw the locus of all these points for e/x_o as the frequency varies, and to observe whether the locus cuts into the circle. The frequency for each point may be written along the locus for reference purposes.

Lead Network Stabilization

The inverse loop transfer function e/x_o for the system of Figure 1 is

$$\frac{e}{x_o} = \frac{1+T_Ap}{1+T_Ap} \times \frac{1+T_Mp}{1} \times \frac{Jp^2}{K_s} \tag{5}$$

in which p is the conventional operator representing differentiation with respect to time. T_B and T_A have the dimensions of time and are network design parameters.

For a frequency response analysis the complex inverse transfer function e/x_o may be obtained from equation 5 by setting $p = j\omega$. For convenience in obtaining a general form suitable for many other servomechanisms, a time τ_o is defined by the relation

$$\tau_o^2 = \frac{J}{K_s} \tag{6}$$

and a nondimensional measure of angular

Figure 2. Servomechanism stabilized by speed feedback through a high-pass filter

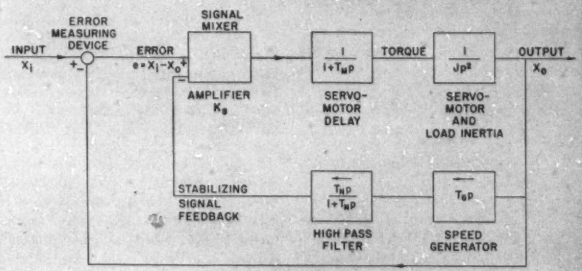

HIGH PASS FILTER:

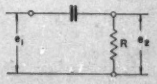

$$\frac{e_2}{e_1} = \frac{RCp}{1+RCp} = \frac{T_Np}{1+T_Np}$$

frequency λ is introduced such that

$$p = j\omega = j(\lambda/\tau_o) \tag{7}$$

The reasons for the choice of τ_o are discussed later. With the substitution from equation 7, equation 5 becomes

$$\frac{e}{x_o} = -\lambda^2 \frac{1+j(T_B/\tau_o)\lambda}{1+j(T_A/\tau_o)\lambda} \times \frac{1+j(T_M/\tau_o)\lambda}{1} \tag{8}$$

This inverse transfer function now can be investigated generally in terms of the three nondimensional ratios T_B/τ_o, T_A/τ_o, and T_M/τ_o. Plots of e/x_o for all possible values of the three ratios involve many curves so that only a few typical ones are shown in Figures 4 and 5. The results obtained from the general curves may be summarized as follows (with a tolerance of about ± ten per cent).

T_B/τ_o and T_M/τ_o represent delays of a similar character, and large values tend to produce a high resonant peak. T_A/τ_o is the stabilizing factor in the system, and if it is too small the resonant peak will be too high.

For a criterion of $|x_i/x_o| > 0.8$, $T_A/\tau_o = 1.5$ is a minimum value even if the delays are zero. For $T_A/\tau_o = 2$, which represents the often quoted critically damped case for a system with negligible delays, the sum of T_B/τ_o and T_M/τ_o may be as high as 0.2, with any division between the two for $|x_i/x_o| > 0.8$. For $T_A/\tau_o = 3$, the sum of the two delays may be as high as 0.25. For higher values of T_A/τ_o the allowable delays gradually decrease, so that for $T_A/\tau_o = 6$, a single delay of 0.19 or two equal 0.06-second delays are satisfactory.

In design the ratios T_A/τ_o and T_B/τ_o are subject to adjustment by the circuit element values of the lead network (Figure 1). By adjustment of the capacitor, T_A and T_B may be varied proportionately within a range such that T_A is not so small as to give insufficient damping nor T_B so large as to make the delay excessive.

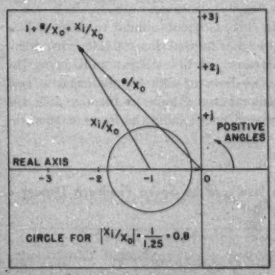

Figure 3. Relation of e/x_o to x_i/x_o

T_B may be made small relative to T_A by using a large ratio between the resistors R_1 and R_2, but this is limited by the loss in gain which must be compensated by the amplifier and by the increase in noise level as discussed later.

T_M however, is determined by the motor and is more or less fixed. Therefore, T_M/τ_o is determined by τ_o, and because T_M/τ_o is limited in all cases to less than 0.25, this implies a limitation on the static sensitivity according to equation 6.

The acceleration lag is also of interest and may be determined directly from the differential equation 5 by setting $x_o = 1/2\, at^2$ representing a constant acceleration and finding the constant error which can maintain this acceleration ($de/dt = 0$). Then

$$e + T_A \frac{de}{dt} = \frac{J}{K_s}\left[T_M T_B \frac{d^4}{dt^4} + (T_M + T_B)\frac{d^2}{dt^2} + \frac{d^2}{dt^2}\right]\left(\frac{1}{2}at^2\right) \tag{9}$$

$$e = \frac{J}{K_s}\, a \tag{10}$$

so that according to equation 2

$$\tau_s^2 = \frac{J}{K_s}. \tag{11}$$

Therefore, according to equations 1, 6, and 11, and the summary of inverse transfer function plots, Table I may be presented.

Speed Feedback Through a High-Pass Filter

In the stabilization scheme of Figure 2, a signal proportional to the output speed is fed back through a high-pass filter to oppose the error signal. A typical high-pass filter is the network shown.

If the high-pass filter is removed, a signal proportional to the speed will be fed back and for constant speed output this signal will have to be balanced by an error signal or speed lag. Therefore, T_G is measured in equivalent radians error per radian per second output speed and has the dimension of time. The high-pass filter is introduced to remove this speed lag and it has a time constant T_N determined by the network circuit constants.

It is well known that for the simple servomechanism without the filter, the speed feedback as determined by T_G must have a certain minimum value for well-damped response. In fact,

$$T_G/\tau_s = T_G \Big/ \sqrt{\frac{J}{K_s}} = 2$$

corresponds to the usually quoted critically damped case when no delays are present. The following analysis determines the effect of the delay T_M and the proper values for T_N and T_G.

The inverse transfer function e/x_o is derived from Figure 2 as

$$\left[e - \frac{T_N p}{1+T_N p} \times T_G p \times x_o\right]\frac{K_s}{1+T_M p} = Jp^2 x_o = \text{torque} \tag{12}$$

$$\frac{e}{x_o} = \frac{Jp^2}{K_s}(1+T_M p) + \frac{T_N T_G}{1+T_N p}\, p^2 \tag{13}$$

τ_s^2 again is defined according to equation 1 as J/K_s and subject to later justification τ_o will be defined by

$$\tau_o^2 = \tau_s^2 + T_G T_N \tag{14}$$

$$(\tau_s/\tau_o)^2 = 1 - (T_G/\tau_o)(T_N/\tau_o) \tag{14a}$$

Placing

$$p = j\omega = j(\lambda/\tau_o) \tag{15}$$

in equation 13 there results

$$\frac{e}{x_o} = -\lambda^2(\tau_s/\tau_o)^2[1+j(T_M/\tau_o)\lambda] - \lambda^2\frac{(T_N/\tau_o)(T_G/\tau_o)}{1+j(T_N/\tau_o)\lambda} \tag{16}$$

or by equation 14a

$$\frac{e}{x_o} = -\lambda^2(\tau_s/\tau_o)^2[1+j(T_M/\tau_o)\lambda] - \lambda^2\frac{1-(\tau_s/\tau_o)^2}{1+j(T_N/\tau_o)\lambda} \tag{17}$$

Combining certain terms in equation 17 yields

$$\frac{e}{x_o} = \left[-\lambda^2\frac{1+j(T_N/\tau_o)(\tau_s/\tau_o)^2\lambda}{1+j(T_N/\tau_o)\lambda}\right] - j\lambda^3(T_M/\tau_o)(\tau_s/\tau_o)^2 \tag{18}$$

The portion of equation 18 in the brackets remains even if the delay T_M/τ_o is zero, and it is analogous in form to equation 8 without delay T_M/τ_o. This is a justification for the choice of τ_o according to equation 14.

Table I. Design Values for a Servomechanism Stabilized by a Lead Network

(a). $\tau_s^2 = \tau_o^2 = \tau_o^2 = J/K_s$

(b). $T_A/\tau_o > 1.5$ if negligible delays are present, but greater than 2 and preferably near 3 if delays are present. This is not a critical condition.

(c). $T_B/\tau_o + T_M/\tau_o \leq 0.25$ leading to

(d). $\tau_o > 4T_M$ as a delay limitation on the static sensitivity and the reduction of acceleration lag.

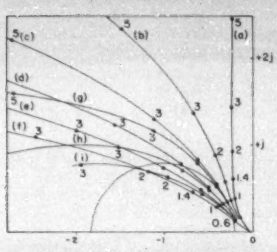

Figure 4. Inverse transfer functions e/x_o for servomechanism stabilized by lead network

$T_A/\tau_o = 2$

Curve	(a)	(b)	(c)	(d)	(e)	(f)	(g)	(h)	(i)
T_B/τ_o	0	0.1	0.2	0.3	0.4	0.5	0.1	0.2	0.3
T_M/τ_o	0	0	0	0	0	0	0.1	0.1	0.1

By analogy with the preceding discussion for a lead network servomechanism the following summary in round numbers may be made, if $T_M/\tau_o \rightarrow 0$:

T_N/τ_o should be at least 2

If $T_N/\tau_o \approx 2$, $(\tau_s/\tau_o)^2$ should be less than $\frac{0.2}{2} \approx 0.1$

If $T_N/\tau_o \approx 3$, $(\tau_s/\tau_o)^2$ should be less than $\frac{0.25}{3} \approx 0.08$

If $T_N/\tau_o \approx 6$, $(\tau_s/\tau_o)^2$ should be less than $\frac{0.19}{6} \approx 0.03$

Because $(\tau_s/\tau_o)^2$ should be less than 0.1, $(T_G/\tau_o)(T_N/\tau_o)$ should be between 0.9 and 1.

Before discussing the effect of the delay T_M/τ_o it is well to interpret the above relations physically. Assuming that T_N and T_G have been set at suitable values according to the condition just mentioned, consider the effect of a variation in the various parameters in conjunction with equation 14.

If the generator voltage T_G is decreased, τ_o^2 will decrease also and eventually $(\tau_s/\tau_o)^2$ will become too large representing too little generator damping and having the same effect as too much delay in the lead network system. If T_G is increased, τ_o will increase, and although $(\tau_s/\tau_o)^2$ will become smaller, T_N/τ_o may become too small. Again there will be too little damping, but in this case it is due to the increased generator voltage increasing the natural period τ_o to such a point that the stabilizing signals cannot pass through the filter in proper phase. This type of resonance often may go unnoticed because of its long period.

If T_N is reduced, τ_o will decrease but at most as the square root so that T_N/τ_o will become too small and $(\tau_s/\tau_o)^2$ too large. If T_N is increased, τ_o will increase almost as the square root, and no harm will be done except to make the system slower and increase the acceleration lag.

If T_N is increased as T_G is decreased inversely, τ_o will remain fixed, and eventually $(T_N/\tau_o)(\tau_s/\tau_o)^2$ will become too large, representing too much delay. Thus a large network time constant cannot make up for a deficiency in generator voltage.

In order to determine the effect of a motor delay T_M/τ_o, it is possible to take plots such as those in Figures 4 and 5 and add the last term of equation 18 for various values of T_M/τ_o. As an example, $T_N/\tau_o = 2$ and $(\tau_s/\tau_o)^2 = 0.05$ yield the same plot as curve *b* in Figure 4. Figure 6 shows the added effect of various values of T_M/τ_o for this same case. In this case T_M/τ_o must be less than about 0.25 in order to remain outside the circle $|x_i/x_o| = 0.8$.

The following summary in round figures may be made of several sets of such curves:

$$\left.\begin{array}{ll}
(a). & \text{If } (\tau_s/\tau_o)^2 \approx 0.1,\ T_M/\tau_o \text{ may be as high as 0.18 if } T_N/\tau_o = 2 \\
(b). & \text{If } (\tau_s/\tau_o)^2 \approx 0.08,\ T_M/\tau_o \text{ must be zero if } T_N/\tau_o = 3 \\
(c). & \text{If } (\tau_s/\tau_o)^2 \approx 0.067,\ T_M/\tau_o \text{ may be as high as 0.25 if } T_N/\tau_o = 2 \\
(d). & \text{If } (\tau_s/\tau_o)^2 \approx 0.05,\ T_M/\tau_o \text{ may be as high as 0.25 if } T_N/\tau_o = 2 \\
 & \text{If } (\tau_s/\tau_o)^2 \approx 0.05,\ T_M/\tau_o \text{ may be as high as 0.13 if } T_N/\tau_o = 3 \\
(e). & \text{If } (\tau_s/\tau_o)^2 \approx 0.033,\ T_M/\tau_o \text{ may be as high as 0.27 if } T_N/\tau_o = 2 \\
 & \text{If } (\tau_s/\tau_o)^2 \approx 0.033,\ T_M/\tau_o \text{ may be as high as 0.15 if } T_N/\tau_o = 3
\end{array}\right\} \quad (19)$$

In general, approximately the same limitation applies to the motor delay in this type of servomechanism as in the lead network type, namely

$$T_M/\tau_o < 0.25 \qquad (20)$$

Equation 13 shows that the lag for a constant acceleration output motion is $(\tau_s^2 + T_G T_N)$ times the acceleration, thus

$$\begin{aligned} \tau_a^2 &= \tau_s^2 + T_G T_N \\ &= \tau_o^2 \end{aligned} \qquad (21)$$

Therefore Table II for this type of servomechanism is equivalent to Table I for the lead network type.

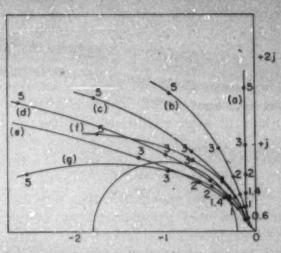

Figure 5. Inverse transfer functions e/x_o for servomechanism stabilized by lead network

$T_A/\tau_o = 3$

Curve	(a)	(b)	(c)	(d)	(e)	(f)	(g)
T_B/τ_o	0	0.1	0.2	0.3	0.4	0.1	0.2
T_M/τ_o	0	0	0	0	0	0.1	0.1

Experimental evidence leads to an even more detailed analysis of this system. If T_G and T_N are increased together, τ_o^2 will increase also so that T_G/τ_o and T_N/τ_o will remain almost constant, but $(\tau_s/\tau_o)^2$ and T_M/τ_o will decrease. This leads to the supposition that the system will become slower but no other trouble will appear. Experimentally, however, the system usually begins to oscillate at a high frequency. This led to an investigation of the effect of a second delay in addition to the motor delay and to the interesting discovery that when $(\tau_s/\tau_o)^2$ is very small the system becomes extremely sensitive to these secondary delays

With a second delay of cT_M seconds in cascade with the motor delay, the inverse transfer function given by equation 18 becomes

$$\frac{e}{x_o} = \left[-\lambda^2 \frac{1 + j(T_N/\tau_o)(\tau_s/\tau_o)^2\lambda}{1 + j(T_N/\tau_o)\lambda} \right] - j\lambda^2(c+1)(T_M/\tau_o)(\tau_s/\tau_o)^2 + \lambda^4 c(T_M/\tau_o)^2(\tau_s/\tau_o)^2 \qquad (22)$$

In this case, plots similar to those of Figure 6 may be used with the last term added. Because the first delay acts to bring the locus down to intersect the negative real axis at some high frequency, and the second delay shifts the locus at this fre-

Table II. Design Values for a Servomechanism Stabilized by Speed Feedback Through a High-Pass Filter

(a). $\tau_s^2 = J/K_s$; $\tau_a^2 = \tau_s^2 = \tau_s^2 + T_G T_N$

(b). T_N/τ_o near 2 allows a maximum delay and is satisfactory for zero delay

(c). $\tau_o > 4T_M$ is the delay limitation

(d). $(\tau_s/\tau_o)^2$ less than about 0.09 if the delay is small, and less than about 0.067 if it is appreciable

Table III. Allowable Values of Secondary Delay in a Servomechanism Stabilized by Speed Feedback Through a High-Pass Filter

$(\tau_s/\tau_o)^2$	τ_M/τ_o	Max Value of Secondary Delay $c\tau_M/\tau_o$ for $\lvert x_l/x_o\rvert \geq 0.8$	Max Value of Secondary Delay $c\tau_M/\tau_o$ for Stability
0.1	0.18		
0.067	0.1	0.09	0.21
	0.2	0.025	0.10
	0.25	0	0.08
0.05	0.1	0.085	0.16
	0.2	0.027	0.08
	0.27	0	0.05
0.033	0.1	0.053	0.09
	0.2	0.021	0.053
	0.29	0	0.03
0.02	0.1	0.031	0.045
	0.2	0.013	0.03

quency along the real axis in the positive direction, there is the possibility that the $|x_l/x_o|=0.8$ circle may be crossed at some high frequency. If the second delay is sufficiently large, the locus may even go through a point to the right of (-1) representing instability.

As an example of this sensitivity to a second delay Figure 7 contains a series of plots with the following values:

$(\tau_s/\tau_o)^2=0.02$
$T_N/\tau_o=2$
$T_M/\tau_o=0.2$
$c=0.05, 0.1, 0.15$

With zero secondary delay the characteristic does not go near the circle $|x_l/x_o|=0.8$, but with a second delay of only $c=0.07$ units relative to the first it crosses the circle, and with a delay of only $c=0.15$ the system is unstable. Because secondary delays of such small value are likely to be neglected, it is important to recognize this sensitivity. The frequency of resonance is so high ($\lambda>10$) that in some applications higher resonances will be allowable, and even systems just on the verge of instability may be acceptable.

Table III is a rough summary of data taken from several sets of such curves ($T_N/\tau_o=2$).

In some cases the second delay will be in the generator feed-back portion of the loop rather than in the forward part. The effects of the two types of delay are very similar and the allowable values are nearly the same for the smaller values of $(\tau_s/\tau_o)^2$.

The Effect of Internal Damping

Some loads have a viscous friction component which requires a torque proportional to speed, and some motors have a torque-speed characteristic with the torque dropping linearly with speed. Both of these characteristics may be treated in the same way and shown to produce a stabilizing or damping action. Some instrument servomechanisms of low performance make considerable use of this type of damping, but it represents a secondary effect only for servomechanisms which are pushed to design limits and must deliver appreciable power to a load. The latter case will be considered here.

The following relation between motor torque and output motion holds:

$$\text{Torque}=Jp^2x_o+fpx_o$$
$$=p^2J(1+f/Jp)x_o \tag{23}$$

where f is the torque per unit speed required by the load, or the drop in torque per unit speed of the motor as measured at the load shaft.

With this new relation, equations 8 and 16 for e/x_o for the lead network stabilization and the speed feed-back stabilization become

$$\frac{e}{x_o}=\frac{\lambda^2[1+j(T_B/\tau_o)\lambda]}{1+j(T_A/\tau_o)\lambda}\times\frac{1+j(T_M/\tau_o)\lambda}{1}\times\frac{1-j(f/J)(\tau_o/\lambda)}{1} \tag{24}$$

and

$$\frac{e}{x_o}=-\lambda^2[1-j(f/J)(\tau_o/\lambda)][1+j(T_M/\tau_o)\lambda)(\tau_s/\tau_o)^2]-\lambda^2\frac{1-(\tau_s/\tau_o)^2}{1+j(T_N/\tau_o)\lambda} \tag{25}$$

Although the exact method for treating these equations is to make plots for all values of the parameters, it is possible to reason the effect of f for certain special cases. One way is to look at the factor $(f/J)\tau_o$ as a partial compensation for the motor delay T_M/τ_o. Thus

$$[1+j(T_M/\tau_o)\lambda][1-j(f/J)(\tau_o/\lambda)]=[1+(T_M/\tau_o)(f/J)\tau_o]+j[(T_M/\tau_o)\lambda-(f/J)(\tau_o/\lambda)] \tag{26}$$

In equation 24 for the lead network type, the delay factor acts principally as a phase shift which tends to bring the plot inside the $|x_l/x_o|=0.8$ circle at frequencies in the region around $\lambda=2$ for $T_A/\tau_o=3$ and around $\lambda=1$ for $T_A/\tau_o=2$, from Figures 5 and 4. If discussion is limited to the cases for which T_M/τ_o and $(f/J)\tau_o$ are only a few tenths, the angle of this phase shift according to equation 26 is approximately $[(T_M/\tau_o)\lambda-(f/J)(\tau_o/\lambda)]$ radians. Consequently near $\lambda\approx1$ a portion of T_M/τ_o equivalent to $(f/J)\tau_o$ is compensated, and near $\lambda\approx2$ a portion equivalent to $1/4(f/J)\tau_o$ is compensated. Thus the allowable motor delay may be increased by these amounts. If the motor delay is negligible, this damping may be looked upon as compensating some of the delay T_B/τ_o or allowing a reduction of some of the stabilizing lead T_A/τ_o.

For the speed feed-back case the effect is slightly different. As the motor delay causes a resonance at high frequencies near $\lambda=5$ in this case, the term $(f/J)(\tau_o/\lambda)$ becomes very small compared to $(T_M/\tau_o)\lambda$. Consequently there is very little delay compensation. However, it does allow higher values for $(T_N/\tau_o)(\tau_s/\tau_o)^2$ or lower values for T_N/τ_o because these are analogous to T_B/τ_o and T_A/τ_o.

Near zero frequency the term $(f/J)(\tau_o/\lambda)$ becomes predominant and the e/x_o plot starts upward along the imaginary axis rather than in the negative direction on the real axis as before. This represents a phase slope at zero frequency for x_l/x_o which is equal to $(f/J)\tau_o^2=f/K_v$. This slope may be shown to equal the lag error per unit velocity for these servomechanisms and indicates why $(f/J)\tau_o$ is small in high performance systems. This speed lag constant f/K_v will determine the necessary value for K_v in some cases rather than either the static or acceleration error limit.

The Transient Response

The justification for setting up criteria for good dynamic response on a frequency analysis basis is that solutions on this basis take considerably less calculation time and give essentially the same results as a transient analysis. Nevertheless it is of interest to show a few transient responses for comparison with corresponding frequency responses.

When the motor delay T_M/τ_o is negligible, the two types under discussion have the same transfer function and differen-

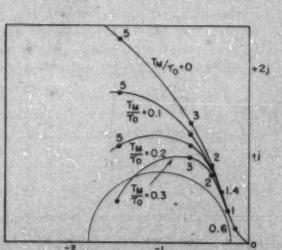

Figure 6. Inverse transfer functions e/x_o servomechanism stabilized by speed feedback through a high-pass filter

$T_N/\tau_o=2$, $(\tau_s/\tau_o)^2=0.05$

tial equation with the following parameters analogous:

$$T_A/\tau_0 \longrightarrow T_N/\tau_0$$
$$T_B/\tau_0 \longrightarrow (T_N/\tau_0)(\tau_s/\tau_0)^2$$
$$T_B/\tau_A \longrightarrow (\tau_s/\tau_0)^2$$

Consequently they will have the same transient responses.

Figure 8 shows the error as a function of time resulting from a suddenly applied input velocity of n radians per second for the case of $T_A/\tau_0=2$ and several values of T_B/τ_0. It will be observed that for $T_B/\tau_0=0.2$ the oscillatory character is barely distinguishable, but it is definitely present for $T_B/\tau_0=0.4$. In the frequency response, $T_B/\tau_0=0.2$ gives a resonant peak $|x_o/x_i|$ of about 1.25, which has been considered good performance, while for $T_B/\tau_0=0.4$ the resonant peak is slightly over 1.5. Thus there is general agreement in the two methods. Sometimes it will be found that simple transient responses mask some of the oscillatory character which is accentuated when several similar servomechanisms are interacting in a common system and two resonant servomechanisms are in cascade.

It is also to be observed that the error peak is roughly $1/2\,n\tau_0$ and that the time required for the transient to die out is about $4\tau_0$ seconds. Therefore there is a dual advantage to making τ_0 low, and the reason for the definition of τ_0 in this particular way is that several different servomechanisms may be placed on a similar basis for comparison. τ_0 has another interpretation in that it is near $1/2\pi$ times the period of oscillation with poor stabilization (T_A/τ_0 or T_N/τ_0 too small).

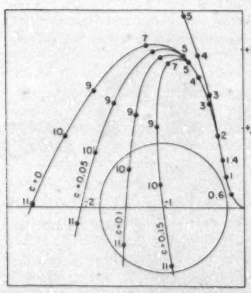

Figure 7. Inverse transfer functions e/x_o for servomechanism stabilized by speed feedback, with secondary delay

$T_N/\tau_0=2$
$(\tau_s/\tau_0)^2=0.02$
$T_M/\tau_0=0.2$

Figure 8. Transient response to a suddenly applied input velocity

Servomechanism stabilized by lead network, with motor delay

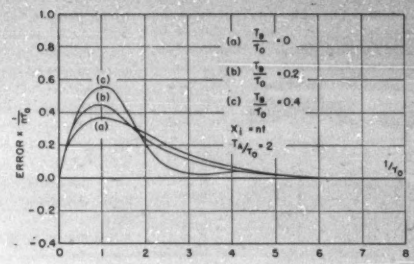

A suddenly applied change in input velocity is a fairly severe disturbance which is not often met in practice. Usually the input motion will be fairly smooth in that there will not be any large changes of acceleration in less than $4\tau_0$ seconds (the transient time), so that the dynamic error will be very closely equal to τ_a^2 times the acceleration. Therefore, the quantity τ_a^2 is a good measure of the dynamic performance of the servomechanism. In the two cases considered τ_s is equal to τ_a, but there are other types which have quantities analogous to τ_s and τ_a but not equal. Therefore, two different symbols have been used to maintain the distinction.

Comparison of the Two Types

The analysis has brought out the fact that the dynamic response can be made essentially the same for the two types, and that improvement in performance is limited by the motor delay according to the relation

$$\tau_0=\tau_s>4T_M$$

As a consequence of this there is little choice between the two if high-speed dynamic response is the difficult specification to meet.

The sensitivity to positional or static errors, however, is different for the two types. For lead network stabilization τ_s is equal to τ_s and limited by the same factor, and therefore $K_s=J/\tau_s^2$, the torque per unit error, is limited by

$$K_s<J/16T_M^2$$

For the speed feed-back type, τ_s^2 must be at least about 11 times smaller and could be many times less than this, limited only by the existence of secondary delays. Consequently, if high static sensitivity is the difficult specification to satisfy, the latter type is preferable.

Because servomechanisms are essentially low-pass filters, they will not follow disturbances which have frequency components above a certain frequency which is proportional to $1/\tau_0$, depending upon how the band width of response is defined. Consequently for equivalent static sensitivities the speed feed-back type is a better filter and has smoother response in the presence of high-frequency spurious error signals. This is sometimes a desirable characteristic when the error measuring device is susceptible to spurious signals.

Some error measuring devices have a serious amount of high-frequency electrical noise or unfiltered ripple which tends to overload the amplifier or motor without producing any average torque. The amplification in the servo loop up to the amplifier output is a measure of the possibility of this type of overloading.

For the lead network stabilization, the high frequency amplification is proportional to

$$K_s\frac{T_A}{T_B}=\frac{J}{\tau_s^2}\times\frac{T_A}{T_B}$$
$$=\frac{J}{\tau_0^2}\times\frac{T_A}{T_B}$$

while for generator feed-back stabilization it is

$$K_s=\frac{J}{\tau_s^2}$$
$$=\frac{J}{\tau_0^2}\left(\frac{\tau_0}{\tau_s}\right)^2$$

and consequently, for equivalent static sensitivity the latter type has less gain and is superior by a factor T_B/T_A, which is less than say 0.09. However, for equivalent dynamic response they are about equal because T_A/T_B and $(\tau_0/\tau_s)^2$ are analogous.

Another type of spurious signal is a low frequency signal which cannot produce torque. For example, a signal 90 degrees out of phase from a true a-c error signal cannot produce torque in an induction motor. The gain for this type is K_s in each case so that the two are equivalent

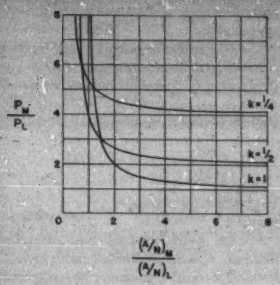

Figure 9. Gearing design curves

on a static sensitivity basis, but the lead network type is superior on an equal dynamic response basis.

Because the error measuring device often is geared down considerably from the motor shaft, there may be a serious amount of backlash between the two which tends to promote oscillations. As the stabilizing signal in the speed feedback type is usually much more directly coupled to the motor, it has less tendency to be disturbed by the backlash of the error signal.

Motor-to-Load Gearing

In the detailed design of a servomechanism the choice of a suitable servomotor and motor-to-load gear reduction is sometimes the source of considerable confusion. An analysis of this problem leads to a means for specifying the applicability of a servomotor for a particular problem and to a procedure for finding the proper gear reduction. In addition it points out the proper direction for improved servomotor development.

The following quantities concerning the load are considered as specified by the application:

F_L = dry friction load including a safety factor
J_L = load inertia
n_L = minimum available load speed
a_L = minimum available load acceleration
e_s = allowable positional or static error due to the dry friction, as measured at the load shaft
e_a = allowable error at the load shaft due to the maximum acceleration. $\tau_a^2 \leq \frac{e_a}{a_L}$

The servomotor is characterized by

F_M = available peak motor torque
J_M = motor inertia
F_M/J_M = maximum free acceleration of the motor, or torque-to-inertia ratio
n_M = maximum speed of the motor, which is discussed in more detail later
T_M = motor response delay

The design problem may be stated as follows. Can proper gearing between the motor and load be found which will allow the servomotor to meet the application specifications?

Let g = gear reduction from the motor to the load.

The first requirement of the gearing is that the maximum motor speed after gear reduction should be not less than the required load speed

$$g = k\frac{n_M}{n_L}, \quad k \leq 1 \tag{27}$$

The second requirement is that the possible acceleration of the motor and load system be not less than a_L. The torque available for acceleration, as measured at the load shaft, is $(gF_M - F_L)$. The effective inertia at the load shaft is $(g^2J_M + J_L)$. Therefore the second condition for the gearing is

$$\frac{gF_M - F_L}{g^2J_M + J_L} \geq a_L \tag{28}$$

By combining equations 27 and 28 and arranging factors

$$\frac{F_M n_M}{(F_L + J_L a_L)n_L}\left[k - k^2\frac{a_L/n_L}{(F_M/J_M)/n_M}\right] - 1 \geq 0, \; k \leq 1 \tag{29}$$

The various factors involved in equation 29 may be given the following interpretations and symbols:

$P_M = F_M n_M$
= peak power output of the motor
$P_L = (F_L + J_L a_L)n_L$
= peak power absorbed by the load
$(A/N)_M = \frac{F_M/J_M}{n_M}$
= acceleration-to-speed ratio of the motor
$(A/N)_L = a_L/n_L$
= acceleration-to-speed ratio of the load

$$\frac{P_M}{P_L}\left[k - k^2\frac{(A/N)_L}{(A/N)_M}\right] \geq 1, \; k = g\frac{n_L}{n_M} \leq 1 \tag{30}$$

Equation 30 may be interpreted with the aid of Figure 9. For each value of $k \leq 1$, any motor which has P_M/P_L and $(A/N)_M/(A/N)_L$ values which lie to the right and above the curve for the corresponding k may be used. Thus the usefulness of a motor is determined by both P_M and $(A/N)_M$ while the difficulty of a set of specifications is measured by P_L and $(A/N)_L$.

Equation 30 may be placed in another form which shows up other aspects of these relations. Thus

$$\frac{P_M}{P_L} \times \frac{(A/N)_M}{(A/N)_L}\left[\frac{k}{\frac{(A/N)_M}{(A/N)_L}} - \left(\frac{k}{\frac{(A/N)_M}{(A/N)_L}}\right)^2\right] \geq 1 \tag{31}$$

Equation 31 has a solution only if

$$\frac{P_M}{P_L} \times \frac{(A/N)_M}{(A/N)_L} \geq 4 \tag{32}$$

Figure 10 illustrates these relations. In view of equation 32 it appears that

$$P_M \times (A/N)_M = F_M^2/J_M$$

is another measure of the usefulness of a motor, and

$$P_L \times (A/N)_L = (F_L + J_L a_L)a_L$$

is a measure of the specification difficulty. Thus a high value for F_M^2/J_M appears to be more valuable for a motor than a high value for the usually specified torque-to-inertia ratio F_M/J_M.

The justification for placing these equations in such a difficult form is that any measure of the performance of a motor must be independent of any gearing placed after the motor. Thus $P_M = F_M n_M$, $(A/N)_M = F_M/J_M n_M$, and F_M^2/J_M are all independent of gearing. A motor disguised by the addition of a gear box is still the same motor and has the same range of application. This is not true for the torque-to-inertia ratio specification.

In addition to its power and acceleration-to-speed ratio, the merit of a motor is measured also by its response delay T_M. For the two types of servomechanism under discussion, T_M must be less than about $0.25\tau_a$, where τ_a is determined by the specifications according to the following relations:

$$\tau_a^2 \leq e_a/a_L \tag{33}$$

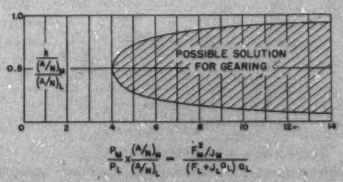

Figure 10. Gearing design curves

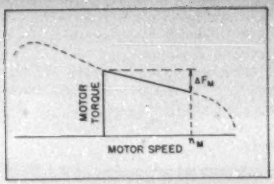

Figure 11. Torque–speed characteristic

$$16T_M^2 \leq \tau_a^2 = \tau_s^2 \text{ for lead network stabilization} \quad (34)$$

$$16\Gamma_M^2 \leq \tau_a^2 = (11 \text{ to, say, } 40)\tau_s^2 \text{ for speed feed-back stabilization}$$

and

$$\tau_s^2 = \frac{J}{K_s} \leq \frac{J_M k^2 + J_L}{F_L} \times e_s$$

$$= \frac{k^2 J_M n_M^3 + J_L n_L^3}{F_L n_L^2} \times e_s \quad (35)$$

If the specifications should call for a τ_a^2 according to equation 33 which is too small relative to T_M^2, there is no choice but to find a new motor with less delay. If, however, it is the specifications according to equations 34 and 35 which are difficult to meet, τ_s^2 may be kept large by setting k as near unity as possible. Another possibility is to add to the motor inertia J_M, provided only that equation 33 is not violated and that $(A/N)_M$ is not reduced too far to make gearing impossible.

A numerical example can illustrate these relations more clearly. Consider the following set of specifications:

$F_L = 5{,}000$ inch-ounces
$J_L = 2{,}000$ inch-ounces per radian per second^2
$a_L = 0.5$ radian per second^2
$n_L = 0.5$ radian per second
$e_a = 0.001$ radian
$e_s = 0.0005$ radian

These specifications determine

$$P_L = (F_L + J_L a_L) n_L$$
$$= (5{,}000 + 2{,}000 \times 0.5)(0.5)$$
$$= 3{,}000 \text{ inch-ounce-radians per second}$$

$$J_L n_L^2 = 2{,}000 \times (0.5)^2$$
$$= 500 \text{ inch-ounce-radians}$$

$$e_a/a_L = \frac{0.001}{0.5}$$
$$= 0.002 \text{ second}^2$$

$$(A/N)_L = a_L/n_L$$
$$= \frac{0.5}{0.5}$$
$$= 1 \text{ per second}$$

These values determine that the motor chosen must have a power at least as large as P_L and a delay T_M less than

$$0.25\sqrt{e_a/a_L} = 0.25\sqrt{0.002}$$
$$= 0.011 \text{ second}$$

Consider a motor with the following characteristics:

$F_M = 10$ inch-ounces
$J_M = 0.002$ inch-ounce per radian per second^2
$n_M = 500$ radians per second
$T_M = 0.01$ second

Then

$$P_M = F_M n_M$$
$$= 10 \times 500$$
$$= 5{,}000 \text{ inch-ounce-radians per second}$$

$$F_M/J_M = \frac{10}{0.002}$$
$$= 5{,}000 \text{ radians per second}^2$$

$$(A/N)_M = \frac{5{,}000}{500}$$
$$= 10 \text{ per second}$$

$$J_M n_M^2 = \frac{5{,}000}{10}$$
$$= 500 \text{ inch-ounce-radians}$$

Therefore

$$P_M/P_L = \frac{5{,}000}{3{,}000}$$
$$= 1.67$$

$$\frac{(A/N)_M}{(A/N)_L} = \frac{10}{1} = 10$$

$$\frac{n_M}{n_L} = \frac{500}{0.5} = 1{,}000$$

Referring these values to Figure 9 indicates that k may be between 1 and 0.64, so that the gearing may be between 1,000 and 640. With these values τ_s^2 may be calculated according to equation 35

$$\tau_s^2 = \frac{k^2 500 + 500}{5{,}000 \times (0.5)^2} \times 0.0005$$
$$= 0.0004 \text{ second}^2 \text{ for } k = 1$$

Thus τ_s may be 0.02 second or somewhat less.

If the lead network type of stabilization is used, $\tau_a = \tau_s = \tau_e$ and each must be greater than $4T_M = 0.04$ second. Therefore, something must be done about increasing τ_s from 0.02 to 0.04. One possibility which often works is to increase J_M by the addition of extra inertia.

With the power ratio $P_M/P_L = 5/3$, the acceleration-to-speed ratio may be decreased to 2.4 (from Figure 9) and still allow a gearing solution $k = 1$. Then

$$\tau_s^2 = \frac{1 \times \frac{5{,}000}{2.4} + 500}{5{,}000 \times (0.5)^2} \times 0.0005$$
$$\approx 0.001$$

$\tau_s \approx 0\ 032$, which is still too small, but J_M cannot be increased further without more motor power.

Consequently, in order to use the lead network stabilization, a motor with less delay must be found or some of the specifications relaxed, possibly by allowing the slightly higher resonance obtained with

$$T_M/\tau_e = \frac{0.01}{0.032} = 0.32$$

In this case the resonance peak is still less than 1.5.

For the speed feed-back type of stabilization, $\tau_a^2 = \tau_e^2$ is limited fairly closely to 0.002 second^2 as it cannot be larger and meet the specifications nor can it be much smaller and still have $\tau_e > 4T_M$. Therefore, τ_s^2 must be less than about $(1/11)\tau_e^2 \approx 0.00018$ second^2. τ_s^2 may be made smaller either by reducing the gear ratio or by setting the value of e_s lower, that is, by increasing K_s. If k is set at its minimum value $k = 0.64$

$$\tau_s^2 = \frac{(0.64)^2 500 + 500}{5{,}000(0.5)^2} \times 0.0005$$
$$= 0.00028 \text{ second}^2$$

τ_s^2 is still too large so that the value of e_s must be decreased, that is, the sensitivity

$$K_s = F_L/e_s$$

must be greater than the static specifications require. But this is no disadvantage except possibly that a less noisy error signal is required.

Motor Torque–Speed Characteristics

Thus far in the analysis a critical discussion of what is meant by peak motor speed n_M has been avoided. The assumption has been made that the motor torque for full excitation is reasonably constant up to a limiting speed n_M. There are several motor types for which this assumption is good; for instance, certain induction motors which have fairly constant torque up to the region of synchronous speed. A-c and d-c motors in which the field is controlled by vacuum tubes and the armature circuit is arranged to keep the current fairly constant and independent of the back electromotive force are also in this class. In the latter case there is either a speed above which it is not considered mechanically feasible to drive the motor or a speed at which the torque falls off fairly sharply because of a rapid increase in windage and hysteresis losses, or a change in circuit conditions.

Other electric motors such as certain induction motors and d-c motors which have their armature voltage controlled

have a torque characteristic which falls off more or less linearly with speed over the useable range, as shown in Figure 11. In this case the analysis is more complicated because there is an error proportional to speed in addition to the static and acceleration errors which must be specified. In forming specifications for a system using a motor of this type, it is necessary to consider such things as what proportions of maximum speed and maximum acceleration are likely to occur simultaneously and whether or not it is allowable to have larger errors at high speed than at low speed.

If the same forward accelerations are desired at all speeds, the problem is somewhat simplified as n_M may be chosen at any value which will give

$$P_M = (F_M - \Delta F_M) n_M$$

and

$$(A/N)_M = \frac{F_M - \Delta F_M}{J_M n_M}$$

values which allow a gearing solution. As both P_M and $(A/N)_M$ decrease with speed, there is a maximum allowable speed n_M which falls on the portion of the curve of equation 30 for $k=1$.

The damping factor f/J used previously for the complete system is

$$\left(\frac{\Delta F_L}{J_L n_L} + \frac{\Delta F_M}{J_M n_M}\right) \text{ second}^{-1}$$

where ΔF_L is the increase in load from zero speed to speed n_L, and ΔF_M is the decrease in motor torque from zero speed to speed n_M. Both factors have the dimension of second^{-1} and may be added directly without the introduction of gear ratios. $\Delta F_M / J_M n_M$ will be always less than

$$\frac{F_M}{J_M n_M} = (A/N)_M$$

and for many cases will be only one-half this value, corresponding to maximum motor power output at speed n_M.

In the absence of a definite application, it does not appear worth while to pursue this analysis further. There is one important class of applications, namely, instrument servomechanisms, to which the gearing analysis does not completely apply as both F_L and J_L are considered negligible, but the same principles should apply.

Other Servomechanism Types

There are several other types of servomechanisms with different physical equipment to which the same basic equations or small variations apply. Some of these will be described briefly.

It has been assumed that the principal delay was in the motor, but the analysis will apply as well to any other equipment with a delay in the same portion of the control loop as the motor.

A form of stabilization similar to lead network stabilization may be obtained if some speed measuring device is placed on both the input and output shafts and the difference in speed $(px_i - px_o)$, which is equal to the error derivative pe, added to the error signal yielding a signal $(1+T_A p)e$. In this case T_B may be taken equal to zero or considered as a secondary delay.

In place of a generator with a high-pass filter producing a signal

$$\frac{T_G T_N p^2}{1+T_N p} x_o$$

it is possible to use an accelerometer with a low-pass filter or a delay network yielding

$$\frac{\tau_a^2 p^2}{1+T_N p} x_o .$$

The same analysis applies, but variation of any of the physical parameters has a different effect on the analysis parameters τ_s, τ_o, T_N/τ_o, and so forth, than previously. The extension is fairly straightforward.

If an inertia J_D is coupled to the servomotor by viscous friction with coefficient f_D, a device known as an inertia damper is obtained. Oil often is used for the viscous coupling so that the torque on the damper inertia is proportional to the difference in speed of the motor and damper. Analysis of this case yields

$$\frac{\text{Motor torque}}{x_o} = p^2 J \left[\frac{J+J_D}{J}\right] \times \left[\frac{1+p\dfrac{1}{f_D} \times \dfrac{JJ_D}{J+J_D}}{1+p\dfrac{J_D}{f_D}}\right] \quad (36)$$

where all quantities are measured at the load shaft, that is, $J = J_L + g^2 J_M$, $J_D = g^2$ (damper inertia), and $f_D = g$ (friction coefficient).

This inverse transfer function is similar to the square bracket of equation 18 and the following analogous relations may be set up:

$$\tau_s^2 \longrightarrow J/K_s$$

$$\tau_a^2 = \tau_o^2 \longrightarrow \frac{J+J_D}{K_s}$$

$$(\tau_s/\tau_o)^2 \longrightarrow \frac{J}{J+J_D}$$

$$T_N \longrightarrow J_D/f_D$$

$$T_G \longrightarrow f_D/K_s$$

and analogous design relations apply. It is interesting that this servomechanism is similar to the speed feed-back type when $T_M = 0$, and $\tau_s^2 \neq \tau_o^2$. However, all delays have an effect similar to that for the lead network type, and in particular, the extreme sensitivity to secondary delays is not present.

Other types have transfer functions different in algebraic form from those given but closely approaching the same form for values of λ greater than some small value, say, 0.5. For these, some of the same design criteria may be used, along with additional ones which allow the various types to converge for $\lambda > 0.5$. Examples of this type are the commonly known integral controls which are best left to a separate paper.

Appendix. Nomenclature

a_L = minimum available load acceleration

$(A/N)_M = \dfrac{F_M/J_M}{n_M}$ = acceleration-to-speed ratio of the motor

$(A/N)_L = a_L/n_L$ = acceleration-to-speed ratio of the load

c = ratio of secondary-to-primary delay

$e = x_i - x_o$ = deviation or error

e_a = allowable error at the load shaft due to the maximum acceleration

e_s = allowable proportional or static error due to dry friction, as measured at the load shaft

F = dry friction torque

f = viscous friction coefficient or torque change per unit change of speed

F_L = dry friction load torque including a safety factor

F_M = available peak motor torque

F_M/J_M = maximum free acceleration of the motor, or torque-to-inertia ratio

g = gear reduction from the motor to the load

J = effective moment of inertia of motor and load

J_L = moment of inertia of the load

J_M = moment of inertia of the motor

K_s = motor torque per unit error, static sensitivity

λ = nondimensional measure of angular frequency

n_L = minimum available load speed

n_M = maximum motor speed

p = differential operator

$P_L = (F_L + J_L a_L) n_L$ = peak power absorbed by the load

$P_M = F_M n_M$ = peak power output of the motor

T_A = circuit time constant

T_B = circuit time constant

T_G = circuit time constant

T_N = circuit time constant

T_M = motor response delay time

$\tau_a = \sqrt{\dfrac{\text{acceleration error}}{\text{acceleration}}}$, a time constant

$\tau_s = \sqrt{J/K_s}$, a defined time constant

$\tau_p = \lambda/\omega$, servo time constant used as a measure for other time constants

x_i = input co-ordinate

x_o = output co-ordinate

References

1. Considerations in Servomechanism Design, S. W. Herwald. AIEE Transactions, volume 63, 1944, December section, pages 871–6.

2. Dimensionless Analysis of Servomechanisms by Electrical Analogy, S. W. Herwald, G. D. McCann. AIEE Transactions volume 65, 1946, October section, pages 636–9.

3. Dynamic Behavior and Design of Servomechanisms, G. S. Brown, A. C. Hall. *Transactions*, American Society of Mechanical Engineers (New York, N. Y.), volume 68, July 1946, pages 503–24.

4. Parallel Circuits in Servomechanisms, H. Tyler Marcy. AIEE Transactions, volume 65, 1946, August-September section, pages 521–9.

5. Frequency Response of Automatic Control Systems, H. Harris. AIEE Transactions, volume 65, 1946, August-September section, pages 539–46.

6. The Analysis and Design of Servomechanisms, H. Harris. *Transactions*, American Society of Mechanical Engineers (New York, N. Y.), volume 69, April 1947, pages 367–80.

Discussion

H. Chestnut (General Electric Company, Schenectady, N. Y.): In the design of servomechanisms, there are employed two basic methods of providing the desired stability and accuracy of an over-all system or for components within a system. In this paper, Herbert Harris points out examples of these basic methods as applied to a torque motor power element with an associated time constant. As is indicated so ably by Harris, the two methods when properly employed produce quite comparable results in many respects. I should like to generalize further the two basic design methods and point out some applications where one or the other method is particularly well fitted. The basic design methods to which I refer have been termed

1. Series means for providing stability and accuracy.

2. Feedback or parallel[1] means for providing stability and accuracy.

These are illustrated by the examples shown in Figures 1 and 2 respectively of Harris' paper. In many high performance servomechanisms both of these means are employed, each being used to provide their desired effect. The automatic control system shown in Figure 3 of George J. Schwartz's paper[2] is illustrative of a servomechanism system in which both series and feed-back stabilizing means are employed.

When series methods are employed, the stabilization is inserted in series with the remainder of the system, and compensation is made for the characteristics of the remainder of the system. As long as the characteristics of the remainder of the parameters of the system are constant and do not vary appreciably with time or operating conditions, the series method may be employed to advantage.

However, if, for example, the gain of the motor K_s were to change, the values of $\tau_s = \tau_o$ and T_m/τ_o would change; as the design values listed in Harris' paper are based on a certain T_m/τ_o ratio, the change in gain will alter the performance of the system directly.

In cases where there are a minimum of spurious higher frequency signals present in the input, this method is advantageous. As pointed out by Harris, these spurious signals may overload amplifier and prevent proper amplification of desired signals. In addition to the use of lead network of the type illustrated in the example used by Harris, series means may include lag networks which decrease the signal transmitted through them at higher frequencies rather than increase them as in the case of lead networks. So-called "integral type" controllers fall into this category. Frequently, combinations of lead and lag networks are used to produce different desired effects in the various frequency ranges included in the input signal to the servomechanism.

The use of cheap reliable network elements in the amplifier stages of a servo amplifier is particularly attractive in that little added equipment or maintenance is required when these series means are employed. However, changes in the gain of the remainder of the system, which generally occur with time, if not with operating conditions, are not mitigated at all by the series stabilizing means. Hence, in large production jobs, where close manufacturing tolerance can be obtained only at additional expense, series stabilization seldom is used exclusively.

Feed-back means are used to provide a net signal to a servo element which is a function of the input to that element and some function of the output of the element. In a sense it is a supplementary closed loop and its performance and stability must be considered in the same careful manner that the over-all closed loop is considered. Three desirable functions which feed-back means can be made to perform are the following:

1. Feedback can minimize the effect of changing gain of an element on the stability and dynamic accuracy of a system.

2. Feedback can be used to reduce the time constant of a servoelement.

3. Feedback can be used to modify the form of a servoelement.

Harris' summary of design information pertaining to the feed-back type of servomechanism illustrates the first point. The

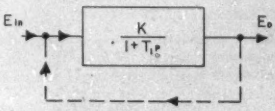

Figure 1. Servo element

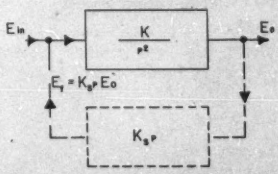

Figure 2. Servo element (top) and feed-back element (bottom)

delay limitation is shown to be imposed by the T_m/τ_o ratio where

$$\tau_o^2 = \tau_s^2 + T_G T_N$$

$$\tau_s^2 = J/K_s$$

$T_G T_N$ is determined by the feed-back parameters.

For good design $T_G T_N$ is shown to be much greater than τ_s^2, greater than nine to one in the illustrative example. Hence changes in τ_s caused by changes in gain K_s represent a smaller percentage change in τ_o and likewise in T_m/τ_o ratio. The feed-back parameters $T_G T_N$ are the dominant factors, and they are quantities which are selected at the discretion of the designer.

Noting that the time lag for constant acceleration output motion is $(\tau_s^2 + T_G T_N)$ times the acceleration, it is apparent that changes in τ_s^2 caused by changes in the gain K_s will not be noticeable because of the high ratio of $T_G T_N$ to τ_s^2. Hence the use of feed-back has reduced the change in the over-all accuracy for high acceleration signals caused by the changes in the gain of the servomotor itself.

Although use has been made of the results of Harris' work on a specific system, a more generalized analysis of feedback reveals the same beneficial results of feedback.

To illustrate the use of feedback in reducing the time constant of a servo element consider Figure 1 of this discussion. A servo element with gain K and a time constant T_1 is shown by the solid lines. The input to the element is E_{in}, the output E_o. Thus

$$\frac{E_o}{E_{in}} = \frac{K}{1+T_1 p}$$

If now the output is fed back to the input as shown by the dotted line, the following equation for the system may be written:

$$\frac{K(E_{in} - E_o)}{1+T_1 p} = E_o$$

Combining

$$KE_{in} = (T_1 p + 1 + K)E_o$$

and finally,

$$\frac{E_o}{E_{in}} = \frac{K}{1+K}\left[\frac{1}{1+\frac{T_1}{1+K}p}\right]$$

Thus the time constant T_1 has been reduced effectively to $\frac{T_1}{1+K}$ by the use of feedback. Because, as is pointed out in Harris paper, the limit on servomechanism performance frequently is caused the value of a

particular time constant, feedback provides a means for reducing the offender.

However, it will be noted that there has been a loss of gain by the same $\frac{1}{1+K}$ factor which must be compensated for elsewhere in the system. Generally amplification can be obtained at low power levels and this is no severe limitation.

Modification of the form of a servoelement is an important application of feedback and Figure 2 of this discussion should serve to illustrate this point. The servoelement shown in solid lines, with input E_{in} and output E_o, has a transfer function.

$$\frac{E_o}{E_{in}} = \frac{K}{p^3}$$

Suppose now the output is fed back through a feed-back element shown by the dotted connection which has as its transfer function

$$\frac{E_f}{E_o} = K_s p$$

The resultant equation for the system with the feedback connected is

$$\frac{E_o}{E_{in}} = \frac{1}{K_s p\left(1+\frac{p}{KK_s}\right)}$$

If $KK_s \gg 1$, then this equation reduces to

$$\frac{E_o}{E_{in}} = \frac{1}{K_s p}$$

and the transfer function has been changed in form from one in which the output acceleration is proportional to the input signal to one in which the output is proportional to the input signal.

As Harris has pointed out, the feed-back signals can be used most effectively when they are used with filters which utilize the feed-back effect only over a limited portion of the frequency range.

Although the use of feedback presents many attractive features, it is important not to gloss over some undesirable items associated with its use. In many cases tachometers or other signal sources are required which add cost and weight and increase the problems of production and maintenance. Frequently, additional wiring is required to bring the feed-back quantities into the amplifier stages. Occasionally, cathode followers, isolating amplifiers, or other means are required to change impedance levels and prevent undesirable interaction of elements. These factors, though not appearing explicitly in the technical analysis, nevertheless figure very prominently in the complete engineering appraisal of a servomechanism system.

Utilizing the concepts of series and feedback methods of stabilization, and using the attenuation-phase shift method described by Mac Coll,[3] one realizes that the use of single *RC* networks has limited somewhat the performance which can be obtained from the servomotor. By employing, on a series basis, two stages of lead networks or the equivalent and providing added gain, the static accuracy and frequency response can be improved. Likewise, by employing two stages of the *RC* network used in the feed-back network and appropriately changing the values of T_N, T_G, and K_s, an improved system utilizing feedback can be obtained. The complexity in analysis required by these added terms would contribute little to the comparison of the two basic servomechanism types performed so capably by Harris. I mention them only as possible means for overcoming some of the design limitations which are dependent on the filter characteristics which are assumed.

In conclusion I should like to take notice of the choice of $M=1.25$ as a design criterion for satisfactory performance. This figure seems to be somewhat lower than generally is considered essential for a system with satisfactory performance. In an actual system, the use of a lower M figure than is necessary means that the speed of response of the system may be impaired or a more elegant and costly design must be employed.

References

1. Parallel Circuits in Servomechanisms, H. Tyler Marcy. AIEE Transactions, volume 65, 1946, August–September section, pages 531–9.

2. The Application of Lead Networks and Sinusoidal Analysis to Automatic Control Systems, George J. Schwartz. AIEE Transactions, volume 66, 1947, pages 69–76.

3. Fundamental Theory of Servomechanisms (book), L. A. Mac Coll, D. Van Nostrand Company, Inc., New York, N. Y., 1945.

H. Tyler Marcy (M. W. Kellogg Company, Jersey City, N. J.): Herbert Harris is to be congratulated for undertaking a direct comparison of two servomechanism types often proposed for the same function.

I should like to indicate another interpretation of two of Harris' equations (8 and 13) which leads more easily to a comparison of the two techniques. If a nondimensional operator γ be defined as $T_M p$ then equations 8 and 13 may be rewritten.

$$\frac{e}{X_e}\frac{K_s T_M^3}{J} = \gamma^3(1+\gamma)\frac{1+\frac{T_B}{T_M}\gamma}{1+\frac{T_A}{T_M}\gamma}$$

$$\frac{e}{X_e}\frac{K_s T_M^3}{J} = \gamma^3(1+\gamma)+\frac{\frac{T_N T_G K_s}{J}\gamma^3}{\left(1+\frac{T_N}{T_M}\gamma\right)}$$

$$= \gamma^3(1+\gamma)\left[1+\frac{\frac{T_N T_G K_s}{J}}{(1+\gamma)\left(1+\frac{T_N}{T_M}\gamma\right)}\right]$$

For the two systems to be nearly alike in resonant characteristics, which has been used as a criterion of similarity, then the comparison of the two techniques reduces to a comparison of the two functions.

$$\frac{J}{K_s T_M^3}\frac{1+\frac{T_B}{T_M}\gamma}{1+\frac{T_A}{T_M}\gamma} \qquad (1)$$

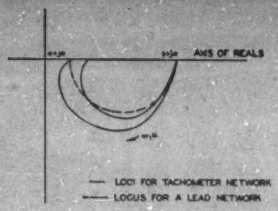

Figure 3

and

$$\frac{J}{K_s T_M^3}\frac{\frac{T_N}{T_M}\gamma^3+\left(\frac{T_N}{T_M}+1\right)\gamma+\left(1+\frac{T_N T_G K_s}{J}\right)}{\frac{T_N}{T_M}\gamma^3+\left(\frac{T_N}{T_M}+1\right)\gamma+1} \qquad (2)$$

Both these functions are familiar when the operator γ is replaced by a complex frequency $j\omega$ and loci drawn. The first is the reciprocal of a lead network and is a semicircle. The second is a form of a matching lead network discussed by Hall.[1] Figure 3 of this discussion shows sketches made of these loci when $J/K_s T_M^3=1$ and an attenuation ratio of five assumed for the lead network.

It will be recognized that there is more freedom in the design of the tachometer feedback as represented by loci for matching lead networks. It at once will be obvious that the two loci can be made to approximate the same phase characteristic over a critical frequency range. This can be done with an increase of the system K_s if an adequate signal level is available from the tachometer as Harris points out.

Reference

1. The Analysis and Synthesis of Linear Servomechanisms (book), A. C. Hall, Technology Press, Massachusetts Institute of Technology, Cambridge, Mass., 1943.

Herbert Harris: The discussions of H. Chestnut and H. Tyler Marcy are quite constructive, and the author has no real disagreement with any of the points presented. Personal preferences as to methods of analysis and to specifications, such as allowable height of resonance peaks, always will be present as long as engineers work in different organizations and on different equipment.

The author wonders whether Chestnut can have any proof of his generalization that feed-back means of stabilization is always less susceptible to the efforts of parameter changes than the series method. These two cases do not prove such a generalization, and it would seem possible to devise contradictions.

The apparent cheapness of network components is often spurious whenever feedback means of stabilization can allow the mechanical system to have less rigidity and more backlash.

An Integrated Control System for Aircraft D-C Generators

A. T. McCLINTON
ASSOCIATE AIEE

Synopsis: This paper describes an electric system for d-c generators used on aircraft that allows physical integration of all control elements normally associated with the control of the generator. The proposed system differs from the present system used by the Army and Navy primarily in that integration has been accomplished in addition to offering automatic control of the generator without a sacrifice in system performance. No attempt has been made to compare this system with present systems. It is the purpose of this paper to describe the individual control elements of the proposed system and to discuss their characteristics.

THE OUTPUT of d-c generators in use at the present time in aircraft is controlled primarily by two elements, namely, a regulator and a relay. The function of the regulator is to maintain the voltage at a predetermined magnitude at some particular point on the electric system for specific conditions of operation of the generator. The principal function of the generator control relay is to connect the generator to the bus whenever the generator is capable of furnishing power to the bus and to disconnect the generator when it is no longer able to furnish power. Controlling this relay by a switch provides a means for manually disconnecting the generator from the bus. Other items normally associated with these control elements are a voltmeter, ammeter, a visual indicator to signal when the generator is disconnected from the bus, and some provision for connecting the equalizer coil to the equalizer bus.

If proper consideration is given to the selection of these control elements and to the configuration of the generator control system, it should be possible to realize the following:

1. System regulation at the aircraft load bus should not be dependent upon the regulator characteristic and line drop but should be governed simply and effectively for any system.

2. Load division should be controlled accurately and readily and should not be dependent upon the proper balance of line resistances and regulator characteristics.

3. The operation of each generator, whether on a single or multigenerator system, should be automatic, thus requiring none of the pilot's or flight engineer's attention.

4. The design and arrangement of the various control elements should permit placing all of these elements into one control panel (in all present installations these generator control elements appear in the aircraft as separate units and frequently in widely spaced parts of the aircraft), so that

(a). Servicing of the aircraft would be simplified.
(b). Possible faults in the control circuit can be determined readily and corrected.
(c). Setting of system voltage would be simplified.

5. The control system would allow bench adjustment of all components. The only adjustment necessary after the control unit is placed in the aircraft would be to set the system voltage.

This, by means of introduction, defines the requirements which the generator control system should meet. In order to satisfy these requirements for system performance, the control elements have been set up as follows.

Voltage Regulator

In order to accomplish the first two requirements for the control system, the voltage regulator should be able to maintain the same no-load voltage for all generators as well as to give approximately the same regulation for each generator comprising the system. If it were possible to obtain identical regulation for all generators, the problem of obtaining proper load division would be simplified greatly. Experience has demonstrated, however, that with present carbon pile regulators the regulation is dependent upon the setting of the regulator as well as upon the particular generator used. One other factor which must be considered is the voltage drop in the power leads from the point of regulation to the point of paralleling the generators.

As a means of providing uniform regulation which is independent of these factors, it is proposed that a carbon pile regulator, equipped with a line-drop compensating coil be used. Such a device was used formerly on the industrial Tirrel-type regulator. Figure 1 shows a schematic diagram of this regulator with the connections to the generator. The voltage signal for the line-drop compensating coil is taken from a potentiometer which is connected across the series field of the generator. Because the drop across the series field is proportional to the generator current, the resultant effect of the line-drop compensating coil on the regulated voltage will be proportional to the generator current. The connections to the potentiometers will allow for either plus or minus compensation; that is, the voltage at the load bus can be made to increase or to decrease with increase in generator current. Thus the regulation of the electric system can be made drooping, flat, or rising; but of greater importance, it can be controlled. This

Paper 47-14, recommended by the AIEE committee on air transportation for presentation at the AIEE winter meeting, New York, N. Y., January 27–31, 1947. Manuscript submitted October 11, 1946; made available for printing November 7, 1946.

A. T. McCLINTON is engineer, aircraft electrical division, Naval Research Laboratory, Washington, D. C.

The author acknowledges the work of J. W. Allen, bureau of aeronautics, Navy Department, Washington, D. C., in the development of the line-drop compensating coil for the carbon pile regulator used on aircraft.

satisfies the first system-control requirement.

The second requirement of the control system is met by the equalizer coil. In addition to the line-drop compensating coil and voltage coil, each regulator is provided with an equalizer coil which is wound in a direction such as to compensate for unbalanced loads between generators. This coil has an amplification factor of approximately ten; that is, 0.25 volt across the equalizer coil will produce a 2.5-volt change in regulated voltage. Equalizer potential is obtained by using part of the voltage drop across the generator series field. An equalizer potentiometer, connected as shown in Figure 1, is used for this. Through the use of this potentiometer it is possible to adjust the equalizer potential to the same value for all generators. The resistance of the grounding circuit (bolts, lugs, and contacts) as well as lead resistance are neutralized through the use of the equalizer potentiometer.

As the regulation of each generator on a system can be controlled by means of the line-drop compensating coil, the setting of the equalizer potentiometer is independent of voltage regulation and thus can be made the same for all regulators on a system. The potentiometer is set to give a potential from tap to ground equal to 1.6 volts at full load on the generator. A voltage of 1.6 volts was chosen rather than some lower voltage because of the fact that better load division results. Because this voltage is compared with a similar voltage on other regulators connected to the equalizer bus, the error signal, for a given percentage load unbalance, is going to be proportional to the total drop across the equalizer potentiometer. It necessarily follows then that if the drop across the equalizer potentiometer is set for 1.6 volts rather than 0.8 volt, the minimum load unbalance detected by the regulator in the system using 1.6 volts will be one-half that of the system using 0.8 volt drop. Thus, better load division will result from the system using the higher equalizing voltage. The magnitude of equalizer potential was limited to 1.6 volts by the fact that the voltage drop across the series field of present standard aircraft generators varies from 1.6 volts to 5.0 volts, and it is desirable to standardize on one voltage setting for all generators.

The selection of an equalizer voltage of 1.6 volts coupled with the high amplification of this equalizer circuit necessitates the removal of this coil from the equalizer bus when the associated generator is disconnected from the load bus.

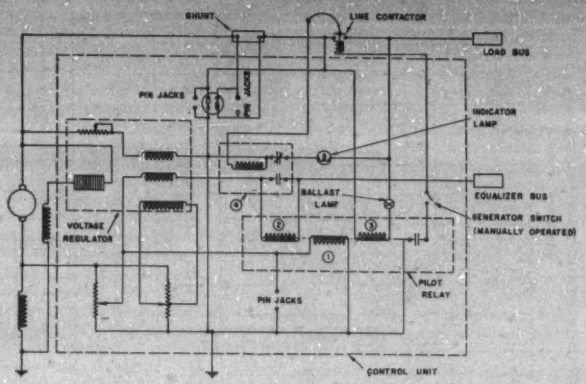

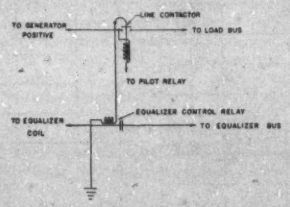

Figure 2. Connections for the equalizer control relay

Figure 3. Schematic diagram of an integrated control system for use with single or multi-generator system

1—Reverse current coil
2—Load differential coil
3—Voltage differential coil
4—Double-pole relay

Equalizer Circuit

In an effort to illustrate the effect of the equalizer coil on bus voltage when the associated generator is disconnected from the bus, Table I is presented. This table, based on an equalizer circuit resistance of 2.0 ohms does not represent the worst possible condition of operation, but demonstrates what is found to be the case in a typical system.

From this it becomes evident that the equalizer coil must be disconnected from its bus when the generator is disconnected

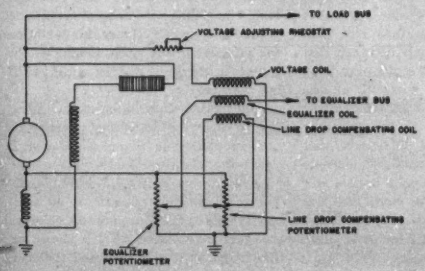

Figure 1. Schematic diagram of the voltage regulator control unit

Table I

Number of Generators in the System	Number of Generators Disconnected From Bus	Decrease in Bus Voltage With Full Load on Remaining Generators*
2	1	3.3
4	1	1.65
4	2	3.3
4	3	4.95

*This is based on the use of equalizer coils in which 0.25 volt causes a 2.5-volt change in regulated voltage; the equalizer potentiometer is set for 1.6 volts at full generator load; the equalizer circuit resistance is considered to be 2.0 ohms (0.4 ohm for each equalizer coil plus 1.2 ohms for interconnections).

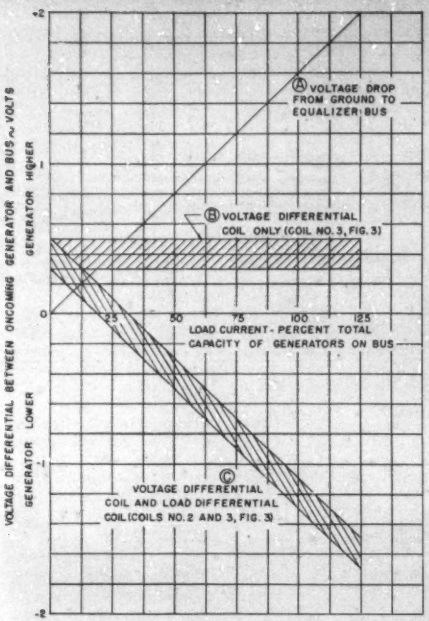

Figure 4. Closing characteristic of pilot relay when used with the integrated control system

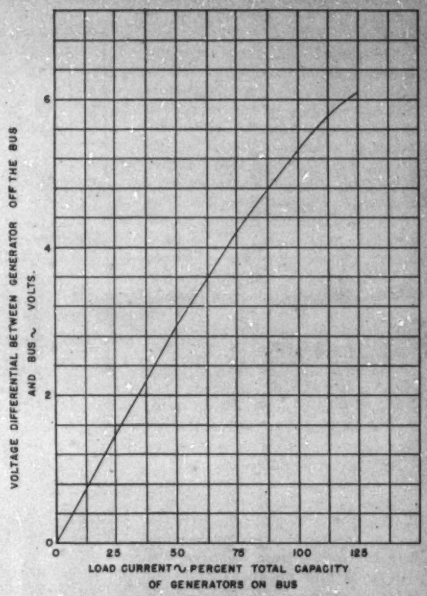

Figure 5. Characteristic of regulator equalizer coils and generator control elements on a multigenerator system

from the load bus. In the proposed system this was accomplished by inserting a relay in the equalizer circuit and connecting its operating coil between the armature of the double-break line contactor and ground (Figure 2). Thus, when the line contactor is open, the equalizer control relay is de-energized. The reasons for using this circuit in preference to several other possibilities will be evident as the complete integrated control system is developed.

Figure 2 immediately brings up another element used for generator control, that is the pilot relay which controls the line contactor.

Pilot Relay

This important item in the control system connects the bus to the generator when it can carry load, and disconnects the generator when it will no longer carry load. The pilot relay developed for use with the proposed system is a polarized device having two identical voltage coils and one current coil. The relay operates on a differential voltage principle, the two voltage coils giving the signal for closing, and the current coil giving the signal for opening the relay on reverse currents. Connections for this relay are shown in Figure 3. Referring to Figure 3, the line contactor coil is energized through the contacts of the pilot relay and a manually operated switch. Coil 2 or 3 will close the relay when the voltage across either coil is at least 0.4 volt and of the proper polarity, or when the algebraic sum of the coil voltages is at least 0.4 volt. Coil 1 will open the relay when no less than 0.08 volt of the proper polarity is impressed across the coil. The generator switch has been inserted to make it possible to remove the generator from the load bus. Referring to Figure 3, it will be noted that one of the voltage coils of the pilot relay connects across the contacts of the equalizer relay, completing the circuit for the equalizer coil to the equalizer bus. Because the load differential coil has a resistance of 20 ohms, the current in the equalizer coil circuit cannot decrease the bus voltage by more than 0.2 volt. This small change in bus voltage resulting from the pilot relay is of negligible magnitude.

The operation of the pilot relay is as follows. (This discussion is based on a 2-generator system although it can be made to apply for any number of generators.) Assume that the equalizer resistors are adjusted for 1.6-volt drop at full load on the generator and that one generator is connected to the bus. When the system load is zero, the voltage from the equalizer bus to ground or across the equalizer relay of the generator off the bus will be zero. Thus, the pilot relay can close only when the voltage of the oncoming generator is at least 0.4 volt higher than the bus voltage. If the system load is one-fourth rated generator load, the voltage from equalizer bus to ground is 0.4 volt. Under this condition the pilot relay will close as long as the generator voltage is at least equal to the bus voltage.

As a further explanation of the operation of this relay, its closing characteristics are plotted in Figure 4. Curve *B* shows the closing characteristic of the pilot relay when only coil 3 is employed. The relay pickup tolerance is approximately plus or minus 0.1 volt which gives the band from 0.3 to 0.5 volt shown on the curve. It should be noted that the

pickup characteristic of this coil is independent of the load on the aircraft bus. When coil 2 is connected also, the characteristic of the pilot relay is dependent upon the system load. The voltage across coil 2 is the same as the voltage drop from ground to equalizer bus, which is shown by curve *A*. As the flux created by the two coils adds algebraically to close the pilot relay, and because coils 2 and 3 are identical, the voltage differential between the oncoming generator and the bus need not be plus 0.4 volt but can be some value less, the amount depending upon the bus load. Because the algebraic sum of the voltages across these coils must be plus 0.4 volt, we need only to subtract the value of voltage appearing across coil 2 from 0.4 volt to get the voltage differential between the oncoming generator and bus which will allow closure of the pilot relay. This is done on Figure 4 by subtracting curve *A* from curve *B* to give the resulting closing characteristic, curve *C*.

The fact that the oncoming generator can have a voltage lower than the bus voltage at the time it is connected to the line brings up the question as to how this generator will be able to carry any of the system load. This is accomplished through the action of the equalizer coils. In way of explanation, let it be assumed that the equalizer coil of a generator is connected to the equalizer bus, but the line contactor of this generator is open. If there is a load on the remaining generators connected to the bus, the current flow in the equalizer circuit will cause an increase in voltage of the generator off the bus (line contactor open) and will cause the voltage of all generators on the bus to decrease. This will result in a new value of voltage difference between the generator off the bus and the bus voltage. The magnitude of this voltage differential caused by action of the equalizer coils is shown in Figure 5. This voltage difference is independent of the number of generators making up the system and the number of generators disconnected from the load bus. As long as the equalizer coils are able to produce a voltage differential which is numerically greater than the values on curve *C*, Figure 4 for corresponding bus load, the oncoming generator will take part of the bus load. A comparison of these curves will reveal that the slope of curve *C* can be increased greatly and still meet these requirements. An increase in the slope of this curve might be desirable in view of the fact that if the increase were accomplished a generator could be paralleled with the bus at lower system loads for a given voltage difference between the oncoming generator and the bus. This can be accomplished by increasing the ampere turns of coil 2, Figure 2; doubling it would double the slope of this curve.

The action of coil 1, Figure 3, is to open the pilot relay on reverse currents; that is, when the generator is no longer capable of carrying load. This coil will open the pilot relay when the voltage drop from the tap on the equalizer to ground is 0.08 volt. As the equalizer potentiometers are adjusted for 1.6 volts at full load on the generator, the pilot relay will open on a generator reverse current equal to five-per-cent rated generator current.

Control Unit

The required generator control unit, as shown on Figure 3, now consists of the

Figure 6A. Load division characteristics of a 2-generator system

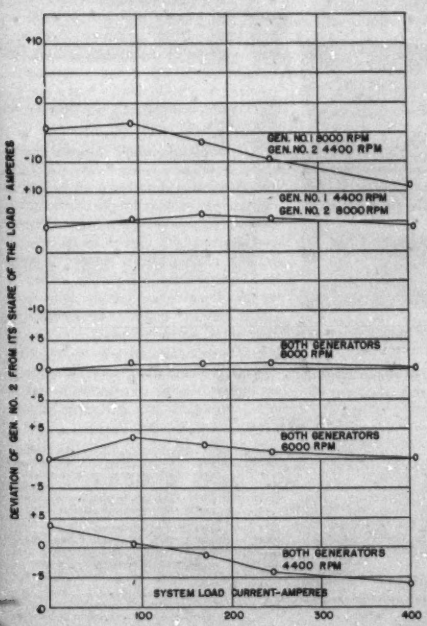

Figure 6B. System voltage characteristics of a 2-generator system

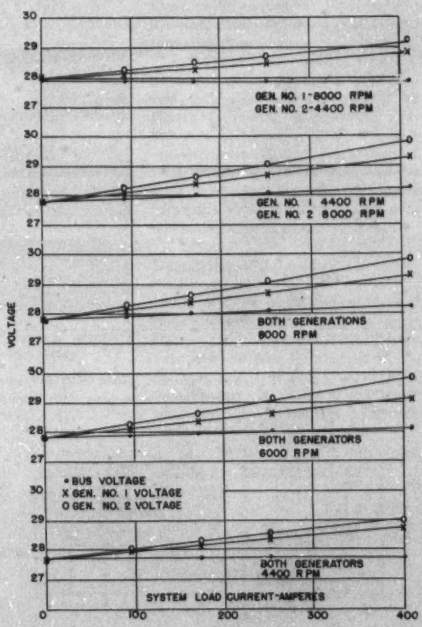

aforesaid voltage regulator, pilot relay, and equalizer control relay in addition to a combination voltmeter and ammeter, a generator switch, an indicator lamp for signaling when the generator is disconnected from the load bus, and pin jacks.

These elements are mounted in one box which can be mounted in the control panel of the aircraft. The ballast lamp is inserted in series with the voltage differential coil to protect this sensitive coil from high reverse voltages. The 50-millivolt shunt and the line contactor are located externally to the control unit to avoid the necessity of having to run the generator current through the control unit.

Load Division

To demonstrate the capabilities of the proposed system to divide the load properly between generators, several tests were made involving different values of line resistance and different size generators. The tests showed that good division would result from the use of this system of parallel operation. Figures 6*A* and 6*B* show results which are typical of a system employing this control unit, where the bus voltage has been adjusted to rise with increase in load. The positive line resistance from each generator to bus was 0.045 ohm and 0.07 ohm, respectively. Ground circuit resistance was approximately 0.001 ohm. The regulator voltage coils were connected to the positive terminal of the generator.

Conclusions

In view of the many operational problems resulting from the use of several individual items of control equipment for aircraft generators, it is desirable that an integrated control system be adopted. It is believed that by the indicated selection and arrangement of control items, a unified system can be constructed which will result in the following:

1. Simplified maintenance problems because of the provision for quick removal of the control elements for bench adjustment.
2. Improved operation arising from a system kept in better adjustment.
3. Reduction in weight and space requirements over that required with decentralized location of devices.

The control system proposed demonstrates that it is possible to build a control unit for aircraft generators that makes the following attainable:

1. Accurate control of the bus voltage by means of control of the system regulation. It is not necessary to rely upon proper regulator adjustment, use of certain generators, or accurately determined line drops.
2. Connection of the bus to the generator when, and only when, it can furnish power to the bus.
3. An automatic system.
4. Better division of load.

No Discussion

The Calibration of Ignition Crest Voltmeters

W. L. DAVIS
MEMBER AIEE

C. E. WARREN
ASSOCIATE AIEE

IN STUDYING the performance of aircraft and automotive types of internal combustion engine ignition systems, ignition crest voltmeters have been used for the measurement of peak voltages at various points in the systems. Several types of meters have been developed for this purpose. Field experience with these meters has shown a considerable variation in reading between the several meters when connected to the same point in the ignition system. In view of the inconsistent performance of the meters, a study was undertaken in which several of the factors influencing the performance of the various available voltmeters were segregated and analyzed separately.

Fundamental Considerations

One of the first factors to be considered in the study of performance of crest voltmeters was the wave shape of the voltages to be measured. Oscillographic records of voltages encountered in both automotive and aircraft engines show that the wave shapes encountered are extremely complex. Figure 1 shows oscillograms of voltages occurring in the ignition system of a typical automotive engine for the firing of one cylinder. Oscillograms of voltages on aircraft engines are similar in nature and complexity. Because of these complexities, it was thought advisable to study the performance of the voltmeters under application of a voltage of relatively simple wave form whose amplitude and shape could be controlled easily. In this way the effects of changing such variables as wave front, duration of peak voltage, and amplitude of peak could be studied. It was decided that equipment should be devised which would produce repetitive voltage surges of simple shape whose wave front, duration of peak voltage, and repetition rate would be independently variable over suitable ranges.

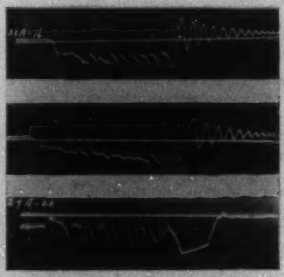

Figure 1. Typical oscillograms of voltages in automotive ignition system

Top and central oscillograms made at spark-coil secondary, bottom oscillogram made at spark plug

Examination of oscillograms of the type shown in Figure 1 showed that the wave fronts most frequently encountered in ignition systems would be included between the limits of 0.5 microsecond to peak voltage and about 25 microseconds to peak. Many of these waves are chopped, and many are oscillatory after reaching peak value. Hence the voltage generating equipment had to be capable of producing these variations in wave shape and wave front without too much change in the equipment. Also, the rate of repetition of voltage surges had to be adjustable over a range from the lowest likely to be encountered in a practical system to some value above which further increases in repetition rate would have no effect on the meter reading. Preliminary experimentation showed that the meters under consideration exhibited no change in reading at repetition rates above 60 per second. The lower limit considered was 7.5 surges per second. A third requirement on the voltage-generating equipment was that successive surges should duplicate each other as to amplitude, wave front, and wave shape.

Description of Apparatus

A study of the oscillograms of Figure 1 reveals that the most frequently occurring wave form is one which rises sharply to a peak and then is "chopped off" as the plug gap arcs over. Other wave forms consist of unidirectional waves which rise to a peak and then decay with

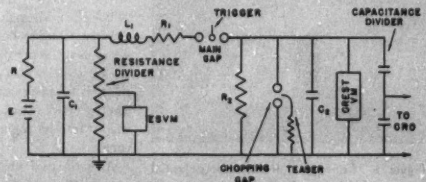

Figure 2. Simplified diagram of surge generator

Paper 47-11, recommended by the AIEE committees on air transportation and instruments and measurements for presentation at the AIEE winter meeting, New York, N. Y., January 27–31, 1947. Manuscript submitted August 23, 1946; made available for printing November 25, 1946.

W. L. Davis was formerly with Ohio State University and is now with Battelle Memorial Institute, Columbus, Ohio; C. E. Warren is professor of electrical engineering, Ohio State University, Columbus, Ohio.

This paper is a co-operative contribution of the Air Materiel Command, Wright Field, Ohio, and The Ohio State University Research Foundation.

or without superposed sinusoidal damped oscillations. These wave forms immediately suggest that a surge generator of the type used for testing power system equipment would be a suitable device for generating surges to be applied to the voltmeters under test. Figure 2 is a simplified circuit diagram of the surge generator used in this equipment.

Capacitor C_1 is charged through R by the source of direct potential E. When the main gap is broken down by a triggering potential, C_1 discharges through R_3 and the resulting surge of potential across R_2 is impressed on the meter. The wave form of the voltage developed across R_2 can be controlled by adjusting the circuit elements L_1, R_1, R_2, and C_2. In general, the time to crest is increased by increasing R_1 and C_2. However, it is not possible to increase the time to crest indefinitely because the voltage dividing action of resistors R_1 and R_2 tends to decrease the amplitude of the surge applied to the meters. The introduction of inductor L_1 results in an oscillatory surge with a frequency of oscillation determined largely by the values of L_1 and C_1. The decrement of the oscillation depends on the values of R_1 and R_2. Independent adjustment of any one part of the wave form is in general not possible, and a surge of desired characteristics must be obtained by a trial and error process with the aid of a cathode-ray oscillograph or by calculation.[1]

The chopped wave which occurs so frequently in ignition systems was obtained with the aid of an auxiliary gap shunted across the output resistor R_2. This gap was adjusted to break down at or near the peak voltage developed across R_2, resulting in a sudden decrease in voltage similar to that which occurs when a spark plug fires. Consistent operation of this gap may be obtained by means of a "teaser" consisting of a small ball or piece of wire placed in the gap and connected to ground through a high resistance.

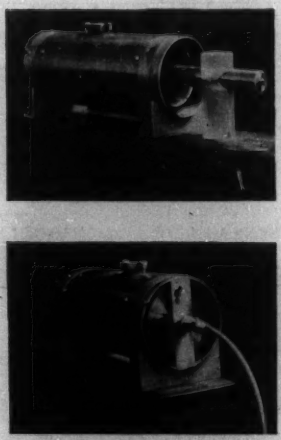

Figure 3. Concentric air-dielectric potential divider for observing surges

Calibration Technique

The accuracy of calibration of the crest voltmeters depends on an accurate determination of the peak output voltage of the surge generator. One possible method for calibrating the output of the surge generator depends on accurate knowledge of the oscillograph deflection sensitivity and the ratio of the capacitor voltage divider (see Figure 3). This method is not entirely reliable as it is difficult to make accurate measurements of the divider ratio because of its low input capacitance. In addition, it has been found that unless the divider is designed carefully, its ratio will be sensitive to surge magnitude and wave shape. Therefore, in view of the uncertainties involved in establishing an accurate value for the divider ratio, a more direct method of calibration was used.

The direct method of calibration is based on the fact that the discharge of a pure capacitance into a pure resistance will produce across the resistance a surge voltage of peak value equal to the maximum steady voltage across the capacitor prior to discharge. If the surge generator circuit elements L_1, R_1, and C_2 of Figure 2 are reduced to zero or to minimum values inherent in C_1, R_2, and auxiliary apparatus, the peak surge voltage developed across R_2 will be within 95 to 99 per cent of the maximum voltage to which C_1 is charged prior to the breakdown of the main gap. The maximum voltage across C_1 prior to gap breakdown is measured by a calibrated resistance potential divider and an electrostatic voltmeter. This technique results in an over-all calibration of the capacitor divider and oscillograph. It has the additional advantage that after a calibration has been established for any set of surge generator constants, the electrostatic voltmeter readings are directly related to peak surge output, and the electrostatic voltmeter readings may be used directly for additional calibration runs.

As indicated previously, the performance of the potential divider coupling the oscillograph to the surge generator output is of considerable importance and must be given careful attention if reliable calibrations are to be achieved. Without going into the details of the design and application of the several types of dividers[2] it can be stated that the capacitor divider is suitable for the range of voltages and surge wave forms encountered in this problem.

Experimentation with several designs of capacitor dividers employing solid low-loss dielectrics and relatively small electrode areas showed that their ratios were sensitive to surge wave shape and magnitude. An analysis of these designs led to the conclusions that their erratic behavior was caused by corona formation at the electrode edges and in the air spaces between the solid dielectric and the electrode surfaces. Therefore, a concentric type divider was constructed in which every effort was made to eliminate series combinations of air and solid dielectric and to provide large smooth areas of electrode surface with air as the principal dielectric. The salient features of this divider are shown in Figure 3.

The divider consists of three concentric cylindrical electrodes. The center high-potential electrode is supported by a large rod of polystyrene. The intermediate electrode is centered with respect to the outer by six small cylindrical pieces of the same material. The cathode-ray deflection plates are connected to the divider output (intermediate and outer electrodes) by a shielded concentric cable whose capacitance forms part of the low side of the divider. Provision is made for connection of mica capacitors between the outer two electrodes in order

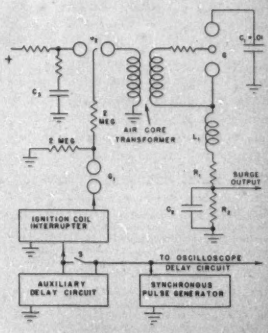

Figure 4. Block diagram illustrating method of synchronizing oscilloscope and surge generator output

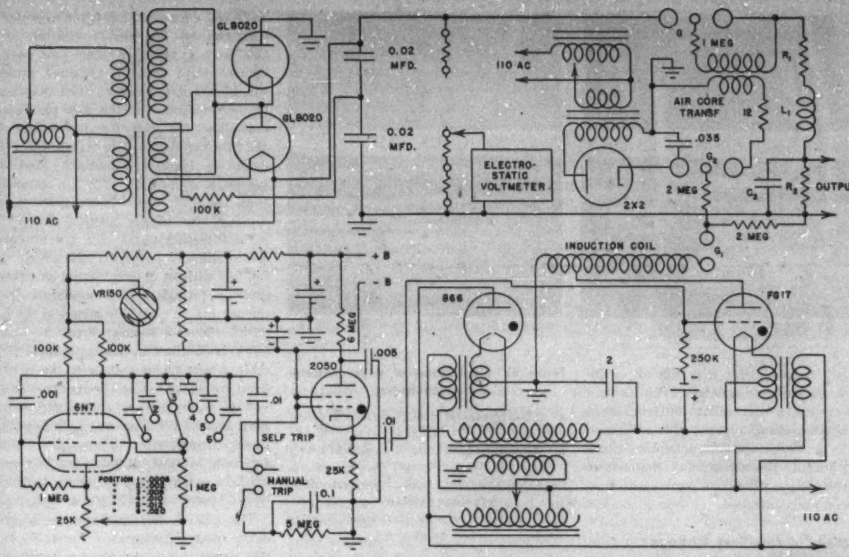

Figure 5. Detailed diagram of surge generator and auxiliaries

Upper left, surge generator power supply; upper right, surge generator; lower left, synchronous pulse generator; lower right, ignition coil interrupter

to adjust the divider ratio. When this divider first was put into operation, erratic results similar to those obtained with previous dividers were observed. However, when the concentric cable connecting the divider to the oscillograph deflection plates was changed from a cable with beaded insulation to one with flexible solid insulation, all evidences of erratic behavior disappeared.

Auxiliary Circuits

As a cathode-ray oscilloscope was used to observe wave shapes and to provide means of voltage calibration, it was necessary to devise auxiliary circuits for synchronizing the oscilloscope with the surge generator output. The total sweep time on some of the shortest duration transients was of the order of three microseconds, so that a rather precise synchronizing method was necessary in order to realize a reasonable percentage of synchronizations. Two synchronizing methods were developed, both of which will be explained by reference to Figure 4.

In the block diagram of Figure 4, the sequence of operation begins with the synchronous pulse generator, whose output is a sequence of positive steep wavefront voltage pulses equally spaced in time. In the first method of synchronizing the switch S is closed, so that the pulses are fed to the ignition coil interrupter and to the cathode-ray oscilloscope delay circuit. Two trains of events are thus initiated, one leading to the breakdown of the main surge generator gap G, the other in starting the oscilloscope beam and sweep circuits. The ignition coil interrupter, which is tripped by the synchronous pulse generator, puts out voltage of rather steep wave front and several thousand volts amplitude. Gap G_1 then breaks down, and gap G_2 is triggered by the steep voltage surge appearing on its teaser. Capacitor C_3 then discharges rapidly through the primary of the aircore transformer, inducing a high voltage of steep wave front in the secondary winding. The sudden voltage surge at the teaser of gap G trips the surge generator. All gaps were adjusted to break down long before their respective tripping voltages reached maximum open-circuit values. In addition all tripping voltages had very steep wave fronts, thereby assuring reliable and consistent gap breakdowns. In the foregoing train of events the principal time delay between the pulse from the synchronous pulse generator and the tripping of gap G occurs during the rise in voltage of the ignition coil interrupter output circuit. In the meantime the same pulse which tripped the ignition coil interrupter has also tripped an electronic delay circuit in the oscilloscope. The output of this delay circuit is a pulse which turns on the oscilloscope beam and sweep circuits. The time delay introduced in the oscilloscope is continuously adjustable over a range of the same order of magnitude as the fixed delay introduced by the voltage rise of the ignition coil interrupter. Thus the time interval between tripping of the oscilloscope beam, and sweep and discharge of the surge generator is controlled by adjustment of the oscilloscope delay circuit.

The second method of synchronizing is illustrated by Figure 4 with switch S open. Here the only change is the addition of an auxiliary electronic delay circuit between the synchronous pulse generator and the ignition coil interrupter. The additional delay circuit adds some flexibility to the system because adjustable delays are then available in both channels. Such an arrangement would have great value where no appreciable delay is inherent in the system. In attempting to synchronize with systems of

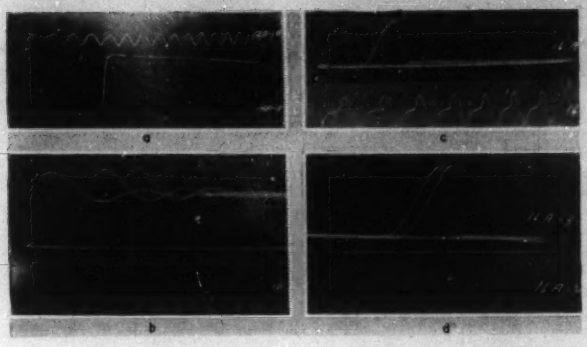

Figure 6. Oscillograms of surge generator output voltages

a—0.5-microsecond front, 1-megacycle timing wave
b—2.0-microsecond front, 1-megacycle timing wave
c—4.0-microsecond front, chopped, 0.2-megacycle timing wave
d—23-microsecond front, chopped, 0.2-megacycle timing wave

small inherent delay it is difficult to adjust the oscilloscope delay circuit for very short delays and still attain consistent synchronization. Hence the additional delay circuit in the system tripping channel permits the use in both channels of longer delays which are more easily produced and controlled.

Details of Auxiliary Circuits

In the following text reference will be made to Figure 5. The high-voltage supply for the surge generator is a voltage-doubling circuit using two type-*GL 8020* high vacuum diodes. Two 25,000-volt 0.02-microfarad capacitors in series constitute the output circuit of the doubler and also serve as the main capacitor of the surge generator. The surge generator is shown in the upper right hand corner of Figure 5 and has been discussed already.

The synchronous pulse generator is shown in the lower left corner of Figure 5. Its power supply is a simple full-wave rectified *R-C* filtered type. The plate supply for the *6N7* is regulated by a *VR-150* regulator tube. In operation the 0.005-microfarad capacitor, connected between ground and the plate of the *2050*, is connected through 6 megohms to the plate supply voltage. If a positive pulse is applied to the *2050* grids, which are biased about 5 volts negative to the cathode, the *2050* suddenly will discharge the 0.005-microfarad capacitor to ground through the 25,000-ohm resistor. In this way a pulse of steep and well-defined wave front is obtained across the 25,000-ohm resistor. The presence of the 6-megohms in the *2050* plate circuit allows the grids to regain control of the tube before the plate voltage can rise again to ignition potential. Positive pulses for tripping the *2050* are obtained from the *6N7*, which is connected as a flip-flop type trigger circuit. The *6N7* cathode-biasing 25,000-ohm potentiometer is adjusted to permit the circuit to flip-flop without external signal on either grid or cathode. The oscillation frequency can be varied by means of the 6-position selector switch. Frequency stability is obtained by adding a small 60-cycle synchronizing voltage to the right-hand grid of the *6N7*. The synchronizing voltage is obtained by capacitance coupling to a 6.3-volt filament winding on the power transformer. Thus, the pulse generator will put out pulses synchronous with the power supply frequency at rates from 60 per second to 7.5 per second.

The ignition coil interrupter is shown in the lower right corner of Figure 5. In this circuit the 2-microfarad capacitor is charged to a direct voltage whose magnitude is controlled by a variable autotransformer. The type *FG-17* thyratron is arranged to discharge the capacitor through the primary coil of an ordinary automobile ignition coil, thus inducing a high voltage in the coil secondary. The *FG-17* is tripped by positive voltage pulses supplied to its grid from the synchronous pulse generator. The induction coil output is used to trip the surge generator as previously described.

The diagram of the auxiliary delay cir-

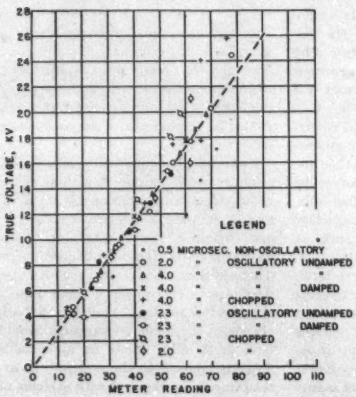

Figure 7A. Calibration data for Hooven electronic voltmeter

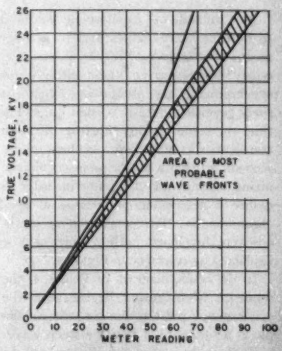

Figure 7B. Calibration area for Hooven electronic voltmeter

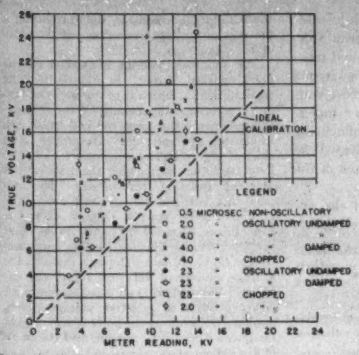

Figure 8A (left). Calibration data for sphere-gap voltmeter

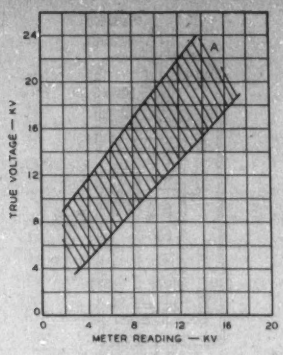

Figure 8B (right). Calibration area for sphere-gap voltmeter

A—Area of most probable wave fronts

cuit is not shown, but it consists of a 1-shot multivibrator[3] utilizing pentodes to produce a square negative pulse whose width or duration is continuously variable over the desired delay range. This pulse is differentiated by a simple capacitance-resistance circuit, so that the output of the delay circuit consists of a negative pulse followed by a positive pulse. The interval between pulses constitutes the required delay.

Results

Figure 6 shows oscillograms of several voltage surges used in crest-voltmeter calibrations. Figure 6*a* shows a 0.5 microsecond wave front with a slowly decaying exponential tail. It is one surge picked at random from a sequence of surges repeating at the rate of 15 per second. Figure 6*b* shows three traces of a 2-microsecond wave with an oscillatory tail. These three waves were also picked at random from a sequence of surges and are shown here to illustrate the accuracy with which the surge generator repeated itself. Figure 6*c* shows a chopped wave with a 4-microsecond front, and 6*d* shows chopped waves with 23-microsecond fronts.

Oscillographic records of the type shown in Figure 6 were used to calibrate several types of crest voltmeters. The results for two of the meters are included here. The Hooven voltmeter (see appendix), whose calibration data are given in Figure 7, is an electronic type meter. Figure 8 shows calibration data for a sphere-gap type meter. In Figures 7*A* and 8*A* are plotted the experimental data for the various wave fronts from 0.5 microsecond to 23 microseconds. The symbols used for each wave front are tabulated in a legend on each figure. For the Hooven meter, whose scale was divided into 100 parts, a dotted straight line was drawn to represent the mean of the data plotted. For the sphere-gap meter the dotted line represents the ideal calibration curve.

For most of the meters investigated, the data for the various wave fronts were quite scattered, so that no single curve could be drawn as a calibration curve for a range of wave fronts or even for a single wave front. Curves for single wave fronts would be of little value anyway unless the wave form of the voltage being measured was known. It was thought that greater utility would result from the pair of lines enclosing the calibration points for the wave fronts most likely to be encountered in ignition voltage measurements. Thus, Figure 7*B* for the Hooven meter has a pair of lines with the area between the lines crosshatched. This area encloses the calibration points obtained for all wave fronts from 2.0 microseconds to 23 microseconds, inclusive, except some of the 2-, 4-, and 23-microsecond chopped waves above 18 kv. The area between the curved line and the upper line of the crosshatched area encloses the points obtained with the 2-, 4-, and 23-microsecond chopped waves. Hence a meter reading of 40 on a wave whose front lies between 2.0 and 23 microseconds would indicate a true peak voltage between about 10 and 12 kv. The calibration area of Figure 8*B* for the sphere-gap type meter is so broad that this meter is virtually useless for general use on systems where the wave front is unknown.

With the type of calibration area described here a meter reading on a typical ignition system can be interpreted to mean that the true peak voltage lies between the upper and lower limits, specified by the crosshatched area of the calibration sheet. The value of any meter for general use on ignition systems can be judged by the interval between the upper and lower limits, or by the width of the crosshatched calibration area. The most suitable meter will have the most narrow calibration area.

In addition to error caused by sensitivity to wave form, a second and perhaps more important consideration is that in most cases met in a practical ignition system the peak voltage being measured is determined by the breakdown potential of a gap, such as a spark plug or distributor gap. It is well known that such breakdown potentials vary considerably on successive breakdowns, and the best that any of the meters investigated can do is to give an average indication depending on the internal circuit and mechanism.

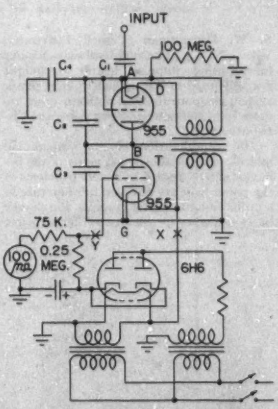

Figure 9. Circuit diagram of Hooven voltmeter

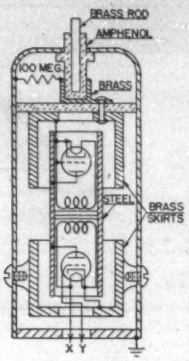

Figure 10. Cross section of part of Hooven voltmeter showing concentric shielded construction

Of the two possible sources of error, the preceding investigation has shown the dependence on wave form. The error resulting from the averaging mechanisms of the meters was not studied.

Conclusions

Circuits and techniques have been described which have proved satisfactory for the production of consistent and accurate potential wave forms adjustable over a considerable range of peak voltage, time to crest, wave shape, and repetition rate. Application of these circuits to the calibration of ignition crest voltmeters has resulted in a better understanding of the various factors influencing meter performance and has indicated the useful range of application of each of the several meters tested.

Several other applications of the apparatus are suggested in the following list:

1. A study of the design and performance characteristics of spark gaps used in various control circuits or as voltage measuring devices.

2. A study of the characteristics of insulation subject to repetitive transient voltages.

3. As a source of transient voltage or current wave forms for use in electrical analogy or electric model computors.

Appendix

Figure 9 shows a circuit diagram of the Hooven voltmeter, developed by F. J. Hooven, Dayton, Ohio and Figure 10 shows a drawing which is a combination cross section and circuit diagram of part of the meter.

The triode T and the diode D are both type *955* miniature triodes. The triode T has a positive voltage applied to its grid. When the plate of T is made negative to the cathode, the potential distribution within the tube will control the grid current, the more negative the plate the smaller the grid current. The microammeter is arranged to read the drop caused by the grid current in the 0.25-megohm resistor, thus providing a measure of the negative voltage at the plate of T.

The unknown voltage is applied at the point marked "input" in Figure 9. The capacitance C_1, which is of the order of two or three micro-microfarads, is the capacitance between the brass rod and brass cup at the top of Figure 10. The upper brass skirt of Figure 10 has capacitance C_3 to the long steel tube containing the triodes and filament isolating transformer. The capacitance between the steel tube and the grounded lower skirt is C_3; and C_4 is the capacitance between the upper brass skirt and the enclosing brass case. The combination of C_1, C_3, C_4, and C_4 forms a capacitance voltage divider of very low input capacitance. The diode D is arranged so that with either positive or negative voltage pulses applied to the input, the point B will always be driven negative to ground, and the plate of T will float at an average negative voltage proportional to the absolute value of peak voltage occurring at point A. The magnitude of the voltage at A determines the microammeter reading as previously described.

References

1. Impulse Generator Circuit Formulas, **J. L. Thomason.** AIEE Transactions, volume 53, 1934, January section, pages 169–76.

2. Theory of Voltage Dividers and Their Use With Cathode-Ray Oscillographs, **M. M. Peters, G. F. Blackburn, P. T. Hannen.** *Journal of Research*, Bureau of Standards (Washington, D. C.), volume 9, July 1932, pages 81–114.

3. Multivibrator Circuits, **M. V. Kiebert, Jr., A. F. Inglis.** *Proceedings*, Institute of Radio Engineers (New York, N. Y.), volume 33, August 1945, pages 534–9.

Discussion

S. W. Zimmerman (Cornell University, Ithaca, N. Y.): The authors show ingenuity in adapting impulse testing technique normally used in testing high voltage power system components to a problem quite remote from the power transmission and distribution field.

This consideration of the voltages in ignition systems shows that many of the behavior effects studied as system problems in the power field are repeated in miniature in ignition systems, as, for example, the change in wave shapes measured in different parts of the system apparent from the records in Figure 1 of the author's paper.

While sphere gaps appear to be unsuitable for means of making measurements in this study because of the wide range of rates of voltage change encountered in this problem, it should not be inferred that they have lost their usefulness as a means of measurement. Clean irradiated sphere gaps in the 10-kv range, for example, generally will have a range of values of impulse spark potential that is more nearly five per cent of the average value for a given wave front than any range that might be implied by reference to the data presented in Figure 8*B*.

The length and character of the connections to the sphere gap will have an effect on the apparent voltage especially where steep wave fronts are involved. The construction of the voltmeter in Figure 10 establishes a means of keeping this lead constant between measurements.

A consideration of the undamped or damped 23-microsecond case of Figure 8*A* appears to indicate a slight discrepancy in the zero setting of the gaps as well as a slight shift in the scale factor of the instrument. The steeper front waves of course will appear to have a higher true voltage because of the characteristic "turn up" of the volt–time curve of the sphere gaps in the shorter time regions. Clean irradiated gaps are expected to be more consistent than some of the chopped wave data shown.

The Cathode-Ray Spectrograph

RUDOLF FELDT
MEMBER AIEE

CARL BERKLEY
NONMEMBER AIEE

IT is now 85 years since Kirchhoff and Bunsen introduced the spectrograph as a tool for analytical research. Despite this long existence, it is only during the last two decades that the spectrograph has developed from a pure research instrument into a tool of more widespread use.

Many types of recording spectrographs are commercially available, and their technical development has paralleled the increasing need for finer and faster instruments. These instruments range from the slow, extremely accurate types requiring tedious photographic procedures to the direct recording photoelectric instruments, as exemplified by the Hardy spectrograph. This spectrograph, which is at present the fastest commercially available instrument, produces a complete spectrum in the order of minutes. Instruments of this kind are rather expensive and require highly trained personnel. This limits their use to a relatively small number of well-equipped laboratories. In addition to this limitation, even the best presently available spectrographic instruments are deficient when the following problems are encountered:

1. Investigation or control of rapidly changing spectra. Examples—rapid chemical reactions, half-lives of compounds, fluorescence, and light sources of varying intensity and color.

2. Problems which require telemetering or simultaneous transmission of spectrographic data to several points. Examples—chemical process control, pyrometry, and transmission from inaccessible locations.

3. Production control.

(a). Where continuous monitoring is desired as in the cases of dye and textile industries.

(b). Where the analysis of a large number of samples is necessary.

(c). Where the use of unskilled personnel is desirable.

Wherever it is found necessary to make such measurements more rapidly and economically, electronic methods will prove a desirable solution.

The use of cathode-ray oscillograph techniques has come into widespread prominence whenever such rapidly acquired information is to be recorded or made visible. Several attempts have been made to produce instantaneous spectrograms on cathode-ray tubes, notably a mechanical scanner using a vibrating prism, by D. Ulrey,[1] and a rotating slit by H. A. Snow (see reference 2). Both of the two mentioned instruments have serious mechanical limitations, inherent in this type of construction. In the instrument to be described the mechanical difficulties have been overcome, and the electrical problems greatly simplified by the use of a mechanically resonant synchronous scanning system.

Problem for Which Developed

This instrument originally was developed to study the color and duration of the light emitted from cathode-ray tube phosphors when excited with electric pulses whose duration was of the order of microseconds. Such problems exist in connection with the observation of radar patterns, the viewing and recording of single and repetitive transients, and in television. With certain modifications this instrument is expected to find, in addition to the usual spectrographic problems, widespread application in problems heretofore difficult to interpret with the usual spectrograph.

General Description of Cathode-Ray Spectrograph

The instrument produces a complete spectrogram within a small fraction of a second. In the present design this value

Figure 1. Schematic diagram of analyzer optical system

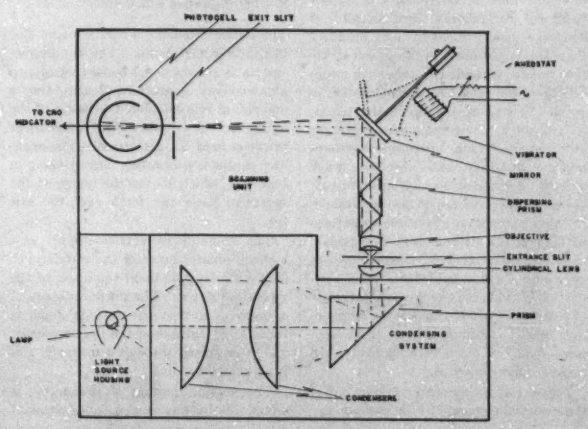

Paper 47-13, recommended by the AIEE committee on instruments and measurements for presentation at the AIEE winter meeting, New York, N. Y., January 27-31, 1947. Manuscript submitted October 3, 1946; made available for printing December 27, 1946.

RUDOLF FELDT and CARL BERKLEY are both with Allen B. DuMont Laboratories, Inc., Passaic, N. J.

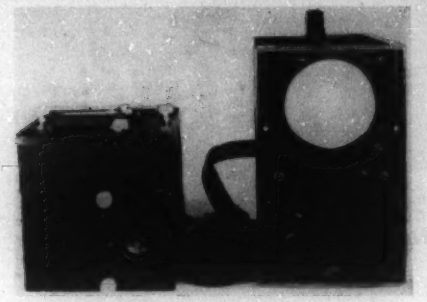

Figure 2(left). Developmental model of the cathode-ray spectrograph

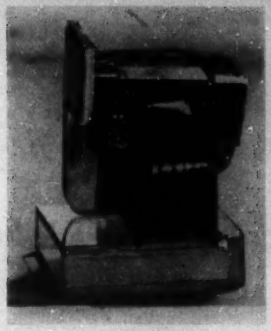

Figure 3. Scanning mirror and vibrator resting on absorption cell

is 1/240 second, but could be either shortened or lengthened if necessary. The record is produced in the form of a luminous pattern on the face of a cathode-ray tube which is used as indicator. Figures 7 through 10 are typical. In general, the instrument is composed of two parts—the analyzer and the indicator unit. The analyzer contains conventional means for dispersion, that is, condensing system, prism, entrance and exit slits. The rapid operation of the analyzer is obtained by the use of a vibrating mirror which scans the image of the spectrum with the aid of an exit slit placed in front of a photocell. This scanning rate is, for convenience, a multiple or submultiple of the power line frequency, and the mirror motion is sinusoidal. The output of the photocell is, consequently, directly proportional to the intensity of any individual part of the spectrum at any given instant in the scanning cycle. This output, after amplification, is applied to the indicator unit which consists of a conventional cathode-ray oscillograph. A deflection proportional to light intensity therefore is obtained in a vertical direction on the cathode-ray tube. A sweep synchronized with the mirror motion is applied to the horizontal deflecting plates. As a result a conventional spectrogram is obtained in which ordinates represent relative intensity and abscissae wave lengths. Because of the high scanning rate the spectrogram obtained on the cathode-ray tube appears as a continuous pattern without flicker. Changes in the spectral characteristic of the light source appear to be recorded instantaneously. The comparison of changes is facilitated by the use of long persistent screens on the cathode-ray tube. Continuous and permanent records may be obtained by conventional photographic procedures.

Figure 1 shows the schematic layout of the essential elements of the cathode-ray spectrograph. A developmental model of the instrument is shown in Figure 2. The indicator, which in this case is a standard DuMont cathode-ray oscillograph modified for the purpose, is connected to the analyzer by a multiconductor cable which can be made of any desired length. The analyzer in turn consists of three interconnected separable units.

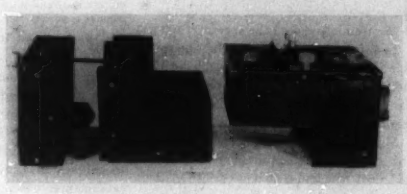

Figure 4. Analyzer unit disassembled. From left to right—light source, condensing system, scanning unit

1. The source.
2. The condensing system.
3. The dispersing and scanning means

The source is usually a concentrated filament projection lamp. The condensing system is conventional consisting of two plano-convex condensing lenses and a cylindrical lens calculated to make all the light enter the entrance slit. A 3-element prism is used for dispersion. The scanning means is a vibrating mirror shown in Figure 3, which moves the image of the spectrum back and forth over the exit slit.

The whole device acts essentially as a monochromator in which the wave length measured depends upon the angle of the vibrating mirror. The mirror consists of a mechanical resonant system which is tuned to a multiple of the line frequency and is energized through a magnetic coil from the power line.

The angular motion of the mirror is adjustable by means of a series rheostat and easily covers the dispersion of the prism throughout the visible range. The photocell used may be any one of the series of 9-stage photomultipliers recently made available. A type *1P22* generally has been used, which, in conjunction with a Wratten number *101* filter, gives an over-all response approximating the visibility function. In order to be able to use the instrument at a location remote from the photocell, which necessarily must be in the proximity of the test object, a cathode follower impedance matching stage is used to feed the signal through the cable into the oscillograph. The oscillograph may be either a-c or d-c coupled. It is preferable to use d-c coupling in order to obtain a fixed reference level. Provision is made for inserting transmission samples or standard absorption cells into the optical path through the top of the analyzer unit. Controls on the analyzer provide for mirror amplitude, entrance slit width, and sensitivity. The slit and sensitivity are adjusted to give maximum resolution, depending on the intensity of the source.

The three units (light source, condensing system, and scanner) may be easily assembled or disassembled at will without tools. Figure 4 shows the three elements of the analyzer unit disassembled, which is done by turning the knurled screws. The ease of separation and replacement of the various units is of considerable

advantage with regard to flexibility of operation. For example, the light source may be removed easily, leaving the condensing system attached. Any other light source for testing or calibration purposes, then may be plugged into the opening of the first light gathering lens in the condensing system. Similarly, the condensing system may be removed and any other optical system whose light transmission characteristics are desired may be used to replace it.

Figure 5. Spectrogram of a cadmium mercury arc used as a calibrating light source

Detailed Description

Some of the particular design features of the previously described parts may be of interest.

Light Source

This instrument was designed to accept light from a cathode-ray tube spot no greater than one centimeter in diameter. Therefore, it is suitable without modification for all other light sources of similar size as arcs, spark gaps, and incandescent filaments. For transmission measurements a concentrated filament projection lamp is used as a source. The color temperature of the lamp may be set by measuring voltage and current. This source may be removed, and a concentrated low pressure cadmium mercury arc may be inserted for wave length calibration. Figure 5 shows the spectral lines of this source.

Scanning Unit

Because the mirror is tuned to mechanical resonance for the frequency desired, it requires only very little energy to produce the necessary amplitude, most of this energy being expended in overcoming air resistance. The actual current through the driving coil is of the order of one milliampere at 110 volts. The corresponding angular deviation of the mirror is 15 degrees. The entire mirror assembly may be rotated about an axis in order to scan about any desired portion of the spectrum. When this is done the wave length scale becomes greatly expanded.

Mechanical Considerations

It is necessary to isolate very carefully the motion of the mirror from the rest of the unit in order to avoid mechanical vibration effects in other parts of the instrument. This isolation is accomplished first by attaching the mirror to a mass which acts as an inductance for this frequency. The rubber grommets then serve to absorb any residual motion at the scanning frequency.

The design of the resonant reed itself presents some interesting problems. The linear sweep, which generally is used with this instrument, is synchronized from the line frequency. The reed is vibrated by the same power source. In order to obtain the largest amplitude possible with the least power dissipated in the magnetic coil, it is necessary that the mechanical Q be very high. However, this makes a limitation on the resolving power that can be obtained on the final instrument. If the Q is made very high, any line frequency change will cause a large change in the phase of the mirror motion with respect to the line. This will be represented on the oscillograph by an apparent change of wave length, as the synchronization of the sweep occurs at almost the same phase of the sine wave over considerable variation in frequency. In the case of line voltage variations, the mirror amplitude will change resulting in a change of the wave length scale. For these reasons it is necessary to control the line voltage very carefully. The Q of the circuit must be made low enough so that phase variations are not serious. Obviously, for power sources having different frequencies, it must be possible to either tune the mirror unit or to replace it by other units of different frequencies. In locations where the line frequency is not sufficiently dependable these difficulties can be eliminated entirely by the use of wave length markers applied as blanking pulses to the grid of the cathode-ray tube. These marker signals may be obtained by optical means.[3]

Photocell

With the present unit, the spectral response ranges available are somewhat limited. It is desirable for many cases to obtain not only the visual response referred to by the use of a suitable filter and photocell combination, but also a flat response characteristic. This can be obtained by changing the optical design in such a way that masks are placed in a stationary focal plane of the spectrum to accomplish this result, or to obtain any arbitrary spectral sensitivity. The masks are superimposed on the real spectrum image so as to reduce the over-all transmission for those wave lengths where it is desired to flatten the peaks caused by the photocell and light source characteristics. Various other methods have been proposed for rapid scanning of the spectrum and indication of the results on a cathode-ray tube. One of these[4] uses a moving prism. The size of the prism required obviously precludes the use of high scanning rates. Another method which has been used by Snow (see reference 2) is one in which a rotating mirror is used. The major disadvantage of this scheme lies in the fact that the spectrum is being scanned by the photocell during only a small portion of the cycle, and this requires the use of wide band amplifiers. Similarly, a mechanical rotating system

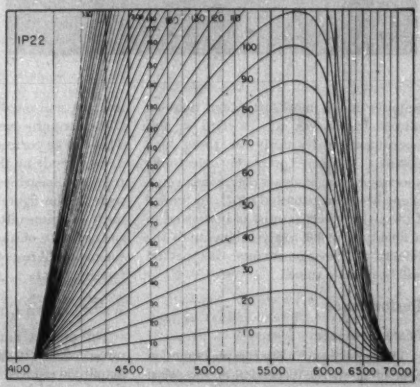

Figure 6. Calibrated wave length and relative transmission scale

Figure 7. Spectrum of tungsten lamp at 3,200 degrees Kelvin and absorption spectrum of chemical solution

Figure 8. Tungsten lamp plus didymium filter

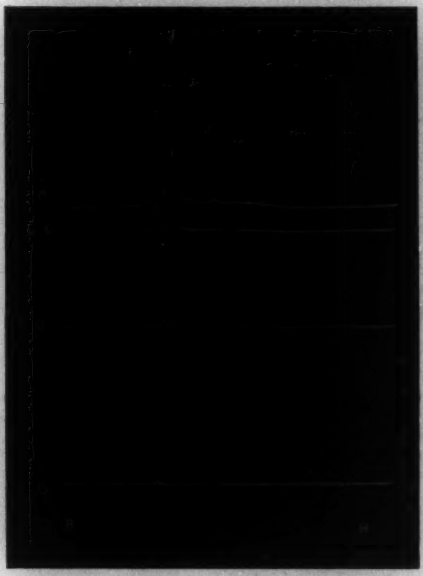

Figure 10 (above). Spectrum of Sylvania recording lamp type *R1130*, at low and high currents

Figure 9 (left). Illumination from mercury arc lamp after 0, 10, 60, and 120 seconds of operation

Figure 11. Spectrogram of light from *P11* fluorescent screen under cathode-ray bombardment—*5FP2* tube, 100 microseconds, 20 volt pulse, 5 kc repetition rate, anode voltage 10 kv

Figure 12 (right). Envelope obtained with nonsynchronous pulses

requires much more attention than an almost frictionless one as used in this instrument, particularly at these high speeds. Another completely electronic spectrographic analyzer using an iconoscope has been patented by H. A. Snow.[5] Unless the spectroscopist is interested in a fidelity of color analysis similar to the fidelity of television images, this method will be of little value.

Performance

Scale Linearity

The scale linearity is a complex function depending on the dispersion of the prism and the sinusoidal motion of the mirror. The net results can been seen in Figure 6. This can be corrected to give almost any desired result by the introduction of arbitrary nonlinearities into the sweep. The scale in the figure permits the measurement of transmittance directly without the necessity of having to compensate for the photocell response, as indicated in the foregoing text.

Wave Length Coverage

The present mirror covers the visible range. Also, it can be rotated and its amplitude reduced to scan a small portion with increased electrical resolution if necessary. Photocells and optics can be used with this system to extend the sensitivity into the ultraviolet, and, to some extent, into the infrared.

Resolution

In the cathode-ray spectrograph, as in other optical instruments, the ultimate resolution is limited by the quality of the optical parts. In the present developmental model the resolution is 35 millimicrons. A second model is expected to have a resolution better than 5 millimicrons.

Sensitivity

It is difficult to state the performance of this device in terms of arbitrary light sensitivities. However, it has been possible to measure the amplitude throughout the visible spectrum of the light from cathode-ray tube phosphors excited by electric pulses as short as one microsecond.[5] This is done by a procedure described in the appendix.

Applications

The cathode-ray spectrograph is not intended to compete with existing spectrographs but rather to make possible spectrographic measurement of sources or samples subject to variations too rapid to be recorded completely by direct photographic methods. In general, this device will find its greatest use in the measurement of similar transient phenomena such as the forementioned spectral distribution of cathode-ray tube pulses, the color of intermittently lit lamps, the color of arcs such as are used in spectroscopy, and the color of flames. Some typical examples follow.

Nonintermittent Light Sources of Varying Intensity. The upper curve in Figure 7 shows the characteristic of an a-c operated tungsten light source operated at 3,200 degrees Kelvin as seen by the spectrograph. The photocell is a type *1P22* whose peak sensitivity approximates that of the human eye. This curve represents the over-all characteristic of the spectrograph when used for transmission measurements, because this is the lamp used in the instrument. The letters *B* and *R* represent the blue and red ends of the spectrum.

Transmission Measurements. Transmission measurements, as percentages, may be made directly by using the scale of Figure 6. The lower curve in Figure 7 shows the transmission of a chemical solution. Figure 8 shows the characteristic of a didymium filter compared with the total characteristic. The peaks and valleys of this spectrum can be used for a rough wave length calibration. These two cases are typical of applications in the chemical and textile industry. The varying color of a dye bath or the strength of a photographic filter may be checked constantly in production by this method.

Slowly Changing Light Sources. Figure 9 shows four spectrograms obtained from a mercury arc light source at different times after starting. It can be seen how the light output increases markedly as the lamp warms up and the mercury vaporizes.

Despite the fact that this light source is intermittent at a rate of 120 cycles per second, a stable picture is obtained because of the synchronization of the mirror frequency with the line. As most light sources are a-c operated, this instrument is a convenient tool for their color study.

Figure 10 shows the spectrogram of the color of the Sylvania recording lamp. The two traces were recorded at low and high currents.

Intermittent Light Sources. Figure 11 shows a type *5FP11* cathode-ray tube pulsed with 100 microsecond flat top pulses at a repetition rate of five kc. Each pulse causes the light output to reach a peak value rapidly corresponding to this portion of the spectrum. This light then decays until the next pulse occurs. Because the pulse length is short with respect to the scanning cycle and the decay is rapid, the individual decay curves are very nearly the decay characteristics for each particular part of the spectrum. If the repetition rate of the pulses is not synchronized with respect to the mirror motion, an envelope of the peaks is obtained, as in Figure 12, which represents the maximum fluorescent light output of the phosphor. This measurement is of importance in the case of the screen materials to be used for continuous film recording.

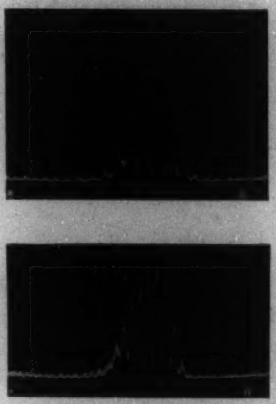

Figure 13. *P7* screen under conditions similar to those in Figure 11 with repetition rates 5 and 10 kc

It also can be seen in Figure 12 that in the center of the spectrum the light energy has no time to decay to zero before the arrival of a new pulse. A second envelope therefore is formed on the bottom which represents the phosphorescence after 1/120 second according to the scanning rate. The amplitude of this second envelope is very small in this case, because the *P11* is a short persistent screen material. This effect is illustrated much better in Figure 13 which shows the characteristic of the long persistent *P7* screen at different repetition rates. The illustrations show clearly the lower efficiency and changed phosphorescent color with increasing repetition rate.

In connection with the usual arc spectroscopy, this method will offer a particular advantage; for example, when a number of compounds are being volatilized in the arc, the presence of interfering compounds may mask a small trace of an impurity. Where this impurity exists in discrete particles, it is possible to take motion pictures during volatilization and to study only the frames which show the characteristics of the desired component.

In connection with the studies of the optimum combustion conditions for jet engines, it is expected that this device will prove useful, particularly when it is desired to use the instrument in the small amount of space available in airborne missiles.

Process Control

This instrument should have wide application in the many chemical and industrial process controls where a continuous indication is required of the state of the product being tested. For example, a reaction may be carried to the correct point, as shown by the spectrogram, and then automatically stopped. This can be done whenever the pattern on the screen reaches a predetermined shape. The indicator, in these cases, may be located in the control room of the plant, while the analyzer is in a remote location.

Transmission From Remote Locations

The possibility of transmitting spectral information in a short time should prove of considerable advantage. This information, of course, can be sent over wires as in the case of the plant, or may be modulated upon a carrier and demodulated at another location, as is desirable in the case of aircraft.

Colorimetry

Analysis. Because this instrument can analyze colors which constantly are changing, it is expected to prove superior in measurements such as the color of television screens. Such colorimetry is,

at present, quite difficult, because of the presence of flicker and the continuous change of color, caused by phosphorescent decay.

International Commission on Illumination Co-ordinates. Because the spectrograms already have been converted to electrical form by this instrument, it becomes very easy to integrate these electrical values by known circuit methods in order to obtain integrated or proportional values, such as are used in the International Commission on Illumination Co-ordinates.

EDUCATIONAL

Finally, this instrument obviously will prove to be a useful tool in the educational and industrial fields where actual graphical demonstrations of color phenomena can be produced and shown to large groups of people with the aid of a projection oscillograph. It has been found that the education of color matchers and similar personnel in the rudiments of color analysis is of considerable help in the manufacture of a more uniform product.[6]

Although the foregoing discussion has been concerned mainly with transmission measurements, it is possible to use the instrument also for reflective measurements as well.

Appendix

In a particular case the energy delivered to screen was

$$10^4 V \times 5 \times 10^{-4} A = 5 \text{ watts}$$

$$= 5 \text{ volt } \frac{\text{coulombs}}{\text{second}}$$

if 1/10,000 of total energy enters the slit for a band centering about 5,500 angstroms and the average energy per photon in this band[6]

$$E = \frac{12.4 \times 10^3}{5.5 \times 10^3}$$

$$= 2.25 \frac{\text{electron volts}}{\text{photon}}$$

The entering power was then

$$\frac{5 \times 10^{-4} \dfrac{\text{volt coulombs}}{\text{second}}}{1.60 \times 10^{-19} \dfrac{\text{coulombs}}{\text{electron}}} \Bigg/ \frac{\dfrac{\text{electron volts}}{\text{second}}}{\dfrac{\text{electron volts}}{\text{photon}}}$$

$$= 1.39 \times 10^{15} \frac{\text{photons}}{\text{second}}$$

For a 10^{-6} second pulse this is 1.39×10^9 photons.

References

1. D. Ulrey. United States patent 2,193,606.

2. THE SPECTROPHOTOMETER IN THE TEXTILE INDUSTRY, Constantine Monego, Werner Von Bergen. *American Dyestuff Reporter*, American Association of Textile Chemists and Colorists (New York, N. Y.), January 4, 1943, pages 2–16.

3. ELECTRONIC EQUIPMENT (book), R. C. Walker. Chemical Publishing Company, Inc., New York, N. Y., 1945. Pages 143–5.

4. Westinghouse Electric Corporation. United States patent 2,193,606.

5. H. A. Snow. United States patent 2,240,722.

6. Discussion by W. M. Scott of INTRODUCTION TO COLOR, Deane B. Judd. American Society for Testing Materials, Philadelphia, Pa., March 5, 1941.

No Discussion

Dimensionless Analysis of Servomechanisms by Electrical Analogy—I

G. D. McCANN
MEMBER AIEE

S. W. HERWALD
ASSOCIATE AIEE

IN a previous paper[1] general solutions were presented in dimensionless form, giving the transient response characteristics of the basic variable-voltage angular-position servomechanisms with simple error control alone and with error control plus optimum anticipation time. This paper continues the analysis for error control servomechanisms having the three most important forms of *RC*-feedback damping; that is, feedback from generator field current, feedback from generator armature terminals, and feedback proportional to the velocity of the regulated system. All solutions were obtained with the mechanical transients analyzer. The actual physical systems together with the equations defining their performance are presented together with the electrical analogies set up on the analyzer. The general solutions are given in dimensionless curve form for the practical range of time constants and damping ratios.

The Servomechanisms and Their Analogies

The dimensionless form used for representing the solutions of such servomechanisms has been treated in detail in references 1, 2, and 3. The basic parameters will merely be tabulated here. Referring to Figures 1, 2, 3, and 4

θ_i = angular position of reference system to be followed

θ_o = angular position of regulated system

$\theta = \theta_i - \theta_o$ = error angle

t_a = armature time constant

t_f = field time constant

K = stiffness constant

I = total system inertia

c = actual mechanical damping of armature circuit

$r = \dfrac{c}{2\sqrt{KI}}$ = ratio of actual to critical damping

$\omega_n = \sqrt{\dfrac{K}{I}}$ = undamped natural frequency of simple error-control system with no time delays

The latter two constants are the basic dimensionless parameters defining the simple error-control system.[3] All time constants are put in dimensionless form[1-3] through multiplication by ω_n.

Also, the actual solutions are obtained for a suddenly applied velocity ω_1 of the system to be followed. Referring to the illustrative solutions for the error angle given on the curves of Figures 5 to 9, the solutions are defined in terms of the crest overshoot θ_{max} and the time t_1. In the curves giving the general solutions, θ_{max} is put in dimensionless form by dividing by θ_{ss} (the steady-state error angle for suddenly applied constant velocity).

$$\theta_{ss} = \frac{2r\omega_1}{\omega_n}$$

The time t_1 is made dimensionless through multiplication by ω_n.

RC-Feedback From Generator Field Current

Figure 2*a* shows a schematic diagram of the actual system. The complete performance equation as shown is derived in the appendix. Only two parameters (in addition to those for the simple error control system) are required to define the system completely. These are the dimensionless constant A_2, which is the voltage gain around the feed-back loop, and the *RC*-feedback time constant t_d which is put in dimensionless form through multiplication by ω_n. The electrical analogy set up on the transients analyzer for obtaining the solutions is shown in Figure 2*b*. Analogy *A* of Figure 1 was used to represent the motor-generator electrical-

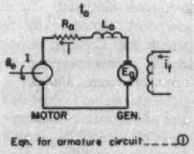

Eqn. for armature circuit ---- ①

$E_g = R_a i + L_a pi + gp\theta_o$

Eqn. for motor torque ---- ②

$bi = Ip^2\theta_o$

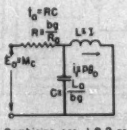

Combining eqn. 1 & 2 as a single torque eqn in terms of θ_o --- ③

$M_c = \frac{bE_g}{R_a} = (1 + t_a p) Ip^2\theta_o + cp\theta_o$

$t_a = L_a/R_a \qquad c = \frac{bg}{R_a}$

ANALOGY A

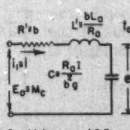

Combining eqn. 1 & 2 as a single torque eqn. in terms of i

$M_c = \frac{bE_g}{R_a} = bi + \frac{bL_a}{R_a} pi + \frac{b^2 g}{R_a I} \frac{i}{p}$

$M_c = b(1 + t_a p)i + c\frac{b}{I}\frac{i}{p}$

ANALOGY B

Figure 1. Derivation of the two electrical analogies used to represent the motor-generator armature circuit and motor torque equations

M_c = control torque

If

$E_g = ai_f$,

$M_c = \dfrac{abi_f}{R_a}$

$= A_1 i_f$

Paper 47-15, recommended by the AIEE joint subcommittee on servomechanisms for presentation at the AIEE winter meeting, New York, N. Y., January 27-31, 1947. Manuscript submitted October 9, 1946; made available for printing November 7, 1946.

G. D. McCANN was formerly with Westinghouse Electric Corporation, East Pittsburgh, Pa., and is now in the department of electrical engineering, California Institute of Technology, Pasadena, Calif.; S. W. HERWALD is with Westinghouse Electric Corporation, East Pittsburgh, Pa.

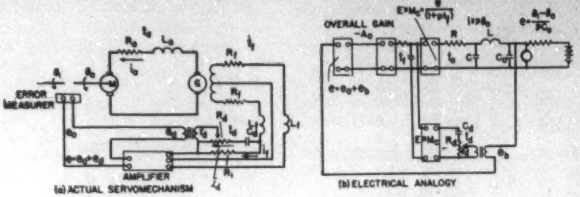

$$M_c = \frac{K(\theta_i-\theta_o)}{(1+t_f p)} - \frac{A\,\frac{r_f}{R_d}\,t_d p M_c}{(1+t_f p)(1+t_d p)}$$

$$E_c = \frac{A_0(\theta_i-\theta_o)}{C_0(1+t_f p)} - \frac{A_2\frac{r_d}{R_d}t_d\, p E_c}{(1+t_f p)(1+t_d p)}$$

$$\frac{K(\theta_i-\theta_o)}{(1+t_f p)} - \frac{A_2 t_d p\left[(1+t_d p)\, I p^2\theta_o + c p\theta_o\right]}{(1+t_f p)(1+t_d p)} = (1+t_d p)\, I p^2\theta_o + c p\theta_o$$

Figure 2 (top). Basic system and analogy for variable-voltage angular-position servomechanism with *RC*-feedback from generator field current

M_c = control torque in pound-feet (see Figure 1)

A = factor relating control torque to amplifier input voltage in pound-feet per volt

A_1 = factor relating control torque to generator field current in pound-feet per ampere (see Figure 1)

A_2 = voltage gain around feed-back loop (dimensionless)

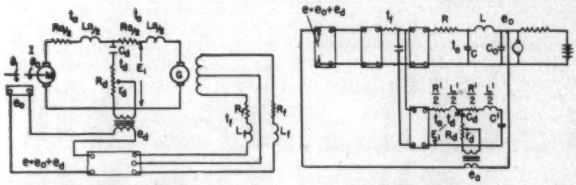

$$M_c = \frac{K(\theta_i-\theta_o)}{(1+t_f p)} - \frac{A_2 t_d p M_1}{(1+t_f p)(1+t_d p)}$$

$$E_c = \frac{A_0}{C_0}\frac{(\theta_i-\theta_o)}{(1+t_f p)} - \frac{A_0\frac{r_d}{R_d}t_d p\, E_1}{(1+t_f p)(1+t_d p)}$$

$$\frac{K(\theta_i-\theta_o)}{(1+t_f p)} - \frac{A_2 t_d p\left[(1+t_d p)\,\frac{I}{2}p^2\theta_o + c p\theta_o\right]}{(1+t_f p)(1+t_d p)} = (1+t_d p)\, I p^2\theta_o + c p\theta_o$$

Figure 3. Basic system and analogy for variable-voltage angular-position servomechanism with *RC*-feedback from generator armature terminals

Assuming equal impedances in motor and generator armatures

mechanical equations. Because of the internal impedance of the amplifier, the voltage at the output terminals of the last stage is not proportional to $E = M_c$. It was therefore necessary to use a parallel stage to supply the *RC*-feedback circuit as shown. If the *RC*-feedback circuit has a high impedance compared to the amplifier impedance, its voltage is proportional to the generator field current through the relation shown in the caption of Figure 1.

RC-Feedback From Generator Armature Terminals

The actual physical system and its electrical analogy are shown in Figure 3. The performance equation is derived in the appendix. The system is defined by the same parameters as used for *RC*-feedback from the generator field current. The only difference is the form of the feed-back damping. In setting up the electrical analogy, the most desirable circuit was found to be one in which the circuit representing the motor-generator armature circuit and motor torque equations was set up in dual using both analogies of Figure 1. Analogy *A* was found most convenient for applying the forcing function (constant ω_i) and for obtaining the error angle control. However, analogy *B* was required to obtain the proper voltage analogous to the generator terminal voltage in providing the *RC*-feedback.

RC-Feedback Proportional to Velocity ($p\theta_o$)

This system and its analogy is shown in Figure 4. As shown by the equation defining performance, the damping component of the control torque can be expressed in terms of the stiffness constant K, the *RC*-circuit constant t_d, and an additional time constant t_n, defined in Figure 4 and derived in the appendix. In the analogy the *RC*-feedback is easily obtained from analogy *A* (Figure 1) by inserting a resistor in the circuit through which the current ($i_1 \equiv p\theta_o$) flows.

Dimensionless Data in Curve Form

The general solutions in dimensionless form giving the optimum damping parameters and the system response are presented in the curves of Figures 5, 6, 7, and 8 for the respective damping ratios of $r =$ 0.2, 0.4, 0.6, 0.8, and 1.0. Each figure

Figure 4. Basic system and analogy for variable-voltage angular-position servomechanism with *RC*-feedback proportional to velocity $p\theta_o$

Kt_n defined as equal to $A\frac{r_d}{R_d}g_t$

t_n is a time constant (see appendix)

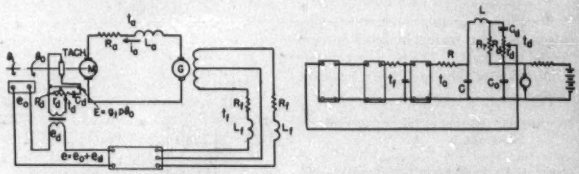

$$M_c = \frac{K(\theta_i-\theta_o)}{(1+t_f p)} - \frac{A\frac{r_d}{R_d}t_d g_t p^2\theta_o}{(1+t_f p)(1+t_d p)}$$

$$E_c = \frac{A_0(\theta_i-\theta_o)}{C(1+t_f p)} - \frac{A_0\frac{r_d}{R_d}R_f r_f p^2\theta_o}{(1+t_f p)(1+t_d p)}$$

$$\frac{K(\theta_i-\theta_o)}{(1+t_f p)} - \frac{K t_n t_d p^2\theta_o}{(1+t_f p)(1+t_d p)} = (1+t_d p)\, I p^2\theta_o + c p\theta_o$$

Figure 5. Dimensionless performance curves and optimum damping parameters for $r = 0.2$

A—*RC*-feedback from generator field current
B—*RC*-feedback from generator armature terminals
C—*RC*-feedback proportional to velocity

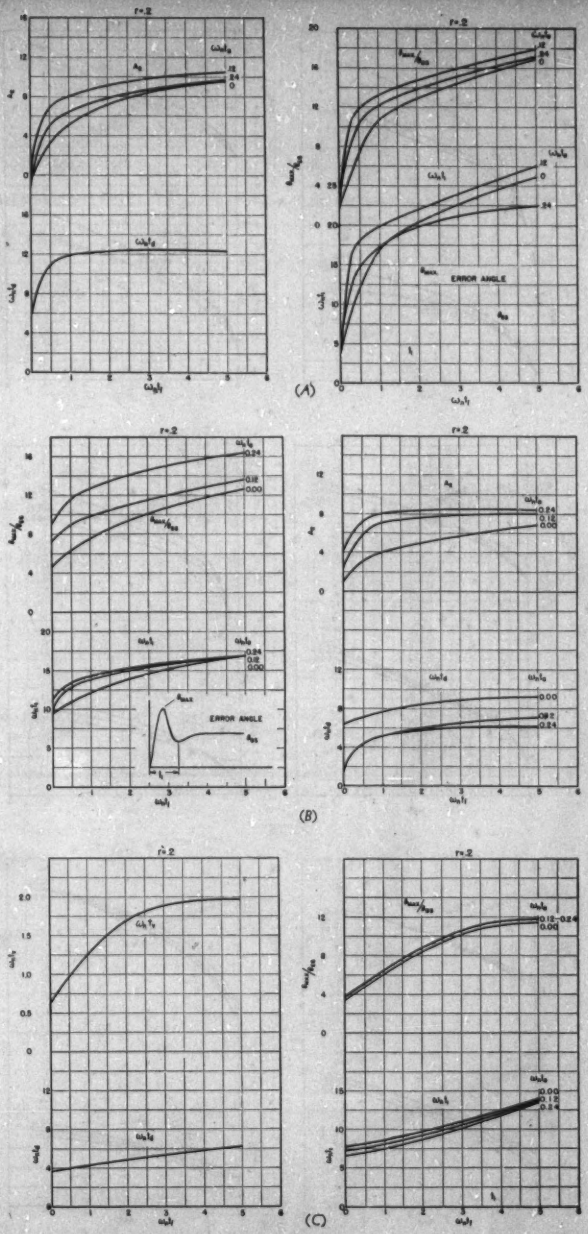

gives solutions for the three types of feedback. There are four sets of curves for each type of feedback and value of damping ratio. Two give the system performance in terms of the ratio of crest overshoot to the steady-state error angle θ_{max}/θ_{ss} (for a suddenly applied constant velocity) and the dimensionless duration of the initial overshoot $\omega_n t_1$. The other to give the optimum values of the time constant of the *RC*-feedback circuit $\omega_n t_d$ and the gain around the feedback loop A_3 for feedback from generator field current and armature terminals or the time constant $\omega_n t_v$ for feedback proportional to velocity.

For the range of parameters covered, damping greater than 85 per cent always could be obtained giving solutions as illustrated. For this reason the per cent damping was not plotted.

Polarity of RC-Feedback

It was found that for a narrow band of parameters, positive feedback gives positive damping with *RC*-feedback from generator field current and from the generator armature terminals. This band is for r less than 0.4 and low values of $\omega_n t_d$ and $\omega_n t_f$ (below about 0.5). A comparison of solutions obtained in this range with both polarities of feedback is given in Figure 10. Positive feedback gives a better solution with much less crest overshoot and more rapid decay to the steady-state value. However, the required amount of feedback is very critical and (as shown by the oscillograms) slightly too much feedback will cause the system to break into relatively high frequency undamped oscillation. For this reason positive feedback will probably seldom provide a practical solution.

Analysis of Data

The principal variations in the system performance as a function of the type of feedback and damping ratio are illustrated by the solutions of Figure 11. The ratio of θ_{max}/θ_{ss} increases with decreasing damping ratio at a rate sufficiently rapid to cause the actual value of θ_{max} to increase slightly. For instance, with case *A* of Figure 11 and $r = 1.0$, $\theta_{ss} = 1$ and $\theta_{max} = 1.9$. For $r = 0.2$, $\theta_{max} = 11.4 \times 0.2 = 2.28$. The ratio of θ_{max}/θ_{ss} at the end of the overshoot (or at t_1) also in-

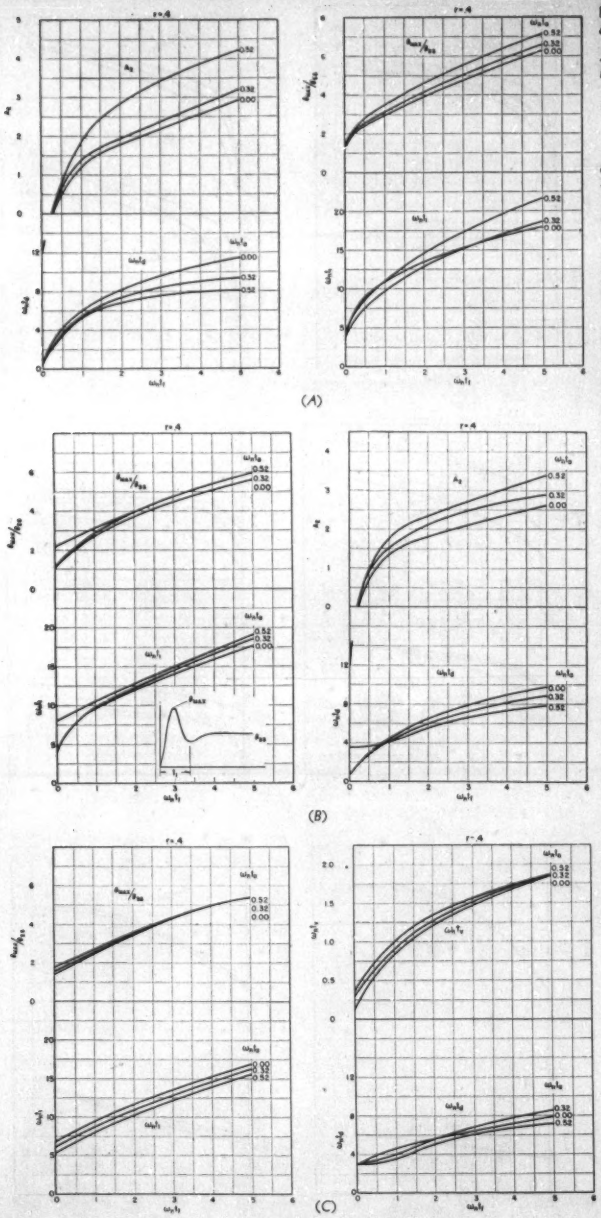

Figure 6. Dimensionless performance curves and optimum damping parameters for $r = 0.4$

A—*RC*-feedback from generator field current
B—*RC*-feedback from generator armature terminals
C—*RC*-feedback proportional to velocity $p\theta_o$

creases with decreasing r, together with the value of $\omega_n t_1$.

Comparison of Types of Feedback

At the lower values of damping ratio, feedback proportional to velocity gives markedly better solutions than for either of the other two types. Referring to Figure 11, it is seen that for $r = 0.2$, this type of feedback gives appreciably lower crest overshoot with shorter times t_1 and markedly lower error at t_1. Feedback from the armature terminals provides somewhat better solutions than from generator field current at the lower values of r. For r greater than 0.8 there is no great difference between the performance with the three types of damping. Feedback from the armature terminals provides a better solution than feedback from the generator field current because of the added delay introduced by the generator armature impedance.

Typical Example

To illustrate how the data presented in Figures 5 to 9 can be used to obtain optimum *RC*-feedback values for a variable-voltage angular-position servomechanism, the following example is given. The values for the basic system parameters are the same as used for determining optimum anticipation time in the previous paper,[1] namely,

$I = 10^{-1}$ pound-inches second^2
$K = 5$ inch-pounds per radian
$R_a = 6$ ohms
$L_a = 0.10$ henry
$R_f = 100$ ohms
$L_f = 15$ henries
$b = 4$ inch-pounds per ampere
$g = 0.6$ volt per radian per second

$$\omega_n = \sqrt{\frac{K}{I}}$$
$$= 7.07 \text{ radians per second}$$

$$c = \frac{bg}{R_a}$$
$$= 0.4 \text{ inch-pound per radian per second}$$

$$r = \frac{c}{2\sqrt{KI}}$$
$$= 0.283$$

$\omega_n t_f = 1.06$
$\omega_n t_a = 0.12$

For the case of *RC*-feedback from the

Figure 7. Dimensionless performance curves and optimum damping parameters for $r = 0.6$

A—*RC*-feedback from generator field current
B—*RC*-feedback from generator armature terminals
C—*RC*-feedback proportional to velocity

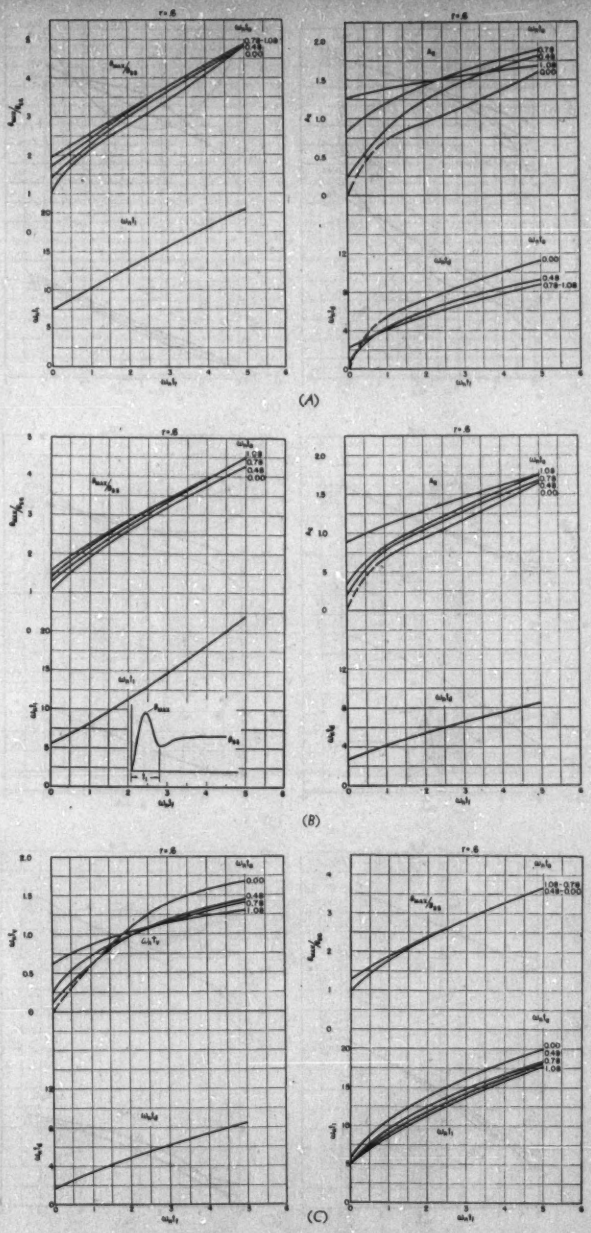

generator field current, interpolating between Figure 5*A* and 6*A* for $r=0.28$

Optimum $\omega_n t_d = 9.6$
$A_2 = 5.3$
$\omega_n t_1 = 15.9$
$\theta_{max}/\theta_{ss} = 9.1$

Therefore, if in the actual servomechanism with the parameters just given the feed-back time constant t_d is made 9.6÷7.07 or 1.35 seconds, and the total gain around the feed-back loop is made 5.3 then time t_1 for the undamped half cycle that occurs with all *RC*-feedback is 15.9÷7.07 or 2.25 seconds. The maximum angular error at the motor shaft θ_{max} for a suddenly applied constant velocity ω_1 is

$$9.1 \times \frac{2r\omega_1}{\omega_n} = 0.725\omega_1$$

The damping after the first overshoot will be very high.

Using *RC*-feedback from the generator terminals for the same servomechanism system and interpolating between Figures 5*B* and 6*B* for $r=0.28$

$\omega_n t_d = 4.9$
$A_2 = 4.8$
$\omega_n t_1 = 11.7$
$\theta_{max}/\theta_{ss} = 7.0$

Then if t_d is made $4.9/7.07 = 0.69$ second and the net gain around the feed-back loop is 4.8, $t_1 = 1.65$ seconds and $\theta_{max} = 0.58\omega_1$. The damping after the first overshoot is high.

Again using the same servomechanism system but making the *RC*-feedback proportional to the output velocity $p\theta_o$ and interpolating between Figures 5*C* and 6*C* for $r=0.28$

$\omega_n t_d = 4.2$
$\omega_n T_v = 1.1$
$\omega_n t_1 = 8.4$
$\theta_{max}/\theta_{ss} = 5.9$

Then if t_d is made equal to 0.59 a second and $T_v = 0.15$ second, $t_1 = 1.2$ seconds and $\theta_{max} = 0.39\ \omega_1$. Again the damping after the first overshoot is high.

In comparing the merits of anticipation[1] and the various means of *RC*-feedback in their benefiting the performance of this particular servomechanism, they should be ranked in this order:

1. Anticipation.
2. *RC*-feedback proportional to output velocity $p\theta_o$.

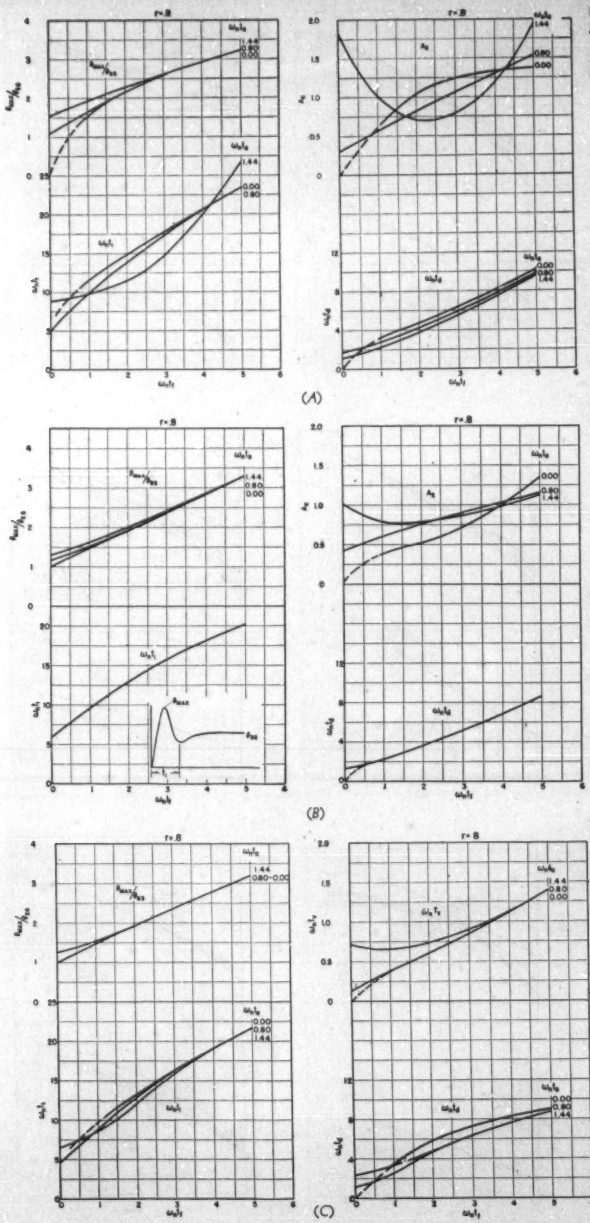

Figure 8. Dimensionless performance curves and optimum damping parameters for $r = 0.8$

A—*RC*-feedback from generator field current
B—*RC*-feedback from generator armature terminals
C—*RC*-feedback proportional to velocity

3. *RC*-feedback from generator terminals.
4. *RC*-feedback from generator field current.

As anticipation requires a d-c amplifier or its equivalent and *RC*-feedback proportional to output velocity $p\theta_o$ usually requires a tachometer, the simplest method to use where the specifications to be met permit is *RC*-feedback from the generator terminals.

It should be understood clearly that the above ranking of performance merit is only for the example given and the ranking for servomechanism systems with different basic parameters may be quite different.

Appendix. Derivation of the Basic Equations for the Various Angular-Position Servomechanisms

RC-Feedback From Generator Field Current

Figure 1 gives the derivation of the two analogous electric circuits used to represent the combined electrical and mechanical equations for the motor and generator armature circuit and motor rotation. For this particular type of *RC*-feedback, analogy *A* was used as shown in Figure 2. Referring to Figure 2 the motion of the system in terms of the controller torque M_c is defined by the equation

$$M_c = (1+t_a p)Ip^2\theta_o + cp\theta_o \tag{3}$$

The controller torque M_c is composed of two components,

$$M_c = M_o + M_d$$

The first term, the error control term derived in reference 1, is

$$M_o = \frac{K(\theta_1-\theta_o)}{(1+t_f p)}$$

Referring to Figure 2 for the derivation of the second term,

$$i_d = \frac{C_d p R_1 i_f}{(1+t_d p)}$$

$$e_d = \frac{r_d C_d R_1 p i_f}{(1+t_d p)} = \frac{R_1 \frac{r_d}{R_d} t_d p i_f}{(1+t_d p)}$$

A = factor relating control torque M_c to amplifier input voltage e (torque÷volts)

A_1 = constant relating control torque M to generator field current i_f (torque÷ampere)

A_3 = gain around the feed-back loop

$$M_d = \frac{-AR_1 \frac{r_d}{R_d} t_d p i_f}{(1+t_f p)(1+t_d p)}$$

$$M_d = \frac{-\frac{AR_1}{A_1}\frac{r_d}{R_d} t_d p M_c}{(1+t_f p)(1+t_d p)} = \frac{-A_3 t_d p M_c}{(1+t_f p)(1+t_d p)}$$

R_1 has the dimension of volts per ampere and thus A_3 is a dimensionless constant. It is actually the voltage gain around the feed-back loop. Thus, as

$$M_c = M_a + M_d = (1+t_a p) I p^2 \theta_o + c p \theta_o \qquad (3)$$

the complete equation becomes

$$(1+t_a p) I p^2 \theta_o + c p \theta_o = \frac{K(\theta_1 - \theta_o)}{(1+t_f p)} - \frac{A_3 t_d p[(1+t_a p) I p^2 \theta_o + c p \theta_o]}{(1+t_f p)(1+t_d p)}$$

RC-Feedback From Generator Armature Terminals

For this type it is assumed that the motor and generator armatures have the same impedances. The terminal voltage is thus given by the equation

$$E_1 = E_g - (R_a/2 + L_a p/2) i_a$$
$$= E_g - R_a(1+t_a p) i_a/2$$

From this a mechanical torque equation can be written.

$$M_1 = \frac{b E_1}{R_a} = M_c - b(1+t_a p) i_a/2$$

Expressing i_a in terms of θ_o (from equation 1, Figure 1),

$$i_a = I p^2 \theta_o / b$$

From equation 3, Figure 1,

$$M_1 = M_c - (1+t_a p) I p^2 \theta_o / 2$$
$$= (1+t_a p) I p^2 \theta_o / 2 + c p \theta_o$$

By analysis identical for the case of *RC*-feedback from generator field current, the control torque can be expressed as follows:

$$M_c = \frac{K(\theta_1 - \theta_o)}{(1+t_f p)} - \frac{A_3 t_d p M_1}{(1+t_f p)(1+t_d p)}$$

$$M_c = \frac{K(\theta_1 - \theta_o)}{(1+t_f p)} - \frac{A_3 t_d p[(1+t_a p) I p^2 \theta_o / 2 + c p \theta_o]}{(1+t_f p)(1+t_d p)}$$

This gives the complete equation

$$(1+t_a p) I p^2 \theta_o + c p \theta_o = \frac{K(\theta_1 - \theta_o)}{(1+t_f p)} - \frac{A_3 t_d p[(1+t_a p) I p^2 \theta_o / 2 + c p \theta_o]}{(1+t_f p)(1+t_d p)}$$

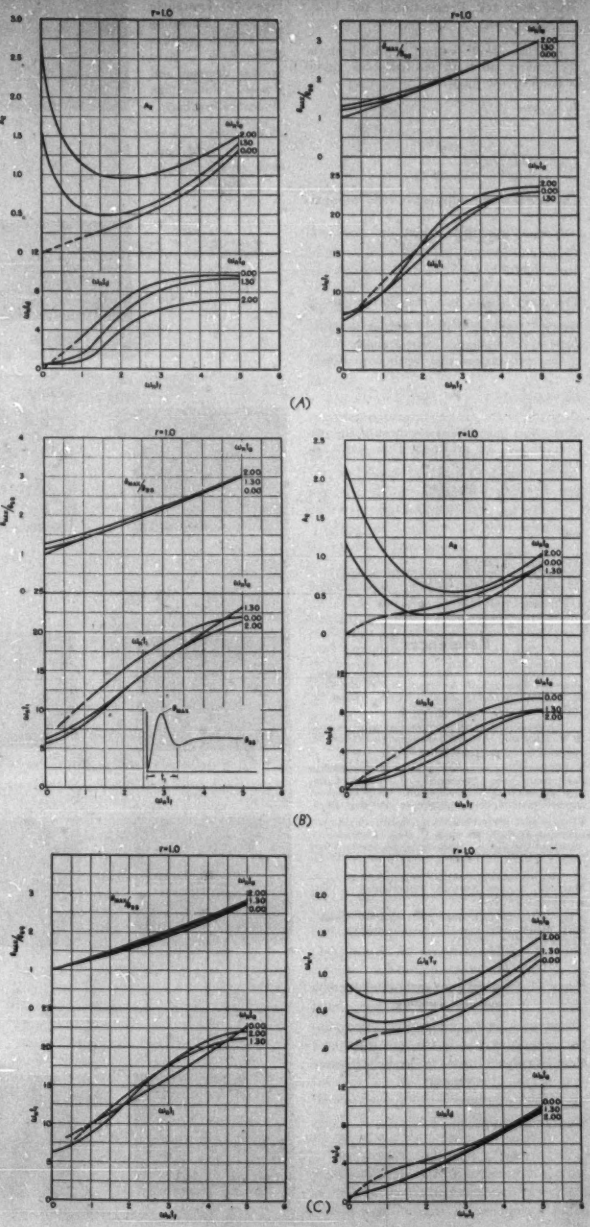

Figure 9. Dimensionless performance curves and optimum damping parameters for $r = 1.0$

A—*RC*-feedback from generator field current
B—*RC*-feedback from generator armature terminals
C—*RC*-feedback proportional to velocity

RC-Feedb ack Proportional to Velocity $p\theta_o$

For this case the voltage applied from the tachometer motor to the feed-back circuit is given by the equation

$$E_t = g_t p\theta_o$$

$$e_d = \frac{r_d C_d g_t p^2\theta_o}{(1+t_d p)} = \frac{\frac{r_d}{R_d} t_d g_t p^2\theta_o}{(1+t_d p)}$$

The torque term resulting from this voltage is

$$M_d = \frac{-A\frac{r_d}{R_d} t_d g_t p^2\theta_o}{(1+t_f p)(1+t_d p)}$$

The term $A\frac{r_d}{R_d} g_t$ has the dimensions of

$$\frac{\text{torque}}{\text{volt}} \times \frac{\text{volt-seconds}}{\text{radians}} = \frac{\text{torque-seconds}}{\text{radians}}.$$

It also can be expressed by the equation

$$K t_v = A\frac{r_d}{R_d} g_t$$

where K is the stiffness constant of the system, and t_v an arbitrary time constant. Thus

$$M_c = \frac{K(\theta_i - \theta_o)}{(1+t_f p)} = \frac{K t_v t_d p^2\theta_o}{(1+t_f p)(1+t_d p)}$$

and

$$\frac{K(\theta_i - \theta_o)}{(1+t_f p)} - \frac{K t_v t_d p^2\theta_o}{(1+t_f p)(1+t_d p)} = (1+t_a p) I p^2\theta_o + c p\theta_o$$

References

1. Dimensionless Analysis of Servomechanisms by Electrical Analogy, **S. W. Herwald, G. D. McCann,** AIEE Transactions, volume 65, 1946, October section, pages 636–9.

2. Considerations in Servomechanism Design, **S. W. Herwald.** AIEE Transactions, volume 63, 1944, December section, pages 871–6.

3. Electrical Analogy Methods Applied to Servomechanism Problems, **G. D. McCann, S. W. Herwald, H. S. Kirschbaum.** AIEE Transactions, volume 65, 1946, February section, pages 91–6.

4. Dynamic Behavior and Design of Servomechanisms, **G. S. Brown, A. C. Hall.** *Transactions*, American Society of Mechanical Engineers (New York, N. Y.), volume 68, number 5, 1946, pages 503–24.

5. Theory of Servomechanisms (book), **L. A. MacColl.** D. Van Nostrand Company, Inc., New York, N. Y., 1945.

6. Automatic Control Engineering (book), **E. S. Smith.** McGraw-Hill Book Company, Inc., New York, N. Y., 1944.

Figure 10. Error angle solutions illustrating case where positive RC-feedback gives positive damping and a better solution than negative feedback

RC-feedback from generator field current, $r=0.2$, $\omega_n t_v = \omega_n t_f = 0$

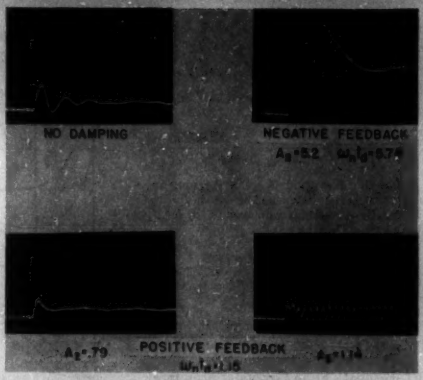

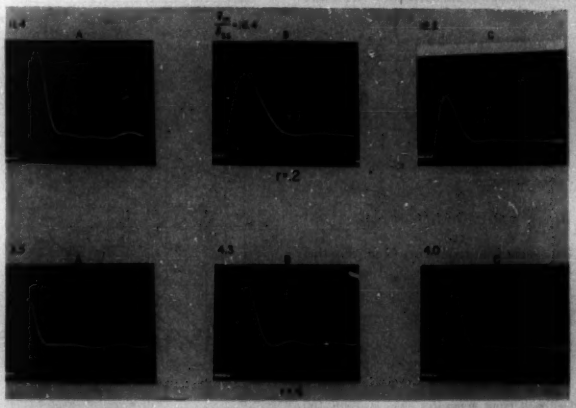

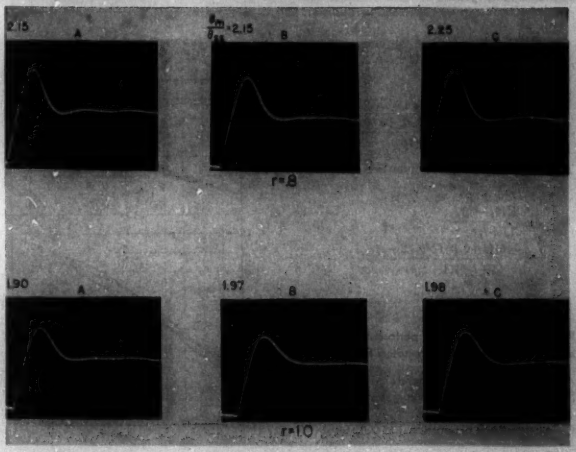

Figure 11. Typical error angle solutions with optimum damping

A—RC-feedback proportional to velocity, $p\theta_o$
B—RC-feedback from generator field current
C—RC-feedback from generator armature terminals

r	$\omega_n t_g$	$\omega_n t_f$
0.2	0	4.26
0.4	0.32	2.12
0.8	0.8	2.65
1.0	1.3	2.7

A 60-Cycle Hysteresis Loop Tracer for Small Samples of Low-Permeability Material

D. E. WIEGAND
ASSOCIATE AIEE

W. W. HANSEN
NONMEMBER AIEE

Synopsis: The basic components of this instrument are

(*a*). A large (35-pound) exciting coil with a pickup coil at its center.

(*b*). An amplifier and integrating circuit.

(*c*). A cathode-ray oscillograph.

The instrument provides a convenient and rapid means of determining the magnetic properties of samples much smaller than can be used conveniently with the ballistic method. Absolute calibration provides greater accuracy and reliability than has been obtained previously in this type of apparatus. Phase errors are reduced to low values through the use of a compensated integrating network with absolute means of adjustment. This network provides a much higher output voltage than the usual circuit and thus makes practicable operation at the power line frequency and the consequent use of an exciting coil of sufficient size to minimize end effect errors and to allow operation at fields as high as 1,000 oersteds for long periods of time.

THIS INSTRUMENT was designed as a research tool in the development of wire for use in magnetic recording and will serve also in connection with process control in the production of this wire. The alloys presently used in the manufacture of recording wire depend on cold working for their magnetic properties, and by measuring these properties at various stages in the drawing process, it is possible to predict the properties of the wire when drawn to the final size. Magnetic measurements on a particular alloy at various diameters in the drawing process, moreover, make possible determining the annealing and drawing schedule required to produce a wire of given magnetic properties.

Of the fundamental magnetic properties in a magnetic recording wire, the residual induction and coercive force seem the most important[1,2] and a recently formed magnetic recording wire standardization committee has set tentative values for these quantities. The equipment for measuring these quantities in the development program of magnetic wire and in the manufacture of this wire must be rugged and simple in operation. It should have sufficient sensitivity to allow measurements on samples consisting of a minimum number of strands of finished wire (0.004-inch diameter). Moderate accuracy is sufficient but the calibrating means should be foolproof and reliable. The cathode-ray oscilloscope hysteresis loop tracer described meets these requirements.

A tester of this same general type but having an operating frequency of ten kilocycles has been in use in the magnetic wire development program at the Armour Research Foundation. Difficulties encountered in the use of this instrument have led to various design improvements in the new tester. Other hysteresis loop tracers of the cathode-ray oscillograph type have been described previously.[2,3]

Experience with the 10-kilocycle tester has shown that, in order to obtain measurements at the intense fields required for saturation of the present magnetic recording wires a much more generously designed field coil would have to be provided. Also, consideration of demagnetizing effects[4] indicated that a much longer magnetizing coil should be used. In the magnetic wire development program, wires as large as 0.040 inch diameter are being studied, and it is these large wires that set the minimum length of the exciting coil.

The size of coil dictated by these two requirements requires for its operation a larger amount of power than can be obtained conveniently from an audio oscillator, and it was this fact that led to choosing the power line frequency as the operating frequency.

Other advantages of this frequency over some higher one are

1. Less trouble caused by stray magnetic fields because all field components are 60 cycles per second (or at most harmonics thereof). Actually it was found practicable to balance out all stray fields with the same device used to balance the air flux in the pickup coil plus a simple phase corrective adjustment.

2. Low stray capacitance effect at low frequency eliminates need for elaborate shielding system.

3. Lower eddy loss in exciting coil makes coil run cooler.

4. Lower reactive component of impedance reduces operating voltage of coil and eliminates need for high voltage insulation. This aids in heat conduction to the coil surfaces and further reduces the temperature rise.

Low operating frequencies in a tester of this type usually impose severe requirements on the amplifier. The gain must be high because the voltage induced in the pickup coil is proportional to the frequency. To keep phase errors small at the operating frequency, the amplifier must have good response at much lower frequencies. The combination of extremely low frequency cutoff and high gain will cause the image on the oscillograph screen to shift up and down with line voltage fluctuations unless special precautions are taken in the design of the amplifier and its power supply.

The severity of these requirements is reduced in the new tester through the use of an improved integrating network which provides at its output terminals a much

Paper 47-18, recommended by the AIEE committee on communication for presentation at the AIEE winter meeting, New York, N. Y., January 27–31, 1947. Manuscript submitted May 2, 1946; made available for printing November 18, 1946.

D. E. WIEGAND and W. W. HANSEN are with the Armour Research Foundation, Illinois School of Technology, Chicago, Ill.

higher voltage than the commonly used circuit.

Experience with the 10-kilocycle tester previously used has shown a very definite need for a calibrating system independent of the use of calibrated samples. Long[3] has pointed out the extreme importance of phase errors when an absolute calibration system is used. An analysis of phase errors in the vertical and horizontal systems, and the use of a phase compensating system whose adjustment is made without reference to the shape of the hysteresis trace, has made possible the use of an independent calibrating system in this tester.

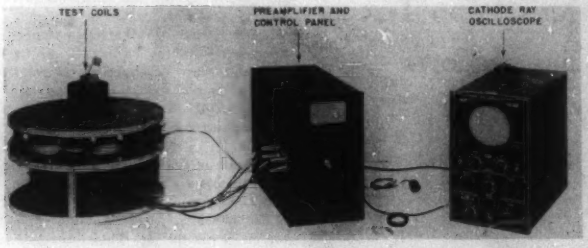

Figure 1. Complete test apparatus

Description

The assembled apparatus is shown in Figure 1 and the circuit diagram and list of component parts in Figure 2. The test coils, control panel, and oscilloscope should be spaced approximately as shown in Figure 1 in order to prevent interaction of magnetic fields between the different parts. The oscilloscope is sensitive to the field of the exciting coil and the leakage field of the variable transformer. The effect of the exciting-coil field on the vertical deflection is balanced out when the balancing mutual inductor is adjusted. Perfect compensation of the effect of the variable transformer field is not practicable as both its magnitude and pattern change with the dial setting. There is no provision for balancing the effect of either field on the horizontal deflection, although such compensation could be provided in case space is at a premium. With the present design and with spacings as shown in Figure 1 or greater, the effect of stray fields is small enough to have no appreciable effect on the accuracy of the measurements.

In Figure 3, the six coils arranged around the exciting coil are mutual inductors which serve to measure the peak current and hence the peak magnetizing force in the exciting coil, to balance the air flux in the pickup coil, and to calibrate the B or vertical scale on the oscilloscope. The coils are wound in pairs to allow making fine adjustment of the mutual inductances by varying the distance between two coils of a pair. Each pair is so connected that the vertical components of field are opposite in the two coils. The central plane of the mutual inductors coincides with the center of the exciting coil and their axes are parallel to and at equal distances from the axis of the exciting coil.

With this symmetrical arrangement, the fields of the mutual inductors cancel at the midpoint of the exciting coil and, therefore, calculating the magnetizing force at the center of the exciting coil from its dimensions and ampere turns is made possible. Furthermore, the external field of the exciting coil has no effect on the secondary voltage of a pair of mutual inductors, thus allowing their adjustment before final assembly.

The Exciting Coil

The exciting coil is designed to operate at a peak magnetizing force of somewhat greater than 500 oersteds continuously without exceeding a 55-degree-centigrade temperature rise. The thermal capacity of the winding is sufficient to allow making measurements at 1,000 oersteds providing the variable transformer is run to zero between tests. Measurements on samples at 1,000 oersteds have been made for periods of several hours and it was found that if this precaution is observed the temperature of the coil does not exceed safe limits.

It is desirable to have the magnetic field along the axis of the exciting coil uniform for as long a length as possible. Changes in field strength cause a distribution of magnetic poles along the length of the sample under test, which reduces the induction in the sample because of demagnetizing action.

Figure 4 shows the field distribution in the exciting coil. Data for this curve were obtained by means of a small exploring coil which was connected to a vacuum-tube voltmeter. Voltage readings were obtained with the exploring coil at various positions along the axis of the exciting coil, with the axes of the two coils coinciding, and with a constant 60-cycle current in the exciting coil. The curve shows the field to be constant within 5 per cent over a length of 6.8 inches.

Measurement of Peak Magnetizing Force

A convenient method of measuring the peak current, and therefore the peak magnetizing force, in the exciting coil is the use of a mutual inductor with its primary winding in series with the exciting coil and its secondary connected to a rectifier type voltmeter.[5] In addition to giving a true reading of peak magnetizing force for all wave forms that are likely to be encountered, this method gives an H scale that is almost linear.

To determine the value of mutual inductance giving a convenient scale factor on the H reading voltmeter, it is necessary to know the ratio of instantaneous values of current and magnetizing force in the exciting coil. Two methods for the determination of this ratio are

1. Take simultaneous readings of alternating voltage across an accurately wound pickup coil inside the exciting coil and current in the exciting coil. The accuracy of this method depends on the accuracy to which the dimensions of the pickup coil are known and the accuracy of calibration of the voltmeter and ammeter. Also, the wave form of current, if nonsinusoidal, may affect the accuracy of the ratio determination.

2. Calculate the ratio of magnetizing force to current from the dimensions of the exciting coil.

Method 2 was chosen in the calibration of this tester. The size of the exciting coil allows the determination of its dimensions to a greater percentage accuracy than those of the much smaller pickup coil in the method 1. Also, the wave form errors of method 1 are eliminated.

The H measuring mutual inductor was adjusted to give a scale factor of 10 on a standard 10/100-volt rectifier type voltmeter. Thus two ranges of magnetizing force readings, 100 and 1,000 oersteds full scale, are provided. Because of the linear relation between peak magnetizing force and average voltage, readings are obtained directly from the voltmeter scale.

Calculation of the required value of mutual inductance is given in Appendix I.

Compensation of Air Flux

The induced voltage in the pickup coil is influenced by the flux through the thickness of its winding and in the space inside the coil as well as the flux in the sample Because only that part caused by the ferromagnetic properties* of the sample is of interest, it is necessary to balance all other flux linkages. In previous testers, this has been done by placing a coil similar to the pickup coil near the pickup coil, both being inside the exciting coil. By adjusting the number of turns in the balance coil it is possible to make its voltage the same as that of the pickup coil with no sample in it. By connecting the two coils so that their voltages oppose, the voltage across the two is zero and the air flux in the pickup coil is effectively balanced out. The balancing operation is a very tedious one as it must be performed with great accuracy because of the large ratio of air flux to sample flux.

In order to provide for an external balance adjustment and to prevent restriction of air circulation on the inside of the exciting coil caused by the presence of an extra coil beside the pickup coil, balancing on the new tester is accomplished by means of an adjustable mutual inductor.

The behavior of the exciting and pickup coils, less sample, is that of a mutual inductor. To balance the air flux, therefore, it is merely necessary to connect a mutual inductor with its primary in series with the exciting coil and the secondary in series-opposing with the pickup coil. If the two mutual inductances are of the same value, the net secondary voltage should be zero.

The required value of mutual inductance was calculated from the dimensions and number of turns in the exciting and pickup coils. The balancing mutual inductor was designed for a somewhat higher value and then trimmed down by removing primary turns. The final balance adjustment is obtained by varying the spacing of the two halves of the mutual inductor.

When the final balance was first attempted, it was found that a residual net voltage of 0.025 volt could not be eliminated by adjustment of the mutual inductor. This minimum residual voltage was obtained with a magnetizing force of 500 oersteds in the exciting coil, and at the same field the voltage across the secondary of the balance coil was only 24.5 volts. The residual voltage was found to be a sine wave of 60 cycles per second and, therefore, was caused by a very slight phase shift (0.058 degree) between pickup and balance coil voltages.

This phase difference is caused by a small amount of mutual resistance which is present in different amounts in the two sets of coils. Mutual resistances are caused by eddy currents in the winding conductors and clamping bolts, which set up spurious magnetic fields having components out of phase with the primary current. These out-of-phase field components induce voltage components in the secondary circuit which are in phase with the primary current.

Although the phase difference caused by these mutual resistances is extremely small, the resulting residual voltage is large enough to affect seriously the accuracy of measurement on small samples.

The residual voltage was eliminated through the use of the mutual resistance coils placed near the ends of the pickup coil (see Figure 5). These coils, when connected across a variable resistance, increase the mutual resistance between the exciting coil and the pickup coil.

When the balancing mutual inductor and the variable resistance are adjusted properly, no residual voltage is detectable with amplifier gain and vertical gain on the oscillograph at maximum. Under this condition 0.0005 volt or greater would be detected.

Integrating Network

The net induced voltage in the pickup and balance coils is proportional to the time rate of change of flux in the sample. As it is desired that the vertical deflection of the oscilloscope beam be proportional to the flux, rather than its derivative, it is necessary to integrate the signal before it is applied to the oscilloscope.

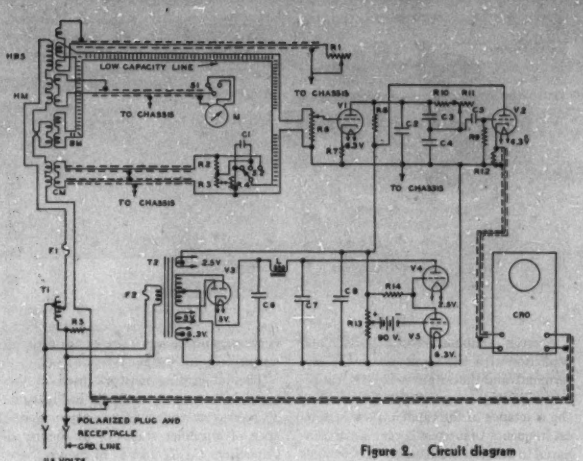

Figure 2. Circuit diagram

HBM—Exciting, induction, and mutual resistance coils
HM—*H* (field measuring) mutual inductor
BM—Balancing mutual inductor
CM—Calibrating mutual inductor
S_1—*H* meter range switch
M—*H* meter (10/100 rectifier type voltmeter, 1,000 ohms per v)
S_2—Measure-calibrate switch
F_1—20-amp fuse
T_1—2 kva 115–0/135-volt variable transformer (type *100 Q*)
F_2—3-amp fuse
T_2—Power transformer 300–0–300 high voltage (Thordarson *T-13R17*)
V_1—*6J5*
V_2—*6J5*
V_3—*5Z4*
V_4—*45*
V_5—*6F5*
CRO—Cathode-ray oscillograph (Dumont type *208B*)
R_1—50-ohm wire-wound rheostat
R_2—50,000-ohm wire-wound resistor
R_3—750-ohm 10-w adjustable resistor
R_4—10-ohm 10-w adjustable resistor
R_5—3 1-ohm 75-w resistors in parallel
R_6—1/2-megohm volume control
R_7—2,000-ohm 1/2-w resistor
R_8—50,000-ohm 1/2-w resistor
R_9—4-megohm 1/2-w resistor
R_{10}—5,000-ohm 1/2-w resistor
R_{11}—0.15-megohm carbon rheostat
R_{12}—2,500 ohm 1/2-w resistor
R_{13}—0.25-megohm potentiometer
R_{14}—0.5-megohm 1/2-w resistor
C_1—0.1-μf paper capacitor
C_2—0.5-μf 600-v paper capacitor
C_3—0.5-μf 600-v paper capacitor
C_4—0.5-μf 600-v paper capacitor
C_5—0.1-μf 600-v mica capacitor
C_6—0.4-μf oil-paper capacitor
C_7—20-μf electrolytic capacitor
C_8—20-μf electrolytic capacitor
L—10-henry 60-ma choke

* The afore-mentioned committee on wire standards has used intrinsic induction B_i as the basis for the proposed values of magnetic properties.

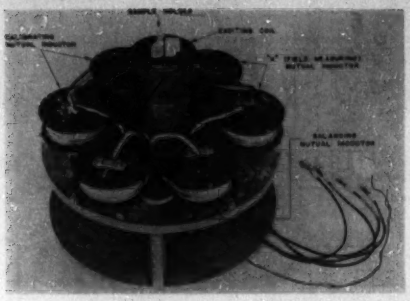

Figure 3. Test coils with upper clamping plate removed

A series combination of a resistor and capacitor with the input across the end terminals and the output across the capacitor will integrate satisfactorily providing the reactance of the capacitor at the lowest frequency of interest is very small compared to the series resistance. This makes the ratio of output to input voltage very small. For instance, if the phase error of the network is to be held to $^1/_2$ degree at the lowest frequency, the output voltage will be only $^1/_{118}$ of the input voltage at this frequency.

A characteristic of this simple circuit is that the phase error will be greatest at the lowest (fundamental) frequency and will be less for the harmonics. It would seem desirable that the reverse be true because, in general, phase errors in the fundamental frequency are of the greater importance.

The integrating network used in the new tester provides a much higher voltage at its output terminals than the simple series circuit and gives zero phase error at the fundamental frequency with slight errors at the harmonic frequencies. The magnitude of these errors at harmonic frequencies depends on the values of capacitances and resistances used in the network, and becomes less as the ratio of output to input voltage is made less.

The integrating network used in the tester is shown schematically in Figure 6. R_e represents the effective output resistance of amplifier stage V_1 in Figure 2. Capacitors C_2, C_3, and C_4 in Figure 2 are shown as C_c, C_b, and C_a in Figure 6. R_b replaces R_{10} and R_{11}.

With the constants chosen in the tester, the phase error is zero at the fundamental frequency (60 cycles per second), 0.3 degree at the third harmonic, and less than this amount for all higher order harmonics. The error in relative magnitude for the fundamental and all harmonics is about 3.5 per cent. The ratio of output to input voltage at the fundamental frequency is 1 to 16.8. An integrating network of the simple series type providing the same voltage ratio would have a phase error of 3.4 degrees at the fundamental frequency.

The steep sides on a hysteresis loop for a sample at saturation correspond to relatively high voltage peaks of very short duration in the pickup coil. Therefore, moderate phase errors in the vertical deflection system may cause serious errors in the location and slope of the sides of the loop with corresponding errors in the coercive force and residual magnetism readings. Moderate phase errors also may cause the appearance of loops at the tips of the pattern on the oscilloscope, but absence of these loops is not an indication that the phase relations for the fundamental and all harmonics are not sufficiently in error to cause serious errors in the readings.

In an instrument having built-in calibration, therefore, it is important to have a phase check other than merely observing the trace on the oscilloscope. This means is provided in the calibration of the instrument (see Appendix III).

A complete analysis of the integrating circuit used in the tester is given in Appendix II.

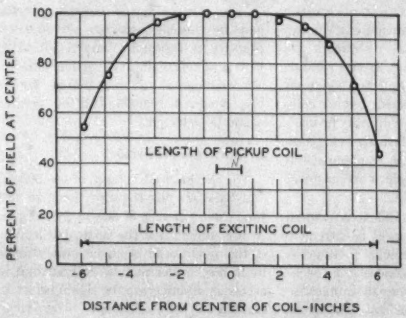

Figure 4. Field distribution along axis of exciting coil

Preamplifier for Vertical Deflection System

The frequency range of the vertical and horizontal amplifiers contained in the oscilloscope used with the tester is from 2 to 100,000 cycles per second. Measurements on the vertical and horizontal systems showed the phase characteristics to be entirely satisfactory. Using these self-contained amplifiers simplifies the design of the equipment external to the oscilloscope.

V_1 in Figure 2 amplifies the signal from the pickup circuit. Its effective output impedance serves as the series resistor feeding C_2, C_3, C_4, R_{10}, and R_{11} of the integrating network.

V_2 is connected as a cathode follower and allows the integrating network to feed into a high impedance (four megohms). This is necessary for proper operation of the integrator. This high value of grid resistor also minimizes the phase error introduced by coupling capacitor C_5. For the values chosen, the phase error is 0.38 degree at 60 cycles per second.

A coupling capacitor to the input stage in the oscilloscope is provided in the oscilloscope so it is possible to feed the voltage across R_{12} (which includes a d-c component) directly to the input terminals.

Cathode by-pass capacitors are omitted in order to eliminate phase errors from this source.

R_6 serves as an input attenuator for the preamplifier. The control is usually set at maximum and the vertical calibration is obtained by adjusting the gain control on the oscilloscope. In testing large samples, V_1 may overload with maximum setting on R_6, and in such cases the R_6 setting should be reduced and the oscilloscope gain setting increased. This procedure is also necessary in testing small samples of relatively high permea-

Figure 5. Detail of sample holder

bility material at beyond saturation excitation conditions. Because of steep sides of the hysteresis loop in such cases, the peak voltage applied to the input of the preamplifier is much higher than would be expected from the height of the oscilloscope pattern.

The extremely low cutoff frequency of the vertical deflection system causes slow variations in the plate supply voltage (such as would be caused by line voltage variations) to be amplified and fed to the vertical deflection plates of the oscilloscope. The result is instability of the position of the hysteresis trace on the screen. The problem is made especially severe because of the action of the integrator which inherently has increasing response with decreasing frequency.

In order to limit these voltage variations to a low value, the self-regulating power supply shown in Figure 2 (lower center) is used. When first built, a glow tube was used for the reference voltage, but the stability of the system was improved when the glow tube was replaced by the 90-volt battery. Since V_1 operates with a negative grid bias the life of this battery should be its shelf life.

There is still some instability of the pattern. Attempts to improve the situation through the use of a constant voltage transformer supplying the power supply of the preamplifier and the oscilloscope resulted in no improvement. With the apparatus in its present form, the pattern is sufficiently stable to allow making measurements on small samples with both R_6 and the vertical gain on the oscilloscope set at maximum. Some trouble may be encountered, however, in taking pictures unless short exposure times are used.

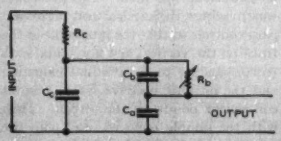

Figure 6. Schematic diagram of integrating network

Calibrating System for Vertical Deflection

Calibration of the vertical system is accomplished by means of the H meter (M in Figure 2) and the calibrating mutual inductor CM. The measure-calibrate switch S_2 removes the calibrating system from the circuit when in the "measure" position. Two calibrating ranges are provided by means of the 100/1 voltage divider (R_2, R_3, and R_4). The capacitor C_1 across R_2 and R_4 corrects for a slight phase error in the voltage divider.

The calibrating mutual inductor was designed and adjusted to give the calibrating formulas

$$H_{cal} = 2a'' B_{cal} \times 10^{-8} \qquad (1)$$

for the "low calibration" position, and

$$H_{cal} = 2a'' B_{cal} \times 10^{-8} \qquad (2)$$

for the "high calibration" position

B_{cal} is the value of B in gausses to be calibrated
a'' is the area of the sample in circular mils
H_{cal} is the required reading of the H meter in oersteds

Sinusoidal wave form of the calibrating current is not required for accurate calibration with the method used in the tester. This is shown in Appendix III, which gives a complete analysis of the calibrating system.

Operation of the Tester

Sensitivity of B and H Scales

With the input attenuator in the preamplifier and the oscilloscope vertical gain control both at maximum, the total vertical deflection (up and down) is 2.56 inches per maxwell. Thus on a single strand of 0.004-inch diameter wire having a saturated residual magnetism of 2,000 gausses (typical for the presently used magnetic recording wire) the height of the hysteresis loop would be about 0.4 inch. This deflection is sufficient for rough measurements but if the full accuracy of the instrument is to be realized, five or more strands of the finished wire should be used. If characteristics of the wire at low inductions are being studied, an even greater number of strands should be used. The opening in the sample holder is large enough to allow the use of 100 strands of the 0.004-inch wire.

With the horizontal gain on the oscilloscope at maximum, the sensitivity of the horizontal system is 0.0129 inch (total left and right) per oersted.

Balance and Phase Adjustment

The balance adjustment is made with no sample in the tester. With the magnetizing force set at about 500 oersteds, and with both vertical gain controls set at maximum, the horizontal gain on the oscilloscope is adjusted to give a pattern about one half of an inch wide. With S_2 in the "measure" position, the position of one of the balancing mutual inductor coils is adjusted to give a pattern of minimum height. If this pattern is an ellipse, the mutual resistance adjustment is varied until a line pattern is obtained. If the line is not horizontal, further simultaneous adjustments of the balance coil and the mutual resistance control are made until a horizontal line pattern is obtained. This completes the balance adjustment.

The phase adjustment is made with the magnetizing force set at 500 oersteds and with no sample in the tester, as before. With S_2 in either of the calibrating positions, and with the horizontal gain control at maximum, the vertical gain controls are adjusted to give a 45-degree pattern. If the "high calibration" setting is used, the B gain control on the control panel must be kept at a low setting to prevent overloading of the preamplifier. If the pattern is an ellipse, the phase adjustment is reset so as to make it a line. This completes the phase adjustment.

Calibration of H and B Scales

The H meter at all times indicates the peak magnetizing force in oersteds in the exciting coil. The calibration of the H scale is accomplished simply by adjusting the horizontal gain control to give a total horizontal deflection equal to the reading

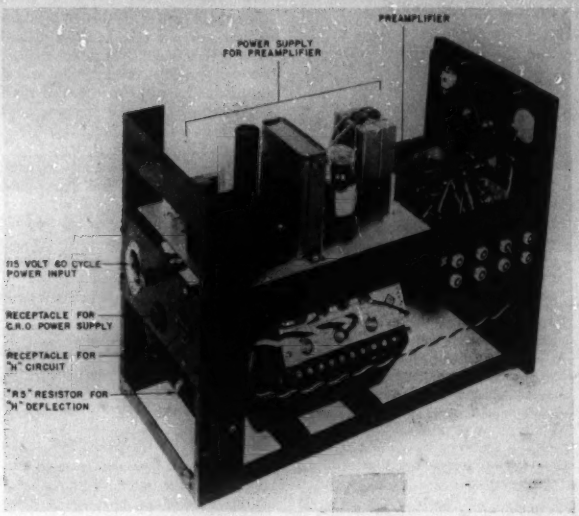

Figure 7. Preamplifier and power supply

of the H-meter divided by a convenient scale factor. This adjustment may be made with or without a sample in the tester.

The B scale calibration is made with no sample in the tester and after the balance and phase adjustments have been made. For small samples of low permeability the "low calibration" position is used, and for larger sample or samples of high permeability "high calibration" is used. Equations 1 and 2 give the relation between the reading of the H meter and the value of B to which the resulting total vertical deflection on the oscilloscope corresponds.

For routine tests on samples whose properties are known approximately, the instrument is precalibrated by adjusting the vertical gain so that a convenient scale factor is obtained. This method allows obtaining the magnetic properties directly from observed deflections on the screen.

For odd samples of unknown properties it is more convenient to calibrate after deflections are measured on the hysteresis loop. This method requires the use of equations 1 or 2 in calculating actual B vulues from the deflections.

In order to prevent excessive errors caused by nonlinearity between oscilloscope deflections and applied voltages, the B and H scales should be calibrated at values near the expected values for the sample. As the residual magnetism and coercive force are usually of most interest, the B and H calibrations should be performed near the expected values of these quantities.

The balance, phase, and calibration adjustments should be checked at frequent intervals to guard against errors resulting from drift or accidental change of adjustment.

Preparation of Samples

To prevent errors caused by self-demagnetization and to allow convenient insertion in the sample holder, samples are cut to a length somewhat greater than the length of the exciting coil (about 15 inches). Samples of finished recording wire are "fished" into lengths of small spaghetti tubing which provide stiffness. Larger samples having sufficient stiffness are put directly into the sample holder. If it is desired to study the variations over a great length of wire, the wire may be threaded through the sample holder. Readings from the hysteresis loop may then be obtained as the wire is pulled through the tester.

Limitations of the Tester

The apparatus was designed specifically for use with the stainless steel wires presently used in magnetic recorders. These alloys have their maximum permeabilities (ranging up to about 15) at about 350 oersteds. The carbon steel wires used in older machines have maximum permeabilities as high as 280 at about 50 oersteds. When these high permeability wires are tested too far above saturation, the hysteresis loop shows evidence of distress. The pickup coil is set into self oscillation and the preamplifier may overload even with the preamplifier gain set at a low value.

The tendency for self-oscillation was reduced by replacing the shielded leads originally used in the pickup circuit by a low capacity line (see Figure 5). This line consists of two number 30 wires spaced about one-quarter inch. Of various filter schemes that were tried, several were successful in eliminating the oscillations but unfortunately yielded coercive readings that were too high. The effect of these filters was to slope off the steep voltage peaks associated with the almost vertical sides of a hysteresis loop at beyond saturation. These filter schemes therefore were discarded as their use would only lead to false confidence in beautiful hysteresis loops at intense fields.

With the apparatus in its present form, the high permeability samples may be tested at sufficiently intense fields to assure saturation, without overloading or self-oscillation difficulties. This is evident from Figure 13.

When high permeability samples are being tested, the vertical gain control on the oscilloscope should be set at maximum and calibration achieved by means of the preamplifier gain control. This will reduce to a minimum the possibility of overloading the preamplifier.

Accuracy

Four samples of widely different magnetic properties were tested in the 60-cycle hysteresis loop tracer and then by means of the familiar d-c method employing a ballistic galvanometer for the induction measurements. Each of the samples consisted of 100 strands of 0.004-inch diameter magnetic recording wire about 16 inches long enclosed in a piece of small spaghetti tubing. To eliminate errors caused by varying sensitivity of the oscilloscope over different regions of the screen, the system of calibrating after the measurement was used. The procedure was to adjust the vertical and horizontal gain controls so that the intercepts of the trace on the vertical and horizontal axes (corresponding to the residual induction and the intrinsic coercive force) were at convenient points on the screen. Then with the sample removed, and with the gain controls undisturbed, the magnetizing force was adjusted to a value providing a horizontal line trace on the screen

whose length was equal to the distance between the intercepts on the horizontal axis of the hysteresis loop. This value of magnetizing force is the intrinsic coercive force for the sample Then, with the switch in one of the calibrating positions, and with the horizontal gain control at zero, the magnetizing force was adjusted to provide on the oscilloscope a vertical line trace whose length was equal to the distance between the intercepts of the hysteresis loop on the vertical axis. The value of residual induction for the sample was obtained by substituting in equation 1 or 2 the area of the sample for a'', the value of magnetizing force determined for H_{cal}. This value of B_{cal} is the residual induction for the sample. Values of maximum induction were obtained by reducing the horizontal gain control to zero and adjusting the vertical gain to provide a vertical line pattern of a convenient length. Then with the sample removed, with the switch in one of the calibrating positions, and without disturbing the gain controls, the magnetizing force was adjusted to provide a vertical line pattern of the same length as before. Substitution of this value of magnetizing force for H_{cal} in equation 1 or 2 gave the value of maximum induction for the sample.

The coil assembly of the a-c tester was used in the d-c ballistic method. The balancing mutual inductor was used to balance the air flux in the pickup coil just as in the a-c method. Calibration of the ballistic galvanometer was accomplished by means of the calibrating mutual inductor. The source of power was a bank of storage batteries. The usual arrangement of switches and rheostats for reversing and controlling the currents in the measuring and calibrating circuits was provided.

The currents in the exciting coil and in the primary circuit of the calibrating mutual inductor were measured by means of ammeters with a guaranteed accuracy of one-half of one per cent of full scale. Values of magnetizing force and galvanometer sensitivity were obtained from these ammeter readings.

With the a-c instrument as described in this paper the accuracy of both induction and magnetizing force calibrations is dependent on the accuracy of the rectifier type voltmeter on the panel. This instrument had been calibrated and provided with a direct reading magnetizing force scale several months prior to the running of the accuracy test. Immediately before running the accuracy test, the calibration of this instrument was rechecked and was found to be in error by a maximum of two per cent of full scale value at certain parts of the scale. In the lower range of the scale, errors in magnetizing force and in the calibration of the induction scale on the oscilloscope could be in error by as much as eight per cent because of this error in calibration of the panel voltmeter.

In order to separate this voltmeter error from other errors, the a-c measurements first were made by relying on the panel voltmeter for all readings and calibrations, and then repeating the measurements with the current in the exciting circuit being measured with a current transformer and a dynamometer type ammeter with a guaranteed accuracy of one quarter of one per cent of full scale. In this case the calibrations were based on the readings of this ammeter. With this method, variations in the wave form of current from a sine wave may cause errors, as the ammeter is sensitive to the rms value while the oscilloscope calibration depends on the peak value of current. The ratio of these values was taken to be the square root of two, the value for a sine wave. It is believed that errors resulting

Figure 8. Control panel

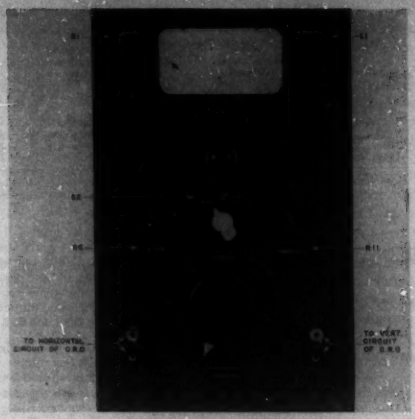

Figure 9. B_r-H curve for medium carbon steel wire

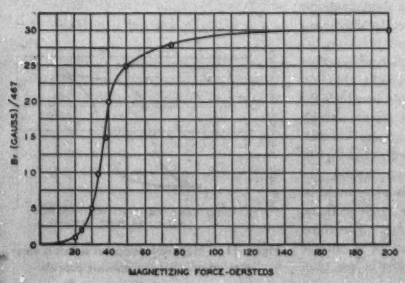

Figure 10. B_r-H curve for stainless steel wire

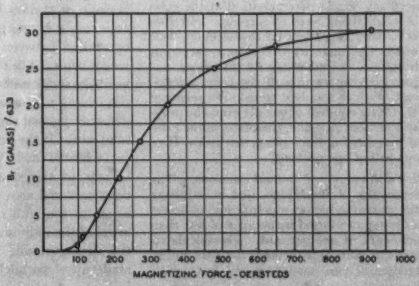

Table I. Comparison of A-C and D-C Ballistic Measurements

Sample Number	A-C Measurements (Panel Voltmeter)				A-C Measurements (Current Transformer and Ammeter)				D-C Ballistic Measurements			
	H_m	H_{ci}	B_r	B_{mi}	H_r	H_{ci}	B_r	B_{mi}	H_m	H_{ci}	B_r	B_{mi}
192	900	280	5,160	5,500	900	272	4,790	5,080	900	276	4,830	5,030
219	900	120	7,040	9,280	900	107	6,740	8,950	900	109	6,920	8,960
702	900	298	1,810	2,190	900	286	1,800	2,140	900	290	1,860	2,110
703	300	38	11,800	17,300	300	36	11,700	17,300	300	35.2	12,000	17,500

H_m = maximum magnetizing force, oersteds
H_{ci} = intrinsic coercive force, oersteds
B_r = residual induction, gausses
B_{mi} = maximum intrinsic induction, gausses

from this assumption are very small, as harmonics in the current caused by harmonics present in the supply voltage are virtually suppressed by the high inductive component of impedance in the magnetizing circuit. Furthermore, the voltage wave form of the 60-cycle power source itself is very nearly sinusoidal.

Results of the comparative measurements are given in Table I.

Samples 192, 219, and 702 are stainless steel magnetic recording wire. Sample 703 is medium carbon steel magnetic recording wire.

Comparison of the d-c ballistic measurements with the a-c measurements based on the panel voltmeter show discrepancies up to nine per cent for induction readings and ten per cent for intrinsic coercive force readings. The maximum discrepancies shown by a comparison of the ballistic measurements with the a-c measurements based on the current transformer and ammeter are 2.7 per cent for induction values and 2.3 per cent for intrinsic coercive force values.

Some errors are common to both the a-c and the ballistic methods and therefore would not be detected by the comparison.

1. *Ratio of magnetizing force to current in exciting coil.* This ratio was assumed to be the same for the a-c and the ballistic measurements and was based on equations 3 and 4 of Appendix I. For a coil of proportions similar to those of the exciting coil, large percentage errors in individual values of b, c, d, and D have a very small effect on the calculated value of K in equation 4. The accuracy of the determination of the ratio of magnetizing force to current is therefore essentially dependent on the accuracy with which the quantity N/b (turns per unit length) is determined. As this value was based on the average of the layer lengths, each of which was determined to an accuracy of at least one-half of one per cent, the probable error in N/b and, therefore, in the ratio of magnetizing force to current is less than one-half of one per cent.

2. *Calibration of mutual inductor.* The sensitivity of the bridge used in adjusting the mutual inductors was sufficient to detect a change in mutual inductance of less than one-tenth of one per cent. The calculated value of mutual inductance depends on the product of two resistances and one capacitance. Calibration of the corresponding components in the bridge is accurate to one-tenth of one per cent for each. Calibration of the mutual inductor therefore is accurate to less than one-half of one per cent.

3. *End effect.* Figure 4 shows that the magnetizing force in the exciting coil at points three inches from the center is about four per cent less than the value at the center. Demagnetizing effects were estimated on the assumption of a sample six inches long in a uniform field. It is quite evident that demagnetizing effects in this hypothetical case are more severe than in the actual case in which the sample extended beyond the ends of the exciting coil, the magnetizing force of which is only four per cent low at three inches from the center and gradually decreases to about one-half value at the ends. Maxwell's equation for the demagnetization factor for an ellipsoid was used in calculating the demagnetizing factor for the assumed 6-inch long sample. The ratio of length to diameter was taken as 6 inches divided by 0.040 inches (diameter of a solid wire having the same cross-sectional area as 100 strands of 0.004-inch diameter wire). That this assumption is also a conservative one is evident from the following considerations.

If the 100 pieces of wire comprising the sample were placed in and parallel to a uniform field with sufficient spacing between wires that for every wire the demagnetizing effect due to poles on the remaining wires is negligible, then the demagnetizing effect on the group of wires would be the same as that on a single wire. If the distance between wires then were decreased gradually, the demagnetizing effect would increase continuously, because of the increasing demagnetizing action on every wire caused by decreasing separation between it and poles on adjacent wires. The demagnetization effect would have for its limiting value that corresponding to the condition in which the wires are pressed together to form a single solid wire. If the pressing operation were performed in such a manner as to keep the lengths of the strands unchanged, the cross-sectional area of this wire would be equal to the sum of the cross-sectional areas of the individual wires. Therefore, the demagnetizing factor for a sample made up of parallel strands is less than that for a solid sample of the same cross-sectional area and decreases as the distance between strands increases.

The demagnetizing effects are most severe in sample 703 because of its higher maximum intrinsic induction. On the basis of the demagnetizing effects calculated in accordance with the above assumptions, the actual magnetizing force present at the center of the sample is 3.7 oersteds less than the value at the same point in the solenoid with the sample removed. This amount of change in magnetizing force near saturation will have an insignificant effect on the intrinsic induction.

The calculated reverse field caused by the residual induction in this sample is 2.5 oersteds. The hysteresis loop for this sample is similar to the one shown in Figure 13. Examination of this figure shows that a reverse field of 2.5 oersteds causes a reduction of 250 gausses from the residual induction value and the error in the residual induction reading due to the demagnetizing effect is about two per cent. For a 10-strand sample of this material, the number ordinarily used in the hysteresis loop tracer, the effect of demagnetization on the residual induction reading would be entirely negligible.

Measurements of intrinsic coercive force are unaffected by demagnetization, because when the intrinsic induction is zero the intensity of magnetization is zero and there are no poles in the sample.

As a check on the various assumptions upon which the calculation of demagnetization effects was based, sample 703 was cut into lengths of one to five inches, inclusive. The value of indicated maximum magnetizing force required to produce an intrinsic induction of 11,300 gausses (the value for maximum susceptibility) was determined for each length by measurement in the a-c tester. The effective magnetizing force was calculated first on the basis of an effective diameter of 0.040 inch, then on the basis of a diameter 1.15 times this value and finally a diameter $^1/_{1.15}$ of this value by deducting from the

Figure 11. Hysteresis loop for stainless steel wire intermediate in drawing process

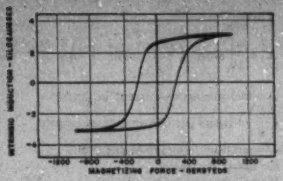

Figure 12. Hysteresis loop for finished stainless steel wire

measured magnetizing forces the corresponding computed values of demagnetizing forces. Results of these measurements and calculations appear in Table II.

For sample lengths approaching the length of the pickup coil, there is an error in induction readings caused by fringing of flux near the ends of the sample. Incomplete linkage of the wire flux with the pickup coil causes measured values of induction to be less than actual values at the center of the sample. Therefore, while the magnetizing force was adjusted for an indicated maximum intrinsic induction of 11,300 gausses for each length, the actual induction for the short samples was greater than this amount. As no correction was made for this error, and as its effect is to make magnetizing force readings too high for the short samples, magnetizing force readings corrected for demagnetization only should increase as the length of the sample approaches that of the pickup coil. In no case should the corrected value decrease as the sample length is decreased.

In Table II the data corrected on the basis of 0.040-inch effective diameter are the same for the 5-inch, 4-inch and 3-inch samples within the limits of experimental error. Data for the 2-inch and 1-inch lengths are high because of the linkage error discussed before.

The data based on the 0.046-inch effective diameter are low at three and two-inches by amounts definitely greater than experimental error. The only explanation of these low values is incorrectness of the assumption of 0.046-inch effective diameter.

Although the data based on the 0.0348-inch effective diameter show continuously increasing values as the sample length is decreased, values for the 5-inch, 4-inch, and 3-inch lengths differ by amounts less than experimental error.

It therefore cannot be concluded from the data whether the 0.040-inch or the 0.0348-inch diameter is more nearly correct. It is definitely shown, however, both by experiment and by the previous analysis, that actual demagnetizing effects in a bundle of wires are less than or equal to the effects as calculated on the basis of an area-equivalent solid wire. The experimental data further show that the true effective diameter for a tight bundle of wires is only slightly less than that of the area-equivalent solid wire. (If experimental errors are neglected, an equivalent diameter about 0.92 times that of the area-equivalent solid wire is indicated.)

Calculations on this basis show that for low permeability materials (for which the tester was designed primarily) no correction need be made for demagnetizing effects. For materials of higher permeability than about 300, demagnetization effects may be calculated as described and if the effects are appreciable corrections may be applied as was done for sample 703.

In Table I discrepancies between the a-c measurements with the current transformer and ammeter and the d-c ballistic measurements are of the order that would be expected in the ballistic method from changes in currents subsequent to their adjustment, due to heating of the rehostats and voltage regulation in the batteries. Actually it was found that in repeating tests under identical conditions, discrepancies on a percentage basis were lower with the a-c method than with the ballistic method.

From these considerations it is evident that errors in measurements on the hysteresis loop tracer are almost entirely due to errors in reading distances on the oscillograph screen, and to errors in the instrument used to measure the peak current in the magnetizing circuit. If the gain controls are adjusted so that the distances being measured on the screen are of the order of three inches, and if reasonable care is taken in measuring the distances, they can be determined to an accuracy of about two per cent.

With the tester as described in this paper it is sometimes necessary to take readings low on the scale of the panel voltmeter. In these cases errors as high as 20 per cent are possible because of reading errors and changing characteristics of the rectifier in the instrument. This error could be reduced to about ten per cent by providing more scales on the instrument.

It is believed that while the combination of a mutual inductor and a rectifier type voltmeter provides a measuring device sensitive to peak currents, greater over-all accuracy would be obtained if the magnetizing current were measured by means of current transformer and ammeter sensitive to rms values (assuming an essentially sinusoidal supply voltage). Panel instruments of this type are available with a guaranteed accuracy of one per cent of full scale. If a current transformer with taps providing full scale ranges of 100, 200, 500, and 1,000 oersteds is used, the maximum error in any current reading need be no more than 2.5 per cent, and magnetic readings to an accuracy of about 5.0 per cent are possible. It is planned to make this change in the instrument.

Results Obtained With the Hysteresis Loop Tracer

Figures 9 and 10 are two of a series of curves that were obtained to compare the recording characteristics of stainless steel and carbon steel wires.

In obtaining these data, ten strands of 0.004-inch diameter recording wire were used. To facilitate comparison of the shapes of the curves, arbitrary gain settings making the B_r deflections the same for all samples at the highest magnetizing force were used. Deflections in tenths of an inch are plotted on the graphs. The vertical scale factors, also shown, allow calculating actual B_r values from the curves.

Photographs of hysteresis loops for various samples are shown in figures 11 to 15 inclusive. Figure 11 shows the loop for a sample of stainless steel recording wire intermediate in the drawing process. The remaining loops are for finished wires. Figures 13 and 14 are for the same sample at different magnetizing forces. A state of near saturation at the

Table II. End Effect Measurements and Calculations (Sample 703)

Length of sample, inches	5	4	3	2	1
Measured maximum magnetizing force, in oersteds, required for 11,300 gausses maximum intrinsic induction	44.0	45.5	48.3	59	210
Maximum magnetizing force corrected for demagnetizing effects: Assumed effective diameter of sample in inches					
0.040	40.7	40.6	40.3	42.7	157.5
0.046	39.8	39.8	39.0	38.3	144.0
0.0348	41.5	41.7	42.0	46.1	168.0

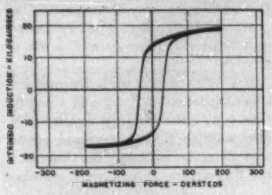

Figure 13. Hysteresis loop for carbon steel wire at 200 oersteds

lesser field is shown by a comparison of the two figures.

Evidence of oscillation in the pickup coil is beginning to appear in the loop for the greater field. These hysteresis loops were obtained with the vertical gain control in the oscilloscope set at maximum, and the control at the input to the preamplifier at a low value. This setting tends to prevent overloading of the preamplifier.

Figure 16 shows evidence of this overloading. This curve was obtained with the same sample and with the same magnetizing force as in figure 14 but with the gain setting on the preamplifier increased and that on the oscilloscope decreased.

Conclusions

The convenience of obtaining measurements from the hysteresis loop on a cathode-ray oscillograph screen has made this general type of apparatus a very useful tool in magnetic measurements when large numbers of samples must be tested. Use of an absolute calibration system and a phase-compensated integrating network with positive means of adjustment has made possible a degree of accuracy and reliability higher than has been possible previously with this general type of apparatus.

Errors in the tester as described are due mainly to inherent errors in the rectifier type voltmeter used to calibrate the vertical and horizontal deflection systems. While in some cases the resulting errors in magnetic readings may be as high as 20 per cent, in most cases they are limited to about five per cent.

Replacement of the rectifier type voltmeter and its associated mutual inductor by a current transformer and ammeter will make possible magnetic readings with a consistent accuracy of five per cent, providing the wave form of the power line voltage is essentially sinusoidal.

In selecting the power line frequency as the operating frequency for the tester the advantages of this and some higher frequency were compared carefully. Some of the more important items of comparison are

A. In favor of a higher frequency

1. Greater volts per turn in pickup coil.

2. If the frequency is near the logarithmic mean of the audio band, materials for use in audio frequency apparatus will be tested more nearly under conditions of use.

3. Greater simplicity of amplifiers and their power supplies.

4. Lower spurious voltages induced by fields of the power line frequency.

B. In favor of the power line frequency

1. Practically unlimited power available without the use of oscillators or motor generator sets—especially important when intense fields are required.

2. Conditions of test more nearly approximate those of the ballistic method. (The truly basic magnetic characteristics of a material are those determined by the ballistic or other d-c method.)

3. Greater number of turns permissible in pickup coil because of lesser effect of distributed capacitance at low frequencies. (*A*–1 is balanced, at least in part, by this consideration.)

4. The two sources of spurious voltage—that caused by stray fields from transformers in the amplifier power supply and from nearby power wiring, and that caused by interaction of the different circuits of the tester at the operating frequency—are both of the same frequency. This fact simplifies the problem of balancing the spurious voltages. (In the tester the air flux balance coils and the mutual resistance adjustment are sufficient in themselves to reduce all residual voltages to negligible values.) If the operating frequency were other than the power frequency, separate adjustments would very likely be required for balancing the effects of the two sources of spurious voltage.

5. Conveniently low operating voltage for the exciting coil without excessive eddy loss in the winding. (If the exciting coil in the tester were operated at 500 cycles per second, the terminal voltage would change from 130 volts to 1,080 volts, and the change in eddy loss would be sufficient to cause a significant increase in power requirements and temperature rise.)

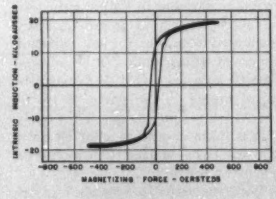

Figure 14. Hysteresis loop for carbon steel wire at 500 oersteds

Appendix I. Calculations for Peak Magnetizing Force Measuring System

Integration along the axial direction and perpendicular to this direction in turn shows the magnetizing force at the center of a solenoid to be

$$H = 0.4\pi K_s\left(\frac{N}{b}\right)i_p \tag{3}$$

where

$$K_s = \frac{b}{2c}\left[\sinh^{-1}\left(\frac{D}{b}\right) - \sinh^{-1}\left(\frac{d}{b}\right)\right] \tag{4}$$

i_p = instantaneous current in amperes

$\left(\frac{N}{b}\right)$ = turns per centimeter of length

D = outside diameter of the coil

d = inside diameter

b = length

c = thickness

H = instantaneous value of magnetizing force in oersteds at the center of the solenoid

The ratio of magnetizing force to current is therefore

$$\frac{H}{i_p} = 0.4\pi K_s\left(\frac{N}{b}\right) \tag{5}$$

or with (N/b) in turns per inch equation 5 becomes

$$\frac{H}{i_p} = 0.495K_s\left(\frac{N}{b}\right) \tag{6}$$

K_s is independent of the dimensions used because only ratios are involved in its determination.

Let the henrys mutual inductance of the H measuring mutual inductor be M_h. If a periodic current having equal positive and negative peaks and which never decreases in the time from negative peak to positive peak nor increases in the time from positive peak to negative peak flows in the primary winding of the mutual inductor, the secondary voltage is given by

$$e_s = M_h\frac{di_p}{dt} \tag{7}$$

where e_s and i_p are instantaneous values of secondary voltage and primary current, and t is time in seconds.

For the time from negative peak to positive peak

$$E_a' = \frac{1}{t}\int_0^{t_1} e_s\,dt \tag{8}$$

where t_1 is the time from negative peak to positive peak, and E_a' is the average secondary voltage over this time.

Substituting equation 7 in equation 8 and remembering that when $t=0$, $i_p=-I_m$ and when $t=t_1$, $i_p=I_m$; where I_m is the absolute value of positive and negative peaks

$$E_a' = \frac{M_h}{t_1}\int_{-I_m}^{I_m} di_p = \frac{2M_h}{t_1}I_m \tag{9}$$

Similarly, for the time from positive peak to negative peak the avera gesecondary voltage is

$$E_a'' = -\frac{2M_h}{t_2}I_m \tag{10}$$

where t_2 is the time from positive peak to negative peak.

The average of the absolute value of volt-

age over a cycle, or any number of complete cycles, is

$$E_a = \frac{E_a' t_1 + |E_a'' t_2|}{t_1 + t_2} = \frac{4M_h I_m}{t_1 + t_2} \tag{11}$$

or, as $\frac{1}{t_1+t_2} = f$ the frequency in cycles per second

$$E_a = 4M_h f I_m \tag{12}$$

Rectifier type voltmeters are regularly calibrated to read the rms value of a sine wave, or $\pi/2\sqrt{2}$ times the average of a wave of any form. Therefore, the reading of such a voltmeter connected to the secondary of the mutual inductor will be

$$E_v = \frac{\pi}{2\sqrt{2}} E_a = \frac{\pi}{2\sqrt{2}} 4M_h f I_m \tag{13}$$

For a scale factor of 10 on the H meter

$$E_v = \frac{H_m}{10} \tag{14}$$

where H_m is the peak magnetizing force in oersteds in the exciting coil.

Substituting equation 14 in 13 and solving for M_h and replacing H_m/I_m by H/i_p

$$M_h = \frac{\sqrt{2}}{20\pi f}\left(\frac{H}{i_p}\right) \tag{15}$$

Substitution of the measured dimensions for the exciting coil in equations 4 and 6 gave

$$\frac{H}{i_p} = 44.2 \tag{16}$$

The required value of M_h therefore is

$$M_h = \frac{\sqrt{2}}{20\pi 60} \times 44.2 = 16.57 \times 10^{-3} \text{ henry} \tag{17}$$

The H measuring mutual inductor was designed for somewhat greater than this value and then adjusted to this value by removing primary turns and, finally, by adjusting the relative position of the two parts of the inductor. A modified Carey Foster bridge[5] was used in making this adjustment.

Appendix II. Analysis of Integrating Network

In Figure 16, C_a, C_b, and R_b may be thought of as a corrective network for the simple series integrator, C_c and R_c, which by itself introduces a serious error at the fundamental frequency due to its small time constant. Actually, however, C_a and C_b add to the capacitance of C_c and serve to increase the time constant as well as serving as a corrective network.

In this network C_a, C_b, and C_c are chosen equal so we may write

$$C_a = C_b = C_c = C \tag{18}$$

and

$$Y_c = Y_a = Y = j\omega C \tag{19}$$

If the network is loaded by an impedance that is very high compared to the reactance of C_a at the lowest frequency, the currents may be represented as shown in Figure 16.

$$i_2 = e_1 Y \tag{20}$$

$$e_2 = e_1 + i_2 Z = e_1 + e_1 YZ \tag{21}$$

$$i_1 = e_2 Y = e_1 Y + e_1 Y^2 Z \tag{22}$$

$$i_1 + i_2 = e_1 Y + e_1 Y^2 Z + e_1 Y = e_1 Y(2 + YZ) \tag{23}$$

$$e_3 = e_2 + (i_1 + i_2) R_c = e_1 + e_1 YZ + e_1 Y(2 + YZ) R_c \tag{24}$$

$$\frac{e_3}{e_1} = 1 + YZ + YR_c(2 + YZ) = 1 + YZ + 2YR_c + YZYR_c \tag{25}$$

Substituting

$$Y = j\omega C$$

and

$$Z = \frac{R_b(1 - j\omega CR_b)}{1 + \omega^2 C^2 R_b^2}$$

$$\frac{e_3}{e_1} = 1 + \frac{R_b(\omega^2 C^2 R_b + j\omega C)}{1 + \omega^2 C^2 R_b^2} + j2\omega CR_c + \frac{R_b(-\omega^3 C^3 R_c^2 + j\omega^3 C^3 R_b R_c)}{1 + \omega^2 C^2 R_b^2} \tag{26}$$

Separating real and imaginary terms

$$\text{Real } \frac{e_3}{e_1} = 1 + \frac{R_b(R_b - R_c)\omega^2 C^2}{1 + \omega^2 C^2 R_b^2} \tag{27}$$

$$\text{Imaginary } \frac{e_3}{e_1} = j\omega C\left[R_b \frac{1 + \omega^2 C^2 R_b R_c}{1 + \omega^2 C^2 R_b^2} + 2R_c\right] \tag{28}$$

Equations 27 and 28 rearranged in terms of ωCR_b and R_c/R_b become

$$\text{Real } \frac{e_3}{e_1} = 1 + \frac{(\omega CR_b)^2}{1 + (\omega CR_b)^2}\left(1 - \frac{R_c}{R_b}\right) \tag{29}$$

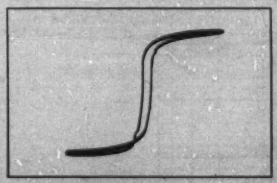

Figure 15. Hysteresis loop for carbon steel wire showing distortion caused by improper adjustment of gain controls

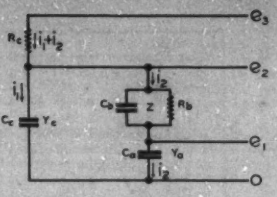

Figure 16. Diagram for analysis of integrating network

$$\text{Imaginary } \frac{e_3}{e_1} = j\omega CR_b\left[\frac{1 + (\omega CR_b)^2 \frac{R_c}{R_b}}{1 + (\omega CR_b)^2} + 2\frac{R_c}{R_b}\right] \tag{30}$$

For perfect integration e_3/e_1 should have no real component, and the error angle θ is given by

$$\theta = \tan^{-1}\left[\frac{\text{real } \frac{e_3}{e_1}}{\text{imaginary } \frac{e_3}{e_1}\frac{1}{j}}\right] \tag{31}$$

Providing θ is not too large

$\left|\frac{e_3}{e_1}\right|$ is given with sufficient accuracy by

$$\left|\frac{e_3}{e_1}\right| = \text{imaginary } \frac{e_3}{e_1}\frac{1}{j} \tag{32}$$

For perfect integration $\left|\frac{e_3}{e_1}\right|$ should vary inversely with ω, or

$$\frac{1}{\omega CR_b}\left|\frac{e_3}{e_1}\right| \text{ should be constant} \tag{33}$$

Using equations 32 and 30

$$\frac{1 + (\omega CR_b)^2 \frac{R_c}{R_b}}{1 + (\omega CR_b)^2} + 2\frac{R_c}{R_b} \tag{34}$$

should be constant

Using the decibel notation

$$20 \log\left[\frac{1}{\omega CR_b}\left|\frac{e_3}{e_1}\right|\right] = \text{decibel attenuation} - 20 \log \omega CR_b$$

$$= 20 \log\left[\frac{1 + (\omega CR_b)^2 \frac{R_c}{R_b}}{1 + (\omega CR_b)^2} + 2\frac{R_c}{R_b}\right] \tag{35}$$

should be constant

The phase error curves in Figure 17 were obtained by substituting equations 29 and 30 in equation 31.

The attenuation data for the curves in Figure 18 were obtained from the left-hand member of equation 35.

Phase error in degrees is given directly in Figure 17. The magnitude error in decibels is given by the deviation of the curves in Figure 18 from horizontal lines.

In the integrating network used in the

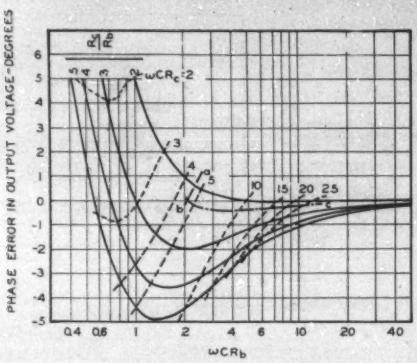

Figure 17. Phase errors in integrating network

Output voltage leads phase of true integration for positive errors and lags for negative

tester, R_c is the effective output impedance of the amplifier stage feeding the network and is therefore fixed, while R_b is adjustable. In actual operation R_b is adjusted to make the phase error zero at the fundamental frequency. The ωCR_c curves (dotted) are shown on Figures 17 and 18 to aid in the analysis of a tester with R_b adjustable and R_c fixed.

Use of the curves will be illustrated by using the constants in the tester described in this paper. Measurements on the V_1 stage showed its effective output resistance to be 24,200 ohms. C is 0.5×10^{-6} farads. So, at the fundamental frequency

$$\omega CR_c = 2\pi 60 \times 0.5 \times 10^{-6} \times 24{,}200 = 4.56$$

Assuming that R_b was originally set too high (R_c/R_b too low), ab (corresponding to $\omega CR_b = 4.56$) is followed downward in Figure 17 until this curve intersects the 0 phase error line. This point, $\omega CR_b = 2.04$, represents the condition of adjustment that gives 0 phase error at 60 cycles per second.

Solving for R_b

$$R_b = \frac{2.04}{\omega C} = \frac{2.04}{2\pi 60 \times 0.5 \times 10^{-6}} \doteq 10{,}830$$

and

$$\frac{R_c}{R_b} = \frac{24{,}200}{10{,}830} = 2.23$$

bc, therefore, gives the phase error in the tester for varying ωCR_b (or varying frequency as C and R_b are now fixed).

If there are no even harmonics in the supply voltage, the first component frequency of importance above the fundamental is the third harmonic. This corresponds to $\omega CR_b = 2.05 \times 3 = 6.12$. At this point bc shows the phase error to be about -0.28 degree. For the higher order harmonics the error becomes gradually less. Note that the phase errors shown are degrees at the particular frequency plotted.

Thus the time error at the third harmonic would be

$$\frac{1}{180} \times \frac{0.28}{360} = -4.32 \times 10^{-6}$$

second rather than three times this value.

With the proper adjustment on R_b, the network will correct for small phase errors in other parts of the B circuit. For instance, the error due to R-C coupling in amplifiers would be corrected by making R_b less than the value giving zero error in the integrator alone, thereby shifting to one of the lower R_c/R_b curves. As the two error curves are of different shapes, the net error will necessarily be zero at the fundamental frequency only. For this reason phase errors in the remainder of the vertical system should be kept as small as possible.

The curve bc in Figure 18 is obtained in a similar manner to bc in Figure 17. A discrepancy of about 0.3 decibel (3.5 per cent) for the third and higher harmonics with respect to the fundamental is shown.

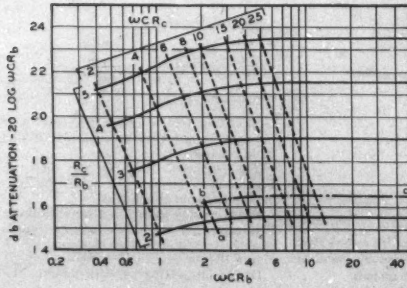

Figure 18. Attenuation in integrating network

Appendix III. Analysis of Calibrating System

The voltage e_p induced in the pickup coil and applied to the input of the preamplifier is

$$e_p = 10^{-8} N_p \frac{d\Phi_f}{dt} \tag{36}$$

where

N_p = number of turns in pickup coil
Φ_f = intrinsic flux in sample
t = time in seconds

But if B_f is the intrinsic induction in the sample

$$\Phi_f = \frac{\pi}{4} \times 2.54^2 \times 10^{-6} a^\pi B_f \tag{37}$$

where a^π is the area of the sample in circular mils and

$$e_p = 10^{-14} \frac{\pi}{4} \times 2.54^2 N_p a^\pi \frac{dB_f}{dt} \tag{38}$$

Neglecting phase and magnitude errors in the preamplifier and integrator, the voltage applied to the cathode-ray oscilloscope input terminals, with switch on "measure" is

$$e_o = K_b \int e_p dt = 10^{-14} \frac{\pi}{4} \times 2.54^2 N_p a^\pi K_b \int dB_f \tag{39}$$

where K_b is an adjustable constant depending on the B gain setting and the characteristics of the preamplifier and integrator.

The vertical deflection of the oscilloscope, again neglecting errors of phase and magnitude in the oscilloscope, is, by integration of equation 39

$$d_v = K_e e_o = 10^{-14} \frac{\pi}{4} \times 2.54^2 N_p a^\pi K_b K_e B_f \tag{40}$$

The constant of integration is necessarily 0 because of the blocking action of coupling capacitors in the amplifiers. K_e depends on the vertical gain setting on the oscilloscope.

Equation 40 shows that the integrator makes the vertical deflection proportional to B_f rather than its time derivative.

With no sample in the tester and with the switch on high calibration the only voltage applied to the input of the preamplifier is that caused by the calibrating mutual inductor, as the induced voltage in the pickup coil is balanced by that of the balancing mutual inductor.

This voltage is

$$e_c = M_c \frac{di_p}{dt} \tag{41}$$

where M_c is the henrys mutual inductance of the calibrating mutual inductor, and i_p is the current in the primary circuit.

Substituting from equation 16 in Appendix I

$$e_c = \frac{M_c}{44.2} \times \frac{dH_{ca}}{dt} \tag{42}$$

where H_{ca} is the magnetizing force in the H coil during the calibration adjustment. The vertical deflection on calibrating is

$$d_{vc} = K_b K_c \int e_c dt$$

$$= \frac{M_c}{44.2} K_b K_c \int dH_{ca}$$

$$= \frac{M_c}{44.2} K_b K_c H_{ca} \tag{43}$$

Equation 43 shows that d_{vc} is proportional to H_{ca} and therefore the trace on the screen should be a straight line during the calibration adjustment. This allows obtaining the proper phase adjustment in the integrator by setting the adjustment so that the trace on the screen is a straight line.

For maximum values in equation 43

$$D_{vc} = \frac{M_c}{44.2} K_b K_c H_{cal} \tag{44}$$

where D_{vc} is the maximum vertical deflection and H_{cal} the maximum magnetizing force. H_{cal} is the value indicated by the H meter as it operates as a peak meter.

It has been stated previously that the calibrating system was to be arranged so that on the high calibrating position

$$H_{cal} = 2a'' B_{cal} \times 10^{-8}$$

Substituting this in equation 44

$$D_{vc} = \frac{M_c}{44.2} K_b K_c 2a'' B_{cal} \times 10^{-8} \tag{45}$$

where B_{cal} is the value of B_i being calibrated. From equation 45 the B_i scale factor is

$$\frac{B_{cal}}{D_{vc}} = \frac{10^8 \times 44.2}{M_c K_b K_c 2a''} \tag{46}$$

Furthermore, this same scale factor is to apply in equation 40 for all values of B_i and d_v so that

$$\frac{B_{cal}}{D_{vc}} = \frac{B_i}{d_v}$$

$$= \frac{4 \times 10^{14}}{\pi \times 2.54^2 N_p a'' K_b K_c}$$

$$= \frac{10^8 \times 44.2}{M_c K_b K_c 2a''} \tag{47}$$

from which

$$M_c = \frac{44.2 \times 10^{-8} \times \pi \times 2.54^2 \times N_p}{4 \times 2} \tag{48}$$

Substituting 16,000, the number of turns in the pickup coil, for N_p

$$M_c = 1.792 \times 10^3 \text{ henry} \tag{49}$$

The calibrating mutual inductor was designed for a somewhat higher value and was then adjusted to this value by removing primary turns and setting the relative position of the two parts of the inductor. The bridge circuit of reference 6, was used in making this adjustment.

When the switch is in the low calibration position, the 100/1 voltage divider is active, and for this position the calibrating formula is

$$H_{cal} = 2a'' B_{cal} \times 10^{-8} \times 10^2$$
$$= 2a'' B_{cal} \times 10^{-6}$$

References

1. Supersonic Bias for Magnetic Recording, Lynn C. Holmes, Donald L. Clark. *Electronics* (New York, N. Y.), July 1945, pages 126–36.

2. A B-H Curve Tracer for Magnetic-Recording Wire, T. H. Long, G. D. McMullen. AIEE Transactions, volume 65, 1946, March section, pages 146–9.

3. B-H Curve Tracer for Lamination Samples, Robert Adler. *Electronics* (New York, N. Y.), November 1943, pages 128–31, 314, 316–7.

4. Magnetic Phenomena (book), Samuel Robinson Williams. First edition, McGraw-Hill Book Company, New York, N. Y., 1931. Pages 37, 210, 211.

5. Tests for Magnetic Properties of Steel (A34–44). American Society for Testing Materials *Standards*, Philadelphia, Pa., 1944, part I, Metals. Page 693.

6. A-C Bridge Methods (book), B. Hague. Fifth edition, Pitman and Sons, New York, N. Y., 1943. Pages 457–9.

Discussion

H. J. McCreary (Automatic Electric Company, Chicago, Ill.): In the Automatic Electric Laboratories we have done some work closely related to this paper.

In the study of magnetic devices employing saturation phenomena, it is sometimes desirable to view the wave shape of the flux against time. For several years we used an exploring coil in series with a high resistance connected to a large capacitor to reproduce by electrical integration in electrical wave form the wave form of the flux through the exploring coil. This device became a tool of more general use about the laboratory and therefore was written up and designated *ELS*-2612, *ELS*-2613, and *ELS*-2614 so that others in the laboratory might make more general use of this test method.

Because of the extreme simplicity of this arrangement, and because of the high impedance across the exploring coil output terminals there is very little reaction of the exploring coil on the flux threading it, and its terminal electromotive force varies almost directly as $d\phi/dt$ 10-8.

It is believed that the comments of Doctor Arthur Bessey Smith and myself as given in *ELS*-2612, *ELS*-2613, and *ELS*-2614 are appropriate additional comments on this paper.

Magnetic Flux on Oscilloscope

Consider one transient, the magnetic flux rising from zero to a finite value. In Figure 1 of this discussion let

ϕ = magnetic flux inside the coil of N turns.
R is a nonreactive resistor which is large enough to dominate the circuit.
C is a capacitor large enough to have a reactance which is small compared to R.
E = electromotive force developed in the coil by the rising magnetic flux.
i = instantaneous current resulting from E.
e is the electromotive force across C resulting from current.

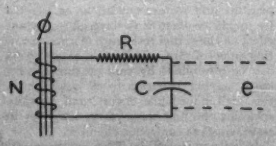

Figure 1

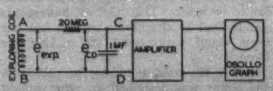

Figure 2

The N-turn coil also must have negligible reactance compared to R. Hence, the whole acts like a noninductive circuit, and the current at any instant will be proportional to E, the electromotive force being generated at that instant by the rising flux ϕ.

The logical development of equation 7 is as follows:

$$e = \frac{q}{C} \tag{1}$$

$$q = \int_0^t i dt \tag{2}$$

Put equation 2 into equation 1.

$$e = \frac{1}{C} \int_0^t i dt \tag{3}$$

$$i = \frac{E}{R} \tag{4}$$

Put equation 4 into equation 3.

$$e = \frac{1}{CR} \int_0^t E dt \tag{5}$$

$$E = 10^{-8} N \frac{d\phi}{dt} \tag{6}$$

Put equation 6 into equation 5.

$$e = \frac{10^{-8} N}{CR} \int_0^t d\phi$$

so that

$$e = \frac{10^{-8}N}{CR}\left[\phi\right] \tag{7}$$

Hence the instantaneous electromotive force e across the capacitor is directly proportional to the magnetic flux ϕ existing at the time t. This is valid under the above conditions and for this first single transient.

Magnetic Flux Intensity Waves on the Cathode Ray Oscillograph

In order to get an oscillogram of the magnitude of flux with respect to time it has been customary in the past to cause a part of the magnetic field to pass through the scope tube and deflect the cathode beam directly, in which case

$$F = BLi$$

However, in the development of electromagnetic apparatus such as relays, stepping switches, and so forth, the magnetic field is often of such a restricted order that the above method of obtaining an oscillogram of the flux variation with time is not practical. In such a case the following method has been found quite practical.

Place an exploring coil about the place in the magnetic circuit where it is desirable to obtain the flux variation.

The voltage generated by the exploring coil is

$$e_{exp} = \frac{d\phi}{dt}10^{-8}$$

$$e_{exp}\,dt \times 10^{+8} = d\phi$$

$$\phi = \int d\phi = 10^{8}\int e_{exp}\,dt$$

Therefore, it is but necessary to integrate the potential e_{exp} electrically with respect to time and place the result on the oscilloscope. The most simple circuit for doing this is shown in Figure 2 of the discussion.

It consists of an exploring coil connected in series with a very high resistance such as 20 megohms and a 1-microfarad capacitor. This circuit then has a time constant of 20 seconds or, in other words, is comparable to that of the needle of the Grassot Fluxmeter.

The vertical oscillograph deflection varies directly as the magnitude of the flux traversing the exploring coil.

Caution: While the time constant of the integration circuit given here is 20 seconds, only the very best cathode ray oscillographs can record accurately frequencies as low as a few cycles per second. Therefore, some discretion must be shown in the selection of an oscillograph which will show accurately the potential across the 1-microfarad capacitor.

Electrical Integration

As mentioned, the potential on the exploring coil terminals when connected to a 20-megohm resistor is practically equal to the electromotive force generated in the coil by the flux change through the coil; that is

$$e = \frac{d\phi}{dt}10^{-8}$$

At frequencies of one cycle per second and greater the potential on the capacitor can never be an appreciable part of the applied potential because the time constant is 20 seconds.

At frequencies of ten cycles per second the potential on the capacitor resulting from accumulated charge through the 20-megohm resistor is so small that it has no appreciable affect on the flow of current caused by the exploring coil. The reactance of 1 microfarad on 10 cycles per second is about 159,000 ohms which, compared to 20 megohms, can be neglected because the voltage drop in the capacitor is about one-half of one per cent of the voltage applied to the circuit.

Therefore, we can conclude that within the accuracy of most indicating instruments the flow of current through the 20-megohm resistor is a direct function of the electromotive force generated by the exploring coil and neglecting the capacitor; that is

$$e_{exp} = ir$$

$$e_{exp} = i\,20\times10^{6}$$

$$i = \frac{e_{exp}}{20\times10^{6}}$$

The voltage on the capacitor is

$$e_{CD} = \frac{Q}{C}$$

where Q is the quantity of charge in coulombs, but

$$Q = \int i\,dt$$

$$Q = \frac{1}{20\times10^{6}}\int e_{exp}\,dt$$

$$e_{CD} = \frac{Q}{C}$$

$$= \frac{1}{C}\,\frac{1}{20\times10^{6}}\int e_{exp}\,dt$$

Therefore e_{CD} is the integral curve of e_{exp}.

Although e_{CD} varies as the flux almost exactly, it is as stated before very small; therefore, it must be applied to a very good amplifier to obtain a voltage large enough to give an appreciable deflection of the cathode ray oscillograph beam.

B. M. Smith (General Electric Company, Schenectady, N. Y.): This paper should be of particular interest to anyone who has made similar measurements and experienced any of the measuring difficulties. The authors are to be commended for their excellent accomplishments and their valuable contributions to the art of magnetic measurements.

As the authors have demonstrated, making magnetic hysteresis loop measurements on a cathode ray oscillograph screen is a very convenient method and greatly facilitates the work where a large number of tests are to be made. This method, however, is not limited to alternating current but has been found very useful for making d-c loops.[1]

One of the errors noted by the authors in the tester was described as being caused mainly by the rectifier type voltmeter, the error being as high as 20 per cent. This is contrary to our experience with this type of instrument which we have found to be accurate within one-half of one per cent at 25 degrees centigrade. Compensation for temperature changes sometimes is incorporated in the instrument. That this accuracy can be obtained is indicated by the recommendations of the American Society for Testing Materials in their test procedures given in *A*34 on magnetic test methods.

The selection of the power line frequency by the authors for the measurement described eliminates many of the difficulties and gives results which were comparable with those obtained by d-c measurements. The question arises, however, as to whether the measurement represents the property of the materials at the higher frequencies at which the recorder wire is supposed to respond. Our experience has been that the frequency response curve for magnetic materials is not related directly to the coercive force obtained at 60 cycles. It depends among other things upon the surface resistivity, size of the wire, as well as the magnetic properties.

The cathode ray oscillograph is also very useful in this work for determining the homogeneity of the wire in its final form.

As a comparator the cathode ray oscillograph should yield very satisfactory results when comparing unknown materials with those which have been tested in service, but this comparison should be made over the frequency range at which the wire is to be used; otherwise it may lead to misleading results.

Reference

1. A New Photoelectric Hysteresigraph, **R. F. Edgar.** AIEE Transactions, volume 56, 1937, July section, pages 805–9.

D. E. Wiegand: Performance of the simple *R-C* integrator described by H. J. McCreary and B. M. Smith is perfectly satisfactory providing the sample under test is relatively large and the voltage to the integrator, therefore, is of a conveniently large value. However, in the case of small samples such as those for which the tester described in the paper was designed, the pickup coil voltage is sufficiently small as to lend great importance to the voltage loss or attenuation in the integrator. It is mainly for this reason that the integrating network described in the paper was used in preference to the simpler one. The output voltage of this network is about 11 times that of a simple *R-C* integrator providing the same maximum phase error.

The value of the integrating resistor in the simple *R-C* network enters directly into the calibration of the instrument. This is evident from McCreary's equations. We would expect severe difficulties in calibration drift caused by changes from the nominal 20-megohm value of this resistor. Temperature and surface conditions as affected by the atmosphere may have an important effect on the actual resistance of a resistor of this order of size. Of course, these errors can be minimized by wax coating the resistor, paying attention to all insulation in this high impedance circuit, and possibly enclosing the first stage of the amplifier in an atmosphere-controlled chamber.

In order to realize the 20-second time constant, it is necessary that the resistance across

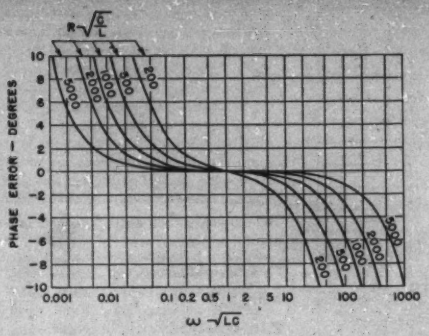

Figure 3

the input of the amplifier, including the leakage resistance of the 1-microfarad capacitor, be high compared to 20 megohms. It may be difficult to obtain a 1-microfarad capacitor having a leakage resistance consistently this high.

A simple *R-C* integrator at the input of the amplifier first was tried in developing our tester. In testing samples at magnetizing forces beyond that required for saturation, it was found that the trace on the oscilloscope screen was wavy at certain parts of the hysteresis loop. It was found that this effect was caused by phase errors resulting from the self-inductance in the pickup circuit. In order to analyze the action of the simple integrating circuit with a series self-inductance, the curves of Figure 3 of the discussion were prepared. In general, the voltage of the pickup coil consists of a fundamental component plus a series of harmonics (usually odd). The voltage relation for any of the frequencies involved is given in equation 1.

$$\frac{V_1}{V_c}=(1-\omega^2LC)+j\omega\sqrt{LC}\,R\sqrt{\frac{C}{L}} \qquad (1)$$

V_1 is the induced (open circuit) voltage in the pickup coil, V_c the voltage across the integrating capacitor, ω the angular velocity corresponding to the frequency of the voltage component, L the total self-inductance in the pickup circuit (henries), C the capacitance of the integrating capacitor (farads), R the total resistance (ohms) in the integrating circuit. In most cases, the integrating resistor is large compared to other resistances in the circuit so that R may be taken as the ohms resistance of the integrating resistor. The curves of Figure 3 are based on equation 1. The tangent of the phase error is the real part of equation 1 divided by the imaginary part.

In the tester as described in the paper, integration is performed after the first stage of the amplifier, and the pickup circuit therefore is loaded only by its own distributed capacitance and by the volume control at the input of amplifier. Even with this arrangement, wavy loops are obtained sometimes when testing samples far beyond saturation. The frequency of these waves was found to be about 14,000 cycles per second. Under these test conditions, apparently, the voltage of the pickup coil has a 233rd harmonic component of sufficient magnitude to excite the pickup circuit at its resonant frequency.

The curves of Figure 3 in this discussion can be used to determine the values of R and C in a simple integrator preceding the first amplifier stage which will perform satisfactorily up to the present limiting frequency of 14,000 cycles per second. The curve for $R\sqrt{\frac{C}{L}}=1{,}000$ shows an error of 0.5 degree at $\omega\sqrt{LC}=0.1$. On this same curve at $\omega\sqrt{LC}=23.3$, 233 times the original value, the error is about 1.3 degrees. The first value corresponds to the fundamental frequency and the second to the 233rd harmonic. Errors within 0.5 degree at the fundamental frequency have been found to produce negligible errors, and the higher phase error at the 233rd harmonic also will have a negligible effect because of the extremely small time-error to which this angular error corresponds.

The self-inductance in the pickup circuit of the tester is about 1.3 henries. Substituting this value for L and 377 for ω in $\omega\sqrt{LC}=0.1$ gives $C=0.054\times10^{-6}$ farad (0.054 microfarad). Similarly, substituting values in $R\sqrt{\frac{C}{L}}=1{,}000$ gives $R=4.9\times10^6$ ohms (approximately 5 megohms).

Placing the integrator ahead of the first stage of the amplifier of course would reduce greatly the problem of amplifier overloading mentioned in the paper. With this location of the integrator, the first amplifier stage would pass the integrated wave (a flat-topped wave) rather than the pip voltage wave of the pickup circuit.

With the integrator at the output of the first stage, however, lower resistances and larger capacitances may be used in the integrating network, and the problem of changes in calibration resulting from surface variations in the resistors is eliminated. With the tester as shown in the paper, providing the gain controls are adjusted properly, samples may be measured well beyond saturation without overloading the amplifier.

With reference to Doctor Smith's comments regarding the 20-per-cent error caused by the rectifier type voltmeter in the tester, in the American Standards for Testing Materials referred to, voltages of the order of 100 volts are measured by the rectifier type voltmeter. In this range of voltage, temperature errors in the rectifier are masked by the relatively large value of series resistance in the voltmeter. In the hysteresis loop tracer, however, it is sometimes necessary to measure values down to a few volts. In this case, the temperature and aging characteristics of the rectifier become much more important, and accurate measurements are difficult. It is believed that the proposed change to a current transformer and ammeter will result in considerably greater over-all accuracy of measurement in the tester.

Doctor Smith infers that it might be desirable to test magnetic recording media at frequencies well up in the audio range rather than at 60 cycles. It is true that the frequency response curve depends on other factors in addition to the basic magnetic properties measured at direct current or a low frequency. If resistivity of the medium in an important factor, it would be desirable to measure this quantity separately and in addition to basic magnetic measurements in a d-c or equivalent tester, rather than making magnetic measurements at a higher frequency, in which case both the resistivity and the basic (d-c) magnetic properties affect the measurements. In general, in studying correlations between basic properties and final performance of a material in order to draw up a specification which will insure satisfactory performance, it is better to measure separately each of the basic factors involved than to measure some quantity which depends on a combination of basic factors.

Shading Coil Calculations for Single-Phase Magnets

C. T. EVANS
FELLOW AIEE

IN a single-phase a-c electromagnet it is customary to provide a shading coil to prevent chatter of the armature against the stationary pole face. Three important affects are produced by the shading coil.

1. At the pole face, the magnetic flux is separated into two parts which are relatively out of phase.

2. The flux density in the "unshaded" area of the pole face is increased.

3. Heating of the magnet is increased because of the watts produced by the current in the shading coil.

Calculation of the watts dissipated in the shading coil and of the instantaneous pull of the magnet are difficult because of the nonlinear relation between the magnetic flux in the steel and the magnetomotive force. It is the purpose of this paper to describe an experimental procedure that has been found useful in the study of this problem, and to offer experimental evidence in support of an approximate method of calculating the shading coil watts.

Theory

Conventional analysis[1] of the shading coil is based on the assumption that saturation of the steel is negligible. In effect it is assumed that the reluctance in the magnetic circuit is constant and is concentrated in the air gap between the pole faces. Experience shows that even with no intentional air gap and with well fitting pole faces there is a reluctance across these surfaces equivalent to that of an air gap approximately 0.001 inch long. Under this assumption, and with sinusoidal flux generated by the exciting coil of the magnet, each of the fluxes and the shading coil current are evidently sine functions.

Figure 1 is a diagrammatic sketch of a single-turn shading coil surrounding approximately two-thirds of the pole face area. The coil passes through a slot dividing the pole faces into the "shaded" area S_2 surrounded by the coil and the unshaded area S_1. Figure 2 is a vector diagram of the magnetomotive forces and of the fluxes across these areas where θ is the phase angle between the fluxes ϕ_1 and ϕ_2, G_2 is the conductivity of the shading coil, ω is the angular frequency, and the total flux ϕ is the vector sum of ϕ_1 and ϕ_2. If $\mathcal{R}_1$ and $\mathcal{R}_2$ represent the reluctances of the two pole areas, and B_1 and B_2 the flux densities, Figure 2 gives

$$\tan\theta = \omega G_2/\mathcal{R}_2 \tag{1}$$

$$\cos\theta = \mathcal{R}_2\phi_2/\mathcal{R}_1\phi_1 \tag{2}$$

$$\phi^2 = \phi_1^2 + \phi_2^2 + 2\phi_1\phi_2\cos\theta \tag{3}$$

Substituting $T = \mathcal{R}_1/\mathcal{R}_2 = S_2/S_1$ in equation 2 and then in equation 3

$$\phi_1^2 = \frac{(1+\tan^2\theta)\phi^2}{(T+1)^2+\tan^2\theta} \tag{4}$$

$$\phi_2^2 = \frac{T^2\phi^2}{(T+1)^2+\tan^2\theta} \tag{5}$$

Watts in the shading coil are evidently

$$P_s = \omega^2 G_2 \phi_{2m}^2/2 \tag{6}$$

If the maximum (peak) flux density in the steel with the shading coil removed ($G_2 = 0$) is represented by B_m, simple substitution and rearrangement of equations 4 to 6 show that the maximum flux density with the shading coil is

$$B_{1m} = B_o B_m$$

Paper 47-17, recommended by the AIEE committee on industrial control devices for presentation at the AIEE winter meeting, New York, N. Y., January 27–31, 1947. Manuscript submitted November 1, 1946; made available for printing November 18, 1946.

C. T. EVANS is consulting engineer, Cutler-Hammer, Inc., Milwaukee, Wis.

and the shading coil watts per square inch of total pole area S are

$$P_s/S = P_o(\omega l_a B_m^2)$$

where

$$B_o^2 = [(1+\tan^2\theta)(T+1)^2] + [(T+1)^2+\tan^2\theta]$$

$B_o = B_{1m}/B_m$ shows the variation of B_{1m} with constant density B_m

and

$$P_o = [T(T+1)\tan\theta]/2\mu[(T+1)^2+\tan^2\theta]$$

P_o = watts per square inch with unit air gap, flux density, and angular frequency

μ = The permeability of air, and l_a the length of the air gap

Thus B_o and P_o depend only on the ratio of pole reluctances (or areas) T and the phase angle θ. The parameters B_o and P_o are plotted in Figures 3 and 4 as functions of θ, and for several values of T. Watts per square inch total pole area reach maximum values at specific phase angles, depending on T, while the flux densities increase with the phase angle.

On the basis of these simplified assumptions it is usual practice to design a magnet for a phase angle between 60 and 70 degrees and a ratio T in the neighborhood of two. Under these conditions reference to Figure 3 shows that the flux density in the unshaded pole area is from 1.66 to 2.15 times the density in the core, as a whole. Thus, if the maximum density B_m is 0.001 weber per square inch, the maximum density B_{1m} indicated for the unshaded area is from 0.00166 to 0.00215 weber (166 to 215 kilomaxwells) per square inch, or from 30 to 70 per cent above the saturation value in the grade of steel ordinarily used for such magnets. From these considerations it is clear that the reluctance of the steel cannot be ignored, nor can it be assumed that the reluctance is constant.

Approximate Solution

Now in dealing with high flux densities, frequent use is made of published data giving the volt-amperes "excitation" per pound of metal for the steel.

Curves giving these volt-amperes as a function of the maximum flux density, and at 60 cycles, are available for the various standard grades of steel. They presuppose sinusoidal flux variations and (tacitly) nonsinusoidal magnetizing forces. The volt-amperes therefore are the product of the rms values of the magnetizing current and induced voltage in a magnetizing coil which would produce the given sinusoidal flux density in a pound of steel.

It would be attractive to work out an approximation for the shading coil watts based on the known values of excitation P_x for the steel, and also based on a vector representation of the fluxes and current as shown in Figure 2. In effect this means that some equivalent fixed reluctance must be substituted for the variable reluctance of the steel, but that the value of this fixed reluctance varies with the maximum flux density. In order to determine the value of this equivalent reluctance it would be convenient to convert the values of volt amperes excitation to rms ampere turns per inch-cube per weber for the steel. A further convenience results if the ampere turns per inch for the steel plus a small per-unit length of air gap is used. For this purpose assume K inches of air gap for each inch of steel.

$\mu = 3.19 \times 10^{-8}$ for air
γ = pounds per cubic inch of steel
σ = stacking factor of the laminations
P_x = volt-amperes per pound of steel
B_m = webers per square inch
$\mathfrak{R}_o = (2\gamma\sigma P_x)/(\omega B_m^2)$ ampere turns per weber per inch-cube of steel
$\mathfrak{R}_o'$ = ampere turns per weber for an inch-cube of steel plus K inches air gap

$\mathfrak{R}_o' = \mathfrak{R}_o + 10^8 K/3.19$

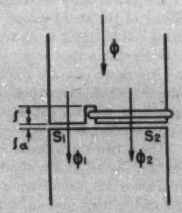

Figure 1. Single-turn shading coil

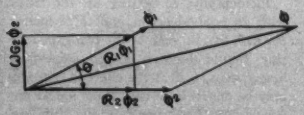

Figure 2. Vector diagram of magnetomotive force and flux

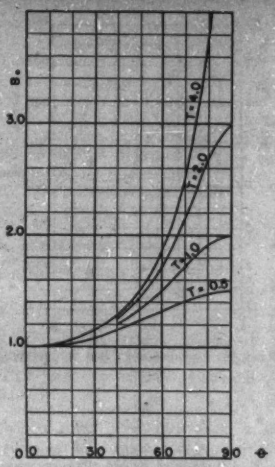

Figure 3. Variation of flux density in unshaded pole area

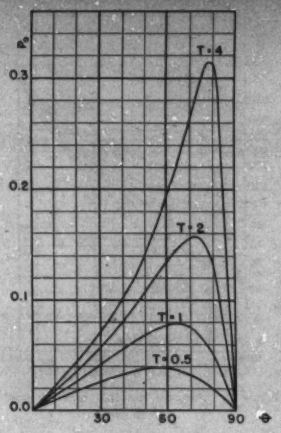

Figure 4. Variation of watts per square inch of pole area

The curves of Figure 5 show $\mathfrak{R}_o' B_m$ as a function of B_m for electrical sheet steel. Now return to the vector relations of Figure 2 and equation 3, noting that

$$\mathfrak{R}_2\phi_{2m} = l\mathfrak{R}_2' B_{2m}$$

with a similar relation for $\mathfrak{R}_1\phi_{1m}$

$$(\mathfrak{R}_1' B_{1m})^2 = (\mathfrak{R}_2' B_{2m})^2 + (\omega S_2 B_{2m} G_2/l)^2 \quad (7)$$

$$\phi^2 = \phi_1^2 + \phi_2^2 + 2\phi_1\phi_2\mathfrak{R}_2' B_{2m}/\mathfrak{R}_1' B_{1m} \quad (8)$$

the conductivity G_2 theoretically should include a term attributable to the watts-per-pound loss in the iron P_r thus

$$G_2 = G_s + (2\gamma\sigma l P_r)/(\omega^2 S_2 B_{2m}^2) \quad (9)$$

where G_s is the conductivity of the shading coil.

However, the last term usually is small compared to G_s, the conductivity of the shading coil, and may as well be omitted considering the degree of approximation involved, so that G_s may be substituted for G_2 in equation 7 without appreciable error. Likewise the iron loss in the unshaded portion can be disregarded.

In practice, the dimensions of the poles, conductivity of the shading coil, and maximum total flux usually are given. To find the watts in the shading coil, proceed by assuming a trial value for B_{2m} and by the curves in Figure 5 find $\mathfrak{R}_2^1 B_{2m}$. Calculate $\mathfrak{R}_1' B_{1m}$ by equation 7 and again by reference to Figure 5, find B_{1m}. Now, multiplying B_{1m} and B_{2m} by the areas S_1 and S_2 of the respective pole sections, find ϕ_{1m} and ϕ_{2m}, and then from equation 8 calculate ϕ_m. If this differs from the actual value of ϕ_m, adjust the trial value of B_{2m} until there is agreement in ϕ_m. The shading coil watts then are

$$P_s = \omega^2\phi_{2m}^2 G_2/2 \quad (10)$$

Measurements made on several commercial magnets of the difference between the watts input with the shading coil in place, and with it removed, gave values for the additional watts attributable to the shading coil agreeing closely with the calculations just outlined. However, it was considered desirable to undertake a more comprehensive study of such magnets, to include effects resulting from variations in physical proportions of the magnet, and to measure the instantaneous flux densities at the pole faces, especially the maximum densities. Although not the subject of the present paper, it may be mentioned in passing that measurement of the instantaneous values of the flux densities have also been used for a general study of the instantaneous magnitudes of the pull developed at the pole faces. The experimental procedure finally adopted permits measurement not only of the instantaneous values, but also of the rms values, as well as direct measurement of the watts over a wide range of physical proportions.

Experimental Procedure

Preliminary tests were made on a large experimental magnet slotted at the pole

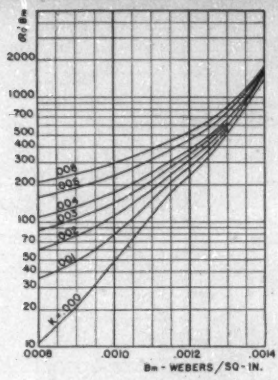

Figure 5. Ampere turns per inch for steel with air gap

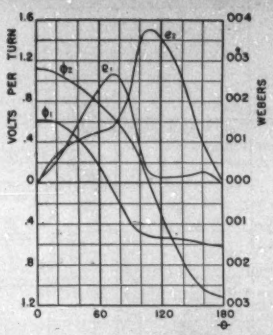

Figure 6. Voltages and fluxes for magnet, Figure 1

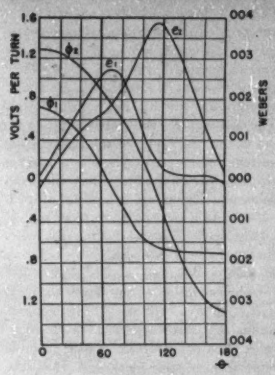

Figure 8. Voltages and fluxes for rings, Figure 7

face to receive a shading coil as well as additional fine wire search coils, by means of which the instantaneous voltages induced by the fluxes in both sections were indicated on an oscilloscope and recorded photographically. Figure 6 shows a trace of the volts per turn in the search coils, as well as the magnetic fluxes obtained by graphical integration of the flux curves. The pertinent data are:

$S_2 = 3$ square inches
$S_1 = 1.37$ square inches
$l = 7/16$ inch
$G_2 = 111$ mhos

The low resistance exciting coil had 245 turns and, for these curves, was energized at 300 volts, 60 cycles.

The technical difficulties attendant on the use of the oscilloscope were such as to suggest a modified arrangement wherein the voltages could be recorded by an oscillograph, particularly as it was desired to obtain a large number of curve traces. Furthermore, with this magnet the effective air gap at the pole faces could not be reduced below approximately 0.001 inch, and could not be controlled easily for larger values.

It was decided to set up an equivalent electromagnetic circuit consisting of two separate laminated steel rings, having separate identical exciting coils connected in series across the a-c source. These two rings represent the unshaded and shaded pole sections, and a resistance shunt, connected across the exciting coil of the "shaded" ring, represents the shading coil. Figure 7 is a diagram of the arrangement. The rings were made by winding electrical strip steel on arbors, with 0.001-inch paper separators between the laminations. Steel rivets were placed around the rings on the center line of the strips to hold them in place and the rings were finally sawed across their diameters. The resulting pole faces were then finished in line, coils inserted, and the rings reassembled with flat insulating plates interposed to control the length of the air gaps. For each ring there are two low-resistance coils of 122 turns each, or 244 turns for the ring. The mean length of the strips for each ring is 32.7 inches and the cross-sectional areas of the unshaded and shaded rings are 1.5 and 3.0 square inches respectively.

A little consideration will show that the differential equation connecting the magnetic fluxes and magnetomotive forces for these rings is of the same form as for the individual sections of the magnet of Figure 1. The resistance of the exciting coils may be neglected if low-resistance coils are used. For the magnet of Figure 1, as the magnetomotive force, integrated over a path from a point in the upper pole to a point in the lower pole is the same, whether the path of integration passes through or outside of the shading coil

$$\mathfrak{R}_1\phi_1 = \mathfrak{R}_2\phi_2 + G_2\frac{d\phi_2}{dt} \tag{11}$$

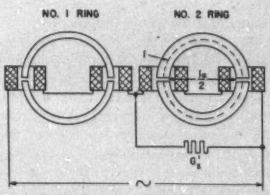

Figure 7. Connections for test of steel rings

For the two rings, moreover, the instantaneous currents

$$i_1 = i_2 + i_s \tag{12}$$

But we have

$$\left.\begin{aligned} Ni_1 &= \mathfrak{R}_1\phi_1 \\ Ni_2 &= \mathfrak{R}_2\phi_2 \\ i_s &= NG_2'\frac{d\phi_2}{dt} \end{aligned}\right\} \tag{13}$$

Substituting equation 13 in 12 gives

$$\mathfrak{R}_1\phi_1 = \mathfrak{R}_2\phi_2 + N^2G_2'\frac{d\phi_2}{dt} \tag{14}$$

In these equations R_1 and R_2 need not be constants, so that the equivalence between the single magnet and the rings of Figure 7 hold regardless of this condition, provided that in each case the $\mathfrak{R}$'s are similar functions of the ϕ's. Thus, if the conductance of the shunt circuit around the exciting coil of ring 2 is multiplied by N^2 and the current in this circuit is multiplied by N, the results are respectively the conductivity and current in an equivalent single-turn shading coil around the shaded pole section, now represented by ring 2. These two rings therefore truly represent the shaded and unshaded pole sections of a magnet, each having an iron path 32.7 inches long, and adjustable air gaps which may be made very short compared to the length of the iron path.

Incidentally, in setting up the rings with an equivalent air gap of K inches per inch length, each of the two gaps in a ring should have a length somewhat longer than $lK/2$ as the effect of fringing may be appreciable with these longer air gaps. The permeance of the fringing path may be calculated by any standard method[1] and the actual air gaps should

be increased by an amount proportional to the per-unit permeance of the fringing path. This increase may amount to 0.2 of the equivalent air gap.

Several advantages accrue from the use of these rings, among which are:

(*a*). There is no unused iron in the rings compared to the return magnetic circuit of Figure 1.

(*b*). The air-gap length may be adjusted so as to study the effect of varying K.

(*c*). With low-resistance exciting coils, the terminal voltages may be assumed to be equal to the induced voltages, and may be recorded on an oscillograph, or the rms values may be measured directly without further amplification.

As an example, Figure 8 shows a trace of an oscillogram of the voltages recorded while testing these rings, with 326 volts, 60 cycles, impressed and with 20.1-ohm shunt around coil 2. The reluctance of the air gaps in ring 1 is 1.16×10^6 ampere turns per weber, and for the (shunted) ring 2, 0.542×10^6 ampere turns per weber. The corresponding values of K are 0.0021 and 0.0017 respectively. By voltmeter measurement there are 224 volts across coil 2, giving 2,490 watts dissipated in the 20.1-ohm shunt.

If the assumption were made that all of the reluctance is concentrated in the air gap, equation 2 would give the phase angle

$$\theta = \tan^{-1}(\omega G_2/\mathfrak{R}_2) = 64 \text{ degrees}$$

Therefore

$$T = 1.16/0.52 = 2.14$$

$$\tan\theta = 2.06$$

The total flux for the two rings

$$\phi_m = 326\sqrt{2}/(244\omega) = 0.00502 \text{ weber}$$

by equation 5

$$\phi_{2m} = \frac{2.14\times0.00502}{[(3.14)^2+(2.06)^2]^{1/2}} = 0.00287 \text{ weber}$$

The rms volts across coil 2 would then be $\omega N\phi_{2m}/\sqrt{2}$, or 186.5 volts, which would produce only 1,650 watts in the 20.1-ohm shunt. This is 23 per cent low compared with the 2,490 watts actually measured.

By making use of the approximations of equations 7, 8, and 9, with a trial value for B_{2m} of 0.00114 weber per square inch, and by reference to Figure 5, with K at 0.0017, $\mathfrak{R}_2'B_{2m}$ is found to be 215. Then with 2,960 mhos for G_2, equation 7 gives 245 for $\mathfrak{R}_1'B_{1m}$. Reference to Figure 5, using 0.0021 for K, then gives 0.0015 for B_{1m}. The corresponding fluxes are

$$\phi_{1m} = 0.00172 \text{ weber}$$

$$\phi_{2m} = 0.00342 \text{ weber}$$

and, using equation 8,

$$\phi_m = 0.005 \text{ weber}$$

This compares with the actual value 0.00502 weber. For a single-turn shading coil having a conductivity, 2,960 mhos, the watts

$$P_s = (120\pi\, 0.00342)^2\, 2{,}960/2 = 2{,}460 \text{ watts}$$

compared with the test value, 2,490 watts. A number of similar calculations and tests give results, comparable within 10 per cent or less in all cases.

With a pair of laminated steel rings, having an appropriate ratio of cross-sectional areas, it is possible to measure the rms volts or current in the shunt circuit by means of ordinary a-c voltmeters or ammeters and thus quickly determine the shading coil watts for any equivalent magnet over a wide range of shading coil conductivities, air-gap ratios, and exciting voltages or frequencies without having to build and test the actual magnet. Other studies, covering a similar range of variations, concerning flux densities or instantaneous pulls readily will suggest themselves.

Conclusion

A procedure has been suggested by means of which the watt loss in the shading coil of a single-phase magnet may be calculated with reasonable accuracy. An experimental method has been described by means of which the validity of these approximate calculations has been confirmed. This experimental method also may be used effectively to study the nonlinear relationships between the magnetic fluxes and magnetomotive forces in single-phase shaded-pole magnets over a wide range of physical proportions.

Appendix. Nomenclature

B_m	= peak flux density for magnet pole as a whole, or when shading coil is removed
B_{1m}, B_{2m}	= peak flux densities, unshaded and shaded poles respectively
B_o	= ratio B_{1m}/B_m
G_s	= conductance of single turn shading coil
G_2	= equivalent conductance of shading coil plus that of the steel in the shaded pole
G_2'	= conductance of the shunt around the coil of ring 2
K	= ratio l_a/l
l	= length of pole (see Figure 1)
l_a	= length of air gap (see Figure 1)
P_s	= watts dissipated in hading coil
P_o	= watts per square inch of total pole area with unit air gap, flux density, and angular frequency
P_r	= watts per pound of steel
P_x	= volt-amperes excitation per pound of steel
$\mathfrak{R}_1$, $\mathfrak{R}_2$	= reluctances of unshaded and shaded poles
$\mathfrak{R}_1'$, $\mathfrak{R}_2'$	= equivalent reluctance of an inch-cube of steel plus K inches of air gap, for the unshaded and shaded poles
$\mathfrak{R}_o$	= equivalent reluctance of an inch-cube of steel, for a given peak flux density
$\mathfrak{R}_o'$	= equivalent reluctance of an inch-cube of steel plus K inches of air gap
S	= combined area of shaded and unshaded poles
S_1, S_2	= areas of unshaded and shaded poles
T	= ratio $S_2/S_1 = \mathfrak{R}_1/\mathfrak{R}_2$
γ	= pounds per cubic inch of steel
θ	= phase angle between ϕ_1 and ϕ_2
μ	= permeability of air
σ	= stacking factor
ϕ, ϕ_1, ϕ_2	= total flux, unshaded and shaded pole flux
ϕ_m, ϕ_{1m}, ϕ_{2m}	= peak values of fluxes

Reference

1. Electro-Magnetic Devices (book), H. C. Roters. John Wiley and Sons, New York, N. Y., 1941.

Discussion

J. E. Ryan (General Electric Company, Schenectady, N. Y.): The conventional method of analyzing shading coil action, neglecting the reluctance of the iron in the vicinity of the butting surfaces, is useful only for visualizing the general effects of the parameters involved. For design, methods akin to C. T. Evans' "approximate solution" have had to be employed, and even then the prediction of maximum quiet pull is not as accurate as that for the shader losses.

The real contribution of this paper is the ingenious equivalent circuit of Figure 7. Working with controllable air gaps and easily measurable quantities, data can be obtained which, when plotted in dimensionless form, will be directly usable in design It should be noted, however, that the equivalent circuit represents none of the iron beyond the depth of the shader slot. Tacitly it is assumed that the flux density is uniform across the section beyond this point. Even if one attempts to allow for the approaches to the shaded and unshaded regions by adding some equivalent length of iron, this is not strictly accurate as the

latter varies cyclically with time. But such refinements are unnecessary because the air gap in an actual magnet is rather indeterminate anyway.

The writer feels that the paper would have been easier to follow if a complete notation had been given at one place, including some subscripts and superscripts not explicitly defined. Also, an appendix containing the complete proof of the similarity of the actual magnet and the equivalent circuit would have been helpful.

There seem to be two errors in the paragraph following equation 14. By independent analysis, the writer has found that

$$G_2 = N^2\left(\frac{S_2'}{S_2}\right)\left(\frac{l_a}{l_a'}\right)G_2'$$

instead of

$$G_2 = N_2 G_2'$$

and that

$$i_s = N\left(\frac{l_2}{l_a'}\right)i_s'$$

instead of

$$i_s = N i_s'$$

where the notation is that of the paper, and primes denote properties of the model.

A further interesting consequence is that

$$P_s = \left(\frac{l_a S_2}{l_a' S_2'}\right)P_s'$$

It is hoped that the author subsequently will present data on the relations between pull, heating, and the various design parameters.

L. A. Doggett (Pennsylvania State College, State College, Pa.): The literature on shading coil design is not very extensive. A brief bibliography of this subject is given on page 22 of bulletin number 52 of the Pennsylvania State College Engineering Experiment Station, entitled "Design of Shading Coils for A. C. Electromagnets." To this list should be added the work of H. C. Roters and now the present paper by C. T. Evans.

In Evans' paper an equivalent electromagnetic circuit has been devised in which the important variables are dualed in a very ingenious manner. The actual magnetic circuit corresponding to Figure 1 consists of two branches in parallel carrying fluxes ϕ_1 and ϕ_2, which in combination yield ϕ. The ϕ_1 branch contains a reluctance $\mathfrak{R}_1$ properly modified to include some iron reluctance. The ϕ_2 branch contains a reluctance $\mathfrak{R}_2$ plus an opposing magnetomotive force caused by the shading coil. Various equivalent circuits have been proposed, notably by Unger, and now by Evans in Figure 7. Figures 6 and 8 substantiate the author's claim as to equivalence. A further equivalence might well be pointed out. If in Figure 8, e_2 and e_1 are added, a very good sine wave of impressed electromotive force is obtained. In Figure 6, where

$$\phi_1 + \phi_2 = \phi$$

$$n\frac{d\phi_1}{dt} + n\frac{d\phi_2}{dt} = n\frac{d\phi}{dt}$$

$$n = 1$$

e_2 plus e_1 also add up to a good sine wave.

Granting that Figure 7 is a satisfactory equivalent, it might be suggested that its use be extended to find out the optimum values of shading coil resistance S_2/S_1 and air gap length for the unshaded part. By optimum values are meant those values which produce a minimum of vibration. To carry out these tests it would be necessary to fasten the lower semicircular cores securely to the laboratory table, whereas the upper semicircular cores should be fastened firmly together but otherwise be free to move. A crystal-type vibration pickup and a cathode-ray oscilloscope may be used to observe the vibration of the upper pair of semicircular cores. The weakness of all analytical methods so far presented lies in their failure to consider the presence of harmonics in the shading coil current. The driving electromotive force of this current, e_2, is far from sinusoidal. However, Evans' experimental arrangement of Figure 7 will have voltage and current wave shapes very similar to those existing in ordinary shading coils.

Finally for the benefit of those investigating this subject for the first time a brief statement of the elementary theory is presented. Using the notation of the present paper, a Kirchhoff's law equation may be set up for the magnetic circuit of Figure 1 Thus

$$-\phi_2\mathfrak{R}_2 - 0.4\pi N_2 i_s + \phi_1\mathfrak{R}_1 = 0$$

If $\phi_1 = \phi_2 \sin \omega t$, then

$$-(\mathfrak{R}_2\phi_2 \sin \omega t - 0.4\pi N_2 G_2(-N_2\omega\phi_2 10^{-8}) \times \cos \omega t + \mathfrak{R}_1\phi_1 \sin (\omega t - \theta) = 0$$

For $\omega t = 0$ and $\omega t = \pi/2$, two important relationships may be derived.

$$\sin \theta = \frac{0.4\pi N_2\omega N_2}{\mathfrak{R}_1 10^8} G_2 \frac{\phi_2}{\phi_1} \qquad (1)$$

$$\cos \theta = \frac{\mathfrak{R}_2\phi_2}{\mathfrak{R}_1\phi_1} \qquad (2)$$

Equation 2 is the same as that in the paper. Equation 1 of the paper may be obtained by the relationship $\tan \theta = \sin \theta / \cos \theta$.

C. T. Evans: As stated in the paragraph following equation 14, the differential equations 11 to 14 are sufficient to prove the equivalence between the ring model and an actual magnet having the same pole dimensions. If one wishes to build a ring model equivalent to any specific magnet, the complete equivalence requires that B_m, ω, K, and T have the same values in the model as for the magnet. Then the following relations hold, where primes refer to the model.

$$P_s'/l'S' = P_s/lS$$
$$G_s' N'^{2} S'/l' = G_s S/l$$

Subscripts for S and l are unnecessary in view of the required invariance of K and T.

Several people have referred to the desirability of developing a criterion for an "optimum" design of a shaded pole. This optimum design would no doubt be such that, given B_m, l, and K, and curves for the reluctivity of the steel, definite values for T and G_s could be derived such that either (*a*) the ratio (minimum instantaneous force)/(watts in shading coil) is a maximum, or (*b*) for a given required minimum instantaneous force per square inch of pole area, the resulting watts in the shading coil per square inch of pole area is minimum. Criterions (*a*) and (*b*) are not necessarily the same. For reasons stated in the paper, ring models would be very helpful in any general investigation of this kind.

A Thrustor Lowering Control System for A-C Crane Hoists

E. L. SCHWARZ-KAST
ASSOCIATE AIEE

THE common interest in a-c lowering controls for crane hoists has increased steadily in the last few years. This trend is very natural because the present power plants are generating a-c power almost universally and conversion into direct voltage is costly and inconvenient.

The General Problem of Lowering Control

For those who do not work every day in this field and are probably not so aware of the problem involved, a brief description of the situation should be given. The problems of speed control for crane hoists are more involved than those for general drives. For speed control of electric drives in general we have to consider load changes ranging from zero to full load. In the case of a crane hoist, the motor load might change from zero to full load during hoisting and from +10 per cent for lowering the empty hook to −64 per cent for lowering the full load.

Another difference between general drives and hoist drives is the fact that in the case of general speed control, failure of the control merely would stop the operation, but usually nothing more would happen. In the case of a crane hoist, failure of the control might cause the abrupt dropping of the load, an extremely dangerous situation. Consequently, in the case of crane hoists the utmost safety in operation is imperative, preceding all other requirements.

Paper 47-19, recommended by the AIEE committee on industrial control devices for presentation at the AIEE winter meeting, New York, N. Y., January 27–31, 1947. Manuscript submitted November 12, 1946; made available for printing December 16, 1946.

E. L. SCHWARZ-KAST is a research electrical engineer with the Armour Research Foundation of Illinois Institute of Technology, Chicago, Ill.

The requirements of a satisfactory hoist control are shown in Figure 1 and are as follows:

1. Safety in operation. Ruggedness and simplicity of apparatus are essential.
2. To hoist all normal loads at slow, medium and high speed.
3. To lower all loads at a slow, medium and high speed.
4. To provide accurate positioning of all loads, overhauling or non-overhauling (so-called inching).
5. To avoid too high currents to reduce heating of motors and apparatus.

With the passing of time the problem of speed control for lowering loads is becoming increasingly difficult. For example, for machine shop cranes the modern machine tools and methods of machining require a greater accuracy of positioning and, on the other hand, there is a general trend toward increase of the full speed for speeding up production to the highest possible degree. The result is that the range of speed control required is increasing steadily.

The Present A-C Lowering Systems for Crane Hoists

The various systems which are at present in use for a-c lowering and which are known most commonly are

1. Oversynchronous lowering with squirrel cage and wound-rotor motors.
2. Multispeed motors, squirrel cage, wound-rotor or combined wound-rotor, squirrel-cage motors.
3. Mechanical load brake, wound-rotor motor and rotor resistors.
4. A-c commutator motor with shunt characteristic and brush shifting.
5. Dynamic braking with wound-rotor or squirrel cage motors and direct voltage applied to the stator windings.
6. Counter-torque (plugging) with wound-rotor motor in combination with oversynchronous lowering.
7. Wound-rotor motor, rotor resistances, and unbalanced voltage, using an autotransformer with multiple taps in one phase.
8. Variable unbalanced voltage. The unbalance is obtained by a saturable reactor in one motor lead. This reactor is saturated automatically in proportion to the motor speed. The rotor voltage is used as a simple and reliable speed indicating means which varies inversely proportional to the speed. The rotor voltage furnishes, through an amplifier, a d-c output inversely proportional to the speed which is used in the reactor for obtaining the necessary unbalance of the primary voltage.
9. Motor-generator set, d-c hoist motor, and variable voltage control. (Ward-Leonard system)

Table I shows the main properties of the various systems and the approximate initial cost of the electrical hoist equipment as compared with the cost of item 1, oversynchronous lowering, which is the lowest and is assumed as 100 per cent. Also, the last column of the table shows the inconvenient features of the various systems. This table shows very clearly that there is a definite demand for an a-c lowering system which is simple, safe, has low current consumption, assures reasonable speed reduction and easy inching, and is inexpensive. It is believed that

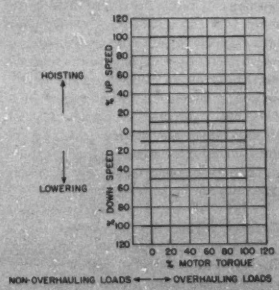

Figure 1. The ideal speed-load diagram for a crane hoist

Table I. Comparison of Common Systems of A-C Lowering

Item	A-C Lowering System	Creeping Speed 64% Negative Load % Full Speed	Current Consumption	Approx. Initial Cost	Safety in Operation	Inching	Notes
1	Oversynchronous lowering	Approx. 105%	Low	100%	Good	Fair	No speed reduction below 105% except by inching.
2	Multi-speed motor	Approx. 25%	Low	150%	Good	Good	Squirrel-cage motor characteristics. Abrupt acceleration no gradual speed increase.
3	Mechanical load brake	Approx. 25%	About 50% of rating	130%	Good	Fair	Assumed best adjustment of the load brake. Continuous wear requires permanent care and adjustment.
4	A-C commutator motor	Approx. 25%	Low	150%	Good	Good	Unconventional, custom-built motor type, maintenance of commutator and brushes, but extremely simple control by brush shifting.
5	Dynamic braking with direct voltage	Approx. 25%	Low	130–150%	Fair	Fair	For overhauling loads only. The necessary rectifier is an additional device, and as such it decreases safety in operation.
6	Counter torque	Approx. 10%	Low	125%	Good	Handicap	Light loads might be lifted. Recommended for predetermined loads.
7	Adjustable unbalance voltage	Approx. 40%	High, up to 230% of rating	130%	Good	Good	The speed reduction at full load is limited. A convenient reduction only obtainable for loads smaller than 60% of full load.
8	Variable unbalance voltage	Approx. 20% with all loads and 30% for light hoist	Line current at lowering can be limited to 125% rated	180%	Fair	Better than number 7	An ingenious system. The characteristics are satisfactory, but the addition of quite a number of apparatus capacitors, transformers, and rectifiers is not very desirable.
9	Ward-Leonard	Approx. 10% with all loads, best speed adjustment, and smooth acceleration	Over-all efficiency is low.	250%	Best	Best	Weight and space requirements of the motor-generator set. Care for commutator and brushes. Standby consumption of motor-generator set is inconvenient.

the Thrustor lowering system which will be described next has these properties to a high degree. The principles of the Thrustor Lowering control are protected to the General Electric Company, and this system has been in use since 1941.

The Thrustor Lowering System

As commonly known, wide range speed reduction can be obtained with a wound-rotor motor and resistors in the rotor circuit, provided the motor is loaded substantially and an appreciable current is flowing through the resistors. Furthermore, it is also commonly known that every crane hoist is equipped with a stop-brake for holding the load at rest at any level. This stop-brake conventionally consists of a brake drum and lined brake shoes, which are pressed by a compression spring on the drum to develop the necessary brake torque. The brake is released electrically by an electromagnetic device such as a solenoid, a torque motor, or a Thrustor. Thrustor is the trade name of an electrohydraulic device developed by the General Electric Company for activating servomechanisms of any kind and especially for brake release.

Figure 2 shows an exploded view of a Thrustor. This device consists of a cylinder in which a piston is traveling. The cylinder below the piston is filled with oil, and a motor driven impeller provides oil pressure in the cylinder to raise the plunger, thus activating the brake release. An adjustment sleeve valve is inserted in the liquid circuit for providing a time delay of the up or down stroke, whenever desired. The impeller motor is a conventional 4-pole 3-phase squirrel-cage induction motor. If the motor is connected to the line, the piston rises and releases the brake; if the motor is disconnected or the power supply should fail, the motor stops, the up-force at the plunger ceases, the piston returns by its own weight supported by the brake spring in its original position, and the brake is applied. Figure 3 shows a Thrustor-operated stop-brake.

In order to understand the operating principles of the Thrustor lowering system, one more fact has to be borne in mind. The Thrustor develops its rated thrust at full speed of the impeller motor. This is the case when the impeller motor is supplied with 3-phase alternating current of rated frequency and voltage. If this motor is supplied with a lower frequency and proportional lower voltage, its speed decreases practically with the frequency. Consequently, the liquid pressure developed by the impeller decreases approximately as the square of the speed and in turn, the thrust operating on the brake lever is reduced very rapidly with the speed. After knowing these facts the operating principle of the Thrustor lowering system can be understood readily.

This system uses a wound-rotor hoist motor for drive and uses the Thrustor-operated stop-brake for development of the temporary motor load which is necessary for the speed reductions desired. This is accomplished in the following way: The control device, drum-controller or magnetic control, connects the hoist motor to the line in the lowering direction and on the first lowering point a higher ohmic resistor is inserted in the rotor circuit to obtain reduced motor torque (about 1/4 of rated torque) and the Thrustor is not connected in parallel with the stator of the motor as usual, but across the rotor of the hoist motor. Rotor voltage and frequency are speed responsive. At synchronous speed both are zero, and at standstill both have the full rated value. Between synchronous speed and zero speed, rotor voltage and frequency vary inversely proportional to the speed.

Figure 4 shows the thrust on the Thrustor *TF*, the force on the brake shoes caused by the brake spring *BF*, and finally, the force available for brake release *BF-TF* in relation to the speed of the hoist motor. In the range *CD* where the thrust of the Thrustor exceeds the force of the brake spring, the brake is released entirely. This is the case as shown in Figure 4, from standstill up to about seven per cent of full speed. With rising speed the force on the brake shoes *BF-TF* increases gradually with the speed. At about 60-per-cent lowering speed the full force is applied on the brake shoes. At actual lowering, on the first lowering point the motor speed increases,

driven by the lowering load, until the brake torque equals the torque developed by the load plus the torque developed by the hoist motor and an equilibrium is established.

Figure 4 shows that relatively small changes of the motor speed cause a very powerful increase of the brake force *BF-TF*. Consequently, the self-adjusting creeping speed is fairly independent of the magnitude of the load.

A similar Thrustor control readily can be provided also at the first hoisting point. The secondary resistor at this point is laid out for starting the full load safely. Figure 5 shows how these self-adjusted creeping speeds on the first hoisting and the first lowering point change with the load from zero to full load. The creeping speed at hoisting changes from 25 per cent at empty hook to 10 per cent at full load, and the creeping lowering speed from 10 per cent at empty hook to 25 per cent at full load. In general this relatively small change in creeping speed is not objectionable even for cranes where a low creeping speed is imperative, as foundry or machine-shop cranes, and there might be only very few special cases where a more constant speed is absolutely necessary.

A very convenient feature of this Thrustor lowering control is that all loads, from empty hook to full load, start positively with the creeping speed on the first point in either direction, lowering and hoisting as well. This makes the so-important inching particularly simple and reliable.

The Electrical Equipment of Thrustor Lowering Control

Figure 6 shows a wiring diagram for an a-c hoist with Thrustor lowering control. All details are conventional parts, with no special custom-built apparatus necessary. The hoist motor is a standard wound-rotor, crane-duty motor. The ohmic values of the secondary resistors are comparable to the conventional resistors, increased in order to provide the small motor torque required at the first lowering position to keep the burden on the Thrustor lowering brake as low as possible. Regular resistors for 150-per-cent starting torque have approximately $0.38E/I$ ohms per phase: in the case of Thrustor lowering at least $0.5E/I$ ohms is recommended and a further reduction of the motor torque by opening one rotor lead. E is the rotor voltage between slip rings at standstill: I the rotor current per slip ring at full load.

The diagram provides for lowering only three steps, which is sufficient for satisfactory crane operation. At the first lowering point the Thrustor brake, connected to the rotor of the hoist motor, acts as a speed responsive automatic brake, and a high ohmic resistor is inserved in the rotor circuit. All loads start at this point, lowering with creeping speed 10 to 20 per cent of full speed. At the second lowering point the Thrustor brake remains rotor connected, but the rotor resistor is lessened; thus motor torque in the downward direction and lowering speed increase with all loads to 50 to 60 per cent. At the third point the Thrustor, now connected to the line, acts like a regular stop-brake; the rotor resistor is short circuited and the motor operates as an asynchronous generator, regenerating the power developed by the lowering load back into the line. In other words, this point provides an over-synchronous lowering and all loads are lowered with 100- to 105-per-cent speed.

Usually the rotor voltage is not identical with the line voltage, and an auxiliary transformer, shown in Figure 6, has to be provided to supply the proper voltage for the Thrustor motor when it is connected to the rotor of the hoist motor.

The following refinement of the Thrustor lowering control is patent protected for the Whiting Corporation, Harvey, Illinois. For hoists having a mechanical efficiency of 80 per cent or higher it can be assumed that very light loads and even the empty hook overhaul the hoist. In this case after releasing the brake all loads start in the downward direction very positively without any motor torque. This system leaves the rotor circuit entirely open on the first lowering point with no resistors in the circuit and only the Thrustor connected to the slip rings. The hoist motor acts merely as a frequency converter for supplying the speed responsive variable frequency for the Thrustor motor. The advantages are as follows: the creeping speed is lower; the burden on the Thrustor lowering

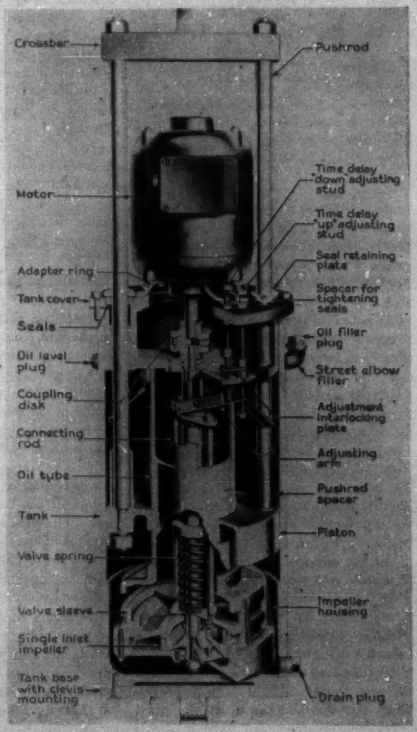

Figure 2. Exploded view of a Thrustor

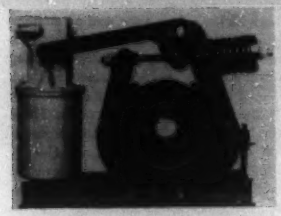

Figure 3. Thrustor-operated stop-brake

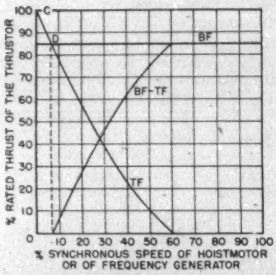

Figure 4. Thrustor lowering. Brake force versus hoist motor speed

BF—Force on brake shoes by brake spring
TF—Thrust of the Thrustor
BF-TF—Acting force on brake shoes (brake torque)

brake is lessened because there is no additional motor torque to take care of; and finally, there is no necessity for any increase of the conventional rotor resistors, because of the Thrustor lowering control.

As mentioned previously the use of the Thrustor regulating brake is not limited merely to lowering; it can be used without any extra cost or additional apparatus for hoisting as well. With the conventional method of using rotor resistors it is not possible to lift all loads with creeping speed on the first controller point, because either the acceleration on light loads is too great or heavier loads do not start at all. Thrustor control allows creeping speed for all loads. As shown in Figure 4, on the first hoisting point the motor is connected in the up-direction, and the resistor is selected so that the full load starts positively at the first point. The Thrustor at the first point is rotor-connected, thus securing a creeping speed of all loads.

Figure 6 shows the wiring diagram using a conventional drum controller. The same operation also can be accomplished readily by magnetic control and a master switch.

As mentioned previously, with this lowering system a creeping speed of approximately 20 per cent of the full speed is readily obtainable. If this range is not satisfactory and a wider speed reduction is required, this can be achieved by arranging a separate small wound-rotor induction motor as a frequency converter and using the rotor voltage of this auxiliary motor instead of that of the main motor for the Thrustor operation. If this auxiliary motor has the same number of poles as the hoist motor and the belt transmission has a ratio two to one, the frequency obtainable at the slip rings of the small motor is double that of the rotor of the main motor and the obtainable creeping speed with Thrustor lowering and full load is about ten per cent of full speed.

For obtaining good results with the Thrustor lowering there is one requirement which the Thrustor has to satisfy. Because of the hydraulic system used the Thrustor needs an appreciable time for its up or down stroke. Furthermore, some Thrustor types are equipped with means for an additional time delay. Experience shows that the operating time of the undelayed normal Thrustor is satisfactory for crane hoist operations. For Thrustor lowering any additional delay beyond the natural time is entirely undesirable and interferes with a satisfactory operation. The omission of the additional time delay also permits an appreciable simplification of the Thrustor for this special use.

The Mechanical Equipment

There are some requirements on the mechanical part of the brake which have to be satisfied in order to secure a successful operation. In the first place, for the sake of safety in operation a larger size brake is necessary. It is customary to select a normal hoist brake for a braking torque about equal to the full rated torque of the hoist motor. In the case of Thrustor lowering, a brake having a brake torque of 150 to 175 per cent of the full motor torque is recommended. However, as will be discussed later, the burden and wear the Thrustor brake is exposed to with this lowering system is unexpectedly light and not at all excessive.

As far as the mechanical part of the brake is concerned, there are some details which are also present in the design of any general purpose crane brake but which are of even more importance in case of Thrustor Lowering. For instance, when lifting the brake lever it is desirable to obtain a gradually decreasing force at the brake shoes. This means a certain proportionality between stroke and brake torque, and any toggle action in the brake linkage is, for Thrustor lowering, entirely undesirable and disturbing. Furthermore, the clearance of the brake shoes should be equalized and kept as small as possible, barely securing entire freedom for the wheel when the brake lever is in the release position. This requirement is also true for every ordinary crane stop-brake.

To secure best service of the Thrustor lowering, it is particularly important to load the Thrustor by the brake springs as near as possible to its full capacity and to select the Thrustor size adequately; only a small safety margin should be allowed. It is clear that the closer the Thrustor is loaded to its capacity, the better the operation of the lowering control.

It is of interest that at the first performances transient changes of the rotor voltage of the hoist motor were expected which might cause disturbing oscillations of the Thrustor brake during the creeping operation. To prevent these oscillations the Thrustor was not rigidly linked with the brake lever, but cushion springs were inserted to consume the oscillations. Actually, such oscillations were not noticeable and in the future these cushions probably will be omitted.

The specific pressure at the brake lining should be about 30 pounds per square inch. This pressure is a good compromise between excess wear resulting from pressure and excess brake shoe area which would reduce the rate of cooling the drum. In addition, it is advisable to arrange a few holes in the web and to insert some pins to give a better air cooling of the drum surface by air radiation and convection.

Conclusions

With every new development, especially in a field of such intense activities and remarkable achievements such as a-c lowering systems, questions have to be anticipated. Prior to the final conclusions some questions which probably may arise will be discussed.

The first logical questions are, "How badly does the Thrustor lowering affect the brake lining? What influence has this lowering system on the wear of the lining? What is the necessary care for maintenance of the brake and for keeping the proper clearance?" Tests and experience prove that the burden on the

brakes under Thrustor lowering is unexpectedly light. For lowering over greater distances or the entire height, the operator does not use the creeping speed. Rather, he will operate longer distances with over-synchronous lowering during which time the brake is entirely released and will use the creeping speed with the lowering brake where it is needed and this, in general, is only a very short portion of the total life. The difference between the burden on a normal stop-brake and a Thrustor lowering brake actually amounts to only a slightly extended braking period. Experience shows also that there is no appreciable difference in temperature rise, wear, and maintenance between a normal hoist stop-brake and a

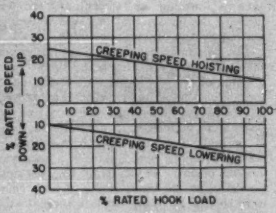

Figure 5. The self-adjusted creeping speeds obtainable with Thrustor lowering brake

properly dimensioned Thrustor lowering brake. In this regard it might be instructive to compare the situation of a Thrustor lowering brake with a mechanical load brake. With the mechanical load brake the braking torque is permanently applied during the entire lowering period, regardless of whether the load is lowered with full speed or with creeping speed, or whether the load-brake torque is needed for speed reduction or not. This results in a permanent wear and power loss. On the other hand, with Thrustor lowering the lowering brake is applied only temporarily when needed for creeping speed. This period is relatively short compared with the full lift.

Another question is, "What happens if, in the case of Thrustor lowering, the power supply fails?"

To ascertain the consequences which a failure of the power supply might have on the Thrustor lowering, a series of tests was performed. To make the investigation dependable a 10-ton hoist having a high mechanical efficiency, over 80 per cent, was selected for the test and was loaded with its rated capacity. Two series of experiments were conducted: one with the hoist at rest and attempting to operate the hoist with one line phase interrupted; in the second series one line phase has been interrupted during hoisting and lowering operations.

The results are shown.

LOAD AT REST, ONE PHASE INTERRUPTED

1. Hoisting, on creeping point—Thrustor motor didn't start and brake remained closed. No movement of the load.

Hoisting, on other points—the same.

Lowering, creeping points—the same.

Lowering, over synchronous point—the same.

ONE PHASE INTERRUPTED WHILE HOISTING OR LOWERING

Hoisting, creeping point—Movement stopped immediately.

Hoisting, other points—Movement stopped immediately.

Lowering, creeping points—Movement stopped immediately.

Lowering, over-synchronous point—This is the case of ordinary lowering and has nothing to do with Thrustor Lowering. The Thrustor motor kept on running but with reduced speed, thus applying the brake partially. The hoist motor continued lowering but with a speed far below synchronous. In this case the Thrustor brake offered an appreciably higher degree of safety than the ordinary solenoid, which might remain completely lifted, even with one phase interrupted.

A third question which might arise is, "What is the behavior of the Thrustor lowering system as far as the inching operation is concerned, a vitally important feature of every hoist control." In this regard this system is especially convenient. As mentioned previously, all loads start up or down with the creeping speed on the first controller point, which facilitates exact inching.

Now to the question of how far the Thrustor lowering satisfies the general requirements for crane hoists which have been mentioned previously. It can be said that the Thrustor lowering meets all the requirements remarkably close.

The table showing the main characteristics of the various a-c lowering systems can be extended now to item 10 for the Thrustor lowering.

Lowest speed at lowering full load 25 per cent without or 10 per cent with frequency conversion.

Lowest speed at lowering light loads 10 per cent without or 5 per cent with frequency conversion.

Lowest speed at hoisting full load 10 per cent or 5 per cent.

Lowest speed at hoisting light loads 25 per cent or 10 per cent.

Current consumption—low.

Initial cost—conveniently low, approximately 125 per cent.

Safety in operation—best.

Inching—best.

However, there are certain limitations in the use of the Thrustor lowering which have to be recognized in order to avoid disappointment. The cases in which the Thrustor lowering does not especially qualify are as follows:

Where a creeping speed in the downward direction lower than 10 or 25 per cent is essential. This might be the case with some high speed hoists.

Where the variations of creeping speed at different loads are objectionable.

Where more speed steps between creeping and full speed are important.

Where regular inspection and maintenance

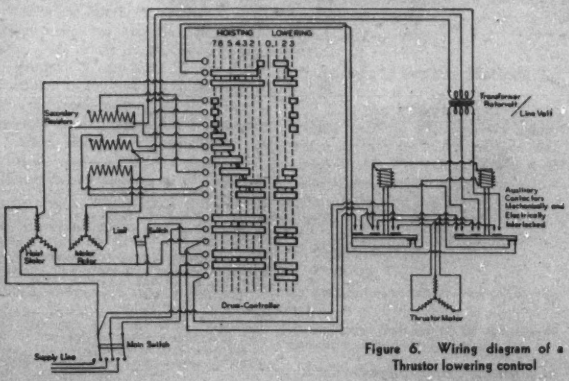

Figure 6. Wiring diagram of a Thrustor lowering control

of the brakes at reasonable intervals cannot be expected.

In general Thrustor lowering is very satisfactory because of its reasonable speed range, simplicity, safety in operation, and low cost.

Finally, one occasional advantage of the Thrustor lowering has to be mentioned. Existing crane hoists can be equipped very readily with this system without difficulties and without great expense.

Discussion

G. W. Heumann (General Electric Company, Schenectady, N. Y.): The author has described for the first time in this country a system of a-c crane hoist control which has found a considerable number of practical applications both here and abroad. To the best of our knowledge, the first commercial installation of a Thrustor load brake was made on a harbor crane near Berlin, Germany in 1935. Since 1941, several hundred boom-type cranes in shipyards and a number of cranes of the traveling type equipped with Thrustor load brakes have been built in this country.

Thrustor load brake control should be considered as a means to decelerate a load from full lowering speed to landing speed. The slow speed obtainable with the load brake should not be used to lower loads over a considerable distance on high-lift hoists, as this would impose an excessive duty on the brake. A certain amount of caution must be exercised by the operator when using the creeping speed point.

When considering the Thrustor load brake system, it must be borne in mind that adjustment of the motor secondary resistor has very little effect on the lowering speed with an overhauling load. The amount of secondary resistance used has a pronounced effect on the kick-off torque which the motor is able to develop, but the effect on the lowering speed under normal load is of no practical consequence.

All energy absorbed by the brake must be dissipated as heat by the brake wheel, and its heat-dissipating ability is the limiting factor determining the selection of brake size for a given application. The author states in his paper that a Thrustor load brake should have a rating of 150 to 175 per cent of motor full-load torque. It would be interesting to know on what grounds this conclusion has been reached. It has been our experience that Thrustor load brakes should be selected for a rating of 200-per cent motor full-load torque.

E. L. Schwarz-Kast: The Thrustor lowering system as pointed out by G. W. Heumann, is not new and has been used in Europe for several years. This paper was written as the result of an installation made in this country in 1939. It is believed that this was the first of its kind in this country.

Heumann's remark, that adjustment of the secondary resistor has very little effect on the lowering creeping speed with an overhauling load, is correct, but it is likewise true, and this is the more important fact which must be kept definitely in mind too, that the use of proper secondary resistor is of great influence on the burden and wear of the Thrustor brake. At lowering overhauling loads with creeping speed the brake has to take over the torque of the load and, in addition, to develop the necessary load for the motor to obtain creeping speed with the secondary resistor in the circuit. The correct rotor resistor for the minimum possible burden and wear on the brake is as follows:

For lowering—The motor must safely start the empty hook in the lowering direction. If the weight of the empty hook is heavy enough to overhaul the hoist, the rotor circuit can remain entirely open (rotor resistor infinite).

For hoisting—The motor must safely start the full load in the upward direction.

It is clear that a too low secondary resistance at lowering with creeping speed will increase the burden and the heat to be dissipated by the brake appreciably.

The recommendation made in the paper, that a Thrustor lowering brake should have a rating of 150 to 175 per cent of full motor torque, was based on actual tests made with a 10-ton hoist. Two series of 200 consecutive stops were performed in a row: one series of normal stops and the others with preceding creeping speed during a generous amount of time. It was found that the temperatures at the brake lining in both cases were nearly the same with a normal stop brake rated 100 per cent and a Thrustor lowering brake rated 150 to 175 per cent of full motor torque. The difference in brake rating obtained by the author and that obtained by Heumann may be because of differences in the secondary resistors used.

Dynamic Braking by Self-Excitation of Squirrel-Cage Motor

A. SRINIVASAN
NONMEMBER AIEE

M. A. THOMAS
MEMBER AIEE

Synopsis: This paper describes a method for calculating the speed–torque curve of a squirrel-cage induction motor when static capacitors are used to produce dynamic braking. The method is simple yet sufficiently accurate for the purpose of selecting equipment for any normal application. The advantages and disadvantages of this method of braking control are compared with those of other methods in use for squirrel-cage motors.

THE USE of static capacitors to produce self-excitation of an induction machine is well known. A number of engineers have realized that this method could be used for dynamic braking, but little application of the principle has been made. If external resistors are connected in parallel with the capacitors, a very great increase in the braking torque can be produced. There are several advantages to be gained by this scheme of braking. A large part of the kinetic energy of the rotating system is dissipated in the external resistors. Braking torque is independent of any power supply. Part or all of the capacitors required may be used during normal motor operation to improve the power factor. The maintenance of mechanical brakes is reduced to a minimum and complicated switching equipment is eliminated. A major disadvantage is the rapid decrease of braking torque as the speed of the motor decreases. In spite of this fact, there are numerous applications of motor control where a careful study of capacitor braking would seem desirable.

Several papers have appeared in technical publications[1,6] in which mention is made of the capacitor braking scheme. So far as the authors are aware, there is no information available as to how the braking torque of a given motor, capacitor and resistor combination may be predetermined. An attempt has been made in this paper to devise a method for calculating the torque–speed characteristic with a minimum of experimental data concerning the motor. A simple graphical scheme is proposed to determine the operating conditions at any selected speed and an approximate value of braking torque is calculated easily. The results of experimental tests conducted on a standard squirrel-cage motor are shown to agree reasonably well with the theoretical calculations.

Comparison of Braking Methods

At least four methods for applying a braking torque to a squirrel-cage induction motor and its load have been discussed in technical articles dealing with the problem of rapidly bringing the motor and its driven load to a stop.

These methods are

1. Mechanical brake.
2. Plugging.
3. Application of direct current to the stator.
4. Induction generator action by means of capacitive excitation.

A brief description and comparison of these schemes will be desirable to show the possible field of application of the method to be described in some detail in this paper.

The mechanical brake, applied by a spring and released by a solenoid operating in parallel with one phase of the motor, provides the simplest type of braking control. It has the advantage that all of the energy absorbed by the brake is dissipated external to the motor. The motor and load are held in position at standstill and this feature makes the mechanical brake an indispensable part of any braking scheme which must provide holding torque at zero or very low speeds. Applications requiring frequent stopping of loads having considerable kinetic energy are likely to result in excessive wear and maintenance cost on a mechanical braking system. Such applications warrant a study of the several electric systems to determine if the advantage to be gained will justify the additional cost and circuit complication of the electrical methods.

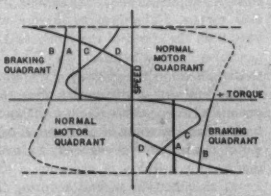

Figure 1. Typical speed–torque characteristics for several types of braking control

A—Mechanical brake
B—Plugging
C—Direct current applied to stator
D—Capacitive braking

Plugging of a 3-phase squirrel-cage motor is accomplished by simply interchanging any two of the supply lines. The surge of current in stator and rotor is somewhat more severe than at starting unless a reduced voltage is provided. For loads having only a small amount of friction torque, the energy which is dissi-

Paper 47-20, recommended by the AIEE committee on industrial control devices for presentation at the AIEE winter meeting, New York, N. Y., January 27-31, 1947. Manuscript submitted November 12, 1946; made available for printing December 16, 1946.

A. SRINIVASAN is with the electrical engineering department, Illinois Institute of Technology, Chicago, Ill.; M. A. THOMAS is with New Mexico State College, State College, N. Mex.

The authors wish to acknowledge with thanks the help of Doctor L. T. Rader, head of the department of electrical engineering, Illinois Institute of Technology, for the suggestion of the problem and for providing all facilities for conducting the experiments in the laboratory.

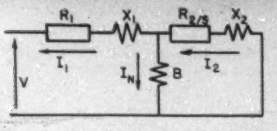

Figure 2. Equivalent circuit of an induction motor

pated as heat in the rotor in braking the load to standstill is nearly three times[3] the kinetic energy of the motor and load. This extreme heating of the rotor would seem to limit the application of plugging of squirrel-cage motors to cases where either low inertia or infrequent stops would make it practical. An additional complication is the necessity of an automatic switch of some kind to remove power at the instant the motor stops, otherwise the motor and load will be brought quickly to full speed in the opposite direction. The magnitude of the braking torque can be controlled only by the application of an adjustable voltage during the braking period.

Application of direct current to one phase of the stator of a squirrel-cage motor will provide a braking torque which can be adjusted quite easily. Heating energy equal to the kinetic energy of the motor and load will be produced in the rotor for applications having a small friction torque. The braking torque will vary with the speed of the motor and in general will follow a characteristic similar to that shown in the diagram of Figure 1.

The difficulty of dissipating any great amount of energy either in a mechanical brake or in the rotor of the squirrel-cage motor has led several engineers to investigate the possibility of operating a motor as an induction generator during the braking procedure and thereby make possible the transfer of power from the machine to an external resistor. Considerable study has been made of the operation of an induction machine with self-excitation supplied by static capacitors.[4] Most of the published information, however, deals with operation at a constant frequency and little has been done on the varying frequency problem of dynamic braking. The self-excitation is known to decrease rapidly with decrease in speed of the motor. However, if braking can be accomplished even to one-half speed, three-fourths of the kinetic energy of the rotating parts will have been dissipated. The application of the method of braking has been handicapped by the fact that no very simple or reliable method has been available for predetermining the speed–torque characteristic which will result from a given motor, capacitor, and resistor combination. The purpose of this paper is to describe a method by which this speed–torque characteristic can be calculated with fair accuracy and with a minimum of test data concerning the motor. Typical speed–torque characteristics for the four methods of braking are shown in Figure 1. A determination of the speed–time characteristic for any given load requires the additional knowledge of only the WR^2 of the load and motor and the load torque. A general method for solution of this problem is given in several standard textbooks[2] dealing with motor applications.

Conventions and Assumptions

The conventional equivalent circuit of the induction motor as shown in Figure 2 will be used as the basis of the analysis. The copper loss in the rotor circuit, however, will be neglected and the current-voltage characteristic of the exciting susceptance B will not be assumed a constant but must vary in accordance with the no-load test data for the motor. The particular volt-ampere characteristic for any motor will depend upon the saturation of the iron of that machine. The wave form of the voltage is nearly sinusoidal[2] and little error is introduced by such an assumption. The frequency is assumed to be that determined by speed alone without regard to slip. This will introduce considerable error at low voltages where the generator action is disappearing, but does permit a simple graphical solution for the operating conditions. A more exact method based on a cut and try solution is available[4] if thought necessary. The voltage drop in the primary impedance caused by the in-phase component of the current through the load resistor is neglected. The very considerable tolerance in the capacitance of capacitor units makes a simple solution sufficiently accurate for the purpose of specifying the capacitors for a given application.

These assumptions reduce the equivalent circuit to the approximate form shown in Figure 3. The symbols have the following meaning:

R_1 = stator resistance in ohms per phase to neutral
X_1 = stator leakage reactance in ohms per phase to neutral, at normal frequency
B = exciting susceptance
C = equivalent capacitance in farads per phase to neutral
R = equivalent resistance of load resistor in ohms per phase to neutral

The actual values of C and R which are connected line to line (and not line to neutral) are respectively one-third and three times their equivalent values as shown in this circuit.

V = terminal voltage to neutral or by assumption of balanced sinusoidal condition is line voltage divided by $\sqrt{3}$
E = air gap induced voltage to neutral
I_1 = primary current per line assumed positive as shown by the arrow

The curve of Figure 4 shows the volt-ampere characteristic of the motor. Data for this curve were obtained by operating the motor at normal speed and without load. A 5-horsepower 850-rpm 220-volt 3-phase 60-cycle squirrel-cage motor was used in the sample calculations and the same motor was used for the experimental checks.

Analysis of the Problem

Consider first the approximate circuit of Figure 3 without the braking resistor. The current I_1 will lead the voltage V by 90 degrees because it is merely the current taken by the capacitor C. The current taken by the motor when running idle with voltage V applied will be near this same current. The voltage E may be expressed as

$$E = V + I_1(R_1 + jX_1)$$

as shown in the vector diagram of Figure 5.

$$E = V - I_1X_1$$

because the component I_1R_1 is at right angles to V and contributes little to the magnitude of E.

In general the air gap induced voltage is a function of flux and speed.

$$E = f(\phi, N)$$

where ϕ and N are flux and speed respectively. Then

$$\phi = g(E/N)$$

The no-load current I_n depends on the flux and hence

$$I_n = h(E/N)$$

Because

$$V = E + I_1X_1 \text{ (numerical addition)}$$

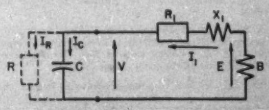

Figure 3. Approximate equivalent circuits for the determination of operating conditions

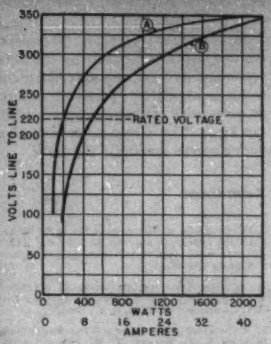

Figure 4. No-load characteristics of induction motor

A—Curve connecting the total no-load watts and line-to-line volts

B—Curve connecting the line current and the line-to-line volts

then we may say that

$$I_n = F(V/N)$$

Either air gap voltage or terminal voltage from test data may be plotted against no-load amperes to represent the given relation. In Figure 6 is shown the curve plotted from data taken on the 5-horsepower motor.

Data taken with capacitive excitation at various speeds checked very accurately with those taken from the usual no-load motor test. The current through the capacitor is

$$I_c = V2\pi fC$$

But

$$f = \frac{P}{120} N(1-S)$$

In the analysis, if slip S is neglected,

$$I_c = \frac{V}{N} \frac{2\pi P N^2 C}{120}$$

where P = number of poles for a given value of speed N and capacitor C this is an equation of a straight line and may be drawn on the plot of Figure 6. The intersection of the curve and straight line will give the no-load operating condition of current and voltage for this speed. Several lines with different slopes representing different speeds or capacitances may be drawn. The slope of the line for a fixed capacitance is seen to vary with the square of the speed.

The power absorbed by the machine from the kinetic energy now may be calculated as the sum of the following three parts:

1. The power to the resistor R is

$$P_r = 3V^2/R.$$

2. The power to R_1 is

$$P_{r1} = 3I_1^2R_1.$$

3. The friction, windage, and core loss P_e read from the test curve obtained at the same time as the no-load saturation curve and shown on Figure 4.

$$P_{\text{Total}} = P_r + P_{r1} + P_e$$

The retarding torque then is obtained from the usual equation

$$T = \frac{7.04 \times P_{\text{Total}}}{N} \text{ pound-feet}$$

The deceleration time is a function of the WR^2 of the motor and driven machines and is also dependent on any friction load which may be present.

A Typical Example

The no-load characteristic of a 5-horsepower 8-pole 60-cycle 220-volt 3-phase squirrel-cage induction motor as obtained from tests is given in Figure 4. The resistance per phase of this motor is 0.375 ohms at 65 degrees centigrade. A calculation of the torque developed with a capacitance of 200 microfarads and a resistance of 120 ohms per phase connected in delta across the lines will be made. The equivalent C and R in the line to neutral circuit of Figure 3 are 600 microfarads and 40 ohms respectively. The current in the capacitor is given by

$$I_c = \frac{V}{N} \times \frac{2\pi P N^2 C}{120}$$

$$= \frac{V}{N} \times N^2 \left(\frac{2\pi \times 8 \times 600 \times 10^{-6}}{120} \right)$$

For $N = 900$ rpm, this reduces to

$$I_c = 203(V/N)$$

This straight line then is plotted in Figure 6 and intersects the curve at $V/N = 0.230$ and $Ic = 46.5$. The voltage to neutral then is $V = 0.230 \times 900 = 206$ volts, or 350 volts line to line. The several power components are

$$P_r = 3 \times \frac{206^2}{40} = 3{,}190 \text{ watts}$$

$$P_{r1} = 3 \times 46.5^2 \times 0.375 = 2{,}430 \text{ watts}$$

From Figure 4, for a line-to-line voltage of 350,

$$P_e = 2{,}200 \text{ watts}$$

$$P_{\text{Total}} = P_r + P_{r1} + P_e = 7{,}820 \text{ watts}$$

The retarding torque

$$T = \frac{7.04 \times 7{,}820}{900} = 61.2 \text{ pound-feet}$$

In a similar way, the torques for speeds of 800, 700, 600 rpm are obtained. The speed at which braking action ceases can be determined by drawing the tangent to the curve in Figure 6. From the slope of the line this speed was found to be 465 rpm. This is the critical speed for the capacitance chosen. The values of torque, voltage, and current for the different speeds are plotted in Figure 7.

An experimental check was made by driving the motor at the different speeds by means of a d-c dynamometer. At speed above the critical speed, the machine rapidly built up voltage when connected to the capacitor-resistor combination. Values of torque, voltage, and current were obtained for each speed. The experimental values are shown by small crosses on the plot of Figure 7; as can be seen, the agreement is satisfactory in most cases.

Solution for Speed–Time Relation

The net friction or overhauling torque of the load as a function of speed and the total WR^2 of the rotating system must be known. Then with the braking torque obtained the net retarding torque T_r will be

$$T_r = T - T_L$$

where T_L is the torque produced at the shaft of the motor by the driven machine. T_r will be represented by a curve and in general will be a function of speed alone.

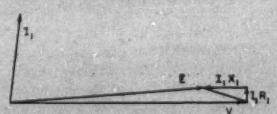

Figure 5. Vector diagram of induction machine at no-load

The usual equation relating T_r and time is

$$(\text{Average})\, T_r = \frac{WR^2 N}{307.8(t)}$$

where N is the change in speed occurring in t seconds. In better form

$$T_r = \frac{WR^2}{307.8} \frac{dN}{dt}$$

expresses the torque as a function of the rate of change of speed.

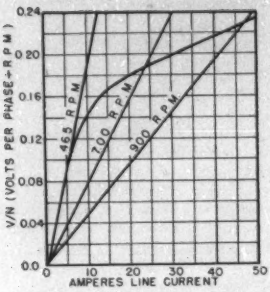

Figure 6. Graphical construction for operating conditions at various speeds

Solving the foregoing equation for time t,

$$t = \frac{WR^2}{307.8} \int_{N_1}^{N} \frac{1}{T_r}\, dN$$

As outlined in reference 2, the integration can be made by a graphic tabular process to obtain the time t for speed to change from N_1 to any other value N.

Conclusions

The capacitor braking scheme has many desirable features for dynamic braking of squirrel-cage induction motors. Although the braking action does not persist till the motor stops, it does dissipate the greater part of the kinetic energy of the rotating system. The analysis proposed in this paper will permit satisfactory prediction of the speed–torque characteristic of any proposed motor and capacitor combination. From the test results it appears that capacitors having a kilovolt-ampere rating of about three times the exciting kilovolt-amperes of the motor will produce an initial retarding torque of double the full load torque. The current and the voltage developed by self-excitation are considerably above the rated values for the motor. The speed, however, is reduced rapidly by this large torque and no damage should result to the motor or associated equipment. A part, or perhaps all of the capacitors needed, can be used for power factor correction during normal running of the motor.

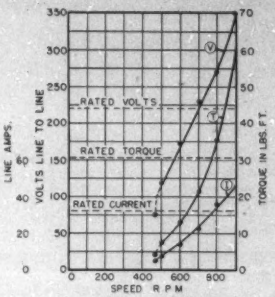

Figure 7. Predetermined characteristics and experimental verification

Firm lines indicate the calculated characteristics
Dotted lines indicate the region of instability

⊗—Test results *T*—Curve of torque
V—Curve of line volts *I*—Line current

References

1. Comparison of Methods of Stopping Squirrel-Cage Induction Motors, **W. I. Bendz.** AIEE Transactions, volume 57, 1938, September section, pages 499–505.

2. Fundamentals of Alternating Current Machines (book). **A. Pen Tung Sah.** McGraw-Hill Book Company, New York, N. Y., 1946.

3. Capacitive Excitation for Induction Generators, **E. D. Bassett, F. M. Potter.** AIEE Transactions, volume 54, 1935, May section, pages 540–5.

4. Self-Excitation of Induction Motors, **C. F. Wagner.** AIEE Transactions, volume 58, 1939, February section, pages 47–51.

5. D-C Braking of Induction Motors, **F. E. Harrell, W. R. Hough.** AIEE Transactions, volume 54, 1935, May section, pages 488–93.

6. Braking of Three-Phase Induction Motor With Static Condensers, **M. Ohtomi.** *Electro-Technical Journal*, Institute of Electrical Engineers (Japan), volume 4, February 1940, pages 29–32.

7. Dynamic Braking, **T. Millar.** *Electrical Review* (London, England), volume 133, December 31, 1943, pages 887–8.

8. Electric Motors in Industry (book), **D. R. Shoults, C. J. Rye.** John Wiley and Sons, Inc., New York, N. Y., 1942. Page 87.

9. Electric Braking Methods—Reversal of Power by Plugging, **E. H. Hornbarger.** *Product Engineering* (New York, N. Y.), volume 15, July 1944, pages 449–51.

10. Dynamic Braking Methods for Stopping Electric Motors, **E. H. Hornbarger.** *Product Engineering* (New York, N. Y.), volume 15, August 1944, pages 524–8.

No Discussion

Dynamic Braking of a Single D-C Series Motor

JOHN D. LEITCH
MEMBER AIEE

Synopsis: Various methods employed in obtaining dynamic braking with a single d-c series motor are discussed. Emphasis is placed on the control of the dynamic braking contactors where braking is required on power failure irrespective of direction of rotation of the motor. The use of polarized spring-closing contactors offers a simple and reliable solution when ruggedness of the equipment is important. Methods of obtaining graduated dynamic braking automatically also are considered.

THE d-c series motor is used widely in steel mills particularly on such auxiliaries as roller tables, blooming mill screwdowns, manipulators and side guards, and on overhead traveling cranes. Many drives require automatic stopping in the event of power failure or the tripping of the overload relay. Such stopping may be obtained by the "setting" of a magnet-operated friction brake, by electric braking within the motor itself, or in many cases, by a combination of both. When electric or dynamic breaking is obtained automatically on power failure, it is referred to as "emergency dynamic braking" to distinguish it from "service dynamic braking" where the necessary switching is controlled by the operator.

Dynamic Braking in One Direction Only

It is a simple matter to provide dynamic braking in only one direction with a single series motor. Figure 1 shows the power circuits of a series motor and a typical reversing controller. Two pairs of reversing contactors, *F* and 1*F* and *R* and 1*R*, a negative line contactor *M*, and an accelerating resistance constitute the essential parts of the controller (the acceleration contactors are omitted from the diagram). Two spring-closing contactors *FB*1 and *FB*2 are shown with their contacts located between the field and armature terminals and including within the loop-circuit so formed, a suitable dynamic braking resistor. On power failure the reversers and the negative line contactor open while the spring closers close.

If the motor is traveling forward (*F* contactors closed) at the instant of power interruption, the counter electromotive force will be in direction 2–1 and current will flow from the armature at 1 through the field in direction 3–4, through the dynamic braking resistor, back to the armature at 2. Thus the current is reversed in the armature and maintained in the same direction in the field, a sufficient condition for developing a braking torque. It can be seen easily that if the motor is traveling in the reverse direction at the instant of power failure, this circuit does not provide dynamic braking as the current is reversed in both the field and the armature.

Dynamic Braking in Both Directions

Obviously a second pair of spring-closing contactors is required to provide dynamic braking in both directions. Figure 2 shows the addition of these two contactors, *RB*1 and *RB*2.

It is necessary that only one pair of spring-closing contactors close on power failure, the *FB*1 and *FB*2 pair when the motion is in the forward direction and the *RB*1 and *RB*2 pair when the motion is in the reverse direction. Various schemes of control have been employed to accomplish this result, the most common being some form of a mechanical latching-out relay which holds out the appropriate pair of spring closers. A typical arrangement of a latching-out relay with four spring closers is shown schematically in Figure 3.

The four spring closers *FB*1 and *FB*2 and *RB*1 and *RB*2 are shown with their contacts open (armatures closed). Each pair is shown with a tie rod which ties the armatures together. The latching-out relay has two coils *RF* and *RR* and a T-shaped armature pivoted at *A*. When the motor is rotating in the forward direction, the coil *RF* is energized and the T-shaped armature engages the tie rod of the contactors *RB*1 and *RB*2 through the hole *C* in the armature. Thus, in the event of power failure while the motor is rotating in the forward direction, *FB*1 and *FB*2 would be allowed to close their contacts while *RB*1 and *RB*2 would not.

It is apparent that some additional control means must be provided which will assure the energization of the appropriate coil *RF* or *RR* of the latching-out relay according to the direction of rotation of the motor. The simplest means is a directional switch mechanically connected to the motor shaft. Figure 4 shows a portion of the control circuit with a directional switch and a latching-out relay.

This method has been used extensively and is free from trouble so long as the directional switch and the latching-out relay are kept in good order. There are some objections to the use of a directional switch from a maintenance point of view, and the latching-out relay is not without mechanical difficulties.

It might be thought at first glance that the directional switch could be elimi-

Paper 47-21, recommended by the AIEE committee on industrial control devices for presentation at the AIEE winter meeting, New York, N. Y., January 27–31, 1947. Manuscript submitted November 6, 1946; made available for printing December 3, 1946.

JOHN D. LEITCH is with The Electric Controller and Manufacturing Company, Cleveland, Ohio.

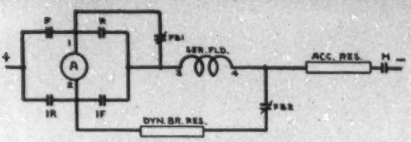

Figure 1. Dynamic braking in one direction

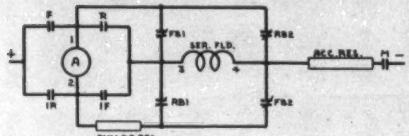

Figure 2. Dynamic braking in two directions

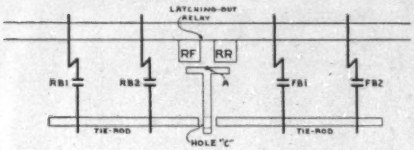

Figure 3. Schematic diagram of latching-out relay

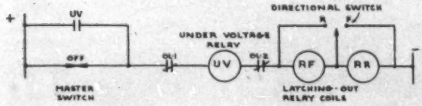

Figure 4. Directional switch used with latching-out relay

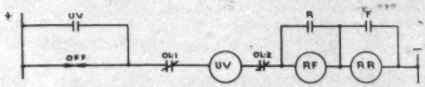

Figure 5. Auxiliary contacts on reversers used with latching-out relay

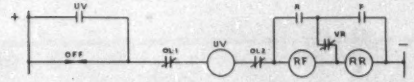

Figure 6. Voltage relay and auxiliary contacts on reversers used with latching-out relay

nated by using auxiliary contacts on the reversers as in the circuit shown in Figure 5. As long as the master switch position is in agreement with the direction of rotation of the motor, the proper coil *RF* or *RR* will be energized. But should the operator "plug" the motor just before power failure, no dynamic braking would result because of closure of the wrong pair of spring closers. In other words, it is essential that the latching-out relay be controlled by the direction of rotation of the motor irrespective of the position of the master switch.

A voltage relay *VR*, having its coil connected across the motor armature, may have its normally closed contacts added to the circuit of Figure 5 as shown in Figure 6. After *VR* has picked up at a low motor speed, there will be no change in the position of the armature of the latching-our relay as long as the motor continues to travel in the same direction even though it is plugged. There is one disadvantage however in that during "drifting" with the master on the "off" point the *VR* relay will open to close its contacts. If the operator then should plug the motor, the latching-out relay would be reversed and should power fail under these conditions, no dynamic braking would be obtained. It is therefore necessary to provide a "teaser field" connection during drifting. This is done by connecting a resistance in series with a contactor between the positive line and the field on Figure 2. This contactor must be energized on the "off" point of the master along with the *M* contactor to provide a current through the field during drifting. This prevents relay *VR* from dropping out during drifting and the difficulty regarding power failure after or during plugging does not arise. The use of a voltage relay in conjunction with the electric interlocks on the reversers suggests the use of a polarized relay, with its coil connected across the armature. The contacts of the polarized relay can be considered identical to those provided by the directional switch shown in Figure 4. Sensitive polarized relays are available which will pick up at a low voltage and hold closed to a very low voltage. Such a relay requires an additional relay to insert a protective resistor in its coil circuit against overheating as the voltage across the motor armature increases with speed. A teaser field contactor and resistor are not necessary with the polarized relay because of its low drop-out voltage.

Polarized Spring Closers

A polarized relay used in conjunction with a latching-out relay is very satisfactory from a circuit point of view, but available polarized relays are far too delicate for use on heavy equipment such as that encountered in a steel mill. The method still has the disadvantage inherent in a mechanical device such as the latching-out relay. If the spring-closing contactors themselves could be polarized, the need for the latching-out relay would disappear and the control would be entirely electrical.

Referring to the circuit in Figure 7, there are four spring closers, *FB*1 and *FB*2, *RB*1 and *RB*2, as shown in Figure 2. One pair only must close its contacts to provide dynamic braking in one direction, the other pair only if the motor is rotating in the reverse direction. Each of the four spring closers has two identical coils referred to as the operating and polarizing coils. The operating coils of all four contactors are connected in series with each other and with a resistor *C* across the control voltage, while the four polarizing coils are connected in parallel and the group connected in series with a resistor *B* across the motor armature.

The system of connecting the two groups of coils is that, for the forward direction of motion, the polarizing coils of the *FB* pair of contactors will be in opposition to the operating coils while both coils on each of the *RB* contactors will be connected additively. Thus, on power failure, with the motor rotating in the forward direction, the *FB* contactors will drop out to close their contacts while the *RB* contactors will be held open by the polarizing coils. In the opposite direc-

tion of motion the *RB* contactors will close their contacts while the contacts of the *FB* pair will remain open.

The spring-closing contactors are somewhat special in that they have a magnetic circuit of low reluctance, and consequently very low drop-out ampere-turns. The coils are good for about 30 volts continuously and must be protected by resistors, hence the use of resistor *C* in the operating coil circuit and the resistor *B* in the polarizing coil circuit. Figure 7 shows two voltage relays *VR*1 and *VR*2 and a time-delay relay *TD* for inserting the protective resistors.

With the master on the "off" point, the *TD* relay is energized through the normally closed auxiliary contacts on *FB*1 and *RB*1. The normally open contacts on *TD* close to short-circuit the resistor *C* permitting the operating coils to open the contacts of all four spring closers. Relay *TD* is de-energized and after a short time delay opens its contacts to insert resistor *C*. The contactors remain closed magnetically with resistor *C* in the circuit. Thus on the "off" point the *UV* relay is closed, the contacts of the four spring closers are open, and the time-delay relay is de-energized.

When the master is moved to any running point, the motor accelerates; relay *VR*2 is the first to pick up inserting protective resistor *B* in series with the polarizing coils of the spring closers. Resistor *B* not only protects the polarizing coils thermally, but also limits the ampere-turns to a value somewhat below that provided by the operating coils. Otherwise one pair of spring closers (that with the coils in opposition) would drop out when the armature voltage increased sufficiently. Resistor *B* will take care of a counter voltage as high as 200 volts but during plugging when the voltage rises above this value, some additional precaution will be necessary. This will be discussed later when a complete controller is described.

Since relay *VR*2 must pick up at a low voltage, it requires an intermittent duty coil. This coil is protected by a second voltage relay *VR*1 which picks up at a somewhat higher voltage to insert resistor *A* in the *VR*2 coil circuit.

On power failure with the motor running in either direction, all contactors drop out magnetically except the appropriate pair of spring closers whose contacts are held open by the polarizing coils. During the short interval from the instant power fails until the dynamic braking circuit is established, this pair of polarizing coils is energized by the low counter voltage obtained from the residual magnetism in the motor field to produce a flux in the contactors in the same direction as their residual flux. The closing of one pair of spring closers removes the polarizing coils from the circuit by the opening of one of its own interlocks. This increases the voltage applied to the remaining pair of polarizing coils since the voltage drop across resistor *B* is reduced. As the motor slows down, relay *VR*2 drops out first (resistor *A* is in series with the coil of *VR*2 as *VR*1 does not open until a much lower voltage is reached). Opening of *VR*2 by-passes resistor *B*, thereby again increasing the voltage to the polarizing coils of the two remaining spring

Figure 8. Graduated dynamic braking, shunt coil spring closer

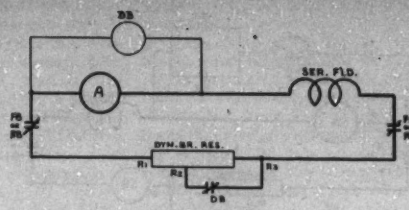

Figure 9. Graduated dynamic braking, spring closer and voltage relay

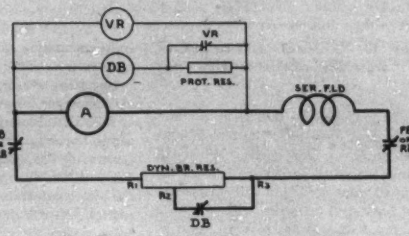

Figure 7. Dynamic braking in both directions with polarized spring closers

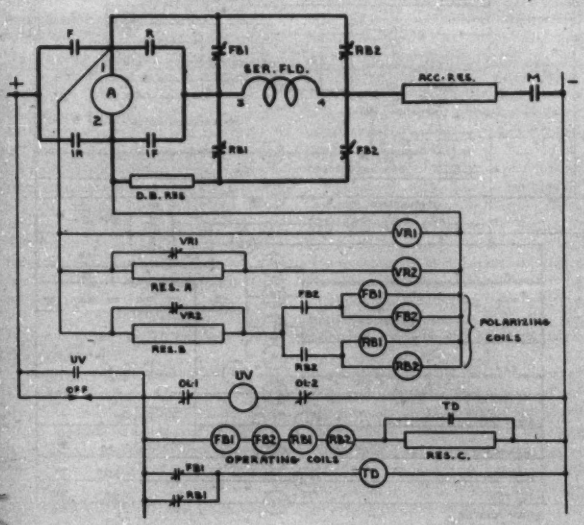

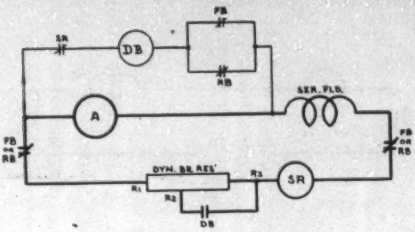

Figure 10. Graduated dynamic braking, series relay and shunt contactor

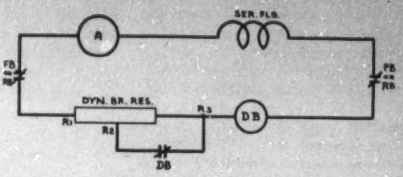

Figure 11. Graduated dynamic braking, series coil spring closer

closers and assuring that their contacts will be held open until the motor slows down to a very low speed. When the voltage across the armature reaches the drop-out value of $VR1$, it will open to bypass resistor A in series with the $VR2$ coil, but $VR2$ will not pick up again at this voltage.

Obviously a teaser field contactor and resistor should be added to Figure 7 to assure a voltage across the polarizing coils and the protective relays during drifting with the master on the "off" point.

Graduated Dynamic Braking

For a given series motor the dynamic braking torque is determined by the speed of the motor at the instant of power failure and by the resistance of the dynamic braking circuit. For reasons of commutation there is a lower limit to the value of resistance that may be used, the choice depending on the maximum anticipated speed. The dynamic braking torque falls off rapidly with motor speed, and if quick positive stopping is desired, it is necessary to short-circuit some of the dynamic braking resistor as the motor slows down.

Figures 8 to 11 inclusive show a variety of methods that have been employed to obtain graduated dynamic braking. Figure 8 shows the use of a spring-closing contactor DB with its coil connected across the motor armature and its normally closed contacts across a portion $R2$-$R3$ of the dynamic braking resistor. Such a contactor can be designed with a drop-out voltage of about 50 volts. Thus when the armature voltage falls to this value during deceleration, the contacts will close to short-circuit resistor section $R2$-$R3$ and increase the dynamic braking torque. Should power fail before the voltage across the armature reaches the pickup value of DB there would be no harm in braking with the lower value of resistance $R1$-$R2$.

On actual test, contactor DB drops out at the instant power fails because of loss of field, but picks up again as the voltage across the armature builds up after the closure of the spring-closing contactors FB or RB. This momentary closure of DB places a definite limit on the value of resistor $R1$-$R2$ from a commutation point of view.

As the motor slows down and DB closes its contacts, the voltage across the armature rises and DB may open and close its contacts two or three times during the interval in which the motor is being brought to rest.

Figure 12. Plugging-reversing controller for single series motor with service and emergency graduated dynamic braking

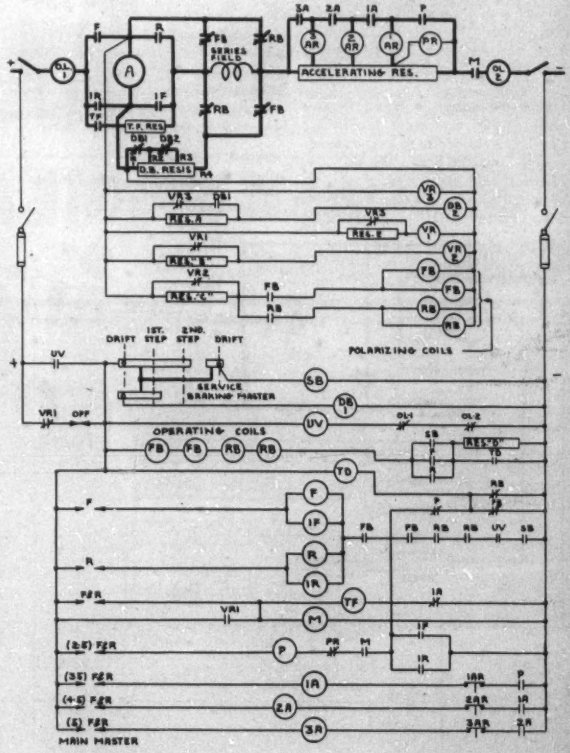

For maximum dynamic braking torque at low speed, it is desirable that resistor *R1-R2* be as low in value as possible. It is therefore desirable that the *DB* contactor remain open during the short interval between loss of power and building up of dynamic braking current. This can be accomplished by using a low voltage coil on *DB* and protecting it with a resistor, at the same time making its magnetic circuit of low reluctance so that its drop-out voltage is but a fraction of a volt. This requires a voltage relay *VR* to insert the protective resistor as shown in Figure 9.

The pickup voltage of contactor *DB* must be below that of relay *VR* so that *DB* will open its contacts before *VR* inserts the protective resistor in series with the *VB* coil. When *VR* picks up, *DB* must continue to holds its contacts open after the protective resistor is inserted. This means that the drop-out voltage of *DB* with protective resistor inserted must be below the pickup voltage of *VR*. With the pickup voltage of *VR* about 70 volts and the drop-out voltage of *DB* (with protective resistor inserted) about 50 volts, this condition is met.

On power failure, the voltage across the armature drops for an instant, *VR* will drop out quickly to by-pass the *DB* protective resistor permitting *DB* to hold its contacts open down to a fraction of a volt. Because of the sluggishness of *DB* in opening magnetically under these conditions, it does not close its contacts during the short interval of low voltage. This permits a lower value of *R1-R2*.

The drop-out voltage of *DB* with protective resistor is about 50 volts. Hence as the motor decelerates to a speed corresponding to this voltage, *DB* drops out to close its contacts. The pickup of *DB* with protective resistor is of the order of 200 volts or more. Hence it will not pick up again as the voltage across the armature increases with increase in dynamic braking current. When the voltage across the armature falls still lower, *VR* relay will drop out to by-pass the *DB* protective resistor. By choosing the drop-out voltage of *VR* below the pickup voltage of *DB* without protective resistor, contactor *DB* will not open its contacts again. Thus the flutter of contactor *DB* during deceleration is eliminated.

It is not intended to present all the possible methods of obtaining graduated dynamic braking automatically. Two other methods are however of interest. The first which has been used for a number of years, employs a series relay and a normally open shunt contactor with its coil connected across the armature as shown in Figure 10. The coil of contactor *DB* is connected in series with the normally closed contacts of relay *SR* and the normally closed auxiliary contacts of the spring closers *FB* or *RB*. Thus when the motor is running the *DB* coil is de-energized. This permits the use of a low voltage coil on the *DB* contactor without need for a thermal protective resistor. The series relay *SR* has its coil connected in the dynamic braking loop.

When power failure occurs, there is a race between the *DB* contactor and the *SR* relay as the current in the dynamic braking loop builds up simultaneously with the voltage across the armature. The small series relay will respond more rapidly than the larger contactor. Consequently *DB* cannot close its contacts until the dynamic braking current has fallen to a value corresponding to the drop-out of the *SR* relay. When the *SR* relay drops out to close its contacts, *DB* will close its contacts to short-circuit part of the dynamic braking resistor *R2-R3*. The current will rise to a value depending on the ratio of *R2-R3* to the total resistance of the loop circuit. If this ratio is high, *SR* may pick up again and drop out *DB*. This will be repeated until *SR* finally stays out and *DB* stays closed. Contactor *DB* must be provided with a low voltage coil and a low reluctance magnetic circuit so that it will stay closed to a low value of voltage.

The pickup voltage of *DB* must be below that corresponding to the drop-out current of relay *SR;* otherwise *DB* would never pick up. Therefore the pickup voltage of *DB* must be still lower relative to that corresponding to the pickup current of relay *SR*. This is on the unfavorable side as far as *SR* winning the race with *DB* is concerned and must be offset by quicker response of *SR* to the rapid rise of current and voltage in the loop circuit immediately following power failure.

The second of the two methods is an exceedingly simple one in that the series relay and shunt contactor of Figure 10 are replaced by a single series coil spring-closing contactor as illustrated in Figure 11. The advantage of this circuit is its simplicity and its freedom from electrical interlocks and protective resistors. The series coil spring-closing contactor has a heavy strap coil of but a few turns and this along with the fact that it is energized only during dynamic braking makes the circuit exceedingly safe from a loss-of-coil point of view.

The one disadvantage of the circuit lies in the possible high inrush of current during dynamic braking just before the spring closer opens its contacts. This places a lower limit on the value of resistor *R1-R2*. The very rapid response of the spring closer to the rapidly rising current makes the duration of the peak current very short. As the motor slows down, *DB* will close its contacts to short-circuit resistor section *R2-R3* and, depending on the extent of the change in the circuit resistance, *DB* may pick up again repeating the operation a number of times as the motor comes to rest. A number of installations using this means of obtaining graduated braking recently have been put in service and no difficulty has been encountered by the fluttering behavior of the contactor during deceleration of the motor.

Plugging Reversing Controller Providing Graduated Service and Emergency Dynamic Braking

To illustrate the application of some of the various schemes set forth, the elementary diagram for a complete plugging reversing controller is shown in Figure 12. This controller provides graduated emergency and service dynamic braking from either direction of motion. The control was designed for use on a coal bridge trolley where the trolley is driven by cables from a motor located on the bridge structure. Magnetic brakes cannot be used without excessive abuse of the cables, and it is desirable that the deceleration of the trolley be as smooth as possible.

The controller is a standard plugging reversing controller with the addition of four polarized spring closers *FB* and *RB* for dynamic braking, a teaser field contactor *TF*, and current limiting resistor. Three voltage relays *VR1*, *VR2*, and *VR3* and a time-delay relay *TD* are included for protection of intermittent duty coils. Two additional spring closers provide graduated dynamic braking and a second master switch is used for service dynamic braking.

It is not necessary to describe completely the operation of the controller as it is a standard controller with additional features which just have been described.

The service braking master provides two points of braking. The first point opens the reversers and permits the appropriate pair of spring closers to close. The dynamic braking resistance is *R1-R4* on this point. The second point closes *DB1* to by-pass resistor *R1-R2* and increases the breaking torque. A third step of braking is provided automatically by contactor *DB2* as described earlier.

The acceleration and plugging of the motor are controlled in the usual manner. The only special feature occurs during

plugging when it is necessary to offset the increase in ampere-turns in the polarizing coils by short-circuiting resistor D in series with the operating coils. This is accomplished by employing normally closed auxiliary contacts on the plugging contactor P in energizing the time-delay relay TD. After the motor has been plugged to rest and accelerated in the opposite direction, TD will open to again insert the protective resistor D.

Should the main master be moved to "off" point with the service-braking master in the "drift" position, the M contactor remains closed and a teaser field contactor TF closes to provide current in the field. This assures voltage on the voltage relays and the polarizing coils of the four spring closers. The M and TF contactors remain closed until the motor speed drops to a value corresponding to the drop-out voltage of relay $VR1$ at which time they open their contacts to remove the teaser field circuit.

In the event of power failure while running or drifting with the master on the "off" point all contactors and relays fall out except the appropriate pair of spring closers and the voltage relays across the armature. Contactor $DB1$ closes its contacts instantly and two steps of dynamic braking are provided automatically by contactor $DB2$.

All of these control schemes have been tested giving results in agreement with the foregoing analyses

No Discussion

Advancements in the Design of Long-Scale Indicating Instruments

R. M. ROWELL
ASSOCIATE AIEE

N. P. MILLAR
ASSOCIATE AIEE

SHORTLY before the war the development of new materials[1] and techniques made it possible to build long-scale instruments for accurate electrical measurements over the widely varying conditions encountered in practice. A complete line of long-scale instruments was designed and built incorporating four new and different mechanisms.[2] These instruments were standardized by the United States Navy for combat vessels as well as for many other naval applications.

Experience gained in the past few years has pointed the way to certain design improvements which seem desirable and which would accomplish the following objectives:

1. Improve the general appearance and ease of reading.
2. Facilitate calibration and adjustments.
3. Improve accuracy under abnormal conditions.
4. Facilitate repairs by making the moving systems more readily removable.
5. Simplify recalibration with existing scales.

The improvements in appearance and readability are described in the following paragraph, while the engineering and design work to accomplish the other objectives are outlined in the description of the individual instruments which follows.

Scale and Cover Design

In the design of modern switchboards considerable attention now is being given to appearance and symmetry as well as to their functional features. The modified instruments therefore have been designed with this fact in mind. With such changes, however, certain features have been incorporated which will aid operators in obtaining quick and accurate readings. Figure 1 shows the appearance of the new line of instruments with plastic covers, although heavy pressed metal covers are available for high-shock applications. The window opening has been beveled to improve readability at sharp angles. The scale numerals have a form and arrangement that make them easy to read, and confusion in associating these numerals with the proper cardinal points is eliminated by wedge-shaped accent marks at these points.

D-C Ammeters, Voltmeters, and Temperature Meters

Improvements in long-scale permanent-magnet moving-coil instruments for d-c use have been directed toward increased permanency of calibration under abnormal conditions and ease of servicing and repair. In such instruments it sometimes is desired to remove the moving system for repair or inspection. This operation usually involves removal and replacement of the center core. This is not serious in the case of conventional 90-degree-scale instruments as any increase in the air gap on one side which affects the torque on the corresponding side of the moving coil results in a decrease in gap on the other side with opposite effect on the moving coil, so that there is no resultant effect on the total torque. On long-scale instruments, however, the moving coils are eccentrically mounted with only one side of the moving coil in the air gap so that any change in the gap affects the scale distribution on both sides. To eliminate the possibility of such distribution changes the magnetic return path is made in a single piece with the center core and the outer ring made of powdered iron sintered in a single mold (see Figure 2). Obviously, this center core must be broken at some point to permit removal of the moving system. Because the magnetic circuit is operated at a high flux density any break in the magnetic core must be made at a point which will have a minimum effect on the total flux density, the stability of the magnet, and the distribution of the scale. Figure 3 shows the magnetic flux paths in this system. It will be noted that the core opens at the top center where it will give the least possible effect because the flux splits at this point to return through the magnet and the outside ring in opposite directions. A small piece of sintered iron is cast onto the frame and fits into the core opening when the frame and moving system are inserted, thus preventing any distortion of scale distribution at this point.

As the electrical losses in this instrument are very low, it has been possible to make most voltmeters with the resistance internal and thus eliminate the rear external-resistance cage. A resistor is provided on the front of the instrument frame

Figure 1. Typical improved design of long-scale instrument

Paper 47-22, recommended by the AIEE committee on instruments and measurements for presentation at the AIEE winter meeting, New York, N. Y., January 27–31, 1947. Manuscript submitted November 1, 1946; made available for printing December 23, 1946.

R. M. Rowell and N. P. Millar are both with the instrument engineering division, General Electric Company, West Lynn, Mass.

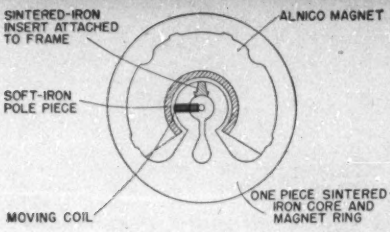

Figure 2. Mechanism of improved d-c instruments

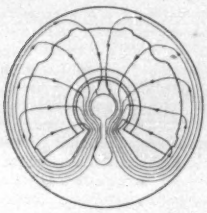

Figure 3. Magnetic circuit of d-c instruments

for adjusting the circuit resistance to compensate for changes which may be made in shunt leads, for example, after the instruments are calibrated originally.

It is felt that this design incorporates the best possible features to obtain high operating torque and torque-to-weight ratio, ease of assembly and repair, and, above all, the most permanent structure possible from the standpoint of mechanical and electrical stability; and a scale distribution that will not change throughout the life of the instrument is assured.

Damping Mechanism for A-C Instruments

All a-c instruments are equipped with an eddy-current damping mechanism of simple construction. It consists of two half-ring Alnico steel magnets with grooves cast in the sides as shown in Figure 4. These two magnets are assembled on the instrument in a circular arrangement directly over a small segmental aluminum disk, which is carried by the moving element. The magnetic circuit is completed through the disk to a soft-iron plate mounted directly below the disk and having the same contour as the magnet. This simple arrangement provides an adequate damping torque throughout 360 degrees of disk movement.

To magnetize these units each magnet is placed in a special magnetizing fixture so designed that a conductor is looped through the grooves in a manner similar to that shown in Figure 5. When a high impulse direct current is passed through the conductor the grooved surface becomes a series of alternate north and south poles. Were it not for the mounting lugs, which are integrally cast with each magnet, the poles would have the same flux distribution. However, the nonuniformity of flux which results does not in any noticeable way affect the over-all damping characteristic. This flux distribution is revealed clearly in Figure 6 by means of an iron-filings pattern taken on such a magnet.

A-C Ammeters and Voltmeters

The use of a long-scale attraction–repulsion iron-vane system for several years has pointed the way to improvements in stability and scale distribution and better control of the latter. In a system comprising four magnetic components, their configuration as well as the spacing between them determine the flux and torque characteristic at any scale point and define the scale distribution of the instrument. Not only is the spacing between the various stationary irons an important factor, but so, also, is the operating radius of the moving vane. To obtain better control of vane dimensions, a new method of mounting was devised in which the mounting bracket was cut from the vane itself and bent over to give a single-piece construction (see Figure 7). This results in better dimensional control radially, and also eliminates any soldering or welding operations on the vane itself with possible introduction of hysteresis effects. The new vane system after final forming requires only a single anneal to bring out its best magnetic characteristics which are no longer jeopardized by subsequent operations.

In the previous attraction-repulsion system, a single repulsion member was used for both ammeters and voltmeters with different attraction irons to obtain the two different types of scale distribution desired. In the new design the two different repulsion irons for ammeters and voltmeters are so shaped as to give the proper scale distribution on the lower half of the scale where their effect is the greatest (see Figure 8). It will be noted that on the ammeter the slope is steeper at the zero end, thus producing a greater torque gradient over the low end of the scale and making possible readings down to ten per cent of full-scale value. On voltmeters, however, conditions are usually different and voltages rarely will vary more than 20 per cent above or below normal established line voltages. The repulsion iron selected for this instrument, therefore, has a straighter slope to produce a gradual opening of the scale from about 20 per cent to the full-scale value, producing a scale which is the most open in the normal operating range. Torque curves (shown in Figure 9), taken at full-scale voltage, indicate the improvement made by the use of the new irons in voltmeters. By straightening these curves any tendency to constriction of the scale distribution around center scale is eliminated.

Improved control of the dimensions and

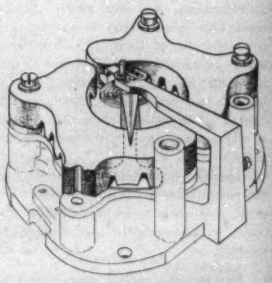

Figure 4. Cutaway section of magnetic damping system

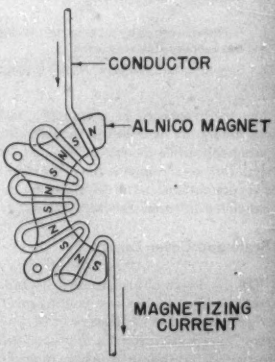

Figure 5. Sketch showing method of magnetizing damping magnets

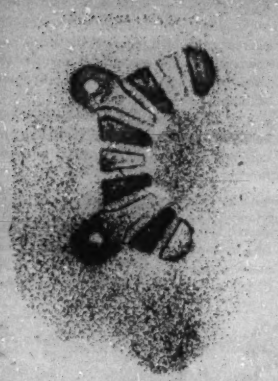

Figure 6. Flux pattern of typical damping magnet

position of the stationary attraction system represents another important improvement in this new design. As indicated by the sketch (Figure 7), the inside of each shield that supports the attraction irons is drawn down to a short tubular section in the center. This results in a stiffer shield with little chance of distortion and at the same time adequately supports the inside of the attraction iron and thus preserves its circular contour. Also, it has been found possible to eliminate the slot through the shield previously used to prevent eddy currents. Because of the high specific resistance of the material used, errors from this source are negligible up to 400 cycles.

To obtain greater control of scale distribution, the full scale ends of the attraction irons have been given an increased slope which gives the instrument greater sensitivity in the upper scale region. This permits a greater adjustment of scale distribution by turning the shields to which the attraction irons are attached, thus making it possible to secure a distribution that is substantially uniform over most of the active range. By forming locating ears which rest against the inside of the shield, the spacing between the attraction irons is held to closer dimensions and thus the duplication and control of scale distribution are facilitated.

Wattmeters and Varmeters

In the design of the new long-scale electrodynamic wattmeters and varmeters of the iron-cored type much thought was given to improved mechanical features as well as to improved performance. In this respect consideration was given to ease of assembly of parts that would greatly facilitate maintenance and service in the field, to more pleasing appearance both inside and outside the instrument, and to better electrical and magnetic characteristics.

The major feature of the redesigned electrodynamic instrument is a unique field coil and laminated-field structure. Figure 10 shows this assembly in detail. The laminations are of a 1-piece construction punched from a new silicon strip steel which permits high flux density and exhibits superior hysteresis characteristics. Care was taken to locate the mounting holes so that losses caused by the mounting rivets would not lessen the efficiency of the magnetic circuit. The laminations are cemented together with a solventless varnish under heat and pressure. This results in a rigid stack of adequately insulated laminations held together without the use of rivets. The only rivets used are the mounting rivets which hold the cemented stack to the support plate as shown in Figure 10. In addition, the field coil after being wound and baked in this new varnish is cast securely to the lamination stack.

The advantages of this method of construction are obvious. Because the solventless varnish is a good heat conductor, the casting of the coil to the laminations permits more efficient heat dissipation and a greater overload rating. Mechanically the cast coil eliminates the use of clips for holding the coil in position and the mold finish presents a pleasing appearance.

Another feature of the mechanical design that will aid the servicing of these instruments greatly is the ability to withdraw the moving system without disturbing the field and coil assembly. In order to realize this objective the die-cast frame is designed so that the frame and moving element are inserted into the hook-shaped section of the lamination assembly. Figure 11 shows this draw-out feature to advantage. All that needs to be done to remove the frame and moving system is to unsolder the lead wires to the moving-system spirals, unscrew the three frame screws, and move the zero regulator until it is restricted by the front jewel support. This removal can be accomplished also with the instrument mounted on a switchboard panel without disconnecting any leads to the base terminals. The draw-out feature has been applied successfully to all instruments that measure single- and polyphase watts and vars.

The moving system and frame assembly are equipped with removable pivots and spring-supported jewels. The pivots are press-fitted into threaded bushings that are screwed into the armature shaft. This permits easy replacement of the pivots if required.

Previous designs always have used external card resistances mounted on the base of the instrument. In the redesign the 120-volt and lower ratings have resistances mounted inside the instrument case. This has made it possible to locate the terminals with increased spacing so that connections can be made more easily and the voltage breakdown value between terminals increased.

The unit lamination and field coil assembly previously described has resulted in a more efficient magnetic circuit. Because of this increased efficiency it has been possible to decrease the field-coil ampere turns and yet obtain a higher torque than that of the previous design. Operating characteristics have been improved thereby, as the ratio of torque-to-weight of the moving system has been increased materially, and the volt-ampere burden of the field coil lowered. Figure 12 gives comparative curves of the field ampere turns versus the torque of the improved and the previous design of electrodynamic system. It can be seen that the field density of the curve A is well be-

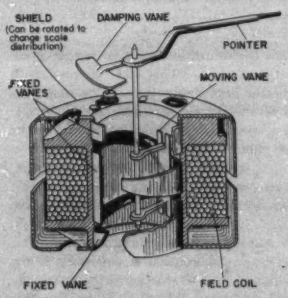

Figure 7. Improved attraction-repulsion mechanism for a-c ammeters and voltmeters

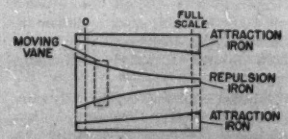

Figure 8(a). Development of repulsion and attraction irons for a-c voltmeter

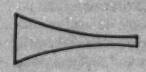

Figure 8(b). Repulsion iron for a-c ammeter

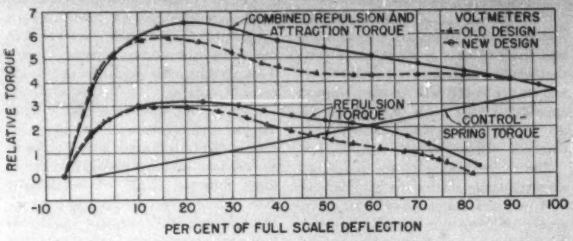

Figure 9. Torque curves of typical a-c voltmeter

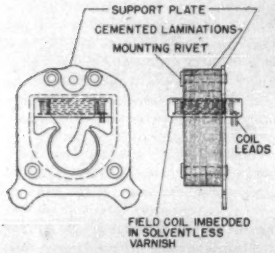

Figure 10. Field coil and lamination assembly for wattmeters and varmeters

low the saturation value for normal operating ranges. This fact, coupled with better heat dissipation in the cast field coil, has permitted a larger overload rating without destroying the linearity of the dynamic-torque characteristic.

As is well known in instrument design, the use of iron in the magnetic circuit causes the current in the potential coil to lag slightly behind the applied voltage. Because iron losses more than cancel this effect, compensation is necessary if the instrument is to read correctly on lagging power factor. This is done by shunting the moving coil and a portion of the series resistance with capacitance until such compensation is attained. No attempt will be made in this paper to discuss the theory of this compensation, as it has been covered adequately in another paper.[2]

Inherent in all iron-clad electrodynamic systems is a small error caused by voltage variation. This may be described as a error caused by the solenoid effect between the potential coil and the core embraced by the coil. Excitation of the potential coil alone results in an upscale torque that tends to move the coil in the direction of maximum flux linkage. The more efficient the magnetic circuit becomes, the more pronounced is this "creep" effect. Because of an increased potential flux of the moving coil at a higher voltage, the indication will be slightly high unless this solenoid effect is compensated.

Voltage error can be reduced substantially

1. By designing the moving system to operate with a minimum potential flux.
2. By adequate compensation.

This compensation takes the form of a coil of suitable turns wound on the central core section and connected in series with the moving coil to produce a flux that opposes the extraneous potential flux causing upscale torque. Therefore, when such an upscale torque increases because of increased voltage, the opposing compensating torque likewise increases for the same reason. This substantially eliminates the voltage-creep effect. Figure 13 is a schematic diagram showing the connections for both power-factor and voltage-creep compensation. This method of compensation has been applied successfully to each element of polyphase wattmeters and varmeters.

Power-Factor Meters

Power-factor meters designed for this line of long-scale instruments operate on the principle of the rotating magnetic vane. The two vanes projecting in opposite directions from the shaft are coupled magnetically by a sleeve of nickel-iron alloy. This is surrounded by a stationary current coil which polarizes the vanes, and the coil and vane assembly is mounted inside a motor-type stator with a polyphase winding.

The ideal power-factor meter will indicate correctly the power factor of the circuit regardless of the amount of current flowing. For various reasons, however, this seldom is achieved in commercial instruments. In the conventional 90-degree type, current is led to the moving coil by means of conducting spirals that exert a constant torque proportional to deflection. As the current in the circuit

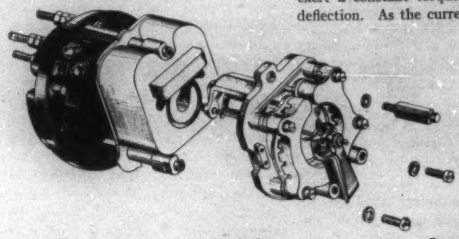

Figure 11. Wattmeter mechanism with frame and moving system removed

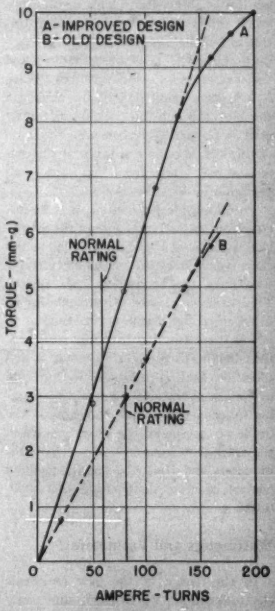

Figure 12. Curves of field ampere turns versus instrument torque

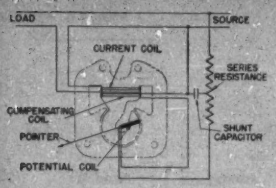

Figure 13. Schematic diagram of connections for power-factor and voltage-creep compensation

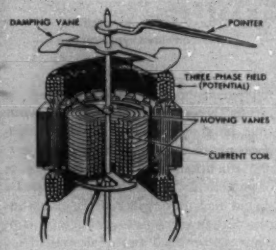

Figure 14. Improved power-factor mechanism showing new vane configuration

decreases, this torque becomes a greater percentage of the total torque and thus influences the indication.

In the rotating-vane power-factor meter there are no conducting spirals, so this source of error is eliminated. There are other effects, however, which tend to produce current errors. Most uncompensated instruments have an error of approximately 0.04 to 0.05 power factor between 1- and 5-ampere calibration values. The sources of these errors were analyzed very carefully and most of these effects were found to be of a minor nature. The major extraneous torque might be described as a hysteresis-motor action tending to cause the moving vanes to rotate with potential alone applied. Although this torque has been reduced to a minimum by the use of well-annealed nickel-iron alloys, it was still appreciable. The hysteretic torque has been measured and compared very carefully with the total instrument torque at one and five amperes respectively. Calculations showed errors approximately of the magnitude of the current errors determined experimentally.

The method of compensating for this hysteretic drag in the new instrument consists of modifying the shape of the rotating vanes and changing the stator ampere-turns. Figure 14 shows the approximate shape of the new moving vanes with their relative position inside the current coil and polyphase stator.

These new vanes saturate at a lower value of current flux so that the torque curve from one to five amperes is much flatter than in the previous design and is almost constant from two to five amperes (see Figure 15). Thus the effect of the hysteretic drag is approximately the same over the current range and is eliminated largely in calibration.

It is apparent that a shift in angular flux position also occurs because of this saturation, because it is possible to overcompensate the instrument and produce errors in the opposite direction. The stator ampere-turns, therefore, have been selected to give a hysteretic torque that results in small errors equal in clockwise and counterclockwise directions.

Figure 16 shows how effectively the new system has reduced these current errors. An instrument of the previous design which had a maximum difference of 4.5 per cent between 1- and 5-ampere readings had its moving vanes replaced with the new style vanes and its stator currents corrected to the new value. It will be seen that the error was reduced to slightly over 2 per cent. By calibrating the instruments at some intermediate value, such as 2.5 amperes, this error can be split so that the total deviation from the correct value is approximately 1 per cent. Although Figure 15 indicates a slight loss of torque at rated current, this is compensated for by the decrease in moving-element weight so that the same torque-to-weight ratio is maintained. It also will be noted that the torque at low current values is increased so that the over-all performance of the instrument is improved materially. The operating range also is extended to lower current values before becoming too sluggish for accurate indication.

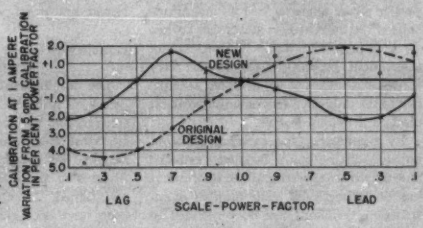

Figure 16. Current-error curves of power-factor meter

Synchroscopes

The synchroscope has essentially the same physical construction as the power-factor meter. It uses the same rotating-vane system, but the polarizing coil is wound for potential instead of current and is directly connected across the line of the running machine. Most synchroscopes are designed for single-phase operation. Hence it is necessary to provide a phase-splitting network in the stator circuit. This network is built into the instrument case in the new design, which offers distinct advantages over the conventional external-impedor type. To make this possible, inductive reactances were replaced by capacitors and combined with resistances in such a manner that quadrature-phase relation and balanced field currents are maintained. Figure 17 is a schematic diagram of the new stator circuit with a corresponding vector diagram. To obtain a lagging current I_2 in stator coil 2 having the same magnitude but 90 degrees out of phase with I_1, it is necessary to place a capacitance in circuit 2. This causes current I_2 to lead voltage V, but lagging is obtained by reversing the connections to stator coil 2. For testing and calibrating purposes some means of adjustment is necessary. This is pro-

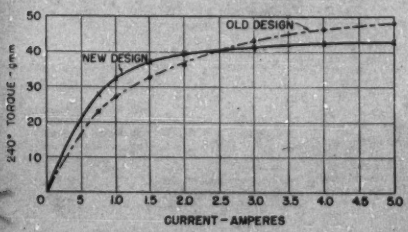

Figure 15. Power-factor meter torque curves

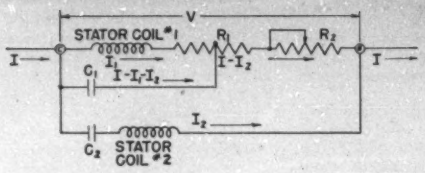

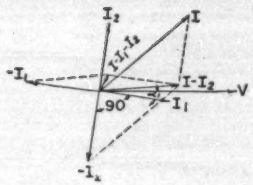

Figure 17. Schematic and vector diagrams of new synchroscope stator circuit

V = line volts (incoming)
I_1 = current in stator coil 1
I_2 = current in stator coil 2
I = total network current
R_1 = fixed center-tap resistor
R_2 = adjusting resistor
C_1, C_2 = capacitors
α_1 = phase angle in stator coil 1 circuit

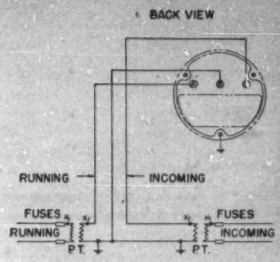

Figure 18. External connections of new self-contained synchroscope

vided by the adjustable resistance R_2. The capacitor C_1 serves to insure the proper phase angle as well as magnitude shift of the current I_1 in stator coil 1 when R_2 is adjusted in test. This resistance adjustment provides a simple and very convenient means of control that is superior to the inductive-reactance adjustment used on previous designs.

By eliminating the external impedor, panel-mounting space has been reduced and the external wiring to the instrument has been simplified. The number of instrument terminals has been reduced to three. Figure 18 shows the external connections to the new design of self-contained synchroscope.

Conclusion

The development of a complete line of long-scale instruments has proved to be a considerable advancement in the field of electrical measurements. In the newly designed instruments all of the desirable features of the initial design have been maintained. Most of the previous limitations have been removed by mechanical improvements that have resulted in greater accessibility and, at the same time, improvements in scale distribution, permanency of calibration under abnormal conditions, and other performance characteristics. Thus these instruments should find even wider fields of usefulness and, in many cases, completely supplant conventional short-scale types.

References

1. Influence of Improved Magnetic Alloys on Design Trends of Electrical Instruments, **M. S. Wilson, J. M. Whittenton.** AIEE Transactions, volume 63, 1944, March section, pages 100–04.

2. Design of Long-Scale Indicating Instruments, **A. J. Corson, R. M. Rowell, S. C. Hoare.** AIEE Transactions, volume 61, 1942, June section, pages 318–27.

No Discussion

Measurement of High Q Cavities at 10,000 Megacycles

R. W. LANGE
NONMEMBER AIEE

Synopsis: Known methods of measuring Q in high Q resonant cavities, together with their accuracies and sources of error are discussed. For relatively low values of Q and of frequency, it is shown that band width methods are more accurate than decrement methods. For values of Q above 30,000 at frequencies above 3,000 megacycles the reverse is true. The significant feature of the present method, the wide range heterodyne decrement method, is that the accuracy is improved by observing the decay over a relatively long interval of time. An absolute accuracy of plus or minus three per cent and a relative accuracy of plus or minus two per cent are achieved. Design features and performance are discussed and constructional details are presented.

THE quality factor of selectivity, Q, is applicable to any form of vibratory or oscillatory system. The defining equation is

$$Q = 2\pi \frac{\text{total energy stored in system}}{\text{energy dissipated per cycle}}$$

The present discussion will be limited to electric systems. When the elements are lumped or when the system may be replaced by lumped constants the equation is simplified. For the simple series resonant circuit the expression becomes

$$Q = \frac{X}{R}$$

where

X = reactance of either the coil or capacitor
R = total series resistance

In any simple resonant system energized by a single frequency the phase shift becomes 45 degrees and the displacement is reduced to 0.707 of its maximum value at two frequencies nearly symmetrical about the resonant frequency and separated by the amount

$$\Delta f = \frac{f}{Q}$$

where

f = resonant frequency

This equation has been used to define the Q of certain complex systems.

The working Q of a system differs from the theoretical unloaded Q by a loading factor controlled by the associated devices. All methods measure the loaded (working) Q. For fixed couplings to electric systems under measurement, the loaded Q depends on the standing wave ratio of the coupled (or connecting) circuits as well as on their nominal impedances. In the specific case of a resonant cavity with input and output couplings fixed by design, the loading depends on the voltage and current relationships existing in the input and output transducers. It is important that these impedances be controlled for all methods of measurement of Q outlined here.

Table I. The Errors for Absolute and Relative Measurements

	Absolute Measurements, Per Cent	Relative Measurements, Per Cent
Measurement of time	±1.7 max; ±0.7 min	±1.7 max; ±0.7 min
Measurement of frequency	±0.05	±0.05
Change of attenuation	±1.25	cancels
Observational error of scope	±0.25	±0.25
Total	±3.25 max; ±2.25 min	±2.0 max; ±1.0 min

Paper 47-23, recommended by the AIEE committee on instruments and measurements for presentation at the AIEE winter meeting, New York, N. Y., January 27–31, 1947. Manuscript submitted November 13, 1946; made available for printing December 19, 1946.

R. W. LANGE is with Bell Telephone Laboratories, Inc., New York, N. Y.

The author wishes to express his thanks to Doctor W. A. Edson, J. P. Kinzer, and I. G. Wilson of Bell Telephone Laboratories for their suggestions and assistance throughout the original design and final completion of this project, as well as the valuable laboratory assistance of Miss M. J. Kilroy.

Band Width Method

Basic Principle

The frequency corresponding to maximum transmission is measured together with the transmission loss. The two frequencies corresponding to a transmission loss three decibels greater are sufficient to give the selectivity from the general equation

$$Q = \frac{f}{\Delta f} \tag{1}$$

Practical Applications

The method is applicable to all forms of four terminal electric networks. It is therefore directly applicable to cavity resonators having two loops or other coupling devices. It is not applied readily to cavities having a single coupling device. The loss usually is determined by means of a heterodyne transmission measuring set. In this way an attenuator operating at the intermediate frequency and having a relatively accurate calibration may be employed. As a difference in frequency is required, each frequency must be known accurately, or, the difference can be measured directly.

For measurement of resonant cavities it is impossible to secure the signal frequency by beating a fixed centimeter oscillator with a calibrated variable frequency signal generator in the 50-megacycle region or lower. This greatly simplifies the problem of determining the frequency difference.[1]

Alternatively a reflex klystron type of centimeter oscillator may be frequency modulated to furnish the pass band picture of the resonant cavity. The frequency swing can be determined by a frequency modulation receiver augmented by a selective amplifier tuned to the klystron modulating frequency.

Accuracy

Consider a case with a value of Q of 30,000 and a midband frequency f of 3,000 megacycles. Then

$$\Delta f = \frac{3{,}000}{30{,}000} = 0.1 \text{ megacycle}$$

$f_2 = 3{,}000.05$ megacycles
$f_1 = 2{,}999.95$ megacycles

If it is necessary to measure Q to plus or minus ten per cent then, allowing all the error in the denominator, Δf must be measured to plus or minus ten per cent. If the frequencies are measured directly then each must be known to plus or minus 5 kc.

Actually the loss cannot be determined exactly at either midband or 3-decibel points. If an error of plus or minus 0.1 decibel is allowed for each of these measurements the uncertainty of the answer is increased by about plus or minus six per cent. To measure absolute values of Q by this method to an accuracy better than plus or minus five per cent requires extreme care and considerable skill in manipulation.

In systems where the Q is low the frequency difference may be determined with negligible error, and the accuracy is limited only by the loss measurements.

Input Standing Wave Ratio Method

Basic Principle

The standing wave ratio of the input device is measured at three or more frequencies in the region of the resonance. The Q of the cavity then is computed from the variation of the standing wave ratio with respect to frequency.

Practical Applications

The method is applicable to any form of cavity having one or more coupling devices. The quantities to be measured are the same as in the band width method—frequency and voltage level. Accordingly the same general techniques are applicable. Because the standing wave ratio is usually high a heterodyne method is desirable.

Accuracy

The same errors appear here as in the band width method. A small difference between two relatively high frequencies must be determined, and voltage levels must be measured with sufficient accuracy to determine the difference between several comparable standing wave ratios. The over-all accuracy is not likely to be better than that of the band width method and easily may be poorer. The principal advantage is that a single coupling device is sufficient to permit a measurement.

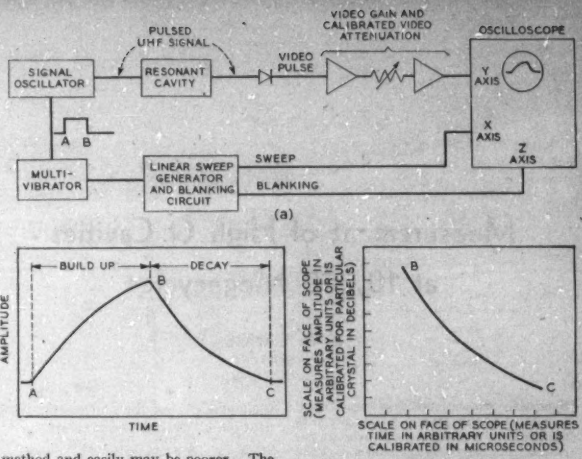

Figure 1. Video decrement method for measuring the Q of resonant cavities

(a). Block diagram of the method
(b). Complete video signal (showing build-up and decay of ultrahigh frequency energy in resonant cavity)
(c). Video decay signal (used in measurement of Q)

Video Decrement Method

Basic Principle

In this method, shown in a block schematic drawing in Figure 1(*a*), the build-up and decay of ultrahigh frequency enery within the resonant cavity is rectified by a crystal detector producing a video signal which is amplified and observed as the vertical deflection on an oscilloscope having a linear time axis. A measurement is made on the oscilloscope of the rate of decay in terms of amplitude in decibels and time in microseconds. The Q may be computed from these quantities and a calibration of the curvature of the crystal characteristic by using the formula

$$Q = 27.3(f)(\Delta t/\Delta db) \qquad (2)$$

where

f = frequency in cycles per second
Δdb = decrement in decibels observed in the time increment Δt seconds

Practical Application

The pulsed ultrahigh frequency signal is applied to the cavity through an input coupling and is delivered to the crystal through an output coupling connection. This method provides a convenient and fairly accurate arrangement for observing decrements. It is quite satisfactory for observing moderately small changes from reference decrements for development work. The signal source should be adequately decoupled from the cavity to prevent pulling. The crystal is operated well under the overload point and sufficiently above the noise level to permit examination of the main mode of the cavity. The video system following the crystal need never be overloaded.

In general, the crystal video output is some exponential function of the ultrahigh frequency input. If absolute measurements are to be made, it is necessary to determine this relationship at the operating signal levels.

The complete video signal observed on the oscilloscope is shown in Figure 1(*b*). The signal oscillator is pulsed on at point A and continues to oscillate to point B, at which time it is pulsed off. The energy within the resonator builds up in the interval A to B and starts to decay at B.

In actual measurement the sweep time axis is delayed or phased with respect to the signal oscillator pulse so the full screen may be utilized in measuring the decay portion B to C.

The initial observation, point B in Figure 1(*c*), is made at or slightly after the instant the signal oscillators stop pulsing. The choice is dependent upon the sharpness with which the signal oscillator is pulsed off. The second observa-

tion point C is made at a point before the decay curve becomes asymptotic to the horizontal reference line. Point C usually is selected three decibels below point B. The Q is computed by equation 2 where the value of db is measured on the vertical calibrated scale and time along the calibrated linear sweep axis.

The method is not directly applicable to cavities having only one coupling device.

Accuracy

For conditions which have been found most satisfactory in the laboratory the error attributed to reading the oscilloscope is plus or minus seven per cent. This can be considered the accuracy of relative measurements of Q.

For an absolute measure of Q the errors involved in calibrating and using the crystal must be added to the foregoing factors. No attempt has been made to evaluate these errors; however it is reasonable to state that this method lacks the accuracy ultimately desired. Error contributed by uncertainty in observation of the frequency is negligible.

No decrement method is applicable to the measurement of low Q systems because of the extremely short time intervals involved and the correspondingly great band widths required.

Heterodyne Decrement Method

Basic Principle

A decrement method is employed to avoid precise measurements of frequency difference. The circuit is shown in block schematic form in Figure 2.

The pulse from the ultrahigh frequency oscillator is applied as a signal to the cavity under test. The decay of energy within the cavity after the signal pulse has ceased is observed through a heterodyne detector circuit ending in an oscilloscope. Two distinct points are observed and compared on the decrement curve. Values of level in decibels and of time result from this comparison and the Q of the cavity is computed from equation 2.

The method differs from the previous one in three important respects.

1. The crystal is energized by a beating oscillator as well as by the signal from the resonant cavity under test. The principal advantage is that the crystal now serves as a linear modulator eliminating the question of crystal exponent.

2. The beating oscillator is pulsed off or shifted in frequency during the main pulse to avoid overload in the intermediate frequency and video systems. Moreover by pulsing the beating oscillator it is practical to employ the method with single-coupling as well as 2-coupling cavities.

3. The range of decrement is increased to approximately 20 decibels so observations of loss and time increments give improved accuracy of Q determination.

The complete build-up and decay of the pulse with the beat oscillator operated continuous wave is shown in Figure 3(a). The signal oscillator pulses on at A and the energy within the cavity builds up from A to B where the signal oscillator is pulsed off. The decay of energy is shown as B to C.

With an ideal beat oscillator pulsed on at time t_0 the decay curve would appear as shown in Figure 3(b) with a sharp increase to full height at t_0. Actually there is a finite build-up time for the beat oscillator during which the energy within the cavity continues to decrease, so that the resultant curve has a gradual build-up from t_0 to t_1 as shown in Figure 3(c) and in Figure 4. (Abnormal intensities were used to facilitate photography.)

The fixed timing spot shown as t_2 in Figure 3(d) appears as an end to the decay trace. This end is sharp and permits an exact alignment of the height of the figure at t_2 with the horizontal reference line on the oscilloscope as shown in Figure 4. (Abnormal intensities were used to facilitate photography.)

The intersection of the fixed timing spot on the decay curve with a reference line on the oscilloscope is adjusted either by changing the precision delay, or the intermediate frequency attenuator, or, within limits, the video gain of the Y axis of the scope. The base line of the image is aligned with the horizontal reference line by vertical positioning on the oscilloscope. The initial observation is made with the maximum loss setting of the intermediate frequency attenuator and the precision delay circuit adjusted to an arbitrary reference point near the minimum delay. The figure is adjusted to a standard height at t_2 by the video gain control. The delay time is read from the dial of the precision delay circuit.

For the second observation at a point later in the decrement curve as shown in Figure 3(e) the intermediate frequency attenuation is reduced and the delay circuit adjusted to provide the same standard figure height at t_2 shown for t_2 in Figure 3(d). The delay time is read from the dial of the precision delay circuit. From the foregoing procedure the change

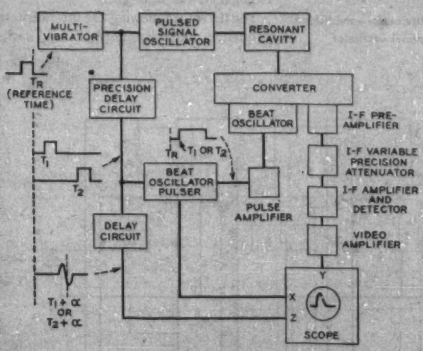

Figure 2. Heterodyne decrement method for measuring the Q of resonant cavities

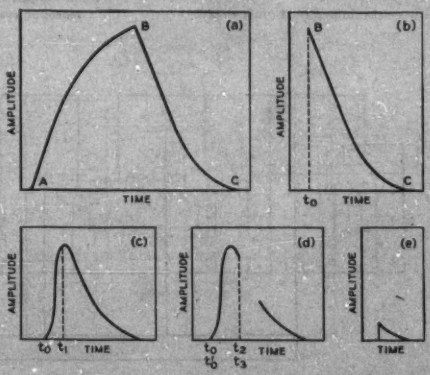

Figure 3. Build-up and decay patterns observed in heterodyne decrement method

in attenuation in decibels and the corresponding time are obtained, and the Q computed from equation 2.

Practical Applications

The present set is used with cavities having 2-coupling devices but it has been modified to operate with cavities having a single-coupling device without serious loss of performance.

The free-running multivibrator shown in Figure 6 sets the repetition rate and pulse length of the signal oscillator and triggers the precision delay circuit. The multivibrator furnishes a flat top pulse with a rise and more particularly a decay in 0.3 microsecond or less.

The signal oscillator uses a velocity variation focused beam oscillator tube in an adjustable cavity. It is pulsed on by a voltage applied to the accelerating anode. This pulse is furnished by a video driver amplifier, integral with the oscillator unit, which amplifies and clips the pulse supplied by the multivibrator. The pulse wave to the accelerator decays in less than 0.1 microsecond.

Excellent frequency and amplitude stability of the signal oscillator is required during the short intervals of measurement (one minute or less) for which the oscillator must remain tuned to the resonant cavity. In the set which was constructed, precautions were taken to obtain a short time frequency stability considerably better than 0.1 megacycle. All voltages, except heater supply, were furnished by well-regulated and filtered power supplies. The heater was operated on rectified alternating current, heavily filtered, to avoid modulation from the heater circuit. All supplies were operated from a voltage regulating transformer. Finally, frequency drift caused by changes in the ambient temperature were eliminated by a draft shield.

Figure 4. Photograph of oscilloscope trace showing complete decay pattern observed in heterodyne decrement method

Figure 5. Photograph of oscilloscope trace showing decay pattern blanked by timing pulse

Amplitude modulation was controlled by the foregoing method and by applying a flat top pulse to the accelerating anode of the signal oscillator. The signal frequency is delivered to the input of the resonant cavity through wave guide or coaxial connections and the output is fed through suitable connections to the converter. It is desirable that the impedance offered to the resonant cavity be that which exists when the cavity is working normally.

The linear converter circuit employs a crystal of the *JAN 1N23B* type in a wave guide mounting. The beat oscillator delivers sufficient power to the converter through a probe inserted in the wave guide or by a directional coupler to operate the crystal at optimum signal-to-noise ratio. The low level signal from the resonant cavity is applied directly to the crystal converter through the minimum loss consistent with obtaining the desired impedance at the output of the resonant cavity. It is a distinct help to adjust the particular crystal in the converter to obtain a low voltage standing wave ratio.

The intermediate frequency output of the crystal is fed directly to a low gain preintermediate frequency amplifier integral with the converter unit and designed to give a good signal-to-noise ratio. The combined unit is a modification of an airborne radar component. The output of the last stage is matched to work directly into a variable intermediate frequency attenuator. The load carrying capacity is adequate to insure constant gain for all signal levels encountered.

The main body of the intermediate frequency amplifier and detector follows the variable intermediate frequency attenuator. The disposition of the gain from the output of the attenuator to the oscilloscope is not critical for the signal level remains unchanged in this portion of the circuit. It is desirable that a good signal-to-noise ratio be obtained in the intermediate frequency amplifier.

The complete intermediate frequency system should provide a moderate band width of two to five megacycles at the 3-decibel points. To ease the requirement on stability of the beat oscillator the mid-band should be flat to a few hundredths of a decibel. A flat band width of 0.5 to 1 megacycle is sufficient.

The detector following the intermediate frequency amplifier normally is back-

Figure 6. Circuit of multivibrator establishing repetition rate of signal oscillator

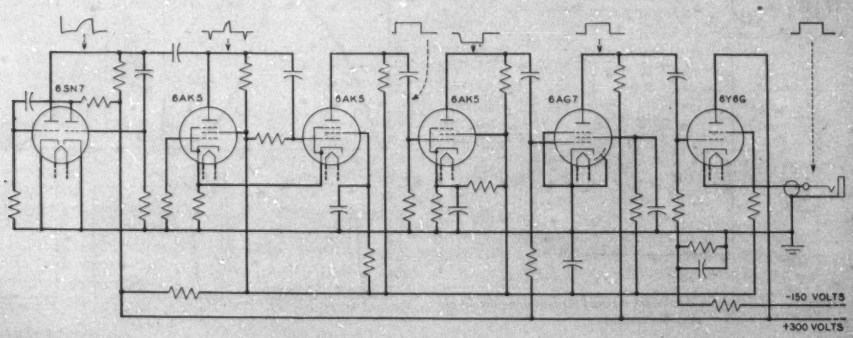

biased and driven by the signal into a square-law region to increase the differential sensitivity.

The beat oscillator is a velocity-variation reflection-type oscillator tube which is pulsed on by a voltage applied to the repeller. This pulse is furnished by a pulse amplifier, associated with the beat oscillator, which amplifies and clips the pulse supplied by the beat oscillator pulser.

As an alternative, the beat oscillator may be frequency modulated to the extent of some ten megacycles by reducing the peak value of the pulse applied to the repeller and making a compensating change in the d-c repeller voltage. The frequency of the beat oscillator is fixed during the interval of measurement as that which produces the required intermediate frequency signal. The frequency modulation shifts the beat oscillator from its off frequency to its on frequency position and maintains that frequency throughout the measurement interval. The operation of the tube in this manner in general reduces the transient intermediate frequency component generated during the build-up of oscillation when the tube is pulsed on. This transient upon conversion is the equivalent of a false signal at the input of the intermediate amplifier.

With either type of modulation of the beat oscillator it is necessary that the frequency remain sufficiently constant to keep the intermediate frequency output of the converter well within the very flat intermediate frequency band. This is accomplished by regulation of the oscillator voltage and the application of a flat top pulse. Further, it is necessary to maintain a constant ambient temperature to eliminate frequency changes. The tube is protected by double thermal shields.

The delay circuit is a monovibrator circuit triggered by the leading edge of the pulse from the precision delay circuit. The output pulse of the delay circuit furnishes a timing spot which is the reference mark on the decay curve appearing on the oscilloscope. Actually the pulse is used to blank the oscilloscope trace providing a sharp end mark on the decrement curve. It is important that the pulse be free of jitter as to time and shape. As shown in Figure 2, it is the sharp transition from positive to a negative voltage that is utilized. Thus the oscilloscope trace is brightened immediately before it is blanked.

For a specific test condition the time delay furnished by the circuit is fixed; however, for general testing it is convenient to have this delay under manual control. The delay may be varied under control of a potentiometer from a minimum of three-fourths to a maximum of five microseconds.

The precision delay circuit, shown in Figure 7, is a monovibrator circuit triggered by the trailing edge of the pulse applied to the signal oscillator. It provides a sharp output pulse accurately delayed from the triggering pulse. The time delay, under manual control of the variable air capacitor C_1, is continuously variable and calibrated. For testing in the 10,000-megacycle range a delay of 1 to 12 microseconds was used.

A commercial 5-inch oscilloscope has been modified for a sweep of five to ten microseconds and for double intensity modulation. Both the normal unblanking during the sweep trace and the reference pulse are applied to the intensity grid of the cathode ray tube.

A special nonglare hood is attached to the oscilloscope to facilitate daylight viewing of the trace. Two pairs of horizontal lines $1^1/_2$ inches apart are scribed on the front and rear surface of an edge-lighted plexiglass plate providing reference lines free of parallax.

Extension of Frequency

By changing the oscillators and converter the set has been applied to the 3,000- and 24,000-megacycle frequency bands. A minor change of components in the precision delay circuit permits adjustment of time delay to the particular frequency and range of Q to be measured.

Sets operating at these frequencies have been constructed and operated over considerable periods.

Accuracy of Measurements

These figures apply to a practical application at about 10,000 megacycles for a range of Q from 45,000 to 150,000.

Measurement of Time. The maximum error in determining the time at one dial setting of the precision delay circuit is ± 0.03 microsecond so that the maximum error of two time measurements in determining Q is $\pm$ 0.06 microsecond.

The least time interval expected is 3.5 microseconds corresponding to a 20-decibel change in the decrement curve of a relatively poor cavity having a Q of 45,000. The error in time measurement is $\pm 0.06/3.5 = \pm$ 1.7 per cent. The maximum time measurement expected is 8.1 microseconds for a Q of 100,000. The error is $\pm 0.06/8.1 = \pm 0.7$ per cent.

Observational Error of the Oscilloscope.

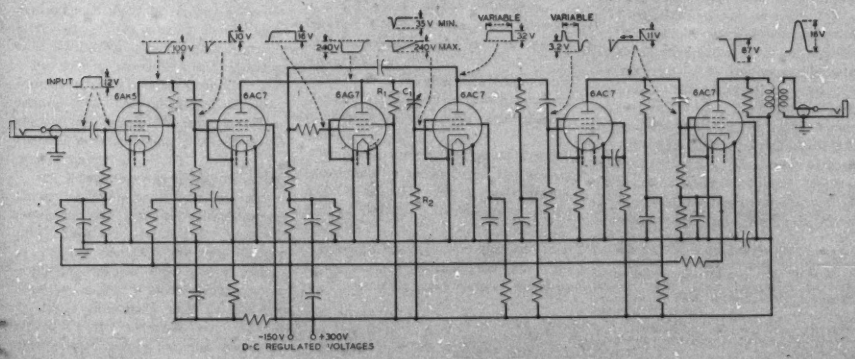

Figure 7. Precision delay circuit used for timing in heterodyne decrement method

R_1, R_2 = precision wire-wound noninductive resistors
C_1 = precision variable air capacitor

a change of one decibel at the intermediate frequency produces a change in video deflection observed on the scope of one-half inch. With this differential sensitivity the spot timing on the decrement curve can be adjusted to the reference line to an accuracy of ±0.05 decibel which is ±0.25 per cent of the 20-decibel change. The adjustment of the base line of the figure to the reference line cancels because consecutive measurements are made with the same adjustment. It is important to note that the oscilloscope is used as a comparison tool rather than for direct measurements which reduces observational errors.

Frequency Error. The error in frequency determination is a maximum of ±0.05 per cent.

Change in Attenuation. The error in the change in attenuation is within ±0.25 decibel which is ±1.25 per cent.

Over-all Accuracy

The errors for absolute and relative measurements are given in Table I.

Conclusion

Sets for the measurement of high Q resonant cavities at about 3,000 and 10,000 megacycles have been built and satisfactorily operated in both the laboratory and in the factory for production testing. A set operating at 24,000 megacycles has been used in the laboratory.

Reference

1. Resonant-Cavity Measurements, R. L. Sproull, E. G. Linder. *Proceedings*, Institute of Radio Engineers (New York, N. Y.), May 1946.

No Discussion

A Polyphase Thermal Ampere-Demand Meter

A. J. PETZINGER
MEMBER AIEE

Synopsis: Reduction of the initial and maintenance costs of the metering equipment required for the measurement of kilovolt-ampere demand has been an objective of the metering industry for many years. The development of a method of measuring polyphase ampere demand has made possible a simple and compact meter which registers kilowatt-hours and indicates maximum ampere demand. A good approximation of true kilovolt-amperes demand is then obtained by multiplying this maximum ampere demand by an assumed base voltage.

KILOVOLT-AMPERE DEMAND long has been one of the quantities which often is involved in billing a consumer for electric service. Undoubtedly one of the factors which has discouraged more widespread measurement of kilovolt-ampere demand has been the fact that the initial cost and maintenance of the metering equipment has been relatively expensive. Recording meters and indicating demand meters are available which measure true kilovolt-ampere demand, and their use is justifiable on large loads. On smaller loads, however, their use may be uneconomical.

For such applications a less expensive form of metering is highly desirable. It is natural that the possibility of using thermal meters should be investigated, as thermal meters require a minimum of maintenance.

One answer to the problem is the thermal kilovolt-ampere demand meter employing the displaced voltage principle. Taps are provided for metering at 100 per cent, 87 per cent, 71 per cent, and 50 per cent power factor. Accuracy is good if the operating power factor is reasonably close to the tap on which the meter is set. Besides the bimetal springs and the associated heaters and boxes, the required parts are two current transformers, two potential transformers, two phase shifting transformers, and facilities for tap changing. (In one form the potential and phase shifting transformers may be combined. For certain capacities the current transformers may be omitted on 3-wire circuits.)

There is, however, another approach to the problem which obtains kilovolt-ampere demand through the indication of a thermal ammeter. This paper deals with such a meter.

Single-Phase Meter

As electric service is supplied at various voltages and from various circuits, ampere demand as such is practically meaningless, unless the voltage is specified. For a given circuit and voltage ampere demand can be converted to kilovolt-ampere demand to provide a common basis. The scale of the meter shown in Figure 1 is, therefore, marked in kilovolt-ampere demand based on the normal circuit voltage.

On 2-wire circuits, the heaters are placed directly in series with the current winding of the watt-hour meter electromagnet.

On 3-wire meters, the use of a 3-wire transformer is necessary, as the heaters must be supplied with a single current which is equivalent to the currents in the two lines.

A simple example will illustrate this. If one heater were used in each line (Figure 2), the total heat generated would be

$$I_1^2R+I_2^2R$$

If $E_{10}=E_{20}=120$ and $E_{12}=240$, the kilovolt-ampere should be the same for $I_1=I_2=10$, $I_3=0$ as for $I_1=I_3=5$, and $I_2=0$, that is, 1.2 kva.

With $R=0.012$, the first case would give heat $=(10)^2\times0.012=1.2$ watts, whereas the second would give $(5)^2\times0.012+(5)^2\times0.012=0.6$ watts. However, if the currents are combined by a 3-wire transformer, each on a 1/1 basis, for example, the result in either event would be a secondary current of ten amperes (Figure 3).

If the voltages are balanced and of nominal value, the meter will read the correct value of kilovolt-amperes. The vector kilovolt-amperes also will be correct, if the power factors of the currents differ, as the transformer secondary current is proportional to the vector sum of the currents I_1 and $-I_3$. The minus sign indicates that the I_3 current is reversed or shifted by 180 degrees, the same angle as that between E_{01} and E_{02}.

Theory of Operation—Polyphase Meters

General

When an attempt is made to use the same principles on polyphase circuits, the problem immediately becomes more complicated. Even three ammeters on a 3-phase circuit do not provide the correct readings unless the load is balanced both as to magnitude and phase angle.

For example, suppose ammeters are placed in each line of a 240-volt 3-phase, 3-wire circuit. A 10-ampere load between lines causes two ammeters to read $10^2R=100R$, or a total or 2.4 for an arbitrary value of $R=0.012$. If the load is ten amperes on each line, the reading will be $3(10^2\times0.012)=3.6$. In the first case, the reading is the same as the kilovolt-amperes; in the second, the reading is 3.6 while the kilovolt-amperes equal 4.16. In this ex-

Paper 47-24, recommended by the AIEE committee on instruments and measurements for presentation at the AIEE winter meeting, New York, N. Y., January 27–31, 1947. Manuscript submitted November 12, 1946; made available for printing December 30, 1946.

A. J. Petzinger is with the meter engineering department, Westinghouse Electric Corporation, Newark, N. J.

Figure 1. A single-phase thermal ampere-demand watt-hour meter with kilovolt-ampere scale

ample, if the meter were adjusted to read kilovolt-amperes correctly on balanced load, it obviously would be incorrect on other loads.

As another example, a network circuit (two phases and neutral of a 3-phase, 4-wire Y circuit) is particularly subject to unbalanced loads and the totalized readings of two meters, one in each phase, give various values depending on the division of load between the phases.

Another consideration is the assumption of a coincident maximum demand on the several meters. This is not necessarily the case. A further objection to the use of a thermal ammeter in each phase is the complication and cost incident to the purchase, installation, maintenance, reading, and billing of such a combination.

If now a single meter is to be used, it is obvious that some method must be found of properly shifting the individual currents by the required amounts and obtaining the vector sum before the result is applied to a thermal unit. It is evident that no combination of the sums or differences of the currents in a polyphase circuit will accomplish this.

Meter for the 3-Phase 4-Wire Delta Circuit

The desired result, however, can be obtained by another method. First it may be well to define the kilovolt-amperes of any circuit. The kilovolt-amperes or vector power is defined as the square root of the sum of the squares of the total active power and the total reactive power. The common methods of measuring kilovolt-ampere conform to this definition.

The basis of the method of phase shifting is the fact that a given current flowing through a resistance will produce a voltage drop in phase with the current, whereas the same current flowing through the primary winding of a mutual inductance will produce an induced voltage in the secondary, which is 90 degrees out of phase with the current. Figure 4 shows the basic circuit for use on a 3-phase 4-wire delta system.

If R_H is open-circuited, the voltage E across the open section is

$$j\omega MI_1 - j\omega MI_3 + I_3R$$

If

$$R = \sqrt{3}\omega M$$

Then

$$E = \omega M(jI_1 - jI_3 + \sqrt{3}I_3)$$

Though it is not an operating condition, a load consisting of resistances between lines and neutral with all line currents of equal magnitude is helpful in visualizing the operation of the circuit. In such a case the kilowatts equal the kilovolt-amperes. Figure 5 shows the vectors for this circuit with the load described. If the single-phase 3-wire portion of the circuit is considered first, it is seen that the voltage derived from current in line 1 is rotated 90 degrees counterclockwise by the mutual inductance, whereas that derived from the current in line 2 is rotated 90 degrees clockwise, with reference to the respective currents. These two voltages are, therefore, in phase and add just as the currents in the case of the single-phase 3-wire ammeter.

The current in line 3 has been assumed to be of the same magnitude as the other two lines, but the voltage, E_{30}, is $\sqrt{3}$ times as large as E_{10} or E_{20}. The voltage derived from line current 3 therefore should be $\sqrt{3}$ times as large as each of the others, and this voltage also should be in phase with the others. A resistance drop of the required magnitude fulfills these conditions ($R = \sqrt{3}\omega M$).

It is apparent that increasing the magnitude of the current in any line will increase the resultant voltage by the proper amount. Also, if any line of the currents has a reactive component, this reactive component will produce a component in the resultant output voltage which is 90 degrees out of phase with the active component of the voltage. The resultant voltage therefore, will be a measure of the circuit kilovolt-amperes if the system voltages are assumed to be balanced and of normal magnitude.

The voltage E is the voltage across R_H assumed as an open circuit. If this open

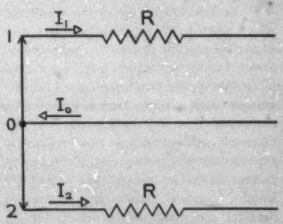

Figure 2. Ammeter for 3-wire service with heater in each leg

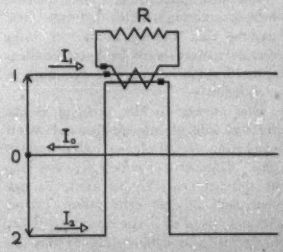

Figure 3. Ammeter for 3-wire service with 3-wire transformer and single heater

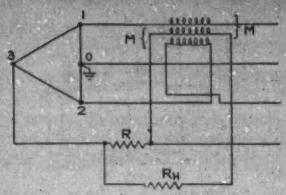

Figure 4. Basic circuit for a polyphase ammeter on 3-phase 4-wire delta service

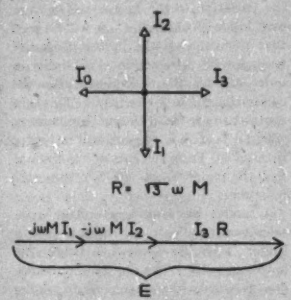

Figure 5. Vector diagram for Figure 4 with each phase resistance loaded to neutral

circuit is closed, the current circulating in the loop will be

$$I_H = E/\sqrt{(R+R_H)^2+\omega^2L^2}$$

where L is the self-inductance of the secondary winding of the mutual inductance, and R_H is the resistance of the heaters of a thermal ammeter unit. The current is, therefore, proportional to the vector kilovolt-amperes of the polyphase circuit at a given voltage, as the loop impedance is constant.

Operation of 3-Phase 4-Wire Delta Meter on Different Loads

Figure 6 shows the vector diagram for various other types of single-phase and polyphase loads, all of which are correctly metered.

It will be noted that the resultant voltage of all kilowatt loads lies along the E_{30} vector, while that of the lagging var load lies along a vector lagging the E_{30} vector by 90 degrees. The vector kilovolt-ampere is, therefore, correct, regardless of what the phase angle of the various loads may be.

In Figure 6 the voltage referred to is the voltage across R_H in Figure 4, if it is assumed to be an open circuit. In Figure 6 the conditions are shown for a balanced polyphase load. In this case $j\omega MI_1$ leads I_1 by 90 degrees, $-j\omega MI_2$ lags I_2 by 90 degrees, and I_3R is in phase with I_3. As shown by the voltage vector diagrams, the sum of these terms $=2\sqrt{3}$ for the values assumed, and this is equal to the kilovolt-amperes of the load.

Figure 6 shows the conditions for a single-phase load across lines 1 and 2. In this case the voltages $j\omega MI_1$ and $-j\omega MI_2$ are in phase and add up to two, which again equals the kilovolt-ampere of the load.

Figure 6 shows the conditions for other single-phase loads. In each case the resultant voltage is the sum of a reactance and resistance term of magnitudes 1 and $\sqrt{3}$ respectively, which gives a resultant of two.

Figure 6 shows a combination of a unity power factor load of 1 kw and 50 per cent load factor balanced polyphase load of $\sqrt{3}$ kva. The vector kilovolt-ampere equals 2.4, and the voltage E likewise totals 2.4. In determining the magnitude of E, the two loads may be treated independently to determine the voltage contributed by each. These voltages, however, must be added vectorially to determine E. As mentioned before, the resultant voltage on a unity power factor load is always along the 3–0 direction, whereas that of reactive loads is along the 1–2 direction in Figure 4.

Other Circuits

For 3-phase 3-wire circuits, the same arrangement can be used, as the neutral current was not involved in the 3-phase 4-wire delta meter.

For network service from a 3-phase 4-wire Y circuit, the diagram in Figure 7 applies.

For 3-phase 4-wire Y service, the circuit shown in Figure 8 may be used. In this case a 3-wire transformer, with polarity as shown, is used to achieve the required shift.

The use of transformers permits the circuits to be modified. The circuits actually used in the various services are shown in Figures 9 to 12. The derivation of these circuits is given in Appendix I.

Application of Symmetrical Component Theory

As stated before, it is assumed that the voltage is balanced. This is an assumption that is common to several forms of kilovolt-ampere metering. For example, a true kilovolt-ampere meter measures the vector sum of the kilowatt and kilovar registrations. The kilovar meter usually employs phase shifting transformers to obtain potentials of the desired magnitude

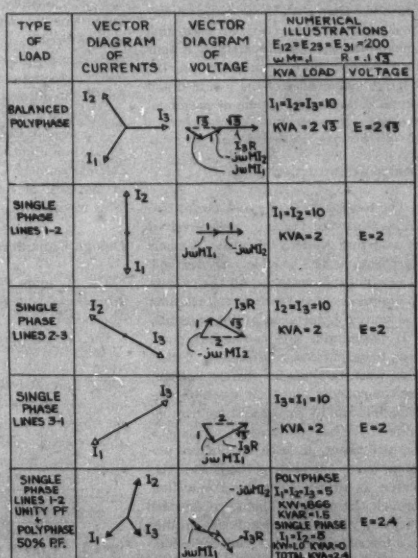

Figure 6. Vector diagram of currents and voltage for various loads on circuit of Figure 4

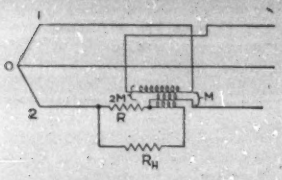

Figure 7. Polyphase ammeter circuit without transformers for network service

and phase. Whenever phase shifting transformers are used, balanced voltages are assumed, and errors result from unbalanced voltages.

A common form of phase shifting transformer, for example, used on 3-phase 4-wire Y circuits, is shown in Figure 13. E_{DE} is the voltage which should be equal to E_{AN} and should lag it by 90 degrees. The error is actually *twice* the negative sequence voltage plus the zero sequence voltage. (See Appendix II.) Similarly for 3-phase 3-wire circuits, the error is twice the negative sequence voltage.

As the meters described measure the positive sequence current, only the positive sequence volt-amperes are measured. The error due to unbalance is, therefore, equal to the negative sequence (and sometimes the zero sequence) volt-amperes. The unbalance error, therefore, is much less than that of conventional var-hour meters. The error in measuring kilovolt-ampere by this method is thus dependent almost completely on the relative magnitudes of the assumed and actual voltages at the time of maximum demand.

Meter Construction

The foregoing circuits and vector diagrams illustrate the principles involved in metering various circuits. Various modifications are possible and desirable in designing the meters. All the circuits in Figures 4, 7, and 8 show the resistors and mutual inductances at line potential.

It is desirable and convenient, however, to use current transformers. Otherwise, when the value of current is large, the components and their assembly become difficult to handle and control because of the heavy cable size. Also, in a thermal meter, if large conductors are connected to the heaters, the heat in the heaters is drawn away by conduction through the cables. This decreases the efficiency with a correspondingly greater watt loss required for full scale deflection. It will be seen that the resistor R, Figure 6, is connected to heater R_H. As will be shown later, the current in the resistor is not the same for equal loads in different phases. This is illustrated by Figure 14. If the heater and resistor are connected by heavy cable, the heat in the resistor will affect that in the heater because of the excellent conduction between them. If current transformers are used, this tendency can be made insignificant.

The use of the current transformers also makes possible variations of the basic circuit as shown in Appendix I.

Figure 15 shows the meter used for 3-phase 3-wire service. The size of the meter is the same as that of 3-element watt-hour meter. The terminal block and trim are the same as the 2-element meter for the same service. All watt-hour meter parts are essentially the same as those of the corresponding watt-hour meter.

To obtain balance between the phases, either the mutual inductance or the resistance must be adjustable. In the meter shown, the iron-cored mutual inductance is adjustable by means of a sliding keeper shunting its air gap. When the meter is calibrated for proper balance, the simplest way is to check the voltage across a heater by means of a vacuum tube voltmeter while single-phase current is passed through successive phases.

Another advantage of using current transformers is that the components—heaters, resistors, and mutual inductances—for the several circuits can be standardized easily. Also various full-scale capacities are possible by changing current transformer ratios without changing the circuit components or the method of assembling them.

The scale of the meter has a basically squared distribution, as do those of other thermal ammeters. It can be calibrated in amperes, or for a given voltage, in kilovolt-amperes.

Design Considerations

The optimum value of the heater resistance can be determined as outlined in Appendix III.

The curves shown in Figure 14 show

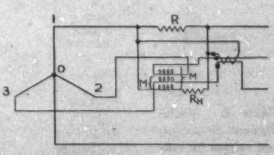

Figure 8. Polyphase ammeter circuit with one transformer for 3-phase 4-wire Y service

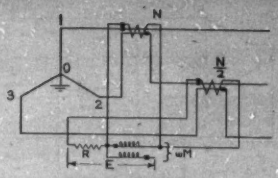

Figure 9. Polyphase ammeter circuit with transformers for 3-phase 4-wire Y service

the variation in the heater and resistor watt loss with variable x. It will be seen that the value of the heater resistance need not be held within close limits in order to keep the deflection within the calibrating range of the meter. This is in contrast to the usual thermal ammeter in which deflection is proportional to heater resistance. From the curves it is evident that the meter is not sensitive to heater resistance.

Actually, ambient temperature considerations make it desirable to use a heater resistance somewhat below the optimum value. The mutual inductance does not vary with the temperature, so the resistor and the heater likewise should have zero temperature coefficient. An unheated bimetal spring opposes the heated spring, thus canceling most of the ambient temperature errors in the springs. However, there still remains a tendency for the deflection to fall off with increasing temperature. It is therefore desirable to use heater material with a slightly positive temperature coefficient and to keep the heater resistance below the optimum value. Then, as the temperature rises, the heater resistance increases slightly, which in turn increases the deflection. Conversely, if the bimetal deflection characteristics were positive, the heater resistance should be kept above the optimum value.

When transformers are used, they may employ different ratios in the different phases. For the circuit shown in Figure 12, assume the transformer ratio for phases 1 and 2 is N_1, and the ratio for phase 3 is N_2. Then

$$R = \frac{N_1}{N_2}\sqrt{3}\omega M$$

Also the optimum value of heater resistance becomes

$$R_H = \omega M\sqrt{3\frac{(N_1)^2}{(N_2)^2}+1}$$

While the efficiency may be decreased, if $N_1/N_2 \neq 1$, there may be compensating

advantages in the standardization of components and ease of manufacturing them.

A study of Figure 14, which applies to the 3-phase 4-wire delta circuit of Figures 4 and 12, discloses interesting information. The heat in the resistor at balanced load is a minimum when $R_H/\omega M=2$. This is to be expected, as the heat in the heater is a maximum at this point. It is important, also to note that the heat in the resistor on full-scale balanced load is much less than the heat in the resistor at one-third scale for any possible single-phase load. The reason is that the current circulated in the heater circuit almost completely cancels the current which would flow in the resistor if the heater circuit were opened. Also, the single-phase load which causes the greatest resistor loss is a load across lines 1 and 3 which, normally, is not an operating condition. Near $R_H/\omega M=2$ the heat in the resistor is almost the same for a load across lines 1–2 as across 2–3. Single-phase loads across lines 1–2 or 1–0 and 2–0 are normal operating conditions.

Similar curves can be drawn for other circuits. In each case, it is usually best to design for the minimum loss in the resistor on balanced load.

As might be suspected, there are numerous circuits which may be used to perform the desired phase shifts on a polyphase circuit. For example, a simple interchange of the function of resistance and reactance (multiplying the equations by $-j$), gives circuits which are entirely practical. One criterion of the relative excellence of different circuits is heat loss in the resistor. On a thermal meter the total heat generated must be limited in order to prevent excessive temperature rise, or to permit operation over wide ambient temperature ranges. One method of controlling this factor is to select the most efficient circuit. Another factor of practical importance is the size of the resistor required, which varies directly with the watt loss. The relative heat in the heater and resistor is, therefore, an important design consideration.

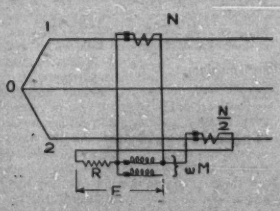

Figure 10. Polyphase ammeter circuit with transformers for network service

Testing

The polyphase thermal ampere-demand meter is tested like other thermal meters, with two exceptions:

1. Balance between phases is adjusted most conveniently by checking the voltage across a heater with a vacuum tube voltmeter when a single-phase load is applied. On the meters described, current in phase 1 feeds only the mutual inductance which is adjustable. The other phases are affected only slightly by the adjustment.

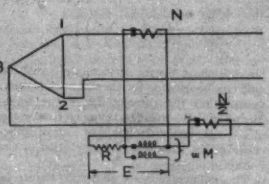

Figure 11. Polyphase ammeter circuit with transformers for 3-phase 3-wire service

2. Full-scale calibration should be set on a balanced polyphase load. A single-phase current can be passed through each phase of the meter in series, direct or reversed, but this is not an operating condition, and full-scale current will not produce full-scale deflection. The use of single-phase current is, therefore, undesirable for calibration.

After a standard has been established it is no longer necessary to control the magnitude and balance of the current exactly, as test meters can be calibrated to read the same as the standard.

Application

One feature of any squared scale instrument which must be recognized is that half of full-scale current corresponds to only one-fourth scale deflection, and so forth. In the case of a 45-ampere full-scale meter, the lowest current marked on the dial is 10 amperes. Also, any error which is independent of deflection causes a relatively high percentage error in terms of the full-scale current at low points on the scale, and small percentage errors at high scale values. An error which at a 15-ampere load would represent a 1-ampere error on the scale would represent only a 0.3-ampere error at a 45-ampere load, as the linear distance between successive ampere points is three times as great at 45 amperes as at 15 amperes.

Conclusion

The meter described in this paper should be useful to those who are searching for more economical means of metering kilovolt-ampere demand on loads which, heretofore, have been too small to justify that type of metering. The use of an assumed voltage perhaps will be looked upon with disfavor in certain quarters. However, it is almost certain that the possibility of measuring kilovolt-amperes to a good approximation at relatively low cost will more than offset any disadvantages of this type of meter.

Appendix I

On a 3-phase 4-wire Y circuit (Figure 9), the currents I_1 and I_3 must be shifted by 120 degrees and 240 degrees, respectively, with reference to I_1. If I_1 is assumed to feed a mutual reactance, it can be seen that the required voltage would be

$$E=-j\omega M\left[I_1+I_3\left(-\frac{1}{2}+j\frac{\sqrt{3}}{2}\right)+I_3\left(-\frac{1}{2}-j\frac{\sqrt{3}}{2}\right)\right]$$

When I_3 is added to and subtracted from the quantity in brackets

$$E=-j\omega M\left[I_1+I_3\left(\frac{1}{2}+j\frac{\sqrt{3}}{2}\right)-I_3\left(\frac{1}{2}+j\frac{\sqrt{3}}{2}\right)-I_3\right]$$

$$=-j\omega M\left[(I_1-I_3)+\left(\frac{I_3-I_1}{2}\right)(1+j\sqrt{3})\right]$$

$$=-(I_1-I_3)j\omega M+\left(\frac{(I_3-I_1)}{2}\right)\times(\sqrt{3}\omega M-j\omega M)$$

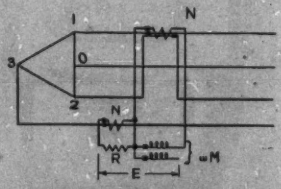

Figure 12. Polyphase ammeter circuit with transformers for 3-phase 4-wire delta service

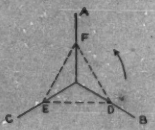

Figure 13. Schematic diagram of phase shifting transformer for 3-phase 4-wire Y service

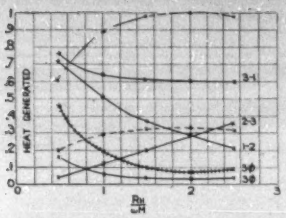

Figure 14. Heat in heater and resistor on various loads for meter of Figure 4 for different ratios of heater resistance to mutual resistance

——— Heat generated in resistor for load giving one-third scale deflection on phase indicated

▬▬▬ Heat generated in resistor for full-scale balanced load

- - - - Heat generated in heater for one-third scale deflection

—·—·— Heat generated in heater for full-scale deflection

Replacing $\sqrt{3}\omega M$ by R yields

$$E=-(I_1-I_2)j\omega M+\left(\frac{(I_2-I_3)}{2}\right)(R-j\omega M)$$

This can be measured by the circuit shown in Figure 9. The turn ratio (primary/secondary) of the transformer in lines 2 and 3 is half that of the transformer in lines 1 and 2.

On 3-wire network service, a similar circuit is shown in Figure 10. The voltage E for this circuit is

$$E=I_1j\omega M-\frac{I_3}{2}(R+j\omega M)$$

where

$$R=\sqrt{3}\omega M$$

or

$$E=j\omega M\left[I_1+I_3\left(-\frac{1}{2}+j\frac{\sqrt{3}}{2}\right)\right]$$

On a 3-phase 3-wire service, the same circuit can be used as for the network service, except that the connections of the transformer in line 3 must be reversed from those of the transformer in line 2 of Figure 10 because of the different phase relation of the voltages.

The connections are shown in Figure 11 where

$$E=I_1j\omega M+\frac{I_3}{2}(R+j\omega M)$$

where

$$R=\sqrt{3}\omega M$$

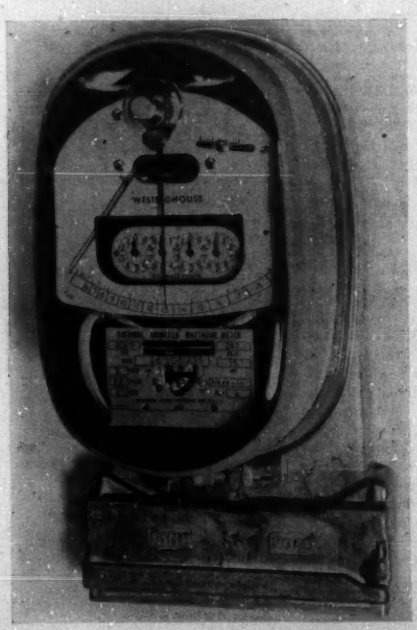

Figure 15. A polyphase thermal ampere-demand watt-hour meter with kilovolt-ampere scale

Appendix II

See Figure 13. For phase A:

Voltage required $=jE_{NA}$

Voltage obtained $=\frac{\sqrt{3}}{3}(E_{NC}-E_{NB})$

$$\text{Error}=\frac{\sqrt{3}}{3}(E_{NC}-E_{NB})-jE_{NA}$$

$$=\frac{\sqrt{3}}{3}E_{NC1}+\frac{\sqrt{3}}{3}E_{NC2}+\frac{\sqrt{3}}{3}E_{NC0}$$

$$-\frac{\sqrt{3}}{3}E_{NB1}-\frac{\sqrt{3}}{3}E_{NB2}-\frac{\sqrt{3}}{3}E_{NB0}$$

$$-jE_{NA1}-jE_{NA2}-jE_{NA0}$$

The sum of the positive (subscript 1) sequence terms $=0$ (first column)

The sum of the negative (subscript 2) sequence terms $=-2jE_{NA2}$ (second column)

The sum of the zero (subscript 0) sequence terms $=-JE_{NA0}$ (third column)

Total error for measurement is therefore $-2\times$negative sequence power$-$zero sequence power, as all phases are analyzed the same way.

Appendix III

For the 3-phase 4-wire delta circuit:

$$E=j\omega MI_1-j\omega MI_3+RI_3$$
$$R=\sqrt{3}\omega M$$

The heater current, on balanced polyphase load

$$I_H=\frac{E}{Z}=\frac{2RI_3}{\sqrt{(R+R_H)^2+\omega^2L^2}}$$

where L is the self-inductance of the secondary winding of the mutual inductance. For equal primary and secondary turns $L=M$

Let

$$\frac{R_H}{\omega M}=x$$

$$I_H=\frac{2\sqrt{3}I_3\omega M}{\sqrt{(R+R_H)^2+\omega^2M^2}}$$

$$=\frac{2\sqrt{3}I_3}{\sqrt{(\sqrt{3}+x)^2+1}}$$

The watts dissipated in the heater

$$W_H=\frac{12I_3^2\omega Mx}{3+2\sqrt{3}x+x^2+1}=\frac{12I_3^2\omega Mx}{4+2\sqrt{3}x+x^2}$$

For a maximum

$$\frac{\partial W_H}{\partial x}=0$$

$$4+2\sqrt{3}x+x^2=2\sqrt{3}x+2x^2$$

$$x^2=4$$

$$x=2=\frac{R_H}{\omega M}$$

Therefore, for maximum efficiency $R_H=2\omega M$.

Discussion

G. G. Waite (Sangamo Company, Ltd., Toronto, Ontario, Canada): In this paper the author has called attention to the merits of measuring demand in amperes. On single-phase circuits this has much to commend it. On polyphase circuits the wisdom is debatable.

Why shy away from scaling the meter in amperes? What is wrong with amperes? Almost any customer can comprehend amperes. Is straightforward simplicity conducive to bad customer relations?

It would seem also that the author, by omitting reference to the $\sqrt{\Sigma I^2}$ type of polyphase demand ammeter, sacrificed unnecessarily the value of his paper. This type of ammeter recognizes unbalance, and for this reason is used in several parts of the world.

The author stresses the economy of his "kilovolt-ampere" ampere-demand meter. In fairness it should be pointed out that the $\sqrt{\Sigma I^2}$ ampere-demand meter is much simpler to build and calibrate.

Wm. C. Downing, Jr. (Sangamo Electric Company, Springfield, Ill.): For the measurement of kilovolt-amperes in single-phase circuits, the use of the thermal demand ammeter, scaled in kilovolt-amperes at a nominal voltage, offers a means of measurement, or approximation, at much lower cost than any device which actually involves the measured voltage. This is due not only to the inherent simplicity of the thermal ampere demand meter but, in part at least, to the difficulty involved in measurement of true kilovolt-amperes in single-phase circuits. Though a thermal kilovolt-ampere demand meter operating upon the displaced voltage principle can be, and is, made to operate on single-phase, to the writer's knowledge, it is not made except for a single power factor condition; as such a meter does not have the flexibility afforded by the various power factor taps of the corresponding polyphase meter, its use for the measurement of single-phase kilovolt-amperes, as such, definitely is restricted. This leaves a considerable gap between the thermal ampere demand meter, scaled for an assumed voltage, and meters which combine power and reactive power to introduce the factor of measured voltage in the measurement of single-phase kilovolt-amperes.

In polyphase circuits, however, this situation is altered by the availability of the displaced voltage type of thermal-kilovolt-ampere demand meter, and it may be questioned, therefore, whether ampere demand, as represented by this very ingenious polyphase meter described by Petzinger, offers appreciable savings in comparison to existing types.

A comparison of the displaced voltage type of thermal kilovolt-ampere demand meter, in which the potential transformers serve also for phase shifting, with the polyphase ampere demand meter shows, on the basis of components: two potential and two current transformers and a tap changing device for the kilovolt-ampere meter; two current transformers, one resistor, and an adjustable mutual inductance for the ampere demand meter. This assumes that substantially the same thermal element is involved in either design; actually, they will differ in detail, as both bimetallic coils must be heated in the former type, whereas only the driving coil is heated in the latter. On the other hand, the problem of thermal lagging, to meet the time interval as defined for thermal demand meters, becomes more difficult for ampere demand, as, due to its inherent square scale characteristic, an ampere demand meter shows less than three fourths of the time interval obtained from a watt demand meter of similar construction. It would be of interest to know, therefore, whether this ampere demand meter can be provided in both 15- and 30-minute intervals, as is the displaced voltage type of instrument.

On the basis of testing, the problem is essentially the same: a complete test means a polyphase test. If, in the manufacture of the displaced voltage type meter, the potential tranformers are tested on polyphase, or by an equivalent single-phase test, then subsequent calibrative testing or checking may be made on single-phase by testing as a watt-demand meter on the unity power factor tap; as the transformers are not subject to change, such a single-phase test is generally adequate. It seems likely that some such method can be developed for the polyphase ampere demand meter, as well, to obviate the necessity of polyphase test.

If, in the matter of accuracy on unbalanced voltages, we accept Petzinger's conclusions that the error in the kilovolt-ampere meter is greater than that of the ampere demand meter, still is it not reasonable to expect that, where the regulation of the supply is such that appreciable voltage unbalance may exist, the departure of the actual voltage magnitude from that assumed may be even more of a factor?

As is pointed out in this paper, any ampere demand meter has, inherently, a square scale, which results in limiting the lower end of the scale to perhaps one fourth or one fifth of the maximum scale value. In contrast to this, the displaced voltage kilovolt-ampere meter has a substantially linear scale and provides, therefore, a useful reading range four to five times as great as that of the ampere demand meter with the same degree of reading accuracy. This means that more different capacities must be available in order to cover adequately a wide range of loads; that the load must be estimated with fair accuracy to permit selection of the proper capacity meter; and that more frequent meter replacement, due to variation of maximum demand, must be expected with the ampere demand meter than with the longer range instrument.

Whether these various factors add up to a more economical method of measuring polyphase kilovolt-ampere demand than with the kilovolt-ampere demand meters currently available is a question that will be decided by time and the requirements of the central station industry. In any event, however, Petzinger's paper presents a new and stimulating solution to the problem of kilovolt-ampere demand measurement; the author is to be congratulated upon it.

A. J. Petzinger: Waite has questioned the desirability of measuring ampere demand on polyphase circuits. There seems to be no fundamental reason why this type of metering should be confined to single-phase circuits.

As far as scaling the meter in amperes is concerned, this is quite possible and, in one respect at least, is desirable. That is, if the meters are scaled in amperes, they may be used on a given circuit regardless of whether the nominal voltage is 115 or 120 volts. On the other hand, present practice, in the United States at least, makes kilovolt-ampere-demand a familiar billing term, whereas, ampere demand is not used so widely. Also, kilovolt-ampere marking is preferable in another respect; namely it is more universal. A demand of a given number of amperes represents one quantity on a 120-volt 2-wire circuit, another on a 240-volt 3-wire single-phase circuit, and still another on a 240-volt polyphase 3-wire circuit. When a kilovolt-ampere scale is used, a given number of kilovolt-amperes represents just that, regardless of type of circuit or voltage.

The operation of the meter described is based on the kilovolt-amperes concept insofar as a given kilovolt-amperes load will produce the same deflection regardless of the current which produced it. For that matter the common single-phase thermal ammeter does likewise. A 10-ampere line to line load indicates 10 amperes on an ampere scale, whereas a 10-ampere line to neutral load indicates 5 amperes. As the actual currents are not being indicated anyway, and as the ampere reading really requires definition, it seems simpler and more direct to use the kilovolt-ampere scale. This, however, is an open question, and the ultimate answer probably will be based on the relative merits in practical application.

Waite suggests the use of a $\sqrt{\Sigma I^2}$ meter and states that this type of meter "recognizes" unbalance. The recognition, however, is of very dubious value. The meter described in this paper recognizes unbalance in the sense that the same kilovolt-amperes load gives the same deflection, regardless of which phase or phases are loaded. The recognition advocated by Mr. Waite merely consists of ignoring this principle and assuming that the arbitrary increased reading on an unbalanced load is a proper penalty for unbalance. This idea contains the following two questionable assumptions:

1. That unbalanced load should be penalized.
2. That the size of the penalty should be in cordance with the reading of a $\sqrt{\Sigma I^2}$ meter.

As to the first, it is not clear why unbalanced loads should be considered so objectionable on polyphase circuits but not on single-phase circuits. In fact, the 3-phase 4-wire delta circuit and the 3-wire network circuit basically are provided for unbalanced loads. It seems contradictory to provide a circuit for combined lighting and power and then to penalize a customer for using the facilities provided.

Waite has not made clear just how such a meter would be used on these nonsymmetric services. On a 3-phase 4-wire delta circuit, for example, the use of equal heaters in each line would encourage loading across 208 volts, as it would cost no more than 120 volts. If the resistance of the heater in this phase were made proportionally larger, it is evident that a single-phase line-to-line load would give different read-

ings, depending on which phase was loaded.

If it were granted that unbalance should be penalized, the second assumption—that the size of the penalty should be in accordance, with the reading of a $\sqrt{\Sigma I^2}$ meter—seems to have no basis other than convenience. It would seem to be a remarkable coincidence, if the meter's reading should provide exactly the desired penalty under all unbalance conditions.

A comparison of the cost of the polyphase ammeter type of kilovolt-amperes meter versus the displaced-voltage type shows, as Downing points out, and as the paper also indicates, that the former requires a mutual reactor and a resistor, while the latter requires two combined potential and phase shifting transformers and a tap changing device. Both require current transformers. However, this enumeration of components does not make apparent the difference in cost or size of these components. The thermal ammeter has a pronounced advantage in both respects. In a combination watt-hour and thermal kilovolt-ampere demand meter, particularly, space is important.

Downing calls attention to the basic difference in time interval of an ammeter from a wattmeter of a given construction. It is possible that development of a 30-minute interval device, if required, may be somewhat more difficult than that of the corresponding wattmeter, but this should not prove at all insurmountable.

As far as the effect of voltage is concerned, the paper merely attempted to show that voltage magnitude was the only factor of any consequence. It should be kept in mind that electricity is distributed on a constant voltage basis and not on a constant power factor basis. A displaced voltage meter, therefore, requires a certain amount of checking to determine the proper tap setting and assumes that the power factor will be reasonably close to the setting.

The paper also called attention to the scale limitations mentioned by Downing. Assuming, as did Downing, that the lower end of the scale would be limited to one fourth of full scale, it is difficult to accept his conclusion that the useful range of a linear scale meter would be four times as great. For example, if the full-scale value of an ammeter were 30 amperes, the lowest reading permissible, on this basis assumed, would be $7^1/_2$ amperes. A linear scale meter, on the equivalent basis, could be read to 2 amperes. The useful range of the ammeter, therefore, would be $22^1/_2$ amperes, whereas that of the displaced voltage meter would be 28 amperes. The range of the ammeter is, therefore, 80 per cent, of that of a linear scale meter. It is doubtful that this would affect the number of capacities required, the estimation of loads, or the frequency of meter replacements to any considerable extent.

The discussions should be of value in clarifying the field of application for the polyphase thermal ammeter. The ultimate decision, of course, will rest with the users, and this meter has been described as a new alternative which undoubtedly will find considerable application.

Electrical Characteristics of the Junction in a Simplified Selenium Rectifier Cell

STEPHEN JAMES ANGELLO
ASSOCIATE AIEE

Synopsis: The selenium-cadmium contact is a simplified version of the commercial selenium rectifier and is studied with the purpose of understanding the physics of contact resistance asymmetry. A theory by W. Schottky, which predicts the contact resistance at zero voltage and the course of this resistance with d-c reverse bias, is not adequate to account for the experimental data. An attempt is made to extend the theory by assuming a fraction of the bromine ions in the selenium to be free. Agreement with experiment is obtained for low voltages at a high temperature, but for high voltages at all the temperatures employed there is marked disagreement. The theory developed is sufficiently general to conclude that the contacts studied have either a polarizable layer less than 10^{-5} centimeter thick between the cadmium and selenium, or there is a mechanism of deactivation of bromine ions at higher voltages. The experiments do not distinguish between the alternatives.

THE PURPOSE of this paper is twofold.

1. To present data on the capacitance and resistance of a selenium-cadmium contact which can be compared with the theoretical predictions made by W. Schottky.[1]

2. To extend Schottky's theory in an attempt to obtain quantitative agreement between the theory and experimental data.

Metallic selenium containing 0.01 per cent by weight of bromine is a semiconductor[2] with a conductivity of approximately 4×10^{-2} mho per centimeter at 25 degrees centigrade. A pure cadmium electrode sprayed on the selenium results in a contact which has a resistance of about 4×10^{4} ohms for one square centimeter at zero volts. The contact resistance is dependent on the voltage applied to the contact and exhibits a remarkable asymmetric variation of values depending on the sense of voltage. Details of the preparation of samples for this work are given in Appendix I.

The simple selenium-cadmium contact should fulfill the conditions on which Schottky's theory is based, but the experimental data are in serious disagreement with predicted results.

Theory

Differential Resistance

Schottky[1] has shown that the relation between the current i through a selenium-cadmium contact and the voltage U applied is

$$i=\sigma_R E_R \frac{1-exp(-U/B)}{1-[exp-(U+V_D)/B]} \tag{1}$$

where

$\sigma_R = n_R e b$
n_R = electron density in the selenium at the metal junction
e = electronic charge
b = electron mobility (average velocity per unit field strength)
$B = kT/e$
k = Boltzmann's constant
T = absolute temperature
$V_D = -B\ ln(n_R/n_R)$
n_R = electron density in the selenium far from the contact
E_R = the electric field strength at the junction

In this paper interest is centered on the high resistance direction for which $U=+U_h$. The constant V_D is known to be much greater than B. Hence

$$i_h=\sigma_R E_R[1-exp(-U_h/B)] \tag{2}$$

An important concept is the differential resistance R defined by

$$R=\left.\frac{dU}{di}\right|_i \tag{3}$$

For the special case of low voltage ($U_h<B$), equation 2 can be written

$$i_h=\sigma_R E_R(U_h/B) \tag{4}$$

and an application of equation 3 yields the resistance at zero volts

$$R_0=\left.\frac{dU}{di}\right|_{i=0}=B/\sigma_R E_R \tag{5}$$

Applying equation 3 to equation 2 permits evaluation of the differential resistance at any voltage in the high resistance direction. The result is

$$R=\frac{2V_D R_0}{B}\frac{(1+U_h/V_D)^{1/2}}{\{1+exp(-U_h/B)\times[(2V_D/B)(1+U_h/V_D)-1]\}} \tag{6}$$

The differential resistance can be measured directly with the a-c bridge described in Appendix II.

Field Strength E_R

Contemporary theoretical discussions of the selenium-cadmium contact agree that the cadmium metal causes an electron redistribution in the selenium at the boundary which results in a thin layer of negative space charge in the selenium. This charge may be associated with ionized bromine which purposely was added to the selenium to modify the electrical properties. Schottky assumes that the bromine ions are distributed uniformly and fixed in position. As there is a space charge density $\rho(x)$ in the boundary layer, the electric field $E(x)$ is given by the Poisson relation

$$\frac{dE(x)}{dx}=-(4\pi/\epsilon)\rho(x) \tag{7}$$

Paper 47-26, recommended by the AIEE committee on electrochemistry and electrometallurgy for presentation at the AIEE winter meeting, New York, N. Y., January 27–31, 1947. Manuscript submitted October 15, 1946; made available for printing December 3, 1946.

Stephen James Angello, formerly a research engineer with Westinghouse Research Laboratories, is now an assistant professor of electrical engineering at the Moore School of Electrical Engineering, University of Pennsylvania, Philadelphia, Pa.

The author gratefully acknowledges the support of Westinghouse Research Laboratories where the work was carried out and the preparation of the selenium-cadmium contacts by Theodore Ebert of the same laboratory.

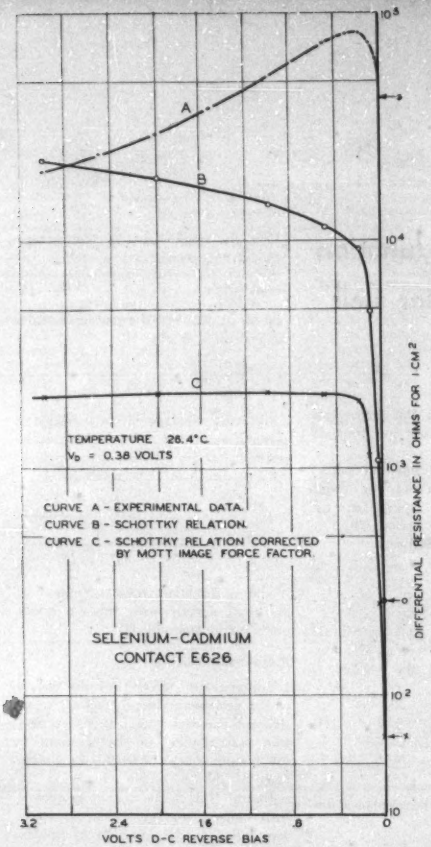

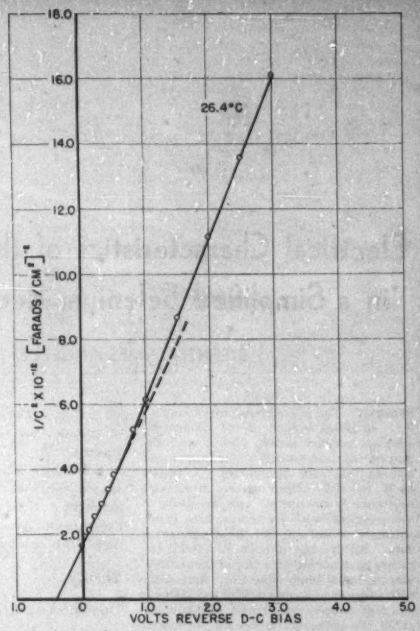

Figure 1 (left). Experimental data compared with data computed from Schottky's formula, equation 6

Figure 2 (above). Selenium-cadmium contact capacity variation with reverse voltage

Selenium-cadmium contact E626

where κ is the dielectric constant of selenium. The development is confined to the case in which $\rho(x)=eN_D$, where N_D is the bromine ion density and is constant through the selenium.

It is convenient to introduce the potential $V(x)$ defined in the usual way so that

$$\frac{d^2V(x)}{dx^2}=(4\pi/\kappa)eN_D \tag{8}$$

Multiplying both sides of equation 8 by dV/dx gives

$$\left(\frac{dV}{dx}\right)\left(\frac{d^2V}{dx^2}\right)=\frac{d}{dx}\left[\frac{1}{2}\left(\frac{dV}{dx}\right)^2\right]=(4\pi/\kappa)eN_D\frac{dV}{dx} \tag{9}$$

Both sides of equation 9 can be integrated to obtain

$$\left(\frac{dV}{dx}\right)^2=(8\pi/\kappa)eN_DV+\text{constant} \tag{10}$$

At a distance from the contact where the cadmium does not affect the electron distribution in the selenium, $V(x)$ and $dV(x)/dx$ are zero. Hence the constant is zero. Finally,

$$E_R=\left.\frac{dV}{dx}\right|_{x=0}=[(8\pi/\kappa)eN_D(V_D+U_h)]^{1/2} \tag{11}$$

Using equation 11, the null resistance of equation 5 becomes

$$R_0=\frac{B}{{}_R(8\pi eN_D/\kappa)^{1/2}V_D^{1/2}} \tag{12}$$

If the quantities N_D and V_D can be found, enough data is available to compute R_0. The theory underlying the determination of these quantities is described in the next section on capacity.

Capacity

The boundary layer of a cadmium-selenium contact behaves as a parallel resistance and capacitor to the alternating voltage employed in the bridge. The capacitance of the contact is given by

$$C=\kappa/4\pi l_k \tag{13}$$

Where l_k is the thickness of the boundary layer, that is, the region influenced by the cadmium. Using the Poisson equation 7 and mathematical manipulation given in Appendix III, the following important result is obtained:

$$\frac{d(1/C^2)}{dU}=\frac{8\pi}{\kappa e}\times\frac{1}{N_D} \tag{14}$$

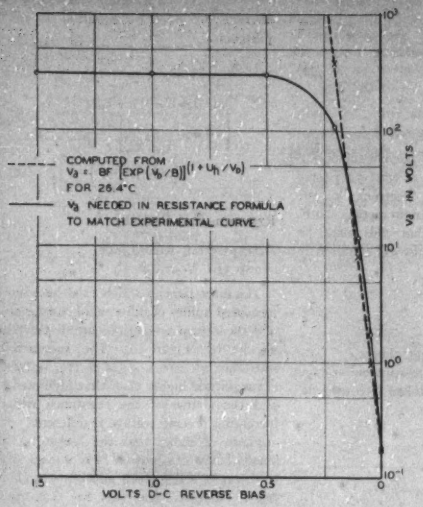

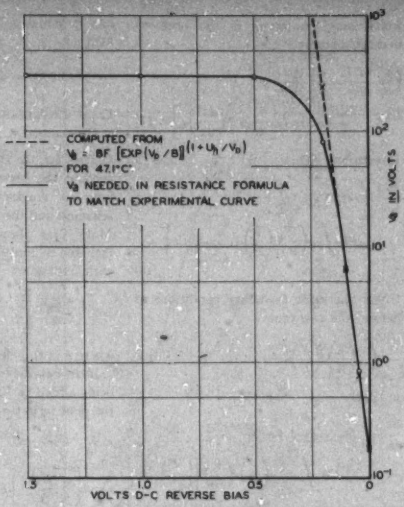

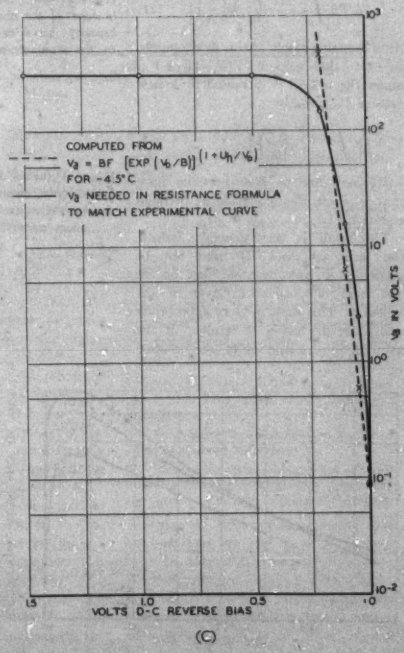

Figure 3. The apparent voltage V_a for three temperatures of the contact

Equation 14 discloses that a plot of the reciprocal of capacitance squared as a function of voltage applied to the contact should be a straight line in this case. The quantity N_D can be computed from the slope. The constant V_D is the intercept of this line on the voltage axis. From equation 1 it can be seen that the junction resistance disappears when $-U=V_D$. This implies that the boundary layer has disappeared and C is infinite.

With the a-c bridge described in Appendix II, both R and C can be measured simultaneously for values of d-c bias voltage applied across the contact.

A New Assumption for the Space Charge

In equation 8, N_D is assumed to be constant. If it be supposed that there is a fraction F of the N_D bromine ions free to move in the electric field $E(x)$, there will be a distribution of charge density $eN_D(x)$ which is dependent on the applied voltage and V_D. The condition may be expressed mathematically as follows:

$$\rho(x)=eN_D[1+F\varphi(V(x)/B)] \tag{15}$$

where φ is any continuous function of $V(x)$. With this added term the determination of E_R may be carried out in a more general way. Equation 8 becomes

$$\frac{d^2V(x)}{dx^2}=(4\pi/\epsilon)eN_D[1+F\varphi(V(x)/B)] \tag{16}$$

which may be solved in the previous manner, namely,

$$\left(\frac{dV}{dx}\right)\frac{d^2V}{dx^2}=\frac{d}{dx}\left[\frac{1}{2}\left(\frac{dV}{dx}\right)^2\right]$$
$$=(4\pi/\kappa)eN_D\left[\frac{dV}{dx}+F\left(\frac{dV}{dx}\right)\varphi\right] \quad (17)$$

Integration yields

$$\left(\frac{dV}{dx}\right)^2=(8\pi/\kappa)eN_D\left[V(x)+FB\int\varphi\left(\frac{V}{B}\right)d\left(\frac{V}{B}\right)+\text{constant}\right] \quad (18)$$

Under the same boundary conditions as before, the constant is

$$-\int\varphi\left(\frac{V}{B}\right)d\left(\frac{V}{B}\right)\Big|_0 \quad (19)$$

so that

$$\frac{dV}{dx}=\left\{(8\pi/\kappa)eN_D\left[V(x)+FB\int_0^{V/B}\varphi\left(\frac{V}{B}\right)d\left(\frac{V}{B}\right)\right]\right\}^{1/2} \quad (20)$$

Finally, at $x=0$

$$E_R=\left(\frac{8\pi eN_D}{\kappa}\right)^{1/2}\left[U_h+V_D+FB\int_0^{V(0)/B}\varphi\left(\frac{V}{B}\right)d\left(\frac{V}{B}\right)\right]^{1/2} \quad (21)$$

An interesting result of this development is that the voltage $V(0)=(U_h+V_D)$ under the radical is increased by a new voltage V_a given by

$$V_a=FB\int_0^{V(0)/B}\varphi\left(\frac{V}{B}\right)d\left(\frac{V}{B}\right) \quad (22)$$

If there are no free bromine ions, that is, $F=0$, then equation 21 becomes equation 11.

The result is very general; indeed, the term $eN_DF\varphi(V/B)$ need not be attributed to free bromine ions, but to any kind of polarizable layer at the junction. This topic is more appropriate under the discussion of results. If the assumption of a fraction of free bromine ions is followed, it is shown in Appendix IV that

$$V_a=BF[\exp(V_D/B)]^{(1+U_h/V_D)} \quad (23)$$

Final Expression for the Differential Resistance

Thus far, the theory has not taken into account the potential of the image force between conduction electrons in the selenium and the cadmium metal. N. F. Mott[3] has shown that this may be included by multiplying σ_R of equation 12 with the factor

$$\exp\left[\frac{e^{3/2}E_R^{1/2}}{\kappa^{1/2}kT}\right] \quad (24)$$

where e is the electronic charge.

If the possibility of an apparent voltage being added to V_D is taken into account, the final form for R_0 is

$$R_0=\frac{B}{\sigma_R\exp\left[\frac{e^{3/2}E_R^{1/2}}{\kappa^{1/2}kT}\right](8\pi eN_D/\kappa)^{1/2}(V_D+V_a)^{1/2}} \quad (25)$$

where E_R is given by equation 21 and R becomes

$$R=\frac{2(V_D+V_a)R_0}{B}\times\frac{[1+U_h/(V_D+V_a)]^{1/2}}{\left\{1+\exp(-U_h/B)\left[\frac{2(V_D+V_a)}{B}\times\left(1+\frac{U_h}{V_D+V_a}\right)-1\right]\right\}} \quad (26)$$

Experimental Results

Differential Resistance and the Voltage V_a

The discrepancies which exist between measured values of differential resistance and theoretical predictions are displayed clearly by Figure 1. The measured resistance at zero voltage is two orders of magnitude higher than that predicted, and the course of the resistance with increasing reverse voltage is different.

Figure 2 shows that the linear $1/C^2$ versus U law of equation 14 is obeyed up to 0.5 volt, after which another straight line is followed. One may say that the slight change in slope indicates a small

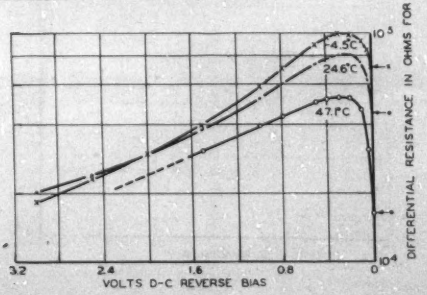

Figure 4 (below left). Experimental resistance data for a selenium-cadmium contact

Selenium-cadmium contact E626

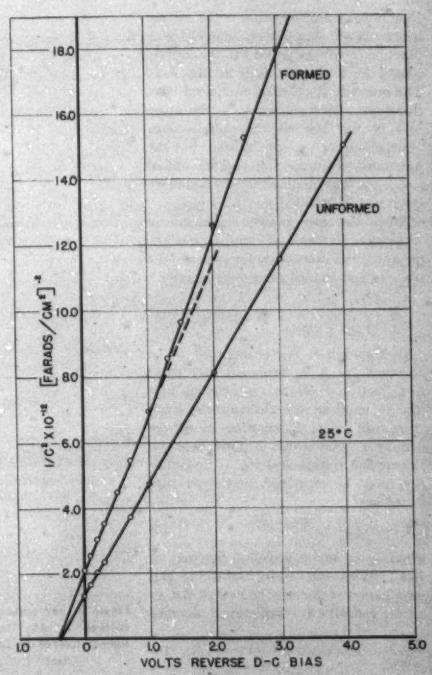

Figure 3 (right). Change in slope of the contact capacity curve caused by the forming process

Selenium-cadmium contact H

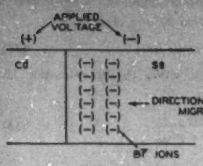

Figure 6 (left). Sense of the electric field in the contact boundary layer for reverse voltage applied

Figure 7 (right). Change in slope of the contact capacity curve caused by heating and exposure to bromine vapor

Selenium-cadmium contact F

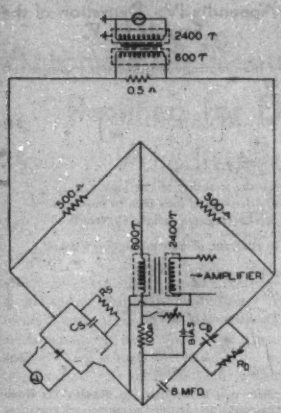

Figure 8 (left). A-c bridge

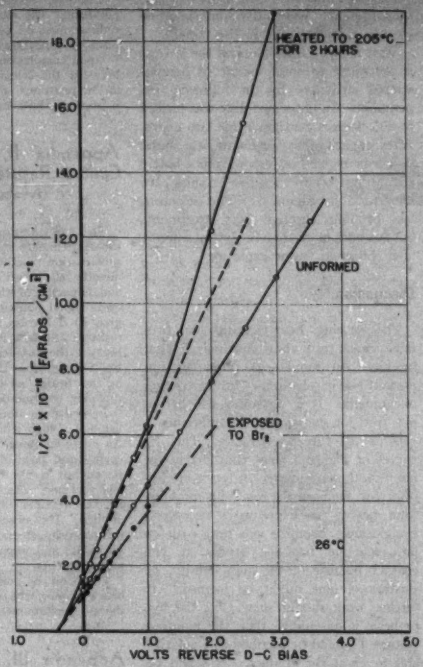

gradient of bromine ion density. Computation yields a value of N_D equal to 1.48×10^{16} ions per cubic centimeter. This agrees well with 2.47×10^{16} found by W. E. Blackburn (in his thesis presented to the department of Physics, University of Pittsburgh, entitled "Temperature Coefficient of Electrical Resistivity for Crystalline Selenium Containing Various Percentages of Bromine") using an electron mobility of one centimeter/second/volt/centimeter given by Schottky.[1] The bromine ions in the boundary layer are all ionized, and Schottky's theory should apply to this case.

The failure of equation 12 to predict the resistance at zero voltage indicates that conditions exist in the contact which have not been considered. The marked effect of small amounts of bromine vapor on the electrical properties of the contact, to be discussed later, lead to the supposition that there are some free bromine ions in the contact. The consequences of this were discussed under "Theory—A New Assumption for the Space Charge." An important result is that V_D is increased by an apparent voltage V_a as set forth in equation 25. It is not at present possible to compute an a priori value for Va using equation 23, because the value of F, the fraction of ions free, is not known. However, if it be assumed that R_0 in equation 25 is the measured value, then V_a can be computed for reverse voltages through equation 23. As the form of the function φ is not certain, it is best to put the measured values of R into equations 25 and 26 to compute V_a as a function of reverse voltage.

Such computations have been made and the results for one sample at three different temperatures is shown in Figure 3. The theoretical expression for V_a is followed up to about 0.2 volt when the contact is at 47.1 degrees centigrade. A rapid deviation occurs at higher voltages. At lower temperatures the exponential law is only approximately obeyed below 0.2 volt. This will be treated further under "Discussion."

The data used in the computations described are plotted in Figure 4. The shape of the curves as well as the null resistance is temperature dependent. It is interesting that the curve for −4.5 degrees centigrade crosses the room temperature curve at about two volts. This phenomenon is probably caused by the image force potential expressed by the Mott factor 24 multiplying σ_R in equation 25.

Effect of Forming, Heat Treatment, and Bromine Vapor on the Bromine Ion Density N_D

Forming is an electrical process whereby the reverse current of a rectifier at a given reverse voltage is caused to decrease permanently. The selenium-cadmium contact sample was formed by a 3-step process.

1. A reverse voltage of 13 volts was applied which gave 2.5 amperes of reverse current initially.
2. The voltage was advanced uniformly to 32 volts in about $2^1/_2$ hours.
3. The rectifier was operated for one-half hour at 32 volts. After this treatment, the current at 13 volts was one-half ampere.

Figure 5 demonstrates clearly that bromine ions are lost to the boundary layer because of the forming treatment. The configuration of signs in the boundary layer when a reverse voltage is applied is shown in Figure 6. One would expect some movement of bromine ions toward

the cadmium. Evidently, some bromine escapes through pores in the metal.

That escape is possible, and the process is reversible to some extent, is demonstrated strikingly by the following experiment. An unformed disk was heated to 205 degrees centigrade for two hours. After capacity measurements, the same disk was exposed to vapor from a bottle containing bromine. The results are illustrated in Figure 7. The selenium lost bromine through heat treatment, but got back more than the initial amount after bromine vapor exposure.

Discussion

The forming, heat treating, and bromine vapor tests show conclusively that bromine ion movement plays an important role in selenium-cadmium contact phenomena. It is not clear whether or not free ion movement is sufficient to explain all the phenomena. The V_a curves of Figure 3 show that if the free ion hypothesis is correct, then a mechanism for temporarily removing bromine from active participation is necessary. For example, bromine ions may coalesce into inactive bromine atoms at the contact because of the high density, or clusters of ions might be formed.[4] If further work should show that the hypothesis is untenable, then the required voltage V_a could be ascribed to a polarizable layer at the contact. It would be of especial interest to try to make a rectifier in vacuum taking care to have no contamination between the cadmium and selenium which would be polarizable. In this case the data should agree better with the Schottky theory, unless free bromine ions have an important effect on the contact resistance.

Appendix I. Preparation of Selenium-Cadmium Contact Samples

The semiconducting material is prepared from pure double-distilled selenium to which is added 0.01 per cent by weight of bromine. An 0.002–0.003-inch layer of this material is spread on a nickel plated iron disk at 350 degrees centigrade and rapidly cooled. The disk is 1/32 inch thick and $2^1/_8$ inches in diameter with a 3/8-inch center hole. Pure cadmium metal is sprayed over 18.7 square centimeters of the surface of the selenium at room temperature. The vitreous modification which results must be converted to the metallic form by annealing below the melting point.

Upon completion of the disk the junction between the selenium and nickel plate is of low resistance and nonrectifying, so that it need not be considered in this paper.

Appendix II. A-C Bridge for Contact Resistance and Capacity Measurements

The special form of a-c bridge used for the experiments is shown in Figure 8. A substitution method is used to obtain directly the equivalent parallel resistance and capacity of the contact. The 1,000-cycle signal generator output is adjusted to give 40 millivolts rms across the 0.5-ohm resistor. Such a low voltage is necessary because the rectifier is a nonlinear element. For voltages less than kT/e it will appear in the bridge as a linear resistance and capacity combination.

In order to obtain an accurate bridge balance, a high gain amplifier is employed. An unconventional feature is that a 1,000-cycle band pass filter is connected across the output to reject noise from the amplifier and rectifier. Electrical noise is generated by the rectifier when reverse voltage is applied. This obscures the bridge null for reverse voltages on the rectifier larger than five volts and impairs the precision of the measurements.

Provision is made for a constant d-c bias voltage on the rectifier without affecting the a-c performance of the circuit.

Appendix III. Capacitance and Bromine Ion Density N_D

Integrating equation 7 across the boundary layer gives

$$E(x) = -\frac{4\pi}{\kappa}\int^{l_k} \rho(x)dx \tag{27}$$

The boundary layer thickness l_k is a function of the applied voltage. Hence it is convenient to change the variable in equation 27 to l_k. Suppose that the integral can be found and is $L(x)$. Then

$$E(x) = (-4\pi/\kappa)[L(l_k) - L(x)] \tag{28}$$

and differentiation with respect to l_k give

$$\frac{dE(x)}{dl_k} = -\frac{4\pi}{\kappa}\frac{dL(l_k)}{dl_k} \tag{29}$$

for a change in $E(x)$ at x. Hence

$$\frac{dE(x)}{dl_k} = (-4\pi/\kappa)\rho(l_k) \tag{30}$$

The change in $E(x)$ at x caused by U is

$$dE(x) = dU/l_k \tag{31}$$

Using equation 30 one obtains

$$dU = (-4\pi/\kappa)\rho(l_k)l_k dl_k \tag{32}$$

Introducing C for l_k through equation 13 results in

$$\frac{d(1/C^2)}{dU} = -\frac{8\pi}{\kappa}\frac{1}{\rho(l_k)} \tag{33}$$

Appendix IV. Derivation of the Formula for V_a

If an ion current i_t exists, it will be given by

$$-i_t = eb_t\left[n_t(x)E_t(x) - B\frac{dn_t}{dx}\right] \tag{34}$$

where

b_t = the mobility of the ions
n_t = density of ions free to move
$E_t(x)$ = the appropriate electric field

In the case of zero voltage, $i_t = 0$ and

$$\frac{dn_t}{n_t} = -\frac{E_t(x)}{B}dx \tag{35}$$

The integral of this is

$$\int_{n_{tx}}^{n_{tH}} \frac{dn_t}{n_t} = ln\left(\frac{n_{tH}}{n_t(x)}\right) = -\frac{V_t(x)}{B} \tag{36}$$

where n_{tH} is the free ion density far from the contact. If the function φ of equation 15 be written as

$$\frac{n_t(x)}{n_{tH}} = \varphi = exp[V_t(x)/B] \tag{37}$$

utilizing equation 36. Then equation 22 becomes

$$V_a = FB\int_0^{(V_D+U_h)/V_D} exp(V_t/B)d(V_t/B)$$
$$= FB\{exp[(V_D+U_h)/B]-1\} \tag{38}$$

Unity can be neglected against $exp(V_D/B)$ which results in

$$V_a = FB[exp(V_D/B)]^{(1+U_h/V_D)} \tag{39}$$

References

1. A Simplified and Extended Theory of the Boundary Layer Rectifier, W. Schottky. *Zeitschrift fuer Physik* (Berlin, Germany), volume 118, 1942, pages 539–92.

2. Modern Theory of Solids (book), F. Seitz. McGraw-Hill Book Company, New York, N. Y., 1940, pages 62–72.

3. The Theory of Crystal Rectifiers, N. F. Mott. *Proceedings*, Royal Society of London (London, England), series A, volume 171, 1939, page 34.

4. The Electrical Conductivity of Zinc Oxide, P. H. Miller. *Physical Review*, American Institute of Physics (New York, N. Y.), volume 60, 1941, page 894.

No Discussion

Automatically Controlled Copper-Oxide Rectifiers for Electroplating and Anodizing Applications

JOSEPH J. BUCKLEY
ASSOCIATE AIEE

IN large electroplating or anodizing installations where the tank current is of the order of thousands of amperes, consideration should be given to a d-c power supply which is completely automatic in its operation. By eliminating the human element, rejects are reduced to a minimum; this in itself frequently justifies the higher initial investment. Moreover, a more uniform quality of work is produced. This paper describes the copper-oxide rectifiers used in applications of this type and several of the more common circuits whereby the d-c output is controlled.

Components

The essential components of an automatically controlled installation are

1. One or more copper-oxide rectifier units.
2. An induction type control.
3. An a-c contactor.
4. An operator's control box.

The first two items will be treated in detail in subsequent paragraphs following a brief résumé of rectifier fundamentals.

Copper-Oxide Rectifier

A fan-cooled basic 3-phase bridge, consisting of six copper-oxide cells, has an almost universally accepted rating of 6 volts direct current. This provides an ample margin of safety between the inverse voltage impressed across the cell when not conducting and the breakdown voltage. By a coincidence, this rating ties in very well with the majority of still tank plating applications, copper, nickel, tin, cadmium, zinc, and so forth, which require a voltage generally between three and six volts.

A sufficient number of cells may be connected in parallel to obtain the desired current rating. A series connection also may be used if higher voltages are required; for example, two cells in series are used for barrel plating or electrolytic cleaning at 12 volts.

Figure 1 illustrates a stack consisting of 26 copper-oxide cells, $4^3/_8$ by 5 inches in size, strung on an insulated bolt and connected in parallel. For simplicity the end brackets are live; thus the stack is connected up at the same time that it is mounted. Six of these stacks comprising a 3-phase bridge, have a fan-cooled rating of 6 volts, 500 amperes maximum. A stack with 4 cells in series and 7 in parallel which is used for anodizing applications at 24 volts (also 40 volts by connecting 2 in series) is shown in Figure 2.

Rectifier Unit

The rectifier unit is a simple assembly of stacks, rectifier transformer, ventilating fan, and air switch. The most popular model for automatically controlled power supplies is shown in Figure 3. It occupies less than seven square feet of floor space, stands five feet four inches high, and weighs about 1,100 pounds. A special foundation for supporting and anchoring the unit is not required. With the exception of the fan, there are no moving parts such as bearings, brushes, or commutator, so that maintenance is reduced to a minimum. As the air enters at the bottom and is discharged at the top, the two banks of stacks are located in the lower part of the unit in order that the operating temperature of the copper-oxide cells will be only 2 to 6 degrees centigrade above the room temperature. Each bank is a complete 3-phase bridge, consisting of 12 stacks similar to those shown in Figures 1 and 2. The rating of each bank is 6 kw direct current. Because the 2 banks can be connected in series or in parallel externally, the unit has a dual output rating such as 6 volts, 2,000 amperes and 12 volts, 1,000 amperes. Above the stacks is a 20-kva 3-phase transformer with 2 secondary windings, each feeding a-c power to a bank. If the fan fails, the air switch will drop down, opening the interlock circuit and disconnecting all units of the installation from the 3-phase a-c supply.

The variation in direct voltage with load current for this unit with a fixed alternating voltage and a load of varying resistance is given at the top of Figure 4. This is an average curve for a new unit. Some units will have a regulation as low as 20 per cent and others after aging may run as high as 38 per cent. If a particular unit is set for 6 volts with a full tank load and the operator starts removing work, the voltage will rise and, if there is no overvoltage relay for protection, the voltage may be as high as 7.5 at light load. This is a very undesirable condition both from the standpoint of the rectifier which has a high inverse voltage impressed across the cells, and the electroplated coating which may be burned or blistered because of the excessive current density. Some method of reducing the alternating voltage, either manually or automatically, as the load is decreased must be employed. A suitable circuit has been developed whereby a special type of motor driven

Paper 47-27, recommended by the AIEE committee on electrochemistry and electrometallurgy for presentation at the AIEE winter meeting, New York, N. Y., January 27–31, 1947. Manuscript submitted October 14, 1946; made available for printing January 2, 1947.

JOSEPH J. BUCKLEY is a design engineer with lighting engineering division, General Electric Company, West Lynn, Mass.

The author wishes to acknowledge his indebtedness to. R. A. Prior of General Electric Company, Pittsfield, Mass., for many helpful suggestions.

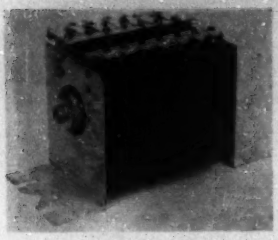

Figure 1. Plating stack consisting of 26 copper-oxide cells in parallel

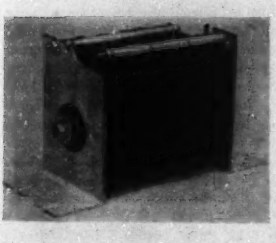

Figure 2. Anodizing stack consisting of 4 copper-oxide cells in series, 7 in parallel

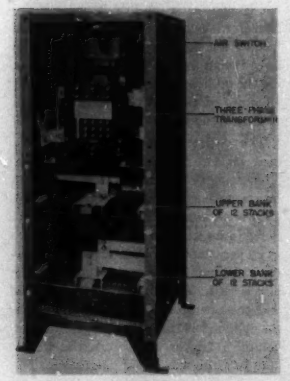

Figure 3. Front view of 12-kw copper-oxide rectifier unit with front panels removed

induction voltage regulator, called an induction type control, automatically maintains a constant direct voltage within limits of $2^1/_2$ per cent or better. A number of installations of this type are now in service and operating very successfully.

Induction Type Control

Induction type controls have been used in conjunction with copper-oxide rectifiers for installations varying from 6 to 210 kw capacity. The size of the control varies depending on the d-c power and also the output range that is maintained; for example, a control which maintains the voltage between four and six volts is relatively small whereas one which holds the voltage anywhere between one and six volts is nearly twice as large. Figure 5 shows a typical one which controls three 12-kw rectifier units. The essential components of the control are the series windings which are connected in series with the control output, and the shunt windings which are connected in Y across the 3-phase a-c supply lines. The voltage induced in each series winding is constant in magnitude but varies in its phase relation with the corresponding supply voltage as the position of the rotor with respect to the stator is changed. The output voltage of the control is the vector sum of the supply voltage and the series winding voltage. As the vector position of the series winding voltage is varied from being in phase to 180 degrees out of phase with the supply voltage by means of the operating motor, the output voltage is decreased continuously from maximum to minimum.

The brain of this type of d-c power supply is the contact-making instrument which is mounted on the panel inside of the control. This consists of a solenoid having an iron core suspended from a spring, and a pivoted beam incorporating a set of single-pole double-throw contacts which is caused to rotate by the up and down motion of the core. A direct or alternating voltage applied to the solenoid causes an upward electromagnetic pull to be exerted on the core. Hence, with normal current through the solenoid, the spring force plus the electromagnetic force just balance the weight of the core, and the beam is horizontal. If the solenoid current deviates from its normal value, either the left or the right hand beam contacts will close, and the operating motor will turn the rotor just enough to correct the situation. Basically then, the contact-making instrument maintains a constant solenoid current.

Control Circuits

By using a solenoid whose voltage drop with normal current through it is slightly less than the minimum rated voltage of a d-c power supply under consideration, and connecting in series with it a variable resistance whose maximum value is such that the voltage drop across it with normal solenoid current flowing is slightly more than the difference between the maximum and minimum rated direct voltages, a constant voltage circuit is created which is completely independent of load resistance variations or line voltage fluctuations. Figure 6 illustrates the principle of operation of the essential elements of such a circuit. For simplicity a single-phase a-c supply is shown and a single-phase bridge rectifier. The motor control relay is added to reduce the current burden of the voltmeter contacts so that the life will be increased greatly. The coils of this relay are energized by the beam contacts and through one or the other of its contacts the necessary current for the operating motor passes. Both the relay and the voltmeter are shown in the de-energized position. Any voltage between the maximum and minimum value is maintained by merely setting the voltage level rheostat. The absolute ratio of maximum to minimum voltage is equal to the ratio of the sum of solenoid and rheostat resistances to solenoid resistance.

When the a-c power of this basic circuit is opened, the "raise" contacts of the voltmeter will close, the "raise" relay coil will be energized (if the no-voltage relay were not in the circuit, the connection between the voltmeter and the "raise" coil would be unbroken), and the rotor will advance all the way to the maximum voltage position without stopping. The next time the a-c power is closed, a high voltage will be impressed on the rectifier for a few seconds until the operating motor drives the rotor back down to the proper point. To prevent this undesirable occurrence, a no-voltage relay is connected into the circuit. When the a-c power is opened, this relay is de-energized, opening the "raise" coil circuit and applying a-c power directly to the "lower" coil. Thus the control resets itself in the minimum voltage position every time the operator presses the stop button at the conclusion of a work cycle. This constant voltage circuit is the most common one for plating applications.

If the control output current is plotted as a function of the direct current, the resulting curve is, for all practical purposes, a straight line passing through the origin. Furthermore, it is independent of the direct voltage. Therefore a circuit which controls the control output current is a constant current circuit. Detail 1 of Figure 6 illustrates how the fundamental constant voltage circuit is modified to accomplish this. That portion of the resistance connected across the current

transformer secondary winding is decreased to increase the direct current. Any current between 40 per cent and rated value is maintained by merely setting the rheostat; by using a multiple winding current transformer, current ranges of 5 to 1 and even 15 to 1 can be controlled. This type of control is used for sulphuric acid anodizing because it is not feasible to impress 18 to 24 volts across the load initially. There would be a heavy overload in current until the oxide film built up sufficiently to increase the load resistance materially. By maintaining the current, the d-c power supply is always within its rating. The circuit also has been used for plating where the work consists of large pieces or a continuous strip. The proper current density is maintained even though the solution varies or the anodes wear down.

It is customary with the chromic acid process to anodize for a definite period of time at 40 volts once the anodic film is established. During the initial build-up period when the load resistance increases many fold, constant current control is best. This enables the build-up to be accomplished in the shortest possible time without overloading the d-c power supply. This requires additions to the fundamental circuit shown in detail 2 of Figure 6. For the first five minutes or so of the anodizing cycle the voltage relay is not energized, and the control circuit is identical with that shown in detail 1 of Figure 6. But once the voltage is up to 40 volts, the relay picks up causing the time switch motor to start and the transfer relay to function. The solenoid is now in series with the voltage level rheostat instead of being in parallel with the current level rheostat, and the contact-making instrument is a voltmeter. At the end of the preset time interval, the time switch shuts off the a-c power, and the control resets itself for the next cycle.

Installation

To obtain the desired tank power, a number of units can be connected together with their outputs in parallel, in series, or by a combination of the first two methods. All the units which make up the installation invariably are connected in parallel on the input side and are supplied with an automatically varying alternating voltage from the induction type control. Anywhere from 1 to 18 units have been used with a single control.

The combined efficiency of such an installation (stack forward and reverse loss, rectifier transformer copper and core loss, induction type control copper and core loss) as a function of direct current both at rated voltage and one-half voltage is shown by curves *A* and *B* in Figure 4. The rectifier fan loss is not included because separate voltage circuits are used for auxiliaries; it is only 2.4 per cent of the rectifier output. The power loss of all other auxiliaries is negligible. The metallic rectifier maintains a high efficiency from very light load to rated load and even at overload, and is superior to all other sources of low voltage d-c power in this respect. It is suited ideally to electroplating and anodizing because the load is likely to vary considerably.

The over-all power factor versus load curves are shown at the bottom of Figure 4. The departure from unity is caused in part by the displacement between voltage and current because of the induction type control and the rectifier transformer and in part by the harmonic content in the a-c line current because of the rectifier. For operation between one-half the rated current and rated current and one-half the rated voltage and rated voltage, the

Figure 4. Voltage of individual unit, overall efficiency and power factor as a function of load

A and *C* = rated voltage, *B* and *D* = one-half voltage

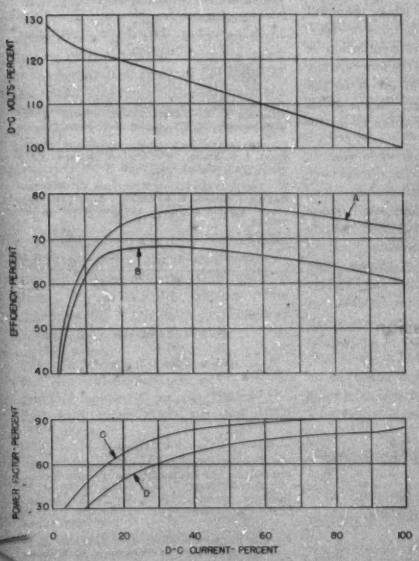

Figure 5. Front view of induction type control with door open exposing control panel

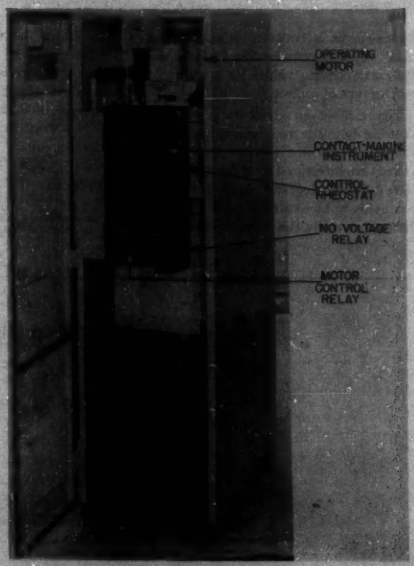

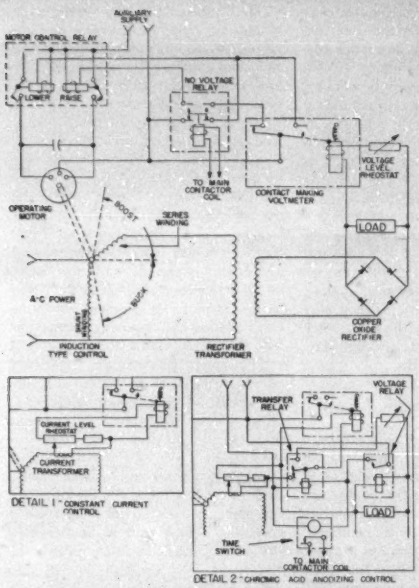

Figure 6. Schematic diagram of fundamental constant voltage circuit

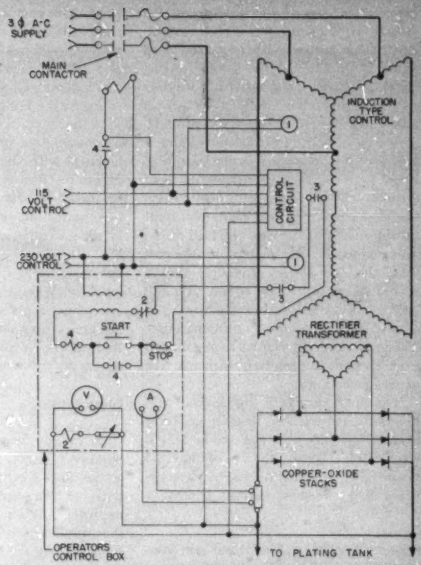

Figure 7. Elementary diagram of complete installation

1 = rectifier fan or control blower
2 = overvoltage relay
3 = air switch or thermal over-temperature switch
4 = auxiliary relay

power factor is between 70 and 90 per cent This is considerably higher than the corresponding values for a saturable reactor type of control.

Figure 7 is an elementary diagram showing how the four components (for simplicity only one rectifier unit is depicted) are integrated to make up a complete d-c power supply. Only the control box needs to be located close to the tank because normally the operator uses only the start and stop push buttons. The rectifier units and the induction type control should be installed in a clean place, preferably a separate room, where they will not be subject to corrosive fumes or excessive moisture and where ventilation is adequate. To make sure the units are not operated at a voltage in excess of the rated value, an overvoltage relay is added with its normally-closed contacts in the interlock circuit.

References

1. Fundamental Characteristics and Applications of the Copper-Oxide Rectifier, C. E. Hamann, E. A. Harty. *General Electric Review* (Schenectady, N. Y.), August 1933, pages 1–8.

2. Characteristics of Copper-Oxide Rectifiers, I. R. Smith. *Westinghouse Engineer* (Pittsburgh, Pa.), August 1943, pages 85–90.

3. The Copper-Oxide Rectifier in Electrochemical Work, I. R. Smith. AIEE Transactions, volume 63, 1944, October section, pages 739–44.

No Discussion

An Analysis of Motor Selection for Brass-Slab Rolling-Mill Service

L. H. BERKLEY
ASSOCIATE AIEE

IT is the purpose of this paper to outline some of the problems and calculations encountered by the author in selecting a motor drive for a brass-slab rolling mill. It is hoped that some of the information given will be useful to other engineers faced with similar problems.

Description of the Rolling Mill

A description of the mill will aid in understanding the problem. (See Figure 1.)

The mill is of an old design but has been kept in excellent running condition. It consists essentially of a 2-stage speed reduction unit to step down from the speed of the motor (600 rpm) to the speed of the rolls ($12^1/_2$ rpm). The intermediate gears rotate at 82 rpm and carry a 14-foot flywheel. There are two stands of 2-high rolls to permit rolling two slabs simultaneously.

Present Motor

The mill is driven at present by a Westinghouse squirrel-cage induction motor, 250 horsepower, 580 rpm, 2,200 volts, 3 phase, 60 cycles, 57.5 amperes. The characteristics of the motor were obtained from the manufacturer as follows:

Full load power factor = 87 per cent
Full load efficiency = 90 per cent
Full load input = 100 per cent, 191 kw
Full load current = 100 per cent, 57.5 amperes
Full load torque = 100 per cent, 2,260 pound-feet
Starting current = 600 per cent, 365 amperes
Starting torque = 110 per cent, 2,490 pound-feet
Pullout torque = 250 per cent, 5,750 pound-feet
Pullout speed = 520 rpm
Pullout power factor = 74 per cent
Pullout efficiency = 63 per cent
Pullout input = 700 kw
Moment of inertia of rotor = 2,300 pound-feet
Weight of rotor = 1,600 pounds

As the effectiveness of the flywheel increases with the slip of the motor driving the mill, the question naturally arises as to why a flywheel was used with a motor having such a small full load slip ($3^1/_2$ per cent). The reason is that the mill originally was driven by a single-stroke Corliss steam engine driving the intermediate shaft at about 80 rpm and the flywheel was necessary to smooth out the load peaks and to help maintain constant speed during the rolling operation. As will be shown later, the power generated by the flywheel during the rolling peak is quite appreciable. The present motor replaced the steam engine in 1917, which necessitated adding the second set of gears, and has been driving the mill at an average of 48 hours per week since then. The motor is living "on borrowed time", so to speak, and it was considered advisable to purchase a replacement to be used in case of breakdown.

Possibilities

In considering the purchase of a new motor, four possibilities were apparent.

1. Standard squirrel-cage induction motor, similar in characteristics to the old motor [NEMA (National Electrical Manufacturers Association) type *A*].
2. High-slip squirrel-cage induction motor (NEMA type *D*).
3. Wound-rotor induction motor.
4. Synchronous motor.

Before a decision was reached, the torque-speed characteristics of each motor had to be considered. From the known data of the present motor, its characteristic was constructed as shown in Figure 2.

The second possibility is the high-slip squirrel-cage motor, whose characteristic also is shown in Figure 2.

The third possibility, the wound-rotor motor, offered the advantages of most rapid acceleration during the starting period and also of variable speed. Because neither rapid acceleration nor variable speed were especially desirable, and because the equipment would be more expensive in first cost and maintenance, the wound-rotor motor was ruled out.

The last possibility, the synchronous motor, looked very favorable as an 80-per-cent-power-factor motor and controls would cost little more than the standard squirrel-cage motor and controls and would offer a leading power of about 150 kva from no load to full load, whereas the induction motor would offer about 100

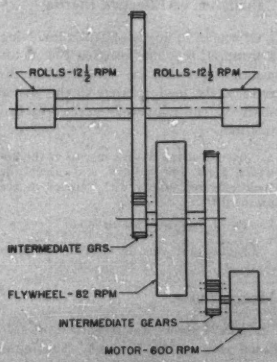

Figure 1. Schematic plan view of mill

Paper 47-28, recommended by the AIEE committee on industrial power applications for presentation at the AIEE winter meeting, New York, N. Y., January 27–31, 1947. Manuscript submitted May 22, 1946; made available for printing November 25, 1946.

L. H. BERKLEY is an electrical engineer with the purchasing department of York-Shipley, Inc., York, Pa.

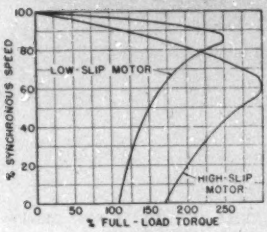

Figure 2. Torque-speed curves of squirrel-cage induction motors

These curves may vary considerably within the same NEMA classification

kva lagging. However, it was decided inadvisable to use the synchronous motor because of the sustained jogging required to remove a slab that may become stuck between the rolls when a coupling breaks. This jogging would all be done on the damper windings of the motor, which could not be made to stand such severe service.

The two remaining possibilities were that of the standard and the high-slip squirrel-cage motors. Before a choice could be made between the two, a load test had to be run and several calculations made.

Load Test. A load test was run using slabs in the hardest condition (just prior to annealing) with results as shown in Figure 3. It should be noted that the maximum input when rolling two slabs simultaneously is about 300 kw. This represents a peak load of about 325 horsepower or about 30 per cent overload on a 250-horsepower motor.

Calculation of Effective Inertia

Of course, in any application involving a flywheel, the first question the motor manufacturer asks is—"What is the inertia of the load referred to the motor shaft?" This may be determined by two methods.

1. By measuring the dimensions of the flywheel, gears, and so forth, and calculating their effective inertia with respect to the motor shaft.
2. By an experimental method.[1]

To check, it was decided to use both methods.

Measurement

Figure 4 shows a simplified cross-sectional view of the flywheel. To obtain the moment of inertia, it is necessary to calculate the weight and the radius of gyration. The rim only will be considered in making these calculations because therein lies about 95 per cent of its inertia.

Radius of Gyration

Considering X as the distance from the end of the flywheel to the center of gravity G, the following equation is obtained from elementary physical considerations:

$$X = \frac{(13\times4^1/_4)(2^1/_8)+(10\times8)(8^1/_4)}{(13\times4^1/_4)+(10\times8)}$$
$$= 5.74 \text{ inches}$$

The radius of gyration R is then

$$R = 86 - 5.74$$
$$= 80.26 \text{ inches}$$

Weight

Cross sectional area $= (13\times4^1/_4)+(10\times8)$
$= 135.2$ square inches

Mean circumference $= 2\pi\times80.26$
$= 505$ inches

Volume $= 505\times135.2$
$= 68{,}250$ cubic inches

Density $= 0.260$ pounds per cubic inch (for cast iron)

Weight $(W) = 68{,}250\times0.260$
$= 17{,}740$ pounds

Moment of Inertia

$$WR^2 = 17{,}740\times\left(\frac{80.26}{12}\right)^2$$
$$= 795{,}000 \text{ pound-feet}^2$$

The effective inertia at the motor shaft is inversely proportional to the square of the speed ratio. Therefore,

$$\text{Effective } WR^2 = 795{,}000\times\left(\frac{82}{600}\right)^2$$
$$= 14{,}900 \text{ pound-feet}^2$$

This is the inertia of the flywheel rim only and does not include the flywheel spokes or the gears of the system.

Experimental Methods

The following formula was derived by the author in reference 1:

$$WR^2(\text{pound-feet}^2) = 21.65\times10^6\times\frac{P_F(KW)}{RPM\times RPM/Sec.} \quad (1)$$

where

WR^2 = effective inertia at the motor shaft including that of motor rotor
P_F = power required to overcome the friction in the motor and load when running at a constant speed (rpm)
RPM = the motor speed at which P_F is measured
$RPM/Sec.$ = the initial rate of retardation of the motor when the driving power is removed

When running the load test, data were obtained which, together with information furnished by Westinghouse Electric Corporation, enabled us to calculate, by means of equation 1 the effective WR^2 of the load as 15,900 pound-feet^2. The details of this calculation may be found with the derivation of equation 1.

The result obtained by the experimental method is 1,000 pound-feet^2 larger than that obtained by measurement. The difference is caused by the flywheel spokes and the gears of the system which were not considered in measurement. In future calculations, the effective inertia of the load will be taken as 15,900 pound-feet^2. Also, the motor rotor and flywheel will be considered as rigidly coupled; that is, they accelerate and decelerate simultaneously.

Flywheel Effect of the Load

Before the proper slip of the motor could be selected, it was first necessary to calculate the effect of the flywheel; that is, the power it generates when the motor slows down. A formula to calculate this power was derived as follows:

The kinetic energy absorbed or released by a flywheel during acceleration or deceleration can be calculated by the following formula:

$$KE = {}^1/_2 I(W_1^2 - W_2^2) \quad (2)$$

where

KE = kinetic energy, foot-pounds
I = inertia of flywheel, slug feet^2
W_1 = initial angular velocity of the flywheel, radians/second
W_2 = final angular velocity of the flywheel, radians/second

The units of inertia and angular velocity may be changed as follows.

1 slug = 32.16 pounds
1 rpm = $2\pi/60$ radians/second
1 radian/second = 30π rpm

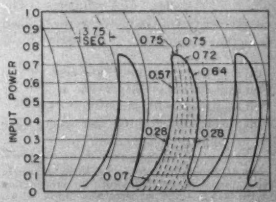

Figure 3. Load test of present motor rolling two slabs

Multiplying factor = 400 kw

Applying these changes,

$$KE(\text{foot-pounds}) = 1.706\times10^{-4}\times WR^2\times(RPM_1^2 - RPM_2^2) \quad (3)$$

If the flywheel reaches its minimum speed in t seconds, the power generated during this period is

$$P(\text{foot-pounds/second}) = 1.706\times10^{-4}\times\frac{WR^2(RPM_1^2 - RPM_2^2)}{t} \quad (4)$$

Since

$1\ HP = 550$ foot-pounds/second

the power generated is

$$HP = 3.102\times10^{-7}\,\frac{WR^2(RPM_1^2 - RPM_2^2)}{t} \quad (5)$$

This formula represents the *average* horsepower developed by the flywheel during the deceleration period. While the instantaneous horsepower will vary considerably during the load peak, the average value is useful to determine the relative effect of the flywheel by comparing with the peak motor load.

To apply the foregoing formula to the rolling mill, the following measurements were made:

Speed of the motor before rolling = 600 rpm
Minimum speed of flywheel during rolling operation (two slabs) = 570 rpm
Time interval required to reach the lowest speed = approximately $2^1/_2$ seconds

The average power generated by the flywheel then is calculated from equation 5 as follows:

$$HP = 3.102\times10^{-7}\,\frac{15{,}900(600^2 - 570^2)}{2.5}$$
$$= 70$$

From the load curve, it is seen that the peak input to the motor when rolling two slabs is approximately 300 kw, which represents about 325 horsepower. The 70 horsepower contributed by the flywheel is 22 per cent of the peak, a very considerable percentage. However, this alone does not tell the complete story. It is necessary to compare the relative energy contributions of the flywheel and the motor. The energy contribution of the flywheel is calculated from equation 3, as follows:

$$KE = 1.706\times10^{-4}\times15{,}900(600^2 - 570^2)$$
$$= 95{,}000 \text{ foot-pounds}$$
$$= 173 \text{ horsepower-seconds}$$

The energy contributed by the motor may be calculated by measuring the area under the motor power curve (Figure 3) in kilowatt-seconds and then converting it to foot-pounds. This was done with a

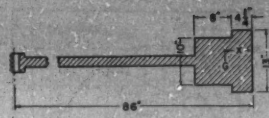

Figure 4. Schematic cross section of flywheel

planimeter and the following results obtained:

Area under power curve:

$A_P = 2.35$ square inches (average)

Area under a chart section 400 kw high by 3.75 seconds wide (1,500 kilowatt-seconds):

$A_{cs} = 3.45$ square inches

Energy absorbed by motor during the load peak:

$$E = \frac{2.35}{3.45}\times1{,}500$$
$$= 1{,}020 \text{ kilowatt-seconds}$$

Assuming 70-per-cent over-all motor efficiency, the power contributed by the motor is

$$P = 0.70\times1{,}020$$
$$= 714 \text{ kilowatt-seconds}$$
$$= 0.198 \text{ kilowatt-hour}$$
$$1 \text{ kilowatt-hour} = 2.656\times10^6 \text{ foot-pounds}$$
$$P = 0.198\times2.656\times10^6$$
$$= 526{,}000 \text{ foot-pounds}$$

The energy contributed by the flywheel (95,000 foot-pounds) is then about 18 per cent of the energy delivered by the motor.

Discussion of Motor Characteristics

After the described tests and calculations had been made, it was felt that some consideration of basic principles would help in making an intelligent choice between the low-slip and the high-slip motors. In rolling and punch press applications having a flywheel, the high-slip motor usually is used for the following reasons:

1. Fuller utilization is made of the flywheel since it is given a chance to release more of its kinetic energy when the motor speed decreases during the load peak. This reduces the peak horsepower required of the motor and therefore the rms horsepower and horsepower rating (this will be explained more fully later). It should be remembered that the energy released by the flywheel is restored to it when the motor speeds up again, so that regardless of which type of motor is used, the total energy delivered by the motor remains unchanged. Also, it should be noted that the flywheel has expended its usefulness when the torque of the motor becomes equal to that of the load and the motor speed becomes constant.

2. The gears between the motor and the flywheel need not be designed to carry as great a peak load since more of the power required will be contributed by the flywheel. This often results in a considerable saving when designing a new piece of equipment.

3. The peak current will be reduced, thus reducing the voltage drop and lamp flicker. In new installations, smaller peak currents mean a reduction in feeder size.

Upon measuring the motor speed with a hand tachometer, it was found to be substantially constant over the middle portion of the rolling period. During this period, the flywheel has very little effect and the motor carries most of the load itself. In other words, the motor torque is almost equal to the load torque and the flywheel contribution is very small. From the previously calculated percentages of the horsepower and energy contributed by the flywheel, it is possible to construct the approximate horsepower–time curves (Figure 5) for the power required to roll two slabs (slab load), the power contributed by the motor (motor load), and the power contributed by the flywheel (flywheel power). The friction power is neglected. Upon inspection of these curves, the following points should be noted:

1. At every point the slab load is equal to the motor load plus the flywheel power. Negative values of flywheel power mean that the flywheel is absorbing energy and accelerating.

2. The energy contributed by the flywheel is equal to the energy absorbed by the flywheel. This must be true because the speed of the flywheel before and after the rolling cycle, and therefore its energy content, are the same.

3. The area under the slab load curve equals the area under the motor load curve, which means that the energy required by

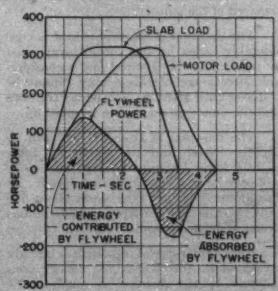

Figure 5. Horsepower–time curves using low-slip motor

Energy contributed by flywheel is about 18 to 20 per cent of motor load

the slab equals the energy supplied by the motor. Neglecting the friction of the system, as we have been doing, this merely follows the law of conservation of energy since the flywheel neither absorbs or contributes energy over a complete cycle.

4. The energy contributed by the flywheel is about 18 to 20 per cent of the motor load (see the preceding text).

5. The motor load continues for about a second after the slab leaves the rolls. Also the peak in this curve lags behind the maximum of the slab load. Both of these phenomena are effects of the flywheel and are caused by the motor trying to restore to it the energy lost during deceleration. The flexibility of the couplings and the rate at which the slab load rises and falls also effect the shape of the curve.

6. From two to three seconds after rolling starts, the power contribution of the flywheel is very small and the motor must carry most of the load itself. Therefore, with a motor having $3^1/_2$ per cent slip at full load, the flywheel does very little toward reducing the load peak.

In view of this point, the next question that comes to mind is—"What will be the effect of a high-slip motor on the load curve?"

The effect of the high-slip motor on the load curves is shown in Figure 6. This motor would have a full load speed of about 560 rpm (seven per cent slip). Comparing the curves with those obtained using a low-slip motor, the following is noted:

1. The maximum horsepower developed by the flywheel, as well as its energy contribution, is considerably greater. As the high-slip motor will slow down at least twice as much as the low-slip motor, it will contribute at least twice as much energy to the load and, consequently, the energy contributed by the flywheel will be about 36 to 40 per cent of the motor load. The flywheel, therefore, reduces the peak of the motor load and also the pullout horsepower required of the motor.

2. The duration of the motor load is considerably longer because more energy must be restored to the flywheel and a considerable percentage of this energy cannot be restored until after the slab leaves the rolls and the motor gets a chance to speed up.

3. The duration of the slab load will be slightly longer and its maximum value slightly lower because the high-slip motor will operate at a slightly slower speed. As the difference in each case is only about five per cent, this does not represent any serious decrease in production.

4. By a similar line of reasoning as already presented in this paper, the energy contributed by the flywheel is equal to the energy absorbed by the flywheel, and also the area under the slab load curve is equal to the area under the motor load curve. Because the energy required by the slab will be the same regardless of the type of motor used, the areas under the slab load curves and, consequently, the areas under

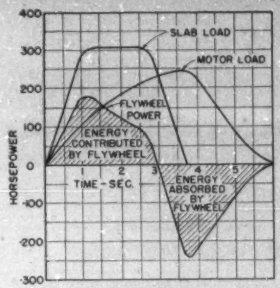

Figure 6. Horsepower-time curves using high-slip motor

Energy contributed by flywheel is about 36 to 40 per cent of motor load

the motor load curves will be equal. (That is, all four areas are equal.)

The effect of the high-slip motor cannot be fully appreciated until its continuous load curve is compared to that obtained with the low-slip motor (Figure 3). To make this comparison, such a load curve is approximated in Figure 7. It is important to note that the curve is much smoother and that it has a lower peak. Also, the areas under both curves for the same number of slabs are equal, and, as the time will vary but a few per cent, the average values will be the same.

Motor Specifications

In order to compare the costs of the high-slip and low-slip motors, it was necessary to determine the complete motor specifications for each case, the horsepower rating, pullout torque, and slip being the most important. The other specifications—synchronous speed, time rating, voltage, frequency—are fixed, while the starting torque is relatively unimportant.

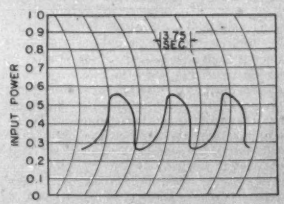

Figure 7. Expected load curve of high-slip motor

Compare with Figure 3—note smoother curve and lower peaks

The motor specifications were determined and outlined as follows.

Low Slip

First, the horsepower rating of the motor, which is equal to the rms of the load curve, must be fixed. Rms horsepower can be approximated as follows:

The rms value is defined briefly as "the square root of the average of the squares." To apply this method, divide the load curve into eight sections, as shown in Figure 3. (Eight sections are chosen for convenience. The accuracy of this method, as well as the result obtained, increases with the number of sections.) To find the rms ordinate of the curve the following formula is used:

$$\text{Rms ordinate} = \sqrt{\frac{(A_1)^2+(A_2)^2+\ldots(A_8)^2}{8}}$$

where A_1, A_2, ...A_8 are the average ordinates for each section. Applying this formula to Figure 3,

$$\text{Rms ordinate} = \sqrt{\frac{(0.07)^2+(0.28)^2+(0.57)^2+(0.75)^2+(0.75)^2+(0.72)^2+(0.64)^2+(0.28)^2}{8}} = 0.56$$

Assuming 70-per-cent over-all motor efficiency,

$$\text{Rms horsepower} = 0.56 \times 400 \times 1.341 \times 0.70 = 210$$

It was considered safe to use a 200-horsepower motor because the mill is idle for short periods of time when the slabs are transported from the receiving to the feeding end, rolls adjusted, waiting for slabs, and so forth.

Secondly, it is necessary to determine the pullout horsepower required of the motor. The maximum power required was approximately 325 horsepower. Since the standard low-slip NEMA class *A* motor usually has a pullout torque of about 250 per cent full load torque, the pullout horsepower of such a motor will be about 425 horsepower (assuming 15 per cent pullout slip) and will be capable of easily carrying the peak load.

Thirdly, the slip of the motor will be specified at approximately $3^1/_2$ per cent.

The complete motor specifications are therefore 200 horsepower, 580 rpm, continuous duty, open type, 40 degree-centigrade temperature rise, pullout torque not less than 250 per cent full load torque, 2,200 volts, 3 phase, 60 cycles.

High Slip

To determine the horsepower rating of the high-slip motor, it was decided to cal-

culate the rms horsepower of the motor load curve of Figure 6. To check the accuracy of this method, the rms horsepower for the low-slip motor was calculated from the motor load curve of Figure 5 and compared with the value obtained from Figure 3. For this purpose, both motor load curves were drawn separately and divided into eight sections each (Figure 8). The rms ordinates were calculated as already explained and found to be as follows:

High-slip motor—159 horsepower
Low-slip motor—211 horsepower

As the value obtained for the low-slip motor (211 horsepower) checked very well from that calculated from Figure 3 (210 horsepower), it was decided that the value of 159 horsepower obtained for the high-slip motor was sufficiently accurate and that the rating of the motor would be 150 horsepower.

The next step was to check whether or not the pullout torque was sufficient. The average power developed by the flywheel using a low-slip ($3^1/_2$ per cent) motor was 70 horsepower and the peak load was 325 horsepower. Using a high-slip (7 per cent) motor, it was considered safe to assume that this peak would be reduced 75 to 250 horsepower (see Figure 6). The pullout torque of a NEMA class *D* motor is usually 300 to 400 per cent full load torque. Assuming a 30-per-cent pullout slip, the pullout power at 350 per cent pullout torque is 368 horsepower, which is quite safe on an expected peak of 250 horsepower.

It should be remembered that the energy required to roll a certain number of slabs is the same, regardless of the type of motor used, and that the energy contributed by the flywheel in the first half of each cycle is restored to it during the

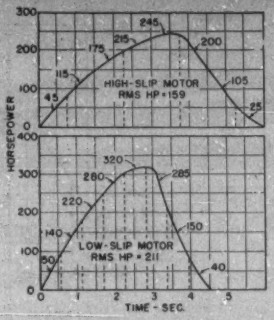

Figure 8. Calculation of rms horsepower from approximate horsepower–time curves

last half. This means that the areas under both motor load curves are the same and that the average horsepowers developed by both motors are essentially the same. The rms horsepower (and therefore the horsepower rating) of the high-slip motor is lower *only because it reduces the magnitude of the load peak.*

The complete motor specifications are 150 horsepower, 560 rpm, continuous duty, open type, 40-degree-centigrade temperature rise, pullout torque not less than 350 per cent full load torque, 2,200 volts, 3 phase, 60 cycles.

Conclusion

Before making the final selection, it is considered advisable to review the three main reasons for using a high-slip motor.

1. Fuller utilization of the flywheel to reduce rms horsepower.
2. Reduction in size of gears between the motor and flywheel.
3. Reduction in peak currents, size of feeders, and sometimes, transformers.

Reduction of rms horsepower may mean a reduction in cost and size of the motor. Reduction in size of gears, feeders, and transformers usually is reflected in a considerable saving.

Investigation of the two remaining possibilities revealed that a 150-horsepower high-slip motor would cost about 15 per cent more and would be larger than a 200-horsepower low-slip motor. In a new installation, the explained savings would more than offset the additional cost of the motor, and the decision unquestionably would be in favor of a high-slip motor. It can be seen, however, that since the gears already were built and the feeders and transformers installed, neither of the three reasons mentioned are applicable in this case. In view of these considerations, and, also, the fact that delivery on the high-slip motor was quoted as twice that of the low-slip motor, it was decided to use a low-slip motor.

It is believed that the methods and calculations explained in this paper can be adapted to many different types of applications involving both new and existing installations. It is a fact well accepted by engineers that time spent in determining, as accurately as possible, the motor size required by a given application is well worth while. Excess horsepower on any induction motor drive is expensive in first cost of motor and control and often entails an additional expense of power-factor correction.

Reference

1. How to Determine WR^2 by Running a Simple Test, L. H. Berkley. *Product Engineering*, New York, N. Y., December 1942, page 704.

Discussion

Fraser Jeffrey (Allis-Chalmers Manufacturing Company, Milwaukee, Wis.): In considering power requirements for intermittent loading with peak conditions occurring at frequent intervals, it is well to work with equivalent horsepower corresponding to rms values of kilovolt-amperes rather than rms values of power directly. This is because the power factor and the efficiency of both synchronous and induction motors vary widely with the load, size, and speed, and the current or kilovolt-amperes will not be proportional to the load.

Thus, the equivalent horsepower rating of a unity power factor synchronous motor necessary to handle a certain highly fluctuating load will be different from the equivalent horsepower rating of an 80-per-cent-power-factor synchronous motor necessary to handle the same load. The same statement is true, although the difference may be less pronounced, when comparing induction motors having different power factor and efficiency curves.

To determine the value of kilovolt-amperes which will give the same average heating as the actual variable kilovolt-ampere input to the motor, the resultant rms kilovolt-amperes will be

$$0.746\sqrt{\frac{\left(\frac{P_1}{\cos\phi_1\eta_1}\right)^2 t_1+\left(\frac{P_2}{\cos\phi_2\eta_2}\right)^2 t_2+\ldots\left(\frac{P_n}{\cos\phi_n\eta_n}\right)^2 t_n}{t_1+t_2+\ldots t_n}} \qquad (1)$$

where

$P_1, P_2 \ldots P_n$ = average load in horsepower for each ordinate section
$t_1, t_2 \ldots t_n$ = time interval of the various ordinates in minutes
$\cos\phi_1, \cos\phi_2 \ldots \cos\phi_n$ = power factor of motor at power loads $P_1, P_2 \ldots P_n$
$\cos\phi$ = full load rated power factor of motor
$\eta_1, \eta_2 \ldots \eta_n$ = efficiency of motor at power loads $P_1, P_2 \ldots P_n$
η = full load efficiency of motor

The equivalent horsepower rating of a motor corresponding to the rms kilovolt-amperes input as per equation 1, that is, the horsepower rating of a motor which, if operated continuously at full load, would show the same average heating as it would

if operated on the load cycle in question, then will be

Equivalent horsepower =

rms kilovolts-amperes from equation 1 $\times \dfrac{\cos\phi \times \eta}{0.746}$ (2)

$$= \cos\phi \times \eta \sqrt{\frac{\left(\frac{P_1}{\cos\phi_1\eta_1}\right)^2 t_1 + \left(\frac{P_2}{\cos\phi_2\eta_2}\right)^2 t_2 + \ldots \left(\frac{P_n}{\cos\phi_n\eta_n}\right)^2 t_n}{t_1 + t_2 + \ldots t_n}} \quad (3)$$

This method of approach may show quite large differences in motor capacities required when the application of different types and different speeds of a-c motors is under consideration.

L. A. Umansky (General Electric Company, Schenectady, N. Y.): The problem of dividing the rolling mill load between the motors and flywheels has been well covered in the literature. The fundamental equations were outlined by Gasche in 1910 before this Institute.[1]

Assuming a rectangular load curve (see Figure 1 of this discussion), with T_1 being the total rolling torque (in pound-feet) and T_0 the initial value of motor torque (when $t=0$), T, the motor torque at any time t (t in seconds, after the beginning of rolling, or after the beginning of interval between passes), may be expressed as

$$T = T_1 - \frac{T_1 - T_0}{e^{At}} \quad (1)$$

and

$$A = \frac{308 T_n}{Wk^2 \times N_s \times S_n} \quad (2)$$

Where

T_n = motor rated torque, in pound-feet
S_n = motor rated slip, in fractions
N_s = synchronous speed in revolutions per minute
Wk^2 = total flywheel effect of rotating parts, in pound-feet^2, referred to motor shaft

If the total load curve is not rectangular but trapezoidal in shape, a somewhat more involved expression can be written readily.

The difference between the total load torque (T_1) and the motor torque (T) is supplied by the flywheel which slows down during the rolling pass and thereby releases a portion of its stored energy. Likewise, during the interval between the passes the excess of motor torque (T') over the friction torque (T_1') goes to accelerate the flywheel.

It is clear that the maximum motor load exists at point B, that is, at the end of the rolling pass. As soon as the metal leaves the rolls, the motor load inevitably goes down. In this respect Figures 5 and 6 of Berkley's paper may be questioned; the motor load is shown as still increasing after its curved crosses the curve of the slab load.

Figure 1

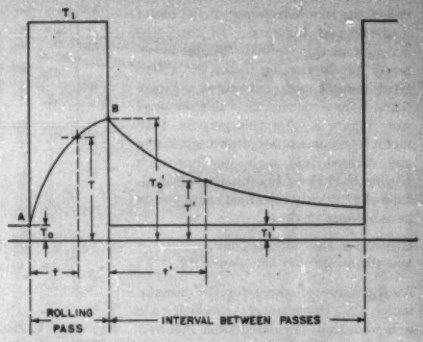

REFERENCE

1. INTERACTION OF FLYWHEELS AND MOTORS WHEN DRIVING ROLL TRAINS BY INDUCTION MOTORS, F. G. Gasche. AIEE TRANSACTIONS, volume 29, part 2, 1910, pages 1385–1402.

J. S. Gault (University of Michigan, Ann Arbor, Mich.): In the analysis of motor and flywheel behavior shown in Figure 5 of the paper, the peak motor load is shown to occur after the rolling is practically finished and about one-half second after the flywheel power has reversed. This is not possible. If the flywheel is absorbing energy, the speed must be increasing, and the motor input power will be decreasing.

The motor peak will come later than the peak rolling load, as stated by Berkley but cannot occur after the slab has left the rolls. The motor peak will be at the point where the flywheel power changes sign, at about 2.5 seconds.

Similarly, in the predicted curves of Figure 6 of the paper, the motor peak should be shown at three seconds instead of 3.7 seconds approximately.

Another point on which there is some question is his dismissal of possibility number 3, the wound rotor induction motor, on the grounds that it was too expensive. This possibility really deserves more consideration. It has all the same advantages shown for the high slip motor, and furthermore, because the rotor losses are not dissipated in the machine, it does not have to be built in an oversize frame. It would seem also that the ability to change speed might be somewhat more valuable in this application than the paper would indicate.

L. H. Berkley: The method of approach, outlined by Fraser Jeffrey, is very valuable and undoubtedly will give a more accurate result. A slight variation of his formula also can be used to advantage in calculating the rms horsepower from Figure 3 of the paper.

Gault is correct in stating that the peak motor load cannot occur after the flywheel power has reversed. As the motor load increases, the motor speed drops, and the flywheel power is positive; when the motor load decreases, the motor speed increases, and the flywheel power becomes negative. Thus, the flywheel power will reverse at the peak motor load.

Also, as stated by L. A. Umansky, the motor load curve cannot increase after it crosses the slab load curve, because the difference in the two curves indicates that the flywheel is gaining energy and the motor speed is increasing. This can occur only when the motor load is decreasing.

An Extension of Impact Speed-Drop Analysis

F. E. CREVER
MEMBER AIEE

WHEN a sudden load change occurs on a d-c motor operating at a given flux there is a transient speed change as a result. Formulas have been available which allow calculation of the transient speed change for a number of years. These formulas do not, however, give as clear a picture of the effect of varying certain factors as might be desired. Also considerable labor is involved in calculating the transient speed change for a given set of values of the determining factors.

It is the object of this study to extend the analysis so that the calculations may be made easily. It is a further object to plot the effect on impact speed drop of varying certain determining factors.

Method of Analysis

The transient speed change is obtained by solution of two differential equations. One is a voltage equation and the other a torque equation. The resulting formula for speed change has been given in other papers but is repeated in the appendix of this paper in order to have all of the information together. From the appendix we take the solution for the case when a damped oscillation is encountered,

$$S=S_o-\frac{\Delta TR}{K_eK_t}\left[1+\frac{1}{\omega t_s}\,\epsilon^{-\alpha t}\cos\,(\omega t+\delta)\right] \quad (1)$$

S = the speed at any time after sudden load change
S_o = the initial speed
ΔT = the suddenly applied torque
R = the motor-armature-circuit resistance
K_e = the motor counter electromotive force per revolution per minute
K_t = the motor torque per ampere
ω = the angular velocity of oscillation

$$t_s=\frac{2\pi}{60}\times\frac{WK^2}{32.2}\times\frac{R}{K_eK_t}$$

= speed time constant
α = the damping factor

$$=\frac{1}{2t_t}$$

$\delta=\cos^{-1}(-\omega t_s)$
t = time in seconds after the load change
$t_t=\frac{L}{R}$ of motor-armature circuit

The general form of the speed change given by equation 1 above is shown in Figure 1*A*. In this illustration are shown also the following factors:

d = the impact speed drop
s = the steady-state speed drop
$d-s$ = the undershoot of steady-state speed on the first downward swing
O_r = the overshoot of the final speed on the first recovery
t_d = the time to reach impact speed drop
t_o = the time to pass through the steady-state speed on the first downward swing
t_r = the time to reach the peak of the first overswing

All of these factors can be obtained by substituting particular values into equation 1 and plotting the speed-time curve.

The impact speed drop d also can be obtained by differentiating equation 1 and equating ds/dt to zero and solving for t_d. Substitution of this value of time into equation 1 will give d the impact speed drop. In this manner we obtain the following relationships

$$\cos\,\omega t_d+\delta=-\sqrt{\frac{\omega^2}{\alpha^2+\omega^2}} \quad (2)$$

$$t_d=\frac{\cos^{-1}-\sqrt{\frac{\omega^2}{\alpha^2+\omega^2}}-\cos^{-1}-\omega t_s}{\omega} \quad (3)$$

$$d=-\frac{\Delta TR}{K_eK_t}\,\epsilon^{-\frac{\alpha}{\omega}\left(\cos^{-1}\sqrt{\frac{\omega^2}{\alpha^2+\omega^2}}-\cos^{-1}\omega t_s\right)}\times\sqrt{\frac{\omega^2}{\alpha^2+\omega^2}} \quad (4)$$

Let us now confine our attention to equation 1 and examine each term so as to see of what each is a function.

Equation 1 can be put in the following form

$$S-S_o=-\frac{\Delta TR}{K_eK_t}\left[1+\frac{1}{\omega t_s}\,\epsilon^{-\alpha t}\cos\,(\omega t+\delta)\right]$$

$S-S_o=\Delta S$ the speed change

$\frac{\Delta T}{K_t}$ = current in the armature required to develop a torque equal to the suddenly applied torque

$\frac{\Delta TR}{K_t}$ = voltage drop resulting from resistance of armature times current required to develop applied torque

$\frac{\Delta TR}{K_eK_t}$ = revolutions per minute change resulting from voltage drop in resistance of armature circuit

This latter factor in per cent of the initial speed is the same as the per cent *IR* drop with respect to the armature applied voltage.

$$\frac{1}{\omega t_s}=2\sqrt{\frac{\frac{t}{t_s}}{4-\frac{t_s}{t_t}}}$$

= a function of $\frac{t_t}{t_s}$ only

$\alpha t=\frac{t}{2t_t}$ This is a function of t and t_t, but if we consider the time t in multiples of one cycle of oscillation the term becomes a function of $\frac{t_t}{t_s}$ only

Paper 47-29, recommended by the AIEE committee on industrial power applications and electric machinery for presentation at the AIEE winter meeting, New York, N. Y., January 27-31, 1947. Manuscript submitted November 18, 1946; made available for printing December 20, 1946.

F. E. CREVER is with the general engineering and consulting laboratory, General Electric Company, Schenectady, N. Y. He was formerly with the steel mill division of the industrial engineering divisions.

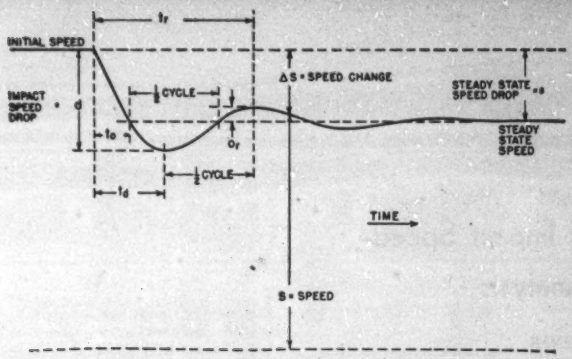

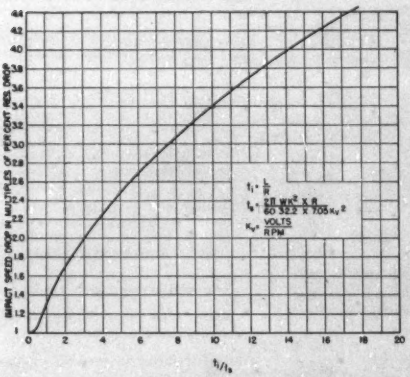

Figure 1*A* (above). General form of impact speed drop with suddenly applied load

Figure 1*B* (left). Impact speed drop as a function of time constant ratio

Figure 1*C* (below). Impact speed drop as a function of time constant ratio to extended scale

IMPACT SPEED DROP CURVES

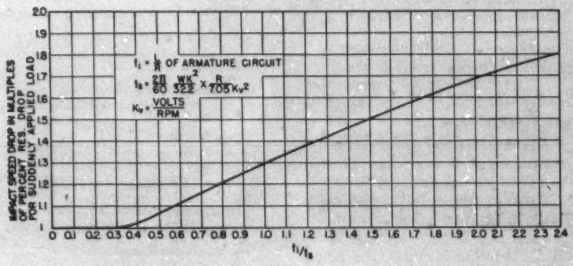

$\delta = \cos^{-1}(-\omega t_s)$

$= \cos^{-1}\sqrt{\frac{t_2}{t_1} - \frac{t_2^2}{4t_1^2}}$ which is a function of $\frac{t_1}{t_2}$ only

ωt is a function of t_1, $\frac{t_1}{t_2}$, and t, but again as in the case of ωt if time is expressed in terms of multiples of the time for one cycle of oscillation the term becomes a function of $\frac{t_1}{t_2}$ only

From this examination we reach the important conclusion that the form of the speed change on impact loading is a function of t_1/t_2 only.

The applied torque and the resistance determine the magnitude as a simple multiplying factor. The values of t_2 and t_1 merely change the time scale and do not alter the form so long as their ratio remains fixed.

Therefore we can calculate the form once for all ratios of t_1/t_2 encountered in practice and plot the values against t_1/t_2.

Now let us concentrate our attention in equation 4 on d the impact speed drop. We again have the same multiplying factor $-\Delta TR/K_eK_t$. The remaining factors are all functions of t_1/t_2 only, which is necessarily so if our conclusions reached from examination of equation 1 are correct. The factors in terms of the ratio of t_1/t_2 are as follows:

$$-\frac{\alpha}{\omega} = \frac{-1}{\sqrt{\frac{4t_1}{t_2} - 1}}$$

$$\sqrt{\frac{\omega^2}{\alpha^2\omega^2}} = \sqrt{\frac{4t_1}{t_2} - 1}$$

$$-\omega t_s = -\sqrt{\frac{t_2}{t_1} - \frac{t_2^2}{4t_1^2}}$$

Therefore, d in terms of multiples of the IR drop is a function of t_1/t_2 only and is plotted so in Figures 1*B* and 1*C*.

The angular velocity ω, the frequency f, and the time for one cycle of oscillation are functions of both t_1/t_2 and the value of t_1 as well.

Therefore, these values are given in Figure 2 as nomographs.

The time t_d to reach impact speed drop is a function of both t_1/t_2 and t_1 and is given in the form of a nomograph in Figures 3*A* and 3*B*. ωt_d is a function of t_1/t_2 only and is plotted in Figure 4.

The time to pass through the steady-state speed on the first downward swing is a function of both t_1/t_2 and t_1, but ωt_o is a function of t_1/t_2 only and is plotted in Figure 5.

The ratio of successive maximum amplitudes of oscillation about the final speed on successive half cycles is $\epsilon^{-\frac{\alpha}{\omega}\pi}$ and is a function of t_1/t_2 only. It is plotted in Figures 6*A* and 6*B*.

The value $(d-s)$ is the underswing of the steady-state speed on the first downward swing and O_f is the overshoot on the next recovery. These are plotted in Figures 7*A* and 7*B* as functions of t_1/t_2.

Explanation of Charts and How to Use Them

To use the charts obtain the following motor data:

Armature-circuit resistance = R ohms

Armature-circuit inductance $=L$ henrys
Motor WK^2 in pound-feet^2. (Include WK^2 of load if any)
Motor speed in revolutions per minute (operating speed)
Motor voltage and rated current V_r and I_r

Then figure the ratio of t_i to t_s from the following formulas:

$$K_s=\frac{\text{volts}}{\text{revolutions per minute}}$$

$$t_i=\frac{L}{R}$$

$$t_s=\frac{2\pi}{60}\frac{WK^2}{32.2}\times\frac{R}{7.05\,K_s^2}$$

$$t_s=0.000461\frac{WK^2R}{K_s^2}$$

The per cent resistance drop of the motor $=I_R=R\times100/V_R$ for rated current or torque.

Impact Speed Drop d

In either Figure 1*B* or 1*C* look up d, the impact speed drop corresponding to the value of t_i/t_s of the motor.

Multiply this value by the per cent resistance drop of the current corresponding to the applied torque, namely,

$$\frac{IR}{V_o}\times100\,\frac{V_r}{V_o}\,\frac{\Delta T}{T_r}\times\text{per cent resistance drop at rated load}$$

where

V_o = operating voltage
V_r = rated voltage
T_r = rated torque
T = suddenly applied torque

This gives the impact speed drop in per cent of the operating speed before impact loading.

Time to Reach Impact Speed Drop

The time t_d to reach the impact speed drop may be obtained in either of two ways depending upon the accuracy required.

For a quick check, obtain ω from Figure 2 by reading the point of intersection on the center scale of a straight line connecting t_i and t_i/t_s on the outer scales.

(The value of f, the frequency of oscillation, also may be read from Figure 2.) The time for one cycle is $1/f$.

Use the value of ω obtained from Figure 2 on Figures 3*A* and 3*B* by laying a straight line between the proper values of t_i/t_s and ω and read t_d in seconds on the right-hand scale.

For higher accuracy look up ω in Figures 3*A* and 3*B* as before and look up t_d in Figure 4. Divide ωt_d by ω to obtain t_d.

Figure 2. Nomograph of frequency of oscillation as a function of time constant ratio and value

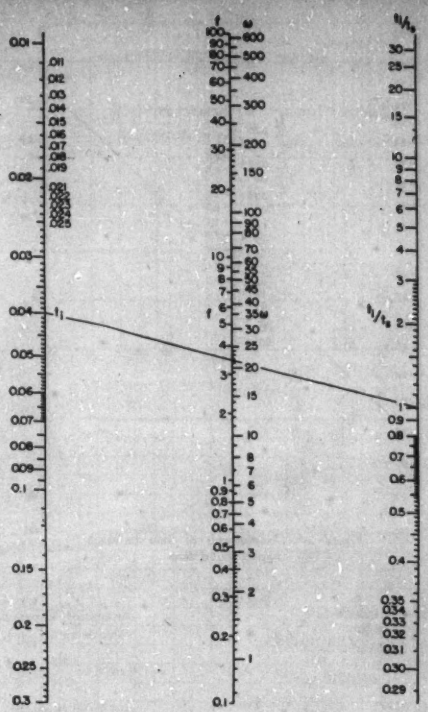

To Draw Complete Speed–Time Curve

Complete the calculations and note the time for one cycle. Successive overswings of the final steady-state speed are in fixed ratio depending upon the value of t_i/t_s as plotted in Figures 6*A* and 6*B*.

Figures 7*A* and 7*B* show both $(d-s)$ and O_r, the first overshoot, in multiples of the per cent resistance drop.

Note that the times of crossing the final steady-state speed value are not spaced halfway between the times at which maximum overswing occurs.

To obtain t_o look up the value of ωt_o (Figure 5) that corresponds to the value of t_i/t_s in question. Divide ωt_o by ω to obtain t_o. Successive time values of crossing the steady-state speed value are obtained by adding the time for one-half cycle to t_o.

Successive values of time at the peaks of the swings are obtained by adding the time for one-half cycle to t_d; thus $t_r=t_d$ plus the time for one-half cycle as shown in Figure 1*A*.

Example of Use of Charts

Consider a motor with pole-face winding rated 8 pole, 1,000 horsepower, 600 volt, 225/730 rpm with the following constants:

$R=0.0180$ ohm
$L=0.0007$ henry
$WK^2=32{,}100$ pound-feet^2
total $WK^2=34{,}300$
load $WK^2=2{,}200$ pound-feet^2

At 225 rpm 600 volts suddenly apply 90 per cent full-load torque.

$$K_s=\frac{600}{225}$$
$$=2.67 \text{ volts per revolution per minute}$$

$$t_i=\frac{0.00072}{0.0180}$$
$$=0.040 \text{ second}$$

$$t_s=\frac{0.000461\times34{,}300\times0.0180}{2.67^2}$$
$$=0.04 \text{ second}$$

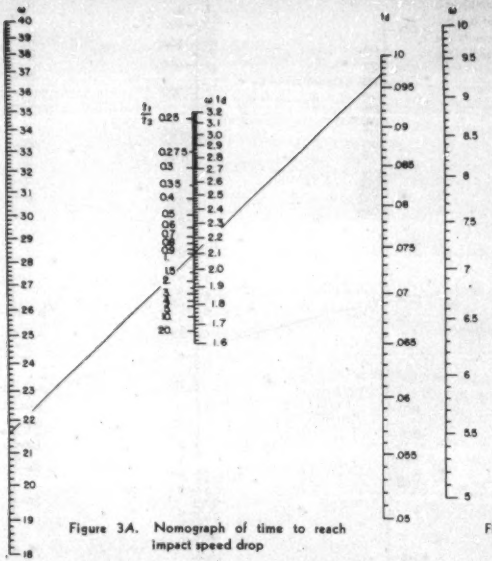

Figure 3A. Nomograph of time to reach impact speed drop

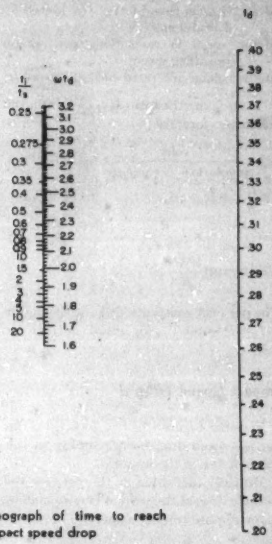

Figure 3B. Nomograph of time to reach impact speed drop

$I_r = 1{,}310$ amperes

$$\frac{I_r R}{V_r} \times 100 = \frac{1{,}310 \times 0.0180}{600}$$
$$= 3.93 \text{ per cent}$$

$$\frac{t_l}{t_s} = \frac{0.04}{0.04}$$
$$= 1.0$$

From Figure 1*C* for $t_l/t_s = 1$, d is 1.3 times the per cent resistance drop. As we are applying 90 per cent load d will be

$0.9 \times 1.3 \times 3.93 = 4.59$ per cent of initial speed

From Figure 2,

$\omega = 21.6$ radians per second
$f = 3.44$ cycles per second
Time for one cycle $= 0.29$ second

From Figure 3*A*,

$t_d = 0.097$ second

Successive peaks occur at

$$\left(0.097 + \frac{0.29}{2} = 0.242\right)$$
$$(0.097 + 0.29 = 0.387)$$

and so forth. From Figure 5

$\omega t_o = 1.05$ seconds

$$t_o = \frac{1.05}{21.6}$$
$$= 0.0486 \text{ second}$$

Successive crossings of the final speed value occur at

$$0.0486 + \frac{0.29}{2} = 0.1936$$

$$0.0486 + 0.29 = 0.338$$

and so forth. From Figure 6*B*, the ratio of the overswing on successive half cycles is 0.164.

The steady-state speed drop is

$0.9 \times 3.93 = 3.54$ per cent

The value of the first underswing below the final speed is

$$d - 3.54 = 4.59 - 3.54$$
$$= 1.05 \text{ per cent}$$

The overshoot of final speed on the first upswing is 1.05×0.164 or 0.172 per cent. The speed at this point will be $3.54 - 0.17 = 3.37$ per cent below the initial speed.

If the first overswing is all that is required the value could have been obtained from Figure 7*B*.

Conclusions

1. The charts give a simple and quick means of drawing the speed change upon impact loading.

2. They also show that both low resistance and low inductance are important to obtain low impact speed drop.

3. While it is theoretically necessary to make $t_s = 4t_l$ giving a ratio of t_l/t_s of 0.25 for nonoscillatory response, the curves show that the response with $t_s = 3t_l$, that is, t_l/t_s 0.333 is so very close to nonoscillatory that it is unnecessary to use any greater value of WK^2 at base speed.

4. The charts should form a basis for a definition of a low impact speed-drop motor when considered in conjunction with motor design data.

Appendix

Let

V = applied armature voltage
K_e = motor counter electromotive force per revolutions per minute
S = motor speed in revolutions per minute
ΔS = motor speed change in revolutions per minute
R = motor-armature-circuit resistance
L = motor-armature-circuit inductance
i = motor-armature current
p = differential operator with respect to time
K_t = motor torque per ampere
T_o = initial load torque
T = applied torque
1 = unit function

$$M = \frac{2\pi}{60} \times \frac{WK^2}{32.2}$$

Assuming the counter electromotive force of the motor per revolutions per minute to be constant, the equations whose simultaneous solution give the transient change in motor

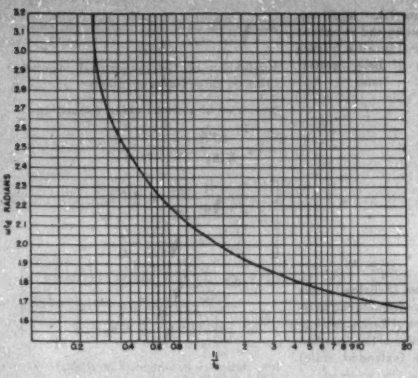

Figure 4. Chart showing product of natural angular velocity and time to reach impact speed drop as a function of time constant ratio

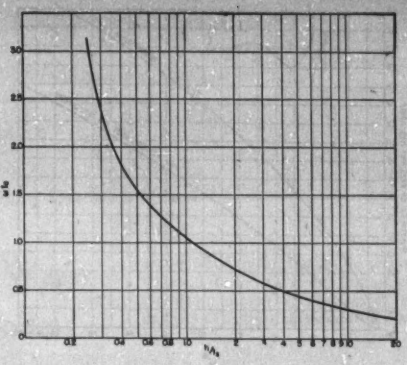

Figure 5 (above, right). Chart showing product of natural angular velocity and time to reach final speed on first downward swing

speed upon suddenly applied load are as follows:

1. By summation of voltages in motor-armature circuit

$$V-K_eS=R_i+Lpi$$

2. By summation of torques on the motor shaft

$$K_ti=T_0+T1+MpS$$

In order to simplify the analysis we may use Δ values to indicate changes and then superpose these on the initial conditions to obtain the complete solution.

The equations then become

$$\begin{aligned}-K_e\Delta S&=(R+Lp)\,\Delta i\\ K_t\Delta i&=+\Delta T1+Mp\,\Delta S\end{aligned}\qquad(5)$$

From equation 5

$$\Delta i=\frac{-K_e\Delta S}{(R+Lp)}\qquad(6)$$

Substituting this into equation 6 for Δi and solving for ΔS we obtain

$$\Delta S=\frac{-T1(R+L_p)}{M_p(R+L_p)+K_tK_e}$$

Divide numerator and denominator by R

$$\Delta S=\frac{-\Delta T1\left(1+\frac{Lp}{R}\right)}{\frac{ML_p^2}{R}+\frac{MR_p}{R}+\frac{K_eK_t}{R}}$$

$$=\frac{-\Delta T1\left(1+\frac{Lp}{R}\right)}{\frac{K_eK_t}{R}\left(\frac{MR}{K_eK_t}\times\frac{Lp^2}{R}+\frac{MR}{K_eK_t}\times P+1\right)}$$

If we let

$$t_t=\frac{L}{R}$$

=current time constant

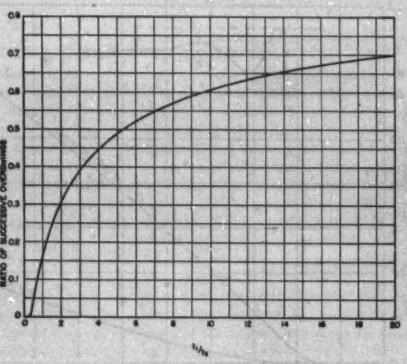

Figure 6A (right). Ratio of successive ½-cycle peak amplitudes of oscillation about final speed as a function of time constant ratio

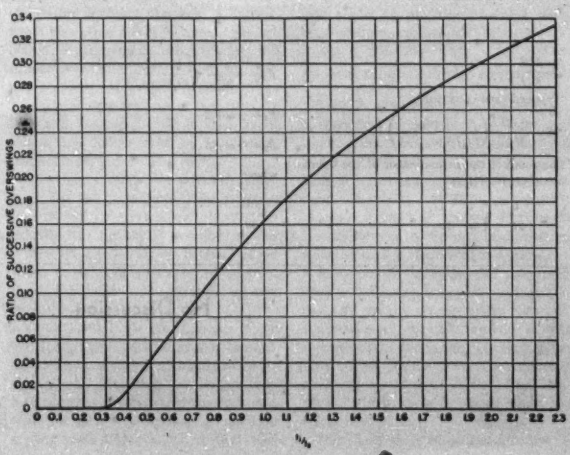

Figure 6B (below). Ratio of successive ½-cycle peak amplitudes of oscillation about final speed as a function of time constant ratio to extended scale

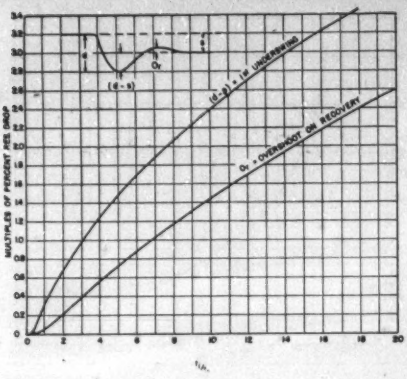

Figure 7A. Initial underswing and overshoot of final speed as a function of time constant ratio

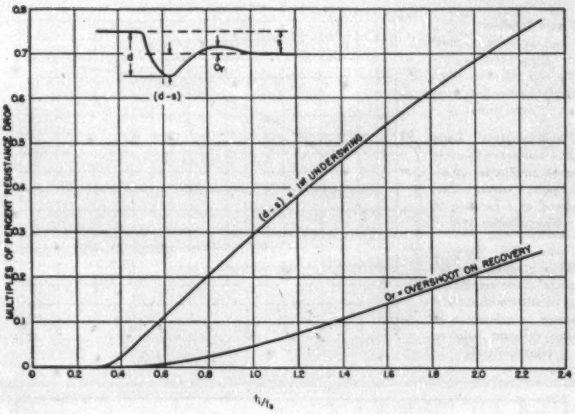

Figure 7B (below). Initial underswing and overshoot of final speed as a function of time constant ratio (extended scale)

$$t_s = \frac{MR}{K_p K_t}$$

= speed time constant

$$\Delta S = \frac{-\Delta TR}{K_p K_t}\left(\frac{1+t_{1p}}{t_1 t_s P^2 + t_{sp} + 1}\right) 1$$

The roots of the denominator of the operational expression are

$$P_1 = -\frac{1}{2t_1} + \sqrt{\frac{1}{4t_1^2} - \frac{1}{t_1 t_s}}$$

$$P_2 = -\frac{1}{2t_1} - \sqrt{\frac{1}{4t_1^2} - \frac{1}{t_1 t_s}}$$

$$P_1 = -\alpha + \beta$$

$$P_2 = -\alpha - \beta$$

where

$$\alpha = \frac{1}{2t_1}$$

$$\beta = \sqrt{\frac{1}{4t_1^2} - \frac{1}{t_1 t_s}}$$

Evaluation of the operational expression takes on three forms as follows:

(a). When $t_s > 4t_1$ both roots are real and negative.

$$\Delta S = \frac{-\Delta TR}{K_p K_t}\left[1 + \frac{\frac{1}{2} + \sqrt{\frac{1}{4} - \frac{t_s}{t_s e}}}{\frac{1}{2}\frac{t_s}{t_1} - 2 - \sqrt{\frac{1}{4}\frac{t_s^2}{t_1^2} - \frac{t_s}{t_1}}} \cdot e^{(-\alpha+\beta)t} + \frac{\frac{1}{2} - \sqrt{\frac{1}{4} - \frac{t_1}{t_s}}}{\frac{1}{2}\frac{t_s}{t_1} - 2\sqrt{\frac{1}{4}\frac{t_s^2}{t_1^2} - \frac{t_s}{t_1}}} \cdot e^{(-\alpha+\beta)t}\right]$$

(b). When $t_s = 4t_1$ both roots are equal.

$$P_1 = P_2 = \frac{-1}{2t_1} = -\alpha$$

and the solution is

$$\Delta S = -\frac{\Delta TR}{K_p K_t}\left[1 - e^{-\alpha t} - \frac{\alpha t}{2} e^{-\alpha t}\right]$$

(c). When $t_s < 4t_1$ the roots are complex and the solution is

$$\Delta S = -\frac{\Delta TR}{K_p K_t}\left[1 + \frac{1}{\omega t_s} e^{-\alpha t} \cos(\omega t + \delta)\right]$$

In this latter case the equation for ΔS is a damped oscillation.

The speed $S = \Delta S + S_0$

or

$$S = S_0 - \frac{\Delta TR}{K_p K_t} \times \left[1 + \frac{1}{\omega t_s} e^{-\alpha t} \cos(\omega t + \delta)\right]$$

References

1. Speed Regulation of Main Roll Drives, L. A. Umansky. Association of Iron and Steel Engineers *Proceedings*, Pittsburgh, Pa., 1927, pages 103–15.

2. Speed Transients of D-C Rolling Mill Motors, L. A. Umansky, T. M. Linville. AIEE Transactions, volume 54, 1935, April section, pages 387–94.

No Discussion

Cathodic Protection of Steel Water Tanks Using Aluminum Anodes

L. P. SUDRABIN
NONMEMBER AIEE

R. B. MEARS
NONMEMBER AIEE

Synopsis: Aluminum alloy anodes have been used in approximately 1,000 installations of cathodic protection of steel water tanks using current from an outside source. From fundamental considerations it would be expected that the loss in weight per ampere hour of current passed from aluminum anodes would be less than one-third the weight loss from steel anodes. This expectation is confirmed in service. In addition, it was found that the aluminum anodes developed a more uniform attack than did anodes of steel or stainless steel. This is desirable because localized attack can result in early anode failure. The corrosion products from the aluminum anodes are white or colorless and adhere to the anodes. In the case of anodes of many other metals the corrosion products are strongly colored and fall off the anodes, thus discoloring or otherwise contaminating the water. Anodes of several aluminum-base alloys all have proved satisfactory in field installations. However, anodes of the aluminum-copper alloys (such as 17*S-T* or 24*S-T*) appear to be superior to anodes of unalloyed aluminum (2*S*) or to aluminum-zinc alloy anodes.

CATHODIC PROTECTION can be obtained either by using direct current supplied by some external source, as by a motordriven generator, or by means of galvanic action resulting from contact with metal that is anodic to the metal to be protected. In this paper attention will be directed mainly to the first, or applied current, method of cathodic protection. In another paper[1] by one of the authors the use of galvanic anodes made of light metals for protecting steel structures was discussed, and in a series of papers[2] by the other author cathodic protection by external current using steel, cast iron, or carbon anodes has been described.

Paper 47-30, recommended by the AIEE committee on electrochemistry and electrometallurgy for presentation at the AIEE winter meeting, New York, N. Y., January 27–31, 1947. Manuscript submitted March 3, 1946; made available for printing December 3, 1946.

L. P. SUDRABIN is a chemical engineer with Electro Rust-Proofing Corporation, Newark, N. J.; R. B. MEARS was formerly with Aluminum Company of America, New Kensington, Pa.

Aluminum has certain inherent advantages for use as anodes with applied current. Its most obvious one is its low electrochemical equivalent. This means that at 100 per cent anode current efficiency a smaller weight of aluminum will be dissolved per ampere-hour of current passed than is the case for any other appropriate metal. The metalloid carbon has a lower electrochemical equivalent than does aluminum. The electrochemical equivalents of several of the common metals and of carbon are given in Table I. From this table it will be noted that one pound of aluminum, theoretically, will supply over three times as many ampere-hours of current as one pound of iron. This means that an aluminum anode only one-third the weight of an iron anode should last longer than an iron anode under similar service conditions.

This lighter weight of equivalent aluminum anodes is important in reducing transportation and labor charges incidental to installation of the anodes. Where the anodes are to be used in elevated water tanks, the ease of handling the lighter aluminum anodes is of particular value.

From Table I, the use of anodes of carbon (or graphite) would appear interesting because of the high electrochemical equivalent. However, anodes of these materials have undesirable physical properties for such applications. In addition, service tests have indicated that such anodes disintegrate rapidly in many waters, probably as a result of attack of the binder followed by sloughing off of unattacked particles of carbon or graphite.

Other Advantages of Aluminum Anodes

Other desirable properties of anodes are that they must not form films of high resistance which would limit current flow. Also, they should corrode uniformly without the development of deep pits. Localized pitting attack can result in complete penetration of the anode and possibly even in corrosion in two before the main mass of the anode has been consumed. This results in great reduction in anode life. As is shown in the examples which are described subsequently, aluminum anodes have proved very satisfactory in both of these respects.

It is also frequently desirable that corrosion products from the anodes do not discolor the water. The corrosion products from aluminum anodes are white or colorless and are, therefore, not as objectionable as are the products from anodes of many other metals.

Application of Cathodic Protection

Since 1935 cathodic protection has been applied as a method of underwater corrosion control to over 4,000 industrial and municipal water storage tanks in the United States and Canada. These tanks range in capacity from only a few gallons to over six million gallons. A typical installation in a hemispherical-bottom elevated tank is illustrated in Figure 1.

Each anode is suspended vertically from a fixed structure such as the tank roof, by means of one-fourth-inch galvanized cable. A strain insulator is used to insulate the anode from the tank structure. The positive lead connection is made to the upper six inches of the electrode, which extends above the high water line.

The electrode is assembled into the re-

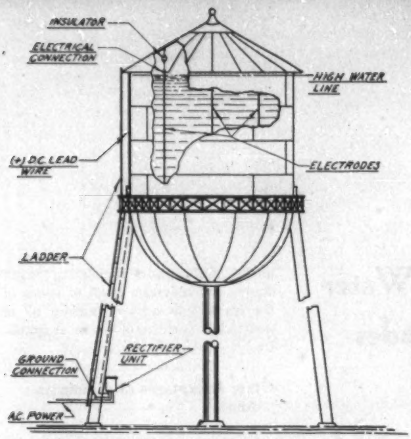

Figure 1. Typical cathodic installation in an elevated tank

Table I. Electrochemical Equivalents of Various Anode Materials

Anode Material	Weight of Material Consumed Per 26.8 Ampere-Hours of Current Passed, Grams	Ampere-Hours Per Pound of Material
Aluminum	9.0	1,552
Graphite	6.0 or 3.0	2,021 or 4,042
Copper	31.8	382
Iron	27.9	436
Lead	103.6	117
Magnesium	12.2	997
Nickel	29.3	416
Zinc	32.7	372

quired length by joining 12-foot long aluminum rod sections end on end with threaded couplings. All couplings are protected by rubber and friction tape. The electrode can be installed and replaced from the tank roof through a 4- or 6-inch-diameter hole cut in the roof adjacent to the point of electrode suspension. The hole cut through the roof is covered with a gasketed plate to prevent birds and debris from entering the tank.

In practice there is no pronounced attack occurring on the anode at the water level. The water level in tanks is rarely kept constant and this operational characteristic probably accounts for the absence of marked attack at the water surface.

However, special care must be given to the taping procedure used to protect the threaded coupling so as to prevent premature local failure of the anode. It has been observed that the longer the taped section on the anode, the greater is the metal wastage immediately adjacent to the tape.

Platinum anodes also have been used to some extent. These have the advantage that they are not attacked appreciably even after prolonged periods of service. However, they have several severe limitations.

1. Because of the high cost of platinum they generally are used in the form of wires of small diameter. This means that higher anode current densities must be used in order to provide equal current to the tank being protected. The higher current densities cause higher IR drops in the water, resulting in higher power costs.

2. Because the platinum is inert, the main anode reaction is the evolution of oxygen. When aluminum anodes are used, the main anode reaction is the dissolution of aluminum. The oxygen evolved from the platinum anode dissolves in the water and increases its corrosiveness. This means, in tanks confining water with a low dissolved oxygen concentration, that higher current densities are required to protect the walls of the water tank and also that steel equipment through which the water from the tank passes will have its corrosion accelerated because of the increased quantities of oxygen dissolved in it.

3. As fine wires of platinum are used there is a definite hazard that they will be broken or bent out of position by ice formation during cold weather.

Beginning in 1939, trial installations were started using aluminum anodes. The results of these trial installations were so promising that early in 1945 the use of aluminum anodes was generally adopted. At the present time aluminum anodes are being used in approximately 1,000 installations of cathodic protection. The results of some typical applications of aluminum anodes are summarized in the following paragraphs.

Example *A*—Two 75,000-Gallon Elevated Sprinkler Tanks

In August 1944 cathodic protection was applied to two 75,000-gallon hemispherical-bottom elevated tanks, which are used for sprinkler water storage at the American Suppliers, Inc. warehouse in Louisville, Ky. These tanks, being alike, lent themselves to study whereby the properties of certain electrode materials could be compared.

Each tank had a single electrode, supported from an insulator, along the vertical center axis of the tank. In one tank the electrode was of seven-eighths-inch-diameter hot-rolled SAE-1020 steel rod submerged for a distance of $21^1/_2$ feet below the high water level. In the other tank aluminum alloy rod (Alcoa 17*S*-*T**) having identical dimensions was used.

An average current flow of 1.60–1.62 amperes was projected from each electrode to the tank. The impressed voltage required to maintain this amperage ranged from 5.0 to 10.0 volts, depending upon variations in conductivity of the water. As the voltage requirements were alike in both tanks, it appears that aluminum does not possess marked electrical valving properties under the conditions of the application.

On February 20, 1945, after the removal of the degradation product, an examination of the aluminum alloy rod

* Composition and properties given in Table II.

Table II. Composition and Properties of Aluminum Alloys

Alloy	Composition	Temper	Typical Mechanical Properties: Tensile Strength, Pounds Per Square Inch	Elongation, Percentage in Two Inches
2*S*	Commercially pure aluminum containing at least 99 per cent aluminum	*O*	13,000	35
		H	24,000	5
72*S*	Aluminum alloy containing 1 per cent zinc	*O*	11,000	35
		H	20,000	5
17*S*	Aluminum alloy containing 4 per cent copper, 0.5 per cent manganese, 0.5 per cent magnesium	*O*	26,000	20
		T	62,000	20
24*S*	Aluminum alloy containing 4.5 per cent copper, 0.6 per cent manganese, 1.5 per cent magnesium	*O*	27,000	19
		T	68,000	19
Alclad 24*S*	This is a duplex product with a 2*S* coating on both sides of a 24*S* core	*O*	25,000	18
		T	64,000	18

Table III. Comparative Anode Performance in Elevated Sprinkler Tanks at Louisville, Ky.

Tank	Anode	Weight, Pounds	Service Hours	Ampere-Hours	Over-all Anode Efficiency, Per Cent
A	1/8-by-21 1/8-inch hot-rolled SAE-1020 steel	43.9	9,100	14,650	77
B	1/8-by-21 1/8-inch aluminum alloy 17*S-T*	15.6	10,600	17,050	81

revealed fairly uniform wastage. The hot-rolled SAE-1020 steel rod was grooved badly with three zones along the length of the rod where premature failure could occur because of localized wastage. This characteristic found in most steel electrodes, including the stainless steels, is especially undesirable since such a failure will result in improper current distribution after the electrode has been shortened.

A marked variation in amperage obtained in relation to applied voltage indicated the failure of the aluminum alloy rod on October 31, 1945. The hot-rolled SAE-1020 steel rod had failed some two months earlier. A performance comparison of 17*S-T* aluminum alloy and hot-rolled SAE-1020 steel rod is shown in Table III, while the composition of the water is given in Table IV. The tanks were kept full by replacing evaporation and leakage losses with Louisville, Ky. water at weekly intervals. Although the water used in filling the tank approaches saturation with dissolved oxygen, it is interesting to note the marked reduction of dissolved oxygen occurring in the water stored in this tank.

Table IV. Louisville, Ky. Water Analysis

Total dissolved solids	221 parts per million
Total hardness	115 parts per million
Total alkalinity	63 parts per million
Chlorides	25 parts per million
pH	8.1
Dissolved oxygen* two feet below surface of water	2.1 parts per million
Dissolved oxygen* in bowl at bottom of tank	1.8 parts per million

* Measured in tank with aluminum anodes.

Table V. Analysis of Deep Well Water

Total dissolved solids	414 parts per million
Total hardness	300 parts per million
Total alkalinity	276 parts per million
Chlorides	20 parts per million
Dissolved oxygen	0.4 parts per million
pH	7.3
Specific resistance at 20 C	1,240 ohms/cm³
Dissolved oxygen in water from bowl of tank	5.1 parts per million

Table VI. Reservoir Water Analysis

Total dissolved solids	42 parts per million
Total hardness	21 parts per million
Total alkalinity	18.6 parts per million
Chlorides	1.9 parts per million
pH	6.6
Specific resistance at 20 C	18,600 ohms/cm³
Dissolved oxygen	5.8 parts per million
Dissolved oxygen in water from bowl of tank	4.2 parts per million

It is interesting to note from Table III that the useful life of the aluminum alloy anode averaged 1,093 ampere-hours per pound of anode weight, whereas the useful life of the steel anode was less than one-third as great (334 ampere-hours per pound of anode weight). The marked superiority of aluminum anodes predicted from fundamental considerations thus actually is obtained in service.

Example *B*—100,000-Gallon General Service Tank

In 1939 the Dayton Power and Light Company found that a 100,000-gallon ellipsoidal-bottom elevated steel tank, erected in 1931, had developed numerous leaks in the bowl. The tank initially had been pointed with two coats of red lead paint. It was desirable to repair the tank with a minimum period during which it would be out of service. Therefore, the perforations in the tank walls were welded shut, and the deep pits were filled by welding. Then cathodic protection was applied. The anodes used initially were of number 303 stainless steel. Protection of the tank was satisfactory, but the anodes had a very short life because they developed severe localized attack. After several replacements, aluminum (2*S*) anodes were installed in 1943. These anodes were definitely more satisfactory because they developed a more uniform attack than did the stainless steel anodes used previously. When this tank was last inspected in 1945, it still was being adequately protected.

The water stored in the tank is from a deep well and has the composition indicated in Table V. The marked increase in dissolved oxygen concentration in water taken from the bowl of the tank can be attributed to the frequent fluctuations in water level which normally occur in tanks used for general service operation.

Example *C*—3,000,000-Gallon Municipal Standpipe

The Pennichuck Water Company of Nashua, N. H. in 1940 erected a standpipe 100 feet in diameter by 50 feet in height, having a capacity of nearly 3,000,000 gallons for water storage. The water confined is the typical New England surface water which has low mineral content but is extremely aggressive because of the high dissolved oxygen concentration and the absence of influencing amounts of cathodic inhibitors such as calcium bicarbonate. The composition is given in Table VI.

In order to overcome the effect of the high specific resistance of this water upon voltage requirements, 1,400 feet of 3/16-by-6-inch Alclad 24*S-T* sheet were used in the electrode configuration within the tank. Eleven volts were required to project a current flow of 30 amperes from the electrode configuration to the tank surface.

Pit depth measurements made with a dial depth gauge in the summer of 1945 indicate a maximum pitting rate of slightly over 0.001 inch per year on the submerged surfaces of the tank. Although

Figure 2. Photograph of portions of anodes of three aluminum alloys (2*S*, 17*S-T*, and 72*S* from left to right) used for 103 days in a 100,000-gallon steel water tank. The anode of 17*S-T* showed the most uniform attack and gave the highest over-all anode efficiency (89 per cent)

Table VII. Comparative Anode Behavior in Water Tank at West Carrollton, Ohio

Material	Service Hours	Ampere-Hours	Theoretical Weight Loss,* Pounds	Actual Weight Loss, Pounds	Over-all Anode Efficiency, Per Cent
2S	2,460	2,460	1.83	2.85	64
17S-T	2,460	2,460	1.83	2.05	89
72S	2,460	2,460	1.83	3.02	61

* Not corrected for presence of alloying constituents.

the applied current is not quite adequate to stifle the corrosion processes in this environment completely, it has reduced the rate of penetration of the steel standpipe to a negligible figure.

Examination of the aluminum alloy sheet electrodes at the end of 14 months operation indicated uniform attack with reasonable certainty of attaining approximately 100 per cent electrochemical electrode efficiency.

It is believed that the use of Alclad 24S-T as the anode material may have been a particularly good choice in this case. As is indicated in Table II, Alclad 24S-T is a duplex material consisting of a central core of an aluminum-copper alloy (24S-T) with a coating on both sides of aluminum. This coating probably resulted in even more uniform attack of the anode surface than would have been the case if plain 17S-T or plain 24S-T had been used as the anode.

Example *D*—100,000-Gallon Sprinkler Tank

A comparison of the electrode characteristics of anodes of three aluminum alloys, namely, 2S, 17S-T, and 72S, was made in a 100,000-gallon hemispherical-bottom elevated tank used for sprinkler storage by the Oxford-Miami Paper Company, West Carrollton, Ohio. Three electrodes—one of each of the types previously mentioned—three-fourths inch in diameter and $26^1/_2$ feet in length were positioned symmetrically within the tank so that identical potential conditions occurred on each electrode. The current flow from each electrode was controlled at one ampere. At the end of 103 days the electrodes were removed and examined. The copper bearing aluminum alloy (17S-T) electrode was found to be covered with an adherent crusty degradation product, including metallic copper particles deposited adjacent to the metal core. The 2S and 72S electrodes were covered with a less adherent and softer degradation product. Except for a few localized pits, the 17S-T had been consumed more uniformly than the 2S and 72S and did not have the intensified attack at the taped joints (Figure 2).

The behavior of the various anodes is compared in Table VII. It will be noted that the 17S-T electrode lost the least weight and had an anode efficiency of 89 per cent. The water confined in the tank is deep well water similar in composition to that stored in the tank of example *B*, in Dayton, Ohio. Evaporation and leakage losses are replaced by weekly filling to the overflow line.

Cathodic protection was applied to this tank in June 1945, at which time tubercles of red rust were observed oozing through breaks in the drying oil type paint film.

The extreme clarity of the water permitted visual examination of the hemispherical bottom of the tank some 30 feet below the water surface. This was also true after the cathodic protection system had been in operation three months, as all of the aluminum electrode degradation product appeared to have adhered to the metal anodes. This adhesion of corrosion products to the aluminum anodes is very desirable. With anodes of some other materials the products fall off and discolor or otherwise contaminate the water.

An examination of the tank at the end of three months of cathodic protection revealed the deposition of scale-forming salts over corrosion product noted earlier. Apparently cathodic processes, which generally produce a predominance of hydroxyl ions, were induced on the areas where the anodic processes resulting in metal wastage had occurred previously. The increase in pH of the rust tubercles caused the precipitation of the calcium and magnesium salts from the water in the form of a white precipitate consisting of $CaCO_3$ and $Mg(OH)_2$. It was interesting to note that none of the scale-forming salts were precipitated adjacent to the metal under the rust. Areas from which tubercles had been removed were found later coated with the white deposit and no further attack had occurred underneath.

Example *E*—Other Applications

In 1941 C. P. Hoover, Columbus, Ohio Water Department, began studies to establish methods for mitigating the corrosion in domestic hot water generating tanks.[3] Among the methods investigated was cathodic protection. A current of 0.35 amperes projected from an electrode centered along the vertical axis of the 30-gallon hot water generating tanks provided complete protection against Columbus, Ohio city water. Chrome steel anodes we found to be less satisfactory than aluminum (2S)—both from the standpoint of electrochemical efficiency, and the introduction of objectionable anode degradation products.

Many institutional and commercial hot water generating tanks now are receiving cathodic protection.

Cathodic protection can be applied effectively to intricate structures such as Dorr Clarifier mechanisms in municipal water treatment plants. An installation made on a 90-foot Dorr Clarifier at the Mahoning Valley Sanitary District, Youngstown, Ohio, reduced the average rate of pitting on the steel members of the rake arms from 0.0009 to 0.0001 inch per month.

Among the other structures submerged in water media to which cathodic protection is being applied are sewage digesters, deep well pumps, lock gates, Spaulding sludge blanket filtration softeners, and so forth. In addition to the applications mentioned previously, pipe line protection against soil corrosion is outstanding.

Cathodic protection provides a desirable electric load for the public utilities as the demand is relatively constant and continuous.

References

1. Light Metals for Cathodic Protection of Steel Structures, R. B. Mears, C. D. Brown. *Corrosion* (Houston, Tex.), volume 1, 1945, 113–18.

2. Cathodic Protection of Steel Surfaces in Contact With Waters, L. P. Sudrabin. *Water Works and Sewerage* (Chicago, Ill.), volume 92, 1945, pages 11, 51, and 147.

3. *Annual Report*, Division of Water, Columbus, Ohio, C. P. Hoover. 1943.

No Discussion

Electrification of the Cotton Industry in the South

S. A. BOBE
MEMBER AIEE

ALTHOUGH the South has advanced industrially in leaps and bounds in the past few years, especially during World War II, cotton still is "king" and remains the major industry. It employs the greatest number of people in manufacturing, 437,000, with a product value of $1^1/_4$ billion dollars. It further accounts for a farm income of $1^1/_2$ billion dollars. There is a total of 1,248 cotton mills of which 75 per cent are in the South.

Cotton accounts for 70 per cent of all textile fibers used, with rayon, wool, and jute accounting for approximately 12, 10, and 8 per cent.

To the electrical industry it represents a total of four million connected horsepower with an annual power consumption of nine billion kilowatt-hours. It uses all electric products from turbogenerators, motors, and lighting to recent installations of radio frequency heating for yarn twist setting.

These large quantities of power are comparatively recent. The industry, being one of the world's oldest, had carried development of mechanical drives to such a point of perfection that the economic necessity for change to electric drives was not as great as in other industries. As a result, the major share of electrification of the cotton industry has taken place in the past 20 or 25 years and still is not completed.

As large quantities of energy were required, early cotton mills, both in New England and the South, were located along streams or rivers. Dams were built and mechanical water wheels installed driving by belts or ropes to mill line shafts. A common arrangement was to have one large grooved rope pulley, driven by the water wheel, located in a ropeway at the end or center of the mill. Ropes then were run in this ropeway from the large pulley to a line-shaft pulley at each floor level. All of the mill equipment then was driven by belts from these line shafts.

With the development of large reciprocating steam engines, mills ceased being dependent on water power and began to move to locations having advantages of raw material and labor supply. This marked the beginning of large scale movement of the industry from New England to the South. The steam engines still used the same power distribution arrangement as the water wheel with usually one large engine driving a complete mill. Such a drive is illustrated in Figure 1.

These large slow-speed steam engines were a very impressive sight with the engine room kept painted and clean and all brass oil cups and governor parts highly polished. Such engine drives now are practically extinct.

The first introduction of electric energy in the cotton mill came as a means to secure safer and better lighting. Small generators were installed driven from the mill line shaft or from small steam engines. The output of these generators was distributed through open knife switch panel boards to drop cords throughout the mill. Some of these original installations, including the drop cords, still occasionally can be found in small mills.

With generators and motors both available, cotton mill operators now found it possible to arrange mills for best equipment location without being limited by a

Figure 1. Reciprocating steam engine driving cotton mill by means of ropes to line shafts at different floor levels

Paper 47-33, recommended by the AIEE committee on industrial power applications for presentation at the AIEE winter meeting, New York, N. Y., January 27-31, 1947. Manuscript submitted November 12, 1946; made available for printing December 9, 1946.

S. A. Bobe is an industrial engineering supervisor with Westinghouse Electric Corporation, Atlanta, Ga.

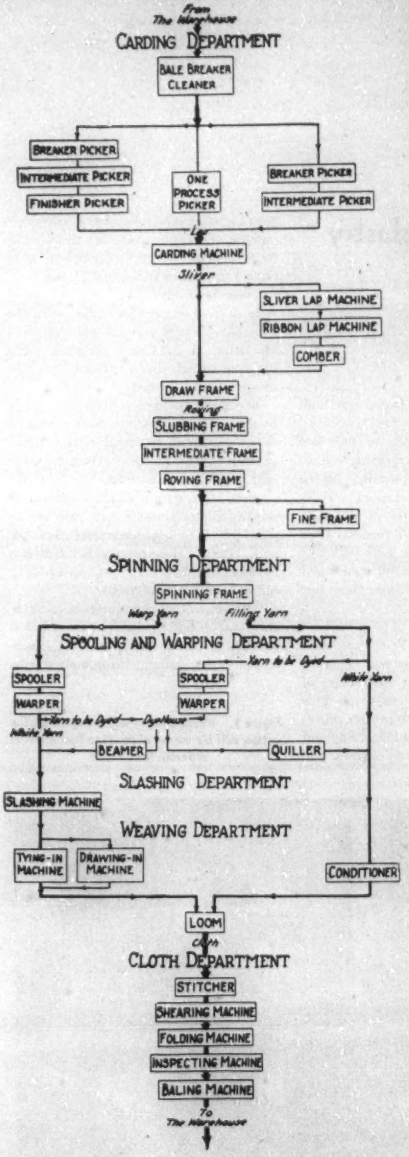

Figure 2. Flow sheet of cotton through a textile mill

Figure 3 (above). Output end of variable voltage sectional motor drive of cloth finishing machine showing last motor and motor-generator set with control

common mechanical drive. This resulted in the water wheels or steam engines being used to drive large generators which supplied electric energy to motors driving short sections of line shafts.

In most cases the early electrified mills were those that generated their own power. It was not until large power systems were organized that mills were able to purchase the large quantities of dependable power required at economical rates. These rates have been decreasing continually and dependability increasing until now most mills can purchase power cheaper than they can generate it. Average mill power costs in the South vary from about one cent per kilowatt-hour for the smaller mills to five mills per kilowatt-hour for the larger users.

The next step from a common line-shaft drive was to provide individual motors on each separate piece of equipment or process. This was a quite logical result as demands were made for higher speeds and cleaner mills. Individual drives gave closer output control by eliminating unpredictable belt slip and permitted unlimited flexibility in arrangement. Machines were arranged for best mill arrangement without concern about drives. As a result all new mills, and almost all old mills, now are nearly completely individually driven. The trend to increase machine speed and output is still continuing, however, and resulting in an increasing kilowatt-hour consumption and investment in machinery per employee.

In the early electrification of cotton mills the question of voltage was given serious consideration and 550 volts adopted as standard for mill distribution. The major reason was saving in copper without increasing costs of motors or con-

trol over 440-volt cost. The rating of 550 volts is now standard in approximately 95 per cent of the mills in the Southeast including both cotton and rayon. Although recent efforts have been made to change this to 440 volts, the textile industry still considers 550 as standard and all new construction continues at 550 volts.

The kilowatt demand of cotton mills will vary from 1,000 for small units to approximately 15,000 for the largest groups. When power is purchased it is brought to the mill at high voltage and then transformed to the mill distribution voltage. The substations usually are owned by a power company. Past practice was to supply a single bank for the complete mill load. This resulted in many transformer banks of 5,000 and 7,500 kva, or even larger, with resultant high currents and high short-circuit capacities. Short-circuit interrupting capacity was not given sufficient consideration always and many present installations do not have adequate protection in this respect. The modern trend is to split up transformer banks into small units of 750- or 1,000-kva capacity and feed portions of the load independently with breakers available for emergency tie-in.

Busses from the transformer secondary winding usually carry the power to a switch room and main distribution board located in the mill. The board includes feeders to the various sections of the mill with indicating and totalizing meters. Past practice was to use manual oil circuit breakers with current limit protection. Modern boards use drawout type air breakers in cubicle construction with both instantaneous short circuit and thermal or inverse time limit feeder protection.

Where modern use of small power transformers is made, present practice tends towards unit substation construction. This includes the transformer, distribution feeder breakers, meters, instruments, and relays all assembled as a factory made unit. This has been carried a step further in some mills now under construction with the unit substation transformer being air cooled or noninflammable liquid cooled, and the complete assembly located inside of the mill.

Power distribution from the switchboard to individual motors is made in the usual manner by conduit feeders, with air breaker or fuse feeder protection. Bus duct has been installed recently in a number of mills in place of conventional conduit and cable. Line starting now is used exclusively for even the largest motors except on some applications such as roving frames where a soft start is required. In these special applications automatic step resistance-type starters now are used.

The average mill will have a connected horsepower of approximately two times the maximum kilowatt demand with the continuous load being nearly equal to the maximum demand. During World War II, and at present, most mills operate 24 hours per day with two full shifts and one part shift. This third shift is used to balance out bottlenecks as very few mills have such a perfect balance of output in all divisions that no shortages result.

Mills having complete individually driven equipment usually have an overall power factor of 75 to 80 per cent. Those with a large share of line shaft drives using higher horsepower motors will average 82 to 86 per cent Some power companies in the Southeast have very attractive power factor rates making the installation of capacitors to correct power factor a high return investment. Most such applications pay for the capacitors in one to two years time. Other utilities provide an optional penalty which they may enforce if the maximum demand power factor drops below 85 per cent. The majority of capacitor installations are of the distributed type with small groups of capacitors being connected to feeders or at larger individual motors.

Cotton Processing

After cotton is picked it is collected loose, in wagons, and taken to the local cotton gin. Here the seed is separated from the fibers by the ginning machine. This machine consists essentially of a series of saws so spaced that the seeds just will pass between the saws. As cotton is fed to the gin the seed is cut out, after which the fibers are carried by suction to the baler. The average bale of cotton weighs 500 pounds but requires 1,500 pounds of cotton bolls before ginning. The other 1,000 pounds are mostly seed with attached short fibers and some small

Figure 4 (above). Picking room showing cotton lap rolls forming at output end

Figure 5 (below). Individual motor driven cotton cards using chain drive from motor to cylinder

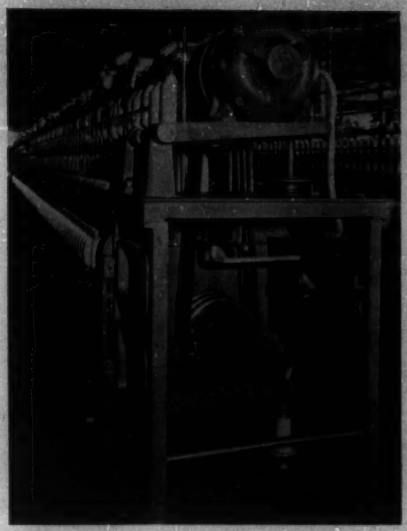

Figure 6 (left). Cotton drawing frame driven by textile gear motor

Figure 7 (right). Spinning frame driven by textile motor with special above-floor mounting and variable pitch V-belt drive

amount of trash. A complete cotton gin, including blowers and conveyors, usually is operated by a 75-horsepower wound rotor motor.

This 500-pound bale of cotton is the standard unit used in records on size of crops, surplus, and manufacturing. It may be stored almost indefinitely without spoiling. The average crop in this country is 10 or 12 million bales of which 8 to 9 million bales are processed.

In converting this 500-pound bale of cotton fiber to cloth there are 45 pounds of waste. It requires approximately 850 kilowatt-hours of electric energy and 100 man hours of labor.

Figure 2 shows a typical flow sheet of a complete cotton mill. All mills do not have all of the operations shown. The more common divisions are yarn mills, cloth mills, and finishing plants. The first group prepares yarn only, starting with baled cotton. This yarn is usually for specialized use such as electrical insulation, sewing thread, tire cord, and knitting. This group uses 18 per cent of the total cotton processed. The second group, which includes the greatest percentage, starts with the raw cotton, follows through all the processes including weaving, but does not dye or print the cloth.

Finishing plants take the woven cloth and wash, bleach, dye, print, fill, and calender as necessary for the various types of cloth called for by the modern market. They usually are separate plants and finish cloth for groups of mills. Their processes involve the use of chemicals, dyes, and large quantities of process steam. Power sometimes is generated as a by-product of this steam but the trend is away from this combination with the decreasing cost of utility power. Electric drives in finishing plants are principally direct current because of the necessity of variable speeds for different weight goods and different finishes. D-c adjustable voltage range drives including several sectional motors operating in tandem are common as most of the washing, bleaching, and dyeing processes are now continuous. Such a range drive is shown in Figure 3.

Mill Drives

As previously mentioned, most all equipment in cotton mills now is driven by individual motors. The major exception has been carding but even this is now beginning to be changed. Electric equipment with standard enclosures is usually satisfactory except in the case of motors. Because of the great amount of free lint, standard open motors will plug up quickly and lose their ability to cool. As a result, most manufacturers make a special textile motor with large ventilating openings and smooth surfaces so that lint easily will pass through the motor without being caught. In the smaller sizes of two horsepower and below, totally enclosed nonventilated assemblies are used. A recent development has been the use of prelubricated sealed ball bearings in textile motors. These bearings do not require any attention, including lubrication, for periods of five years or longer and result in a cleaner mill.

A breakdown of power consumption in an average mill shows the largest share, or about 50 per cent of the total, is used in spinning. The next largest is 20 per cent for weaving. The remaining 30 per cent is divided between opening, picking, carding, drawing, roving, warping, slashing, and miscellaneous uses such as lighting, ventilation, pumps, and elevators.

To show more clearly how horsepower is distributed in what might be called an average mill, Table I lists the actual installed horsepower in one such mill.

Opening and Picking

This operation involves taking the baled cotton, breaking it loose, fluffing, beating, cleaning, and forming a thin layer about 40 inches wide which is called a lap and collected in a roll. This involves the use of 3-, 5-, and $7^1/_2$-horsepower

Table I. Distribution of Horsepower in a Typical Cotton Mill

Demand, 948 Kw

	Connected Horsepower	Percentage of Connected Horsepower
Opening and picking	215	8.0
Cards	505	18.7
Drawing	15	0.6
Roving	40	1.5
Spinning	1,117	41.5
Warping	20	0.8
Slashers	30	1.1
Weaving (looms)	400	14.9
Miscellaneous	345	12.9
Total	2,687	100.0

Figure 8. Installation of twisting frames driven by textile motor

motors of 1,160- and 1,750-rpm speeds. The motors are line started and usually interlocked in sequence as the process includes air and belt conveyors which must be protected against overflow. A typical picking room is shown in Figure 4.

Cards

Cotton cards still usually are driven from a line-shaft drive with 30 to 50 cards tied to a single line shaft driven by a single motor. Average 40 or 45 inch cards require $1^1/_4$ horsepower for normal running. Two problems complicate the use of individual card motors.

1. The requirement of a high breakaway and accelerating torque necessary because of the large diameter and weight of the cylinder.

2. The close overload protection which must be provided because of frequent card packing and quick overload build-up.

When using a $1^1/_2$-horsepower motor, which is ample for normal running, the starting torque must be at least 300 per cent of full load to provide for breakaway and acceleration. Overload relays used must permit the long accelerating period of approximately 30 to 45 seconds and still be sensitive to both quick or slow overload build-up. A standard thermal overload device must be supplemented by shunts or a thermostat on the motor itself.

The average cotton card cylinder with its driven pulley operates at a speed of 165 rpm, and is driven by a 870- or 1,160-rpm motor. The required power will vary as the square of the cylinder operating speed. Cotton mills will have from 50 to 500 cards, depending on the size of the mill and the quality of yarn being made.

Figure 9 (below). Curves used in estimating horsepower requirements of spinning frames

A—2-inch diameter ring
B—$2^1/_2$-inch diameter ring
C—3-inch diameter ring

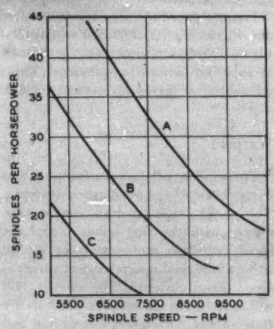

The output of the card is in the form of a fleecy strand of cotton about one inch in diameter and called a sliver.

Control equipment is commonly a magnetic or manual line starter with some reversing device as the card must be reversed for stripping or cleaning. A typical individually driven card is shown in Figure 5.

Drawing

After carding, the cotton fibers may be combed to eliminate short fibers, as in the case of fine combed yarns, or go direct to drawing frames. At the drawing frames the fibers are aligned further and straightened by means of a series of rolls each of which runs faster than the preceding one. With the rolls being spaced greater than the longest fiber length this results in a further drawing and straightening of individual fibers.

This operation uses only a small amount of power. Floor mounted gear motors or low speed textile motors drive the frame shafts which operate at 250 rpm. The average requirement is six sliver deliveries per horsepower. Motors are usually line-started. Figure 6 shows a typical installation using a gear motor.

Roving

The next operation involves roving which combines the required number of fibers for the weight yarn to be made, further draws the yarn, and slightly twists while winding on large bobbins in preparation for spinning. Average roving frames require 3- and 5-horsepower textile motors with speeds of either 870 or 1,160 rpm. It is necessary that roving frames start slowly since the yarn is yet very soft with no twist and low strength and may be broken easily. This soft starting

Figure 10. Drum driven warper

Figure 11. Output end of variable voltage sectional driven slasher with core driven beam

is accomplished either by using a closely applied motor with low starting torque and line-starting or a larger motor with primary resistance type starter.

Spinning

This is the operation wherein the greatest percentage of power in a cotton mill is consumed. The yarn is pulled by a set of rolls which further draw the fibers and feed to a spindle rotating at high speeds, in the order of 7,000 to 10,000 rpm, depending on yarn weight. A small traveler which rotates in a ring guide around the spindle acts as a guide for the yarn.

Average spinning frames consist of 200 to 250 spindles. There may be differences in the size of bobbins, spindle speeds, and amount of twist obtained. Required horsepowers for individual motor drives range from $7^1/_2$ to 20 horsepower at 1,750 rpm with some at 1,160 rpm. Textile-type motors must be used since the lint content in the air is quite high. Line-starting is standard with combination starters usually mounted on the end of the frame. The horsepower required varies about as the 1.5 power of spindle speed. Other factors effecting the horsepower are ring diameter, amount of drawing effect of feed rolls, and size of yarn handled.

There are two general types of spinning called filling and warp. Filling spinning is for yarn used in the woof or cross threads in cloth. It is usually lighter and is usually spun onto bobbins used in loom shuttles. Warp yarns are usually heavier with more twist and wound on larger bobbins.

Another variation of spinning is twisting which combines and twists spun yarns together to get greater weight or strength. These machines are essentially duplicates of spinning frames except that no drawing is included in the feed rolls.

After yarns are twisted they are completed except for any treatment that may be required to prepare them for weaving. In the case of the filling or woof none is usually necessary. Warp yarns, however, must be wound on beam rolls of approximately the width of the cloth to be woven. Further, the individual yarns are sized or starched to give them greater strength and abrasion resistance. This is necessary in weaving for the yarn to withstand the shuttle friction.

Figure 7 shows a cotton spinning frame and Figure 8 an installation of twisters. Figure 9 shows a typical set of curves used in applying motors to spinning. These are simplified curves for normal applications.

Warpers

The winding of the yarn from bobbins or spools onto beams is done on a warper. This may be either a drum or core type warper with the first using a constant speed induction motor and the second either multispeed squirrel cage or variable-speed direct current. The average mill will have two to ten warpers. Motors are three or five horsepower line-started and equipped with brakes for quick stopping. Drop wires automatically stop the warper whenever a feed thread is broken. Figure 10 shows a typical warper installation.

Slashing

The operation of yarn starching is known in textile terms as slashing and the machine as a slasher. Any faulty slashing is quite costly in that it results in excessive loom stoppages with loss of production and lower grading of cloth because of more warp knots. To provide more exacting tension and speed control a modern slasher drive uses adjustable voltage direct current with sectional motors and a tension regulated beam windup.

The slasher consists of a stand on which unstarched beams are mounted, a size box with rolls for depositing wet starch on the warp, a set of steam drying cylinders or a hot air drying chamber, a delivery roll for pulling the yarn and a beam roll for winding up the finished warp. Individual motors are applied to the size box, delivery roll, and the beam in order to provide tension control between these sections. Occasionally motors also are applied to cylinders. Because of low driven speeds required, gear motors usually are used with floor mounting and driving by chain to their respective rolls The starch and delivery rolls are usually 9 inches in diameter and the beam roll starts on a 6-inch core and builds up to between 24 and 30 inches when full. Usual speeds are four to five yards per minute for creeping and threading with operating speeds of 20 to 65 yards. Some newer slashers are operated as high as 100 yards per minute. A typical slasher would have a $1^1/_2$-horsepower motor on the size box or boxes, a 3-horsepower motor on the delivery roll, and a 5-horsepower motor on the beam windup.

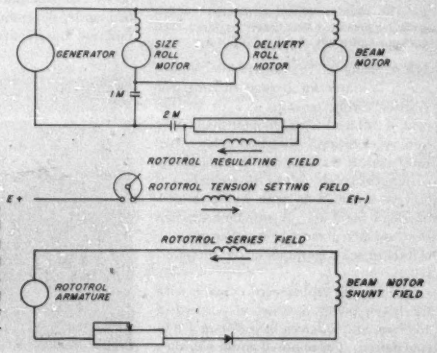

Figure 12. Elementary diagram of sectional driven slasher showing arrangement of rotating regulator field circuits. Series and regulating fields are accumulative and tension field differential

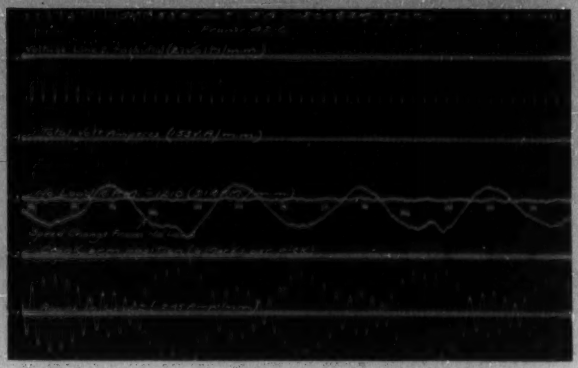

Figure 13. Oscillograph of test on $1^1/_2$-horsepower 6-pole motor driving a loom at 160 picks per minute with low slip rotor and showing regeneration each pick

The beam windup motor must operate over the entire speed range of the slasher with either an empty or full beam and maintain constant a preset yarn tension. It replaces a slip clutch on the old mechanical drives which permitted greater slippage as the beam filled up. This resulted in uneven winding tension with soft and hard spots in the finished beam and tangles and breaks at the loom.

A five-to-one speed range motor by field control is used with the shunt field, energized by a Rototrol (rotating regulator). The Rototrol has three fields.

1. A differential pattern field excited from the constant potential exciter and in series with a tension adjusting rheostat.
2. An accumulative field sensitive to beam motor armature current.
3. The usual series field to obtain amplification.

The Rototrol maintains constant armature current with changing speed by changing the motor field current. This results in varying motor output torque as necessary to maintain constant yarn tension with changing diameter.

The control includes necessary starting equipment for the motor generator set, a motor operated rheostat to give smooth acceleration and deceleration, tension control stations for each motor, a preset speed control rheostat, and several "start-stop-slow" pushbuttons. Figure 11 shows the output end of a slasher showing the beam and control station. Figure 12 is an elementary diagram of the electric equipment.

Weaving

All yarn processing as described is necessary to prepare cotton so that it finally may be woven into cloth. The operation of weaving is still the same as in ancient days in that a shuttle must be thrown between warp threads alternately from one side to the other. Now, however, it is done at high speeds by machines rather than slowly by hand.

An average cotton mill will have from 400 to as high as 3,000 looms. Many still are driven by line shafts and flat belts but the number is being reduced steadily.

The present standard motor drive is an enclosed nonventilated motor mounted on the loom and driving by pinion a loom main gear. These main gears average about 175 teeth. The motor pinion will vary as determined by loom and motor speeds. For ordinary cloth of weights similar to sheeting, looms will operate at 175 to 210 picks, or shuttle throws, per minute. For heavier goods or intricate weaves the speed will be reduced to possibly as low as 100 picks for heavy duck.

When first individually motorized, the majority of looms required 1/2- and 3/4-horsepower motors. Since that time loom speeds have increased steadily until at present the 1-horsepower rating is most common with some $1^1/_2$ and 2 horsepower, but no new installations are below 1 horsepower.

The atmosphere in a weave room is very linty and it is necessary to protect the motors. As loom motors are small, totally enclosed motors rather than lint-free were adopted as standard. These motors, however, are rated at a 40 degrees centigrade continuous rise rather than the usual 55 degrees centigrade. There are two reasons for this rating

1. The motor must be able to pull the loom during the breaking-in period when the great number of new tight bearings cause extra loading.
2. A loom load is of pulsating nature and the motor losses and heating are higher than for an equivalent steady load.

Early loom motors used standard motor parts which were usually of low inertia and resulted in the motor passing from motoring to regeneration with each loom pick. This is illustrated clearly in Figure 13 which is an oscillograph of such a motor in operation. As a result of considerable study and test, present motors have a more nearly correct balance of motor inertia to match the loom, eliminating the regeneration and increasing motor effi-

Figure 14. A modern weave room installation with individual motor on each loom

ciency on this type of load. Efficiency is an important factor where hundreds of motors are operated in a single room.

Individual loom motors are controlled by manual switches at the motor which include some thermal device for overload protection. Several motors are grouped on a common feeder protected by an air circuit breaker located in a distribution panel. The number of motors tied to one feeder is determined by the size of circuit breaker permitted by the wire used and thermal capacity of the individual motor starter thermal overload elements. This feeder breaker must hold in when the looms all are line-started simultaneously. With 1-horsepower 550-volt motors, eight usually are grouped together on one 25-ampere breaker. It usually works out for a convenient physical arrangement that about 50 looms can be handled from one panel board. The feed to this panel board is supplied through a magnetic contactor so as to give undervoltage protection and permit starting of the group from one push-button station. A modern weave room is shown in Figure 14.

Conclusion

This has been a brief outline of cotton manufacturing with the object of showing the importance of the industry as an electric power consumer and user of electric equipment. All types of electric equipment are used from central station generating equipment through motors and control to modern electronic devices.

The industry is vitally interested in new developments such as new motor insulation, unit substations, dielectric heating, electrostatic air cleaning, air conditioning, and electronic drives.

References

1. Loom Motor Research Moves Into the Weave Room, E. S. Lammers, C. G. Veinott, *Cotton* (Atlanta, Georgia), November 1941, page 59.

2. Economics of the Cotton Textile Industry (book), Jules Backman, M. R. Gainsbrugh. National Industrial Conference Board (New York, N. Y.), 1946.

Discussion

A. T. Bacheler (Westinghouse Electric Corporation, East Pittsburgh, Pa.): I first want to congratulate Bobe on his fine paper on the electrification of the cotton industry in the South.

There are a few items which might be discussed in greater detail than was possible in his paper. Bobe mentioned the regulation of warp tensions at the slasher beam, using the armature current of the beam motor as the cue to the tension obtained. In some instances this is not a sufficiently accurate indication of the tension from empty to full beam to produce the desired results especially when regulating for light tension on drives designed to permit greater tensions to be obtained. One of the factors producing error is the no load current of the motor, and this is especially true at light tension where the tension load may not be much greater than the losses. At full field the no load current of the motor is much less than at weak field since the windage of the motor, friction, and core losses are greater at the higher speed. Also, when gearing is used, the gearing losses, including churning of oil and friction at the oil seals, must be considered. These losses also increase at the higher speeds of the beam motor. Therefore, if the regulator maintains constant armature current, the tension at empty beam will be less than at full beam. A satisfactory solution to this problem has been devised and consists of a circuit which reduces automatically the value of regulated armature current as the beam builds up. Thus, the tension is held much closer to the desired optimum value from empty to full beam without the use of dancer rolls or other devices operating on the diameter of the beam.

It might also be desirable to mention electronic applications which are being made in the textile industry in the South. I shall mention two typical applications.

An all-electronic warper drive has been built and installed in one of the southern mills. The armature power and field excitation of the direct current drive motor are both provided by grid controlled mercury arc rectifiers operating from the alternating current power supply. This drive is essentially a standard electronic drive combined with an electronic speed regulator to hold warp speed constant. A pilot generator is used to indicate warp speed, and the speed range for warp speed and build-up on the beam is obtained by a combination of armature voltage and field control. Several more of these electronic units are being built.

An electronic relay has been developed for use on loom, warper, and knitting machine stop motions involving drop wires or other contact making devices which operate when a thread is broken. Sometimes these devices do not make contacts of low enough resistance to operate magnetic relays. The electronic relay has been designed to overcome these difficulties and provides reliable operation on contacts of high resistance due to dirt and lint. This relay uses a thyratron tube whose firing is initiated by the drop wires connected in the high impedance grid circuit. In the plate circuit of the thyratron is a small magnetic relay which handles the control circuit which stops the drive.

A modification of the electronic relay has been applied to loom bobbin feeler mechanisms, where the time of electric contact between feeler and bobbin is too short and the resistance may be too high for dependable operation of a magnetic relay. As soon as the yarn on the bobbin runs out, firing of the thyratron is initiated by the feeler which makes contact with the bobbin. A high resistance of the order of half a megohm is placed in the thyratron grid circuit so that the actual contact resistance becomes negligible. The thyratron operates on direct current and, once fired, keeps on conducting until a magnetic relay in the plate circuit has picked up. The magnetic relay initiates a change of bobbin and deenergizes the thyratron so it will be ready for the next operation.

The Physics of Electronic Semiconductors

G. L. PEARSON
NONMEMBER AIEE

SEMICONDUCTORS have a number of unique properties which make them useful in the design of electric circuit elements. Their electrical resistivities near room temperature fall in the range 10^{-2} to 10^{-4} ohm-centimeters. In comparison, the resistivities of typical metals in this temperature range are around 10^{-6} ohm-centimeters and those of insulators between 10^{6} and 10^{15} ohm-centimeters or higher. The electrical resistivities of semiconductors and insulators decrease rapidly with rise in temperature, while those of metals increase relatively slowly. The resistivities of dry rectifiers, which consist of a metal in contact with a semiconductor, may change by a factor of 1,000 as the sign of the applied potential is reversed. The purpose of this paper is to outline the present theories relating to semiconductors and to correlate these with quantitative experimental data obtained on some typical semiconducting samples.

Semiconductors may be classified on the basis of their current carriers into electronic, ionic, and mixed conductors. In ionic and mixed conductors, ions are transported through the solid, thus changing the composition of the material. As this leads to unstable characteristics, only those substances in which the current is carried solely by electrons will be discussed here.

As early as 1900 Drude[1] suggested that the high electrical conductivity of metals (low resistivity) was due to the large number of so-called free electrons. These electrons are free in the sense that under the action of an electric field they move through the crystal lattice, thus carrying a current. Their number is of the order of one per atom or approximately 10^{23} per cubic centimeter in most metals, and this density does not change appreciably with change in temperature. In the modern theory of semiconductors and insulators as proposed by Wilson[2-4] around 1930, it is shown that most of the electrons in these substances are bound to their respective atoms, thus leaving only a small fraction of the electrons (1 per 10^{8} to 10^{9} atoms) free to conduct current. Furthermore, the number of such electrons increases rapidly with increase in temperature, thus accounting for the high negative temperature coefficient of resistance in semiconductors and insulators.

The physical picture of a metal consists of an electron gas formed by the free electrons in which the positive ions float. As the ions repel each other, they tend to arrange themselves so as to use their space to the best advantage, which requires that they take up some close-packed crystal arrangement such as body-centered cubic, face-centered cubic, or close-packed hexagonal. By means of X-ray analysis Grimm[5] has determined, as shown in Figure 1*B*, the electron charge density in the metal magnesium for the base plane of the close-packed hexagonal lattice. This figure is drawn to scale, the unit being angstroms (1 angstrom $= 10^{-8}$ centimeter). It is seen that the valence electrons give a uniform negative charge in which the positive magnesium ions are imbedded. The heavy density near the lattice points is from the electrons bound to the ions. Figure 1*A* gives the electron density in the insulator diamond as determined by Grimm for the 110 plane of the face-centered cubic lattice. Although the positive carbon ions are imbedded in the negative charge of the valence electrons, it is seen that spherical symmetry is lacking and the electrons are concentrated along the shortest paths between atoms.

Band Theory of Solids

If all of the charge in the electron gas were free to move through the lattice under the influence of an electric field, Figures 1*A* and 1*B* indicate that diamond and magnesium should be equally good conductors. Measurements show, however, that at room temperature magnesium is more conducting by a factor of 10^{18} and therefore we must add something to our picture to explain this enormous difference. This was one of the major problems of the physics of solids which had to wait until the advent of quantum mechanics around 1930 for a solution. Although the problem is now completely solved, the solution is so wrapped up in mathematical language that it can not be presented here. It can be said that solids, like free atoms, are pictured as having a large number of discrete energy states with one and only one electron allowed in each individual state. These energy states arrange themselves into bands, the structure of which determines the properties of the solid. Just as automobiles in a parking lot are unable to move when they are parked bumper to bumper, so the electrons in a solid are immobile when every energy state in the band is filled with an electron. When there are unoccupied states in the band, the electrons move under the action of an electric field and the material is a conductor. A semiconductor has only a few electrons in a conduction band (a band with energy states only partially filled) at room temperature, but this number increases with increase in temperature. These ideas are represented graphically in Figure 2 where the black areas represent

Paper 47-34, recommended by the AIEE committee on basic sciences for presentation at the AIEE winter meeting, New York, N. Y., January 27-31, 1947. Manuscript submitted October 31, 1946; made available for printing December 5, 1946.

G. L. PEARSON is with Bell Telephone Laboratories, Inc., Murray Hill, N. J.

Acknowledgment is made to J. H. Scaff and H. C. Theuerer for furnishing the silicon samples described in this paper and to E. F. Kingsbury for contributing Figure 5*A*. A great deal of helpful criticism was received from J. Bardeen during the preparation of this paper.

allowed energy levels filled with electrons, the white areas represent forbidden regions where no energy states exist, and the shaded areas represent conduction bands. Energy is plotted vertically on an arbitrary scale. The width of the forbidden region may vary from zero to ten electron volts (one electron volt is the energy required to move one electron through a potential difference of one volt). Figure 2*A* indicates the conditions existing in an insulator where all the electrons are in filled bands and the forbidden region is so wide, several electron volts, that thermal agitation is incapable of exciting electrons from the filled band into the conduction band. In a semiconductor (Figure 2*B*) the energy gap between the filled and conduction bands is small, one electron volt or less, so that electrons from the completely filled band may be thermally excited to the conduction band, thus producing a conductivity which increases with temperature. In some metals such as magnesium, the energy gap between the filled and unfilled bands is zero as shown in Figure 2*C*, and in others such as the alkali metals the lower band is only half filled with electrons (Figure 2*D*). In either case conduction is good at any temperature.

Semiconductor Classifications

More detailed representation of the electron arrangements in the energy bands of chemically pure semiconductors and of those containing small amounts of different types of impurities are shown in Figure 3. Figure 3*A* is for pure semiconductors which have been termed intrinsic. At any temperature T an average number n of electrons are excited thermally from the lower filled band to the upper band. Conduction then can take place both by means of the electrons in the upper band and holes in the lower band, which is now not quite full. In the latter mechanism the sign of the carrier charge appears to be positive.

In most semiconductors the conductivity is highly dependent on the impurities present in the sample. By impurities we mean added foreign atoms, physical defects in the lattice, or differences from stoichiometric composition. It is assumed that the impurities introduce extra energy states in the normally forbidden region between the bands as shown in Figures 3*B* and 3*C*. Electrons in these impurity states are localized in the neighborhood of the impurity and cannot take part in conduction. Two types of impurity are possible. In the donator or N-type shown in Figure 3*B* the impurities carry extra electrons with them and usually have energies near the conduction band. Since the energy gap E_1 is much less than E, electrons are thermally excited at lower temperatures than in an intrinsic semiconductor. At very low temperatures the extra electrons are all bound to the impurity atoms; at higher temperatures these electrons are thermally excited to the upper band where they may conduct. At still higher temperatures the donator electrons may all become excited so that the number of conduction electrons remains constant with further increase in temperature until the thermal energy becomes great enough to excite intrinsic electrons from the lower band. An impurity semiconductor turns into an intrinsic semiconductor at high temperatures. At low temperatures the number of excited impurity states and, therefore, the conductivity at a given temperature increase with the amount of impurity present.

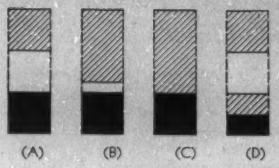

Figure 2. Energy level diagrams for solids

The clear regions are forbidden, the dark areas are allowed and full, the shaded areas area allowed but empty

A. An insulator
B. A semiconductor
C. A metal with overlapping filled and conduction band
D. A metal with half filled band

In the acceptor or P-type impurity semiconductor shown in Figure 3*C*, the extra states lie near the filled band. At very low temperatures these states are all empty, but on heating, electrons from the lower band are excited into them. Although the excited electrons are bound, hole conduction is possible in the lower band.

In an intrinsic semiconductor the conduction is by an equal number of electrons and holes, in an N-type conduction is solely by electrons at low temperatures and by electrons and holes at high temperature, and in a P-type solely by holes at low temperatures and by electrons and holes at high temperatures. In addition to explaining the magnitude of the conductivity and temperature coefficient, we will see that this picture clarifies certain anomalies in the Hall and thermoelectric effects in semiconductors.

Electrical Resistivity

Wilson's theory shows that for intrinsic semi-conductors the specific resistance

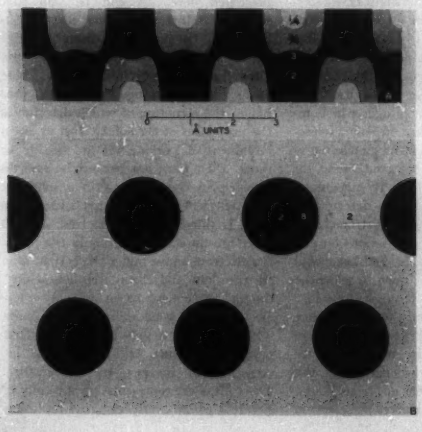

Figure 1. Electron charge densities in an insulator and a metal

The numerical values give the number of electrons per atom in the space corresponding to each intensity of shading

A. Diamond
B. Magnesium

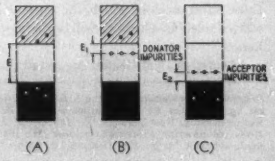

Figure 3. Energy level diagrams for semiconductors

A. Intrinsic semiconductor
B. N-type impurity semiconductor
C. P-type impurity semiconductor

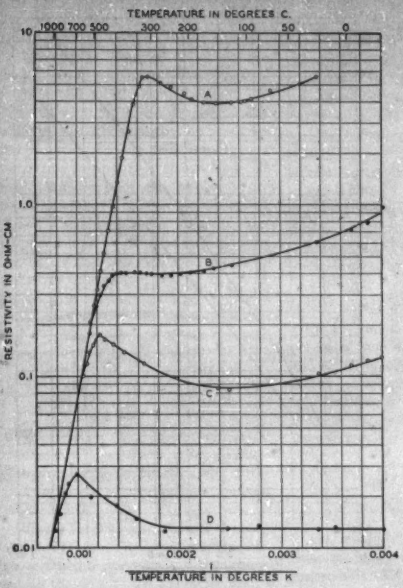

Figure 4. Logarithm of the resistivity of various specimens of silicon as a function of inverse absolute temperature

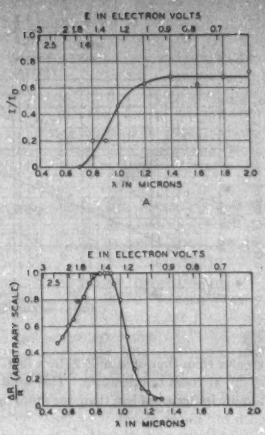

Figure 5

A. Photo transmission in a thin silicon film as a function of wave length

B. Photo conductivity in a thin silicon film as a function of wave length

ρ in ohm-centimeters is

$$\rho = Ae^{E/2kT} \qquad (1)$$

where A is a factor which varies relatively slowly with temperature, T is the temperature in degrees Kelvin, k is Boltzman's constant (8.69×10^{-5} electron volts per degree), and E is the energy gap between the two bands in electron volts. From equation 1 it can be seen that a plot of log ρ versus $1/T$ for an intrinsic semiconductor should give a straight line the slope of which is equal to $E/2k$ or 5,750 times E in electron volts. Figure 4 is such a plot for silicon containing different amounts of impurity. Curve A was obtained from measurements made on a block of silicon prepared from a melt of high purity material obtained from du Pont. Curve D is from a block of the same material to which 0.03 atomic per cent of boron had been added. Curves B and C were obtained from silicon samples containing intermediate amounts of unknown impurities. At the higher temperatures the resistivities of all the samples fall on the same straight line in accordance with our picture of semiconductors in the intrinsic range. The slope of this line indicates that the energy gap between the filled and unfilled bands in silicon is 1.2 electron volts. At lower temperatures the resistivities do not continue to follow the intrinsic line, but branch off at increasingly higher temperatures with increase in impurity. In the branch curves, the number of intrinsic electrons and holes becomes small compared with the number excited from impurity states and the resistivity is determined by the amount of impurity present. The decrease in resistivity just beyond the branch point is not associated with a change in the number of excited impurity states, but rather arises from a decrease in mobility resulting from the heat motion of the ions in the lattice.

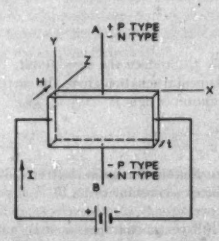

Figure 6. Schematic circuit arrangement for the measurement of Hall coefficient in semiconductors

Sign conventions are as shown

This is a complicated story and will not be discussed here. On going to still lower temperatures the impurity resistivity increases and an estimate of the energy gaps E_1 or E_3 can be made from the slopes.

Although sample A is the purest silicon we know how to prepare, even this material must contain some impurity, as defined above. At room temperature the addition of three boron atoms for each 10,000 atoms of silicon in sample D reduced the resistivity by a factor of 500 as compared with sample A. This indicates that A is pure to about one atom in five million so far as conductivity is concerned. If absolutely pure silicon, which followed the intrinsic line to room temperature, could be obtained its resistance would be

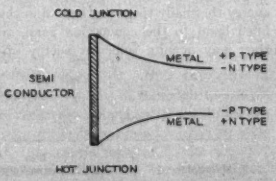

Figure 7. Schematic circuit arrangement for the measurement of thermoelectric power in semiconductors

Sign conventions are as shown

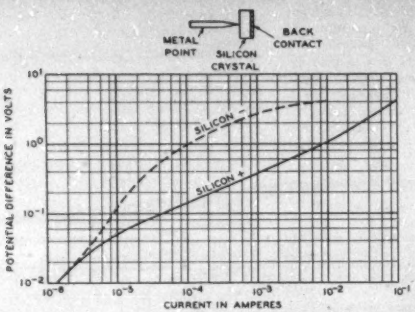

Figure 8. Logarithmic plot of the current versus voltage characteristic for a P-type silicon point contact rectifier

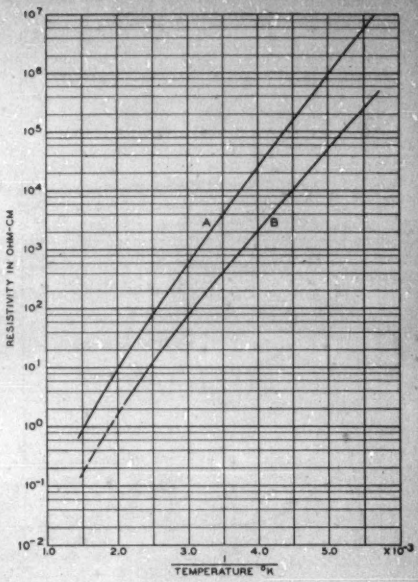

Figure 9 (right) Logarithm of the resistivity of two thermistor materials as a function of inverse absolute temperature

greater than that of sample D by a factor of 10^7 at room temperature. This would require impurity of less than one atom for each 10^{11} silicon atoms.

Resistivity measurements such as those shown in Figure 4 have been made on other materials which have intrinsic characteristics. The values of the energy gap E in electron volts are shown in Table I. Diamond, of course, is an insulator at ordinary temperatures but it, like most other insulators, has a high negative temperature coefficient of resistance and shows intrinsic characteristics at very high temperatures.

The values of the energy gaps E_1 and E_2 due to impurities can be deduced in like manner from measurements made at low temperatures. As these vary both with the variety and amount of impurity, no quantitative values will be given, although in general they lie between 0.001 and 0.3 electron volt.

Photo Effect

In addition to an increase in conductivity with rise in temperature, many semiconductors show increased conductivity on exposure to light of the proper wave length. This arises from the fact that just as electrons can acquire enough energy thermally to excite them from the filled band to the conduction band, so they may acquire sufficient energy optically to produce the same result. The fundamental equation giving the energy of a quantum of light is

$$E = \frac{hc}{\lambda} \qquad (2)$$

where E is the energy in electron volts, h is Planck's constant (4.1×10^{-15} electron volt per second), c is the velocity of light (3×10^{10} centimeters per second), and λ is the wave length of the optical radiation in centimeters. The energy of a light quantum in electron volts according to equation 2 is 1.236 divided by the wave length of the radiation expressed in microns (1 micron $= 10^{-4}$ centimeter). The wave length of the sodium D line in the yellow part of the visible is 0.589 micron and the quantum energy is 2.1 electron volts, which is sufficient to excite electrons from the filled to the conduction band in germanium, silicon, cuprous oxide, and boron, but is insufficient to excite electrons in diamond. Radiation of 1.5 microns, situated in the infrared, has a quantum energy of 0.82 volt and cannot excite any of the semiconductors shown in Table I excepting germanium. By equation 2 only wave lengths shorter than 1.05 microns have energy equal to or greater than the 1.2 electron volt energy gap in intrinsic silicon. Light longer than this wave length should pass through silicon without absorption but shorter wave lengths should be absorbed and cause photoconductivity. Figure 5A is a plot of the ratio of the light transmitted to the light incident on a thin film of silicon as a function of the wave length λ expressed in microns. At wave lengths longer than 1.2 microns the transmission is about 67 per cent, the remainder being reflected. At some wave length between 1.0 and 1.2 microns, absorption sets in and the transmission falls off with decrease in wave length. Figure 5B, which was obtained by Teal[9] and his collaborators, gives the ratio of the change in resistance to the dark resistance when light of constant energy per square centimeter but varying wave length falls on a film of high purity silicon. It is seen that the resistivity is little affected by long wave-length radiation, but photoconductivity sets in around 1.2 microns and increases sharply below 1.0 microns. The decrease in photoconduction below 0.8 microns is not completely understood, but it is thought the large absorption in this wave-length region keeps the excited electrons near the surface where they recombine with the ions before producing photoconduction.

Table I

Material	E in Electron Volts
Diamond[3]	7
Boron[3]	2
Cuprous oxide[7] (Cu_2O)	1.4
Silicon	1.2
Germanium[8]	0.76

The Hall Effect

Fundamental information about the mechanism of conduction in semiconductors can be obtained from studies of the Hall effect. In 1879 Hall[8] discovered that a potential difference may be produced across a strip of metal which is carrying a current by placing the strip in a magnetic field. Consider a rectangular plate in the plane $Z=$ zero, with edges parallel to the X and Y axes as shown in Figure 6. If a current I from an external battery flows in the X direction and the sample is placed in a magnetic field H in the Z direction, a transverse electric potential V is produced between the terminals A and B. The magnitude of this potential in volts is given by the equation

$$V=\frac{10^{-8}RIH}{t} \tag{3}$$

where I is the current in amperes, H the magnetic field in gausses, t the thickness of the sample in centimeters, and R the Hall coefficient in centimeters cubed per coulomb.

The Hall effect occurs because the magnetic field causes the electrons in the sample to travel in curved paths, thus charging up the sides of the conductor until a transverse electric field exists of just the right magnitude to cancel the effect of the magnetic field and make the electrons travel through the solid undeviated. Under the conditions shown in the figure, the terminal A should be negative with respect to terminal B. In many metals and semiconductors this is the case, but in others the sign is reversed. The so-called anomolous Hall effect (reversal of sign in some materials) was not understood until the advent of Wilson's band theory of solids and semiconductors. In the light of this theory, N-type samples give the correct sign since conduction is by free electrons in the upper band but P-type samples give the reverse sign as conduction is by holes (equivalent to an electron with a positive charge) in the lower filled band.

The number n of free electrons or holes per cubic centimeter in semiconductors can be deduced from Hall measurements because the theory shows that

$$n=\pm 3\pi/8eR \tag{4}$$

where R is the Hall constant in centimeters cubed per coulomb, e is the electronic charge (1.59×10^{-19} coulomb), the minus sign is for electrons, and the plus sign for holes. Putting in the values of the constants we find that n is equal to $7.4\times10^{+18}$ divided by R. Hall measurements on the silicon samples C and D of Figure 4 at room temperature gave R values of $+6.5$ and $+0.5$ centimeter cubed per coulomb respectively, which indicates 1.1×10^{18} and 1.5×10^{19} holes per cubic centimeter. Although the impurity of sample C is unknown, that in sample D is 3 boron atoms for each 10,000 silicon atoms. As there are 5.2×10^{22} silicon atoms per cubic centimeter, this means that 1.7×10^{18} atoms of boron are present in this sample and that each boron produces approximately one hole.

The conductivity σ of an electrical conductor is given by

$$\sigma=nev \tag{5}$$

where n is the number of current carriers per cubic centimeter, e is their charge, and v their mobility in centimeters per second per volt per centimeter. Combining equations 4 and 5 we see that the mobility of the holes or electrons in a semiconductor is

$$v=\frac{8R\sigma}{3\pi}$$
$$=0.85R/\rho \tag{6}$$

The mobilities of the holes in silicon samples C and D at room temperature are, respectively, 55 and 33 centimeters per second per volt per centimeter. In intrinsic semiconductors where electrons and holes are both present at the same time, the Hall coefficient is[3]

$$R=-\frac{3\pi(n_1C^2-n_2)}{8e(n_1C+n_2)^2} \tag{7}$$

where n_1 is the electron density, n_2 the hole density, and C the ratio of the electron mobility to the hole mobility. As C is generally greater than one, intrinsic semiconductors show the negative sign.

The value of the mean free path of the current carriers is shown from the theory to be

$$l=\frac{2\times10^{-7}R(2\pi mkT)^{1/2}}{\pi e\rho} \tag{8}$$

where l is the mean free path in centimeters, M is the mass of the carrier ($m=9\times10^{-28}$ grams for electrons and is assumed to be the same for holes), and the remainder of the constants are as previously defined. Substituting in these values we see that

$$l=3.5\times10^{-10}T^{1/2}R/\rho \tag{9}$$

At room temperature the mean free paths of silicon samples C and D are, respectively, 4×10^{-7} and 2.3×10^{-7} centimeter. These are approximately 10 times greater than the lattice constant of silicon which is 5.4×10^{-8} centimeter.

The Thermoelectric Effect

When a semiconductor is connected between two metal wires as shown in Figure 7, a thermoelectric voltage is produced when the junctions are at different temperatures. The sign of the potential is dependent on whether the semiconductor is N- or P-type, the polarity being as shown in the figure. Intrinsic semiconductors give the same sign as N-type. The thermoelectric power for some semiconductors may be as high as one millivolt per degree centigrade, which is greater than that obtained from most metal thermo-junctions by a factor of 200. For pure hole or pure electron conduction the magnitude of the thermoelectric power Q in volts per degree centigrade difference in temperature between the junctions is[10]

$$Q=\frac{1}{e}\left[\log_e n/T^{3/2}-\frac{\log_e 2(2\pi mk)^{3/2}}{h^3}\right] \tag{10}$$

Putting in the appropriate values for the constants we see that

$$Q=6.3\times10^{-4}-8.6\times10^{-5}\log_e RT^{3/2} \tag{11}$$

Reference to the original paper should be made for a treatment of simultaneous electron and hole conduction.[10] Experimental determinations of the thermoelectric powers in silicon samples C and D at room temperature gave 0.92 and 0.44 millivolt per degree centigrade, respectively.

Rectification

When a metal point is placed against an impurity semiconductor as shown in Figure 8, the combination has a nonlinear current versus voltage characteristic and acts as a rectifier. For a P-type sample the current is large when the semiconductor is made positive and the metal point is negative, but is small when these polarities are reversed. For an N-type sample the sign of the effect is reversed so that the current is large when the semiconductor is negative. The plot in Figure 8 was obtained with a tungsten point pressed against silicon sample D which, according to the Hall measurements described, is P-type.

It is impractical within the scope of this paper to give a thorough exposition of rectifying action; however, the following simplified description will convey some of the general features of the theory.[11] Electrons which are thermally excited from the filled band to the acceptor impurity levels produce positive holes in the filled band and charge the acceptor centers negatively. The positive holes in the contact area drift away, thus leaving next

to the metal a negatively charged barrier layer from 10^{-4} to 10^{-4} centimeter in thickness. This barrier layer is a region of high resistivity so that when an external voltage is applied between the metal point and the back electrode, almost the entire drop is across the layer. If the external voltage is poled to make the semiconductor negative, the barrier layer increases in thickness and the resistance goes up. If the semiconductor is made positive the barrier layer becomes thinner and disappears entirely for a sufficiently high applied voltage. This is the direction of low resistance and high current. The case of an N-type semiconductor in contact with a metal is analogous. When electrons are thermally excited from donator levels to the conduction band, the donator levels are left positively charged. Electrons are depleted from the boundary layer, leaving an excess of positively charged donators. A positive external voltage applied to the semiconductor increases the thickness of the barrier and a negative voltage decreases the thickness, thereby permitting a large flow of current.

Thermistors

Thermistors, or *therm*ally sensitive re*sistors*, are circuit elements made of semiconducting materials whose electrical resistances vary rapidly with temperature.[13] The semiconducting materials used in the construction of thermistors include sintered mixtures of nickel oxide (NiO), manganese oxide (Mn_2O_3), and cobalt oxide (Co_2O_3). Figure 9 is a plot of log ρ versus $1/T$ for two compositions which have been extensively used to date. Curve A is for a binary mixture of manganese and nickel oxides and curve B is for a ternary mixture of manganese, nickel and cobalt oxides. These semiconducting materials are unique in that small changes in their composition and impurity content have relatively little effect on their electrical characteristics. This is a particularly useful property as it permits the large scale manufacture of a reproducible product.

The specific resistances at room temperature of the materials A and B are 250 and 2,000 ohm-centimeters respectively, and the corresponding values of E as calculated by equation 1 are 0.68 and 0.60 electron volts. It must be pointed out, however, that the energy band picture of solids is not applicable to these thermistor materials as each of the ingredient oxides have partially filled conduction bands like the metals of Figure 2D and therefore, according to the band theory, should be metallic conductors. This fundamental discrepancy was first pointed out by De-Boer and Verwey.[13] Although these authors have derived a theory different from that of Wilson to explain the electrical properties of this class of materials, it will not be discussed here.

Conclusion

The band theory of solids is capable of explaining such fundamental properties of electronic semiconductors as

(1). The dependency of specific resistance on impurity content.

(2). The negative temperature coefficient of resistance.

(3). The sign of the Hall and thermoelectric effects.

(4). The direction of rectification.

Measurements of the specific resistance and the Hall constant enable one to calculate the density, mobility, and mean free path of the electric carriers as a function of temperature and impurity.

References

1. Zur Elektronentheorie der Metalle, **P. Drude.** *Annalen der Physik* (Leipzig, Germany), volume 1, 1900, pages 566–613.

2. Semiconductors and Metals (book), **A. H. Wilson.** The University Press, Cambridge, England, 1939.

3. The Modern Theory of Solids (book), **Frederick Seitz.** McGraw-Hill Book Company, New York, N. Y., 1940.

4. Electronic Processes in Ionic Crystals (book), **N. F. Mott, R. W. Gurney.** The Clarendon Press, Oxford, England, 1940.

5. Anorganische Riesenmolekülle, **H. G. Grimm.** *Die Naturwissenschaften* (Berlin, Germany) volume 27, January 6, 1939, pages 1–11.

6. Modern Theory of Solids, **Frederick Seitz, R. P. Johnson.** *Journal of Applied Physics* (New York, N. Y.), volume 8, March 1937, pages 186–99.

7. Zur Elektrischen Leitfähigkeit von Kupfer(I)xydul, **W. P. Juse, R. W. Kurtschatow.** *Physikalische Zeitschrift Der Sowjetunion* (Moscow, U. S. S. R.), volume 2, 1932, pages 453–67.

8. Electrical Properties of Germanium Alloys—I. Electrical Conductivity and Hall Effect, **K. Lark-Horovitz, A. E. Middleton, E. P. Miller, I. Walerstein.** *Physical Review* (New York, N. Y.), volume 69, March 1946, page 258.

9. A New Bridge Photo Cell Employing A Photo Conductive Effect in Silicon. Some Properties of High Purity Silicon, **G. K. Teal, J. R. Fisher, A. W. Treptow.** *Physical Review*, (New York, N. Y.), volume 69, June 1946, page 686.

10. Theory of Thermoelectric Power in Germanium, **V. A. Johnson, K. Lark-Horovitz.** *Physical Review* (New York, N. Y.), volume 69, March 1946, page 259.

11. Schottky's Theories of Dry Solid Rectifiers, **J. Joffe.** *Electrical Communication* (New York, N. Y.), volume 22, 1945, pages 217–25.

12. Properties and Uses of Thermistors—Thermally Sensitive Resistors, **J. A. Becker, C. B. Green, G. L. Pearson.** AIEE Transactions, volume 65, 1946, November section, pages 711–25.

13. Semiconductors With Partially and Completely Filled 3d-Bands, **J. H. DeBoer, E. J. W. Verwey.** *The Proceedings of the Physical Society* (London, England), volume 49, August 31, 1937, pages 59–71.

No Discussion

A 3,000 Horsepower Diesel-Electric Locomotive for the Seaboard Air Line Railway

D. R. STAPLES
NONMEMBER AIEE

T. L. WEYBREW
NONMEMBER AIEE

C. A. ATWELL
MEMBER AIEE

A 3,000-horsepower Diesel-electric locomotive has been built recently by the Baldwin Locomotive Works and Westinghouse Electric Corporation for the Seaboard Air Line Railway. This locomotive is the largest and most powerful Diesel-electric locomotive which has ever been built in a single unit.

The purpose of this paper is to describe certain features of this locomotive and discuss their advantages over existing types of locomotives.

General Description

The locomotive is of the articulated truck type, having two main trucks and two swivel trucks, one at each end. Each of the main trucks has four axles, each equipped with a traction motor. The main-truck frame castings extend to the ends of the locomotive and carry the couplers for pulling the train. The two main truck frames are connected at the center of the locomotive by means of a flexible hinge. The two swivel trucks have two axles each and are located at the ends of the locomotive. They are connected to the main truck frames by center pins.

The locomotive cab structure is of welded construction, made of welded plates and structural members. It includes a truss at each side of the locomotive, built up of welded structural shapes. It contains the operating compartment and the equipment compartments separated by partitions. It is supported by the main trucks on center pins and spring plunger-type side bearings.

The power plant consists of two 1,500-horsepower Diesel engines. The engine is the 4-cycle type having eight cylinders in line and is equipped with an exhaust gas-type Buchi supercharger. The rated speed is 625 rpm. Each engine drives a direct-connected generator. Each generator furnishes power to the four traction motors mounted in the truck directly below each power unit.

Features of Locomotive

A locomotive of this type has many advantages which are not available in other types of Diesel-electric locomotives.

As mentioned above, the main truck frames carry the couplers for hauling the train. Also, these main truck frames are connected at the center of the locomotive. Because of this arrangement, the stresses resulting from pulling and bumping the train are absorbed by the main trucks and are not transmitted to the cab structure. The truck frames are very heavy cast steel structures and the stresses do not produce high deflections. The cab structure, however is of light construction relative to the truck frames, and in locomotives in which the pulling and bumping stresses are transmitted to the cab there will be much greater deflection.

The tracking qualities of this type of locomotive are recognized to be of the best. Many of the electric locomotives operating in this country have a similar truck arrangement. These electric locomotives have been recognized as having superior riding and tracking qualities. Good tracking reduces the blows and stresses on the rails and the maintenance required on the road bed.

Resulting from the large number of axles, the weight per axle is extremely low. On this locomotive, the weight per axle is approximately 50,000 pounds, which is very low for a locomotive of this size and capacity. Low weight per axle is very desirable in order to reduce stresses on the rails particularly at high speeds. Low weight per axle also reduces track maintenance.

The large number of axles also permits the application of eight traction motors. This results in a universal locomotive which can be used either in high-speed passenger service or heavy freight service in mountainous territory, by simply changing the traction motor gearing. For example, when this locomotive is equipped with gearing for heavy freight service, the tractive effort at the continuous rating of the electrical equipment is 85,600 pounds with a maximum locomotive speed of 65 miles per hour. Gearing also can be supplied which will result in a maximum speed of 120 miles per hour and a continuous rating of 44,000 pounds. Intermediate gearing between the above limits can be supplied also. The foregoing indicates the wide range of service for which this locomotive is suitable.

In this type of running gear, there is practically no transfer of weight from one axle to other axles when starting a heavy train. This permits each axle to develop its full adhesive tractive effort and results in the locomotive's developing the maximum tractive effort for starting the train. On some types of locomotives particularly those having short 2-axle trucks and short over-all length there is a considerable tendency to shift weight from one axle to the next axle. This is mainly because of the moment set up by the pull of the train at the coupler. This reduction in weight on some axles will decrease the tractive effort which these axles can exert and thus decrease the total tractive effort of the locomotive.

Paper 47-36, recommended by the AIEE committee on land transportation for presentation at the AIEE winter meeting, New York, N. Y., January 27-31, 1947. Manuscript submitted November 13, 1946; made available for printing December 9, 1946

D. R. Staples is with the Baldwin Locomotive Works, Eddystone, Pa. T. L. Weybrew and C. A. Atwell both are affiliated with Westinghouse Electric Corporation, East Pittsburgh, Pa.

Figure 1. The 3,000-horsepower Diesel-electric locomotive built for Seaboard Air Line Railway by Baldwin-Westinghouse

Figure 2. The 1,500-horsepower power plant undergoing load test

The water and fuel oil tanks are located in the base of the cab structure. This permits the application of very large capacity tanks. This locomotive is provided with fuel tank capacity of 3,500 gallons and water capacity of 2,500 gallons. These are very large capacities and fulfill the requirements of practically any railroad. However, if the need should arise, this type of design permits the application of larger tanks. The fuel oil tanks, being located in the cab frame, are protected from the roadbed by the main trucks. This protects the fuel oil tanks from damage resulting from minor accidents and articles thrown up from the roadbed. In several cases, where the fuel oil tanks have been located underneath the locomotive, minor accidents have punctured the fuel oil tanks with resultant serious damage from fire.

This type of locomotive permits arranging the equipment in the cab so that the train heating boiler can be located adjacent to the operating compartment. In this location, the fireman can control and observe the operation of the train heating boiler without leaving his operating position.

The arrangement of the locomotive permits connecting two 3,000-horsepower locomotive units to obtain a single unit 6,000-horsepower locomotive. The running gears of the two 3,000-horsepower units can be connected with a permanent drawbar. The cabs of the two units can be connected with any of the usual type of flexible connections.

This locomotive is the shortest 3,000-horsepower unit yet available. Expressed in other words, the ratio of horsepower to unit length of locomotive is the highest of any locomotive yet built. A locomotive of minimum length has many advantages to a railroad, for example, ability to use existing turn tables and shop facilities, and to occupy a minimum length of station platforms.

Generating Unit

The generator is mounted on the Diesel engine bed which, in turn, is supported resiliently on the locomotive frame. The rotor is bolted to the flanged end of the engine crankshaft and is supported by the engine main bearing and the single generator bearing at the commutator end. The generator shaft extends beyond the bearing and is fitted with a pulley and Vee-belt drive for the exciter-generator unit mounted on top of the main generator. The air compressor is driven also by the generator shaft extension through a flexible coupling. The engine turbocharger is mounted on top of the main generator to the left of the exciter-generator unit.

The generator frame is rolled from plate and butt-welded to form the barrel. The bearing and brush holder support is formed by a plate welded into the barrel. This method of construction is simple and produces a strong rigid frame. It is lighter than the more common type with a bolted-on bearing support. The roller bearing is carried in a cartridge bolted to the end plate. This cartridge need not be disassembled to remove the rotor from the frame. The cartridge is opened only when necessary to inspect and repair the bearing itself. The bearing is of the double spherical self-aligning type. Ample labyrinths are provided in the inner and outer caps to prevent the escape of grease from the bearing.

In contrast to the usual side-supported brush holders, on the generator they are supported at the end of the brush box. The space around the commutator is less obstructed, and the brushes are more accessible for inspection and maintenance. Double brush holders are used, having two narrow brushes side by side. Each brush has its own pressure finger. This design results in better contact between the brushes and the commutator than obtained with single wider brushes and reduces commutator maintenance.

The generator operates as a separately excited motor using power from the storage battery to start the Diesel engine. During this time, most Diesel locomotive generators are excited by a series winding on the main poles, which is used only for this purpose. No such series winding is needed on this generator. The main field winding is used instead for excitation during engine starting. The generator is smaller in diameter and lighter because the series field is omitted.

The exciter-generator unit operates at 3.6 times the engine speed and consists of two machines mounted in a single frame

assembly. The shaft with the two rotors is carried on two roller bearings, one of which is a thrust type. A dual fan mounted on the shaft between the two rotors draws air through the two machines and exhausts it radially through openings in the frame at the center of the unit. The exciter portion of the unit is a 6-pole machine, four poles of which have a single winding separately excited from the storage battery. The other two poles have double windings. One of these is self-excited, being connected across the exciter armature. The other is excited separately being connected in series with the main-generator armature. The exciter supplies excitation power to the main generator field. This combination of fields and a careful design of the magnetic section of the exciter produce a generator output voltage which varies inversely with current. Such an output characteristic closely matches the Diesel engine loading requirements. This is known as the Westinghouse differential exciter system. Because the desired voltage characteristics are produced by the exciter, the main generator needs no differential series winding. The space which would be required for this winding and its insulation from the separately excited winding is not needed, and the generator is small and light for its rating when its relatively low speed is considered.

The generator portion of the exciter-generator unit has a capacity of 9 kw and supplies power at 75 volts for lighting, battery charging, and locomotive control circuits. It is a separately excited 4-pole machine. The voltage of this machine is held constant by a voltage regulator for engine speed varying between 250 and 625 rpm.

Traction Motor

The locomotive has eight axle-hung traction motors, four of which are on each locomotive truck. The motor is of the series six-pole type and is ventilated separately. Its power is transmitted by a spur pinion on the motor shaft to the gear on the axle. The motor has a rolled steel barrel with a cast-steel commutator end-housing welded to the barrel to form an integral rigid assembly. The pinion end-housing is fitted to the barrel and bolted in place. This latter housing is removed when disassembling the motor. Access to the commutator and brushes is afforded by two large openings, one on the top and one at the bottom.

The brush holders are the usual railway-motor type except that the brushes are split to form two narrow brushes operating under a single pressure finger. This construction has lengthened the brush life and reduced commutator maintenance.

The bare motor weighs 7,380 pounds complete with gearing and has a rating of 650 horsepower output. On this basis, a very favorable ratio of less than 11.5 pounds per horsepower is obtained. This figure is reduced to less than 10 pounds per horsepower when gearing is eliminated from this comparison. Approximately one-half this horsepower output per motor is required on this locomotive. Hence, long life and low maintenance are expected.

This design of locomotive is intended for slow-speed freight service as well as on higher speed passenger trains. In freight service, high tractive effort is important. The maximum reduction gear ratio includes a 15-tooth pinion which is of conventional design. The pinion is shrunk on the motor shaft and replaced readily when worn. With this gear ratio the motor produces a tractive effort at continuous rating of 10,700 pounds or 85,600 pounds for the locomotive. This is unusually high for a lightweight motor using conventional gearing.

Engine Load Control

The cumulative and opposing fields of the exciter cause the voltage curve produced by the generator to take the shape *C* in Figure 3. This curve is at full speed but only at a definite temperature of the generating units and at a particular setting of the exciter field resistor. Lower equipment temperature causes a higher curve and loads the engine beyond its capacity and pulls down its speed. For any equipment temperature the generator output characteristic is fixed at a certain horsepower. The engine speed may be pulled down by its inability to develop this horsepower for several reasons such as valve or ring leakage, defective injectors, or high intake air temperature. It is desirable to regulate automatically the load on the engine to match closely its power output as shown by curve *B*. This result is obtained by

1. A carbon pile type rheostat called a carbonstat, electrically connected in series with the exciter battery field.
2. A pilot valve mounted on and operated by the governor.
3. A metering valve.

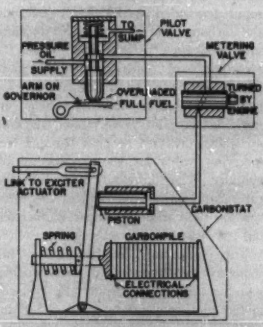

Figure 4. Schematic diagram of engine load control system

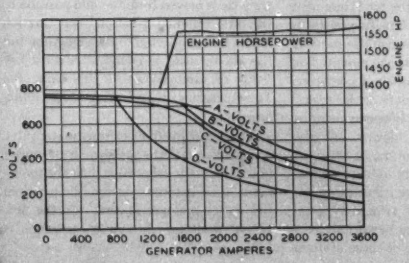

Figure 3. Result of engine load control at full engine speed

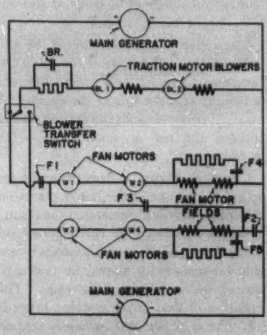

Figure 5. Blower motors and radiator-fan motor circuits

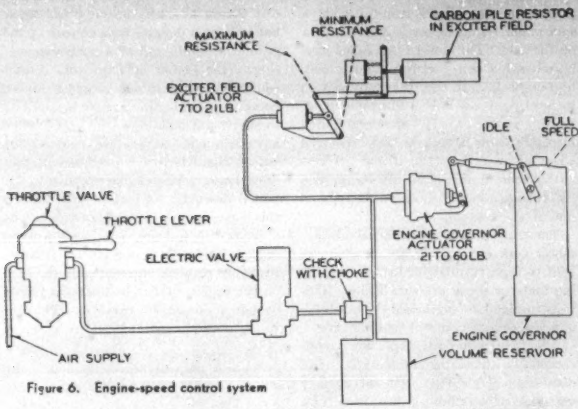

Figure 6. Engine-speed control system

This system is shown in Figure 4. At light loads, indicated by less than full fuel input demanded by the engine governor, the carbonstat is compressed to its minimum resistance by a spring. When the governor load tends to demand more horsepower than the engine can develop at its full fuel input, an arm on the governor lifts the pilot valve piston, allowing oil under pressure to pass through the metering valve to the carbonstat oil cylinder. The oil pressure compresses the carbonstat spring and reduces the pressure on the carbonpile rheostat, increasing its resistance, decreasing the exciter voltage and the load demand. This sequence continues until the demand matches the engine output. If the locomotive and, hence, the generator load decreases, the governor drops the pilot valve piston, relieving the oil pressure in the carbonstat cylinder, reducing the carbonstat resistance until demand and engine output match again.

The metering valve determines the rate at which the oil can flow into or out of the carbonstat cylinder, and, hence, the rate of loading or unloading of the engine. A rotary type valve gives the desired timing without the use of small passages or chokes.

Curve *B*, Figure 3, was obtained by actual test of one of the power plants on this locomotive and represents the results obtained in service by this engine load control system. The corresponding engine horsepower is shown by curve *E*, plotted on an exaggerating scale. The variation of load in the working range is less than 0.75 per cent, which is beyond the accuracy of the test equipment used. Curves *A* and *D* indicate, respectively,

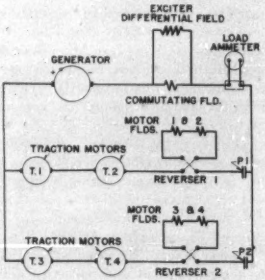

Figure 7. Connections of main generator and traction motors

the upper and lower limits of the loading system. Wide variation in engine power is permitted, therefore, without overloading or underloading the engine.

Auxiliary Motors

The fans which draw air through the engine-cooling radiators are driven by four vertical series d-c motors, each rating 33 horsepower. The fan is mounted on the armature shaft. The two centrifugal blowers which furnish ventilating air to the traction motors are mounted on the floor at the center of the locomotive. Air is forced through ducts in the underframe and sliding joints to openings in the traction motors. The blowers are also driven by series d-c motors.

Motor drive generally is accepted as preferable to a belt drive from the engine for such auxiliaries, but several types of power supply are favored by various locomotive builders. Most of these systems require an extra generator to supply power to the auxiliary motors. On this locomotive, this power is supplied by the main generator. This arrangement eliminates the extra generator on each power plant, which reduces cost and maintenance. The system efficiency is improved also, because the main generator efficiency is better than that of a smaller machine. The motors are designed to operate two in series so that the windings are more rugged and less likely to break.

The traction motor blowers operate whenever the engines are running so that the motors are ventilated during locomotive coasting and idling periods. The fan motors operate in three different combinations depending on the amount of radiator cooling required. The proper combination is selected automatically by thermostat switches actuated by the temperature of the engine-cooling water. For slow speed operation, the four motors are connected in series. The medium speed is obtained with two motors connected in series, and high speed is obtained by shunting the series field sets one half of full strength.

Figure 3 shows the wide range of generator voltage depending on locomotive speed. The auxiliary motors are designed for full speed operation at 600 generator volts which is the continuous rating point. To prevent motor overload, the field shunt is removed automatically above 600 volts by a relay controlling the *F*4 and *F*5 contactors. This system in conjunction with automatic shutter control regulates the temperature of the engine-cooling water very closely under all conditions of load and ambient temperature and without attention from the engineman.

Engine Speed Control

The control of application of power, more commonly termed, the throttle, is entirely pneumatic. When the locomotive is standing still, the Diesel engines are operating at the idling speed. When the throttle is moved from the idle position to the first running position, the traction motors are connected to the generator and the exciter field is energized with a low value of excitation. At this time, the Diesel engines are operating at the idling speed.

The throttle valve is a pneumatic valve designed so that the pressure in the outlet pipe is directly proportional to the movement of the handle. In the idle position, the outlet pressure is zero. In the first power position, the outlet pressure is seven pounds.

Movement of the throttle valve beyond the first power position operates the exciter field actuator as indicated on Figure 6. Operation of the exciter field actuator increases the pressure on the exciter field carbonstat, thereby increasing the excitation of the exciter. At 21 pounds the exciter receives full excitation, and further movement of the throttle valve operates the engine governor actuator to increase the Diesel engine speed.

This system results in a smooth even rate of power application without jerks or sudden changes. It permits the locomotive to exert full tractive effort for starting the train because it is possible to approach more closely the slipping point of the wheels by applying the power at a uniform rate than is the case when the power is applied in large steps It will be noted from Figure 6 that check valves with chokes and volume reservoirs are supplied in the air line to the actuators. These devices prevent a too rapid increase in rate of applying power which could occur if the operator moved the throttle handle too fast. Such operation tends to produce slipping of the wheels and reduces the tractive effort which the locomotive can develop.

It will be noted also that electric valves are supplied in the air lines. The purpose of these valves is to control wheel slippage. It may be, when starting a heavy train on a slippery rail, that the wheels slip in spite of the best care of the operator to prevent this condition. When wheel slippage occurs, the voltage of the motor geared to these wheels increases rapidly. Electric relays are provided which detect this increase in voltage and operate to close a control circuit. This control circuit energizes the electric valve, thereby shutting off the supply of air and exhausting the air line to the governor actuator. This reduces the engine speed, thereby reducing the amount of power supplied to the traction motors. When the slipping ceases, the electric valve is de-energized, air pressure is applied to the engine governor actuator, and the engine speed builds up to that corresponding to the setting of the throttle valve.

The system of wheel slip control is entirely automatic and requires on action by the operator. When wheel slippage occurs, the power is reduced automatically on the slipping motors. When the slippage ceases, power is reapplied automatically to these motors. With this system, the reduction in power is under control of the Diesel engine governor. This prevents any tendency of the Diesel engine to overspeed, which would be the case if the load were removed quickly by such means as opening the electric circuits. Overspeeding of the Diesel engine is likely to trip the engine overspeed governor, thereby stopping the Diesel engine.

This system of wheel slip control reduces jerks and bumps in the train, ordinarily caused by wheel slippage. The rate at which power is reduced to the traction motors is controlled by limiting the rate at which air is exhausted from the governor actuator. The rate at which power is reapplied to the traction motors is controlled also by the rate at which air is allowed to flow into the governor actuator. The control of air flow results in a smooth even reduction in power followed by a smooth even reapplication of power.

No Transition

The main electric circuits of this locomotive are extremely simple. See Figure 7. Each generator furnishes power to four traction motors. The four traction motors are connected permanently in a series-parallel arrangement. One of the important features of the permanent motor connections is that a perfectly smooth acceleration of the train is obtained. On a locomotive which includes a change from one motor combination to another, it is always necessary to reduce the power when making the transition. This reduction in power coupled with the subsequent reapplication of power results in a jerk throughout the train.

The permanent motor connections make it easier for the engineman to operate the locomotive. Only one lever, the throttle lever, is required for complete control of the power of the locomotive. It is not necessary to reduce power and operate a transition lever at the proper operating point while accelerating the train. On locomotives which require a transition, the engineman must observe the ammeter to determine when operating conditions are correct to make the transition. A transition must be made when the train is accelerating from standstill and when the train is decelerating because of ascending a grade. Failure to make the transition at the correct operating point may result in damage to the electric equipment.

Another benefit of the permanent motor connections is that the electric circuits are much simpler and more easily understood. Also, fewer pieces of electric equipment are required, which results in reduced maintenance expense.

The series-parallel connection of traction motors also stabilizes the electrical transmission when starting a heavy train. If the wheels geared to one traction motor start to slip, the current through the two motors in this circuit decreases. Due to the constant horsepower characteristics of the generator, a reduction in current is accompanied by a rise in voltage. A rise in generator voltage, however, causes a rise in current in the remaining two motors in the parallel circuit. This rise in current limits the rise in generator voltage and stabilizes the electrical conditions.

This locomotive has been in both passenger and freight service for several months and has demonstrated its practical advantages. Its performance has been observed by many railroad men, and their satisfaction has resulted in orders for similar units from several railroads. The Seaboard Air Line Railway also has ordered a number of duplicate units.

No Discussion

Higher Voltage Copper-Oxide Rectifiers

I. R. SMITH
ASSOCIATE AIEE

THE FIRST metallic rectifier to be accepted generally in the United States for industrial and power uses was the copper-oxide rectifier. Such applications for this rectifier began to be made in 1927, and since that time literally millions of these rectifiers have been put in service. The story of the remarkable development of the copper-oxide rectifier has been told many times. Suffice it to say here that the original optimism as to its long life, dependability and suitability for industrial use has long since been justified. So far as life is concerned, it may still truly be said that its life is indefinitely long—there is still no indication that there is any limit to the life of a copper-oxide rectifier that has been properly designed, applied, and used. Figure 1 shows a typical life test curve, covering a period of 15 years of operations. In this curve a preliminary aging period can be observed, followed by a great reduction in the rate of aging so that output remains practically constant for many years.

The earliest examples of these rectifiers were simple stacks of $1^1/_2$ inch diameter cells, sometimes with small radiating fins, which were generally rated at about 3 volts, 1/4 ampere direct current per basic rectifier (single phase bridge). As time went on some increase in these ratings was obtained by means of improving the cooling. Large diameter fins, coupled with metal spacers to get proper fin spacing for maximum cooling effect, brought the rating in a single phase bridge up to 4.5-volt 1/2-ampere d-c output per cell. An additional increase resulted from the use of forced cooling, using small propellor type fans, which permitted outputs of 5 volts, 1 ampere per cell, again from a single phase bridge. At this point, however, a limit was reached. Unless one were willing to go to the impracticable expense of refrigeration, there was nothing more that could be done to increase the output ratings.

Rectifier ratings are based on the losses which have to be dissipated and the ability of the rectifier structure to get rid of them without reaching a temperature at which the rectifier may become unstable or suffer excessive deterioration in characteristics. So when the structure of the rectifier has been developed to its maximum heat dissipation capability, further improvement can only come by reduction in losses, or in other words, by improvement in rectifier characteristics.

Research into the problem of improving the quality of the copper-oxide rectifier has been going on ever since its discovery in 1921. It is fairly general knowledge by now that the process of making a copper-oxide rectifier involves the use of a particular type of high purity copper, which is oxidized at a temperature not far from its melting point, subsequently annealed at an intermediate temperature, and then quenched in water. The process is relatively simple on the surface, although the most careful control is required at all points to get consistently good results. When carried out properly, the process results in a cell with a thin coating of cuprous oxide, tightly adherent to the copper base. The copper-cuprous oxide combination made in this way is inherently a rectifier, requiring no additional operation, such as forming, to enhance its rectifying characteristics.

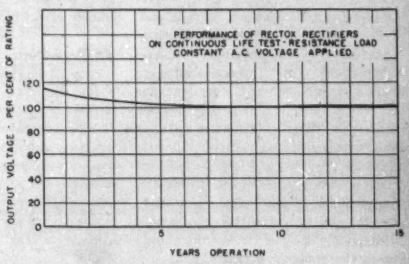

Figure 1. Performance on life test of standard copper-oxide rectifiers on resistance load with fixed a-c input voltage

Figure 2. Special double stack type Q copper-oxide unit, designed for forced cooling

Paper 47-25, recommended by the AIEE committee on electrochemistry and electrometallurgy for presentation at the AIEE winter meeting, New York, N. Y., January 27-31, 1947. Manuscript submitted October 29, 1946; made available for printing December 11, 1946.

I. R. Smith is manager, rectifier and brake section, motor engineering department of Westinghouse Electric Corporation, East Pittsburgh, Pa

Figure 3. Rear view of power cubicle, radio station *KDKA*, showing forced-cooled copper-oxide stacks at rear

The research programs that were laid out embraced all phases of the problem. Most effort however was directed toward the process itself, with the chief aim being to produce improvement in the reverse resistance which would allow higher voltage ratings, since this was felt to be the most fruitful field in which to work.

The first tangible result of this work then was a new process of manufacture known as the vacuum-preanneal process. In this process the copper blanks, after the initial cleaning step, were placed in a vacuum furnace and maintained at a high temperature and a relatively high vacuum for a considerable period. Then they were put through the normal oxidation, annealing and quenching steps, as before.

This process produced cells having roughly four times the reverse resistance of the standard cells, with forward resistance approximately twice that of the standard cell. This was the sort of change needed to permit operation at higher cell voltages. It was found by appropriate life tests, that these cells could be safely operated at the same current as the standard cells, and at twice the voltage. Maximum ratings were obtained with forced draft, for which condition an operating rating of 20 volts direct current per basic rectifier (three phase bridge) was reached.

Production of these cells began on a small scale in 1939. The first installation in the field was made at radio station *KDKA*, at Saxonburg, Pa., in June 1939. This was a fan-cooled rectifier designed to deliver continuously 3,000 volts, 1.4 amperes direct current. It was a 3-phase bridge-connected rectifier, in which the cells were operated at 20 volts, 0.7 ampere direct current each.

Performance of the rectifier was so satisfactory that in the new *KDKA* station then being built at Allison Park, Pa., all of the rectifiers up to 3,000 volts direct current were of the new higher voltage copper oxide cells. Figure 2 shows the type of unit construction developed for this installation and others like it, while

Figure 4. Rear view of type *TBM-10* Navy power pack, with forced-cooled copper-oxide stacks

Figure 3 shows an inside view of a power cubicle at *KDKA*, in which two 3,000-volt rectifiers can be seen mounted in an air duct in the floor. Air is blown up through the stacks and exhausted at the top of the cubicle.

Because all of the equipment at this station was forced-air cooled, the requirement of forced air cooling for the copper-oxide rectifiers did not add to the ventilating expense, in view of the relatively small amount of air required and the low pressure drop through the units.

The satisfactory performance of these

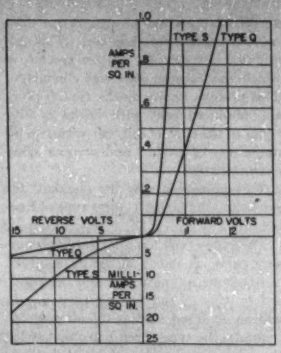

Figure 5. Volt-ampere curves, type *S* and type *Q* copper-oxide rectifier cells

rectifiers resulted in their being adopted as standard in all Westinghouse commercial transmitters above 5 kw. The volume of production of these transmitters was such that it absorbed the entire available production of the vacuum-preannealed or type *H* cells, up to the time when the war put an end temporarily to the manufacture of commercial radio equipment.

The war however brought on a great demand for all types of radio equipment among the more important of which were the Navy shore and ship transmitters of all types. These were normally powered by multiple voltage motor-generator sets, in which a serious production bottleneck quickly developed. Fortunately the type *H* Rectox units in the various commercial transmitters had by this time piled up a very successful performance record, so that it was felt to be proper to suggest the copper-oxide rectifier to the navy as an alternate source of power. A sample power pack was submitted and approved, and a program adopted of using rectifier power packs for shore stations, thus freeing the motor-generator set production for ship use. Nearly 40,000 stacks containing some $3^1/_2$ million cells were supplied for this program, requiring a shop set-up with eight vacuum furnaces at the peak of production.

Figure 4 shows a rear view of one of the power packs developed for Navy use. This was known as the type *TBM-10*, and contained four copper-oxide rectifiers with outputs of 3,000 volts, 0.35 ampere, 2,000 volts, 0.75 ampere, 1,000 volts, 0.1 ampere and 275 volts, 0.6 ampere, all assembled in the same block of stacks and cooled by a single fan.

During this time continued research was going on, spurred by the fact that the

vacuum process was proving rather difficult to control for shop use. This culminated in a new, far simpler process, in which the vacuum step was eliminated. This process, known as the type Q process, produced cells with initial quality equal to the type H cell, but with greater uniformity of product and superior aging characteristics.

This process is now the standard for producing the higher voltage type of Rectox cells.

The type Q cell has a forward volt-ampere curve as shown in Figure 5, where also is shown a typical curve for the standard or type S cell for comparison. It will be observed that at 0.5 ampere, for example the type Q cell has about twice the voltage drop as does the type S standard cell.

In the reverse direction, typical curves also are shown in Figure 5. Here the type Q cell may be seen to have about four times the resistance of the type S at a given voltage, say 15 volts.

The same output voltage ratings then were adopted for the type Q cell as for the type H, namely double the ratings of the standard cells for any given constructions, with the current ratings being the same as for the type S. The over-all voltage regulation of the type S and Q rectifiers is about the same, since the higher resistance of the type Q cell is offset by the smaller number of cells required for a given voltage output.

Typical efficiency curves are shown in Figure 6, again comparing the standard to the higher voltage type. There will be observed a slight improvement in efficiency resulting from the improved reverse characteristic.

The forward aging of the two types is identical. Aging in the forward direction for the copper-oxide rectifier, it will be remembered, is strictly a function of the temperature of the stack. At any normal temperature, then, the change in resistance for both types will follow the same curve.

Applications of these higher voltage cells have so far been largely in the radio-broadcasting field, where large numbers of stacks are operating at voltages up to 3,000 volts direct current. In this field they have shown outstanding advantages, such as simplicity of control, instant starting, elimination of any warm-up period, elimination of filament windings, and particularly freedom from maintenance and unpredictable failures. The original rectifiers which were installed in November 1939 at *KDKA*, for example, have completed seven years of service at 18 hours per day, without failure. In fact the forward aging so far has been so slight as not to have been noticed by the station operators.

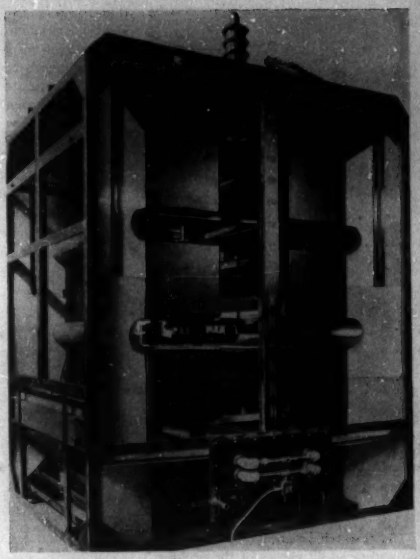

Figure 7. A totally enclosed 75-kv 0.25-ampere d-c forced-cooled copper-oxide rectifier

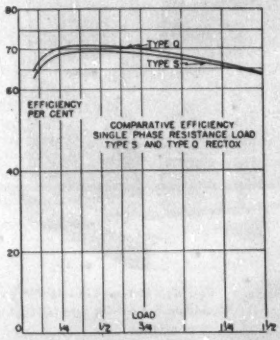

Figure 6. Comparative efficiencies, type S and type Q copper-oxide rectifiers, stacks only

Another interesting application for the higher voltage cells was a 70-kv 1/4-ampere d-c totally enclosed rectifier, used in fly ash precipitation. This unit, shown in Figure 7, with covers removed, was also a forced-cooled rectifier, a recirculating system with heat exchanger being used.

The type Q cell can of course be used in nearly all ordinary rectifier applications. The tendency has been to use it for the higher voltage work, where the greatest savings can be shown, so that it is in these applications that the bulk of the production so far has been used.

This development is another indication that the metallic rectifier, copper-oxide type, is still expanding its field of usefulness. Each increase in output rating widens the range of application. What the future may bring it is still too early to say, as there is no indication that the copper-oxide rectifier has reached a limit in output ratings beyond which there can be no further increase.

No Discussion

Developments in Diesel-Electric Traction-Generator Excitation Control Systems

C. A. BRANCKE
ASSOCIATE AIEE

G. M. ADAMS
ASSOCIATE AIEE

Synopsis: The introductory review covers the major inherent and external regulating excitation systems which have been developed for use on Diesel-electric locomotives. A recently developed amplidyne excitation system using saturable core reactors and selenium rectifiers to obtain definite generator field and armature current limits is described in detail. Used in conjunction with a speed sensitive power plant regulator it provides complete and flexible engine control over its entire operating range of speed and power. Maximum flexibility of motive power is provided by safe and complete remote control which permits operating several locomotive units in multiple.

SEVERAL different excitation systems have been used during the past 35 to 40 years on gas and Diesel-electric cars and locomotives. Most of these have been of the inherent regulating type, depending upon built-in generator or exciter characteristics. Very few have been externally controlled, and most of these have been limited to applications using relatively large power plants.

Inherent Regulating Systems

The earliest excitation system, as used on the first gas-electric rail cars, consisted of a shunt wound generator with a self-excited exciter. Output was controlled by manually changing engine speed and generator field resistance independently. This system was used with apparent success over a period of approximately ten years when this activity was interrupted by World War I.

The next system used on gas-electric rail cars consisted of a generator with two shunt field windings, both of which were energized from a separately (battery) excited exciter. One generator field winding was connected directly across the exciter and the other was connected in series with the control battery, and thus furnished excitation only when the exciter voltage was above battery voltage. The exciter also had a series differential field winding which carried generator armature current, thus producing a drooping generator characteristic. This resulted in a system which was very sensitive to engine speed. It would reduce load rapidly with slight reductions in speed, thus always balancing near rated engine speed regardless of temperature or engine changes.

The excitation system used on the earliest Diesel-electric switching locomotives was similar to this, differing only by elimination of the battery field and by winding the series differential field on the traction generator instead of the exciter. These changes both were made because of battery charging considerations, as considerably more operation at reduced engine speeds is obtained inherently on a switching locomotive. The battery was charged through a carbon pile regulator from the exciter.

The auxiliary requirements on Diesel-electric switchers soon led to the adoption of a constant voltage supply for battery charging, air compressor, traction blowers, and radiator fan motors, at which time the exciter was eliminated. The traction generator then was changed to a combination of self and separate excitation, still retaining the series differential field. While the speed-loading characteristic was not quite as good as that obtained by using a separate exciter, it proved to be satisfactory for this type of service.

Still another arrangement was introduced at about this same time for use on lightweight low-powered locomotives, which is still used extensively today. This consisted of a self-excited shunt generator with an auxiliary (battery excited) "teaser" field winding (which was used only during starting at low generator voltages). This system depends upon an appreciable amount of engine stalling to obtain suitable generator characteristics and engine utilization. In the present-day applications the teaser field has been eliminated and equivalent results obtained by interconnecting the battery in the self-excited field circuit through suitable resistors.

One of the most popular inherent regulating excitation systems is that using the "split-pole" exciter. This consists of a conventional shunt generator but the main poles of the exciter are "split" so that the series differential field can be wound on a part of each pole. The shunt

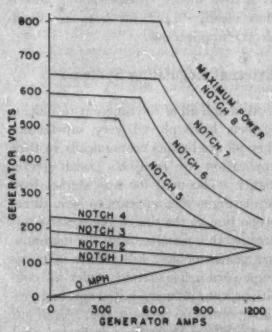

Figure 1. Generator output curves obtained with speed sensitive control

Paper 47-37, recommended by the AIEE committee on land transportation for presentation at the AIEE winter meeting, New York, N. Y., January 27-31, 1947. Manuscript submitted November 12, 1946; made available for printing December 9, 1946.

C. A. BRANCKE is with General Electric Company, Erie, Pa., and G. M. ADAMS, formerly of the same company, is now with Boeing Aircraft Company, Seattle, Wash.

The authors acknowledge the assistance of O. A. Keep and J. C. Aydelott.

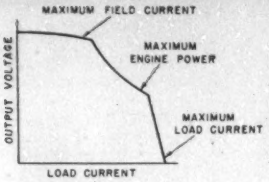

Figure 2. Generator output curve determined by various limitations

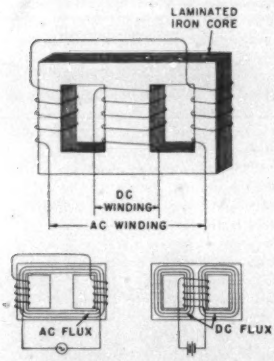

Figure 3. Saturable core reactor showing flux produced by a-c and d-c windings

winding encircles the complete pole, the same as in a conventional machine, and is primarily battery excited although it usually has, in addition, a self-excited connection through relatively high resistance. This results in a generator characteristic which has practically constant kilowatt output over a two to one range in current. It is also highly speed-sensitive and is thus ideally suited for use on Diesel-electric applications.

External Regulating Systems

Although all of the inherent regulating systems have proved very satisfactory they all are limited economically in their application to relatively small power plants. The need for an external load regulating system appears to be in direct proportion to the size of the power plant because this permits using the minimum size generator and still results in maximum permissible output under all conditions, thus reducing initial cost and providing optimum performance. All of our studies along these lines indicated that engine speed was the basic function upon which such a system should be based as this always would result in maximum power output, regardless of variations in temperature, altitude, fuel, or engine ability.

Our first application of this type was on a rail car powered by a 535-horsepower 950-rpm gasoline engine and consisted of a conventional shunt generator which was separately excited from a constant voltage source through a face-plate rheostat. The rheostat arm was driven by a governor actuated servo motor, thus regulating the excitation as a function of engine speed. These controls were effective over the entire engine speed range and included a variable fuel limit, thereby limiting engine torque to safe values at all speeds.

Shortly after this we made a similar application on a 115-ton switching locomotive with an 825-horsepower 500-rpm Diesel engine. Generator characteristics for this locomotive are shown in Figure 1. This locomotive also used a separately excited shunt generator and a face-plate rheostat. The rheostat arm, however, was electrically controlled by a contacting mechanism or switch attached to the engine governor output shaft so as to respond to very minute changes in engine speed. This "speed" switch controlled the magnet valves of a balanced air engine which operated the rheostat arm. Quick response was obtained when increasing excitation by momentarily connecting an auxiliary contact brush on the rheostat arm, which was positioned several bars in advance of the main contact brush. Stability was obtained by means of an anticipating solenoid on the speed switch, which was energized only when the high speed contact was closed. This solenoid opposed the governor spindle movement and temporarily displaced it sufficiently to cause premature opening of the high speed contact. This permitted rapid movement of the rheostat arm while approaching its ultimate position after which a notching effect was obtained until the final balancing point was reached. Variable fuel limit was obtained by repositioning the stationary contacts for each engine operating speed, thus forcing the electric controls to operate at proper fuel setting for each operating speed. Automatic traction motor transition was provided, the forward transitions being made whenever maximum generator excitation was obtained, as indicated by the rheostat arm position. Because no differential field was used, the generator volt-ampere characteristics for all field settings were very flat, with the voltage decreasing very slightly with increasing current, governed entirely by internal resistance and armature reaction. There was therefore no inherent limitation in generator current. Wheel slipping provided the necessary protection against excessive generator current when the motors were in series and a current relay was provided to initiate backward motor transitions whenever maximum generator current was obtained with the traction motors in parallel.

Amplidyne Excitation System

A recently developed system uses a shunt generator and an amplidyne exciter. The exciter, together with its associated control equipment, always furnishes the proper current for the shunt field of the traction generator. This system, in conjunction with the power plant regulator, automatically regulates the excitation to provide optimum locomotive performance without exceeding

1. Maximum available engine power.
2. Maximum traction generator load current.
3. Maximum traction generator field current.

The limitations imposed by the engine are obvious. Generator armature current must be limited to prevent overheating or excessive sparking. Several load current limit settings are desirable to provide the operator with controlled tractive effort for proper locomotive operation. The generator field current is limited to permit using minimum field structure and to limit the maximum generator voltage. Figure 2 shows the resulting generator characteristics at rated engine speed when observing these limitations.

Saturable Core Reactors

A brief review of the characteristics of a saturable core reactor probably will be helpful before attempting to describe the complete system.

The reactors used in this system have a 3-legged iron core with series connected a-c windings on the two outer legs, and one or more d-c windings on the center leg as illustrated by the upper portion of Figure 3. The a-c windings create alternating flux in the outer part of the core only, whereas the d-c windings create flux in all parts of the core, including the center leg, as shown in the lower portion of Figure 3. The d-c windings are used to saturate the core to varying degrees. Any saturation of the core reduces the amount of a-c flux produced by a given alternating current. As the alternating voltage across the reactor will be proportional

to the a-c flux, the voltage across the a-c winding will decrease as the d-c flux increases, assuming constant alternating current in the windings.

Basic Regulating Circuit

The basic regulating circuit is shown in Figure 4 and consists of two saturable core reactors *XA* and *XB*, with their a-c windings connected in series across a constant alternating voltage supply. The d-c winding of reactor *XB* is connected in series with a calibrating resistor across a constant direct voltage supply. The current to be controlled, *I*, is fed through the d-c winding of reactor *XA*. When *I* is zero, there is no d-c flux in reactor *XA*, whereas reactor *XB* has a definite preset d-c flux. Because the sum of the alternating voltages is constant, we then will have more alternating voltage on *XA* than on *XB* As current *I* increases, the alternating voltage on *XA* decreases, whereas the alternating voltage on *XB* increases. When current *I* increases to the point where the d-c flux in reactor *XA* equals that in *XB*, the alternating voltages will be equal. As *I* increases beyond this point, the alternating voltage across *XA* continues to decrease and the alternating voltage across *XB* continues to increase. Thus for any given setting of the calibrating resistor, the alternating voltage across reactor *XB* is always proportional to direct current *I* in reactor *XA*. This voltage is rectified by means of a full wave selenium rectifier and fed into the exciter field control circuit to regulate excitation as a function of any desired current *I*.

It also should be noted that this arrangement permits control of the excitation circuit without any electric connection between it and the controlling function. It is thus possible to obtain a regulating force for use in the relatively low voltage excitation system which is proportional to any desired current *I*, regardless of its voltage, merely by providing suitable insulation on the d-c winding of reactor *XA*.

Basic Excitation System

Figure 5 shows the basic excitation system for a typical locomotive application with the approximate voltages indicated for various parts of the circuit. A 400-cycle 115-volt alternator, driven by a 74-volt d-c motor, is used to energize the primary winding of transformer *T1*. This transformer has three secondary windings; one is wound for 25 volts and the others for 55 volts each. The 25-volt winding is connected to full wave selenium rectifier *R1*, which furnishes 20-volt d-c power supply to load control potentiometer *125* and its series connected resistor *120*. Filter reactor *164* is inserted in the d-c feed circuit to reduce the a-c ripple. The output of potentiometer *125* is connected to amplidyne field *F1-F2* and its series connected resistor *152*. This resistor has approximately four times the ohmic value of field *F1-F2*. Thus the maximum field voltage that ever can be obtained is only 20 per cent of the d-c supply, or 4 volts. Under this condition the voltage drop across resistor *152* is 80 per cent of the d-c supply, or 16 volts.

The amplidyne exciter field resistor circuit was designed to obtain a maximum exciter field current equivalent to twice that normally required for any steady state full output condition, thereby providing rapid generator response whenever increased excitation is required. This "forcing" action is even greater at all other points of operation on the generator characteristic where lesser excitation is normally required. The field current therefore always is limited under full output steady state conditions to 50 per cent or less of the maximum obtainable. Thus the field voltage is never more than two volts under any steady state full load condition, and the voltage across resistor *152* is never less than 18 volts. With this field circuit arrangement it can be seen that if the voltage drop across resistor *152* could be increased by some external means to 20 volts, the exciter field voltage would be reduced to zero. It is therefore only necessary to increase the voltage across resistor *152* approximately 10 per cent to obtain 100 per cent reduction in excitation.

Such a high rate of response was made possible by the use of the amplidyne exciter and its previously developed stabilizing circuit. This consists of an additional winding (not shown in Figure 5) connected in series with a capacitor across its output circuit, and is thus only effective during a change in exciter voltage. Its polarity is such as always to oppose any change in exciter voltage, whether it be increasing or decreasing. The opposing action is also proportional to the rate of change and thus always provides proper stabilizing action.

Because the input to amplidyne field *F1-F2* is but one watt for steady state full output conditions, very low energy control devices, inherently small and lightweight, can be used. All of the static devices, consisting of a transformer, reactors, rectifiers, and resistors, are assembled in one group on the panel shown in Figure 6.

Generator Load Current Limit

The a-c windings of saturable core reactors *X1* and *X2* are connected in series across one of the 55-volt secondary windings of transformer *T1*. The d-c winding of reactor *X2* is connected in series with its calibrating resistor *156* across the 74-volt locomotive battery, thus establishing its amount of saturation. The d-c winding of reactor *X1* is connected in series with resistor *116* across the commutating pole field of the main generator. Resistor *116* provides temperature compensation. It is designed to heat up and increase its resistance at approximately the same rate as the generator commutating pole field. The current flowing through the d-c winding of reactor *X1* is therefore proportional to generator armature current. With no current flowing in the generator, there will be no current in the d-c winding of reactor *X1* and hence minimum saturation. Having previously set the saturation in reactor *X2* we then obtain minimum voltage across the a-c windings of reactor *X2* and connected rectifier *R3*. The output voltage of rectifier *R3*, if disconnected from the system, would be far below that being obtained across resistor *152*, to which it is normally connected. Rectifier *R3*, however, blocks any reversal of current; hence this connection has no effect on the amplidyne field circuit under these conditions. As generator load current builds up, the alternating voltage across *X2* increases and finally reaches a

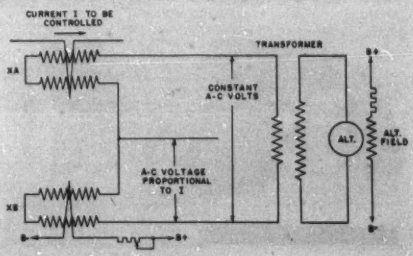

Figure 4. Basic regulating circuit

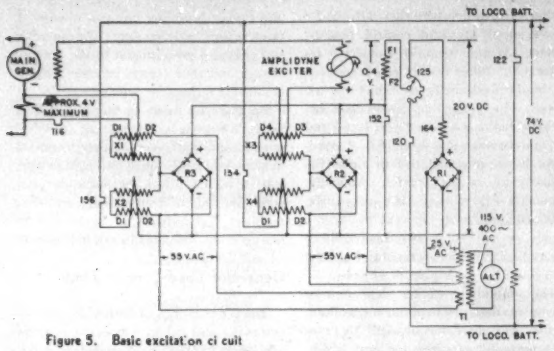

Figure 5. Basic excitation circuit

point where the d-c output voltage of rectifier *R3* is just equal to the drop across resistor *152*. Any further increase in generator load current then will increase the d-c output voltage of rectifier *R3*, thus forcing additional current flow through resistor *152* and increasing its voltage. This increase in voltage reduces the voltage across amplidyne field *F1-F2*. This action continues until the amplidyne excitation has been reduced to the point where it is just sufficient to maintain the current flowing in the generator armature. A very sharp cutoff is obtained for, as previously pointed out, only a 10 per cent increase in voltage is required across resistor *152* to reduce amplidyne excitation to zero. Thus, when sufficient current flow is obtained to increase the voltage drop across resistor *152* by one-half volt (less than three per cent), the amplidyne excitation will be reduced to 75 per cent of the maximum ever required for any steady state full output condition. As the a-c voltage across reactor *X2* is proportional to generator load current, it can be seen that less than three per cent increase in load current will be required to obtain 25 per cent reduction in amplidyne excitation. Because the traction generator normally is being operated quite low on its saturation curve whenever load current limit is effective, this slight change in load current will produce approximately the same high percentage change in generator voltage. Thus the generator volt–ampere characteristics are very steep at the high current ends of the curves. This is of particular value on locomotive applications because this always will permit the operator to work very close to the adhesion point without danger of slipping the drivers, regardless of rail condition.

Generator Field Current Limit

The a-c windings of saturable core reactors *X3* and *X4* are connected in series across the other 55-volt secondary winding of transformer *T1*. This pair of reactors, together with rectifier *R2*, regulate the amplidyne excitation as a function of generator field current in exactly the same way as reactors *X1* and *X2*, together with rectifier *R3*, regulate the amplidyne excitation as a function of generator load current. When the generator field current reaches its limit setting, rectifier *R2* starts "spilling" and regulates the amplidyne excitation, thereby providing a ceiling on generator field current. Reactors *X2* and *X4* are exact duplicates. Reactors *X3* is identical with *X1* except that its d-c winding is designed to carry full generator field current but the d-c winding on *X1* only carries a small percentage of the generator load current.

These two limit circuits are entirely independent and have no effect on each other. Therefore, when operating at high load currents, the generator field current is relatively low so that the alternating voltage across reactor *X2* is high (and regulating), whereas that across *X4* is low. This low voltage on *X4* has no effect on the excitation because blocking rectifier *R2* prevents any reversal of current in this circuit. Likewise, when operating at high generator field current, the load current is relatively low and the alternating voltage across *X4* is high (and regulating), and that across *X2* is low. Blocking rectifier *R3* then prevents any reversal of current because of low alternating voltage on *X2*.

Load Control

If only load current and field current limits were provided, we would obtain maximum generator characteristics which would be very flat at the high voltage end, and very steep at the high current end. Under these conditions it would only be possible to utilize full engine output at some one point, without seriously overloading the engine at other points. These two limits therefore are designed to produce generator characteristics which at rated speed over an appreciable range of current, demand more power than the engine can develop. The power plant regulator (which is described in detail in a separate paper[1]) then reduces the excitation as necessary over this range as a function of engine speed. This is accomplished by potentiometer *125*, which reduces the d-c supply voltage to the amplidyne field circuit whenever the generator load demand exceeds engine ability. The composite curve shown in Figure 2 is the result of all three of these "limit" circuits.

Locomotive Application

Almost all Diesel engines can operate successfully over a 3-to-1 speed range. Advantage is taken of this variable speed characteristic to obtain variable power output easily and economically. Standard practice for several years by most manufacturers of Diesel-electric road locomotives has established the use of eight throttle handle notches for obtaining eight different engine operating speeds on units which are operated in multiple. The amplidyne excitation control circuits

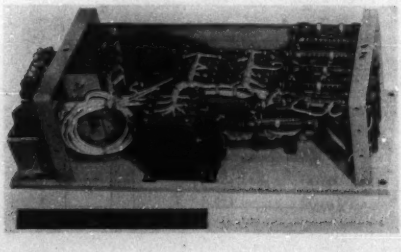

Figure 6. Excitation control panel

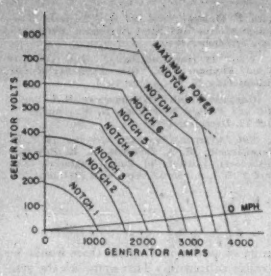

Figure 7. Generator output curves for all notches

therefore were designed on this same basis in anticipation of probable requests by ultimate customers to operate in multiple with existing locomotives. Thus, while we use but one fixed generator field current limit setting, we have a total of eight different load current limit settings. This, in conjunction with the different engine speeds and fuel limit settings, results in eight different generator output curves as shown in Figure 7. Resistor *156* shown in Figure 5 is commutated to obtain a different current limit setting on each throttle handle notch by remotely controlled relays which also commutate resistors for simultaneously changing the engine speed and fuel limit settings.

The advantages of the load current limit feature can be seen by comparing these curves with those shown in Figure 1. When starting from rest, the generator load consists of the resistance of the traction motors together with connecting cables, and can be represented by the straight line extending from the origin, which is marked "0 mph." When starting the locomotive, the throttle handle is notched out until sufficient current is obtained to develop the tractive effort necessary to start moving the train. As soon as the train starts moving, the equivalent resistance of the generator load increases rapidly because of the counter electromotive force being developed by the traction motors. Thus, with the generator characteristics shown in Figure 1 the load current drops off rapidly as the locomotive starts moving with resultant immediate reduction in tractive effort whereas the load current and tractive effort are maintained nearly constant with generator characteristics shown in Figure 7.

A-C Excitation Source

The alternating voltage developed by the 400-cycle alternator will be affected by variations in locomotive control battery voltage as well as its own temperature and loading. Variations in this a-c supply voltage will cause corresponding variations in the alternating voltage across the saturable reactors. These variations are nullified by providing a d-c supply to the exciter field resistor circuit which varies in exactly the same way. This is the reason for using rectified alternating current fed from the same transformer that supplies the reactors, rather than battery supply for the excitation circuit. With this arrangement the limit settings are changed only slightly by all the variations in a-c supply voltage normally obtained in service, and are not of sufficient magnitude to be of any consequence.

Dynamic Braking

During dynamic braking, all traction motor fields are connected in series across the traction generator and their armatures are connected to the braking resistors which dissipate the energy developed by the motors.[2]

Under this condition the generator output is very low, being practically negligible at top locomotive speed where minimum motor excitation is required, and but 15 to 20 kw at lower speeds where maximum motor excitation is needed. The maximum generator current ever required is approximately one-fourth of that used during motoring, while the maximum voltage is but four to five per cent of maximum motoring voltage. The Diesel engine therefore is operated at idling speed and the traction generator series cranking winding is inserted into the circuit to obtain as much inherent stability as possible. It also must be possible to change the traction motor excitation very gradually to permit obtaining any desired braking rate, up to the maximum, at any locomotive speed. The same rectifiers and reactors are used to control the generator current output during braking as are used during motoring, but the controlling circuits are rearranged because of the lower range in generator armature currents and the necessity of providing fine graduations in current limit settings. This is accomplished by adding a modulating d-c winding to reactor *X1* and connecting it, as well as the d-c winding on reactor *X2*, to a resistor network so arranged that the current limit setting can be changed by varying the potential applied at one point of this circuit. The operator then can adjust the excitation to suit any requirement by varying the potential at this point. This is done by a controlling potentiometer which is operated by the braking control handle. The variable voltage appearing at the brush arm of this potentiometer is applied to one of the control train wires. Simultaneous recalibration of the current limit settings on any number of locomotive units operating in multiple thus is obtained by merely varying the voltage applied to this one train wire. The energy involved is so low that a relatively small potentiometer is only slightly affected by the number of units operating in multiple. Because the amplidyne field current is regulated automatically to maintain a definite generator armature current for each setting of the braking handle, the system is not affected by changes in engine speed or changes in temperature, both of which would seriously upset any Ward-Leonard system.

Conclusions

This latest excitation control system contains several new features which result in improved performance as well as reduced maintenance and higher locomotive availability. These consist of

1. *Engine Protection.* All engine limitations are observed, thus providing reduced torque at reduced speeds and controlling the loading to maintain proper speed on each notch, regardless of changes in temperature, altitude, fuel, or changes in engine ability. It is flexible and readily conformed to suit any reasonable engine speed-torque characteristic. Additional functions can also be readily incorporated; for example, reduction in loading in event of high engine temperatures. These protective features should result in long life and low engine maintenance, together with improved performance.

2. *Generator Protection.* Limiting the maximum load current and the maximum field current greatly reduces the possibility of overheating the generator. The load current limit also limits the commutation duty for which the generator must be designed.

3. *Controlled Tractive Effort.* By providing several different generator load current limit settings, the operator always can obtain the desired tractive effort. This should improve locomotive performance, especially when starting a heavy train. As the excitation is regulated as a function of generator output, this automatically eliminates any variations in this output because of variations in excitation voltage supply, machine temperature, or individual generator characteristics.

4. *Minimum Size and Weight Control Devices.* The amplidyne exciter requires very low energy input, thereby permitting the use of high safety factors in designing and still obtaining unusually small and lightweight devices.

5. *Low Maintenance.* The transformers, reactors, rectifiers, and resistors used in the

limit circuits have no moving parts and thus require minimum maintenance. Being static, the possibility of trouble is reduced greatly, and should result in increased locomotive availability.

References

1. A Power Plant Regulating System for Diesel-Electric Locomotives, **C. B. Lewis.** AIEE Transactions, volume 66, 1947, pages 242–246.

2. Braking Resistors and Control for Diesel-Electric Locomotives, **E. F. Weiser.** AIEE Transactions, volume 66, 1947, pages 229–232.

3. Brill Governor Controls Speed and Regulates Engine Load, **Charles Guernsey.** *Automotive and Aviation Industries* (Philadelphia, Pa.), December 14, 1929, pages 873–4.

4. Control Features of 115-Ton, 800-Hp Diesel-Electric Locomotive on Erie Railroad, **C. A. Brancke.** *General Electric Review* (Schenectady, N. Y.), August 1933, pages 364–7.

5. The Amplidyne—A New Tool of Many Uses, **F. Mohler.** *Iron and Steel Engineer*, Association of Iron and Steel Engineers (Pittsburgh, Pa.), September 1940.

6. What Is the Amplidyne? How Does It Work? **Fremont Felix.** *General Electric Review*, (Schenectady, N. Y.), August 1943.

7. Understanding the Amplidyne, **H. L. Smith.** *Mill and Factory*, New York, N. Y., volume 33, page 92, December 1943.

8. The Amplidyne System of Control, **E. F. W. Alexanderson, M. A. Edwards, K. K. Bowman.** *Proceedings*, Institute of Radio Engineers (New York, N. Y.), volume 32, September 1944, page 513.

Discussion

Lanier Greer (General Electric Company, Erie, Pa.): Since the days of the first gas-electric rail cars and locomotives, the desirability of a power unit control and generator excitation system which would accurately control engine speed and loading regardless of variations in temperature, fuel, altitude and engine ability has been acknowledged. This has become more important with the advent of the Diesel engine and with the increased speed and power of these engines. Inherent regulating systems, although rugged and simple, have been proven to be inadequate for the modern high-speed high-power Diesel engine. This has made it necessary to find an external regulating system which accurately will control and impart the desired characteristics to the engine generator combination. Such a system is described in the paper under discussion and has advantages for each major piece of rotating apparatus. These accrue as simplicity of design, lighter weight, lower initial cost, better performance, and lower maintenance.

The source of power for the Diesel-electric locomotive is the Diesel engine and if it is not properly regulated and protected the maximum amount of work cannot be performed. If the control system of the power unit as a whole is such as to allow the engine to operate under optimum conditions at all times, the best possible performance will be obtained. By accurately controlling speed, loading, and temperature of the engine under all conditions of operation, as is done by the system under discussion, engine maintenance will be kept low, time between overhauls will be increased and engine performance will be improved.

Mechanical power produced by the engine is delivered to the generator which converts it into electric energy. The generator is simplified by accurately controlling the maximum load current to a value which gives adequate starting tractive effort, when applied to the traction motors, and by limiting this current to a definite maximum. This reduces the possibility of excessive sparking due to overload current.

By externally controlling and limiting the field current (maximum voltage on the high voltage end of the engine generator volt ampere curve) the size of the generator field structure is kept to a minimum because a simple single exciting winding can be used on the main poles. This reduces the amount of insulation in the coils and increases the heat transfer coefficient. By keeping the field current constant, from maximum full utilization to maximum locomotive speed, field heating is controlled and damage to the fields from this cause is minimized. Controlled field current (maximum voltage) keeps the peak volts per bar within reasonable limits and reduces generator flashing.

Accurate control of load and field current makes possible the use of a simple salient pole single armature generator over a wider range of power and speed than would be possible otherwise. This simplifies the generator manufacture and reduces the initial cost. A generator without compensating windings is also an advantage to the operator because it is easy to maintain and repair.

The voltage and load current of the generator are supplied to the motors which drive the locomotive. Controlled load current applied to the traction motors protects them from sparking due to overloads. Also controlled field current on the generator gives controlled voltage on the motors and limits the peak volts per bar to a reasonable value which keeps flashing on the motor at a minimum. This reduction in flashing and sparking reduces heating, gives longer life and helps to keep motor maintenance low.

Therefore, a system of power plant regulation used in conjunction with a generator excitation system such as described in the paper by C. A. Brancke and G. M. Adams does these three things for the major pieces of rotating apparatus.

1. Gives better prime mover performance.

2. Makes possible a simpler lighter-weight and smaller traction generator.

3. Keeps the maximum that is demanded from the traction motors to a reasonable value.

These things combined give lower initial cost, better locomotive performance, longer life, lower maintenance and better availability.

Braking Resistors and Control for Diesel-Electric Locomotives

E. F. WEISER
NONMEMBER AIEE

Synopsis: This paper covers the general scheme and performance of a new dynamic braking system for heavy Diesel-electric road locomotives and a description of design features of the newly developed braking resistor unit.

MANY of the new Diesel-electric road locomotives appearing on American railroads are being equipped with dynamic braking. This enables the locomotive to hold back or to stop as well as to accelerate the train. Attractive savings appear in lowered wheel and brake shoe maintenance and faster schedules.

"Grinding to a stop" is a hackneyed literary phrase, but unfortunately it is a correct technical description of conventional railway brakes in action. Replacing brake shoes and worn and cracked wheels represents a major item in car maintenance. The danger of a train running away on long mountain grades because of overheated brakes losing their effectiveness often dictates speed limits as low as 15 miles per hour with frequent stops to cool the brakes. Faster schedules are possible when the locomotive can absorb all or part of the power generated by the descending train.

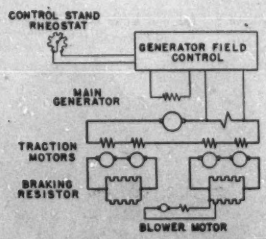

Figure 1. Control and power connections during dynamic braking

Generating 1,490 kw of power in the crowded interior of a modern locomotive presents a number of engineering problems, and getting rid of a like amount presents another, for a Diesel-electric locomotive cannot return power to an overhead system as an electric locomotive can.

Braking Scheme and Circuits

The general scheme of dynamic braking employs the traction motors as generators with their fields separately excited to provide control (see Figure 1) and a resistor to dissipate the power generated. Excitation of the motors during braking is accomplished by connecting all motor fields in series with the propulsion generator which is capable of supplying the low-voltage, high-current excitation required by the series traction motor fields. The braking can then be controlled by varying a rheostat in the main generator excitation system. Switching equipment is required in the main power circuits to make up the excitation circuit of the motors and connect the traction motor armatures to the braking resistors. Additional switching in the control circuits sets up the main generator excitation and engine speed control circuits.

Interlocked separate controller handles for motoring and braking require the operator only to return the motoring handle to the "off position" and notch up on the brake handle to brake, being careful not to exceed the motor rated current as registered on his instrument panel ammeter.

Figure 1 shows a simplified circuit diagram of the connections during braking. The generator field control system regulates a constant selected output current to the traction motor fields, independent of minor variations in engine speed, motor field coil temperatures and other variables, using the voltage drop through the generator commutating field coils as an indication of current.

Since the adhesion of the locomotive to the rails is sufficient to generate full motor rated current, and therefore torque, the maximum braking rate is determined by the traction motor ratings. On a 3-cab 6,000-horsepower locomotive this fixes the braking horsepower per cab at slightly over 2,000 horsepower, 1,490 kw, due to the transmission losses which aid during braking.

The tractive effort available for braking is shown in Figure 2 for various speeds. Since, during braking the transmission losses are aiding the braking, the braking tractive effort available is actually higher than the motoring effort at the same speed. With dynamic braking, the locomotive with the assistance of the train's rolling friction can brake the train down a grade without assistance from the air brakes at a higher speed than it can pull the train up the same grade.

The requirements for a braking resistor are that it dissipate 1,490 kw of power in as small as possible space in the already crowded cab and that weight and cost be kept to a minimum.

Resistor Design

The functions of the resistor are

1. To convert electric energy into heat.
2. To take the heat away from the locomotive.

An air-cooled, forced-ventilated design was selected for development because of the unavailability of other cooling mediums on Diesel-electric locomotives and

Paper 47-38, recommended by the AIEE committee on land transportation for presentation at the AIEE winter meeting, New York, N. Y., January 27-31, 1947. Manuscript submitted November 12, 1946; made available for printing December 6, 1946.

E. F. Weiser is affiliated with the engineering division of the General Electric Company, Erie, Pa.

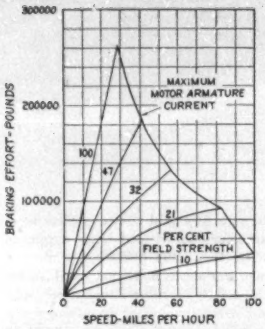

Figure 2. Tractive effort versus speed during dynamic braking in a 2,000 horsepower locomotive

because space limitations demanded operation of the resistor elements at an intensity of heat transfer unobtainable with natural convection.

The problems which emerged during development were primarily those of a heat exchanger rather than a resistor. The final design consists of a double ended, axial flow fan and motor unit, diffusers, tunnel type resistor grids, and discharge elbows. Figure 3 shows the components installed in their mounting frame which forms part of the locomotive cab roof. The discharge elbows, not shown, are incorporated in the locomotive cab roof. The assembly pictured is removable as a unit. Its length is 11 feet 2 inches.

Primary consideration was given to maintaining an air path through the system of constant cross section without turns to reduce eddys and velocity head losses in the air stream. The elimination of eddys and unequal air velocities through the bank of resistors is vital to elimination of hot spots in the resistor bank which would limit the intensity at which resistor grids could be operated.

Two factors determine the quantity of air required: the amount of heat to be carried away and the temperature to which the air may be raised. For standard air conditions the following equation gives the approximate relationship of cubic feet per minute, kilowatts, and allowable temperature rise C in degrees centigrade:

$$C = \frac{1750\ (KW)}{CFM}$$

The permissible temperature rise is limited by the temperature that the discharge elbow and the paint on the adjacent cab roof can withstand. Limiting this rise to 100 degrees centigrade fixes the air requirements at approximately 26,000 cubic feet per minute to remove the 1,500 kw of power from the locomotive.

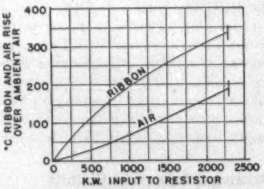

Figure 4. Temperature rise of ribbon and air versus kw input for 2,000 horsepower locomotive resistor

The use of such a volume of air made it inadvisable to draw the resistor cooling air from inside the cab, its inlet louvers and filters being already taxed by the requirements of the engine and the generator and motor ventilation. The location of the resistor over one side aisle between the engine and the outside wall enables it to draw its air directly from the outside, to pass it through the resistors and to discharge it vertically through the cab roof.

The fans require 74 horsepower but by connecting the series-wound fan motor in parallel with a section of the resistor it uses part of the power being dissipated. The motor can thus be connected permanently in parallel with its section of resistor eliminating all danger of control failure. This means that the voltage supplied to the blower motor is proportional to the current in the resistor. However, the combined characteristics of the fan loaded series motor, resistor heat transfer and fan discharge result in a temperature versus power curve for the resistor of the type shown in Figure 4 from which it can be seen that the highest kw input region of the curve results in the highest resistor temperature in spite of the resulting higher fan motor voltage and speed in that region.

The terminus of the curve is the point at which the fan motor reaches its maximum permissible speed, limiting the input to the resistor to the kw which produces this speed. Operation of the resistor at altitudes of 7,500 feet in some mountain passes would result in higher fan motor speed than at sea level due to reduced fan load in the rarified atmosphere. Allowance has been made in selecting the fan speed at normal resistor input, 1,490 kw, to insure against overspeed under adverse conditions. To protect the motor against overspeed, a voltage relay is connected across the motor terminals and is set to operate at maximum permissible motor voltage, flashing a warning light near the operator who must correct the condition by reducing the excessive braking rate.

The motor fan unit, shown in Figure 5, is rated at 26,000 cubic feet per minute at 11 inches of water static pressure at 3,500 rpm. Originally developed as a traction

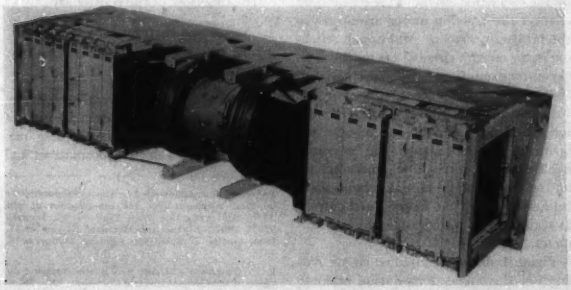

Figure 3. Assembly of blower, diffusers, and resistors in their mounting frame

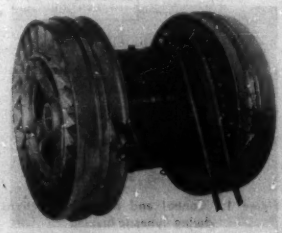

Figure 5. Fan and motor unit showing fans and contravanes

motor blower, the unit is extremely compact and light in weight for its output. Its small size makes possible an equally important weight saving in the supporting cab structure. The fans are of axial flow type and use curved stationary entry vanes which direct the entering air at the correct angle for efficiency at the high output pressure.

The conversion of the toroidal section of the air stream from the fan into a square section suitable for the resistor is accomplished in a diffuser pictured in Figure 6. Concentric baffles divide the air from the fan and distribute it over the square outgoing section assuring an equal air velocity to all resistor ribbons and elimination of eddys which would recirculate air through portions of the resistors resulting in hot spots.

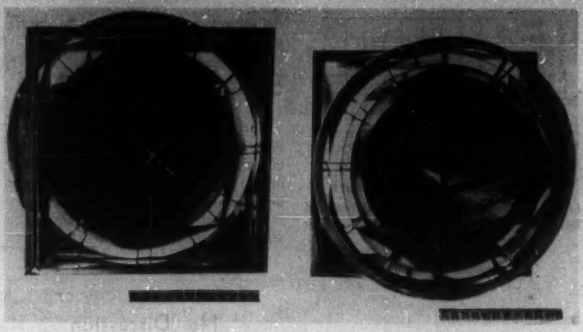

Figure 6. Two views of diffuser showing inlet and outlet ends

Grid Units

Sixteen resistor grids, eight at each end of the fan unit, make up the resistor proper. Figure 7 shows a single grid. The frame of the grid, which is of insulating material, encloses the resistor element and forms the duct which confines the cooling air stream when stacked with succeeding units. The mounting lugs form both the electrical and mechanical connections. Removal of any unit can be accomplished by removing two bolts and sliding the unit out without disturbing adjacent units.

Parallel strips of a chromium-aluminum-iron alloy resistance material, connected in series, form the resistor element. Conventional supporting tie rods with their mica insulation were eliminated when tests showed ribbon temperature in in the lee of the tie rod ran just twice that in areas not blanketed by tie rods. This single innovation resulted in a 50 per cent reduction in the ribbon area and resistor cubic volume required at no increase in maximum ribbon temperature. By forming each resistance strip into a shallow V cross section which nests with adjacent strips, sufficient mechanical rigidity was obtained and the increased turbulence in the air stream materially increases the heat transfer from the ribbon to the air stream.

The resistance element is fastened in its frame at only two points, the outgoing terminals. Guide pins at the ends of each strip project into clearance holes in the insulation, frame supporting the resistance strips without restricting their endwise expansion, which amounts to 0.1 inch at 375 degrees centigrade rise. All ribbon buckling forces are thus effectively eliminated and it is possible to space the resistance strips closely, effecting a saving in the cubic space required for the resistors.

The use of rolled strip provides grids far superior to castings in durability and resistance to cracking from vibration. Thin rolled sections also provide greatly increased heat radiating surfaces over that of cast section grids. Each of the 16 units contain 42 strips of resistance material presenting 5,855 square inches of radiating surface to the air stream. Each square inch of surface radiates approximately 17.5 watts per square inch. The connectors brazed between ribbons are of heavy section which conduct heat away from the joint and assure joint temperatures substantially lower than that of the ribbon proper.

The air stream passing through the resistor increases progressively in temperature, volume, and velocity. Each successive grid is thus subjected to a higher ambient air temperature, however, the temperature rise of each grid over that of the air emerging from it is substantially the same for all layers. The maximum temperature is experienced by the last grid and is the sum of the outgoing air temperature and the rise of the ribbon over the air passing it. The temperature difference between the ribbon and the air passing it may be viewed as the potential required to force the heat from the ribbon into the air stream. Thus the more heat being transferred per unit area, the higher the required temperature differential. However, the two major factors reducing this differential are air turbulence and velocity. The use of the nesting V cross section ribbons forces the passing air to change direction and assures turbulence. The effect of velocity is illustrated in Figure 8, the higher the air velocity the lower is the necessary temperature differential.

With a given air flow the velocity can be increased by reducing the cross-sectional area of the resistor tunnel. Increasing the velocity, however, increases the fan pressure required to force the air through the resistor and limits the practical velocity to that corresponding to the available fan pressure. In the resistor designed, the air enters the resistor bank at 4,400 feet per minute and leaves at approximately 6,600 feet per minute after heating and expanding. This exit velocity, which is 75 miles per hour in a vertical direction, effectively removes the heat from the vicinity of the locomotive and all trailing cabs and cars, fulfilling

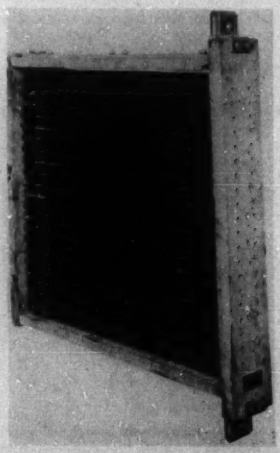

Figure 7. Tunnel type grid unit

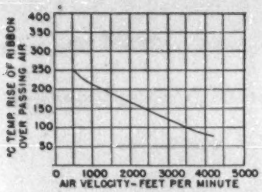

Figure 8. Temperature differential required between ribbon and air for one grid unit at 100 kw input

the second major requirement of the resistor, that of getting rid of the heat.

Conclusions

The design can be summarized as a high-velocity air-colled resistor in which major attention has been given to air flow, heat transfer, and the removal of the heated air from the locomotive.

Incidental features include air intake screens, air velocity actuated shutters to protect the exit end of the resistor from the weather while the resistor is not in use, and drains in the exit elbows. The shutters and drains permit the use of air exits which do not project from the cab roof and thus greatly improve the appearance of the locomotive. Some installations incorporate connections to the resistor which makes it possible to load the engine, for test purposes, through the main generator, which is an invaluable aid to the maintenance shops.

No Discussion

Developments in Control Systems for Diesel-Electric Locomotives

M. D. HENSHAW
NONMEMBER AIEE

Synopsis: In the years 1945 and 1946 we have seen the completed development of new and larger Diesel engines designed specifically for use in main line Diesel-electric locomotives. Application of the larger electric transmission systems required for converting the engine power into tractive effort at the rail has presented new control problems, in the solution of which many new developments in circuits, apparatus, and manufacture have been made.

TWO TYPES of main line locomotives were in manufacture prior to World War II. One of these was a 2,000-horsepower unit frequently used in pairs in passenger service. Each cab included two separate 1,000-horsepower power plants with the generators independently connected to pairs of traction motors on three axle trucks, the center axle being an idler. Duplicate installations were required of mechanically driven air compressors, of the engine water and oil cooling systems, and of the electric auxiliaries and control. Only the master controller, the storage battery, and the air brake system served both power plants in common. No dynamic brake installations had been developed for these units.

A second type appeared in 1940 which utilized a single 1,350-horsepower power plant in each cab. The generator supplied power to four traction motors, of which there were two each on the two axle trucks. No idler axles were used. Dynamic braking was available as a holding brake on long grades. This size locomotive found wide application in freight service in spite of the low power rating which required from three to four coupled cabs to handle the service.

The arrival of new Diesel engines of 1,500- and 2,000-horsepower ratings in 1945 and 1946 greatly broadened the field of application of single power plant per cab locomotives. Improvements in traction motors and generators for these locomotives have produced higher ratings so that in some cases three 1,500-horsepower cabs will perform the same service formerly done by four 1,350-horsepower cabs. In high speed passenger service on most eastern railroads, two 2,000-horsepower cabs suffice and the two power plants involved constitute a distinct saving in fuel, lubrication, and maintenance costs in contrast with the four smaller power plants used on the older type of 2,000-horsepower locomotives.

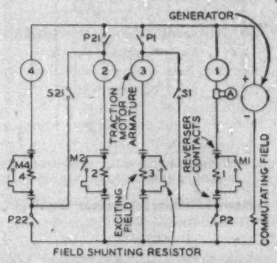

Figure 1. Power connections—motoring

Connections	Contactors Closed S1	P1	P2	S21	P21	P22	M1	M2	M3	M4
Series parallel FS1		●			●					
Series parallel FS2		●			●			●	●	●
Parallel FS1			●	●		●				
Parallel FS2			●	●		●	●	●	●	●

Although some of the new engines operate at higher speeds than have been used before in main line locomotives of comparable power, the design emphasis was placed on long life with minimum replacement of wearing parts. This in turn has constituted a challenge to the control engineer to produce new standards in handling of these larger power units.

As far as possible, circuits and apparatus have been designed to fit both the 1,500- and 2,000-horsepower units. This is of benefit not only in reducing the first cost, but also in simplifying the maintenance, servicing, and renewal parts problems.

Power Circuits—Motoring

The new single power plant 1,500- and 2,000-horsepower units both employ four series wound traction motors, powered from a single main generator.

Conventional series-parallel and parallel motor connections are used (see Fig-

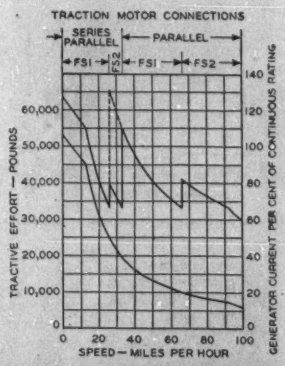

Figure 2. Typical speed-tractive-effort curve for 2,000-horsepower unit showing relation of generator current to speed

Paper 47-40, recommended by the AIEE committee on land transportation for presentation at the AIEE winter meeting, New York, N. Y., January 27–31, 1947. Manuscript submitted November 12, 1946; made available for printing December 6, 1946.

M. D. HENSHAW is with the engineering division, General Electric Company, Erie, Pa.

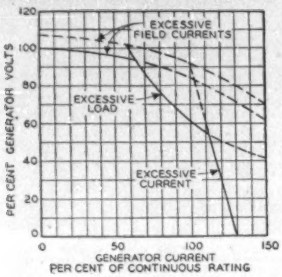

Figure 3. Typical generator characteristic for 2,000-horsepower unit

ure 1) with a single step of resistor shunting of the motor fields.

Field shunting is analagous to the overdrive commonly used on some types of automotive vehicles. It extends the range in locomotive speed over which full power can be obtained from the generator within its current and voltage limits.

Formerly applied only in the high speed (parallel) motor connection, field shunting now also is used in the low speed (series-parallel) connection as shown in Figure 2. The locomotive is operated up to a higher speed before transfer to parallel is required, and the parallel connection is established at a lower value of generator current as indicated by the dotted lines. As the limiting current rating in parallel is that of the generator and not that of the motors, the use of the field shunting step in series parallel results in a reduction in generator rating, with resultant savings in weight and size.

Excitation System

One of the chief problems in control for Diesel locomotives is the matching of the generator demand to the load the Diesel engine can carry over the required volt-ampere range.

On early units this was attempted by giving the generator output a hyperbolic pattern, obtained by various schemes of self and separate excitation or in conjunction with special exciters.

The pattern obtained usually was subject to variation from temperature changes in the equipment itself, from battery voltage change, or from misadjustment. None of the schemes recognized any change in engine ability, such as might be caused by faculty fuel injection equipment. When such faults occurred, or when the electric equipment was cold, the engine became overloaded and stalled in speed. This in turn frequently aggravated the condition and contributed to early failures.

As the art advanced, external regulating schemes began to demonstrate their superiority over those using inherent generator patters. Out of the wealth of ideas advanced and tried, two distinct trends became evident.

1. The Diesel engine designer showed willingness to operate his engine at a fixed speed with fixed fuel injection and to accept whatever loading could be applied within these limits.

2. As a corollary to the first, the control designer became conscious that engine speed with fixed fuel injection is the best measure by which to adjust the generator demand.

It is with these elements in mind that the new excitation system for these locomotives has been designed.

The solid line curves in Figure 3 show the nominal generator output, with recognition of desired field current and armature current limits corresponding to the generator load demand which can be carried by a 2,000-horsepower engine operating at top speed.

No attempt is made to develop this as an inherent pattern, but instead the generator and exciter are arranged for an output shown by the top dotted curve, considerably in excess of all three limits. The setting is made high enough so that

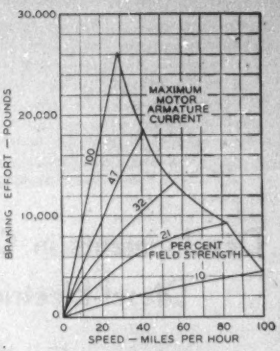

Figure 6. Typical speed–braking-effort curve for 2,000-horsepower unit

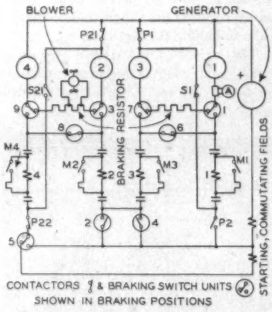

Figure 5. Power connections—braking

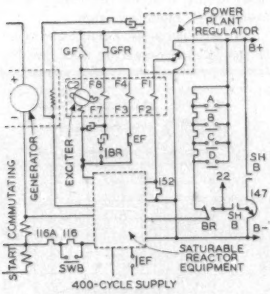

Figure 4. Elementary connections for excitation system

EF—Exciter field relay
GF—Generator field contact
GFR—Field discharge resistor
BR—Braking relay
SWB—Braking switch
A, B, C, D—Sequence relays
147—Breaking potentiometer
116—Temperature compensating resistor
SH, B—Contact on controller, closed when selector handle is in braking zone

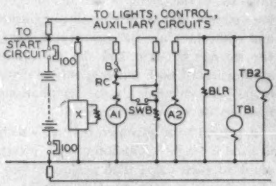

Figure 7. Auxiliary power circuits

A1—Auxiliary generator for battery charging
A2—Auxiliary generator for blowers
B—Battery charging contactor
RC—Reverse current relay
X—Voltage regulator
SWB—Interlock on braking switch
TB1, TB2—Traction motor blower
BLR—Blower warning relay
100—Battery switch
□—Circuit breaker

all variations with temperature and with commercial tolerances between machines still will exceed the three limits.

Dependence then is placed on the power plant regulator to reduce the exciter excitation to the point where the generator demand will not stall the engine or to adjust it upward to the point where full fuel injection is obtained. In this manner the proper load limitation, shown by the solid hyperbolic curve in Figure 3, is obtained. The actual loading obtained will depend on the engine condition and other factors such as fuel and air temperature, but in any event the engine speed and fuel injection will be obtained at proper levels.

Further dependence is placed on the saturable reactor equipment to control the exciter excitation so that the desired limits of generator field and load current are not exceeded.

Exciter

An amplidyne exciter is used in the new excitation system. This is its first application in the railway locomotive field.

Full advantage is taken of the amplification factor in that all control devices are of small size and thus can be suitably located. For instance, the load control potentiometer is mounted directly on, and is operated by, the engine servo unit. Conventional capacitors are used for stabilizing purposes.

Excitation Circuits

The elementary connections are shown in Figure 4. The amplidyne exciter is connected to the generator shunt field through a contactor, with discharge resistor across it, and through one element of the saturable reactor equipment. This is for signaling excessive field current.

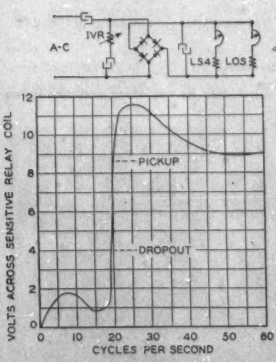

Figure 8. Typical connections and characteristic curve for tuned frequency relay equipment

Figure 9. Locomotive overspeed relay equipment

Antihunt field *F7-F8* is connected across the exciter armature through a stabilizing capacitor. During dynamic braking, an additional capacitor is added by contacts of the braking relay.

Suicide field *F3-F4* is used in conjunction with the exciter field relay to reduce quickly the generator field current to zero when the throttle is closed.

The control field *F1-F2* is energized from the locomotive battery through the load potentiometer on the power plant regulator and through resistor *152*.

To signal excessive generator current, the voltage drop across the generator commutating field is fed through resistors *116* and *116A* to an element of the saturable reactor equipment.

When the saturable reactor equipment receives a signal of excessive current either in the generator field or load circuit, a counter voltage is applied to resistor *152*, thereby reducing the *F1-F2* excitation to a value needed to observe the required limit.

During motoring, sequence relays *A*, *B*, *C*, or *D* operate to change the battery circuit bias on the saturable reactors to establish the desired generator load current limit for each throttle position.

During dynamic braking, an interlock on the braking switch cuts out resistor *116* to establish the lower current limit required. The braking relay connects the saturable reactor bias circuit to potentiometer *147*. This potentiometer is operated by the controller selector handle, and the voltage established on train wire 22 modifies the braking current limit simultaneously on all connected locomotive units.

The saturable reactor windings are insulated suitably so that the generator and battery circuits are not connected electrically.

The load potentiometer in the power plant regulator operates to control *F1-F2* field excitation so as to maintain whatever load the engine can carry at the specified speed.

When the traction motor demand is less than the engine can carry, the power plant regulator reduces the engine fuel to maintain the desired engine speed. Under this condition the load potentiometer is at the maximum voltage position.

As the motor load increases, more fuel is admitted to the engine up to the maximum value permitted. Load demands beyond this point produce an internal overtravel of the servo unit, which in turn operates the load potentiometer towards the reduced voltage position to lower the *F1-F2* excitation as required.

A feature of this system is the capacitor feedback from the generator shunt field amplidyne exciter circuit to the power plant regulator. Any large voltage

Figure 10. Axle generator for tuned frequency relay systems

change appearing in this circuit, such as occurs when the field contactor is opened momentarily during motor transitions from series parallel to parallel, signals the regulator in advance of the actual load change on the engine. Anticipatory regulator action thus is initiated, and any transient engine speed increase is prevented during the transitions. This feature is an improvement over older sys-

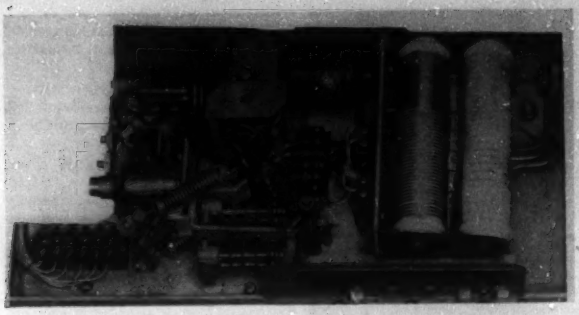

Figure 11. Water temperature relay

tems where the engine sometimes tripped out on overspeed during motor transitions.

Further details of the operation of both the saturable reactor equipment and of the power plant regulator will be found in other papers.

Dynamic Braking

With the development of a new air-cooled braking resistor of high capacity, dynamic braking is now available for the new locomotives of a rating limited only by the capacity of the traction motors themselves.

Power braking circuits are shown in Figure 5. An air-operated braking switch establishes the power braking circuits. This switch is interlocked suitably to insure its operation only when there is no power in the circuits. Each pair of motors is connected across half of the braking resistor. A blower motor with dual fans receives its energy from taps on one of the resistor halves. The blower speed is proportional to the energy being dissipated in the resistor.

The series fields of all four traction motors are connected across the generator through its starting field. This field acts differentially and allows the generator to be operated well up on its saturation characteristic, thereby providing maximum inherent stability.

Control of dynamic braking is obtained by operation of the selector handle on the master controller. This handle operates potentiometer *147* in Figure 4 to obtain any definite braking effort required. This voltage, appearing on the saturable reactor equipments on all connected cabs, establishes identical current limits on all the generators, and thus sets duplicate excitation levels on all traction motors.

The loadmeter, in front of the operator, is his guide as to the amount of dynamic braking. This meter, connected to a shunt in series with the Number 1 motor, indicates the actual braking current.

The amount of braking effort obtained at a fixed current depends on the locomotive speed as shown in Figure 6. A fixed selector handle position gives a braking characteristic as designated by the several curves for various percentages of field strength.

The system is stable. Any tendency for the locomotive to speed up is counteracted by increased braking effort, without movement of the selector handle. This is true up to the point where maximum motor armature current is reached and is indicated by a red band on the loadmeter. Further speed increase beyond this point must be met by a handle movement to reduce the dynamic braking, or by an application of the air brake, or by both.

Auxiliary Power Circuits

Although conventional battery charging circuits are used, new connections and equipment are involved in the air-cooling of the traction motors (see Figure 7).

The exciter, battery charging, and blower generator machines are gear driven from the end of the main generator. This eliminates difficulties and failures encountered with the V-belt drive formerly used. It also permits location of the blowers to best advantage.

A d-c system is used for the blowers because of its simplicity and for the important reason that its voltage level, and hence the blower speed and motor cooling can be raised during dynamic braking for a higher rating.

During motoring, the blower generator voltage varies with engine speed. During dynamic braking, with the engine at idling speed, an interlock on the braking switch commutates the blower generator field resistor so as to obtain approximately three-fourths of maximum air-cooling in the traction motors.

Tuned Frequency Equipment

The wartime development of tuned fre-

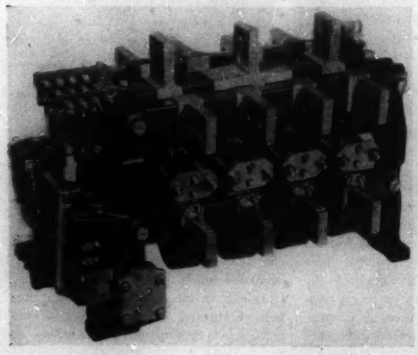

Figure 12 (left). Motor reverser

Figure 13 (below). Typical relay for amplidyne excitation system

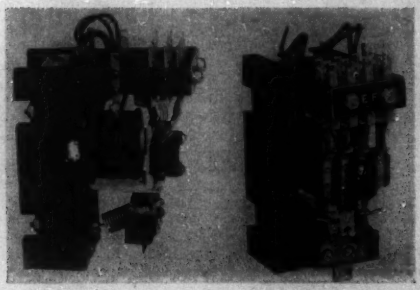

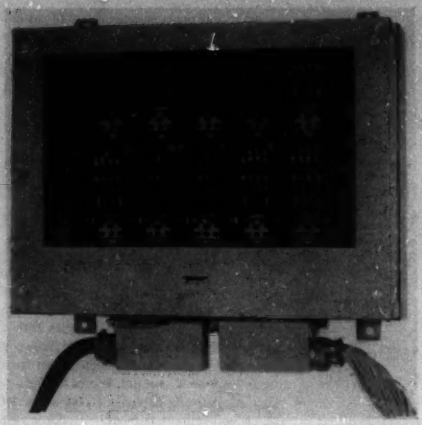

Figure 14. Dust-tight equipment box

quency systems and of low energy relays have produced equipments suitable for handling a variety of tasks not attempted before on Diesel locomotives.

Prewar 2,000-horsepower passenger locomotives were equipped with voltage biased current relays for automatically transferring from series to parallel motor connections. These relays were not suited to handle backward transitions from parallel to series. It was the operator's responsibility to retard the throttle handle and to drop the relay back to the lower connection.

The 1,350-horsepower freight unit depended solely on manual operation of the selector handle for initiating the transitions. Results were satisfactory as long as the operator moved the handle at the correct locomotive speed. When he erred, the results in terms of shock on the train, and in the electric equipment, were most undesirable.

Figure 8 shows the connections and

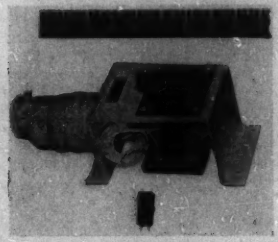

Figure 15. Motor cutout switch

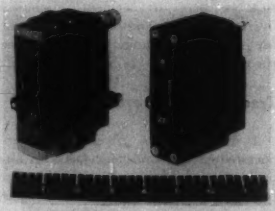

Figure 16. Circuit breakers

characteristics of a typical element of the new tuned frequency equipment. An axle driven permanent-magnet-rotor a-c generator supplies power with voltage and frequency proportional to speed.

A combination of reactors and capacitors, tuned to peak sharply at the desired speed and to maintain approximately the maximum output for frequencies above the peak value, operate a low energy relay through a rectifier. The sharpness of the curve is such that the pickup and dropout of the relay are within five per cent, in terms of locomotive speed. This means that transitions from series parallel to parallel can be set for 33 miles per hour and the reverse at 31.5 miles per hour. The low energy relay action is relayed to the locomotive control circuits.

By using similar equipments, each tuned to operate at the proper speed, completely automatic forward and backward transfers including field shunting can be had. On locomotives so equipped, the selector handle then is used as a restrictive lever to hold the connections at a lower level, if desired.

Similar equipments have been developed for locomotive overspeed protection. The circuit at the top of Figure 8 shows a double relay equipment *LS4* being arranged to operate a warning light at a speed just below that where *LOS* operates to cut off the engine power and to apply the air brakes.

Figure 9 shows a single stage locomotive overspeed relay equipment.

Figure 10 shows the axle generator developed to operate tuned frequency equipments. This is a permanent magnet 14-pole rotor with a 3-phase Y-connected stator, rated 50 volt-amperes for speeds from 15 to 120 miles per hour, with wheels from 36 to 42 inches in diameter. The unit is self-contained with its own shaft and bearings and mounts on the locomotive journal-box cover. The drive is by a double spline shaft, removable from the outside through the generator hollow shaft which enables the unit to be tested without moving the locomotive.

The application of tuned frequency equipments is not limited to that of motor transitions and locomotive overspeed. Similar equipments can be applied to modulate the locomotive and train air brakes for constant rate deceleration. The generator has sufficient capacity to operate a variety of these equipments, plus a speedmeter of the frequency responsive type.

Water Temperature Control

The new engines require a precise control of cooling water temperature. One

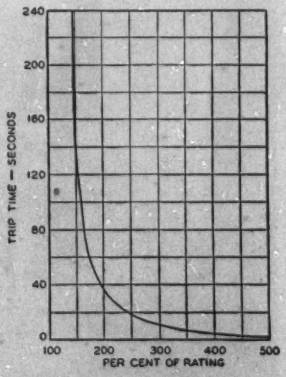

Figure 17. Typical circuit-breaker inverse time trip characteristic

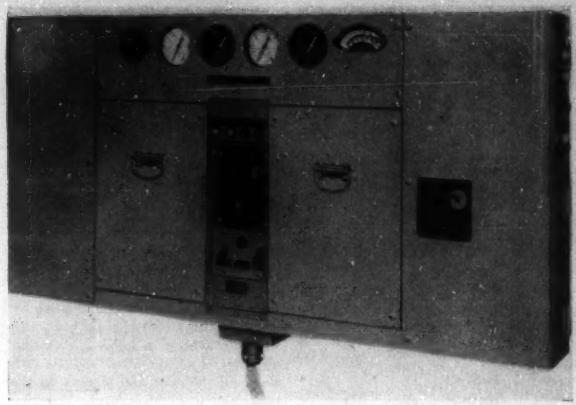

Figure 18. Engine control panel

type of locomotive utilizes a radiator fan mechanically driven from the engine through an eddy current clutch. Modulation of the clutch excitation varies the degree of slip and affords a simple method of controlling water temperature.

Figure 11 shows a relay developed for this purpose. A vapor filled bulb and bellows system operates a set of contacts to advance or retard a motor driven rheostat for changing the clutch excitation. A suitable bias arrangement minimizes overtravel and undertravel, and means are provided for manual operation of the rheostat in the event of motor failure.

Traction Motor Reverser

A new butt-type silver-contact air-operated reverser was developed to obtain a small unit for handling four motors. It occupies the same space as formerly was required by the 2-motor drum-type reverser (See Figure 12).

Each layer is, in effect, a double-pole double-throw switch with a common contact and occupies a $3^1/_2$-inch vertical space. The contact pressure of 40 pounds is sufficient for the 1,000-ampere rating. An ingenious arrangement of the operating mechanism holds the unit in either of its two closed positions should the air pressure fail.

Control Relay

A new medium energy control relay was developed to match the rating of the amplidyne control circuits as shown in Figure 13.

This standard relay has four double-throw contacts, each with 10 amperes continuous rating and 0.5 ampere inductive interrupting capacity at 75 volts direct current. Space is provided in the base for one or more capacitors which, when connected across a contact, increases inductive interrupting capacity to 5.0 amperes at 75 volts direct current.

The operating coil rating is 7.5 watts. A variety of special forms were developed from the standard form including one with a latch to hold the armature in the energized position, another with less contacts for low energy operation.

Because of the type of contact used, these relays usually are mounted in a dust-tight enclosure.

Relay Box

Typical of the new practice of grouping related devices in a unit assembly is the relay box shown in Figure 14. This enclosure, with a glass inspection panel in the cover, houses all traction control re-

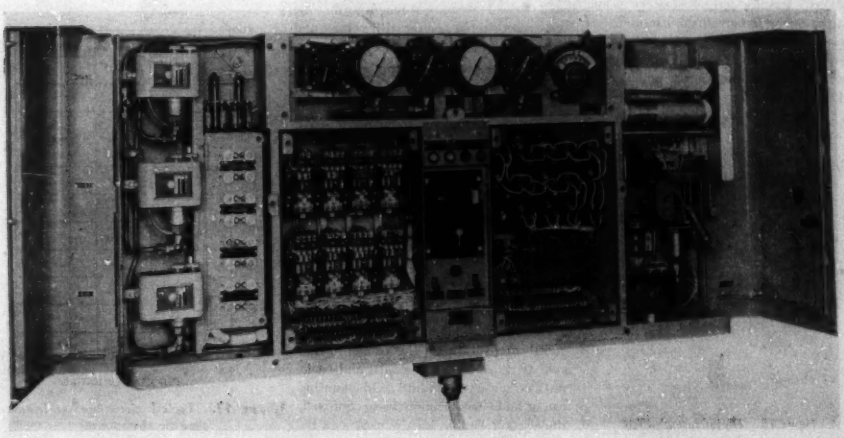

Figure 19. Engine control panel with doors opened

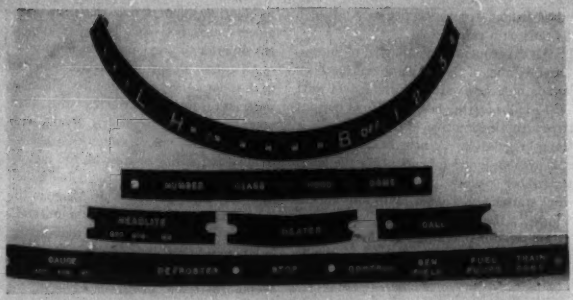

Figure 20. Laminated plastic indicators

lays with associated resistors, capacitors, and rectifiers.

All circuits enter the box through quick removable connectors. Replacement of the complete box involves only disconnecting the connectors and the removal of the four mounting bolts.

This arrangement facilitates a quick changeout of the complete box in the event of trouble and a more leisurely correction of the fault at a central servicing point.

Motor Cutout Switch

An interesting adoption of the wartime-developed small switch unit for low energy control circuits (see Figure 15) incorporates eight single-pole double-throw units in a cam operated device for cutting out the individual traction motors.

A multipoint connector connects all circuits to the unit and facilitates a quick disconnect in case of trouble.

Previous locomotives have used relatively large open-front knife-blade switches for this purpose, requiring an excessive amount of panel space.

Circuit Breakers

Until the present time, circuit protection on Diesel locomotives has been by fuses. Although these fuses have served their purpose well, there have been many cases of road delays and failures because of blown fuses which the crew could not locate or for which there was no replacement on board.

The arrival of the wartime-developed low-voltage circuit breaker has made it possible to eliminate completely all fuses on the new locomotives (see Figure 16).

These breakers are indicating, tripfree, and have sufficient shock resistance for locomotive service. They are available in ratings from 15 to 200 amperes, 75 volts direct current. The inverse trip time current characteristic of a typical unit is shown in Figure 17. Tests have shown an ability to interrupt the maximum short circuit to be expected on the locomotive battery circuits.

Most types use a thermal trip, and because of the effect of ambient temperatures care must be taken not to locate the units too close to any local heat; for example, the steam heat generator.

Engine Control Panel

A further example of co-ordinated grouping of related devices in a unit assembly is the engine control panel shown in Figures 18 and 19.

Included are gauges and switches formerly mounted in an unsightly manner on the side walls of the engine room. The new panel mounts all gauges, switches, and indicating devices needed for checking the engine operation, together with electric controls for the power plant regulator. The rotary switch on the front center is used for starting and stopping the engine. Intermediate positions are provided whereby the engine can be operated at partial speed and load, as when wearing in a new part.

A multipoint connector is used for all electric circuits into the panel and facilitates panel changeout in event of trouble.

Lighting

A number of lighting developments have been applied to the new locomotives.

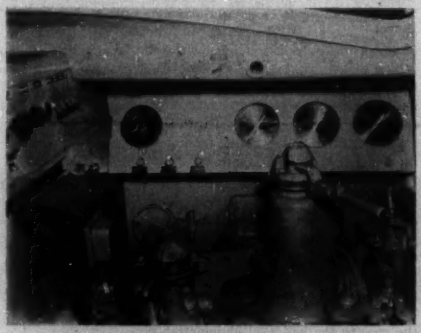

Figure 21. Operator's view of control stand and of instruments on the dashboard

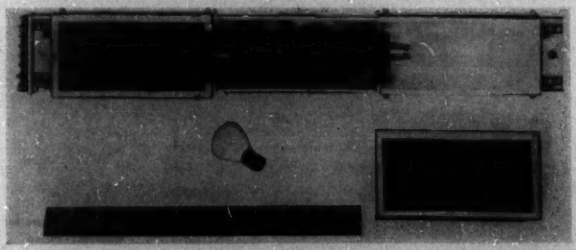

Figure 22 (below). Fixture for ultraviolet lamps

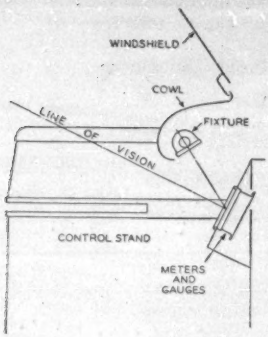

Figure 23. Section through cowl showing installation of fixture for ultraviolet lamps

Laminated plastics are used for control and position indicators (see Figure 20). This material has a black face on a white translucent back. Letters are engraved through the black layer and show as white in the daytime. They may be rear illuminated at night, as at the operator's position (see Figure 21).

Ultraviolet lighting (black lighting) has been applied to the electric instruments and air gauges on the dashboard in front of the operator. The wartime-developed *RP-12* fluorescent bulb was found satisfactory for the 75-volt d-c circuits when used with proper resistor control. A fixture (Figure 22) was arranged with suitable reflectors and filter glasses for mounting under the cowl (see Figure 23).

Instrument and gauge scales were finished in black with letters and figures engraved into the surface. Fluorescent paints in various colors were applied to the engraved markings and to the pointers. The ultraviolet illumination at night is not only pleasing to the operators, but is a real aid to the dark adaptation of the eyes to the low level illumination of the distant track, particularly at high speeds on a rainy night.

An experimental installation of fluorescent lighting of the engine rooms has been made on a few units. Standard 14-watt *T-12* bulbs are operated on direct current from the locomotive battery through a lamp regulator. A new fixture (Figure 24) was designed for mounting the lamp in rubber sockets. Mounts for the thermal starter and ballast lamp also are included. If no unusual troubles develop from the d-c operation, further applications may be made as the improved illumination and lower energy consumption are attractive features.

Apparatus Installation

Complete co-operation between the locomotive builders and the control engineers made possible a layout of apparatus superior to previous arrangements.

All traction control items are mounted in the contactor compartment. The compartment frame forms the rear wall of the operating cab. The design details were worked out in such a fashion that the assembly and wiring is done on the factory floor (see Figures 25 and 26). The finished assembly then is lowered into place in the cab, cables and wiring are connected. This method has produced a real saving in labor and time over previous methods.

The entire locomotive cable and wiring arrangement was designed according to the plans shown in Figure 27. Emphasis was placed on apparatus location that would give the shortest possible runs, consistant with location of devices entirely in three control centers. These are the control stand, the contactor compartment, and the engine control panel. The actual conduit locations follow closely the details shown on the plan.

New developments in solderless terminals were applied to all sizes of wire and cable (see Figure 28). These include swedge-on terminals for 750,000-circular-mil wire and indented terminals on number 16 wire. The labor saving inherent in this development is large and a better

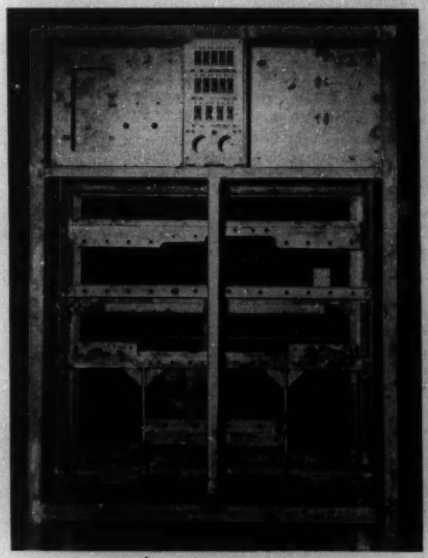

Figure 25. Contactor compartment frame

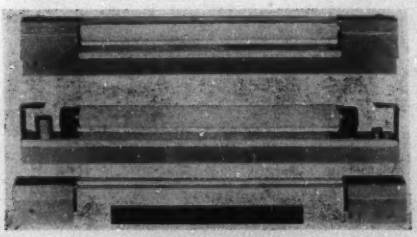

Figure 24. Fixture for fluorescent lamp

quality job results. This is especially true of the large cables because the terminal application must be made after the piece has been pulled through its conduit. Often the cable ends are hard to reach and present real gymnastic problems to the workman with a solder pot. The portable press die presents no such problem.

Conclusions

The arrival of new and larger Diesel power units for locomotive service has required that new standards be created in precision of control of engine speed, engine loading, and in such associated matters as control of temperature of engine cooling water. Generator and motor improvements likewise have required more precise handling of the rotating electric equipment.

To meet these new requirements there have been many new developments. These consist of new excitation circuits, a new power plant regulator, an improved dynamic braking control, an automatic transition control, a new water temperature control, together with new apparatus and applications in the locomotive itself.

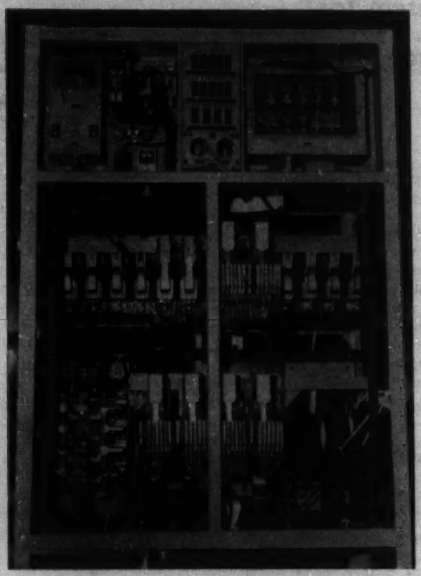

Figure 26. Contactor compartment with apparatus installed and wired

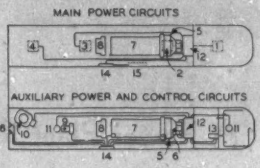

Figure 27. Wiring plan

1, 2, 3, 4—Traction motors
5—Main generator
6—Exciter, auxiliary generators
7—Engine
8—Air compressor
9—Clutch and gear box for radiator fan
10—Steam generator
11—Traction motor blowers
12—Contactor compartment
13—Control stand
14—Engine control panel
15—Battery
16—Train line receptacles

Figure 28 (below). Solderless terminals

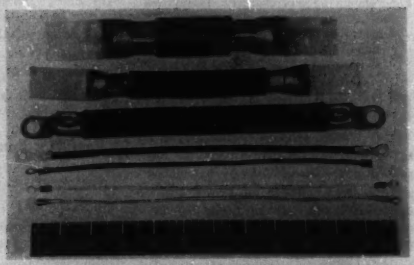

No Discussion

A Power Plant Regulating System for Diesel-Electric Locomotives

C. B. LEWIS
MEMBER AIEE

Synopsis: This paper describes a new power plant regulating system which incorporates speed and load control, recognizes the ability of the engine, permits maximum utilization of the engine's power, and protects the engine from harmful overloads. The ability of the regulator to schedule permissible engine fuel as a function of engine speed allows it to be used with the latest type engines employing supercharger. The system permits remote and multiple-unit operation and provides a high degree of plant protection against damage because of failures.

IN the adaptation of Diesel-electric power plants to locomotives, the problem of remote semiautomatic control is primordial. With few exceptions the present-day Diesel-electric locomotive consists of a number of power plants operating in multiple and under the control of a single operator who must be sufficiently free from mechanical chores to be able to devote maximum attention to the rail ahead and the speed of his train.

The control of locomotive speed is accomplished best by the control of locomotive power and this done by manual movement of a master controller handle which will modulate simultaneously the power of all units.

The individual power plants necessarily must be under the jurisdiction of some sort of regulator which will enable the unit to maintain a power level in correspondence with the setting of the master controller. The configuration of this regulating system is the chief concern of this paper.

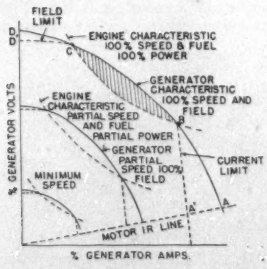

Figure 1. Power plant volt-ampere characteristics

Summary of Regulator Functions

The regulator controls power plant output by

1. Controlling engine speed.
2. Controlling load by matching generator demand with engine ability.
3. Controlling engine torque as a function of engine speed (fuel limit).

The regulator also allows multiple unit operation and remote control. Finally, it protects the power plant by

1. Providing automatic shutdown against

(a). Overspeed.
(b). Low lubricating oil.
(c). Control failures.

2. Reducing power during unusual conditions as

(a). Overtemperature.
(b). During motor cutout.

Description of Regulator Functions

Speed Control

In the design of a regulator, the characteristics of the engine and electric transmission must be considered objectively. The characteristic of a Diesel engine at a constant speed is one of constant power or, in terms of the generator input, constant volt-amperes. The volt-ampere characteristics of a shunt generator with constant speed is shown in Figure 1 along with the engine characteristic. The power delivered by the power plant is controlled readily by controlling engine speed.

Load Control

In order to provide for full utilization of engine power over as wide a range of locomotive speed as possible, the generator characteristic must be altered to coincide with the engine characteristic over as wide a range in generator voltage as is possible. This can be accomplished between points B and C by a reduction in the generator field using engine speed as a reference. It should be pointed out that, if the generator characteristic is above that of the engine, the engine would be forced to run in a bogged condition or at a speed lower than that called for, which is harmful to the engine and results in decreased power. However, if the generator characteristic is lower than the engine characteristic, the full power ability of the engine would not be utilized. It is possible by means of the proper connection of the traction motors and their associated control to remain on the constant horsepower portion of the engine-generator curve (between B and C Figure 1) over an appreciable range in locomotive speed. The speed range which can be covered depends upon the gearing, the design of the electric machines, and the proper motor switching, and is beyond the scope of this paper.

Further consideration of the power plant characteristics, reveal that the output of a Diesel is not always the same at a given speed but is dependent on engine

Paper 47-39, recommended by the AIEE committee on land transportation for presentation at the AIEE winter meeting, New York, N. Y., January 27-31, 1947. Manuscript submitted November 12, 1946; made available for printing December 6, 1946.

C. B. Lewis is with the transportation control engineering division of General Electric Company, Erie, Pa.

Figure 2. Tachometer-generator and over speed switch (typical engine mounting)

wear, ambient temperature, and calorific yield of the fuel. The generator characteristic is also variable and is influenced by the temperature of the copper in both generator and exciter. This is further evidence that the regulator should perform the function of load control which will match the generator and engine characteristics at all times while operating in the region of constant power.

Engine wear is a primary factor and it is desirable to run the engine at the lowest possible engine speed commensurate with the power requirements set by the master controller.

Fuel Limit

This brings into consideration another item which is particularly important with the use of the larger more powerful supercharged or mechanically aspirated engines of the type now being used in locomotives and that is the reduction in fuel necessary with reduced engine speeds. The air density of the cylinder charge and the amount of excess air for cooling valves and pistons decreases with speed as well as the amount of cooling water and oil. Therefore the permissible maximum fuel charge must be decreased in order to maintain safe mean-cycle temperatures. This makes it very desirable to schedule the engine fuel (torque) as a function of engine speed. The same considerations apply to a "bogged" or overloaded engine. Because the engine is running at a speed below that called for, the engine temperatures are certain to increase. A "bogged" engine not only means lowered performance but is one of the principal causes of engine failure. It is important, therefore, that the regulator does not allow the engine speed to fall off.

Multiple-Unit Operation and Remote Control

In multiple-unit operation each power plant must be operated up to the limit of its individual abilities and the division of load should be made on that basis. Inasmuch as all of the plants are operated remotely, the same operating signal from the master controller must be provided to all engines.

Automatic Shutdown

A very necessary consideration in a remotely controlled plant is automatic protection of important apparatus. Protection against overspeeding of the power plant, loss of lubrication, and loss of engine control should be provided as simply and reliably as possible and should shut down the power plant. As the electric drive is freewheeling, this can be done only at the expense of the complete loss of tractive power and the addition of the rolling resistance of the dead unit.

Reduction of Power Because of Unusual Conditions

Other conditions which may not warrant the complete shutdown of a unit but for which protection must be provided are high engine temperature and the loss of a traction motor. The modern Diesel-electric locomotive is equipped with automatic temperature control of a very reliable nature; however, should the engine temperature rise above the safe operating range, a reduction in the permissible torque (fuel) of the engine should be made without affecting the engine speed. By so doing, the heat rejection of the engine may be reduced sufficiently to return the temperature to a safe value and the unit left in operation. A cab warning also should be provided and if the high temperature persists the operator can shut down the unit before serious damage may be caused.

During operation with a traction motor

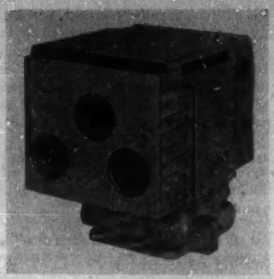

Figure 3. Power plant regulator (back view)

cutout, the remaining motors and the generator should be protected from overcurrents by reducing the engine torque (fuel) without affecting the speed. The reduction in power resulting should be sufficiently large so that the remaining motors operate at normal power.

Description of the Regulating System

The regulating system consists of the following devices:

Engine Driven Tachometer-Generator and Centrifugal Overspeed Switch

The tachometer-generator (see Figure 2) provides the speed signal to the regulator by producing a voltage proportional to speed. A 3-phase a-c machine with a permanent magnet rotor has been chosen because the output characteristics can be maintained uniformly among machines. Because the machine is engine mounted, the absence of brushes is an advantage. A visual indication of engine speed readily is provided at the engine panel by using a frequency-sensitive drag-type indicator driven by the tachometer-generator.

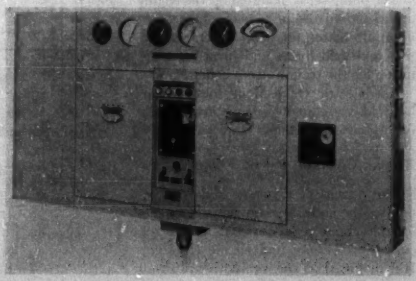

Figure 4. Engine control panel

The centrifugally operated switch is used to interrupt the holding coil on the regulator clutch and remove the engine fuel whenever the engine overspeeds. In case of an overspeed trip, the switch must be reset manually before the engine can be restarted.

Army-Navy connectors are used to facilitate the electrical connection and minimized "wiring errors" by maintenance personnel.

An Engine Mounted Regulator or Governor

This device (see Figure 3) incorporates

1. A speed responsive servo unit which controls engine fuel and generator excitation.

2. A positioning mechanism which serves as a fuel limit.

3. A magnetically latched spring restored clutch which overrides the speed servo unit and will remove the engine fuel whenever the holding coil current is interrupted.

4. A hydraulic pressure regulator which maintains the pressure on the hydraulic source for the speed servo unit and fuel limit. As this device is separate from the tachometer-generator, it can be located on the engine wherever it is most convenient to the fuel control system.

The use of an amplidyne exciter makes possible the control of generator excitation and load control by a small commutator type rheostat driven directly by the speed servo unit. This arrangement provides a very fast acting load control using little power and occupying a relatively small space.

The hydraulic supply to the regulator is provided readily by a d-c driven auxiliary motor pump set which has two pumps, one for use as a fuel transfer pump to supply fuel to the engine injection pumps and the other for pumping a good grade of light lubricating oil from a small reservoir to the regulator. This insures an ample supply of oil to provide proper regulation during transients regardless of engine speed.

The pump set is mounted off the engine and if desired also may incorporate a 400-cycle alternator for main generator current and field limits and furnish the ignition for the train heating boiler.

The electric connections to the regulator also are made in an Army-Navy connector for maximum convenience.

Engine Control Panel

This panel (see Figures 4 and 5) incorporates the necessary control components for the engine regulator, remote control, engine protection, and engine cranking. It is mounted on the locomotive cab wall as near to the regulator as possible to minimize the lengths of the connections, particularly those for pressure and temperature, so the operator may observe the action of the regulator during engine starting.

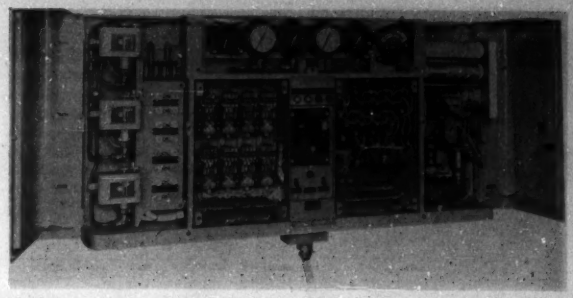

Figure 5. Engine control panel (covers removed and showing apparatus)

A plug connector is used for the connection of electric circuits. In detail the panel contains the following:

1. The engine control switch used for starting the engine, for controlling engine speed for testing purposes, and for switching the control to the master controller for actual locomotive operation.

2. The combined speed and fuel limit setting resistors and commutating relays. Four relays are used to commutate resistance in the regulator circuits to set the speed and the fuel limit in a manner to give eight steps of engine power. While it is possible to provide the regulator with the proper signal for either a step or a modulated control in a variety of ways, the relay scheme is the one that was first used on Diesel-electric locomotives and must be adhered to as standard if the newer locomotives are to be trained with the older ones without duplication in systems.

3. Tachometer-generator rectifier and safety relay. The a-c output of the tachometer-generator is rectified to provide a d-c signal to the solenoid operated pilot valve in the regulator. The safety relay de-energizes the clutch holding coil in case of circuit failure to shut down the engine.

4. Stabilizing capacitors for the speed control element of the regulator.

5. Indicating and signal devices for indica-

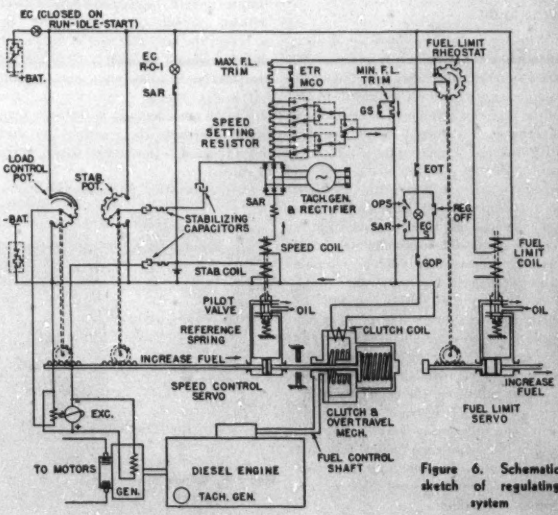

Figure 6. Schematic sketch of regulating system

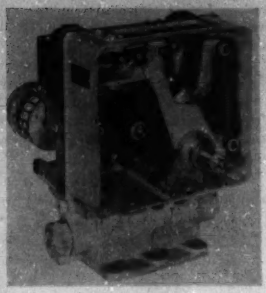

Figure 7. Power plant regulator (covers removed to show details of safety clutch)

tion of power plant condition in the form of

(a). Engine speed indicator.

(b). Lubricating oil pressure gauge and low lubricating oil pressure switch with warning light.

(c). Pressure gauge for fuel oil header pressure.

(d). Engine temperature gauge and temperature limit switch with warning light and the relay necessary for fuel limit reduction.

(e). A boiler flame outlight also is included in the panel because of convenience of location.

(f). A signal relay to sound a warning gong in case of failure and an engine stop relay which provides shutdown of all units at once from a push button located on the master control stand.

Description of Operation

The operation of the system can be explained best by referring to Figure 6 which is a schematic sketch of the system.

Speed Control

The tachometer-generator produces a d-c signal in the solenoid which operates the pilot valve of the speed servo unit. The solenoid force is compared with the force of a reference spring and during balance conditions the pilot valve is lapped and the power piston is stationary. Because the force level for equilibrium is a constant, the speed circuit current is constant and the engine speed is determined by the circuit resistance and is proportional to it.

Load Control

A speed change will cause a corrective movement of the power piston and depending on the generator demand will regulate either the engine fuel or the generator field. Regulation of engine fuel will take place until the motion of the fuel control shaft is arrested by the fuel limit stop, after which the power piston can continue to move through the overtravel spring and reduce generator excitation by means of the load control potentiometer. The potentiometer is provided with blank sections so the generator has full field until the fuel limit is reached. When the plant is operating on the constant power characteristic, the engine speed is maintained by regulating on the generator field; the speed control servo unit is working in the overtravel region and the generator demand is made equal to the engine ability.

Because the power piston of the servo unit has no restoring force, the governor is isochronous and has no speed droop with load.

Inasmuch as the regulator is isochronous some stabilizing means is necessary, and this is accomplished by an antihunt winding in the control solenoid to which stabilizing signals are fed

1. As a rate of change of engine torque by the capacitor tie from the stabilizing potentiometer.

2. As a rate of change of speed by the capacitor tie from the tachometer-generator.

A blocking rectifier is provided to make the rate of response in the turn-on direction slower than in the turn-off direction.

A load anticipation signal is provided by the capacitor tie from the positive side of the exciter which is particularly helpful during motor switching in minimizing transient regulation.

Fuel Limit

The fuel limit mechanism, for mechanical expediency, consists of a power cylinder and solenoid valve, which is a duplicate of the ones in the speed servo unit. This system functions as a positioning system for the fuel stop which schedules engine torque as a function of speed. Inserting resistance in the speed circuit to increase the called for speed effectively removes resistance from the fuel limit circuit and the resultant increase in solenoid current causes the power piston to drive the fuel limit rheostat and insert resistance to rebalance the system. Schematically the stop is shown on the power piston of the fuel limit servo unit. In the actual regulator, however, the fuel stop takes the form of a cam, which together with a matching rheostat gives the desired torque schedule for the particular engine.

Multiple-Unit Operation and Remote Control

For multiple-unit operation, four train wires for the speed setting relays are required to each unit and the engine control switch *EC* must be switched to the run position.

If a new engine port must be run in at reduced speed and power, leaving the *EC* on position 6, this will cause the engine to follow the master controller up to the sixth notch but will hold the unit at sixth notch speed and power when the master controller is in the seventh and eighth positions.

Engine Protection

Interruption of the clutch holding coil circuit will remove the fuel from the engine by releasing an overriding spring and shut down the plant.

Figure 7 shows a view of the regulator with covers removed, showing the clutch, overtravel spring, and regulator interlock.

Power plant shutdown protection specifically provided for is

1. Engine overspeed (*EOT* contacts).
2. Low lubricating oil (*OPS* contacts).
3. Control failures.

(a). Loss of speed circuit (*SAR* contacts).
(b). Loss of regulator oil (*GOP* contacts).

Unusual Operating Conditions

During high temperature operation, the engine temperature relay *ETO* (actuated by a temperature bulb) commutates resistance in the maximum fuel limit trimmer circuit and reduces the fuel to a value corresponding to 75 per cent torque.

During motor cutout, the motor cutout switch *MCO* commutates resistance in the maximum fuel limit trimmer circuit and reduces the power to 75 per cent (for a 4-motor system).

The engine must be started by the operator from the engine control panel. After energizing the control circuit and starting the fuel transfer regulator oil pump set, the engine switch is turned to

Figure 8. General view of typical installation of regulator and tachometer-generator on engine

the idle position. This energizes the stabilizing coil and causes the power piston to close the clutch and the regulator "off" interlock and energize the clutch coil circuit. By pulling the *EC* switch handle away from the panel, the generator starting contactor energizes the auxiliary starting field and motors the generator. At the same time the stabilizing forcing circuit is removed and the power piston goes to the full "on" position. While the handle is in this position, the oil pressure switch *OPS* and the safety relay contact in the clutch circuit is by-passed by an *EC* switch contact and as the fuel turns on the regulator "off" interlock is opened (its sole purpose being to provide overlap in switching the coil circuit). After the engine fires and runs at idle speed, the oil pressure switch and the safety relay close, which permit the *EC* handle to be released, thereby disconnecting the generator from the battery and the engine left running at idle.

During cranking the engine starting contactor interlock *GS* short-circuits the minimum fuel limit trimmer so the engine can be started more quickly than would be possible on the normal fuel allowed for low speed operation.

To operate the power plant from the master controller, the *EC* switch is turned to "run" and the plant is ready for locomotive operation.

When it is desirable to test the engine, the speed can be controlled from the panel with five steps including idle and full speed being available.

Applications of the regulating system have been made to a number of power plants, both military and commercial, gas-electric and Diesel-electric, and operating experience indicates high reliability and improved performance.

Figure 8 shows application of the regulator and tachometer to a large new type Diesel engine for locomotive use.

The flexibility of arrangement possible because the regulator is separate from the speed measuring means will facilitate future application to a wide variety of power plants.

Discussion

T. H. Murphy (American Locomotive Company, Schenectady, N. Y.): The power plant regulating system outlined by Lewis' paper has been used in a considerable number of American Locomotive-General Electric Diesel locomotives. The equipment has been used on two sizes of engines, the larger being rated at 2,000 horsepower. The regulating and control system and rotating equipment had to be made as light and effective as possible, because the large engine was used in a single cab locomotive unit of 2,000-horsepower capacity with two 3-axle swivel trucks.

The regulating equipment outlined by the paper permitted minimum size generator as all special regulating fields were omitted from this unit. Also, the equipment does not include an inherently regulated exciter, but only the amplidyne exciter which is controlled through the regulator. Therefore, the rotating equipment is of minimum weight, assisting materially in the design of the complete locomotive to maintain a low weight per axle.

Previous control and governing systems have been completely separated with one set of equipment to provide proper generator regulation or loading and the other set to provide correct governing of the engine. The system in question combines both so that the governing of the engine and regulation of the generator is performed by what might be called the governing unit for the whole power plant. The governor functions without speed droop. Combined with the generator regulation to prevent engine overloading, are such added features as a current limiting device, a voltage limiting device, and an engine fuel limit, together with the so-called throttle and engine alarm systems integrated with the regulator.

The system is very quick acting and the control of power very uniform. This is difficult to explain by use of any circuits, diagrams or description other than to state that the system works to maintain a uniform tractive effort on the locomotive during acceleration once the operator has selected the desired operating point. The constant tractive effort related as it is to wheel slippage and other factors, tends to give very uniform performance of the locomotive and enables the operator, with a minimum of skill, to get the maximum at starting. This condition has been very noticeable on actual locomotives in service with maximum tonnage trains started without any difficulty on severe grades.

Extreme care has been used in applying the regulator to the engine to avoid installing it where it would be subjected to the greatest heat or to either lubricating or fuel oil. The locations of both the tachometer-generator and governor are shown clearly by the photographs. The structure of the units has been made so that the insulation is particularly impervious to the action of heat and oil such as might be obtained on an engine application. The current limit feature has given added safety against false operation such as with locked brakes and, of course, it is set above the wheel slippage point of the locomotive. This feature is inherently related to the constant tractive effort or constant accelerating current feature which gives the uniform accelerating characteristics to the locomotive.

The earliest schemes of regulating devices were with straight generator field control, and later developments include control systems of the differential regulation type. These two schemes had independent engine governors. Following the generator field and differential control schemes, came the so-called speed controls. This power plant regulating system is based inherently on speed regulation which seems established through the locomotive industry as the best established means for this purpose.

T. R. Rhea (General Electric Company, Schenectady, N. Y.): I am not familiar with locomotive power plants, but these regulators or electro-hydraulic governors have been applied to Diesel-electric oil-well-drilling rigs.[1] Perhaps a discussion of the operation of this Diesel-electric drilling rig with its governing system will assist in emphasizing some of the points made in Lewis' paper.

This drilling rig consists of three 700-horsepower Diesel engines, each driving a 400-kw d-c generator and each provided with the electro-hydraulic governor described by Lewis. These engines are run over a speed range of 450–900 rpm, depending upon the desired output. For hoisting, all three generators are paralleled and supply a 1,000-horsepower motor; while for drilling, they are separated and supply individual mud pumps and rotary table motors.

Since the driller does not have time in his normal operations to attend to the paralleling of the engines, the governor attends to this function automatically and insures that all of the engines carry the proper shares of the load.

The second great advantage is the load-limit feature of the governor that prevents the engines from being overloaded no matter how heavy a pull or lift the driller is trying to make on the engines. The third advantage of this governing system on the drilling rig is that it permits the engines to run at half speed a great part of the time.

The governor or regulator on the drilling rig described does not have such features as engine overspeed and engine temperature since these are taken care of by other devices and are not considered necessary.

The governors have been in successful operation on the drilling rig now for a number of months and it is expected that they will show considerable advantage in engine maintenance and fuel savings over previously used unregulated systems.

Reference

1. Modern Diesel Electric Drilling Rig, T. R. Rhea. AIEE Transactions, volume 65, July section, pages 447–53.

Modern Car Equipment for New York City's Subway System

B. F. CORDTS
NONMEMBER AIEE

TO meet the increasing need for additional car equipment, the Board of Transportation has placed orders for 400 subway cars to be operated on the BMT and IND divisions, and for 100 subway cars to be operated on the IRT division of the New York City Transit System.

These cars when put into operation should provide the traveling public with

1. Better lighting.
2. Better riding qualities.
3. Smoother acceleration and deceleration.
4. Reduction in noise.
5. Other items for passenger comfort.

Each of the five items will be discussed in detail after a few remarks about the cars in general.

The arrangement of the floor plan of the new cars remains essentially the same, that is, the 60-foot car for the BMT and IND divisions will have a floor plan similar to the present IND cars. This floor plan was selected by a committee of experts after an exhaustive study back in 1927. The investigation involved passenger movements through various sized openings, door spacing at the platforms, and the arrangement of seats in the car.

Comparative estimates were made for line capacity and operating efficiency for most of the 75 or more different arrangements considered. Their sound judgment in the selection made has been justified amply by actual performance in service over the past 14 years. The dimensions and arrangement of the new IRT car also follow the latest type built in 1939. These cannot be changed in width, height, or length because of limitations of the present subway structure.

Wherever possible the body structure and equipment of both types of cars have been made standard to take advantage of the full benefits of such standardization. An artist's sketch of the exterior of this car is shown in Figure 1.

Lighting

The need for better car lighting has been recognized by car designers and, as more efficient lamps were developed, higher light intensities became possible without increasing the number of lamps. The improvement from the 5 circuits of 36-watt 5-in-series lighting to the 22-in-series 1.6-ampere lamps was a long step in the right direction. Based on their respective nominal ratings, the lumen output was increased from 9,125 to 15,455. This represented an increase of 69 per cent for approximately the same wattage.

With the introduction of fluorescent lamps, a new source of light, ideally adaptable to car lighting, presented itself. Tubes of fluorescent light placed end to end for the length of the car provided a distribution of light impossible to obtain by any other means.

The problem then became one of selecting the type best suited to the specific requirements of subway service. The two types of fluorescent lamps are classified as hot cathode and cold cathode, each having several desirable and undesirable characteristics. Without going into the details of the investigation and tests conducted to determine which type would be better, the cold cathode lamp was selected for the following reasons:

1. Long life.
2. Life independent of frequency of starting.
3. Instant starting.

These characteristics are most important in subway operation, particularly items 2 and 3, as the number of third rail gaps caused by section breaks and crossovers is very high. For example, on the IND division between 207th Street, Manhattan, and Rockaway Avenue, Brooklyn, 27 interruptions were recorded. This is a run of 19 miles. Based on 60,000 miles per year and the same rate of interruptions, the lamp would be started 85,000 times. This is far above the number of starts any of the present hot cathode lamps could withstand.

The new car will have 24 72-inch cold cathode lamps operating on 600 volts direct current. These lamps have a lumen output of 1,600 when operating at 110 milliamperes and with their ballasts

Figure 1. An artist's idea of the general perspective of the new car

Paper 47-43, recommended by the AIEE committee on land transportation for presentation at the AIEE winter meeting, New York, N. Y., January 27-31, 1947. Manuscript submitted November 13, 1946; made available for printing December 13, 1946.

B. F. CORDTS is with the New York City Transit System, New York, N. Y.

have an over-all wattage of 66. Compared to the old IND car using 22 1.6-ampere lamps in series, an increase of 148 per cent in lumen output is obtained for an increase of 65 per cent in power consumption.

Resistances were used in the circuit in place of two small ballast lamps as we felt that the variation in light output, shown on curves in Figure 2, caused by voltage variation was not sufficient to warrant the added maintenance that would be entailed by the use of the small ballast lamps and sockets. Voltage fluctuations are of relatively short duration, although the swing may be large, ranging from 400 to as high as 750 volts.

The circuit for the cold cathode lamp on 600 volts is shown in Figure 3.

Riding Qualities

The subject of riding qualities always has been a problem to the designer. For many years good or bad riding qualities were a matter of personal opinion, and there was no instrumentation available for measuring these factors. This was the first difficulty Professor C. F. Hirshfeld encountered when he undertook the work for the Presidents' Conference Committee which led to the now well-known PCC trolley car. By placing various types of people, young, old, thin, fat, and so forth, on a vibrating table controlled insofar as amplitude, frequency, and direction of movement are concerned, he was able to establish what he termed an "average comfort zone." This zone was determined by curves of amplitudes and frequencies in vertical, horizontal, and longitudinal directions. Instruments were developed to measure and record the various factors.

Many tests were conducted on subway cars and the records analyzed to see what the effects of various changes made in the truck had upon the riding qualities of our own cars. From these tests certain factors were found to be desirable and were incorporated in the new design.

Without going into the details of each item, the following changes from present construction were made:

	New Cars	Old Cars
Truck frame	Cast steel	Built-up
Bar	Equilizer	Arch
Springs	Coil	Elliptic
Center plate	Conical	Flat
Shock absorbers	Vertical and lateral	None
Bearings	Roller	Plain
Insulation	Rubber*	Rubber

* Increased over old cars.

Add them all together and they "spell" better riding.

Acceleration and Deceleration

Considerable thought and study were given to the question of acceleration and deceleration—first to determine the desirable rates and then to methods of obtaining and controlling them. Rates of 2.5 miles per hour per second acceleration and 3 miles per hour per second deceleration were selected.

The extreme rate used for the PCC car, principally on account of the desirability of maintaining its position in street traffic, was not deemed necessary for subway operation for the following reasons:

1. *Increased Power Required.* Power peaks would be increased materially if higher acceleration rates were used. This high demand on power generating stations during morning and evening rush hours would affect their operation, and in the case of purchased power would raise the total rate. The power rate is computed monthly from two factors—the maximum kilowatt demand for one hour and the total energy furnished in kilowatt-hours. Roughly, the proportion of each factor is 50 per cent of the total.

2. *Complete Change of Type of Control.* Rheostatic control with a large number of steps would be necessary for the higher rates of acceleration to provide the small current increments required to keep it smooth, and also to avoid the difficulties encountered in transition from series to parallel at the high rates. A saving of approximately four to five per cent in power can be made by using series-parallel control. In addition, a switching notch for short movements of cars, such as are necessary for coupling cars, is provided, and a slow speed running notch at the full series position is also available. Facilities in the shops for maintaining unit switch type control and the familiarity of maintainers with this type of control also were considered in making our decision.

3. *Comfort of Passengers.* The comfort of passengers, of course, is of prime importance in the sale of transportation. With large numbers of standing passengers, and with others on longitudinal seats and on seats facing in the opposite direction of travel, we felt that accelerating rates in excess of 2.5 miles per hour per second were too high.

4. *Relatively Small Increase Obtained.* Analysis of typical speed time curves indicated that in changing the acceleration rate from 2 miles per hour per second to 2.5, the average increase in schedule speed is 1.3 per cent. From 2.5 to 3, the increase is less than 1 per cent. Applying this figure to average schedule speeds of say 20 miles per hour for local service, the result is 20.2 miles per hour, or a saving of 36 seconds in one hour of running. This certainly is not worth the added cost and possible discomfort to passengers. From three miles per hour per second up, the law of diminishing returns goes to work with increasingly poor results, insofar as scheduled speeds are concerned.

Deceleration received the same consideration and a dynamic rate of three miles per hour per second for seated load conditions was selected for the following reasons:

1. *Increased Size of Motors Required.* Since the required capacity of the motors is determined by the combined accelerating and dynamic braking duty, higher braking rates would necessitate larger motors, involving additional costs and weights.

2. *Change of Control.* Dynamic braking was not carried to zero resistance on the new

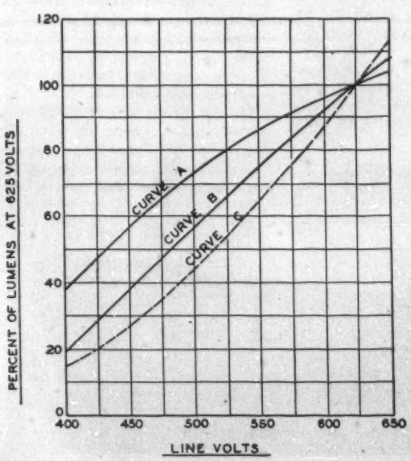

Figure 2. Comparison of light output with variation of line voltage using different types of ballast

A—Incandescent lamp ballast

B—Fixed resistor ballast

C—Typical incandescent lamp

equipment on account of the large number of steps required in the lower speed ranges. It starts to fade at about ten miles per hour at which time air is applied and used to the final stop. Combining the dynamic and air at this point permits time enough so that the blending is perfectly smooth. The amount of work left for the air brake is a very small percentage of the total. Assuming a stop were made from 40 miles per hour and that air did all the work below ten miles per hour, only a little over six per cent of the kinetic energy would be dissipated by the brake shoes.

3. *Comfort of Passengers.* The same comments apply here as in the case of acceleration. A maximum rate of three miles per hour per second is maintained on account of the signal control and, where full load conditions reduce the dynamic rate, sufficient air is used to supplement the dynamic braking so that the rate of the operator is calling for is maintained.

4. *Relatively Small Increase in Schedule Speeds.* Here also the law of diminishing returns applies. Because of the short interval involved in braking, any increase above the three miles per hour per second rate would be even less effective than a corresponding increase in acceleration.

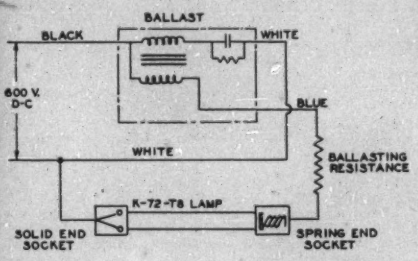

Figure 3. Circuit diagram of cold cathode lamp with fixed resistor ballast

Reduction of Noise

Certainly the desirability of noise reduction in subway operation is not controversial, though some of the previous items may be. It is a difficult job to do effectively on account of the enclosed structure which permits sound waves to reverberate with very little absorption, but every effort was made to obtain the best results possible. Without developing new features, the specific details of our efforts toward noise reduction in these cars are as follows:

1. *Use of Rubber.* Rubber is used at important points of contact such as between the equalizer and the journal box, the truck frame and the equalizer spring, the bolster and the bolster spring, and the bolster and bolster guides. This should insulate the car body from the high frequency vibrations effectively and materially reduce impact forces.

2. *Motors and Gears.* Motors are truck mounted, being hung on the transom and connected to a separate gear unit through a flexible coupling. This reduces the unsprung weight and prevents the transmission of road shocks from the wheels and axle to the motors.

High angle helical gears running in oil were selected for quietness and low tooth loading. They are single reduction for simplicity and low cost. Motors and gear units are equipped with antifriction bearings throughout, so that accurate clearances can be maintained. This is very important on account of the high rotor speeds and small air gaps.

3. *Lateral Shock Absorbers.* The older subway cars had a tendency to nose, causing lateral motion of the car body when certain factors reached a resonant stage. A long series of tests lasting over several years developed information which led to changes in basic truck design and to the adoption of a lateral shock absorber between the truck bolster and the side frame. On tests conducted with this application the striking of the bolster against the side frame was eliminated.

4. *Center Plates.* Conical center plates on bronze bearings and in an oil bath will reduce the slap between the body and the truck center plates. This construction also will reduce the force required to turn trucks on curves, resulting in lower flange pressures of the wheel against the rail, thereby reducing squealing and increasing the life of both the wheel flanges and rail heads.

5. *Dynamic Braking.* The use of dynamic braking will reduce the number of shoe applications to the wheels, and also the shoe pressures. As explained under deceleration, only about six per cent of the total work required to be done in stopping the train will be done by the brake shoes, thus eliminating most of the frictional noises between shoes and wheels.

6. *Brake Cylinders Mounted on Trucks.* Brake cylinders have been mounted on the trucks, thus avoiding the use of foundation brake rigging on the body.

The noise level of operation within the subway structure with present equipment averages 89 decibels. The elimination or reduction in magnitude of the foregoing factors will have a noticeable effect in lowering the noise level.

Other Features of the New Cars

In the first part of this paper the four major changes in the newest cars were discussed in detail. This section will cover a summary of the smaller items which will add to the comfort of passengers.

Four motors per car, one per axle, were selected so that accelerating and braking loads would be distributed evenly and kept within the normal adhesion factor of wheels and rail.

Thermostatic control of heat will provide more uniform temperatures and utilize the body heat of passengers during crowded periods. Tests indicate that heaters are "off" 75 per cent of the rush hour period. This will reduce power costs through the reduction of the "maximum demand" peak.

Eight 10-inch horizontal fans will provide a much better distribution of air than the five fans blowing vertically in the old cars. With fans blowing vertically about 30 per cent of the car area is in a high velocity downward air stream and the balance of the car has very little air movement. The horizontal fans will move air over every passenger location, seated or standing.

An effort was made to improve the cleanliness of both the car and the subway proper. The car interior is designed for easy cleaning. All surfaces were kept as smooth as possible, and corners were coved and rounded. Exhaust ventilation will improve cleanliness of the ceiling. Dynamic braking will reduce the amount of iron dust from brake shoes and wheels. Completely sealed gear cases will eliminate the grease drip which is so objectionable.

Plastic seat coverings, impervious to all common acids and alkalies, will be used in the upholstery of the cushions and backs. It is colorful, easily cleaned, and well able to take the daily wear and tear without becoming shabby.

Additional space for passengers was obtained by changes in car body construction. Narrower side posts and recessing interior finish under window sills provided wider aisles as well as longer seat cushions. Wider door openings will facilitate the interchange of passengers.

The color scheme for the interior has not been decided definitely, but it is anticipated that the scheme selected will be pleasing to the passengers.

Discussion

G. M. Woods (Westinghouse Electric Corporation, East Pittsburgh, Pa.): The use of four high-speed spring-borne motors, instead of two axle-hung motors, on the New York, N. Y., subway cars is of great interest to electrical engineers engaged in transportation work. The conditions of operation are extremely severe and the effects of any apparatus failure in this service are so far-reaching that the greatest care in the selection of equipment must be exercised.

The application of high-speed motors was initiated on light-weight surface cars some 20 years ago. Today, all modern street cars have high-speed spring-borne motors. The 25 multisection cars of the New York city transit system employ high-speed motors with gear unit drives. These cars represent the only commercial application of this type of equipment to rapid transit service. On the new cars for the BMT and IND divisions, the load per axle will be 25 per cent greater than on the multisection cars and the motors will have one-third more capacity.

The application of motors to all axles gives traction on all wheels. This makes dynamic breaking and the higher rates of acceleration discussed by Cordts practicable. The motors are desigued for 300 volts and are connected two in series for 600 volt operation. The 300-volt motor compared to the 600-volt motor is more stable, has better commutating characteristics, and its commutator and windings are mechanically stronger. Peak voltages in dynamic braking are much lower.

The motor has a 1-hour rating of 100 horsepower and 300 volts at 1,175 rpm. The motor alone weighs 1,770 pounds and the gear unit with suspension bolt and coupling weighs 1,010 pounds. The maximum safe speed with worn wheels is 55 miles per hour.

Single reduction gear units are used. The gear case is of cast steel and the gears and tapered roller bearings are oil lubricated. The gears have a 4-inch face, 5.25 diametral pitch and 21-degree helix angle.

The couplings are of the internal-external gear type. The internal teeth are in a pair of cylindrical sleeves bolted together through flanges at their inner ends. The external teeth are on a pair of pinions, one on the motor shaft and one on the pinion shaft of the gear unit. The external teeth are so shaped that the pinions can swivel freely with respect to the internal teeth throughout the required angle.

L. G. Riley (Westinghouse Electric Corporation, East Pittsburgh, Pa.): From the standpoint of the motor control equipment, the discussions in this paper covering the characteristics of acceleration and deceleration are very interesting.

Riding comfort is influenced by the rates of change of speed, and also by the total number of notches or steps in the controlling system. In going to a 2.5 miles per hour per second starting rate, as compared to the 1.75 rate used on the present IND system, the number of notches will be more than doubled. This is probably more than would be required for the increase in rate alone, but is justified to obtain increased riding comfort and to limit the power peaks.

Dynamic braking will be controlled by the same switching apparatus as is used for acceleration and with the equivalent number of notches.

In developing the detail characteristics for new cars, the board of transportation engineers have very properly taken into account the shop and operating problems involved in adding new equipment to the existing system.

One of these features is the use of practically identical arrangements for the operating cabs, including the location and functioning of the power and brake levers.

This makes it necessary to combine the control of the dynamic and air brake systems on a single brake lever in a manner to insure that each will automatically do its allotted share of the braking duty.

During the initial application and build-up, air will be locked out of the brake cylinders by dynamic load current, except for the small amount required to maintain the full rate on cars having more than the average seated passenger load.

The lock-out feature will be nullified when the speed drops below 10 miles per hour and brake cylinder air will be admitted to make up for the gradual loss of dynamic retardation and to complete the stop. Full use of the self-lapping air brake system will thus be made available for graduation and for spotting the train at the station markers.

Control of power application, with running positions for switching, series and parallel, will also be identical, so that there will be only minor changes in the training of operators.

Special 10-Car Train for the New York City Transit System

J. J. SINCLAIR
NONMEMBER AIEE

IN AN EFFORT to obtain for the subways of New York, N. Y., a most modern type of car, the Board of Transportation has designed a car for use in an experimental 10-car train, embodying many special features not heretofore used in one application in a transit vehicle. Figures 1*A* and 1*B* show artist's rendering of side elevation and interior, and Figure 2 shows plan, side, and end elevation of this proposed subway car.

It is proposed to make their performance and appearance as attractive as possible to the traveling public.

The motor control has been designed so as to give smooth acceleration of $2^1/_2$ miles per hour per second; higher rates would not seem desirable for rapid transit service where comparatively infrequent stops are concerned.

Dynamic braking has been provided, supplemented by air brakes. All axles are driving axles which permit an even distribution of tractive effort and the elimination of wheel slippage.

The motors are of 100-horsepower capacity, full spring supported and capable of producing a maximum dynamic rate of 3 miles per hour per second with a full seated load and interlocked to provide a maximum available dynamic brake with a minimum amount of air required.

The dynamic brake interlock with electropneumatic and pneumatic brakes provides sufficient air brake to produce a retardation rate of 3 miles per hour per second on a fully loaded car for maximum normal service rate.

An automatic emergency pneumatic and electropneumatic brake is available at any time through the emergency position of the brake valve handle, the deadman controller, conductor's valve, track trip or parting of the brake pipe or brake pipe hose.

There are many features included in the design of the car body and trucks which are of special interest where the complete performance of the car is involved, and these are as follows:

Body Construction

Body construction is of aluminum high-tensile low-alloy steel, or stainless steel, or combinations thereof, to obtain a light weight body of strength comparable with the present IND division subway cars.

General Dimensions

The general dimensions of these cars will remain the same as those on the IND division, which are governed by tunnel and subway construction clearances. The roofs will be of turtleback design and, as far as practical, have a streamline appear-

Figure 1*A* (above). Artist's rendering of side elevation of proposed new special car

Figure 1*B* (below). Artist's rendering of interior of proposed new special car

Paper 47-44, recommended by the AIEE committee on land transportation for presentation at the AIEE winter meeting, New York, N. Y., January 27–31, 1947. Manuscript submitted November 13, 1946; made available for printing December 13, 1946.

J. J. SINCLAIR is with the New York City Transit System.

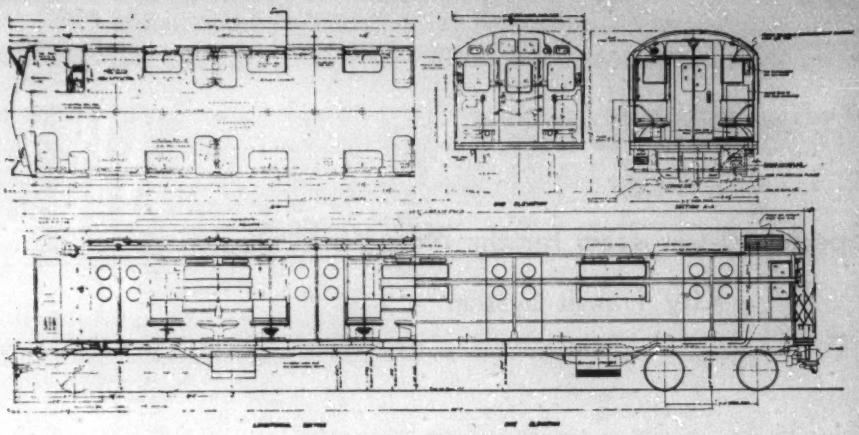

Figure 2. Plan, side, and end elevation of proposed new special car

ance. Anodized aluminum or stainless steel mouldings on the exterior of the cars add to the general exterior appearance.

The general floor plan remains practically the same as in present cars. Past experience leads us to believe the present arrangement of seating is the most practical for quick loading and unloading of cars in New York subway service.

Such a floor plan, in combination with the doorways which have been increased from 46 inches to 50 inches, provides for a uniform distribution of passengers.

Changes in seat frame construction were found desirable to provide for the installation of outlets required in combination with the ducts for forced ventilation.

Seat upholstering is of the most modern material and color selected to obtain a most pleasing effect in combination with the general scheme of interior decoration.

Three wide windows on each side of the car, each having an upper half as a drop sash and the lower half stationary, will give standing passengers, as well as seated passengers, a better view of stations along the route. Two circular windows in each door add to the general appearance of the car.

The flooring is of magnesite on truss plate construction. Parting strips and special treatment of color in combination with the interior color scheme of the car has been given considerable thought in order to obtain a most pleasing effect.

Forced Ventilation and Heating

Forced ventilation is one of the outstanding features of these cars. By the use of blowers concealed in the ceiling at each end of the car, air is taken from the car interior through a large grill, passed over four 36-inch 25-watt sterilizing lamps and then into a plenum chamber between the ceiling and the roof sheets, thence out into the car as recirculated air, distributed uniformly throughout the length of the car by means of specially designed distributors. The blower motors are of 300-volt type, connected two in series on the 600-volt d-c line. When operated at 1,750 rpm on full field, each will deliver 2,660 cubic feet per minute. Provision has been made, however, for tapping the fields of these motors by the use of a contactor under thermostatic control. This provision contemplates the requirement of more air delivery by the blowers on excessively hot days and crowded car conditions. It is believed that by setting the thermostats at 85 degrees Fahrenheit, the motor fields will be tapped and the air delivery of each blower will be increased from 2,660 cubic feet per minute to 3,320 cubic feet per minute, and the speed from 1,750 to 2,200 rpm with 600 direct volts on the line. The fields are tapped automatically by the thermostatic control, governed by temperature in the respective cars.

It will be noted that the capacity of this recirculated air system with blower motors in full field is calculated at 5,320 cubic feet per minute total per car, which is increased to 6,640 cubic feet per minute on tapped field. Since a certain amount of fresh air will enter the car at station stops and through windows when open, a large proportion of this recirculated air will be fresh air.

In addition to the air movement obtained by this recirculating system, fresh air is drawn into a plenum chamber near the roof at each end of the car by two 1,500-cubic-feet-per-minute blowers mounted on the car underframe. This fresh air intake which is controlled by a system of dampers and thermostats, is passed through precleaning tubes which take out dust particles down to 10 microns; then over Precipitron units where fine particles are ionized and deposited on plates of opposite polarity, and finally over sterilizing lamps before entering ducts for distribution to air distributors mounted underneath the longitudinal seats of the car.

There are a total of 14 such outlets, and back of them in the air ducts are located strip heaters for heating this air during the heating season. This heating system is under thermostatic control and the total output is 18.2 kw per car with the heater elements connected in four circuits of seven elements in series on each circuit.

The outlets for this fresh air system have been designed so as to direct the air toward the floor fanned out to 180 degrees to be effective in producing a warm floor in the heating season and supply heated air at low velocity to the maximum number of passengers. The calculated velocity of this air on leaving the distributor will be not more than 210 feet per minute. Actual tests in a mockup car section indicate that this air velocity will not be disturbing to passengers, and will be comforting at their feet level in inclement weather.

The fresh air system will add a maxi-

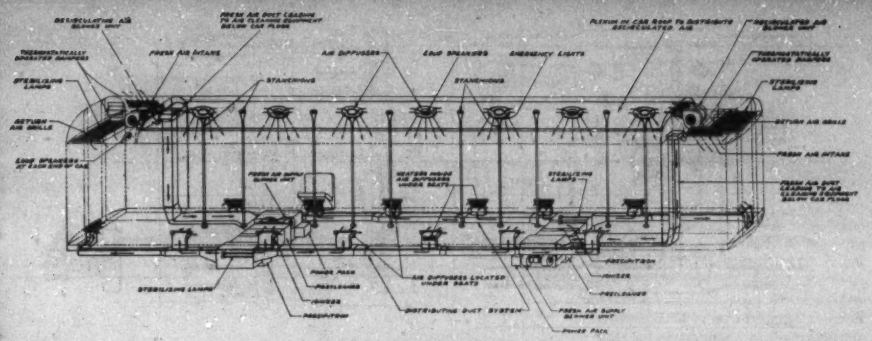

Figure 3. Schematic diagram of ventilation, air filtering, and sterilization in proposed new special car

mum of 3,000 cubic feet per minute of fresh filtered and sterilized air to the car, making a total of 9,600 cubic feet per minute maximum of recirculated and fresh air turbulence within the car. See schematic diagram shown in Figure 3.

Lighting

Cars are illuminated by means of fluorescent lighting. Two rows of fixtures extend for the full length of car on either side of the centerline of the ceiling, and two crosswise fixtures are placed one at each end, providing 17-foot candles on the reading plane throughout the car.

Each row of lighting fixtures in the ceiling contain eight 72-inch hot-cathode tubes of 38-watt rating at 118 volts alternating current, two lamps per ballast with instant starting. Two 42-inch lamps are mounted cross-wise at the ends of the car, each with a rating of 25 watts, 118 volts, alternating current, with a starter for each lamp. These lamps are so distributed in each phase of a 3-phase, 118 volt circuit as to reduce to a minimum any stroboscopic effect.

Station Announcing System

A station announcing system is provided, having reproducers mounted in the ventilating air distributors along the centerline of the ceiling, with one microphone mounted on each end of the car at corner posts at the cab side on the outside, which is a convenient location for trainmen in announcing station stops before doors are opened and after they have closed. All microphones in the train will be dead except the operating microphones at the time of announcement. This is accomplished by a foot switch mounted in the trainman's step, and an interlock in the door control drum switch.

Only one train-line wire is used throughout the train, connected to an amplifier in each car. These amplifiers operate from the 32-volt car battery. There is a semi-fixed volume control provided in the amplifiers to be adjusted to suit the service.

Electric Door Operators

Electric door operators are included instead of air-operated equipment originally considered for these cars. They operate the doors at the same over-all speed for both opening and closing as the air operators. The motors are wound with Class B insulation, and will not be damaged by interruption of door movement throughout the door operating cycle.

Motor Alternators

All power for fluorescent lighting, including exterior car lighting, side sign lights, illuminated maps, sterilizing lamps, Precipitrons, and car battery charging, is obtained from a motor alternator. The motor alternator has a full load rating of 4.2 kva at 90 per cent power factor, and 118 volts, 60 cycles, 3 phase. The 32-volt car battery obtains its charge through a 3-phase full wave rectifier using selenium rectifier units and having a two-step charging rate. A regulator automatically chooses the charging rate depending on the condition of the battery. The motor alternator maintains an alternating voltage at 60 cycles plus or minus 2 cycles under all conditions of load with a d-c supply voltage of 450 to 650 volts maximum. With unusual supply voltage swings of 400 to 750 volts direct current, the frequency is maintained at 60 cycles plus or minus 4 cycles. In order to maintain the frequency and voltage, expecially for interior lighting in passing over gaps in the third rail with a maximum interruption in d-c supply of 10 seconds, a flywheel is included on the shaft of this motor alternator.

Trucks

Two types of light weight trucks of special design are being considered for these cars. (See Figures 4 and 5). They embody new features for rapid transit service, such as the elimination of the full elliptic bolster springs, spring planks, and swing links. The bolsters are supported at each end by helical springs with lateral and vertical movement controlled by lateral and vertical shock absorbers as well as by rubber pads between the transom and bolster.

Hypoid gearing with right angle drive through flexible shafts, and couplings will apply power to each of the car axles from the 100-horsepower motors mounted on the truck frames.

All journal bearings are of the roller type. All wheels are 34 inches in diameter, and are of the resilient type, designed for a maximum wheel load of 14,500 pounds.

It is believed that with the generous amount of rubber included in these trucks in combination with resilient wheels and flexible drive, stresses in truck frames will be minimized, nosing reduced, and much quieter performance obtained.

With completely sealed gear cases and roller bearings, oil or grease drip to the trainways will be eliminated.

Noise reduction is one of the outstanding features of these trucks. With the elimination of practically all brake rigging and simplified truck construction, comparatively quiet performance is expected.

All axles are driving axles, and each

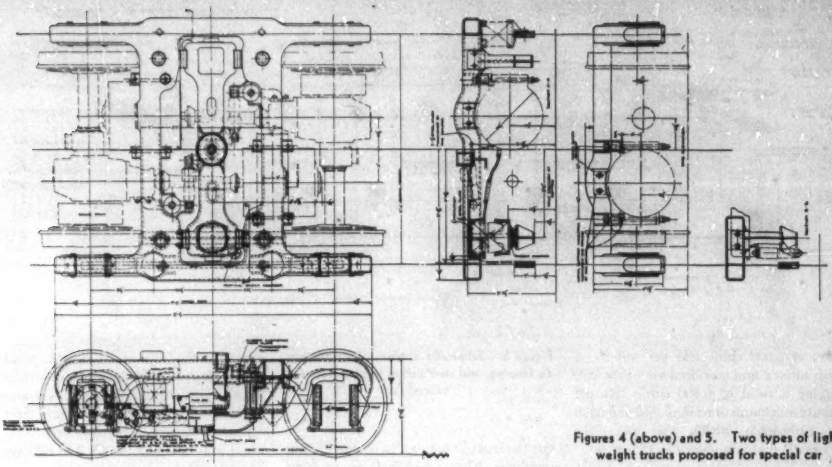

Figures 4 (above) and 5. Two types of lightweight trucks proposed for special car

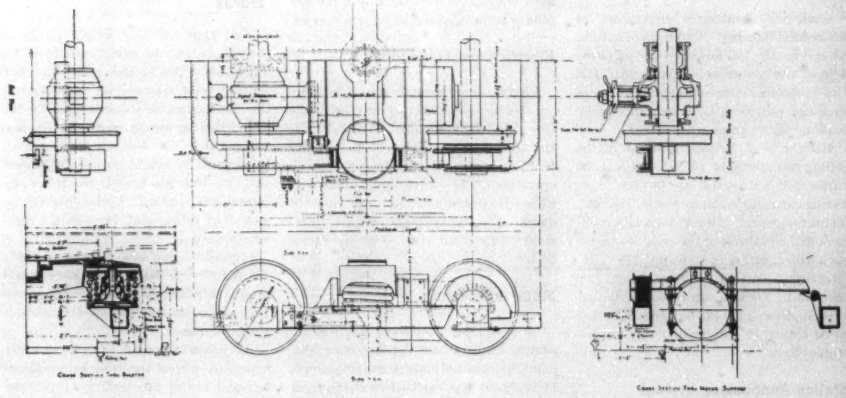

axle will be equipped with an air-operated drum brake which supplements the dynamic brake obtained from the driving motors. Provisions have been made for obtaining full braking rates in the event of failure of the dynamic braking, which normally will do all the braking down to a speed of 10 miles per hour when the drum brake will engage to make the stop. Under heavily loaded conditions the drum brakes in combination with the dynamic brake will maintain the three miles per hour per second braking rate as a maximum service rate. Any degree of service braking below the maximum rate is available as determined by the brake valve handle position in the normal service quadrant zone.

Discussion

G. M. Woods (Westinghouse Electric Corporation, East Pittsburgh, Pa.): The motors of the cars described by Sinclair will be similar to those of the cars covered by Cordts except they will be mounted at right angles to the axles and will drive through hypoid gears. The accelerating and braking rates will be the same on all cars but the balancing speed of the experimental cars will be slightly higher than the others because of the lower weight. The rates of acceleration and braking selected are believed to be as high as practicable for the conditions of operation.

An Improved Automatic Circuit Recloser

J. M. WALLACE
ASSOCIATE AIEE

Synopsis: Several years of field experience with automatic circuit reclosers indicated room for worth-while improvements in the existing design. This earlier recloser incorporated time-lag tripping characteristics to allow co-ordination with other reclosers and with fuse links. The improved design helps reduce outage time by extending the range of co-ordination with fuses by means of high speed tripping and reclosing. This paper describes the new recloser and points out the application of its new features.

Recloser Operating Characteristics

Early Recloser

IN 1941 an automatic recloser with inverse-time-lag tripping was described to the Institute.[1] This paper proposed several methods of using the recloser described to sectionalize radial distribution systems. One method was the extension of the reclosing function to the fuse cutouts which are located on the load side of the recloser. To obtain this operation, the fuse link and recloser combination is selected so that for a fault on the load side of the fuse the recloser will interrupt the circuit before the fuse link is damaged. If the fault is temporary, the line is re-energized on reclosure without a needless fuse operation. If the fault is permanent, the fuse is blown on the second or third successive reclosure because of the heat stored in the fuse link by the fault current on the previous operations. The fuse cutout then isolates the fault in the conventional manner, and the recloser can re-energize the rest of the distribution system which it controls.

The recloser described at that time has been in successful operation for more than six years. Co-ordination of reclosers with each other is foolproof provided they are located in descending order of ampere rating proceeding away from the power source. However, the co-ordination of reclosers with fuses in the manner described is sometimes difficult to achieve over a sufficiently wide range of fault currents.

Improved Characteristics Needed

To improve co-ordination of reclosers and fuse links, the tripping characteristics of the recloser should be changed from all time-lag to high-speed (instantaneous) tripping on the first and second operations followed by time-lag tripping operations until lockout. In this fashion, fuses may be protected by the recloser over a wider range of fault currents. However, the reclosers forming the main line of the distribution system should utilize time-lag tripping on all operations. These are the reclosers located at the first two or three points proceeding outwardly from the power source. In this fashion, the backbone of the distribution system is kept stiff and the entire system will not suffer power interruptions from troubles which should be confined to the branches. Smaller sizes of reclosers protecting branches can use the high speed tripping as power interruptions, thereby, are confined to the branches and are not communicated to the entire system.

The co-ordination of fuse links and reclosers must be planned adequately by the use of proper time–current curves. Because of the fast-blowing characteristics of small fuse links, it is impossible to protect them with the larger sizes of reclosers as fault currents on branches near the power source are likely to blow the fuse link in the first half cycle. Thus, even though the substation recloser is set for instantaneous tripping, it cannot protect the small branch fuse and the only result is to cause many needless interruptions affecting the entire systems.

Characteristics Required of Instantaneous Recloser

A study of the literature applying to the reclosing of transmission and distribution lines after faults shows the following cycle to be ideal for the small automatic recloser when using instantaneous tripping:

1. Instantaneous first trip followed by high speed reclosure.
2. Instantaneous second trip followed by time delay reclosure.
3. Time-lag third trip followed by time delay reclosure.
4. Time-lag fourth trip followed by lockout.
5. Time-lag on first trip followed by lockout on manual reclosure.

First Operation

The instantaneous tripping characteristic on the first operation is desirable because it insures the protection of small fuse links over a wide range of fault currents. This is the problem involved in extending the reclosing feature to the fuse cutout.[1] To enhance the value of the high-speed first trip, it should be made extremely fast in order to limit the damage to conductors by power arcs. In G. A. Matthews' paper on the "burn-down" characteristics of conductors, he stated that "to prevent burn-down of covered wire and to hold the arc damage within admissible limits, power arcs must be limited to one-half to two cycles (60-cycle basis) over-all time, depending upon the size of conductors and arc current. Bare conductors are less liable to serious arc damage owing to the phenomenon of arc travel and to the self-extinguishing characteristic of arcs on such conductors."[2]

The desirability of high speed reclosure

Paper 47-50, recommended by the AIEE committee on protective devices for presentation at the AIEE winter meeting, New York, N. Y., January 27–31, 1947. Manuscript submitted October 23, 1946; made available for printing November 25, 1946.

J. M. Wallace is section engineer in the switchgear and control engineering department of Westinghouse Electric Corporation, East Pittsburgh, Pa.

after the circuit is cleared was shown many years ago.[3] Experience over a considerable period of time has proved the usefulness of rapid reclosure in minimizing system disturbances and in reducing inrush currents after the outage. The reclosing time on circuits where the small automatic recloser may be used can be made as short as ten cycles with expectation of complete deionization of the flashover region.[4] It is obvious that a 10-cycle outage on lighting loads is so short as to be considered a "flicker" rather than an outage. Most motors will operate through such an interruption with only a small change in speed. Consequently, if the reclosing time is made very short, the line inrush current will be small compared to that which would result for a longer outage period.[5] In addition it is felt that if reclosure after the first operation is not high speed, there is a good probability of retripping an instantaneous recloser because of inrush currents.

Figure 2. Cross section of recloser

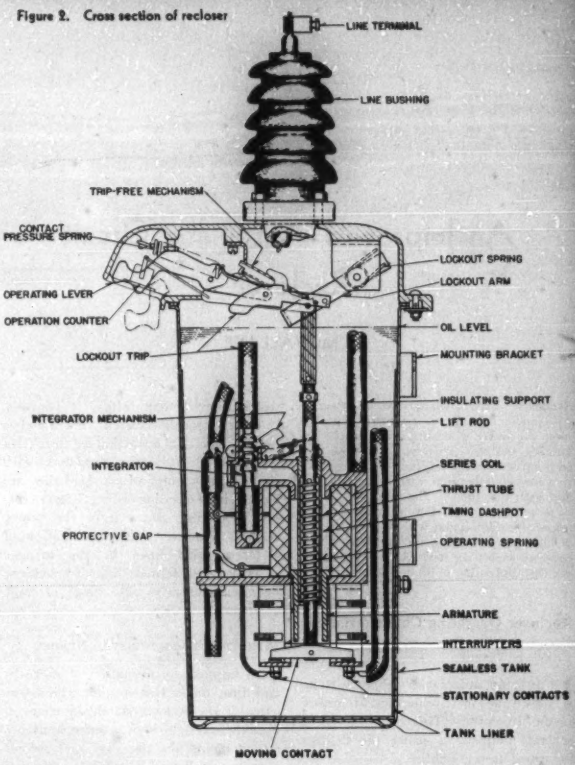

Second Operation

The characteristic on the second operation also should be instantaneous as some of the faults will not be cleared on the first operation, and others will be repetitive lightning strokes.[6] Field tests over a number of years have shown that about 80 per cent of all faults are cleared on the first operation and about ten per cent are cleared on the second operation of the protective device. Consequently, if the instantaneous tripping characteristic is maintained for the second operation, an additional ten per cent of the fuse cutout operations can be prevented. The reclosing time after the second operation should be long, however, in order to insure clearing of the fault in the case where the necessary deionization time exceeds that allowed on the first reclosure. Also, if the next tripping operation is to be time delay, a slower reclosing time and larger inrush currents will not interfere with re-energizing the system.

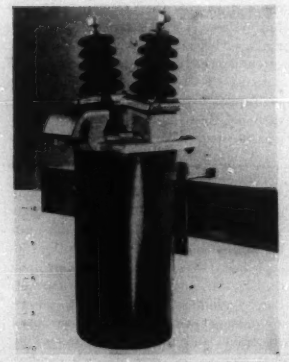

Figure 1. Improved recloser mounted on 4-by-5-inch crossarm

Third Operation

On the third operation the time-lag tripping characteristic is essential to allow sufficient time to blow the fuse link in the protected fuse cutout and isolate a fault beyond it.[7] In addition, it is desirable to insure pickup of the load.[8] In some instances it may allow enough time for burning the fault clear, and in these cases an interruption of the power arc is required before the line can be re-energized successfully. For this reason, the third operation should be followed by time delay reclosure to allow time for mechanical separation of foreign agents such as tree branches.

Lockout and Manual Reclosure

The last operation before lockout should be time lag to insure pickup of the load after the fuse link has blown or tree branch dropped clear. Similar reasoning applies to the tripping characteristics on manual reclosure after lockout. If the fault has been cleared, the time-lag tripping will allow the line to be re-energized. If, however, the fault is still on the line, the recloser should lock out after the first operation to prevent needless contact and oil deterioration.

New Recloser

A new recloser has been developed to meet the foregoing requirements. Its general appearance is shown in Figure 1. In order to meet safety requirements of

direct pole mounting, the recloser is encased in a metal tank which may be grounded. The operating coil is protected by an internal lightning protective gap connected directly across the coil thus eliminating the necessity for external gaps. The mounting brackets are welded to the drawn steel tank and allow use of various types of hangers. The operation counter is mounted in an extension of the top casting in order that it may be seen easily even from the ground. The top cover is held in place by clamps which allow it to be rotated to the most convenient position for manual operation.

Figure 2, a sectional drawing of the recloser, shows the mechanism in its normal current carrying position. The circuit is from the upper line terminal through the coil to one stationary contact, through the moving contact to the other stationary contact, and back to the other line terminal. The armature of the coil furnishes the entire work required for operation of the recloser. On overload it is drawn upward by the coil and compresses the operating spring. As it reaches the end of its stroke, the thrust tube connects solidly with the shoulder on the operating rod and starts the contacts traveling upward. Because of the arrangement of the mechanical linkage of the contact pressure spring, the contact force decreases rapidly as the contacts move upward and drops to zero in about 5/8-inch travel. Consequently, the operating spring will force the moving contact to travel to the end of its stroke as there is no opposing force from the contact pressure spring. This arrangement of the contact pressure spring reduces the work required from the coil to a minimum and helps to attain high speed on tripping. In addition, it helps to insure positive operation

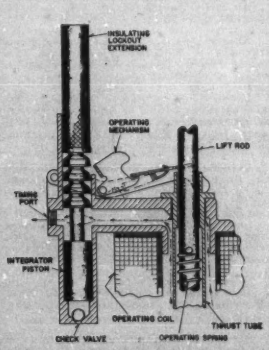

Figure 3. View of integrator and timer assembly

Figure 4. Oscillogram showing timing of operation to lockout. Sections of oscillogram showing open circuit conditions have been deleted

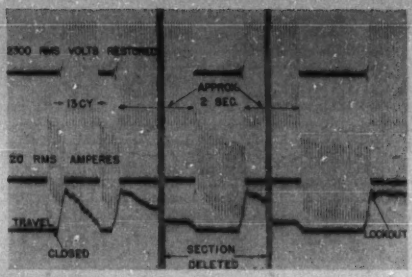

Figure 5. Oscillogram showing interruption on first operation at 1,200 amperes, 8 per cent power factor, 7,200 volts

when only a relatively small operating force is available as is the case with this class of equipment.

On each operation of the recloser the integrating piston is advanced one notch by its mechanism, being held in position by oil trapped by the check valve. After a successful reclosure of the circuit, the integrator will settle slowly to its starting position as the trapped oil leaks away. However, four successive openings will cause it to advance continuously until it breaks the lockout toggle, thus moving the operating level downward to indicate lockout and to hold the contacts in their open position. It is seen that the reclosure is tripfree as it is impossible to hold it closed by means of the operating lever.

As may be seen in Figure 3, the integrator performs the additional function of controlling the timing cycle of the recloser. As with the earlier model, the armature is a relatively close fit in its guiding tube and consequently must force oil in and out of the dashpot thus formed. When the integrator is in its initial position, this dashpot is freely vented through the timing port, as shown by the arrows, thus allowing instantaneous tripping. As there is nothing to prevent immediate flow of oil back into the dashpot, the recloser immediately resets. On the second operation, the timing port is not closed until the last half inch of armature travel, thus again allowing an instantaneous tripping operation. On reclosure, as the timing port has been closed by the integrator, the armature is restrained in its downward motion. Consequently, the contacts will move towards their closed position at a slow rate along with the armature until the contact pressure spring starts to leave its "dead center" position. The rapidly increasing force characteristic of the contact pressure spring causes it to accelerate the contacts rapidly, slightly compressing the operating springs, and gives snap action on reclosing. On the third and fourth operations the vent remains closed so that time lag is afforded on both tripping and reclosing.

To meet the requirements for a recloser utilizing time lag on all operations, the recloser is supplied with a plug in the timing port so that no dashpot venting can take place and all operations both opening and reclosing are time delay. This meets the requirements for substation and main line installations as described previously. In order to change to the instantaneous cycle described in the paper, it is necessary only to remove and discard the plug, an operation readily done in the field at installation.

The recloser utilizes a modified Deion grid to insure interruption at the end of the first half-cycle of arcing. This minimizes oil consumption and reduces wear on the silver tungsten contacts. The contact structure is arranged to give self-aligning action.

Standard current ratings for the re-

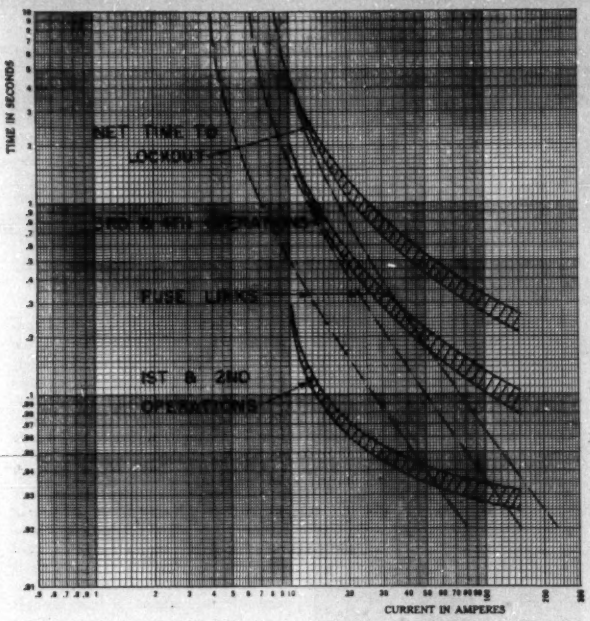

Figure 6. Time–current curve for 5-ampere recloser

Note co-ordination with conventional fuse links

closer are 5, 10, 15, 25, and 50 amperes with corresponding interrupting ratings of 150, 250, 375, 600, and 1,200 amperes at 15 kv. The basic insulation level is 95 kv. These ratings are met by the use of five different interchangeable coils for use in the same recloser structure. Coils are protected by a novel type of protective gap mounted under the oil on the coil frame. As the protective gap is thus insulated from ground, it can have a very low breakdown value compared to the 95-kv basic insulation level required for a grounded gap. Because of the low breakdown of the protective gap, very little stress is placed on the coil insulation. As the protective gap is in shunt relationship with the coil, surge currents are by-passed by the coil through the gap and power follow current is interrupted easily by the protective gap and shunted back into the coil. This direct connection of coil and protective gap allows each to help the other efficiently.

Recloser Performance

A complete cycle of recloser operation to lockout is illustrated by Figure 4. Although the current shown is but twice the minimum tripping current of the recloser, the high speed tripping time is only six cycles. Note that reclosure takes place in 13 cycles after the first interruption. Figure 5 shows an oscillogram of an interruption at 1,200 amperes, and it will be noted that total clearing takes place in two cycles. Note that the contacts separate in one cycle and that two half-cycles of arcing takes place. The test circuit has a high rate of rise-of-recovery voltage and the test power factor was eight per cent lagging. On a circuit having a lower rate of rise-of-recovery voltage or with a higher power factor, such as would be encountered on most distribution systems, arcing time limited is usually limited to one-half cycle giving a total clearing time of 0.024 seconds at maximum fault current. Figure 6 shows a time–current curve for the 5-ampere recloser and includes curves for standard fuse links. This shows that they can be protected on the first and second operations of the recloser and blown by the third operation throughout a wide range of current. Thus the co-ordination described in the beginning of the paper is achieved.

Conclusions

Field experience for more than six years shows the advantages to be gained by the use of a small automatic circuit recloser on a-c distribution systems. Co-ordination to extend the reclosing feature to the fuse cutout has proved itself quite valuable. The revised recloser still includes the time-lag of the previous model for co-ordination of reclosers with each other. In addition, by simple field adjustment, the new recloser can be made to co-ordinate with fuses under wider ranges of fault currents than were previously possible.

With the instantaneous tripping characteristic followed by instantaneous reclosing, 80 per cent of the temporary service interruptions now experienced with conventional automatic circuit reclosers will be eliminated effectively. Further advantage of the instantaneous tripping is the reduction of damage to the conductors and the system on temporary faults. These new factors will aid in the co-ordination of radial distribution systems and will increase the benefits obtained from this type of protective device.

References

1. An Automatically Reclosing Breaker for Co-ordinating Distribution Systems, **H. L. Rawlins, J. M. Wallace.** AIEE Transactions, volume 60, 1941, December section, pages 1021–4.

2. Power Arc-Over on Overhead Distribution Lines and Newly Developed Equipment for Protection Against Conductor Burndown From That Cause, **G. A. Matthews.** AIEE Transactions, volume 60, 1941, pages 596–604.

3. Many Interruptions to Electric Power Supply Are Avoidable, **Robert Treat.** *General Electric Review* (Schenectady, N. Y.), volume 37, April 1934, pages 162–4.

4. Keeping the Line in Service by Rapid Reclosing, **S. B. Griscom, J. J. Torok.** *The Electric Journal*, volume 30, May 1933, pages 201–04.

5. Factors Contributing to Improving Electric Service by Means of High-Speed Switching and Utilization of Stored Energy, **J. T. Logan, John H. Miles.** AIEE Transactions, volume 60, 1941, December section, pages 1012–16.

6. Immediate Initial Reclosure of Oil Circuit Breakers, **D. C. Prince, A. E. Anderson.** *General Electric Review* (Schenectady, N. Y.), volume 38, June 1935.

7. Improved Fault Protection for Rural Distribution Systems, **A. Van Ryan.** AIEE Transactions, volume 64, 1945, May section, pages 261–3.

8. Motor Inrush Following Distribution Outage, **Ernest O. Painter.** *Electrical World* (New York, N. Y.), volume 124, September 1945, pages 78–80.

9. Experience With Oil Circuit Reclosers on REA Systems, **Lee M. Moore, Bruce O. Watkins.** AIEE Transactions, volume 62, 1943, August section, pages 531–5.

Discussion

C. E. Asbury (The Commonwealth and Southern Corporation, Jackson, Mich.): It is encouraging that further progress is being made in oil circuit recloser development. In some of the earlier designs, tripping operations were either all instantaneous or all time delayed. Either of these arrangements usually could be worked in a system to co-ordinate with backup protection but could not be made to select properly when the recloser was used as a backup device or a protected device. That is, it was very difficult to obtain proper selectivity with fuses on the load side of the recloser. In this paper Wallace has pointed out that this type of co-ordination often depended on heat storage in the fuse elements during successive operations of the recloser. The amount of heat stored between successive operations of the recloser may be very small and unreliable for co-ordination purposes, as there is a cooling period of the fuseable element while the recloser is open and as most of the heat dissipation of the fuseable element is due to conduction, which may be quite rapid, depending on the mass and temperature differential of the surrounding metallic parts of the cutout. The necessity for improving the design of the recloser to permit proper co-ordination of fuses has been recognized, and successful application has been made of a number of reclosers having the first one or two tripping operations high speed followed by one or more time-delayed tripping operations. It is encouraging to find another manufacturer of reclosers changing design to incorporate this desirable feature.

As the main purpose of making the first two tripping operations fast is to allow more time between the fast and time-delayed tripping operations for proper fuse co-ordination, why should not the fast tripping operations be designed for 1 or 2 cycles instead of from 2 to 15 cycles as shown in Figure 6? Referring further to Figure 6, a band is shown for the time–current characteristic. Are these bands intended to allow for manufacturing tolerances or for performance variation due to temperature changes or some other cause?

What is meant by the "net time to lockout" time–current characteristic in Figure 6, and how is this characteristic established?

The cycle of operations listed as 1–5 in Wallace's paper are all important, and for most applications are desirable features to incorporate in a recloser. Wallace points out that in certain applications it may be desirable to modify these characteristics to make all tripping operations time delayed to prevent undesirable tripping of a recloser on the first instantaneous operation due to faults on branches that have small fuses. Item 5, which provides one time lag tripping operation when reclosed manually following a lockout, appears to be a new feature in this recloser that is not available in most other designs, and this likewise is a very desirable characteristic. Even though there have been many improvements in the design of reclosers during the few years of their development, there are still a number of quite important characteristics that should be given consideration in their design for additional improvement. These additional desirable characteristics may be listed as follows:

1. The original designs were intended for application on rural lines having relatively low short-circuit capacity. The interrupting rating for this class of recloser is too low for very general application on distribution circuits. With growing demands which will require larger supply banks and heavier power sources, the short-circuit capacities for distribution as well as for rural service are quite likely to increase considerably in the next few years. This will limit further the application of reclosers, unless their interrupting ratings are increased. It would be interesting if Wallace could point out how much the interrupting capacity could be increased, if any, by permitting the recloser to trip one time on an instantaneous operation, reclose at the end of a time delay of approximately 30 cycles, and then, if the fault is persistent, trip on one time delay operation and lockout. A recloser adjusted for this type of operation might be used in a number of applications where the interrupting rating is somewhat higher than those stated in the paper.

2. The continuous current ratings for the class of recloser described in the paper are too low, especially for application of the lower voltage distribution systems such as 7,200 volts and less.

3. The time delay used for tripping has not always been found consistent and reliable enough in reclosers in general. As these reclosers must select with relays and fuses, they should have a time–current characteristic at least as accurate as a fuse, and preferably approaching that of an overcurrent relay. The recloser described by Wallace uses an oil dashpot for timing, which undoubtedly will be affected appreciably by variations in temperature. In addition to using oil dashpots, some manufacturers have used timing escapements, which are in general inconsistent and unreliable when produced on a mass basis and usually are subject to hanging and binding, which may cause failures to reclose or trip. Oil dashpots, air bellows, and escapement methods of timing were attempted in the earlier design of protective relays and found to be unreliable and were superseded by more accurate timing arrangements. It would be very desirable if a more accurate and reliable timing principle could be selected for the tripping function of oil circuit reclosers. It would be interesting if Wallace could point out what variation due to wide ranges in temperature (100 to 0 degrees Fahrenheit) he has found in the time–current characteristic of the recloser. Oil circuit reclosers could be applied more intelligently by the users if the manufacturers would publish time–current characteristics showing the effect of temperature on their timers used for tripping. This could be represented by a band on the time–current curves, so that proper allowance could be made by the user when the device is co-ordinated with the time–current characteristics of fuses and relays.

4. The application of reclosers would be simplified, and probably increased, if a more flexible arrangement could be provided for their settings. A reliable external pickup adjustment and time lever setting for shifting the time–current characteristic is desirable to provide more flexibility in the co-ordination of various makes of reclosers with various makes of fuses and relays.

5. Most reclosers are designed with solenoids connected in series with the line, so that overcurrent in the solenoid operates the plunger. As the plunger moves into the coil, the impedance of the coil changes which makes it impractical in most instances for testing on a low voltage test source. It is quite difficult to check the pickup or time–current characteristics of these devices on high voltage test sources, and it would be very desirable if the design of the timing device could be such as to permit testing in the field with a low voltage test source using ordinary relay testing equipment, such as a load box and cycle counter.

It is hoped that these desirable characteristics can be incorporated in the design as a result of advancement in the art and, with the aid of increased production, that they will not necessarily result in any appreciable increase in price.

Figure 5 of Wallace's paper shows one interruption of 1,200 amperes at 7,200 volts which occurred in about 2 cycles. Have any tests been made on the recloser at 1,200 amperes on 15 kv where it was required to produce its complete sequence of two fast and two time-delayed tripping operations to lock out?

G. Fred Lincks (General Electric Company, Pittsfield, Mass.): Wallace's paper points out the benefits that will be obtainable when reclosers and fuses can be co-ordinated, so that the reclosers clear all nonpersistent faults on the entire circuit and so that the main line sectionalizing fuses, the branch fuses, and in some cases even the transformer fuses operate only on persistent faults to isolate a small section of the circuit. This will be spoken of hereafter as the "modern concept" of distribution overcurrent protection. In addition to the improved service continuity attainable, he stresses the value of the initial instantaneous opening in the prevention of line burn-down. However, in his recommendations on the application of reclosers, he would apply reclosers so that the benefits of the modern concept are obtained only at the outer end of the circuit and on the small percentage of the branches which are long enough to justify the use of reclosers.

Wallace recommends the use of time delay opening on all operations on the first two or three reclosers from the power source on the main feeder and, we assume, the use of fuses on all of the many short branches connected directly to the main feeder, with these fuses co-ordinated to clear both nonpersistent and persistent faults before operation of the recloser. He premises these recommendations on a desire to avoid power interruptions to a majority of the consumers on the circuit resulting from faults occurring on short single-phase branches. He does not mention, and may have overlooked, that with the modern concept of fuse-recloser co-ordination, a fault on these single-phase branches causes only one, or possibly a succession of two or three, momentary power interruptions before the fault clears itself or the branch fuse blows and also that these momentary outages affect about one third of the consumers on a rural 4-wire circuit. One third of the consumers are affected only by faults on

branches connected between the first and second reclosers, and the number of consumers subjected to momentary power interruptions is much less for faults on branches beyond the second or the third recloser. He indicates that possibly an influencing factor in guiding his proposal is the inability of higher rated reclosers, when used close to the power source, to protect associated lower rated fuses used at the branch junctions. Such protection of the branch fuses is necessary on the initial two instantaneous openings with the modern fuse-recloser co-ordinated setup. But, why use small fuses, unless this is a limitation of Wallace's recloser.

It has been shown[1] that automatic reclosing equipment for protecting short branches affords very little benefit to the over-all service continuity of the whole system because of the few consumers on the branch who are affected by the prolonged outages caused by nonpersistent faults on the branch. However, the individual consumers on these branches benefit from automatic reclosing on the branches, and relatively large savings can be effected in the expense for restoring service and in the automotive miles traveled.[2]

Generally, application limitations or requirements make it necessary to locate reclosers from 10 to 15 to 25 miles apart on the main feeder. Thus the first two or three reclosers from the power source control long sections of the 3-phase feeder plus the numerous short single-phase branches connected thereto. The combined mileage of the feeder and these branches represents at least 20 to 25 per cent of the total mileage on the circuit and an equal percentage of the consumers. Thus, with Wallace's scheme, at least 20 to 25 per cent of the consumers would get an inferior grade of service continuity, and the restoration expense would be increased in order that the other consumers need not be subjected to the additional momentary power interruptions from faults occurring on only one third or less of all the short single-phase branches connected to the main feeder.

With reclosers spaced 15 to 25 miles apart, the problem of locating faults quickly makes it imperative to sectionalize further the main feeder. With the modern concept, fuse–recloser co-ordination will permit this additional sectionalizing of the main feeder between reclosers, using fuses which melt only to clear persistent faults in the section they protect. Wallace's scheme does not permit such advantageous sectionalizing and, thus, would impair further the service continuity to a majority of consumers on the circuit below that possible under the modern concept.

Fuse–recloser co-ordination studies made on four or five rural circuits with different types and makes of reclosers operating on the modern concept make very understandable the limitations Wallace faced in applying his recloser. However, these studies indicate that the co-ordination of the reclosers with branch fuses, either close to the source of power or out on the line, is entirely practical if the reclosers have the right characteristics. Also, with the right characteristics it is practical to fuse sectionalizing points between reclosers and to connect these section fuses in series with branch fuses, both of which are protected properly by the reclosers. In addition it is possible to co-ordinate with internal fuses found in both early and recent vintages of distribution transformers.[3]

Another apparent oversight in Wallace's recommendation that the first two or three reclosers from the power source on the main feeder should have all time-delay openings is that the advantage of preventing line burn-down on the backbone of the feeder was not considered. Initial instantaneous opening, in preventing some burn-downs of the main line, avoids long outages to a majority of the consumers.

Thus, while the elimination of a few momentary power interruptions to a number of consumers is advantageous, as suggested by Wallace, it appears that the sacrifices in impaired service continuity, in increased restoration expense, and in the possibility of more line burn-downs on the backbone of the system are too high a price to pay for just preventing a few clocks from showing the red flag. Thousands of reclosers which operate instantaneously have been performing successfully for years in clearing nonpersistent faults at all locations on rural lines. A few may have locked open by inrush currents from motor starting after prolonged outages, but not following a momentary opening as is suggested by Wallace. Therefore, the best distribution overcurrent protection practice appears to be that of applying all fuses and reclosers on the circuit in accordance with the modern concept and making certain that the characteristics of the recloser permit the full advantages to be obtained with such an application.

References

1. Relative Value of Different Types of Overcurrent Protection for Distribution Circuits, G. F. Lincks. AIEE Transactions, volume 61, 1942, January section, pages 19–26.

2. Relative Expense for Service Restoration With Different Types of Overcurrent Protection for Distribution Circuits, G. F. Lincks, C. R. Craig. AIEE Transactions, volume 61, 1942, November section, pages 813–21.

3. Discussion by G. F. Lincks of Sectionalizing and Internal Transformer Fusing on Rural Power Circuits, Bruce O. Watkins. AIEE Transactions, volume 66, 1947, pages 388–9.

Leonard M. Olmsted (Duquesne Light Company, Pittsburgh, Pa.): The recloser described in this paper has characteristics far better suited to the requirements of distribution circuit protection than its predecessor described in the 1941 paper.[1] It shows recognition of certain difficulties encountered by distribution engineers and marked improvement in several respects. Though small self-contained devices of this sort can not be expected to satisfy all the requirements of all possible applications, it seems probable that further consideration of application problems may encourage the development of reclosers suitable for use in many places where this recloser would not be satisfactory.

In the first place, the paper discusses the desirability of characteristics such that the recloser will operate initially fast enough to protect small fuse links and to prevent the burning down of covered wire. Before lockout, however, the accumulated effect of successive operations must be sufficient to operate the largest fuses on the load side of the recloser, as otherwise a faulted transformer or branch line could hold a large portion of the circuit out of service. Distribution engineers frequently select a minimum fuse size determined as a compromise between transformer protection and unnecessary operations caused by lightning surges or customers' trouble, and use this size on the two or three smallest sizes of transformers. For somewhat larger transformers, the fuse size is increased more or less as a function of the transformer current rating. In planning the application of reclosers to a specific distribution circuit, it is not unusual to find transformers ranging in size from $1^1/_2$ to 15 kva with several sizes of primary fuses, possibly also line fuses, with which the recloser is expected to co-ordinate successfully.

At distribution voltages of 7,200 or higher, it may be that only a small range of fuse ratings is encountered and that such recloser characteristics as those of Figure 6 in the paper are satisfactory. On 2,400–4,160-volt circuits, however, it is not uncommon to find fuses ranging from 5 or 10 amperes up to 25 or 30 with which the recloser must co-ordinate on the basis of protecting the smallest fuse on its initial operation and clearing the largest fuse before lockout. Assuming that its time–current characteristics are proportional to Figure 6, then co-ordination with a 10-ampere fuse would require a recloser not larger than about 40-ampere rating, and such a recloser could not clear reliably a larger fuse than perhaps 20 amperes. The ratio between maximum and minimum fuse sizes appears to be two to one, where the application requirements are more on the order of four to one. From this viewpoint, it would seem that the new recloser, though it is superior to its predecessor, still is imperfectly suited to the requirements for extensive use on the lower voltage distribution circuits, where a larger recloser with greater spread between initial operation and lockout is desired. This problem was recognized several years ago by at least one industry association which urged the development of larger reclosers for such applications.

Another problem encountered in the application of reclosers to lower voltage circuits is safety to operating personnel. It is customary to work on lines and pole-mounted equipment energized at voltages up to 5,000 without interrupting service, by applying protective covering to all "live" conductors and equipment. In this respect, the new recloser shows a marked improvement over the earlier design, in that the top casting is insulated from line potential. The lineman still has limited access to operate the device by hand, however, and must climb close to the top casting to read the operation counter. Under these conditions, interrupting capacity is an important factor in safety to personnel; the present maximum of 1,200 amperes greatly impedes the application of reclosers to 2,400–4,160-volt circuits.

After extensive investigations, one large power company has concluded that the length of rural 2,400–4,160-volt circuits must be restricted to approximately 20 miles, if the desired degree of service continuity is to be attained. Because of sparse loading, many circuits must exceed this length and can be expected to provide satisfactory service continuity only if automatically sectionalized in such a manner that no fault can involve more than 20

miles of circuit. Many reclosers could be applied advantageously in such a program, provided they can be designed with a suitable time–current characteristic and sufficient interrupting capacity.

REFERENCE

1. AN AUTOMATICALLY RECLOSING BREAKER FOR CO-ORDINATING DISTRIBUTION SYSTEMS, J. M. Wallace, H. L. Rawlins. AIEE TRANSACTIONS, volume 60, 1941, December section, pages 1021–4.

R. F. Quinn (General Electric Company, Schenectady, N. Y.): Wallace's paper, and particularly the characteristics claimed for the recloser, have been studied with regard to the actual problem of co-ordinating protective devices on a rural distribution feeder. As a result of this study, the following questions have arisen:

1. What does the shaded area shown on the recloser time–current curves in Figure 6 indicate?

2. What is the effect on the instantaneous opening time–current curve and on the time delay opening time–current curve of ambient temperatures ranging down to −10 degrees Fahrenheit and up to 120 degrees Fahrenheit?

3. If the shaded area referred to in question 1 does not include over-all service temperature effects, how should the user factor these effects to obtain proper co-ordination of fuses with reclosers as discussed by Wallace under the heading, "Improved Characteristics Needed"?

4. What is the resetting time of the mechanism after the first opening, if it is assumed that the fault is cleared by the one operation? What is the resetting time after the second and third openings, assuming successful reclosure in either case?

It is believed that Wallace will recognize that the answers to these questions are very pertinent to any sound engineering application of reclosers for rural line sectionalizing. It is better for the user to evaluate these factors with full knowledge of their effect on the ultimate co-ordination that will be realized, than to overlook these effects and run the risk of malfunction of the intended scheme of operation.

Max W. Rothpletz (Rural Electrification Administration, Washington D. C.): It is gratifying to note the operating characteristics which are incorporated in the oil circuit recloser described by Wallace. The sequence of two fast and two time-delayed openings, together with the time-lag tripping on manual reclosure, should make this a very desirable recloser for sectionalizing rural power lines.

The problem of co-ordinating fuses with oil circuit reclosers has been a serious one on rural circuits; co-ordination of distribution transformer weak links with reclosers has been particularly difficult to obtain. For example, the weak link in one make of 3-kva transformer has a time–current characteristic such that the 5-ampere recloser described in the paper will trip on time delay before the link will blow on currents less than about 21 amperes, or the recloser would lockout, in accordance with the curves shown, before the link fails on currents less than about 15 amperes. If the time delay were increased, so that the recloser would open in about 10 seconds at minimum tripping current, this co-ordination problem would be largely solved.

Our data on inrush currents are not complete enough to warrant drawing any definite conclusions; however, it appears that a time of at least two seconds at minimum tripping current is required to permit the recloser to pick up loads.

W. J. Rudge (General Electric Company, Pittsfield, Mass.): Under the paragraph headed "New Recloser" the author states, "In order to meet safety requirements of direct pole mounting, the recloser is encased in a metal tank which may be grounded. The operating oil is protected by an internal lightning protective gap connected directly across the coil, thus eliminating the necessity for external gaps."

I would like to ask the author to explain how a protective gap which is placed directly across the series coil, and can only limit the impulse voltage across the coil, eliminates the necessity for lightning protection of the major insulation of the recloser, particularly since the author points out that the tank may be grounded.

If flashover takes place on the load side bushing of the recloser, the recloser itself would be expected to clear the fault. However, if flashover takes place on the source side bushing of the recloser, it would be necessary to depend on some other recloser or fuse nearer the power source to clear the fault. This latter case would cause an interruption to a part of the system which could be avoided by proper lightning protection of the recloser.

Roy M. Smith (Railway and Industrial Engineering Company, Greensburg, Pa.): The operating characteristics of the new automatic circuit recloser are most interesting. However, we cannot agree that the cycle of two instantaneous trips followed by two time lag trips to lockout is by any means "ideal."

While everyone will agree that an instantaneous trip followed by a fast reclosure is desirable to prevent the unnecessary blowing of fuses, there seems to be little justification for the second instantaneous trip. An inspection of Figure 6 of the author's paper indicates some margin for fuse co-ordination between the first instantaneous trip and the third time lag trip, although apparently only one or two fuse ratings could be accommodated—and then for only a portion of the current range. As the first trip is not particularly fast, as compared with the damaging time for a fuse, it is difficult to see how the second instantaneous trip can be made to co-ordinate, for it will be faster than the fuses for small currents, and slower for larger currents.

It would appear that an improvement in operating duty cycle might be the following:

1. Instantaneous first trip followed by high speed reclosure;

2. Time-lag trip followed by time-delay reclosure;

3. Time-lag trip followed by lockout.

With such a duty cycle, it would be possible to protect one or two fuses for transient faults and to blow them on permanent faults without an unnecessary lockout. At the same time, permanent faults on an unfused portion of the circuit would be given two opportunities to burn clear. With such a duty cycle the system would be subjected to less shock, and yet full protection would be obtained.

We note that the timing characteristics of the new recloser appear to be somewhat erratic. While the time curves in Figure 6 are shown as a band, similar to fuse curves, they apparently should be considerably wider to accommodate the variations normally expected with a dashpot timer.

For example, the paper indicates that the oscillogram in Figure 4 was taken on a 5-ampere recloser at 20 amperes, but the times shown do not fall within the bands of Figure 6. The time for the first two instantaneous trips are shown as 0.1 second, but the curve in Figure 6 shows a time between 0.06 second and 0.073 second, or an average of 0.067 second. This is an error of 50 per cent.

Likewise, Figure 4 shows a time lag of 0.3 second for the third trip and 0.4 second for the fourth, although Figure 6 gives an average time of 0.52 second or an error of 42 per cent in the worst case. Perhaps the inconsistency is due merely to temperature error, but some explanation would be desirable, as it would be difficult to co-ordinate the recloser with a fuse from the data given.

A. Van Ryan (Kyle Corporation, South Milwaukee, Wis.): The development of automatic circuit reclosers came about through the knowledge that by far the greatest majority of faults occurring on rural distribution systems are of a transient nature. These faults, once cleared, permit automatic restoration of service.

Fuses do not have the ability to interrupt automatically and restore service indefinitely, and, as pointed out by Wallace, cannot be depended on to co-ordinate with automatic circuit reclosers having single time–current characteristics.

However, low revenue does not warrant the cost of automatic reclosers on small branches extending from the main lines as well as from the main branch lines, and thus inexpensive fuse cutouts are used at these points on the system.

To permit the use of fuses and yet provide complete protection, the automatic circuit recloser having dual time–current characteristics was developed. A recloser of this type was described to the Institute in 1945.[1] Such reclosers have been in use for somewhat more than two years and have proved their ability to interrupt and restore service upon the occurrence of transient faults and to isolate permanent faults to a small locality. In a distribution system so arranged, the transient faults are cleared, and service is restored, by the automatic recloser; the permanent faults are cleared and isolated by the recloser or the fuse, depending upon which one of these protects the faulted section.

Thus, although it may seem desirable to protect the main lines with automatic reclosers having delayed time–current characteristics to prevent short interruptions of service and thus give the main lines so-called "backbone," it appears that this will cause unnecessary blowing of fuses on the small branches of the main lines.

The reason for this, as pointed out, is that fuses and single time–current characteristic reclosers will not co-ordinate with one another over a wide enough range of fault currents. It is, in fact, the reason why dual time–current characteristic reclosers were developed. In other words, what is good for the branch lines is good for the main lines. Thus, it appears that dual time–current characteristic automatic reclosers must be used throughout, if fuses are to be used in conjunction with them. That part of the system protected for its transient faults by an automatic circuit recloser by necessity will have an outage of very short duration when a transient fault occurs.

Automatic circuit reclosers are used in series on distribution systems. For this reason they must co-ordinate with one another as well as with the fuses they protect against transient faults.

If, after a permanent outage, a recloser has only one retarded time opening characteristic, all related reclosers having substantially instantaneous time–current characteristics will operate until they too fall into retarded time characteristics. If a dual time–current recloser not so arranged for its first operation after manual reclosure is substituted, it often will reduce the current, during the time of the first two reclosures, to such a value that it is below the value which will cause the backup recloser to operate. Besides this, it has in reserve another retarded characteristic opening, should the first one fail to pick up the starting load. It is, therefore, not clear that this feature of the described recloser is desirable.

Wallace is to be congratulated on the work he has done on his recloser, so that it too has satisfactory tripping characteristics for co-ordination with fuse cutouts.

Reference

1. Improved Fault Protection for Rural Distribution Systems, A. Van Ryan. AIEE Transactions, volume 64, 1945, May section, pages 261–3.

J. M. Wallace: Asbury suggests that the speed of the first tripping operation be increased. It should be pointed out that in small automatic reclosers, all of the energy to operate the recloser is taken from the circuit by means of a series coil. On low currents, there just is not sufficient energy available to operate the recloser in the short time that Asbury suggests. Of course, by going to additional complications, high speed tripping might be realized, but this in turn probably would result in a higher cost for this type of device. It is believed that in general the operation of the device is satisfactory for most locations and, that the increased cost would not be welcomed by the user, even though it did result in somewhat better characteristics. In some locations the increased cost would be justified, and perhaps a new device will be developed to meet these requirements.

The second question asked by Asbury is the reason for the bands on the time–current characteristics curves. These bands are intended to show manufacturing tolerances.

The third question is about the "net time to lockout" characteristic. The net time to lockout consists of the sum of the tripping time at any current for all four operations. In other words, it represents the total time of flow of fault current to lock out the recloser. Contrary to Asbury's statement that the heat loss from a fuse link is extremely variable, experiments have shown that on larger sizes of fuse links, above 5 amperes, with interruptions of less than two seconds on each flow of fault current, there will be less than 5 per cent of the heat lost. Consequently, in considering this problem, it is possible to co-ordinate over a somewhat wider range of current by considering the heat that is stored in the fuse link.

Asbury asked whether the interrupting rating of the recloser could be increased by limiting its operation to two interruptions. For the recloser described in the paper, no increase could be realized, and it is the author's belief that the same is true of other reclosers. In order to build a recloser which will operate satisfactorily, it is necessary that the interruptor be cleaned completely or flushed after each interruption, and, consequently, the duty on the interruptor is not reduced greatly by limiting the number of interruptions.

Asbury asks whether tests have been made at 1,200 amperes and 15 kv. In reply we would state that the recloser has been tested successfully at 1,200 amperes, 20 per cent power factor, and with 13,800 volts across the single pole.

Lincks discusses the so-called modern concept of distribution overcurrent protection. It should be noted that the modern concept was introduced first by H. L. Rawlins and the author of the present paper in 1941 when a recloser using all time lag characteristics was described to the Institute. At that time it was shown how a fuse link could be protected on its first operation and blown before lockout of the recloser by means of stored heat in the fuse. This method of co-ordination is satisfactory over a range of current which admittedly is somewhat limited when compared with the combination of instantaneous and time lag trips shown in the present paper. However, the range of current is satisfactory for many locations and will take care of many of the short branches, which Lincks states will not be protected adequately.

Also, Lincks' discussion overlooks the number of short branches which require no fusing and the number of short branches which can be co-ordinated with the time lag reclosers. He concludes with a statement that at least 20 to 25 per cent of the consumers would get an inferior grade of service continuity. Perhaps this should be restated that 5 to 10 per cent of the consumers would get an inferior grade of service continuity rather than the 25 per cent, as he has overlooked the afore-mentioned conditions. The author still believes that, in order to prevent an inferior grade of service continuity of the whole system by having momentary outages experienced by simultaneous tripping of reclosers and by additional operation and lockout of reclosers, it is worth having a somewhat inferior grade for the 5 to 10 per cent of the consumers mentioned. After all, this so-called inferior grade of service is still as good as that which these customers have been getting for the last several years. Consequently, it is hard to believe that very many complaints would be heard from these particular customers, especially as more than half of the system would have an increased class of service at the expense of this 5 per cent. It still is believed that the "backbone" of the system should be kept stiff.

Olmsted practically confines his discussion to 2,400–4,160-volt circuits. Admittedly, circuits of this nature are higher current circuits than the 7,200-volt circuits on which this recloser is expected to operate. For these lower voltages, the current rating should be increased somewhat and the interrupting requirements probably should be increased also. Whereas we agree that it is desirable to develop reclosers for this service, so far it has not been proved that their application would result in a rather wide market. It should be realized that, with devices of this type, the development and tooling is necessarily quite expensive, and in order to produce any reasonable cost it is necessary that the number of units produced be high. Perhaps, as more users become familiar with the problem set forth by Olmsted and begin to accept his viewpoint, the market for such a device will grow to a point where a manufacturer will become interested in developing a device specifically for these voltages.

Quinn questions the effect of ambient temperature on the recloser. The temperature effects are not critical over a range from 40 degrees Fahrenheit to 100 degrees Fahrenheit. Most of the operations of the recloser will take place in these temperatures as found in the United States. These are temperatures experienced during the lightning season. If sufficient margin is allowed between the fuse links and recloser, proper operation will take place over a wider temperature range. Although it is realized that the recloser will change time characteristics with temperature change, it also should be realized that there will be corresponding change in the fuse link characteristic. This will help to offset the difficulties pointed out by Quinn.

Quinn questions the resetting time of the mechanism after a successful reclosure. This time is approximately 15 seconds per step, which means that after one reclosure, 15 seconds is required to reset, and after three interruptions, 45 seconds is required.

Rothpletz has pointed out the difficulty of co-ordinating the reclosers with the so-called "weak link" in the transformers. This co-ordination problem is serious, and it is agreed that attention must be given to the subject. However, an immediate solution is readily available to the operators by use of a larger size of recloser. If the 3-kva transformer will not co-ordinate with a 5-ampere recloser, it is possible to use a larger rating of recloser where this problem must be solved.

Rothpletz mentions the data on inrush current and states that for the recloser to pick up load it ought to take at least two seconds at minimum tripping current. The earlier recloser which preceded the one in the present discussion had time–current curves which met this requirement, and to the best of our knowledge there never has been any operating trouble experienced in picking up load. The present recloser meets Rothpletz's requirements in that it has exactly two seconds at its minimum tripping current for load pickup.

The discussion by Rudge is correct

in that the protective gap across the coil does not eliminate the necessity for lightning protection of the distribution circuit or of the recloser. However, the paper did not infer that such protection was unnecessary but stated that the coil itself is furnished protection, which is superior to that supplied by external lightning gaps. External gaps or arresters must meet the basic insulation level of the system, and so they permit far higher surge voltages to appear across the coil than are experienced when the internal coil protective gap described in the paper is used. However, this internal gap is purely for the purpose of preventing surge voltages on the coil itself and obviously has no effect on the over-all system.

The discussion presented by Smith contained two principal points. The first is a question of the need for the second instantaneous trip. The need for this second trip is occasioned by repetitive lightning strokes. Operating experience and lightning studies both have indicated occasions when lightning strokes will take place in the same area in fairly rapid succession. Because of the length of the time required for a recloser to recycle to its initial position, about 10 seconds, it is desirable to have two chances of rapid clearing of the temporary fault. Smith's second point is that the recloser is inconsistent in its time–current characteristics. He refers to the oscillogram, Figure 4, where there is a variation between the operating time of the recloser on its first and second and its third and fourth operations. However, when variations in asymmetry of the different operations shown on the oscillogram are taken into account, the actual variations fall within those shown in Figure 6.

The discussion by Van Ryan is similar to that of Lincks in that he argues that instantaneous tripping should be used on all reclosers rather than as suggested by the author. However, Van Ryan does not present any new evidence which has not been taken into consideration.

Van Ryan states that the recloser ought not to have a time-lag operation when it is being closed after a lockout. He makes this statement on the basis that it is necessary to get co-ordination between main line reclosers, and he adds that the two instantaneous reclosures may be sufficient to reduce the line inrush current to a point at which it can be handled without the necessity of using time lag on the recloser. Experience with tests in the field have shown that this is not the case. In one test, after a 1/2-hour outage, an instantaneous recloser tripped or "chattered" approximately 15 times before the line was re-energized. This certainly indicates the need for time lag on re-energization of the line. In turn, if time lag is used, the recloser will cause an instantaneous recloser preceding it to trip out. In fact, a 5-ampere time-lag recloser can cause a 25-ampere instantaneous recloser to trip. This is one more reason why it is desirable to use time-lag tripping for the backbone of the system in order to prevent such useless operations when re-energizing the system.

Can the Trolley Coach Compete Economically With the Gas or Diesel Bus Where No Overhead Facilities Exist?

J. H. GAUSS
NONMEMBER AIEE

Synopsis: Each type of local transit vehicle has its proper place in the picture of modern transit. This position is determined by sound economics, including complete depreciation on all equipment and facilities. The attractiveness of trolley coach service and its corresponding low operating cost enable this type vehicle to compete favorably with either the gas or Diesel bus even though new power and distribution facilities are required.

MANY factors affect the location of the nerve center of our modern city, one of the most important of which is its urban transit system. Without adequate local transit service, the flow within the city stops. The congestion of cars and more cars clogging streets, parking lots, and garages is one of the first reasons business men shift to new locations. A business ceases to be one, if people cannot get to it. You have seen business districts shift within a city. What once was the heart of a growing city now may have comparatively little value. The heart has shifted to a more desirable location.

Superhighways and freeways have been built and expanded to improve approaches to the city. Actually, streets within the city are fixed basically and do not lend to this improvement. The result is that the external highway improvement adds to the downtown traffic congestion.

Of late, people have become more aware that the problem is basically one of moving people, not vehicles. The search has been for transit equipment that will move people with an economic utilization of available street space.

Selection of Proper Vehicle

In selecting the proper transit vehicle, many widely different factors must be considered, ranging from public preference to fundamental economics. The public's interest in this problem is that they have a short wait for a transit vehicle and that it takes them safely, quickly and quietly to their destination. Public officials and local business men are interested in that the transit system takes them and their workers to their stores and factories and then maintains a rapid turnover of shoppers to the business districts. The transit operators are interested in supplying the above service at a reasonable profit to themselves.

Combining all of these varied requirements of a transit service, there remains the problem of selecting a vehicle that best will suit the desires of all people concerned. Our present consideration is the economics of this operation.

Each of the standard existing types of urban transit vehicles, namely the mechanical bus, trolley coach, Presidents' Conference Committee cars, and rapid transit trains, has its proper economical application. Primarily this application depends upon the density of traffic to be handled. Those familiar with New York City have seen or have been a part of the terrific crowds handled by the subway system. It is difficult to imagine any other vehicle that would move this volume of people adequately. It would require 20 4-lane highways to handle this crowd were they to move by private automobile. This is based on the national average of 1.7 people per car. Those familiar with Washington, D.C., Boston, Mass., or Pittsburgh, Pa., know what a PCC car can do and how many people can be crammed into it during the rush hour. Again, it is hard to imagine smaller vehicles doing that job. If these people all traveled by private automobile, it would require a 9-lane highway to handle the raffic that is now handled by carline.

The Trolley Coach

The trolley coach's economic field of service is those trunk lines that do not justify PCC car operation but do justify a large size vehicle (37–44 passengers). There is another way of expressing this

Figure 1. A trolley coach operating in Kansas City, Mo.

Paper 47-45, recommended by the AIEE committee on land transportation for presentation at the AIEE winter meeting, New York, N. Y., January 27–31, 1947. Manuscript submitted October 30, 1946; made available for printing December 6, 1946.

J. H. Gauss is with the General Electric Company, Erie, Pa.

Figure 2. A trolley coach operating in Denver, Colo.

traffic density bracket. Where a rush hour headway of from two to ten minutes is required, the trolley coach is the most economical transit vehicle. There is still another yardstick. Where a traffic density of from 400 to 2,000 passengers per hour is to be handled, the trolley coach is the most economical vehicle. One trolley coach line can handle the people that a 7-lane highway normally handles by private automobile. For lines of lighter service than those listed above, the mechanical bus is best suited.

With the foregoing background as a general installation guide, one gets a rough idea as to which vehicle to consider most seriously when studying vehicle application to various lines. Under no circumstances can any guide or rough yardstick of this sort be applied to a specific line for the final and definite vehicle selection. A very complete traffic study followed by a simple economical analysis of the proposed vehicle applied to each line is the only sure way of assuring economy of service.

As a means of illustration, we can assume a line in an average American city, ten miles long round trip. A traffic study has indicated that this line requires 44-passenger vehicles operating on a 4-minute rush hour headway. The problem is "Which vehicle can serve this line most economically?"

Number of Vehicles Required

The first step is to determine the number of vehicles required for the line. Table I indicates that 14 44-passenger trolley coaches are required to handle the traffic. To do the same job, 16 44-passenger mechanical busses would be necessary. Because of normal maintenance, wrecks, reconditioning, and so forth, two spare trolley coaches, or three mechanical busses should be purchased, making the total number of vehicles required 16 trolley coaches or 19 busses. Table II indicates the annual number of miles, hours, and passengers handled by each type of vehicle.

The basis of comparison used in Tables I and II bears explanation. All trolley coach data for this entire study were taken from a report published in Bulletin 707 by the American Transit Association in July 1946, covering the operation of large size trolley coaches by 24 transit companies in 1945. This bulletin gives a very accurate set of figures for up-to-date trolley-coach operation.

No such comprehensive data are available for large size mechanical busses. However, the figures used in this study are all based on those of actual operation of large busses. You will note that where it requires but 14 trolley coaches for revenue service, it requires 16 busses. The trolley coach is able to maintain a faster schedule speed in similar service than that of a large size bus because of its almost unlimited power availability for acceleration. The electric motor in the trolley coach operates at between 150 and 200 per cent load for a short period of time during acceleration, making possible a faster and smoother coach pickup and enabling operation at a faster schedule speed. On the other hand, a 44-passenger mechanical bus with seated load is sluggish getting under way, especially if operating on a slight up-grade and does not have the reserve power required to hold its place with other traffic.

In addition to the fact that the trolley coach is inherently a faster accelerating vehicle, other features of its construction assist it in maintaining a faster schedule speed. For example, the trolley coach generally has a 30 per cent wider aisle and wider doors than mechanical busses, enabling the movement of passengers on and off the coach to be speeded up considerably, thereby reducing stop time and increasing schedule speeds.

For these reasons, the schedule speed of the bus in this report is assumed to be ten per cent less than that of the trolley coach. This has the effect of requiring more busses to do a given service than trolley coaches, which has been borne out on many properties.

Table I. Number of Vehicles, Miles, and Hours

	Hours	Head-way	Trolley Coaches	Vehicle Miles	Vehicle Hours	Busses	Vehicle Miles	Vehicle Hours
Weekdays								
A.M. peak	2	4	14	300	28	16	300	32
P.M peak	2	4	14	300	28	16	300	32
Base	14	6	10	1,400	140	11	1,400	154
Night	6	16	4	225	24	4	225	24
				2,225	220		2,225	242
Sundays and Holidays								
Base	16	8	7	1,200	112	8	1,200	128
Night	6	16	4	225	28	4	225	24
				1,425	140		1,425	152

Average schedule speed: trolley coach—10.6 miles per hour; bus—9.5 miles per hour.

Table II. Annual Vehicle Miles and Hours

	Days	Miles: Trolley Coach	Miles: Bus	Hours: Trolley Coach	Hours: Bus	Passengers: Trolley Coach	Passengers: Bus
Weekdays	308	685,000	685,000	67,700	74,600	5,110,000	4,600,000
Sundays	52	74,000	74,000	7,280	7,900	552,000	497,000
Holidays	5	7,100	7,100	700	760	53,000	48,000
Total	365	766,100	766,100	75,680	83,260	5,715,000	5,145,000

Trolley coach—7.46 passengers per mile; bus (ten per cent less than trolley coach)—6.71 passengers per mile.

Most trolley coach operators maintain 2.5 to 7 per cent spare trolley coaches. In this study we have used two spare coaches, or 14 per cent, which is high. As more vehicles were applied to other lines this percentage would reduce in favor of a reduced first cost. We have included three spare busses, or 18 per cent, which is also high by about the same ratio. Fifteen per cent spares for bus operation is normal.

A recent study made of 11 properties disclosed that these properties maintained an average of 2.4 per cent spare trolley coaches and 15.3 per cent spare busses. Seattle, operating 307 trolley coaches, maintain only 2.6 per cent spares. Similarly, they operate approximately 300 busses and maintain 12 per cent spares. For our small operation, two spare trolley coaches and three spare busses seem reasonable.

The miles and hours figures of Table II were obtained from Table I. The ATA bulletin, previously referred to, stated an average passenger loading of 7.46 passengers per mile which results in 5,715,000 annual trolley coach passengers.

Time and again on properties where trolley coaches have replaced busses, passenger revenue has increased materially. Where trolley coaches have replaced street cars and busses have replaced street cars on similar lines, the increased riding on the trolley coach lines has been greater than that on the bus lines. Because of the long life and constant operating characteristics of the trolley coach, it is able to hold its increased revenue through its entire life which is not the case with a bus. Further, the trolley coach, having wider aisles and being a more roomy vehicle over-all, is able to carry approximately ten per cent more people during rush hour than a similar seating capacity bus. These combined characteristics enable us to justify a ten per cent minimum revenue differential in the favor of the trolley coach; consequently there is a difference in annual passengers carried between the two vehicles.

As a summary of the study thus far, we find that to handle this 10-mile route, it requires 16 trolley coaches operating 766,100 miles and carrying 5,715,000 passengers per year. To do the same job, it requires 19 busses operating 766,100 miles and carrying 5,145,000 passengers per year.

Investment

The next factor to consider is the investment required for each type of operation. Table III covers the trolley coach investment and Table IV the bus investment. All costs are as of September 1946; so they are comparable to each other. The bus and trolley coach cost are averages of bids of seven and four builders, respectively, on an actual installation.

Table III. Trolley Coach Investment

Capital Investment	
16 trolley coaches at $16,300.00 (14 revenue service + 2 spares)	$261,000.00
5 miles 2-way overhead	89,000.00
5 miles 2-way feeder	14,440.00
1 1/2 500-kv substations	56,000.00
1 garage and facilities	40,000.00
Total	$460,440.00

Table IV. Bus Investment

Capital investment	
19 busses at $15,300.00 (16 revenue service + 3 spares)	$290,500.00
1 garage and facilities	60,000.00
1 bus storage garage and maneuvering area	60,000.00
Total	$410,500.00

The trolley coach substation cost is worth a comment. The capacity required for this one operation is a 500-kw station located near the center of the line. The reliability record of a modern rectifier station is 99+ per cent; however, sufficient stand by capacity must be available in case of a fault. Consequently, 1 1/2, 500-kw units are included. We can assume safely that one stand-by station could serve three similar lines. In actual practice where a large network is electrically connected together, this cost might be further reduced. Similarly, were this a single self-supporting line, two 500-kw stations would need to be installed, increasing the substation cost to $76,000.00.

You will note that the garage facilities for the trolley coach are considerably less than for the bus. This is justified for several reasons. Maintenance of trolley coaches is a relatively small portion of their operating cost. The absence of an engine is a great factor in this cost reduction. Further, an average trolley coach is approximately 2,000 pounds heavier than a bus. This weight is in axles and construction in general, giving a sturdier and more dependable vehicle. These factors combine to require less maintenance work and hence less maintenance facilities. This is further borne out by the number of spare vehicles required for service as explained above.

For operation in colder climates, this differential is further increased. Trolley coaches can be stored out of doors with absolutely no serious effect on starting or performance. On the other hand, most properties arrange for heated storage facilities for busses to enable reasonable starting characteristics. In southern climates where this storage is not necessary, the investment for bus garage would be approximately $60,000.00 Therefore, to summarize the investment needed to put either type of vehicle in operation, trolley coaches can be put into service for an investment of $460,440, and busses can be put into the same service for an investment of $410,500.

Operating Costs

Now that we have our investment figures for the two proposed vehicles, there remains the comparison of actual operating cost versus income. Operating costs consist of two major items, namely, fixed charges and operating expenses. First, we will consider fixed charges.

Tables V and VI show the fixed charges for each of the proposed systems. Depreciation is figured by dividing the first cost by the number of years of expected life. You will note that the expected life of the trolley coach is 12 years, while the expected life of the mechanical bus is only 8 years. This is based on actual practice of the transit industry at large. The rate of depreciation varies from 12–8 to a 20–10 ratio. For example, Boston, Mass., and Baltimore, Md., depreciate trolley coaches in 12 years and busses in 8 years. Des Moines, Iowa, depreciates trolley coaches in 20 years and busses in 10 years. Cleveland, Ohio, depreciates trolley coaches in 15 years and busses in 10 years. Our choice of 12 years for trolley coaches and 8 years for busses is reasonable.

Table V. Trolley Coach Fixed Charges

Depreciation	
Coaches (12 years)	$21,750.00
Overhead (20 years)	4,450.00
Feeder (20 years)	720.00
Substations (20 years)	2,800.00
Garage (50 years)	800.00
Total	$30,5200.00
Interest (average two per cent per year)	9,2000.00
Total annual fixed charges	$39,720.00

Table VI. Bus Fixed Charges

Depreciation	
Busses (8 years)	$36,400.00
Garage and facilities (50 years)	1,200.00
Garage storage (50 years)	1,200.00
Total	$38,800.00
Interest (average two per cent per year)	8,200.00
Total annual fixed charges	$47,000.00

Table VII. Trolley Coach Operating Expenses

	Cents	Per Vehicle Mile
Maintenance expense		
Ways and structures	1.29	
Equipment	4.12	
Power	.09	
Total		5.50
Operating costs		
Power	4.17	
Conducting transportation (drivers, and so forth)	13.9	
General and miscellaneous (claims, general office, salaries, and expenses, and so forth)	5.2	
Traffic	.06	
Total		23.33
Total operating expense (Not including taxes)		28.83 cents per mile

Table VIII. Bus Operating Expenses

	Cents	Per Vehicle Mile
Maintenance expense		
Bodies and chassis	4.65	
Tires and tubes	1.1	
Miscellaneous	2.4	
Total		8.15
Operating costs		
Fuel and oil	5.0	
Conducting transportation (drivers, and so forth)	14.6	
General and miscellaneous (claims, general office, salaries, and expenses, and so forth)	5.2	
Traffic	.06	
Total		24.86
Total operating expense (Not including taxes)		33.01 cents per mile

The depreciation rate for the remainder of the electric equipment and garages needs little explanation except that they represent a fair cross section of the industry in general.

Interest is assumed at an average of two per cent per year of the original investment. Obviously the interest rate is larger; however, as the investment is depreciated the payment becomes considerably less, and consequently, this is a simple way of expressing an average interest charge.

Totaling the fixed charges, we find that the trolley coach operation will cost $39,720 per year against $47,000 per year for the busses in fixed charges. This means that in spite of the higher first cost, because of the longer life of the trolley coach they actually cost $7,280.00 less per year than do the busses in fixed charges.

The next step in total operating cost is the operating expense. This includes the actual day-by-day expenses such as maintenance, fuel, drivers, and so forth. Tables VII and VIII list these items for the trolley coach and bus, respectively. Again the trolley coach figures were obtained from the ATA bulletin and represent a fair average of 24 operating companies operating large trolley coaches. The maintenance cost for ways and structures is 1.29 cents per mile. This cost is considerably higher than one would expect for new overhead as used for this illustration. The figure, 1.29, undoubtedly includes repairs to converted street car overhead and general rehabilitation. New modern overhead would not exceed $0.75 mile maintenance; however, the published figure is used herein.

Bus expense data were obtained by averaging a number of bus operating reports. In comparing figures of this sort, care must be taken to obtain data pertaining to vehicles of the same seating capacity operating on lines of similar traffic density, (both passenger and other vehicles), and operating over streets of the same general width, profile, and state of repair. Each of these factors seriously affects both operating expenses and schedule speed ability. It is obviously unfair to compare a 44-passenger vehicle with 36-passenger vehicle. It is also obviously unfair to compare two vehicles of the same size, one operating in congested areas and the other operating over wide free streets with few stops.

The foregoing figures are comparable as they represent data taken from lines operated under similar conditions.

By comparing Tables VII and VIII we find that the trolley coach costs 28.83 cents per mile to operate excluding taxes, while the bus costs 33.01 cents per mile excluding taxes. Basically the difference is found in maintenance and operators' wages.

You will recall in the first part of this paper we included additional garage and maintenance facilities for the busses. These added facilities are justified by the above maintenance costs. Because of the simplicity of the electric drive, the more sturdy construction of the trolley coach itself, and, further, the absence of engine vibration affecting vehicles, bodies, and chassis, the maintenance costs are considerably less for the trolley coach than for the mechanical bus operating as outlined above.

Summarizing thus far, we find that to operate trolley coaches on this line we must make a considerably larger initial investment than is required for busses. For this larger investment we will receive greater revenue. We also find that because of the longer life of the trolley coaches, annual fixed charge cost for the trolley coach operation will be considerably less than that for the bus operation. Further, we find that the actual operating expenses for the trolley coaches will be considerably less per year than those for the busses.

Table IX. Trolley Coach Annual Statement

	Cents Per Mile		Annual
Passenger revenue		50.9	$390,000.00
Expenses			
Operating expenses	28.83		
Fixed charges	5.17		
Total	34.00	34.00	
Net revenue		16.90	
Taxes	8.09	8.09	
Operating expense	42.09		322,500.00
Operating income		8.81	$ 67,500.00
Per cent return on investment		14.6 per cent	

Table X. Bus Annual Statement

	Cents Per Mile		Annual
Passenger revenue		45.8	$351,000.00
Expenses			
Operating expenses	33.01		
Fixed charges	6.14		
Total	39.15	39.15	
Net revenue		6.65	
Taxes	3.20	3.20	
Operating expenses	42.35		325,500.00
Operating income		3.35	$ 25,500.00
Per cent return on investment		6.2 per cent	

Annual Statement

The final analysis for our economic study is the annual statement. In the annual statement, Tables IX and X, the operating income is balanced against the total operating costs. After deducting operating expenses, fixed charges and taxes, the trolley coach operation leaves an operating income of 8.81 cents per mile or $67,500.00 per year. Expressed as a per cent of the initial investment, this is a return of 14.60 per cent.

The bus annual statement indicates an operating income of 3.35 cents per mile or $25,500 per year which in turn represents a return of 6.2 per cent on the original investment.

It is interesting to note that the trolley coach net revenue before deducting taxes is approximately two and one-half times the corresponding bus figure. This is obviously because of a combination of higher income and less operating expense.

Taxes used in this analysis represent the total of vehicles, facilities, and revenue

taxes, the basic figure of 8.09 cents per mile for the trolley coach being obtained from the ATA bulletin. As there is no ready means of computing bus operation taxes, the ratio of taxes to net revenue was maintained in both annual reports; hence total bus taxes are reduced considerably as a result of a reduced net revenue.

Conclusion

In conclusion, to answer the question asked by the title of this paper, the trolley coaches not only can compete with the bus under the conditions where no overhead or substation equipment exists, but they offer the most economical and satisfactory service.

Discussion

L. W. Birch (Ohio Brass Company, Mansfield, Ohio): Following a hearing before the Public Utilities Commission of New Jersey in June 1938, concerning the possible fire hazard introduced by 2-wire trolley coach overhead systems, the commission's subsequent ruling was rendered negatively. The overhead wires were not considered a hazard. Testimony was given during this hearing that indicated aerial ladders could be raised along the route and that there would be no impediment to fire fighting. It was also stated by several witnesses from operating companies that only in very rare cases have wires been cut to facilitate fire fighting. The negative wire located on the building side is usually 13 feet from the curb line, thus providing 20 to 25 feet between this wire and the building walls.

Radar Technique in an Industrial Control

W. D. COCKRELL
MEMBER AIEE

FOR a long time, industrial electronic engineers and communication engineers have felt that their circuits and techniques had little in common, that the one dealt with low frequencies and high power, whereas the other dealt with high frequencies and often with signals of extremely small power. However, with the development of such special communication fields as radar and loran, it has been found that many new circuits have been adopted in the communication field which are also quite useful in the industrial field. Therefore, it is highly desirable that the progressive electronic engineer in either field keep close contact with developments in the other so that he may take advantage of those which he may use best. Circuits such as square-wave circuits, clippers, blocking timing, and counting circuits normally associated with radar have an equally important place in industrial electronic circuits. In fact, the circuit to be described was designed before the war and before the present radar circuits were made available to the industrial engineer.

Typical Industrial Application—Photoelectric Side-Register Control

In the paper and printing industry, on slitting and processing machines where an accurate alignment of a web or strip is required, it is very desirable that the strip be wound or unwound so that its edge or a line of printing on it shall follow an exact path. Such a machine is shown in Figure 1. The basic mechanical operation will be seen more clearly from the simplified sketch of Figure 2. A photoelectric scanning head, shown in the center above the strip, views the strip edge or a printed line. Any deviation from the correct path is signaled to the electronic control panel at the right to excite an amplidyne generator. The amplidyne drives a correcting motor which moves the feed roll sidewise to correct the position or register of the strip.

Photoelectric Scanning Method

The photoelectric means developed to accomplish this result operates as follows: Because the most sensitive phototubes change their characteristics slowly over a period of time, it is desirable to operate on a sudden change of light, rather than on a continuous amount of light. To obtain a sudden change of light reaching the phototube, as reflected from the printing or edge of web, an optical system is used. It consists of four lenses mounted on a disk which is turned by a synchronous motor. The image of a lamp filament is projected through the lens onto the paper, and as the lens moves this small spot of light describes a quarter circle. Figure 3 shows a typical unit with cover removed. As the rotor of the small synchronous motor turns in accord with the electric voltage wave form, the position of the spot at any instant is related directly to the instantaneous value of the voltage driving the motor. Therefore, as the spot sweeps past the change in color corresponding to the register point, the change of phototube signal may be matched in time with the instantaneous value of the a-c voltage. In this way, a corrective action may be set up if the register point is not in its correct

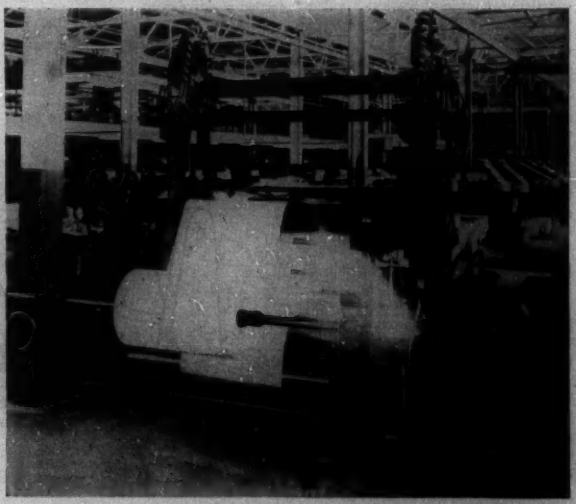

Figure 1. A side-register control installation

Paper 47-47, recommended by the AIEE committee on industrial control devices for presentation at the AIEE winter meeting, New York, N. Y., January 27–31, 1947. Manuscript submitted November 13, 1946; made available for printing December 19, 1946.

W. D. Cockrell is in the industrial engineering division of General Electric Company, Schenectady, N. Y.

position. The photoelectric scanning head including the optical system and phototube is set up so that the correct register position corresponds approximately to the midpoint of the light arc.

The principle of determining accurately the arrival of an electric pulse is fundamental in radar. Although here such extreme accuracy is not needed, we must determine times before, as well as after, the reference instants.

The use of the rotating-lens optical system to operate a reversing motor on an on-off basis is not new, but the circuits developed to provide a signal proportional to the direction and amount of misregister do involve a number of radar-like circuit elements and should be of interest. A previous system provided only that if the light spot occurred earlier or later than a critical phase angle that the correcting motor would be driven in a forward or reverse direction. However, inherent hunting action caused an excessive wear on the correcting mechanism and was not completely satisfactory. A circuit was needed which could apply a correction nearly proportional to the distance away from register so that the corrective action might be smooth and the motor might remain at standstill when no correction was needed.

Circuit Requirements

As outlined briefly, we must compare

1. An amplified phototube signal which has a comparatively steep wave front at the instant the light spot crosses the edge of the material or the printed line which will be used for register. Because the width of the line is indeterminate, and the surface over which the light passes afterwards cannot be controlled, it is desired to eliminate the phototube signal for the rest of the cycle as soon as the register signal has been obtained.

2. The instantaneous value of the sine wave alternating voltage which is indicative of the position of the moving light spot.

Our first step is to change the phototube signal into a uniform pulse and to eliminate all of the undesirable signals which the phototube may pick up.

Input and Pulse-Forming Circuit

In order to transform the somewhat indefinite signals coming from the phototube amplifier into a consistent signal, our first step is to use them to trigger a square-wave or gate circuit. Referring to Figure 4, we see that the circuit consists of a twin triode tube *3V* with common cathode resistor *11R*, and with the grid of the second triode driven from the anode of the first by a voltage divider, *13R* and *14R*, to provide snap action from full current to cutoff whenever the first grid passes a critical voltage. Switches are provided in the phototube amplifier so that the triggering signal is always in a positive direction.

The small circles at the top of the figures enclose oscilloscope traces of typical wave forms at the points indicated.

The Circuit Action—The Signal Trips

Before the circuit is tripped, the first triode *3aV* is normally nonconducting while the second *3bV* is conducting with zero grid voltage. When a positive pulse is applied by the phototube amplifier to the grid of the first tube through the capacitor *4C*, the first tube *3aV* begins to conduct, its anode potential drops to that of the cathode, and the grid of the second tube, through the voltage divider *13R* and *14R*, is driven sharply negative cutting off the second triode. The cathodes fall in potential permitting full current to flow through the first triode *3aV*. This instant in the operating cycle is shown at point *A* in the oscillograph traces above the diagram.

The grid of tube *3bV* is driven well negative below the *3aV* grid return point, *40*, so that no further action of the phototube amplifier will be effective to cut off the first tube. If the signal from the phototube amplifier should go very negative as shown in the oscillograph trace, the rectifier element of *4aV* limits the voltage to nearly that of point *40* and prevents any further negative swing.

Thus, we have accomplished the first requirement of obtaining a definite signal from the phototube and preventing any further signals from causing operation. We have developed a triggered gate circuit with rectifier blocking of reverse action.

Circuit Resetting Means

However, in order to make the circuit alive for the next cycle, we must reset it. This is done by means of an a-c voltage obtained from the transformer *2T* and the phase-shift circuit *13C* and *44R* which provides a sine wave of the proper magnitude and phase.

Rectifier *4bV* is so connected that during the positive part of this sine wave *4bV* is not conducting and the reset circuit is disconnected. However, as this reset voltage swings negative (as it does near the end of the light-beam sweep) *4bV* conducts and so makes the grid of *3aV* very negative. This stops *3aV* from conducting and resets the circuit. Furthermore, so long as the reset voltage is negative, *3aV* cannot conduct and signals from the phototube remain ineffective until the reset voltage again swings positive and releases the *3aV* grid. Point *B* on the oscillograph traces indicates the beginning of the reset time.

The Pulse or Pip Circuit

The signal which we wish to use as the indication of the instant of tripping is a

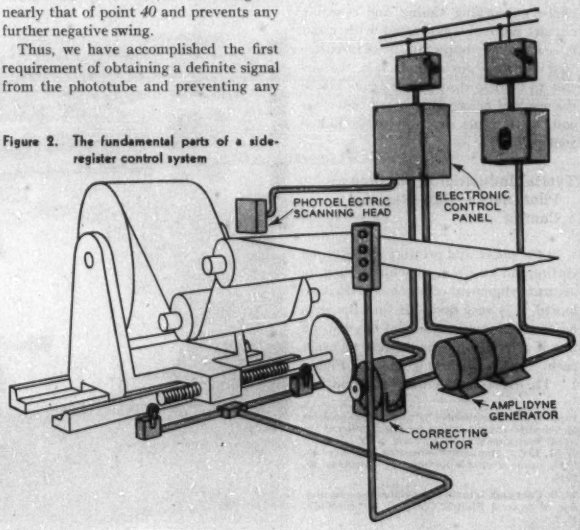

Figure 2. The fundamental parts of a side-register control system

Figure 3. A photoelectric scanner with rotating lens system

A (left). Unit with cover removed

B (right). Sketch of optical system

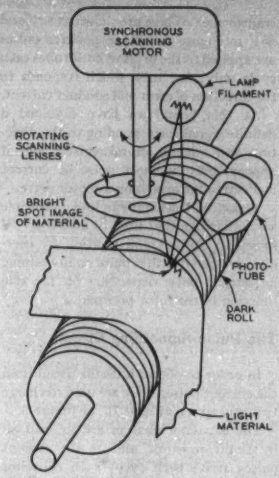

very sharp pulse of positive voltage. This is obtained by coupling a very small capacitor to the anode of the second tube *3bV* so that the output plate of the capacitor will be drawn quickly positive when the tube *3bV* stops conducting but will recharge rapidly to its original condition. The voltage appearing at the output of this portion of the circuit is shown in the right-hand oscillograph trace.

The output signal from this portion of the circuit consists of a single uniform pulse, accurately timed to the passage of the light spot past the paper edge or register line. This occurs once each electric cycle.

Error Detection Circuit

In this circuit (Figure 5), we compare the instant of passage of the light spot past the register line, as indicated by the uniform pulse which we have produced and the relative position of the light spot in its sweep, as determined by the instantaneous value of the voltage driving the synchronous motor. Because this voltage is a sine wave, which we may change in magnitude or reverse in phase easily by means of transformers, it provides a very desirable signal for our purpose. The relation between the voltage wave and light spot may be preset by the location of the lens disk on the motor shaft.

In practice, we confine ourselves to a 90-degree arc of movement. Because the scanner motor operates at 1,800 rpm, this allows 1/2 cycle (at 60 cycles) for operation. In a properly phased sine wave, the voltage swings from a positive maximum through zero to a negative maximum. If we apply this sine wave to the anode of a tube and use the pulse on the grid to permit conduction at the proper instant, we will release a brief surge or current corresponding to the instantaneous voltage applied. Thus, if we should phase our optical system so that the correct register point corresponds to the zero voltage of the sine wave, we can obtain a current flow proportional both to direction and distance from register.

Because an electronic tube is a rectifier and cannot pass current in both directions, we use two tubes: one which is supplied with voltage from one phase, and the other from the opposite phase of the

Figure 4 (left). Input and pulse-forming circuits

Figure 5 (right). Error-detection circuit, for polarity and magnitude

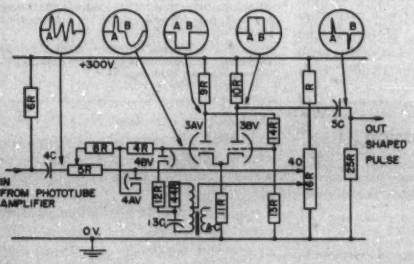

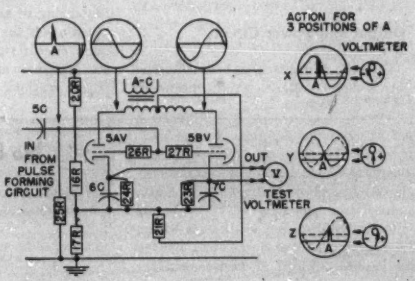

transformer. These are shown as *5aV* and *5bV* in Figure 5. If the positive pulses are applied to the grids of both tubes each cycle only that tube which responds to the direction of error will conduct current.

At this point, we have obtained a definite signal corresponding to the direction and amount of misregister, but it appears only as short pulse of current ineffective for operating a motor drive.

This circuit element employs a principle somewhat like that used to match a *PPI* sweep to the antenna position by energizing a selsyn with a pulse and obtaining an output pulse depending on the sine function of the rotor position.

The Pulse-Smoothing Circuit

In order to obtain a useful signal from the current pulses, they are used to charge two capacitors, *6C* and *7C*, of Figure 5.

The capacitor charges are drained off by shunt resistors, and as the current pulses arrive each cycle, each capacitor assumes a fairly constant voltage proportional to the charge received. The output from this part of the circuit is taken from the positive plates of the capacitors. The voltage between these leads is a comparatively smooth direct voltage indicating both by magnitude and polarity the amount of misregister.

The oscilloscope traces and voltmeters at the right in Figure 5 indicate three possible actions of this circuit. At the top, *X*, the pip has occurred before the zero point of the a-c cycle so that the left-hand tube *5aV* has conducted, charging *6C*. We will assume that the pointer of a zero-center voltmeter applied across the output leads would swing to the left.

For condition *Y*, the register is correct. The pip cuts the a-c wave at the zero-voltage point, and small equal charges appear on both *6C* and *7C*. The voltmeter indicates zero.

Finally, at *Z* the pip occurs late. Tube *5bV* charges *7C* and the voltmeter pointer swings to the right.

Output and Power Circuit

Once the misregister has been converted into a direct voltage, several means are available to provide power for the correcting motor. These include power electronic circuits, electromagnetic means, and the usual rotating exciters, and d-c generators. In this particular application, we will assume a fast-response generator, requiring low excitation power, known as the amplidyne.

The two balanced control fields which excite the amplidyne are supplied by a pair of output pentode tubes. These, in turn, are fed by a balanced voltage amplifier whose grids are responsive to the capacitor potential indicating the misregister. This voltage-amplifier stage consists of a balanced cathode-follower circuit sometimes given the descriptive name long-tailed pair. This circuit is coming into widespread use to provide symmetrical deflection for the plates of the cathode-ray-oscilloscope tube employed in radar, television, and many other fields.

Circuit Refinement

In an article devoted to the fundamental features of a circuit it is always desirable to eliminate those subordinate circuits which, while necessary in a practical design, tend to confuse a newcomer who wishes to trace the fundamental circuits. In the commercial equipment, there are rectifiers to supply direct voltage and filters for obtaining good wave form. Stabilizing or anti-hunt circuits are provided to obtain fast response with maximum circuit stability. Motor switches and protection are needed as well as push-button stations to permit manual operation of the correcting motor while setting up the equipment.

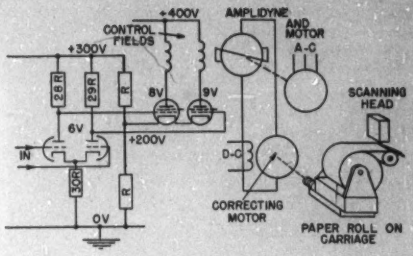

Figure 6. Output circuits and mechanical system

Conclusion

In this description of a typical industrial electronic application, we have tried to show that the elementary electronic tube circuits familiar to the radar man are not limited to one field only, but can be combined and arranged to serve many functional requirements. In industrial electronics, as in other fields, we obtain the most satisfactory results by breaking the problem down to its basic functions so that each tube circuit has but one job to do. These basic elements then may be combined to obtain the final results. Often in adding together the components, we are able to combine one or more functions without loss of operating efficiency. However, this can be done safely only if the essential functions for each circuit are kept clearly in mind.

References

1. A Position Regulator for Paper Slitters, **F. H. Gulliksen.** AIEE Transactions, volume 57, November 1938, pages 634–6.

2. The *SCR-584* Radar. *Electronics*, New York N. Y., volume 18, November 1945, page 104, December 1945, page 104, and volume 19, February 1946, page 110.

3. Radar on 50 Centimeters, **H. A. Zahl, J. W. Mardiettl.** *Electronics*, New York, N. Y., volume 19, January 1946, page 98, and February 1946, page 98.

4. The *MPG-1* Radar, **H. A. Straus** and others. *Electronics*, New York, N. Y., volume 18, December 1945, page 92, and volume 19, January 1946, page 110.

5. Loran Indicator Circuit Operation, **D. Davidson.** *Electronic Industries*, New York, N. Y., volume 5, March 1946, page 84.

No Discussion

A Balanced Amplifier Using Biased Saturable Core Reactors

H. S. KIRSCHBAUM
ASSOCIATE AIEE

E. L. HARDER
MEMBER AIEE

THE balanced amplifier using biased saturable core reactors was developed in the course of development of an impedance type regulator. Vacuum tubes were excluded from the latter device because of shock involved in the particular application, and it was essential that the amplifier also be nonelectronic. However, in addition to its shockproof characteristics, the resulting amplifier has unlimited life and a number of other features which suggest its use for a variety of other applications. It therefore was felt desirable to present the engineering features of this amplifier to the Institute.

The amplifier was required to amplify a small d-c signal of the order of 0 to 0.0004 watt to approximately 100 times this value. It also should handle 10 to 100 times this power with about the same amplification. It should be duodirectional, reversing the output for a reversal of input. The time delay was required to be not greater than two cycles (60-cycle basis) for certain applications but was permitted to be as great as one second in others.

A study first was made of the conventional saturable core reactor in a miniature size and it was found that 0.0004 watt was insufficient d-c excitation on the d-c leg of the reactor to produce enough flux density to have any material effect on the a-c legs.

Figure 1 shows the characteristic of a typical saturable core reactor. When used in the circuit shown, the power amplification is of the order of 20 to 40 times greater in region 2 of moderate d-c excitation than in region 1 of low d-c excitation.

The possibility of biasing the reactor to operate in the high amplification region was considered. However, with the extremely small signal power of 0 to 0.0004 watt superposed on the comparatively large bias power of a few watts, the signal of course, would be indistinguishable from small variations of the bias power supply. Bias by permanent magnet provided some interesting possibilities. However, the real answer to the problem was found in the form of a balanced amplifier design.

Balanced Amplifier

The amplifying element of the amplifier circuit consists of a 3-legged reactor as described by Aggers and Pakala.[1] This reactor is illustrated in Figure 2(*a*) and consists of a 3-legged core with one coil on each of the outer legs and two (or more) coils on the inside leg. The reactor coils (those on the outside legs) are connected so that the a-c flux Φ_A passes around the outside iron path as shown in Figure 2(*a*). None of this flux enters the center leg. The coils on the center leg carry direct current which sets up a flux Φ_D, which has a path through both outside legs thus permitting control of the degree of saturation of the iron of the a-c flux path. By controlling the saturation of the core, the permeability of the iron, and, as a consequence, the reactance of the reactor are under control. By varying the ampere turns on the center leg, the reactance of the reactor can be varied over a 30- or 40-to-1 range. The foregoing description is qualitative to the extent that the a-c and d-c magnetomotive forces are not superposable. Figure 2(*b*) illustrates the schematic equivalent circuit of the saturable core reactor, and it will be used to represent the reactor in the work which follows.

If the reactor is connected to a sine-wave voltage source as shown in Figure 3, and the alternating voltage across the reactor and the d-c amperes in one of the coils on the center leg are varied over wide limits, a family of curves as shown in Figure 4 will be obtained. The reactor current I_A will contain odd harmonics because of the saturation of the iron core. However, there will be no even harmonics because of the parallel connection of the a-c coils. The harmonic content will depend upon the extent of a-c and d-c saturations in the core.

The push-pull arrangement which is to be analyzed is illustrated in Figure 5. This amplifier consists of two biased saturable core reactors supplied by a 3-winding transformer which is used to isolate the reactor circuits. The bias is introduced in order to have an initial d-c saturation of the core, this being necessary for the successful operation of a push-pull amplifier and to obtain high amplification of small signals. The reactor currents are rectified before being passed through the load resistance, and, as a consequence, the abscissa and ordinates of Figure 4 are expressed in average instead of effective quantities. The rectified current of one of the reactors is passed through half the load resistance, and the rectified current of the other reactor is passed through the other half of the load resistance in such a way that the net voltage across the resistance is zero, when the control current I_C is zero.

As there is inherent unbalance in the amplifier, caused by slight differences in the reactors and so forth, initial balancing action is obtained by means of the resistor R_D. This refinement may be dispensed with where the amplifier output is not required to be zero at zero input.

When current is passed through the

Paper 47-48, recommended by the AIEE committee on industrial control devices for presentation at the AIEE winter meeting, New York, N. Y., January 27–31, 1947. Manuscript submitted November 6, 1946; made available for printing January 6, 1947.

H. S. KIRSCHBAUM, formerly with Westinghouse Electric Corporation, East Pittsburgh, Pa., is now with Research Foundation, Ohio State University, Columbus, Ohio. E. L. HARDER is with Westinghouse Electric Corporation, East Pittsburgh, Pa.

The major portion of this paper is abstracted from a thesis, "A Static Power Amplifier Employing Saturable Reactors" by H. S. Kirschbaum, submitted to the University of Pittsburgh in partial fulfilment of the requirements for the degree of master of science.

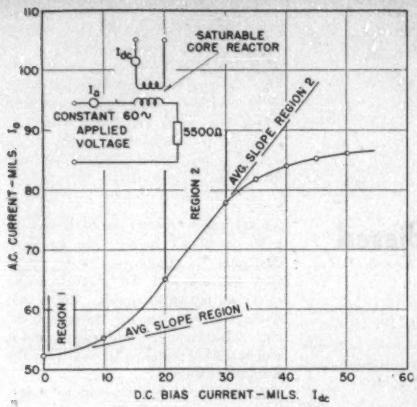

Figure 1. Characteristics of a typical saturable core reactor

Slope 2 = 6.5 × slope 1
Power amplification in region 2 is $(6.5)^2 = 42$ times that in region 1

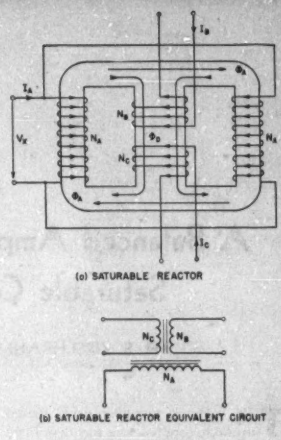

Figure 2 (right). Saturable reactor

Figure 3 (below). Test circuit for determination of reactor characteristics

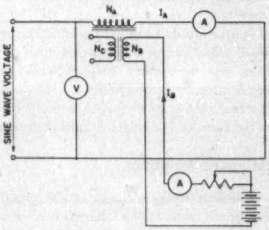

control coil circuit, the bias ampere turns on one reactor are aided by the control coil ampere turns, and those on the other reactor are bucked by the control coil ampere turns. Thus one of the reactances decreases and the other increases. This unbalance in reactance causes a net voltage to appear across the load resistance. Because this load resistance generally will be a coil, the net average ampere turns of which will perform some useful function, the useful power input to the coil will be $V_R^2/2R$.

This device is a true d-c amplifier having no lower frequency limit and yet having complete isolation of output and input circuits, a feature much sought after in certain electronic amplifiers. It, of course, does have limitations for signals of more than a few cycles per second, as will be outlined later.

In Appendix I, the amplification of the amplifier is determined analytically in terms of constants of the reactor obtained from the characteristic curves shown in Figure 4. The voltage across the total load resistor $2R$ as a function of the control current I_C is

$$V_R = 2R\left[\frac{N_C X_O Z_{MO}}{N_B(R^2 + X_O X_{DO})}\right] I_C \tag{1}$$

and the power amplification is

$$A = \frac{R}{R_C}\left[\frac{N_C X_O Z_{MO}}{N_B(R^2 + X_O X_{DO})}\right]^2 \tag{2}$$

The symbols used are defined in Appendix IV.

From equation 2 it is obvious that if R were either zero or infinite, the amplification of the amplifier would be zero. There must be some value of R between zero and infinity which will give the maximum amplification. This optimum resistance is found by differentiating equation 2 with respect to R and setting the differential equal to zero. Solving for R yields

$$R_{opt.} = \sqrt{\frac{X_O X_{DO}}{3}} \tag{3}$$

It is a well-known characteristic of saturable core reactor amplifiers that if the d-c excitation is low, the center core is unsaturated and the time constant is long. The bias windings, therefore, not only greatly increase the amplification, but also reduce time constant, or increase the speed of action. Of course, a limit is reached, above region 2 in Figure 1, where a further increase in bias would improve the speed only at the expense of a decrease in amplification.

The time constant of the d-c input control circuit is the principal time delay involved in the device. Note that net coupling with the bias winding is substantially zero because of the equal and opposite coupling on the two cores. The time constant of the amplifier can be reduced by inclusion of resistance in the input circuit at the expense of reduction of over-all gain. In Appendix II, the following equation is developed for the time constant of the control circuit:

$$T_C = \frac{4X_O}{2\pi f R_C}\left[\frac{N_C}{N_A}\right]^2 \tag{4}$$

By the addition of another coil on the center leg of the reactor, positive (or negative) feedback can be introduced as shown in Figure 6. The output voltage sends a current I_F through the feed-back coils on the center leg in a direction to aid the control coil. Thus the amplifier will supply a portion of the energy necessary to sustain its output. This connection is stable up to the point where the amplifier supplies 100 per cent of this energy. Negative feedback can be secured by reversing the connections at the feed-back input as shown by the dotted lines in Figure 6.

The power amplification and time constant with feedback as developed in Appendix III are

$$A = \frac{A_O}{\left[1 \pm \frac{KN_F}{2R_F N_C}\right]^2} \tag{5}$$

$$T = \frac{\left[1 + \frac{R_C N_F^2}{R_F N_C^2}\right]}{\left[1 \pm \frac{KN_F}{2R_F N_C}\right]} T_{CO} \tag{6}$$

where

A_O and T_{CO} are the amplification and time constant without feed-back

R_F and N_F are the resistance and turns of the feed-back coil per reactor

$$K = \frac{2RN_C X_O Z_{MO}}{N_B(R^2 + X_O X_{DO})} \tag{7}$$

Table I. Amplifier Power Amplification

Method	Power Amplification
Calculated (equation 2)	187
Test (without filters)	169
Test (with filters)	266

For positive feedback the negative sign is used in equations 5 and 6, and the positive sign for negative feedback. The use of feedback permits wide control of the amplification and time constant of the amplifier. However, it must be borne in mind that the use of positive feedback gives greater amplification with the sacrifice of greater time constant and negative feedback gives a smaller time constant with a smaller amplification.

Experimental Confirmation of Analytical Results

Two reactors as described in the preceding section were built and tested to check the foregoing analysis. Illustrated in Figure 7 are the reactor core and coil data, the coils being wound as shown in Figure 2(*a*). The resistance of each a-c coil is 6.0 ohms, or 3 ohms for both coils in parallel, which is negligible when compared with the load resistance generally used with these reactors. Because the two reactors are duplicates, only one of them was tested in accordance with Figure 3. The current I_A was measured with a rectifier type ammeter, the current being expressed in average amperes, whereas the voltage V_X was measured with an iron vane type of voltmeter, the average voltage being determined by dividing the measured voltage by 1.11. The reactor characteristics as obtained are plotted in Figure 8. These data cover a range of reactance of over 30 to 1.

Using the two reactors, the circuit of Figure 5 was tested with the reactors operating initially at the point marked 0 in Figure 8. The voltage across the 210-ohm load resistance is plotted, as curve *A* in Figure 9, as a function of the control coil current I_C. The calculated curve, using equation 1, agrees within five per cent of the test up to a load voltage of 35 volts. At this point, the reactors cease to operate on the straight line portions of their characteristics, and the output voltage is no longer a linear function of the input current. The theoretical curve is above the test curve because of the resistance of the a-c coils and the selenium rectifier and also because of the leakage reactance of the transformer. These tend to reduce $\Delta I_A/I_C$ at the operating point.

By placing second and fourth harmonic filters across the total load resistance, as shown in Figure 5, the load voltage can be increased by approximately 25.5 per cent with a consequent increase of 58 per cent in power amplification. Table I lists the power amplifications on the linear portions of curves *A*, *B*, and *C* of Figure 9.

The amplifier circuit with the filters is not amenable to analysis; however, experience has shown that a gain of roughly 50 per cent can be expected in power amplification when they are used.

The reactors were operated at the point $V_{XO}=71.0$ volts, $I_{AO}=0.338$ ampere, $I_{BO}=50$ milliamperes, and the load resistance varied. Figure 10 illustrates the variation in amplification with load resistance, the optimum resistance being 230 ohms. At the point of operation, X_O is 210 ohms and X_{DO} is 360 ohms, which give an optimum resistance by equation 3 of 160 ohms. From the results of this test, equation 3 should be rewritten

$$R_{opt.}=0.76\sqrt{X_O X_{DO}}$$

This discrepancy between theory and test is not important because, near the peak of the amplification curve, it takes a wide variation in resistance to cause an appreciable change in amplification. The difference in amplification between the true optimum and calculated optimum resistances is only nine per cent.

Figure 11 illustrates the response of the amplifier to a suddenly applied direct voltage at the input terminals (for three different operating points) plotted as a deviation of output voltage from the ultimate output voltage on semi-log paper.

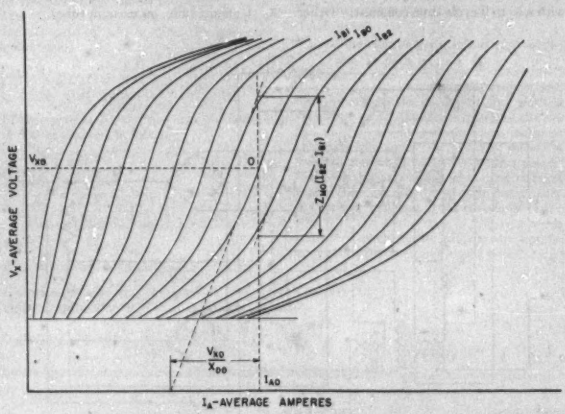

Figure 4. Reactor characteristics

Figure 5 (below). Amplifier circuit

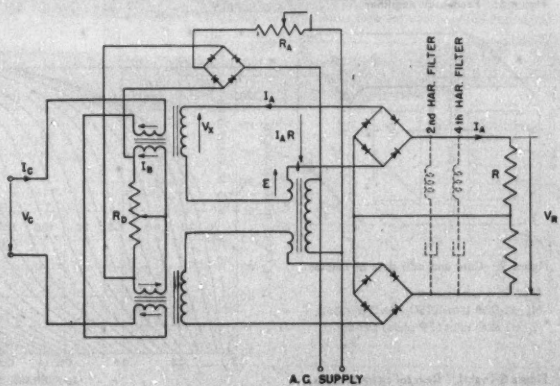

From these curves, the amplifier time constants can be obtained. There is a slight subtransient effect at the beginning of the transient which probably is caused by eddy currents set up in the core of the reactor. The time constants so obtained are plotted in Figure 12 as a function of X_0. There is good agreement between test and theory, the maximum deviation being about 15 per cent.

Conclusions

The performance of the typical amplifier described may be summarized as an amplification of 150 to 250 for input signals as low as 0 to 0.0004 watts, with a time constant of 60 to 90 cycles. The amplification and time constant can be reduced proportionately by introduction of resistance; for example, to 15 to 25 with a 6- to 9-cycle time constant. Other sizes are, of course, feasible. By using two or more stages the over-all time delay can be reduced without reducing the power amplification.

The amplifier described should find its principle field of application where one or more of the following features are needed, and where the time delay involved can be tolerated:

1. True d-c amplifier, with no lower frequency limitations.
2. Complete conductive isolation of input and output circuits.
3. Operation to low input signals 0 to 0.0004 watt.
4. Amplification almost independent of variation of a-c supply.
5. Amplification almost independent of variation of bias supply.
6. Shockproof.
7. Unlimited life, no vacuum tubes.

A possible application is the regulating circuit shown in Figure 13. In this application the output of an impedance type regulator of low output is amplified to supply the field of a main exciter Rotorol. This requires reduction of amplification to improve the time constant. In another system, quick compounding is used to provide the major correction and slow accurate follow-up uses the full available amplification of the saturable core amplifier. The authors believe, however, that there are numerous other applications where the characteristics enumerated will be of value.

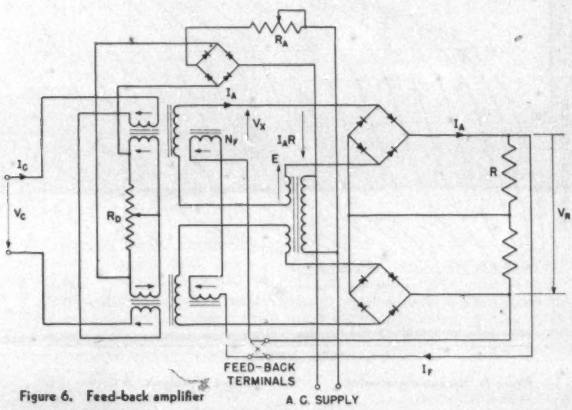

Figure 6. Feed-back amplifier

Appendix I. Amplification

In Figure 5 the total voltage at the secondary winding of the power supply transformer divides between the saturable reactor and the load resistor R. This voltage E will be assumed to remain constant for small variations of the current I_A.

Referring to Figure 14, the (average) voltage vector diagram of the circuit, the following equation can be written:

$$I_A^2R^2+V_X^2=E^2 \tag{8}$$

which when differentiated with respect to I_A gives

$$2I_AR^2+2V_X\frac{dV_X}{dI_A}=0 \tag{9}$$

Rearranging,

$$\frac{dV_X}{dI_A}=-\frac{R^2}{(V_X/I_A)} \tag{10}$$

Referring to Figure 4, the characteristic curves of the reactor, the initial operating point (no signal input to the control winding) is indicated by the point 0. Using the subscript 0 for all reactor quantities at this point, equation 10 can be rewritten

$$\left[\frac{dV_X}{dI_A}\right]_0=-\frac{R^2}{X_0} \tag{11}$$

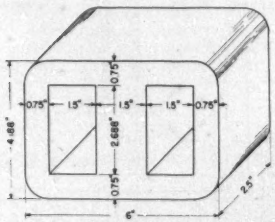

Figure 7. Core and coil data of reactor

N_A—366 turns per coil
N_B—1,200 turns (150 ohms) per coil
N_C—3,200 turns (79 ohms) per coil

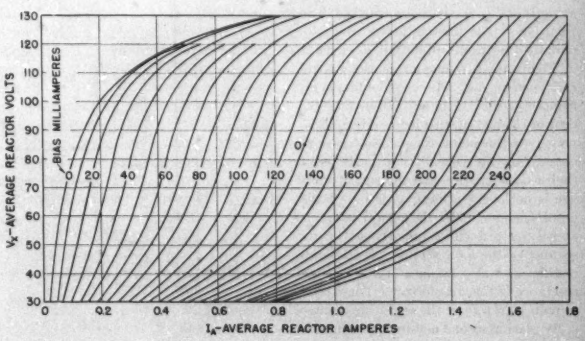

Figure 8 (right). Reactor characteristics

where

$$X_O = \frac{V_{XO}}{I_{AO}} \tag{12}$$

The expression for a small deviation in the voltage across the reactor can be derived from equation 11. It is

$$\Delta V_X = \left[\frac{dV_X}{dI_A}\right]_O \times \Delta I_A = -\frac{R^2}{X_O} \times \Delta I_A \tag{13}$$

The center-leg excitation of the reactor is contributed by two windings, the bias winding which contributes I_{BO} and the control winding which contributes ΔI_B. Because, in general, the control coil turns will not equal the bias coil turns,

$$\Delta I_B = \frac{N_C}{N_B} I_C \tag{14}$$

where

N_C are the control coil turns
N_B are the bias coil turns

Over a considerable portion of the family of curves of Figure 4, the curves are very nearly parallel straight lines, and they can be represented by the following equations:

$$I_A = I_{AO} + \Delta I_A$$
$$I_B = I_{BO} + \Delta I_B \tag{15}$$

$$V_X = V_{XO} + \Delta V_X$$
$$\Delta I_A = \frac{\Delta V_X + Z_{MO} \times \Delta I_B}{X_{DO}} \tag{16}$$

where

$$Z_{MO} = -\left[\frac{\partial V_X}{\partial I_B}\right]_{I_A = I_{AO}} \tag{17}$$

$$X_{DO} = \left[\frac{\partial V_X}{\partial I_A}\right]_{I_B = I_{BO}} \tag{18}$$

Equation 16 is the equation of a family of parallel straight lines with the point I_{AO}, V_{XO} taken as the origin. Z_{MO} is called the mutual transimpedance of the reactor and

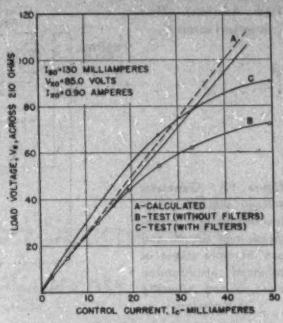

Figure 9. Amplifier output versus input

X_{DO} is the dynamic reactance of the reactor at the operating point. Substituting equations 13 and 14 into equation 16, and solving for the ratio of ΔI_A to I_C at the operating point yields

$$\left[\frac{\Delta I_A}{I_C}\right]_O = \frac{N_C X_O Z_{MO}}{N_B(R^2 + X_O X_{DO})} \tag{19}$$

From equation 19, the power amplification A can be derived as follows:

$$A = \frac{2R}{2R_C}\left[\frac{\Delta I_A}{I_C}\right]_O^2 = \frac{R}{R_C}\left[\frac{N_C X_O Z_{MO}}{N_B(R^2 + X_O X_{DO})}\right]^2 \tag{20}$$

where

R_C is the control coil resistance of one reactor.

Equation 19 also may be used to find the voltage across the total load resistance:

$$V_R = 2R \times \Delta I_A = 2R\left[\frac{N_C X_O Z_{MO}}{N_B(R^2 + X_O X_{DO})}\right] I_C \tag{21}$$

Appendix II. Time Delay

Because the control coil circuit of the amplifier has inductance, the control coil current will lag behind the signal voltage applied to the input terminals. The amount of this lag is the time constant of the amplifier and is the ratio of the control coil inductance to its resistance. The presence of both d-c and a-c fluxes in the core of the reactor makes the calculation of the d-c flux extremely tedious.[3] However, an approximate method for calculating the inductance of the control coil can be developed by determining the average permeance of the iron path which is traversed by the a-c flux. The average reactance of the reactor is a measure of this permeance. Solving for this permeance,

$$P_O = \frac{X_O}{2\pi f N_A^2} \tag{22}$$

where

P_O is the average permeance of the a-c flux path
N_A are the reactor turns effective throughout the path

In saturable reactors of normal proportions, the physical length of the a-c flux path is very close to 1.5 times the length of the d-c flux path. In addition, the cross-sectional area through which the d-c flux passes is twice that through which the a-c flux passes. However, the permeance of the center leg is higher (because of lower average flux density in this leg) than that of the remainder of the core. If the permeance of the center leg were very much greater, the average permeance of the d-c flux path would be $4P_O$:

$$P_C = 4P_O = \frac{4X_O}{2\pi f N_A^2} \tag{23}$$

where

P_C is the average permeance of the d-c flux path

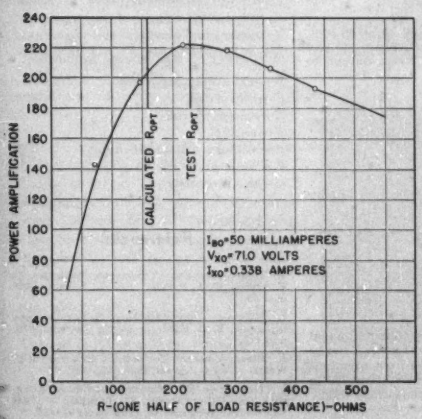

Figure 10 (left). Power amplification versus load resistance

Figure 11. Load voltage versus time for suddenly applied signal

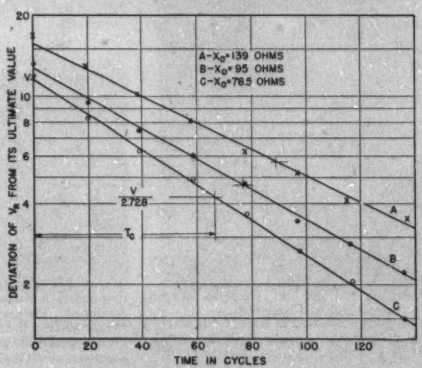

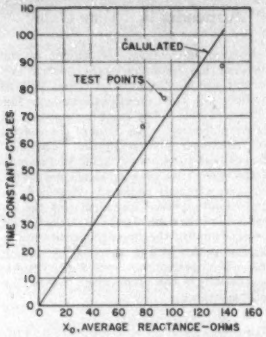

Figure 12 (left). Time constant versus X_O

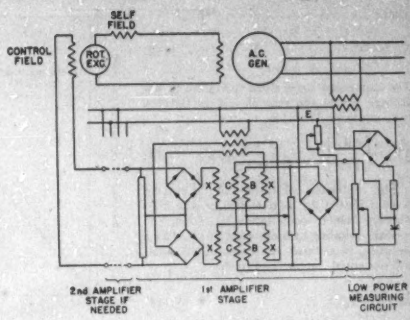

Figure 13. Generator voltage regulating system having low power measuring circuit and one or more stages of balanced amplification using biased saturable core reactors

From equation 23 the inductance of the control coil is

$$L_C = N_C^2 P_C = \frac{4X_O}{2\pi f}\left[\frac{N_C}{N_A}\right]^2 \tag{24}$$

And the time constant of the control coil is

$$T_C = \frac{L_C}{R_C} = \frac{4X_O}{2\pi f R_C}\left[\frac{N_C}{N_A}\right]^2 \tag{25}$$

The coupling of the control coil with the bias coil in one reactor is cancelled out by the coupling in the other reactor, because the control coils are wound in aid of the bias coil on one reactor and in opposition on the other.

Appendix III. Feedback

From Figure 6, which shows the equivalent circuit of the amplifier with positive feedback, the power amplification and time constant can be determined by solving for the output voltage of the amplifier as an operational function of the input voltage.

The voltage equations in the control and feed-back circuits for a suddenly applied voltage V_C are

$$V_C = 2R_C I_C + 2L_C p I_C + 2Mp I_F \tag{26}$$

$$V_R = 2R_F I_F + 2L_F p I_F + 2Mp I_C \tag{27}$$

where

$p = d/dt$

From equation 1,

$$V_R = \frac{2RN_C X_O Z_{MO}}{N_B(R^2 + X_O X_{DO})}\left[I_C + \frac{N_F}{N_C} I_F\right] \tag{28}$$

Letting

$$\frac{2RN_C X_O Z_{MO}}{N_B(R^2 + X_O X_{DO})} = K \tag{29}$$

$$V_R = K\left[I_C + \frac{N_F}{N_C} I_F\right] \tag{30}$$

Assuming 100 per cent coupling between the control and feed-back coils,

$$L_F = \left[\frac{N_F}{N_C}\right]^2 L_C \tag{31}$$

$$M = \frac{N_F}{N_C} L_C \tag{32}$$

Equations 26 and 27 now can be rewritten by substituting equations 30, 31, and 32 into them.

$$V_C = 2R_C I_C + \frac{2L_C}{K} p V_R \tag{33}$$

$$V_R = 2R_F I_F + \frac{2N_F L_C}{KN_C} p V_R \tag{34}$$

The currents I_C and I_F can be eliminated between equations 33 and 34 with the aid of equation 30. Solving for V_R,

$$V_R = \frac{K/2R_C}{\left\{\left[1 - \frac{KN_F}{2R_F N_C}\right] + T_{CO}\left[1 + \frac{R_C N_F^2}{R_F N_C^2}\right] p\right\}} V_C \tag{35}$$

where

$T_{CO} = \frac{L_C}{R_C}$, the control coil time constant without feedback

The power amplification can be found from equation 35 by setting p equal to zero and solving for the ratio of power output to power input

$$A = \left[\frac{V_R}{V_C}\right]^2 \frac{2R_C}{2R} = \frac{A_O}{\left[1 - \frac{KN_F}{2R_F N_C}\right]^2} \tag{36}$$

where

$A_O = \frac{K^2}{4RR_C}$, the power amplification without feedback

$$T_C = \frac{\left[1 + \frac{R_C N_F^2}{R_F N_C^2}\right]}{\left[1 - \frac{KN_F}{2R_F N_C}\right]} T_{CO} \tag{37}$$

In a similar manner the amplification and time constant with negative feedback can be developed. They will differ from equations 36 and 37 only in that the negative sign in the denominators of these equations will be positive.

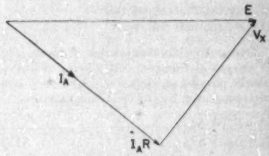

Figure 14. Vector diagram of amplifier circuit

All voltages and currents are average

Appendix IV. Nomenclature

N = turns
I = current
V = voltage
E = supply transformer secondary voltage
X = reactance
R = resistance (when used without subscript it is the load resistance)
Z_M = mutual transimpedance of the reactor
X_D = dynamic reactance of the reactor
A = power amplification

Subscripts have the following significance:

O = at the operating point
C = control coil
X = reactor a-c coil
F = feedback
A = reactor a-c and load circuit
B = bias oil
R = load resistor

References

1. Direct-Current Controlled Reactors, **C. V. Aggers, W. E. Pakala.** *Electric Journal*, 1937, page 55.

2. Effect of Direct Current in Transformer Windings, **E. L. Harder.** *Electric Journal*, 1930, page 601.

3. Direct-Current Controlled Reactor, **E. C. Wentz.** *Electric Journal*, 1931, page 561.

4. Theory of D-C Excited Iron-Core Reactors and Regulators, **A. Boyajian.** AIEE Transactions, volume 43, 1924, pages 919–36.

Burning of Wood Structures by Leakage Currents

PAUL M. ROSS
MEMBER AIEE

Synopsis: Wood pole or structure fires of leakage-current origin have caused serious wood-member damage and service interruption. These fires often occur at the end of prolonged dry periods. Operating experience indicates surface tree carbonization on crossarms and pocket burning at the crossarm-pole junction to be the two general types of burn damage. Pocket burning on some properties has been responsible for the larger part of the cases that required wood-member replacement. Laboratory tests conducted on approximately 200 specimens indicate that a coincident occurrence of dry wood and selective wetting of pole and crossarm surfaces by a light rain or fog, wind directed, which leaves a dry wood area in series with the leakage path, can result in a fire of a pocket type. This dry area, being high in resistance in comparison with adjacent series wetted-wood surfaces, results in a voltage concentration across the dry zone. If the dry zone is sufficiently short for a given circuit voltage, electrical breakdown occurs across the dry zone. This electrical breakdown being located favorably in dry wood and encouraged by a breeze may result in a pocket burn. Shunting devices which by-pass leakage currents around dry high resistance areas have proven successful in laboratory tests in eliminating pocket fires within the by-passed zone.

PRACTICAL and prime objectives in the operation of power lines are continuity of service and the prolonged life of physical equipment. One of the several causes that may prevent the realization of these objectives is the burning of wood structures by leakage currents. Because the majority of the medium voltage lines on this continent are constructed on wood poles, this constitutes a considerable problem.

Pole or structure fires may be caused by power-frequency leakage currents which flow over the surface of contaminated insulators and through supporting wood members. In some localities these fires may occur at infrequent intervals and are only an incidental nuisance. In others they may occur frequently and may be of such a character as to result in the complete loss of the crossarm and pole and cause a prolonged service outage.

Field Operating Conditions

Pole fires usually are preceded by three general conditions.

1. They are preceded by a prolonged dry period in which the wood members dry out.
2. During this dry period contamination accumulates on the insulator surface. The accumulated contamination layer reduces the surface leakage resistance of the insulator, particularly when it becomes dampened. The contamination may be salt deposits in coastal areas, dust on the plains, or smoke and other air-borne by-products from industrial establishments.
3. The dry period is followed by a fog, misty rain, or even snow.

Any fires that result may become evident shortly after precipitation has occurred, or they may not break out into the open until a later time or even until after precipitation has stopped.

Figure 1 shows carbonized surface burns on crossarms which were caused by leakage currents. The tree-like appearance of the burn patterns suggests that this be called tree burning. This type of burning is quite common. It usually does not result in burn damage sufficiently extensive to require replacement of the wood members.

Figure 2 illustrates burn damage on a pole and on a crossarm, which occurred at the gain areas. The burns are pocket-shaped and extend into the body of the members; they are not confined primarily to the surface as are tree burns. The

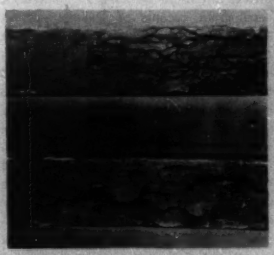

Figure 1. Typical cases of carbonized tree burns shown on crossarms which have been removed from service installations

Figure 2. Typical carbonized pocket burns on a pole and crossarm removed from a service installation

Paper 47-49, recommended by the AIEE committee on power transmission and distribution for presentation at the AIEE winter meeting, New York, N. Y., January 27-31, 1947. Manuscript submitted November 13, 1946; made available for printing December 5, 1946.

PAUL M. ROSS is superintendent of the high-voltage laboratory of the Ohio Brass Company, Barberton, Ohio.

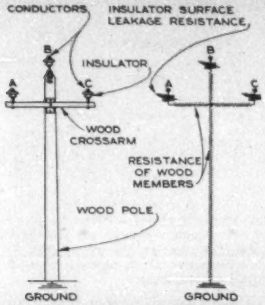

Figure 3. A schematic circuit diagram illustrating the series-circuit relation of insulator-surface leakage resistance with supporting wood members

burn damage in these cases occurred predominately on one side of the through-bolt. Pocket burning does not occur as often as tree burning, but when it does it is more likely to result in the need for replacement of the wood members. One property has estimated that approximately three-fourths of their cases of burn damage which required wood member replacement have been of the pocket-burn type. The specimens in Figures 1 and 2 were removed from service installations.

The foregoing are the general conditions that are the setting for wood burning of leakage current origin. The number of pole fires is small relative to the total number of circuit-pole-years of operation. This suggests that because the probability of a fire is small, a coincidence of unfavorable conditions is required to produce the event. Therefore, there is a need for finding the combination of conditions which may result in a fire.

Laboratory Approach to the Problem of Pocket Burning

The magnitude of leakage currents that flow through a porcelain-wood combination is controlled principally by the total resistance of the wood plus the surface leakage resistance of the insulator. It is controlled largely under the lesser contamination conditions by the insulator. The insulator and the supporting wood members therefore comprise a series circuit. This is illustrated in Figure 3. Any leakage current that might flow from phase *A* conductor to ground, for example, must flow through the surface leakage resistance of the insulator and then through the crossarm and pole resistance.

Leakage currents have been found by measurement to be surges.[1] Magnetic oscillogram records of leakage current surges taken in our laboratory show that the surges vary in magnitude of maximum current, frequency of occurrence, and time duration of individual surges. This investigation was started by the use of surges that were controlled in these three variables. It was found that the burn damage obtained with these surges could be duplicated in a shorter time by the use of a continuous-power frequency leakage current. Therefore, for the purpose of speeding up the investigation, a constant leakage alternating current of ten milliamperes was used. This is a typical value that may be expected in service.

In order to cause the leakage current to be controlled principally by a circuit element other than that of the wood resistance (thereby simulating the presence of an insulator with a constant leakage resistance) an impedance was inserted in series between the test transformer and the wood specimen. This test arrangement is shown in Figure 4. With the wood specimen in Figure 4 jumpered out, the test transformer voltage was adjusted so as to cause ten milliamperes to flow through the series impedance. It was found when the jumper was removed and the previously established transformer voltage reapplied that if the wood specimens were dry, the wood resistance was exceedingly high[2] and by itself limited the current through the series circuit to values less than one-half milliampere. If only one longitudinal surface of the same wood specimen were dampened the leakage current through the circuit would rise immediately to approximately ten milliamperes, thereby indicating the wood resistance had decreased through a wide range.

Figure 5 illustrates the nature of the influence of moisture content on the electrical resistance of wood. These data were obtained from reference 3 which states, "A surface film of moisture caused by condensation or rainfall will lower the resistance of the surface of a dry piece to that of a piece with a moisture content of 25 per cent or more." The ordinates in Figure 5 are relative resistance ratios based on the resistance at 25 per cent moisture content as unity. Depending upon the length of the drying period and the surrounding atmospheric conditions,

Figure 4. The test arrangement used to investigate the influence of surface moisture on wood resistance

1. Voltage control variable-voltage transformer
2. Test transformer
3. Transformer voltage
4. Series impedance
5. Wood test specimen, one foot long
6. A-c milliammeter

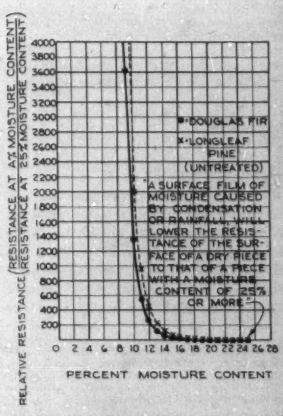

Figure 5. The influence of moisture content on the electrical resistance of wood

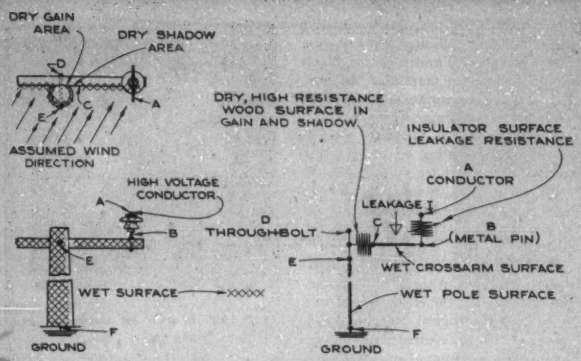

Figure 6. A schematic series-circuit diagram illustrating the reduction in surface resistance of dampened wood and the relative lack of reduction in dry shadow or gain area

the moisture content of the wood may reach values as low as ten per cent. If this were assumed to be the case, the wetting of one surface of a piece of wood would reduce that surface's resistance in the order of 1,200 or 1,400 to 1.

Figure 6 shows a portion of a wood structure consisting of a wood pole, a wood crossarm, and a porcelain pin type insulator mounted on a steel pin. The direction of a light wind is assumed relative to the structure. With this air movement direction the surfaces indicated by the cross marks will become dampened selectively. A schematic series circuit of this physical arrangement is shown to the right. The insulator surface leakage resistance is indicated between the conductor and the metal pin. That portion of the crossarm which is dampened is represented as a low resistance. Similarly, the dampened portion of the pole surface extending either to another phase or to ground is represented as a low resistance.

There remains, however, a connecting area between the end of the wetted portion of the crossarm surface, point *C*, and the nearest electrode which is the crossarm and pole through-bolt *D*. This area has not been dampened because of the particular air movement direction and therefore has a high resistance. This high resistance area consists of the pole shadow on the crossarm with respect to the air movement direction and the dry gain area between the crossarm and pole. The flow of leakage current through this series circuit causes a large *IR* voltage drop to appear across the dry high resistance area.

To verify, experimentally, the existence of a voltage concentration across the dry zone, equipotential lines in the electrostatic field surrounding a specimen were located and plotted. Figure 7 was obtained by these measurements. This is the top view of an untreated dry pine pole which was gained and fitted with a section of dry Douglas-fir crossarm. The flat steel plate was the voltage application electrode. Twelve kv was applied at this point. A circumferential copper braid band, located one foot below the through-bolt, was the ground electrode. The 25 per cent (3 kv), 50 per cent (6 kv), 75 per cent (9 kv) equipotential lines first were determined for the dry condition.

The same specimen then was wetted selectively as it might occur with the assumed air movement and moisture direction of Figure 6. The pole surface was dampened from the through-bolt to the ground band. About six inches of the face of the crossarm extending from the voltage application electrode was wetted. There remained the dry wind-shadow of the pole on the crossarm and the dry arm-to-pole-gain area. The equipotential line locations for this wetted condition are plotted in solid lines. A large change in the electrostatic field is indicated by comparing the dotted line map with the solid line map. The wetted pole surface being low in resistance has placed the through-bolt at near ground potential. In effect, the wetted crossarm surface has extended the voltage application electrode to the edge of the wetted area. As a result, a voltage concentration zone as shown in

Figure 7. The influence of dampened pole and crossarm surfaces in forming a voltage concentration zone at the gain

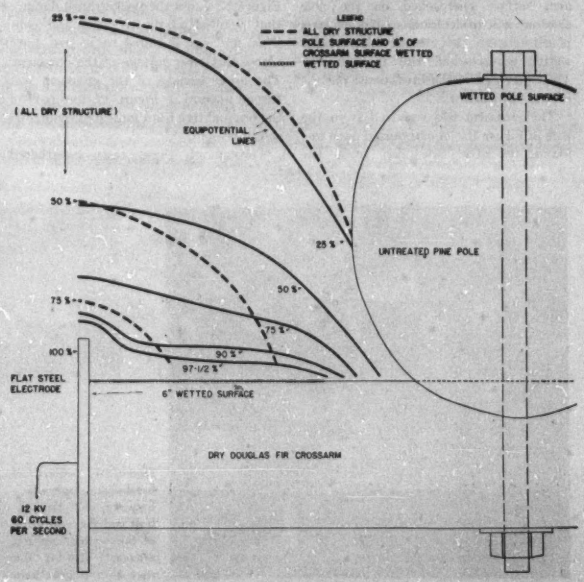

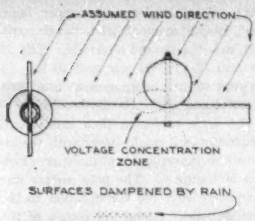

Figure 8. These selectively dampened pole and crossarm surfaces cause a voltage concentration to occur across the dry series zone

Figure 8 appears between the end of the wetted crossarm surface and the through-bolt.

Figure 9 shows the crossarm and pole arrangement used in the equipotential line-mapping tests. The pole surface and crossarm were wetted by a light finely divided mist applied from an air-operated spray gun. The wind direction was simulated by a fan. The front of the pole was dampened between the through-bolt and the grounded band, and it therefore had a low resistance. The arm also had been dampened from the steel electrode to the edge of the pole shadow. The pole shadow and gain were dry. As the light water spray was continued the dampened arm surface encroached on the pole shadow until an electrical breakdown took place between the nearest edge of the wetted surface and the through-bolt. The outer end of the breakdown path is indicated by arrow.

The crossarm was removed from the pole in Figure 10. A carbonized path was found to have developed from the through-bolt across the gain. The mating crossarm burn, indicated by arrow in Figure 11, extended from the through-bolt out to the wetted portion of the arm. Drying of the arm surface occurred at the outer end of the crossarm burn.

In Figure 12 the structure was reassembled and the test continued. The current flowing was ten milliamperes, 60 cycles per second, as controlled by the series impedance. Encouraged by the breeze, open flames appeared in about ten minutes.

Figure 13 was taken by looking along the crossarm toward the pole. A pocket was burning into the crossarm and into the pole at the original carbonized path locations. The fire continued without the help of leakage current at this stage.

Figure 14 shows the pocket burn that formed to the left of the through-bolt in the pole and to the right of the through-bolt hole in the crossarm. These pockets are similar in appearance and location to those found on the field burned specimens shown in Figure 2.

If the direction of the air movement is changed so that the crossarm and pole become dampened as shown in Figure 15, a voltage concentration zone occurs across the lower side of the crossarm and from the through-bolt toward the wetted pole surface below. A fire that resulted from these conditions is shown in Figure 16. Figure 17 shows the pocket burn damage that resulted on the crossarm and pole. This fire was initiated by a tree burn across the lower surface of the crossarm. The lower surface of the crossarm was turned upward in Figure 17, and part of the original tree burn indicated by arrows is still present.

Throughout these tests, weathered crossarm and pole sections were used. The large hole at the right end of the crossarm in Figure 17 was used previously for a wood pin when the arm was installed in service. The through-bolt hole used in these tests is indicated by asterisk.

The preceding examples of burn damage are typical of the many obtained during the investigation. Controlled leakage current surges produced the same type of damage.

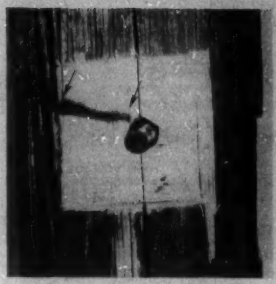

Figure 10. The resulting carbonized path across the pole gain

Figure 11. The mating carbonized path on the crossarm surface

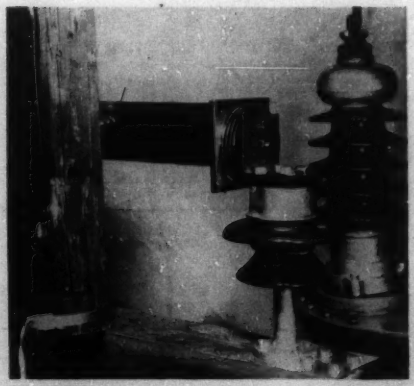

Figure 9. Electrical breakdown took place between the through-bolt and the near edge of the wetted crossarm surface. This is the start of a pocket burn

Remedial Devices for Pocket Burning

Voltage concentration across high resistance sections may be avoided if a low resistance shunt is placed in parallel with them. Figures 18 through 21 show four

possible shunting arrangements. The assumed air movement direction and the resulting selective wetting are the same as in Figures 15 and 16. The shunting devices are also effective on other air movement directions such as Figures 8 and 9.

In Figure 18 leakage currents originating on the crossarm leave the wet and conducting surface at *A* and enter the circumferential arm band *B*, flow through crossarm jumper *C* to the through-bolt *D*, flow the length of the through-bolt and enter the pole jumper *E*, flow through pole jumper *E* to pole band *F*, then flow around pole band *F* to the wet and conducting pole surface at *G*. These interconnected bands thereby present a low resistance path which shunts the leakage currents past the dry high resistance shadow and gain area.

The completeness of the previous banding arrangement might be simplified as shown in Figures 19 through 21. These devices are connected to the through-bolt and extend beyond shadow areas onto the pole and crossarm.

Pocket burns have not occurred within the shunted area while using these de-

Figure 12 (left). Open flames appeared in about ten minutes

Figure 13 (right). A pocket burn developed on the pole and crossarm at the location of the original carbonized paths

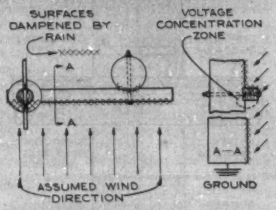

Figure 15. This assumed wind and rain direction casts a relatively dry crossarm shadow on the pole. In addition to the shadow the gain is dry. A voltage concentration occurs across these dry zones

Figure 14. The pocket burn that formed in the pole and crossarm

Figure 16. A pocket burn developing from the conditions assumed in Figure 15

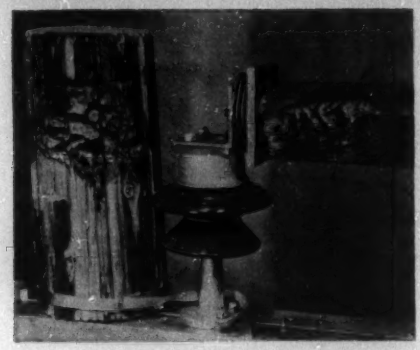

Figure 17. The pocket burn that resulted in the pole and crossarm

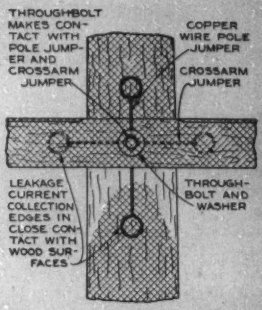

Figure 20. A pair of wires with leakage-current collection loops at the ends may be used as shunts

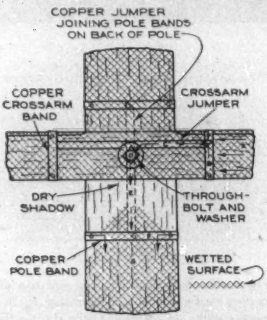

Figure 18. A banding arrangement that shunts leakage currents past dry high resistance shadow and gain areas

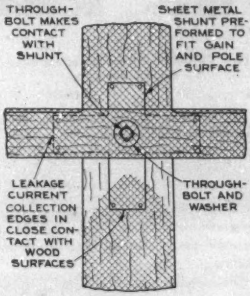

Figure 19. A metal gain-plate shunt

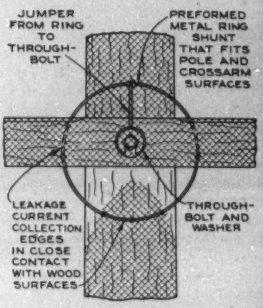

Figure 21. A preformed ring may be used as a shunt

vices during laboratory tests. To obtain this result it is necessary that the leakage current collecting edges of the devices be located outside of all wind shadows of either crossarm or pole and be terminated snugly against the wood's wetted surfaces.

Shunting devices possess certain disadvantages.

1. They may reduce in small degree the impulse insulation contributed by the wood structure.

2. The elimination of high resistance areas may tend to increase the magnitude of leakage current because this magnitude is controlled partially by the wood structure resistance.

3. If improperly designed and applied, the shunting devices may cause an aggravated tree-burning condition at the current collection edges of the shunting electrodes.

4. The shunts, being metallic, are subject to corrosion, and therefore the life of the device should be questioned in relation to the structure it is protecting.

Experience gained from actual installations will be required in order to evaluate the relative merits and demerits of these devices.

A second approach to the elimination of a voltage concentration zone is through the use of wood treatments which would increase dry wood conductivity. Various other forms of remedial devices undoubtedly will suggest themselves to the practical operator. The final forms will be dictated by cost and expected life.

Conclusions

1. Operating experience indicates the consequences of pocket burns to be more expensive than tree burns.

2. Laboratory tests indicate that a coincident occurrence of the following conditions may result in pocket burn.

(a). Dry low-conductivity wood.

(b). The selective wetting of the pole and crossarm surface by a precipitation which leaves dry high resistance zones in series with low resistance wet sections of the leakage path.

(c). A dry zone which is sufficiently short so that the circuit voltage will cause electrical breakdown to occur across it.

3. Laboratory tests show that metallic shunting devices which by-pass leakage currents around high resistance dry zones are effective in preventing pocket burns within the shunted zone.

4. The selection of a final form of remedial device will be dictated by the initial and installation cost of the device itself and its expected life in relation to the structure it is protecting.

References

1. The Characteristics and Performance in Service of High-Voltage Porcelain Insulators, J. S. Forrest. *Journal*, Institution of Electrical Engineers (London, England), volume 89, part II, number 7, February 1942, pages 60–80.

2. The Electrical Resistivity of Resin-Treated Wood and Laminated Hydrolyzed-Wood and Paper-Base Plastics, Richard C. Weatherwax, A. J. Stamm. AIEE Transactions, volume 64, 1945, December section, pages 833–8.

3. Wood Handbook (book). Prepared by Forest Products Laboratory, U. S. Dept. of Agriculture (Washington, D. C.), pages 43–5.

Discussion

L. D. Cronin (Ebasco Services, Inc., New York, N. Y.): A short time ago I inspected several poles where burning by leakage currents has occurred and I can assure Ross that the types of wood burning which he has produced in the laboratory are very similar to those actually occurring in the field at least in so far as the pole is concerned. The arms had been replaced in the locations which I inspected. Ross has provided a very logical explanation of the occurrence of pocket burns at or near the junction of the pole and the crossarms. His paper represents a real contribution to the knowledge of the subject.

It would have been very helpful if the metal braces ordinarily used on distribution circuits had been included in the test setup so that their effect could have been determined. It may be noted that the braces provide a metallic path for the leakage current around the high resistance "shadow" area in the same manner as the shunting devices described in the paper. Perhaps the reason that the braces do not prevent burning in the shadow area is that there is insufficient contact area on the arms and on the pole at the end of the braces. The use of bands around the arm and around the pole at the ends of the braces and electrically connected thereto, might make it possible to accomplish the desired shunting of the danger area in a simpler and easier manner.

W. H. Wickham (Commonwealth Edison Company, Chicago, Ill.): Ross' paper suggests two points which merit further consideration.

1. The importance of the resistance of the junction between pole and crossarm in limiting the current in the porcelain–wood circuit.

2. The importance of selective wetting as a factor in producing burning of the wood members.

In selecting a value of series impedance to be used in the test circuit Ross has assumed that the resistance of the wet wood circuit is of no importance in controlling the leakage current and, with the test arrangement shown in Figure 4 of the paper, this is the case. However, for the test arrangement of Figure 9, this may not be the case. In fog or misty rain the gain surface on the pole and the surface of the crossarm in contact with the pole remain relatively dry. Furthermore, at this junction some of the current must take a path across the grain of the wood in passing from the crossarm to the pole. So, even though wetting reduces the resistance of the individual wood members to a low value, the resistance at the junction between the two may remain relatively high. These conditions would suggest that a much lower series impedance would more nearly represent field conditions and would change the behavior of the wood portion of the circuit.

The higher resistance of the wood circuit in the gain area gives the voltage concentration necessary to produce burning without selective wetting. This accounts for the occurrence of wood burning in fog conditions, with practically no wind, where selective wetting can hardly take place.

F. E. Andrews and **R. W. Caswell** (Public Service Company of Northern Illinois, Chicago, Ill.): The paper by Ross is a valuable contribution to the knowledge and information on a very troublesome operating problem which heretofore has had inadequate investigation as a general technical subject.

During the past ten years we have experienced about 60 cases of pole fires on 33-kv lines due to leakage currents under the field conditions referred to by Ross. About two-thirds of the cases occurred during 1944 and 1945. This concentration of troubles probably resulted from a combination of weather conditions especially conducive to creating the necessary leakage and an acceleration of dirt deposits under wartime industrial conditions. This illustrates the erratic expectancy of this type of trouble. Several years may pass with very little of it, to be followed by an epidemic within a few months to one or two years following.

In addition to the burning at junction of pole and crossarm, we have had vertical corner poles burned at the bolt used for attachment of the dead end insulators to the pole. Approximately one-third of our fires have been on vertical corner poles.

Our experience indicates that the use of more porcelain insulation than normal does not prevent pole fires. Fires have occurred on poles in 33-kv lines using 35-, 45-, and 55-kv pin-type insulators, and at strain insulator dead ends on vertical corner poles with widely varying amounts of insulation. This insulation has varied from a minimum of two $6^1/_2$-inch spaced units to a maximum of 5. Three units are normal either with $5^3/_4$- or $6^1/_2$-inch spacing. Fires due to leakage have occurred with both types of insulators.

Many of these fires have been in areas that are not considered as excessively dirty. We have not been able to determine that the presence or absence of creosote treatment of poles and arms has any important influence on their susceptibility to fires, as fires have occurred on both treated and untreated poles and arms.

We have found that the presence of a static wire ground lead on a pole does not prevent fires at junction of the arm and pole. In addition to burning at junction of pole and arm, we have experienced burning off of the crossarm about midway between the insulator and the pole.

During the past two years we have installed some band arrangements following the same principle as shown by the author's Figure 18. However, we wrapped the pole and arm with small soft drawn copper wire, usually Number 18. The small wire is used in preference to a strap because it is believed that the wire will provide a more intimate contact with the wood surface over a longer period of time than straps which may not so closely follow the contour of the wood surface. We have also used this wire method to connect the pole to the insulator hardware at vertical corners. So far we have had no fires on poles protected in this manner, but we consider that our operating experience is insufficient to assume that this remedial measure is fully effective.

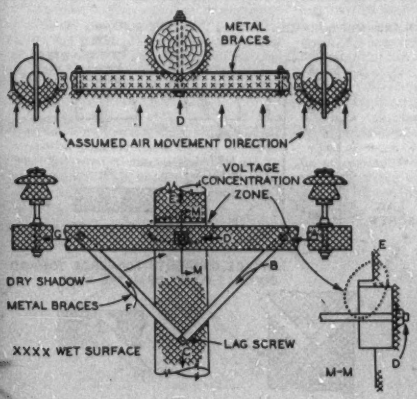

Figure 1. Metal braces provide low resistance shunt paths for the current flow direction *A-B-C*, also *A-B-F-G*, but not *A-D-E*

H. E. Weaver (Public Service Company of Northern Illinois, Maywood, Ill.): Ross should be commended for his paper and this discussion is in the nature of a corroboration rather than a criticism of the paper.

Ross used ten milliamperes of leakage current in order to get results quickly, but, in independent laboratory studies that we have made, we got fires with eight milliamperes, found that with three milliamperes burning would continue slowly and quietly, and that with one milliampere of leakage current the carbon in the charred spots would continue to glow.

Apparently leakage currents of ten milliamperes frequently occur in practice. After periods of dry weather, the surface resistance of line (37 kv) insulators, when sprayed with distilled water, was found to be the order of 0.2 to 20 or more megohms with an appreciable percentage falling in the one half to one megohm class. The appearance of the insulators is often unreliable as a means of estimating its wet surface resistance.

For convenience, Ross used an imped-

ance, between the testing transformer and the wood circuit, to simulate an insulator. On some of our tests, we used a regular line insulator in series with the wood circuit. Burning could be established and maintained, after spraying water on insulators that had accumulated storeroom dust for a period of two months, and burning could easily be started when using insulators that had been removed from service near a chemical plant, even after they had been flushed off with water.

Of the methods of mitigating burning, which were mentioned in the paper, our tests tended to show that banding the pole and arm would be the most effective for it seemed easier to maintain good contact with the wet surfaces.

M. S. Oldacre (Commonwealth Edison Company, Chicago, Ill.): It is obvious to anyone who has seen the demonstration of the work described by Ross that a real contribution has been made to our knowledge of the pole burning problem. This discussion is to suggest some of the other phases of the problem that exist.

The insulator is a very important part of the leakage circuit under ordinary conditions, but under wood burning conditions seems to become a negligible factor. Thus there is a field for insulator development for specially contaminated areas. The requirements seem to be that a reasonable portion of the surface remains dry under all conditions or that there be enough leakage surface so that the current will be less than enough to cause burning.

It would seem that the surface conductivity of the pole and cross arm is of vastly more importance than the conductivity of the mass of the wood. That is, there should be no great difference in the burning characteristics of so-called dry or wet wood if the surface conditions were suitable to cause burning. If this statement is not correct, there would undoubtedly be many cases where the shunting devices across the joints would be ineffective. Actually the shunting devices perform as expected if their condition remains as good as when installed.

More knowledge is still needed on this subject and it is suggested that some of the factors to be considered are:

1. Effects of different surface treatments or impregnations of poles and arms.
2. Shunting devices of low cost and easy application that will remain effective during the life of the poles and arms.
3. Consideration of insulator design to secure an effective dry area under all conditions.
4. Selection of insulators that will give enough leakage surface to prevent burning under contaminated conditions. This would assume that insulators could be washed or otherwise cleaned prior to the period of the year when contamination is likely to contribute toward burning of the wood.
5. On double circuit lines the location of the corresponding phases of the two circuits should be selected to avoid concentration of leakage current at any one connection.

The ultimate solution to the problem may be a combination of results from the above items as the cost of making the changes must not be overlooked.

Paul M. Ross: The nature of the questions and character of the comments given by the various discussers of this paper indicate that they have given careful consideration to the various phases of the problem of pole and crossarm burning.

Cronin has requested an explanation of the shunting action afforded by metal braces. Figure 1 of the discussion presents a typical pole and arm construction including the use of metal braces. An air movement direction has been assumed which is parallel with the conductors. If the air movement carries with it a form of precipitation, the indicated areas of the structures will become dampened and these wetted wood portions will therefore have relatively low resistance. Assuming that leakage current flows from the right-hand insulator, it would flow in direction *A*, through the conducting surface of the wetted arm to the brace, then down the brace in direction *B* and leave the brace on the wetted and conducting pole surface in direction *C* in order to reach another phase or grounded point below.

If the leakage current path is from phase-to-phase between the right-hand insulator and the left-hand insulator, the leakage currents would flow from *A* down the brace in direction *B*, up the left-hand brace in direction *F* and through the wetted arm surface in direction *G* to the left-hand insulator. This latter path is in parallel with the low resistance wetted arm surface joining the two insulators. In these two cases the braces do provide a shunting action.

If, however, the leakage current flows between the right-hand insulator and either some other phase or a grounded point higher on the pole, the leakage current would flow in direction *A* and *D* through the wetted surface of the arm and then must leave the arm surface and flow thru the wet conducting surface of the pole *E*. Unless the arm fits snugly into the pole gain, a gap may exist between the top of the arm and the pole surface as shown in section *M-M*. If there is such a discontinuity in the wetted conducting surfaces between the arm and the pole, a voltage concentration zone will appear at that point and this zone is, therefore, a possible pocket burn location. The braces in this case do not provide a shunt for the leakage current around this voltage concentration zone because the wet surface of the pole above and below the arm is interrupted by the dry shadow of the arm and the gain.

In Figure 2 of the discussion, the assumed air-motion direction causes the pole structure to be wetted on the opposite surface from that in Figure 1. In this case the metal braces provide a shunt path by-passing the high resistance shadow zone between the arm and the pole for leakage currents flowing from the right-hand insulator to the left-hand insulator. The braces do not, however, provide a low resistance shunt if the leakage current flow is either to another

Figure 2. Metal braces do not provide a complete low resistance shunt path for either current flow directions *A-B-C-D* or *A-E-F-D*

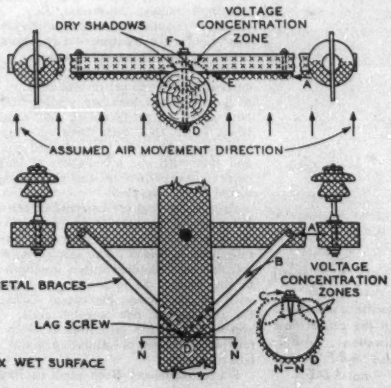

Figure 3. Leakage current density is greatest at edges of metal parts. Drying proceeds faster in wood areas *A* adjacent to metal parts. Tree burning develops across *A*

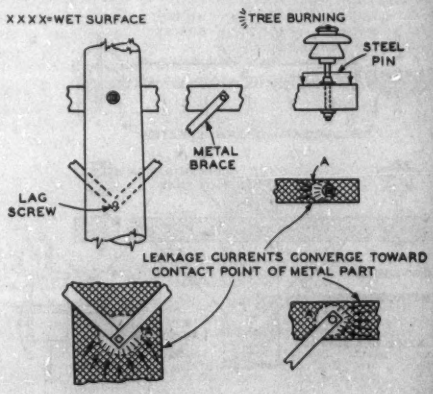

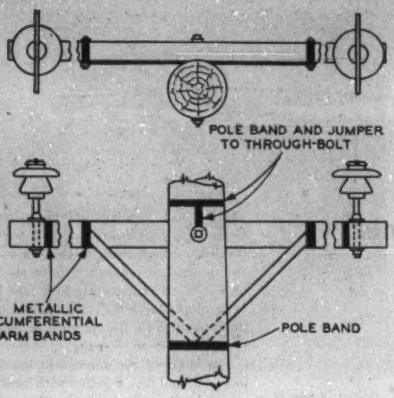

Figure 4. Suggested method for reducing tree burning at metal attachment points

phase or to ground at a location above or below the crossarm.

There are two surface paths available by means of which the leakage current starting from the right-hand insulator in direction *A* may reach the wet conducting surface *D* of the pole. The current may flow downward through the metal brace in direction *B* to lag screw *C*. In order to reach the low-resistance wetted surface of the pole *D*, as shown in section *N–N*, the currents must flow through the dry, high resistance areas on the back of the pole.

The second path is indicated in the top view of the structure. The leakage currents might flow from the right-hand insulator in direction *A* to the edge of the wetted conducting surface of the arm at point *E*. They must then flow thru the dry, high resistance, shadow zone in order to reach the thru bolt, the outer end of which is terminated in the wet conducting surface *D* of the pole.

Voltage concentration zones, therefore, exist between point *E* and the through bolt and on both sides of lag screw *C* in section *N-N*. These voltage concentration zones are subject to burning tendencies.

Laboratory tests on an arrangement electrically similar to Figure 2 have indicated that electrical breakdown will occur in the direction of the grain from point *E* to the through-bolt in preference to the circumferential direction from the lag screw *C* to the edge of the wetted pole surface.

The grain structure of the wood in the arm is usually continuous while in the case of the circumferential direction around the pole from lag screw *C* the surface may not be continuous. It is usually interrupted by checks or cracks in the pole surface. The presence of cracks in the pole surface requires a higher voltage to cause electrical breakdown across a given circumferential distance in comparison with an equal distance along the grain of the crossarm. Pocket burning may develop at both locations. However, I would expect a greater number of cases to develop at the dry shadow area of the pole on the crossarm in comparison with the lag screw *C* location.

Under light precipitation conditions in which evaporation from the wood surfaces, due to the I^2R loss of the leakage current flow in these surfaces, exceeds the precipitation rate, localized drying will take place at these areas and tree burning may develop across the dry sections. Figure 3 of the discussion illustrates this condition at the contact between metal attachment parts of steel pins or braces on arms or poles.

Remedial banding methods similar to those suggested by Cronin are presented in Figure 4 of the discussion. Bands have been located at all metal attachment points. These bands when applied snugly to the wood surfaces decrease the leakage current density at the current collection edges of the bands and thereby tend to avoid localized drying and subsequent tree burning at these locations. To accomplish this result it is necessary that the current collection edges of the bands make good contact with the wood surfaces. In addition, the pole bands provide low resistance shunt paths around the dry high resistance voltage concentration zones in Figures 1 and 2.

The presence of the pole and arm bands do not detract from the impulse insulation strength of the structure in an important degree. If wood braces are used in place of the metal braces in order to increase the impulse insulation of the structure, it is suggested that the banding procedure shown in Figure 4 be used at the insulator and brace attachment points on the pole and the crossarm. In addition, a shunting arrangement similar to that shown in Figures 18 to 21 of the paper, be included at the pole to arm junction.

In reply to Wickham's question concerning the series impedance used in Figures 4 and 9 of the paper, we varied the magnitude of this impedance during part of our nonreported tests. During these particular tests we maintained the applied voltage constant from the test transformer and varied the magnitude of the impedance. Once electrical breakdown had taken place across the dry, high resistance, voltage concentration zones, the current magnitude that flowed thru the combination of series impedance and wood structure was controlled principally by the series impedance. The current magnitude that flowed after electrical breakdown were 2, 5, 10, and 20 milliamperes depending upon the magnitude of the series impedance. The general location of the burn damage in all cases was the same. The higher current magnitudes produced a given amount of burn damage in a shorter time than did the lower current magnitudes.

I believe Wickham has suggested the proper explanation for wood burning under fog conditions in which no particular part of the structure may become more wetted than others due to the absence of air movement, vertical convection or otherwise. Under these light wetting conditions the junction between the pole and the crossarm would be expected to remain dry and, therefore, have high resistance. If this high resistance section occurs as a part of a series leakage current circuit, a voltage concentration will appear across it, possibly accompanied with electrical breakdown and pocket burn damage. This situation would be aggravated by the presence of a gap between the arm and the pole due to either loose hardware or a loose fit similar to the condition illustrated in section *M-M*, Figure 1. I would not expect the fog to penetrate into these confined spaces without the aid of air movement.

I wish to thank Andrew, Caswell, and Weaver for the description of their laboratory tests and their field experiences including the use of banding arrangements. Our research efforts closely parallel their laboratory work and the general test findings are in good agreement.

Oldacre has made several valuable suggestions as to desirable future research work on this subject. These points also constitute a good criterion to follow in selecting materials for transmission line use from present designs when it is desired to avoid wood pole burning.

Some Recent Developments in the PCC Car

S. B. COOPER
NONMEMBER

Synopsis: The PCC (Presidents' Conference Committee) car was developed about ten years ago as a result of a co-operative research program by the major transit operating companies and manufacturers. This paper briefly reviews the history and experience with the car and outlines the recent changes and improvements. New performance curves are included.

THE PCC car is the result of a co-operative research program started in 1929 under the name of the "Electric Railway Presidents' Conference Committee." Rising costs and declining revenues indicated the urgent need of improvement over existing cars and of some degree of standardization of design so that cars and their equipment could be produced in manufacturing quantities instead of in small individual lots.

The committee was formed by a group of the presidents of the larger city transit systems, and the activity was financed by contributions from these operating companies and from the principal manufacturers interested in the car and equipment business.

Professor Clarence F. Hirshfeld was selected as chief engineer. Under his direction the program began with a careful study of the characteristics of then existing cars, their shortcomings, and the specific need for improvement that would make the streetcar more efficient and appealing to the riding public and would put its design and construction on a manufacturing basis.

The work of the committee and the resulting car have been described in previous Institute papers. It is the purpose of this paper to review the progress and developments since the last papers were presented and to indicate the trends which further developments may be expected to follow.

The first PCC cars were ordered early in 1935, and during the years from then until 1944 about 2,500 cars were placed in service on 16 properties in the United States and Canada. This period covered the latter years of the depression and the early years of the war. It was recognized that following the war there would be an increased demand for equipment to replace older rolling stock worn out by intensive use during the war period. A program was started to review and evaluate the experience with the cars up to that time and to establish the objectives of further developments and improvements to be incorporated in the postwar designs. This program resulted in the production of a sample 1945 model car which was placed in service on the lines of the Pittsburgh Railways Company in October 1945. The principal improvements may be outlined as follows.

Body changes were made to improve passenger comfort and aisle width by making seat spacing and post spacing the same. This makes it possible to move the seat cushion closer to the side wall of the car and to obtain a greater effective aisle width. Standee windows now have been adopted as a standard feature, making it possible for the standing passengers to see out without stooping.

The slope of the windshield has been increased and this, together with improvements in the "shadow apron" over the operator's desk, greatly reduce windshield reflections and improve the operator's view of the street at night. The shape and location of the front corner posts have been altered so as to minimize the "blind spots" and increase safety. The operator's position has been raised and moved forward somewhat to give him a better view of the area immediately in front of the dash. Detail improvements in doors, door mechanisms, and so forth, tend toward easier entrance and exit.

In spite of the fact that the original PCC car had a system of ventilation that took 1,200 to 1,500 cubic feet per minute of air out of the car, it has been recognized for some time that further improvement in car ventilation was desirable. It was felt that a definite circulation of additional fresh air would add materially to passenger comfort.

As the result of a considerable amount of experimental development, a system of ceiling ventilation is now available as an optional feature. A longitudinal roof monitor with louvered sides extends almost the entire length of the car roof. This is divided by cross barriers into alternate intake and exhaust sections. Three or four vertical motor driven fans,

Figure 1. Car 1600 of Pittsburgh Railways Company, the first postwar model

Paper 47-41, recommended by the AIEE committee on land transportation for presentation at the AIEE winter meeting, New York, N. Y., January 27-31, 1947. Manuscript submitted November 13, 1946; made available for printing December 6, 1946.

S. B. Cooper is a transportation engineer with the industry engineering department, Westinghouse Electric Corporation, East Pittsburgh, Pa.

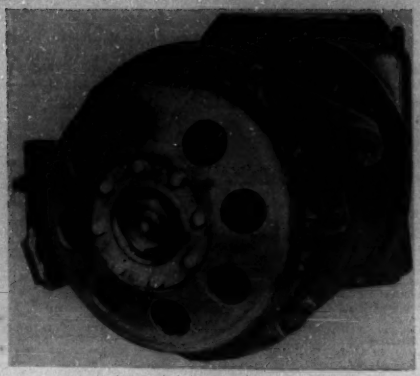

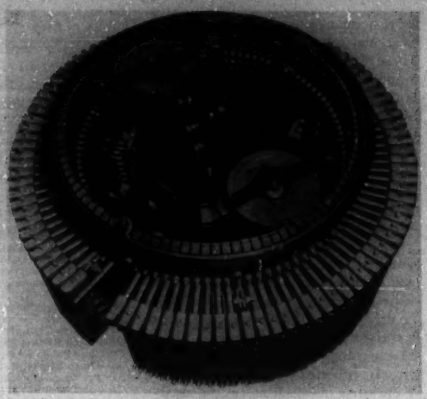

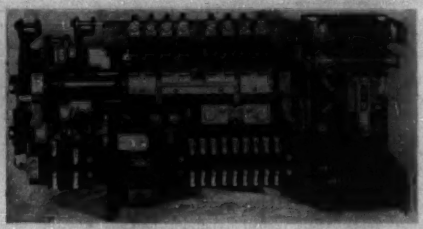

Figure 2 (above, left). Type 1432-J motor showing drum brake mounted

Figure 3 (above, right). Accelerator viewed from below

Figure 4 (left). Combined master and brake controller

spaced along the ceiling of the car, draw their air from the intake sections of the roof monitor and discharge it directly into the car through diffusion grilles. These grilles are so arranged so as to direct the air flow out along the ceiling line, downwards diagonally, and along the sides of the car to give a definite feeling of air movement but without direct blast or draft effect. The roof monitor and fan intakes are arranged to trap and drain moisture. The space between the ceiling and the car roof is used as an exhaust duct communicating with the outlet sections of the monitor. The fan motors are connected in series across the line and are arranged for thermostatic control of fan speed—the speed being increased with higher outdoor temperatures. At top speeds these fans introduce a total of 12,000 to 14,000 cubic feet of fresh air per minute into the car. Experience with this system to date indicates that it may be entirely possible to operate with permanently closed windows.

This ventilation system has brought with it a change in the motor-generator-blower system of equipment ventilation and car heating. The air exhausted from the car by the motor-generator blower now is drawn partly through air intake grilles in the side lining of the car in the area opposite the center doors and immediately above the motor-generator-blower compartment, and partly from the center door step-well through the space between the car floor and the accelerator support plate. The motor-generator set now has a blower on each end. Each of these two blowers has its runner and housing partitioned by a divider plate, giving in effect two sections to each blower. In each one, the outer section farthest from the motor-generator set draws its air through louvered openings in the outside of the car and discharges it into a duct under the car floor leading to the two traction motors on the adjacent truck.

The inner section of each blower draws its air from the car body through the paths described and discharges it directly into the equipment compartment over the accelerating and braking resistors. From this space it is blown into cross ducts just ahead and back of the step-well section, and then directed by the thermostatically controlled dampers either to outside air in nonheating season or to the longitudinal sill ducts on *both* sides of the car in the heating season.

Because in summer weather the car body is under pressure ventilation from the ceiling fans, the side sill heater ducts also serve as air outlets from the car, further improving body ventilation and avoiding any possibility of damper leakage permitting warm air entering the car from the equipment.

Auxiliary heaters are mounted in the air stream on the outlet side of the blowers so that in case of a blockade or in case of infrequent stop service, where acceleration or braking resistor losses are insufficient to maintain comfortable car temperature, these auxiliary heaters are cut in automatically.

The heating and ventilating control is arranged to provide a definite sequence of operation of auxiliary heat, damper control, and steps of ceiling fan speed so as to provide for proper heating, cooling, and ventilation of the car throughout the range of operating temperatures.

Important improvements have been made in braking. The cost, complication, and maintenance of compressor, reservoirs, valves, piping, and cylinders of the air brake system seemed out of line with the small amount of work required for completion of the stop below the speed of dynamic fade-out and for holding the car at stops. In addition, it had proved quite difficult to keep the brake levers and shoes of the air operated wheel brakes

from accumulating clearances caused by wear and consequent noise and rattles. These reasons led to investigation of other forms of supplementary mechanical brakes. In 1939 the St. Louis Public Service Company purchased 100 cars of the all-electric type. The performance of these and of the second hundred purchased in 1941 was so successful that the initial skepticism of the industry was overcome and all-electric operation now has been adopted as standard.

On this type of car the air operated shoe brakes bearing on the wheel tread have been replaced by drum brakes carried on the coupling at the motor end of the drive shaft. Two forms of brakes are in current production and use—an internal expanding and an external contracting. In either case, either of two forms of operating mechanism can be used—spring application and solenoid release or solenoid application and spring release, with special means provided for spring application in case of failure of control power. This makes it possible to do away with the former hand brake for parking the car in sidings or yards as, with either form of brake or operating mechanism, opening the brake solenoid control circuit gives a spring applied brake without battery drain.

The necessity for finding room for the brake drum at the drive end of the motor was what first brought forced motor ventilation into consideration. The traction motor was shortened by omitting its internal ventilating fan. Since that time the obvious advantages of forced motor ventilation have become more generally recognized, and no doubt it would be continued today for its own merits entirely aside from the question of brake drum space. Forced ventilation keeps the motor under pressure, thus tending to keep dirt and water out rather than sucking them in as under "natural" ventilation. Also, the uniform continuous flow of cooling air independent of speed has proved much more effective than the widely fluctuating amount of air resulting from the internal fan at varying speeds.

While the original spring solenoid brake in St. Louis was quite successful, it was felt that for general application as standard equipment for hilly as well as flat cities a brake of greater holding power was necessary, and also that the drum brake should have sufficient thermal capacity for making the stop in case of failure of the dynamic brake. It seemed obvious that the drum brake would have the best chance of success in general application if its normal duty were reduced to the lowest possible level.

This led to the development of "extended dynamic" braking, wherein the dynamic brake is carried down almost to standstill, actually to about one mile per hour. This development was carried out with the co-operation of the engineers and staff of the Pittsburgh Railways Company and has proved remarkably successful. This limits the normal duty on the drum brake almost entirely to holding at stops and therefore reduces the wear on shoes and drums to a point within the practical limits of a short travel device like a solenoid.

Improvement also has been made in the "easy shut-off" by introducing resistance into the circuit before opening the line switch. This feature adds materially to passenger comfort during "on and off" operation behind slow traffic or with the nervous type of operator who, in spite of training and instruction to the contrary, will start and shut off two or three times while waiting for the traffic light to signal "go."

A combined master and braking controller simplifies installation and maintenance by providing permanent line up between the limit relay and the cams on the power and brake controllers.

The trend at present is toward the use of deion type circuit breakers in place of fuses for both 32- and 600-volt circuits.

Table I. PCC Cars in North America as of November 1946

Transit Company	Total Number	On Order	In Operation
Baltimore Transit Company, Baltimore, Md.	275	0	275
Birmingham Electric Company, Birmingham, Ala.	48	48	0
Boston Elevated Railway, Boston, Mass.	271	21	250
Chicago Surface Lines, Chicago, Ill.	683	600	83
Cincinnati Street Railway Company, Cincinnati, Ohio	53	25	28
Cleveland Transit System, Cleveland, Ohio	50	50	0
City of Shaker Heights, Department of Transportation, Cleveland, Ohio	25	25	0
Dallas Railway and Terminal Company, Dallas, Tex.	25	0	25
Department of Street Railways, Detroit, Mich.	80	78	2
Johnstown Traction Company, Johnstown, Pa.	17	17	0
Kansas City Public Service Company, Kansas City, Mo.	99	41	58
Los Angeles Railway Corporation, Los Angeles, Calif.	165	40	125
Louisville Railway Company, Louisville, Ky.	25	25	0
Twin City Rapid Transit Company, Minneapolis, Minn.	91	90	1
Mexico City Tramways, Mexico City, Mexico	1	1	0
Montreal Tramways, Ltd., Montreal, Canada	18	0	18
New York City Transit System, Brooklyn, N. Y.	100	0	100
Pacific Electric Railway, Los Angeles, Calif.	30	0	30
Philadelphia Transportation Company, Philadelphia, Pa.	470	210	260
Pittsburgh Railways System, Pittsburgh, Pa.	566	0	566
St. Louis Public Service Company, St. Louis, Mo.	300	100	200
San Diego Electric Railway Company, San Diego, Calif.	28	0	28
San Francisco Municipal Railways, San Francisco, Calif.	15	10	5
Capital Transit Company, Washington, D. C.	490	0	490
Toronto Transportation Commission, Toronto, Canada	390	100	290
British Columbia Electric Railway Company, Vancouver, Canada	36	0	36
Total	4,350	1,481	2,869

Figure 5. Speed, time, and distance curves

Weight of empty car, lb	36,000
Average passenger load, lb	6,000
Equivalent rotation allowance, lb	5,600
Motors per car	4
Motor type	*1432-J*
Gear ratio	7.17 to 1
Wheel diameter, in.	25
Accelerating rate, mphps	3.5
Average voltage	550
Train resistance	Davis plus 6 lb per ton
Grade and curve resistance	0

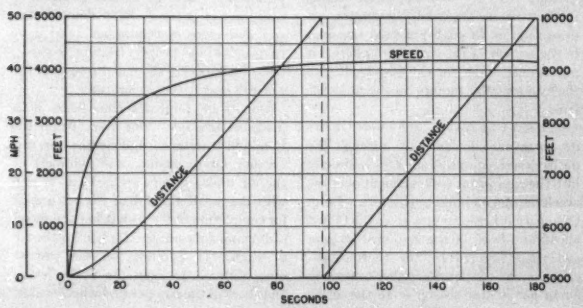

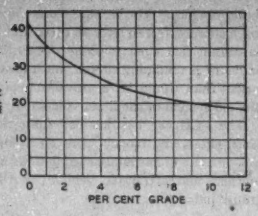

Figure 6. Balancing speeds on grades

Weight of empty car, lb	36,000
Average passenger load, lb	6,000
Motors per car	4
Motor type	*1432-J*
Gear ratio	7.17 to 1
Wheel diameter, in	25
Average voltage	550
Train resistance	Davis plus 6 lb per ton

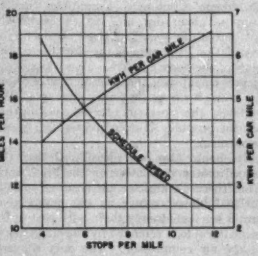

Figure 7. Surface car operating characteristic

Weight of empty car, lb	36,000
Average passenger load, lb	6,000
Equivalent rotational allowance, lb	5,600
Motors per car	4
Motor type	*1432-J*
Gear ratio	7.17 to 1
Wheel diameter, in	25
Acceleration, mphps	3.50
Breaking, mphps	3.15
Average voltage	550
Train resistance	Davis plus 6 lb per ton
Grade resistance, lb per ton	
Coasting	25 per cent of moving time
Coasting rate, mphps	0.415

A trip is indicated by the position of the handle, making it easier for the operator to locate quickly the circuit in trouble. Pushing the handle to "off" and then to "on" is easier and quicker than hunting for and replacing fuses.

Detail improvements have been made in the motor—a longer commutator permits larger brush area and increased brush life. Greater protection over the front commutator V-ring minimizes the damage resulting in case of motor flashing. Better insulation on both armature and field coils has lengthened coil life and reduced chances of breakdown.

Many control details have been improved as a result of the accumulated experience with the earlier cars. Silver faced wiping type control fingers and interlocks, improved type limit relay contacts and similar developments have increased reliability further.

Improvements in wiring and layout worked out in co-operation with the wiring committee and the engineers of the car builders have resulted in better equipment arrangement and installation and reduction in the number of pieces to be housed, mounted, and wired.

A new design of truck has been completed so there are now two sources of supply.

Car Performance

With the various modifications, car weights have tended to increase. At the present time standard single-end single-unit cars are coming through at about 36,000 pounds empty weight. Also, the equivalent weight addition for rotational or flywheel effect has been increased by the addition of the drum brake on the drive shaft and by some increase in the weight of the resilient wheels. Car performance based on these current weights and on the corresponding rates of acceleration and braking are shown on the accompanying curves.

Figure 5 shows the speed time and distance curves for a 36,000-pound car with an average load of 6,000 pounds up to balancing speed on level track.

The balancing speeds on grades up to 12 per cent are shown in Figure 6.

Schedule speeds and propulsion power consumption for varying stops per mile from 4 to 12 are shown in Figure 7. These are based on an acceleration rate of 3.5 miles per hour per second, dynamic braking at 3.15 miles per hour per second, coasting for 25 per cent of moving time and 7-second stops.

All curves are based on train resistance curve shown in Figure 8 plus six pounds per ton for resilient wheel resistance.

The number of cars in service and on order is the best possible testimonial to their success. Table I shows the cars now in service and on order by properties. This seems quite an impressive showing when it is recalled that the period covered included the latter years of the depression and the war years with material and production restrictions.

There is still much transit rehabilitation work to be done. No doubt many existing car lines in smaller cities or secondary and cross-town lines in the larger cities will be changed over to trolley coach or motor coach operation. The modern street car, however, remains a most efficient vehicle for heavy trunk route service in the large cities, in the field where density of riding is too high for a 40- or 44-passenger vehicle and not high enough to justify real rapid transit subways. There is growing recognition of the fact that street congestion is largely a function of the number of vehicles, and attempting to handle large numbers of people in private automobiles or in small capacity transit vehicles is neither efficient nor economical. City planners now recognize the prime importance of mass transportation in our cities. Along with plans for freeways and super highways, consideration is being given to the needs of the great number of people who necessarily will continue to depend on public transit. In a number of instances, plans are being studied for rail rapid transit, in conjunction with the freeways, where stations are arranged for convenient interchange with feeder lines for local distribution.

The PCC car equipment already has been developed for multiple unit operation, first for Pacific Electric Railway in Los Angeles and later for Boston Elevated Railway. The 50 cars recently placed in service on Cleveland Transit System all are equipped for multiple operation. Couplers can be added whenever the contemplated plans for rapid transit are completed. The city of Shaker Heights has just ordered 25 PCC cars arranged for operation in trains on their system operating from Cleveland terminal over private right of way out into Shaker Heights.

Chicago Rapid Transit has on order four experimental articulated cars of PCC type modified for their type of service and other developments are under way toward the development of larger capacity trucks

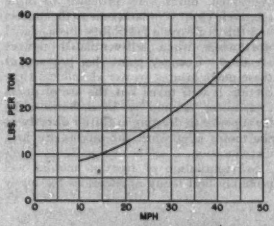

Figure 8. Estimated train resistance

Davis-21 ton car. Resilient wheel allowance not included

and equipment to apply the basic ideas of the PCC to heavy service.

Foreign cities are showing considerable interest in this type of car, and it confidently may be expected that many cars of this type will be used abroad.

Future developments probably will trend toward weight reduction by the use of lighter metals, continuing effort for greater passenger comfort and appeal, and also for the simplification and the further reduction of maintenance and inspection work.

The results obtained certainly bear out the hopes and expectation at the start of the committee's program. The cars have shown great passenger appeal and have met with almost unanimous public approval. The advantages of standardized design of body trucks and equipment, permitting minor modifications without too great change in major tooling, have been obvious. To be sure costs have risen sharply, but so have all costs, and it is certain that even at today's costs the industry is obtaining cars at much lower prices than would have prevailed under the old system of small individual lots.

The PCC car has justified fully the time, effort, and money spent on its development and has established itself as an efficient and attractive vehicle for the transit industry.

Discussion

John C. Aydelott (General Electric Company, Erie, Pa.): Cooper has mentioned the reason why forced ventilation was adopted for the traction motors of the Presidents' Conference Committee car and some of the good points of this system. It may be in order to say a few words in general in favor of self-ventilation, that is ventilation by a fan mounted on the shaft of each motor armature.

It is interesting to compare the amount of dirt which accumulates in two different types of motors in the subway in New York, apparently as a result of the system of ventilation. In both cases the motors referred to are modern high speed motors, those which are force ventilated are, in fact, an adaptation of the Presidents' Conference Committee car equipment and have been observed to be much dirtier than those on other equipments which are self-ventilated. Cooper speaks of the "widely fluctuating amount of air resulting from the internal fan at varying speeds". Apparently, the occasional high velocity blast of air which passes through the self-ventilated motors at high speed scavenges the dirt from the motors much more effectively than does the relatively slow steady stream of air passing through the forced ventilated motors. The effectiveness of both systems of ventilation as far as cooling is concerned is attested by the fact that there have been very few insulation failures in either application.

The provision of clean ventilating air is not an exclusive feature of the forced ventilation system. When the motors on the Presidents' Conference Committee cars were self-ventilated, ducts were provided to bring relatively clean ventilating air to the motors and this is always a possibility if considered worthwhile when self-ventilated motors are used. Cooper's point that pressure in these ducts insures greater cleanliness than suction is well taken but the use of ducts even under vacuum has been shown to be far superior to drawing in the air directly at the motor inlet when the motors are in a dirty location.

Self-ventilation of traction motors will probably find many applications for many years to come. High speed motors in particular lend themselves to the use of self-ventilation. Certain double reduction motors recently developed for use on industrial diesel locomotives are self-ventilated and have proved to be very successful with this type of ventilation. The fact that the motors are used with double reduction gearing is important as it means that even at very low locomotive speed the motors are revolving rather rapidly and ventilating themselves very effectively. In many cases these motors are used one to a locomotive and the simplicity of the self-ventilation system as compared to the use of a separate blower and the necessary ducts is obvious. In addition to simplicity the self-ventilation system also has an element of certainty to recommend it. There are fewer places where the system can go wrong. Whenever the motor is turning over it is providing its own ventilation.

Forced ventilation has its uses but consideration should also be given to the lower cost and simplicity of the self-ventilation system where it can be used.

Cooper's paper is concerned primarily with Presidents' Conference Committee cars and Presidents' Conference Committee car equipment and in this connection he mentions several applications of this equipment to rapid transit service. It might be well to point out that the traction equipment now being developed for the new subway cars described in the papers presented by B. F. Cordts and J. J. Sinclair at another session of this meeting should also find wide use on other rapid transit properties in this country. This equipment developed for rapid transit use is more powerful than the Presidents' Conference Committee equipment and is capable of handling the somewhat larger cars and high speeds usually associated with rapid transit operation.

S. B. Cooper: Our experience with forced ventilation on the Presidents' Conference Committee cars is quite definitely contrary to that indicated in Aydelott's interesting discussion. Direct comparison of natural and forced ventilated motors, duplicates in all respects except ventilation, on similar cars in the same service in the same city shows a definite advantage of forced ventilation in

1. Cleaner motor interior.
2. Fewer motor failures due to moisture in bad weather.
3. Materially lower temperature rise.

There can be no question of the value of the duct arrangement used on the older Presidents' Conference Committee cars to supply "clean dry air" to the naturally ventilated motors. This drew air for motor ventilation from outside the skirt line at the ends of the body bolsters. This was a great improvement over the older method of drawing motor air from the under-floor area. We believe the present forced ventilation scheme provides an even greater step of improvement.

It should also be remembered that the forced motor ventilation on the Presidents' Conference Committee car required no additional blower motor as the motor generator set was already there with part of its mechanical load removed by the elimination of the air compressor. The only net addition, then, was a small increase in blower size and some additional duct work—surely a small price to pay for the marked benefits obtained.

So far as "certainty" is concerned, if the motor generator set should fail, the car should not be run in any case because of absence of resistor ventilation. Such failures have been quite rare and it is difficult to see how any other failure could interfere with motor ventilation.

Admittedly, many successful applications of self-ventilated traction motors have been and will, no doubt, continue to be made, especially where cost and simplicity are paramount considerations. However, where a driving means for the blower is already available, the net added cost and complication for forced ventilation seems very small in proportion to the obvious benefits.

I had no intention of implying that the Presidents' Conference Committee equipment could take over the whole rapid transit field. There are, however, some types of rapid transit or semi private right-of-way running where weights and service requirements are within the capacities of PCC equipment where advantage can be taken of this very interesting development.

Automatic Control of Air Switches for Line Sectionalizing and Load Transfer

F. W. RICH
ASSOCIATE AIEE

M. S. KIRWEN
ASSOCIATE AIEE

Synopsis: The considerations involved in the design and application of automatic control of air switches are discussed in this paper with the thought that they might be used to guide designers and engineers who encounter similar problems. Three air break switch control schemes are described and the diagrams involved are shown. These control schemes were designed to provide automatic switching as follows:

1. Load transfer with synchronism check interlock, using direct current for operation and control.
2. Line sectionalizing and subsequent load transfer, using direct current for operation and control.
3. Load transfer, using alternating current for operation and control.

The description outlines the operation of the various control devices for manual switching and for automatic switching which occurs during fault conditions.

IN the application of automatic switches for transferring load, consideration should be given to the relative costs of air break switches versus oil circuit breakers. This is especially true when the circuit or circuits under consideration, at some future date, might become the source for important load centers. It is not the intent of the authors to discuss the costs nor to outline the relative advantages of one type of switching scheme over another. It might be pointed out, however, that automatic air break switches can be installed readily in such a manner that, when the circuit conditions warrant, oil circuit breakers can be added and the original air break switches used for by-pass switching.

Paper 47-51, recommended by the AIEE committee on automatic stations for presentation at the AIEE winter meeting, New York, N. Y., January 27-31, 1947. Manuscript submitted October 31, 1946; made available for printing November 25, 1946.

F. W. RICH and M. S. KIRWEN are both with The Commonwealth and Southern Corporation, Jackson, Mich.

The principal function of an automatic load transfer scheme is to transfer a load from a preferred source, upon failure of voltage on the preferred line, to an emergency source, thus restoring service to the station. The second function is to transfer the load back to the preferred source upon restoration of voltage on the preferred line. This latter transfer should be made without interruption to service which necessitates paralleling the two lines for a short time during the transfer.

The principal function of an automatic line sectionalizing and load transfer scheme is to first sectionalize the line by opening both line switches upon failure of voltage on the bus, followed by the closing of one of the switches when voltage is restored on one section of the line, thus restoring service to the station. If desired, normal service can be restored by additional provisions in the control scheme for closing the second line switch when voltage is restored on its section of the line.

In the design of automatic air break switch control schemes, the first consideration is the potential source to be used for operation and control. Some schemes require a source of potential independent of the lines being switched while others can be operated with duplicate sources, one connected to each of the two main transmission lines. Another important consideration is the completion of a transfer, once it is started, or to set up the control so that a transfer will take place when one of the lines is energized. Another consideration is flexibility. Power circuit conditions change rapidly and it becomes necessary to change the automatic control to meet the new requirements of the power circuits. The control scheme should be such that the new requirements can be met with the minimum number of changes.

In the installations which will be described the main power sources are protected by oil circuit breakers which are equipped with reclosing relays and the normal circuit protective relays.

Time delay features are incorporated in the air break switch control schemes to prevent unnecessary switching caused by transient faults and to co-ordinate the timing of the transfer switching with that of the source oil circuit breakers.

Automatic Control of Air Switches for Load Transfer With Synchronism Check Interlock—D-C Operation and Control

This control scheme (see Figures 1 and 2) includes the general requirements previously outlined for automatic load transfer schemes. There also is provided a synchronism check interlock to block an attempt to parallel the two sources during switching operations unless they are in synchronism.

Normal Conditions

Station *L* normally is served from station *OC* which in turn is served from a 69,000-volt transmission line connecting stations *OR* and *P*. Oil circuit breakers 488 at station *OR* and 588 at station *P* normally are closed and are reclosed manually after automatic tripping. Oil circuit breakers 177 at station *OC* and 188 at station *OR* normally are closed with control arranged for one immediate reclosure after automatic tripping and two time delay reclosures. The total reclosing cycle is approximately $2^1/_2$ minutes. At station *L* motor operated air break switch 152 normally is closed and 252 normally open with their controls arranged for automatic switching.

Automatic Switching for Fault Conditions

1. *Failure of Line Potential.* Failure of voltage on the incoming line from station *OC* causes, after a time delay of approximately three minutes, the opening

of switch 152 followed by the closing of switch 252. This switching is initiated by the de-energized contact of auxiliary line voltage relay *UV-X* which is normally energized through energized contracts of line voltage relays *UV*-1 and *UV*-2.

2. *Return of Line Potential.* Return of potential on the line from station *OC* causes, after a short time delay, switch 152 to close, which for a few seconds parallels the two sources, followed by the opening of switch 252, thus restoring normal service. This operation is initiated by the energized contacts of relays *UV*-1 and *UV*-2 and is interlocked with synchronism check relay *SCR*.

Failure of voltage on the incoming line from station *OC*, which caused the original switching operation, might have resulted from the tripping of breaker 177 at station *OC* or from the tripping of breakers 488 and 588 at stations *OR* and *P*. The instructions for switching on the 69,000-volt line after a trip-out call for first closing breaker 488 at station *OR* followed by synchronizing and closing breaker 588 at station *P*. Because of the possibility of the reverse switching operations, that is, closing switch 588 before 488, thus energizing station *L* from a different generating source, and in order to serve stations *OC* and *L* from station *P* in an emergency with switch 488 open at station *OR*, the automatic control at station *L* is provided with a synchronism check relay. This relay blocks an attempt to parallel the two sources during this switching operation unless they are in synchronism. One coil of the synchronism check relay is connected to the bus potential transformer and the other to one phase of the line potential transformers.

3. *Failure of Bus Potential Following Line Potential Failure.* Failure of voltage on the incoming line from station *OR* after switching operation 1 has taken place causes no further switching. If this conditions still exists when voltage is restored on the line from station *OC*, switch 252 will open and 152 will close. This operation is initiated by auxiliary line voltage relay *UV-X* and bus voltage relay *UV*-3.

4. *Failure or Restoration of Potential During Switching Operations.* In the foregoing three switching operations, it is assumed that the initiating voltage conditions continue until a switching operation is completed. In switching operation 1, if line potential is restored on the line from station *OC* before relay *TD* completes its timing cycle, no switching will take place. If line potential is restored after *TD* contact closes but before 152-*b* contact is closed, switch 152 will open, 252 remains open and 152 will reclose by the operation of relay *CX*-1*A* as in switching operation 3. In switching operation 2, if voltage again fails on the incoming line from station *OC* before the contact of the synchronism check relay *SCR* closes, no switching takes place. If voltage fails on this line after relay *CX*-1 has closed its contacts, switch 152 will close and 252 will open. Under this condition switching operation 1 will be repeated.

In switching operation 3, if voltage fails on the incoming line from station *OC* after relay *TX*-2*A* contact closes but before 252-*a* closes, switch 252 will open but will reclose by the operation of relay *CX*-2 as in switching operation 1.

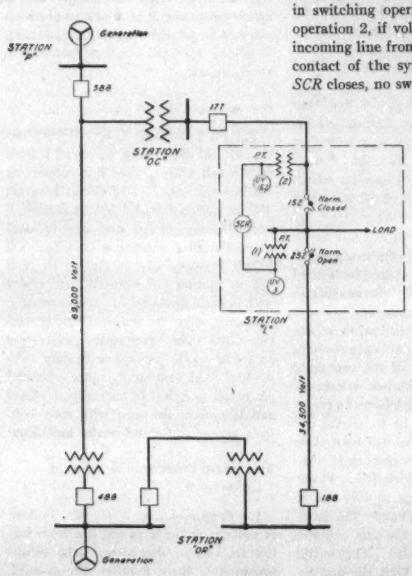

Figure 1. A 1-line diagram of station *L* and connected system

Control Schedule

In the operation of the switch mechanism, the motor circuit is held closed mechanically and the brake is held in the released position until the mechanism has reached its full angular travel. It is, therefore, unnecessary for the control switch or control contacts to remain closed in order to complete a closing or opening operation.

Manual. Turn the "automatic-manual" switch 43 to the "manual" position. Since the manual operation of each switch is identical, the following description will be confined to the operation of switch 152.

To close or open switch 152, energize relay *CC*-152 or *TC*-152 by operating control switch *C*-101 or *T*-101. This operation closes contact *CC*-152 or *TC*-152, energizes the motor *M* and mechanically releases the motor brake. At the end of the closing or opening operation a cam unlatches contact *CC*-152 or *TC*-152. Contact *CC*-152 or *TC*-152 therefore opens and the motor brake is applied. Relay *CC*-152 or *TC*-152 is de-energized when control switch *C*-101 or *T*-101 is released or by the operation of contact 152-*bb* or 152-*aa*.

The air break switch also may be operated by means of a hand crank. For hand operation an interlock is provided in the motor and brake circuit which serves as a safety feature in the event manual operation of the switch is necessary. This interlock is attached to the emergency hand crank guard. The guard must be moved aside before the hand crank can be attached. This operation opens the motor circuit and releases the brake. A mid position of the guard is the locked-out position. In this position, the brake is engaged but the motor switch is open. The guard may be padlocked in this position so that it can be used as a lockout while working on the motor mechanism or on the line.

Automatic. With air break switch 152 closed, 252 open, turn the "automatic-manual" switch to the "automatic" position. Relay *UV-X* is energized

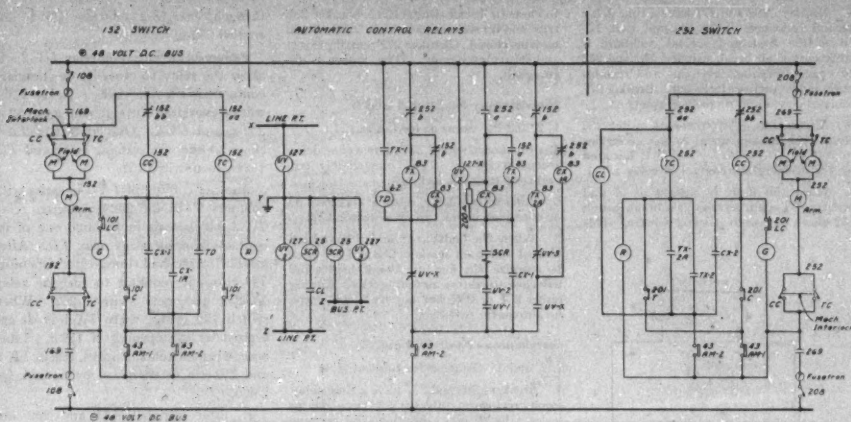

Figure 2. Schematic diagram of station *L*. Load transfer scheme with synchronism check interlock using direct potential for operation and control

through an energized contact of relays *UV*-1 and *UV*-2 in series.

Failure of Line Potential. Failure of potential on relay *UV*-1 or *UV*-2, or on both relays simultaneously, allows the de-energized relay or relays to open their energized contact, after a time delay, to de-energize relay *UV-X*. A contact of *UV-X* closes to energize relay *TX*-1 through contact 252-*b*. A contact of *TX*-1 energizes relay *TD*. After a time delay of approximately three minutes, *TD* contact closes to energize *TC*-152 to open switch 152. When contact 152-*b* closes, relay *CX*-2 is energized through the de-energized contact of *UV-X*. *CX*-2 contact closes to energize *CC*-252 to close switch 252. When switch 252 closes, relay *CL* is energized through contact 252-*aa*. An energized contact of *CL* energizes relay *SCR*.

Return of Line Potential. If, after switch 152 is open and 252 is closed, relays *UV*-1 and *UV*-2 close their energized contacts, voltage relay *UV-X* will be energized. If line potential and bus potential are approximately equal in magnitude and in phase, relay *SCR* contact will close to energize relay *CX*-1 through 252-*a*, *UV*-1, and *UV*-2 contacts. *CX*-1 seals in through one of its contacts. The purpose of this seal-in is to allow the transfer to be completed if line voltage fails during the transfer. Another contact of *CX*-1 energizes *CC*-152 to close switch 152. After switch 152 closes, relay *TX*-2 is energized through *CX*-1, 152-*a* and 252-*a* contacts. *TX*-2 contact closes to energize *TC*-252 to open switch 252.

Failure of Bus Potential. If, after switch 152 is open and 252 is closed, voltage fails on the bus and relay *UV*-3 closes its de-energized contact, no switching takes place. Subsequently, if voltage is restored on the line, relay *UV-X* is energized after a time delay through energized contacts of *UV*-1 and *UV*-2. Relay *TX*-2 is energized through contacts *UV*-3, *UV-X* and 152-*b*. *TX*-2*A* contact closes to energize *TC*-252 to open switch 252. After switch 252 opens, relay *CX*-1*A* is energized through contacts 152-*b*, 252-*b* and *UV-X*. *CX*-1*A* contact energizes *CC*-152 to close switch 152.

Automatic Control of Air Switches for Line Sectionalizing and Subsequent Load Transfer—D-C Operation and Control

This control scheme (see Figures 3 and 4) was designed for a station connected to a normally closed transmission loop and provides for first sectionalizing the line upon failure of voltage on the bus and subsequently transferring the load to one section of the line. One potential transformer on the preferred section of the line and one potential transformer on the bus are used for this scheme. If voltage returns on the station *OR* section of the line, the load will be transferred to this source. If potential fails to return on this section of the line within the time required for the line voltage relay to close its de-energized contact, the load will be transferred to the section served by station *W*. This control scheme is not fully automatic under all conditions. If transfer is first made to station *W*, restoration of voltage on station *OR* section of the line will close the loop automatically for normal operation. If, however, transfer first is made to station *OR*, the loop will not be closed automatically.

Normal Conditions

Station *FB* normally is served from a 34,500-volt closed transmission loop fed from station *OR*. This loop has automatic sectionalizing oil circuit breakers at station *W*. Oil circuit breaker 288 at station *OR* normally is closed with control arranged for one immediate reclosure after automatic tripping and one time delay reclosure. Oil circuit breaker 277 at station *W* normally is closed with control arranged the same as breaker 288. At station *FB* motor operated air break switches 152 and 252 normally are closed with control arranged for automatic switching for voltage failure and for voltage restoration.

Automatic Switching for Fault Conditions

Fault at A

1. Breakers 288 and 277 open and immediately reclose. If the fault is cleared, no further switching occurs.

2. If the fault is sustained, breakers 288 and 277 again are tripped.

3. After a time delay, air break switches 152 and 252 open. This switching is initiated by bus voltage relay *UV*-2.

4. Breakers 288 and 277 have a time delay second reclosure. (The elapsed time between the first and second reclosure is sufficient for air break switches 152 and 252 to open.) Breaker 288 trips and remains open and its recloser locks out. Breaker 277 remains closed and its recloser resets.

5. After a time delay, air break switch 252 closes (152 remains open) to restore service to station *FB*. This switching is initiated by the de-energized contact of relay *UV*-1.

6. When the fault is cleared at *A* and breaker 288 again is closed, air break switch 152 closes to restore normal service. This

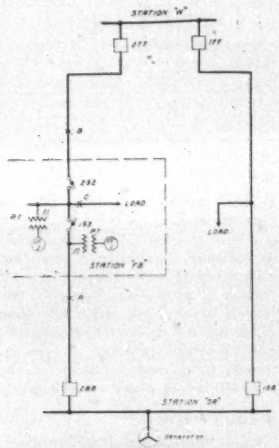

Figure 3. A 1-line diagram of station *FB* and connected system

switching is initiated by the energized contact of relay *UV*-1.

Fault at B

1, 2, and 3. Same as for fault at *A*.

4. Breakers 288 and 277 have a time delay second reclosure. Breaker 277 trips and remains open and its recloser locks out. Breaker 288 recloses and its recloser resets.

5. After a time delay, air break switch 152 closes (252 remains open) to restore service to station *FB*. This switching is initiated by the energized contact of relay *UV*-1.

6. When the fault at *B* is cleared and breaker 277 again is closed, no automatic switching occurs. Manual switching at station *FB* is required to restore normal service.

Fault at C—Bus Fault

1, 2, and 3. Same as for fault at *A*.

4. Breakers 288 and 277 close on the time delay second reclosure and remain closed.

5. Relay *UV*-1 closes its energized contact to close air break switch 152. Breaker 288 trips and its recloser locks out. Switch 152 remains closed. Breaker 277 remains closed and its recloser resets. The station is de-energized.

Simultaneous Faults at A and B

1, 2, and 3. Same as for fault at *A*.

4. Breakers 288 and 277 have a time delay second reclosure. They immediately trip and their reclosers lock out.

5. After a time delay, relay *UV*-1 closes its de-energized contact to close switch 252.

6. When the faults at *A* and *B* have been cleared and both breakers 288 and 277 close to energize the line, air break switch 152 will close to restore normal service. Closing either 277 or 288, but not both, will cause no automatic switching.

Simultaneous Faults at A and C

1, 2, and 3. Same as for fault at *A*.

4. Breakers 288 and 277 have a time delay second reclosure. Breaker 288 trips and its recloser locks out. Breaker 277 remains closed and its recloser resets.

5. After a time delay, relay *UV*-1 closes its de-energized contact to close switch 252. Breaker 277 trips and its recloser locks out. Subsequent closing of breaker 288 causes no further automatic switching.

Fault at B or C Subsequent to a Fault at A

1. Breaker 277 trips and recloses twice if the fault does not clear and its recloser locks out. No automatic switching occurs at station *FB*.

Fault at A and C Subsequent to a Fault at B

1. Breaker 288 trips and recloses twice if the fault does not clear and its recloser locks out. No automatic switching occurs at station *FB*.

Failure of Voltage on Line Voltage Relay UV-1 When Switches 152 and 252 Are Closed

1. No automatic switching occurs.

Failure of Voltage on Bus Voltage Relay UV-2 When 152 and 252 Are Closed

1. After a time delay relay *UV*-2 closes its de-energized contact to open switches 152 and 252. Switch 152 immediately recloses. Switch 252 remains open. No other switching occurs.

CONTROL SCHEDULE

The operation of the switch mechanism is the same as previously outlined for the control scheme shown in Figure 1.

Manual. The manual operation of switches 152 and 252 is the same as previously outlined for the control scheme shown in Figure 1.

Automatic. With air break switches 152 and 252 closed, turn the "automatic-manual" switch 43 to the "automatic" position. Relay *CX*-1*A* will be energized through energized contact *UV*-2 and contact 252-*a*.

Failure of potential on relay *UV*-2 will allow the relay to close its de-energized contact after a time delay. Relay *TX*-1 will be energized through contacts 152-*a*, 252-*a*, and *UV*-2. One contact of *TX*-1 closes to energize opening relay coil *TC*-152 to open switch 152.

Another contact of *TX*-1 in series with contacts *UV*-2 and 252-*a* energizes relay *TX*-2 which seals in through one of its contacts and energizes relay *TD*. After switch 152 has had time to start opening, *TD* closes its contact to energize relay *TC*-252 to open switch 252. When switch 152 opens, relay *TX*-1 is de-energized by the opening of 152-*a*. Likewise, when switch 252 opens, relays *TX*-2 and *TD* are de-energized by opening of 252-*a*.

If, after switches 152 and 252 are opened, relay *UV*-1 has its energized contact closed, or again closes it before it has time to close its de-energized contact, relay *CX*-1 will be energized through energized contacts *UV*-1 and 152-*b*. *CX*-1 contact in series with 252-*b* energizes *CC*-152 to close switch 152.

If, after switches 152 and 252 are opened, relay *UV*-1 does not close its energized contact but after a time delay closes its de-energized contact, relay *CX*-2 will be energized through contacts 152-*b* and 252-*b* in series with *UV*-1 de-energized contact. A contact of *CX*-2 completes *CC*-252 closing relay circuit to close switch 252.

If, after switch 252 has closed automatically, voltage is restored to relay *UV*-2, the relay will close its energized contact to energize relay *CX*-1*A*. Subsequently, if relay *UV*-1 again is energized to pick up relay *CX*-1, *CC*-152 will be energized through contacts *CX*-1 and *CX*-1*A* to close switch 152. However, if closing of switch 252 does not re-energize *UV*-2 and consequently *CX*-1*A*, the energizing of relay *UV*-1 will cause no switch operation because of the fact that relay *CX*-1*A* is de-energized and its contact in switch 152 closing circuit is open.

Automatic Control of Air Switches for Load Transfer—A-C Operation and Control

This control scheme (see Figures 5 and 6) is designed to include the general requirements previously outlined for automatic load transfer. In addition, control devices are provided so that either one of the sources of power supply may be selected as the preferred source. The

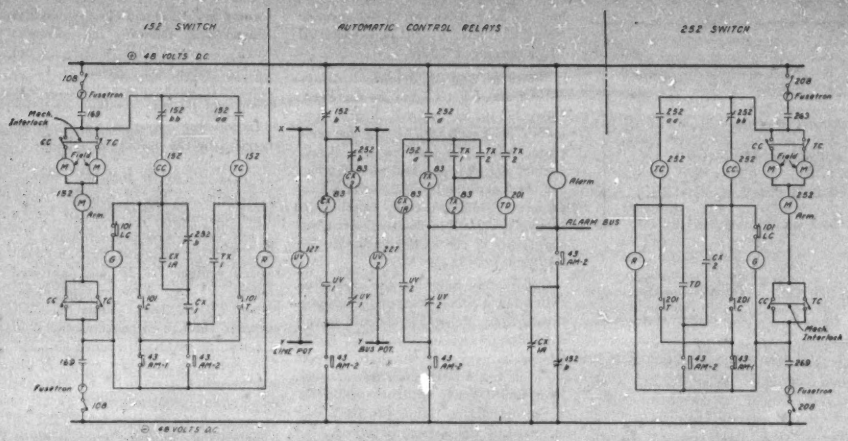

Figure 4. Schematic diagram of station *FB*. Line sectionalizing and subsequent load transfer scheme using direct potential for operation and control

emergency line must be energized in order to perform an automatic transfer of load.

The operating and control potential is obtained from the line potential transformers. The complete control and operating equipment for each switch is located in the switch mechanism housing. Certain interlock wiring is provided between the switches in order to obtain proper sequence of control potential during switching operations.

Normal Conditions

Oil circuit breakers 188 and 288 normally are closed with controls arranged for one immediate reclosure after automatic tripping and two time delay reclosures. Line *A*, the preference line, has its motor operated air break switch 152 closed with control arranged for automatic switching to line *B* in the event of a voltage failure on line *A*. When normal voltage is returned to line *A*, switch 152 will close and switch 252 will open.

Automatic Switching for Fault Conditions

Fault at A

1. Breaker 188 opens and immediately recloses. If the fault is cleared, no further switching occurs.

2. If the fault is sustained, breaker 188 again opens and after a time delay recloses. If the fault still persists, the opening and reclosing cycle is repeated and the automatic recloser locks out.

3. During the previous switching, relays *UV*-1*A* and *UV*-1*B* closed their de-energized contacts. This operation energizes relay *TD*-202. The timing cycle of relay *TD*-202 is such that its contact will not close until after the automatic reclosing relay on breaker 188 has locked out. After the forego-ing timing cycle is completed, the energized contact of relay *TD*-202 closes and energizes relay *TC*-152. Switch 152 will open and the closing circuit for switch 252 is made through 152-*b*. Switch 252 therefore will close. During this operation, it is assumed that line *B* has normal voltage.

4. When the fault is cleared at *A* and breaker 188 is closed, relays *UV*-1*A* and *UV*-1*B* close their energized contacts to close switch 152. Closing potential is obtained from line *A* potential transformer.

5. Immediately after switch 152 is closed, a circuit is set up through 152-*a* to open switch 252.

Fault at B

With emergency line *B* serving station *X* and line *A* out of service because of fault conditions, switch operations are as follows:

1. Same as fault at *A*, except refers to breaker 288.

2. Same as fault at *A*, except refers to breaker 288 and station *X* is de-energized because line *A* is out of service.

3. In the meantime, if the fault has been removed from line *A* and breaker 188 again is closed, switch 252 will open and switch 152 will close, thereby energizing station *X*.

Fault at C

1, 2, and 3. Same as for fault at *A*.

4. The fault at *C* has not been removed; therefore, during the previous operation, switch 252 closed into the fault and breaker 288 opened. Breaker 288 immediately reclosed.

5. Same as fault at *A*, item 2, except refers to breaker 288 and station *X* is de-energized because line *A* is out of service.

6. When the fault is cleared, breakers 188 and 288 are closed by the operators at the terminal station. Switch 152 will close and switch 252 will open thereby restoring normal conditions.

Simultaneous Faults at A and B

1. Breakers 188 and 288 immediately trip and reclose automatically.

2. If the faults are sustained, the breakers again open and reclose after a time delay. If the faults still persist, the opening and closing cycle is repeated and the automatic reclosers lock out and prevent further automatic switching. During this time no automatic switching has occurred at station *X*. Station *X* therefore is de-energized.

Control Schedule

The operation of the switch mechanism is the same as previously outlined for the control scheme shown in Figure 1.

Manual. The manual operation of switches 152 and 252 is the same as previously outlined for the control scheme shown in Figure 1 except that each switch is provided with an "automatic-manual" switch 143 and 243.

Automatic—With Line A Preferred. With switch 152 closed, turn the "automatic-manual" switches to the "automatic" position. The "line preference" selector switch 95, located in 252 switch mechanism housing, should be turned to the "preference" position.

Failure of Line A Potential. Failure of potential on line *A* causes relays *UV*-

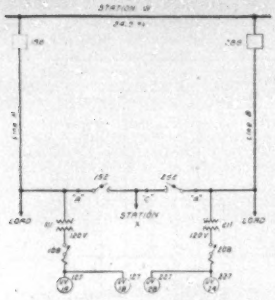

Figure 5. A 1-line diagram of station X

1A and UV-1B to close their de-energized contacts. Relay TD-202 is energized through de-energized contact UV-1B and energized contact UV-2A. After a time delay, contact TD-202 closes. Relay TC-152 is energized through energized contact TD-202 and de-energized contact UV-1A. This operation energizes motor M-152 and the switch starts to open. After the switch opens completely, relay TC-152 is de-energized by the opening of 152-aa.

Immediately following the opening of switch 152, a circuit is set up for closing switch 252. Relay TD-202 still is energized and its contact is closed. Relay CC-252 is energized through 152-b in series with contacts TD-202, UV-1B, and UV-2A. After switch 252 is closed completely, relay CC-252 is de-energized by the opening of 252-bb.

Return of Line A Potential. Relays UV-1A and UV-1B again are energized. Relay TD-102 is energized through contacts UV-1A and SS-X (of the line preference relay 83). After a time delay, contact TD-102 closes and sets up a circuit through contacts UV-2B and SS-X to energize CC-152 to close switch 152. Relay CC-152 will be de-energized at the completion of the closing operation by the opening of 152-bb.

Immediately following the closing of switch 152, a circuit is set up for opening switch 252. Relay TD-102 still is energized and its contact is closed. Relay CC-252 is energized through contact 152-a in series with contacts TD-102, SS-X and UV-1A. At the completion of the opening operation CC-252 is de-energized by the opening of 252-aa.

Automatic—With Line B Preferred. With normal conditions existing, turn the "line preference" selector switch 95 to the "emergency" position. Relay TD-202 is energized through contacts SS2-95 and UV-2A. After a time delay, contact TD-202 closes and sets up a circuit through contacts UV-1B and SS2-95 to energize CC-252 and close switch 252.

Immediately following the closing of switch 252, a circuit is set up for opening switch 152. Relay TC-152 is energized through contacts 252-a, TD-202, SS2-95 and UV-2A. At the completion of the opening operation, CC-152 is de-energized by the opening of 152-aa.

Failure of Line B Potential. Failure of potential on line B potential transformer causes relays UV-2A and UV-2B to close their de-energized contacts. Relay TD-102 is energized through de-energized contact UV-2B and energized contact UV-1A. After a time delay, contact TD-102 closes. Relay TC-252 is energized through energized contact TD-102 and de-energized contact UV-2A. This operation energizes motor M-252 and the switch starts to open. After the switch opens completely, relay TC-252 is de-energized by the opening of 252-aa.

Immediately following the opening of the switch 252, a circuit is set up for closing switch 152. Relay TD-102 still is energized and its contact is closed. Relay CC-152 is energized through 252-b in series with contacts TD-102, UV-2B and UV-1A. After switch 152 is closed completely, relay CC-152 is de-energized by the opening of 152-bb.

Return of Line B Potential. Switch and relay operations are the same as outlined in the two paragraphs following "Automatic—With Line B Preferred."

Figure 6. Schematic diagram of station X. Load transfer scheme using a-c potential for operation and control

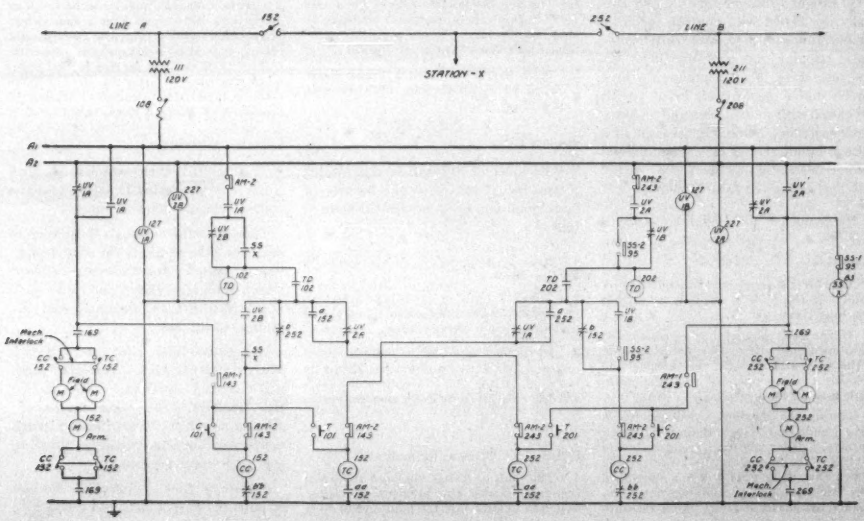

Conclusions

The three control schemes described were designed to meet specific system operating requirements. However, other system requirements can be met readily with a minimum number of changes in the control wiring. It is advisable to keep the design of an air break switch transfer scheme simple and inexpensive as the load center might develop beyond the limits of air break switches. In this event it would be necessary to replace the air break switches with more adequate and more costly equipment such as oil circuit breakers.

Appendix. Nomenclature of Schematic Diagrams

a = auxiliary switch contact—closed when device is in energized or operated position

aa = auxiliary switch contact—closed when operating mechanism of main device is in energized or operated position

b = auxiliary switch contact—closed when device is in de-energized or non-operated position

bb = auxiliary switch contact—closed when operating mechanism of main device is in de-energized or non-operated position

AM-1 = automatic manual switch—contact closed in manual position

AM-2 = automatic manual switch—contact closed in automatic position

C = close contact of control switch

CC = air break switch closing relay

CL = auxiliary relay used to energize synchronism check relay

CX-1, *CX*-1*A* = auxiliary relays for closing switch 152

CX-2 = auxiliary relay for closing switch 252

G = green indicating lamp

LC = lamp cutoff contact on control switch

M = air break switch operating motor

R = red indicating lamp

SCR = synchronism check relay

SS-1 = line preference selector switch contact—closed when line *A* is preferred ("preference" position)

SS-2 = line preference selector switch contact—closed when line *B* is preferred ("emergency" position)

SS-X = line preference selective control auxiliary relay

T = trip or open contact on control switch

TC = air break switch opening relay

TD = timing relay with time delay closing contacts, instantaneous reset

TX-1 = auxiliary relay for opening switch 152

TX-2, *TX*-2*A* = auxiliary relays for opening switch 252

UV-1, *UV*-2, *UV*-3 = line or bus voltage relays

UV-1*A*, *UV*-2*A* = line undervoltage relays for line *A*

UV-1*B*, *UV*-2*B* = line undervoltage relays for line *B*

UV-X = line voltage auxiliary relay

25 = synchronism check relay

43 = control transfer switch

83 = selective control relay

95 = line preference control transfer switch

101, 201 = control switches

201, 202 = time delay closing relays

108, 208 = control power switches

111, 211 = control power transformers

127, 227 = undervoltage relays

127-*X* = undervoltage auxiliary relay

143, 243 = control transfer switches

152, 252 = air break switches

169, 269 = interlock switches—open only when crank is inserted to operate mechanism by hand

Discussion

G. E. Heberlein (Railway and Industrial Engineering Company, Jeannette, Pa.): F. W. Rich and M. S. Kirwen's paper is particularly valuable in illustrating solutions to very common operating problems, providing improved service reliability on low voltage transmission lines. Little has been published on the extent of automatic switching and sectionalizing schemes and few engineers appreciate how widely used are such automatic air break switching installations. In general terms, most of the larger eastern utilities, having a large number of 33-kv or equivalent transmission lines, have from a few to dozens of these installations. K. Reardan of the West Penn Power Company stated that his company has 43 automatic switching installations. I am informed that one of the southern utilities has made over 200 installations during the past 20 years. I would like to comment, summarizing the experience gained from various operating engineers as to their preferences and needs, regarding automatic switching equipment of this type.

The application of such equipment is, of course, to improve service for the least capital investment, commensurate with the value of service rendered. Such installations involve air break switches, voltage sources, and the automatic relay equipment. For the lower voltage distribution lines, potential transformers are relatively inexpensive and can be used to provide both voltage indication and operating source for motor operation. For the usual transfer installation, the operation is only required when one or the other line is energized and as such, the operating source is available. In many cases, sectionalizing has been accomplished by means of spring operated switches with motor reclosing after the line again becomes energized.

In addition to the transfer and sectionalizing equipment described in the paper, many utilities are using special forms of automatic switching equipment. These schemes include:

1. Sectionalizing on overloads, where an air break switch is used to open a live line on overload. Equipment used is usually post-type current transformers with induction-type overcurrent relays, with conventional motor operated switches. Such switches may be of a special type for air break load interruption.

2. Sectionalizing of a line after a predetermined number of overloads, such operation is a dead line switching, usually after one, two, or three trippings of the associated feeder breaker. Equipment used includes special relays to record the number of overloads and timing the resetting.

Other automatic switching schemes combining features of the above have also been used.

While operating requirements vary widely and sometimes complicated schemes must be used, engineers tend toward greatest reliability through the use of simpler relaying equipment. By using a motor mechanism with a clutch which disconnects the air break switch drive from the mechanism, including the limit and auxiliary switch, testing of the automatic installation can be done without requiring operation of the air break switch. This permits going through a complete sequence without disturbing the position of the air break switch or requiring the switching of any lines.

The authors show the use of switch *169* as well as some auxiliary relays to insure completion of certain sequencing. By using motor mechanisms with contactors equipped with sealing-in contacts, which become de-energized by the motor limit switch at the end of the operating travel and the use of electrically operated brakes, simplification can be attained.

In general, Rich and Kirwen's schemes have been used by the majority with some simplification attained through the use of some of the features outlined. More specifically, in these change-over and sectionalizing schemes potential transformers are connected to the incoming lines ahead of the air break switches and only two undervoltage relays are used. The change-over schemes are usually arranged that the back transfer from the emergency to the preferred line takes place by paralleling the lines in case the emergency line is energized. Otherwise, the emergency line air break switch opens up before the preferred line switch closes. Naturally, a synchronism-verifier, connected directly to the potential transformers on the two lines, is required when there is a possibility of the lines not being in synchronism.

These schemes have varied in timing from 20 cycles to 60 minutes, depending upon the system conditions. This requires specific relays for these timing purposes. When the time delay for the change-over is not over 80 seconds, a long-time, geared induction type undervoltage relay is used for timing. If the required time is over 80 seconds, or a predetermined accurate time is required for back transfer switching, instantaneous undervoltage relays in con-

nection with long range mechanical timers are used. For accuracy purposes, the timers are driven by synchronous motors and are supplied with a vibrator type rectifier in case an alternating current supply is not available. Wherever possible, the operating mechanism contactor coils are energized directly by the voltage relay contacts.

The general preference seems to be to forego the use of indicating lamps on the relay equipments as they are only valuable during the time of testing of the equipments. Most engineers seem to prefer the seal-in type of control so that manual operation is completed without the need for holding the control switch in the operated position.

The general acceptance of this form of automatic control indicates satisfactory and reliable operating performance. With such widespread usage of automatic equipments and the diversity of conditions and schemes used, a symposium of the existing practices and experiences would be desirable.

R. S. Smithley (nonmember; Duquesne Light Company, Pittsburgh, Pa.): The automatic control of air switches or nonautomatic breakers for line sectionalizing or load transfer on the system of the Duquesne Light Company is based upon the procedure which would be followed by an operator in restoring service. The schemes ordinarily do not check line potential before a transfer is made. In general, 3-phase potential from the low voltage side of the nonautomatic station bank is employed for the supply to the undervoltage relays. An arbitrary sequence of sectionalizing is set up based upon the probability of a permanent fault occurring in the longer line section.

Two schemes performing the same functions as the schemes used by the authors for automatic control of air switches for line sectionalizing and subsequent load transfer, and automatic control of air switches for load transfer only, will be contrasted with those of the authors.

Referring to Figure 3 of the paper, and using the authors' designation of stations and switches, the sequence of operations used by the Duquesne Light Company to restore service is as shown in Table I of the discussion.

The sequence at station *FB* is controlled by two undervoltage relays making their de-energized contacts at 15 seconds and 45 seconds. Should the station become energized before either of these timers close their de-energized contacts, the sequence of operation at station *FB* is discontinued. The air break switches or the nonautomatic breakers at station *FB* are operated from a battery.

The scheme used by the Duquesne Light Company for automatic control of air switches for load transfer accomplishes the same result as the authors' scheme illustrated in Figure 5. Referring to this figure, and again using the authors' designation of stations and switches, the sequence of operation to restore service is as shown in Table II.

The scheme of load transfer when the station is fed as a double tap normally operated from one of two lines, consists fundamentally of transferring the station to the reserve line after it is shown that the fault on the regular line is permanent. The transfer is made by means of undervoltage relays at the station *X*. Should the regular line be returned to service on the instantaneous reclosure, the undervoltage relays at station *X* will not have closed their de-energized contacts, and therefore station *X* will continue to be served from the regular line. The air break switches or nonautomatic breakers at station *X* are operated from a battery.

Normal running order is not restored after damage has been repaired for either of the schemes described above. It is felt that travelling operators will have to perform the necessary switching to block the equipment out of service before repairs to the damaged lines can be made. Therefore, these same operators will restore the lines or stations to their normal running order after the damage has been repaired.

Table II. Automatic Control of Air Switches for Load Transfer*

Station W	Station X
(Normal Running Order is with breakers *188* and *288* closed)	(Normal Running Order is with air break *152* closed, *252* open)
Breaker *188* trips	
Reclose *188* instantaneously	
Breaker *188* trips if fault is permanent	
	Open *152* in 15 seconds Close *252* after *152* opens

* The two lines to which the taps are made are not necessarily from the same station.

Table I. Automatic Control of Air Switches for Line Sectionalizing

Station OR	Station FB	Station W
Breaker *288* trips		Breaker *277* trips Reclose *277* instantaneously Breaker *277* trips if fault is permanent in either line section
	Open *252* in 15 seconds	
Reclose *288* in 30 seconds		
	If permanent fault is between stations *W* and *FB*, service is now restored to station *FB*	
If fault is permanent between stations *OR* and *FB*, breaker *288* trips		
	Close *252* in 45 seconds Open *152* in 45 seconds	
		Close *277* in 60 seconds
	If permanent fault is between stations *OR* and *FB*, service is now restored to station *FB*	

S. C. Killian and **M. Stene** (Delta-Star Electric Company, Chicago, Ill.): Rich and Kirwen have made a worthwhile contribution to the literature by discussing in detail, line sectionalizing and transferring by air switches. Since this method of switching came into general use only a few years ago, there has not been a completely detailed sequence of operations for any particular scheme available for reference. Only manufacturers had literature available and that covered more generalized cases than those the authors have analyzed. Sectionalizing and transferring by this means presents an economy as compared to oil circuit breakers and more use of this method will doubtlessly be made, especially when lines are pulled into lightly loaded areas and where revenue does not justify the use of more expensive oil breakers. Other combinations of switching are being devised regularly, all based somewhat on the theory outlined by the authors. As an example, in a ring system, the scheme can be used to isolate a faulted section by progressive reclosing and then locking out.

With specific reference to each of the automatic switching sequences described in this paper, the following may be of particular interest. In the event of a bus fault at station *L*, Figures 1 and 2, breakers *177* and *188* will lock out. If either or both of the 34.5-kv lines have other load taps, the addition of a sequence lockout may be desirable to prevent complete outages at these load taps. The sequence lockout provides for automatic opening and lockout of both switches in the event of immediate voltage failure when either switch closes automatically. With the potential transformers located as shown in Figure 1 of the paper, this sequence lockout would apply only on closing switch *152*. However, both switches would be locked out, so that service could be restored to other load taps on both 34.5-kv lines. This sequence lockout is automatically reset when either switch is manually closed to a live line.

Referring to Figures 3 and 4 of the paper, it is presumed that the potential transformer is located on the low side of a transformer connected to the bus and that this was dictated by cost considerations. The authors state that this scheme is not fully automatic under all conditions but it is obvious that if both potential transformers were also located on the line side of the switches, fully automatic operation could be obtained.

It should be noted that the a-c load transfer scheme, Figures 5 and 6 of the paper, with the addition of a synchronism check relay will accomplish the same switching sequences as shown in Figures 1 and 2 without the need for a d-c source. This scheme

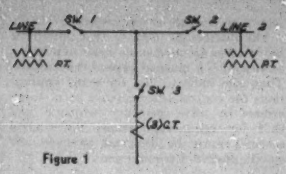

Figure 1

using alternating potential for operation and control has been used by our company. Motor mechanisms for this application have been built with oversize housings with space available for relays and control switches. Two such mechanisms are used for an alternating transfer scheme, or with slight modifications, for the load transfer scheme shown in Figure 6 of this paper.

The automatic switching schemes described by the authors are for single-phase control only—that is, one potential transformer for each line. The use of two potential transformers for ungrounded systems or three for grounded systems should be given consideration. We have had several instances in which single-phase control was chosen and failure to operate and consequent outage has resulted when line wires have broken. Additional potential transformers and relays have then been installed to prevent such failures.

The authors have made no mention of switching schemes using fault current through current transformers as a means of locating and clearing faulted line sections. A typical method using three motor-operated air switches is shown in Figure 1 of the discussion. The tap in this case is on a tie line with all switches normally closed. One potential transformer is used on each line and a current transformer on the load tap. Switches *1* and *2* open on loss of voltage after time delay providing fault current has not flowed through the tap. Restoration of voltage to either line causes reclosure of one switch. A synchronizing check relay allows the second line switch to close only when line *1* and *2* are in synchronism. The switch on the tap opens only on loss of voltage after fault current has flowed through the tap current transformers. With fault current through the tap, subsequent loss of voltage within a predetermined interval of time causes switch *3* to open and lock out; switches *1* and *2* are locked in and remain closed for sufficient time to allow the breakers to reclose and restore service through the tie line.

The use of air switches and motor operating mechanisms for this type of service reflects the faith that has grown up in the utility field in these two devices. The air switch, expected to stand out in all varieties of weather year after year with little or no maintenance, has become a highly reliable piece of apparatus, as has the motor mechanism.

K. N. Reardon (West Penn Power Company, Pittsburgh, Pa.): The very splendid paper written by Rich and Kirwen concerning the automatic control of air switches brings to attention the automatic air switch as a device of efficiency and economy in the maintenance of power supply and in the location of faults on line sections. The authors have well covered three types of applications by incorporating in their control schemes actions and safeguards required by their system operating procedure. It is natural and customary for control engineers to design circuits to duplicate automatically the functions that would be performed manually by an operator. At first judgment, it seems that too many provisions have been included in the schemes to take care of reasonable eventualities. However, as stated in the authors' conclusions, the three control schemes were designed to meet specific system operating requirements. Simplicity of control scheme is recommended by them and with that recommendation everyone will concur. Sometimes an operating department tends to burden control specifications by demanding that the circuits cope with more unusual than usual situations. A reasonable balance of probability will often result in circuit simplification without sacrificing reliability and essential requirements.

The West Penn Power Company has been applying automatic switches steadily since 1925 when the first installation of a directionally controlled spring operated type was made. There are now in active service 43 automatic air switch installations of which 19 are of the sectionalizing type, 16 of the transfer type, 7 of the isolating type, and 1 of the by-pass type. Two are in 132-kv service, one in 4,000-volt service, one in 33-kv service, and 39 in 25-kv service.

The transfer type and the sectionalizing type have become definitely standardized by us. The transfer type is operated by an alternating current supplied from small transformers on the incoming line. The sectionalizing type is operated by a 48-volt battery supply. Relay and control equipment has been reduced to a minimum. Fortunately we have not found it necessary to use synchronism check relays nor have we, except in one instance, found it necessary to return a transferred customer automatically to a preferred source as soon as that preferred source became available. The customer remains on the source to which he is transferred until an operator manually restores him (without interruption) to the preferred source.

Upon loss of power the automatic transfer type station will always transfer itself to its second available source of power provided that that second source is energized. The automatic sectionalizing type station will always pick itself up upon whichever line becomes energized and will close the sections together if both become energized. If a fault occurs on the bus between the automatic air switches of either transfer type or sectionalizing type, both air switches will, after unsuccessful attempt to re-energize the bus, open and remain open until manual switching is performed. With both switches thus locked open it is evident that all sections of the line can be energized from their respective sources of power.

Our method of operation differs in an outstanding point from that of Rich and Kirwen. There is no need of co-ordination of timing between the operation of the breakers and the feed points in the operation of the automatic air switches, except that the breaker should not close until the air break switches have opened, that is, the first reclosure should not be less than about three seconds. We do not delay the operation of our air-switches until tests are made by the automatic breakers at the source stations. Instead, the transfer type installation at once transfers its load to the second source; the sectionalizing type at once opens both of its air-switches. The action in both cases is initiated by an undervoltage time delay relay set to close its contacts in one second at zero volts. The load of the transfer type installation is thus re-energized within three seconds; the load of the sectionalizing installation is energized after an interruption not exceeding about nine seconds. If both line sections become energized, the two air-switches will close restoring the entire line to service in the case of the sectionalizing type of installation.

F. W. Rich and M. S. Kirwen: The authors wish to express their appreciation to G. E. Heberlein, R. S. Smithley, S. C. Killian, M. Stene, and K. N. Reardon for their discussions of this paper and for their valuable contribution to the information available on the general subject of automatic control of air switches.

As emphasized by Reardon, the control schemes presented in the paper were designed to meet specific system operating requirements. No reference was made to the more general types of control schemes in use. The outline of the general control schemes presented by the discussers together with the operating experiences given is valuable data. Also the special automatic control features such as sectionalizing on overload, sectionalizing after a predetermined number of overloads, and the use of the fault current through current transformers as a means of locating and clearing a fault, should prove of interest to control engineers.

Conditions frequently arise which might justify the use of current transformers in the tap line to locate a fault on that line. In a transfer control scheme such a fault would cause an unnecessary trip-out on the emergency line. In cases where there is considerable exposure on the tap line and where fuses in the tap cannot be co-ordinated with protective relays on the main line breakers it would seem that this additional feature should be given consideration. Whether or not the additional motor operated air break switch suggested by Killian and Stene for this purpose can be justified is questionable. The control of the two motor-operated air break switches could be arranged to lock out in the open position, on overcurrent, for faults on the tap line.

Reardon indicates that, in the control schemes used by the West Penn Power Company, the operation of the automatic air switches is not delayed until tests are made on the line by the automatic breakers at the source stations. It would seem that the probability of a fault being cleared on the first reclosure of a source breaker would justify testing the line before an automatic transfer could take place.

The authors wish to clear up some points in the control schemes presented by them which have apparently been misunderstood. Killian and Stene stated that these control schemes were for single phase control only, that is, one potential transformer for each

line. The control scheme shown in Figures 3 and 4 of the paper uses 3-phase line potential. Loss of potential, either single phase or 3-phase, will initiate a transfer to the emergency source. The transfer back to the preferred source will not be made unless 3-phase potential is available on the preferred line. The nature of the load at this station justified this additional protection. Heberlein, in commenting on the methods described by the authors for the completion of certain sequencing, has apparently overlooked the fact that motor mechanisms with contactors equipped with sealing-in contacts which become energized by the motor limit switch at the end of the operating travel are employed in these control schemes. Also Heberlein overlooks the fact that *169* and *269* are interlock switches which are open only when the crank is inserted to operate a mechanism by hand.

The discussions indicate that automatic air switches are used extensively to improve service with a nominal capital expenditure. They also indicate that for many applications the control schemes have been standardized by some operating companies and that for other applications the control schemes must be designed to meet the specific operating requirements.

Recent Developments in Track Brakes and Drum Brakes for PCC Cars

S. J. VOUCH
NONMEMBER AIEE

ONE of the factors which has made the President's Conference Committee car so successful is the effective braking system which has been incorporated into its design. This paper explains details of construction and characteristics of two component parts of the braking system—the magnetic track brake and drum brake, which recently have undergone extensive design changes.

The braking system often is taken as a matter of course while actually it is of great importance in that it permits the operator to use the accelerating and speed characteristics of the equipment to their fullest extent with confidence that he can stop as fast as any vehicle in his path. Without this confidence the operator would proceed in a timid fashion accelerating at a lower rate and running at reduced speed so as not to be taken unaware by some unexpected change in traffic conditions requiring a quick stop. As a consequence schedule speed would be reduced because the operator would not be able to use with safety the schedule ability provided by the motive equipment.

The major portion of the braking duty is performed by the motors acting as generators to produce a dynamic brake down to a car speed of about one mile per hour at which point the drum brakes automatically take over as the dynamic brake fades out. These two forms of braking depend upon the adhesion between the wheels and rails for their effectiveness, but the track brake presents an entirely separate friction surface to the rail, making it an important emergency brake particularly under slippery rail conditions. It is brought into play whenever the operator depresses the brake pedal beyond the maximum dynamic brake position, and thus can be applied any time operating conditions warrant its use.

Magnetic Track Brake

The track brake system includes four electromagnetic brake shoes, a controller, and resistances for varying the excitation from the car battery. Each shoe normally is held in equilibrium by a pair of springs so the bottom of the shoe is about three-eighths inch above the rail surface, the shoe being suspended between the wheels on one side of the truck, as shown in Figure 1. In effect the shoe is a long narrow electromagnet consisting of a coil held between fixed steel side plates to which are bolted renewable steel wearing strips as indicated in Figure 2. When the coil is energized from the 32-volt car battery it is pulled down to the rail by its own magnetism, gripping the rail with a force proportional to the current flowing in the coil.

The two shoes on each truck are tied together mechanically by a steel framework which holds the shoes in alignment along the rail and also provides a rigid surface so the drag exerted by the track brakes can be transmitted to the truck structure.

Because of the exposed location of the track brake shoes, the coil is subjected to direct wheel wash and in the winter months this may include salt water splash, slush, snow, mud, and so forth. During inclement weather the coil receives a constant barrage of these elements, any one of which may be detrimental to its continued functioning.

Previous construction included a steel spool body on which the coil was wound, with a copper strip encircling the winding; the whole assembly being put through a vacuum varnish treatment for waterproofing. In order to provide a better protection against failure from the causes mentioned a new method of coil construction has been developed wherein the coil is encased in a nonmagnetic stainless steel shell hermetically sealed to prevent the entrance of foreign matter.

Figure 1. Truck for PCC car showing track brake shoe suspended from springs and actuator for drum brake

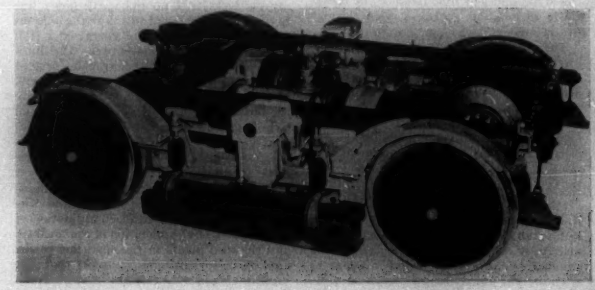

Paper 47-42, recommended by the AIEE committee on land transportation for presentation at the AIEE winter meeting, New York, N. Y., January 27–31, 1947. Manuscript submitted November 6, 1946; made available for printing December 6, 1946.

S. J. VOUCH is with transportations divisions, General Electric Company, Erie, Pa.

The author wishes to acknowledge the assistance of J. F. Tritle, designer of the braking equipment described, in preparing this paper.

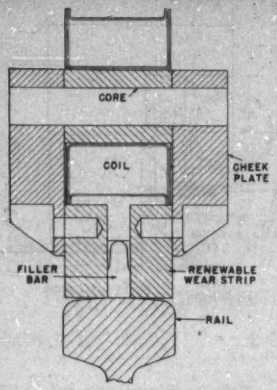

Figure 2. Cross section of track brake shoe

Accelerated life tests on coils of this construction indicate this improvement will result in greatly increased reliability in service. Figure 3 shows a cross section cut from a completed coil with the winding and method of sealing the edges of the case visible. Among other problems encountered in working out this construction was a suitable means of bringing the power lead through the case (the negative lead is grounded internally). This was

Figure 3. Section cut from completed track brake coil to show method of sealing edges of case

accomplished by building a female receptacle in one end of the case so a plug connection could be used on the end of the cable. A gland nut and tapered rubber bushing provide a seal at this point. This construction is of value in that it also permits easy replacement of damaged leads.

Figure 4 shows a typical pull characteristic, measuring the force required to pull the shoe from a machined surface on a 130-pound rail as the coil excitation is

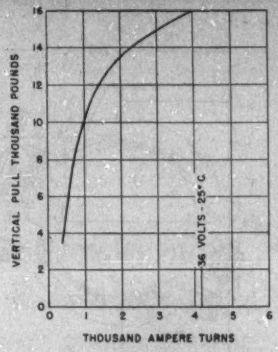

Figure 4. Typical pull curve for track brake shoe

varied. While this type curve forms a useful basis for comparing characteristics of various designs under static conditions, it does not give a true picture of performance under service conditions, mainly because of two variables, rail condition and car speed.

It has been found that the surface of the shoe soon conforms to the contour of the rail head after it has been in service for a while, which results in greater retardation because of the reduction in air gap when the shoe is in contact with the rail. However variations in rail condition over the system will produce some variation in re-

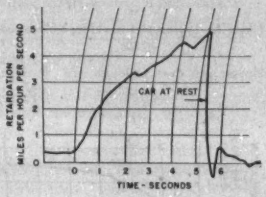

Figure 5 (right). Retardation curve, track brakes alone

Maximum rate, brake applied at zero time, 17 miles per hour car speed

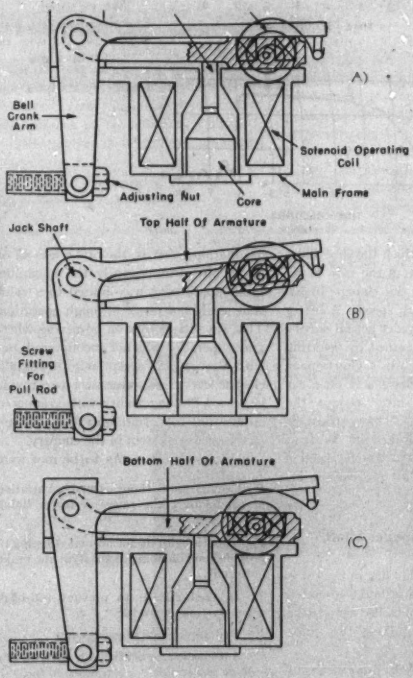

Figure 6. Diagrammatic sketch of brake actuator positions

A. Brake released—holding coil energized, operating coil de-energized

B. Normal brake application—both coils energized, operating coil current determines amount of braking

C. Emergency or parking application—both coils de-energized (spring applied), full brake

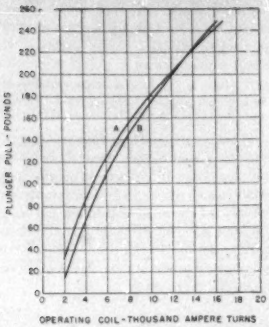

Figure 7. Typical pull curves for brake actuator

Plunger gap *A*—One-fourth inch *B*—One-half inch

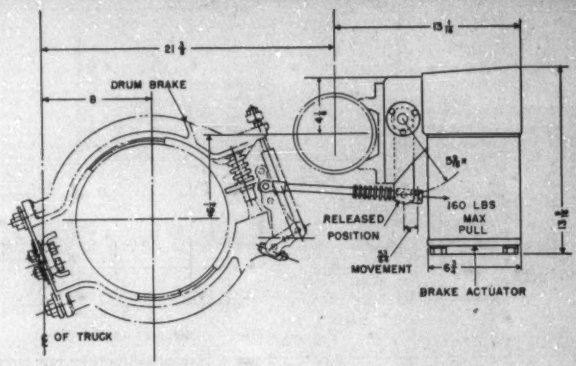

Figure 8. Relative position drum brake and actuator in truck

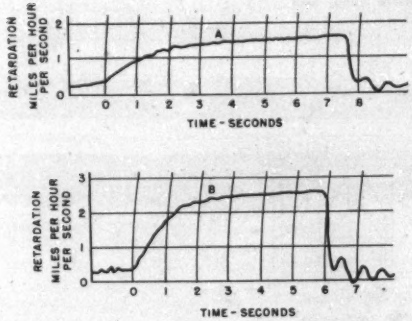

Figure 9. Retardation curves, drum brakes alone

A—Low rate, brake applied at zero time, 10 miles per hour car speed

B—Intermediate rate, brake at zero time, 13 miles per hour car speed

sults. The speed at which the shoe slides over the rail also affects the rate of retardation because of the change in coefficient of friction with speed. A better picture of operation under actual service conditions may be obtained by referring to Figure 5. This shows a chart made with a recording accelerometer on a car and therefore takes into account the variables mentioned. The pattern is typical of the track brake, the deceleration increasing rapidly as the car speed is reduced and coefficient of friction increased.

Drum Brake on Propeller Shaft

Final stopping and holding of the car is accomplished by a drum brake mounted on each drive shaft, controlled by a brake actuator shown just above the track brake in Figure 1.

Previous designs included no means of graduation; that is, the brake was all on or all off. Consequently the maximum brake application was limited to a value that would not result in rough operation. This was satisfactory on properties where grade operation was not encountered, but with the general acceptance of the all-electric car it was necessary to provide increased braking ability with graduated application to permit operation on any street railway system in the country.

General requirements to be met were

1. Graduation without excessive variation in results over the range of brake lining wear.

2. Smooth build-up for normal stopping to provide good blending as the dynamic brake faded out.

3. Delayed release to prevent roll-back when starting on grades.

4. Fast application in emergency.

5. Automatic application on loss of low voltage power.

These requirements were met as follows:

1. A magnetic circuit design generally as indicated in Figure 6 produces pull characteristics as shown in Figure 7.

2. The inductance of the solenoid operating coil inherently results in a smooth build-up for normal operation.

3. By arranging the control to short-circuit the solenoid coils in the pedal release position, the flux decays slowly resulting in a gradual release of braking effort.

4. A separate holding coil when de-energized causes emergency springs to apply the brakes in 0.02 second as compared to normal application time of one second.

Although the drum brake normally is used only for the final stop and for parking, the control is arranged to apply it automatically if the dynamic brake should fail. The accelerometer charts show this condition and it is interesting to note the brake block material used has a nearly constant coefficient of friction with change in speed. This characteristic can be varied readily by changing the composition of the brake lining material to produce a rising coefficient of friction as car speed decreases.

Conclusions

The variety of braking means provided on the modern street car permits the operator to use the full capacity of the motive equipment with safety under present-day traffic conditions.

Design of an electric brake actuator has replaced the air brake used on street cars for many years. Automatic application of the drum brakes on failure of low voltage power has made it possible to eliminate the hand brake for parking. A total of 1,703 all-electric PCC cars are in service or on order.

Investigation of Silicone Insulation on High-Temperature Railway Motor

GEORGE GRANT, III
ASSOCIATE AIEE

T. A. KAUPPI
ASSOCIATE AIEE

GRAHAM LEE MOSES
MEMBER AIEE

Synopsis: Thermal aging and humidification tests are reported on a silicone insulated railway motor. This included 1,675 hours at a temperature of 285 degrees centigrade with 46 cycles of severe humidification. Loss of initial moisture resistance was observed but no operating failure occurred. No change occurred in the heat dissipating characteristics of the machine. Finally, the motor was dismantled and the insulation examined in detail. Thermal aging data are interpreted.

A comprehensive test program was begun in November 1943 to determine behavior of silicone insulating materials in electric motors. The program had as its main objectives to determine the relation between operating temperature and service life for silicone insulated motors and to obtain a comparison between the behavior of class *A*, class *B*, and silicone insulated motors when subjected to the same type of test cycle. Most of the equipment used consisted of induction motors, which have been operated at temperatures ranging from 200 to 310 degrees centigrade; this portion of the test program is not complete because of insufficient motor failures. One piece of equipment used, however, consisted of a silicone insulated street railway motor, and this motor has had over two years of accelerated testing.

The accelerated testing method used was based on the belief that moisture or humidification could be used to detect insulation faults. The testing cycle, then, consisted of periods of high-temperature operation of the motor, alternated with periods of severe humidification during which the condition of the insulation could be determined. In order to obtain test results in a reasonable length of time, the relatively high operating temperature of 285 degrees centigrade was selected. This temperature, chosen on the basis of laboratory tests and previous motor tests, proved to be sufficiently high to produce changes in insulation characteristics within 400 hours of aging. It was low enough, however, so that factors other than electrical insulation, such as commutation and bearings, did not interfere with the test.

Figure 1 shows the physical arrangement used to test the motor, loading it during the high-temperature run by a belt-connected generator.

Table I. Temperature Test Results

	Test Before Aging, October 29, 1943	Test After Aging, May 31, 1946
Line current	135	135
Line volts	302	294
Main field current	118	118
Speed (rpm)	1,820	1,822
Rise by resistance, C		
Main field	154	142
Commutating field	135	149
Armature	92.5	83.5

Description of Apparatus

The railway motor chosen for the test was the one used at that time on standardized Presidents' Conference Committee street cars. The motor has a normal continuous rating of 46 horsepower on 300 volts at 1,820 rpm in accordance with AIEE Standard 11. Under these conditions, the armature and commutating field currents are 135 amperes and the main field current is 118 amperes.

The mechanical design of the motor was unchanged including the copper sections and insulation thicknesses. The only changes made were to utilize silicone treated and bonded materials (mica, fiber glass, and asbestos) wherever possible. Full details are given in Appendix I.

Test Results

The test cycle consisted of a heat run at 285 degrees centigrade by resistance to age the insulation, followed, after cooling, by a severe humidification to facilitate the detection of possible insulation faults.

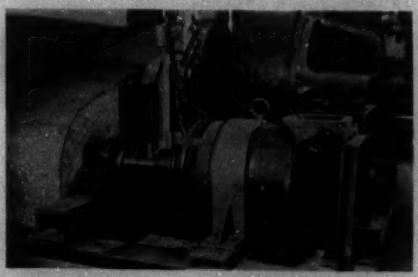

Figure 1. Silicone-insulated railway motor on life test in laboratory

Paper 47-53, recommended by the AIEE committee on land transportation for presentation at the AIEE winter meeting, New York, N. Y., January 27–31 1947. Manuscript submitted November 13, 1946; made available for printing December 5, 1946.

George Grant, III, electrical engineer, and T. A. Kauppi, manager of product engineering, are both of Dow Corning Corporation, Midland, Mich.; Graham Lee Moses is manager of development insulation section, a-c engineering department, Westinghouse Electric Corporation, East Pittsburgh, Pa.

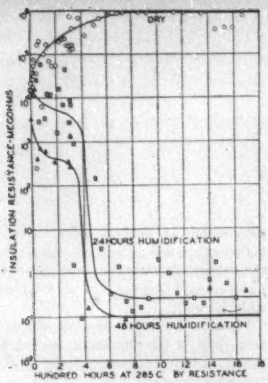

Figure 2. Insulation resistance data for various conditions of humidification plotted as a function of aging at 285 degrees centigrade

The humidification was followed by a drying run at relatively low temperature to eliminate the possibility of steam pockets causing faults which later might be interpreted as the result of aging. A full description of the procedure may be found in Appendix II.

The complete data are shown in the curves of Figures 2 through 7.

Figure 2 shows how the insulation resistance, both dry and humidified, varied with aging. It will be noted that the dry values tend to increase gradually to a maximum and continue with little change. But in the case of the humidified values, an initial high degree of moistureproofness is retained for something over 300 hours. At this point, the insulation resistance and moistureproofness quickly reach a minimum value which continues from there with little change.

Figure 3 shows that capacitance values reduce slightly with aging but offer little to correspond to the sudden loss in insulation resistance after humidification.

Figure 4 shows that a slight improvement in dry dissipation factor is gained upon aging. However, the values of wet dissipation factor show a retention of initial moistureproofness for approximately 350 hours, at which point it suddenly is lost.

Figures 5, 6, and 7 show the variation in insulation resistance, capacitance, and dissipation factor with time of humidification for three different stages of aging. These indicate, by their slope, the rate and, by ultimate values, the degree of moisture penetration.

Visually, the condition of the insulation did not change a great deal throughout the test period. Regular inspections were made before each humidification and a tendency for the silicone to lighten in color in the hotter spots was noted. No crazing, cracking, or loosening of the insulation was noted.

No trouble was experienced with bearings, grease, brushes, or commutation. This lack of trouble should be attributed to the cooling system of the motor. The cooling air was drawn in over the commutator, brush rigging, and brackets to bearing supports, effectively cooling them as well as the bearings.

After 46 cycles of heat and humidification, totaling 1,675 hours of operation at 285 degrees centigrade by resistance, the aging was discontinued and the unit examined Figure 8 shows the condition of the stator assembly at this point.

A temperature test disclosed that the heat dissipating ability of the winding had remained essentially unchanged by the severe accelerated aging test (see Table I).

A measurable increase in field resistance occurred during the test period; 2.23 per cent in the main field and 2.75 per cent in the commutating field. However, this is not of sufficient magnitude to cause any trouble and is, in fact, within normal manufacturing tolerances. Further, it must be remembered that this motor was run at a temperature well in excess of that contemplated for actual service to determine what does happen at such high temperatures and accelerated thermal aging. This high temperature definitely would accelerate resistance increase of the copper which is caused by oxidation.[6]

Table II. Dielectric Test Results

Motor Winding	Voltage: Held (One Min)	Voltage: Breakdown
Armature	2,200	2,600
Commutating field	2,200	2,600
Main field	5,400	5,800

Winding Breakdown Tests

Step-by-step (1-minute) dielectric tests were made on each winding separately with the results as shown in Table II.

After the armature was stripped, the individual coils were given a high potential test to breakdown between turns. This was a momentary test starting at 200 volts and increasing in 200-volt steps. The results of this test are shown in Table III.

Final Examination of Winding

Upon completion of all tests, the motor was disassembled and coils removed in

Figure 3. Capacitance changes with aging under varying humidity conditions

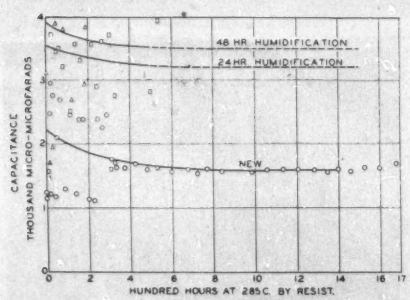

Figure 4. Effect of thermal aging and humidification on dissipation factor of silicone insulation

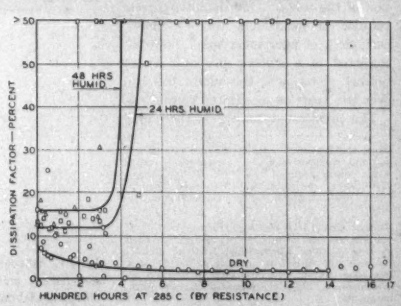

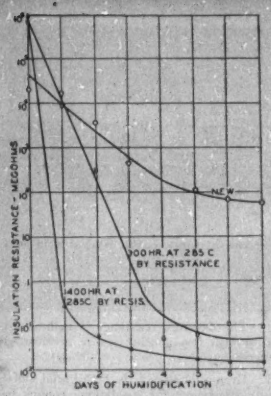

Figure 5. Effect of time of humidification on insulation resistance at several stages of thermal aging

steps to permit detailed examination of the insulation.

Figure 8 shows the condition of the field coils in the stator. In a number of spots, the final coat of varnish had begun to flake off. At the hottest spots (under wiring) there was evidence of more serious degradation of the varnish film as the color had lightened considerably and the varnish had become very brittle. However, in most places, the film was intact and in very good condition. The iron surfaces of the stator were well covered and essentially rustfree.

Figure 9 shows individual field coils with the ground insulation partially cut away. The insulation was flexible and still well bonded. No serious signs of degradation were observed.

A cross section of a main field coil is shown in Figure 10. The conductors were well bonded and the silicone filling cement (in the bevel) was solid. There was no evidence of insulation shrinkage or loosening throughout the coil structure.

The armature assembly is shown in Figure 11 in a partially dismantled condition. There were no visible signs of silicone insulation deterioration. The coils and insulation were flexible. Wires of the coils were well bonded. Engineers examining the motor were of the opinion that almost no aging had occurred on the armature insulation, which had operated considerably cooler than the fields. Only the wedges showed serious evidence of thermal aging and these were made of phenolic bonded asbestos laminate. The outer edges of the punchings were seriously rusted, indicating exposure to high humidity.

Discussion

The data on insulation condition show that a high degree of moistureproofness was attained in the motor as constructed. The loss of moistureproofness at approximately 350 hours of aging indicates that one or more faults developed in the continuity of the insulation structure permitting an increase in both rate and degree of moisture penetration to the conductors. However, additional aging produced little change in degree of penetration as seen in Figures 2, 3, and 4, but did produce an increase in rate as shown in Figures 5, 6, and 7. The fact that the rate of moisture penetration continued to increase steadily after 350 hours of aging indicates that new paths for moisture penetration were being developed by the heat aging. This was confirmed finally by the cracks and crazing discovered in hot spots during stripping of the winding.

Table III. Momentary Test Results

Breakdown Test Voltage	Number of Failures
200	2*
1,400	6
1,600	51
1,800	16

* Believed to have been damaged during removal.

If the rate of moisture penetration had not increased after the initial loss of moistureproofness, it would have been concluded that the 350-hour point was not a true turning point but an accidental one caused by an isolated crack in the insulation.

Comparing the various types of insulation measurements, it is seen that insulation resistance and dissipation factor give a true measure of the insulation condition only when the motor has been exposed to moisture. Capacitance changes are not great and do not appear to be significant either wet or dry. In view of this, when measuring the insulation condition of a silicone insulated motor, a low reading of insulation resistance will mean danger, but a high value does not mean the unit is in good shape unless it is known to have been exposed to high humidity. An excellent indication of condition is the ratio of change in insulation resistance or dissipation factor in going from a dry to a wet condition.

The concept of lightening in color is new with silicones. The organic types of resins used for insulation carbonize upon heat aging and produce free carbon which is black and a comparatively good conductor of electricity. However, silicones decompose into silica which is white and an insulator. Hence lightening in color is evidence of thermal aging with silicones.

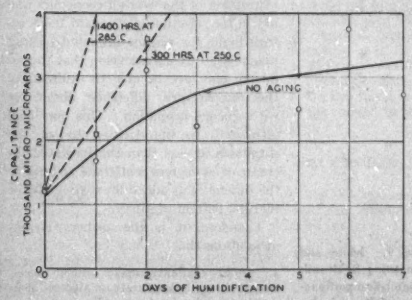

Figure 6. Changes in capacitance with time of humidification at several stages of thermal aging

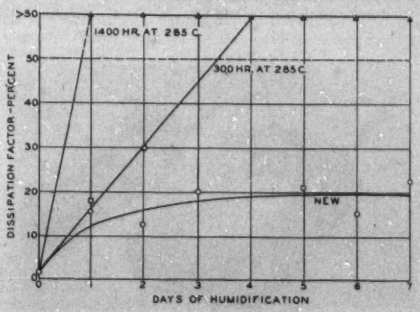

Figure 7. Dissipation factor changes with time of humidification at several stages of aging

Figure 8. Stator assembly after completion of 1,675 hours aging at 285 degrees centigrade

Furthermore data on this have been reported.[6]

In interpreting the thermal aging data from this test, the authors have followed the current concept of the thermal aging of insulation. This is based on the assumption that aging is a logarithmic function of temperature with the life being halved for a given temperature increment.[7] Pursuing this line of reasoning, the curve shown in Figure 12 was constructed as follows:

1. The point at which the loss of moisture resistance was noted is plotted as point *A*. This is considered "minimum life" at 285 degrees centigrade (by resistance).

2. The end of the test is plotted as point *B* and is considered as probable "average life" in view of the field winding condition at the end of the test.

3. Two parallel curves are drawn through these points (*A* and *B*) with a 12-degree-centigrade slope for 2-to-1 life expectancy change.

This is believed to be reasonably conservative in extrapolating toward lower temperatures as tests on materials and laboratory specimens indicate a value of ten degrees centigrade for half life.

Other tests have indicated that silicone insulation will have at least equal thermal endurance to class *B* insulation at 50 degrees centigrade higher temperature. Other recommendations to the AIEE have been made on this basis.[3] It therefore appears reasonable to examine such an increased temperature value in the light of this test. Adding 50 degrees centigrade to the current class *B* insulation standards for railway apparatus (AIEE Standard 11) would be equivalent to a peak temperature of 220 degrees centigrade or a normal temperature of 205 degrees centigrade (both observable values by resistance).

Figure 12 predicts that 36,000 hours operation at 205 degrees centigrade (observable temperature) will be required to reach the condition resulting in loss of initial moisture resistance, which is assumed to be minimum thermal life of the insulation. The average life represented by the final condition observed in this test would be at least four times as great.

In a necessarily simplified approach to an approximation of service life, it was assumed a railway motor is at normal operating temperature 25 per cent or less of each year. (This value was based on the advice of several railway application engineers.) On this basis, a silicone insulated motor would retain its original moisture resistance for over 16 years. This leads to the conclusion that, insofar as the silicone insulation is concerned, present temperature limits for class *B* insulation could be increased by 50 degrees centigrade for silicone insulation, and that reasonable thermal life is to be expected.

Conclusions

The tests reported herein are on a single railway motor which does not permit specific conclusions. However, the broad test program has indicated the following general conclusions:

1. Excellent initial moisture resistance.

Figure 9. Main and commutating field coils with insulation partly removed (after aging)

Figure 10. Cross section of aged main field coil

2. The moisture resistance is maintained at a high level during severe accelerated thermal aging.

3. Even after loss of the high initial moisture resistance, the insulation remains in operable condition throughout considerable additional thermal aging and exposure to extremely severe humidity conditions.

4. The thermal endurance indicated by these tests is such that reasonable life expectancy is predicted for silicone insulation at 50 degrees centigrade above the present temperature limits for class *B* insulation.

5. Improved thermal endurance of silicone insulation may be utilized to increase thermal life expectancy of insulation to many times that of class *B* insulation under the same temperature conditions.

Recommendations

Selection of specific railway temperature standards for silicone insulation should await further tests by other engineers, as it is recognized that a single test does not provide sufficient background for concrete recommendations of standards.

It would be of considerable value if design engineers would analyze various types of electric railway machines to determine what advantage in design may be gained from increase in operating temperature. This would permit sound evaluation of the over-all economics and aid in the selection of standard temperature limits for silicone insulated railway machinery. It may develop that the industry may not be able to utilize fully the temperature difference obtainable with silicone insulation. This may lead ultimately to the decision to set the standards at less than the indicated increase of 50 degrees centigrade and utilize the difference as added life expectancy or thermal margin of safety.

Therefore, it is the authors' recommendations that

1. Other engineers make similar accelerated thermal aging tests on silicone insulated apparatus for future discussion.

Figure 11. Partly disassembled armature after completion of test

2. Design engineers study various designs of apparatus to evaluate what advantage, if any, may be derived in size, weight, and rating through operation at higher temperatures.

3. The committee on land transportation sponsor further papers on this problem and discussions at future meetings.

Appendix I. Description of Apparatus

Armature Coils

Conductors were 0.144-inch square wire, glass covered, and treated with silicone varnish (*DC-990-A*). Ground insulation consisted of $2^1/_2$ turns of glass-backed mica wrapper 0.008 inch thick. The glass cloth was silicone-varnish sized and a silicone bond was used. Binder tape was fiber glass, sized with silicone varnish (*DC-990-A*). The coils were vacuum and pressure impregnated with silicone varnish at 70 per cent solids (*DC-990-A*).

Main and Commutating Field Coils

These coils were made of strap conductors, separated by a single thickness of glass-backed mica tape (0.007 inch thick, silicone bonded, and sized). Chamfer of the main field coil was filled with an asbestos and silica cement with a silicone resin bond. Ground insulation consisted of two half-lapped layers of thick glass-backed mica tape (0.007 inch thick, silicone bonded and sized). Binder tape was fiber glass sized with *DC-990-A*. These coils were vacuum and pressure impregnated with *DC-990-A* at 70 per cent solids.

Insulation details for winding the armature were made of glass-backed mica and asbestos cloth, silicone sized and bonded. For slot wedges the best available grade of asbestos cloth, laminated phenolic, was employed as no silicone bonded laminates were available at that time. Coils were soldered in the commutator necks with high melting solder (304-degree-centigrade solidus temperature).

Both armature and stator were dipped twice in *DC-990-A* silicone varnish (at 50 per cent solids). Subsequently, after preliminary testing, an additional dip and bake was applied to both armature and stator.

The Commutator

The commutator was insulated with mica bonded with a high-temperature synthetic shellac substitute. The bars were made of silver-bearing hard-drawn copper to avoid softening during the high-temperature bake or during operation. During all baking cycles, the commutator nut was loosened to relieve the V-binding from pressure strains.

Appendix II. Details of Thermal Aging Test

Heat Run

Each test cycle began with an aging heat run. The motor was overloaded and its ventilation restricted in order that the test temperature, 285 degrees centigrade, be reached as rapidly as possible. This was done to minimize the effective aging on the insulation during this time. Upon reaching 285 degrees centigrade, the ventilation was restored to normal and the load reduced to that required to hold this temperature in both fields. The temperature then was maintained for six hours in the initial runs. On succeeding runs this time was increased in steps. When a duration of 72 hours was reached, no further increase was made. During the 18–22 hours required to cool from the heat run to room temperature, readings of insulation resistance, capacitance, and dissipation factor were taken at 20 degrees centigrade intervals. These data were used for correcting the readings to 25 degrees centigrade.

In order to obtain the same temperature in the two fields, it was necessary that some of the current be shunted around the main field.

Heat Run Data

The following data were obtained on the heat run with 310 volts direct current, 1,650 rpm:

Main field = 285 degrees centigrade by resistance

Commutating field = 285 degrees centigrade by resistance

Armature = 180 degrees centigrade by resistance

Commutator = 150 degrees centigrade by thermocouple

Front bearing = 80 degrees centigrade by thermocouple in grease

Rear bearing = 95 degrees centigrade by thermocouple in grease

Outside frame = 150 degrees centigrade by thermocouple

Cooling air rise = 36 degrees centigrade (average of six thermocouples, 14 to 53 degrees centigrade)

Humidification

Upon reaching room temperature, the motor was placed under humidification for 24 hours. This was accomplished by covering the air exhaust and placing a tank over the air intake of the motor. In the tank a regulated quantity of air was bubbled through a bath of water five to ten degrees centigrade above ambient. This wet air then passed into the interior of the motor. Thus this method was extremely severe, as the winding acted as a condenser, causing the water in the air to form into rivulets and droplets on the insulation as well as produce a high humidity ambient atmosphere.

After 24 hours of humidification, the insulation resistance, capacitance, and dissipation factor were checked and a 5-minute high potential of 500 volts alternating current applied between windings and ground. This was followed by a 5-minute no-load run (125 volts, the maximum permissible without causing overspeed). The insulation readings and high potential then were repeated.

Originally it was planned that the insulation resistance, capacitance, and dissipation factor be studied on the main field, commutating field, and armature. However, it soon was found, because of the exposed lead ends, brush rigging, commutator, and other unavoidable bare copper, that the severe

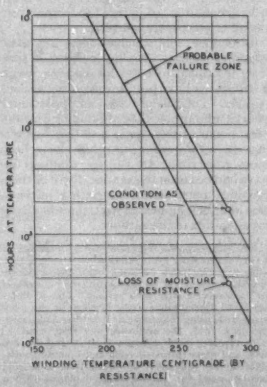

Figure 12. Thermal aging curve interpreting test results

humidification caused these values in the commutating field and armature to vary beyond the range of available instruments. The complexity of these leakage circuits precluded satisfactory guarding. Hence the data here presented are those obtained from the main field whose leads extend outside the motor, thus avoiding leakage from bare copper inside the wet motor.

Drying

After the readings at the end of humidification, the motor was prepared for another heat run by drying it. This consisted of running 2 hours at 90 amperes, 250 volts producing a slow rise to 75 degrees centigrade. The load then was raised to 120 amperes, 300 volts producing an ultimate temperature of 130 degrees centigrade. This was held 8 to 16 hours. The motor then was considered ready to start a new cycle with the next heat run.

Preliminary Test

In order to bring the unit to a dry condition, it was run 8 hours at 120 amperes on 300 volts causing a temperature of 130 degrees centigrade. While cooling from this run, readings were taken as in the heat runs. Upon reaching room temperature, humidification was started and continued for one week. Daily readings of insulation resistance, capacitance, and dissipation factor were taken and the high potential test of 500 volts alternating current applied. At the end of the week, the no-load run (125 volts) was made. The insulation readings and high potential test were repeated and the motor dried as outlined earlier. This preliminary run provided a bench mark for comparison of data obtained as aging progressed. This 1-week humidification was repeated at 300 and 1,400 hours of aging as well as several 48-hour humidifications. These were run to broaden the over-all picture.

Appendix III

With reference to the values given in the paper the following items should be noted:

1. All resistance, insulation resistance, capacitance, and dissipation factor values are corrected to 25 degrees centigrade.

2. Insulation resistance values are 1-minute 500-volt direct current.

3. Capacitance and dissipation factor values were obtained with a low-voltage 60-cycle bridge.

4. Winding temperatures are all resistance values. The operating values on the main and commutating fields were obtained at frequent intervals by the voltmeter-ammeter method. These values were checked regularly by using the resistance at zero time, extrapolated from the cooling curve obtained with a Kelvin bridge. This bridge method also was used in obtaining the armature temperature.

References

1. Organo-Silicon Compounds for Insulating Electric Machines, **T. A. Kauppi, G. L. Moses.** AIEE Transactions, volume 64, 1945, March section, pages 90–3.

2. The Application of Silicone Resins to Insulation for Electric Machinery, **J. DeKlep, L. R. Hill, G. L. Moses.** AIEE Transactions, volume 64, 1945, March section, pages 94–8.

3. Silicone Insulation Proved by Test, **T. A. Kauppi, George Grant, G. L. Moses, R. F. Horrell.** *Westinghouse Engineer* (Pittsburgh, Pa.), September 1945.

4. Standard for Wet Tests. AIEE Standard 29, November 1941.

5. American Standard for Rotating Electrical Machinery on Railway Locomotives and Rail Cars and Trolley, Gasoline-Electric and Oil-Electric Coaches. AIEE Standard 11, March 1943.

6. Silicone-Resin-Treated Magnet Coils, **Graham Lee Moses, Julius J. Torok.** AIEE Transactions, volume 65, 1946, July section, pages 412–16.

7. Synthetic Insulation and the 10 Degree Rule, **G. L. Moses.** *Westinghouse Engineer* (Pittsburgh, Pa.), July 1945.

8. Silicone Insulation for Railway Motors, **G. L. Moses.** *Railway Mechanical Engineer* (New York, N. Y.), October 1944.

Discussion

N. J. Greene (National Electric Coil Company, Columbus, Ohio): It is evident that the authors have devoted a tremendous amount of time and energy to the laboratory investigation of silicone treated and bonded insulating materials and windings. They have presented a summary of this information in a manner that should certainly stimulate further work along similar lines by both manufacturers and users who are desirous of increasing temperature rating of electrical apparatus.

Of the 300 odd silicone, mica, and glass windings we have supplied, ranging in sizes from fractional to 1,800 horsepower, about a half dozen have been returned for various reasons. This has provided an opportunity of determining how they are standing up and what some of their good and bad features may be. The operating results have been most gratifying. Of the six windings we have had occasion to examine, three of them provided particularly interesting information and they support in part, the laboratory investigation of the authors.

1. A 30-horsepower d-c crane motor operating on a very severe duty cycle provided an excellent test. Over a period from 1942 to 1945, the armature winding roasted out 21 times with an average of 50 days service after each rewind. The windings are class *B* insulation, of the usual mica and glass insulation, using conventional varnishes and bonds. On July 1945, the armature and field windings were replaced with silicone treated and bonded mica and glass insulated coils and operated satisfactorily for 312 days, at which time a bearing failure caused the winding to be damaged. Upon examination, the silicone, mica and glass insulation showed no perceptible deterioration. The same motor is again operating with silicone mica and glass and it has been in service now for 324 days. With the proper bearing maintenance, we would expect it to provide several years of service.

2. An 800-horsepower 1,800-rpm wound rotor induction motor driving an induced draft fan on top of a boiler in a powerhouse provided field test under high ambient temperature operation and also one where both a high speed rotating element and stationary element incorporated silicone, mica and glass insulated coils. After approximately six months operation, the rotor developed trouble due to squashing out of some of the silicone treated glass insulation on the rotor winding jumpers connecting to the slip rings. The winding itself was in excellent condition but the point of high mechanical stress had to be re-enforced with a melamine glass laminate supporting member in order to provide a safe job. It was interesting to observe that the silicone varnish showed no tendency of slinging off the rotor when operating at 10,000 feet per minute peripheral speed.

3. Of the several approximately 450-horsepower high-speed d-c traction armatures in service, one of them developed some difficulty at the commutator where the leads are soldered to the risers after 200,000 miles service. This provided an opportunity to remove several coils and thoroughly examine the condition of the band insulation, the coil insulation, and the copper at the coil corners, for copper fatigue. We had been concerned about copper fatigue at the high stress joints because of the almost complete annealing by virtue of the several bakes at 500 degrees Fahrenheit. It was a pleasure to learn that the insulation, copper, and the entire winding assembly was in by far the best condition that has been observed on an armature operating under similar conditions. There was almost a total absence of mica powdering as is customary where there is considerable winding motion and where conventional insulating materials are used in traction service.

M. R. Hanna (General Electric Company Erie, Pa.): The very excellent heat endurance reported in this paper is in full accord with results obtained on a number of machines of various types insulated in the same manner. The introduction of silicone has made possible a very considerable advance in the design of high-temperature insulation systems. However, to keep our thinking straight and to avoid possible costly failures from incorrect applications of silicone, we should bear in mind that silicone is not employed as a primary dielectric in these successful insulation systems. In other words, this is not silicone insulation but mica insulation treated with silicone.

The fact that none of the silicones now known are suitable for use as a primary dielectric does not minimize their importance in the mica-silicone insulation systems. Silicone treatment perfectly supplements mica by excluding moisture and preventing the shifting of mica flakes. Silicone is unique in its ability to perform this essential function at temperatures in excess of class *B* insulation operating limits.

The practical fabrication of mica-silicone insulations presents a number of new problems and it may be some time before the economics of this application of silicone become clear.

Graham Lee Moses: There were several points raised in the discussion which need some comment or clarification. It is true that the silicone varnishes in current use do not have as good solvent resistance as the best synthetic organic varnishes. However, those now available have solvent resistance equivalent to that of oleo-resinous varnishes which were reasonably satisfactory in this respect as demonstrated by many years experience.

A question was raised concerning the physical characteristics of silicone varnish

films at elevated varnish temperatures. It must be remembered that there are a number of different silicone varnishes having a variety of characteristics. Therefore, one generally can be selected having properties which are peculiarly suited to the application. *DC-993* silicone varnish has satisfactory hot film strength when properly baked. As in conventional organic varnishes no one silicone varnish has all of the desirable properties for every insulation application; therefore judgment must be exercised in the selection of the proper silicone varnish for each specific application.

Hanna's comments emphasize two important points on which there is general agreement.

1. Silicone insulation should include mica to provide the basic dielectric strength. The term "silicone insulation" was used to imply that silicone resin bonds and treatments are substituted for the organic resin bonds in an insulation system consisting of mica, glass, and asbestos in much the same manner as a class *B* insulation system. The term "silicone insulation" was used in this paper because of the lack of an AIEE insulation class. Currently, the Institute is in the process of defining and classifying this new form of insulation as class *H*.

2. All of the problems of applying and utilizing silicone insulations, especially mica-silicone combinations have not been solved. Many of the silicone insulation components are rather fully developed but there is still considerable work to be done on silicone-mica materials for use in commutators. Furthermore, the problem of attaching coil leads to commutators in railway type motors is a difficult problem requiring further attention. General usage on traction motor armatures is therefore further away than on some other types of electrical apparatus.

Automatic Switching Schemes for Capacitors

W. H. CUTTINO
ASSOCIATE AIEE

IMPROVEMENTS in design and reduction in cost within the past ten years have given increased recognition to the capacitor as an efficient, economical, and reliable generator of kilovars. The reduction in cost and increase in reliability resulted in more application investigations which revealed the economic possibilities of the capacitor as a useful tool for releasing system capacity, improving voltage regulation, reducing losses, and improving power factor.

The recognition of these many benefits has led to a rapid increase in the size and number of capacitor installations. When more and more capacitors are added to a system with widely varying loads, a situation may be reached where their effect becomes objectionable during certain operating conditions. It is therefore desirable to obtain the benefits of additional capacitor correction without the objectionable features. The maximum benefits can be obtained by adjusting the capacitor kilovars to the correct value at the proper time. When capacitor kilovars installed are greater than the light load reactive kilovars, it is usually desirable to have the capacitor kilovars reduced at light load to avoid objectionable overvoltage or excessive leading kilovars. The line losses are at a minimum when the capacitor kilovars are the same as the load kilovars. If voltage regulation is the primary objective, then the capacitor kilovars should be adjusted to hold the circuit voltage within the set limits. Unlike the ordinary voltage regulator, however, the adjustable capacitor improves the voltage regulation on both the supply and load side by reducing the current flowing in the supply feeders. If the primary objective is to keep the kilovolt-ampere demand to a minimum or to keep the over-all power factor within certain limits, the capacitor kilovars may be adjusted in response to a kilovar regulating relay or a power factor regulating relay. When the need for adjustable capacitor kilovars is established, then the question arises as to the most economical arrangement that will give the desired operating results.

The capacitor kilovars may be adjusted automatically by varying the voltage on the capacitor or by varying the amount of capacitors connected to the circuit. The amount of capacitors may be varied by automatically switching in equal or unequal steps in response to circuit conditions or they may be switched by the same switching means controlling the load for industrial plants. Switched capacitors also may be used to increase the effective range of a voltage regulator efficiently. In some instances, it is desired to have a kilovar generator which can furnish leading and lagging kilovars. This may be accomplished by a combination of capacitor, reactor, and automatic tap changing transformer; by a combination of capacitor and synchronous condenser; or by a combination of directly connected capacitors and reactors. These various schemes now will be discussed.

Indirectly Connected Capacitors

Variable Voltage Method

It is well known that the kilovars supplied by a given size capacitor vary as the square of the voltage applied. Consideration therefore has been given to varying the voltage applied as a means of adjusting the capacitor kilovars. The voltage applied to the capacitor may be varied by means of a tap changing transformer as illustrated in Figure 1*A* or by means of an induction regulator as shown in Figure 1*B*. By the use of either of these methods, the capacitor kilovars can be adjusted readily into small increments. The losses of the transformer or regulator add to the capacitor losses to substantially increase the over-all losses for the installation.

In general, reasonably coarse adjustment of the capacitor kilovars is found to be entirely satisfactory and the cost of directly connected capacitors with switches for each step is less expensive than the combinations of capacitor with tap changing transformer or capacitor with induction regulator.

If the repetitive switching duty on the breakers for directly connected capacitors cannot be tolerated because of a highly fluctuating load, then consideration should be given to capacitor with tap changing transformer or capacitor with induction regulator. In this connection, it should be remembered that if multistep automatic control is used to initiate the adjustment of capacitor kilovars, the kilovar increments should be in equal steps. To accomplish this with a tap changing transformer requires voltage steps of unequal values because the capacitor kilovars vary as the square of the voltage applied. If the capacitor kilovars are to be varied in $12^1/_2$-per-cent steps from zero to 100 per cent then the voltage steps must be 0, 35.4, 50, $61^1/_4$, 70.8, 79, 86.7, $93^3/_4$, and 100 per cent.

Directly Connected Capacitors

Switched in Equal or Unequal Steps

The capacitor kilovars usually are adjusted by switching the capacitors in equal steps as illustrated in Fgure 2*A* with a circuit breaker for each step. The control with master relay which will meet the operating requirements most economically will determine whether the capacitors are switched automatically in response to voltage, current, kilovar, or power factor.

Paper 47-54, recommended by the AIEE committee on automatic stations for presentation at the AIEE winter meeting, New York, N. Y., January 27–31, 1947. Manuscript submitted November 15, 1946; made available for printing December 18, 1946.

W. H. Cuttino is with Westinghouse Electric Corporation, East Pittsburgh, Pa.

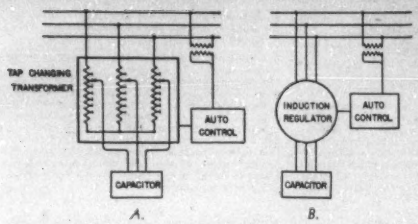

Figure 1. Variable voltage method of control is seldom used for adjusting capacitor kilovars

A. Tap changing transformer varies voltage on capacitor

B. Induction regulator varies voltage on capacitor

Voltage control may be used to remove capacitors at light load if the supply voltage is regulated and the bus voltage varies owing to regulation. It also may be used for switching capacitors to regulate the feeder or bus voltage. Current control may be used to remove capacitors at light load if the supply voltage is nonregulated and the load power factor is reasonably constant with variation in loading. Kilovar control may be used to remove capacitors at light load when the supply or bus voltage is regulated or nonregulated and also may be used for switching capacitors to regulate kilovars or power factor. The band width or spread adjustment of the master relay of the automatic control panel always must be larger than the effect of the largest capacitor being switched. Maximum flexibility and minimum operating duty on the switch therefore are obtained by having the capacitors arranged in equal switching steps. This also permits the user to standardize on a certain size capacitor rating and vary the number of capacitor steps at a particular location depending upon requirements. If conditions change for any reason, the capacitors may be relocated as requirements may dictate.

To obtain a finer degree of control, it sometimes is proposed to switch the capacitors in unequal steps as illustrated in Figure 2*B*. Although a maximum number of kilovar values can be obtained with a minimum number of switches, there will be many more instantaneous changes and some of these will be greater than if the capacitors were switched in equal values. Figure 2*B* shows how the capacitors may be divided into three unequal values of 14, 28, and 58 per cent and switched to obtain seven values in steps of approximately 14 per cent. The maximum momentary disturbance occurs when switching from 42 to 58 per cent when the *C* switch closes and the *A* and *B* switches open, or when switching from 58 to 42 per cent when the *C* switch opens and the *A* and *B* switches close. The increased number of switching operations inherent with this scheme always cannot be tolerated. There are 22 switching operations for one complete cycle of switching for the unequal steps as compared with six for the equal steps. The *A* switch of the unequal step group operates 14 times during a complete cycle of switching, while the *A* switch of the equal step group operates only twice.

Figure 2. Directly connected capacitors divided into equal switching steps is a common method of adjusting capacitor kilovars. Capacitors divided into unequal switching steps seldom is used

A. Capacitors divided into equal steps

A, closed = 33 1/3 per cent
A and *B*, closed = 66 2/3 per cent
A, *B*, and *C*, closed = 100 per cent

B. Capacitors divided into unequal steps

A closed = 14 per cent
B, closed = 28 per cent
A and *B* closed = 42 per cent
C, closed = 58 per cent
A and *C*, closed = 72 per cent
B and *C*, closed = 86 per cent
A, *B*, and *C*, closed = 100 per cent

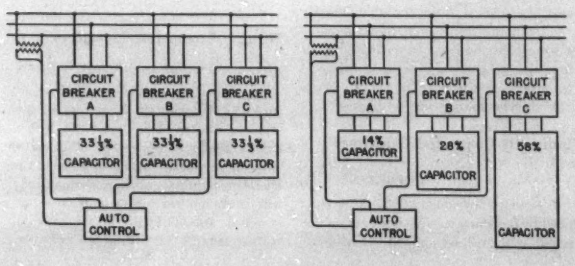

Switching Capacitors With Motors

In general, capacitors should be applied as near the load as practical. If it is found desirable to switch the capacitor with variation in load for an industrial plant, consideration should be given to distributing them out on the circuit and connecting them directly to the motor terminals as shown in Figure 3*A*. The capacitors then will be switched "off" and "on" with the motor without additional switching equipment.

The size of the capacitor switched with the motor switch should be selected to avoid excessive overvoltage caused by self-excitation and excessive transient torque. Charts[1] are now available listing the maximum capacitor size that should be switched with a given size motor. When capacitors are connected to the motor terminals, the line current drawn is less than without the capacitors. The overload devices, therefore, should be selected on the basis of the reduced line current if proper protection is to be obtained.

To avoid excessive overvoltage or excessive transient torque, it may be desirable in some cases to use a separate switch for the capacitor as shown in Figure 3*B*. In the interest of economy, the motor control may be used to initiate the opening and closing of the capacitor switch.

Capacitors Increase Effective Range of Voltage Regulator

When a voltage regulator is used for regulating line voltage, its effective range can be increased by adding a switched capacitor. The capacitor, unlike the ordinary voltage regulator, improves the voltage on both the supply and load side of the installation by reducing the current flowing in the supply feeders and lowering the losses in the circuit. The adding or removal of the capacitor increases or decreases the general voltage level of the circuit a given amount.

Figure 4 shows a regulator with limit switches arranged to initiate the closing or opening of the capacitor switch. When the regulator reaches the maximum "boost" position, the capacitor switch closes to increase the voltage level and the regulator and then backs up until the regulating relay is satisfied. However, as the regulator reaches the maximum "buck" position, the capacitor switch

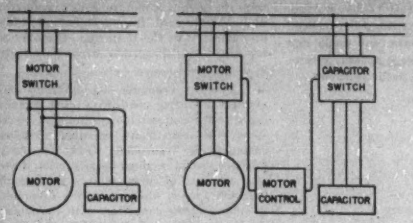

Figure 3. Capacitors switched "on" and "off" with the induction motor for adjusting the capacitor kilovars

A. Motor and capacitor switched as a unit eliminating a separate switch for capacitor
B. Separate switches for motor and capacitor operated simultaneously by motor control

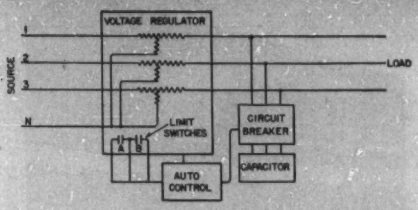

Figure 4. Switching capacitors extend effective range of voltage regulator

A. Limit switch on regulator closes when regulator reaches maximum boost position to close the capacitor switch
B. Limit switch on regulator closes when regulator reaches maximum buck position to open the capacitor switch

opens decreasing the voltage level and the regulator reverses its travel and backs up until the regulating relay is satisfied. If adding or removing the capacitor changes the voltage level five per cent, then the effective range of the regulator is changed by this amount.

If it is desired to minimize the voltage change produced by switching the capacitor as one group, then the capacitor can be divided into several smaller groups each with switches and let the limit switches initiate a sequencing device to obtain selective switching of the capacitor groups.

Supplying Adjustable Leading and Lagging Kilovars

Capacitor, Reactor, and Transformer Combination

Capacitors rapidly have been replacing synchronous condensers for providing bulk wattless power or kilovars for voltage regulation and power factor correction. There are many applications of synchronous condensers at the ends of power transmission lines where it is necessary to adjust the kilovars supplied over a wide range including positive and negative values. For this purpose, standard synchronous condensers are provided with 50 per cent lagging reactive capacity as well as 100 per cent leading reactive capacity and can be varied between these limits.

A capacitor, reactor, and tap changing transformer have been proposed for performing essentially the same functions as the synchronous condenser. One scheme is shown in Figure 5*A*. This involves a tapped shunt winding, a capacitor, a reactor, and a tap changing mechanism which can vary the capacity kilovars from 100 per cent of the capacitor rating to zero by changing taps. A transfer switch is provided to transfer from capacitor to reactor when the tap changer reaches the bottom of the travel, whereupon the same tap changer operating on the taps of the same shunt winding can be used to increase the lagging kilovars from zero to full rating of the shunt reactor. If the capacitor kilovars is 100 per cent and the reactor 50 per cent, this combination will cover the usual range of the standard synchronous condensers.

A very similar scheme was described by Butler and Foster.[2] This arrangement omitted the transfer switch and connected the capacitor in series with the reactor and the combination in parallel with the transformer winding. The common point between the reactor and capacitor is connected to the tap changer. Although this eliminates the cost of a transfer switch, the advantage is counteracted by adding operating losses and increasing the size of the transformer.

Directly Connected Capacitors and Reactors

The tap changing transformer equipment adds considerable expense to an installation. If the repetitive switching duty can be handled satisfactorily by a breaker and there are not a great number of switching steps required, then directly connected capacitors and reactors as shown in Figure 6 are less costly than the

Figure 5. Adjustable leading and lagging kilovars provided by capacitor and reactor with tap changing transformer or with capacitor and synchronous condenser

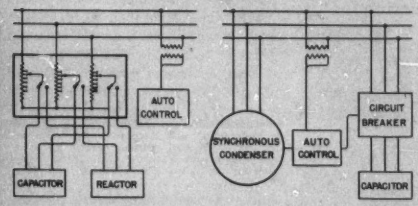

A. Tap changing transformer capacitor-reactor combination
B. Synchronous condenser and capacitor combination

Figure 6. Adjustable leading and lagging kilovars furnished by switching directly connected capacitors and reactors

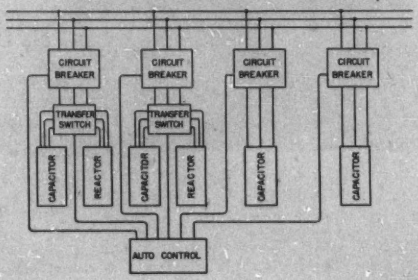

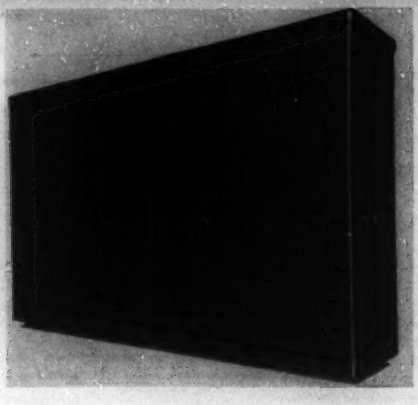

Figure 7. A 1,260-kilovar 13.8-kv outdoor capacitor with oil circuit breaker and single step voltage control for automatic switching

schemes involving the tap changing transformer. It will be noted that transfer switches are added to permit one breaker being used for switching either a capacitor step or a reactor step. The directly connected capacitors and reactors eliminate the losses of the tap changing transformer and also have the advantage that they can be added to or subtracted from readily.

Capacitor and Synchronous Condenser Combination

A synchronous condenser lends itself well to control of kilovars where a large range of leading to lagging is required. It also provides a means of improving system stability or smoothing out voltage dip where these features are desired. Capacitors, however, are less expensive, easy to install, lower in losses, and are added to or subtracted from easily.

The combined advantages of the two types of equipment have been realized[3] by adding capacitors to an existing synchronous generator installation. The capacitor may be used primarily as a base correction with the synchronous condenser output varying to meet the variations of kilovar requirements with changing load conditions.

Figure 5*B* illustrates the combination of synchronous condenser and capacitor. If the load kilovar requirements vary over a wide range, it may be desirable to switch the capacitors automatically in addition to the variations obtained from the synchronous condenser. This can be accomplished by means of limit switches on the synchronous condenser control—one limit switch to close as the control approaches the maximum "boost" position to initiate the closing of the capacitor switch and another limit switch to close as the control approaches the maximum "buck" position to trip the capacitor switch.

Conclusions

1. Maximum benefits with increased use of shunt capacitors require that more consideration be given to switching them automatically.

2. The size and number of adjustable capacitor kilovars should be selected to keep the voltage, power factor, or kilovar demand within desired limits. Usually, coarse adjustment of the capacitor kilovars will meet the operating requirements satisfactorily. In this case, the small steps readily obtainable with the induction regulator or tap changing transformer are not a feature of importance.

3. Generally, economic considerations and average operating conditions favor switching directly connected capacitors in equal steps with electrically operated switches automatically controlled. Other switching schemes should be given consideration if the load consists of large motors with good diversity factor, which is usually favorable to switching the capacitors with the motor or if the expected repetitive switching duty is sufficiently high to make the application of breakers questionable.

4. Capacitors may be considered in combination with reactors or synchronous condensers for supplying leading and lagging kilovars.

5. The operating conditions and requirements will determine which type of automatic control should be used.

References

1. Use the Right Capacitor With Induction Motors, **J. B. Owens.** *Factory Management and Maintenance* (New York, N. Y.), May 1945.

2. Static Phase Modifier, **J. W. Butler, L. W. Foster.** *General Electric Review* (Schenectady, N. Y.), March 1943.

3. Capacitors on 24 Kv as Adjunct to Condensers, **E. R. Smith, N. J. Roberts, H. R. Vaughan.** *Electrical World* (New York, N. Y.), November 1945.

4. Automatic Control and Switching Equipment for Capacitor Banks and Its Application, **T. W. Schroeder, W. C. Bloomquist.** AIEE Transactions, volume 63, 1944, September section, pages 649–54.

5. Extending the Use of Shunt Capacitors by Means of Automatic Switching, **W. H. Cuttino.** AIEE Transactions, volume 63, 1944, September section, pages 674–8.

6. When and How to Switch Capacitors Automatically, **W. H. Cuttino.** *Factory Management and Maintenance* (New York, N. Y.), July 1945, pages 148–52.

7. Selection and Application of Automatic Control for Capacitors, Parts I, II, and III, **T. W. Schroeder, W. C. Bloomquist.** *General Electric Review* (Schenectady, N. Y.), October and December 1945, March 1946.

8. Application of Capacitors for Power Factor Improvement of Induction Motors, **W. C. Bloomquist, W. K. Boice.** AIEE Transactions, volume 64, 1945, May section, pages 274–8.

9. Capacitor Installation at Newport News, **V. R. Parrack, E. L. Harder.** AIEE Transactions, volume 63, 1944, pages 1165–73.

No Discussion

Laboratory Aids for Electromechanical System Development

GEORGE C. NEWTON, JR.
ASSOCIATE AIEE

W. T. WHITE
NONMEMBER AIEE

Synopsis: Laboratory aids for development of electromechanical systems are described in this paper. Standardized components for "mocking up" complex electromechanical systems have proved to be time-saving aids in laboratory work at the Sperry Gyroscope Company, Inc. Illustrations are shown of laboratory setups using these components and descriptions are given of the more generally used mechanical and electronic components.

THE PURPOSE of this paper is to describe a set of standardized components used by engineers at the Sperry Gyroscope Company, Inc. for mocking up electromechanical systems. These components enable laboratory tests to be conducted for such systems long before the completion of the product designs and the construction of pilot models. With the standardized components it is possible to construct a dynamic system similar to the electromechanical system of the product under development. Such a dynamically similar system is termed a "mockup" and the components are called mockup components.

The relation between the mockup and the system it represents is analogous to that between a "breadboard" of a radio receiver and the product receiver as finally manufactured. The breadboard receiver can be made to represent the production receiver as accurately as necessary by refining the networks used to study the effects of stray capacitance and so forth. Likewise, a mockup can be made to represent an electromechanical system as closely as desired by properly introducing stray effects such as backlash and elasticity in gear trains, nonlinearities in signal-producing elements, and various types of friction loading.

As currently practiced, the mockup technique is not an analytical tool in the same sense as differential analyzers,[1] transient analyzers,[2] network analyzers and the various mathematical methods[3] used in the analysis of electromechanical systems. It is not an analytical tool any more than pilot-model testing is. Rather, the mockup technique is a means whereby certain results, in the past usually obtained from tests conducted on a pilot model, may be anticipated by corresponding tests of a dynamically similar system which can be constructed and modified with relative ease. If pilot models could be built with a hundredth of the effort and in a hundredth of the time currently necessary, they would be used in preference to mockups and no need for mockups would exist. A mockup attempts to represent the actual system dynamics as closely as necessary so that the results obtained are truly indicative of system operation. However, for application of an analytical tool the system must be idealized, and the results may be significantly nonindicative of system operation.

To understand more fully the position of a mockup in the development of a product involving an electromechanical system, consider the phases through which such a development passes. Specification, conception, analysis, design, pilot-model construction, test, modification, and reproduction are the major phases. If a mockup phase were to be included, it would be inserted between the analysis and design phases. By adding this phase, which includes a certain amount of testing much benefit may result through

Figure 1. Demonstration servomechanism

Paper 47-52, recommended by the AIEE joint subcommittee on servomechanisms for presentation at the AIEE winter meeting, New York, N. Y., January 27-31, 1947. Manuscript submitted October 31, 1946; made available for printing December 4, 1946.

GEORGE C. NEWTON, JR. is with the Sperry Gyroscope Company at Garden City, N. Y.; W. T. WHITE is with the same company at Great Neck, N. Y.

improvement of design and the consequent reduction of expense and time lost in the testing and modification phases. It is to be emphasized that the mockup phase does not supplant the analysis phase and that any and all techniques ordinarily used in analysis also will be appropriate when the mockup phase is included. The mockup phase is merely a way of making the pilot-model dynamics available for test much earlier than otherwise would be possible.

It is recognized that the mockup technique has stimulated the development of a set of components which may be used for many purposes not directly connected with their original function. These components may be used in the construction of differential analyzers and other analytical aids. They may be used as an educational medium to help engineers and students appreciate more keenly the problems of dynamics.

The mockup components described in this paper are relatively simple in design; the fundamental ideas could be embodied much more elegantly. However, the best way to present the basic ideas seems to be by showing their present embodiment and allowing the reader to make his own abstractions.

Mechanical Mockup Components

Figures 1 and 2 illustrate mockup components in use. As can be seen, the components form a precision "mechano" set with an electronic addition. They may be classified broadly into mechanical and electronic categories. Together with a few special parts manufactured by the laboratory technician and special assemblies peculiar to the system being represented, such as electric motors, hydraulic apparatus, integrators, and gyroscopes, the standard components make possible the mocking up of almost any electromechanical system. After one is familiar with the components, the method of using them follows directly from the signal schematic of the system being represented; therefore this aspect of the mockup technique need not be discussed here.

The standardized mechanical parts are classified as

1. Foundational components, Figure 3.
2. Apparatus-mounting components, Figure 4.
3. Rotational components, Figure 5.
4. Bearing brackets, Figure 6.
5. Special hardware, Figure 7.

Only typical examples of the more frequently used items are shown.

Many of the features of these parts are obvious. They are simple in design, rugged, and easy to manufacture. But their form is not entirely arbitrary. For example, the base plates shown in Figure 3 appear arbitrary in design. They are nothing more than plates with holes

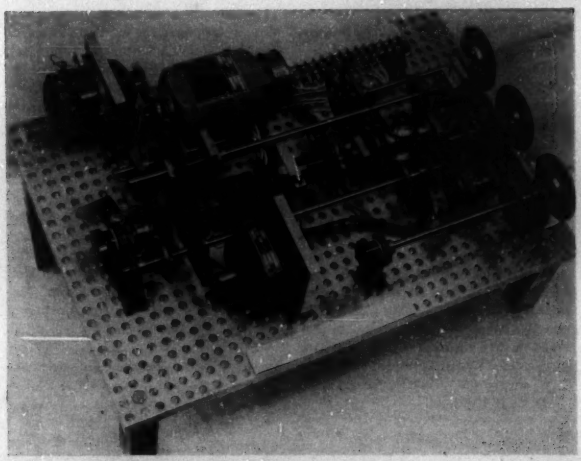

Figure 2. Demonstration servomechanism, mechanical assembly

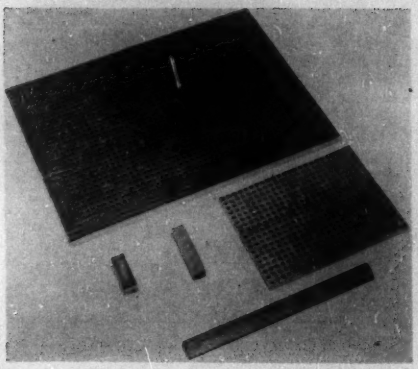

Figure 3 (below left). Foundational components, base plates and stand-offs

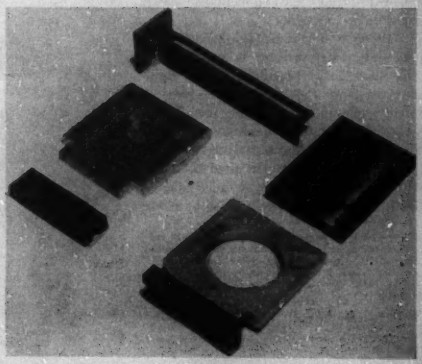

Figure 4 (below right). Apparatus-mounting components

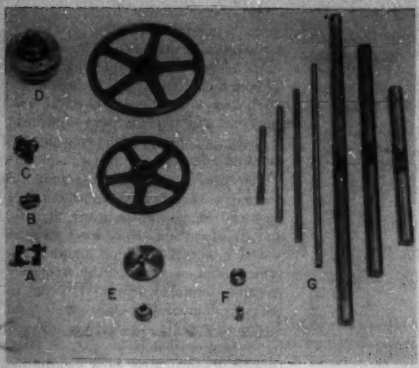

Figure 5. Rotational components

A—Clamp
B—Collet boss
C—Collet boss and clamp assembled
D—Differential
E—Gears
F—Bushing and collar
G—Shafts

Figure 6 (below). Bearing brackets

Figure 7 (below right). Special hardware

A—Shims
B—Clamp blocks
C—Dog
D—T-slot bolt

drilled in them; yet some of the thoughts entering into their design are

1. Material—should be lightweight, rigid, and have a reasonably hard surface.

2. Hole spacing—should permit flexibility of adjustment of all parts, yet not require more holes than necessary.

3. Tapped holes versus nuts and bolts—the convenience of not working below the plate must be weighed against the cost and disadvantages of tapped holes (such as dirt causing stripped threads and the impossibility of using T-slotted pedestals).

4. Size—the plates of various sizes should form a related series and individually be convenient in use with other components.

It was decided that slotted plates were not desirable because of the large portion of plate surface removed and because of cost. Aluminum alloy was chosen as the material. In particular *24ST* sheets, 5/8-inch thick, are used for all but the largest plates. A square hole-spacing of 1/2-inch center-to-center distance was selected after consideration of the other components. Drilled holes 9/32-inch diameter are used to pass, with ample clearance, 1/4-inch bolts. The size series 9 by 12, 12 by 18, 18 by 24, 24 by 36, and 36 by 48 inches was adopted; each plate's size is equivalent to two of the smaller size plates and one-half of the corresponding larger size plate.

Apparatus such as self-synchronized motors, small motors, and potentiometers are mounted on plates to which are fastened pedestals (see Figure 4). The pedestals have T-slots milled lengthwise to receive bolt heads. The nuts are tightened from below the base plate upon which the plate-pedestal assembly rests. The infrequent contingency of the pedestal slot not coinciding with a row of holes is met by clamping the pedestal with dogs, bolts, and clamp blocks shown in Figure 7. A universal pedestal with two T-slots is shown in Figure 4. This has tapped holes to aid in mounting apparatus which cannot be mounted by the plate method.

A basic consideration in the design of rotational components and bearing brackets is the shaft size. On the predication that the standard inch-type ball bearing would be used, it was decided to standardize on 1/4-, 3/8-, and 1/2-inch nominal diameter shafts. The greatest portion of the shafting of any mockup is of the 1/4-inch size. The shafting is stainless steel drill-rod, ground to a diameter sufficiently less than nominal to slide through a ball bearing without undue force. Standard short lengths are stocked, as well as commercial lengths, from which a desired nonstandard length may be cut; examples are shown in Figure 5.

The gears adopted for mockup use are 48-, 32-, and 20-diametrical pitch, $14^1/_2$-degree pressure angle. Most of the gearing is 48-pitch and attempts are made to stock these gears by 1-tooth steps from 10 through 200. Other pitches are stocked less completely. The number of gears stocked in any size is determined by expected frequency of use.

The fastening of gears to shafts has been a problem. Setscrews are easily shaken loose unless a type is used that mars the shaft. Provision of flats on the shafts is expedient but not entirely effec-

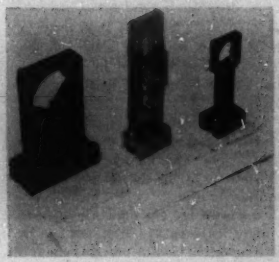

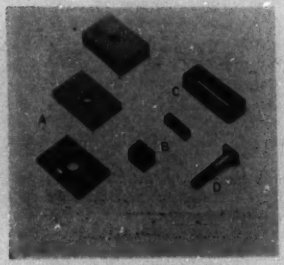

Figure 8

(*a*)—*EMC* cathode follower
(*b*)—*EMC* amplifier

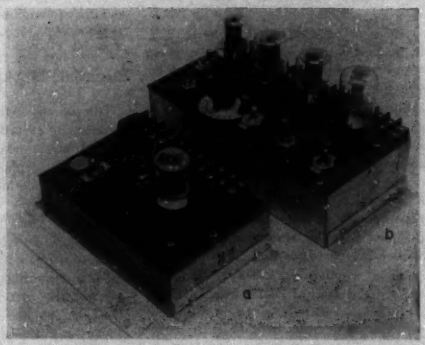

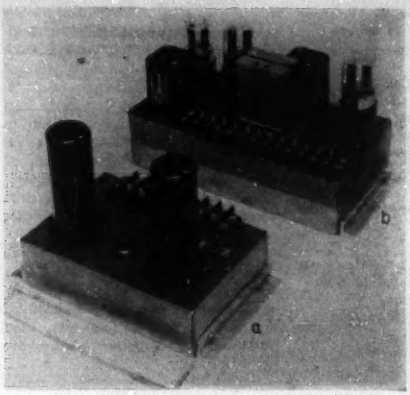

Figure 9
(*a*)—*EMC* output stage
(*b*)—*EMC* demodulator

tive (grooves may be more effective but they are difficult to machine). The use of clamps and collet-type bosses has been very satisfactory. The clamps and bosses are shown in Figure 5. Bosses are machined in quantity and installed on gears by pressing (and pinning if necessary). With this design of fastening, round shafts are used and no flats or grooves are required.

Bosses can be used as collars in most situations. However, if space is limited, the simple ring collar shown in Figure 5 may be used. The latter is held by brass setscrews which do not mar the shafts.

An assortment of bushings to fit 1/4-inch bored gears to smaller shafts used on self-synchronized and other motors is valuable. Since the use of bushings ordinarily requires setscrew fastening of gears to the undersized shafts, the bushings are provided with holes to pass the setscrews (see Figure 5).

The bearing brackets shown in Figure 6 are designed to receive inch-type ball bearings. The standard brackets are designed for $2^1/_4$-inch shaft center height above the base plate. This permits swinging 48-pitch gears of more than 200 teeth. The base of the bearing block is T-slotted and may be used as a clamping surface. Generally, it is best to make mockups with all shafts in a single plane if possible. However, if shafts must pass over one another, or if a height different than $2^1/_4$ inches is used, standard brackets may be shimmed or recourse had to the adjustable-height bearing bracket shown in Figure 6. The larger bearing bracket shown in Figure 6 will accommodate bearings for 1/2-inch nominal diameter shafts; 3/8-inch shafts are made to fit 1/2-inch bearings by means of collar bushings. The ball bearings used in the bearing brackets and other parts usually are hand lubricated.

Figure 7 illustrates the special hardware necessary for use with mockup components. The square-head T-slot bolt is designed to fit the slots of pedestals and bearing brackets. A 1/4-inch 28-pitch thread is used. The shims are made in a variety of thicknesses up to one-half inch for supporting bearing brackets and other uses; the holes provide passage for bolts. Also shown are examples of clamp-blocks and dogs for mounting items that cannot be held by T-slot bolts.

Electronic Mockup Components

The success of the mechanical mockup components stimulated the development of electronic mockup components for use in electromechanical system mockups. To save engineering on system mockups, the development of standardized electronic units was justified. Such apparatus can be serviced by technicians and stocked in quantity so that failures will not delay experimental work on the mockup system. After successful system operation is obtained, the electronic-mockup-component units (abbreviated *EMC* units) can be replaced with prototype product units of the same over-all performance, but vastly simplified and diminished in weight and size.

The *EMC* units are classified as follows:

1. Cathode followers, Figure 8 part *a*.
2. Amplifiers, Figure 8 part *b*.
3. Output stages, Figure 9 part *a*.
4. Demodulators, Figure 9 part *b*.
5. Power supplies, not illustrated.

A cathode follower frequently is required for measurements and occasionally for isolation of networks. The *EMC* cathode follower is shown in Figure 8 part *a*. This cathode follower has a single-ended input and a single-ended output. Two stages are used to permit zero adjustment of the output signal without changing the input impedance.

The *EMC* amplifier, Figure 8 part *b*, is designed to sum six single-ended (or three push-pull) signals, phase invert, amplify, and transform impedance level. Figure 10*a* is a simplified circuit showing the principles of operation. The frequency response, shown by Figure 11, is flat in the range of interest for electromechanical system operation. The gain is adjusted by a control switch in discrete steps (spaced approximately in a logarithmic series) from a minimum gain of unity to a maximum gain of 40. The amplifier uses an inverse feed-back arrangement to accomplish the summation and the gain is varied by changing the feed-back ratio. To compensate for level changes in power-supply voltages and push-pull input signals, a tube has been incorporated to measure output level variations and apply corrections to the cathode of the second amplifier tube. A cathode-follower output tube is used. The input impedance is 1.2 megohms per input terminal; the output is push-pull with an impedance of 20,000 ohms over-all. Plus and minus voltages with respect to ground must be supplied to the amplifier; these are required because of the resistance coupling used between stages which makes response possible at zero frequency. The amplifier is used wherever voltage amplification, signal addition (or subtraction), signal inversion, or frequency-sensitive amplifiers are needed in system mockups. Circuits which typify its use with networks of specified frequency characteristics are shown in Figure 10*b*. The circuits correspond to the conventional lag and lead networks.[4,5]

An output stage, Figure 9 part *a*, is used to translate voltage signals into push-pull current signals for operation of small field-controlled servomotors and the like. The *EMC* output stage uses two beam-power tubes, type *6L6*, to provide a push-pull output; push-pull input signals must be supplied.

In electromechanical system work it is often necessary to convert self-synchronized signals, or suppressed carrier signals, back to their fundamental form. This is accomplished by demodulation in which a carrier or reference signal is supplied in addition to the suppressed carrier signal. The *EMC* demodulator is shown in

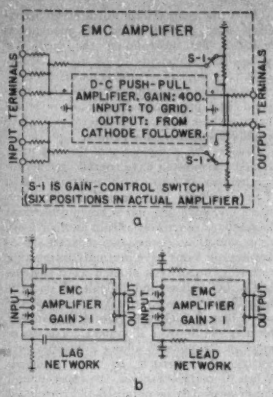

Figure 10 (left)

(*a*)—Simplified schematic *EMC* amplifier
(*b*)—*EMC* amplifier used to form lag and lead networks

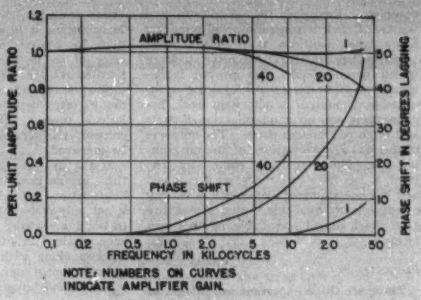

Figure 11. Frequency response of EMC amplifier

Figure 9 part *b*. The single-ended input signal is amplified and supplied through a signal transformer to the full-wave detector tubes. The output may be either push-pull or single-ended.

To supply the plus and minus voltages required for the electronic units, regulated low-impedance power supplies are used. The plus and minus voltages most frequently used are ±200 to ±300 volts. One supply is used for the positive voltage and a second supply appropriately grounded is used for the negative voltage. Power supplies are rated for 240 milliamperes at 300 volts with a ripple of less than one millivolt rms. The source impedance is a function of frequency, but never exceeds 25 ohms and generally is much lower. The voltage is adjustable over the range of 200 to 350 volts.

Generally, a conventional unregulated power supply is used for the *EMC* output stage.

Connections are made to all electronic components by means of screw-type terminals. In a mockup the units generally are fastened to a plywood panel and the proper interconnections are made by push-back wire. When a large number of wires join a single terminal, a piece of bus wire is screwed to the terminal and the wires soldered to the bus wire. Much thought has been given to the possibility of using plug connectors and racks with only the signal terminals exposed, but this has not been undertaken because it would reduce the flexibility of unit application.

It will be noted that the *EMC* units comprise nothing new; they are of conventional design. What is new, perhaps, is the idea of having such units available in quantity. The engineer then may construct complex circuits using as fundamental elements these units rather than the separate circuit elements.

Mockup Component Problems

Mockup components have associated with them certain problems. There is a tendency to expand the line of standard parts to include items infrequently used. The basic principle underlying the mockup component idea is to have standardized, simple parts that can be put together quickly in a multitude of ways to serve a maximum number of uses. It is necessary to consider this principle before a new component is added to the standardized line. Another problem arises when, after a component is adopted as standard, a proposal is made to replace it with a part of superior design. The choices are

1. Adopt the new part and scrap the old one.
2. Adopt the new part and retain the old one.
3. Do not adopt the new part.

Generally, for the sake of economy, decision 2 or 3 is made. If decision 2 is made, an extra item is added to the line. If decision 3 is made no progress results.

In a large organization there may arise the problem of enforcing standardization. Engineers are essentially individualists and prefer to use their own ideas. Not infrequently some one will design and have built his own line of parts without consulting others. This is serious if company-wide exchange of parts is desired.

Conclusion

The mechanical and electronic mockup components have great utility in laboratories where electromechanical systems are developed. Once the initial investment has been made, complex systems may be mocked up rapidly at small cost. The components save much engineering time by making it possible for technicians to service and maintain system units. A considerable reduction in time for mockup construction is achieved by having available a stock of parts. This eliminates the repetitious designing and building of parts with substantially similar function for each mockup. When a mockup has served its purpose, it may be disassembled and the parts returned to stock for subsequent use.

References

1. A New Type of Differential Analyzer. V. Bush, S. H. Caldwell. *Journal*, Franklin Institute (Philadelphia Pa.), volume 240, October 1945, pages 255–326.

2. Electrical Analogy Methods Applied to Servomechanism Problems, G. D. McCann, S. W. Herwald, H. S. Kirschbaum. AIEE Transactions, volume 65, 1946, February section, pages 91–6.

3. Dynamic Behavior and Design of Servomechanisms, G. S. Brown, A. C. Hall. *Transactions*, American Society of Mechanical Engineers (New York, N. Y.), volume 68, July 1946, pages 503–22.

4. Application of Circuit Theory to the Design of Servomechanisms, A. C. Hall. *Journal*, Franklin Institute (Philadelphia, Pa.), volume 242, October 1946, pages 279–307.

5. The Comparison of Two Basic Servomechanism Types, H. Harris, Jr. AIEE Transactions, volume 66, 1947, pages 83–92.

Discussion

Robert F. Garbarini (Sperry Gyroscope Company, Great Neck, N. Y.): The laboratory aids for electromechanical system development which are described in the paper of Newton and White had their beginning in the computer engineering department of the Sperry Gyroscope Company. Prior to 1942, mockups of new devices were laid out on the drafting board, the parts sketched and manufactured. Since parts such as shafts, bearing blocks, and motor mounts were not designed for general use, they would be scrapped after the tests were

complete. Realizing the handicaps and wastes of such a procedure, and requiring more rapid solutions to problems, some engineers began to make their own stocks of useful parts. These soon proved inadequate in a laboratory that was doing an increasing amount of development work, because there was no standardization of parts and often not enough parts. The outcome of this was a systematic set of mockup components. Now, shafting comes by the yard, it has flats for set screws if required and has one standard diameter. A variety of adapters are available so that almost any gear which may be available in stock can be used.

Advantages

There are three important advantages of these laboratory aids which make them of value to the company, to the engineer, and to the customer who is paying for the development:

1. They make available a saving of time in both the shop and the laboratory where the mockup must undergo numerous tests and changes.

2. They make available a financial saving because of the saving in time and the continued usefulness of the parts.

3. By far the most important advantage is that uncertain devices or entire instruments may be tested before design layouts have progressed too far. It can prove embarrassing to an engineer to find that he has underestimated the required size of motor and does not have enough room for a larger one. These circumstances come about when production motors are available which are on the border line of having sufficient torque. Usually the next size motor is too large so that either a new motor must be developed or a chance must be taken with the smaller one.

Typical Applications

These laboratory aids are not the only ones that are used in instrumentation. The aids are used in conjunction with component such as multipliers, dividers, integrators, vector resolvers, and optical elements for mocking up a variety of instruments.

Data Systems. A complete electromechanical data system can be mocked up in a matter of a half day. In this case the transmitter synchro mechanism could be driven by a Scotch yoke mechanism which would provide a sinusoidal input. The amplitude can be varied by means of a screw driver adjustment, and the frequency changed by adjusting the speed of the angular drive motor of the Scotch yoke. The data receiver synchro mechanism is positioned by an amplifier-controlled servomotor and gearing. With the flexibility afforded by the laboratory aids, it is easy to change gear ratios, inertia, viscous damping, friction and backlash.

Thus, it is possible to study the frequency response of the system with different parameters.

Computing Circuits. A very important application of the laboratory aids is in the development of complicated electromechanical computing instruments which have to meet severe specifications as to weight, size, and accuracy. Such a computing instrument may consist of several servomotors and any number of mechanical computing elements such as adding differentials, multipliers, integrators, and polar converters, all connected in closed loops. Since allowable size determines scale factors, which in turn determine the errors caused by backlash and machining inaccuracies, it is quite difficult to determine by analysis just what the probable error of an instrument will be. This is particularly the case under dynamic conditions because the sensitivity of the servomotors often depends on how much backlash is present. If the backlash is decreased, the servomotor performance can be improved.

If the new instrument is complex, and there are no previous instruments of similar functions available for obtaining data, it not only is desirable but often necessary to build a working mockup. The experience obtained in studying and testing the mockup along with careful analysis, provides sufficient data for preparing sound proposals and design information.

R. S. Edwards (Sperry Gyroscope Company, Inc., Garden City, N. Y.): The paper of G. C. Newton and W. T. White presents a new type of tool for use in engineering laboratories involved in the development of electromechanical devices. The mockup components described in the paper have been used quite widely in several of the laboratories of the engineering department of the Sperry Gyroscope Company, Inc.

The widest use of these components has been in the system study work and preliminary test work of complicated electromechanical systems such as gun-sight computers, antiaircraft computers, and bombsights.

Most apparatus of this type involves the use of servomechanisms which often become quite complicated. A method of servomechanism analysis that is widely used at the present time is the sinusoidal input, frequency response method which has been discussed by G. S. Brown, A. C. Hall, H. Harris, and others. This method lends itself very well to the experimental approach and the experimental approach in turn is easily carried out with the aid of the mockup technique described by White.

The frequency response method of servomechanism analysis involves the determination of transfer loci or input to output ratios and phase angles as a function of frequency for the various components making up the servomechanism loop. Since servomotors and signal devices are often electromechanical devices the mockup components described by White are valuable for performing the necessary tests. Plates and brackets are available for holding the units properly and any necessary gearing is easy to install. The electronic mockup components ease the problem of measurement. The generation of proper input signals is also eased by the use of both mechanical and electronic mockup components. Although transfer functions can usually be determined analytically, it is always wise to check the results experimentally and often the experimental values are more accurate. When the transfer loci of the components of the servomechanism loop are determined experimentally, the subsequent analysis of the loop as a whole is much simplified.

The problem of experimental verification of the results of the loop analysis is also much easier if a laboratory well stocked with mockup components is available.

Once the general form of the servomechanism loop is determined the mockup is valuable for determining the particular values of components to be used. Allowable tolerance of components that determine gain of servoamplifiers and time constants and proportionality factors of stabilizing networks may be determined quite readily by experimental testing.

Present day equipments of the sort mentioned above often have complicated servomechanism systems with multiple loops. These multiple loops usually occur when there are one or more servomechanism loops that are entirely within another loop, or as sometimes occurs, two separate servomechanism loops have mutually interacting terms. The analysis of such servo systems is a rather tedious and difficult job particularly if conditions are to exist in each of the servo loops which will give optimum performance of the over-all system. The use of mockup components allows a practical experimental approach to this problem. When properly organized, the experimental data can usually be obtained and correlated in less time than an analytical approach can be made.

There are other aspects of electromechanical systems which cannot wait for pilot model production. One of these deals with the co-ordination and time constants of the operator of the equipment since in many cases the operator is included in the over-all servomechanism loop where he is required to perform tracking or similar operations. The use of a flexible electromechanical mockup permits a wide experimental investigation of this problem.

As pointed out by White, the use of mockup components in servo and other problems is not in itself an analytical tool but rather a time-saving device whereby the necessary answers can be obtained long before a unit reaches the pilot model stage.

The speed with which a mockup can be made and proved is of great importance in the initial examination of a problem. Most engineers dealing with complicated electromechanical equipment, having made an analysis of the problem, have been confronted with the question, "Yes, I understand all you have on paper, but will it work?" A working mockup which can be built in a short time is a decided asset in such cases.

Donald L. Herr (Control Instrument Company, Inc., Brooklyn, N. Y.): White's methods of utilizing relatively fixed components for assembly in laboratory mockups of servomechanisms is ingenious and no doubt efficient in programs of a highly related nature and where such laboratory mockups can be relied upon and utilized safely in the development of a complete servomechanism. We, of the Control Instrument Company, have developed and are using a method of servomechanism synthesis to which White's laboratory mockup technique in some cases lends itself quite well. Such cases are where certain components of the entire servomechanism are relatively fixed from the beginning of the problem and it is desired to rapidly investigate the effects upon performance of other variable components introduced into the system. It is believed that the Control

Instrument Company synthesis method may be found fundamentally of interest and value.

It is necessary to go back to some fundamental considerations. We cannot, it seems to me, place great emphasis upon structural or configurational difference in servomechanisms as a basis for differentiating between servomechanisms. Actually, of course, the structural configuration of a servomechanism is chosen because of the engineering advantages resulting from the use of available components which appear in those arrangements, whereas, mathematically, servomechanisms fundamentally differ only as they differ in their over-all transfer functions. For any given transfer function, there is an infinite variety of structural configurations which will give rise to that same transfer function. It is, however, the over-all transfer function which specifies the accuracy and stability of the servomechanism, regardless of how it is physically obtained as an engineering structure. So rather than continue to speak about the properties of each individual case of actual servomechanisms, which leads us into many detailed considerations characteristic largely and only of each individual physical servomechanism, a fundamental method of synthesis is to start with the loop transfer function, having the properties which satisfy the stability and accuracy requirements of a particular application, and then attempt to synthesize the servomechanism to that loop gain function and its corresponding system response function. The method is as follows.

Mathematically, the loop gain functions proceed from the simplest type involving only a constant divided by some positive power of the periodicity to those involving a constant times a ratio of one polynomial in real frequency to another, in which the roots of numerator and denominator may or may not be placed in evidence. Loop transfer functions, mathematically, are more complex the more terms or roots there are in the numerator and denominator functions. We may exhaustively examine all of the properties of such ratios of functions for each successive case of increasing complexity. In doing so, we start out on the basis that we desire to synthesize a system having a certain degree of stability, as indicated by its maximum value of system response function, and fulfilling a certain accuracy requirement, which establishes the value of the constant multiplier of the ratio of polynomials. These may be called the steady-state stability and accuracy requirements. In any particular application, the steady-state stability and accuracy requirements may be sufficient to form the basis of our synthesis. However, in certain applications, the percentage overshoot and time of build-up of the transient response may be the determining factor, so long as the system is characterized as stable.

If we now view the servomechanism as a low-pass filter, we can somewhat arbitrarily say that we desire to synthesize those servomechanisms which meet either the steady-state stability and accuracy requirements or which meet the transient response requirements with stability and that, in either case, we desire our servomechanism, or low-pass filter, to be of the "minimum band width type". In other words, we desire to synthesize that servomechanism which, when viewed as a low-pass filter, has the narrowest pass band consistent with fulfilling whatever stability and accuracy requirements must be met in a particular situation.

On this basis we have found it possible to take successively more complex, physically realizable transfer functions and, on a normalized frequency basis, elicit the values of the design frequencies in the loop transfer function around which the servomechanism is synthesized. When this has been done a servomechanism results which is of the "minimum band width type" and which meets whatever accuracy and stability requirements are specified.

The mass or structure that is controlled is itself, of course, an element in the servomechanism and, very often, is "something which is handed to us" and which cannot be changed but which must be controlled by the closed loop system we build around it. It is necessary to obtain the frequency response characteristic, in amplitude and phase, of any such fixed elements, remove this transfer function from the idealized transfer function which we have chosen from a tabular array as being the simplest which satisfies the prescribed accuracy and stability requirements on a "minimum band width" basis, and then the residual problem of design becomes that of synthesizing the remainder of the idealized transfer function. At this point we have available the infinite number of possible circuit configurations to synthesize this portion of the chosen over-all transfer function.

By use of the mockup technique, similar to that described by White, certain of the physical components in the remaining portion of the idealized transfer function are of fairly universal application such as modulators, demodulators, filters, stabilizing networks. Only the appropriate gain levels need be established and a residual stabilizing or equalizing network be synthesized.

In conclusion we should like to point out that this method of synthesis places in glaring evidence the very close interconnection between the transient overshoot and time of build-up, on the one hand, and the degree of stability of the system, as indicated by the maximum value of steady-state θ_o/θ_i, and the gain level or steady-state accuracy factor, on the other hand

The Economies of Using Capacitors in Amounts to Require Automatic Switching

J. W. BUTLER
FELLOW AIEE

AT PRESENT price levels, capacitors generally can be justified in quantities considerably in excess of what electric systems can permit to be connected permanently. The average price of kilovars today, as supplied by capacitors, is one quarter of the price of 15 years ago, while other system equipment has increased in price 25 to 30 per cent during the same period. Obviously this lower price level greatly increases the economic sphere of application. It is believed that, if the economics of capacitors at their present price level are to be realized fully, switching procedures should be adopted more widely to allow for the use of larger quantities than the system can accommodate in permanently connected equipments.

The availability in general, and during these times in particular, of reliable factory assembled capacitor equipments complete with circuit breaker and automatic control makes this form of kilovar supply a full-grown economic tool of the distribution and subtransmission engineer. It allows him to design in more detail toward the desirable objective of having at the dispatcher's complete control the basic system kilovar generation, which, as will be shown, makes for maximum system economies.

On the Economic Operating Power Factor

Trite as it may be, the question, "How much of my high-priced system investment should be used to generate and transmit and distribute 10-dollar kilovars?" has not been answered very thoroughly by system planning and operating engineers. At the time of peak load, system capacity has its highest value, so it follows that minimum kilovar transmission generally should prevail at this time. The problem is to determine how many kilovars should be generated at this time by the powerhouse and transmitted to the load, and how many kilovars should be supplied in the load areas. Two approaches that may be taken to help answer this question are offered.

Thermal Limited Equipment

Allocate Kilovar Usage of System Capacity on the Basis of Its Use of System Thermal Capacity. The heating in a piece of electric equipment carrying a load, kilovolt-amperes, is proportional to (kilovolt-amperes)^2. The heating caused by the kilovar in this kilovolt-ampere load is proportional to (kilovars)^2, and that caused by the kilowatt load is proportional to (kilowatt)^2. This follows from the fundamental relation.

$$kva^2 = kw^2 + kvar^2$$

Therefore, the per unit heating, or thermal capacity used by kilovars is equal to

$$\frac{kvar^2}{kva^2} = \sin^2\theta \qquad (1)$$

and, as the per unit kilovar flowing is equal to

$$\frac{kvar}{kva} = \sin\theta \qquad (2)$$

Paper 47-55, recommended by the AIEE committee on automatic stations for presentation at the AIEE winter meeting, New York, N. Y., January 27–31, 1947. Manuscript submitted November 1, 1946; made available for printing December 26, 1946.

J. W. Butler is with the capacitor section of the General Electric Company, Pittsfield, Mass.

it follows where equation 1 is divided by equation 2, that the per unit thermal capacity used *per kilovar* of load is equal to sin θ.

If S equals value of system in question in dollars per kilovolt-ampere and C equals cost of capacitors in dollars per kilovar, the economic operating condition, exists when

$$S(\sin\theta) = C \qquad (3)$$

That is, when the dollars per kilovar charged for use of system thermal capacity equal the cost of load area kilovar generation, the economical value of kilovars then are flowing through the system.

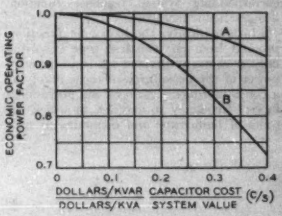

Figure 1. System operating power factor at which investment usage by kilovars equals the cost of capacitors

A—Based on thermal capacity usage by kilovars

B—Based on kilowatt capacity usage by kilovars

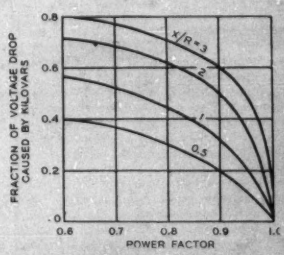

Figure 2. Fraction of total voltage drop in various conductors caused by kilovars

From equation 3 it follows that

$$\cos\theta = \sqrt{1-(C/S)^2}^{*} \qquad (4)$$

= the economic operating power factor by definition, consistent with the assumptions

This relation is plotted in Figure 1 as curve *A*.

Allocate Kilovar Usage of System Capacity on Basis of Its Use of System Kilowatt Capacity. Consider a system or portion of a system operating at its kilovolt-ampere rating at any given power factor. As a system is designed and operated primarily for the purpose of supplying kilowatts to the load requirements, it appears logical to allocate against kilovars, a usage of system capacity according to the relation,

kva − kw = system kilowatts capacity used by kilovars, where kilovolts-amperes and kilowatts are absolute values

If the cost of the system in question is S dollars per kilowatt, then it follows that

$$\frac{S(\text{kva}-\text{kw})}{\text{kvar}} = \text{dollars per kilovars chargeable for their usage of the system investment} \qquad (5)$$

When this charge for use of investment is equal to the cost of supplying kilovars in the load area, it will be said, by definition, that the system is operating at its economic power factor.

Equating equation 5 to C, the cost per kilovar when supplied in the load area, dividing through by the kilovolt-ampere, and rearranging yields

$$\frac{1-\cos\theta}{\sin\theta} = C/S \qquad (6)$$

solving

$$\cos\theta = \frac{1-(C/S)^2}{1+(C/S)^2} = \text{economic operating power factor, by definition, consistent with the assumptions} \qquad (7)$$

This relation is plotted in Figure 1 as curve *B*.

The results of this analysis are reasonable when applied where capacity really is needed, as the effects of kilovars on voltage drop and losses—both important—have been neglected. The results, however, are worthy of further consideration.

Numerical Application. Consider a transmission line over which kilovars are being transported from a generating plant, where kilovars can be produced relatively inexpensively. Each kilovar being transported is stepped up through a high voltage substation. It then is stepped down possibly three times before it gets to the load. These substations conservatively cost an average of $15 per kilovolt-ampere, which gives a figure of $60 per kilovolt-ampere for substation investment through which these kilovars flow during peak load in getting to their destination. Kilovars can be supplied in the load area by capacitors for $10 per kilovar. Hence, referring to Figure 1, curve *B* (the more conservative of the two curves), for a C/S of 0.167 (10/60), it is seen that the power factor should be 0.95 to make the investment charge equal the capacitor cost.

It appears reasonable to say, therefore, that, where substation capacity really is needed, its use for supporting the transportation of kilovars cannot be justified below some value on the order of 95 per cent power factor. These figures indicate that a much broader use of load area kilovar supply can be justified than now is practiced. The trend, however, is definitely toward higher system operating power factors, as indicated to a certain extent by the industry in adopting an 0.85 power factor turbine generator in place of the previous 0.8 power factor unit in general use.

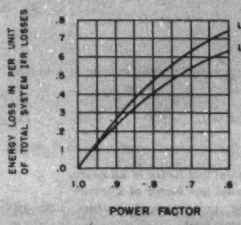

Figure 3. Energy loss reduction by power factor improvement in terms of total system I^2R losses

L_p = kilowatt current loss factor
L_q = kilovar current loss factor

Where Voltage Drop Is Limiting Factor

In system elements where voltage drop is the limiting factor—such as overhead lines—it appears logical to charge kilowatts and kilovars for use of the investment for that particular equipment on the basis of the portion of the voltage drop which they produce. With this assumption, a reasonably direct analysis can be made for determining overhead line investment usage by kilovars.

An approximate but convenient expression for voltage drop is

$$V_d = I(R\cos\theta + X\sin\theta) \qquad (8)$$

I = amperes
R = resistance
X = reactance
θ = power factor angle

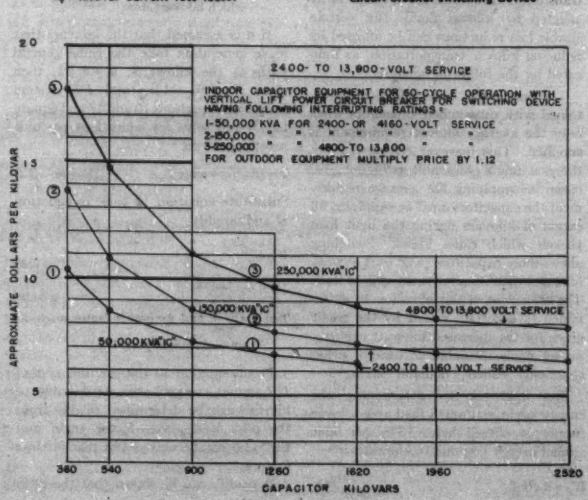

Figure 4. Approximate price in dollars per kilovar versus equipment rating with power circuit breaker switching device

* This relation was first derived in an unpublished manuscript by L. R. Janes, Public Service Company of Northern Illinois by an entirely different approach using differential calculus.

The fraction of the total drop caused by kilovar current is

$$V_q = \frac{N \sin \theta}{\cos \theta + N \sin \theta} = \frac{N \tan \theta}{1 + N \tan \theta} \tag{9}$$

Equation 9 is plotted in Figure 2.

Numerical Application. Consider an overhead line with $X/R=3$. From Figure 2 it is seen that one half the voltage drop is caused by kilovars at 95 per cent power factor. In other words, one half the line investment should be charged against kilovar usage of the line at the relatively high power factor of 95 per cent. Another line having $X/R=2$ will show that one half the investment is chargeable at 90 per cent power factor.

From such fundamental consideration, one readily may determine whether it is economical to use the line to transport kilovars from a relatively inexpensive source to the load, or to generate them near the load with supplementary kilovar generation, such as capacitors.

Energy Losses Due to Kilovar Transportation

Another closely related and important angle to the kilovar supply problem is that of energy loss reduction. It is not uncommon to find that the total kilowatt-hour loss in a system closely approximates the residential kilowatt-hour sales. All of these losses obviously are not retrievable, as power current losses and transformer iron losses are not necessarily affected by kilovar flow. But certain sizable loss reductions can be affected by reducing kilovar transportation, as indicated by the following analysis.

The maximum loss reduction is obtained with unswitched capacitors when only the average kilovar requirement is supplied. This, however, obviously is not the maximum obtainable reduction, because in supplying the average requirement the capacitors must be supplying an excess of kilovars during the light load periods which cause losses. Switching allows more capacitors to be used at peak load and then removes them at light load. The economies of this measure are determined to a certain extent by the credit given for the increased kilowatt capacity saving made available at time of peak, commonly called "demand saving".

One approach to determining the energy savings through load area kilovar supply is offered here. The per unit annual energy loss due to kilowatts is

$$W_p = \mathrm{kw}^2 k_1 L_p \tag{10}$$

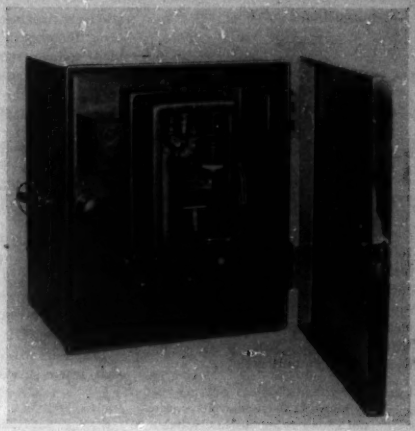

Figure 5. Automatic single-step voltage control for capacitor switching

and the per unit annual energy loss due to kilovars is

$$W_q = \mathrm{kvar}^2 k^2 L_q \tag{11}$$

where

L_p = annual loss factor of kilowatts
L_q = annual loss factor of kilovars
Kw = per unit annual system kilowatt peak load
Kvar = per unit annual system kilovar peak load
k_1 = equivalent per unit resistance through which kilowatts flow
k_2 = Equivalent per unit resistance through which kilovars flow

If it is assumed that the kilovars that leave generators take the same general paths as the kilowatts, $k_1=k_2=k$, then since $W_P+W_Q=1.0=$ total I^2R system losses, add equations 10 and 11 and equate to 1.0 and solve for equivalent per unit resistance, to get

$$k = (K_w^2 L_p + \mathrm{kvar}^2 L_q) \tag{12}$$

Substitute equation 12 back in equation 11 and simplify

$$W_Q = \frac{1}{\dfrac{L_p}{L_q}\dfrac{1}{\tan^2 \theta} + 1} \tag{13}$$

$\tan \theta = \dfrac{\mathrm{kvar}}{\mathrm{kw}}$ and θ = power factor angle at time of system peak load

From equation 13 the per unit system I^2R annual energy losses attributable to kilovars can be determined readily from the peak load power factor angle and the ratio of the active and reactive loss factors.

It readily can be shown that the ratio $R=L_p/L_q$ should lie between 0.6 and 0.9 for actual system load patterns. Using these two limits for the loss factor ratio, the curves in Figure 3 are plotted.

Numerical Application

The following figures apply to an actual system:

Peak load—87 000 kw at 0.85 power factor.

Annual I^2R energy losses—40,000,000 kilowatt-hours

Referring to Figure 3, by improving from 0.85 to 0.90 power factor, approximately ten per cent of the annual I^2R losses are saved. This is assuming the ratio of the active and reactive loss factors remains constant, which would be the case only if the kilovar supply were controlled in infinitely fine steps, so as not to alter the kilovar load pattern and thus maintain the loss factor. If capacitors were being used for this kilovar supply, some would be applied unswitched and some would be switched in finite steps, hence the kilovar loss factor actually would reduce and the ratio of loss factors would increase, which is in the direction of a larger energy saving. Therefore, it appears reasonable to use the 10-per-cent saving figure in going from 0.85 to 0.90 power factor. This represents a 4 million kilowatt-hour saving, in this case, and at four mills, an annual saving of $16,000 is realized.

To improve the power factor from 0.85 to 0.90, and realize these savings 12,000 kvars would need to be supplied near the load. If capacitors were used at $10 per kilovar installed, and a per unit

annual carrying charge of 12 $^1/_2$ per cent applied, the carrying charge would be $15,000 per year. Under these conditions the capacitors are justified strictly on loss savings. This is not unreasonable, as a few large scale installations of this nature actually have been made and proved in on loss savings alone. Assuming the assumptions were sufficiently off to introduce a 50 per cent error, it still indicates that load area kilovar supply could be half paid for by loss savings—a factor which often is ignored.

Analyses need to be made for each individual system for accurate figures, but certainly these savings are important and should not be overlooked in the quest for lower cost power.

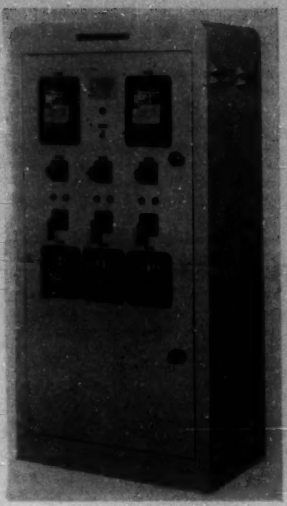

Figure 6 (left). Three-step automatic kilovar control for capacitor switching

Figure 7 (right). Auto-Switch capacitor equipment, rated 180 kva, 2,400–4,160Y volt, 3 phase, 60 cycle, complete with capacitor units, fuses, and oil switch with automatic control and potential transformer

On Establishing a Practical Minimum Load Power Factor

The requirement for switching capacitors develops when the kilovar supply at time of peak load exceeds the desirable kilovar supply at time of minimum load. The kilovars to be switched are equal to the difference between the peak load and light load requirements. Therefore, to be conservative (on the low side) on estimates of the switched capacitors, the unswitched requirements should be as great as practicable. The amount of unswitched capacitors a system can accommodate generally is governed by two conditions.

Voltage Considerations

When all links of a system are operated at unity power factor during light load period, the system is operating with what is termed a *flat voltage*. Under this condition there is no voltage rise along any line such as a circuit or feeder. This is an extremely acceptable operating condition. In fact, it is not uncommon for certain feeders in a system to operate during light load with a rising voltage gradient due to the amount of permanently-connected capacitors. For purposes of this discussion, unity power factor or flat voltage operation as an average in the system will be taken as the ultimate for light load operation. Few operating companies have attained this goal in their kilovar supply program.

Stability Considerations

It generally is considered by operating engineers that unity power factor operation of generators at light load is acceptable from the system stability standpoint. Some feel this is going a bit too far, while others, when adequate voltage regulators are used under certain conditions, will allow their generators to operate slightly underexcited. This subject is a complete one in itself and has been treated elsewhere,[1,2] but for the purpose at hand, suffice it to say that unity power factor generator operation at light system load will be taken as the limiting condition in the application of uncontrolled kilovar supply.

The Necessity of Switching Capacitors

Operating data of systems indicate the full load kilovar requirement to be on the order of three times the light load requirement. The first part of this analysis established that peak load power factors of approximately 95 per cent are in the economic realms of possibility. Approximately one kilovar requirement accompanies every kilowatt of load, and, as at 95 per cent power factor the kilovars equal 1/3 of the kilowatts, it follows that a value of regulated kilovars that is economically feasible is one approximating the light load requirement, or about one third of the total. If these kilovars are to be supplied by capacitors, they must be controlled by switching and if the kilovar supply is to follow the load pattern requirement and keep within circuit loading and voltage requirements, automatic switching is the answer. If these kilovars are supplied by synchronous condensers, the automatic voltage regulator will control them in accordance with requirements.

Where Do Capacitors and Where Do Synchronous Condensers Fit Into This Picture?

This additional kilovar generating capacity, over and above the amount that can be installed on an unswitched capacitor basis, can be divided roughly into two categories.

1. Kilovar generating capacity is characterized by a need for constant and finely controlled adjustment with changing system conditions. The range of this adjustment will include, not only going to zero output but also to reverse to take care of light load or loss of load conditions. It also involves the requirement that the kilovar generator deliver sudden increases in kilovar output as required by system conditions, such as loss of transmission lines. In general, these broad requirements are associated with

kilovar generators associated with major transmission and therefore appear in fairly large unit blocks. The foregoing is a rough description of the system requirement that tends to indicate the synchronous condenser as the proper kilovar generator.

2. There are many locations on the average power system, generally in the distribution and subtransmission areas, where kilovar generation under load conditions is justifiable to a point where it often will seem embarrassing from a system operating standpoint under light load or loss of load conditions if the generation is maintained. These locations generally tend to indicate the need for kilovar generators in smaller blocks than when associated with the major transmission, and, therefore, still tend to fall in the capacitor class. Of course, even here, if synchronous condensers are available on a major transmission, they will be able in some degree to compensate for the overgeneration of kilovar by the capacitors under light load conditions and thus tend to allow more unswitched capacitors.

The type of kilovar supply chosen is based, for the latter category, on first cost, and such items as availability, flexibility, and maintenance, all need to be factored into the broad economic picture. Based on installed cost only, capacitors are favored in banks up to approximately 15,000 kilovar, and their availability at present is materially better due to general manufacturing conditions. Also, as a 10,000 or 15,000 kilovar capacitor, as contrasted with the condenser, initially or later can be broken down into smaller units and located near the kilovar requirement in case of changed conditions, the flexibility factor is in its favor. Even if a consenser is to be used later, the availability and flexibility factor may justify the capacitory on a temporary basis.

Fineness of voltage control, as offered by the condenser, may be advantageous in many instances. The capacitor, however, does not provide what would be called *coarse* voltage control for many applications. For example, a 15,000 kilovar bank probably would be located at a point in a system which would supply a short circuit of approximately 250,000 kva. Hence, if the capacitor bank is switched in six 2,520-kva steps, each step would give a voltage change of only one per cent. This voltage change would be a maximum at the capacitor location and would diminish as the electrical distance from the bank is increased. Such an operating result would need to be considered and judged on its own merits for the individual case.

Cost of Switching Capacitors

There is a general misconception extant that switching capacitors is an expensive procedure. In the smaller equipments, the cost per kilovar can become relatively large, but in larger substation equipments, where the controlled banks are used, the cost is quite small. Good estimating figures[3] for switched equipments are given in Figure 4. Factory-built housed equipments without circuit breakers range from $5 per kilovar for the 5-kv class up to $6 per kilovar for the 15-kv class. When these figures are compared with those in Figure 4, the cost for switching readily is seen for the different sizes.

These prices do not include automatic control. Estimated prices for various types of control and different number of steps are given in Table I.

Table I. Approximate Price of Indoor Automatic Capacitor Control Equipments[3]

Number of Steps	Voltage	Current	Kilovar
1	$300	$300	$400
2	600		700
3	650		750
4	700		800
5	750		850

For outdoor enclosure add $75.

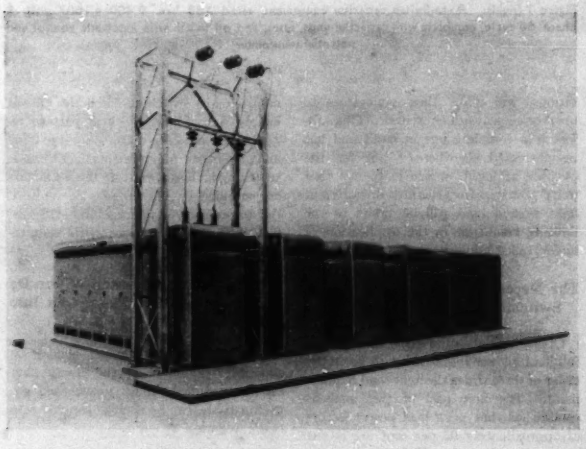

Figure 8. Capacitor installation totaling 15,120 kilovars

Made up of six large outdoor floating-neutral type equipments, throat connected, each rated: 2,520 kilovars, 13,800 volts, 3 phase, 60 cycles, each with built-in type *AM-15-250* Magne-blast circuit breaker electrically operated for automatic control

Typical Switching Equipments and Installations

Figures 5 to 8 illustrate a few equipments and show how they go together in a substation installation.

Conclusions

1. The basic load kilovar requirement of a system generally can be most economically supplied by capacitors.

2. The capacitor's reliability, cost, and flexibility have resulted in one of the most economic tools that is now available to the system planner and designer. And its availability due to favorable manufacturing conditions at present makes it attractive even on a temporary basis, where a condenser may be used later.

3. Capacitors generally are justified in the system design and operation pattern in such quantities as to require switching.

4. The cost of switching is so small it is not a deterrent or a controlling factor in an economic analysis, the main criticism being the system's ability to accommodate the stepped control as contrasted with the fine control a condenser gives with an automatic generator voltage regulator.

References

1. Kilovar Supply on Public Service Electric and Gas System, H. K. Sels. *Bulletin*, Edison Electric Institute (New York, N. Y.) November, 1943.

2. Capacitors, Condensers, and System Stability. J. W. Butler, T. W. Schroeder, W. Ridgway AIEE Transactions, volume 63, 1944, pages 1130–8.

3. Selection and Application of Automatic Control for Capacitors. W. C. Bloomquist, T. W. Schroeder. *General Electric Review* (Schenectady, N. Y.), March 1946.

Discussion

W. R. Brownlee (Commonwealth and Southern Corporation, Jackson, Mich.): It is believed that the advantages of switched capacitors as a useful tool in system planning generally are recognized, and they justly are finding a place on power supply systems as a source of reactive power along with unswitched capacitors on distribution lines, synchronous condensers at strategic locations, and the synchronous generators themselves. Certain cautions must be observed in determining the "most economical power factor" of power supplied by the generating units.

In the case of some older plants and systems, which may have been planned and designed without proper regard to or sufficient knowledge of kilovar requirements, surprisingly high power factors at the generators may be justifiable. However, the enormous increase in generating capacity in recent years results in power supply systems with a substantial proportion of modern efficient generating units and associated equipment, with ample opportunity to take full account of kilovar requirements and to produce balanced designs. Accordingly, there should be no limitations in the kilowatt producing ability of these plants because of the necessity of supplying also the designed amount of kilovars. Therefore, any investment savings credited to the installation of switched capacitors must be confined to the transmission and subtransmission systems, usually extending no further than the low voltage distribution substation busses.

With the economical loading of transmission systems, substantial amounts of kilovars will be required at points other than the load centers. Certainly the kilovars required for the magnetizing current and I^2X loss of step-up transformers of generating plants can be supplied most economically by the generators, even if the respective kilovar production costs were equal. Substantial amounts of kilovars also will be required for the net reactive "loss" in a transmission line, and this is supplied more economically from the generating end. These and similar extra kilovar requirements may account for a generated power factor (including condensers and capacitors as "generators") as low as 80 per cent, with a power factor at the subtransmission stations of as high as 90 per cent. Thus the economical power factor at a typical generating station may be more nearly on the order of 85 to 88 per cent, rather than 95 per cent as advocated by the author.

The examples used to illustrate the curves and equations may be misleading, because they consider the *total* transmission system investment rather than the *incremental* investment which might be required to transmit certain portions of the system kilovar supply. For example, the cost of transformers themselves may increase about as the square root of the kilovolt-amperes rather than the first power, and other items of substation expense may not be increased at all by moderate increases in substation kilovolt-amperes. Similar reasoning applies to transmission lines.

T. W. Schroeder (United Light and Railways Service Company, Davenport, Iowa): It is interesting to note from Butler's analyses and examples that the economic system power factor is creeping ever nearer unity, as the ratio of system investment per kilowatt to kilovar generation cost per kilovar increases. The fact that the cost of automatic switching equipment does not add greatly to the price per kilovar of capacitor banks in reasonable sizes certainly should further the use of comparatively large blocks of switched capacitors on electric utility systems generally now and in the future.

The present high value of the system investment to kilovar generation cost ratio leads to two conclusions, namely,

1. That a large share of the kilovar requirements of large commercial and industrial loads should be supplied near the load.

2. That the comparative cost of furnishing the kilovar component of these loads is small.

These conclusions lead to the reasonableness of the view that the utility rather than its commercial or industrial customers, is in the best position to supply the load kilovars, because in general

1. The utility can supply the kilovar requirements at lowest cost, from an over-all utility–customer viewpoint, because it can do the job with larger blocks of kilovar generation and fewer total kilovars by reason of diversity of load requirements.

2. The utility logically should have control of the system kilovar generation, particularly as economics dictate the use of greater quantities of controlled kilovar generation, such as switched capacitors.

Exceptions to this reasoning will occur, of course, such as cases where the customer requires the kilovar generation in his own plant for benefit to his own system, and where large amounts of synchronous drive equipment are used.

On the basis of the foregoing reasoning, it also develops that the utility's charge to customers for kilovars will be small, as compared with the kilowatt charge. It may be small enough to justify its complete omission from the rate structures in the interests of simplicity—thus doing away entirely with the cumbersome appendage of the "power factor clause." This actually has come about in the case of one of the United Light and Railways' Systems' properties.

Energy Losses Due to Kilovar Transportation

In substantiation of Butler's discussion pointing out that large scale capacitor installations may be justified on the basis of energy loss reduction alone, an actual case may be cited.

System Data

1. System generation at peak load—130,000 kw

2. Power factor of generation at peak, without capacitors—82.4 per cent

3. Power factor of generation at peak with 27,540 kilovars of capacitors installed—94.0 per cent.

4. Calculated loss reduction at peak with 27,540 kilovars capacitors—1,275 kw.

5. Estimated installed cost of capacitors (10,260 kilovars in outdoor units on distribution circuits and 17,280 kilovars in substation banks)—$222,421.

6. Average annual load factor—approximately 50 per cent.

7. Estimated system equivalent hours (number of hours per year maximum load must prevail to give same losses as actual load—depends on shape of load curve)—2,800.

Assumptions

1. Energy production cost—$0.003 per kilowatt-hour.

2. Generating station investment—$165 per kilowatt on firm capacity.

3. Fixed charges on investment—12.5 per cent.

Calculation of Loss Savings and Comparison With Capacitor Investment

Annual Saving in System Losses	
2,800×1,275=3,570,000 kilowatt-hours at $0.003	$10,710
Demand Saving Due to Released Generating Capacity	
1,275×$165=$210,375 at 12.5 per cent	$26,297
Total gross annual savings	$37,007
Investment Charge on Capacitors	
$222,421 at 12.5 per cent	27,802
Net Annual Savings	$ 9,305

It will be noted that an evaluation of the release of generating plant capacity was included on this analysis.

Using Figure 3 of Butler's paper, improving the power factor from 0.824 to 0.94 results in a reduction of energy loss of

0.25 per unit for $L_p/L_q=0.6$
0.22 per unit f r $L_p/L_q=0.9$

The actual calculated loss reduction at peak for the case cited here is from 4,655 kw to 3,380 kw, or 0.274 per unit.

Minimum Load Power Factor

As an indication of the possibilities of high power factor system operation the St. Joseph Light and Power Company, St. Joseph, Mo., may be cited as an example. This is an urban type system of peak load (1946) of approximately 30,000 kw. In recent years, to make maximum use of system capacity for kilowatt transportation, unswitched capacitors have been installed on 4-kv and 12-kv busses and feeders in amounts totaling approximately 10,000 kilovars. Heavy load power factor varies from 0.87 to 0.95.

Two generators, a 7,500-kw 0.7-power-factor and a 10,000-kw 0.8-power-factor machine, are normally in operation during light load. Both machines feed a common 4-kv bus. Excitation is provided from an exciter bus supplied by a dual-driven motor-generator set. The exciter bus voltage is controlled by a direct-acting type generator voltage regulator.

Minimum load generator operation has been underexcited slightly and at present is very near unity power factor to slightly overexcited. Minimum load is about 12,000 kw.

No particular difficulty has been experienced with this type of operation. Light load system voltage is controlled by reduction of generator bus voltage on a clock schedule. It is probable that future large

capacitor installations on the system will employ automatic switching equipment.

J. W. Butler: It has been the general rule with operating companies in the past to design a power station with boiler, feed water, and such facilities to enable the prime mover to deliver kilowatts equal to the kilovolt-ampere rating of the generator. Obviously, there have been some exceptions to this practice. In the general case, therefore, if the designed amount of kilowatts are to be obtained, some kilovars must be provided from auxiliary sources. The ability to increase the kilovar capability by increasing the hydrogen pressure in hydrogen-cooled generators is taken advantage of by some companies. These considerations obviously all should be factored in the individual problem. I believe Brownlee's discussion, wherein he referred to stations having "substantial proportion of modern efficient generating units and associated equipment, with ample opportunity to take full account of kilovar requirements and to produce balanced designs" concerned modern stations or possibly those still in the design stage. To this I very well agree. There are, however, a very large number of older stations wherein valuable designed kilowatt capacity is "bottled up" by kilovars. To these older stations, I do not believe the principle of "incremental costs" should be applied in the process of justifying or not justifying capacitors. If by removing said kilovars, additional kilowatts become immediately available, then the actual value of these kilowatts at present time rather than their incremental costs should determine the choice.

It is truly refreshing to see a representative of an operating company offer the philosophy outlined in the first part of Schroeder's discussion. And this writer feels it to be a definite forward step for a utility to abandon the so-called "power factor clause," as has been done by one of the United Light and Railways' properties.

It is gratifying to obtain actual system data regarding loss savings obtained through the application of capacitors and check them with a generalized approach. An explanation of Schroeder's use of Figure 3 of the paper may be in order.

As energy loss = peak loss $\times$ 8,760 $\times$ loss factor, the data in Figure 3 can be used to estimate peak kilowatts loss as well as annual energy loss. As outlined under "Numerical Application" of the energy loss savings section of the paper, the ratio of the loss factors (Lp/L_q) will actually increase when capacitors are applied, instead of remaining constant due to the change made in the kilovar pattern. Therefore, using the lower limit of the loss factor ratio ($Lp/L_q = 0.6$), as the "before" condition, and using the upper limit as the "after" condition, we obtain a peak loss saving of 0.28 per unit when improving power factor from 0.824 to 0.94. This is surprisingly close to the figure of 0.274 per unit actually calculated by Schroeder with detail system data.

The operating data of the St. Joseph Light and Power Company system should be useful. It substantiates the philosophy that light load power factors of around unity to be entirely practicable from the operating standpoint. And the value of capacitors required to bring the light load condition to approximate unity very closely checks that value given in the paper under the section "The Necessity of Switching Capacitors," namely, a value equal to approximately one third of the peak kilowatt load.

Testing Governor Performance on Electric Power Systems With Improved Instruments

J. E. ALLEN
MEMBER AIEE

W. B. HESS
NONMEMBER AIEE

FOR GOVERNORS to perform well it is essential that they possess certain operating characteristics at the time of installation and throughout their operating life. Heretofore such characteristics have been difficult to measure. This paper describes governor-testing methods and instruments, applicable to both steam and hydro units, which mark a distinct advance in the technique of governor testing.

Historical

When the governors were installed at the Safe Harbor hydroelectric plant, starting in 1931, they were tested under operating conditions by using the oscillograph to record instantaneous frequency without the inherent lag common to instruments employed up to that time.[1] The records, showing, among other things, frequency and gate opening as a function of time were analyzed subsequently by plotting simultaneous values of these two variables as functions of each other to secure diagrams* known as figures of Leaute.[2] These diagrams of frequency versus gate, recurring because of the governor's adjusting itself to each change of frequency, proved extremely valuable, first in detecting the imperfections in the governor operation, and later as a measure of characteristics desired in a governor. However, the hand plotting was so laborious and slow that it became highly desirable to develop an instrument which would accomplish automatically the same as an X-Y recorder; and thus it immediately would give the results in a manner similar to the familiar steam-engine indicator card diagrams. This requirement was met satisfactorily by an instrument completed in 1940. The equipment has been developed since to record diagrams of frequency as a function of kilowatt output of the generator. The usual strip chart records of frequency, gate-operating piston, and kilowatts as a function of time are recorded simultaneously with the same instrument.

Scope of Paper

The first part of this paper is intended to describe the mechanical and electrical features of a new frequency recorder, the essential element in the instrument for automatically plotting the diagrams of frequency versus operating piston, or frequency versus kilowatts. The equipment for recording kilowatts also is described. The second part of the paper describes the results obtained when using the instrument as an aid in the maintenance of governors and for measurement of their operating performance. Examples of card diagrams obtained under operating conditions will be given.

Results

The card diagrams of frequency versus operating piston and frequency versus kilowatts have proved to be the best means thus far devised for measuring over-all governor performance. The most important characteristics, such as sensitivity, dead band, speed droop, and regulation are readily apparent on these diagrams. Such factors as friction, lap, compensation, maladjustments, and so forth give characteristics readily recognized and evaluated by experience. The instrument has served as a valuable guide in detecting and correcting governor difficulties, because the results are immediately available.

Terms and Definitions

In the past considerable confusion has arisen from the fact that definitions pertaining to the subject of speed regulation and governing have not been standardized. There is a joint committee of the American Society of Mechanical Engineers and the AIEE now engaged in this task, and consequently for this paper it is necessary to make some arbitrary definitions solely for the purpose of describing the results obtained by test.

Sensitivity and Dead Band

Dead band is considered to be that band of frequency variation in which there is no corresponding movement of the operating piston. In actual operation the governor is subjected to a complex succession of frequency variations during which the governor continuously is adjusting itself. Consequently it becomes difficult in tests of this kind to distinguish the dead band as defined. Furthermore the unavoidable lag in the gates or valves while attempting to follow the frequency gives the diagram a width over and above that which would be caused by the dead band alone. The term sensitivity as used in this paper will refer to the total width of the diagram even though caused partly by dead band and partly by lag in the governor response.

Speed Droop and Regulation

Speed droop refers to the relationship between the frequency and operating-

* These diagrams of frequency versus gate are in effect an incremental portion of the speed droop curve. They would consist of straight lines in the case of an ideal governor, but because of compensation and mechanical imperfections they assume the shape of hysteresis loops.

Paper 47-56, recommended by the AIEE committee on power generation for presentation at the AIEE winter meeting, New York, N. Y., January 27–31, 1947. Manuscript submitted November 12, 1946; made available for printing December 5, 1946.

J. E. Allen is chief of tests at the Pennsylvania Water and Power Company, Baltimore, Md. W. B. Hess is test engineer at the Safe Harbor Water Power Corporation, Safe Harbor, Pa.

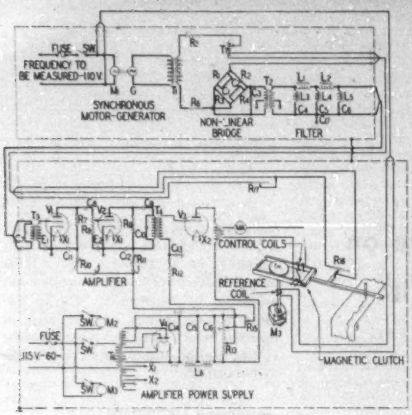

Figure 1. Schematic diagram of frequency recorder

R_1, R_4—Linear resistances
R_2, R_3—Nonlinear resistances
R_5, R_6—Nickel temperature-compensating resistances
R_{14}—Bridge-balancing slide wire
R_{17}—Pen-positioning rheostat
T_1—Impedance-matching transformer for changing sensitivity
M_1—Synchronous motor, 110 volts, 60 cycles, 0.5 ampere
M_2—Chart-drive motor
M_3—Disk-drive motor, 60 rpm

piston travel expressed in per cent of normal speed and full piston travel. Regulation substitutes the generator output in place of the operating piston. The distinction between the two terms arises from the fact that kilowatts are not in many cases proportional to piston stroke. Incremental speed droop and incremental speed regulation are the slopes of these curves at any point in question.

Steady State Values

Definitions referring to governor performance have been expressed as steady state values, assuming that the equipment could be subjected to a constant or controlled frequency. In operating tests such a condition never exists and in the following tests it will be seen that as a result of a complexity of transient phenomena the diagrams become modified greatly, primarily by the compensation introduced and other mechanical imperfections. The test results under normal operating condition, therefore, cannot be considered equivalent to steady-state values.

Description of Frequency Recorder

The principal feature of the governor-testing equipment is a new direct-writing frequency recorder, certain features of which have been described briefly in an AIEE discussion,[2] and having the following specifications:

1. Rectangular co-ordinate strip chart 6 inches wide with $4^1/_2$ inches pen travel.
2. High sensitivity, usually 1.0 inch deflection per 0.1 cycle, but adjustable from 0.33 to 1.65 inches per 0.1 cycle. Scale is linear.
3. Maximum pen speed 5.5 inches per second.
4. No hunting and overshoot less than three per cent of full scale deflection at maximum pen speed. When recording frequency, overshoot is negligible.
5. Chart speed is 3 inches per minute.
6. Stylus-type ink pen.
7. Large pen actuating force available, permitting an additional stylus pen to be attached to the pen arm for automatic plotting of frequency versus piston travel on a drum attachment.
8. Sturdy construction to meet the requirements of field testing without sacrificing high sensitivity.

Principle of Operation

The frequency sensitive circuit comprises a small 1,800-rpm 60-cycle-to-60-cycle synchronous motor generator set in which the generator voltage is proportional to the speed or frequency of a synchronous motor driving it. The latter is energized from the source to be measured, such as the system or from the main generator potential transformers in case the unit being tested is isolated from the system. The generator, which is a 60-cycle permanent-magnet type, energizes a nonlinear bridge having its two opposite arms made of a material whose resistance varies inversely with current. Balance at a given voltage or frequency is accomplished by means of an external resistance in series with the bridge. When the frequency changes, the corresponding change in voltage from the a-c generator unbalances the bridge. Balance is restored by changing the resistance in series with the bridge. Thus, the incremental value of resistance required to maintain bridge balance is a measure of the frequency change, and meter calibration becomes a simple function of a linear slide-wire rheostat. See schematic diagram, Figure 1.

The bridge automatically is kept in balance as the frequency varies by means of a high-speed servomechanism or clutch which actuates the slider on the calibrated rheostat *R-16* The clutch functions in a manner similar to a 2-phase reversible motor One winding is energized from the a-c source to be measured and the other winding from an amplifier connected to the bridge output through appropriate harmonic filters. A 180-degrees-phase-angle reversal occurs at the bridge output terminals as the frequency or voltage varies above or below a given initial balance point. This phase reversal provides the directional means for balancing the bridge automatically as the frequency varies. A pen attached to the slider in combination with a strip chart provides the means for recording frequency with respect to time

Magnetic Clutch

The important feature of the recorder is the high-speed reversible magnetic clutch also shown in Figure 1. Essentially it consists of a driving member in the form of a magnetic disk, revolving at 60 rpm, which engages a driven member consisting of a magnetic fork, the prongs of which are hinged and rub with metallic friction against opposite sides of the periph-

Figure 2. Close-up view of magnetic clutch

A—Laminated magnetic fork
B—Reference coil
C—Control coil
D—Rotating magnetic disk, 1.75-inch diameter
E—Slide wire
F—Aluminum guide and support for fork

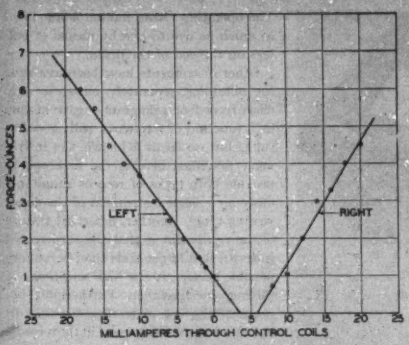

Figure 3. Linear force exerted by fork at standstill as a function of current through control coils

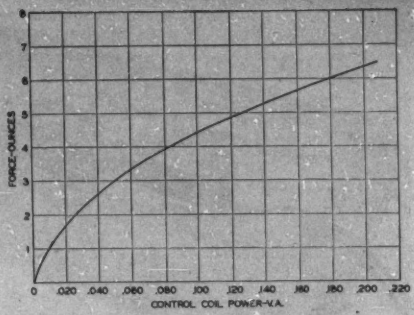

Figure 4. Linear force exerted by fork at standstill as a function of power input to control coils

ery of the disc. The rubbing friction is controlled primarily by the magnetic attraction between the fork and disc as a result of the alternating current in the reference coil near the disc. Both prongs or legs of the fork are attracted to the disc with equal force, but the disc tends to drive one leg of the fork in a direction opposite to the other leg; consequently, the differential force is zero, and there is no tendency for the fork to move in either direction. If, however, the series-connected control coils become energized because of a bridge unbalance, in proper phase-relation to the reference coil, the magnetic attraction between the two legs of the fork and the disc will be unbalanced. This creates an unbalance in rubbing friction between the two legs and causes the fork to move in a given direction. Reversing the polarity of voltage energizing the control coils will reverse the direction of motion. Linear motion of the fork thus takes place when the frictional forces between the two legs of the fork become unbalanced because of current through the control coils. Effective damping action is provided by the frictional drag or braking effect of one leg opposing the desired motion initiated by the other leg. Hunting and overshooting thus are minimized. Figure 2 shows the magnetic clutch with the driving disc, magnetic fork, reference winding, control coils, and slide wire.

A large force is available for overcoming bearing and pen friction. This force was measured by holding the fork at standstill and passing alternating current through the control coils; a linear relation was found as shown in Figure 3. Because of saturation taking place above 30 milliamperes the maximum measured force was from eight to nine ounces. For a given power input to the control coils below saturation, the large force available for actuating a slide wire, inking pens, and so forth is shown in Figure 4. It is seen that a force of four ounces requires less than 0.1 volt-ampere input. This good performance is realized because the clutch functions as an electromechanical amplifier. Friction between the two legs of the fork may be unbalanced as shown in Figure 3, but this in no way impairs operation because sufficient amplifier gain always is used to maintain negligible pen dead band at bridge balance.

It is well to point out that magnetic clutches in general are capable of very high rates of acceleration, stopping, and reversal. For instance, a recorder employing a magnetic clutch has been described which responds to a frequency as high as 60 cycles per second.[4] Reversing motors have a relatively high inertia and low efficiency as compared to magnetic clutches. The clutch described in this paper requires only one control winding and a simple a-c amplifier to effect directional control in contrast to other types which have two independent electric windings with complicated amplifiers.

General Description

A general view of the recorder is shown in Figure 5. A second stylus pen on an extension records frequency versus operating piston on a large 4.25-inch diameter drum attached to the same end of the cabinet. This cabinet also houses the

Figure 5. Frequency recorder with drum attachment for recording frequency versus operating piston

A—4.25-inch diameter drum actuated by operating piston
B—Wire connected to operating piston
C—Frequency pen *D*—Counterweight

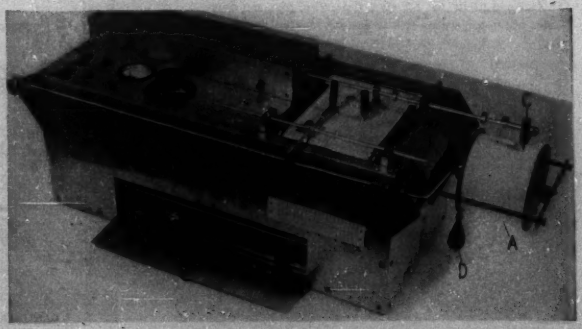

Figure 6. Synchronous motor generator set in cabinet

amplifier and its power supply. It will be noted that a third stylus pen has been provided to record the piston travel on the same strip chart with frequency. This pen and the drum both are actuated from a common wire attached to the operating piston. Thus, two types of records are obtained simultaneously

1. A strip chart showing the variations in frequency and operating piston with respect to time for determining dead time and rate of response.

2. A card diagram of frequency versus operating piston from which sensitivity, dead band, and speed droop may be obtained readily.

A separate cabinet shown in Figure 6 houses the small synchronous motor generator, nonlinear bridge, and harmonic filter. Various sensitivities are obtained from 0.33- to 1.65-inch deflection per 0.1 cycle by changing taps on the impedance matching transformer *T-7* in Figure 1. The proper phase angle between the control coils and reference coil for maximum force is obtained by adjusting the angular position of the synchronous motor shaft with respect to the a-c generator shaft. The operating piston motion is amplified as much as five to one by means of pulleys on the end of the drum.

Other instruments have been available for obtaining separately either a strip chart record[5] or a diagram of gate motion as a function of frequency with good results,[6] but, so far as is known, the instrument described here is the first one to provide both types of records simultaneously on a single instrument of the direct writing type. Another important feature of the equipment is that the card record is drawn to a larger scale than heretofore possible because of the high sensitivity of the frequency recorder. Furthermore, because of the use of rectangular co-ordinates no distortion is present in the records. It should be recognized, however, that this equipment was designed primarily for testing over-all governor performance under actual regulating conditions and is not intended to replace other methods for making more detailed analysis of phenomena such as relay and pilot valve motion, pressure, power output, rapid transient response, and so forth.[7]

Frequency Deviation Meter

No attempt has been made to calibrate the meter in terms of absolute frequency, because the application intended did not justify this refinement. It is primarily a frequency deviation meter and provision has been made by means of a variable resistance *R-17* in series with the

Figure 7. Frequency recorder with attachments for recording kilowatts and incremental speed regulation

A—4.25-inch diameter drum actuated by the recording wattmeter
B—Wire connected to operating piston
C—Frequency pen
D—Counterweight
E—Slide wire rheostat for recording wattmeter
F—Reversing motor
G—Rack and pinion for actuating slide-wire, pen, and drum

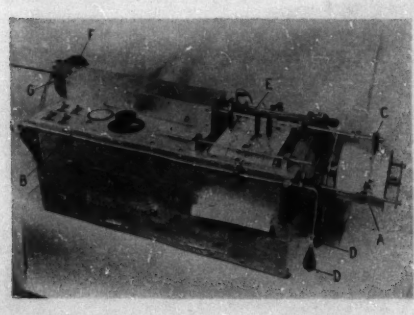

Figure 8. Typical power output versus gate-opening curves for Kaplan, propeller, and Francis turbines

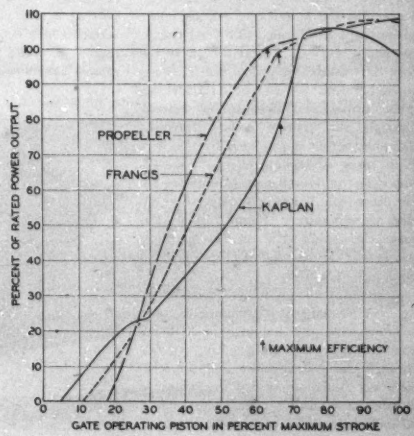

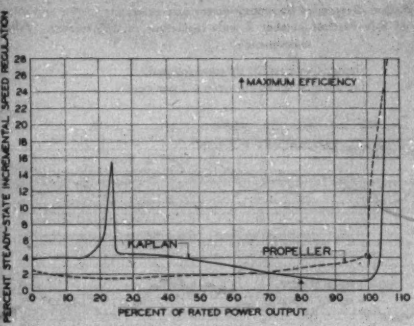

Figure 9. Typical steady-state incremental speed-regulation curves for Kaplan and propeller turbines based on 5-per cent speed droop

bridge to shift the pen to any desired position on the chart.

Temperature Compensation

Because of the negative temperature coefficient of resistance of the two nonlinear arms in the bridge, it has been necessary to compensate the recorder for changes in ambient temperature. This has been accomplished by the use of nickel compensating resistors *R-5* and *R-6* connected in series with the bridge. Drifting because of temperature, except for a warming up period of about 20 minutes, has been reduced to a negligible value for ordinary room temperature variations. It has not been necessary to compensate the a-c generator for ordinary room temperature variations.

Analysis of Records

Strip Charts

The strip-chart records of frequency and piston motion need not be discussed to any extent because their analysis requires no special technique. It should be emphasized that they provide a valuable adjunct to the drum records by permitting an analysis to be made of dead time and rate of response.

Incremental Speed Droop

The card obtained from the drum consists of a multiplicity of diagrams superimposed on a common axis. By means of pulleys on the drum the piston travel is amplified so that the diagrams are greatly elongated and resemble an ellipse, with the major axis representing the slope of the speed droop curve. The diagrams are the result of the governor's responding to the frequency changes taking place on the system under normal operating conditions. A sufficient number of them is required to establish the slope of a common major axis, and ordinarily only five to ten minutes are required, depending on the system frequency changes. After the card is detached, a line or common major axis is drawn through the diagrams by visual inspection and its slope, expressed in per cent incremental speed droop, is determined by applying the proper multiplying factor between piston and drum motion. No replotting and no further working up of data are necessary. Typical cards with sample calculations are shown in Figures 13–14.

Sensitivity and Dead Band

The frequency change corresponding to the vertical width of the diagrams measured at the minor axis is considered a measure of sensitivity. Good or bad governor performance usually is interpreted as being a function of the total width and shape of the superimposed diagrams. Once an acceptable standard has been established the card diagrams and strip chart records become an important adjunct to the routine maintenance of governors.

Dead band may be obtained by noting the vertical portion of those loops in which there is no change in gates or valves for a given frequency change

Direct Recording of Incremental Speed Regulation

The speed droop obtained in the above manner obviously will be based on the travel of the operating piston or gate. If desired, incremental speed regulation may be obtained by referring to a test curve of gate travel versus kilowatts output at the point of test. However, this practice is somewhat inaccurate and laborious, and therefore further developments in instruments were made for the direct measurement of frequency versus kilowatts on a single card so that incremental speed regulation may be obtained readily without additional plotting. This is accomplished by actuating the drum by

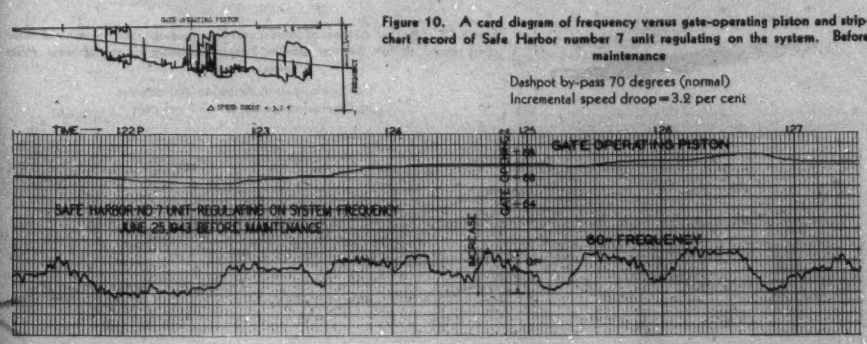

Figure 10. A card diagram of frequency versus gate-operating piston and strip-chart record of Safe Harbor number 7 unit regulating on the system. Before maintenance

Dashpot by-pass 70 degrees (normal)
Incremental speed droop = 3.2 per cent

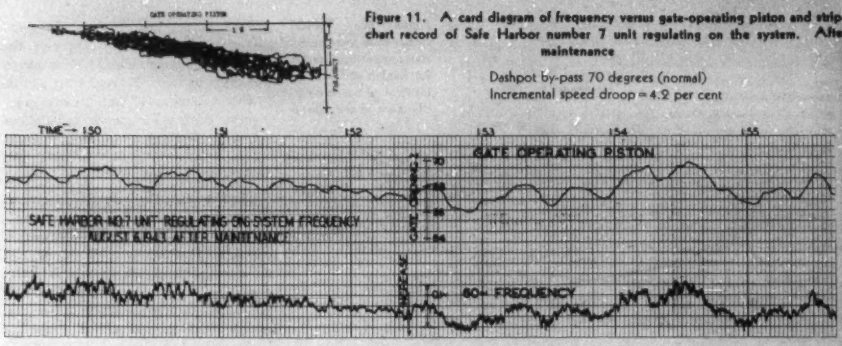

Figure 11. A card diagram of frequency versus gate-operating piston and strip-chart record of Safe Harbor number 7 unit regulating on the system. After maintenance

Dashpot by-pass 70 degrees (normal)
Incremental speed droop = 4.2 per cent

means of a special recording wattmeter having high sensitivity, large torque, and negligible time lag. Such a recorder in combination with the drum and frequency meter is shown in Figure 7.

The recording wattmeter is restricted in its application to small direct currents or potentials such as are available from telemetering circuits. Advantage was taken of a General Electric Company torque balance telemeter installed on each generator at Safe Harbor. These telemeters are a source of direct current proportional to the kilowatt output. The special recorder employs a null balance system whereby the voltage drop across a fixed resistance in the telemeter output circuit is used to buck a reference voltage in a self-balancing potentiometer circuit. A slide wire rheostat calibrated in kilowatts keeps the potentiometer in balance as the telemeter output varies. A 2-phase reversible motor energized from an a-c amplifier automatically actuates the slider on the balancing rheostat. A converter of the vibrating reed type changes the unbalanced direct voltage to alternating current. The motor, amplifier, and converter are standard components made by the Brown Instrument Company for their "Electronik" recording instruments. The slider on the above rheostat has a pen attached for recording on the same strip chart with frequency, as shown in Figure 7. A rack and pinion couples the motor shaft to the slider and pen, and also to the drum through a system of counterweighted pulleys for mechanical amplification as shown in Figure 7. Maximum pen speed is 1.4 inches per second. It will be noted that a third pen has been added to record operating piston motion on the strip chart simultaneously with kilowatts and frequency.

The cards obtained have rectangular co-ordinates and are quite large because of the high sensitivity of recording both frequency and kilowatts. The combined instrument thus gives two types of records simultaneously

1. A strip-chart record of frequency, piston motion, and kilowatts with respect to time.

2. A card diagram of frequency versus kilowatts from which incremental speed regulation may be obtained readily without any further plotting.

The card is worked up in the same manner as a frequency versus operating-piston card by visually drawing a line or common major axis through the superimposed figures and calculating its slope after applying the proper instrument calibrations for frequency and kilowatts.

In addition to testing the individual units in the above manner, the generator output telemeters were totalized so that the incremental speed regulation of the entire plant was recorded on a single card.

Testing Applications

The equipment has been used extensively in checking governor performance at the plants of the Safe Harbor Water

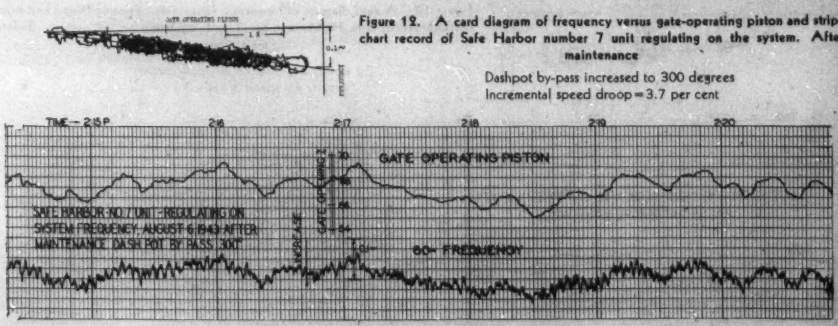

Figure 12. A card diagram of frequency versus gate-operating piston and strip-chart record of Safe Harbor number 7 unit regulating on the system. After maintenance

Dashpot by-pass increased to 300 degrees
Incremental speed droop = 3.7 per cent

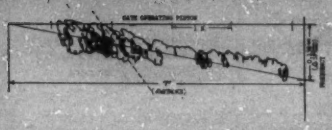

Figure 13. A card diagram of frequency versus gate-operating piston and strip-chart record of Safe Harbor number 4 unit regulating on the system

Original dashpot, drum ratio = 4.8, total stroke = 29.625 inches, rated speed = 60 cycles

Incremental speed droop = 4.7 per cent

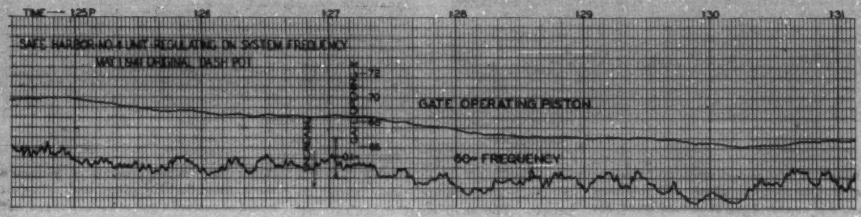

Power Corporation and Pennsylvania Water and Power Company. The Safe Harbor station contains seven 42,500-horsepower Kaplan and two 3,100-horsepower Francis units. All machines have Woodward governors with motor-driven fly balls. At Holtwood there are ten units of the Francis-type rated from 13,500 to 20,000 horsepower. The governors are all I. P. Morris double-floating lever-type with mechanically-driven flyballs. There are two 12,500-kilowatt turbogenerators in the steam station with General Electric Company governors.

These plants are a part of the interconnected systems comprising most of Federal Power Commission areas *5* and *6*. Geographically these areas include Eastern Pennsylvania, New Jersey, Maryland, Delaware, and the District of Columbia. The usual generating capacity of the group is in excess of 4,000,000 kw. There is no automatic frequency control; average frequency for electric time is regulated manually by a designated station with all other frequency regulation taken by the individual unit governors.

During the low river flow periods the hydro units at Safe Harbor and Holtwood have the governors free to assist the other stations on the interconnected system in regulating frequency. On an average year this amounts to about 75 per cent of the time at Safe Harbor and less than 50 per cent of the time at Holtwood. For effective regulation and economy of operation it is important to have correct governor action free of hunting, creeping, and other irregularities. To this end the testing equipment has been a valuable aid in locating malperformance and in measuring the effect of adjustments and corrective measures. It is not within the scope of this paper to discuss the effects of governor performance on system operation as the subject has been covered competently by others.[8]

Speed Droop and Regulation of Hydraulic Turbines

Because the greater portion of this work has been in connection with governors on hydraulic units an explanation of some of the characteristics of these machines may be helpful to those who are not familiar with this type. It has been the practice of the manufacturers to base the speed droop characteristics of the governor on percentage of gate stroke rather than power output. This relationship on the more recent governors is substantially a straight line over the full range of

Figure 14. A card diagram of frequency versus gate-operating piston and strip-chart record of Safe Harbor number 4 unit regulating on the system

Positive centering dashpot, drum ratio = 4.8, total stroke = 29.625 inches, rated speed = 60 cycles

Incremental speed droop = 3.2 per cent

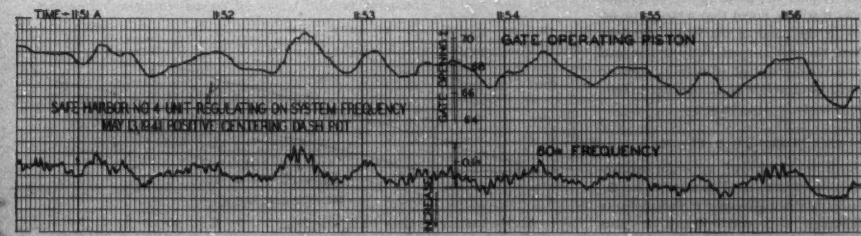

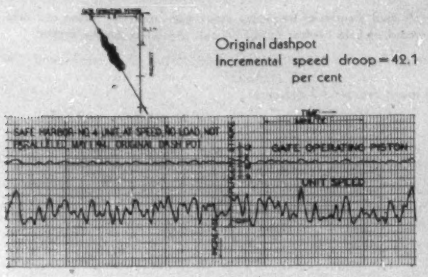

Figure 15. A card diagram of frequency versus gate-operating piston and strip-chart record of number 4 unit at no-load speed, not paralleled

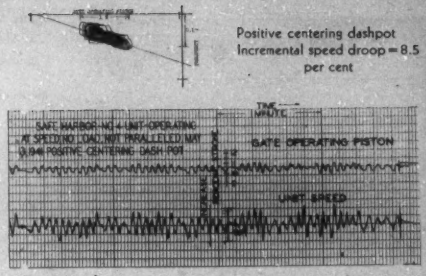

Figure 16. A card diagram of frequency versus gate-operating piston and strip-chart record of number 4 unit at no-load speed, not paralleled

gate stroke and therefore is proportional for equal increments of gate stroke. However, there may be considerable variation in incremental speed regulation over certain ranges of gate travel because the power output of a hydraulic turbine is not a linear function of gate opening over the full range. Figure 8 illustrates typical curves of gate-power relation for three different types of turbines. By combining the information of Figure 8 with the speed droop characteristic of the governor a speed–power curve can be obtained; the slope of this curve at increments of power output establishes the incremental speed regulation curve. The steady-state incremental speed regulation for the Kaplan and propeller types with an assumed linear speed droop of five per cent is shown in Figure 9. Because the characteristics of the Francis turbine are similar to the propeller type the incremental regulation curve will be practically the same.

The speed droop characteristics of a governor may be modified to compensate for the nonlinear power-gate curve. Within the normal operating range of the Kaplan units the compensation would be gradual and of a low order. However, with respect to the propeller or Francis types it will be noted that a steep rise occurs at the point of maximum efficiency where the unit is most likely to regulate. From the standpoint of stability, caution should be exercised in attempting to fully compensate for the steep rise.

Routine Maintenance Checks

Routine checks of governor performance have been used as a guide for determining when governor maintenance or adjustment is needed. Figure 10 shows the performance of a governor before a periodic maintenance and inspection period. The strip chart indicates very poor governor action in that the gate-operating piston has a tendency to follow only the general trend of the average frequency and offers little helpful operation in regulating the swings. The card diagram of frequency versus operating piston, taken simultaneously with the strip chart, shows a very insensitive governor with the average width of diagrams approximately 0.10 cycle per second or 0.17 per cent of rated speed. The straight vertical lines extending across the diagram are, according to definition, dead band. This type of diagram is indicative of friction in the primary elements of the governor.

Maintenance inspection revealed friction in the main-relay valve-packing gland, the ball-head bearings, compensating dashpot plungers, and also an 0.08-inch off center setting of the small dashpot plunger. The charts of Figure 11 show the operation of this same governor after the above conditions were corrected. The strip chart shows a decided improvement in governor performance with the gate piston following all of the major frequency swings with little time delay. The card diagram indicates an average sensitivity of 0.05 cycle per second or 0.08 per cent of rated speed. The actual dead band is 0.025 cycle per second or 0.04 per cent of rated speed.

Effect of Compensation

The variation in the width of the minor axes of the different superimposed loops is quite evident in Figure 11 A portion of it was the result of overcompensation on the higher rates of frequency change To illustrate, Figure 12 shows a test with the compensation reduced by opening the dashpot by-pass; the figures are more uniform and not nearly so wide. The strip chart also shows a more active governor with the gate following even the small fringe variations in frequency

Compensating Dashpot Investigation

One of the problems encountered at Safe Harbor was that of sluggish response to the load adjusting control. After the initial movement the turbine gates had a tendency to creep making it difficult to adjust the unit loading promptly and accurately. Test results showed that this

Figure 17. A card diagram of gate-operating piston versus blade angle of Safe Harbor number 1 unit taken at slow traversing speed

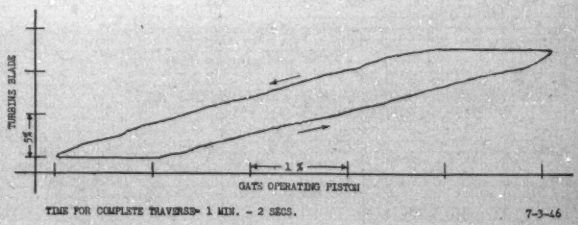

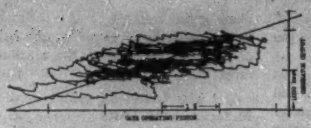

Figure 18. A card diagram of gate - operating piston versus generator output and strip-chart record of Safe Harbor number 5 unit regulating on the system

Kilowatts per per cent stroke = 445

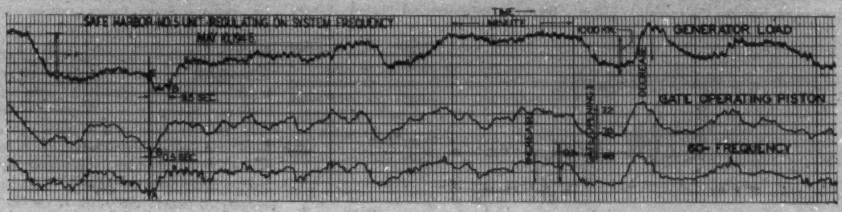

Figure 19. A card diagram of frequency versus total load and strip-chart record of Safe Harbor station regulating on the system

Head = 55 feet
Load range = 170–185 megaw atts
Incremental regulation = 2.70 per cent

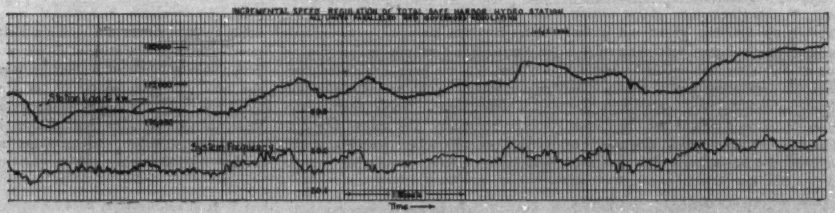

same response prevailed when the machine was regulating frequency See Figure 13. Note the poor governor response and gradual drift in the gate motion. The card diagram illustrates very erratic governor action; the small complete loops occurring either side of the central axis indicate false movements coming from the compensating mechanism. The steep droop characteristics of the larger loops, designated by the dashed line, are also indicative of trouble coming from the same source.

Further investigation showed the spring on the compensating dashpot plunger was failing to bring the mechanism to a definite center position, thereby establishing with each speed change a different neutral position for several of the governor components. This particular dashpot design employed a spring which in neutral position should have been in zero tension, and, therefore, the slightest friction caused it to position itself to one or the other side of actual center. Furthermore, the low order of centering force exerted by this particular spring application produced spasmodic motion and produced the erratic diagrams pointed out previously.

The dashpot was replaced with a positive centering type in which the spring always is exerting a force to hold the plunger in central position against a positive stop, thereby minimizing the effect of friction. The results of operation after this change are shown in Figure 14.

Tests made at no-load speed with the generator off the bus after the dashpot change indicated better speed control and a very drastic change in droop characteristics. See Figures 15 and 16. The incremental speed droop of the original dashpot was increased greatly because of the effect of friction. To provide a cushion effect minimizing swings on sudden load rejection, the speed droop has been increased purposely to approximately 10 per cent in the 0 to 15 per cent gate opening range. Note that the diagram with the positive centering type of dashpot shows a much lower speed droop than the original dashpot, and the actual measurement now checks the

Figure 20. A card diagram of frequency versus gate-operating piston of Holtwood number 5 unit regulating on the system

Gate opening 73 per cent, drum ratio = 4.8, total stroke = 23.5 inches
Incremental speed droop = 4.6 per cent

nominal value. It has been found that friction regardless of its origin tends to increase the incremental speed droop.

Lost Motion Recording

Many times the advantages of a good governor are lost because of play in the mechanism between the operating piston and the gates, blades, or valves controlling the speed or load. The percentage effect may be appreciable on small movements such as are required on system frequency regulation. A very accurate evaluation of the amount of lost motion between the operating piston and blades on a Kaplan unit has been obtained by means of X-Y recording, whereby motion from the operating piston rotates the drum as one axis, and motion from the blades actuates a pen as the other axis. The width of the elliptical diagram is a measure of the magnitude of lost motion. Such a diagram taken at slow traversing speed is shown in Figure 17. Subsequent studies have shown the lost motion to be in the Kaplan control valve and in the Kaplan mechanism itself

Power Response

In our work we have carried the study with X-Y recording from the motion of the operating piston to the power output of the generator. Thus in Figure 18 the generator output is recorded as a function of operating piston motion under regulating conditions. Instead of the expected nearly straight line characteristic with a slope of 1,200 kw per per cent stroke, as indicated by calculations, the diagram is wide, irregular, and with an average slope of only 445 kw per per cent stroke.

The strip-chart record of frequency, gate, and power output, Figure 18, shows the relative time lag between the operating piston and power output. It will be noted that the piston responds to the frequency within 0.5 second as shown at B, but the power at C still is dropping from the previous frequency change at A and does not respond in the proper direction until at D, 9.5 seconds after the frequency change. This example was exceptional; on the average the lag appears to be five six seconds.

A small portion of the lag can be ascribed to inertia of the control system and transient hydraulic effects; the greater part, however, is the result of lost motion between the gates and blades. Consequently, the sensitivity is decreased and the per cent incremental speed regulation increased as much as three times the calculated value.

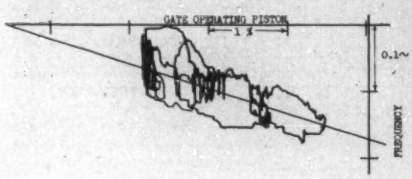

Figure 21. A card diagram of frequency versus gate-operating piston of Holtwood number 5 unit regulating on the system

Gate opening 29 per cent, drum ratio = 4.8, total stroke = 23.5 inches
Incremental speed droop = 6.2 per cent

To reduce the degree of overspeed on our Kaplan units the closing time of the blades has been increased to 15 seconds as compared to 6 seconds for gate closure. No time lag has been introduced purposely which would retard the initial blade movement. Under normal frequency regulation, the above slow traversing times have been found by actual test to have little or no effect on the blade or gate response because the rate of frequency change does not require either of them to travel near the maximum rates.

Miscellaneous Tests

Incremental Speed Regulation of Safe Harbor Station

Where telemeter totalizing equipment is available regulation diagrams can be made of an entire station or group of stations. Figure 19 is a diagram of the Safe Harbor station with all units paralleled and governors regulating. The power lag described in the previous discussion can be seen on the strip chart; it is reflected also in the width of the diagram and higher than calculated per cent regulation. However, the actual slope or incremental speed regulation is still only 2.7 per cent, and the governors are seen to be very responsive to frequency changes

Holtwood Hydro Units

Figure 20 shows incremental speed droop diagrams from a 12,000-kw Holtwood hydro unit operating at 73 per cent gate. Figure 21 shows a diagram from the same unit operating at 29 per cent gate; note the difference in sensitivity at these two gates. The unit seldom is operated at this low gate, and the increased friction in the working parts of

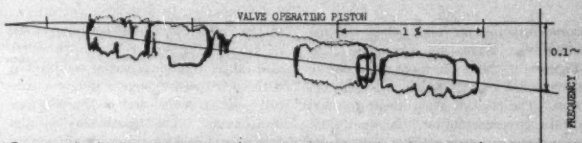

Generator load = 95 per cent rating, drum ratio = 31.75, total stroke = 6.5 inches
Incremental speed droop = 4.5 per cent

Figure 22. A card diagram of frequency versus valve-operating piston of Holtwood Steam Station number 15 unit regulating on the system

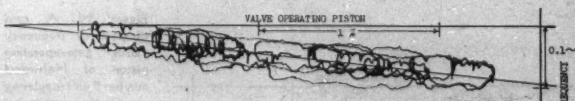

Generator load = 95 per cent rating, drum ratio = 42.34, total stroke = 6.5 inches
Incremental speed droop = 5.3 per cent

Figure 23. A card diagram of frequency versus valve-operating piston of Holtwood Steam Station number 16 unit regulating on the system

the governor because of inactivity is quite evident.

Holtwood Steam Plant

By including additional step pulleys in the setup, thereby further amplifying the drum motion, diagrams can be made on steam units with relatively small total stroke. Diagrams, Figures 22 and 23, were made on the Holtwood steam turbines where the total travel of the valve operating piston is 6.5 inches.

Compensating Dashpot Oil

Seasonal temperature changes and the resulting effect on the viscosity of the compensating dashpot oil have a decided effect on the performance characteristics of the hydro governors. This condition can be remedied by changing the adjustments on the dashpot or using heaters in cold weather; however, our experience has shown that standardization of settings is desirable. At the present time tests are being made on the more constant viscosity silicone oils.

Conclusions

1. Improved instruments for testing governors have been described and numerous examples shown of applications to hydro and steam units. These examples demonstrate that the many factors affecting governor performance are shown readily and can be evaluated by the card diagrams and strip chart records. The effects of maintenance, adjustments, and corrective measures therefore are determined quickly and easily.

2. The method of testing with card diagrams of frequency versus gate offers a convenient means of establishing practical governor performance standards and maintaining them throughout the life of the equipment.

3. Adoption by the industry of methods of testing similar to those described in this paper would provide a common basis for analyzing governor performance. More general use of this method of testing would be promoted by the early adoption of suitable terms defining the characteristics of the frequency versus gate diagrams obtained under operating conditions.

References

1. Oscillograph Analyzes Governor Performances, J. E. Allen. *Power* (New York, N. Y.), volume 78, November 1934, pages 610–12.

2. Les Régulateurs de Vitesse des Turbines Hydrauliques (Hydraulic Turbine Governors), P. Cayère. *Arts Et Métiers*, September–October 1937.

3. Discussion by J. E. Allen of Prime-Mover Speed Governors for Interconnected Systems. AIEE Transactions, volume 60, 1941, pages 729–30.

4. A High Speed Level Recorder for Acoustic Measurements, E. H. Bedell. *Bell Laboratories Record* (New York, N. Y.), November 1934, page 75.

5. The Field of System Governing, Albion Davis. *Transactions*, American Society of Mechanical Engineers, volume 62, number 3, April 1940, pages 207–19.

6. Discussion by R. Sheppard and C. Concordia of A Turbine-Governor Performance Analyzer. AIEE Transactions, volume 61, 1942, pages 393–4.

7. A Turbine-Governor Performance Analyzer, W. O. Osbon. AIEE Transactions, volume 60 November 1941, pages 963–7.

Discussion

G. J. Vencill (Union Electric Company of Missouri, St. Louis, Mo.): It is apparent that the authors have considerable interest in the subject of governor analysis and testing from the time and effort that must have been required to develop the equipment used. They are to be complimented on the soundness and completeness of their presentation. The use of such instruments in testing governors to determine the need for and effectiveness of maintenance work should eliminate practically all the uncertainty usually present in such determinations. Without definite information on governor performance, it is so easy to assume that as long as it is quiet it is good.

Our company has fitted a General Electric photoelectric frequency meter with an auxiliary table to make the diagrams of frequency versus operating piston position, and has found it useful in tracing locations of trouble. The simultaneous recording of the strip chart and diagrams, while convenient, is not regarded as necessary, since the same actions recur indefinitely and can be recorded separately. We have not made direct comparisons of kilowatt output with frequency, but think it would be very desirable to do so since that is really the ultimate result of the regulating action.

The frequency–gate diagrams provide a very simple means of analysis where the governor has no compensation as is usually the case with a steam turbine. Where compensation is used, the shape of the diagram will depend considerably on the speed with which frequency changes, and the characteristics of the frequency pattern. This would need to be taken into consideration when drawing conclusions from the records. In any case the strip chart record is necessary to determine time lag.

Figure 1 of this discussion is two sample diagrams showing performance of two steam unit governors on our system, both of which are quite sensitive.

Figure 1. Sample performance diagrams

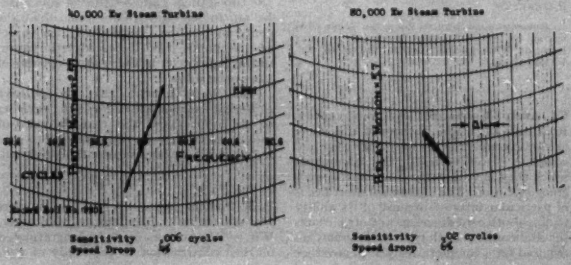

R. Sheppard (nonmember; General Electric Company, Schenectady, N. Y.): The contribution of the speed governor controlling the steam or hydro unit once its generator is phased in with a large interconnected system of relatively constant average frequency is largely determined by the governor's ability to accurately respond and correctly direct the positioning of the inlet valves in response to the minute and relatively slow frequency variations constantly occurring. The dead band of the governor mechanism, as defined by reference 1, is the total magnitude of the sustained speed change within which there is no resulting measurable change in the position of the governor controlled valves. This dead band or insensitivity of the governing mechanism is the one characteristic which has so much to do with the width of the frequency fringe drawn by instantaneous frequency recorders on so-called constant frequency systems. Automatic frequency control or careful manual control can do little to narrow the characteristic system fringe band however well they may maintain the average frequency. It is believed that a reduction of such frequency fringe bands on existing systems is possible and may slowly come about as additional new prime movers with governors of small dead band are added to systems.

At least two central station systems have undertaken a limited program of replacing a few older governors having poor dead band characteristics with modern accurate low dead band governors. The improvement and effect upon the frequency band will be carefully studied when these replacements are installed. It is hoped that tie-line and frequency regulation will be simplified and made easier by the conversion of an appreciable portion of the steam prime mover capacity to such low dead band characteristic governors.

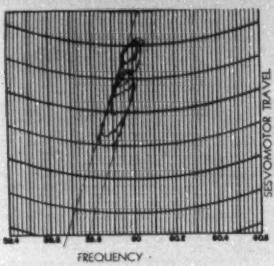

Figure 2. Steam turbine servopiston travel versus system frequency showing poor dead band of older type governor

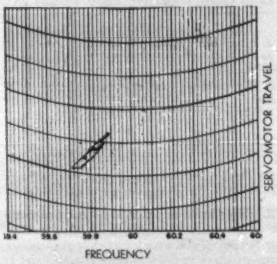

Figure 3. Steam turbine servopiston travel versus system frequency showing reasonable dead band of an oil relay governor

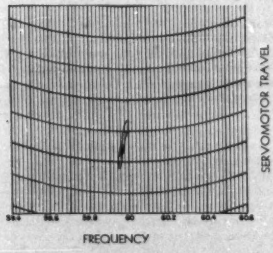

Figure 4. Steam turbine servopiston travel versus system frequency showing good dead band of improved oil relay governor

The development of instruments described by the authors, and their use to study the insensitivity of governor mechanisms has assisted governor manufacturers in the improvement of their product. Such studies for the most part have first been conducted in hydro and steam stations. The writer and his associates have used a photoelectric straight dead band diagram recorder similar to the early type first developed by Allen. Governor mechanisms of some 60 large steam turbines and seven hydro units have been studied on their respective power systems. These studies clearly revealed which types of speed governors had consistently poor sensitivity and those which were superior. The knowledge gained from such studies has materially aided in the adoption of improved governors and the rejection of those with poor sensitivity.

Figures 2–5 are examples of governor dead band hysteresis cards of progressively smaller dead band governors. All have been taken on steam units whose governors unlike those of hydro units had no time delay speed compensating dashpot mechanism, and in general, each had a nominal 5 per cent over-all steady-state speed regulation. Any small time lags in the positioning of the servo motor piston were largely due to the normal time for oil to flow through the relays to restore the servo pilot back to port equilibrium. In steam turbine governors of the non-compensated type these time lags are small.

Figure 2 illustrates the dead band of a governor which, although it exhibited no instability and suffered no noticeable difficulties, contributed little to the accurate regulation of the system and certainly aggravated the characteristic frequency fringe of the system to which it was attached. Unfortunately the nature of the inherent friction and drift in the governor of this example was of such a nature that little if anything could be done to improve it as far as maintenance attention or parts replacement are concerned.

Figure 5 is an unusual governor mechanism and approaches the ideal in accuracy and dead band. Notice the momentary deviations from the true speed-travel line caused by rather fast frequency changes of very small magnitude.

The new instrument described by the authors which simultaneously records the frequency and load as a function of time on a strip chart plus the $X-Y$ gate-frequency hysteresis loops should be very helpful in interpreting the dead band loops since it is believed the rate at which the frequency is changing has some bearing on the dead band width. It is suggested that the authors take a series of gate position dead band cards of only long enough time duration to permit the pen to form one or two loops. These cards could then be studied knowing the rates at which frequency was changing. Thus, for a given governor there could be established the relation between effective dead band and rate of change in frequency.

The authors are to be congratulated for their valuable work in the development of speed governing of large central station prime movers.

REFERENCE

1. RECOMMENDED SPECIFICATION FOR SPEED GOVERNING OF PRIME MOVERS INTENDED TO DRIVE ELECTRIC GENERATORS. AIEE STANDARD 600, JULY 1944.

C.L. Avery (Woodward Governor Company, Rockford, Ill.): The authors of this paper are to be complimented on a very clear and complete description of the instrument which they have developed for testing governor operation. The instrument described is of particular interest because of its ability to draw both card diagrams and strip charts simultaneously. Both types of diagrams are required for a complete analysis of governor

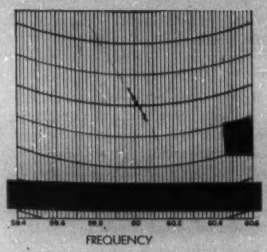

Figure 5. Steam turbine servopiston travel versus system frequency showing unusually small dead band of an improved oil relay governor

operation, hence the ability to make both types of records at the same time considerably reduces the testing time.

While the authors state that "no attempt has been made to calibrate the meter in terms of absolute frequency," and it is evident that meter drift during the time to make a run is negligible, it would be of interest to know what the drift over an extended period of time would be. It is distinctly of advantage to be able to shift the position of the pen on the chart, and it should be noted that such a shifting of the pen does not affect the sensitivity of the instrument.

A program of periodic testing of governing equipment is to be strongly recommended as a means of determining when the operation is becoming so erratic that maintenance work should be done. By such a program, incipient difficulties can be detected and the necessary maintenance performed before system operation is adversely affected.

The diagrams showing the contrast between the operation of unit 4 with the original dashpot (Figures 13 and 15 of the paper) and with a positive centering dashpot (Figures 14 and 16 of the paper) are very interesting. The positive centering dashpot was first used at Safe Harbor, Pa., and is of especial advantage on a very active load such as is supplied by the Safe Harbor Plant. The difference in construction of these two types of dashpots is illustrated by Figures 6 and 7 of the discussion. The transmitting plunger e of the regular type (Figure 6) is returned to its null position by the push-pull spring a whereas the plunger of the positive centering type is returned to null position by the two springs b and c either of which can be separately adjusted for preload at the centering position. Incidentally, the values of "dashpot by-pass" indicated on the figures of this paper refer to the relative opening of the needle valve d.

The charts indicate that the positive centering dashpot allowed a larger opening of the by-pass and also that the ratio of movement of the receiving plunger f to gate travel may have been substantially reduced.

B. R. Nichols (nonmember; Allis-Chalmers Manufacturing Company, Milwaukee, Wis.): The authors are to be congratulated on their contribution to the study of gov-

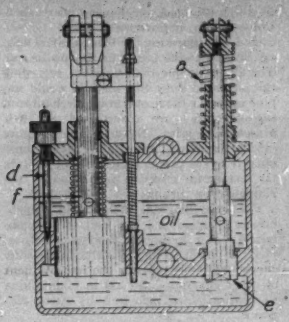

Figure 6. Dashpot construction

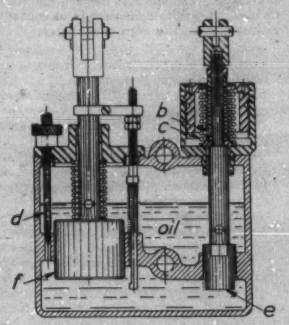

Figure 7. Dashpot construction

ernor performance, and the development of the simplified highly sensitized recording instrument for recording the performance of governors operating under field conditions.

This type of work should be encouraged, particularly among the operating department of power companies not only to learn more about the requirements of new governors, but also to improve the performance of existing governors.

The writer has observed that there are many governors, particularly of the older installations, throughout the country that are not performing correctly. Some of these governors have never been adjusted correctly because of various reasons, others have been adjusted to improve a particular condition without regard for other operating conditions. A common adjustment of this type among some operators is to tighten the dash pot by-pass valve if the turbine gates swing too much when the unit is off the line, instead of investigating the cause of the swings.

In order to obtain the best performance from the governors on a system, it is necessary to make numerous observations of the load and frequency characteristics of the system. These studies often require considerable time and for these reasons the studies can best be made by power company engineers, equipped with the proper instruments, and, as pointed out by the authors, it would be relatively easy to make routine maintenance checks on the governors after a governor performance record has been made with the most satisfactory governor adjustments. The instrument developed by the authors, combining high sensitivity with both strip chart and card diagram records should be very satisfactory for this type of inspection.

With reference to the authors' comments on the compensating dashpot, our experience has shown the necessity of a definite centering device if the governor is to accurately respond to system speed changes. This centering spring should exert a force at center position which is considerably greater than the viscosity drag of the oil film between the cylinder and piston and other functional forces in the mechanisms which are operated by the dashpot.

The rigidity of the restoring mechanism between the governor and turbine shifting ring is also of importance for accurate positioning of the governor mechanism during operation.

We have whenever possible used the rod and lever type of restoring mechanism because this type of mechanism, if properly designed, will transmit the shifting ring motion to the governor very accurately.

The cable type relay must have a heavy weight or spring attached to one end to maintain a tension in the cable.

This mass has to be accelerated when the shifting ring moves in a direction to lift the weight and when moving in the reverse direction of the movement of the weight must be quickly stopped at the end of the shifting ring movement. The inertia of this mass changes the tension of the cable.

The change of tension on the cable is more pronounced on the governors that respond quickly to system speed changes.

The spring method of maintaining cable tension reduces the inertia effect on the cable tension, but the spring must be made with many coils to keep the difference in cable tension at a minimum between the ends of the relay strokes. This condition requires a long spring which is difficult to locate in the governor assembly.

Paragraph 3 of the authors conclusion is a very worthy suggestion. The industry can, however, avoid many of the disappointments of the past by setting forth an acceptance test code which will state the governor performance that is expected when the governor is installed. This code should also provide suitable time and conditions for these tests. Quite frequently a customer will spend millions of dollars and years of time to develop and build a power project, but when one of the last phases of completion arrives, that of adjusting the governor, he is so eager to start generating kilowatts that he cannot spare another day to properly test and adjust the governor. This is one of the reasons why he sometimes discovers at a later date, and to his disappointment, that his governor is not performing as he had expected it to perform.

F. Oppenheimer (Pennsylvania Water and Power Company, Baltimore, Md.): The testing method described applies only when the unit is on system but can be applied over full frequency range (that is, equal to speed droop, say 5 per cent) if a means is available to load the unit at frequencies of 95 per cent of normal. This is not usually possible, but several other schemes can be used which give similar data over the full range. Scheme 1 consists of driving the ballhead of the unit being tested from a separate source of adjustable frequency while the main generator itself is on the system carrying load. The frequency could be varied over a range sufficient to change the main generator output from full load to no load. Scheme 2 consists of again driving the ballhead at variable frequency but with the main unit shut down This is not true operating condition but will give piston stroke versus frequency. Scheme 3 consists of taking two generating units off the line, shutting steam or water off one of them and driving it by means of the other unit. Full range of speed variation is possible (by throttle or hand control of the driving unit if necessary) but again this is not under true operating condition. Just which of the three schemes, if any, is used

Figure 8A. Incremental speed droop of the Safe Harbor unit 5

2:25 PM–2:32 PM, December 9, 1946
Dashpot by-pass = 70 degrees (normal)
Incremental speed droop = 3.5 per cent

Figure 8B. Performance diagrams of governor operation after periodic overhaul

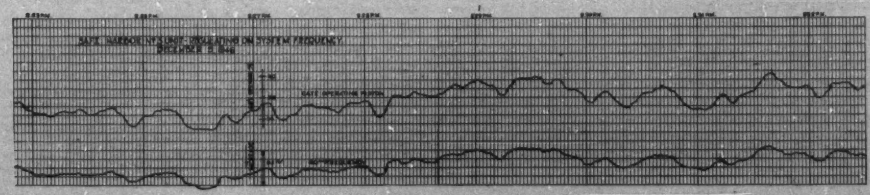

eventually must be determined by the desires of the individual.

It is logical to inquire of what practical use are instruments and test methods described in the paper. An example of the practical results of routine testing is indicated by Figure 8 of the discussion which shows the performance of the governor of a waterwheel after a periodic overhaul. We try to test governors before and after such outages in the hope of detecting imperfections which may need special attention during the outage and then to make sure the governor is at least no worse than before. A glance at this chart gives an immediate impression of good operation without even measuring it. The experienced eye would see high sensitivity, narrow speed droop curve, and small time lag.

J. E. Allen and W. B. Hess: Precise temperature compensation was not attempted and therefore some drift, as referred to by Avery, would be expected if the temperature change was sufficiently large. Tests have shown that, after the initial warming up period of about 20 minutes, the drift during the period of governor test was negligible. No tests have been made for an extended period.

The suggestion submitted by Sheppard concerning single loop diagrams has been used successfully in making studies of units running at speed no-load off the bus. This diagram has led to improvements in speed control for synchronizing. The spiral type of diagrams obtained by manually disturbing a governor are also valuable for investigation of unstable conditions.

Six of the Kaplan units at Safe Harbor, Pa., have the rod and lever type connections between the gate links and the blade control valve; one unit has weighted cable connections. So far as lost motion is concerned, our tests indicate very little difference between the two types. The greatest amount of the time lag has been found in the blade control valve lap and lost motion between the gate operating piston and the gate link to which the blade mechanism is attached. Considerable improvement could be obtained by connecting the blade control linkage directly to the gate operating piston rod. There is some question, however, regarding the increased duty this method would impose upon the blade operating mechanism if the governors are maintained at their present sensitivity. Nevertheless, it is quite evident that the gates and blades must operate in the proper relationship to obtain the maximum effective regulation of the Kaplan type turbine.

The card diagram included in Oppenheimer's discussion is the best thus far obtained on a hydraulic turbine governor. Past experience and continued routine checks will assist greatly the improvement of other governors and aid in maintaining the performance indicated by these diagrams.

Appreciation is expressed to the authors of the excellent discussions which have been submitted. The subjects covered and additional descriptive material submitted greatly increase the scope of the paper.

Automatic Control of Hydroelectric Generating Stations

M. J. BROWN
MEMBER AIEE

W. A. DERR
ASSOCIATE AIEE

Synopsis: This paper discusses hydroelectric station equipment, operating procedures and the factors involved in applying automatic control. Hydraulic governors and the types of water wheels (impulse, reaction, fixed propeller, and adjustable propeller) are described from the electrical engineer's viewpoint. A typical automatic control diagram is shown for each of the two methods commonly employed for accelerating the generator and synchronizing it with the system. In one method, termed self-synchronizing, the machine circuit breaker is closed at less than synchronous speed, and the machine synchronizes after its field is applied. In the other method, automatic speed matching and synchronizing equipment bring the machine on the line at correct voltage and phase angle. Considerations involved in applying supervisory control to automatic hydroelectric stations are presented.

HYDROELECTRIC STATIONS are particularly well adapted to automatic control. As they are justified economically only if their operating expenses are in keeping with the value of their generating capacity, many small installations must be completely automatic to compete commercially with other sources of power. An important consideration is the random availability of their generating capacity. Except in large installations, hydroelectric power must be considered as an auxiliary to steam power. It can be used either for short periods when extra generating capacity is needed, or for long periods when an abundance of hydraulic power is available. Automatic control of hydroelectric stations is favored by the relative simplicity of control of both the prime mover and the stored hydraulic energy which drives it.

Paper 47-57, recommended by the AIEE committee on power generation for presentation at the AIEE winter meeting, New York, N. Y., January 27–31, 1947. Manuscript submitted November 8, 1946; made available for printing December 26, 1946.

M. J. Brown and W. A. Derr both are with the Westinghouse Electric Corporation, East Pittsburgh, Pa.

Station Elements

The elements controlled in an automatic hydroelectric station are the headwater valves or gates, the hydraulic turbine gates or jets, the turbine governor, the lubrication system, the water wheel generator, and the switchgear. The latter includes control relays, protective relays, the voltage regulator, the generator field circuit breaker, and the generator line circuit breaker.

Each of the foregoing elements has a particular function in the over-all operation. The headwater valves, or gates, render the hydraulic equipment inoperative and conserve water during shutdown periods. The turbine gates under the control of the governor admit water in proportion to the load requirements of the turbine. The lubrication system establishes a lubricating film on the bearings during starting, maintains it during operation, and circulates the lubricant so that it can be cooled. The switchgear provides control and protection. The voltage regulator controls the excitation of the machine in keeping with the voltage requirements and demand for reactive power output of the generator. The generator field circuit breaker provides a means of field interruptions during faults, and thereby minimizes damage to the generator and other equipment. The generator line circuit breaker serves to connect the generator to the system after the generator has been started. It also disconnects the generator from the system prior to shutdown or following an electrical fault.

Headwater Control

The headwater gates, or valves, may be of various designs. They have been built in the form of needle or conical plug valves, butterfly valves, gate valves, and sluice gates. These gates are operated either electrically or hydraulically. No details of the cont ol of these gates are included in the following description, because the control is straightforward and can be added to the other operating functions without difficulty. There also may be requirements for the control of diversion and reject spill gates. These requirements are similar to those for headwater gates.

Hydraulic Turbines

The arrangement and location of a hydroelectric power plant will depend upon the developed head, river flow conditions, means of introducing water to the plant, means of conducting water from the plant, and the total installed capacity. Although these factors do not affect automatic control directly, they do determine the equipment that will be used, and this in turn will have its bearing on the demands placed upon the automatic control.

It is the turbine design and the associated governor equipment that will be of most interest to the electrical engineer. Turbines will be of one of four types, three of which are shown in Figure 1. Installations using a high speed input (above approximately 800 feet) generally will employ impulse or Pelton turbines, one type of which is shown in Figure 1*A*. In the moderate head installations (range of approximately 60 to 800 feet), the reaction or Francis type turbine, Figure 1*B*, usually will be encountered, and on low head installations (below approximately 70 feet) the fixed and adjustable blade propeller or Kaplan type turbines, Figure 1*C*, will be found most frequently. Often, the hydraulic engineer has a choice between the use of a reaction type turbine or propeller type turbine. The propeller type turbine will operate at a higher speed (approximately 50 per cent).

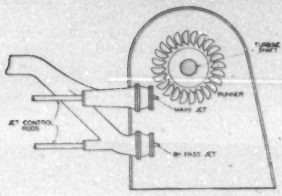

A (left). Impulse type
B (below). Reaction type
C (right). Adjustable propeller type

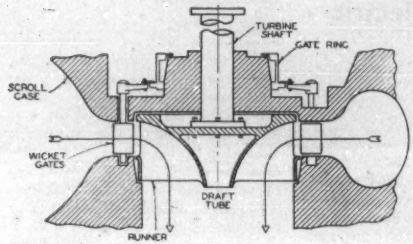

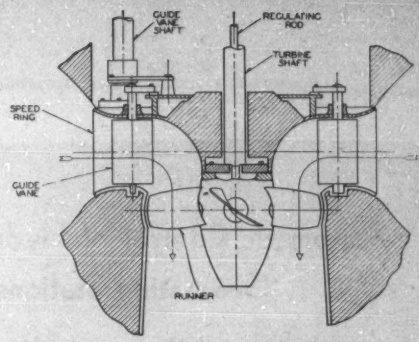

Figure 1. Three types of water wheels

The Water Wheel Governor

The water wheel governor has a multiplicity of tasks assigned to it. It is the central control point for the prime mover operation and is the device through which the automatic starting and stopping equipment functions in its relations with the prime mover. The duties performed by the governor are as follows:

1. Initiation of water flow to the turbine at start and its discontinuation when stopping. This in practice will be the opening or closing of the wicket gates, guide vanes, or jets, of the reaction, propeller, or impulse turbine, as the case may be. This particular function is executed under the direction of the automatic equipment on the switchboard.

2. Control of turbine speed

A. During starting. The governor, in one method of starting controls the turbine speed under the direction of a speed matcher on the governor or on the switchboard. In an alternative method of starting, the governor brings the machine to full speed without any attempt to match existing line frequency.

B. After the generator is on the line. In those cases where the hydroelectric generator parallels with a large system, its turbine speed will be determined by system frequency. However, in the case of an isolated generator or one which represents a large portion of system capacity, the system frequency and turbine speed can be determined by the governor of that machine alone.

3. Control of the turbine loading. The governor must provide means by which the turbine will take on or drop off load as the load on the generator or system changes. It also must provide an adjustment which will determine how the turbine will share load changes with other power sources.

4. In some special cases it provides means for operating the generator as a synchronous condenser at normal frequency with no flow of water to the turbine and at the same time provides for opening the gates in the event that frequency drops

As practically all automatic hydroelectric stations will be connected to large systems, it will be of interest to examine the operating requirements of a hydroelectric station when operating as part of such systems. Consider Figure 2. This is a diagram showing the characteristics of two generators, having respectively one per cent and two per cent speed droop, connected to a large system. The large system approaches an isochronous characteristic in that it operates with little change in frequency as load changes. As long as system frequency remains constant, the load supplied by generators *1* and *2* will be constant and of the value indicated by point *a*. If the system frequency drops, generator *1* with one per cent speed droop will show a considerable change in load as indicated by the intersection of the dotted line with the characteristic line of generator *1*. The load on this machine will increase from the value indicated by point *a* to that of point *c*. However, generator *2* with a two per cent speed droop will show less change in load with change in system frequency. The speed droop characteristic of the governors, therefore, should be adjustable so that load changes will be taken on generators which can accommodate them best. Governor sensitivity, which is a nonadjustable factor, figures in the distribution of load changes. The more sensitive governor will respond to frequency changes faster and by being more prompt will cause its prime mover to take a greater share of the load changes than the prime mover controlled by a less sensitive governor.

The Lubrication System

The lubrication system includes the facilities required for lubricating both the turbine and generator.

In most cases the generator lubrication system is self-contained and, therefore, does not require auxiliary pumps. However, horizontal generators may have high pressure bearing lift pumps for use during starting. Likewise, some high speed generators will use pumps for circulating the lubricant after the machine is running.

Automatic control must consider the operating requirements of the lubrication system during start, running, and shutdown.

Water Wheel Generators

Water wheel generators fall into one of two general classes, depending upon whether they have horizontal shafts or vertical shafts. In general, the impulse turbine installations require horizontal shaft machines and develop speeds between 300 and 1,000 rpm. The other turbine types require vertical shaft machines, which they drive at speeds ranging generally from 100 to 300 rpm. Either type is subject to severe overspeeds, and rotors are constructed to withstand the resulting stresses.

The slow speed of rotation demands high excitation current for the generator field. This reflects on the ratings of the field circuit breaker equipment and has a bearing on the voltage regulator application.

The automatic sequence in some cases places demands on the amortisseur winding for synchronizing torque. When

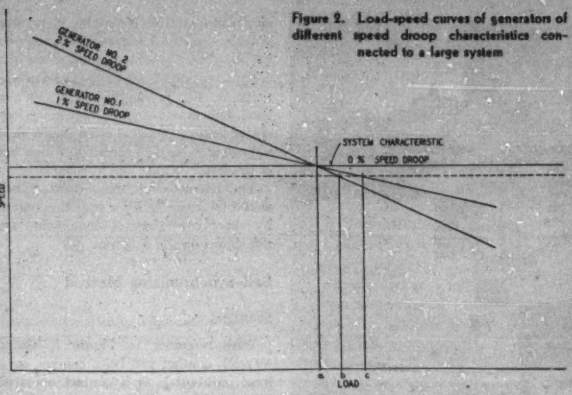

Figure 2. Load-speed curves of generators of different speed droop characteristics connected to a large system

control of this type is contemplated, the capacity of the amortisseur winding must be investigated to determine its adequacy.

A water wheel station is shown in Figure 3. The switchgear is located adjacent to the left wall. The governor cabinets are located in front of the switchgear opposite each generator. A cross section of a station of this type is shown in Figure 4.

Exciters for water wheel generators may be direct connected, belted, geared, or motor driven by an electric or water motor. The direct connected exciters are preferred because of their greater reliability.

Switchgear

Under the general heading of switchgear comes a variety of devices which may be considered the nerve center of the entire plant. This equipment performs extensive functions and is tailored to fit the operating methods adopted for the station.

The automatic hydroelectric unit by definition is one in which the generator is started and put on the line following an impulse received from a control device. The operating methods established for a particular hydroelectric generating plant will determine the origin of the starting impulse.

The starting impulse may be given by a local operator, by a remote operator through supervisory control equipment, or it may be given automatically by a float switch in the forebay, a time switch, or other device.

Regardless of the type of starting means employed, automatic units are protected continuously by devices which cause shutdown under abnormal conditions. After shutdown by protective devices, units which are started by a local operator or by supervisory control equipment usually must be given another starting impulse to restart the unit, regardless of the reason for shutdown Units which are started by a float switch, time switch, or other automatic device usually restart automatically after shutdown by protective devices when normal conditions again exist. When automatic restarting is employed, caution must be exercised in the design of the protective system, so that repeated unsuccessful attempts at restarting are not encountered.

There are two methods employed for accelerating and synchronizing a hydroelectric generator with a system. One method is known as self-synchronizing, and the other as automatic synchronizing.

In the self-synchronizing method, the generator circuit breaker is closed after the turbine has accelerated to approximately 95 per cent of synchronous speed. Field is applied after the generator circuit breaker is closed. For this type of synchronizing, the generator field is equipped with an amortisseur winding to develop synchronizing torque.

Self-synchronizing should be employed only on units which constitute a relatively small percentage of the total system capacity, as with this method a considerable amount of synchronizing power is exchanged with other units on the system. Self-synchronizing a large unit results in an appreciable voltage disturbance, therefore, it seldom is employed for units having more than 5,000 kw output

The automatic synchronizing method employs automatic speed matching and synchronizing equipment. This equipment connect the generator to the line at the proper speed, voltage, and phase angle.

The automatic synchronizing method makes it possible to connect a unit to a line with the least possible disturbance, regardless o the size of the unit. Automatic synchronizing is superior to manual synchronizing and often is employed in stations which do not have an automatic starting sequence.

After an automatic unit is in operation, the real and the reactive power delivered to the system may be controlled by a local operator, or by a remote operator through supervisory control equipment. Real power may be regulated automatically by load control devices or equipment responsive to headwater level.

The control equipment preferably is

Figure 3. Hydroelectric station showing generators, governor, and switchgear

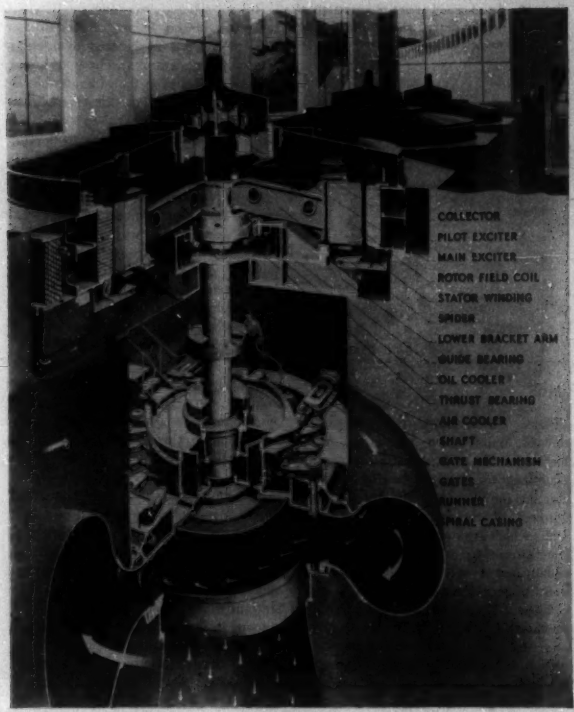

Figure 4. Cutaway view of hydraulic turbine and connected generator

battery operated, as in general it is not desirable to depend upon the availability of a-c power for control functions.

Figure 5 shows the front and rear view of a typical tunnel type switchboard for an automatic hydroelectric station.

Automatic Sequences for Controlling Hydroelectric Stations

The following description treats independently the starting sequences for self-synchronizing and automatic synchronizing of hydroelectric generators. The schemes described are typical and would be altered in practice by changes in details to suit each particular application. The diagrams and description of operation apply to those automatic stations having a local operator, or those stations remotely operated through supervisory control. The diagrams and description apply to stations using reaction type turbines. The basic scheme involved can be modified to meet the operating requirements of the other three types.

Figure 6 shows a single line diagram which applies for either of the two methods of control; Figure 7 is a control diagram for the self-synchronizing method; and Figure 8 is a control diagram for the automatic synchronizing method.

Single Line Diagram

Figure 6 indicates the main connections of a hydroelectric generator, being of large enough size to warrant the use of a pilot exciter as well as a main exciter. Direct connected exciters are indicated.

A direct connected permanent magnet generator for operation of the governor flyball motor also is indicated. The governor flyball motor often is operated from potential transformers connected to the generator.

Instrumentation for local indications of electrical quantities is simple. Generator voltage, current, kilowatts, kilovars, and kilowatt-hours and bus voltage are the a-c quantities of interest. A synchroscope usually is supplied to provide a local indication of synchronism. Generator field current and main exciter field voltage are the d-c quantities which are of interest.

The telemetering transmitters, which would be desirable for a station operated by supervisory control equipment, are not shown on the diagram.

Self-Synchronizing Method

Starting

With reference to Figure 7, the *1 START* contact can be a contact on a local pushbutton or a contact operated by supervisory control equipment. If the lockout relays *86E* and *86N* are reset, the machine speed contact *14* closed, the generator circuit breaker *41* open, and, if the protective contacts connected across the coil of master relay *4* are open, master relay *4* will be energized. When master relay *4* picks up, it seals itself in around the momentarily closed *1 START* contact, as well as the *14* and *41* contacts. It will remain picked up unless short-circuited by the *1 STOP* contact, any one of the protective devices connected across the coil, or de-energized by either of the lockout relays *86E* or *86N*.

A make contact of relay *4* sets up a circuit to all the devices operated in the starting sequence. Relay *88QX* is operated immediately after *4* picks up to start operation of the bearing oil pumps. Incomplete sequence timing relay *48* likewise is energized immediately.

Adequate bearing oil pressure closes contacts *63QB*, and *63QX* is picked up. A contact of relay *63QX* energizes the governor solenoid *65S*, and the water wheel gates start to open under the control of the governor.

When the generator has reached 95 per cent of synchronous speed, contact *13Y* closes, which completes a circuit to the closing relay of the generator circuit breaker *52*. Closing of the generator circuit breaker completes a circuit to the closing relay of the generator field circuit breaker *41*. Thus, the generator is connected to the system at slightly less than synchronous speed, and its field is applied immediately thereafter. The field circuit breaker de-energizes the incomplete sequence relay.

After the generator is connected to the system, the load can be adjusted by means of the governor synchronizing motor, or it can be arranged to take a

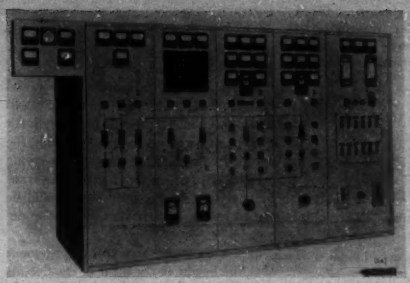

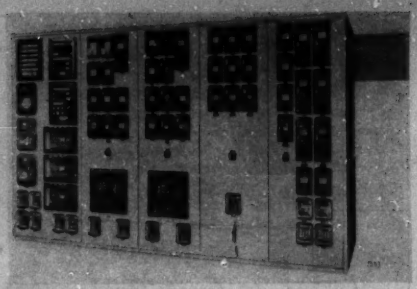

Figure 5. Front (left) and rear view (right) of a typical tunnel type switchboard for a hydroelectric station

load automatically, depending on the governor load limit setting.

STOPPING

The *1 STOP* contact can be a contact on a local pushbutton or a contact operated by supervisory control equipment. When the *1 STOP* contact is closed momentarily, it short-circuits relay *4* and causes its release.

When relay *4* releases, it de-energizes the governor solenoid *65S* and the bearing oil pumping motor relay *88QX*. A time delay circuit not shown continues the oil pump motor operation for a definite period of time after the release of relay *88QX*. Release of the governor solenoid causes the turbine gates to start to close. When the gates reach the no-load position, gate contact *33NL* closes. Closing of this contact completes a circuit which sequentially trips the generator circuit breaker and the field breaker. Thus the generator is disconnected from the system with no disturbance, as the load had been dropped gradually before the generator circuit breaker was opened.

The turbine gates continue to move until they reach the fully closed position. When the gates are closed completely, gate interlock *33Z* operates brake relay *20*, providing contacts *14*, *4*, and *52* are closed. Through circuits not shown, relay *20* causes the turbine brakes to be applied for a definite period of time, assuring that the machine is brought to a stop.

Automatic Synchronizing Method

STARTING

It will be noted from Figure 8 that the circuit for energizing relay *4* is the same as shown in Figure 7, except that it is unnecessary to check the position of the field circuit breaker *41* before starting. When relay *4* picks up, it seals itself in around the momentarily closed *1 START* contact as well as the contact of device *14*. Just as in Figure 7, it will remain picked up, unless short-circuited by the *1 STOP* contact, any one of the protective devices connected across the coil, or de-energized by either of the lockout relays *86E* or *86N*.

The operation up to the energizing of relay *63QX* is the same for automatic synchronizing as for self-synchronizing.

When relay *63QX* picks up, the governor solenoid *65S* is energized, automatic synchronizing and speed matching auxiliary relay *25X* is energized and the generator field circuit breaker *41* is closed. Thus, the water wheel gates start to open under the control of the governor, the generator field current builds up as the exciter comes up to speed, and the speed matching and automatic synchronizing equipment is energized.

As the generator comes up to speed, the speed matching equipment functions to match the generator frequency with the line frequency, and the voltage regulator adjusts the field current for line voltage.

When the instantaneous frequency difference and the phase angle difference are satisfactory for proper synchronizing with the system, automatic synchronizing contact *25* is closed to energize the generator circuit breaker closing circuit. Closing of the generator circuit breaker de-energizes relay *25X* and takes the automatic synchronizing and speed matching equipment out of service.

The incomplete sequence relay is de-energized when the generator reaches 95 per cent speed. The synchronizing time is variable and hence is not included in the over-all timing of device *48*.

Where it is required that the generator energize a dead bus, the contact of relay *25* in the foregoing description must be paralleled by a contact of a dead bus relay in series with a synchronous speed contact.

STOPPING

The normal shutdown by operation of the *1 STOP* contact is exactly the same as was described previously for the self-synchronizing system.

Hydraulic Governor

The over-all arrangement of the mechanical parts of a typical hydroelectric station is shown in Figure 9. On the shaft of the water wheel generator, a permanent magnet generator is shown. Three-phase power from this generator drives a flyball motor at a speed synchronous with that of the generator shaft. The flyballs deliver an indication to the governor in proportion to their speed of rotation. This indication is applied to the power cylinder and amplified by hydraulic means. Compensating devices provide the antihunting characteristics of the governor. Within the mechanism there are facilities for changing speed, limiting gate opening, and controlling the speed droop characteristic of the governor.

The pilot valve of the servomotor is controlled by the motion of the rod connected to the flyballs. This pilot valve controls the relay valve which in turn controls the power cylinder that operates the gates.

The mechanical feedbacks from the relay valve and power cylinder are used to operate the mechanism which obtains a motion of the power cylinder proportional to the motion of the speeder rod and at the same time allows the speeder rod to respond to the resulting change in speed without further change in gate position.

The power for the operation of the relay valve and power cylinder is obtained from an oil pump which stores oil in a tank against a head of air.

Details of governor operation are of

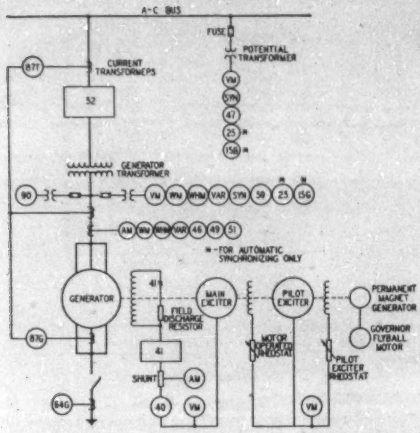

Figure 6. Single line diagram of a single unit hydroelectric generating station

interest because the automatic control functions with it. Figure 10 is an arrangement of devices analogous to an actual governor. In practice the linkages and compensator take a form more convenient and practical.

Assume, in Figure 10, that the speeder rod is in a given position, the floating lever is level, the pilot valve is on neutral, the relay valve is on neutral, and the power cylinder is in a given position.

Now assume that the flyballs depress the speeder rod in response to an increase in speed. The left end of the floating lever is depressed, pivoting about point *A*. The pilot valve is pushed to the close position by rod *1*. The relay valve, under force of hydraulic pressure received from the pilot valve, travels to the close position and through bell crank *1* lifts the pilot valve to the neutral position by pivoting lever *1* around point *C*. The relay valve stays at the closed position admitting oil under pressure to the power cylinder, driving the gate rod in closing direction. In response to this motion, bell crank *2* drives the pistons of the compensator upward in unison against spring pressure. This causes the floating lever to pivot about point *D* raising rod *1* and the pilot valve to the open position. The relay valve in response to this action, moves towards the open position but halts at neutral when its motion, transmitted through bell crank *1* lowers the pilot valve to neutral. The governor thus has moved the gate rod a definite distance in response to a definite motion of the speeder rod.

The next sequence of events prevents a change in gate rod position, as the speeder rod changes position in response to the asked for decrease in speed. Following the action described in the last paragraph, the floating lever is subject to a spring pressure tending to lower its right end and a change in flyball pressure, due to decreasing speed, that tends to raise the left end. An adjustment of the needle valve in the compensator can be made, so that the right end of the lever will lower at a rate matching the rising of the left end as the floating lever revolves about point *B*. When this condition exists, rod *1* will not move, and therefore, no gate motion can result from the speeder rod movement.

In Figure 11 further details of the governor are shown. Speed or load adjustment is accomplished by changing the speeder spring pressure. This is done remotely from the governor by energizing the synchronizing motor. This motor drives a lead screw upon which is mounted a traveling nut. The base of the speeder spring is raised by the traveling nut to increase its pressure and lowered to decrease it. Limit switches sometimes are provided to limit the range of speed adjustment.

Speeder spring pressure also is raised and lowered by the action of the speed droop mechanism. As the power cylinder moves in a direction to open the gates, the speed droop mechanism decreases spring tension, thereby satisfying the governor balance at a lower speed than would be the case if there were no speed droop device.

It will be noted from this arrangement that the height of the orbit of the flyballs and the corresponding position of the speeder rod depends upon the speed of the flyballs and the speeder spring pressure. As the spring pressure is increased, the turbine will be required to take more load at a given speed. Likewise, at a given load, such as would be experienced during starting, increased spring pressure develops increased speed.

Since the operating speed varies only slightly during normal operation, the position of the speeder rod will be an index of the load being carried. Consequently, a load limit device can be made to operate on the speeder rod merely by limiting its excursion toward the open position.

The automatic starting and stopping control works on the mechanism of the load limit device.

To put the turbine in operation, the starting solenoid must release the gate lock and open the gates quickly to the point at which the wheel starts turning.

If a permanent magnet generator is employed to drive the governor flyball motor, the governor takes a control as soon as the generator starts to rotate. However, if the governor flyball motor is energized from potential transformers connected to the generator, the gate open-

Figure 7. Typical schematic diagram for self-synchronizing starting method

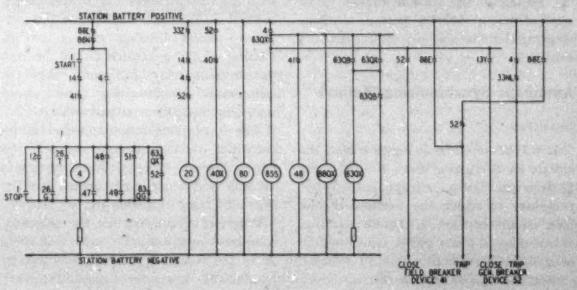

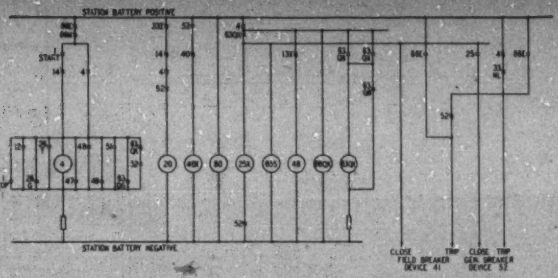

Figure 8. Typical schematic diagram for automatic synchronizing starting method

ing is under control of a timer until excitation appears and makes voltage available to the governor flyball motor.

With reference to Figure 11, operation of the starting solenoid actuates a valve which causes the pilot and relay valves to be energized and the gate lock released. Another valve releases the pressure in the control cylinder, and the spring attached to the control level causes it to descend rapidly until it engages the timer. The descent is slower after the timer is engaged and thereby limits turbine acceleration until the exciter voltage builds up.

To shut down the turbine it is required that the gates be closed slowly to the no-load position before the circuit breaker opens. De-energization of the solenoid opens a valve which allows the control lever to raise slowly and close the gates. The oil to the gate lock cylinder, pilot valve and relay valve is shut off slowly. Spring pressure firmly applies the gate lock and maintains it a long as the machine is shut d.wn.

Contacts are connected to the gate rod and are used with the automatic control to indicate zero gate opening and full-speed no-load gate opening. Contacts for operating the automatic control functioning in response to speed changes are provided on either the generator shaft or the permanent magnet generator shaft.

Voltage Regulator

A voltage regulator applied to a hydroelectric generator provides a method of maintaining a desired voltage at that point and of adjusting for the amount of reactive power which it is desired to have the generator furnish. The latter adjustment is made possible by the fact that a change in the field current of a generator connected to a system does not change its load but does change its power factor. A decrease in the generator field current makes its power factor less lagging, and an increase in its field current makes its power factor more lagging. Thus, to vary the reactive load taken by the generator, it is merely necessary to change the adjustment of the voltage regulator

A typical voltage regulator, suitable for either automatic or self-synchronizing is shown in Figure 12. It is brought into service by the closing of generator circuit breaker *52*, providing the transfer switch is in the regulating position. The regulator transfer switch has "Manual", "Indicating," and "Regulating" positions. In the "Manual" position, the motor-operated rheostat may be raised or lowered by hand through the contacts *CSR* and *CSL* of a local control switch. In the "Indicating" position, the voltage regulator performs all its functions, except that it does not move the motor-operated rheostat. In the "Regulating" position, the voltage regulator is in full operation.

The d-c motor which drives the motor-operated rheostat has a split series field. Energization of the armature in series with one field will raise excitation, the other will lower excitation. Limit switches prevent excessive travel of the mechanism. Cam switches are connected in the rheostat motor circuit to run the rheostat to the no-load position after the generator field circuit breaker *41* opens on shutdown. It is sometimes preferred to have the regulator in service before the generator is connected to the line. For such operation, the cams can be eliminated on the exciter field rheostat, and the voltage adjusting rheostat can be equipped with cams to return the motor-operated voltage-adjusting rheostat to the no-load position when the machine is shut down. For either arrangement, no-load field excitation is present during starting of the generator.

Contactors *NR* and *NL* control the exciter rheostat motor under direction of the voltage element of the regulator. The latter is connected to generator potential transformers as shown in Figure 12.

An indication comes from the voltage regulator element that a raise in excitation is necessary by the closing of contact *VR*. Contactor *NR* is picked up by this action, and it operates the motor-operated rheostat and antihunt coil *NH*. The latter functions to open contact *VR* mechanically before a rise in voltage is effected by the generator. Contact *VR* closes again, if, after a time delay, an adequate rise in voltage is not effected. Similarly, a demand for reduction in voltage involves contact *VL*, contactor *NL* and antihunt coil *NH*.

Sudden wide changes in voltage demand more rapid changes in excitation than normal operation through the motor-operated rheostat will provide. In this

Figure 9. General schematic of water wheel governor

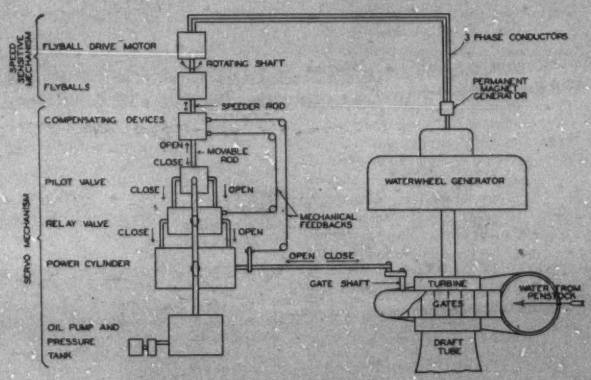

case, contacts *AR* and *AL* operate the quick raise contactor *QR* or the quick lower contactor *QL*. These contactors energize the antihunt coil *QH* and also switch the field forcing or field reducing resistors into the circuit.

With generators operated in parallel, the division of kilowatt load between the machines is unaffected by the voltage regulator, but the division of reactive power is affected directly by the operation of the regulator. In cases where the reactive drop between generators is low, such as in feeding a bus directly and not through transformers, satisfactory operation may be obtained by giving the regulator a drooping characteristic from a cross current compensator energized from a current transformer.

The motor-operated voltage-adjusting rheostat shown in the circuit of the voltage element of the regulator in Figure 12 provides a means of setting the regulator to regulate the voltage at the value at which it is to be maintained. If there is an operator at the station, the voltage-adjusting rheostat need not be motor operated. If the station is to be remotely controlled, the voltage adjusting rheostat will be motor operated when the reactive power flow is to be adjusted remotely and manually operated when a fixed setting is adequate.

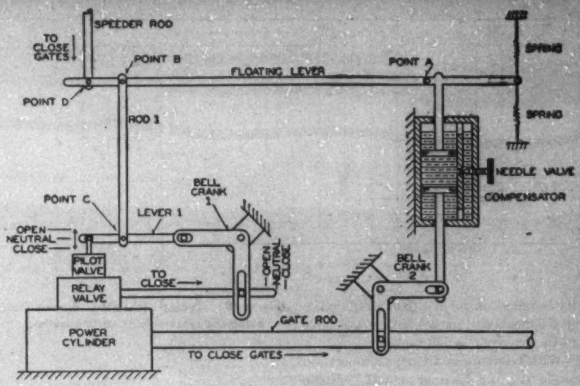

Figure 10 (above). Details of mechanism for moving gate rod

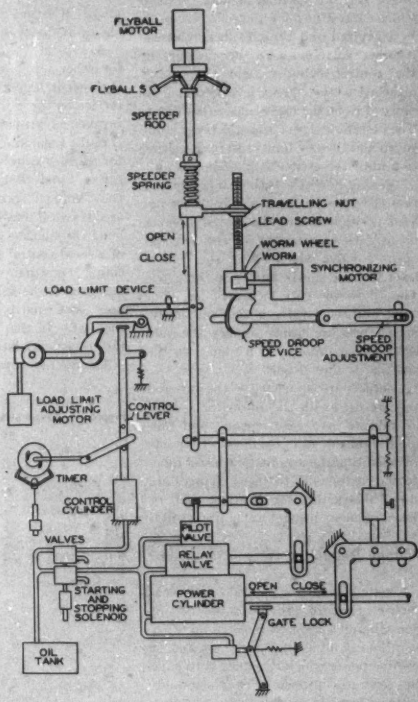

Figure 11. Control devices of a hydraulic governor

Automatic Synchronizer and Speed Matcher

Figure 13 shows the connections of a speed matcher and an automatic synchronizer. It will be noted from this diagram that the speed matcher and automatic synchronizer are put into service when relay *25X* is energized.

The balanced torque type speed matcher indicated is a device in which two synchronous motor-driven centrifugal devices develop opposing torques on a balanced beam. When the torques are unbalanced, the beam will close one or the other of two contacts, depending upon which torque is the greater. These contacts are connected to auxiliary relays *15BX* and *15GX*. Contacts of relays *15 BX* and *15GX* operate in the circuit of the governor synchronizing motor to raise or lower the speed of the generator. Thus, the speed matcher properly adjusts the speed of the generator, so that the automatic synchronizer can close the generator circuit breaker.

An automatic synchronizer should meet the following requirements:

1. The circuit breaker closing coil should be energized at an exact time in advance of synchronism, so that the time consumed by the circuit breaker in closing is just equal to the time consumed by the generator in arriving at exact synchronism.

2. The synchronizer should close the circuit breaker only if the frequency difference between the two voltages is less than a predetermined value.

These requirements are met by the automatic synchronizer shown in Figure 13. The synchronizer is connected to the generator and bus potential transformers to give a dark lamp beat voltage across dry-type full-wave rectifiers *1* and *2*. The

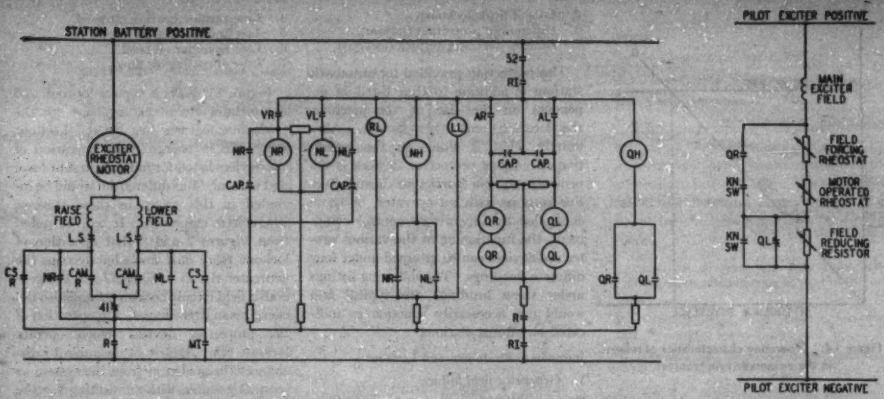

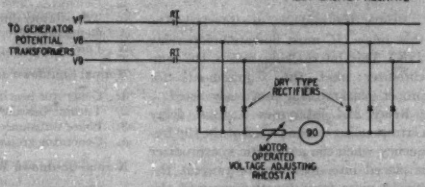

Figure 12. Typical voltage regulator schematic

dry type rectifier output voltage is essentially a pulsating direct voltage of sine wave form, having a frequency equal to the frequency difference between the generator and bus voltages.

A constant negative bias is applied to triode *1* through adjustable resistor *X* and a constant negative bias is applied to triode *2* through adjustable resistor *Y*.

The output of rectifier *2* provides a negative bias for both the triodes which is proportional to the phase angle difference between the generator and bus voltages. Thus, minimum negative bias is obtained when the phase angle difference is zero. This being the only varying bias on triode *2*, adjustment of resistor *Y* makes it possible to have relay *25C* energized at any desired phase angle difference between the two voltages.

Triode *1* is furnished with a second varying bias from the output of rectifier *1*. When the frequency difference is zero, the voltage across capacitor *C* is equal to the output voltage of rectifier *1*. When the phase angle between the generator and the bus voltages is changing from 180 degrees towards zero, the output voltage of rectifier *1* decreases, leaving the voltage of capacitor *C* higher than the output voltage of the rectifier. The amount the capacitor voltage is higher than the rectifier voltage under this condition is proportional to the frequency difference. The discharge current of the capacitor *C* produces a voltage drop across resistor *Z*, the magnitude of this voltage being proportional to the frequency difference. The voltage across resistor *Z* provides a varying bias to triode 1 in addition to the varying bias provided by the output of rectifier *2*. Thus, triode *1* is provided with a bias that varies with the actual phase angle difference, as well as the rate at which the phase angle is changing. Resistor *X* is adjusted so that the constant negative bias provided is just low enough to operate relay *25B* at zero phase angle difference when the frequency difference is zero. Relay *25B* then will operate at an advanced phase angle position, the amount of advance being proportional to the frequency difference. The amount of phase angle advance desired is obtained by adjustment of resistor *T*.

Figure 15 indicates the operating characteristics of relays *25B* and *25C*. Relay *25B* closes its contacts at a phase angle in advance of synchronism proportional to the frequency difference between the two voltages according to line *a*. Relay *25C* closes its contacts at a fixed phase angle in advance of synchronism according to line *b*. The intersection of lines *a* and *b* of Figure 14 indicates the maximum frequency difference between the two voltages at which the circuit breaker will be closed.

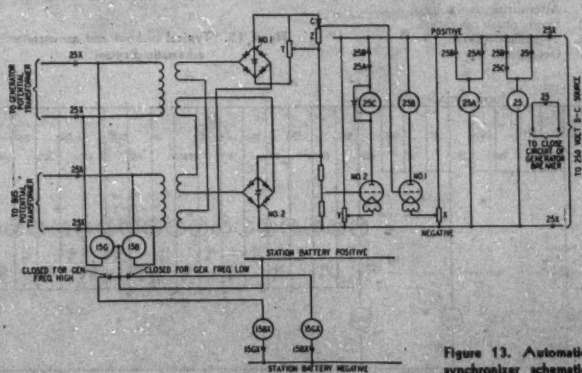

Figure 13. Automatic synchronizer schematic

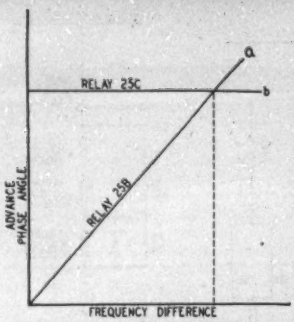

Figure 14. Operating characteristics of relays in the automatic synchronizer

Relays *25B* and *25C* are interlocked so that relay *25C* must operate before relay *25B*. This interlocking makes the synchronizer meet the requirements for proper synchronizing previously listed.

Relay *25A* interposes a time delay corresponding to one period of the slip frequency when the automatic synchronizer is placed into operation to prevent the synchronizer from functioning until the voltages on the component parts are stabilized.

Relay *25* is energized by relays *25B* and *25C* to energize the generator circuit breaker closing circuit. This relay can not be energized if either of the triodes fail.

Protection

The American Standards Association lists the following minimum protection for automatic hydroelectric generators.

1. Alternating overvoltage.
2. Single phase operation.
3. Thermal overload.
4. Overspeed.
5. Loss of field (lockout).
6. Differential protection (lockout).
7. Bearing overtemperature (lockout).

The protection provided for automatic stations in addition to that listed is dependent on the size of the machine, the location, and other factors. Also, exactly what is done on the operation of various protective devices is dependent on the particular installation. For stations with an operator, or those controlled by supervisory control equipment, the functioning of the various protective devices can be grouped under four different headings. The following listings under these headings are typical and would not necessarily function as indicated on all installations.

Immediate Shutdown and Lockout

1. Generator field failure.
2. Generator differential relay operation.
3. Transformer differential relay operation.
4. Generator overvoltage.
5. Low station battery voltage.

Normal Shutdown and Lockout

1. Generator bearing overtemperature.
2. Turbine bearing overtemperature.
3. Phase unbalance.
4. Generator ground relay operation.

Normal Shutdown Without Lockout

1. Overspeed.
2. Generator thermal overload.
3. Governor oil pressure failure.
4. Single or reverse phase.
5. Generator overcurrent.
6. Transformer overtemperature.
7. Generator winding overtemperature.
8. Incomplete starting sequence. (Often used to lockout).
9. Bearing oil pressure failure. (Often used to lockout).

Annunciator and Alarm—No Shutdown

1. Loss of generator bearing cooling water.
2. Loss of turbine bearing cooling water.
3. Low generator bearing oil level.
4. Low turbine bearing oil level.
5. Low transformer oil level.
6. Low governor oil level.
7. Loss of cooling air flow.

Figure 15 shows a typical lockout and annunciator circuit arrangement for the protective features just listed. Lockout relay *86E* is energized by operation of the devices listed for immediate shutdown and lockout. Bus differential would be included in this group in those stations where it is employed. It will be noted from Figures 7 and 8 that operation of lockout relay *86E* immediately trips the generator circuit breaker *52* and the generator field circuit breaker *41* and also de-energizes master relay *4*. On operation of the protective devices which operate lockout relay *86E*, it is desirable to disconnect the generator from the system as soon as possible without waiting for the turbine gates to reach the no-load position.

Lockout relay *86N* is energized by operation of the devices listed for normal shutdown and lockout. As shown in Figures 7 and 8, operation of relay *86N* only opens the circuit to the master relay *4*. The shutdown for this operation is the same as a shutdown by operation of the *1 STOP* contact as previously described.

Lockout relays *86E* and *86N* both must be reset manually before the generator can be restarted.

The protective devices for normal shutdown without lockout operate directly on master relay *4*. Figures 7 and 8 show each of these protective devices short-circuiting the coil of relay *4* to cause it to release and open its seal-in contact. Shutdown thus follows the same procedure as for shutdown by operation of the *1 STOP* contact. When shutdown results from any of these conditions, the unit can be restarted without the necessity of manually resetting any devices.

The last group of protective devices listed only operate annunciator drops and

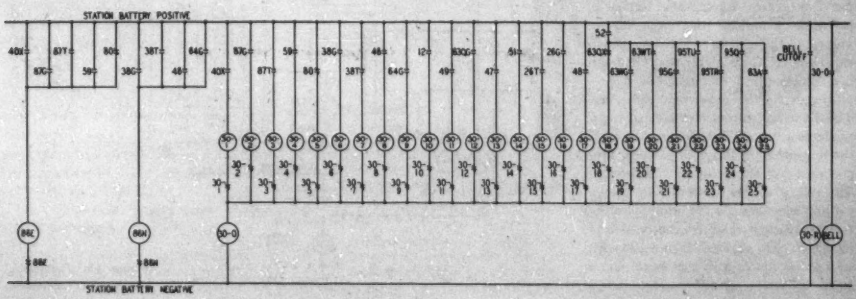

Figure 15. Typical lockout and annunciator schematic diagram

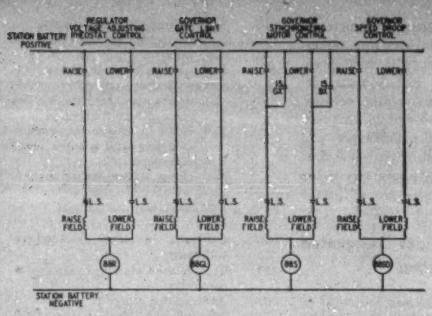

Figure 16. Schematic diagram for motor operated controls

sound an alarm as shown in Figure 15. All of the other protective devices which shutdown the unit also are shown operating annunciator drops and sounding the alarm.

The annunciator consists of drops and a latching type alarm relay *30*. Operation of any of the protective devices energizes an individual drop in series with the operating coil *30O* of the latching relay. Operation of the annunciator drop opens its circuit. Operation of relay *30* completes a circuit to the alarm bell.

Closing the bell cutoff contact energizes the reset coil *30R* of the latching relay and silences the alarm.

Governor and Regulator Control

Figure 16 shows split series field motors for the four controls which make it possible to adjust for the desired operating characteristics. The *Raise–Lower* contacts indicated can be contacts of local control switches or contacts actuated by supervisory control equipment. It is to be noted that the governor synchronizing motor also is controlled by contacts of the speed matcher when automatic synchronizing is employed.

Supervisory Control

Remote control equipment often is applied to automatic hydroelectric stations. Economic considerations usually dictate the use of supervisory control equipment to provide the necessary controls and indications.

Supervisory control equipment as manufactured today can be operated over a single pair of telephone wires, a power-line carrier channel, or a space radio channel. The single channel means is all that is required for the necessary controls, amp indications, and selective telemetering indications. This is indicated in block diagram form in Figure 17.

1. *Start-Stop* control of generators with supervision of generator circuit breakers.
2. Control of governor synchronizing motors with simultaneous telemetering of real power output.
3. Control of regulator voltage adjusting rheostats with simultaneous telemetering of reactive power output.
4. Control and supervision of other circuit breakers in station.
5. Supervision of generator lockout.
6. Supervision of annunciator.
7. Supervision of *Local-Remote* transfer switch.
8. Telemetering of bus voltage.
9. Telemetering of headwater level.
10. Communication.

Other functions which may be performed by the supervisory control are dependent on the requirements of the particular installation. The following additional functions sometimes are provided by the supervisory control equipment.

1. Control of governor gate limit with simultaneous telemetering of gate limit position.
2. Control of governor speed droop with telemetering of speed droop position.
3. Control and supervision of headwater gates or valves.
4. Control of diversion and reject spill gate position with simultaneous telemetering of gate position.
5. Supervision of door giving access to hydroelectric station.

The supervisory control equipment at the hydroelectric tation usually is inco porated as part o the local control and protective relaying switchboard. The supervisory control and telemetering equipment is shown mounted on the left-hand panel of the rear view in Figure 5.

Figure 18 shows the front and rear view of a typical supervisory control dispatching office unit. The supervisory control keys and lamps, as well as the telemetering receivers, are mounted on the front stationary panel, and the supervisory control relays are mounted on the rear swing panel.

Conclusion

Modern automatic generating stations are the result of the technical advances in this field that have been made over a period of more than 25 years. The reli-

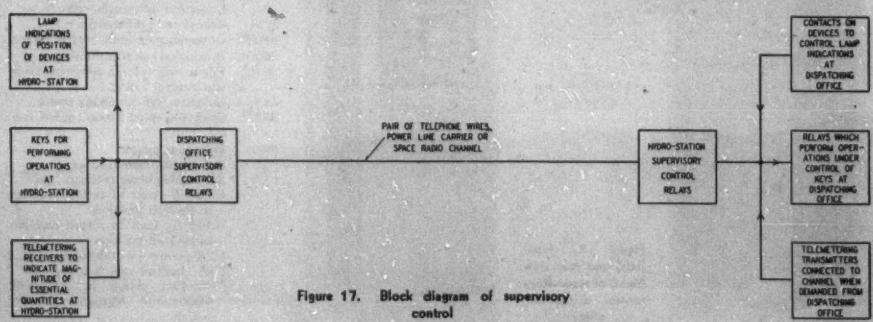

Figure 17. Block diagram of supervisory control

able performance and satisfactory operation of automatic control on small machines has led to its use with progressively larger sizes.

The justification of automatic control is purely economic. While in most cases a direct reduction of operating costs are obtained, there are others where the economies are realized indirectly.

The factors which must be studied by the engineer contemplating or designing an automatic hydroelectric station are as follows:

1. Type of hydraulic turbine.
2. Type of hydraulic governor.
3. Size of generator.
4. Design of generator.
5. Size of system.
6. Impedance of interconnection to system.
7. Operating requirements.
   - (a). Point of control.
   - (b). Personnel in attendance.
   - (c). Telemetering requirements.
   - (d). Type of channel used for remote control and telemetering.
   - (e). Conditions under which machine is started and stopped.
   - (f). Dispatching and loading program.

Devices are available for building control around any reasonable operating requirement for ordinary generating equipment. Modern facilities for telemetering and supervisory control over wire, power-line carrier channels, or radio channels enable the designer to include many desirable features in the operating scheme. Advances in relay and switchboard construction have made maintenance and operation simpler, and at the same time have brought improved appearance to the control room.

Appendix. Devices Designated in Figures

1. Start—stop elements.
4. Master relay.
12. Generator overspeed contact (closes at 125 per cent synchronous speed).
13X. Generator synchronous speed contact (open at 95 per cent synchronous speed and above).
13Y. Generator synchronous speed contact (closed at 95 per cent synchronous speed and above).
14. Generator underspeed contact (closed at 50 per cent synchronous speed and below)
15B. Speed matcher bus motor.
15BX. Speed matching auxiliary relay (to lower speed).
15G. Speed matcher generator motor.
15GX. Speed matching auxiliary relay (to raise speed).
20. Generator brake timing relay.
25. Automatic synchronizer.
- *25A* delays synchronizing for one cycle of heat frequency.
- *25B* closes in advance of synchronism proportional to frequency difference.
- *25C* closes at fixed phase angle in advance of synchronism.

25X. Auxiliary relay to energize device *25*.
26G. Generator winding overtemperature relay.
26T. Transformer winding overtemperature relay.
30. Annunciator relay.
- *30I* individual drops.
- *30O* operate coil to sound alarm.
- *30R* reset coil to silence alarm.

33NL. Interlock closed from zero to no-load opening of turbine gates.
33Z. Interlock closed at zero opening of turbine gates.
38G Generator bearing thermal relay.
38T. Turbine bearing thermal relay.
40 Field failure relay.
40X. Auxiliary timing relay for device *40*.
41. Generator field circuit breaker.
46. Generator phase balance relay.
47. Single and reversed phase relay.
48. Incomplete sequence timing relay
49. Generator thermal overload relay.
51. Generator overcurrent relay.
52. Generator circuit breaker.
59. Generator overvoltage relay.
63A. Cooling air flow relay.
63QG. Governor oil pressure relay.
63QB. Bearing oil pressure relay.
63QX. Auxiliary relay for device *63QB*.
63WG. Loss of generator bearing cooling water relay.
63WT. Loss of turbine bearing cooling water relay.
64G. Generator ground current relay.
65S. Governor solenoid (energized to open gates de-energized to close gates).
80. Station battery undervoltage relay.
86E. Lockout relay—immediate tripping of generator circuit breaker (electrically operated, manually reset).
86N. Lockout relay—normal shutdown (electrically operated, manually reset).
87G. Generator differential relay.
87T. Transformer differential relay.
88GL. Governor gate limit control motor.
88QX. Bearing oil pump motor relay.
88R. Regulating voltage adjusting rheostat control motor.
88S. Governor synchronizing motor.
88SD. Governor speed droop control motor.
90. Voltage regulator.
- *AR*—quick raise contact.
- *AL*—quick lower contact.
- *CAM–R*—cam to return rheostat to no-load position.
- *CAM–L*—Cam to return rheostat to no-load position.
- *CSR*—control switch raise.
- *CSL*—control switch lower.
- *I*—contact closed in indicating position of regulator transfer switch.

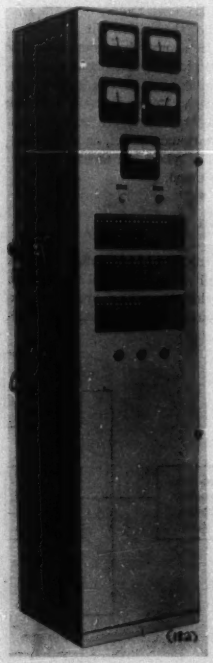

Figure 18. Front (left) and rear view (right) of supervisory control dispatching office

LS—limit switch.
M—contact closed in manual position of regulator transfer switch.
NR—normal raise contactor.
NL—normal lower contactor.
NH—Antihunt coil (normal raise and lower contacts).
QH—Antihunt coil (quick raise and lower contacts).
QR—quick raise contactor.
QL—quick lower contactor.
R—contact closed in regulating position of regulator transfer switch.
RL—red light indicating raise required.
LL—green light indicating lower required.
VR—raise contact (voltage element).
VL—lower contact (voltage element).
95G. Generator bearings low oil level contact.
95Q. Governor low oil level contact.
95TR. Transformer low oil level contact.
95TU. Turbine bearings low oil level contact.

References

1. Automatic and Partial Automatic Hydroelectric Plants, *Proceedings*, 53rd Convention National Electric Light Association, 1930, pages 557–75.

2. Hydroelectric Power Plants, A. H. Frampton. Electrical Engineering, volume 65, April 1946, pages 151–9.

3. Electrical Transmission and Distribution Reference Book (book). Westinghouse Electric Corporation, Pittsburgh, Pa. Chapter 7, Machine Characteristics.

4. Governing the Pickwick Landing Hydro Turbine, J. J. Ring. *Power* (New York, N. Y.) November 1941, pages 98–100.

Discussion

R. M. Alspaugh (Tennessee Valley Authority, Knoxville, Tenn.): This paper by Mr. Brown and Mr. Derr on the automatic control of generating stations is most timely. Present high operating costs and growing pressure to reduce power rates have stimulated a keen interest in changing old stations and designing new stations for automatic and supervisory control. The early installations of such equipment were limited to stations of small capacities, but the present trend is to employ automatic control for larger generating units.

The authors have done an excellent job of summarizing the many items to be considered in the application of automatic control for unattended hydroelectric plants. They have emphasized that the responsibility of the control engineer does not stop at the switchboard. A thorough knowledge of the operating features of all major powerhouse equipment is necessary for the proper application of automatic control.

Little has been published on automatic control installations during recent years. It is hoped that the present paper will stimulate sufficient interest to encourage the preparation of similar papers, especially papers on recent installation and operating experience of stations under automatic and supervisory control.

To date, the Tennessee Valley Authority's experience with unattended generating plants has been limited to the Ocoee number 3 plant which has one 30,000-kva generating unit and which was put in operation April 30, 1943. The excellent performance of this station has encouraged the consideration of supervisory and automatic control for several existing substations and two new hydroelectric stations.

It now is planned to use automatic starting equipment in an unattended plant consisting of two 27,800-kva generating units and full automatic control for a new single-unit plant of 38,888-kva capacity. The first plant will have direct wire supervision from a control building in the immediate vicinity. The second plant will be supervised from this same control building by power line carrier channels over a 17-mile 66-kv transmission line.

The control features of the Ocoee number 3 plant and its operating record have been discussed.[1] It is suggested that the latter paper and a recent article[2] are references for the present paper.

References

1. Supervisory Control of 30,000-Kva Hydroelectric Plant, C. W. Bohner, A. P. Maness. AIEE Transactions, volume 65, 1946, June section, pages 337–42.

2. Automatic Hydro Stations Prove Profitable, G. C. George, S. O. Schamberger. *Electric Light and Power* (Chicago, Ill.), December 1946.

The Voltage Drop in the Welder Throat Loaded With Ferromagnetic Materials

G. M. STEIN
MEMBER AIEE

Synopsis: The magnetic flux distribution in a welder throat, containing two steel sheets, is calculated as a potential field. On this basis, the flux density in the sheets and the flux change caused by their presence in the throat are computed, and furnish the voltage drop caused by the sheets if they would be unsaturated. Actually, the sheets are saturated, and this condition is considered by approximating the magnetization curve of the welding material with a broken line. The corresponding voltage components are calculated for various dimensions of the throat and of the sheets, for different positions of the sheets in the throat, and for different welding currents, and agree satisfactorily with test results.

THE resistance welding machine can be considered as a single phase transmission system. Its power is supplied through the welding transformer and the welder throat represents the transmission line; the welding spot can be considered as the load. Each of these three elements will consume a resistive and reactive voltage component whereby the over-all efficiency is relatively low and the regulation becomes very high as compared with a regular power transmission system.

The voltage components in the throat and in the welding spot essentially determine the required kva rating of the transformer, and are, therefore, of special interest for its designer

In a paper by J. J Riley and C. E Smith,[1] these two voltages have been determined experimentally. The welder throat offers hereby a special problem because the material to be welded very often extends deeply into this transmission line and its magnetic flux distribution and its voltage drop are altered considerably. It shall be the object of this paper to calculate this influence of the welding materials on the fields and voltages of the welder throat, and to compare the computed values with the test results obtained by Riley and Smith [1]

The calculation is made under the assumption of a inusoidal current–time curve. According to Figure 1, introduce

I = welding current (amperes effective)
a = horn spacing (inches)
D = diameter of throat bars (inches)
t = thickness of each of the two steel sheets to be welded (inches)
a_1; a_2 = distances of sheets from each throat bar (inches)
b = width of sheets (inches)
d = distance of sheets in throat (inches)

Calculation of the Field

The current loop of the welder throat, shown in Figure 1, represents the excitation of the magnetic flux in the steel plates. In this capacity, the loop can be considered as being composed of three separate sections which are the vertical inner end of the throat, the vertical electrode holders, and the two horizontal throat bars. Imagine that these three sections excite three separate fluxes in the plates which can be calculated. Such an analysis is made below for the flux excited by the horizontal current flow, and shows that this flux alone is saturating the section of the steel plates which is extending into the welder throat. Consequently, the additional excitation, resulting from the two vertical current flows in front and back, will have only a secondary effect on the flux and on the voltage drop created by this section of the plates. The load, represented by the rest of the steel which remains outside the throat, will be minor as compared with the effect of the inside portion on the power supply unless the sheets extend only a short distance into the throat; but then the whole influence of the work pieces on the performance of the welder is so small that it will be of no particular interest to the designer. For these reasons, only the horizontal current flow is considered in the excitation of the plates.

The magnetic flux, entering the iron, depends on the field distribution in the surrounding air space. In the calculation of this latter field, the steel sheets are assumed to be of infinite permeability so that their surface is on equal potential. As a result, all instantaneous values of the fluxes and flux densities are proportional to the instantaneous welding current, and change with the time in sine waves, if the current waves are undistorted. The effect of a saturation of the steel sheets will be taken care of later.

Because only the space inside the welder throat is considered, and, because

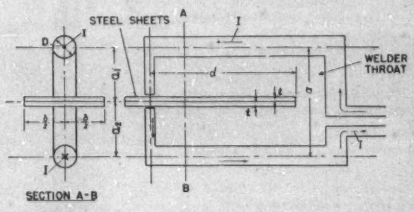

Figure 1. Position of steel sheets in welder throat

Paper 47-62, recommended by the AIEE committee on electric welding for presentation at the AIEE winter meeting, New York, N. Y., January 27–31, 1947. Manuscript submitted October 18, 1946; made available for printing December 30, 1946.

G. M. Stein is with Westinghouse Electric Corporation, Sharon, Pa.

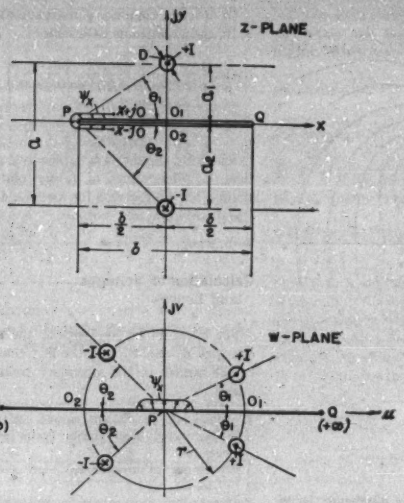

Figure 2. The conformal transformation

its end effect is neglected, the condition of infinitely long bars and sheets can be substituted; that is, a 2-dimentional magnetic field is computed in an x–y plane located perpendicular to the third bars, as shown in Figure 2. The cross section of these bars is approximated by a circular form in whose center the current I can be considered as concentrated for the determination of the magnetic field outside the copper. The steel sheets are replaced by a single line P–Q over which the currents $+I$ and $-I$ appear under angles Θ_1 and Θ_2. By introducing a complex variable $z=x+jy$, the x–y plane becomes a z plane, and can be transformed conformally into the upper half of an auxiliary w plane of $w=u+jv$ by the function

$$w=r\sqrt{\frac{b/2+z}{b/2-z}} \qquad (1)$$

derived in Appendix I. In this w plane, the sheets appear as the whole u axis, and their edges P and Q are shifted into the zero point and into the infinity. The currents $+I$ and $-I$ are located on a circle of the radius r with P as center and appear under the angles Θ_1 and Θ_2 over the u axis. This circle corresponds to the y axis in the z plane, and intersects the u axis in O_1 and O_2 which are the upper and lower midpoints of the plates in the z plane.

In the z plane and in the w plane, the steel sheets represent an equipotential line of the magnetic field. Consequently this boundary can be replaced in the w plane by the images of $+I$ and $-I$ obtained with respect to the u axis with the same sign. In this way, solve for

φ = potential function (gilberts peak value)
ψ = flux function (maxwells/centimeter, peak value)

in the w plane

$$\chi=\psi+j\varphi=0.283I\times \log\frac{(w-re^{+j\theta_2})(w-re^{-j\theta_1})}{(w+re^{-j\theta_2})(w+re^{+j\theta_1})} \qquad (2)$$

By substituting w of equation 1, this field is transformed into the z plane. By this method and for the example $a_1=a_2$ and $b/a=2$, the flux distribution of the w plane is plotted in Figure 3, and the corresponding actual throat field of the z plane is constructed in Figure 4, as explained in Appendix II.

In order to compute

B_x = flux density in steel plates at x (gausses peak value)
B_m = maximum value of B_x on center line of plates (gausses peak value)

find the flux ψ_x, entering the plates between $x+j$ O and $x-j$ O, as

$$\psi_x=\psi(x;\ y=-O)-\psi(x;\ y=+O) = \chi(x-jO)-\chi(x+jO) \qquad (3)$$

and obtain

$$B_x=0.198(\psi_x/t) \qquad (4)$$

Combine also

$$\lambda=a_1/a_2$$

$$\tan\theta_1=\frac{a}{b}\times\frac{2\lambda}{1+\lambda}$$

$$\tan\theta_2=\frac{a}{b}\times\frac{2}{1+\lambda}$$

$$\tan\theta=\frac{a}{b},\ \text{for}\ \theta_1=\theta_2=\theta\ \text{or}\ \lambda=1 \qquad (5)$$

and derive, according to the equations 1 to 4,

$$B_x=0.112\frac{I}{t}\times\left(\tanh^{-1}\sqrt{\frac{1-\left(\frac{2x}{b}\right)^2}{1+\left(\frac{a}{b}\frac{2\lambda}{1+\lambda}\right)^2}}+\tanh^{-1}\sqrt{\frac{1-\left(\frac{2x}{b}\right)^2}{1+\left(\frac{a}{b}\frac{2}{1+\lambda}\right)}}\right) \qquad (6)$$

Table I. Comparison of Calculated Values With Test Results of the Resistive and Reactive Voltage Components Caused by Two Steel Sheets

Distance in Throat d=30 Inches

Sample Number	Thickness of Each Sheet t (Inches)	Secondary Welding Current I (Amperes)	Horn Spacing a (Inches)	Sheet Width b (Inches)	Reactive Voltage V_{XS} (Volts) Tested	Reactive Voltage V_{XS} (Volts) Calculated	Resistive Voltage V_{RS} (Volts) Tested	Resistive Voltage V_{RS} (Volts) Calculated
1	0.090	15,000	8	36	1.82	2.02	0.48	0.47
2	0.090	15,000	8	18	1.66	1.62	0.31	0.21
3	0.090	15,000	8	9	1.08	1.02	0.14	0.10
4	0.119	18,000	8	36	2.42	2.59	0.68	0.78
5	0.119	18,000	8	18	2.10	2.02	0.42	0.36
6	0.119	18,000	8	9	1.42	1.35	0.21	0.14
7	0.119	18,000	8	36	2.42	2.59	0.68	0.78
8	0.090	15,000	8	36	1.82	1.98	0.46	0.43
9	0.060	12,000	8	30	1.21	1.29	0.24	0.17
10	0.032	8,300	8	36	0.69	0.75	0.09	0.06
11	0.119	18,000	16	36	2.41	2.02	0.72	0.72
12	0.090	15,000	16	36	1.83	1.53	0.46	0.40
13	0.060	12,000	16	30	1.22	0.95	0.25	0.15
14	0.032	8,300	16	36	0.59	0.57	0.09	0.05

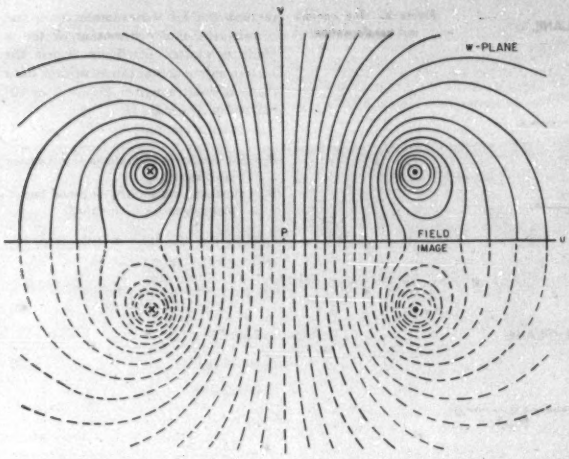

Figure 3. Magnetic flux distribution in the auxiliary w plane for $a_1=a_2$ and $b/a=2$

Introduce the factor

$$f_1=\sinh^{-1}\left(\frac{b}{a}\,\frac{1+\lambda}{2\lambda}\right)+\sinh^{-1}\frac{b}{a}\,\frac{1+\lambda}{2}$$

$$f_1=2\sinh^{-1}\frac{b}{a},\ \text{for } \lambda=1 \qquad (7)$$

f_1 is given in Figure 5 as function of b/a for $\lambda=1, 2, 4, 6$. The substitution of f_1 transforms the equation 6 for $x=0$ into

$$B_m=0.112\,\frac{I}{l}\,f_1 \qquad (8)$$

In order to find

ϕ = flux change caused by steel sheets (maxwells peak value)

determine

ϕ_s = total throat flux with steel plates (maxwells peak value)

ϕ_o = total throat flux without steel sheets (maxwells peak value)

and compute

$$\phi=\phi_s-\phi_o \qquad (9)$$

In particular, calculate

$$\phi_s=2.54d\left\{\chi\left[z=-j\left(a_2-\frac{D}{2}\right)\right]-\chi\left[z=+j\left(a_1-\frac{D}{2}\right)\right]\right\} \qquad (10)$$

according to equations 1 and 2, and obtain

$$\phi_o=0.722dI\log\left\{\frac{[1+\cos(\theta_1+\theta_2)]\times[1+\cos(\theta_1-\theta_2)]}{1/2[\cos(\theta_1-\theta_2)-\cos(\theta_1+\theta_2)](\cos\theta_1\cos\theta_2)^2}\left(\frac{b}{D}\right)^2\right\} \qquad (11)$$

The complex potential function, representing the field in an infinitely long welder throat without steel sheets, has the form

$$\chi_o=\psi_o+j\varphi_o=0.283I\log\left(\frac{z-ja_1}{a+ja_2}\right) \qquad (12)$$

from which ϕ_o is derived, like ϕ_s in equation 10, as

$$\phi_o=0.722dI\log\left(\frac{2a}{D}\right)^2 \qquad (13)$$

In order to compute ϕ from equations 9, 10, and 13, introduce the factor

$$f_2=\log\left\{\frac{1+\cos(\Theta_1-\Theta_2)}{[1-\cos(\Theta_1+\Theta_2)]\sin\Theta_1\sin\Theta_2}\right\}$$

$$f_2=4\log\frac{1}{\sin\Theta},\ \text{for } \Theta_1=\Theta_2=\Theta \text{ or } \lambda=1 \qquad (14)$$

in which Θ_1, Θ_2, and Θ are given by equation 6. The values of f_2 are plotted against b/a in Figure 5 for $\lambda=1, 2, 4, 6$. Use these curves and compute

$$\phi=0.722dIf_2 \qquad (15)$$

Calculation of Voltages and Losses

For unsaturated steel sheets, the flux densities B_x and B_m and the flux change ϕ will furnish in the secondary welding circuit

V = total voltage change caused by unsaturated steel sheets (volts peak value)

λ = reactance of unsaturated steel sheets (ohms)

P = total eddy current losses in unsaturated steel sheets (watts)

In the calculation of these values introduce also

W_x = specific eddy current losses in unsaturated steel sheets at x (watts/cubic inches)

F = frequency (cycles/second)

ρ = resistivity of steel sheets (ohms/cubic centimeters)

Note further that any change of the ratio $\lambda=a_1/a_2$, that is, of the position of the sheets between the throat bars Figure 1, is, according to Figures 5 and 6, of little influence on the values of the factors f_1 and f_2. Consequently, B_m and ϕ_s

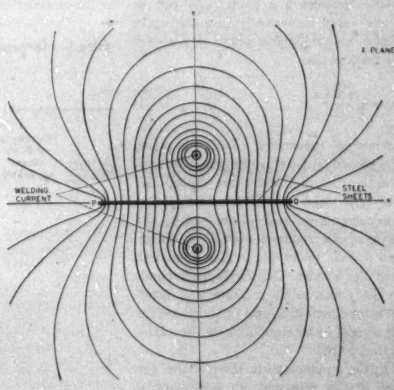

Figure 4. Magnetic flux distribution in the z plane of the welder throat for $a_1=a_2$ and $b/a=2$

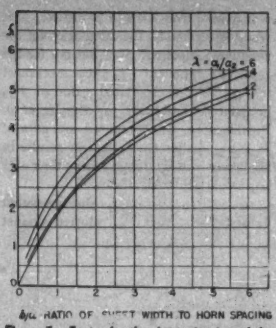

Figure 5. Factor for the determination of the flux density in the steel sheets

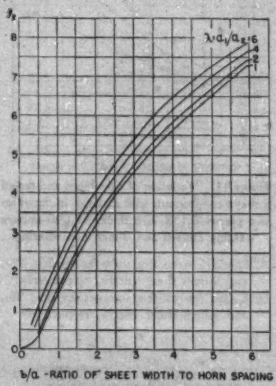

Figure 6. Factor for the determination of the flux change caused by the steel sheets

given by equations 8 and 15, and the steel sheet voltages, derived from B_m and ϕ, will be almost independent of this location of the load, as also claimed by the paper of Riley and Smith.[1] Therefore the remaining part of the analysis can be confined to the condition $a_1 = a_2$, or $\lambda = 1$, that is, to a centered position of the plates.

Approximate further the reactive component of the steel sheet voltage by the total voltage V and write

$$V = 4.44 10^{-8} F\phi$$
$$X = V/I \tag{16}$$

Substitute equation 15, and obtain

$$V = 3.2\ 10^{-8} F d f_3 I$$
$$X = 3.2\ 10^{-8} F d f_3 \tag{17}$$

Note that X is independent of I.

If the steel sheets are insulated from each other and skin effect is neglected, W_x can be written[2]

$$W_x = 0.0174 \frac{F^2 t^2}{\rho} B_x^2 \tag{18}$$

and furnishes

$$P = 2db \int_0^1 W_x d(2x/b) \tag{19}$$

In this equation, combine the factor

$$f_3 = \int_0^1 (B_x/B_m)^2 d(2x/b) \tag{20}$$

B_x/B_m and $(B_x/B_m)^2$ are given by equations 6 to 8, and are plotted in Figure 7 against $2x/b$ for $\lambda = 1$ and for $b/a = 0$, 1 and 4. A numerical integration of these curves furnishes f_3 as function of b/a in Figure 8. In this way, combine equations 18 to 20 into the form

$$P = 0.0348 \frac{F^2}{\rho} f_3 d b^3 B_m^2 \tag{21}$$

in which B_m has to be computed according to equation 8. For an estimate of the numerical range of this B_m, use $I/t =$ 84,000 to 250,000 and $b/a = 1.1$ to 4.5 according to Table III and Figures 12 and 13 of the paper of Riley and Smith.[1] With these values, obtain $f_1 = 1.4$ to 4.5 for $\lambda = 1$ from Figure 5, and find $B_m = 13{,}000$ to 126,000 gausses. Consequently, B_m will exceed the saturation limit of the steel sheets (about 20,000 gausses) in most cases.

In order to account for this saturation, the magnetization curve of the steel sheets, that is, its flux density B as function of its field strength H, is approximated by the broken line shown in Figure 9 in which B has the limit[4]

β_∞ = saturation value of the intrinsic flux density in the steel sheets (gausses)

The corresponding time values B_{Tm} and V_T of the maximum flux density and voltage of the steel sheets are plotted in Figure 10 against ωT ($\omega = 2\pi F$ and T = time in seconds) for a sinusoidal current I_T. In this chart, B_{Tm} assumes a trapezoidal shape, and V_T has a rectangular form which extends up to

$$T_\infty = \sin^{-1}\left(\frac{\beta_\infty}{B_m}\right) \approx \frac{\beta_\infty}{B_m} \tag{22}$$

The shape of the curves agrees with those shown in Figure 19 of the paper of Riley and Smith.[1] In the approximation shown in Figure 10, compute

V_e = total effective value of V_T (volts effective)
V_1 = fundamental value of V_T (volts effective)

and find

$$\left.\begin{aligned} V_e &= V\sqrt{\frac{4}{\pi}\sin^{-1}\frac{\beta_\infty}{B_m}} \approx V\sqrt{\frac{4}{\pi}\frac{\beta_\infty}{B_m}} \\ V_1 &= V\frac{4}{\pi}\frac{\beta_\infty}{B_m} \end{aligned}\right\} \tag{23}$$

which furnishes

$$V_e^2 \approx V_1 V \tag{24}$$

The voltage V_1 also may be written, according to equations 8, 17, and 23,

$$V_1 = 0.365\ 10^{-8} F \beta_\infty f_4 d t, \text{ for } f_4 = f_3/f_1 \tag{25}$$

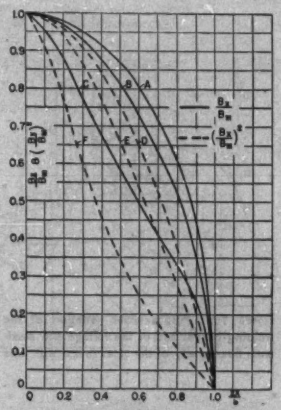

Figure 7. Distribution of the flux density in unsaturated steel sheets for $\lambda = a_1/a_2 = 1$

A and D — $b/a = 0$
B and E — $b/a = 1$
C and F — $b/a = 4$

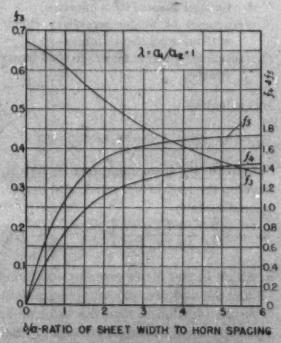

Figure 8. Factors for the determination of the eddy current losses and of the voltage components caused by the steel sheets

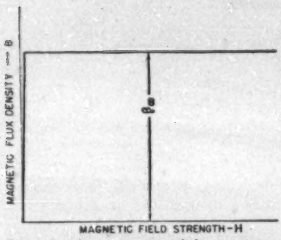

Figure 9. Approximation of the magnetization curve of steel including saturation

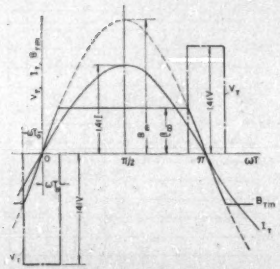

Figure 10. Approximate variation of the welding current and of the voltage and maximum flux density of the steel sheets with time

and is independent of I. For $\lambda=1$ take f_4 from Figure 8.

Introduce further

V_{XS} = reactive voltage component caused by steel sheets (volts effective)

V_{RS} = resistive voltage component caused by steel sheets (volts effective)

X_o = reactance of welder secondary circuit without steel sheets (ohms)

P_e = actual eddy current losses in steel sheets (watts)

and calculate

$$V_{XS}=\sqrt{(IX_o+V_1)^2+(V_e^2-V_1^2)}-IX_o$$

Substitute V_e^2 from equations 16 and 24, develop the root into a series, and derive, approximately

$$V_{XS}=V_1\left[1+\frac{1}{2}\frac{IX-V_1}{IX_o+V_1}\right] \tag{26}$$

in which V_1 and X are given by equations 17 and 25, and are, like X_o, independent of I. In addition to this, the value of V_1 is usually small as compared with IX and IX_o so that V_{XS} will change only little with the welding current I, in conformity with the findings of Riley and Smith.

For the computation of

$$V_{RS}=P_e/I \tag{27}$$

determine

$$P_e=P(V_e/V)^2 \tag{28}$$

by equations 17, 21, and 23, and obtain the approximation

$$V_{RS}=49.6\times10^{-4}\frac{F^2}{\rho}\beta_m f_5 bdI^2\times\left[1+13.3\left(\frac{\beta_m t}{IJ_1}\right)^2\right] \text{ for } f_4=f_1f_3 \tag{29}$$

which depends on I only slightly, as in the paper of Riley and Smith. For $\lambda=1$ obtain f_4 from Figure 8.

Comparison of Calculated Values With Test Results

With this analysis, compare the empirical formulas

$$V_{XS}=0.63Id+2I$$
$$V_{RS}=0.59t^{3/2}Id \tag{30}$$

developed by Riley and Smith[1] for the construction of their nomogram (Figure 21) for b=36-inch wide sheets. For a=8-inch horn spacing, that is, for $b/a=4.5$, take $f_2=6.2$ from Figure 6 for $\lambda=1$, and find $f_4=1.4$, $f_5=1.7$ from Figure 8. Choose further $B_m=20{,}000$ gausses and $\rho=12\times10^{-6}$ ohms/cubic centimeter as average properties of the sheet steel. Introduce these values into equations 17, 25, 26, and 29, and find for $F=60$, cycles/second

$$X=11.9\times10^{-6}d$$
$$V_1=0.61dI$$
$$V_{XS}=0.61dI\left[1+\frac{1}{2}\frac{IX-V_1}{IX_o+V_1}\right]$$
$$V_{RS}=1.82dI^2\left[1+4.1\left(\frac{t}{I}\cdot10^4\right)^2\right] \tag{31}$$

The calculated expression for V_{XS} is quite similar to the empirical value and the calculated expression of V_{RS} varies with the second power instead of the 3/2 power of the sheet thickness t. This difference may be in some extent caused by skin effect which is not considered in the analysis.

On the same basis, that is, for $B_m=20{,}000$, $\rho=12$, and $F=60$, the test results of V_{XS} and V_{RS}, given in Figures 12 and 13 of the paper of Riley and Smith,[1] and some additional experimental data are compared in Table I, for $d=30$ inches with a calculation made according to equations 17, 25, 26, and 29 developed in the foregoing text. In this tabulation, the test values of sample numbers 7 to 14 change very little if the horn spacing is increased from $a=8$ to 16 inches. This result is verified by the calculation for the resistive component V_{RS}, but not for the reactive component V_{XS} of the steel sheet voltage as the calculated value of V_{XS} is reduced noticeably for the larger a. Furthermore, the computed amounts of V_{RS} are smaller than the test results in the lower voltage range where their size has no particular significance.

In addition to this, the measured values of V_{XS} and V_{RS}, plotted against

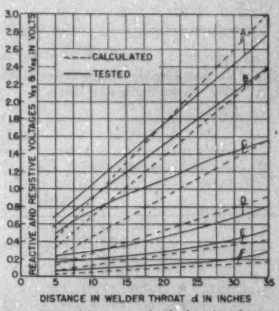

Figure 11. Variation of calculated and tested voltage components with distance in throat for two pieces 0.118 inch thick, 18,000-ampere welding current and 8-inch horn spacing

A, B, and C = reactive voltages for 36-, 18-, and 9-inch sheet widths, respectively

D, E, and F = resistive voltages for 36-, 18-, and 9-inch sheet widths, respectively

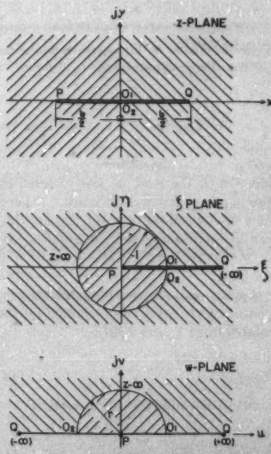

Figure 12. Development of the conformal transformation

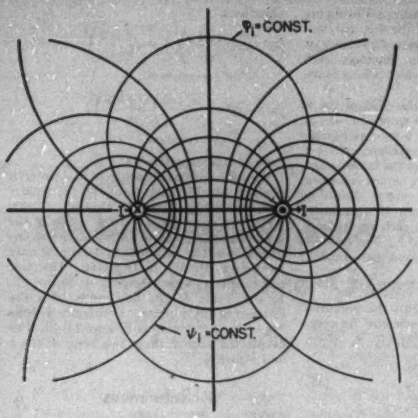

Figure 13. The magnetic field of an individual double line

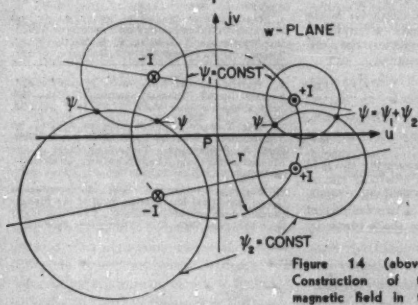

Figure 14 (above). Construction of the magnetic field in the auxiliary w plane

d for $t=0.118$ inches in Figure 13 of the paper of Riley and Smith [1] are compared with the corresponding calculated amounts in Figure 11 of this paper. These voltages are taken at $I=18{,}000$ amperes welding current and $a=8$-inch horn spacing. In the lower range of d, the computed voltage drops of Figure 11 are smaller than the test results, because the effect of the currents in the vertical electrode holders has been neglected in the calculation. This discrepancy is unimportant because for small distances d the values of V_{XS} and V_{RS} remain low, and, therefore, can have only a reduced influence on the over-all welding characteristic.

Appendix I. The Conformal Transformation

The conformal transformation, represented by equation 1, can be derived in two steps.

In the first step, the left half of the s plane, Figure 2 of the welder throat, is transformed into the interior of a unit circle in the center of a ζ plane of $\zeta=\xi+j\eta$, as shown in Figure 12.

This is done by the equation

$$\zeta=\frac{b/2+s}{b/2-s} \tag{32}$$

Hereby the imaginary axis of the s plane becomes the circumference of the circle in the ζ plane and the real axis of the two planes are transformed into each other. In particular, the edges P and Q of the steel sheets appear in the points zero and infinity of the ζ plane. The outside of its circle corresponds to the right half of the s plane so that the whole s plane is transformed uniquely into the whole ζ plane.

By a second transformation

$$w=r\sqrt{\zeta} \tag{33}$$

also shown in Figure 12, the inside of the unit circle in the ζ plane is reduced to the

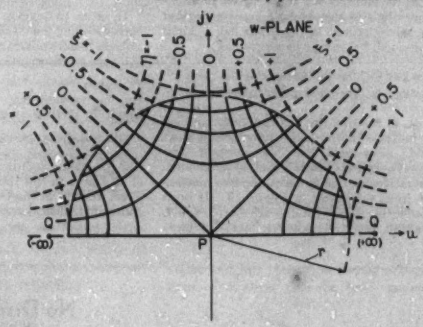

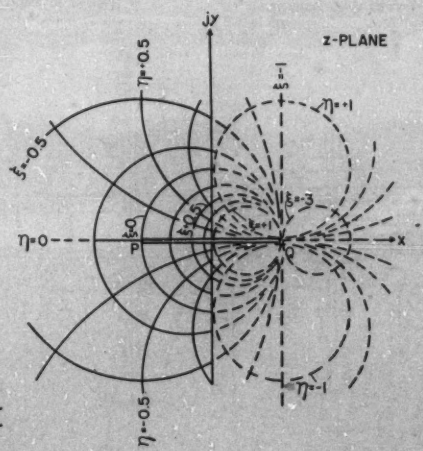

Figure 15. The coordinates of the conformal transformation

inside of one-half circle of the radius r in the auxiliary w plane of Figure 2. This half circle corresponds also to the left half of the z plane. As a result, the total z plane will go over into the upper half of the w plane, the real axis of which becomes the section P–Q of the steel plates, if the two transformations of equations 32 and 33 are combined into

$$w = r\sqrt{\frac{b/2+z}{b/2-z}} \tag{1}$$

Appendix II. A Graphical Method of Field Plotting

The magnetic flux distributions, shown in Figures 3 and 4 in the w plane of $w=u+jv$ and in the z plane of $z=x+jy$, are obtained by a graphical procedure. The field $\chi=\psi+j\varphi$ is excited in the w plane of Figure 2 by two double lines, that is, by a double line with the currents $+I$ and $-I$ located in the upper half of the w plane and by another such line located in the lower half. Their individual fields may be written as

$\chi_1=\psi_1+j\varphi_1$, for the upper double line
$\chi_2=\psi_2+j\varphi_2$, for the lower double line

if ψ_1, ψ_2 describe the flux functions, and φ_1, φ_2 indicate the potential functions of each field. The field lines ψ_i=constant and φ_i=constant ($i=1$ or 2), excited by an individual double line, are forming two families of circles, as shown in Figure 13. If both double line fields χ_1 and χ_2 are plotted in the w plane, their intersections furnish the resultant field χ. This is illustrated in Figure 14 by the construction of the flux distribution $\chi(u, v)$. The individual circles χ_1=constant and χ_2=constant intersect each other in points $\chi=\chi_1+\chi_2$ which belong to the resultant field, Figure 3.

In order to transform this field of the w plane into the z plane, the variable $\zeta=\xi+j\eta$ of the ζ plane (Figure 12) is used as parameter, that is, curves ξ=constant and η=constant are constructed in the w plane and in the z plane where these curves represent the special co-ordinate systems shown in Figure 15. The field then is transferred point by point from one such co-ordinate system into the other.

In the w plane, (obtain from equation 33)

$$\zeta=(w/r)^2 \tag{34}$$

This function $\zeta(w)$ represents the potential field in an inner corner whereby its components

$$(u/r)^2-(v/r)^2=\xi=\text{constant}$$
$$2(u/r)(v/r)=\eta=\text{constant} \tag{35}$$

form two families of hyperbolas

In order to develop the character of the corresponding ξ–η co-ordinate system in the z plane, its zero point is shifted into the point Q by the transformation

$$z=z-b/2 \tag{36}$$

Equation 32 then may be written

$$\zeta^*=-(\zeta+1)=b/z^* \tag{37}$$

The function $\zeta^*(z^*)$ is representing the field of a dipole in the point $z^*=0$ of the z^* plane, that is, in the point Q of the z plane. This dipole field consists of two families of circles which are given in the z plane by equations

$$\left(x-(b/2)\ \frac{\xi}{\xi+1}\right)^2+y^2=\left(\frac{b/2}{\xi+1}\right)^2,$$

for ξ=constant

$$(b/2-x)^2+\left(y-\frac{b/2}{\eta}\right)^2=\left(\frac{b/2}{\eta}\right)^2,$$

for η=constant (38)

derived from equation 32.

The calculations are confined to a centered position of the steel plates in the welder throat shown in Figure 1, that is, to fields which are symmetrical to the y axis of the z plane shown in Figure 2. Under this condition, it will be sufficient to determine only the field in the left half z plane. This half plane corresponds, according to Figure 12, to the inside of the half circle with the radius r in the w plane. Consequently, the ξ–η co-ordinate systems (Figure 15) have to be plotted only in these two areas of the z and w planes.

References

1. Influence of Magnetic Materials on the Welding Characteristics of Resistance Welding Materials J. J. Riley, C. E. Smith. AIEE Transactions volume 65, 1946 December section, pages 852-60.

2. Properties and Testing of Magnetic Materials (book) Thomas Spooner, McGraw-Hill Book Company New York N. Y., 1927 page 26.

3. The Theory of Functions as Applied to Engineering Problems (book), R. Rothe, F. Ollendorff, K. Pohlhausen. Technology Press of the Massachusetts Institute of Technology, Cambridge, Mass., 1942.

4. Magnetic Circuits and Transformers (book), Electrical Engineering Staff of the Massachusetts Institute of Technology, John Wiley and Sons, Inc., New York, N. Y. 1944, pages 8 and 21.

No Discussion

Modern Bearing Practice for Vertical Water Wheel Generators

C. M. LAFFOON
FELLOW AIEE

R. A. BAUDRY
MEMBER AIEE

IN THE United States approximately 80 billion kilowatt-hours of electric energy were produced in 1945 by hydroelectric power stations. This represents 35 per cent of the total electric energy produced by the electrical utilities industry in the country.

Water power resources are determined by nature, and the hydroelectric engineer has very little control over the quantity of water and the pressure heads available. Consequently, the hydroelectric turbine must be designed and proportioned to suit existing conditions. As a result, there is a wide range in speeds for which hydroelectric generating equipment must be designed in order to obtain economically the maximum power from the installation.

As the available head of water is normally small and the vertical type hydroelectric unit offers the greatest opportunity in utilizing the largest portion of the head, the use of this type of unit has become accepted practice.

The vertical type hydroelectric unit requires guide bearings to position the rotating parts and a thrust bearing to support the weight of the rotating parts and the thrust load due to the water head. It is normal practice for the thrust bearing and its supports to be provided as a part of the generator. The speed and proportions of the turbine and generator parts are such that one guide bearing normally is required for the turbine and one or more for the direct coupled generator.

The need for bearings of greater size and capacity has necessitated improvements in design, manufacturing procedures, and lubrication. The required information has been obtained from laboratory tests and field experience.

A better understanding of the performance requirements of vertical water wheel generator thrust bearings has made possible the development of simple, compact machines which are less costly to erect, easier to operate, and have increased performance reliability.

Bearing Arrangement

Three principal types of bearing arrangement, as shown schematically in Figures 1, 2, and 3 have been developed to meet the operating requirements of water wheel generator units for a wide range in dimensions, proportions, weights, and speeds.

For high speed units for which the ratio of rotor diameter to core length is small, two forced lubricated sleeve guide bearings are placed on the shaft as close as possible to the rotor, and the thrust bearing is located above the generator. This arrangement, which is shown in Figure 4, makes possible the use of the minimum size guide bearings with minimum friction losses. A rather complex lubricating and cooling system is needed for this arrangement.

Figure 1 (left). Schematic picture of high-speed vertical water wheel generator unit

Figure 2 (center). Schematic picture of medium speed vertical water wheel generator unit

Figure 3 (right). Schematic picture of Kaplan type water wheel umbrella type generator unit

1. Turbine guide bearing
2. Generator lower guide bearing
3. Generator upper guide bearing
4. Thrust bearing

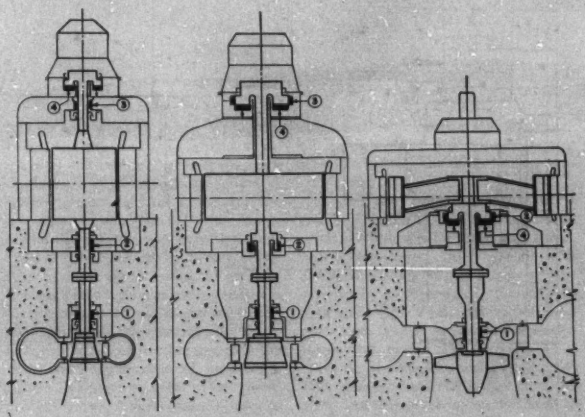

Paper 47-58, recommended by the AIEE committee on power generation for presentation at the AIEE winter meeting, New York, N. Y., January 27-31, 1947. Manuscript submitted November 14, 1946; made available for printing December 30, 1946.

C. M. LAFFOON is manager of the a-c engineering department of the transportation and generator division, and R. A. BAUDRY is manager of the mechanical development section of the a-c engineering department, Westinghouse Electric Corporation, East Pittsburgh, Pa.

The authors acknowledge the assistance of H. R. Criner, formerly of the Westinghouse Electric Corporation, and of their other associates in the company.

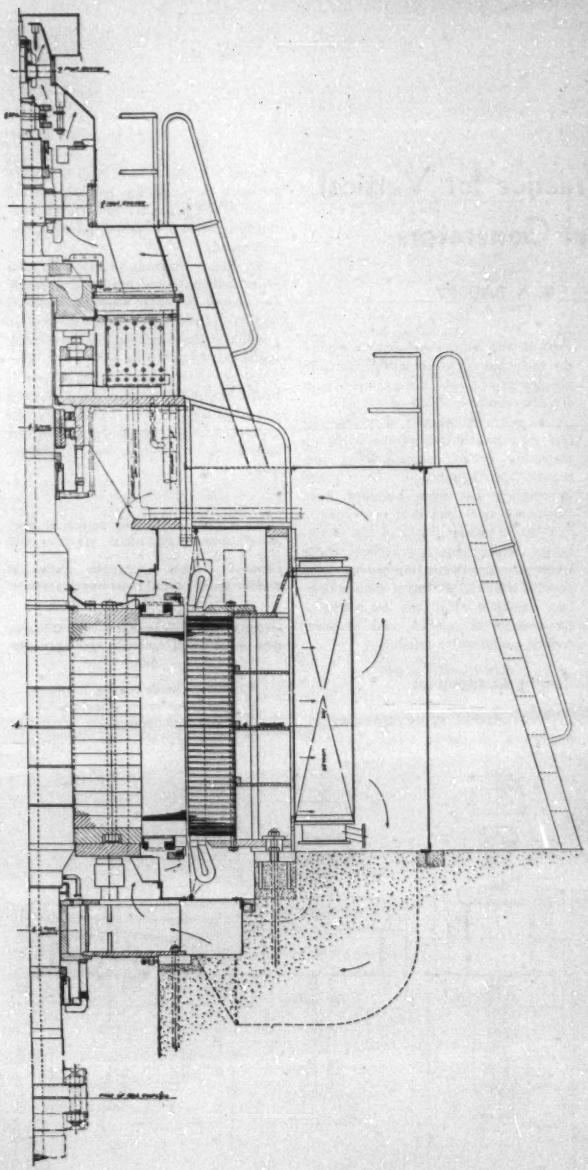

Figure 4. High speed vertical water wheel generator with sleeve type guide bearing

On medium speed machines with a higher ratio of rotor diameter to core length, a similar bearing arrangement still is maintained, but the guide bearings are designed to operate in an oil bath, thus eliminating the usually complicated lubricating system. A machine of this type is shown in Figure 5. With this design, the guide bearing losses are somewhat higher than for a sleeve guide bearing placed on the shaft but are kept within reasonable limits by the use of pivoted pads which have a high carrying capacity and make possible a smaller bearing area.

For low speed units with a still higher ratio of diameter to core length, the single guide bearing type generator is used extensively as its low height makes possible a power station of much lower head room. This type of water wheel generator commonly is known as the "umbrella type." The thrust bearing is placed under the rotor; the single guide bearing of the pivoted pad type is placed at the periphery of the thrust bearing runner and operates in the same oil bath, thus reducing to a minimum the bearings and lubricating system of the machine as shown in Figure 6. When provided with a rigid support, the thrust bearing of the umbrella type generator provides a very large stabilizing effect. Any unbalanced magnetic force acting on the rotor pushes it against the guide bearing and produces an overturning moment, which is opposed by the weight of the rotating parts and hydraulic thrust as shown in Figure 7.

The usual small distance between the transverse axis of the rotor body and the transverse axis of the guide bearing, the large thrust bearing diameter, vertical load, and the thin rigid oil film separating the bearing parts provide a large factor of safety against the overturning of such a rotor. It can, for practical purposes, be considered as built-in with the supporting lower bracket. This structure is much more rigid than the shaft, and a very rigid lateral support thus is obtained for the rotor. Some very large generators have been tested in the shop at overspeed when operating with only the single combined thrust and guide bearing. Similar operation can be obtained in the field, if it should become necessary to disconnect the generator from the turbine and operate it separately as a synchronous condenser, or to measure the generator friction and windage losses.

Bearing Design and Manufacture

With the continuous increase in size of hydroelectric generating units, machines now are built with thrust load well above

1,000 tons and requiring large thrust bearing approaching ten feet in diameter. The design, manufacturing, and operation of such large bearings have brought many new problems which have been solved successfully following many laboratory and field tests. Such tests have shown that the performance of a thrust bearing during the starting period can be very critical, unless a satisfactory finish, quality of oil, and temperature of the oil are provided or controlled.

In order to perform satisfactorily, the thrust bearing runner and pads also must be provided with adequate supports which permit the bearing to remain permanently under alignment and have uniform pressure distribution and loading on the supporting pads. These problems have been discussed by the authors.[1]

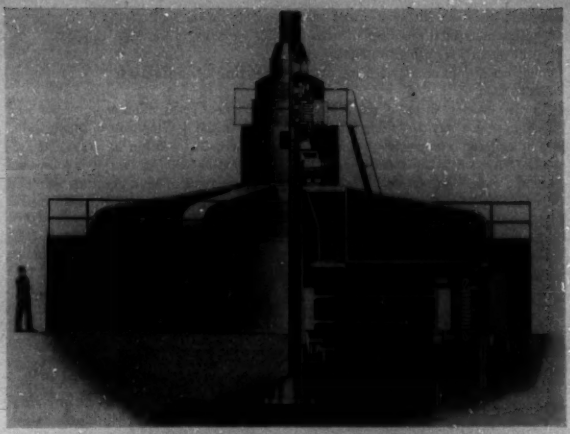

Figure 5 (above). Medium speed vertical water wheel generator with guide bearings operating in oil bath

Figure 6 (below). Umbrella type generator with a single guide bearing combined with the thrust bearing

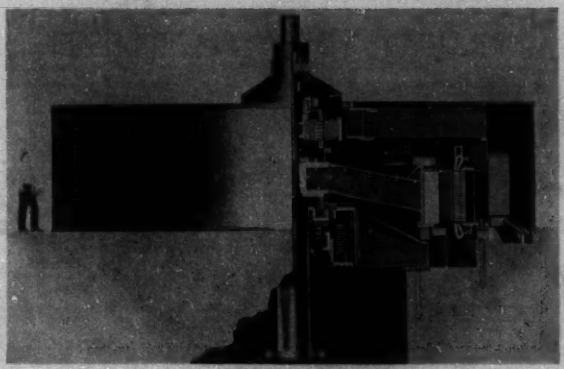

Thrust Bearing Arrangement

When placed above the generator, the thrust bearing runner is made in one piece and supported by a rigid supporting collar mounted on the shaft. In order to permit the dismantling of the generator, this collar must be removable. In the early designs, it was secured to the shaft by means of a heavy steel nut, which was tightened by means of a ram. With this design, it was very difficult to insure a tight fit between the collar and the shaft under all operating conditions. With a small settlement of the foundation, or even with the normal alignment tolerances, a small wobble between the shaft and the collar could not be avoided and resulted frequently in wear showing in the form of red rust at the contact between these parts. This type of wear which is found frequently on many types of machines is now the object of considerable research work. The wear is caused by minute sliding motion, as low as a few millionth of an inch, between surfaces under pressure, and is better known under the name of "fretting corrosion".[2]

This kind of wear is difficult to eliminate completely but can be reduced to a negligible amount, if the press fit between the thrust collar and the shaft is appreciably larger than the disturbing forces produced under operating conditions. A very successful attempt to fasten the collar on the end of the shaft was made by the use of high strength bolts which were tightened by means of electric heaters. The stretch of the bolt indicates the magnitude of the assembling force which was kept at double the value of the maximum thrust load. On large bearings, this design proved somewhat unwieldy and was replaced by the design shown in Figure 8 where the thrust collar has a tight fit on the shaft and is pressed against the shaft shoulder by means of high strength steel levers which are deflected a given amount by relatively small bolts. This design can be assembled very easily with a minimum of effort and makes the end of the shaft available for mounting the exciters. With umbrella type generators, the thrust bearing collar need not be removed to permit dismantling the machine and, therefore, can be forged in one piece with the shaft, thus eliminating an undesirable joint. However, experience has shown that this type of thrust collar also must be made with sufficient rigidity to prevent minute slips which would result in fretting corrosion between the thrust bearing support parts.

A hard close-grained material, which can be polished readily and is hard to scratch, is desirable for heavy duty thrust bearing application. Alloy cast iron with a chilled bearing surface has been very satisfactory for this service. Several runners made from steel forgings and steel plate have been in satisfactory operation for several years. The performance of these runners has been comparable with that obtained from chilled cast iron runners. All thrust bearing runners must be

annealed to relieve internal strains when the rough material is produced in order to prevent distortion during subsequent machining operations and after being placed in service.

Thrust bearing shoes or pads are designed in such a way that the deformation due to load and temperature gradient will not interfere with the formation of the oil film. Steel plate or steel forgings are adequate for this purpose because of their high modulus of elasticity and the ease with which babbitt can be applied to them. Tin base babbitt is needed and normally is used for water wheel generator guide and thrust bearings. Because of the scarcity of tin, a set of thrust bearing pads was made with arsenitic lead base babbitt, containing practically no tin, for trial use on a large water wheel generator. This unit was installed in 1943 and has been in satisfactory operation since.

The pivoted pads of most thrust bearings used with hydroelectric generators are in most cases supported on individual jack screws. They provide a simple and rugged means for adjusting the load uniformly on the pads, and for determining the elevation of the rotating parts.

Bearing Manufacture

In recent years, much progress has been made in the development of manufacturing methods to obtain surfaces of the required quality. For this purpose, special machine tools of high accuracy are used and enclosed in an air-conditioned room, which is maintained at constant temperature and supplied with filtered air. This eliminates the dust particles which are usually present in the air of the average manufacturing plant and scratch the bearing surface during the polishing operation.

The roughness of the surface is measured by means of a profilometer which indicates the rms of the profile of a chosen section. Laboratory and field tests have indicated that roughness values of ten microinches or less are sufficient and satisfactory

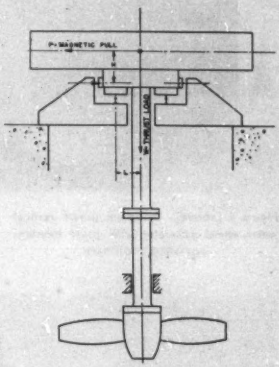

Bearing Operation

The pivoted-pad thrust bearing has an excellent record of reliability when properly installed, lubricated, and maintained. It gives years of service with practically no wear; many bearings inspected after more than 20 years of service currently show the original machining marks on the babbitt. At normal operating speed, the bearing surfaces are separated by an oil film from a clean oil supply system. The only wear occurs during the starting and stopping periods. The finish of the bearing surfaces and the oiliness of the lubricant are very important, particularly for bearings which are started

Figure 7 (above). Stabilizing effect of rigidly supported thrust bearing

Rotor is stable for $W \times L > P \times H$

$W \times L$ is always several times larger than $P \times H$

Figure 8 (below). Modern thrust bearing runner held on shaft by means of preloaded flexible keys

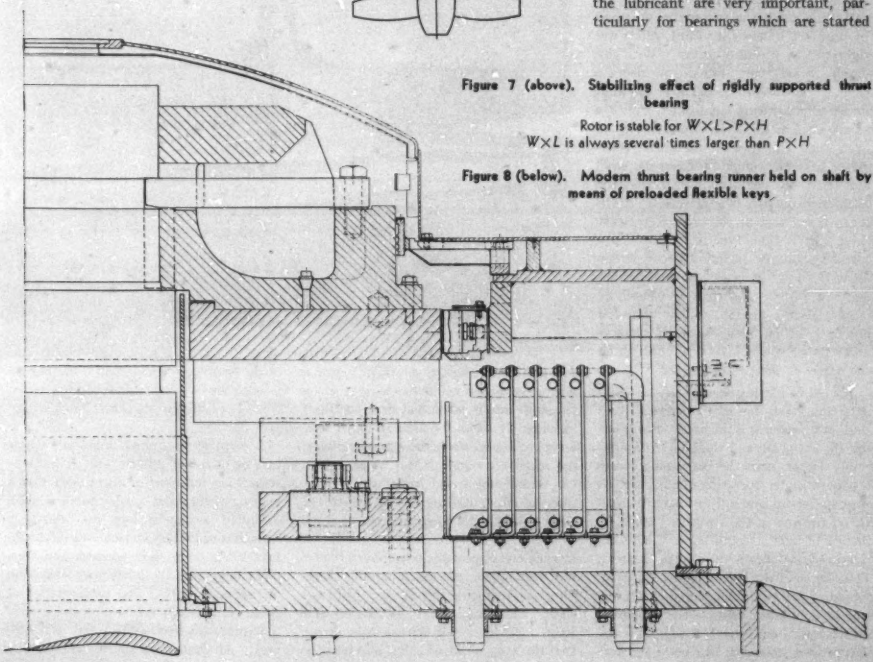

frequently. Laboratory and field tests show that the coefficient of friction is much higher when starting than when stopping. When starting, the bearing runner is not carried on an oil film until a speed of 20 to 30 rpm is reached; but when stopping, it still is carried on an oil film down to a speed of one rpm. The coefficient of friction during the starting period for a small laboratory model and a large thrust bearing in the field are given in Figure 10.

The smoothness of the rubbing surfaces and the oiliness of the lubricant improve appreciably with time. Therefore, when placing a machine in service, several temporary measures can be taken to increase the factor of safety during this period in which the machine is submitted to many starts at high temperature during the dryout.

As shown in Figure 11, the speed at which the bearing rides completely on an oil film increases rapidly with the temperature of the lubricant to such an extent that with a high starting temperature, a failure is likely to occur. Therefore, it is very important not to attempt to start a water wheel generator unless the temperature of the oil is kept at a relatively low value; that is, 45 degrees centigrade or lower.

Many horizontal electric machines are provided with oil pressure under the journal when starting, in order to reduce the starting friction forces and keep to a minimum the current inrush. This feature reduces greatly the strain on the bearing. Oil pressure lift is not necessary on water wheel generators, as there is ample power to break away the bearing. Furthermore, the installation of oil lift on the several tilting pads of a thrust bearing is rather complicated although it has been done on a few vertical motors where low starting torque was required. The same effect can be obtained, however, by jacking up the rotor with the hydraulic jacks normally provided. Oil thus is introduced between the bearing surfaces, and an oil film is maintained during an appreciable time after the jacks are released. If the machine is started immediately, the starting coefficient of friction is reduced to a value comparable with that obtained with oil pressure lift. This method of starting when used for the first 40 or 50 starts increases the factor of safety of the bearing while the bearing surfaces and lubricant are improving.

Variation of the Hydraulic Thrust Load as a Function of the Blade Angle in Kaplan Type Water Wheels

The coefficient of friction during the starting period shown on Figure 10 was obtained in the field by means of electromagnetic strain gauges, which were mounted on the generator shaft in position to measure the angular and axial deformations of a given section of the shaft. These deformations are proportional to the torque and axial load acting on that section of the shaft and were

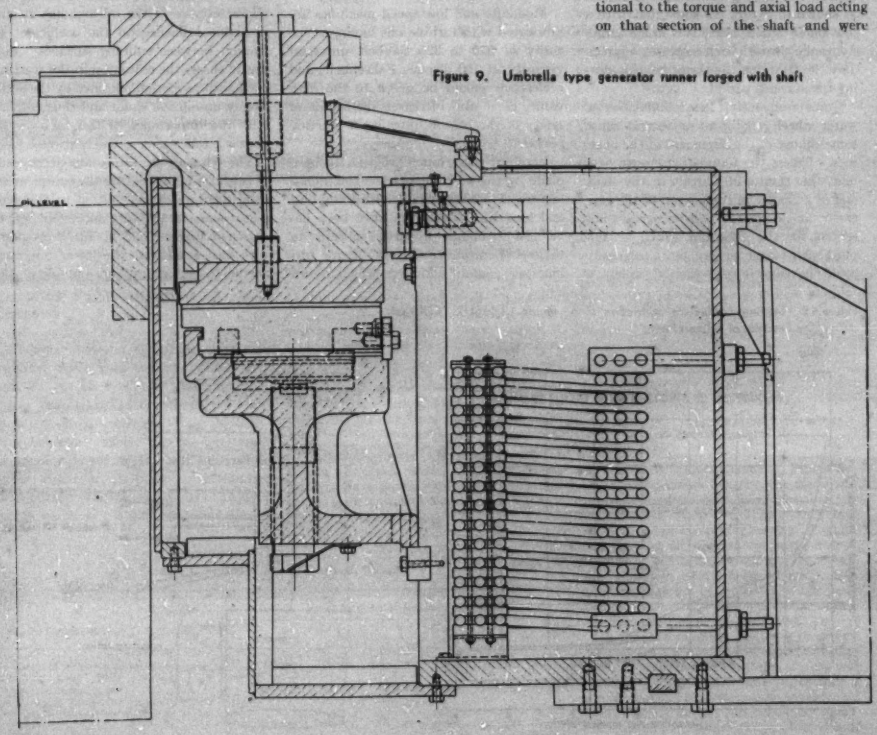

Figure 9. Umbrella type generator runner forged with shaft

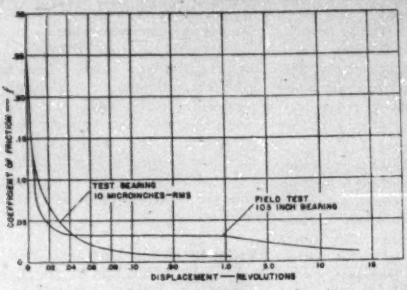

Figure 10. Starting coefficient of friction of thrust bearing model and of 105-inch thrust bearing

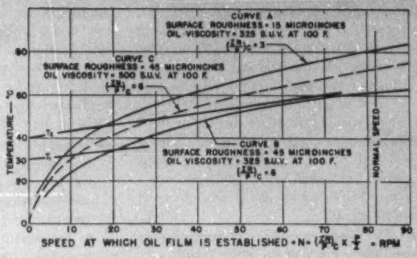

Figure 11. Speed at which thrust bearing is carried entirely by an oil film

$P = 250$ pounds per square inch for all curves
$(ZN/P)c$ = characteristic number ZN/P when oil film is established

recorded by means of an oscillograph for different angular displacements and speeds of the rotor.

Several starting tests, which were made with varying blade angle indicated as shown in Figure 15, show that with a low blade angle, there is a much larger hydraulic thrust which increases appreciably the strain on the thrust bearing during the starting period.

Quite frequently, the foundations of water wheel generators settle and cause some change in the alignment of the bearings. Unless the foundations move as a unit, this results in a strain in the shaft and in a change in the air gap of the generator and exciters. This is usually not serious for the generator which is supplied with a large air gap, but a rub easily could develop in the exciter, unless a check is made when a foundation settlement is suspected. The distance between guide bearings being usually relatively large, an appreciable misalignment can occur before large strains are produced in the shaft or excessive loading is imposed on the bearings.

Lubrication

Moderate and low speed machines are lubricated with turbine oils having a viscosity of 275 to 325 Saybolt universal viscosity at 100 degrees Fahrenheit, and preference should be given to the high value, as it also increases the factor of safety of the bearing during the starting period.

In recent years, much progress has been made by the oil companies in the manufacture of oils having increased stability and long life. Additives have been developed to obtain properties suitable to various operating conditions. Some turbine oils contain additives which retard oxidation, reduce foaming, or prevent oxidation in the presence of water. This latter agent also increases the oiliness characteristics of the oil and has an appreciable influence on the coefficient of friction between rubbing surfaces. Figure 12 shows the reduction in the starting coefficient of friction obtained by the addition of an oiliness agent and thus emphasizes the importance of this factor with respect to the safety of the bearing.

The oil seals are important accessories of bearings in preventing the escape of oil from the lubricating system to the generator housing. A very successful seal is shown on Figure 13. This seal is provided with two chambers, the lower one connected to the atmosphere outside of the

Figure 12. Starting coefficient of friction as a function of oiliness factor

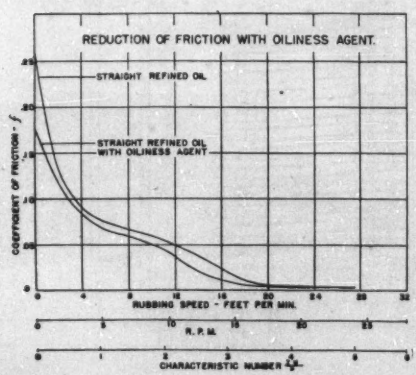

Figure 13 (right). Oil seal

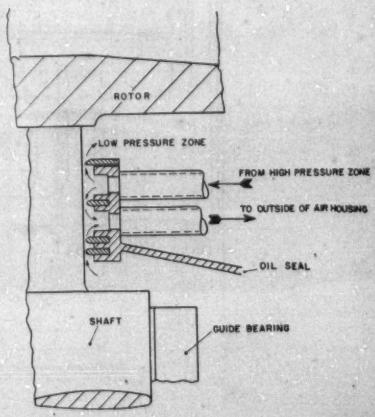

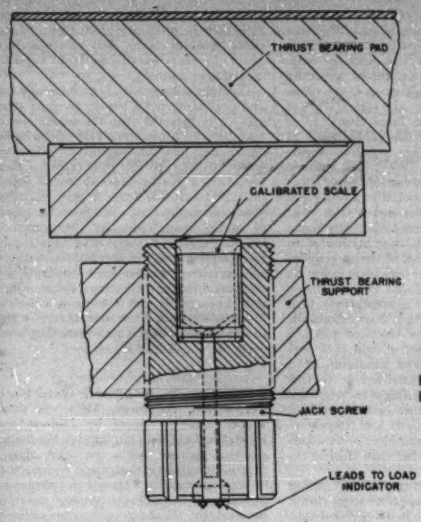

Figure 14 (left). Calibrated scale placed in jack screw

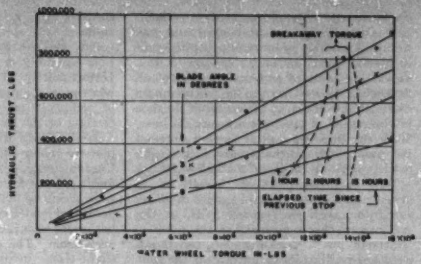

Figure 15. Variation of the hydraulic thrust as a function of the blade angle of a Kaplan water turbine

bearing housing, thus equalizing the pressure at this point and in the bearing housing to the pressure at the inner oil guard near the shaft. The upper chamber is connected to the highest pressure zone in the machine which forces the air to flow into the lower chamber and thus prevent positively any oil vapor from being sucked into the generator.

Adjusting the Load on Thrust Bearing Pads Supported on Jack Screws

Most pivoted-pad thrust bearings are provided with jack screws, which are used to get the rotating parts at the proper height and to distribute the load on all pads as uniformly as possible. Every erector usually has his preferred scheme for adjusting the loading on the pads. However, in order to determine the accuracy of several methods of adjusting the height of the pads, individual calibrated scales were placed at the center of each of the jack screws of a thrust bearing as shown in Figure 14. These scales are made of a high strength steel cylinder on which is cemented a resistance wire strain gauge. Each scale was calibrated in a testing machine in order to obtain a high accuracy.

In Table I are given the loads obtained in all the jack screws by each of the three following adjusting methods:

1. Each jack screw was tightened by means of a wrench and a sledge hammer; the maximum variation from the average was 11.1 per cent of the average and 7 per cent at the second try.

2. The rotor was set and leveled on blocks; then the pads were tightened snug against the thrust bearing runner. The maximum variation from the average was 11.7 per cent.

3. After the water wheel was connected to the generator shaft, the jack screws finally were adjusted by means of the strain gauges with a variation of plus or minus 2 per cent of the average.

Table I. Loads Obtained in Jack Screws

Method of Tightening Jack Screws	Load on Each of Six Jack Screws					
	1	2	3	4	5	6
By means of wrench and sledge hammer	61,000	68,000	57,000	59,050	61,000	64,800
Rotor set level. Pads tightened snug against runner	60,400	69,500	63,800	57,200	68,500	66,500
Water wheel connected to shaft. Jack screws adjusted by means of strain gauges	93,100	96,600	94,800	89,800	90,500	93,500

Conclusion

Laboratory and field tests have contributed to a better understanding of the problems involved in the design and manufacture of thrust bearings and their application to water wheel generators of various characteristics.

These tests also indicate many operating requirements which increase considerably the factor of safety of water wheel generator thrust bearings, and their use is recommended as a means of extending the life of bearing parts.

References

1. Performance of Vertical Water Wheel Generator Thrust Bearings, C. M. Laffoon, R. A. Baudry, P. Heller. *Transactions*, American Society of Mechanical Engineers (New York, N. Y.), volume 69, May, 1947.

2. An Investigation of the Fretting Corrosion of Closely Fitted Surfaces, G. A. Tomlinson, P. L. Thorpe, H. J. Gough. Institution of Mechanical Engineers (London, England), March 1939.

Discussion

E. I. Pollard (Elliott Company, Ridgeway, Pa.): The authors mention the use of oil pressure applied directly to the bearing surfaces as a means of reducing the torque required to break away the bearing. Though this method of reducing the coefficient of friction at standstill, by using a high pressure pump to establish an oil film before starting, may not be a cure-all, it has some definite advantages for generator thrust bearings that should be considered.

In the first place the operating procedure for starting the unit can be made less complicated than use of the jacks to raise and lower the rotor before starting, as it is a simple matter to start a motor-driven pump unit. Safety devices can be applied easily; for example, a pressure switch often is used

on horizontal bearing applications to indicate that pressure is established and may be interlocked to prevent starting the unit in case of pump or motor failure. Check valves are used to prevent reversal of oil flow when the unit is running, as this would diminish the oil film at the center of the shoe in the region of the high pressure oil inlet. With the pressure switch located between the pump and the check valves, it can be used to indicate failure of a check valve.

With oil pressure applied directly to the bearing surfaces there is no danger of lifting the rotor more than a few mils, as the gallons-per-minute capacity of the pump is relatively low. Consequently, the pump need not be shut down until after the unit is up to a safe speed.

After a vertical generator has been at standstill long enough to squeeze out most of the oil from between runner and babbitt, the suction force between shoe and runner is quite large. If the rotor is raised up too rapidly by means of the jacks, there is danger of this suction force pulling the babbitt loose from the shoes. This hazard is eliminated if oil pressure first is applied directly to the bearing surfaces.

The authors discuss adjustment of the thrust load between the various shoes and refer to checking the adjustment by means of strain gauges. When a high pressure oil lift system is used, it also can serve as a convenient method of checking adjustment of load by comparing pressures in the oil lines to the various shoes with the unit running at reduced speed.

R. O. Standing (nonmember; Hydro-Electric Power Commission of Ontario, Toronto, Canada): The importance which the authors attach to the rigid and tight-fitted thrust collar is of special interest, as, in the experience of the Hydro-Electric Power Commission of Ontario, a considerable proportion of all troubles encountered in vertical thrust bearings is attributed to the so-called loose fit between collar and runner plate.

Not only does the loose fit promote "fretting," or pitting, of the collar bore and the shaft, which in the case of the latter may lead to an expensive remachining operation if allowed to continue indefinitely, but also it promotes pitting of the lower surface of the collar and the mating upper surface of the runner plate. This is especially true if the collar has become "cocked" on the shaft, or the plane of the stationary rubbing surface has for any reason deviated from the normal with respect to the rotating axis.

The Commission has upwards of 100 vertical thrust bearings in operation, some of these, including the largest (500 tons capacity), having been in operation more than 20 years. Eighty of these are of modern design, and of this number approximately half are pivoted-shoe type and half spring-supported.

Generally speaking, the trouble most frequently encountered is common to both types, and, strangely enough, this is not outright failure of the bearing, but what is called "near failure" and is found by inspection. These near failures manifest themselves, after approximately ten years of bearing service, as pitting of the shaft, collar, and runner plate as described previously, and abnormal wear of the babbitted rubbing surface, usually at the outer periphery. Except for the effect of the loose collar, this pitting is attributed to either poor assembly or poor alignment, or both. Unfortunately, it is not known generally what proportion of these errors is the result of defective assembly and alignment or settling of the machine foundations.

With regard to the rubbing surfaces of pivoted-shoes, operating engineers of the Commission do not share the authors' findings as to wear. Invariably these shoes show a central hollow spot after a prolonged period of service. This means that wear has occurred as is confirmed readily by visual inspection. The condition is attributed to slight elastic deformation of the shoe under load. It has not led to difficulty, however.

Experience indicates that modern thrust bearings will operate for surprisingly long periods under conditions of poor alignment. Knowledge of this fact tends to produce carelessness during erection, and it is suggested that more cases of misalignment in modern machines are attributable to this circumstance than to settling of foundations. Eventually however, misalignment will lead to failure and costly repairs, and it is therefore unwise to erect a machine, or to maintain it, on any basis other than that of extreme accuracy.

As a means of reducing pitting resulting from the relative movement between thrust collar and runner plate, it is suggested that these two might be bolted together. As a means of reducing the effect of misalignment of the guide bearings, it is suggested that the increasingly popular practice of using the thrust collar as the journal of the upper guide bearing, (that is, placing the upper guide bearing as near as possible to the plane of the thrust bearing rubbing surface) is a step in the right direction. With this arrangement the generator lower guide bearing becomes the principal source of misalignment. If this bearing be given maximum permissible clearance, the effects of foundation settlement are reduced materially. Actual cases have arisen in the Commission's experience where an increase in the clearance of this bearing has produced notable improvement in unit operation. It is suggested for the average modern machine of appreciable size, the bore of this bearing may exceed the diameter of the shaft by 0.012 inch plus 0.0005 inch per inch of diameter in excess of 12 inches.

In the matter of adjusting the pivoted-shoe type bearing, it is pointed out that, regardless of the method used, the ultimate requirement is that the shaft be plumb and the rubbing surfaces normal to it. Very satisfactory results have been obtained by the expert with the sledge hammer after the precaution of treating the bearing rubbing surfaces and the jack screws with lubricant is taken. The adjustment of the bearing is complete when the segments have been sledged up all around and the shaft is found plumb, as determined by a rotational test. The importance of the rotational test as a means of checking this operation, and of checking the alignment, can not be overemphasized.

The Commission's practice in thrust and guide bearing lubrication for a great many years has been the use of mineral oil of viscosity 250 (Saybolt universal viscosity) at 100 degrees Fahrenheit. No additives are employed. The neutralization value of these oils is maintained below 0.5 by treatment, where necessary, with the activated earth process. Some oils, however, have given 20 years service without requiring special acid treatment.

Outright failures have been relatively few, and practically none has occurred at start-up. It is believed that the liberal use of lubricants on the rubbing surfaces on installation and on other appropriate occasions has contributed to this good record. Jacking of the rotor to establish an oil film is resorted to after lengthy shutdowns. Preventative maintenance has been the means of saving many bearings from outright failure. However, there have been a relatively large number of near failures, and it is this experience that has led to the inevitable conclusion that accuracy must be the watchword in assembly and alignment, as well as in manufacture, if these bearings are to give the prolonged service for which they obviously are capable.

B. Van Ness, Jr. (Safe Harbor Water Power Corporation, Baltimore, Md.): A study of the excellent paper by Laffoon and Baudry can not help but impress the hydroelectric engineer with the high degree of attention given to design and manufacture of bearings today. This was not always so. In the early days, thrust bearings were not supplied by the generator manufacturers, and those which were available became increasingly inadequate as the size of machines increased. When the first five main units at Holtwood were placed in operation in 1910 and 1911, roller type thrust bearings were used, these having been selected over the then prevalent oil pressure bearings because of the increased thrust load on the slow speed low head units. The roller thrust bearings had only one virtue; when failure took place it was gradual, and it was possible to shut a machine down without damage to parts other than the bearing. An average of five or six and a maximum of fifteen overhauls per unit per year is recorded.

In 1912 Professor Albert Kingsbury made application for a trial installation of one of his bearings in a Holtwood unit; in view of the bad record of the roller bearings such an installation was made. Interestingly enough, the first bearing failed after about two hours of operation. Professor Kingsbury was not discouraged explaining that the time allowed him had not been sufficient for a thorough scraping in of the bearing. The damaged parts were returned to his shops for reconditioning and on June 26, 1912, were reinstalled in the unit and put on load. This Kingsbury thrust bearing, the first to be applied to a vertical hydroelectric unit, is running today, almost 35 years from the date of its installation. Its installation marked the beginning of a new era in the fundamentals of bearing design and operation.

In 1931–1932 when the Safe Harbor station was brought into service with the first large Kaplan water wheels in the United States, our record of 20 years successful operation with Kingsbury thrust bearings was marred. Three bearings failed in quick succession.[1] The difficulty was established as caused by the extraordinary thrust at starting, which is characteristic of the Kaplan water wheel at too low blade angle.

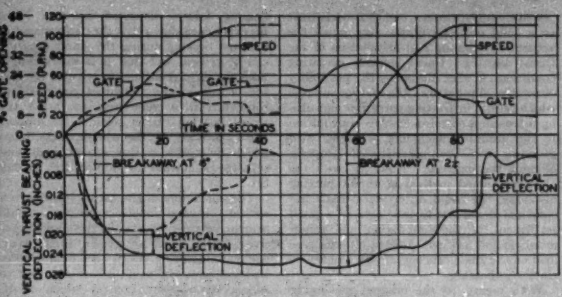

Figure 1. Curves showing the effect of blade angle on starting duty of 42,500 horsepower hydraulic turbine

--- 6-degree blade angle
— 2¼-degree blade angle

This was aggravated by bearing surfaces not adequately polished. With correction of these difficulties, reliable and continuous thrust bearing service has been restored.

In our 1932 investigations to determine the cause of failures, the additional starting duty, as a function of decrease in blade angle, was shown clearly. By means of an electric strain gauge mounted on the bearing bracket support, the vertical deflection or relative hydraulic thrust, together with speed and gate opening, were recorded by the oscillograph during the transient starting period. Comparative tests at two blade angles are shown in Figure 1. It is seen that, at breakaway, a 2¼-degree blade angle increases the hydraulic thrust approximately 50 per cent over that of a 6-degree blade angle, the latter our present operating adjustment for starting. This is in good agreement with the author's data given in Figure 15, which shows the increased starting duty in a much more comprehensive form.

In our newer units the thrust bearings are located below the rotors, as, interestingly enough, they were in the older Holtwood machines. In the 25-cycle single-phase generators at Safe Harbor, an additional guide bearing is used above the rotor. This has seen so little duty that it has not been necessary to operate the water cooling system; it serves purely as a steady bearing in case of short circuit.

We have had one case of unsatisfactory performance in the 60-cycle machines, which have the combined thrust and guide below the rotor, this occasioned by the simultaneous burning open and grounding of the field. The failure caused an unbalanced side thrust on the rotor and damaged slightly the main exciter, the rotating parts of which rubbed against the stationary.

The authors mention the advisability of jacking the rotor of a vertical unit in order to establish an oil film after an extended period at rest. This is not possible with all designs. In some units the runner plate is fastened to the thrust blocks by sliding dowels and remains in contact with the shoes when jacking takes place. In units where the runner plate is fastened to the thrust block, we have known shoes to adhere to and rise with the runner plate during jacking.

We have had some experience with the need for providing ventilation of the bearing oil pots, a point mentioned in the paper. On the 60-cycle machines at Safe Harbor, it has been necessary to operate an aspirator to produce a negative pressure sufficient to remove the oil vapors from the bearing pot, but difficulty has been experienced in disposing of these vapors We are planning to apply electrostatic precipitation to the vapor discharge from the bearing pots of these units.

REFERENCE

1. Discussion by **P. M. Hess** of Safe Harbor Project. AIEE TRANSACTIONS, volume 52, 1933, pages 186–8.

T. W. Gordon (nonmember; General Electric Company, Schenectady, N. Y.): Under the heading "Bearing Manufacture" the authors indicate the necessity of special machine tools and an air-conditioned room supplied with filtered air and maintained at constant temperature for obtaining a satisfactory finish on thrust bearing runners. We would like to point out that a fully air-conditioned room may not be a rigid requirement for producing good surfaces on thrust bearings. In the manufacture of large thrust bearing runners at Schenectady, two principal factors have contributed to high quality and consequent successful performance. These are, the precision boring mill, in use since 1940, with suitable tools and the protection of this equipment from the dirt and chips found in the ordinary large shop. Cleanliness must prevail, but constant temperature is not required. This work can be done with the usual variation in temperature of a machine shop.

In this paper and in another paper by the same authors presented in December 1946, at the annual meeting of the American Society of Mechanical Engineers in New York (reference 1 of the paper), attention is called to the severity of the duty on large thrust bearings at the time of starting. When a new thrust bearing is being put in service, it has been standard practice to assemble it with grease or heavy oil between the rubbing surfaces for the initial start, often made after standing under load for several weeks. Although it is recognized that the first few starts may be critical for any bearing, we expect that a good bearing will make all starts subsequent to the first without damage and at any prevailing temperature of oil or bearing parts.

As mentioned by the authors, high pressure oil has been used on horizontal bearings, but only to reduce the power inrush at starting. Up to the present, this has not been considered worth while in hydroelectric generators where there is plenty of power to start. However, in the case of the new 65,000-horsepower motor-driven pumps for Grand Coulee, high pressure oil will be pumped between the thrust bearing surfaces to float the rotor, so that two pumps may be started more easily together from one 108,000-kva generator.

In cases where it is desirable for one reason or another to separate the bearing surfaces and establish an oil film before rotation occurs, we understand that the authors favor raising the rotor with the oil jacks or brakes to allow oil to flow between the bearing surfaces. Instead of pumping high pressure oil into the brakes or jacks, we favor what seems like the simpler method of pumping the oil direct to the bearing to form a film. The first method requires opening the turbine gates very quickly after the pressure on the jacks is released, whereas, with the second method, the operator, after starting the high pressure pump, can give all his attention without haste to starting the turbine. The pump may be left running until after the generator is on the line. As is done in some synchronous condenser stations, a signal or relay interlock may be installed at the turbine control board to make sure the bearing oil pump is started first.

On an experimental bearing installed temporarily at the Bonneville station of the United States Engineers in 1939, the latter scheme was given a good trial and found to be very satisfactory. The thrust bearing at Bonneville was the General Electric Company's spring supported type 112 inches in diameter with the stationary babbitted surface in 12 segments. Each segment had a suitable recess in the babbitt to which high pressure oil was pumped to float the rotor. The 12 segments were connected in multiple to a common header running around the periphery of the bearing in the oil housing. A check valve was included in the line to each individual bearing segment, and oil was furnished for the starting period by a pump good for 5 gallons per minute at 1,000 pounds per square inch. The distribution of oil to the various segments was satisfactory without metering nozzles. As the oil film in the thrust bearing was formed, the rotor rose about 0.006 inch, the pump pressure dropped to 350 pounds per square inch, and the starting friction was reduced to a very small figure. The usual groan and vibration present in starting a standard bearing was absent as the 1,500,000-pound rotor turned noiselessly on the high pressure film

C. M. Laffoon and R. A. Baudry: The authors agree with E. Pollard that the use of oil pressure lifting to reduce the starting torque is not a cure-all. Oil lifting normally is used when there is not sufficient torque to start the machine, as is the case with synchronous condensers or motors. Several pivoted-pad type thrust bearings thus have been equipped for this application.

To apply oil lift on a pivoted-pad bearing, it is necessary to connect an oil pressure pipe to the center of each pad and to provide for a check valve in each connection. It is also desirable to have at least two oil pumps to insure a uniform oil film on all the pads. All these connections must be perfect, as any leakage would relieve the pressure at the center of the pad and thus prevent formation of the oil film. Furthermore, should the oil pressure be permitted to leak under the babbitt, the latter would be lifted, and an immediate failure of the bearing would result.

The authors are favoring lifting the rotor by means of the oil jacks which are provided with all large water wheel generators. The operation can be performed automatically and very rapidly by adding a very simple electric control, thus reducing the friction torque to a value close to the one obtained by means of oil pressure lift and without the added complex equipment with the increased risk of failure.

It is not believed that an oil pressure lift system would be practical to check the adjustment of the individual pads, as it is believed more practical to do this operation before the oil pot is filled with oil. The resistance wire strain gauges provide a more precise means of adjusting the load, although they were used principally to determine the degree of accuracy obtained by the conventional methods, which apparently are satisfactory.

Years of experience show the necessity of having the rotating parts of a bearing machined accurately. The fastening of the thrust bearing runner to the shaft in such a way that the contact surface is always under relatively high pressure, and thus equivalent to a solid unit, facilitates very much the accurate machining and installation of the thrust bearing. Under normal operating conditions, it also eliminates the possibility of relative slip between the mating surfaces which results in fretting corrosion and ultimate looseness of the assembly. In addition to this accurate machining, we agree with Standing for the necessity of properly aligning the machine. However, with the afore-mentioned method of thrust bearing fastening, the usual water wheel shaft has sufficient flexibility to take care of a small settlement of the foundation and minor misalignment without causing an excessive load on the guide bearings or any damage to the thrust bearing.

With regard to the original machining marks on the thrust bearing pads being present after 20 years operation, the authors did not intend to convey the impression that there is no wear at all, because results of laboratory tests show that during the initial starts, there is an appreciable wear of the high spots on the pads. With very smooth runner this wear is very small, but quite frequently with such a surface, after many years of operation, the original machine marks can be seen between these worn spots. The central hollow spot mentioned by Standing is believed to be caused by the crowning of the pad resulting from the thermal gradient across the thickness of the latter.

Van Ness's history of the development of the pivoted pad thrust bearing agrees very well with the authors' experience. Although they are not familiar with the detail of the Kingsbury type thrust bearing failure discussed by Van Ness, his experience shows that the performance of a thrust bearing during the starting period can be critical and that it is warranted to take special precautions to increase the factor of safety. In machines designed for rotor lift, it is very easy to fasten the thrust bearing runner against its support and to provide, on the pad supports, stops which limit the motion of the pads and separate them from the runner after a small lift.

The machining of the thrust bearing in a special air-conditioned room was made principally to eliminate the dust and abrasive particles which are present in the average manufacturing plant. As a completely enclosed room was used, it was very easy to add a temperature control which maintained a constant temperature. We agree with Gordon that the small temperature variation obtained in the average machine shop would be satisfactory. The practice of using grease or heavy oil protects the bearing for one start only. As our laboratory tests (reference 1 of the paper) show that there is an appreciable wear of the bearing surface during the first five starts, it is believed worth while to lift the rotor for the first 20 or 30 starts and thus increase the factor of safety of the bearing during this critical period. The authors agree with Gordon that a good bearing should be able to make all starts subsequent to the first, without damage at any prevailing oil temperature, and without lift or oil pressure starting; however it is felt to be good practice to adopt operating procedures which produce the maximum factor of safety at practically no additional cost.

The Interruption of Charging Current at High Voltage

W. M. LEEDS
MEMBER AIEE

R. C. VAN SICKLE
FELLOW AIEE

Synopsis: The switching of high-voltage transmission lines and underground cables occasionally produces overvoltage surges on electric power systems. While operating experience generally has been satisfactory voltages of 66 kv and below, there have been transient disturbances of considerable magnitude at the higher voltages. The length of many of the transmission lines and the importance of maintaining continuity of service on heavily loaded interconnections have stimulated a critical analysis of the problem. However, in contrast to the extreme overvoltages predicted by theoretical studies, a review of several hundred field tests over the past ten years, including many tests with voltage records by cathode ray oscillographs, discloses practically no cases of line or bus surge voltages on solidly grounded systems reaching transient peaks as high as $2^1/_2$ times normal line-to-ground crest voltage.

This paper attempts to evaluate the effect of both the circuit constants and the characteristics of the various types of interrupters used in modern high voltage oil circuit breakers on the magnitude of switching surges. Particular attention is given to the advantages and disadvantages of such special breaker modifications as auxiliary oil flow pistons or low ohmic value resistors in parallel with the main arc extinguishing devices.

HIGH voltage circuit breakers are designed primarily to interrupt heavy short circuit currents in as short a time as possible. However, this emergency duty is required only rarely, and it is important that routine switching operations should be accomplished also with a minimum of disturbance. For instance, it has long been recognized that capacitive current switching, such as the opening of charging current to a long transmission line or a bank of capacitors, involves certain peculiarities not associated with load current or fault interruptions. While circuit breakers on low voltage circuits handle capacitive currents easily with practically no arcing, delayed restriking of the arc in the breaker often is observed when opening the charging current to high voltage transmission lines and cables. The resulting system disturbances appear to give rise occasionally to voltage surges several times the normal system voltage.

Their magnitude and how frequently they occur are of great importance.

When the problem of intermittent arcing in a power system is approached mathematically or by the use of a network calculator, the arcing and dielectric recovery characteristics of the circuit breaker must be assumed. Since the highest possible voltages are of most interest, the breaker is usually assumed to restrike and clear at just those instants which lead to maximum overvoltage, even postulating sometimes an arbitrary forcing of the current zero. Thus, while these studies are of great value in determining the effect of variations in the system constants, they do not duplicate actual multiple restriking. Field tests with accurate voltage records are necessary to determine how the breakers perform and the voltages which may be produced. Over the past decade arc-rupturing devices, particularly for the higher voltage circuit breakers rated 115 kv to 287 kv, have undergone many changes in design, and it seems pertinent at this time to take stock of the present situation as regards actual breaker performance when interrupting capacitive currents.

We have studied oscillograms made during the interruption of charging currents, both during field tests on systems and in a laboratory, and have been impressed with the consistency with which the breaker avoids behaving in the manner which produces maximum overvoltages. The oscillograms show that breakers on grounded systems, even though they restrike several times, seldom produce voltages higher than $2^1/_2$ times normal, although values of 4 to 5 times are possible.

Analysis of Charging Current Interruption Problem

The phenomena associated with the interruption of capacitive currents may be described more clearly by considering a specific circuit such as that of Figure 1 in which a lumped capacitance C is connected to a high voltage a-c bus through a circuit breaker B. The small parallel capacitance C_s represents the capacitance of the bus together with that of the directly connected equipment. The series inductive reactance between the generated voltage and the bus, while often quite small in comparison with the capacitive reactance, is a factor which should not be neglected as will be shown in the following discussion.

Figure 1*b* illustrates the time variation of the voltage to ground on both the bus side and capacitor side of the breaker for an opening operation in which one restrike occurs under the unfavorable condition of nearly a full half-cycle pause in the charging current. It is further assumed that the breaker characteristics are such that the restrike current is extinguished after only one-half cycle of oscillation at the frequency determined by the series inductance L and the sum of the capacitances C and C_s. The result of the restrike and the voltage overswing is to leave the capacitor C charged to a voltage between two and three times the crest voltage before the breaker opened.

Figure 1*c* shows the voltage conditions directly across the breaker contacts as a function of time. It is to

Paper 47-59, recommended by the AIEE committee on protective devices for presentation at the AIEE winter meeting, New York, N. Y., January 27–31, 1947. Manuscript submitted November 13, 1946; made available for printing December 13, 1946.

W. M. Leeds is a development engineer and R. C. Van Sickle is a design engineer, both with Westinghouse Electric Corporation, East Pittsburgh, Pa.

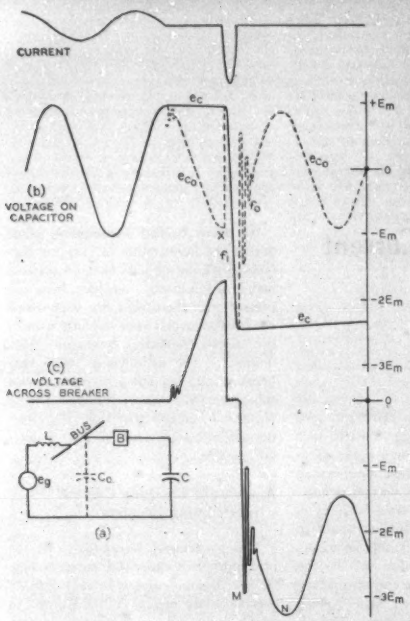

Figure 1. Interrupting the charging current of capacitor. Overvoltage produced by arc current restrike at X, extinguished after half-cycle oscillation at frequency f_1 determined by L and $C+C_c$. Bus voltage oscillation frequency f_o determined by L and C_c

be noted particularly that at current zero where the charging current is first interrupted, the bus voltage undergoes a small transient resulting from the sudden shift of potential to that of the generator following the disappearance of the voltage rise that had existed because of charging current flowing through the series inductive reactance. This transient is usually neglected, but with power supplied from a relatively high impedance source its magnitude may be such as to encourage immediate harmless restrikes and avoid delayed restrikes which could lead to high overvoltage surges.

One half cycle after the current zero, the difference of potential across the breaker contacts reaches approximately twice the crest value of the voltage at which the capacitor is left charged. It is assumed now that the dielectric strength between the breaker contacts is just insufficient to hold this voltage, and an arc reignition or restrike occurs. During the time that the resulting current surge is flowing through the breaker as the capacitor potential attempts to adjust itself to the instantaneous generator voltage, the voltage across the contacts is only the arc drop which is almost negligible for short gaps. Just after this current is extinguished, the bus voltage swings back to the generator voltage in a high frequency oscillation determined by L and C_c only. Following this transient the voltage across the breaker builds up to a value between three and four times normal crest as the generator voltage reverses polarity at fundamental system frequency. If, now, a second restrike were to follow the first at the next crest of the generator voltage, the swing in capacitor voltage could carry it to a crest value between four and five times normal. This phenomenon of cumulative build-up of voltage by intermittent arcing in an a-c circuit charging a capacitance has been discussed many times before the AIEE.[1,2,3]

In the simple capacitive circuit of Figure 1 there would be no limit to the voltage which could be attained by repeated restriking under the most unfavorable conditions. However, if the effects which damp the high frequency transients during restriking are taken into account, a limiting voltage is reached which is a maximum regardless of the number of restrikes. This ultimate value, expressed as a multiple of the system crest voltage, depends upon the damping of the transient restrike current and on the magnitude of the arc voltage drop in the circuit breaker. In Figure 2 is shown the maximum voltage on the capacitor which can be attained for various damping factors and various values of arc voltage. These results are calculated using the assumption that the breaker is capable of a large number of successive restrikes at the crest of the voltage wave, and that the restrike is interrupted each time after just one half cycle of the high frequency.

The voltage which appears across the breaker immediately after one of these interruptions as shown after the restrike in Figure 1*c* is a transient determined by the constants of the circuit on the supply side of the breaker and by the voltage left on the capacitance being disconnected. An initial high frequency crest M is followed by a normal frequency crest N one half cycle later at which time the next restrike is assumed to take place. Cumulative effects result in a proportionately greater increase in the first of these two voltage crests, so that sooner or later the first peak becomes greater than the second. Under these conditions it would seem logical to expect either a restrike at the first crest M which would at once reduce the voltage on the capacitor or, if no restrike occurred at M, none should occur at the subsequent crest N a half cycle later at an equal or lower voltage. In fact, as the dielectric strength of the breaker contact gap is known to increase with time, the limitation in consecutive restrikes should be reached when the voltage at M is still some fraction such as 0.8 of the voltage at N. On the assumption that the same damping factor applies to both the transient voltage on the capacitor during the restrike and to the transient recovery voltage across the breaker just after the restrike, it is possible to add two limiting curves to Figure 2. Curve B shows the maximum voltage on the capacitor which can be reached if the breaker can withstand as much voltage at M as it needs to restrike at N, and curve C shows the maximum voltage which can be reached if the breaker can withstand at M only 0.8 of the voltage required to restrike at N. The first condition indicates that the maximum voltage that can be reached is about 5.0 times the normal crest of line to ground voltage and the second condition gives 4.3 times.

The probability of these theoretical limits being reached is apparently rather small, even though only a few restrikes may be required to produce them.

It often happens that the oscillatory

Table I. High Voltage Line Dropping Field Tests

Test Series	Line Voltage, Kv	Line Length, Miles	Number of Tests	Restrike Time for Max Voltage,† Cycles	Max Voltage ÷ E_M Bus Mag*	Bus CRO‡	Line CRO‡
A	287	90	4	5	1.54		
B	287	90	4	4.5	1.48		
		180	1	6	1.57		
C	287	90	7	5.5	1.73		
		180	2	2.5	1.60		
D	287	90	3	5	1.47		
		180	2	6	1.50		
E	287	90	3	1	1.30		
		180	4	1	1.15		
F	287	90	7	1.5	1.35		
		180	3	1	1.15		
G	287	90	6	3	1.46	1.14	1.38
		180	6	3.5	1.16	1.18	1.24
H	287	90	6	2.5	1.22		
		180	3	3.0	1.08		
I	230	246	1	6		2.0	
		118	1	7.5		2.2	
		23	2	6		1.2	
J	230	55	4	2.5			1.83
		125	6	4.5			1.78
		253	6	3.5			1.97
K	230	70	16	4	1.93	1.77	2.12
L	230	50	4	3	2.00		
		135	3	2	1.90		
M†	230	133	6	1.5		1.20	1.55
N††	230	133	10	Grounded		2.1	2.0
(Parallel resistance)		133	5	Grounded		1.2	1.0
		133	4	Neutral reactor		4.4	4.4
(Parallel resistance)		153	5	Neutral reactor		2.0	1.7
		233	5	Grounded		1.6	1.9
(Parallel resistance)		233	5	Grounded		1.6	1.6
(Parallel resistance)		233	7	Neutral reactor		2.0	1.7
O	230	99	12	2.0	1.2		
P	230	183	25	0.5	1.6		

† Restrike time is measured from the time the contacts part.

* Mag signifies data from magnetic oscillograms.

‡ CRO signifies data from cathode ray oscillograms.

Magnetic oscillograph records series *A* to *H* were made from 16.3 kv bus, others from high voltage bus.

current surge at the time of a restrike is not interrupted at the first high frequency current zero but continues for several half cycles or is not extinguished at all until the next system frequency current zero. Under these conditions the capacitor voltage is brought back closer to the bus voltage and previous cumulative voltage is partly or completely wiped out. Figure 3 shows a high power laboratory test switching approximately 45 amperes of capacitive current at 66 kv single phase. The record of voltage across the circuit breaker indicates a restrike after the voltage had built up to about 1.6 times normal crest. The restrike current was not interrupted until after three half-cycles of high frequency, and the next voltage crest of normal frequency reached a peak of 2.3 times normal without further restriking.

An analysis of the most probable restrike conditions requires some knowledge of the rate at which the dielectric strength is built up between the contacts of a circuit breaker immediately following current zero. Although this is a function of the type of circuit breaker and the manner in which the arc is deionized and interrupted, certain conclusions may be drawn from rather simple assumptions. Figure 4 shows the voltage rise across the breaker together with a family of curves representing the rise of dielectric strength immediately following the initial interruption of charging current. At current zero, the dielectric strength is considered to be a definite value, depending in magnitude upon the contact separation and the intensity of deionizing activity. The initial slope of the dielectric recovery curve may be expected to be fairly steep, but later the curve tends to level off at the breakdown strength of the deionized and increasing contact gap. The subsequent slope depends on such factors as the rate of replacement of gas dielectric by oil dielectric and by the speed of contact opening.

If the interrupting effectiveness is low or if the current zero occurs only a small fraction of a cycle after contact parting, a harmless restrike may take place in a very short time on the high frequency voltage kick at the beginning of the recovery voltage wave as at point *A*. With greater contact separation, restriking may occur after, say, one quarter of a cycle as at point *B*. With greater interrupting effectiveness or more contact separation as indicated by curve *C*, the interruption will be complete without any restriking. It is evident that the bending over of the voltage wave at crest makes it unlikely that a restrike will occur just at crest or later. Actual circuit breaker tests show that most restrikes occur before the voltage across the breaker builds up to a value as high as twice normal crest, thus tending to avoid those conditions which lead to extremely high overvoltage surges. Consequently, the probability of having a succession of restrikes with the voltage across the breaker building up each time to the maximum crest is rather remote. Figure 5 shows a cathode ray oscillogram of a laboratory test in which one restrike occurs on the first high frequency transient and then one after about one-quarter cycle of the slower rising normal frequency recovery voltage. It has been found advisable when making laboratory tests checking the interrupting performance of a circuit breaker on charging current to have the impedance of the power source less than ten per cent of the capacitive reactance being switched in order to avoid such a large initial high frequency kick that restriking tends to occur either on this oscillation or not at all.

The analysis given above applies to the switching of large static capacitor banks such as are used for power factor control, or as used in high power laboratory tests arranged to simulate the switching of high voltage transmission lines. High voltage cables of short length can be considered also as lumped capacitances insofar as the interruption of charging current is concerned.

Transmission Line Switching

If a long transmission line is substituted for the lumped capacitance, the general operation of interrupting charging current is similar, although there are detail differences which may be of considerable importance. Figure 6 indicates the transient voltage variations of the bus and line potentials that may be expected with a single arc restrike approximately one-half cycle following current zero. The most obvious difference between this operation and the switching of a lumped capacitance is the more abrupt change in the voltage and current at the beginning and end of a restrike because of the characteristics of traveling waves on a transmission line. The magnitude of the surge current is equal to the potential difference across the breaker at the restrike instant divided by the surge impedance of the line (approximately 500 ohms).

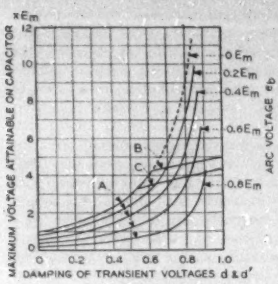

Figure 2

Curves *A* show maximum voltage attainable as a function of arc voltage magnitude and transient damping factors, assuming repeated restriking during interruption of capacitor charging current. Additional limits are indicated by curve *B* calculated for zero arc voltage on basis of breaker not restriking at voltage crest *N* (Figure 1) when equal to or less than high frequency crest *M* previously withstood. Upper limit curve *C* applies if breaker dielectric strength is assumed to increase at least 25 per cent from *M* to *N*. Damping factors *d* and *d'*, with and without capacitor *C*, assumed equal

The duration of the restrike current pulse is primarily a function of the line length, representing the time for a wave to travel the length of the line, reflect, and return to the circuit breaker, with a small additional time interval for the current to fall to zero depending on the amount of series inductance in the source. During the traveling of the wave there is an appreciable amount of attenuation which reduces the amplitude of the overvoltage at the breaker when the wave returns. If there is appreciable series inductance in the source, the rate of change of voltage on the bus during a restrike will be slowed down, the equivalent time constant being approximately L/Z where Z is the surge impedance of the line. Taking into consideration the bus capacitance C_e results in a superimposed oscillation on the rising surge voltage and current as indicated in Figure 6. Provided that the restrike current is extinguished after only one-half cycle, the voltage oscillation immediately following has a frequency and damping coefficient dependent on the constants of the circuit on the bus side and independent of whether a transmission line or capacitance is on the other side of the open contacts of the breaker.

Figure 7 is a reproduction of the oscillographic record for one phase of a typical field test interrupting 155 amperes of charging current to 183 miles of line with a bus voltage of 241 kv. Voltage across the breaker was measured from the amplified potential difference taken from capacitance dividers utilizing the potential taps on the capacitor-type high voltage breaker bushings. A standard bushing potential device and current transformer were used to obtain the records of the bus voltage and line current.

A single restrike took place approximately 0.2 cycle after a current zero. The surge current was interrupted after a single pulse, the bus voltage swinging momentarily about 35 per cent above the voltage immediately after the line was dropped but only 20 per cent above the voltage on the bus while charging current was flowing. The maximum voltage across the breaker one-half cycle after the restrike was two and one-half times the final bus voltage. Insofar as disturbance to the system is concerned this particular operation would be of negligible importance, being comparable to the voltage fluctuations to be expected during the energizing of the line.

Functioning of Various Types of Interrupting Devices

High voltage circuit breakers are designed primarily to interrupt short-circuit currents quickly and effectively. Although their ability to handle charging current generally has been taken for granted, specific modifications to improve this function may be justified in some cases provided that high current arc rupturing performance is not jeopardized.

The ideal type of circuit breaker from the point of view of opening charging current is one which will develop dielectric strength at a sufficiently rapid rate so that even if a current zero occurs just after contact parting, the dielectric strength will keep above the rising recovery voltage, and thus no restrike will occur. At moderately low voltages, such as 2,300 to 15,000 volts, the standard oil circuit breaker conforms very closely to this ideal, except perhaps when switching large capacitor banks rated in excess of 10,000 kva.[4] At higher voltages, more contact breaks in series or higher contact opening speeds may be used to avoid restriking. Another method is to provide a high velocity oil flow suitably directed into each gap, so that in a very small interval of time after current zero the contact gaps are filled with high dielectric strength oil. Such breakers have been built commercially,[5] but they are costly because of the large number of contact parts and the very great amount of mechanical effort required to produce high velocity oil flow in all of the contact breaks.

It is instructive to consider the early types of high voltage oil circuit breakers with either plain or quick-break contacts, which in spite of a dozen restrikes or more seldom seemed to produce appreciable overvoltages. The rate of recovery of dielectric strength was so low in these breakers that during the first few inches of arc length drawn by the opening contacts, restrikes occurred with very short current zero pauses and therefore with no overvoltage produced. Even when sufficient arc length had been attained to be almost capable of holding the recovery voltage, the probability of interrupting the restrike current at the first current zero was rather low because of the high rate of voltage rise just after the return of the traveling wave on the line. In general, the lack of effective arc control contributed to random restriking of the arc which made it extremely unlikely that even two consecutive restrikes would occur under the special conditions required for cumulative build-up of high voltage. Appreciable arc voltage for the long arcs at the time of the later restrikes might be expected to contribute some voltage limiting effect, although the curves in Figure 2 indicate that even fairly high arc voltage does not have a very important influence unless other damping factors are quite strong. The introduction of highly effective deionizing structures has made it possible to interrupt quite high rates of rise of recovery voltage with relatively short arc length, so that one or two successive restrikes with interruptions of the surge current at the first current zero have become more common.

The majority of arc extinguishing devices on high voltage breakers at the

Figure 3. Interruption of 45 amperes capacitor-charging current at 66,000 volts. Single arc restrike is extinguished after three half cycles of high frequency surge current. Voltage across breaker is increased by charge trapped on capacitor

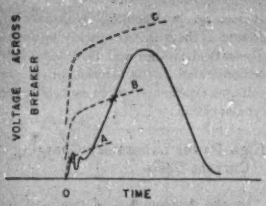

Figure 4. Typical transient recovery voltage across breaker following current zero when interrupting capacitor charging current

Dotted curves indicate dielectric recovery of arc space for different contact separations. Restrikes will occur under condition *A* and *B*, but not for recovery condition *C*

present time are of the self-generated flow type. These may be separated into two distinct classes, those with a single break per interrupting unit and those with at least two series breaks for each interrupting unit, one of which is a pressure generating break for providing oil flow into one or more interrupting breaks. The first of these two classes of interrupters obtains a high degree of gas turbulence and deionizing activity by various arrangements of baffles and vents, in certain constructions using magnetic action[6] to keep the arc and oil in close proximity. However, the interrupting effectiveness decreases very rapidly as the current to be opened decreases in value, so that in interrupting magnetizing or charging current, the dielectric developed per inch of contact gap is only slightly greater than with plain breaks. However, by using a considerable number of units in series and operating at high speed, the interrupting effectiveness may reach a value where the number of restrikes even at very high voltage amounts to only one or two.[7]

The second class of interrupters also has a reduced deionizing activity at lower current, although not nearly to the extent of the first class. If the pressure generating gap is made relatively long, even though the pressure produced for driving oil into the second break decreases as the current goes down, tests show that the required flow for effective deionization also decreases with current, so that the arcing time is only slightly longer at low currents than when interrupting short-circuit current.[5,9]

Even though several restrikes during the interruption of charging current in actual practice rarely produce voltage surges above twice normal crest voltage, the desirability of reducing the number of restrikes to a minimum makes the use of an auxiliary oil flow piston driven by springs or other definite mechanical force appear attractive. Where only two interrupting units are used per breaker pole, the voltage gradients developed at a current zero immediately after contact separation could be rather high. However, very satisfactory performance has been shown when an oil flow piston is used with a delayed action so that a minimum gap will be obtained before attempts to hold voltage are made.[10] At any current zeroes coming at the prepumping interval the arc will, of course, reignite at a very low voltage. At the next current zero after the pump has gone into action, because of adequate contact separation, the interrupter will be able to hold the double voltage occurring one half cycle later.

Compressed air circuit breakers have interrupting characteristics approaching those of forced oil flow or impulse type oil circuit breakers. However, when the number of breaks for high voltage ratings is reduced to a minimum, delayed action may be desirable for these air blast breakers also in order to avoid attempts to clear at very short contact spacings. This has been arranged in at least one commercial interrupter[11] by allowing the moving contact to act as a valve, letting it practically fill the orifice until a certain separation has been obtained. When the orifice is unplugged by the contact, air flow starts and interruption will occur usually at the next current zero.

Use of Parallel Resistance

Resistance in parallel with the arc extinguishing devices may be used for two distinct purposes, according to the value of resistance employed. High resistance, from several hundred thousand ohms up to one or two megohms per interrupter,[8] is used primarily to assure substantially equal division of voltage among the several series breaks. This provides the most effective utilization of all contact gaps, and therefore keeps the number of arc reignitions to a minimum when interrupting either short-circuit current or line-charging current. Because of the relatively low power loss during the few cycles that such resistors are in the circuit, their physical dimensions may be made quite small. Also the opening of the residual resistor current, being only a small fraction of an ampere at high power factor, presents no difficulty as the main breaker contact disconnects from the interrupting units.

If, now, the value of the resistance is brought down to between a few hundred and several thousand ohms it will fall in a range recommended[12,13] for reducing overvoltage surges during the interruption of charging current. When the extinction of the arc between the breaker contacts inserts such a resistor in the circuit, instead of the transmission line being left isolated, it still will be connected to the bus, but now through series resistance. Taking a value for the resistance two or three times the capacitive reactance of the line, the a-c line voltage gradually will settle down to less than half its normal value. However, what happens to the voltage across the breaker contacts (that is, across the resistor) in the transient period during the first half cycle after current zero is of the most interest. Instead of building up to twice normal crest as shown in Figure 1*c* for the case without the resistor, the potential of the line will fall sufficiently so that a somewhat lower maximum of perhaps only one and one-half normal crest voltage is reached. This, naturally, decreases the probability of restriking and also lowers the magnitude of the overswing of the line voltage perhaps 20 per cent should the restrike occur. The resistor, however, does not introduce additional damping in the oscillation of the voltage when a restrike does occur, because the surge current

Figure 5. Cathode ray oscillogram of voltage across circuit breaker during interruption of capacitor charging current, illustrating restriking conditions indicated in Figure 4

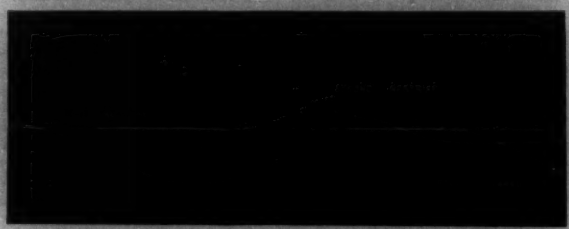

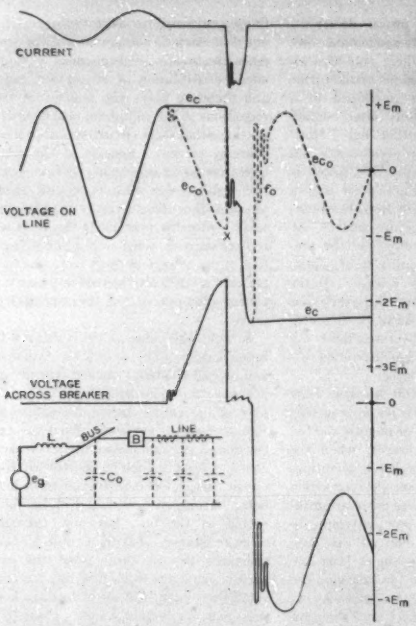

Figure 6. Interrupting charging current of transmission line with one restrike occurring at X and producing overvoltages

Similar to Figure 1 except for modifications in transient voltages and currents because of distributed capacitance and inductance of line and resulting traveling wave effects

temporarily short circuits the parallel resistor.

On the other hand, when energizing a capacitance load, the resistor is inserted first and then short circuited by the contacts. This sequence tends to reduce the voltage oscillation and current surge normally produced should the line be connected at a time when the bus voltage is at crest value. Another incidental advantage of the resistor is the damping effect on the recovery transient when opening short-circuit currents. For those less effective interrupters which are sensitive to high voltage-recovery rates, this action may be beneficial.

There are, however, some disadvantages in using these low ohmic value resistors which should not be overlooked entirely. Adequate thermal capacity requires relatively large physical dimensions, which in some cases may reduce electrical clearances within the breaker. Also, the magnitude of the resistor current is comparable with that of line charging currents, and the circuit, therefore, should not be considered interrupted until after the resistance circuit is broken, which usually requires several additional cycles of interrupting time. During the interruption of this residual resistor current, restrikes may occur although the amplitude of the voltage surges is not likely to be important unless the resistance has a value somewhat below the preferred range of approximately two to three times the capacitive reactance of the line being switched.

Arcing in the disconnect gap provided in oil circuit breakers below the interrupting units contaminates what was intended to be a clear oil break, and delays the removal of the high voltage gradient from the main contact gaps after the interruption of a heavy short circuit. Resistor currents of only 40 to 50 amperes are still high enough to sustain an ionized flashover path on a transmission line until interrupted by the breaker so that the additional time for opening this current increases by approximately that amount the minimum permissible interval before line re-energization on a high speed reclosing duty cycle.

In connection with the use of resistors, the beneficial effect of a grounded neutral transformer connected to the far end of a line or cable being switched should be mentioned. Under these conditions, instead of the line being left isolated at high potential, the charge has an opportunity to leak off through the transformer which approaches a shunting resistance to ground as the iron core quickly saturates. Theoretical studies and field tests have demonstrated a definite reduction in overvoltages experienced when switching this type of circuit.

High Power Laboratory Charging Current Tests

In the development of new and improved high-voltage arc-rupturing devices, the high power testing laboratory[14] has proved to be an indispensable tool. Short-circuit interrupting ability may be demonstrated over a wide range of currents and voltages and voltage-recovery rates. High current transformers have made possible adequate checks on short time current ratings. However, in the demonstration of transmission line switching, a number of difficulties arise.

First, the amount of capacitance required to simulate a long high-voltage transmission line is by no means inconsiderable. A 3-phase capacitor bank taking 200 amperes at 230 kv (80,000 kva) to represent approximately 260 miles of line would cost in the neighborhood of $750,000 and would occupy the space of a fair-sized building! Actually, the situation is not too serious, as it is practical to test single phase only, and because the test is only momentary it is possible to obtain the higher currents by operating the capacitors at over twice normal voltage, representing an increase of four times in the kva. However, under these circum-

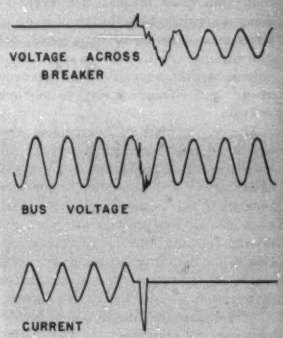

Figure 7. Tracing of oscillogram of field test disconnecting 183 miles of 230-kv line

Single restrike leaves line charged slightly above normal crest voltage, increasing voltage which appears across breaker. Oscillation in bus voltage is not over 15 per cent above normal crest

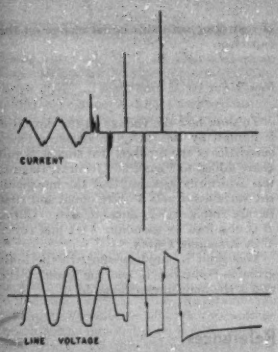

Figure 8. Tracings of oscillograms of field test disconnecting 50 miles of line at 230 kv

In spite of six restrikes, four of which are extinguished at first zero of surge current, maximum voltage attained on line is less than twice normal crest of line-to-ground voltage

stances the capacitors must be protected from overvoltage surges by series damping resistors and protective gaps so that cumulative buildup of voltage is avoided. Thus, the effects of repeated restriking are not checked in the higher current range, although the tests do determine fairly accurately the probability of an initial restrike.

It should also be noted that traveling wave phenomena are not simulated accurately, so that the ultimate verification of charging current interrupting performance should be carried out on an actual power system. Network calculator studies likewise only approximate traveling wave conditions, but they are very helpful in checking the effects of various system connections,[3] in spite of the uncertainty caused by the necessity of predicting the way in which the breaker will function.

In spite of these limitations in facilities, it has been found that the high voltage interrupters developed and checked in the laboratory perform very satisfactorily in the field when applied on transmission line switching duty.

Field Testing of Charging Current Interruption

It has been shown in Figure 2 that repeated restriking of an arc during the interrupting of charging current theoretically might produce overvoltage surges above four times normal line to ground crest voltage. However, records of hundreds of field tests on solidly grounded systems rarely have shown voltages on either line or bus above two and one-half times normal. In Table I are presented data taken from a large number of these tests showing the maximum voltages measured with either magnetic type or cathode ray oscillographs. Several different types of high voltage interrupters are included with arc restriking conditions varying from no restrikes at all to six or seven cycles of repeated restriking.

One fairly severe example of restriking is shown by Figure 8, the record of a charging current interruption of 37 amperes of current for a 50-mile section of 230 kv line. Six reignitions of the arc current may be observed, the last four restrikes being spaced at approximately half cycle intervals with the unfavorable condition of successive interruptions after only a single surge of restrike current. Although the line voltage built up cumulatively at each restrike the maximum potential reached was still appreciably less than twice normal line-to-ground crest value.

Close examination of the arc reignitions shows that in each case the contact gap broke down before the potential across the breaker had reached the maximum possible value. This illustrates very clearly the general conclusion that the dielectric build-up characteristics of high voltage circuit breakers just does not provide the restrike timing required to develop the theoretical voltage ceilings of four to five times normal voltage for grounded neutral systems.

Conclusions

As the severity of switching duty has increased, improved circuit breakers have been developed which give better performance not only on fault interruption but also on charging current interruption. While it is possible to construct breakers that are capable of interrupting charging currents even at the highest voltages without any restriking, such extremes are not usually necessary. For instance, a single restrike will not produce hazardous overvoltages on solidly grounded systems. A number of breaker designs incorporating such features as delayed-action oil-flow pistons or extra high-speed multibreak contacts are available which do not restrike more than once after an appreciable pause in the current. While certain sequences of repeated arc restriking and clearing can produce surge voltages over four times normal line-to-ground crest voltage, numerous field tests demonstrate that in service such sequences seldom are produced. For the rare instances that may occur, protective gaps or lightning arresters can be relied on to protect important pieces of equipment.

Resistances of a few thousand ohms connected in parallel with the breaker contacts, in spite of certain inherent disadvantages, may be used to reduce not only the probability of arc restriking when interrupting charging currents but also the magnitude of the overvoltage surges. They also serve to limit the moderate voltage surge that may accompany the energizing of a capacitive load. On systems having appreciable impedance in the neutral and where long lines or cables are to be switched, consideration may well be given to the use of such resistances.

Because of the difficulty of simulating transmission lines in laboratories, field tests of charging current interruption are of very great value. Fortunately considerable data have been obtained already but more field tests are desirable to establish with greater certainty the probability of severe overvoltage surges. Such information will assist both system engineers and circuit breaker designers to determine the emphasis which should be placed on obtaining special features, such as resistors or limited restrike performance, in high voltage switching equipment.

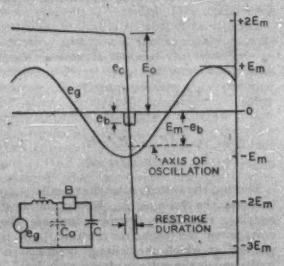

Figure 9. Breaker *B* opening charging current of capacitor *C*. During restrike, arc voltage e_b shifts axis of oscillation from E_m to $E_m - e_b$

Appendix I. The Effect of Arc Voltage During a Restrike

In the circuit of Figure 9 for a breaker *B* opening the charging current of a capacitor *C*, the arc voltage, e_b, is in series with the generated voltage. During the relatively short time consumed by one-half cycle of a restrike, the arc voltage is opposed to the

generated voltage, and both voltages can be considered constant. Consequently, the effect of the arc voltage is the same as an equal reduction in the generated voltage. This reduces the initial amplitude of the transient voltage by the value of the arc voltage and reduces the value of the voltage reached by two times the arc voltage.

If E_o is the voltage on the capacitor C prior to the restrike, the transient voltage, e_c, during the first half-cycle of high frequency can be written

$$e_c = (E_m - e_b) - (E_m + E_o - e_b) \cos t / \sqrt{LC}$$

The maximum voltage is reached at $t = \pi \sqrt{LC}$.

$$e_{c_{max}} = 2E_m - 2e_b + E_o$$

Appendix II. The Effect of Arc Voltage and Circuit Resistance During a Restrike

Arc voltage and circuit resistance limit the maximum voltage which can be reached by an unlimited number of restrikes at just those instants which give maximum increase in the voltage on the capacitor.

The voltage e_c on a capacitor, during a half-cycle of a restrike is given by the following equation taken from Appendix I and modified to include the damping effect of circuit resistance. It is assumed that the resistance is not high enough to make an appreciable correction to the oscillation frequency.

$$e_c = (E_m - e_b) - (E_m + E_o - e_b) \times \epsilon^{-\frac{R}{2L} t} \cos t / \sqrt{LC}$$

The maximum value is reached when $t_1 = \pi \sqrt{LC}$.

Let

$$d = \epsilon^{-\frac{R}{2L} t_1} = \epsilon^{-\frac{\pi RC}{2}}$$

$$e_{c_{max}} = E_m - e_b + dE_m + dE_o - de_b$$

$$e_{c_{max}} = (E_m - e_b)(1+d) + dE_o$$

Because the voltage after the restrike $e_{c_{max}}$ becomes the voltage, E_o, before the next restrike, successive restrikes increase the voltage on the capacitor until a limit is reached at which the voltage before a restrike equals the voltage after a restrike.

Then

$$E_o = e_{c_{max}}$$

$$e_{c_{max}} = (E_m - e_b)(1+d) + de_{c_{max}}$$

$$e_{c_{max}} = \frac{1+d}{1-d}(E_m - e_b)$$

The curves A of Figure 2 are plotted from this equation.

Appendix III. The Effect of the Dielectric Strength Recovery in the Breaker on the Maximum Voltages Attainable by Repeated Restriking

After a breaker in a capacitive circuit interrupts a restrike current surge, leaving a charge on the capacitor, the breaker is subjected to a high-frequency transient recovery voltage as shown in Figure 1*c*. The amplitude of this transient voltage is a function of the charge left on the capacitor. If the charge is increased, the crest of the transient recovery voltage will be increased by a greater amount than the voltage crest which is available a half-cycle later to produce the next successive restrike under the assumed conditions for maximum cumulative build-up of voltage. The maximum transient recovery voltage, reached after a half-cycle of high frequency, is

$$e_t = (E_o - E_m)(1+d')$$

where

E_o is the voltage on the capacitor.

E_m is the crest of the generated voltage.

d' is the damping factor (Appendix II) for the circuit with the breaker open.

$$d' = \epsilon^{-\frac{\pi R' C'}{2}}$$

The voltage across the breaker, at the end of a half-cycle of system frequency when a restrike is assumed to occur, reaches a peak.

$$e_s = E_o + E_m$$

The ratio, k, of these voltages is

$$k = \frac{e_t}{e_s} = \frac{(E_o - E_m)(1+d')}{E_o + E_m}$$

As shown in Figure 4, the dielectric strength of a breaker increases during the half-cycle following a restrike. Therefore, a restrike on the system frequency voltage crest should not occur if the crest voltage is less than or equal to the high frequency transient recovery voltage peak; that is, if k is equal to or greater than one. To allow for an increase in dielectric strength during this period, some lower value of k such as 0.8 can be chosen.

The maximum voltage at which a restrike can occur on the system frequency voltage to produce an increase in capacitor voltage, is therefore a function of k, and can be expressed as follows by rearranging the formula for k

$$E_o = E_m \frac{d'+k+1}{d'-k+1}$$

The maximum voltage which can be reached by restriking is therefore the result of restriking with this initial charge on the capacitor.

$$e_{c_{max}} = (E_m - e_b)(1+d) + dE_m \frac{d'+k+1}{d'-k+1}$$

To show how the voltage on the capacitor is limited by the dielectric recovery characteristics of the breaker, two curves B and C are added to Figure 2. To draw them it was arbitrarily assumed that the independent variables d and d' were equal and that the arc voltage e_b was equal to zero. Curve B is obtained by assuming $k = 1$ and curve C by assuming $k = 0.8$.

This limit is supplementary to the limit given in Appendix II and the lower of the two is the maximum attainable.

References

1. Voltages Induced by Arcing Grounds, **J. F. Peters, J. Slepian.** AIEE Transactions, volume 42, 1923, April section, pages 478–93.

2. Circuit Breaker Recovery Voltages, **Robert H. Park, Wilfred F. Skeats.** AIEE Transactions, volume 50, 1931, March section, pages 204–38.

3. Power-System Transients Caused by Switching and Faults, **R. D. Evans, A. C. Monteith, R. L. Witzke.** AIEE Transactions, volume 58, 1939, August section, pages 386–94.

4. Tests and Analysis of Circuit-Breaker Performance When Switching Large Capacitor Banks, **T. W. Schroeder, E. W. Boehne, J. W. Butler.** AIEE Transactions, volume 61, 1942, November section, pages 821–31.

5. Circuit Breakers for Boulder Dam Line, **D. C. Prince.** AIEE Transactions, volume 54, 1935, April section, pages 366–72.

6. Recent Developments in Arc Rupturing Devices, **R. C. Van Sickle, W. M. Leeds.** AIEE Transactions, volume 51, 1932, pages 177–84.

7. Tests of 230-Kv High-Speed Reclosing Oil Circuit Breakers, **A. C. Schwager.** AIEE Transactions, volume 63, 1944, November section, pages 784–8.

8. A Multionifice Interrupter for High-Voltage Oil Circuit Breakers, **L. R. Ludwig, W. M. Leeds.** AIEE Transactions, volume 62, 1943, March section, pages 119–25.

9. Dethermalizing Arc Quenchers, **Lloyd F. Hunt, Fred H. Cole.** AIEE Transactions, volume 62, 1943, November section, pages 720–4.

10. High-Voltage Oil Circuit Breakers for Rapid Reclosing Duty, **A. W. Hill, W. M. Leeds.** AIEE Transactions, volume 63, 1944, March section, pages 113–18.

11. A Three-Cycle 3,500-Megavolt-Ampere Air-Blast Circuit Breaker for 138,000-Volt-Service, **H. L. Byrd, Ben S. Beall.** AIEE Transactions, volume 64, 1945, May section, pages 229–32.

12. Influence of Resistance on Switching Transients, **R. C. Van Sickle.** AIEE Transactions, volume 58, 1939, August section, pages 397–404.

13. Switching Overvoltage Hazard Eliminated in High-Voltage Oil Circuit Breakers, **L. F. Hunt, E. W. Boehne, H. A. Peterson.** AIEE Transactions, volume 62, 1943, February section, pages 98–106.

14. High Capacity Circuit-Breaker Testing Station, **J. B. MacNeill, W. B. Batten.** AIEE Transactions, volume 61, 1942, February section, pages 49–53.

Discussion

Philip Sporn and **H. P. St. Clair** (American Gas and Electric Service Corporation, New York, N.Y.): The authors of this paper have added some important data and conclusions in regard to the problem of interrupting charging current in long high-voltage lines. We should like to suggest that the successful elimination of switching surge overvoltages higher than say, two times normal, if this can be assured through modern breaker developments, may have very great economic significance.

Insulation levels at present are determined by voltages originating in lightning and switching surges, and by the level of protection afforded by lightning arresters. While the arrester must withstand the maximum dynamic or 60-cycle overvoltage which can be imposed upon it at its point of application, and this voltage has nothing to do with switching surges, it very well may be that the ultimate elimination of excessive switching surge overvoltages will permit a substantial reduction in insulation generally because lightning overvoltages are of so much shorter duration than switching surges and hence much less destructive to arresters. While this reasoning applies particularly to station apparatus, a reduction in insulation levels of transmission lines may be feasible also because lightning effects can be controlled pretty well, first, by design in regard to shielding and tower footing resistance, and second, by the use of ultrahigh speed reclosing. Obviously, shielding and tower-footing resistance cannot control the effects of switching surges.

Some 20 years ago one of the discussers of this paper first presented to the Institute a paper entitled "Rationalization of Transmission System Insulation Strength." The ideas developed there not only found general acceptance but later as they were further developed served as the basis for modern ideas of insulation co-ordination which have contributed both to the improved technical performance and economic soundness of modern transmission systems. But, while the ideas with regard to insulation levels needed had been developed soundly, the levels subsequently adopted were determined by experience, both analytical and pragmatic, in the operation of systems with breakers as then existed.

It would appear therefore, that the time is fully ripe now for a re-evaluation of the whole problem in the light of new concepts for controlling the magnitude of switching surges by the use of modern breakers. We have indeed here the possibility of savings which will be of tremendous economic importance to the entire electric power industry.

A second point we should like to mention in connection with this paper has to do with field testing of circuit breakers. As is well known, we in our own organization have carried out field tests on various occasions during the past 20 years and have advocated persistently the making of such tests as a necessary supplement to factory laboratory procedure in the proving and perfecting of new circuit-breaker developments. With this background, therefore, we are pleased to note that for the first time, we believe, the authors have given unqualified recognition to the need for field testing programs to supplement factory testing facilities. We are glad to welcome the Westinghouse Company into the fold.

E. C. Starr (Oregon State College, Corvallis, Oreg.): This paper is of particular interest because of the data given in its Table I on measured overvoltages arising from switching surges. It appears that previous estimates of switching-surge voltages caused by restrikes in breakers interrupting the charging current of long high-voltage lines may require a downward revision. Most lines of the voltage class reported in this table operate so near the corona level that any large increase in voltage requires a large power input. Because the mechanism involved in these switching surges is not adaptable to transferring large amounts of power, excessive voltage rises are suppressed effectively. Figure 8 of the paper bears out this analysis. The rate of free decay of voltage on the open line when considerably above normal is shown to be very rapid indicating high losses which decrease rapidly as the voltage is reduced.

A careful consideration of such data may lead to the adoption of lower normal-frequency line insulation levels where lightning is not the determining factor. Increased economies thereby may be effected.

It would be interesting to know the magnitudes of voltages appearing at the far ends of the lines corresponding to the values given for the interrupted ends in Table I. If the authors have obtained such data, a general summary or discussion would be appreciated. If these data have not been obtained previously, consideration should be given to recording open-end voltages in future charging-current interrupting tests.

I. B. Johnson (General Electric Company, Schenectady, N. Y.): The authors' paper on the interruption of charging current at high voltages is indeed a timely review and summarization of some of the knowledge on the subject. The basis of the authors' evaluation of the relative cost and use of multibreak high-speed oil impulse breakers of the stored energy type, however, appears to be somewhat questionable. These breakers do more than interrupt line charging current without any difficulty pertaining to switching surges These breakers of high-speed operation, which improve system stability, reduce damage from dynamic current following faults, and reduce maintenance because of the short arcing time and slight oil deterioration, have demonstrated their superiority by their operation in the field. It is expected that the superiority will become more evident at a higher voltage such as 360 kv.

In the authors' conclusions regarding overvoltages from restriking it is stated, "For the rare instances that may occur, protective gaps or lightning arresters can be relied on to protect important pieces of equipment." It is to be realized that, as transmission line voltages and distances increase, the capacitive energy stored in the line will tend to increase as the square of the voltage and as the first power of the line length. This will increase considerably the discharge duty requirements of arresters in the event of arrester operation by a switching surge. Also, for breakers using no shunting resistance across the interrupting contacts, transient analyzer studies indicate in an extreme case of switching 400 miles of line that the degree of overvoltage and the degree of arrester duty are not as great when restriking occurs for maximum voltage across the breaker contacts a half-cycle after interruption of charging current at a current zero as when restriking occurs sooner at a lower voltage than the maximum voltage possible across the breaker contacts. Because of the possible random nature of the phenomenon when allowed to occur, it is probable that designing breakers with a more positive reliability against restriking is to be preferred for long distance transmission systems that may operate up to such levels as 360 kv in order to guarantee further the protection of the essential line insulation and terminal equipment of such systems from the effects of switching surges.

E. W. Boehne (Massachusetts Institute of Technology, Cambridge, Mass.): The authors are to be congratulated on an interesting paper. They re-emphasize the importance of the capacitance switching problem in high-voltage breakers. Attention is drawn to the statistical observation that field tests do not give rise to the magnitude of surges obtained on theoretical considerations. This is of great practical significance, however, care must be taken to be assured that the field results studied give a fair sample of the probable field conditions. The conservatism of the authors on this point is not of the same type as is expressed by the ultimate user who does not wish to base the performance of his equipment upon the average to be expected but is more concerned with the worst probable condition to be encountered.

Experience shows that early random restriking is comparatively harmless and in some respects a desirable characteristic if restriking is associated with large capacitive currents, and that if the available capacitance current is reduced the restriking is further delayed into the more dangerous regions. Hence each breaker will experience its most vulnerable condition at some nominal value of leading current which may be considerably less than the capacitive current encountered in the average installation. This characteristic of high-voltage breakers, when interrupting capacitive currents, must be recognized to evaluate properly the material presented and to formulate adequate factors of safety for all eventual applications of the breaker.

High-voltage circuit breakers having two breaks per pole enjoy a distinct advantage over single-break breakers when interrupting capacitive currents. This is primarily true of the more modern breakers having arc control devices and specifically true of those breakers whose arc control devices possess low resistivity by means of resistance coatings or resistors of less than 25 megohms. Such breakers divide the voltage more or less equally between the two breaks. It is interesting to point out, however, that at the instant the double voltage appears across the single pole of a double-break breaker during a capacitive interruption, the distribution would be 50-50 across the two breaks on the basis that the intermediate crosshead held no charge at this instant.

This is the inherent voltage distribution across any 2-break breaker pole whose breaks are identical and arranged symmetrically, and where plus E volts is applied to one terminal and minus E volts applied to the other, and is independent of the amount of resistance across the breaks. These considerations become important from the standpoint that the breaker having two breaks per pole is most efficient, voltage wise, when interrupting capacitive currents. Their substitution with breakers having but one break per pole and required to interrupt capacitive currents requires close analysis and test to insure their proper field application. Fortunately those breakers of this type are primarily of the impulse type or equipped with resistors which provide adequately for this contingency.

The authors' recommendation of resistors between two and three times the capacitive ohms to neutral is of interest and agrees quite well with the nominal value of 2.1 times the capacitive ohms to neutral suggested in 1945. This result stems from the equation

$$B^2 = \epsilon^{\frac{2}{B}}$$

Where B is the ratio of ohmic resistance to capacitive ohms to neutral. The solution of this equation for this ratio is 2.11. This value of resistance will permit the line charge to drop to zero in just one-half cycle following the interruption of leading current. As pointed out then, and in the present paper, resistances just above and below this value will be found of suitable protective value, the variation usually depending upon the type of interrupter, speed of contact separation, nature of the circuit, and the type of grounding employed.

T. M. Blakeslee (Los Angeles Department of Water and Power, Los Angeles, Calif.): The Leeds and Van Sickle paper presents a timely summary of the situation regarding charging-current interruption. Their thorough mathematical analysis takes into account more factors than the basic treatment presented in the Sadler and Blakeslee paper.[1] Because these additional factors indicate slightly lower overvoltages, operating men should be encouraged as the situation is not quite as bad in those cases where these factors are applicable.

The paper, however, is characterized by an attitude of hopeful optimism that is dangerous for the operating engineer. His must be the pessimistic point of view. He knows by painful experience that if it is possible to happen, some day it will. There are many random things that the operating engineer cannot control as exemplified by troubles resulting from lightning, severe storms, or falling airplanes, but if he could control these things at a reasonable cost he certainly would do so, in order to approach more closely his goal of uninterrupted power service.

When breakers that do not restrike while interrupting charging currents can be obtained at a reasonable cost they will be used. In the meantime the self-extinction-principle circuit breaker, or as Leeds and Van Sickle call it, the "self-generated flow" type is still used extensively and while giving excellent performance on short-circuit currents, admittedly it restrikes when handling charging currents. Freedom from trouble resulting from these restrikes is a gamble and therefore cannot be guaranteed.

The application of resistors to this type of circuit breaker is a means of limiting overvoltages resulting from restrikes. It is reasonable that the operating engineer should use this panacea for troubles from charging-current interruption to the utmost possible within the limits of design and cost. He thus can get the guarantee of immunity he likes to have rather than live in the hope that trouble will not occur.

REFERENCE

1. RESISTORS FOR 138-KV CABLE SWITCHING, **E. K. Sadler, T. M. Blakeslee.** AIEE TRANSACTIONS, volume 66, 1947, pages 39–50.

W. M. Leeds and **R. C. Van Sickle:** The design, application, and use of electrical apparatus progresses as more and more facts become known. As Philip Sporn, H. P. St. Clair, and E. C. Starr have mentioned, the less the uncertainty, the less the allowance that has to be made for it. The interruption of charging currents at high voltage involves complicated phenomena and is best studied through actual tests on high-voltage circuits. This has resulted in the several series of tests which produced the data summarized in Table I of the paper. This compilation of available pubilshed and unpublished data covers various types and makes of breakers. Further field testing to increase our knowledge of charging current interruption and the performance of new interrupters is certainly desirable and additional data on voltages at the open end of the circuit as suggested by E. C. Starr should be obtained.

As emphasized by I. B. Johnson, the paper points out that the difficulty of interrupting charging current increases with voltage and current, and in addition, it points out and discusses the solutions which are available without emphasis upon the merits of a particular one. Interruptions without restrikes is an obvious solution, but not the only one. Interruptions accomplished by inserting one or more steps of resistance is another solution and limits the overvoltages which can be reached when restriking occurs. Even without the resistors in the circuit breaker, resistance and damping effects are present in the circuit and exert an influence on any restrike as discussed in the paper and as added to by Starr's remarks on corona losses. The particular solution which may be best depends on an evaluation of the disadvantages as well as the advantages of the various schemes.

The longer the line, the longer the time interval required for a surge to travel to the end of the line and back. For the longer lines, the time becomes an appreciable part of a cycle, and the system voltage changes considerably during a restrike as can be shown easily. This and the additional attenuation reduce the maximum voltage which can be produced and, as Johnson pointed out, move the restriking point producing the maximum voltage to a voltage occurring before the maximum crest is reached. Consequently, the charging current of long lines will be correspondingly large and more difficult to interrupt, but the voltages which can be reached by a single restrike will be less than on a shorter line.

The paper does not indicate a change in our attitude toward field testing. We have participated in many field tests and still believe in obtaining as much field data as possible to demonstrate circuit breaker performance on line-charging currents and on short-circuit interrupting capacities beyond those obtainable in our high power laboratory.

However our experience has shown that when the field tests are within the interrupting capacities tested in the laboratory, they have closely confirmed the laboratory performance, and usually have provided no additional significant data.

We hope the paper has accomplished its purpose in calling attention to the data obtained on field tests and to the discrepancy between calculated and measured maximum voltages and in analyzing some of the breaker and circuit characteristics which control the voltages reached during charging current interruption.

Sectionalizing and Internal Transformer Fusing on Rural Power Circuits

BRUCE O. WATKINS
MEMBER AIEE

Synopsis: This paper discusses the co-ordination of internal transformer fuse links with line sectionalizing devices on 7.2/12.5-kv multigrounded neutral rural lines, and methods for improving this co-ordination and the electric service to farm areas.

An internally mounted primary fuse link is an integral part of the transformer on a large number of the transformers supplied to rural electric systems. In the interests of more adequate sectionalizing and less interrupted power aimed toward the improvement of electrical service to the farm consumer the following suggestions are made:

1. Internal links of various transformer manufacturers should be standardized.

2. The rating of the link in the conventional internally-fused-type transformer should be no greater than that in the entirely self-protecting type of the same rating.

3. The characteristics of the internal link should be designed for better co-ordination.

4. The characteristics of sectionalizing reclosers should be designed for better co-ordination.

5. System studies should give consideration to proper co-ordination of reclosers and transformer protective equipment.

ONE OF the principal means for maintaining as continuous electrical service as possible consists in sectionalizing the system so that trouble in one area will be isolated and not affect other areas. Perhaps the greatest difficulty confronting the engineer in the solution of sectionalizing problems on rural distribution systems stems from one fact that economics severely limit the use of relays or other expensive devices, and resort must be made to fuses, series coil trip circuit breakers, and so forth. In spite of these difficulties, a reasonably good co-ordination job is generally possible. Line sectionalizing on rural systems has trended toward use of the automatic reclosing circuit breaker, which has materially improved electric service.[1] New designs of "reclosers" are expected to further increase continuity of service.[2]

The co-ordination of rural type primary transformer protection and line sectionalizing devices is a field which offers promise for material reduction in consumer outage time. This applies particularly to the internally fused transformer. When an individual transformer fails it is highly desirable to automatically disconnect it from the line since failure of a transformer over-current protective device to clear before the line sectionalizing unit opens results in an outage on the entire line, putting a group of consumers out of service until the faulty transformer is located.

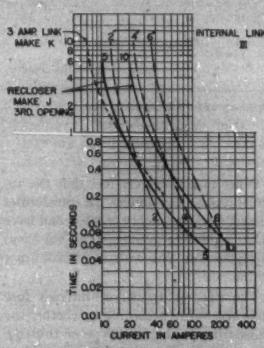

Figure 1. Co-ordination of internal transformer links and reclosers

Application of internal link III: link 2, for 1½, and 5 kva, and link 4, for 7½ and 10 kva ratings for *ESP* type over No. 6,000,000 and *CIF* type over No. 7,316,000. Also for 3 kva *ESP* type No. 6,000,000 to 7,660,000 and *CIF* type less than No. 7,316,000. Link 6 for 5 kva *ESP* type under No. 6,000,000, *CIF* type under No. 7,316,000, 25 kva *ESP* type over No. 6,000,000 and 25 kva *CIF* type over No. 7,316,000. All for transformers of Make *B*

An attempt will be made to crystallize and systematize the questions involved, establish the problems and offer suggestions for improvement of existing conditions of transformer protective device and line sectionalizing device co-ordination.

Definitions Used in This Study

An external fuse link is one external to and in series with the distribution transformer on the source side.

An internal fuse link is a fuse on the source side, placed in the transformer, usually under oil, by the transformer manufacturer, and is an integral part of the transformer. It is also called a weak link by some engineers.

An entirely self-protecting (*ESP*) transformer means a transformer containing an internal primary fuse link and a secondary breaker, both mounted inside the transformer.

A conventional internally fused (*CIF*) transformer means a transformer with an internal link but no internal secondary breaker.

Co-ordination and External Transformer Over-Current Protection

For external primary fuses, the fuse size is readily changeable, and for established recommended fuse ratings, co-ordination with reclosers having time delay opening is not a great problem. For example, in Figure 1, a 3-ampere fuse of make *K*, which is one of the slower acting makes, will co-ordinate with a 5-ampere make *J* recloser up to about 18 amperes on the third recloser opening (first time de-

Paper 47-60, recommended by the AIEE committee on protective devices for presentation at the AIEE winter meeting, New York, N. Y., January 27-31, 1947. Manuscript submitted September 4, 1946; made available for printing December 11, 1946.

BRUCE O. WATKINS, formerly an engineer with the Rural Electrification Administration, is now an engineer with A. B. Chance Company, Centralia, Mo.

Table I. Internal Fuse Characteristics

Transformers Furnished to Rural Electrification Administration Financed Systems From 1936 to 1946

| Transformer Manufacturer's Designation—Serial Number | Current, Amperes | | |

Table I (continued). Internal Fuse Characteristics

Transformers Furnished to REA-Financed Systems From 1936 to 1946

	Transformer Manufacturers' Designation—Serial Number	Current, Amperes																	
		5 Kva								7 1/2 Kva									
	Time, Seconds	300	100	10	5	1	0.5	0.2	0.1	300	100	10	5	1	0.5	0.2	0.1
A	No. 2,222,500 to 2,500,000	14.5	15	16.5	17.5	25	30	40	52	20	20	23	25	28	46	62	80
A	No. 2,500,000 to 3,536,360	12	13	16	17.5	25	30	42	60	16	17	22	23	35	43	62	90
A	No. 3,536,360 and over	12	13	16	17.5	25	30	42	60	16	17	22	23	35	43	62	90
B	*ESP* type less No. 6,000,000	33	33	35	38	63	83	130	180	41	41	44	48	82	120	175	250
B	*ESP* type No. 6,000,000 and over	12	12	13	14	19	25	36	49	22	22	23	24	38	50	75	101
B	*CIF* type less No. 7,316,000	33	33	35	38	63	83	130	180	51	51	56	62	120	150	230	320
B	*CIF* type No. 7,316,000 and over	12	12	13	14	19	25	36	49	22	22	23	24	38	50	75	101
C	*ESP* type	12	12	15	16.5	24	30	42	52	16	16.5	20.5	23	36	45	64	85
C	*CIF* type	21	22	28	32	55	75	120	165	30	31	40	46	82	115	175	240
D	less No. 1,850,465	18	18	20.2	21.5	29				29	32	37	38	52.5			
D	No. 1,850,465 and over	18	18	20.2	21.5	29				42	44	52	55	76			
E	*ESP* type	12	13	16	17.5	25	29	42	60	16	17	22	23	34	42	62	90
E	*CIF* type		21	22	23	26	30	36		21	22	23	26	30	36		
F	*ESP* type	12	13	16	17.5	25	29	42	60	16	17	22	23	34	42	62	90
F	*CIF* type	32	34	34	36	38	48	60		54	58	59	60	64	79	99	
G	*ESP* type less No. 273,400	12	13	14	17	26	32	43	55	15	15	19	22	36	46	65	85
G	*ESP* type No. 273,400 and over	13	13	16	17.5	25	30	42	60	15	17	22	23	35	43	62	90
G	*CIF* type less No. 393,000	29	31	33	50	68	108	160		42	45	51	88	120	195	295	
G	*CIF* type No. 393,000 and over	8	8.8	9	13	17	28	42		42	45	51	88	120	195	295	
H	*ESP* type		15	16.7	25.7	31.7*	45*	60*			19	22.2	36	45*	66*	91*	
H	*CIF* type	9	9.4	9.7	11	11.5	12.8	14		9	9.4	9.7	11	11.5	12.8	14	

* Estimated.

Internal links for the 10-kva rating are the same as for the 7 1/2-kva rating, except for the following makes:

Manufacturer *B CIF* less No. 7,316,000; Manufacturer *C CIF*; Manufacturer *D CIF* less No. 1,850,465; Manufacturer *F CIF*; Manufacturer *G CIF* less than and over No. 393,000.

The links in the above makes of 10-kva transformers are larger than the links in the same make of 7 1/2-kva transformers.

furnished by the same manufacturers.

Taking the 5-kva transformer for example, the *CIF* type link is about twice as large as the *ESP* type for manufacturer *C*, but the *CIF* type link is smaller than the *ESP* type link for manufacturers *E*, *G*, and *H*. In general, the *ESP* type is now more standardized than in 1943.

It also can be observed that some of the *CIF* links and some of the older ESP links are so large that fault currents on rural systems are frequently insufficient to blow the link at all.

Results of Diversity Between Internal Links in the Co-ordination of Links and Line Sectionalizing Devices

Figures 1 and 2 show how the make *J* recloser time delay operation co-ordinates with certain internal links. Where the fuse and recloser curves cross determines a minimum current point. For currents greater than this value, proper co-ordination will occur, but for currents of lesser value it will not. Table II is made up from a comparison of various reclosers and internal fuse links. Table II*A* is made up using the first time delay opening curve (third opening) of the make *J* recloser. Subsequent time delay openings are not considered in the co-ordination of the fuse and recloser. This method was used because it is not known just how heat is dissipated in a fuse under oil, and because the use of an automatic disconnecting or isolating device on branch lines would make such an operation desirable in case the recloser had two fast and two time delay openings to lock-out. Table II*A* may also be used for the first opening of the make *A* recloser, as the characteristics are very similar. However, the later device has four time delay openings, and the factor of safety in clearing a fuse before recloser lockout would therefore be greater. Table II*B* is made up for the first opening of the make *B*. This recloser has four fast openings to lockout, and hence, is much more difficult to co-ordinate.

Use of Table II

The table shows the minimum fault current for which various internal fuses will be cleared before the recloser operates (see above for details of operation). If the minimum calculated fault current is less than the value in the table, the co-ordination described above is not assured. Spaces with dashes indicate that no such co-ordination is possible. For example, for a make *B* 1 1/2-kva transformer, *ESP* type, less than serial number 6,000,000, the fault current must be greater than 80 amperes if a 5 ampere make *J* recloser is not to open on its time delay operation. If a make *B* recloser is used, co-ordination is not possible. The higher the figure in the table, the more difficult is the co-ordination.

By comparing these tabular figures, the problems of co-ordination with various makes of internal links becomes very apparent.

Solution of Co-ordination Problems on Existing Installations

Examination of the system by use of these tables will show where trouble may be expected.

Table IIA. Co-ordination of Reclosers and Internal Links

Minimum Current, Amperes, for Which Internal Fuse Will Clear Before Recloser Opens on Time Delay

Make *J* and Make *A* Reclosers**

Transformer Rating	Recloser Ratings 5	10	15	25	Recloser Ratings 5	10	15	25	Remarks
Make *A*	*ESP* type and *CIF* type less No. 2,500,000				*ESP* type and *CIF* type No. 2,500,000 and over				
$1^1/_2$ kva	10*	20*	30*	50*	18	20*	30*	50*	$1^1/_2$ kva *ESP* type of serials between 2,500,000 and 3,536,360 will co-ordinate with 5 amperes recloser down to 10 amperes
3	42	20*	30*	50*	18	20*	30*	50*	
5	42	20*	30*	50*	45	20*	30*	50*	
$7^1/_2$	85	42	30*	50*	130	35	30*	50*	
10	85	42	30*	50*	130	35	30*	50*	
Make *B*	*ESP* type less No. 6,000,000				*ESP* type No. 6,000,000 and over				
$1^1/_2$ kva	80	20*	30*	50*	28	20*	30*	50*	
3	80	20*	30*	50*	28	20*	30*	50*	3 kva at serials 7,660,000 and over same as serials less than 6,000,000
5	220	135		50*	28	20*	30*	50*	
$7^1/_2$		260		50*	150	56	30*	50*	$1^1/_2$ kva *ESP* type of serials between 6,000,000 and 7,316,000 will co-ordinate with 5 amperes recloser down to 10 amperes
10		260		50*	150	56	30*	50*	
	CIF type less No. 7,316,000				*CIF* type No. 7,316,000 and over				
$1^1/_2$	28	20*	30*	50*	28	20*	30*	50*	
3		56	30*	50*	28	20*	30*	50*	
5		220	135	50*	28	20*	30*	50*	
$7^1/_2$				250	150	56	30*	50*	
10				480	150	56	30*	50*	
Make *C*	*ESP* type				*CIF* type				
$1^1/_2$ kva	10*	20*	30*	50*	10	20*	30*	50*	
3	18	20*	30*	50*	150	20*	30*	50*	
5	45	20*	30*	50*		190	30*	50*	
$7^1/_2$	130	35	30*	50*			270*	50*	
10	130	35	30*	50*				210	
Make *D*	*CIF* type less No. 1,850,465				*CIF* type No. 1,850,465 and over				
$1^1/_2$ kva	10*	20*	30*	50*	130	23	30*	50*	No *ESP* types made
3	47	20*	30*	50*	130	23	30*	50*	
5	130	23	30*	50*	130	23	30*	50*	
$7^1/_2$		200	60	50*			220	60	
10			220	60			220	60	
Make *E*	*ESP* type				*CIF* type				
$1^1/_2$ kva	18	20*	30*	50*	11	20*	30*	50*	$1^1/_2$ kva *ESP* type prior to 1944 will co-ordinate with 5 ampere recloser down to 10 amperes
3	18	20*	30*	50*	11	20*	30*	50*	
5	45	20	30*	50*	28	22	30*	50*	
$7^1/_2$	130	35	30*	50*	28	22	30*	50*	
10	130	35	30*	50*	28	22	30*	50*	
Make *F*	*ESP* type				*CIF* type				
$1^1/_2$ kva	18	20*	30*	50*	11	20*	30*	50*	$1^1/_2$ kva *ESP* type less No. 755,849 will co-ordinate with 5 ampere recloser down to 10 amperes
3	18	20*	30*	50*	26	22	30*	50*	
5	45	20*	30*	50*	55	36	35	50*	
$7^1/_2$	130	35	30*	50*	140		78	62	
10	130	35	30*	50*		115	85	60	
Make *G*	*ESP* type less No. 273,400				*ESP* type No. 273,400 and over				
$1^1/_2$	10*	20*	30*	50*	18	20*	30*	50*	
3	18	20*	30*	50*	18	20*	30*	50*	
5	45	20*	30*	50*	45	20*	30*	50*	
$7^1/_2$	130	35	30*	50*	130	35	30*	50*	
10	130	35	30*	50*	130	35	30*	50*	
	CIF type less No. 393,000				*CIF* type No. 393,000 and over				
$1^1/_2$	10*	20*	30*	50*	10*	20*	30*	50*	
3	130	25	30*	50*	130	20*	30*	50*	
5		200	40	50*		20*	30*	50*	
$7^1/_2$				50*				50*	
10				350				350	
Make *H*	*ESP* type				*CIF* type				
$1^1/_2$	10*	20*	30*	50*	10*	20*	30*	50*	
3	14	20*	30*	50*	10*	20*	30*	50*	
5	52	20*	30*	50*	10*	20*	30*	50*	
$7^1/_2$	130	35	30*	50*	10*	20*	30*	50*	
10	130	35	30*	50*	10*	20*	30*	50*	

* Minimum trip current of recloser.
** First opening for make *A* recloser. Third opening for make *J* recloser.
The *ESP* type is one transformer with an internal fuse link and secondary circuit breaker.
The *CIF* type transformer is one with an internal link, but no secondary circuit breaker.

If the internal fuse link will not clear properly, there are three alternatives

1. Move the transformer so that it is behind some larger recloser, or to some point where the minimum fault current is greater, or both.

2. Install a larger recloser, or one with greater time delay if the requirements for co-ordination on the primary lines can still be met.

3. Install an external fuse link of smaller rating than the internal link. In the case of the *ESP*-type transformer, make sure that this external link will co-ordinate with the secondary breaker. When using external secondary protection, co-ordinate such protection with the primary fuse.

Most of the difficulties will occur with the transformers manufactured prior to 1943, and the *CIF* type.

It might be pointed out that in the case where a recloser with one or two fast openings and subsequent time delay openings is used, it would be desirable to install single shot fuses or branch lines to clear permanent faults. The transformer internal link should clear before the branch line fuse, and the branch line fuse should clear before the recloser locks out. A greater margin for co-ordination between the internal link and the recloser should therefore be applied.

It would also be very helpful if some satisfactory but inexpensive transformer failure indicating device could be developed which could be attached to all transformers. Thus, although improper co-ordination might prevent automatic transformer disconnection, at least the transformer which failed could be easily located. This would save considerable outage time.

Suggestions for Steps to Be Taken in Future Development

The main co-ordination difficulty is clearing internal transformer links with the smaller ratings of reclosers. Unfortunately, most of the lower rating reclosers are out on the fringes of the system, where nonco-ordination will result in long outage time and costly maintenance. The transformer kilovolt-ampere ratings of greatest number on rural power systems are probably the $1^1/_2$, 3, and 5. The minimum line-to-ground current (considering 40 ohms fault resistance) on most 7.2/12.5-kv multigrounded rural systems runs around 20 amperes. It is therefore highly important to be able to automatically disconnect a 5-kva or lesser rating transformer before the smallest rating recloser operates for fault currents down to 20 amperes. This

Table IIB. Co-ordination of Reclosers and Internal Links

Minimum Current, Amperes, for Which Internal Fuse Will Clear Before Recloser Opens

Make *B* Recloser

Transformer Rating	Recloser Ratings 6	12	25	50	Recloser Ratings 6	12	25	50	Remarks
Make *A*	*ESP* and *CIF* types less No. 2,500,000				*ESP* and *CIF* types No. 2,500,000 and over				
1½ kva	17*	30*	65*	130*	85	30*	65*	130*	1½ kva *ESP* type of serials between 2,500,000 and 3,536,360 will co-ordinate with 6 ampere recloser down to 17 amperes
3	120	52	65*	130*	85	30*	65*	130*	
5		52	65*	130*		80	65*	130*	
7½		140	65*	130*		200	65*	130*	
10		140	65*	130*		200	65*	130*	
Make *B*	*ESP* type less No. 6,000,000				*ESP* type No. 6,000,000 and over				
1½ kva		120	65*	130*	85	30*	65*	130*	3 kva serials 7,660,000 and over same as serials 6,000,000 and less
3		120	65*	130*	85	30*	65*	130*	
5			280	130*	85	30*	65*	130*	1½ kva *ESP* type of serials between 6,000,000 and 7,316,000 will co-ordinate with 6 ampere recloser down to 28 amperes
7½			460	130*		200	65*	130*	
10			460	130*		200	65*	130*	
	CIF type less No. 7,316,000				*CIF* type No. 7,316,000 and over				
1½ kva	85	30*	65*	130*	85	30*	65*	130*	
3		200	65*	130*	85	30*	65*	130*	
5			280	130*	85	30*	65*	130*	
7½				460		200	65*	130*	
10				850		200	65*	130*	
Make *C*	*ESP* type				*CIF* type				
1½ kva	17*	30*	65*	130*	80	30*	65*	130*	
3	85	30*	65*	130*		210	65*	130*	
5		80	65*	130*			250	130*	
7½		200	65*	130*			400	130*	
10		200	65*	130*			510	370	
Make *D*	*CIF* type less No. 1,850,465				*CIF* type No. 1,850,465 and over				
1½	60	30*	65*	130*		180	65*	130*	No *ESP* types made
3	140	80	65*	130*		180	65*	130*	
5		180	65*	130*		180	65*	130*	
7½			300	130*			480	130*	
10			480	130*			480	130*	
Make *E*	*ESP* type				*CIF* type				
1½ kva	85	30*	65*	130*	17*	30*	65*	130*	1½ kva *ESP* type prior to 1944 will co-ordinate with 6 ampere recloser down to 17 amperes
3	85	30*	65*	130*	17*	30*	65*	130*	
5		80	65*	130*	50	30*	65*	130*	
7½		200	65*	130*	50	30*	65*	130*	
10		200	65*	130*	50	30*	65*	120*	
Make *F*	*ESP* type				*CIF* type				
1½ kva	85	30*	65*	130*	17	30*	65*	130*	1½ kva *ESP* type of serials No. 756,649 or less will co-ordinate with a 6 ampere recloser down to 17 amperes
3	85	30*	65*	130*	36	30*	65*	130*	
5		80	65*	130*	100	70	65*	130*	
7½		200	65*	130*		170	65*	130*	
10		200	65*	130*			170	130*	
Make *G*	*ESP* type less No. 273,400				*ESP* type No. 273,400 and over				
1½ kva	17	30*	65*	130*	85	30*	65*	130*	
3	85	30*	65*	130*	85	30*	65*	130*	
5		80	65*	130*		80	65*	130*	
7½		200	65*	130*		200	65*	130*	
10		200	65*	130*		200	65*	130*	
	CIF type less No. 393,000				*CIF* type No. 393,000 and over				
1½	85	30*	65*	130*	85	30*	65*	130*	
3		180	65*	130*		30*	65*	130*	
5			280	130*		30*	65*	130*	
7½				400				400	
10				700				700	
Make *H*	*ESP* type				*CIF* type				
1½ kva	17*	30*	65*	130*	17*	30*	65*	130*	
3	80	30*	65*	130*	17*	30*	65*	130*	
5		75	65*	130*	17*	30*	65*	130*	
7½		200	65*	130*	17*	30*	65*	130*	
10		200	65*	130*	17*	30*	65*	130*	

* Minimum trip current of recloser.
The *ESP* type is one transformer with an internal fuse link and secondary circuit breaker.
The *CIF* type transformer is one with an internal link, but no secondary circuit breaker.

problem involves consideration as follows:

1. Standardization of Internal Links

The present differences in electrical characteristics between links of various transformer manufacturers is an almost intolerable situation.

Discussing the *ESP* type for the moment, standardization of internal links should be carried out as soon as possible. So far as primary line co-ordination is concerned, the lower ampere rated link for a particular transformer size, the better. If the link is too small, fusing might occur due to surges, but with the $1^1/_2$-kva transformer links now generally used, such trouble has not been encountered. The only other requirement is that the link co-ordinate with the secondary breaker.

Suggested requirement: Internal links in transformers up to and including 5-kva 7,200-volt rating, shall clear the circuit in less than one second for a current of 20 amperes.

2. Improvement of the Fuse Link Characteristics

The link could be improved by changing the shape of the time current characteristics. In Figures 1 and 2, if the top, or low current portion of the internal link curve were swung to the left, resulting in less slope to the curve, the co-ordination with primary sectionalizing devices would be improved, and at the same time the bottom, or high current portion could remain as at present for proper co-ordination with the secondary breaker, and adequate surge absorbing characteristics.

3. Improvement of Recloser Characteristics

If the minimum tripping current of the lowest rated recloser were increased to 15 amperes, the situation would be greatly improved (See Figure 2.) This would permit the present make *J* recloser characteristic to co-ordinate with the present 5-kva make *A* link down to about 24 amperes. By increasing the opening time delay, similar results could be obtained. Both minimum tripping current and time delay could be increased.

Suggested requirements: (*a*) The lowest ampere rating of recloser shall have a minimum tripping current of not less than 15 amperes, or (*b*) reclosers shall trip in not less than one second for a current of 4.5 times *normal load* current, or (*c*) a combination of both; *b* or *c* are preferable, because consideration of inrush currents after re-energization indicates

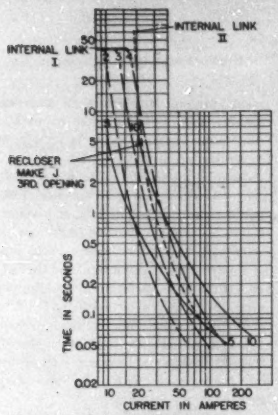

Figure 2. Co-ordination of internal transformer links and reclosers

Application of internal link I: link 2 for $1^1/_2$ and 3 kva, link 3 for 5 kva and link 4 for $7^1/_2$ and 10 kva ratings for *ESP* type transformers at present date. For transformers of makes *A*, *E*, *F*, *G* and *C*. Also *CIF* type of make *A*. Application of link II: Link for $1^1/_2$, 3, and 5 kva *CIF* type transformers of make *D*

the necessity of increased time-delay in recloser opening.

4. *CIF*-Type Internal Links

If a low ampere rated internal link is used, it may blow on secondary short circuits if there is no secondary protection. In most cases a blown link makes it necessary to take the transformer to the shop for link replacement. However, unnecessary outages to numerous consumers by an internal link which caused an entire line section to be de-energized is undoubtedly more costly to the rural consumers and power supplier than the replacement of one fuse link. Co-ordinated sectionalizing to provide as continuous service as possible to the majority of rural consumers on a rural power circuit is more important than consideration of one consumer or one transformer. (In rural areas there is generally one consumer per transformer.) A low rating internal link may also prevent some transformer failures. It would therefore seem that the internal link in the *CIF* type should be no greater than that in the *ESP* type. Two of the manufacturers are already using the same rating of link regardless of the transformer type, and two others use a smaller link in the *CIF* type.

At the same time, it is not felt that, generally speaking, the internal fuse should be of such low rating as to provide any great amount of secondary short circuit protection to the transformer. Usually low ratings will lead to an excessive number of difficult fuse replacements.

Suggested requirement: The time for the *CIF* type transformer internal link to clear shall not be more than ten per cent greater nor 15 per cent less than the time to clear, at the corresponding current, of an internal link in corresponding *ESP* transformer ratings.

In using such links, the engineer should recognize the fact that the link may occasionally blow due to a secondary fault, if there is no secondary protection. This may be prevented by using some external secondary protection, such as a fuse, or the secondary protection may be omitted and blowings due to secondary faults accepted. Table III gives the approximate service distance in feet within which the internal link on the make *B* type CIF transformer would be blown. A metallic fault at any service distance up to the figure shown would melt the link for the service size indicated. The 120-volt faults will probably be in the majority.

Table III. Distance From Transformer in Which a Fault Will Melt the Internal Link

Make *B* type CIF transformer

Transformer Size, Kva	Service Size	Maximum Service Distance (in Feet) of Fault to Melt Internal Link: 120 Volt Faults	240 Volt Faults
$1^1/_2$	No. 8	0	0
$1^1/_2$	No. 6	0	0
3	No. 6	0	160
3	No. 4	0	240
5	No. 6	80	320
5	No. 4	120	500
$7^1/_2$	No. 4	50	240
$7^1/_2$	No. 2	70	350
10	No. 4	80	280
10	No. 2	130	400

Transformer Protection

It must be recognized that few of the internal fuse links discussed above will provide adequate protection to the transformer from secondary short circuits. Referring to Table III, for example, the internal link offers protection to the associated transformer against secondary faults for service distances of lesser length than those shown. It can be seen that this protection is not very great, particularly for the 120 volt faults. Other makes, using smaller links, will of course provide more protection, but at the same time probably require more replacement.

References

1. Procedure for Making a Sectionalizing Study. *Technical Standards Bulletin 4A*, United States Department of Agriculture, Rural Electrification Administration (Washington, D. C.)

2. Experience With Oil Circuit Reclosers on REA Systems, **Lee M. Moore, Bruce O. Watkins.** AIEE Transactions, volume 62, 1943, August section, pages 531–5.

3. Engineering Memorandum 21R3, United States Department of Agriculture, Rural Electrification Administration (Washington, D. C.)

Discussion

G. Fred Lincks (General Electric Company, Pittsfield, Mass.): Watkins' paper deals with a very pertinent overcurrent protection problem on rural distribution circuits. Possibly, if anything, he has understated the importance of making certain that the internal fuses in distribution transformers are properly co-ordinated with the fuses and reclosers at branch junctions and at sectionalizing points in the main feeder. It is not only the cases where the internal fuse in a faulted distribution transformer fails to clear ahead of the branch or sectionalizing fuse or recloser that must be considered. Wherever such a hazard of incorrect co-ordination exists, operating experience has shown that many hours of trouble crews' time is spent disconnecting transformers from the line only to find a fault not readily discernible, in some other place than within a transformer.

In suggesting further improvement in the time–current characteristics of internal fuses Watkins recognizes the difficulty of obtaining proper co-ordination of these internal fuses with recloser and fuses at branch junctions and line sectionalizing points. Through the years, thousands of transformers of early and recent vintage having internal fuses with different time–current characteristics have been scattered all over many rural distribution systems. Originally in presenting the data on internal fuses[1] it was hoped that a knowledge of the time–current characteristics of the different fuse sizes used in each vintage of transformer, as determined by serial number, would aid in securing proper co-ordination. However, further experience indicates that the climbing of poles to determine the serial number or date of manufacture of these thousands of individual transformers in service involves so much expense that in many cases it may be impracticable to know the exact size of internal fuse in each transformer. Without a knowledge of the size of the internal fuses, the necessary proper co-ordination must be based on the fuses in the earliest of this type

of transformer on the circuit, which have the slowest time-current characteristics. Improving the internal fuse characteristics by the method suggested by Watkins, or otherwise, offers no solution to having to base co-ordination studies on the earlier designs if the new transformers are scattered along the circuit among the older transformers with internal fuses, as will be done in most cases.

The foregoing discussion is not intended to discourage further development of internal fuses and improvement in their characteristics, but rather to introduce a word of caution into any thinking that such improvements will act as a solution for any present inability to obtain co-ordination of internal fuses with branch or section fuses or reclosers on the line. Improvements were made in 1939 by decreasing the fuse size used in each different kva rating of transformer. However, this change did not ease the co-ordination problem, because as stated previously, it is not practical to determine readily and at reasonable cost the size of internal fuse in each transformer mounted on a pole in service, and even if this were practical, the internal fuses in any earlier transformers on a circuit will continue to dictate the rating of the branch or section fuse or recloser that must be used on the line. Thus the co-ordination problem with internal fuses today is no different on most of those circuits where they are used than when the problem was discussed originally in 1937[2], except that today there are many more transformers with internal fuses installed.

Watkins may have had this in mind when he asked for the development of an inexpensive transformer failure indicating device. Some users of transformers with internal fuses are solving their co-ordination difficulties by using external fuses at trouble points.[3] Watkins' comments on such use of external fuses would be interesting. Also, why he believes the development of a new device is necessary and how much he thinks it can be used in view of the foregoing discussion.

It appears that the solution of the problem of co-ordination with internal fuses must be solved by providing the right characteristics in the reclosers so the recloser clears all non-persistent faults on the entire circuit and the fuses operate only on persistent faults to confine prolonged outages to a few consumers. The solution must provide not only for the co-ordination of reclosers with internal fuses, but also, of internal fuse to branch fuse, branch fuse to line sectionalizing fuse and line sectionalizing fuse to recloser. The changes in the recloser minimum pick-up and time-current characteristics suggested by Watkins might be a step toward the solution of this co-ordination problem but experience in making co-ordination studies on rural circuits indicates his suggestions do not offer the final solution. They may increase the hazard of improper recloser-to-recloser co-ordination.

References

1. Line Sectionalizing with Internally Fused Transformers, G. F. Lincks. *Distribution* (Schenectady, N. Y.), January 1945.

2. Trends in Distribution Overcurrent Protection, G. F. Lincks, P. E. Benner. AIEE Transactions, volume 56, 1937, pages 138–52.

3. Co-ordination Gains with External Primary Fuses Applied to Transformers Having Self-Contained Protection, R. F. Quinn, J. R. Burkhart. *Distribution* (Schenectady, N. Y.), April 1947.

L. A. Finzi (Carnegie Institute of Technology, Pittsburgh, Pa.): Watkins' paper contains interesting information. He mentions that no fuse failures due to lightning surges have been observed in any of the *ESP* transformers of his survey. This is the more remarkable as some of the links listed in Table I for such transformers are characterized by i^2t short-time values as low as 60 amperes²-seconds. The question arises whether this favorable performance may be related to the fact that *ESP* transformers have a well co-ordinated secondary breaker and whether all this may help to throw some new light on the whole problem of fuse failures in connection with lightning surges.

It is customary to explain such failures by saying that some part of the lightning current may search some path to ground through the primary winding of the distribution transformer, while the lightning arrester operates and even more importantly when it stops conducting before exhaustion of the tail of the discharge. Initially the inductance of this winding is very high, but it decreases towards the air-core inductance value as some lightning current penetrates the winding and begins to saturate the core. In addition to this penetration current there is then also an unusually high magnetizing current delivered by the power line into the saturated transformer and so all together there is an undesirable loading of the transformer primary fuse.

This process of penetration, however, is comparatively slow; it may require a few thousand microseconds. On the other hand the speed of propagation of the lightning overvoltages over the line is about 1,000 feet per microsecond; thus quite a large number of distribution transformers in the territory should be affected simultaneously. Moreover a good path to ground is offered immediately by the secondaries of the power transformers feeding the line, since they have a much larger rating and since their primaries are nearly short circuited through the low impedance of the generating system. The penetration current available for each of the many distribution transformers may be then quite small, while the inrush of magnetizing current will be also limited by the general voltage regulation which is likely to occur in a rural line if too many transformers actually become saturated simultaneously.

But some other factors also may enter the picture. When the lightning strikes high voltages appear in the secondary distribution circuits because of electrostatic and electromagnetic transformer coupling and also because of direct induction in secondary overhead loops. Some weak spot of the secondary insulation may fail, generally by flashover, as we all may have noticed in our homes when a lightning strikes nearby. When such a failure occurs, the affected transformer becomes particularly likely to drain the lightning penetration currents, since its inductance decreases to the leakage inductance value right away. On top of this, a power fault current also will flow through the fuse while the line regulation is no longer such a limiting factor as before, since now only one or a few of the transformers of the territory are likely to be affected in this way.

If this is actually a reason for primary fuse failure, we should expect that a transformer with a well co-ordinated secondary breaker be less inclined to develop such troubles and this is just what Watkins' results seem to indicate. I realize that these considerations may appear somewhat too far fetched at this time. Certainly more field data, properly co-ordinated, are needed before any entirely satisfactory explanation may be worked out for this complicated question of lightning fuse failures. While we should congratulate Watkins for his excellent survey, we should beg him—as well as any other member who may be in the position to do so—to extend systematically the field investigation to this particular aspect of the fusing problem and to present the information to the Institute.

W. A. Sumner (Westinghouse Electric Corporation, Sharon, Pa.): Watkins' paper is a valuable contribution to this subject. The manufacturers welcome his study as it presents information which has been rather difficult for them to obtain but which nevertheless is needed badly in order to make their apparatus of greatest usefulness. Since the paper deals with primary circuit co-ordination problems, the author has quite rightly confined his discussion to the protective elements involved. However, the major equipment investment in a rural power circuit is the transformer. Therefore, this important piece of equipment should also be given careful consideration.

We agree with Watkins that similar characteristics of internal protective links in transformers of different makes would be of material benefit in laying out and operating rural power circuits. A good start has already been made, as can be seen by referring to Table I of his paper. Of the seven manufacturers of completely self-protecting transformers, six are shown to make the same application of links for current production in the 3- to 10-kva range of sizes. It is also believed that all these six have now changed their $1^1/_2$-kva ratings over to use the 3-kva link. The modern link characteristics of the seventh manufacturer of *ESP*'s, although having a somewhat different overall shape, agree very closely with the others through a portion of the range tabulated. We feel, therefore, that there is really a greater similarity of internal link characteristics in modern *ESP* transformers than might be indicated on the surface by the paper. It should be noted that the field

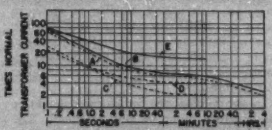

Figure 1. Co-ordination curves for a typical transformer rating, which show current-time characteristics for a 5-kva 7,200-volt CSP transformer starting at no load 25 degree centigrade ambient temperature

A—Signal light *C*—35 ampere quick-lag
B—Trip of breaker *D*—60 ampere fuse
E—Protective link

situation is alleviated somewhat further by the fact that the *ESP* transformers represent a large portion of the total number of transformers equipped with internal links and the majority of *ESP* transformers in service undoubtedly would contain the modern links as most of the changes were made a number of years ago.

We also concur in the recommendations for a much closer agreement between the links used in the *CIF* and those of the *ESP* transformers; in fact, Westinghouse designs have always used the same link in both types of transformers. The field service record of this arrangement has been satisfactory.

As to the fixing of the protective link levels, it is our opinion that the levels of the *ESP* designs have been wisely chosen. A study of the co-ordination curves for a typical transformer rating will show what is involved. Curve *A* in Figure 1 of this discussion is the signal light load-time curve. This represents the thermal capacity of the transformer windings, based on the American Standards Association recurrent temperature schedule,[1] in the useful loading band, and for shorter times conforms to the characteristic shape of fuse curves generally available for sectionalizing purposes. Curve *B* is the trip curve of the breaker. This is set higher than the signal curve to give an emergency operating band, and by tripping at these higher loads which produce winding temperatures corresponding to the ASA emergency temperature schedule,[1] the breaker prevents winding burnouts. The position of the breaker curves also provides excellent co-ordination with the secondary overcurrent devices commonly used, such as shown in curves *C* and *D*. To drop the breaker curves any lower would deprive the purchaser of the full value of his transformer investment in short-time overload capacity, and would make co-ordination with the secondary overcurrent devices uncertain. With the breaker curves thus fixed, it then becomes a matter of judgment and experience in selecting the protective link curves in such a manner as to give satisfactory co-ordination with the breaker. In the original *CSP* transformer—brought out several years before the Rural Electrification Administration—a wide margin was taken between the breaker and the link. For instance, the current required to clear the 5-kva link in one second was 86 times full load, rather than 38 times full load current. With continued experience, it was found the precision of the internal breaker would permit fixing the link curve much more closely to the breaker curve, so that today we have a close relation as shown in curve *E*. With this arrangement, the full thermal capacity of the winding has been made available and good co-ordination between the breaker and protective link has been secured.

In our opinion, the transformer should be the starting point in this problem. The author's suggestions—that internal links through 5 kva, 7,200 volts clear the circuit in less than one second for a current of 20 amperes and that changes in shape of the link curves be made to effect over-all improvement in system operation—these are recommendations worthy of careful consideration but should also be studied from the viewpoint of the transformer. We, therefore, believe it is wise to add to the author's recommendations on internal links one more—that any changes in the protective link to improve primary circuit co-ordination be made in such a way that the availability of the full thermal capacity of the transformer and satisfactory co-ordination with secondary overcurrent devices will be retained.

Reference

1. American Standards for Transformers, Regulators, and Reactors, C57.1–.3, November, 1942, pages 83–88.

J. M. Wallace (Westinghouse Electric Corporation, East Pittsburgh, Pa.): Watkins has made a thorough study of the problems involved and has made certain recommendations. I am particularly interested in his recommendations regarding reclosers. His first point is that the lowest rating of recloser should have a minimum tripping current of 15 amperes. I certainly agree that if the industry needs this action such a change can be made and is quite practical. It has been suggested that a change be made in the present 5 ampere rating to change its minimum tripping current but I would suggest that instead, we change our recloser to be rated at 7.5 amperes. In this way, the customer is given the benefit of the increased ampere rating of the recloser and at the same time the requirements of the increased tripping current are met.

Watkins' second recommendation was that the time delay of the recloser should be increased. This is rather difficult to accomplish and would probably mean the modification of the recloser to use some sort of intricate clock work mechanism which would undoubtedly increase its cost. I am not sure that the industry would want this change if it were reflected in an increased cost of reclosers.

One of the things which has been brought out in Watkins' paper is that in studying these co-ordination problems, different devices should not be compared on the basis of ampere rating only, as this is apt to be quite misleading. There seems to be a considerable tendency in the industry to make the assumption that a 5-ampere fuse will co-ordinate with a 10-ampere recloser, without any reference to the time-current curves of the device. I would just like to point out that it is absolutely necessary that proper use of time-current curves be made in all co-ordination studies as the time-current curves are the real story of what the devices do and are the only practical way in which co-ordination can be properly planned.

Max W. Rothpletz (Rural Electrification Administration, Washington, D. C.): This paper is very timely in setting forth the problems of co-ordinating internal fuses with oil circuit reclosers and should be given very careful attention by both transformer and recloser manufacturers.

The paper points out that many fuse links do not co-ordinate with reclosers on the low current end of the time-current curves. This lack of co-ordination is particularly undesirable because of the tendency of transformers to fail by progressive increases in fault current. That is, the fault begins by a fault across a few turns and gradually involves more and more turns. For such faults if the recloser operating time for currents slightly greater than the minimum tripping current is less than the clearing time for the internal fuse, the recloser will probably lock out and the faulted transformer will be very difficult to locate.

C. E. Asbury (The Commonwealth & Southern Corporation, Jackson, Mich.): The difficulties pointed out by Watkins are very troublesome to protective and distribution engineers and it would be very desirable if something could be done to standardize on the rating and time current characteristics of fuse links as well as the general principles to be followed when fusing distribution and rural transformers. The problem of wide spread variation in time current characteristics need not be limited to internal fusing of transformers as it applies to fuse links in general and can also be very troublesome where external fusing of transformers is used.

The difficulties arising when fusing the primary side of distribution and rural transformers might be divided into three groups:

1. Differences in time-current characteristics and ratings of the various manufacturers' fuse links (despite several years of joint attempts of standardization).

2. Differences of opinion as to the purpose of the transformer primary fuse.

3. The present time-current characteristic of standard fuse links is not of the proper shape to parallel the thermal curve for distribution transformers and thus do not provide reasonable thermal protection, especially on the smaller sizes of transformers. An improved time-current characteristic is also needed to provide proper surge ability of standard distribution fuse links especially in the lower ampere ratings.

This first problem of difference in ratings and time-current characteristics is under study by a joint committee of the Edison Electric Institute and the National Electrical Manufacturers' Association and a proposed standard for distribution fuse links has been set up which defines the time current characteristic limits to fall within a specified band. It is hoped that this band width in its accepted form will be narrow enough and definite enough to be a great aid in fuse link application and co-ordination. These proposed ratings and characteristics have been designated as *E* ratings. The present accepted fuse link standard known as 100 per cent or *N* ratings permit wide variations in time-current characteristics to exist. One manufacturer for instance publishes two types of *N*-rated links having time-current characteristics such that a 65 ampere *N*-rated link in the one type coincides with a 100-ampere *N*-rated link in the other type. The result is that if the same ampere ratings in the two types are applied to the protection of a given transformer, radically different time-current characteristics are obtained.

Our second point mentioned that makes co-ordination difficult is the reason for the primary transformer fuse and which part of the electrical system it shall be intended to protect.

As pointed out by Watkins, some place fuses on the primary side of the distribution transformer on the theory of protecting the primary distribution circuit against faults in the transformer. When such practice is followed, a fusing factor (which is the num-

ber of times the fuse rating is of transformer full load current) may be 2, 3, 4, or even higher. Others attempt to place fuses on the primary side of distribution transformers to provide as much thermal protection for the transformer as possible for overload and for secondary faults. This usually results in a much lower fusing factor, usually in the order of 1.25 to 2, depending upon the particular individual's judgment. If this latter practice is followed of using a fusing factor rather low to protect for overload and secondary faults, it is quite likely that primary fuses will be blown more frequently and thus where internal fusing is used extended outages would result unless the internal fuse can be designed for quick replacement in the field. In order that a more systematic and perhaps intelligent fusing practice can be followed by the manufacturers using internal links, it appears that a standard basis for fuse link ratings and time-current characteristics must be established and an agreement reached on the fusing factors to be applied.

Watkins recommends that internal fuse links and oil circuit reclosers be designed having time-current characteristics suitable for better co-ordination. In this we concur and it would be very desirable if this new design could be similar in characteristic to that chosen for distribution fuse links used for sectionalizing and external transformer fusing. It would be ideal if internal fuses, all distribution fuse links, and oil circuit reclosers time-current characteristics could have a similar shape and all be parallel to the thermal curve for distribution transformers. Such characteristics should provide adequate thermal protection for distribution transformers and also should be designed to provide sufficient time delay at high currents to give adequate surge capacity in the smaller ampere ratings.

In conclusion I would like to emphasize the need for (*a*) an agreement on transformer fusing practice to be followed by the industry, and (*b*) adoption of similar time current characteristics having close tolerances for these various distribution protective devices. These would be important steps in the art of distribution and rural line protection. Such steps would eliminate many of the co-ordination problems for the distribution engineer and reduce the number of interruptions to customers' service.

R. O. Loomis (Georgia Power Company, Atlanta, Ga.): Watkins' paper presents the problems involved in making the fuse link an integral part of a distribution transformer. Such links do not protect the line against failure of a transformer bushing, which has caused much trouble on older transformers. Regardless of arguments for and against use of internal links, I believe we should approach the problem with the usual criteria that the best solution results in the least total customer hours of interruption for a reasonable cost.

Some people believe (*A*) this condition obtains when the transformer fuse is the maximum size which can be cleared by the next sectionalizing device ahead of it, regardless of the size of transformer. Such fuses usually provide no protection to the transformer itself. This theory would not lend itself to standardization of internal fuses since they are used on lines of varying capacity. Other people use various smaller transformer fuses, down to (*B*) those which protect the transformer regardless of customer hours of interruption. It is rather unlikely that everybody will agree on a standard internal link, but REA may be able to set a standard for themselves which will be accepted by the industry if they develop a logical standard.

Our records and experience seem to show that theory *A* results in best service at least cost, and therefore we do not use internal fuses at all ordinarily, but perhaps a strictly logical internal fuse would be desirable.

The following should be considered:

1. Since fuse links are the universal low cost protective device on distribution systems, the shape of fuse link curve should be standardized first and other devices, such as pole top breakers, relays, and internal fuses should be made to fit. Since all distribution circuits contain transformers, I suggest that the standard shape of fuse curve should approximate the heating curve of distribution transformers. It is obvious that the shape of curve followed by internal links should be standardized.

2. In the interest of standardization the size of link in a given size of transformer should probably be standardized.

3. The use of internal links is not consistent with the logic of theory *A*. Therefore the size of link should veer more to theory *B*.

4. Since REA systems like most other systems are growing in capacity, a standard set by the low capacity ends of the system will become too small in the future.

5. Generally speaking, the larger the transformer fuse the fewer unnecessary outages occur.

6. It is suggested that the size and shape of curve of internal links be just below the breakdown point of the transformer. It is believed that this point will be far above the safe heating curve of the transformer. Such a transformer would hang onto the load almost to the point of failure but a blown link would be easier to repair than a failure. Such a link should satisfy those holding both theory *A* and *B*.

7. Stamp the size link on the transformer name plate; for example, "Internal fuse—5 amperes at 10 seconds."

It is suggested that such a standard would be used somewhat as follows:

For the majority of locations the internal fuse would be satisfactory. Wherever the link is too large for use beyond a certain sectionalizing device, all transformers would be equipped with an external fuse of such size as to co-ordinate with the sectionalizing device. This fuse size would be used on all such transformers regardless of size and the fuse size would be specified by the engineer making the co-ordination study. It would not be changed until system changes made another co-ordination study necessary, at which time perhaps all such external fuses could be removed.

Such an internal fuse might be desirable on all transformers regardless of type of transformer or fusing practices of the company.

M. M. Samuels (Rural Electrification Administration, Washington, D. C.): Watkins made a very creditable presentation by crystallizing a confused situation. Even though he does not offer any solution of the problem, the facts are so presented that it should not be too difficult for the interested parties to get together and arrive at a solution.

The paper gives the impression that the manufacturers are responsible for the confusion. This is not the case. The manufacturers would soon standardize on something if the majority of their customers would tell them definitely what they require. It is another one of the many cases that presented themselves lately to demonstrate the need of a co-operative research association, participated in by all electric utility operating organizations, to do the type of research which cannot be done in the factory but which must be done on the operating systems. No one individual system has either the staff or the budget to undertake such research.

A confusion, similar to the one brought out by Watkins, prevails in the secondary protection field. When the type of transformer which Watkins identified as *ESP* is used, there is frequently installed a so-called service protection on the transformer pole, within reach by the customer, in series with the breaker within the transformer. In addition we have a service entrance protection within the house, so that we have three overcurrent protective devices in series in the same circuit. This is brought about partly by code requirements, partly by operating requirements and partly by sheer foolishness. Some means should be found to simplify this silly arrangement and find a way to get along with one protective device. Code or no code, when there is a service entrance protection on the pole, it is silly to require another one in series in the house, and if a service entrance protection is required on the pole it should be possible to make its characteristics so that it takes care of all the protection now furnished by the breaker inside the transformer and so eliminate that breaker.

Recently carrier and similar equipment have been added to the service transformer pole, with additional fuses, gaps, capacitors, and chokes, and making the transformer distribution pole look like a Christmas tree which was decorated by a child. The whole arrangement looks amateurish at its best. The whole problem of primary and secondary protection for rural distribution transformers should be subjected from scratch to a clean engineering study which should culminate in a neat, competent, co-ordinated design all around.

Bruce O. Watkins: In reply to Linck's discussion, although it would be impractical to ascertain the serial numbers of all transformers at one time by field inspection it should be possible for line crews to locate most of them when on other duties in various areas. Many companies have card records of transformer installations and in these cases co-ordination studies could be made easily. Those companies who do not keep such records would probably find it helpful to start doing so. It should be possible to obtain better co-ordination by shifting transformers, although it is granted that such shifting would necessarily cover a long period of time. In any case, the fact that mistakes in internal fuse ratings were made in the past should not deter the improvement in co-ordination which can be brought about by changes now.

The difficulty with external fuses on small transformers of 7.2-kv voltage is that to prevent unnecessary fuse blowing due to surges, the fuse link rating has to be so high that it no longer offers adequate protection to the transformer against secondary faults. Under this condition, the operator

might as well use an internal fuse, which is considerably less expensive, and resort to some sort of secondary protection.

The suggestions on recloser characteristics were made assuming that proper recloser-to-recloser co-ordination could also be achieved.

No REA data yet exists as to fuse failures due to lighting. (Finzi's comments.)

In reply to Sumner's comments, it is felt that continuity of service to as many consumers as possible may be of more importance than obtaining all the short time overload capacity inherent in each transformer, although the later is important from an investment standpoint. It is felt that the system as a whole, not the individual transformer, should be the basic consideration. However, much could be done in improving co-ordination, still retaining the present secondary breaker characteristics, by following the suggestion made in the original paper on improving the internal link characteristics.

In regard to Wallace's comments, so long as the minimum trip current is increased, it matters little as to the method, whether by recloser rating increase, or otherwise. Increased cost of reclosers would probably be welcomed if the recloser were correspondingly improved.

I agree entirely with Loomis that the over-all effort should result in the least total customer hours of interruption, consistent with reasonable costs. Loomis indicates that his company disregards transformer size when fusing, and bases fuse ratings on sectionalizing. This is along the lines of our thinking, but it is not readily apparent why this philosophy necessarily eliminates the use of internal fuses. If the fuse does not protect the transformer, it might as well be internal. Failure in the bushing is probably less serious now than formerly. A fuse link characteristic approaching that of the transformer, as suggested by Asbury and Loomis would probably be helpful.

The comment made by Loomis—under point 4, that systems are growing rapidly, is quite true, and it may well be that future problems will be concerned with the high fault currents rather than the low ones. However, the low fault currents generally occur at the greatest distance from the maintenance center, and may cause more outage time. Point 7, requiring the fuse size to be on the name plate is also good, except that the name plate is already crowded.

In applying reclosers to systems, probably the one-fast-opening two-time-delay-opening recloser would be almost as satisfactory from the standpoint of clearing temporary faults, and would be more satisfactory from the standpoint of hunting, co-ordination, and so forth than the two-fast-opening type.

In regard to Samuel's comments, some means probably should be used to better co-ordinate field experience and research with new designs. It is also true that lack of standardization exists with regard to secondary breakers and house protective devices. The same might be said of expulsion-type lightning arresters.

Electrical Characteristics of Resistance Welding Tools

E. M. CALLENDER
ASSOCIATE AIEE

Synopsis: Methods of measurement and calculation of resistance welding tools, particularly for the large group of nonstandard type portable welding guns, are contained in this paper. Electrical characteristics have considerable bearing on

1. Kilovolt-amperes at an installation.
2. Required secondary voltage of the welding transformer.
3. Efficiency of the tool.

Timesaving means for either measurement or calculation provide accuracies well within the average requirements of the engineer. The approximation calculation of inductance is semiempirical in nature to facilitate computation of tool or cable reactance and can be extended in principle to various types of welding equipment.

BY practical necessity the average resistance weld is made in a lengthy looped circuit that gives rise to high kva demands, low power factor, and large inefficiency. The load itself, comprising two or more pieces of relatively thin sheets to be welded, is frequently an insignificant part of the total secondary circuit resistance. The characteristics of permanent type welders are available from the manufacturer in many cases. However, the welding engineer, both designer and user, often has a vital interest in the large class of welding tools known as portable welding guns, whose installations include water-cooled cables of 4- to 20- (or more) foot lengths. The reason these cannot be standardized is that a vast number of specialized yokes (welding arms of such guns) are required "to reach into" all the spots which require welding by the builder of large sheet structures. The impedance of the welding transformer secondary circuit is vital both to users who must select the proper rated welding transformer for the job and to designers who seek to provide better efficiencies and power factor loads.

Most technical papers deal with highly theoretical calculation of inductance.[1] Several reasons are given for avoiding this in the present case.

1. The results are more rigorous and time consuming than justified.
2. The particular geometries and conditions may impose problems of solution which leave certain factors rather screened. Thus, for example, the cross section of an arm may be of such physical shape as to complicate greatly the current distribution within it. Or it may vary in cross section along its length, further complicating the analysis.
3. Practical errors, such as unaccounted contact resistances, dimensional error, may detract from the accuracy of a highly mathematical calculation. However, regardless of the method employed for obtaining the result, it is essential to take into account all the various factors which enter, so that the accuracy may be appraised and improved whenever possible by corresponding correction factors.

The groundwork for calculating inductance as described herein is based on the simple theoretical case for an infinite pair of lines. With that consideration suitable correction factors then are developed as required for the various special problems encountered with welding tool configurations.

A system of a-c measurement was devised to provide reasonably accurate measurements of the low order impedance, resistance, and reactance of welding tools of cables. Such measurements proved of great value in correlating the mathematical work, and test results are reported here to substantiate the methods described.

Figure 1 shows a large welding tool with smaller ones. The basic motive in the design does two things.

1. It allows the exertion of a large force (many hundred pounds) in opposing electrodes that close to grip the spot being welded.
2. It causes the large welding current (several thousand amperes) to thread through opposite sides of the work sheets.

Most portable guns are used in 60-cycle

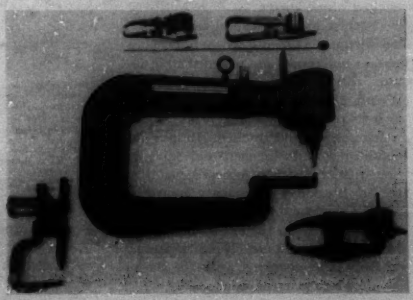

Figure 1. Typical portable welding tools. Illustrated in the center is a large C-type 32-inch-throat steel tool having copper bus on inside path. In the lower left hand corner is a smaller tool similar to a C-type and three small X-type tools also are shown

Paper 47-63, recommended by the AIEE committee on electric welding for presentation at the AIEE winter meeting, New York, N. Y., January 27-31, 1947. Manuscript submitted November 4, 1946; made available for printing December 30, 1946.

E. M. CALLENDER is with The Budd Company, Philadelphia, Pa.

The author wishes to thank Doctor C. A. Adams for guidance. He also wishes to thank the following men: T. A. Rich, General Electric Company, Schenectady, N. Y., for loan of light beam wattmeter which was tried out; H. Van Sciver and A. C. Johnson, for certain early work; and, finally, The Budd Company, who sponsored this study.

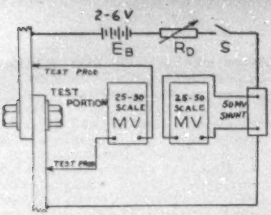

Figure 2A. Measurement circuit for low d-c resistance values

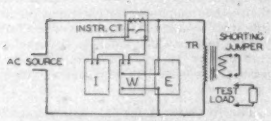

Figure 2B. Customary circuit for a-c measurement of welder electrical characteristics

installations, and, because the tool resistance and reactance will vary with other types of welders,[2,3] their current wave characteristics must be dealt with in a special manner not treated here.

Electrical Measurement

Resistance and reactance are the vital welding tool electrical characteristics. These are obtained most readily from impedance and power factor measurement. Accuracy will be limited to the precision with which the latter values can be obtained in measurement.

From a comparison standpoint, and to ascertain contact resistances, it is occasionally desirable to make d-c resistance measurements.[4,5] This can be done in another manner according to Figure 2A, using two millivolt meters of good accuracy and preferably of high resistance so as to minimize the effect of lead length and potential contact resistance. The method is well known.

The first method investigated for a-c measurement is mentioned only because certain test results are recorded from its use. Briefly, it is the measurement, (Figure 2B) made on the primary side of a low reactance welding transformer which was well underexcited. Results are obtained by measurement and subtraction with and without observed load by the substitution of a secondary jumper in place of the load. Consistent fair results are obtained when the magnitudes of resistance and reactance being measured are very large compared with the short-circuited secondary impedance.

The method of a-c measurement recommended by the author is shown in Figure 3. The impedance voltage drop is taken directly across the terminals of the tool and amplified by a potential step-up transformer as this low voltage drop may range from a few volts down to several millivolts at the lower limit. If the potential transformer is provided with several ratios, it is possible to read the voltmeter and wattmeter near full scale. It should be apparent that the measurement is strictly one for obtaining impedance and power factor.

Results of measurement are obtained from the following equations:

$$Z_m = \frac{E_m}{P_t \cdot I_m \cdot C_t} \tag{1}$$

$$PF = \frac{W_m(P_t \cdot C_t)}{E_m \cdot I_m(P_t \cdot C_t)} = \cos\theta \tag{2}$$

$$x = Z \cdot \sin\theta \tag{3}$$

$$r = Z \cdot \cos\theta \tag{4}$$

Meter errors affect the values in different degrees. Thus, maximum per-cent errors for accurately read meters of one-half per cent accuracy and transformers, whose included error is assumed negligible, are shown in Table I.

A description of the component instruments is desirable. The loading is kept very moderate on the potential transformer to minimize phase and ratio errors. For this reason the suggested values are 1,000 ohms per volt for the voltmeter and 100 ohms per volt for the wattmeter. The particular portable wattmeter used in tests had a maximum rating of 10 volts (510 ohms) for the potential coil and three amperes for the current coil. The existing current transformer used was 5,000/5, which limited the weld tool current to 3,000 amperes. To obtain a suitable a-c voltmeter complying with the resistance requirement and one-half per cent accuracy, a thermocouple meter with scale ranges of 3–10–15 volts is desirable.

Electronic filament transformers of good construction were used for the potential transformers. Although the excitation, loading, and potentials for these are low, the reactance of the low winding may detract somewhat from their accuracy. Ratios of step-up of 50 to 1 may be required on small tools whose heating

Table I. Meter Errors*

Item	Case I, E±, I∓, W∓, Per Cent	Case II, E∓, I∓, W±, Per Cent	Case III, E±, I±, W±, Per Cent
Z	1	0	0
PF	0.5	1.5	0.5
x	1.5	1.5	0.5
r	1.5	1.5	0.5

* Maximum per cent error for accurately read meters of one-half per cent accuracy and transformers whose included error is assumed negligible. Measurement circuit is Figure 3.

Table II. Guide for Obtaining K_s, λ_h'', λ_s'' and Inductance

To Obtain	$\frac{D}{R}$	$\frac{S}{D}$	$\text{Log}_e \frac{D}{R}$	K_s	Install Values in Equations 9 and 10 (Below)
λ_{sh}''	$\frac{S_s}{R}$	$\frac{S_h}{S_s}$	from Fig. 13	from Fig. 7	$\lambda_{sh}''=0.508\left(K_t\cdot\frac{1}{4}+K_{ch}\cdot\log_e\frac{S_s}{R}\right)$
λ_{ss}''	$\frac{S_h}{R}$	$\frac{S_s}{S_h}$	from Fig. 13	from Fig. 7	$\lambda_{ss}''=0.508\left(K_t\cdot\frac{1}{4}+K_{ss}\cdot\log_e\frac{S_h}{R}\right)$
Example					
λ_{sh}''	$\frac{10}{2}=5$	$\frac{25}{10}=2.5$	1.6	0.82	$\lambda_{sh}''=0.508\left(0.9\times\frac{1}{4}+0.82\times1.6\right)=0.80$
λ_{ss}''	$\frac{25}{2}=12.5$	$\frac{10}{25}=0.4$	2.4	0.51	$\lambda_{ss}''=0.508\left[0.9\times\frac{1}{4}+0.51\times2.4\right]=0.72$

The representation of various dimensional symbols are given in Figures 4 and 7, as well as nomenclature. For determining λ_{sh}'' and λ_{ss}'' the length of path need not be exact. To determine L the exact length of chosen path is imperative.

Numerical example: A closed rectangle of circular cross section with miterd corners in which $S_h=25$, $S_s=10$, $R=2$ (diameter 4 inches), $K_t=0.90$. An opening of 4 inches is on one horizontal side.

$$L_{uh}=\frac{2S_h\cdot\lambda_{sh}''}{100}+\frac{2S_s\cdot\lambda_{ss}''}{100} \text{ (similar to equation 6)}$$

where sides have identical characteristics; otherwise, adjust so that true length of path is summated. Thus

$$L_{uh}=\frac{[(2\times25)-4]0.80}{100}+\frac{2\times10\times0.72}{100}=0.51uH$$

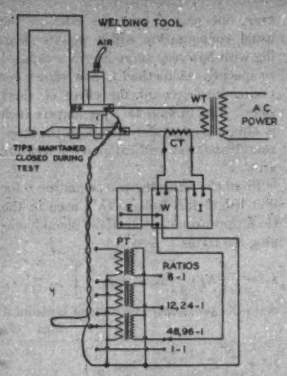

Figure 3. Proposed circuit for a-c measurement of electrical characteristics by potential drop

constant may not allow a large current during measuring time and which do not have large potential drops to start with. The maximum ratio used in tests later shown was 16.3 step-up.

Besides the induced potential pickup in the leads discussed in Appendix I the following factors are summarized to aid in accurate measurement:

1. Meters and transformers should be calibrated at frequent intervals and correction charts used.

2. Power source for measurement must be dependable in frequency and of sine wave form.

3. Extraneous steel must not be in proximity with measured piece, and tests should be conducted above concrete floors, which may contain pipes and so forth, and not on such floors.

4. Temperature of the measured pieces has a direct bearing on the result and should be noted and maintained as constant as possible.

5. In order that phase angle error is negligible in wattmeter, the potential coil should have a large R/X ratio.

6. The position of potential pickup leads has a definite bearing in reactance measurement, as taken up in Appendix I.

7. Voltmeter and wattmeter loading on the potential transformer should be kept extremely low. A low reactance potential transformer is preferable to the one earlier mentioned.

Calculation of Inductance by Approximation Method

This method is used for obtaining workable values of inductance of welding tools, cables, and other electrical heavy current conducting paths. A thorough understanding of various factors in a given estimate often will allow a crude evaluation to be made in one's mind with astonishingly close approximation. Through use of charts and tables a better computation can be made, yielding results that are entirely adequate for most uses. A typical welding tool such as we are dealing with is shown dimensioned in Figure 4.

In the rough approximation an average value of flux linkage per ampere inch is assigned and multiplied by length of path; thus

$$L = \lambda''(2S_h + 2S_v)\frac{10^6}{10^9}\ \text{microhenry} \qquad (5)$$

Actually the unit flux linkage will vary over parts of most circuits dealt with, and the equation for the close approximation becomes

$$L = \frac{1}{10^3}[\lambda_h''\cdot(S_{h1}+S_{h2}) + \lambda_v''\cdot(S_{v1}+S_{v2}) + \lambda_o''\cdot(S_o + \ldots.]\ \text{microhenry} \qquad (6)$$

in which λ_h'' and λ_v'' will be analyzed later.

Ability to obtain a working accuracy is predicated on

1. The logarithmic character of the flux linkage outside the conductor (when $u_m = 1$) maintains the values in a relatively narrow working range.

2. The most doubtful item, the internal linkage within the conductor, is a comparatively small value (when $u_e = 1$) and does not influence the resultant value greatly.

Now in cases where u_e or u_m are large (steel members conducting or in the vicinity of current) the foregoing stipulations are no longer true. It is an object of this paper to bring out the influence of steel members in welding tools by analysis and test results so that a working approximation can be evolved for such cases.

Table III. Typical Measurement Data

Data for Table IV Line	Meter Volts	Meter Amp	Meter Watts	C_1	P_1	$Z_p = \frac{E}{I \cdot C_1}$ Ohms	$r_p = Z_p$ Cos θ_p Ohms	$X_p = Z_p$ Sin θ_p Ohms	Power Factor	$r_a = r_p$, a Microhms	$X_a = x_p$, a Microhms	L_a, Microhenrys	Estimated Effective Length Path, In.	λ'' Per Amp In., Maxwells	R_{ac} Per Yoke, In.
1	9.5	2.11	34	10/5	—	2.25	1.91	1.2	0.847	2,350	1,480	3.91			
(60 cycle)	9.25	4.1	144	20/5	—	0.565	0.533	0.19	0.947	655	230	0.61			
Result										1,695	1,250	3.3	43	7.7	39.2
2	23.5	1.75	124	20/5	—	3.36	2.53	2.2	0.755	3,100	2,700	2.4			
(180 cycle)	9.8	3.37	98	20/5	—	0.727	0.522	0.482	0.741	640	600	0.53			
Result										2,460	2,100	1.87	43	4.3	57.0
13	8.7	5.6	40.0	—	—	1.55	1.3	0.78	0.845	1,458	965	2.3			
(60 cycle)	9.3	8.04	66.0	—	—	1.16	1.02	0.53	0.884	1,138	657	1.58			
Result										320	308	0.72	36	2.0	8.9

	Measurement by Figure 3: Meter Volts	Meter Amp	Meter Watts	C_1	P_1	$Z = \frac{E}{I \cdot PC_1}$	—	—	Power Factor = $\frac{W}{EI}$	r = Z Cos θZ, Microhms	x = Sin θ, Microhms	L_a, Microhenrys	Estimated Effective Length Path	λ'' Per Amp In.	R_{ac} Per Yoke, In.
14	2.0	4.75		2,500/5	—										
			2.2	5,000/5		.842	—	—	0.465	390	745	1.98	105	1.80	3.7
1 (Table V)	8.55	2.4	1.7	5,000/5	16.3	.219	—	—	0.0826	18.1	218	0.58	55.5	1.045	0.326
13	8.65	1.92	2.5	5,000/5	16.3	.276	—	—	0.15	41.4	275	0.74	55.5	1.33	0.745

Measurement by Figure 2(b).

Heading includes date, place, purpose of test, test number, meters and equipment listed, characteristic data of transformers, voltages, frequency, and so forth, for example, welding transformer ratio 28.5/1.

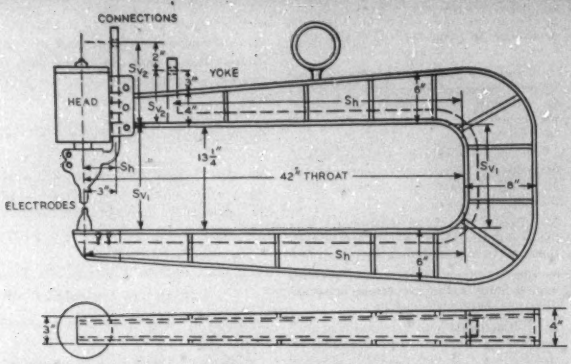

Figure 4. Sketch of large size welding tool of stainless steel fabrication with copper bus inside

However, many tools do not make use of the rigidity of steel because of their moderate size. On large tools using steel for strength and an inside copper conducting path it is safe to say that, the influence of steel on flux linkage (inductance) with many designs, often is minor in effect.

We are dealing with almost closed loops that differ greatly from transmission lines. In Appendix II is given the flux linkage per ampere inch for infinite length conductors. Integration for flux linkage within a rectangle is very involved. However, for point of simple illustration consider a tool *abcd* as shown in Figure 5A. Recalling Ampere's law for magnetic gradient at some point p with respect to a single conductor,

$$dH_p = \frac{I \cos\theta \, ds}{4\pi D^2} \qquad (7)$$

Through proper integration this becomes

$$H_p = \frac{I}{4\pi r}(\sin\theta_2 - \sin\theta_1) \text{ ampere turns per inch} \qquad (8)$$

The influence of magnetic components at single points taken by superposition, first with respect to the infinite lines, one at a time, then with respect to current flowing only in *abcd*, gives rather apparent implications. Thus, by removing all lines external to *abcd*, considerable reduction in intensity, hence flux, results inside the rectangle. It also will be apparent that those points in the vicinity of a conductor have intensity values approaching that received from an infinite length conductor. Thus, from Figure 5*A* for the single conductor of length *ab*, a greater inclusion of magnetic component results at point p_1 than at p according to equation 8. Actually, when S_{ab} is 15 times D_p the error in intensity for any chosen point p is less than one per cent in using the infinite conductor magnetic gradient value rather than that value for length *ab*, which is the actual condition. Thus in some cases relatively short lines are not in great error when assigned flux linkage values the same as for infinite line. However, one pair of opposite sides of the usual configuration which we are dealing with has very short length compared to spacing. A method is now shown for taking into account the effect of short sides. Flux linkage (λ'') per ampere inch is obtained separately for both the horizontal and the vertical pair of welding arms.

From the foregoing text, equation 6 for unit length flux linkage (λ'') used in the close approximation method should employ the terms

$$\lambda_h'' = \frac{3.2}{2\pi}\left[K_t \cdot \frac{1}{4} + K_{e(h)} \cdot \log_e \frac{S_v}{R}\right]$$

maxwells per ampere inch along horizontal sides (9)

$$\lambda_v'' = \frac{3.2}{2\pi}\left[K_t \cdot \frac{1}{4} + K_{e(v)} \cdot \log_e \frac{S_h}{R}\right]$$

maxwells per ampere inch along vertical sides (10)

The next part is devoted to analyzing the factors K_e and K_t and special effects of geometry, high permeabilities, and other influences.

Internal Flux Linkage and Factor K_t. Internal self flux linkage will be defined here as that flux all or part of whose path passes through the conductor to encircle

Figure 5A. Analogy for component effect from perpendicular pairs—infinite lines versus rectangle

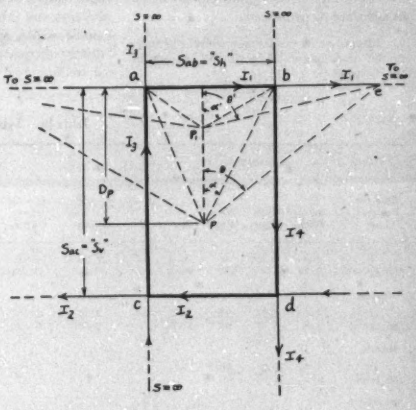

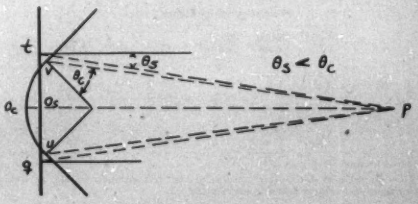

Figure 5B. Effect of round comer on flux linkage by comparison to straight wire

Table IV. Results of Tool Measurements

Line	Tool	*Description	Test Circuit	Z, Ohms × 10^{-6}	Power Factor	E_{dc}	I_{ac}, Microhenrys	X, Microhenrys	L_t, Microhenrys	Measurement Per Unit Length: Avg $\lambda^{\prime\prime}$ Amp-In., Maxwells	Avg I_{ac} In.	Temp., F	Comparison by Approximation: $\lambda^{\prime\prime}$ Amp-In., Maxwells	I_{ac} In., Microhenrys	Comparison by Calculation, L_t, Microhenrys
Solid steel—copper tool (Figure 8) during various stages of copper plating															
1	Fig. 8	A	Fig. 2B	—	—	—	210	1,670	1,250	3.3	7.7	30.2	room		
2	Fig. 8	B	Fig. 2B	—	—	—	210	2,460	2,100	1.9	4.3	57	room		
		(180 cycles)													
3	Fig. 8	C	Fig. 2B	—	—	—	190	1,210	636	1.6	3.8	28.3	room		
4	Fig. 8	D	Fig. 2B	—	—	—	180	205	0.54	1.25	4.2	room			
5	Fig. 8	E	Fig. 3	.210	0.51	53.8	107	181	0.48	1.12	2.5	—	—	—	0.437
6	Fig. 8	F	Fig. 3	.220	0.645	58.8	142	168	0.44	1.02	3.3	—	—	—	0.437
7	Fig. 8	G	Fig. 3	.394	0.74	172	291	181	0.70	1.16	4.8	—	—	—	0.65
8	Fig. 8	H	Fig. 3	.357	0.756	172	270	235	0.69	1.16	4.5	—	—	—	0.65
Fabricated tool (Figure 9) of steel sides and copper bars (box)															
9	Fig. 9	I	Fig. 2B	—	—	36.3	118 (?)	193 (?)	0.51 (?)	1.29 (?)	2.95 (?)	room	—	—	—
		(see note 1)													
10	Fig. 9	J	Fig. 3	.173	0.204	36.3	52	164	0.435	1.09	1.30	room	$[\lambda_4 = 1.14,\ \lambda_5 = 1.1]$	1.19 (r_{dc})	0.446
11	Fig. 9	K	Fig. 3	.373	0.73	.111	273	254	0.67	1.15	4.7	room	$[\lambda_4 = 1.14,\ \lambda_{5_1} = 1.1,\ \lambda_{5_2} = 1.07]$	1.19 (dc)	0.446
Fabricated steel box tool before and after copper spray															
12	—	L	Fig. 2B	—	—	—	400	990	790	1.9	5.2	27.5	room		
13	—	M	Fig. 2B	—	—	—	280	320	308	0.72	2.0	8.9	room		
Large steel tool (Figure 1) with copper bus															
14	Fig. 1	N	Fig. 3	.842	0.465	—	390	745	1.98	1.80	3.7	87	1.8	2.0 (r_{dc})	2.2
Stainless box tool similar to Figure 4 (except 26 in. throat for line 15 only)															
15	—	O	Fig. 3	.450	0.486	—	219	394	1.05	1.19	2.5	—	1.3	3.2	1.01
16	Fig. 4	P	Fig. 3	.744	0.432	—	322	670	1.78	1.48	2.60	83	1.5	3.2	1.74
17	Fig. 4	Q	Fig. 3	.585	0.404	—	237	534	1.42	1.38	2.33	83	...		
18	Fig. 4	R	Fig. 3	.147.5	0.646	—	95	—	—	—	4.5	.230			
2 to 12-foot 400,000-circular mil water-cooled cables (ends bolted)															
19	3-in. spaced	S	Fig. 3	18.0	0.792	—	14.3	11.1	2.97	1.03	0.496	85	1.04	—	3.0
20	6-in. spaced	S	Fig. 3	21.7	0.725	—	15.7	15.0	3.96	1.38	—	85	1.40	—	4.02
21	12-in. spaced	S	Fig. 3	23.0	0.66	—	15.1	17.2	4.58	1.59	—	85	1.75	—	5.04

* Description

A—Yoke alone measured (see note 2). Steel 5/8″ thick. Length path taken as 43 inches. 60-cycle test.
B—Same as *A* except 180-cycle test. Could not later renew 180-cycle tests.
C—Same as *A* except copper plated 1 to 2 mils on surface.
D—Same as *A* except copper plated about 30 mil average on surface.
E—Same as *A* except copper plated about 60–80 mil average. Only test shown using light beam wattmeter.
F—Same as *E* except without light beam wattmeter.
G—Complete tool measured. Same as *E* except with bronze mechanical air head. Length path taken as 63 inches.
H—Complete tool measured. Same as *G* except insert *F* for *E*.
I, J—Yoke alone measured (see note 2). Copper bar 3 by 1/4 inches. Length path taken as 40 inches. 60-cycle test.
K—Complete tool measured. Same as *J* except bronze mechanical air head included. Length path taken is 60 inches.
L—Yoke alone measured (see note 2). The steel box structure, 3 inches high by 2¼ inches across, is a type similar to Figure 9. Length path taken is 36 inches.
M—Same as *L* except copper sprayed about 1/32 inch on surface.
N—Complete tool measured. Steel box section tool with sides 6 inches average and top or bottom ranging from 2¼ to 3⅓ inches. Copper strap inside 1¾ by ¼ inch. Length path taken as 105 inches.
O—Complete tool measured. Stainless box section tool with 26½-inch throat depth. Internal copper bus is probably 1⅜ by ¼ inch. Length path 78 inches.
P—Complete tool measured. Stainless box section tool with 42-inch throat. Internal copper bus is probably 1⅜ by ¼ inch.
Q—Yoke alone measured (see note 2).
R—Resistance of mechanical air head across electrodes (contact resistance) measured disregarding *X* value.
S—Water cooled cables 12 feet each whose jackets were 3 inches in diameter with spacing varied. Resistance variation is caused by high contact resistance of bolted joint.

Note 1. Accuracy for method Figure 2*B* may be within ten per cent except for line 9, and for method Figure 3 should be better than five per cent in many cases.
Note 2. Measuring yoke alone is for tool circuit with omission of upper electrode and mechanical air head.

some portion of current. Internal flux linkage in a round solid conductor of zero frequency current having uniform current density is found to be

$$\lambda_i'' = \frac{3.2}{2\pi} \cdot \frac{1}{4} \text{ maxwells per ampere inch} \quad (11)$$

for $u_c = 1$ and zero effective proximity to other conductors (see Appendix II). This small internal unit value per single side of a loop to be practical must include some multiplying factor K_t that can be made to account for skin effect and proximity effect according to methods and tables provided in references 6–12. Still other factors are involved in unequal current distribution such as lower resistance of shorter inside path, uneven geometry, and steel near the conducting cross section. These factors are sometimes negligible. For example, proximity effect (proportional to current squared and inversely as distance) has little effect when D/R is greater than six. K_t will influence equations 9, 10, and 11 in such a way as to reduce the λ_i'' value (for skin effect in nonmagnetic circuits) and to increase it when iron is in proximity to the conductor.

Cross sectional geometries vary from those that are simple and symmetrical to others shown comparatively in Figure 6. Requirements of the longer yokes are for lower unit deflections and better structural strengths, which necessitate a high moment of inertia and a resort to steels as mechanical members. Copper then is co-ordinated as the electrical conducting medium. That steel can be employed with copper for Figures 6*C*, 6*D*, 6*G*, 6*H*, and 6*I* without large increase in inductance will be verified by test data. We are not concerned particularly with the case of steel as a current conductor, be-

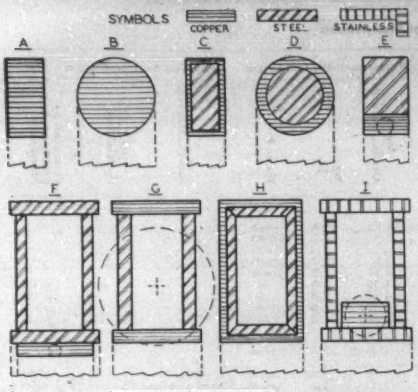

Figures 6A to 6I. Various types of welding arm cross sections and materials as designated

cause extreme losses and temperature rise prohibit its use. K_f is found experimentally to vary between approximately 10 and 60 for various "all steel" configurations or for conductors surrounded mostly or wholly by steel.

The air cylinder which often surrounds a current carrying member can be a very doubtful item when made of steel as it is on large tools. One such example is Figure 1. For that length of current path threading a steel bracket, recommended values for K_f are suggested as 30 to 60 for steel.

External Flux Linkage and Factor K_e. K_e is the correction factor used in equations 9 and 10 for the external flux linkage. It is obtained from the curves shown in Figure 7, which covers a practical range of geometries. A tabulation form for working out inductance values along with a specific example is found in Table II. Theoretical flux linkage and factor K_e are worked out in Appendixes II and III, respectively. An outstanding ratio D/R is seen to be important in determining external flux linkages. R is found to relate particularly to the permeance path adjacent to the conductor, while D determines the flux inclusion between conductors.

It will be apparent that the radius R shown in Figure 7, although suitable for simple circular cases, will not have significant meaning for many of the geometries of Figure 6. However, it may be possible to choose an equivalent circle in such special cases so as to provide an approximating R value. The purpose of such a circle is to establish the equivalent averaging flux permeance path in the vicinity of the conductor. By using an equivalent circle the equations retain simplicity and the approximation is still satisfactory in accuracy.

In a more extended approximation the lumped correction for a slight amount of steel adjacent to the conductor occasionally can be made by reducing the size of the equivalent circle (see Appendix IV).

It will be noticed that permeability μ was not shown as a multiplier in the equations. It would be unsatisfactory to do so because the permeability ratio has no fixedness, at least not for steel. Instead, because most of the materials are close to unity permeability, an allowance for steel (widely different from unity) is by careful choice of correction factors.

Rounded corner paths should have a slightly lower value for flux linkage per ampere inch, hence lower K_e than straight conductors, according to the indication given by Figure 5*B*. Here the magnetizing force is less at some point p taken well outside the point of center of radius for a curve line than for some compared straight side of equal length by reason of the deviation of magnetic compouents from normalcy. The geometric deviation is θ_c compared to θ_s at the end points as shown in Figure 5*B* and at corresponding points between. However, the corners are usually a small part of the total perimeter, and neglect of this correction will not result in any great error if the straight side value of flux linkage is used.

Of greater importance is the actual length of path to use in calculating inductance, particularly for tools such as illustrated in Figure 6*G*. This path is not to be confused with an average current path but is that path at which the kernel

Table V. Measured and Calculated Values of Special Laminate Test (Figure 10) Using Alternating Potential Drop Measurement (Figure 3)

			Measured								Comparison by Approximation Calculation		
Line	Test Figure Reference	Potential Points [See Fig. 10(h)]	Z, Microhms	Power Factor	r_{ac}, Microhms	x, Microhms	L, Microhenrys	Avg λ / Amp-In.	Avg r_{ac} / In.	Temp, F	Avg λ / Amp In.	r_{ac} / In.	L, Microhenrys
1	10(a)	E_4F_4	219	0.0826	18.1	218	0.58	1.045	0.326	100	1.21	0.354 d-c.	0.675
2	10(a)	E_2F_2	222	0.0965	21.3	219	0.58	1.046	0.374	102			
3	10(a)	D_1F_1	53	0.148	7.8					105			
4	10(a)	C_1D_1	7.7	0.42	3.23								
5	10(a)	E_4C_1	33.6	0.162	5.4								
6	Total inside path by parts.	Compare with line 1.			16.43								
7	10(a)	D_2F_2	25.8	0.44	11.3					105			
8	10(a)	C_2D_2	6.4	0.58	3.7								
9	10(a)	E_2C_2	15.7	0.416	6.55								
10	Total outside path by parts.	Compare with line 2.			21.55								
11	10(b)	E_4F_4	930	0.642	600	715	1.9	3.4	10.8	230			
12	10(b)	B_2A_2	913	0.69	630	660	1.75	3.2	11.3	235			
13	10(c)	E_4F_4	276	0.15	41.4	275	0.74	1.33	0.745	110	1.55	—	0.858
14	10(d)	E_4F_4	254	0.167	42	250	0.664	1.2	0.76	92	1.42	—	0.78
15	10(e)	A_4B_4	297	0.274	84	285	0.756	1.33	1.475	90	1.42	—	0.81
16	10(f)	E_4F_4	278	0.403	112	254	0.675	1.21	2.02	86	1.42	—	0.737
17	10(g)	E_4F_4	2.440	0.84	2.050	1.330	3.52	6.3	37	300			

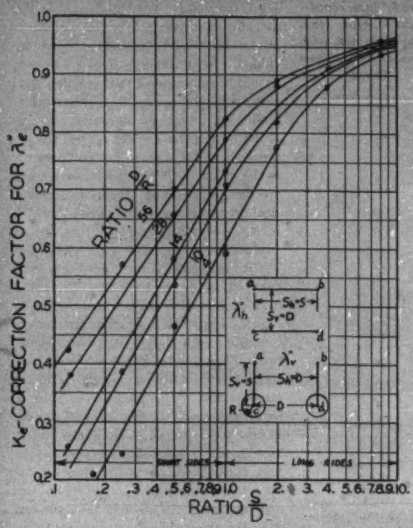

Figure 7. Correction factor K_e for external flux linkage for short pairs of sides. Used with Table II

of zero-flux-linkage cur ent line occurs as inductance is the objective (see Figure 14*A*). The center of a properly located equivalent circle may provide a good path for some configurations.

It is not within scope to consider effects of magnetic materials in proximity to the welding gun during welding.[13]

Calculation of Resistance

In general the problems relating to internal flux interlinkages extend to the calculation of resistance. The simple cross sectional unit permeable type tools allow skin effect and proximity effect to be accounted for and give reasonable resistance evaluations by using the earlier noted references 6–12. Rectangular copper bars form the yokes in many small tools and are readily calculable.

Combination material tools of steel and copper present no special problem for resistance calculation in at least three cases, Figures 6*C*, 6*D*, and 6*E*, if the current through the steel part is of negligible quantity.

The resistance of other types is more difficult to calculate because of the following possibilities encountered:

1. Nonuniform current distribution across current path from the same causes outlined in the preceding section.

2. Varying cross sectional area with respect to current path.

3. Steel losses.

4. Current path sometimes taken through welding gun pressure head, which may be a large nonuniform section difficult to calculate.

5. Contact resistances (both connections and electrode tips).

In considering the foregoing generalities the best line of approach is to deal with the specific case, weighing the relative effect of various factors entering into the resistance calculation to ascertain its justification. If the result appears indefinite or of doubtful accuracy, resort can best be made to measurement of resistance.

Resistance calculation should begin by obtaining the d-c resistance for the portion of the cross section in which alternating current will flow. The skin and proximity effects then must be evaluated and the a-c resistance obtained for the particular frequency.[6–11] The resistance formula for an averaging uniform section is

$$r_{ac} = K_r \cdot r_{dc} = \frac{K_r \rho}{A}(2S_h + 2S_v + \ldots) + r_e \quad (12)$$

where

$K_r = K_{sk} \cdot K_{pr}$

The equivalent resistance r_e for iron losses caused by steel close to current carrying members must be included.

Specific d-c resistivity is given as a guide in Table VI for several materials used in welding arms. The weld material resistance is composed of body resistance, sheet-to-sheet, and sheet-to-electrode contact resistance, all in series. Welding

Table VI. Electrical Resistivities of Welding Tool Materials

Welding Tool Material	Resistivity at Room Temperature, Microhms Per Cm³	Magnetic Susceptibility**
Elkaloy *A*,		
Wrought	2.05	diamagnetic
Mallory *J*		
Cast	2.15	paramagnetic
Wrought	2.3	paramagnetic
Mallory *53*		
Cast	4.3	paramagnetic
Wrought	4.3	paramagnetic
Mallory *73*		
Cast	8.6	diamagnetic
Wrought	7.5	diamagnetic
Mallory *100*		
Cast	3.8	paramagnetic
Wrought	3.45	paramagnetic
Copper		
Cast*	2.15	diamagnetic
Wrought	1.75	diamagnetic
Typical high tensile		
Manganese bronze	12.5 per cent conductivity in per cent IACS	
Typical aluminum Bronze (equal to Ampco *18*)	12.2 per cent conductivity in per cent IACS	
Typical aluminum Bronze (equal to Ampco *21*)	10.2 per cent conductivity in per cent IACS	
Hikonite Grade†		
10W3	5.75	paramagnetic
20W3	5.95	paramagnetic
3W53	5.75	paramagnetic
10W53	6.15	paramagnetic
TC-5	3.65	paramagnetic
TC-20	5.4	paramagnetic
TC-53	8.6	paramagnetic

* Electrical resistivity of copper castings varies rather widely and is dependent upon the degree of deoxidation, type of deoxidizer, and the amount of residual deoxidizer in the casting. The value given is typical of a so-called high quality casting.

** Essentially the permeabilities are in the order of unity for these materials.

† Other materials used for spot welding electrodes for high resistance work sheets, or for projection welding, flash welding and butt welding dies.

Figure 8. Steel copper-plated C-type tool measured in test, with magnetic field shown (inset)

sheet resistances vary greatly with materials, setup conditions, hot and cold sheet-to-sheet contact resistance values, and so forth, which differ widely. A very crude estimate would place the weld resistance range between 4 and 250 microhms with aluminum (prepared) at a low end range (4–80 very approximate), carbon steel next (10–100 very approximate), and stainless steel having higher values (40–250 very approximate). The cold contact resistance is normally higher than the hot value and for stainless steel, may, be five or more times the hot contact resistance in many instances. This large reduction of resistance during the early stages of current flow is mostly offset by the resistance rise of the body material under high temperatures.

Heating of welding tools involves very special consideration because of the wide latitude of duty cycle, cooling, and so forth, and will not be considered here.[14]

Results of Measurement

Measurements were taken on a variety of welding tools to indicate electrical characteristics along the lines described and, although not made with high laboratory precision, are representative and form a basis for comparison. Results were obtained for circuits of Figures 2*B* and 3. In most cases four measurements were taken for each test and with good agreement. In the interest of clarity representative full data is shown in Table III, and one result of each test is shown in Tables IV and V.

Table IV gives the final test result and description for all welding tools measured. Lines 1 to 8 are progressive changes in electrical characteristics during the copper plating of a solid steel tool yoke, Figure 8. The final conclusion on this experimental study for lines 1 to 8 was that excellent electrical characteristics combined with mechanical strength could be obtained with this cross section (Figure 6*C*). Eddy current effect in the sides of tool helps to reduce internal flux, as seen by the few lines going through the yoke (Figure 8 inset showing magnetic pattern.[15] Comparison then is made to a fabricated steel tool (Figure 9) and magnetic pattern (inset). It will be noticed that the internal flux tends to cancel to some extent because of unidirectional divided current. A low flux linkage per inch measured indicates only slight inductive effect caused by the steel sides.

Other tool tests are shown, some of all steel construction, and in several cases with comparisons by approximation calculation. In such calculation only d-c resistance has been indicated. Measurements and subsequent calculation regarding resistance verifies the danger of any attempt to calculate it in the vicinity of steel unless the iron losses are properly included. In considering lines 15 to 18 it should be remembered that stainless steel (unless highly annealed) has a permeability much higher than utility, and this probably accounts for a larger flux linkage per inch. Flux linkage in many cases is in the order of 1.15 maxwells per ampere inch length. Notable exceptions are for a steel type such as Figure 1 (line 14), which is 1.89 maxwells, and for the various steel tools.

The artificial laminated yoke constructed as shown in Figure 10(*h*) and measured in the various arrangements, Figures 10(*a*) to 10(*g*), offers further information even though not a tool structure. The influence of various steel-copper combinations is shown by measurement, and results are given in Table V for cross sections varying from all copper, Figure 10(*a*), to all steel, Figure 10(*g*). Here again the flux linkage per ampere inch varied from about one maxwell for all copper to about 1.2 for several of the combinations. An all steel assembly ran from three maxwells (large section) to six maxwells (small section.) The results in lines 6 and 10 show the totalizing of resistance by partial summations without detrimental effect from inductance pickup in the leads.

Considerable review and comparison by the reader for Tables IV and V is necessary in order to gain an idea of the various factors influencing inductance and resistance.

Summary

The main method of measurement described can provide at least a fair accuracy upon correct application and will obtain low order values of impedance, resistance, and reactance for resistance weld-

Figure 9. Fabricated steel and copper bar C-type tool measured in test, with magnetic field shown (inset)

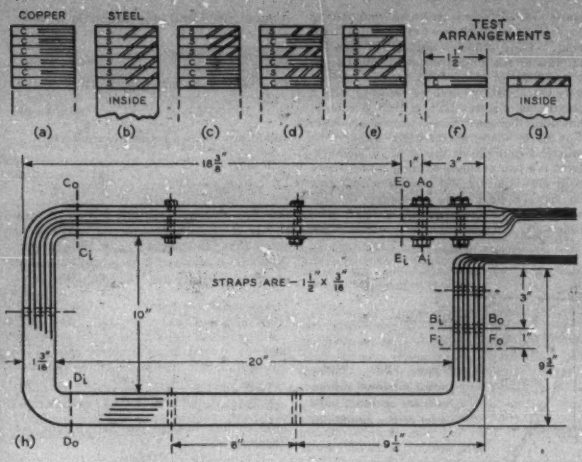

Figure 10

a to *g*—Laminate section test combination identified

h—Assembly of laminate rectangle for measurement work. Measurement points taken at planes A, B, C, D, E, and F

ing tools or other electric equipment. Such measurement becomes a valuable adjunct, when studying welding tools, for the purpose of establishing semiemperical formulas or for gaining familiarity with their electrical characteristics. The method of measurement is straightforward, and, by referring to Appendix I, a further description of potential lead connections (the only difficult part) is shown. Current and potential transformer ratios and phase angles influence the accuracy in the customary manner.

Welding tools have a relatively large span between opposite conductors, which reduces the importance of two factors; namely, geometric mean distance and current distortion from proximity effect. These factors are for most cases negligible. Other factors, such as skin effect and effect of short pairs of lines, can be taken account of in accordance with the text and provide good approximation calculations within the scope of the method.

A summary for procedure in calculating inductance is as follows:

1. Obtain all dimensional, cross sectional, and other specific data of welding tool.

2. Choose equivalent circle (R_e), if required, according to context and also to Appendix IV. Determine kernel and assign path around tool for inductance.

3. Determine correction factors K_1 and K_2 for all required corrections.

4. Obtain flux linkage per ampere inch for the horizontal pair of arms and repeat for the vertical pair, using equations, references 6–12 and charts given.

5. Take into account the air cyclinder section (if steel), round corners, and length of path.

6. Calculate resultant total inductance from equation 6.

A summary for procedure in calculating resistance is as follows:

1. Obtain all dimensional, cross sectional, and specific data of tool.

2. Find out if a calculation of resistance appears feasible.

3. Proceed to calculate d-c resistance of the cross section that carries alternating current and determine average length of current path to be used; or (as an alternative) obtain resistance by measurement.

4. Apply necessary corrections.

5. Calculate a-c resistance which must include equivalent iron loss (resistance r_e), if present. Such calculation must take into account variations in cross section, correct length, and special variations such as electrode contact resistance.

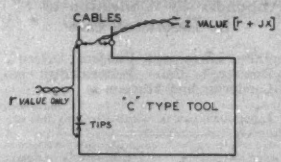

Figure 11A. Potential prod pickup positions for typical measurement on C-type tool

Figure 11B. Potential prod pickup position for measurements on X-type tool

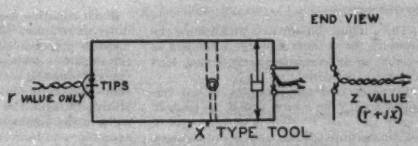

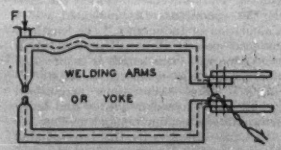

Figure 11C. Diagram showing imaginary pickup loop for measuring reactance value (coupling is unity)

Appendix I. Potential Pickup Leads for Measurement

Twisted pair and spread leads are used for taking the potential drop of the welding tool or test piece as shown in Figures 11 and 12. Extremely moderate loading is stipulated for the potential transformer so that very little current will be taken by primary, and suitable connections are made directly to the tool terminals as desired.

Induced voltage pickup with respect to the leads is now considered.[14] As a starting point it will be well to note that induced pickup, whatever it may be, should not influence resistance measurements if all measuring circuit apparatus is reasonably precise and correctly chosen. This is apparent when it is remembered that the intent of the method is to break down the impedance into r and x values. However, for z and x measurements the effect of induced pickup is vital.

The leads are connected in close proximity to opposite sides of the tool circuit and theoretically must close a loop which includes all the flux interlinkages for which x is being measured. By referring to Figure 11*C* it is seen that this loop is really homogeneous to the welding circuit itself, which acts as a "search coil" for flux. To disconnect the test leads and run a wire around the

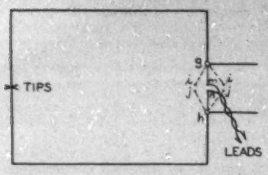

Figure 12A. Error of potential pickup leads not in a straight line is seen a function of tool size

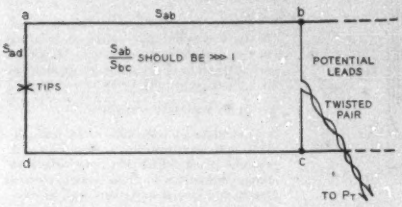

Figure 12B. Widespread potential pickup leads are operative only under certain conditions

welding tool would be a poor substitute as the coupling would not be perfect because of internal conductor flux. Therefore proper placement of test leads will give Z measurements as well as r and x values if the subsequent discussion is borne in mind.

A list of rules in connection with utilizing potential pickup leads is as follows:

1. The spread leads should be straight, perpendicular to, or at least symmetrical with the current paths being spanned.

2. The twisted pair should be carried away perpendicular to the spread leads and to the plane of the welding tool (see Figure 11B).

3. The twisted pair terminus at leads is preferably in the center between the wires, although because the induced voltage is unidirectional this is not an absolute requirement.

4. For Z and x values it is desirable that the pickup leads be short (a shall part of the total circuit measured).

5. Measurement for r alone does not require these stipulations with the same rigor.

6. Measurement for x along one arm alone is of theoretical interest only.

There follow illustrations which show the necessity for as short a pickup lead span as feasible, or at least a low ratio of such lead length to tool perimeter.

Consider that the accuracy is not impaired greatly for a large tool if the leads in Figure 12A take position gi or hj instead of gm, hm because the flux area is not changed appreciably. Such would not hold for very small tools or for Figure 12B as drawn. Therefore some guide for accuracy is derived from considering the enclosing area and, in addition, the relative proportion of length of pickup leads to the total enclosing circuit.

The error imposed by pickup leads can be visualized in another way. Induced voltage in lead bc of Figure 12B is that from interlinkages from opposite side ad as the horizontal arms cancel their induction in bc. But to provide accurate measurement the voltage induced in bc must be zero, because side ad has no adjacent conductor in juxta position and hence has a large external field. Thus induced voltage in lead bc implies in the measurement a smaller external field for side ad than exists. Hence only fair accuracy could be obtained with a circuit as Figure 12B, which accuracy, however, becomes more precise as ratio S_{ab}/S_{bc} is made increasingly large. One practical example in this kind of measurement is a pair of single welding cables where their close spacing and relative length give no conceivable inaccuracy caused by this effect. The foregoing text points out a possible slight discrepancy in measurements for Figures 11A, 11B, 11C, 12A, and 12B and tools where a gap occurs at the terminus. However, where the pickup leads are short compared to the total loop as in most all practical cases, this error will be so diminished as to be of no importance.

Appendix II. Derivation of λ'' for Theoretical Case

Infinite Lines and Uniform Current Density; Unit Permeability of Conductor and Medium

Inductance can be defined by any one of three equations, namely,

$$L = 2\mathcal{E}/i^2 \tag{20}$$

$$L = (d\varphi/di)10^{-8} \tag{21}$$

$$L = e/(di/dt) \tag{22}$$

Each equation says the same thing in a different manner. Where flux linkage produced is proportional to current, these relationships can hold for a-c as well as the d-c (zero frequency) case. However, because skin effect as produced in large conductors always changes the proportionality internally in the conductor, we should start by assuming a uniform current density throughout the conductor. As indicated under "Calculation of Inductance," the length of conductor pair is vital to the unit length inductance, and such length is assumed of infinite equivalent compared to lengths D and R. Other assumptions maintained are sine wave known frequency and unity permeability of conductors and medium.

The first objective is the internal flux linkages per unit length in one of the conductors. Making use of the practical unit for magnetomotive force and considering the latter in terms of energy or work around a magnetic circuit, the magnetic gradient at any point R_p is

$$H = I/2\pi R_p \tag{23}$$

By straight relationship for $u = 1$

$$B = 3.2H \tag{24}$$

and at any point p inside the conductor

$$B_p = \frac{3.2I_{(R_p)}}{2\pi R_p} \tag{25}$$

the flux density per unit length at any radius R (within conductor). It will be noted that the current $I_{(R_p)}$ is that proportion of total current I (one ampere) assumed of uniform density over the conductor, or

$$I_{(R_p)} = I \cdot \frac{R_p^2}{R_o^2} \tag{26}$$

Then

$$d\varphi'' = B_p dR \cdot 1 = \frac{3.2}{2\pi} \cdot I_{(R_p)} \cdot \frac{dR}{R_p} \tag{27}$$

Internal flux linkage per unit length per conductor is

$$I_{(R_p)} \cdot d\varphi'' = \frac{3.2}{2\pi} \cdot I^2_{(R_p)} \cdot \frac{dR}{R} \tag{28}$$

or

$$d\lambda_i'' = \frac{3.2}{2\pi} \cdot I^2 \cdot \frac{R^3 dR}{R_o^4} \tag{29}$$

considering (R_p) as R henceforth. Because $I = 1$

$$\lambda_i'' = \frac{3.2}{2\pi R_o^4} \int_0^{R_o} R^3 dR$$

$$= \frac{1}{4} \cdot \frac{3.2}{2\pi R_o^4} \left[R^4 \right]_{R=0}^{R=R_o} \tag{30}$$

$$= \frac{3.2}{2\pi} \cdot \frac{1}{4}$$

$$= 0.508 \cdot \frac{1}{4} \tag{31}$$

External flux linkage is taken in similar manner, remembering that the entire current is linked by flux and also is linked by certain flux from the opposite conductor, which for opposite direction current has reversed induced electromotive force sign.

$$\lambda_e'' = \frac{3.2}{2\pi} \int_{R_o}^{R(\text{large})} I_1 \frac{dR}{R} - \frac{3.2}{2\pi} \int_D^{R(\text{large})} I_2 \frac{dR}{R} \tag{32}$$

$$= \frac{3.2}{2\pi} \log_e \frac{R}{R_o} - \log_e \frac{R}{D} \tag{33}$$

$$= \frac{3.2}{2\pi} \cdot \log_e \frac{D}{R_o}$$

$$= 0.508 \log_e \frac{D}{R_o} \tag{34}$$

$$\lambda''(\text{total}) = \lambda_i'' + \lambda_e = 0.508 \left[\frac{1}{4} + \log_e \frac{D}{R_o} \right] \tag{35}$$

for unit permeability both for conductor and medium. The value of $\log_e D/R_o$ is plotted

in Figure 13 and also the flux linkages per ampere inch per conductor for various ratios of D/R_o.

Hollow Conductor—Internal Flux Linkages for Hollow Circular Conductor

Where the conductor is circular but hollow, the equation for internal flux linkages (for u_m, $u_g = 1$) is

$$\lambda_i'' = \frac{3.2}{2\pi}\left[\frac{R_i^4}{(R_o^2 - R_i^2)^2} \cdot \log_e \frac{R_o}{R_i} - \frac{1}{4}\,\frac{3R_i^2 - R_o^2}{R_o^2 - R_i^2}\right] \qquad (36)$$

where R_i and R_o are inner and outer radii respectively (see reference 7 section 14, page 45). For various inside radii the portion in the bracket ranges from 0 for infinitesimal shell to 0.25 for solid conductor.

Rectangular Conductor—Internal Flux Linkages for Hollow Circular Conductor

A square conductor does not differ greatly in internal flux interlinkages from that of a circle and can be the same for this approximation. The equivalent circle for the square may be approximated closely by taking the radius as $a/\sqrt{3}$ (see Figure 14*A*). If the equivalent circle is used, an approximation value K_i for skin effect can be obtained from reference 6.

A long rectangular bus (Figure 14*B*) gives about twice the value for internal flux linkage as for the circular conductor when the current is assumed uniform. However, skin effect, tending to crowd the current on the ends of the bus will tend to reduce the value somewhat and should be corrected for. An equivalent circle for obtaining K_e alone would have slightly less a diameter than the long side of the bus. To approximate K_e and K_i together, the diameter would be about two-thirds the long side. Variations between a square and narrow bus must be treated accordingly.

Appendix III. Method for Obtaining Inductance

Correction factor K_e (as shown in Figure 7) is devised to take into account the end effect for short pairs of lines and the sides of welding tools. The method established for obtaining this plot for K_e shown in Figure 7 is merely to take a derived equation for inductance of a short pair and work out the corresponding plots for various relationships. This equation given in reference 17 is as follows:

$$L = 4U_m\left(\sqrt{S^2+D^2} - \sqrt{S^2+R^2} + R - D + S\log_e\frac{S+\sqrt{S^2+R^2}}{R} - S\log_e\frac{S+\sqrt{S^2+D^2}}{D}\right) + u_c S \qquad (37)$$

The assumptions applying are

1. Permeability of medium u_m and conductor u_c are unity.

2. The last term relating to internal flux will be omitted because we are correcting only for the external flux linkage.

3. Round solid conductor is the only case for which the equation is exact, and caution is imposed on use of the resulting factor K_e for other than round shapes (see Appendix IV).

4. By maintaining a ratio for D/R of at least four to one the practical influence of proximity effect and geometric mean distance is minimized so that they impose no important errors.

5. The conductor must carry uniform density current. The latter is an original assumption; but because only the external flux is resolved in the method, this assumption is noted only for correlation with the foregoing equation.

Curves plotted in Figure 7 clearly show the narrowness of the correction factor for wide ranges of D/R. This is one indication that the use of equivalent circles may be justified. The curves also indicate the degree toward which the dimensional relationship is approaching the infinite length conductor case. Thus, at ratio $S/D = 10$ a correction of only five per cent is required from that of the infinite pair.

With regard to the accuracy of this procedure and resulting chart for K_e in Figure 7 it merely will be stated that comparative calculations for it against both experimental results and theoretical formulas give close agreement. Any error in the chart would tend to be more severe for low values of K_e, which are for relatively shorter portions of the total circuit.

Appendix IV. Equivalent Circles in Approximating Steel Close to Conductor

A reduced size equivalent circle may be tried for a moderate amount of steel plate next to the conductor. Such philosophy is based on

1. Very limited permeance increase at the section produced by the steel, which must have a low ratio of path to air path.

2. The field although most intense next to the conductor, representing just a fraction of the total flux linkages, as an integration will show. A calculation of permeance in this vicinity with and without steel will predict its influence.

Steel exerts a large influence when sandwiched along the extent of the copper bus. Here close section permeance is increased greatly and also are the flux linkages. When dealing with a condition of this kind, the equivalent circle should define the limit of external flux linkages only, and a correction factor K_i should be worked out for the remaining portion of the increased internal flux.

The location of the kernel as shown in Figure 14*A* is important, as this is the point at which the flux centers and has a bearing on where an equivalent circle ought to be located. Other reference is made to "Rectangular Conductor." Appendix II and Figures 14*A*, 14*B*, 14*C*. The degree to which a reduced circle will alter flux linkages can be determined for Figure 13 for varying R. Because of the logarithmic character, these circles are not supercritical;

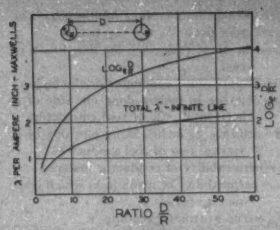

Figure 13. Value of flux linkage per conductor per ampere inch for infinite length pair, and also the value of log. D/R_o plotted

and an integral value of 2-inch diameter was used for line 10, Table IV and a 1-inch diameter for line 14, together with $K_i = 3$ and K_i (head) = 40.

Appendix V. Nomenclature

a = transformer ratio—connected primary/-connected secondary
B_p = flux density maxwells per square inch at any point p
C_t = current transformer ratio
D = distance in inches between centers of a pair of conductors whose flux linkage is being determined
$\mathcal{E}$ = energy stored magnetically
H_p = magnetic potential gradient in ampere turns at any point p
I = total assigned current in a conductor
I_{Rp} = fraction of total I with assumed uniform current density to some radius R_p
I_m = true ammeter reading
E_m = true voltmeter reading
K_e = correction factor for external flux linkage λ_e''
K_i = correction factor for internal flux linkage λ_i''
K_{sk} = correction factor for skin effect (resistance)
K_{pr} = correction factor for proximity effect (resistance)
λ'' = flux linkages (maxwells) for current in a conductor per ampere inch
λ_e'', λ_i'' = external and internal flux interlinkages, respectively
λ_h'', λ_v'' = flux interlinkages (maxwells) along horizontal and vertical sides, respectively, of a welding tool
L = inductance in microhenrys
l = length of a magnetic path
P = permeance
ρ = electrical resistivity in circular mil inches
PF = power factor
P_t = potential transformer ratio = $1/a$
R_o = radius of an equivalent circle for obtaining λ_e''
R_o = radius to outside surface of conductor
R_p = arbitrary radius to any point p, (omitting the p at times)

r = resistance in microhms (unless otherwise specified)

r_e = equivalent resistance for iron losses in tool

S = distance along conductor side in inches

S_h = distance in inches along one side of a horizontal pair of tool conductors

S_v = distance in inches along one side of a vertical pair of tool conductors

u_c = permeability of conductor material

u_m = permeability of medium in which conductor resides

W_m = true wattmeter reading

x = reactance in microhms unless otherwise specified

Z_m = impedance in microhms by measurement

θ = power factor angle and also angle of component comparison

θ_c = extreme angular deviation from normal for curved line with respect to a common remote point p

θ_s = extreme angular deviation from normal ($\theta_s < \theta_c$) for straight line with respect to a common remote point p

φ = flux

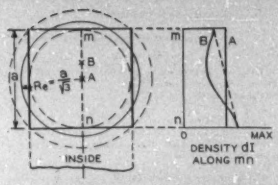

Figure 14A. Square copper conductor shown with equivalent circle, kernel, and plot of artificial current density variation

A—Designation of zero magnetic kernel and current density plot along *mn* for uniform current density distribution

B—Designation of zero magnetic kernel and current density plot along *mn* for nonuniform current distribution caused by skin and proximity effect. Proximity effect alone would be more nearly the dotted line shown

Figure 14B (above left). Rectangular horizontal flat copper conductor and field

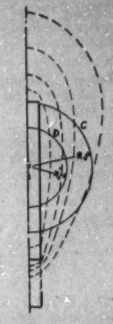

Figure 14C (above right). Rectangular vertical flat copper conductor and field

C—Equivalent circle for external flux linkage

D—Equivalent circle approximating both external and higher internal flux linkage

References

1. The Design of Bus-Bar Industrial Distribution Systems: An Epitomization of Available Data, **Thomas James Higgins.** AIEE Transactions, volume 64, 1945, pages 385–400.

2. Scope and Limitations of Stored Energy Type Spot Welding Equipment, **G. S. Mikhalapov, C. N. Weygandt.** *Welding Journal*, American Welding Society (New York, N. Y.), November 1940.

3. Small Portable Condenser Welding Set, **E. M. Callender.** *Welding Journal*, American Welding Society (New York, N. Y.), October 1944, pages 882–90.

4. Measurement and Effect of Contact Resistance in Spot Welding, **Robert A. Wyant.** AIEE Transactions, volume 65, 1946, January section, pages 26–33.

5. Contact Resistance Measurements as Control for Preweld Cleaning of Aluminum Alloys, **G. W. Scott, Jr., E. B. Charles.** *Welding Journal*, American Welding Society (New York, N. Y.), January, 1944.

6. Standard Handbook for Electrical Engineers (sixth edition), edited by **Archer E. Knowlton.** McGraw-Hill Book Company, New York, N. Y., 1933, section 4–33.

7. Electrical Engineers Handbook (third edition), edited by Harold Pender. John Wiley and Sons, Inc., New York, N. Y., 1936, section 3–22.

8. Standard Handbook for Electrical Engineers (seventh edition), edited by Archer E. Knowlton. McGraw-Hill Book Company, New York, N. Y., 1941. Section 4–29.

9. Skin Effect in Tubular and Flat Conductors, **H. B. Dwight.** AIEE Transactions, volume 37, 1918, pages 1379–1403.

10. Skin Effect and Proximity Effect in Tubular Conductors, **H. B. Dwight.** AIEE Transactions, volume 41, 1922, pages 189–98.

11. Skin Effect in Rectangular Conductors, **H. C. Forbes, L. J. Gorman.** AIEE Transactions, volume 52, 1933, pages 516–19.

12. Geometric Mean Distances for Rectangular Conductors, **H. B. Dwight.** AIEE Transactions, volume 65, 1946, August–September section, pages 536–38.

13. Influence of Magnetic Materials on the Welding Characteristics of Resistance Welding Materials, **J. J. Riley, C. E. Smith.** AIEE Transactions, volume 65, 1946, December section, pages 852–60.

14. Rating of Electric Equipment Under Intermittent Load, **Myron Zucker.** AIEE Transactions, volume 63, 1944, November section, pages 778–83.

15. Mapping of Fields, **Ernst Weber.** AIEE Transactions, volume 53, 1934, pages 1563–70.

16. The Measurement of Large Varying Currents, **A. C. Johnson.** AIEE Transactions, volume 65, 1946, January section, pages 8–11.

17. Electric and Magnetic Fields, **S. S. Attwood.** John Wiley and Sons, Inc., New York, N. Y. Section 177, page 207, equation 248.

18. The Origins and Developments of the Concepts of Inductance, Skin Effect, and Proximity Effect, **T. J. Higgins.** *American Journal of Physics*, American Institute of Physics (New York, N. Y.), volume 9, 1941, pages 237–46.

19. Bessel Functions for Calculating Skin Effect, **H. B. Dwight.** *Electrical World*, New York, N. Y., volume 79, 1922, page 964.

20. Inductance of Hollow Rectangular Conductors, **T. J. Higgins.** *Journal*, Franklin Institute, Philadelphia, Pa., volume 230, 1940, pages 375–80.

21. Formulas for the Geometric Mean Distance of Rectangular Areas and of Line Segments, **T. J. Higgins.** *Journal of Applied Physics*, American Institute of Physics (New York, N. Y.), volume 14, 1943, pages 188–95.

22. Reactance Values for Rectangular Conductors, **H. B. Dwight.** *The Electric Journal* (Pittsburgh, Pa.), volume 16, 1919, pages 255–6.

23. Electric and Magnetic Fields (book), **S. S. Attwood.** John Wiley and Sons Inc., New York, N. Y., 1932 and 1941.

24. Electrical Measurement (book), **F. A. Laws.** McGraw-Hill Book Company, New York, N. Y., 1917 and 1938.

No Discussion

Experience With Single-Pole Relaying and Reclosing on a Large 132-Kv System

J. J. TRAINOR
MEMBER AIEE

C. E. PARKS
MEMBER AIEE

Synopsis: Three full years of operating experience with single-pole switching on five 132-kv transmission lines totaling 331 miles in length is presented and analyzed. Total number of faults for the period studied was 59, of which 54 were of temporary nature. Of these 54 temporary faults, 42 involved only one phase and ground, and 38 successful single-pole fault clearing operations were experienced. Conclusions are that singlepole switching has numerous advantages over multipole high-speed switching in that better system stability is realized by its use, longer phase de-energization time permits greater time for dissipation of ionized gases at the point of fault, and over-all system disturbance is minimized during fault clearing operation.

FOR the past 12 or 15 years, the great advantages to be obtained from the use of ultrahigh speed reclosing on large capacity power transmission lines have been appreciated fully.[1] Until five years ago, however, this high-speed reclosing was limited to simultaneous multi- or 3-pole reclosing. On March 13, 1941, the Public Service Company of Indiana placed in service a revolutionary installation of single-phase or so called single-pole reclosing on a 50-mile single circuit 132-kv line between the Lenore substation at Indianapolis, Ind., and the New Castle substation at New Castle, Ind.[2] This type of reclosing differs from the formerly mentioned 3-pole reclosing in that only the faulted phase is tripped and reclosed simultaneously at both terminals of the transmission line in event of a single-phase-to-ground fault on the line. During the short interval of time the faulted phase is open, either parallel transmission line paths or the ground itself will assume the load current of the interrupted phase.

The original installation of single-pole reclosing was made on the basis that greater system stability would obtain from this method of switching than from 3-pole switching.[3] The transmission line on which this form of protection was applied first acted as the major tie between the Chicago, Ill., and northern Indiana systems and the Cincinnati, Ohio, Louisville, Ky., and Tennessee Valley Authority southern systems, and the proper maintenance of stability between these systems during fault conditions was of prime importance to proper system operation of all parties in the interconnected system. As the system developed, additional 132-kv transmission lines were constructed which knit together more closely than ever the Public Service Company's system with the large northern and southern 132-kv systems. It was felt that the advantages to be derived from the use of single-pole reclosing greatly outweighed those to be secured from 3-pole reclosing; hence single-pole reclosing was installed on all these later transmission line developments.

Much information and data have been published on the subject of high-speed breaker reclosing.[3,4] The choice of the method and speed of reclosing may be governed mainly by the consideration of the events which take place during the de-energization or "dead" time of the line in question. During this dead time two things are taking place which have a direct bearing on the problem. The systems which supply the opposite terminals of the line under consideration may be drifting apart in phase angle, and the more rapid the reclosing, the less system

Figure 1. Simplified 3-pole and single-pole systems

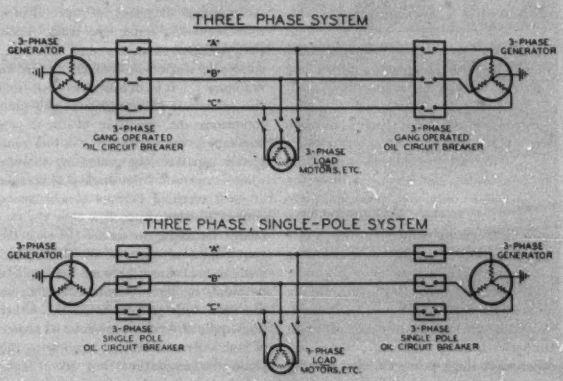

Paper 47-67, recommended by the AIEE committees on power transmission and distribution, and protective devices for presentation at the AIEE winter meeting, New York, N. Y., January 27-31, 1947. Manuscript submitted October 29, 1946; made available for printing December 18, 1946.

J. J. TRAINOR is the chief engineer of Public Service Company of Indiana, Inc., Indianapolis, Ind., at which company C. E. PARKS is assistant system operating engineer.

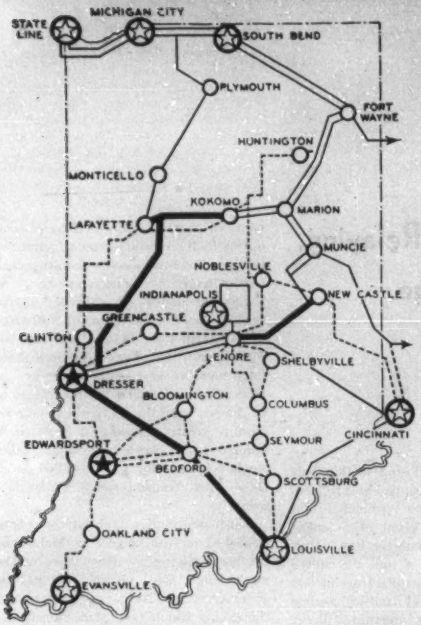

Figure 2. Major high-voltage interconnected lines of the Public Service Company of Indiana, Inc., and neighboring systems

shock that will be encountered when the systems are brought together again. This speed of reclosing, however, definitely is limited by the fact that sufficient dead time must be allowed to permit the ionized gases at the point of fault to disperse in order to prevent restrike of the fault arc. This latter consideration usually has been the limiting factor in governing the speed of reclosing. The final choice in the matter is often a compromise between the maximum reclosing time that may be tolerated from a system stability standpoint and the minimum reclosing time that will result in not too many fault arc restrikes.

Single-pole switching results in much less voltage and power flow disturbance than is caused by multipole switching because of the fact that synchronizing power flows over the remaining two phases left in service. The drift in phase angle between the two terminals of a line thus equipped is retarded, permitting phase de-energization times in the order of 100 per cent over the time normally allowed for 3-pole switching, still maintaining better system stability than with the latter form of reclosing. Stated another way, single-pole switching permits the transfer of larger blocks of power over major transmission lines with less chance of system instability and less chance of arc restrike on faults which involve one phase and ground. Actual operating experience indicates that approximately 75 per cent of all transmission line faults on the type of transmission line construction which is employed on this system are single phase to ground.

Simplified diagrams of two electric transmission systems, one using 3-pole gang-operated breakers and the other employing single-pole breakers, are shown in Figure 1. It is, of course, evident from this schematic diagram that under fault conditions the operation of the 3-pole breakers at each terminal of a line completely separates the generating sources, whereas operation of a single-pole breaker at each terminal permits synchronizing current to continue to flow over the two phases remaining in service between the two points of generation. The intermediate load shown between the two line terminals in Figure 1 would have to be provided with proper switching, either single-pole or 3-pole, to remove its source of fault current to the system during the phase de-energization time on a high-speed operation of the terminal breakers. Should single-pole switching be employed at this intermediate load point, the effects of a single-phase-to-ground fault on the transmission system would have little effect on the load. This might be a vital point for consideration in supplying some types of loads.

Three-pole high-speed switching is employed also on the Public Service Company system. The New Castle terminal of the Muncie 132-kv line, the Clinton terminal of the Lafayette 66-kv line and the two terminal breakers on the Kokomo-Huntington Junction 66-kv line are operated in this manner.

Locations of Installations

Following the original installation of single-pole reclosing on the Lenore–New Castle 132-kv line, similar equipment was installed on the following newly constructed 132-kv lines:

1. Bedford–Louisville* (59 miles) on January 20, 1944.
2. Kokomo–Lafayette (39 miles) on February 29, 1944.
3. Dresser (Terre Haute)–Bedford (68 miles) on March 10, 1944.
4. Dresser–Lafayette (101 miles) on March 31, 1944.

A map of the major transmission lines in service in Indiana is shown in Figure 2.

* The Louisville terminal of this line is at the Paddys Run Station of the Louisville Gas and Electpany, one of the electric systems with which the Public Service Company of Indiana interconnects.

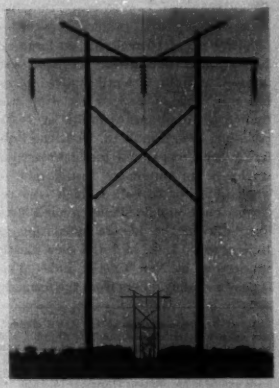

Figure 3. Wood-pole construction and conductor arrangement of Kokomo–Lafayette 132-kv line. No static wire

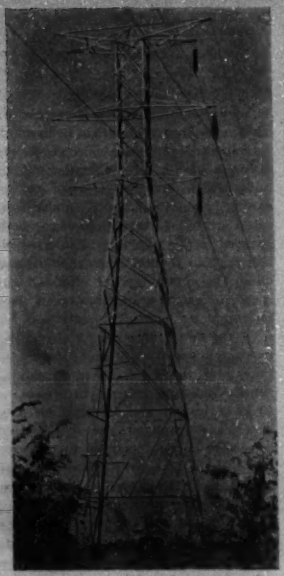

Figure 4. Tower construction and conductor arrangement of Lenore–New Castle 132-kv line

All the transmission lines on which single-pole switching is employed are wood-pole constructed single-circuit lines (Figure 3) except the Lenore–New Castle line which is of steel tower construction (Figure 4). Each line is equipped with well-placed static wire protection except the Kokomo–Lafayette line which has no static wire. A 14-mile tap line is connected approximately half way between Dresser and Lafayette and serves a customer who has installed a 3-pole reclosing 132-kv breaker at his substation. Thus the total circuit mileage of the 132-kv transmission system which is operated single-pole reclosing is 331 miles.

The 132-kv system of the Public Service Company of Indiana, Inc., is operated with each of its 132-kv power transformer bank neutrals solidly grounded.

Protective Relays

The relay installation at each of the ten single-pole line terminals is practically identical.[5] It consists of the standard power-line carrier pilot relay protection with the addition of a phase-selector relay (Figure 5) which recognizes the faulted phase and causes it to trip individually in the case of a single phase to ground fault. The electrical quantities which are employed in the phase-selector relay are

1. Negative sequence current.
2. Zero sequence current.

The negative sequence current is obtained from a negative sequence filter circuit. The development of the vector quantities of these two[5] shows that it is possible for only one phase element of the phase selector relay to close its contacts on a single-phase-to-ground fault, the other two elements being actuated in the nonoperating direction. On any type of fault other than one which involves only one phase and ground, all three poles are tripped. In the latter case, all three poles reclose high-speed simultaneously.

The additional maintenance required for the single-pole relay scheme is but little greater than for the standard carrier pilot relay scheme used for 3-pole tripping. The component parts which have been added to the standard scheme are only modifications of standard relay elements; hence their testing is relatively simple and can be performed with the usual test equipment.

The physical layout of the relay panels for two circuits at the Lafayette substation is shown in Figure 6. The protective relay (and metering) panels are located to the right and left of a panel which carries the breaker reclosing and auxiliary relays for both the Dresser and Kokomo circuits.

Oil Circuit Breakers

The oil circuit breakers located at the terminals of the single-pole operated lines are standard 35-cycle breakers, and all but three of them are operated pneumatically.[6] Each pole is equipped with a standard breaker operating mechanism with a central air compressor for the three mechanisms. A typical installation of the single-pole breaker is shown in Figure 7.

Operating Experience

A summary of the operating experience of the single-pole equipment in rather detailed form by line is given in Table I. From the data which Table I provides, it will be seen that by far the largest percentage of the faults experienced occurred on the Kokomo–Lafayette line. As mentioned before, this line has no static or ground wire. All hardware on each pole structure is solidly grounded on this line as it is on each of the other wood-pole constructed transmission lines. The static wire was omitted intentionally at the time the Kokomo–Lafayette line was constructed in order to provide accelerated information on the performance of the single-pole reclosing equipment, and the information thus obtained has been of great value. It might be mentioned that only one case of conductor burning has been observed on the line, even with all its operational record, and this particular case was not of such severity to cause the line to be removed from service for repair except at a convenient time. Insulator damage caused by flash-overs is no more severe on this line than on a line protected by static wire and in the majority of cases, a patrol of the line after an operation reveals absolutely no damage resulting from its momentarily faulted condition.

An analysis of the data contained in Table I, providing operating information on all five 132-kv lines now equipped with single-pole tripping and reclosing for the total number of years the equipment has been in service is summarized as follows:

1. Total number of operations resulting from fault 59
2. Number of operations under temporary fault conditions 54
3. Number of temporary single-phase-to-ground faults 42

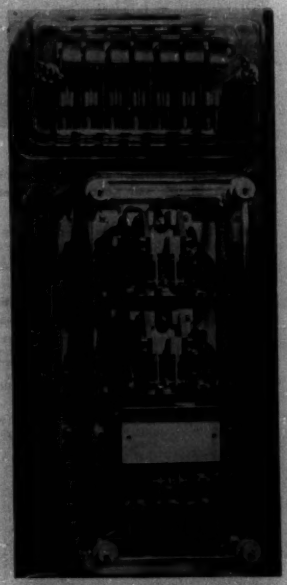

Figure 5. Close-up of phase-selector relay

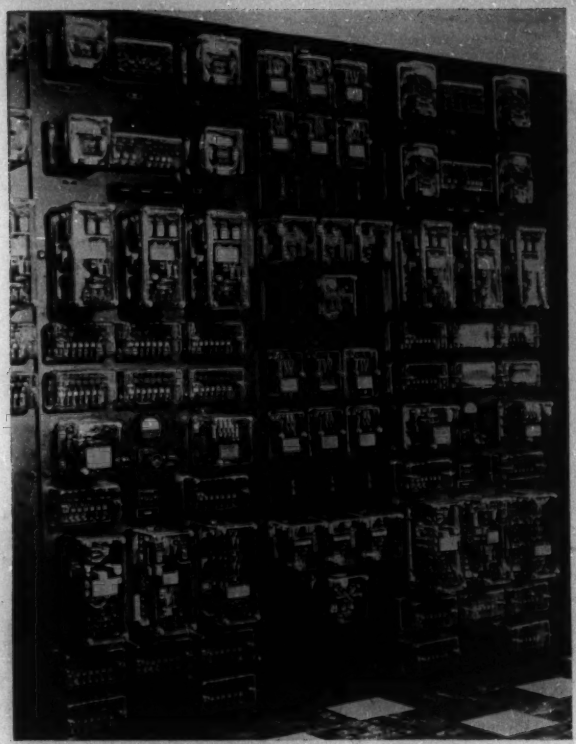

Figure 6. Panel arrangement of carrier pilot relays on Dresser and Kokomo circuits at Lafayette

Phase-selector relay at lower right. Reclosing relay panel for both circuits in center

4. Number of successful single-pole reclosing operations.....38
5. Number of unsuccessful single-pole reclosing operations..... 7
6. Number of temporary multiphase faults 12
7. Number of successful 3-pole reclosing operations.....3
8. Number of unsuccessful 3-pole reclosing operations.....4
9. Number of permanent faults.....5

An explanation of the nomenclature used in the above data might be in order. A temporary fault is one which exists only during a specific relay operation. Thus faults which clear to permit proper reclosing or faults that restrike under high-speed reclosing operations are both grouped in this category. Faults which still exist on the line when the operator closes the circuit breaker after a high-speed reclosing operation has taken place are considered permanent faults.

Of the seven unsuccessful single-pole reclosing operations, three occurred at times when the line was faulted permanently, and four occurred because of restrike of the fault arc. Of the three cases of permanent fault, two were attributable to a steel derrick boom contacting one phase of the Dresser–Bedford line, and one was caused by a tree limb blowing into one phase of the Bedford–Louisville line.

With regard to the considerable difference to be noted between the twelve temporary multiphase faults as compared to only three successful 3-pole reclosing operations, it will be observed from Table I that seven of these multipole operations were nonreclosing because of the lack of the 3-pole reclosing feature on the Kokomo–Lafayette line terminal circuit breakers at the time these faults occurred. Since that time, 3-pole reclosing has been incorporated in the control of the circuit breakers at these terminals.

The summary of the operating data indicates that there were a total of four unsuccessful 3-pole breaker reclosing operations on the five lines for the three years covered by this report. Two of these four lock-out operations were caused

Table I. Summary of Actual Operations Under Fault Conditions of Single-Pole High-Speed Reclosing Oil Circuit Breakers

Line	Year	Total Number of Operations	Number of Operations Under Temporary Fault Conditions	Number of Temporary Single-Phase Faults	Number of Successful Single-Pole Operations	Number of Unsuccessful Single-Pole Operations	Number of Temporary Multiphase Faults	Number of Successful 3-Pole Operations	Number of Unsuccessful 3-Pole Operations	Permanent Faults
Kokomo–Lafayette	1944	11	11	11	9	2				
	1945	23	23	16	14	2	7	Not equipped		
	1946	11	11	10	10		1		1	
Dresser–Bedford	1944	2	1			1	1	1		1
	1945	No operations								
	1946	2	1			1	1	1		1
Bedford–Louisville	1944	2	1			1	1	1		1
	1945	1	1	1	1					
	1946	1							1	1
Dresser–Lafayette	1944	No operations								
	1945	1	1	1	1					
	1946	1	1				1		1	
Lenore–New Castle	1944	2	1	1	1				1	1
	1945	1	1	1	1					
	1946	1	1	1	1					
Total		59	54	42	38	7	12	3	4	5

by restrike after the line was reclosed high-speed following the original fault. The remaining two unsuccessful reclosing operations were caused by a permanent fault existing on the line, one occurring when the hardware of an insulator string failed on the Bedford–Louisville line allowing a phase conductor to contact ground and another conductor, and the other occurring when an airplane crashed into the Lenore–New Castle line breaking two phase conductors. Table II provides analysis of this data in a slightly different manner and reference to that table is suggested.

While the single-pole relaying was placed in service on the Lenore–New Castle line in 1941, it will be observed from the data given in Table I that the record does not cover any time previous to 1944. Actually there were four operations on this line during the three years not shown, each operation being incorrect. These incorrect operations were all directly traceable to electrically and mechanically defective equipment in the relay scheme and the breaker control wiring; hence their inclusion in this paper would serve only to cloud the real intent and purpose of the analysis which is made of the operation of the equipment. On one of these four occasions, a fault outside the protected section of line caused the breaker at Lenore to trip because of poor contact adjustment on the directional element of the distance relay at Lenore. Two other incorrect operations were caused by an electric breakdown between two wires in the negative sequence filter because of improper winding and impregnation of the filter coils at the factory. The fourth incorrect operation was caused by a poor connection in the breaker closing control circuit at Lenore. All these conditions were corrected immediately, and no further trouble of this or any other nature has been experienced since.

Analysis of the Operating Data

An analysis of the operating data obtained is presented in Table II on a percentage basis. Considering the total number of operations of all the equipment involved in this study for the 3-year period, 1944–1946, it will be seen that 91.6 per cent of all faults on the lines were of temporary nature. Of the total 59 faults which were experienced, 76.3 per cent or 45 faults involved only one phase and ground. Of these 45 phase-to-ground faults, successful single-pole reclosure was experienced in 84.4 per cent or 38 of the cases, the arc re-established itself after reclosure in 8.9 per cent or four cases, and 6.7 per cent or three cases were faults of permanent nature.

Of the total 14 faults which involved more than one phase, seven occurred on a line where no provision for 3-pole reclosing had been made. Of the seven multiphase faults which occurred on lines equipped for 3-pole as well as single-pole reclosing, three successful 3-pole reclosures were experienced for a percentage of 42.8 per cent. The fault arc re-established itself in two cases or 28.6 per cent of the total number of operations, and permanent faults existed also in two cases. Had the Kokomo–Lafayette line been equipped for 3-pole reclosing, it is definitely felt that a large percentage of the seven temporary faults which occurred on this line would have resulted in successful reclosing operations, making for a much better showing for 3-pole reclosing operation.

Because by far the largest number of operations resulting from flashover studied occurred on the Kokomo–Lafayette 132-kv line, the operational record of this line might be considered separately from the other four lines involved. All 45 faults on this line were of a temporary nature, and 82.3 per cent of the faults occurring involved only one phase and ground. Of these temporary 37 faults, 89.2 per cent were cleared successfully and reclosed high-speed single-pole. This figure well indicates the advantages to be realized by the use of single-pole reclosing and conclusively demonstrates its effectiveness. On two separate occasions, oscillograms taken at the time of operation of this line under fault conditions have indicated that a fault on one phase was cleared and reclosed to be followed immediately 10 cycles later by a fault on another phase, which in turn tripped and reclosed successfully. If 3-pole tripping and reclosing had been employed on this line, it is very doubtful if a successful reclosing operation on such a fault would have been experienced. Oscillograms obtained during actual fault conditions are shown in Figures 8 and 9.

The average loads carried on each of the five lines involved in this study is in the order of 25,000 kw. However, a number of these operations occurred when the lines were carrying approximately 40,000 kw. Under no operation has system instability been noted. The system voltage disturbance at the time of single-pole action is extremely light and is scarcely discernable even at the terminal stations involved.

Some fear was expressed at the time of the introduction of the single-pole method

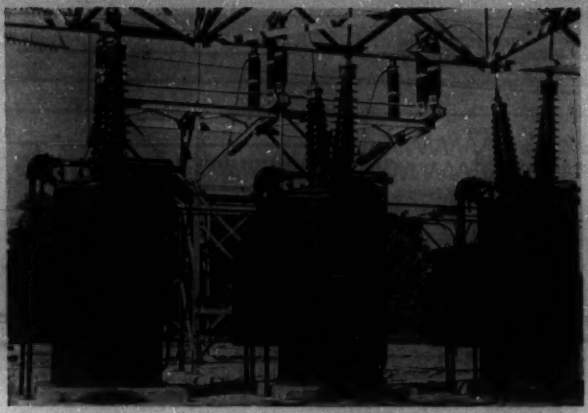

Figure 7. Close-up of 132-kv single-pole reclosing breakers at Bedford

Table II. Analysis of Reclosing Operations

A. Single-phase faults (76.3 per cent of all faults)		
Successful reclosures	38	84.4 per cent
Arc re-established	4	8.9 per cent
Permanent faults	3	6.7 per cent
	45	100.0 per cent
B. Multiphase faults (23.7 per cent of all faults)		
Successful reclosures	3	42.8 per cent
Arc re-established	2	28.6 per cent
Permanent faults	2	28.6 per cent
	7	100.0 per cent
Multiphase faults with no 3-pole reclosing	7	
	14	

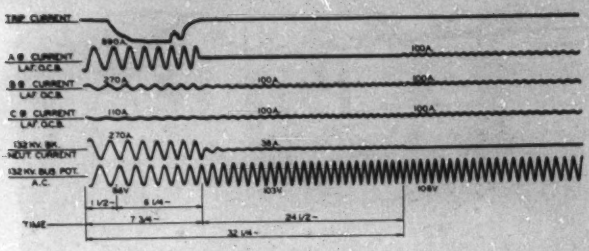

Figure 8 (above). Typical oscillogram showing single-pole reclosing breaker operation for a temporary *A* phase-to-ground fault

Relay operating time	$1^1/_2$ cycles
Fault clearing time	$7^3/_4$ cycles
Reclosing time	$24^1/_2$ cycles

Figure 9 (below). Oscillogram showing relay and breaker operation for 3-phase fault which restruck on *A* phase at time of reclosing

Relay operating time	$1^1/_4$ cycles
Fault clearing time	8 cycles
Reclosing time	24 cycles

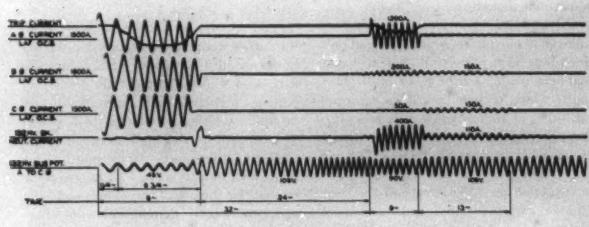

of operation of transmission lines that the tripping of one phase would cause inductive interference on parallel communication circuits or would bring about ground relay co-ordination problems on other transmission circuits which terminate at the same station where the single-pole operated breakers were located. There absolutely has been no evidence that such undesirable conditions as this exist. Concern was expressed also that the capacity coupling between the two energized phases and the de-energized phase during a single-pole fault clearing operation would tend to maintain the fault arc long enough that successful reclosing of the isolated phase could not be accomplished. There has been no direct evidence of such a condition existing and it is felt that this problem is one of not too great concern in the application of single-pole operation, except possibly on very long transmission lines.

Summary and Conclusions

During the past three years, invaluable operating experience has been accumulated in the use of single-pole high-speed reclosing of 132-kv transmission lines on a large interconnected power system. From the data obtained, the following conclusions may be drawn:

1. Of all faults caused by flashover on 331 miles of 132-kv line, incorporating five separate line sections on the system under study, 76.3 per cent involved only one phase and ground.

2. Successful single-pole tripping and reclosing was recorded in 84.4 per cent of all cases of single-phase-to-ground faults.

3. No evidence has been produced for line distances up to 100 miles that indicates that the fault arc is maintained on one phase by its capacity coupling to other phases during single-pole operation.

4. No evidence of system instability has been observed during or immediately following a single-pole reclosing operation even with large amounts of power flowing over the faulted line.

5. Use of single-pole reclosing for single-line-to-ground faults permits longer de-energization periods with greater system stability than does 3-pole reclosing, making for less chance of restrike.

6. Very little system voltage or power flow disturbances have been noted during single-pole tripping and reclosing operations.

7. No difficulty was experienced with communication circuit inductive interference or ground relay co-ordination on other adjoining transmission line circuits because of single-pole operation.

8. The relaying equipment involved in faulted phase selection is simple and reliable and requires no special maintenance. The additional equipment required to operate single-pole instead of 3-pole reclosing on line terminals requires only slightly more maintenance than does the conventional equipment.

9. Single-pole reclosing for this system has all the advantages that are to be realized by the use of 3-pole reclosing and in addition possesses a number of advantages that are not enjoyed by the latter scheme.

10. It is felt that further data which will be accumulated in succeeding years will prove conclusively that single-pole relaying and reclosing have taken their just place in modern power system equipment. Further application of single-pole reclosing is planned on at least three 132-kv lines now proposed for construction on the Public Service Company of Indiana, Inc., system.

References

1. Nine Year's Experience With Ultra-High-Speed Reclosing of High Voltage Transmission Lines, **Philip Sporn, C. A. Muller.** AIEE Transactions, volume 64, 1945, May section, pages 225–8.

2. High-Speed Single-Pole Reclosing, **J. J. Trainor, J. E. Hobson, H. N. Muller, Jr.** AIEE Transactions, volume 61, 1942, February section, pages 81–7.

3. Hi-Speed Reclosing, **J. E. Hobson.** *Proceedings* of the Midwest Power Conference, volume 5, 1942, pages 156–64.

4. Analysis of the Application of High-Speed Reclosing Breakers to Transmission Systems, **S. B. Crary, L. F. Kennedy, C. A. Woodrow.** AIEE Transactions, volume 61, 1942, June section, pages 339–48. *General Electric Review* (Schenectady, N. Y.), volume 45, March 1942, pages 173–85.

5. Relays and Breakers for High-Speed Single-Pole Reclosing, **S. L. Goldsborough, A. W. Hill.** AIEE Transactions, volume 61, 1942, February section, pages 77–81.

6. Reclosing Single-Circuit Tie Lines, **H. N. Muller, Jr., W. W. Parker.** *Westinghouse Engineer* (East Pittsburgh, Pa.), volume 5, March 1945, pages 60–3.

7. Hi-Voltage Interconnections Made Reliable By Single-Pole Switching, **J. J. Trainor, H. N. Muller, Jr.** *Power Plant Engineering* (Chicago, Ill.), volume 48, June 1944, pages 77–9.

8. Single-Pole Fault Clearing for Greater Stability, **J. E. Hobson, H. N. Muller, Jr.** *Westinghouse Engineer* (East Pittsburgh, Pa.), February 1942, pages 23–5.

9. Single-Phase Switching Applied to 132 Kv, **J. J. Trainor.** *Electrical World* (New York, N. Y.), volume 115, May 17, 1941, page 1667.

10. Five Year's Experience with Ultra-High-

Speed Reclosing of High Voltage Transmission Lines, Philip Sporn, C. A. Muller. AIEE Transactions, volume 60, 1941, May section, pages 241–6.

11. Experience With Ultra-High-Speed Reclosing of High Voltage Transmission Lines, Philip Sporn, C. A. Muller. AIEE Transactions, volume 58, 1939, December section, pages 625–36.

12. Ultrahigh-Speed Reclosing of High-Voltage Lines, Philip Sporn, D. C. Prince. AIEE Transactions, volume 56, 1937, January section, pages 81–90.

13. First Report of Power-System Stability, AIEE Subcommittee on Interconnection and Stability Factors. AIEE Transactions, volume 56, 1937, February section, pages 261–82.

14. Keeping the Line in Service by Rapid Reclosing, S. B. Griscom, J. J. Torok. *Electric Journal*, volume 30, 1938, May section, pages 301–4.

15. Electrical Transmission and Distribution Reference Book (book). Westinghouse Electric Corporation, East Pittsburgh, Pa., 1942, Chapter 8, page 207.

Discussion

J. G. Holm (Gibbs and Hill, Inc., New York, N. Y.): It has been a recent contention of a great many engineers that single-pole reclosing of power transmission lines is better from the viewpoint of maintaining stability in lines where stability is a problem, that it is somewhat more successful in clearing system faults, and that it could be used to advantage in cases where fault clearing produces large mechanical forces in the circuit breakers. Of these, the authors discussed in their paper only the effect of single-pole reclosing on fault clearing and although the reclosing time of their circuit breakers is rather slow, being of the order of 25 cycles, the percentage of successful reclosures of single-phase faults on the entire system is 84.4 per cent.

This result is obtained at the expense of costlier circuit breakers, somewhat costlier relaying, and at the cost of greater space required, none of which has been evaluated in the paper. It is probably correct to say that in longer or heavier lines, where stability is a problem and its advantages may be evaluated, single-pole reclosing and relaying is ultimately more economical and in the shorter lines it is more expensive than the 3-pole reclosing and relaying, where systems of similar general design and construction are compared. But it is true that the selection of the breaker is not made on the basis of costs alone.

It seems to me, however, that the novelty of results reported by the author lies in another direction. If the operating results obtained on the Kokomo–Lafayette 132-kv 39-mile single-circuit wood-pole line, the only line in the system not equipped with ground wires, are calculated separately from the rest of the system, then the percentage of successful reclosures of single-phase faults rises to 89.2 per cent. It is true that on this line the number of such faults is far greater than on other lines of the system, perhaps because of the absence of ground wires, but what of it once the faults have been cleared so successfully without any ill after-effects? With this percentage of successful reclosures there is not much margin left for an improvement that could be had from the installation of ground wires on this line. Similarly, operational statistics obtained on other systems shows that on lines equipped with ground wires and using 3-pole breakers the percentage of successful reclosures exceeds this figure by an amount so small that it may be considered to be within the limits of ever-present errors. It is in the fact that on the Kokomo–Lafayette line no ground wires were provided, with results in successful single-pole reclosures of single-phase faults better than on the remaining parts of the system, that may lie the major significance of the paper.

Should these results be sustained by further operational experience, the benefit obtained from ground wires will have to be reexamined. The additional costs connected with single-pole reclosing and relaying may be more than compensated by economies obtained from savings in ground wires and supporting structures. Trial installations on longer lines located in regions where atmospheric disturbances generally encountered are of a serious nature may be worth while. A revision of transmission line protection in the light of recent developments in circuit interruption and relaying may then come to be in order, and the authors' paper may be a forerunner of a coming modified outlook on the protection of high voltage lines.

W. A. Derr (Westinghouse Electric Corporation, East Pittsburgh, Pa.): The Public Service Company of Indiana pioneered the application of single-pole switching on high voltage transmission lines and the paper presented by Trainor and Parks gives conclusive evidence to substantiate previously made claims for this type of switching.

Loss of tie lines and system shock have been reduced greatly in the past years by the use of ultrahigh-speed 3-pole reclosing. However, the speed of reclosing is limited by the de-energized time necessary to prevent restriking of the arc. The paper presents proof that temporary single-phase faults can be cleared successfully without noticeable system disturbance even with 35-cycle single-pole reclosing breakers, because of the flow of synchronizing power over the unfaulted phases.

The authors point out that a single pole is tripped and reclosed on single-phase-to-ground faults, and that all three poles are tripped and reclosed on all other faults. Because approximately 75 per cent of transmission line faults are single-phase-to-ground, the installations described should provide the optimum in system stability for approximately 75 per cent of their faults. The average installation probably does not warrant the individual consideration of the remaining 25 per cent of transmission line faults. However, a relaying scheme is available which provides for tripping a single pole on phase-to-ground faults and phase-to-phase faults, two poles on double-phase-to-ground faults, and three poles on 3-phase faults. When an arrangement is used which provides for tripping and reclosing one, two, or three poles of the breaker it is known as selective pole switching. With selective pole tripping with solidly grounded neutrals, some synchronizing power continues to flow over the tie line for all except 3-phase faults.

Eric T. B. Gross (Illinois Institute of Technology, Chicago, Ill.): Ultrahigh-speed reclosing has proved to be an economical solution at system voltages of about 110 kv and up, and this paper shows that its refinement into single-pole reclosing has brought additional advantages. It is quite safe to say, however, that ultrahigh speed reclosing would be too expensive at lower voltages. The question remains, therefore, how a similar degree of reliability and continuity of service could be achieved at lower voltages, in particular in subtransmission and distribution systems. In Table I of this discussion it is indicated what influence ultrahigh speed reclosing has on various important factors, and how it compares with resonant neutral grounding by means of ground fault neutralizers (*GFN*) which are designed for extended time rating.[1] It can be seen that the application of ground fault neutralizers brings all the advantages of ultrahigh speed reclosing at reasonable cost. Recent installations of ground fault neutralizers, designed for extended time rating, in

Table I. Comparison of Ultrahigh Speed Reclosing (*UHSR*) and Resonant Grounding

Influence on	3-Phase UHSR	Single-Phase UHSR	Resonant Grounding
Stability	Improved	Considerably improved	No problem at all No short circuit
Breaker operation	Operated under short circuit	Operate under short circuit	No operation No short circuit
Generator shaft	To be considered	Small	None
Reclosing torque			
Arc at point of fault	Extinguished by breaker operation	Extinguished by breaker operation	Self extinguishing
Relaying	Carrier current needed	Carrier current preferable	Regular type
Continuous fault	Line out of service	Line out of service	No interruption if *GFN* properly designed
Equipment required	For each feeder or line section	For each feeder or line section	One or a few coils only
Economy above and at 110 kv	Reasonable	Reasonable	Reasonable
Economy below 110 kv	Expensive	Expensive	Reasonable, inexpensive for lower voltages

a 13.8-kv system and in a 6.6-kv underground cable system indicate the practicality of such schemes.

REFERENCE

1. NEUTRAL GROUNDING DEVICES, AIEE Standard 32, 1947.

Frank V. Smith (Sargent and Lundy, Chicago, Ill.): Since the tests on the original single-pole reclosing installation in 1941, transmission and protection engineers have been looking forward to a record of the performance of the system over a period of years. The authors have done a service to the industry by the presentation of this material.

In essence, the record shows that no difficulties have been experienced with single-pole reclosing. The relays and circuit breakers have performed satisfactorily, and no interference has been found with communication circuits.

Comparison with 3-pole reclosing is inevitable. The single-pole system is more costly both with regard to breakers and relays. On short lines where the operation of the two systems will not be very different, the difference in cost may not be justified.

On long lines, however, where stability is a factor, the advantage of the system is apparent. Studies on the calculating board are sometimes startling in demonstrating the marked reduction in angle of swing that results when only one pole is opened on a single-phase-to-ground fault. Units that would fall out of step with the opening of all three poles can be held together sometimes with little disturbance to the remainder of the system with single-pole reclosing. Where the stability problem is important, the application of this system should be studied carefully.

One by-product of the paper is of interest in indicating the effect of ground wires. The record shows that for the circuit without ground wires there were 38 outages per hundred miles per line per year while on the remainder of the system this figure was 1.6, a ratio of 24 to 1. It would be interesting to know if the authors feel that there were any other factors contributing to the difference in performance of these lines.

Philip Sporn and **J. H. Kinghorn** (American Gas and Electric Service Corporation, New York, N. Y.): In considering the results obtained by Trainor and Parks with single-pole relaying and reclosing it must be borne in mind that the reclosing time employed is not ultrahigh speed in the modern sense of this term. As indicated by their oscillograms the reclosing time from energization of trip coil to re-establishment of the transmission circuit is $30^3/_4$ cycles for either a single-pole or a 3-pole operation. This compares with 18 cycles for the ultrahigh speed 3-pole reclosing equipment now in service. The effect on system stability of this relatively long reclosing time for single-pole switching can be evaluated only by a detailed study of the specific system involved. It may be that in single-pole action it affords a degree of stability comparable to that which would exist with 18-cycle 3-pole reclosing. On the other hand this longer reclosing time can be detrimental only when all three phases are involved.

Assuming for the purposes of discussion, and it is a major assumption, that the two switching methods are comparable, the record of experience which Trainor and Parks have presented is one which is bound to be of interest because it is the most comprehensive information which has yet been made available, showing the results obtained with this variant of ultrahigh speed reclosing. It is indeed encouraging to note that the relaying equipment, which is certainly more complicated than that required for conventional 3-pole switching, has proved reliable and that after the initial troubles were eliminated no incorrect operations have been experienced.

It is of interest to make a few comparisons with previously published results obtained with 3-pole reclosing. For all system faults including both temporary and permanent ones single-pole switching is 84.4 per cent successful when operations involving only one phase are included, and 78.9 per cent successful when those involving more than one phase are added in. Straight 3-pole switching, however, shows 89.8 per cent successful. If permanent faults are omitted then single-pole switching for short circuits involving only one phase becomes 90.5 per cent successful and when short circuits involving more than one phase are added in, it becomes 87.2 per cent. This compares with 91 per cent for 3-pole switching. It thus appears that the record for faults involving only one phase approaches that obtained for 3-pole switching, but for faults involving more than one phase the record has not been so good. Perhaps the accumulation of a greater number of operations will improve this figure in the future.

While such a comparison is of interest in determining relative service improvement obtained by use of single-pole and 3-pole ultrahigh speed reclosing, it apparently leads to the conclusion which logically could have been expected since the inception of the two schemes that given reliable equipment properly maintained there will be very little difference in performance so long as system stability limitations are not exceeded. There is probably room for both systems, and the basic question in choosing between them then becomes one of determining how often the added complication of single-pole reclosing is justified.

As to that it is interesting to note that the authors have concluded that single-pole reclosing has all the advantages of 3-pole and a number of others besides. As opposed to this the disadvantage of increased cost and complication of relaying must be considered. Furthermore the data indicate that its performance is not yet equal to that of 3-pole reclosing particularly when multipole operations are involved. It would appear that 3-pole switching with its comparative simplicity and lower cost is preferable for applications where its reclosing speed, which is 18 cycles at present and is expected to be less in the near future, is sufficient for maintaining stability. For those applications where 3-pole reclosing cannot maintain stability single-pole may offer advantages.

The conclusion is drawn also by the authors that single-pole reclosing for single line-to-ground faults permits longer de-energization periods with greater system stability than does 3-pole reclosing, making for less chance of restrike. There is nothing in the data given which bears out this conclusion. The percentage of successful single-pole reclosures on temporary faults is 90.5 per cent as compared with 91 per cent for 3-pole indicating that the chance for restrike is low in either case.

Anticipation of results of future data is a doubtful basis from which to draw conclusions, and it would be much better to let the available data speak for itself. Frankly it is worth pointing out that there is at least the possibility if not the prospect of single tank high-voltage switches which would spread further the cost differential in favor of 3-pole switching. For the present it would appear that this conclusion is warranted and is fully borne out by the records: for overhead high voltage lines there is nothing known or available that will produce as much improvement in continuity of supply for dollar of investment as ultrahigh speed reclosing. For practically all purposes normally encountered 3-pole reclosing will do the job more simply, more economically, and perhaps more effectively, than single-pole. For exceptional cases the additional cost and involvement of single-pole reclosure may be justified. The records offered so far seem to indicate that they will be few and far between.

J. J. Trainor and **C. E. Parks:** The authors wish to thank the various contributors to the discussion of this paper. The following, in part, answers some of the questions raised.

The authors agree with J. G. Holm that significance may well be attached to the feature of the paper explaining the operation of a transmission line in the 132-kv class which is not equipped with a ground wire. This fact has led the authors to believe that there may be merit in the thought of the exclusion of ground wires on transmission lines, particularly those operated single-pole reclosing, and we are seriously considering the exclusion of ground wires on a number of transmission lines which are proposed for construction on the system of the Public Service Company of Indiana, Inc.

At the time single-pole relaying was introduced, the selective pole method of tripping mentioned by W. A. Derr had not been fully developed. This method of tripping, while possessing slightly more complexity of control than the standard single-pole scheme, certainly may have some advantages in specific cases over the standard scheme. It might be pointed out, however, that oscillograms taken on a majority of the faults covered in this paper have not indicated once that the fault originated as phase-to-phase or 2-phase-to-ground. Several simultaneous 3-phase faults have been observed, particularly on the Kokomo–Lafayette circuit.

With reference to Eric Gross' comments, it is certainly true to say that generally, on systems with voltages below 110 kv, the expense of single-pole reclosing may not be justified, and ground fault neutralizers may be the answer in the protection of the system. This may be particularly true on a system which is being proposed or which is now operating ungrounded. For a system operated with numerous transformer bank neutrals solidly grounded and with its

lightning protection equipment installed on the basis of that condition, it would be very costly to convert from a solidly grounded to a resonant neutral grounded system.

The Public Service Company of Indiana, Inc. well appreciates the advantages of the ground fault neutralizer on its ungrounded 33-kv system. There are at present five of the neutralizers in operation, protecting approximately 1,400 miles of 33-kv line.

As explained by Frank V. Smith, comparison of the additional cost of single-pole reclosing over 3-pole reclosing is to be expected. It has been the authors' observation over a number of years of experience in the utility business that as new developments are made in electric equipment, developments which will improve service and general system operation, these developments are adopted as general system standards. The question might be asked, "Where would we be today with overcurrent relay protection on our transmission lines?" It has been improvement and development in every field of the industry that has made possible the large interconnections existing today. As each improvement has been made, the question is asked, "Will it benefit general system operation?" The matter of price is usually secondary and further usually is outweighed completely by the increased advantages to be secured by the employment of equipment which will provide more satisfactory and stable service.

The startling results, mentioned by Smith, which have been observed on calculating board studies on the great advantages to be obtained from single-pole operation, have been well borne out by actual operating experience.

Smith further points out that "where the stability problem is important, the application of this system should be carefully studied." This is certainly true. However in the authors' opinion, wherever general system operating improvement is desired, single-pole relaying should be seriously considered as a means toward this end.

Smith questions whether any other factors might contribute to the great difference in the operational records of the Kokomo–Lafayette line compared to the other lines, besides the fact that this line is not equipped with ground wires. One factor that certainly would contribute to the number of operations experienced would be that this line runs from west to east, thus receiving continuous exposure from lightning storms in the area whose general direction of movement is also from west to east. Past years' records on system weather indicate that the area in which the Kokomo–Lafayette line is located is more subject to lightning than any other area on the system. This fact would further have bearing on the number of observed operations on this line.

Philip Sporn and J. H. Kinghorn point out that the reclosing time for single-pole operation discussed in this paper is in the order of 30 cycles compared to 18 cycles for ultrahigh speed 3-pole reclosing. An extensive study of the system of the Public Service Company of Indiana, Inc. was made at the time of the original single-pole installation, and it was proven that the same system stability would obtain whether 30-cycle single-pole reclosing or 18-cycle 3-pole reclosing were employed in the clearing of single-phase-to-ground faults. By means of the former method of switching more dead time will be allowed for fault arc deionization, and certainly much less maintenance will be required to keep the oil circuit breaker in proper operating condition, providing the reclosing time specified.

The discussers point out that the records of operation for the single-pole installations compare very favorably with those previously published on 3-pole reclosing. This is of course true; however, the records themselves do not tell the complete story. It is quite evident that considerably better general system operation, less general system disturbance at the time of fault, results from the use of single-pole switching.

Sporn and Kinghorn cite the increased cost and complication of relaying of the single-pole over 3-pole reclosing. It should be pointed out again that, in order to obtain more satisfactory operation and hence better service conditions on a given system, the farsighted engineer will realize that any improvement usually must be associated with increased costs for various phases of the complete project. In the case of large capacity high-voltage transmission lines, over the past several years considerable additional money has been invested in making such lines perform more satisfactorily. Improving the terminal facilities by the installation of either 3-pole or single-pole switching must result in more cost and possibly some more maintenance, but such increased costs are very small when compared with the total complete project cost. It is a known fact that the rapid advancement in the art of electric generation and transmission in the last decade has resulted in the introduction of new and more satisfactory equipment, working toward the betterment of system operation and improvement to service. This development has naturally caused some increased first costs and some small increased operating costs. For these reasons, the authors fail to see how too much emphasis may be placed reasonably on first cost of single-pole reclosing equipment compared to 3-pole reclosing when, by the use of single-pole equipment, so much is to be realized in general system benefits.

The single-tank high-voltage oil circuit breaker which Sporn and Kinghorn mention as being a "possibility if not a prospect" is unknown to the authors. However the development of air-blast air-operated breakers in the 132-kv class seems to be the forerunner in this field and under the present method of operation, these breakers if applied to single-pole reclosing would cost no more than they would adapted to 3-pole reclosing.

The authors strongly feel that the advent of the use of single-pole reclosing spells a new era of development in the art of improved system reliability and performance and that it is a further step in the advancement of the industry.

Functionalized Resistance Welding Control

C. B. STADUM
ASSOCIATE AIEE

W. E. LARGE
NONMEMBER AIEE

E. C. HARTWIG
NONMEMBER AIEE

Synopsis: In the past, it has been necessary because of unco-ordinated circuit design to build synchronous-precision welding controls which were useful for only one application. By redesigning the welding control circuits and mechanically separating each basic electrical function, a versatile line of welding controls has been obtained. This paper describes some of the redesigned circuits in the new line of welding controls.

ANY synchronous-precision welding control system must consist of

1. A power circuit to handle the large current in the primary of the welding transformer.

2. A "firing" circuit to initiate the power circuit.

3. A heat control circuit which controls the amount of current flow.

4. A coupling circuit which isolates the "firing" circuit from the timing and sequencing circuits.

5. A timer circuit.

If a spot timer is used, some type of sequence timer generally is required to coordinate the mechanical action of the welding machine with the electrical function of the control. Figure 1 shows how the several functions can be combined in different manners to obtain the desired type of control.

The redesigned sequence timers are superior to those built in the past because the stability of their circuits has been increased by use of voltage regulator tubes which nullify the effect of power line voltage changes and surges.[1] Unit contact pressure of relays used in the timers had been increased which reduces maloperation caused by foreign materials between the contacts.

The Synchronous-Precision Spot Timer

In the spot timer diagram shown in Figure 4, bias supplies have been shown as batteries and minor electrical components have been omitted in the interest of simplicity. The critical grid voltage of the thyratrons as been assumed equal to zero. Before the start of weld time, $1TU$ is not conducting because the alternating voltage on its grid is 180 degrees out of phase with its anode voltage and because the rectifying action of the grid develops a negative voltage across $1C$. $1C$ receives its negative voltage when the grid voltage becomes positive which causes a unidirectional current flow from the grid to the cathode. $3TU$ is held nonconducting because of the high negative bias on its control grid. After the "squeeze" time relay $1CR$ in the sequence timer has been energized, its contact operating on the phase shift circuit in the grid circuit of $1TU$ shifts the phase of the grid voltage so it becomes positive for a few degrees at the start of the positive anode voltage. This allows $1TU$ to conduct which starts two actions.

1. The pulsating output voltage energizes the welding transformer through intermediary circuits.

2. The timing action is started through the timing components $2C$ and $1P$.

$1P$ is actually five resistors which may be short-circuited by five toggle switches to give a 1-to-30-cycle timing range in 1-cycle steps. The length of time it takes $1TU$ to charge $2C$ to a value of voltage which exceeds the bias on $3TU$ determines the length of the weld time. This time is determined by the setting of $1P$. The greater the resistance, the longer the time; the smaller the resistance, the shorter the time. $3TU$ will conduct only when its control grid is made positive by the increasing voltage on $2C$ and when its shield grid is positive. The shield grid voltage is phase shifted to 150 degrees leading the anode voltage. Thus $3TU$ can start conduction only in the 0–30 degrees range. Start of conduction of both $1TU$ and

Figure 1. A synchronous-precision welding control consists of (1) a power circuit, (2) a "firing" tube panel, and (3) a timer panel (and a sequence timer and current regulator if they are required)

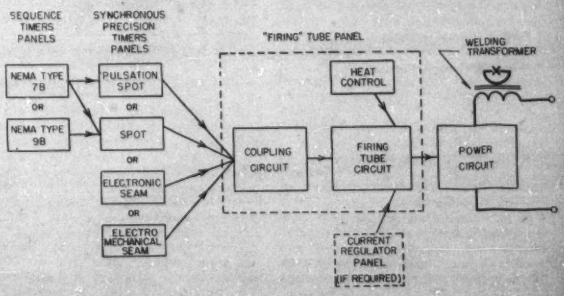

Paper 47-64, recommended by the AIEE committee on electric welding for presentation at the AIEE winter meeting, New York, N. Y., January 27–31, 1947. Manuscript submitted November 13, 1946; made available for printing December 3, 1946.

C. B. Stadum, W. E. Large, and E. C. Hartwig are all with Westinghouse Electric Corporation, East Pittsburgh, Pa.

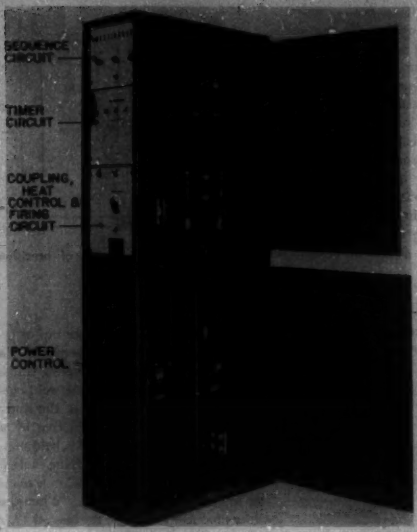

Figure 2. Assembly of functional panels in a typical synchronous-precision control

$3TU$ in only the 0–30 degrees range assures consistency of timing and uniformity of wave shape of the output voltage—necessities for synchronous-precision timers. When $3TU$ conducts, it reduces the output voltage to the arc drop of the thyratron which stops the welding current and also energizes $2CR$ in the sequence timer. This enables the sequence timer to progress through its functions. At the end of the function of "hold", $1CR$ is de-energized which stops the conduction of $1TU$ and $3TU$ in addition to discharging $2C$, which resets the circuit for the next weld. The purpose of $2TU$ is to prevent $2C$ from discharging during the half cycles when $1TU$ is not conducting. $2TU$ which is a twin diode also serves as the rectifier for the bias in the grid of $3TU$. Oscillograms of the operation of the spot timer panel are shown in Figure 5.

Figure 3. Side view of control panels in a welding control combination

The Seam Timer

The seam timer panel shown schematically in Figure 6 provides alternate "on" and "off" periods of a length required by the welding schedule. Prior to initiation of the timer by $1CR$, $10TU$ is held nonconductive by its negative bias $2B$ and $11TU$ is held nonconductive by its self bias which is identical with the bias on $1TU$ in the spot timer panel. When $1CR$ is energized by the operator, $11TU$ starts conducting at the start of the positive half cycle of its anode voltage. Conduction by $11TU$ creates a half wave voltage pulse across the output voltage terminals which, through intermediary circuits, starts the welding current. Conduction of $11TU$ also charges the "on" timing capacitor $6C$ through the variable timing resistors $5P$. When $6C$ is charged to a value which exceeds the negative bias $2B$ in the grid of $10TU$, $10TU$ will conduct.

In the grid circuit of $10TU$ is also a half wave voltage which is 180 degrees out of phase with the anode voltage on $10TU$. The purpose of this voltage is to assure that $10TU$ will start conducting only at the beginning of its positive anode voltage. When $10TU$ conducts, the output voltage is reduced to zero since the output voltage terminals are connected to the cathodes of the two conducting thyratrons supplied from the same source and having the same arc drops. When both $10TU$ and $11TU$ conduct, the welding current stops. Conduction of $10TU$ also starts the "cool" timing action by charging $5C$ through the variable timing resistors $4P$. When $5C$ has received a sufficient charge to overcome bias $3B$, $15TU$ immediately will discharge $6C$ through $3R$. The voltage developed across $3R$ by the discharge exceeds the bias on $14TU$ which discharges $5C$ through $2R$. The simultaneous discharge of the two timing capacitors to zero voltage readies the circuit for another "heat-cool" action which continues until the operator's relay $1CR$ is de-energized. This action stops $11TU$ and discharges the two timing capacitors. $12TU$ and $13TU$ prevent $5C$ and $6C$ from discharging through the output circuit during the half cycles when they are not

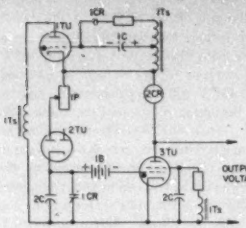

Figure 4. Schematic diagram of precision spot weld timer

The components on this panel are shown schematically on Figure 8. The purpose of the coupling circuit is to transform the half wave pulses from the timer circuit into an electrically symmetrical output to be applied to the "firing" circuit. A secondary purpose is to isolate the high power circuits electrically from the precision timing circuit and other circuits which the welding operators adjust. This insures that electrical disturbances and the high voltage in the power circuit will not endanger the operator or cause maloperation of the precision circuits.

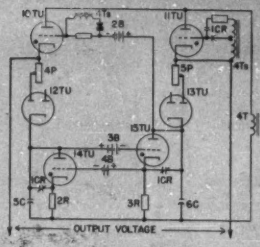

Figure 6. Schematic diagram of precision seam weld timer

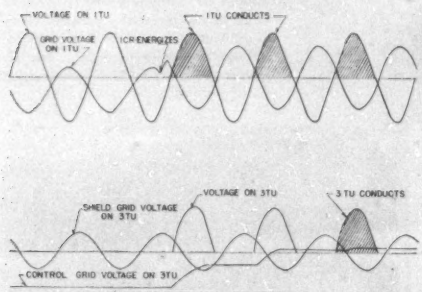

Figure 5. Voltages appearing in the synchronous-precision spot timer

being charged. The second anode of the twin diode serves as rectifiers to supply direct current for biases $2B$ and $3B$.

The timing resistors in the seam timer are five precision resistors which can be short-circuited by toggle switches. Such an arrangement gives both "heat" and "cool" circuits a 1-to-30-cycle timing range in 1-cycle steps.

The Pulsation Spot Timer Circuit

By adding a counting circuit to the "heat-cool" of the seam timer circuit, a pulsation spot timer can be obtained. At the end of each "cool" period, a voltage indication is taken from $2R$ by the discharge of $5C$. This voltage triggers a thyratron in the counting circuit which gives a discrete charge to a capacitor. After this increasing charge has overcome a negative bias in the grid of another thyratron, a continuous voltage is supplied to the "heat-cool" circuit to prevent it from operating.

The "Firing" Tube Panel

Common to all synchronous-precision timers is the coupling circuit, the heat control circuit, and the "firing circuit" which have been combined on one panel.

The primary of $2T$, the coupling transformer, normally is energized by $1T$ through $1R$. The secondary voltage prevents conduction of welding current by preventing the "firing" thyratrons from conducting. During the weld time, both $4TU$ and $5TU$ which are connected in inverse parallel conduct and act like a closed single pole switch. Because during conduction of $4TU$ and $5TU$, $2TP$ is connected between the center tap of transformer $1T$ and the center tap of resistor $1R$ which is connected across $1T$, no voltage appears across the coupling transformer. This action starts the weld current. Prior to the initiation of the timer panel, $4TU$ is held nonconductive by a bias in its grid circuit. $5TU$ is held nonconductive by a grid rectifying action which charges both $3C$ and $4C$ in a manner to keep the grid negative. When the timer produces its pulses, the bias on $4TU$ is overcome and $4TU$ conducts. The voltage thereby produced across half of $1R$ is rectified by the dry type rectifier, which action charges $3C$ to a polarity opposite its normal polarity. $4C$ is not charged appreciably by this action as the resistor in series with it gives the combination a relatively low time constant. When the anode of $5TU$ becomes positive, the tube will conduct since the charge on $3C$ has made the grid positive. $4TU$ and $5TU$ continue to conduct as long as $4TU$

Figure 7. Voltages appearing in precision seam timer

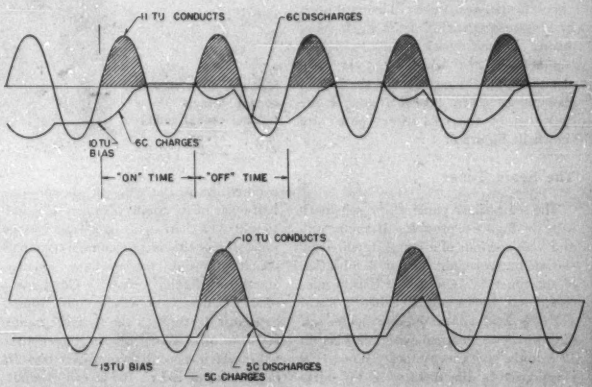

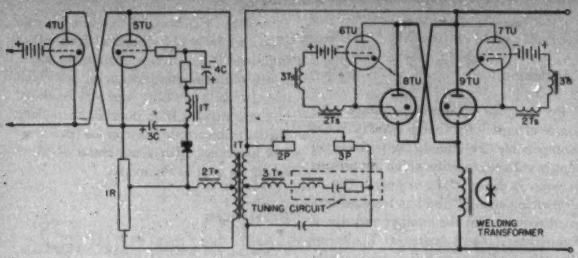

Figure 8 (above). Schematic diagram of (1) power and "firing" circuit, (2) heat control circuit, and (3) coupling circuit

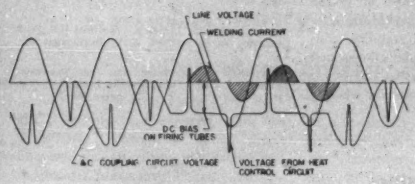

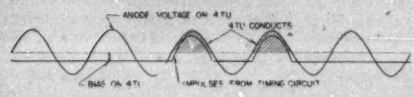

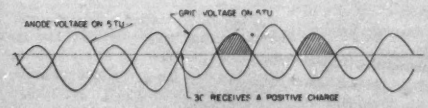

Figure 9. Voltage appearing in the synchronous "firing" tube panel

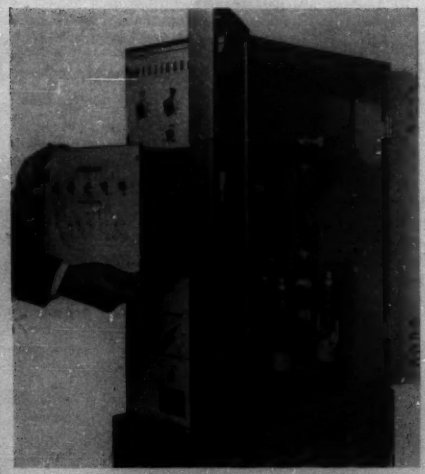

Figure 10. Adding or substituting of control functions can be accomplished in functionalized welding control

receives pulses from the timing circuit. When the pulses stop, the grid of $4TU$ can no longer become positive and this tube can no longer conduct. Stopping of $4TU$ discontinues the voltage which charged $3C$. Because this charging action has stopped, $1T$ in the grid of $5TU$ recharges $3C$ negatively and $5TU$ stops conduction.

Stopping of the coupling circuit tubes causes a voltage again to be impressed on $2TP$ which stops the welding current.

The normally present coupling circuit voltage in the grids of $6TU$ and $7TU$, the "firing" tubes, is 180 degrees out of phase with the anode voltage of each tube. In addition to this voltage, there is also a negative d-c bias and a positive peaked voltage from the heat control circuit. The sum of the direct and alternating voltages is sufficient to keep the grids of these tubes negative in spite of the positive peak of voltage from the heat control. When the coupling circuit voltage is reduced to zero by the action of the timer, the peaked voltage is great enough to overcome the d-c bias which causes $6TU$ and $7TU$ to conduct and "fire" the ignitrons. Oscillograms of the action of coupling and firing tube circuit are shown in Figure 9.

A peaked heat control voltage with its steep wave front was chosen in order to insure precise starting of the firing tubes in spite of possible variations of critical grid voltages of the tubes or possible unsymmetrical circuit conditions. The heat control circuit and peaking transformer are conventional types, a description of which can be found in the literature.[3] A tuning circuit has been included in the heat control circuit to give the necessary 45-to-135 degree shift of peaked voltage. (This is the shift required to vary the current of a high power factor welding machine from 100 to 20 per cent of maximum current.) Without the tuning circuit, the shift would be from 135 to 225 degrees because the peaks are produced when the current through the transformer is approximately zero—the 90 degree point on the applied voltage wave. $2P$ is the heat control potentiometer which shifts the phase of the peaked voltage to vary the firing point and consequently the current in the welding transformer. $3P$ is the potentiometer which limits the maximum advanced phase position of the peaks to a point on the voltage wave which corresponds to the power factor angle of the welding machine. If the peaks are allowed to be further advanced than the power factor angle, transients will appear in the welding current.

The ignitrons $8TU$ and $9TU$ receive their ignitor impulses from $6TU$ and $7TU$

by the familiar "anode firing" manner.[3] When the grid of $6TU$ is positive and its anode is positive, it will conduct and its associated ignitron $8TU$ will "fire" and allow current to pass through the welding transformer. When $8TU$ conducts, the voltage across $6TU$ falls to the arc drop of $8TU$. This stops conduction of $6TU$.

Other Control Circuits

It has been found necessary to complete the complement of controls to be used either with or in addition to the circuits mentioned. These include

1. "Firing" tube circuit for series capacitor applications.
2. Current regulator.
3. Tempering sequence.
4. A-c forge timer.
5. D-c precision forge timer.
6. Foot switch attachments.

Conclusion

By using an alternating voltage as a source of supply for timing circuits, it has been possible to eliminate the problems of supply voltage stability which are present in controls using a d-c supply. Use of alternating current also has resulted in a great reduction in the number and size of component parts. Judicious choice of the values of the electrical components has made it possible to meet all of the National Electrical Manufacturers Association's specifications of stability, consistency, and precision under all specified varying voltage conditions.

By designing new circuits for welding controls with each major function capable of being physically separated from other functions, it has been possible to assemble panels of the functions in enclosures which increase the versatility and serviceability of the control. It is possible to replace old controls, or substitute or add new control functions, with a minimum of effort as can be seen in Figure 10.

References

1. Timers for Welding Control, S. A. Clark. *Electronics* (New York, N. Y.), November 1942, pages 65–9.

2. Theory and Application of Electron Tubes (book), H. J. Reich. McGraw-Hill Book Company, Inc., New York, N. Y., 1939, pages 445–51.

3. Theory and Application of Electron Tubes, H. J. Reich. McGraw-Hill Book Company, Inc., New York, N. Y., 1939, pages 486–7.

No Discussion

Grounding of Instrument Transformer Secondary Circuits

AN AIEE COMMITTEE REPORT

THE AIEE relay subcommittee has reviewed current practices and thoughts on grounding of instrument transformer secondary circuits for the purpose of disclosing shortcomings in certain methods and recommending preferred practices. Members of the working group were asked to

1. Outline briefly the practices followed in their organizations.
2. Describe any adverse experience that may have been encountered.
3. Present their opinions on the subject.

The information in their replies was summarized and copies of the findings sent to all members of the relay subcommittee, some of whom responded with additional suggestions. Where the term instrument transformer is used, it is intended to include both current and potential transformers. Following is a summary of the information received.

Summary of Information Received

General Opinions

Agreement was unanimous that instrument transformer secondary circuits should be grounded for safety of personnel and equipment; also that station ground copper should not be depended upon to complete any part of the secondary circuits of current transformers. Agreement was general that the latter principle should apply also to potential transformers, but in the absence of adverse experience one company uses the station ground copper for this purpose except where long secondary runs to directional relays are involved.

Single Point and Multipoint Grounding

Single point grounding refers to the existence of only one ground connection on a secondary wiring system involving either a single instrument transformer, a set of transformers on a polyphase circuit, or interconnected sets of transformers such as may be used for differential relays. Multipoint grounding refers to the presence of two or more ground connections on such a secondary wiring system.

With the secondary circuit grounded at only one point, the secondary wiring does not parallel the station ground copper and run the risk of carrying a portion of the fault current which may cause incorrect relay operation or possibly burn off secondary wiring at some point. Where multigrounding is used there is also the risk that the ground relay may be shunted inadvertently through incorrect connection. Testing the secondary circuits with a megohm-meter to detect accidental grounds or deterioration of insulation is facilitated when the circuits can be isolated by removal of a single ground connection. This ground connection should not be removed while the instrument transformers are energized.

Experience

Operating companies with multigrounded instrument transformer installations reported isolated cases of trouble that were suspected of having been caused by the presence of more than one ground on a particular secondary circuit. The troubles were remedied by removing all but one ground from each circuit involved. As would be expected from the nature of the problem and confirmed by experience, relays in current circuits are more likely to be influenced by the effects of multigrounding than relays in potential circuits because current relays will respond to smaller values of foreign potential that may be introduced into their circuits from multigrounding. Short-circuiting of a potential relay by incorrect application of several grounds will cause immediate fuse blowing whereas similar short-circuiting of a current relay may not be recognized at once. No experience was cited to show that single point grounding ever resulted in faulty operation of equipment or hazards to personnel that multigrounding would have prevented.

Practices Followed

Although it was admitted to be theoretically desirable to ground the secondary circuits of instrument transformers at only one point irrespective of whether single sets of transformers or interconnected groups are involved, multigrounding has existed on some installations for many years without ill effect. On this basis several thought it unnecessary to change existing installations from multi- to single-point grounding where no adverse experience has been encountered but would recommend single-point grounding for new installations. One correspondent inferred that single-point grounding presents increased hazards, particularly to test men who may remove the ground connection.

Location of Single Ground Point

Considerable advantage is gained in operating and maintenance practices by placing grounds at points convenient for checking and removal when the secondary circuits are to be tested with a meg-

Paper 47-65, recommended by the AIEE committee on protective devices for presentation at the AIEE winter meeting, New York, N. Y., January 27-31, 1947. Manuscript submitted November 14, 1946; made available for printing December 12, 1946.

This report was prepared by a working group on grounding of instrument transformer secondary circuits of the relay subcommittee, AIEE committee on protective devices, consisting of H. R. Paxson (M'40, sponsor), senior engineer, inside plant section, electrical engineering division, Philadelphia Electric Co., Philadelphia, Pa.; R. E. Cordray (M'43), in charge of relay engineering, General Electric Co., Philadelphia, Pa.; G. B. Dodds (M'45), relay protection and section engineer, planning and development department, Duquesne Light Co., Pittsburgh, Pa.; E. L. Harder (M'41), central station engineer, Westinghouse Electric Corporation, East Pittsburgh, Pa.; E. L. Michelson (M'44), senior engineer, Commonwealth Edison Co., Chicago, Ill.; K. N. Reafdon (M'45), switchgear engineer, West Penn Power Co., Pittsburgh, Pa.

ohm-meter. The two preferred locations are at the instrument transformers or at the switchboard. Opinion, however, was divided on which to use because various reasons were advanced for each. It appears that no fixed rules can be applied, and decision must be based on local conditions for particular installations and individual preferences. Although many existing installations are grounded at the instrument transformer secondary terminals, the general trend is toward grounding at the switchboard. This is brought about probably by the greater use of relay schemes involving interconnected current transformers.

Advantages cited for grounding at the switchboard were

1. The ground is at a convenient point for checking or removal when the insulation of the secondary wiring is to be tested.

2. Greater safety is afforded personnel.

3. There is less likelihood of a ground connection being burnt off because of the failure of a current or potential transformer.

4. This is the preferred location for fault bus systems in order that the instrument ground will be remote from the fault bus ground.

5. Most comprehensive protection is provided for differential relay circuits because, electrically, the switchboard is centrally located with respect to the current transformer secondary-wiring circuits.

One operating company with current transformer secondary circuits grounded at the switchboard prefers, where a ground relay is used, to ground the junction point of the phase leads before the common return passes through the ground relay. This practice is based on the theory that an accidental ground on any single secondary conductor will not render both the ground relay and a phase relay simultaneously inoperative. However, each current transformer secondary winding has the impedance of the phase relay or relays and instruments, when used, interposed between one end and ground and the impedance of the ground relay interposed between the other end and ground.

One switchboard manufacturer provides an instrument transformer ground on factory-assembled switchboards at the switchboard for remote instrument-transformers provided by the customer but recommends its removal if the secondary circuits are grounded elsewhere; final decision is left to the discretion of the customer.

Where grounds are made at switchboards the ground connection should be placed in such a manner that it goes directly to a recognized ground bus and should not be looped about in such a way that any instrument transformer can be disconnected inadvertently from ground.

The principle reason advanced for placing the ground connection at the instrument transformer terminals was that in case of transformer failure the fault current would not travel to the switchboard to reach ground. In some cases a ground at the instrument transformers facilitates checking the continuity of the common return wire which does not carry any current of fundamental frequency under normal load conditions.

Testing of Secondary Circuits

Attention was called to the fact that many so-called relay troubles are not relay troubles at all but result from troubles in the external circuits. Because faulty system operation may result from trouble in secondary circuits, it is important that they be tested periodically to detect open circuits, short circuits, accidental grounds, and deteriorated insulation. Testing the secondary circuits with a megohm-meter was recommended strongly; also the relay tester often can recognize faulty current transformer circuits by observing the difference in current required to operate each relay when it is isolated from the secondary circuit and again when it is connected to its current transformers; the current in the second case should be only slightly greater. There was one suggestion that periodic testing of secondary circuits be included as a definite recommendation.

Conclusions

The conclusions reached from the foregoing are embodied in the following recommended preferred practices:

1. The cases of instrument transformers always should be grounded.

2. The secondary circuit of a single instrument transformer, or that of a set of interconnected instrument transformers, always should be grounded and at only one location, that location to be either in close proximity to the instrument transformer secondary terminals or at the switchboard. When a neutral secondary wire exists, that wire preferably should be grounded.

3. Station ground copper should not be depended upon to complete any part of instrument transformer secondary circuits; the connection should be made always with an insulated wire.

4. When current transformers are mounted remote from the switchboard panel, and if they are to be grounded at the current transformers, a current transformer neutral ground bus should be used to which the neutral points of all current transformers in an interconnected group are connected. This bus should be grounded at only one point and should be a conductor as large or larger than the secondary phase conductors. It should be insulated and connects all neutral points to a common ground in such a manner that the ground connection will not be removed unintentionally by the operation of any testing devices. The connection from the neutral bus to ground may or may not be insulated.

5. When instrument transformers are mounted back of the switchboard, the ground connection may be made to the panel ground bus. Ground connections for any transformer or set of transformers should not be made both at transformer ground bus and panel ground bus because of the possibility of difference in potential between the two ground busses as a result of the impedance of ground connections. This precaution is recommended primarily to assure accuracy of instruments and meters and correct performance of protective relays.

6. Certain types of secondary circuit interconnections, such as for current totalizing or differential relaying, should have their ground connection preferably at the switchboard panel. Delta-connected current transformers used in conjunction with wye-connected current transformers to supply transformer differential protection are grounded through the coils of the differential relays to the neutral of the wye-connected transformers.

7. To minimize the possibility of secondary circuit trouble interfering with the performance of instruments, meters, and relays, the instrument transformers and their secondary circuits should be tested at periodic intervals for short circuits, open circuits, accidental grounds, and deterioration of insulation.

The Shunt Tube Control of Thyratron Rectifiers

J. A. POTTER
NONMEMBER AIEE

Synopsis: The magnitude control of thyratrons in regulated rectifiers is accomplished effectively by the use of a shunt tube bridged across the d-c output and resistance coupled to the thyratron grids. The shunt tube grid operates from the output of a regulating feedback amplifier to give precision voltage regulation and highly improved dynamic response to transients, as well as electronic ripple suppression. Extensive application of this recent development has been made in supplying plate power to video and d-c amplifiers for radars and computers. Closely regulated d-c power for electronic equipment is not unduly costly when the shunt tube technique is applied.

WITH the increased acceptance of thyratrons for power rectification in communication power supplies, an abundance of ingenious and valuable circuits has been devised in the course of attempts to take full advantage of thyratron properties. The incentives for these improved d-c power supply techniques have been the desirability of, and in some systems, a dire need for

1. A highly constant voltage.

2. A very low interference content (a-c ripple).

These have been attained in spite of the gradual and abrupt changes in operating conditions encountered in a-c operated power supply systems which must be fully automatic once initial adjustments have been made.

Paper 47-66, recommended by the AIEE committee on electronics for presentation at the AIEE winter meeting, New York, N. Y., January 27–31, 1947. Manuscript submitted November 8, 1946; made available for printing December 23, 1946.

J. A. POTTER is a member of the technical staff, power development group, Bell Telephone Laboratories, Inc., New York, N. Y.

The author wishes to acknowledge the helpful advice of D. E. Trucksess of Bell Telephone Laboratories, Inc.

Fluctuations hardest to overcome and offering the greatest challenge are those occurring in the source of a-c power, such as voltage and frequency variations; those in the amount of d-c load current drawn; and those appearing in ambient temperature and humidity. Devices with the ability to reduce to any degree output changes caused by these fluctuations are termed regulated rectifiers, and in this field thyratrons have found wide usage because they are efficient rectifiers whose output can be controlled and adjusted by a negligible amount of power in their grid circuits.

The application of the controlling voltage to the thyratron grids has been accomplished with extremely simple circuits, with extremely intricate ones, and with those only moderately complex; but in all cases the control signal voltage is made to vary in order to overcome variations in one or more of the operating conditions. Writings on grid controlled rectifiers indicate that, in the minds of those skilled in the art, there are two distinctive methods of controlling thyratrons

1. Phase shift control, which means that the grids receive an alternating potential made to vary in phase with respect to the plate circuit voltage.

2. Magnitude control,[1] whereby the grid potential, usually direct current, is adjustable in magnitude only.

Circuits are not uncommon where a combination of phase shift and magnitude control is used to accomplish certain effects, and this involves both direct and alternating current in the grid circuit. Also, there are sometimes advantages to using nonsinusoidal signals. But a thyratron rectifier, in almost every instance, can be identified adequately as either magnitude or phase shift controlled. The large number of different regulating circuit configurations found useful all must produce an output for the thyratron grids, and the character of this output classifies the system.

A recently developed circuit which takes full advantage of magnitude operation is described as shunt tube controlled, because its characterizing difference from the many other configurations is the employment of a vacuum tube whose plate circuit is connected as a shunt on the regulated output.[2] The shunt tube method arose to meet requirements which could not be met economically with other practicable circuits for certain wartime radar amplifier 300-volt plate supplies, and subsequently has been used extensively for this purpose as well as in other war projects, such as computers. An inherent limitation to thyratron rectifiers is that there is only one opportunity in each half-cycle (single phase) of input voltage to modify output voltage. Therefore, the effectiveness of grid control, while adequate for regulating the average output, will not diminish transients beginning at points in the half-cycle after the thyratron fires. The prime function of the shunt tube is to eliminate such variations and so provide a high degree of output stability.

Another power supply means used extensively for this type of service is the series tube[3–5] regulated rectifier, and is so termed because the plate circuit of one or more vacuum tubes is connected in series with the load. Such rectifiers give excellent performance and are quite satisfactory for low current drains, where efficiency is no object. But the high power requirements of some electronic devices bring power consumption to the fore as a principal design consideration; and it is in this field that the relatively high efficiency of the shunt tube regulated rectifier proves most valuable.

A variety of regulating circuits have been used with the shunt tube; and various auxiliary schemes have arisen to obtain special performance features. For instance, a pentode as the shunt tube permits a secondary signal input to the

screen-cathode circuit. This has been suggested as a means to improve regulation in a typical rectifier, as a line voltage change compounder. However, the principal features of the shunt tube regulator can be discussed best by taking a power triode as the shunt tube, and showing the regulating circuit as an undescribed entity. No matter what may be the variety of features within the regulating circuit, the desired effect is to provide automatically the required variable cathode-grid potential to the shunt tube. In order to build from the simpler to the more involved, we first shall show a shunt tube regulating circuit, Figure 1, without thyratrons,[3] and then show the addition of thyratrons in Figure 2. A complete regulated rectifier circuit, the first developed and now widely used, is shown in Figure 3. Figure 4 shows an improved arrangement using a 2-stage regulating amplifier.

The basic idea of the shunt tube voltage regulator is shown in Figure 1. The tube plate current is a load on the unregulated power supply, which is in parallel with the useful regulated output load. The regulating circuit is sensitive to output voltage changes, and automatically adjusts the cathode-grid voltage to throttle the plate current as required. A certain amount of internal impedance in the d-c power supply is indispensable, and if it is not of sufficient magnitude it must be supplemented with a series resistor. The drop across this resistance is subtracted from the power supply voltage to give the output voltage. Because the tube plate current flows through this resistance, any change in it causes a change in the drop, and by this means affects the output.

With suitable components for a given application, the regulating circuit will produce a grid voltage change in response to any slight output deviation from the desired regulated value. This change has the sense needed to change the plate current to oppose output voltage variations.

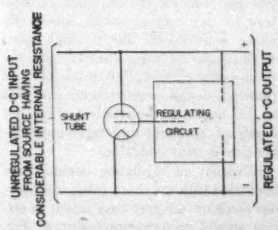

Figure 1. Basic circuit for the shunt tube voltage regulator

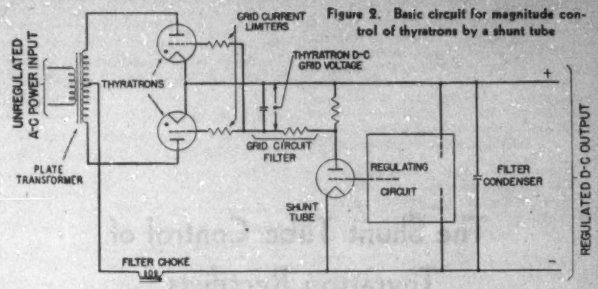

Figure 2. Basic circuit for magnitude control of thyratrons by a shunt tube

In high-gain regulating circuits the output voltages variations are infinitesimal, as an infinitesimal signal is sufficient to control the shunt tube plate current. In such systems the output drift or any other departure from regulated voltage is almost entirely a function of the regulating circuit properties, as long as the shunt tube plate current is not called upon to reach zero nor a higher value than its rating.

The basic regulated thyratron rectifier circuit employing a shunt tube (Figure 1) is shown in Figure 2. The input power is supplied from a commercial unregulated a-c source, and the thyratrons are connected to the plate and filter coils and to the d-c load in the conventional manner. The drop across a coupling resistor in the plate circuit of the shunt tube is the voltage available for the thyratron grids, and a grid circuit filter is used to suppress alternating current at this point.

The shunt tube is controlled by the regulating circuit and has the same effect as in Figure 1; but the voltage across the added coupling resistor, being proportional to the shunt tube plate current, provides a control path for adjusting the thyratron output in response to load voltage changes. That is to say, the output voltage is regulated automatically by the amplified feedback of its changes, acting to control the plate current in the thyratron tubes. This control is phased for negative feedback and so keeps the output voltage constant except for the amount of change required for input to the regulator. These changes, amplified in the regulator circuit, finally appear as changes in drop across the resistor. This voltage controls the point of time in each cycle at which each of these tubes fires, and so has control over the average output voltage. It will be noted that the amplified effect of only the average change in output voltage reaches the thyratron grids since the line-frequency and double-line-frequency components are suppressed by the low pass filtering effect of grid circuit resistance-capacitance filter. However, this does not mean that the regulator circuit fails to respond to higher frequency output voltage changes. These higher frequency changes are taken care of by the shunting effect of the shunt regulator tube across the impedance of the swinging filter coil. In practice, the ripple suppression and response to counteract abrupt line and load changes is effective over a very wide range of frequencies because the thyratrons take care of d-c and low frequency changes, the shunt tube covers an intermediate range, and the final filter capacitor removes high frequency variations. The effectiveness at intermediate frequencies is limited, however, by the response characteristic of the regulating circuit amplifier and the capacity of the shunt tube. The shunt tube average current is a drain on the total direct current available from the thyratrons, and so decreases the efficiency somewhat from what is attained in some other magnitude controlled rectifiers. However, tube current required for effectiveness in most applications is only about 1/12 of the useful output current and is outweighed by far by the improved dynamic response it provides. Where more capacity for dynamic response is required, more than one shunt tube is operated in parallel.

The selection of the shunt tube (or tubes) and its operating conditions so that the peak shunted current obtainable is somewhat higher than the maximum instantaneous load current change anticipated is a convenient rule of thumb for optimum design.

A regulated rectifier circuit, complete except for filament supply and thyratron cathode preheating means, is given in Figure 3. Nothing is added to Figure 2 except the details of the regulating circuit and a stage of filtering. The added filter

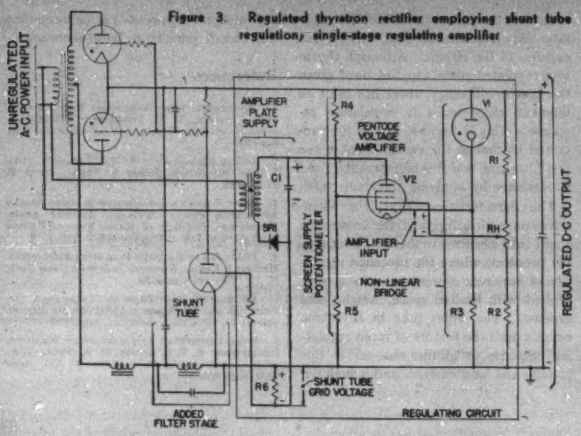

Figure 3. Regulated thyratron rectifier employing shunt tube regulation, single-stage regulating amplifier

stage is tuned to antiresonance at twice the line frequency, because this component requires greatest attenuation and otherwise would overload the shunt tube.

The regulating circuit may be considered a nonlinear bridge working into a d-c amplifier. The nonlinear bridge includes a reference voltage in the form of the drop across a cold-cathode gas filled tube, to which a fraction of the output voltage is compared. The difference between these two voltages is the input to the d-c amplifier; the output of the d-c amplifier is the shunt tube grid voltage. The cold cathode voltage regulating tube *V1*, resistors *R1*, *R2*, *R3*, and potentiometer *RH* make up a nonlinear bridge. Three of the arms of this bridge are linear resistors; the fourth is the voltage regulator tube, which is nonlinear in that the voltage drop across it remains essentially constant with currents varying within its operating range. The output voltage of the rectifier is applied to the input corners of this bridge. Potentiometer *RH* provides an adjustment to allow for manufacturing variations in the characteristics of component parts, so that the unbalance voltage at the galvanometer corners of the bridge may be adjusted to the voltage required for the control grid of the amplifier tube *V2* (about 1.5 volts) to which it is applied.

The *V2* pentode is used to amplify the voltage from the galvanometer corners of the nonlinear bridge. The cathode and the suppressor grid are at a potential above ground equal to the voltage across *R3*. Resistors *R4* and *R5* provide a suitable screen potential. A plate supply is furnished by a transformer winding and a half-wave selenium rectifier *SR1*, and appears across capacitor *C1*. *V2* works into resistor *R6*, which couples it to the shunt tube.

An improved regulating circuit employing a high gain amplifier, and its use as a grid signal supply for the shunt tube is given in Figure 4, and, as in Figure 3, the filament supply and starting time delay for thyratron cathode preheating are omitted. The circuit outside the regulating circuit is the same as shown in Figure 3 except that the series element in the added filter stage is a resistor instead of a tuned inductance for the sake of economy and to improve shunt tube effectiveness over a wider frequency range of ripple suppression.

Equipments incorporating the features of Figure 4 have been found to vary from the output voltage setting about 0.25 per cent with the fluctuations in operating conditions encountered in military service. The component of ripple voltage present in the output is less than 0.01 per cent. The nonlinear bridge circuit configuration here differs from that of Figure 3 by the location of the nonlinear element *V1* and the addition of two resistors *R7* and *R8*. These are needed to divide the reference voltage potential of *V1* to provide a suitable potential for the cathode of the first amplifier stage. In the 2-stage voltage amplifier, *R9* couples the first to the second stage; and *R6* couples the second stage to the shunt tube grid-cathode circuit. Capacitors *C2* and *C3* by-pass the attenuating effect of the nonlinear bridge resistors upon alternating voltage components of the output fed into the regulating amplifier, and are a considerable factor in the high degree of ripple and other noise suppression attained.

Because this regulating system is in a general sense a negative feed-back amplifier of high gain, the techniques to prevent the tendency to oscillate must be applied. All that is needed here is a resistor and capacitor (not shown) connected to feed-back a signal from the output to oppose and damp out any parasitic oscillation that may appear.

Among the other regulating circuits successfully employed in shunt tube applications, most notable are various cathode follower amplifiers[3,4] using dry cells or nonlinear elements as reference voltages. Chiefly a problem of amplifier design, the regulator can take one of many forms,

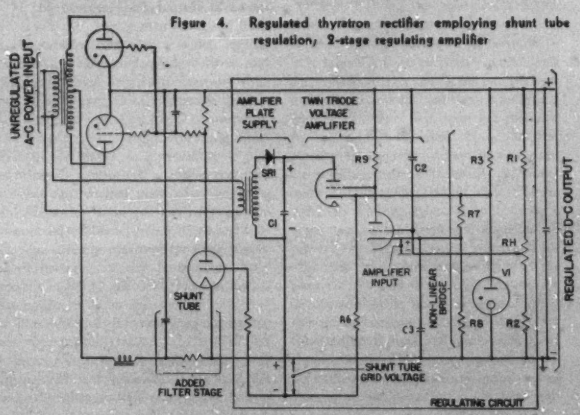

Figure 4. Regulated thyratron rectifier employing shunt tube regulation, 2-stage regulating amplifier

according to requirements, the available auxiliary components, and the ingenuity of the designer. In general, the more closely regulated the output must be, the higher the gain in the regulating circuit, and the more exacting are the requirements for the elements. And conversely, if desire for economy and less stringent requirements permit, a very simple regulating circuit will be found most practicable.

The thyratron not only is an efficient rectifier but also affords means of controlling the rectified current it passes. In many regulating circuits[8] using uncontrolled rectifier elements such as diodes or dry disks, the regulating elements must be inserted in series with the main power circuit and thus introduce considerable additional losses. This flow of the power in tandem through both rectifier and regulator also increases the size, weight, and expense of the circuit. Although thyratron-regulated plate supplies have given the best in efficiency, there has been an inherent sluggishness in regulating response. This is because of the time required to change the energy level in the first filter coil, which is indispensable, and is overcome by applying the shunt tube.

The characteristics of thyratrons themselves undergird the gratifying answer the shunt tube circuit is to the d-c power supply problems where the precision regulation of hundreds of watts must be accomplished with limited space, weight, and expense. The shunt tube in thyratron circuits adds the feature of rapid regulating response to abrupt changes in line voltage and load current, and a high degree of ripple suppression at no more than a moderate penalty to basic economies.

References

1. Regulated Tube Rectifiers Using Magnitude Control, D. E. Trucksess. *Bell Laboratories Record* (New York, N. Y.), September 1938, page 24.

2. United States patent 2,377,370, June 5, 1945, Voltage Regulation, James A. Potter, David E. Trucksess.

3. Basic Theory and Design of Electronically Regulated Power Supplies, Anthony Abate. *Proceedings*, Institute of Radio Engineers (New York, N. Y.), July 1945, page 478.

4. Features of Cathode Follower Amplifiers. Herbert J. Reich. *Electronic Industries* (New York, N. Y.), July 1945, page 74.

5. Regulated Rectifiers in Telephone Offices, D. E. Trucksess. AIEE Transactions, volume 61, 1942, August section, pages 613–17.

6. Some Industrial Applications of Selenium Rectifiers. S. V. C. Scruby, H. E. Girot. *Electrical Communication* (New York, N. Y.), April 1939, page 366.

Electronic Constant-Current Motor Systems

O. W. LIVINGSTON
MEMBER AIEE

BEFORE the development of electronic tube control the adjustable voltage system consisting of a d-c motor energized from an adjustable voltage d-c generator driven by a separate d-c or a-c motor, was generally considered to be one of the most flexible drives for adjustable speed applications. It was only natural that the initial electronic tube motor controls would develop along similar lines.

An adjustable voltage system, as most commonly employed is basically an adjustable voltage d-c supply for a shunt wound d-c motor. At any fixed d-c voltage it is basically a constant speed drive which is capable of supplying either positive or negative torque with only a small speed change. When positive torque is supplied power flows from the motor generator set to the drive motor. If the load has an overhauling characteristic the motor speed increases only slightly to permit its voltage to exceed that supplied by the motor generator set, and the current and power flow is reversed.

Under these conditions the drive motor becomes a generator, the normal generator of the motor generator set becomes a motor, and the motor of the motor generator set becomes a generator or alternator pumping power back into the supply line.

If, as is conventionally done, we supply the armature of a d-c shunt wound drive motor from a controlled rectifier we may supply any desired direct voltage to the motor armature and control its speed in a manner similar to the variable voltage system as long as we are supplying power to the motor. However, if the load of the drive motor becomes overhauling, it is not possible to reverse the current in the d-c circuit to provide negative torque, since a simple rectifier unlike a d-c machine basically permits current flow in only one direction. While it is possible and practical in some instances to supply the drive motor from two paralleled reversely connected, controlled rectifiers so that the motor current may flow in either direction, this increases the size of the power unit and the complexity of the control, to prevent or minimize circulating current between the rectifiers. To overcome these difficulties an electronic constant current control system was developed which overcomes many of the disadvantages cited.

Basic Constant Current Principle

In this system, the armature of a conventional d-c shunt motor is excited from a constant current source which in this case is a phase controlled rectifier and regulator which adjusts the output voltage to whatever value necessary (within the designed voltage limits) to maintain the average d-c current constant. The field of the motor is supplied by a pair of reversely connected controlled rectifiers so that any desired positive or negative value may be attained. These reversely connected rectifiers present the same problems as already outlined for their use in the armature, but due to smaller power requirements of the field these problems are no longer as serious.

This system is inherently an adjustable constant torque system. If the field flux is set at zero it is obvious that zero motor torque will be developed. If the field flux is made either positive or negative a positive or negative motor torque will be developed, which if the motor were connected to a rising torque characteristic load such as a fan, would cause positive or negative rotation at increasing speed until the load torque equaled the constant torque developed by the motor. The constant current armature rectifier will automatically adjust its voltage as the counter electromotive force of the motor builds up so that the current flow remains constant. At zero speed the output voltage is very low—just enough to supply the IR and brush drop. As the motor speed increases the rectifier voltage increases proportionally. Since negative rotation is accomplished by reversing the field, the counter electromotive force always has the same polarity and the rectifier voltage is positive, indicating positive power for motoring in either direction.

If however, the drive motor is excited to give positive torque and the machine is mechanically rotated in the negative direction by an external driving device the counter electromotive forceof the machine will be reversed, and will be in the direction to increase the armature current flow. In order to keep the armature current constant it will be necessary for the output voltage of the rectifier to go to a negative value, or to act as an inverter.

Figure 1 shows this relation for a particular value of armature current and field current which produces a fixed torque.

It is well known to those familar with controlled rectifier operation but perhaps unfamiliar to others that there is no fundamental difference between a controlled rectifier and an inverter. If a controlled rectifier is supplying a load having sufficient inductance to maintain the direct current continuous and an ability to reverse its voltage (that is to become a generator rather than an absorber of power), the average output voltage of the "rectifier" may become negative after the phase of the grid is retarded beyond the 90 degree lagging point. Figure 2 shows the instantaneous output voltage for three different values of phase retard in a simple 2-tube (diametric) circuit assuming sufficient inductance and suitable load characteristics to maintain the load cur-

Paper 47-99, recommended by the AIEE committee on electronics for presentation at the AIEE winter meeting, New York, N. Y., January 27-31, 1947. Manuscript submitted November 14, 1946; made available for printing December 23, 1946.

O. W. LIVINGSTON is with the industrial control engineering department of General Electric Company, Schenectady, N. Y.

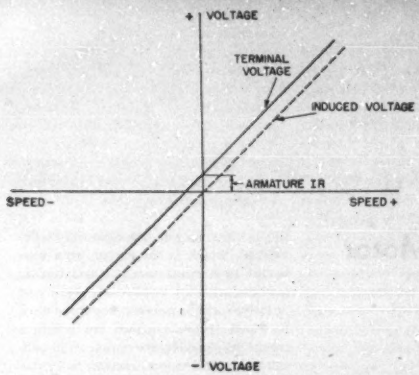

Figure 1. Relation between armature voltage and motor speed, operating at constant armature and field current

rent continuous. Figure 2*a* indicates an average voltage that is positive for a small angle of phase retard. Figure 2*b* shows that the average value of output voltage is zero for a phase retard of 90 degrees, and Figure 2*c* shows that the average d-c voltage is negative for values of phase retard between 90 and 180 degrees. From analytic considerations neglecting regulation in the rectifier and tube drop the relation of output voltage to "full on" voltage of such a rectifier may be shown to be

$$E_{d\alpha} = E_{do} \cos \alpha$$

Figure 3 shows this relation on both rectilinear and polar co-ordinates. While insufficient inductance in the armature circuit may cause the current to become discontinuous so that the above relations are no longer completely accurate, it is still possible to invert and pump back when the counter electromotive force of the motor reverses.

Constant Torque Circuit

Figure 4 shows an elementary diagram of a simple constant torque motor control. For ease in understanding, the circuit may be broken down into several functional components. The anode transformer together with the armature tubes *VT*1 and *VT*2 and the field tubes *VT*3 and *VT*4 supply the armature and field respectively of a d-c motor. For simplicity the field rectifier is shown uncontrolled and the field current varied by the rheostat 3*R*. Obviously a field reversing contactor or switch could be added if both positive and negative torques were desired.

The grid control of the armature rectifier is affected by the grid transformer 2*T* which in turn is energized by the simple *R–L* phase splitting circuit involving the resistor 12*R* and the a-c winding of the saturable reactor *SRAC*.

A special current transformer 3*T* having two primaries one in series with each of the armature tubes is used to obtain a current signal. The secondary of the transformer is shunted by a resistor 11*R* and the secondary voltage rectified by the tube *VT*8. The output of this rectifier, which is essentially proportional to the current of the main armature rectifier, is then filtered and used to affect control of the tube *VT*7. It will be seen that the grid voltage of tube *VT*7 is the result of two signals: the positive "turn on" voltage from the potentiometer 8*R*, and the negative "turn off" voltage from the armature current signal rectifier. The magnitude of these two voltages and the relative value of their "feed resistors" 7*R* and 9*R* determine the grid voltage of *VT*7. Under steady operating conditions an equilibrium is reached in which the current through the tube *VT*7 is sufficient to produce the phase shift which produces the required output voltage which in turn causes the required armature current to flow and produces the correct armature current rectifier output voltage to maintain the grid voltage at the required value. If however, for any reason, such as a change in the motor load, the armature current decreases the negative current signal voltage would decrease and the grid of *VT*7 would become more positive. This would result in more anode current through *VT*7, increased saturation in the saturable reactor, a phase advance in the grid excitation, greater rectifier output voltage, which would finally cause the armature current to increase until it attained substantially its former value. Similarly an increase in armature current would have the reverse action of these components so that the current would be reduced to substantially its initial value.

Obviously this is a very simple armature current regulator which can be adjusted to any desired value of armature current by means of the potentiometer 8*R*. This control then gives the motor a constant torque characteristic which may be set to any value by adjusting either the field strength or the armature current. Figure 5*a* shows the idealized speed torque characteristics possible by different per unit armature currents with full field. It should be noted that once the torque setting is made, the motor will develop this torque regardless of the direction of rotation within the motor rating. The dotted line at top and bottom of the curves represent rated armature voltage which occurs at full basic speed if full field excitation has been maintained. Figure 5*b* shows the family of curves resulting from regulating the armature current at one fixed value and adjusting the field for definite values of either positive or negative flux. In this case the per unit armature voltages at the various operating points are indicated by the dotted lines. It is interesting to note that the voltages which are proportional to input power at constant armature current are positive in the first and third quadrants, which are the normal motoring quadrants, and negative in the second and fourth quadrants, which are the generating quad-

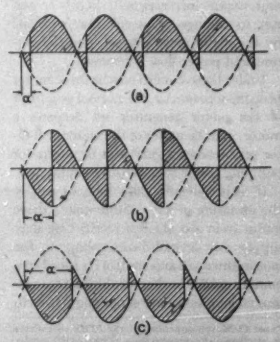

Figure 2. Output voltage wave shapes of diametric controlled rectifier assuming continuous current flow in the load for several values of phase retard

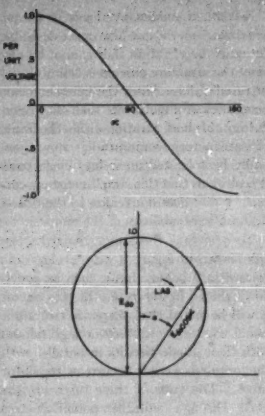

Figure 3. Per unit output voltage of controlled rectifier versus phase retard for continuous current conduction

A—Rectangular co-ordinates
B—Polar co-ordinates

rants. It is seen that if reduced torque is obtained by field weakening it is possible to run the machine above basic speed provided that the load torque is reduced correspondingly without exceeding rated armature voltage. This of course is similar to the constant horsepower obtained in the field weakening range in the more familiar constant voltage operation.

Constant Speed Control

Figure 6 shows the main power circuits of a simple constant current motor speed control consisting of a controlled rectifier supplying the armature and a pair of reversely connected controlled rectifiers supplying the field so that either positive or negative field current may be supplied. Small resistors in the output of the two field rectifiers minimize any circulating current between them due to any "overlapping". The grid control is affected by means of saturable reactor phase splitting circuits which may be individually controlled by means of the respective saturable reactor d-c windings. As in the previous circuit current transformers in the anode of the armature tubes in cooperation with a rectifier and filter provide a d-c control voltage proportional to armature current.

Figure 7 shows the control circuit used to control the power circuit shown in Figure 6 to obtain speed control. The left hand tube *VT*8 is employed in the armature current regulator as previously explained. To obtain speed control a d-c tachometer mounted on the motor shaft is compared with the d-c speed signal determined by the setting of the potentiometer *R*22 and the difference or "error" fed to the grid circuit of the amplifier tube *VT*9. The tubes *VT*9 and *VT*10 have a large common cathode resistance and operate basically as a type of phase inverter sometimes called a "long tailed pair". The output of these two tubes, which move in opposite directions as the input to the grid of *VT*9 is changed, are coupled by means of potentiometers to the saturable reactor tubes *VT*11 and *VT*12 which, through their respective saturable reactor phase shift circuits, control the negative and positive field rectifiers.

Let us consider the zero speed equilibrium conditions. The potentiometer *R*22 is in midposition so that the voltage of the slider to the middle voltage bus is zero. The output of the tachometer is zero. Thus the grid potential of the tube *VT*9 is the same as that of *VT*10. Since their inputs are balanced the output voltages are the same and the saturable reactor tubes are each passing a very small but equal current so that there is zero field voltage and current. Under this condition the motor stands still even though the preset armature current is flowing since if there is no field there can be no torque.

If now the speed control potentiometer is turned so as to give positive voltage with respect to the middle bus the equilibrium is destroyed. As the grid of tube *VT*9 is made more positive by this action its anode current increases and its anode potential decreases. Due to the coupling in the common cathode or "tail" the anode current of *VT*10 decreases and its anode potential increases. This action decreases the small current in the negative saturable reactor tube *VT*11 to zero and increases the current in the positive saturable reactor tube. This causes the negative field rectifier to be turned completely off and the positive field rectifier to be turned on. This in turn produces positive field current, positive torque, and motor rotation in the positive direction. As the motor speed increases the tachometer voltage rises, tending to counteract the positive voltage of the speed signal supplied by the potentiometer *R*22. Finally another new equilibrium is reached in which the tachometer voltage has increased sufficiently to bring the grid of tube *VT*9 almost back to its initial condition. It must generally be very slightly higher than formerly however so that sufficient net positive field still remains on the motor to produce the necessary torque to maintain that speed. If the load torque is now increased the motor speed decreases by only a small amount to permit the grid voltage of *VT*9 to rise slightly so that the necessary increase in positive field and torque may be supplied. Since only a small change in grid voltage of *VT*9 is necessary to obtain large changes in field it will be seen that such a device will give good speed regulation as the load torque is increased.

Now suppose that the load torque were decreased and even finally made negative. The first tendency would be for the speed to start to rise. As soon as the tachometer had risen a short distance however, the field excitation would first be reduced to zero and then reversed giving rise to a negative torque which would be increased until it was equal to the "overhauling" torque of the load. Under this condition

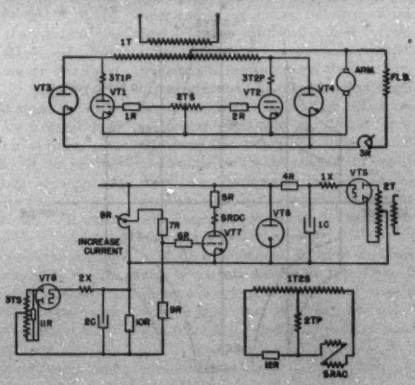

Figure 4. Simple constant torque motor control

the induced voltage in the motor would reverse, but since the constant current armature regulation always functions to maintain the current constant, we would find that the power flow had reversed and the armature controlled rectifier would be actually operating in the normal inverter quadrant. Thus it is possible to maintain substantially constant speed from full positive to full negative torque.

In a similar manner it may be seen that if the speed control potentiometer is suddenly moved to a lower positive speed the field excitation will temporarily reverse to apply negative torque, which is in effect regenerative braking until the machine has reached the lower speed at which time the positive field will be reestablished at a value required to satisfy the load torque at this speed. If the speed control potentiometer is turned so as to give a negative voltage the system regulates at a negative speed or the motor reverses. In this case the tachometer voltage reverses but the sense of all the voltages is such that no switching is necessary. When running in the negative direction with a power absorbing load we find we must exert negative torque or have a net negative field. A negative rotation and negative field results in a normal positive counter electromotive force on the motor. Any change in the nature of the load so as to make it overhauling, which would tend to increase the speed in the negative direction will result in the field excitation changing from negative to positive which reverses the induced voltage in the motor and the constant current rectifier again becomes an inverter to absorb the necessary power to maintain the speed.

Thus this equipment is a very simple reversible motor control capable of responding to a "speed voltage" signal of relatively small power, and capable of either supplying or absorbing power to maintain the desired speed. This system has many desirable characteristics but has several disadvantages which lead to the modification given in the next section.

Modified Constant Current System

Several disadvantages of the previous system will be evident. First, if it is necessary to obtain full output from the machine it will be necessary to set the constant current control at rated current. This means that we will have full load armature copper loss whether the machine runs at full load or at fractional load, at full speed or at zero speed.

Second, if sudden overloads of torque are thrown on the machine or are desirable for quick acceleration they cannot be met since the armature current is definitely set at rated value. Since the inherent characteristics of a motor are such that overcurrents of short duration within the limits of satisfactory commutation may generally be tolerated on a duty cycle basis it is obvious that this simple constant current system does not realize to the fullest degree the capabilities of the motor.

To overcome these objections the circuit shown in Figure 8 was developed to control any power circuit such as previously shown in Figure 6. In this circuit it will be noted that there are two additional triodes known as "forcing" triodes with their anode circuits in parallel with the original constant current regulator tubes. The grids of these tubes are excited through suitable potentiometers from the anodes of the original "long tailed pair" in the speed regulation circuits and so biased that with that circuit at or near balance they are cut off. Under that condition the original constant current tube has full control of the armature circuit rectifier and maintains constant current. However, this current may now be set at a low value such as one-half or one quarter rated current so that the heating effect will be greatly reduced. If the load applied to this system is low such that the required torque may be produced with the reduced current the system will operate substantially as a constant current system. However, as more and more torque is demanded by the load the field excitation is increased more and more until full field has been reached. If the torque increases beyond this point the motor speed will start to decrease further causing still more unbalance of the output of the "long tailed pair". It will be seen that this unbalance is also producing a grid voltage change on the grids of the armature forcing tubes. One has been getting more negative and the other less negative. However, their bias or "take over" adjustment has been such that they remained non-conductive during the range of unbalance necessary to obtain full field. If however, the motor torque is insufficient and the unbalance becomes greater one of these tubes starts passing current which increases the current in the armature saturable reactor and increases the armature current sufficiently to produce the required torque. Thus after maximum field is reached in either the positive or negative direction, either the positive or negative armature current forcing tube increases the armature current to whatever value required even if

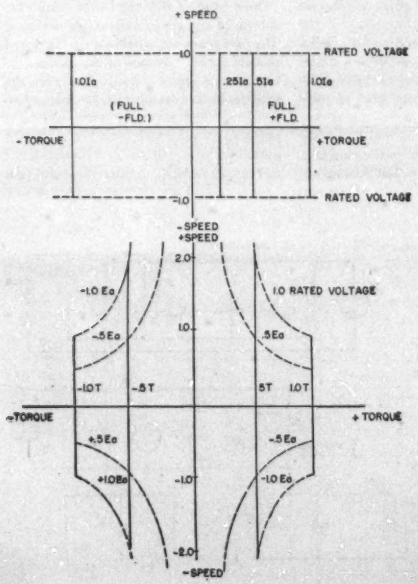

Figure 5. Speed torque relations

A—With full field and several armature currents
B—With full armature current and several different field currents

several times normal. In order to limit this current under forcing conditions to a value which is safe for the motor commutation it is necessary to add an absolute current limit "take over" circuit including the two diodes with their respective anodes connected to the grids of the two "forcing" tubes. As long as the current signal is sufficiently small, the potential of the cathode of the "take over" diodes will be well above the middle supply bus so that their anodes which are connected to the grids of the forcing tubes will be negative with respect to their cathodes. Since no appreciable reverse current may flow the current limit circuit is essentially disconnected. However, if the armature current continues to increase, the diode cathodes continue to fall until finally the cathode becomes more negative than one of the forcing tube grids. This results in a current from anode to cathode and since the diode has relatively low impedance in this direction and the current limit network is relatively "stiff" compared to the potentiometer supplying the forcing tube, the grid of the forcing tube is pulled negative and it tends to regulate at this maximum current limit.

It is quite evident that this system of operation can be modified by reducing the initial constant current to as low a value as desired—even to zero. In such an arrangement the constant current regulator tube may actually be omitted and all armature current is due to operation of the "forcing tubes" after full position or negative field has been called for.

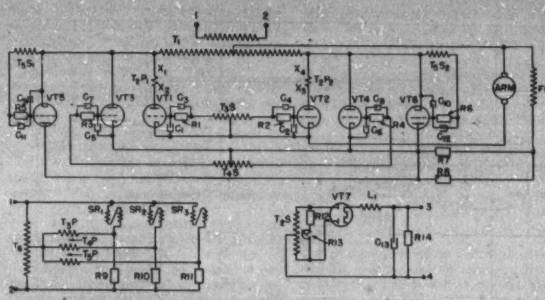

Figure 6 (above). Main power circuits of a simple constant current motor speed control

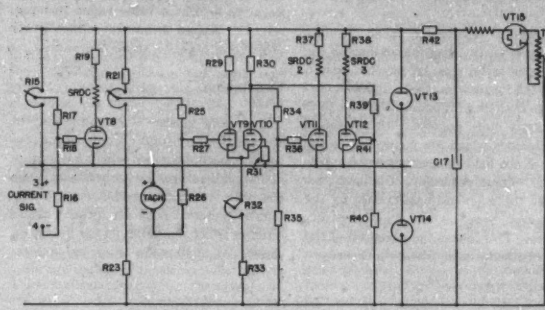

Figure 7 (below). Control circuit for constant current reversible speed control

Operation of Speed Control Systems Above Basic Speed

In the foregoing description of speed control systems no mention was made of operation above basic speed. In some cases if acceleration is very slow, as when a slow-speed motor-operated speed control is used, it may be possible to run above basic, but if the speed control may be turned quickly the desired speed will not be attained. This may be explained in the following way in the simple constant current system.

Let us assume that the speed potentiometer is suddenly turned to three times basic speed with the motor at standstill. Almost immediately we get full positive field and the motor starts to accelerate. As the motor speed increases the armature voltage increases and the rectifier voltage must also increase to maintain constant current. At base speed the armature voltage reaches the full rating of the machine. If the rectifier has the ability to go to higher voltage it may continue to rise in speed; however, if it must go to three times basic, it would mean that both the armature voltage and the rectifier would have to go to three times rated voltage. After reaching the required speed the field would be reduced since only load torque must be developed and if the load was within the rating of the motor the armature voltage would drop to within the rating. However, this would not be a very uneconomic design because even if the motor could stand the overvoltage it would require a rectifier of three times the voltage rating just to take care of the acceleration. If the rectifier did not have this voltage capacity the rectifier voltage would rise with the armature until it reached its ceiling. It would then no longer be possible to maintain the current constant, and as the counter electromotive force continued to rise the current would fall to a value just sufficient to supply the motor losses and the motor would operate as a simple constant potential motor with full field and an armature voltage equal to the maximum rectifier voltage, far under the speed desired.

In order to overcome this difficulty it is necessary to reduce the field excitation so that the induced voltage in the motor may not appreciably exceed its rated value in spite of the fact that the main speed regulator has not reached equilibrium and is demanding full accelerating field. This is possible if a field current "take over" is incorporated which weakens the field whenever the armature voltage gets too high. This in effect, regulates the armature voltage at some reasonable value such as 110 per cent. Of course this reduces the torque but if the load is within the machine rating at three times basic speed it must not exceed one third basic torque so the motor will successfully accelerate to any operating point within its rating.

While a number of different methods may be used to accomplish this Figure 9 shows a simple field "take over" system using a magnetron and two "take over" diodes operating on the positive and negative field saturable reactor tubes in such a manner that the armature voltage may

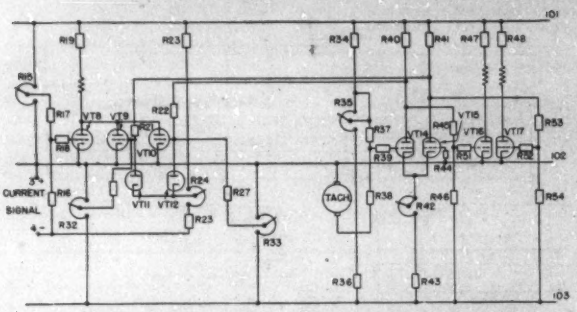

Figure 8. Modified constant current control circuit employing armature forcing

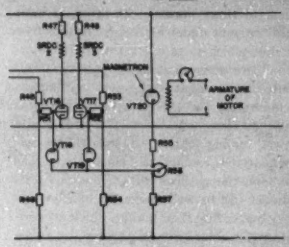

Figure 9. Magnetron "take over" to limit armature voltage

be limited to any desired value. As may be seen from the diagram as long as the armature voltage is below the desired value the magnetron passes sufficient current so that the cathodes of the take over diodes are quite positive with respect to their anodes which are connected to the grids of the field saturable reactor tubes. As the voltage, regardless of polarity, increases the magnetic field traversing the magnetron increases and its current decreases. This lowers the potential of the diode cathodes and when the armature voltage gets high enough they start pulling the grids more negative. This tends to regulate either the positive or the negative field at a value which just permits the desired armature voltage either positive or negative to be maintained.

Conclusion

A general system of constant current and modified constant current motor control has been described which has certain definite advantages for use with electronic control. A simple constant current system has inherent constant torque characteristics which simplifies its use in certain classes of application such as maintenance of tension. As an adjustable speed drive it has the same characteristics of the variable voltage system with a minimum complement of power tubes. Many other circuits and systems based on these fundamental methods have been devised which would be beyond the scope of this paper. At the present time the author is aware of about 50 or 60 installations of this general type in operation or about to go into operation ranging in size from about 1/4 to $7^1/_2$ horsepower. At some future date it may be possible to present more complete data on particular applications covering such points as speed of response, stability, economics and operating experience.

Discussion

K. P. Puchlowski (Westinghouse Electric Corporation, East Pittsburgh, Pa.): O. W. Livingston has presented a very interesting paper which describes circuits and systems possessing rather uncommon and advantageous characteristics. His system has a property of "stiffness", that is, of holding nearly constant speed of motor at a preset value equally well in the case of positive torques (motoring) as in the case of negative torques (overhauling), where braking through inversion and regeneration is obtained in an apparently continuous manner.

Regeneration through inversion in rectifier-motor systems has been known and used commercially for quite a time. In most cases, however, reconnection of the motor armature with respect to the rectifier by means of a reversing contactor was used, combined, of course, with armature constant current regulation. Field reversing as means of obtaining proper polarity of the generated voltage, necessary for regeneration, also was known, but was limited mostly to cases where fast reversing of the motor was required.

Livingston's system introduces that particularly welcome continuity in performance and general adaptability to an extended range of torques, both positive and negative. It would be interesting to have some of the performance characteristics of the system, such as experimental speed-torque graphs for different speed settings. Unfortunately, such characteristics have not been included in the paper.

I would like to make a few critical remarks concerning those portions of the paper which do not seem to be sufficiently clear or are somewhat misleading.

Although I completely agree with the author that there is no fundamental difference between a controlled rectifier and an inverter, I must disagree with the author's presentation of the phenomena which take place in a controlled rectifier with inductive load. This applies particularly to the last paragraph of the second section of the paper and to Figures 2 and 3. The negative average output voltage of a rectifier cannot be obtained by merely delaying the firing angle, regardless of how inductive the load is. The negative average output voltage necessary for regeneration, where the direction of flow of energy must change and become from the load into the line, requires a source of energy in the load circuit. A motor driven by an overhauling load, and operated as a generator is an example of such a source of energy. Inductance is not a source of average energy in the sense that it cannot supply the energy which was not delivered to it by the rectifier during the preceding half-cycle. We may speak of a period of inversion in a rectifier-inductance system where over a certain portion of the negative half-cycle the rectifier output voltage becomes negative, and some of the energy supplied to the load during the preceding half-cycle is returned to the line. However, inversion as a continuous average phenomenon in an inductive load circuit as shown in Figure 2c of the paper is non-existent and contrary to the principle of conservation of energy.

Figure 2a gives a correct representation of the case of continuous conduction with a resistive-inductive load of the rectifier. There, of course, the rectifier output voltage is positive. Figure 2b represents the border case of continuous conduction where with the angle of ignition of 90 degrees continuous conduction is obtained only with purely inductive load, that is, with the impedance angle of the load equal to 90 degrees. Figure 2c is incorrect, since with the angle of ignition of more than 90 degrees the conduction of a symmetrical 2-phase rectifier will become discontinuous, regardless of the value of inductance of the load. At no time the rectifier output voltage will be negative, and consequently Figure 3a is also incorrect.

The problem of current regulation as described by the author is not very clear. Regulation for constant armature current with constant excitation of the motor is possible only during acceleration or deceleration

of the motor or, under steady state conditions, only when the load itself has a consistently rising torque-speed characteristic such as in fans, for example. In the latter case, if constant current or constant torque regulation is provided, the motor will accelerate to a speed at which the load torque will become equal exactly to the torque developed by the motor. However, in the majority of cases the load torque is a rather indefinite quantity and is not a function of speed. In that case it is not possible to speak of motor torque regulation since the motor torque always depends on the load torque and not on the properties of the motor control circuits. Consequently, the author's general statement that Figure 4 represents an armature current or torque regulator which can be adjusted to any desired value of armature current or torque should be properly qualified. It seems that terms like "constant torque system" should not be used indiscriminately and should be avoided unless proper qualifications and limitations are given.

The problem of ignition control of the armature rectifier tubes during inversion is not presented very clearly. From the diagrams and from the author's description of the circuits it appears that a conventional resistance-adjustable inductance phase-shift circuit for the alternating grid voltages is used. However, it is known that such a control scheme may present difficulties during inversion, particularly when the angle of ignition is to be delayed to the vicinity of 180 degrees or beyond that point. Apparently capacitors $C3$ and $C4$ together with resistors $R1$ and $R2$ in Figure 6 provide the necessary negative direct-voltage component in the grid circuit of the armature rectifiers. However, this important point is not clarified nor is it mentioned that the grid transformer $T3$ is apparently a peaking type transformer rather than the conventional sine-wave type.

As far as the application of Livingston's system is concerned, it seems that one of the most promising fields is small and medium size hoists and, of course, any other applications where overhauling loads occur frequently or where regenerative braking under various conditions is required. It seems, however, that tension regulation mentioned by the author requires some further clarification. For example, maintenance of constant tension in the section between the mill or pinch rolls and the take-up reel calls for a constant horsepower reel drive rather than a constant current drive. This is normally accomplished at constant armature voltage by maintaining the armature current constant through field control rather than armature control. Such a system, of course, is entirely different from the one described by the author.

O. W. Livingston: These remarks will be chiefly directed at clearing up any possible confusion regarding the points brought up in K. P. Puchlowski's discussion.

Puchlowski points out that the wave shape and voltage relations shown in Figures 2 and 3 cannot be continuously obtained with a simple energy absorbing circuit no matter how large the value of inductance. We are entirely in agreement with Puchlowski and in the discussion stipulated that the load have "an ability to reverse its voltage (that is to become a generator rather than an absorber of power)." However, since we may not have emphasized this point sufficiently we wish to again call it to the reader's attention.

Perhaps a few additional words of explanation regarding the constant torque system such as shown in Figure 4 would prevent a misunderstanding. The author intended to imply that in using such a system it would be connected to a load having an appropriate rising torque versus speed characteristic such as for example a fan. As Puchlowski points out it is only possible to maintain constant current and constant torque generation in the motor as long as it is balanced either by the load torque or the accelerating torque of the motor and load. If the load torque was not capable of absorbing the motor torque, the system would continue to accelerate until the top voltage of the rectifier was reached after which the armature current would necessarily fall off since the regulator has "run out of range". In any application of this nature the load must be studied and care taken to insure stable operating conditions in the same way an application of a series d-c motor must be considered.

The grid circuits shown for the armature tubes are typical of those normally used in a simple diametric circuit. The actual grid voltage obtained, while not always a sine wave due to the odd harmonics introduced by the saturable reactor phase shift, is essentially positive for 180 degrees and negative for 180 degrees. It can be seen that as long as the current is continuous in the load circuit it is not necessary to retard the phase more than 180 degrees—in fact it must never reach 180 degrees since this would require zero commutating and deionization time. In practice it is found that by the selection of a suitable resistor in series with the a-c winding of the saturable reactor the maximum phase retard with zero d-c saturating current may be limited to 160 or 170 degrees to give sufficient time for successful inverter commutation. Under these conditions it may be seen that the positive values of grid voltage coincide with the angle of tube conduction which is essentially 180 degrees. At the end of commutation the grid becomes negative so that when positive anode voltage again appears across the tube, the grid will have attained control. Thus it is not essential in the diametric inverter with restricted phase retard to supply peaked grid voltages or d-c bias. However, when dealing with a polyphase rectifier having angles of conduction less than 180 degrees, it is essential that the grid must remain in the permissive initiation condition (open angle) not in excessive of the angle of conduction plus the inverter phase angle of advance:

$$\text{Grid open angle} \leq \frac{2\pi}{\rho} + \theta$$

Under these conditions the capacitors $C3$ and $C4$ may be used to add negative grid rectification bias which is one method of decreasing the open angle of the grid. In the circuit in question, however, these capacitors might be omitted without impairing the basic operation of the circuit.

As Puchlowski points out that there are certain types of tensioning control which involve winding up or removing material from a reel in which the effective radius of the material changes. In this type of application if the reel is core driven, and the constant tension function in the web must be imparted by this reel machine the drive, neglecting friction, requires constant horsepower rather than constant torque. However, there are other tensioning applications in which tension is imparted to the web by motorized constant diameter pinch rolls, capstans, swifts or by surface drive of reels in which constant torque is required. In these latter cases the simple constant current system may be applicable. It should also be noted that this system may be readily adapted to maintain constant power by using a circuit similar to the tachometer speed circuits but arranged to regulate armature voltage instead of tachometer voltage. This then permits adjustment for either a constant positive or negative power so that the equipment may be used as the tensioning control for either building up or paying off a reel. It also permits rapid change from either motoring to overhauling or vice versa as may be required if inertia compensation is required for rapid starting and stopping of the web without excessive tension or slack.

The full field of application of these systems will probably be determined by experience with their performance, and a consideration of their cost compared with competitive devices. It would seem that their basic field of usefulness would be in that class of application that requires frequent and rapid reversals of torque. In this field it will be in competition with conventional and special variable voltage control. Considerations of performance and economics may be required in individual applications.

The Stromberg-Carlson XY Dial Telephone System

H. R. REED
MEMBER AIEE

Synopsis: This paper describes a flat type of step-by-step switch and its associated equipment which recently has been introduced in the United States for dial telephone switching systems. "Truly, this (the automatic telephone system) seems the very high-water mark of human creative power." This remark was made by Doctor J. A. Fleming, the eminent British electrical engineer, about 1920 when referring to the step-by-step and other dial telephone systems. The step-by-step system, which previously had been developed by Strowger and others,[1] at that time was being widely installed in England and other locations, both here and in Europe, and since has become the most universally adopted method of dial switching.

IN GENERAL, there are three fundamentally different methods of dial telephone switching that have proved commercially successful and which are used throughout the world today. In one method, the switch used for connecting a calling subscriber's line with link circuits and the switches used for connecting those link circuits with the called subscriber's line are power driven and are not controlled directly by the dial pulses sent from the calling station. In another method, there are no "switches" in the ordinarily accepted meaning of that term; switching operations are performed entirely by relays or relay type selecting units. The third method, step-by-step, has switches which are driven by magnets individual to each switch and controlled directly by dial pulses sent from the calling subscriber's station.

Paper 47-76, recommended by the AIEE committee on communication for presentation at the AIEE winter meeting, New York, N. Y., January 27-31, 1947. Manuscript submitted October 18, 1946; made available for printing December 4, 1946.

DOCTOR H. R. REED is chief telephone engineer, Stromberg-Carlson Company, Rochester, N. Y.

The step-by-step dial telephone system, representing as it does over 75 per cent (15,000,000) of the world's dial telephones, remains for most installations the most economical and efficient type of dial switching system for both large and small communities. The numerous installations of this type of dial switching equipment throughout the world attest to its reliability, economy of operation, and complete flexibility to satisfy all types of customers' requirements as well as the varying demands of complicated networks.

Fundamentally, the step-by-step dial telephone system is a unit system; that is, there is no common equipment upon which the operation of all the switches depend, with the exception, of course, of the office power plant. Additions and rearrangements are made easily by installing switches and other associated circuits or they in turn can be rearranged easily to fit the varying requirements of networks which are changing to meet different traffic conditions. It is thought that a general description of the step-by-step system would be of some value to the reader and there follows, therefore, a brief résumé of its fundamental principles.

Step-by-step dial telephone systems consist of the familiar subscriber's telephone instruments equipped with dials, together with central office switching equipment. The switching equipment consists of either a line switch individual to each subscriber's line or a line finder common to more than one subscriber's line, together with associated first and succeeding selectors and connectors. After the individual line switch has operated to select an idle first selector or after an idle line finder has operated to find the calling subscriber's line and thereby connect him through to an associated idle first selector, dial tone is received and the subscriber proceeds to dial the wanted number. The first digit dialed sets the wipers of the first selector opposite the level corresponding to the digit dialed, whereupon a hunting action takes place to select a trunk to an idle second selector or to the next switching unit in the switch train. The second digit is dialed and the wipers of the second selector are set opposite the level corresponding to the digit dialed; a hunting action again takes place in exactly the same manner as in the case of the first selector. The procedure is repeated until all of the selections are made excepting that to the individual subscriber's line and his particular ringing frequency or code, if he is one of several on a party line. In the case of a single party line, the two remaining digits of the called subscriber's number are dialed and the wipers of the connector switch are set, successively, opposite the level corresponding to the tens digit of the called line and then on the contacts corresponding to the units digit of the called line, whereupon ringing of the called line takes place. In the event that the called subscriber is one of several persons on a party line, a final frequency or code selecting digit is dialed by the calling subscriber and an additional selector switch is operated to select the desired means of ringing the bell at the called station.

It can be seen from the foregoing text that each "rank selection" is sufficient unto itself; that is, the subscriber dials a digit and the entire ensuing operation is performed completely within the switching circuit in question. A series of relays, associated with that switch, operate and in turn transmit the impulses received from the calling subscriber's dial to the stepping magnets of the switch which, in turn, set the wipers opposite the level corresponding to the digit dialed. In the case of the connector, similar operations take place except that, unlike the "rank selection" switches, the wipers of the connector are set both opposite the level and on the particular contact dialed, completely under the control of the calling subscriber's dial, there being no hunting

Figure 1. The *XY* switch

action over the contacts of the particular level selected. The line finder is a non-numerical switch; that is, it performs neither a level-selecting operation nor a contact-selecting operation under the control of the calling subscriber's dial. This switch is started by the removal of the handset of the telephone at the calling subscriber's station, and the wipers are operated to connect to the calling line without that subscriber's intervention. Line switches perform in a similar manner, except that they are individual to the calling line rather than common to a group of calling lines.

This paper describes a new and different type of step-by-step switch and related system, utilizing modern methods and materials to produce the desired functional operations quickly and economically. The equipment is lighter in weight and requires less floor space than any other type of dial system equipment and has many novel features which provide great ease for additions and changes caused by fluctuating traffic loads and plant rearrangements.

Most step-by-step systems are arranged on a decimal basis in that the subscriber lines or trunks are divided into groups of ten (or multiples of ten) units. For instance, most variations of the step-by-step switch have the bank contacts arranged in ten levels of ten contacts each. In the *XY* system this method has been adopted because it has been found that the convenience of locating the called contact together with the inherent simplicity of the circuits makes its adoption most desirable. Other systems have been designed, however, using a greater number of contacts on each level.

The XY Switch

The Stromberg-Carlson *XY* system can be described best by first discussing the *XY* switch, shown in Figure 1, which is the heart of the system. This switch first was developed by Telefonaktiebolaget L. M. Ericsson of Stockholm, Sweden and obtains its name by virtue of the fact that the wipers, during the movement to a desired position, traverse first in a direction to the right of the observer and then away from him which, in the right-hand rectangular co-ordinate system, are *X* and *Y* directions, respectively.

A carriage, which takes the two motions, has two pairs of wipers mounted on it for tip, ring, sleeve, and hunt connections. These wipers are bifurcated, employing twin contacts that make connection directly to bare wires which run in banks behind the switches. The bare wires are arranged in molded frames (Figure 2) which are mounted rigidly to the cells which in turn hold the switches, as shown in Figure 3. The multiple will accommodate up to 50 switches with only one set of soldered connections, if need be. Experience has demonstrated that the contacts established between the moving wipers and the wires of the multiple are such that contact disturbances are nonexistent.

The switches are mounted in die-cast aluminum cells, each cell capable of mounting two switches, and are connected to their associated relays by means of plugs and jacks. Because of the ease with which switches can be added to a unit, only those switches which are needed to accommodate current traffic need be mounted at the time of the installation and additional ones added as traffic conditions increase. The switches are removed very easily from the cells for routine inspection, a duty which is simplified greatly for the operator as the unit is built up on a flat plate making all parts readily accessible for examination and cleaning.

The details of switch operation are seen best by reference to Figures 4 and 5. The carriage is driven by the cog roller (or tubular shaft) assembly which slides along the shaft during the *X* motion. The cog roller is a double-cut tubular gear with ratchet teeth cut parallel to its length and rack teeth cut as rings. The annular rack teeth mesh with and are driven in the *X* motion by the sprocket. For stepping in the *X* direction, the *X* magnet, located in the upper left corner of the mechanism plate, operates through a pawl the ratchet wheel on the sprocket assembly. By repeated pulses the magnet steps the cog roller assembly along the shaft, positioning the wipers on the carriage successively before each wire bank

As the *XY* switch is 100 point, the *X* motion is given ten steps (plus one which provides for marking overtravel) and the *Y* motion ten steps, thereby making possible the selection by the wipers of any one of 100 lines. An eleventh step in the *Y* direction again marks overtravel. Because four wipers are involved and each wiper has its own set of 11 wires, 44 rows of wires each 11 deep are lined up along the front edge of the mechanism plate, immediately before the wipers. The 11 pairs of wires that are lined up before a pair of wipers are molded in plastic and constitute a wire bank.

To mark the level of *X* travel for finder operation, timing, or discriminatory purposes, another wiper enters a separate or twenty-third bank called the *X* bank. This wiper is operated by a pinion assembled to the sprocket through a rack to which it is attached. Thus, as the *X* magnet steps the sprocket, both the cog roller and *X* wiper rack move. The layout of wires in a complete multiple is shown in Figure 6.

When the *X* wiper has found the proper level, thereby positioning the wipers on the carriage before the proper wire banks,

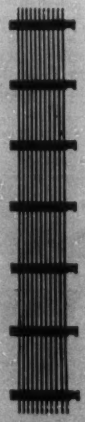

Figure 2. Molded wire bank

the X magnet is de-energized and the Y magnet takes over. The Y magnet is located in the lower central portion of the mechanism plate. In stepping, its pawl operates directly on the ratchet teeth of the cog roller, turning it, and thus driving the wipers into the wire banks through the rack and pinion arrangement of the carriage, as shown in Figures 4 and 5.

The X position of the wipers is shown by reference to a scale attached to the mechanism plate (see Figure 5) and the Y position by reference to a numbered drum located on the tubular shaft assembly Thus the position of the wipers is determined directly and quickly.

It should be recognized that the momentum of the switch, if not arrested, would carry each step beyond its limits This is realized more easily when one considers that the stepping is in the order of 50 per second and the X and Y motions both are completed before the mind can register the start. In order to stop the X motion at each step, the end of the armature of the X magnet engages a tooth of the sprocket at the bottom point of the armature travel. The sprocket motion is locked, therefore, each time the X magnet completes a pulse. In the Y motion, a cam on the underside of the Y armature operates against a member called the stop bar. This stop bar is rocked forward at each downward stroke of the Y armature. A knife edge on the stop bar engages a ratchet wheel on the end of the cog roller locking the rotation of the cog roller, and thus the advancement of the wipers at the completion of each Y armature stroke.

Most dial switching mechanisms of the step-by-step type use "pulse assist" on the switches. This is necessary if the switch is equipped with only a simple interrupter that breaks the magnet current at a certain position of the armature travel and remakes the connection at the same place during the armature return Such a unit produces flutter of the armature, instead of a full powerful pulse, unless there is pulse assist. The pulse assist in some systems is in the form of an outside time delay and in others this time delay is achieved through lost motion in the interrupter. The Stromberg-Carlson XY switch achieves this pulse assist by the use of "snap-action" interrupters. The linkage employed on the unit is such that the current remains flowing through the magnet until the power stroke is completed and then the current is held off until the armature has returned to its stop. Separate leads are brought out through the plug (and jack) from the magnet coils and interrupters so that the switches may operate with or without self-interruption, depending upon the particular circuit requirements. If the switches are used as line finders or selectors, self-interruption is employed. For the numerical movement (as in connectors) or for finding the proper level in selector operation, the stepping is obtained by means of impulses to the X and Y magnets.

Four sets of control springs, in addition to the snap-action interrupters are used in the XY switch

1. X off-normal
2. Y off-normal.
3. Overflow.
4. Release.

The first three are mounted on a common assembly located in the lower left-hand corner of the mechanism plate and the release springs are mounted on a separate assembly located near the release magnet (see Figure 5).

The X and Y off-normal springs perform similar functions, that of informing the relay equipment associated with each switch as to the position of the brushes or wipers. Operation of the X off-normals for instance, indicates that the switch has taken at least a single step in the X direction. Operation of the Y off-normals similarly indicates that at least a single step has been taken in the Y direction.

The circuit function of the off-normals differs in each use of the switch but, in general, indicates that it has either moved in one direction and now should move in another or all necessary motion has taken place. There is, however, one circuit function common to all switches and that is to remove current from the release magnet when the brushes have returned to the normal position. When the release signal is given, current is kept on the release magnet until the switch is fully home and then is removed to avoid unnecessary current flow and heating. Both the X and Y off-normals are used in this function since the switch can be moved independently in either direction.

In the event of certain incorrect dial manipulations or an all-trunks-busy condition, hunting switches may progress the entire length of the bank without encountering a stopping signal. Unless some means of correction were provided, they would continue to hunt vainly until the circuit was de-energized. Overflow springs, arranged to operate in the ex-

Figure 4. Tubular shaft assembly

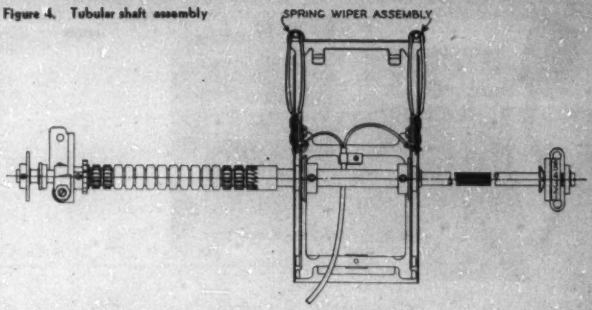

Figure 3. XY switch in cell

treme position of the brushes in either the X or Y directions (namely the eleventh X or Y step), interrupt the magnet current in order to stop useless stepping instantly and permanently until the switch is released.

The release springs have two important functions in connection with the release of the switch.

1. It is necessary to continue the release signal until the switch is fully home despite any immediate re-energization of the circuit which might occur.

2. There must be positive protection against premature seizure of a switch before it is fully home.

In the XY switch, the first is accomplished by a release spring contact establishing a self-locking electric circuit which keeps the driving pawls removed from the ratchet wheel (X motion) and the cog roller (Y motion). The lock is interrupted when the switch returns home. The second function is performed by a second release spring which maintains a busy indication until the switch is home, thus preventing its seizure until everything is perfectly normal. The Y return movement of the carriage is performed by a spring coiled in the tubular shaft of the cog roller and the X movement by a spring coiled around the shaft of the sprocket assembly.

It is to be emphasized that all Stromberg-Carlson XY switches are identical whether they be used as line-finders, selectors, or connectors. The variations in functional operation are obtained by virtue of the relays to which a switch is connected and not by the switch itself.

The A-Type Relay

The A-type relay is a general purpose relay designed to meet exacting circuit and field operating requirements in Stromberg-Carlson telephone switching systems. The A-type relay can accommodate 18 "make" contacts or the equivalent occupied space in break, change-over, or make-before-break contacts.

The magnetic circuit is of a conventional telephone relay type using a core and frame of equal length and an L-shaped armature. The core is threaded and secured to the frame by a nut, which allows the coil to be changed easily, if required, without disturbing the spring pile-ups. The armature pivots on a knife edge of the frame and is held in place by a spring retainer (see Figure 7). The spring retainer rests on an edge of the armature which is formed carefully in line with the axis of rotation of the armature, thereby reducing to a minimum the effect of friction upon armature operation. Bending of the armature under heavy loads, thus losing motion at the contacts, is kept small by stiffening the armature with a support which also serves to adjust the length of the air gap.

The spring combinations employ the precious metal twin contacts which have proved so reliable in the telephone operating field. The two tines on each bifurcated spring which bear the contacts are designed to allow the independence of motion necessary to give true twin-contact operation.

The stability of contact adjustment is maintained in A relays by a rigid mechanical arrangement of the heavy springs The stationary heavy springs are located by a stepped-phenolic spring stop which rests against the clamping plate. The clamping plate is held rigidly by a mounting screw and metal spacer which rests between the clamping plate and the relay frame. The heavy springs thus are held firmly in position at a point near the contact end.

A stepped-phenolic continuous pusher is used that is not fastened to the springs and has only line contact with them. This type pusher greatly reduces friction and pusher wear, thus insuring maintenance of contact force and relay timing Because the springs are independent, the effects of wear of the contact or of the pusher at one spring will not affect the adjustment of any other spring.

For the occasional field adjustments and especially for functional and manu-

Figure 5. XY switch assembly

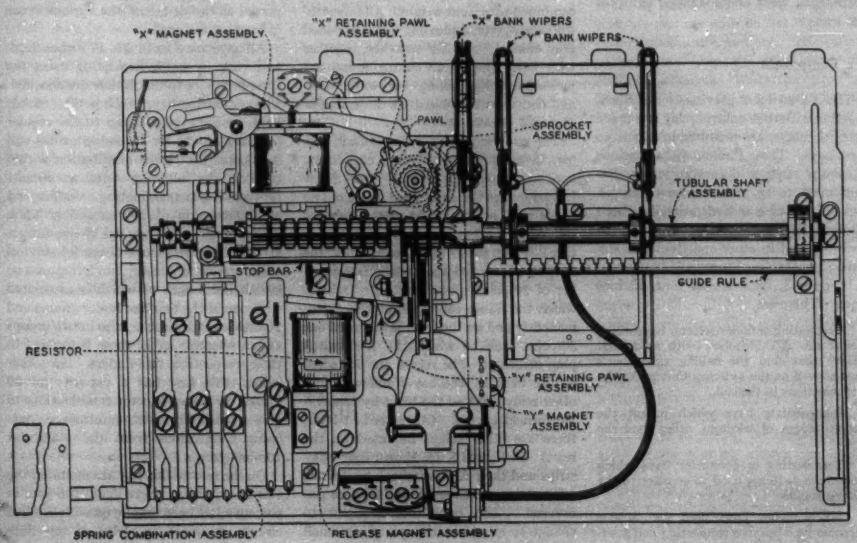

facturing advantages, features such as the removable armature, coil and core, the adjustable armature air gap, and the "residual" screw were incorporated in the design. The spring retainer allows the armature to be removed from the relay for cleaning or removal of a coil. By unsoldering the wires to the coil terminals, which are on the spool head as shown in Figure 7, and removing the core nut with a screwdriver, the coil and core can be removed without disturbing either the relay frame or the spring combination wiring. After a coil and core have been replaced, it may be necessary to readjust the armature stroke but this is done easily by turning the armature support screw.

On fast-releasing relays, a small hard nonmagnetic disk is welded to the armature to limit the operated air gap. This disk is used in preference to a screw because it will maintain its thickness after a larger number of armature operations than would be possible with a screw. Also, a screw having an area comparable to that of the disk would remove too much magnetic material from the flux path.

On slow-releasing relays it is necessary to use an operated air gap of approximately 0.001 inch. A welded disk of this thickness is impractical and a residual screw is used to obtain such a small projection. As the release time of the slow release relays increases beyond usable limits faster than other relays, the residual screw must be made to compensate for mechanical wear and magnetic aging of the iron.

XY Equipment

The XY switches previously described, together with their control relay sets made up of A relays, are mounted in frames to form bays. These frames assume various sizes and shapes depending upon the equipment to be mounted on them. A high degree of standardization has been attained, however, by the common use of ironwork and in other constructional details.

In general, bays are of four distinct types. These are

1. Originating or finder-selector bays which mount the XY switches (with associated relays) that find the calling subscriber's lines as well as the switches that make the first selections in the call.

2. Intermediate bays which mount the various stages of selectors, other than the first.

3. Terminating or connector bays which mount the switches used to connect to the desired parties.

4. Miscellaneous bays used for various purposes such as cross-connecting and grading of selector multiples, mounting of interoffice trunk circuits, power charge and discharge units, and wire chief test facilities.

Figure 6. Arrangement of XY switch in multiple

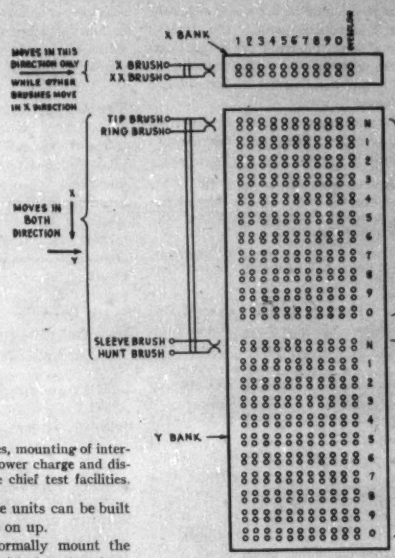

Exchanges using these units can be built in sizes from 60 lines on up.

All bays which normally mount the switch cells together with the relay plates associated with the XY switches, are constructed of formed-up sheet metal, a special section like a capital C being employed as the frame uprights. Strong cross members are made from folded-up sheet metal which provide great rigidity combined with light weight. All bay ironworks are given a pleasing finish of baked gray enamel. All XY switches, together with their respective circuit units, are jack mounted, enabling them to be easily and conveniently placed on the frame or removed therefrom.

The relay mounting strips contain one, two, or three rows of A relays, capacitors, and associated apparatus. The 2-row strip occupies the equivalent space of two single rows or the height of the 2-switch cell, while the 3-row strip is equivalent to three single rows. On the rear of the strip are mounted the appropriate number of 30-point plugs to fit into jacks to which the frame cabling is attached permanently and on the front is mounted one 30-point jack to which the XY switch plug attaches. The relays are protected on the back by the bay framework and other relays and on the front by removable formed covers. (As described later, there are other relays mounted on the rear.) In Figure 8 are shown four relay strips and their XY switches; two of the relay strips are covered and two are uncovered. The only tool required to change or to add a relay plate is a small screwdriver. It is this ease of removal and additions which makes the Stromberg-Carlson XY system so flexible with regard to traffic growth and rearrangement. This fact will become more apparent as the details of the various types of bays are outlined.

All bays are 8 feet high, 17 inches deep, and vary in width depending upon the type of service to which they are adapted. The originating bay, which is $46^1/_2$ inches wide, mounts, in addition to the regular terminal blocks for incoming cables and fuse panel for power distribution within the bay, the following switching circuits for handling the originating or calling end of a maximum of 100 subscriber lines. On the front of the bay are 20 line-finders arranged in two groups of ten line-finders each, one dual allotter consisting of two circuit units each of which is associated with one of the two line-finder groups and 20 first selector circuits, also in two groups of ten selectors each, these being tied to their respective line-finders. In other words, this bay has a capacity of 20 "links" or finder-selector combinations to give a possibility of 20 simultaneous outgoing connections from the particular 100-line group.

On the rear of this bay are mounted the 100 line circuits. Here again the jack-in principle has been employed with the line circuits mounted in strips of ten lines

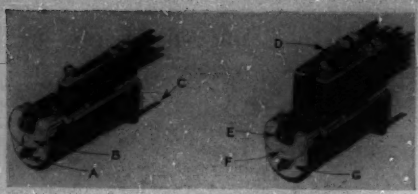

Figure 7. *A*-type relay

A—Residual screw
B—Armature support
C—Coil terminal
D—Clamping plate
E—Spring retainer
F—Armature support screw
G—Armature

each. There is also capacity on the back of the bay for a total of three reverting call circuits used to complete calls between two parties on the same line, one busy verification selector, the use of which will be explained later, and one common timing and alarm circuit.

As all of the foregoing equipment, with the single exception of the dual allotter, is jack mounted, it is very easy to cater to traffic changes and to exchange growth or reduction. The traffic of an original installation may be such as to justify, for instance, only 14 links per 100 lines, in which event only the first 14 line-finders (and of course their respective first selectors) need be equipped—the unequipped positions being covered with simple blanks. Sudden changes in traffic may require the addition or removal of several of these links to continue economical or satisfactory operation. This is accomplished by simply jacking in or out the required number of line-finder-selector combinations. In the same manner a partially equipped bay (from a line standpoint) may be added to at any time by merely jacking in new line-relay strips made in units of ten lines each.

The intermediate, or selector, bays are of two basic types, single-sided and double-sided. The single-sided bay uses the same framework as the originating bay, whereas the double-sided bay, using a similar iron framework, is arranged to mount units on both front and rear. *XY* switches together with their respective circuit plates can be mounted on both front and rear of these bays because there is no individual line equipment to be mounted as in the case of the originating bays. The double-sided bay is $60^3/_4$ inches wide. The single-sided intermediate bay will mount one, two, three, or four groups of ten selectors each or one or two groups of 20 selectors each. The double-sided bay will mount from one to eight groups of ten selectors each or one to four groups of 20 selectors each. The actual number of selectors equipped is dependent upon traffic conditions.

Terminating bays are similar to the intermediate bays in that they also are made up in two types, single-sided and double-sided. The single-sided bay is $57^1/_2$ inches and the double-sided bay is $71^3/_4$ inches wide. The single-sided unit can be equipped with either one or two groups of ten connectors each or one group of 20 connectors, whereas the double-sided unit accommodates from one to four groups of ten connectors each or either one or two groups of 20 connectors each. Here again the number of connectors actually supplied in each group depends on the type of service of the group and the relative amount of terminating traffic therein.

All of the circuit units just described are jack mounted and therefore, as in the originating bay, it is quite easy to cater to variations in traffic loads.

The ease of installation of an *XY* system becomes apparent when one considers, for instance, the small amount of work to be done by the installer on an originating bay. It is only necessary for him to connect the terminating cables, to jack-in the respective line-finder units, first selector units, line circuit units, and other miscellaneous units, and to add the necessary fuses, lamps and caps, and dummy mounting plates. In order to facilitate handling and installation, the bays are shipped with all permanent wiring, jacks, switch cells, wire banks, and fuse panel mounted and the various relay mounting strips and *XY* switches are shipped separately.

Circuit Features

The fact that the jack-in principle has been used whenever possible in the design of the *XY* system equipment has led to many economies and features in the design of circuits. The line circuits, jack mounted in strips of ten, may be of the 2- or 3-relay types, the latter providing lock-out service. Both, however, are mounted on interchangeable mounting plates which permit the percentage of lock-out type lines in an originating bay to be changed at will from 10 to 100 per cent in multiples of 10 per cent. This is an especially valuable feature in small community dial offices where the number of rural lines (normally provided with lockout service) may decrease or increase depending on the growth of the town.

Any line may be provided with coin-box tone by changing a strap on the line circuit and in this way postpay type coin boxes can be installed on any line.

The first selector, which may be used for local or incoming service, can be restricted from hunting on any specified level by a strapping operation on the *X* "direction-locating" bank (see Figure 6). A similar strapping operation serves to make the selector drop back from a specified level or levels. These features are of great value in networks where changes occur in trunk routing, dialing conditions, or revenue determining factors.

The dual allotter normally has ten line-finders associated with each of its two units. If trouble occurs in either unit then all 20 line-finders are transferred automatically to the remaining unit. When the operator wishes to work on this troublesome unit, or for routine checking, he need only flip a double-throw key to the proper position and thereby busy-out that unit and place the 20-line-finders on the other. While the key is in the off-normal position, a display lamp on the right-hand end of the mounting plate is lighted. The only effect of this change-over is a slight increase in finding time.

The reverting call circuit is designed to allow two subscribers on the same line to call one another by dialing a special number consisting of a preliminary digit followed by the last digit of the calling subscriber's number and the last digit of the called subscriber's number. The calling party then hangs up and both subscribers' bells ring. When the call is answered the bells cease ringing and the calling party thereby is informed. Another form of revertive calling is described with the connector circuit.

Selectors mounted on the intermediate bay perform in much the same manner as those described as first selectors.

Connectors may be of various types depending on the kinds of service which they may perform. These services are party-line ringing of either the harmonic or code types, *PBX* trunk hunting, conversation timing from one or both ends, and reverting call by directory number. Party line ringing may be of the 2-, 4-, 5-, or 10-party full selective or 10- or 20-party semiselective types employing multifrequencies or combinations of long and short rings to secure the desired party. *PBX* trunk hunting allows the assignment of successive numbers to a business establishment, hospital, or other similar institution whose telephone needs are such as to justify two or more consecutive

telephone lines. In this service the connector tests the first line and, if busy, tests the second line and so on until a free line is found. If all of the lines in the group are busy, a busy tone is returned to the calling subscriber. Normally when the first line is called, testing commences over the entire group. As a feature for night service, however, if any line other than the first in the group is called that line only is tested and, if busy, the proper tone is returned. This feature allows the listing in the telephone directory of all telephone lines except the first as night lines for particular individuals and at such times they receive the benefit of individual line service.

The conversation timing feature allows for precision timing of telephone calls either when originated by or completed to subscribers on party lines. This timing may be of any predetermined duration and a warning tone may be given to both parties at any set time during the timed interval. A special feature of the *XY* system is that any line may be equipped with time cancelling; that is, calls originated by or completed to this line have the timing feature cancelled and conversation may continue uninterrupted for any desired period.

Reverting call by directory number differs from the method previously described in that it is not necessary for the calling subscriber to dial a special number. He merely dials the number of the wanted subscriber and upon receiving busy tone hangs up. After an interval which he assumes is sufficient for the called party to have answered, he again removes his receiver and conversation commences if the called party has answered.

Figure 8. Relay mounting strips

The busy verification switch train allows an operator or the wire chief to verify the busy or idle condition of a particular subscriber's line. This is valuable where a party, after repeated attempts to reach an indicated busy line, requests verification of that busy condition from the operator. The wire chief also may use this switch train to perform the various electrical tests necessary to routine and maintain subscribers' lines properly. The person using the busy verification train can listen to a conversation in progress and also may speak to the talking parties to advise them that an urgent call is awaiting.

Conclusion

The features of the *XY* switch and system that make it readily adaptable to dial telephone exchanges of all sizes and possible growths are

1. The universal nature of the switch, the same switch being used as line-finder, selector, or connector.

2. Its compactness; being smaller than any other switch, smaller switching equipment and exchange buildings can be realized.

3. Its bare wire multiple which yields economies in wiring.

4. Its package type units which readily allow for exchange growth and standardization.

5. Its plug and jack mounted units, which give flexibility, provide for fluctuations in traffic conditions, and simplify routining.

References

1. Fifty Years of Electricity (book), J. A. Fleming. Iliffe and Sons, Ltd., London, England.

2. Applicability of Automatic Switching to All Classes of Telephone Service, Arthur Bessey Smith. AIEE Transactions, volume 38, part 2, 1919, pages 1567–1604.

3. A Modern Automatic Telephone Apparatus, W. Lee Campbell. AIEE Transactions, volume 29, part 1, 1910, pages 55–106.

4. A Study of Multioffice Automatic Switchboard Telephone Systems, W. Lee Campbell. AIEE Transactions, volume 27, part 1, 1908, pages 503–51.

5. Crossbar Dial Telephone Switching System, F. J. Scudder, J. N. Reynolds. AIEE Transactions, volume 58, 1939, May section, pages 179–92.

6. Machine Switching Telephone System for Large Metropolitan Areas, R. B. Craft, L. F. Morehouse, H. P. Charlesworth. AIEE Transactions, volume 42, 1923, pages 187–204

Arc-Back Testing of Graphite

WM. E. PAKALA
MEMBER AIEE

C. J. CUCULLU
NONMEMBER AIEE

Synopsis: This paper describes a mercury-vapor tube and associated circuits used to obtain the arc-back rate of various grades of graphite which might be applied in ignitrons and other types of electronic tubes. The methods of test and results obtained are included. The tests indicate that the arc-back rate of a graphite anode can be reduced by degassing at 1,800 degrees centigrade and that this improvement is maintained at room temperature and at atmospheric pressure. It also is shown that anodes when not in operation get charged with arc-back causes of two classes—those that can be removed readily by heating and those that persist regardless of heating and apparently are removed by the arc-back itself.

THE ARC-BACK by definition[1] is a "failure of the rectifying action which results in the flow of a principal electron stream in the reverse direction, due to the formation of a cathode spot on an anode."

Because the unwanted cathode spot forms on the anode, considerable thought has been given to this electrode of a mercury-arc tube. Several arc-back tests[2-1] have been made in the past and the results of these tests have been very useful, especially in the power rectifier field.

All the primary causes of arc-back probably are not known. Those causes, which are known from tests to exist are given in items 1 and 2. These two causes seem to be the ones most substantiated by experiment and by general experience with mercury vapor rectifier tubes. The others are causes about which we know very little and which probably occur very infrequently in tubes with shields and baffles.

1. Insulating or semiconducting particles or patches on the anode surface.[6] According to Kingdon and Lawton,[3] these particles are charged by positive ions until breakdown occurs from the charged mass to the anode proper. In this paper, test data are given which show that by placing small insulating particles on an anode surface the arc-back rate can be increased greatly.

2. The presence of conducting particles on the anode, such as small globules of mercury. If a mercury globule leaves the anode during the time ionization is present, an arc-back is formed. This action is similar to breaking an electric circuit, because the globule is collecting ions and a current flows from it to the anode. Tests are given in this paper (see Figure 5) which indicate that mercury droplets are a cause of arc-back.[7] Numerous arc-backs were seen to start at tiny mercury globules[8] on the anode surface.

3. Thermal emission from anode.

4. Gas bursts from anode or other parts of tube causing intense local ionization.

5. Effects of radiation and particles of mercury and other materials from the tube cathode on the anode surface.

6. Field emission at anode independent of foreign particles adhering to the anode.

The forenamed causes are primary causes. What the actual arc-back rate will be depends on several secondary factors, such as vapor pressure, foreign gas pressure, maximum anode voltage, anode current density, ion density, the deionization rate, the initial inverse voltage, the

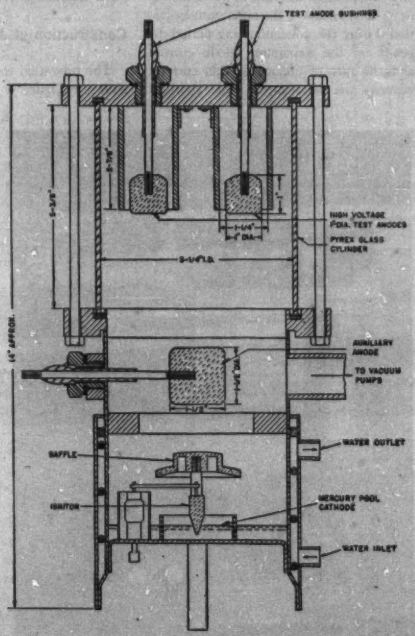

Figure 1. Tube used for testing anode materials

Paper 47-71, recommended by the AIEE committee on electronics for presentation at the AIEE winter meeting, New York, N. Y., January 27-31, 1947. Manuscript submitted November 6, 1946; made available for printing December 21, 1946.

Wm. E. Pakala and C. J. Cucullu are both with Westinghouse Electric Corporation, East Pittsburgh, Pa.

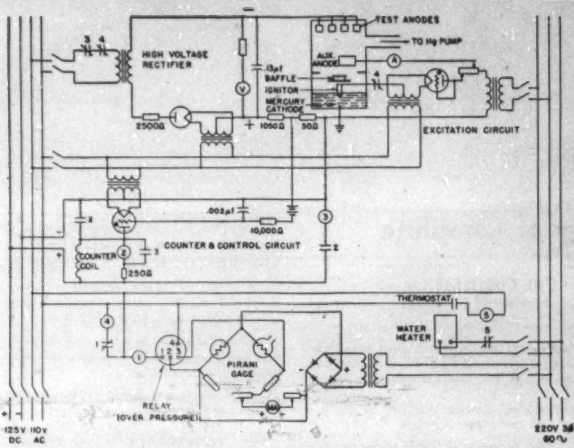

Figure 2. Test circuit diagram

rate of rise of the initial inverse voltage, and surging. Some of these factors depend on the circuit[8] used with the tube and others are a function of the tube design. For instance, the maximum ionization during the nonconducting period depends on the maximum anode current and the rate of change of this current, whereas the deionization time constant depends on the tube design and vapor pressure near the anode.

This paper covers primary causes inherent to the anode. The test apparatus described is intended to indicate the arc-back characteristics of anode materials.

Construction of Arc-Back Tester

The tube used to test sample anodes is shown in Figure 1. The lower portion of the tube is a water-cooled ignitron and the upper portion is a glass cylinder with a steel top plate and four bushings for testing four samples singly or in parallel. As can be seen from Figure 2, the ignitron portion of the tube is operated from 220 volts, 60 cycles using anode firing with a thyratron. The one inch diameter by one inch long test anodes are connected to the negative side of the output of a high voltage rectifier. The positive ion current is supplied by the low-voltage excitation arc to the auxiliary anode and its average density at the test anode is limited to 0.043×10^{-3} ampere per square centimeter, which is somewhat higher than the average ion density to the anode in power rectifier ignitrons.

When an arc-back occurs, it is counted and the primary circuit of the high voltage transformer is opened and immediately closed. The voltage and positive ion current of the test anodes, the water rate, and the auxiliary anode current are kept constant throughout a test run. The complete apparatus is shown in Figure 3.

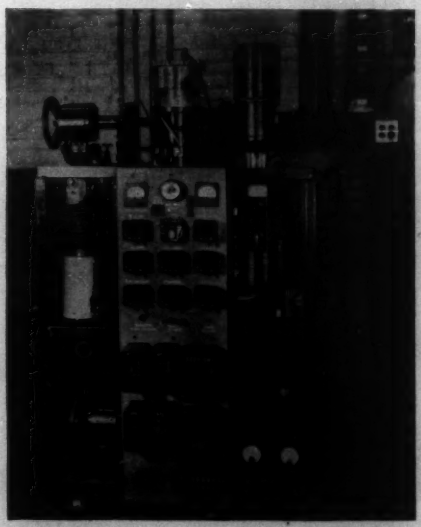

Figure 3. Arc-back test apparatus

Method of Testing

Before anodes are connected to high voltage to determine the arc-back count they are current degassed in the test bottle at 700 degrees centigrade for 30 minutes. This degassing is similar to degassing of anodes in rectifier tubes and results in a low foreign gas pressure (0.1 micron) in the test bottle. After degassing, the anodes are connected to high voltage and are ready for the arc-back test. Six runs are made on each sample of graphite. The first run is made with all four anodes in parallel, and the next four on each anode individually to make certain that no one anode has a much higher rate than any one of the other three. These five runs tend to get rid of any spurious impurities on the surface of the anode thus insuring that the sixth and final test, which is made with all four anodes in parallel, gives an arc-back rate indicative of the quality of the graphite. The values for the sixth run are always less than those of the first, but no further reduction is obtained by additional runs. All tests last for 24 hours, and the rate used to define the quality of the anode material is obtained from the number of arc-backs occurring in the last 16 hours. Occasionally a standard sample is used to make sure that the test device is normal.

Results Obtained With Tester

The average arc-back rate as obtained for the last 16 hours of the sixth run are

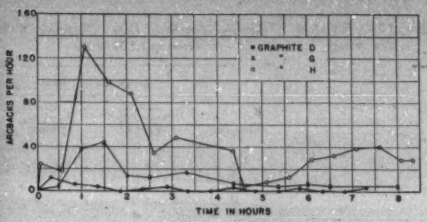

Figure 4. Comparison of three grades of graphite

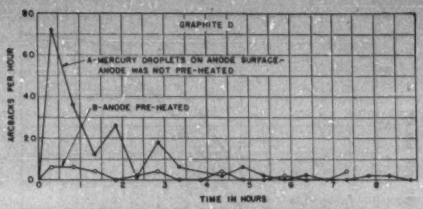

Figure 5. Effect of preheating of anodes

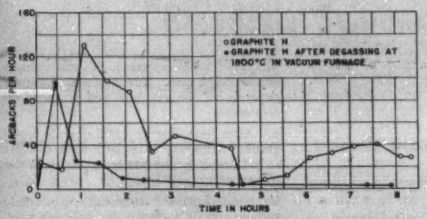

Figure 6. Effect of degassing at 1,800 degrees centigrade

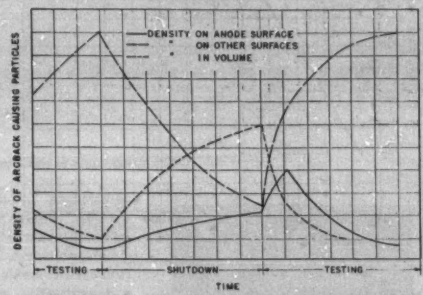

Figure 7 (right). Changes in volume and surface density of particles

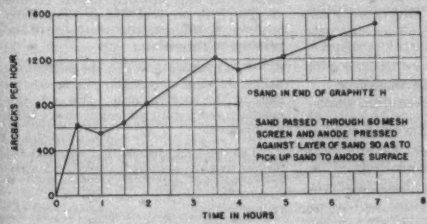

Figure 8. Effect of insulating particles (sand) on the arc-back rate

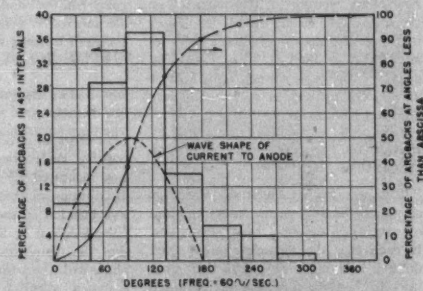

Figure 9 (right). Arc-back distribution

given in Table I for various grades of graphite indicated as *A*, *B*, *C*, and so forth. The effect of degassing and decontaminizing at 1,800 degrees centigrade is given for grades *G* and *H*. All grades of grahite which were degassed at this temperature were improved even after they had been treated at 700 degrees centigrade. Apparently, the higher temperature removes most of the impurities in the graphite which are conducive to arc-back. It was found that after an anode is degassed at 1,800 degrees centigrade it can be left at room temperature and at atmospheric pressure for several weeks without affecting its final or steady state value.

It will be noted from curves shown in Figures 4, 5, and 6 that all samples have a transient arc-back rate which is several times higher than the final value. This transient effect occurs after every shutdown although the tube is maintained continually at a low pressure. In plotting curves, the arc-back rate is for the time interval between the points on the curves.

Curves *A* and *B* of Figure 5 show how the transient value is reduced by preheating the anodes. The higher transient rate shown by curve *A* is caused by mercury droplets on the anode surface. The transient effect observed for the preheated test, curve *B*, is perhaps caused by charging of anode with semiconducting or conducting particles other than mercury.

These particles reach the anode perhaps when the tube is not in operation or after applying high voltage to the test anodes. In either case, an arc-back charge, which cannot be removed completely by heating, is built up on the anode surface. When the tube is not in operation, the number of particles in the volume may increase because they are uncharged and leave the surfaces. They then remain in the volume until the density of the particles corresponds to the "pumping speed" of the walls for uncharged particles. Then on application of ionization and voltage to the anodes some of these particles are swept to the anode resulting in a transient arc-back rate. The pumping speed to the surfaces also is increased by the ionization and the electric field, thus resulting in a gradual decrease in the num-

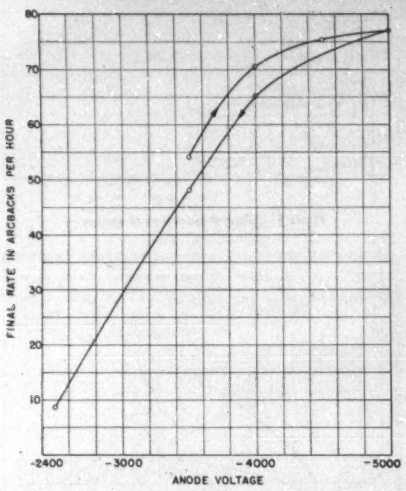

Figure 10. Effect of anode voltage

Table I. Arc-Back Data Obtained With Tester at 3,500 Volts

Graphite	Arc-Backs Per Hour: Before Degassing, 1,800 C	Arc-Backs Per Hour: After Degassing, 1,800 C
A	0.5	
B	0.7	
C	0.8	
D	1.3	
E	1.4	
F	2.0	
G	9.0	1.2
H	18.0	1.3
I	8.7	
J	18.4	

ber of particles in the volume and a corresponding increase in the particles on the surfaces, including the anode. Those reaching the anode gradually are removed by arc-backs. The changes in density of arc-back causes in the volume and on the surfaces is shown in a very approximate manner in Figure 7.

Effect of Particles on the Anode Surface

Tests were made to determine the effect of nonconducting, semiconducting, and conducting particles on the anode surface. In each case the particles were passed through a 60-mesh sieve and then were stuck to the test anode, in this case grade *H*, by simply pressing the anode against a layer of these particles. The nonconducting material (sand) was the only one which greatly increased the arc-back rate. Figure 8 shows the curve obtained for a run of seven hours. The rate continually increases and is very much higher than was obtained in an earlier test of grade *H* (see Figure 4). One explanation of the effect of particles on an anode is described by Kingdon and Lawton.[2] They state that the anode has "small regions which are in such poor electrical contact with the anode that the positive ions from the residual ionization are driven on these regions when the anode is made negative, and that if the number of these ions is sufficient the region will become charged positively, cause field emission from the electrode, and lead to failure." After completion of the foregoing test the anodes were cleaned with a file and tested again. This cleaning was sufficient to bring the arc-back rate back to its normal value.

Arc-Back Distribution With Ion Current

In order to obtain data as to effect of positive ion current, the ignition angle was measured for 176 arc-backs. The distribution of these arc-backs and relative position of the positive ion current pulse is given in Figure 9, which shows that the distribution curve is almost in phase with the positive ion current. This is a good indication that the magnitude of ionization is a major electronic factor in the initiation of an arc-back.

Effect of Anode Voltage

The effect on the final arc-back rate of increasing and decreasing the negative potential of the anode can be seen from Figure 10. This curve indicates that the arc-back rate increases with the voltage and that operation at the higher voltages improves the performance of the anodes at lower voltages.

Conclusions

1. The tester described is found useful in the control of the quality of anode material and in determining the procedures required to build ignitrons of more uniform quality.

2. Degassing and decontaminizing graphite at 1,800 degrees centigrade *in vacuo* reduces the arc-back rate. The reduction obtained depends on the graphite and its previous treatment.

3. After degassing at 1,800 degrees centigrade, anodes may be exposed to air and yet a reduction in the arc-back rate will be measured.

4. Insulating particles placed on the anode surface greatly increase the arc-back rate, whereas conducting particles (steel was used) do not.

5. Anodes of all grades have the highest rate at the beginning of a test. This transient effect indicates that anodes become charged with arc-back causes either from space or by diffusion from the inside of the graphite to the surface.

6. With mercury drops on the anode, arc-backs are more numerous and appear to start at the mercury drop. The rate decreases rapidly until all visible drops have disappeared.

7. The arc-back distribution obtained indicates that the positive ion current density is a major electronic factor in initiating arc-backs.

References

1. Report on Proposed Standard for Pool Cathode Mercury-Arc Power Converters, AIEE Number 6. June 1946.

2. The Relation of Residual Ionization to Arcback in Thyratrons, **K. H. Kingdon, E. J. Lawton.** *General Electric Review* (Schenectady, N. Y.), volume 42, 1929, pages 474–3.

3. Phase Occurrence of Arc-Backs in High-Current Mercury-Arc Rectifiers, **W. E. Pakala, W. B. Batten.** AIEE Transactions, volume 59, 1940, June section, pages 345–8.

4. The Phase of Arc-Back, **A. W. Hull, F. R. Elder.** *Journal of Applied Physics*, American Institute of Physics (New York, N. Y.), volume 13, March 1942, pages 171–8.

5. Development of Excitron-Type Rectifier, **H. Winograd.** AIEE Transactions, volume 63, 1944, pages 969–78.

6. Mercury-Arc Power Rectifier (book), **O. K. Marti, H. Winograd.** McGraw-Hill Book Company, Inc., New York, N. Y., 1930. Page 41.

7. Maintenance of Rectifiers on Electrochemical Installations, **J. E. Housley, G. N. Hughes.** AIEE Transactions, volume 65, 1946, July section, pages 436–41.

8. Rectifier-Circuit Duty, **C. C. Herskind.** AIEE Transactions, volume 63, 1944, March section, pages 123–8.

Television Equipment for Broadcast Stations

WALTER L. LAWRENCE
ASSOCIATE AIEE

THE PROMISED advent of commercial television service on a nationwide scale makes timely a discussion of the apparatus available for equipping television broadcast stations.

Framework for a national television service was set up in the winter of 1945 by 406 channel allocations in the first 140 metropolitan districts of the United States made from the 13 channels established by the Federal Communications Commission for commercial television broadcasting. The metropolitan districts vary in population from 11,690,500 for New York City to 62,000 for Pueblo, Colorado, and comprise 48 per cent of the population of the United States.

The filling in of the framework thus established has progressed, up to November, 1946, with the granting of 42 licenses or station construction permits, which assure television service within the near future to 23 metropolitan districts comprising 26.6 per cent of the population. Of the first 16 metropolitan districts only Pittsburgh is not represented by licenses, station construction permits, or applications.

To furnish television broadcasting at the service standards required for commercial operation, all stations must provide reliable, consistent operation. Such operation requires the integrated functioning of many pieces of equipment which are somewhat more complex than the analogous units for sound broadcasting. Reliable and consistent operation of the equipment throughout its useful life is facilitated if the various units are product design equipment. By product design is meant equipment that is produced in quantities to the same design. This type of production affords relatively large amounts of money for engineering design and development to obtain the required degree of performance. However, since the development costs are spread over a number of units, so that each unit bears only its proportionate fraction of the development expense, product design is economically feasible.

The purpose of this paper is to discuss various units available for equipping commercial television broadcasting stations.

Division of Equipment

Television station equipment is divided into studio equipment and transmitting equipment.

A simple method of classifying these two divisions uses as a basis the type of signal current utilized in each division. Studio equipment utilizes video frequencies, which cover the band from 30 cycles to 4.5×10^6 cycles. Transmitting equipment utilizes radio-frequency carriers in the range of 44 to 216 megacycles, which are modulated by visual and aural signals. Regarding the system as a whole, this method of classification draws the dividing line at the input to the broadcast transmitter. This division is analogous to that currently prevailing in the sound broadcasting field where we have studio or speech input equipment separate from transmitting and radiating equipment.

Paralleling the division just specified is the spatial division of the system—both for sound and television broadcasting—in which the studio equipment is confined almost wholly to the studio building, while the transmitting apparatus is housed in a transmitter enclosure. The location of the studio is dictated largely by publicity considerations, and accessibility for talent. Considerations relating to the efficacy with which the electromagnetic disturbance that constitutes the signal can be radiated into free space govern the location of the transmitter enclosure.

The description of equipment which

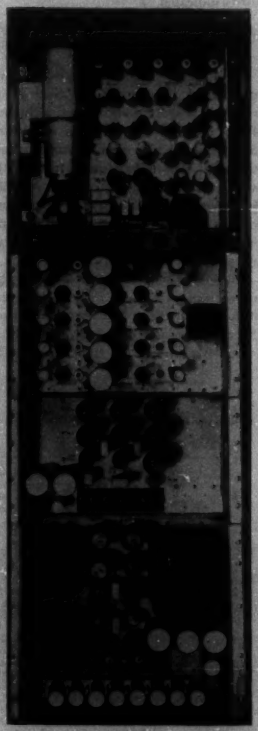

Figure 1. Monoscope camera, distribution amplifier, and regulated power supplies

Paper 47-72, recommended by the AIEE committee on communication for presentation at the AIEE winter meeting, New York, N. Y., January 27–31, 1947. Manuscript submitted November 13, 1946; made available for printing December 12, 1946.

WALTER L. LAWRENCE is in the engineering products department of the RCA Victor Division of the Radio Corporation of America, Camden, N. J.

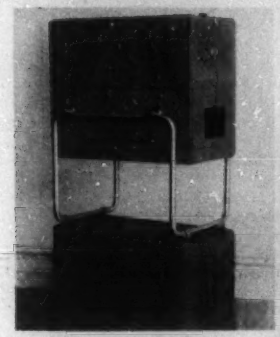

Figure 2. Television film camera

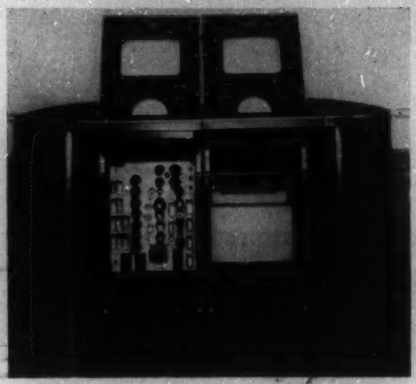

Figure 3. Television film camera control

follows is divided into the two main categories indicated

Studio Equipment

The primary function of studio equipment is to transform an optical image which is a space variation of light and shade into a time variation of electric intensity, or video wave. An auxiliary function of studio equipment is the switching of video signals so that the desired signal from any of the various sources of program material, either local or remote, can be selected and fed to the transmitter.

In general, the production of a video wave from an optical image is accomplished by setting up a charge distribution, the space variation of which corresponds to the pattern of light and shade in the optical image. Precisely timed excursions of an electron beam over the charged surface remove the distribution. As a result of the removal, a time variation results in the electrical condition of one of the elements of the pickup tube. The video wave thus produced is the studio equipment signal current.

Studio equipment starts with the camera or cameras containing the television pickup tube, proceeds through camera control units, synchronizing signal generators, video amplifiers and associated video switching equipment for multicamera and multistudio operation, and ends with a stabilizing amplifier. This latter unit is used at the input of the visual transmitter to minimize transient disturbances that may be introduced by the switching process. Ancillary studio equipment includes film projectors in both 16 and 35 millimeter sizes, monoscope cameras, monitors for observing the picture and wave-form qualities of the video signal at various points, and associated electronically regulated power supplies for furnishing plate power to the various units.

The lighting equipment required for future television studios will be similar in kind and amount to that required for photographic studios. The required general level of illumination for these studios will be of the order of 50 footcandles. This illumination may be obtained from any of the conventional sources. If fluorescent tubes are used, to eliminate flicker, they should be 3-phase units, closely spaced. The movable lighting equipment for obtaining dramatic effects by artistic use of highlights and shadows also can be of the conventional type.

Table I lists the various units required for operation from the four general sources of program material. The sources are listed in the order of increasing complexity of operation.* The list is cumulative, that is, the units listed under succeeding headings are to be added to those under the earlier headings.

The equipment most used by operating personnel—cameras, camera controls, and switching facilities—is so packaged and mounted as to facilitate their tasks (Figures 3 and 4). The auxiliary equipment, which does not require extensive or frequent adjustment, such as power supplies, video amplifiers and synchronizing signal generator, is rack mounted.

There are four general types of television cameras, namely: monoscope,

Table I

Source	Units
1. Network	Monitor, monoscope camera, synchronizing generator, equipment to switch between network and monoscope camera
2. Film	Film projectors, film camera, monitors, equipment to switch between film camera, network and monoscope
3. Remote pickup	Field cameras and controls, field synchronizing generator, field switching unit if more than one camera is used, relay equipment if no coaxial cable is available from pickup point to control room, equipment to switch between remote source, film camera, network, and monoscope
4. Studio	Studio cameras and controls, studio lighting, equipment to switch between studio, remote source, film camera, network and monoscope

* Note that network operation is assigned to the position of least complexity from the viewpoint of the network affiliate station operator or the user of network program material, rather than from the viewpoint of the network operator whose function it is to produce the network program material.

Figure 4. Image Orthicon field camera

Table II

Item	Conventional Film Projector	Television Film Projector	Reason
Projector drive	Induction motor	Synchronous motor	Frame frequency must be rigidly locked to vertical blanking pulse frequency, which in turn is locked to power supply frequency.
Shutter	Open 50 per cent of frame time. Operating frequency 48 cycles.	Open 6–8 per cent of frame time. Operating frequency 60 cycles.	Image must be projected on iconoscope during vertical blanking time, that is, time during which iconoscope scanning beam flies back from bottom to top.
Intermittent motion	Uniform film dwell time with operating frequency of 24 cycles.	Even frames dwell 50 per cent longer (1/36 second) than odd frames (1/48 second) to give average operating frequency of 24 cycles.	Preserves average frame rate while adhering to 60 cycle vertical scanning frequency required by 30 frame, 2:1 interlaced scanning which is standard for television.

film, field, and studio. A monoscope camera (Figure 1) produces a fixed test pattern which is a collection of wedges, circles, and lines designed to accentuate the most common aberrations of television systems. The signal is generated by scanning with an electron beam a plate on which is engraved the desired test pattern. Such a signal is used for system testing, since its invariant character permits quantitative measurements to be made at different times. Test signal also is transmitted for the purpose of installing and setting up receivers. A monoscope camera is the simplest television camera.

A television film camera (Figure 2) produces video signals from motion picture images projected on its pickup tube. An iconoscope is used as the pickup tube, as experience has shown that the gamma characteristic of the iconoscope best complements the gamma normally obtained from film, and the low sensitivity of the iconoscope is of no moment with the high intensity of light available from motion picture projectors. The camera contains the required circuits for deflecting the scanning beam and video amplifiers to increase the amplitude of the signal obtained from the iconoscope. The associated film camera control (Figure 3) contains shading circuits to correct the dark spot or spurious signal which is characteristic of iconoscopes. It contains also the monitoring equipment to view the picture and waveform quality of the video signal, and the required power supply. The camera and camera control are connected by a suitable cable permitting flexibility in their relative positions.

Field cameras (Figure 4) are designed with a view to compactness and portability. As it is not possible to control the lighting for remote pickups, these cameras are equipped with the newly developed Image Orthicon pickup tube, whose sensitivity is comparable to that of the human eye. The four-position lens turret is provided to permit rapid selection of various types of lenses to meet the wide variety of optical conditions encountered in remote pickup work. An electronic viewfinder which furnishes the cameraman an image produced from the signal supplied by the camera is provided to facilitate focusing of the camera and to overcome the limitations (such as parallax, dimness of image, and necessity for camera lens and viewfinder lens focusing synchronization) which are inherent in all optical viewfinders.

Figure 5 is a photograph of a two-camera set of field pickup equipment with the various suitcase size units identified. The functional relationships of the various units of field pickup equipment are shown in Figure 6.

Studio cameras are larger and heavier than field cameras because for the former portability is not an essential requirement. These cameras usually are mounted on dollies or self-propelled pedestals to obtain the mobility necessary for securing different camera angles. Figure 7 shows a view of a prewar camera mounted on a pedestal. Prewar cameras used the iconoscope, as the more sensitive type of pickup tube had not been developed before the war. Studio cameras with improved sensitivity are promised and when they are available, it is reasonably certain that the required lighting levels in television studios will be reduced by a factor of at least ten from that required for prewar iconoscope cameras. This reduction in lighting load should reduce the cost of studio construction for two reasons:

1. The cost of the lighting equipment and the required electric wiring would be reduced substantially.

2. The size of the air conditioning equipment necessary to obtain satisfactory temperatures in the studio would be reduced.

An additional continuing economy would obtain from the lessened cost of power for both lights and air conditioning.

Figure 8 shows a synchronizing generator. It is the function of this apparatus to produce the accurately timed series of pulses which control the excursion of the scanning electron beam in the cameras. These pulses also are added to the video signal before it is fed into the transmitter and are transmitted along with the video information. In the receiver, the pulses

Figure 5. Field pickup equipment, two camera equipment setup

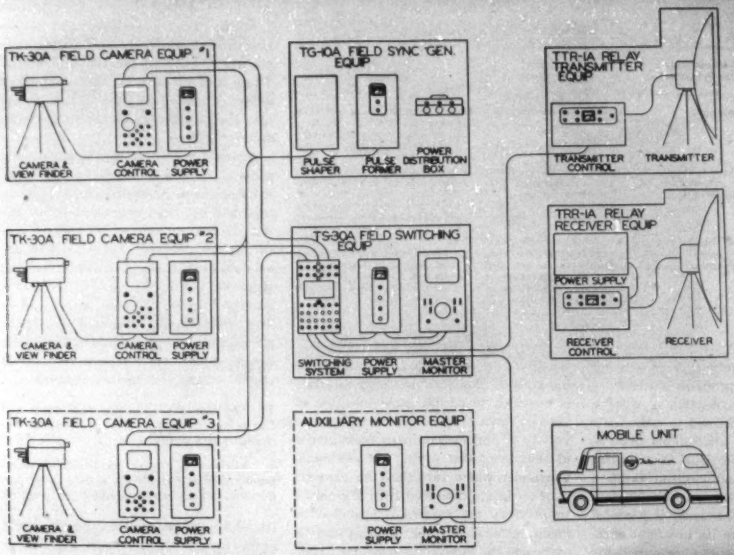

Figure 6 (left). Field pickup equipment block diagram

Figure 8 (below). Synchronizing signal generator

are used to synchronize the excursions of the scanning beam in the receiver kinescope with those of the pickup tube beam. The field synchronizing generator is a duplicate of the studio synchronizing generator in its circuits. For convenience it is broken into two units called a pulse shaper and a pulse former (Figure 5).

Television film projectors, in both 35 and 16 millimeter types, differ from conventional projectors in the items and for the reasons listed in Table II. Figure 9 shows a 16 millimeter projector mounted on a pedestal.

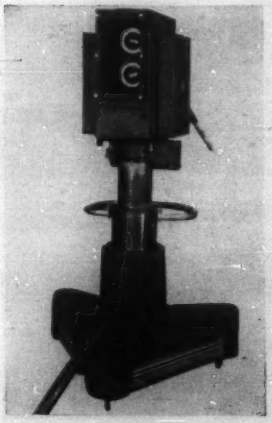

Figure 7. Iconoscope camera

Distribution amplifiers, shown in Figure 1, are used where it is desired to supply several signals from a common source, that is, where branch connections are necessary. They consist of five unity gain video amplifiers mounted on the same chassis. Provisions are made for paralleling either the input or output of several amplifiers. The amplifiers accordingly can be used as mixers, that is, for adding synchronizing signal to video signal; or they may be used as multiple feeds, that is, to feed synchronizing pulses from a single synchronizing generator to several cameras.

Electronically regulated plate power supplies, two of which are shown in Figure 1, are used to supply plate current for the electron tubes in various equipments. Electronic regulation maintains the voltage output constant with variations in load current. As the ratio between these two quantities is a measure of the effective internal impedance of the power supply, the stabilization of the voltage output tends to eliminate the undesirable coupling between different units when fed for a common power supply. The effective internal impedance of these units is measured in tenths of ohms

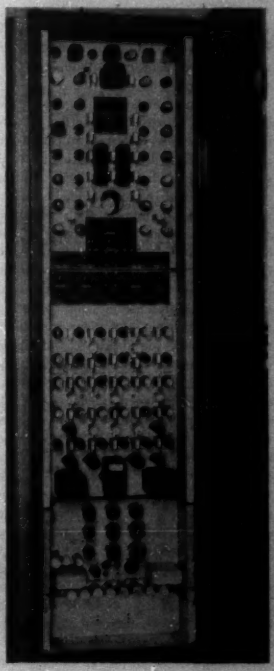

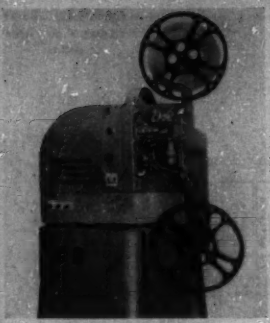

Figure 9 (above). 16-millimeter television film projector

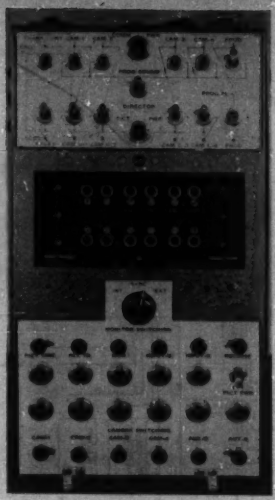

Figure 10 (right). Operating controls, field switching system

and this low value is maintained over the wide band of frequencies occupied by video waves.

As an example of switching equipment, the switching system for the remote pickup equipment shown in Figure 5 may be mentioned. As may be deduced from the close-up view of the operating panel in Figure 10, it is, in effect, a complete control center for a remote pickup operation. The following functions are performed by this unit:

1. Switching is provided for a maximum of four cameras. When one particular camera is selected, tally lights at the front and rear of the camera, and at the switching system are lighted automatically to indicate to cameraman, control operator, and performer the selection of that camera. Additional switching is provided for the two auxiliary video inputs.

2. The master monitor associated with the switching system can be switched to the outgoing picture line, to either of the auxiliary inputs, or to a signal obtained from the relay equipment.

3. A complete audio switching system is provided to permit intercommunication between the various operating personnel. In addition, program sound is distributed to such personnel. The headsets worn by operating personnel supply program sound to one ear and intercommunication or order wire sound to the other ear.

All of the studio and control room interunit connections carrying video information must be made with coaxial cable in

Table III

Frequency, Megacycles	Antenna Sections	Channel	Relative Gain: Television	Relative Gain: Frequency Modulation
54–66	3	II	3.6	3.0
		III	4.0	
66–88	3	IV	3.6	4.5
		V	4.1	
		VI	4.4	
174–216	6	VII	7.2	3.6
		VIII	7.4	
		IX	7.6	
		X	7.8	
		XI	8.0	
		XII	8.3	
		XIII	8.6	

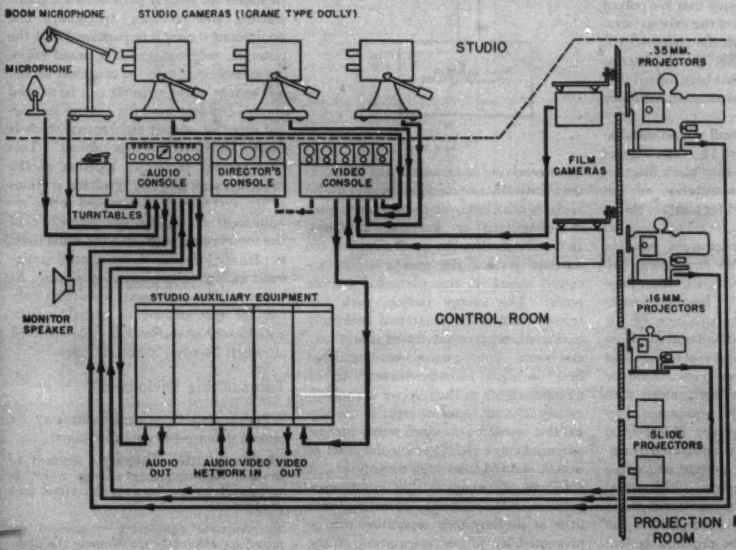

Figure 11. Small studio equipment layout

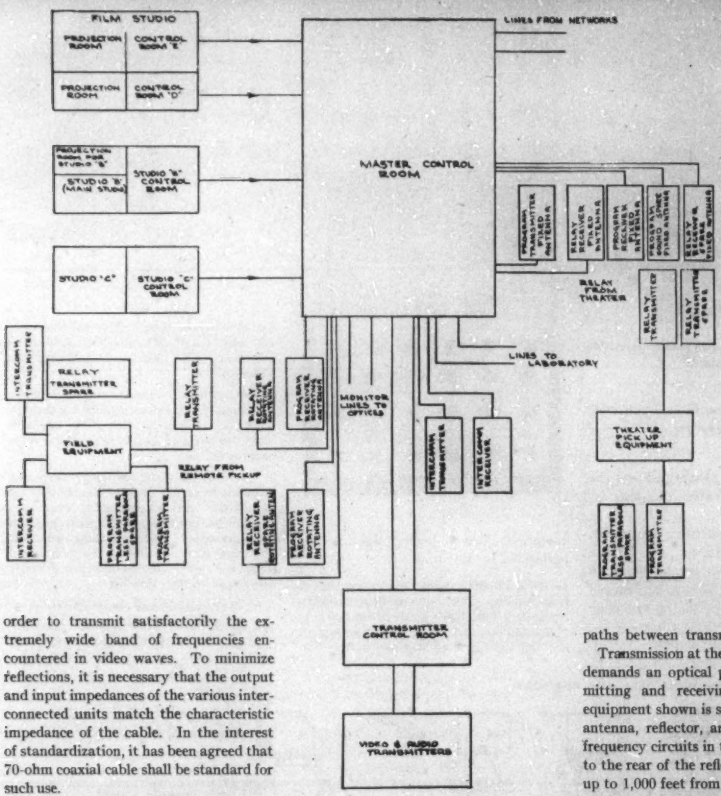

Figure 12. Block diagram of large station

order to transmit satisfactorily the extremely wide band of frequencies encountered in video waves. To minimize reflections, it is necessary that the output and input impedances of the various interconnected units match the characteristic impedance of the cable. In the interest of standardization, it has been agreed that 70-ohm coaxial cable shall be standard for such use.

An example of a small studio installation is shown in Figure 11, while Figures 12 and 13 show the master block diagram and a pictorial representation of the main studio equipment for a rather elaborate installation.

The inclusion of microwave relaying equipment with studio equipment violates the rules for classifying the equipment suggested in the preceding paragraphs. However, the smallness of the signal powers involved and a recognition that this equipment is a replacement for coaxial cable offers some justification for considering relay equipment along with studio equipment. This equipment, Figure 14, is a superfrequency (6,500–7,050 megacycles) frequency-modulated transmitting and receiving system employing highly directive antennas. The actual power output of the transmitter is of the order of 0.1 watt. However, due to the high directivity of the antenna system (both receiving and transmitting antennas are identical), a tremendous gain in useful signal is achieved over that obtained with non-directional or isotropic antennas. It is obvious that the more directive the antenna system, the greater is the received signal at the particular remote point. The energy (which, with isotropic antennas is scattered uniformly over a sphere) is concentrated into a narrow beam. For the equipment illustrated here, the signal actually delivered to the r-f input circuit of the receiver is approximately 25×10^8 times as great as the signal that would be obtained were isotropic antennas employed. Such is the order of benefit secured from high directivity. A corollary advantage is that interference between relay systems operating with little or no frequency separation can be prevented by proper orientation of the paths between transmitter and receiver.

Transmission at these super frequencies demands an optical path between transmitting and receiving antennas. The equipment shown is so packaged that the antenna, reflector, and associated radio-frequency circuits in the container affixed to the rear of the reflector can be located up to 1,000 feet from the control and signal input or output equipment which is housed in the rectangular cabinet. This arrangement facilitates location of the radiation emitting and receiving portions of the system with due regard to the requirement of optical characteristics of the intervening path. At the same time, it permits location of the control equipment at convenient operating points. At present, this equipment is suitable only for the transmission of visual signals. Satisfactory operation has been obtained at ranges between 15 and 20 miles.

Transmitting Equipment

The transmitting equipment may be broken down into two sub-groups:

(*a*). Transmitter—equipment required to produce high-frequency energy which is modulated by the appropriate visual and aural signals.

(*b*). Antenna equipment—equipment required for efficiently transferring the high-

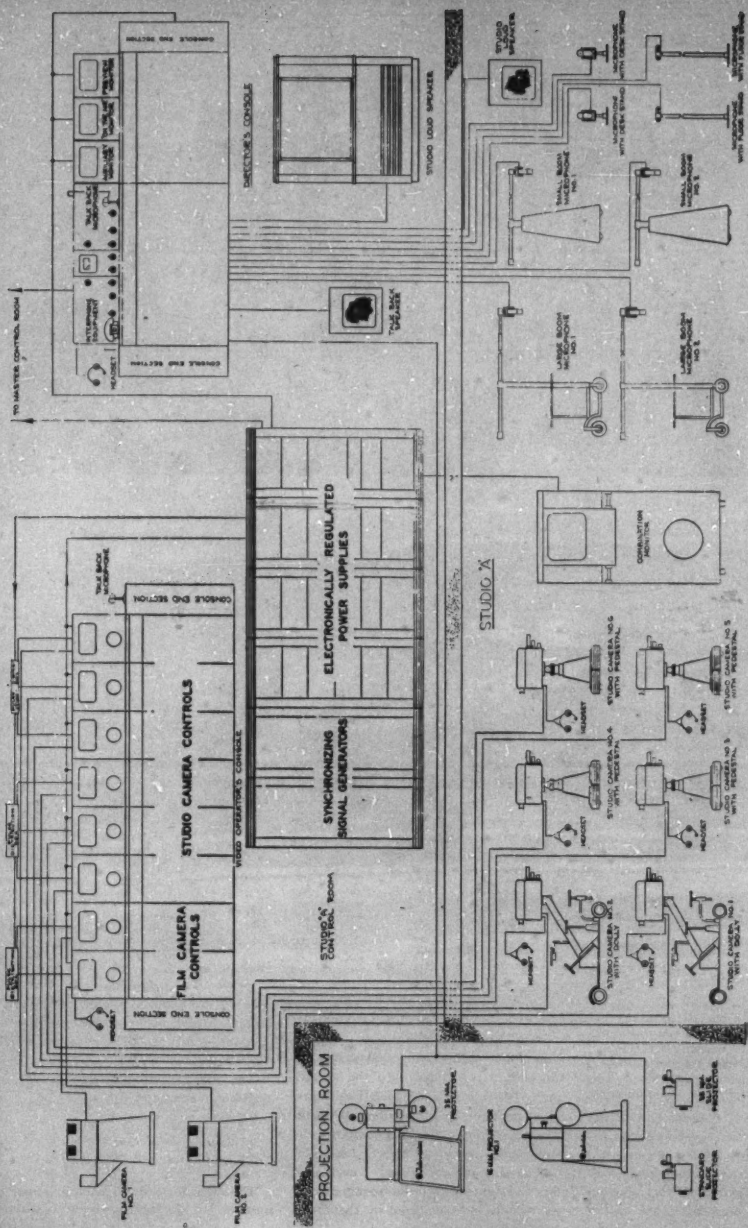

Figure 13. Large studio equipment layout

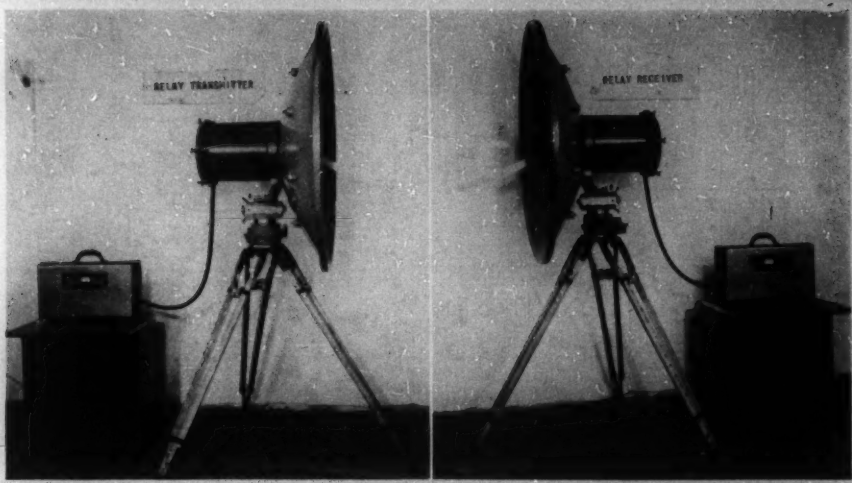

Figure 14 (above). Super frequency television relay equipment

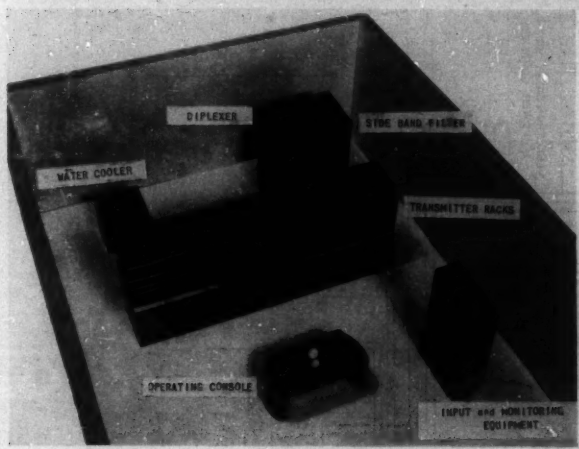

Figure 15. Television transmitter and associated equipment

frequency energy produced by the transmitter from ohmic conductors into free space. It should be noted that this definition of radiation is valid only for that lower portion of the electromagnetic spectrum currently utilized for radio communication.

The type *TT-5A* television transmitter covers all 12 of the television channels from 54 to 216 megacycles now assigned by the Federal Communications Commission for commercial metropolitan television station operation. For ease of operation, inspection and maintenance convenience in shipment and installation, and economy in manufacturing, the transmitter is divided into the several units shown in Figure 15. The transmitter assembly is contained in an assembly of eight racks. In these racks are the necessary electronic tubes with their associated components and power supplies to produce two radio-frequency carriers which are modulated by the visual and aural signals. The input signals to the transmitter are at standard studio levels—1.5 volts peak to peak for the visual and +10 decibels, approximately three volts, for the aural. The output of the transmitter is two modulated carriers—5-kw peak for visual and 2.5-kw peak for aural. Amplitude modulation is used for the visual carrier, while the aural carrier is frequency modulated with a maximum swing of ±25 kc.

A convenient grouping of the controls required for starting the transmitter and observing its performance is afforded by the control console. The centrally positioned video monitor may be switched to check the visual signal at several points in the transmitter.

Input and monitoring equipment racks contain units necessary for observing and checking the transmitter output—carrier frequency and modulation monitors and their auxiliary apparatus and a stabilizing amplifier to remove disturbances due to switching, and so forth from the incoming video signal.

The antenna equipment consists of three components:

1. Antenna.
2. Diplexer.
3. Required transmission line.

The super turnstile antenna possesses a number of advantages as a radiating

Figure 16 (above). Television super turnstile antenna

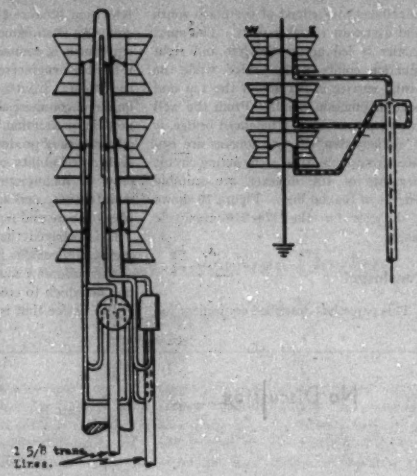

Figure 17. Schematic and layout of super turnstile antenna

Schematic diagram of radiators of antennas for range of 54 to 88 megacycles. Diagram shows *E–W* radiators; *N–S* radiators are fed similarly, but with 90-degree phase displacement. The power gain of the super turnstile antenna is the same as the power gain of an equivalent turnstile antenna with dipoles spaced at one half wave length intervals

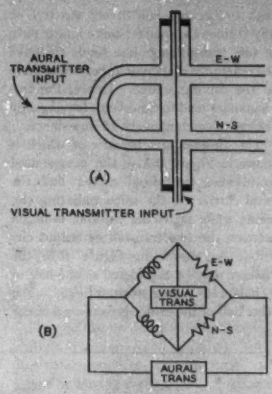

Figure 18. Functional diagram of diplexer

The schematic is shown in *A* and the equivalent circuit is indicated in *B*. *E–W* and *N–S* are the turnstile antenna east-west and north-south radiators respectively

structure for television. Those advantages of the most importance to television are

1. Adequate broadband characteristics.
2. Structure inherently adapted to the simultaneous radiation of two carriers from the same elements.
3. Esthetically satisfactory appearance.

Other advantages which are not peculiar to television are

4. Absence of tuning or other field-made adjustments.
5. Mechanical ruggedness.
6. Radiators attached to supporting pole without insulators. Thus there are no insulators required to withstand mechanical stresses.
7. Moderate wind loading.

Briefly, the super turnstile antenna consists of a central supporting pole to which are attached layers or sections of radiators. Each section consists of four vertical sheet-like radiators set at 90-degree intervals around the pole. The radiators are fabricated to be electrically equivalent to a current sheet while keeping the wind resistance at a minimum. The shape of the sheet is dictated by the two requirements of uniformity of impedance with minimum reactance over the desired band and the need to obtain such suitable value for the radiator impedance as will simplify the paralleling of radiators in several sections. Figure 16 shows a super turnstile antenna, while Figure 17 shows the connections for feeding three sections of east-west or north-south radiators. The bandwidth performance of the antenna may be judged from the fact that only three different antennas are required to cover the twelve metropolitan commercial television channels. See Table III.

For feed purposes, each section is treated as two perpendicular dipoles, the east-west radiators being fed by one coaxial feeder and the north-south radiators being fed by a second coaxial feeder. As in all turnstile radiating systems, the two sets of radiators—north-south and east-west—are fed by separate transmission lines. By making one of these lines a quarter-wave length longer than the other, a 90-degree phase displacement is secured between the currents in the two sets of radiators. The effect of this phase displacement is to give a radiation pattern in the horizontal plane that is essentially circular.

This quadrature phasing of the radiator pairs improves the constancy of impedance over a wide band. If the radiators

Figure 19. Diplexer for television channels VII [illegible] to XIII

tend to become inductively reactive in any region, the quarter-wave longer path of one transmission line tends to make the reactance of its pair appear capacitive to the driving source. Hence, the two reactances tend to cancel out, leaving only the resistive component of impedance.

The diplexer, a schematic of which is shown in Figure 18A, is the device used to impress the visual carrier and the aural carrier on the same radiating elements while providing suitable isolation between the two transmitter output circuits. As shown in Figure 18B, the diplexer may be considered as one-half of a balanced Wheatstone bridge. The other half of the bridge is composed of the impedances-to-ground of the north-south and east-west radiator pairs. The aural carrier is fed across the left and right junction points of the bridge, while the visual carrier is fed across the top and bottom junction points. From the well known properties of a balanced bridge, it is obvious that the two sources are isolated from each other. The actual circuit elements of the diplexer are suitable lengths of coaxial lines. Figure 19 shows a diplexer for the 174–216-megacycle range.

Conclusion

This paper has described equipment for television broadcasting stations which is complete from camera to antenna. The equipment is commercial in character as it has been engineered to the standards of consistent, trouble-free operation required of commercial broadcasting, and is now in production. The units possess advantages of product design equipment, such as reliability of performance, economy of manufacture, accessibility for maintenance, and adequate reliable supplies of spare and replacement parts.

It is believed that the availability of such equipment as items in current production affords a sound technical foundation on which to erect a commercial television service that is national in scope.

No Discussion

Postwar Television Receiver Design

D. W. PUGSLEY
ASSOCIATE AIEE

THE new postwar television receivers include many new design features and characteristics which result in a much superior product to the consumer, not only from the standpoint of performance, utility, and reliability, but also from the standpoint of minimum obsolescence. It is the purpose of this paper to discuss some of these new design features which a progressive manufacturer certainly will include in his product to assure maximum customer satisfaction.

Receiver Types

The majority of receivers in this postwar era fall into two major categories known as direct view and projection. Direct view receivers, as the name implies, are receivers designed to allow the user to view the picture directly on the screen of the picture tube. In the projection type receivers, however, the picture is formed first on the screen of the cathode-ray tube, and then is magnified optically and projected onto a viewing screen. In most, if not all, cases the screen is a part of the cabinet and is not a separate detachable piece such as is used with home movie projectors.

The indirect view receiver, which was quite common before the war, is now largely obsolete. This was a type wherein the picture formed on the screen of the tube was viewed not directly, but by means of a plane mirror set at an angle of 45 degrees to the vertical.

A fourth type, which has no particular name, is a modification of the direct view type wherein the picture is viewed through a large "magnifying glass" or condensing lens which is placed directly in front of, and close to, the picture tube. This type is seldom used, primarily because the condensing lens limits the field of vision quite considerably.

External Design Features

Figure 1 shows a new direct view television receiver, and Figure 2 shows a new projection type receiver.

Both of these figures show the receivers in an operating condition, that is, with doors open, the controls accessible, and the screen visible. Inasmuch as the television screen, when not in use, has a rather nonharmonious appearance when compared with the rest of the furnishings of an average living room it becomes necessary, in the better receivers, to provide some means for covering the screen.

At least one satisfactory method for direct view receivers is to provide doors on the cabinet. Such an arrangement is shown in Figure 3, which is the receiver shown in Figure 1 except that the doors are closed.

This particular receiver provides standard broadcast radio reception in addition to television operation. Controls are so grouped that by opening only one door, as shown in Figure 4, complete broadcast receiver operation is possible.

In the case of the projection receiver the covering of the screen is a more difficult objective to achieve. The picture, being large, has the possibility of being viewed by a large number of people at the same time provided the screen is not placed so low as to make it difficult for more than one row of people to see it simultaneously. However, a high screen is not conducive to a well-balanced piece of furniture. Therefore it appears obvious that the screen, ideally, should be capable of folding in or sliding into the cabinet when not in use.

Figure 5 shows the receiver of Figure 2 with its screen in closed position. In this particular receiver the problem was solved by having the so-called "doghouse" so arranged that it can be elevated into position. The "doghouse" houses the screen and a large flat mirror. More will be said about these components later.

The system of folding first the mirror and then the screen into the cabinet was one method of solution that was tried first, but this was found to have the objection of creating a hazard. The mirror and the screen are quite heavy, thus giving rise to the constant danger of having one or the other slip out of a person's hand, resulting in shattered glass or physical injury.

In the receiver of Figure 6, these objections were overcome completely by having the "doghouse" balanced by counterweights, thus making it very easy to lift or lower the screen and mirror. A force of only about $4^1/_2$ pounds is required to raise or lower the entire mechanism although the total weight is 40 pounds.

There is also an "anti-finger-pinching" device connected with this mechanism which prevents the lid from coming down on a person's fingers when lowering the screen. This is shown in Figure 6.

Chassis and Circuit Design

The design features discussed up to this point are largely functional. Operating convenience and safety are obtained as well as good appearance.

Attention now will be directed to electrical and mechanical features of the television chassis.

Figure 7 shows the chassis of the direct view receiver of Figure 1. This chassis is complete, (except for a shield which was removed) and has all the components on it necessary for both television and standard radio broadcast reception, except for

Paper 47-73, recommended by the AIEE committee on communication for presentation at the AIEE winter meeting, New York, N. Y., January 27–31, 1947. Manuscript submitted November 13, 1946; made available for printing December 10, 1946.

D. W. PUGSLEY is with the General Electric Company, Bridgeport, Conn.

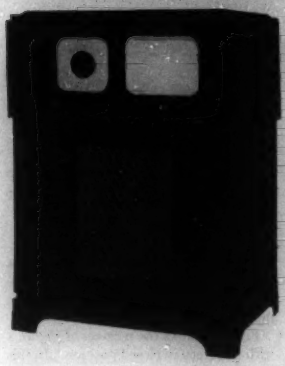

Figure 1. Direct view television receiver

the loudspeaker which necessarily is mounted to the cabinet for accoustical reasons. As can be seen, even the cathode-ray tube is mounted securely on the chassis. It is left there even during shipment. This has proved to be a real step forward from the old prewar scheme of shipping the tube separately from the chassis.

From the technical standpoint there are a number of interesting and vitally important new design considerations which must be given full consideration when designing any really worth-while present-day television receiver. Some of these items are of extreme importance in that they affect not the user's reception, but may interfere seriously with a neighbor's television or radio reception. Many readers will recall that during the early days of radio a very cheap but very sensitive circuit known as the superregenerative detector was put into many radios. This circuit worked well as far as receiving signals was concerned, but unfortunately it also radiated spurious signals of its own, through the antenna, with the result that neighboring receivers for blocks around were filled with miscellaneous whistles and squeaks. This circuit subsequently was outlawed.

A similar condition can exist with television receivers unless proper design considerations are taken into account by all receiver manufacturers. However, in the case of television receivers this condition is more serious in that even though a straight superheterodyne receiver is used intolerable interference may result. In this case it is the local oscillator radiation that causes the trouble. This is demonstrated by the following example. If a receiver is operating on television channel 2 (54–60 megacycles) and has the standard RMA (Radio Manufacturers' Association) intermediate frequency with the sound intermediate frequency at 21.9 megacycles, then the local oscillator frequency is 81.65 megacycles. This is only 100 kc away from the sound carrier of channel 5, which is at 81.75 megacycles, and thus easily can cause interference to a neighboring receiver attempting to operate on channel 5, unless the radiation is held down to reasonable levels. There are other such combinations possible. In some cases it is the picture that is interfered with rather than the sound. Also, of course, if a lower intermediate frequency is used the combinations are more numerous. Properly designed receivers will have the radiation from the local oscillator reduced to such a level that neighboring receivers are not bothered.

Figure 3. Direct view television receiver with the doors closed

RMA has taken cognizance of the oscillator radiation situation, and has issued memoranda to manufacturers strongly stressing the need for mutual co-operation in the design of receivers which will not cause serious radiation interference.

One of the best ways, and almost the only practical way, of reducing oscillator radiation to reasonable levels is to provide a properly designed radio-frequency stage in the input section of the receiver. This of course adds cost that otherwise would not be necessary, but which is essential to the public's best interests. It will be most unfortunate if some manufacturers seize upon this condition as affording a source of lucrative cost reduction.

Another source of interference that may come from some poorly designed sets is the type of radiation that is created by some types of radio-frequency or "fly-back" high voltage supplies when

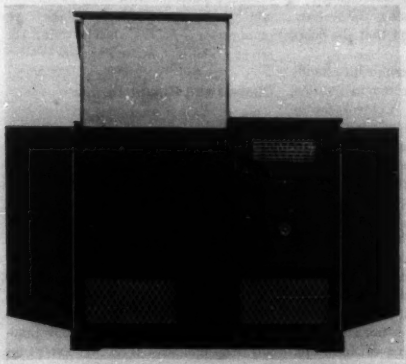

Figure 2 (left). Projection television receiver

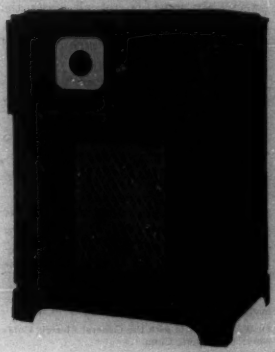

Figure 4 (right). Direct view television receiver radio operation

not properly shielded. This type of interference does not bother television receivers, but does play havoc with radio receivers in the immediate area. Here again this source of annoyance is eliminated completely in reputable receivers which incorporate adequate shielding.

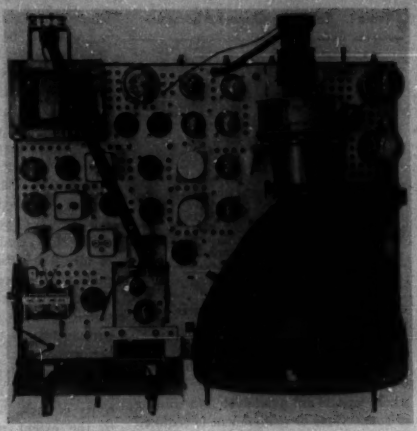

Figure 7. Top view of television chassis

High Voltage Supplies

The high voltage supplies of the new television receivers are quite interesting.

It was the custom in prewar receivers to use a 60-cycle type of supply wherein a high voltage power transformer was used with a conventional rectifier circuit to obtain the necessary high direct voltage for the final anode of the picture tube. In prewar receivers this voltage was usually in the order of 2,000 to 5,000 volts, but in modern receivers it is seldom less than 6,000 volts and may run as high as 12,000 volts on direct view receivers, and 30,000 volts on projection receivers.

To a power engineer it undoubtedly sounds like heresy to consider generating such voltages in a cabinet in a person's home.

As a first reaction it would appear that the use of such high voltages necessarily would entail large bulky equipment, and also would be extremely dangerous. If the obsolete prewar 60-cycle supplies still were used that would be true. However, with the type of supply described in this paper, this danger has been eliminated because this supply cannot deliver a dangerous amount of current before the voltage drops to a very low level. A typical regulation curve is shown in Figure 8.

In this type of supply the voltage is generated by vacuum tube circuits operating at relatively high frequencies. An oscillator tube incorporates a tuned tank circuit in its plate as shown in Figure 9. The frequency of this oscillator usually lies in the range between 30 and 500 kc. As shown in the figure there is an extension on the plate winding which raises the voltage to the desired value. This voltage then is rectified as shown, filtered, and supplied to the final anode on the picture tube. Usually about 8,000 to 10,000 volts can be obtained in this fashion.

For protection type receivers voltages in the order of 27,000 to 30,000 volts are necessary. This voltage is obtained from a similar circuit except that voltage multiplying is employed. Figure 10 shows the schematic diagram of such a circuit.

The equipment required by such a type of supply is surprisingly small and compact. Figure 11 shows a typical supply which delivers 30,000 volts. This figure shows all the major components except for the coil which is not visible.

Figure 5. Projection television receiver with screen and doors closed

Figure 6. Device to prevent lid from closing on fingers

Tuner Units

Another interesting feature of present-day television receivers is the tuner unit. Present-day frequency allocations call for 13 different television channels distributed in the spectrum from 44 to 216 megacycles. Table I indicates the specific channels.

Frequency allocations are such that there will be a maximum of eight channels assigned to any major metropolitan area.

Any worthy design of television receiver must be designed so as to allow op-

Table I. Television Channel Allocations

Channel Number	Frequency Band, Megacycles
1	44–50
2	54–60
3	60–66
4	66–72
5	76–82
6	82–88
7	174–180
8	180–186
9	186–192
10	192–198
11	198–204
12	204–210
13	210–216

eration on any of the 13 channels. The best designs of receivers provide 13 operable channels all permanently connected and aligned for use. Such a set is usable at any place in the country where signals are available. No shifting of connections or realignment is required if the purchaser moves to a new location.

Some receivers will be provided with only 8-channel selection positions. Each position, however, will be adjustable to two or more different channels. With this type of receiver it will be necessary for the service man to align each receiver for the particular stations in the area, somewhat like setting up push buttons on a radio receiver. The 8-channel selector method, while it is less expensive than the 13-channel system, does have the disadvantage that the service man must readjust the positions if the owner moves to a new area. Also there may be areas between large cities, such as Philadelphia and New York, where acceptable signals could be received from each city. In this case it may be found that the 8-channel positions are inadequate.

Some receivers incorporate a continuous tuning mechanism which tunes continuously from 44 to 216 megacycles. These have the advantage of not requiring a switch, but have the disadvantage of tuning over a large portion of the radio spectrum wherein there are no stations, and thus restricting the usable portions of the scale. Also, positioning accuracy requirements are quite stringent.

A tuner unit incorporating all 13 channels preset need not be extremely complicated or bulky. Figure 12 shows such a unit used in General Electric receivers. A 17-position selector switch is used, thus enabling the incorporation of all 13 television channels as well as radio and phonograph services if desired. The coils for each channel are extremely simple as can be seen, and each is aligned permanently at the factory for optimum performance.

A distinct advantage of using separate coils for each channel is that the selectivity of each channel can be controlled to the extent needed. Selectivity requirements may be different for some channels than for others. For instance, using the standard RMA intermediate frequency it is possible for high powered frequency modulated stations in the band from 88 to 108 megacycles to lie on the image frequency of television channels 1 and 2. When individual coils are used for each channel this problem is solved readily by increasing the selectivity of these two channels to the degree needed. In the particular tuner unit shown, the normal image attenuation of each channel is about 50 decibels, but for channels 1 and 2 it has been increased to 75 decibels. Since at least 30 decibels difference between a desired and an interfering signal is needed before the interfering signal starts to become objectionable this leaves about 45 decibels to account for difference in field strengths of the two signals. This means that if a receiver were located at equal distances from a television transmitter and a frequency modulated transmitter on the image frequency than the frequency modulated transmitter would have an effective power of over 30,000 times that of the television transmitter before it would start to cause objectionable interference.

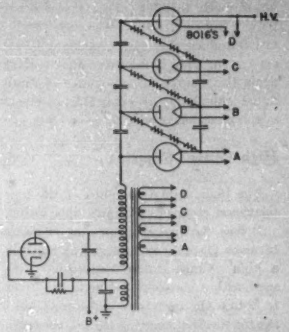

Figure 10. Schematic diagram for projection receiver high voltage supply

Synchronization

Another circuit of particular interest in many new television receivers is the "AFC sync." circuit. In unabbreviated language this means "automatic frequency control synchronization" and is applied to the horizontal scanning circuits. The use of this circuit eliminates the characteristic scalloped edge effect so typical of prewar receivers. It also enables the receiver to maintain excellent synchronization right through very bad bursts of noise such as electrical or automotive ignition interference. The improvement is really amazing, and actually has to be seen to be appreciated.

In brief the circuit operates by utilizing a direct voltage derived from the average frequency of the horizontal synchronizing pulses for controlling the frequency of the line scan oscillator. As this average frequency is not disturbed to any appreciable effect by scattered bursts of noise,

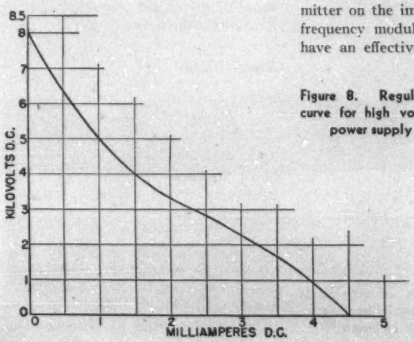

Figure 8. Regulation curve for high voltage power supply

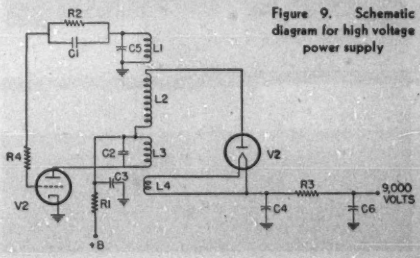

Figure 9. Schematic diagram for high voltage power supply

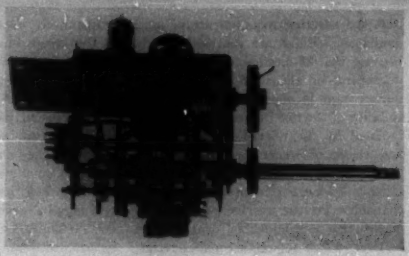

Figure 11 (above). High voltage power supply

Figure 12 (right). Tuner unit

the receiver maintains excellent synchronization right through the noise.

Intermediate Frequencies

With the advent of the new and higher frequency allocations for television it became necessary to change the intermediate frequencies used in receivers. Prewar intermediate frequencies usually lay in the region from 8 to 12 megacycles, but most modern receivers have an intermediate frequency considerably higher. The RMA has standardized on an intermediate frequency such that the sound carrier lies between 21.25 and 21.9 megacycles, and the picture carrier between 25.75 and 26.4 megacycles. This obviates a lot of difficulties encountered with the old prewar intermediate frequencies such as interference from high powered short-wave transmitters and poor image rejection. It also helps immensely in the problem of reducing local oscillator radiation.

Optical Systems for Projection Receivers

The most popular type of optical system in use in projection receivers today is a reflective system, known as the Schmidt system. Figure 13 shows the essential elements of a Schmidt system. It can be seen that light from the picture which is formed on the face of the picture tube is collected by the spherical mirror and reflected back to focus on the picture screen. In the process the light passes through the aspheric corrector lens which corrects for spherical aberration of the spherical mirror, and is turned at right angles by the flat mirror set at 45 degrees. Picture sizes of 16 by $21^1/_2$ inches are commonly used although larger ones are possible. The Schmidt system is characterized by its simplicity and its high light efficiency. Apertures equivalent to approximately $f0.9$ are attainable.

Some refractive systems are being used in projection receivers. Here a lens system similar to that in the ordinary picture projector is used to collect light from the picture tube face and focus it on the picture screen. To date refractive systems have suffered by comparison to the Schmidt because they have a smaller effective aperture, thus giving a picture which is less bright. Also, they result in barrel distortion when used with the standard projection tube, since this tube has a convex face, and the refractive system requires a flat face, or ideally a concave face tube. Attempts made to eliminate this distortion by the use of field flattening lenses have not been entirely successful to date. Undoubtedly a suitable tube can be developed and produced when the refractive system is developed to the point where it will be equivalent to the Schmidt reflective system in cost and performance.

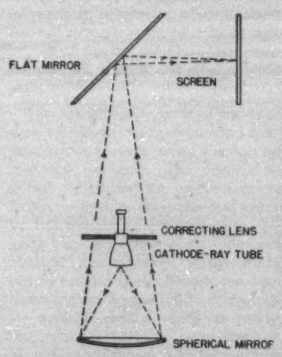

Figure 13. Elements of Schmidt reflective system

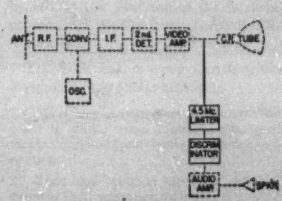

Figure 14. Block diagram of interchannel sound system

Intercarrier Sound System

An item which is of particular interest for the future is a new method recently proposed to industry by R. B. Dome of the General Electric Company for deriving the sound signal in a television receiver. This new system is known as the intercarrier sound system.

In past and present television receivers the sound signal is received, amplified, and heterodyned by the same radio frequency circuits and tube employed for the picture signal. The sound signal ordinarily then is separated from the video early in the video intermediate frequency stages. It then is amplified in its own intermediate frequency channel and detected.

In the intercarrier sound system, however, the sound signal is not separated from the video in the intermediate frequency channel at all. Instead, both the sound carrier and the picture carrier are allowed to be detected in the second video detector. These two carriers beat together to produce a 4.5-megacycle beat note since the two carriers are separated by 4.5 megacycles. This 4.5-megacycle beat note will be frequency modulated with the audio modulation of the original sound carrier.

This 4.5-megacycle carrier is separated conveniently from the video signal at the input to the picture tube. It then is amplified, limited, and detected as is a conventional frequency modulated signal. Figure 14 shows a block diagram of the system.

The chief advantage of this system is

that the exacting requirements of local oscillator stability are removed largely because the 4.5-megacycle carrier is independent of the local oscillator frequency and is dependent only on the stability of the two carrier frequencies as radiated by the television transmitters, and these, of course, are crystal controlled. Thus it is only necessary to have a stable 4.5-megacycle discriminator and channel. To the receiver owner this means that objectionable drift of the receiver, which sometimes makes retuning necessary, is almost eliminated. This is a tremendous help.

For best operation some minor additional requirements are placed on the transmitter. One of these requirements is that there be no frequency or phase modulation of the picture carrier. Another is that the picture carrier not be allowed to drop to zero at any time, even when transmitting white. Standards for these items are being sponsored by RMA, and when they finally are adopted by the Federal Communications Commission and industry then the intercarrier sound system may be incorporated in most receivers. It appears that such standards will be adopted soon. The adoption of these additional standards in no way will cause obsolescence of present-day receivers.

As a concluding remark the author should like to emphasize that well-designed postwar television receivers are much superior to the prewar receivers both because of improved circuit techniques, as partly discussed in this paper, and also because of greatly improved picture tubes which afford much greater brilliance, detail, and contrast. This is especially noticeable in regards to fine detail, and contrast. Therefore it behooves a prospective purchaser to be certain he buys a strictly modern receiver, incorporating the latest advances in the art, if he does not wish to be doomed to disappointment. Very excellent television reproduction is now an established reality, but it can be obtained only by using well-designed receivers.

No Discussion

Television Network Facilities

L. G. ABRAHAM
MEMBER AIEE

H. I. ROMNES
ASSOCIATE AIEE

Synopsis: This paper describes television network facilities which are needed to connect studios and other pickup points to transmitters in the same and in distant cities, and discusses their transmission characteristics. Short-haul television circuits may be by microwave radio or over wire circuits. Long-haul television connections may be by radio relay or over coaxial systems of the type originally developed for carrier telephone circuits. Transmission requirements include adequate frequency band, accurate gain and phase equalization, and freedom from interference resulting from excessive noise, crosstalk, or modulation. Radio and wire systems are under development to provide extensive high-quality television networks.

MORE than a quarter of a century of experience in the broadcasting of sound programs has demonstrated the necessity for interconnection of broadcasting stations. Only because the same program thus can be brought simultaneously to millions of listeners is it economically possible to present famous orchestras, singers, actors, and comedians. In no other way can on-the-scene sports and news events be brought to a nationwide audience. Television, with its still more costly programs and its even greater effectiveness for on-the-scene events, obviously also will require network interconnections if it is to become the important source of information, education, and entertainment that is predicted.

The provision of these network facilities will be a big job. Indicative of the magnitude of the undertaking are the present-day sound program networks which may serve well as a pattern for future television networks. These sound program networks reach into every section of the country, serve more than 95 per cent of the approximately 1,000 standard broadcasting stations and employ 135,000 miles of program facilities. They represent an investment which is about one-half as much as the total investment by all of the nation's broadcasters in transmitters, studios, and other physical plant.

The normal development of transmission facilities to handle the nation's communications needs is paving the way for television networks. The tremendous growth in demand for communications has encouraged the development of means for transmitting many telephone or telegraph messages over a single wide-band channel. The number of messages which can be handled simultaneously has been increasing year by year until now channels are available each of which can handle hundreds of telephone conversations. Television, which uses a frequency space equal to that of hundreds of telephone messages, can be carried over this same kind of very wide band channel, and thus benefit by the joint use of the facilities provided for the many other communications needs.

Television station connection facilities divide naturally into two classes.

1. Short-haul circuits from program pickup point to studio, from studio to associated transmitter, and from studio to network connection.

2. Long-haul circuits between different cities to form television networks.

Three methods are available for providing these circuits—wire pairs, coaxial cables, and radio. In a comprehensive network, all three of these methods may be used.

Short-Haul Television Circuits

Balanced Pairs

Wire pairs in ordinary telephone cables are used quite generally for television circuits within cities. They require certain special preparation, such as removal of bridged taps, removal of loading, special splicing between cables to obtain the most favorable routing, and in some cases special measures to reduce noise. Amplifiers are provided at short intervals to provide good signal-to-noise ratio, the exact spacing depending principally upon the wire gauge and the availability of suitable amplifier locations. For a typical case, the loss at four megacycles averages about 60 decibels per mile and an amplifier spacing of about one mile is used. Telephone buildings sometimes are not available at the desired amplifier locations, so use has been made of rented space adjacent to the cable routes. Amplifiers are now under development which can be placed in manholes if necessary and can have power for their operation sent to them over telephone pairs.

Where several television services are needed along a route or where a lower loss facility is advantageous, polyethylene-string-insulated shielded pairs of the type shown in Figure 1 are being included in certain new local cables to form backbone television networks within large cities. These have a loss at four megacycles of about 18 decibels per mile, and any desired number can be placed in a cable without crosstalk difficulty.

Coaxial cables are being used for relatively short video circuits, generally with arrangements to reduce the effect of low-frequency noise induction.

About 30 short-haul television circuits ranging in length up to more than ten miles have been in use during the past year, employing these different kinds of wire facilities. Some of them have been in service for regularly recurring programs over a period of several years. The

Paper 47-74, recommended by the AIEE committee on communication for presentation at the AIEE winter meeting, New York, N. Y., January 27-31, 1947. Manuscript submitted November 14, 1946; made available for printing December 11, 1946.

L. G. Abraham, coaxial systems engineer, is with Bell Telephone Laboratories, Inc., New York, N. Y.; H. I. Romnes, radio engineer, is with American Telephone and Telegraph Company, New York, N. Y.

Figure 1. Video balanced pair

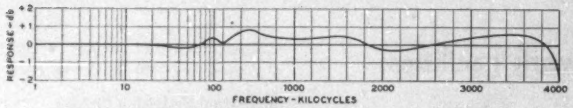

Figure 2. Attenuation characteristics of typical local video circuit

characteristics of a typical circuit of this type are shown in Figure 2.

Microwave Radio

Radio facilities for short-haul television circuits are described in a companion paper.[15] They are especially promising for unusual geographical situations, and while the present system is applicable primarily to permanent installations, they also would be useful for temporary pickups. When a pickup of a special news or sports event from a given spot occurs only occasionally, the radio link may be advantageous because it can be installed more quickly than a permanent type of wire link. Also, for a case like that between several Hollywood studios and their proposed Mount Wilson broadcasting stations, wire video circuits would require a long and circuitous route, with many amplifiers, whereas a single link direct radio path can be obtained. However, radio circuits at microwave frequencies need line-of-sight transmission paths. Fading effects must be taken into account by allowing margins over the requirements for normal conditions. Through use of highly directive antennas, low power can be used and difficulties with interference and ghosts resulting from reflections minimized. These radio circuits have been used successfully for several pickups and demonstrations, an interesting example being a 2-link circuit between West Point and New York. In some cases, combination wire and radio circuits have been used, the wire video facilities being employed to reach favorable radio sites.

Long-Haul Television Circuits

For television circuits interconnecting studios in different cities, coaxial cable and radio relay are the most suitable methods. It is quite possible that a comprehensive broad-band communication network in the future will consist of combinations of these facilities, each being used where conditions are best adapted to it. The status of the microwave radio relay first will be described briefly and then the coaxial cable system will be reviewed in some detail with special emphasis on the features of interest for television transmission.

Microwave Radio Relay

Radio operation at frequencies below about 30 megacycles has been used for point-to-point communications for many years. However, it has been applied principally where the use of wire lines was impracticable. Wire communication channels have desirable characteristics which have heretofore been lacking in radio, that is, an unlimited number can be established, the energy is precisely directed, they can be made very stable, and noise and interference can be controlled. With the development of techniques permitting the use of frequencies of thousands of megacycles, radio is beginning to approach wire lines in these respects. These improved characteristics permit the extension of radio over long distances by the use of repeaters, a method which has long been used for wire lines.

Experiments are now under way to determine the practicability of radio relay from the standpoints of cost, performance, and reliability. As part of the Bell System experiments, a full scale radio relay system is being established between New York and Boston. Some interesting features of this system are

1. It will employ seven intermediate radio repeater points, the average spacing being about 27 miles for a total circuit length of about 230 miles. These repeaters are located on high points of ground so that a direct line-of-sight path is available between adjacent repeaters.

2. The system will employ frequencies in the vicinity of 4,000 megacycles. A total of four channels will be established, two in each direction of transmission. A frequency assignment 20 megacycles wide has been obtained for each channel. It is probable that frequency modulation will be used and that a usable frequency band of at least four megacycles will be obtained for television transmission. Tests also will be made in the transmission of large bundles of telephone circuits.

3. The antennas will be horns with 10- by 10-foot apertures equipped with metal lenses to focus the radio waves.[13] These antennas give a gain of about 40 decibels, so that the normal attenuation of a 30-mile path between transmitters and receivers equipped with such antennas is less than 60 decibels. With a suitable allowance for fading, a satisfactory signal-to-noise ratio can be obtained for the number of sections involved in this experiment using transmitting power in the order of one watt.

It is expected that the New York–Boston system will be in experimental service before the middle of 1947. A similar system having four links looped back and forth between New York and Murray Hill, N. J., for a total length of 85 miles, has been undergoing tests for a number of months. Preliminary indications are that satisfactory television operation between New York and Boston can be provided by this means.

Coaxial Cable Systems

Coaxial cable systems now have gone far beyond the experimental stage so that more can be said about them than about radio relay. Several hundred miles of this cable have been in commercial use for telephone purposes for a number of years and great progress has been made in the construction of a nation-wide coaxial cable network since the war. As of January 1, 1947, about 4,000 route miles of coaxial cable had been placed in the ground and construction is continuing. Figure 3 shows the cables now in place or under construction and the extensions planned for the next three or four years. The coaxial routes shown on this map total about 12,000 miles. It is expected that early 1948 will see the Southern coaxial cable route ready for telephone service to points as far west as Los Angeles, and that by the end of 1948, the Central coaxial route will extend from New York to Chicago and St. Louis. The whole program indicated on the map may be completed by 1950.

Coaxial cable between Philadelphia and New York was used for experimental television service in 1940 when the proceedings of the Republican National Convention at Philadelphia were transmitted

to New York and broadcast by the National Broadcasting Company's television station. Following the war, these experiments were expanded, and now television circuits are in experimental service in both directions between New York and Washington. More than a hundred programs have been transmitted over these circuits, including such outstanding events as the National Broadcasting Company's pickup of the Army–Navy games from Philadelphia in 1945 and 1946, the inauguration of the new Dumont Studios, and Columbia Broadcasting System's test programs in full color.

The general features of coaxial systems have been covered in previous papers.[12] However, certain changes have been made and a brief review may be of interest in considering their use for television transmission.

The construction of the coaxial conductors and their arrangement in a cable are shown in Figure 4. The present standard coaxial line has an outer conductor with an inner diameter of 0.375 inch rather than the 0.27-inch diameter described in previous papers. Polyethylene rather than hard rubber is used now for the insulating disks which are 0.08 inch thick and are placed one inch apart. This larger size coaxial conductor has about 70 per cent as much attenuation per mile as the smaller, thus permitting wider spacing of repeaters.

Most cables contain eight coaxial conductors together with a number of paper-insulated wires for maintenance purposes. Layers of ordinary telephone pairs may be placed around the coaxial core for short-haul service needs. These cables are buried directly in the ground or placed in underground conduit. When placed in conduit, the cable may have a plain lead sheath or, in addition, may use corrosion protection. When buried, the cable is protected against corrosion and, in addition, may have lightning protection in the form of thermoplastic layers and a copper jacket or mechanical protection in the form of steel tapes or wires.

Figure 5 shows the impedance, attenuation, and phase delay characteristics of the 3/8-inch coaxial cable up to five megacycles. Limited measurements up to several thousand megacycles indicate that coaxial cables can be used for much wider frequency bands, the main inhibiting factor being that the attenuation increases about as the square root of the frequency.

Figure 6 shows the general layout of coaxial systems. Present arrangements provide a usable frequency band from about 64 to 3,100 kc and employ repeaters on 0.375-inch coaxial lines at about 8-mile intervals. Most of these are auxiliary repeaters which are housed in small closed huts not requiring heat or power connections. These huts are designed to have very small inside daily temperature fluctuations which, combined with the general use of underground cable, reduce over-all transmission variations caused by temperature changes in a short period to such small proportions that good equalization can be maintained. Auxiliary repeaters are fed 60-cycle a-c power over the central conductors of the coaxial cables from main repeater stations which are spaced up to 165 miles apart.

Variations in loss caused by temperature and other changes are compensated for by regulators associated with alternate repeaters which continuously and automatically measure the output level of a 2,064 kc pilot frequency and adjust the amplifier gain to maintain a substantially constant output level. Supplementary regulation and equalization is provided at the main repeater stations under control of four pilot frequencies sent over the coaxial line at 64, 556, 2,064 and 3,096 kc.

The 64–3,100-kc frequency band provided by the present coaxial line may be used either for telephone or for television transmission. When used for telephone service, terminals are provided for up to 600 circuits as required. When used for

Figure 3. Coaxial cable and radio relay networks—January 1, 1947

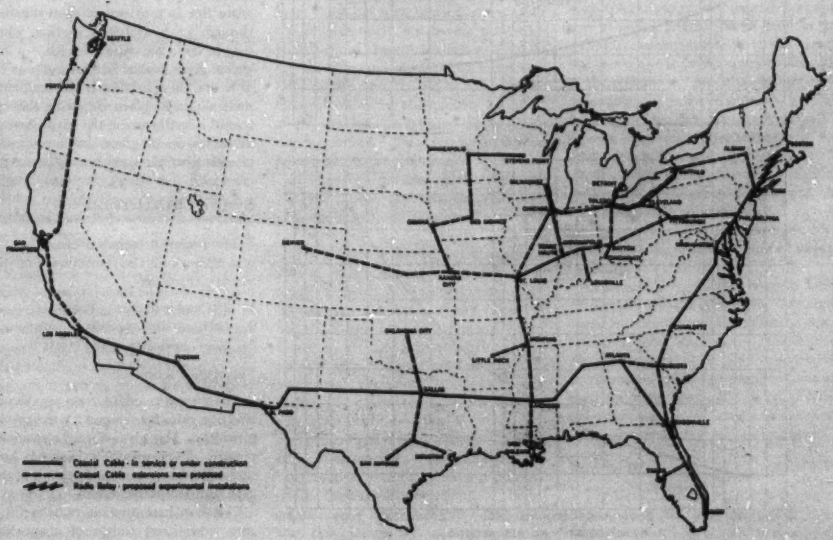

Figure 4. Makeup of coaxial cable

Figure 5 (below). Characteristics of 0.375-inch coaxial cable

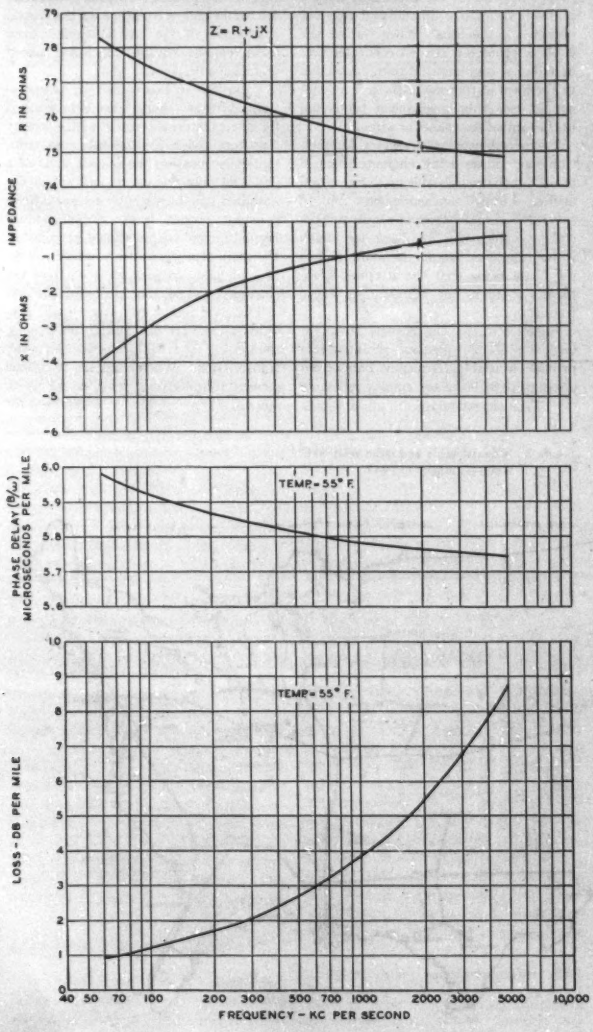

television service, the video signals to be transmitted are moved by double modulation to a carrier frequency of 311 kc, with the upper side band extending to about 3,100 kc and a vestigial lower side band extending down to about 200 kc. At the receiving end, the signals are restored to the video range by two more steps of modulation.

Sound for the television program is provided in the range from 76 to 88 kc by means of single side-band program terminals which give an 8-kc band. Wider bands can be provided if needed.

Many features have been included in the system to insure continuity of service. The cables generally are buried deep in the earth or put in conduit, are protected against corrosion, lightning, or mechanical damage, as described previously, and are maintained under gas pressure with alarms to indicate any leak in the outer sheath, so that repairs can be made before failure occurs. Each stage of amplification in the repeaters has parallel tubes and one tube in any stage may fail to function without interrupting service. Pilot alarms at each auxiliary repeater warn the nearest attended station of excessive pilot frequency deviations. The power supply is arranged so that if commercial power fails, a-c power will be supplied automatically from large storage batteries through rectifier-inverters or motor generators. Gas engine generators are available if the commercial power should be off for some time. Finally, a spare line is provided in each direction through each switching section, which may be up to 200 miles in length. Whenever a given coaxial line fails or gets out of limits, the spare line is switched automatically in its place so quickly that not a word is lost in any of the telephone conversations in progress, and an alarm is given so that the trouble may be cleared.

System Characteristics

The principal technical characteristics of a network for the transmission of television pictures are

1. The usable frequency band.
2. Echoes and gain and phase deviations.
3. Noise, modulation, and crosstalk.

Frequency Band

The present coaxial system provides an effective video band about 2.8 megacycles in width. This gives a very respectable picture. Even color television has been transmitted over a 450-mile circuit of this type with acceptable results.

The short-haul wire and radio facilities give video band widths of about four

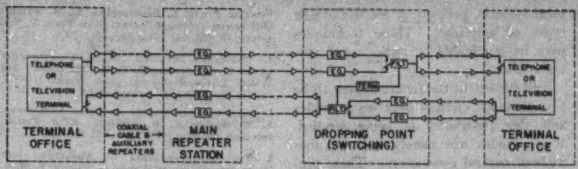

Figure 6 (above). General layout of coaxial cable systems

Figure 7 (below). Attenuation and phase deviation of New York–Washington television circuit

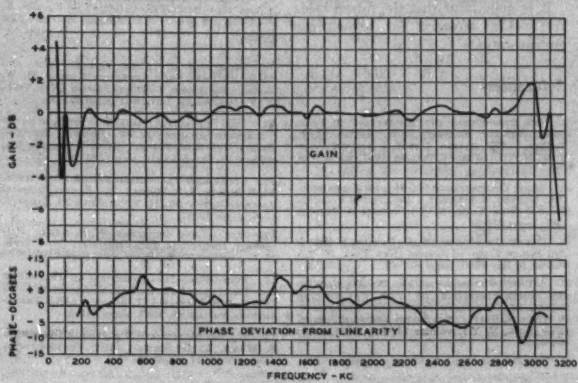

megacycles, and the same band width is contemplated for the long-haul radio relay system to be tried out between New York and Boston.

Echoes, Gain, and Phase Deviations

Echoes caused by reflections from objects in a radio transmission path or from impedance irregularities in a coaxial cable cause ghosts in television pictures. These reflections also cause deviations in the gain and phase characteristics of the circuits. Conversely, gain and phase deviations resulting from causes other than reflections give the same sort of picture ghosts as do echoes resulting from reflections.

A large echo with a delay of, for example, three microseconds, produces a ghost about one-half inch to the right of the original object on a 10-inch picture screen. Such ghosts may be positive, (for example, a dark ghost of a dark object), or negative, (for example, a light ghost of a dark object). They may have a frequency characteristic caused by greater reflections in one part of the band than in another. For example, a high-frequency echo might reproduce completely a ghost of a thin vertical line such as a flagpole, but the ghost of a wider object would show only at its edges. However, with only fairly low video frequencies (that is, near the carrier) present in the echo, the wide object might have a large ghost but with blurred edges, while the flagpole might not have a noticeable ghost. Very short delay echoes produce picture ghosts so slightly displaced that they merely blur the edges of the sharp discontinuities in the picture or affect overshoots which outline such sharp discontinuities. Therefore somewhat greater amounts are allowable.

It is possible to analyze the measured gain and phase characteristics of a circuit and predict the magnitude and placing of the resultant picture ghosts. For example, if there is a ±0.8-decibel gain deviation with a corresponding ±6-degree phase deviation, each recurring regularly, the picture will have ghosts about 20 decibels down lagging the main signal. However, if the gain deviations were present without the phase deviations (or vice versa), there would be both lagging and leading ghosts, each weaker than the single ghosts just described.[8]

Gain and phase deviations in the video band at frequencies below the line scanning rate of ±15.75 kc have a different effect than such deviations at higher frequencies. This is because they distort the pictures by making successive horizontal lines fail to match up. Also, the use of vestigial side-band transmission requires special attention to phase deviations at frequencies near the carrier to insure that the two frequencies on either side of the carrier combine properly to form one in the final picture.

Ghosts in television broadcast reception have been the subject of considerable investigation, and means for minimizing these effects are an important part of the broadcasting and receiving aspects of television. The magnitude of the echoes normally encountered in coaxial cables are much smaller, but to provide good transmission over long distances, echoes caused by reflections are reduced by careful manufacture and installation of the coaxial cables. Tests to check this feature are made by means of the pulse echo method as described in a forthcoming paper.[14] The desired gain and phase characteristics are obtained by means of gain and delay equalizers introduced at the main repeater stations. Figure 7 shows the over-all gain and phase deviations obtained on a 225-mile New York–Washington television circuit. Television pictures have been transmitted experimentally over 800-mile circuits with satisfactory results.

Noise, Modulation, and Crosstalk

Systematic noise caused by harmonics of 60 cycles may produce very objectionable patterns on the picture, and resistance noise may produce general fuzziness and a boiling effect. Noise may be reduced by raising the level of the signal, but this tends to increase the modulation in the repeaters. Modulation may show up as spurious patterns generally associated with sudden changes in picture brightness or may cause interference with the pilots which are used for regulating the circuit. Also, modulation into the sound program channel may occur. On the New York–Washington coaxial circuit, a ratio of peak video signal-to-peak noise of about 54 decibels was obtained experimentally.

Crosstalk from another system tends to produce interference which shimmers, causes moving diagonal patterns, or superimposes a weak copy of the picture from the other system. This requires special attention when ordinary telephone pairs are used for video circuit. Where shielded pairs are used and in coaxial cables crosstalk is not generally a serious problem.

Future Prospects

The trend to wider and wider frequency bands no doubt will continue. These wider bands will be needed to handle the

ever increasing demand for communications and perhaps for greater definition or color television. Such wider band circuits are already under development by the Bell System.

Short-haul video circuits now generally transmit up to about four megacycles, but very short studio-transmitter links have been equalized up to ten megacycles. If such very wide band video links are needed for general local use, they can be provided by wire or radio.

The radio relay system being tried out between Boston and New York is designed for 4-megacycle television transmission over about 250 miles. Further developments are expected to make possible considerably longer circuits and, in the more distant future, wider frequency bands.

A new coaxial system now under development will use the present coaxial cable, and will permit one direction of transmission for several hundred telephone channels plus a wide band television channel on each coaxial line. If still wider bands are needed for color transmission or for greater detail pictures, this system could provide a band of the order of seven megacycles if used only for television purposes. Very much wider bands could be provided over coaxial systems, perhaps by the use of new types of amplifiers. These techniques may be applicable to radio relay systems also.

Still further in the future appear to be long distance circuits over wave guides and this possibility is being studied. Wave guides are merely hollow tubes without central conductors. These provide transmission paths for enormously wider bands sealed away from interference of all sorts.

It is quite clear that the future holds promise for advances far beyond our present status.

References

1. The Production and Utilization of Television Signals, **F. Gray, J. W. Horton, R. C. Mathes.** *Bell System Technical Journal* (New York, N. Y.), volume 6, October 1927, pages 560–603.

2. Wire Transmission System for Television, **D.K. Gannett, E. I. Green.** *Bell System Technical Journal* (New York, N. Y.), volume 8, October 1927, pages 616–32.

3. Delay Measurements, **H. Nyquist, S. Brand.** *Bell System Technical Journal* (New York, N. Y.), volume 9, July 1930, pages 522–49.

4. A Theory of Scanning and Its Relation to the Characteristics of the Transmitted Signal in Telephotography and Television, **P. Mertz, F. Gray.** *Bell System Technical Journal* (New York, N. Y.), volume 13, July 1934, pages 464–515.

5. Systems for Wide Band Transmission Over Coaxial Lines, **L. Espenschied, M. E. Strieby.** *Bell System Technical Journal* (New York, N. Y.), volume 13, October 1934, pages 654–79.

6. Crosstalk Between Coaxial Transmission Lines, **S. A. Schelkunoff, T. M. Odarenko.** *Bell System Technical Journal* (New York, N. Y.), volume 16, April 1937, pages 144–64.

7. Analysis and Design of Video Amplifiers, **S. W. Seeley, C. N. Kimball.** *RCA Review*, volume 2, October 1937, pages 171–83.

8. The Interpretation of Amplitude and Phase Distortion in Terms of Paired Echoes, **H. A. Wheeler.** *Proceedings*, Institute of Radio Engineers (New York, N. Y.), volume 27, June 1939, pages 359–84.

9. Effect of the Quadrature Component in Single Side-Band Transmission, **H. Nyquist, K. W. Pfleger.** *Bell System Technical Journal* (New York, N. Y.), volume 19, January 1940, pages 63–73.

10. Relations Between Attenuation and Phase in Feed-Back Amplifier Design, **H. W. Bode.** *Bell System Technical Journal* (New York, N. Y.), volume 19, July 1940, pages 421–54.

11. The Subjective Sharpness of Simulated Television Images, **M. W. Baldwin, Jr.** *Bell System Technical Journal* (New York, N. Y.), volume 19, October 1940, pages 563–86.

12. Television Transmission Over Wire Lines, **M. E. Strieby, J. F. Wentz.** *Bell System Technical Journal* (New York, N. Y.), volume 20, January, 1941, pages 62–81.

13. Metal-Lens Antennas, **W. E. Kock.** *Proceedings*, Institute of Radio Engineers (New York, N. Y.), volume 34, February 1946, page 85W.

14. Pulse Echo Measurements on Telephone and Television Facilities, **L. G. Abraham, A. W. Lebert, J. B. Maggio, J. T. Schott.** AIEE Transactions, volume 66, 1947, pages 541–8.

15. A New Microwave Television System, **J. F. Wentz, K. D. Smith.** AIEE Transactions, volume 66, 1947, pages 565–70.

No Discussion

A New Microwave Television System

J. F. WENTZ
MEMBER AIEE

K. D. SMITH
NONMEMBER AIEE

Synopsis: A microwave point-to-point radio system is described which is designed for the transmission of television programs. This system is intended to supplement wire facilities for local distribution of television signals from pickup points to studios or from studios to broadcast transmitters and to long distance network terminals. The circuits and equipment are described in detail. Performance obtained in tests during 1946 is given.

THE EXPECTED DEVELOPMENT of a national television network consisting of coaxial cable and radio relays will require, in addition to the intercity facilities, means for connecting pickup points with studios, and studios with transmitters or other switching points. These may be provided by wire lines or radio links, whichever proves to be more practical. In the past, wire lines equipped with video amplifiers have provided most of these end connections.[1] The advent of microwave techniques makes it feasible to utilize radio for these terminal connections where this method of transmission is suited to the purpose.

This system was designed by Bell Telephone Laboratories, particularly for fixed locations where the transmitter or the pickup point might be so isolated that wire video lines would not be practical. It was designed as a single link system, but in experimental tests has been operated with two links in tandem.

Method of Operation

This system operates on a frequency modulation basis, using frequencies from 3,900 to 4,400 megacycles. A 4–5-megacycle video signal can be accommodated.

In order to provide protection from extraneous interference and to minimize the chance of interference with other microwave systems which might be operating nearby at approximately the same frequency, it is proposed to utilize shielded lens antennas.[2] However, on short links where local conditions permit, less directive parabolic reflectors may be used. More than one channel may be multiplexed on the same antenna and this system provides pairs of filters for 2-channel operation. Of the two presently used pairs one is located at 3,930 and 4,130 megacycles, the other at 3,970 and 4,170 megacycles.

Transmitter

The microwave transmitting equipment for one channel in a cabinet attached to the rear of the antenna is shown in Figure 1. The video signal can be transmitted to it over a short length of coaxial cable making it possible to locate the control and power supply equipment in a sheltered position. This cabinet is shown on Figure 2. The present design has separate transmitting and receiving antennas, but each terminal can be equipped with filters for two one-way channels on the same antenna.

The microwave oscillator is adjustable to the allotted station frequency and determines the midband frequency which is transmitted. Metering circuits are provided for indicating departures from the designated frequency during idle periods in the program. A functional diagram of the transmitter is shown in Figure 3.

Receiver

At the receiving end, the radio frequency components again are located in a cabinet directly behind the antenna which is multiplexed for 2-channel reception. This terminal is shown in Figure 4. In addition to the radio frequency detector and beat frequency oscillator, this cabinet contains several stages of intermediate frequency amplification to permit locating the main intermediate frequency amplifier and control equipment at some distance from the antenna. The control

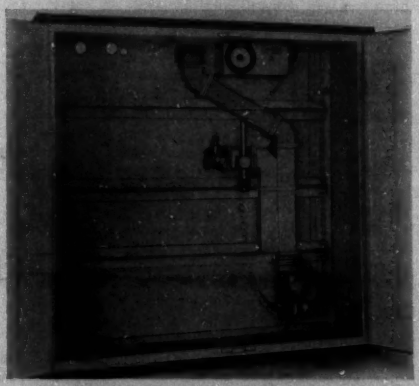

Figure 1. Transmitter radio frequency cabinet

Paper 47-75, recommended by the AIEE committee on communication for presentation at the AIEE winter meeting, New York, N. Y., January 27–31, 1947. Manuscript submitted originally November 15, 1946; final manuscript made available for printing January 17, 1947.

J. F. Wentz and K. D. Smith are both with Bell Telephone Laboratories, Inc., New York, N. Y.

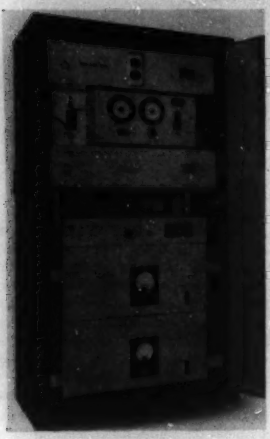

Figure 2. Transmitter control cabinet

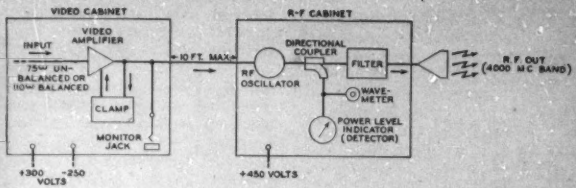

Figure 3. Transmitter—block diagram

cabinet is shown in Figure 5. The intermediate frequency is 65 megacycles, determined by means of an automatic frequency control circuit operating on the receiving beat frequency oscillator. Intermediate frequency and video amplification following the second detector is sufficient to deliver a 1-volt peak-to-peak signal to audio or video line equipment. The complete functional diagram of the receiver is shown in Figure 6.

Power Supply

The system operates from a 115-volt 60-cycle supply. This supply will be quite variable both in voltage and frequency in certain locations so the equipment has been designed with regulated rectifiers and line voltage regulators so as to eliminate fluctuations in the radiated frequency and transmission characteristics over a wide range of supply voltages.

Transmitter Details

The transmitter, shown in functional diagram on Figure 3, is arranged for single channel operation. The video signal on either balanced (110-ohm impedance) or unbalanced (75-ohm impedance) cable is applied through an adjustable attenuator to the video amplifier. The equipment is designed to accept the standard input signal of 2.00 volts peak to peak with an allowable range of 0.75 volt to 10.0 volt peak to peak.

The 3-stage video amplifier uses two *6AC7* tubes and one *6AG7*, with cathode feed-back coupling. The grid resistor of the third stage is shunted by a germanium crystal diode to improve performance at high signal levels. Output from the amplifier is obtained from a *6AG7* cathode follower, which feeds the repeller of the transmitting tube through a short length of *RG-63/U* cable. The cathode of this tube is connected through the load impedance to a regulated, but adjustable, −250-volt power supply, and adjustment of this voltage may be used to vary the operating frequency of the transmitter through a small range. A monitoring jack is provided to allow inspection of the signal actually being supplied by the video circuit to the radio frequency equipment.

The cathode follower output tube also feeds a 2-stage voltage amplifier and diode "clamp" circuit, connected in such a manner as to bring the potential of the cathode follower grid to the negative supply voltage during the start of each horizontal synchronizing pulse. The function of this clamp circuit is to establish an arbitrary reference voltage (direct current) for each picture line, and therefore to minimize low frequency distortion or interference.

Radio Frequency Unit

Figure 1 shows the transmitter radio frequency cabinet with doors opened. This cabinet has reserve space to allow installation of equipment for a second channel, using the same antenna. The transmitter tube is mounted in a shield can attached to the 1-by-2-inch wave guide at the lower right of the cabinet. This tube is similar to the beat oscillators used in radar receivers but operated at a higher power level. Figure 7 shows a typical curve of the change of frequency of the transmitting tube and the power output variation as a function of repeller

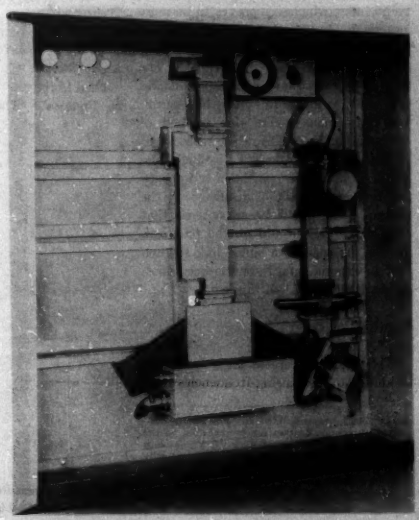

Figure 4. Receiver radio frequency cabinet

Figure 5. Receiver control cabinet

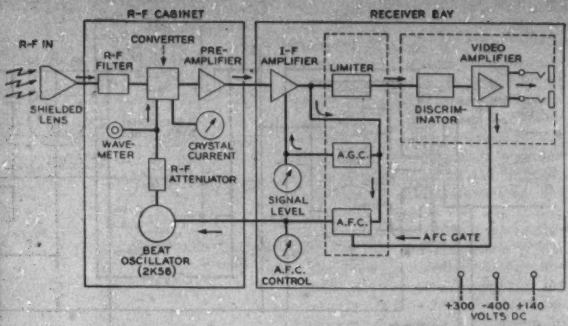

Figure 6. Receiver—block diagram

voltage. The modulating voltage normally used with the system is ten volts, peak to peak, giving a total frequency swing of four to five megacycles. The available radio frequency output power over this range is about 0.4 watt.

From the transmitting tube the modulated radio frequency energy travels in wave guide through a directional coupler to the antenna. The directional coupler is a device which feeds a small portion of the outgoing energy into the monitor circuit, which consists of an absorption frequency meter and crystal rectifier. Meters are provided for reading the crystal current in the radio frequency cabinet and in the video control cabinet. Means also are provided to connect a frequency and power measuring test set for maintenance checks and for calibration of the transmitter.

Two types of antenna may be used with the system. For long hauls, a shielded lens antenna of aperture ten feet square is desirable. A smaller shielded lens antenna of aperture five by seven feet can be used under less severe requirements. For temporary circuits over short distances, a parabolic screen antenna of 57-inch diameter may be used. The gains of these antennas, referred to an isotropic radiator, are 39, 35, and 33 decibels, respectively.

Transmitter Power Supply

The power supply voltages for the transmitter are obtained from three separate regulated rectifiers, one for each voltage required. The transmitter tube requires plus 450 volts, while the repeller electrode operates at about minus 250 volts. The video amplifier is operated at plus 300 volts. As the 10-volt modulation voltage is applied to the repeller, already at a high negative voltage, it is evident that very good power supply regulation must be maintained to prevent modulation of the output frequency by power supply ripple or line fluctuation. In addition, when transmitting television pictures, the picture content will affect the video amplifier plate current drain so that rapid load fluctuations cannot be avoided. Figure 8 shows a circuit diagram of one of the power supplies. Regulation is obtained by series regulating tubes, controlled by a 2-stage high gain d-c amplifier. The line voltage ripple in the 300-volt output is reduced to about one millivolt, and the impedance looking back into the power supply is less than one-half ohm at frequencies less than ten kc. The other rectifiers are similar.

Receiver Details

Figure 4 shows the receiver radio frequency cabinet with doors opened. The received energy passes in wave guide through a directional coupler and channel separation filter into a balanced crystal converter. The filter consists of two resonant wave guide sections, separated by a short length of wave guide. The converter is a wave guide hybrid structure which minimizes the beat oscillator energy in the signal path, prevents loss of signal energy in the beat oscillator path, and gives some balance against beat oscillator noise at signal frequency. The 65-megacycle intermediate frequency output is obtained at a 75-ohm impedance level by means of tuned transformer windings built into the converter.

Repeller voltage of the beat oscillator tube is used for manual tuning, for automatic frequency control, and to sweep the frequency for alignment of the receiver. The beat oscillator output is fed through an adjustable wave guide attenuator and an absorption frequency meter to the converter. The crystal current of either crystal may be read on meters in the radio frequency and video cabinets, and this current is used for

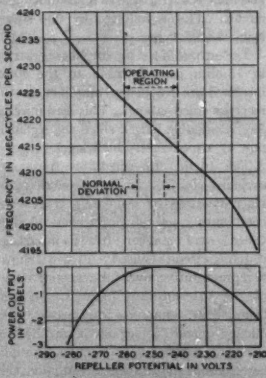

Figure 7. Transmitter—frequency deviation and power output

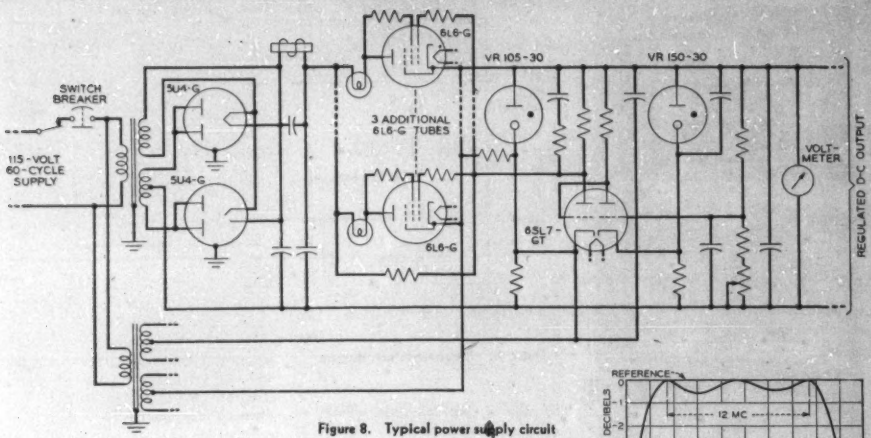

Figure 8. Typical power supply circuit

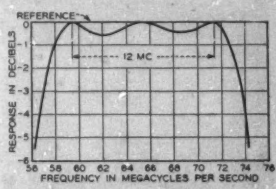

Figure 9. Receiver response at intermediate frequency output

indication of frequency meter resonance. The beat oscillator operates above the signal frequency and is so adjusted that the intermediate frequency output during the synchronizing pulse is 63 megacycles. As the transmitter is so connected that white or positive picture signals cause a reduction of signal frequency, the variation of intermediate frequency will be from 63 megacycles upward to about 68 megacycles during scanning of a white element of the picture.

The intermediate frequency preamplifier which follows the converter has three stages, giving a gain of about 35 decibels with a band width of about 14 megacycles. The first stage of this amplifier is a *6J4* tube in a grounded grid circuit. This is followed by two stages using *6AK5* tubes.

The output of the preamplifier is carried in 75-ohm coaxial cable to the main intermediate frequency amplifier in the receiver video cabinet. This lead may be any reasonable length since the signal is now at a moderately high level.

The main intermediate frequency amplifier consists of a *6J4* grounded grid stage followed by six *6AK5* stages. A combination of single tuned, double tuned and stagger tuned interstage coupling circuits is used. Figure 9 shows a representative over-all response curve of the intermediate frequency system from signal input to intermediate frequency output. The maximum gain of the main intermediate frequency amplifier is about 60 decibels. Normally, this circuit operates with considerably less gain, because of operation of the automatic gain control circuit.

The intermediate frequency amplifier is followed by a 2-stage limiter, using *6AK5* tubes. Because of the broad band and necessarily low impedance of these circuits, germanium crystal diodes are used as the nonlinear elements in the limiter circuit. Figure 10 is a simplified schematic diagram of the limiter. The plate of the first *6AK5* is transformer coupled to a pair of biased germanium crystals which present a fairly high impedance for signal voltages less than the bias value, and quite a low impedance for voltages greater than the bias value. In the circuit shown, the clipping level is about two volts peak to peak for the first stage, and about six volts peak to peak for the second stage. In the latter, the diodes are effectively across an inductive plate load. The stage following the limiter circuit contains an output network which delivers about one volt rms into the discriminator. Figure 11 shows limiter output versus input response at the center and at the edges of the intermediate frequency band.

The automatic frequency and gain control circuits also are activated from the intermediate frequency amplifier. The input amplifier drives a discriminator network which provides a sharp crossover characteristic centered at approximately 63 megacycles. This feeds a balanced grid leak detector which delivers at its plates a differential voltage proportional to the deviation of the frequency from 63 megacycles. This voltage drives a d-c amplifier and cathode follower which feeds the repeller of the radio frequency beating oscillator. A meter is provided to show the amount of control action being exerted by the automatic frequency control circuit, and thus the relative drift between the transmitting and receiving radio frequency systems.

As the automatic frequency control

Figure 10. Limiter circuit

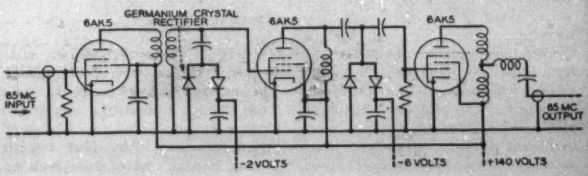

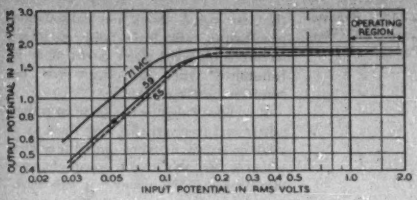

Figure 11. Limiter characteristic

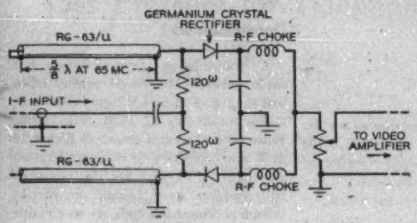

Figure 12. Discriminator circuit

must operate at a point in the signal which has the same frequency regardless of signal content, the first stage of the automatic frequency control circuit is gated by means of a positive pulse applied to its screen. This gate pulse, which is generated in the video amplifier, permits the automatic frequency control amplifier to pass a burst of intermediate frequency signal to the discriminator circuit only during a short portion of the line synchronizing pulse. A switch is provided which permits operation of the system on manual tuning when this is desired. A second switch provides a test condition by means of which the frequency characteristics of the limiter and intermediate frequency stages may be determined. The latter superimposes about 20 volts of 60-cycle alternating current on the normal repeller voltage of the beat oscillator, which sweeps it through its normal tuning range at a 60-cycle rate. By sending an unmodulated radio frequency test carrier into the converter and suitable detecting equipment, visual alignment of the intermediate frequency system can be made.

The automatic gain control circuit consists of a single-stage intermediate frequency amplifier feeding a crystal detector, a 2-stage d-c amplifier and cathode follower output tube. The cathode follower output is a voltage inversely proportional to the average amplitude of the intermediate frequency signal, and this is used to control the screen voltage of the first three *6AK5* tubes in the main intermediate frequency

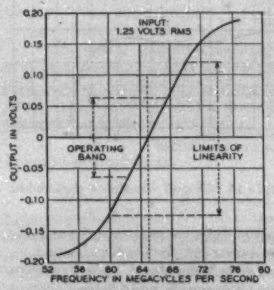

Figure 13. Discriminator response

amplifier. The operating level of the automatic gain control system is adjusted by changing the bias of the first tube of the d-c amplifier. A meter on the operating panel indicates the intensity of the signal being received.

The discriminator circuit is shown in simplified form in Figure 12. The discriminator frequency sensitive elements are two pieces of coaxial cable, each five-eighths wave-length long at 65 megacycles. One of these sections is open-circuited, the other is short-circuited. As the intermediate frequency is increased, the impedance presented by the open-circuited line will decrease, while that of the short-circuited line will increase, and as the intermediate frequency is decreased the reverse action will occur. As the germanium crystal rectifiers are connected across these line sections and are poled oppositely, the combination will provide the usual discriminator characteristic as shown in Figure 13. This circuit has been found easy to adjust and stable in operation.

The discriminator output feeds the video amplifier through a gain adjusting potentiometer, variable over a range of about ten decibels in steps of one decibel. This amplifier is a 3-stage cathode coupled feed-back circuit with provisions for either 110 ohms balanced or 75 ohms unbalanced output. The maximum gain is about 20 decibels and the maximum output about two volts peak to peak in the 75-ohm load.

A portion of the output of the video amplifier is used to drive an additional stage, which feeds a clipper tube, so arranged as to transmit only the peaks of the synchronizing pulses. These are used to trigger a blocking oscillator, which delivers gating pulses of about 1.5 microseconds duration to the automatic frequency control circuit. The constants of the circuit are so chosen that in the absence of any signal, the blocking oscillator will gate the automatic frequency control circuit at a rate slightly slower than the line frequency.

The receiver power supplies are generally similar to those used in the trans-

Figure 14. Receiver on Mount Wilson (Hollywood, Calif.)

Figure 15. Repeater on "Crows Nest" (West Point, N. Y.)

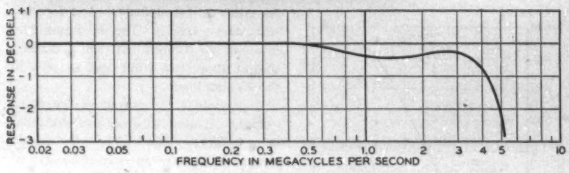

Figure 16. Over-all transmission characteristic

mitter, a separate regulated rectifier being used for each voltage required. The first two stages of the receiver video amplifier are operated with a d-c heater supply to minimize hum.

Test and Alignment

Desirable test equipment consists of a radio frequency signal generator, a frequency-power meter, a video test signal generator, and intermediate frequency detector unit, a test oscilloscope, and radio frequency and intermediate frequency attenuators. A picture monitor is also desirable but not necessary. A vacuum tube voltmeter and d-c analyzer are convenient for trouble shooting.

The procedure used in setting up a link for operation would depend on local conditions and type of antenna. Generally, a telephone order wire would be useful in orienting the transmitter antenna for maximum energy at the receiver end. The receiver antenna, of course, may be oriented by observation of the received signal level. A video test signal is applied next and examined with an oscilloscope at the receiver. If the received signal is consistently strong, the test signal shows no transmission peculiarities, and little noise or interference is observed when carrier alone is transmitted, then the circuit may be considered satisfactory.

If no line-of-sight exists between transmitter and receiver, this may show as a weak or erratic signal or one with echoes which is very sensitive to small changes of transmitted frequency. A sun flash from a hand mirror may be of assistance in checking a doubtful path.

Demonstration

A transmission demonstration was made between Hollywood central office and the top of Mount Wilson in southern California on July 17, 1946. The Mount Wilson installation is shown in Figure 14 as it was used for a later demonstration on August 22, 1946.[3] On this occasion, two systems were looped on Mount Wilson so that both ends were available at the Hollywood end.

While the equipment is not strictly portable, it was moved to other locations to pick up important events in the fall of 1946. Some of the earliest ones were at the Los Angeles Coliseum on August 25, 1946, Burbank (Lockheed Airport) on September 9, 1946, and Pomona on September 15, 1946. Later a 2-link system was set up between the United States Military Academy at West Point and New York and used first on October 5, 1946, for the Army-Cornell football game. Figure 15 shows a repeater installation on top of "Crows Nest" mountain. Figure 16 shows an over-all transmission characteristic of the system from transmitter video input to receiver video output.

References

1. Television Transmission Over Wire Lines, **M. E. Stieby, J. F. Wentz.** *Bell System Technical Journal* (New York, N. Y.), January 1941.

2. Metal Lens Antennas, **W. E. Kock.** *Proceedings*, Institute of Radio Engineers (New York, N. Y.), November 1946.

3. Television Link Test in Southern California, **Paul B. Wright.** *Communications* (New York, N. Y.) October 1946, pages 15 and 55.

No Discussion

Gas Pressure for Telephone Cables

R. C. GIESE
MEMBER AIEE

Synopsis: Communication cables consist of a number of electric conductors insulated from one another and encased in a metal sheath. This encasement is subjected to numerous hazards, such as those caused by electrolysis, crystallization, various kinds of mechanical damage, and lightning burns. Any damage to the sheath which will permit water to enter the cable will decrease the effectiveness of the insulation material and thus cause an impairment or an interruption to the service. The entrance of moisture through small openings in the sheath can be materially retarded when the space inside the cable, not occupied by the conductors or insulation, is filled with a gas maintained under controlled conditions. Nitrogen is the gas usually used for this purpose because it is inert and does not combine chemically with the conductors or insulation. In addition the use of the gas provides a method of locating openings in the sheath by means of a pressure gradient, which is a material aid in cable maintenance.

IN 1926, the idea of making the cables gastight and maintaining them under continuous internal pressure was conceived along with the plan of providing some form of mechanical device which could be connected permanently to the cable and so arranged that a decrease of pressure would operate an electric alarm. The first work done in the field employing these principles was in the early part of 1927, using dry nitrogen gas. From that date to the present time, there has been a continued development in the technique of employing gas under pressure for the purpose of keeping moisture out of the cables and as a means of locating small openings in the sheath.

Service Considerations

In utility work, service is the commodity offered to the customer and reliability of service is a prime consideration in marketing service.

With the advent of carrier development, the number of circuits carried in a cable increased tremendously and the importance of avoiding interruptions to service increased proportionately. This is exemplified by the 225 voice frequency circuits afforded by a full size cable, which compares with a circuit possibility of over 2,000 for a cable of the same size containing coaxials and paper insulated conductors operated on a carrier basis.

To protect this concentration of circuits from interruption, all of the long toll cable plant is maintained under gas pressure. As of March 31, 1946, the status of this work is indicated in Table I.

Layout Considerations

In order to apply gas under pressure to the practical maintenance job, it has been found desirable to install gastight plugs, at intervals, which will confine the gas to a limited length of cable. Figure 1 presents a picture of a typical gas section.

The length of cable included in one gas section will depend upon the resistance to the flow of gas in the cable and the degree of protection required. In general, this length is between 50,000 and 60,000 feet, but sections as short as 25,000 feet, or as long as 34 miles have been employed in actual practice.

Because the gas is placed in the cable so as to prevent moisture from entering through small openings in the sheath, it is essential that a certain limited pressure range be maintained. In order to determine when this pressure has reached the minimum limit, a low pressure warning device, called a contactor, is provided at regular intervals. This unit consists of a Bourdon tube and electric contacts with associated mechanical features, arranged in such a way that the electric contacts normally are held open by the pressure of the gas. When the pressure falls below a certain predetermined value, the contacts close and place a short circuit across a pair of conductors, called the "alarm pair", which operates an alarm in an adjacent attended office. Assuming a normal underground or buried gas section of 60,000 feet, one such contactor usually is placed about 5,000 feet from each end of the gas section and four others are spaced uniformly along the cable at 10,000-foot intervals.

To provide a means of measuring the pressure of the gas, valves similar to those used in automobile tires are spaced fairly uniformly along the cable about 3,000 feet apart. Some deviation from this spacing, however, is permitted if the location of the valves can be made more accessible to the maintenance personnel Such valves also are provided at the location of each contactor and on each side of the gastight plugs.

Table I. Miles of Toll Cable Maintained Under Gas Pressure

	Toll Cable Maintained Under Gas Pressure		
	Total Miles	Miles Under Pressure	Percentage of Total
Aerial	18,629	13,245	71.1
Underground	12,230	9,784	80.0
Buried	9,547	9,318	97.6
	40,406	32,347	80.1

In addition to contactors and valves, there also is provided at each contactor location a means whereby the maintenance forces can connect a telephone to a pair of conductors and establish communication between these points and an attended telephone office. The pair of wires in the cable for this communication is commonly referred to as a "talking pair,"

Paper 47-37, recommended by the AIEE committee on communication for presentation at the AIEE winter meeting, New York, N. Y., January 27–31, 1947. Manuscript submitted November 12, 1946; made available for printing December 12, 1946.

R. C. GIESE is with American Telephone and Telegraph Company, New York, N. Y.

The author wishes to express his appreciation to colleagues in his own organization for their assistance in the compilation of data and preparation of the paper.

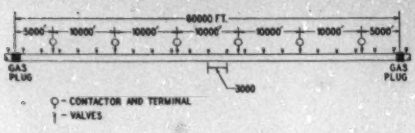

Figure 1. Typical cable gas plug section showing plugs, valves, contactors, and terminals

which is stubbed out of the cable and connected to a terminal in a watertight housing.

Pressure Ranges Used in Cable Work

The alloys used in cable sheath and sleeves will withstand satisfactorily a unit stress of about 150 pounds per square inch without undue elongation. Stresses in the walls of cylindrical objects, such as sheath and sleeves, caused by internal pressures, can be computed from the formula

$$P = 2ST/d$$

where

P = internal pressure in pounds per square inch
S = unit stress in pounds per square inch
T = wall thickness of the cylinder in inches
d = inside diameter of cylinder in inches

Applying the formula to both sheath and sleeves shows that the sleeve is controlling and that a $4^1/_2$-inch sleeve limits the pressure to a maximum of ten pounds per square inch.

It does not appear desirable to establish a nominal cable pressure equal to this maximum permissible sustained pressure of ten pounds per square inch because of the likelihood of exceeding it as a result of an incorrect estimate of the temperature during charging, creepage of pressure regulators, and so forth. Accordingly, a 1-pound tolerance has been established, resulting in a nominal cable pressure of nine pounds per square inch.

From a protection to service standpoint, experience has indicated that a buried or underground cable is fairly well protected, if the average pressure between a plug and a leak does not drop below two pounds per square inch, which is sufficient to withstand a hydrostatic head of four feet of water. For aerial cables this limit is reduced to one pound per square inch, as it is not necessary to keep out a head of water and the one pound per square inch is usually adequate to prevent moisture from being drawn into the cable at a sheath break with the temperature swings normally encountered.

In addition to these upper and lower limits, some pressure range must be available to take care of normal losses between recharging periods, protection to service, contactor adjustment limits, and so forth. The pressure values used in practice are summarized in Table II.

Fundamental Theory

General familiarity exists regarding the laws governing the flow of water through pipes, and the analogy between this action and that of the transmission of an electric current over a conductor. In each case the rate of flow between any two points of the system depends upon the difference in pressure and the flow resistance offered by the conducting medium. The resistance to the flow is affected by such factors as the configuration, kind, and size of the conducting material.

The flow of gases through pipes behaves in a very similar manner. In looking at the cross section of a cable, the space under the sheath appears to be filled; however, the space between insulated conductors and the porosity of the insulation account for 50 to 70 per cent of the total volume, so that the cable is in reality a pipe partly filled with various types of materials. The air or gas space around the conductors provides numerous paths for the flow of gas, which in turn offer considerable resistance to the flow. Figure 2 shows the cross section of two cables—one containing paper insulated conductors and the other containing coaxial conductors.

It has been found experimentally that within the range of pressures normally employed in cable work, the volume of gas flowing through a given length of a particular cable under steady flow conditions is approximately proportional to the pressure drop over the length. The ratio between pressure drop and volume of flow is called pneumatic resistance and this relationship may be expressed mathematically as

$$R = P/F, \text{ or } P = FR$$

where

P = pressure drop in pounds per square inch per 1,000 feet of cable
F = volume of flow in cubic feet (at atmospheric pressure) per hour
R = total pneumatic resistance

It will be noted that this formula is analogous to Ohm's Law for an electric circuit—$R = E/I$.

The total pneumatic resistance R of a cable can be determined by applying gas to one end of a length of cable, with the other end open. After a steady flow has been established, the volume of gas used over a fixed period of time, with the pressure constant during this period, is read and recorded. From these data and the formula $R = P/F$ the value of total pneumatic resistance is calculated.

The values of total pneumatic resistance R for any two cables cannot be compared directly, because the sizes of the cables may be different. Also two cables of the same size but of different makeups will not have the same total pneumatic resistance. It is apparent, therefore, that some basic unit of cable pneumatic resistance must be established and that all other cables must be equated in terms of this basic cable. To this end, unit pneumatic resistance has been defined as the resistance offered to the steady flow of gas by 1,000 feet of a cable of unit cross sectional area (1-inch diameter inside sheath) and of such core structure that the steady rate of gas flow through it will be one cubic foot (at atmospheric pressure) per hour for each pound of admission pressure. Such a basic cable is said to have a pneumatic resistance of one.

Table II. Normal Maintenance Pressures Used on Cables

	Underground or Buried Cable	Aerial Cable
Maximum charging pressure	10	7
Nominal pressure	9	6
Recharging pressure	7	4
Contactor operating pressure	6	3
Minimum pressure	2	1

The above values are the corrected equivalent at a temperature of 60 degrees Fahrenheit.

The resistance of electric conductors is based on the specific resistance of a sample of the conducting material of unit length and unit cross sectional area. The total resistance of a unit length of conductor is equal to its specific resistance divided by the area of the cross section of the conductor. In similar manner, the total pneumatic resistance R of a unit length of a particular cable will be the specific or unit pneumatic resistance (the resistance per unit of cross sectional area) divided by the cross sectional area inside the sheath. If a cable of one inch diameter under the sheath is considered as having unit cross sectional area, the relation between the total pneumatic resistance R

and specific or unit pneumatic resistance r of a cable will be

$R = r/d^3$, or, by transposition, $r = Rd^3$

where

d = outside diameter of the lead sheath in inches (as sheath thickness increases with core diameter, the outside sheath diameter, for practical purposes, can be used in the expression for core area instead of the diameter inside the sheath) and both R and r are expressed in units of pneumatic resistance.

With total resistance R of a given cable determined from field test, the unit resistance r can be calculated. This value of unit resistance r then can be compared directly with the unit resistance of any other cable for the comparison of gas flow characteristics. This unit pneumatic resistance is used in determining proper maintenance procedures, which depend upon such factors as the rate of propagation, the permissible gas loss consistent with adequate protection to service, the shape of the leak gradient, and the time for equalization after charging.

Corrections for Pressure Measurements

Pressure measurements are made under varying temperatures and barometric conditions, at different altitudes, and by various types of instruments. Such readings could not be compared or used on maintenance work unless they all are referred to a common reference base. Such a base has been established using 60 degrees Fahrenheit for temperature, sea level for elevation, and 30 inches of mercury for barometric pressure.

Variations in Pressure Caused by Changes in Temperature

Cables are subject to rapid and rather wide variations in temperature but the volume of the gas remains almost constant because the expansion and contraction of the cable sheath caused by temperature variations are so small as to be negligible. Because changes in temperature do not materially change the volume of the space occupied by the gas it is evident that changes in temperature will cause changes in pressure. This can be expressed by the equation $T_1/T_2 = P_1/P_2$, where pressures and temperatures are expressed in absolute values.

Pressures normally are measured as pounds above one atmosphere, which is 14.7 pounds per square inch absolute at sea level at a temperature of 60 degrees

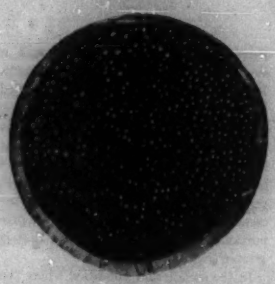

Figure 2. Cross section of two cables—one containing paper insulated conductors and the other containing coaxials and paper insulated conductors for control purposes

Fahrenheit. Figure 3 shows a family of curves based upon the foregoing equation. As an example, consider a cable with a pressure of 17.7 pounds per square inch absolute at a temperature of 60 degrees Fahrenheit. This would equal a measured pressure of 3 pounds per square inch above one atmosphere at sea level. If the temperature of this cable were increased to 100 degrees Fahrenheit, the

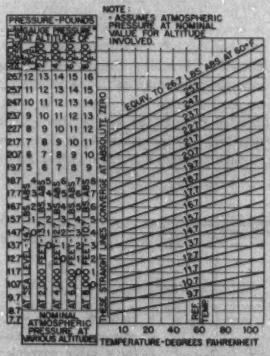

Figure 3. Family of curves of pressure versus absolute temperature

absolute pressure would then be 19.1 pounds per square inch, which is 4.4 pounds per square inch above one atmosphere at sea level.

An approximate rule for temperature changes is that a 25-degree-Fahrenheit change in temperature will change the measured pressure one pound per square inch.

From the foregoing text, it should be quite evident that when measuring the pressure of the gas in a cable it is imperative to take into account the cable temperature at the time the pressure measurement is made.

Variations in Pressure Caused by Changes in Weather

The absolute pressure exerted by the atmosphere may vary from hour to hour and may reach a magnitude of one pound per square inch in 24 hours during rapid changes in weather conditions.

The measurement of the gas pressure in a cable usually is made with some form of mechanical pressure gauge or by an open-end manometer. Such measurements actually indicate the difference in pressure of the gas in the cable and the pressure of the atmosphere at that location. It would be possible to measure the absolute pressure of the gas in the cable by using a vacuum-sealed type of manometer similar to a mercury barometer. Because of the length of such an instrument and the difficulty of its operation under field conditions, it has been found more practical to measure the difference in the two pressures.

As the cable forms a closed gas chamber and is not influenced by changes in barometric pressure, a comparison of readings taken before and after changes in the barometric pressure may lead to the conclusion that the pressure in the cable has changed. Therefore, for accurate comparison of measurements of gas pressure, which are required in certain maintenance operations, it is necessary to correct for barometric variations, which may be a positive or a negative value, from the standard of 30 inches (14.7 pounds per square inch) of mercury.

Variation in Pressure Caused by Changes in Altitude

At sea level, under normal 30-inch barometric pressure, the pressure of one atmosphere is 14.7 pounds per square inch and represents the pressure exerted by the weight of the column of air above the earth. At altitudes above sea level this weight becomes less because of a decrease in the height of the column of atmosphere

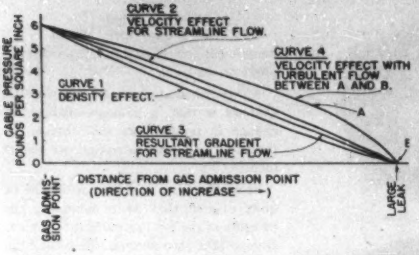

Figure 4. Steady flow gradients

and the change in its density. For altitudes of 8,000 feet or less, that is, in the practical range where cables may be installed, the effect of changing density is too small to be significant. Accordingly, a uniform change in weight of atmosphere with change in elevation of one-half pound per square inch per 1,000 feet is used.

Where a cable is placed over terrain which has changes in elevation, the measuring devices will reflect the changes in atmospheric pressure, but are complicated further by the fact that the column of nitrogen gas in the cable also has weight. At 9 pounds per square inch pressure, the weight of a column of nitrogen 1,000 feet high is 0.8 pound per square inch; at 6 pounds per square inch pressure, this weight is 0.7 pound per square inch. In practice, tables are used to correct for the combined effect of the weight of the nitrogen in the cable and the change in the weight of the column of air outside the cable. For a cable maintained at a pressure of 9 pounds per square inch, this correction amounts to 0.3 pound per square inch per 1,000-foot change in elevation.

Effects of Compression, Density, and Velocity

The structure of a given make-up of cable is essentially uniform in all parts of its length. The amount of friction or resistance offered to the flow of gas at any point along the length of a cable, therefore, will depend on the number of the molecules of gas coming in contact with the surfaces of the cable core as well as the manner in which contact is made. Broadly speaking, friction is determined by the density of the gas and its velocity of flow. The density of the gas varies in proportion to its absolute pressure. At low velocities, the flow is streamline and friction is approximately proportional to velocity. At higher velocities, flow becomes turbulent and friction becomes proportional to a power of velocity that is greater than one.

In the steady flow condition where the input pressure is 6 pounds per square inch, the densities of the gas at the input and exhaust ends of the cable will be in the ratio of (14.7 + 6) to (14.7 + 0) or approximately 1.4. The friction or pressure drop in the foot of cable adjacent to the gas admission point, therefore, should be 1.4 times that in the foot of cable adjacent to the exhaust end. The effect of density on the steady flow gradient can be approximated as shown by curve 1 of Figure 4, which is constructed so that its relative slope varies continuously from 1.4 at the admission point to 1.0 at the exhaust end. This indicates that the variation in density tends to make the gradient concave upward in shape.

The volume of a given quantity of gas is inversely proportional to its absolute pressure. Thus a cubic foot of gas admitted to the cable at 6 pounds per square inch gauge pressure at the input end becomes 1.4 cubic feet of gas as it is exhausted through the leak at atmospheric pressure. As the gas expands during its passage through the cable (which has a constant volume per unit of length) its velocity increases from a relative value of 1.0 at the admission point to 1.4 at the exhaust end. The friction or pressure drop per unit of length will vary accordingly as approximated by curve 2 of Figure 4, which is constructed so that its relative slope varies continuously from 1.0 at the input end to 1.4 at the exhaust end. Curve 2 indicates that the variation in velocity tends to make the gradient concave downward.

At low velocities where flow is streamline and resistance is proportional to the first power of velocity, the effects of changing density and velocity should be of about the same magnitude and should counterbalance each other so that the resultant gradient is substantially a straight line, curve 3 of Figure 4.

Because the velocity of flow increases as the gas approaches the leak, streamline flow conditions prevail in the input end of the test section while at the same time turbulent flow is occurring in the end of section adjacent to the leak. Under these circumstances, the friction or pressure drop per unit of length is greater in the portion of the cable subject to turbulent flow and the gradient representing the velocity effect assumes the general appearance indicated by curve 4 of Figure 4. This, of course, will overbalance the density effect and the resultant gradient is concave downward.

From the foregoing, it is apparent that the normal pressure gradient toward a leak in a cable is concave down, with the steepest part of the gradient occurring immediately adjacent to the leak. This contrasts with the straight line pressure drop gradient along a uniform conductor in an electric circuit.

Effect of Leaks and Method of Location

Effect of Leaks

When stable gas pressure conditions prevail in a gastight cable the gas distributes itself evenly throughout the gas section and the pressure gradient (neglecting temperature and altitude effects) becomes essentially a straight line as shown in Figure 5.

When a leak occurs, the cable pressure at the leak is reduced and gas flows toward the leak from points of higher pressure on each side. This causes a progressive drop in pressure away from the leak in both directions and the sources of gas at initial pressure become farther and farther removed from the sheath opening. As a result, the shape of the gradient changes continuously after a leak occurs.

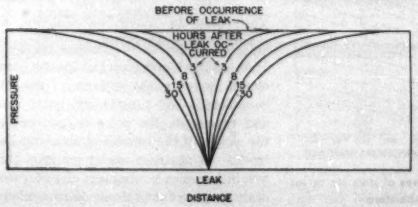

Figure 5. Leak gradients—variation with time for a cable containing paper insulated conductors

At any elapsed time, however, the gradient, unless disturbed by influences other than the leak, will be of the general characteristic shape shown in Figure 5, that is, concave downward with increasing slope as the leak is approached. Stoppages or irregularities in the cable's structure, temperature variation, addition of gas, incomplete equalization, and loss of gas caused by other leaks will distort the shape of the gradient.

Normal gradient shape is controlled by the unit pneumatic resistance of the cable, size of leak, elapsed time after occurrence of the leak, initial cable pressure, and position of the leak with respect to the ends of the gas section.

An instantaneous picture of the pressure relationship at any given time, within the disturbed distance, is known as a true leak gradient. In order, therefore, to secure a true leak gradient, it would be necessary to obtain simultaneously a large number of pressure readings at short spacings along the cable. This is impractical and various methods have been devised to attain a close approximation to this conditions.

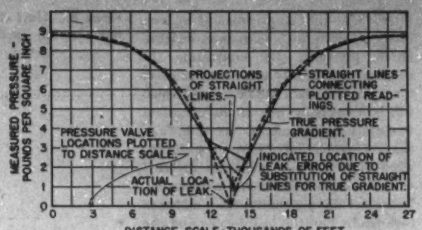

Figure 6. Large true leak gradient and simulated practical equivalent

General Principles of Leak Location

The shape of the pressure gradient always reflects the various influences that are acting on the gas in the cable. When a large leak is the only factor disturbing the equalized pressure conditions, the gradient will assume the characteristic shape shown in the dashed lines on Figure 6.

Leak location by means of pressure measurements is based on the principle of obtaining the closest possible approximation of the shape of the true gradient so that the point of lowest pressure—which occurs where the gas is escaping through a leak—can be determined accurately. To facilitate this process, permanent valves are installed at about 3,000-foot intervals along the cable. When the pressures measured at these valves are plotted and connected with straight lines as shown on Figure 6, an approximation of the true gradient shape is obtained. By projecting the lines from the two points of lower pressure until they intersect, as shown by the dotted lines of Figure 6, the approximate location of the leak is indicated. This technique is quite satisfactory where a large leak occurs in a long gas section which is not affected severely by temperature changes.

In the case of small leaks the pressure at the leak will not drop to atmospheric pressure, so that there is less difference in pressure between the normal sustained pressure and the pressure at the leak; this results in a very flat gradient, and perhaps there is not a sufficient pressure drop between adjacent valves to observe a difference in reading on the manometer. Where such leaks are encountered, they must be allowed to remain until they enlarge with time, or more sensitive instruments must be used.

There are various conditions tending to produce significant variations from a true leak gradient which may be summarized as follows:

1. Temperature changes which cause the pressure in the cable to vary appreciably during the period while leak location readings are being made.
2. The loss of gas through the leak during the interval required to make successive readings, because simultaneous readings usually cannot be made.
3. The gas lost in applying and removing the measuring device to and from the cable at each reading point
4. Lack of instrument sensitivity, personal errors in reading instruments, and cleanliness of the mercury and tube of the manometer.
5. Irregularities in a gas section such as a partially plugged splice, a second leak, or a change in the cable make-up.
6. Lack of complete equalization, encountered particularly in combination aerial and underground gas sections, where temperature variations establish shifting pressure heads.

Various means have been devised and are in use for minimizing the effects of the above conditions and they are discussed under "Leak Location Methods."

As a general rule it is advisable for one man to make all the pressure readings, make them as rapidly as possible consistent with accuracy, and to have a uniform interval between the readings. The points then are plotted on a graph paper, using the vertical co-ordinate for pressure and the horizontal co-ordinate for distance and joined by straight lines. By inspection of the gradient, it is possible to note whether it approximates a true gradient; that is, the steepness of the gradient should increase on each side as the location of the leak is approached. If these conditions prevail, the projections are made from the two lower measured points to determine their point of intersection, which should be the location of the leak on the horizontal distance scale. The leak then can be located by soaping the cable at the indicated location and observing for bubbles. If the gradient secured does not approximate a true gradient, the irregularities first must be cleared, the cable recharged, and new pressure gradient data taken.

Leak Location Methods

2-Cable Method. Where there are two cables on the same route, with identical layouts, and one of them develops a leak, pressure readings can be taken on both cables instead of only on the leaky cable. Both cables will have their measured pres-

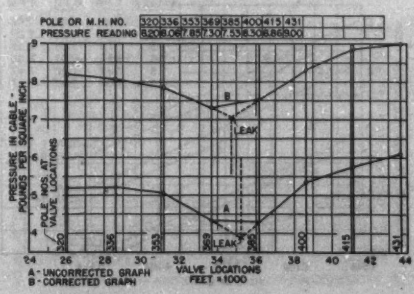

Figure 7. 2-cable method of leak location

sures affected in a similar manner by temperature, elevation, and changes in barometric pressure. By subtracting the readings on the leaky cable from those of the good cable, data will be secured which will be essentially free of the effects of temperature, barometric pressure, and changes in elevation. However, such data when plotted would afford an inverted gradient which might result in confusion. To correct this possibility, ten is added to each reading on the leaky cable and the readings on the good cable subtracted from these new leaky cable values, thus affording data for a normal leak gradient. As an example, if the leaky cable reading in pounds per square inch is 5.20 and the good cable reading is 7.0, the value to be plotted would be 5.20 plus 10 minus 7, or 8.20.

Curve *A* of Figure 7 shows the gradient obtained from pressure readings made only on the leaky cable, which are affected by changes in temperature, barometric pressure, and elevation. Curve *B* of Figure 7 shows the gradient obtained by the 2-cable method in which these variations were eliminated, resulting in a more accurate location of the gas leak.

This method is particularly valuable on aerial cables and cables which traverse terrain of varied elevation.

2-Tank Method. In this method a tank of gas is connected to the cable on each side of the leak and at a sufficient distance away to permit a reading at three valve points on each side of the leak. Gas is allowed to flow from each tank toward the leak until steady flow conditions have been established, as indicated by no change in the reading in pressure of a valve location over a 15-minute period. Gradient readings then are taken and plotted for a leak location under stable gas flow conditions. A modification of this method is employed during cable construction; this entails joining three unspliced lengths of cable with lead pipe, the center section being the one showing leakage. The ends and junctions afford reading points for gradient data.

Figure 8. Short circle leak location method

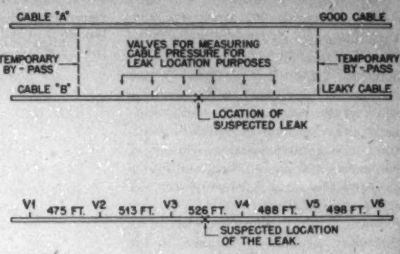

Short-Circle Method. This is an adaptation of the 2-tank method which can be used on multicable routes. The good and leaky cables are joined together with a temporary by-pass on each side of the leak, as shown in Figure 8.

This method, in addition to tending to stabilize the gradient because of the larger reservoir of gas (two cables) available for supplying the gas lost through the leak, is used also where more than one leak exists in a cable. The method eliminates any distortion of the gradient from a second leak or irregularity which might be located beyond the temporary by-passes.

2-Direction Method. This method requires starting on one side of the suspected leak, reading the pressure along the cable toward the leak at three or more valve locations, then reading at three valve points beyond the leak; after reading at the farthest valve point, all the previous valve points are read in the reverse order. Average the two readings at each valve point and plot the resulting values. If the travel time in each direction is the same and the interval between readings is uniform, the resulting gradient is approximately the same as if all readings were secured simultaneously, and, therefore, correction is made for the effect of a pressure drop caused by the loss of gas through the leak during the interval required to make the readings. The 2-direction method requires more time for obtaining readings and averaging them, and does not correct for temperature, altitude, or barometric changes.

Time-Pressure Method. This method is a refinement of the 2-direction method. It requires that four sets of readings be made at three valve locations on each side of the suspected leak location, taking each set in the same direction, and recording the time the readings were made as well as the pressures measured. Graphs then are made of the four readings taken for each valve point by plotting pressure against time as shown in Figure 9.

The curves plotted for each valve point should be similar if no other irregularities exist, and an occasional error in reading or recording can be detected immediately by observing a dissimilarity of the curves. Vertical time lines then are drawn through the plots to secure equivalent instantaneous values of pressure at each valve location. These data are shown tabulated in Figure 9.

Leak gradients then can be plotted from these data as shown in Figure 10.

Effectively this method provides data for any number of leak gradients using theoretical simultaneous readings at all valve points. The leak location for all gradients can be averaged.

This method, while requiring more time and work, affords greater accuracy and is considered warranted where a cable is in conduit or buried where it is desirable to keep digging to a minimum in locating and clearing a leak. This method, however, does not correct for temperature, altitude, or barometric variations.

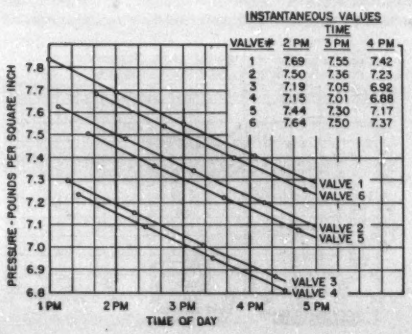

Figure 9. Time-pressure curve—pressure point plot

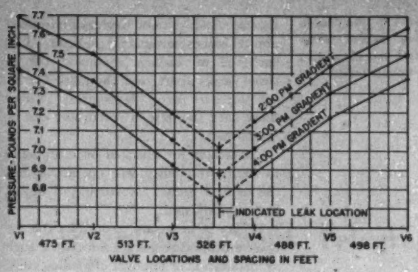

Figure 10. Time—pressure curve—leak gradients

Where pressure drops between 3,000-foot spaced valves are appreciable, it may be desirable to install intermediate valves, so as to reduce the spacing between reading points and thereby improve the accuracy of the resultant location.

Charging and Recharging Cables With Gas

Cables are charged initially to a pressure of one pound per square inch above nominal pressure, that is, to ten pounds per square inch in underground or buried cable and to seven pounds per square inch in aerial cable. When the pressure drops to seven pounds per square inch on underground and buried cable and to four pounds per square inch on aerial cable, because of seepage losses, the cable is recharged to the initial pressures.

Standard points for the admission of gas are established by dividing the gas section into equal lengths of $1^1/_2$ to $2^1/_2$ miles and locating the admission point at the midpoint of each such section. It has been found by field test that the time required to charge or recharge a cable to an equalized condition depends on the number of charging points, being about inversely proportional to the square of the number of charging points. For example, it will take one-ninth the time to charge a gas section with three charging points as would be required using only one charging point.

In practice, tables are used for setting cylinder regulators at the pressure required to provide the ultimate equalized pressure desired at the equivalent of 60 degrees Fahrenheit and 30 inches barometer. Also, elevation changes in a given gas section must be considered, the cylinders at higher elevations being set at correspondingly lower values to correct for the weight of the column of nitrogen gas.

Before charging it is desirable to know how much gas will be required. A basic unit has been established arbitrarily and it is called the charging constant, designated K. It is defined as the number of cubic feet of gas required to raise the pressure in 1,000 feet of cable one pound per square inch. This can be determined by field test on one cable. For other cables, the value of K then can be determined, because the gas capacities and charging constants are closely proportional to their cross sectional areas or to the squares of their respective diameters; that is, $K_1/(d_1)^2 = K_2/(d_2)^2$. Knowing K for any given cable, the length of the gas section and the average pressure increase which the charging must accomplish, the required volume of gas needed in the cylinders can be determined from the formula

$$G = KL(P_e - P_a)$$

where

G = cubic feet of gas to be admitted
K = charging constant
L = length of cable in thousands of feet
P_a = average pressure of gas section at start of charging
P_e = average desired equalized pressure of gas section at end of charging

On multiple cable routes where two cables form part of the same circular gas section, connection is made to both cables at each charging point, thus simplifying the charging and reducing the number of cylinders required.

The charging gradient, if measured during the charging interval, would be similar to an inverted leak gradient.

Design Considerations

The design and layout of gas sections are predicated upon securing adequate protection to service, consistent with cost and simplicity of maintenance effort.

Figure 11, curve B shows the time required for the average pressure between a large leak and the end of the gas section to fall from nine to two pounds per square inch. The vertical ordinate for any distance, therefore, indicates the elapsed hours following the occurrence of a leak during which the cable will be protected by a reservoir of gas with an average pressure head in excess of two pounds per square inch.

With a contactor set to operate at six pounds per square inch and cable maintained at a nominal pressure of nine pounds per square inch, some time will elapse after the occurrence of a leak before the cable pressure at the contactor reaches the six pounds per square inch operating value; this time varies, depending upon the proximity of the contactor to the leak. Figure 11, curve A shows this time–distance relation for a contactor spacing of two miles throughout the section, except for the first contactor which is located one mile from the end of the gas section.

The time available for location and clearance of a leak located at any distance from the end of the gas section can be secured by noting the hours on the vertical ordinate between the two curves A and B in Figure 11. This time, which is known as permissible delay time, is zero at the end of the gas section and increases to well over 100 hours for leaks occurring beyond the second contactor.

It would be possible, of course, to increase contactor spacing, but the contactor operating time goes up in proportion to the square of the distance to the leak, as shown by the dashed extension

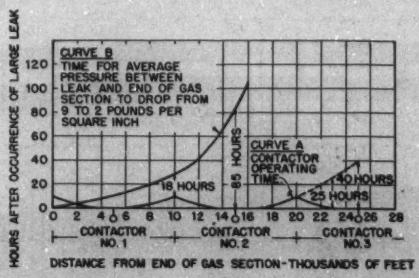

Figure 11. Delay time and contactor-operating time

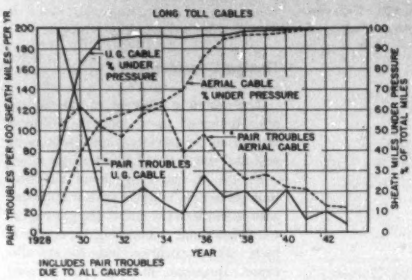

Figure 12. Progress of placing cables under pressure and contrasting trouble results

on curve *A* in the lower right hand corner of Figure 11.

In practice it has been found to be expedient to establish a uniform spacing of about 10,000 feet for contactors on underground and buried cables and about 16,000 feet for aerial cables. This spacing is halved at the end of a gas section, for the reasons outlined. Wherever possible, two cables on the same route are connected together to form a circular or continuous gas section, thus eliminating the vulnerable end section where pressures drop rapidly and deplete the reservoir of gas available to protect service. With the contactor spacings fixed and uniform, the permissible delay interval in responding to contactor operations can be set safely at a fixed interval of about 70 hours in a circular gas section. In a straight gas section this 70-hour interval also is used for most of the contactors, with a reduced interval for contactors located near the end of the section. Thus, for the most part, simplicity and uniformity in spacing and contactor response time is achieved. The 70-hour interval, during which the leak must be located and cleared (or more gas added to the section), was selected to permit scheduling work in an orderly manner, during daylight hours on regular working days.

When cable length makes it impractical to form a long gas section, several cables may be connected together to secure the larger reservoir. Where short isolated cables only are involved, a reservoir of gas adjusted to feed continuously at nominal cable maintenance pressure may be connected to the cable. Various control measures, such as contactors and reservoir exhaustion indicators, are used on such installations.

Maintaining Cables Under Pressure

After a cable has been charged with gas and equalized, it is necessary to determine when recharging will be necessary, in order to schedule the work and to insure that it is done before the average cable pressure drops to contactor operating pressures and false alarms occur. This is accomplished by reading the pressure at regularly spaced valves about 18,000 feet apart, averaging them and correcting the readings to 60 degrees Fahrenheit and 30 inches barometric pressure. Two such sets of readings are made, two or three weeks apart, and the rate of average pressure drop determined. From these data the date of recharging can be established.

Contactors are checked once annually to insure that they will operate within the desired limits. If outside of limits, they are adjusted.

It may be necessary to open a cable for reasons other than gas pressure work, such as installation or removal of loading coils, or clearance of conductor trouble, resulting in a loss of gas. Tables have been prepared indicating how long splices may be left open in various parts of a gas section without endangering service. Where splices are open longer than established by these limits, cylinders of gas must be attached to the cable to keep the pressure within safe limits. After the cable is closed, the lost gas is restored.

Trouble Results

Figure 12 shows the results attained on the longer toll cables during the past 18 years in reducing the pair troubles per 100 sheath miles of cable contrasted with the progress of placing cables under gas pressure. These troubles include failures from all sources, such as total failures from foreign workmen severing cables, which account for some of the trouble peaks during periods when a large portion of the cable was already under pressure. With the training programs now being given on gas pressure and improvement in maintenance methods, still further reductions in troubles are anticipated and fuller more-comprehensive coverage of the maintenance job is anticipated.

No Discussion

Frequency Shift Telegraphy—Radio and Wire Applications

J. R. DAVEY
NONMEMBER AIEE

A. L. MATTE
MEMBER AIEE

Synopsis: Frequency shift telegraphy is described and compared with amplitude modulation telegraphy under various conditions found in radio and wire transmission. Experimental data are given to demonstrate the influence of various design factors on the over-all performance under these conditions. It is shown that the most outstanding characteristic of the frequency shift method is its ability to accept large and rapid changes in signal amplitude. Frequency shift telegraphy thus proves to be of great advantage for use in the high-frequency radio range. Frequency shift telegraphy also shows an advantage over amplitude modulation telegraphy with respect to noise. For applications where the level variations are small or slow, the advantage of the frequency shift method over amplitude modulation is relatively small.

DURING World War II, single-channel and multichannel frequency-shift radio telegraph systems proved of the utmost importance in providing the Allied Powers with a world-wide automatic printing telegraph network for handling with precision, secrecy, and dispatch the unprecedented volume of traffic engendered by a war of global extent. It is expected that the next few years will witness a greatly expanded application of this method of operation by commercial telegraph companies and others interested in long distance telegraphy.

Frequency shift carrier telegraphy (FS) may be applied to any carrier telegraph circuit, but, as will appear later, it provides particularly striking advantages in high-frequency radio transmission. For some other radio frequency ranges and for wire-line operation, the conditions are such as to limit the advantages of the FS method. The main advantages of the FS over the amplitude modulation method are a greater ability to accept rapid level changes, which results in better stability and lower distortion, and an improvement in signal-to-noise ratio, which permits a reduction in carrier amplitude. It is therefore of particular importance where automatic printing is desired over high-frequency radio circuits. When it is necessary to transmit through very high noise levels, low speed AM signaling with aural reception of an audio beat note remains the superior method.

FS is a form of frequency modulation in which signaling is accomplished by shifting a constant amplitude carrier between two frequencies representing, respectively, the marking and spacing conditions of the telegraph code. Frequency variations in FS telegraphy correspond to amplitude variations in AM telegraphy (continuous wave); thus the signal transitions in FS are represented by frequency–time transients, while in the AM case they are amplitude–time transients. Since

Figure 1. Amplitude of side-band components

(a). Square-wave amplitude modulation
(b). Square-wave frequency modulation

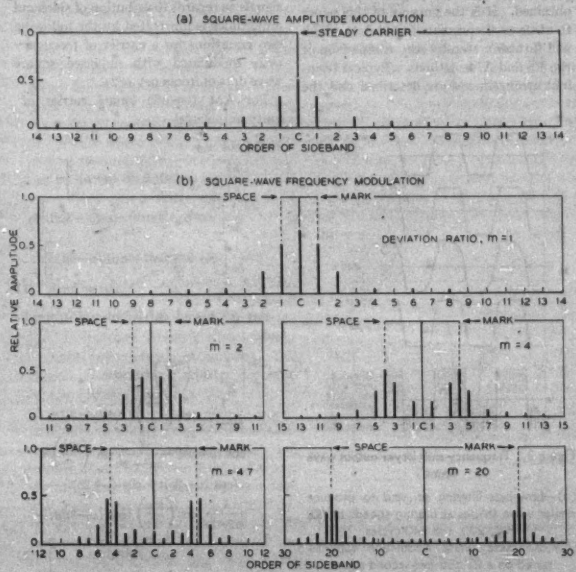

Paper 47-78, recommended by the AIEE committee on communication for presentation at the AIEE winter meeting, New York, N. Y., January 27–31, 1947. Manuscript submitted November 14, 1946; made available for printing December 5, 1946.

J. R. DAVEY and A. L. MATTE are both members of the technical staff of Bell Telephone Laboratories, Inc., New York, N. Y.

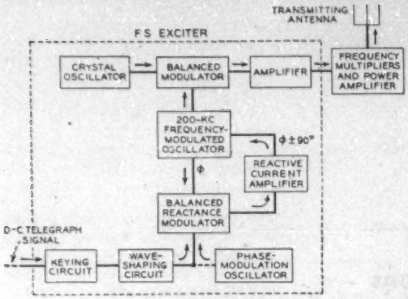

Figure 2. Block diagram of a typical FS transmitter

AM telegraph is the more common system, a discussion of the FS method involves numerous comparisons between the two systems. The merits of a telegraph system must be judged on its ability to combat the various adverse conditions encountered in the transmission medium and in the terminal apparatus. In general these adverse conditions involve variations in amplitude, frequency, and phase of the signals and the presence of extraneous signals and noise.

In the course of the development of a number of FS radio teletypewriter systems, a large amount of information concerning the characteristics and design parameters of such equipment has been obtained. It is the purpose of this paper to abstract therefrom selected data which will furnish a step-by-step comparison of the FS and AM methods. Typical terminal arrangements are described and the effects of varying certain design factors are illustrated by experimental data. Although the material presented applies largely to high-frequency radio telegraph, much of it is of a general nature, and with proper interpretation applies to other frequency ranges and transmission media and to cases in which the telegraph modulated carrier may be a subcarrier or one of several subcarriers.

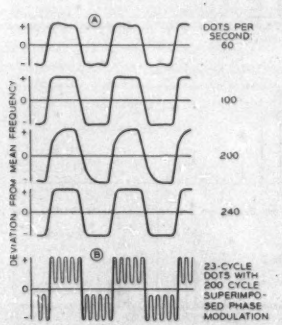

Figure 3. Frequency shift keyer output wave forms

(*a*)—Low-pass filtering adjusted to produce similar wave shapes at dotting speeds of 60, 100, 200, and 240 cycles

(*b*)—200-cycle phase modulation superimposed on a 23-dots-per-second signal

General Discussion

Sideband Energy Distribution

The difference between FS and AM signals as regards distribution of sideband amplitudes is illustrated by the following two equations for a carrier of frequency $\omega/2\pi$ modulated with unbiased square wave dots of frequency $\rho/2\pi$.

For AM (on-off) keyed carrier of unity amplitude[1]

$$e = 0.5\cos\omega t + \frac{1}{\pi}\left[\cos(\omega+\rho)t + \cos(\omega-\rho)t\right] - \frac{1}{3\pi}\left[\cos(\omega+3\rho)t + \cos(\omega-3\rho)t\right] + \frac{1}{5\pi}\left[\cos(\omega+5\rho)t + \cos(\omega-5\rho)t\right]\ldots \quad \text{and so forth} \qquad (1)$$

For FS keyed carrier of unity amplitude[2]

$$e = \frac{2m}{\pi}\left[\frac{1}{m^2}\sin\left(\frac{m\pi}{2}\right)\cos\omega t + \frac{1}{m^2-1^2}\cos\left(\frac{m\pi}{2}\right)(\cos(\omega-\rho)t - \cos(\omega+\rho)t) - \frac{1}{m^2-2^2}\sin\left(\frac{m\pi}{2}\right)\times(\cos(\omega-2\rho)t + \cos(\omega+2\rho)t) - \frac{1}{m^2-3^2}\cos\left(\frac{m\pi}{2}\right)(\cos(\omega-3\rho)t - \cos(\omega+3\rho)t) + \ldots\right] \qquad (2)$$

where m is the deviation ratio $= \dfrac{\text{frequency shift}}{2\times\text{signaling speed}}$.

Typical side-band amplitudes calculated from these formulas are shown in graphical form in Figure 1. In the case of FS keying, the relative amplitudes of the side bands vary considerably as the amount of frequency shift is changed. For miscellaneous signals these line spectra do not exist, but they do indicate the general distribution of energy over the band for a given signaling speed.

Methods of Modulating the Carrier

In AM telegraphy the carrier usually is modulated by simply interrupting it for the spacing condition. This is sometimes referred to as "on–off" keying. For low power and low frequencies the carrier may be keyed directly by electrical contacts.

A more universally applicable method is to use vacuum tubes or other nonlinear elements to interrupt the carrier effectively. In some instances it is practical to start and stop an oscillator source of carrier.

The usual radio telegraph transmitter consists of an oscillator followed by a number of cascaded stages of amplification and frequency multiplication arranged to reach the desired output frequency and power. For on–off keying the carrier usually is interrupted by suitably varying the plate or grid voltage of one or more of the stages.

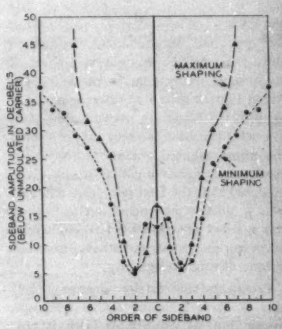

Figure 4. Effect of shaping FS transitions on amplitude of radiated side bands

100 dots per second and 500-cycle frequency shift

The maximum and minimum wave shaping conditions correspond to those used with 60 and 240 dots per second respectively in Figure 3(*a*)

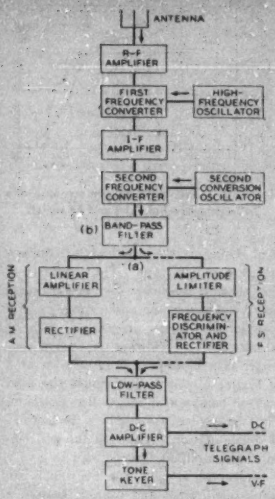

Figure 5. Block diagram of a typical receiving arrangement for either AM or FS telegraph signals

There are two general methods of obtaining frequency modulation

(*a*). The frequency of an oscillator may be modulated directly by suitably varying the frequency-determining circuit.

(*b*). The output of a constant-frequency oscillator may be shifted in phase at such rates of change as to produce indirectly the desired frequency variations.

In the latter case the marking and spacing intervals of an FS signal would be formed by periods of constant rate of phase charge versus time. Square-wave reversals therefore would require a triangular shaped wave of phase versus time. Because the transmission of long periods of steady mark or space would therefore involve huge phase swings, the modulator would have to be able to produce a steady phase rate of change. A phase modulator capable of performing in this way while not producing undesirable phase discontinuities at the signal transitions becomes rather impractical. For this reason FS telegraphy usually utilizes the direct frequency modulation method. This may be accomplished conveniently by the use of a reactance modulator which, by injecting a reactive component of current into the tuned circuit of the oscillator, varies the resonant frequency thereof. Such a modulator may be made linear so that a frequency shift proportional to the input voltage to the reactance modulator is obtained.

To apply FS telegraph signals to a radio transmitter the regular exciter oscillator is either replaced or modified by an arrangement providing a source of radio-frequency excitation that can be shifted in frequency in accordance with the telegraph signal. All the stages are operated with full radio-frequency excitation continuously to produce a constant amplitude carrier.

As a matter of expediency frequency shift keying has sometimes been provided by switching between two independent sources of carrier current separated in frequency by the desired shift. In such a case the frequency transitions involve sudden phase discontinuities of random values. This results in the instantaneous frequency swinging considerably outside the steady-state mark and space frequencies. If the band is wide, such as is the case in a radio transmitter, there results a very broad side band radiation capable of causing severe interference to adjacent channels. If the band is narrow, as might be the case where sending filters are employed, the interference is eliminated but the amplitude transients resulting from the sudden phase shifts are capable of producing considerable distortion

Restriction of Transmitted Band

As seen before, square-wave modulation results in a wide spread of side-band components which are of sufficient amplitude to interfere seriously with adjacent channels unless greatly attenuated. The transmitted band may be restricted either by the use of a band-pass filter centered about the carrier frequency or by a low-pass filter to suitably shape the modulating wave form. Band-pass filters are usually used if the power level is low and the frequency low enough to permit suitable filter construction. For multichannel systems the use of band-pass filters also permits efficient paralleling of the transmitting channels. For radio transmitters with a transmitted power measured in kilowatts, and with a frequency of several megacycles which is frequently changed to best suit the prevailing conditions, shaping of the modulating wave is the more practical method of restricting the transmitted band.

Insufficient attention has been given in the past to the envelope shape of the signals from on-off keyed radio transmitters. With the ever increasing crowding of frequency assignments, it becomes more and more important to restrict the emission of unnecessary side bands arising from keying. The envelope shape in on-off keying may be controlled by properly shaping the modulating grid or plate voltage wave. It is important that the stages following the keyed stage or stages be nearly linear, otherwise the wave shaping will be largely destroyed. In the case of frequency shift keying, however, the wave shaping is preserved after passage through class *C* amplifier or multiplier stages, and these may be operated for maximum efficiency. The greater ease of producing and maintaining the desired wave shaping, so necessary for close frequency spacing of channels, is one of the outstanding advantages of frequency-shift keying

Apparatus

Typical FS Exciter for Radio Telegraph

A typical FS exciter arrangement such as is used often with radio telegraph transmitters is shown in Figure 2. A d-c telegraph wave, after suitable shaping, is caused to frequency-modulate an intermediate frequency of 200 kilocycles which, in turn, amplitude-modulates a radio frequency from a crystal-controlled oscillator. The upper side band of this latter modulation is an FS signal and is selected and amplified sufficiently to drive the first amplifier or multiplier stage of

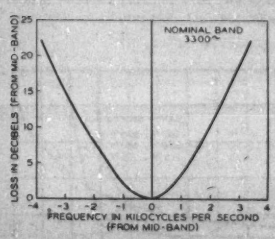

Figure 6. Intermediate frequency selectivity characteristic of radio receiver

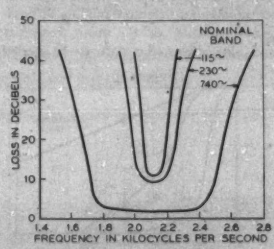

Figure 7. Attenuation versus frequency characteristics of band-pass filters shown at (b) in Figure 5

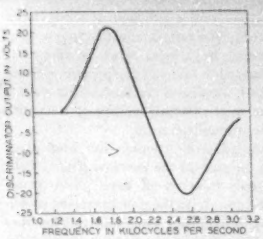

Figure 8. Linear discriminator characteristic

the transmitter. The 200-kilocycle oscillator is frequency-modulated by a reactance modulator which, by feeding a leading or lagging quadrature component of current into the oscillator tuned circuit, decreases or increases the frequency. By operating the reactance modulator within its linear range the frequency shift wave form is made the same as the d-c telegraph wave form into the modulator. A d-c amplifier stage, designated "keying circuit," is provided to furnish a modulating wave effectively isolated from an plitude and wave front variations of the incoming telegraph signals. The d-c telegraph signals may be polar or neutral and often are obtained from a tone demodulator unit which allows keying from a remote point by voice frequency telegraph. The amount of frequency shift is adjusted by an amplitude control in the quadrature feed-back path to the 200-kilocycle oscillator. The shift thus may be varied continuously or in definite steps to allow for subsequent frequency multiplications, by suitable attenuation controls. Controlling the shift in this manner keeps the instabilities of the reactance modulator a constant percentage of the frequency shift, which wou'd not be the case if the shift were adjusted by varying the amplitude of the modulating wave. The use of a balanced instead of an unbalanced reactance modulator minimizes variation of the mean frequency and also allows the shift to be varied without effecting the mean frequency.

The frequency-shift signal transitions are wave-shaped to restrict side-band radiation by means of a low-pass filter in the d-c telegraph signal path to the reactance modulator. The low-pass filtering is made adjustable to accommodate a range of signaling speeds. Frequency versus time wave forms from an exciter of the type described are shown for several keying speeds in Figure 3a. The effect of wave shaping on the side band components in the radio frequency output of such an exciter is shown in Figure 4.

Phase modulation readily may be added to the signal in this type of exciter by superimposing the desired sine wave modulating frequency on the telegraph signal wave input to the reactance modulator, as indicated in Figure 2. Figure 3*b* shows the keyer output wave form with superimposed phase modulation. The use of this type of phase modulation is considered later.

To obtain optimum results in FS radio telegraph transmission and to allow close spacing of channels, a high degree of frequency stability is necessary. An over-all frequency stability of ±100 cycles is desirable in a system using a value of frequency shift between 500 and 1,000 cycles. A frequency shift exciter of the type described previously, with the crystal oscillator and 200-kilocycle FS oscillator located in a temperature-controlled oven, usually has a frequency stability such that the mean radio-frequency carrier frequency may be held to within ±50 cycles up to frequencies of 20 megacycles over ordinary periods of operation on any one frequency. One of the advantages of this type of exciter is that small inaccuracies in crystal frequencies may be compensated for by adjusting the mean frequency of the 200-kilocycle oscillator.

Receiving Terminal Arrangements

Typical receiving terminal arrangements are shown in the block diagrams of Figure 5. Up to point *a* in the arrangements the FS and AM systems are identical, being of the usual high-frequency superheterodyne type. The output from the second frequency-conversion stage may be either in the audio range or at a considerably higher frequency, such as 50 kilocycles. Following the second converter is a band-pass filter (shown at *b* in Figure 5) which determines the final over-all band width before demodulation. The two systems differ only in the method of demodulation. The AM (on–off) signals are amplified and rectified to give a d-c telegraph signal. The FS signals are amplitude-limited and passed through a frequency discriminating network and then rectified to give a d-c telegraph signal. Beyond this point the two systems are again identical. The d-c signals pass through a low-pass filter to remove carrier ripple and higher frequency noise components and then are amplified to a suitable level to operate automatic recording or printing apparatus. The d-c signals also may be used to modulate an audio frequency so as to pass the signals to a remote point by multichannel voice frequency carrier telegraph methods.

The radio receiver portion of the terminals up to point *a* should be designed to have low noise and good selectivity. Extreme high-frequency oscillator stability is necessary for either system if narrow band-width operation is to be maintained without constant attention. An over-all frequency stability of ±50 cycles is desirable for the receiving terminal over a period of six to eight hours. Sufficient selectivity and amplifier capacity should be provided at all points to prevent over-

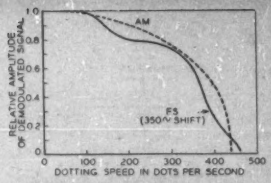

Figure 10. Over-all frequency response of a 740-cycle band to AM and FS signals

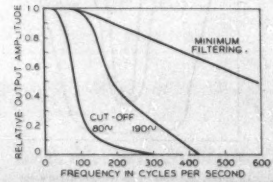

Figure 9. Attenuation versus frequency characteristics of low-pass filters

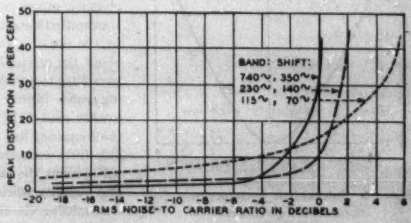

Figure 11. Peak distortion versus thermal noise for FS transmission

80-cycle cut-off low-pass filter

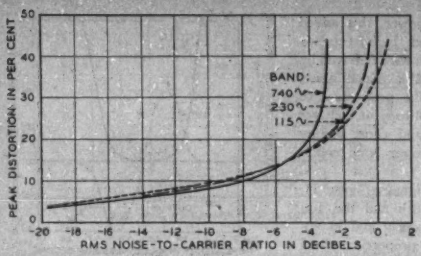

Figure 12. Peak distortion versus thermal noise for AM transmission

80-cycle cut-off low-pass filter

loading by unwanted signals or loss of automatic gain control. In the following discussion those portions of the terminals beyond the second frequency converter will be given major attention.

Experimental Transmitting and Receiving Arrangements

For the laboratory transmission studies described in the following sections, the transmitter and receiver were located nearby and connected together by means of an amplitude modulator and associated with various sources of noise designed to simulate quantitatively and under controlled conditions the variations which would be encountered in the actual medium.

Throughout the tests, 7.42-unit start–stop signals were used unless otherwise stated, and the speed was 60 words per minute (23 dots per second). Their peak distortion and bias were measured on a cathode-ray tube telegraph distortion measuring set.

An exciter of the type shown in Figure 2 was used as a source of signals. A frequency of 6.4 megacycles was employed, with the radio receiver connected to the exciter output through an amplitude modulator. This modulator was an electronic circuit permitting amplitude modulation of a frequency shift signal to produce unequal mark and space amplitudes. This modulator also was used to amplitude-modulate a single frequency for the AM portions of the measurements.

A temperature-limited diode together with a 2-stage tuned amplifier was used as a source of thermal noise centered around 6.4 megacycles. A polar relay driven by 60-cycle alternating current and arranged to produce sharp polar impulses from the discharge of small capacitances connected to its contacts was used as a source of impulse noise. The noise level was adjusted by an attenuator and mixed with the 6.4-megacycle carrier of the exciter. A minimum amount of wave shaping was used, so that the modulation may be considered as having been essentially square wave.

Receiving Arrangements. The experimental data submitted in the following discussion was obtained from reception through a laboratory setup essentially like that shown in Figure 5. The radio receiver proper was a commercial type of high-frequency superheterodyne. The output of the second frequency converter was in the audio frequency range, which enabled the use of various band-pass filters at *b* of the type used in voice frequency telegraph systems. The amplitude limiter was effective over an input range of −60 dbm* to above +20 dbm. The pass-band characteristics of the radio receiver and of the several band-pass filters used in position *b* are shown in Figures 6 and 7, respectively. Unless otherwise stated, the frequency shift signals were centered about 2,125 cycles and were demodulated by a linear discriminator centered about 2,125 cycles, as shown in Figure 8. The characteristics of the low pass filtering are shown in Figure 9. These low-pass filters were adjusted by oscillographic observation of the signal wave form and had cutoff characteristics giving very little characteristic distortion.[3] The d-c amplifier was a high-gain nonlinear type designed so as to have a square wave output having transitions established by the passage of the demodulated voltage wave through a narrow amplitude range. The amplitude and wave-front slope of the demodulated wave thus had no effect on the output wave form and could not affect the distortion measuring equipment.

*The symbol *dbm* signifies decibels referred to one milliwatt.

Experimental Results

Band Width Before Demodulation

The band width before demodulation determines the amount of noise and interference which is to be accepted along with the desired signal and thus largely determines the signal-to-noise condition at the antenna at which the system fails to receive intelligence. The band width at this point (point *a* in Figure 5) also limits the signaling speed capabilities of the system. In the following experimental data the values of band width were measured between the points of 6 db loss above that at midband.

Effect on Signaling Speed. For both methods of signaling considered here the band width must be at least twice the maximum signaling speed in dot-cycles per second, but it is found that signal distortion rises rapidly for a band width less than three times the maximum signaling speed, and that a factor of at least four

Figure 13. Peak distortion versus impulse noise for FS transmission

80-cycle cut-off low-pass filter

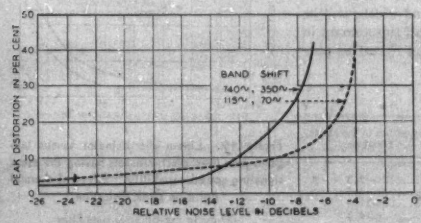

Figure 14. Peak distortion versus impulse noise for AM transmission

80-cycle cut-off low-pass filter

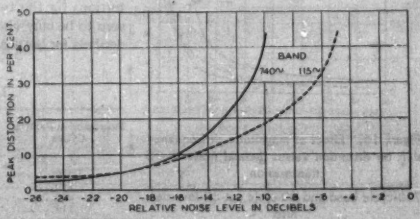

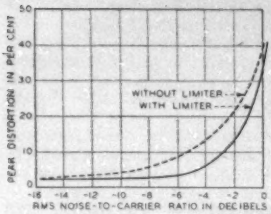

Figure 15. Effect of the limiter on distortion versus thermal noise for FS transmission

740-cycle band, 350-cycle frequency shift, 80-cycle cut-off low-pass filter

times is indicated for a system which is to have reasonably low distortion with any margin of safety. The signaling speed capability of a given band width is nearly the same for FS signals as for AM (on-off) signals. In Figure 10 is shown the over-all signaling frequency response to FS and AM signals for a nominal band width at point *a* of about 740 cycles. It will be noted that the FS method is but slightly inferior and that both systems fail at a signaling frequency of approximately one-half the band width.

Effect on Noise. The effect of thermal noise on distortion for band widths of 115, 230, and 740 cycles is shown in Figures 11 and 12. The rms noise-to-carrier ratios indicated in the figures were measured in the 3,300-cycle band of the radio receiver in all cases. The actual noise-to-carrier ratio existing in the transmission band used was lower and may be obtained from Table I. These values are from rms measurements.

For AM signals, Figure 12, varying the band width has little effect when the telegraph signal distortion is less than 15 per cent. Although the wider bands accepted more noise power, this added noise merely produced high-frequency noise components which were removed by the low-pass filter. This added noise, however, does cause the peak noise to exceed the signal amplitude at a lower noise-to-carrier ratio and cause failure before that for a narrower band condition.

In the case of FS signals, Figure 11, changing the band width and the frequency shift simultaneously and in approximately the same proportion alters the whole distortion characteristic. At low noise levels a wider band with a greater frequency shift gives an improved signal-to-noise condition. However, as the noise level is increased the wider band causes the peak noise to exceed the carrier at a lower noise level than with a narrower band. Thus a change to a wider band gives less distortion at low noise levels and more distortion at high noise levels. This results in a much more sharply breaking distortion characteristic for the wider band. This behavior is typical of frequency modulation systems in general.

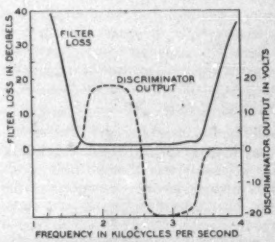

Figure 17. Characteristics of 1,920-cycle band-pass filter and associated discriminator consisting of two band-pass filters

Although the noise actually passed by the 740-cycle band filter was approximately eight decibels above that passed by the 115-cycle band filter, the difference in the failure points (35–40 per-cent distortion) for the two band widths will be seen to be only about half this amount in decibels for both AM and FS. This phenomenon is typical of carrier telegraph systems when compared at the same signaling speed. This means that it is not particularly beneficial to decrease band width to obtain lower distortion under high noise conditions. The main reason for narrow bands is for more economical use of frequency space.

Table I

Pass Band at Point a, Cycles	Correction to Be Made, Decibels
1,920	−2.3
740	−6.5
230	−11.6
115	−14.3

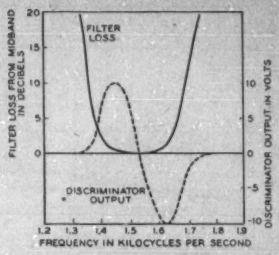

Figure 18. Characteristics of 295-cycle band-pass filter and associated discriminator consisting of two band-pass filters

As to the comparison between FS and AM, the FS method has an advantage of 2.5 to 4.5 decibels at a distortion of 35 to 40 per cent, corresponding to the selector failure point of the usual teletypewriter. From a signal-to-noise standpoint it is thus seen that the gain in changing to the FS method is approximately equal to the resulting increase in average transmitted power of about three decibels. A comparison at a lower distortion such as 15 per cent shows an advantage of four to six decibels. At a still lower distortion the 740-cycle band, because of the higher deviation ratio, shows an improvement of over ten decibels. In this region the slopes of the curves make accurate comparisons impossible due to the masking effect of other sources of distortion. These large improvements at low noise levels are similar to those associated with

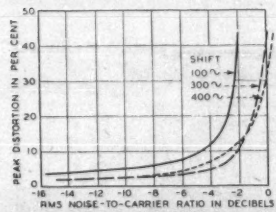

Figure 16. Effect of magnitude of frequency shift on distortion versus thermal noise in FS transmission

740-cycle band and 80-cycle cut-off low-pass filter

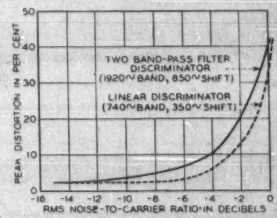

Figure 19. Linear discriminator versus two band-pass filter discriminators having the same signaling speed capability. Effect of thermal noise on peak distortion

80-cycle cut-off low-pass filter

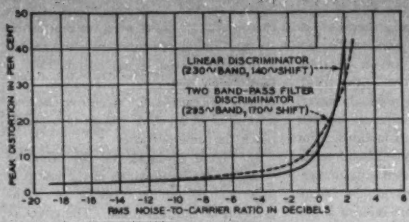

Figure 20. Linear discriminator versus two band-pass filter discriminator with equal bandwidths. Effect of thermal noise on peak distortion

80-cycle cut-off low-pass filter

wide-band FM broadcast systems. However, in carrier telegraph transmission the criteria are so different that the difference between a nearly perfect circuit and one of small distortion is not of great importance except when a large number of telegraph sections are to be operated in tandem. From a practical standpoint the improvement in signal-to-noise is not more than about six decibels for equal band widths.

In Figures 13 and 14 similar characteristics are shown for impulse noise. The noise level values of these curves are purely relative as no attempt to measure the peak noise was made. The comparisons between AM and FS, and between different band widths, agree closely with those for thermal noise.

Effect of Limiter on Signal-to-Noise Ratio

The limiter in the FS system is a high-gain nonlinear amplifier which delivers to the frequency discriminating networks an essentially square wave having transitions coinciding with the passage of the instantaneous voltage of the input carrier signal through zero. The limiter thus passes only the frequency or phase changes of the carrier signal. Noise voltages which are small compared to the signal cause approximately linear phase modulation of the signal and this is passed through the limiter. The amount of frequency deviation thus imparted to the carrier by a given component of noise is proportional not only to its amplitude but also to its frequency separation from the carrier. This gives rise to the so-called "triangular noise spectrum"[4] when a linear frequency discriminator is used. If the limiter is removed from the frequency shift terminal, the noise components in phase with the carrier, as well as those in quadrature therewith, are allowed to reach the frequency discriminating network. For a balanced type discriminator this increases the demodulated noise for small amounts of noise about three decibels. Figure 15 shows the effect of removing the limiter from the circuit. The limiter is seen to have little effect on the failure point, but an improvement of two to four decibels is shown in the 5- to 12-per cent distortion region.

Other beneficial effects resulting from the use of a limiter are discussed under "Level Variations".

Demodulation of Frequency Shift Signals

It is desirable that the frequency discriminating network be of the balanced type having two branches, allowing differential combination of the two rectified outputs. This minimizes the response to amplitude modulation not eliminated by the limiter. Two general types of networks have been in common use for FS telegraph. One consists of two band-pass filters centered about the mark and space frequencies respectively and effectively dividing the total band into halves. The other consists of a 2-branch network, each branch of which has a varying amplitude characteristic extending over the complete transmission band and usually well beyond. The amplitude-versus-frequency characteristics of these two branches have opposite slopes and are of such shape that differential combination of their rectified outputs results in an approximately linear voltage-versus-frequency curve, passing through zero at midband (Figure 8).

In Figure 17 is shown the characteristic of a 2-band-pass filter type of discriminator which was used in early frequency shift terminals. The characteristic is fairly flat near the mark and space frequencies so that this type of discriminator does not produce a triangular noise spectrum. In Figure 18 is shown the type of discriminator characteristic obtained by the use of two narrow band-pass filters. In this case there is no broad flat region around the mark and space frequencies and an intermediate type of characteristic (approaching the linear type) is obtained.

With the linear type of discriminator (Figure 8) the demodulated noise has the well-known triangular spectrum and as illustrated previously, the signaling speed capability is essentially the same as an AM system of equal band width.

To compare experimentally these two general types of discriminators, a 740-cycle band system with linear discriminator and 350-cycle shift was compared with a system with a band width of about 1,900 cycles, a discriminator consisting of two 740-cycle band-pass filters, and an 850-cycle shift. The results are shown in Figure 19. The two systems are seen to reach failure distortion values at the same signal-to-noise point, with the linear discriminator becoming about three decibels superior at distortions around

Figure 21. Effect of low-pass filter cut-off frequency on distortion in the presence of thermal noise

740-cycle band

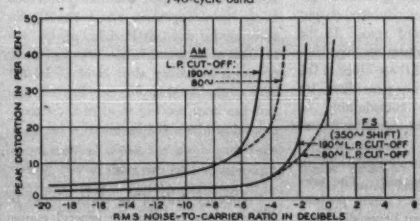

Figure 22. Effect of low-pass filter cut-off frequency on distortion in the presence of impulse noise

740-cycle band

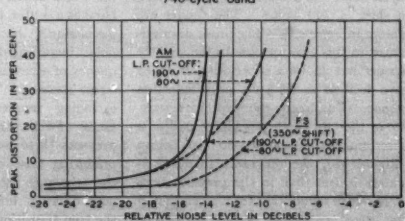

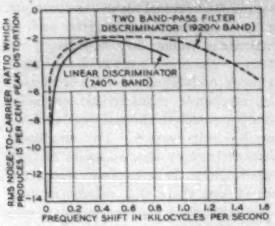

Figure 23. Effect of magnitude of frequency shift on distortion produced by thermal noise

80-cycle cut-off low-pass filter

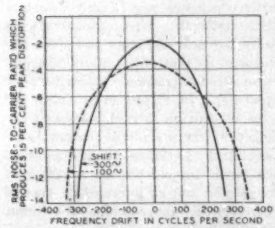

Figure 24. Effect of frequency drift on distortion produced by thermal noise in FS transmission

740-cycle band and 80-cycle cut-off low-pass filter

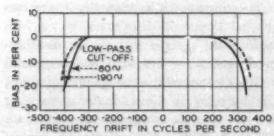

Figure 25. Signal bias versus frequency drift for AM transmission in a 740-cycle band

five per cent. A second comparison was made using roughly equal band widths. A 295-cycle band with a discriminator consisting of two band-pass filters and 170-cycle shift was compared with a 230-cycle band with a linear discriminator and a shift of 140 cycles. The results are shown in Figure 20. The linear discriminator in this case appears to fail slightly sooner but shows a superiority of about two decibels in the 5 per cent distortion region. Due to the rounded characteristic of the two band-pass filters used as a discriminator in the second comparison (Figure 18), the difference in discriminators is less than in the previous test. It has been found[5] that for a given signaling speed capability almost twice the band width is required if a 2-band-pass-filter discriminator is used instead of the linear type. This added band width does not appear to cause any loss in signal-to-noise capabilities as to the failure point. The less sharp breaking point, however, makes the linear discriminator superior for moderate and low distortions. For a system occupying a given band width the 2-band-pass-filter discriminator provides some improvement at the failure point but is still somewhat inferior to the linear discriminator at moderate distortions. More importantly the 2-band-pass-filter discriminator impairs the signaling speed capabilities to an extent which depends upon the shape of the cut-off of the filters used.

Band Width After Demodulation (Low-Pass Filtering)

In an AM system the low-pass filtering after demodulation can to a large degree make up for a greater than necessary band width before demodulation. During marking intervals the added noise admitted by a wide band causes noise in the demodulated output at frequencies higher than the signaling frequency and this can be filtered out, unless the noise is so great as to over-modulate the carrier. During spacing intervals there is no carrier and hence only the noise is rectified. Added noise admitted by a wide band causes not only higher frequency components in this rectified noise, which may be filtered out, but also an increase in the d-c component. This tends to cause marking bias of the received signals as the noise level increases.

In an FS system where the carrier is present continuously, the added noise from a wider band produces high-frequency noise components in the demodulated output which can be filtered out by the low-pass filter if the noise level is low. As the noise level increases there are short intervals when the noise envelope exceeds the carrier. The action of the limiter is to give preference to the greater signal, in this case the noise, and as the noise will appear to the discriminator as a carrier fluctuating around mid-band as a center, the demodulated output momentarily dips toward zero. As the noise increases, the duration and frequency of occurrence of these holes in the signal increase. The low-pass filter, by excluding frequencies considerably in excess of the maximum signaling speed, prevents these holes in the signal from producing false or extra transitions in the telegraph signal output. The low-pass filtering, however, cannot prevent the true transitions from being displaced by this type of noise component because the signal is obliterated momentarily. Its most important function is to prevent a breakup in the signal output until a fairly high distortion is reached. For noise peaks exceeding the carrier the low-pass filter of an AM system also serves much the same purpose.

In Figure 21 is shown the effect of changing the band width of the low pass filter in an FS and in an AM system in the presence of thermal noise. The effect of a narrower low-pass filter is seen to consist mainly in shifting the breaking point toward a higher noise level. Similar characteristics for the case of impulse noise are shown in Figure 22.

Magnitude of Frequency Shift in Relation to Band Width

A frequency shift transient in a band of given width has a wave shape much like that of an amplitude transient in the same band provided the shift is symmetrical and not over 50 per cent of the band width.[6] If the frequency shift approaches the total width of the band, the transient is of such shape as to cause distortion and to make the system more susceptible to noise. A very small shift results in a low amplitude of demodulated signal, which is more readily distorted by noise and biased by frequency drifts. It is of interest, however, that the signal-to-noise ratio of the demodulated signal is not proportional to frequency shift for high noise conditions. As described before, noise peaks tend to reduce momentarily to zero the output from a balanced discriminator. The amplitudes of the dips or holes are thus about one-half of the demodulated signal amplitude for any value of shift. This tends to maintain a constant signal-to-noise condition and this characteristic is illustrated by Figure 16, in which the breaking point with a 100-cycle shift occurs only two decibels before that with a 400-cycle shift although the difference in actual signal amplitude is 12 decibels. Figure 23 shows the effect on signal-to-noise ratio of progressively varying the frequency shift while the band width is kept constant. There is a fairly broad region in which the signal-to-noise ratio is little affected by the amount of frequency shift. For optimum results a frequency shift of 50 to 60 per cent of the band width is indicated, and this has been used in most of the experimental results given herein.

Frequency Instabilities

Frequency drift of the carrier input to the receiving terminal in general causes

biased signals, and if severe enough results in failure of the system.

In Figure 25 is shown the effect of frequency drift on signal bias in an AM system. In an AM system little bias is produced until the carrier reaches the cutoff region of the filter. The bias then becomes rapidly negative due to the increased loss and decreased amplitude of demodulated signal. When an automatic gain control arrangement is used, the bias becomes positive due to a distorted envelope shape. The demodulated wave form determines the degree of sensitivity to frequency drift and depends on the band width both before and after demodulation.

In an FS system using a linear discriminator, frequency drift changes the d-c component of the signals and thus changes the operating point on the demodulated wave. The amount of bias depends upon the slope of the wave front and is thus affected by the amount of low-pass filtering. The effect of frequency drift on bias for a number of FS systems is shown in Figures 26 and 27. If a 2-band-pass filter type of discriminator is used, the system is insensitive to moderate frequency drifts because of the flat pass bands, as illustrated in Figure 26. The relative shape and amplitude of the signal from a linear discriminator does not change appreciably with frequency drift; only a d-c displacement occurs. This makes it desirable to have the low-pass filter coupled to the output amplifier by a network which passes only the useful signaling frequencies and blocks the d-c and very slow drift components. When this is done the effect of frequency drift on bias is not greatly different from that for an AM system, as may be seen by comparing the dotted curves on Figures 26 and 27 with Figure 25.

The general method of performing this d-c elimination is illustrated in the block diagram of Figure 29. The output from the low-pass filter is passed through a coupling network which blocks the d-c and passes the useful signaling frequencies. The output of the coupling network is passed through a positive feed-back nonlinear amplifier which has but two output conditions representing the mark and space of the telegraph signal. The feed-back network passes d-c and low frequencies so as to just compensate for the loss of the coupling network. The time constant of the coupling network may be large enough so that the signal wave form into the d-c amplifier is practically the same as at the output of the low-pass filter. The operating point on the demodulated wave may be readily

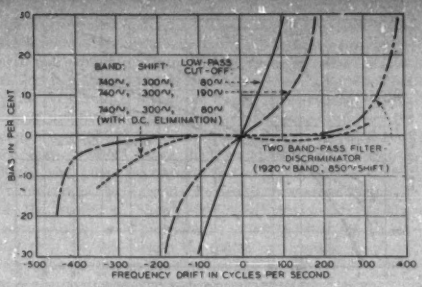

Figure 26. Signal bias versus frequency drift for FS transmission

Wide filter bands

adjusted by adjusting the bias voltage at the input to the d-c amplifier. This arrangement differs from the impulse type of d-c elimination, in which the demodulated wave form is effectively differentiated to form pulses but a fraction of a unit dot in length.

When d-c elimination is used, operation with FS signals decentered in the pass band causes little bias, but it does cause a loss in signal-to-noise ratio, especially at high noise levels. Due to the effect of noise peaks in causing a dip toward zero in the demodulator output, the effect of noise becomes exaggerated during the signal condition which is farther from midband. This change in signal-to-noise condition with frequency drift is shown in Figures 24 and 30. A comparison between a 2-band-pass-filter discriminator and a linear discriminator with d-c elimination as regards frequency drifts in the presence of noise is shown in Figure 31.

Radio telegraph systems operating in the high-frequency region require a high degree of frequency stability if narrow band widths are to be used. Because of the several frequency conversions involved, a number of different oscillators or frequency sources are involved, but usually the major burden of frequency stability rests on the transmitter exciter and the high-frequency beating oscillator of the receiver.

Various methods of automatic frequency control may be used to hold the carrier input to the demodulator at the correct frequency. In the case of FS signals, the control may be arranged to operate only on the marking frequency or to utilize both the mark and space conditions. It is preferable to have inherent frequency stability rather than to compensate for the drift at the receiving end as it is difficult if not impossible to provide an automatic frequency control which will not reduce the transmission capabilities of the system in the presence of noise and other interference. Best results are obtained if the frequency stability is high enough to require only a very slow correction, which usually dictates some mechanical rather than electronic tuning arrangement. Manual retuning may be found satisfactory where stability is reasonably good, provided care is taken in making the adjustments. Suitable frequency stability with the retention of flexibility in frequency adjustment may be obtained by frequency sources making use of a combination of

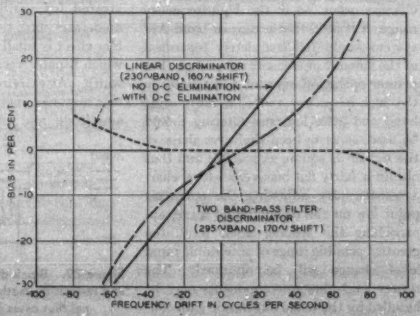

Figure 27. Signal bias versus frequency drift for FS transmission

Narrow filter bands

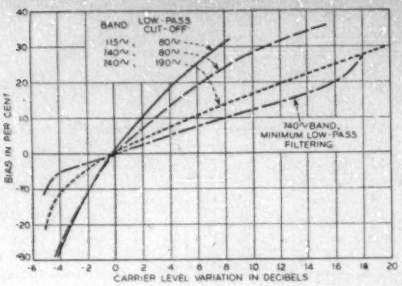

Figure 28. Signal bias versus carrier level variation for AM transmission

crystal oscillators and high stability variable oscillators of lower frequency.

Level Variations

Extreme and rapid variations of received level exist in high-frequency radio transmission. It is upon the ability to accommodate these level variations that the merits of a high-frequency radio telegraph system must largely be judged. FS telegraph shows its outstanding advantage in this respect.

To obtain zero-bias signals and optimum signal-to-noise conditions, in an AM system, the operating point must be near the half amplitude point on the demodulated wave. This means that complete failure will result for a drop in level of six decibels unless some compensating arrangement is provided. The slope of the bias-versus-level characteristic depends upon the slope of the demodulated wave, which in turn depends on the band width of the system and upon the degree of low-pass filtering. The bias-versus-level characteristics of some AM systems are shown in Figure 28. Where the level variations are relatively slow compared to the signaling speed, automatic gain control circuits can be used to maintain a nearly constant level into the demodulator. However, where large rapid level changes occur, as in the high-frequency range, it is seen that a narrow-band AM system would fail completely regardless of the amount of transmitted power. For printer operation over an AM system in the high-frequency range, a fairly wide band and little low-pass filtering should be used, so as to keep the wave shape of the signals as square as possible and thus obtain a fairly flat bias-versus-level characteristic. By adjusting the operating point low on the demodulated wave, approaching the spacing noise level, the greatest possible range of acceptable rapid level change will be obtained. The slower level change components may be handled by the usual automatic gain control circuits. This will cause the bias of the signals to average marking somewhat, but the peak distortions will be kept to a minimum.

In an FS system no bias is produced so long as both the marking and spacing frequencies are affected alike, with their received levels remaining equal. Such nonselective fading conditions cause no distortion even when they occur at quite rapid rates. If a balanced type of discriminator is used, amplitude limiting is not essential to obtaining this immunity from nonselective variations in attenuation. It is only when the mark and space levels are different that bias results. In Figure 32 are shown bias versus mark-to-space level ratio characteristics both with and without a limiter. More bias exists when there is no limiter because the amplitude of the demodulated wave is directly affected and consequently the low-pass filtering also becomes a factor. With a limiter the amplitude of the demodulated wave is held constant and the amount of low-pass filtering has no effect on bias. Some bias is still produced, however, due to the differently shaped frequency transients in the pass band of the receiving system when a level change occurs at the moment when the frequency changes. In Figure 33 this bias effect is demonstrated for various band widths. For moderate mark-to-space level ratios the bias effect is small and linear, with a slope which usually varies inversely with band width. At extreme level differentials the bias may rise very rapidly because of the amplitude and phase characteristics of the input pass band; transients from the greater amplitude condition may interfere severely with the lower amplitude condition. For the types of band-pass filters used in the tests it appeared that the amount of level difference required to produce 20-per-cent bias did not change greatly with band width. Severe wave shaping of the signal at the transmitter was found to be an aid in reducing the bias effect due to such transients, but the characteristic distortion became too great to give any practical improvement.

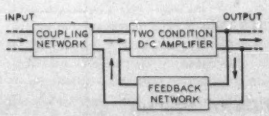

Figure 29. Block diagram of d-c elimination and restoration method used to minimize signal bias caused by frequency drift

The fading modulator used in obtaining the data for Figure 33 caused no change in phase. Selective fading over an actual radio circuit would involve considerable phase shift and greater distortion might be expected. The data of Figure 32 were obtained by use of the phase control associated with the crystal filter of the radio receiver to vary the loss-versus-frequency characteristics of the receiving pass band and thus cause unequal mark and space amplitudes. This method gave an amplitude and phase characteristic for the transmission band more like that over an actual radio circuit.

Multipath Propagation Effects

The rapid fading conditions prevailing in the high-frequency range are brought about by multipath propagation. Under such conditions, the signal induced in a receiving antenna by a distant transmitter may be the resultant of two or three separate waves each propagated over a different path. If two waves arrive over paths differing in length by an odd number of half wave lengths, the resulting 180-degree phase difference causes maximum cancellation. However, if the paths differ in length by an integral multiple of whole wave lengths, the waves arrive in phase and maximum reinforcement results. The difference in path lengths may at times be as great as 500 to 1,500 kilometers (delay times of two to five milliseconds) which in the high-frequency region corresponds to thousands of wave lengths. Under these maximum conditions waves at one frequency may arrive in-phase while waves at a frequency a few hundred cycles away may arrive in phase opposition. Because the path lengths are constantly changing, the transmission at a given frequency is subject to wide variations in amplitude and phase with time. When the difference in path lengths is not great enough to cause frequencies in one portion of a communication channel to fade differently from those in another portion, the term "nonselective" or "flat" fading is applied.

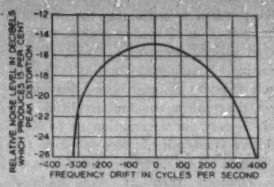

Figure 30. Effect of frequency drift on distortion produced by impulse noise in FS transmission

740-cycle band, 100-cycle frequency shift, 80-cycle cut-off low-pass filter

When the difference in path lengths becomes great enough to cause considerable amplitude or phase distortion over the transmission band, the term "selective" fading is used. As the propagation paths existing at a given moment vary for different antenna sites, the fading patterns obtained from two or three antennas separated by several wave lengths usually show a considerable phase difference, so that a given frequency is not likely to fade into the noise level at all antennas simultaneously. By employing separate receivers for each antenna and suitably combining or selecting the demodulated outputs, a system is obtained which is much less susceptible to fading. Such a method is called space diversity reception. Inasmuch as fading over a given combination of paths is highly selective with respect to frequency, much the same effect is obtained by frequency diversity reception. When this method is employed, the intelligence is transmitted on two or more frequencies simultaneously, and then received by separate receivers from a single antenna and the resulting demodulated signals combined or selected as for space diversity.

In telegraph transmission large differences in delay over two separate propagation paths cause the telegraph signal transitions to arrive at different instants over the two paths. Thus, there are intervals of overlap when a marking condition is received over one path and a spacing condition over a second path. When two components of nearly equal amplitude arrive at nearly 180-degree phase difference, a signal transition may involve large and sudden amplitude and phase changes. The resulting transients in the band-pass networks of the receiving equipment may cause fortuitous distortions considerably greater than the difference in delay times over the two paths. The wider the pass-band of the receiving system the shorter the duration of these fortuitous transients, and hence the less the distortion. This phenomenon is one of the determining factors in the selection of band width and frequency shift to be used in a given application of FS telegraphy. It becomes of increasing importance when the circuits are long and at higher signaling speeds such as are used in time-division multiplex methods.

In an AM system the effect of large differences in path lengths is usually a filling in of the spacing intervals with resulting marking bias. In an FS system the overlap time and associated transients may add to either marking or spacing intervals in a random fashion, depending on the amplitude and phase conditions at each transition. The overlapping of the mark and space frequencies in FS transmission can sometimes be heard in an AM receiver as short pips of audio tone at each transition, the audio tone being the beat between the two frequencies.

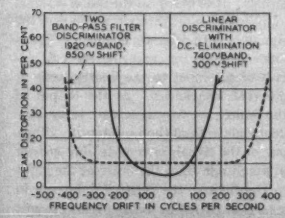

Figure 31. Linear discriminator versus two band-pass filter discriminators when frequency drift occurs in the presence of thermal noise

—4 db rms noise-to-carrier ratio

Use of Superimposed Phase Modulation

Superimposed phase modulation sometimes has been employed as a simple means of achieving a certain amount of frequency diversity both in AM and FS telegraph systems. This consists in causing the radiated signal to oscillate continuously through a small phase angle at a rate relatively high compared to the dotting speed. Phase modulation spreads the energy of the signal over a wider frequency band so that the complete loss of the signal through selective fading becomes less probable. The spectra generated by sinusoidal phase modulation of 1.0, 1.4, and 2.0 radians are shown in Figure 34. Most of the energy is seen to be concentrated in the carrier and first order side bands. Less than 1.0 radian of modulation results in too little amplitude of the side bands, while more than 1.5 radians results in too wide spread of energy outside the first order side bands. The center three components are equal at about 1.4 radians. In the case of FS, the phase modulation frequency appears as a variation in amplitude of the signals from the discriminator. For AM no additional amplitude variation is caused by the phase modulation if there is no selective attenuation in the medium, but if such exists, the phase modulation frequency or a multiple thereof appears in the rectified signal. To permit these unwanted amplitude variations to be removed by the low-pass filter so as not to break up the signals, the phase modulating frequency should preferably be ten or more times the maximum signaling frequency.

A test of superimposed phase modulation on FS signals was made over a radio circuit approximately 200 miles in length. A frequency shift of 850 cycles, and one radian of 200-cycle phase modulation, was used. A 60-word-per-minute test sentence was transmitted and received without space diversity.

It was found over a period of several hours that the phase modulation, on the average, gave a decrease in printed errors of about 50 per cent when the error rate was in the proximity of one to two per cent. For short intervals the reduction in errors was often considerably greater. The use of 200-cycle phase modulation when space diversity is used provides little or no improvement and is therefore undesirable.

A more effective way of employing phase modulation with FS signals would be to use a phase swing of ±1.4 radians at a frequency of two to three times the frequency shift and to demodulate the three major components of the signal separately, thus obtaining in effect a triple frequency diversity system. This, of course, involves quite a wide transmitted band, but it might be of use in cases where space diversity is impossible, such as on board ships. When a space

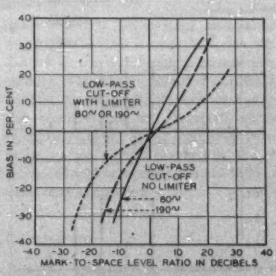

Figure 32. Signal bias versus mark-to-space level ratio in FS transmission

740-cycle band, 350-cycle frequency shift

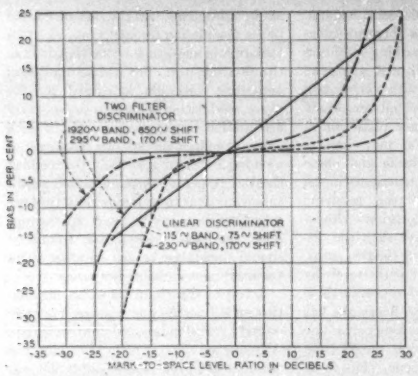

Figure 33. Signal bias versus mark-to-space level ratio in FS transmission

80-cycle cut-off low-pass filter

diversity arrangement is feasible it is much to be preferred.

Diversity Operation

To obtain reliable operation in the high-frequency range it is common practice to employ space diversity reception. The use of frequency diversity, with the increase of transmitted power and greater frequency space required, is seldom justified if space diversity reception can be arranged. For AM radio telegraph, double or triple space diversity receiving arrangements are used frequently. Because an FS signal generally covers more frequency space, it is even more likely to be mutilated by selective fading than an AM signal. It has been found, however, that a double space diversity system for FS signals usually gives sufficient diversity action provided it is of a type that permits switching between channels at signaling speed without appreciable distortion. This is necessary because it is a frequent occurrence that the mark of one channel may fade, leaving a good space, while the opposite may occur on the second channel. Since an FS system can accept rapid level changes, the main purpose of diversity methods is to insure that both the mark and space portions of the signal will be received above the noise level. In the case of AM telegraph, because it cannot accept rapid level changes, diversity operation is important not only in keeping the signal above the noise but also in averaging out some of the rapid level changes. For this reason AM systems usually show considerable improvement in going from double to triple diversity. It would be expected that a like change would show much less improvement in an FS system.

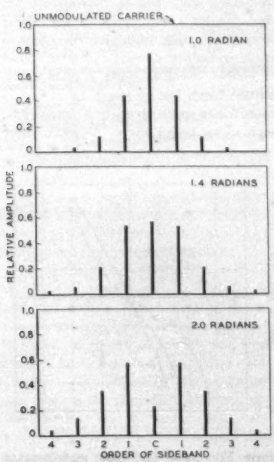

Figure 34. Frequency spectra for sinusoidal phase modulation

Diversity Channel Selection

The method employed to combine or select the channels of a diversity system is of great importance. For an AM system the relatively simple method of using a common load circuit for the diode detectors of the diversity channels generally is used. By deriving a common automatic-volume-control voltage from the combined output and by properly adjusting the receiver sensitivities, a fairly constant output is obtained. The parallel connection of the diode detectors causes the stronger signal to block the weaker signal effectively, thus giving a fairly sharp diversity selection characteristic. The problem of combining the diversity channels of an FS system is more complicated mainly because of the amplitude limiting. If amplitude limiting is used in each diversity channel before demodulation, the resulting constant amplitude signals convey no information as to their relative amplitudes as received from the antennas. Any diversity selection must be obtained then by some indirect method. It is necessary to furnish some selecting device as the noise from a faded channel, if added directly to a good signal from another channel, will cause high distortion.

In an early frequency shift system employing a 2-band-pass-filter discriminator (shown previously in Figure 17), it was found that for a poor signal-to-noise condition the sum of the outputs of the mark and space rectifiers increased above that for a good signal-to-noise condition. This increase was utilized to suppress the output of the poorer channel and emphasize that of the better channel. Although neither the degree of diversity selection nor the speed of response was as good as might be desired, fairly satisfactory results were obtained.

Another method which has been used involves the derivation of control currents or voltages proportional to the amplitudes of the incoming signals, which in turn select the better diversity channel by some type of gate action. The time constants of the control circuits must be low enough to permit switching at signaling speed without introducing considerable distortion. The gate circuits also must be of a type which does not introduce interfering transients or otherwise allow the control voltages or currents to interfere with the signal. This method permits very sharp diversity selection and has the capability of approximating ideal results although it becomes somewhat involved in a practical form.

A considerably simpler method has been used in some of the more recent FS terminals. It is based on the use of a signal amplitude limiter through which pass the signals of both diversity channels. This is made possible by arranging the two signals at the input to the limiter to be at different frequencies. At the output of the limiter the two signals are separately demodulated and then combined. When one of the signals is considerably greater in amplitude than the other at the input to the limiter, the relative difference in level is increased by an additional amount of about six decibels at the limiter output. The limiter output may be considered as the stronger signal frequency-modulated by the weaker signal. For small modula-

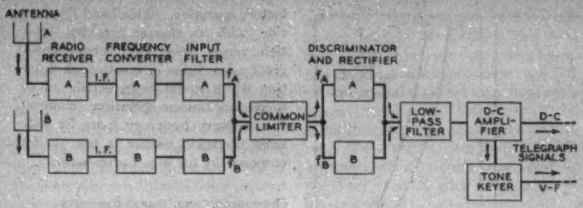

Figure 35. Block diagram of dual-diversity FS receiving system using a common limiter

tion indices, the amplitude of the first order side band is approximately one-half the modulation index, thus explaining the six-decibel added difference in level at the limiter output. As the input levels approach equality, the added level difference decreases to zero. A block diagram indicating the arrangement of such a diversity system is shown in Figure 35. Tests were made of both parallel and series connections of the two discriminator outputs. With a parallel connection the discriminator having the greater output blocks the rectifier output of the other discriminator, and thus gives a sharp diversity selection characteristic. However, the level ratio of the channels at which a switch takes place is affected not only by the ratio at the limiter input but also by frequency drift and discriminator slope. With the series connection, only the input level ratio at the limiter input affects the diversity switching; this arrangement therefore was selected as the preferred method although its selection characteristic is not sharp. The series and parallel combining characteristics are shown in Figures 36 and 37.

Various tests were made on a terminal having a 1,500-cycle band width and using the series combining method to determine the signal-to-noise characteristics under different conditions of diversity fading. A frequency shift of 850 cycles was used and the midband frequencies of the two diversity channels at the common limiter input were 30 and 35 kc. Figure 38 shows the distortion versus signal-to-noise ratio characteristics of each channel separately and in diversity combination for various relative level conditions of the two channels. During diversity operation equal noise levels were maintained in the two channels and various combinations of level differences of the two channels were preserved as the whole signal level combination was varied. The level differentials are indicated in the figure for each curve. The signal-to-noise level scales refer to the highest level portion of the diversity signal. As the amplitude modulator which was used to simulate the selective fading did not produce phase shifts or transmission delays as would actually exist over high-frequency radio circuits, the actual distortions shown by the curves are optimistic.

The ideal diversity selection circuit theoretically should give a signal-to-noise characteristic identical to that of a single channel under the signal-to-noise condition corresponding to the signal of the best momentary reception. It will be seen that the test results of Figure 38 approach this limit within two or three decibels at a peak distortion of 20 per cent. Part of this difference is caused by the dissimilar band-pass characteristics of the two channels of the experimental unit used for the tests and part caused by the lack of an extremely sharp diversity selection. It should be pointed out that the conditions under which the theoretical maximum diversity signal-to-noise condition may be reached are very hard to obtain in practice. If the noise levels in the two channels are not equal, and if the diversity selecting method at all times does not select exclusively the channel with the greater signal, the distortion characteristic will deteriorate accordingly. Because the automatic-volume-control sensitivities of two radio receivers may differ considerably, the noise levels cannot be maintained closely the same, and usually no provision is made for determining the noise level except by ear. The slightly better diversity action which can be obtained theoretically therefore is believed to be of doubtful usefulness under actual operating conditions. The common limiter method has the advantage of being simple in that the diversity action is obtained in the transmission circuits directly and no added switching circuits or adjustments are required. Tests of this type of diversity selection in the field have indicated a marked superiority over earlier FS terminal equipment.

In connection with the use of a common limiter, care must be taken in the selection of the two channel frequencies. Frequencies having nearly integral ratios such as 3:5 and 5:7 produce disturbing amplitude modulation of the demodulated signal. The frequencies should be chosen so as to avoid low integral ratios; then all amplitude modulations are negligible or easily filtered out. Where frequency drift is to be allowed for, the frequencies should be chosen so as not to approach a low integral ratio at any place in the expected drift range.

If the radio receivers associated with a space diversity FS system have automatic gain control it must be a common control so the receivers will change gain equally. The use of common automatic volume control prevents overloading of the receivers as the received signal strength varies. If no common automatic volume control is available, the receivers should be operated in the manual gain control condition.

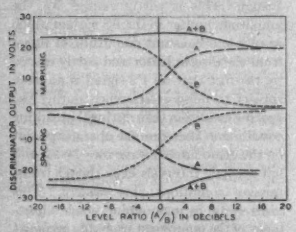

Figure 36. Diversity combination characteristic obtained by series addition of discriminator outputs

Levels measured at output of 400-kc intermediate frequency amplifier

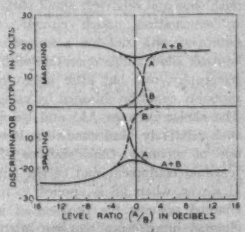

Figure 37. Diversity combination characteristic obtained by parallel addition of discriminator outputs

Levels measured at output of 400-kc intermediate frequency amplifier

Conclusions

General Comparison of FS and AM Carrier Telegraphy

The foregoing sections have compared the characteristics of AM and FS carrier

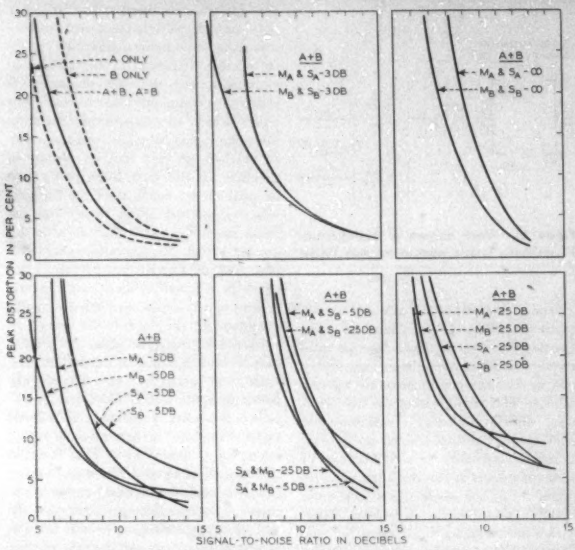

Figure 38. Peak distortion versus signal-to-noise ratio characteristics for dual-diversity operation with a common limiter

Signal-to-noise measured at output of 400-kc intermediate frequency amplifier

telegraph transmission under various conditions. Whether or not FS would prove to be the preferable method for a specific communication use depends largely on the transmission medium and the quality of transmission desired. As regards frequency space requirements, both methods provide essentially the same signaling speed capability for a given band width.

As to the ability to transmit through noise, FS has an advantage of three to four decibels at distortions approaching the failure point when equal band widths are compared. At lower distortions the advantage of FS is six decibels or more so that it is attractive in this respect for tandem operation of several telegraph sections where regeneration of signals is not practiced. When frequency space permits wider bands, with correspondingly increased frequency shifts, the signal-to-noise advantage of FS over AM increases for low noise levels. Wide-band FS therefore provides a means of obtaining higher quality circuits if the noise level is not too great.

The AM method is basically less susceptible to frequency variations than is the FS method. However, as has been illustrated, frequency drift can be compensated for by d-c elimination so as to make FS comparable to AM in this respect.

FS transmission is essentially immune from effects of nonselective level variation, even when extremely rapid, and in this characteristic displays its most outstanding advantage over AM.

Operation Over Wire Circuits

A wire circuit usually provides a transmission medium having a low noise level with slow and relatively small variations in attenuation. Such circuits, when equipped with suitable automatic gain control, allow stable operation with AM telegraphy, and but little improvement probably could be obtained by using FS. The choice between AM and FS under such relatively ideal conditions becomes one of economic considerations of the terminal equipment and carrier supply. However, when FS is applied to multichannel systems the problem of interchannel interference requires attention. For wire circuits having high noise levels or sudden changes in attenuation, the use of FS instead of AM provides considerable improvement, and in severe cases the FS method may be a necessity for satisfactory operation. Wide-band FS operation, with its sharper breaking distortion versus noise level characteristic, gives a low value of rms-to-peak distortion which would be especially advantageous for tandem operation. However, the necessary frequency space for wide-band operation usually is not justified economically for wire line operation.

Operation Over Radio Circuits

For operation over radio circuits providing stable conditions similar to those on wire circuits, the FS method does not show a great advantage over the AM method. In the case of long distance telegraphy in the high-frequency range, however, FS shows a marked advantage over AM. This is because of the rapid fading and high noise conditions which commonly prevail in the high-frequency region. The amount of rapid variation in marking level that an AM system can accommodate is less than the difference between marking and spacing levels that an FS system can tolerate. In the worst case of selective fading, the level differences between the mark and space frequencies might approach values equal to the short time level swings of a single frequency, but in general would be less. A given condition of selective fading thus causes less distortion in an FS system than in an AM system. FS allows the use of narrow bands without much loss in signal quality in the presence of fading, whereas AM does not. FS therefore is essential for satisfactory operation of closely spaced narrow-band high-frequency radio channels. Where frequency space is not restricted and wider bands are used to permit considerable frequency drift, the improvement afforded by FS over AM is materially less. To obtain optimum results from an AM system, however, requires more careful adjustment and more attention than does an FS system. This is partly caused by the amplitude limiter in the FS system which results in a constant amplitude of signal from the discriminator and partly caused by the fact that an FS signal is no more subject to noise interference during the spacing condition than during the marking condition. Therefore the operating point on the demodulated wave may be set and left for long intervals even though transmission conditions vary widely. This greater ease in maintaining good adjustment of the equipment probably accounts for some of the apparent improvement in changing from an AM to an FS system.

It should be noted that a system may fail either because of level variations well above the noise level or because of the

signal becoming submerged in noise. If a system fails because it can accept only moderate level variations, an increase in transmitted power will provide no improvement since the level variations will remain the same as before. However, a system which can accept very wide variations in level will show improvement upon increasing transmitted power up to the point where no failures occur because of an unfavorable signal-to-noise ratio.

The over-all improvement obtained in changing from AM to FS radio telegraph sometimes is expressed as a ratio of transmitted powers required to give equivalent transmission results over the two systems. Such a ratio fluctuates widely depending upon the prevailing conditions. With little fading the improvement ratio will be caused mainly by the better signal-to-noise obtained with FS and may be less than five decibles. Under severe fading conditions no amount of power may give good results with AM while FS may be satisfactory. Thus the power ratio would become infinite. By making a long-time comparison, an average power ratio figure may be found which gives equal average error rates in the printed copy from each system. Such tests[7] between a triple space diversity AM system and a double space diversity FS system have indicated a power ratio of 11 decibels in favor of the latter when the error rate was 0.1 to 0.5 per cent.

When the two systems thus are made equal by adjustment of transmitted power, more errors caused by the signal becoming submerged in noise occur in the FS system to compensate for a larger number of errors in the AM system because of rapid level changes. Often the reason for changing a radio telegraph system from AM to FS is to increase the reliability of the circuit and not just to save transmitted power.

To insure a definite improvement in such cases the carrier level should not be decreased more than about six decibels.

References

1. Certain Topics in Telegraph Transmission Theory, H. Nyquist. AIEE Transactions, volume 47, 1928, pages 617–44.

2. Frequency Modulation, Balth. van der Pol. *Proceedings*, Institute of Radio Engineers (New York, N. Y.), volume 18, July 1930, pages 1194–1205.

3. Measurement of Telegraph Transmission, H. Nyquist, R. B. Shanck, S. I. Cory. AIEE Transactions, volume 46, 1927, pages 367–76.

4. Frequency Modulation Noise Characteristics, M. G. Crosby. *Proceedings*, Institute of Radio Engineers (New York, N. Y.), volume 25, April 1937, pages 472–514.

5. Performance Characteristics of Various Carrier Telegraph Methods, T. A. Jones, K. W. Pfleger. *Bell System Technical Journal* (New York, N. Y.), volume 25, July 1946, pages 483–531.

6. Transients in Frequency Modulation, H. Salinger. *Proceedings*, Institute of Radio Engineers (New York, N. Y.), volume 30, August 1942, pages 378–83.

7. Observations and Comparisons on Radio Telegraph Signaling by Frequency Shift and On-Off Keying, H. O. Peterson, J. B. Attwood, H. E. Goldstine, G. E. Hansell, R. E. Schock. *RCA Review* (Camden, N. J.), March 1946, pages 11–31.

Discussion

F. B. Bramhall (Western Union Telegraph Company, New York, N. Y.): J. R. Davey and A. L. Matte are to be complimented on an excellent report of perhaps the most comprehensive engineering investigation and comparison of frequency modulation and amplitude modulation in audio frequency telegraphy ever undertaken.

That there be no confusion about the terms employed, it should be pointed out that FS as used in this paper is quite synonymous with FM as used in a paper[1] by J. Edwin Boughtwood and myself. Davey and Matte report the advantages of FM over AM almost precisely the same as announced in the earlier paper.

Since in a nationwide communication network, several sections of carrier channels are commonly tied together end on end, I prefer to consider the improvement in disturbance susceptibility at a noise-signal ratio much lower than the point of complete failure. On wire carrier circuits, a deviation ratio of unity is commonly employed in order that channels may be stacked closely together and spectrum utilization may be efficient. Within the range of disturbances which may reasonably be encountered on such circuits, FM will withstand as shown in both papers, 8 or 9 decibels more disturbance than AM. This is essentially the same whether the disturbance be fluctuation noise or impulse noise. The freedom from level changes, rapid or slow, is of course complete. I question whether any transmission media is dependably so quiet and so stable through all seasons and in all circumstances that substantial benefit is not derived from FM.

The telegraph company pioneered in the use of FM on wire circuits, its first commercial circuits of this type being inaugurated in 1938. Since that date, practically all of the older AM equipment has been replaced, until recent expansion runs the channel miles of FM telegraph into the hundreds of thousands. The improvement both in transmission efficiency and in circuit continuity is little short of revolutionary.

Reference

1. Frequency-Modulated Carrier Telegraph System, F. B. Bramhall, J. E. Boughtwood. AIEE Transactions, volume 61, 1942, January section, pages 36–9.

Lloyd Espenschied (Bell Telephone Laboratories, Inc., New York, N. Y.): Most ideas are older than one realizes at first, and it may be of interest to recall some of the earlier proposals for the frequency shift kind of telegraph signaling.

We find the idea coming into the picture in a crude sort of way with the very birth of the electromagnetic telegraph. Steinheil, in one of the most classical papers of telegraph literature, in 1839 describes a d-c pulse-type of telegraph system in which the polarity of the pulses, plus and minus, was employed for marking and spacing. In receiving his signals, he sought to relieve the eye from reception by having the signal operate a sounding device and thus appeal to the ear. He says, in fact, that he would like to make his system "copy the most perfect of all methods of communication—speech, in which the sound as it falls on the ear of itself arrests the attention, and is at once understood."[1] But, of course, electric telegraphy had not yet grown up to the higher frequencies whereby speech could be accommodated, and the telephone was not yet invented!

But Steinheil did go on and do the best he could to address the message to the ear, and free the eye for writing it down. One of the schemes he describes is that of causing the plus and minus impulses to clang bells of two different frequencies.[2] I suppose such a rendering might be called ding-dong telegraphy.

Of course Steinheil was not passing his two different frequencies over the line; his dots, plus and minus, occupied one and the same near-zero frequency slit on the line.

A case in which the two different frequencies were passed over the line is that disclosed by Elisha Gray in 1875 in his patent 166,095, entitled: "Electric Telegraph for Transmitting Musical Tones." For transmitting he employed two vibrators, tuned to different frequencies, each with its transmitting key, so that the two channels could be played upon as desired. For receiving he employed an electromagnetic diaphragm sounding box arrangement capable of taking both frequencies. As to the use of his apparatus, he says that "letters and signals can be represented by tones differing in pitch; or the ordinary Morse signals can be made by short and long interruptions in a prolonged tone of the same pitch, ...". At the time, Gray's invention represented but one of the many ideas that were being entertained along in the 1870's of multitone transmission for various purposes, for musical effects, for multiplex telegraphy and for the transmission of speech, as it turned out. The technique then being experimented with, of vibrating reeds and electromechanical resonators, was participated in by a number of notable inventors such as Varley and LaCour in Europe, and Gray, Bell, and

Edison over here. Out of it came mainly telephony. The distance to which telegraphy had been stretched in actual practice by that time was so great as to cause the higher attenuation of these tone frequencies to be fatal at the time. There was no amplifier, and the receiving apparatus was not sufficiently sensitive to cause line noise to be controlling, and of course radio was not yet known.

We now realize that what enables us to use the noisy and wobbly channels that we do in long distance transmission, especially in radio, is Doctor deForest's grid controlled vacuum tube amplifier, for which he so properly this very week has been awarded the Institute's Edison Medal. It is this, the amplifier, which redeems the weak signals with which we work, and in doing so draws up from the bottom of the channel Nature's dregs. Hence the effort of modern engineers to combat the noise and instability problem as exemplified by reverting, unconsciously I am afraid, to ideas of long standing, now applying quantitatively our present high frequency electronics, as so well exemplified in the present paper.

References

1. Upon Telegraphic Communication, Especially by Means of Galvanism, Doctor Steinheil. The Annals of Electricity, Magnetism, and Chemistry; and Guardian of Experimental Science, London, England, volume 3, July 1838–April 1839, page 441.

2. Same as reference 1, pages 443–4, 449, 517, and 520.

Some Modern Techniques in Ocean Cable Telegraphy

C. H. CRAMER
MEMBER AIEE

Synopsis: Transmission on long nonloaded submarine telegraph cables has been improved by application of efficient signal-shaping amplifiers, replacing electromechanical types of receiving equipment; also by duplex balances of greater accuracy through use of new artificial line networks and new methods of balancing. With these improvements it became practicable to change from cable code recorder operation to printer operation and at the same time to obtain higher quality of transmission at increased speeds

THE STATE of the art in ocean cable telegraphy has been recorded at intervals in the literature of the Institute and elsewhere through the early nineteen thirties.[1,2] It is the purpose of this paper to give an account of some of the more recent developments which have been devoted almost exclusively to the improvement of transmission in one of the oldest of the electric signal mediums, the non-loaded submarine telegraph cable.

The limitations of the earliest methods of cable operation were largely determined by the available operating equipment. The receiving instrument first used on the transatlantic cables was the mirror galvanometer, a moving-coil instrument. By reason of its sensitivity and favorable signal-shaping characteristics, the moving-coil type of receiving equipment remained in a dominant position in nonloaded cable operation until relatively recent years. The mirror galvanometer was followed by the siphon recorder which provided a permanent record of the received signals. In turn the recorder was supplemented by magnifiers of various types which amplified the received signals before passing them to the recorder; and by the sensitive cable relays such as the drum relay and the gold wire relay which made possible the abandonment of manual relay operation at repeater stations. All of these instruments were of the moving-coil type. Application of these developments and the regenerative repeaters which followed, extending over the years to the period immediately after World War I, brought about substantial increases in signaling speeds. Recorder operation was still universal requiring manual transcription of messages from the recorder tape at the receiving terminal.

The success of printing telegraph systems in land-line operation had engaged the attention of cable engineers but trial printer operation on cables while showing promise indicated generally the necessity for improved signal transmission before the automatic system could be entirely satisfactory.

Because of the fragility of the moving-coil equipment and the gain limitations of the magnifiers, the potentialities of the vacuum tube in ocean cable telegraphy were recognized early in the development of the electronic art. However, the efforts of 1918–19 toward application of vacuum-tube signal-shaping amplifiers did not produce performance justifying the replacement of magnifiers. The principal reasons for this result were the high disturbance levels generally existent on duplexed nonloaded cables at that time, comprising natural or static interference and duplex unbalance; and the lack of electric networks with shaping and discrimination characteristics better than or even equal to the characteristics of the mechanically-tuned moving coil. Certain practical apsects of the problem also then presented difficulties which subsequently disappeared when improved magnetic materials and electronic components became available.

The continuously-loaded telegraph cable with its promise of considerably higher signaling speeds, which became practical with the invention of permalloy, emphasized the limitations of recorder operation and electromechanical terminal equipment. Necessity thus brought about the concurrent development of a signal-shaping amplifier and a multiplex printer system suitable for high-speed loaded-cable operation. The laying of the first loaded cable in 1924 between New York and Horta, Azores Islands, and its immediate success are a matter of communications history.[3] The amplifiers and other terminal and repeater equipment[4,5] which formed an important part of that project contributed in no small degree to the over-all success of the undertaking. The several later loaded cables were provided with amplifiers of essentially the same design. Most of these amplifiers are still in operation with a continuous record of excellent service. It may well be said that the loaded-cable circuits established a new high standard in reliability, continuity and quality of day-to-day cable operation.

Following the period of preoccupation with loaded-cable developments and as the success of the new operating methods and equipment became evident, efforts toward improvements in the operation of the nonloaded cables were renewed. The end results of these developments, which may now be regarded as substantially completed, have been successfully applied to a considerable extent in the North Atlantic cable system of the Western Union Telegraph Company. Installations were intensified during the war in the course of which the developments were made available to the Com-

Paper 47-79, recommended by the AIEE committee on communication for presentation at the AIEE winter meeting, New York, N. Y., January 27–31, 1947. Manuscript submitted November 12, 1946; made available for printing December 10, 1946.

C. H. Cramer is with the Western Union Telegraph Company, New York, N. Y.

The author appreciates the opportunity to present an account of developments which embrace the collective achievements of a number of his associates in the Western Union Telegraph Company. Work leading to the frequency analysis of duplex balance networks was initiated by J. W. Milnor.

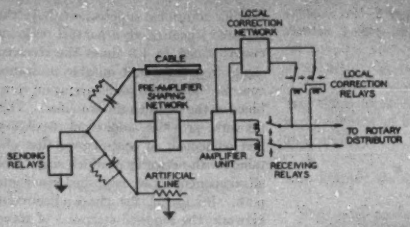

Figure 1. Typical application of signal-shaping amplifier on duplexed nonloaded cable

mercial Cable Company and they were utilized in the rehabilitation and extension of the cable system of the Alaska Communication System.

The program has included conversion from cable code recorder operation to 5-unit code printer operation; the replacement of magnifiers with vacuum-tube signal-shaping amplifiers which also makes possible use of sturdy land-line type polar relays instead of the mechanically-delicate cable relays; and improvements in duplex artificial line networks and in the technique of balancing. The advantages of more completely automatic operation have thus been made available and at the same time circuit speeds have been increased and circuit and equipment maintenance at the cable stations have been reduced.

The Printer System

In view of the high capital cost of the long nonloaded ocean cable and its relatively low signaling speed, the message output of the circuit is a matter of great importance and thus it is ordinarily essential to use a signaling code with a minimum number of time units per character. For this reason much work has been done on cable printer systems based on various nonuniform codes which average fewer units per character than the Baudot 5-unit uniform code. These systems[6,7] have been tried experimentally and some have had practical application. However early experiments with printer operation on Western Union cables, confirmed by experience with the loaded-cable circuits, favored the adoption of the 5-unit code with a method of transmission, used also on the loaded cables, which effectively overcomes the relative inefficiency of the code.

The printer system which has been standardized for nonloaded cables does not differ fundamentally from the loaded-cable system but it resembles the land-line multiplex more closely. It utilizes land-line types of transmitters, rotary distributors, synchronizing mechanisms, and printers, thus gaining the advantages of uniformity. It differs in two respects from normal land-line practice. It is applied to single-channel as well as to multi-channel operation whereas the land-line system employs start-stop 7-unit code printers for single-channel applications. Secondly, on long cables the printer signals are transmitted at a speed such that pulses of unit or dot length are received at very small amplitude and may be regarded as completely missing. The receiving networks are adjusted to respond to signals two or more units long and thus for purposes of signal reception the fundamental received frequency is one-half the transmitted dot frequency. The receiving relay operates as a 3-position relay and remains at the zero position for dot signals. The dots are reinserted synchronously by the receiving rotary distributor.

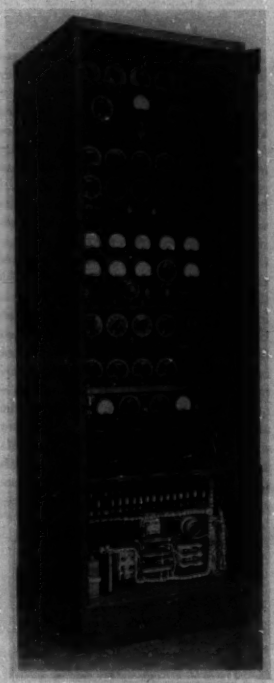

Figure 2. Signal-shaping amplifier for long nonloaded cables

It might appear at first glance that the attenuated-dot method of transmission would double the cable output as compared with normal multiplex transmission in which all signal elements are received at full amplitude. That must be regarded as a limit which may be approached but cannot be fully realized because with attenuated-dot transmission the received signals are more susceptible to interference and somewhat more difficult to shape. This device does permit a substantial increase in the letters-per-minute circuit speed, amounting to about 80 per cent over that possible with normal transmission, and thus in effect it shortens the code.

The cable printer system has all the elements of flexibility of the land-line multiplex; that is, individual channels may be terminated, extended or combined with other channels as required to meet traffic conditions and the transmission speeds of the available circuits. Varioplex methods may be applied to obtain subchannels for use as direct point-to-point or customer-to-customer circuits where the full capacity of a channel is not required.

Signal-Shaping Amplifier for Long Nonloaded Cables

The requirements of a signal-shaping amplifier which will permit satisfactory printer operation on long non-loaded cables at the highest practicable speeds are severe. The more important of these are

1. A higher standard of accuracy is necessary than for recorder operation in which manual transcription of received signals affords the opportunity to correct transmission errors. A higher standard of continuity and reliability of operation is also now required, determined in part inherently by automatic operation and in part by various present-day competitive and economic conditions. Amplifiers and other operating equipment should thus require a minimum of skilled attention.

2. In transmission, signals are subjected to heavy distortion resulting from unequal attenuation and phase shifting of their component frequencies. At present operating speeds, the attenuation of the higher-frequency components of a signal pulse as compared with the lower-frequency components

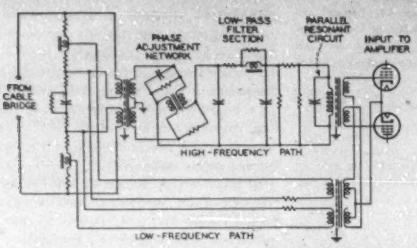

Figure 3. Pre-amplifier signal-shaping network

differs as much as 11.5 napiers (100 decibels). The signal-shaping network must equalize or restore these components to an approximation of the original amplitude and phase relationships.

3. To reduce susceptibility to interference to a minimum, the shaping network must pass only the narrowest band of frequencies consistent with a satisfactorily-low degree of characteristic distortion. The network must cut off somewhat sharply above the band to discriminate against extraneous interference and duplex unbalance voltages. It must also reject direct currents as well as alternating currents of near-zero frequency to discriminate effectively against earth currents, particularly during the abnormal conditions accompanying magnetic storms.

4. In the case of duplex-operated cables—and almost all nonloaded cables are at least held available for duplex operation—the shaping network should be electrically symmetrical with respect to the duplex bridge or electrically isolated from it so that the network and the amplifier do not of themselves contribute to the duplex unbalance. Signal-shaping amplifiers meeting this requirement, including spare equipments, may be assigned interchangeably to various cable circuits without requiring readjustment of balances.

5. The network elements must be provided with a considerable degree of adjustability. Approximate network constants may be calculated but the optimum values must be determined for each cable by manual adjustment.

6. The amplifier should be provided with sufficient gain and output to operate rugged polar relays of the general type standard in land-line telegraphy.

The signal-shaping amplifier which is now regarded as standard for long nonloaded cables meets the requirements detailed above and may be viewed, at least for the present, as a satisfactory conclusion of several years of laboratory development and field operating experience. A standard installation, Figures 1 and 2, includes a primary or pre-amplifier shaping network, an amplifier unit, receiving relays, and a secondary shaping or local correction network which supplies low-frequency components of the signals rejected by the pre-amplifier network.

The pre-amplifier network, Figure 3, when correctly adjusted, passes a band which includes all of the higher-frequency components of the signals required for good signal shape, properly proportioned and phased. Frequencies below the fundamental received frequency are heavily attenuated, with almost complete rejection in the range of earth current disturbances. The first branch of the network, symmetrically arranged and directly connected across the duplex bridge, together with the effective capacitance of the cable circuit, is tuned to about 1.5 times the received frequency. The following elements of the network are isolated from the first branch by shielded transformers so that the effect on duplex balance is negligible whatever their arrangement. In one path the lower frequency components are passed to the amplifier input with little or no further shaping. Higher-frequency components are further shaped in the second path which includes a bridge-type phase-adjusting network, a low-pass filter section for additional suppression above the required signal band, a parallel resonant circuit tuned to 1.5 times the received signal frequency, and suitable resistance controls. The two paths are again combined at the input to the amplifier. This network provides additional flexibility and refinement of control over that obtained with networks in which shaping of all components is accomplished in a single path. By use of the phase-adjustment network, the required steepness of wave front is secured with less of the higher-frequency components thus narrowing the band at the upper end and discriminating more effectively against interference. The network frequency response given in Figure 4, which includes the characteristics of the amplifier as described below, is typical of those obtained in actual operation.

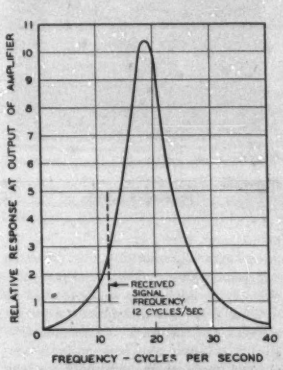

Figure 4. Frequency characteristic of signal-shaping amplifier

Printer operation: attenuated-dot transmission, 575 letters per minute (dot frequency, 24 cycles per second)

The three-stage resistance-capacitance-coupled amplifier is of a push-pull type with two stages of voltage amplification. The time constant of the interstage coupling is such as to suppress frequencies below those transmitted by the shaping network. This effectively eliminates disturbances or sways which might otherwise result from power supply variations. The maximum voltage gain of the amplifier is about 83 decibels. The available overall gain for the higher-frequency components, including the input transformer, is about 103 decibels. This provides a reasonable margin above the maximum gain likely to be required for the most severe conditions of application. The output of the amplifier is adequate for the operation of modern land-line type polar relays. Following usual cable practice the normal receiving relay circuit comprises a pair of standard 2-position relays functioning together as a 3-position relay. This circuit is readily converted for optimum reception of 2-current signals.

A long square-top signal transmitted from the far end of the cable is reproduced at the receiving end as shown in Figure 5. The signal as it appears at the output of the pre-amplifier network, 5*C*, rises to maximum amplitude in the time of the shortest received signal and then decays to zero. At this point signals of the fundamental received frequency are fully shaped and suitable for operation of the receiving relays but longer signals would be badly distorted because of the deficiency of low-frequency components. These components are restored by the local correction network, Figure 1, under control of the receiving relays. The shaped local correction voltage, 5*D*, is added to the received signal in the grid circuit of the output stage resulting in the

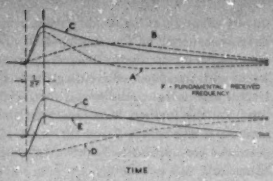

Figure 5. Received signal resulting from transmission of long signal

A—Component through high-frequency path of pre-amplifier network
B—Component through low-frequency path of pre-amplifier network
C—A+B
D—Component supplied by local correction network
E—Complete signal, C+D
F—Fundamental received frequency

fully-shaped signal, 5*E*, which, if required, will hold at constant amplitude indefinitely.

The general method of shaping involving local correction, while considerably refined in the present application, is not new. It was normally utilized in some degree in the magnifier shaping systems. It differs from the method employed in the loaded-cable amplifiers in which essentially all shaping is accomplished in pre-amplifier and interstage networks with, however, some deficiency in the very-low-frequency components. The advantages over the latter method include, in addition to the relative immunity from low-frequency disturbances mentioned previously:

1. Simplification of amplifier design and increased amplifier stability, since the amplifier is not required to pass the lowest signal frequencies;

2. The received signals are not subject to "wandering zero", the slow transient resulting from signal combinations in which the polarities are unbalanced

Duplex Operation

Since duplex operation of non-loaded cables normally affords greater total message capacity, that method is usual unless abnormal transmission and traffic conditions favor one-way operation. With modern amplifiers in use, extraneous interference and duplex unbalance levels determine the top signaling speeds. If unbalance is the principal factor, maximum capacity is obtained with the speeds in the two directions unequal; for example, two printer channels in one direction and a single channel in the opposite direction. Parenthetically, it may be remarked that in addition to the transmission factors, efficient utilization of operating personnel is also a factor in determining channel speeds and maximum circuit capacity. The importance of duplex unbalance as a limiting factor has been reduced in recent years through improvements in artificial line networks and balancing methods.

The Duplex Balance

The basic ocean cable artificial line, Figure 6*A*, has changed little in form since the early days of duplex operation. The lumped series resistance and shunt capacitance elements, simulating the conductor resistance and the capacitance of the cable, have varied somewhat in fineness of subdivision over the years. In some instances greatly increased adjustability has been provided. It has been well established in theory[1] and practice, however, that the very fine subdivisions employed throughout many of the existing artificial lines are unnecessary from the standpoint of balance accuracy. Further, the size of the lumps may be progressively enlarged along the artificial line, since the accuracy with which the cable must be matched decreases as distance (and attenuation) from the head of the artificial line increases. Modern artificial lines of American design follow this pattern and have the advantage of simplified and less costly construction.

Although the basic artificial line simulates directly only the d-c resistance and the capacitance of the cable, the circuit parameters include inductance and effective resistance which vary with frequency because of the characteristics of the earth return path[8] and are commonly termed the sea-return impedance. These factors, Figure 7, although small and generally of minor effect on signal transmission, are of considerable importance in balancing, particularly in high-accuracy balancing of the near end of the cable. Inductive networks have been added to artificial lines in various forms[9,10] and while theoretically an accurate simulation of the sea-return impedance can thus be obtained it is difficult practically to provide inductors or inductive networks which have the required characteristics and ease of manipulation. Artificial line modifications of that type have not proved to be a satisfactory method for obtaining balances of the order of accuracy now demanded.

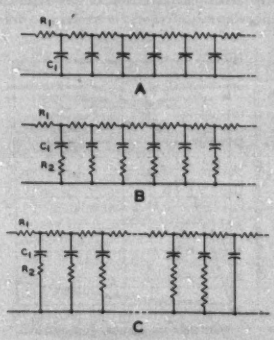

Figure 6. Artificial line networks

A—Basic artificial line
B—With uniform R_2 added to simulate inductance
C—With tapered R_2 to simulate inductance and effective resistance

Simulation of Sea-Return Impedance

Milnor has shown[1] that in a uniform network of the form illustrated in Figure 6*B*, the resistances R_2 in series with the capacitors provide a match of the cable inductance L if

$$R_2 = \frac{L}{R_1 C_1} - R_1/4 \qquad (1)$$

and R_1, C_1 are equal to the corresponding cable parameters. The balance is correct for all frequencies if L is constant. Actually the inductance varies with frequency as indicated in Figure 7. While for this reason the uniform network is not a complete answer it can be applied to a very limited extent at the head of the artificial line with some beneficial results at the frequencies requiring the greatest accuracy of balance. Another factor which limits the use of the network is that its propagation constant differs substantially from that of the cable and hence affects the balance of the following sections of artificial line, particularly as the cable is commonly not uniform as to core size, armoring, and so forth.

More recently it has been found that if R_2 is tapered as in Figure 6*C* the sea-return impedance is simulated over a relatively wide band of frequencies and further that there is no important change in the propagation constant of the section of artificial line to which it is applied. The taper which has provided the best results experimentally may be defined by the empirical equation

$$L_1 = K_1 e^{K_2 d} \qquad (2)$$

in which L_1 is the apparent value of inductance to be balanced, d is the distance

from the head of the artificial line (or cable) and K_1, K_2 are constants related to the parameters of the cable. Now, with values of R_2 calculated by substituting L_1 for L in equation 1, a balance of both inductance and effective resistance is obtained. For optimum results the taper should be terminated at a critical distance from the head of the artificial line, dependent also upon the cable parameters. Empirical equations for this relationship may likewise be set up. Experimentally, the point of termination is determined by inserting R_2 section by section until the cumulative added impedance equals the difference in impedance between the cable and the basic artificial line. The section of artificial line thus modified corresponds to the first 100 to 150 nautical miles of cable and the number of resistors added is usually less than ten. For some types of cable it may be advantageous to insert a second taper system to increase the accuracy of matching at the lower frequencies.

Figure 8 shows comparative residual unbalances with the artificial line set to match only the d-c resistance and the capacitance of the cable and after the insertion of the tapered resistance. It should be noted that neither of these conditions represents a balance sufficiently accurate for duplex operation. They are instead only foundations upon which the operating balance may be built.

Under the first condition, reduction of the unbalance is accomplished by a series of time-consuming cut-and-try compromise adjustments which must provide a sea-return impedance balance as well as refinement of the resistance-capacitance balance. The necessary compromises frequently result in a considerable distortion of the resistance-capacitance ratio in some sections of the artificial line.

In the second case, where the initial balance includes a simulation of the sea-return impedance approximating in accuracy that of the other components, refinement of the balance is less difficult, requires less time and a final balance of greater accuracy can be obtained.

Frequency Analysis of Unbalance and Application of Resonant Corrective Networks

The conventional method of balancing involves transmission of slow reversals and observation of the residual unbalance transient by oscillograph or ink recorder while adjusting the artificial line. In the final stages of the adjustment, unbalance resulting from transmission of signals at operating speeds is also observed. Adjustment in this manner of the basic artificial line or any of its modifications eventually reaches a point where further reduction of the unbalance becomes impracticable. The limit occurs on specific cables at different levels of balance. The limit may be determined by one or more of such factors as inadequacy of artificial line, masking effect of extraneous interference, inability of the technician, however skilled, to make further beneficial adjustments by cut-and-try methods or by mental analysis of the unbalance transient.

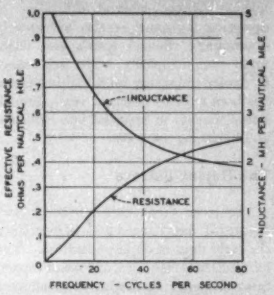

Figure 7. Inductance and effective resistance or sea-return effects of a common type of cable

These barriers have been lowered by a new approach to the problem in which corrective resonant networks are applied, each supplying an impedance which can be effectively controlled as to magnitude and width of frequency band. The networks are designed in accordance with a frequency characteristic of the residual unbalance. Methods involving frequency analyses of the residual unbalance have been used[11] in the step-by-step development of synthetic balancing networks with the object of avoiding the relatively expensive conventional artificial line. In the method here presented the artificial line is retained and the resonant networks are applied to improve existing balances.

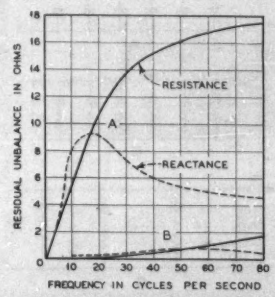

Figure 8. Frequency characteristic of unbalance

A—Basic artificial line set to simulate d-c resistance and capacitance of cable
B—With tapered resistance R_2 added (Figure 6C)

The frequency characteristic which is the basis of the method may be obtained by a mechanical harmonic analysis of an oscillographic record of the unbalance transient or the effective residual impedance unbalance at the head of the artificial line may be measured directly across the duplex bridge through the important frequency range. The first procedure has the advantage, perhaps useful under special conditions, of permitting the analysis to be carried out at a location away from the cable station. The electrical measurement, which is now used exclusively in practice, requires considerably less time and it is more accurate since extraneous interference is rejected by sharply selective filters.

The preferred network, of the parallel-resonant type, and the manner in which it is inserted in the cable circuit are illustrated in Figure 9. The network consists of a variable air-gap transformer with low-inductance primary and a high-inductance secondary tuned to the desired frequency and suitably damped to obtain the required impedance characteristic. A single network is effective over only a part of the frequency range and for best results several networks may be required, some in series with the artificial line, some in series with the cable, as the artificial line impedance at different frequencies is deficient or excessive. The low-inductance primary, usually from a fraction of a millihenry to several millihenries, and its low d-c resistance are desirable to avoid unwanted effects on signal transmission and balance. The high-inductance secondary permits tuning at the low frequencies involved with practical sizes of capacitors.

Figure 10 shows the frequency characteristic of the unbalance on a typical circuit adjusted for best balance and before the application of corrective networks; and the unbalance on the same circuit after the insertion of the networks indicated in Figure 9. It is to be noted that the balance has been improved not only within the most important frequency band but that the greatest reduction has been made at the higher frequencies. The high-frequency unbalance, largely ignored previously and although heavily attenuated by the signal-shaping network

has affected operating balances by reason of its magnitude. The final balance following the insertion of resonant networks is obtained by minor adjustments of the usual artificial line controls. An important further advantage of this method of balance refinement is that the work may be carried on without disturbing the existing operating balance, so that the circuit may be quickly returned to operation if required. Also the networks can be designed and checked to a large extent independently of the cable circuit and thus without interruption of circuit operation.

While the frequency-analysis technique is essential in the design of resonant balance networks, it has proved to be very valuable in balancing work generally. For example, development of the tapered sea-return impedance correction would have been difficult if not impracticable if the study had been limited to transient effects.

The Cathode Ray Oscilloscope in Balancing

The cathode ray oscilloscope, when provided with the slow sweep necessary for the very low frequencies encountered, has proved to be an important and versatile adjunct in balancing work. Compared with electromechanical types of oscillograph it is more convenient to use and reduces the time required for balancing since the effect of an adjustment can be observed immediately. It is free of the frequency limitations of ink-writing recorders. By use of a retentive-screen tube and superposed traces of the unbalance transient, the effects of interference are more readily discounted. It is particularly suited to observing abnormal unbalance effects such as polarity distortion in which transmitted pulses of opposite polarity produce unlike unbalance transients.

Interference

Crossfire between cables is not unusual where two or more cables land at the same point and may of necessity be laid with small separation between cables. Such interference is controlled readily by use of simple corrective networks at the cable stations. The most difficult crossfire condition results when two cables, landing at different points, have been laid closely parallel or with a small-angle crossing some distance from the landing points. In such instances correction requires a more complex network including a delay network and a wire connection between

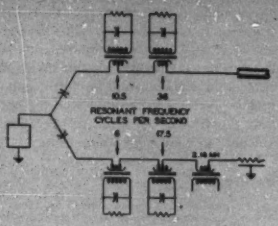

Figure 9. Typical installation of resonant balance networks

the cable stations. One correction of this type has been applied effectively in which the cable stations are located about 30 miles apart.

With the means now available for improved balances and for correction of crossfire, extraneous interference, mostly of natural origin, becomes, in general, the most important factor preventing further increases in speed. Natural interference is picked up in the shallow-water end section of cable and its magnitude, depending upon the depths and distances encountered, varies widely from cable to cable. Receiving earths of the nonloaded cables are generally located at distances up to several miles from shore. The cable conductor and the earth con-

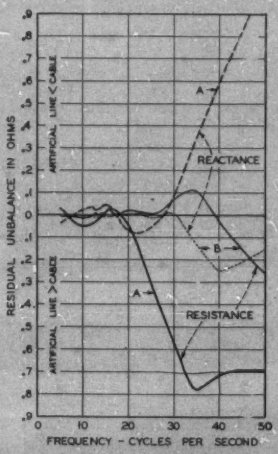

Figure 10. Frequency characteristic of unbalance on a transatlantic cable

A—Before insertion of networks as shown in Figure 9

B—After insertion of networks as shown in Figure 9

nection are carried to the earthing point in twin-core cable which provides a considerable reduction of the interference within that section. Reduction of the existing levels of interference could obviously be accomplished by extending the twin-core sections but that, unfortunately, is costly. Some improvement has been obtained by increasing the sending voltages which until recent years were conservatively restricted to about 50 volts. In the Western Union cable system voltages of 90 to 120 are now in common use.

Conclusion

All of the transatlantic nonloaded cables of the Western Union Telegraph Company have been converted from cable code recorder operation to 5-unit code printer operation. The Commercial Cable Company has installed like equipment on two of its transatlantic circuits supplementing an earlier installation of 5-unit code equipment of different design on a third circuit. The advantages of more completely automatic operation, greater flexibility including use of sub-channeling methods such as the varioplex, and uniformity with land-line multiplex printer systems have been obtained, while at the same time the message-handling capacity of the cables has been generally increased. Improved signal transmission insuring the success of the conversion has been obtained through use of vacuum tube amplifiers and improved signal-shaping networks, more accurate duplex balances, and by reduction of crossfire and use of increased sending voltages which provide a better signal-to-interference ratio.

Signal-shaping amplifiers of the type described in this paper are in use on all of the long nonloaded cable sections of Western Union's North Atlantic system and short-cable amplifiers, of which several types are available to meet a range of requirements, are in operation on the short connecting cables of the system. The Commercial Cable Company has amplifiers installed and in course of installation on the long and short cable sections making up four of its transatlantic circuits.

The new resonant-network balancing method has been applied by the Commercial Company to three main circuits involving 14 cable sections. Utilization of the latest balancing methods in the Western Union system has been more gradual because existing balances had been improved by use of modern types of observing instruments in conjunction with conventional balancing procedures and

by application of forerunners of the methods described in this paper. Of greatest technical interest perhaps are the results obtained with the new methods on the Commercial Company's heavy-core cable laid in 1923 between Canso, Nova Scotia and the Azores. On low-resistance cables, sea-return impedance effects become relatively more important, particularly in view of the higher signaling speed. Theoretical indications of difficulty in balancing cable of this type for the expected speed were confirmed in practice. Experience with an inductive balancing network[10] was unsatisfactory and its use had been discontinued. In the course of the present work the balances were refined with resonant networks, supplemented at the Azores end only by an early version of the tapered sea-return impedance correction. As a measure of the improvement obtained, the previous 2-channel recorder speeds of 550 and 575 letters per minute eastward and westward respectively were increased initially to 600 letters per minute in each direction and the performance of the circuit was substantially improved. The ultimate speed in printer operation, when 3-channel multiplex equipment is available, is expected to be 750 letters per minute in each direction.

On the duplex-operated nonloaded cables of the Western Union system the sum of the letters-per-minute speeds in the two directions now averages in printer operation more than 40 per cent above the previous recorder speeds. The average net increase in the message capacity of these cables, taking into account the short cuts, abbreviations, and so forth, commonly practiced in recorder working but not practicable in printer operation, amounts to more than 30 per cent.

References

1. Submarine Cable Telegraphy, **J. W. Milnor**, AIEE Transactions, volume 41, 1922, pages 20–38.

2. Submarine Telegraphy in the Post-War Decade, **I. S. Coggeshall**. AIEE Transactions, volume 49, 1930, pages 476–85.

3. The Loaded Submarine Telegraph Cable, **O. E. Buckley**. AIEE Transactions, volume 44, 1925, pages 882–91.

4. The Application of Vacuum Tube Amplifiers to Submarine Telegraph Cables, **A. M. Curtis**. *Bell System Technical Journal*, volume 6, 1927, pages 425–41.

5. Automatic Printing Equipment for Long Loaded Submarine Telegraph Cables, **A. A. Clokey**. *Bell System Technical Journal*, volume 6, 1927, pages 402–24.

6. Printing Telegraph on Nonloaded Ocean Cables, **Herbert Angel**. AIEE Transactions, volume 46, 1927, pages 884–95.

7. Direct Printing Over Long Nonloaded Submarine Telegraph Cables, **M. H. Woodward, A. F. Connery**. *Electrical Communication*, volume 10, 1931–32, pages 210–19.

8. Transmission Characteristics of the Submarine Cable, **J. R. Carson, J. J. Gilbert**. *Journal of the Franklin Institute*, volume 192, 1921, pages 705–35.

9. The Newfoundland-Azores High-Speed Duplex Cable, **J. W. Milnor, G. A. Randall**. AIEE Transactions, volume 50, 1931, pages 389–96.

10. Balancing Cables by Inductive Networks, **M. I. Pupin**. Electrical Engineering, volume 50, 1931, pages 935–38.

11. The Simulation of Long Submarine Cables, **H. Salinger, H. Stahl**. *Elektrische Nachrichten-Technik*, volume 3, 1926, pages 296–306.

Discussion

J. J. Gilbert (Bell Telephone Laboratories, New York, N. Y.): A point of particular interest in this paper is the progress that has apparently been made in improving duplex balance. The use of impedance measurements in this process is undoubtedly a real step in advance and represents an interesting break with tradition. Until comparatively recently in the long history of the submarine cable art it was customary to analyze problems on a transient basis rather than in terms of steady state conditions. Some years ago it was demonstrated that steady state methods, involving measurements and computations with sinusoidal currents, furnished, when properly interpreted, the most exact means of designing cables and associated apparatus. In some problems, such as those associated with the high speed permalloy loaded cable, most of the important design factors such as sea-return impedance and eddy current and dielectric losses were not at all amenable to treatment by transient methods but could be readily dealt with by steady state methods. In duplex unbalance investigations the transient method probably still has certain practical uses, but it is evident that for fundamental work in the subject steady state methods offer great advantages.

A Carrier Telephone System for Rural Service

J. M. BARSTOW
ASSOCIATE AIEE

THE POSSIBILITY of supplying telephone service over power lines to rural customers in sparsely settled areas first was considered seriously by engineers of Bell Telephone Laboratories in 1936. A brief investigation at that time indicated that the transmission of voice frequencies directly over the power wires was impracticable because of the high transmitting power necessary to override ambient noise levels. As static and power system noise generally decrease with increasing frequency, attention thereafter was focused on the possibilities of carrier current methods.

A technique for the transmission of carrier currents over high-voltage power lines had been established previous to 1936, but the communication circuits so provided were relatively expensive and were generally in a class with long distance toll telephone circuits. They were used chiefly for relaying, telemetering, or speech communication between widely separated power stations.

Carrier current technique in the telephone field also had reached a high degree of development by 1936, but its use was confined to relatively expensive long distance toll circuits. Thus the rural power line carrier system, as conceived at that time, represented the first attempt, in the United States at least, to devise a carrier system which might in some situations compete from a cost standpoint with conventional voice frequency facilities.

The entry of the United States into the war in 1941 made it necessary to defer further work on the rural power line carrier project because of the diversion of development effort at the laboratories to war projects. By that time, however, the project had been carried to a point where it seemed that there was a good chance for success. A great deal of work had been done co-operatively with the Rural Electrification Administration on power line transmission characteristics at carrier frequencies, and tentative requirements had been established on auxiliary apparatus to be applied to the power lines to make them suitable for carrier transmission. Experimental carrier equipment also had been assembled and tested successfully in the field.

Early in 1945 the project again was taken up by a small group of engineers at the laboratories. In order to satisfy with the greatest speed the portion of the large postwar demand for telephone service that could be served economically by power line carrier, the engineers assigned to the project set about the design of a system representing the best compromise that could be effected quickly among cost, performance, and ruggedness, giving great weight to reliability. Between January 1945 and October 1946 a system known as the *M1* carrier telephone system was developed and is being manufactured by the Western Electric Company. Experimental models have been tested under field conditions, with subscriber participation, and have been found to perform satisfactorily.

The transmission of carrier frequencies over a ramified network designed for the distribution of 60-cycle energy at relatively high voltages is in itself a rather complicated problem, and the effort on the power line carrier project therefore has been divided between

1. The devising of methods of treating the power system to provide a suitable carrier transmission path.

2. The developement of the carrier system itself.

The results of these two phases of the work will be described in succeeding sections of this paper.

Treatment of Power System

The transmission characteristics of a power system at carrier frequencies are quite different from those at 60 cycles. This is primarily caused by the fact that the lines are "electrically long" at carrier frequencies; that is, the physical length of the lines may be many times the carrier wave length, whereas at 60 cycles the line length is a very small fraction of the transmitted wave length. This may be appreciated by noting that the wave length at 60 cycles is about 3,000 miles, whereas the wave lengths of the carrier frequencies of interest here vary from less than one-half mile to slightly over one mile. Furthermore, whereas power line carrier systems heretofore have been operated over long relatively "smooth" transmission lines, power distribution systems involve many serious electrical irregularities.

Figure 1 illustrates the actual layout of a portion of a representative single-phase rural distribution system. The pole-head diagram in the upper right hand corner shows the type of construction generally employed in rural areas and with which the power line carrier project mainly is concerned. The upper wire is a phase wire operating at a 60-cycle voltage of about 7 kv above ground, while the lower wire is a neutral wire which generally is grounded at frequent intervals. It will be noted that the network shown in Figure 1 is characterized by many

Paper 47-80, recommended by the AIEE committee on communication for presentation at the AIEE winter meeting, New York, N. Y., January 27–31, 1947. Manuscript submitted November 14, 1946; made available for printing December 11, 1946.

J. M. BARSTOW is with Bell Telephone Laboratories, Inc., New York, N. Y.

The author wishes to give credit to those who have invented, designed, and devised the components of the system and without whose work the system would not have taken its present form. These men are A. J. Aikens, J. M. Dunham, R. C. Edson, J. W. Emling, L. B. Hochgraf, W. E. Kahl, B. McWhan, and J. W. Geils. Appreciation is expressed to these men and also to P. W. Blye, under whose general direction the work was done, for making this paper possible and for their constructive criticisms on its form and content.

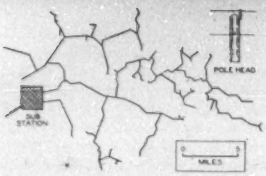

Figure 1. Rural power distribution lines

branches and taps over which telephone service may or may not be required.

From a carrier transmission standpoint, in a system such as that shown in Figure 1, every branch and tap, whether used for carrier transmission or not, is a potential source of high attenuation. For example, it is well known that, with its far end open, a transmission line one-quarter wave length long looks virtually like a short circuit from its transmitting end. An unused branch, therefore, one-quarter wave length long at a particular carrier frequency may produce almost a short circuit across the main transmission path at that frequency. It has been found practicable greatly to reduce adverse transmission effects resulting from reflections at electrical irregularities by the use of carrier frequency choke coils and carrier frequency terminations at strategic points in the power system. These terminations, as well as the various coupling units which will be described, are connected to the primary phase wire (normally 7.2 kv above ground) through 2,000-micromicrofarad capacitors, one type of which is illustrated in Figure 2.

The manner of applying coupling capacitors, carrier frequency terminations, and choke coils is described more completely in another paper,[1] and will be treated only summarily here. In general, only a portion of a power system network is used for carrier transmission, and within the boundaries of the portion a "main line" is selected, along which carrier telephone service is to be provided. Service also is provided to branches and taps to the main line. The following summary describes the treatment applied to the power network in order to provide satisfactory carrier transmission. The treatment is illustrated in Figure 3.

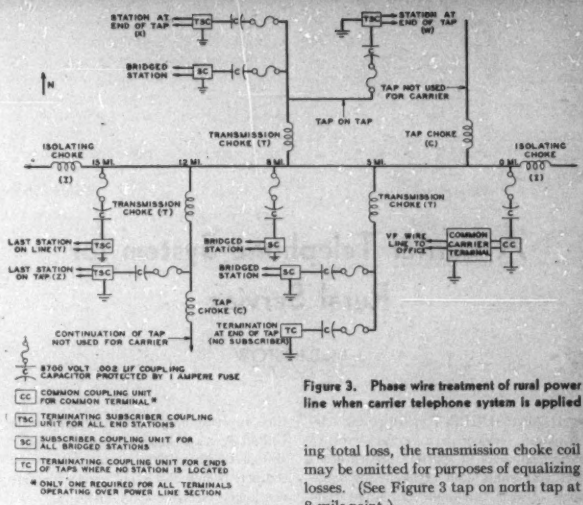

Figure 3. Phase wire treatment of rural power line when carrier telephone system is applied

Summary of Power Line Treatment

1. Main line used for carrier transmission.

(*a*). Always terminated at carrier frequencies in approximately characteristic impedance (500 ohms) at each end.

(*b*). Isolating choke coils (10 millihenrys) applied at ends as required. Tap chokes (2.5 millihenrys) may be used when 60-cycle current rating is sufficient.

2. Taps not used for carrier transmission.

(*a*). Choke coil always applied at tap point. Tap chokes normally used, but isolating choke may be used if 60-cycle current rating of the tap choke is insufficient for the tap.

3 Taps used for carrier transmission.

(*a*). Always terminated at carrier frequencies in approximately characteristic impedance at, or beyond, the location of last subscriber.

(*b*). Transmission choke (0.6 or 0.3 millihenry) used at each tap point.

An exception would be as follows: at a point where the loss caused by the insertion of a transmission choke coil would produce a loss to the connected stations such that the total loss exceeds the limiting total loss, the transmission choke coil may be omitted for purposes of equalizing losses. (See Figure 3 tap on north tap at 8-mile point.)

By the use of these arrangements, carrier telephone systems may be applied to rural power distribution systems having maximum over-all lengths of from 10 to 20 miles, depending mainly on number of taps, ground resistivity (with which transmission loss varies directly), and type and size of line wire. Maximum over-all permissible line losses are about 40 decibels (including losses caused by taps).

Transmission measurements at carrier frequencies on actual rural power distribution lines have shown that the treatments outlined in the foregoing paragraphs are very necessary to obtain satisfactory carrier system operation. Figure 4 is an illustration of the attenuations measured before and after treatment on a 14-mile line with a normal number of branches and tap, located west of Hutchinson, Kans. This line was very similar to the 15-mile line shown in Figure 3.

Description of M1 Carrier Telephone System

General

The technique employed in the *M1* system is double side-band amplitude modulation with transmitted carrier. This technique generally is conceded to be somewhat more susceptible to noise than single side-band or phase modulation techniques, but its simplicity and low cost together with the ease with which it could be integrated with present Bell System local plant signaling and supervisory

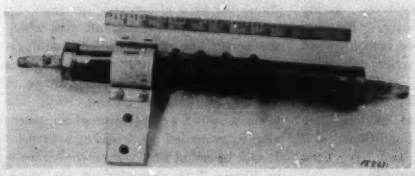

Figure 2. Coupling capacitor

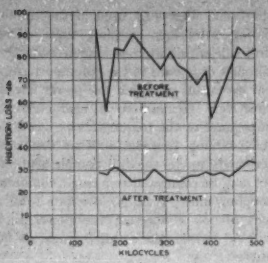

Figure 4 (left). Attenuation – frequency characteristics of 14-mile power line

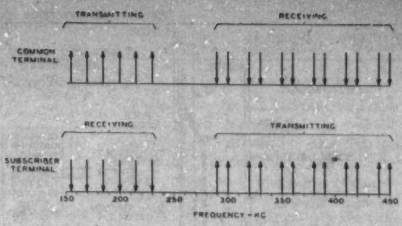

Figure 5 (right). Frequencies employed by *M1* carrier telephone system

methods were large factors in its selection.

The frequencies used lie between 150 and 455 kc. At frequencies below 150 kc, coupling problems become increasingly difficult, and at frequencies above 455 kc high line attenuation and interference from broadcasting stations would limit the usefulness of the system.

Six 2-way channels are provided within this band, each making use of three carrier frequencies. The frequency allocations are shown in Figure 5. Any subscriber's receiving frequency may be associated with any pair of subscriber's transmitting frequencies (shown ten kc apart in Figure 5) to form one 2-way channel. The second subscriber's transmitting frequency is needed when making a reverting call; that is, when one party calls another party on the same channel. The manner of using these three frequencies is described in a later paragraph.

Each 2-way carrier channel is connected to the telephone central office via a voice frequency line, as shown in Figure 3 and may be thought of as an extension of that line. One channel of the carrier system consists of a common terminal, coupling arrangements to the power line, including a common carrier coupling unit, and the associated subscriber station equipments including coupling units and subscriber terminals. There are as many subscriber terminals associated with one common terminal as there are "parties on the line" in ordinary voice frequency terms. Assuming eight parties per 2-way channel a complete carrier system would serve 48 subscribers (6 channels, 8 parties per channel). A common carrier coupling unit will take care of from one to six common terminals while each subscriber coupling unit is designed to accommodate only one subscriber terminal.

The system is designed to operate in either manual or dial central office areas. Divided code ringing is provided; that is, simultaneous ringing occurs for half the parties on one channel. Optional wiring is provided to enable full code ringing to be used also.

Sixty-cycle power is required at each subscriber's terminal and at the common terminal. Under standby conditions a subscriber terminal uses about seven watts of power. While being used for speech transmission and reception, a subscriber terminal consumes energy at the rate of about 25 watts. Under standby conditions, the common terminal uses 16 watts and under full operating conditions, uses about 30 watts.

Figure 6 shows the principal elements of the *M1* carrier telephone system and illustrates their manner of use. The equipments used at a subscriber's location are as follows:

1. A telephone set.
2. A subscriber carrier terminal consisting of a carrier-frequency oscillator, modulator, transmitting amplifier, receiver amplifier, demodulator, filters, relays, power supply, and associated equipment.
3. Carrier drop wire (not the power service wire) connecting the subscriber terminal through the usual station protector to the coupling unit at the coupling unit pole (this pole is usually the nearest high-voltage power pole).
4. A subscriber coupling unit including selective filters, relay, carrier-frequency transformer, and associated safety switch and protectors.
5. A 2,000-micromicrofarad high-voltage coupling capacitor.
6. A fuse interposed between the capacitor and the power phase wire.

The equipments used at the common terminal point where connection is made to a voice-frequency pair to the central office are as follows:

1. A fuse connected between the phase wire and a 2,000-micromicrofarad high-voltage coupling capacitor.
2. The common coupling unit consisting of a carrier transformer and associated safety switch and protectors.
3. Common terminal drop wire for transmitting carrier frequencies between the coupling unit and the common terminal (This wire will be only a few feet long when the terminal and the coupling unit are mounted on the same pole, but may be up to 1,000 feet in length where required.)
4. The common terminal itself, consisting of an oscillator modulator, transmitting amplifier, two receiving amplifiers, demodulators, ringing circuit, filters, relays, hybrid coils for combining the incoming and outgoing signals on the same voice frequency line, power supply, and other associated apparatus.

Coupling Units

Four different coupling units have been standardized for the *M1* carrier telephone system. Each coupling unit is housed in a galvanized iron coupling unit box as illustrated in Figure 7*B*.

Subscriber Coupling Unit

This coupling unit is used for bridging subscribers and is designed so that it produces only a small bridging loss on the main line or tap to which it is connected. Figure 7*A* shows a circuit diagram of the coupling unit. *FL1* is a broad band filter passing all frequencies in the band 150–455 kc.

FL2 and *FL3* are narrower filters, *FL2* being capable of transmitting either of the two transmitting frequencies associated with the subscriber terminal and *FL3* tuned to pass the receiving frequency. The receiving filter is connected between *FL1* and the drop wire at all times, while the transmitting filter is connected only when relay *RL1* is operated, which occurs only when the subscriber is using his telephone.

The impedance which *FL3*, in combination with the subscriber terminal, drop wire, and *FL1*, bridges across the power line at all times is about 3,000 ohms at the receiving frequency and a much higher impedance at all other frequencies. Similarly, *FL2* in combination with the subscriber terminal, drop wire, and *FL1* bridges the line with 750 ohms at the transmitting frequencies and with a much higher impedance at all other frequencies, during the time that the telephone is being used. When the subscriber is not using the telephone, the bridging loss on the line caused by the transmitting

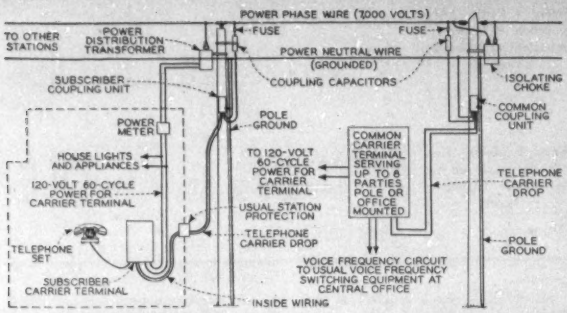

Figure 6. Principal elements of the M1 carrier telephone system

Figure 7A (below). Subscriber coupling unit circuit diagram

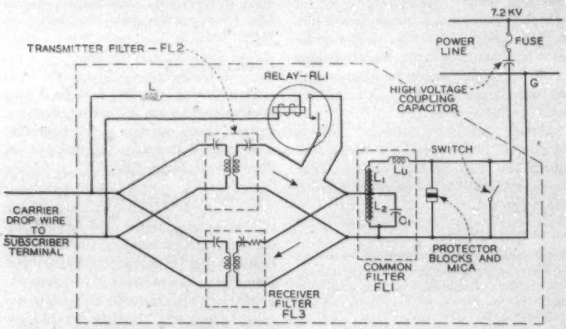

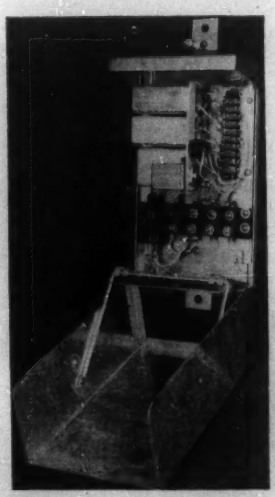

Figure 7B (left). Subscriber coupling unit assembly

branch of the coupling unit is negligible because *RL1* is not operated.

Terminating Subscriber Coupling Unit

This coupling unit is similar to the subscriber coupling unit except that *FL1* has a different stepdown ratio and is terminated on the drop side in 100 ohms. This effectively terminates the line or tap to which it is connected in characteristic impedance at all frequencies during standby condition and at all but the particular subscriber transmitting frequencies when the telephone is in use. At the transmitting frequencies the line is terminated in about one half of its characteristic impedance while the telephone is in use, and a small irregularity is caused thereby.

Common Coupling Unit

This coupling unit, because it may be common to six channels, employs only the broad filter *FL1* used in the terminating subscriber coupling unit. The drop side of this filter is connected directly through drop wire to the common terminal by means of which the power line is effectively terminated in characteristic impedance at the frequencies assigned to the common terminal. Other common terminals up to the full complement of six may be connected to a single common coupling unit. If all six common terminals are so connected, the power line will be terminated at all frequencies of interest.

Terminating Coupling Unit

This coupling unit is identical with the common coupling unit except that 100 ohms is connected across the drop side of the common filter *FL1*, thus terminating the power line in approximately characteristic impedance.

Subscriber Terminal and Telephone Set

The block diagram shown in Figure 8*A* will serve to show the principles of operation of the subscriber terminal and telephone set without going into detail concerning the electronic circuits involved. Photographs of this equipment are shown in Figures 8*B* and 8*C*.

The frequency of the transmitting oscillator is controlled by one or the other of two crystals corresponding to the two frequencies allotted for transmission purposes to a single subscriber terminal. The power amplifier consists of a single stage, operating class *A* with a maximum of two watts carrier output. Under standby conditions, no carrier is generated or transmitted because of the open filament circuit of the power tube and the high positive bias applied to the heated filament of the oscillator modulator tube. The output filter is broad enough to pass either of the transmitting frequencies but narrow enough to prevent effectively unwanted harmonics from being transmitted.

The receiver employs two tubes and associated filters as indicated. Automatic gain control is provided which keeps the range of voice frequency levels at the demodulated output within about three decibels for a range of input levels of 30 decibels, assuming a constant percentage modulation. A sensitive relay operates from the d-c component of the demodulated signal, and is associated directly with the ringer and frequency control circuits. The receiver is energized at all times to receive signals. Under standby condition, however, the potential applied to the screen of the second

receiving tube is 60-cycle alternating potential derived from the 60-cycle power supply, so that the receiver is able to receive signals only if the time of arrival of the signals coincides with the time of arrival of the positive potential from the 60-cycle power supply. This method of energization during standby periods provides for divided code ringing as explained later.

When the handset is lifted from the cradle to originate a call or in response to a ring, six functions are performed as follows:

1. A connection is made which provides the telephone transmitter unit with normal current.

2. The oscillator modulator and power amplifying stages are energized completely. The frequency of the oscillator has been predetermined according to whether or not a sufficient magnitude of carrier energy at the receiving frequency was on the receiver input before the receiver was lifted. If no receiving carrier (or an insufficient amount of the receiving carrier) was on the receiver input, the normal frequency is generated. If a sufficient amount of receiving carrier was on the receiver input, the reverting frequency is generated.

3. The frequency control is disabled. If the preselected frequency was normal frequency, it will remain normal frequency. If the preselected frequency was reverting frequency, it will remain reverting frequency as long as sufficient carrier at the receiver's frequency is present at the input to the terminal. If the receiving carrier disappears or is reduced below a receivable level, the transmitting frequency will return to normal and will remain normal even though a sufficient magnitude of receiving carrier later appears. These functions are performed by relays.

4. A few watts of a-c power are applied through the drop wire to the coupling unit to operate the relay in the transmitting circuit.

5. The potential applied to the screen of the second receiver tube is changed from alternating to positive direct potential.

6. The demodulated voice frequency output of the carrier frequency receiver is connected through to the telephone receiver.

Under these conditions the terminal is arranged both to receive and transmit. In a manual area further signaling is accomplished verbally in the usual manner. In a dial area the subscriber operates his dial in the usual manner which alternately opens and closes the plate supply to the modulator section of the oscillator modulator tube. This causes carrier to be sent out during the closed periods of the dial contacts but to be cut off during the open periods of the contacts. This signal is received at the common terminal and produces alternate "closures" and "opens" in the d-c path associated with the voice frequency loop, thus operating the central office dial equipment in the normal manner.

Common Terminal

The important functional characteristics of the common terminal may be described with the aid of the block diagram shown in Figure 9*A*. A common terminal assembly is shown in Figure 9*B*.

In the standby conditon, both the reverting and normal frequency receivers are energized completely to receive signals. The filaments of the transmitter tubes are heated and plate power is applied, but the grids are biased negatively to such an extent that no carrier is transmitted. The transmitter can be made to put out carrier either by the ringing control circuit or by the normal receiver control circuit.

When ringing power is applied between either or both of the voice frequency loop wires and ground, the ringing control operates to apply pulses of normal bias to the grids of the transmitter tubes. These pulses have a 30-cycle frequency and are synchronized with the 60-cycle supply used to supply power for the terminal. The particular phase of the 60-cycle power with which the pulses are synchronized depends on which of the two line relays associated with the ringing control is pulled up by the applied ringing power; that is, the relay connected between tip side of the line and ground, or the relay connected between the ring side of the line and ground. The pulses that are transmitted when the tip relay operates cause ringing at all sub-

Figure 9B. Subscriber terminal and telephone set

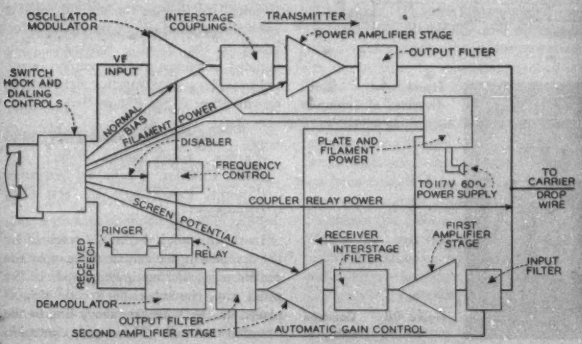

Figure 9A. Block diagram of subscriber terminal and telephone set

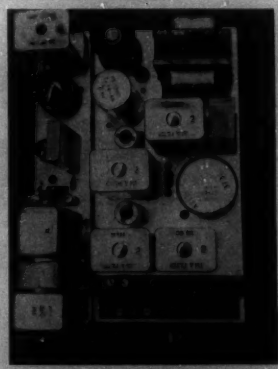

Figure 9C. Subscriber terminal assembly

scriber terminals poled so as to be enabled on the phase of 60 cycles corresponding to the tip pulses, and, similarly, when the ring relay operates, ringing is caused at all subscriber terminals correspondingly poled. If both tip and ring relays operate, ringing is caused at all subscriber terminals on the channel.

The limiter associated with the oscillator modulator stage of the transmitter operates by separating the voice frequency output of the stage from the carrier output, rectifying it and applying the resulting direct current via the limiting circuit shown in the diagram to the hybrid coil where it is applied to biased varistors shunting a coil winding. When the direct potential associated with the returned direct current is sufficient to overcome the bias on the varistors, the current passes through them in the forward direction reducing their resistances, shunting the coil, and reducing the speech level transmitted to the oscillator modulator over the transmitting branch.

When an adequate amount of normal carrier receiver current is received at the terminal, the normal receiver control operates to disable ringing control and to establish normal grid bias on the transmitter tubes. The normal receiver control also transfers the voice frequency loop to the pad and hybrid line circuit and makes the d-c closure, giving the supervisory signal to the local office and setting up conditions for speech transmission or further signal transmission either verbally or by dialing.

When revertive frequency carrier is applied to the terminal, the revertive receiver control bridges the demodulator voice frequency output across the receiving branch of the hybrid circuit and destroys part of the network balance in order to secure better transmission from the receiving to the transmitting branch of the hybrid on reverting calls.

Over-all Method of Operation

Figure 10 illustrates the manner of using the three frequencies allotted to a 2-way channel. In this figure, *F1* is the subscriber's normal transmitting frequency, *F2* is his reverting transmitting frequency, and *F3* is his receiving frequency. The system is so designed that the subscriber makes a call in the same manner that he would use if he were making a call on a voice frequency line. To the operator in the local office, signals received are the same as those received if the subscriber were located on the voice frequency line connecting the local office with the common terminal. The following paragraphs will describe in detail the procedures used when

1. A call is originated from a carrier party to a voice frequency party or another carrier party on a different channel.

2. A carrier subscriber receives a call through the local office from a voice frequency party of another carrier party not on his own channel.

3. One carrier party calls another carrier party on his own carrier channel (reverting call).

Call From Carrier Subscriber to a Voice Frequency Party (or Carrier Party Not on His Own Channel)

The carrier subscriber lifts his telephone from the cradle, thus energizing his own carrier transmitter. Assuming that the channel was not busy at that time, carrier frequency *F1* is selected and is transmitted over the power line and is received by the normal receiving amplifier and detector associated with the common terminal. The normal receiver control operates, establishing normal common terminal transmitting condition at frequency *F3*, and making a d-c closure on the voice frequency line to the central office. This lights the operator's signal or in the case of a dial office returns dial tone. The dial tone or speech from the operator is transmitted to the subscriber's location where it is received over the subscriber's station equipment.

The subscriber then places the call in the usual way either verbally or by dialing. If he dials, pulsed carrier is transmitted to the common terminal and, through the normal receiver control and associated closure circuit connected to the voice frequency line, operates the office dial equipment in the usual way. When the call is completed and the carrier subscriber hangs up, the switch hook operation will turn off his oscillator. The absence of received carrier at the common terminal will release the normal receiver control relays and restore the common terminal to the standby condition. The standby condition at the common terminal provides a disconnecting signal at the central office. (See Figure 10a).

Call From Voice Frequency Subscriber to Carrier Party (or From Carrier Party to Another Carrier Party Not on His Own Channel)

In this instance the call is received by the operator at the central office or by the central office dial equipment, and, in the usual way, the subscriber's code ring is placed on the voice frequency line to the common terminal. The ringing control in

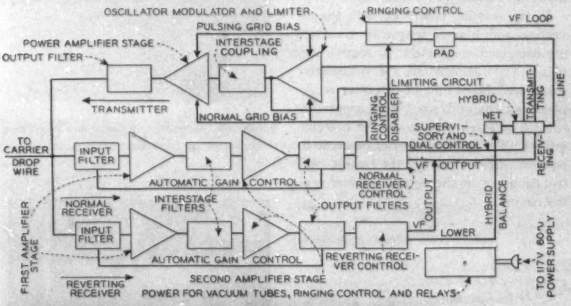

Figure 9A. Block diagram of common terminal

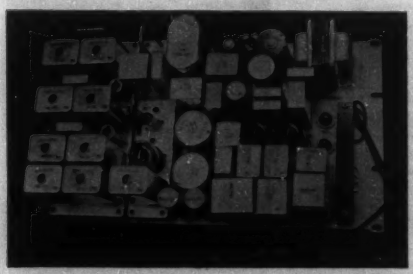

Figure 9B. Common terminal assembly

the common terminal operates to cause the transmitter to send out carrier at *F3* pulsed at a 30-cycle rate, the pulses being synchronized with the 60-cycle power supply. Assume that the tip relay in the ringing control circuit operates. All subscriber terminals assigned to this channel, with 60-cycle power poled so as to be responsive to ringing initiated by the relay on the tip side of the line, will ring and all similar subscriber terminals with 60-cycle power poled so as to be responsive to ringing initiated by the relay on the ring side of the line will not respond. In case the central office has facilities for sending out a guard ring on the ring side of the line when a party on the tip side is being called, this would be accomplished by applying 20-cycle power to the ring side of the line at some time during the code ring of the party called, either at the same time that a 20-cycle spurt was being placed on the tip side of the line or at a different time. In either case the ringing equipment in the common terminal of the carrier telephone system will respond and the guard ring will be transmitted.

The subscriber whose code is rung lifts his telephone receiver, thus energizing his oscillator so that it transmits *F1* which is returned to the common terminal, received by the normal receiving amplifier and through the normal receiver control disables the ringing control, puts normal bias on the transmitting tube grids, and by the closure of the d-c voice frequency line circuit trips the ringing. The call then is established. At the completion of the call, restoration of the carrier subscribers handset to the cradle de-energizes his transmitter, which causes the relay in the normal receiver control at the common terminal to release, restoring the system to normal.

Call From One Carrier Subscriber to Another Carrier Subscriber on the Same Channel—Reverting Call

In this case (Figure 10*b*) the calling subscriber raises his handset and places his call in the same manner as that used when placing a call to a voice frequency subscriber. The carrier subscriber, however, should know that he is calling another subscriber on his own carrier channel and as a result of that knowledge should replace his handset as soon as he has placed the call. If he does not do this, a manual operator probably will ask him to hang up, or, in the usual case, the dial equipment at the central office will send him busy tone because he has made his channel of the carrier system busy. As soon as the operator or the dial equipment at the central office receives the signal that the calling party has hung up, the called party's ring will be placed on the line. The ring will go out in the same manner as if the called party were being called by a voice frequency subscriber.

Figure 10. Manner of using frequencies allotted to 2-way channel, M1 carrier telephone system

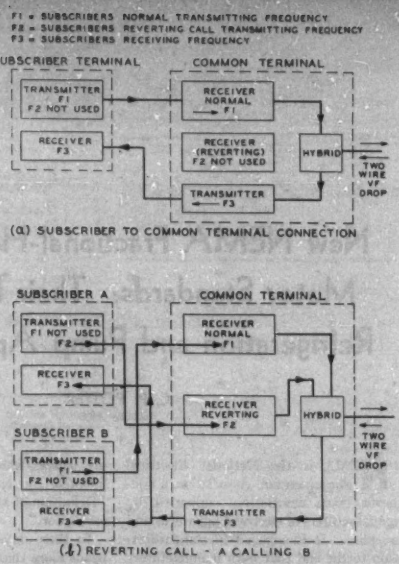

When the called party answers, he establishes a connection by means of his own normal transmitting frequency *F1* to the common terminal and gives indication to the central office that the call has been answered. The transmitter at the common terminal will be placed in the operating condition at frequency *F3* as before. The calling party, hearing the code ring or guard ring stop, assumes that the called party has answered and raises his handset. (If the calling party is on the other side of the line and no guard ring is transmitted to subscribers on that side of the line, the common practice is to wait a reasonable length of time before raising his handset.) In the foregoing sequence of operations, the calling party raises his handset the second time after the transmitter at the common terminal has been energized by virtue of normal received frequency from the called party. Therefore the calling party's frequency selector has operated so that when he raises his handset his oscillator modulator and selective amplifier are energized at frequency *F2* under the control of the reverting frequency crystal. This frequency will be transmitted to the common terminal receiver and will cause the reverting receiver control to operate. This will connect his voice frequency output across the receiving branch of the hybrid and will alter the network balance. This establishes the connection completely.

As may be seen by Figure 10*b*, transmission from subscriber *A* to subscriber *B* is via *F2* to the common terminal and via *F3* back to *B*. Transmission from subscriber *B* to subscriber *A* is via *F1* to the common terminal and via *F3* to subscriber *A*. Each subscriber hears his own transmission as side tone. If either the calling or the called party hangs up under these conditions, the party remaining on the line either will stay on, or revert to, the normal transmitting frequency. When the second of the two subscribers hangs up, the common terminal will return to the standby condition because the absence of the received carrier will restore all operated relays to the nonoperated position.

Reference

1. Application of Rural Carrier Telephone System, E. H. B. Bartelink, L. R. Cook, F. A. Cowan, G. R. Messmer. AIEE Transactions, volume 66, 1947, pages 511–17.

No Discussion

New NEMA Fractional-Horsepower Motor Standards; Their Effect on Refrigeration and Pump Applications

C. P. POTTER
FELLOW AIEE

"NEMA is the National Electrical Manufacturers Association, a non-profit trade association, supported by manufacturers of electrical apparatus and supplies. It is engaged in standardization to the end that both manufacturers and users of electrical apparatus may be informed of the best practices in the industry.

"NEMA Standards represent the result of many years of research and investigation by this organization, its predecessors, its Sections, and Committees. They have been developed through continual consultation among manufacturers, users, and national engineering societies, and represent practices that are both practical and economical in manufacture which, when utilized by the industry, have resulted in improved quality of electrical apparatus."

The foregoing paragraphs are quoted from the NEMA motor and generator standards. The latter also defines a small-power motor as one "built in a frame smaller than that having a continuous rating of 1 hp, open type, at 1700-1800 rpm." Small-power motors are known more familiarly as fractional horsepower motors, and for all practical purposes, fractional horsepower motors are those which are included in the range from 1/20 to 3/4 horsepower inclusive. The new fractional horsepower motor standards which we propose to discuss are those which recently have been adopted by NEMA and are entitled "Definition of Motor Output" and "Service Factor."

In these days, the general public depends more than they realize on the successful operation of fractional horsepower motors. It would be very interesting to take a census of all these motors and make a list of their application. This list would include

Washing machines
Ironing machines
Stokers
Oil burners
Blowers
Unit heaters
Evaporative coolers
Circulating pumps for heating systems
Domestic water pumps
Sump pumps
Gasoline dispensing pumps
Air compressors
Coffee and meat grinders
Domestic and small commercial refrigerators
Room coolers

It is quite obvious that the removal of these motors from our domestic economy would be felt severely, and it also would be very inconvenient for all of us if these motors and the devices which they operate were not thoroughly reliable and dependable.

There are millions of these motors in operation in the United States at the present time, and the public has become accustomed to having them operate night and day with few interruptions. This indicates that the motor manufacturers have done a good job in producing reliable motors and motors which have good operating performance. Every fractional horsepower motor has a horsepower rating stamped on its name plate and this would seem to be a rather definite indication of its capabilities. However, this is not necessarily true, because motor characteristics frequently are modified to suit the desires of the manufacturer of the devices which they operate. Some of these modifications are logical, some are not.

An open type fractional horsepower motor (and most of them are open type), with good operating characteristics, usually has a temperature rise somewhat less than 40 degrees centigrade. Manufacturers of motor driven devices which are used in highly competitive fields, have found this out, and have applied these motors so that they carry considerable overloads. When this is done, it is necessary to increase the starting torque and breakdown torque of these motors so that if operating conditions should become abnormal, or if the voltage should become low on the customer's premises, the motor will operate in spite of these handicaps. There have been instances where this practice has been carried too far, with the result that some of these fractional horse-power motors do not have the life expectancy which they would have if they were designed and applied more conservatively. Unfortunately, NEMA standards have not been sufficiently definite on the subjects of fractional horsepower torque and overload, and the reason for adopting the two new NEMA standards previously mentioned, is to promote a more logical design and application of fractional horsepower motors so as to serve the best interest of all parties concerned.

Breakdown Torques

As indicated previously, the breakdown torques of single-phase fractional horsepower motors have varied considerably depending upon customers' requirements. As a result a motor obtained from one manufacturer might be perfectly satisfactory for a given application, while a motor of the same type and horsepower rating furnished by another manufacturer might be entirely unsuitable. This has

Paper 47-93, recommended by the AIEE committee on electric machinery for presentation at the AIEE winter meeting, New York, N. Y., January 27-31, 1947. Manuscript submitted October 18, 1946; made available for printing December 16, 1946.

C. P. Potter is chief engineer, electrical engineering division, Wagner Electric Corporation, St. Louis, Mo.

Table I. Single-Phase Fractional Horsepower Motors Defined in Terms of Breakdown Torque

	Revolutions Per Minute					
Synchronous rpm	3,600	3,000	1,800	1,500	1,200	900
Approximate full load rpm	3,450	2,850	1,725	1,425	1,140	850
Brake Horsepower Rating	Breakdown Torque Oz-Ft					
1/20	2.0– 3.7	2.4– 4.4	4.0– 7.1	4.8– 8.5	6.0–10.4	8.0–13.5
1/10	3.7– 6.0	4.4– 7.2	7.1–11.5	8.5–13.8	10.4–16.5	13.5–21.5
1/4	6.0– 8.7	7.2–10.5	11.5–16.5	13.8–19.8	16.5–24.1	21.5–31.5
1/3	8.7–11.5	10.5–13.8	16.5–21.5	19.8–25.8	24.1–31.5	31.5–40.5
1/2	11.5–16.5	13.8–19.8	21.5–31.5	25.8–37.8	31.5–44.0	40.5–58.0
3/4	16.5–21.5	19.8–25.8	31.5–40.5	37.8–48.5	44.0–58.0	58.0–77.0
1/3	21.5–31.5	25.8–37.8	40.5–58.0	48.5–69.5	58.0–82.5	
3/4	31.5–44.0	37.8–53.0	58.0–82.5	69.5–99.0		
1	44.0–58.0	53.0–69.5				

Note 1. Small-power single-phase induction motors shall be rated primarily on the basis of breakdown torque. The value of breakdown torque for the purpose of defining horsepower rating shall fall within the above ranges.

Note 2. Breakdown torque range includes the higher figure, down to, but not including the lower figure.

made it necessary for purchasers to test each manufacturer's motor on his device before he can be sure that it will do the job. In order to correct this difficulty, NEMA has defined single-phase fractional horsepower motors in terms of breakdown torque as shown in Table I.

This table allows every purchaser to determine the breakdown torques he may expect to obtain when buying motors of a given horsepower rating from any motor manufacturer and provides a definite basis for applying them.

Service Factors

It is presumed, of course, that the manufacturer of any device which is driven by a fractional horsepower motor, will know quite accurately the load imposed upon the motor by this device. If he has information from the motor manufacturer or from the Motor and Generator Standards which will assist him in determining the safe overload which the motor will carry, he will quite likely select a suitable horse power rating, and that is the reason for establishing service factors for fractional horsepower motors.

Service factor is a number by which the horsepower rating should be multiplied in order to determine the maximum safe load which may be applied to the motor. For instance, if a 1/2-horsepower motor has a service factor of 1.25, this motor will safely carry 0.625 horsepower. The service factors for fractional horsepower single-phase motors, which recently have been adopted, are given in Table II.

These service factors were obtained by determining the overloads which produce a 50-degree centigrade rise on motors having an actual temperature rise at full load of 40 degrees centigrade, and are intended to be used only where the voltage and frequency are held within close limits and

Table II

Horsepower	Service Factor for General Purpose 40 C Induction Motors
1/20	1.4
1/10	1.4
1/8	1.4
1/4	1.35
1/3	1.35
1/2	1.35
3/4	1.25
1	1.25
1 at 3,600 rpm only	1.25

The temperature rise on which the nameplate rating is based shall be no more than 40 degrees centigrade for all coil windings. This low limiting temperature rise is provided to allow a greater factor of safety where the service conditions are unknown.

When authorized by the manufacturer such a motor may be operated (at rated voltage and frequency and in an ambient temperature not exceeding 40 degrees centigrade) at a continuous load greater than rated load determined by the above service factors.

It is recommended that the service factor shall be marked on the name plate in addition to the rating.

where the temperature surrounding the motor (known as the ambient temperature) does not exceed 40 degrees centigrade.

The statement has been made that an open type fractional horsepower motor with good operating characteristics may have a temperature rise somewhat less than 40 degrees centigrade. The service factors were determined by assuming that the temperature rise at full load is 40 degrees centigrade. It is quite obvious, therefore, that the use of the service factor may not absorb all of the thermal capacity of the motor, or, in other words, it may be possible to use still higher overloads on certain applications without damage to the motor. The question may be asked therefore, why conservative service factors have been chosen. There are several reasons.

1. It is felt that a factor of safety should be allowed to take care of low-voltage, abnormal

Table III

Rated Horsepower	Locked Rotor Current in Amperes 115 Volts	230 Volts
1/4 and smaller	20	10
1/4	23	11.5
1/3	31	15.5
1/2	45	22.5
1/4	61	30.5

Table IV

Code Letter	Kva Per Horsepower *
A	0 – 3.15
B	3.15– 3.55
C	3.55– 4.0
D	4.0 – 4.5
E	4.5 – 5.0
F	5.0 – 5.6
G	5.6 – 6.3
H	6.3 – 7.1
J	7.1 – 8.0
K	8.0 – 9.0
L	9.0 –10.0
M	10.0 –11.2
N	11.2 –12.5
P	12.5 –14.0
R	14.0 –and up

* Locked kilovolt amperes per horsepower includes the lower figure, up to but not including the higher figure.

operating conditions, and high ambient temperatures. Electrically driven devices which have wide distribution are quite likely to be installed in rural communities where the voltage conditions may be bad, and where the cost of servicing these devices may be very high. It therefore seems to be economically sound to choose service factors which give the motor manufacturer, the machinery manufacturer, and the user a chance to operate successfully under adverse conditions. Figure 1 has been prepared to show the effect of voltage variation on the temperature rise of a typical fractional horsepower motor. This indicates quite clearly that a motor which will operate satisfactorily at a reasonable overload and at normal voltage may have a dangerous temperature rise under abnormal voltage conditions.

2. The maximum efficiency of single-phase motors occurs approximately at the overload allowed by these service factors. If, therefore, the machinery manufacturer is interested in obtaining the best possible over-all efficiency, it will be to his advantage to operate the motor at these service factors. Figure 2 shows a typical performance curve for a 1/3-horsepower single-phase motor which now has a service factor of 1.35. It will be noted that the maximum efficiency occurs at 135 per cent of full load, and that the speed of the motor at this load is still quite high.

3. When excessive overloads are applied to any single-phase motor, the speed of the motor decreases considerably, and this affects the operation of the driven machines. For example, if the speed of a motor driving a refrigeration compressor or pump drops

too much, the output may be reduced to a point which makes it unsatisfactory to the user.

4. There is a definite relationship between breakdown torque and locked current. There is a growing tendency on the part of power companies to limit the applications of motors on the basis of locked current rather than on the basis of horsepower rating. Motors with greater service factors must have more breakdown torque, resulting in higher locked currents, and it is possible that these currents sometime may cause trouble by failing to meet the requirements of the local power companies.

Locked Rotor Currents

The maximum values of locked rotor currents for single-phase motors have been standardized, and are shown in Table III. It might be worthwhile to call attention to the fact that 1/2- and 3/4-horsepower motors have had code letters stamped on their name plates for several years, and that in the near future motors smaller than one-half horsepower also will have the code letters stamped on the nameplate. The code letters are determined from Table IV, and it is evident that motors with code letters at the beginning of the alphabet have lower locked currents than those at the middle or end.

A manufacturer of refrigeration equipment or pumps may agree with all of these statements and at the same time may feel that the new NEMA standards will cause him a great deal of expense and inconvenience and may make it necessary

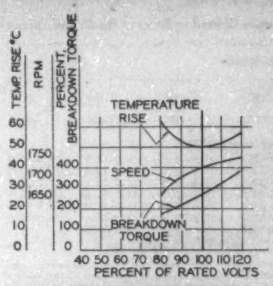

Figure 1. Effect of abnormal line voltage on temperature rise, speed, and breakdown torque of a typical 1/3-horsepower single-phase 60-cycle 1,725-rpm motor operating at 135 per cent rated load at rated voltage

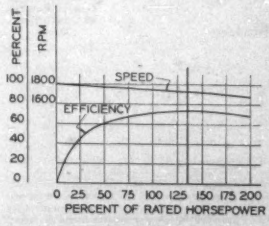

Figure 2. Speed and efficiency versus per cent of rated horsepower of a typical 1/3-horsepower single-phase 60-cycle 1,725 rpm motor

to use larger and more expensive motors for driving his equipment. The new NEMA standards do not require any changes in the performance or capacity of motors which have been established on their applications and which are giving good service. The standards provide a consistent method of designating the rating of such motors without making any changes in the motors except perhaps the horsepower stamping on the name plate.

It is quite unlikely that any motor user will be required to make any changes in the applications of motors which have been applied on a sound basis and whose life has been satisfactory. In cases where the user is buying motors which have greater breakdown torques than those covered by NEMA standards, it will be necessary, after a suitable period of time, to stamp the nameplates of these motors properly. Certainly, all new applications should be made on the basis of the new NEMA standards, and if this is done we will have the following results:

1. The user will be supplied with motors which have a long life and will not cause losses as a result of fire or stoppage of production.

2. The application engineer and the manufacturer will be able to select the proper motor without having to test each application.

3. The power companies will be able to connect these motors to their circuits, and feel sure that their equipment is adequate and that the operation of the motors will not cause annoyance to their customer.

No Discussion

Application of Rural Carrier Telephone System

E. H. B. BARTELINK
ASSOCIATE AIEE

L. E. COOK
FELLOW AIEE

F. A. COWAN
FELLOW AIEE

G. R. MESSMER
ASSOCIATE AIEE

Synopsis: This paper deals with the application of a carrier system developed primarily for providing rural telephone service over power distribution circuits in areas where this means of extending telephone service may be more attractive than other available methods. The modifications required in the power circuits to permit carrier frequency transmission are described, including the effect of these modifications on the operation of the power system. Construction features also are discussed. The use of the rural carrier telephone system over open wire telephone pairs is discussed briefly.

DEVELOPMENTS in conventional methods of extending rural telephone service using open wire line construction have been described.[1] These methods include the use of long span construction on separate poles or on poles used jointly to provide power and telephone service. To provide service in those areas where the circuit lengths between subscribers are relatively long, means for the joint use of both poles and conductors of rural power systems have been developed. These means employ carrier transmission technique and this paper describes its application both to rural power lines and to telephone pairs.

As a result of co-operative arrangements made by the Bell System through the Edison Electric Institute and the Rural Electrification Administration, detailed tests were conducted on several rural power systems to determine

1. The characteristics of rural power systems at carrier frequencies.

2. The modifications necessary in the power systems to permit their use as a medium for carrier transmission.

3. The adequacy of experimental terminal and power line equipment design for the carrier telephone system.

As a result of this work carrier telephone equipment has been designed for commercial application. This equipment constitutes the rural carrier telephone system.[2]

The primary purpose of this paper is to explain methods and considerations involved in the application of such a system to rural power lines. In applying the carrier system it is necessary to modify the power line to enable it to be used as a medium for carrier transmission, to provide terminal equipment for the transmitting and receiving of the carrier signals and means for coupling the terminal equipment to the power lines. Figure 1 illustrates the arrangement of this equipment on the power line. The principal components that make up the carrier system are listed as follows:

1. Common carrier terminal—used to connect the carrier channels with the central office.

2. Common coupling unit—used to connect the common terminal to the coupling capacitor.

3. Subscriber carrier terminal and telephone set.

4. Subscriber coupling unit—used to connect the subscriber terminal to the coupling capacitor.

5. Coupling capacitors—used to connect the coupling units to the power lines.

6. Series chokes—used to modify the power lines for satisfactory carrier transmission.

7. Sectionalizing networks—consist of series chokes and shunt capacitors and used where two carrier systems are operated on adjacent sections of the same power system.

The carrier system is for use primarily over power lines of the multigrounded

Paper 47-81, recommended by the AIEE committee on communication for presentation at the AIEE winter meeting, New York, N. Y., January 27–31, 1947. Manuscript submitted November 13, 1946; made available for printing December 10, 1946.

E. H. B. BARTELINK is radio engineer with the General Telephone Corporation, New York, N. Y.; L. E. COOK is general engineer with Ebasco Services, Inc., New York, N. Y. and chairman for the Edison Electric Institute of the joint subcommittee on rural telephone service by carrier on power circuits of Edison Electric Institute and Bell System.; F. A. COWAN is transmission engineer with American Telephone and Telegraph Company, New York, N. Y. and chairman for the Bell System of the joint subcommittee on rural telephone service by carrier on power circuits of Edison Electric Institute and Bell System; and G. R. MESSMER is an engineer with Rural Electrification Administration, United States Department of Agriculture, Washington, D. C.

The technical data included in this paper have been furnished through the co-operation of Bell Telephone Laboratories, Inc., and a number of operating power and telephone organizations whose contributions are gratefully acknowledged.

Table I. Summary of Characteristics of Chokes Installed on Power Lines

Type of Choke	Continuous Current Rating, Amperes	1-Second Short-Circuit Current Rating, Amperes	Nominal Inductance, Millihenrys	60-Cycle Impedance, Ohms	Temperature Rise With Rated Current, Degrees Centigrade	Impulse Breakdown Voltage of By-Pass Gap, Kv	Weight Pounds
Isolating*	10.0	500.0	10.0	0.9+j4.5	50	30**	60
Tap	4.0	500.0	2.5	0.4+j0.95	25	21	12
Transmission	4.0	500.0	0.6	0.2+j0.23	10	21	8
	4.0	500.0	0.3	0.1+j0.12	7	21	7

* Minimum withstand requirements of isolating choke assembly with case grounded are 35 kv dry for one minute, 30 kv wet for 10 seconds and 95 kv on impulse.

** In addition to 3/4-inch by-pass gap, gaps with electrode spacing of approximately 2¾ inches are connected between each bushing and ground. These gaps are protected by insulating shields and break down at approximately 75 kv.

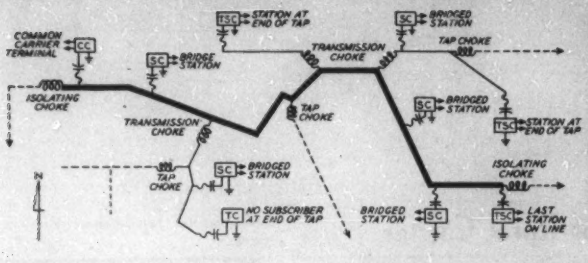

Figure 1. Arrangement of equipment on rural power line modified for carrier transmission

neutral type operating below 8,700 volts between phase wire and neutral. Under favorable conditions, its application can be extended to unigrounded lines without primary neutral conductors, provided the phase-to-ground voltage does not exceed 8,700 volts. The series chokes available at present can carry from four to ten amperes continuous load current and maximum short-circuit currents of 500 amperes for one second. The carrier system also can be applied to telephone pairs as discussed later

This system, operating in the 150- to 455-kc band, can provide a maximum of six 2-way telephone channels over a given section of power line. Each channel can be considered equivalent to a voice frequency telephone pair and can serve as many parties as requirements and ringing facilities at the central office permit. For each channel used, a separate common carrier terminal is required. Provision can be made for connecting the common terminal over a voice frequency circuit to the regular rural line equipment in any type of dial, common battery manual, or magneto exchange. Operating procedures on all types of calls are the same as for rural wire lines in the same exchange.

The 120-volt 60-cycle power supply for the subscriber carrier terminal is obtained from a convenience outlet at the subscribers' premises. The power requirements of the subscriber terminals range from 7 watts in the stand-by condition to a maximum of 25 watts in the talking condition.

Common carrier terminals can be installed in central offices in cases where proximity of the central offices to the power lines permits. In other situations the terminal is installed at a convenient point on or adjacent to the power line and the 120-volt 60-cycle power supply is obtained from the power system through a conventional service connection. Power requirements for the common carrier terminal range from 16 watts per carrier terminal in the stand-by condition to about 30 watts per carrier terminal in the talking condition

Modification of Power Lines

A section of rural power line which is to be used for carrier transmission can be considered as consisting of a main line with a number of taps of different lengths connected to it. Such a system is shown schematically in Figure 1. Each tap, irrespective of length, represents a source of impedance irregularity and loss to carrier transmission over the main line. To minimize the effect of these taps on the carrier transmission and to provide for dividing the power lines into carrier sections, chokes are used in series with the phase wire of taps at the point where they connect to the main line, and in series with the phase wire of the main line at the ends of carrier sections.

Figure 2. Isolating choke

Three general types of chokes are provided.

1. Isolating choke.
2. Tap choke.
3. Transmission choke.

Table I summarizes the more important characteristics of these chokes.

The isolating choke is primarily for use at the end of a carrier section to confine the carrier transmission within the section. Figure 2 illustrates an isolating choke. It is mounted in an oil-filled 2-bushing metal container which may be grounded. Insulators are required in series with the phase wire at each isolating choke location. The installation and connections of the choke to the phase wire and for grounding the case may be in accordance with the normal practices of the power organizations.

The tap choke is used primarily where taps are to be connected to the main line and no telephone subscribers on the tap are to be served. The coils are coated with a dry type of dielectric material and enclosed in a sealed container. Figure 3 shows an example of an installation of a tap choke. The choke coil is supported by a pin type insulator which provides insulation to ground, mounted at the end of a double arming bolt. The design of the choke is such that it can be installed or removed by hot line tools if necessary.

The transmission choke is provided for regulating the carrier transmission on taps over which telephone subscribers are served. This choke is similar in appearance to the tap choke. The mounting arrangements are the same as for the tap choke.

Isolating chokes can be used in the place of tap chokes where the load current is above four amperes. Tap chokes

Figure 3 (left). Tap choke installed at same pole as pole top reclosing circuit breaker

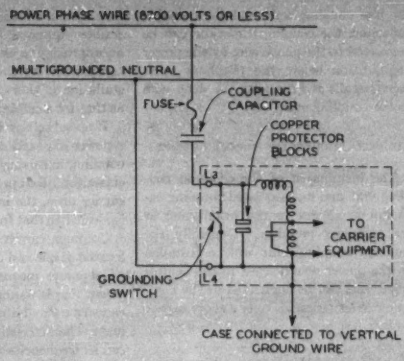

Figure 4 (right). Connections of coupling capacitor and line coupling unit to power line

can be used in place of isolating chokes where the load current is four amperes or less, except where a sectionalizing network is required. Isolating chokes can be used in parallel where the load current exceeds the 10-ampere limit, except in sectionalizing networks.

The 60-cycle ratings of the chokes have been selected with the objective of causing a minimum effect on the operation of the power system (and at the same time obtaining the required carrier frequency characteristics). The maximum impedance of any of the chokes is about $0.9+j4.5$ ohms at 60 cycles. In some cases three or four chokes may be placed in series with a phase wire between the power source and loads. In situations such as this, the line impedance may be increased sufficiently that the impedance of the chokes should be considered in short-circuit current or voltage regulation studies on the system. The resistive component of the impedance of the chokes is relatively low and, therefore, the energy loss is small.

The coupling capacitor (designed primarily for connecting the coupling units to the power lines) has a capacity of 2,000 micromicrofarads and is rated at 8.66 kv. It will withstand a rms 60-cycle voltage of 35 kv for 1 minute when dry and 30 kv for 10 seconds when wet, and has an impulse voltage strength of not less than 95 kv when tested with a 1.5x40 microsecond wave. The impedance of the capacitor at 60 cycles is about 1,300,000 ohms and, consequently, the 60-cycle current is about 5 milliamperes. A fuse with a rating up to 3 amperes may be used in the connection between the capacitor and phase wire.

As shown in Figure 4 the coupling unit is connected in series between the capacitor and ground. The normal 60-cycle voltage drop across the coupling unit is less than 1 volt. The copper protector blocks with 0.01-inch separation break down at around 1,200 volts and thus protect the coupling unit for abnormal voltage conditions.

A grounding switch is provided to ground the capacitor lead solidly when maintenance work in the coupling unit is required.

Coupling capacitors and coupling units are used to provide coupling for subscriber stations, common carrier terminals, and terminating units. The installation of these units for the three cases will be discussed.

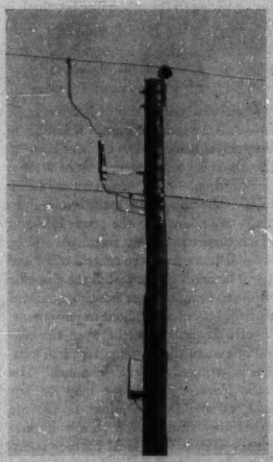

Figure 5. Coupling capacitor and subscriber coupling unit installation

Subscriber Station Couplers

The installation usually is made on the primary pole nearest the telephone subscribers' premises. It consists of a coupling capacitor and fuse, a line coupling unit, and a telephone drop wire to the premises. In many instances this installation will be on the same pole as a distribution transformer, but it may be on a pole having only primary conductors. Figure 5 shows a typical installation for a subscriber's station. The grounded capacitor bracket supports the capacitor in a vertical position above the neutral conductor. The fuse is connected between the top terminal of the capacitor and a hot line clamp or connector which connects to the phase wire. The bottom capacitor terminal is connected to the line coupling unit with number 10 insulated wire over which wood molding is placed. The line coupling unit is mounted at least 40 inches below any power attachment or equipment (secondary, neutral, transformer case, and so forth). The metal case of the coupling unit is connected to the pole ground wire with a short jumper while another lead from within the coupling unit is connected directly to the neutral conductor as shown in Figure 4. This double grounding arrangement insures that the coupling unit will remain grounded even if one of the ground connections becomes open. Where a coupling capacitor is installed, a pole ground is required. In cases where a distribution transformer protected with external fuse cutout is located on the pole where the coupling capacitor and the coupling unit are to be installed, it sometimes may be practicable to utilize the same fuse to protect both the capacitor and distribution transformer.

After completing the installation of

the line coupling unit and the coupling capacitor, the coupling capacitor can be connected to the phase wire by the power organization before the telephone company installs and connects the drop wire to the coupling unit.

Common Carrier Terminal Coupler

The installation of the common coupling unit and its associated coupling capacitor is similar to the installation at the customer premises. Generally the common coupling unit will be installed on the power pole nearest to the central office, and will be connected to the common carrier terminals over a short carrier drop.

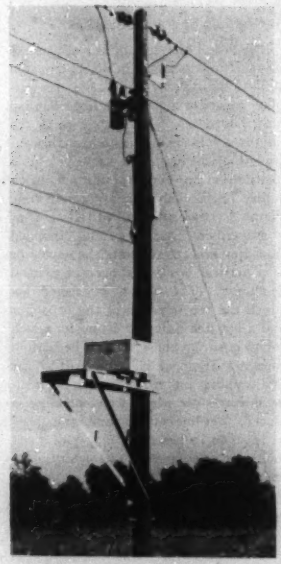

Figure 6. Isolating choke, coupling arrangement, and common carrier terminal installation

Terminating Unit

The ends of a power line section and of taps over which carrier telephone service is to be provided must be terminated in approximately the characteristic impedance of the power line. When a telephone subscriber is located at the end of a tap or carrier section, a terminating subscriber coupling unit is utilized. This unit is similar to the subscriber coupling unit and, in addition to coupling the subscriber terminal equipment, provides an approximate characteristic impedance termination for the power line. The installation of this equipment is the same as that for a subscriber station.

If no subscriber is located at the end of a power line section or tap, a terminating coupling unit is installed with a coupling capacitor. Except for the absence of the carrier drop, the installation of this unit is similar to that for a subscriber station.

Common carrier terminals usually are located at one end of a carrier section and no separate means for terminating the power line is required, since the common carrier terminal always provides approximate characteristic impedance at the carrier frequencies used.

Carrier Equipment

Installation of the carrier terminal equipment on the subscribers' premises and at the common terminal end of the power line is made as follows:

Subscriber Station

The subscriber carrier terminal is installed in the same manner as a conventional telephone wall box at a location close to a 60-cycle power outlet, and the combined telephone set is located conveniently near the subscriber terminal. The installation of the carrier drop from the coupling unit to the subscribers' premises, and of the station protection and inside wiring to the subscriber terminal, is the same as for a voice frequency rural station.

Common Terminal

If circumstances permit, it is desirable to install the common carrier terminals in the central office and to connect them to the common coupling unit over a short carrier drop. This arrangement facilitates installation and maintenance. In many cases, however, the power line over which carrier is to be transmitted will be some distance from the central office and it will be necessary to install the common terminals in an outdoor housing mounted near the base of a telephone or power pole. A voice frequency pair between the central office and the common terminal location is required for each channel. The voice frequency facilities may be the same as would be required to provide satisfactory transmission to a voice frequency station with local battery transmitter supply and located at the same point as the common terminals. A single carrier drop is used to connect as many as six common terminals to the common coupling unit. Each common terminal is provided with a 120-volt 60-cycle power supply. Figure 6 shows one of the earliest installations of a pole mounted common carrier terminal and associated coupling arrangements.

Carrier Frequency Losses

With the modifications described previously, the impedance of a single-phase multigrounded neutral power line in the 150–455-kc frequency range is approximately 500 ohms. The carrier frequency loss of the line depends upon a number of factors, the more important of which are the earth resistivity in the vicinity of the power line and the type of conductor used for the phase and neutral wires. The effect of these factors is illustrated by the curves shown in Figure 7. As shown in curve *A*, the loss per mile for number 6*A* Copperweld-copper or number 4 aluminum-cable-steel-reinforced conductors ranges from about 0.8 decibel at 150 kc to about 1.7 decibels at 450 kc, under conditions of low earth resistivity. Under other conditions, the losses may be substantially higher, as shown in the figure. Data from additional installations will provide a more reliable basis for evaluating the effects of various factors on the loss.

In addition to the line losses, the overall loss from the common carrier terminal to the subscriber terminal is affected by various bridging losses and by the losses through the coupling units. Bridging losses are contributed by taps used for carrier transmission, by taps not used for carrier transmission which are equipped with tap chokes, and by distribution transformers on the power line. Figure 8 shows the bridging loss introduced by a transmission tap. The transmission choke also introduces a loss to transmission to stations on the tap, as shown in Figure 9. The bridging loss of taps isolated from the carrier path by tap chokes is ordinarily of the order of 0.1 to 0.2 decibel each. The bridging loss from a distribution transformer of 5 kva rating or smaller is also about 0.1 to 0.2 decibel Larger transformers probably will introduce higher losses, and it may be found necessary to connect them to the power line through chokes.

The reactance of the operating coil used in reclosing oil circuit breakers may introduce a loss to carrier transmission of the order of 10 decibels. Preliminary information indicates that this loss may be reduced to about 0.5 decibel by shunting a noninductive 50-ohm resistance around the

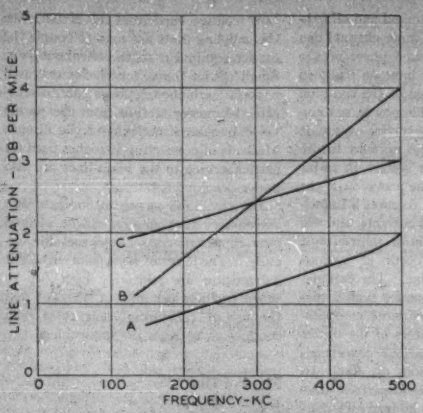

Figure 7 (above). Carrier frequency loss per mile versus frequency for various line conductors and different ground resistivity conditions

A—Number 6A Copperweld-copper or number 4 aluminum-cable-steel-reinforced conductor in locality with 10 to 30 meter-ohms ground resistivity

B—Number 6 Amerductor in locality with 500 to 1,500 meter-ohms ground resistivity

C—Number 6 steel conductor in locality with 5 to 25 meter-ohms ground resistivity

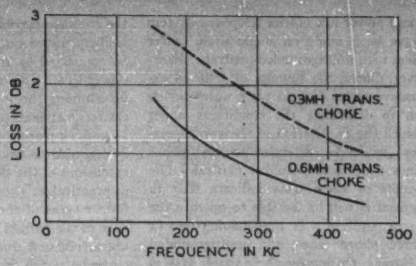

Figure 8. Carrier frequency loss to main line transmission introduced by tap equipped with transmission choke

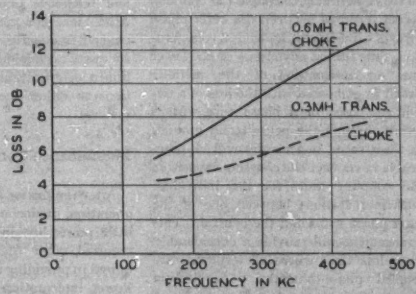

Figure 9 (right). Carrier frequency loss to station on tap introduced by transmission chokes

operating coil. Methods of mounting the resistance and its effect on the reclosing circuit breakers operation are being studied.

Design Considerations

The performance of the rural carrier telephone system may be affected by atmospheric static, by noise caused by power line sources, and by near-by radio stations or other carrier systems operating in the same frequency range. The effects of atmospheric static are dependent on the severity and duration of thunderstorms, on the ground resistivity in the vicinity of the power line, and also on the frequency at which the carrier channel is operated. In regions of comparatively low ground resistivity, of the order of 50 meter-ohms, and where the atmospheric static is low, adequate signal-to-noise ratios usually can be secured with carrier losses up to 48 decibels (exclusive of coupler losses) from the common carrier terminal to the most remote station. For normal static areas, these losses are reduced six to eight decibels. For very low ground resistivity areas (below 25 meter-ohms) the limiting losses may be about three decibels higher than those specified for 50-meter-ohm ground. Where the ground resistivity is comparatively high, the limiting losses must be reduced, possibly by as much as ten decibels. Further experience in applying the carrier system under different conditions will be helpful in establishing more definite limiting losses.

While the maximum noise on the carrier channels ordinarily will occur only during peak periods of atmospheric static, there may be cases where noise will occur from power line sources. These sources are the same as those that may create interference with radio reception, such as punctured or cracked insulators, or loose hardware, and their location and elimination is handled in accordance with usual power system practices.

Signals from near-by radio stations or carrier systems operating in the same frequency range as the rural carrier telephone system in some cases may be a possible source of interference with telephone transmission. In engineering applications of the carrier system, it will be desirable to avoid using carrier channels which operate at the same frequencies as radio stations in the vicinity of the power line. The design of the carrier equipment which provides the possibility of associating any pair of transmitting frequencies with any receiving frequency, as described in the companion paper,[8] facilitates the most effective use of the available frequency space which is free from external interference. The avoidance of the use of affected channels will reduce further the possibility of interference with radio stations through operation of the low powered carrier system.

As at present designed, only one 6-channel carrier system can be applied successfully to any single section of power line. However, it appears practicable to operate carrier channels at the same frequency on adjacent power line sections, provided suitable carrier frequency sectionalizing networks are inserted between the power line sections. The degree of effectiveness required of the sectionalizing networks will vary depending upon the cross talk requirements in each case. While the development work on these networks has not been completed, it is expected that they generally will consist of isolating chokes as series elements in combination with coupling capacitors as shunt elements.

So far most of the applications of the

rural power line carrier telephone system have been made on single-phase power lines with multigrounded neutrals. However, during the summer of 1946 an extensive series of field tests were carried on to determine the conditions under which the application of the carrier system might be extended to multiphase lines with multigrounded neutral. The results of these tests indicate that in general it will be feasible to operate the carrier system over lines having two or three phase wires and multigrounded neutral. Ordinarily the carrier system will be coupled from one phase wire to neutral, and under this condition the line loss usually will be about the same as for the single-phase line. In some cases it may be found desirable to couple the common carrier terminal between the outer phase wires of a line having horizontal configuration, thus taking advantage of the lower line loss attenuation of the metallic circuit as compared with the loss of a circuit composed of a phase wire with a return through the neutral and ground. In these cases, it generally will be practicable to connect the coupling capacitors and coupling units for the individual subscriber stations between one of the outer phase wires and the neutral. This arrangement will provide a considerably lower loss than where all terminals are coupled phase-to-neutral. Application of a carrier system is planned on a 3-phase power system without primary neutral. Preliminary information indicates that phase-to-phase coupling for the common carrier terminal with phase-to-ground coupling of subscriber stations may be feasible. The metallic circuit transmission characteristics are expected to be comparable with those obtained on the multiphase line with primary neutral.

The application of a rural carrier telephone system to a particular power system requires a knowledge of the physical characteristics and layout of the power line, including all branches, the locations of prospective telephone customers to be served by the carrier system, as well as information regarding the earth resistivity, severity of atmospheric static, and location of near-by radio stations operating in the same frequency range as the carrier system. With a knowledge of the line losses caused by the power line conductors and the various bridged taps, transformers, and so forth, it should be possible to apply isolating, tap, and transmission chokes, and terminations to provide for satisfactory carrier transmission from the common terminal to any proposed customer. Divided code ringing can be provided by the carrier system if the common carrier terminal and all subscribers served on the same channel can be connected to the same phase of the power line. This may have an effect in determining the location of the common carrier terminal on the power system. In making plans for the carrier system, it is desirable to take into account future extensions of the power system, in so far as practicable. Also, the provision of the proper types of chokes requires a knowledge of the normal load currents, and the magnitude and duration of short-circuit currents which may occur at various points on the power line. The completion of satisfactory plans for such a carrier installation requires close co-operation between the engineers of the power and telephone organizations concerned. Also, since the conditions are likely to change frequently, it is important that adequate arrangements be made for continued co-operation in engineering additions to either the power or telephone systems.

Maintenance Considerations

After the carrier telephone system is in operation, under usual conditions very little power line maintenance should be required other than that normally required in providing reliable power service. Power interruption to a telephone subscriber will cause an interruption to the subscriber's telephone service. Power interruption to a common carrier terminal will make inoperative all telephones on the carrier channel. When maintenance work is required, close co-operation is desirable between local maintenance forces of the power system and telephone company. This will include arrangements for clearing of troubles, replacements of capacitors (or fuses) and chokes, advance notification of planned power system interruptions, and correction of power line conditions which create interference with carrier transmission.

Application to Telephone Pairs

While the rural carrier telephone system is designed primarily for use over power lines, it is expected that it also will be found useful as a means of providing additional circuits over rural open wire telephone lines. One such application already has been made and the results are satisfactory.

The same carrier equipment is used for both power line and telephone line service with the exception of the coupling capacitors and heavy duty series chokes. Low voltage capacitors associated with the coupling units are used to couple the carrier equipment to the telephone pair. Small carrier frequency chokes are used in series with the telephone pair to separate the carrier section from the purely voice frequency portions of the circuit. Methods of connecting branches used for carrier service to the main lines are also under development.

Data available at present indicate that satisfactory transmission can be secured over copper or copper-steel metallic circuits. The losses of steel pairs with light galvanizing are relatively high (up to seven decibels per mile at 450 kc) and the use of substantial lengths of such conductors appears impracticable.

Field of Use

The ultimate field of use of the power line carrier telephone system in comparison with other means of extending rural telephone service will depend on several factors, which can be evaluated accurately only after considerable experience with the carrier system has been obtained. These factors include

1. The cost of the equipment for the carrier system.
2. The arrangements which are worked out between the telephone and power organizations in connection with this type of service.
3. The demand for rural telephone service in areas more remote from existing telephone facilities.
4. The operating and maintenance experience with the carrier system. (Probably the most important factor.)

The results of preliminary studies of the probable field of use for the carrier system have indicated that it will be most attractive where the prospective telephone customers who are served by power distribution lines are remote from existing telephone pole lines. In general the carrier system appears worthy of study in cases where the prospective telephone customers are separated by distances of the order of one-half mile or more.

In deciding whether rural service should be extended by carrier or by wire, the relative flexibility of the carrier system deserves particular consideration. Telephone service can be furnished from any channel to customers located anywhere along the section of the power system which has been modified for carrier transmission. This permits maximum utilization of the carrier channels installed initially and facilitates adding additional customers.

Conclusion

Several installations of the rural carrier system already have been made in various parts of the country and the experience to date has been generally satisfactory. The early installations are providing valuable experience in installation, operation, and maintenance of the system under a variety of conditions. Improvements in the carrier system and in its application to power and telephone lines can be expected to result from this experience.

References

1. Joint Use of Pole Lines for Rural Power and Telephone Services, J. W. Campbell, L. W. Hill, L. M. Moore, H. J. Scholz. AIEE Transactions, volume 66, 1947, pages 519–524.

2. A Carrier Telephone System for Rural Service, J. M. Barstow. AIEE Transactions, volume 66, 1947, pages 501–507.

Discussion

J. M. Dunham (Bell Telephone Laboratories, Inc., New York, N. Y.): The four types of choke coils used in equipping a rural power line for carrier were designed to meet certain requirements regarding impulse voltages, load, and short-circuit currents. While design tests were considered sufficient for load requirements, all types of choke coils from production are being tested for specified short-circuit currents and impulse voltages.

The short-circuit tests include, first, a preheating of the coils to operating temperature at normal loads, and then the application of 500 amperes for one second. This is a rather severe test as short-circuit currents of this magnitude and duration will not be encountered frequently in contemplated rural power line carrier applications.

Impulse voltage tests using a $1^1/_2$x40-microsecond wave are made at voltages above the breakdown of protective gaps on the coils. Gaps are blocked or removed for these tests. On the isolating choke, which has a protective gap from each terminal to the grounded tank and a third gap across the coil, three impulse tests are made. Each terminal of the coil is tested to ground and one test is made with voltage applied across the coil. These test voltages are 95 kv from terminals to ground and 55 kv across the coil. Impulse tests are made following short-circuit tests so that any movement of parts, resulting from the short-circuit current, which affects the impulse strength may be detected.

The authors have given temperature rises of choke coils when carrying normal rated load. These temperatures are conservative for class *A* insulation. Also, in the isolating choke, glass or glass and mica insulation is used throughout which puts the insulation of this coil in class *B*. Accordingly, while revised ratings have not yet been specified, indications are that the isolating chokes could be rated at 15 amperes continuous. The corresponding temperature rise for this current is 85 degrees centigrade as against about 50 degrees centigrade for 10 amperes.

Although the smaller chokes were designed for 4 amperes continuous current, the short-circuit requirement of 500 amperes for one second was the controlling factor in determining the size of the coil conductors. The isolating choke and the smaller chokes are wound with the same size conductors, equivalent to about number 11 American Wire Gauge. This size conductor on the small choke coils makes it possible to increase their continuous current rating above those originally specified. Although the smaller choke coils are wound with glass tape insulation, the phenol fiber used in assembling the coil is the limiting factor in the allowable temperature rise or rating of the coils. On a basis of 55 degrees centigrade rise, for class *A* insulation, the tap choke could be rated at 7 amperes, and the transmission chokes at 9 amperes (0.6 millihenry) and 10 amperes (0.3 millihenry).

Because, on some power lines equipped for carrier, peak loads may exceed the aforementioned choke coil ratings, curves of short-time overload currents will be made available.

W. R. Brownlee (Commonwealth and Southern Corporation, Jackson, Mich.): The application of joint rural carrier telephone systems is a welcome development in the general program of extending communication facilities throughout rural areas. Certain operating considerations warrant further study and improvement.

The development of methods and procedures for investigating failures of the communication channel is needed urgently. There does not seem to be any adequate method of determining in all instances whether a communication failure is the result of devices and equipment maintained and operated by the communication company or of one of the several pieces of equipment maintained and switched by the electric power company. Accordingly, it may be difficult to decide which maintenance crew should investigate first.

The authors mention the possibility of interfering noise from cracked insulators, line hardware, and so forth, on the power system, and indicate that these may be handled in accordance with usual practices. One common method for locating interference involves a momentary interruption of the power line, noting whether or not the interfering noise disappears at the same instant. Such a method cannot be used to determine whether the trouble is originating on the distribution circuit, as de-energizing such a circuit also interrupts power supply to the carrier telephone equipment.

Another operating feature of the joint carrier system is that, in the event of a power failure, the customer cannot use his communication facilities to notify anyone.

S. C. Bartlett (American Gas and Electric Service Corporation, New York, N. Y.): The paper appears to be a very complete discussion of the subject. There are, however, one or two points I thought worthy of further comment. In the first place the probable field of application should be considered. The authors mentioned that this system particularly was adapted for those areas having long circuit lengths between customers. A system such as this, which is actually joint use of both poles and conductors, appears to be practical, at least under present economic considerations in areas where subscriber density does not exceed one or two per mile. In the territory served by the American Gas and Electric System, for instance, we find practically no areas of such low density. However, to make sure all technical advances such as this one are available to our customers, we are co-operating with the telephone company in the selection of test sites. It is our hope that at least four such installations will be made during 1947. There is always the possibility that economic considerations may change, making the scheme practical in areas of higher density.

From the point of view of the carrier current engineer familiar with performance of carrier telephone equipment on high tension transmission lines, the over-all performance of this rural telephone system is very impressive. On main transmission lines we are forced to use a system which was designed for transmission of 60-cycle energy with no consideration of the characteristics at carrier frequencies. The resulting peaks and valleys in the transmission characteristic of the average power line are frequently so sharp that even the narrow side bands we need for intelligible speech cannot be passed without bad distortion. On a high voltage system the cost of corrective measures is usually so great that they are not employed.

On this rural telephone equipment, however, because of its lower voltage, it is entirely practical to provide proper terminations, traps, and so forth so that the resulting performance is very satisfactory. In fact, observations by listening to conversations on these circuits gives the impression that the quality is fully as good as that obtainable on ordinary open wire telephone lines

P. A. Jeanne (Bell Telephone Laboratories, Inc., New York, N. Y.): Reclosing oil circuit breakers used on rural power lines have operating coils connected in series with the line. These coils, particularly those of smaller ratings, cause rather large transmission losses at the frequencies of the *M1* carrier system. One type of reclosing oil circuit breaker, for example, produced a 10-decibel loss at 150 kc. Means for reducing the loss from this type of equipment have been given considerable study. Transmission computations indicated that the loss would be reduced sufficiently if the "recloser" was

shunted by 50 ohms, either in the form of a resistor or a capacitor of equivalent impedance at the lowest frequency of the carrier system.

A 50-ohm resistor has little affect on the 60-cycle ratings of even the smallest size recloser. Of course, it would be desirable, from the standpoint of convenience of application to existing breakers, to connect a resistor or capacitor across the terminals of the recloser. However, a resistor so connected would prevent isolation of the line, and a capacitor, in case of its failure, would energize the line at full potential even though the breaker were open. These difficulties may be avoided if space and adequate dielectric clearance are available for connecting a resistor or capacitor across the operating coil inside the recloser.

The most logical choice for the by-pass element would be a capacitor, providing one of high enough dielectric strength and one small enough to fit into available space could be provided. It was desired, insofar as possible, to use the same type of by-pass element for the various types of reclosers now in the field. Some types of reclosers have their operating coils shunted with lightning protective elements but others do not. Partly because of this latter consideration, that is, lack of lightning protection around coils, and partly because of availability in suitable shapes, a 50-ohm 125-watt plaque-type resistor has been used with reclosers so far modified. The wattage rating is several times as high as that required by the continuous rating of reclosers. However, the resistor must withstand the load imposed on it during faults. The heaviest duty on the resistor occurs when it is used with the smallest rating of recloser. For example, when used with a 3-ampere recloser carrying rated current, the resistor load is approximately 40 watts compared with 35 kw for 0.17 second under maximum interrupting current conditions, if the recloser goes through its complete cycle to lockout. The duty on the resistors decreases quite rapidly with increase in the rating of the recloser, which is a fortunate circumstance as only a small per cent of the reclosers in service are of the lowest ratings.

By-pass resistors increase somewhat the operating temperatures of the reclosers. Except possibly for the 3-ampere rated reclosers it does not appear that this increased temperature rise will be a limiting factor for reclosers now in the field. This matter is still under study.

Pending final solution of this problem, which is being studied co-operatively with manufacturers, and to facilitate modification of recloses in the field, modification kits containing the resistor and necessary mounting brackets, and so forth, are being provided for the more frequently encountered reclosers now in the field. Information has been received concerning several new models of reclosers now under development and the manufacturers have been asked for recommendations as to suitable carrier by-passing means. Where designs have not progressed too far it is hoped that provision might be made for the necessary elements and thus simplify this problem in the case of the newest designs.

Lee E. Cook: The comments of the discussers are timely and constructive. Discussions by J. M. Dunham and P. A. Jeanne exemplify continuing progress in betterment of the devices. With respect to the comment by W. R. Brownlee, the excellent co-operation that has existed between power and telephone operating folks will be fruitful in operating and servicing the carrier system.

Urban joint use of poles for electric and telephone lines has been practiced effectively and beneficially for many years. However, until recently opportunities for benefits in the rural situation have not been so apparent. The rural carrier system offers opportunity for joint use in the more sparsely settled areas with substantial savings indicated in construction materials and operating requirements.

Equipment already in service gives reasonable appearance, and experience to date indicates acceptable operating characteristics from both the telephone and power points of view. Undoubtedly with the great public interest and apparent future demand for utility services on the farm, and with the economies afforded by the carrier telephone system on rural power lines, the system will find considerable application.

Joint Use of Pole Lines for Rural Power and Telephone Services

J. W. CAMPBELL
MEMBER AIEE

L. W. HILL
MEMBER AIEE

L. M. MOORE
FELLOW AIEE

H. J. SCHOLZ
FELLOW AIEE

THE use of poles to carry both power and communication circuits is not new, having been employed before 1890. There are today more than 6,000,000 poles used jointly by power and telephone organizations in the United States. The great bulk of these poles are located in urban areas where the voltages of the power circuits concerned are generally less than 5,000 volts and the span lengths between poles generally do not exceed about 150 feet.

As power and telephone lines were extended into rural territory, new problems were encountered in the application of joint construction because of the use of longer spans and higher voltages for the power circuits and the increased noise induction in the necessarily longer exposures. However, progress in the art through co-operation of the telephone industry with the Edison Electric Institute and the Rural Electrification Administration has brought about the developments reviewed in this paper which now make long span higher voltage rural joint use feasible where conditions are favorable.

Higher Voltage Joint Use

A report[1] covering the safety features of joint use of poles by telephone circuits and 6.9- or 13.2-kv power circuits was issued in 1937. This report opened the way for a pattern which now facilitates joint use where power circuits of more than five kv are involved. One important condition which this pattern includes is that provision be made for co-ordinated electrical protection. This includes arrangements whereby the supply circuit will be de-energized promptly in the event of contact with the telephone plant, and the resulting voltages on the telephone plant in the event of accidental contact will be within the range of safe operating characteristics of telephone protective equipment. The 5th edition of part 2 of the National Electrical Safety Code provides that where this condition exists, grade *C* construction may be employed. This has an important bearing on the present problems involved in long span rural joint use.

Joint use of poles for telephone circuits and power circuits operating at voltages over five kv has been employed on a general basis in a number of urban localities, and there are now in the order of 100,000 or more poles involved in such construction. In a majority of these cases, the telephone circuits are in cable, the sheaths of which may be effectively grounded, thus affording a low impedance path to ground in the event of accidental contact. Where open-wire telephone circuits are involved, 3-kv carbon gap protectors, described later, are associated with the telephone open wires for the same purpose. Wherever practicable the cable sheaths and the protectors are connected to grounds which are connected also to the multigrounded neutral of the supply circuit.

Some of these higher voltage joint use installations in urban areas have been in service for ten years or more, so that in approaching the rural joint use problem, a considerable background of experience is available so far as co-ordination of electrical protection is concerned. Experience from these cases as to noise co-ordination is applicable less directly to the rural situation.

High Strength Wires

Some 25 years ago there began to be used types of wire which, while relatively small, had sufficient strength and conductivity for the construction of power lines with much longer spans between poles than the spans which predominate in urban areas. These wires are generally of the stranded type in which strength is provided by one or more strands containing steel, and their use has made practicable a considerable reduction in the cost of pole plant. There are also available both steel and copper-covered steel telephone wires which are suitable for long span construction.

Joint Pole Practices

In considering the long span construction an attempt was made to approach the matter from the standpoint of the representative typical situation rather than the most adverse situation. It was assumed that both the power and telephone wires would be of the high strength types and, therefore, their sag characteristics would not differ sufficiently to cause contacts in the span under ice and wind loading or temperature changes if reasonable separations were provided at the poles. It was assumed also that a very large percentage of the rural power circuits concerned would consist of one phase wire located on a pin at the top of the pole and a multigrounded neutral located below it on a separate pin or on the secondary rack, or that the primary circuit would consist of two or more primary wires located on a crossarm at the top of the pole and that the multigrounded neutral, if present, would be located on the same crossarm or on the pole below the crossarm. Practices for joint use were prepared,[2] the major provisions of which (with

Paper 47-82, recommended by the AIEE committee on communication for presentation at the AIEE winter meeting, New York, N. Y., January 27–31, 1947. Manuscript submitted November 13, 1946; made available for printing December 15, 1946.

J. W. Campbell is outside plant engineer of the American Telephone and Telegraph Company, New York, N. Y. L. W. Hill is president of the Carolina Telephone and Telegraph Company, Tarboro, N. C. L. M. Moore is with the technical standards division of the Rural Electrification Administration, United States Department of Agriculture, Washington, D. C. H. J. Scholz is a supervising engineer of the Commonwealth and Southern Corporation, Birmingham, Ala.

respect to the vertical separations between the power and telephone conductors at the pole and in the span) are given as follows. Because of limited experience with joint use in long spans, these practices are still tentative and are subject to modification in the light of experience obtained from their use.

1. The minimum vertical separations between supply and telephone wires at the pole and in the span comply with the provisions of the National Electrical Safety Code. These minimum vertical separations for supply circuits 0 to 8,700 volts are 40 inches at the pole and 30 inches in the span; for supply circuits over 8,700 volts, 60 and 45 inches, respectively. All voltages are the highest voltages between wires on the pole head.

2. In addition the minimum vertical separations at the pole are so adjusted that under conditions of 60 degrees Fahrenheit, no wind and final unloaded sag, no supply conductor of 0 to 750 volts shall be lower at any point in the span than a straight line (line-of-sight) joining the points of supports of the highest communication cable or conductor on adjacent poles, and no supply conductor of more than 750 volts is lower at any point in the span than 30 inches above such line-of-sight.

3. An exception is made in the case of the line-of-sight requirement where a power circuit multigrounded neutral is located on the pole below the primary wires and secondary wires are not present. Where such construction exists the normal separations as regards the neutral apply, that is, 40 inches between the neutral and telephone wire or cable at the pole and 30 inches in the span, provided also that the line-of-sight requirement for separation between the primary wires and the telephone wires or cables, as per item 2, is met also.

4. The requirements just reviewed are based on the use of high strength conductors for both the power and telephone circuits, and when supply conductors having greater sag increases under temperature or loading are employed further increases in separation at the pole may be required.

As will be noted, item 2 provides a line-of-sight basis for determining separations between power and telephone conductors at the pole. The objective is to provide separations between the power and telephone conductors so that during wire stringing and repair operations, telephone wires will not be swung into contact with energized power conductors if reasonable procedures are followed in such work. Where a multigrounded neutral is located below the energized power conductor, therefore, a somewhat relaxed requirement is practicable, as indicated in item 3. It is possible that as experience is gained with long span construction, further simplification can be effected.

The minimum size of power wire recognized by the National Electrical Safety Code for grade *C* construction is number 8, American Wire Gauge medium-hard drawn copper. Where this wire is used in spans exceeding about 150 feet, it is necessary to provide more than 40 inches separation between the power and telephone wires at the pole to meet the 30-inch separation requirement in the span. High strength wires as usually strung have, of course, much smaller sags than medium-hard drawn copper and therefore, can be used in longer spans without the necessity of increasing the separation at the pole. As will be seen therefore, the necessity of adjusting the separation at the pole depends in large measure upon the power wires employed and the tension to which they are strung. The line-of-sight formula given in item 2 can be considered as generally applicable. However, for spans such as usually are employed in urban areas, the separations provided by the NES Code have proved to be adequate and satisfactory. In the practical case, for vertical configuration with the phase wires at the top of the pole and the multigrounded neutral located three or four feet below, normal separations at the pole can be employed often for spans exceeding 200 feet and in some instances exceeding 300 feet. A factor which has bearing on the design of joint use lines is that, for noise induction reasons, the separations between the power and telephone circuits should be kept uniform as far as practicable without incurring undue costs or construction difficulties. It is believed that as experience is gained it will be practicable to prepare pole-head diagrams which can be used for all but a few exceptionally long spans which may require special consideration.

Another factor which is involved in long span construction is clearance above highways and ways generally. The NES Code specifies minimum clearances for both power and telephone wires along, or crossing highways, driveways, and so forth, but does not cover ways generally such as across fields. The NES Code also requires that for spans exceeding 175 feet in the heavy loading district, 250 feet in the medium loading district, or 350 feet in the light loading district, certain increases in clearance shall be provided. Across fields or other ways which may be traversed by loaded vehicles or farm machinery adequate ground clearance should be provided. Ground clearances, together with the separations between supply and telephone conductors serve, in large measure, to determine necessary pole heights for joint lines. As span lengths are increased, pole heights and, therefore pole costs, increase and, as would be expected, a span length is ultimately reached where economies begin to decrease. In the practical case, however, topography, highways, locations of customers, and other factors generally result in span lengths well under this economic limit.

As will be observed, the separations specified are based on the final unloaded sag of the supply conductors. This recognizes that in long spans there is often considerable difference between the stringing sag and the sag after the wires have been subjected to ice and wind loading.

Table I. Summary of Measurements at Selma, Ala.

(Alabama Power Company and Southern Bell Telephone and Telegraph Company)

Length of Exposure	Ground Return; $I \cdot T = 90$;** Voltage TIF = 19: Receiver Noise (Dba)*	Ground Return; $I \cdot T = 90$;** Voltage TIF = 19: Noise-to-Ground (Dba)	Ground Return; $I \cdot T = 275$;† Voltage TIF = 12: Receiver Noise (Dba)*	Ground Return; $I \cdot T = 275$;† Voltage TIF = 12: Noise-to-Ground (Dba)
Circuit 1—				
16 miles	14	44	18	54
Circuit 2—				
5 miles	14	32		

* With tube station sets and well-balanced carrier-operator equipment.

† $I \cdot T$ constant throughout exposure.

** $I \cdot T$ at start of exposure; tapers to zero at end.

Notes:

Receiver noise measured at last station on circuit with *HAI* weighting.

Noise-to-ground measured at outer end of circuit with *FIA* weighting.

$I \cdot T$ and voltage *TIF*—tentative 1941 weightings.

Recheck after about 16 months of operation indicates slightly lower receiver noise with about same noise-to-ground.

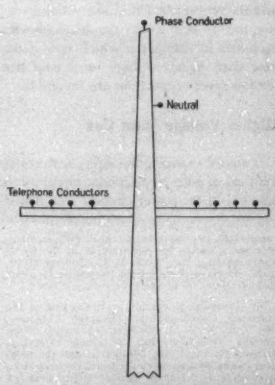

Figure 1. Typical pole head for rural joint use

Table II. Summary of Measurements at Centerville, Ala.

(Alabama Power Company and Southern Bell Telephone and Telegraph Company)

Length of Exposure	Ground Return; I·T = 200;** Voltage TIF = 20		Ground Return; I·T = 1,000;† Voltage TIF = 35	
	Receiver Noise (Dba)*	Noise-to-Ground (Dba)	Receiver Noise (Dba)*	Noise-to-Ground (Dba)
Circuit 1—				
8.7 miles	10	41	23	60
Circuit 2—				
7.5 miles			19	56

* With tube sets and well-balanced carrier-operator equipment.

† $I \cdot T$ constant throughout exposure.

** $I \cdot T$ at start of exposure; tapers to zero at end.

Notes:

Receiver noise measured at last station on circuit with *HA1* weighting.

Noise-to-ground measured at outer end of circuit with *F1A* weighting.

$I \cdot T$ and voltage *TIF*—tentative 1941 weighting.

Information concerning the sag characteristics of the various types of wire used for rural construction is provided by the wire manufacturers.

Instances of Long-Span Joint Use

There are a number of existing installations where long-span joint construction has been employed as the best engineering solution of specific problems. The present objective is to work out arrangements whereby such joint use may be entered into more generally in rural areas much as it is now carried out in urban areas. In this connection five installations have been given specific study during the past two years, and have furnished data of considerable value. Three of these are located in Alabama, in the medium and light loading districts, one in South Dakota and one in Minnesota, the latter two being in the heavy loading district. In the Alabama installations, the spans average about 400 feet with maximum spans ranging between 600 and 800 feet. In the installations in South Dakota and Minnesota, the spans average around 320 feet, with maximum spans about 400 feet. One of these five installations was completed in the summer of 1945, and has proved satisfactory since that time. The other four have been completed only recently.

Table III. Summary of Measurements at Webster, S. D.

(Lake Region Electric Association, Inc., and Northwestern Bell Telephone Company)

Length of Exposure	Ground Return; I·T = 45;‡ Voltage TIF = 25		Ground Return; I·T = 350;ϕ Voltage TIF = 12	
	Receiver Noise (Dba)*	Noise-to-Ground (Dba)	Receiver Noise (Dba)*	Noise-to-Ground (Dba)
Circuit 1—				
11 miles**	10	31	15	53
Circuit 2—				
9.5 miles**	10	32	14	50
Circuit 3—				
1 mile†	<0	22		

* With tube sets and well-balanced carrier-operator equipment.

† Exposed to two phases throughout.

** Exposed five miles to two phases; remainder to single phase.

‡ $I \cdot T$ at start of exposure; tapers to zero at end.

ϕ $I \cdot T$ constant throughout exposure.

Notes:

Receiver noise measured at last station on circuit with *HA1* weighting.

Noise-to-ground measured at outer end of circuit with *F1A* weighting.

$I \cdot T$ and voltage *TIF*—tentative 1941 weightings.

Telephone Circuit Noise

Rather complete measurements of noise and power system influence have been made in the five joint-use installations mentioned previously. The results of these measurements are summarized in Tables I–V. Explanations of some of the terms used in these tables are contained in the appendix.

In these tables noise values corresponding to two conditions of power circuit influence are given. In all cases, the lower of the two $I \cdot T$[4] values and the noise associated with it represent normal conditions; the higher $I \cdot T$ and associated noise values represent a condition existing when the magnetic influence was increased artificially for test purposes by connecting a shunt capacitor across the power circuit at the end of the exposure. This was done in order to determine the increase in receiver noise resulting if the power circuit influence, as measured by ground return $I \cdot T$, were to increase for one reason or another. The effect of the capacitor on the voltage *TIF*[4] was in most cases small compared to the change produced in the $I \cdot T$ values; in some cases it decreased, and in some it increased when the capacitor was applied.

The general indications in this connection are summarized in Table VI which shows for the five cases, the relationships between $I \cdot T$, noise-to-ground, and receiver noise. It will be noted that in general the noise-to-ground follows the $I \cdot T$ reasonably closely; in fact, because the telephone circuits are essentially grounded at the central office, the noise-to-ground measured at the outer ends of the circuits is probably a better indication of the average $I \cdot T$ through the exposure than the recorded $I \cdot T$ measurements. On the other hand, the receiver noise increases less than the noise-to-ground, a fact which appears to indicate that for the cases studied, reasonably large increases in power system influence, at least to the extent that influence is measured by $I \cdot T$, will not result necessarily in high receiver noise.

The reasons for the relatively small increase in receiver noise compared to the increase in noise-to-ground with increasing $I \cdot T$, were not conclusively determined by the measurements made. A reasonable explanation appears to be that with the low values of $I \cdot T$ existing under normal conditions, the receiver noise primarily results from electric induction. Therefore, increasing the $I \cdot T$ will not directly affect the receiver noise until the $I \cdot T$ becomes high enough to be controlling.

Tables I–V give a good indication of the effectiveness of the methods used to keep receiver noise low. One of the best overall single indicators of the effectiveness of these methods is the ratio of receiver noise to noise-to-ground. The test results indicate that ratios in the order of −36 decibels (about 1 to 60) are obtained commonly where the $I \cdot T$ is fairly high and that ratios as high as −42 decibels (1 to 120) can be obtained in some cases. Ratios of these orders should be adequate in any but the most severe exposures and should continue to result in noise on rural joint-use circuits which compares favorably with that on urban party line circuits in cable.

Among the reasons why these favorable noise conditions are obtained is that in joint use, the exposures can be made very uniform, an arrangement which facilitates obtaining a high degree of effectiveness of telephone circuit transpositions. A particularly high effectiveness is obtained where the *R*1 system[2] with tandem brackets is used, because this system provides frequent transpositions and an average wire spacing of only about seven inches. While this system was developed primarily for telephone circuits on separate lines its effectiveness and ease of installation recommends it for joint use. Also, many of the exposures involve single-phase common-neutral power circuits with vertical configuration (see Figure 1) for which the direct metallic circuit induction into a horizontal joint-use telephone pair is inherently low.

The low receiver noise values noted in the tables, of course, can be obtained only when the telephone circuits are very well balanced. For example, the use of

directly grounded ringers (without tubes) of even the highest impedance types available is likely to increase the receiver noise in the order of ten decibels or more. Likewise, central office unbalances of the type frequently encountered and which are unimportant in connection with urban telephone service may produce, in rural service, increases of the order just mentioned.

It may be well to point out that the need for co-ordinat on between the power and telephone circuits is not confined to joint use; it applies also when telephone circuits are on separate lines exposed to power circuits. The noise-to-ground on a telephone circuit at 50-foot separation from a power circuit is in the order of four decibels less than on one in joint use with power circuit having the same ground return *I-T*. Thus there is in general only about 4 decibels difference in the noise because of unbalances in the two cases, a difference which rarely would make a significant difference in the measures which would need to be applied to obtain co-ordination.

Electrical Protection

As pointed out earlier, the types of construction, clearances, and so forth, used in joint-use lines are such as to minimize the chances of contact between power and telephone circuits. Experience with several million joint poles in other circumstances indicates that the frequency of occurrence of such contacts will be very low, but electrical protective arrangements are incorporated which will provide a high degree of safety if a contact does occur.

These protective arrangements are

1. In the power system, fuses, circuit breakers, or other devices which will de-energize reliably and promptly the power wire in the event of a ground fault of relatively low impedance.

2. In the telephone system, protective gaps connected between the telephone circuit and the common neutral (or other low resistance ground) at intervals such that the impedance presented to ground by the telephone plant if a contact occurs will be low enough to insure proper operation of the power protective devices.

As a general rule, the relaying and fusing arrangements used by power organizations for their own purposes are more than adequate to provide prompt and reliable de-energization if a contact occurs. In any event, any changes which might be desirable, in general, would be in line with trends in power circuit protection.

The protective gaps used on the telephone circuits usually are *99A* protectors. As shown in Figure 2, the *99A* protector consists of three rugged carbon cylinders enclosed in a weatherproof container and separated so that the breakdown voltage between them is about three kv rms. Any two of the cylinders can be connected to a pair of line wires, the third being connected to ground. Placing *99A* protectors at about 1/2-mile intervals usually will provide sufficiently low impedance to insure proper operation of the power protective arrangements for a contact at any point.

Occasionally, in connection with the use of *99A* protectors, consideration needs to be given to their current carrying capacity. The currents which these protectors will carry for three successive shots are about as shown in Figure 2*B*. The power relaying and fusing arrangements used for power purposes in rural areas usually will provide adequate co-ordination with these characteristics.

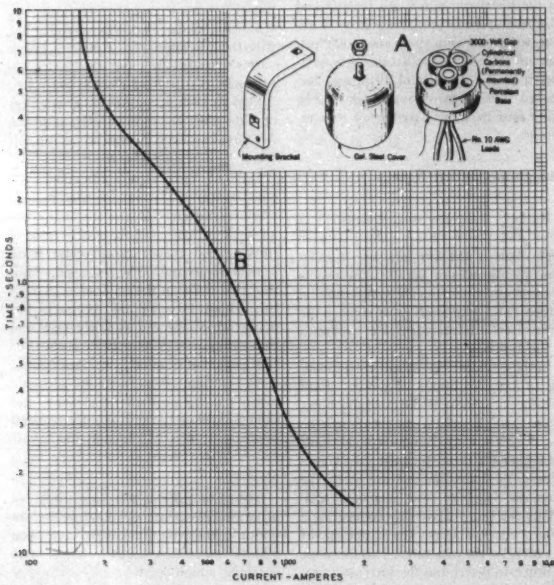

Figure 2. Current carrying ability of 99A protector

A—*99A* protector disassembled for illustration

B—Approximate current-carrying ability of *99A* protector, each of three successive shots

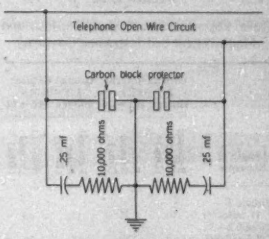

Figure 3. Schematic diagram for drainage device

The *99A* protectors also can be used often to advantage on separate telephone lines involved in crossings with rural power circuits.

In case the telephone circuit should become disconnected from the central office equipment and the entrance cable for any reason, there may be a fairly high 60-

Table IV. Summary of Measurements at Alexander City, Ala.

(Alabama Power Company and Southern Bell Telephone and Telegraph Company)

Length of Exposure‡	Ground Return; I·T = 120**; Voltage TIF = 9		Ground Return; I·T = 300†; Voltage TIF = 11	
	Receiver Noise (Dba)*	Noise-to-Ground (Dba)	Receiver Noise (Dba)*	Noise-to-Ground (Dba)
Circuit 1—				
12 miles	10	36	11	47
Circuit 2—				
11.5 miles	10	35	11	46
Circuit 3—				
6.5 miles	10–14	28	10	35

* With tube sets and well-balanced carrier operator equipment.

† $I \cdot T$ constant throughout exposure.

** $I \cdot T$ at start of exposure; tapers to zero at end.

‡ Includes 2.8 miles with low $I \cdot T$(32) for all test conditions.

Notes:

Receiver noise measured at last station on circuit with *HA1* weighting.

Noise-to-ground measured at outer end of circuit with *F1A* weighting.

$I \cdot T$ and voltage *TIF*—tentative 1941 weighting.

cycle voltage between it and ground because of electric induction under normal operating conditions. This voltage regulates through a very high impedance consisting of the capacitance to ground of the circuit so that only small current can be drawn. However, with long exposures, such currents can cause annoying electric shocks and in extreme cases cause false bell ringing or even damage to station ringers.

While the occasions on which circuits are disconnected from central office equipment and entrance cables are infrequent, electrical drainage has been used to limit the open-circuit voltage. The devices which have been used to date consist of a capacitor of 0.25 microfarads and a resistor of 10,000 ohms from each wire to ground. The arrangement is shown in Figure 3. These devices usually are installed at about 5-mile intervals. They also can be used to advantage in some cases on separate telephone lines exposed to power lines.

Summary

While experience to date is still limited, it definitely has demonstrated the feasibility of higher voltage long span joint use in rural areas. Economic studies still in progress indicate that where new extensions are to be made to provide both power and telephone service, worthwhile economies can be realized in most cases by such joint construction. Where power lines already extend over the area, modification of such lines to accommodate communication circuits of course will introduce an additional element of cost. Even in this case, however, it appears that there will be an over-all economic advantage in favor of joint use as compared to separate lines.

The relative field of application of joint use and of the carrier system discussed in a companion paper[3] must be determined by experience. It is evident that they will supplement one another and taken together will further promote communication coverage of rural areas.

Appendix. Qualitative Explanation of Certain Terms Used in Tables I–V

While the terms used in noise induction work have been publicized widely, a few brief qualitative explanations may be of some use to those who are not familiar with the work.

The term, receiver noise, refers to the noise in the receiver of a telephone set, that is, the noise which is heard by the customer.

Table V. Summary of Measurements at Pipestone, Minn.

(Southwest Minnesota Electric Co-operative and Northwestern Bell Telephone Company)

Length of Exposure	Ground Return; I·T = 200;†** Voltage TIF = 11		Ground Return; I·T = 600;† Voltage TIF = 12	
	Receiver Noise (Dba)*	Noise-to-Ground (Dba)	Receiver Noise (Dba)*	Noise-to-Ground (Dba)
Circuit 1—				
14.5 miles	15.5	40	18	60
Circuit 2—				
13.0 miles	7.5	40	18	60

* With tube sets and well-balanced carrier-operator equipment.

† Average $I \cdot T$ through exposure.

** $I \cdot T$ near start of exposure; tapers to zero at end.

Notes:

Receiver noise measured at last station on circuit with *HA1* weighting.

Noise-to-ground measured at outer end of circuit with *F1A* weighting.

$I \cdot T$ and voltage *TIF*—tentative 1941 weightings.

It is measured by measuring the audio-frequency voltages existing across the receiver terminals caused by induction (or some other noise source) using an instrument (usually a 2-type noise measuring set) which weights the various frequencies in accordance with their relative interfering effects and takes account of the impedance-frequency and efficiency characteristics of the receiver, because these characteristics affect the power at the receiver input and output, for given voltages across the receiver.

Noise is expressed in decibels with relation to a small reference value. The number of decibels above this reference value is called "dba" to distinguish it from the numerous other uses of the term decibel. For receiver noises up to about 17 dba the resulting impairment of telephone transmission is less than one decibel. For noises above 17 dba the impairment increases with increasing noise but not as rapidly as the noise until rather high levels are reached.

In a metallic telephone circuit, the noise voltages existing between either (or both) of the wires and ground are much larger than those between the two wires of the circuit or across the telephone receiver, ratios of between a hundred and several thousand to one being common. Therefore, if the noise to ground were to be measured with a noise measuring set having the same order of sensitivity as is used for receiver noise measurements, a very wide range instrument would be required and the quantities measured might be unwieldy. Also, in many cases, it is desirable to measure noise to ground without changing the magnitudes of the noise voltages. For these reasons, in noise-to-ground measurements, the sensitivity of the measuring set is decreased and the desired high impedances obtained by using a 100,000-ohm noninductive resistance input circuit and utilizing the voltages across only 600 ohms out of this total.

The term tube station set refers to a type of equipment used at customers' premises in which a cold cathode gaseous type tube is inserted in the ringer-to-ground connection so that this connection is open during the talking intervals and the ringer produces no unbalance during these intervals. When ringing voltages are applied, the tube breaks down so that the ringers can operate.

The term $I \cdot T$ means the product of rms current and its TIF,[4] (telephone influence factor). Voltage TIF is the telephone influence factor of the voltage.[4] They are, respectively, over-all indications (linear) of the magnitudes and frequencies of the harmonics in the power line currents and the power line voltages. Ground return $I \cdot T$ pertains to those harmonic currents which go out over the power wires and return through the ground

Table VI. Comparison of Increases in Noise to Ground and Receiver Noise With Increase in I·T

Test Location	I·T Lower Value*	I·T Higher Value	I·T Increase Ratio	I·T Increase Db	Increase, Db Noise to Ground	Increase, Db Receiver Noise
Selma	45	275	6	15.5	10	4
Centerville	100	1,000	10	20	19	13
Webster	22	350	16	24	23	5
Alexander City	60	300	5	14	11	1
Pipestone	100	600	6	15.5	20	9–10

* One-half the values recorded in Tables I through V on assumption that average magnitude in exposure is one-half that at start.

The *HA1* receiver and *F1A* line noise weightings refer to the conditions when the noise measuring set is so adjusted that the individual frequencies are weighted in accordance with their interfering effects with the newer types of telephone station equipment using *HA1* receivers and *F1A* transmitters Tentative 1941 weightings refer to tentative telephone influence factor (*TIF*) weightings which are consistent with *HA1* and *F1A* noise weightings. These *TIF* weightings have not been standardized yet but are used quite widely in field investigations partially to secure data on which to base ultimately a standard set of weightings.

References

1. Joint Use of Poles—Telephone Circuits and 6.6 and 13.2 Kv Power Circuits—Safety Features. Provisional Report 19 by the Joint Subcommittee on Development and Research of the Edison Electric Institute and the Bell Telephone System. Edison Electric Institute (New York, N. Y.), Publication number E4.

2. Part 5 of Joint Pole Practices for Supply and Communication Circuits, a tentative report for field trial. Joint Committee on Plant Co-ordination of the Edison Electric Institute and the Bell Telephone System, May 1946. Edison Electric Institute (New York N. Y.) Publication number M12.

3. Application of Rural Carrier Telephone System, E. H. B. Bartelink, L. E. Cook, F. A. Cowan, G. R. Messmer AIEE Transactions, volume 66, 1947, pages 511–518.

4. Inductive Co-ordination Aspects of Rectifiers, AIEE Committee Report. AIEE Transactions, volume 65, 1946, July section, pages 417–36.

Discussion

H. A. Enos (American Gas and Electric Service Corporation, New York, N. Y.): This discussion concerns the portion of the paper which covers the structural requirements of the proposed part 5 of the joint use practices. I am particularly interested in the application of these structural requirements to actual situations in the field.

A partial study of the wide variety of conditions which may exist in the field has led to some interesting conclusions. It is true that for a given pole top arrangement and specific power and telephone conductors there will be relatively few span lengths under which the addition of telephone conductors, on one level, will require more pole height than would be required with those particular power conductors alone. This is only true, however, for perfectly level ground and where each pole is separately engineered. A superficial examination of the requirements of the proposed part 5 for separations at the pole would lead to the conclusion that the determination of pole heights with these requirements is a relatively simple matter. Further study, however, will disclose that it is, on the contrary, a rather complicated process.

Under part 2 of the safety code for the shorter span lengths it is possible to determine pole height quite simply by adding up the required separations at the pole, together with the normal communication wire sag and the depth of pole setting, and come out with a fairly standard pole height for a certain pole top arrangement. Under the requirements of part 5 it is not such a simple matter. Depending upon the type of power circuits involved, the pole height changes for every change in span length, and for every change in kind of conductor, both power and telephone; it is also different depending on whether the lowest power conductor is secondary, multigrounded neutral, or primary. Then again if the common neutral is on the side of the pole below the primary, a check will have to be made to see whether the sag of the primary wire or the sag of the neutral is the governing factor and, in addition, bearing in mind that the separation at the pole must be sufficient to provide a minimum of 30 inches separation between the multigrounded neutral and the telephone conductor at 60 degrees Fahrenheit with no wind. If there is a secondary below the multigrounded neutral the separation at the pole will have to be such as to provide not only a separation equal to the final unloaded 60 degrees sag of the secondary wire but, also in order to comply with the safety code, it will be necessary to make a further check to see that a minimum of 30-inches separation at any point in the span is maintained between the lowest secondary wire and the highest telephone wire at 60 degrees Fahrenheit with no wind. In other words, it cannot be determined easily which condition will be the governing factor in determining the separation. Furthermore both the power company engineers and the telephone company engineers will have to be thoroughly conversant with the sagging practice of both companies, under all conditions for all conductors which are likely to be used, in order to determine the required separations.

It will require considerable study but it is probably worthwile doing to try to evolve some simpler means of determining separations at the pole, not only to avoid the necessity for detailed engineering of each span but also to make the application of the joint use practices sufficiently simple and at the same time safe, so as to insure that the necessary calculations will be made and not by-passed because they are complicated and onerous. Whether such a simplification of the method would result in less economy is hard to determine until the necessary investigation has been carried through to a conclusion

Rural Radiotelephone Experiment at Cheyenne Wells, Colo.

J. HAROLD MOORE
ASSOCIATE AIEE

PAUL K. SEYLER
NONMEMBER AIEE

S. B. WRIGHT
MEMBER AIEE

Synopsis: The first rural party-line telephone service by radio installations operating on the subscribers' premises was inaugurated August 20, 1946. This paper describes the equipment used, how it operates, and the results obtained during the preliminary testing and the initial period of regular operation. Radio is one of several new methods which the Bell System is exploring in its program for extension of telephone service in rural areas. It is expected that experience gained in this experiment will aid in developing a standard rural radiotelephone system.

IN connection with studies of the practicability of utilizing radio for extending telephone service to remote areas, a rural subscriber radiotelephone experiment has been undertaken by the Bell Telephone Laboratories and The Mountain States Telephone and Telegraph Company, with subscriber participation, in the vicinity of Cheyenne Wells, near the eastern border of Colorado.

As indicated in the general layout map, Figure 1, eight ranches are served, four being reached directly by radio and the remaining four being served by wire line extensions from the radio equipped location most remote from the central office. The complete installation comprises an 8-station party line that functions in much the same manner as a conventional party line, and since August 20, 1946, has been providing regular telephone service to the eight ranches involved.

The Cheyenne Wells locality was selected for the experiment because it is sparsely settled and does not now have telephone or power distribution lines in the outlying areas; furthermore, a number of ranchers in this area had indicated a desire to obtain telephone service. The ranches involved in the trial are located from 11 to 21 miles southeast of the town, and the propagation paths between antennas at the central office and the various ranches are somewhat poorer than line-of-sight over relatively flat and open terrain.

The experiment was undertaken using frequencies in the 44–50-megacycle band because equipment designed for mobile systems could be modified to accomplish the desired result and was readily available. The 44–50-megacycle band is one of a number of locations in the spectrum where provision is made for rural telephone service under the Federal Communications Commission's frequency allocation plan. One transmitting frequency is employed at the central office terminal, and two other frequencies are required for the subscribers' transmitters. The second subscriber frequency is utilized only for reverting calls between subscribers on the same system, in a manner similar to that described in a companion paper[1] discussing the *M1* carrier telephone system.

Operation of System

The system is designed to operate as a common battery signaling rural line with a standard appearance in a manual telephone switchboard. Subscriber stations are called by the telephone operator of this board using 20-cycle code ringing. Each station telephone set is provided with a call key which forms part of the switchhook assembly of an otherwise standard combined telephone set. The contacts of the call key are arranged to provide for listening only when it is not operated, and to provide for simultaneous talking and listening when operated. It may be operated by the subscriber when the handset is off its cradle, and is restored automatically when the instrument is replaced. Its purpose is to turn on the system, and its use reduces the likelihood of accidental operation of the system and interference with calls in progress, and facilitates making reverting calls by permitting monitoring while the called station is being rung.

Figure 2 shows a diagram of the electrical arrangement. Each subscriber station is connected over a pair of wires through a cutoff relay to a hybrid coil, with branches leading to the radio transmitter and receiver. Associated with the hybrid coil and cutoff relay are devices for converting d-c signals to transmitter carrier, for translating received carrier to direct current and for resupplying 20-cycle ringing current. Several subscribers may be served from one radio-equipped terminal, the connection being extended by a wire line as illustrated. The central office installation includes a radio transmitter and two radio receivers connected to branches of a hybrid coil, which is associated with a pair of wires leading to a jack in the switchboard and relays for converting and translating direct current and for converting 20-cycle current to carrier pulses. Normally all the receivers are energized ready to receive a call and the transmitters are turned off.

To make a call, a subscriber lifts his handset from its cradle and listens. If the circuit is busy, he replaces the handset; if the circuit sounds clear he operates the call key. This closes the wire line through the telephone and operates a relay which causes the radio transmitter to emit carrier at the regular frequency. A

Paper 47-83, recommended by the AIEE committee on communication for presentation at the AIEE winter meeting, New York, N. Y., January 27–31, 1947. Manuscript submitted November 14, 1946; made available for printing December 4, 1946.

J. HAROLD MOORE is with the American Telephone and Telegraph Company, New York, N. Y.; PAUL K. SEYLER is with The Mountain States Telephone and Telegraph Company, Denver, Colo.; and S. B. WRIGHT is with the Bell Telephone Laboratories, Inc., New York, N. Y.

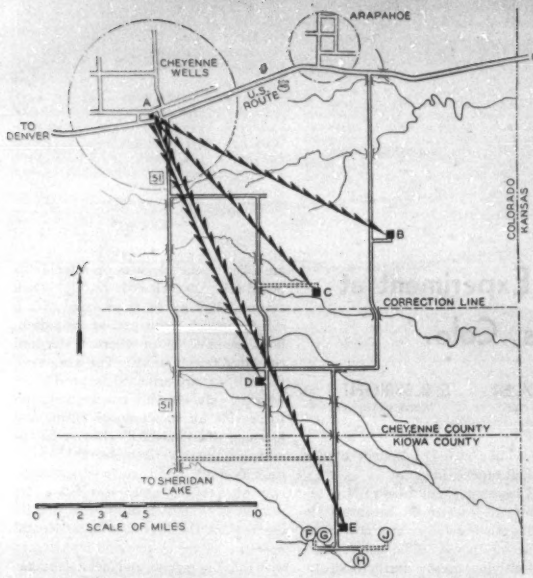

Figure 1. General layout

A—Telephone central office in town of Cheyenne Wells, Colo.

B, C, D, E—Ranches on party line connecting to central office by radio

F, G, H, J—Ranches connecting to ranch *E* by wire line and thence by radio to central office

portion of this carrier reaches the regular central office receiver and operates a relay which starts the central office transmitter and closes the switchboard loop causing the line lamp in the switchboard to glow. (This is the condition illustrated in Figure 2.) The operator plugs in the switchboard cord and completes the call through the switchboard in normal fashion. When the call is ended, the subscriber replaces the handset on the cradle, which automatically restores the call key, opening the wire line and thus releasing the relays and turning off both the subscriber's and the central office transmitters.

On a call for a station from the switchboard, the operator connects the calling cord to the line jack and rings the desired code. This operates a polar relay intermittently, causing the central office transmitter to emit pulses of carrier frequency at a rate determined by the frequency of the ringing current. This causes operation of relays in the subscriber's radio equipment and the bells ring at all the subscribers' stations. In the interval between rings, all relays are restored to normal, and the central office carrier is turned off. Upon hearing his code, a subscriber answers by lifting his handset and then his call key, which turns on his transmitter. Reception of his carrier at the regular central office receiver causes the central office transmitter to emit steady carrier, as in a call originating at his station.

On a reverting call, that is, a call between subscribers on the same system, the subscriber placing the call restores his call key while the operator rings the called station. When the called party answers, operation of his call key locks in his transmitter on the regular frequency and in turn causes the central office transmitter to be turned on. The transmitters of all the subscribers whose call keys are normal are automatically made ready to

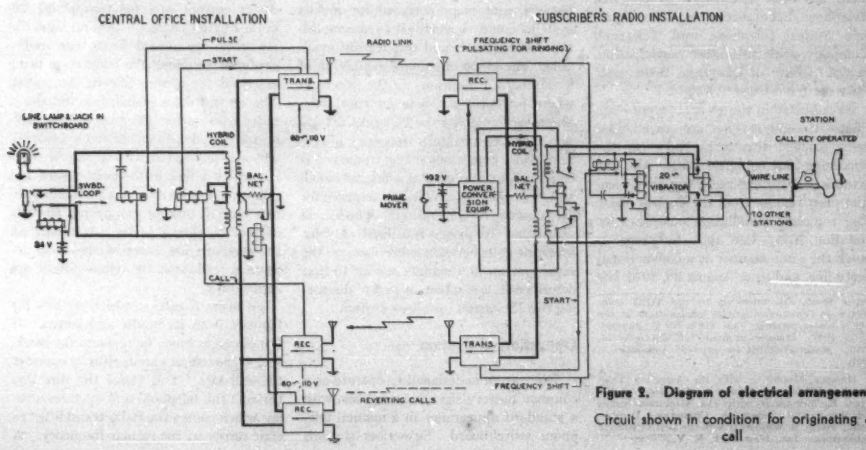

Figure 2. Diagram of electrical arrangement

Circuit shown in condition for originating a call

operate at the alternative subscribers' frequency by the presence of continuous carrier from the central office transmitter. When the calling party hears the called party answer, he operates his call key, which causes his transmitter to emit the alternative frequency which is received at the central office in the second receiver. Each subscriber hears the other by retransmission from the central office transmitter. Reception of the alternative frequency at the central office operates a relay which changes the impedance of the balancing network at the hybrid coil so as to provide this retransmission at the proper strength.

Description of Equipment

In the Cheyenne Wells system the central office frequency is 44.2 megacycles supplied by a crystal controlled transmitter with maximum rated output of 60 watts. The carrier is keyed by 20-cycle input for signaling, and frequency modulated with maximum deviation of ±15 kc by speech. Both the transmitter and receivers, which are also crystal controlled, are powered from commercial 60-cycle 110-volt supply. The antennas are vertically polarized half-wave coaxial type, fed by 72-ohm flexible polyethylene insulated coaxial cable 0.405 inch in diameter. The transmitting antenna is clamped to the top of a guyed 90-foot wooden pole. The two receiving antennas are mounted on crossarms atop a similar pole 50 feet away from the transmitting pole.

At the subscriber stations, the regular and alternative frequencies are 49.0 and 49.2 megacycles respectively, and are supplied from crystal-controlled transmitters having maximum rated outputs of 10 watts. Transmitters are frequency modulated by speech with maximum deviation of ±15 kc; signaling is by unmodulated carrier. Receivers are also crystal controlled. Antennas of the type used at the central office and some experimental *J*-type antennas are mounted on poles which range from 25 to 60 feet in height, depending on the distance from the central office. As shown in Figure 3, the transmitting and receiving antennas are supported by the same pole at opposite ends of a pair of crossarms. Lightning protection is provided by an air gap at the feed point of the coaxial antenna, and copper wires leading from the antennas to ground rods at the bases of the poles. These wires are bonded to the cable sheath.

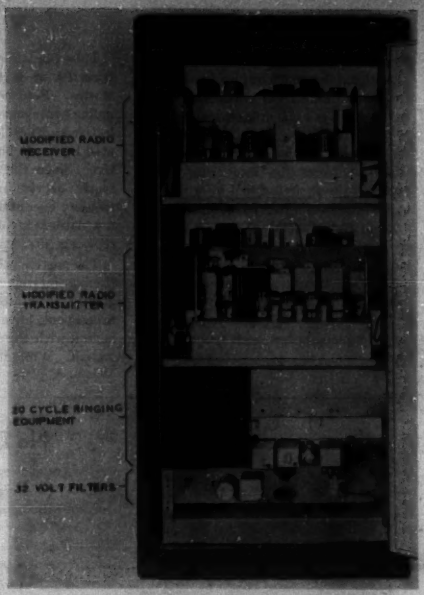

Figure 4. Subscribers' equipment cabinet—radio side

Power for operating the subscribers' radio and station equipment is supplied from customer owned power plants having 32-volt batteries which are charged by wind-driven and supplementary gasoline engine driven generators. Utilization of 32 volts to supply the vacuum tubes in the radio sets is accomplished by a combination of 100-cycle synchronous vibrators together with transformers and filters, by metallic disk rectifiers supplied with 100 cycles by the vibrators, and by a 32–400-volt dynamotor for the transmitter plate supply. A source of 20-cycle ringing current controlled by incoming carrier pulses is supplied by a 20-cycle synchronous vibrator circuit. Figure 4 shows the manner in which the modified mobile radio and telephone signaling equipment has been assembled on the customers' premises. The cabinet also contains the power conversion equipment and normally is locked for protection.

Figure 3. Most remote radio-equipped ranch

Results of Operation

During the period of preliminary tests of this system in Colorado during June and July of 1946, principal difficulties encountered were the following:

1. Sporadic interference from frequency modulation broadcast stations.

2. **Bell taps from local thunderstorms.**

Initially, intermittent interference from frequency modulation broadcast stations in the order of 1,000 miles from Cheyenne Wells was encountered. The interference was observed at the subscriber locations, where at times the interfering carrier exceeded the desired signal from the central office transmitter by as much as 10 decibels and, therefore, captured the subscribers' receivers. From a survey, frequencies lying between the frequency modulation broadcast frequency assignments finally were selected—44.2, 49.0, and 49.2 megacycles, and operation at these frequencies has been found free of interference.

False operation of the subscribers' bells occurred at first during local thunderstorms. Replacement of the initial signaling arrangement with one which is selective to 20-cycle pulses and is not operated by single bursts, proved quite effective. Since the system was placed in regular service in August 1946, the only troubles encountered have been of a minor nature, involving tube and vibrator replacements.

The participating ranchers, whose continuing interest and co-operation have greatly facilitated the progress of this experiment, have expressed general satisfaction with the service provided by this system. While it is, of course, too early to draw any general conclusions from the rural radio experiment described here, the results of utilizing, for the first time in history, radio installations on the subscribers' premises for furnishing regular telephone service are encouraging. It is expected that the experience gained will aid in developing a standard rural radiotelephone system especially designed to meet the requirements of this type of service.

Reference

1. A Carrier Telephone System for Rural Service, J. M. Barstow. AIEE Transactions, volume 66, 1947, pages 501–07.

No Discussion

A Magnetic Compass With Cathode-Ray Sensing Element

WALDO H. KLIEVER
NONMEMBER AIEE

RICHARD R. SYRDAL
NONMEMBER AIEE

THE remote indicating compass which has been named "Cathotrol", was developed to meet the need for an aeronautical one which would place the sensing element away from the engines and instrument panels and other disturbances, and produce an accurate remote indication on the panel as well as provide for automatic control. It was developed for airplanes but obviously permits other applications. Various other methods were considered and tested in our laboratory, including

1. Magnetic needle with photoelectric pickup.
2. Magnetic needle with capacitor pickup.
3. Magnetic needle with potentiometer pickup (like German Patin type).
4. Magnetic needle with inductive pickup.
5. Rotating inductor coil.
6. A-c saturated ferromagnetic inductors.

For advantages enumerated in the following text it was decided to concentrate on developing the cathode-ray method. Some work by others[1-3] has been done previously on cathode-ray compasses.

Principle of Cathode-Ray Compass

It is well known that when a cathode-ray oscilloscope is moved to different positions in the laboratory the image, in general, is displaced on the screen because of deflection of the cathode rays by the earth's magnetic field. This effect, generally considered undesirable, is used to operate the cathode-ray compass. Instead of a screen the tube has four target plates (Figure 1) which collect the beam current. The tube is mounted vertically so that only the horizontal component of the earth's magnetic field deflects the beam. The deflection is always at right angles to the field, that is, toward the west, if the beam is directed downward. This deflection causes the current to vary in the respective target plates.

The system of measurement considers these plates in opposing pairs. To facilitate measurement and amplification the cathode-ray beam is modulated in intensity with 400-cycle alternating current. Each opposite pair of plates is connected in a push-pull circuit and the output representing the difference in current between the plates is proportional to the component of the magnetic field at right angles to the line through the centers of those plates.

We obtain, thus, two outputs proportional to two components H_x and H_y of the earth's horizontal magnetic field. If the tube is so aligned, for example, that H_x is parallel with the longitudinal axis of the plane, and H_y with the lateral, we have sufficient information to determine the plane's magnetic heading. The resolving mechanism to accomplish this will be described after we look at the cathode-ray tube in more detail.

Cathode-Ray Tube Design

The first cathode-ray compass models were made with tubes of the type used in oscilloscopes, except having target plates instead of a screen. They were up to 17 inches long over-all with sockets, were dependent upon high potentials of one to two thousand volts, and were designed for pin-point spots with currents of only a few microamperes.

The first model was made with the tube horizontal and driven about a vertical axis by a servo motor. This motor obtained its signals from a target plate divided into upper and lower halves and drove the tube to the position in which the beam would line up with the horizontal component of the earth's field, corresponding to equal currents in the two halves of the target. In the second model a tube of similar design was mounted vertically to eliminate the need for rotation.

While these models worked, it was obvious that tubes designed for oscilloscopes were not at all suited to our requirements, and that the basis for a good cathode-ray compass lay in the development of more appropriate tubes. In initiating a new tube design in our own tube research laboratory the following conditions were imposed:

1. Much smaller size.
2. Lower accelerating voltage.
3. Beam current measured in milliamperes instead of microamperes with larger focal spots permitted.
4. Suitability for a-c modulation of intensity.

With regard to size, the present tube is one inch in diameter and seven inches long over-all with sockets. The deflection of the beam in a magnetic field varies as the square of the length, but there is also resultant gain because of the fact that the focal spot is reduced in diameter so that more current is transferred between target plates for any given deflection. There is no evidence that the present size represents a practical limit.

The most important change was in the construction of the gun itself. To obtain larger beam currents the efficiency, that is, the ratio of target to cathode current,

Paper 47-84, recommended by the AIEE committee on electronics and the AIEE joint subcommittee on electronic instruments for presentation at the AIEE winter meeting, New York, N. Y., January 27-31, 1947. Manuscript submitted November 13, 1947; made available for printing January 6, 1947.

WALDO H. KLIEVER, director of research, and RICHARD R. SYRDAL, senior design engineer, are both with Minneapolis-Honeywell Regulator Company, Minneapolis, Minn.

The authors wish to acknowledge the contributions of many people to this development, especially those of Ralph Squier, assistant director of research, Merle Ludwig, design engineer, both of Minneapolis-Honeywell Regulator Company, and Doctor Henry Hartig of the University of Minnesota.

Figure 1. Diagram showing the working principle of the cathode-ray compass

had to be improved. It was not necessary to have a pin-point focal spot; and rather, the circuit which does not involve rebalance requires that the spot have sufficient dimensions to provide linear output over the desired deflection. Opening the apertures of a standard type gun did not give the desired improvement. The correct potential distribution to "direct" the electrons through small apertures was found by using a cupped grid on nearly the same plane with the cathode and also imposing a curve on the first anode. Others[4,5] have done work on rectilinear electron flow using shaped electrodes with good results. A curved electrode also has been used for focusing X rays.[6]

The new electron gun is shown diagrammatically in Figure 2. Tests of this tube show an available target current of better than 1.5 milliamperes at 300 volts with 95 per cent of the cathode current reaching the targets as against about 20 per cent for ordinary cathode-ray tubes. Figure 4 shows the cathode current and the target current plotted against the grid voltage for this tube. The ratio of target current to cathode current is shown on the same graph.

Figure 3 shows the appearance of the tube which has been made up with two local sockets, one end furnishing connections to the cathode-ray gun and the other one furnishing leads to the four target plates. It may be of interest also to note here that the target plates are bevelled so that they overlap one another to prevent the loss of any electrons between the plates. This was found desirable not only because of the loss of current but because the stray electrons produced undesirable charges at other points of the tube. It also has been found very important to coat the inside of the glass with conducting coating to prevent charging of the glass and resultant shift in the balance point. This coating is connected to the last anode.

Additional tests have been conducted to determine the characteristics of this tube. Figure 5 shows the variation of target current with target potential for several grid voltages. There is noticeable secondary emission at low voltages. Figure 7 shows the effect of different load resistors in the target circuit.

The tube has a focal spot about 10 millimeters in diameter and deflects about 1.6 millimeters with earth's horizontal field of 0.16 gauss, when operating at 300 volts. It operates in the model with 50 per cent modulation, with 400-cycle alternating current on the grid, and a total average current of 0.5 milliampere. Under these conditions the difference of alternating current between target plates at right angles to 0.16 gauss is about 6 microamperes through an effective impedance of 160,000 ohms, or after the transformers, 0.25 volt across 10,000 ohms.

Cathode-Ray Tube Mounting

Figure 7 shows how the tube is mounted in a nonferrous metal housing on gimbals to maintain its vertical position. Connections are made through flexible leads. The tube is supported by rubber clamps against the glass and the sockets, instead of being supports as in normal tube practice, are floating on the tube. In order to minimize the number of flex leads a voltage divider (Figure 9) also is made part of the tube mounting.

Obtaining Compass Angle From Component Outputs—The Square Potentiometer Resolver

As already indicated, the tube gives us two components of the earth's magnetic field and leaves us with the problem of converting this information into the angle of the principal magnetic vector. Perhaps the resolvers should be called synthesizers for this reason. The square potentiometer resolver is composed of two wire wound cards of approximately square dimensions

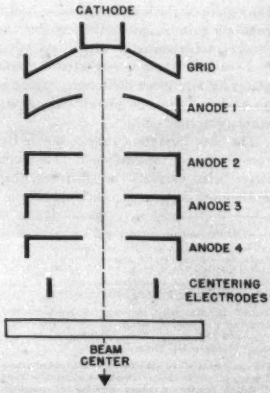

Figure 2. Sectional diagram of cathode-ray gun

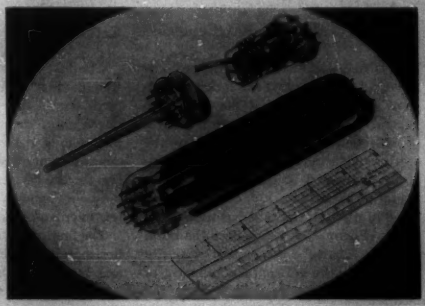

Figure 3. Cathode-ray compass tube

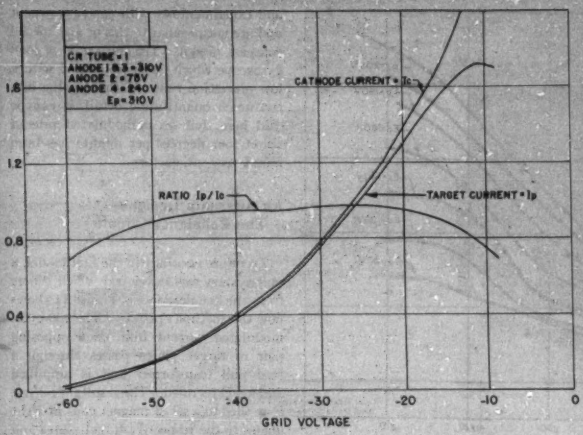

Figure 4. Curves showing efficiency of cathode-ray gun in transmitting cathode current to targets

with a wiper which rotates in a circle as shown in Figure 8 (upper part). When a voltage is applied across one of these potentiometers, which is grounded at the center of the circle, then the voltage between the wiper and ground will vary as the sine or cosine of the angle of the wiper, depending upon the position from which the angle is measured. As used with a compass, the two potentiometers are connected to the tube through transformers as shown in Figure 8. The theory of operation is as follows (Figure 8): if we refer to the two axes as the x and y axes, with x being the direction of maximum deflection for north heading, then the x potentiometer has a voltage across it equal to

$$V_x = 2KH \cos \theta$$

where

K is a proportionality constant depending on the deflection sensitivity, focal spot, and transformer characteristics
θ is the angle that the earth's horizontal magnetic field of intensity H makes with the forward direction of the tube

Similarly, the voltage across the y potentiometer is

$$V_y = 2KH \sin \theta$$

Now if we let the angle of the potentiometer wipers be represented by ϕ, then the voltage between the wipers will be given by

$$V = V_y \cos \phi - V_x \sin \phi$$
$$= KH \sin \theta \cos \phi - KH \cos \theta \sin \phi$$

It will be noted that this voltage is equal to zero when θ is equal to ϕ. It also can be shown that the voltage reverses sign when ϕ is made greater or less than θ. This gives us the signal necessary for controlling the servo mechanisms to drive the potentiometers until V equals zero in which case the angle of the potentiometer is a measure of the angle of the magnetic field.

Another interesting variation of the square potentiometer involves two straight line potentiometers making up opposite sides of a square which is completed by solid conductors across the other two sides. This is illustrated in Figure 8 (lower part). Considering only the first 45 degrees, it will be noted that the x potentiometer varies as the tangent of ϕ, while the y potentiometer is constant. This gives us the equation

$$V = KH \sin \theta - KH \cos \theta \tan \phi$$

This gives the same balance point as the previous equation as shown if we multiply through by cosine ϕ.

Obtaining Compass Angle From Component Outputs—The 2-Phase Synchro Resolver

In the 2-phase synchro resolver the principle is very much the same as with the square potentiometer except that it is the magnetic coupling of the output coil with the two input coils which varies according to the sine and cosine laws. This device also has been tested and found satisfactory for operation with the compass.

The Complete Circuits and Operation

Having studied some of the principles and components of this compass, we show in Figure 9 a schematic diagram of the complete system. The voltage divider is in the tube mounting to save flexible leads and minimize stray pickup. The two coupling transformers are within a few feet of the tube as it was considered undesirable to use long target current leads because of their high impedance. The amplifier and power supply unit is illustrated in Figure 10.

A procedure has been developed for no field centering of the beam and for adjusting the compass to level suspension in the gimbals. If no field free space is available the former can be checked by lining up the tube parallel with the magnetic field as determined by varying the accelerating voltage.

Compass Leveling Errors and the Slave Gyroscope

Any magnetic compass gives a correct reading of the direction of the earth's horizontal field only if it is level. It can be shown that the azimuth error E caused by east or west tilt B is given by

$$\tan E = \tan D \sin B$$

where

D is the angle of dip

At Minneapolis this means that one degree tilt produces 2.7 degrees error in azimuth reading, which is very important.

One possible solution is to maintain the compass vertical with a vertical gyroscope but we preferred to keep all iron away from the tube. As the compass was designed for use with our autopilot, which already has a directional gyroscope, it has proved advantageous to mount the compass pendulously in gimbals and slave the gyroscope to it by means of a precession motor in the gyroscope operated by the compass signals. The operation of this system is very similar in principle to that of a gravity erection system on a vertical gyroscope—the signals to the gyroscope are not instantaneously correct because of accelerations of the airplane, but they generally have an accurate average, and the gyroscope has the ability to integrate them to obtain the average. During periods of known long-time accelerations, such as in turns, the precession is switched off.

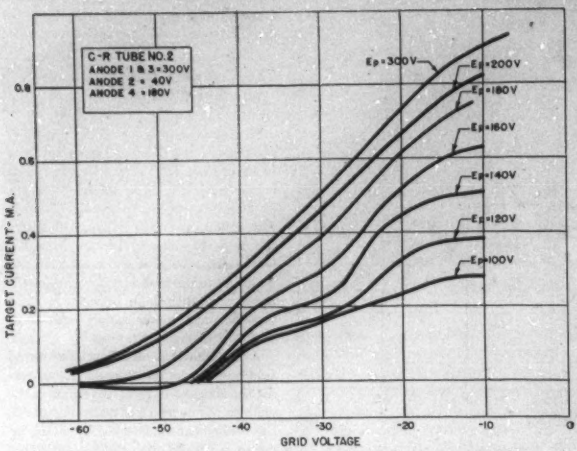

Figure 5. Curves showing characteristics of tube with various target potentials. Note secondary emission effects when *Ip* is below potential of anode 4

As in the vertical gyroscope analogy, there are possible conditions of feedback between the gyroscope precession system and the airplane controlled by the gyroscope. We will try to explain this condition briefly for the compass. When flying north, consider a slight bank introduced by, say, rough air. The plane starts to turn in the bank, which tilts the compass. The latter, caused by the resulting azimuth error, calls for precession of the directional gyroscope which calls for more turning of the plane through the autopilot. After reaching the angle off course corresponding to the bank called for by the rate of precession, the process reverses and a continuous hunt follows. In flying south the feedback is negative, and there is stability. In flying east or west this azimuth hunt is not a problem, but some temporary changes in heading can result from longitudinal accelerations because of changes in power or attitude. These effects have been studied both theoretically and experimentally with good agreement and are not peculiar to this or any special compass design. The answer is a good gyroscope which can be operated with a low precession rate. Without going into too much quantitative detail, it can be said here that an unmodulated rate of about four degrees per minute has been found very satisfactory.

An Alternate Design—The Rebalance Circuit

To insure accuracy in the first model, a null system was developed which differs from the one described. Figure 11 shows how this method operates. The 400-cycle modulated current from each opposing pair of target plates passes through a push-pull transformer and is amplified and again rectified. The resultant output is applied to a set of magnet coils at right angles to the respective target plates and operates to neutralize the component of the earth's field in question. It has been found practical to rebalance to about one or two per cent of the original tube output, the remaining amount being necessary to operate the amplifier. This is done in both the x and y axes, and the two d-c rebalance currents are an accurate measure of the two components of the earth's field. For example, they may be the fore and aft and the lateral components with respect to the airplane. From this it is possible to get considerable in-

Figure 6. Curves showing variation of target current with load resistors

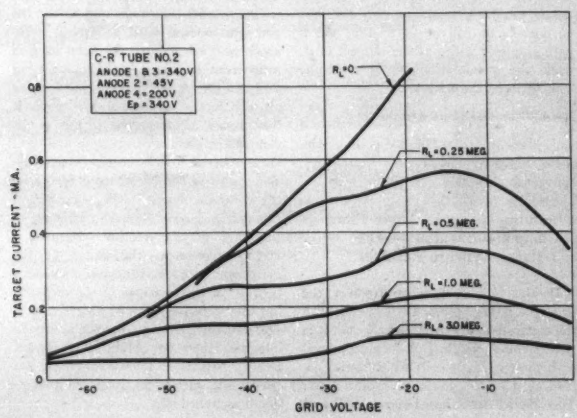

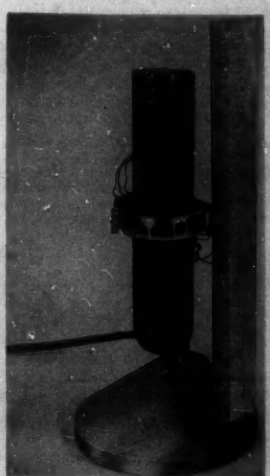

Figure 7. Mounting of compass tube

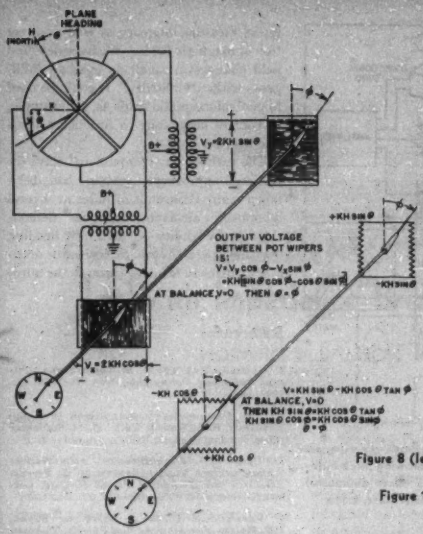

Figure 8 (left). Diagram showing operation of square potentiometer resolvers

Figure 10 (right). Cathode-ray compass power supply and amplifier

formation; for example, we could determine the total intensity of the earth's horizontal field if desired. Because in a compass we are interested only in angle, we can read this with no more additional equipment than a ratio meter using the two direct currents. This meter, shown diagrammatically in Figure 11, consists essentially of two coils at right angles and a permanent magnet. However, it usually is desired to obtain an electric signal to drive a control motor or slave a directional gyroscope, and in this case the same resolvers previously described are used. Both the direct motor-driven indicator and the slave gyroscope also are shown in the figure.

This null method is adaptable to almost any desired accuracy but it has been found for practical purposes in an aeronautical compass that the linearity of response in the two axes can be made sufficiently accurate to use the tube current directly. This very considerably simplifies the machinery required in the system as it eliminates rebalance coils, four flex leads, two amplifier channels and phased rectifiers with filters for going from alternating to direct current for the two rebalance coils, and a vibrator or other device for converting direct to alternating current for amplification to operate the gyroscope or servo motor.

Figure 9. Simplified diagram of circuit of cathode-ray compass and slave gyroscope system

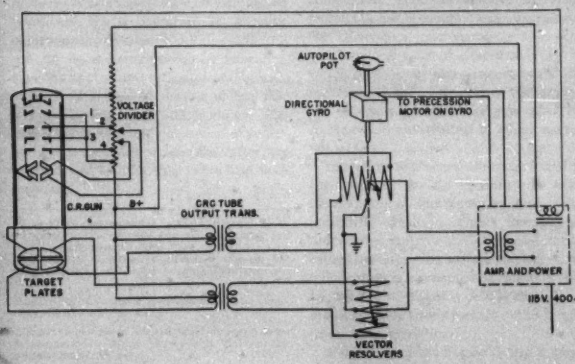

Advantages and Other Applications

With regard to accuracy, we have talked with many pilots and they agree that they do not read compasses to better than one degree and that closer readings do not have much meaning because of uncertainties in drift. Therefore we have aimed at plus or minus one degree accuracy in the design, and we are well within this around the 360-degrees circle. However, the sensitivity is better than 0.25 degree, and the consistency of holding a course is considerably better than one degree. This accuracy is easily obtainable, and it has not been considered warranted to take the extra steps necessary to improve it for this particular application.

For use as an aeronautical compass the cathode-ray system appears to have the following desirable features:

1. There is no iron in the system to distort the earth's field or get magnetized or demagnetized.
2. There is no northerly turning error of the type found in needle compasses.
3. The electron beam has negligible time lag.

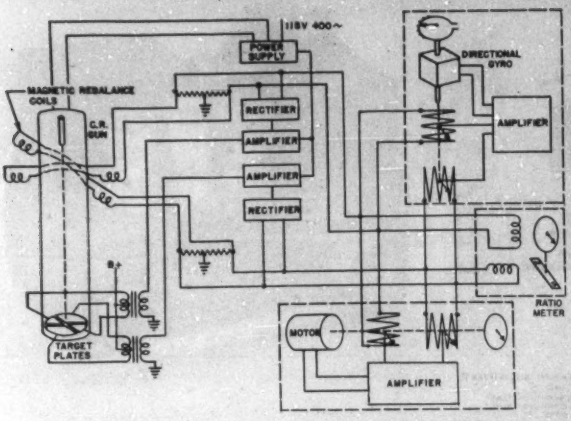

Figure 11. Diagram of cathode-ray compass circuit with null rebalance showing three independent methods of output—slave directional gyroscope, ratio meter, and servo motor

4. The output in each axis is linear with magnetic field to values beyond the maximum horizontal field of the earth, so that it becomes easy to measure angles to the desired accuracy specified in the foregoing text.

5. There is reasonable independence of readings from either voltage changes or field intensity changes. With changes of voltage of 25 per cent the changes in the angle have been consistently less than one-half degree. As mentioned under "The Complete Circuits and Operation," changes of voltage are used in one method to establish the zero adjustment.

6. The tube and system are rugged.

In closing it may be worth suggesting other possibilities for the tube. It can be driven with motors in both axes to align itself with the earth's field. This might be helpful in determining dip and latitude. With controlled voltage or rebalance coils it can measure intensity as well as direction of magnetic fields. We have detected field changes as small as one-half milligauss without difficulty. It could be used to control magnetic fields as, for example, to control large coils to produce a field-free space.

The cathode-ray compass and slave directional gyroscope system has been flown many thousands of miles in several laboratory airplanes. It has demonstrated the ability to maintain heading over long periods and to determine accurate changes in heading through the autopilot.

References

1. Cathode-Ray Tubes, **M. Von Ardenne.** Pitman Publishing Corporation, New York, N. Y. 1939, pages 162, 358.

2. The Cathode-Ray Oscillograph in Radio Research, **R. A. Watson Watt.** H. M. Stationery Office, London, England 1933.

3. Über die Ausmessenden magnetischer Felder mittels Elektronenstrahl, **E. Brüche.** *Zeitschrift fuer Technische Physik* (Leipzig, Germany), volume 12, 1931, page 94.

4. Rectilinear Electron Flow in Beams, **J. R. Pierce.** *Journal of Applied Physics*, American Institute of Physics (New York, N. Y.), volume 2, 1940, pages 548–54.

5. Some Notes on the Design of Electron Guns, **A. L. Samuel.** *National Electronics Conference Proceedings*, Chicago, Ill., volume 1, 1944, pages 48–61.

6. A High Voltage Demountable X-ray Tube, **Waldo H. Kliever.** *Review of Scientific Instruments*, American Institute of Physics (New York, N. Y.), volume 10, 1939, pages 126–8.

No Discussion

Electronic Null Detectors for Use With Impedance Bridges

HORATIO W. LAMSON
MEMBER AIEE

THE ADVANCEMENT of the science of electronics in the past decade has permitted the development of several types of null detectors for indicating a balanced condition of various forms of impedance-measuring bridges or for use with other a-c networks in which it is desired to establish zero potential difference between two points. It is the purpose of this paper to describe certain forms of these devices which have proved especially useful.

Indicating Systems

An integral part of any null-balance detector must be a system which is responsive to an alternating voltage. The actual indicating device may be either aural or visual in character.

For a-c networks which are excited at some audio frequency to which the human ear is relatively sensitive, say from 300 to 5,000 cycles per second, the use of ordinary headphones is a well-established practice. When operating in a noisy environment, or when the long continued use of headphones becomes fatiguing, some form of visual indicator is required. The use of a visual indicator is desirable when operating below 300 or above 5,000 cycles per second and demanded at superaudible frequencies unless the latter are heterodyned to afford an audio beat-note response.

Paper 47-85, recommended by the AIRE committee on electronic instruments for presentation at the AIRE winter meeting, New York, N. Y., January 27–31, 1947. Manuscript submitted October 28, 1946; made available for printing December 30, 1946.

HORATIO W. LAMSON is with General Radio Company, Cambridge, Mass.

The author wishes to acknowledge the many helpful suggestions of his colleague, R. F. Field, in the preparation of this paper.

One form of visual indicator which long has been used at lower frequencies, predominately at 60 cycles per second, consists of a galvanometer which is responsive directly to alternating current. This may be either an Einthoven (vibrating-string) or a vibrating coil galvanometer, both of which have a permanent magnetic field. If a suspended coil galvanometer supplied with a synchronously excited a-c field from a laminated core and giving a steady deflection is used, a polarized detector, discussed later, is obtained.

Because of its inherently high sensitivity a d-c microammeter of the D'Arsonval type is used extensively. In this case the indicating instrument must be preceded by some form of rectifier. A single rectifying element gives half-wave rectification. More efficient full-wave rectification can be obtained with two elements, provided that a transformer having a center-tapped secondary winding is employed. To avoid the need for such a transformer and still achieve full-wave rectification it is common practice to have the D'Arsonval microammeter G constitute a cross branch of a rectifier bridge in which each of the four arms consists of a rectifying element, usually of the copper-oxide type, as shown in Figure 1. This combination constitutes, in effect, an a-c voltmeter.

Extensive references are to be found in the literature to a-c vacuum-tube voltmeters,[1] any of which may be used as the indicating device. These instruments universally employ a D'Arsonval meter calibrated either in rms or peak volts, and rectification is accomplished electronically by the use of either a simple diode or a multielectrode tube operating with a nonlinear characteristic.

A diode rectifier, Figure 2, has a small slope at the origin of its current-voltage characteristic which makes it relatively insensitive as a null indicator unless it is followed by d-c amplification. When an a-c input signal is applied to a multielectrode tube, an increase in plate current results if the tube has a fixed negative bias, Figure 3, while a decrease in plate current occurs if the tube is functioning as a grid-leak detector, Figure 4. The initial (no signal) plate current is offset either by mechanically depressing the zero of the D'Arsonval meter, or by a suitable compensating circuit such as indicated in Figure 5. For use as null indicators, the customary vacuum-tube voltmeter circuits sometimes are modified to produce a logarithmic response for reasons discussed later. The arrangement of Figure 4, in which rectification occurs in the grid circuit, is inherently more sensitive than that of Figure 3. The circuit of Figure 3, however, can be made to have a higher input impedance than those of Figures 2 and 4.

As a result of self-capacitance a copper-oxide rectifier becomes increasingly less sensitive above 50 kc, while the vacuum-tube rectifier loses sensitivity above 100 megacycles. When operating at ultra-high frequencies to obtain a minimum of

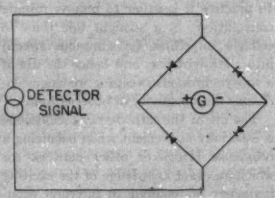

Figure 1. Rectifying bridge with D'Arsonval galvanometer

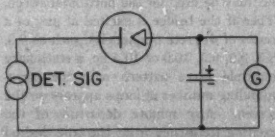

Figure 2. Typical diode rectifier

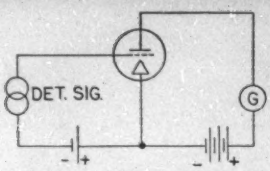

Figure 3. Triode detector (fixed negative bias)

self-capacitance and to produce a rectifier of minimum physical dimensions, a single small crystal of silicon or germanium with a fine wire contact point has proved successful.

A convenient and very compact form of visual indicator is to be found in the "magic eye" as exemplified by the type *6E5* electron ray tube. This unique tube has a small conical-screen electrode, which appears as an illuminated annulus except for a sharply defined dark or shadow sector. When subjected to an alternating voltage, the radial boundaries of this shadow area become blurred and the angular opening of the totally dark sector diminishes as the applied signal is increased. Bridge balance thus is indicated by a "wide awake" appearance, that is, maximum dark area with sharply defined boundaries.

The ordinary cathode-ray oscilloscope frequently is used as a visual null-balance indicator. It is customary to apply the detector voltage from the bridge to the vertical deflecting plates and to sweep the spot horizontally at the same or some lower frequency. A lower sweeping frequency gives a multiple-wave pattern on the screen which is reduced to a horizontal straight line when the bridge is balanced. In practice it is easier to remove minute convolutions in a straight line than to collapse an ellipse (synchronous sweep) into a straight line, and hence the use of a subsynchronous sweeping frequency increases the sensitivity of observation.

The use of the cathode-ray oscilloscope is especially convenient when balancing a resonance bridge or other network for which an exact knowledge of the exciting frequency is required to interpret accurately the data obtained. A precisely known "standard" frequency, say one kc, may be used for the horizontal sweep. Then if the bridge is excited at any of a series of discrete frequencies, such as 8.0, 8.5, 9.0, 9.5, 10.0 or 10.5 kc, a stationary multiple wave pattern with the corresponding number of loops appears on the screen. Any minute departure of the exciting frequency from the true desired value is immediately observable as a slow phase progression in the screen pattern. Thus the exciting frequency may be monitored accurately to the desired value at the time each bridge balance is made.

Sensitivity Controls

Most forms of indicating devices give an "off-scale" deflection if subjected to an excessive voltage when the impedance bridge is considerably off-balance. This condition, which may be detrimental to the device itself and which hinders the initial balancing operations, may be eliminated by providing a manually operated sensitivity control designed to apply only a portion of the voltage from the bridge to the indicator and thus reduce its sensitivity below the maximum value. Sensitivity may be adjusted progressively, or by discrete steps. Methods are available for giving the indicating device an automatic sensitivity control by causing its response to be logarithmic rather than linear in character, a procedure commonly designated as automatic volume control. An example of this will be cited later.

When using headphones, a form of response control sometimes is employed to prevent an uncomfortable signal in the head phones with large detector signals. Reduced to its simplest terms this consists merely of shunting the headphones with a thyrite or varistor element whose admittance increases with the voltage applied across it. Series impedance in the generator is essential for its operation. For this purpose a nonrectifying network composed of oppositely oriented copper-oxide rectifiers also may be used. Such a network easily may be obtained by taking the rectifier bridge mentioned and tying together its two d-c and its two a-c vertices respectively as shown in Figure 6.

Selectivity Requirements

Many impedance networks when balanced to the fundamental components of the exciting frequency are not balanced simultaneously to the harmonic components thereof, which may be present in the voltage exciting the bridge. Or, assuming pure sine-wave excitation, if any of the network elements (such as iron-cored inductors) possess nonlinear impedance characteristics, unbalanced harmonic components are generated thereby. Then, when the bridge is balanced completely to the fundamental, these residual components prevent an absolute null response of the indicating system and render the determination of true balance quite difficult. It becomes, therefore, highly desirable to provide the indicating device with selectivity, that is, frequency discrimination, attenuating all voltage components other than the fundamental frequency used in exciting the bridge.

Vibration galvanometers mechanically tuned to the fundamental frequency possess considerable inherent selectivity. The average headphones are constructed to give a maximum response at about one kc and, together with the response curve of the human ear, exhibit an inherent selectivity in the neighborhood of that frequency. Headphones also possess an additional pseudoselectivity in that a skilled operator can balance out the fundamental while ignoring higher harmonics. Most visual indicators, such as vacuum-tube voltmeters, possess no inherent selectivity.

The selectivity of any indicator may be increased electrically by the use of filter networks peaked at the fundamental frequency or designed to attenuate all harmonic components thereof.

Selection of an Indicating System

All null indicators may be classified either as power-operated or voltage-operated types. Power-operated indicators, which include a-c galvanometers, headphones, and copper-oxide rectifiers, have relatively low impedance values and derive their energy from the bridge circuits. Their sensitivity rating thus is determined by the minimum input power required to give a perceptible response. When used with low impedance bridges their voltage sensitivity values also become significant. A maximum sensitivity may be attained by the use of a suitable transformer to match the impedance of the detector to the output impedance of the bridge system viewed from the detector vertices.

Voltage operated indicators, such as vacuum-tube voltmeters, the electron-ray tube, the cathode-ray tube, and *any* indicator preceded by a vacuum-tube amplifier, are energized by a separate source (*B* battery or equivalent) and, in general, have input impedance values which are quite large compared to the output impedance of the bridge so that their application does not appreciably modify the

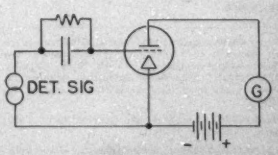

Figure 4. Triode detector (grid-leak type)

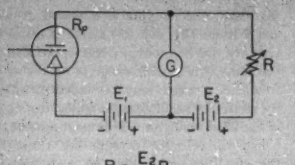

Figure 5. Method for balancing d-c component of plate current

Table I

Indicator	Impedance, Thousands of Ohms	Cycles Per Second	Microvolts	Micromicrowatts
Einthoven galvanometer	4	100	100	2.5
Einthoven galvanometer	4	300	800	160
Vibrating coil galvanometer	0.7	60	17.5	0.44
Suspended coil galvanometer	0.012	60	0.08	0.0003
Headphones	20	1,000	400	2.4
Rectifier bridge	25		5×10^4	10^3
Tube voltmeter			2×10^4	
Electron-ray tube			3×10^4	
Cathode-ray tube			2×10^6	

output terminal voltage of an unbalanced bridge. It is thus desirable to rate the sensitivity of this type in terms of the minimum input voltage required to produce a perceptible response. This sensitivity usually may be augmented by using a step-up input transformer, the turns ratio of which frequently is limited by transformer imperfections to something less than that corresponding to impedance matching. To cover a wide frequency range this ratio may not much exceed 3/1, while for spot-frequency operation this ratio may be made as high as 10/1, or perhaps 30/1 for low impedance bridges.

While the choice of an indicating system for balancing an impedance bridge frequently is dictated by the instruments which are available or most readily obtainable, the following rough values of sensitivity for the types discussed may prove of interest. In Table I voltage sensitivities are given in microvolts and power sensitivities in micromicrowatts required to give a perceptible response.

In Table I the data for the a-c galvanometers are based upon a 1-millimeter deflection with a 1-meter scale distance. Headphones having an impedance of 20,000 ohms and an a-c resistance of 6,000 ohms give a threshold of audibility at 1 kc with a current of about 0.02 microampere. The copper-oxide rectifier bridge produces a rectifier current of 2 microamperes, 1 per cent of full scale deflection on a 200-microampere D'Arsonval instrument. Thirty millivolts changes the shadow angle of an electron-ray tube by about 1 degree while a perceptible deflection is obtained on the screen of a typical cathode-ray tube with a signal of 2 volts on the deflecting plates.

For balancing, at 1 kc, any impedance bridge whose output voltage is not lowered significantly by the addition of 20,000 ohms, it appears that headphones are 34 decibels (50 fold) more sensitive than a vacuum-tube voltmeter, 37.5 decibels more sensitive than the electron-ray tube, 42 decibels more sensitive than the rectifier bridge specified, and 74 decibels more sensitive than the cathode-ray tube.

Sensitivity Requirements

The sensitivity of the null detector required for balancing an impedance bridge depends upon the composition of the bridge network, the magnitude of the incremental changes which can be made in the components of the network, the magnitude of the exciting voltage, and the precision of balance desired. The required detector sensitivity may lie within the wide limits of 1 microvolt and 100 millivolts. For any given bridge less detector sensitivity is required as the exciting voltage is raised. There are, however, practical limitations to such a procedure; for example, dissipation ratings of resistors, dielectric strengths of capacitors, and voltage coefficients of iron-cored inductors when it is desired to measure their inductance as close as possible to initial permeability.

The voltage sensitivity required for any given impedance bridge using a voltage-operated detector may be computed as follows: let E be the terminal voltage of the exciting generator and E_d be the minimum detectable output voltage required to balance the bridge and obtain a specified fractional precision δ of either the resistive or reactive component of the unknown element. Let A and B be the impedance values of two arms across which the generator is placed and ρ equal the ratio A/B or its reciprocal. Then, for a high impedance detector,

$$E_d = \frac{E\rho\delta}{(1+\rho)^2} \tag{1}$$

provided that A and B are both resistive or both reactive, and

$$E_d = \frac{E\rho\delta}{1+\rho^2} \tag{2}$$

if A is resistive and B is reactive or vice versa.

As an example, consider the detector sensitivity necessary to measure to 0.00001 the dissipation factor of a 1-microfarad capacitor on a Schering bridge excited with 150 volts at 1 kc. A bridge ratio ρ of 1,000 is to be used, and it can be shown that the numerical precision of the dissipation factor is equal to the fractional precision δ of the resistive balance. Using the first equation E_d is seen to be 1.5 microvolts.

Consider also the measurement of inductance to 0.01 per cent on the Owen bridge set up for a ρ value of 20, when the exciting voltage is limited to 5 volts. Using the second equation E_d equals 25 microvolts.

Use of Amplification

Although any of the indicating systems described may be used directly as a null-balance detector, in general, their maximum sensitivity as indicated by the foregoing data will be less than that required to balance the bridge with the desired precision.

To enhance the precision of balance by giving the complete detector system a sensitivity exceeding that inherent in the indicator alone, it is now quite universal practice to add a vacuum-tube amplifier to the indicating device. This may be either a d-c amplifier following the rectifier element and magnifying its output signal, or an a-c amplifier interposed between the detector terminals of the bridge and the actual indicating device. In the latter case sensitivity control may be accomplished by a manual adjustment of the amplifier gain or partial automatic volume control may be used to prevent

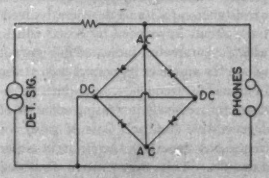

Figure 6. Automatic volume control with headphones

off-scale deflections. Pronounced automatic volume control should be avoided because it would render small changes in large input signals difficult to observe and hinder initial balancing operations.

In the two examples cited, an amplifier voltage gain of 270/1 would be required if headphones were to be used in balancing the Schering bridge, and a gain of 1,200/1 if the Owen bridge is to be balanced with an electron-ray tube.

The use of an a-c amplifier offers the additional advantageous feature in that further selectivity may be incorporated into the amplifier itself. This often has been done by resonance methods such as the addition of a parallel inductance and capacitance antiresonant network into the input or output circuit of one or more of the amplifier stages. Changes in the resonant (maximum gain) frequency, of course, may be made by appropriate modifications in the values of either or both reactive elements. The components of such an antiresonant circuit should have high values of storage factor Q at the resonant frequency. The resonant impedance of this circuit should be a proper compromise between a value too high (loss of selectivity versus harmonics) and a value too low (excessive insertion loss). The location of such a resonant circuit in the amplifier is significant. If introduced at or near the output end, strong harmonics may tend to overload the amplifier and render more difficult the initial balancing operation. If introduced too near the input of the amplifier, the inductor of the antiresonant circuit may pick up sufficient fundamental voltage directly from the exciting generator or elsewhere to give a false balance of the bridge and yield erroneous data. This situation is especially troublesome when balancing a 60-cycle network, as most laboratories are permeated with a significant 60-cycle electromagnetic field. An astatic inductor, such as one which is wound symmetrically upon a toroidal iron core with no air gap, has been found highly beneficial for this purpose.

Elimination of inductive pickup and certain other advantages may be accomplished in a selective amplifier by the use of a resistance-capacitance degenerative feedback circuit introduced by Scott[3] which, with the parameters indicated in Figure 7, allows the amplifier its normal gain at the fundamental frequency, but which introduces progressively increasing amounts of degenerative feedback (loss of gain) for frequencies departing therefrom in either direction. This degenerative feedback must be applied over an odd number of direct-coupled amplifier stages to function

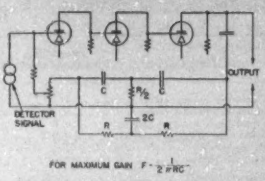

Figure 7. The degenerative amplifier

in the manner indicated. The frequency value for maximum gain may be changed by modifying appropriate R and C elements in the degenerative network while maintaining the proper relationships between them.

The a-c amplifier may be given a pronounced degree of selectivity at a single frequency, say 100 kc, by the use of piezoelectric quartz crystals as indicated in Figure 8. These have such sharp resonant peaks, because of their high storage factor values, that combinations of two or more crystals slightly detuned from each other frequently are used to produce a response curve having a flat top a few cycles in width.

When any form of indicator is preceded by a vacuum-tube amplifier, the composite sensitivity of the combination cannot be increased indefinitely by raising the gain of the amplifier. A limiting value is reached when extraneous voltages, caused by thermal agitation in resistors or tube noises, obscure the desired minimum value of detector signal. Because these extraneous voltages cover a wide frequency spectrum, good selectivity, that is, a narrow band width, is quite essential in using a high gain amplifier.

Heterodyne Detectors

For many applications a null detector which is tunable over a wide range with uniform selectivity is desired. Consequently, it is common practice when working with frequencies below 20 kc to mix the detector signal with that from an independent tunable oscillator, and to amplify (and subsequently rectify) the resulting summation signal produced by the heterodyne action between the detector signal and that from the local oscillator. In this manner a tunable low-frequency detector is achieved in which a

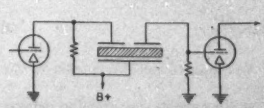

Figure 8. Amplifier with piezoelectric tuning

high and efficient gain is obtained at a single frequency, say 100 kc. The sensitivity of this heterodyne detector remains the same over a wide range of operating frequencies, which may be varied at will by relatively small changes in the tuning of the local oscillator. This arrangement, using piezoelectric crystals for tuning the amplifier and calibrated as a voltmeter, has been used successfully as a wave analyzer.

When operating at radio frequencies, the superheterodyne principle, extensively used in radio receivers, may be employed. In this case the detector signal likewise is mixed with the signal from a tunable local oscillator to give a constant difference or intermediate frequency which may be of the order of 450 kc at which efficient and selective amplification is obtained. This amplified intermediate frequency signal then may be rectified and applied to a D'Arsonval meter. More commonly, it is applied to a second oscillating detector tube and heterodyned again down to an audio frequency whereat it may be observed aurally in headphones or a loudspeaker, or visually by a D'Arsonval meter in a rectifier bridge.

A superheterodyne radio receiver thus becomes an excellent null detector for balancing impedance bridges at radio frequencies. It has been shown by Sinclair[2] that if the balance of the radio frequency bridge is frequency sensitive, it is essential to excite the bridge with an unmodulated radio frequency generator and to employ the necessary heterodyne action in the receiver, rather than to apply any modulation to the signal exciting the radio frequency bridge. In the latter case the bridge cannot be balanced simultaneously at the carrier and the side-band frequencies. When a radio receiver is used as a null detector, it is best to omit automatic volume control and to monitor its gain to provide the desired degree of sensitivity.

Technique of Bridge Balance

The complete balance of any impedance bridge requires the adjustment of two impedance elements of the bridge circuit. Manipulation of each element controls a component of the detector voltage. These two components have approximately a quadrature phase relationship. The balancing procedure, using any ordinary type detector, consists of an alternate adjustment of these bridge elements through progressively reducing minima of detector response until both quadrature voltages (and hence the total observed voltage) are brought to zero value. This is a some-

what troublesome procedure, especially with those types of bridge circuits which inherently possess a "sliding zero", meaning that the adjustment of one of the elements affects the values of both voltage components so that the initially apparent balance value of either element is displaced from its ultimate true balance magnitude.

A Polarized Null Detector

To facilitate the balancing operation the author has developed[4] a polarized null detector employing a small cathode-ray tube as the indicating device. The bridge detector voltage, suitably magnified by a degenerative amplifier, is applied to the vertical deflecting plates. The exciting voltage is passed to the horizontal deflecting plates through an adjustable phase-shifting network, Figure 9, first introduced by Turner and McNamara.[5] Thus the phase of the horizontal sweep with respect to the vertical spot motion produced by the amplified detector signal may be varied at will. With the bridge off-balance, an elliptical pattern having inclined axes appears on the screen. In general, the manipulation of either bridge control towards balance simultaneously will reduce the tilt of the ellipse and shorten its minor axis.

If, however, the horizontal sweeping voltage is adjusted to become in exact quadrature to either one of the amplified components of the detector voltage, then any variation of that voltage component will vary uniquely the length of the minor axis of the ellipse without changing the inclination angle of the axes, while any variation of the second component of the detector voltage will tilt uniquely the ellipse without changing its minor axis. In such a polarized detector, the two components of the detector voltage may be observed separately and one bridge control (chosen at will) may serve to align the major axis of the ellipse horizontally, while the other bridge control reduces the ellipse to a horizontal straight line at balance. This procedure is analogous to what may be accomplished by using a suspended coil galvanometer having a field synchronously excited with the proper phase.

A polarized detector possesses two other advantages. If the value of only one of the balancing controls is required for the desired bridge data, a complete balance of the second control is not necessary. Thus the ellipse may be collapsed into a straight line without bothering to obtain an exact horizontal alignment of this line. Most detectors embodying a high gain amplifier require a suitable gain control which must be monitored to give increasing sensitivity as the balancing operation proceeds, or else amplifier overloading will make it difficult to approach balance with either control when, initially, both controls are considerably off-balance. This polarized detector may be left at full sensitivity at all times. Amplifier overloading results in a distorted loop pattern which, however, undergoes a sudden definite change in its configuration as either control is passed through its approximate balance position. An over-all sensitivity of about 100 microvolts is attained.

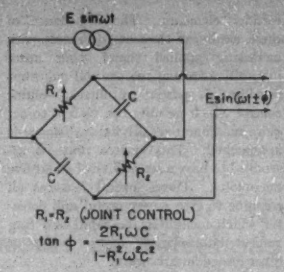

Figure 9. Adjustable phase-shifting network

A Polarized and Directional Null Detector

The author more recently has developed another form of polarized detector which has the additional feature of being directional.[6] This arrangement likewise embodies a suitable degenerative amplifier, but the indicating device is a center-scale-zero d-c galvanometer of the D'Arsonval type. This galvanometer G, as shown in Figure 10, constitutes the cross-branch of a "modulation bridge" or ring modulator having a copper-oxide rectifier element in each of its four arms and discussed by Hellman[7] and Caruthers.[8] The amplified detector signal is applied to two opposite corners of this bridge. A suitable polarizing voltage obtained from the exciting generator is applied in pairs to all four corners of the modulation bridge through resistors R_a, R_b, and R_c as indicated in Figure 10. Note that this ring modulator is quite different from the rectifying bridge shown in Figure 1.

Analysis of the operation of such a modulation bridge shows that when either the polarizing signal, or the detector signal is applied individually, no response occurs in the galvanometer. However, if both of these signals are applied simultaneously, the galvanometer response will be proportional to the product of those components of each signal which are either in phase or directly opposite in phase. Hence there will be no response on the galvanometer when the detector voltage is zero. A phase-shifting network, mentioned in the foregoing text is used to give, by throwing a switch, two alternative phases Θ and $\Theta + \pi/2$ to this polarizing voltage. The angle Θ is set so that, for each switch position, the polarizing voltage corresponds to one of the quadrature components of the detector voltage. In this manner the galvanometer can be made uniquely responsive to either bridge control, thus furnishing a polarized detector. In addition, the position (left or right) of the galvanometer needle, when the modulation bridge is polarized correctly, indicates at once the direction in which the corresponding control of the impedance bridge should be turned to proceed towards balance. This is the convenient directional feature of this detector which, of course, is possessed by the familiar center-scale-zero galvanometer used to balance a d-c Wheatstone bridge.

The operation of the modulation bridge, essentially, affords additional selectivity to this system at the frequency of the polarizing voltage which is the fundamental frequency exciting the impedance

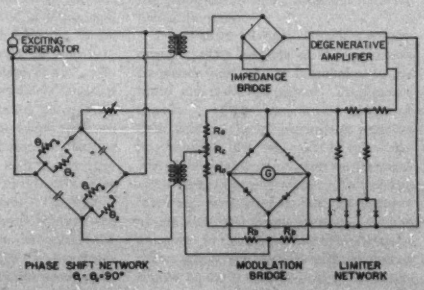

Figure 10. A polarized and directional null detector

bridge. Even harmonics are obliterated completely because, during a cycle of the polarizing voltage, they are just as much in phase as out of phase with the polarizing voltage and thus integrate to a null response on the d-c meter. Odd harmonics are attenuated because, as their phase progresses with respect to the simultaneous phase of the polarizing cycle, their components in quadrature with the latter contribute nothing to their integrated response on the meter.

To avoid the necessity of monitoring the amplifier gain, the system is given an approximately logarithmic response to the detector voltage by interposing a resistive network between the amplifier and the modulation bridge. Each shunt arm of this limiter network contains a paralleled pair of oppositely-directed copper-oxide rectifier elements. The impedance of these nonlinear elements decreases with increasing applied signal, thus automatically reducing the over-all gain, but providing a partial automatic volume control which permits the system to acquire maximum sensitivity as balance is approached. This system may be assembled to have a sensitivity of about five microvolts. These several features all combine to give a very useful null detector which facilitates the rapid and convenient balancing of an a-c bridge or other impedance network.

References

1. Vacuum-Tube Voltmeters 1941 (book), **John F. Rider**. John F. Rider, Inc., New York, N. Y.

2. A New Type of Selective Circuit and Some Applications, **H. H. Scott**. *Proceedings*, Institute of Radio Engineers (New York, N. Y.), volume 26, February 1938, pages 226–35.

3. Impedance Measurements, **Donald B. Sinclair**. *Communications* (New York, N. Y.), volume 19, July 1939, pages 5–9.

4. An Electronic Null Detector for Impedance Bridges, **Horatio W. Lamson**. *Review of Scientific Instruments*, American Institute of Physics (New York, N. Y.), volume 9 September 1938, pages 272–5.

5. An Electron Tube Wattmeter and Voltmeter and a Phase Shifting Bridge, **H. M. Turner, F. T. McNamara**. *Proceedings*, Institute of Radio Engineers (New York, N. Y.), volume 18, October 1930, pages 1743–7.

6. A Method of Measuring Magnetic Properties of Small Samples of Transformer Laminations, **Horatio W. Lamson**. *Proceedings*, Institute of Radio Engineers (New York, N. Y.), volume 28, December 1940, pages 541–8.

7. The Modulator Bridge, **Reinhard K. Hellman**. *Electronics* (New York, N. Y.), volume 11 March 1938, pages 28–30.

8. Copper-Oxide Modulators in Carrier Telephone Systems, **R. S. Caruthers**. AIEE Transactions, volume 58, 1939, June section, pages 253–60.

No Discussion

Pulse Echo Measurements on Telephone and Television Facilities

L. G. ABRAHAM
MEMBER AIEE

A. W. LEBERT
NONMEMBER AIEE

J. B. MAGGIO
NONMEMBER AIEE

J. T. SCHOTT
NONMEMBER AIEE

Synopsis: Pulse echo measurements have been used on telephone and television facilities since 1940 to locate impedance irregularities and control quality in manufacture and installation. These sets send a pulse into a line and observe on an oscilloscope the echoes returned from irregularities. The shape and width of the pulse, the rate at which it is repeated and the pulse magnitude are important in determining the accuracy of the results and the requirements of the measuring apparatus. The "coaxial pulse echo set" is used for factory and field testing of coaxial cables. The "Lookator" was developed for use on much narrower band systems such as spiral-four field cable and open wire lines.

THIS paper describes means of making pulse echo measurements on telephone and television facilities to locate irregularities and to control quality in manufacture and installation. The first practical use of this sort of measurement started in 1940[1] to control the manufacture of coaxial cable facilities by means of the "coaxial pulse echo set." This set has been improved and its use extended to include field testing of coaxial cables during and after installation to insure proper installation methods, to set deviation limits, to locate irregularities, and so forth. The second practical device is the "Lookator," built for the Signal Corps during the war to test spiral-four field cable, open-wire lines; and other facilities and to locate gross troubles and irregularities in such lines. The two devices have quite different frequency ranges and equipment requirements, but are basically similar in their general principles of operation.

The first part of this paper discusses general principles and limitations of such sets, the second part discusses the coaxial pulse echo set and the third part discusses the Lookator.

General

Figure 1 shows the general operating features of both types of pulse echo set. The base oscillator controls the device which originates the pulses, sending such pulses into the test line once every base oscillator cycle. It also controls the sweep generator, which in turn controls the horizontal progress of the trace on the cathode-ray oscilloscope, with one complete horizontal sweep every base oscillator cycle. The transmitted pulse goes through the hybrid coil and out over the connected line. Irregularities in the line reflect echoes toward the sending end, which are amplified and delivered to the vertical plates of the scope, thereby controlling the vertical motion of the cathode-ray trace. With a regularly repeated sweep and transmitted pulse, the result is a stationary trace on the scope with the horizontal scale showing time or distance along the test line and with the vertical height showing the magnitude of any irregularities causing echoes. The hybrid coil and balancing network reduce the part of the original pulse that enters the receiving circuit directly so that overloading due to this pulse does not occur, thus making electronic cutoff during the transmission of the pulse unnecessary. A terminating network at the far end of the line may be adjusted to terminate the line as well as possible, thus reducing the echo returned from the distant end. Alternatively, the normal working termination may be used, or under some circumstances the distant end echo may be ignored since it is separated in time. The adjustments of the balancing network and terminating network for minimum original pulse and distant end echo also indicate the impedances of the input and distant ends of the line, respectively.

By means of the phase shifter between the base oscillator and the sweep generator, the horizontal position of the pattern may be shifted back and forth as desired. A comparison of the phase shift setting which, say, lines up the part of the original pulse across the hybrid with a reference point and the later setting, which lines up the echo from an irregularity at the same reference point, determines the delay from the sending end to the irregularity and therefore the distance to the irregularity.

The pulses used with these devices are d-c pulses rather than a-c pulses such as are used in radar. Figure 2 illustrates the approximate appearance of a repeated d-c pulse wave versus time. Here d is the pulse width normally measured at half of the maximum amplitude of the pulse and $D=1/f_r$ is the pulse spacing or repetition time, with f_r being equal to the repetition frequency. These two factors plus the pulse shape and amplitude entirely define the pulse.

The Fourier analysis of such a succession of pulses consists of the repetition frequency and all its harmonics to infinity, plus a d-c component. To preserve the shape of the transmitted pulses or their echoes, the measuring set and the line on which it is used must be relatively free of delay and gain distortion throughout a wide frequency band. If excessive distortion were present, various amounts of the distorted frequencies would seem to appear in the part of the cycle between pulses where the current without echoes should be zero, thus confusing the inter-

Paper 47-86, recommended by the AIEE committee on communication and the AIEE joint subcommittee on electronic instruments for presentation at the AIEE winter meeting, New York, N. Y., January 27–31, 1947. Manuscript submitted November 14, 1946; made available for printing December 19, 1946.

L. G. Abraham, A. W. Lebert, J. B. Maggio, and J. T. Schott all are with Bell Telephone Laboratories, Inc., New York, N. Y.

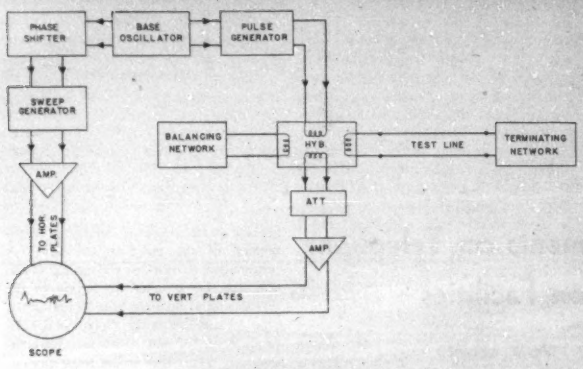

Figure 1. Block diagram of pulse echo sets

pretation when echo currents are received in that interval.

The choice of a repetition frequency depends upon a number of factors. The time between pulses must be long enough or the repetition frequency low enough so that all echoes it is desired to inspect and any longer delay echoes which are large enough to cause interference are returned before a second pulse is sent out. At the same time, the repetition frequency must be high enough so that excessive low frequency delay or gain distortion will not be encountered in the line or measuring set.

The pulse width for a given shape needs to be small in order to accurately locate irregularities, to separate nearby irregularities and to observe the impedance over the desired frequency range for the facility in question. At the same time, the pulse should not be any shorter than is necessary, since for a given pulse shape the effect of line distortion and of measuring set distortion at high frequencies increases as the pulse width decreases.

A resistance irregularity returns a copy of the arriving pulse and the accuracy of location is generally inversely proportional to the pulse width. In addition, when reactance irregularities are encountered, as will be discussed later, the echo of a pulse assumes a shape which is approximately that of the derivative of the original pulse shape with both a maximum and a minimum. Under such circumstances, the maximum and minimum of the pulse echo are each roughly one-quarter pulse width from the true location, for the shapes of pulses considered most desirable.

If two irregularities are close together in a line, a wide pulse will return an integrated total of the irregularities and the two may be very difficult to separate. This is because the return of the two echoes may differ in time by only a fraction of a pulse width so that the lesser echo may be hidden within the greater or, if both echoes are approximately the same size, only a single irregularity may seem to be present. In theory, with two such similar irregularities, the returned echo trace will be wider than with one irregularity and the two might be separated by means of that information. In practice, with different types of irregularities and with many small irregularities present, it is very difficult to separate irregularities which are much less than one pulse width apart.

In order to inspect the entire frequency range of interest on the line being tested, it is desirable to have harmonics present over this entire range. This is particularly true if types of irregularities are present which vary in magnitude over the frequency range. On the other hand, it is desirable to have the magnitude of the harmonics decrease as quickly as possible above the range of interest because

1. Such harmonics return irregularity information which may be misleading.

2. Line distortion generally is greater there than within the important range.

3. The requirements on the delay and gain characteristics of the measuring set extend up to the point at which the relative power in the higher harmonics becomes small enough to be neglected.

The shape of the distribution of such harmonics is determined by the pulse shape. In general, the simplest thing to use is a half sine wave pulse and an approximation of this has generally been used in devices built to date. However, from theoretical considerations, the raised cosine-wave pulse should be considerably better than a half sine wave pulse and either of these much better than a rectangular pulse. A Gaussian law pulse is probably also good and may be easier to handle analytically. Figure 3 shows four pulses that were considered in some detail in selecting an optimum pulse.

Figure 4 shows the distribution of harmonics of these various pulses plotted against the relative frequency of the harmonics. All harmonics are assumed to be positive in magnitude although alternate groups would have different signs. At a relative frequency of 1.0, the absolute frequency is $1/d$ (see Figure 3) for these pulses and the first zero magnitude occurs at this point. The amplitudes are all expressed in decibels down from the magnitude of the repetition frequency current.

It may be seen that the distribution of the harmonics up to a relative frequency of 1.0 is about the same for all the pulses, thus making them about the same from the standpoint of the criterion that they should cover all parts of the desired frequency range approximately equally. The main differences between the harmonic distributions for the various pulses are at higher frequencies which are important because there the harmonics may be distorted in amplitude or phase by the line or by the measuring equipment. When the power in these harmonics is quite small, it does not matter what is done to them in phase or extra loss or whether or not small amounts of extra gain are inserted. Eliminating the higher harmonics completely would be equivalent to adding similar harmonics of equal magnitude but 180 degrees out of phase. If such an addition is far enough down in magnitude, no effect will be observed on the oscilloscope. No amount of phase shift can be any worse than this.

Just how far these harmonics must be down in a particular case is a complex combination of the hybrid balance at high frequencies, the irregularities in the line at such frequencies, the sensitivity of the measuring set, the rate at which further harmonics decrease, the way in which the remaining currents add, and so forth. As a first approximation, suppose it is assumed that when the harmonics beyond a given frequency are 30 decibels down, the higher frequencies may be ignored as far as loss or phase distortion is concerned.

On this basis, the loss and phase distortion may be neglected for the raised cosine wave above a relative frequency of

about 0.9, for the half sine wave above a relative frequency of 1.5, for the isosceles triangle above a relative frequency of 1.6 and for the rectangular pulse above a relative frequency of about 10. These figures show in a rough way the relative difficulty of building satisfactory measuring equipment for the different pulse shapes. For example, if a receiving amplifier well equalized for gain and phase up to 5 megacycles were needed for a given width of raised cosine pulse, the half sine pulse of the same width would need an 8-megacycle amplifier, an isosceles triangle pulse of that width a 9-megacycle amplifier and a rectangular pulse of that width about a 50-megacycle amplifier.

Similarly, the weighted average line attenuation to a pulse is decreased by shaping the pulse in this way, even before the distortion becomes noticeable on the oscilloscope. Experiment has shown noticeable reduction in the pulse attenuation of a given type of coaxial cable for slightly more optimum pulse shapes. In looking at irregularities at considerable distances, the better shape of pulse is doubly important because the reduced attenuation permits the pulse echo to be larger as received and also because the total noise is less due to the reduced frequency band necessary in the receiving

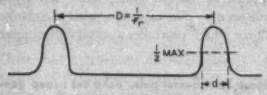

Figure 2. Repeated pulses

circuit. Practically, the pulse attenuation and pulse delay are determined experimentally by measurements on lines. The pulse loss per mile decreases as the length of line increases, particularly for the first part, because the higher frequencies disappear soon and further attenuation acts on lower and lower frequencies where the average attenuation is less.

It is possible to insert equalizers in the sending or receiving circuit to correct for the line distortion to a pulse echo from any particular point. This is of somewhat limited value, in general, however, because nearby echoes then are more distorted. A compromise value is often worth while.

The pulse magnitude to be used is partly a question of the needed signal-to-noise ratio for echoes versus the line and set noise, partly a question of what voltage is permissible on the lines, and partly a matter of the magnitude which it is practicable to get from available tubes with available power supplies, and so forth. Within these limits, the higher the pulse magnitude is made, the better, because higher magnitudes permit overriding noise and using minimum gain in the receiving circuit, but this should not be done at the expense of distorting the pulse.

Description of Coaxial Pulse Echo Test Set

The present coaxial pulse echo test set represents continued development of the original circuit which was first used in 1940 for factory testing of coaxial cables. There have been changes in the direction of increasing the sensitivity and accuracy of measurement and the ease of measurement.

On a smooth line, the present measuring equipment can detect an isolated irregularity which gives a reflection approximately 100 decibels below the test pulse. The location of an irregularity is dependent upon a number of factors such as pulse width and the nature of the irregularity. With the 0.25-microsecond pulse in the present field test equipment, the position of an isolated irregularity not too distant from the sending end may be measured to about plus or minus 50 feet. Complex echoes make recognition and isolation of irregularities considerably more difficult and in the usual length of manufactured cable, echoes approximately 75 decibels down from the transmitted pulse are about the determinable minimum.

Figure 1, which is a general schematic diagram of the pulse echo sets, is representative of a coaxial pulse echo set. In the coaxial set, however, a compensating network to be discussed later is shunted across the coaxial cable at the sending end. The following is a detailed description of a Bell Laboratories model used to measure coaxial cables in the field.

Figure 5 is a schematic diagram of the pulse and sweep generators. The wave shapes indicated near the several components serve to represent the approximate shapes of the waves with no attempt being made to indicate their relative magnitudes or durations. The oscillator which is a sine wave resistance capacitance oscillator is arranged to furnish either 56, 13, or 3.3 kc. The rates at which pulses are generated and at which the horizontal sweep is repeated are both controlled by the particular oscillator frequency and are thereby kept in synchronism.

To generate the pulses required, the sine wave is first squared in an overloaded amplifier, clipped, and used to trigger a start-stop multivibrator circuit. The output of the multivibrator is connected to a circuit tuned to produce the desired pulse width of 0.25 or 1.5 microseconds (a 0.08-microsecond pulse is now under development). A damping diode is also connected across the tuned circuit. The normal response of the tuned circuit to the square pulse output of the multivibrator would be a train of oscillations. However, the diode acts to absorb the energy in the tuned circuit after the first half cycle in the negative direction, which occurs at the front edge of the multivibrator pulse, and to greatly reduce the output by absorbing the energy in the trailing edge of the multivibrator pulse. The resulting pulse at the output of the tuned circuit is approximately a half sine wave and is fed into a pulse amplifier which includes an output stage biased beyond cutoff. This serves to remove most of the residual undershoot due to the imperfect damping action of the diode.

The output of the pulse amplifier is connected to the hybrid coil circuit by means of an output transformer. The high impedance side of the transformer is terminated in a resistance so that its output looks like approximately 75 ohms. The transformer is designed to deliver 35- to 40-volt positive pulses to a 75 ohm load.

The portion of the base oscillator output which is used to derive the horizontal sweep of the oscilloscope is first fed through a phase splitting and inverting circuit and a variable phase shifting circuit. The latter is a standard 4-stator variable capacitor where quadrature voltages are applied to the four plates and a single rotor used as a pickup device. The varying positions of the rotor give a change in phase over the full 360 degrees. The output of the phase shifter is ampli-

Figure 3. Pulse shapes

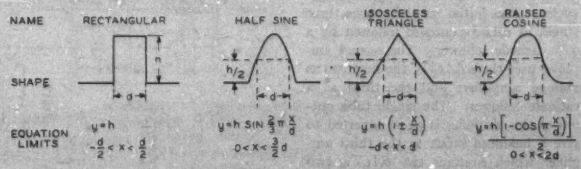

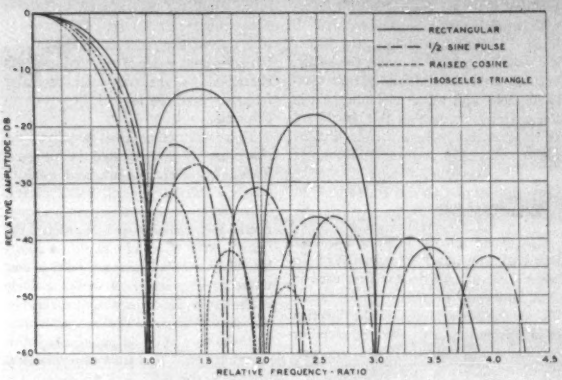

Figure 4. Distribution of harmonic frequencies of various shapes of repeated pulses

fied, squared, and differentiated to give positive and negative short pulses which are applied to a clipper tube. The positive pulse is flattened while the negative pulse is amplified and used to trigger the multivibrator which in turn drives a sweep generator tube. The length of the sweep is determined by the length of the multivibrator pulse. The sweep generator is a switching tube which is normally conducting and which is driven beyond cut-off by the output of the multivibrator. A capacitor in its plate circuit charges exponentially toward the positive plate supply voltage when the tube is cut off and by using only a small portion of the exponential rise a reasonably linear sweep is secured.

The vertical deflection system for the cathode-ray oscilloscope employs essentially a 12-tube amplifier which is composed of three individual amplifiers for practical reasons. The amplifier combination has a reasonably constant time delay up to 5 megacycles and a gain characteristic which is flat to within plus or minus 2 decibels between 2.5 kc and 5 megacycles. Above and below this frequency band, the gain of the amplifier decreases gradually, the 10-decibel points being at approximately 1 kc and 10 megacycles. The initial amplifier uses three stages of *6AK5* pentodes followed by a *6J6* cathode follower. The second amplifier uses three *6AC7*'s, the first two as voltage amplifiers and the third as a cathode follower. The single tube output of this amplifier is phase inverted to give a balanced input to the third amplifier which contains two *6AC7*'s, two *6AG7*'s and an *829* tube to provide three balanced stages of amplification. The vertical deflection plates of the 5-inch cathode-ray tube are connected to the plates of the *829* output stage.

The 4-winding hybrid coil (Figure 1) is used to transmit the pulses to the cable under test and to balance them out of the vertical deflecting circuit. A variable attenuator at the input of the vertical deflecting circuit serves as a gain adjustment and calibrating device. Since, in general, the cable under test is not directly accessible to the terminals of the test set, a 50-foot length of flexible coaxial cable is included for connection to the test sample. To simplify the balancing problem, an identical electrical length of flexible cable is used to connect the balancing network to the conjugate winding of the hybrid coil.

In order to secure the desired balance of approximately 80 decibels, the balancing network would be necessarily complex since it must match the cable resistance and reactance to a high degree of accuracy over a wide frequency range. However, the use of a compensating network, as discussed later, serves to make the combination of the cable and network look like a pure resistance. The balancing network, therefore, can be a simple resistance network as shown in Figure 6. A small variable capacitor is included to correct any small deviations in cable reactance, and so forth.

The cable under test also must be terminated accurately if large terminal reflections are to be eliminated. A complex terminating network which matches the cable impedance closely over a wide range of frequencies is necessary in this case. Figure 7 illustrates a typical network.

As indicated in the general discussion, the application of a pulse to a resistance does not change the general shape of the pulse. The impedance of a coaxial cable, however, is not a pure resistance since it contains both resistance and reactance components. When a pulse is applied to coaxial cable, pulse distortion will occur. For example, when a voltage source which produces a small rectangular

Figure 5. Coaxial pulse echo set sweep generator and pulser

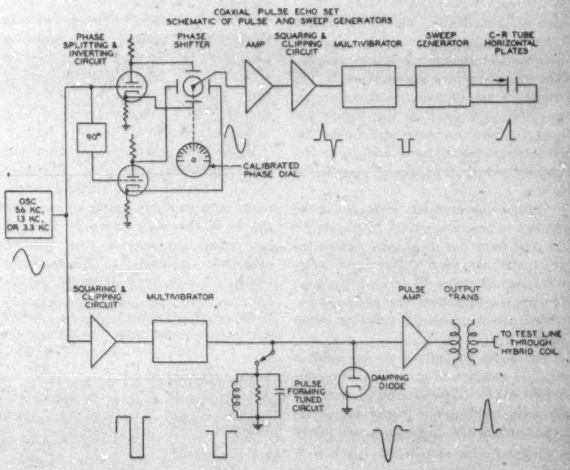

pulse of voltage is connected in series with a coaxial cable terminated in characteristic impedance, computations indicate that the resulting current produces a voltage across the near end of the coaxial cable which does not restore to zero immediately at the end of the pulse. It does fall to a small value and then decreases very gradually. A network (shown in Figure 8) called a compensating network is therefore connected in parallel with the cable under test. This combination looks effectively like a pure resistance over the frequency band involved. The use of this network for all practical purposes eliminates the pulse distortion from this source and, as indicated previously, permits the use of a very simple balancing network.

For quality control of manufactured cables, it is desirable to note the magnitude of the echoes as well as their position in the reel. The magnitude of echoes is measured by initially opening or shorting the line side of the hybrid coil. This permits the pulse normally applied to the cable to be transmitted to the vertical deflection system. With an 80-decibel loss in the input variable attenuator, the variable gain control in the vertical amplifier is adjusted for a reference deflection. The hybrid coil is then reconnected to the coaxial under test and the magnitude of any echo may be determined by adjusting the variable attenuator for reference deflection. The difference in attenuator readings is then directly the ratio of the reflected pulse to the applied pulse.

Measurements of distance to an irregularity are made with the phase shifter in the sweep circuit. Several methods of doing this are possible. For the set now being used in the field, the phase dial is divided into uniform divisions. Calibration curves for the several pulse widths and sweep lengths showing the experimental relationship between phase dial divisions and known lengths of cable have been prepared. A small mismatch is inserted at the input of the section under test by degrading the balance across the hybrid with the balancing network. The reading of the phase dial to bring the initial echo to a reference line on the scale is then noted. The phase dial reading required to bring any particular irregularity to the same reference line is also noted. Distance along the cable to any irregularity may then be determined by converting the two phase-dial read ngs to feet and taking the difference between them.

Another method, where the length of the cable under test is known, is to degrade the balance across the hybrid coil with the balancing network to give a well defined echo at the sending end, and to adjust the phase dial so that this echo coincides with a vertical line on the oscilloscope scale. The terminating network may then be adjusted to give a sizable echo at the end of the cable section. The phase dial is readjusted to bring the terminal echo to the reference line on the scale and the reading noted. The difference between the two phase-dial readings is the length of the cable in phase-dial divisions. With the networks restored to their normal operating condition, the phase-dial reading required to bring any particular irregularity to the reference vertical line is noted. The difference between this phase-dial reading and the phase-dial reading locating the near end of the cable is the distance to the irregularity in phase-dial divisions. The distance to the irregularity in feet is then determined by proportion. This method is less accurate than the preceding one because it assumes a linear relationship between length of cable in feet and the phase-dial readings.

In manufacture, the usual reel length of coaxial cable is approximately 500 to 1,500 feet and the set has been used extensively with this length of sample. It may also be used as a field test set where the lengths of cable in question may be up to that between repeaters, or about eight miles. The sensitivity for echoes returned from considerable distance is, of course, considerably less due to the attenuation of the pulses in the cable.

The round trip pulse attenuation per unit length varies with the total length from the sending end to the irregularity Table I shows typical values determined for nominal 0.25- and 1.5-microsecond pulse widths on various lengths of 0.27- and 0.375-inch polyethylene disk insulated coaxials.

Figure 9 shows irregularities on a reasonably smooth cable and on a cable which has several fair sized irregularities. The pictures were taken from each end of the two-1,265-foot cables. Those pictures designated "feeding inner" indicate

Figure 9. Coaxial echo traces

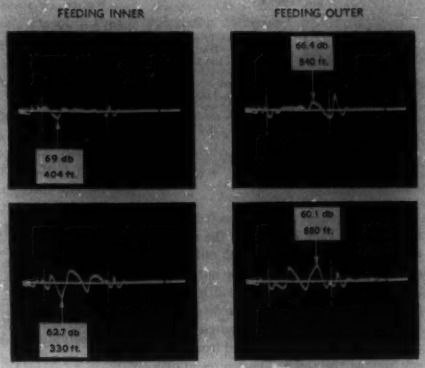

Figure 6 (right). Balancing network

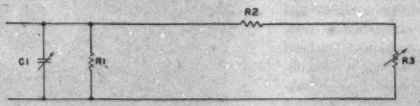

Figure 7 (right). Terminating network for 0.27-inch polyethylene coaxial cable

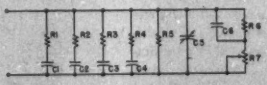

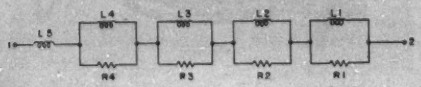

Figure 8 (left). Compensating network for 0.27-inch polyethylene coaxial cable

Table I

	Round-Trip Attenuation—Decibels Per 100 Feet		
Distance to irregularity, Feet	1,000	2,000	20,000
0.27-inch coaxial, 0.25 microsecond	0.22	0.21	0.15
0.375-inch coaxial, 0.25 microsecond	0.15	0.15	0.11
0.375-inch coaxial, 1.5 microseconds		0.10	0.07

that the echo set was connected to the inner end of each coaxial on the reel and for those designated "feeding outer" the echo set was connected to the outer ends. The 0.25-microsecond pulse width and the 56-kc repetition rate were used to obtain these pictures. The designated echoes are the same echoes measured from opposite ends of the reel. The figures in decibel indicate the magnitude of the echo at the point at which it exists. The locations in feet are the distances from the measuring end of the circuit. It is interesting to note that the peak of the echo in each case turns over, that is, is of opposite sign, when measured from opposite ends of the reel. This would indicate that these were impedance irregularities, that is, a change in characteristic impedance so that the pulse went from low to high impedance when sent from one end and from high to low impedance when sent from the other end.

Lookator

An example of the practical application of the echo time measuring technique as a fault finding means on voice frequency telephone circuits is found in the Lookator.[2] When connected to a telephone circuit of favorable characteristics, the Lookator shows departures from the normal impedance of the circuit along its length by means of a trace on a cathode ray tube. If steady or swinging faults of a magnitude sufficient to cause appreciable impedance irregularities are present, their general nature can be at once detected and their distance from the Lookator measured. The device is thus a fault locator that permits the operator in effect to "look" out over the circuit and it seemed appropriate to call the instrument a Lookator.

Figure 10 shows a front view of the Lookator with cover removed and ready for use. A 110-volt a-c power source capable of supplying 150 watts is required for operation. The instrument is shown housed in a carrying case approximately 19 by 19 by 15 inches and weighs approximately 100 pounds complete with case.

Figure 11 shows the functional setup used in locating faults by connecting the Lookator directly to a 2-conductor telephone circuit. The bridge-stabilized 220-cycle oscillator feeds through a zero adjustment circuit into a pulse generator where the oscillator frequency controls the repetition rate. The pulses, having individually the approximate shape of a positive half-sine 3-kc wave, are delivered to the line through a hybrid coil at a peak voltage of about 20 volts. An adjustable balancing network is provided which can be set to balance the particular type of line being measured. A balance setting sufficient to introduce an additional loss of 25 to 30 decibels in the pulse energy that passes directly across the hybrid coil into the receiving amplifier will permit, without overloading, sufficient receiving sensitivity for ordinary fault finding. The pulses returning as reflections from faults in the line enter the receiving amplifier and appear as vertical deflections on the screen of the cathode ray tube.

A second oscillator output feeds through the measuring circuit into the sweep circuit where it controls the frequency of the horizontal sweep. The zero adjusting circuit and the measuring circuit provide individual continuous control of the phases of the voltages supplied to the pulse sending and sweep circuits respectively, thus permitting the times at which electrical events in these circuits take place to be adjusted with respect to each other. A simple procedure measures the round-trip time of the repeated pulses in terms of difference in phase between sending and measuring circuits. The result can be read from a single dial with arbitrary scale divisions. The fault distance is then obtained from a substantially linear plot between dial divisions and distances obtained experimentally or by simple proportion when compared to the dial reading for an artificial fault introduced at a known distance along a particular line. The use of two phase adjustments permits measuring between any points along a circuit since the zero point can be set at any point desired along the circuit.

The original requirement to which the Lookator was built specified operation particularly on loaded spiral-four cable (*CC358*), having a nominal velocity of 18,000 miles per second. This 4-conductor cable is made in one-quarter mile lengths with bayonet connectors at the ends. Locations were required to be made over a length up to 35 miles with a desired accuracy of plus or minus one quarter-mile loading section. In addition, it was desired to operate the fault finding gear through carrier repeaters and other line equipment having a lower cut-off in the order of 200 cycles. A 200-cycle repetition rate would permit measurement of a total length of 45 miles without overlapping of pulses. A repetition rate of 220 cycles was selected so as to place the oscillator frequency equally distant from the harmonics of 60- or 50-cycle power supply. If noise is present on a faulty circuit, this prevents the possibility of power harmonics synchronizing

Figure 10. Front view of Lookator with cover removed

with the sweep which would cause troublesome standing patterns and possibly interfere with measurements. The 220-cycle rate permits measurements on circuits up to approximately 40 miles long.

After some experience with an experimental model, a further requirement was added, namely, operation on copper open-wire lines. The velocity of transmission for these circuits is in the order of ten times that of spiral-four cable. A different set of circuit elements for oscillator, phasing, and sweep circuits would ordinarily be indicated for open wire measurements in order to reduce cramping of the scale. In the instrument described here, however, only a single combination was provided, resulting in considerable simplification in equipment and operation, and retaining sufficient accuracy to meet requirements.

The relatively flat attenuation and velocity characteristics of spiral-four cable and copper open-wire over a range of 200 cycles to, say, 16 kc, allows operation over the required circuit lengths with a permissible amount of distortion of the pulse. If this same proportioned pulse were applied to a circuit of widely differing high frequency attenuation characteristics, the top of the returning pulse might become too rounded to use for measuring. Again, if it were contemplated to use this technique on circuits of very short electrical length, the measurement of much shorter time intervals would require a change in design of some of the apparatus components.

The measuring procedure is as follows: After turning the instrument on, with no line connected, a trace appears on the cathode-ray tube screen as shown in Figure 12*A*. The sharp projection above the horizontal is the measuring pulse that has passed across the hybrid coil because of the unbalance resulting from the open circuited line terminals. After placing the *MEASURE* dial on zero, the *INITIAL ZERO* dial is turned until the peak of the measuring pulse moves behind the vertical index line as shown in Figure 12*B*, thus setting the instrument on zero in preparation for a measurement. The circuit to be tested is then connected by operating the *TEST* key. Assuming a proper network setting, the original pulse at its normal position is now greatly reduced by the increased loss across the hybrid coil. If a fault is present, it will appear in some characteristic fashion on the trace, and in a position along the trace that represents the distance to it. The height of the pattern can be adjusted for examination. Figure 12*C* illustrates an open (both wires) in a spiral-four cable pair 11 miles from the Lookator. To measure the distance to this fault, the *MEASURE* dial is turned to move the pattern toward the index line until the peak of the pattern aligns with the index line as shown in Figure 12*D*. The reading of the *MEASURE* dial is an indication of the distance to the fault.

From the standpoint of a measurement of time, one turn of the *MEASURE* dial represents 1/220 second, or 22.7 microseconds for each division of the 220 division dial. Each division of the dial represents approximately 0.2 mile of spiral-four cable or 2.0 miles of copper open wire. Although the base width of the half-sine measuring pulse extends over several dial divisions, proper placement of the pulse tip permits a duplication of readings within 0.2–0.3 dial division, or a time of approximately 5 microseconds.

Examples of several types of faults on spiral-four cable are shown on Figure 13 which illustrates the possibilities of identifying the nature of the faults. For the patterns shown, the balancing network has been adjusted off-balance intentionally to show the original pulse at the left of a sufficient height to indicate its position with reference to the trouble pattern. With the network properly adjusted, the original pulse becomes very small when the test line is connected. An open is indicated in Figure 13*A*, a short Figure 13*B*, and a missing loading coil in Figure 13*C*. The latter trace shows an open at the end of the 20-mile circuit in addition to the missing loading coil 10 miles out. This illustrates the ability of the Lookator to "look" through faults that are not gross faults and show others farther along on the circuit. The faults can be readily located whether they are steady or intermittent. Noise would tend to broaden the trace but even considerable amounts would not seriously interfere with the location of the irregularities.

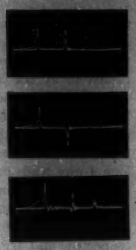

Figure 13. Examples of faults on spiral-four cables

A—Open circuit (two wires)
B—Short circuit
C—Missing loading coil

A supplementary terminating unit, although not required for the operation of the Lookator, is of assistance in definitely identifying a particular defective 1/4-mile section of spiral-four cable. This device can be connected into the cable at any of the bayonet connector points by inserting the unit between the two connectors. Test keys permit the circuit being tested to be connected back upon the opposite pair or toward either pair beyond, thus providing an option of several terminations. If a fault is indicated at the Lookator with the pair in question connected normally through and disappears when terminated otherwise, then the fault is beyond this particular connection point. If, after connecting the terminating unit at a point farther along the circuit, the fault remains showing regardless of the termination employed, then the fault is between the Lookator and the terminating unit.

Figure 14 shows a special application for locating troubles in spiral-four cable beyond the first repeater section by measuring through one or more spiral-four carrier repeaters. The hybrid coil and

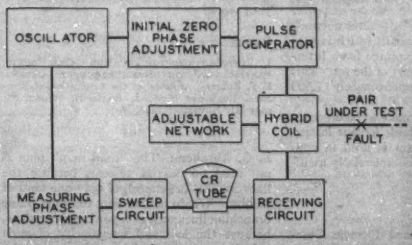

Figure 11 (right). Block-schematic diagram of Lookator for testing 2-wire circuit

Figure 12 (left). Example of Lookator measuring procedure

A—Measuring pulse
B—Adjust initial zero
C—Connect line and note fault
D—Measure distance to fault by turning measure dial until fault pulse aligns with index line

network circuit in the Lookator are switched out, and a small hybrid unit containing the equivalent equipment is connected in at the intermediate repeater point preceding the section in trouble. The Lookator in this case is connected on a 4-wire basis with the sending and receiving sides of the carrier system used as long 4-wire leads to the hybrid coil circuit. The Lookator zero is set with the faulty circuit disconnected from the hybrid unit. The circuit beyond is then connected, and the result given by the Lookator is in terms of distance beyond the repeater point where the hybrid unit is being used. It is not expected that the nature of the faults will be as clearly defined in this type of measurement as when testing directly into a line. This is because of distortions which result when operating through the intermediate repeaters with normal line settings.

If the Lookator could always connect directly to a line of the same makeup throughout its length, conditions would be relatively simple. Unfortunately this is not always realized. On open wire, for instance, short runs of entrance cable, submarine cable, or insulated field wire may be encountered. Since there is an impedance change at points where the circuit changes, these irregularities will appear in the Lookator trace of the overall circuit. In addition, since the velocity through different types of facility will not be the same, the slope of the calibration curve will change when the facility changes. For such cases, a sort of road map interpretation of the Lookator trace will be necessary. If calibration or reference measurements are made at any convenient time to locate the strategic points on the circuit where the makeup changes, these readings will serve as a guide to sectionalize trouble along the line. If then a reading is obtained between two reference points where the circuit makeup remains the same, distance within the section may be obtained by simple proportion, since the dial is approximately linear with distance between section reference points.

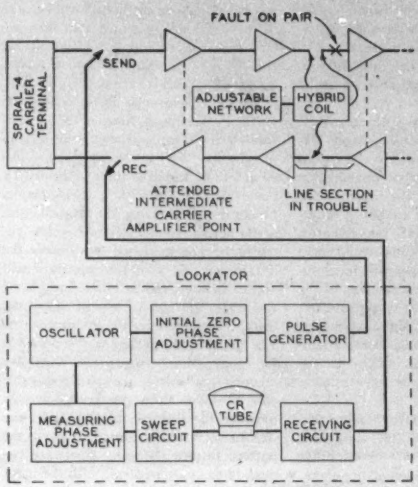

Figure 14. Block schematic of Lookator for testing through a repeater

Conclusion

The use of repeated pulses to locate irregularities and to determine their magnitudes has proved worth while. Further development to widen the fields of usefulness of such devices and to use them for somewhat different purposes is in progress.

References

1. United States patent 2,345,932. K. E. Gould. March 26, 1941.

2. The Lookator, J. T. Schott. *Bell Laboratories Record*, volume 23, October 1945, pages 379–83.

Discussion

B. G. Ballard (National Research Council, Ottawa, Ontario, Canada): The National Research Council of Canada has developed a transmission line fault locator employing a pulse-echo technique very similar to the telephone line fault locator described in the paper. Three of these devices have been constructed and are in use on both overhead and underground power lines. The results have been encouraging. Reflections are obtained from all discontinuities on the line including transpositions, and it has been found advisable in some cases to compare the reflections on a faulty line with those which were recorded when the line was in perfect condition.

Instead of a phase shift arrangement for determining distance, the National Research Council fault locator employs a ranging pip generated in a "phanastron" linear control delay circuit. This method has the advantage that the whole width of the oscillographic screen can be in use while measurements are being made, and it is possible to view the echo pattern of the whole line while making a distance measurement on any irregularity. It does not preclude the expansion of the sweep to any desired degree for examination in detail of a particular echo, and it allows equally accurate distance measurements to be made while the sweep is thus expanded. In addition, as the lines being tested normally have some interfering voltage at power frequency induced on them, a filter network has been provided in our unit which is capable of preventing this voltage from interfering with the receiver part of the set. This filter will withstand approximately 1,500 volts.

No attempt has been made to incorporate the oscillograph in the fault locator instrument itself and the latter is used in conjunction with standard commercially available oscillographs.

Harry R. Meahl (General Electric Company, Schenectady, N. Y.): May I direct your attention to some of the work done in England as reported by Roberts?[1]

This method has apparently been found quite valuable in spite of the fact that it has been necessary to make what they have called a "road-map" of their distribution system. This was made necessary, of course, by the many interconnections of transmission lines having unlike characteristic impedances and, therefore, propagating the pulses with different velocities.

Have you had a similar experience in your work?

Reference

1. New Methods for Locating Cable Faults, Particularly on High-Frequency Cables. F. F. Roberts. *Journal* of the Institution of Electrical Engineers (London, England), volume 93, part III, November 1946.

L. G. Abraham: The "road map" plan is not used on coaxial systems because the lines consist, in general, of only one kind of facility. We do not, in long toll lines, have branching lines such as a power system does, because the loss and irregularity of such junctions are prohibitive. In open wire systems, however, where loaded or nonloaded entrance cables, open wire pairs of different gauges and spacings are used, the road map is used both to determine which echoes are due to new irregularities and to assist in locating them more accurately.

Effective Resistance of Isolated Nonmagnetic Rectangular Conductors

HERBERT B. DWIGHT
FELLOW AIEE

WHEN a long straight conductor carries alternating current, the reactive voltage drop is not the same at different parts of the cross section. This results in nonuniform current density and an increase in the effective resistance. Values of the resistance ratio R_{ac}/R_{dc} have been computed for round conductors and for groups of such conductors, and the computed values have been confirmed by measurements.

For rectangular conductors, complete computations are not available and reliance must be placed to a considerable extent on measured values of the resistance ratio. Determinations of this ratio have been published in a number of papers and are now sufficient to give numerical values for almost any case encountered in practice.

In order to correlate the various determinations and to show where the frequency is too low for the use of high-frequency formulas, it is desirable to collect the values of resistance ratio in one family of curves, as shown in Figure 1. It has been shown that for any conductor or group of conductors, of a given shape, there is a definite value of the resistance ratio R_{ac}/R_{dc} for each value of f/R_{dc} where f is the frequency. This has been called the principle of similitude, and it is true at all frequencies. It makes it possible for measurements made at low frequencies to be plotted and compared on the same sheet with those made at higher frequencies.

It has been shown further that for very high frequencies where the distortion of current is so extreme that the current flows chiefly in the skin of the conductor, the resistance ratio is proportional to $(f/R_{dc})^{1/2}$. If this quantity is used as a base, the curves become straight lines when the frequency is high. Because of some calculated expressions for skin effect, it has been customary to use $\omega = 2\pi f$, and to plot ratios for rectangular conductors on a base of

$$P = (8\pi fab/\rho)^{1/2} \qquad (1)$$

The meaning of the letters is given under Figure 1.

A very complete set of curves for nonmagnetic rectangular conductors has been published by Forbes and Gorman.[1] This forms the basis of Figure 1. For comparison, three low-frequency curves published by Kennelly, Laws, and Pierce[2] are shown by dotted lines, for $b/a = 8$, 16, and 24. The first two curves are seen to agree closely with the others, as was shown by Forbes and Gorman in their Figure 4. The left-hand curve of measured values for square wire indicated by small triangles, given by Arnold,[3] confirms the corresponding curve by Forbes and Gorman. A curve for very thin strip ($b/a = 238$) is plotted below the other curves. This is taken from Figure 22 of a paper by Kennelly and Affel.[4]

The straight, broken lines in the right-hand part of Figure 1, which are asymptotes of the curves, now will be described. A theoretical paper on this subject has been published by J. D. Cockcroft.[5] It gives, in his equation 6, in the notation of this paper, the following solution which he stated to be for extremely high frequencies:

$$R_{ac}/R_{dc} = \frac{\Phi(b/a)}{\pi}\left(\frac{4\pi fab}{\rho}\right)^{1/2}$$

$$= \frac{\Phi(b/a)}{\pi 2^{1/2}} P \qquad (2)$$

$$= 2^{1/2}\pi^{-3/2}(E - k'^2K)^{1/2}(E' - k^2K')^{1/2}(K + K')P \qquad (3)$$

where

$\Phi(b/a)$ is a function, given by equation 3, of b and a the width and thickness of the metal strip conductor
K and K' are complete elliptic integrals of the first kind to moduli k and k'
E and E' are corresponding integrals of the second kind
$k' = (1 - k^2)^{1/2}$

The modulus k may be considered as a parameter. It is not given explicitly in terms of a and b, but a and b are given by

$$a = \text{thickness of strip} = 2(E' - k^2K')/k \qquad (4)$$

$$b = \text{width of strip} = 2(E - k'^2K)/k \qquad (5)$$

where

k^2 is greater than 1/2

Values of Φ (b/a) may be read from Figure 2.

The resistance ratio for a given value of b/a is plotted against P for each curve in Figure 1, and for this equation 2 or 3 gives a number multiplied by P. For the various values of b/a this gives straight lines through the point (0, 0), the origin of co-ordinates (not shown on Figure 1 but somewhat below it). Portions of these straight lines are plotted as broken lines on the right-hand part of Figure 1. They are seen to be in good agreement with most of the curves of Forbes and Gorman, Figure 1, at the right-hand end of the curves where the frequencies are high.

A set of measurements at about six megacycles has been published by W. Jackson,[6] and it confirms the results of equations 2 and 3 in the range $R_{ac}/R_{dc} =$ 40 to 90. These results are plainly much beyond the range of Figure 1.

It is evident from Figure 1 that the broken line asymptotes give values of R_{ac}/R_{dc} which are consistent with the measured values when R_{ac}/R_{dc} is greater than about 2.6, but below that value the test curves bend away from the asymp-

Paper 47-88, recommended by the AIEE committee on basic sciences for presentation at the AIEE winter meeting, New York, N. Y., January 27–31, 1947. Manuscript submitted August 10, 1946; made available for printing December 10, 1946.

HERBERT B. DWIGHT is a professor of electrical engineering at Massachusetts Institute of Technology, Cambridge, Mass.

totes; and when R_{ac}/R_{dc} for thin strips is as small as 1.5 the values given by the asymptotes bear almost no relation to the measured values. In fact, the asymptotes if continued a little farther to the left, give values of R_{ac}/R_{dc} which are less than one, and that is plainly out of the question.

An example of the usefulness of the curves of Figure 1 is to be found in Table II of a paper by Smith, Gregory, and Lynn.[7] Four measurements of skin effect ratio of rectangular copper conductors were made, as follows: $R_{ac}/R_{dc}=1.235$, 1.20, 1.525, and 1.45 for values of $P=2.7$, 3.3, 4.7, and 5.6, respectively. The values of b/a were 42 and 58, or an average of 50, for which an asymptote is drawn in Figure 1. The readings would be expected to lie between the curves for $b/a=24$ and 238, and they are reasonably close to that. However, the values of R_{ac}/R_{dc} are much less than 2.6 and for thin strips, as can be seen from Figure 1, there can be no expectation of making these readings correspond with the calculated asymptote, as was attempted by the authors of the paper. The asymptotes should be used only in the range where they are valid.

In order to interpret and correlate the curves of Figure 1 to some extent, it is useful to examine the curve of Figure 3, which gives the calculated resistance ratio of two equal tubes forming a return circuit, the axial separation of the tubes being four times the radius, and the thickness being 0.005 times the diameter.

This curve is computed from equation I of a paper by S. P. Mead,[8] which states that the resistance ratio of a tube in a return circuit of two parallel tubes is equal to the resistance ratio of the tube when it is isolated; that is, its skin-effect ratio, multiplied by a proximity-effect factor, formulas and curves for which were given.

The skin-effect resistance ratio R_{iso}/R_{dc}, for a very thin isolated tube, is given by curve A, Figure 4. This is taken from the curve for $t/d=0$ published by the writer,[9] d being the outside diameter of the tube. Dividing the values in Figure 3 by those of curve A, Figure 4, the proximity-effect ratio is obtained, as plotted in curve B, Figure 4.

The curve of Figure 3 thus is seen to show first proximity effect and then at higher frequencies it shows also skin effect. The example was chosen especially so that the proximity effect would appear separately.[10]

By proximity effect, the current is crowded to the adjacent parts of the two tubes in the case of a return circuit, or to the more remote parts of the cross sections in the case of two tubes connected in parallel. The amperes per millimeter of circumference are not constant, and at extremely high frequencies become the same in proportion as the density of charge in the capacitance problem of the same conductors. This is because a magnetic line of force cannot cut through the metal at extremely high frequency but must be parallel to the metal surface. In an electrostatic capacitance problem the equipotential lines are parallel to the metal surface, which is itself an equipotential line. Therefore, the electrostatic field map around the conductor has the same shape and proportions as the magnetic field map around the same conductor at extremely high frequency. This is a well-known principle in high-frequency skin-effect calculations, and was quoted and used in the paper by J. D. Cockcroft.[5]

The loss at any point caused by a certain value of amperes per millimeter of circumference is obtained by using the skin-effect calculation as if the tube were isolated. For high frequencies, the penetration formula may be used. By this, the loss is the same as if the current flowed in the outer skin of the conductor to a depth δ, the "effective penetration depth," where

$$\delta=\left(\frac{\rho}{4\pi^2 f}\right)^{1/2} \text{ centimeters} \qquad (6)$$

where

f = frequency
ρ = resistivity in abohms per centimeter cube

If the amperes per millimeter of periphery in the case of an isolated thin strip were uniform, the current would crowd

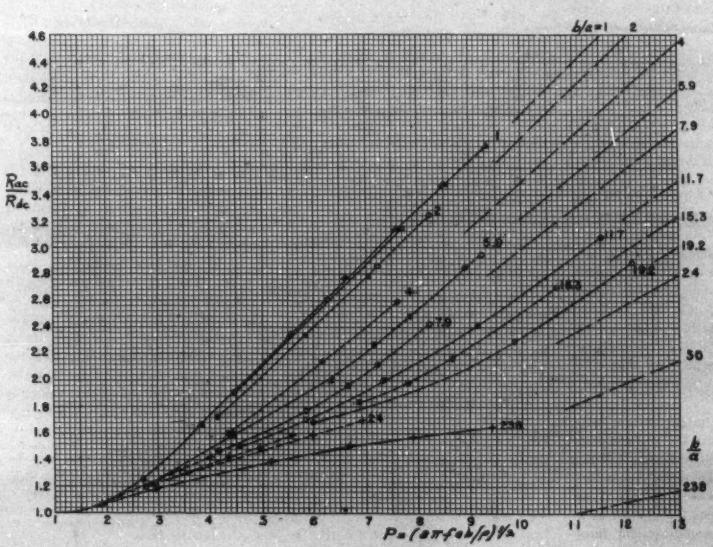

Figure 1. Resistance ratios of isolated nonmagnetic rectangular conductors

a = thickness of conductor, centimeters
b = width of conductor, centimeters
f = frequency, cycles per second
ρ = resistivity, absolute electromagnetic units

Figure 2. Values of the function Φ (b/a) for use in equation 2

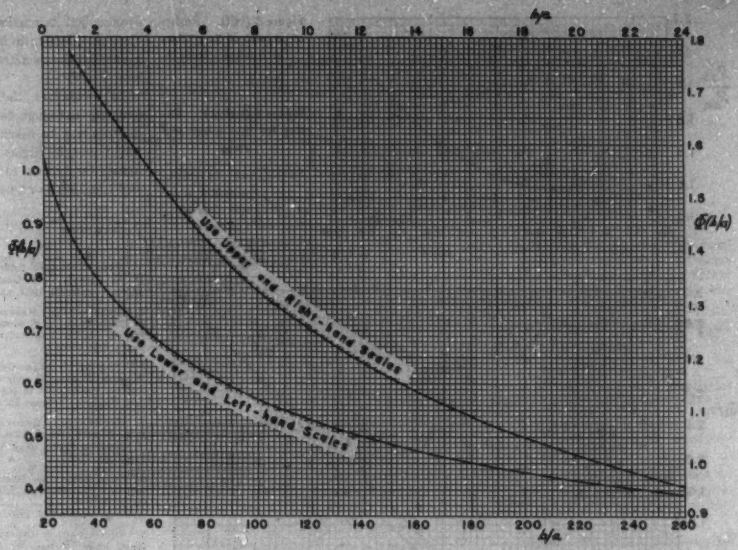

into the skin of the conductor on all sides, and the skin-effect resistance ratio at high frequencies—by the penetration formula—would be the ratio of ab, the cross section of the strip, to $2\,(a+b)\delta$, the cross section of the skin of thickness δ. This ratio is

$$\frac{ab}{2(a+b)\delta}=\frac{ab}{2(a+b)}\left(\frac{4\pi^3 f}{\rho}\right)^{1/2} \tag{7}$$

when a and b are the thickness and width of the strip and where δ is given by equation 6.

For the present purpose, the increase in resistance of an isolated strip caused by crowding of current toward the skin, at constant amperes per millimeter of periphery, may be called "skin effect" and the ratio of increase caused by crowding of current toward the edges, producing changes in the amperes per millimeter from one part of the periphery to another, may be called "edge effect".

Because conditions at a given part of a thin flat strip are the same as for a tube with very large radius ($t/d=0$) and with the same amperes per millimeter of surface, the skin-effect ratio of the strip may be read from curve A, Figure 4. For large values of the ratio the straight-line extension of curve A, given by equation 7, may be used. This ratio then should be multiplied by the edge-effect ratio, in order to obtain the measured resistance ratio, just as for the pair of tubes of Figure 3 the skin-effect ratio is multiplied by the proximity-effect ratio to give the complete, or measured, resistance ratio.

It may be seen from curve A, Figure 4, that for values of $\dfrac{ab}{2(a+b)\delta}$ less than 0.5 the increase caused by skin effect is almost zero, and all the increase in resistance in such cases would be caused by edge effect.

In order to show an example of the latter case from one of the curves of Figure 1, it is necessary to express equation 7 in terms of the constant of equation 1,

$$P=\left(\frac{8\pi fab}{\rho}\right)^{1/2}$$

Equation 7 then becomes

$$\left(\frac{8\pi fab}{\rho}\right)^{1/2}\frac{1}{(a+b)}\left(\frac{\pi ab}{8}\right)^{1/2}$$
$$=\frac{P}{a+b}\left(\frac{\pi ab}{8}\right)^{1/2} \tag{8}$$

Considering the curve for $b/a=238$ in Figure 1, the largest value of P on the curve is 9.4

$$\frac{ab}{2(a+b)\delta}=\frac{P}{a+b}\left(\frac{\pi ab}{8}\right)^{1/2}$$
$$=\frac{9.4}{239}\left(\frac{\pi 238}{8}\right)^{1/2}$$
$$=0.38$$

As this is less than 0.5, the measured curve for $b/a=238$ shows edge effect only, just as curve B of Figure 4, or the first part of the curve of Figure 3, shows proximity effect only.

By equation 2 the product of skin-effect ratio and edge-effect ratio for extremely high frequency is

$$\frac{\Phi(b/a)}{\pi}\left(\frac{4\pi fab}{\rho}\right)^{1/2}$$

Dividing this by the skin-effect ratio for extremely high frequency, namely, equation 7, the high-frequency edge-effect ratio is

$$\frac{\Phi(b/a)}{\pi}\left(\frac{4\pi fab}{\rho}\right)^{1/2}\times\frac{2(a+b)}{ab}\left(\frac{\rho}{4\pi^3 f}\right)^{1/2}$$
$$=\frac{\Phi(b/a)}{\pi^{1/2}}\times\frac{2(a+b)}{(ab)^{1/2}} \tag{9}$$

Because this is independent of f, the edge-effect ratio approaches a maximum value, just as the proximity-effect ratio of a pair of tubes does in curve B, Figure 4. There is a different maximum value of edge-effect ratio for each value of b/a.

The maximum value of the edge-effect ratio for $b/a=238$ is, by equation 9,

$$\frac{0.40\times2\times239}{3.14\times1.77\times15.4}=2.2$$

The measured curve for $b/a=238$ in Figure 1 shows that it is beginning to bend over to the right, but it would have to be extended to much higher frequencies be-

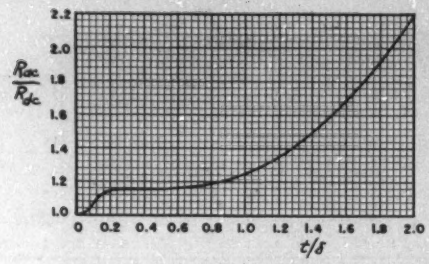

Figure 3 (left). Resistance ratio of two tubes in a return circuit

Figure 4 (below). Ratios for thin tubes and strips

t = thickness of tube, centimeters
a = thickness of strip
b = width of strip
f = frequency
δ = penetration depth

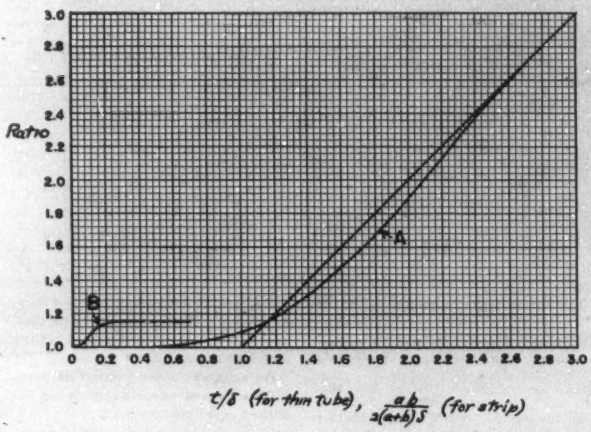

fore it would approach its maximum value 2.2. Therefore, the curve for $b/a = 238$ cannot be expected to approach its asymptote (shown on the lower right-hand corner of Figure 1) or to agree with equation 2 or 3 until much larger values of P are reached than are shown on Figure 1; that is, until the edge-effect ratio has approached its maximum value and until the skin-effect ratio is large enough to be given by the penetration formula, equation 6 or 7.

In conclusion, the resistance ratio of isolated nonmagnetic rectangular conductors may be taken from Figure 1, and for frequencies higher than shown by that figure, for b/a up to about 24, Figure 2 and equation 2 or 3 may be used.

References

1. Skin Effect in Rectangular Conductors, **H. C. Forbes, L. J. Gorman.** AIEE Transactions, volume 52, 1933, pages 516–19.

2. Experimental Researches on Skin Effect in Conductors, **A. E. Kennelly, F. A. Laws, P. H. Pierce.** AIEE Transactions, volume 34, 1915, pages 1953–2018.

3. The Alternating-Current Resistance of Hollow, Square Conductors, **A. H. M. Arnold.** *Journal*, Institution of Electrical Engineers (London, England), volume 83, 1938, page 537.

4. Skin-Effect Resistance Measurements, **A. E. Kennelly, H. A. Affel.** *Proceedings*, Institute of Radio Engineers (New York, N. Y.), volume 4, 1916, page 523.

5. Skin Effect in Rectangular Conductors at High Frequencies, **J. D. Cockcroft.** *Proceedings*, Royal Society of London (London, England), series A, volume 122, 1929, page 533.

6. Skin Effect in Rectangular Conducyors at High Frequencies, **W. Jackson.** *Philosophical Magazine* (London, England), series 7, volume 18, 1934, page 433.

7. Electrical Resistance of Permalloy Strips, **A. W. Smith, J. H. Gregory, J. T. Lynn.** *Journal of Applied Physics*, American Institute of Physics (New York, N. Y.), volume 17, 1946, page 33.

8. Wave Propagation Over Parallel Tubular Conductors, **S. P. Mead.** Bell System Technical Journal (New York, N. Y.), volume 4, 1925, page 327.

9. Electrical Coils and Conductors (book), **H. B. Dwight.** McGraw-Hill Book Company, New York, N. Y., 1945. Figure 3, page 222.

10. Letters to the Editor, Skin Effect in Conductors of Given Shape, **H. B. Dwight.** *Electrical Engineering*, volume 52, 1933, pages 724–5.

No Discussion

Liquid Cooling of A-C Turbine Generators

CARL J. FECHHEIMER
FELLOW AIEE

THE foresight of a number of engineers, a little less than a quarter of a century ago, led to the successful development of hydrogen-cooled turbine generators. Until some 15 years ago many operating and manufacturing engineers were skeptical about the safety of hydrogen as a cooling medium. Today those fears are dispelled and practically every large turbine generator built recently in the United States is hydrogen-cooled.

By contrast, the writer ventures to say, present-day engineers look askance at the idea of liquid cooling, especially for the rotors of turbine generators. It is feared that the liquid can not be made to pass into, through, and out of, a high speed rotor without giving trouble.

From the standpoint of gains to be achieved, provided the mechanical difficulties can be overcome, it is at least as large a step from hydrogen to liquid cooling as it was from air to hydrogen cooling. This paper covers the gains to be expected, and proposed methods of surmounting mechanical difficulties. The paper is almost entirely nonmathematical, although a great deal of time was given to calculations of 100,000-kva 80-per-cent power factor generators at 1,800 and 3,600 rpm.

Gains by Liquid Cooling of Turbine-Generator Rotors

It is recognized that, aside from magnetic saturation and mechanical stresses, it is the temperature rise of the rotor winding that imposes the limitation as to the over-all dimensions when the load current lags behind the voltage. For to decrease the D^2L it is necessary to increase the ampere turns, and that gives rise to increased I^2R loss. Thus, one principal gain to be affected by liquid cooling of the rotor is that the I^2R loss can be increased for a given temperature rise, and the machine can be made smaller, lighter, and cheaper for a given rating.

A second important gain is that the rotor copper temperature will be nearly uniform, both radially and longitudinally, and consequently there should be no damage or deformation resulting from differential expansion and contraction, as in gas-cooled rotors, as was brought out in the papers by Noest [1] Juhlin,[2] and Coates and Pyle.[3]

A minor advantage is that the temperature of the copper and the steel above that of the entering liquid can be predicted within only a small percentage of error, if the losses and the various constants of the materials are known. With gas cooling, the highly turbulent flow in some places, the consequent uncertain heat transfer rates, and the complex heat flow defy calculation.

Gains by Liquid Cooling of Turbine-Generator Stators

For the stator, either transformer oil or Pyranol may be used. The gains are

1. For a given internal stator diameter (determined by the previously chosen rotor external diameter), and for given magnetic densities and voltage, the stator external diameter can be made smaller than for gas cooling. This is explained under the section entitled "Mechanical Construction of the Stator."

2. The stator copper temperature is nearly uniform.

3. There is absolutely no corona.

4. The stator may be wound for considerably higher voltage than is practical with gas cooling.

5. Fairly accurate temperature predetermination can be made.

6. The rate of flow of the liquid can be regulated readily, and thereby the temperature rise of the stator winding can be controlled to a large extent.

7. The internal reactances are higher than with gas-cooled machines, thereby admitting of smaller external reactors, or possibly their omission. (This is because the number of effective stator ampere conductors is larger with liquid cooling.)

Mechanical Construction of the Rotor

The same liquid is used repeatedly in a closed-circuit system. In the external part of the circuit, not shown in the illustrations, the liquid is cooled in some established heat exchanger, and in series therewith is a pump and some device for removing entrapped air (or other gas). The latter is needed when the machine is started, and probably may be by-passed when the machine has attained full speed. The front end is shown in Figure 1*B*, and the turbine end in Figure 1*A*. Figure 2 shows the end elevation. In Figure 3 a second scheme for connecting the shaft and rotor duct parts of the liquid circuit is shown. The drawings are intended to convey to the reader the construction and are only partly proportional to a machine's dimensions.

Referring to Figure 1*B*, the stationary metal tube *A-B*, which clears the bore in the shaft, is welded to the plate *C*, which in turn is bolted to a rigid stationary plate *D*. The liquid flows from *A* to *B* and is discharged near *B* into the pocket *E*. It then passes through the radial holes *F* and *G*, into the casing *H*, then flows radially outward and then into

Paper 47-95, recommended by the AIEE committee on electric machinery for presentation at the AIEE winter meeting, New York, N. Y., January 27-31, 1947. Manuscript submitted October 30, 1946; made available for printing December 16, 1946.

CARL J. FECHHEIMER of Milwaukee, Wis., is a consulting engineer.

The author acknowledges with appreciation the suggestions of K. L. Hansen, Forrest Nagler, E. F. Vilter, and Arthur Simon, as well as the co-operation of C. M. Laffoon and of some members of the staff of the Armour Research Foundation.

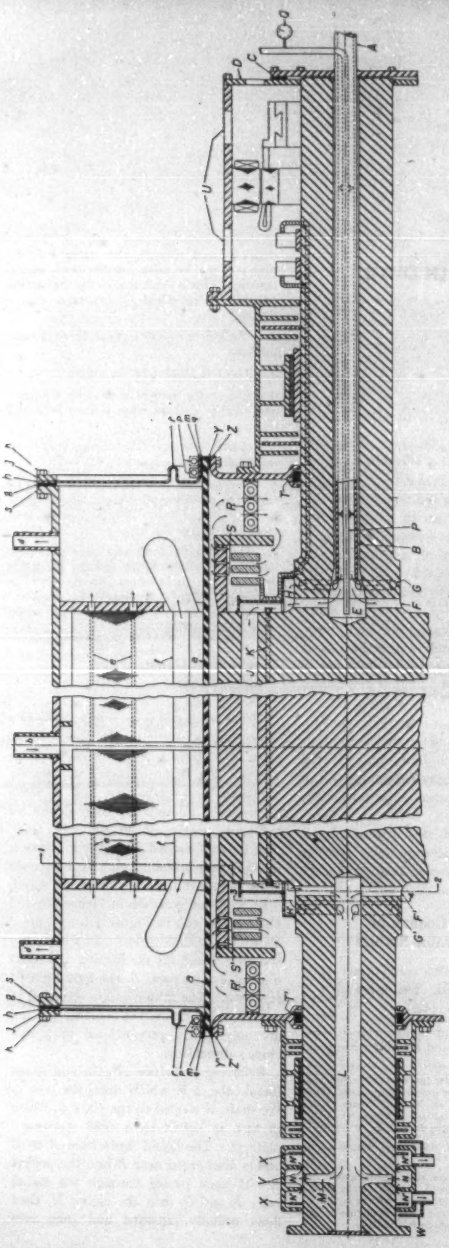

Figure 1A. Turbine end. Side elevation

Figure 1B. Front end. Side elevation

Figures 1A and 1B. Liquid-cooled turbine-generator rotor

axial ducts J and K. These ducts J and K are the main cooling ducts and extend the full axial length of the rotor body. The liquid then flows radially inward to H', (Figure 1A), through radial holes G' and F', then axially through the hole L in the shaft, to the discharge radial holes M. It then collects in the annular space, N, and later it passes through the external pump the heat exchanger in the external part of and circuit, back to the entrance tube A-B.

During the passage of the liquid through the rotor body, the centrifugal action thereon at the incoming end (H to J and K) is balanced substantially by the centrifugal action at the leaving end (J and K to H'). However, the head generated in the centrifugal pump at M is not balanced at the other end. This head generated from the shaft bore to the shaft external periphery is considerably more than is needed to overcome the sum of the hydraulic resistances opposed to the flow of the coolant from the entrance at E to the discharge in L.

The large centrifugal action between the shaft bore and the rotor ducts will cause entrapped gases to collect in the pocket E at the incoming end, (Figure 1B) The gases then are drained off through the small stationary tube P and can be allowed to issue through a suitable trap, not shown (Supports for tube P from the tube A-B are indicated.) A pressure gauge Q may be added to indicate the pressure at E To insure that the gases escape, the pressure at E should be slightly above atmospheric pressure, but should not be so high as to cause the liquid to flow out between the shaft bore and the external periphery of the tube A-B. The pocket E is enlarged (shown tapered) so that centrifugal action will cause the liquid to flow into the radial holes F and G and not into the annular space between the shaft bore and the tube A-B even with the pressure in E slightly above that of the atmosphere.

There may be several locations for the outlet ducts F and G, one being shown in Figure 1B. In some instances it may be advantageous to locate both the F and G ducts at the larger bore beyond the taper Also, the number of rows and number of ducts indicated are mere suggestions. At the turbine end (Figure 1A), no taper is shown, and the F' and G' ducts terminate at a shaft bore which is slightly smaller than the bore beyond the taper at the front end. This smaller bore is desirable as it increases the rigidity of the structure slightly, but it also reduces the pressure in the bore L. When a machine is designed, the proportions of such parts can be determined readily, and the en-

Figure 2. Front elevation

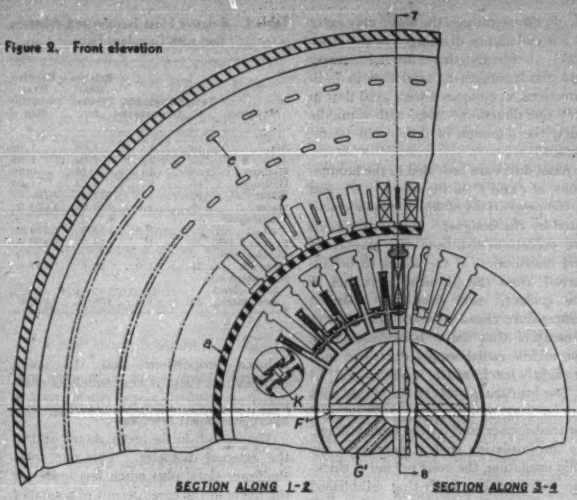

gineer should not have difficulty in deciding whether or not to make the shaft bore at the turbine end similar to that at the front end, or even to make the turbine end bore larger, so as to increase further the pressure there.

There is appreciable resistance to the flow of the liquid through the rotor ducts, and the resultant loss of head is sufficient to reduce the pressure in the shaft bore at the turbine end to a value below atmospheric; but with suitable proportions the pressure there should be appreciably above a vacuum. Thus, a reasonable loss of head through the rotor ducts is of the order of 20 feet, and with 34 feet of water as atmospheric pressure, added to the positive head at E, there is still ample pressure above vacuum.

If the shaft diameter is determined by an usual value of working stress in torsion for the transmitted load, for a large generator at either 3,600 or 1,800 rpm, the head generated by centrifugal action at M is several times the equivalent of sea-level atmospheric pressure. Consequently, there would be danger of cavitation in the shaft bore at the turbine end if there were no provision for absorbing the additional head. This is secured by restricting the discharge ducts near the shaft periphery, as shown, by means of orifices. To insure against cavitation at the entrance of the radial ducts M, the velocity of the liquid is made low by making the entrance section relatively large, and then curving, so as gradually to accelerate the liquid. The curved portion terminates in a cylinder which continues to the orifice near the external diameter of the shaft. By applying Bernoulli's equation at several shaft diameters, the proportions of the ducts joining M with N can be made such as to insure that pressure will be well above vacuum at all points, generally increasing with diameter.

After the liquid is discharged from M, it enters the annular space N at high velocity. This space fills rapidly and the liquid whirls and most of its kinetic energy is dissipated, and goes into heat. The calculated mean temperature rise of the liquid caused by this loss usually will be less than one degree centigrade. This means also that the power required to drive the centrifugal pump M is small and decreases the generator efficiency by an extremely small amount.

The liquid next passes through the restricted areas V between the two annular spaces N and N' and is finally discharged from the bottom of N' into suitable pipes, whence it flows into the heat exchanger and external pump, and is returned to the entrance tube at A. The whirling rings X should prevent the axial escapement of liquid while the rotor is running at normal speed. When getting ready to run at or near standstill, there may be a small escapement of liquid. Practically all of this may be caught in the gutters W and returned to the main part; the very small amount that still might leak out during the starting period may be caught and drained. There also may be a little leakage near the entrance at C, although this can be substantially eliminated by suitable gaskets between the plates C and D. It will be noted that at standstill, or very low speed, the flow is produced by a low-pressure external pump. Consequently, the volume of flow is less than when running at normal speed, and the leakage is very small. Although the volume of flow is less at very low than at normal speed, the temperature rise of the copper (above the ingoing coolant) for a given I^2R loss should be nearly the same, because the duct surface temperature drop and temperature rise of the coolant are small, and there is negligible pole face loss at very low speed.

The ducts in the rotor body, J and K, (Figure 1B) are shown as rectangular in section. Other suitable section, as trapezoidal, may be chosen. They are machined (by milling or planing) from the external cylindrical surface, and the outer parts of the J-ducts are filled subsequently by steel pieces, suitably welded in place. The small ducts, K, below the winding slots are cut in after machining the main winding slots, and their outer parts are covered then with suitable thin plates welded in place at the bottom of the main slots. (In the patents* circular holes instead of rectangular ducts are shown, but the difficulty in drilling long holes in a solid rotor precludes their use.) One of the larger ducts is in each of the rotor teeth, and in the central pole adjacent to the last slots. A small duct is located below each rotor slot. If the rotor is built of plates, circular holes can be drilled, and to prevent leakage of the liquid at the junctions of plates, thin walled metal tubes are pushed into the ducts, and they then are welded at the ends of the rotor body.

One way of constructing the casings H and H' is shown in Figures 1A and 2. They are fabricated entirely of steel sheets of such thickness that the stresses therein caused by liquid pressure and their own centrifugal forces will be of the usual order for safety. With the construction shown in Figure 3, the engineer is cautioned to keep the stresses and velocities conservative.

In order to absorb the heat generated in the coil ends of the rotor windings, the gas at the ends is caused to circulate by centrifugal action, passing through holes, S, in the retaining rings, and passing over the surfaces of circularly bent tubes and between fins on the tubes R and R', in a continuous closed circuit. These

* United States Patents 2,381,122 and 2,285,960.

finned tubes are stationary and are suitably supported, as indicated. Water or other liquid is circulated within these coils to absorb the heat. The finned tubes may be placed in some other location in the gas stream.

In order to reduce the windage loss, to improve the heat conductivity of the insulating wall in the rotor slots, and to improve the heat transfer between rotor coil ends and the circulating gas, and between that gas and the finned tubes R and R', the rotor is operated preferably in a hydrogen atmosphere. Safe operation is assured by extensive experience, during the past 15 years, with hydrogen-cooled turbine generators. The gland seals for minimizing the escape of hydrogen and infiltration of air are indicated at T and T'. There are several successful schemes for constructing the gland seals, all employing a lubricating liquid, and as details for the several constructions differ, they are not shown at T and T'.

With this construction, calculations of the heating of the rotor coil ends in one atmosphere of hydrogen, when suitable blocking is provided to insure high gas velocities adjacent to the coil surfaces, indicate that when running those parts will have about the same order of temperature rise as the copper in the embedded parts.

Fitting snugly in the stator bore is a cylinder a of insulating material such as micarta. The flanged disks Z and Z' are bolted to this cylinder, being separated therefrom by suitable gaskets, Y and Y'. Thus, a, Y, Z, and T (and a, Y', Z', and T') form the inner sides of the structure wherein the hydrogen gas is retained.

In Figure 1*B* a suggestion is given as to how the rotor leads may be brought out from the winding to the collector rings. A direct-connected exciter is shown also; evidently, the omission of the exciter would not entail difficulties. Openings at U admit of inspection and replacement of the brushes on the commutator and collector rings.

It is important that all welds be leakless, and that they be tested with great care.

Mechanical Construction of the Stator

The liquid-cooled stator is illustrated in Figures 1*B*, 1*A*, and 2. The coolant is an insulating liquid, either transformer oil or Pyranol, which is circulated in a closed system, with an external pump and a suitable heat exchanger in series, the latter two being omitted in the illustrations. As shown, the liquid enters at the middle, at b, and is discharged at both ends, at d and d'. For some ratings, the liquid may enter at one end and be discharged at the other end. (Evidently there are advantages and disadvantages to axial flow in both directions, as compared with axial flow in only one direction. Also, with a middle duct, the direction of flow could be reversed.)

Axial ducts are provided in the laminations, at e and f* in Figures 1*B*, 1*A*, and 2, the proportions of which can be calculated by the designer. Such proportions are predetermined from the magnitude and distribution of the losses to be absorbed, from the physical properties of the coolant,† and from the assumed temperature rises. For the 100,000-kva generators that have been calculated, one middle radial supply duct, one inch or slightly less in width, is ample.

The insulating walls of the stator coils can be made of materials like those used for transformer coils for the same voltage. As the insulating coolant permeates the solid insulation, the volts per mil of thickness can be taken to be that established by good transformer design. The wall thickness is then less than with air or hydrogen as the cooling medium. The thermal conductivity is improved over that in air, and should be at least as good as in hydrogen. Furthermore the liquid coolant reduces the lamination temperature below that obtainable with hydrogen. As a duct is in each tooth (f in Figures 1*B* and 2, the coolant is close to the coil, and the thermal drop in the steel teeth (in the favorable planes of the laminations) is not large. Consequently, the permissible thermal drop through the insulating wall may be higher than for hydrogen. From these several considerations it will be seen that the watts per square inch of copper surface (and the current density) may be higher with the liquid coolant. Therefore, the slot size, for a given number of ampere-conductors per slot, may be reduced considerably. As the rotor ampere-turns are higher, the total number of stator ampere-conductors is also higher, with liquid cooling. Even so, it will be found that the stator slot depth may be less than with gas cooling.

Owing to the much better thermal properties of the coolant (giving greatly improved heat absorption and heat transfer), the ducts (e and f) may be of such reduced proportions that the space occupied by them is very small as compared with the space for the ducts in a hydrogen-cooled machine.

Table I. Relative Heat Transfer and Absorption with Turbulent Flow

Medium	Temp, C	Pressure, Atmospheres	Relative Heat Transfer	Relative Heat Absorption
Air	40	1	1.00	1.00
Air	25	1	1.04	1.08
Hydrogen	40	1	1.46	0.99
Hydrogen	40	2	2.53	1.98
Water	20	1	530.0	3,700.0
Water	40	1.0	653.0	3,670.0
Transformer oil	25	1.0	51.6	1,570.0
Pyranol 1,488	25	1	58.2	1,450.0
Turbine bearing oil	21	1.0	29.6	1,440.0
50 per cent ethylene glycol and water	25	1.0	268.0	3,240.0

The ducts f, in the teeth, do not add to the external diameter. This fact, plus shallower slots, plus much less space for the ducts in the core, permit of a smaller external diameter of the stator laminations for given internal diameter, magnetic densities, and stator voltage, as stated in the paragraph on "Gains by Liquid Cooling of Turbine-Generator Stators."

In Figures 1*B* and 1*A* the stator is closed at each end by the diaphragm, h, which is separated from the frame flanges, by means of a fluid tight, oil resisting gasket, g. The rings, j, are interposed between the heads of the bolts, k, and the outer surfaces of the diaphragms, h. The diaphragms may be provided with one or more circular corrugations, r, to increase their flexibility and prevent high stresses arising from transient pressure caused by a fault. The diaphragms have axial flanges, m, whose internal diameter is nearly the same as the bore of the stator laminations, and are separated from the cylinder, a, by means of gaskets, q. These flanges are pressed hard against the cylinder a through q by means of two clamp rings, p, (Figures 1*B* and 1*A*). The flanges for these two rings are not in the same location circumferentially to insure positive pressure on the gaskets for all peripheral positions, and thereby prevent leakage of oil.

An advantage of the high dielectric strength of the stator coolant is that the stator can be wound for higher voltage than is the present practice in the United States. Thus, in some instances, step-up transformers may be eliminated. Furthermore, oil avoids corona formation. The damage arising from corona in air is well known. (Although corona is present

* The f ducts are shown rectangular, but they may be advantageously trapezoidal, with sides parallel to the slot sides.

† The physical properties are: Specific gravity, specific heat, thermal conductivity, and viscosity. Consideration is given to them under the section entitled "Heat Absorption and Heat Transfer." The values of the properties may be found in authoritative tables and other publications. See equation 2 under "Heat Absorption and Heat Transfer."

with high voltage when hydrogen is the cooling medium, it is generally believed that then corona is not damaging.)

The designer is sometimes in a quandary with large machines, especially for 2-pole, as to how to secure a sufficiently small number of stator conductors with the desirable star connection when the voltage is of the order of 13,800. When the stator voltage is raised, this difficulty is reduced. Also, the switch-gear costs may be, and bus copper weights are, reduced by adopting a higher voltage.

Heat Absorption and Heat Transfer

The heat absorption rate is

$$\frac{\text{Heat absorbed per unit of time by coolant}}{\text{Volume per unit time of flow} \times \text{degrees temperature rise of the coolant}}$$

It can be shown easily that for a given volume flow per unit of time and temperature rise of the coolant

$$\text{The heat absorption rate is proportional to } C_p\gamma \tag{1}$$

C_p is the specific heat (at constant pressure for a gas), and γ is the weight density of the coolant.

The heat transfer rate is

$$\frac{\text{Heat transferred per unit of time}}{\text{Surface of duct} \times \text{degrees temperature difference}}$$

An equation for turbulent flow inside smooth ducts, checks for which against many experimental data are given by McAdam.[4]

$$\frac{hD}{k} = 0.023\left(\frac{\xi DV}{\mu}\right)^{0.8}\left(\frac{\mu C_p}{k}\right)^{0.4} \tag{2}$$

To assist the reader, the units in the centimeter-gram-second system are added as follows:

h = heat transfer coefficient (gram calories ÷ seconds × square centimeters × degrees centigrade)

D = diameter of duct, if circular, or $= \frac{4 \times \text{section}}{\text{perimeter}}$ for other shapes (centimeters)

k = thermal conductivity of the coolant (gram calories ÷ second × centimeters × degrees centigrade)

ξ = mass density of the coolant (gram mass per cubic centimeter = nearly to specific gravity)

V = mean velocity of the coolant (centimeter per second)

μ = viscosity of the coolant (Poise = dyne-second per square centimeter)

C_p = specific heat at constant pressure of the coolant

The coefficient 0.023 should be increased for rough or laminated ducts. The equation is written in the form given in equation 2, because each of the three groups is dimensionless and is significant unto itself, and each is named after an outstanding investigator; the first after Nusselt, the second after Reynolds,‡ and the third after Prandtl. (Consistent units must be used in each of the three groups).

With the same values of D and V, for comparison of heat transfer rates with various coolants, h is then proportional to

$$\xi^{0.8}k^{0.6}(C_p/\mu)^{0.4} \tag{3}$$

Evidently, the cooling is dependent upon these two: the heat transfer and the heat absorption rates. In Table I are given their relative values for a few fluids as referred to air at 40 degrees centigrade and at one atmosphere pressure, as obtained from equations 1 and 3. The values of the physical properties were obtained from various publications or by correspondence with producers.

It will be noted from Table I that the gains to be affected by some liquids over air or hydrogen are enormous. At present many engineers are justifiably pleased with the gains of hydrogen over air, and especially if the pressure of hydrogen is about twice that of the surrounding air. But such gains are insignificant when contrasted with liquids, especially with water. To be sure, the volume per unit of time, as adopted for machines, with liquids, would be much less than with gases. The velocities would be lower also and the duct sections and surfaces smaller, but even so, with entirely practical values, the temperature rise of the coolant, and the thermal drop from the duct surface to the coolant are much smaller than with gases.

In order to save space, in Table I only two petroleum oils are included: transformer oil and turbine bearing oil; transformer oil because either it or its equivalent, Pyranol, is a suitable coolant for the stator, and turbine bearing oil because it is used by some generator manufacturers as the bearing lubricant for large turbine generators. Oils are inferior to water as coolants, but greatly superior to gases. It should be noted that for the stator the velocity and volume of the coolant are controlled readily, and the temperatures are measured easily. Thereby the velocities can be raised, if need be, to insure turbulent flow.

It would be desirable to operate the rotor-cooling system in parallel with the lubricating system. Unfortunately, the viscosity of the bearing oil considered is such that the flow in the ducts probably would be laminar, and therefore the heat transfer rate would be lower then given in Table I, for which turbulent flow was assumed. Other petroleum oils have been given consideration, and it appears that some of them have possibilities. The low flash point and consequent fire hazard of kerosene prompted its exclusion, although it is excellent as a coolant.

Ethylene glycol plus an inhibitor is used extensively with water as an anti-freeze in automobile cooling systems. For this application it has splendid properties from the thermal standpoint. It is highly hygroscopic. It is listed in Table I for dilution with an equal weight of water. When a suitable inhibitor is added there should be extremely small corrosive action of the steel surfaces.

Some special silicones may prove to be suitable for the rotor, and studies of the properties of the 500 series** with about 2 centistokes kinematic viscosity were made. That and other silicones may warrant further investigation.

Without doubt, water is the best liquid coolant for the rotor from the thermal standpoint. The objection that may be raised is that it might cause corrosion or scaling of the steel surfaces. However, assurance has been given by a water-treatment expert chemist that, with a suitable inhibitor, and with the conditions obtaining in this application, such will be practically negligible. These conditions are

1. Only distilled or deionized water with proper inhibitor will be used.
2. It will operate only in a closed system.
3. The temperature of the liquid will not exceed 70 degrees centigrade in any place in the closed circuit.

The Reynolds number with water is so high as to insure desirable turbulent flow in the ducts.

In Table II are given the calculated temperature drops in a 100,000-kva 80 per-cent power factor 3,600-rpm turbine-generator rotor at full load, with water as the coolant. The velocity in the ducts is about six feet per second, and the total water volume about 0.69 cubic foot per second. The properties of the water are those for 20 degrees centigrade, which are less favorable for heat transfer than for higher temperature. (See Table I.)

It will be recognized that

1. The percentage drop through the insula-

‡ It is well known that to secure turbulent flow the Reynolds' number should be greater than about 2,000 to 3,000 for smooth ducts.

** This is the designation of the Dow-Corning Company.

tion is large because the I^2R loss per inch of length axially is higher than in a gas-cooled rotor. This means more ampere-turns and larger kilovolt-amperes for a given D^2L.

2. The small temperature rise of the coolant (2×1.3 degrees) means that the temperature axially for the full length of the rotor body is nearly uniform.

3. With the small mean drop in the teeth is associated a small difference radially, of the order of only 4.5 degrees centigrade. These two small (axial and radial) temperature differences mean that the steel and the copper temperatures are each nearly uniform throughout the embedded portions, although the copper is necessarily considerably hotter than the steel.

An important point is that with the large drop through the insulation there should be substantially uniform thermal conductivity of the insulating wall in order that this drop will not vary.

Temperature Distribution in and Deformation of Rotor Windings

Deformation of the rotor windings produced by the temperatures in combination with long lengths and large centrifugal forces, in gas-cooled machines, is brought out in three papers and in the discussions thereon.[1,2,3]

If the copper is preheated at standstill, or at very low speeds, so that full-load copper temperature is attained then, and the rotor then is brought up to speed, without change in temperature, after which the same, or nearly the same, temperature is maintained, and if the cooling, (that is, ventilation in gas-cooled rotors) is the same at very low speed as at full speed, and if the copper and steel temperatures are uniform (though different from each other) then there will be no deformation because of expansion or contraction of the copper. (This assumes that the copper is not bound longitudinally by adhesion to the slot sides, which experience indicates is not the case). Then the copper expands uniformly as a unit, for its entire radial depth (while at, or near, standstill), and there are no forces to alter the axial length after normal speed is attained.

These conditions cannot be met in large modern gas-cooled machines, because

1. Such machines, as built in the United States are provided with internal fans, and therefore the ventilation can not be the same running as at standstill.

2. The temperature distribution of the copper when running is not uniform either radially or axially.

The two conditions however, can be nearly met in liquid-cooled turbine-generator rotors. It will be recognized that for small changes in temperatures there is also a small internal stress in the copper (with no change in length) for which, even with soft annealed copper there should be no plastic deformation. (With soft copper the proportional limit is not clearly defined.) Thus, if we take conservatively the proportional limit of soft copper to be 5,000 pounds per square inch, the modulus of elasticity 15,000,000 pounds per square inch, then the strain at this stress is $5{,}000/15{,}000{,}000 = 0.00033$ inch per inch. For a coefficient of expansion of 0.000017 inch per inch per degree centigrade, the temperature change corresponding to this stress $= 0.00033 \div 0.000017 = 19.4$ degrees centigrade.

Table II. Thermal Drops in a Turbo-Rotor With Water as Coolant

	Degrees Centigrade	Per Cent
Mean temp. rise of liquid	1.30	1.89
Surface drop at ducts	1.20	1.74
Mean drop in steel in teeth	4.80	6.96
Mean drop through insulation wall	61.60	89.41
Total	68.90	100.00

According to calculations, with water as coolant, the radial differences of copper temperature can be kept to less than five degrees centigrade, and the calculated difference between the steel temperature at standstill and when running is of the order of only two degrees centigrade, assuming excitation for full load in either case. It seems highly probable that there should be no deformation with water as the coolant, with careful proportioning, and with proper preheating,* and with soft copper, provided the current in the rotor winding is maintained constant when running. This latter condition will be considered now.

If after attaining steady-state temperatures at full load, the load is decreased, one helpful procedure is to keep the rotor current from falling by allowing the reactive kilovolt-ampere to increase, and decreasing it on paralleled synchronous machines. Recognizing that this can be done generally only to a limited extent, another possibility is to decrease the rate of primary water in the heat exchanger, so as to increase the temperature of the entering coolant.

Thus, for the rotor whose thermal drops are given in Table II, if the load decreases from full load to 70 per cent, at the same power factor of 80 per cent, the rotor amperes being dropped accordingly to about 83 per cent of those at full load, and the primary water supply is decreased so as to maintain the same rotor copper temperature, but with higher steel temperature, the calculated steel temperature will rise from 7.3 to 26.6 degrees centigrade above the ingoing coolant temperature. (The steel temperature rise is taken as the copper rise — the drop through the insulation.) If centrifugal forces of the copper in the slots (pushing against the wedges, which expand axially with the steel), produce an axial elongation of the copper with the steel, the following are the results: Taking the linear coefficient of expansion of steel to be $11.5/10^6$ inch per inch per degrees Centigrade, the steel expands $(11.5/10^6)\ (26.6-7.3) = 222/10^6$ inch per inch. With the modulus of elasticity of copper of 15×10^6 pounds per square inch, the tensile stress in the copper because of this enforced elongation $= (222/10^6)(15 \times 10^6) = 3{,}340$ pounds per square inch.

This should be well within the proportional limit, but the question of creep and relaxation may arise. From data in a paper by Evan A. Davis,[5] the creep for 24 hours at a stress of 4,000 pounds per square inches and at 165 degrees centigrade is $1.91/10^4$ inch per inch. (165 degrees is considerably higher temperature than anticipated. All calculations are believed to be well on the safe side.) In a rotor 100 inches from the center line to the end of the rotor body this will cause a creep of 0.0191 inch,† and for 3,340 stress it is only about 0.016 inch, based on the assumption that the creep is proportional to the stress. During the relaxation period this creep will largely disappear, so that it is believed that there should not be any trouble from this source, even with soft copper, provided the precautions as given in the foregoing are observed. Further drop in kilowatts may be secured by increasing the reactive load. As an additional safeguard, hard-drawn copper may be used, as is the present practice, although that may prove to be unnecessary.

The Coates and Pyle[3] formula for computing the differential temperature between the copper and the steel is

$$\text{Temperature rise of the copper} - \frac{115}{170} \times \text{temperature rise of the steel}$$

where $115/10^7$ and $170/10^7$ are expansion coefficients of the steel and copper, respectively. Applying this equation for the above, the differential rise will de-

* Preheating is further considered under "Starting a Liquid-Cooled Turbine-Generator."

† The rotor body length for the 100,000 kva at 3,600 rpm is appreciably less than 200 inches.

crease from 63.9 to 50.9 degrees centigrade, or a change of 13 degrees, when the load is reduced to 70 per cent of full load. This change is considerably less than 19.4 degrees, corresponding to 5,000 pounds per square inches. The stress is $5{,}000 \times 13.0/19.4 = 3{,}340$ pounds per square inch the same as computed above.

It should be noted that the coolant temperature in no case should be elevated sufficiently to risk boiling when in the shaft bore near the turbine end where the pressure is below atmospheric pressure. At present it is believed that if the water temperature does not exceed 65 degrees centigrade, for which the vapor pressure is 3.62 pounds per square inches absolute, there should be sufficient margin. With the pressure at E (Figure 1B) of $14.7 + 2 = 16.7$ pounds per square inches absolute, and duct resistance drop of 20 feet (8.65 pounds per square inches), the pressure in L (Figure 1A) is $16.7 - 8.65 = 8.05$ pounds per square inches absolute, or considerably above 3.62.

Returning to the example, and referring to Table II, with reduced load and 83 per cent rotor amperes, the mean temperature rise of the liquid is raised from 1.3 degrees (for full load) to 22.5 degrees for the reduced load and the same copper temperature.

$$26.6 - (0.83)^2\ (1.2 + 4.8) = 22.5$$

If at full load the temperature of the liquid going into the rotor is 40 degrees centigrade, then at reduced load the temperature of the liquid at L (Figure 1 A)

$$= 40 + 22.5 + (0.83)^2(1.3)$$

$= 63.4$ degrees centigrade, which should be safe, as the boiling temperature for 8.05 pounds per square inches is 84 degrees centigrade

With hydrogen for the coolant, with high ratings at 3,600 rpm, and with the great effort that is being made to reduce the D^2L, there may be high local temperatures in the rotor copper, even with hydrogen at two atmospheres. It is the writer's opinion that recent large 2-pole rotors built in the United States with hydrogen cooling are not operated at as high average temperatures as those built in Great Britain for air cooling. However, those in this country are for 60 cycles, as contrasted with 50 cycles in England, and the recent maximum kilovolt-ampere ratings here are at least three times those for machines whose data appear in the Coates-Pyle paper. Is it not likely that in those very large American machines there is the possibility of serious deformation, even when wound with hard-drawn copper?

Coates and Pyle[3] state: "The temperature difference between the top and bottom turns was sufficient to discolor materially the bottom turns, the color change fading toward the top turns, which were the same color as when wound." One of the discussers (Horsley) stated: "The controlling factor is not the copper to iron temperature difference, but the temperature gradient in the copper in a radial direction." Another discusser (Kilner) told of the softening of hard-drawn copper.

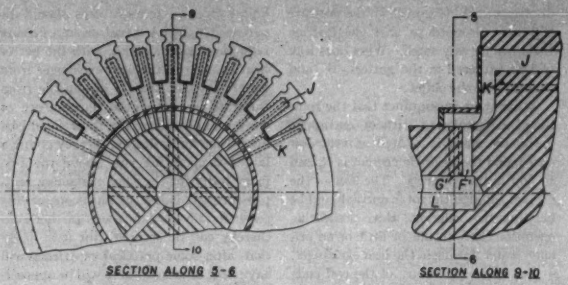

Figure 3. Alternative method for joining rotor ducts

At the present writing there is no intention to state what are the limits of either hydrogen- or liquid-cooled rotors. But it seems evident that dangers from deformation can (with reasonable and relatively simple precautions, as given previously) be eliminated from a liquid-cooled rotor. Also, short-time large changes in rotor current will not cause deformation, owing to the storage of heat in the copper. These statements are for soft copper, and limits as to change in rotor current are greatly increased with hard-drawn copper.

Some years ago an experimental and analytical study was made of ventilation of turbine-generator rotors. While a report was written, the findings were not published. It is beyond the scope of this paper to go into lengthy explanations of the factors that are productive of inequalities of distribution of gas volumes, as an entire paper could be written on that subject. It is unfortunate that, while in operation under load there is no practical means for measuring the rotor copper and steel temperatures at selected points, as on stationary apparatus. While it may be possible to obtain an approximate estimate of the gas volumes for each radial vent duct and the volumes in the axial ducts, the highly turbulent states and resultant uncertain heat transfer rates, together with the complex heat flow, make the calculation of local temperatures well-nigh impossible.

It is interesting that the temperatures produced by the I^2R loss may be measured at selected points in a liquid-cooled rotor at standstill, with results that are within a small percentage of those at full load. (Precautions to avoid pitting of the collector rings must then be observed.)

Starting a Liquid-Cooled Turbine Generator

The following procedure is suggested at this time:

In a new machine, initially all ducts are filled with air. The insulating liquid coolant for the stator is caused to circulate with the aid of the external pump, there being a suitable vent outside to allow air to escape; (later a valve in the vent is closed to prevent escapement of liquid). It is advisable to cause the liquid to enter a vacuum tank, or other deaerating device, before it passes into the stator, so as to exclude the air. Moisture should be removed also, as is the usual practice with transformers. The suggestion is offered to have instruments to indicate the pressure and volume of flow at all times. The coolant should be in the stator long enough to insure that it has penetrated the insulating walls before the machine is started.

Hydrogen should be introduced around the rotor and maintained for a sufficient length of time for it to penetrate the rotor's insulating walls. With the rotor stationary, the rotor coolant should be circulated long enough to insure the expulsion of air everywhere, the initial procedure being similar to that for the stator. If water is the coolant, it should be distilled or de-ionized and treated with a suitable inhibitor. The volume of liquid per unit of time at standstill will be less than when running. The pressure needed for driving the liquid through the ducts at standstill is not large, and suitable gaskets are provided between plates C and D (Figure 1B) to eliminate leakage, or reduce it to a very small amount. At the

discharge at N' (Figure 1A), the pressure will have dropped so that the leakage there will be very small. What does leak will be gathered in the gutters, W, and drained into the outlet.

When there is assurance that the rotor liquid is circulating without entrapped gases, the rotor is rotated at very low speed, and then electric current is caused to flow in the windings. The flow of the coolant through the rotor ducts should be maintained. During this preheating operation there should be little or no primary water flowing in the heat exchanger, so that the temperature of the coil ends will not differ greatly from that of the embedded parts. The resistance of the winding should be measured by voltmeter-ammeter method at various times, and it is advisable to have a continual check on the resistance when at full speed. The temperatures of the ingoing and outgoing liquid should be recorded also on a chart.

When full-load rotor copper temperature is attained, the rotor should be brought up to speed, care being taken to adjust the excitation so as not to generate too high voltage. The generator should be synchronized rapidly and loaded, so that there will not be a large change in rotor temperature. The flow of primary water in the heat exchanger should be started or increased when full speed is approached. As previously pointed out, small temperature changes will not produce plastic deformation of the copper. If future experience so dictates, the deaerator may be bypassed; similarly for the stator deaerator.

Notes on Size of Machine

Attempts have been made to compare the calculated rotor and stator diameter squared times length for 100,000 kva, 80-per-cent power factor, 13,800 volts, 3 phase, 60 cycle for 1,800 and 3,600 rpm for liquid-cooled machines with hydrogen-cooled machines at one and at two atmospheres. It is believed that the designs of the liquid-cooled machines are conservative; the calculated rotor temperature rises above the ingoing liquid for 3,600 rpm are given in Table II. For this speed the calculated short-circuit ratio is 0.83. The D^2L's are around 80 per cent of those for hydrogen-cooled machines for two atmospheres, or about 66 per cent of hydrogen cooled generator for one atmosphere.

It should be noted that the limitation is not the average rotor copper temperature, but the maximum rotor temperature. With the small differences in copper temperatures, in liquid-cooled machines, higher average temperatures should be permissible, which would mean a further reduction in D^2L. Also, with the better heat transfer in the heat exchanger from water to water than is obtainable from water to hydrogen, the temperature of the coolant entering the rotor should be lower than for hydrogen, thereby giving a larger temperature rise above the primary water for the same maximum temperature. It is beyond the scope of this paper to indicate how much further gain thereby can be secured, but it is likely that, after some practical experience will have been obtained, there will be appreciable further reductions in D^2L.

Comparison of Constructions for Hydrogen- and Liquid-Cooled Machines

For a given D^2L, there are some added costs, and some reduced costs of liquid-cooled generator contrasted with hydrogen-cooled, as follows:

Liquid-cooled machine reduced costs:

1. Omission of internal fans.
2. Omission of internal end-bell walls.
3. Omission of large internal coolers (heat exchangers).
4. Omission of multiplicity of vent ducts for stator and rotor.
5. Omission of duct work for flow of coolant to and from internal heat exchanger.

Liquid-cooled machine added costs:

1. Machining of ducts in rotor (nearly offset by machining of rotor vent ducts for hydrogen).
2. Welding of ducts and casings (Figures 1A, 1B, 2 and 3) which must be leak-proof.
3. Micarta cylinder (or equivalent) in stator bore added.
4. External heat exchangers for stator and rotor, and internal heat exchangers R and R'. (These will be offset probably by the internal heat exchanger for hydrogen.)
5. Pumps and deaerators for both stator and rotor.

The writer is unable at present to give a comparison in dollars, but he is of the opinion that for equal D^2L there will be little difference in first cost. But the smaller D^2L for liquid-cooled machine should make the cost appreciably lower, nearly in proportion to the D^2L. Of course, the reduction in floor space is important to the power company.

A Few Notes and Acknowledgments

Thought has been given to liquid cooling for many years. The writer first began giving serious consideration to practical means for constructing liquid-cooled turbine generators after reading a paper by A. B. Field,[6] who suggested the use of the insulating cylinder in the stator bore, and an insulating liquid for the stator coolant. No machines, nor models of machines, so far have been constructed according to descriptions in this paper.

Doctor S. H. Mortensen, commenting upon an address on liquid cooling at a meeting of the Edison Electric Institute Electrical Equipment Committee in May 1946, pointed out that while liquid cooling "might appear rather radical, the initiation some years ago of hydrogen, rather than air, cooling was likewise looked upon as a radical step." He remarked that "while the present proposal will require a great deal of effort and much research, it may well mark the beginning of a new period in turbogenerator development."

It is the writer's opinion that two models should be constructed and tested in order to check the calculations. One should simulate the rotor's hydraulic circuit, and the other the rotor's heat circuit. The hydraulic model would be advisable in order to make certain that the hydraulic system will function properly in a large generator. The expense of constructing and testing such a model would be relatively small. It could be built of pipes and plates, suitably fabricated, to which a limited amount of machining would be added.

In the hydraulic model, and perhaps in the first machine, the determination of the rate of flow as affected by the diameter of the orifices at the outlet from the shaft, could be obtained by means of orifices of several diameters drilled into plugs that would be screwed successively into the shaft.

References

1. Prevention of Rotor-Winding Deformation on Turbogenerators, **John G. Noest.** AIEE Transactions, volume 63, 1944, July section, pages 514–19.

2. Deformation of Turbo Alternator Rotor Windings Due to Temperature Rise, **G. A. Juhlin.** *Journal* Institution of Electrical Engineers (London, England), 1939, pages 544–52.

3. The Operation of Large Turbo-Alternators to Reduce Rotor Winding Deformation, **R. H. Coates, B. C. Pyle, and Discussers.** *Journal* Institution of Electrical Engineers (London, England), part II, 1946, April section, pages 192–212.

4. Heat Transmission (book), **W. H. McAdams.** Second edition, McGraw-Hill Book Company, Inc. (New York, N. Y.), 1942. Page 158.

5. Creep and Relaxation of Oxygen Free Copper, **Evan A. Davis.** *Journal of Applied Mechanics* (New York, N. Y.), June 1943, pages 101–5.

6. Large Alternators, **A. B. Field.** *Transactions* of the First World Power Conference, volume III, 1924, pages 791–806.

Discussion

S. H. Mortensen (Allis-Chalmers Manufacturing Company, Milwaukee, Wis.): C. J. Fechheimer's paper presents a number of interesting features obtainable by substituting liquid cooling for gas cooling in large turbogenerators. Some years ago a European firm designed and built turbogenerators with water-cooled rotors. However, as the design proved costly the project was abandoned. The author demonstrates advantages accruing from the use of water or oil for cooling generators. A number of features mentioned in the paper invites discussion but for reasons of time and space limitations the following remarks are limited to some of the mechanical features in the author's proposed 3,600-rpm generator design. The possibility of obtaining smaller and lighter generators with liquid cooling is demonstrated as is the possibility of building machines of very large capacities with present-day materials. This feature will become increasingly important as requirements for generator capacities exceeding those obtainable with high pressure hydrogen cooling arises. For the time being, however, it appears that the simple hydrogen-filled generator operating with gas pressures of 15 pounds per square inch or higher can be built for capacities well over 100,000 kw and fulfill all requirements encountered so far.

To compete in ratings that come within the range of hydrogen ventilation the liquid-cooled machine must show lower costs, not only of required materials but also of labor involved. To this end the mechanical construction of generator parts should be as simple as possible. In the proposed design a number of features are involved which might cause difficulties; for example, machining the longitudinal cooling ducts through the rotor teeth represent a problem. Drilling holes through a long rotor without excess drill run-out could not be accomplished with common shop practice. If, instead of drilling, the ducts were obtained by planing, the moisture-tight closing of the top of the duct by welding hardly might be considered the best engineering practice in highly stressed rotors. The use of nonmagnetic tubes in the stator bore would introduce difficulties with installing the rotor without injuring the tube. Further a reliable oil seal between the end of the tube and the stator end covers would not only be costly but also a possible source for oil leakage which in turn might cause outages. The oil seal proposed at the inner end of the bearing will require an elaborate design to insure against oil getting from the bearing into the machine and saturating the rotor. Furthermore, if the rotor is hydrogen-cooled as proposed, the hydrogen seal required between the shaft and stator end cover will be located in a position most difficult for assembly and inspection. The usual complement of seal- and hydrogen-control auxiliary would be required also. The use of hydrogen requires an explosion-safe generator construction which would introduce difficulties with the use of a nonmagnetic tube in the air gap.

The above are some of the features in the proposed design that is suggested to the author for further consideration both from an engineering and cost point of view.

The proposed design needs simplification but so did a great many of the complex solutions suggested during the past 50 years to turbogenerator designers for turbogenerator improvements.

It would be possible to build generators along the lines suggested by modifying some of the ideas set forth by Fechheimer. However, the proposed construction based upon present-day shop practice would be so expensive as to limit the application of this type of cooling to generators of capacities too large for gas cooling or to installations where space requirements are at a premium. However, further developments also may alter this condition.

M. D. Ross (Westinghouse Electric Corporation, East Pittsburgh, Pa.): The design proposed in C. J. Fechheimer's paper brings up many interesting features which deserve study. The use of liquid cooling for the stator of a rotating machine is, so far as I know, something that has not been tried in actual practice. Liquid cooling of the rotor was tried in Europe about 25 years ago but was abandoned because of certain difficulties in these early machines. I would be interested to know whether Fechheimer has investigated these early liquid-cooled rotor designs and whether his design overcomes the problems encountered in the earlier designs.

When the idea of using hydrogen as a cooling medium was advanced in the early twenties, a number of problems had to be overcome before a commercial product could be produced.

These problems included suitable sealing glands, a gas-tight enclosing structure, gas coolers, and suitable gas metering and control equipment. Solution of those problems covered a period of over ten years and involved a very considerable development expense by the manufacturers before hydrogen-cooled turbine generators were put in operation. The design for the liquid-cooled machine would seem to entail solving as many problems as were involved in the development of hydrogen cooling. Whether the reduction in size would justify the development expense involved is a debatable item.

In evaluating the gains in reducing the size of the generator it should not be lost sight of that further reductions in size from those now established for hydrogen-cooled designs probably will involve increases in generator losses. We are already at the point in the design of hydrogen-cooled machines where increasing the output will increase the losses faster than the output increase, resulting in a lower efficiency.

So far as the United States is concerned, there has been little tendency to distribute large blocks of power at voltages up to 33 kv direct from the generator as is done in Europe in many cases. It usually has been found more economical to generate at voltages up to 16 kv and step up the voltage through a transformer than to generate at voltage without the transformer. Should this condition change in this country, the oil-insulated stator would certainly be a help in designing suitable high voltage windings.

Fechheimer should be congratulated on the very thorough way in which he has discussed the problem of liquid cooling, and the suggestion made here should stimulate further analysis of this type of design.

H. D. Taylor (General Electric Company, Schenectady, N. Y.): The considerable reduction in dimensions and weight of the active material in turbine generators claimed by C. J. Fechheimer undoubtedly can be achieved by liquid cooling somewhat along the lines he describes. Also such other advantages as uniformity of temperatures in both rotor and stator seem quite reasonable to expect. Numerous studies of various forms of liquid cooling have been made in the past, and these ideas were promoted actively within the General Electric Company by the late Henry M. Hobart, who was quite an enthusiast on the subject. Actual trials have been made from time to time. Tests on a water-cooled turbine-generator rotor made in 1915 are described in D. S. Snell's discussion of this paper. In 1926 tests were made in Schenectady on an oil-cooled stator arranged with an insulating cylinder in the air gap. This machine functioned quite satisfactorily, but the development did not proceed farther at that time, partly on account of the fire hazard, and partly because no demand developed for the extra high generator voltages originally contemplated. The development of Pyranol would now eliminate the fire hazard. A quite different type of liquid cooling was applied to one of the first large 3,600-rpm generators made by General Electric Company, a 50,000-kva unit for the Logan Station of the American Gas and Electric Company, installed in 1937. In this machine, the usual gas ducts in the stator core were replaced by water-cooling pads, through which distilled water was circulated, with a heat exchanger in the external circuit. The rotor runs in hydrogen. This unique generator has operated very satisfactorily for nearly ten years. This construction has not been repeated because its manufacture was not economical, and the more conventional hydrogen-cooled machines proved entirely satisfactory.

The present cooling system used on hydrogen-cooled machines is basically simple,—all the heat being gathered by one medium. Fechheimer's proposal involves three media: oil for the stator, water for the rotor body, and hydrogen for the air-gap and rotor ends. The complicated construction required inside the machine, and the additional auxiliary equipment required outside, for such a combination, would involve not only a substantial cost increase to offset the reduction in active material of core and coils, but would offer numerous opportunities for operating troubles, such as leakage inside the machine, failure of the auxiliaries, or inaccessibility for inspection and service. In short, it appears doubtful to the write whether the gains to be realized would be worth the complications and the possible sacrifices in reliability, which after all is probably the most important quality required in these large generators. Much more developmental work and actual service experience would seem to be necessary before liquid cooling can be adopted generally for turbine generators.

E. D. Huntley (General Electric Company, Schenectady, N. Y.):

1. In the event of a leak in the rotor-cooling circuit, or if for some other reason water is shut off, what kilovolt-ampere capacity in per cent of rating could be expected?

In the beginning considerable importance was attached by some to this factor for air operation of hydrogen-cooled generators. With the proved reliability of hydrogen-cooling systems less emphasis is now being placed on this factor.

2. From reading the paper, I am not sure whether the author is recommending preheating of liquid-cooled generators because of necessity or because the features of liquid cooling render it more feasible. With liquid cooling capitalized to give approximately double the temperature drop between conductor and rotor body although having nearly uniform radial and axial conductor temperature, is it expected that preheating would be necessary?

On the basis of experience obtained during the last five to ten years it is the general feeling that old very large gas-cooled machines, having so-called soft rotor conductors, will be kept out of trouble by preheating, even with frequent starts and stops. With machines of up-to-date design having conductors with improved physical properties obtained by alloying and some degree of cold work and with further progress realized in obtaining more uniform temperatures, preheating is considered beneficial but not necessary.

D. S. Snell (General Electric Company, Schenectady, N. Y.): The great advantage of liquid cooling over gas cooling for the rotors of turbine generators has long been recognized, and many attempts have been made to obtain a practical design that would permit the utilization of this type of rotor cooling. One of the earliest attempts along this line was made by General Electric Company in 1915, when a 7,812-kva 80-per-cent power factor 1,800-rpm turbine generator was built with a water-cooled rotor. This machine was tested at the factory both with air cooling and with water cooling with results which clearly proved the efficacy, although not the practicability, of this type of cooling for generator rotors. Some of the results of these tests and the conclusions obtained therefrom are presented in this discussion.

The construction of the water-cooled rotor is partially illustrated in the sectional view in Figure 1 of this discussion. Sixteen $1^1/_4$-inch diameter axial holes were provided in the rotor body below the coil slots through which the cooling water was circulated, these holes being supplied from a $3^1/_4$-inch hole in bore of shaft through 16 connecting radial holes located at the turbine end of the rotor body; the discharge from the axial holes was carried to an annular space at bore of shaft through 16 other radial holes, located at the collector end of rotor body. Water was supplied to the $3^1/_2$-inch hole in shaft bore through a pipe entering from the collector end, the end of this pipe inside the bore carrying a friction seal against the bore surface. The annular space around the feed pipe, between seal and collector end of shaft, provided a passage for carrying to the outside the water discharged from the axial holes.

The principal data from the heating tests

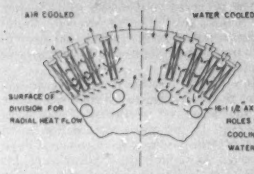

Figure 1. Partial cross section of a water-cooled rotor for a 4-pole 7,812-kva 1,800-rpm turbine generator, showing paths for heat flow from winding to the cooling medium for rotor cooled with air and for rotor cooled with water

on this generator, made both with air cooling and with water cooling, are summarized in Figure 2 of this discussion. The temperature rise of the field winding by resistance and of the armature winding and iron by temperature detectors from the tests are shown for different intensities of loss on the outside surface of field or armature coil. These temperature rises are all given with respect to the temperature of ingoing cooling water, the rises with air cooling having been reduced to this basis by assuming that a surface air cooler is provided and adding to the measured temperature rises above inlet air an assumed difference of seven degrees centigrade between inlet air and inlet water. The tests with water cooling were all made with the same water velocity (0.34 foot per second) in the axial holes.

It is shown in Figure 2 of this discussion that for a loss intensity on field coil surface corresponding to rated field current in air, the use of water cooling in place of air cooling reduced the average temperature rise of the field winding above inlet water by about 20 degrees centigrade, while for the same temperature rise of field winding as at rated load in air, water cooling of the rotor would permit an increase of about 28 per cent in watts per square inch of field coil. For the armature there is also a reduction in temperature rise of the winding and iron when water cooling is supplied for the rotor, because of the reduction in the temperature rise of the air in the air gap effected through water cooling of the rotor.

The considerable reduction in temperature of the rotor winding of the test generator effected with water cooling may be explained readily by calculating the different temperature drops in the thermal circuit for the two conditions shown in Figure 1 of this discussion. Considering two tests with the same kilowatts input to the field winding, the one made with air cooling, the other with water cooling, the calculated temperature rise of the body part of field winding with air cooling was 90.3 degrees centigrade above inlet air and with water cooling 60.2 degrees centigrade above inlet water. With air cooling the calculated temperature drops were as follows:

Insulation—33 degrees
Tooth iron—11 degrees
Gap surface—17.2 degrees
Air rise plus rise from pole face loss—29 degrees

With water cooling the calculated temperature drops were

Insulation—30 degrees
Tooth iron—16 degrees
Water film—14.2 degrees

It will be apparent from this analysis that the rotor temperature with water cooling could have been reduced further had it been possible to obtain higher water velocities in the axial ducts, thus reducing the drop in water film; also the provision of cooling ducts in the rotor teeth, as well as below the slots as suggested by Fechheimer, would have eliminated most of the drop in tooth iron. However, trouble was experienced in the operation of the test machine because of entrapment of air in the water passages, causing unbalancing of the rotor, and making higher velocities unobtainable; and no practical method was thought of for providing passages for the cooling water in the rotor teeth.

The tests on the generator provided with water-cooled rotor confirmed the view that substantial gains in output from a given weight of material are possible with liquid cooling, but also revealed many obstacles to the practical application of this cooling method, obstacles which up to the present have appeared to be insurmountable. Also, considering that the principal temperature drop in the thermal circuit of the rotor, the drop in insulation, is reduced by nearly one half by the use of hydrogen in place of air as the cooling medium, the use of liquid cooling for the rotor interior to obtain a reduction in the remaining temperature drops at present does not appear to offer sufficient advantage over the use of hydrogen cooling for both interior and exterior of the rotor to offset the complication involved.

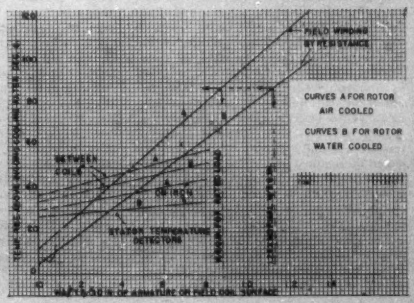

Figure 2. Temperature rise of field winding by resistance and of armature by temperature detector for different watts per square inch of armature and field coil for a 7,812-kva 1,800-rpm turbine generator with rotor arranged for water cooling. From tests with rotor air cooled and with rotor water cooled. Temperature rises with air cooling given above water entering surface coolers

C. J. Fechheimer: Attention has been called by M. D. Ross and S. H. Mortensen to the fact that liquid cooling of turbine-generator rotors was tried in Europe, and H. D. Taylor and D. S. Snell inform us that it was tried in 1915 at the company with which they are associated. I presume that the European machines were built by the Parsons Company. Figure 3 of this discussion is a photograph from the Parsons British patent number 16,986 of 1914. It appears evident that the General Electric experimental rotor construction was the same as Figure 3, except for a detail of the cooling ducts.

Replying to D. S. Snell, it was because the seriousness of air getting into the water passages was recognized that I provided for its prevention, first by using a deaerator while at rest, and second, when running, by draining out air through the small tube, shown in Figure 1 in the paper. I am quite certain that it was not air entrapment alone that prevented securing of a higher water velocity. Before the water emerges it must flow through the annular channel, *n*, (Figure 3 of this discussion), between the bore in the shaft and the external surface of the pipe. The water enters this region in an axial direction, but the circular movement at the shaft's bore soon causes the water to move in a helical path, and the pitch of the helices becomes very short before the water leaves the annular channel. The effect is to create high fluid resistance which opposes the flow, and this is the principal reason why the water velocity was so low. The temperatures were consequently higher than they should have been.

Another reason why there was not a greater gain over the air-cooled rotor was that the distance that the heat had to flow to the ducts was greater than desirable. Snell recognizes the importance of having ducts in the teeth in addition to those below the slots, and states that most of the thermal drop in the teeth thereby would have been eliminated. Yet, with all these unfavorable conditions, about 28 per cent more watts per square inch were obtainable than with air cooling. I estimated that for the same temperature rise as in that test, about five times as high watts per square inch are obtainable with my proposed water cooling as in the experimental rotor with water cooling.

Other objectionable features in the Parson's construction are that the inner rubbing seal *w* (Figure 3 of the discussion) would be liable to become troublesome, and the radial holes *h* become too crowded near the shaft bore. There was not a sufficiently great reduction in temperature to warrant its use.

Snell stated that "the principal drop in the insulation is reduced by nearly one half by the use of hydrogen in place of air." In the calculations of the liquid-cooled rotor in a hydrogen atmosphere I have assumed that the thermal conductivity of the insulation is increased by 50 per cent over that in air, which figure is based upon some early tests. If the conductivity is as high as Snell states, there would be further improvement and the D^2L could be reduced more.

Mortensen believes that there may be difficulty in machining the longitudinal ducts and welding them subsequently in the rotor. An experienced manufacturing engineer told me that they could be cut readily on a milling machine, but not on a planer. An authority on welding stated that the welding for the ducts in the teeth does not present difficulties. It is doubtful whether the stresses are increased thereby, and in case of doubt, relief can be secured by heating after welding. The sections in the teeth are such as to secure lower stresses adjacent to the ducts than at the bottom of the teeth.

When installing the rotor, the nonmagnetic tube should be protected with metal or other material, which subsequently could be removed. I disagree about the high cost of the seal at the end of the tube, and I see no reason why it cannot be made leakless. There is now an oil seal at the end of a bearing in a hydrogen-cooled generator, and its relation to the hydrogen gland is the same in the design that I propose. Windows in the structure not shown in the drawing, would admit of inspection of the outside of the gland seal, and parts adjacent thereto. The present hydrogen-cooled generators are as inaccessible as the proposed liquid-cooled generators would be; yet they are considered to be safe.

If the parts that enclose the hydrogen are to be explosion-proof, that is a far simpler problem than in the large diameter stators with hydrogen on the inside, in which the enclosing end bells must be curved and ribbed, and constitutes a rather expensive construction. The forces acting on the enclosing end in a liquid-cooled generator are much lower, as the diameter is smaller. The stress produced in the nonmagnetic tube in the event of an explosion in the 100,000-kva 3,600-rpm generator, with an internal pressure of 100 pounds per square inch, and 0.75-inch thick tube, would be only 2,600 pounds per square inch.

I do not believe that the criticisms about high cost are justified. There are some items that will cost more and some less than for hydrogen cooling. In the comparison in the paper I failed to include the lower cost of the outer end bells referred to above. The auxiliaries for the liquid-cooled generator are small and should not be costly.

Answering H. D. Huntley, there necessarily would be a large reduction in capacity if the water is shut off. After a little experience, the liquid-cooled generator should prove to be at least as reliable as one cooled with hydrogen. I believe that preheating is important for a large rotor with a large number of ampere-turns, in order that the copper will have expanded to the same dimensions at or near standstill, as would correspond to the temperatures when running.

H. D. Taylor's comments on the work of the late eminent H. M. Hobart, and upon the tests on an oil-cooled stator are very interesting. His remarks about the complications and auxiliaries remind me that we accept complications and auxiliaries for large steam boilers and steam turbines. Also, we do not now know how well the very large hydrogen-cooled generators at two atmospheres will withstand the test of time.

The efficiency of a liquid-cooled turbine generator probably would be about the same as one cooled with hydrogen. In the latter the maximum efficiency occurs at an appreciable overload, for which the constant and variable losses are equal. Hence a decrease in constant losses and increase in variable losses would lower the maximum efficiency point. This would apply to the liquid-cooled machine, the iron and windage losses being decreased, and the I^2R and stray losses being increased.

Experience has shown that two paths for the air were insufficient for large stators. In the rotors, however, there is no feasible way to increase the number of parallel paths, and regardless of size, the cooling gas enters only at the two ends. The ducts in the teeth or below the slots can not be made of sufficient cross section for cooling long rotors, especially those with deep slots and large I^2R loss. The gas temperature is then too high as the middle of the rotor is approached to be effective for cooling. Yet it is the cooling in those ducts which must be depended upon to help secure an approximation of uniform temperature radially. With water the heat absorption per degree rise is so large that the coolant's temperature rise is very small. (See Tables I and II of the paper.)

Since writing the paper a few minor points have occurred to me as follows:

The calculations of the 100,000-kva, 3,000-rpm generator were based upon very conservative assumptions. If the water volume were reduced to one half, the total temperature rise of the rotor copper would be increased by only about 3.5 degrees, and the fluid resistance drop would be decreased to about 5 feet. The pressure in the shaft bore near discharge then would be nearly atmospheric.

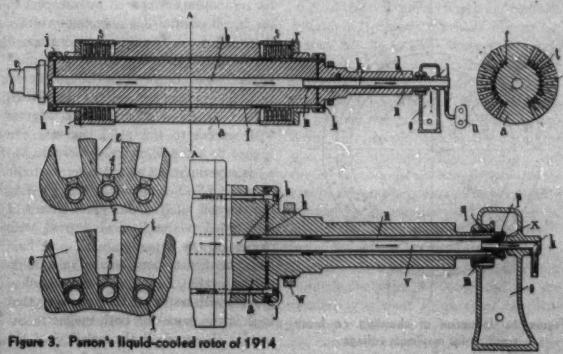

Figure 3. Parson's liquid-cooled rotor of 1914

It may be advisable to attach stationary gutters to the plate D, like W, at the turbine end, so that the water that might leak between the shaft bore and the plate C, with the rotor stationary, can be caught and drained back into the system.

Difficulty might be experienced in drawing up the bolts which secure the insulating tube a to the flange Z. These two parts could be fitted firmly to each other and held together with bolts, without a gasket between them. A gasket then can be placed at the end and held securely with a steel ring suitably bolted in place.

It is important to note that in the proposed construction there are no rubbing seals, such as are liable to be troublesome.

The Multistage Rototrol

M. M. LIWSCHITZ
MEMBER AIEE

THE amplidyne is a 2-stage amplifier with a pole ratio of 1:1; that is, in the amplidyne both stages of amplification have the same number of poles. Another kind of a 2-stage amplifier, is the 2-stage Rototrol. This new type of 2-stage amplifier has a pole ratio of 1:2. It is the aim of this paper to describe a multistage Rototrol, an amplifier with more than two stages of amplification. It will be shown that a 4-pole d-c machine may be adapted to operate as a 3-stage amplifier with pole ratios of 1:1:2, and that, in general, a d-c machine with p poles may be made to operate as a $(p\text{-}1)$-stage amplifier.

Possible Number of Stages of Amplification

A rotating amplifier with m stages of amplification contains m magnetic circuits interlinked with a single armature. The m magnetic circuits having in part different number of poles should not interfere with each other; that is, the iron should have no saturation. It is evident that the number of brush studs necessary for all magnetic circuits will be a minimum, namely, equal to that necessary for the magnetic circuit with the largest number of poles, and that the arrangement for good commutation will be the simplest if the brush studs necessary for the different magnetic circuits are made to coincide. The conditions under which this occurs and also the maximum possible number of stages of amplification will be discussed.

The winding used is a lap winding, without equalizers. The coil pitch is made equal to the pole pitch of the magnetic circuit with the largest number of poles. The winding is then fractional-pitch (chorded) with respect to all other magnetic circuits.

In general, for a full-pitch winding, the coil pitch is equal to $360/p$ mechanical degrees; the lower layer is moved with respect to the upper layer $360/p$ mechanical degrees, and the brush position for maximum voltage is shifted $180/p$ mechanical degrees with respect to the pole axis. When the winding is chorded β mechanical degrees, the coil pitch is equal to $(360/p-\beta)$ mechanical degrees; the lower layer is moved with respect to the upper layer $(360/p-\beta)$ mechanical degrees, and the brush position for maximum voltage is shifted $(180/p-\beta/2)$ mechanical degrees with respect to the pole axis. Consider Figure 1 which shows a 2-pole magnetic circuit and a chorded armature winding. Upper and lower layers of only one path are shown. The chording is β degrees and the brush position for maximum voltage is shifted $(90-\beta/2)$ degrees with respect to the pole axis. If a position of the brushes is assumed other than that shown in the figure, it will be found that the electromotive force is smaller than for the position shown. Also it will be found that when the brushes are in the position ab, the electromotive force induced between them is zero; that is, the brush position for zero voltage is shifted with respect to the brush position for maximum voltage by $2(180/p-\beta/2)$ mechanical degrees.

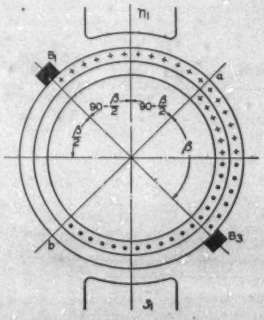

Figure 1. Influence of chording on brush position for maximum voltage

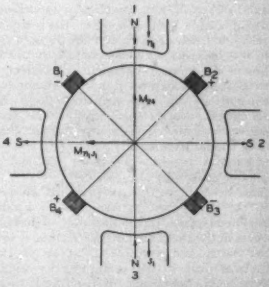

Figure 2. A 2-pole magnetic circuit superimposed on a 4-pole magnetic circuit

In Figure 1 the chording β is assumed 90 mechanical degrees and the brush position for maximum voltage is shifted $(180/2-90/2) = 45$ mechanical degrees with respect to the pole axis n_1s_1. In Figure 2, a 2-pole magnetic circuit (n_1-s_1) is superimposed on a 4-pole magnetic circuit ($NSNS$). Because the winding has the coil pitch of the 4-pole circuit, it is chorded 90 mechanical degrees with respect to the superimposed 2-pole flux, and the brush position for maximum voltage is $(180/2-90/2) = 45$ mechanical degrees with respect to the poles n_1s_1; that is, it is the same for both magnetic circuits. However, if the polarity of the

Paper 47-96, recommended by the AIEE committee on electric machinery for presentation at the AIEE winter meeting, New York, N. Y., January 27-31, 1947. Manuscript submitted September 18, 1946; made available for printing December 10, 1946.

M. M. Liwschitz is professor of electrical engineering at Polytechnic Institute of Brooklyn, Brooklyn, N. Y. and is also consulting engineer for Westinghouse Electric Corporation, East Pittsburgh, Pa.

The author expresses his appreciation to H. S. Kirschbaum of Westinghouse Electric Corporation for calculation of the example and of Figure 8 in the text.

brushes B_1 and B_3 is minus with respect to the 4-pole magnetic circuit, it is for these brushes minus and plus, respectively, with respect to the superimposed 2-pole magnetic circuit.

The superimposed 2-pole flux (Figure 2) does not induce an electromotive force between the brushes B_2 B_4, because these brushes are moved $2(180/2-90/2) = 90$ mechanical degrees with respect to the brushes B_1 B_3. In general, the smallest number of field coils will be necessary in the amplifier, when each magnetic circuit is arranged to induce voltage between as many brushes as it has poles. This is achieved when all magnetic circuits are symmetrical with respect to the armature winding; that is, when for each magnetic circuit all armature paths have the same number of turns.

Consider the magnetic circuit with the largest number of poles p_1. Because for this magnetic circuit the winding is full-pitch ($\beta=0$), the distance between pole axis and brush axis (for maximum voltage) is $\alpha_1=180/p_1$ mechanical degrees. The width of an armature path, in each layer, is $b_1=360/p_1$ mechanical degrees. For any other magnetic circuit with p_2 poles ($p_2<p_1$) with respect to which the armature winding is symmetrical, the width of an armature path in each layer, is $b_2=360/p_2$ mechanical degrees, and, therefore, the chording is $\beta_2=b_2-b_1=360(1/p_2-1/p_1)$ mechanical degrees. The distance between pole axis and brush axis (for maximum voltage) is for this magnetic circuit

$$\alpha_2=\frac{180}{p_2}-\frac{\beta_2}{2}$$
$$=\frac{180}{p_2}-180\left(\frac{1}{p_2}-\frac{1}{p_1}\right)$$
$$=\alpha_1$$

It is the same as for the magnetic circuit with the largest number of poles.

The superimposed 2-pole flux n_1 s_1 in Figure 2 produces a voltage between the brushes B_1 B_3. The load circuit is connected to the brushes B_1 B_3 and B_2 B_4. The voltage induced between the brushes B_1 and B_3 by the 2-pole flux n_1 s_1 produces a circulating current through the armature and these brushes. The axis of the armature magnetomotive force $M_{n_1 s_1}$ resulting from this circulating current coincides with the axis of the poles 2 and 4 and produces a second superimposed 2-pole flux. This flux induces an electromotive force between the brushes B_2 B_4 which are brushes of same polarity with respect to the 4-pole flux *NSNS* and the load circuit. Therefore, a second circulating current will flow through the armature,

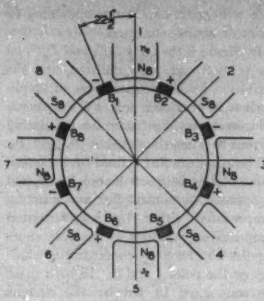

Figure 3. A 2-pole magnetic circuit superimposed on an 8-pole magnetic circuit

but this one will flow over the brushes B_2 B_4. The armature magnetomotive force M_{24} produced by this circulating current has its axis along the axis of the flux n_1 s_1 and counteracts this flux. The armature magnetomotive force M_{24} must be compensated as exactly as possible. If the circulating current between the brushes B_2 B_4 (Figure 5) is used to excite the field coils of the 4-pole magnetic circuit, the 4-pole machine, Figure 2, is able to operate as a 3-stage amplifier with the following three stages of amplification:

1. Control coils producing the 2-pole flux $n_1 s_1$ and the armature between brushes $B_1 B_3$.

2. 2-pole flux produced in the axis of the poles 2 and 4 by the circulating current between $B_1 B_3$ and the armature between brushes $B_2 B_4$.

3. 4-pole flux excited by the circulating current between $B_2 B_4$ and the armature between brushes $B_1 B_3 B_2 B_4$.

The connections of the field windings are shown in Figures 5 and 6.

If control coils are arranged on the poles 1 and 5 of the 8-pole machine, Figure 3, a 2-pole flux n_2 s_2 will be superimposed. This flux induces an electromotive force only between the brushes B_1 B_5. Because these brushes have the same polarity with respect to the 8-pole flux, a circulating current will flow in the armature over these brushes. The armature flux caused by the circulating current has its axis in the pole axis 3–7. The circulating current B_1 B_5 can be used in order to excite another 2-pole or 4-pole superimposed flux giving one more stage of amplification. In this case the armature flux through the poles 3–7 produced by the circulating current B_1 B_5 must be compensated. Instead of using the circulating current for feeding of field coils, the

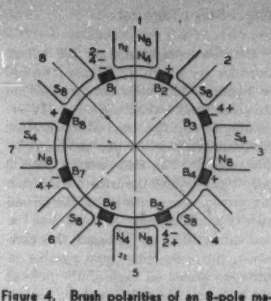

Figure 4. Brush polarities of an 8-pole machine with superimposed 2-pole and 4-pole magnetic circuits

brushes B_1 B_5 can be short-circuited and the armature flux through the poles 3–7 can be used as superimposed 2-pole flux. It will produce a voltage between the brushes B_7 B_3 which are again brushes of the same polarity with respect to the 8-pole flux. The circulating current through the brushes B_7 B_3 can be used in order to excite a further 2-pole or 4-pole superimposed flux giving a further stage of amplification.

Figure 4 shows the brush polarities for the 8-pole flux, for a 2-pole flux superimposed on the poles 1 and 5, and for a 4-pole flux superimposed on the poles 1, 3, 5, and 7. The 4-pole flux induces voltages only between the brushes B_1 B_3 B_5 B_7. The polarity of the brushes B_1 B_5 is minus with respect to the 4-pole as well as with respect to the 8-pole flux. However, the brushes B_3 B_7 have the polarity plus with respect to the 4-pole flux and minus with respect to the 8-pole flux. The armature currents resulting from the 4-pole flux are, therefore, circulating currents able to produce another stage of amplification. The total number of stages of amplification possible in an 8-pole machine is 7, namely, four 2-pole stages, two 4-pole stages and one 8-pole stage. In general, the possible number of stages is

$$S=p_1\left(\frac{1}{2}+\frac{1}{4}+\frac{1}{6}+\frac{1}{8}+\ldots\right)$$

Only those terms have to be counted which yield an even integer or one. The first term gives the number of 2-pole stages, the second term the number of 4-pole stages, and so forth. For example, a 4-pole machine has $4/2=$ two 2-pole stages of amplification and $4/4=$ one 4-pole stage of amplification.

The 3-Stage Rototrol

Two coil arrangements for the 3-stage amplifier are shown in Figures 5 and 6. In Figure 5 field coils are arranged on the poles 2 and 4 which are fed by the circulating current $I_{B_1B_3}$, and which increase the armature reaction flux produced by this current. The field coils on poles 2 and 4 together with the armature reaction flux provide the excitation of the second stage of amplification. In order that the load current does not influence this excitation, two coils with equal number of turns are placed on each of the poles 2 and 4 (C_2 and D_2, and C_4 and D_4, respectively). The two C-coils as well as the two D-coils are connected in series and the lead to the load is connected to a tap between the C-coils and D-coils. The four coils are wound in the same direction so that they cancel out on each pole with respect to the load current I_4, while all four coils add up with respect to the exciting current $I_{B_2B_4}$. The coils C_1 to C_4 and D_1 to D_4 which are fed by the circulating current $I_{B_1B_3}$ and provide the excitation for the third stage of amplification are connected in a manner similar to that of the coils C_2C_4 and D_2D_4.

If the C-coils and D-coils in the circuit B_2B_4 all have the same number of turns, the machine operates as a pure amplifier and all circuits carry no current under steady-state conditions. If operation as a generator under steady-state conditions is desirable, either the coils C_1 to C_4 and the coils D_1 to D_4, in the B_2B_4 circuit, have to be given different numbers of turns or four special coils have to be placed on the poles 1, 2, 3, and 4 to provide self-excitation. These coils may be series or shunt-connected.

In Figure 6 the coils C_2C_4 and D_2D_4 on the poles 2 and 4 are omitted, and the excitation for the second stage of amplification is provided only by the armature flux resulting from the circulating current between the brushes B_1 and B_3.

The armature flux caused by the circulating current between the brushes B_2 and B_4 opposes the control flux and must be compensated either by a distributed compensating winding in the pole shoes of poles 2 and 4 or by concentrated windings on the poles 1 and 3. In both cases the coils must be fed by the current $I_{B_1B_3}$. Because the amplification of the 3-stage amplifier is very high, the compensation of the armature reaction is not so critical as in the 2-stage amplifier, under stable operating conditions.

Under transient conditions, the current distribution in the armature is not symmetrical. To provide good commutation, several commutating coils are needed on each interpole as in the 2-stage Rototrol.

The 3-Stage Rototrol under Transient Conditions

The transient conditions will be investigated for the arrangement shown in Figure 6 under the assumption that special series coils are provided for self-excitation under steady-state conditions.

Because the control coils on poles 1 and 3 make these poles north and south, while the C and D coils and also the series field coils make these poles north and north, there is no mutual induction between the control coils and the C and D coils or series coils. However, mutual induction exists between the control coils and the resultant of the armature between the brushes B_2B_4 and the compensating winding, if the compensation is not perfect. Further, mutual induction exists between the C and D coils and the series field coils.

In Figure 7 the different circuits are denoted by *0*, *1*, *2*, and *3*. The fluxes caused by armature reaction are represented by the coils AR_{13} and AR_{24}. CF is the control field, CW the compensating winding, and SF the series field for self-excitation. With the assumption that the compensation is not perfect, the voltage equations for no-load are

$$e_0 = R_0 i_0 + L_0 p i_0 - M_{02} p i_2 \tag{1}$$

$$K_0 i_0 - K_a i_2 = R_1 i_1 + L_1 p i_1 \tag{2}$$

$$K_1 i_1 = R_2 i_2 + L_2 p i_2 - M_{20} p i_0 \tag{3}$$

$$K_2 i_2 = e_2 \tag{4}$$

where $K_0 i_0, K_a i_2, K_1 i_1$, and $K_2 i_2$ are rotational electromotive forces. For load conditions, equations 3 and 4 become

$$K_1 i_1 = R_2 i_2 + L_2 p i_2 - M_{20} p i_0 + M_{12} p i_1 \tag{3a}$$

$$K_2 i_2 + K_a i_2 = R_1 i_1 + L_1 p i_1 + M_{12} p i_2 \tag{4a}$$

Further there exists a relation between e_0 and i_2 which depends upon the application of the Rototrol. For example, when it is applied to voltage control, this relation can be assumed as

$$\begin{aligned} e_0 &= -A e_4 \\ &= -A K_2 i_2 \end{aligned} \tag{5}$$

where e_4 is the deviation from normal of the generator voltage.

Equations 1, 2, 3a, and 4a can be solved for i_2. With

$$T_0 = \frac{L_0}{R_0}$$

$$T_1 = \frac{L_1}{R_1}$$

$$T_2 = \frac{L_2}{R_2}$$

$$l_{12} = \frac{M_{12}}{K_2}$$

the current i_2 becomes

$$i_2 = \frac{[K_0 K_1 + R_1 M_{20} p(1+T_1 p)][K_2(1-l_{12} p)]}{D(p)} e_0 \tag{6}$$

where

$$\begin{aligned} D(p) = {} & R_0 R_1 (1+T_0 p)(1+T_1 p) \times \\ & [K_2 M_{12} p(1-l_{12} p) + R_2(1+T_2 p) \times \\ & (R_2 - K_a + L_2 p)] - (R_2 - K_a + L_2 p) \times \\ & [K_0 K_1 M_{20} p - K_a K_2 R_0 (1+T_0 p) + \\ & (M_{20} p)^2 R_1 (1+T_1 p)] \end{aligned} \tag{7}$$

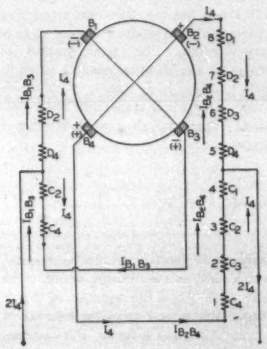

Figure 5. Coil arrangement for the 3-stage Rototrol

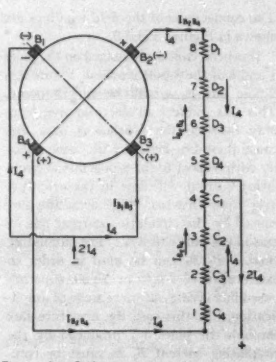

Figure 6. Coil arrangement for the 3-stage Rototrol

For perfectly compensated armature reaction caused by the circulating current $I_{B_1B_3}$

$$M_{23} = M_{30} = K_a = 0$$

and

$$i_3 = \frac{K_6K_1K_2(1-t_{32}p)}{D'(p)}e_0 \tag{8}$$

where

$$D'(p) = R_6R_1(1+T_6p)(1+T_1p)\times\{K_3M_{32}p(1-t_{32}p)+R_3(1+T_3p)\times(R_3-K_4+L_3p)\} \tag{9}$$

EXAMPLE: 3-STAGE ROTOTROL APPLIED TO VOLTAGE CONTROL

The following constants apply to a large turbogenerator:

$R_f = 14.7$ ohms (Resistance of control field coils)
$R_r = 14.7$ ohms (Resistance of regulator for maximum power transfer)
$R_6 = 14.7+14.7 = 29.4$ ohms
$L_6 = 3.90$ henrys
$K_6 = 17.9$ volts per ampere
$R_1 = 0.0176$ ohm
$R_3 = 0.0214$ ohm
$L_1 = 0.00188$ henry
$L_2 = 0.00289$ henry
$K_1 = 0.366$ volt per ampere
$K_2 = 0.653$ volt per ampere
$R_4 = 0.286$ ohm
$L_4 = 0.865$ henry
$K_3 = 21.0$ volts per ampere
(Proportional to slope of saturation curve at normal voltage of the generator)
$K_4 = 0.286$ volt per ampere
$M_{23} = 0.0010$ henry
$M_{30} = 0.0045$ henry
$K_a = 0.012$ volt per ampere
$T_6 = 0.133$ second
$T_1 = 0.107$ second
$T_3 = 0.135$ second
$t_{32} = 0.00153$ second

The Rototrol is slightly undercompensated. However, it will be assumed at first that the compensation is perfect, that is, $M_{30} = M_{02}$ and K_a will be set equal to zero. Equations 5 and 8 yield then

$$AK_6K_1K_2K_3(1-t_{32}p)+D'(p) = 0 \tag{10}$$

Inserting equation 9 for $D'(p)$ and substituting the system constants,

$$p^4+24.57p^3+200.0p^2+540.5(1-13.83A)p+4{,}886{,}000A = 0$$

With this equation in general form

$$a_0p^4+a_1p^3+a_2p^2+a_3p+a_4 = 0$$

the system will be stable, if

$$a_1 > 0$$
$$a_1a_2-a_0a_3 > 0$$
$$a_3(a_1a_2-a_0a_3)-a_4a_1^2 > 0$$
$$a_4 > 0 \tag{11}$$

The first condition is satisfied. The second condition

$$a_1a_2-a_0a_3 = 24.57\times 200-540.5(1-13.83A) > 0$$

is satisfied by any positive value of A. The third condition is satisfied when $A < 0.000801$. The fourth condition is satisfied when $A > 0$.

Putting $A = 0.000801$, the highest frequencies can be found for which the system is stable.

$$p^4+24.57p^3+200.0p^2+534.5p+3{,}194 = 0$$
$$p = -12.29 \pm j5.40$$
$$p = 0 \pm j4.66$$

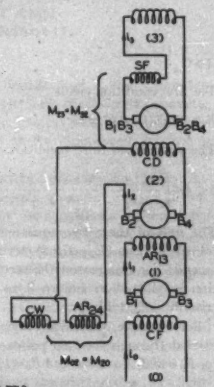

Figure 7. The circuits of the 3-stage Rototrol for calculating the transient conditions

That is, in this case there is a highly damped oscillation of 0.860 cycle per second and an undamped oscillation of 0.743 cycle per second.

Experience has indicated that satisfactory damping will be obtained, if A is made 30 to 40 per cent of the critical value. The response to a sudden change of reference voltage will be determined for $A = 0.00025$ by the methods developed by Gardner and Barnes.

The transfer function for the controlled system is

$$G_{12}(p) = \frac{K_6K_1K_2K_3(1-t_{32}p)}{D'(p)} \tag{12}$$

and for the controller is

$$G_{24} = -A \tag{13}$$

Substituting these equations into equation 48[1] with $D_1(p) = 0$ and $D_2(p) = 1/p$ (unit disturbance)

$$e_4(p) = \frac{D'(p)}{p[D'(p)+AK_6K_1K_2K_3(1-t_{32}p)]} \tag{14}$$

Substituting the system constants here,

$$e_4(p) = \frac{p^3+24.57p^2+200p+540.5}{p^4+24.57p^3+200p^2+538.6p+1{,}221.5}$$

or

$$e_4(p) = \frac{(p+7.52)(p+7.69)(p+9.35)}{[(p+11.03)^2+14.01][(p+1.253)^2+7.426]}$$

From the operational form of e_4, $e_4(t)$ can be found by the Bromwich integral

$$e_4(t) = \frac{1}{2\pi j}\int_{Br_1} e^{zt}e_4(z)dz$$

Figure 8 (below). Response of the 3-stage Rototrol of the example to sudden change in reference voltage

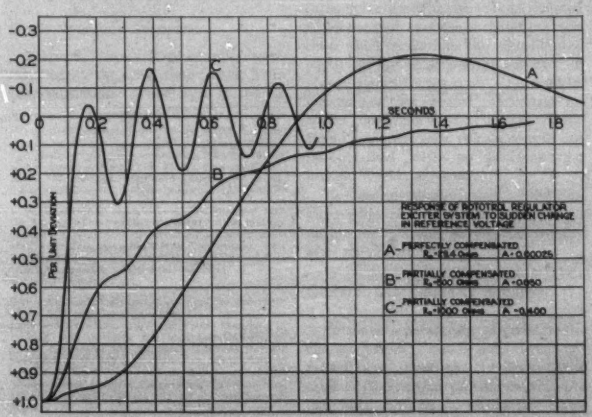

$$e_a(t) = 0.244e^{-11.98t} \times \sin(3.743t + 81.5 \text{ degrees}) + 1.287e^{-1.938t} \times \sin(2.725t + 37.44 \text{ degrees})$$

This function is plotted as curve A in Figure 8. For a response similar to that shown in this figure, the 2-stage Rototrol needs a regulator with about 30 times as much voltage amplification as the 3-stage Rototrol.

The imperfect compensation now will be taken into account. Equations 6 and 7 for i_2 will be used and for the constants $M_{20} = M_{02}$ and K_a the values given previously will be substituted. It should be pointed out that these values for M_{20} and K_a represent the difference of two large and nearly equal quantities and are, therefore, not very reliable For instance

$$M_{02} = 0.0739 - 0.0694 = 0.0045 \text{ henry}$$

where the first term is the mutual inductance between the armature and control coils and the second term is the mutual inductance between the compensating winding and the control coils. The compensation which corresponds to $M_{02} = 0.0045$ henry is 94 per cent.

From equations 5 and 6

$$AK_s[K_0K_1 + R_1M_{20}p(1+T_1p)]K_2 \times (1 - t_{ad}p) + D(p) = 0 \quad (15)$$

Inserting equation 7 for $D(p)$ and substituting the system constants,

$$p^5 + 17.04[1 + 0.01505R_0 - 0.00057A]p^3 - 511[1 - 0.00855R_0 - 0.0122A]p^2 + 225.7[R_0 - 33.0A]p + 4{,}900{,}000A = 0$$

For reasons which will become apparent later, R_0 has been left as a general constant to be varied.

The stability conditions, neglecting the relatively small A terms in the first two brackets, are

$$\left[38.57(1 - 0.00855R_0) + \frac{R_0 - 33.0A}{1 + 0.01505R_0}\right] < 0$$

$$\left[(R_0 - 33.0A) + \frac{27{,}920A(1 + 0.01505R_0)^2}{(R_0 - 33.0A) + 38.57(1 - 0.00855R_0) \times (1 + 0.01505R_0)}\right] > 0$$

$$A > 0$$

The first condition yields

$$R_0 > 279.8(1 - 0.0778A)$$

The second and third conditions yield

$$0 < A < \left[\frac{R_0(R_0 - 279.8)(R_0 + 27.78)}{1{,}308(R_0^2 + 118.0R_0 + 4{,}100)}\right]$$

The first of these two equations is contained in the $(R_0 - 279.8)$ term of the second; for this reason the second equation is plotted in Figure 9 as the sole criterion of stability.

For example, the calculation has been carried through for two points, namely, for $R_0 = 500$, $A = 0.050$ and $R_0 = 1{,}000$, $A = 0.40$, respectively. The result in the first case is

$$e_a(t) = 1.024e^{-8.778t} + 0.0799e^{-2.938t} \times \sin(27.99t - 17.5 \text{ degrees})$$

and in the second case

$$e_a(t) = 0.9722e^{-9.347t} + 0.3157e^{-1.149t} \times \sin(28.28t + 5.04 \text{ degrees})$$

In both these cases the contribution of the fourth root is negligible.

These two responses are plotted in Figure 8 as curves B and C along with the response of the perfectly compensated 3-stage Rototrol exciter system (curve A). As mentioned previously, these two curves cannot be trusted quantitatively, because M_{20} and K_a are not trustworthy as a result of the nearly perfect compensation. However, the analysis shows that negative damping caused by partial compensation can be made negligible by supplying the control field from a high resistance source. Such a high resistance in the control field circuit has the advantage of reducing the control field time delay but has the disadvantage of increasing the power of the regulator. For the same response, the 3-stage Rototrol always will need a regulator with less power than the 2-stage amplifier, or for the same power of the regulator it always will be faster than the 2-stage amplifier.

Reference

1. Transients in Linear Systems, Volume I, M. F. Gardner and J. L. Barnes. John Wiley and Sons, Inc., New York, N. Y., 1942. Page 193.

No Discussion

Field Investigation of Lightning Surges at Substations

I. W. GROSS
FELLOW AIEE

G. D. McCANN
MEMBER AIEE

THIS investigation, undertaked through co-operative efforts of the American Gas and Electric Service Corporation and the Westinghouse Electric Corporation, was begun in 1939 with the original purpose of studying the frequency, magnitude, and wave shape of the lightning currents discharged by lightning arresters in stations. The results obtained after the study had been in progress three years were reported in an earlier paper.[1] Five surge-current measuring stations were set up originally at different 3-phase arrester locations in substations of The Ohio Power Company in Ohio, and the Appalachian Electric Power Company in Virginia. The arrester current studies have been continued with certain changes in the location and character of the recording stations. Also, the scope of the investigation has been increased to include the measurement of the crest surge voltages at the terminals of both the arresters and the transformers being protected.

Description of Investigation

In the initial stages,[1] the investigation was conducted at two substations of The Ohio Power Company and three of the Appalachian Electric Power Company. At the end of the 1942 lightning season the installations in Virginia were discontinued and the investigation in Ohio amplified with additional recording instruments installed at the two substations already under study, and the addition of recording equipment at a third station. Pertinent information on the characteristics of the substations, the years under study, and the frequency of arrester discharges are given in Table I. The basic surge-current recording installations originally consisted of a high-speed fulchronograph and surge crest ammeter links in the ground lead of each arrester phase leg and a slow-speed fulchronograph, surge-crest ammeter links, and a magnetic surge front recorder in the common arrester ground. In addition, cathode-ray oscillographs were connected in the common ground at the Twin City and Stone Creek substations. These installations and the recording instruments have been described previously in detail.[1,2] As indicated in Table I magnetic surge front recorders were installed in each arrester phase leg and removed from the common ground at the two Ohio substations at the start of the 1943 lightning season. Photographic surge current recorders[3] were installed also in the common ground to record the very low magnitude continuing surge currents and power follow.

Surge Voltage Recorders

Magnetic surge voltage recorders were installed at the same time in the Twin City substation. These were located at each terminal of the transformer and arrester to measure the phase-to-ground surge voltages at these six locations. Similar installations were made at the Stone Creek substation, and the Midvale substation at the beginning of 1944. The complete recording installation at Midvale consists of the voltage recorders and surge crest ammeter links in the arrester ground leads. The surge voltage recorder is shown schematically in Figure 1*A* with an actual installation illustrated in Figure 1*B*. It consists of a noninductively wound resistance, small low inductance coils for magnetizing magnetic links, and dry-disk rectifiers to prevent reversal of the magnetizing field polarity. The crest magnitude of both polarities of the voltages is recorded through two sets of the coils and rectifiers. The potentiometer is isolated from the line with a special arrester-type gap set to break down at voltages ten per cent below that of the actual arrester at the station. This gap will quench the very low power follow current through the resistor, thus permitting a lower power rating on the potentiometer. The shunt capacity of the rectifiers is such that a small percentage of reverse current is permitted to flow through the magnetizing coils for very high frequency oscillations. However, through the use of multiple links situated in different parts of the magnetizing coils these small oscillations can be calibrated partly for giving an over-all accuracy of plus or minus 20 per cent. It should be pointed out that because the voltage recorder gaps break down at a lower voltage than the arrester gaps, voltage records can be obtained with no accompanying arrester discharge record.

The field installations were serviced on an average of once every week or two during the lightning season, and usually after each lightning storm.

General Discussion of Records

Fifty-five separate sets of arrester discharge current records have been obtained now, involving 112 single-phase arrester records that provide data on 153 individual component discharges The

Paper 47-97, recommended by the AIEE committees on protective devices and power transmission and distribution for presentation at the AIEE winter meeting, New York, N. Y., January 27–31, 1947. Manuscript submitted October 11, 1946; made available for printing December 13, 1946.

I. W. Gross is an electrical research engineer with the American Gas and Electric Service Corporation, New York, N. Y. G. D. McCann, formerly affiliated with Westinghouse Electric Corporation, East Pittsburgh, Pa., is now with the department of electrical engineering, California Institute of Technology, Pasadena, Calif.

The authors acknowledge the co-operative assistance of the field organizations of The Ohio Power Company and Appalachian Electric Power Company in making and servicing the field installations, of G. D. Lippert of the American Gas and Electric Service Corporation in co-ordinating the field work, and of Edward Beck and O. Ackerman of the Westinghouse Electric Corporation for their contributions in the lightning arrester and oscillograph fields.

Table I. Summary of Installations

	Substations of The Ohio Power Company			Substations of Appalachian Electric Power Company			
	Twin City Substation	Stone Creek Substation	Midvale Substation	Huntington Court Substation	Christiansburg Substation	Reusens Substation	Rocky Mount Substation
Type of station	Delta	Delta	Delta	Grounded Y	Delta	Delta	Delta
Miles to nearest grounded source	20	10	20	0	0.6	82	25
Circuit voltage	33 kv	33 kv	33 kv	12 kv	12 kv	132 kv	33 kv
Arrester type	Line	Line	Station	Station	Line	Station	Station
Arrester rating	30 kv	30 kv	37 kv	12 kv	12 kv	109 kv	30 kv
Arrester ground resistance, ohms	0.5	1.8		0.7		0.4	0.2
Earth resistivity, meter ohms	15–40	15–70		55–220		45–250	120–220
Conductor length, from lightning arrester to transformer, ft	50	32	80			6	
Number of lines	2	2	2	2	1	2	1
Type of lines	Wood	Wood	Wood	Wood	Wood	Steel grounded	Wood
Period under investigation	1940–1946*	1940–1946*	1944†–1946	1939–1943	Mid 1939–Mid 1941	1940–1943	Mid 1941–1943
Number of years of study	6	6	2	4	2	3	1½
Number of composite 3-phase records**	22	20	6	2	1	6	9
Apparatus standard basic impulse level, kilovolts	200	200	200	110	110	650	200
Number of records exceeding basic impulse level if no arresters	15	12	3	1	1	4	9
Number of discharges per individual arrester pole	35	28	5	2	3	14	25
Average discharges per year — phase 1	1.83	1.83	1.50	0.23	0.5	1.67	6
Average discharges per year — phase 2	2.0	1.50	0.50	0.23	0.5	1.67	5.33
Average discharges per year — phase 3	2.15	1.33	0.50	0	0.5	1.33	5.33

* At start of 1943 season magnetic surge front recorders were put in each arrester phase leg ground lead; also surge voltage recorders were installed (see text).

† Surge voltage recorders and magnetic links only were installed (see text).

** Includes those for which only voltage surges were recorded.

frequency, magnitude, and wave shape of these data are summarized in Tables I through IV together with Figures 2 through 6. Illustrative surge current records are shown in Figures 7 and 8. Figure 8*B* is of interest as it is one of the most complete records obtained.

Twenty-two sets of surge voltage records have been obtained. These are included in Table I. As indicated in Table IV, arrester discharge currents were recorded for only eight of the surge voltage records, as the remaining surges were not severe enough to produce measurable arrester discharges. For the last two years reported here the lightning seasons have not been very severe in the Ohio region, and only a few of the higher current surge records have been obtained.

The distribution of arrester discharge frequency is summarized at the bottom of Table I and in Figure 2, which compares the average annual frequency of per phase arrester discharges with that obtained in other investigations. The discharge frequency is markedly higher for this investigation probably because of the fact that the recording stations were chosen from past records which showed more than the average number of surges.

Twenty-four of the 51 composite surge current records involved all three phases, 14 two phases, and 13 only one phase. Because any one record may be the result of several strokes, analysis of the individual components is of greatest significance. Thirty-six or 22.5 per cent of the 153 component discharges were of positive polarity.

Crest Magnitude of Discharge Currents

Percentage distribution curves giving the frequency of occurrence of crest magnitudes are shown in Figure 3. They are plotted both for individual components and for the maximum component of each phase record. It is of interest that the two curves are quite close together. It is also interesting that there is fairly good agreement with the Gross and McMorris curve obtained from a considerably larger number of substations. The higher percentage of low magnitude records as obtained by them is primarily the result of their higher limit of sensitivity which was about 300 amperes as compared to about 50 amperes for the data reported here. This indicates that although (as shown by Figure 2) the stations of this study have greater than average lightning exposure from the standpoint of frequency of surges, the percentage of surges producing discharges above a given magnitude is not appreciably different. Although it is known that higher currents can occur in arresters at stations, the highest so far measured in this investigation out of 153 component discharges is 9,600 amperes. The maximum positive polarity surge current recorded is 2,800 amperes (see record 340, Figure 7 and Table IV), and only 9 per cent of the positive surges exceeded 500 amperes. This together with the much higher percentage of positive records (30 per cent) as compared to those for direct strokes (5 to 10 per cent)[5,6] indicates that most of the positive records result from surges induced by indirect strokes.

Wave Fronts

The wave front data as obtained with the magnetic surge front recorder and cathode-ray oscillograph are listed in Tables II and III, respectively. Probability curves plotted from these data are shown in Figure 4 compared with a curve for direct strokes. All cathode-ray oscillograms are for the current in the common arrester ground. The surge front recorder data contain records of both the common ground currents and the individual arrester phase leg currents as shown in Table II. The previously described phenomena[1] of the initial steep front as the arrester starts to discharge are verified further by the more recent data. This is illustrated by the oscillograms of Figure 7, most of which had initial rates of rise too steep to be recorded. All surges below 500 amperes have fronts less than 0.5 microsecond, and all but one below 1,000 amperes had fronts less than one microsecond. This effect is shown quite clearly by the two curves of Figure 4. One of these applies to all surge front records and the other to those above 500 amperes for phase leg currents and

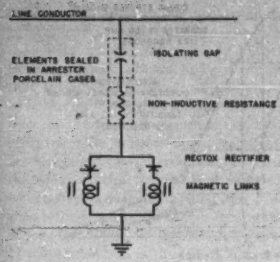

Figure 1

A (left)—Schematic diagram of surge voltage recorder installation

B (right)—Photograph of surge voltage recorder installation

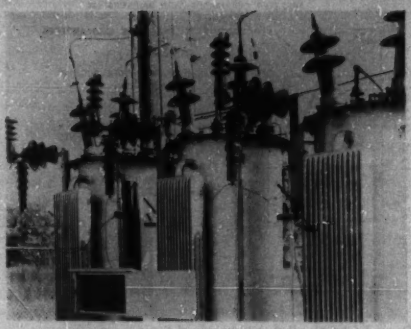

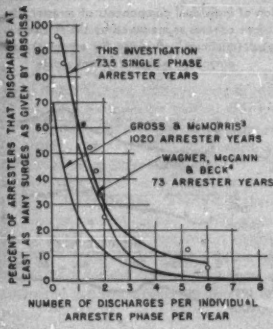

Figure 2 (left). Probability curves showing average frequency of arrester discharges

Figure 3 (right). Probability curves of crest magnitude of arrester discharge currents

Figure 4 (below, right). Probability curves of effective fronts of arrester discharge currents as compared with direct stroke data

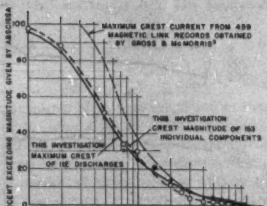

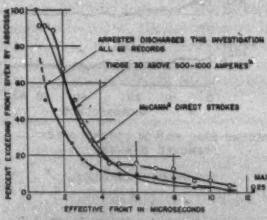

Table II. Arrester Discharge Current Surge Front Data as Obtained With Magnetic Surge Front Recorder

Phases Discharged	Record Number	Nominal System Kilovolts	Crest Current, Amperes	Surge Front, Microseconds	Average Rate of Rise, Amperes Per Microsecond
With recorders in common ground only*					
3	92	33	−9,600	3.7	−2,500
3	77	33	−6,500	4.4	−1,480
2	87	33	−5,150	8.8	−585
3	73	33	−3,650	6.6	−555
2	91	132	−3,150	Over 25	Less 125
3	66	33	−2,000	8.3	−240
3	55	33	−1,600	2	−800
3	165	33	−1,100	1.8	−610
3	108	132	−1,100	2.5	−440
3	206	33	−1,900	1.2	−1,580
2	234	132	−1,100	2.8	−390
With recorders in all three-phase legs†					
327—phase 1		33	−1,000	1.8	−555
2			−800	1.5	−535
3			−650	1.5	−430
294—phase 1		33	−550	0.5	−1,100
2			−200	Less 0.5	Over −400
3			0		
304—phase 1		33	−1,800	1.8	−1,000
2			−2,500	2.9	−860
3			−2,500	3.2	−780
403—phase 1		33	−5,000	2.2	−2,300
2			−7,600	2.4	−3,200
3			−3,100	2.7	−1,150
404—phase 1		33	−1,700	1.8	−950
2			−1,700	1.7	−1,000
3			0		
428—phase 1		33	−1,700	3.0	−570
2			−1,540	3.5	−440
3			−1,700	3.0	−565

* In addition, there were ten records with crests below 1,000 amperes and fronts less than one microsecond.

† In addition, there were six recorded phase discharges with crests less than 500 amperes and fronts less than 0.5 microsecond.

Table III. Arrester Discharge Current Surge Front Data Obtained With Cathode-Ray Oscillographs in Common Arrester Ground

Phases Discharged	Record Number	Nominal System Kilovolts	Crest, Amperes	Surge Front, Microseconds	Amperes Per Microsecond
3	77	33	−6,500	3.5	−1,850
3	206	33	−1,900	1.0	−1,900
1	304d*	33	−1,800	10.0	−180
1	311a*	33	−1,200	2.0	−600
3	327	33	−2,500	1.5	−1,670
	340*	33	+2,800	2.3	+1,220

* Not recorded with magnetic surge front recorder. In addition, there were 27 component discharges recorded and having fronts less than one microsecond that were not recorded with magnetic surge front recorders.

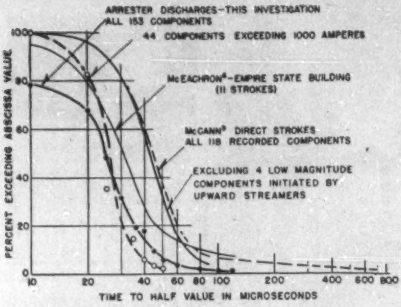

Figure 5 (above). Probability curves of times to half value of arrester discharge currents as compared with direct stroke data

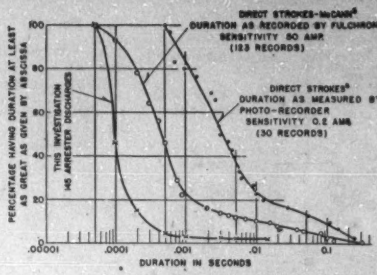

Figure 6 (above). Probability curves of duration of individual components of arrester discharge currents as measured by the fulchronograph (minimum sensitivity 50 amperes) and compared with direct stroke data

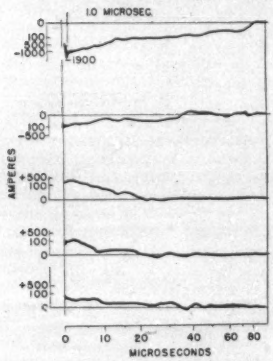

RECORD 206 FILM 58 STONE CREEK
REMOVED 8-4-42

(7A, above) (7B, below)

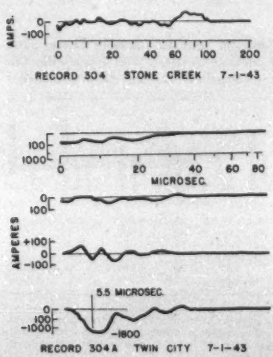

RECORD 304 STONE CREEK 7-1-43

RECORD 304A TWIN CITY 7-1-43

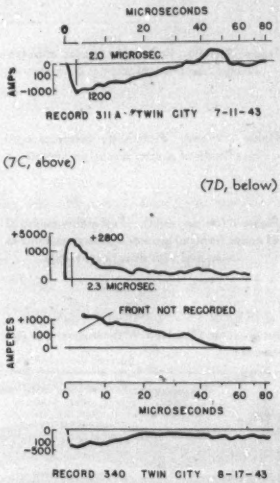

RECORD 340 TWIN CITY 8-17-43

Figure 7. Illustrative cathode-ray oscillograms showing current in common arrester neutral

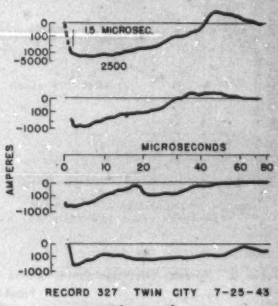

RECORD 327 TWIN CITY 7-25-43

(8B, above)

Figure 8. Typical composite record as obtained with fulchronographs, cathode-ray oscillograph, and photographic surge current recorder. See Tables II, III, and IV for additional data on surge fronts and crest voltages

(8A, below)

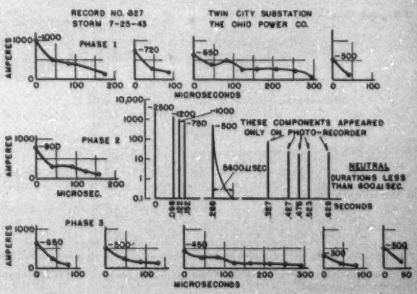

above 1,000 amperes for the common ground current data. Comparison with the direct stroke curves shows rather close agreement. It would be expected that the lower magnitude surges would have shorter fronts than direct strokes, as they do. It would be expected also that except for the arrester discharge effect, arrester surges would have longer fronts than direct strokes because of attenuation with wave propagation along the line. This is borne out by the higher percentage of long fronts and the maximum front of 25 microseconds as compared to 10 microseconds, the maximum recorded for direct strokes.[5]

Times to Half Value

The times to half value data of this study have been plotted in Figure 5 to show the effect of current magnitude. Direct stroke curves are plotted also for comparison. These curves show a larger percentage of shorter tails for lower magnitude arrester surges and considerably shorter tails for arrester surges as compared to direct strokes. The first of these differences may be caused by the sensitivity limit of the recording instruments.[1,3] However, it is thought that the shorter tails for the arrester discharges as compared to direct strokes are also the result of the fact that most severe surges result from direct strokes to the line that initially feed high current into the arrester until a line flashover occurs, at or close to the point of stroke contact. Then the lower impedance flashover path carries most of the surge current in effect robbing the arrester.

Duration of Component Discharges

Such a phenomenon is indicated also by the duration data of Figure 6. The durations as recorded by the fulchronograph with a sensitivity limit of 50 amperes are considerably lower than for direct strokes. Only ten per cent of the recorded components exceeded a duration of 300 microseconds. Another factor that previously has been shown to shorten the duration of the low magnitude continuing currents through the arresters is the system grounding.[1,4,7] The systems[1] under study are all solidly grounded. Fifty per cent of the higher current discharges were quite short (100 microseconds or less). More detailed data on the lower magnitude surge and power follow currents are given in a companion paper.[8]

Crest Surge Voltages and Arrester Protection

The surge crest voltage records are summarized in Table IV together with the crest magnitudes of the arrester currents wherever a surge was accompanied by an arrester discharge. This occurred for only 8 out of the 22 cases where voltages were recorded as the latter two lightning seasons covered by this study have been very mild.

To compare the recorded field records with the performance of the arresters, actual laboratory tests were made of the arresters at two of the substations, Twin City and Stone Creek. Typical oscillograms from these tests are shown in Figure 9. This gives the higher breakdown voltages recorded with a maximum of about 100-kv crest. Examination of the records shows that the crest voltages at the transformer terminals are frequently somewhat higher than at the respective arrester terminals. In Table I is given the length of phase conductors between the arresters and transformers. The highest voltage recorded at the transformers is 155 kv. This is about 48 per cent above the laboratory test breakdown voltage of

Figure 9. Laboratory oscillograms showing discharge voltage characteristics of the 30-kv line type arresters at Twin City Substation

Table IV. Summary of Crest Voltage Records

Record Number	Crest Voltage and Current at Arrester: Phase 1 Amp	Phase 1 Kv	Phase 2 Amp	Phase 2 Kv	Phase 3 Amp	Phase 3 Kv	Crest Kilovolts at Transformer: Phase 1	Phase 2	Phase 3
Twin City substation									
304a	0	− 92	−1,800	− 96	0	No disch.	− 88	− 65	− 60
311b	0		+ trace	+100	0	No disch.	+102	No disch.	+ 95
327	−1,000	−125	−800	−135	−650	−127	−127	−140	−145
340	0		+2,800*	+ 98	0	− 98	+ 90	− 95	No disch.
408	0	+ 96	0	+129 −120	0	+ 90 −97	+110 −155	+113 −145	+109 −115
433	0	+ 79 −137	0	No disch.	0	No disch.	+ 80 −148	+ 99 − 95	+100 −116
469	0	No disch.	0	No disch.	0	+ 90	Recorder out of order		
474	0	+ 95	0	No disch.	0	+ 85	No disch.	+100	+ 87
483	0	No disch.	0	+110	+220	+110	+110	+110	+100
485	+185	+110	0	+ 85	+100	+115	+ 95	+100 −110	+110
Stone Creek substation									
441	0	No disch.	0	No disch.	0	No disch.	+100 −129	+115 − 72	+ 95 −153
450	0	No disch.	0	No disch.	0	No disch.	+ 97 −132	+ 82 −132	−105
470	0	− 90	0	−100	0	No disch.	+ 95 −105	+ 90 −110	−105
471	0	No disch.	0	No disch.	0	No disch.	+ 95	No disch.	+100
475	0	No disch.	0	No disch.	0	+ 70	No disch.	+ 95	+ 90
482	0	No disch.	0	− 90	0	No disch.	No disch.	−100	− 95
484	0	No disch.	0	+ 8[illegible]	0	+ 90 −100	No disch.	+ 95 −105	+ 85 −105
Midvale substation									
441a	0	+125	0	No disch.	0	No disch.	+ 86 −115	No disch.	No disch.
472	+575	+110	+400	+110 −110	+775	+100 −75	+105 − 75	+ 9[illegible]	+100 − 95
473	0	+ 87 −100	0	No disch.	0	No disch.	+ 90 −1[illegible]	No disch.	No disch.
476	0	+ 95 −110	0	No disch.	0	No disch.	+ 90 −105	No disch.	No disch.
486	−500	+110 −100	0	+115 − 90	0	+ 90 −95	+ 90 −100	+ 95 −105	+105 − 90

* See record 340 Figure 7*D*, front of one discharge not recorded.

the arrester alone, and 8 per cent above the voltage actually recorded across the arrester and its grounding circuit for this surge. The highest ratio obtained between the transformer and arrester voltages occurs for record 450 in which the arrester recorder gap did not discharge, but 132 kv was indicated at the transformer terminals. The highest voltage recorded at the arrester terminals was 137 kv. Because the basic impulse level for 33-kv equipment is 200 kv, a good margin of protection is indicated for all surges so far measured.

It is of interest to consider the number of arrester discharges produced by surges that might have damaged the transformer insulation if arresters had not been present. A basis for such a determination has been given already.[1] In Table I are listed the composite records that had any discharge currents sufficiently high to indicate a voltage in excess of the basic impulse level with no arresters connected. Forty-five of the 66 composite records had currents above this critical value. Seventy-five per cent of the 153 recorded discharge current components were above this critical value.

Summary and Conclusions

1. A 9-year lightning investigation has been conducted at seven substations on 12- to 132-kv systems. The bulk of the data was obtained at 33-kv substations connected to non-ground wire lines. The frequency of arrester discharges, the polarity, magnitude, and wave shape of the discharge currents, and the crest magnitude of the surge voltages at both the arrester and transformer terminals have been recorded. One hundred twelve single-phase arrester discharges were recorded providing data on 153 individual surge components. Twenty-two composite crest voltage records were obtained.

2. The average frequency with which a single-pole arrester discharges varied from 0.2 to 6 times per year with a general average of about two per year. Thirty per cent of the surge components were of positive polarity. The maximum recorded positive discharge current was 2,800 amperes. The maximum negative discharge current was 9,600 amperes.

3. The wave shapes of the lightning discharge currents were of the same general character as for direct strokes. However, the fronts, times to half value, and measurable durations were markedly shorter. The wave fronts are characterized by an initial high rate of rise as the arrester starts to discharge, and low magnitude surges have very short fronts.

4. The wave fronts ranged from less than 0.5 microsecond to one maximum value of over 25 microseconds, but only 10 per cent exceeded 6 microseconds, with 80 per cent less than 2 microseconds. For those surges of sufficient magnitude that the fronts could be recorded the highest average rate of current rise was 3,200 amperes per microsecond for a surge with a crest of 7,600 amperes. The times to half value ranged from less than 5 to 120 microseconds. Only 10 per cent exceeded 45 microseconds whereas about 50 per cent of the direct stroke discharges are indicated to exceed this value. The measurable durations are considerably shorter than for direct strokes with a maximum of 15,000 microseconds and only 10 per cent exceeding 250 microseconds.

5. The fact that nearly one-half (75 of 153) of the current components measured through the arresters would have permitted surge voltages above the apparatus basic impulse level, if the arresters had not been present, indicates that the arresters are supplying the required protection.

6. Surge voltage values at the transformer terminal were measured as large as 32 per cent greater than at the arrester for the same surge, thus indicating the necessity of locating arresters close to the apparatus they are intended to protect, if the maximum protection is to be obtained under field conditions.

Inductive voltage drop in the arrester leads and high rates of voltage rise of surges are indicated from the data (Table IV) wherein voltage drops higher than the arrester characteristic were measured across the arrester plus 30 feet of ground lead.

References

1. Field Investigation of the Characteristics of Lightning Currents Discharged by Arresters, I. W. Gross, G. D. McCann, Edward Beck. AIEE Transactions, volume 61, 1942, May section, pages 266–71.

2. Instruments for Recording Lightning Currents, C. F. Wagner, G. D. McCann. AIEE Transactions, volume 59, 1940, pages 1061–8.

3. Lightning Currents in Arresters at Stations, I. W. Gross, W. A. McMorris. AIEE Transactions, volume 59, 1940, August section, pages 417–22.

4. Field Investigations of Lightning, C. F. Wagner, G. D. McCann, Edward Beck. AIEE Transactions, volume 60, 1941, pages 1222–9.

5. The Measurement of Lightning Currents in Direct Strokes, G. D. McCann. AIEE Transactions, volume 63, 1944, pages 1157–64.

6. Lightning to the Empire State Building, K. B. McEachron. AIEE Transactions, volume 60, 1941, September section, pages 885–9.

7. Lightning and Lightning Protection on Distribution Circuits, R. C. Bergvall, Edward Beck. AIEE Transactions, volume 59, 1940, August section, pages 442–9.

8. Field Research on Lightning Arrester Discharges, G. D. McCann, Edward Beck. AIEE Transactions, volume 66, 1947, pages 825–30.

Discussion

J. H. Hagenguth (General Electric Company, Pittsfield Mass.): The paper gives a valuable addition of data showing the crest values of lightning discharges through arresters in stations. With crest values of the order of 10,000 amperes, the modern arrester is capable of keeping the line voltage in the station well below the basic insulation levels.

Of considerable interest are the results of the voltage measurements with the magnetic surge voltage recorders, which, in general, indicate that the arrester is holding line voltage to about 50 per cent of the basic insulation level on the 33-kv delta system even though wood-pole lines are used. It is not stated whether ground wires are used near the stations.

It is, however, unfortunate that the accuracy of the recorder is not better than plus or minus 20 per cent. Theoretically, it has long been known that long connections between arrester and transformer should be avoided, because for steep-fronted waves the voltage at the transformer may be considerably in excess of the arrester voltage. If definitive proof of overvoltages at the transformer terminal were obtained, this would constitute a valuable confirmation of the theory as well as an indication of the steepness of the voltage waves entering the station.

Judging from the test results shown in Figure 9 of the paper, the variation in gap spark-over voltage of an individual arrester is relatively small, varying between 90 and 99 kv or plus or minus five per cent for six impulses and a maximum of 106 kv for the wave-shape calibration. Assuming that the arresters for phases one, two, and three of Table IV of the paper were not changed during this investigation, it is difficult to see why the arresters should not discharge even though the voltage measured across the arrester was as high as 137 kv. Likewise, an arrester discharge of 1,800 amperes resulted in a voltage measurement of 96 kv, while 800 amperes through the same arrester caused a drop of 135 kv. One reason for this might be the inductive drop in the arrester lead. However, with a 2,800-ampere discharge and only a slightly lower rate of current rise, only 98 kv was recorded. It would seem, therefore that the voltage recorder accuracy is not sufficiently high to draw conclusions as to actual arrester discharge voltages.

Likewise, of course, the readings at the transformers may be affected similarly. Thus, while an increase in voltage at the transformer of 32 per cent over the arrester is stated in the paper, the actual increase may have been considerably less. It is hoped that the accuracy of this device, which seems to be a very simple means of determining line voltages, can be improved if further measurements are to be made. From the over-all point of view of insulation and test levels, it is very important that accurate statistical facts become available.

P. L. Bellaschi (Westinghouse Electric Corporation, Sharon, Pa.): This contribution by I. W. Gross and G. D. McCann adds further, and significantly, to the knowledge of lightning surges at substations. Only too often in prior field investigations entirely disproportionate attention has been given to the lightning-current phase of the problem

and not enough to lightning-surge voltages From this as well as the prior contributions by Gross and Lippert[1,2] pertinent data on lightning-surge voltages at substations become available.

These recent field investigations on lightning should give industry a further opportunity to compare and assess present practices in relation to actual service conditions and from all this it may be possible to rationalize further our present methods and ways of doing things. When viewed in the light of these recent findings, it would seem that the present reference values as now in use for purposes of insulation co-ordination and testing, for instance the $1^1/_2$x40 microsecond wave and the steepness of front in front-of-wave voltage testing, do not appear too far from the mark on the whole.

There are a few questions I would like to raise on this paper that might clarify further the significance of the data presented. In Table IV of the paper under the column entitled "Crest Kilovolts at Transformers," is it correct or incorrect to construe that the corresponding voltages at the three transformer terminals appear simultaneously? Second, in Table I of the paper the impulse levels indicated as 200 kv, 110 kv, and 650 kv refer, respectively, to the 34.5-kv, 15-kv and 138-kv classes. Glancing at Figure 1*B* one would get the impression that some of the station apparatus apparently antedates the time when present basic impulse levels were established. Is it possible that the impulse levels of the stations in question actually are lower than present basic impulse values because of the presence of apparatus of old vintage?

Are we to conclude from Table I of the paper that had the lightning arresters been removed or were not present, failure of the apparatus would have resulted? Finally, referring to Table IV of the paper, some discrepancies appear to exist between the voltage records on the arresters and corresponding voltages recorded at the transformers, which may be accountable to the inherent difficulties in measurement encountered in the field. Perhaps the authors may have some comments on this point.

I was much interested to note in this paper that considerable importance is attached to the lead effect. This is a matter to which much study and attention have been given during the past 15 years. For instance, in many of the large and small transformers now built arresters are installed on the tank proper as integral parts of the transformer installation, thus minimizing lead-drop voltages and to that extent enhancing the degree of protection attainable.

REFERENCES

1. LIGHTNING INVESTIGATION ON 132-KV TRANSMISSION SYSTEM OF AMERICAN GAS AND ELECTRIC COMPANY, I. W. Gross, G. D. Lippert. AIEE TRANSACTIONS, volume 61, 1942, April section, pages 178–85.

2. LIGHTNING INVESTIGATION ON 132-KV SYSTEM OF AMERICAN GAS AND ELECTRIC COMPANY, I. W. Gross, G. D. Lippert. AIEE TRANSACTIONS, volume 64, 1945, February section, pages 76–84.

E. C. Starr (Oregon State College, Corvallis, Oreg.): This paper is a distinct contribution to the growing fund of information in the field of transmission-circuit protection. The quantitative data presented make it possible to analyze rather completely the performance of a number of lightning arresters in several substations having moderately severe lightning exposures. The number of installations studied and the period of time covered should give the data obtained a fairly representative cross section.

Several noteworthy observations can be made. Among them are

1. The arresters afforded definite protection to the transformers with which they were associated.

2. The maximum discharge currents recorded were low in comparison with a substantial percentage of direct-stroke currents.

3. The surge voltages appearing at the transformers were, on an average, essentially the same as those appearing at the arresters.

The following tentative conclusions might be drawn from these observations: when the discharge currents involved are relatively small, such as those associated with traveling waves or light direct strokes, the protection afforded by lightning arresters is excellent. This would indicate that from the standpoint of apparatus protection the practice of employing lightning arresters in conjunction with ground wires over the substation and extending out on all radiating lines at least a few thousand feet is satisfactory. A good common ground for all apparatus and arresters at the station is necessary. It is not shown that the arresters would fail to provide protection in the event of moderately severe direct strokes to unshielded substation conductors. The authors' comments will be appreciated.

The relatively low order of all recorded arrester discharge currents in comparison with direct-stroke data indicates that little, if any, field information has been obtained on the performance of arresters under close proximity direct-stroke conditions. It is recognized that the stricken conductors as well as the arrester grounds provide stroke discharge paths, but the relative impedances are such that, in the absence of insulation flashover, the arrester should discharge the major portion of the current.

Although it is recognized that ideally the arrester should be connected by leads of minimum length directly across the insulation to be protected, the data presented in this paper indicate that even in the 33-kv voltage class, lead lengths up to 80 feet between arrester and transformer have little if any influence on protection. The average ratios of transformer surge voltages to corresponding arrester voltages in Table IV of the paper are as follows:

Twin City substation (18 cases, arrester distance 50 feet)—1.025

Stone Creek substation (7 cases, arrester distance 32 feet)—1.13

Midvale substation (15 cases, arrester distance 80 feet)—0.985

Thus the greatest arrester distance, with 15 cases included in the average, gave the lowest voltage ratio, a value less than unity.

It is significant to point out that the largest and smallest voltage ratios recorded were within the stated limits of accuracy (plus or minus 20 per cent) of the measuring equipment, and hence should not be given too much individual weight.

Previous studies of lightning arrester performance employing artificial surges[1] indicated that the method of lightning arrester connection has a very important influence on the voltage developed across protected equipment some distance beyond. Thus if the *V* connection is employed in which the arrester, with very short leads, is shunted between the line and a common ground, the surge voltage developed even 120 feet beyond the arrester at the end of an open line is very little higher than that across the arrester for traveling waves of moderately steep fronts. The presence of a transformer on the end of the line would reduce this voltage because of the capacitance of the bus, bushing, static plate, shields, and so forth.

These points are brought out because of the desirability at times, for various reasons, of locating the arresters a short distance from equipment to be protected. The authors' comments will be appreciated together with a description of the exact methods of lightning arrester connections employed in the substations named above.

REFERENCE

1. FIELD TESTS ON THYRITE LIGHTNING ARRESTERS USING ARTIFICIAL LIGHTNING OF 1,500,000 VOLTS, E. B. McEachron, E. J. Wade. AIEE TRANSACTIONS, volume 50, 1931, pages 479–89.

Philip Sporn (American Gas and Electric Service Corporation, New York, N. Y.): The report on lightning conditions at stations and the duty on arresters given in the authors' paper, indicates clearly that definite progress has been made in obtaining accurate knowledge so necessary to apply lightning protection on a sound engineering basis.

As far back as 1927 we initiated an intensive study of protection of equipment by the then available lightning arrester. It was soon apparent that the arrester could be, and should be, reduced in rating and thus increased in protective value if it were to provide the protection against lightning of which it was capable. At that time we decided to really put the lightning arrester to work. As a result arrester ratings on our 132-kv system were reduced drastically with a very appreciable lowering of the protective level, and with a substantial margin of protection between the arrester and equipment. The next step was a study of arrester protective levels and equipment impulse strength with the result that some 13 years ago we placed in service on our 132-kv system a transformer with closely coupled arresters, the arresters being mounted directly on the transformer tank. Thus protected, the transformer was actually impulse-tested in the factory and the protective value of the arrester and satisfactory impulse strength of the transformer definitely proved. This transformer with closely coupled arresters was placed in service in the field and is operating still without any trouble having been experienced to date either on the arrester or the transformer proper.

The practice of closely coupling arresters to equipment is now standard practice in our company. It is significant, also, that the practice of using derated arresters having lower protective levels has now spread and is being followed on a number of other power systems. This does not apply to the practice of checking insulation co-ordination by actually impulse-testing large and important high voltage transformers with steep front,

chopped, and full wave lightning surges which we have followed for some 12 years or so. But it has seemed to me that proper protection involves three important elements:

1. Knowledge of the insulation strength of the transformer.

2. Knowledge of the arrester protective level.

3. A relationship between the two to allow an appropriate margin between them.

Testing assures this. Such tests have picked out imperfections in design and faulty workmanship and material, and our experience shows that they are thoroughly justified. The results of this practice, which, as stated, has been followed for over 12 years on our 132-kv system, have produced economies not only in the cost of arresters and transformers, but also complete freedom from failures of equipment protected in this way.

It will be noted from Table I of the paper that in four of the seven stations where tests were conducted, the arresters have reduced ratings even though the transformer bank where the arresters are located is delta-connected. In other words, the solid grounding of the system itself still has permitted the use of reduced rated arresters even at delta transformer banks.

The application of reduced rated arresters offers two advantages: one is the greater protection of equipment, which is particularly valuable where older equipment with insulation strength not equal to present-day values is in service, but still has years of useful life; and the other is that by reducing the arrester rating within practical limits, lower insulation than is generally recognized as standard in transmission practice today can be used. This latter advantage is one which needs to be given more consideration and actively explored under present conditions to effect greater economy in cost of system transmission and distribution facilities, and to improve continuity of service. Field experience data of the type presented by the authors should be of value in helping this work along.

I. W. Gross: J. H. Hagenguth has pointed out that the lightning arresters as used on the 33-kv system hold the voltage to about 50 per cent of the basic insulation level. The basic insulation level for a 33-kv system is 200 kv, and the recorded voltages shown in Table IV of the paper average about 50 per cent of this value. In setting up the protection that has to be supplied against impulse voltages in a station due consideration must be given to the few high voltage surges as well as the average values which appear throughout the year. It should be mentioned also in this connection that although the transformers were delta-connected, the system itself operated with a solidly grounded neutral and the arresters were rated 30 kv. This is a so-called reduced rated arrester as compared with the 37-kv nominal rating which is standard throughout the industry for the isolated neutral system, thus providing additional margin between the arrester and transformer.

Regarding ground wire protection at stations, only in two cases (Midvale and Reusens) were ground wires installed.

The accuracy of the voltage recorders used to determine voltage at the arrester and tranformer has been commented on by several discussers. It was hoped that although the accuracy of these instruments was not all that could be desired, some useful information such as trends could be established which might be used as worth-while support of theory.

Hagenguth has pointed out the small variation (plus or minus five per cent) on the gap breakdown of the arrester characteristic which is shown in Figure 9. It is recognized, of course, that with average distribution arresters, gap breakdowns and IR drops can vary much more than this between different arresters.

While a great deal of speculation can be gone into to justify the variation in readings shown in Table IV of the paper, two points must be recognized: first, that the voltage-measuring device does not have the accuracy of commercial indicating instruments; and second, that commercial arresters do vary one from another as has been pointed out in past Institute committee reports on arrester discharge characteristics.

P. L. Bellaschi raised a question concerning Table IV of the paper as to whether the voltages given are simultaneous in all three phases. It would be too optimistic to say, "yes," but it is a fact that these voltages were obtained at regular field inspection periods and can be assumed to have occurred during the same lightning disturbances; however, they might have occurred during one lightning storm but separated by several seconds or minutes. There was no timing device used to accurately tie the records together.

It was also possible, as pointed out by Bellaschi, that the impulse levels of the equipment in the station may not conform to present-day standards. Some may be lower and some are known to be higher.

Bellaschi has asked also if it is reasonable to assume that failure of apparatus would have resulted if no lightning arresters had been present. The number of failures without arresters, of course, cannot be predicted. The point which we attempted to make was that the basic insulation level of voltages would have been exceeded in a number of cases; but whether the apparatus would have failed would depend, of course, on a number of other factors such as impulse strength of the equipment including not only its safe limit but its single shot breakdown.

E. C. Starr has pointed out that the maximum arrester discharge currents were quite low in comparison with direct stroke currents such as measured on transmission lines and in towers. This is to be expected and seems to indicate that at the stations covered by this investigation direct strokes are very rare, at least.

As pointed out in the paper, the objective was to study field lightning conditions in and adjacent to stations and determine the duty on protective devices and their ability to perform. With measuring instruments available for determining the characteristics of lightning currents and voltages, it is well known that accuracies of measurements do not approach those of commercial indicating instruments and errors in the order of 10 to 20 per cent in measured values may well appear. To attempt to draw any hard and fast conclusions with data so obtained requires a considerable amount of study, analysis, and screening of data, and consideration of theoretical aspects if worth-while results valuable to future use are to be expected.

Several of the discussers have commented on the variation in surge voltages recorded at the arrester and transformer terminals, although the two pieces of equipment were located some 30 to 80 feet apart. It was pointed out that the highest ratio voltage (with the transformer being the higher) was 132 per cent. This general result can be expected from theory if the incoming voltage surge is steep and also checks quite well with laboratory tests where voltages under somewhat similar conditions have appeared at the transformer terminal in the order of 150 per cent of that measured at the arrester where the arrester was 50 feet distant from the transformer.

While the records have been presented as obtained in the field, and discussed in the light of the authors' analysis, it is appreciated that others may wish to place different interpretations on some parts of the data. It should be pointed out, however, and this is backed by a great deal of experience in lightning field investigation work, that while a great deal of data must be obtained on any particular feature under investigation, the average values in any particular case are apt to be misleading or certainly may result disastrously if due consideration is not given to the maximum values. This has been appreciated in insulator mechanical strength where a weak link in the insulator string can put an entire transmission line out of service. Likewise, the average ratio of voltages at the transformer to those measured at the arrester is a figure which must be used with care; otherwise, the infrequent high voltage at the transformer, which is indicated from our data as possible, may result in station equipment failure which is intolerable.

Starr has summarized some of the modern thinking on the protection of equipment within the station by pointing out the desirability of shielding the line as it enters the station, the necessity for good grounds, and the desirability of short leads between the arrester and equipment. Just how far each one of these features is to be carried must be determined by local conditions, the degree of protection desired, and the importance of protecting equipment in service.

Regarding the methods of lightning protection in the stations reported in the paper, the practice has been followed of using the lowest rated arrester consistent with the system over voltages expected and placing the arrester as close as practical to the equipment which it is intended to protect. It must be recognized that in any station there are other pieces of equipment and apparatus in addition to the transformer such, for example, as fuse mountings, disconnecting switches, bus insulators, potential transformers, and in larger stations, circuit breakers and coupling capacitors. It is impractical, not economical, and not necessary, as shown by experience, to place an arrester at each one of these pieces of equipment, and final decision is usually left to the experience and judgment of the designing engineer. The general practice on which lightning arrester protection in stations of the system under investigation is applied is outlined in the discussion by Philip Sporn.

Photographic Study of Lightning

J. H. HAGENGUTH
MEMBER AIEE

THE lightning investigation in Pittsfield was started in 1935 for principally two reasons:

1. To obtain information on lightning strokes to open country as a check or supplement to the Empire State investigation.[1, 2]

2. To obtain a large amount of statistical material concerning lightning characteristics.

For this purpose cameras were chosen as the principal means of investigation. Cameras have the advantage of giving a very great range of observation, and therefore are well adapted to obtaining data on a large number of strokes. Cameras have, however, certain limitations which will be discussed in the text.

The investigation was carried on for seven consecutive years. The investigation gradually was discontinued during 1940 and 1941, and completely halted in 1942 on account of the war.

In this paper only the most important items will be discussed. Such items as the intensity of the lightning stroke throughout its length, the relative intensity of multiple current peaks, and so forth will be discussed in a later paper.

The valley around Pittsfield is at an elevation of about 1,100 feet above sea level. This valley is bounded by the Taconic Hills (elevation—2,200 feet) in the west, Washington Mountain (elevation—2,200 feet) in the east, Mount Greylock (elevation—3,500 feet) in the north and a host of lesser hills in the south, and it is part of the Berkshire Hills.

The average number of days per year during which thunder is heard, recorded over a period of 30 years by the United States Weather Bureau, is 27 days.

For the purpose of this investigation an observatory was built and special cameras were used.

Observatory

In 1935 a lightning observatory was built on top of one of the office buildings of the General Electric Company in Pittsfield, Massachusetts. The observatory is shown in Figure 1. It has essentially three parts. On the platform below the structure the multiple stroke camera is mounted. A ring equipped with a series of small holes and fed with high pressure air is provided to produce a curtain of air around the camera and thus keep the rain away from the lenses. Directly above the camera is a small room from which the camera can be operated and which also serves as a recording station. Above this well the main part of the observatory contains 16 windows, providing an unobstructed view of the surrounding country towards the hills, ranging from 5 to 20 miles. In the center of this room curtains can be lowered to provide a dark room for changing films.

Figure 1. Lightning observatory erected at Pittsfield works of the General Electric Company for study of lightning and thunderstorms

The observatory is mounted on four posts, and all wiring, supply piping, and guying is arranged in line with these posts; likewise, the two lightning rods shown in Figure 1. Thus, a minimum of interference with the field of view of the camera is attained.

Cameras

The principal camera used for this investigation was the multiple stroke camera. This camera is shown in Figure 2. It has 12 lenses which cover the whole horizon. The fields covered by adjacent lenses overlap slightly. The film is stored on two spools inside of the revolving drum, a storage spool and a take-up spool. To obtain photographs the film is wound around the outside of the large drum (right of Figure 2) which has a periphery of 100 centimeters and is driven at 78.26 revolutions per minute by means of a constant-speed phonograph motor.

The lenses have stops of $f7.9$ to $f32$. For night photographs, the largest stops were used. Each lens covers a field of 56 by 75 centimeters on the film.

A second camera which proved of considerable value was a stereoscopic camera with two Tessar $f4.5$ lenses, with focal lengths of nine centimeters, each lens projecting an image of 52 by 55 centimeters on the film. The photographs taken with this camera have served two purposes: one to provide a still image of

Paper 47-98, recommended by the AIEE committees on power transmission and distribution, and protective devices for presentation at the AIEE winter meeting, New York, N. Y., January 27–31, 1947. Manuscript submitted November 12, 1946; made available for printing December 11, 1946.

J. H. HAGENGUTH is in charge of the high voltage engineering laboratory of General Electric Company, Pittsfield, Mass.

The author wishes to express his appreciation to Doctor K. B. McEachron, who was the director of the investigation; C. J. Kettler and W. L. Lloyd Jr., who were responsible for the design of most of the equipment used; and J. C. Russ, H. G. Sokop, A. P. Rohlfs, W. B. Brown, W. C. Russell, and C. McIntosh, who were active with observation and reports.

Figure 2. Multiple stroke camera—interior view

the strokes photographed, and the other to obtain a relatively good measure of the location of the ground terminal of the stroke by means of the stereoscopic viewer.

During several years a medium-speed Boys camera was operated also because of the ease with which its film can be changed and because a similar camera was in use at the Empire State investigation. This camera is shown in Figure 3 and has been described elsewhere.[2] A high-speed Boys camera has been used[3] for several years. The results obtained with this camera were not of sufficient value to warrant a description.

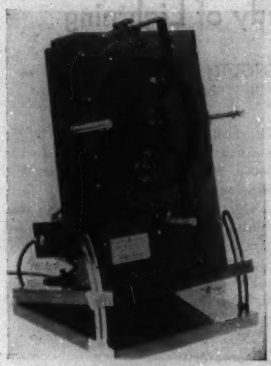

Figure 3. Medium-speed Boys camera. Bottom lens rotates at 120 revolutions per minute

Auxiliary Equipment

A direction finder, graduated in degrees, was used to determine the angular position of the strokes with respect to the observatory. This finder was placed in the window facing the storm center and the pointer adjusted at the time of the lightning discharge. The number of the window and the degrees indicated by the finder resulted in a relatively good positioning of the stroke in a radial direction.

A stop watch was used to time the stroke and thus obtain the approximate distance of the stroke from the observatory. This is, of course, a fairly rough measure because it not only depends on the reaction time of the person using the watch, but also to a considerable extent on the configuration of the stroke relative to the laboratory. Some strokes have horizontal parts of considerable length, and the top and bottom portion may have different distances from the observatory. In general, the stop watch will be operated when the first thunder is heard which should result from the closest portion of the stroke.

In spite of the inaccuracy this method has proved to be very successful when checked against actual distances known because of the damage produced by the stroke. For instance, for an actual stroke distance of 4,400 feet, a distance of 4,700 feet was determined by stop watch. In general, the accuracy was of the order of plus or minus 20 per cent. This could be improved materially in those cases where stereoscopic photographs of the stroke were available.

A dictating machine with lapel microphone was used to take all records during the storm. These were later transcribed. This has proved itself to be a very reliable and speedy method of recording.

Discussion of Results

The principal results to be obtained from a photographic and visual investigation of lightning are

Multiplicity of strokes.
Duration of strokes.
Time interval between current peaks.
Continuity of strokes.
Current peaks.
Branching.
Leaders.
Cloud-to-cloud strokes.
Stroke height.
Stroke density.

These are discussed in the following paragraphs.

Multiplicity of Strokes

Figure 4 shows a composite plot of multiple stroke data by various investigators. The curve marked "McEachron —619 photographs"[4] gives the results of this investigation. Because of restriction of the photographic method, these are minimum values. While there is considerable difference between individual curves,[5,6,7] it is evident that approximately 50 per cent of all strokes have two or more current peaks. If the strokes are adjusted for visibility during the storm and distance from the observatory, the 50-per-cent point from this investigation falls more nearly on three or more current peaks.

A typical multiple stroke is shown in Figure 5 which shows the beginning and the end of a 22-current-peak stroke to ground. To conserve space the intermediate portions are not shown. The timetable for their discharge is given in Table I. The maximum number of current peaks in a stroke recorded during this investigation is 26.

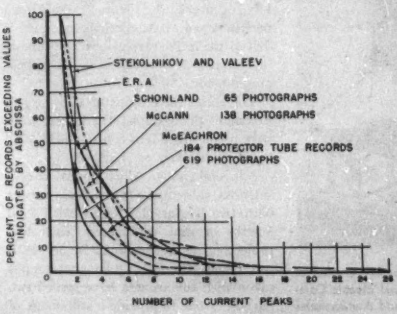

Figure 4. Number of current peaks in lightning strokes. (All photographs are of strokes to open ground)[4]

Duration of Strokes

Figure 6 shows stroke durations as obtained by various investigators.[4,5,6] The

curve marked "McEachron—619 photographs" gives the results of this investigation. The values are minimum values. The maximum duration obtained was 0.80 second. As pointed out under camera limitations the actual maximum duration may have been considerably greater. Fifty per cent of all cloud-to-ground strokes had a duration of at least 600 microseconds. From data not shown, using selected strokes only, 50 per cent had a duration of 3,500 microseconds or more. On the basis of multiple strokes only, 50 per cent had a duration of at least 12,000 microseconds. The strokes were selected for good visibility and relative closeness to the observatory. These strokes comprise about eight per cent of all strokes.

It is of interest to note that the duration of a stroke is largely independent of the number of current peaks. This is indicated by Figure 7 showing the limits obtained for the duration of strokes having a given number of current peaks. A stroke with two current peaks may have a duration of a few hundred microseconds and also as high as 500,000 microseconds. However, as the number of current peaks increases, a marked increase in minimum duration is indicated.

Time Interval Between Current Peaks

Figure 8 shows the values obtained by various investigators.[4,5,8] The curve marked "McEachron—939 values" was obtained from this investigation. This curve shows that 50 per cent of the values are 15,000 microseconds or greater. A maximum of 500,000 microseconds was recorded.

The photograph in this case gives maximum values. The Pittsfield curve shows a large number of current peaks occur at time intervals of 1,000 microseconds or less. In the long time interval range, the results of different investigators are of the same order of magnitude.

Persistence of Illumination

Of late years the continuing type of current discharge has become of considerable importance. It has been proved by McEachron[1] that current flow as indicated by oscillographic measurements is coincident with illumination of the stroke path as indicated by the photographic camera. Therefore, persistence of illumination in the present investigation can be considered as current flow and the existence of a continuity of current.

However, the data obtained, which give uninterrupted persistence in a stroke, and shown in Figure 9 are minimum values and definitely too low. The current in continuing discharges is of relatively low amplitude, and conditions must be very favorable if a current of less than ten amperes can be photographed if the stroke distance is in excess of a few thousand feet. The curve shows that 30 per cent of the current peaks had a persistence of at least 100 microseconds, 5 per cent—10,000 microseconds, with a maximum persistence of at least 500,000 microseconds.

General Discussion of Value of Camera Investigation

As stated, the camera is capable of taking a vastly larger number of lightning stroke photographs than can be obtained with measuring devices such as oscillographs, magnetic links, fulchronographs and others in fixed positions. This is of great value from an economic point of view to obtain a large amount of statistical data in a relatively short time. As long as the limitations of this method are kept in mind the results are of considerable value to increase our knowledge of the lightning stroke phenomena.

Figure 5. Record of 22-discharge multiple lightning stroke taken with multiple stroke camera

The limitations of the camera study are principally the sensitivity of the camera lenses and films. Also, the intensity of the light received at the camera will be a function of the haze, fog and rain existing between the camera and this stroke channel. Because the amount of light available from the stroke decreases at a rate between the square of the distance and the distance, it is apparent that a current peak of threshold intensity at a distance of one mile will not record when a stroke of equal intensity has a distance greater than one mile.

Consequently, the number of current peaks recorded for strokes at great distances may be too small because current peaks of low current amplitude may not be recorded. This readily accounts for the apparent lower record of number of current peaks for the Pittsfield investigation as compared with results from other

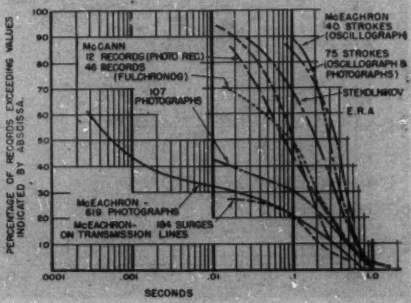

Figure 6. Total duration of lightning strokes to ground. (All photographs are of strokes to open ground)[1]

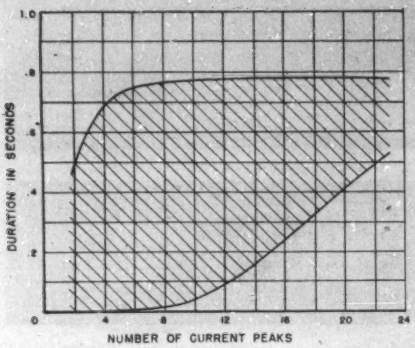

Figure 7. Multiple strokes—relation between number of current peaks and duration

investigations (Figure 4). However, the larger number of strokes photographed would be expected to cancel out some of the differences because of other causes. Likewise, the persistence of illumination obtained from all films must be considered much too short, because the currents involved generally are of much lower order than the current peaks. It is, however, significant that even on this basis, five per cent of the strokes exceed 10,000 microseconds. Similarly, the total duration of strokes gives minimum values partly because the last few weak current peaks may not be recorded and persistence of illumination towards the end of the stroke may be of insufficient intensity. The Pittsfield curve of Figure 8 probably is too low at the short time duration, principally because of inability of the camera used to record the persistence of illumination.

It is of some interest that the duration and number of current peaks obtained on a line equipped with expulsion protector tubes and by photographs in Pittsfield check fairly closely indicating that the photographic results have considerable value as far as effects of lightning strokes on transmission lines are concerned

Current Peaks

One of the very difficult tasks to determine from the photographs is the amount of current flowing in the stroke. As a result of the war and reconversion conditions, this has not been done, but it is hoped to obtain such data and report it at a later time. Doctor J. W. Flowers has done preliminary work from records of strokes to the Empire State Building which gives very promising results.[10]

There are, however, a few obvious observations which can be made. In general, the first current peak in a multiple stroke indicated the highest intensity, and therefore, presumably the highest current amplitude. In a few strokes, the subsequent current peaks had as high or even higher intensities. In Figure 5, current peak *F*, is of considerably higher intensity than the first current peak *A*.

In many of Malan and Collens'[9] photographs, the intensity of light given off by the return stroke channel decreases abruptly when reaching branches. In this investigation the change in intensity along the channel is not nearly as great, indicating some considerable differences in the mechanism of the stroke. It is quite probable that the change in illumination is not because of the branches, but rather caused by availability of charges in the ground. In many of Malan and Collens' photographs it definitely appears as if the charges in the ground were insufficient to neutralize the stroke channel charges and the return stroke of high amplitude degenerates into a cloud-to-ground discharge of low amplitude, similar to the Empire State strokes. Further studies along this line will be made on the available photographs.

Branching

It has been established from field and laboratory data that branching is always in the direction of propagation of the leader strokes, and, therefore, branching indicates whether a stroke started at the cloud or from the ground. In this investigation an attempt has been made to evaluate branching statistically. It was found that if all strokes were taken into account, about 50 per cent of the strokes showed downward branching, indicating the cloud as the stroke origin. From se-

Figure 8. Time interval between successive discharges of multiple strokes[4]

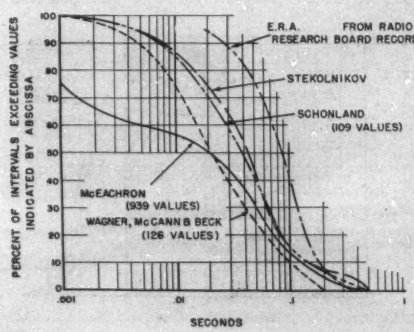

Figure 9. Persistence of illumination of lightning strokes

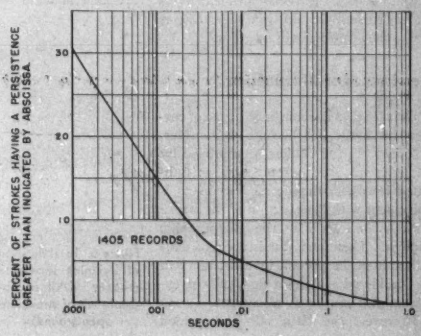

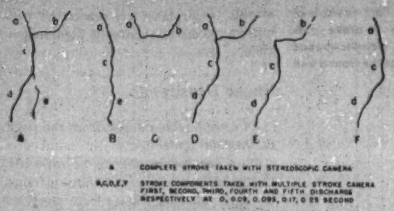

Figure 10. Example of change of stroke path of a cloud-to-ground stroke at cloud end as well as at ground end of stroke

lected photographs, 94 per cent showed downward branches, while 6 per cent did not show any branches. It is assumed that if conditions were perfect some downward branching would appear on all strokes indicating that all strokes started at the cloud.

Quite a number of the still photographs show upward branching, mostly close to the cloud. In all such strokes where the time sequence of the stroke components is available, it can be shown that the apparent branching results from either a cloud-to-cloud discharge, which later developed during the sequence of the stroke as shown in Figure 10, or a change of cloud terminal, or a combination of these conditions.

The branching on cloud-to-ground strokes usually occurs on the first current peak only, although a few records were obtained where branching occurred on subsequent current peaks.

In many of the strokes the branches are of considerable length (Figure 11) without contacting the ground; in other strokes two ground termini result (Figure 12) where *A* is the still image. Under the conditions of two ground termini, these may be established simultaneously (Figure 12) or may be the result of change in stroke path (Figure 13). The largest horizontal separation between two ground termini of a stroke was recorded as 8,000 feet.

In no case have upward streamers been recorded. Figure 14 shows a stroke to a patch of weeds about 20 feet from the lakeshore, approximately 1,200 feet from the observatory (Stroke *A*, still image A_1–A_3, two close current peaks taken by rotating lens). It is interesting to note that neither of the two tall smoke stacks—the further one is approximately 400 feet from the stroke terminus—show signs of upward streamers. The stroke proper indicates a split about 10 feet up from the water extending for a distance of approximately 28 feet, with a maximum separation of about 4 feet. This may indicate upward streamers of about 38 foot lengths, or it might have been produced by wind action changing the stroke path. Such splits have been identified as the terminus of a streamer with long laboratory discharges.

Schonland[7] mentions the large number of air discharges which were observed during his investigations. In this investigation only very few streamers from the cloud not connected with a cloud-to-ground stroke were observed. It is quite likely that these are streamers from a cloud-to-cloud discharge with insufficient energy available to reach the ground.

Leaders

Of considerable interest in the explanation of the formation of the lightning stroke are the leaders. In this investigation the results obtained were not as numerous as for the other stroke characteristics, principally on account of the photographic limitations. However, 54 leaders were photographed and could be analyzed as to the velocity of propagation. The values are shown in Figure 15 and indicate a range of values similar to those found by Schonland[7] and others.[1]

The curve marked "initial continuous leaders" undoubtedly represents initial stepped leaders; the steps, however, could not be identified from the photograph.

A relation of about 1:10 exists between the velocity of propagation of the initial leaders, preceding the first current peak in a stroke, and subsequent leaders, preceding the remaining current peaks in the stroke.

Figure 11. Lightning stroke showing profuse branching of great length

Figure 12. Lightning stroke with two ground termini occurring within not more than 200 microseconds (*A*—still image)

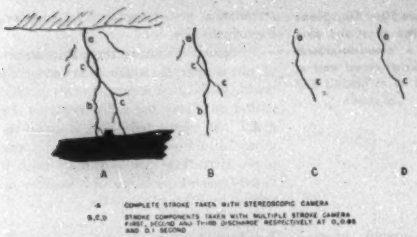

Figure 13. Example of change in stroke path of a cloud-to-ground stroke at the ground end

Figure 14. Lightning stroke to a patch of weeds about 20 feet from the lakeshore. Bottom end of still image *A* gives indication of possible upward streamer

Two stepped leaders were photographed which are not included in Figure 15. They had a velocity of propagation of 1.6 feet per microsecond and 3 feet per microsecond.

The velocity of the return strokes could be measured in four cases, with an average of 209 feet per microsecond, a minimum of 136 feet per microsecond, and a maximum of 253 feet per microsecond.

Cloud-to-Cloud Strokes

The number of cloud-to-cloud strokes photographed is of the order of 20 per cent of the cloud-to-ground strokes. The data obtainable from the photographs are very meagre because very little of the stroke path is visible. In most cases the cloud-to-cloud discharges were of the continuing type, although in one case a distinct number of weak current peaks were visible. A few leaders were observed with estimated velocity of propagation of the order of the initial leaders of the cloud-to-ground strokes. However, the calculation of the velocities is much more uncertain than for cloud-to-ground strokes because the distance of the stroke to the camera is very difficult to determine accurately.

Stroke Height

Of more than academic interest is the height of lightning strokes. An attempt has been made in this investigation to obtain statistical data which are shown in Figures 16 and 17.

The largest number of strokes have a height above ground of between 2,000 and 7,000 feet. Fifty per cent are longer than 4,000 feet, and the maximum measured was 16,000 feet.

These measurements are based on the height of the stroke up to the bottom of the cloud. In many cases the strokes extend high up into the cloud as indicated by the illumination visible above the cloud.

Therefore, the values shown are minimum values. These statistics are of particular interest in the study of lightning effects on airplanes. From the data obtained it is quite evident that airplanes flying even at 16,000 feet altitude are subject to cloud-to-ground discharges. Evidence obtained from airplanes indicate that a considerable percentage of strokes to airplanes are associated with current peaks of relatively high magnitude.

Stroke Density

Of considerable interest from the point of view of protection is the number of strokes per square mile to be expected. Golde[8] has made a very skillful attempt to determine such values from statistics obtained on transmission lines. The results obtained in Pittsfield by photographic and visual observation, principally during night storms, are shown in Figure 18. The data are plotted as strokes per square mile against various size areas over which the strokes were averaged. Thus, if only strokes over an area with a radius of one-half mile were counted or an area of 0.75 square mile, a density of 19 strokes per square mile was obtained in 1938 and 10.2 in 1939. If, however, a larger radius was used, say three miles or an area of 28.2 square

Table I. Timetable of Lightning Stroke

Current Peak Number	Time Interval Microseconds	Duration Microseconds
1	0	0
2	27,600	27,600
3	3,000	30,600
4	44,400	75,000
5	35,800	110,800
6	75,700	186,500
7	2,500	189,000
8	36,000	225,000
9	500	225,500
10	19,200	244,700
11	236,600	481,300
12	5,400	486,700
13	28,600	515,300
14	600	515,900
15	900	516,800
16	900	517,700
17	62,100	579,800
18	14,300	594,100
19	30,400	624,500
20	26,100	650,600
21	34,300	684,900
22	2,500	687,400

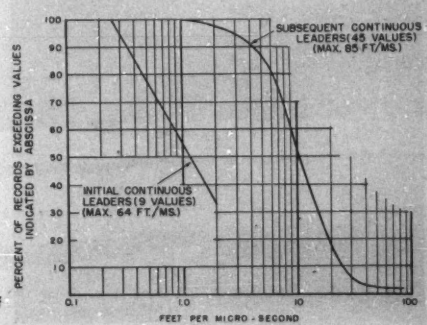

Figure 15. Velocity of leaders

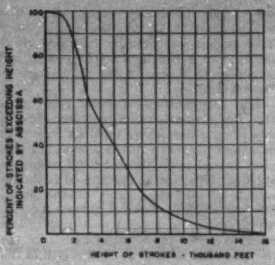

Figure 16. Vertical height of cloud-to-ground strokes—5-year average (181 strokes)

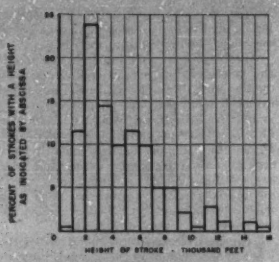

Figure 17. Vertical height of cloud-to-ground strokes—5-year average (181 strokes)

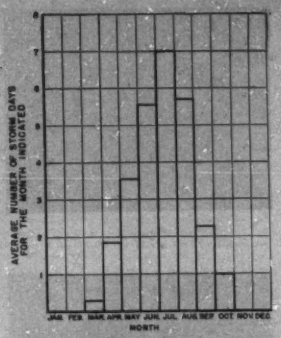

Figure 19. Storm day expectancy chart. Average storm days per month from 7-year investigation (1935–1941)

miles, stroke densities of only 2.9 and 4.4 strokes per square mile were obtained for 1938 and 1939, respectively.

This, of course, indicates that it not only is very difficult to obtain accurate values by observation but that the number of strokes in a given area vary widely. If a still smaller circle with a radius of 1,200 feet or 0.16 square mile is used, an average of 45 strokes per square mile per year was obtained in a three-year period, the maximum being 65 and the minimum 19. A period of three years, of course, is not sufficiently long to judge for a long-time average. It is, however, significant that extraordinary high stroke densities can occur.

It should also be mentioned that the observatory and its lightning rods with a height of 129 feet and two nearby smoke stacks never once have been struck during the seven years as was verified by magnetic links. On the other hand, a 180-foot high radiator of the local radio station has been struck three times in four years while under observation. This radiator is only 2,000 feet away from the observatory.

Such observations make it very difficult to reconcile the value of statistical evidence as far as the protection of single objects is concerned.

Storm Days

This investigation would not be complete without an evaluation of the number of storm days in the various years. The average per month over the 7-year period is shown in Figure 19. It shows that June, July, and August are by far the most productive months. The average number of storm days per year was found to be 27.2, with a minimum of 22 storm days and a maximum of 43 storm days. These results check the 30-year average of the United States Weather Bureau very well.

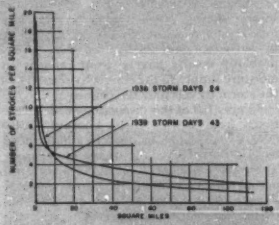

Figure 18. Number of lightning strokes per square mile as affected by area of observation (cloud-to-ground strokes)

Conclusions

1. The photographic method gives a very good tool to obtain a considerable number of valuable statistical information on the characteristics of lightning strokes at minimum expense.

2. It has been confirmed that a large number of strokes have long durations and that continuing currents are of frequent occurrence, both factors being important in the operation of transmission and distribution circuits.

3. The investigation has shown that lightning phenomena in Pittsfield are of essentially the same character as in other parts of the world.

References

1. Lightning to the Empire State Building, **K. B. McEachron.** *Journal of the Franklin Institute* (Philadelphia, Pa.), volume 227, number 2, February 1939, pages 149–217.

2. Lightning to the Empire State Building—II, **K. B. McEachron.** AIEE Transactions, volume 60, 1941, September section, pages 885–90.

3. Lightning Recording Instruments, **J. H. Hagenguth.** *General Electric Review* (Schenectady, N. Y.), volume 43, 1940, numbers 5 and 6, pages 195–201 and 248–55.

4. Lightning, **K. B. McEachron.** Encyclopaedia Britannica, Encyclopaedia Britannica Company Ltd. (New York, N. Y. and London, England).

5. The Lightning Discharge, **C. E. R. Bruce, R. H. Golde.** *Journal of the Institution of Electrical Engineers*, volume 88, part II, number 6, December 1941, pages 487–505.

6. The Measurement of Lightning Currents in Direct Strokes, **G. D. McCann.** AIEE Transactions, volume 63, 1944, pages 1157–64.

7. Progressive Lightning—II, **B. F. J. Schonland, D. J. Malan, and H. Collens.** *Proceedings*, Royal Society of London (London, England), series A, number 877, volume 152, November 1935, pages 595–625.

8. The Frequency of Occurrence and the Distribution of Lightning Flashes to Transmission Lines, **R. H. Golde.** AIEE Transactions, volume 64, 1945, pages 902–10.

9. Progressive Lightning—III—The Fine Structure of Return Lightning Strokes, **D. J. Malan, and H. Collens.** *Proceedings*, Royal Society of London (London, England), series A, number 909, volume 162, September 1937, pages 175–203.

10. Lightning, **J. W. Flowers.** *General Electric Review* (Schenectady, N. Y.), volume 47, 1945, number 4, pages 9–15.

Discussion

E. A. Evans (General Electric Company, Pittsfield, Mass.): J. H. Hagenguth has shown that a photographic and observational study of lightning can yield information of substantial value to the electrical industry.

One very important result of such a study is that it gives the investigator a vivid conception of the physical and electrical characteristics of thunderstorms which he cannot secure by any other means. It will help him to plan and interpret the measurements which must be made to arrive at a quantitative understanding of lightning phenomena. It will also help in evaluating the results of

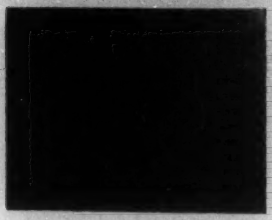

Figure 1

Figure 2

Figure 3

Figures 1–3. Discharges influenced by the proximity of two discharge centers

laboratory tests and the conclusions appearing in the literature which have been based on idealized thunderstorm models.

An observer who studies lightning under the conditions of unrestricted vision and on the scale of the investigation described in this paper soon sees that conditions in actual thunderstorms are far from the idealized diagrams shown in the literature. He sees that thunderstorms frequently have several active discharge centers and that several storm clouds can pass over a region at approximately the same time each with its active storm centers. These clouds often become so intermingled that it is impossible to tell where one ends and the other begins. The charged regions in these clouds interact on each other to produce lightning discharges under complicated and continually changing electric field conditions. To complicate the picture still further, each center of charge accumulation has its own life history during which it may be relatively inactive for a period, then increase greatly in activity, and finally die out. This probably results largely from changes in moisture supply to the convective centers as the storm travels over the country.

Figures 1–3 of this discussion,[1] which were taken from Devil's Head Lookout, Colorado, are examples of discharges influenced by the proximity of discharge centers. These three discharges were taken within a period of approximately three minutes Figure 1 was a cloud-to-cloud discharge between two near-by centers. The next discharge, about a minute later, was not photographed. The next two discharges, which occurred about one minute apart, are shown in Figures 2 and 3. In Figure 2 the discharge started from the left-hand center and terminated under the right-hand center. In Figure 3 the discharge started from the right-hand center and terminated beneath the left-hand center. (Figure 3 has been retouched to improve reproduction.)

It is of interest to note that these photographs were taken in the daytime. This was done by timing the period between several previous discharges and opening the camera shutter a few seconds before a discharge was expected. Discharges from any one center frequently occur at regular enough intervals so that this can be done. This method was used by me many times during two 3-month periods spent in observation of thunderstorm phenomena at Devil's Head.

The superposition of fields from more than one charged region probably explains why electric fields of low intensity have been measured frequently at the ground just previous to and at the time of cloud-to-ground strokes. The field at the ground is the resultant of all fields acting at the point. Strongly charged regions of opposite polarity acting on the same point on the earth can result in a very low field there, even though the field close to each charged region in the cloud may be of sufficient strength so that discharges are occurring from it to ground. This condition was shown to occur at Devil's Head in 1930 by corona measurements from a fine wire when two storm clouds met near the lookout. The corona current measurements showed that one of the centers was positive and the other negative. Both were discharging to ground.

Hagenguth found stroke durations lasting as long as 0.8 second. Figures 4*A*–4*C*[1] of this discussion show stroke durations of 0.2 0.3, and 0.6 second obtained at Devil's Head. Initial breakdown occurred at the extreme left of each picture. These pictures were obtained by swinging the camera through an angle of about 60 degrees in one second. Even longer times were experienced visually. On several occasions, while watching one discharge center, a discharge occurred from a center in back of me. I had time to turn completely around and observe the discharge.

Another indication of the duration of some discharges is given by one of the methods used to photograph lightning in the daytime. This method was based on the fact that discharges at any one time from one center are usually a mixture of single and so-called fast-multiple discharges or, less frequently are predominately of the slow-multiple type. A fast-multiple discharge is one which lasts a very small fraction of a second. A slow-multiple discharge is one which lasts a large fraction of a second. When slow-multiple

Figure 4. Moving camera records of multiple discharges

Initial breakdown occurred at the extreme left of each figure

A—Multiple discharge lasting approximately 0.2 second

B—Multiple discharge lasting approximately 0.3 second

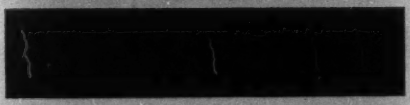

C—Multiple discharge lasting approximately 0.6 second

(A)

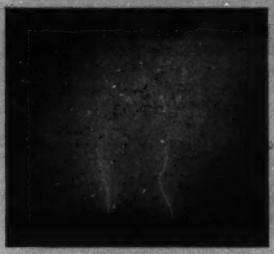

(B)

Figures 5A and 5B. Lightning discharges having multiple ground termini

Figure 6. Lightning striking plains in eastern Colorado

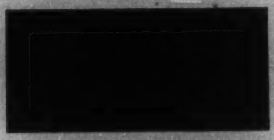

Figure 7. Lightning striking in foothills of Colorado Rockies

discharges predominated, I frequently photographed lightning discharges by tripping the shutter by hand upon seeing the start of the discharge. This procedure resulted in catching some of the later components of the stroke.

Hagenguth's Figures 12 and 13 of the paper show discharges which had two ground termini. While not common, these discharges occur sufficiently often so that the electrical industry should be familiar with them as an aid in interpreting certain field experiences. Two other such photographs obtained at Pittsfield in 1934 are shown in Figures 5*A* and 5*B* of this discussion. In Figure 5*A* the discharge struck the ground at three and possibly at four points. In Figure 5*B*, which was the next discharge from this center, the discharge struck the ground at two points.

These multiple termini discharges have been photographed also in Colorado.[1] Figure 6 of this discussion shows a stroke which struck the plains of eastern Colorado at two points. A third branch nearly reached the ground.

Figure 7[1] shows another such discharge with two ground termini which struck in the foothills just east of the front range of the Rocky Mountains about halfway between Denver and Colorado Springs.

In this discussion the following points have been covered:

1. The value of a photographic and observational study of lightning in giving the observer a clear conception of actual conditions in thunderstorms has been pointed out.

2. An example has been shown of the influence of field conditions on the path taken by lightning discharges.

3. A suggestion has been advanced explaining why, as frequently observed, lightning discharges can occur to ground during periods when the field at the ground is very low.

4. Stroke durations in Colorado have been shown to be of the same order as in Pittsfield, Mass.

5. Further evidence on strokes with multiple-ground termini has been presented showing that these occur both in Pittsfield, Mass. and in Colorado sufficiently often so that their existence should be kept in mind by the electrical industry in interpreting field experiences.

REFERENCE

1. A STUDY OF THE MECHANISM OF THE LIGHTNING DISCHARGE, **E. A. Evans.** *Stanford University Bulletin* (Stanford, Calif.) fifth series, number 158, July 31, 1933.

J. H. Hagenguth: I want to congratulate E. A. Evans on the fine work he has done in Colorado in photographing lightning discharges, and the good information he obtained from these studies.

Of particular interest are the photographs taken during the daytime by timing the opening of the camera shutter from corona observations.

There is no question that by means of photographic studies of lightning valuable information can be obtained concerning many of the characteristics of the stroke.

Accuracy of Temperature Measurements on Coil Surfaces

H. MARTIN BEEDE
NONMEMBER AIEE

BERNARD M. CAIN
MEMBER AIEE

Synopsis: In this paper the authors show the relationship to be expected between observations of surface temperature rise by various methods of measurement. Predictions based on laboratory tests are shown to be borne out by practical tests on induction motors. The data presented provide a basis for comparing a number of methods of temperature measurement from the standpoint of repetitive accuracy and the degree to which they indicate the true surface temperature.

THE NEED for data showing the basic relationship between observed values of surface temperature for different methods of observation has been suggested at numerous conferences concerned with the establishment of temperature standards. This paper has been written for the purpose of discussion of the basic problem of temperature measurement and to demonstrate by test data the limits of accuracy for various methods of observing the temperature of the surfaces of insulated coils and other parts of electrical devices. The work in this paper is limited to surfaces which remain stationary thus permitting the temperature measuring device to be in place during the entire test. Particular attention is given to surface temperature measurements of induction motor stators.

The results of tests made by the authors (see Tables I and II) show that the difference between indicated temperature and true surface temperature varies greatly with the type of temperature sensitive element used and the means of attaching it to the surface. Errors appear to be greatest for mercury-in-glass thermometers regardless of the method of mounting. Minimum error was obtained by using thermocouples made from small wire (10-mil diameter) embedded in a metal pellet and attached with a pliable plastic compound, and covered with a felt pad. When thermocouples made of larger wire were used, the error under some conditions was as great as with mercury-in-glass thermometers.

For mercury-in-glass thermometers the average indicated temperature rise was found to be about 85 per cent of the true temperature rise of the surface. Furthermore, the results show that thermometers such as those tested almost never will indicate nearer than about 90 per cent of the true rise while the minimum indication might be as low as 80 per cent of the true rise.

When using 10-mil thermocouples enclosed in a small lead pellet and mounted with a special putty and a felt covering, the average indicated temperature rise was found to be about 99 per cent of the true rise. The minimum ever to be expected for this method would be about 95 per cent of the true rise.

To obtain the foregoing results the authors planned a series of tests to determine the normal error of observation for a number of devices installed in several different ways for observing the surface temperature of a coil of insulated copper wire in still air. The laboratory tests were made in still air rather than moving air because temperature standards for electrical devices are based on shut down temperatures, not running temperatures, unless the latter happen to be higher.

Types of temperature sensitive exploring devices vary from relatively large glass thermometers to relatively minute ther-

Table I. Summary of Data From Test Coil Arranged in Order of Increasing Correction

	Type of Temperature Sensitive Element	Method of Application	Average Correction Per Cent of Rise	Standard Deviation Per Cent of Rise
1.	10-mil thermocouple, small pellet*	Duxseal** under felt†	0.9	1.4
2.	10-mil thermocouple, small pellet	Felt	1.1	1.2
3.	10-mil plain thermocouple	Putty	1.9	1.5
4.	10-mil plain thermocouple	Duxseal	3.2	2.0
5.	10-mil plain thermocouple	Felt	3.5	3.9
6.	20-mil thermocouple, large pellet	Felt	3.8	3.1
7.	10-mil thermocouple, small pellet	Duxseal	3.9	1.1
8.	10-mil thermocouple, small pellet	Putty	4.7	2.4
9.	20-mil plain thermocouple	Putty	4.9	1.8
10.	20-mil thermocouple, large pellet	Putty	5.3	2.7
11.	20-mil thermocouple, small pellet	Duxseal under felt	5.9	1.6
12.	20-mil thermocouple, large pellet	Duxseal	7.6	1.4
13.	20-mil plain thermocouple	Anatone	8.5	2.6
14.	20-mil plain thermocouple	Duxseal	8.8	2.6
15.	20-mil thermocouple, small pellet	Duxseal	10.5	2.0
16.	Thermometer‡	Putty	13.4	1.6
17.	20-mil plain thermocouple	Felt	13.6	3.4
18.	Thermometer‡	Felt (extra large)	14.9	2.8
19.	Thermometer‡	Duxseal	15.7	1.4
20.	Thermometer‡	Felt	16.8	3.2

* Junction enclosed in a cast lead pellet 1/4 by 3/16 by 1/16 inch.

** Duxseal is a trade name for a special putty described in text.

† Felt pads 1 by 1 by 1/8 inch.

‡ Mercury-in-glass thermometer 0–110 degrees centigrade, 1/4 inch diameter by 6 inches long

Paper 47-94, recommended by the AIEE committee on electric machinery for presentation at the AIEE winter meeting, New York, N. Y., January 27–31, 1947. Manuscript submitted November 13, 1946; made available for printing December 20, 1946.

H. MARTIN BEEDE and BERNARD M. CAIN are both with the General Electric Company, West Lynn, Mass.

The authors wish to express their appreciation for the assistance given by F. O. MacFee, Jr., C. M. Wheeler, and C. Mathews in planning and carrying out the test program on which this paper is based.

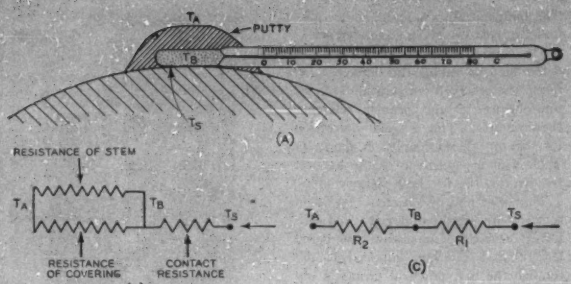

Figure 1. Simplified diagram of the thermal elements of a typical thermometer installation. The parallel resistances shown in *B* are combined in C to give a single resistance

mocouples. Also, the methods of applying these exploring devices to surfaces vary widely. For the studies reported in this paper the authors tested a total of 20 different combinations.

A comparison of various methods of observing the temperature rise of stationary surfaces in electric apparatus from the standpoint of basic accuracy and reliability should evaluate the following requirements:

1. From the standpoint of accurate correlation of data, it is important that the average departure of the indicated temperature from the true temperature be as small as possible.

2. From the designer's standpoint, an important feature of temperature measurement is ability to obtain the same temperature reading each time the test is repeated. A factor representing the degree of dispersion is therefore important.

Laboratory tests were conducted in such a manner that it was possible to determine the average departure from a reference temperature very close to the true temperature. It was also possible to determine the standard deviation or dispersion factor (see the appendix) for each method of measurement. The results are shown in Table I.

A series of tests also were taken on open induction motors comparing two methods of surface measurement. The laboratory tests showed that one of these methods had high basic accuracy while the other had relatively low basic accuracy. The results which are shown in Table II agree closely with the laboratory tests.

Analysis of Temperature Measurement Problem

In order for any device to measure the temperature of a surface such as the surface of a coil, it is necessary for the temperature sensitive portion of this device to be at the same thermal level as the surface. An analysis of this problem from a temperature and heat flow viewpoint can be presented by referring to the typical thermometer installation (Figure 1*A*) and accompanying heat flow circuit of Figure 1 showing the thermal resistances involved. Figure 1*B* shows the major resistances which must be considered. Figure 1*C* shows these combined into two basic resistances R_1 from the surface to the bulb and R_2 from the bulb to the air. The temperature of the bulb T_B will be at some temperature between the surface temperature T_S and the temperature of the surrounding air T_A. The bulb temperature T_B will approach the surface temperature T_S as the ratio R_1 to R_2 approaches zero.

To minimize the resistance R_1 between the bulb and the surface it is necessary to make sure that adequate contact is provided between the bulb and the surface. To make R_2 large it is necessary to provide insulation over the bulb.

The matter of insulating the bulb from the air is a very critical part of temperature measurement. If too much insulation is applied the temperature of the surface under the insulation will be increased. If too little insulation is used the ratio R_1 to R_2 will be such that T_B will not approach T_S. The selection of the material used in applying the bulb to the surface is therefore extremely important. An ideal material would be one having high thermal conductivity. The material then would take on the temperature of the surface being measured. However, no such plastic material is known. Another ideal insulation would be one which provided good thermal conductivity between the bulb and the surface but had low conductivity from the bulb to the air. This suggests the use of two materials such as putty with a felt covering. The last method together with several others was tried out in the laboratory tests.

Laboratory Tests

The usual procedure for determining the accuracy of any measuring device involves taking a number of successive measurements of the same quantity. This procedure becomes impractical for this type of temperature measurement because adhesive cement and other material used in applying the temperature sensitive element cannot be removed completely. Successive measurements therefore would be influenced to some extent by the previous measurement.

To avoid the problems of successive measurement at a single point a method was devised for making ten simultaneous

Table II. Comparison of Two Methods of Surface Temperature Measurement on a Number of Induction Motors

Frame Size	RPM	Average Temperature Rise* Method A	Method B	By Resistance	Rise A Divided by Rise B	Rise A Divided by Resistance Rise	Rise B Divided by Resistance Rise
204	1,200	31.5	33.8	32.6	0.934	0.970	1.039
254	1,200	26.5	29.8	28.0	0.890	0.945	1.061
254	1,800	54.8	59.8	64.0	0.916	0.855	0.934
254	1,800	30.5	34.3	31.0	0.890	0.984	1.105
254	1,800	43.3	49.4	49.5	0.877	0.930	1.060
254	1,200	27.0	28.6	32.0	0.944	0.844	0.894
254	1,800	43.3	49.5	50.0	0.874	0.865	0.990
284	3,600	83.8	99.8	98.0	0.840	0.855	1.018
284	3,600	43.3	42.3	45.0	1.025	0.961	0.939
324	1,200	26.0	31.9	31.5	0.816	0.826	1.012
324	1,200	31.4	34.0	38.0	0.923	0.825	0.895
324	1,200	43.1	50.5	55.0	0.854	0.784	0.918
326	3,000	42.3	44.0	44.0	0.960	0.960	1.000
326	1,200	30.5	35.0	33.0	0.806	0.925	1.060
326	3,000	37.0	42.8	42.5	0.866	0.871	1.005
				Average	0.895	0.894	1.003
				Standard deviation		0.064	0.064

* Temperature rise shown is the average of four readings, two on each end of stator.
Method *A* corresponds to item 17 and method *B* to item 1 in Table I.

measurements on a uniform surface. These then would be equivalent to ten successive measurements at a single point. The surface used for the purpose was made to simulate the surface of the winding of an electric machine. This was done by winding a large coil approximately ten inches in diameter by ten inches long using number 16 enameled copper wire. The wire was wound one-half inch deep on a wood spool and was treated with insulating varnish. Figure 2 is a photograph of this coil with five types of thermocouple installations ready for testing, each type located in a separate band. For each class of installation there are ten thermocouples installed around the circumference of the coil.

Each installation in a group of ten was located on the same circumferential strip of coil surface, as shown in Figure 2. The reference temperature for the group was determined by embedded thermocouples wound in place under the two outer layers of the coil. There were three such thermocouples for each test group equally spaced around the circumference making a total of 15 reference thermocouples for the entire coil. It was recognized that the temperature of the point where the reference thermocouples were located would be slightly higher than the temperature at the surface. However, this difference would be small because of the high thermal conductivity of the copper. The precise difference between the reference temperature and the true surface temperature of course could not be determined, but the data show that it would be less than one per cent. The temperature of the coil also was determined by resistance measurement as a check on the reference thermocouples and the results obtained agreed very closely.

The coil was heated by direct current. It was placed in a vertical position as shown in Figure 2 and located so that convection cooling would be uniform. The surface temperature for the tests was approximately 100 degrees centigrade with an ambient temperature of approximately 25 degrees centigrade. The temperature was found to be quite uniform over any given circumference.

The correction shown in Table I was determined by taking the difference between the observed temperature and the temperature of the nearest reference thermocouple. The average correction for the ten thermocouples is shown in Table I as a percentage of the average temperature rise for these thermocouples.

The selection of different types of temperature sensitive devices and different methods of mounting was based largely on a program intended to determine the best practical means of obtaining accurate measurements on coil surfaces. The device must be applicable to production testing and for this purpose it should be

1. Inexpensive.
2. Easy to install correctly by relatively inexperienced workers.
3. Easy to read correctly and accurately.
4. Applicable to any size machine.
5. Small in size in order to fit into relatively inaccessible places.
6. Designed so that it will not change appreciably the thermal characteristics of the body under test.
7. Capable of withstanding the temperatures encountered.
8. Able to adhere to surfaces in any position.
9. Noninjurious to the surfaces where it will be used.

Figure 3 shows four of the types of temperature measuring devices used in the investigation. The various combinations of device and method of application are listed in Table I.

A special putty known as Duxseal compound was used for comparison with ordinary putty because it does not soften at elevated temperature and because it can be used on commutators without leaving an objectionable oil deposit. Duxseal is a trade name for a compound used for sealing the space between cables and the inside of the duct in electrical conduits. Felt, held by adhesive at its edges, was used over the putty to provide stronger adherence to the surface and to provide surface insulation. Small diameter thermocouple wire (10-mil) was used to reduce conduction along the wire and because it is more flexible and hence easier to use. Thermocouples enclosed in pellets to increase the contact surface of the thermocouple junctions were used to improve the probability of good surface contact. Without the pellet there is always the possibility that a small movement of the junction might easily change its temperature a considerable amount. This is especially true when thermocouples are used under felt without putty. Table I shows that the installations using felt alone tend to have the greatest standard deviation.

The method of applying mercury-in-glass thermometers might be improved by further study. However, the limited use of this method did not appear to justify further work on it.

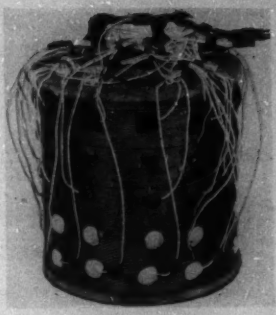

Figure 2. Coil used in laboratory tests for evaluating basic accuracy of various methods of observing surface temperature. Photograph shows five sets of thermocouples ready for testing five different methods of measurement

Tests on Induction Motors

In order to obtain practical data for comparing two methods of temperature measurement on induction motors a series of heat runs was made on 15 different open motors under various operating conditions. The tests were conducted by several different operators over a period of three months. Duplicate sets of four thermocouples each were installed for each test. One set consisted of four 20-mil thermocouples under felt corresponding to item 17 of Table I. The other set consisted of four 10-mil thermocouples in small lead pellets covered

Table III. Standard Deviation for Rise by Resistance

	Standard Deviation for One Reading, Per Cent	Standard Deviation for Average of Four Readings,* Per Cent	Standard Deviation of Ratio of Surface to Resistance, Per Cent	Standard Deviation of Rise by Resistance,** Per Cent
Method *A*	3.4	1.7	6.4	6.17
Method *B*	1.4	0.7	6.4	6.35

* The standard deviation for the average of four readings is the standard deviation for individual readings divided by the square root of four.

** The standard deviation for rise by resistance is computed by taking the square root of the difference of squares of the second and third columns.

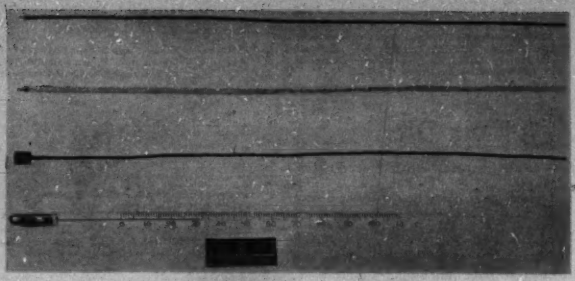

Figure 3. Thermometer and thermocouples used in tests. Top to bottom these are 10-mil thermocouple, 20-mil thermocouple, 10-mil thermocouple enclosed in small lead pellet (1/4 by 3/16 by 1/16 inch), mercury-in-glass thermometer

with Duxseal and a felt pad corresponding to item 1 of Table I. The two sets were installed in pairs consisting of one of each type. Figure 4 shows one end of a motor with the end shield and rotor removed and with the two sets of thermocouples in place. One of each type of thermocouples may be seen at the top and at the left side of the end winding. Additional thermocouples were installed on the opposite end not visible in the photograph making a total of eight thermocouples. The results of the induction motor tests are shown in Table II.

The grand average for the ratio of the rise by plain thermocouple to the rise by pellet thermocouple for all the induction motor tests was 0.895. That is, the pellet type thermocouple installed under Duxseal and felt indicated on an average a 10.5 per-cent higher temperature rise than the plain thermocouples installed under felt. From Table I the laboratory tests would indicate that this difference would be 13.6 per cent minus 0.9 per cent, or 12.7 per cent, which is a very reasonable agreement.

Comparison of the rise by resistance with rise by the two thermocouple methods gives a very interesting result. The laboratory tests indicate that method *B* is much more accurate than method *A*. (See standard deviation in Table I.) However, Table II shows that the standard deviation, or dispersion factor for the ratio of surface rise to resistance rise is the same for both methods. This can be explained by computing the standard deviation for the resistance measurement from the data by both methods. The results are essentially the same for each and are shown in Table III.

The standard deviation for rise by resistance thus computed refers to the relationship between observed rise by resistance and true surface temperature. It therefore includes both testing error and variation caused by differences in the machines tested. How much each contributes to the variation cannot be determined without further data.

Conclusions

Accurate measurement of surface temperature is not a simple matter of applying a thermometer to the surface. To obtain an accurate measurement it is necessary to give careful consideration to the design of the temperature sensitive element and the method of applying it to the surface. Methods which are commonly accepted may upon close examination prove to be less reliable than is desired.

To measure surface temperature accurately the following are important:

1. It is necessary to have a low thermal resistance between the temperature sensitive element and the surface. A thermocouple having its junction enclosed in a metal pellet or soldered to a metal tab will provide a good contact if held firmly against the surface.

Figure 4. Induction motor with end shield and rotor removed showing installation of thermocouples for comparing two methods of applying thermocouples

2. The temperature sensitive element must be held firmly against the surface. This can be done by covering it with a pliable but fairly firm putty which will not soften at the temperature to be measured. Wires leading from the thermocouple junctions should be sufficiently flexible so that there will be no tendency for stiffness of the wire to lift the junction off the surface.

3. It is necessary to provide a good thermal insulation between the temperature sensitive element and the surrounding air. Although the putty covering may be adequate for this, it is advisable to provide an additional covering of thin felt larger than the pad of putty and attached to the surface by adhesive cement at its edges. In addition to providing thermal insulation this felt covering gives added assurance that the putty will not become loose. Without this covering the temperature sensitive element may become dislodged sufficiently to cause an error and yet not be noticeably loose. Use of small size wire (approximately 10-mil diameter) for thermocouples is also important. Large wires provide a relatively low resistance path from the junction to the surrounding air. Use of small wire greatly increases the thermal resistance of this path.

Appendix. Explanation of the Use of Standard Deviation

The deviation of an individual observation is the amount that the observed value differs from the average of a number of observations. The "standard deviation" is calculated by taking the rms of the deviations for all the observations. Standard deviation has a known relation to the distribution of the data only when the distribution follows a normal symmetrical pattern.

Data conform to a normal distribution when each observation has an equal chance of being above or below the average. An observation of temperature however theoretically cannot be greater than the true temperature although it might be any amount less than the true temperature depending upon the accuracy of the method. Temperature readings therefore will have a skewed rather than a symmetrical distribution.

The authors have chosen to ignore the fact that errors in temperature measurement follow a skewed distribution. By applying the usual rules for normal distributions it has been possible to demonstrate relationships between various methods which are qualitatively correct although not precisely exact. The values of standard deviation which are shown in the tables are an index to the degree of dispersion of the data. They should not be used in the usual sense of standard deviation.

References

1. Investigation of Hot-Spot Temperatures in Fractional-Horsepower Motors, L. H. Hirsch, R. F. Munier, M. L. Schmidt, L. W. Wightman, J. S. Himebrook, T. C. Lloyd, O. G. Coffman, C. P. Potter. AIEE Transactions, volume 64, 1945, March section, pages 128–36.

2. Investigation of Hot-Spot Temperatures in Integral-Horsepower Motors, L. E. Hildebrand, B. M. Cain, F. D. Phillips, W. R. Hough, J. G. Rosswog, C. P. Potter. AIEE Transactions, volume 64, 1945, March section, pages 124–8.

3. Determination of Temperature Rise of Induction Motors, E. R. Summers. AIEE Transactions, volume 58, September section, 1939, pages 459–67.

4. Measurement of Temperature in General-Purpose Squirrel-Cage Induction Motors, C. P. Potter. AIEE Transactions, volume 58, 1939, September section, pages 468–72.

5. Some Problems in the Standardization of Temperature Ratings of Fractional-Horsepower Motors, Cyril G. Veinott. AIEE Transactions, volume 59, 1940, pages 1055–61.

6. Temperature Limits and Measurements for Rating of D-C Machines, F. A. Compton, Jr. AIEE Transactions, volume 62, 1943, December section, pages 780–5.

Discussion

C. P. Potter (Wagner Electric Corporation, St. Louis, Mo.): This paper demonstrates quite clearly that it is necessary to take certain precautions in order to obtain true measurements of the temperatures on coil surfaces. If this information had been available before earlier tests were made,[1,2] it is quite likely that the results obtained would have been more consistent.

The tests which were reported by the writer at that time were made using thermocouples 12½ mils in diameter which were inserted in the crevices between adjacent coils and then covered with a layer of sealing compound which becomes quite hard and is not affected by temperatures ordinarily obtained in motor windings.

Beede and Cain recommend the use of a lead pellet covered with putty and felt, and because of the fact that we have not tried this method, we do not know whether it will give results comparable with those which we obtained.

It seems quite likely that every company employs a slightly different method of attaching and protecting thermocouples in temperature tests and it would be well worthwhile for all of us to compare the methods we have been using with those proposed by the authors of the paper.

Beede and Cain are to be congratulated for attacking the fundamental problems involved in the measurement of surface temperatures, and completing the record by submitting the results of their tests. It is hoped that more and more motor designers will become interested in the apparently simple problem of determining motor winding temperatures, and that the literature on the subject will soon be quite complete.

References

1. Investigation of Hot-Spot Temperatures in Integral-Horsepower Motors, L. E. Hildebrand, B. M. Cain, F. D. Phillips, W. R. Hough, J. G. Rosswog, C. P. Potter. AIEE Transactions, volume 64, 1945, March section, pages 124–8.

2. Investigation of Hot-Spot Temperatures in Fractional-Horsepower Motors, L. H. Hirsch, R. F. Munier, M. L. Schmidt, L. W. Wightman, F. S. Himebrook, T. C. Lloyd, O. G. Coffman, C. P. Potter. AIEE Transactions, volume 64, 1945, March section, pages 128–36.

John L. Fuller (Reliance Electric and Engineering Company, Cleveland, Ohio): The paper has pointed up the need of more accurate than usual method of temperature measurement on electric apparatus. It also shows that properly measured surface temperature rise on induction motors is nominally equivalent to rise by resistance.

Our experience over the last three years using thermocouples instead of thermometers for engineering test data has proved that far greater consistency of results can be obtained by this means. Thermocouples of 0.020-inch diameter and a plastic putty have been used. A few tests using 0.010-inch thermocouples with lead pellets secured from Beede and Cain have shown that approximately 10 per cent higher rise may be obtained for a well ventilated open motor, whereas the difference compared with the larger thermocouple wire becomes much less for a totally enclosed fan cooled motor.

As a laboratory check, tests were made to compare how well various thermocouples might follow a changing temperature. To accomplish this, a long brass strip of uniform cross section was heated by passage of current. A thermocouple was soldered into a small hole and was assumed to read the true temperature. Two other couples were placed adjacent and within 1–4-inch of the soldered-in couples, and all three covered with a single piece of putty. Starting from room temperature, the strip was heated at various rates. Results are shown in Table I.

These results show a very definite advantage when measuring rapidly changing temperatures in the use of a small couple, and some advantage for the lead pellet. Presumably more advantage for the lead pellet would show up when taking temperatures of a surface having a lower heat conductivity than the brass strip investigated.

The adoption of a standard for apparatus temperature limits equal to those for rise by resistance when using this applied detector method seems justifiable.

Table I

Initial Rate of Rise, C Per Minute	Time, Minutes	True Rise, C	Rise for 0.020-inch Couple Touching Strip		Rise for 0.010-inch Couple Touching Strip		Rise for 0.010-inch Thermocouple in Lead Pellet Touching Strip	
			C	Per Cent of True	C	Per Cent of True	C	Per Cent of True
8	0	0	0		0		0	
	1	8	4.5	56.2	6	75	7	87.5
	3	20	15.5	77.5	18	90	19.5	97.5
	5	26	23	88.5	24	92.4	26	100
	7	29.5	27	91.5	28.5	96.5	29.5	100
	9	31	29.5	95.2	31	100	31	100
22	0	0	0		0		0	
	1	22.5	13	57.8	17.5	77.9	20.5	91
	3	51.5	40.5	78.6	47	91.3	49	95.1
	5	65	57	87.7	61	94	63	97
	7	71.5	65	91	69	96.5	70	98
	9	74.5	69.5	93.3	73.5	98.6	73.5	98.6
60	0	0	0		0		0	
	1	60	33	55.0	53	88.4	57	95
	3	84.5	67.5	80	79.5	94	80.5	95.2
	5	106	93.5	88.2	102	96.2	103.5	97.7
	7	117	105	89.8	114	97.5	114.5	97.9
	9	121.5	112	92.2	120	98.8	120	98.8
76	0	0	0		*	*	0	
	1	76	39	51.3	*	*	70	92.1
	3	129	102	79	*	*	125	97
	5	157	138	87.9	*	*	152	96.8
	7	171	153	89.5	*	*	167	97.8

*No data available.

Internal Corona Discharges in Insulated Cables

E. W. GREENFIELD
MEMBER AIEE

IN recent years there has been considerable interest in the study of internal discharges associated with electric apparatus operating at high-voltage stresses. Experience has indicated generally that insulated cables or other electric apparatus have a higher mortality rate when operated with internal discharges present. Usually such discharges take place at an interface between gas and liquid or solid, the gas phase becoming ionized and thus conductive. All organic materials in the discharge area suffer profound chemical and physical changes because of the localized heating and electronic bombardment. Progressive damage with resulting premature failure of the insulation then occurs.

Early investigation[1] disclosed that electric discharges always produced high-frequency components in the voltage wave. The magnitude of these ripples is influenced by the electrical stress and volume of ionized regions, whereas the range of frequencies is determined by the distribution of relaxation times of the many local discharge circuits. The detection and measurement of internal discharges therefore simplified to the detection and measurement of the discharge harmonics in the voltage or current wave applied to the object under test.

In 1933, Paine, Tykociner, and Brown[2] developed several forms of discharge bridges and applied these to cable. In 1936 Armon and Starr[3] described a number of practical cable discharge-detecting circuits and for the first time utilized the Schering bridge as a means to suppress extraneously-produced harmonics. Quinn[4] used a simple high-pass filter and cathode-ray oscilloscope to detect discharges in transformer bushings and other high-voltage equipment. Extending Armon and Starr's technique, Whitehead and Shaw[5] described studies of internal discharges in paper-cable models using the Schering-bridge type detector.

Regardless of differences in method and apparatus there is, however, common agreement as to the importance of suppressing discharges within electric equipment and cables. In the latter particularly, it is agreed that internal discharges must be absent at maximum operating voltage, if the cable is to realize its good inherent properties and ultimate life.

In 1938, the author became interested in the use of an internal discharge detector for determining cable quality. Whereas power factor and dielectric loss for many years have been used as criteria of high-voltage cable quality, for the most part it is the interpretation of these parameters in terms of gaseous ionization which has given them their practical significance. In many cases where the correlation has not been clear, the interpretation has been misleading. On the other hand, direct detection and measurement of internal discharges are readily accomplished, and interpretation of the records unmistakable.

A simplified form of internal discharge detecting and measuring equipment has been developed, based principally upon Arman and Starr's original circuit. This equipment has been used for the past five or six years in the evaluation of type *CB* (carbon-black) impregnated-paper-insulated cable.[6] In this application, the outstanding beneficial effects obtained by incorporating highly adsorbent conductive carbon-black paper tapes within the structure of an impregnated-paper cable have been demonstrated conclusively. Also, interesting information has been recorded regarding deterioration produced by silent discharges, associated with the so-called solid ionization within the insulation.

Paper 47-91 recommended by the AIEE committee on power transmission and distribution for presentation at the AIEE winter meeting, New York, N. Y., January 27-31, 1947. Manuscript submitted November 8, 1946; made available for printing December 18, 1946.

E. W. GREENFIELD is engineer-in-charge, electrical laboratory, Anaconda Wire and Cable Company, Hastings-on-Hudson, N. Y.

The author is indebted to many of his engineering associates who have assisted in the development and construction of the detector, test program, and preparation of this paper and wishes to make specific acknowledgements to A. E. Widmer, D. G. Clute, G. E. Kinsley and E. S. Rohrbach, all with Anaconda Wire and Cable Company, Hastings-on-Hudson, N. Y.

Corona Detection and Measurement

The final form of the internal corona detector was controlled by three principal considerations:

1. To be completely self-contained and portable.
2. To be applicable to all types of cable (within its voltage range) including flexible rubber or synthetic-insulated and shielded as well as lead-covered cable.
3. To be applicable to paper-cable model tests where the sample is set up in separate sealed containers.

As shown in Figure 1, the final equipment consists of four component parts; power, high-voltage, bridge, and detector circuits. Figure 2 shows the completed self-contained unit.

Although the circuit diagrams are almost self-descriptive, a few remarks concerning some of the special features will be required.

Power Circuit

The filter and isolating transformers (items *F* and *T*) were found of benefit in decreasing audio- and radio-frequency disturbances from the power line.

High-Voltage Circuit

The high-voltage transformer was designed especially for this installation, taking every precaution to make the windings and terminals corona-free. Enclosing copper electrostatic shields grounded to

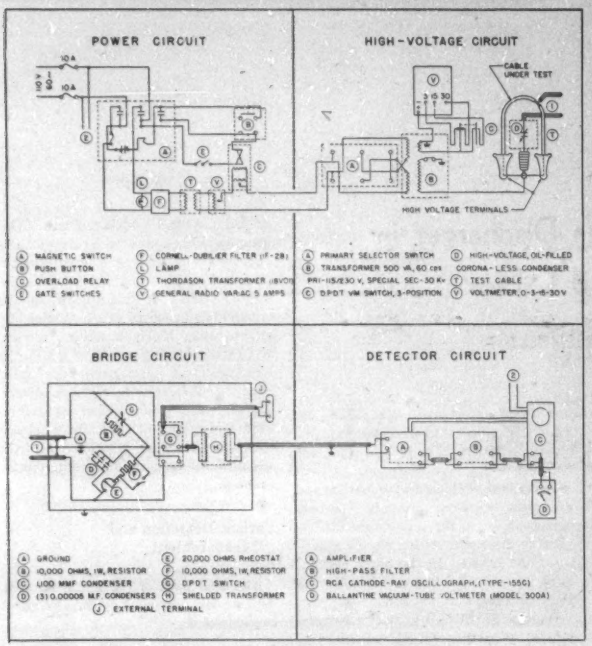

Figure 1. Wiring diagram, internal corona detector

core and case are used between the primary and secondary windings. As shown in Figure 3, the high-voltage terminal of the transformer connects directly to the high-voltage side of a corona-free oil-filled variable capacitor through a 30-kv oil-filled bushing. This capacitor consists of a fixed (lower) and a movable (upper) brass plate each 1/2-inch thick and ten inches in diameter with all edges rounded. An approximate rule for setting the capacitor plates is to allow 10,000 volts for each 0.100 inch of plate separation. The capacitor is filled with a high-grade insulating oil (Dow Corning silicone fluid number 500 has been found satisfactory).

Figure 3 shows the high-voltage corona-free terminals mounted one at each end of the 30-kv bushing arms. These terminals, called flower pots, were designed especially for sheathed cable testing. Figure 4 shows a cross section of a flower pot. The terminal is made of brass machined to a log-log flare to obtain constant longitudinal stress on the dielectric medium below the discharge point up to 30 kv. A banana jack is located in the bottom of the holder with a guide (of insulating material) to facilitate the insertion of the cable end. One or more cylindrical polystyrene barriers are placed in the oil space extending almost to the top of the terminal. This allows free passage of oil (through small openings) but provides barrier action to prevent oil ions from lining up. The terminals may be filled with clean dry transformer oil before testing, but silicone fluid will be found more satisfactory and durable. Each flower pot may be rotated readily about its support and drained into the catch pans shown in Figure 3.

Bridge Circuit

The bridge circuit shown in Figure 1 contains two arms which are in the high-voltage compartment. One consists of the high-voltage oil-filled capacitor and the other, the cable or model under test. Shielded leads, as shown in Figure 3, connect the cable sheath and the movable plate of the capacitor to opposite corners of the Schering bridge. The junction of the low-voltage arms is grounded, and leads from opposite corners of the bridge are brought to a double-pole double-throw switch which connects directly to either an external terminal for amplification calibration determination or to a special shielded bridge transformer which permits operating the oscillograph and amplifier at ground potential. The low-voltage bridge arms are located in a doubly shielded section at the upper right of the cabinet.

Detector Circuit

From the shielded transformer the output is fed directly to a flat voltage resistance–capacitance amplifier with a maximum gain of 400. This unit provides sufficient gain over and above the oscillograph amplification to detect the smallest types of relaxation oscillation (frequencies determined by $1/RC$ of the discharge circuit). The amplifier is varied by screwdriver control through a small opening in the side of the cabinet. A calibration terminal can be used to determine or set the over-all amplification of the amplifier and oscillograph. This is accomplished by placing a known source of 1,000-cycle voltage across an attenuating network and varying the gain to give the required sensitivity in microvolts per inch. From the amplifier the circuit is continued to a 3-section high-pass filter which has a very sharp cutoff at 1,000 cycles. It has a stop band from 60 cycles through the first 11 harmonics with an attenuation of over 45 decibels. The output of the filter goes directly to the cathode-ray oscillograph.

For quantitative determination of the volume of ionization taking place in the discharge, a sensitive vacuum-tube voltmeter is inserted in parallel with the oscillograph. This instrument has a range from 30 microvolts to 100 volts, with high input impedance, and permits obtaining a value for ionization which is proportional to the average value of the complex discharge voltage wave (including harmonics) up to 150 kilocycles.

Table I

Cable Sample Group Number	Description
LL-1 and *2*	Standard solid-type cable with round, stranded conductor; no conductor shielding
LL-3 and *4*	As above, except conductor shielded with intercalated aluminum-foil-backed paper (foil side inwards) and similar outside core shielding (foil side outwards)
LL-5 and *6*	Type *CB* cable (carbon-black tapes replace three insulating tapes over the conductor and three insulating tapes over the core)

Theory of Operation

Operation of the circuits used is comparatively simple. Sixty-cycle voltage applied to the upper and lower corners of the bridge produces a voltage across the detector terminals proportional to the unbalance in magnitude and phase between the high-voltage capacitor and the test object. Manipulation of resistance and capacitance elements in the low-voltage arm restores bridge balance, and the voltage across the detector terminals will be reduced to zero provided there are no harmonics present in the bridge currents. Whereas the capacitance balance of a Schering bridge is universal for all frequencies, the phase-angle balance is unique. Therefore, perfect balance is obtained only for the condition that no harmonics are present. When discharges occur in the test sample, the fundamental is modulated by unit functions which produce a varying degree of higher frequency waves, and it is the in-phase or loss components of these high-frequency discharge waves which pass through the bridge into the detecting circuits. The function of the high-pass filter is to remove any of the usual harmonics which may be present in the applied voltage from the transformer.

Applied Voltage

Discharges occur initially on the peaks of the voltage wave, and as the voltage is increased the region of discharge spreads. Hence, it is the peak value of the applied voltage which is of most importance in determining discharge characteristics. For this reason, the voltmeter is calibrated in rms volts determined from peak readings obtained by means of a precision high-voltage crest-voltmeter.

Sample Preparation and Measurement

If the cable to be tested is sufficiently flexible, it is wrapped loosely about the high-voltage capacitor, and both ends suitably prepared to eliminate end discharges are inserted in the oil-filled terminals. Larger lead-covered cables are formed into inverted U shapes and the ends brought through bushed holes in the top of the cabinet down into the high-voltage terminals.

Where the cable under test is inserted directly into the high-voltage compartment, end preparation is very simple. The conductive sheath is cut back about $3^1/_2$ inches, belled out slightly, a foil cylinder partly inserted, and then bent back over the sheath edge to form a smooth rounded surface. Finally, a standard banana plug is attached to the conductor. When the test cable must be located externally to the unit, special high- and low-voltage leads are used to extend the sample arm of the bridge. The high-voltage lead is more than 0.6 inch in diameter and sufficiently smooth so that it produces no discharges up to 30 kv. It is necessary to insure that the whole high-voltage system external to the test cable itself be free of electric discharge at the maximum test voltage.

With the test cable connected into the bridge circuit, a moderate voltage is applied and the Schering bridge balanced for both phase and magnitude until a perfectly smooth straight line is obtained on the screen of the oscilloscope as shown in Figure 5*a*. The voltage is increased then until the first signs of a ripple or a pip or jagged saw teeth appear. This is the initiation voltage. The voltage then is decreased slowly until all signs of ripple disappear. This is termed the extinction point. The latter always occurs at a lower value because of the reduced energy required to maintain the ions in motion. Figure 5*b* shows the oscilloscope screen after the voltage has been increased somewhat beyond the initiation point.

Once the discharge is started, the vacuum-tube voltmeter is connected into the oscilloscope circuit, and ripple potential may be measured directly because the gain of all amplifiers is known from previous calibration.

A word about over-all gain is required. It appears certain from our experience that the determination of discharge initiation and extinction voltages is somewhat dependent on the amount of amplification provided by the detection system. Electric discharges in minute voids distributed within the insulation apparently go through all the phases of dark discharge, brush, and finally visual corona as the stress is increased gradually. Each of these stages introduces harmonics on the voltage and current waves which progressively increase in amplitude and frequency characteristics. The higher the gain, the lower the order of discharge which can be detected. Sufficient gain must be available so that the start of true ionization can be observed. On the other hand, excessive gain will show apparent discharges which actually may be of an electronic nature rather than the more commonly considered relaxation type because of ionization. For this work a maximum gain of about 250-microvolts-per-inch oscilloscope deflection has been adopted.

Type CB Cable Tests

In a previous paper,[8] it was shown that the application of carbon-black paper tapes, containing an enormous surface area of a special electrically conductive and chemically adsorptive colloidal carbon, produced impregnated-paper cable which was in every way superior to standard types. It is known now that carbon-black tapes of correct composition, quantity, and distribution in the cable

Figure 2. Internal corona detector

Cable sample is totally enclosed in high-voltage compartment while test is being conducted

Figure 3. High-voltage test compartment internal corona detector

Shows high-voltage capacitor, flower-pot high-voltage corona-free terminals, and cable sample under test

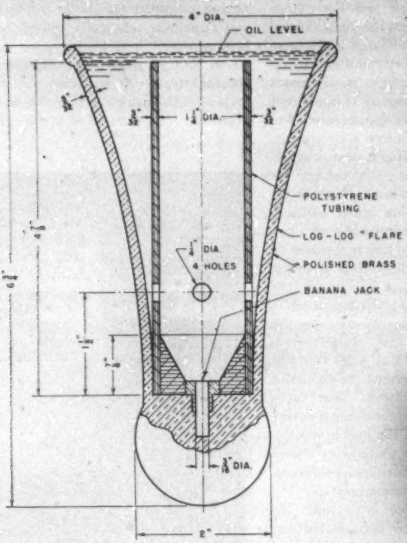

Figure 4. High-voltage corona-free terminal

Internal corona detector

Figure 5 (below). Oscillogram of internal corona. Polyethylene-insulated coaxial cable

a—Trace on oscillograph screen after balancing bridge at a voltage below discharge initiation point
b—Trace of discharge waves at a voltage 25 per cent above initiation point
c—Timing wave, 1,000 cycles per second

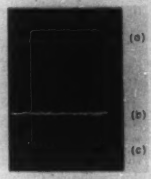

structure exert a 4-fold benefit as explained in the following:

1. Avidly adsorb oxidation products produced in the oil as a result of heat, stress, and catalysis. Reduce formation of metallic soaps (copper and lead) by screening the electrode metals. Adsorbed products (electrolytes) held outside of dielectric field influence because of shielding by high conductivity of carbon.

2. Eliminate strand stress concentrations at conductor thus reducing maximum stress by more than 25 per cent. Eliminate possibility of stress between loose sheath and insulated core. Because the carbon-black tapes form the cable's electrodes, the fit of the paper insulation to the electrodes is better than that obtained by any other means not excepting highly polished metal cylinders.

3. The high stress electrode is transferred from a metal (copper) with a high-work function to a nonmetal (carbon) with a low-work function. This has an important influence on the character of the electric discharge. At a given gradient, the discharges from carbon are much less severe than those from copper.

4. Impulse strength of the cable insulation is increased because the carbon-black tapes act as distributed series resistors of sufficient value to damp the wave fronts of surges of external origin.

The internal corona detector described in the afore-mentioned has been found very useful to evaluate type *CB* cable. Several of these experiments, involving both cable and models, are described as follows:

Cable Tests

A number of lengths of single-conductor impregnated-paper lead-covered cable were prepared. See Table I. These cables all were rated nominally at 12 kv; all had 4/0 American Wire Gauge standard stranded conductors, 0.172-inch paper insulation (including *CB* tapes), 0.086-inch lead sheath.

Table II is a summary of the cable constructions and calculated operating voltage stresses. The standard construction shows the highest maximum stress as a result of strand concentrations. However, the decrease in actual insulating wall for the other constructions partially offsets their strand shielding features so that the maximum stresses are not greatly different for all cable types. (For higher voltage cable (thicker walls), this is not true; strand shielding reduces maximum stress very appreciably.)

Particular care was exercised to secure uniform high-quality taping, 60/40 per cent overlays with butt spaces varying from 0 to 5 per cent maximum; all sections were taped in one length. The cables were dried and impregnated together in a single tank under standard treatment procedures.

After routine factory acceptance tests to Association of Edison Illuminating Companies specifications, two 12-foot lengths of each construction were subjected to thermal aging cycles as follows:

1. Initial measurements of power factor, corona initiation and extinction voltage, and volume of discharge at twice operating voltage, all at room temperature.

2. Ends sealed with foil and sealing tapes and cables placed in an aging oven held at 125 degrees centigrade for 5-, 15-, and 30-day periods, respectively.

3. After each aging period the cables were removed from the oven, allowed to cool for 24 hours and then remeasured per item 1.

Table IV is a summary of the results obtained during the heat-aging tests; the averaged results of each construction are shown graphically in Figures 6*A* and 6*B* These results are indeed striking. All cable lengths started with power factors very nearly equivalent, variations in the same type exceeding differences between types. The corona initiation voltage, however, showed distinot differences by type. The standard cable exhibited start of discharge at less than twice operating voltage. The foil-backed paper conductor-shielded construction was appreciably better, discharge beginning at almost 20-per-cent higher voltage. The type *CB* cable with carbon-black tape electrodes showed no internal discharges up to almost three times operating voltage and in this respect was much superior to either of the other types. The initial volume of discharge (as defined by the effective

Table II. Cable Construction and Operating Voltage Stresses

Cable Sample Group *LL*

Cable Sample Number	Construction	Insulation Thickness: Total Mils	Insulation Thickness: Effective Mils	Operating Voltage Stress: Average Volts Per Mil	Operating Voltage Stress: Maximum Volts Per Mil
LL-1 and *2*	Standard	172	172	40.0	66.0
LL-3 and *4*	Conductor shielded (foil-backed paper)	172	152	46.0	58.5
LL 5 and 6	Type *CB*	172	142	48.5	61.0

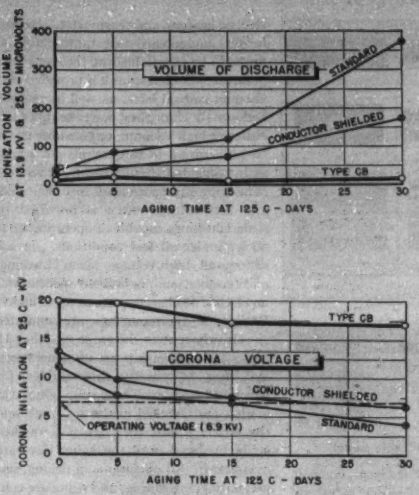

Figure 6A. Ionization characteristics during aging sealed paper-lead cable samples (group *LL*)

Ionization volume and corona initiation voltage

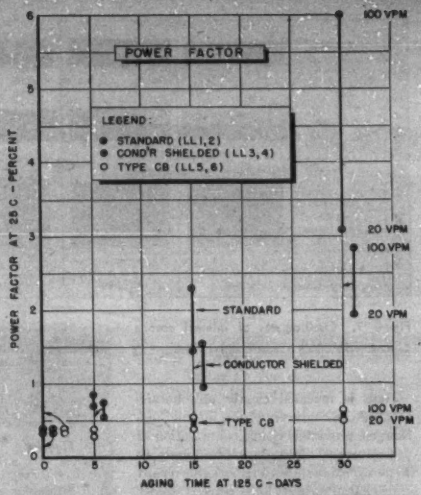

Figure 6B. Ionization characteristics during aging sealed paper-lead cable sample (group *LL*)

Power factor at 20 and 100 volts per mil

microvolts of the in-phase discharge harmonics at twice operating voltage) also showed large differences as would be expected considering the observed initiation voltages.

Progress of aging at 125 degrees centigrade showed deterioration of electrical characteristics in all the cables under test, the amount varying widely among the three constructions. At the end of 15 days, the standard cable showed initiation of internal discharges at operating voltage and at the end of 30 days the initiation point had dropped to 4.0 kv, less than 60 per cent of operating voltage. During this same period, the volume of discharge increased almost 15 times. The foil-backed paper conductor-shielded cable also showed a continuously decreasing initiation point and after 22 or 23 days aging exhibited internal discharges at operating voltage. The volume of ionization rose steadily to over six times initial, and the disruptive character of the discharge was emphasized. Only the type *CB* cables exhibited discharge stability. During the entire aging period the initiation voltage was reduced by only 3 kv, from approximately 20 to 17 kv. The volume of discharge remained remarkably low throughout the test as expected because the initiation point never dropped as low as 14 kv, the applied voltage at which volume of discharge was determined.

Figure 6*B* shows how the power factor varied during the aging period. The increase in gaseous ionization is shown clearly by the relative values of power factor at 100 and 20 volts per mil for each cable type. Reference to Table II indicates that the maximum stress at operating voltage (6.9 kv) for all cables was approximately 66 volts per mil. Therefore, because the corona initiation voltage after the first few days of aging had decreased in the case of the standard and foil-backed paper conductor-shielded cables to below 10 kv, power factor measurements at 100 volts per mil were made under discharge conditions whereas at 20-volts-per-mil measurements they were not. This accounts for the good agreement between power factor and discharge measurements. In the case of type *CB* cables, there were no measurable discharges at 100 volts per mil at any time Hence the power factor difference between 100 and 20 volts per mil remained unchanged, and the relatively small increase in power factor level must be accounted for by chemical changes alone.

Figure 7 is a group of oscillograms taken during the course of the cable tests. Each row represents a single cable as designated and the photographs from left to right were taken initially and after 5 days, and 30 days aging. These oscillograms were made immediately following the tests described above with all cables at room temperature. The upper trace in each picture is the result of internal discharges within the cable; the lower trace is a 1,000-cycle timing wave. All oscillograms with the exception of the 30-day aged standard cable were taken at a gain level of 250 microvolts per inch; the exception was made at one half that gain.

Table III. Cable Model Construction and Test Voltage Stresses

Cable Model Set *R*

Cable Model Number	Construction	Effective Insulation Thickness, Mils	Test Voltage Stresses: Average Volts Per Mil	Test Voltage Stresses: Maximum Volts Per Mil
R-5	Type *CB*	63	100	105
R-6	Conductor shielded (foil-backed paper)	63	100	105
R-7	Tinned cylindrical conductor	63	100	107
R-8	Standard	63	100	126

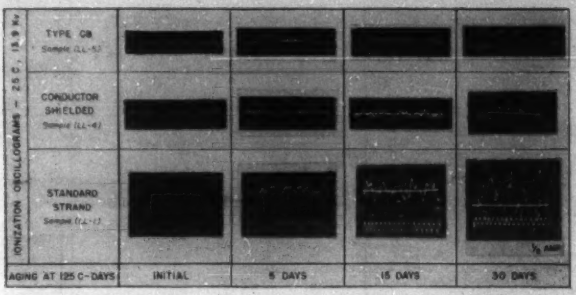

Figure 7. Oscillograms of internal corona
Sealed paper-lead cable samples (group *LL*)

Here is revealed clearly and unmistakably the character of the internal discharges, providing visible confirmation of the numerical data shown in Figure 6. Type *CB* cable shows a remarkable record of discharge stability; the trace is almost flat initially, and at the end of the 30-day period its harmonic content is still negligible. On the other hand, the standard cable shows a small amount of discharge initially and this increases in intensity and complexity to a point where the amplification had to be reduced in order to photograph the trace amplitude. The foil-backed paper conductor-shielded cables after starting with almost no trace of discharge soon developed a very high-frequency type of wave shape containing sharp pulses repeated at one-half to one millisecond intervals. The harmonic amplitudes increased with aging so that at the end of the 30-day interval, discharge could be classed as very severe.

Cable Model Tests

In these tests on cable, the aging was so conducted as to emphasize gaseous ionization as well as the effect of high temperature. Heating of the sealed cables for long periods of time caused sheath expansion and creep with consequent redistribution of impregnant, formation of voids, and so forth. In addition, chemical reaction of the cable materials with residual air and gases was greatly accelerated at 125 degrees centigrade. The tests described later were made on a group of cable models, continuously immersed in oil so that gaseous ionization as such was suppressed. On the other hand, the models were aged at high temperature with continuously-applied electrical stress, and the tanks in which they lay were exposed to air during this time. Hence, oxidation and electrolytic ionization were the factors emphasized.

Figure 8. Typical cable model
16 inch, 4/0 American Wire Gauge, stranded, 60 to 70 mils insulation, fully shielded and guarded

Four cable models (set *R*) were prepared each with different treatment of its conductor. These models are similar in design to those previously described.[6] Briefly, they are paper tape-wound on a lathe and equipped with outer electrodes by hand. The insulation is wrapped cable fashion on a 16-inch long number 4/0 American Wire Gauge stranded conductor with 60 to 65 mils of high-density (air resistance, 250 seconds per mil) wood-pulp insulating paper, 60/40 per cent overlay, 0.5-per-cent butt space. A 5 $^1/_8$-inch outer wrapping of perforated lead foil acts as the low-voltage electrode or sheath, and, on both sides of this, 5$^1/_2$-inch flared paper end-re-enforcements are installed to permit operation up to 30 kv. Guard electrode foils cover the re-enforcements and overlap the main electrode slightly. Figure 8 shows a typical cable model completed and ready for test.

The equipment used for treating and testing these models has been built especially for this purpose. There are two 12-gallon storage and degasser tanks equipped with vacuum pump, heaters, resistance thermometers, and oil atomizing devices for properly storing, degassing, and dehydrating the impregnant. The oil is piped from these tanks to each or all of four square-section test tanks in which the dry cable models are mounted. These test tanks are mounted in an insulated air bath provided with circulating blowers, electric heaters, and thermostat. Booster heaters under each test tank enable all tanks to be maintained at the same temperature. Each test tank is provided with vacuum and oil inlets as well as metallic bellows so that they may be operated either at high vacuum, or constant gas or oil pressure up to 200 pounds per square inch. Shielded circuits bring a-c and d-c measuring and guard leads into the tanks, and high-voltage entry is provided by sealed bushings capable of operating up to 40 kv under all test conditions. In addition, all high-voltage leads, bushings and terminations are built to operate with no electric discharges present up to 30 kv. Resistance thermometers are mounted closely adjacent to the cable models. All tanks and components are of monel metal and may be quickly disassembled for cleaning before each test run. Once the models are installed in the test tank and the covers sealed they are not touched again by hand until the aging tests are completed. All operations of drying, impregnating, measuring, and aging are controlled externally. The model accelerated life testing (*MALT*) unit thus permits control to the closest degree possible of the variables entering into the manifold operations of assembly, treating, testing, and aging of impregnated-paper cable. Figure 9 is a general view of the *MALT* unit, and Figure 10 is a bird's-eye view looking into the test tank group showing the cable models in place ready for sealing and processing.

Difference in make-up of the four models in set *R* were as follows:

Model *R-5* had two 5-mil carbon black tapes wound over the stranded conductor prior to applying insulating tapes; this is the usual type *CB* model.

Model *R-6* differed in that a highly polished heavily tinned solid copper cylinder was used in place of the usual stranded conductor. No carbon black types used.

Model *R-7* had two aluminum-foil-backed paper tapes over a stranded conductor with metallic side toward the conductor; this is the usual type of conductor-shielded model.

Model *R-8* represented standard construction, stranded conductor with no shielding of any kind.

Table III is a summary of model constructions and calculated average and maximum test voltage stresses.

After mounting in their individual test tanks, the models were dried at 105 degrees centigrade at a vacuum of 600 microns mercury for a period of 30 hours. They then were impregnated under these conditions with high-grade cable oil having a power factor of 0.0015 at 50 volts per mil and 85 degrees centigrade, and a vis-

cosity of 96 seconds Saybolt (0.187 poise) at 100 degrees centigrade. After impregnation but still under vacuum, the temperature was allowed to drop slowly and electrical measurements made at five points. At the end of the temperature run the models were supplied with a continuous source of dry air at atmospheric pressure, the temperature increased to 100 degrees centigrade, a potential of 6.3 kv applied to give 100-volts-per-mil average stress, and the life test started. At 2-week intervals a cold cycle was obtained. During this time, the temperature was lowered to ambient temperature over a 24-hour period.

During aging of the models, power factors, capacitances, and insulation resistances were measured. In addition, the internal corona detector was used to determine corona initiation and extinction voltages and volume of discharge at three times test voltage, or 18.9 kv. Oscillograms of the discharge traces at 18.9 kv also were taken at intervals during the test. In order to establish a reasonable time limit for these tests, it was decided to remove any model whose 100-degrees-centigrade power factor reached five per cent or more or whose volume of discharge reached 500 microvolts or more.

The history of the aging is well represented by the changes in electrical characteristics shown summarized in Figure 11*A* (ionization data) and 11*B* (dielectric data). The tests lasted for more than 90 days during which time model *R-8* (standard) was removed after 27 days and model *R-7* (conductor shielded) after 71 days both having attained high values of power factor and internal discharge. At the start of the test all initiation voltages were well above test voltage, the tinned cylinder conductor being highest and the plain stranded standard conductor lowest. At the end of only five days, the initiation voltage of the standard model had fallen to test voltage level, and consequently its aging proceeded under discharge conditions which continuously increased in severity, as shown by the volume of discharge curve.

The conductor-shielded model *R-7*, after 40 days aging, showed a sharp decrease in initiation voltage to the test voltage level. Thereafter the volume of ionization increased rapidly, being reflected also in a sharp power factor increase. Models *R-6* (cylinder conductor) and *R-5* (type *CB*) both performed excellently. Neither was under particularly active discharge throughout the test, but at the end of 92 days the type *CB* model showed the highest initiation voltage and lowest volume of discharge. The large difference in power factor between these two models at the end of test cannot be explained by differences in their discharge characteristics but rather by differences in deterioration of impregnant. The impregnant in the type *CB* model was protected by the adsorbing properties of the colloidal carbon and was therefore in much the best condition.

Perhaps the best view of the tests is shown by the series of oscillograms in Figure 12 taken during the course of aging. The upper group was made at 100 degrees centigrade, the lower during the room temperature cooling cycles. For the initial and 5-day pictures the gain was set at 250 microvolts per inch, but beyond this time it was necessary to reduce it to 500 microvolts per inch in order to accommodate the large discharge amplitudes developed by some of the models. Starting with complete freedom from discharge harmonics, there developed a wide divergence of behavior between the several models. The standard model showed up poorly, whereas the type *CB* model exhibited almost complete ionization stability. The foil-backed paper conductor-shielded model, although starting well, soon was in trouble and developed considerable internal discharge as shown by the long spiked streamers in the oscillograms. The tinned cylinder conductor showed up very well as far as the 50-day point; thereafter the oscillograms show development of appreciable discharge. The oscillograms taken at room temperature show much less discharge than at 100 degrees centigrade. This would appear to indicate that the oil bath surrounding each model actually supplied oil to the cable structure as it breathed.

Figure 9. Model accelerated life test (MALT) general view

Oil treatment tanks, model test tanks (behind screen), and control panel

Figure 10. Model test tanks (MALT) bird's-eye view

Models mounted and ready for processing

As each model was removed from test, the insulation was dissected carefully for examination and tape-by-tape power factor tests. Visual examination revealed carbonization of the paper and thickening of the impregnant at the oil channels for the first three paper layers from the conductor in the standard construction. The conductor-shielded model showed carbonization of the paper along the edges of the foil backing. The discharge here was evidently very intense because the adjacent paper showed some dendritic patterns. No carbonization was found in the tinned cylinder model, but the impregnant near the conductor was darkened as was also the case for the two previously described models. The carbon-black model showed no evidence of stress on the paper or any impregnant deterioration except at the outside tape where the model was in immediate contact with the bath oil.

Results of radial (tape-by-tape) power factor tests are shown in Figure 13. In the main, these simply corroborate the findings previously indicated. It appears definite that the carbon-black tapes act to keep the impregnant in good condition in the oil channels near the conductor region in addition to reducing the discharge intensity.

Discussion and Summary

A portable self-contained apparatus has been developed which permits rapid and accurate quantitative determination of

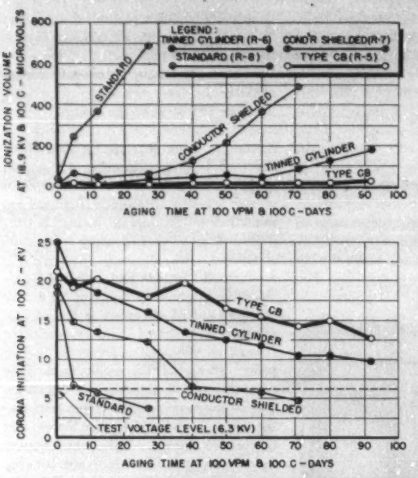

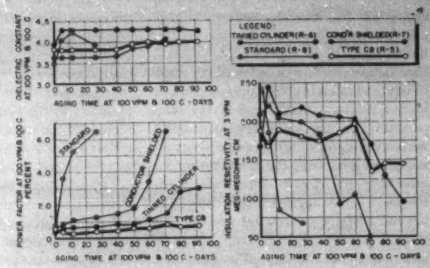

Figure 11*A* (left). Electrical characteristics during aging cable models (set *R*)

Ionization volume and corona initiation voltage

Figure 11*B* (above). Electrical characteristics during aging cable models (set *R*)

Dielectric constant, power factor, and insulation resistivity

Figure 12 (below). Oscillograms of internal corona cable model (set *R*)

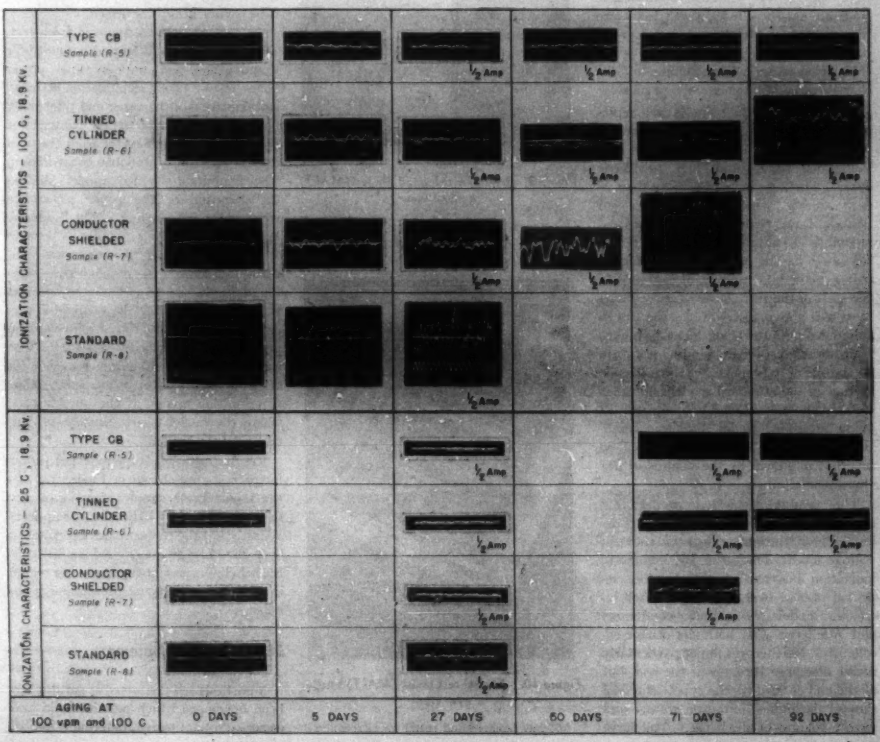

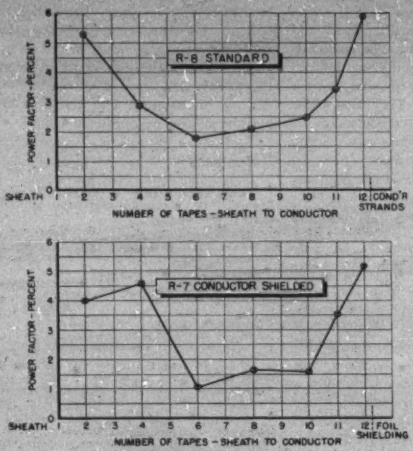

Figure 13A. Radial power factor after aging cable models (set *R*)

100 volts per mil, 60 degrees centigrade

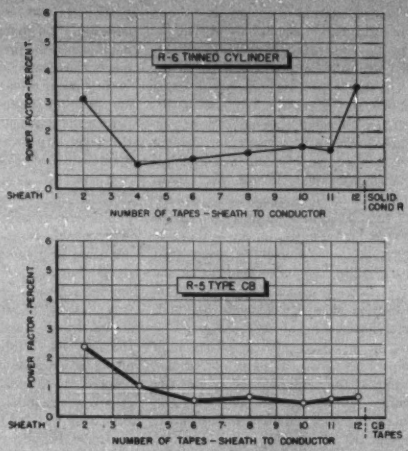

Figure 13B. Radial power factor after aging cable models (set *R*)

100 volts per mil, 60 degrees centigrade

internal corona within insulated cable. The present equipment is limited to 30 kv but could be modified readily for use at higher voltages. Minor modifications also can be made to apply the method to capacitors, transformers, and other forms of high-voltage electric apparatus.

Two applications of the internal corona detector in the study of type *CB* cable have been presented. In one case lead-covered cable was used and the test conducted so as to emphasize void formation as well as thermal deterioration. Under these conditions, the standard (unprotected) stranded construction deteriorated steadily to a point where it supported intense internal discharges below rated operating voltage. Conductor shielding by means of metal foil-backed paper tapes, while helpful in reducing the rate of deterioration, also was found to permit development of destructive internal discharges the character of which appears to be somewhat different than for unprotected strands. The remarkable stabilizing effect of carbon-black protected cable, shown clearly in Figure 7, appears to be the result of

1. Reduction of stress at the smoothed conductor electrode.
2. Suppression of discharge intensity at the carbon-black electrode.
3. Maintenance of good impregnant quality by adsorption of electrolytes.

Presumably all cables had impregnant movement and void formation alike. It also appears likely that void formation contributing most importantly to internal discharges occurred right at the conductor electrode. Here it is that the sharp metallic edges of the foil-backed tapes must have discharged directly across the voids and oil channels. The increase in power factor at low stress of both standard stranded and conductor-shielded cables also indicates, in this case, a certain amount of deterioration of the impregnant which contributed further to the discharge.

The model tests were conducted under what amounts to oil-filled cable conditions with the exception that the bath oil (reservoir) was exposed continuously to oxidation at elevated temperature. In this case, too, it was shown that the de-

Table IV. Internal Corona During Thermal Aging

Cable Sample Group *LL*

Cable Sample Number	Construction	Per Cent Power Factor at 20–25 C: 20 V Per Mil	Per Cent Power Factor at 20–25 C: 100 V Per Mil	Corona Voltage in Kilovolts: Initiation	Corona Voltage in Kilovolts: Extinction	Ionization Volume at 2×Operating Voltage Stress in Microvolts
Initial						
LL-1	Standard	0.381	0.411	11.5	10.1	35
LL-2	Standard	0.322	0.391	11.7	9.8	33
LL-3	Conductor shielded	0.373	0.397	12.7	11.5	24
LL 4	Conductor shielded	0.355	0.394	14.1	12.9	30.5
LL-5	Type *CB*	0.816	0.362	21.7	20.1	12.5
LL-6	Type *CB*	0.341	0.355	18.9	18.0	18
Aged at 125 C for 5 days						
LL-1	Standard	0.678	0.809	7.7	7.0	78
LL-2	Standard	0.750	0.921	7.8	7.1	94
LL-3	Conductor shielded	0.552	0.707	9.9	9.0	41
LL 4	Conductor shielded	0.559	0.797	9.5	8.9	52
LL 5	Type *CB*	0.378	0.408	21.0	18.9	12.5
LL-6	Type *CB*	0.364	0.399	18.5	17.5	20
Aged at 125 C for 15 days						
LL-1	Standard	1.85	2.37	6.5	6.2	124
LL-2	Standard	1.09	2.14	6.9	6.0	118
LL-3	Conductor shielded	0.942	1.41	7.4	6.9	77
LL 4	Conductor shielded	0.999	1.65	7.9	7.0	81
LL-5	Type *CB*	0.405	0.631	18.1	17.2	13
LL-6	Type *CB*	0.392	0.433	16.5	15.4	13
Aged at 125 C for 30 days						
LL-1	Standard	3.79	7.04	3.9	3.7	452
LL-2	Standard	2.44	4.98	4.1	3.7	291
LL-3	Conductor shielded	1.99	2.87	5.9	5.4	171
LL 4	Conductor shielded	1.85	2.91	6.2	5.1	185
LL 5	Type *CB*	0.571	0.699	17.5	16.5	18
LL-6	Type *CB*	0.447	0.581	16.5	15.5	25

tection of internal discharges is a direct clue to insulation condition and that the type-*CB*-cable principle provides perhaps the best insulation protection.

The steady decrease in corona initiation voltage and increase in volume of discharge with aging time appears to correlate closely with power factor increase and to some extent with insulation resistance decrease. Because the careful thorough method of impregnation and the fact that the models all operate continuously in hot-oil baths appear to preclude any appreciable amount of gassy void formation, it must be concluded that the observed effects are caused principally by production and action of ions in the liquid. Deterioration of the impregnant in the butt spaces under high stress and high temperature produces ions, and it appears that the more ions the greater the volume of discharge and the higher the losses. One known source of these ions is through the interactions of the electrode metals and oil which form metallic soaps and organic electrolytes. The ions bombard the fibre structure at definite portions of the potential wave build-up depending on temperature, stress and number of ions present. The bombardments cause unit function discontinuities in the current wave corresponding to each ion group discharge. They also cause permanent damage by carbonization, to the paper structure as was very evident upon dissection of the models.

Where ion generation or mobility was reduced, there immediately was found less discharge and lower losses. For example, every model showed much less internal discharge at room temperature than at elevated test temperature. This might not have been the case if dealing with true gaseous ionization. Also where strand stress was reduced as in the case of the foil-backed tape conductor-shielded model the ion generation and mobility was reduced, and hence the volume of discharge was reduced. In addition, where the stress was reduced further and the electrodes heavily tinned (cylinder construction) the oil deterioration again was reduced and consequently the ionization was less. The carbon-black protected model is unique, however. In addition to reducing the stress greatest locally, the colloidal carbon also reduces free ions by adsorbing them within its structure out of the electric field, so that ion production not only is retarded but also actually may be reduced by continued aging.

References

1. Oscillograph Study of Corona, **Edward Bennett.** AIEE Transactions, volume 32, 1913, pages 1787–1809.

2. Investigation of Cable Ionization Characteristics with Discharge Detection Bridge, **J. T. Tykociner, H. A. Brown, E. B. Paine.** *Bulletin 260*, University of Illinois Engineering Experiment Station, (Urbana, Ill.) September 1933. (See also *Bulletin 259* and *Bulletin 278*.)

3. The Measurement of Discharges in Dielectrics, **A. N. Arman, A. T. Starr.** *Journal*, Institution of Electrical Engineers (London, England), volume 79, July 1936, page 67.

4. A Method for Detecting the Ionization Point on Electric Apparatus, **G. E. Quinn.** AIEE Transactions, volume 59, 1940, December section, pages 680–2.

5. The Detection of Initial Failure in High-Voltage Insulation, **J. B. Whitehead, M. R. Shaw, Jr.** AIEE Transactions, volume 60, 1941, June section, pages 267–72.

6. The Type CB Impregnated-Paper Cable, **Samuel J. Rosch.** AIEE Transactions, volume 59, 1940, pages 1041–9.

Discussion

Herman Halperin (Commonwealth Edison Company, Chicago, Ill.): This paper presents a report on further progress on a subject that we were interested in as a project of the Utilities Research Commission some 20 years ago, as indicated in references by the author. At that time, we found that the apparatus developed at the University of Illinois was not suitable for detecting ionization in ordinary lengths of cable several hundred feet long. Can the author's apparatus be used for such applications? I should think this apparatus could be adapted to advantage in testing other insulation than cable insulation.

It is gratifying to me to learn that the author's test indicates a definite advantage in using conductor shielding. We have been specifying this construction for the past few years as a result of accelerated aging tests made on samples of cable with two types of conductor shielding. In these tests we have found no particular difference between the two types of shielding, although the tests have been rather severe from both the standpoints of voltage and conductor temperatures. Perhaps longer tests or more severe tests would bring out some differences. We have a number of lengths of 3-conductor cable with reduced insulation in service on 12-kv lines, and the results of examinations and tests of these cables after having been in service over a period of years may be of assistance in connection with the points raised by the author.

Regarding the author's tests on the samples of cable, he indicated that the cables had a rating of 12 kv although the insulation thickness was 172 mils. That was the rating a few years ago, but for the past $1^1/_2$ years the rating for that insulation thickness has been almost 15 kv.

In the model tests, the author states that the conditions amount to oil-filled cable conditions, except that the oil is exposed to oxidation. Such test conditions give some information, but I think that more convincing information comes from tests on cable with simultaneous application of heating and cooling and overvoltage.

E. C. Starr (Oregon State College, Corvallis, Oreg.): The principles embodied in E. W. Greenfield's equipment for the detection of corona discharges are very useful and have been employed in a modified form over a long period of time. The simplest application is perhaps that in which the charging current (or part of it) of a section of cable, insulated or bare, or other high-voltage apparatus, is coupled inductively to the input circuit of a radio receiver. This receiver then responds to the abundant radio-frequency components of the corona current. The audio output then can be used to drive a loudspeaker or an oscillograph. In a properly cleaned-up set-up, the inception of radio interference in the 500- to 1,500-kc band is coincident with the start of ordinary corona. This is a simple application of a band-pass filter to remove the large normal-frequency charging current and to pass the *r-f* components resulting from corona.

If it is desired to separate all ionization-current components from the normal charging current or $C(de/dt)$ components, a simple balancing circuit can be employed. The composite charging or dielectric current of the test specimen is passed through a non-inductive resistor which also carries the charging current of an ionization-free capacitor supplied with a voltage from the test source but with phase shifted 180 degrees. To effect complete balance of the normal charging current

$$C_1E_1 = C_2E_2$$

where the subscripts one and two refer to the test specimen and balancing capacitor, respectively. The voltage drop across the resistor is then caused by ionization-current components only and may be observed directly or amplified as required. This scheme has been employed to study radio interference caused by conductor and insulator corona.[1]

Corona discharges can be produced in which no high-frequency current components exist. If the discharge is caused to occur from an electrode of high specific resistance, some semi-conducting material such as carbon-black paper tape, the electron avalanches responsible for the current surges that give rise to the high-frequency components cannot occur. Radio interference or high-frequency currents are then no longer an indication of ionization or corona discharges. The second method described is better adapted to detecting discharges of this character. The necessary resistivity of electrode material to produce this type of discharge in air is of the order of 200,000 ohms per inch cube.

The periodic nature of the discharges recorded in some of Greenfield's observations are somewhat similar to the periodic

character observed in a study of high-voltage d-c point discharges.[3] It was found that the burst frequency, both positive and negative, was related to the type of electrode employed and to the magnitude of discharge current.

REFERENCES

1. SOME CHARACTERISTICS OF A-C CONDUCTOR CORONA, F. O. McMillan. AIEE TRANSACTIONS, volume 54, 1935, March section, pages 282–92.

2. HIGH-VOLTAGE D-C POINT DISCHARGES, E. C. Starr. AIEE TRANSACTIONS, volume 60, 1941, pages 356–62.

Roger M. Peirce and Victor Siegfried (Electrical Cable Works, American Steel and Wire Company, Worcester, Mass.): The author has presented a clear and complete description of a very useful tool to aid in the effective use of insulation in the design of electric cable. He is to be congratulated on a skilled development of pioneer circuits to give a highly sensitive detection system. The bridge type of circuit probably is most desirable in a highly refined type of equipment. The device should be applicable to all forms of dielectrics whether in insulators, capacitors, alternators and motors, transformers, or cable constructions. Our experience with a similar, though simpler, detector has led to placing a great deal of confidence in the determination of corona starting voltage as a measure of quality of design. We would not recommend it at this time as a standard for purchase specification, however, because of the many factors which may be involved that are not too clearly definable nor sufficiently familiar throughout the industry.

In the manufacture of radar pulse cable during the war, using this method showed conclusively the need for a low-resistance conducting rubber (100 ohms per inch cube) supplementary shielding between the insulation and the copper braid. Conducting rubber of too high resistance (10,000 ohms per inch cube or higher), or just bare insulation and copper braid in contact, reduced the voltage of corona starting below tolerable levels.

The use of end-bells as described should prove very helpful, and we are glad to have a design that will reduce the time factor and suppress incipient corona at the ends, where spurious discharges may discredit the design of the cable itself unfairly.

The corona starting voltage tester should be used more widely in the art of dielectrics. Lest the formidability of the bridge circuit used in the Greenfield apparatus seem a barrier to prospective users, we offer the simplified circuit of Figure 1 of this discussion which has been found adequate for cable testing up to 25-kv and sufficiently sensitive to detect even minor deficiencies. This circuit is very similar to that described by Miller[1] in connection with elimination of radio interference from porcelain insulators.

A corona detector depends on the voltage drop appearing across a radio-frequency inductance carrying the 60-cycle charging current of an air capacitor energized by the same voltage source which produces the corona in the specimen. The corona disturbance is mirrored in this inductance, as a circuit of low impedance for high frequencies is formed in the right hand loop of the system shown in Figure 1 of this discussion.

This circuit employs a corona-free capacitor and a battery-operated radio receiver as its principal components. Both are readily obtainable and should permit application of this tool even for a field investigation. Audio response can be used in the radio, although the cathode-ray oscilloscope is a valuable option so as to know what types of discharges are involved and thus distinguish corona from line disturbances. The magnitudes of the L and C values shown are quite flexible but should be chosen to give a resonant frequency of about one megacycle to provide maximum sensitivity where the harmonic components of corona discharge are richest. The choke is desirable but not vitally necessary, as it serves only to increase sensitivity through directing the high frequency currents into the inductance of the detector, rather than permit them to be bled to ground through the capacitance inherent in transformer windings. It is most effective if its L is several times that of the main detector inductance.

Although this circuit does not balance out the 60-cycle voltage, its effect on the measurements is negligible, as the trace on the cathode-ray oscilloscope is only slightly ripply because of it.

The material presented in the paper regarding the use of carbon black paper shielding is to be commended also. We are in entire agreement with the assertions of the second and third benefits made in the paper in "Discussion and Summary" from our own test data which show decreased deterioration of paper cable under aging tests where carbon black paper is incorporated in the insulation.

The importance of good bonding between the conductor and the dielectric cannot be over-emphasized. This is the most strategic place to avoid ionization because of the higher gradients involved. Shielding materials of the same physical characteristics will expand and contract in conformity with the rest of the insulation and thus ease the transition from conductor to insulating paper regardless of load cycle performance. This is likewise true on the outer surface of the insulation, where other materials always may not be in intimate contact with the dielectric under all conditions.

Figure 1. Corona starting voltage detector

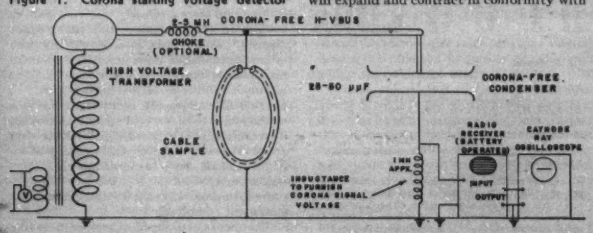

REFERENCE

1. ESTABLISHED METHOD OF MEASURING RADIO INTERFERENCE, Charles J. Miller, Jr. *Electrical World* (New York, N. Y.), volume 3, March 11, 1939, pages 690–2.

F. H. Gooding (The Okonite Company, Passaic, N. J.): E. W. Greenfield has developed methods of detection and measurement of ionization in dielectrics stressed at 60-cycle voltages in which he seems to have divorced very effectively the high-frequency component of the charging current from the 60-cycle component. The visual recording of the high frequency oscillations resulting from ionization may lead to the possibility of analysis of the type or radial location of the ionizable spaces, or to discrimination between electronic ionization in oil-filled cavities and gaseous ionization in void spaces. The principles involved in the measurement are not new, but freedom from corona discharge up to 30 kv and the high sensitivity are notable improvements.

The essential difference between Greenfield's measuring circuit and that of Arman and Starr is that Greenfield uses his Schering bridge to balance out the 60-cycle component, whereas Arman and Starr use their bridge for balancing out the high-frequency voltages resulting from discharges in the circuit external to the specimen under test. The author relies on conducting surfaces of large radius, immersed in dielectric solids or liquids. The English authors record measurements up to 100 kv on cables and up to 600 volts per mil on capacitors. It is possible that at values of voltage above say 50 kv, it may be desirable to balance out the discharges from the high-voltage transformer and leads rather than to try to eliminate them by changes in design.

The change in power factor as the voltage is increased in perfectly impregnated cable may become a factor of importance in high-voltage cable, and the apparatus described seems to be particularly well suited for this type of measurement, especially because of its sensitivity.

The comparisons made between test results on a conductor wrapped with metallized paper and one wrapped with carbon black paper may be very misleading. The precise method of application of metallized paper tapes over the conductor, and the type of tape used, have been the subject of years of research involving extended stability and aging tests, and the comparison with carbon black paper has not been overlooked. Intercalation of metallized paper tapes has long been discarded, as it presents a saw-tooth electrode surface to the insulation. Instead, two metallized papers are applied with an open gap in such a way as to maintain contact with the conductor, and a third metallized paper is then applied, with the metal side toward the conductor and having a very small gap between turns. This results in the conductor being sheathed in an almost perfectly smooth tube of aluminum with no sharp edges projecting into the

paper dielectric, and yet permitting impregnation of the conductor by way of the narrow gap between the turns of the wrapping. Impregnation of the conductor has been found to be important, particularly as it provides a reservoir of oil for the inner papers. The unexpectedly high ionization after five days on the tinned cylinder (sample *R-6*), as reflected in the oscillograms of Figure 12 of the paper, is no doubt a consequence of a gas film formed at the surface of the unperforated cylinder after impregnation, although the gas ultimately may dissolve in the oil.

Aging tests carried out by Balsbaugh and others have shown that oil heated with copper deteriorates much less when cable paper is immersed in the oil, the paper absorbing products which contribute to dielectric loss or conductivity in the oil. Advantage has been taken of this phenomenon in using special paper for backing the metal foil which not only forms a barrier between the highly catalytic copper conductor and the inner layers of insulation, but which also absorbs the deterioration product such as metallic soaps formed by chemical reaction between the copper and oil.

The effectiveness of the metallized paper layers in maintaining low power factor and ionization has been well demonstrated. Two lengths of cable so protected were held at 100 degrees centigrade in an oven for one year. At the end of this time, the power factors were 0.34 per cent and 0.33 per cent, respectively. A standard aging test applied to 12-kv cable for 26 days with maximum temperatures of 115 degrees centigrade on the conductor resulted in power factors of 0.5 per cent at 25 degrees centigrade and ionization of 0.1 per cent; at 115 degrees centigrade the power factor was 0.8 per cent and the ionization was 0.5 per cent. These values are much lower than indicated for shielded conductor cable in Figure 6*B* of the paper. The power factor values of paper tapes, measured by a utility after their own aging test had been applied to a cable, are only a fraction of the values presented in Figure 13*A*, and the upturn at the electrode surfaces is insignificant when the correct kind of metallized paper and the proper method of application are used. Also a sufficient number of these papers must be used so that the outer surface is not corrugated with strand ridges.

The carbonization of the paper along the edges of the foil backing reported by the author seems to confirm the unsuitable wrapping method, which results in salient metallic edges. Carbonization has never been found in cables wrapped with metallized paper tape as described herein.

It is stated in the paper that the carbon black tapes act as series resistors of sufficient value to damp the wave fronts of surges of external origin. Is it possible that the series resistance of the carbon black tapes damps the oscillations resulting from the ionization which are being measured, so that they are already attenuated or reduced by the time they arrive at the surface of the copper conductor?

Finally, the intercalated metallized paper construction has been found to present a barrier to the necessary flow of oil radially between the stranded conductor and the insulation as the cable is heating and cooling, and for this reason also this construction is unsuitable.

With reference to the conditions of aging, while some accelerated temperature aging may be desirable, reactions may occur at 125 degrees centigrade or in the presence of air which have little relation to what takes place in a cable in which the upper temperature limit is probably 85 degrees centigrade and in which the oxygen content is less than one-tenth of one per cent.

While taking issue with some of the author's constructions and preparation of cable ends for typical dielectric tests, we are indebted to him for the development of a piece of apparatus that appears to have great possibilities for detecting and evaluating the earliest stages of gaseous ionization, and ionization in the oil. The latter we may perhaps justly refer to as electrolytic ionization.

W. A. Del Mar (Phelps Dodge Copper Products Corporation, Yonkers, N. Y.): New apparatus for telling us what is happening inside a cable is always welcome and usually serves a useful purpose for a time but does not survive unless of proven reliability. The several predecessors of E. W. Greenfield's apparatus have had local use in certain laboratories but have not commanded sufficient confidence to come into more general use.

The reason, I believe, is that too much confidence should not be placed in any apparatus of very high sensitivity for detecting and measuring ionization caused by the liability of the instrument to show something that is not ionization.

As an instance of this, I will raise three questions about one set of readings in Table IV of the paper.

1. The ionization volume is the voltage across the oscilloscope at twice the operating voltage or at $2\times12/\sqrt{3}=14$ kv. The type *CB* cables, however, do not begin to ionize until voltages of 16.5 to 21.7 kv are reached. How can ionization require such a high voltage to start if there is considerable volume of ionization at a lower voltage?

2. Referring to the initial readings of Table IV of the paper, although ionization volume is apparently two or three times as great on the standard cables as on the *CB* cables, this is not reflected in the rise in power factor. This is shown by Table I of this discussion.

Another circumstance that makes me suspicious of this highly sensitive apparatus is the strange form of the waves in Figure 7 of the paper. These should be compared with the form in Figure 5 of the paper. It will be noted that whereas Figure 5 of the paper shows very high frequencies, a mere fuzz, in fact, compared with the 1,000-cycle timing wave, Figure 7 of the paper shows a series of distorted waves of about 180-cycle frequency. These are not characteristic of ionization, as revealed in our laboratory tests, although the ripples on them may be, and these ripples are common to all three types of cable. One cannot help suspecting that a third harmonic from the supply system is sneaking around the wave filter. We have made innumerable oscilloscope studies of paper cables and have always found ionization to be characterized by a high frequency fuzz like Figure 5 of the paper.

Table I

Cable Number	Cable Type	Power Factor 100 V Per Mil	Power Factor 20 V Per Mil	Power Factor Diff.	Ionization Volume	Ratio of Ionization Volume to P. F. Diff.
LL-1	Standard	0.411	0.381	0.030	35	1,170
LL-2	Standard	0.391	0.322	0.069	33	480
LL-5	*CB*	0.362	0.316	0.046	12.5	270
LL-6	*CB*	0.355	0.341	0.014	18	1,285

How are these variations in the ratio from 270 to 1,285 to be explained?

3. Again referring to Table IV of the paper, how are the variations in initial ionization volume of *CB* cable to be explained unless either the over-all gain of the oscilloscope had changed or unless the apparatus was subject to extraneous influence?

I have confined my remarks to the *LL* or 12-foot samples as I think that the *R* tests on 16-inch samples have little or no significance because of the presence of oxygen in the oil, oxygen in such quantities not being present in operating cables because the degasification of oil and the evacuation and carbon dioxide treatments they receive in manufacture.

In one sense, the term standard cable used by Greenfield is rather unfortunate because the data presented are pertinent only to high-voltage cables, and, in general, such cables are shielded with a copper shielding tape which prevents ionization between insulation and sheath, whereas his standard cables had no such protection. If he had made tests on such a shielded cable, it would have been easier to differentiate between ionization at the conductor and that at the lead. We made a large number of load cycle tests on 3-conductor cable having 122 mils instead of 172 mils of insulation and provided with a copper shielding tape over the insulation. These cables were tested at 24,000 volts and at temperatures ranging from 20 degrees centigrade to 115 degrees centigrade for over 30 days and suffered no increase of power factor measured at 60 degrees centigrade, and actually had a drop in ionization as the test proceeded

We also have made many load cycle tests to 85 degrees centigrade on cables with 220 mils of insulation at 203 volts per minute maximum stress lasting up to 300 days during the course of which ionization developed and became fairly intense. Examination invariably revealed waxing but not carbonization. Greenfield's model cables showed carbonization after operation for only 27 days at 126 volts per mil. Our cable compound contained rosin; Greenfield's, apparently, did not. I cannot help wondering what was wrong with the author's standard cables.

Some of the discussers have referred to metallized paper conductor shielding as if its function were primarily to give a smooth surface to the conductor and thus reduce stresses. While this is undoubtedly one of its functions, a more important one, in my opinion, derives from the fact that the aluminum foil is cemented to the paper, so that no discharges can occur from the face of the metal to oil or void space. Although a metallic edge is exposed, I have never seen any evidence of deterioration starting at an edge. Indeed, tests to check this characteristic of metallized paper have just been reported from our Laboratory and confirm the statement completely.

The metallized paper, therefore, acts like

the *CB* paper, as an inhibitor of electronic avalanches and, therefore, adds to the dielectric strength both at 60 cycles and on impulse test.

Edwin J. Merrell (Phelps Dodge Copper Products Corporation, Yonkers, N. Y.): E. W. Greenfield is to be commended for his excellent arrangement of the tools now available for the study of corona discharge in cables. In our research work we have employed circuits virtually equivalent and other variations as well, and likewise have found that study of the characteristics of cable discharge provides much information helpful to carrying on the development of dielectrics in general.

Unfortunately, we cannot agree that the tests to which Dr. Greenfield has applied his corona study are particularly pertinent to the evaluation of cable quality or stability. Thus, both his methods of cable aging are essentially ways of inducing excessive and unlikely chemical breakdown and degradation; in the 125 degrees centigrade case, of the paper component; and in the 100 degrees centigrade exposure to air, of the oil and the paper. The end result is that he has employed an electrical measuring means to illustrate the affects of chemical aging.

While we appreciate the many valuable aspects of experiments of this nature, we are inclined to consider them in a secondary sense when judging cable constructions. Of primary concern is a demonstration of electrical stability on long time load cycle tests of actual cable, at two to three times rated voltage continuously, and temperature cycled daily between ambient and maximum rated conductor temperature by passage of conductor loading current.

A. D. Pettee (General Cable Corporation, New York, N. Y.): The author is to be congratulated in having prepared an interesting and provocative paper. Because he has selected conditions for his tests on actual cables and models which are definitely outside of the normal operating ranges, he has made it quite difficult to evaluate his results on short notice by comparison with existing test data which have generally been obtained under conditions which more nearly approach those occurring in normal operation. I have, however, a few test data which are pertinent.

Of particular interest is the rapid increase in the low voltage power factor of the metallized tape shielded cable sample as shown in Figure 6*B* of the paper. This is explained by E. W. Greenfield as "a certain amount of deterioration of the impregnant which contributed further to the discharge." Without speculating as to the reason for this, I have taken the liberty of plotting the 20-vpm power factors at 25 degrees centigrade of the type *CB* cable and the metallized paper tape shielded sample as shown in Greenfield's Figure 6*B*, and have superimposed on this plot the low voltage power factor at room temperature and at 125 degrees centigrade of a cable recently tested in our research laboratory (Figure 2). This test was made for another purpose but the conditions were sufficiently close to those of Figure 6*B* of the paper to be of interest. This 40-foot length had metallized paper

Figure 2. Low voltage power factor during aging of paper lead cable samples

Figure 3 (below). Effect of aging at 100 degrees centigrade change of power factor at 100 degrees centigrade with time of aging

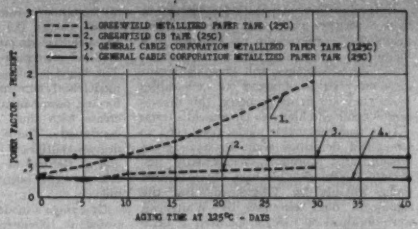

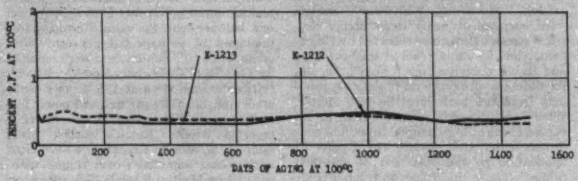

tape strand and insulation shielding, was provided with a loose sheath to facilitate drainage, was suspended as an inverted U with open ends, and aged without voltage at a temperature of 125 degrees centigrade for 41 days.

Due to three cooling periods, the cable had ample opportunity to breathe in air from the room. The sustained low voltage power factor value of 0.32 per cent at room temperature and of 0.65 per cent power factor at 125 degrees centigrade illustrate the fact that insulation which is stable under these very adverse conditions can be manufactured with metallized paper shielding tape and without the use of carbon black paper.

Supplementary evidence that the power factor of impregnated paper cable made without carbon black shielding does not necessarily rise under severe heat aging conditions is found in tests of the power factor of sealed samples aged continuously at 100 degrees centigrade without voltage. We have found with Doctor Davidson that this is a very sensitive and informative test. The low voltage power factors in this case have been measured at 100 degrees centigrade over a period of more than four years. Figure 3 shows power factor curves which are outstandingly flat for a test of such severity and duration.

Radial tape-by-tape power factor readings taken before and after aging also furnish reliable evidence of the effect of aging cycles. Figure 4 shows the initial and aged radial power factor at 60 degrees centigrade on a length of our standard 12-kv cable shielded with metallized paper tape. These data were reported originally by Halperin and were published first in a paper.[1] The cyclic aging test was of the combined heat and voltage type designed to break the cable down in about 30 days. The test voltage was in the order of 240 volts per mil on the net insulation wall. The flat curves before and after aging are practically coincident and show the degree of stability which may be attained with metallized tape shielding. I might add that the metallized paper shielding tapes on this cable were applied in a

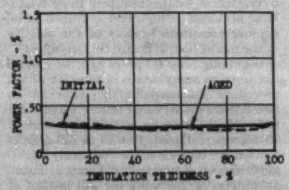

Figure 4. Radial power factor at 60 degrees centigrade before and after accelerated aging test on type H cable with conductor shielded with metallized paper tape

manner different from that described by Doctor Greenfield for his tests.

I have not attempted in this brief discussion to evaluate the merits of carbon black paper shielding, but simply have tried to suggest that there is still much to be explained satisfactorily concerning the practical aspects of Doctor Greenfield's reported differences in the effect of heat aging and differences in ionization in cable made with metallized paper and carbon black paper shielding.

REFERENCE

1. CONDUCTOR SHIELDING IMPROVES PAPER CABLE, **Faucett, Atkinson.** *Electric Light and Power* (Chicago, Ill.), July 1940.

R. W. Atkinson (General Cable Corporation, Bayonne, N. J.): Shielding of insulation commonly has been understood to refer to the Hochstadter construction, where a metal or metallized paper surrounds the insulation. It is worthy of emphasis that the present discussion has to do with shielding over the stranded conductor—under the insulation. The chief function of such conductor shielding is, however, the same as for the Hochstadter shielding; namely, the elimination of stress from insulation that is electrically weak. This is illustrated in Figures 5 and 6 presented herewith.

Extensive laboratory testing and long time field experience show that Doctor Greenfield's data concerning cable shielded with metallized tape are wholly nonrepresentative. As a colleague will give significant data on what is obtained on such cables when they are made properly, this discussion is confined chiefly to Greenfield's tests.

It is true that cable model tests such as Greenfield describes seem to have great possibilities. Moreover, some very important information has been obtained with them, notably by Whitehead. But the significant data obtained by Whitehead were obtained on models operated at little above room temperature (40 degrees centigrade). Moreover, Whitehead's models were operated at many times higher electrical stresses than these reported by Greenfield; thus, for a much shorter time to failure and giving much less time for oxidation and for diffusion of oxygen and oxidation products from the bath into the test sample. When such models are operated in an exposed bath at high temperatures, new conditions enter that vitiate the results in application to the operation of sheathed cables. Thus, the value and importance of Whitehead's data (including those Whitehead obtained at high temperatures) in no manner constitute support of the validity of the model tests reported by Greenfield.

Beginning fully 20 years ago, we carried out tests on many scores of samples with a procedure substantially the same as on Greenfield's model cable tests. Chiefly our tests differed from his in that they were at 75 degrees centigrade instead of 100 degrees centigrade, and extended for many thousands instead of hundreds of hours, and were at a stress of 250 volts per mil instead of 100. The results were very similar. The dissolved oxygen and oxidation products diffused into the cable strand, deteriorated, and continued the migration into the test dielectric, raising the power factor for some saturants even to fantastic values. After a rather extended experience with these tests, we concluded they were a waste of time. We concluded that they have little more relation to cable operation than would, for example, tests made to study the behavior of the oil as an automotive lubricant. Greenfield says he used "good" cable oil. Suppose we do not dispute that; where is the significance of his using "good" oil, when that is mixed promptly with seriously deteriorated oil? For our part, we were reluctant to abandon a lot of data that, at first, had seemed so valuable, but it was a great deal better to stop fooling ourselves with tests that had no relation to cable operation.

It should be noted in passing that it is possible to use a cable saturant which is far more resistant to the conditions of Greenfield's tests than that he used. It may be of interest to compare some of the data presented in advocacy of carbon black with what can be obtained without carbon black but with a different saturant. We started with a piece of insulated unimpregnated cable having metallized paper shielded strand. Models from this length were prepared and saturated under laboratory technique and then tested in an exposed bath of the impregnating oil at 125 degrees centigrade and at 125 volts per mil. Three similar samples were prepared, one being maintained without voltage except during power factor measurements, the other two with voltage. Initially, after 7 days, and after 10 days, the power factor at 100 degrees centigrade and 100 volts per mil was 0.48 per cent plus or minus 0.05 per cent. The highest value was for the unstressed model, and there appeared a slight tendency for the power factor on all samples to decrease with time. These tests are being continued. The power factor at about 30 degrees centigrade of these models initially, and at the end of the 10 days, was about 0.32 per cent both at 20 and 100 volts per mil.

Greenfield's models were maintained and tested at 100 degrees centigrade and 100 volts per mil. His *CB* model seems to have had an initial power factor of slightly over one half per cent, the value decreasing to a minimum of perhaps 0.3 per cent after about 11 days. Similar data were reported by Greenfield's associate, Rosch.[1] Rosch's tests were carried on at 125 degrees centigrade and 125 volts per mil, and power factor shown for 100 degrees, as were the tests reported herein. Rosch's carbon black samples, as well as Greenfield's were cited to show their superiority over samples without carbon black. Rosch's Figure 3 shows an initial 100 degrees centigrade power factor of substantially zero, 6 per cent in 5 days, and about 8 per cent in 10 days.

The impregnant used in our aforementioned tests, based upon the evidence of extensive experience and of a large number of tests of various significant types, is outstanding in its properties as a cable saturant. However, we have not considered that the evidence of the open bath model test adds particularly to other pertinent and complete evidence of the remarkable practical value of this saturant. Likewise, we do not consider that the evidence furnished concerning such tests by Rosch and Greenfield alone is sufficient to condemn their oil as an unsatisfactory cable saturant.

Sources of error in Greenfield's ionization data on cable samples are not so easily determinable from the data presented. However, entirely aside from the wholly contrary data of our tests, the inherent evidence of his tests shows clearly that his relatively poor showing for the metallized paper shielding is attributable to some major variable not intended in the test procedure. This may be shown by specific reference to the initial ionization tests.

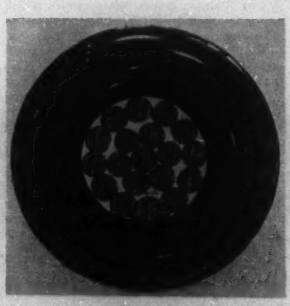

Figure 5. Styrene wafer of cable

Even with his freshly prepared cables, the *initial* ionization voltages of the unshielded, the metallized paper shielded, and the *CB* cables are reported in the ratios of approximately 1.0, 1.2, and 2.0, respectively That is, the first two differ from each other by a relatively insignificant amount, but differ greatly from the third, the *CB* model. Consider this result in the light of the geometry of these cables. Refer to Figure 5 of the discussion showing a styrene wafer of a cable of the dimensions described by Greenfield. Halation makes the butt spaces in the insulation appear fainter and wider than they are in fact. It is easy to observe that their radial depth is very small compared with the size of the interstices of the strands. The sketch in Figure 6 of the discussion shows these relative dimensions with greater clarity. In the cable shielded with either metallized paper or *CB*, the inner two or more tapes are conducting, and the depth of film subject to liquid or gaseous ionization is confined to the depth of the butt spaces. In the cable without shielding, the much greater depth in the strand interstices is under stress and subject to liquid or gaseous ionization. It is not surprising that (as reported by Greenfield) ionization in this space in the unshielded cable occurs at perhaps half the voltage required to produce ionization in the cable shielded with *CB*, where the ionization can occur only in the thin butt spaces. But if there are no differences not covered in the description, the geometries of the metallized paper and *CB* cables are alike. The matter of the voltage for initial ionization "the initiation voltage" is not particularly affected by any stated differences in the cables. The "work function" of the carbon and metal is not pertinent to the initial ionization, nor is the "distributed series" resistance of the *CB*, whether or not it should have an effect on the amount of ionization after that has started. Moreover, sharp edges can not be argued within the dimensions of the spaces. I do not believe Greenfield will attribute the difference on *these* tests to sorption characteristics of the *CB*. In short, there are no inherent differences due to type of these two shielded cables that can explain the large difference in initial ionization of the freshly prepared sample. However, there are various inadequacies of the preparation of the cable samples which, if present, well might produce results of the nature he has reported. Thus, there might be mentioned, for example (1) possible failure to assure that the foil of the strand shielding is in electrical contact with the conductor, (2) possible difference in degree of impregnation arising from improper control of saturating procedure. It is incredible that such results would be reported in an AIEE paper without proper care having been taken in these respects, but, to me, a reasonable analysis of the geometry, even without our extensive and wholly contrary data, makes it even more incredible that the initial ionization values reported are representative of the two types of shielded cable and are not the results of some inadvertently introduced and unrecognized test condition. Of course, whatever unintended, and thus undescribed, test condition produced the change in initial properties, it readily can have lead to increasing differences in performance during the course of the testing.

Taking up one other phase, one seems to

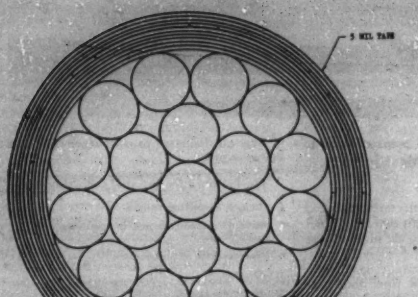

Figure 6. Scaled cross section of taped insulated conductor

19 wire, 4/0 American wire gauge

read between the lines that Doctor Greenfield's expectation that "Impulse strength of the cable insulation is increased since the carbon-black tapes act as distributed series resistors of sufficient value to damp the wave fronts of surges of external origin" may be an afterthought—perhaps a pious hope. No data are given, and such practical and theoretical data as we have challenge the conclusion. From the theoretical (or test) standpoint, does Doctor Greenfield consider that his conclusion applies to frequencies, such as are encountered in switching, and does he consider that the resistivity is high enough to produce the required damping directly over a strand wire on which the tapes chance to press tightly? If there is sufficient resistance in this location, what is the case where the charging current must be carried not merely radially but also circumferentially, as in the space between strands or perhaps where one or more consecutive strands may chance not to make contact? May not the resistance here be too high and the space not be shielded effectively, resulting in an arc—actually a large area of arcing—from the conductor to the *CB* tape? Would he consider such arcing objectionable? Finally, if the resistance is sufficiently high always to accomplish damping at switching frequency, will it not be so high that at lightning frequency many areas will behave as though not shielded at all? Doctor Greenfield's statement concerning impulse strength hardly can be considered seriously without further data or analysis.

REFERENCE

1. THE TYPE CB IMPREGNATED PAPER CABLE, **Samuel J. Rosch.** AIEE TRANSACTIONS, volume 59, 1940, pages 1041–50.

James Bower, Jr. (General Cable Corporation, Bayonne, N. J.): In the outline of his internal corona detector, Doctor Greenfield describes a high pass filter connected between the amplifier and measuring circuit "which has a very sharp cutoff at 1,000 cycles," yet most of his oscillograms consist to a large extent of irregular waves seeming to be at frequencies much below 1,000 cycles.

The circuit described is adapted to the measurements which the author intended to make (gaseous ionization measurements), but apparently it does not so function, in that the filter permits frequencies below 1,000 cycles to pass through. His filter appears to be poorly designed, or it is being by-passed. He may believe that the type of measurements he has obtained has more value than those he originally attempted. If this is the case and he wishes to study conditions other than internal gaseous ionization, then his circuit needs modification for facility of interpretation. Some of his oscillograms appear to have considerable 1,000 cycle pickup, possibly from the timing frequency.

The measuring device is shown as a Ballantine vacuum-tube voltmeter, model *300A*. The minimum reading of this instrument, according to the manufacturer's catalogue, is 1 millivolt. The paper indicates sensitivities to 30 microvolts. Has he obtained this sensitivity with catalogue instruments, perhaps by means not explained?

Our laboratory has used for voltages up to 30 kv a very simple ionization detector similar to that described by Quinn (reference 2 in Greenfield's paper). In this no bridge balance is made. The detector is made to reject the low frequencies, actually leaving, however, a very appreciable fundamental frequency. Ionization is shown by high-frequency oscillations at the crest of the 60-cycle waves.

Figure 7 shows this unit in operation on polyethylene radar cable, for which it has been extensively used. Though it is much simpler in design and operation than Greenfield's bridge, it seems very satisfactory up to 30 kv for this type of cable.

The author, properly, goes to some length to emphasize that, for his ionization tests, it is necessary to eliminate completely ionization in the terminations, leads, and supply circuit. This follows from the fact that the method cannot distinguish between ionization in the specimen under test and ionization on the test terminals, the leads, or even the source of supply. The author suggests that his test method may be applied directly at voltages above the 30 kv, the maximum value at which his tests have been made. This is true, except for the vital qualification that the difficulty of eliminating ionization on the terminals, leads, and source increases rapidly with increased test voltage.

We greatly reduce the effect of ionization in the leads by use of a device proposed and used by Whitehead. A source of external corona which Whitehead calls a "spark generator" is connected deliberately to the high voltage leads for a preliminary balance at voltages below that at which measurements are to be made, and the bridge is balanced to be insensitive to this discharge, though remaining sensitive to cable ionization.

We have measured ionization by means of this method up to 75 kv. For such measurements the standard capacitor has been a high voltage high gas pressure cable equipped with capacitor terminals. The capacitor terminals are important here not from the standpoint of dielectric strength but as a

Figure 7. Ionization detector

convenient means of freeing the terminations from corona for voltages upward of 75 kv. The supply voltage is from a 250-kv transformer that is essentially corona-free also at least upward of 75 kv.

We have used this device for measuring ionization in a high gas pressure cable. We have varied the ionization point of the cable by varying the gas pressure and thus could make a critical study of the ionization measurements. In comparison with 60-cycle power factor measurements, the ionization detector method was found to give results quite comparable to the 60-cycle measurements with which it was compared, though it was somewhat more sensitive.

The difficulties produced by ionization external to the sample under test result is a serious limitation of the practical usefulness of the ionization detector, though it has some uses in supplementing 60-cycle determinations.

A. E. Widmer (Anaconda Wire and Cable Company, Hastings-on-Hudson, N. Y.): It was near the close of 1943 that the armed services altered the *JAN-C-17* coaxial cable specifications to include an internal corona test for the majority of the required cable types. This corona limitation usually stated that, at a certain specified minimum voltage, the cable should be free of corona. Corona-free operation was deemed essential, as the ionic bombardment occurring during the discharge eventually would cause failure because of the waxy nature of the polyethylene insulation. In addition, the many harmonics present resulting from the corona discharge would interfere with the signal transmission requirements.

The first equipment used by the Anaconda Company for corona testing of coaxial cable was placed in operation about February 1944. This consisted of a single "flower pot" placed atop the high voltage terminal of a test transformer. The associated Schering Bridge, amplifier, and oscillograph were placed outside the test area. This arrangement was employed until portable equipment similar to that described was completed.

The standard *RG*-type cable lends itself readily to this type of test. The end preparation is most simple, consisting of $4^1/_8$ inches of jacket removal followed by a wrap of marker tape over the braid $3^1/_2$ inches from the end. The braid is removed to within an inch of the wrap and then fanned out and folded back. After the loose ends have been bound down firmly, the braid termination presents a smooth rounded appearance, causing no danger of external corona discharge when inserted into the special oil-filled high voltage terminals. A single General Radio type *274/U* plug with all sharp edges machined smooth is soldered to the inner conductor. Both ends are prepared in this way, and in addition about 1 inch of jacket is removed for lead connection to one corner of the bridge circuit. Figure 8 shows completed end preparation of an *RG-8/U* coaxial cable.

The cable simply may be wrapped around the high-voltage corona-free capacitor and fed directly into the "flower pots," or, as in the case of larger diameter cables, where sharp bends may cause the solid inner conductor to pull away from the insulation, the samples are formed into an inverted U and allowed to pass through two large holes in the top of the detector to the high voltage terminals.

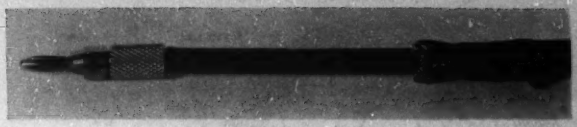

Figure 8. Completed end preparation of an *RG-8/U* cable

All types of coaxial cables have been tested with this equipment from diameters of 0.200 inch to 1.20 inches and with corona requirements from 2,000 volts to 14,000 volts.

During the war period, this equipment was used mainly for production control work on coaxial cable. Operators could be trained in a few hours to prepare and test cable samples. A person need have very little technical background to observe and record the voltage readings.

Such test methods allow checking for voids in the insulation due to improper cooling or extrusion practice, also for loosely extruded cores or inner braids which are not tight.

Cable in process also may be spot-tested for corona value. That is, cable without a wire braid cover can be placed in a water bath, if care is taken to prevent air bubble formation along the insulation and it is tested quite rapidly. This test repeated at night upon a cable with many voids will cause the sample to glow brightly.

The equipment described is simple to operate, and in the case of coaxial cable, sample preparation is simple. Tests can be made rapidly and reproduction of results has been proved.

B. Jore (Anaconda Wire and Cable Company, Hastings-on-Hudson, N. Y.): The author has shown ably the usefullness of the internal corona detector in laboratory investigations. My purpose in presenting this discussion is to give an example of how the detector can be of great service to the production man in selecting the proper manufacturing procedures.

During the investigation of polyethylene insulated power cables, we found that the length of time a cable could withstand a specified voltage varied considerably on samples from different runs. Adjacent samples then were subjected to test with the internal corona detector, and we found that those performing poorly on the long time tests showed internal corona at voltages below the test voltage.

The internal corona consisting of electronic and ionic bombardment in the voids, create sufficient heat to melt the polyethylene in local spots and finally result in complete breakdown of the insulation.

It is known that polyethylene has a relatively high coefficient of thermal expansion, hence, if improperly cooled, voids are created especially near or at the conductor surface. This void formation is particularly serious in cables with small conductors and a ratio of over-all diameter to conductor diameter in excess of 3.

The factors affecting void formation are

1. Length of cooling trough.
2. Actual temperature and temperature gradient of cooling water.
3. Temperature of conductor.
4. Die design.
5. Extrusion speed.

Varying these conditions, corona discharges were detected at voltages as low as 2.5 kv, whereas in other samples of the same type and size, no corona was detected at 30 kv.

In this manner the internal corona detector was a valuable tool in selecting extrusion conditions that produced cables with no corona discharge at voltages well above the rated value. This in turn assures satisfactory service performance of the cable.

E. W. Greenfield: The many discussions and the wide range of comments contained therein indicate considerable interest in the subject matter. This is, of course, gratifying to the author. It is hoped that the use of internal corona detecting devices will increase and that more exact information thus will be obtained as to the electrical performance characteristics of insulated cables. With regard to the general question of type *CB* versus ordinary conductor shielding, it is of interest to note that the latter was not used to any extent in this country prior to the introduction of type *CB* cable.

In reply to Halperin, it is my belief that this ionization (corona) detector can be used, if suitably modified, for testing ordinary lengths of cable several hundred feet long. For cable on a reel, we have applied the Schering bridge balancing technique successfully, using arms which can carry the higher current adequately. Where the cable is installed, we have experimented with draining off some of the sheath current and analyzing this for harmonics. In this case the filter circuit should be arranged to pass only frequencies greater than several hundred kilocycles. By this means it may be possible to measure the corona current in a given length of the cable, as terminals and/or joints can become effective impedance barriers at these high frequencies, thus isolating the particular length of cable. It would be of great interest if this phase of the use of corona detectors could be investigated thoroughly.

The equipment is adapted very readily to the determination of corona discharges in bushings, circuit breakers, transformers, capacitors, and other similar electrical structures. All that is required is that the apparatus to be tested shall form one high voltage arm of the Schering bridge. Care should be taken to make the high voltage leads to the sample under test corona-free.

Halperin points out that the test data indicate definite advantage for conductor shielding. I agree with him, but wish to emphasize again that there are several types of conductor shielding available. Of the types used, the intercalated foil-backed paper types appear to be less effective than type *CB* cable, in which perfect conductor shielding is obtained as only one of many benefits.

The model tests and oven-aged cable tests cited in this paper were set up specifically to investigate *internal ionization*. To the best of our knowledge to date, no such data have been obtained on any cable tested with simultaneous application of heating and cooling and overvoltage. We agree that such cyclic-loading tests most nearly simulate service conditions. The superiority of type *CB* cable in this type of test was reported to the Institute previously (see reference 6 of the paper, Figures 12 and 16) Additional confirmatory data are being prepared for presentation.

Starr states that, if the electrode resistivity is greater than about 200,000 ohms-inch, the discharge will give no avalanche bursts of electrons, and thus no high-frequency components will be found. This thought-provoking discussion indicates that he has made experiments in this connection which certainly should be published. We, too, believe that, as electrode resistivity goes up, the avalanche bursts decrease and the oscillatory character of the discharge decreases, but it would seem to follow also that the destructive energy of the discharge also will decrease. That this is so is demonstrated amply by the condition of the impregnated paper in the sample protected by carbon black compared with those having metallic electrodes. The resistivity of our carbon-black tapes is on the order of 50,000 to 100,000 ohms-inch. It is not desirable to use higher resistivity because of its possible influence in increasing power factor and reducing shielding action.

Peirce and Siegfried describe a choke type corona point detector which was used extensively on radar cable testing during the war and now is used in power cable development. The equipment described is quite interesting and resembles somewhat that described by Quinn (reference 4 of the paper). However, as in that case, incomplete elimination of the 60-cycle component probably reduces the sensitivity severely. Even if the radio receiver is tuned sharply to some narrow high-frequency band, there still must be considerable 60-cycle modulation. Also, does the operator have to take readings at various settings of the receiver tuning circuit in order to explore the character of the ionization?

We are very happy to find confirmation of our data from the discussers on their own aging tests on cables. It should be pointed out, however, that the special feature of carbon-black paper in adsorbing impurities must not be overlooked; it often has been demonstrated and may be demonstrated readily in their own tests.

Conductor shielding by means of intercalated foil-backed tapes, which Gooding says "was discarded years ago," was copied for purposes of these tests from commercial cables recently fabricated by other manufacturers. We agree that this construction has serious limitations, as brought out in the paper. The particular construction described by Gooding as incorporating filtering in addition to shielding characteristics is not a construction used generally by the cable industry. As a matter of fact, it is a proprietary construction. We are interested to note that this is an acknowledgment of one of the advantages of the type *CB* cable principle, in which a highly adsorbing medium is used to protect the cable dielectric. It is of further interest to note the relative complexity of this design as compared with the exceedingly simple type *CB* application.

As I understand it, there are two purposes in Gooding's shielding design. The first is the use of a metallized layer to act as an electrostatic shield in order to prevent the filter medium he employs from becoming part of the electric field. The second is the use of a metallized shield in order to force the fluid medium longitudinally through the filter tapes. With this construction, it appears that the metallized layer is used in a manner which does not comprise a true electrostatic shield, as the metallized tape is separated both from the high voltage conductor and the sheath by the filter medium. As the filter medium consists of paper, the metallized tape will take up a voltage which is a function of the thickness of the filter aid and the over-all dimensions of the cable. In this respect, the metallized tape is neither a shield nor is the filter medium free from the electric field. Only if the filter medium has sufficient conductivity, will the voltage difference between the metallized tape and the conductor be small enough to give the tape shielding effects. In this case, however, the necessity for the foil backing is not obvious. Of course, if the outer filter tapes are intercalated with a metallic shielding tape, such as used in type *H* cable, shielding then will be achieved at that point.

With regard to the barrier action of the metallized-foil layer, it is believed that this is indeed a disadvantage rather than an improvement. Gooding's theory of contamination apparently is based on the production of contaminated oil at the copper and lead only. Thus, by interposing "barriers," he desires to hold this contaminated oil in these regions. We believe the fluid dielectric is everywhere within the cable exposed to contaminating influences and that this contamination is a function of the impurities in the paper, the electric fields, and the presence of metals. Hence, we would suppose an ideal system would permit as accessible a flow as possible for diffusion of the dielectric fluid through and in continuous contact with the filter medium. If liquid is forced to travel longitudinally, it definitely will not travel longitudinally through the tapes but will by-pass it and travel along the faces of the tapes. It is therefore evident that a system such as suggested by Gooding will have much less filter surface readily available for adsorption than the construction as embodied in our carbon-black design.

Regarding damping of external oscillations, there are no oscillations due to external causes in the apparatus nor connecting circuits. This is checked carefully prior to any test. The means for doing this are readily available within the equipment itself. Any discharge damping occasioned by the carbon black is that which occurs within the insulation itself.

With reference to the conditions of aging, accelerated temperature aging at 125 degrees centigrade was conducted on sealed cable samples within which the conditions closely approximate those in actual service. Air (oxygen) was excluded by sealing, and the temperature is not too much higher than that permitted for emergency operation. Furthermore, all cable constructions were tested alike, therefore the results are comparative.

Del Mar indicates that he does not believe internal corona detecting equipment is very reliable and, therefore, should prove of little help in evaluating cable constructions. His appears to be the only dissenting voice with regard to the value of this tool. I do not hesitate to say that in its present form the internal corona detector can be much improved. However, I believe such improvement eventually will come and that internal corona measurements will become equally as important and as widespread as the accepted use of power factor. In fact, one of Del Mar's associates (E. J. Merrell) has indicated in his discussion that the use of the corona detecting equipment is very helpful in carrying on development in cables.

Referring to data presented in Table IV in the paper:

1. As pointed out in the paper, discharges in paper cable go through all stages of intensity, and the limit of their detection becomes a function of instrument sensitivity In the case cited, the initiation voltage is determined by observation of the cathode-ray oscilloscope screen; the volume of ionization is read from the vacuum-tube voltmeter whose limit of sensitivity is between 12 and 15 microvolts. Therefore, readings below 20 microvolts do not represent "considerable" volume of ionization, but, rather, are near the limit of sensitivity of the apparatus and represent little, if any, relaxation discharges.
2. Del Mar's arbitrarily calculated ratios have no significance, as the power factor change between two voltages may or may not bear a relation to internal discharge. When the discharge arises from gaseous ionization, there *is* a directional relation between power factor increase and discharge, but the quantitative relation varies considerably with local conditions. When the discharge is electrolytic in nature or there is moisture present, the power factor will show little rise, although considerable discharge may be present. Armon and Starr in their paper (see reference 3 of the paper) give a number of examples of this.
3. Variations in initial ionization volume of type *CB* cable are minor and are explained by the fact that the values lie close to the limit of sensitivity of the equipment. Also, the data presented represent tests on different cable samples.

Referring to the wave forms shown in Figures 5 and 7, as noted, the high-frequency components in each of the cable or cable model types displayed are quite different. For example, in the 5- and 15-day aging of sample *LL-4* (Figure 7) there are many exceedingly sharp-pointed "fuzz" groups, as Del Mar terms them, and again in many of the pictures shown in Figure 12. With regard to the lower-frequency components present, these appear to be due to the periodic nature of the discharges (as also pointed out by another discusser, E. C.

Starr). By this it is implied that the high-frequency needles and ripples represent the individual discharges and the lower-frequency periodicity, found only in the poorer cases, represents the burst frequency of the grouped avalanches. Careful examination of these cases reveals no uniformity between samples nor even in a single sample. They definitely bear no systematic relation to the usual harmonics of the 60-cycle source. Even a casual observation confirms the fact that these burst periodicities are not present initially but only appear when appreciable discharge has developed.

I would like to point out that, in the case of the models, the paper clearly indicates that all samples have a 2-mil perforated foil electrode bound down tightly over the insulation. This foil electrode is unquestionably superior to the usual intercalated copper shielding tape, insofar as providing ionization suppression between insulation and electrode. Generally, commercial single-conductor cables do not have a supplementary shielding tape between insulation and lead sheath at voltages below 40 or 69 kv and in many cases not even at 69 kv.

We are interested in the cyclic loading data presented by Del Mar but are at a loss as to how to draw comparisons with our results, as his cables are of various sizes and contain an entirely different impregnant. The fact that on his 300-day load test he obtains intense ionization, and as a result finds waxing of his compound "but no carbonization," would indicate his cables to be far from stable. Our own load-cycle tests on type *CB* cable under more severe loading conditions never have revealed any appreciable ionization nor any waxing of the compound. The fact that carbonization may be obtained in a nontype *CB* model test derives from the essentially greater severity of this test.

If cementation of the foil to the paper does not permit gaseous (void) ionization at this interface, it certainly does not prevent discharges of other types involving electrolytic material. In addition, although Del Mar claims never to have seen it, we have, on a number of occasions, observed the carbonization damage to the paper in the regions opposite the sharp metallic edges caused by outward curling of the foil backing. This happens particularly when the cable is bent or handled but is also present in carefully made laboratory samples. We also have observed rather high power factors associated with the paper backing of the foil. As this paper backing is unshielded, it contributes to the over-all losses of the insulation. In the case of rosin-blended compounds used with aluminum foil-backed tapes as conductor shielding, we also have observed electrolytic action between the aluminum foil edge and the copper conductor. This resulted in rather heavy black spiral markings on the conductor surface.

Accelerated tests, questioned by Merrell, in general are a means to an end. Admittedly they may not simulate service aging conditions. Model tests are designed specifically to accentuate the effects of certain variables under controlled testing conditions. On this basis, the results obtained are comparable, and they readily may be interpreted in terms of cable operation.

We agree that long-time cyclic-load tests of actual cable are very valuable, probably more so than any other single test. However, they also are accelerated tests, and the conditions of testing are not entirely standardized throughout industry. Nevertheless, they do more nearly approach service operating conditions. The results of such tests on type *CB* cable were presented to the Institute in paper reference 6. With reference to Pettee's discussion in general, it is improper engineering analysis to plot together data taken with dissimilar apparatus, dissimilar test structures and dissimilar variables of construction. In the case of the inverted U test, Pettee obviously is describing a cable impregnated with a so-called nonmigrating compound, which cannot be compared with those impregnated with a light mineral oil as used in our tests. It would appear that this impregnant is of a synthetic origin probably one of the hydrogenated high polymers recently made available to the industry. These impregnating oils have been evaluated in our laboratories with results similar to those presented by the discusser.

The oven-aging tests on sealed cable samples reported in the paper were essentially the same as those previously sponsored by the Brooklyn Edison Company (Doctor Davidson), except that in our case we used a slightly higher temperature (125 degrees centigrade versus 100 degrees centigrade) in order to keep the testing time within reasonable limits. In addition we used a much more sensitive measuring technique (internal ionization versus power factor) to evaluate the effects of the accelerated aging.

Regarding the radial power factor data obtained on a 30-day cyclic-loading test, the reference cited covers tests on cables incorporating changes in impregnant, paper, and construction. It is not clear that the flat radial power factor curve was entirely due to the foil-backed paper tape conductor shielding, nor is it clear that the particular curve referred to applies to all three conductors of the cable or is limited to just one.

In the first two tests outlined by Pettee, no electrical stress was applied to the samples. Hence, these tests have little or nothing to do with conductor shielding properties and are largely tests of the saturant stability (both as to oxidation and mechanical movement) which was outside the scope of our paper. The foil-backed paper tapes for the tests described in our paper were obtained from the same source and applied in the same manner as observed in recent General Cable Company paper-lead cables.

The use of models in cable research has taken much unwarranted abuse from Atkinson and other discussers. It is significant to realize that most of those who discount model tests have used them extensively, and by their own admissions are continuing to do so. The results obtained with our carefully designed models, tested in accordance with a carefully thought out program are far from worthless. It is only by means of such tests that the multiple variables entering into cable construction and operation can be controlled reasonably. Although the conditions imposed on models may be very severe, it is to be appreciated that control models carried with each new development serve to form an accurate base line for estimating the efficiency of any new design. Oxidation is an enemy to cable saturants. In the cable model tests conducted by Whitehead, as in those conducted by the author, the models were exposed continuously to dry atmospheric air. Thus the ability of a given design to withstand the effects of oxidation are evaluated readily. How much better it is to make such tests in the form of cable models than in the form of beakers of oil in an aging oven. In the cable model the various components of a cable and their geometry are correct, and the techniques for measuring the effects are perfected. Again in the study of ionization the drained model provides the closest control of the void-forming variables entering than any other form of such testing. Of course, it is necessary that the interpretation of the results of model testing be carried out udiciously. In this same respect it is necessary to interpret carefully the results of cyclic load tests on cables when predicting their behavior under service conditions. In our laboratory, the model tests serve to complement tests carried out on commercial size cable under cyclic loading conditions.

I do not believe that Whitehead's work, for example, with MacWilliams on the effects of long-time stress and high temperature on cable models[1] is worthless. Here he shows that at high temperatures the rate of deterioration of impregnated paper may be many times that at 40 degrees centigrade and also that oxygen actually played a small role and electrolytic dissociation a primary role. I also would remind the discusser that my paper discusses results of tests on actual cable as well as cable models.

Regarding the model-test data presented by the discusser, we wish to point out again that attempting to compare results of dissimilar tests can lead to misleading conclusions. Our tests were not made to evaluate the impregnant. We used a good quality light mineral oil for *all* the tests presented in this paper, so that it would constitute one of the uniform, controlled variables in the test. The main object of the tests was to determine differences in internal ionization with different cable constructions, and all other factors in the test setup were maintained constant, so that only those factors which were varied deliberately would have a bearing on the comparable results obtained. When a different type of impregnant has been used, *numerical* values of the results have been different. No matter what impregnant is used, we doubt seriously that there would be any change in *relative* results.

In the case of the sealed cables, the corona initiation voltage at the start of the test was in the ratio of 1.0–1.2–1.7 (not 1.0–1.2–2 as indicated by Atkinson). For the models the ratio was 1.0–1.1–1.2. The discussion on cable geometry presented by the discusser is voluminous but not completely understandable, and hence I cannot comment on it. However, the difference in corona initiation voltage as between the carbon-black model and the model equipped with foil-backed conductor shielding is primarily due to the sharp edge of the intercalated foil (as corroborated by Gooding's comment). Secondarily, it is due to the difference in the character of the electrode, namely metallic, as compared with carbonaceous. Furthermore, the adhesive between the paper and the foil backing is a high-loss material and must contribute materially to electrolytic ionization. The use of noninter-

calated tape application, indicated by the discusser as being their present practice, may tend to minimize the effect of curled foil edges, but it certainly cannot obviate other deficiencies due to the *character* of the tapes.

Atkinson's implications as to test technique and sample preparation are not warranted by the facts and in deed are irrelevant.

Regarding the impulse strength of type *CB* cable, the discusser seems to have missed the point of the argument entirely. The series resistance of the carbon-black tapes referred to is to be considered longitudinally along the cable. A lightning or switching surge propagates a steep wave front down the cable, which is accentuated further by reflections from impedance discontinuities such as terminations and joints. The steep wave front and high frequency currents must be attenuated by the resistance of the conductor and losses in the dielectric. In the case of a type *CB* cable, it is considered that the longitudinal attenuation of a surge may be much more rapid. The high-frequency currents flow mostly on the outside of the conductor, where are located the carbon-black tapes, and, as their resistivity is much higher than that of copper, the attenuation must be much greater. Atkinson is referred to the paper by Komives,[2] in which surge tests were made on type *CB* cable among others. Here the type *CB* cable gave values which were considerably better than for standard construction (breakdown stress in type *CB* approximately 30 per cent higher than in standard construction).

Reference also to data presented by McCabe[3] shows that the impulse strength of type *CB* cable is 35 per cent higher than that of standard cable, whereas similar cables with foil-backed paper conductor shielding made by two different manufacturers gave $17^1/_2$ and 32 per cent increase respectively. The low value obtained on one of the foil-backed paper shielded samples was ascribed to the formation of wrinkles in the foil-backed tapes, thus forming a sharp discharge surface.

Further evidence of the effective selective damping or attenuation of steep-fronted (high frequency) waves is given by the performance of the "lossy" radar cable developed by the Anaconda Company (patent applied for). In this construction, *CB* tapes are applied under the outer conductor of the coaxial cable. Attenuation increases of 10 to 100 times can be obtained, depending on the longitudinal resistance of the *CB* tapes. At frequencies below one megacycle, however, the presence of the *CB* tapes causes no increase in attenuation.

With regard to whether or not the *CB* tapes have sufficient conductivity to constitute an effective shield, this has been demonstrated repeatedly. Data have been published in two papers (reference 6 of the paper and the paper) and well established in service by over five million feet of installed cable.

Regarding the design of the filter circuit mentioned by Bower, we believe it is more than adequate. It consists of a 3-stage ladder-type unit with tunable elements and is adjusted to give over 45-decibel attenuation against 60 cycles, and the first 11 harmonics thereof. It was made by one of the foremost filter design laboratories in the country. With regard to the 1,000-cycle pickup, this was impossible as the timing waves were not obtained simultaneously but made after the discharge trace was photographed.

The model *300-A* Ballantine vacuum-tube voltmeter is supplied with a decade amplifier (model *220*), so that the combination has a minimum reading of ten microvolts. The sensitivity of the equipment (the readable difference voltage) is in the order of ten microvolts.

It is agreed that the type of apparatus described by Quinn is simpler in construction than the bridge equipment. It is, however, not simpler in operation. The greatest trouble with this equipment is its lack of sensitivity. In this respect it is so sharply limited by the fact that a large 60-cycle component is always present that it is generally not usable for nongaseous types of discharges. With regard to the bridge method used by Bower, I do not wish to detract from Doctor Whitehead's work in the least. However, it is necessary to point out that the credit for developing a bridge balanced on an extraneous source of high-frequency disturbance must go to Arman and Starr, who published this work in great detail in their paper (reference 3 of the paper). My objection to this circuit is that the bridge must be balanced on a band of frequencies resulting from the extraneously produced discharge. The inphase components of a great proportion of these frequencies thus may ride through to the detector circuit. Indeed, where possible, it seems much the preferred method of cleaning up the external circuit, so that no corona within the limit of voltage of the equipment is present.

References

1. Temperature and Electric Stress in Impregnated-Paper Insulation, J. B. Whitehead, W. H. MacWilliams, Jr. AIEE Transactions, volume 61, 1942, January section, pages 10–13.

2. Impulse Strength as a Measure of Cable Quality, L. I. Komives. AIEE Transactions, volume 60, 1941, October section, pages 929–34.

3. Minutes of the 24th Meeting of the Transmission and Distribution Committee. Edison Electric Institute (New York, N. Y.), 1941. Appendix III.

Machine Computation of Power Network Performance

L. A. DUNSTAN
ASSOCIATE AIEE

Synopsis: The planning of modern power system expansion demands that voltages, phase angles, power flow, and reactive power flow throughout the network be determined in advance of actual system changes. Determination by calculation of these quantities increases in difficulty to such an extent, as the system increases in size, that, for large interconnected systems, it heretofore has been considered necessary to use a network analyzer for this work. Since the first a-c network analyzer was put in service at the Massachusetts Institute of Technology in 1929 the scale model method of handling complex power system problems has grown in popularity, and the number and size of analyzers in the United States has been increasing steadily. To date, 14 network analyzers have been constructed, and more are on order, all at a total cost approaching two million dollars. A widespread, but misguided, belief prevails among power system engineers that the foregoing problems are not solvable practically except with the aid of an analyzer. It is the purpose of this paper to set forth certain principles and methods which so facilitate the handling of problems of power flow in networks that the mathematical solution appears more feasible than the analyzer solution. The methods and equations presented in this paper have been tested by recomputing an actual network analyzer study by mathematical means for comparison. Data and answers from this study are tabulated in this paper. The mathematical solution was first made with a key calculating machine. It later was recomputed by punched-card accounting machines to determine experimentally the time required and to standardize card design, coding, plugboards, and machine sequences to be suitable for the solution of any power network. It was deemed advisable to limit this paper to the electrical and mathematical features of the method rather than to lengthen it unduly with the many details of card design, coding, and machine sequences. Although many papers have stressed the saving of time by computing network problems with the network analyzer, it is the belief of the author that, as mathematical understanding of the problems increases and machines for computation are improved, this saving of time will so diminish as to favor the mathematical solution over the analyzer solution. The sample study presented in this paper indicates that load studies may be computed in about the same time that they are presently being solved with the aid of network analyzers, and that the mathematically computed solution will be of greater accuracy and will have been computed with less chance for error than the analyzer solution. If the network problem to be solved is extremely large, or contains a number of phase-shifting transformers, the advantage of the mathematical solution over the analyzer solution further increases. The aforementioned standards of speed and accuracy may be reached by performing the computations in the mathematical method with standard punched-card accounting machines.

Paper 47-87, recommended by the AIEE committee on basic sciences for presentation at the AIEE winter meeting, New York, N. Y., January 27-31, 1947. Manuscript submitted November 6, 1946; made available for printing, December 26, 1946.

L. A. DUNSTAN is an engineer in the electrical division, bureau of power, Federal Power Commission, Washington, D. C.

The author is indebted to the Bonneville Power Administration for the test study solution as worked on their network analyzer. Appreciation also is expressed for the assistance given by Doctor Paul Herget, director of the Cincinnati Observatory, in the accomplishment of the punched-card computations.

Statement of Problem

THE method of solving power networks described in this paper has been designed to fit a standardized problem, assuming that certain quantities are known and that certain other quantities are desired. In case the actual knowns and unknowns fail to fit the standardized problem, it is necessary to assume values to convert the problem to standard form and to check the answers against the desired knowns. Methods are described in the paragraphs on "Making Changes" which may be used to check the reasonableness of assumed values by computing some few answers which are critically dependent upon the assumed values without computing the entire network.

The standardized problem consists of a set of known values, a set of answers to be computed, and a set of conditions to be satisfied by the answers:

Known values:

(*a*). The circuit of the network.

(*b*). The resistance of each impedance.

(*c*). The reactance of each impedance.

(*d*). The capacitive susceptance of each impedance.

(*e*). The voltage ratio of each transformer.

(*f*). The phase shift of each transformer.

(*g*). The power load (or generation) at each bus in the network except one which is reserved to take up the slack due to system losses. This bus is referred to as the "slack-take-up bus."

(*h*). The reactive power load (or generation) at each bus in the network except one.

(*i*). The voltage at any one bus in the network.

(*j*). The phase angle at any one bus in the network.

Answers to be computed:

(*k*). The power flow at each end of each impedance.

(*l*). The reactive power-flow at each end of each impedance.

(*m*). The voltage at each bus.

(*n*). The phase angle at each bus.

Conditions to be satisfied:

(*o*). The summation of power at each bus must equal zero, that is, the power entering any bus must equal the power leaving it.

(*p*). The summation of reactive power at each bus must equal zero.

(*q*). Around each loop the summation of voltage drops must equal zero.

(*r*). Around each loop the summation of phase angle drops must equal zero.

These four conditions to be satisfied are merely restatements of the laws of Kirchhoff; that the summation of all currents at a point must equal zero, and that the summation of all voltages in a circuit must equal zero. Each of the two laws breaks into two conditions; the current is divided into two rectangular components, for each of which the law must hold; and the

voltage is broken into two polar components, and again the law must hold for each component. For purpose of application of the law regarding voltages in a circuit, "circuit" means loop in the network, rather than the actual power circuit through loads and generators, for the concept of a power network being represented by a single-line, single-phase common-ground network.

Initial data for the sample problem are given in Figure 1 and in Tables I and II. Figure 1, the master diagram, gives the circuit of the network; this is item *a* of the known data. Table I indicates the line data corresponding to items *b*, *c*, and *e* of the known data; and Table II indicates the bus data corresponding to items *g* and *h* of the known data. Line numbers and loop numbers in Table I and bus numbers in Table II are taken from the master diagram, Figure 1. It should be noted that item *d* of the known data, namely, the capacitive susceptance of each impedance, is not given in the line data, but instead the susceptance has been distributed among the busses and is included in the bus data because information was furnished the author in this form. Item *f*, the phase shift of each transformer, has been omitted from the initial data since the sample study contained no phase-shifting transformers. Item *i* of the original data for the sample study, the voltage at any one bus in the network, was 1.0700 per unit volts at bus number one; and item *j*, the phase angle at bus number one, was 0.7156 radians.

As in the case of network analyzer solutions, it is most convenient to work in the per unit system. Thus, all voltages, impedances, susceptances, powers, and reactive powers are expressed in the per unit system. For the sample problem, the power base was 50,000 kva and the voltage bases are as indicated for each bus in Table II. Because of the method of working with the small differences between the tangents and angles, it is necessary that phase angles be expressed in radians.

Master Diagram

The master diagram, Figure 1, provides the link between the power network under consideration and the sequence of computations required to solve it, just as the plugging diagram in network analyzer studies serves to co-ordinate the network analyzer units with the actual system being studied. The network is so thoroughly coded by means of the master diagram that computations may proceed for any desired set of loadings and transformer ratios without ever referring back to the master diagram. Despite the thoroughness with which the network is coded, the construction of a master diagram is a simple task which may be accomplished by mere inspection and marking on a single-line diagram.

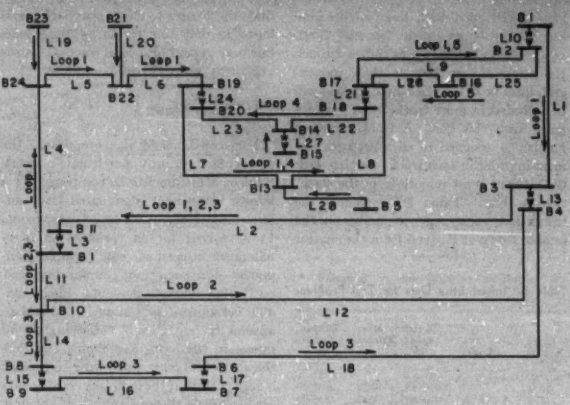

Figure 1. Master diagram for test problem

The following information is indicated on, or derivable from, the master diagram:

(*a*). Each network element is assigned either a bus number or a line number. All network elements having a direction of flow of power or reactive power are assigned line numbers. Bus numbers are assigned to: points in the network where loads, generators, synchronous condensers, or susceptances are attached, junction points, and any other points at which it is desired to compute voltage.

(*b*). Each loop in the network is assigned a loop number.

(*c*). The network is divided into "tracks," each of which is assigned a track number.

(*d*). A positive direction of flow is indicated for each network element bearing a line number. The positive direction of flow serves also to differentiate between the two ends of lines, sending and receiving.

(*e*). Each network element in each track is assigned a track sequence number.

The combination of line numbers, bus numbers, loop numbers, track numbers, and track sequence numbers is sufficient to describe a network completely. Given this information, one could draw the single-line diagram for the most complex network. The positive direction of flow was not included in the foregoing data because the positive direction is indicated by the track sequence numbers.

Certain precautions should be observed when preparing a master diagram. The arrows indicating positive direction of flow, in any loop, must be all in the same direction, either clockwise or counterclockwise. Since there should be only one positive direction for any particular line, attention should be given to the meshing of loops so that no arrows conflict. This point is illustrated in Figure 1 by the manner in which loop 3 was meshed with loops 1 and 2. After loops 1 and 2 had been meshed and the decision made to make loop 3 a counterclockwise loop, it was necessary that loop 3 include lines 2, 3, 11, 14, 15, 16, 17, 18, and 13. Had it been decided to make loop 3 a clockwise loop it would have been necessary to include lines 12, 18, 17, 16, 15, and 14 in this loop. It is of some advantage to choose loops so that they mesh with as few other loops as possible, as this has the effect of increasing the number of zero coefficients in the sets of symmetrical simultaneous equations which will arise in the solution.

In network computation, tracks serve the dual function of referring all loads and losses to the slack-take-up bus, and of referring a voltage or a phase angle at the slack-take-up bus to all points throughout the network. Tracks start either with the ends of radial lines, at loop junctions where the directional arrows divide as opposed to the confluence of directional arrows, or at the slack-take-up bus for loops containing this bus. They then proceed throughout the network following the directional arrows toward the slack-take-up bus. Directional arrows on radial lines must be toward the slack-take-up bus. Thus, the number of tracks equals the number of loops plus the number of radial lines; and

loop tracks start with lines; and radial line tracks start with busses. Obviously, tracks will merge as they approach the slack-take-up bus so that, in general, lines near the slack-take-up bus will be included in more tracks than lines remote from this bus. A track sequence number is assigned to each network element in order in each track, starting with the element most remote from the slack-take-up bus. Table III indicates the tracks and track sequence numbers in the sample study as derived from the master diagram, Figure 1. Note that each bus is listed in only one track, although each line may appear in several tracks. This is explained under "Load-Loss Flows."

Table I. Initial Line Data for Test Problem

Line Number	Loops	Resistance (b)	Reactance (c)	Voltage Ratio (e)
1	1	0.0112	0.0720	0.0000
2	1 2 3	0.0080	0.0500	0.0000
3	1 2 3	0.0000	0.1200	−0.0800
4	1	0.0120	0.0400	0.0000
5	1	0.0080	0.0330	0.0000
6	1	0.0125	0.0490	0.0000
7	1 4	0.0250	0.0380	0.0000
8	1 4	0.0110	0.0160	0.0000
9	1 5	0.0190	0.0560	0.0000
10	1	0.0000	0.0270	0.0500
11	2 3	0.0240	0.0760	0.0000
12	2	0.0390	0.1240	0.0000
13	2 3	0.0000	0.0420	0.1400
14	3	0.0490	0.1560	0.0000
15	3	0.0000	0.3100	−0.0300
16	3	0.0840	0.2240	0.0000
17	3	0.0000	0.3900	0.0000
18	3	0.0570	0.1790	0.0000
19		0.0625	0.2000	0.0000
20		0.0220	0.0700	0.0000
21	4	0.0000	0.0820	0.0000
22	4	0.0190	0.0300	0.0000
23	4	0.0210	0.0320	0.0000
24	4	0.0000	0.0600	−0.0500
25	5	0.0195	0.0620	0.0000
26	5	0.0024	0.0080	0.0000
27		0.0000	0.1220	0.0000
28		0.0310	0.0520	0.0000

Table II. Initial Bus Data for Test Problem

Bus Number	Susceptance (d)	Power (g)	Reactive (h)	Base Voltage
1	0.1400	(Slack-take-up bus)		200.00
2	0.0000	−1.8400	0.7000	100.00
3	0.2400	2.4800	0.6800	200.00
4	0.0400	−1.2000	−0.6000	100.00
5	0.0500	1.3000	0.0800	100.00
6	0.0200	0.0000	0.0000	100.00
7	0.0000	−0.0400	0.0000	57.40
8	0.0200	0.0000	0.0000	100.00
9	0.0000	−0.5000	0.0800	57.40
10	0.0500	−0.4400	−0.1900	100.00
11	0.1000	0.0000	0.0000	200.00
12	0.0200	−0.2200	−0.1000	100.00
13	0.0400	0.0000	0.0000	100.00
14	0.0000	0.0000	0.0000	50.00
15	0.0000	−0.8400	−0.2100	3.96
16	0.0000	−0.9600	−0.0400	100.00
17	0.0000	−0.7800	−0.6000	100.00
18	0.0000	−0.5200	0.4200	50.00
19	0.0300	0.0000	0.0000	100.00
20	0.0000	−0.7600	0.1400	50.00
21	0.0000	−0.4400	0.0000	100.00
22	0.0500	0.0000	0.0000	100.00
23	0.0300	−0.8200	−0.1200	100.00
24	0.0500	0.0500	0.1500	100.00

Load-Loss Flows

For convenience in computing, the power flow in any particular network element is assumed to be composed of: a known component, designated the load-loss component; and a set of components to be solved for as variables in loop-balancing equations, one variable component for each loop containing that particular network element. Each variable component is assumed to circulate around its loop, thereby satisfying, for all busses in the loop, Kirchhoff's law that the sum of all currents flowing to a point is zero. Thus, if the load-loss components are also made to satisfy this law, the flow obtained by combining the components likewise will satisfy it. The set of load-loss power flows is any set of flows satisfying equation 1 of the appendix for each bus in the network, and equation 7 for each line.

Consider, for example, that the simple 2-loop network shown in Figure 2 were to be solved in such a manner that the summation of the products of flows times reactances for lines in each loop be zero. No losses are assumed for this case, that is, the input of 50 equals the sum of the loads. A diagram similar to Figure 3 might be drawn by inspection, and the simultaneous equations written and solved. It is the function of load-loss flows to systematize the derivation of the equations in Figure 3, and the function of the master diagram to obviate the necessity of computing on the diagram in this figure. In the simultaneous equations in Figure 3, the coefficients of the variables a and b are the sums of the reactances of the lines in each loop containing these variables, and each equation contains a constant term which may be computed by summing the products, for each line in the loop, of the reactance times a flow computed from the network loadings. This latter flow is termed the load-loss flow.

Figure 4 is a master diagram for the network shown in Figure 2 and is used as the basis for the complete network coding tabulated in Table IV. This table also lists the line reactances (symbolically) and the bus loads. Table V illustrates the computation of load-loss flows by arranging lines and busses by tracks in order of track sequence numbers, taking progressive totals of loads down each track, and, finally, combining the progressive totals by line numbers. Note that these load-loss flows are the same as those computed by inspection in Figure 2.

In the general case, line losses must be considered as well as bus loads in computing load-loss flows, and, for reactive load-loss flows, $E^2(1/2)\Sigma Y$ (the charging kilovolt-amperes, see Appendix I, symbols) for each bus also need be included. Thus, when taking progressive totals down a track, all three of these quantities must be included in the totals instead of merely the loads which were used for simplicity in the illustrative case of Figure 2. It is also important that no duplication exist in the progressive totals, that is, each bus load, line loss, and bus $E^2(1/2)\Sigma Y$ be added only once. Duplication in loads may be avoided simply by listing each bus in only one track, as was done in the example in Tables IV and V, but, since lines may not be omitted from tracks, duplication in line losses is avoided best by assigning each line loss to a specific

Table III. Tracks in the Test Problem

Sequence	Track 1	Track 2	Track 3	Track 4	Track 5	Track 6	Track 7	Track 8	Track 9
1	L 01	L 11	L 14	L 21	L 25	B 23	B 21	B 15	B 05
2	B 03	B 10	B 08	B 18	B 16	L 19	L 20	L 27	L 28
3	L 02	L 12	L 15	L 22	L 26	L 05	L 06	L 23	L 08
4	B 11	B 04	B 09	B 14	L 09	L 06	L 07	L 24	L 09
5	L 03	L 13	L 16	L 23	L 10	L 07	L 08	L 07	L 10
6	B 12	L 02	B 07	B 20		L 08	L 09	L 08	
7	L 04	L 03	L 17	L 24		L 09	L 10	L 09	
8	B 24	L 04	B 06	L 07		L 10		L 10	
9	L 05	L 05	L 18	L 08					
10	B 22	L 06	L 13	L 09					
11	L 06	L 07	L 02	L 10					
12	B 19	L 08	L 03						
13	L 07	L 09	L 04						
14	B 13	L 10	L 05						
15	L 08		L 06						
16	B 17		L 07						
17	L 09		L 08						
18	B 02		L 09						
19	L 10		L 10						

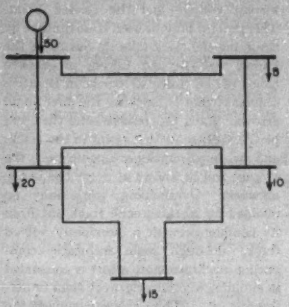

Figure 2. Circuit and loadings for explanation of "load-loss flows"

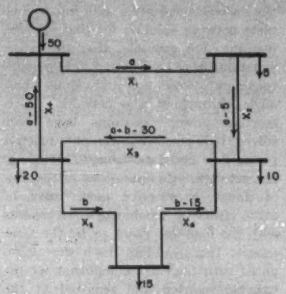

Figure 3. Solution of Figure 2 by inspection

$$0 = aX_1 + (a-5)X_2 + (a+b-30)X_5 + (a-50)X_4$$

$$0 = (a+b-30)X_5 + bX_6 + b - 15)X_4$$

or

$$0 = (X_1 + X_2 + X_5 + X_4)a + X_5b - 5X_2 - 30X_5 - 50X_4$$

$$0 = X_5a + (X_5 + X_6 + X_4)b - 30X_5 - 15X_4$$

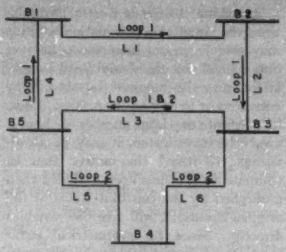

Figure 4 Master diagram for Figure 2

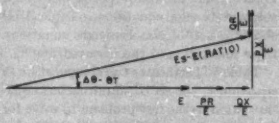

Figure 5. Vector diagram, basis for equations 11 and 12

track. As illustrated by the example, loads must be assigned a negative sign for computing load-loss flows. From this, it follows that line losses must also be negative, while generation and $E^2(1/2)\Sigma Y$ must be positive.

Although each line has two load-loss flows, the receiving flow being less than the sending flow by the line loss, the procedure outlined here will compute only the receiving load-loss flow. The procedure was so devised because all equations are based upon computing with receiving end quantities, and the sending load-loss flows are unnecessary. If they are desired, however, they may be computed either by adding losses to receiving load-loss flows, or by making a double entry of each line in each track for progressive totals, assigning the line loss always to the entry with the higher sequence number.

Table VI shows the load-loss power flows for the first approximation in the computation of the sample problem. The sending and receiving load-loss flows are equal in this case because of the initial assumption of zero power loss for the first approximation which is explained under "Successive Approximations."

Solutions About Loops

The satisfaction of conditions q and r, that around each loop the summation of voltage drops ($\Sigma\,\Delta E$) and phase angle drops ($\Sigma\,\Delta\theta$) must equal zero, leads to the simultaneous solution of loop equations in ΔE and in $\Delta\theta$. By the method of successive approximations, the solution to make the summation of the voltage drops zero about loops is a separate process from the solution to make the summation of the phase angle drops zero about loops, the former involving a set of reactive power loop equations and the latter involving a set of power loop equations. Thus, each set of simultaneous equations contains only one variable for each loop, instead of two as would be the case if both the summation of ΔE and $\Delta\theta$ were made zero in a single step. Further simplification is effected by holding the voltage, power loss, reactive power loss, and trigonometric functions to be known quantities, thus making the simultaneous equations linear.

The sets of simultaneous equations to solve for Pv or Qv are obtained by summing up the values of the parts of equations 26 or 31 for all of the network elements in each loop. Thus, an equation will result for each loop, and, in general, these equations must be solved simultaneously. It is possible to visualize a network in which none of the loops meshes with any of the other loops and for which the equations would not have to be solved simultaneously but this would be a special case of zero coefficients. The coefficients of the variables in the power equations are seen to be the summations of X' for all network elements in the loop through which the particular variable flows, and, for the reactive power equations, these coefficients are the summations of X''. X' and X'' are defined in equations 14 and 16, respectively, of the appendix. Thus, the summation of X' or X'' for any loop must be largest for the variable flowing around that loop, and the summation of X' or X'' for any other variable must be the same as the summation of X' or X'' for the given variable in the loop equation for the other variable. Therefore the sets of simultaneous equations must be symmetrical, because, wherever two loops mesh, in each loop equation the coefficient of the other variable must be the sum of the common reactances X' or X''. Similarly, wherever two loops do not mesh, the sum of the common reactances is zero, and zero coefficients appear in the equations. The solution to any of the sets of simultaneous equations is much simplified by the symmetry and by the presence of zero coefficients.

Although two approximations of a network solution are required to give network analyzer accuracy, and two approximations necessitate the solution of four sets of simultaneous equations, the solution of the equations is usually a small portion of the whole network solution. In the solution to the test problem of 5 loops, 24 busses, and 28 impedances, using a desk calculating machine, the solution to the simultaneous equations took between two and three per cent of the total computing time. However, as the network to be solved grows larger, the importance of simultaneous equation solution increases, because, for symmetrical equations, the difficulty of solution varies with the cube of the number of variables, whereas the rest of the work will vary directly with the size of the network.

In making changes in a computed solution, the simultaneous equation solution may assume greater importance, because only a small amount of additional computation may be required to obtain the equations or to expand the results. Thus, if the effects of a large number of changes are to be investigated, it may be of advantage to invert the matrix, that is, compute a set of coefficients which, when multiplied by the constant terms of the original equations, will give the variables directly. Since, for symmetrical equations, the inverted matrix is also symmetrical, the amount of computation required to invert the matrix is only slightly greater than the computation in a single solution to the equations. Table VIII shows a set of simultaneous equations, their solution, and the inverted matrix.

Table VII indicates the computation of equation 1, the set of simultaneous equations used in the test problem to solve for P_v (the power component circulating about each loop) in the first approximation. In this computation $X'=X$, and the constant term is obtained by summing $P_{LL}X$. Table VIII shows these equations and their solution. If the variables in this table are combined with the load-loss power flows in Table VI, the first approximation of power as given in Table IX will be obtained.

Expansion of Loop Solutions

After the simultaneous loop equations have been solved, it is necessary to expand the variables and other data into a complete network solution for that approximation. For example, after the power equations have been solved, it is possible to compute power flow and voltage phase angle throughout the network. After reactive power equations have been solved, it is possible to compute reactive power flow and bus voltage throughout the network. Computations of the flow of power or reactive power may be made either by combining the variables with the load-loss flows, or by the same process that load-loss flows were computed with the extra component for the variable inserted and removed at the proper place in each loop track.

Having obtained the flow of power, or reactive power throughout the network, $\Delta\theta$ or ΔE, as the case may be, can be computed for each line by equations 28 or 33. Assume, for example, that ΔE had been computed for each line, and it is desired to compute E for all busses. The voltage at each point in the network is computed from the known voltage in the initial data by subtracting from the known voltage all voltage drops (ΔE) in a path following the directional arrows from the known voltage to the particular point. Since ΔE is a voltage drop from sending to receiving end of a line, it also may be viewed as a voltage rise from receiving to sending end. Thus, the voltage at the desired point in the network also could be obtained by adding to the known voltage all voltage drops in a path opposite the directional arrows between the known voltage and the desired point. This process may be used to advantage by assuming the slack-take-up bus to be the known voltage and taking progressive totals of ΔE down all tracks in negative sequence, that is, bucking the directional arrows. Each progressive total then will be the voltage at that point in the track, and, when all tracks are completed, the voltage will be known at every bus in the network. Overlapping work may be avoided by working each track out from its confluence with a previously solved track, although with automatic computing machines more effort is consumed in avoiding overlapping work than in performing it. This process makes the tracks and track sequence numbers serve a dual function: by summing the tracks in positive sequence, loads and losses are all referred to the slack-take-up bus; by summing the tracks in negative sequence, a voltage or phase angle at the slack-take-up bus is referred to all busses in the network.

Obviously, the foregoing method of computing voltages throughout the network, using a starting voltage and a ΔE for each line, will work equally well for computing phase angles throughout the network, using a starting phase angle and a $\Delta\theta$ for each line. When computing E or θ, it is desirable to close all loops to check that the summation of ΔE and $\Delta\theta$ equals zero about each loop.

Successive Approximations

Equations must be set up and values of P and Q solved for so that conditions o, p, q, and r are all satisfied. Rigorous equations for a direct solution for P and Q throughout the network would be difficult to solve; hence, a method of successive approximations has been developed. It may be demonstrated for any power network that the phase-angle drop for most network elements is more dependent upon the flow of power than upon the

Table IV. Coding of Simplified Example Shown in Figure 2

Line Data			Bus Data		Track Data		
Line	Loops	Reactance	Bus	Load	Sequence	Track 1	Track 2
L 1	1	X_1	B 1	Slack	1	L 1	L 5
L 2	1	X_2	B 2	−05	2	B 2	B 4
L 3	1 2	X_3	B 3	−10	3	L 2	L 6
L 4	1	X_4	B 4	−15	4	B 3	L 3
L 5	2	X_5	B 5	−20	5	L 3	L 4
L 6	2	X_6			6	B 5	
					7	L 4	

Table V. Computation of Load-Loss Flows by Combining Tracks

	Track 1			Track 2			Load-Loss Flow	
Element	Sequence	Load	Progressive Total	Sequence	Load	Progressive Total	Line	Flow
L 5				1		00	L 5	00
B 4				2	−15	−15		
L 6				3		−15	L 6	−15
L 1	1		00				L 1	00
B 2	2	−05	−05					
L 2	3		−05				L 2	−05
B 3	4	−10	−15					
L 3	5		−15	4		−15	L 3	−30
B 5	6	−20	−35					
L 4	7		−35	5		−15	L 4	−50

Table VI. Load-Loss Power Flows in First Approximation

Line	P_{LL}	Line	P_{LL}
1	0.0000	15	0.0000
2	0.3000	16	−0.5000
3	0.3000	17	−0.5400
4	0.0800	18	−0.5400
5	−0.6900	19	−0.8200
6	−1.1300	20	−0.4400
7	−3.2500	21	0.0000
8	−1.9500	22	−0.5200
9	−3.6900	23	−1.3500
10	−5.5300	24	−2.1200
11	0.0000	25	0.0000
12	−0.4400	26	−0.9600
13	−2.1800	27	−0.8400
14	0.0000	28	1.3000

flow of reactive power, and, similarly, voltage drops are more dependent upon the flow of reactive power than upon the flow of power. This circumstance may be used to advantage by holding Q to be a known constant and P the variable to be solved for when equating $\Sigma\,\Delta\theta$ to zero about each loop, and by holding P a known constant and Q the variable to be solved for when equating $\Sigma\,\Delta E$ to zero, thus having the number of simultaneous equations and variables by performing these solutions separately. Further simplifications result from holding the voltage, power loss, reactive power loss, and trigonometric functions to be known quantities when computing any one successive approximation.

The successive approximation method involves a series of steps as follows:

(*a*). Assume a set of voltages and power and reactive power flows.

(*b*). Compute power losses for each network element.

(*c*). Compute an improved power flow, incorporating the computed losses and making the summation of the phase-angle drop zero around each loop.

(*d*). Compute reactive power losses for each network element, using the assumed voltage, reactive power flow, and the improved power flow.

(*e*). Compute bus charging reactive power, using the assumed voltages.

(*f*). Compute an improved reactive power flow, using the computed losses and improved power flow, and making the summation of the voltage drops zero around each loop.

(*g*). Compute the voltage E and the phase angle θ throughout the network, using the improved values of power flow and reactive power flow.

The cycle should now be restarted, using the improved values of power flow, reactive power flow, and voltage.

Convenient initial assumptions for network solution by successive approximations are $P = 0$; $Q = 0$; and $E = 1$, throughout the network. Even using such crude starting values, it was found that the first approximation was of sufficient accuracy for purposes of adjusting the study to fit desired operating conditions, and the second approximation was of approximately the same accuracy as the network analyzer solution. In most cases it is believed that a third approximation would be of greater accuracy than are results obtainable from any network analyzer thus far developed. Computation of the first approximation is considerably simpler than the computation of the second, and any succeeding approximation, because of the initial assumptions of zero flow.

The initial assumptions mean, physically, that power losses are zero, voltages are constant at the nominal value throughout the network, tangents of phase angles due to impedance drops are equal to the angles (or that the differences between angles and tangents cancel around each loop), and that phase shifts due to reactive power flow are zero (or cancel around each loop). Power systems ordinarily are designed to have small power loss and good regulation.

Table VII. Computation of Coefficients for Simultaneous Equations

Line	Loops	Pr_1	Pr_2	Pr_3	Pr_4	Pr_5	K
1	1	0.0720					0.0000
2	1 2 3	0.0500	0.0500	0.0500			0.0150
3	1 2 3	0.1200	0.1200	0.1200			0.0360
4	1	0.0400					0.0032
5	1	0.0330					−0.0228
6	1	0.0490					−0.0554
7	1 4	0.0380			0.0380		−0.1235
8	1 4	0.0160			0.0160		−0.0812
9	1 5	0.0560				0.0560	−0.2066
10	1	0.0270					−0.1493
(Equation 1)		0.5010	0.1700	0.1700	0.0540	0.0560	−0.5346

Table VIII. Simultaneous Equations, Inverted Matrix, and Variables

	Pr_1	Pr_2	Pr_3	Pr_4	Pr_5	K
Equation 1	0.5010	0.1700	0.1700	0.0540	0.0560	= 0.5346
Equation 2	0.1700	0.4120	0.2880	0.0000	0.0000	= 0.0952
Equation 3	0.1700	0.2880	1.5470	0.0000	0.0000	= 0.4599
Equation 4	0.0540	0.0000	0.0000	0.2880	0.0000	= 0.3410
Equation 5	0.0560	0.0000	0.0000	0.0000	0.1260	= 0.2143
Solution	0.7989	−0.2817	0.2619	1.1545	1.3457	

Inverted matrix

K_1	K_2	K_3	K_4	K_5	P_T
2.5463	−0.9830	−0.0968	−0.5329	−1.1317 =	0.7989
−0.9830	3.1697	−0.4831	0.2057	0.4368 =	−0.2817
−0.0968	−0.4831	0.7483	0.0203	0.0430 =	0.2619
−0.5329	0.2057	0.0203	3.9875	0.2369 =	1.1545
−1.1317	0.4368	0.0430	0.2369	8.4395 =	1.3457

Table IX. Convergence of Power Flow From Initial Assumption to Second Approximation With Network Analyzer Power Flows for Comparison

	Per Unit System			Actual		Network Analyzer Actual*	
Line	Initial P	First P	Second P	Second P	Second Ps	P	Ps
1	0.0000	0.7989	0.9143	45.72	46.12	49	50
2	0.0000	1.0791	1.1121	55.61	56.08	54	55
3	0.0000	1.0791	1.1121	55.61	55.61	52½	54
4	0.0000	0.8789	0.9402	47.01	47.48	46½	47
5	0.0000	0.1089	0.1252	6.26	6.27		7
6	0.0000	−0.3311	−0.3206	− 16.03	− 15.96	− 15	
7	0.0000	−1.2966	−1.2233	− 61.17	− 58.93	− 60	− 58
8	0.0000	0.0034	0.0226	1.13	1.22	3	3
9	0.0000	−1.5454	−1.6485	− 82.43	− 80.06	− 82	− 80
10	0.0000	−4.7311	−4.9172	−245.86	−245.86	−245	−244
11	0.0000	−0.0198	−0.0576	− 2.88	− 2.87	− 6	
12	0.0000	−0.7217	−0.7846	− 39.23	− 38.12	− 43	− 42
13	0.0000	−2.1998	−2.2727	−113.64	−113.64	−119	−118
14	0.0000	0.2619	0.2612	13.06	13.24		15
15	0.0000	0.2619	0.2612	13.06	13.06	13½	15
16	0.0000	−0.2381	−0.2437	− 12.19	− 12.94		− 12
17	0.0000	−0.2781	−0.2837	− 14.19	− 14.19	− 15½	− 15
18	0.0000	−0.2781	−0.2861	− 14.41	− 14.19	− 15½	− 15½
19	0.0000	−0.8200	−0.8649	− 43.25	− 41.00	− 42	− 40½
20	0.0000	−0.4400	−0.4443	− 22.22	− 22.00	− 23	− 22
21	0.0000	1.1545	1.2760	63.80	63.80	67	67
22	0.0000	0.6845	0.7438	37.19	37.80	39	40
23	0.0000	−0.5055	−0.0980	− 4.90	− 4.81	− 3	
24	0.0000	−0.9655	−0.8580	− 42.90	− 42.90	− 41½	− 41
25	0.0000	1.3457	1.3926	69.63	71.44	70	72
26	0.0000	0.3857	0.4322	21.61	21.63		22
27	0.0000	−0.8400	−0.8400	− 42.00	− 42.00	− 42	− 42
28	0.0000	1.3000	1.2476	62.38	65.00	63	65

* Blanks indicate that values were not read in analyzer study.

Generally, they operate with small angles between busses, usually less than 10 degrees and seldom exceeding 35 degrees. Phase shifts due to reactive power flow are also negligible compared with those due to power flow because, for most network elements, resistance is smaller than reactance and reactive power flow is smaller than power flow. Thus, although the first approximation for power flow is computed from very rough initial assumptions, it is fairly accurate, and all subsequent computations for power and other network quantities have better starting values than the first power computation.

The symbols and equations are discussed in detail in Appendixes I, II, and III. Equations for ΔE and $\Delta\theta$ were derived from the vector diagram, Figure 5. This vector diagram illustrates that, for any line, the sending voltage equals the receiving voltage plus the impedance drop, and shows the impedance drop divided into components expressed in terms of power and reactive power. In order to make the equations for ΔE and $\Delta\theta$ general, the effects of transformer ratio and transformer phase shift were considered. The analytical network solution makes use of the fact that the equations derived from Figure 5 are general and may be used for either positive or negative values of power flow, that is, the receiving end may be physically either a receiving or a sending end.

The fact may be noted that the transformer ratio in equation 31, and all other equations in which it appears, is multiplied by the receiving voltage. This has the effect of putting all of the transformer impedance before the ratio, speaking in terms of the directional arrows in the master diagram. The problem of exact placement of the ratio in a transformer is not discussed in this paper, but it was found expeditious to standardize computations by assuming the ratio to be at the receiving end. A more general representation of the transformer would use two impedances in series with the ratio between (at the receiving end of the first one, according to the standardized methods herein), as this would allow any desired apportionment of transformer impedance between primary and secondary.

The equations used to carry through the steps in one cycle of the method of successive approximations are shown in Appendix III, and consist of equations 5, and 26 through 34. The first step is to compute power loss from equation 5, which is merely the familiar I^2R equation with I expressed as two perpendicular components, P/E and Q/E. Power loss must be zero for the first approximation, if the initial values of P and Q are zero. Load-loss power flows are next computed by arranging losses and loads in tracks by track sequence numbers, taking progressive totals down the tracks, and combining the progressive totals by line numbers as discussed under "Load-Loss Flows." Having the load-loss flows, P_v for each loop may be computed from equation 26, solving this equation simultaneously for all loops. In the first approximation, QR' and the trigonometric function $(\Delta\theta' - \tan\ \Delta\theta')$ are zero, and X' is equal to X in equation 26. Thus, for the first approximation for cases containing no phase-shifting transformer, equation 26 breaks down into the familiar device of power engineers, of making the summation of PX zero about power loops. Having obtained P_v, the improved values of P, $\Delta\theta$, and θ throughout the network are computed from equations 27, 28, and 29, using methods discussed under "Expansion of Loop Solutions."

A similar process is used to obtain improved values of Q and E throughout the network. First, reactive power loss is computed for each network element by equation 30, which is the ordinary I^2X equation with I expressed as two components, P/E and Q/E. Load-loss reactive flows are then computed, using the reactive power losses, the reactive loads and generation from the initial data, and the $E^2(^1/_2)\Sigma Y$ reactive power generated at each bus. Having the load-loss reactive power flows, Q_v may be computed for each loop from Equation 31, solving this equation simultaneously for all loops. Equations 32, 33, and 34 may then be used to determine reactive power flow and voltage throughout the network. The computed values of power flow, reactive power flow, voltage, and phase angle throughout the network may then be used in place of the initial assumptions to obtain improved values by repeating the cycle.

The trigonometric functions sec $\Delta\theta'$ and $(\Delta\theta' - \tan\ \Delta\theta')$ must be evaluated in order to carry through the steps just outlined. Experience indicated that it was most convenient to evaluate these functions by using the first two or three terms, as necessary, of the infinite series when computing with key calculating machines, but with automatic punched-card accounting machines, the functions were evaluated most readily by preparing punched-card tables, so that angles could be sorted into the tables and desired functions reproduced automatically. Since the punched-card accounting machines were not capable of division,

Table X. Convergence of Reactive Power Flow From Initial Assumption to Second Approximation With Network Analyzer Reactive Power Flow for Comparison

	Per Unit System			Actual		Network Analyzer Actual*	
Line	Initial Q	First Q	Second Q	Second Q	Second Qs	Q	Qs
1	0.0000	0.3188	0.2854	14.27	16.06	7½	10½
2	0.0000	0.1631	0.1413	7.06	10.11	7	10½
3	0.0000	0.1234	0.1149	5.74	12.25	5	
4	0.0000	0.0933	0.0936	4.68	6.27	6½	8
5	0.0000	0.0684	0.0657	3.29	3.32		5
6	0.0000	0.0994	0.1043	5.22	5.46	8	
7	0.0000	0.3538	0.3620	18.10	20.78	19	21
8	0.0000	0.4159	0.4528	22.64	22.77	24	24
5	0.0000	−0.3491	−0.3261	−16.31	−11.68	−13	− 8
10	0.0000	−0.5785	−0.5115	−25.58	3.34	−18	8
11	0.0000	−0.0808	−0.0881	− 4.41	− 4.37	− 6	
12	0.0000	−0.2552	−0.2492	−12.46	− 9.20	−13	− 9½
13	0.0000	+1.0174	−1.0211	−51.06	−38.84	−48	−38½
14	0.0000	−0.0409	−0.0451	− 2.26	− 1.78		− 3
15	0.0000	−0.0422	−0.0396	− 1.98	− 1.10	− 2	3
16	0.0000	0.0251	0.0298	1.49	2.02		2
17	0.0000	−0.0051	0.0049	0.25	1.49		2
18	0.0000	0.0011	0.0186	0.93	1.51	1	2
19	0.0000	−0.2245	−0.2335	−11.68	− 4.57	−10	− 6
20	0.0000	−0.0136	−0.0124	− 0.62	0.00	− 1	0
21	0.0000	0.0938	0.0879	4.40	10.43	4	10½
22	0.0000	0.5017	0.4850	24.25	25.40	23	24
23	0.0000	0.2042	0.1818	9.09	9.17	8½	
24	0.0000	0.2883	0.2777	13.89	16.09	14½	17
25	0.0000	0.2130	0.1996	9.98	15.36	8	13
26	0.0000	0.1718	0.1581	7.91	7.98		5
27	0.0000	−0.2961	−0.3017	−15.09	−10.50	−14½	−10½
28	0.0000	0.0221	0.0472	2.36	5.88	3	6

* Blanks indicate that values were not read in analyzer study.

punched-card reciprocal tables were prepared, also to be consulted mechanically.

The rapid convergence of the various quantities as solved for by the method of successive approximation is illustrated in Tables IX, X, and XI which show: the initial assumptions; the computed first and second approximations; the second approximations converted from the per unit system to actual values; and, for comparison, the answers as read from the network analyzer. It is believed that the second approximations and the network analyzer answers, as presented in these tables, are of approximately equal accuracy because the answers agree closely, and the slight differences are comparable with known inaccuracies in the network analyzer solution. Network analyzer errors may be detected in cases where the flows entering and leaving busses do not check exactly, and cases of power losses in units for which the initial data indicate zero resistance. High losses occur in the transformers where the resistance should be about one per cent of the reactance, but the network analyzer reactance unit has a ratio of resistance to reactance of about four per cent, and especially in transformers where an autotransformer unit was used in the network analyzer to obtain the proper ratio, due to losses in the autotransformer unit.

Making Changes

One frequently cited disadvantage of mathematical methods of power network solution is the difficulty in making changes in a study once it has been completed. Experience indicates, however, that changes may be made readily in a completed, or partially completed, solution being computed by the methods outlined in this paper. The general method of solution may be divided into three processes:

(*a*). The funneling of a vast quantity of data into a set of simultaneous equations.

(*b*). The solving of the set of simultaneous equations.

(*c*). The expansion of the simultaneous equation solution into a vast quantity of network answers.

When it is desired to investigate the effect of a change in a network study, the information usually desired is the effect of the change upon a very limited number of network quantities. This problem may be solved readily by building upon a previously computed solution, because the amount of additional information to be incorporated into the simultaneous equations is limited and the equation solution need be expanded only to the extent necessary to obtain the desired information.

For example, suppose it were desired to investigate the effect of a change in a reactive power load on the voltage at a particular bus. Only the track containing the given load will be altered; loadings in all other tracks remain the same. The changed reactive load will alter by a constant amount the load-loss flow in all lines in the track containing the given load, between this load and the slack-take-up bus. This will affect only the constant terms in the loop reactive flow equations for the loops containing these few lines. The change in these constant terms may be computed by summing the X'' for this group of lines by loops and multiplying the sums by the reactive load change. After solving the simultaneous equations, the voltage drops (ΔE) need be computed for only the lines in a path between the lead-off voltage and the particular bus desired. This whole computation is extremely simple as compared with the initial solution of the whole network. The solution to the simultaneous equations may be readily built upon a previous solution, if only the constant terms are altered, and it may be that all of the variables need not be solved for to compute the desired voltage. If the matrix had been inverted, no simultaneous equations would have to be solved to compute the effect of the change.

The effect of altering a transformer ratio is less difficult to determine than the changing of a load, since changing the ratio merely changes by a constant amount the constant terms in the simultaneous reactive flow equations for loops containing the transformer. Similarly, altering the phase shift of a transformer merely changes the constant terms in the simultaneous power flow equations by a constant amount for loops containing the phase-shifting transformer.

The effect of changing a network impedance is somewhat more difficult to evaluate than the changing of loads or ratios. This change will alter not only the constant terms in equations for loops containing the given impedance, but also the coefficients of variables. The solution to the set of simultaneous equations is, therefore, more difficult in this case.

Attention is directed to the fact that this discussion of the effect of a change upon a computed network solution is based upon starting with the computed solution and working through a small portion of a single approximation. If greater accuracy is desired, other successive approximations must be solved,

Table XI. Convergence of Bus Voltage From Initial Assumption to Second Approximation and Bus Phase Angles and Charging Kilovolt-amperes With Network Analyzer Answers for Comparison

	Per Unit System			Actual			Network Analyzer Actual		
Bus	Initial E	First E	Second E	Second E	Second θ Deg	*E² (1/y)ΣY	E	θ	E² (1/y)ΣY
1	1.0000	1.0700	1.0700	214.00	41.00	8 015	214	41	8
2	1.0000	1.1124	1.1178	111.78	34.31		112	35	
3	1.0000	1.0366	1.0385	207.70	37.78	12.895	209½	38	13
4	1.0000	1.1379	1.1464	114.64	32.49	2.590	116	33½†	3
5	1.0000	1.1176	1.1231	112.31	33.05	1.875	112	34	2
6	1.0000	1.1235	1.1358	113.58	30.18	1.260	115	31	1
7	1.0000	1.1274	1.1418	65.54	25.18		66.3	26	
8	1.0000	1.0747	1.0888	108.88	26.35	1.155	110	27	1
9	1.0000	1.1145	1.1307	64.90	22.59		65½	23½	
10	1.0000	1.0818	1.0950	109.50	28.46	2.925	110½	29	3
11	1.0000	1.0183	1.0213	204.26	34.82	5.185	206½	35	5½
12	1.0000	1.0751	1.0875	108.75	28.33	1.155	109½	29	1
13	1.0000	1.0737	1.0831	108.31	29.98	2.305	108	30½	2
14	1.0000	1.0273	1.0367	51.84	24.17		52	25	
15	1.0000	0.9963	1.0058	8.98	18.44		3.96	19	
16	1.0000	1.0693	1.0783	107.83	30.34		108	31	
17	1.0000	1.0670	1.0761	107.61	30.20		108	31	
18	1.0000	1.0547	1.0648	53.24	24.85		53½	25½	
19	1.0000	1.0560	1.0687	106.87	27.19	1.675	107½	28	2
20	1.0000	1.0250	1.0329	51.65	24.58		52	25	
21	1.0000	1.0468	1.0603	106.03	24.72		106½	25	
22	1.0000	1.0570	1.0699	106.99	26.32	2.795	108	27	3
23	1.0000	0.9762	0.9892	98.92	17.72	1.430	102†	18½	1½
24	1.0000	1.0602	1.0729	107.29	26.50	2.810	108	27	3

* Computed from first approximation of E.

† It is believed that this voltage was read or transcribed incorrectly.

necessitating complete solutions to the network instead of short-cutting from the change to its effect as illustrated above.

Conversion and Correction of Answers

After the computation of a network has progressed to the point where the solution is of sufficient accuracy and bears sufficient similarity to the desired conditions, the results need be converted to a form readily presentable for reports or other purposes. This process involves: correcting reactive power flows for $(^1/_2)E^2Y$, adding a constant angle to all phase angles to make the lowest one zero in some cases, converting data from the per unit system to actual quantities, converting phase angles from radians to degrees, and listing the answers in suitable form. All of this work may be done mechanically. Only the "correction" of reactive power flows will be discussed further.

The solution of a power network, using nominal pi representation for the transmission lines, introduces a problem in that the reactive power flow in each end of each line is in error by the amount $(^1/_2)E^2Y$ and the busses each have an extraneous reactive power load of $E^2(^1/_2)\Sigma Y$. In the case of network analyzer solutions, this situation frequently is left uncorrected, and improper line flows and extraneous bus loads are recorded. This is done to save time, thought, and calculation by avoiding the necessity of apportioning each bus reactive power among the various lines attached. In the case of the analytical solution, however, the reactive flows in lines may be readily corrected by mechanical computation. The computation consists merely of a set of multiplications to obtain the product $(^1/_2)E^2Y$ for each end of each line, and a set of additions to combine $+(^1/_2)E^2Y$ to the reactive power flow at the receiving end of each line, and $-(^1/_2)E_s^2Y$ to the reactive power flow at the sending end of each line.

Punched Card Equipment and Methods

The International Business Machines equipment consisted of a 601 multiplying punch, 405 tabulator, 513 reproducing summary punch, and 080 sorter. These machines are briefly described as follows:

Multiplying Punch. This machine is designed to multiply groups of numbers which it reads from a card, and to punch the resulting product in the same card. The capacity of the machine is limited to 8-digit factors and a 16-digit product. At least 1,125 computations per hour may be performed when operating with 4-digit multipliers, the actual speed being somewhat higher owing to machine cycles being eliminated whenever zeros appear in the multiplier. The multiplying punch is also capable of addition, and certain combinations of multiplication and addition of groups of numbers read from a card may be performed and the result punched in the same card.

Tabulator. The tabulator is a combined adding, subtracting, and printing machine designed to read groups of numbers from cards, and also to respond to control punches in the cards. Groups of numbers on a single card may not be added together, but rather these numbers may be added to groups of numbers on other cards passing through the machine. By connecting the tabulator to a reproducing punch, summary cards may be punched with the same totals being printed, the process being termed "summary punching." The tabulator functions at speeds up to 150 cards per minute when merely accumulating, and at slower speeds when printing totals or when summary punching.

Reproducing Summary Punch. This machine is used to perform reproducing, summary punching, and gang punching. Reproducing is transcribing all, or any part, of the information punched on one set of cards into another set of cards, either in the original or in an altered sequence. Summary punching is the punching of a set of totals accumulated on the tabulator into a set of cards. Gang punching is the punching of identical information, copied from a master card, into a group of detail cards. The reproducer operates at 100 cards per minute for reproducing and gang punching.

Sorter. The sorter serves to divide a set of cards into several sets in accordance with the number punched in a particular column. If the several sets are then arranged in order into a single set, the original set of perhaps random sequence will have been rearranged into numerical sequence of the numbers in the particular column sorted on. The sorted set may be resorted in accordance with the number punched in another column to give a resulting set arranged in numerical sequence of 2-digit numbers formed by the two columns sorted on. Thus, 999 cards may be sorted from random sequence into numerical sequence by sorting three times, first on the units column, next on the tens column, and finally on the hundreds column. Since the sorter operates at 400 cards per minute, this process would take $7^1/_3$ minutes. The cards may be sorted into either positive or negative sequence, depending upon whether the sorted sets are arranged in positive or negative sequence. The sorter is used either for arranging a set of cards into a desired sequence, or for separating a set of cards into several sets.

It is necessary that each card used in computing bear sufficient coding that the quantity on the card can be identified, and that the card may be sorted into any sequence required for computing. Positive identification is possible from the line number (or bus number) on each card and a set number consisting of a number for each set of cards required in an approximation plus an approximation number. The line or bus members, loop numbers, track numbers, and track sequence numbers comprise the coding necessary for sorting the cards into sequences required for computing.

Each item of initial data is key punched into a separate set of cards. Thus, items *b* through *j* in "Statement of Problem" are punched in nine sets of data cards. The initial data also contain sets of cards showing the base voltage for each bus, blank line cards for all tracks, blank line cards, blank bus cards, and breaker cards (control cards to be sorted in at the end of each track to clear the tabulator total before starting another track).

After initial data cards are prepared, computation of load-loss power flows is the first step in the network solution. Initial data bus cards containing power loads, item *g* in "Statement of Problem," together with the blank line cards for all tracks and the breaker cards are sorted into the order of track sequence numbers, considering the track number as the first digit (two digits had there been more than nine tracks) of a larger sequence number. This large set of cards, made up from the three smaller sets, then is run through the Tabulator, taking a progressive total for each line number and summary punching the progressive totals. The summary punched cards next are sorted by line numbers and the sorted set then run through the tabulator, this time taking a total each time the line number changed, and summary punching the totals. This second set of summary punched cards will contain the load-loss power flows for the first approximation as shown for the sample problem in Table VI, and may now be run through the reproducer with the set of initial data cards containing the reactance of each line, to transcribe the load-loss flows and reactances to a set of cards for multiplying. A run through the multiplier produces the product $P_{LL}X$ on this set of cards, which is then ready to sort by each loop number in turn and tabulate, thus giving the constant terms for the set of simultaneous power equations for the first approximation. This is the manner in which the -0.5346 in equation 1 in Tables VII and VIII was computed. The coefficients of the variables in the simultaneous equations are obtained by sorting by each loop a set of cards containing reactances, and then resorting the cards in each loop by each of the other loops, tabulating the results of each sorting. A schedule of operations similar to the

foregoing, but resulting in the preparation of 50 sets of cards, is involved in the computation of one complete approximation of a network solution.

For purposes of division and trigonometric functions, punched-card tables were prepared. The multiplying punch required two plugboards, one to multiply field I equals field II times field III, and the other to interpolate the tables of reciprocals, sec $\Delta\theta'$, or (tan $\Delta\theta' - \Delta\theta'$). The reproducer required three plugboards, one for summary punching or for gang punching from the tables, another for reproducing card identification and field I into field II or field III, and another for reproducing and gang punching the information for a given line into enough cards to accommodate all the loops containing that line. The tabulator board was arranged to perform either of two operations, depending upon the shifting of the total control impulse. In one case, it performed ordinary accumulation and summary-punched the results by control groups. In the other case, it tabulated the coefficients of the simultaneous equations to be solved, and printed them in suitable form.

Nearly all of the operations are illustrated in the computation of $X' = X + (E^2 + PR + QX)$. With reference to Table XII, all the punches in the fields II and III were obtained on nine separate reproducer runs, reproducing from whichever set of cards already contained these quantities in field I. Thus, field III in set 248 was reproduced from field I in set 247. Field 1 of sets 218, 238, 241, and 249 was obtained by multiplying field II times field III. Set 247 was obtained by sorting and tabulating sets 218, 238, and 241, and summary punching the results. Set 248 was sorted into the reciprocal table, gang punched, and multiplied using the interpolating plugboard.

Every operation was reduced to a routine, requiring only the changing of plugboards and following of a fixed schedule. Fifty sets were required for one complete approximation, and two approximations were sufficient to give the results with the required accuracy.

General Discussion

The multitudinous numerical computations involved in the solution of a network by the method outlined in this paper may be handled expeditiously by punched-card accounting machines of the variety in daily use in most cities throughout the United States, and, in fact, in use for billing and payroll purposes in many of the larger power companies. While it is not this paper's purpose to imply that accounting machines are ideally suited to the solution of network load studies, it is maintained that such machines can solve load studies without limitation as to size, and that load studies of the size and complexity presently being handled by network analyzers can be solved in comparable time with accounting machines. Progressively superior machines for computing purposes constantly are being developed, and if such a machine were peculiarly adapted to the solution of power system problems, in all probability it could out-perform a network analyzer in speed, accuracy, versatility, and perhaps cost.

Table XII. Sample Sets of Computing Cards

Set	Field I	Field II	Field III
218..	PR	...R...	P
238..	E^2	...E...	E
241..	QX	...X...	Q
247..	$(E^2+PR+QX)$		
248..	$1/(E^2+PR+QX)$	.....	$(E^2+PR+QX)$
249..	X'	...X...$1/(E^2+PR+QX)$	

The test problem discussed herein was solved in approximately 70 hours computing time with a desk calculating machine, but required only 10 hours to compute using a punched-card tabulator, sorter, multiplier, and reproducer. Of such 10 hours, the machines were idle approximately one-third of the time because of time consumed in card handling, checking, and analysis. A total of approximately 4,000 cards was used in computations. Among the discoveries during the punched-card computation of the test problem, in addition to minor improvements in the system, was the fact that a larger study, perhaps ten times larger, would be a more appropriate size for the method. The test study had 28 impedances and 24 busses, so that many of the operations were performed on only 24 or 28 cards which would run through the reproducer in about one quarter of a minute, or through the multiplier in about $1^1/_2$ minutes. A larger study could be performed more efficiently because the time of starting and stopping the machines would be a smaller percentage of the operating time, and the running time would be long enough for the operator to prepare the next run, or perhaps to keep two or more machines running simultaneously.

Comparison of the mathematical method of network load studies with the network analyzer method indicates certain advantages and disadvantages of each over the other. The methods are not directly comparable since, with a calculating board, some solution to the network is always available for the reading whenever the board is plugged and energized, and the problem is to adjust the board so that the solution fits the desired loading and voltage conditions. With the analytical method the solution is not available until computed, but the computed solution will fit the desired loading with great precision. Small changes may be made readily in a board solution at the time it is in progress, but such changes would require some portion of the computed solution to be rerun, although, if the computing cards are preserved, the change may be made at any subsequent time. The board solution is subject to human errors of plugging, setting, and reading which are not detected readily, whereas, in the punched-card solution, all transcribing and computing, except for the punching of the original data, is done mechanically and may be listed mechanically for future reference and checking. The initial data and final answers may be printed in a form suitable to be incorporated into a report directly from the cards used in computing; whereas, with an analyzer solution, it is customary to have the answers drawn up in the drafting room for reports. Because of the greater accuracy of the computed solution, power losses may be tabulated for all network elements, and, if desired, losses attributable to any particular load may be ascertained by computing load studies with and without the particular load.

A special advantage of a punched-card solution to a network is that all of the punched-card computations may be listed mechanically, and the list preserved for future reference. If, then, a modification of the original study be desired at some future time, the original computations may serve as a basis and the few required additional computations may be performed conveniently with a desk calculating machine. The methods outlined under "Making Changes" may be used for this purpose.

The advantages and disadvantages of the analytical method over the network analyzer method of making load studies may be summarized briefly:

ADVANTAGES

1. Greater accuracy.
2. Less chance for error.
3. Neatness of automatically printed data and answers.
4. Easier and more effective filing of data for use in subsequent studies.

5. Computations may be automatically listed so that a study may be easily modified with a desk calculating machine at any subsequent time.

6. Reactive flows in lines may be automatically "corrected" for $(^1/_2)E^2Y$.

7. No limitation to the size of the network analyzed.

8. Phase-shifting transformers offer no special difficulties.

9. Nontechnical help can perform computations.

DISADVANTAGES

1. The computed solution is more difficult to modify than the network analyzer solution at the time it is being prepared.

2. The computed solution has not yet been systematized and mechanized for fault studies and transient stability studies.

3. Computed solutions lack a psychological advantage enjoyed by network analyzer solutions where in measurements are taken on an actual electric circuit.

Appendix I. Symbols

R = resistance of an impedance
X = reactance
Y = susceptance
$(^1/_2)\Sigma Y$ = susceptance at a bus (for nominal pi representation of lines the bus susceptance equals half the sum of the susceptances of all lines connecting to the bus)
P = receiving power
Q = receiving reactive power (lagging power factor if P and Q have same sign)
E = receiving voltage
θ = phase angle of receiving voltage
P_s = sending power
Q_s = sending reactive power
E_s = sending voltage
θ_s = phase angle of sending voltage
ΔP = power loss $(P_s - P)$
ΔQ = reactive power loss $(Q_s - Q)$
ΔE = voltage drop $(E_s - E)$
$\Delta\theta$ = phase angle drop $(\theta_s - \theta)$
Ratio = transformer buck in direction of arrow in Figure 1 $(E_s/E - 1)$
θ_t = phase angle buck in direction of arrow in Figure 1 due to phase-shifting tranformer (fixed component of $\Delta\theta$ for phase-shifting transformer)
P_{LL} = load-loss power
Q_{LL} = load-loss reactive power
P_{v_1}, P_{v_2}, etc. = a power flow circulating around loops 1, 2, etc., to be solved for as a variable in equations to make $\Sigma\Delta\theta = 0$ around those loops
Q_{v_1}, Q_{v_2}, etc. = a reactive power flow circulating around loops 1, 2, etc., to be solved for as a variable in equations to make $\Sigma\Delta E = 0$ around those loops

In these symbols the receiving and sending end refers to the head and tail ends, respectively, of the directional arrows in the master diagram (Figure 1), irrespective of the actual direction of power flow.

Appendix II. Equations

From conditions o and p in "Statement of Problem":
At each bus

$$\Sigma P = 0 \tag{1}$$

$$\Sigma Q = 0 \tag{2}$$

From conditions q and r in "Statement of Problem":
Around each loop

$$\Sigma\Delta\theta = 0 \tag{3}$$

$$\Sigma\Delta E = 0 \tag{4}$$

Loss equations:

$$\Delta P = (P^2 + Q^2)R/E^2 \tag{5}$$

$$\Delta Q = (P^2 + Q^2)X/E^2 \tag{6}$$

Line equations:

$$P_s = P + \Delta P \tag{7}$$

$$Q_s = Q + \Delta Q \tag{8}$$

$$E_s = E + \Delta E \tag{9}$$

$$\theta_s = \theta + \Delta\theta \tag{10}$$

From vector diagram, Figure 5,

$$\Delta\theta = \left(\tan^{-1}\frac{PX - QR}{E^2 + PR + QX}\right) + \theta_t \tag{11}$$

$$\Delta E = (E + PR/E + QXE/)\ \sec\ (\Delta\theta - \theta_t) + (E)\ (\text{Ratio}) - E \tag{12}$$

For simplification let

$$\Delta\theta' = \Delta\theta - \theta \tag{13}$$

$$X' = X/(E^2 + PR + QX) \tag{14}$$

$$R' = R/(E^2 + PR + QX) \tag{15}$$

$$X'' = (X/E)(\sec\ \Delta\theta') \tag{16}$$

$$R'' = (R/E)(\sec\ \Delta\theta') \tag{17}$$

Substituting equations 13 through 17 into equations 11 and 12

$$\Delta\theta = \tan^{-1}(PX' - QR') + \theta_t \tag{18}$$

$$\Delta E = PR'' + QX'' + E(\sec\ \Delta\theta' + \text{Ratio} - 1) \tag{19}$$

Let P in equation 18 and Q in equation 19 equal, respectively,

$$P = P_{LL} + P_v \cdots \tag{20}$$

$$Q = Q_{LL} + Q_v \cdots \tag{21}$$

where $P_v \cdots$ or $Q_v \cdots$ represents the sum of P_v or Q_v for all of the loops which include the particular line for which P or Q is being solved by equations 20 or 21.

Substituting equations 20 and 21 into equations 18 and 19

$$\Delta\theta = \tan^{-1}(P_{LL}X' + P_v \cdots X' - QR') + \theta_t \tag{22}$$

$$\Delta E = PR'' + Q_{LL}X'' + Q_v \cdots X'' + E(\sec\ \Delta\theta' + \text{Ratio} - 1) \tag{23}$$

Substituting equations 22 and 23 into equations 3 and 4, around each loop

$$0 = \Sigma[\tan^{-1}(P_{LL}X' + P_v \cdots X' - QR') + \theta_t] \tag{24}$$

$$0 = \Sigma[PR'' + Q_{LL}X'' + Q_v \cdots X'' + E(\sec\ \Delta\theta' + \text{Ratio} - 1)] \tag{25}$$

Appendix III. Network Solutions by Successive Approximation

In these equations the asterisk indicates an improved approximation of a quantity computed from previous approximations.

Power and Angle Solution

$$\Delta P = (P^2 + Q^2)R/E^2 \tag{5}$$

From equation 24 by separating the variables from the knowns, and by substituting for the angle, the tangent of the angle plus the difference between the angle and its tangent in the previous approximation around each loop,

$$0 = \Sigma P_v^* \cdots X' + \Sigma(P_{LL}X' - QR' + \theta_t + \Delta\theta' - \tan\ \Delta\theta') \tag{26}$$

where the quantity after the first summation sign is composed of the products of variables times reactances, and the quantity after the second summation sign is a constant. The summation of the reactances by loops in each loop, as illustrated for loop 1 in Table VII, forms the coefficients for a set of simultaneous equations.

From equation 20

$$P^* = P_{LL} + P_v^* \cdots \tag{27}$$

From equation 22 with substitution for the angle, the tangent of the angle plus the difference between the angle and i s tangent in the previous approximation

$$\Delta\theta^* = P^*X' - QR' + \theta_t + \Delta\theta' - \tan\ \Delta\theta' \tag{28}$$

From equation 10

$$\theta_s^* - \theta^* + \Delta\theta^* \tag{29}$$

Reactive Power and Voltage Solution

From equation 6

$$\Delta Q = (P^{*2} + Q^2)X/E^2 \tag{30}$$

From equation 25 by separating the variables from the knowns, for each loop,

$$0 = \Sigma Q_v^* \cdots X'' + \Sigma[P^*R'' + Q_{LL}X'' + E(\sec\ \Delta\theta'^* + \text{Ratio} - 1)] \tag{31}$$

where the quantity after the first summation sign is composed of the products of variables times reactances, and the quantity after the second summation sign is a constant.

From equation 21

$$Q^* = Q_{LL} + Q_v^* \cdots \tag{32}$$

From equation 23

$$\Delta E^* = P^*R'' + Q^*X'' + E(\sec\ \Delta\theta'^* + \text{ratio} - 1) \tag{33}$$

From equation 9

$$E_s^* = E^* + \Delta E^* \tag{34}$$

Cycle may be restarted using P^*, $\Delta\theta^*$, Q^*, and E^* in place of previous assumptions.

Discussion

R. B. Squires and **H. P. Peters** (Westinghouse Electric Corporation, East Pittsburgh, Pa.): This paper gives a very interesting method for simplifying the mathematical analysis of network performance. The author compares his method with the network calculator solution, which has been the only practical means of solving complicated networks easily and accurately. Since the writers of this discussion are associated closely with network calculators and have participated in over 500 calculator studies they feel justified in taking certain exceptions to the author's comparisons.

The claim of greater possible accuracy with a mathematical solution is undoubtedly true. However, the data used in calculator studies are always more inaccurate than the answers obtained. For instance, if future loads are used in the study, as they usually are, they must be estimated. The chance of the load growing exactly as predicted is very remote. Probably a more practical definition of accuracy would be the accuracy of the differences between two or more conditions using the same general set of load and line impedances. The network calculator will give these differences very accurately.

The chance for error on the network calculator, with two operators checking each other, is very remote. The possibility of an occasional incorrect instrument reading is always present, but these are usually simple to correct.

Most power system engineers prefer to have the results of their studies plotted on a copy of the system diagram. With the Network Calculator this can be done directly, and, with a little care, in sufficiently neat manner to be put directly into a report. The tabulated data obtained from the machine calculation would have to be transcribed onto a diagram before it could be analyzed satisfactorily. Thus the tabulated data are a disadvantage, rather than an advantage, of the machine method.

The problem of the distribution of charging current to give correct line readings has been solved on several network calculators now under construction by the inclusion of pi circuits. These circuits consist of an impedance circuit with an adjustable capacitor at each end. Circuit readings are made outside the capacitors so that the values obtained are true line values. One of the new network calculators has 72 such circuits. On calculators not equipped with pi circuits, the line charging correction often is neglected, as it would have a negligible effect on the line current. In the Northwest systems, with which the author had most of his calculator experience, the high voltages and long lines of course required that this correction be made.

The sample problem cited is not the usual problem encountered in power system work. This problem has the following known quantities: the load kilowatts or kilovolt-amperes, the generator kilowatts and kilovars, the transformer taps, and the voltage at one bus. The problem as usually encountered has the following known quantities: the load kilowatts and kilovars, the generator kilowatts (but not kilovars, except for maximum values) and the voltage at several busses (usually generator busses). The unknown quantities in the sample problem are the voltages at all the busses and the kilowatt and kilovar flow in the lines. In the usual problem the unknowns are, in addition to these: the transformer tap settings and the generator kilovars. The addition of these unknowns will complicate materially the mathematical solution.

The time comparison between the mathematical and network calculator methods is interesting. The author solved the problem by use of machines in ten hours. This presumably means starting from complete basic data. Starting from the same point the writers set this problem up on a network calculator and obtained an answer in two hours with the result plotted in final form on the system diagram.

Over half of this time was consumed in setting up and checking the network and the impedances. Subsequent studies could have been made in much less time.

This is not, however, a good comparison. With the usual power system problem, one finished network calculator study actually may be equivalent to several studies. For instance, if optimum transformer taps are to be determined, it may be done very rapidly by trial and error methods on the network calculator, whereas by mathematical calculation each tap change would require a set of calculations, and a new solution to the sets of simultaneous equations involved. This same condition would arise if capacitors were being distributed through a network to maintain a required voltage level or generator loading. Most power system engineers will agree that a network calculator study usually is not made to determine how a system will perform with a given set of conditions, but to determine what conditions must be met for satisfactory operation of the system. For this type of problem mathematical solution cannot compare with network calculator solution.

F. S. Rothe (General Electric Company, Schenectady, N. Y.): In this paper the author has shown that, given a set of known values in a power system network, with the aid of standard punched card accounting machines one can calculate the power and reactive flow throughout the network and obtain the voltages at the various busses. As an example, a small network problem was computed in a time of ten hours. Based on these data, the author has concluded that load studies of the size and complexity now being handled by a-c network analyzers can be solved in comparable time with accounting machines. We do not feel that this conclusion is justified from the data for two reasons.

First, certain values in a power system network which the author has assumed as known are in fact not generally known. They are the voltage ratio of each transformer and the reactive generation at each generator bus. Instead bus voltages more often are known at several points in the network and the reactive generation and transformer ratios are adjusted to obtain these desired voltages. This would make the computation by machines a cut and try procedure unless another method of calculation could be found which would make use of these known values of bus voltage. In any case, it is probable that the time of solution would be increased, whereas on the network analyzer the time is decreased if the voltages at a number of generator busses are known.

Second, comparisons involving time to do a problem are very hard to make without knowing all the factors included. However, we do not believe that the author has given sufficient data to substantiate his statement that accounting machines can handle a network problem in comparable time to an a-c network analyzer. For example, the figure of ten hours given for the time of solution of the sample problem on accounting machines is at least double the time required for the solution of the same problem on any modern a-c network analyzer.

In addition to the question of the relative efficiency of the two methods as applied to the solution of load flow problems, there is, as the author has pointed out, a very decided psychological advantage in favor of the network analyzer since it bears such a close resemblance to the actual power system both in the similarity of its elements and in their operation

Although, for these reasons accounting machines may not be well suited to the solution of load studies on power networks, we do wish to point out that there is a wide range of problems for which they are especially well suited. Such problems include those which can be solved by equivalent electric circuits but which are beyond the range of accuracy or size of present network analyzers.

C. H. Hoffman (Public Service Electric and Gas Company, Newark, N. J): This paper is a timely reminder that a network analyzer is not the only method of solving networks, although most engineers familiar with network-analyzer technique probably will be reluctant to change to punched-card computation. The fact that the computed solution is more difficult to modify, as pointed out by the author, constitutes a serious disadvantage in the study of complex interconnected systems.

One of the advantages of the network analyzer is the ease with which adjustments can be made to arrive at satisfactory operating conditions for future system arrangements. Even after considerable experience with analyzer studies of one system, it is not possible to forecast exactly the combination of generator outputs, bus voltages, and transformer taps most satisfactory for system arrangements involving previously unstudied facilities. Before obtaining the first balanced condition which justifies a complete set of readings, it is usually necessary to make a dozen or so minor changes from the original assumptions of tap settings, synchronous-condenser outputs, and generator outputs, as spot checks of critical locations indicate changes are necessary. The network analyzer is ideal for this purpose, since the spot checks are made readily, and the effects produced by adjustments are available immediately on the meters.

A second advantage of the analyzer is its flexibility when there are more specified conditions to be met simultaneously than are mathematically permissible. Generator output conditions frequently are specified in voltage as well as in megawatts and in megavars, voltages have to be maintained at more than one bus in the network, and even the duties of the slack-take-up bus may be

assigned to several generator busses. Obviously, it is not possible to meet exactly all of these conditions. The result must be a compromise, obtained by a number of small departures from the specified values. The analyzer permits making the required adjustments simultaneously so that, as far as practicable, the departures are few in number, small in magnitude, in the preferable direction, and remote from the area of interest.

These two important advantages of the analyzer solution should be given consideration when any further development is made in the method of machine computation.

J. B. Ward (Purdue University, Lafayette, Indiana): This paper presents a very interesting application of network theory and a promising contribution to power system analysis. The following comments come to mind in studying this new method:

1. The author claims greater accuracy of results as one of the advantages of his method over the network analyzer solution, yet the accuracy of the machine computation depends on the convergence to a true solution of a series of successive approximations. The question naturally arises as to means of evaluating the maximum error in any line flow or bus voltage upon the completion of one approximation to determine the necessity of carrying through another approximation.

2. In many system planning studies approximate projected loads are used, and as a result a high degree of accuracy is of little significance.

3. Frequently in a study of proposed lines and system connections the performance of a once familiar system is changed drastically. Establishing a satisfactory operating condition may involve considerable trial and error adjustment of tap settings, capacitor loadings, and source voltages. In other words, the boundary conditions or known values are not established definitely at the beginning of the study. It seems that the network analyzer solution gains a definite advantage in speed and convenience in studies of this type.

4. One of the major assets of the machine computation method is that it offers a solution to the difficult problem of accurately determining system losses.

Lester LeVesconte (Sargent and Lundy, Chicago, Ill.): The author has presented a very interesting system which probably will be useful in some companies having access to the necessary machines and having personnel with sufficient interest in the method to master and understand the technique. It is questionable if the system could be set up on a co-operative basis between several companies, similar to several of the network calculator arrangements, because of the difficulty of the power system engineers in presenting the basic data to an operator not thoroughly familiar with the system. This observation is based on experience in operating a network calculator. It is an exceptional case that can be set up and operated correctly without some changes in the original data, the need for such changes becoming evident as the adjustments are being made. The fact that the power system engineer can observe the operation of the system in units with which he is familiar, and detect the need for changes during adjustment, is an advantage far greater than psychological as listed by the author in the last statement of the paper.

Although greater accuracy can be obtained by computation, from the practical standpoint an accuracy greater than that of the original data is not justified and most network calculators easily can equal that.

While there may be less chance for error after the cards have been started through the machines, there are all the same chances for error in the preparation of the data and less chance of detecting the errors during the process.

Although the automatically printed data and answers may be neat, the significance of the answers can not be understood thoroughly until they are plotted on a system diagram. On modern network calculators the readings are recorded directly on the diagram where they are immediately available for analysis.

Glenn W. Bills (Bonneville Power Administration, Portland, Ore.): It is my belief that the author has devised an excellent tool in the study of power system networks. Such a unique use of an accounting machine might have caused many who read his paper or heard the presentation to overlook the powerful method of analysis inherent in his use of successive approximations together with the logical approach used in setting up the load flow study. His treatment of the problem is superior to that which uses the accounting machine only as a device to solve the determinants of the groups of simultaneous complex linear equations. In most load studies, it is impossible to arrive at a practical solution from a rigorous approach on the first attempt because of certain conditions, such as bus voltage limitations, which must be met. Dunstan's technique is much like that used on the calculating board where the final system equilibrium is achieved by a cut and try process involving the manipulation of board generators and the adjusting of load units. Of course the increase in the number of board units needed to satisfy the representation of a load flow problem makes this board procedure somewhat tedious and involved.

The fact that for the machine computation an increase in size of the network to be studied results only in the increase of coding cards and computation time is interesting to us who are in direct contact with network analyzers. We have found that as the interconnected systems of the Northwest have expanded, not only have the fixed number of board elements created limits, but that the time required for adjusting complex networks increases rapidly, and skilled and alert operators are essential to obtain the most efficient use of the board. In fact, we have been considering schemes which would make board balancing easier and faster. One idea that seems time saving would be the use of negative resistors in parallel with capacitor units to represent system generators. Then by using one board generator for that machine in the system which takes up the slack real and reactive power, the balancing should be much more rapid than when attempting to juggle 18 board generators. This method parallels that used by Dunstan in his employment of a slack-take-up bus.

It must be admitted that phase-shifting transformers have not been represented easily in network analyzers but, fortunately, few systems have required such transformers. However, the use of stable negative resistances together with the use of accurate transformer equivalents should eliminate the troubles previously experienced when phase-shifting transformers appeared in networks being studied and were placed on the board.

One disadvantage of the Dunstan process which should have been noted under "disadvantages" is that a check on line loadings and bus voltages is not possible at all times as they are on a network analyzer.

One distinct advantage which Dunstan claims for the machine computation is that the wearisome and time consuming recording and transcribing of load studies is eliminated. To prepare a report from the accounting-machine results, the various network values for voltage and power flow would have to be placed in a one-line diagram of the system under consideration. We understand that since the paper has been presented, a modification in card coding makes it possible to print results directly on the circuit diagram which eliminates much chance for error and greatly speeds the preparation of reports.

A special advantage of the mathematical procedure is in the determination of power system losses. Network analyzers, though possessing good accuracy for most network quantities are unable to discern accurate differences in system losses for different loading conditions. In attempting to find the exact losses attributable to Bonneville Power Administration transfer loads (BPA loads carried by and on other utilities through a power exchange agreement), the network analyzer has not been entirely adequate.

It seems probable that this mathematical method could be extended to short-circuit studies. This would indeed be a boon to power system engineers, since such computations are extremely tedious on large systems, and because of mutual inductance effects between lines in some systems, ordinary short-circuit calculating boards are inadequate to cope with the problem.

It is our belief that Dunstan has a method for solving network problems which will be of considerable value to power system engineers. Electric utilities which have no network analyzers, but do have access to accounting machines should welcome this contribution to power system theory.

It is felt that a more exhaustive study should be made to determine the relative advantages of Dunstan's procedure when compared to the a-c network analyzer method. This comparison should include time required to prepare the study, make it, and evaluate the results. It may be that one method is outstanding for certain fields of investigation while the other is superior along other lines of investigation.

Joseph J. A. Jessel (Federal Power Commission, Washington, D. C.): Perhaps the most important factor in Dunstan's technical paper is the organization and presentation of circuit analysis in a systematic manner. This makes possible the solution of many ordinary, though tedious, problems by means of ordinary business machines with the employment of nonengineering operators once the basic data are set up. This, in turn, makes the method generally usable to a greater percentage of the electric utility engineers.

It is well to note that the method of analysis developed by Dunstan is well adapted to the relative magnitude of circuit constants usually prevalent in most electric networks. It appears, however, for low-voltage rela-

tively high-resistance networks without transformers in any of the loops, that the convergence of the approximate to the nearly correct answers may be at a slower rate than ordinarily expected and the number of successive approximations may have to be increased by one to yield results comparable to those obtained for the more common high-voltage networks. Perhaps Dunstan has given consideration to this matter and his comments thereon could be rather enlightening.

Myron M. Moore (Federal Power Commission, Washington, D. C.): It appears that the author of this paper has developed a mathematical process which, in addition to enabling him to mechanize the calculation of system load studies on existing punched card machines, also simplifies the calculations to the point where it is practical to perform such network calculations on standard desk-type calculating machines with considerable facility.

I have used the author's method for calculating a family of load studies on a network of two loops and eight busses for the purpose of planning a representative system for transmitting specified amounts of power to several given load centers. I found that the first approximation gave adequate indication of the division of load on various lines, voltages, and angular displacement for planning circuit capacities and load reactive requirements. After making changes indicated by several first approximations the general characteristics needed for the system were determined; the second approximation gave the refined answers for the load flow diagram.

It will be noted that by the author's method the line losses can be obtained with reasonable accuracy. In the use of the calculating board, the readings cannot be relied upon to give losses since meter accuracy as well as the interpolation required in reading meters may make loss calculation by this method unreliable.

In the calculation of studies "by hand" on standard calculating machines all sorting, multiplication, and addition must be performed by the operator for each step. In this manner the fallibility of the human element causes errors which require time to locate and correct. The introduction of standardized procedures set up on plugboards, which are simple to install and remove from the machines, throws the responsibility for sorting and setting up multiplications on the machine. This eliminates the weakness of the human element in the chain of calculations and since the machine performs the operations faster than can be done by hand operation, it cuts down the time required two-fold.

It is noticed in Tables IX and X that values of P and Q may vary from 10 to 15 per cent between the first approximation and the second approximation. It would be of interest to see the third approximation compared to the second approximation. This comparison would probably be of only academic interest since the author claims, and the tables tend to verify the statement, that the convergence toward actual value is rapid. The proof would be more convincing if the third approximation were given to indicate just how rapid the convergence was.

Walter C. Johnson (Princeton University, Princeton, N. J.): The author is to be congratulated for bringing a fresh point of view to a subject in which the methods of computation have been regarded as very nearly fixed. His paper is significant not only because of its particular subject matter, but also because it is one of the first reconsiderations of old engineering problems in the light of the methods made available by present day digital computing devices. Recent developments in the field of computers will undoubtedly stimulate further re-evaluations of this kind.

I believe it helps in fixing a perspective to remember that no new method of computation ever has displaced an old one completely. Even the ancient abacus is still a useful device, to judge by newspaper reports. The introduction of a new method results in a temporary readjustment, after which the old methods and the new serve side by side and are utilized in a complementary manner. It appears that digital methods will be essential in problems where high accuracy is necessary, but that analogy devices will continue to be useful in many applications where moderate accuracy is adequate. This seems to be true in the present proposal, where the analogy method still offers certain advantages in the way of speed and flexibility. However, new computing devices now are being developed, and this field will bear close watching by the many engineers who have to struggle with difficult problems in computation.

J. M. Shepley and **C. B. Walton** (nonmembers; Federal Power Commission, Washington, D. C.): The mathematical solution of problems in connection with power networks operating under steady load conditions differs from those involving pure impedance networks because in the former load points are specified which have given values of real and reactive power regardless of the voltages at these points. The nature of such problems makes them practically impossible of solution in closed form whereas the solutions for the impedance network problems can be made in closed form.

Practically all mathematical solutions of the power network problems fall into two groups, namely, the superposition method and the impedance method, the former being generally recognized as the more practical method of the two. The superposition method yields answers which are approximately correct but successive applications of the method are required to get more accurate answers. In this method a number of complicated a-c networks having one source of supply and one load are solved and the solutions are grouped together for a composite solution. Needless to say these manipulations involve a great deal of work using the algebra of complex numbers, usually requiring numerous Y-delta and other circuit transformations, and, when successive applications are required for a more accurate solution, the required time and effort usually becomes prohibitive. The Hardy-Cross method found in recent years to be useful for network analyses offers another possible means of solution by successive approximations but appears to be a difficult method to apply to the type of problem at hand. By manipulating with single loops instead of all loops simultaneously the Hardy-Cross solution converges too slowly.

The author of this article has devised herein a new successive approximation method of solution for this problem which utilizes no complex algebra and which takes advantage of the fact that the power angles throughout the network mostly are dependent upon real power flows while voltage drops throughout the network mostly are dependent upon reactive power flows, and hence the solution converges rapidly. The author has also systematized the steps of the problem thereby reducing the amount of time and work involved immensely. He has also adapted it for use with machine computers thereby further reducing the time and effort required once familiarity with the method has been acquired.

The presently accepted means for solving power network problems is of course the network analyzer. In order to make the author's method acceptable it is not necessary for it to compete with the analyzer for solving problems particularly suited to that machine. As the author has shown, there are certain problems which fall outside the capacity of the analyzer, or for which greater accuracy than that obtainable from the analyzer is desired; the author's method offers a practical solution for these problems.

L. A. Dunstan: The author is indebted to the discussers for bringing out points which were not covered adequately in the paper.

Squires, Peters, and Rothe suggest that the knowns and unknowns in the standardized problem discussed do not fit the usual knowns and unknowns in actual system studies. They point out that generator reactive power, and transformer ratios and phase shifts, ordinarily are not known in advance, and, ordinarily, the voltages, or voltage limits, are known for more than one bus. The problem was standardized in the manner described in the interest of logic to avoid giving data in a heterogeneous fashion, that is, reactive loads at some busses and voltages at others, although the problem readily may be set up in other manners if so desired. It has been the author's experience that frequently more conditions are to be satisfied than are necessary for complete mathematical description of the problem. This situation is resolved with a calculating board by cutting and trying until the board operator is satisfied with the balance. It was the writer's thought that, although the standardized problem may not fit the desired, cutting and trying with computing machinery is quite feasible just as with the network analyzer.

The thought also arises that perhaps the knowns and unknowns commonly used for network analyzers have been influenced by that instrument's greater facility in handling data in one form than in another form. Thus, 18 years of network analyzer experience to date may have influenced the engineer's thinking, and have caused more attention to be paid to voltmeters than to varmeters. It has been the author's experience in studies involving generators at the end of long high-voltage transmission lines that, in some cases, the generator reactive power was more to be watched than its voltage, in order to avoid having the generator drawing excitation from the line and operating with such a weak field as to endanger stability. The relative paucity of studies containing

phase-shifting transformers also tends to bear out the thought that perhaps studies have been tailored to fit the analyzer, since phase shifters offer considerable difficulty in analyzer work.

The afore-mentioned discussers, and, in addition, Hoffman and Ward, point out that frequently analyzer studies involve cutting and trying which is carried out more readily with an analyzer than by computation. The author is cognizant of this fact, and the paper mentions it as a disadvantage. However, the section entitled "Making Changes" mentions the many short cuts which may be used to advantage. The short cuts are based on computing a small portion of a single approximation from an existing solution. This corresponds in a sense to the network analyzer practice of making a change and reading its effect roughly without bothering to rebalance the system. Thus, although changes, are not as readily computed as they may be read with an analyzer, the computation method is not impractically slow. The multiple-track method of coding a network was described in the paper rather than the single-track method (which is considerably faster than the multiple-track method) because multiple tracks allow the effects of changes in loads or generation to be investigated quickly. Several discussers have mentioned the ease with which transformer tap changes may be investigated with an analyzer. Significantly, changes in transformer taps (or changes in phase shifter settings) are the types of changes most readily investigated by computation methods. The computation of the effect of a tap change upon a single reactive power flow or upon a single voltage may be reduced to a single multiplication and addition by manipulation with an inverted matrix. A complete listing of all flows and voltages as a result of a tap change may be obtained with relatively few machine steps. This simplicity may be obtained by using a previously computed inverted matrix and by taking advantage of the fact that a separate set of flows and drops *due to the change only* may be computed and combined with the previous answer to obtain the new answer.

Discussers have mentioned that the sample problem, which was computed in ten hours, could be solved in considerably less time with an analyzer. Squires and Peters report that they set up, balanced, and read the study in two hours. This time comparison is not unfavorable when it is considered that two men, with an experience of 500 studies, using an equipment designed especially for the purpose managed in two hours (four man-hours) what one man, not an electrical engineer and with no previous network analyzing experience, pioneering with new techniques, and using accounting equipment of not the most modern type, managed to compute in ten hours. Consideration of the fact that 28 lines having a power flow and reactive flow at each end, and 24 busses having a voltage, phase angle, and charging power, results in 184 readings indicates that the analyzer operators were fairly busy during the two hours. As pointed out in the paper, the computation method is more efficient for large studies than for small ones because the set up and card handling time becomes a smaller percentage of the total time as the study becomes larger. Much of the computing time was devoted to multiplication. Two-punched card multiplying machines have been developed which are considerably faster than the one used for the sample study. One of these machines is capable of multiplying six times faster than the machine used, and the other operates about twice as fast and is capable of performing short sequences of computations including multiplication, division, addition, and subtraction in a single run of cards through the machine. Use of these improved machines undoubtedly could speed the computation method.

LeVesconte, Bills, Squires, and Peters have mentioned that answers to a load study cannot be analyzed properly in tabular form and must be transferred to a system diagram for study. It has been determined that system diagrams may be prepared to a suitable scale with directional arrows in the assumed positive direction so that prints may be run through the tabulator and all network quantities printed directly on the diagram in the proper place. Card coding for this operation is not complex, and, once it has been fitted to a system diagram, the same diagram and coding may serve for innumerable studies. Little imagination is required to note that special type bars with directional arrows could eliminate the printing of negative quantities and would result in a printed study in the form with which power engineers are now accustomed.

Bills suggests that the method might be extended to short-circuit studies. Although this is quite possible, as is the derivation of a method of computing swing curves, little attention has been given this matter by the writer.

Jessel, Ward, and Moore suggest that, since the method is a successive approximation method, attention should be given to the matter of the convergence of the approximate answers to the correct answers. One method of checking the accuracy of any particular approximation is to carry through more approximations until the point is reached where an approximation repeats the previous one. It is unfortunate that equipment was not available to the writer for carrying through more approximations. Studies may be proposed for which there is no answer, and, obviously, the method would not converge for such situation. It is possible to visualize a situation near the border line between possible and impossible operating situations for which successive approximations might be erratic rather than converging. As Jessel points out, the method will converge more slowly for systems having high resistance to reactance ratio, but it is the thought of the writer that power networks usually contain enough transformers with high reactance and negligible resistance to bring the relative magnitude of circuit constants into favorable range for the method.

Moore mentions his experience with carrying through the steps with a desk calculating machine. It is the thought of the writer that an accurate study, computed and listed for all steps by accounting machines, could serve as a basis for future hand computed modifications performed with key calculating machines. From this standpoint, a mechanically computed study is of considerably greater future usefulness than a network analyzer study.

Johnson makes general comparison between digital computing and analogy devices. He points out that recent developments in the field of computers should stimulate further investigation as to the value of analogy methods. It is the belief of the author that presently developed computers may compete economically for much of the work now being performed with analogy devices, especially the more expensive devices such as network analyzers, wind tunnels, and model basins.

Field Research on Lightning Arrester Discharges

G. D. McCANN
MEMBER AIEE

EDWARD BECK
MEMBER AIEE

FOR the past seven years the Westinghouse Electric Corporation, in co-operation with a number of public utility companies, has been engaged in a study of the frequency, magnitude, and wave shapes of the lightning currents discharged by arresters, both in substations and on distribution circuits. This paper presents a summary and analysis of all of the data obtained in this investigation, including data previously published.[1,2] Because of the many variables and the fortuitous nature of lightning discharges, the data have been collected and presented on a statistical basis. An investigation of such wide scope covering the effects of the various types of systems located in different areas of the country is possible only through the co-operation of a number of utilities whose help is acknowledged gratefully. The co-operating utilities are listed in Tables I and II, together with a summary describing the system, the type of lightning recording installations, and the period for which the stations were under study. The number of substations investigated was 19, with operating voltages from 6,900 to 138,000 volts, providing data on 133.5 single pole arrester years of operation. The distribution arrester study was conducted on six systems ranging from 2,300 to 6,900 volts, covering 160 arrester years of operation.

The recording instruments used and details of the installations have been described in earlier papers.[1-4] In most of the substations the recording instruments consisted of high speed fulchronographs, surge crest ammeter links, and surge indicators in each arrester phase leg with a slow speed fulchronograph, surge crest ammeter links, a surge indicator, and a magnetic surge front recorder in the common arrester ground lead. This type of installation is designated in Table I as 3-phase fulchronograph. Modifications and additions to the equipment are noted in the tables. It should be noted that the sensitivity limits of the instruments, excepting the photographic surge current recorder is of the order of 50 amperes. The photographic recorder can register currents from 150,000 amperes to as low as 0.2 ampere, thus assuring the recording of the total duration of the discharges including power follow current.

Number of Records Obtained

The data obtained on lightning arresters in stations comprise 226 records of single pole arrester discharges having a total of 294 individual components. Ninety distribution arrester records were obtained with 114 individual components. Statistical summaries of the frequency of arrester discharges, number of components recorded, crest magnitude, polarity, fronts, times to half values, and durations are given in the curves of Figures 1 to 8, inclusive.

The curves of Figure 1 show the probability of the average number of discharges per single pole arrester per year over the period for which each arrester was under observations. The maximum number of discharges recorded for arresters in stations was six in contrast to two for distribution arresters. Fifty per cent of the arresters in stations discharged an average of $1^1/_2$ times per year compared to $^1/_2$ discharge per year for distribution arresters. These curves are not necessarily typical of an average group of arresters since the recording stations are at locations known to be subject to especially severe lightning conditions. Comparison of the two curves shows that the station arresters discharged more frequently. This has been shown also by earlier data and would be expected from the consideration that, in general, there is a lower density of station arresters per mile of line than for arresters on distribution circuits. However, distribution arresters are usually lower in voltage ratings and will discharge for a higher percentage of disturbances. The first factor appears to have more weight.

Number of Components

The number of components per composite record obtained by the fulchronographs and by the photographic recorders in substations is shown in Figure 2. It is recognized that the data may be subject to corrections since it is possible that the effects of more than one stroke may be recorded. It was not practical to service the distribution arrester stations as frequently as the substation installations, therefore, such data on distribution arresters have not been considered sufficiently significant to be included in the curves. The installations in substations were serviced on an average of about once a week and usually after every storm. For purposes of comparison, Figure 2 also includes the probability curves for the number of components in direct strokes. The photographic recorder data obtained on two systems (see Table I) indicate a larger number of components probably because the photographic recorder measures currents too low in magnitude and duration to be detected by the fulchronograph. There are several factors that cause the arrester data to differ from the direct stroke curves. The arrester data, as recorded by the fulchronograph, shows less components than measured in direct strokes probably because not all the com-

Paper 47-99, recommended by the AIEE committee on protective devices for presentation at the AIEE winter meeting, New York, N. Y., January 27–31, 1947. Manuscript submitted November 7, 1946; made available for printing January 2, 1947.

G. D. McCANN, formerly with Westinghouse Electric Corporation, is in the department of electrical engineering, California Institute of Technology, Pasadena, Calif.; EDWARD BECK is section engineer, switchgear engineering department, Westinghouse Electric Corporation, East Pittsburgh, Pa.

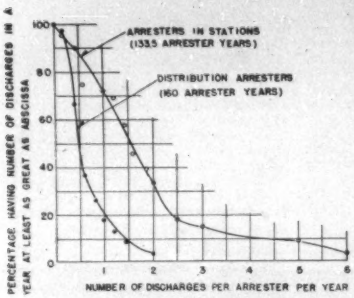

Figure 1. Average number of single-pole arrester discharges per year in the period under observation

ponents were detected and probably because not all stroke components produce arrester discharges. The photographic recorder curve lies above the direct stroke curves in certain regions. This may be due to the fact that the effects of several strokes were obtained on one record.

Crest Magnitude and Polarity

Probability curves on the crest magnitudes of arrester discharges are given in Figures 3 and 4. Comparisons are made on the basis of the types of installations studied and the polarity of the discharge currents. Although lightning arresters in stations discharge more frequently, crest magnitudes are lower than in distribution arresters. It is of interest that the curves for the crests of the individual components do not differ much from those for the maximum components in each record. The highest crest current so far recorded is 10,000 amperes. It must be recognized, however, that considerably higher current than this can occur infrequently.

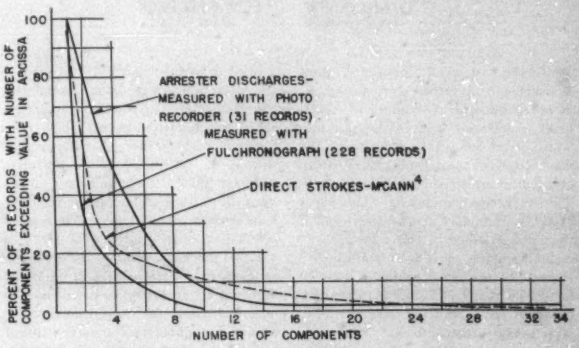

Figure 2 (below). Statistical distribution of the numbers of components in records of arrester discharge currents

The curves of Figure 4 show a higher number of negative currents than positive as would be expected. The maximum positive current recorded was 2,800 amperes whereas the maximum negative current was 10,000. Twenty-six per cent of the individual components recorded were positive, whereas the direct stroke data[4] indicate that not over 5–10 per cent of all direct stroke components are positive. The greater number of positive currents in arresters is the result of surges induced by nearby strokes, a considerable number of which appear to be of sufficient magnitude to discharge arresters.

Wave Fronts

The data on wave fronts are summarized in Figure 5. The maximum recorded wave front was 25 microseconds as compared to 10 microseconds for direct strokes.[4] It has been shown previously[5] that the low current discharges have fronts usually less than 1 microsecond in

Table I. Recording Installations on Arresters at Substations

Company	Description of Station	Type of Installation	Years Under Study
1. American Gas and Electric Co.			
(a). Appalachian Electric Power Co.	Two 12-kv; one grounded Y, one delta; grounded system wood poles	Three-phase fulchronograph	1939, 1943
	One 33-kv delta grounded system, wood poles; One 138-kv delta grounded system, steel towers with ground wire	Three-phase fulchronograph	1941, 1943
(b). The Ohio Power Co.	Two 33-kv delta grounded system, wood poles	Three-phase fulchronograph; cathode-ray oscillograph*	1940, 1946
2. West Penn Power Co.	Three 25-kv delta resistance grounded system, wood poles	Three-phase fulchronograph plus photographic recorders†	1939, 1946
3. Consumers Power Co.	Two 44-kv delta system, wood poles	One is 3-phase photographic recorders and surge-crest-ammeter links; other has photographic recorders and surge-crest-ammeter links; in ground only	1943, 1946
4. Monongahela Power Co.	One 22-kv delta system, wood poles	Three-phase fulchronograph	1939, 1943
5. Duquesne Light Co.	Two 22-kv delta resistance grounded system, wood poles	Fulchronograph in common neutral	1939, 1941
6. Mississippi Power Co.	One 110-kv grounded Y, wood poles	Three-phase fulchronograph	1939, 1941
7. Georgia Power Co.	Two 9-kv delta, wood poles	Three-phase fulchronograph	1939, 1941
8. Lower Colorado River Authority	One 132-kv grounded Y, wood poles, two ground wires	Three-phase fulchronograph	1941, 1944

* Cathode-ray oscillograph installed in common arrester ground.

† Photographic surge current recorders in each arrester phase leg at two of the substations.

Table II. Recording Stations at Distribution Arresters

Company	Description of System	Type of Recording Instruments	Years Under Study
1. Wisconsin Public Service Corp.	6.9 kv, wood pole, single phase, delta source	10 with fulchronographs and surge crest ammeters; 10 with photographic recorders, surge-crest-ammeter links, and integrators	1940–1945
2. South Carolina Electric and Gas Co.	4.6 kv, wood pole, single phase, delta source	12 with fulchronographs and surge-crest-ammeter links	1939–1943
3. Union Electric Co. of Missouri	4.16 kv, wood pole, single-phase extension from grounded-Y source	4 with fulchronographs and surge-crest-ammeter links	1942–1944
4. Green Mountain Power Co.	2.3 kv, wood pole, single phase, delta source	2 with fulchronographs and surge-crest-ammeter links	1942–1945
5. Houston Lighting and Power Co.	12 kv, wood pole, grounded-Y source	3 with fulchronographs and surge-crest-ammeter links	1941–1945
6. Public Service Co. of Northern Illinois	2.4 kv, wood pole, single phase, delta source	2 with fulchronographs and surge-crest-ammeter links	1941–1943

duration. In higher current discharges also, the current initially rises more quickly for a short period. This is brought about by the abrupt change in surge circuit resulting from the sudden spark-over of the arrester gap. This effect is shown clearly in Figure 5 by the curves for discharges below 1,000 amperes. Because of attenuation by wave propagation, it would be expected that the higher current discharges would have longer fronts than direct strokes. This is indicated also by the curves for discharges in excess of 1,000 amperes. One surge of less than 1,000-ampere crest had a front of 20 microseconds.[3] As shown by the cathode-ray oscillogram in reference 2 it has an abrupt front followed by slow rate of rise to the crest.

Times to Half Value

Figure 6 gives the data on times to half values for arrester discharges as compared to direct strokes. The times to half value for arresters in stations are shorter than for distribution arresters or direct strokes. There are several factors that may cause the wave shape of the tail of arrester discharges to differ from those of direct strokes. The lower magnitude surges, in general, should show shorter tails because of the sensitivity limit of the fulchronograph and also because an appreciable number of surges are induced by indirect strokes. Such induced surges have shorter tails than direct stroke currents.[5] Conversely, attenuation from propagation will tend to make the times to half value greater. However, direct strokes close to arresters, if they cause line flashover, usually should shorten the times to half value of the arrester discharge because the flashover path, if of low impedance, will tend to rob the arrester of current. The data for both types of arrester installations, substation, and distribution were analyzed in terms of those records above 1,000 amperes, and all records. The distribution arrester data showed little effect and was not plotted separately. However, the station data showed shorter tails for the lower magnitude surges.

Duration of Components

Figures 7 and 8 summarize the data on durations of individual component discharges as recorded with the fulchronograph and photographic surge current recorder. Of particular interest is the markedly greater durations recorded with the more sensitive photographic recorder.

Figure 3 (below, left). Statistical distribution of the crest magnitudes of the currents discharged in single-pole arresters

Measured by fulchronograph and surge crest ammeter links

Figure 4 (right). Comparison of crest magnitudes of positive and negative currents discharged through single-pole arresters

Figure 5 (below, right). Statistical distribution of the durations of the fronts of the currents discharged by arresters, measured by the magnetic surge front recorder

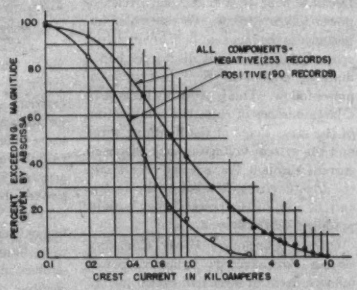

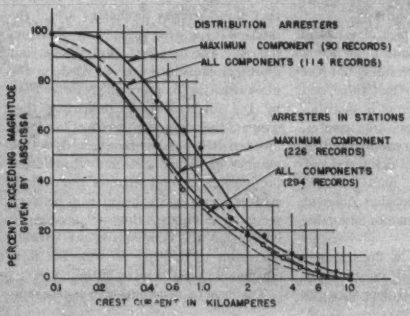

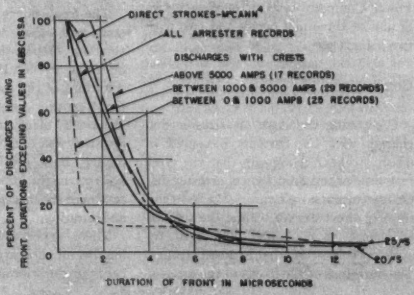

The curves for distribution arresters show longer durations than those for arresters in stations, and the Wisconsin Public Service Corporation data show appreciably longer durations than for any other system. The maximum durations as recorded by the fulchronograph are of the order of 15,000 microseconds for arrester discharges as compared with 300,000 microseconds for direct strokes. Only ten per cent of the discharges in stations exceeded a duration of 250 microseconds as recorded by the fulchronograph whereas ten per cent of the distribution arrester discharges showed durations ten times as long and direct strokes 100 times as long.

Photographic surge current recorder data were obtained at substations on two systems. A segregation of these is given in Figure 8 as shown by Table I. These two systems are similar except that the West Penn Power Company system is resistance grounded through 18 ohms while the Consumers Power Company system is ungrounded. Also, they are in different parts of the country. On the Consumers Power Company system more records per arrester-year were obtained with more component discharges per record. The Consumers Power Company data also show somewhat longer durations with a maximum of 34,000 microseconds. The discharge producing this record contained a little over three half cycles of power follow current. Of particular importance is the fact that only about 25 per cent of the component discharges had a duration equivalent to a half cycle of power follow. This is probably because in a large number of cases the combination of the wave shape of the lightning surge and the system voltage is such that zero current through the arrester occurs and the arrester clears itself before the normal current zero of the power follow current produced by the system.

On the Consumers Power Company system three records indicated power follow current of three half cycles and six of two half cycles. On the West Penn Power Company system there were two of almost three half cycles and two with two half cycles.

Figure 6. Times to half crest value of all individual components as recorded by fulchronographs

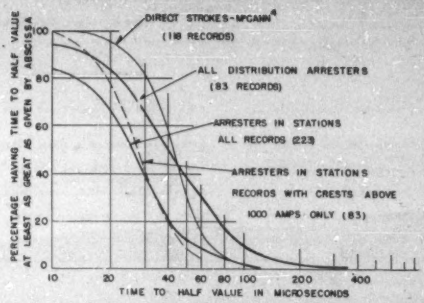

Figure 7 (below). Statistical distribution of the durations of all components of records of arrester discharge currents

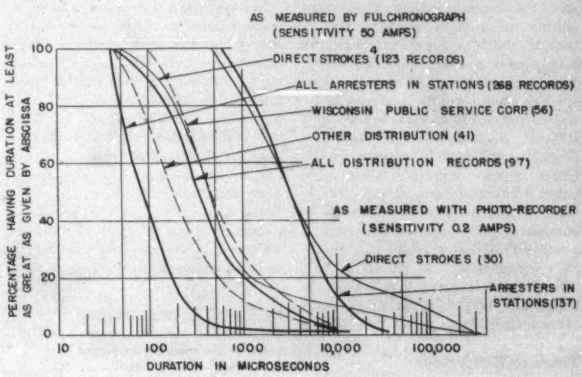

Conclusions

Comparing the data on arrester discharges with the currents measured in direct strokes,[4] it appears that the crest magnitudes and durations of arrester discharge currents are appreciably less than those in direct strokes. Thus, the amount of charge or coulombs discharged by arresters is less than that in direct strokes. The durations of the fronts of the arrester currents are, except for the low current discharges, about the same or longer than those in direct strokes. The average time to half value of currents in distribution arresters is of the order of that in direct strokes, but for currents in arresters in stations, it appears to be less. A higher percentage of positive currents were found in arresters than in direct strokes, and about 14 per cent of the negative discharge currents were higher than the highest positive current.

The frequency with which arresters in stations discharge was found to be higher than for distribution arresters, but the crest magnitudes, times to half value, and durations of the components in distribution arrester discharges are greater. Practically all of the data on distribution arresters was obtained on delta systems. Similar data on 4-wire multigrounded systems might show somewhat different results in the matter of time to half value and duration.

There appears to be a considerable number of discharges with crest magnitudes or durations or both less than the sensitivity of the fulchronograph. These currents would be of the order of 50 amperes or less or shorter than 20 or 30 microseconds. Such discharges probably are caused by low voltage surges of the order of the spark-over voltages of the arresters resulting from induced voltages or system disturbances.

From the data obtained on the probability of multiple strokes as indicated by the number of components, it is likely that some arrester discharges are of the multiple type with more than one component. The data of Figure 4 show that more components were recorded by the more sensitive photographic recorder than by the fulchronograph indicating that many of the components were of low magnitude. It is possible that records with a number of components may have been produced by several separate and distinct strokes occurring in the interval between servicing as Figure 4 does not necessarily imply that the components are entirely the result of multiple strokes, but it is concluded that a number of them are.

The data on distribution arresters indi-

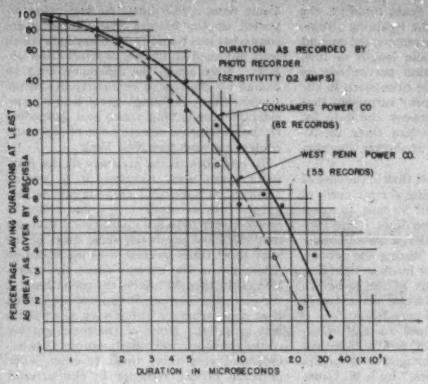

Figure 8 (right). Statistical distribution of durations of arrester discharge currents on two different systems as measured by the photographic surge current recorder

cate some important differences between systems. On the Wisconsin Public Service system the records indicate that the frequency of arrester discharge, the crest magnitude of current, and the time to half value are of the same order as on the other distribution systems studied. The durations, however, were two and three times as great indicating a greater proportion of discharge currents with long tails and greater charge. The Wisconsin Public Service study was carried out in a small area where lightning arresters have been damaged, and the region is one of high soil resistivity which may affect the lightning current wave shape. The system was delta at the time the study was carried on. This will tend to increase the probability of long tailed arrester currents, but practically all of the other distribution systems were delta also, so that this is not the principal reason.

The photographic recorder data indicated that about 25 per cent of the components have durations equivalent to a half cycle of 60 cycles. This indicates that many discharges are not accompanied by full power follow. This has been suspected from certain laboratory tests. Some discharges indicate more than a half cycle of power follow. This can be caused by a long tailed discharge which keeps the arrester in its conducting state or it may be the result of restriking of arresters. Laboratory tests indicate that restriking is probable when the system voltage applied to the arrester terminals exceeds the arrester rating.

The duty on lightning arresters apparently varies from place to place and from year to year. There is no typical discharge current. However, it appears that the tests recommended in the AIEE Standards for lightning arresters are sufficiently severe to assure good lightning arrester performance. While it is recognized that discharges more severe than any recorded in this investigation may occur occasionally, this probability appears to be small. The principal risk of damage to lightning arresters resides in an unrecognized or unforseen system voltage condition that applies voltage to the arrester line and ground terminals in excess of its rating.

References

1. Field Investigations of Lightning, **C. F. Wagner, G. D. McCann, Edward Beck.** AIEE Transactions, volume 60, 1941, pages 1222–30.

2. Field Investigations of the Characteristics of Lightning Currents Discharged by Arresters, **I. W. Gross, G. D. McCann, Edward Beck.** AIEE Transactions, volume 61, 1942, May section, pages 266–71.

3. Instruments for Recording Lightning Currents, **C. F. Wagner, G. D. McCann.** AIEE Transactions, volume 59, 1940, pages 1061–8.

4. The Measurement of Lightning Currents in Direct Strokes, **G. D. McCann.** AIEE Transactions, volume 63, 1944, pages 1157–64.

5. Induced Voltages on Transmission Lines, **C. F. Wagner, G. D. McCann.** AIEE Transactions, volume 61, 1942, pages 916–30.

Discussion

S. B. Howard (General Electric Company, Pittsfield, Mass.): The data presented by McCann and Beck on the crest magnitude of discharge currents through arresters in stations check closely with that reported by Gross and McMorris in 1940.[1] The highest crest current recorded in the earlier investigation was 15,000 amperes, with 3.5 per cent of the 459 recorded discharges having a crest value at least as great as 5,000 amperes. A maximum of 10,000 amperes is reported by McCann and Beck, with 4 per cent of the 226 recorded discharges having a crest value at least as great as 5,000 amperes. About 25 per cent of the recorded discharges in both investigations had a crest value at least as great as 1,500 amperes.

The data from several investigations have established that the crest values of arrester-discharge currents will be much lower than the crest values of the currents in direct lightning strokes, when considered on an expectancy basis. However, it is of interest to compare the times to crest of the arrester-discharge currents, as reported by McCann and Beck, with similar data on direct lightning strokes reported by K. B. McEachron in 1941.[3] For times to crest of three microseconds or more, the data from the two investigations show a high degree of conformity; for example, 80 per cent of the recorded direct-stroke peaks and 70 per cent of the recorded arrester-discharge currents reached crest in not more than three microseconds, with 97 per cent and 90 per cent, respectively, reaching crest in not more than six microseconds. However, McEachron found that approximately 30 per cent of the recorded direct-stroke current peaks had a time to first crest not greater than 0.5 microseconds, whereas none of the arrester-discharge currents reported by McCann and Beck reached crest in less than 0.5 microsecond.

The McEachron data on the time to crest of direct-stroke currents were obtained by oscillograph, while most of the data on arrester-discharge-current fronts presented by McCann and Beck apparently were obtained by magnetic surge-front recorders. In view of this fact, I would like to ask the authors if the characteristics of the latter instrument might not have affected seriously the measurements in the region below about three microseconds, and possibly have created an artificial "threshold" of 0.5 microsecond for the time to crest of the recorded arrester-discharge currents.

McCann and Beck conclude that the duration of arrester-discharge currents are appreciably less than those of direct-stroke currents. While this may be true as regards total duration, I would like to point out that the times to half value of the two currents are comparable, even for discharges through arresters in stations. Over the range from 10 to 40 microseconds, which includes 75 per cent of the data on time to half value from either investigation, a comparison of McEachron's measurements on direct strokes with those on station-arrester-discharge currents reported by McCann and Beck shows that the percentile curves of time to half value check within 20 per

cent between the two investigations.

In conclusion, McCann and Beck are to be congratulated for bringing these data to the attention of the industry. I am sure that the information will be of great interest to both users and manufacturers of lightning protective equipment.

REFERENCES

1. LIGHTNING CURRENTS IN ARRESTERS AT STATIONS, I. W. Gross, W. A. McMorris. AIEE TRANSACTIONS, volume 59, 1940, August section, pages 417–22.

2. LIGHTNING TO THE EMPIRE STATE BUILDING, K. B. McEachron. AIEE TRANSACTIONS, volume 60, 1941, September section, pages 885–90.

G. D. McCann and **Edward Beck:** Howard has pointed out the difference between the statistical data on the times to crest of lightning arrester discharge currents shown in Figure 3 of the paper, and the data reported by McEachron on time to crest of the currents in direct strokes to the Empire State Building. In our opinion differences in the measurements are to be expected. In the case of the Empire State Building, the current is measured at the lightning stroke. In the case of lightning arresters, the current usually arrives over some length of line, hence there is attenuation particularly of currents which may have been steep in the stroke. It does not appear surprising that there is a similarity between the data for times to crest greater than three microseconds and a difference at shorter times because of this effect.

Moreover, it is probable that in the case of the Empire State Building steeper rates of rise may occur than in strokes to open ground or to transmission lines. The Empire State Building is a large metallic mass which becomes charged during the process of charge separation that leads to lightning strokes. The upper part of the structure may discharge into the stroke channel very quickly after contact has been made.

In regard to the times to half-value, reference to Figure 5 of AIEE technical paper 47-97, "Field Investigation of Lightning Surges at Substations," by I. W. Gross and G. D. McCann, indicates considerable similarity between the data for arrester discharges, McEachron's data, and the McCann data. The times to half-value reported on the Empire State Building are somewhat less than the McCann data which were obtained on strokes to much lower objects. Here again, the differences may be caused by the special characteristics of the Empire State Building: great height, considerable conducting mass, and grounding to the widespread counterpoise of pipes and cables that underlies New York.

In reference to the accuracy of the magnetic surge front recorder, it is not as accurate as a reliable cathode-ray oscillograph. Its accuracy is less for times to crest shorter than 0.5 microsecond than for longer times. However, since most of the very short times to crest were measured on discharges of low current where the operation of the arrester affects the wave shape of the discharge current, it was not considered that great accuracy at the very short times was essential. None of the oscillographic records of the arrester discharge currents has indicated very short times to crest. The presence of the recorder in the arrester ground lead circuit will not affect the character of the surge current as the recorder is of negligible impedance.

The Equivalent Circuit of the Capacitor Motor

SHELDON S. L. CHANG
STUDENT MEMBER AIEE

BASED on the cross-field theory of the capacitor motor[1] an equivalent circuit is derived from which the following are obtained:

1. A method for performance calculation which involves no more than a few hours labor for the complete speed, torque, efficiency, power factor curves.

2. An accurate and comparatively simple expression of the maximum torque of the capacitor motor. (See equation 36.)

3. An approximate and very simple expression of the maximum torque for design estimations. (See equation 42.)

4. A condition for good efficiency and low noise which allows itself to be expressed very simply in terms of motor constants. (See equation 35.)

5. An expression for the pulsating torque at any speed. (See equation 45.)

6. A comparison of the equivalent circuits of the capacitor motor, the polyphase motor, and the plain single-phase motor, which is not only an interesting correlation of the fundamentals but also enables a designer to know what he can and ought to expect from his designs.

The Equivalent Circuit

The equivalent circuit of Figure 1*A* and the corresponding torque equation 1 are derived from the fundamental equations of the cross-field theory. Because the derivations are not essential to the understanding of the circuit, and hence the capacitor motor, we shall start from the equivalent circuit itself. Readers interested in the derivations are referred to Appendix I at the end of this paper. At present it is only necessary to state the following:

1. In deriving the equivalent circuit and the torque equation from the cross-field theory, no assumptions or approximations have been made. The equivalent circuit is as exact and general as the cross-field theory itself.

2. The cross-field theory does not take into account the existence of two separate skin effects in rotor conductors or the effect of space harmonics. When these effects are considerable, the cross-field theory and, therefore, the equivalent circuit would not hold good. In general, if there are two or more coils per phase per pole, and if the frequency is not high enough to give unusual skin effects, the equivalent circuit can be expected to give accurate results.

Figure 1*A* is the equivalent circuit of a capacitor motor with both the capacitor phase and main phase connected to the same power source. However, in setting up an equivalent circuit in which current from both phases must feed into the rotor circuit, represented by one set of constants, such rotor currents must be represented as in phase with each other on the circuit to correspond to the actual motor condition of being in time quadrature. This can be done by using the j-operator on the capacitor winding applied voltage, even though it must be kept in mind that the two windings actually are connected to the same source. Because motor performance can be identified by volts per turn, the correct effect of the capacitor winding (with different number of turns) requires that the capacitor winding be divided by the ratio a. Hence the actual applied voltage on the capacitor winding is multiplied by $-j/a$ through these considerations.

The circuit parameters of Figure 1*A* are characteristic reactances and resistances of the capacitor motor. The reader is referred to the table of symbols at the end of this paper for their significance. For any capacitor motor it is only necessary to solve the circuit of Figure 1*A* for I_z', I_y, I_c', I_m from which the torque, line current, efficiency, power factor, and so forth are calculated readily.

The iron loss is represented by the real components of Y_m and Y_z. Because the iron losses are proportional to the square of the air-gap voltages E_m and E_z for a good range of voltage, this approximation can be expected to hold for the entire performance range, that is, $0.7 < S < 1$. The friction and windage losses should be deducted from the generated torque.

$$T = RI^2 + \frac{2r_2}{1+S} I_z' I_y \times \cos(I_z', I_y) \text{ synchronous watts} \quad (1)$$

The torque equation 1 consists of two terms. The first term is the power absorbed by the virtual resistance R. It represents the major part of running torque but vanishes as R vanishes at zero speed. The second term represents exclusively the starting torque. Its effect on the running torque usually amounts to only a few per cent for an adequately designed motor. An examination of this second term shows

1. When the angle between I_z' and I_y is small, the second term is positive, and the generated torque in synchronous watts is higher than the energy absorbed by the virtual resistance R. Better efficiency would be realized under this condition.

2. When the angle between I_z' and I_y is larger than 90 degrees, the second term is negative. The total current I is reduced also. The torque would be small, and the efficiency would be poor.

Physically, a small angle between I_z' and I_y means that the capacitor phase and the main phase are matched so that they supply the virtual load R jointly. If a flow of energy exists either from the capacitor phase to the main phase or vice

Paper 47-101, recommended by the AIEE committee on electric machinery for presentation at the AIEE winter meeting, New York, N. Y., January 27–31, 1947. Manuscript submitted October 28, 1946; made available for printing December 9, 1946.

SHELDON S. L. CHANG is a design engineer at Robbins and Myers, Inc., Springfield, Ohio. This paper is based on research for a doctoral thesis, 1947, Purdue University, Lafayette, Ind.

The writer is indebted to T. C. Lloyd of Robbins and Myers, Inc., for his valuable advice and discussions.

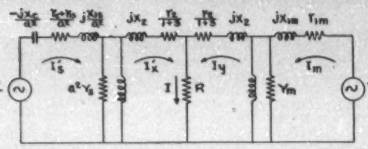

Figure 1A. The equivalent circuit for the capacitor motor. On this diagram

$R=\frac{Sr_2}{1-S^2}$

$I=I_x'+I_y$

Capacitor winding current $=I_s'$

$=\frac{jI_s'}{a}$

Main winding current $=I_m$

Line current $=I_s+I_m$

Line voltage $=V$

Figure 1B (below). Equivalent rotor circuit of the capacitor motor

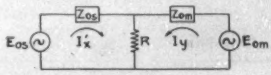

Figure 2. Simplified equivalent circuit viewing from the rotor. This circuit gives correct rotor currents for various speeds but gives no idea what the stator currents are

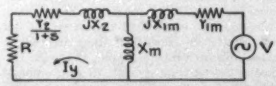

Figure 3. Approximate equivalent circuit at maximum torque point. The capacitor phase is assumed to supply its own magnetization current, the iron loss, and the friction and windage loss

versa, the angle between $\boldsymbol{I}_x'$ and $\boldsymbol{I}_y$ would be larger than 90 degrees, and the efficiency would be poor.

A relationship between the motor constants which guarantees satisfactory operation in this light will emerge from later developments.

Solution of the Equivalent Solution

The circuit of Figure 1*A* can be solved readily by taking the voltage and currents at the virtual resistor R as a starting point. Either looking into the right or into the left from this virtual resistor, we see a T-circuit connected to a power source. Let the voltage across R be called $\boldsymbol{E}$. The voltage $\boldsymbol{E}_m$ across the magnetizing branch $\boldsymbol{Y}_m$ is then

$$\boldsymbol{E}_m=\boldsymbol{E}+\boldsymbol{I}_x\boldsymbol{Z}_s' \tag{2}$$

The current in the magnetizing branch is $\boldsymbol{I}_m-\boldsymbol{I}_y$, and this current should be equal to $\boldsymbol{E}_m\boldsymbol{Y}_m$. So we get

$$\boldsymbol{I}_m-\boldsymbol{I}_y=\boldsymbol{E}_m\boldsymbol{Y}_m \tag{3}$$

The above equation is converted readily into

$$\boldsymbol{I}_m=\boldsymbol{I}_y+\boldsymbol{E}_m\boldsymbol{Y}_m \tag{4}$$

The terminal voltage V is equal to $\boldsymbol{E}_m$ plus the voltage drop across the impedance $\boldsymbol{Z}_{1m}$.

$$\boldsymbol{I}_m\boldsymbol{Z}_{1m}+\boldsymbol{E}_m=V \tag{5}$$

substituting equation 2 in equation 4 we get

$$\boldsymbol{I}_m=\boldsymbol{I}_y(1+\boldsymbol{Y}_m\boldsymbol{Z}_s')+\boldsymbol{E}\boldsymbol{Y}_m \tag{6}$$

Substituting equation 6 in equation 5 we get

$$V=\boldsymbol{E}(1+\boldsymbol{Z}_{1m}\boldsymbol{Y}_m)+\boldsymbol{I}_y(\boldsymbol{Z}_s'+\boldsymbol{Z}_{1m}+\boldsymbol{Z}_{1m}\boldsymbol{Y}_m\boldsymbol{Z}_s') \tag{7}$$

Eliminating $\boldsymbol{I}_y$ between equation 6 and equation 7

$$V(1+\boldsymbol{Y}_m\boldsymbol{Z}_s')-\boldsymbol{I}_m(\boldsymbol{Z}_s'+\boldsymbol{Z}_{1m}+\boldsymbol{Z}_{1m}\boldsymbol{Y}_m\boldsymbol{Z}_s')=\boldsymbol{E} \tag{8}$$

Equations 7 and 8 can be written as

$$\boldsymbol{I}_y=\boldsymbol{Y}_{tm}V-\boldsymbol{Y}_{om}\boldsymbol{E}=\boldsymbol{I}_{om}-\boldsymbol{Y}_{om}\boldsymbol{E} \tag{9}$$

$$\boldsymbol{I}_m=\boldsymbol{Y}_{em}V-\boldsymbol{Y}_{tm}\boldsymbol{E}=\boldsymbol{I}_{em}-\boldsymbol{Y}_{tm}\boldsymbol{E} \tag{10}$$

where

$$\boldsymbol{Y}_{tm}=\frac{1}{\boldsymbol{Z}_s'+\boldsymbol{Z}_{1m}+\boldsymbol{Z}_{1m}\boldsymbol{Z}_s'\boldsymbol{Y}_m} \tag{11}$$

$$\boldsymbol{Y}_{om}=(1+\boldsymbol{Z}_{1m}\boldsymbol{Y}_m)\boldsymbol{Y}_{tm} \tag{12}$$

$$\boldsymbol{Y}_{em}=(1+\boldsymbol{Z}_s'\boldsymbol{Y}_m)\boldsymbol{Y}_{tm} \tag{13}$$

$$\boldsymbol{I}_{om}=\boldsymbol{Y}_{tm}V \tag{14}$$

$$\boldsymbol{I}_{em}=\boldsymbol{Y}_{em}V \tag{15}$$

The same procedure can be applied to the circuit to the left of R and we obtain

$$\boldsymbol{I}_x'=\boldsymbol{I}_{os}-\boldsymbol{Y}_{os}\boldsymbol{E} \tag{16}$$

$$\boldsymbol{I}_s'=\boldsymbol{I}_{es}-\boldsymbol{Y}_{ts}\boldsymbol{E} \tag{17}$$

where

$$\boldsymbol{Y}_{ts}=\frac{1}{\boldsymbol{Z}_s'+\boldsymbol{Z}_{1s}'+\boldsymbol{Z}_{1s}'\boldsymbol{Z}_s'a^2\boldsymbol{Y}_s} \tag{18}$$

$$\boldsymbol{Y}_{os}=(1+\boldsymbol{Z}_{1s}'a^2\boldsymbol{Y}_s)\boldsymbol{Y}_{ts} \tag{19}$$

$$\boldsymbol{Y}_{es}=(1+\boldsymbol{Z}_s'a^2\boldsymbol{Y}_s)\boldsymbol{Y}_{ts} \tag{20}$$

$$\boldsymbol{I}_{os}=\boldsymbol{Y}_{ts}\left(-j\frac{V}{a}\right) \tag{21}$$

$$\boldsymbol{I}_{es}=\boldsymbol{Y}_{es}\left(-j\frac{V}{a}\right) \tag{22}$$

Adding equations 16 and 9

$$\boldsymbol{I}=\boldsymbol{I}_x'+\boldsymbol{I}_y=(\boldsymbol{I}_{os}+\boldsymbol{I}_{om})-\boldsymbol{E}(\boldsymbol{Y}_{os}+\boldsymbol{Y}_{om})=\boldsymbol{I}_o-\boldsymbol{E}\boldsymbol{Y}_o \tag{23}$$

where

$$\boldsymbol{I}_o=\boldsymbol{I}_{os}+\boldsymbol{I}_{om} \tag{24}$$

$$\boldsymbol{Y}_o=\boldsymbol{Y}_{os}+\boldsymbol{Y}_{om} \tag{24a}$$

From equations 10 and 17

$$\boldsymbol{I}_{\text{line}}=\boldsymbol{I}_m+j\frac{\boldsymbol{I}_s'}{a}=\left(\boldsymbol{I}_{em}+\frac{j\boldsymbol{I}_{es}}{a}\right)-\left(\boldsymbol{Y}_{tm}+\frac{j\boldsymbol{Y}_{ts}}{a}\right)\boldsymbol{E} \tag{25}$$

Substituting the relation $E=IR$ in equation 23 we obtain

$$\boldsymbol{I}=\frac{\boldsymbol{I}_o}{1+R\boldsymbol{Y}_o} \tag{26}$$

For a given motor at a given speed $\boldsymbol{I}_o$ and $\boldsymbol{Y}_o$ can be calculated by going through equations 11–15, 18–22, and equations 24 and 24*a*. From equation 26 we obtain $\boldsymbol{I}$ and $\boldsymbol{E}$. From equations 9, 10, 16, and 17, $\boldsymbol{I}_y$, $\boldsymbol{I}_m$, $\boldsymbol{I}_x'$, $\boldsymbol{I}_s'$ can be calculated. The generated torque is calculated from equation 1. The efficiency and power factor are evaluated from $\boldsymbol{I}_m$, $\boldsymbol{I}_s$ and the torque. But $\boldsymbol{Z}_s'$ is dependent on S through the term $r_2/1+S$. That means that all the $\boldsymbol{Y}$'s are dependent on S, and it is therefore necessary to recalculate for every point on the performance curve if an exact result is required. However, sufficiently accurate results can be attained by using

$$\boldsymbol{Z}_s'=0.55r_2+jx_2 \tag{27}$$

As S varies from 0.7 to 1, $r_2/(1+S)$ varies from 0.59 r_2 to 0.50 r_2. The approximate equation 27 introduces an error of at most 0.05 r_2 to Z_s'. Its effect on the currents and torque are well below one per cent.

With the introduction of the approximate equation 27, it is only necessary to calculate equations 11–15 and 18–22 once for a motor. After that calculation of performance is no more complicated than for a balanced polyphase motor.

A few samples of such calculations are given under Appendix II.

The torque expression corresponding to equation 27 is

$$T = RI^2 + 1.1 r_1 I_x' I_y \cos(I_x', I_y) \tag{28}$$

Designer's Formula for Good Efficiency

From the point of view of a designer, it is not desirable to have all of the operating characteristics of a proposed design unknown until a complicated calculation has been made. However, if the angle between I_x' and I_y is made small, we can be certain that the efficiency of the motor would be somewhere near the highest obtainable under the lamination and capacitor restrictions. The relation between the angle (I_x', I_y) and the efficiency is seen first from equation 1 and will be illustrated more completely later, where comparisons between the capacitor motor, polyphase motor, and plain single-phase motor are made.

A condition between the motor constants which predicts a small angle between I_x' and I_y for all speeds is derived as follows. Multiplying equation 9 by Z_{om} which is the reciprocal of Y_{om}, we obtain

$$\begin{aligned} E &= I_{om} Z_{om} - I_y Z_{om} \\ &= E_{om} - I_y Z_{om} \end{aligned} \tag{29}$$

Similarly, equation 16 becomes

$$E = E_{os} - I_x' Z_{os} \tag{30}$$

Equations 29 and 30 lead to the equivalent circuit of Figure 2. If the angle between I_x' and I_y is made small for all values of R, it should be small for $R = \infty$ under which conditions $I_x' + I_y = 0$, or $I_x' = -I_y$. That means, when $R = \infty$, both I_x' and I_y must vanish, or they must be equal and opposite to each other. The latter possibility is inconsistent with the assumed condition of a small angle between I_x' and I_y. The former possibility leads to

$$E_{os} = E_{om} \tag{31}$$

If equation 31 holds, we have from equations 29 and 30

$$I_y = \frac{E_{om} - E}{Z_{om}}$$

$$I_x' = \frac{E_{om} - E}{Z_{os}}$$

Therefore the angle between I_x' and I_y is the angle between Z_{om} and Z_{os} and our condition, that the angle between I_x' and I_y should be small for all speeds, is equivalent to

1. $E_{os} = E_{om}$
2. The angle between Z_{om} and Z_{os} is small.

These two conditions lead to one condition between the motor constants. By definition and equations 14 and 12

$$\begin{aligned} E_{om} &= I_{om} Z_{om} \\ &= Y_{1m} V \frac{1}{Y_{om}} \\ &= \frac{V}{1 + Z_{1m} Y_m} \end{aligned} \tag{32}$$

A similar set of equations leads to

$$E_{os} = \frac{-j\dfrac{V}{a}}{1 + Z_{1s}' a^2 Y_s} \tag{33}$$

Substituting equations 32 and 33 into condition 1, we obtain

$$ja(1 + Z_{1s}' a^2 Y_s) = 1 + Z_{1m} Y_m \tag{34}$$

By definition $Z_{1s}' = (Z_{1s} + Z_c)/a^2$; equation 34 reduces to

$$ja(1 + (Z_{1s} + Z_c) Y_s) = 1 + Z_{1m} Y_m \tag{35}$$

Z_{om} and Z_{os} in terms of the motor constants are, by definition,

$$\begin{aligned} Z_{om} &= \frac{Z_1' + Z_{1m} + Z_{1m} Z_1' Y_m}{1 + Z_{1m} Y_m} \\ &= \frac{Z_{1m}}{1 + Z_{1m} Y_m} + Z_1' \end{aligned}$$

$$\begin{aligned} Z_{os} &= \frac{Z_c' + Z_{1s}' + Z_{1s}' Z_1' a^2 Y_s}{(1 + Z_{1s}' a^2 Y_s)} \\ &= \frac{Z_{1s}'}{1 + Z_{1s}' a^2 Y_s} + Z_c' \end{aligned}$$

If equation 35 is satisfied, the angle between $Z_{om} - Z_1'$ and $Z_{os} - Z_c'$ would be

$$\begin{aligned} &\angle(Z_{om} - Z_1') - \angle(Z_{os} - Z_c') \\ &\quad = \angle Z_{1m} - 90 \text{ degrees} - \angle Z_{1s}' \end{aligned}$$

In general, the angle of Z_{1m} is in the range of $+20$ degrees to $+50$ degrees, corresponding to a range of $r_1/x = 0.4$ to 1.4. The angle of Z_{1s}' is around -70 degrees. Therefore the two vectors $Z_{om} - Z_1'$ and $Z_{os} - Z_c'$ deviate in general not more than 30 degrees. Hence Z_{om} and Z_{os} deviate in general not more than 30 degrees.

The above deductions establish the condition represented by equation 35 as the necessary and sufficient condition for good efficiency over a whole range of speeds. However, because of the fact that Z_{os} is much larger than Z_{om}, the condition of equation 35 is not too critical. We can obtain a good motor whenever the relation is nearly satisfied.

Readers familiar with circuit theories easily may observe that equations 9, 16, 29 and 30 are Thevenin's theorem in its constant-current and constant-voltage forms. The equations 10 and 17 are direct results of the reciprocal theorem. All the equations listed in the preceding section and the first part of this section can be verified from circuit theories.

The Maximum Torque

It seems that any attempt to derive an exact expression for maximum torque of a capacitor motor is bound to lead to complicated calculations with third order equations. The equivalent circuit theory is certainly no exemption if the circuit of Figure 1*A* and the torque expression of equation 1 are used without approximations. But such a procedure is hardly justifiable, because some unaccountable factors may introduce an error far larger than an approximation of Figure 1*A* and equation 1 introduce. These factors are

1. The two separate skin effects of the rotor.
2. The variation of stator and rotor resistances as a result of temperature variations.

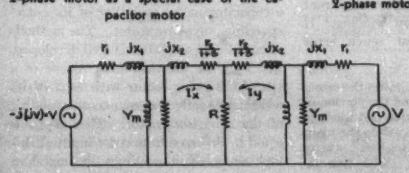

Figure 4. The equivalent circuit of a balanced 2-phase motor as a special case of the capacitor motor

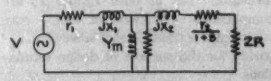

Figure 5. The equivalent circuit of a balanced 2-phase motor seen from each phase

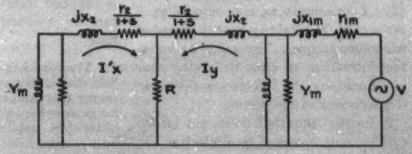

Figure 6. The equivalent circuit of a plain single-phase motor as a special case of the capacitor motor

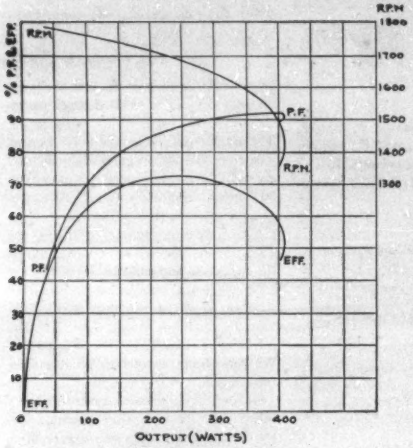

Figure 7. Performance curves of Morrill's 1/4-horsepower 4-pole motor

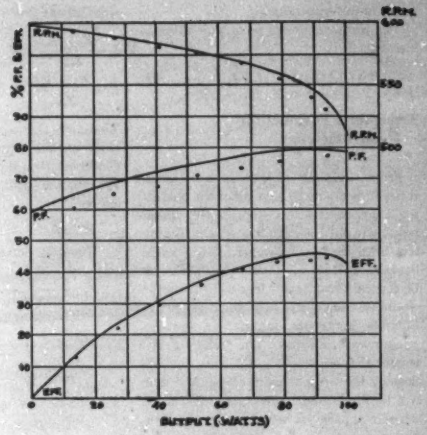

Figure 8. Performance curves of a 12-pole 1/10-horsepower motor

3. The effect of space harmonics.

4. The variation in air-gap length resulting from temperature variations of stator and rotor. This variation is especially appreciable under successive starting.

The combined effects of these factors introduce an error which may well amount to a few per cent.

The maximum torque can be evaluated readily by assuming

1. The approximate equations 27 and 28.

2. The variation of the term $1.1 r_2 I_x' I_y \times \cos(I_x', I_y)$ can be neglected so that we can assume the maximum torque occurs when RI^2 is maximum.

From equation 26 it is evident that RI^2 is maximum when $R = \frac{1}{Y_o}$. Hence

$$T_{max} = \frac{I_o^2}{Y_o}\left|\frac{1}{1+\frac{Y_o}{Y_o}}\right|^2 + 1.1 r_2 I_x' I_y \cos(I_x', I_y) \quad (36)$$

I_x' and I_y are evaluated at $R = \frac{1}{Y_o}$

In general, the term $1.1\ r_2\ I_x'\ I_y \cos(I_x', I_y)$ amounts to not more than 5 per cent of the total torque at the speed of maximum torque. Neglecting its variation introduces an error well below that introduced by the factors mentioned at the beginning of this section.

A further simplified maximum torque expression is obtained by neglecting the second term completely. Then equation 36 becomes

$$T_{max} = \frac{I_o^2}{Y_o}\left|\frac{1}{1+\frac{Y_o}{Y_o}}\right|^2 = K_t \frac{I_o^2}{Y_o} \quad (37)$$

The coefficient K_t depends on the angle of Y_o only. Let θ be the angle of Y_o, then

$$K_t = \left|\frac{1}{1+\frac{Y_o}{Y_o}}\right|^2 = \left|\frac{1}{1+e^{j\theta}}\right|^2 = \left(\frac{1}{2\cos\frac{\theta}{2}}\right)^2 \quad (38)$$

Equation 37 is simple enough to apply when the preliminary calculations have been made to determine the performance. But as both I_o and Y_o are complicated expressions of motor constants, this formula is still somewhat unwieldy for the purpose of design estimations.

In general, at the speed of maximum torque, the major portion of rotor current is supplied from the main winding. It can be assumed without much error that

1. The capacitor phase supplies the cross-field magnetizing current and the portion of energy that overcomes friction and windage losses as well as iron losses, while the main phase alone supplies the power that converts into a measurable torque. With this assumption, the equivalent circuit becomes that of Figure 3.

2. The maximum torque occurs at the speed of maximum rotor input.

From Figure 3 it is clear that not all the rotor input converts into torque expressed in synchronous watts.

$$\text{Rotor input} = I_y^2\left(R + \frac{r_2}{1+S}\right) \quad (39)$$

$$\text{Synchronous watts} = I_y^2 R \quad (40)$$

Dividing equation 40 with equation 39 we have

$$\frac{\text{Synchronous watts}}{\text{Rotor input}} = \frac{R}{R+\frac{r_2}{1+S}} = \frac{\frac{Sr_2}{1-S^2}}{\frac{Sr_2}{1-S^2}+\frac{r_2}{1+S}} = S \quad (41)$$

Equation 41 is useful in establishing a relation between the maximum torque of a capacitor motor and that of its corresponding polyphase motor. The methods of calculating the latter is well developed. Let T_{2max} be the maximum torque of a straight 2-phase motor with each of its windings exactly the same as the winding of the capacitor motor. Then T_{2max} is equal to the maximum rotor input of this 2-phase motor or two times the maximum

rotor input of the capacitor motor. From equation 41 we have

$$T_{max} = S\frac{T_{2max}}{2}$$
$$= 0.5ST_{2max} \tag{42}$$

Equation 42 is verified for a number of cases. The agreement between the tested and calculated values turns out surprisingly well. A numerical comparison between equations 36, 37, 42, and a tested result will be given in Appendix III.

It is important to note that the speed for maximum rotor input of a capacitor motor is not the same as that of its corresponding 2-phase motor, and the S in equation 42 stands for the former. Let S_2 denote the speed of the 2-phase motor at which its rotor input per phase is equal to the rotor input of the capacitor motor of Figure 3 at speed S. The rotor resistance reflected to the stator is, for the capacitor motor, $R+\frac{r_2}{1+S}=\frac{r_2}{1-S^2}$, and for the 2-phase motor per phase, $\frac{r_2}{1-S_2}$. Equating these two expressions we get

$$S^2 = S_2 \tag{43}$$

The starting torque of a capacitor motor is obtained readily by substituting $S=0$ into equation 1. We get

$$\text{Starting torque} = 2r_2 I_{20}'I_{y0}\cos(I_{20}', I_{y0}) \tag{44}$$

where I_{20}', I_{y0} are values of I_2', I_y, $S=0$. I_{20}' and I_{y0} are the same as I_{os} and I_{om} of the preceding section with $Z_2'=r_2+jX_2$. But in calculating I_{os} and I_{om} for performance calculation the approximation of equation 27 for Z_2' is used, and that leads to somewhat different values of I_{os} and I_{om}. However the latter values can be used in equation 44 to yield an approximate result.

The Pulsating Torque

If the effects of space harmonics are neglected, the generated torque of a capacitor motor consists of a constant component and an a-c component of twice the frequency of the power source. The amplitude of the pulsating torque is defined as

$$T_p = \frac{\text{Maximum instantaneous torque} - \text{minimum instantaneous torque}}{2}$$

The above definition implies that if $T_p > T$, the constant component of the generated torque, the instantaneous torque is negative for some part of a cycle.

In Appendix V, a relationship between T_p and the rotor currents is derived as presented in the following:

$$T_p = R\left|I_y^2 - I_x'^2\right|$$
$$= E\left|I_y - I_x\right| \tag{45}$$

Both I_y and I_x' are a-c vectors of effective values as used throughout this presentation. The difference between the squares of these two vectors is a vector difference. Equation 45 is as exact as the cross-field theory.

By comparing equation 45 and equation 1, a picture of the instantaneous torque can be visualized. The comparison is made for three different cases.

1. The angle between I_x' and I_y is 90 degrees. This implies as a special case that one of the two currents is zero. Equation 1 reduces to

$$T = RI^2$$
$$= R\left|I_x' + I_y\right|^2 \tag{46}$$

$$\frac{T_p}{T} = \frac{\left|I_y^2 - I_x'^2\right|}{\left|I_y + I_x'\right|^2}$$
$$= \frac{\left|I_y - I_x'\right|}{\left|I_y + I_x'\right|}$$
$$= 1 \tag{47}$$

The vector sum and difference of two vectors 90 degrees apart from each other have the same magnitude.

Equation 47 implies that the instantaneous torque is zero at some instant during the cycle, but it is never negative.

2. The angle between I_x' and I_y is larger than 90 degrees. In this case, the term

$$\frac{2r_2}{1+S} I_x' I_y \cos(I_x', I_y) < 0$$

and

$$\frac{T_p}{RI^2} = \frac{\left|I_y - I_x'\right|}{\left|I_y + I_x'\right|} > 1.0$$

Because a smaller quantity plus a negative quantity is still smaller, T is smaller than T_p. The instantaneous torque is negative during some part of a cycle.

3. The angle between I_x' and I_y is smaller than 90 degrees. In this case

$$\frac{2r_2}{1+S} I_x' I_y \cos(I_x', I_y) > 0$$
$$RI^2 > T_p$$
$$\therefore T > T_p$$

The instantaneous torque is always positive.

It is clear from the above comparison that a small angle between I_x' and I_y is desirable not only to maintain good efficiency but also for quiet operation without excessive vibration. A motor so designed is smoother running and favorable to long bearing life.

Reduction to Polyphase

A polyphase motor can be considered as a special case of a capacitor motor in which

1. Two identical windings are used.
2. $Z_c = 0$
3. A voltage jV is applied to the capacitor phase instead of V.

Making the corresponding changes in Figure 1A, we obtain the diagram of Figure 4.

To prove that Figure 4 is exactly the polyphase circuit diagram, two points need to be established.

1. The apparent rotor resistance seen from each phase is $\frac{r_2}{1-S}$.
2. The generated torque in synchronous watts as given in equation 1 is equal to the rotor input.

Because the circuit of Figure 4 is entirely balanced, it can be split into two, each of which is as shown in Figure 5.

The apparent rotor resistance is

$$\frac{r_2}{1+S} + 2R = \frac{r_2}{1+S} + \frac{2Sr_2}{1-S^2}$$
$$= \frac{r_2}{1-S}$$

That establishes the first point.

The second point is a consequence of the following general theorem:

The generated torque of a capacitor motor in synchronous watts is equal to or less than the rotor input of the said motor at said speed; the equality holds if, and only if, $I_x' = I_y$.

Rotor input from Figure 1A is

$$\frac{r_2}{1+S} I_x'^2 + \frac{r_2}{1+S} I_y^2 + RI^2$$

Table I

Method	I_m	I_x	Input	Net Output
Morrill[3]	$2.47\angle 59°3$ min	$0.948\angle 38°46$ min	221+24	177
Lyon and Kingsley[3]	$2.67\angle 55°48$ min	$0.935\angle 38°40$ min	239	165
Punga[4]	$2.57\angle 56°30$ min	$0.948\angle 40°50$ min	234	162
Cross-field[1]	$2.64\angle 58°36$ min	$0.954\angle 39°0$ min	233+24	177 to 179.8
Exact Circuit	$2.59\angle 56°$	$0.950\angle 39°$	240	168
Approximate Circuit	$2.57\angle 57°$	$0.950\angle 39°$	236	165

Generated torque by equation 1 is

$$RI^2+\frac{2r_2}{1+S}I_x'I_y\cos(I_x',I_y)$$

The difference of these two expressions is rotor input − generated torque in synchronous watts =

$$\frac{r_2}{1+S}[I_x'^2+I_y^2-2I_x'I_y\cos(I_x',I_y)]$$

$$=\frac{r_2}{1+S}[I_x'-I_y]^2\geq 0 \qquad (48)$$

The equality sign holds when, and only when, the two current vectors I_x' and I_y are equal.

From equation 45 of the pulsating torque it is clear that a non-pulsating torque is obtained when, and only when, the two current vectors I_x' and I_y are equal. The significance of this fact and the foregoing theorem is twofold.

1. This verifies the equivalent circuit of Figure 1, the d-c torque equation 1, and the pulsating torque equation 45 in the known special case of a balanced polyphase motor.

2. This proves that the highest efficiency and the smoothest running condition of a capacitor motor are realized for a certain speed, if the two current vectors equal each other at that speed.

In general, it is not possible to realize this quasi-polyphase condition for all speeds. But it always can be realized at any single designated speed if we are free in choosing the capacitor and the capacitor winding.

Reduction to Plain Single-Phase

A plain single-phase motor is equivalent to a capacitor motor in which the capacitor impedance approaches infinity. With this modification the equivalent circuit of Figure 1*A* reduces to that of Figure 6. This diagram has been derived from a number of different sources. In effect it may be derived from both the revolving-field theory and the cross-field theory.

Showing I_x' on this diagram in the direction indicated for the capacitor motor, it now takes a negative value. Hence it is evident that the angle between I_x' and I_y is always larger than 90 degrees. That implies that the efficiency of a plain single-phase motor is lower than that of a properly designed capacitor motor and that there is always some instant of time in each cycle in which the instantaneous torque is negative.

The comparisons so far show that in all respects, torque, efficiency, and constancy of torque in the capacitor motor are in between the polyphase and plain single-phase motors. The difference of the three types of motors is smaller if the per-unit rotor resistance and the per-unit magnetizing admittance are smaller. The advantages of a capacitor motor over a plain single-phase motor are better realized when these quantities are high.

However, an inadequately designed capacitor motor is more likely to lead to very poor results than a plain single-phase motor. Because the per-unit magnetizing admittances are usually much smaller than unity, I_x' is in general a small quantity. That insures an upper limit for T_y and a lower limit for the efficiency. In an inadequately designed capacitor motor, transfer of energy between the main phase and the capacitor phase usually takes place. In such cases

Table II. Detailed Calculations

1	2	3	4	5	6	7	8	9	10
S	R	RY_o	$1+RY_o$		I^2R	$(1-S)I^2R$	Net Output	E = IR	Y_mE
0.99	205	33.8/−50.6	22.4−j26.1	0.503/3.2°	52	51	38	103/3.2°	15.65/−44.8°
			34.4/−49.4°						11.1−j11.02
0.98	101	16.55/−50.6	11.6−j12.9	1.00/1.8°	101	99	86	101/1.8°	15.35/−46.2°
			17.35/−48°						10.62−j11.09
0.96	50.4	8.31/−50.6°	6.27−j6.42	1.92/−0.6°	186	178	165	97/−0.6°	14.75/−48.6°
			8.99/−45.6°						9.75−j11.05
0.93	28.4	4.68/−50.6	3.97−j3.62	3.22/−3.8°	294	273	260	91.4/−3.8°	13.9/−51.8°
			5.37/−42.4°						8.60−j10.91
0.90	19.5	3.22/−50.6	3.04−j2.49	4.40/−6.8°	377	339	326	85.8/−6.8°	13.03/−54.8°
			3.93/−39.4°						7.51−j10.64
0.85	12.6	2.08/−50.6	2.32−j1.61	6.13/−11.4°	474	402	389	77.3/−11.4°	11.72/−59.4°
			2.82/−34.8°						5.96−j10.1
0.80	9.16	1.51/−50.6	1.96−j1.17	7.59/−15.4°	526	421	408	69.5/−15.4°	10.56/−63.4
			2.28/−30.8°						4.77−j9.52
0.75	7.06	1.165/−50.6	1.74−j0.90	8.83/−18.9°	550	412	399	62.3/−18.9°	9.47/−66.9°
			1.96/−27.3°						3.72−j8.70

11	12	13	14	15	16	17	18
I_m	jY_LE	ϵ	I_{line}	Input	Power Factor	Efficiency	Revolutions Per Minute
0.05−j2.18	0.707/178.4°	0.782+j0.639	0.832−j1.74	91.6	0.432	41.5	1,782
2.18/−88.7°	−0.706+j.020	1.01/39.2°	1.93/−64.4				
0.53−j2.11	0.694/177	0.768+j0.623	1.30−j1.49	143	0.656	60.0	1,764
2.18/−75.9°	−0.692+j.036	0.99/39.1°	1.98/−49°				
1.40−j2.15	0.665/174.6	0.738+j0.596	2.14−j1.55	236	0.810	70.0	1,728
2.57/−57°	−0.662+j.063	0.950/39°	2.64/−35.9°				
2.55−j2.29	0.628/171.4	0.697+j0.565	3.25−j1.72	337	0.883	73.9	1,674
3.43/−41.9°	−0.621+j.094	0.898/39°	3.67/−28°				
3.64−j2.56	0.590/168.4	0.654+0.541	4.30−j2.02	473	0.905	68.9	1,620
4.45/−35.2°	−0.578+j.118	0.850/39.5°	4.75/−25.2°				
5.19−j3.1	0.530/163.8	0.585+j0.511	5.78−j2.59	636	0.913	61.1	1,530
6.06/−30.8°	−0.509+j.148	0.776/41.2°	6.34/−24.1°				
6.38−j3.68	0.477/159.8	0.523+j0.494	6.90−j3.18	759	0.91	53.8	1,440
7.36/−30°	−0.447+j.165	0.720/43.4°	7.60/−24.7°				
7.43−j4.50	0.428/156.3	0.468+j0.487	7.90−j4.01	869	0.893	46.0	1,350
8.69/−31.2°	−0.392+j.172	0.676/46.1°	8.86/−26.9°				

Table III

1 S	2 R	3 $1+RY_0$	4 I	5 E	6 EY_{1e}	7 I_{line}	8 I^2R	9 Torque	10 Output	11 Input	12 Eff.	13 Power Factor
0.995	.997	25.3−j31.5	0.10/6.3°	99.7/6.3	2.62/−51.3°	0.81−j1.09	10	0	0	93.1	0	0.595r
		40.4/−51.3°			1.64−j2.04	1.36/−53.4°						
0.98	.247	7.0−j7.8	0.387/2°	95.7/2°	2.52/−55.6°	1.03−j1.05	37	27	26.5	118.4	22.4	0.684
		10.47/−48°			1.42−j2.08	1.47/−46.1°						
0.96	.122	3.96−j3.86	0.733/−1.7°	89.4/−1.7°	2.35/−59.3°	1.25−j1.11	65.5	55.5	53.3	144	37	0.749
		5.53/−44.3°			1.20−j2.02	1.67/−41.6°						
0.93	.69	2.68−j2.18	1.17/−6.9°	80.8/−6.9°	2.13/−64.5°	1.53−j1.21	94.5	84.5	78.6	176	44.6	0.784
		3.46/−39.1			0.92−j1.92	1.95/−38.4°						
0.90	47.4	2.15−j1.50	1.55/−11.1°	73.5/−11.1°	1.932/−68.7°	1.75−j1.33	114	104	93.5	201	46.5	79.6
		2.62/−34.9°			0.70−j1.80	2.20/−37.2°						
0.85	30.6	1.743−0.967	2.04/−17°	62.5/−17°	1.645/−74.6°	2.01−j1.55	127.5	117.5	100	231	43.3	0.792
		1.99/−29°			0.44−j1.58	2.54/−37.6°						

I_x' is nearly equal to $-I_y$; T_y is inflated while efficiency is depressed.

Conclusion and Acknowledgment

The equivalent circuit introduced in this presentation is by no means limited to the study of capacitor motor alone. By modifying constants of the auxiliary phase it can be used to study the resistive split-phase and the inductive split-phase motors.

The maximum torque equation 42 and the good efficiency equation 35 can be used as a starting point for capacitor motor design. These will be studied in detail in a companion paper.

Appendix I. Derivation of the Equivalent Circuit

This analysis is based on seven equations from the cross-field theory. They are

$$E_m+I_mZ_{im}=V \tag{49}$$

$$E_s+I_s(Z_{1s}+Z_c)=V \tag{50}$$

$$\frac{E_s}{a}+jS(-E_m+jI_yX_2)=aZ_sI_x \tag{51}$$

$$-E_m+iS\left(-\frac{E_s}{a}+iaI_xX_1\right)=-I_yZ_r \tag{52}$$

$$E_m=Z_m(I_m-I_y) \tag{53}$$

$$E_s=Z_s(I_s-I_x) \tag{54}$$

$$T=aE_mI_x\sin(E_m,I_x)+\frac{E_s}{a}I_y\times \sin(I_y,E_s) \tag{55}$$

The subscripts m and s denote the main and capacitor windings, respectively. The subscripts 1 and 2 denote stator and rotor circuits. I_x and I_y are rotor currents in the capacitor and the main axis. I_m and I_s are the stator currents. E_m and E_s are the air-gap counter electromotive forces in the main and capacitor windings. E_m, I_y, Z_{im}, Z_m, Z_s are in main winding terms. E_s, I_x, Z_{1s}, Z_s are in starting winding terms. For the detailed meaning of these symbols, the reader is referred to the nomenclature at the end of this paper.

Each of the Z's, E's, I's is a vector quantity. The line voltage V is taken as a reference vector for the voltage and currents. Therefore its angle is zero.

All equations connecting these vectors and their conjugates are understood to be vector equations, and the rules governing vector sum, difference, multiplication, and division are implied.

Whenever the plain magnitude of such vector expressions is referred to, the absolute sign // is used. The vector operation rules still hold within these two bars.

Equations 49 and 50 are stator equations. Equations 51 and 52 are rotor equations with due account of the speed electromotive forces. Equations 53 and 54 express the magnetizing effect. Equation 55 is a scalar expression of the torque. In vector form equation 55 becomes

$$T=\text{Real part of}\left[-j\left(aI_x \operatorname{conj} E_m-I_y \operatorname{conj}\frac{E_s}{a}\right)\right] \tag{56}$$

Equations 51 and 52 can be solved for E_s and E_m and yield

$$\frac{E_s}{a}=\frac{jSr_2}{1-S^2}I_y+jaX_2I_x+\frac{r_2}{1-S^2}aI_x \tag{57}$$

$$E_m=\frac{-jSr_2}{1-S^2}aI_x+jX_2I_y+\frac{r_2}{1-S^2}I_y \tag{58}$$

with the introduction of the symbols

$$R=\frac{Sr_2}{1-S^2}$$

$$Z_s'=\frac{r_2}{1+S}+jX_2$$

$$E_s'=-\frac{jE_s}{a}$$

$$I_x'=-iaI_x$$

The equations 57 and 58 become

$$E_s'=(Z_s'+R)I_x'+RI_y \tag{59}$$

$$E_m=(Z_s'+R)I_y+RI_x' \tag{60}$$

Equations 59 and 60 are recognized readily as the mesh equations of the circuit shown in Figure 1*B*.

Equation 56, in terms of the new notation E_s', I_x', becomes

$$T=\text{Real part of }[I_x' \operatorname{conj} E_m+I_y \operatorname{conj} E_s'] \tag{61}$$

Note that $\operatorname{conj} E_s'=\dfrac{j \operatorname{conj} E_s}{a}$.

Substitute equations 59 and 60 into 61.

$$\begin{aligned}T=&\text{Real part of }[I_y(\operatorname{conj} Z_s'+R)\times \\ &\operatorname{conj} I_x'+RI_y \operatorname{conj} I_y+I_x'\times \\ &(\operatorname{conj} Z_s'+R)\operatorname{conj} I_y+RI_x' \operatorname{conj} I_x'] \\ =&\text{Real part of }[\operatorname{conj} Z_s'(I_y \operatorname{conj} I_x'+ \\ &I_x' \operatorname{conj} I_y)+R(I_y \operatorname{conj} I_y+I_y\times \\ &\operatorname{conj} I_x'+I_x' \operatorname{conj} I_y+I_x' \operatorname{conj} I_x')] \\ =&\text{Real part of }[\operatorname{conj} Z_s'(I_y \operatorname{conj} I_x'+ \\ &I_x' \operatorname{conj} I_y)+R(I_y+I_x')\operatorname{conj}(I_y+I_x')]\end{aligned} \tag{62}$$

Note that $I_y \operatorname{conj} I_x'+I_x' \operatorname{conj} I_y=2I_x'I_y\times \cos(I_x', I_y)$. The real part of the expression on the left of equation 62 is equated to T.

$$T=\frac{2r_2}{1+S}I_x'I_y\cos(I_x,I_y)+R|I_y+I_x'|^2$$

This is the torque equation 1.

Multiply equations 50 and 54 with $-j/a$ and note that

$$E_s'=-\frac{jE_s}{a}$$

$$I_s'=-jaI_s$$

$$I_x'=-jaI_x$$

$$E_s+'I_s'\left(\frac{Z_{1s}}{a^2}+\frac{Z_s}{a^2}\right)=\frac{-jV}{a} \tag{63}$$

$$E_s'=\frac{Z_s}{a^2}(I_s'-I_x') \tag{64}$$

The equations 63, 64, 49, and 53 can be used to add stator parameters to the rotor circuit Figure 1*B*. The result is Figure 1*A*.

Appendix II. Example of Performance Calculation

To illustrate the application of the equivalent circuit theory in performance calculation, two examples of calculations are shown in this section. One is the motor for which constants are given in Morrill's paper.[3] The other is a 12-pole motor with very low magnetizing reactance for which ordinary approximations do not hold.

Example 1

The values for this 1/4-horsepower 110-volt motor are

$r_{1m}=2.02$
$r_{1s}=5.12\times1.18^2$
$\quad=7.13$
$r_2=4.12$
$r_e=9.00$
$X_{1m}=2.79$
$X_{1s}=2.31\times1.18^2$
$\quad=3.22$
$X_2=2.12$
$X_e=-172.0$
$a=1.18$
$X_m=66.8$
$X_s=92.9$
$\quad=66.8\times1.18^2$
Friction and windage loss = 13 watts
Iron losses = 24 watts
$\quad=110^2\times.001\times2$

From these values, and making the approximation of equation 27

$Z_3'=2.27+j2.12$

The iron loss is absorbed in each of the magnetizing branches as a conductance of 0.001 mho.

$a^2Y_s=Y_m$
$\quad=0.001-j0.015$

The approximation, generated torque $=RI^2$, is used for the calculation of performance curves. For the point $S=0.04$, an exact calculation is made, and both the results are compared with results of former papers on the same motor. See Table I.

The differences between the results of the equivalent circuit and the cross-field theory originate from the fact that in the former the iron loss is taken care of by the conductive component in the magnetizing admittance, while in the latter, the iron loss is treated as an additional loss to the power source.

The small deviation between the exact and approximate results justifies the use of these approximations. The approximate methods for performance calculation is given below. From

(11) $Y_{1m}=0.152/-48.0°$
(12) $Y_{om}=0.159/-49.5°$
(13) $Y_{sm}=0.1572/-49.8°$
(14) $I_{om}=16.7/-48.0°$
(15) $I_{sm}=17.3/-49.8°$
(18) $Y_{1s}=0.0081/85.2°$
(19) $Y_{os}=0.0070/-75°$
(20) $Y_{ss}=0.0084/83.4°$
(21) $I_{os}=0.755/-4.8°$
(24) $I_o=17.3/-46.2°$
(24a) $Y_o=0.165/-50.6°$
(22) $\frac{jI_{os}}{a}=0.664/83.4°$
(18) $\frac{jY_{1s}}{a}=0.00686/175.2°$

Then calculate

(2) $=\frac{4.12S}{1-S^2}$
(3) $=(2)\times Y_o$
(4) $=1+(3)$
(5) $=I_o/(4)$
(6) $=(5)^2\times(2)$
(7) $=S\times(6)$
(8) $=(7)-13$ watts
(9) $=(5)\times(2)$
(10) $=Y_{sm}\times(9)$
(11) $=I_{sm}-(10)$
(12) $=0.00686/175.2°\times(9)$
(13) $=0.664/83.4°-(12)$
(14) $=(13)+(11)$
(15) = real part of $(14)\times110$
(16) = cosine of angle of (14)
(17) $=\frac{(8)}{(15)}$

It is advisable to calculate each step for different slips at the same time. The result is plotted in Figure 7.

Example 2

In this example, an actual motor is calculated with measured constants. The result is compared with experiment. In case only the line current instead of the two separate currents is of interest, the process of performance calculation can be simplified considerably. This will be illustrated in this example. A 1/10-horsepower 12-pole 115-volt 60-cycle motor has the following constants,

$Z_c=22-j660$
$X_{1m}=14.0$
$X_{1s}=106$
$R_{1m}=12.1$
$R_{1s}=121$
$R_2=10.0$
$X_2=10.0$
$a=3.13$
$a^2Y_s=Y_m$
$\quad=0.0012-j0.0154$
$F\&W=10$ synchronous watts

From

(27) $Z_3'=5.5+j10.0$
(11) $Y_{1m}=0.0306/-51°$
(12) $Y_{om}=0.0380/-58.9°$
(13) $Y_{sm}=0.0355/-54.3°$
(18) $Y_{1s}=0.0169/72.5°$
(19) $Y_{os}=0.00478/10.5°$
(20) $Y_{ss}=0.0196/69.2°$
(24a) $Y_o=0.0399/-52.4°$
(14) $I_{om}=3.52/-51°$
(21) $I_{os}=0.62/-17.5°$
(24) $I_o=4.05/-46°$
(25) $Y_{1s}=Y_{1m}+\frac{jY_{1s}}{a}$
$\quad=0.0263/-57.6°$
(25) $I_o=V\left(Y_{sm}+\frac{Y_{ss}}{a^2}\right)$
$\quad=2.45-j3.13$

Then calculate

(1) $=S$
(2) $=\frac{10S}{1-S^2}$
(3) $=1+(2)\times Y_o$
(4) $=I_o/(3)$
(5) $=(4)\times(2)$
(6) $=(5)\times Y_{1s}$
(7) $=I_o-(6)$
(8) $=(4)^2\times(2)$
(9) $=(8)-10$ watts
(10) $=(9)\times(1)$

The result is plotted in Figure 8 and compared with experimental values, which are shown as dots on Figure 8.

Appendix III. An Example of Maximum Torque

For the two motors specified in Appendix II, the maximum torques are calculated with different formulas, and the results are compared with experimental value for the 12-pole motor. See Table IV. The values of $R=1/Y_o$, I_2', and I_y are calculated by (9) and (16), respectively. The exact coincidence between the experimental value and the accurate formula is by chance. It is, however, interesting to note that in these widely different cases the formula $0.5ST_{2max}$ still holds good. It has been verified for a number of other cases; the agreement between the $0.5ST_{2max}$ value and the measured values is always within ten per cent. (The only exception is this quoted 12-pole motor, which shows a difference of about 11 per cent).

The starting torque of this 12-pole motor is calculated and compared with experiment. I_{om} and I_{os} are calculated on the approximation $Z_3'=0.55r_2+jX_2$.

Appendix IV. Comparison Among Polyphase, Capacitor, Plain Single-Phase Motors

The maximum torque, the torque at four per cent slip (with F and W deducted), and the pulsating torque at four per cent slip are calculated for Morrill's motor, operating

1. As a 2-phase motor with the winding of each phase exactly as the main winding.
2. As a capacitor motor.
3. As a plain single-phase motor.

The results are tabulated. See Table VI.

Appendix V. Derivation of Pulsating Torque Expression

A set of complex instantaneous current and voltage vectors is defined as

$i_m=\sqrt{2}I_m\epsilon^{-jut}$
$i_s=\sqrt{2}I_s\epsilon^{-jut}$
$e_s=\sqrt{2}E_s\epsilon^{-jut}$
$e_m=\sqrt{2}E\epsilon^{-jut}$

The real part of these vectors represents the instantaneous values of voltage and currents.

A complex instantaneous current vector multiplied by an impedance vector forms a complex instantaneous voltage vector. The sum or difference of two complex instantaneous vectors forms a complex instantaneous vector, the real part of which represents the sum of the two instantaneous values. However, the product of two such vectors is utterly meaningless, and the real part of the product does not represent the product of the two instantaneous quantities, because the product of the associated imaginary parts of the two vectors is real and inseparable from the product of the real parts.

Such difficulties can be met by the use of complex conjugate vectors to eliminate the imaginary part. For instance, if we want to find the instantaneous value of the product of a current and a voltage, we need only separate the real part from the product.

$$i_x \frac{e+\text{conj}\, e}{2}$$

The instantaneous torque in synchronous watt is

$$T_{iss} = -\omega\left(\varphi_m a i_x - \frac{\varphi_s}{a} i_y\right) \tag{65}$$

where φ_m, φ' are the total flux linkage of main winding and capacitor winding with the rotor, respectively. Both φ_m, φ', and ix, iy are real instantaneous values. If we introduce the notation of complex a-c vectors, the foregoing equation becomes

$$T_{iss} = \text{real part of}\left[-\frac{\omega}{2}\left\{a i_x(\varphi_m + \text{conj}\,\varphi_m) - \frac{i_y}{a}(\varphi_s + \text{conj}\,\varphi_s)\right\}\right] \tag{66}$$

Because

$$e_s = -\frac{d\varphi_s}{dt} = j\omega\varphi_s$$

$$e_m = j\omega\varphi_m$$

$$\text{conj}\, e_s = -i\omega\, \text{conj}\,\varphi_s$$

$$\text{conj}\, e_m = -j\omega\, \text{conj}\,\varphi_m$$

Equation 66 becomes

$$T_{iss} = \text{real part of}\left[-\frac{i}{2}\left\{a i_x(\text{conj}\, e_m - e_m) - \frac{i_y}{a}(\text{conj}\, e_s - e_s)\right\}\right] \tag{67}$$

By definition

$$e_s = \sqrt{2}E_s e^{-j\omega t}$$

$$e_m = \sqrt{2}E_m e^{-j\omega t}$$

$$\text{conj}\, e_s = \sqrt{2}\,\text{conj}\, E_s e^{j\omega t}$$

$$\text{conj}\, e_m = \sqrt{2}\,\text{conj}\, E_m e^{j\omega t}$$

Equation 67 becomes

$$T_{iss} = \text{real part of}\left[-j\left\{a I_x \,\text{conj}\, E_m - \frac{I_y}{a}\,\text{conj}\, E_s\right\}\right] + \left[i\left\{a I_x E_m - \frac{I_y}{a} E_s\right\} e^{-2j\omega t}\right] \tag{68}$$

Table IV

Formula	Max Torque of Merrill's Motor	12-Pole Design Max Torque
(36) $RI^2 + 1.1 r_3 I_3' I_y \times \cos(I_3' I_y) - F\&W$	566	121
(37) $RI^2 - F\&W$	542	115.5
(42) $0.55 T_{max}$	561	108
Experimental Value		121

Table V

Method	Formula	Starting Torque Synchronous Watts
Exact calculation	$2 r_s I_{sa}' I_{ya} \times \cos(I_{sa}' I_{ya}) - F\&W$	25.2
Approximate calculation	$2 r_s I_{om} I_{os} \times \cos(I_{om}, I_{os}) - F\&W$	26.4
Measured by test		25.6

Table VI

Type Motor	Max Torque	Torque at 4-Per-Cent Slip	Pulsating Torque at 4-Per-Cent Slip
2-Phase Motor	1,520		0
Capacitor Motor	566	173	144
Plain Single-Phase Motor	489	141	300

All the values are in synchronous watts.

The first term is the constant torque as given in equation 56, and the second term is the pulsating torque. The amplitude of the pulsating torque is

$$T_p = \left|a I_x E_m - \frac{I_y}{a} E_s\right| = \left|I_x' E_m - I_y E_s'\right| \tag{69}$$

Substituting equations 59 and 60 into equation 69 we get

$$T_p = R\left|I_x'^2 - I_y^2\right|$$

as the cross products cancel each other.

Appendix VI. Nomenclature

V = applied volts (Used as reference vector)

E_m = the counter electromotive force in the main axis

$Z_{1m} = r_{1m} + jX_{1m}$ = the local impedance of the main stator winding

Z_2 = the rotor impedance in main winding terms $= r_2 + jX_2$

E_s = the counter electromotive force of the starting winding

$Z_{1s} = r_{1s} + jX_{1s}$ = the local impedance of the stator starting winding

Z_c = capacitor impedance $= r_c - jX_c$

I_m = the stator current, main axis

I_x = the stator current, starting axis

I_y = the stator component of the rotor current, main axis

I_z = the stator component of the rotor current, starting axis

Z_s = magnetizing impedance in the S-axis

Z_m = the magnetizing impedance in the M-axis

Y_m = magnetizing admittance of main winding $= \dfrac{1}{Z_m}$

Y_s = magnetizing admittance of capacitor winding $= \dfrac{1}{Z_s}$

$a = \dfrac{\text{effective starting winding turns}}{\text{effective main winding turns}}$

$S = \dfrac{\text{actual revolutions per minute}}{\text{synchronous revolutions per minute}}$

$Z_2' = \dfrac{r_2}{1+S} + jX_2$

(Its approximate expression $= 0.55 r_2 + jX_2$)

$Z_{1s}' = \dfrac{1}{a^2}(Z_c + Z_{1s})$

$Z_m = Z_{1m} + Z_2' + Z_{1m} Y_m Z_2'$

$Y_{1m} = \dfrac{1}{Z_{1m}}$

$Y_{om} = (1 + Z_{1m} Y_m) Y_{1m}$

$Y_{om} = (1 + Z_2' Y_m) Y_{1m}$

$Z_{om} = \dfrac{1}{Y_{om}}$

$Z_{12} = Z_{1s}' + Z_2' + Z_{1s}' Z_2' Y_s a^2$

$Y_{1s} = \dfrac{1}{Z_{1s}}$

$Y_{os} = (1 + Z_{1s}' a^2 Y_s) Y_{1s}$

$Y_{os} + (1 + Z_2' a^2 Y_s) Y_{1s}$

$Z_{os} = \dfrac{1}{Y_{os}}$

$Y_o = Y_{os} + Y_{om}$

R = virtual load resistance $= \dfrac{S r_2}{1 - S^2}$

I_{om} = short-circuit current at R from main phase alone

I_m = values of I_m when R is short-circuited

I_{os} = short-circuit current at R from capacitor phase alone

I_{os} = values of I_s' when R is short-circuited

I_o = short-circuit current at R $= I_{os} + I_{om}$

I = current through virtual load R

E = back electromotive force across R

E_{om} = main phase open-circuit voltage, defined as I_{om}/Y_{om}

E_{os} = capacitor phase open-circuit voltage, defined as I_{os}/Y_{os}

I_s' = capacitor winding current in main winding terms with 90 degrees backward phase shift $= -jaI_s$

I_r' = capacitor axis rotor current in main winding terms with 90 degrees backward phase shift
$= -jaI_r$

T = d-c component of the generated torque

T_{max} = maximum d-c torque of the capacitor motor

S_2 = per unit speed of equivalent polyphase motor

T_{2max} = maximum torque of the 2-phase motor, the windings of which are identical with the main winding of the capacitor motor

T_p = amplitude of the pulsating torque

F & W = friction and windage

References

1. The Cross-Field Theory of the Capacitor Motor. A. F. Puchstein, T. C. Lloyd. AIEE Transactions, volume 60, 1941, February section, pages 58–62.
2. The Revolving Field Theory of the Capacitor Motor. Wayne J. Morrill. AIEE Transactions, volume 48, 1929, April section, pages 29–38.
3. Analysis of Unsymmetrical Machines. W. V. Lyon, Charles Kingsley, Jr. AIEE Transactions, volume 55, 1936, May section, pages 471–476.
4. Das Stromvektordiagram des Einphasen-Motors mit Kapazitat in der Hilfsphase. F. Punga. *Archiv fuer Elektrotechnik*, Berlin, Germany, volume 18, 1927, page 267.

No Discussion

Air-Borne Magnetometers for Search and Survey

E. P. FELCH
MEMBER AIEE

W. J. MEANS
NONMEMBER AIEE

T. SLONCZEWSKI
Membership Application Pending

L. G. PARRATT
NONMEMBER AIEE

L. H. RUMBAUGH
NONMEMBER AIEE

A. J. TICKNER
NONMEMBER AIEE

Synopsis: Air-borne magnetometers developed during the war for the detection of submerged enemy submarines now have become important tools for aerial geophysical exploration. The instruments described utilize the second harmonic outputs produced by the magnetic field in saturated core inductors for field measurement and for control of servo stabilizing systems acting around two axes to maintain the measuring element in alignment with the earth's field. The field to be measured is compared continuously with that produced in the measuring inductor winding by an accurately controlled direct current. The sensitive element usually is towed in a bombshaped bird sufficiently removed from the airplane to escape the effects of its magnetic field. A continuous record is produced which, when keyed with position records obtained by photography or shoran, may be used in the preparation of maps of total magnetic field intensity.

MAGNETIC measurements have played an increasingly important part in geophysical exploration since the seventeenth century, when iron ore bodies were located in Sweden with the help of crude compasses and magnetic dip needles.[1]

In recent years magnetic methods have been employed by geophysicists in reconnaissance of extensive areas to designate limited sections for intensive study by more elaborate methods. The presence of certain anomalies in the intensity of the earth's magnetic field often can be correlated with features of the subsurface structure associated with petroleum or minerals.[2] Many deposits of iron ore, oil, copper, and gold have been located with the aid of magnetic surveys.[3]

Until recently, magnetic surveys have been carried out on the ground with magnetometers requiring accurate leveling upon a firm base.[4] Mapping of an area has involved correlation of a multitude of discrete measurements at accurately spaced stations. A typical survey employing quarter-mile spacing might proceed at a rate of five miles of contour or about $1^1/_2$ square miles per day in favorable terrain.

Employing the air-borne magnetometer, the United States Geological Survey and the Naval Petroleum Reserves have been able to cover as much as 1,000 miles of contour per day over inaccessible terrain. An additional advantage of the aerial method resides in the continuous nature of the record and freedom from the influence of surface magnetic irregularities.

The impetus for the development of practical air-borne magnetometers or magnetic air-borne detectors (MAD in naval parlance) was furnished by the advent of the submarine menace of World War II. Many agencies set to work upon the problems involved, with their efforts co-ordinated by the United States Navy and by NDRC (National Defense Research Committee of the Office of Scientific Research and Development). Aided by their previous experience in magnetic research and development, the Bell Telephone Laboratories, General Electric Company, and Gulf Research and Development Company were progressing on NDRC contracts well before the Pearl Harbor attack.

The Airborne Instruments Laboratory, operated by the Columbia University Division of War Research, produced *AN/ASQ-1* systems employing multiwinding balanced peak-type magnetometer elements similar to those described by Vacquier.[5]

The development carried on by the Bell Telephone Laboratories under contract with the Naval Ordnance Laboratory led to the manufacture of the *AN/ASQ-3* and *-3A* systems by the Western Electric Company for the United States Navy Bureau of Aeronautics. These instruments employ single-winding second-harmonic-type magnetometer elements. This paper is concerned with the *AN/ASQ-3* and *-3A* systems and the subsequent modifications of the latter for use in geophysical exploration. These are popularly called "aerial doodlebugs".

Paper 47-104, recommended by the AIEE committees on communication, electronics, and instruments and measurements for presentation at the AIEE winter meeting, New York, N. Y., January 27-31, 1947. Manuscript submitted December 3, 1946; made available for printing December 19, 1946.

E. P. Felch, W. J. Means, and T. Slonczewski are with Bell Telephone Laboratories, Inc., New York, N. Y.; L. H. Rumbaugh is with the Naval Ordnance Laboratory, Washington, D. C.; L. G. Parratt and A. J. Tickner, with the Naval Ordnance Laboratory during the war, are now at Cornell University, Ithaca, N. Y. and the Western Electric Company, Inc., Hollywood, Calif., respectively.

This air-borne magnetometer development involved close co-operation among many different organizations. Some of these organizations with the names of the individuals active in the direction of this particular work are listed below.
Naval Ordnance Laboratory, Doctor R. B. Valle, Jr.; Bell Telephone Laboratories, Inc., W. J. Shackelton; United States Geological Survey, J. R. Balsley, Jr.; Naval Petroleum Reserves, Commodore W. G. Greenman, United States Navy; Project Sail, Experimental Flight Group, United States Navy, Captain D. E. Wait, United States Navy; Bureau of Aeronautics, United States Navy, Commander J. W. Joyce, United States Naval Reserve; Western Electric Company, Inc., C. T. Prendergast; Aero Service Corporation, Homer Jensen.

The Air-Borne Magnetometer

Air-borne magnetometers measure the variation in the magnetic field at the detector as it is moved through space. This variation is recorded as a function of time, and when the speed of the vehicle is known, and the scales are adjusted properly, the record gives a magnetic profile of the path.

The Saturated Inductor

The method of detection consists of placing in the field under investigation an

open core of high permeability and easily saturable magnetic material and superposing on the unknown field a sinusoidal magnetomotive force large enough to saturate the core. The electromotive force produced by the time variation of the flux in the core in a winding surrounding it, then is fed into an electronic circuit where its wave shape is analyzed in such a manner as to indicate the magnitude of the field producing the flux.

The operation of such saturated inductor may be understood by considering that the flux density B produced in a magnetic material by a field H is an odd function of the field. Analytically, neglecting hysteresis, this is expressed by

$$B = b_1 h + b_3 h^3 + b_5 h^5 \ldots \quad (1)$$

where the coefficients b are determined by the shape and the material of the core. If

H = the field to be detected
H_o = the impressed field
$p = 2\pi$ times the frequency of the impressed field

we have

$$h = H_o \cos pt + H \quad (2)$$

By inserting this value of h into equation 1, expanding the binomials, expressing the powers of the cosines as cosines of multiples of p, and collecting the terms of the same frequency, we get

$$\begin{aligned} B = {} & (b_1 + \tfrac{3}{2} b_3 H_o^2 + \tfrac{15}{8} b_5 H_o^4 + \ldots) H + \\ & (b_3 + \tfrac{10}{2} b_5 H_o^2 + \ldots) H^3 + \\ & (b_5 + \ldots) H^5 + \Big[b_1 H_o + \tfrac{3b_3}{4} H_o^3 + \\ & \tfrac{10 b_5}{16} H_o^5 + \ldots) + (3 b_3 H_o + \\ & \tfrac{30 b_5}{4} H_o^3 + \ldots) H^2 + \\ & (5 b_5 H_o + \ldots) H^4 + \ldots \Big] \cos pt + \\ & \Big[\Big(\tfrac{3}{2} b_3 H_o^2 + \tfrac{20 b_5}{8} H_o^4 + \ldots \Big) H + \\ & \Big(\tfrac{10 b_5}{2} H_o^2 + \ldots \Big) H^3 + \ldots \Big] \cos 2pt + \\ & \Big(\tfrac{b_3 H_o^3}{4} + \tfrac{5 b_5}{16 H_o^5} + \ldots \Big) + \\ & \Big(\tfrac{10 b_5}{4} H_o^2 + \ldots \Big) H^3 + \ldots \Big] \cos 3pt + \\ & \Big[\Big(\tfrac{5 b_5}{8} H_o^4 + \ldots \Big) H + \Big(\ldots \Big) H^3 + \\ & \ldots \Big] \cos 4pt + \Big[\Big(\tfrac{b_5}{16} H_o^5 + \ldots \Big) + \\ & \Big(\ldots \Big) \times H^3 + \ldots \Big] \cos 5pt \quad (3) \end{aligned}$$

Figure 1. Idealized and measured magnetization characteristics of inductor. The hysteresis effect is neglected

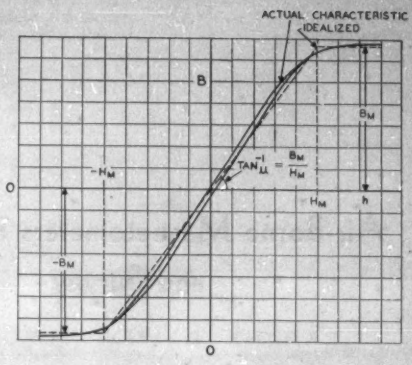

Figure 2 (below)

(*a*). Variation of flux with time for an idealized *B–H* characteristic

(*b*). Electromotive force per turn corresponding to variation of flux in Figure 2(*a*)

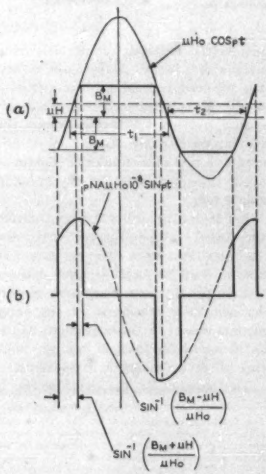

This can be written in a simpler form.

$$B = B_0(H_o, H) + B_1(H_o, H) \cos pt + B_2(H_o, H) \cos 2pt + B_3(H_o, H) \times \cos 3pt + B_4(H_o, H) \cos 4pt \quad (4)$$

Here the B's with even subscripts are odd functions of H and even functions of H_0 while the B's with odd subscripts are even functions of H and odd functions of H_0.

The electromotive force per turn obtainable in the winding is then

$$e = 10^{-8} A\, dB/dt$$

where

A = the effective cross sectional area of the core

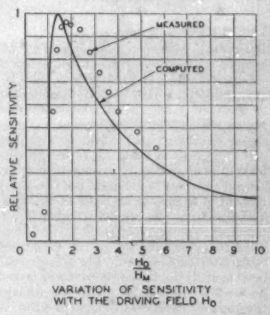

Figure 3. Variation of inductor sensitivity with driving field

Inserting the value of B in the foregoing expression we get

$$e = -10^{-8} A (pB_1 \sin pt + 2pB_2 \sin 2pt + 3pB_3 \sin 3pt + 4pB_4 \sin 4pt) \quad (5)$$

Because every one of the coefficients B is a function of H, any one of them or combinations of them may be used for the purpose of detection. Use can be made of the even and odd function properties of the coefficients to build multiple element detectors in which the even harmonics are segregated from the odd harmonics. However, the *ASQ-3* and *-3A* systems use a single frequency, the second harmonic, for detection. While a multi-frequency broad-band detector utilizes more of the available energy, it presents the problems of broad-band amplification and balance for both amplitude and phase. The single frequency system, although using a smaller source of energy, benefits from the simplicity of narrow-band amplification, lends itself to a de-

sign free from balance requirements in manufacture or in flight, and is adapted to efficient production and inspection methods. It permits the use of a 2-terminal inductor, markedly simplifying design.

The Sensitivity of a Single Frequency Detector

The series representing the values of the coefficients B in the foregoing discussion, although convenient for qualitative analysis, converge too slowly for the purpose of investigation of the sensitivity, when applied to measured characteristics.

Simpler results are obtained by resorting to Fourier analysis. Figure 1 shows a typical field strength—flux density characteristic as obtained from measurement, together with a simplified characteristic composed of straight lines on which the analysis is based. In Figure 2(*a*) is shown the variation of the flux with time for the simplified characteristic when a sinusoidal field $H_0 \cos pt$ is impressed upon the inductor which is placed in a field H. The flux is seen to alternate between positive and negative values over unequal time intervals t_1 and t_2. Figure 2(*b*) shows the corresponding variation in the electromotive force per turn and gives the limits of integration for the coefficient of the Fourier series. For the second harmonic we get

$$e_2 = \frac{2pNA\mu H_0 10^{-4}}{\pi} \int_{-\frac{\pi}{2}-\sin^{-1}\left(\frac{Bm+\mu H}{\mu H_0}\right)}^{\frac{\pi}{2}+\sin^{-1}\left(\frac{Bm-\mu H}{\mu H_0}\right)} \sin x \sin 2x \, dx$$

The integration, which can be performed easily, gives

$$e_2 = \frac{4pNAH_0 10^{-8}}{3\pi}\left(\left[1-\left(\frac{H_m+H}{H_0}\right)^2\right]^{3/2} - \left[1-\left(\frac{H_m-H}{H_0}\right)^2\right]^{3/2}\right)$$

The sensitivity of the instrument is defined by the derivative of the output electromotive force with respect to the field. For small values of field this is approximately

$$\frac{de_2}{dH} = \frac{8pNA\mu \times 10^{-8}}{\pi} \times \frac{H_m}{H_0}\sqrt{1-\left(\frac{H_m}{H_0}\right)^2}$$

The agreement between the computed and the measured values (see Figure 3) shows that the possibilities of the method of detection were fully exploited by the present design, that the simplified idealized characteristic is adequate for the purpose of approximate analysis, and that there is no point in trying to obtain sharper saturation characteristics, because the sharpest possible characteristic has little more sensitivity than the actual one.

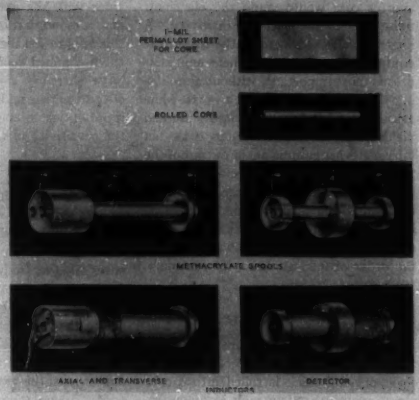

Figure 4. Details of construction of inductor

A more elaborate computation, based on a better approximation to the B–H curve, $B = k \tan^{-1}(h/a)$ where k and a are empirical constants, yields results not much different from the foregoing one. An analysis based on a double characteristic, accounting for the hysteresis loop, yields the result that the hysteresis does not affect the foregoing results. Further analysis reveals that keeping the inductance of the inductor constant, at the optimum value from the circuit design standpoint, the sensitivity is independent of the cross section of the core and increases with its length. For mechanical reasons small inductors are desirable, and for this reason the length of the core was limited to $1\frac{1}{2}$ inches.

In examining the result of the foregoing analysis for factors affecting the sensitivity of the instrument, it is important to remember that μ is not the permeability of the material of the core. The latter is high while the length of the core is small. As a result of the large demagnetizing factor of the core, μ depends on its shape and very little on the permeability of the material. The curve showing the variation of the sensitivity with the input current exhibits a maximum, a circumstance which is exploited by operating the inductor at the maximum sensitivity point in order to make it fairly independent of voltage variations in the driving oscillator.

Assuming an optimum circuit design the sensitivity is limited by the highest impedance which can be maintained at the grid of the first vacuum tube with a satisfactory stability. At constant impedance, the sensitivity increases with the length of the core and is affected very little by its cross sectional area. In a well-balanced design the core length will be such that the magnetic noise at the inductor caused by uncontrollable motions of the inductor in the earth's field and the motion of nearby magnetic objects is somewhat larger than the electronic noise in the detecting circuit. A

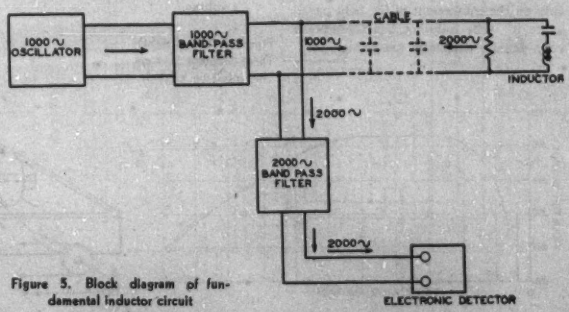

Figure 5. Block diagram of fundamental inductor circuit

shorter core would cause the electronic noise to limit the over-all sensitivity. A longer core would increase the size of the equipment at the point where compactness is most important, without simplifying the amplifier design by a worth-while amount. The 1.5-inch length adopted yields a sensitivity of better than ten microvolts per gamma at the output of the 2,000-cycle filter. A third source of noise limiting the sensitivity of the instrument is found in the Barkhausen effect. This is, at present, much lower than the over-all noise of the system in flight which is of the order of 0.25 gamma. (1 gamma = 10^{-5} oersted)

Construction of the Inductor

Figure 4 shows the construction of typical inductors. A strip of permalloy sheet one mil thick is rolled into a core about one tenth of an inch in diameter. The use of the thinnest practicable material reduces the eddy current losses. The rolled core has barely more than one convolution. An inside turn would be shielded by the outside convolution and would not add to the sensitivity, but would increase the required driving power.

Although the sensitivity of the inductor differs little for different materials as pointed out, the driving power required by the inductor does depend on its choice. The best material was found to be standard *4-79* molybdenum permalloy. After the core is annealed, it is slipped over a glass tube which then is inserted in a lucite spool as shown. The spool carries a single winding which is used both to feed the input current to the inductor and to detect the useful output. In static field measuring applications this same winding also carries the direct current for nulling and compensation purposes.

With the proportions of the cylindrical core as shown, the output of the inductor is independent of the field at right angles to the axis of the cylinder and depends only on the component of the field parallel to it. The inductor has therefore a very definite magnetic axis which coincides with the axis of the cylinder. It also is found that to a sufficient degree for this application the output is proportional to the applied field. For any field H we have therefore $e = H \cdot D$ where e is the output voltage and D is a constant vector representing in magnitude and direction the sensitivity of the inductor.

Inductor Circuit

The circuit to which the inductor is connected consists of a 1,000-cycle oscillator which feeds the driving current to the inductor through a filter which eliminates all other frequency components, the most important of which is the second harmonic which could add a spurious signal to the useful output of the inductor. The current is fed over a long cable as shown in Figure 5 which removes the inductor from the vicinity of the rest of the apparatus and its magnetically disturbing effects. The second harmonic current generated in the inductor returns over the same conductors and is fed into the electronic detector through a narrow pass and filter which eliminates all frequency components except the second harmonic. In particular it eliminates the 1,000-cycle current from the oscillator and the third and other order harmonics generated in the inductor. Each filter offers a high impedance in the attenuation band so as not to introduce an insertion loss to the other. The large capacitance of the cable presented a problem which was solved by absorbing it as a part of the filter configuration.

The nonlinearity of the inductor as an inductance has brought about a special filter design problem because the reactance of the inductor also forms part of the filter network. This difficulty was turned to advantage by designing the input filter as a voltage regulator so as to make the inductor output independent of the driving voltage. The relation between the driving voltage and the inductor output is shown in Figure 6.

Even this refinement is not sufficient to provide the required output stability with extreme variations of the voltage of some airplane power supply systems. For this reason the oscillator output is regulated by an automatic level control. The control voltage is obtained by rectifying the alternating plate voltage of the oscillator output stage.

Orientation of the Inductor

In the design of air-borne magnetometers the proper selection of the inductor axis is a matter of primary importance because the variation ΔH to be measured is usually small in comparison with the total value of the field.

This can be seen by considering that as the instrument is carried from O to O' (Figure 7) the component of the field along the axis of the detector changes

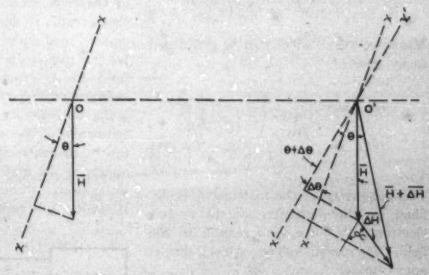

Figure 7. Inductor orientation error

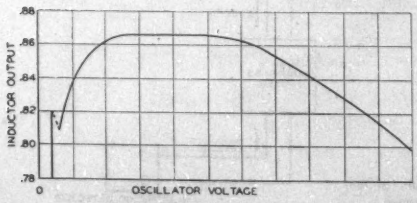

Figure 6 (below left). Variation of inductor output with driving voltage

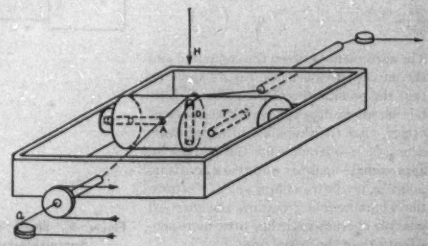

Figure 8 (below right). Three-inductor system mounted on gimbals

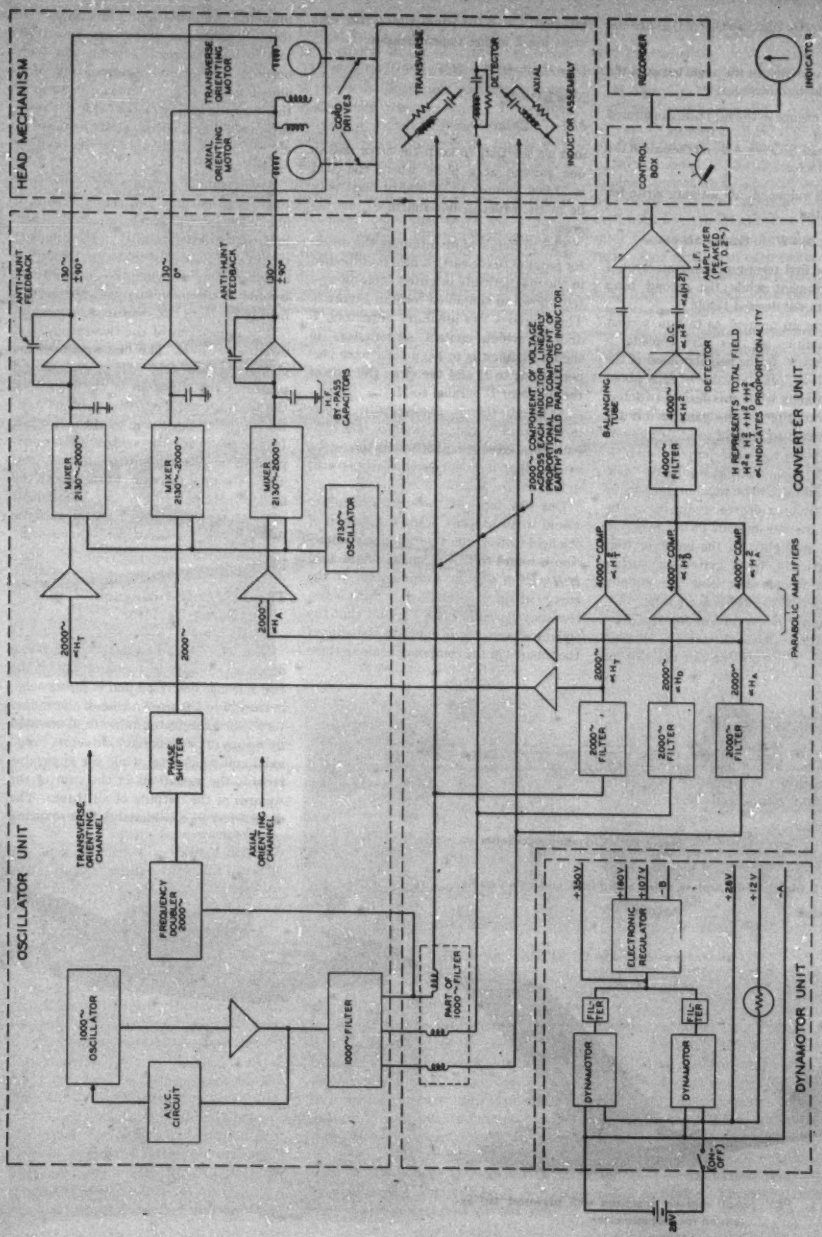

Figure 9. Block schematic diagram of AN/ASQ-3 system

from $H \cos \Theta$ to $H \cos (\Theta + \Delta\Theta) + \Delta H \cos \alpha$ where

$\Delta\Theta$ = the variation in the angle between the field and the detector

ΔH = the change in the field being measured and

α = the angle between ΔH and the axis of the detector

For small values of $\Delta\Theta$ we may write for the variation

$$\Delta(H \cos \Theta) = H \sin \Theta \Delta\Theta + \Delta H \cos \alpha$$

where the first term represents an error of the instrument while the second term represents the desired result.

To form an opinion as to how serious the difficulties are, we may consider a specific case. In the neighborhood of the city of New York the value of H is about 57,000 gamma while it is desired to detect a field variation of one gamma. If the x-x axis were to be held so as to measure the component of ΔH perpendicular to H the variation $\Delta\Theta$ that would be tolerable would have to be small in comparison with 0.001 of a degree, requiring a stability of motion difficult to achieve, particularly in flight. If the inductor were held vertically, by a gyroscope, such a situation would exist near the equator where the earth's field is horizontal.

The form of expression for the error given indicates that the error is smallest for $\Theta = O$. We now can not use this expression for computing the error, but must use a higher approximation

$$\delta H = H \sin \Theta \Delta\Theta + (H/2) \cos \Theta (\Delta\Theta)^2$$

Now if $\Theta = O$,

$$\delta H = \quad 2)(\Delta\Theta)^2$$

and we see that to keep the error within one gamma at a place where the field is 57,000 gamma the stability need only be of the order of one fourth of one degree.

This principle of maintaining the detector parallel to the earth's field is embodied in the magnetically oriented detector system shown in simplified form in Figure 8. This employs two auxiliary inductors, T and A, which control servomotors in such a manner as to keep their axes perpendicular to H and therefore the axis of the inductor D parallel to H.

Although this is theoretically a perfectly sound system, in practice it is difficult to build a sufficiently sensitive servo system that does not require adjustment in flight.

One way to avoid the servo difficulties would be to measure a scalar function of the field instead of a vector. Such a function is found to be the square of the field $H \cdot H = H^2$, a quantity proportional to the energy of the magnetic field. Such a system may be built using the fact that the square of a vector is equal to the sum of the squares of the components along three mutually perpendicular directions. If three inductors are mounted with their axis in an orthogonal system, and their outputs are squared electronically, and added to produce an indication proportional to the energy of the field, this indication will be independent of the position of the axis and therefore of the position of the system.

A few simple computations show that the requirements for the mechanical alignment of the three inductors, their linearity, and the stability of the squaring circuits are too severe to be practical, except in the case when the angle formed by one of the inductors with the earth's field is less than two degrees.

The indications of the two systems are essentially alike. The first measures the change in the field ΔH. The second measures the variation in the energy of the field $\Delta H^2 = 2H\Delta H$ which differs from the preceding expression by the factor $2H$. In the first case the sensitivity is independent of the magnitude of the field; in the second it increases linearly with the field. If, however, a proper adjustment of the scales is made, the indications of the two systems for small field changes are the same.

The AN/ASQ-3 Magnetic Air-Borne Detector

The *AN/ASQ-3* magnetic air-borne detector employs a combination of the two schemes described and is shown schematically in Figure 9. One of the inductors, called the dector inductor, is oriented by means of two auxiliary inductors called axial and transverse, while the apparatus records the variations in the sum of the squares of the outputs of all three. The device may be considered to be a squaring

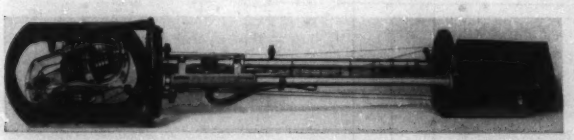

Figure 10. Orienting mechanism

Figure 12 (right). *TBF* airplane flying a bird from underwing cradle

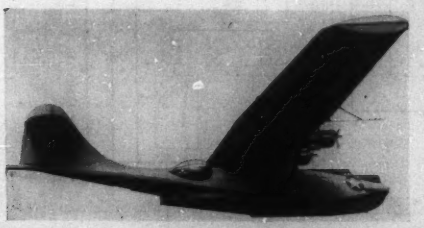

Figure 11. *PBY* patrol airplane equipped with plywood tail extension for magnetometer

Figure 13. Inductor mounting with three orthogonally disposed inductors, drive pulley, and slip rings

detector with partial orientation to keep it in the most favorable operating position, or a magnetically oriented detector with a compensating system for disturbances caused by small deficiencies in orientation.

Electronic Circuits

Each of the three orthogonal inductor outputs is connected through a 2,000-cycle filter to the grid of a separate vacuum tube. These tubes have a substantially parabolic grid voltage-plate current characteristic. If a is the coefficient of the square term in the expression for the plate current in the tube, then the 2,000-cycle tube inputs $e_d = H_d \cos 2pt$, $e_t = H_t \cos 2pt$, and $e_a = H_a \cos 2pt$ will produce a combined plate current which will have components $\alpha/_2 H^2 + (\alpha/2) H^2 \cos 4pt$ because $H_d^2 + H_a^2 + H_t^2 = H^2$.

From this it follows that either a direct current or a second harmonic 4,000-cycle current may be used to obtain a response proportional to the square of the input. The objection to the use of direct current is that it is superposed on the zero input space current of the tube. This is not only large, but is not very stable. It is affected by variations in the supply voltages, by accelerations, and by the rotation of the tube in the magnetic field of the earth. The fourth harmonic current is free from these objections.

The outputs of the three parabolic tubes are combined as shown on Figure 9 by connecting their plates together at the input of a 4,000-cycle filter. This rejects unwanted modulation products and delivers across the low frequency amplifier input a voltage which is proportional to the energy of the field, and, as stated above, independent of the orientation of the detector in the earth's field. The 4,000-cycle voltage is linearly rectified and the resulting direct voltage is blocked by a capacitor while the low frequency signal passes through an equalizer which determines the frequency response of the detector. The output is recorded on an Esterline-Angus ink recorder. A meter which may be observed by the pilot is connected in series with the recorder. A control box permits the operator to adjust the sensitivity of the instrument to 10, 25, 50, or 200 gamma full scale.

As shown on Figure 9 the inputs to the amplifiers which energize the servomotors are in parallel with the inputs of the squaring tubes. The frequency of the signal is lowered to 130 cycles by heterodyning against a 2,130-cycle oscillator. The driving motors are of the induction type with a very light aluminum cup type rotor to provide a high torque-to-inertia ratio. One winding of each motor is supplied by the signal which originates in the inductors, and which changes in sign when the angular departure of the inductor from the equilibrium positions is reversed. The other windings of the motors are energized by a voltage obtained from a modulator in which the second harmonic of the inductor driving oscillator is heterodyned against the 2,130-cycle oscillator. This system has the advantage that, once the phase difference between the two motor windings is adjusted to quadrature, it remains constant and independent of variation in phase in either oscillator. In order to obtain dynamic stability without sacrificing the

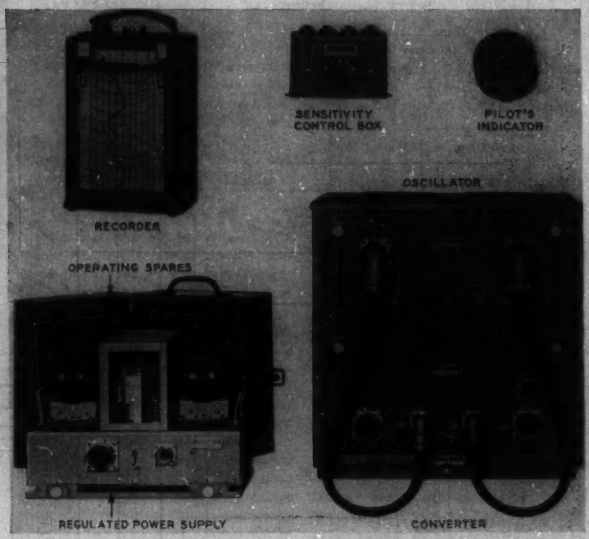

Figure 14. AN/ASQ-3 system electronic units

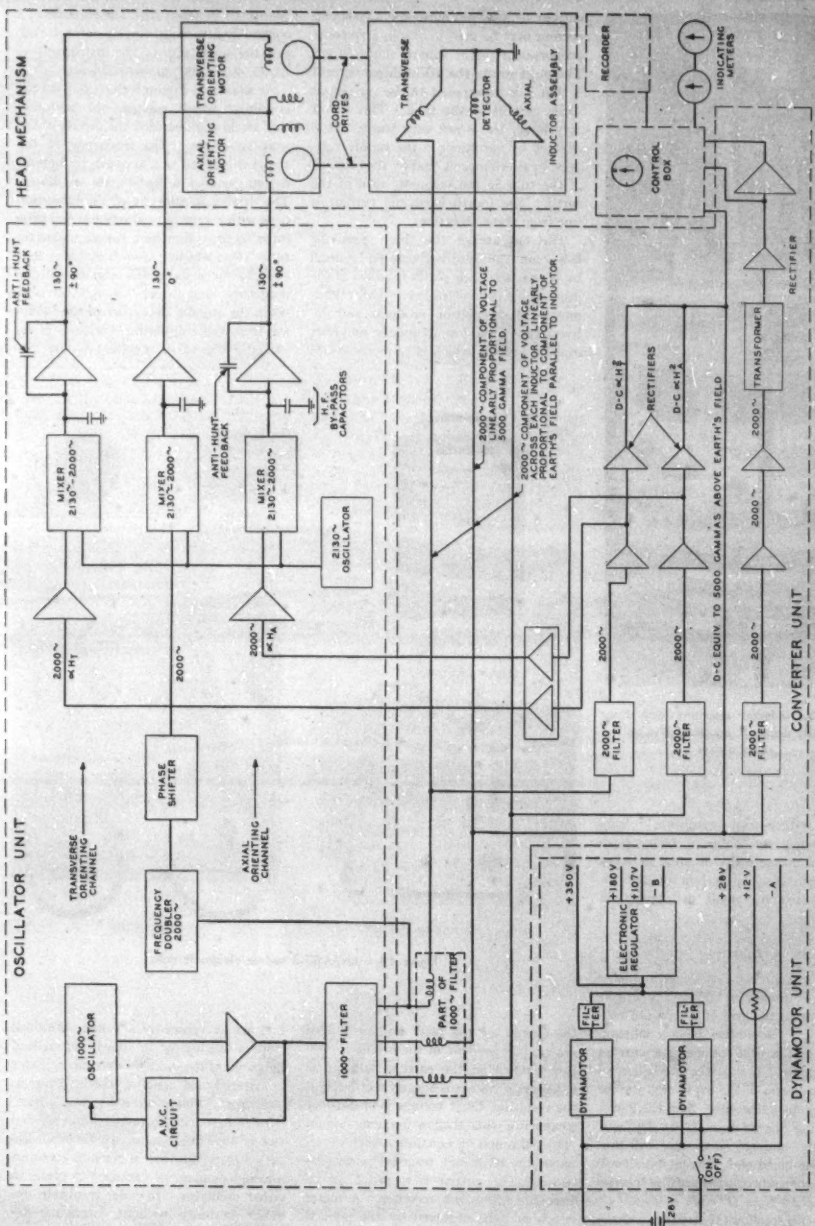

Figure 15. Block schematic diagram of AN/ASQ-3A system

speed of response, a capacitor connected from the rotor winding to the preceding amplifier feeds back the motor electromotive force which is induced by the rotation of the armature. This dynamic feedback introduces damping which prevents hunting.

Power for the operation of the entire system is derived from the 28-volt aircraft supply through a dynamotor unit. Because in actual practice the 28-volt supply often fluctuates violently, an electronic voltage regulator and a ballast lamp for regulation of the filament current of the critical tubes are provided.

Mechanical Construction

The mechanical design of the system is governed by the necessity of preventing magnetic disturbances from reaching the inductors.

The closest disturbing magnetic mass happens to be that of the servomotors which in the interest of good servo performance cannot be too far from the inductors. A satisfactory balance of these conflicting factors was obtained by mounting the motors and the inductors at opposite ends of an aluminum framework less than three feet long as shown in Figure 10. At this distance the magnetic effect of the motors is not negligible but can be compensated readily although the length of the cord drive is not excessive.

This entire unit called the "orienting mechanism" is located as far as possible from magnetic parts of the airplane, particularly the engines. In a large airplane such as the *PBY* sufficient isolation is obtained by mounting the unit in a plywood tail extension as shown in Figure 11. The electronic apparatus then is mounted forward in the airplane.

Towed Bird

In the case of smaller airplanes such as the *TBF* the unit is housed in a streamlined nacelle called a "bird" towed about 70 feet beneath the airplane (Figure 12).

Aerodynamic stability is achieved by attaching the towing cable by gimbals on the geometrical axis of the bird slightly ahead of and above the center of gravity and ahead of the center of pressure. By the addition of lead weights it is possible to adjust the center of gravity so that the gimbal suspension can be mounted conveniently on the frame as shown on Figure 10. This arrangement gives the bird a small component of lift which facilitates handling in flight. The bird itself is made of resin bonded molded plywood to which is attached a rugged aluminum tail section. The nose is removable to provide access to the mechanism. A

Figure 16. Control box of *AN/ASQ-3A* system

manually operated winch equipped with a brake, ratchet, and slip rings is used to lower the bird from a cradle in the bomb bay or beneath the wing.

The towing cable which is less than one-half inch in diameter contains seven conductors which convey the currents to the three inductors, return their outputs, and energize both of the 2-phase servomotors. The ground conductor of silicon bronze also serves as the strain member.

The Orienting Mechanism

The inductors are mounted in a cylindrical block of cast methacrylate shown in Figure 13. Because of its homogeneity this material possesses 3-dimensional stability to a satisfactory degree. Four slip rings are provided for taking off the connections. These slip rings are gold-plated phenol fiber in order to reduce the volume conductivity, which causes eddy current difficulties. Monel metal ball bearings at each end of the inductor mounting fit into beryllium copper pivot screws in a methacrylate inner gimbal which in turn rotates in similar bearings in the outer gimbal frame. Rotation about the two perpendicular axes is effected by two cord drive systems one of which passes through the hollow bearings in the outer gimbal ring. This feature together with the slip rings permits unlimited rotation about both axes, so that under no circumstances can the system become locked.

The cord drive which combines the attributes of low inertia and flexibility of arrangement employs a nylon covered linen cord which is both long wearing and relatively immune to the effects of humidity. Tensioning devices on the drive unit provide uniform cord tension without introducing elasticity in the servo system.

From the kinematic properties of the gimbal structure shown in Figure 8, it follows that the velocity of turning of the outer gimbal ring may approach infinity as the direction of the field approaches the direction of the outer gimbal axis. Such a situation could arise near the equator where it is horizontal. To avoid this, an alternative mounting position is provided by simply rotating the entire unit by 90 degrees so that the outer axis becomes vertical. Then for similar reasons the mechanism can not be used far from the equator. However, the two mounting positions have a generous zone of more overlap.

Electronic Units

The electronic units are housed in shock-mounted frames as shown in Figure 14. The main electronic unit is in two drawer sections. The upper one called the oscillator contains the driving oscillator and servo amplifier while the lower or converter contains the detector and squaring circuits. Only the small sensitivity control box and the recorder need be located at the operator's position.

The AN/ASQ-3A System

The *AN/ASQ-3A* system was developed for applications at lower aircraft speeds which required an extension of the frequency range downward. It is capable of measuring changes in static field strength. The basic principles and most of the apparatus units are identical to those employed in the *AN/ASQ-3* system. The principal departures in design involve a different converter unit and the addition of a control box.

As shown on the block schematic diagram, Figure 15, the field in the detector inductor is reduced to approximately 5,000 gamma by a d-c suppression current flowing in the inductor winding. This direct current is obtained from a dry cell battery and a calibrated current control network in the control box. The 2,000-cycle output of the detector inductor which is linearly proportional to this 5,000-gamma residual field is amplified and linearly rectified. This rectified voltage is amplified in a d-c amplifier and applied to the recorder and indicating meters. Hence, as long as the suppression current remains constant, the recorder and meters indicate changes in the magnitude of the earth's field.

In contrast with the *AN/ASQ-3* the sensitivity of this system is independent of the field strength. The suppression current may be adjusted by controls to permit operation in ambient fields of 25,000 to 75,000 gamma.

The squaring arrangement for compensation of small angular motions differs considerably from that used in the *AN/ASQ-3* system. The 2,000-cycle outputs of the axial and transverse inductors are amplified and rectified by parabolic rectifiers. The output currents of these rectifiers which are proportional to the squares of their inputs are added to the suppression current in the detector inductor. Although this compensation method is based on an approximation, it is entirely adequate for angular departures up to two degrees. A series resistor ganged to the coarse suppression current control serves to proportion the compensating current to the ambient field.

The control box shown in Figure 16, in addition to the fine and coarse suppression current controls, includes a sensitivity control and a selector which provides three optional frequency responses. The lowest extends the response downward to direct current, while the other two have blocking capacitors which obviate the necessity of frequent suppression current adjustments at higher aircraft speeds.

The oscillator unit, orienting mechanism, power unit, and recorder are similar to those shown in Figure 14.

The Air-Borne Magnetometer for Geophysical Exploration

The air-borne magnetometers which have been used by the United States Navy and the United States Geological Survey of the Department of the Interior for geophysical exploration are modified *AN/ASQ-3A* systems.

In geophysical application the instrument measures changes in the absolute magnitude of the earth's magnetic field. To obtain the desired precision of plus or minus one per cent plus one gamma for measurement of changes in field it is necessary to maintain the suppression current to better than 0.01 per cent in spite of wide variations in ambient temperature.

The *AN/ASQ-3A* system is provided with a special control box for geophysical use and the converter unit is slightly modified. Advantage is taken of the fact that a maximum sensitivity of 50 gamma full scale is adequate compared with the 10 gamma full scale sensitivity of the *AN/ASQ-3A*. The introduction of additional feedback at several points in the circuit improves the stability of the converter with respect to supply voltage changes and shock so that such effects are less than one gamma.

The suppression current is derived from a large $22^1/_2$-volt dry battery in a thermally insulated portable box. To insure stability a constant current of 700 microamperes is drawn continuously from this battery, even when the instrument is not in use. By preaging this battery and maintaining its temperature above 50 degrees Fahrenheit, it is possible to reduce the current drift to less than 0.01 per cent per hour over a useful battery life of over six months.

The special control box shown with the complete geophysical instrument on Figure 17 is equipped with a 3-decade suppression current control having steps of 50, 500, and 5,000 gamma. A mechanical linkage between the dials steps the next higher dial automatically one position as each is turned through step nine to step

Figure 17 (above). *AN/ASQ-3A* system modified for geophysical use, with control box, battery box, winch, and bird

Figure 18. Installation of geophysical instrument in United States Geological Survey airplane (looking from rear)

Note winch at right, bird in bomb bay rack below electronic units, and control box and recorder forward

zero. A thermal compensation scheme maintains the required accuracy of the current control resistors with ambient temperature changes. The sensitivity control provides normal recorder scales of 100, 200, 500, 1,500, and 5,000 gamma full scale. These values may be halved if desired by an adjustment in the converter. Flexible shaft connections are attached to all four controls so that a number stamping device may be used on the recorder to indicate the control settings. Three indicating meters on the control box monitor the airplane power supply voltage, the suppression current, and the recorder indication.

An installation in a United States Geological Survey airplane is shown in Figure 18. This *SNB* airplane is particularly well adapted to this work because of its range, performance, and the built-in bomb bay.[6]

Similar installations have been made in *R4D* (Douglas *DC-3*) airplanes for the 1947 United States Navy expedition to the Antarctic.

The noise level of the geophysical instrument in flight is less than one gamma. Instrument drift is less than ten gamma per hour and the accuracy of measurement of field changes is in the order of one per cent. In practice it has been found that this performance is ample for magnetic mapping even in areas of low magnetic gradients.[7,8]

References

1. Terrestrial Magnetism and Electricity (book), edited by J. A. Fleming. McGraw-Hill Book Company, New York, N. Y., 1939.

2. Exploration Geophysics (book), J. J. Jakosky. Time-Mirror Press, Los Angeles, Calif., 1940. Page 53, "Magnetic Methods."

3. Choice of Geophysical Methods in Prospecting for Ore, Hans Lundberg, Basil T. Wilson, H. Stewart Scott. *Mining and Metallurgy*, American Institute of Mining and Metallurgical Engineers (New York, N. Y.), volume 26, August 1945, page 387.

4. Manual on Geophysical Prospecting With the Magnetometer, J. Wallace Joyce. United States Bureau of Mines, 1937.

5. United States patent 2,406,870, September 3, 1946, V. V. Vacquier, assigned to Gulf Research and Development Company.

6. The Airborne Magnetometer, *Mining Congress Journal*, American Mining Congress (Washington, D. C.), volume 32, July 1946, pages 48–9, 50, 55.

7. The Airborne Magnetometer, a New Aid to Geophysics, A. W. Knoerr. *Engineering and Mining Journal* (New York, N. Y.), volume 147, June 1946, pages 70–5.

8. The Airborne Magnetometer, J. R. Balsley, Jr. Geophysical Investigation Preliminary Report Number 3, United States Department of Interior Geological Survey, Washington, D. C.

No Discussion

A Design Method for Capacitor Motors

T. C. LLOYD
MEMBER AIEE

SHELDON S. L. CHANG
STUDENT MEMBER AIEE

IN designing a permanent split capacitor motor, the designer is faced with many choices. Both main and auxiliary windings are to be determined, as well as the rating of the capacitor. Any tentative design might prove unsatisfactory because of a poor selection of windings, an incorrect ratio of turns, or excessive voltage across the capacitor. Even a satisfactory design might lead to the suspicion that a more favorable arrangement might have resulted in a reduced capacitor size or a less expensive motor.

By the equivalent circuit for the cross-field theory and the analyses which result from it, certain relationships are clarified so as to simplify greatly the choices of the designer.

It will be shown in this paper how the main winding can be designed directly to yield a desired maximum torque. It can be proven that the maximum torque of a capacitor motor is practically independent of the auxiliary winding. With the increased emphasis in the industry on defining the horsepower of a motor by maximum torque bands, this method of design seems doubly desirable.

Several methods are available for calculating the starting torque of a permanent split capacitor motor. The designer is more frequently interested in the reverse problem of determining the winding and the capacitor necessary to yield a predetermined starting torque and starting current.

It is possible to prepare a set of curves based on ratios of winding parameters which enable the auxiliary winding to be selected. The derivation of such data is given here. Because of the apparent range of winding and capacitor combinations which can give the desired results, the prepared curves offer the double benefit of saving time in calculation, and showing more readily the effect of varying factors under the designer's control.

The equivalent circuit for the capacitor motor has indicated desirable ratios of constants for minimum torque pulsation and maximum efficiency. Possible combinations of auxiliary winding and capacitor can be examined in light of these ratios to obtain predetermined results.

Rotor Current From the Auxiliary Phase

It has been shown in a previous paper[1] that the capacitor motor equivalent circuit can illustrate the change in performance from plain single phase to perfect polyphase by the change in position and magnitude of the rotor current I_x' arising from the auxiliary winding. The highest efficiency and lowest pulsation in torque is realized when I_x' is nearly equal to, and in phase with, the similar rotor current I_y from the main phase.

However, because I_x' is nearly independent of speed, while I_y varies from five to twenty times in magnitude (over the speed range) the approximate realization of this balanced condition at the full-load point would mean that I_x' is relatively unimportant at the pull-out point. It can be assumed that the auxiliary phase supplies the cross-axis magnetization current, as well as the friction, windage, and core losses at the point of pull-out. The energy transferred to the rotor from the main phase is converted to the measurable torque. For such a case, the maximum torque is

$$T_m = 0.5S \cdot T_{m2} \tag{1}$$

where

S = the speed (as a decimal fraction) at which the maximum torque o the capacitor motor occurs

T_{m2} = the maximum torque of a 2-phase motor with windings identical to the main phase of the capacitor motor

The maximum torque of a permanent split capacitor motor is always more than that obtained from plain single-phase motor action although less than the 2-phase value. This increase results from the necessity for the plain single-phase motor to supply its own cross-magnetizing exciting current and losses.

The pulsating torque has been shown to be dependent upon the relative magnitude and position of the two rotor currents, I_y and I_x'. As investigated in numerical examples in this paper, the pulsating torque in synchronous watts equals

$$T_p = R|I_y^2 - I_x'^2| \tag{2}$$

These quantities can be further identified by reference to Figure 1.

Calculation of Maximum Torque

The maximum torque of a 2-phase motor in pounds-feet can be calculated readily.

$$T_{m2} = \frac{7.05V^2}{\text{Synchronous speed } (R_1 + \sqrt{R_1^2 + X^2})} \tag{3}$$

Or by a more accurate formula

$$T_{m2} = \frac{7.05V^2K_rK}{\text{Synchronous speed } (X)} \tag{4}$$

where

$$K_r = \frac{X_0 - X}{X_0}$$

X = total leakage reactance, main winding, and rotor

X_0 = total reactance

Paper 47-102, recommended by the AIEE committee on electric machinery for presentation at the AIEE winter meeting, New York, N. Y., January 27–31, 1947. Manuscript submitted October 28, 1946; made available for printing December 9, 1946.

T. C. LLOYD is chief engineer of Robbins and Myers, Inc., Springfield, Ohio, where SHELDON S. L. CHANG is an engineer.

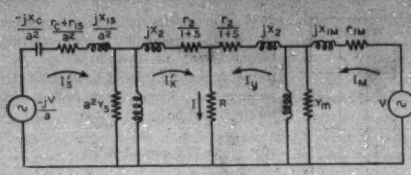

Figure 1. The equivalent circuit of the capacitor motor. (Cross-field theory)

$$K=\frac{1}{\beta}+0.1(1-K_r^2)$$

$$\beta=\frac{R_1}{X}+\sqrt{\left(\frac{R_1}{X}\right)^2+1}$$

By transformation, the leakage reactance necessary to produce a desired maximum torque is[2]

$$X=\frac{7.05V^2K_rK}{\text{Synchronous speed } T_{m2}} \tag{5}$$

With the permeance of all leakage paths equal to P_L, it follows that

$$X=2\pi fC^2P_L10^{-8} \tag{6}$$

Method

It is assumed that the main winding for a capacitor motor is unknown, but that the lamination stack and a tentative rotor cage have been selected. It is then possible (through selecting a relative distribution for the winding) to determine R_1/X, R_2/X, K_r.

The desired maximum torque is T_m. This can be obtained by designing the winding to yield a 2-phase torque.

$$T_{m2}=\frac{T_m}{0.5S} \tag{7}$$

The slip at which the maximum torque occurs in a 2-phase motor is

$$s=\frac{R_2/X(5-K_r)}{4\sqrt{(R_1/X)^2+1}} \tag{8}$$

The speed (as a decimal fraction) at which a capacitor motor displays maximum torque is then approximately

$$S=\sqrt{1-s} \tag{9}$$

By equations 5 and 6 it follows that the series conductors needed to produce this torque are

$$C=\sqrt{\frac{X10^8}{2\pi fP_L}} \tag{10}$$

An example of these calculations is given in Appendix I.

Verification of Assumptions

The fact that most acceptable capacitor designs are so proportioned as to yield negligible effect from I_s' at the point of maximum torque can be investigated in two ways.

1. A group of existing motors, used industrially and designed with no reference to this procedure, is analyzed in Table III.

2. A design in which ratios of turns between auxiliary and main windings (and also capacitor ratings) are changed over a considerable range has been investigated for maximum torque under each condition. These data are presented in Appendix II and show only a few per cent change for the range of designs made.

Table III shows tests and calculations on seven capacitor motors of various speed and horsepower ratings. Calculated maximum torque values based on equation 1 compare favorably with test values of column (2) of the table. It is of interest to note how much the capacitor motor offers over the plain single-phase values as shown by the ratios of column (6).

Calculation of Auxiliary Winding

The method followed in determining the capacitor winding is based on the viewpoint described below.

1. The main winding has been fixed by the maximum torque.

2. The size of the capacitor (although not always the allowable voltage rating) has been assumed. Any system which makes X_c a dependent variable is likely to require recalculation because capacitors are usually purchased in definite steps of ratings. The time involved in investigating a second capacitor size, if necessary, is not great, if a definite value can be assigned in the initial calculations.

3. The starting torque required for the design is used as the basis for determining the auxiliary winding.

4. A definite area has been allowed in the stator slots for auxiliary winding. A winding distribution is assumed. Without knowing the number of turns it is still possible to calculate

$$\frac{R_s}{X_s}=\frac{R_{1s}}{X_s}+K_r\frac{R_{2s}}{X_s} \tag{11}$$

5. Because of the possible difference in winding distributions, the ratio of rotor resistance to total leakage reactance in auxiliary winding terms may be different from R_2/X.

6. A system of curve sheets plotted for various values of R_m/X and R_s/X_s is advocated as a time-saving device. A brief derivation of the equations is given in Appendix III and one curve sheet is shown in Figure 2.

7. Choices in number of turns required for the desired starting torque can be shown by the curves as to the effect on the noise, pulsating torque and voltage across the capacitor, to enable an intelligent choice to be made.

Procedure

The starting torque in ounce-feet is

$$T_s=\frac{K_cC_sK_r}{\sqrt{X}}\times\frac{R_s}{X} \tag{12}$$

where

$$K_c=\frac{V^2}{\text{Synchronous speed }\sqrt{X_s}} \tag{13}$$

The term C_s is read from Figures 2

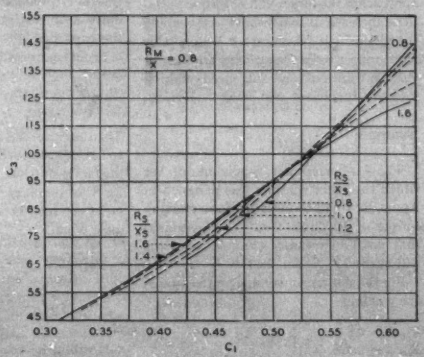

Figure 2. The relation between ratio of transformation and starting torque is a function of these C_s, C_1 curves

or 3. C_3 is plotted as a function of C_1 defined as the ratio

$$C_1 = a\sqrt{X/X_c} \tag{14}$$

The value of C_3 necessary to produce a required starting torque with a fixed capacitor is obviously

$$C_3 = \frac{T_s \text{ synchronous speed } \sqrt{X_c X}}{V^2 K_r R_s/X} \tag{15}$$

This is independent of the ratio of turns but is influenced as the square root of the capacity reactance.

From the correct curve for R_s/X_s and R_m/X, the value of C_1 pertaining to C_3 can be read.

Then the ratio of effective conductors in the auxiliary winding to effective conductors in the main winding is

$$a = \sqrt{\frac{X_s}{X}}\, C_1 \tag{16}$$

It has been shown from the equivalent circuit[1] analysis that the efficiency, torque pulsations, and motor noise are influenced by the ratio of certain constants. The significant ratio is (refer to Appendix V)

$$1/8 < \frac{X_s}{a^2 X_o} < 1 \tag{17}$$

Because

$$C_1 = a\sqrt{\frac{X}{X_c}}$$

It follows that

$$C_1 = \sqrt{\frac{a^2 X_o}{X_c}}\sqrt{\frac{X}{X_o}}$$

$$\cong (1 \text{ to } 1.5)\sqrt{\frac{X}{X_o}} \tag{18}$$

When C_1 falls close to the smaller value, the efficiency is higher, and the pulsations reduce to a very small value. As C_1 approaches the larger value, torque pulsations increase in magnitude, approaching the plain single-phase case. Beyond this point, one winding may load another at various values of load and speed, making for very inefficient and noisy operation.

Example

The $^1/_4$-horsepower 8-pole motor for which the main winding was designed in Appendix I will be designed for a starting torque of 10 ounce-feet. It is assumed that an 8-microfarad 330-volt capacitor will be used. X_c equals 331.

For the slot area available for the auxiliary winding

$R_{1s}/X_s = 0.842$
$R_{2s}/X_s = 0.425$

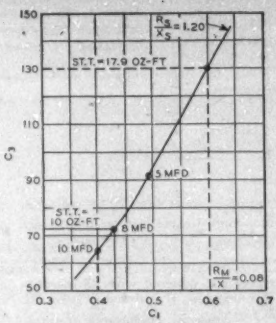

Figure 3. C_1 versus C_3 curve for one value of R_m/X and R_s/X_s

Then from equation 11

$R_s/X_s = 1.20$

From equation 15 the correct value of C_3 to yield 10 ounce-feet of starting torque is

$$C_3 = \frac{10.0 \times 900 \times \sqrt{331 \times 5.92}}{110^2 \times 0.84 \times 0.54} \text{ or } 72.5$$

Refer to Figure 3 which reproduces from the complete curve sheet the value R_s/X_s of 1.20 pertaining to this problem. For $C_3 = 72.5$, C_1 is read as 0.43.

Check the allowable values of C_1 from equation 18.

$$C_1 \cong (1 \text{ to } 1.5)\sqrt{\frac{X}{X_o}}$$

$$\cong 0.4 \text{ to } 0.6$$

Dotted vertical lines are drawn in at these values on Figure 3. Note that this design is close to the point of maximum efficiency and minimum torque pulsation. The design is probably satisfactory but still must be investigated for voltage across the capacitor.

From equation 16 it follows that

$$a = \sqrt{\frac{X_s}{X}}\, C_1 \text{ or } 3.21$$

Then because the main winding is known to have 732 series conductors with a winding factor of 0.831, and the winding factor for the auxiliary winding is 0.985, the series conductors of the auxiliary winding must equal

$$C_s = aC\frac{K_{wm}}{K_{ws}}$$

$$= 3.21 \times 732\,\frac{0.831}{0.985} \text{ or } 2{,}000$$

It will be noted, of course, that a varies as C_1. On this design it would be possible to obtain considerably higher starting torque, going to $C_3 = 130$ before performance became inferior to plain single-phase motor action. By proportion, the torque would be

$$10 \times \frac{130}{72.5} \text{ or } 17.9 \text{ ounce-feet}$$

With C_1 going to 0.6, the turn ratio a becomes 4.5. The effect of this ratio will be investigated later.

Effect of Change in Capacity

The effect of capacitor rating is well illustrated by these curves. Consider that the use of 5- and 10-microfarad capacitors are to be investigated for this motor. Because C_3 varies as the square root of the capacity reactance

$$C_3(5 \text{ microfarads}) = \sqrt{\frac{530}{331}} \times 72.5 \text{ or } 91.6$$

$$C_3(10 \text{ microfarads}) = \sqrt{\frac{265}{331}} \times 72.5 \text{ or } 64.7$$

The corresponding values of C_1 can be read from Figure 3.

Note that the 5-microfarad capacitor can produce the desired torque but only at the expense of motor noise and efficiency. Ten microfarads produce practically negligible pulsating torque.

Change in Resistances

Referring to the more complete curve sheet of Figure 2, it will be noted that a change in R_s has little effect on C_1, and therefore is unimportant so far as the starting torque is concerned. But in order to achieve best efficiency with little torque pulsation it is important to keep the current densities in the main and auxiliary windings as close as possible at the full load point. Equation 18 with $C_1 = \sqrt{X/X_o}$ is intended to give a small angle between I_x' and I_y for all speeds. It gives no idea of their relative magnitude. Too little copper for the auxiliary phase causes, not only excessive heating of the auxiliary winding and poor efficiency, but also increased torque pulsation resulting from reduced I_x'.

In case of a many-pole motor, where X/X_o is as high as 0.3 or more, a good motor can usually be obtained by using the same winding distribution and same amount of copper in both main and auxiliary phases. In case of a motor with fewer poles, where X/X_o is low, the amount of copper in the auxiliary winding should be reduced to give approximately equal current densities in both windings. In this

respect, the permanent split capacitor motors should be different from the capacitor start motors, where the amount of copper of the starting winding is usually one third to one quarter of that of the main winding. In the latter case, the auxiliary phase is cut off during running while in the former it continues to carry the load as long as the motor is energized. Any advantage of the capacitor motor over a plain single-phase motor would be nullified, if too high a current density exists in the auxiliary phase.

Starting Current

The locked rotor current of a capacitor start motor is the vector addition of both winding currents. Usually the capacitor winding current is small enough and of such phase position as to add little to the total. Then

$$I_T \cong I_M = V\frac{C_4}{X_m} \tag{19}$$

$$C_4 = \frac{1}{\sqrt{1+(R_m/X)^2}} \tag{20}$$

C_4 can be read from Figure 4.

Voltage Across the Capacitor

While the equations for plotting the torque curves involve the ratio C_2 (which gives a measure of voltage across the capacitor) actually this voltage is always low at the starting point in permanent split capacitor motors. Hence it is not as significant as the running voltage, which may limit the design. As the voltage at no load can be determined more readily through solution of the equivalent circuit, this voltage will be calculated. It is usually slightly higher than the full-load value. The relative change is shown in Appendix VI.

At no load, consider that the equivalent circuit can be reduced to the form shown in Figure 5. Solving for V_c, we obtain

$$V_c \cong \frac{V(1+jaK_r^2)}{1+j\omega C[R_{1s}+a^2(R_2+R_{1m})+j(X_s+a^2X)]} \tag{21}$$

$$\cong \frac{V(1+jaK_r^2)}{1+\frac{a^2X}{X_c}\left[-2+j\left(\frac{R_m}{X}+\frac{R_{1s}}{X_s}\right)\right]} \tag{22}$$

This equation is derived in Appendix IV.

Either form of this equation can be used as convenient. For the example given above

$$V_c = \frac{110(1+j3.21\times0.84^2)}{1+377\times8\times10^{-6}\times2.31^2\times5.92\times[-2+j(0.797+0.842)]} = \frac{110\times2.48}{0.707} \text{ or 385 volts}$$

The use of 5 microfarads, for the same starting torque resulted in a transformation ratio of 4.62. In this case

$$V_c = \frac{110(1+j4.62\times0.84^2)}{1+377\times5\times10^{-6}\times4.62^2\times5.92\times[-2+j(0.797+0.842)]} = \frac{110\times3.41}{0.652} \text{ or 574 volts}$$

It is obvious that if 330-volt capacitors are to be used, the use of an 8-microfarad rating is necessary to keep within the allowable overvoltage range; 5 microfarad would require a special capacitor.

Figure 4. Curve for determination of starting current in main winding

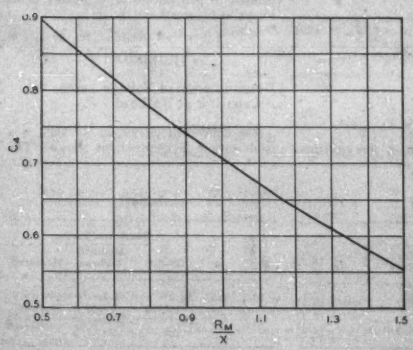

Conclusion

A method of design has been shown here whereby the maximum torque of a permanent split capacitor motor can be used to determine the main winding and the starting current.

The auxiliary winding can be determined from a predetermined value of starting torque, selecting the ratio of transformation and hence the number of conductors, on that basis. However, if starting torque is not critical it is possible to determine the ratio of transformation needed to give a good balanced operation with maximum efficiency.

For any combination of main and auxiliary windings it is possible to determine by methods shown here, the maximum torque, the starting torque and current, the voltage across the capacitor at no load, and the relative degree of torque pulsation and efficiency. All of these can be found without detailed solution of the equivalent circuit

Appendix I

Example of Main Winding Designs

A $^1/_4$-horsepower 8-pole 60-cycle motor of the permanent split capacitor type is to be designed for a maximum torque of 54 ounce-feet (3.37 pound-feet). The main winding is to be determined

The cage is tentatively selected and the stator winding distribution is assumed. Calculated ratios of constants which result from the lamination and core length are

$R_1/X = 0.344$
$R_2/X = 0.54$
$K_r = 0.84$

From equation 9 the fraction of synchronous speed at which maximum torque occur is

$$S = \sqrt{1-0.535} = 0.68$$

Where the slip at which the 2-phase motor maximum torque occurs

$$S = \frac{0.54}{\sqrt{(0.344)^2+1}} \cdot \frac{.5-0.84}{4} = 0.535$$

The winding must be designed for a 2-phase maximum torque as determined from equation 7.

$$T_{m2} = \frac{3.37 \text{ pound-feet}}{0.5\times0.68} = 9.9 \text{ pound-feet}$$

To yield this torque requires a main winding with a leakage reactance (equation 5).

$$X = \frac{7.05\times110^2\times0.84\times0.74}{900\times9.9} = 5.92 \text{ ohms}$$

Where

$$\beta = 0.344+\sqrt{0.344^2+1} \text{ or } 1.399$$

$$K = \frac{1}{1.399}+0.1(1-0.84^2) \text{ or } 0.74$$

The permeance of all leakage paths has been calculated as 2.93 and hence the series conductors of the main winding should be (equation 10)

$$C = \sqrt{\frac{5.92\times10^6}{377\times2.93}} \text{ or } 732$$

Calculated in the usual manner, the winding constants are then

$R_1 = 2.04$
$R_2 = 3.20$
$X = 5.92$
$X_s = 37.1$

This winding will produce a maximum torque of 54 ounce-feet when supplemented by any reasonable capacitor winding. (Test value was 54.0 ounce-feet).

Appendix II

Influence of I_s' on the Maximum Torque

Analytical and experimental data indicate that within practical ranges of design, the rotor current supplied by the auxiliary winding has little influence on the maximum torque. The point will be further illustrated by investigating the $^1/_6$-horsepower 8-pole motor used elsewhere in this paper as an example, and also through calculations on a $^1/_8$-horsepower 4-pole design.

Changing the capacitor but keeping the starting torque constant through ratio change modifies the equivalent circuit constants and naturally affects the running performance. For a constant starting torque of 10 ounce-feet the $^1/_6$-horsepower motor displays values as shown in Table I.

On a $^1/_8$-horsepower 4-pole motor a somewhat similar investigation is made and indicates a similar agreement.

Appendix III

Derivation of Curves for Starting Torque

The fundamental starting torque equation as used here is

$$T_s = 2aK_rR_sI_sI_M \sin\theta_{ms} \quad \text{(synchronous speed)} \tag{23}$$

The problem is to express this in terms of ratios of constants, eliminating the ratio of transformation a, or rather absorbing it in such a manner that it need not be known to use any of the other ratios.

After this equation is expanded into ratios, a suitable range of values can be assumed, the resulting terms calculated, and plotted as curves.

Let

$$C_1 = \sqrt{\frac{X_s}{X}}.$$

Then

$$X_c' = \frac{Xa^2}{C_1^2}$$

or

$$a = C_1\sqrt{\frac{X_c}{X}}$$

Where

X_s = the total leakage reactance of the auxiliary winding and rotor, in auxiliary winding terms

Figure 5

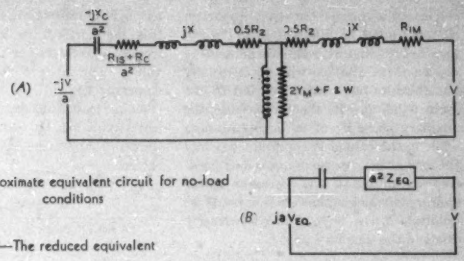

A—The approximate equivalent circuit for no-load conditions

B—The reduced equivalent

X_c = the reactance of the capacitor

Let

$$C_2 = \frac{V_c(\text{the voltage across the capacitor})}{V}$$

Then

$$I_s = \frac{C_2V}{X_c}$$

Let

$$C_4 = 225.4C_1C_2\frac{X}{Z_M}\sin\theta_{ms}$$

Where

Z_M = the total impedance of the main winding circuit

$$= \sqrt{(R_1+K_rR_2)^2+X^2}$$

Let

$$C_4 = \frac{X}{Z_M} = \frac{1}{\sqrt{1+\left(\frac{R_M}{X}\right)^2}}$$

The starting torque in ounce-feet is then

$$T_s = \frac{V^2K_rC_2}{\text{Synchronous speed}\sqrt{X_cX}}\frac{R_2}{X} \tag{24}$$

or

$$T_s = \frac{K_cC_4K_r}{\sqrt{X}}\frac{R_2}{X} \tag{25}$$

where

$$K_c = \frac{V^2}{\text{Synchronous speed}\sqrt{X_c}} \tag{26}$$

This is the final form of the equation.

But to prepare curve data in a straightforward manner, all of the C constants given here should be expressed as functions of angles which can be assumed as the independent variables. The method is:

Conversion of Constants

Define the angle θ_s as that by which the auxiliary winding current leads the applied voltage. Then

$$\tan\theta_s = \frac{X_c - X_s}{R_s}$$

or

$$C_1 = \frac{1}{\sqrt{1+\frac{R_s}{X_s}\tan\theta_s}} \tag{27}$$

Define the angle θ_2 as that between the voltage across the auxiliary winding and the auxiliary winding current Then

$$C_2 = \frac{\tan\theta_2 + \tan\theta_s}{\sec\theta_s} \tag{28}$$

$$= \left(1+\frac{R_s}{X_s}\tan\theta_s\right)\frac{\cos\theta_s}{R_s/X_s} \tag{29}$$

For any assumed value of R_m/X, the angle which the main winding current makes with the applied voltage is fixed Call this θ_m.

$$\theta_m + \theta_s = \theta_{ms}$$

For corresponding values of R_m/X and R_s/X_s, as assumed, C_2 and C_4 can be calculated to plot curves of C_4 versus C_1 as shown in Figures 2 and 3.

Appendix IV

Determination of Voltage Across the Capacitor at No Load

The equivalent circuit, at no load, is a modification of Figure 1, as shown The

Table I

Microfarads	C_2	C_1	a	Per Cent Max Torque	I_{os}
5	91.6	0.49	4.62	102.2	1.066/−18.2°
8	72.5	0.43	3.21	100	1.063/−12.2°
10	64.7	0.40	2.67	96.3	1.16 /−12.2°

Table II

Microfarads	a	Maximum Torque Circuit	Maximum Torque Modified 2-Phase	Maximum Torque Measured
16	1.83	38.2 = 100%	38.5 = 100%	38.2 = 100%
24	1.50	39.5 = 103.3%	38.5 = 100.7%	

value of R is so chosen as to absorb only the friction and windage loss. An approximation can be made, so that the circuit condenser conveniently to that shown in Figure 5A. Now the middle branch absorbs both magnetizing currents and the core, friction and windage losses. This circuit in turn is equivalent to that of Figure 5B.

Then

$$V_{eq}=\frac{V}{1+YZ_1} \tag{30}$$

$$Z_{eq}=Z_2+\frac{Z_1}{1+YZ_1} \tag{31}$$

$$i_c=\frac{jaV_{eq}+V}{Z_c+a^2Z_{eq}} \tag{32}$$

$$V_c=\frac{jaV_{eq}+V}{1+j\omega CZ_{eq}a^2} \tag{33}$$

As an approximation, it follows that

$$V_c=\frac{V(1+jaK_r^2)}{1+j\omega C[R_{1s}+a^2(R_{1M}+R_k)+j(X_s+a^2X)]} \tag{34}$$

Appendix V

Favorable Ratios of Constants

In reference one the following equation is derived as a condition for good efficiency and low pulsating torque under the lamination and capacitor size restrictions. The angle between I_s' and I_Y would be small for all speeds when this equation is satisfied.

$$ja[1+(Z_{1s}+Z_c)Y_s]=1+Z_{1M}Y_M \tag{35}$$

Usually

$$a^2Y_s=Y_m$$

and

$$\frac{X_{1s}}{a^2}=X_{1m}$$

Making these substitutions in equation 35, dividing by Y_m, letting $\frac{1}{Y_m}=R_{mm}+jX_{mm}$, and neglecting R_c, we obtain

$$ja\left[R_{mm}+\frac{R_{1s}}{a^2}+j(X_{1m}+X_{mm})-j\frac{X_c}{a^2}\right]=R_{mm}+R_{1m}+j(X_{1m}+X_{mm}) \tag{36}$$

Equating real and imaginary components we get

$$a\left(R_{mm}+\frac{R_{1s}}{a^2}\right)=X_{1m}+X_{mm}=X_o \tag{37}$$

and

$$\frac{X_c}{a^2}-X_o=(R_{mm}+R_{1m})\frac{1}{a}\cong\left(R_{mm}+\frac{R_{1s}}{a^2}\right)\frac{1}{a}=\frac{X_o}{a^2} \tag{38}$$

Equation 38 reduces to

$$\frac{X_c}{X_o}=a^2+1 \tag{39}$$

Equation 37 is not a critical condition, because any rotor load component current taken by the windings can be similarized by a conductance parallel to Y_m or Y_s and absorbed by it. That makes R_{mm} a dependent variable fixed by a rather than an independent variable fixing a. Equation 39 should be used to fix the turn ratio a. However, in absorbing the load component of current into Y_m or Y_s, the effective value of X_o is reduced to approximately $1/\left(1+\frac{R_m^2}{X_o^2}\right)$ of its normal value. Because its normal value rather than this reduced value is used in design calculations equation 39 should be replaced by

$$\frac{X_c}{X_o/\left[1+\left(\frac{R_{mm}}{X_o}\right)^2\right]}=a^2+1 \tag{40}$$

or

$$\frac{X_c}{X_o}=\frac{a^2+1}{1+\left(\frac{R_{mm}}{X_o}\right)^2}\cong a^2 \tag{41}$$

The condition expressed by equation 41 is desirable from the efficiency and constancy of torque viewpoint but is undesirable from the viewpoint of starting torque. An increased turn ratio usually results in higher starting torque.

The upper limit of a is fixed by $a^2=\frac{2X_c}{X_o}$.

Referring to the equivalent circuit, this condition means that the capacitive admittance neutralizes the magnetizing admittances of both the main and capacitor phases. Thus instead of being magnetized by the main phase, the capacitor phase magnetizes the main phase. The main phase current becomes the power component alone. In spite of increased power factor, this type of operation approaches plain single-phase operation so far as the efficiency and pulsating torque are concerned.

Appendix VI

Torque Pulsation, Efficiency and Transformation Ratio

The statement has been made throughout this paper that the change in capacitor, and ratio of transformation between auxiliary winding and main winding affect the pulsating torque, noise, and efficiency.

The approximate rule has been developed in Appendix V, that for workable results

$$1/2<\frac{X_c}{a^2X_o}<1$$

or in terms of the constant C_1 used for calculating starting torque

$$C_1\cong(1\text{ to }1.5)\sqrt{\frac{X}{X_o}}$$

It has been pointed out that when the lower value is used for C_1, the efficiency is high and the pulsating torque is a minimum. Actually this desirable condition results from the relationship of I_s' and I_Y, and it is obviously impossible for a fixed relationship to be maintained over the entire working range of speed, because I_Y varies so much more widely with the load than does I_s'.

This entire field remains to be illustrated by numerical work. The 1/4-horsepower 8-pole motor will be used, and the circuit calculated for 4-per cent slip. Designs utilizing five, eight, and ten microfarads will be shown. As an aid to the reader in further investigation, detailed tabulation of significant quantities will be given.

Results shown in Table IV require comment. At a speed of $S=0.96$, the most favorable ratio of X_c/a^2X_o results in a minimum pulsating torque of 129 synchronous watts. This can be zero at some other speed. The unfavorable ratio resulting from five microfarads gives a pulsating torque of 406 synchronous watts, or 3.15 times as high. For the eight microfarads actually used in the design, the pulsation is not zero but is comparatively low.

Statements made concerning efficiency are effectively illustrated. The unfavorable ratio of constants resulted in a motor with only 49.0 per cent efficiency as against 60.5 for the ten microfarads case and 57.1 for the compromise design.

It is interesting to note also that the voltages across the capacitor reduce from the approximate no-load values. That is, at no load the voltage across the 5-microfarad capacitor was 574 volts, versus 500 at $S=0.96$. Similarly the 8-microfarad capacitor calculated 385 at no load and 320 at $S=0.96$. This is of some importance in keeping below maximum safe values on motors such as fan-duty types, in which no-load operation can not occur.

Table III. Torque Comparisons Fixed Main Winding and Rotor Winding

Item	Max. Torque Calculated $I_s'=0$	Max. Torque Tested Capacitor Motor	Max. Torque Plain Single Phase	Max. Torque 2-Phase*	% Max. Torque 2-Phase / Capacitor	% Max. Torque Single Phase / Capacitor
1	6.83	6.50	2.66	17.6	271	243
2	2.16	2.05	1.10	5.6	272	186
3	9.50	9.80	5.65	24.9	255	174
4	21.00	20.00	15.6	52.0	260	128
5	72.00	71.00	44.2	186.0	262	172
6	53.80	54.20	43.1	132.4	245	126
7	38.50	38.20	30.2	95.6	250	127

* Using two windings identical to the main winding, or a capacitor winding designed for perfect balance at the maximum torque point.

Table IV

Rating—1/4 Horsepower, 8 Poles, 110 Volts, 60 Cycles

Item	$R_1=2.04$ $R_2=3.20$ $X=5.92$	$K_T=0.84$ $X_2=37.1$ $R_{1a}/X_1=0.842$	$R_{2a}/X_2=0.42$ $R_2/X_1=120$
a	2.67	3.21	4.62
Mld	10	8	5
Y_m	$0.294/-86.1°$		
Z_1'	$3.45/59.3°$	$3.45/59.3°$	$3.45/59.3°$
Z_{TM}	$3.57/56.0°$		
Z_{TM}	$4.10+j6.08$		
Y_{TM}	$0.136/-56°$		
I_{om}	$14.95/-56°$	$14.95/-56°$	$14.95/-56°$
Z_{a}'	$34.9/-79.9°$	$31.8/-79.2°$	$22.7/-75.4°$
Y_{TS}	$0.0282/78.8°$	$0.0311/77.8°$	$0.0448/71.8°$
I_{os}	$1.16/-11.2°$	$1.063/-12.2°$	$1.066/-18.2°$
Speed	0.96	0.96	0.96
I	$2.39/-3.4°$	$2.38/-4.5°$	$2.47/-9.1°$
I_x'	$0.50-j0.08$	$0.31-j0.27$	$-0.54-j1.33$
I_y	$1.88-j0.06$	$2.06+j0.08$	$2.97+j0.94$
E	$93.8/-3.4°$	$93.3/-4.5°$	$97.0/-9.1°$
EI	224 watts	222 watts	240 watts
$1.1R_2I_x'^2$	3.3 watts	2.2 watts	−10 watts
Friction	7 watts	7 watts	7 watts
Output	211 watts	208 watts	214 watts
I_x	$1.07+j0.212$	$0.95+j.09$	$0.924-j0.194$
I_m	$2.1-j3.0$	$2.36-j2.94$	$3.05-j2.0$
I_{line}	$4.22/-41.3°$	$4.36/-40.7°$	$4.53/-29°$
Input	349 watts	364 watts	437 watts
Eff	60.5%	57.1%	49.0%
Z_p	129 syn. watts	167 syn. watts	406 syn. watts
V_c	290	320	600
Xo			
a^2X_s	1.000	0.865	0.670

See reference one for complete explanation of these symbols.

Appendix VII. Nomenclature

V = applied volts

V_c = the voltage across the capacitor

E = the back electromotive force across R

I_M = the stator current, main axis

I_s = the stator current, auxiliary axis

I_y = the stator component of the main axis rotor current

I_x' = the rotor current of the cross axis in main winding terms, with 90 degrees backward phase shift

I_T = the total motor current at starting

I_{om} = the short-circuit current at R from the main phase

I_{os} = the short-circuit current at R from the auxiliary phase

I = the current through the load resistance R

T_m = the maximum torque of the permanent split capacitor motor

T_{m2} = the maximum torque of the 2-phase motor

T_s = the starting torque

T_p = the pulsating torque

R_1 = the stator winding resistance

R_{1a} = the stator winding resistance, auxiliary phase

R_c = the resistance of the capacitor

R_2 = the rotor resistance in main winding terms

R_{2a} = the rotor resistance in auxiliary winding terms

X = the total leakage reactance main winding terms

X_s = the total leakage reactance auxiliary winding terms

X_{mm} = the magnetizing reactance of the main winding circuit

X_o = the sum of magnetizing and leakage reactances

X_c = the reactance of the capacitor

a = the ratio of transformation, auxiliary to main windings

C = the series conductors of the main winding

C_s = the series conductors of the auxiliary winding

K_{wm} = the winding factor, main

K_{ws} = the winding factor, auxiliary

S = actual speed/synchronous speed

s = the slip as a decimal fraction

Y_m = magnetizing admittance of main winding

Y_s = magnetizing admittance of the auxiliary winding

References

1. The Equivalent Circuit of the Capacitor Motor, Sheldon S. L. Chang. AIEE Transactions, volume 66, 1947, pages 631–40.

2. Some Aspects of Electric-Motor Design—Polyphase-Induction-Motor Design to Meet Fixed Specifications. T. C. Lloyd. AIEE Transactions, volume 63, 1944, January section, pages 14–20.

Discussion

P. H. Trickey (Diehl Manufacturing Company, Somerville, N. J.): In our experience with capacitor motors, we have found that we can change the shape of the speed–torque curve, particularly regarding the speed at maximum torque, by varying the capacitor, from a shape very much like that of a single-phase motor when small capacity is used, to a shape more nearly like that of a polyphase motor when large values are used. Many unit heater 3-speed motors have high values of rotor resistance and many control motors have resistances even higher. The 2-phase slip at maximum torque may be as high as 1.5. I would like to ask the authors three questions:

1. Does the method of this paper apply only to capacitor motors with low rotor resistances and low values of capacitance, such as single-speed motors, or will it apply to control motors balanced near stand-still?

2. How should equation 9 of the paper, $S=\sqrt{1-s}$, be interpreted or used when s is greater than 1.0?

3. Does this paper give a means of obtaining quickly the no-load watts and amperes?

Sheldon S. L. Chang: The scope of application of the design paper is limited by the assumptions made in deriving equation 42 of the paper. Quoting reference 1 of the companion paper,[1]

"The capacitor phase supplies the cross-field magnetizing current, and the portion of energy that overcomes friction and windage losses as well as iron losses, while the main phase alone supplies the power that converts into a measurable torque."

"It is further assumed that the maximum torque occurs at the speed of maximum rotor input."

Quoting the design paper,

"However, because I_x' is nearly independent of speed, while I_y varies five to twenty times in magnitude, the approximate realization of this balanced condition at the full-load point would mean that I_x' is relatively unimportant at the pull-out point."

From the foregoing, it is clear that the design method is subjected to two limitations:

1. The motor is designed with a view of good efficiency and is balanced at the full-load point and thereabouts.

2. The rotor resistance is not too high, so that the point of maximum rotor input is not far away from the point of maximum torque. This point will be better defined in the following discussion.

It should be emphasized that the condition of balance at the full-load point or thereabouts as defined in this paper with the angle of I_x' and I_y in view imposes no limitation on the capacitor size if the starting torque is not fixed. A small capacitor with more turns or a large capacitor with fewer turns, as governed by equation 17, gives good performance at no-load and full-load points, with the starting torque varying as the square root of the capacity, approximately.

P. H. Trickey's statement about the effect of the capacitance on the shape of speed–torque curve of a motor with fixed windings, particularly regarding the speed at the maximum torque, is true and clear. But from a practical point of view, when a small capacitor is used so that the shape of the speed–torque curve is very much like that of a plain single-phase motor, would not a proper increase in the number of

turns of the starting winding increase both the starting torque and full-load efficiency? When a large capacitor is used, so that the shape of the speed–torque curve is very much like that of a polyphase motor, would the watts and vibration at no load and full load be acceptable without a proper decrease in the number of turns of the starting winding? The authors wonder how many motors are on the market which belong to the extreme.

A capacitor motor with too few turns in the starting winding is of little or no use. The capacitor-start induction-run motors have too many turns if judged from the same point of view as for the permanent capacitor motors. As the point of view is different, this class of motors is not discussed here.

The approximations made in this paper are in view of obtaining a simplified and usable maximum torque expression. Although each approximation may not be correct in itself, their errors usually oppose each other. For instance, the speed of the maximum torque as given by equation 9 of the paper is lower than the actual speed. But the maximum rotor input is always higher than the rotor input at the maximum torque point. The net effect is that the expression of the maximum torque holds for a larger range than the expressions for speed and rotor input at the maximum torque point.

In our experience, for the motors with 2-phase slip at maximum torque less than 0.5, the approximation is reliable. With this value in between 0.5 and 0.7, the result is fair. With this value larger than 0.7, the approximation no longer holds. The limitation on the 2-phase slip at maximum torque in turn fixed the limitation on the rotor resistances.

However, the only class of motors which call for a high rotor resistance and an earlier balance are the torque motors which are used in such a fashion that the time of acceleration and the time of running are comparable, and to which the control motors Trickey mentioned belong. As in the case of the multispeed motors for the unit heater or other fan and ventilating duties, it sometimes has been the practice to use low resistance rotors to obtain high efficiency at the high-speed operation. The other speeds are obtained by weakening the main winding by either introducing an extra inductance or by using series and parallel connections. Only the high speed is higher than the speed of maximum torque while the other speeds are lower than the speed of maximum torque. Because the torque required to run a fan varies as the square of the speed, the operating points at the low speeds are stable enough.

The advantage of this fashion of speed control lies in the fact that its high-speed efficiency is high, and it is the high-speed efficiency which determines the maximum temperature rise. In designing a motor for continuous running at substantially constant loading for a given maximum temperature rise, it is not the horsepower rating but the total loss which determines the amount of material required to build such a motor. For instance a motor of 70-per cent efficiency requires about $6/7 \times 3/4 = 64$ per cent of the material of a motor of 60-per cent efficiency of the same horsepower to give the same dissipation per unit weight. If a high rotor resistance is used to lower the speed of maximum torque to a point lower than the low speed, the high speed efficiency would be reduced seriously. Far more material would be required to prevent overheating at high speed as compared with the former method. The latter method gives better efficiency at lower speeds, but the loss at low speeds are low anyway.

Whereas the torque motors are not treated in this paper, their design can be facilitated by the analysis introduced in the companion paper.[1] The problem of designing a torque motor is to accelerate a given inertia from rest (or full speed in the opposite direction) to full speed within given duration of time with as little total loss as possible. For a polyphase motor, in which the rotor input is equal to the torque in synchronous watts, the rotor loss during the accelerating period is approximately equal to the energy stored in the moving mass. For a single-phase motor the difference between the rotor input and synchronous watts is $\frac{r_2^2}{1+S}\,|I_x'-I_y|^2$, and this loss is added to the rotor. The problem would become

1. To allocate more loss to the rotor as compared with that to the stator, and
2. To minimize the value $|I_x'-I_y|$ at various speeds.

The variation of speed of maximum torque with capacitor size can be explained by the companion paper.[1] The maximum torque occurs at the speed where R is equal to Y_o. As Y_{os} varies with the capacitor size, so does the speed. But in this connection, the neglecting of the variation of the term, $\frac{2r_2}{1+S} I_x I'_y \cos(I_y I_x')$ introduces also more error in the speed location than in the value of maximum torque.

This paper does not give a means of obtaining quickly the no-load watts and amperes. However if the motor satisfies the condition represented by equation 17 of the paper, and at full-load point the current densities in the main and auxiliary windings are nearly equal, the motor would give no-load watts somewhere in between that of the same motor operated as a plain single-phase motor and that of the 2-phase motor depending on the value of the significant ratio introduced in equation 17 of the paper. The no-load amperes in the main winding would be lower than that of a plain single-phase motor. The no-load amperes in the starting winding is given by equation 34 of the paper.

In the companion paper,[1] a method can be evolved to calculate the exact no-load watts and amperes of any capacitor motor, no matter whether equation 17 of the paper is satisfied or not. It is given in the following. At no-load point

$$T = RI^2 + \frac{2r_2}{1+S} I_x' I_y \cos(I_x', I_y) - F \text{ and } W = 0$$

$$I_y \cong -I_x' \cong \frac{E_{om} - E_{os}}{Z_{om} + Z_{os}} = \frac{\frac{I_{om}}{Y_{om}} - \frac{I_{os}}{Y_{os}}}{\frac{1}{Y_{om}} + \frac{1}{Y_{os}}} = \frac{I_{om} Y_{os} - I_{os} Y_{om}}{Y_o}$$

$$RI \cong V\left(\frac{X_{mm}}{X_o}\right)$$

$$S \cong 1$$

After I_y and $-I_x'$ are calculated in the above equation, R can be determined by

$$R = \frac{V^2\left(\frac{X_{mm}}{X_o}\right)^2}{I_y^2 r_2 + F \text{ and } W}$$

After R at the no-load point is obtained, the no-load performance can be calculated just as other load points are calculated.

Reference

1. The Equivalent Circuit of the Capacitor Motor, Sheldon S. L. Chang. AIEE Transactions, volume 66, 1947, pages 631-40.

Power Distribution in Textile Plants

J. D. McCONNELL
ASSOCIATE AIEE

THE RECORD of change and growth in the textile industry, particularly in the South, is tied closely to the history of availability and application of electric power. The first cotton mills were located on water power sites by reason of having to be within mechanical transmission distance of the power source. The high atmospheric humidity of such locations was known to be needed for the proper processing of cotton and was also a factor. The development of the steam engine was the first step made in moving the mills away from streams, though before the advent of mechanical air conditioning efforts were made to locate mills in geographical areas of high humidity. The first mechanical air conditioning came just after the advent of a reasonably economical steam engine and the industrial migration away from the streams started. In the early days in the South, availability of labor in locations immediately adjacent to the proposed mill was not too much of a factor as it was standard practice to build villages at the mills for the help to live in because towns were small and widely separated as in any essentially rural economy.

As high voltage transmission of power became practical and economical and its availability increased in the South, textile plants began to be built with the availability of labor considered as more of a factor. The advantage of nearness to raw material supply is obvious.

Lighting

The first major application of electricity in textile plants was for lighting. Oil lamps and gas lamps were the first lighting means used; but these offered obvious hazards from fire in an industry that works a material that catches fire at a low temperature and burns, when loose and fluffed, at a very high rate. Rather early applications of the enclosed arc lamps therefore were made and this lamp was used widely until about 1912, the last arc lamps in a southern cotton mill being removed in this year.

Incandescent lamps then were applied and a great deal of trouble was had in getting satisfactory life from the early ones with their brittle filaments. As the history of change in industries shows that much progress is made because of pressure for development from the final user, it is only fair to assume that the textile industry helped to apply the pressure for development that resulted in the ductile tungsten filament for incandescent lamps. It also appears reasonable to assume that there was pressure for development in this field from the groups carrying insurance on mills because fire in the early plants was much more of a hazard than it is today, though it still is a considerable risk compared to other important industries.

The textile industry has been quick to adopt the latest lighting developments, and is today one of the important users of the fluorescent lamps as the seeing tasks in many departments of textile mills are quite severe. The severity of these seeing tasks has caused intensities of illumination to climb steadily, a recent modern mill specification calling for an intensity of 40-foot candles in a fine-goods weave room with the fixtures calculated on a basis of 65 and 70 per cent for dirt, utilization, and aging.

Electric Drives

The first completely electrically driven cotton mill of record was put into operation in Columbia, S. C., April 15, 1894. The motor installation in this plant comprised 17 65-horsepower 550-volt 3-phase 36-cycle motors with a no-load speed of 535 rpm. These motors were fed by two 550-kw water-wheel-driven generators. The motors were of internal resistance construction, operated line shaft groups by either counterbelts or direct connection to the line shaft and ran until 1927. Some of the engineering decisions made in favor of electric drive are quoted in the following paragraph from the memoirs of one of the men associated on the project.

> Theoretically the manufacturing buildings should be located between the canal and the river, but in this case such an arrangement was impracticable, as the only space for this purpose was inadequate. Moreover, the Congaree River was subject to severe freshets. There was, however, an ideal mill site on an elevation about 700 feet from the canal, which would avoid all danger of freshets and which would permit the location of the mill adjacent to the railroad. In order to use the canal for power purposes it would be necessary, however, to locate the wheel pits beneath the mill and carry the penstocks from the canal to the mill and build a tailrace from the mill under the canal to the river. As an alternative a wheelhouse might be erected between the canal and the river, and the power transmitted to the mill by rope drive. Another alternative was to drive the mill by steam power. Either alternative would involve a large expenditure, and the use of a steam plant would have resulted in the abandonment of the canal and the water rights.

After presentation of the motor drive idea to the designing engineer, and his recommendation of it, the treasurer of the mill asked where he could inspect such an installation. He was told that no such installation had ever been made, and after only a moments conversation with the engineer decided to risk the operation of this mill on a theory.

Distribution Systems—Voltages and Frequencies

It is interesting to note that these motors were designed for 550 volts, still the standard voltage used in the textile

Paper 47-103, recommended by the AIEE committee on industrial power applications for presentation at the AIEE winter meeting, New York, N. Y., January 27–31, 1947. Manuscript submitted November 18, 1946; made available for printing December 30, 1946.

J. D. McConnell is with Proximity Manufacturing Company, Greensboro, N. C.

industry, and apparently based on some engineering decision made in the very early days. Alternating current also was chosen, and this decision was taken when the a-c-d-c question was productive of violent argument. Between this early choice of voltage and today's present standardization to all practical purposes on 550-volt 3-phase 60-cycle current is a record of trying many voltages, frequencies, and phase arrangements. All of the following types of current have been operated in southern textile mills between these two times—on voltages 1,040; 2,080; 2,200; 550; and 220 volts. As to frequencies, 25, 40, 50, $66^2/_3$, and 60 cycles have been used. Two-phase current, mostly 4-wire and some 3-wire, has been used though 3-phase 3-wire current long has been popular and is now almost standard. The early choices of frequencies were guided in great measures by lamp flicker.

Textile Machinery Requirements

The present design of textile machinery and its associated electrical equipment was in large part evolved through pressure for change from the following factors:

1. Increased production.
2. Reliability.
3. Safety from fire.
4. Ease of installation and maintenance.

The pressure for increased production per hour of operation or per unit of mill area took the form of increasing the operating speed of the machinery and increasing the package size of the product made. These two factors operated in different proportions in the various departments of the mill, increase of operating speed being greater than increase of package size in the weave room and the situation being reversed in the spinning room. In the roving, drawing, carding, and picking departments the changes have been minor in package size, the speeds have increased some, and the most marked tendency has been to cut out as many processes as possible in the path from bale of cotton to finished product.

The development of the high speed loom and the general increases of loom speeds in the late 1920's to middle 1930's changed many weave rooms from belt to individual motor drive, as belt drive has not proved generally satisfactory for speeds above the range of 160 to 170 picks per minute.

In the spinning room, ring sizes and spindle speeds were increased in step until we have reached a temporary maximum today of about 8,000 rpm of the spindle in a ring about 3 inches in diameter, with a yarn weight on the bobbin of nearly half a pound on number 10 (coarse) yarn. A spinning frame must be stopped to remove the full bobbins and replace them with "empties" and most efforts have been aimed at making this stopping time as productive as possible in pounds of yarn yielded by running the frame a long time between doffs.

Both of these trends increase the amount of power per unit of area in the mill and have been factors in increasing the amount of power needed in the textile country. Replacing the textile machinery of 25 years ago with the machinery of today would increase the demand for power almost 20 per cent in any given spinning and weaving plant.

From the standpoint of reliability, pressure from the textile industry was probably not much greater than from other industries, except for the development of small control equipment, sleeve bearings from which oil would not siphon out, and for small motors that would stand shock loadings. The reliability of cables in standard insulations when properly installed has been satisfactory. The mechanical reliability of motors used on individual drives with short centers and rather high belt tensions has been increased markedly by the increasing use of ball bearings for such motors.

Continuous Power Supply

The matter of a constant power supply is dealt with differently in mills that generate all or a part of their power and those that buy from a public utility. In those that generate, a schedule of dropping load either manually or by relays usually is set up, and in mills that purchase power the installation of time-delay undervoltage devices is very common, particularly because automatic reclosing breakers have become common on utility systems. These devices enable the production machinery to coast over a failure of short duration, and some comments on the action of various machines under power failure conditions will explain their worth.

A power failure in the opening and picking departments is not too severe in its effect on the stock or the machines, because these rooms usually can be restarted without the machinery choking up or making an uneven product. This situation does not apply in the card rooms, where machine speed must be held even, where group drive is very nearly standard practice, and where starting duty is quite severe because of the fly-wheel-type load of the carding engine. A power failure in a card room calls for all the belts to be pried manually onto the loose pulley of each card before the shafting can be started and the cards put back to running.

Somewhat the same line of reasoning applies on the fly or roving frames used in the next process, though these machines are started more easily than a card.

Spinning frames usually can be stopped without too much damage to the stock in process, restarting the room requiring only that the operator go to each machine and start it.

Stopping looms properly requires skill and timing on the part of the operator, and if a power failure occurs there is a fair prospect of having looms stopped in such position that the operator manually must put each machine in proper position for starting and then set it going, thus costing seriously in production.

In those parts of the plant either dyeing or processing goods across heated cylinders, there is prospect of ruining the goods by too long exposure to heated cylinders or having goods in a dye bath so long that the shade becomes uneven.

Also in connection with reliability, the trend on the protective elements of motor control has swung very strongly to thermal overload equipment designed to heat in step with the motor load and to trip at motor heating safe limit. As much textile machinery is quite long, is set on floors subject to settling, and has many bearings on long shafts, overloads can creep up on motors by reason of slow changes in building alignment. Also, it is much easier to match protective equipment to starting conditions with this type of overload device and lint collections do not jam it easily.

Fires From Electrical Causes

The question of safety from fires which started from electrical equipment entered in the change of feeder design from open wiring to the present universally used conduit wiring. It also has had its effect on questions of motor control and protective equipment design because the lint that flies from the cotton being processed will get into control equipment, and if kindled by an arc will add its share of ionized gas to that contained in the control cabinet and help push the equipment to a condition that could mean a flashover with attendant projection of hot gas from the control case. This question also has contributed largely to changes in motor design so motors will not offer places where lint can collect and either become mechanically jammed between moving surfaces that through rubbing

will raise its temperature to the kindling point or be exposed to sparks from brush arrangements that would set it afire.

Also to be considered from the fire standpoint is the question of what happens to electrical apparatus when thoroughly doused by sprinkler heads opened by a fire, or by fire buckets and extinguishers. This was probably one of the things that led to the early adoption of completely enclosed control equipment in the cotton mills.

On the factors of ease of installation and maintenence, it is interesting to note that the present combination line starter with magnetic switch and short-circuit protective equipment installed in the same case is a development coming from the textile industry. This construction offers a number of advantages in ease of mounting and wiring and in ease of replacements of parts. Because textile mills are by nature units containing many similar machines this development has proved to be logical, and has been accepted rather widely in other industries.

Feeder Design

The feeders employed in cotton mills followed, in general, the design of the shafting they in effect replaced. The feeders in the early mills were of radial design, often quite large, and grew longer as the mills grew. Because transformer banks furnished by the public utilities were quite large many of the 600-volt feeders were installed in sizes from 500,000 to 1,000,000 circular mils with an eye to putting up as much copper as possible for a labor dollar spent. The first wiring was open on porcelain cleats tied to the building structure with lag screws and had slow-burning insulation. The problems of carrying many such feeders through parts of the mills where fires occurred rather often, and in carrying these feeders from floor to floor of multistory mills, often caused installations that were none too safe from the standpoint of fire or mechanical damage. Conduit construction then became standard as it is today.

One problem that exists in certain parts of the cotton mill that does not appear to be common to any other industry is one of floor and structure vibration. The loom throws an oscillating load on the floor supporting it which is transmitted not only to the main span elements of the structure but also to the walls and through the walls to the roof. This vibration is at a frequency, in general, in time with the oscillation of the loom lay, or shuttle guide, and increases and decreases in intensity as the looms in a given area swing into and out of synchronism. It is quite common to see weave rooms with an easily detectable motion by either eye or feel, and in severe cases the wiring in the conduit can be bounced around enough to cause abrasion on the conductor jackets. This often leads to grounds on the system where wiring comes through conduit bushings or similar fittings. Also in connection with feeder design is the problem of sealing the wiring from entrance of water if the wiring is run on the ceiling of a room to feed motors on the floor above and a fire on the top floor floods the floor from open sprinklers.

As mills grew the radial feeders became longer and longer, and 600-volt feeders over 1,100 feet long and in sizes up to 1,000,000 circular mils are in operation today. It is interesting to note that the present economic length of 600-volt feeders has been calculated as 700 feet.

Capacitors have been used on long feeders not only for the power factor correction commonly associated with their application, but for voltage control.

Switchgear Interrupting Capacity

Handling feeder power in such large blocks as indicated, particularly when a plant is fed by a large transformer bank has put many textile mills in the position of not having enough interrupting capacity in their switchgear to handle the short-circuit currents that can obtain if trouble comes on one of these large feeders.

For many years trouble did not occur with such installations in small mills because the public utilities supplying the power were operating rather long radial feeders whose characteristics served to limit short-circuit currents to the capacity of existing protective equipment. This condition has been changed in recent years by stiffening the high-voltage backbone of the public utility systems, and the ratio of protective equipment interrupting capacity to short-circuit amperes available has changed markedly.

This change, and the recognition of its consequences, has led the cotton mills to start installation of unit substations fed from a mill-owned 13-kv or 2,200-volt circuit, the feeders being equipped with modern air circuit breaker equipment, usually of draw-out design. This breaker by its speed of action has served to limit the severity and consequent damage of short circuits by decreasing the total amount of power fed into an arc over its duration time, the severity of a failure as a cause of fire apparently being tied rather closely to the total amount of power liberated in an arc and also to its attendant projection of hot gas out of an enclosure.

Control Design and Duty

It is interesting to note the changes in control design that have occurred in the cotton mills, the first application of individual-drive control equipment being a direct operated shipper-rod oil switch which was applied about 1923. This application of a direct operated switch was primarily a price consideration as the smallest contactor available at that time was 75-ampere rating and cost $35.00. The progression from this direct operated switch was to the combination starter and a shipper-rod switch carrying control current only. This type of switch commonly is applied on spinning frames, twisters, and roving frames.

From the standpoint of control duty, some of the cotton mill applications, particularly on spinning frames, are quite severe. In the operation of setting up the spinning frames for removing the full bobbins, an operation called doffing, the motor is started repeatedly while the ring rail carrying the spinning rings is worked down to low elevation. This calls for the magnetic switch to take about a dozen shots of locked-rotor current, or very nearly this current, within a minute. This is a duty that older magnetic control and direct operated control often failed on but the modern contactors handle very satisfactorily.

Fly Lint

Many of the problems concerning the operation of electric equipment in a cotton mill arise by the nature of the cotton fiber that allows us to make yarn and cloth of it. A cotton fiber is a somewhat flattened cylinder in section, quite kinky, and resembles a dried pea hull more than anything else. Both the roughness of the fiber surface and its kinkiness make individual fibers cling one to the other.

This property makes cotton fibers felt or form a mat that will increase in thickness if additional fibers float by and touch the surface of the mat. This mat is quite a good heat insulator, and the felting action complicates the operation of any air cooled apparatus in a cotton mill, particularly any depending on rather small ventilating ducts and low velocity air currents. One of its few advantages is that it can be made into a self-building filter layer.

Atmosphere Control

Power distribution in a cotton mill has a most interesting sequel in the question of atmosphere control from the standpoint of temperature and humidity. A very small percentage of the power going into a cotton mill goes into actual work done in stretching the cotton or in sliding the fibers one across the other to draft a strand of cotton into a finer yarn. The major part of the power goes to mechanical friction in the bearings of the machines and into whipping the air surrounding a strand of rapidly moving yarn. Almost all the power going into a given area of the mill therefore appears as mechanical heat in this room because the stock does not take any appreciable heat out of the room in moving to the next process. To keep the individual fibers contained in a strand of yarn it is necessary that the static generated by slipping one fiber over another be kept at a minimum and this is handled by keeping the humidities in the rooms rather high, the humidities in the various departments of the mill running from 60 to 80 per cent relative. To maintain this humidity requires spraying water into the air by one means or another and the latent heat demand of transferring this sprayed water from the liquid into the vapor phase sops up a portion of the heat liberated. If adequate ventilation is maintained through the room and the proper amount of water sprayed, it is therefore possible to chill the air in the room by evaporative cooling to a temperature of some 16 degrees above outside wet bulb temperature. With an outside average wet bulb in the summer months of 72 degrees Fahrenheit, as exists in the Piedmont region of North Carolina, this gives an average temperature in the room of 88 degrees Fahrenheit. Some of the synthetic fibers that now are being run either alone or in combination with cotton do not run well at such temperatures, requiring a maintained temperature of approximately 80 degrees in the room under operating conditions. Maintaining these conditions calls for mechanical refrigeration and it is worthy of note in this connection that the design of a mill now under construction calls for roughly 1,000 kw of motor load on the processing machinery and a 400-horsepower motor load from the air conditioning compressor only. This is a development that reasonably can be expected to progress as more information is obtained on economies of operation effected by better temperature control, as employee comfort and efficiency becomes more of a factor, and will bring into the mills motors and control larger in size than have been used for manufacturing purposes previously.

Conclusion

It appears safe to state that the trend in power usage in the cotton textile mills is upward both from the standpoint of killowatts per square foot of mill area and per employee. This trend will increase in rate of change as various mechanical limitations to higher speed in the textile machinery are removed by future developments. The speed, for instance, on spinning frames now is limited by the traveler-and-ring assembly used in spinning and the yarn tension that can be carried. The speed of looms at present is limited by braking methods on the shuttle and to some extent by the weight of the reciprocating parts of the loom. In other machinery speeds are limited not only by the tensions that the strand of fibers can carry, but also by questions of bearing and gear design in the details of the unit.

Coupled with these possibilities should be considered the fact that the cotton industry is not static in its pressure for development, and that other branches of the textile industry are just as aware that there is constant change in the competitive situation and customer demands. It is also well to note that this industry, which for many years had few technical men working in it, now recognizes the importance of the engineering and research approach to its problems.

The industry has built few new plants in recent years and for a very long time will be restricted by having to use existing buildings, some of them 75 years old. Some new plants now are being built in a windowless completely-air-conditioned design with the machinery functionally arranged with ease of transport of stock in process as a prime consideration. The full impact of recent developments probably will not be felt for three to five years, but the industry is conversant with such things as infrared and radio frequency heating, control of static electricity by high-voltage and radioactive ionization, stroboscopic observation and photography, the application of vacuum tube devices for measurement and control of temperature, moisture content, machine speed, and color values. Many more could be mentioned, concerned with what are rather narrow details of the industry's operation, but from the mass of these small changes will come the next great advances.

No Discussion

Voltage Changes Caused by Resistance Welding Loads

I. B. JOHNSON
MEMBER AIEE

H. A. PETERSON
MEMBER AIEE

C. M. RHOADES, JR.
ASSOCIATE AIEE

A CONSIDERABLE NUMBER of utility and industrial power engineers have raised questions regarding the effect of resistance welding machine loads in producing voltage changes in the system supplying power to the welders. This paper will present data, largely in the form of curves, relating to the effects of the following types of welding loads:

1. Single-phase electronically controlled welders operated from 3-phase systems through delta-delta and Y-delta step-down transformer connections.

2. Electronically controlled resistance welders equipped with series capacitors for reduction of kilovolt-ampere demand and improvement of power factor.

3. Leading-power-factor loads obtained by the use of series capacitors for overcompensation of welder reactance.

4. Three-phase electronic frequency converters. *Such converters rectify 3-phase a-c power to single-phase low-frequency power thereby reducing the amount of reactive kilovolt-amperes required to circulate welding current through the inductive secondary circuit.

Resistance Welding

Resistance welding is a process of welding under pressure with the heat for the weld produced by the flow of current through the resistance of the metal parts being joined and the resistance at their area of contact. No metal is added to the weld so that the weld nugget is the same as the parent metal. A resistance weld is made in a fraction of a second. The majority of welding machines in use today are single-phase spot and seam welders, operated directly from industrial 3-phase or single-phase power systems, which in turn usually are fed from 3-phase utility distribution lines.

As a result of the speed of this process and the short heat time—such as approximately one-half second for a spot weld in one-eighth-inch sheet steel—accurate control of the timing and the amount of current is an absolute necessity if welds of uniform strength are to be obtained. Electronic contactors and timers make possible this accurate control.

An ignitron contactor for current control of a single-phase welder, as shown in Figure 1, is used to control the flow of current to the welder while auxiliary electronic controls are used to initiate and time the duration of this current. Ignitron contactors consist of two sealed ignitrons connected in parallel, with the anode of one connected to the cathode of the other, so when each has passed a half wave of current of the correct polarity a complete cycle of current has been applied to the welder.

The amount of current passed by an ignitron contactor can be reduced by retarding the starting point of current during each half cycle, beyond the point of current zero at the natural power factor angle. This is effected by means of electronic controls connected in the ignitor circuits of the ignitrons. Controls used for this purpose are called phase-shift heat controls. Such control often is used for fine variations of the current of spot welders after coarse adjustment has been made by means of taps on the primary of the welder transformer, although full reduction of current can be obtained by phase-shift control alone. Seam welders normally are furnished without primary taps so that all control of current is obtained by phase shift.

When phase-shift control is used, the wave form of current is not sinusoidal, as will be evident from inspection of current traces in Figure 2, showing discontinuity of current during each half cycle of time. A logical question arises as to what is the effect of such current in producing voltage drop which might influence lights, other resistance welders, or other electric equipment.

Figure 1. Ignitron contactor with electronic heat control

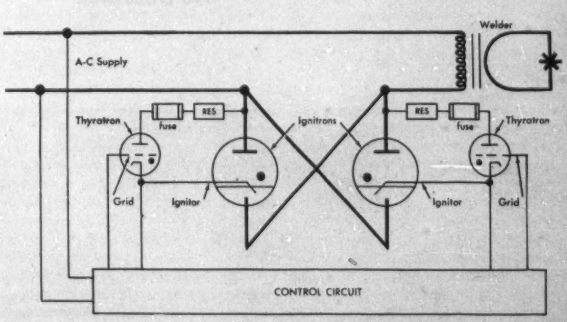

Paper 47-61, recommended by the AIEE committee on electric welding for presentation at the AIEE winter meeting, New York, N. Y., January 27-31, 1947. Manuscript submitted November 13, 1946; made available for printing December 4, 1946.

I. B. JOHNSON and H. A. PETERSON are both in central station engineering divisions and C. M. RHOADES, JR. in industrial engineering divisions of General Electric Company, Schenectady, N. Y.

The authors wish to acknowledge the assistance of J. Wilson of central station engineering divisions in observing transient analyzer results.

Voltage Change Caused by Single-Phase Sine-Wave Current

As a basis of reference for voltage changes caused by the nonsinusoidal current produced by phase control, those changes caused by sine-wave single-phase currents flowing in a 3-phase system are shown in Figure 3. It is to be noted that a single-phase load produces voltage changes in all three line-to-line voltages of a 3-phase system. The nature of the change will depend upon the magnitude and power factor of the single-phase current, as well as upon the magnitude and reactance-to-resistance ratio of the impedance of the supply lines and transformers. Figure 3 indicates the line-to-line voltages at the single-phase load. The same curves will apply for voltage changes on the system near the utility substation, provided the intervening voltage transformations are made through delta-delta connected transformer banks. As an example consider the case of a welder drawing 100 kva at 0.4 power factor from a 3-phase system having a short-circuit capacity of 20,000 kva and with system X/R ratio of one to one. The ratio of single-phase kilovolt-amperes of the welder to the 3-phase short-circuit kilovolt-amperes is 0.005 per unit. Multiplying this figure by the ordinates read from the curves in Figure 3, the voltage changes per unit voltage drop are as follows:

Loaded phase = 0.0094
Lagging phase = 0.0008
Leading phase = 0.0039

It will be noted that the limiting voltage drop occurred on the loaded phase and was read from the curve at a point on a solid line. The other line-to-line voltages were not limiting and were read from portions of the curves formed by broken lines.

If there is a Y-delta transformation between the power system and the welder, the voltage changes on the primary can be determined from Figure 4. With a Y-delta transformation, the primary voltage changes are not the same as with a delta-delta transformation. Using the same example as previously used, the voltage changes per unit voltage drop are as follows:

Voltage $BC = 0.0086$
Voltage $CA = 0.0054$
Voltage AB = no change (multigrounded system)

The effect of other load power factors and line X/R ratios will be apparent from a study of the curves given in Figures 3 and 4.

These curves have been calculated upon the assumption of equal positive and negative phase sequence impedance. It should be noted that voltage drop has been plotted as the positive ordinate and voltage rise as the negative ordinate. As most of the voltage changes will be voltage drops, this convention makes possible easy reading of the curves.

The curves also have been calculated on the basis of the assumption that the principal change in voltage is in phase with the reference voltage and that any right-angle component of voltage can be neglected. This is true for small voltage changes, which are generally the only changes that can be tolerated on resistance welding systems and on power distribution systems supplying both welders and other loads.

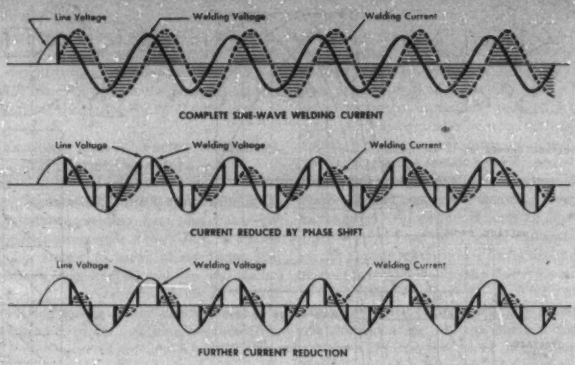

Figure 2. Heat controlled current waves

Method of Determining Voltage Changes Caused by Phase Controlled Current

Accurate calculation of voltage changes caused by phase controlled current cannot be made easily. Furthermore, it is tedious and costly to run tests on welders with different power factor and where line impedance must be varied to obtain various X/R ratios normally encountered in practice. Instead a circuit was set up on the transient analyzer[1] to duplicate in miniature the welder and line circuits as shown in Figure 5. Thyratrons were used in place of ignitrons and, because the circuit voltage was low, batteries were connected in series with each thyratron to cancel out the voltage drop across the tube so that this loss would not affect the value of load impedance. The rms voltage was measured at the load with constant voltage maintained at this point for all conditions of load. The difference between the no-load and full-load rms voltages divided by the welder voltages considered as unity gave the per-unit voltage change. The voltage changes have been expressed by curves both as per-unit change per 0.01 system impedance or as a factor which is multiplied by ratio of single-phase welder kilovolt-amperes divided by the 3-phase system short-circuit kilovolt-amperes to obtain per-unit voltage change.

Voltage Changes Caused by Phase Controlled Current

Using the miniature system, tests were made to determine the effect of phase controlled welder current. With a range of welder power factor between 0.2 and 0.8, the limiting voltage changes were found to occur on the loaded lines and are shown in Figure 6. In Figure 7 are shown the changes in the three line-to-line voltages, either at the welder or on the distribution system, without Y-delta transformation. It will be noted that the line-to-line voltage changes are reduced almost linearly with current.

Welders With Series Capacitors

Series capacitors have been used for power factor correction of individual resistance welders with considerable success.[2,3] The circuit is shown in Figure 8. One electronic welder control is used to control the series circuit of welder and capacitors. The more common arrangement is to provide sufficient capacitors of the proper voltage rating to cancel out the reactance of the welder, thus correcting the power factor to unity. The relationships between the current and various voltages existing in the series resonant

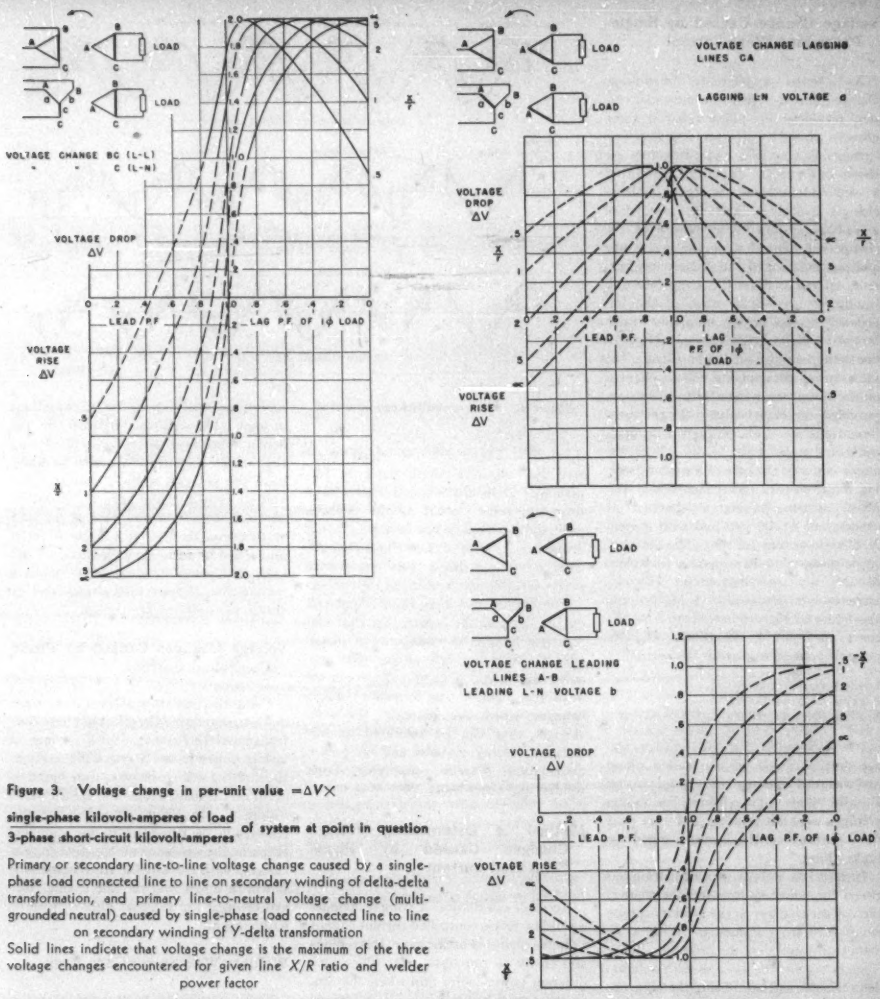

Figure 3. Voltage change in per-unit value $= \Delta V \times \dfrac{\text{single-phase kilovolt-amperes of load}}{\text{3-phase short-circuit kilovolt-amperes of system at point in question}}$

Primary or secondary line-to-line voltage change caused by a single-phase load connected line to line on secondary winding of delta-delta transformation, and primary line-to-neutral voltage change (multi-grounded neutral) caused by single-phase load connected line to line on secondary winding of Y-delta transformation

Solid lines indicate that voltage change is the maximum of the three voltage changes encountered for given line X/R ratio and welder power factor

circuit are shown in Figure 8 also. A charge is maintained on the capacitor units between welds so that synchronous starting can be effected, thus making every half cycle of current the same, even during a short heat time.

It can be appreciated that because it is necessary for capacitor reactance to balance the welder reactance in order to achieve unity power factor, any change in welder reactance, such as might be occasioned as a result of changing the transformer turn ratio to effect change of welder heat, would disturb the circuit and cause relatively large change in current. Therefore, it is the usual practice to operate the welders as much as possible at one welder transformer tap setting and with fixed arrangement of the arms of the welder, so as to keep the reactance as nearly constant as possible. Under this condition, it is necessary to make adjustments of welder current by means of phase-shift heat control.

With series capacitors applied to correct the circuit to unity power factor, the limiting voltage change without Y-delta transformation increased as the welder current was reduced by phase-shift heat control. The maximum limiting voltage change was found to occur at rms currents between 0.8 to 0.9 of full sine-wave current. A typical set of curves is shown in

Figure 9. It will be noted that here the drop on the loaded lines of the circuit with no Y-delta transformation increases to a value 1.43 times greater than the voltage drop at full-wave current, even though the current has been reduced to 0.9 per unit.

With the Y-delta transformation between load and system, the limiting voltage changes on the system were reduced at reduced current for variations of welder power factor of from 0.2 to 0.8 and all line X/R ratios.

The ratios of limiting voltage changes with phase controlled current to the limiting values of the changes with sine-wave current without Y-delta transformation are summarized in Figure 10 for various uncorrected welder power factors and system X/R ratios when series capacitors are used to correct to unity power factor. Using the previous example of a 100-kva 0.4-power-factor welder on a 20,000-kva short-circuit system, with X/R ratio of 1 to 1, the uncorrected welder caused a limiting line drop of 0.0094 per unit. With series capacitors used to correct to unity power factor, the maximum drop with sine-wave current is $1.41 \times 0.40 \times 0.005 = 0.0028$ per unit. To determine the limiting drop with phase controlled current, multiply the drop on the loaded line by the factor 1.15 taken from Figure 10 to get a limiting drop of 0.032 per unit. Since phase control is used on nearly all series capacitor welders, it would not be correct to figure on more than a 3-to-1 improvement from the use of series capacitors for this particular set of conditions.

Leading Power Factor Operation With Series Capacitors

Occasionally, when a system feeding a resistance welding load has relatively more resistance than reactance, correction of a welder to unity power factor still leaves considerable drop on the loaded line. Then it sometimes is suggested that leading power factor operation be obtained to cancel out this resistance drop. From the curves in Figure 3 for no Y-delta transformation, the voltage change on the other pairs of lines probably will become limiting so that not much improvement can be gained. However, if leading power factor operation is used, the tests which were made show that the voltage changes occurring when current is reduced by phase control are greater than the limiting values at sine wave and, more important, the limiting drops are, in general, greater than those that would have occurred if correction had been made to unity power factor only. Figure 11 will serve to illustrate the behavior of a series capacitor circuit applied for 0.9 power factor leading where the welder alone has a power factor of 0.2. Figure 11 shows the wave form of phase controlled currents and also shows the corresponding voltage changes for system X/R ratio of 5 to 1. Here when the current supposedly was reduced by retarding the firing point of the electronic contactor, the rms current actually increased to a maximum of 1.16 per unit and did not return to unity until the firing point was retarded about 90 degrees. At this point, the maximum voltage drop exceeded the limiting voltage drop with sine-wave current by about 20 per cent.

In explanation of the effect of phase controlled current to increase voltage changes when series capacitors are used, the effect of phase control can be considered as increasing the reactance of the

Figure 4. Voltage change in per-unit value

$$= \Delta V \times \frac{\text{single-phase kilovolt-amperes of load}}{\text{3-phase short-circuit kilovolt-amperes of system at point in question}}$$

Primary line-to-line voltage change caused by single-phase load connected line to line on secondary winding of Y-delta transformer bank

Solid lines indicate that voltage change is the maximum of the two voltage changes encountered for given line X/R ratio and welder power factor

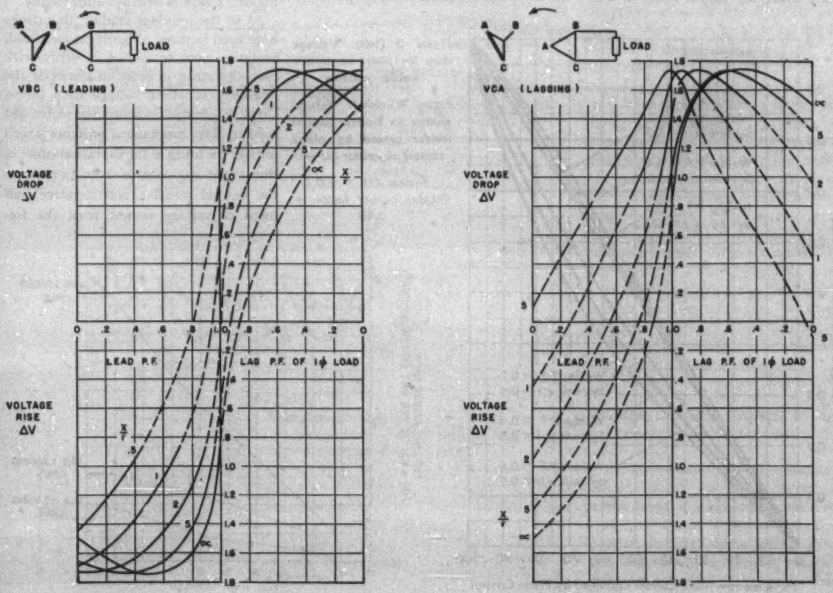

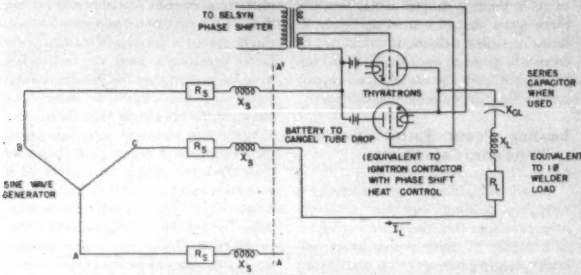

Figure 5. Miniature system studied

In this system voltages were measured at the sine-wave generator terminals and at A–A′ to determine system voltage changes produced by phase controlled resistance welder load

System impedance $= R_S + jX_S$

Welder circuit impedance $= R_L + j(X_L - X_{CL})$

circuit and hence introducing lagging power factor where unity or leading power factor was obtained with full sine-wave current. The effect of this lagging power factor is to increase voltage drop even though the current may have been reduced by phase control. While voltage change can be calculated approximately on this basis, the curves given in this paper indicate more correctly the actual changes which occur.

Low-Frequency Welders

Operation of a welder from a low-frequency power supply reduces the reactive kilovolt-ampere drop in the secondary circuit of the welder. As most single-phase a-c welders operated at line frequency have a fairly low power factor as a result of the inductance of the secondary arms which are spaced some distance apart, it will be seen that improvement in the kilovolt-ampere demand of a welder can be effected through the use of low frequency. In order to obtain low-frequency power, 3-phase 60-cycle power is rectified and applied to the primary winding of the welder transformer. Welding current flows in the secondary windings as the current builds up in the primary winding. Voltage of opposite polarity from the rectifier then is applied to the welder transformer so that current is built up in the opposite direction, thus obtaining a low-frequency alternating welding current. A typical converter consists of a 3-phase single-way rectifier with a pair of oppositely connected ignitrons connected to each of the three secondary windings of the transformer.

The problems of applying such converters for resistance welding have been discussed in a previous paper by R. L. Longini.[4] In that paper there were given data on the relative voltage drop produced by the load drawn by such frequency converters applying low frequency to resistance welding machine for one X/R ratio of line impedance. Although the voltage change produced by such loads on a 3-phase system can be calculated, such procedure becomes quite tedious when attempting to evaluate the effect of changing the frequency, the reactance-to-resistance ratio of the low-frequency load, and the reactance-to-resistance ratio of the 3-phase line impedance. However, by representation of the system in miniature on the transient analyzer as shown in Figure 12, results were obtained readily.

As in the previous studies, thyratrons were used in place of ignitrons and small batteries were connected in series with each thyratron in order to eliminate the relatively constant voltage drop across the tube. A small synchronous motor was used to drive mechanical switches which initiate the firing of the thyratron tubes in the proper sequence in order to produce the desired positive and negative half loops of voltage output from the fre-

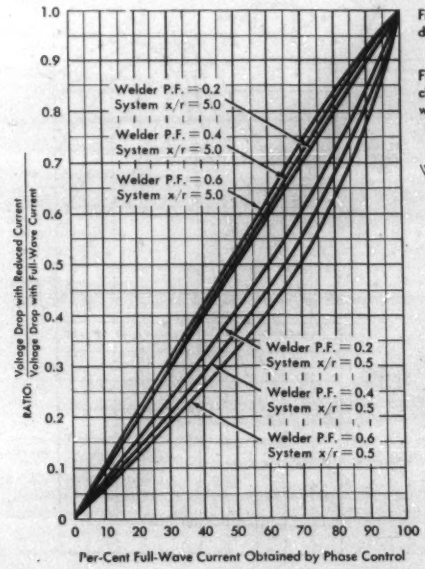

Figure 6 (left). Voltage drop for phase controlled welder currents

Figure 7 (below). Voltage change on 3-phase lines at welder caused by phase control of welder current

System $X/R = 2.0$
Welder power factor = 0.40

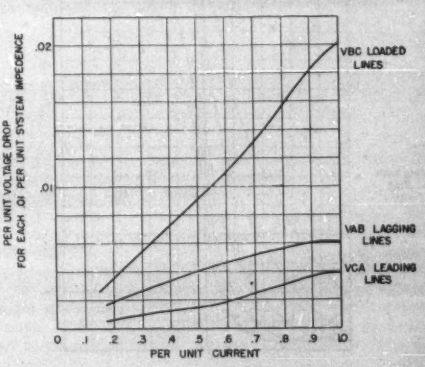

quency converter. By making appropriate changes in the gearing between the synchronous motor and the mechanical switches, various low frequencies were obtained.

Control of voltage output from the frequency converter was obtained by phase control of the rectifying tubes, by means of a small self-synchronous transmitter which can be rotated to displace the thyratron grid voltage with respect to the anode voltage and thus reduce the amount of voltage rectified by each tube.

In Figure 13*A* it is shown how each positive and negative loop of low-frequency voltage is obtained from the frequency converter. Here for 60-cycle loops make one-half cycle at low frequency. For this combination, the low frequency is exactly 20 cycles per second. The voltage loops making up each half cycle are seen to be the same for each half cycle of the low-frequency current. Unequal currents, therefore, exist in the 3-phase 60-cycle line. This is illustrated by the oscillograms of Figure 13*B* and 13*C* showing the low-frequency load current and the 3-phase line currents.

As the voltage can be rectified only in integral numbers of loops of 60-cycle voltage, some frequencies will be found to give equal values of 60-cycle line current, while other frequencies will give unequal currents. As the frequency is reduced, the amount of inequality in the 3-phase line currents will be reduced because of the increased number of 60-cycle loops going to make up each half cycle of the low frequency. When the number of 60-cycle loops equal $N \times 3$ or $N \times 3$ minus 1 equal currents will flow in the 3-phase lines. When the number of 60-cycle loops equal $N \times 3$ plus 1, the currents will be unequal. For example, equal currents are obtained at $25^5/_7$, $13^{11}/_{13}$, $10^{10}/_{17}$, and $5^{30}/_{31}$ cycles per second of low-frequency power. Unequal line currents would be obtained with 20, 12, and $8^4/_7$ cycles per second. These inequalities in the line current have a slight effect in producing unequal line-to-line voltage drop on the 3-phase lines as will be shown later.

As pointed out in the previous paper by R. L. Longini, when the inductance and resistance of the welder circuit are such that upon reversal of the low-frequency voltage the current requires longer than 1/120 of a second to decay to zero, the thyratron continues to conduct even though the voltage is building up in the opposite direction. One thyratron then carries single-phase 60-cycle power which is applied across the primary of the welder transformer. Such a condition has been designated as a commutation fault. This condition persists until the current goes to zero at which time the negative half cycle of voltage is applied to the welder transformer at low frequency. In general, this condition is not encountered on low-frequency systems where the power factor of the load at 60 cycles is above 25 per cent. Commutation faults can be eliminated by means of inverter operation of the rectifier which permits the energy stored in the magnetic circuit of the welder to be returned to the 3-phase lines while rectifier current decays to zero. However, in studies made in this paper, no inverter operation of the rectifiers was provided and welder impedances were used which did not cause commutation faults.

Table I. Comparison of Per-Unit Maximum Voltage Drops for Series Capacitor and $13^{11}/_{13}$-Cycle Low-Frequency Welders

60-Cycle Single-Phase Load of 100 Kva at 0.40 and 0.60 Power Factor Short-Circuit Kilovolt-Amperes of Line = 20,000

Line x/r	Low-Frequency Welders: 45.3 Kva, Single Phase R = R (60 Cycles)	36.6 Kva, Single Phase R = 0.75R (60 Cycles)	Series Capacitor, 40 Kw, Single Phase
0.5	0.0033*	0.0026	0.0036**
2.5	0.0028	0.0023	0.0027
5.0	0.0025	0.0021	0.0020
	62.6 Kva, Single Phase	**48.5 Kva, Single Phase**	**60 Kw, Single Phase**
0.5	0.0047	0.0036	0.0053
2.5	0.0040	0.0031	0.0040
5.0	0.0035	0.0027	0.0028

* $\frac{45.3}{20{,}000} \times 1.46$ (Figure 15—$X_L/R_L = 0.53$) $= 0.0033$

** $\frac{40}{20{,}000} \times 1.786 \times 1.0$ (Figure 10—power factor $= 0.4$) $= 0.0036$

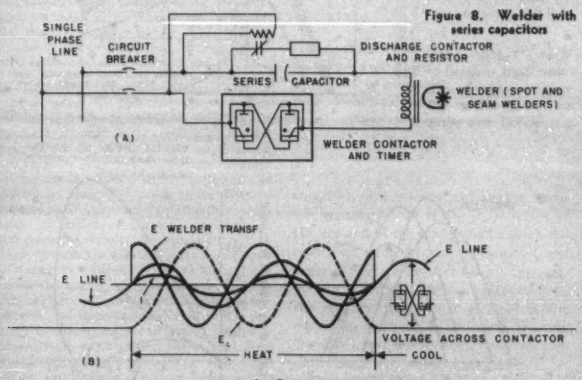

Figure 8. Welder with series capacitor

A—Circuit

B—Instantaneous voltages

C—Vector relations. For 100 per cent power factor

$I = \frac{E_{line} - \text{Ignitron arc drop (15 volts)}}{R}$

$I = \frac{V}{R}$

Power factor of welder alone $= \cos \phi$

$E_W = \frac{V}{\cos \phi} = \frac{V}{\text{Power factor}}$

$E_C = E_W \times \sin \phi$

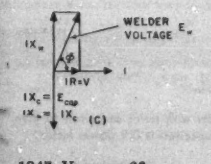

Voltage Changes Caused by Low-Frequency Converter Loads

Before indicating voltage changes obtained caused by low-frequency converter loads, it is necessary that a reference load or base be defined for the purpose of plotting system voltage changes and load currents in per-unit values. In order to make the procedure for the de-

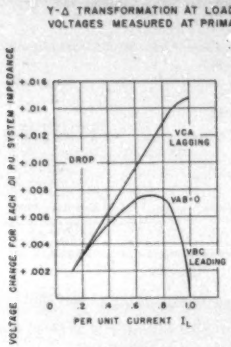

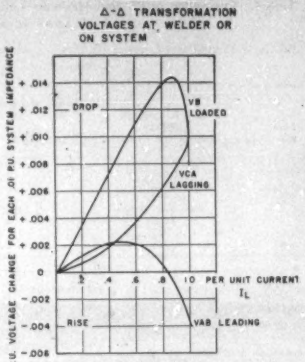

Figure 9. Voltage changes on 3-phase lines when welder with power factor = 0.40 is corrected to unity power factor by series capacitors and current is reduced by phase control

System $X/R = 2.0$

termination of voltage changes similar to the calculations made on a welder drawing a single-phase load from the 3-phase system as described in the earlier part of this paper, the base load was taken as the single-phase low-frequency kilovolt-amperes calculated on the basis of the required current (effective) and the impedance at the low frequency selected.

Since the voltage wave and resulting current wave are non-sinusoidal, the actual single-phase low-frequency kilovolt-amperes will be in excess of the calculated kilovolt-amperes based on the impedance at low frequency. The harmonic currents and the voltages add to the kilovolt-amperes calculated. Also, as is well known, the 3-phase kilovolt-amperes resulting from rectified load is in excess of the kilovolt-amperes of the load. For a 3-phase single-way rectifier without any losses in the rectifying transformer or in the tubes, the ratio between the 3-phase kilovolt-amperes and the rectifier output kilowatts is 1.21. If to the foregoing values are added the losses in the rectifier transformer and tubes, it is obvious that the 3-phase kilovolt-amperes drawn from the lines will be somewhat greater than the calculated single-phase kilovolt-amperes of the welder. The voltage changes measured on the analyzer were those caused by the total 3-phase kilovolt-amperes but have been expressed in terms of the calculated single-phase kilovolt-amperes of the welder.

Certain assumptions concerning the similarity between an actual welder and representation of this circuit in miniature were made.

1. The resistance of the welder was represented as a constant value for the fundamental and harmonic of the low frequency. Actually, the secondary resistance of a welder varies with frequency because of the skin effect of the current which flows in the large arms of the welder. The amount of such variation in the resistance will depend upon the frequency and the size of the welder arms and will vary for various types of welders. However, as the principal kilowatt loss is caused by the fundamental current and resistance, the error caused by variation in the amount of loss due to harmonic currents which flow in the secondary circuit of the welder is not large and is well within the limits of accuracy claimed for this analyzer. Actual calculation of the harmonic currents and losses based on oscillo-

Figure 10. Maximum 3-phase line voltage drop caused by current of phase controlled welder with series capacitors for correction to unity power factor. Delta-delta transformation

Maximum drop in per unit of maximum drop on any pair of lines with full sine-wave current

When Y-delta transformer bank is ahead of welder, maximum primary voltage drop occurs at full sine wave

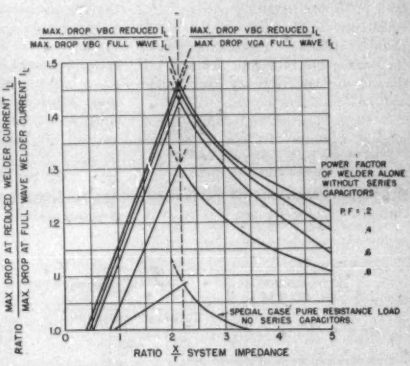

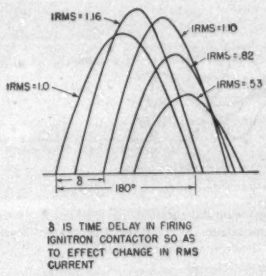

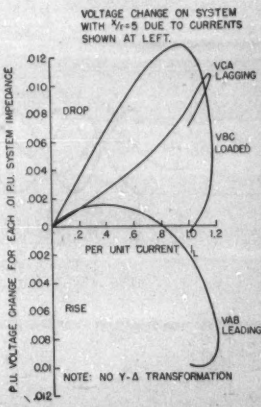

Figure 11. Half cycle current traces of phase controlled welder with series capacitors to give 0.9 power factor leading. Welder power factor without capacitors is 0.2 power factor

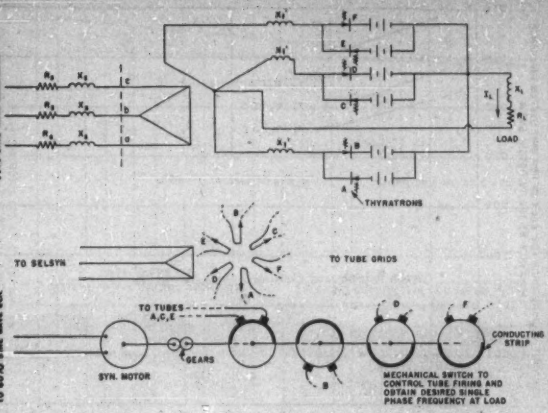

Figure 12. Miniature system studied

Resistance welding loads using 3-phase to single-phase frequency converters

graphic measurements of a low-frequency welder substantiate this.

2. The inductance of the secondary circuit is constant. Here again changes in the path of the fundamental and harmonic currents will produce slight changes in the flux linkages or inductance; effectively, however, the reactance varies almost linearly with frequency. Constant inductances were used in the transient analyzer study.

3. Regulation of the rectifier will be approximately 25 per cent when drawing maximum welder current. As welders are operated intermittently economy dictates that the welder and frequency converter be overloaded above the continuous capacity during the short weld time. Losses in the system are naturally greater under this condition and 25-per-cent regulation is reasonable. In this paper, regulation is defined as 100 times the ratio of the calculated voltage drop through the rectifier when considered as a straight rectifier divided by the voltage across the welder. This voltage is equal to the product of rms current and low-frequency load impedance referred to the primary of the welder transformer. For a 3-phase single-way rectifier, the voltage drop would be the sum of the resistance, commutation, and ignitron arc drops which can be calculated as follows:

$IR = I$ (effective) $\times$ resistance in ohms per phase of the rectifier transformer windings and secondary leads referred to the secondary winding of the transformer

Commutation drop for 3-phase single way rectifier $= \dfrac{I(\text{effective}) \times 3}{2\pi} \times$ reactance per phase of the rectifier transformer windings referred to the secondary winding

Arc drop = approximately 15 volts constant drop for ignitrons

For the miniature circuit used, the commutation voltage drop was approximately one-half of the total drop.

The per-unit voltage drops determined from the tests with representative systems in miniature are shown in Figures 14, 15, and 16 for load frequencies of $8^4/_7$ (unequal line currents), $13^{11}/_{13}$ (equal line currents), and 20 (unequal line currents) cycles as functions of the X/R ratios of the line and of the welder load. With the calculated low-frequency kilovolt-amperes of the welder as base kilovolt-amperes and for a 25-per-cent regulation in the rectifier transformer and tubes, the curves are remarkably similar in showing the maximum drops which occur on any of the three line-to-line voltages.

Except for line impedances with high X/R ratios, the results indicated that maximum drops occurred at maximum current and not at reduced current obtained by phase control as illustrated in Figures 17*A* and 17*B*. These figures show also the unbalanced voltage drops resulting from the unbalanced line currents. For comparison, Figure 17*C* shows the balanced voltage drops obtained at the frequency of $13^{11}/_{13}$ cycles and Figure 17*D* shows the greater unbalance in voltage changes at the frequency of 20 cycles. Tests indicated that the magnitude of the voltage changes on the 3-phase line were not affected by a Y-delta transformation between the line and the primary winding of the frequency converter.

Comparison With Actual Welder

Tests on a welder operated from a $25^5/_7$-cycle frequency converter served to substantiate the results of the tests made on the analyzer. At this frequency, the welder power factor was 0.5, calculated regulation was 25 per cent, the X/R ratio of the line impedance was 3.8 to 1. The voltage change per 0.01 line impedance was 0.015. The miniature system, with the same relative impedances, gave a voltage change of 0.014, showing very good agreement.

Comparison of Low-Frequency Welder With Series Capacitor Welder

Comparison of the effect of the load drawn by a frequency converter supplying power to a welder with the effect of a single-phase series capacitor corrected welder can be made only if the impedance of the welder at low frequency is known. It is particularly necessary that the re-

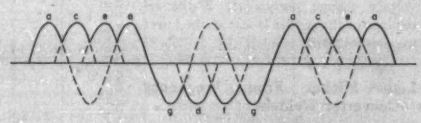

Figure 13*A*. Twenty cycles per second alternating voltage obtained from frequency converter

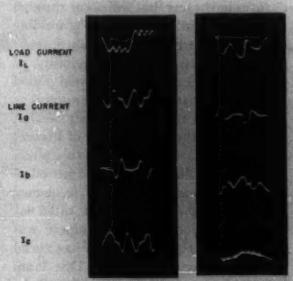

Figure 13*B* (above right). Full heat welder load current and system line currents for unity power factor load at 20 cycles

Figure 13*C* (above left). Full heat welder load and system line currents for welder $X/R = 2$ at 20 cycles

sistance of the welder at low frequency be determined accurately. Because this resistance may vary with frequency and because the ratio between 60-cycle resistance and the resistance at low frequency will vary for the various types and models offered by the many builders of resistance welders, exact data must be obtained from the manufacturer. However, if the calculated kilovolt-amperes as defined in the paper is known, the effect of this load can be determined from the data in this paper.

To illustrate the use of the data, comparison will be made between a welder equipped with series capacitors to improve the single-phase load to unity power factor with this same welder operated from a frequency converter delivering $13^{11}/_{13}$-cycle power to make the same weld. The demand of the welder at 60 cycles without series capacitors will be 100 kva at 0.4 power factor. The comparison will be for the case where there is no change in the resistance of the welder and for the case where there is a 25-per-cent reduction in the secondary resistance of the welder when operated at $13^{11}/_{13}$ cycles. Table I gives this comparison as well as a comparison based upon a welder power factor of 0.6 at 60 cycles. These comparisons indicate that the voltage changes for the two methods of reducing the welder load are very nearly the same for line X/R ratios in excess of 2.5. For lower ratios, the low-frequency welder causes less voltage change particularly if the resistance of the welder is less at the lower frequencies used.

Light Flicker From Frequency Converter Welders

In addition to the periodic voltage changes in the line that will occur through the starting and stopping of the welding current and which may produce light flicker, there is also the possibility of voltage variations during the weld period because of variations in the line current as reflected from the low-frequency welder, as shown in the oscillograms of Figures 13*B* and 13*C*. To determine this possibility of light flicker during the period of continuous operation of the frequency converter, a fluorescent lamp rated at 8 watts, 115 volts, and 0.14 ampere was placed across the 3-phase line just ahead of the frequency converter. This lamp indicated to several observers for all the low frequencies considered in this paper that

1. For a 10-per-cent drop in line voltage, there was appreciable and objectionable flicker.

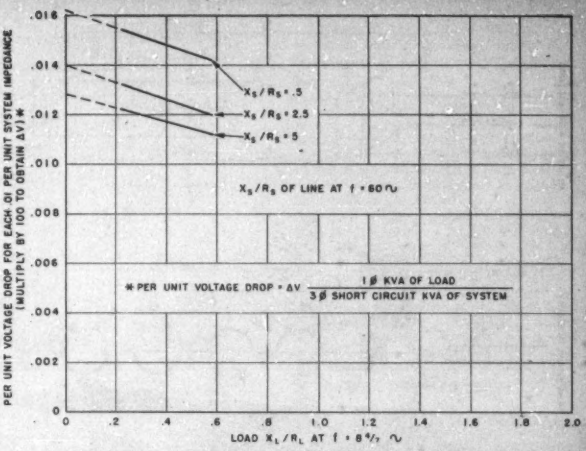

Figure 14 (above). Maximum system line voltage drop versus X_L/R_L of low-frequency welder operated at $8^4/_7$ cycles

Figure 15 (below). Maximum system line voltage drop versus X_L/R_L of low-frequency welder operated at $13^{11}/_{13}$ cycles

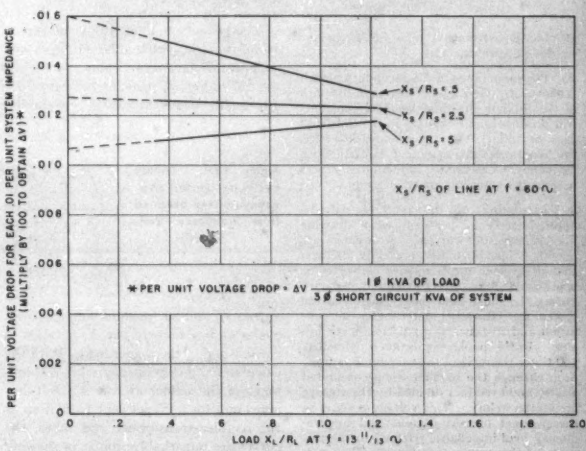

2. For a 1-per-cent drop in line voltage, there was a perceptible flicker that bordered on the region of objectionability.

3. For line drops below one per cent, flicker bordered on perceptibility.

Summary and Conclusions

1. Voltage changes caused by a single-phase load on a 3-phase system can be determined for sine-wave currents from Figures 3 and 4. These curves show the effect on the line-to-line voltages of Y-delta transformation and delta-delta transformation between the distribution line and the load.

2. The effect of electronic controls used to vary the current or "heat" of a single-phase resistance welder, when used without series capacitors, does not increase the voltage changes above those encountered at full sine-wave current for the same welder transformer tap setting. This applies both with and without a Y-delta transformation and for line-to-line and line-to-neutral voltages.

3. When series capacitors are used with electronically controlled single-phase welders

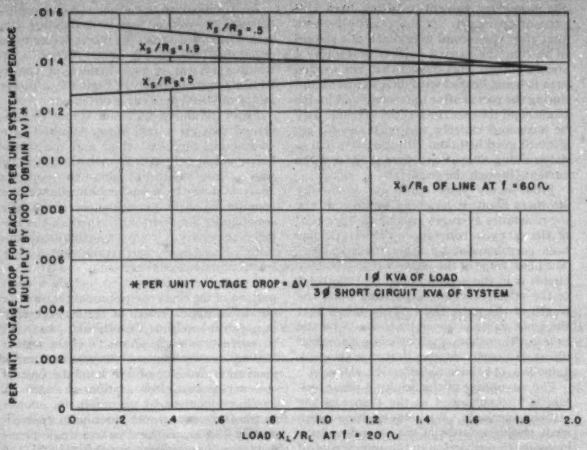

Figure 16 (above). Maximum system line voltage drop versus X_L/R_L of low-frequency welder operated at 20 cycles

to correct the load to approximately unity power factor, the limiting rms voltage change on the 3-phase lines occurs

(a). At reduced currents obtained by phase control for line-to-line voltages at the primary winding of a delta-delta and at the secondary windings of delta-delta or Y-delta transformations.

(b). At reduced currents obtained by phase control for line-to-neutral voltages at the primary winding of a Y-delta transformation.

(c). At full sine-wave current (100 per cent with phase control) for line-to-line voltages at the primary winding of a Y-delta transformation.

4. Overcompensation of resistance welders by the use of series capacitors to obtain leading power factor does not reduce the magnitude of the limiting voltage change on the 3-phase system. For low $X-R$ ratios of the system impedance, where overcompensation would be used to reduce voltage drop on the pair of lines feeding a welder, the limiting voltage drop with phase controlled current can be nearly 25 per cent greater than the limiting drop when capacitors are used to correct only to unity power factor. Therefore, reliance on overcompensation to minimize line voltage changes should be avoided.

5. The data given in this paper can be used to determine the voltage changes caused by a low-frequency welder load provided the impedance and primary current of the welder at low frequency are known. With the kilovolt-amperes determined from these known conditions used as base kilovolt-amperes, the line-to-line voltage changes on the 3-phase 60-cycle system can be determined directly from the curves given in this paper. The curves indicate voltage changes caused by 3-phase kilovolt-amperes of a converter with 25-per-cent regulation. If the calculated regulation differs from 25 per cent, the 3-phase kilovolt-amperes and the voltage changes for the same single-phase low-frequency kilovolt-amperes will be changed proportionately.

6. The maximum voltage changes per ampere of 3-phase line current are approximately the same for the range of frequencies and power factors of the low-frequency loads studied.

7. Comparison between single-phase series capacitor welders and low-frequency welders only can be made with accurate information available regarding the impedance of the low-frequency welder. It is not advisable to use the data on a 60-cycle welder translated to lower frequency without checking the correctness of this procedure with the welder manufacturer. A complete comparison between the two systems must include an analysis of the cost of equipment required to obtain the desired improvements.

References

1. An Electric Circuit Transient Analyzer, H. A. Peterson. *General Electric Review* (Schenectady, N. Y.), September 1939.

2. Power-Factor Correction of Resistance-Welding Machines by Series Capacitors, L. G. Levoy, Jr. AIEE Transactions, volume 59, 1940, pages 1002–09.

3. Application of Series Capacitors to Resistance Welding Machines, R. M. Partington. *Welding Journal* (American Welding Society, New York, N. Y.), January 1943.

4. Line Drop Produced by Resistance Welders, R. L. Longini. AIEE Transactions, volume 64, 1945, September section, pages 619–23.

Figure 17. System line voltage drops versus low-frequency phase controlled welder current in per unit of maximum current without phase control

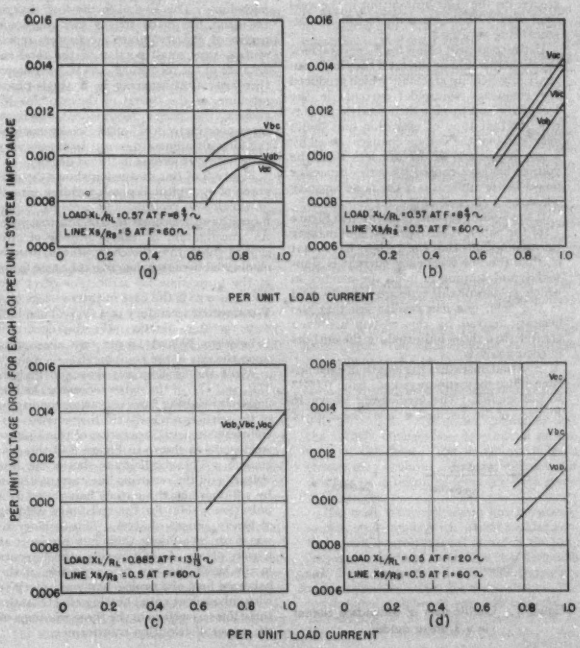

Discussion

J. L. Solomon and William J. Farrell (nonmembers; Sciaky Brothers, Inc., Chicago, Ill.): The authors have in this paper given us an excellent analysis of the possibility and extent of line drop due to various types of resistance welding loads through the use of various types of welding apparatus. They point out very well the advantages as well as the disadvantages in some of the systems used to lower the voltage changes in the power supply system.

In the case of series capacitor power factor correction equipment, they point out very definitely that under the best possible conditions, that is correction to unity power factor, one would not expect more than one-to-three ratio in voltage drop between series capacitor power factor corrected and uncorrected welding apparatus. They also bring out the point that as the phase shifting is increased in order to lower the heat in the secondary of the welder, the reactance of the load is increased, which in effect lowers the power factor of the load, thus cancelling out in part what benefits may be derived in the installation of series capacitor equipment.

This effect may be appreciable, since no welding transformer is ever designed so that it is used in production at its maximum output, which means that during the actual welding operation the phase shift dial is normally set at somewhere around 70 per cent. The peak currents that result from this phase shift operation therefore, are greater for the same heat output in the weld than would be the case where full 180 degrees firing were used.

In the treatment of low frequency welders, the authors would be correct if they had been analyzing welding machines which produced low frequency sinusoidal currents in the secondary and in fact their analysis is correct for that type of operation and shows very well that the voltage changes caused by a low frequency welder are less than the voltage changes caused by series capacitor power factor apparatus of the same capacity when the X/R ratio of the line is below 2.5.

If the 3-phase system, illustrated in Figure 12 of the paper, is analyzed without making the assumptions that the authors have, that is, that the low frequency current is sinusoidal, and keeping in mind the manner in which welders of this type are actually used in the field, one can readily see that the benefits derived by this system are even greater than those indicated by the authors in their analysis.

In actual operation the length of each on-time pulse may run anywhere from 0.0833 to 0.2 second. The oscillogram shown in Figure 1 of this discussion shows the shape of the secondary current resulting from this type of operation. It can readily be seen that after the second hundredth of a second of on-time the current reaches practically a steady state. This means that the welded area is being heated with direct current and during the period after the second hundredth of a second the reactance of the machine may be neglected entirely and only the d-c resistance need be taken into consideration in determining the power required to force the current through the secondary circuit.

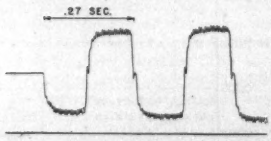

Figure 1. Oscillogram of secondary current in a 3-phase welder

From many tests made at the Sciaky Brothers plant, it has been found that the d-c resistance averages around 43.5 per cent of the 60-cycle resistance. This ratio has been corroborated by other investigators.[1] The peak value of the pulse in the secondary circuit is in the neighborhood of 1.05 to 1.1 of the effective value, depending upon the length of the pulse time. This means that the peak value is lower than would be the case in the authors analysis using sinusoidal pulses of current since in that case the peak value is 1.414 times the effective value.

The advantage of the Sciaky 3-phase system is also enhanced as the throat of the machine increases. With single-phase equipment the impedance of the secondary loop increases in proportion to the square root of the throat area; however, the difference in the d-c resistance between an 18-inch throat machine and a 48-inch throat machine is no more than a few microhms. On an 18-inch throat machine, the d-c resistance will be approximately 35 microhms depending upon the size of the machines, whereas a 48-inch throat machine may measure 40 microhms. This is due to the fact that as the arms are made longer the additional length of the secondary conductors represents a very small portion of the total resistance of the secondary circuit. It follows therefore, that whereas in a single-phase machine, as the throat of the machine increases, the power requirements increase correspondingly; in a 3-phase Sciaky machine the kilovolt-ampere demand increases very little with an increase in throat depth.

Figure 2 of this discussion shows the diagram of a typical 3-phase welding circuit in which the rectifier and welding transformer have been combined on one iron core. An examination of the operation of this system shows that the commutation drop is eliminated because when two tubes are firing at the same time no saturation effect can take place as is the case in the two legs of a Y-connected secondary of a typical one-half wave rectifier. Furthermore, the regulation is between 10 and 15 per cent depending upon the size of the equipment.

While the oscillograms shown in Figures 13B, and 13C of the paper represent the line currents resulting from operating conditions of the authors analysis, the line currents encountered in actual operation of this 3-phase welder are as shown in Figure 3 of this discussion. This oscillogram shows the line voltage and the resulting line current drawn by a 3-phase machine when being used as a pulsation welder for the resistance welding of heavy gauges of steel. The oscillogram was made by a Power Company Engineer at a users plant. As can be seen, the currents in the three lines are representative of the balanced load of a typical half wave rectifier with subsequent equal heating effects on the three lines as well as in the three windings of the power distribution transformer.

An examination of the phase relationships between the voltage and corresponding current wave trace shows the power factor to be approximately 85 per cent. When a 6-winding system is used instead of the 3-winding system shown in Figure 2, a power factor of 90–95 per cent is obtained.

From the above discussion it may be concluded that the actual power required by a commercial 3-phase welder and the subsequent voltage changes are substantially less than those resulting from the authors analysis since the secondary impedance of a commercial 3-phase welder is practically equal to its d-c resistance, whereas, the impedance resulting from the authors, calculations is based upon their assumption of a low frequency sinusoidal current.

It may be of interest to include a comparison of the costs of equipment required to obtain an improvement in the voltage drop in a typical welding installation. In order to correct a single-phase 60-cycle welder having a power factor of 30 per cent, and a maximum demand of 285 kva, the cost of the series capacitor equipment and its auxiliary equipment required for power factor correction would amount to approximately $3,600; as the standard single-phase welder will cost approximately $3,600, the corrected equipment represents an increase of almost 100 per cent. The addition of the corrective equipment would reduce, under optimum conditions, the voltage change in the line to one-third of what it was in the uncorrected condition.

A 3-phase welder of the same welding capacity would cost a total of approximately $5,800. This represents a total investment of only 80 per cent of the total cost of a single-phase capacitor corrected machine. Comparing a welder having an uncorrected power demand of approximately 1,900 kva with a 3-phase machine of the same capacity the total investment for the 3-phase machine represents approximately 68 per cent of the series capacitor corrected single-phase machine.

The 3-phase machine in both cases will create voltage changes in the line of only one-fourth to one-sixth of that which would be caused by the uncorrected single-phase welder.

Reference

1. Electric Coils and Conductors (book), Herbert Bristol Dwight. McGraw-Hill Publishing Company, 1945.

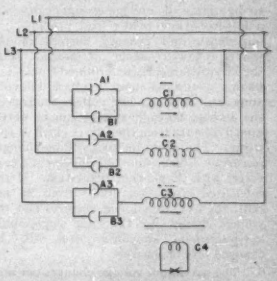

Figure 2. Typical 3-phase welding circuit

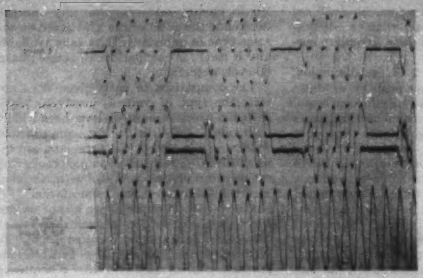

Figure 3. Oscillogram of 3-phase welder operation

Harold Cole (The Detroit Edison Company, Detroit, Mich.): The authors of this paper have made a definite contribution toward a better understanding of how welder loads affect power supply systems. The paper, with its abundance of supporting curves and data, should prove of particular value to utility engineers in analyzing their own power systems with respect to welder loads.

The authors employed a convenient tool in making their calculations and in setting forth results; namely, the per unit method of expressing voltage and the per unit system impedance. This method of expression appears to be replacing the familiar per cent method. It is not necessary to go into the advantages of either system since both say the same thing and give the same answers. However, it is believed that the thought in the paper under discussion could have been more quickly grasped by a wider range of readers if one or two simple examples had been added. For instance under "Voltage Change Due to Single Phase Sine-Wave Current" the voltage changes in the various phases of a three-phase system which are caused by a single-phase welder load are discussed. The results are given in per unit voltage drop. If an example had been given that said in effect; for a 3-phase supply voltage of 440 volts the actual voltage drop would be 440 $\times$ .0094 = 4.14 volts on the loaded phase for the above problem; it is believed all readers would have found the common denominator more quickly. This comment seeks to prove the old rule that simple examples are always too few and does not detract in any way from an excellent paper.

The subject of the low frequency welder is one which will bear considerable thought by utilization engineers. The advantages of this type of welder are readily apparent in that power factor is improved and the power inrush reduced for a given operation. Furthermore, the advantage of using 3-phase power lies in balanced loads and reduced voltage drop per phase compared to a single-phase welder on the same kilovolt-ampere base. These advantages, however, are offset to some extent by the fact that the 3-phase circuit supplying the low frequency welder may be subject to cyclic voltage flicker. In other words, these welders may draw 3-phase current with a frequency of from 2 to 18 times per second with the attendant voltage drops. Voltage fluctuations which occur in this range are more noticeable than single voltage dips. Voltage fluctuations which occur about eight times per second present a voltage flicker which is exceedingly irritating to lighting customers.

As has been pointed out earlier in this discussion, a given kilovolt-amperage of load can be handled with a lower voltage drop from a 3-phase supply than from a single-phase supply; namely, about one-half the single-phase drop. However, for cyclic voltage flicker in the order of eighth per second, the maximum allowable voltage drop on The Detroit Edison System is limited to about one-fourth the voltage drop which would be caused by a single-shot or non-cyclic welder. It is apparent, therefore, that even though the power factor is improved and the load is fed 3-phase, that under certain cyclic operating conditions that fewer kilovolts-amperes may be available for the 3-phase low-frequency welder than for the single-phase welder with its high current inrush and low power factor.

Our experience is quite limited with the low frequency welder up to this time. A recent discussion with an industrial concern had to do with low frequency welder that had a 3-phase demand occurring 7.5 times per second which is at the most critical part of the cyclic range. Low frequency welders will undoubtedly find their proper place in welding operations due to their many advantages. However, utilization engineers must carefully check the welder operating characteristics to insure that the welder and job in question do not impose undesirable voltage fluctuations on the supplying circuits and substation buses even though the demand is relatively low.

I. B. Johnson, H. A. Peterson, and **C. M. Rhoades, Jr.**: Cole has pointed out that some readers may not have understood the use of the per unit system in representing system voltage changes. It was the hope of the authors that, by giving several examples, the use of the system would be clear but, if not, Cole's example should help and we thank him for it. Actually one is interested in the per unit or per cent changes in voltage and not the actual number of volts change, in determining the effects on lights and other machines.

With regard to Cole's reference to the advantage of 3-phase load and the reduced voltage drop compared to a single-phase welder on the same kilovolt-ampere base, it should be pointed out that the single-phase kilovolt-amperes used as a base in representing the low frequency load is not the same as the 3-phase kva resulting from this single-phase load. With a 3-phase single-way rectifier applied as a frequency converter without any losses in the rectifying system, the 3-phase kva would be approximately 1.25 times the low-frequency single-phase kilovolt-amperes. In order to compare the effects of low-frequency single-phase kilovolt-amperes and single-phase 60-cycle kilovolt-amperes, the comparison must be made on the basis of the impedance of the welders when doing the same welding job, as was pointed out in the paper.

The voltage changes indicated for the low frequency system are those measured by a voltmeter which was not responsive to the variation in voltage during the weld time resulting from reflections of the low frequency current in the 3-phase lines. Since the low frequency current varies during each half cycle, the 3-phase system experiences load changes at twice the frequency of the low frequency system. The effect of the variation of line to line voltages for different root-mean-square voltage drops was summarized in the paper.

The effects of lower frequencies than $8^8/_7$ cycles per second and discontinuous half cycles of low frequency current would be to aggravate the variation in 3-phase line voltages during weld time so that a root-mean-square voltage drop of one per cent probably would cause objectionable flicker whereas, with continuous alternating current as obtained with the frequency converter used in the tests, the flicker of the fluorescent lamp was just perceptible at one per cent change.

The authors have a number of comments to make to clarify the discussion presented by Solomon and Farrell, and will reply to the questions in the order raised.

The example given in the paper showing three-to-one improvement in line drop through the use of series capacitor power factor corrected welder was one example only based upon certain welder and line constants, and should not be used to summarize the results given in this paper which presents data to determine voltage changes for any conditions which may be encountered. Another example might be a welder drawing 100 kva single-phase at 0.20 power factor with system X/R = 1.0 short circuit kva of 20,000 and with delta–delta transformation between line and load. The drop due to this load is 1.6$\times$0.005 or 0.008 per unit. The maximum voltage drop when series capacitors are used with electron heat control to adjust the welding current would be 1.41$\times$0.2$\times$0.005$\times$1.17 or 0.0017 per unit. Here the improvement on voltage drop would be 4.7-to-1.

The authors agree that most welder transformers are not used in production at maximum output. Series capacitors are usually selected for the production condition and the voltage changes are determined on the basis of this load. The maximum voltage change may occur at a reduced current and this can be determined from the data given in this paper.

The tests on a miniature low frequency system were made with nonsinusoidal currents such as are obtained in one of the low-frequency systems described by Solomon and Farrell, as well as the low-frequency welder actually tested by the authors. The low-frequency kilovolt-amperes referred to and defined in the paper is merely a tool to tie down the impedance of the welder. Ad-

mittedly the impedance of various makes of welders will be different at low frequency just as the kilovolt-amperes will differ at 60 cycles when different welders develop the same secondary or welding current. The results given in the curves show the effect of the non-sinusoidal currents and voltages as illustrated by the typical oscillograms of Figures 13*B* and 13*C*.

If the time of each current pulse is 0.0833 to 0.2 second as suggested, then we assume that the low frequencies involved range between 6 to 2.5 cycles per second. The oscillogram in Figure 1 of the discussion represents current at 4 cycles per second. This current varies exponentially during each half cycle. While the secondary current approaches a constant value at the end of each half cycle, it would be interesting to see the corresponding primary line currents for this condition, since constant current through the welder transformer might saturate the core with consequent increase in the primary current and decrease in the secondary voltage. If such saturation exists in a practical case, then the voltage changes due to the welder load will be greater than those determined by the analysis given in this paper.

The resistance of large conductors, such as the arms of a welder, is not appreciably greater at five to ten cycles per second than when passing direct current; therefore, the use of d-c resistance as suggested by Solomon and Farrell is permissible. In the comparison of a low-frequency welder, the authors assumed a condition where the resistance of the electrodes and work pieces was 50 per cent and the resistance of the arms was 50 per cent at 60 cycles per second. At low frequency the resistance of the arms was assumed to decrease 50 per cent while the electrodes and work resistance was assumed to stay constant as a result of the highly concentrated cross section as compared with the welder arms. Thus the total resistance at low frequency would be 75 per cent of the 60 cycle resistance.

As was pointed out previously, this analysis is based on nonsinusoidal currents so that the discussion of peak currents is not relevant.

The resistance of a welder does not change appreciably with increased throat depth. A machine with 48-inch throat depth will have greater reactance than a machine with 18-inch throat; therefore, the reactive kilovolt-amperes required will be greater. This increased kilovolt-amperes of a single-phase 60 cycle machine is compensated for by using more capacitors to bring the power factor near unity. The demand is then proportional to the resistance of the welder and the deep throat machine will not draw much more load than a shallow throat machine for the same secondary currents.

Referring to Figure 2 of the discussion, the circuit with the three primary windings on the core of the welder transformer is still a rectifier circuit and commutation losses are present. Without going into the theory of rectification, it can be stated that the voltage drop during commutation is due to the transfer of a finite current from one winding to another. This causes an inductive drop proportional to the leakage inductance in the circuit in which the current is changing. With the system shown in Figure 2, current must transfer from one winding to another at a time when the current is not zero. The commutation drop will depend upon the construction of the transformer and the coupling between the primary coils. Since the welder transformer must transform low frequency voltage, the core must be larger than an equivalent 60 cycle rectifier transformer, and the leakage inductance of the coils will probably cause comparable commutation voltage drops. In no type of rectifier system is the commutation drop due to saturation of the transformer core.

The line currents shown in Figure 3 of the discussion are similar to Figure 13*B* of the paper except that the low frequencies are different. Both rectifier systems are 3-phase single-way type.

Power factor of nonsinusoidal currents and voltages as shown in Figure 3 of the discussion, cannot be determined by phase relationship. For a rectifier the power factor of the 3-phase load is determined by the fundamental definition of power factor; namely, the ratio of average kilowatts divided by the 3-phase kilovolt-amperes. As was shown in the paper, the power factor of a 3-phase single-way rectifier is approximately 85 per cent.

The authors wish to state again so that there is no misunderstanding, that they have not indicated the 3-phase load of any low frequency system except in the comparison in Table 1 which was based on certain assumptions regarding the resistance of the circuit. The data has been presented to permit determination of the effect of the 3-phase load of a frequency converter when the impedance of the welder at low frequency is known and the regulation of the frequency converter system is known. The equivalent low-frequency kilovolt-amperes based on fundamental components of current and voltage at this frequency has been used as a convenient tool in expressing the impedances and desired weld current of the low-frequency welder so that any one can determine the effect of the load based on the same type of impedance data as is available and is used for calculations of single-phase 60-cycle welders.

The comparison of costs given does not state the type of controls involved. Synchronous precision controls have been widely used with series capacitor compensated welders. The cost of the necessary capacitors, discharge resistor, capacitor racks and synchronous precision control with National Electric Manufacturers Association 7*B* sequence control required for a spot welder which would draw 285 kilovolt-amperes at 0.30 power factor is approximately $3,000. Without series capacitors, a synchronous precision control with NEMA 7*B* sequence control for the spot welder without series capacitors would cost approximately $1,450. The approximate additional cost of series capacitors and control equipment would be $1,550 rather than $3,600. The authors are not in a position to comment on the cost of a welding machine when series capacitors are used, but believe that a few hundred dollars should take care of the additional charge for the higher voltage transformer required.

If nonsynchronous welder controls were used with the uncorrected welder, the cost of the controls would be approximately $800 so that the extra cost for capacitors and synchronous precision control would then be $2,200 rather than $3,600.

One other comment is in order since it bears upon a point made by Cole in his discussion. In Figure 3 of the discussion by Solomon and Farrell, the primary line current is applied to the primary of the welder transformer in pulses to obtain each half cycle of four-cycle-per-second current. The primary line current does not flow for two 60 cycle periods between each half cycle of load current.

In the analysis made by the authors using the transient analyzer, there were no periods during which the control was shut off as shown in Figure 3. Therefore, the variation in primary line voltage at a frequency of 8 cycles per second will be greater than that observed by the authors. The reaction of a fluorescent lamp at various root-mean-square voltage changes as recorded in the paper will not apply for current pulsations similar to those shown in Figure 3 of the discussion.

In conclusion the authors believe that the data given in the paper is representative of the performance of all the types of welder systems described in the paper and as further outlined by those who have submitted discussions.

Radio-Noise Influence of 230-Kv Lines

H. L. RORDEN
MEMBER AIEE

THE DIFFICULTIES of obtaining materials during recent years have made it necessary to economize in the design of new transmission facilities. During war conditions the Bonneville Power Administration undertook such limited means as were possible to determine if economies could be effected in transmission line design without lowering standards of service. One of the first departures from previous practice involved the use of wood poles for transmission of power at 230 kv. Design of the first line of this type on the Bonneville-Coulee system was based on previous practice of similar installations in other parts of the United States. This 230-kv line is 184 miles long, contains H-frame structures with 22-foot conductor separation, 1.108-inch aluminum-cable steel-reinforced conductor, uses 13 standard $5^3/_4$-inch suspension insulators, and is not protected with ground wires. It was built to relieve a serious bottleneck during the war emergency.

When the materials' situation became critical, it became apparent that considerable further saving could be effected if the conductor diameter and spacing, as well as the insulation level, could be reduced. These three items were considered in the light of the hazards that would be involved by their further reduction. Twenty-two-foot conductor separation required spliced crossarms which were initially expensive and difficult to replace when repairs were necessary because of lightning flashovers. The question of conductor separation also involved transmission reactance and losses, mid-span flashovers, safety to personnel when working on energized lines, and radio interference. Thirty-six-foot arms were available in one piece and even 40-foot arms sometimes were obtainable. The number of insulators used involved cost and delivery of the insulators, structure height, and number of structures per mile necessary to maintain required ground clearances at mid-span. Since ground wires are not used for other than station protection on the Bonneville system, insulation levels involved more consideration of the magnitude of switching surges than lightning flashovers. Conductor diameter involved losses, economic loading, and radio interference.

Wherever possible, repairs on both 115- and 230-kv lines of the Bonneville system are made with the lines energized. It is therefore necessary for maintenance crews to climb poles and towers with lines energized and to use hot-line equipment. This practice has proved most satisfactory and economical, and permits continuity of service, but safety to personnel must be considered in the design of such transmission facilities. This involves both the insulation level and conductor separation.

Selection of the insulation level was based on experience with 115-kv circuits and 230-kv test installations. Most of the lightning hits to the system are direct strokes to conductors, and as far as is known, these hits always result in flashovers to ground; although occasionally there is no power-follow arc and consequently no outage occurs. Except in experimental areas,[1] the stroke usually follows over the insulators and crossarms and down the pole of wood-pole lines. Because the number of suspension units in this path is a small part of the total insulation for lightning, the adopted level is based on switching surges and possible pole fires as well as safety to personnel. Sufficient data have been obtained from protective gaps on the system to conclude that switching surges rarely, if ever, reach three times normal. Pole fires have occurred when a large percentage of the insulators were shattered from lightning, so that the remaining units and the wet crossarm and pole sustained heavy leakage currents to ground.

Suspension insulators are one of the lesser sources of radio disturbances, irrespective of whether they contain special treatment. The common types of suspension clamps, containing two U bolts which protrude below the nuts, are worse offenders than the insulators. This source of disturbance is not of much consequence on steel towers, because of tower shielding, but it is appreciable on wood pole lines.

The questions of conductor diameter and separation are complicated by several variables, all of which should be weighed in proportion to their importance. Reduction of diameter, which is also considered to mean reduction of cross section, increases corona as well as line resistance and reactance. The change in reactance is not of great importance, but increased losses, including a decrease in the firm capacity of the line, must be balanced by the reduction in first cost to be economically justifiable. The first cost includes not only that of the conductor, but also involves pole height and number of structures per mile.

Reduction of conductor separation also increases corona losses but involves a decrease in reactance, resulting in a slight increase in the stability limit. The saving in first cost may include width of the right of way but is mainly confined to length of crossarms, which is important if it involves the difference between 1-piece versus spliced arms. Further reduction below the maximum commonly available length of 1-piece crossarms involves little improvement in cost and probably increases the hazard to personnel beyond desirable limits.

Mid-span flashovers are not considered of importance in the selection of conductor separation. Close observations over the entire system during recent years have shown that if mid-span flashovers have occurred at all, they are too rare to be important in the design of lines.

Radio-noise influence was of major con-

Paper 47-92, recommended by the AIEE committees on communication and power transmission and distribution for presentation at the AIEE winter meeting, New York, N. Y., January 27-31, 1947. Manuscript submitted November 15, 1947; made available for printing January 6, 1947.

H. L. Rorden is protection engineer, Bonneville Power Administration, Portland, Oreg.

cern in the question of conductor diameter and separation. It generally was believed that a reduction of these factors should result in increased noise levels as well as increased losses. Data are available on losses that could be anticipated,[2] but considerable concern was expressed over possible increases in radio-noise levels. A considerable portion of the Bonneville transmission system traverses sparsely settled areas at a considerable distance from broadcasting stations. The lines are relatively close to some dwellings in rural areas, and it was considered of paramount importance to keep radio-noise influence in these areas within an acceptable minimum. Complete data on radio interference from high-voltage lines were not available, and so an investigation was undertaken to determine whether radio noise is a serious item in the design of high-voltage lines.

Method of Measurement

Measurements of radio-noise influence during this investigation were confined to a Ferris type radio-noise and field-strength meter containing means for calibrating the receiver gain so that the meter reading is proportional to the input. This instrument is equipped with an antenna of such length that the calibrated meter reading is proportional to the microvolts of field strength per half meter. The instrument reads both crest and integrated values so that readings could be obtained proportional to the radio noise as well as the average field strength. Since the major objective of the investigation was the determination of radio interference to domestic receivers, the data given here are in terms of radio noise or crest values. After conducting preliminary tests over the broadcast range, a frequency of 800 kc was adopted, it being near the center of the band. Frequently throughout the tests readings were taken at various frequencies in order to ascertain that no radical differences existed from the data obtained at 800 kc.

It was found that in order to eliminate radio interference entirely from ordinary domestic receivers it is necessary to maintain a signal strength of the broadcasting station of at least 40 times that of the interference. Fair reception is possible at a ratio of 25 to 1. Reception is practically impossible at a ratio of 10 to 1. These ratios involve variables which may alter them to some degree depending upon local conditions, but it is believed that they represent a fair average. In areas remote from transmitting stations it was considered necessary to maintain lower levels of interference than can be tolerated in metropolitan areas because of the greatly reduced signal strength of broadcasting stations in the remote areas.

The method of measurement consisted of placing the Ferris meter at predetermined positions on the ground with respect to the transmission line. In the accompanying data the point on the ground directly beneath the outer conductor is taken as the reference, measurements being made from that point, moving away from the transmission line and at right angles thereto.

The map of Figure 1 illustrates the general location of the high-voltage transmission system of the Bonneville Power Administration in 1946. The 230-kv system from Grand Coulee to Spokane,

Figure 1. Location of Bonneville–Coulee transmission system (1946)

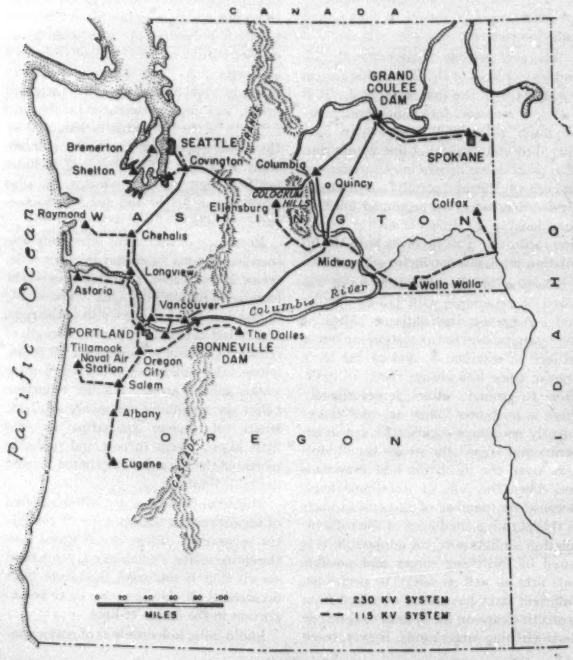

Figure 2. Corona radiation—Covington–Grand Coulee line 1

November 20, 1944, 2:30–6:40 a.m., curves corrected for background noise
Conductor: Aluminum cable steel reinforced, 1.108-inch outside diameter, 26 strands aluminum, 7 steel, 27-foot separation, 41 feet high
Weather: Fair, barometer 29.8 inches, temperature 38–22 degrees Fahrenheit
Test frequency: 800 kc

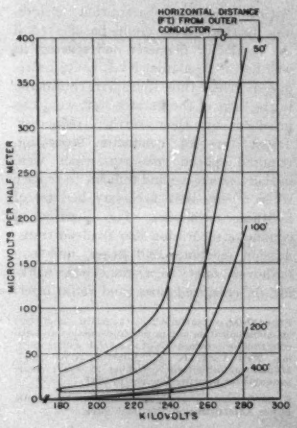

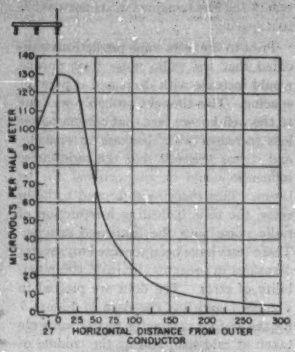

Figure 3. Corona radiation—Midway–Columbia line

January 15, 1946, 12 noon
Excitation: 236 kv
Conductor height: 47.5 feet
Weather: Clear, barometer 28.6 inches, temperature 24 degrees Fahrenheit
Test frequency: 830 kc

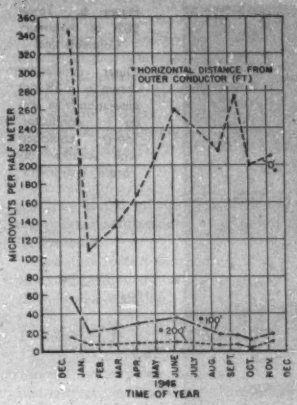

Figure 4. Corona radiation—Midway–Columbia line

Conductor height: 47.5 feet
Line excitation: 236–240 kv

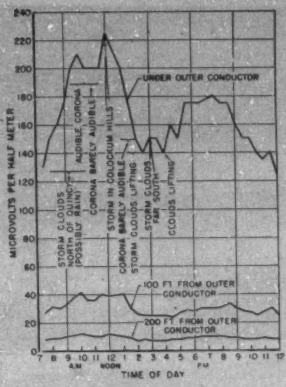

Figure 5. Hourly variation in corona radiation—Midway–Columbia line

April 2, 1946
Excitation: 239–241 kv
Conductor height: 46.5 feet
Weather: Cloudy, barometer 28.6 inches, wind 1–7 miles per hour

Covington, and Vancouver, all contain parallel circuits. The wood-pole line previously mentioned is the second Coulee-Covington line.

Levels Within the Induction Field

The curves of Figure 2 illustrate the radio noise measured at mid-span on a steel-tower line that had been in service for several years (Coulee-Covington number 1). These data illustrate the limited distance through which energy is radiated within the field of direct induction. The normal operating potentials on the Bonneville system range from about 222 kv to 244 kv at different points on the system. It is apparent that for fair weather the radio-noise influence is well below the knee of the curve for all distances beyond 100 feet from the outer conductor. At 200 feet the line excitation could be increased to about 260 kv without the increase in noise departing substantially from a linear relation.

Corona loss measurements also were made on this line using commonly available instruments and instrument transformers. In fair weather the losses per 3-phase mile measured as low as 0.6 kw, and in inclement weather that was general throughout the area, as high as 12 kw. A relatively large tolerance probably should be allowed for the low reading, but the high value is believed to be within ten per cent.

One-Inch Conductor

Based on the data of Figure 2, a 230-kv line was constructed with a 1-inch diameter aluminum-cable steel-reinforced conductor. This is the line between Midway and Columbia of Figure 1. Because of its importance to the war emergency, it is a steel-tower line and differs from earlier practice only in the conductor diameter. The conductor contains 54 strands of aluminum and 7 of steel. Conductor separation is 27 feet. Although considerable concern was expressed over the use of this conductor because of possible radio noise, early tests with line potentials of 240–243 kv proved that the design constituted good engineering practice so far as radio-noise influence is concerned.

The curve of Figure 3 illustrates a test that was made on the afore-mentioned line within two months after it was energized. These data show that even when this line was new radio noise emanating therefrom was not substantially higher than that of the weathered line of Figure 2, which uses a larger conductor. For all distances beyond 200 feet the measured difference is negligible. Although there is somewhat greater conductor height for Figure 3, other data show that this difference apparently is not of great importance.

Of particular interest in Figure 3 is the lower noise level measured under the center conductor than that measured under the outer conductor. Figure 3 also shows the rapid attenuation of the induction field, the noise influence falling to about three per cent of its maximum measured value in 300 feet.

The Midway Columbia line, containing the 1-inch conductor, has been used for repeated tests of radio-noise influence in the interest of design of future lines. Figure 4 illustrates data obtained on this line at approximately monthly intervals since the line was energized and extending over a period of approximately 11 months. It was anticipated initially that these data should result in a curve decreasing with time, perhaps nearly exponentially, ultimately arriving at a minimum level that should be substantially constant. It is generally believed that new conductors are subject to some corona radiation which recedes with time, and it was expected that the radio noise would be proportional thereto. The purpose of the test was to determine how long it takes for the corona level to become stable and constant. Irregularities were expected, but the data differ considerably from that which was anticipated. The results may be influenced by weather changes between winter and summer. However, they are of interest because of the extreme reduction in the measured noise level that occurred early during the tests and the gradual recovery to a more or less uniform average that followed. The measured points of Figure 4 are joined by lines, but the data

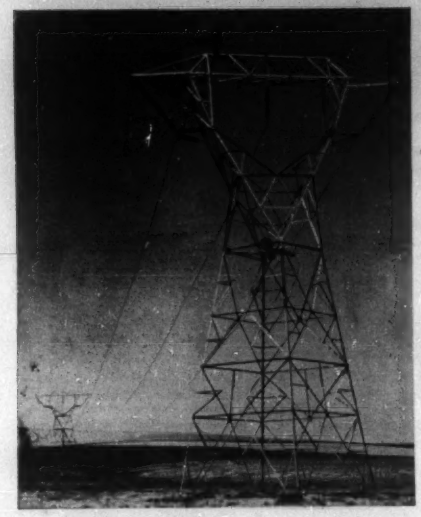

Figure 6. Tower 202 of Midway–Columbia line

Outer conductors drawn in to 18-foot separation from center conductor. Tower equipped with weather recording instruments

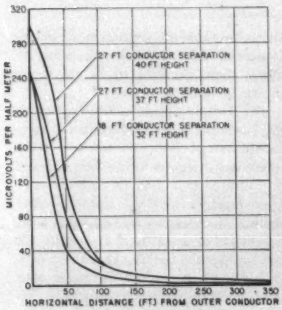

Figure 7. Corona radiation

18-foot versus 27-foot conductor separation
Measured at mid-span, September 12, 1946
Excitation: 235 kv
Test frequency: 800 kc
Weather: Fair, barometer 28.1 inches, temperature 71–76 degrees Fahrenheit, wind 3 miles per hour

probably do not represent a continuous curve.

Hourly Variation

The curves of Figure 5 illustrate the data obtained on one of several continuous runs made to observe hourly variations in radio interference. These curves illustrate the differences that occurred in noise level due to a storm at some distance from the test location. While the weather in the test area was generally cloudy during the run, no rain fell. The storm was estimated to be about 15 miles distant in a straight line from the test area, but was over lines of the 230-kv system, some 25 to 30 miles distant along the transmission line. It seems probable that electrostatic influence was projected along the transmission line since the noise level decreased in the usual manner when the meter was placed at increasing distances from the line. The background noise level at the test area did not increase. Corona on the conductors became audible at the test area although there was no change in weather, and the storm remained at a considerable distance. Transformer connections on the 230-kv system are all grounded Y, the nearest being about 60 miles from the storm area and about 30 from the test area.

Eighteen-Foot Conductor Separation

An area including four consecutive towers on the Midway-Columbia line was selected for determining the effect of reduced conductor separation. In this area the outer conductors were drawn toward the towers, as is illustrated in Figure 6, so that the conductor separation for three spans was approximately 18 feet. The rest of the line remained at its normal 27-foot spacing.

Prior to the tests some predictions indicated that the radio noise from corona would increase with decreased conductor spacing. This thought probably was due to the well-known fact that corona power loss increases with decrease in spacing, and it was believed that the radio-noise influence would be proportional to the losses. This theory was proved to be in error, the tests indicating a reduction of radio noise with the decreased spacing These tests have been repeated on several occasions in order to eliminate the possibility of error. The data are plotted in Figures 7 and 8. The data of Figure 7 for the 18-foot conductor separation were taken at mid-span and at the middle of the three 18-foot spans. The 27-foot data were taken in the second span beyond the three with reduced spacing (three spans away from the 18-foot data). Similar readings were taken at distances of approximately 3, 7, and 10 miles from the 18-foot area in order to be assured that the radiated noise was not unusually high in spans adjacent to the test area. The conductor height was slightly greater for the 27-foot span than for the 18-foot. A lower noise influence ordinarily would be expected from the higher conductor.

Tests also were conducted opposite towers in the test area at both 18- and 27-foot separation. Results are plotted in Figure 9. Actually only the points have significant value, although they are joined by straight lines. The noise level in all instances, including both the 27- and 18-foot areas, was considerably lower opposite the towers than at mid-span, as is evident by comparing Figures 8 and 9. For instance, at towers *201* and *202* directly under the conductor, the measured noise level was 25 and 20 microvolts per half meter, respectively, as is shown in Figure 9. At mid-span between these two towers and directly under the conductor, as is shown in Figure 8, the level was about 250 microvolts per half meter. This general relation was observed consistently throughout the tests.

Figure 9 shows that radio-noise influence, measured at towers where conductor separation is 27 feet, is considerably higher than it is at towers within the 18-foot area. Directly under the towers whe e the conductors hang at their normal 27-foot separation, corona is hardly audible in fair weather. At the towers where the conductors have been drawn in to 18-foot separation, there is considerable audible corona at all times. Personnel climbing the towers report that the field strength at some considerable distance

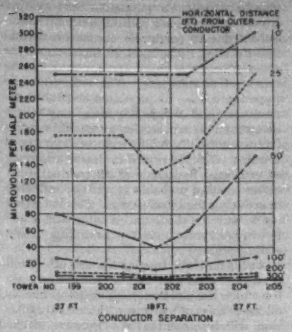

Figure 8. Corona radiation opposite mid-span

18-foot versus 27-foot conductor separation
September 12, 1946
Excitation: 233 kv
Test frequency: 800 kc
Weather: Fair, barometer 28.1 inches, temperature 86–84 degrees Fahrenheit, wind 17 miles per hour

below the conductor is very much greater on the towers having the conductors drawn in to 18 feet where they are about five feet from the nearest tower steel.

It is apparent from the foregoing results that the radiated radio-noise influence is not proportional to corona. It is also apparent that the energy radiated into space is reduced by drawing the conductors toward the grounded steel towers, although the electrostatic field between the conductor and the grounded steel is increased very considerably.

Analytical Verification

Although these data are contrary to commonly advanced theory, they are not difficult to understand from hindsight analysis. C. M. Sorvaag, of the Bonneville staff, has advanced the following explanation for this phenomenon.

It is a well-known fact in the field of radio communications that an open 2-wire radio-frequency transmission line will radiate an amount of radio-frequency energy depending upon line spacing, wave length, power transmitted, and other circuit conditions. With a properly terminated, balanced, open 2-wire radio-frequency transmission line under conditions of fixed frequency and power, the amount of radio-frequency energy radiated will be inversely proportional to the square of the conductor spacing. At decreasing values of conductor spacing, the radiation will decrease and more energy will be propagated down the line. Practically zero radiation would exist when the 2-wire line is resolved into a coaxial type of transmission line, and all of the radio-frequency energy is transmitted down the line except for line losses.

Radiation from a nonresonant open 2-wire transmission line can be expressed by the following equation:[3]

$$P = 160I^2\left(\frac{\pi a}{\lambda}\right)^2$$

where P is the power radiated; I is the line current; and a/λ is the conductor spacing in wave lengths. From this relation it is apparent that the power radiated is proportional to $(a/\lambda)^2$ where a is the conductor separation and λ is the wave length of a component of radio noise. So far as radiated radio noise is concerned, we consider for the sake of simplicity that only two wires of the transmission line are affected and that the corona will be a point discharge, or simply a random radio-frequency generator between the two conductors. In this case a portion of the radio-frequency component of the corona will be radiated and the remaining radio-frequency energy will be propagated down the transmission line in both directions, and the amount of radiated energy will be governed by the aforementioned equation.

This theory of reduced radio noise with decrease in transmission line spacing is verified by the data obtained with the 27-foot and 18-foot separation. According to the equation, the noise in the radiation field should decrease by a factor of 2.25. The data show the noise level decreased by a factor of approximately 2 with the 18-foot spacing.

Summary and Results

This investigation has resulted in design of 230-kv H-frame wood-pole lines including 11 insulator units, 18-foot conductor separation, and 1-inch-diameter conductor. Radio-noise influence ordinarily is not considered to be a limiting factor in high-voltage transmission line design. Suspension insulators are not responsible for radio-noise levels emanating from high-voltage lines, even though the line-end unit may be stressed to the corona limit. Static discharges can be severe offenders, and hardware is sometimes responsible.

Selection of conductor size should be based on losses and system characteristics rather than on radio-noise levels.

Safety to personnel working on energized lines rather than radio noise or mid-span flashovers is considered to be the limiting factor in conductor separation.

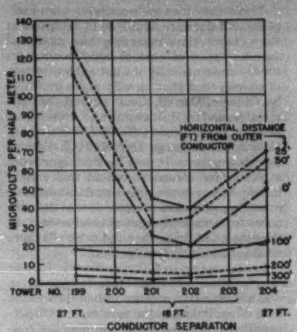

Figure 9. Corona radiation opposite towers

18-foot versus 27-foot conductor separation
September 12, 1946
Excitation: 237 kc
Test frequency: 800 kc
Weather: Fair, barometer 28–27.9 inches, temperature 85–70 degrees Fahrenheit, wind 7–11 miles per hour

References

1. Wood-Pole Line Protection Without Ground Wires, H. L. Rorden. *Electrical World* (New York, N. Y.), December 9, 1944.

2. Empirical Method of Calculating Corona Loss From High-Voltage Transmission Lines, J. S. Carroll, M. M. Rockwell AIEE Transactions, volume 254, 1937, pages 558–65.

3. Transmission Lines for Short-Wave Radio Systems, E. J. Sterba and C. B. Feldman *Proceedings*, Institute of Radio Engineers (New York, N. Y.), volume 20, July 1932.

Discussion

A. E. Davison (Hydro-Electric Power Commission of Ontario, Toronto, Ontario, Canada): Some of the students and cadet engineers, who are giving attention to radio interference and to higher voltage generally, are discussing the point, given suitable conductor diameters, of how effectively voltage might be raised on certain of the 230-kv groups of lines on this continent. For instance, if switching surges are not of great duration, then it may be possible to raise the voltage on some 230-kv designs to as much as, say, 350 kv. Has the author or have others any experience or comments in that connection?

These same men are wondering what literature and data are available to designers at the present time regarding the merits of various types of smooth-body conductors versus concentrically wound cables—other, of course, than that already made available by Oldacre, Carroll, Cozzens, and their associates, and by B. Hanning and those whom he quotes in a recent CIGRE (International Conference on Large Electric High-Voltage Systems) paper. It may be that figures are available for corona threshold and corona losses; however, are sufficient data available regarding radiation of these corona disturbances from various types of conductor? In the opinion of the author and others, is there need for further investigation?

In the opinion of the author, is further investigation of radio interference from transmission lines required when the limited field of radiation and attenuation, with perpendicular distance from the line, are considered?

To some degree, at least, the author raises the old controversy of the merits of steel versus wood supports. Does the author or others know of any data available and investigational work being done on the effectiveness of tuned circuits and natural frequencies within adjacent steel or other metal fabrications stimulated or energized by radiations from corona? Is it possible that natural frequencies of these tuned circuits within steel structures may account for an important part of transmission line radio interference generally? Do those who are working with this subject generally see a need for further study along these lines? Also, is it considered as a fact that steel structures, such as transmission towers, function as considerable absorbers of corona radiation?

Another question raised by these students is: What is the shielding effect of such paralleling grounded metal works as a suitable grounded static wire supported by wood or other like structures having high insulation values at low frequencies? Does this vary greatly from the absorbing capacities of static wires when supported by a considerable metal network such as steel towers?

With reference to Sorvaag's work on the effects of conductor spacing upon radio interference, has it been assumed that the radio-frequency energy produced will remain constant during the change in spacing? Is it the opinion of the author and his associates that the total radio interference energy produced by corona—that is, the sum of the transmitted energy, the absorbed energy, and the radiated energy—is independent of the corona disruptive voltage and the corona losses? Would it appear that further investigational work should be done on these relationships? Are there any suggestions as to how this subject should be approached, either theoretically or in practical testing?

G. B. Tebo of the Hydro-Electric Power Commission of Ontario and his associate, G. R. Slemon, raise the point that surge impedance will drop from 408 ohms for the 27-foot spacing to 384 ohms for the 18-foot spacing. This impedance may have a bearing upon the reflection of incoming radio interference waves, corona-generated or otherwise. Is this reflection considered important by the author in his conclusion regarding reduced radio interference with reduced conductor spacing?

E. H. Grosser, Jr. (Commonwealth Edison Company, Chicago, Ill.): This discussion will be limited to the radio-noise influence measurements described in the paper. Similar measurements were made by Commonwealth Edison Company in 1940 in connection with the design and operation of the Powerton-Crawford 220-kv transmission line, and partial data were given in an AIEE paper[1] describing that line.

Results of some very extensive tests on other high-voltage lines also were presented[2] by a committee before the Edison Electric Institute in 1940. These showed particularly the characteristic rapid attenuation of radio noise away from transmission lines.

In our case, we wished to determine the possible effect of radio interference on the communication and beam facilities of the airlines. Even prior to construction of the line, preliminary study was made with the co-operation of the Civil Aeronautics Authority by measuring the radio noise resulting from existing 132-kv lines when flights were made at low altitudes over these lines. Such interference was found to be negligible over the frequency bands involved.

After placing our 220-kv line in service, the investigations were continued and measurements made on the ground at various locations to determine (*a*) noise levels under the line at various radio frequencies from 150 kc to 125 megacycles and under various weather conditions, and (*b*) the decrease in noise levels normal to the line.

Radio noise was found to be most severe at the lower frequencies, particularly at the extreme lower end of the broadcast band. At higher frequencies the noise levels dropped off very rapidly. For example, the radio noise at 10 megacycles was only one or two per cent of that measured at 300–500 kc. This gave assurance that the aviation radio facilities, using the higher frequencies were not likely to be disturbed by proximity of a 220,000-volt transmission line.

The effect of weather conditions was perhaps not as large as had been anticipated. However, the rainy weather radio noise turned out to be roughly in the order of five times that measured in dry weather. Directly under an outer conductor at mid-span we measured, at about 350 kilocycles, a radio noise of around 700 to 800 microvolts per meter in fair weather, and about 4,000 microvolts per meter while it was raining.

Measurements transverse to the line showed, for instance, in fair weather at about one megacycle: directly under the outer conductor, 450 microvolts per meter; 100 feet out, 85 microvolts per meter; and 300 feet and beyond, from 10 to 15 microvolts per meter. These data show very close agreement with those presented by Rorden, in spite of the considerable difference in design of the two lines.

REFERENCES

1. POWERTON-CRAWFORD 220-KV LINE—DESIGN AND CONSTRUCTION FEATURES, M. S. Oldacre, F. O. Wollaston AIEE TRANSACTIONS, volume 60, 1941, pages 1108–20.

2. *Bulletin*, Edison Electric Institute (New York, N. Y.), October 1940, page 490.

E. C. Starr (Oregon State College, Corvallis, Oreg.): The data presented in this paper are very interesting and indicate that we should expect no particular fair-weather broadcast-frequency radio-interference difficulties due to conductor corona on normal 230-kv lines. The reduced interference for the section with closer spacing may be the result of two factors. The reduced surge impedance due to increased insulator capacitance and reduced spacing may reflect away from the test section a part of the interference normally fed in from other parts of the line. The decreased radiation efficiency at broadcast frequency of the conductors at closer spacing probably is a major influence in reducing the interference. This is further borne out by the reduced interference between conductors where a cancelling action should occur.

At higher radio frequencies this effect will be less pronounced and at the frequencies for which the conductor spacing approaches odd multiples of half wave, the lateral radiation will be accentuated. Because of the increasing use of high radio frequencies, this effect may be important and the interference spectrum should be explored at least somewhat beyond the television frequencies. It is probable that because of the nature of the source of the interference, it will decrease in magnitude with increased frequency. However, there may be some critical regions, and it is felt that the whole spectrum should be explored before final or general conclusions are drawn.

H. L. Rorden: Some of the questions raised by Davison are beyond the scope of the investigation, and therefore our comments must be based on analyses rather than on definite knowledge of the phenomenon. Such analyses are useful in supplying us with foresight of what might be expected. However, results described in the paper have convinced us that the only sure guide is experience. With this in view Mr. Davison's questions will be commented upon in the order given.

The question of insulation levels and the possibility of raising voltage on the existing system has been given considerable study by the Bonneville Power Administration. We hope to publish information of this nature in connection with our experimental lightning protection program at a later date. Since the Bonneville transmission system is not protected with overhead ground wires, the question of insulation levels differs somewhat from that of lines which are so protected. Our present trend is toward the use of high-speed reclosing circuit breakers, in lieu of ground wire protection. Although we have no definite proof, our observations and studies lead us to believe that we may expect practically all direct strokes to conductors to result in flashovers. Raising the insulation level, even beyond present limits of practice, would afford only partial protection, if any. We therefore are considering basing our insulation levels on a safe margin above switching surges plus a necessary tolerance for units that may be broken by lightning. We consider it all important to adopt a level that will permit the line to be re-energized before repairs are made, when a lightning flashover occurs. On this basis we believe that many of our present lines are overinsulated for 230-kv and also that the conductor diameters are adequate (although perhaps not the most economical) to permit them being used at higher voltages. We are not prepared to say that an increase

of 50 per cent, as suggested by Davison, can be effected without any change in the transmission system. However, we are thinking in terms of 25 to 33 per cent. We believe our insulation is adequate for these increased levels and that the radio noise will not be of serious concern.

Some *HH* conductor is in use on the Bonneville system, and the few tests that were made on this conductor indicate a little lower radio noise level. We have relied on data of the authors mentioned by Davison for losses and have no other publications to suggest. We believe that we have sufficient data to assure us that radio noise generated by corona is not a limiting factor in the design of high-voltage transmission facilities. However, as previously stated, the real answer is experience and further investigation could reveal additional useful data.

Further study might be necessary for exact data in the event a transmission line is located unusually close to radio or other communication facilities. We believe that there are other limiting factors controlling the design of transmission facilities which make it unnecessary to consider radio noise generated by corona. For instance, when conductors are of such diameter that they are economical for a given voltage and loading of a transmission system, they should be adequate so that radio noise need not be studied further. Also, if conductor separation is adequate for tower clearances and for safety to personnel working on energized lines, it will not be necessary to give serious consideration to radio interference emanating from the lines. As stated by Davison, the field of radiation and attenuation perpendicular to the line is very limited for noise generated by corona. Static discharges caused by loose or too close hardware, particularly on wood-pole lines, generate radio noise that radiates farther and at greater intensity than does that generated by corona.

From the results of this investigation it appears that the effect of steel towers or of reducing conductor separation is to change the dielectric field about the conductor, that although more corona is generated, there is no increase but probably a decrease in the amount of energy radiated perpendicularly from the line. From a comparison of Figures 8 and 9 it is apparent that the energy radiated from the line opposite steel towers is very much less than that radiated at mid-span. In this sense, steel towers act as an absorber of corona radiation, probably due to a considerable change in the configuration of the dielectric field which more than oversets the increase in the amount of corona generated by proximity of the conductors to the grounded metal. We are not aware of any work being done on the possibility of tuned circuits existing within the steel structures of transmission systems. It is our belief that since steel towers represent a relatively low impedance to ground, any energy that might be generated by tuned circuits within the structures does not transmit a great amount of energy into the power system to be radiated as radio interference. However, further study of this phenomenon seems very much in order.

We believe the use of grounded static wires will decrease the radio noise by shielding to some degree similar to that provided by steel towers. In some of the early investigations, it was found that the noise emanating from the line was considerably higher opposite wood poles than opposite steel structures. The data are not directly comparable because of the difference of conductor height at the structures. We are inclined to the opinion that the effect of the static wire itself would not be influenced by the supporting structure as long as the static wire is grounded at the structure. It seems that the proximity of other energized conductors has some shielding influence on the radiated energy and therefore a grounded static wire should perform similarly.

We believe that the random radio-frequency energy is dependent upon the amount of corona present. In the tests the corona increased with the decreased spacing and, correspondingly, the radio-noise energy produced must have been increased. However, due to the smaller spacing, a greater amount of energy was propagated down the line, and apparently enough less was radiated to offset the increased radio noise generated. The propagated radio-noise energy is probably dissipated quite rapidly as it travels down the line, and the line thus acts as an absorber. This would appear to be an excellent topic for further study which might be conducted to best advantage in a laboratory where conditions may be controlled.

The change in surge impedance by abruptly reducing conductor separation from 27 to 18 feet results in a reflection coefficient of about 2 $^1/_2$ per cent, which would have a negligible effect on reflecting radio noise disturbance from other parts of the system. Since the transition in the test area was not abrupt, it can be considered as an impedance matching device which should tend to reduce the reflection coefficient for radio frequency to a very small value.

Grosser's concurrence that our results agree with those obtained by the Commonwealth Edison Company some time ago lends added confidence to our conclusions. We are particularly interested in his data up to 125 megacycles. Our tests were limited to the broadcast frequencies for reasons stated, but there are undoubtedly some cases where higher frequencies may be of importance. General analysis indicates that the radiated energy should decrease with increasing frequency. Grosser's verification of this fact is very helpful and minimizes the necessity for additional data at the higher frequencies.

Grosser's mention of weather conditions is also of interest. We do not believe it is economical to design transmission lines to have low corona losses in inclement weather and therefore our comparisons were made under fair weather conditions. Although much higher levels exist in the rain near the line, the radiated energy is attenuated very rapidly. The wet noise level may be five times as high as the dry level within the induction field near the conductor, but it falls to less than twice the dry value at about 300 feet from the line. Figure 5 of the paper shows that although considerable abrupt variation in the noise level may exist under the conductor, at 200 feet the curve is fairly smooth and flat. We believe that, in general, radio noise generated by corona is not nearly as serious an offender as that generated by static discharges, both near the source and at a considerable distance from the line.

Grosser's results in part answer the questions raised by Starr. There is undoubtedly much yet to be learned about radio noise, and an investigation of the entire spectrum should be of considerable academic value. Our results give us sufficient confidence to use where possible to effect economies in the design of high-voltage lines, and we are further encouraged by Grosser's remarks. But development must continue if we are to continue to progress. Therefore, while we build our facilities on the basis of present knowledge, it is always in order to investigate further into the unknown.

Electric Drives for Textile Finishing Ranges

R. B. MOORE
ASSOCIATE AIEE

H. C. UHL
MEMBER AIEE

THE CONTINUOUS finishing of textiles with machines operated in tandem, or "in range," requires carefully co-ordinated, adjustable-speed machine drives. Electric drives, as compared to mechanical drives, generally offer several advantages, and are used predominantly on modern range installations. Of the electric systems, d-c drives are most generally suitable and most widely used, although a-c drives are used advantageously under certain circumstances. There are several types of co-ordination control that may be used on range drives, each type having certain advantages and disadvantages, depending on the basic type of range drive used.

This paper gives general information on textile ranges, basic requirements of range drives, basic considerations in selecting drive equipment, comparison of electric and mechanical drives, description of various types of electrical drives and co-ordination control, and recommendations for selecting proper equipment for specific conditions.

General Information on Textile Ranges

For a number of years the trend in textile finishing operations has been away from "batch" to "continuous" processing. In the batch system each lot of cloth is put through various separately operated processing machines, and is rolled-up or folded-down after each operation before being transported to the next machine. In the continuous system each lot of cloth is passed continuously and without intermediate handling through a line-up of machines called a "range." In more precise terms, a textile range consists of two or more cloth finishing machines, or elements of a single machine, arranged to operate in tandem on a common length of fabric passing without interruption through each of the machines, or elements, in succession.

Primary reasons for putting finishing machines in range are the speeding-up of production and the general streamlining of finishing operations. Handling of the fabric between operations is largely eliminated, resulting not only in improved product quality but also in large savings in man-hours and floor space. The orderly arrangement of machines and the elimination of handling equipment contribute greatly to the appearance of the finishing room and to the improvement of working conditions. All of the above advantages of range operation are realized in the form of increased output, improved quality, lowered costs, and increased profits.

Among the machines commonly operated in range, in a variety of combinations, are mangles, pads, washers, soapers, saturators, tenters, dryers, dye-units, recuperators, calenders, squeezers, batchers, folders, reels, and pilers. With the notable exception of the tenter, the machines named above have various types of rolls or cylindrical surfaces around which or between which the fabric passes for purposes of immersion, impregnation, drying, squeezing, nipping, etc. These machines are essentially friction loads, and usually require very nearly constant torque for driving at any speed. The tenter, which is used for straightening and stretching fabric to width, may require more torque at reduced speed when increased weft tension is placed on heavy fabrics. Maximum range operating speeds usually are limited by such considerations as the ability of machines to wash or dry the cloth satisfactorily, to retain the liquids used in the process, or in some cases to withstand the mechanical stresses caused by high speeds. Range speeds of 50 to 150 yards per minute are common and speeds of 200 yards per minute are not unusual. Equipment for speeds up to 300 yards per minute is now being manufactured for a type of high-speed bleaching range. The power required to drive textile finishing machines rarely exceeds 50 to 60 horsepower per machine, with the large majority of machines requiring from 5 to 25 horsepower. A few range elements, such as winders, reels, batchers, folders, pilers, and light squeezers, may be driven by 1- to 3-horsepower units. Tenters and calenders take the most power, frequently needing 30 to 60 horsepower. Medium loads are usually encountered on mangles, pads, washers, dryers, and heavy squeezers, with about 15 horsepower being a good average value. Of course, the total power required to drive an entire range will vary over wide limits depending on the type and number of machines involved, 30 to 100 kw being sufficient to accommodate the majority of modern ranges.

The commonly used finishing machines may be arranged in an almost limitless variety of combinations, each depending on the particular variation of a general type of range. Functions generally performed in range operation include bleaching, mercerizing, washing, dyeing, printing, and plain finishing. Figure 1 contains a schematic diagram of a typical range for finishing narrow sheeting. Drive equipment is not shown.

Drives for Textile Ranges—General

In selecting the proper drive for a finishing range, there are two basic require-

Paper 47–32, recommended by the AIEE committee on industrial power applications for presentation at the AIEE North Eastern District meeting, Worcester, Mass., April 23–25, 1947. Manuscript submitted November 15, 1946 and originally presented at the AIEE winter meeting, New York, N. Y., January 27–31, 1947, as a miscellaneous paper. Made available for printing March 12, 1947.

R. B. Moore is application engineer with the General Electric Company, Schenectady, N. Y., and H. C. Uhl is district application engineer with General Electric Company, Atlanta, Ga.

ments which must be satisfied regardless of the type of drive used.

1. The drive must be capable of covering the range of speed needed for any type and weight of fabric for which the equipment is intended.

2. The individual machine drives must be co-ordinated accurately to insure proper relative speeds and fabric tension at every point along the entire range, not only for steady range speeds but also during periods of acceleration and deceleration.

With reference to the requirements described above, the two main considerations in deciding on a range drive are:

1. What fundamental type of drive will be used?

2. What type of control will be used for co-ordinating the individual machine drives?

Mechanical drives and electric drives have been used for textile ranges. Considering that nearly all motive power in modern textile mills is furnished by electric motors (excepting some steam turbines), it sometimes becomes difficult to accurately differentiate between "electric" and "mechanical" drives. Therefore, these definitions will be used throughout the following discussion.

1. An electric range drive is one in which co-ordination is effected by adjustment of the speeds of the individual range motors.

2. A mechanical range drive is one in which co-ordination is effected entirely by adjustment of the mechanical ratios between the drive(s) and the individual range units.

The following is a list of mechanical and electric types of drives which might be used for textile ranges. Although there are other electric drives that might be mentioned, this list is limited to the four types that have been most successfully used.

Mechanical drives

1. Line shaft
2. Individual

Electric drives

1. Adjustable voltage (direct current)
2. Constant voltage (direct current)
3. Brush shifting type *BTA* (alternating current)
4. Turbine-electric (alternating current)

With the line-shaft drive, there is a single power unit driving a line shaft which runs the length of the range, and the individual range elements are driven from this line shaft through adjustable-ratio mechanical reducers. In the case of the range with individual mechanical drive, there is a separate constant-speed power unit, such as an induction motor, for each range element with the entire speed control obtained from the adjustable-ratio mechanical reducers.

In contrast, all of the electric range drives have individual, adjustable-speed driving units on each range element, obviating the necessity for any adjustable mechanical ratios.

Comparatively speaking, the mechanical drives are cumbersome, noisy, and expensive to maintain, whereas the electric drives are characterized by mechanical simplicity, flexibility, and adaptability to several different types of co-ordination control. The shafts, gears, belts, and pulleys commonly associated with adjustable-ratio mechanical drives are replaced by wires and rheostats in the electric system. A few points of comparison of electric and mechanical systems are

1. Relative speed adjustment on electric drives is generally easy to obtain by variation of the individual motor speeds, whereas relative speed adjustment on mechanical drives requires the use of mechanical ratio changers, usually regarded with disfavor. Electric drives are much more suitable for various types of co-ordination control, upon which relative speed adjustment depends. Some types of co-ordination control, as will presently be described are entirely unsuited for mechanical drives.

2. In some processes, it is occasionally desired to disconnect or by-pass certain of the range elements and to operate the others. Although this can be accomplished on mechanical drives by belt-shifting or unclutching, it can usually be done more simply on electric drives by electric disconnecting switches. There will be some maintenance on belts and clutches, but the maintenance on disconnecting switches is nil.

3. On electric drives, it is possible to use indicating instruments to show the loads

Figure 1. Schematic diagram of typical range for finishing narrow sheeting

Drive equipment not shown

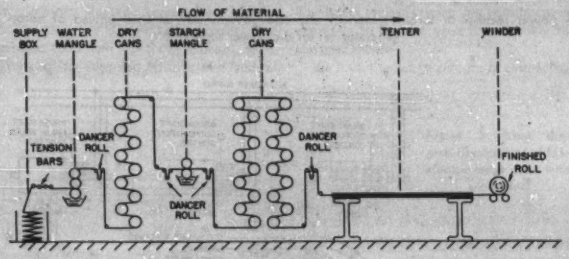

Figure 2. Line diagram illustrating adjustable-voltage d-c range drive with motor-generator set for d-c power supply

A controlled power rectifier or turbine-generator set, also shown, may be used instead of motor-generator set for d-c power supply

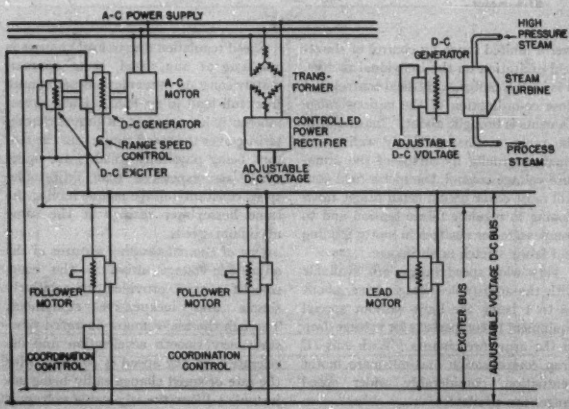

on the various motors. This not only helps to indicate the power requirements of the individual machines, but also serves to warn the operators of abnormal operating conditions which could conceivably be due to faulty machinery or improper use of the machinery. Such individual machine load indication on mechanical line-shaft drives cannot be realized.

4. The flexibility of individual electric motor drive is often an aid in the design and layout of the ranges and the buildings themselves. On the other hand, the use of a line shaft becomes a great hindrance when it is desired to lay out the range when all of the machines are not in a straight line or on the same floor of the building.

5. From the standpoint of appearance, neatness, quietness, space economy, and safety to personnel, it is conceded generally that the electric range drive is superior to the mechanical drive because of the elimination of a considerable amount of mechanical rigging around the machines.

Because of the many advantages of electric drives of this type, they are now used on textile ranges almost to the complete exclusion of mechanical drives. Among the electric drives, the direct-current types, particularly the adjustable-voltage system, have the most universally suitable characteristics and have been most widely used. However, the alternating-current drives definitely have their proper places of application. Therefore, the remainder of this paper will be devoted to detailed analyses of the four direct and alternating current types of drives and the various schemes of co-ordination control which may be used. The co-ordination control systems will be discussed separately from the drive types.

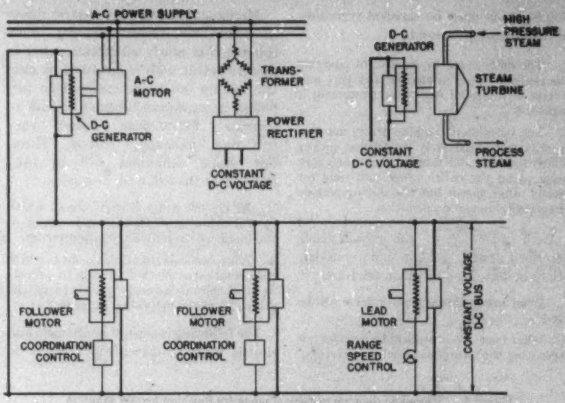

Figure 3. Line diagram illustrating constant-voltage d-c range drive with motor-generator set for d-c power supply

A power rectifier or turbine-generator set, also shown, may be used instead of motor-generator set for d-c power supply

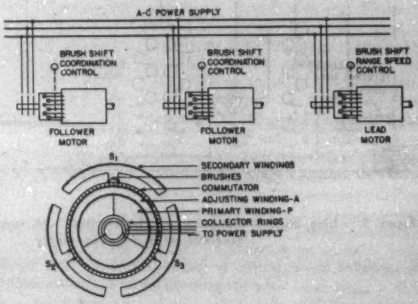

Figure 4. Line diagram of range drive with type *BTA* brush-shifting a-c motors, and schematic diagram of *BTA* motor

Adjustable-Voltage D-C Drives

The one line diagram in Figure 2 illustrates the equipment and connections for the adjustable-voltage type of drive. As shown in the diagram a motor-generator set is used to convert a-c power to adjustable-voltage d-c power. The conversion may also be effected by turbine-generator sets or by controlled electronic rectifiers.

The armatures of all the range motors are connected to the adjustable-voltage bus through a common controller. Excitation for the generator and the range motors may be supplied from a common, constant-voltage exciter, as shown, or may be obtained from separate, adjustable-voltage exciters, depending on the type of co-ordination control employed.

Over-all speed control of the range is obtained by rheostatic adjustment of the armature voltage, which is common to all the range motors. In addition, speed control on the individual motors is obtained over a limited range by control of shunt-field excitation on the individual motors. It is by this motor-shunt-field control that close co-ordination of the various range elements is brought about. Inasmuch as the range motors are fairly well co-ordinated initially by virtue of the armature-voltage control, the motor-field control must cover only a small range, functioning to regulate fabric tension and to compensate for changes in motor loading and fabric stretch or shrinkage.

Very wide speed ranges are available with the adjustable-voltage drive, about 15 to 1 being the limit without special equipment to compensate for voltage drop in the armature circuits. With this *IR* drop compensation and adequate motor ventilation, considerably wider speed ranges are available.

Speed regulation due to load changes is adequate at any speed, being approximately constant in revolutions per minute from full load to no load. These drives inherently have a constant-torque characteristic over the speed range, and the motors, being physically smaller, are somewhat less expensive than adjustable-speed constant-voltage motors having the same horsepower ratings at the same maximum speeds.

One of the outstanding features of the adjustable-voltage drive is the easy, smooth control provided by relatively simple and inexpensive equipment. Through the use of motor-operated rheostats very smooth acceleration and deceleration to any speed is possible, with the rate of speed change easily being adjustable. When the adjustable-voltage is

supplied by a motor-generator set, accurately controlled deceleration is obtainable with regenerative braking, an inherent characteristic. Rapid stopping also can be realized by dynamic braking.

The system is adaptable to control from a number of duplicate pushbutton stations at different locations. Speed indicators and load indicators for the various machines are frequently provided inasmuch as they give a good picture of the performance of the drive.

Motors may be removed from range operation, but may not be operated independently unless separate additional control and other d-c power supply are provided.

Inasmuch as the adjustable-voltage conversion apparatus is usually purchased for a specific range drive, good judgment must be used in choosing equipment with sufficient capacity to take care of possible future additions to the range.

In certain ranges having a large number of machines, it is sometimes advantageous to "sectionalize" the drive by dividing the motors into two or three groups, each group being supplied with power from a separate generator. This scheme has been used with marked success on a number of new continuous peroxide-bleaching ranges, in which there is a large amount of fabric "storage" between sections. The multigenerator drives on these bleaching ranges contribute to ease of operation and increased production by providing flexibility in an operation that may require different speeds in each section or may require some sections to be shut down while others are operating.

Constant-Voltage D-C Drives

Figure 3 illustrates the equipment and connections for this type of drive. As the name indicates, there must be available a source of constant voltage d-c power in sufficient quantity to drive the entire range. This d-c power generally has been supplied from motor-generator sets, as shown, but some plants have used turbine-generator sets or mercury-arc rectifiers. The latter type of conversion equipment is expected to become used more widely in the near future.

Each of the range motors is connected to the constant-potential bus through suitable starting control. Individual controllers or a common controller may be used for all the motors, depending on the degree of flexibility desired. Motors which are to be removed from range on occasion, and operated independently should have their own individual controllers. Excitation for the range motors may be supplied from the constant-voltage bus, as shown, or may be obtained from separate, adjustable-voltage exciters, depending on the type of co-ordination control employed.

Speed control on the motors is obtained by adjustment of the shunt-field excitation. This includes not only over-all speed control of the range but also co-ordination adjustments on the individual motors. In order to simplify the range control, it is common practice to have the co-ordination control cover the entire field-control range on a motor. However, this has the disadvantage of throwing the complete job of speed control on the co-ordination equipment, and the drive tends to be less stable than the adjustable-voltage type.

This type of drive is suitable for an operating speed range up to four to one in standard designs. Wider speed ranges can be obtained, but the motor designs are special and have a considerably higher cost. Speeds below basic speed, or minimum rated speed, can be obtained by means of series armature resistors, but efficiency and speed regulation become very poor under these conditions. Furthermore, the use of armature resistors greatly reduces the effectiveness of shunt-field control, and co-ordination of the range motors is likely to become difficult. Therefore, speeds below basic speed are not used commonly except intermittently for setting-up or threading-in operations

The adjustable-speed motors used in these constant-voltage drives inherently have a constant-horsepower characteristic over the normal speed ranges. Thus, more torque is available at low speed than at high speed, although this is no particular advantage except in a few applications. Because of this characteristic, these motors have a larger physical size and are more expensive than constant-torque motors having the same horsepower ratings at the same maximum speeds.

Smooth speed control is a feature in the field-control range, but favorable accelerating characteristics up to basic speed are difficult to obtain while the armature starting resistance is being removed in steps. Regenerative braking is available down to basic speed, and dy-

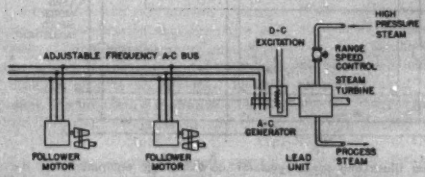

Figure 5. Line diagram illustrating turbine-electric range drive with a-c motors

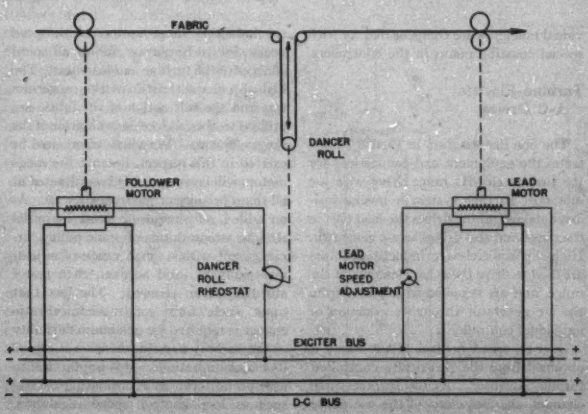

Figure 6. Line diagram illustrating dancer-roll co-ordination equipment for d-c range drive

namic braking may be used for stopping the drive from any speed. In comparison to other electric range drives, the control for the constant-voltage type is somewhat more complex and expensive.

Brush-Shifting Type BTA A-C Drives

In Figure 4 is a one-line diagram showing the equipment and connections for the *BTA* motor range drive. In this type of drive, 3-phase a-c power is used directly without any conversion equipment. Each of the range motors is connected to the a-c power line through its own individual controller. The system is quite flexible, and, if desirable, individual machines may on occasion be omitted from range operation and used independently without undue complication.

All speed control in the normal range is obtained by shifting of the brushes on the commutators. In this respect the *BTA* drive is similar to the constant-voltage d-c drive in which all normal speed control is accomplished by change in motor shunt-field excitation.

Operating speed ranges of three to one and four to one are available, with the three to one range being less expensive than the four to one range. As in the case of the constant-voltage d-c motor drive, speeds below basic speed may be obtained by use of resistors, this time in the motor secondary circuits. Speeds down to 50 per cent of basic speed are possible on an intermittent basis, speed regulation and efficiency being quite poor under these conditions.

Type *BTA* motor drives are suitable for constant-torque loads over the speed range. Being equipped with slip-rings, brushes, and two rotor windings, in addition to the commutators, type *BTA* motors are a little more expensive than constant-torque d-c motors. The individual controllers are relatively simple and inexpensive.

Although acceleration from basic speed upwards may be very accurately controlled, slow and smooth acceleration from standstill up to basic speed is difficult to obtain. For deceleration, regenerative braking is available down to basic speed. Dynamic braking may be obtained by using specially designed motors or by applying direct current on one phase of the primary of standard motors. However, the additional expense and complications of arranging for dynamic braking on *BTA* range drives is considerable, and all of the existing ranges of this type are allowed to coast to a standstill from basic speed. Unequal coasting times on individual machines are compensated for with special coasting relays in the controllers.

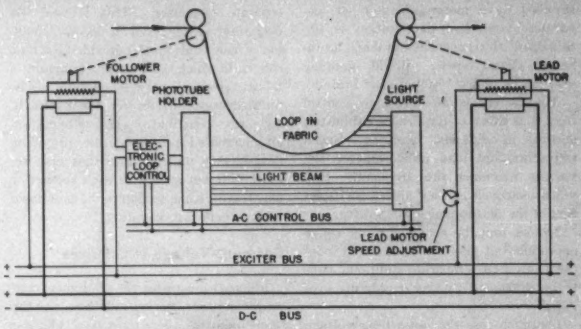

Figure 7. Line diagram illustrating photo-electric loop control used for co-ordinating elements of a d-c range drive

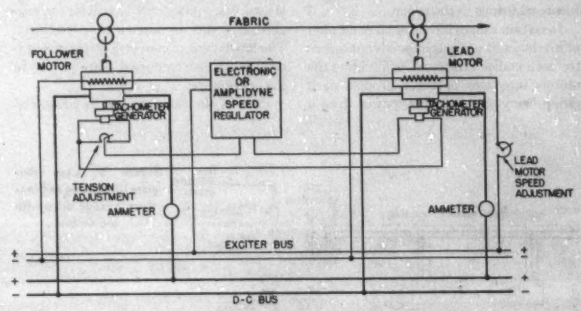

Figure 8. Line diagram illustrating speed-regulator co-ordination equipment for d-c range drive

Turbine-Electric A-C Drives

The one line diagram in Figure 5 illustrates the equipment and connections for the turbine-electric range drive with a-c motors. In this system a mechanical-drive steam turbine drives the lead unit in the range and also drives an a-c generator. High-slip squirrel-cage induction motors are used to drive the other elements of the range, and are supplied with power from the a-c generator through a common or individual controller.

Over-all speed control of the range is obtained from the electrically controlled turbine governor. As the turbine speed changes, the frequency of the a-c power generated changes in proportion. Thus, the induction range motors, with speed responsive to frequency, follow all speed changes of the turbine and lead unit. The high-slip characteristics of the range motors and the belt action of the fabric are utilized to obtain close co-ordination of the range elements. Very little effort need be exerted in this respect, because the range motors will be very nearly co-ordinated at all times because of the frequency tie. As an added refinement to assist in initial set-ups, some kind of cone-pulley arrangement with a small range of adjustment may be used between each motor and the driven element. The fact that some such form of mechanical-ratio change is required for maximum flexibility of the turbine-electric a-c drive is one of its major limitations. It is impractical to use special forms of coordination control such as loop control, speed regulators, strain regulators, and current regulators,

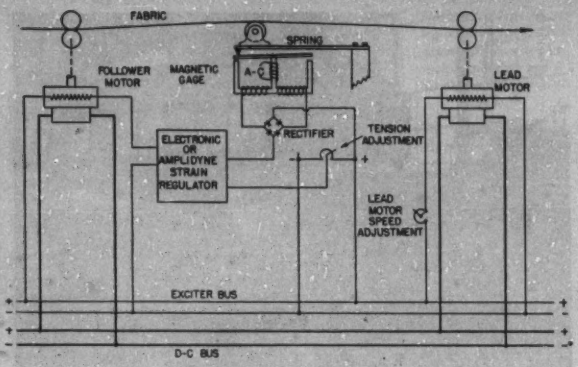

Figure 9. Line diagram illustrating use of strain regulator for controlling tension between elements of a d-c range drive

as will be described presently, for relative speed adjustments between the range elements.

Wide speed ranges, on the order of 15 to 1, are possible and very smooth acceleration and deceleration characteristics are easily obtainable with proper control on the turbine. Rapid stopping of a drive of this type may be accomplished by dynamic braking the a-c machines. To obtain this dynamic breaking effect, the steam is shut off from the turbine, the field of the a-c generator remains excited, and a 3-phase resistor of proper capacity is connected across the a-c bus, which is common to the generator and all of the follower motors. Stored energy of the entire drive, including the turbine rotor, is dissipated in this braking resistor, with the follower motors acting as induction generators excited from the rapidly decreasing a-c bus voltage. Regenerative braking is not feasible because power cannot be pumped back through the steam turbine.

The adjustable-frequency drive inherently has a constant-torque characteristic over its speed range.

The squirrel-cage induction motors are quite inexpensive, as is the a-c control. However, the turbine, the turbine governor, and the a-c generator are relatively expensive from the standpoint of first cost. The importance of first cost, though, becomes less because the turbine exhaust steam may be recovered for process operations. The need for process steam not readily available from other sources generally decides the question of consideration of a turbine-electric drive.

Although the turbine-electric drive has been described as an a-c electric system, it is possible to drive a d-c generator from the lead unit and to use d-c follower motors on the range elements. However, this would actually be a special form of the adjustable-voltage d-c drive, and rarely would seem to be justified because it offers no appreciable advantages over a straight adjustable-voltage d-c drive and because it results in a slightly more complicated mechanical and electric system than a straight adjustable-voltage d-c drive. Thus, if process steam is needed and if a simple turbine-electric a-c drive is not adequate, the conventional adjustable-voltage d-c drive with a turbine-driven generator set may be the best solution.

As in the case of the adjustable-voltage d-c drive, the rating of the turbine and a-c generator should be carefully considered from the standpoint of capacity to accommodate possible future additions to the range.

Types of Co-ordination Control

The fact that the various elements of a textile range are individually driven makes necessary some provision for co-ordinating the range motors to maintain correct relative speeds and fabric tension between elements. There are a number of methods by which the elements of an electric range drive may be co-ordinated, several of which will be described in this paper. Following is an outline of the types to be discussed.

Regulated systems

1. Dancer rolls (compensating gates)
2. Photoelectric loops
3. Speed regulators
4. Strain regulators
5. Current regulators

Unregulated systems

1. With shunt motors
2. With "soft" motors

By "regulated system" is meant one in which the range motors are continuously controlled by automatic, closed cycle, regulating equipment. It follows, then, that an "unregulated system" has no such regulating equipment.

Figure 10. Line diagram illustrating use of current regulator for controlling tension on centerwind reel at end of an adjustable-voltage d-c range drive

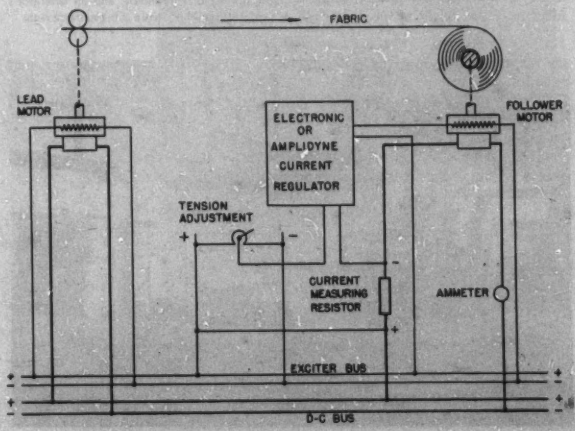

Dancer Rolls

In the textile finishing industry dancer rolls, often called compensating gates, are the oldest and most widely used method of range-drive co-ordination. Each roll is supported in a loop of fabric between successive elements of the range and is mechanically connected by chain and sprocket to a speed-changing device on one of the motors, all motors thus arranged being known as "follower" motors. Figure 6 illustrates one type of dancer-roll and rheostat mechanism. One motor, known as the "lead" motor, will not be associated with a dancer roll, and its speed will determine the over-all speed of the range. Obviously, a dancer roll will rise or fall if fabric is removed from the loop faster or slower than it is fed into the loop. As the roll changes position, it will drive the speed-changing device on the motor it controls. Thus, the dancer roll will always assume a position so that cloth is removed from and fed into the loop at the same rate, and the range elements on either side of the loop are said to be co-ordinated.

In view of the fact that dancer rolls take up space and require maintenance and proper installation, they have been much maligned of late. Whereas this criticism is understandable, the fact remains that dancer rolls give the simplest, least expensive, most accurate simultaneous control of speed and tension, automatically compensating for changes in fabric stretch or shrinkage and for changes in relative motor speeds due to any causes. The average speed control is 100 per cent accurate, and the tension on the fabric is definite and unvarying under steady-state conditions, being a function of the weight of the dancer-roll equipment. The amount of tension can be changed by altering the weight on the dancer roll.

This type of co-ordination control is adaptable to any of the types of adjustable-speed drives already described. On the direct-current drives, the dancer rolls control rheostats, and on the *BTA* drives, they shift brushes.

Figure 12. Mercerizing range drive of Figure 11, viewed obliquely against the direction of fabric flow as the fabric leaves the tenter on the right and enters the recuperator on the left

The splashproof d-c motors, 40 horsepower on the tenter and 15 horsepower on the recuperator, drive the machines through V-belt drives

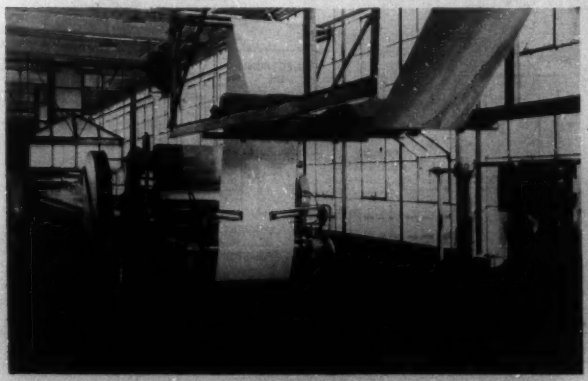

Figure 11. Adjustable-voltage d-c mercerizing range drive, in large Southern finishing plant, viewed obliquely in direction of fabric flow, with caustic pad in foreground and tenter in left background

At the left of the pad is its $7^1/_2$-horsepower splashproof driving motor, and an operator's control panel is visible at the extreme right

Photoelectric Loops

This type of control is similar in many respects to the dancer-roll control, but is devoid of the mechanical objections of the dancer-roll equipment, since the regulating equipment involves no moving parts. A loop in the fabric acts to intercept a portion of a wide beam of light, as indicated in Figure 7. The voltage output of the photoelectric control, and therefore the motor excitation, is a function of the amount of light reaching the phototubes. Thus, the speed of the motor being controlled from the loop depends on the position of the bottom of the loop, just as the position of the dancer roll in the discussion above determined the speed of the motors. The loop will always assume a depth that gives a balance between the rates of fabric motion into and out of the loop, and the motors on either side of the loop are properly co-ordinated.

The fabric tension in a system of this type may be zero, or may be made any desirable amount by supporting a properly weighted roll in the loop. Obviously, for best results, the fabric should be closely woven in order that the light beam may be cut off sufficiently to give control. For loosely woven fabrics which will not

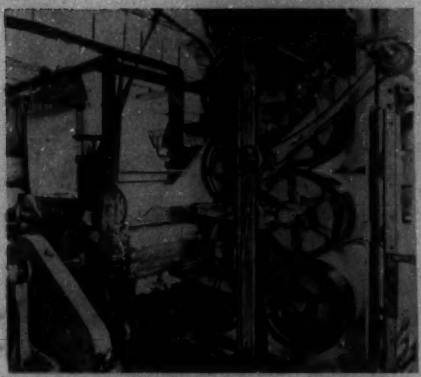

Figure 13. View showing 10-horsepower STA motor driving a set of drying cylinders and a 2-roll mangle in a finishing range

The dancer roll, visible in the lower right corner, acts to control the speed of the motor relative to other motors in the drive, using the visible chain-and-sprocket arrangement to shift the brushes on the commutator

Figure 14. Part of a turbine-electric a-c range drive viewed across the top of a tenter, with the mechanical drive turbine in the background

The turbine drives the a-c generator (partly visible) directly, and drives the tenter from the shaft extension on the rear end of the a-c generator

speed reference in this case could be the voltage from a tachometer generator driven by the lead unit in the range, or it could be a master, adjustable reference voltage against which the speeds of the lead unit and all the follower units could be matched. The one line sketch of Figure 8 illustrates a type of speed-regulating control.

For fast, accurate speed control, the regulating equipment must have quick response and high amplification characteristics in order to operate with very small error signals. Electronic regulators and dynamo-electric regulators of the amplidyne type have these characteristics, and give very accurate control.

Speed regulation of this type offers an excellent means of controlling stretch, but because of the very flat speed-load characteristic, it is not necessarily a good way of directly controlling fabric tension. In other words, a small change in speed between range elements may result in a much larger change in tension, depending in part on the stretch characteristics of the particular fabric.

This kind of speed-regulation equipment is ideally suited to d-c drives, being somewhat easier to use on the adjustable-voltage system where only a small amount of speed control is necessary on the motor shunt fields. Speed regulators of this type are not recommended for the a-c systems included in this article because of the problems encountered in translating the error signals into the mechanical motion necessary for speed correction.

cut off much light, special arrangements with auxiliary equipment may be made.

Photoelectric co-ordination of range elements is readily achieved on direct current drives, and although possible on the a-c drives, it is not so easily adaptable and is not recommended.

Speed Regulators

Straight speed-regulating equipment on the individual motors may be used for co-ordinating elements of range drives. In this system the speeds of the individual machines are compared with a speed standard, and any difference between the actual machine speeds and the speed standard are amplified and fed back into the individual motor speed control in a closed loop regulating circuit. One way of picking up speed signals from the individual machines is through the use of tachometer generators, the voltages of which are proportional to speed. The

Figure 15. Three cloth-printing ranges in large Southern plant

View perpendicular of direction of fabric motion to illustrate use of dancer roll and rheostat co-ordination control. The dancer rolls, rheostats, and chain drives are visible near the top of the illustration

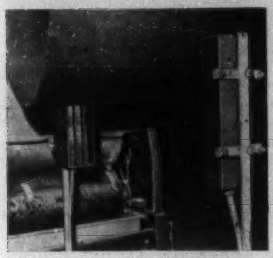

Figure 16. Photoelectric loop control on new dyeing range in a New England plant

The fabric loop, maintained between two successive range elements, acts to intercept part of the light beam between the light source on the left and the phototube holder on the right, the speed of the controlled motor being a function of the amount of light reaching the phototubes

Figure 18. Motor-generator set and d-c control panel for the adjustable-voltage mercerizing range shown in Figures 11 and 12

This 1,800 rpm set consists (left to right) of a 125-horsepower induction motor, a 75-kw d-c generator, and a 3-kw overhung d-c exciter

Strain Regulators

In certain finishing processes, fabric tension is rather critical and must be controlled accurately. For this accurate work, special equipment may be used actually to measure and control fabric tension between elements. In this system, the cloth may be passed over a roll and the deflection of the member on which the roll is mounted may be measured by some form of strain gauge, the voltage output of which will depend on the amount of gauge motion, and, hence, fabric tension. By means of a rheostat an adjustable tension reference may be established against which the output of the strain gauge will be compared. The difference voltage is amplified and fed back into the motor speed-control circuit so as to maintain the selected tension. Figure 9 shows the elements of a system using strain regulators. As in the case of speed regulators described before, electronic or amplidyne control may be used for very close regulation of tension.

Although not recommended for the a-c drives described, this kind of tension control is well suited to d-c drives, being somewhat easier to use for range coordination on the adjustable-voltage type.

Figure 17. Close-up view of adjustable-voltage d-c soft-motor drive on continuous dyeing range in large Southern bleachery, showing 3-horsepower splashproof gear-motors direct connected to squeeze rolls

Near the top of the photograph are the load-indicating ammeters and directly above the motors are the tension-adjusting rheostats for the respective motors

Current Regulators

Fabric tension between range elements may sometimes be controlled indirectly by means of motor-current regulators. This system, which is suitable only on the adjustable-voltage d-c type of drive, uses an amplidyne or electronic closed loop regulating circuit for motor shunt-field control in maintaining constant motor-armature current. The one-line schematic diagram of Figure 10 illustrates the current regulator. Obviously, if current control is to give accurate tension control, most of the motor load current must be due to tension. Therefore, the system is at its best only on drives where the friction component of the load is quite low. This kind of tension control is well suited for centerwind reels, a type of load requiring approximately constant horsepower for constant tension as the reel diameter builds up, for one given speed of fabric.

Unregulated Systems

There are types of finishing ranges in which there is no necessity to maintain extremely accurate control over speed or tension between range elements. In these cases, no automatic regulators are necessary, and manual control plus the inherent motor characteristics are relied on entirely.

Shunt Motors

One example is a type of continuous peroxide bleaching range in which the

cloth is handled in slack-rope form without tension between sucessive range elements. A large number of these ranges with adjustable-voltage d-c drive are being installed throughout the country today. Since the cloth is slack between machines, speed regulators are about the only automatic co-ordination control that could be used. However, since there is considerable slack-cloth storage between machines, such fine speed control is superfluous, and the co-ordination control is therefore obtained from manual rheostats.

Soft Motors

Another example is the so-called "soft motor" adjustable-voltage d-c range, of which a considerable number have recently been installed. Motors for these drives have been purposely designed so that their speeds will change considerably with load, compound windings being used to give this characteristic. Fabric tension between successive machines can be adjusted according to the manual setting of the individual motor shunt-field rheostats. Any tendency for individual motor speeds to drift initially will cause more or less fabric tension between the particular machines, and this change in fabric tension will be reflected in the loads on the individual motors. A motor attempting to speed up, for example, therefore will take more load and due to the drooping characteristics will tend to slow down, thereby taking on less additional load than would be the case if the speed remained unchanged. At the same time, the temporary increase in load on one motor would mean the temporary decrease of load on some other motor, which would promptly tend to speed up slightly. Thus, the whole system tends to be more or less self-regulating, with the "belt" action of the fabric and the inherent motor characteristics being utilized in holding the entire drive together. Obviously, this kind of soft-motor drive must be considered carefully and properly engineered. Also, for the most part, applications have been restricted to motors below 20 horsepower since the soft-motor drive is likely to be most successful where the driving motors fall in the lower horsepower ratings. The reason for this is the fact that "over-motoring," which occurs frequently, is a greater disadvantage in the large horsepower ratings since more tension is likely to appear in the fabric if the individual motor speeds should be inclined to drift.

Figure 19. View of d-c magnetic controller for adjustable-voltage range drive consisting of 14 motors totaling 102 horsepower

This controller, which includes dynamic braking and jogging features, is typical of the simple, inexpensive controllers furnished on adjustable-voltage range drives

Table I. Co-ordination Control Selection Chart

Type of Range Drive	Type of Co-ordination Control: Dancer Roll	Photo-electric Loop	Speed Regulator	Strain Regulator	Current Regulator	Soft Motor
Adjustable voltage, direct current	XX	XX	XX	XX	XX	X
Constant voltage, direct current	XX	XX	X	X	—	—
Type *BTA* alternating current	XX	—	—	—	—	—
Turbine-electric alternating current	—	—	—	—	—	X

XX—Very good
X—Good
—Not recommended

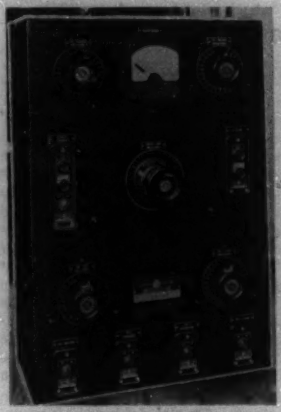

Figure 20. Operator's control panel for adjustable-voltage d-c continuous peroxide bleaching range drive in large Southern plant

Panel includes control stations for starting and stopping the motor-generator set, the entire range drive, and individual range motors. Also included are rheostats for speed control on the entire range and the individual motors as well as a cloth-speed indicator

How to Select Proper Type of Drive

Since there is such a variety of drives and co-ordination equipment available for textile finishing ranges, some kind of guide for making proper selections to meet specific requirements should be helpful to those concerned with the application of such equipment. Although there will always be special cases and exceptions to broad generalizations, the following should be useful in making preliminary decisions regarding the suitability of the various drive systems. It is recommended that final selection of equipment be based on studies and specific proposals made by electrical engineers specializing in textile-mill applications.

1. *Adjustable voltage (direct current).* For wide speed ranges, regardless of type of available power supply; where very smooth acceleration and/or deceleration is a requisite; where range operation at creeping speeds may be necessary for moderately long time intervals; for moderate speed ranges when drive is composed of a large number of motors over which the expense of the power conversion equipment may be spread.

2. *Constant voltage (direct current).* For speed ranges up to four to one and where enough constant-voltage d-c power is already available without adding to the capacity of the d-c system. If additional generating equipment is required and/or a large number of range motors are involved, it may prove advantageous to consider an adjustable-voltage system.

3. *Brush shifting type BTA (alternating current).* For speed ranges up to four to one; where a-c but no d-c power is available; where the number of range units is small. If a large number of range motors are involved, it may be advantageous to consider an adjustable-voltage d-c system.

4. *Turbine-electric (alternating current).* Where low-pressure process steam, not readily available from other sources, is needed and where the simple co-ordination control of the a-c system is sufficient.

In addition to these considerations, the type of co-ordination control desired may be a decisive factor in selecting the type of drive. Table I lists the various kinds of co-ordination control with indication of suitability of the control for the different kinds of drives, based on accuracy adaptability, and stability.

No Discussion

Fundamental Basis for Distance Relaying on 3-Phase Systems

W. A. LEWIS
FELLOW AIEE

L. S. TIPPETT
NONMEMBER AIEE

FOR THE PROTECTION of transmission lines against short circuits and ground faults, it is desirable to have a system of relays which will divide all faults on the line it protects, regardless of type or system conditions, into two classes: one, those which occur between the relaying station and the next sectionalizing point on that line, and two, all other faults. It is also desirable that this classification be performed instantaneously, so that the section in trouble may be isolated immediately, thus reducing the damage at the point of fault and the shock to the remainder of the system, and in general permitting operation nearer the stability limit. The quantities which may be utilized for classification are currents, voltages, the phase relations between them, and time. The demand for high speed of fault isolation, rendered acute by the development of high-speed circuit breakers, largely has disqualified time as a fundamental means of discrimination, leaving only the other three.

For protection of single lines, the nearest approach to this ideal, exclusive of pilot-wire or superposed high-frequency methods, has been obtained by the use of distance relays. For parallel lines a somewhat closer approach has been obtained by means of balanced-current relays. However, additional protection is required for single-line operation and to take care of the possibility of simultaneous faults on both lines, for which distance relays are well suited. Therefore, if the distance relays are made sufficiently accurate and rapid, the balanced-current relays may be dispensed with or provided for backup protection only. A systematic and comprehensive analysis of the voltages and currents which may be used to operate the distance relays, to determine their suitability and the results which may be expected, has not appeared previously. The aim of this paper is to provide such an analysis.

Distance relays consist of two basic types: impedance relays and reactance relays. The impedance relay compares the magnitudes of the voltage and the current, the ratio being the indicated impedance. The reactance relay compares the magnitude of that component of the voltage 90 degrees out of phase with the current and the magnitude of the current, the ratio being the indicated reactance. Since the original presentation of this paper, several modified types of relays have been developed, having characteristics which are modifications of, or combinations of, the characteristics of impedance or reactance relays. The purpose of these special types has been to minimize the danger of undesired relay operation during load swings or other system disturbances, while retaining or improving the ability of the relay to operate for faults in the protected zone with fault resistance present.

Under line-to-line fault conditions on an individual single-phase line, the indicated impedance is equal to the actual impedance of the circuit from the relay to the fault, plus the effect of any fault impedance which is present. On polyphase systems the ratio is not necessarily equal to the circuit impedance, but may be affected in various ways by the type of fault, the system load, and other conditions external to the section being protected, as well as by the fault impedance. As the impedance in the fault is primarily resistance, it generally is assumed that a relay operating on the reactive component of the impedance will be unaffected by the fault resistance. On a radial single-phase system this is quite generally true, but, if the fault is fed from two or more points or if a polyphase system is involved, it does not follow necessarily. Current flowing through the fault resistance produces a voltage drop in phase with it. This voltage drop is added to the line drop and thus affects the voltage at the relay. Unless the current through the relay is exactly in phase with the current through the fault, the fault resistance drop will have a component 90 degrees out of phase with the relay current thus producing an effect similar to reactance in the line. This apparent reactance can be either positive or negative thus making possible an increase or decrease in the indicated reactance and adversely affecting the relay operation. If the fault resistance becomes very large in comparison with the reactance of the transmission line section, this effect becomes quite serious and may prevent the application of the relay in some cases, particularly on very short lines.

Because the circuit impedances are not absolutely invariable and the relaying indications not an absolutely accurate measure of the distance to the fault, it has been found impractical with distance relays to classify all faults into the two classes specified. For faults near the remote end of the section, the relay is unable to determine whether the fault is just within or just beyond the end of the section. Hence, an intermediate class has been introduced to include faults in the immedate neighborhood of the end of the section on either side. If a fault falls in the first class, the circuit breaker is tripped instantly. If a fault falls in the second or intermediate class, a definite

Paper 47-66, recommended by the AIEE committee on protective devices for presentation at the AIEE winter meeting, New York, N. Y., January 27-31, 1947. This paper is based on one originally presented at the AIEE Middle Eastern District meeting, March 11-13, 1931. Manuscript submitted November 14, 1946; made available for printing December 12, 1946.

W. A. Lewis is dean of the graduate school, Illinois Institute of Technology, Chicago, Ill., and consultant for the Armour Research Foundation; L. S. Tippett, formerly switchboard engineer, Westinghouse Electric Corporation, is now with Westinghouse Rosebery Proprietary, Ltd., Waterloo, Australia.

The authors acknowledge the co-operation and encouragement of H. A. Travers, S. L. Goldsborough, and the late R. D. Evans and L. N. Crichton.

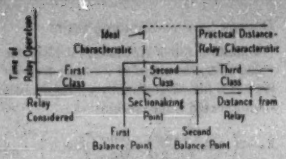

Figure 1. Ideal and practical distance relay characteristics

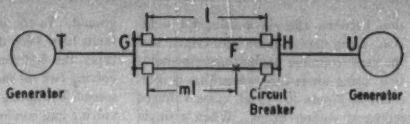

Figure 2. Single-line diagram—assumed equivalent system

time delay is introduced before the circuit breaker is tripped, and if the fault falls in the third class, the circuit breaker either is not tripped or is tripped only after a considerably greater time delay. This is shown in Figure 1. If the fault is beyond the end of the section, it will be cleared by other circuit breakers and relays before the expiration of the time delay, and the relay will reset. If the fault is just within the section, the relay will trip the circuit breaker at the end of the time interval. Thus, the final classification for faults in the intermediate group is made in conjunction with the operation of other circuit breakers and relays during a short time interval.

When impedance or reactance relays are used, the fault belongs in the first class, if the indicated impedance or reactance is below a definite lower limit; in the intermediate class, if the indicated quantity lies within two given limits; and in the third class, if it exceeds the upper limit. It will be convenient to call the points at which faults must occur in order to produce the limiting values of indicated impedance or reactance "balance points," as for such faults the relay just balances between one type of operation and another. To achieve the ideal, it is necessary to make the first balance point coincide exactly with the remote end of the section. In practice this is not possible, but in order to prevent false operation, and give full protection, the first balance point never must extend into the adjoining section, and the second balance point in the adjoining section never must extend into any other section. The smaller the variations in balance point position, the closer the balance points may be located to the remote end of the section, and the more nearly the relaying system approaches the ideal.

It is not essential for the second balance point to be located close to the end of the first section, as advantage may be taken of its presence in the adjoining section to provide backup protection for a portion of the second section, in case the circuit breakers in that section fail, for any reason, to open when they should. However, it is highly desirable that the variation be kept to a minimum, so that a short section of line may follow a long one without danger of the balance point moving out of the section, or extending beyond the first balance point of the relay protecting that section.

If the quantity indicated by the relay is constant for all faults in any given location, but increases as the distance to the fault increases, and decreases as the distance to the fault decreases, it is obvious that the balance points may be fixed accurately. If the quantity is variable for different faults at the same location, the balance points will shift an amount depending upon the maximum variation. It is, therefore, important to eliminate or reduce the variations in indicated impedance or reactance as far as is practicable.

The quantities which would be indicated by the two basic types of relays under different fault conditions are determined in the paper in terms of the circuit constants and fault currents, and a comparison is made to show the possible variations. The methods which will result in smaller variations are pointed out.

For the purpose of developing the necessary formulas, a typical 2-circuit transmission system has been assumed, as shown in Figure 2, with a source of power at each end of the line. The 2-circuit line between stations G and H has been shown in detail, with bussing of the two lines assumed at these points. The remainder of the system at each end has been represented by a single equivalent circuit and a single generator. In general, any section of a system may be represented in this manner for short circuits outside the section so simplified, although the constants of the equivalent circuit and equivalent generator may change. If there are ties between the two generating stations other than the lines shown, provided these ties are so remote that they do not have appreciable mutual coupling with the two lines considered, the effects may be taken into account by giving to the constants of the equivalent circuit and the equivalent generator variable values, such that at every instant the voltages and currents flowing from the simplified portion of the system into stations G and H are the same as those occurring under the actual conditions. This is always possible, although the practical application may be quite difficult. For our purposes, it is necessary only to know that the representation is possible, the actual values of the equivalent circuit constants being required only in special cases. Adequate neutral grounding is assumed at both ends of the system, although from the standpoint of the following theory it may be either solid or through impedance.

Shunt loads and distributed capacitance have been neglected, for simplicity, in line with the usual practice in the calculation of short-circuit currents, although later the effects of loads will be discussed. However, the simplification of assuming both generating sources in phase is not permissible, as phase relations have an important bearing on the results.

The use of symmetrical components for the determination of short-circuit currents during unbalanced faults is now well known, but the application to the determination of voltage conditions is not so widespread, due to the fact that the voltages are not required so often. For present purposes the voltages at relaying points are of particular importance, and, as the relaying voltages generally will be compared with the relaying currents, it is desirable to know the voltages in terms of the fault currents and the constants of the circuit, instead of in absolute values, thus facilitating the comparison. In the appendixes, the voltages at relaying points, line to neutral and line to line, as well as their symmetrical components, have been worked out in terms of the fault currents and circuit and fault impedances for all the common types of faults. In the body of the paper these voltages will be compared with the fault currents to determine the impedance or reactance indicated by the relay which should be operated for the particular fault, and comparisons drawn for possible relay connections.

The notation used is that of symmetrical components with additional subscripts to indicate the particular point or path involved. The notation is given in Appendix I.

For simplicity in writing the equations, the single-subscript method of indicating delta voltages has been used. The rela-

tion between the single-subscript notation, using capital-letter subscripts, and the more common double-subscript notation, using lower-case subscripts, is indicated in Figure 3. In all cases voltages represent voltage drops. When a single lower-case subscript, a, b, or c, is used, the voltage drop from that phase to neutral is intended. When two lower-case subscripts are used, the voltage drop from the first subscript to the second is meant. The corresponding relation for the single capital subscript is shown in Figure 3. A small plus sign indicates the terminal of higher potential when the corresponding voltage is positive.

It is necessary to set up the sequence networks for the assumed system. The networks are shown in Figures 4, 5, and 6, and the steps involved are explained in Appendix II. Here also the fault currents at relaying stations are set up in terms of their symmetrical components for the various types of faults. Certain instrument current transformer connections, which will be used, give different relaying currents, and these likewise are worked out assuming a 1-to-1 transformer ratio. The actual relaying currents may be obtained by dividing by the transformer ratio. The connections considered are shown in Figures 7, 8, and 9.

The use of a single set of relays for protection against all types of faults has not been found possible yet. One set of relays is required to protect against faults involving two or more line conductors, and another set of relays is needed for protection against faults between one conductor and ground. It is also possible, by means of a set of transfer relays, to use a single set of distance relays, connected in one way for faults involving two or more conductors, and in another way for faults involving one conductor and ground. In the following discussion, the faults have been divided into two general types, the first consisting of line faults involving two or more conductors, and the second consisting of ground faults involving one conductor and ground.

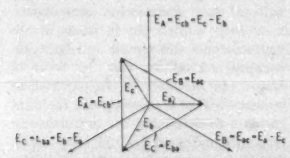

Figure 3 (above). Voltage vector diagram showing convention in choosing delta voltages

Figure 4 (below). Positive-sequence network for assumed system

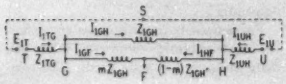

Line Faults—Star-Current Relaying

The earlier connection of impedance or reactance relays for protection against line faults made use of the delta voltage and the line current for operating the relay. The phase relations usually were chosen so that the current lagged the voltage by 30 degrees at unity power factor. This connection is shown schematically in Figure 10, only the connections for the impedance element being given. By using the quantities given in the appendixes, the impedance or reactance given by this connection may be determined. In setting up the sequence expressions, line faults involving only two conductors are assumed to occur between conductors b and c. The delta voltage of this phase at the relaying point G is then E_{AG}. The line current which lags the voltage by 30 degrees at unity power factor and flows from G to the fault is $(-I_{bGF})$.

Line-to-Line Faults

Equation 106 of Appendix III gives the value of E_{AG} in terms of $(-I_{bGF})$ for this type of fault. Dividing this voltage by the relaying current $(-I_{bGF})$ gives the relay impedance Z_R, indicated by the relay at G which should trip, as

$$Z_R = 2\left(mZ_{1GH} + \frac{R_S}{2}\right) + 2\frac{I_{bHF}}{I_{bGF}}\frac{R_S}{2} + \frac{I_{aGF}}{I_{bGF}} mZ_{1GH} \quad (1)$$

An impedance relay, of course, responds to the magnitude, and a reactance relay to the imaginary or reactive component of the foregoing vector expression.

To facilitate comparison it is also desirable to write this expression when the fault impedance is zero. In that case

$$Z_R = 2mZ_{1GH} + \frac{I_{aGF}}{I_{bGF}} mZ_{1GH} \quad (2)$$

If the circuit breaker at H is open, I_{bHF} and I_{aGF} are zero, and equation 1 becomes

$$Z_R = 2\left(mZ_{1GH} + \frac{R_S}{2}\right) \quad (3)$$

With no fault resistance this becomes

$$Z_R = 2mZ_{1GH} \quad (4)$$

Double Line-to-Ground Faults

Equation 130 of Appendix IV gives the value of E_{AG} in terms of $(-I_{bGF})$ for this type of fault. Dividing by $(-I_{bGF})$ gives the indicated impedance as

$$Z_R = 2\left(mZ_{1GH} + \frac{R_S}{2}\right) + 2\frac{I_{bHF}}{I_{bGF}}\frac{R_S}{2} + \frac{I_{aGF}}{I_{bGF}} mZ_{1GH} - \frac{3I_{bGF}}{I_{bGF}}\left(mZ_{.GH} + \frac{R_S}{2}\right) - \frac{3I_{0HF}}{I_{bGF}}\frac{R_S}{2} \quad (5)$$

As in the preceding case, an impedance relay indicates the magnitude, and a reactance relay the imaginary component of the foregoing vector expression.

If the fault resistance is zero this becomes

$$Z_R = 2mZ_{1GH} + \frac{I_{aGF}}{I_{bGF}} mZ_{1GH} - \frac{3I_{bGF}}{I_{bGF}} mZ_{1GH} \quad (6)$$

If the circuit breaker at H is open, these expressions simplify, as I_{aGF}, I_{bHF} and I_{0HF} are zero, giving

$$Z_R = 2\left(mZ_{1GH} + \frac{R_S}{2}\right) - \frac{3I_{bGF}}{I_{bGF}}\left(mZ_{1GH} + \frac{R_S}{2}\right) \quad (7)$$

and for zero fault resistance giving

$$Z_R = 2mZ_{1GH} - \frac{3I_{bGF}}{I_{bGF}} mZ_{1GH} \quad (8)$$

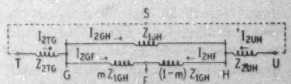

Figure 5 (above). Negative-sequence network for assumed system

Figure 6 (below). Zero-sequence network for assumed system

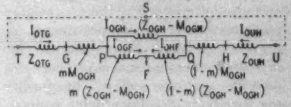

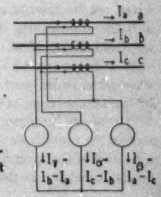

Figure 7. Delta-connected current transformers

Three-Phase Faults

Equation 146 of Appendix V gives the value of E_{AG} in terms of $(-I_{bGF})$ for this type of fault. Dividing by the relaying current $(-I_{bGF})$ gives

$$Z_R = 2\left(mZ_{1GH}+\frac{R_S}{2}\right)+2\frac{I_{bHF}}{I_{bGF}}\frac{R_S}{2}+\frac{I_{aGF}}{I_{bGF}}\left(mZ_{1GH}+\frac{R_S}{2}\right)+\frac{I_{aHF}}{I_{bGF}}\frac{R_S}{2} \quad (9)$$

If the fault resistance is zero, this becomes.

$$Z_R = 2mZ_{1GH}+\frac{I_{aGF}}{I_{bGF}}mZ_{1GH} \quad (10)$$

In this case, however, because of the fact that the fault is symmetrical, we have the following relations between the currents

$$I_{aGF}/I_{bGF} = I_{aHF}/I_{bHF} = \alpha$$

Also

$$2+\alpha = \sqrt{3}e^{j30°}$$

These expressions then become

$$Z_R = \sqrt{3}\left(mZ_{1GH}+\frac{R_S}{2}\right)e^{j30°}+\sqrt{3}\frac{I_{bHF}}{I_{bGF}}\frac{R_S}{2} \quad (11)$$

and, when the fault resistance is zero,

$$Z_R = \sqrt{3}mZ_{1GH}e^{j30°} \quad (12)$$

If the circuit breaker at H is open, I_{bHF} and I_{aHF} are zero, and equations 9 and 11 become, respectively,

$$Z_R = 2\left(mZ_{1GH}+\frac{R_S}{2}\right)+\frac{I_{aGF}}{I_{bGF}}\left(mZ_{1GH}+\frac{R_S}{2}\right) \quad (13)$$

and

$$Z_R = \sqrt{3}\left(mZ_{1GH}+\frac{R_S}{2}\right)e^{j30°}$$

Equations 10 and 12, being independent of currents from H, are unaffected by the opening of the circuit breaker at H.

Comparison

First consider that the fault impedance is zero. Comparison of equations 2, 6, and 10 shows that the first term of each, $2m\ Z_{1GH}$, is the same and, therefore, independent of the type of line fault. Moreover, it is equal to twice the line-to-neutral impedance between the relay and the fault, and so is proportional to the distance from the relay to the fault. However, each of these expressions contains one or more additional terms which involve not only the constants of the line but the currents in the remaining line conductor and in the ground, if any is flowing there, as well as the current in one of the faulted conductors. In a balanced 3-phase fault, definite relations exist between the currents in the line conductors, and the ground current is zero, so that in this case the value of the additional terms may be determined. This is done in equation 12. For both line-to-line and double line-to-ground faults, the currents in the unfaulted conductor and in the ground are determined by conditions external to the section being protected, and are subject to variations over wide limits. The current in the unfaulted conductor may be positive, negative, or zero, depending upon load conditions, exchange of synchronizing power, positions of circuit breakers at other points on the system, and so forth. The current in the ground during double faults is also subject to considerable variation, depending upon the relative impedances to phase and to ground current. These variations cause corresponding variations in the value of Z_R, affecting both impedance and reactance relays. The exact range of variation is difficult to determine for the general case because of the wide range possible in the magnitudes and phase angles of the currents involved. But a difference between maximum and minimum values of 25 per cent of the magnitude or reactive component of the first term is easily possible. As will be shown later, all the variations introduced by the preceding factors may be eliminated by changing the relay connections, so that it is not essential to analyze these limits very carefully.

After the circuit breaker at H has opened, Z_R becomes definite for both line-to-line and 3-phase faults, but is still variable for double line-to-ground faults. The corresponding values are given by equations 4, 8, and 12. As an impedance relay is unaffected by the 30-degree rotation of equation 12, the indicated impedance is reduced from $2mZ_{1GH}$ to $1.73\times mZ_{1GH}$, a reduction of approximately 15 per cent. The reactance relay is affected by the phase relations, so that the reduction in reactance depends upon the phase angle of Z_{1GH}. If the phase angle is less than 75 degrees, the reduction is less than 15 per cent, and, if the angle is greater than 75 degrees, the reduction is greater than 15 per cent.

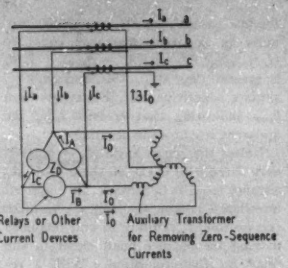

Figure 8 (above). Delta-connected device with zero-sequence filter

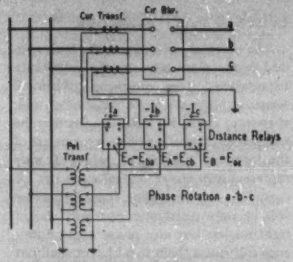

Figure 10 (above). Distance relay connections for line-fault protection, using line currents

Figure 9 (below). Special current transformer connection for ground fault protection

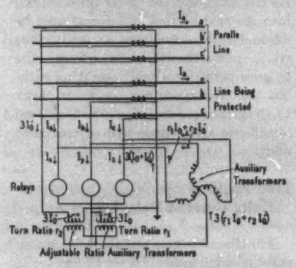

Figure 11 (below). Preferred distance relay connections for line-fault protection using delta-connected current transformers

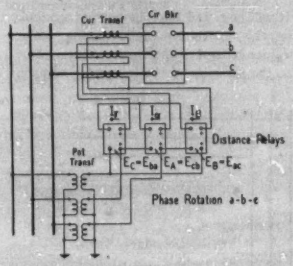

Effect of Fault Resistance

The effect of resistance in the fault is to add two or more terms to the impedance expressions. One of these additional terms is always a pure resistance, and, therefore, adds at right angles to the reactance. The other term or terms are of the form $(I_n/I_{bGF})(R_S/2)$, where I_n may represent any one of several currents. If I_n and I_{bGF} are in phase, these terms also will be pure resistances and will add at right angles, but any phase angle difference will cause them to add vectorially at an angle differing from 90 degrees. Let the phase angles of I_n and I_{bGF} be θ_n and θ_{bGF} with respect to some arbitrary common reference. Then these terms may be expressed in the form

$$(I_n/I_{bGF})(R_S/2)\cos[(\theta_n-\theta_{bGF})+ j\sin(\theta_n-\theta_{bGF})]$$

It will be noted that the current symbols in this expression indicate the scalar values instead of the vector values. Due to the presence of the imaginary term in the last parenthesis, this expression contains an apparent reactance equal to $(I_n/I_{bGF})(R_S/2)\sin(\theta_n-\theta_{bGF})$. If θ_n is greater than θ_{bGF}, this apparent reactance is positive, but, if θ_n is less than θ_{bGF}, indicating that I_n lags I_{bGF}, the apparent reactance is negative.

Unless the phase angle $(\theta_n-\theta_{bGF})$ is very large, the effect of these fault resistance terms is to increase the indicated impedance, making the fault appear more remote than it actually is, and therefore moving the balance point closer to the relay for that condition. With a reactance relay the first resistance term has no effect. However, the additional terms may cause either an increase or a decrease, depending upon phase relations between currents, so that the balance point may be shifted in either direction. As the balance point never must extend into the next section, allowance must be made for this condition in setting the relay, and, therefore, in general the balance point for a fault occurring without fault resistance may be made closer to the next sectionalizing point with an impedance relay than with a reactance relay.

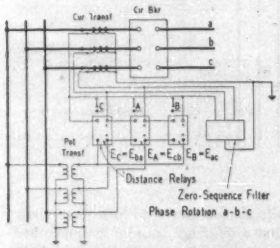

Figure 12 (above). Distance relay connections for line-fault protection using delta-connected relays and zero-sequence filter

Figure 13 (below). Distance relay connections for single line-to-ground faults using current compensation

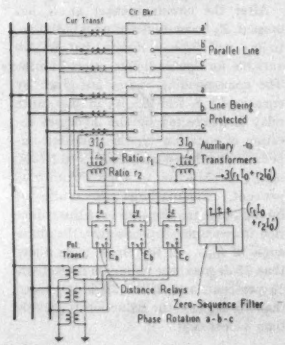

Line Faults—Delta Current Relaying

The clue to a means of obtaining a constant relaying indication for all line faults is given by comparing equations 100, 124, and 143 which give the delta voltages at G on the faulted phases for line-to-line, double line-to-ground, and 3-phase faults expressed in terms of the corresponding currents obtained from delta-connected current transformers.

Figure 14. Distance relay connections for single line-to-ground faults using voltage compensation

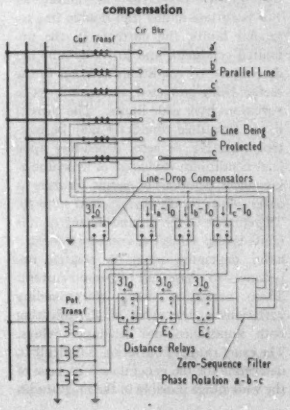

For line-to-line faults equation 100 gives

$$E_{AG}=I_{aGF}\left(mZ_{1GH}+\frac{R_S}{2}\right)+I_{aHF}\frac{R_S}{2} \qquad (15)$$

For double line-to-ground faults equation 124 gives

$$E_{AG}=I_{aGF}\left(mZ_{1GH}+\frac{R_S}{2}\right)+I_{aHF}\frac{R_S}{2} \qquad (16)$$

For 3-phase faults equation 143 gives

$$E_{AG}=I_{aGF}\left(mZ_{1GH}+\frac{R_S}{2}\right)+I_{aHF}\frac{R_S}{2} \qquad (17)$$

These expressions are all the same. It is evident, therefore, that if I_{aGF} is used for the relaying current instead of $(-I_{bGF})$, the same fundamental expression will be obtained for all types of line faults at a given location. If the circuit breaker at H is open, the relay indicates for all three types of faults

$$Z_R=mZ_{1GH}+\frac{R_S}{2} \qquad (18)$$

This expression consists of an impedance term which is directly proportional to the distance to the fault and a variable fault resistance term. Hence, with the remote circuit breaker open, a reactance relay will receive a constant indication for all line faults which is proportional to the distance to the fault. The impedance relay will receive an indication which may vary somewhat due to the presence of fault resistance, and the variation depends upon the relative magnitudes of the line resistance plus fault resistance and the line reactance. However, it should be noted that only one half of the fault resistance from conductor to conductor should be used to compare with the positive-sequence, or line-to-neutral, impedance of the line in determining the effect of fault resistance on the indicated impedance.

When the circuit breaker at H is closed, the vector impedance is affected, of course, by the current from the remote end, and Z_R becomes

$$Z_R=mZ_{1GH}+\frac{R_S}{2}+\frac{I_{aHF}}{I_{aGF}}\frac{R_S}{2} \qquad (19)$$

Here again, if I_{aHF}/I_{aGF} is not a pure number, which may be the case due to differences in phase, the reactance relay also is affected, so that it is not altogether free from the effects of fault resistance so long as the fault is fed from two or more points. However, all other fundamental-frequency variations are eliminated, rendering the relay free from conditions of the

system external to the protected section.

Two methods are available for obtaining the proper current. The necessary current transformer connections are shown in Figures 7 and 8. The first method consists of connecting the current transformers in delta and the relays in Y, in accordance with Figure 7. Connections for a set of three relays using this connection are shown in Figure 11. The second method consists of connecting the current transformers in Y and the relays in delta, in accordance with Figure 8. Connections for three relays using this connection are shown in Figure 12. In this case, the currents through the relays are I_A, I_B, and I_C, which are equal to one third of the currents obtained by the method of Figure 7. Hence the impedance indicated by the relay is three times as great, other conditions remaining the same, as it is using the delta-connected current transformer scheme. When the system has a grounded neutral, a zero-sequence filter is required with the connection of Figure 12 to provide a path for the zero-sequence or residual current. One form of such a filter is shown in Figure 8. Any grounding transformer connection is suitable for this purpose, so that several other designs are possible.

Ground Faults—Conventional Distance Relaying

It generally is recognized that the high value of resistance which may be present in ground faults is sufficient to eliminate the ordinary impedance relay from consideration. However, the use of a relay which effectively eliminates the resistance component often is considered, and an analysis of the available currents and voltages during ground faults is, therefore, pertinent. It is customary to use the line-to-ground potential and line current for energizing the relay, although use of the residual current has been suggested. In setting up the conditions for this type of fault in Appendix VI, the fault is assumed to occur on conductor a. The line-to-neutral voltage on the faulted phase is, therefore, E_{aG}. Equation 159 of Appendix VI gives the value of E_{aG} during this type of fault. Using the line current, I_{aGF}, for tripping, the indicated impedance is

$$Z_R = mZ_{1GH} + R_G + \frac{I_{aHF}}{I_{aGF}}R_G + \frac{I_{0GF}}{I_{aGF}}m(Z_{0GH} - Z_{1GH}) + \frac{I_{0GH}}{I_{aGF}}mM_{0GH} \quad (20)$$

It is evident that this quantity is affected by the fault resistance, the residual current in the line being protected, and by the residual current in the parallel line.

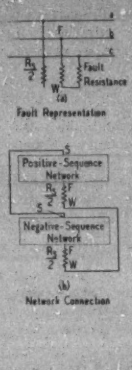

Figure 15 (above, left). Representation of line-to-line faults

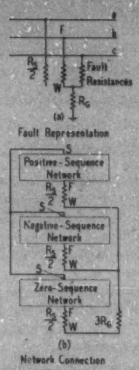

Figure 16 (above, right). Representation of double line-to-ground faults

Where two lines parallel each other at close spacings, the zero-sequence mutual impedance between the lines becomes quite appreciable in comparison with the self-impedances, and, when m is large, that is, when a fault occurs near the remote end of the section, the value of I_{0GH}/I_{aGF} becomes of the order of one third on a normally designed system, so that an important term is added. However, if the parallel line is not in service, this term is not present, and considerable variation in the indicated impedance is possible. Of course, if only a single line is involved, this term will not enter in any case.

The variable term $(I_{0GF}/I_{aGF})m \times (Z_{0GH} - Z_{1GH})$ is also a source of trouble, as the ratio (I_{0GF}/I_{1GF}) is not fixed by conditions within the section itself, unless there is only one path for the fault current to take, true in this case only after the circuit breaker at H has opened. In general, where the fault is near the remote end of the section, the ratio (I_{0GF}/I_{aGF}) often will be less than one third when the circuit breaker at H is closed, and equal to one third when the circuit breaker at H is open, causing an increase in impedance due to the opening of the circuit breaker, at which time a decrease is much to be preferred if any change must occur. The value one third given for the ratio (I_{0GF}/I_{aGF}) is imposed by the conditions at the fault when the fault current comes entirely from one point. When the fault current divides and comes from two or more points to the fault, the proportion of the current in the conductor which is residual or zero sequence depends upon the relative impedance to phase and ground currents in that branch, and, due to the fact that the impedance of the transmission line is much higher to ground current than to phase current, a relatively greater portion of the residual current usually will come from the end of the line nearer the fault

The variations in indicated vector impedance discussed affect the indicated reactance in much the same proportions, so that the use of a reactance relay presents no advantages when considered from the standpoint of these errors alone, and the justification for such a relay rests on the fact that it reduces the effect of the two resistance terms

Use of the residual current does not give any improvement over the use of line current, as the voltage E_{aG} is not directly proportional to the residual current, even when fault resistance is neglected, and a detailed analysis of this method therefore is not included

Ground Faults—Improved Distance Relaying

From what has preceded it is evident that the use of either impedance or reactance relays in the manner suggested will not be entirely satisfactory, and methods for improving the performance are necessary if the distance principle is to find extensive application for ground faults. As the currents and voltages which are available at the relaying station do not give satisfactory indications as they stand, it may happen that they may be modified in accordance with known characteristics of the circuits to give more suitable quantities. Modification may be made in either the current, or the voltage, or both. In any case much improved performance may be obtained.

Current Compensation

Equation 159, giving E_{aG} during this type of fault, may be written in a different form by factoring mZ_{1GH} out of all terms except those involving R_G. We obtain

$$E_{aG} = \left(I_{aGF} + I_{0GF}\frac{(Z_{0GH} - Z_{1GH})}{Z_{1GH}} + I_{0GH}\frac{M_{0GH}}{Z_{1GH}} \right) mZ_{1GH} + (I_{aGF} + I_{aHF})R_G \quad (21)$$

If now we are able to use for tripping a current I_r defined by the equation

$$I_r = I_{aGF} + I_{bGF}\frac{Z_{0GH} - Z_{1GH}}{Z_{1GH}} + I_{0GH}\frac{M_{0GH}}{Z_{1GH}} \quad (22)$$

we obtain a very simple result, as follows

$$Z_R = mZ_{1GH} + \frac{I_{aGF} + I_{aHF}}{I_r}R_G \quad (23)$$

The first term of this expression is directly proportional to the distance from the fault to the relay and is independent of conditions external to the section being protected. The second term is a function of the fault resistance and has the effect of a pure resistance if $(I_{aGF}+I_{aHF})$ is in phase with I_r. As, in general, all the impedances involved in equation 22 will have nearly the same phase angle, unless the line resistances are very large, and also, as I_{aGF}, I_{bGF}, and I_{0GH} are usually nearly in phase for this type of fault, this will be nearly true. In general, the variations in phase will be of the same order as those occurring between corresponding currents in the preceding analysis of line faults. Hence, for faults having fault resistances in the same proportions, just as satisfactory protection can be obtained for ground faults as for line faults, using distance relays. However, the fault resistance generally reaches considerably higher values, so that the variations will be somewhat larger than the minimum obtainable on line faults, and a relay which is substantially unaffected by fault resistance generally will be required.

There are several methods of obtaining the current I_r for relaying purposes. Where the line resistance is not too large, it will be satisfactory to assume that $(Z_{0GH}-Z_{1GH})$, M_{0GH}, and Z_{1GH} are all in phase. If this is true, the ratios of these quantities, appearing in equation 22 for I_r, become pure numbers or transformer ratios, so that these currents may be added to the relay currents by means of transformers of corresponding ratio energized from the residual currents in the two lines respectively. For this purpose, the relays may be provided with additional current coils which carry the added currents. Another method is to introduce these currents directly into the normal coil by means of the zero-sequence filter, according to the scheme of Figure 9. The connections for a set of relays using this method are shown in Figure 13. The currents flowing through the relays become I_x, I_y, and I_z, given by equations 62, 63, and 64 in which $r_1 = |(Z_{0GH} - Z_{1GH})|/(Z_{1GH})$ and $r_2 = M_{0GH}/Z_{1GH}$.

Where the resistances in the lines are large, correction for phase-angle differences in the impedances may be required. Various means of making this correction are possible, but they introduce considerable complication and are not considered here.

Voltage Compensation

It has been stated earlier in this paper that it is desirable to obtain a constant relay indication for all faults in a particular location and that this indication should be proportional to the distance from the relay to the fault. This is a sufficient condition to establish the balance points accurately and divide the faults into the proper classes, but with relays operating on the balance-point principle it is not a necessary condition. It is, however, necessary for the relays to receive a constant indication for faults at the chosen balance points. For faults at other locations, it is immaterial whether the indication is proportional to the distance from the relay to the fault or not, provided the indication given does not exceed the limits provided by faults at the balance points. This is due to the fact that a distance relay of the balance-point type will trip with practically a constant speed for all faults within the limits of the class in which the fault falls, regardless of whether the indicated value is well within the class or near the limits.

Use is made of this principle in applying voltage compensation to distance ground relays. In analyzing this application, the relaying, voltage E_{aG} may be expressed more conveniently in the form given by equation 167 in Appendix VI as

$$E_{aG} = (I_{1GF}+I_{2GF})mZ_{1GH} + I_{0GF}mZ_{0GH} + I_{0GH}mM_{0GH} + 3(I_{0GF}+I_{0HF})R_G$$

If I_{0GF} is used for energizing the relay, considerable error and variation will be produced by the terms not proportional to I_{0GF}. However, for faults at particular locations, these terms, other than the resistance term, may be removed by means of line drop compensators. Let us assume that the fractional distance to the first balance point is n. Then we may subtract from the relay voltage the quantity

$$(I_{1GF}+I_{2GF})nZ_{1GH} + I_{0GH}nM_{0GH}$$

If a fault occurs at the balance point, $m=n$, and we have

$$E_{aG} = I_{0GF}nZ_{0GH} + 3(I_{0GF}+I_{0HF})R_G \quad (24)$$

If I_{0GF} is used for relaying current, the measured impedance becomes

$$Z_R = n\,Z_{0GH} + 3R_A + 3\frac{I_{0HF}}{I_{0GF}}R_G \quad (25)$$

This value of Z_R is composed of a definite impedance $n\,Z_{0GH}$, a pure resistance $3R_G$, and a term which may have a reactance component unless I_{0HF} is exactly in phase with I_{0GF}. The factor 3 enters here in connection with the resistance, making the apparent resistance much larger, but the impedance term in this case is Z_{0GH}, which is usually three or more times the positive-sequence impedance for the line, Z_{1GH}, so that the ratio of resistance to reactance in Z_R for a given value of R_G is not increased, over that obtained by current compensation, and, therefore, the errors introduced by the difference in phase of I_{0HF} and I_{0GF} will be of about the same percentage as before.

If the fault occurs at some other location, m is no longer equal to n, and Z_R becomes

$$Z_R = mZ_{0GH} + 3R_G + 3\frac{I_{0HF}}{I_{0GF}}R_G + \frac{I_{1GF}+I_{2GF}}{I_{0GF}}(m-n)Z_{1GH} + \frac{I_{0GH}}{I_{0GF}}(m-n)M_{0GH} \quad (26)$$

The two additional terms are positive for m greater than n and negative for m less than n, so that, for faults beyond n, Z_R increases by a greater percentage than m does, and for faults nearer than n, Z_R decreases by a greater percentage than m Hence, as m becomes quite small, the impedance may become negative. As the reactance elements of most reactance relays will trip for negative reactance, this introduces no difficulty so long as the

Figure 17 (below, left). Representation of 3-phase faults

Figure 18 (below, right). Representation of single line-to-ground faults

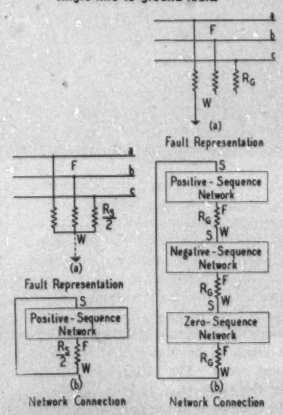

directional element is not energized from the compensated voltage and operates properly.

With the foregoing scheme, four compensators are required per group of three ground relays. Three of these compensators must be energized from the positive- and negative-sequence components of the current in the corresponding line conductors and the remaining compensator from the residual current in the parallel line. The current $(I_{1GF}+I_{2GF})$ is equal to $(I_{aGF}-I_{0GF})$ or in other words the required current may be obtained by removing the zero-sequence component from the line current. This may be accomplished by means of the zero-sequence filter previously described. Use of this method of compensation is made in the relay connections shown in Figure 14. However, the current through each relay is $(3\ I_0)$ so that the indicated impedances are one third of the values given by equations 25 and 26.

Other schemes of compensation may be utilized, making use of line current, residual current or any of the symmetrical components of the line current for tripping the relay, and eliminating the terms in the voltage not proportional to the distance from the fault by means of compensators.

Operation of Ground Relays on Line Faults

Operation of ground relays upon the occurrence of line-to-line faults is not to be expected, unless the fault current is very large, because the line-to-ground voltage maintains a large proportion of its normal value, and the indicated impedance or reactance is, therefore, usually sufficiently great to prevent operation. In the few cases where the line-to-line fault currents are large enough to operate the ground relays, it is almost certain that the corresponding line relay also should operate, so that false tripping will not occur, but indication of a more severe fault involving ground occasionally may be obtained. The indicated impedance or reactance is not fixed by the impedance of the line and fault, but is affected by the remainder of the system, so that determination of the actual value requires consideration of each individual case.

Double line-to-ground and 3-phase faults previously have been classed as line faults. However, operation of the ground relays upon the occurrence of such faults normally will take place, and an analysis of the operation is required. Analysis is given only for ground relays provided with compensation as described.

Double Line-to-Ground Faults

The fault is assumed to occur between conductors b and c and ground. Hence, the relaying voltages are E_{bG} and E_{cG}, given by equations 122 and 123. Factoring out mZ_{1GH}, as was done during the analysis of current compensation for single line-to-ground faults, we obtain

$$E_{bG}=\left[I_{bGF}+I_{0GF}\frac{(Z_{0GH}-Z_{1GH})}{Z_{1GH}}+I_{0GH}\frac{M_{0GH}}{Z_{1GH}}\right]mZ_{1GH}+(I_{bGF}+I_{bHF})\frac{R_g}{2}+(I_{0GF}+I_{0HF})3R_G \quad (27)$$

$$E_{cG}=\left[I_{cGF}+I_{0GF}\frac{(Z_{0GH}-Z_{1GH})}{Z_{1GH}}+I_{0GH}\frac{M_{0GH}}{Z_{1GH}}\right]mZ_{1GH}+(I_{cGF}+I_{cHF})\frac{R_g}{2}+(I_{0GF}+I_{0HF})3R_G \quad (28)$$

Except for the fault resistance terms, the foregoing equations are of exactly the same form as would be obtained for single line-to-ground faults on the corresponding phases. Hence, exclusive of the fault-resistance terms, if the relaying currents are equal to the expressions in brackets, the same indicated impedance is obtained for double line-to-ground faults as for single line-to-ground faults. If the circuit impedances are such that we may assume $(Z_{0GH}-Z_{1GH})$ and M_{0GH} in phase with Z_{1GH}, these currents reduce to I_{bGF} and I_{cGF}, as given by the connections of Figure 13 and equations 63 and 64, r_1 and r_2 being $|(Z_{0GH}-Z_{1GH})|/Z_{1GH}$ and M_{0GH}/Z_{1GH} respectively. Under these assumptions Z_R for the two relays becomes

$$Z_{R(b)}=mZ_{1GH}+\frac{I_{bGF}+I_{bHF}}{I_{bGF}}\frac{R_g}{2}+\frac{I_{0GF}+I_{0HF}}{I_{bGF}}3R_G \quad (29)$$

$$Z_{R(c)}=mZ_{1GH}+\frac{I_{cGF}+I_{cHF}}{I_{cGF}}\frac{R_g}{2}+\frac{I_{0GF}+I_{0HF}}{I_{cGF}}3R_G \quad (30)$$

For this type of fault, the currents in the line conductors are usually considerably out of phase with the residual currents, and the relay currents, being made up of both, will be intermediate in phase between the two. Hence the individual resistance terms never will appear as pure resistance but will have reactance components. However, as the relaying current has a phase position intermediate between the line and residual currents, it will lead one and lag the other, so that the reactance effects will tend to compensate. Therefore, the amount of variation introduced into the indicated reactance usually will be small, unless the two resistances R_g and R_G run to opposite extremes or are large in comparison with the reactance of the line.

A similar analysis may be given for voltage compensation. The line-to-neutral voltages expressed in the most convenient form are given by equations 132 and 133. With the scheme of compensation shown by Figure 14, the voltages subtracted from the line-to-neutral voltages will be $(a^2I_{1GF}+aI_{2GF})\ nZ_{1GH}+I_{0GH}nM_{0GH}$ and $(aI_{1GF}+a^2I_{2GF})n\times Z_{1GH}+I_{0GH}\ n\ M_{0GH}$ respectively.

The resultant relay voltages become

$$E_{bG}=I_{0GF}(mZ_{0GH}+3R_G)+3I_{0HF}R_G+(I_{bGF}+I_{bHF})\frac{R_g}{2}+(a^2I_{1GF}+aI_{2GF})\times(m-n)Z_{1GH}+I_{0GH}(m-n)M_{0GH} \quad (31)$$

$$E_{cG}=I_{0GF}(mZ_{0GH}+3R_G)+3I_{0HF}R_G+(I_{cGF}+I_{cHF})\frac{R_g}{2}+(aI_{1GF}+a^2I_{2GF})\times(m-n)Z_{1GH}+I_{0GH}(m-n)M_{0GH} \quad (32)$$

As $3I_{0GF}$ is the relaying current, the indicated impedances become

$$Z_{R(b)}=\frac{mZ_{0GH}}{3}+R_G+\frac{I_{0HF}}{I_{0GF}}R_G+\frac{I_{bGF}+I_{bHF}}{3I_{0GF}}\frac{R_g}{2}+\frac{a^2I_{1GF}+aI_{2GF}}{3I_{0GF}}\times(m-n)Z_{1GH}+\frac{I_{0GH}}{3I_{0G}}(m-n)M_{0GH} \quad (33)$$

$$Z_{R(c)}=\frac{mZ_{0GH}}{3}+R_G+\frac{I_{0HF}}{I_{0GF}}R_G+\frac{I_{cGF}+I_{cHF}}{3I_{0GF}}\frac{R_g}{2}+\frac{aI_{1GF}+a^2I_{2GF}}{3I_{0GF}}\times(m-n)Z_{1GH}+\frac{I_{0GH}}{3I_{0GF}}(m-n)M_{0GH} \quad (34)$$

Here again, exclusive of resistance terms, for a double line-to-ground fault at the balance point, that is, for $m=n$, the indicated impedances are the same as would be obtained for a single line-to-ground fault on the same conductors. However, the resistance terms involving $R_g/2$ may be a source of considerable error whenever R_g becomes large in comparison with Z_{0GH}, as $(I_{bGF}+I_{bHF})$ and $(I_{cGF}+I_{cHF})$ will be considerably out of phase with I_{0GF}, thereby producing an apparent reactance which will be positive in one phase and negative in one other.

Three-Phase Faults

On 3-phase faults, using current compensation, the compensated relaying

currents do not differ from the phase currents, as no ground or zero-sequence current flows. For the same reason the zero-sequence impedance does not appear, so that the indicated impedance on phase a will be

$$Z_R = mZ_{1GH} + \frac{R_S}{2} + \frac{I_{aHF}}{I_{aGF}}\frac{R_S}{2} \tag{35}$$

with a similar expression for each of the other phases.

Using the scheme of voltage compensation described, the relays will not be operated, as the zero-sequence current is used, and this current is zero for a balanced 3-phase fault.

From the foregoing it appears that, fundamentally, the proposed schemes of ground relaying are not affected adversely by line faults, if the fault resistances are relatively small or bear certain relations to each other, but, if the fault resistances are large, the possibility of considerable variations appears during double line-to-ground faults, thus requiring larger margins in setting or introducing the possibility of false tripping. On relatively short lines, where the fault resistance may become large in comparison with the line impedance, it may be desirable to lock out the ground relays upon the occurrence of double line-to-ground or 3-phase faults, this being accomplished satisfactorily in most cases by the use of simple voltage relays operating on line-to-ground voltage, locking out the ground relays when low voltage occurs on any two phases.

Operation of Line Relays on Ground Faults

Operation of line relays upon the occurrence of ground faults is very improbable as the line-to-line voltage is affected but slightly by a single line-to-ground fault. Here again the values indicated by the line relays are not fixed definitely by the fault and section impedances but depend upon the remainder of the system as well, so that the values must be determined individually in each case, whenever this question must be answered.

Effect of Loads

In the preceding discussion and analysis, the system load has been neglected. However, the equations in the appendixes for voltages and currents at the fault, and at a relaying point on the faulted line, have been derived in a perfectly general manner from the conditions at the fault, and are independent of the network external to the two lines between G and H. As it is assumed that no loads will be connected to the lines between G and H, the equations are valid whether loads are included or not. However, the loads will affect, to some extent, the current and voltage distribution in the network and, therefore, the actual values of the voltages and currents entering the equations. The expressions for impedance on the faulted phase do not involve explicitly any voltage expressions but do involve certain current ratios, and these ratios will be affected somewhat by the loads. If the delta-current relaying methods are used for line faults and the current-compensation method for ground faults, as previously described, these current ratios enter only in the fault-resistance terms and have no effect if the fault resistances are zero. If the voltage-compensation method is used for ground faults, the same is true for faults at the balance point, and it is unlikely that the effect of load will cause any serious difficulty for faults that are not close to a balance point. Hence, with these methods of relaying, the system load affects the relaying indications only in so far as the redistribution of fault current changes the effect of fault resistance.

Summary

In the preceding investigation the quantities upon which distance relays must depend for their operation have been determined for all possible types of faults occurring at a single location. It has been shown that the quantities obtained by the use of earlier distance relay connections for both line and ground faults do not give the closest approach to the desired result, a constant indication for all types of faults at a given location. It has been shown further that, by the use of different connections and certain auxiliary apparatus, a constant relaying indication may be obtained by the line relays for all types of line faults and by the ground relays for all types of faults involving ground, if the fault resistance is zero, and, if the fault resistance is not zero, that smaller deviations from the normal value will be obtained for a given fault resistance. The analysis has been based upon the assumptions of sine wave currents and voltages, constant circuit impedances, and negligible distributed capacitance in the faulted sections of line. It has been assumed further that the fault impedance is resistance only and that it is effectively constant throughout each cycle. All of these assumptions, except perhaps the latter, are reasonably valid as far as relaying is concerned, although some consideration must be given to the d-c component of the short-circuit currents with very high-speed relays. Sufficient data are not yet available to state the characteristics of fault impedances definitely, but undoubtedly further information will be obtained from future investigations. Until more accurate data are available, certain margins determined by experience must be provided in relay settings to allow for deviations from the assumptions.

If the suggested connections are used, the vector impedance which is indicated by the voltage and current applied to the relay on the faulted phase, at least for all faults near the first balance point, will consist essentially of three terms, when the fault is fed from both ends of the section. They are: a circuit impedance term which is proportional to the distance from the relay to the fault, a fault resistance term, and a term proportional to the fault resistance multiplied by the vector ratio of two currents. An impedance relay operates upon the magnitude of the vector sum of the three terms, and, as the two resistance terms are nearly at right angles to the impedance term, the magnitude of the sum will be greater than the magnitude of the circuit-impedance term, although the increase will be much less than the added resistance terms, unless the latter are very large. To maintain a balance at the relay, the circuit-reactance term must decrease as the fault-resistance terms increase, so that the effect of fault resistance is to shift the balance point toward the relay. A reactance relay, on the other hand, operates on the reactive component of the three terms, and, therefore, is unaffected by the first fault-resistance term. However, the second resistance term will have an apparent reactance if the two currents involved in the ratio are out of phase, and this apparent reactance may be positive or negative, depending upon which current leads in phase. Hence the balance point may be shifted in either direction by the presence of fault resistance. Although the actual shift usually will be less with a reactance relay, the fact that it may be in either direction must be taken into account, so that where the fault resistances are moderate in comparison with the reactance of the section, the impedance relay usually will give as satisfactory protection as a reactance relay. However, where the fault resistances are larger, as on ground faults, the increases in impedance become so great that the ordinary impedance relay is disqualified.

In the preceding analysis, all current

and voltage transformer ratios have been assumed as unity. In setting the relays, the current and voltage transformer ratios must be taken into account. It is customary also to set the relays under the assumption of zero fault resistance, choosing a balance point under this condition which gives a suitable margin for the variation introduced by fault resistance. If n is the fraction of the section from the relay to the balance point, r_v the ratio of the circuit voltage, line-to-line for line faults, line-to-ground for ground faults, to the voltage impressed on the relay circuit, and r_c the current transformer ratio, the actual settings of the relays will be as given below for the different suggested connections. If the voltage is obtained from high-voltage potential transformers, as shown in the diagrams, r_v is simply the potential transformer ratio. For line relaying using delta-connected current transformers (Figure 11), and for ground relaying using current compensation (Figure 13), the relay should be adjusted to balance for an impedance

$$Z_R = nZ_{1GH}r_c/r_v \tag{36}$$

For line relaying using delta-connected relays (Figure 12), the relays should balance for an impedance

$$Z_R = 3nZ_{1GH}r_c/r_v \tag{37}$$

For ground relaying using the suggested scheme of voltage compensation, the relays should balance for an impedance

$$Z_R = nZ_{0GH}r_c/(3r_v) \tag{38}$$

The settings for both balance points of a 3-zone relay will be made in the same manner, a different value of n being used in the two cases.

Application

Distance relaying for protection against line and ground faults is suitable for general application to either single- or multiple-circuit lines, the only theoretical limitation being the variations in the balance-point locations introduced by the effects of fault resistance. Either the first or second balance point may be the limiting factor. The first balance point always must remain in the protected section, and the second balance point in the adjacent section. Furthermore, for general application the second balance point never must extend beyond the first balance point of the relay at the next sectionalizing point, or both circuit breakers will be tripped for some faults. The shorter the line sections become, the more difficult these conditions are to fulfill, so that a certain minimum length of section or impedance is required. This minimum depends upon such factors as short-circuit current distribution and the fault resistances encountered, so that it cannot be fixed definitely.

Because of the higher values of fault resistance generally met during ground faults, distance ground relaying cannot be applied to lines as short as the minimum which can be protected satisfactorily by distance line relaying. However, where the lines are sufficiently long, this type of protection may offer substantial advantages. High-speed ground relaying of single lines is difficult by the customary overcurrent methods, as the ground current may vary over wide limits for a fault in a given location, thus requiring selective time settings to obtain discrimination. Either compensated current or compensated voltage methods of distance relaying appear to be well suited for this purpose.

The current compensation method also appears to be well adapted to cases where grounded-neutral power transformers are made an integral part of the line and the high-voltage circuit breakers are omitted. This case is particularly difficult to relay by ordinary methods of ground-fault protection, as, after the low-voltage circuit breaker at one end is open because of a fault near that end, most of the ground fault current continues to flow from the grounded-neutral transformer at that end, making it very difficult to open the circuit breaker at the opposite end. As the compensated distance relay measures the impedance or reactance from the relay to the fault, independent of the relative distribution of line and ground current, it is essentially unaffected by such system connections. The particular compensated voltage method described is not well suited to this application because of the low ground current available for operating the relays at the end remote from the fault, but a compensated voltage method using line current for relay operation instead of ground current, also would give good results

It should be pointed out that this analysis has considered only the possible accuracy, and has not taken into account the performance of the relay itself, its design, its simplicity, its reliability, or its speed of operation. All of these factors are important and must be taken into account in a final choice of the type of distance relay to be used for a given application.

The equations derived in the appendixes giving the voltages and currents at relaying points in terms of circuit impedances and conditions at the fault have been used in the paper only for the purpose of determining the performance of distance relays. However, they may be found useful for many other purposes and constitute a contribution to the further development of the method of symmetrical components.

Conclusions

This analysis has shown:

1. That the earlier conventional methods of distance relaying are subject to errors other than those caused by fault impedance.

2. That these errors may be eliminated in relays protecting against line faults by the use of "delta relaying." Delta relaying may be obtained either by connecting the current transformers in delta or by connecting the current windings of the relays in delta, using a suitable zero-sequence filter.

3. That these errors may be eliminated in relays protecting against ground faults by the use of current or voltage compensation and, therefore, that distance relaying is suitable for ground fault protection, if the impedance of the section being protected is sufficiently great.

4. That the limitation in the application of distance relaying is the error introduced by the presence of fault impedance, which will decrease with increasing section impedance, and that this limitation affects distance relays of both the impedance and reactance types, although to a different extent.

5. That distance relaying may be made to approach even closer to the desired relaying ideal and that within the limits of its application it should give satisfactory protection, regardless of generator capacity or system conditions.

Appendix I. Notation

$a = e^{j120} = -0.5 + j0.866$

F = physical point of fault along transmission line

G = substation where relaying is considered

H = substation at opposite end of line section

P, Q = equivalent junction points in zero-sequence network

S = equivalent point of zero potential

T = equivalent point of application of E_{1T}

U = equivalent point of application of E_{1U}

W = equivalent point of fault when fault resistance is present

E_{1T} = equivalent positive-sequence generated voltage of part of system feeding station G

E_{1U} = equivalent positive-sequence generated voltage of part of system feeding station H

E = voltage symbol, with subscript notation as follows:

First subscript:

a, b, or c = line-to-neutral voltage of corresponding phase

A, B, or C = line-to-line voltage of corre-

sponding phases, *cb*, *ac*, *ba* respectively. See Figure 3

1, 2, 0 = symmetrical components of line-to-neutral voltage, phase *a* as reference

Second subscript:

F, *G*, *H*, *W* = point at which voltage is measured

I = current symbol, with subscript notation as follows:

First subscript:

a, *b*, or *c* = line-to-neutral current in corresponding line

A, *B*, or *C* = line-to-line or delta current of corresponding delta phase, obtained by delta connection of relays. See Figure 8.

α β, or γ = delta current obtained from delta-connected current transformers. See Figure 7

x, *y*, *z* = relaying currents obtained from the connection of Figure 9

1, 2, 0 = symmetrical components of line-to-neutral current, phase *a* as reference

Second and third subscripts:

GF, *HF*, *GH*, *TG*, *UH*, *SG*, *SH*, *FW*, and so forth = stations between which current flows. Assumed positive direction of current is from station of first letter to that of second.

Z = impedance symbol, scalar value, with subscript notation same as for ***Z***

Z = impedance symbol, vector value, with subscript notation as follows:

First subscripts, if only one:

R = impedance indicated by relay for various types of faults

D = impedance of current winding of relays or other current devices

First subscript, if more than one:

1, 2, 0 = sequence of current with which impedance is to be used

Second and third subscripts:

GF, *HF*, *GH*, *TG*, *UH*, *SG*, *SH* = stations between which impedance is measured. Between stations *G* and *H* value is for one line only

M_{0GH} = zero-sequence mutual impedance between the two parallel lines from *G* to *H*

R_g = fault resistance for line faults between two line conductors

R_G = fault resistance for ground faults

m = fraction of the distance from *G* to *H* at which fault is assumed to occur

n = fraction of the distance from *G* to *H* at which the first balance point is located

r_p = potential transformer voltage ratio

r_c = current transformer current ratio

r_1, r_2 = auxiliary transformer turn ratios, See Figures 9 and 13

Appendix II. Network Representation and Fault Currents

In order to calculate the fault currents and voltages during unbalanced faults, by the method of symmetrical components, it is necessary to set up sequence networks for the flow of positive-, negative-, and zero-sequence currents, corresponding to the system under investigation. The positive- and negative-sequence networks comprise a group of impedances having a branch corresponding to every branch of the single-line diagram. Synchronous machines are represented by their equivalent circuits for a single phase, with single-phase voltages inserted at the proper point. As synchronous machines generate only positive-sequence voltages, generated voltages appear only in the positive-sequence network.

The positive- and negative-sequence networks, for the system shown in Figure 2, are given in Figures 4 and 5, respectively. In the positive-sequence network, two voltages, E_{1T} and E_{1U}, are inserted to represent the voltages generated by the equivalent synchronous machines at *T* and *U* respectively. The impedance of each branch of the networks is represented by the symbol ***Z*** with three subscripts, the first a number indicating the sequence network in which the impedance appears, and the second and third the points between which the impedance is measured. As E_{1T} and E_{1U} are expressed in terms of line-to-neutral voltage, the other terminals of these voltages are connected to the common neutral *S* of the positive-sequence network. In the negative-sequence network, these voltages are equal to zero, so that the terminals *T* and *U* may be omitted and the impedances connected directly to the corresponding point *S*. For all static apparatus the negative-sequence impedance is equal to the positive, so that the branches between *G* and *H*, corresponding to the transmission line, will have the same impedance as in the positive-sequence network. This has been represented by substituting Z_{1GH} for Z_{2GH} in Figure 5. The fault is assumed to occur at *F*, intermediate between *G* and *H*, at a fraction *m* of the distance from *G* to *H*. As the impedance from *G* to *H* of one line has been taken as a unit, and as, neglecting distributed capacitance, the impedance is proportional to the distance, the impedances from *G* to *F* become mZ_{1GH} and from *F* to *H* become $(1-m)Z_{1GH}$. As the branches between *T* and *G* and between *H* and *U* contain synchronous-machine impedances, they will in general be different for the different sequences.

The zero-sequence network is made up only of those branches which may carry current having an earth-return path, and, therefore, in general it has a smaller number of branches. The corresponding impedances are also usually quite different and generally larger, although in certain special cases such as grounding transformers, the zero-sequence impedance to ground may be less than the corresponding positive- and negative-sequence impedances. The zero-sequence network for the system shown in Figure 2 is given in Figure 6. As adequate grounding has been assumed at each end of the system, branches are required from *G* and *H* to *S*. In the positive- and negative-sequence networks, the mutual impedance between two parallel lines is generally small enough to be neglected, but in the zero-sequence network this is not true, because of the great distance between the conductors and the ground return, as compared with the spacing between the two parallel lines. Because of the common use of the earth return and ground wires, the mutual impedance also may contain a resistance component. The mutual impedance is represented by the vector symbol M_{0GH}.

It is well known that two circuits, having a mutual impedance between them and connected together at one end, may be replaced by three impedances connected in star, the branch connected to the original junction being equal to the mutual impedance and the other branches being equal to the original branches minus the mutual impedance. Use is made of this property in setting up the zero-sequence impedances between stations *G* and *H* and the fault *F*. The symbols for impedance are similar to those used in the positive- and negative-sequence networks, except that the first subscript is now 0 instead of 1 or 2.

The current flowing in the various branches of the networks is indicated by the symbol ***I*** with three subscripts, the first a number (1, 2, or 0) indicating the sequence of the current, and the second and third letters indicating the stations between which the current is flowing, the assumed positive direction being from the station indicated by the first letter toward the one indicated by the final letter.

If the currents and voltages at various points in the sequence networks are known, the actual currents and voltages in the three phases at corresponding points in the actual system may be found by combining the currents and voltages according to relations that follow. Phase *a*, line-to-neutral, has been assumed as reference, and the phase rotation is assumed to be *a*, *b*, *c*. Then

$$E_a = E_1 + E_2 + E_0 \tag{39}$$

$$E_b = a^2E_1 + aE_2 + E_0 \tag{40}$$

$$E_c = aE_1 + a^2E_2 + E_0 \tag{41}$$

and

$$I_a = I_1 + I_2 + I_0 \tag{42}$$

$$I_b = a^2I_1 + aI_2 + I_0 \tag{43}$$

$$I_c = aI_1 + a^2I_2 + I_0 \tag{44}$$

The voltages between lines, or delta voltages, defined in accordance with the vector diagram of Figure 3, may be determined by subtracting the phase voltages in pairs, as follows. In performing the subtraction it is convenient to make use of the following relations concerning the vector ***a***

$$1 - a = j\sqrt{3}a^2 \tag{45}$$

$$a - a^2 = j\sqrt{3} \tag{46}$$

$$a^2 - 1 = j\sqrt{3}a \tag{47}$$

Thus:

$$E_A = E_c - E_b = j\sqrt{3}(E_1 - E_2) \tag{48}$$

$$E_B = E_a - E_c = j\sqrt{3}(a^2E_1 - aE_2) \tag{49}$$

$$E_C = E_b - E_a = j\sqrt{3}(aE_1 - a^2E_2) \tag{50}$$

For the purposes of relay operation, it will be desirable to consider three special forms of current transformer connection,

as shown in Figures 7, 8, and 9. In the following analysis it will be assumed that the main current transformer ratio is 1-to-1, so that the results will be the same as if the actual line currents had been manipulated. In actual cases the currents in the secondary circuits can be obtained by dividing by the current transformer ratio. In Figure 7 the current transformers are connected in delta, and leads from the corners of the delta are taken to current utilizing devices, connected in star. With this connection the leads carry currents which are the differences of the line currents taken in pairs. It will be noted that these currents are of the same mathematical form as the delta voltages E_A, E_B, and E_C, and the corresponding currents are designated by I_α, I_β, and I_γ, determined as follows

$$I_\alpha = I_c - I_b = j\sqrt{3}(I_1 - I_2) \tag{51}$$

$$I_\beta = I_a - I_c = j\sqrt{3}(a^2 I_1 - a I_2) \tag{52}$$

$$I_\gamma = I_b - I_a = j\sqrt{3}(a I_1 - a^2 I_2) \tag{53}$$

In Figure 8, the utilization devices are assumed to have identical impedances, Z_D, and are connected in delta. At the corners of the delta, the line currents I_a, I_b, and I_c are introduced. This delta connection offers no path to any residual or zero-sequence current in the line conductors, so that, if the system is grounded, allowing zero-sequence current to flow in the line, some additional path must be provided for this current. It is also desirable that this additional path pass as little positive- and negative-sequence current as possible. These conditions are satisfied by means of the small interconnected-star transformer bank shown. Any other grounding transformer connection may be used as well for this purpose, as it is the function of a grounding transformer to offer very high impedance to all but zero-sequence currents.

The currents in the branches of the delta may be denoted by the symbols I_A, I_B, and I_C. Following the convention previously adopted, I_A is the current in the delta branch opposite the line a, and so forth. Writing the equation for the voltage drop around the delta, we obtain

$$(I_A + I_B + I_C) Z_D = 0 \tag{54}$$

or

$$I_A + I_B + I_C = 0 \tag{55}$$

The interconnected-star transformer or, more generally, the zero-sequence filter bypasses all of the zero-sequence currents and, if properly designed, only a negligible portion of the positive- and negative-sequence currents, so that at the junction of the delta we may write

$$I_B - I_C = I_a - I_0 = I_1 + I_2 \tag{56}$$

$$I_C - I_A = I_b - I_0 = a^2 I_1 + a I_2 \tag{57}$$

$$I_A - I_B = I_c - I_0 = a I_1 + a^2 I_2 \tag{58}$$

These four equations, of which only three are independent, may be solved for I_A, I_B and I_C, giving

$$I_A = j\frac{\sqrt{3}}{3}(I_1 - I_2) = \frac{I_\alpha}{3} \tag{59}$$

$$I_B = j\frac{\sqrt{3}}{3}(a^2 I_1 - a I_2) = \frac{I_\beta}{3} \tag{60}$$

$$I_C = j\frac{\sqrt{3}}{3}(a I_1 - a^2 I_2) = \frac{I_\gamma}{3} \tag{61}$$

The connection of Figure 9 is adapted particularly to altering the zero-sequence component of current through the relay, which may be desirable because of the difference between Z_{0GH} and Z_{1GH}. Residual current may be introduced not only from the line being protected but also from a parallel or other adjacent line. Adjustable-ratio auxiliary transformers serve to introduce the desired proportions. Let r_1 and r_2 be the turn ratios of the auxiliary transformers, and $3I_0$ and $3I_0'$ be the currents in the primaries of these transformers, the primed symbol indicating the current from an adjacent line. Then the current feeding the neutral of the interconnected-star transformer is equal to $3(I_0 r_1 + I_0' r_2)$. The interconnected-star transformer divides this current into three equal portions, so that $(I_0 r_1 + I_0' r_2)$ is added to the line current in each relay. Let us designate these currents I_x, I_y, and I_z respectively

$$I_x = I_a + I_0 r_1 + I_0' r_2 \tag{62}$$

$$I_y = I_b + I_0 r_1 + I_0' r_2 \tag{63}$$

$$I_z = I_c + I_0 r_1 + I_0' r_2 \tag{64}$$

Equations 42, 43, and 44 for I_a, I_b, and I_c, equations 51, 52, and 53 for I_α, I_β, and I_γ, equations 59, 60, and 61 for I_A, I_B, and I_C, and equations 62, 63, and 64 for I_x, I_y, and I_z apply in general and for unbalanced faults involving ground. During line-to-line faults on an otherwise balanced system no ground current flows so that $I_0 = 0$, and equations 42, 43, and 44 become

$$I_a = I_1 + I_2 \tag{65}$$

$$I_b = a^2 I_1 + a I_2 \tag{66}$$

$$I_c = a I_1 + a^2 I_2 \tag{67}$$

Equations 62, 63, and 64 become

$$I_x = I_a = I_1 + I_2 \tag{68}$$

$$I_y = I_b = a^2 I_1 + a I_2 \tag{69}$$

$$I_z = I_c = a I_1 + a^2 I_2 \tag{70}$$

During balanced 3-phase faults, both I_2 and I_0 are zero, so that the foregoing become

$$I_a = I_1 \tag{71}$$

$$I_b = a^2 I \tag{72}$$

$$I_c = a I \tag{73}$$

$$I_\alpha = j\sqrt{3} I_1 = 3 I_A \tag{74}$$

$$I_\beta = j\sqrt{3} a^2 I_1 = 3 I_B \tag{75}$$

$$I_\gamma = j\sqrt{3} a I_1 = 3 I_C \tag{76}$$

$$I_A = j\frac{\sqrt{3}}{3} I_1 = \frac{1}{3} I_\alpha \tag{77}$$

$$I_B = j\frac{\sqrt{3}}{3} a^2 I_1 = \frac{1}{3} I_\beta \tag{78}$$

$$I_C = j\frac{\sqrt{3}}{3} a I_1 = \frac{1}{3} I_\gamma \tag{79}$$

$$I_x = I_1 \tag{80}$$

$$I_y = a^2 I_1 \tag{81}$$

$$I_z = a I_1 \tag{82}$$

The foregoing values are general and apply at any location. Hence, the expressions for the corresponding currents between particular points may be obtained by adding the proper subscripts, in accordance with Appendix I.

Appendix III. Line-to-Line Fault

Assume that a line-to-line fault has occurred at point F of one of the parallel lines of Figure 2, between conductors b and c, and that a fault resistance R_S is present between the two conductors. It will be convenient to consider that a resistance $R_S/2$ is connected to each line conductor at F and that at a point W the remaining terminals of the resistors on phases b and c are connected together, as shown in Figure 15a. This device has the advantage of making the system symmetrical up to the point W, at which point we have

$$E_{bW} = E_{cW} \tag{83}$$

$$I_{bFW} = -I_{cFW} \tag{84}$$

and

$$I_{aFW} = 0 \tag{85}$$

Resolving the currents into symmetrical components, we obtain

$$I_{1FW} = \frac{1}{3}(a - a^2) I_{bFW} = -I_{2FW} \tag{86}$$

$$I_{2FW} = \frac{1}{3}(a^2 - a) I_{bFW} = -I_{1FW} \tag{87}$$

$$I_{0FW} = 0 \tag{88}$$

As the system is assumed symmetrical at all other points, the fact that $I_{0FW} = 0$ requires that $E_0 = 0$ and $I_0 = 0$ over the entire system.

Resolving the voltages into symmetrical components gives

$$E_{1W} = \frac{1}{3}(E_{aW} - E_{bW}) = E_{2W} \tag{89}$$

$$E_{2W} = \frac{1}{3}(E_{aW} - E_{bW}) = E_{1W} \tag{90}$$

$$E_{0W} = \frac{1}{3}(E_{aW} + 2E_{bW}) = 0 \tag{91}$$

Hence

$$E_{aW} = -2E_{bW} = -2E_{cW} \tag{92}$$

and

$$E_{1W} = E_{2W} = -E_{bW} = -E_{cW} = E_{aW}/2 \tag{93}$$

These conditions will be satisfied if the networks are connected as shown in Figure 15b.[1-4]

As the system is symmetrical elsewhere, the sequence currents flow independently,[1-4] and the sequence potentials at point G may be obtained by adding to the sequence voltages at W the sequence voltage drops between W and G. The currents flowing from F to W are the sums of the currents flowing

from G to F and H to F. Making these substitutions, we obtain

$$E_{AG}=I_{1GF}\left(mZ_{1GH}+\frac{R_S}{2}\right)+I_{1HF}\frac{R_S}{2}+E_{1W} \quad (94)$$

$$E_{1G}=I_{2G}\left(mZ_{1GH}+\frac{R_S}{2}\right)+I_{2HF}\frac{R_S}{2}+E_{1W} \quad (95)$$

$$E_{0G}=0 \quad (96)$$

The phase voltages at G become, from equations 39 to 41 and 48 to 50,

$$E_{aG}=I_{aGF}\left(mZ_{1GH}+\frac{R_S}{2}\right)+I_{aHF}\frac{R_S}{2}+2E_{1W} \quad (97)$$

$$E_{bG}=I_{bGF}\left(mZ_{1GH}+\frac{R_S}{2}\right)+I_{bHF}\frac{R_S}{2}-E_{1W} \quad (98)$$

$$E_{cG}=I_{cGF}\left(mZ_{1GH}+\frac{R_S}{2}\right)+I_{cHF}\frac{R_S}{2}-E_{1W} \quad (99)$$

$$E_{AG}=E_{cG}-E_{bG}=I_{\alpha GF}\left(mZ_{1GH}+\frac{R_S}{2}\right)+I_{\alpha HF}\frac{R_S}{2} \quad (100)$$

$$E_{BG}=E_{aG}-E_{cG}=I_{\beta GF}\left(mZ_{1GH}+\frac{R_S}{2}\right)+I_{\beta HF}\frac{R_S}{2}+3E_{1W} \quad (101)$$

$$E_{CG}=E_{bG}-E_{aG}=I_{\gamma GF}\left(mZ_{1GH}+\frac{R_S}{2}\right)+I_{\gamma HF}\frac{R_S}{2}-3E_{1W} \quad (102)$$

For convenience in connection with star-current relaying connections, it is desirable to rewrite the foregoing in a different form. As $I_0=0$ everywhere during this type of fault, we may arbitrarily write $(I_{aGF}+I_{bGF}+I_{cGF})(mZ_{1GH}+R_S/2)+(I_{aHF}+I_{bHF}+I_{cHF})(R_S/2)=0$.

Subtracting this equation from the foregoing gives

$$E_{AG}=-2I_{bGF}\left(mZ_{1GH}+\frac{R_S}{2}\right)-2I_{bHF}\frac{R_S}{2}-I_{aGF}\left(mZ_{1GH}+\frac{R_S}{2}\right)-I_{aHF}\frac{R_S}{2} \quad (103)$$

$$E_{BG}=-2I_{cGF}\left(mZ_{1GH}+\frac{R_S}{2}\right)-2I_{cHF}\frac{R_S}{2}-I_{bGF}\left(mZ_{1GH}+\frac{R_S}{2}\right)-I_{aHF}\frac{R_S}{2}+3E_{1W} \quad (104)$$

$$E_{CG}=-2I_{aGF}\left(mZ_{1GH}+\frac{R_S}{2}\right)-2I_{aHF}\frac{R_S}{2}-I_{cGF}\left(mZ_{1GH}+\frac{R_S}{2}\right)-I_{cHF}\frac{R_S}{2}-3E_{1W} \quad (105)$$

As $I_{aGF}+I_{aHF}=I_{aFW}=0$ equation 103 simplifies to

$$E_{AG}=-2I_{bGF}\left(mZ_{1GH}+\frac{R_S}{2}\right)-2I_{bHF}\frac{R_S}{2}-I_{aGF}mZ_{1GH} \quad (106)$$

Appendix IV. Double Line-to-Ground Fault

Assume that a double line-to-ground fault has occurred at point F of one of the parallel lines of Figure 2, between conductors b and c, that a fault resistance R_S is present between the two conductors, and that a fault resistance R_G occurs between some point of R_S and ground. Representation of the most general case requires that the point of connection of R_G may be at any point of R_S, but in order to obtain a simple analysis, it is necessary for R_G to be connected to the mid-point of R_S. In most practical cases, it is expected that either the resistance between phases will be small, or that the two parts will be nearly equal, so that the case assumed is sufficiently general for most purposes. It is convenient to consider again that a resistance of $R_S/2$ is connected to each line w re at the fault, and at a point W, the remaining terminals of the resistors on phases b and c are connected together and to one terminal of R_G, the remaining terminal of R_G being connected to ground. This is shown in Figure 16a.

Then at the point W, we have

$$I_{aFW}=0 \quad (107)$$

$$E_{bW}=E_{cW}=(I_{bFW}+I_{cFW})R_G \quad (108)$$

Resolving the currents into symmetrical components gives

$$I_{1FW}=\frac{1}{3}(aI_{bFW}+a^2I_{cFW}) \quad (109)$$

$$I_{2FW}=\frac{1}{3}(a^2I_{bFW}+aI_{cFW}) \quad (110)$$

$$I_{0FW}=\frac{1}{3}(I_{bFW}+I_{cFW}) \quad (111)$$

From which

$$I_{1FW}+I_{2FW}+I_{0FW}=0 \quad (112)$$

and

$$I_{bFW}+I_{cFW}=3I_{0FW} \quad (113)$$

Resolving the voltages into symmetrical components gives

$$E_{1W}=\frac{1}{3}(E_{aW}-3I_{0FW}R_G) \quad (114)$$

$$E_{2W}=\frac{1}{3}(E_{aW}-3I_{0FW}R_G) \quad (115)$$

$$E_{0W}=\frac{1}{3}(E_{aW}+6I_{0FW}R_G) \quad (116)$$

from which

$$E_{1W}=E_{2W}=E_{0W}-3I_{0FW}R_G \quad (117)$$

These conditions may be satisfied by connecting the networks as shown in Figure 16b.[4] As all networks are symmetrical up to the point W, we may write the expressions for the voltages at the point G by adding the proper sequence voltage drops. Remembering that the currents through the resistances $R_S/2$ are made up of the corresponding currents from G to F and H to F, we obtain

$$E_{1G}=I_{1GF}\left(mZ_{1GH}+\frac{R_S}{2}\right)+I_{1HF}\frac{R_S}{2}+E_{1W} \quad (118)$$

$$E_{2G}=I_{2GF}\left(mZ_{1GH}+\frac{R_S}{2}\right)+I_{2HF}\frac{R_S}{2}+E_{1W} \quad (119)$$

$$E_{0G}=I_{0GF}\left(mZ_{0GH}+\frac{R_S}{2}+3R_G\right)+I_{0HF}\left(\frac{R_S}{2}+3R_G\right)+I_{0GH}mM_{0GH}+E_{1W} \quad (120)$$

The line-to-neutral and line-to-line voltages may be obtained by substituting in equations 39 to 41 and 48 to 50

$$E_{aG}=I_{aGF}\left(mZ_{1GH}+\frac{R_S}{2}\right)+I_{aHF}\frac{R_S}{2}+I_{0GF}(mZ_{0GH}-mZ_{1GH}+3R_G)+3I_{0HF}R_G+I_{0GH}mM_{0GH}+3E_{1W} \quad (121)$$

$$E_{bG}=I_{bGF}\left(mZ_{1GH}+\frac{R_S}{2}\right)+I_{bHF}\frac{R_S}{2}+I_{0GF}(mZ_{0GH}-mZ_{1GH}+3R_G)+3I_{0HF}R_G+I_{0GH}mM_{0GH} \quad (122)$$

$$E_{cG}=I_{cGF}\left(mZ_{1GH}+\frac{R_S}{2}\right)+I_{cHF}\frac{R_S}{2}+I_{0GF}(mZ_{0GH}-mZ_{1GH}+3R_G)+3I_{0HF}R_G+I_{0GH}mM_{0GH} \quad (123)$$

$$E_{AG}=E_{cG}-E_{bG}=I_{\alpha GF}\left(mZ_{1GH}+\frac{R_S}{2}\right)+I_{\alpha HF}\frac{R_S}{2} \quad (124)$$

$$E_{BG}=E_{aG}-E_{cG}=I_{\beta GF}\left(mZ_{1GH}+\frac{R_S}{2}\right)+I_{\beta HF}\frac{R_S}{2}+3E_{1W} \quad (125)$$

$$E_{CG}=E_{bG}-E_{aG}=I_{\gamma GF}\left(mZ_{1GH}+\frac{R_S}{2}\right)+I_{\gamma HF}\frac{R_S}{2}-3E_{1W} \quad (126)$$

For convenience in connection with star-current relaying connections, it is desirable to rewrite the foregoing in different form. As $I_{aGF}+I_{bGF}+I_{cGF}=3I_{0GF}$ and $I_{aHF}+I_{bHF}+I_{cHF}=3I_{0HF}$, we may write arbitrarily

$$(I_{aGF}+I_{bGF}+I_{cGF}-3I_{0GF})\times\left(mZ_{1GH}+\frac{R_S}{2}\right)+(I_{aHF}+I_{bHF}+I_{cHF}-3I_{0HF})\frac{R_S}{2}=0$$

Subtracting this identity from the foregoing give:

$$E_{AG}=-2I_{bGF}\left(mZ_{1GH}+\frac{R_s}{2}\right)-2I_{bHF}\frac{R_s}{2}+(3I_{bGF}-I_{aGF})\left(mZ_{1GH}+\frac{R_s}{2}\right)+(3I_{bHF}-I_{aHF})\frac{R_s}{2} \quad (127)$$

$$E_{BG}=-2I_{cGF}\left(mZ_{1GH}+\frac{R_s}{2}\right)-2I_{cHF}\frac{R_s}{2}+(3I_{cGF}-I_{bGF})\left(mZ_{1GH}+\frac{R_s}{2}\right)+(3I_{bHF}-I_{bHF})\frac{R_s}{2}+3E_{1W} \quad (128)$$

$$E_{CG}=-2I_{aGF}\left(mZ_{1GH}+\frac{R_s}{2}\right)-2I_{aHF}\frac{R_s}{2}+(3I_{aGF}-I_{cGF})\left(mZ_{1GH}+\frac{R_s}{2}\right)+(3I_{aHF}-I_{cHF})\frac{R_s}{2}-3E_{1W} \quad (129)$$

As $I_{aGF}=-I_{aHF}$, equation 127 may be simplified to

$$E_{AG}=-2I_{bGF}\left(mZ_{1GH}+\frac{R_s}{2}\right)-2I_{bHF}\frac{R_s}{2}+3I_{bGF}\left(mZ_{1GH}+\frac{R_s}{2}\right)+3I_{bHF}\frac{R_s}{2}-I_{bGF}mZ_{1GH} \quad (130)$$

For studying ground relaying, it is desirable to have the line-to-neutral voltages expressed in terms of the symmetrical components of current. This may be done by substituting for the line currents in equations 121 to 123 inclusive, giving

$$E_{aG}=(I_{1GF}+I_{1GF})\left(mZ_{1GH}+\frac{R_s}{2}\right)+(I_{1HF}+I_{1HF})\frac{R_s}{2}+I_{0GF}\times\left(mZ_{0GH}+\frac{R_s}{2}+3R_G\right)+I_{0HF}\left(\frac{R_s}{2}+3R_G\right)+I_{0GH}mM_{0GH}+3E_{1W} \quad (131)$$

$$E_{bG}=(a^2I_{1GF}+aI_{1GF})\left(mZ_{1GH}+\frac{R_s}{2}\right)+(a^2I_{1HF}+aI_{1HF})\frac{R_s}{2}+I_{0GF}\times\left(mZ_{0GH}+\frac{R_s}{2}+3R_G\right)+I_{0HF}\left(\frac{R_s}{2}+3R_G\right)+I_{0GH}mM_{0GH} \quad (132)$$

$$E_{cG}=(aI_{1GF}+a^2I_{1GF})\left(mZ_{1GH}+\frac{R_s}{2}\right)+(aI_{1HF}+a^2I_{1HF})\frac{R_s}{2}+I_{0GF}\times\left(mZ_{0GH}+\frac{R_s}{2}+3R_G\right)+I_{0HF}\left(\frac{R_s}{2}+3R_G\right)+I_{0GH}mM_{0GH} \quad (133)$$

Appendix V. Three-Phase Fault

Assume that a 3-phase fault has occurred at point F of one of the parallel lines of Figure 2, between all conductors and ground, and that a fault resistance $R_s/2$ is present between each conductor and ground. In the general case, the fault resistances will not be exactly equal, but the treatment of the general case is much more complicated, and the case of equal resistances is probably sufficiently general for our purposes. Making use of the previous assumption that a resistance $R_s/2$ is connected to each conductor at the fault, we may consider the remaining terminals connected together and to ground at point W, as shown in Figure 17a. Then we have

$$E_{aW}=E_{bW}=E_{cW}=0 \quad (134)$$

$$I_{aFW}+I_{bFW}+I_{cFW}=3I_{0FW}=0 \quad (135)$$

From symmetry

$$I_{2FW}=0 \quad (136)$$

These conditions are represented by the connection of Figure 17b. Hence,

$$E_{1G}=I_{1GF}\left(mZ_{1GH}+\frac{R_s}{2}\right)+I_{1HF}\frac{R_s}{2} \quad (137)$$

$$E_{2G}=0 \quad (138)$$

$$E_{0G}=0 \quad (139)$$

and

$$E_{aG}=I_{0GF}\left(mZ_{1HG}+\frac{R_s}{2}\right)+I_{aHF}\frac{R_s}{2} \quad (140)$$

$$E_{bG}=I_{0GF}\left(mZ_{1HG}+\frac{R_s}{2}\right)+I_{bHF}\frac{R_s}{2} \quad (141)$$

$$E_{cG}=I_{cGF}\left(mZ_{1GH}+\frac{R_s}{2}\right)+I_{cHF}\frac{R_s}{2} \quad (142)$$

$$E_{AG}=I_{\alpha GF}\quad Z_{1GH}+\frac{R_s}{2}\Big)+I_{\alpha HF}\frac{R_s}{2} \quad (143)$$

$$E_{BG}=I_{\beta GF}\left(mZ_{1GH}+\frac{R_s}{2}\right)+I_{\beta HF}\frac{R_s}{2} \quad (144)$$

$$E_{CG}=I_{\gamma GF}\left(mZ_{1GH}+\frac{R_s}{2}\right)+I_{\gamma HF}\frac{R_s}{2} \quad (145)$$

As the system is everywhere symmetrical, $I_{aGF}+I_{bGF}+I_{cGF}=0$, hence $(I_{aGF}+I_{bGF}+I_{cGF})(mZ_{1GH}+R_s/2)=0$. Likewise $(I_{aHF}+I_{bHF}+I_{cHF})(R_s/2)=0$. Subtracting these expressions from the foregoing equations, we obtain the useful forms given below as

$$E_{AG}=-2I_{bGF}\left(mZ_{1GH}+\frac{R_s}{2}\right)-2I_{bHF}\frac{R_s}{2}-I_{aGF}\left(mZ_{1GH}+\frac{R_s}{2}\right)-I_{aHF}\frac{R_s}{2} \quad (146)$$

$$E_{BG}=-2I_{cGF}\left(mZ_{1GH}+\frac{R_s}{2}\right)-2I_{cHF}\frac{R_s}{2}-I_{bGF}\left(mZ_{1GH}+\frac{R_s}{2}\right)-I_{bHF}\frac{R_s}{2} \quad (147)$$

$$E_{CG}=-2I_{aGF}\left(mZ_{1GH}+\frac{R_s}{2}\right)-2I_{aHF}\frac{R_s}{2}-I_{cGF}\left(mZ_{1GH}+\frac{R_s}{2}\right)-I_{cHF}\frac{R_s}{2} \quad (148)$$

Appendix VI. Single Line-to-Ground Fault

Assume that a single line-to-ground fault has occurred at a point F on one of the parallel lines of Figure 2, between conductor a and ground, and that a fault resistance R_G is present. It is convenient to assume that a resistance R_G is connected to each conductor at F and at a point W the other terminal of the resistance attached to conductor a is grounded, as shown in Figure 18a. Then the system is symmetrical up to the point W. At W we must have

$$I_{bFW}=I_{cFW}=0=I_{bGF}+I_{bHF}=I_{cGF}+I_{cHF} \quad (149)$$

and

$$E_{aW}=0 \quad (150)$$

Resolving into components, we have

$$I_{1FW}=\frac{1}{3}I_{aFW}=I_{2FW}=I_{0FW}=I_{1GF}+I_{1HF}=I_{0GF}+I_{2HF}=I_{0GF}+I_{0HF} \quad (151)$$

$$E_{1W}=\frac{1}{3}(aE_{bW}+a^2E_{cW}) \quad (152)$$

$$E_{2W}=\frac{1}{3}(a^2E_{bW}+aE_{cW}) \quad (153)$$

$$E_{0W}=\frac{1}{3}(E_{bW}+E_{cW}) \quad (154)$$

so that

$$E_{1W}+E_{2W}+E_{0W}=0 \quad (155)$$

These relations will be satisfied by connecting the sequence networks as shown in Figure 18b. It is immaterial, as far as the actual system is concerned, whether a resistance R_G is connected between each pair of networks as shown, or whether a resistance $3R_G$ is inserted between terminal F of the zero-sequence network and S of the positive-sequence network, as is more common.[4] However, as some use is made in this analysis of the voltages at the terminals of the fictitious resistances connected to conductors b and c, the representation shown is preferred in this case.

Adding the voltage drops from G to W, we may obtain the voltages at G as

$$E_{1G}=I_{1GF}(mZ_{1GH}+R_G)+I_{1HF}R_G+E_{1W} \quad (156)$$

$$E_{2G}=I_{2GF}(mZ_{1GH}+R_G)+I_{1HF}R_G+E_{2W} \quad (157)$$

$$E_{0G}=I_{0GF}(mZ_{0GH}+R_G)+I_{0HF}R_G+I_{0GH}mM_{0GH}+E_{0W} \quad (158)$$

$$E_{aG}=I_{aGF}(mZ_{1GH}+R_G)+I_{aHF}R_G+I_{0GF}m(Z_{0GH}-Z_{1GH})+I_{0GH}mM_{0GH} \quad (159)$$

$$E_{bG}=I_{bGF}(mZ_{1GH}+R_G)+I_{bHF}R_G+I_{0GF}m(Z_{0GH}-Z_{1GH})+I_{0GH}mM_{0GH}+j\sqrt{3}(aE_{1W}-a^2E_{2W}) \quad (160)$$

$$E_{cG}=I_{cGF}(mZ_{1GH}+R_G)+I_{cHF}R_G+I_{0GF}(Z_{0GH}-Z_{1GH})+I_{0GH}m\times M_{0GH}-j\sqrt{3}(a^2E_{1W}-aE_{2W}) \quad (161)$$

$$E_{AG}=I_{aGF}(mZ_{1GH}+R_G)+I_{aHF}R_G+j\sqrt{3}(E_{1W}-E_{2W}) \quad (162)$$

$$E_{BG}=I_{bGF}(mZ_{1GH}+R_G)+I_{bHF}R_G+j\sqrt{3}(a^2E_{1W}-aE_{2W}) \quad (163)$$

$$E_{CG}=I_{\gamma GF}(mZ_{1GH}+R_G)+I_{\gamma HF}R_G+j\sqrt{3}(aE_{1W}-a^2E_{2W}) \quad (164)$$

As $I_{bGF}=-I_{bHF}$ and $I_{cGF}=-I_{cHF}$, further simplification of equations 160 and 161 may be made, giving

$$E_{bG}=I_{bGF}mZ_{1GH}+I_{bGF}m(Z_{0GH}-Z_{1GH})+I_{0GH}mM_{0GH}+j\sqrt{3}(aE_{1W}-a^2E_{2W}) \quad (165)$$

$$E_{cG}=I_{cGF}mZ_{1GH}+I_{cGF}m(Z_{0GH}-Z_{1GH})+I_{0GH}mM_{0GH}-j\sqrt{3}(a^2E_{1W}-aE_{2W}) \quad (166)$$

For certain purposes it is desirable to have the foregoing voltages in terms of the symmetrical components of currents instead of the line currents. It also will be more convenient to combine all the resistance terms, making use of the relation that $I_{1GF}+I_{1HF}+I_{bGF}+I_{bHF}=2(I_{bGF}+I_{bHF})$. Substituting and combining, we obtain

$$E_{aG}=(I_{1GF}+I_{1GF})mZ_{1GH}+I_{0GF}mZ_{0GH}+I_{0GH}mM_{0GH}+3(I_{bGF}+I_{bHF})R_G \quad (167)$$

$$E_{bG}=(a^2I_{1GF}+aI_{bGF})mZ_{1GH}+I_{bGF}mZ_{0GH}+I_{0GH}mM_{0GH}+j\sqrt{3}(aE_{1W}-a^2E_{2W}) \quad (168)$$

$$E_{cG}=(aI_{1GF}+a^2I_{bGF})mZ_{1GH}+I_{bGF}mZ_{0GH}+I_{0GH}mM_{0GH}-j\sqrt{3}(a^2E_{1W}-aE_{2W}) \quad (169)$$

References

1. Method of Symmetrical Co-ordinates Applied to the Solution of Polyphase Networks. **C. L. Fortescue.** AIEE Transactions, volume 37, 1918, pages 1027–1115.

2. Studies of Transmission Stability, **R. D. Evans, C. F. Wagner.** AIEE Transactions, volume 45, 1926, pages 51–80.

3. Calculation of Single-Phase Short Circuits by the Method of Symmetrical Components, **A. P. Mackerras.** *General Electric Review* (Schenectady, N. Y.), volume 29, April 1926, page 218; July 1926, page 468.

4. Symmetrical Components, **C. F. Wagner, R. D. Evans.** *Electric Journal*, March 1928, page 151; April 1928, page 194; June 1928, page 307; July 1928, page 359; September 1929, page 426; December 1929, page 571.

5. Modern Requirements for Protective Relays on Important System Interconnections, **O. C. Traver, L. F. Kennedy.** AIEE Transactions, volume 49, 1930, pages 1226–31.

6. High-Speed Protective Relays, **L. N. Crichton.** AIEE Transactions, volume 49, 1930, pages 1232–8.

7. Fundamental Basis for Distance Relaying, **W. A. Lewis, L. S. Tippett.** Electrical Engineering, volume 50, June 1931, pages 420–2.

8. Operating Experience With Reactance Type Distance Relays, **E. E. George.** AIEE Transactions, volume 50, 1931, pages 288–93.

9. New High-Speed Distance Relay, **S. L. Goldsborough, W. A. Lewis.** Electrical Engineering, volume 51, March 1932, pages 157–60.

10. A High-Speed Reactance Relay, **A. R. van C. Warrington.** Electrical Engineering, volume 52, April 1933, pages 248–52.

11. Symmetrical Components (a book), **C. F. Wagner, R. D. Evans.** McGraw-Hill Book Company, Inc., New York, N. Y., 1933.

12. Control of Distance-Relay Potential Connections, **A. R. van C. Warrington.** AIEE Transactions, volume 53, 1934, pages 206–13; discussion pages 465–6, 617.

13. Distance-Relay Action During Oscillations, **E. H. Bancker, E. M. Hunter.** AIEE Transactions, volume 53, 1934, pages 1073–80; discussions, pages 1320–2, and volume 54, 1935, pages 216–18.

14. High-Speed Distance Relay, **L. N. Crichton.** *Electric Journal*, volume 32, December 1935, pages 537–42.

15. Performance of Distance Relays, **G. Calabrese.** AIEE Transactions, volume 55, 1936; pages 660–72; discussion pages 1254–5.

16. A Comprehensive Method of Determining the Performance of Distance Relays, **J. H. Neher.** AIEE Transactions, volume 56, 1937, pages 833–44; discussion page 1515.

17. High-Speed Relaying, **W. A. Lewis.** *Proceedings*, Midwest Power Conference, volume 5, 1942, pages 137–55.

18. Distance Relaying With Low-Tension Potentials, **J. L. Blackburn.** *Westinghouse Engineer*, Pittsburgh, Pa., volume 3, 1943, pages 61–4.

19. Performance Requirements for Relays on Unusually Long Transmission Lines, **F. C. Poage, C. A. Striefus, D. M. MacGregor, E. E. George.** AIEE Transactions, volume 62, 1943, June section, pages 275–83; discussion pages 422–5.

20. Protective Relaying for Long Transmission Lines, **A. R. van C. Warrington.** AIEE Transactions, volume 62, 1943, June section, pages 261–8; discussion page 427.

21. Staged Fault Tests of Relaying and Stability on Kansas–Nebraska 270-Mile 154-Kv Interconnection, **C. W. Minard, R. B. Gow, W. A. Wolfe, E. A. Swanson.** AIEE Transactions, volume 62, 1943, pages 358–67.

22. The Principles of High-Speed Relaying, **W. A. Lewis.** *Westinghouse Engineer*, Pittsburgh, Pa., volume 3, August 1943, pages 91–4; November 1943, pages 131–4

23. Circuit Analysis of A-C Power Systems (a book), **Edith Clarke.** John Wiley and Sons, Inc., New York, N. Y., 1943.

24. A Distance Relay With Adjustable Phase-Angle Characteristics, **S. L. Goldsborough.** AIEE Transactions, volume 63, 1944, pages 835–8; discussion, page 1471.

25. Compensators for Distance Relaying, **J. L. Blackburn.** *Electrical World*, volume 122, 1944, July 22, pages 146–8–50; August 19, pages 112–3; September 16, p. 112.

26. Impedances Seen by Relays During Power Swings, With and Without Faults, **Edith Clarke.** AIEE Transactions, volume 64, 1945, pages 372–84; discussion page 471.

27. Operating Experience With Distance Ground Relays, **W. A. Wolfe.** AIEE Transactions, volume 65, 1946, page 458.

Discussion

C. G. Dewey (General Electric Company, Philadelphia, Pa.): In connection with the discussion of fault resistance, it is worth noting that there is nearly the same disadvantage in having the second zone balance point to retract to a point within the first section, as for the first zone balance point to extend into the second section. The former also may cause loss of selectivity, which would mean losing power unnecessarily at some substation.

Even if it is granted that the balance point for no arc resistance can be set nearer the end of the section for the impedance relay than for the reactance, the protection is not necessarily better. This advantage is lost directly on arcing faults, as such faults cause an automatic retraction of reach in the impedance relay, particularly on short lines.

E. L. Harder (Westinghouse Electric Corporation, East Pittsburgh, Pa.): The method of symmetrical components now enters vitally into the design and application of nearly every piece of equipment that goes into an electric power system. It is used in determining the short-circuit currents for which the generators and transformers must be braced. It is used in determining the interrupting duty of the circuit breakers and fuses. It enters into the application of lightning arresters and protector tubes, and into the insulation of transformers and other equipment. However, nowhere has the method of symmetrical components contributed quite so much as in the field of protective relaying. For in this field it has become the indispensable tool for visualizing, as well as computing, the currents and voltages during fault conditions, which are the fundamental basis of relay operation.

The introduction of the method of symmetrical components by the late Doctor Fortescue was followed by its expansion and development into a general industry tool by many of his associates, notably by Wagner and Evans, who developed and first presented in book form the working data and methods for treating machines, lines, and transformers. Wright, under their direction, and Kilgore determined the sequence impedances of machines by test and calculation.

It perhaps is not surprising, therefore, that this paper, an excellent contribution of symmetrical components to the relaying field, has come from the hands of a man who was closely associated with Doctor Fortescue, Wagner, and Evans.

At the time of the writing of this paper the symmetrical component method was in quite common use for relay current calculations. However, distance relays, particularly of the high-speed type, were in their infancy, and little was known of the merits of different arrangements. Expression of the relay balance points in terms of the sequence impedances and currents of the system, provided, as the title implies, "A Fundamental Basis for Distance Relaying."

It showed immediately that the delta currents should be used to avoid a 15 per cent difference in the reach of the relay for 3-phase and line-to-line faults. It provided an accurate basis for appraising the relative merits of reactance and impedance relays. In this paper appear the fundamental formulas that show the two ways to make

ground distance relays measure correctly. Subsequently ground distance relays have been developed along both of these lines.

The work is so systematic, so thorough, and so fundamental that it stands today, as when written—the fundamental basis for distance relaying.

Edward W. Kimbark (Northwestern University, Evanston, Ill.): The new presentation and publication of an AIEE paper 16 years after it was first presented at an AIEE meeting and published in pamphlet form is, I believe, without precedent. The paper (31-61) first was presented during a period of depression when, for economy, many AIEE papers, including this one, were published in abstract in ELECTRICAL ENGINEERING. The unprecedented action now puts this paper on permanent, accessible record, where it deserves to be.

The passage of 16 years has but confirmed earlier judgment that this paper by Lewis and Tippett is the classic paper in the field of power-system circuit theory as applied to predicting the behavior of protective relays. Nothing equalling it in this field had appeared before, and very little such has appeared since. Attempts to analyze the behavior of directional elements as Lewis and Tippett analyzed distance elements have produced results far less clear-cut than theirs. Only two other outstanding analyses in this field come to the mind of this discusser. They are the analyses of relay characteristics made by Neher[1] and Warrington[2] and the analysis of impedances seen by relays during swinging and out-of-step conditions made by Miss Clarke.[3]

Since the first publication of the paper by Lewis and Tippett, the following related developments have occurred:

1. The relay connections recommended in the paper have been used widely for phase relays and, to a lesser extent, for ground relays.

2. The analysis was extended by Calabrese[4] to cover the case of relays on the side of a Y-delta-connected power transformer bank away from the fault.

3. An alternative method of obtaining the effect of delta currents, or differences of two line currents, was devised, in which the relay had two current windings each carrying one of the line currents.

REFERENCES

1. A COMPREHENSIVE METHOD OF DETERMINING THE PERFORMANCE OF DISTANCE RELAYS, J. H. Neher. ELECTRICAL ENGINEERING, volume 56, July 1937, pages 833–44.

2. A CONDENSATION OF THE THEORY OF RELAYS, A. R. van C. Warrington. *General Electric Review*, Schenectady, N. Y., volume 43, September 1940, pages 270–3.

3. IMPEDANCES SEEN BY RELAYS DURING POWER SWINGS WITH AND WITHOUT FAULTS, Edith Clarke. AIEE TRANSACTIONS, volume 64, 1945, pages 372–84.

4. PERFORMANCE OF DISTANCE RELAYS, G. Calabrese. ELECTRICAL ENGINEERING, volume 55, June 1936, pages 660–72.

Short-Circuit Requirements for Transformers

A. N. GARIN
MEMBER AIEE

SYSTEM FAULTS impose a great variety of short circuits on the windings of 3-winding transformers. Because of the excellent service record of modern transformers their ability to withstand these short circuits is often taken for granted. If, however, the suitability of a given transformer for use on a given system is questioned, a rational answer can be given only when the impedances between all windings are known, so that the magnitudes of short-circuit currents in them can be calculated, and when the maximum current that each winding can withstand without injury is also known. The information on impedances, if not immediately available, can be obtained from the manufacturer of the transformer, and the ability of each winding to withstand short-circuit current could be assumed to be as specified by the standards of the American Standards Association.[1] Unfortunately, the present American Standards on short circuits are inadequate and subject to misinterpretation, particularly in the case of line to ground faults on Y-connected windings of transformers provided with delta connected stabilizing windings.

The purpose of this paper is to point out the inadequacies of the present standards on short circuits and to submit recommendations for their revision.

A brief review of the physical factors involved may be helpful in focusing once more our attention on a transformer problem that has been somewhat neglected in recent years.

Short-Circuit Currents

To begin with it must be clearly understood that the present discussion is limited to short-circuit currents resulting from system faults external to the transformer.

For an external fault the magnitude of symmetrical short-circuit currents in all windings of a transformer on the faulted system can be readily calculated, provided the impedances of the system and the impedances between all windings of the transformer are known. For unbalanced faults such calculations are greatly facilitated by the now well-known method of symmetrical components,[2] with both the transformer and the system replaced by their equivalent circuits. The familiar 3-terminal equivalent circuit[3] may be used to represent Y-Y-delta connected 3-winding transformers for all 3 sequences, although when the transformers are of 3-phase construction in some cases better accuracy will be obtained if a special 4-terminal equivalent circuit[4] is used in the zero sequence network. The peak value of the transient currents in all windings is obtained by assuming the short-circuit currents to be initially completely displaced from zero.

It should be realized that the information on short-circuit currents given by this process is somewhat over-simplified due to the implicit assumption that the vector sum of the ampere turns in all windings of a transformer remains equal to zero during the short-circuit transient. Actually the transient is quite complicated since several coupled circuits of different time constants are involved, and moreover for autotransformers, and in the case of unbalanced faults, there is always a possibility of partial saturation of the magnetic circuit with a corresponding increase in magnetizing ampere turns. It would be impractical to make allowance for these complications in a routine calculation, the more so because many other design factors besides the impedances between the windings would have to be taken into acount.

A study of short-circuit currents in windings of representative transformers due to faults on representative systems leads to the following conclusions:

1. Under the most unfavorable conditions short-circuit currents in transformer windings due to unbalanced system faults are substantially equal to short-circuit currents caused by balanced three phase faults. Thus in an investigation conducted on the pessimistic basis of fully maintained line voltages and no external impedances whatever there is no need of calculating any unbalanced faults and complete information will be obtained from the much simpler calculation of balanced three phase faults only. As an example, in the case of a Y-Y connected transformer with a delta connected stabilizing winding the maximum value of the current the stabilizing winding may have to carry during line to ground faults on the lines of Y-connected windings may be determined by calculating the following balanced three phase short circuits that would be possible if the terminals of the stabilizing winding were brought out:

(a). Short circuit on the stabilizing winding, or on both the stabilizing winding and the first Y-connected winding, with voltage maintained on the second Y-connected winding, and

(b). Short circuit on the stabilizing winding, or on both the stabilizing winding and the second Y-connected winding, with voltage maintained on the first Y-connected winding.

2. Many autotransformers and some 3-winding transformers, particularly those in which one winding is smaller than either of the others, if calculated on the basis of fully maintained system voltages will be found to have short-circuit currents in some winding in excess of the accepted permissible limit of 25 times normal load current, which is based on the usual interpretation of the present American Standards. The continued successful operation of these units suggests either the presence of sufficient system impedances, or large design safety margins, or both. It would appear, therefore, that only in exceptional cases could there be any justification for specifying designs with the short-circuit requirements for any winding in excess of 25 times normal load current of that winding.

Paper 47-105, recommended by the AIEE committee on electric machinery for presentation at the AIEE North Eastern District meeting, Worcester, Mass., April 23–25, 1947. Manuscript submitted February 11, 1947; made available for printing March 19, 1947.

A. N. GARIN is an electrical engineer with General Electric Company, Pittsfield, Mass.

3. Under representative conditions unbalanced system faults result in considerably lower short-circuit currents in transformer windings than balanced three phase faults. This justifies the well-established practice of making the delta-connected stabilizing windings of Y-Y-connected transformers and autotransformers of smaller size than the main windings since the stabilizing windings carry short-circuit currents only during line-to-ground faults and do not participate in balanced 3-phase short circuits on the lines of the main windings.

Ability to Withstand Short-Circuit Currents

The danger of short circuit currents is in their thermal and mechanical effects, both of which are proportional to the square of the magnitude of the currents, but in other respects follow different laws and depend on different design factors.

On the basis of all heat being stored in the copper, the temperature rise of the winding carrying the short-circuit current is directly proportional to the duration of the short circuit and is practically independent of the short-circuit currents in the other windings of the transformer.

Leaving aside such secondary factors as eddy losses, absorption of heat by the surrounding insulation, and slight variations in initial temperature, the final temperature reached by the copper depends only on the current density during the short circuit and on its duration. The current density, therefore, is the only design information needed to establish with acceptable accuracy the thermal short-circuit limits of a given transformer.

Mechanical stresses imposed on a winding by short-circuit currents have their maximum value during the first cycle of the current and diminish as the displacement of the current with respect to zero decreases with time; their magnitude for any winding depends on short-circuit currents in all windings of the transformer.

The magnitude, distribution, and direction of mechanical stresses in the windings carrying short-circuit currents depend on the shape, arrangement, and configuration of windings, so that the same value of short-circuit ampere turns may result in entirely different forces if the windings are of different type or of different proportions. The ability to withstand these stresses is determined by the structural characteristics of the windings, which must be known in great detail, since a local deformation or distortion may be as fatal to the transformer as a displacement of a complete winding. Obviously, fairly complete design information must be available even to estimate the ability of a given transformer to withstand mechanically short-circuit currents of a specified magnitude.

Continuous Kilovolt-Ampere Rating and Short-Circuit Kilovolt-Ampere Rating

It is perhaps natural to think that in a 3-winding transformer with windings of different continuous kilovolt-ampere capacity the maximum short-circuit kilovolt-amperes that each of the three windings is capable of withstanding would be approximately proportional to its rating. Broadly speaking, on the basis of everything else being equal, that is not far from the truth.

It is true, for instance, that it would be difficult to make a very small tertiary winding of a large transformer self-protecting under short circuit, even if there were no upper limits to the acceptable reactances from this tertiary to the main windings of the transformer. In this case, thermal requirements would present no serious problem since the short-circuit current density could be kept down to a permissible value by designing for sufficiently high reactances, but mechanical requirements would be difficult to satisfy. Small windings tend to be weak mechanically, and high values of reactance usually result in very large forces per ampere turn of current, so that reduction in short-circuit current due to high reactance does not necessarily reduce the forces. A familiar example of disastrous results that may be expected when the winding carrying the short-circuit current is very small and has very high reactance is an internal fault involving a small portion of a primary or secondary winding. Instead of resorting to some very special construction to make a very small winding self-protecting under short circuit it has been found more economical to make it larger and use the normal construction. Hence, the generally accepted practice of never making any winding of a multi-winding transformer, with terminals brought out, smaller than 35 per cent of the rating of the largest winding.

The same practice has been extended to delta connected stabilizing windings of Y-Y connected transformers and autotransformers. Since in many cases stabilizing windings are not provided with external leads, the intent has been not to give them any continuous load carrying capacity but to assure obtaining the ability to withstand short-circuit currents normally expected from a winding of this kilovolt-ampere rating. There have been cases where, obviously following the same line of reasoning, purchasers specified stabilizing windings of larger then the minimum 35 per cent size, although they either had no way of loading them, or planned only to use them to carry very small station loads.

As a matter of fact, there is, of course, no definite relation between the continuous kilovolt-ampere ratings of windings, which depend on their ability to dissipate heat, and what might be called the short-circuit kilovolt-ampere ratings of the same windings, which depend on their ability to store heat and to withstand mechanical stresses. Such definite relation could exist only on the basis of everything else being equal which is seldom the case with modern transformers with their complicated windings, wide variety of physical arrangements of coils, and wide range of normal current densities, often influenced by the method of cooling.

In view of this, the practice of specifying the desired ability of a winding to withstand short circuit by giving it a fictitious, or real, continuous kilovolt-ampere rating should be abandoned and the short-circuit rating should be specified directly as so many kilovolt-amperes, or so many times some reference kilovolt-amperes, for so many seconds.

Stabilizing Windings

Delta connected stabilizing windings of Y-Y-connected transformers, already referred to several times to illustrate the salient points of the above discussion, deserve further attention, not only because of their inherent importance, but also because they are not covered specifically by the present American Standards.

Complete self-protection against line to ground faults can be economically justified in exceptional cases only and, therefore, need not be the basis of a general specification. As demonstrated by the service record of many years on a great variety of systems, and as confirmed by fault current calculations for representative cases, the usual 35 per cent capacity stabilizing winding is adequate for most applications. The American Standards should legitimize and clarify this well-established design practice. The required rules should specify, however, the minimum permissible short-circuit kilovolt-ampere rating of stabilizing windings and not their continuous kilovolt-ampere rating, since, first, a continuous kilovolt-ampere rating is not a reliable measure of the ability to withstand short-circuit currents, and second, there can be no justification for designing a winding for continuous loading when such loading is

either impossible or not required. For example, in the case of a 10,000 kilovolt-ampere Y-Y-connected transformer with a stabilizing winding, the rules should give the minimum size of the stabilizing winding not by specifying for it a 3,500-kva continuous rating, but by specifying a short-circuit rating of 3,500 × 25 or 87,500 kva for two seconds. Since 0.35 × 25 = 8.75, this minimum permissible 2-second short-circuit rating of the stabilizing winding is equal to 8.75 times the continuous kilovolt-ampere rating of the main windings. A smaller stabilizing winding would not be furnished even if transformer impedances were sufficiently high to limit the short-circuit kilovolt-ampere in the stabilizing winding to less than 8.75 times the continuous kilovolt-ampere rating of the main windings. Naturally, in such a case the actual short-circuit current could be carried for longer than 2 seconds. If, in the present example, the short circuit was limited by transformer impedances to 70,000 kva in the stabilizing winding it could be carried for 3 seconds (see part 1*B* under Recommended Revision of American Standards on Short Circuits).

For autotransformers the practice has been to provide stabilizing windings equal to at least 35 per cent of the equivalent size of the autotransformer windings. As for transformers, the American Standards should give this minimum size in short-circuit kilovolt-amperes and not in continuous capacity kilovolt-amperes. Since the equivalent size of an autotransformer is always smaller than its output rating, the minimum short-circuit rating of stabilizing windings in autotransformers will be smaller than in transformers of the same output rating. Thus if the 10,000 kva Y-Y-connected unit of the above example were a 66- to 44-kv autotransformer, the equivalent size of the autotransformer windings would be 3,333 kva, and the minimum short-circuit rating of the stabilizing winding would be 3,333 × .35 × 25 = 29,167 kva, or 8.75 times the equivalent size of the autotransformer, for 2 seconds.

Obviously all the Standards can do is to indicate the minimum short-circuit rating for stabilizing windings consistent with good design practice. They can not attempt to specify the short-circuit rating actually required in a given case. This decision must be left to application engineering. Indiscriminate acceptance of the minimum stabilizing winding size regardless of the values of reactance between the windings of the transformer, or autotransformer, and regardless of system reactances, would mean that in some cases short-circuit currents permitted by these reactances would be larger than the windings could be expected to withstand. It is hoped, therefore, that the recommended practice of giving the stabilizing windings a definite short-circuit rating would call attention to this most important criterion of the design and result in heavier windings being specified whenever needed.

While it is true that in autotransformers the per cent reactances between the stabilizing windings and the Y-connected windings, based on the output kilovolt-amperes of the unit, are usually much higher than in transformers, the resultant reduction in fault currents in many cases may be insufficient to justify the reduction in the minimum size of stabilizing windings indicated by the present practice. Because of this, short-circuit ratings of the stabilizing windings of autotransformers should be given special attention.

The Present American Standards on Short Circuits

The present American Standards[1] are clear when applied for balanced 3-phase short circuits on two-winding transformers. They are subject to misinterpretation and may be actually misleading when applied for three-winding units, and particularly for unbalanced faults on units with stabilizing windings when these windings have no definite continuous kilovolt-ampere rating.

The very title of the rules, "Permissible Duration of Short Circuit," suggests that they are based primarily, if not exclusively, on thermal considerations, an attitude that may have had some justification at the time when the rules were first formulated because of relatively high current densities then in use. The rules begin with the statement:

> Transformers shall be capable of withstanding short circuits on any secondary winding or windings without injury for the time-periods given below, with rated line voltages maintained on all windings intended for connection to external sources of power. See exceptions listed in Table I. Intermediate values may be determined by interpolation. The initial current is assumed to be completely displaced from zero insofar as determining the mechanical stresses.

Table I

Per Cent Impedances	Rms Symmetrical Short-Circuit Current to Be Withstood	Time Period in Seconds
4 or less	25 times rated current	2
5	20 times rated current	3
6	16.6 times rated current	4
7 or more		5

If the reader stops at the end of the first paragraph, just before the tabulation, and ignores for the time being the reference to the time-periods, he gets the impression that a stabilizing winding, being a part of a transformer, must be capable of withstanding any kind of a fault at the terminals of Y-connected windings, with maintained voltage "on all windings intended for connection to external sources of power." Some engineers have claimed just that. But the framers of the rules meant something else, as indicated by the tabulation following the first paragraph. This tabulation is directly applicable only to 2-winding transformers. The important point for the present purposes is that, apparently, when the impedance is less than 4 per cent, the windings of a 2-winding transformer are not required to withstand more than 25 times rated current. What justification is there, then, to expect the stabilizing winding to be capable of withstanding more than 25 times its rated current?

The term "rated current" itself is not very clear. What is to be taken as rated current for transformers with various increased kilovolt-ampere ratings, by means of supplemental methods of cooling? What should be taken as rated current of a stabilizing winding without a continuous kilovolt-ampere rating?

The next two paragraphs read:

> For transformers having three or more windings, the time for which the transformer shall be capable of withstanding a short circuit is dependent upon the maximum current which can flow in any short circuited winding with rated voltage maintained on all other windings intended for connection to an external source of power.
>
> Each winding shall be considered separately and the ratio of maximum short-circuit current in a winding to its rated current shall be used in the table to obtain the permissible duration of short circuit for that winding.

It would seem desirable to clarify and rewrite these paragraphs. Line to ground faults and stabilizing windings are ignored completely, since the stabilizing winding during a line to ground fault cannot be identified either as an excited, or as a short-circuited winding in the ordinary meaning of these terms. The assumption the rules make that the maximum possible current in a winding will necessarily flow when this winding is short-circuited and the other windings are excited is incorrect. In some cases the maximum value of current occurs when the winding in question is one of the excited windings and some other winding is short circuited.

The rules, as written, are concerned only with the duration of the fault and do

not cover specifically the case when the current in some winding during some condition of short circuit is larger than 25 times normal.

The concluding paragraphs are:

Exceptions:

(*a*). The combined impedances of transformers and directly connected apparatus shall be considered as limiting the short-circuit current of transformers which are directly connected to other apparatus possessing inherent impedance and located only a few feet from the transformer and connected to it by buses or cables so arranged that there will be no practical possibility of short circuit occurring between them.

(*b*). Autotransformers, being series apparatus, are liable to exceptionally severe short circuits unless protected by current limiting means. Because of the cumulative detrimental effects of successive severe short circuits, it is practically impossible to determine by tests the maximum safe short-circuit current that this class of apparatus will withstand successfully. It is recommended, therefore, that current limiting reactors be installed where necessary to limit the short-circuit current to 25 times rated current.

The first paragraph does not call for any comments, the second one makes the reader wonder why "the cumulative detrimental effects of successive severe short circuits" are worse for autotransformers than they are for transformers and why the recommendation on the use of current limiting reactors—assuming that such recommendations belong in American Standards—should be limited to autotransformers if the Standards do not require the windings of transformers to be capable of withstanding more than 25 times rated current.

Recommended Revision of American Standards on Short Circuits

The intention of the revision being suggested is not to alter the spirit of the present rules, but only to clarify them and thus reduce the possibility of misinterpretation when the rules are applied to multi-winding transformers and autotransformers, and for unbalanced, as well as balanced, short circuits. The following revision is suggested:

1. Transformers shall be capable of withstanding without injury short circuits on any external terminals with rated line voltages maintained on all terminals intended for connection to external sources of power, provided:

(*A*). The magnitude of the symmetrical current in any winding of the transformer resulting from the external short circuit does not exceed 25 times the base current of the winding (see Parts 2 and 3).

(*B*). The duration of the short circuit is limited to the following time periods listed in Table II. Intermediate values may be determined by interpolation. The initial current is assumed to be completely displaced from zero.

2. The base current for any winding is equal to its rated current, except as noted in 3.

For self-cooled transformers with increased kilovolt-ampere ratings obtained by supplementary cooling means the base current shall be taken at the self-cooled rating.

3. In the following special cases the base current for the winding specified may be larger than its rated current;

(*A*). For multiwinding transformers the base current for any winding provided with external terminals, and for a delta-connected stabilizing winding without external terminals, shall not be taken at less than 35 per cent of the kilovolt-ampere rating of the largest winding of the transformer.

(*B*). For Y-Y-connected autotransformers:

(*a*). The base current for a delta-connected stabilizing winding, with or without external terminals, shall not be taken at less than 35 per cent of the equivalent transformer kilovolt-amperes of the autotransformer windings.*

(*b*). The base current for the common winding shall be equal to the maximum current in the common winding when carrying any simultaneous loads authorized by the nameplate.

(*c*). The base current for the series winding shall not be taken at less than 35 per cent of the kilovolt-ampere capacity of the common winding or of the delta-connected winding, whichever one is the larger.

4. The combined impedance of transformers and directly connected apparatus shall be considered as limiting the short-circuit current of transformers which are connected in series with other apparatus possessing inherent impedance, located only a few feet from the transformers, and so connected to them that there will be no practical possibility of the loss of this additional series impedance.

Table II

Symmetrical Current in Any Winding	Time Period in Seconds
25 times base current	2
20 times base current	3
16.6 times base current	4
14.3 or less times base current	5

* Equivalent transformer kilovolt-amperes of autotransformer windings equals 1/2(total kilovolt-amperes of series winding plus total kilovolt-amperes of the common winding), where total kilovolt-amperes of each winding is given by the product of the maximum voltage times the maximum current of the winding.

References

1. Standards for Distribution and Power Transformers, ASA-C-57, 1942, page 29.

2. Method of Symmetrical Coordinates Applied to the Solution of Polyphase Networks, C. L. Fortescue. AIEE Transactions, volume 37, 1918, page 1027.

3. Theory of Three-Circuit Transformers, A. Boyajian. AIEE Transactions, volume 43, 1924, pages 508–28.

4. Zero-Phase Sequence Characteristics of Transformers, A. N. Garin. *General Electric Review*, March and April 1940.

No Discussion

Hiperco—A Magnetic Alloy

J. K. STANLEY
NONMEMBER AIEE

T. D. YENSEN
MEMBER AIEE

DURING the war considerable effort was expended in developing a high magnetic saturation alloy for electric apparatus in which a saving in weight or volume would be important, as in aircraft or submarines. Research work finally led to the development of an alloy suitable for such applications, in which cost is of secondary importance.

It has been known for a long time that iron-cobalt alloys in the range of 30 to 40 per cent cobalt have the highest magnetic saturation value so far attained,[1, 2] namely, a ferric induction, $4\pi I_s$* of about 24,200 as compared with 21,600 for iron, 21,000 for low silicon (1 per cent) iron, and about 19,000 for high silicon (4 to 5 per cent) iron. The gain in saturation over standard electrical grade sheet (1 per cent Silicon) thus amounts to about 15.0 per cent, and for high silicon grades to about 25 per cent. (See Figure 1.) This increase in saturation, coupled with an even higher increase in induction for $H = 10$ to 400, can by proper design, be translated into savings in weight of motors and generators of 20 to 25 per cent.

There are two reasons which have retarded the application of iron-cobalt alloys in the electrical industry. One is the high cost of cobalt ($1.50 per pound at present), and the other is the difficulty of fabrication, because the alloy, as ordinarily made, is too brittle to work either hot or cold. Even vacuum fused ingots, made from high purity iron and cobalt are usually "hot short," as metallurgists would say, making it difficult to hot work the alloy to desirable shapes. Although this was done in 1915,[3] it was not until 1932 that the Bell Telephone Laboratories succeeded in preparing an iron-cobalt alloy with good hot working properties and one whose magnetic quality was unimpaired by the alloy addition, using vanadium and quenching.[3] For the purpose of providing aircraft with lighter generators and motors, the Westinghouse Research Laboratories undertook in 1940 the problem of developing an iron-cobalt alloy which could be processed commercially in wide strip from which armature and pole pieces could be punched and having losses comparable with those of 1-per cent Silicon-iron, which was then commonly used.

Paper 47-125, recommended by the AIEE committee on electric machinery for presentation at the AIEE summer general meeting, Montreal, Quebec, Canada, June 9–13, 1947. Manuscript submitted November 14, 1946; made available for printing April 11, 1947.

T. D. YENSEN is manager of the magnetic department of the research laboratories, Westinghouse Electric Corporation, East Pittsburgh, Pa. J. K. STANLEY is also with the Westinghouse Electric Corporation, East Pittsburgh, Pa.

* I_s = saturation intensity of magnetization.

Composition of Material

Of the numerous additions to the binary alloys that were tried, only two alloying elements were found to be useful in making the alloys workable, namely vanadium and chromium. The addition of these elements is beneficial also in that they greatly increase the electrical resistivity of otherwise very low resistivity alloy, as shown in Figure 2. One per cent vanadium or 0.5-per cent chromium

Figure 1. Effect of elements on the saturation values of iron

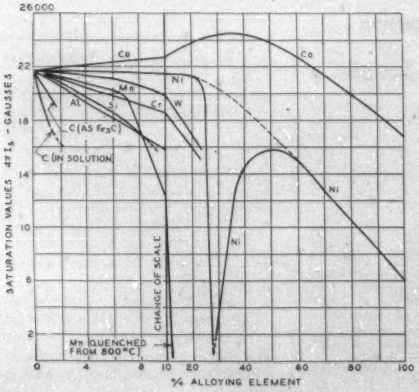

Figure 2 (below). Effect of elements on the electrical resistance of iron

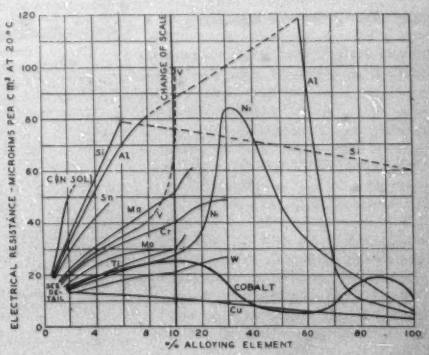

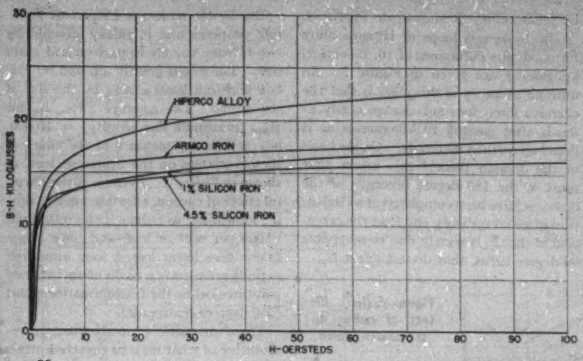

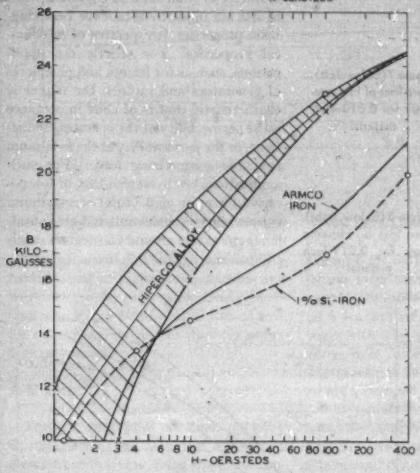

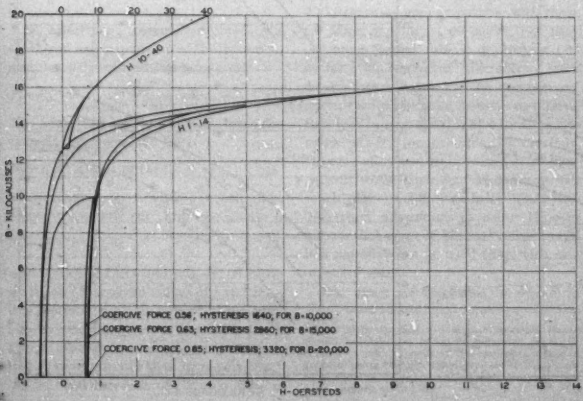

Figure 3 (above). Comparison of B–H curves of Armco and silicon-iron to Hiperco alloy

Figure 4 (left). Variation in B–H curves of Hiperco alloy

Figure 5 (below). Hiperco alloy hysteresis loops for 10, 15, and 20 kilogausses

double the resistivity of the 35 per cent cobalt alloy, that is, increase it from about 10 to about 20 microhms per cubic centimeter. High resistivity is desirable for a-c applications to reduce eddy current losses.

The composition selected for the alloy is

Cobalt: 34.5–35.5 per cent
Chromium: 0.4–0.5 per cent
Iron: balance

The cobalt content is kept as low as possible without sacrificing maximum saturation because of the cost of cobalt. The trade mark Hiperco has been adopted as the trade name of this alloy and has been registered with the United States Patent Office.†

Hiperco alloy has been commercially made in 6-inch strips in two thicknesses, 0.017 inch and 0.025 inch. In the laboratory the material has been reduced to 0.001 inch without difficulty. In the cold rolled condition, the material can be readily punched.

Magnetic Properties

Hiperco alloy, like other soft magnetic materials, must be annealed to remove strains and induce grain growth, so that low losses and good permeabilities can be realized. Experimental work has shown that the optimum magnetic properties are obtained by annealing in hydrogen below the transformation range, which is located in the neighborhood of 950 degrees centigrade, its exact location depending on the composition.

D-C Data

The d-c measurements were carried out on baby Epstein strips (0.04 by 3 by 28 centimeters or 0.017 by $1^{3}/_{16}$ by 11 inches) in a 25-centimeter Epstein frame described by Burgwin[4] using the ballistic method.

The data obtained are initial and maximum permeability, the magnetization curve, and the hysteresis loop.

The initial and maximum permeabilities of Hiperco alloy are approximately

$\mu_0 = 650$
$\mu_{max} = 10{,}000$

varying considerably with composition and heat treatment.

† A distinction should be drawn between cobalt-iron and cobalt-steel. The cobalt-iron alloy is essentially nonhardenable and low in carbon. Cobalt-steel is strictly a hardenable alloy of different composition containing carbon. Cobalt-iron is a "soft" magnetic material (low hysteresis) while cobalt-steel is a "hard" or permanent magnetic material (high hysteresis). The discussion here will cover only cobalt-iron.

The average magnetization, or B–H,‡ curve of Hiperco alloy is shown in Figure 3 in comparison with those for common soft magnetic materials. This curve shows the superiority of Hiperco alloy for high density applications. It also shows that good permeabilities are obtainable at lower magnetizing forces; for example the permeability of Hiperco alloy for H = 10 is 1,700 to 1,800. The expected range in permeability is shown in Figure 4.

‡ These symbols conform to the units adopted in 1930 by the International Electrotechnical Commission. In the centimeter-gram-second electromagnetic system the magnetizing force H is in oersteds and the magnetic flux density B is in gausses.

The hysteresis loops of Hiperco alloy for maximum inductions of 10, 15, and 20 kilogausses are given in Figure 5. An unusual property of this alloy is that the coercive force does not change nearly as much after passing 10 kilogausses as it does for common materials. On the basis of the domain theory[5] this means that most of the 180 degree reversals of the domains have been completed at an induction of 10 kilogausses, and that the extension of the tip is merely due to reversible 90-degree turns, that do not affect H_c.

The hysteresis loss is a structure sensitive property and is chiefly affected by two factors, namely impurities and grain size. The loss is greatly affected by carbon and to a lesser extent by the size of the grains. The coercive force, H_c for B_{max} (maximum flux density) = 10,000, is a convenient measure of the effect of these variables on the hysteresis loss, as shown in Figure 6. Because of the harmful effect of carbon, efforts are made, during annealing, to reduce it to a minimum (0.005 per cent or less) and since larger grains give lower losses, long annealing periods are used (up to 50 hours) at temperatures below the transformation point (950 degrees centigrade).

These magnetic properties are representative of what may be expected, when efforts are made to obtain the best magnetic properties, irrespective of mechanical properties. For strictly d-c applications, such as for frames and polepieces of generators and motors, the magnetic characteristic that is of chief importance is the permeability at the operating inductions, or the permeability at the maximum available magnetizing force. For such applications low hysteresis loss, or low coercive force, or high initial or maximum permeability is irrelevant, and an annealing temperature around 750 degrees centi-

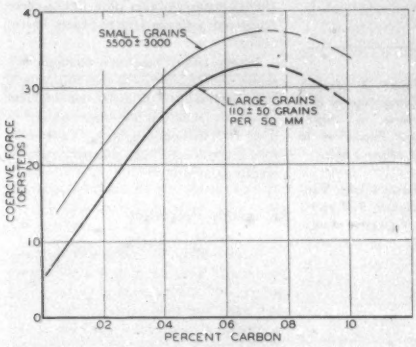

Figure 6 (left). Effect of carbon on the coercive force

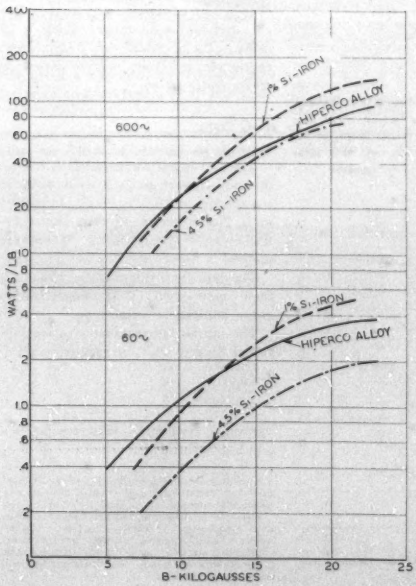

Figure 7 (below, left). Core loss of Hiperco alloy for 0.010-inch material

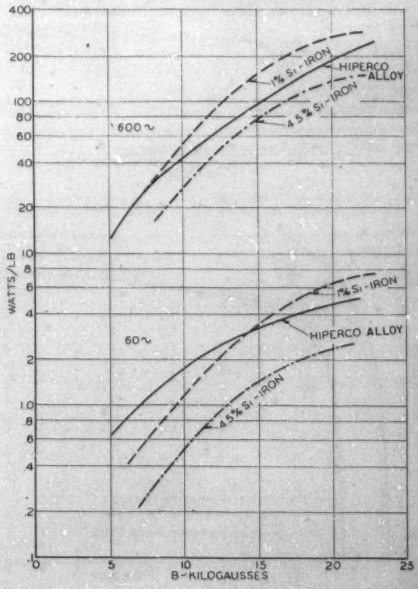

Figure 8 (below, right). Core loss of Hiperco alloy for 0.017-inch material

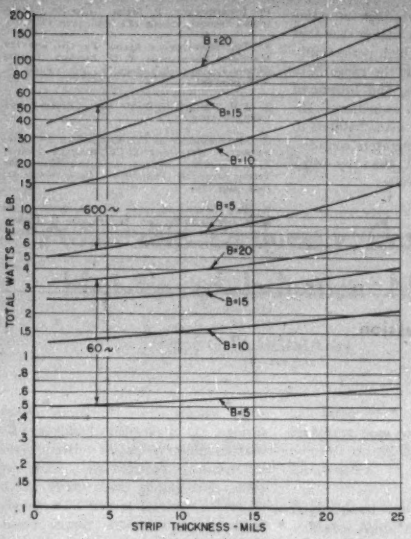

Figure 9. Effect of strip thickness on losses of Hiperco alloy

grade to relieve the rolling strain is sufficient. For magnetizing forces above 20 oersteds this will give as high permeability as annealing at higher temperatures and will preserve the good mechanical properties, which may be of greater importance for frames and polepieces than for armature punchings.

A-C Data

The a-c data were obtained on baby Epstein strips, also tested in a 25-centimeter Epstein frame, using the procedure discussed in reference 4.

In alternating current machines the total iron loss is made up of the hysteresis and the eddy current losses

$$P_e = P_h + P_e \tag{1}$$

The hysteresis loss has already been discussed. At frequency f it is

$$P_h = K \times f \times (\text{area of the loop}) \tag{2}$$

where K is a proportionality factor. The eddy current loss per cubic centimeter is

$$P_e = \pi^2 f^2 t^2 B^2_{max}/6\rho \tag{3}$$

where t is thickness and ρ is electrical resistivity. For given values of f and B_{max} it is therefore possible to control the eddy loss by varying t and ρ, but since t is a squared factor, it is usually easier to control P_e by means of t than by means of ρ.*

The total core loss of Hiperco alloy is shown for 60 and 600 cycles in Figures 7 and 8, Figure 7 for 0.010-inch strip and Figure 8 for 0.017-inch strip. While the figures show that lower losses apparently can be obtained with high silicon-iron (4-5 per cent silicon) rolled to 0.010 inch than with the same gauge of Hiperco alloy, it is impractical to use the high silicon iron at flux densities above 19,000 gausses, because the exciting current becomes prohibitive. For this reason the losses for 1-per-cent silicon-iron should be used for comparison. With 1-per-cent silicon-iron, 0.010 inch thick, the losses at 20 kilogausses are comparable with those for Hiperco alloy at 60 cycles, but they are much higher (about double) at 600 cycles. If 1-per-cent silicon-iron were used at 20 kilogausses, the magnetizing current would be over 13 times as high as that for Hiperco alloy. Also for the same value of H, for example 30 oersteds, Hiperco alloy can be operated at 20 kilogausses while 1-per-cent silicon-iron will reach only 15,500, a ratio of 1.3 to 1.0. The chief advantage in using Hiperco alloy is thus evident, because considerably less material can be used than with any ordinary alloy.

The effect of thickness is shown in Figure 9 for four inductions: 5, 10, 15 and 20 kilogausses, and for two frequencies: 60 and 600 cycles. The curves show much greater thickness effect for 600 cycles than for 60 cycles, because eddy losses predominate at the higher frequency, and these vary as the square of the thickness

Mechanical Properties

Hiperco alloy can be readily forged or rolled at elevated temperatures (900–1,200 degrees centigrade), and, by taking certain precautions, it can be cold rolled to any desired gauge. In the cold rolled state its mechanical properties are sufficiently good, so that it can be sheared or punched without difficulty

Yield Point†	80,000–95,000 pounds per square inch
Ultimate Strength	100,000–120,000 pounds per square inch
Elongation	6–8 per cent
Modulus	30.6×10^6 pounds per square inch
Endurance Limit**	63,000 pounds per square inch

To obtain good magnetic properties the strip or punchings must, of course, be annealed in order to remove strains and impurities and to produce large grains. As already mentioned, the above mechanical properties are largely preserved, if an annealing temperature of 750 degrees centigrade is not exceeded.

When the best magnetic properties are desired, as in a-c applications, annealing temperatures around 900 degrees centigrade are required for long periods, resulting in grain growth, lower strength and lower ductility. Representative mechanical properties after such annealing are

Ultimate strength	60,000–80,000 pounds per square inch
Elongation	3–5 per cent
Endurance limit	30,000 pounds per square inch

These mechanical properties are good enough for use in rotating machines even if operating at 3,600 rpm. However, the annealed material is very notch sensitive, so that it must be handled with care. If a tooth is bent 90 degrees, for example, it will probably break upon straightening.

* It is probable, that a domain orientation factor should be added, as privately suggested by G. C. Richer, to take account of the assumption that in domains going through 180-degree shifts B_{max} is always equal to B_{sat}, (saturation flux density), thus increasing the eddy loss.

† Hiperco alloy does not have a definite yield point, and for this reason the yield point is taken at an arbitrary set of 0.2 per cent.

** The endurance limit was determined on "as forged" material. The values were determined on a standard R. R. Moore type of testing machine, which applies a constant moment to a specimen 3⅞ inches in length and 0.273 inch minimum diameter.

Summary

Hiperco alloy is an improved iron-cobalt alloy specifically developed for electric machinery applications, where weight or space is at a premium. The basic composition is 34.5–35.5 per cent cobalt with an alloying element such as chromium added to improve hot and cold workability and increase electrical resistance. Processes have been developed whereby the alloy can be cold rolled to any desired gauge.

Because of its high magnetic saturation value (over 12 per cent higher than that of iron), its unusually high permeability for magnetizing forces in the range $H = 10$ to $H = 400$ oersteds, and because of its low losses at high inductions, Hiperco alloy will enable manufacturers to produce motors and generators considerably lighter in weight than by using present standard materials.

References

1. Sur le Champs Magnetiques Obtenus Avec un Electroaimants Muni des Pieces Polaires en Ferrocobalt, P. Weiss. *Comptes Rendus* (Paris, France), volume 156, 1913, page 1970.

2. The Iron-Cobalt Alloy, Fe, Co, and Its Magnetic Properties, T. D. Yensen. *General Electric Review* (Schenectady, N. Y.), volume 18, 1915, page 881.

3. J. H. White, C. V. Wahl. United States Patent 1,862,559, 1932.

4. Measurement of Core Loss and A-C Permeability With the 25-Cm Epstein Frame, S. L. Burgwin. *Bulletin*, American Society for Testing Materials (Philadelphia, Pa.), volume 41, 1941, page 779.

5. The Magnetization of Polycrystalline Iron and Iron-Silicon Alloys, G. C. Richer. *Journal*, Iron and Steel Institute (London, England), volume 40, 1944, page 93.

No Discussion

Adjustable Frequency Control of High-Speed Induction Motors

G. W. HEUMANN
MEMBER AIEE

THE simplest type of electric motor available to industry is the squirrel-cage induction motor. A minimum number of leads are required to connect the motor to its power supply and control equipment. Except for cases where the power supply system imposes certain limitations only one single 3-pole contactor is required to start and stop the motor.

Control by Adjustable Frequency

The principal limitation imposed on the use of squirrel-cage motors, when connected to commercial constant frequency lines, is that they are constant speed motors. The operating speed of the motor is slightly below its synchronous speed, which is fixed by the line frequency and the number of poles for which the motor windings are laid out. Once a motor is built, nothing can be done to adjust its speed except by changing the frequency of the a-c power supply.

Line frequency determines the highest speed for which an induction motor can be designed. On a commercial 60-cycle power system, the highest speed attainable is 3,600 rpm which is the synchronous speed of a 2-pole motor. Higher speeds could be attained if the frequency were raised above 60 cycles, and the only limitation would be the design of the motors and the power supply systems.

Thus the provision of an adjustable frequency system would enable squirrel-cage induction motors to operate as adjustable speed motors over a wide speed range and at speeds in excess of 3,600 rpm. The aviation industry has found numerous applications for high-speed adjustable-speed squirrel-cage motors, and rather elaborate power supply systems have been developed to provide the required range and accuracy of motor speed control.

High Speed Squirrel-Cage Motor Applications

Rapid advances in the design of aircraft during recent years have made it necessary to construct huge wind tunnels for testing the aerodynamic behavior of airplanes. Scale models are used, and to obtain aerodynamic data on the airplane models which are equivalent to the expected performance of the actual airplanes, it is necessary to drive the model propellers at speeds greatly in excess of propeller speeds of the actual airplanes. During a test run in the wind tunnel it must be possible to adjust and maintain accurately the propeller speed so that speed and power input into the propeller can be measured. Shown in Figure 1 is an airplane test model with a propeller which is driven by a squirrel-cage motor assembled in the nacelle of the model. Such motors are calibrated on dynamometers or torque stands so that the electrical input of the motors and their speed during a wind tunnel test can be used to determine the propeller torque required by the actual plane.

A typical motor for powered model testing is shown in Figure 2. In order to fit such motors into the limited space available on the airplane models, their physical dimensions have been reduced to the barest minimum. The specific loadings of the active materials have been made much higher than on conventional induction motors, and the stators are water cooled to carry away the heat generated by the losses. Motors of this general construction have been built for speeds up to 80,000 rpm at 1,330 cycles.

Larger motors frequently are used to test full size propellers whether inside or outside a wind tunnel. Figure 3 is a view of two 375-horsepower motors assembled as a dual unit for testing contraturning propellers. The view shows the motors mounted on a torque stand for calibrating. Their top speed is 6,000 rpm at 400 cycles. Still larger squirrel-cage motors have been built for adjustable speed testing of compressors and gas turbines. A typical design is shown in Figure 4 which is a 3,000-horsepower motor rated 3,600 rpm at 120 cycles. It is forced ventilated by a blower mounted on top of the stator frame.

Although the aviation industry has so far provided the broadest field for the application of such motors, applications in other industries will probably be found as time goes on.

Basic Requirements of Adjustable Frequency Systems

As electric power is readily available in large blocks and at low cost wherever industrial plants exist, adjustable frequency is obtained from power conversion equipment. Alternators and frequency converters, driven by adjustable speed electric motors, are the two fundamental types of conversion apparatus in use. Thus control of frequency is accomplished by control of the speed of the driving motor of the conversion set.

The maximum frequency to be attained is governed by the design and rating of the motors used for a particular application. Flexibility is a prime requirement

Paper 47-106, recommended by the AIEE committee on industrial control devices for presentation at the AIEE North Eastern District meeting, Worcester, Mass., April 23–25, 1947. Manuscript submitted February 2, 1947; made available for printing March 7, 1947.

G. W. Heumann is in the control engineering division of General Electric Company, Schenectady, N. Y.

The author wishes to acknowledge that C. C. Clymer, industrial engineering divisions, General Electric Company, Schenectady, N. Y., first proposed the use of frequency converters for the control of high-speed model testing motors. Acknowledgement is made to J. Muncey, Cornell Aeronautical Laboratory, Buffalo, N. Y., for Figure 1.

Figure 1. Airplane scale model with motor-driven propeller

Figure 2. Squirrel-cage induction motor for airplane model testing, rated 250 horsepower, 10,800 rpm

for testing equipments and thus it is necessary to vary frequency over a wide range, generally six to one or more, in a practically infinite number of steps. During a test it is necessary to maintain the test motor speed accurately so that the testing equipment operates at a stable test point and precision measurements can be taken. Thus, frequency not only must be adjusted at a desired value but also must be regulated accurately at the set value.

Adustable speed d-c shunt motors with adjustable voltage control are used most generally for driving the frequency conversion machines because such driving systems are ideally suited for wide speed ranges and accurate speed control. Speed is adjusted by adjusting the voltage applied to the armature of the d-c motor, and within the range of speed control the drive system is able to produce constant torque, in other words, the output of the adjustable frequency system in kilowatts changes in proportion to frequency. If a wider speed range is desired, an additional four-to-one speed range can be gained by weakening the d-c motor shunt field. However, within the field weakening range the drive system produces constant horsepower which means the kilowatt output of the adjustable frequency system stays constant.

Another problem which has to be given careful consideration is the control of the voltage of the adjustable frequency power system. The torque produced by a squirrel-cage induction motor is determined by its air gap flux and its rotor current. When a squirrel-cage motor is connected to an adjustable frequency power source, the voltage applied to the motor stator terminals should change in proportion to frequency in order to maintain constant air gap flux which enables the motor to develop its rated torque over its speed range. It has become cutomary to rate adjustable frequency motors in terms of volts per cycle rather than in terms of volts. If an adjustable frequency system is used to supply power to motors of different size or manufacture it must be possible to adjust the volts per cycle of the system. Voltage drifts due to natural regulation of the power conversion apparatus should be minimized to enable the squirrel-cage motors to develop their full rated torque and to prevent their being overheated. Hence provision should be made not only to control volts per cycle over a certain range but also to maintain volts per cycle close to the set value regardless of the frequency and the load of the system.

Synchronous Alternator Sets

Figure 5 is an elementary diagram of the principal circuits of an adjustable frequency control system utilizing an adjustable speed alternator as a power source. The system is self-contained and does not require any auxiliary power source in addition to the general purpose a-c power supply in the plant.

Power is taken from the constant frequency a-c system through a constant speed motor generator set consisting of an a-c driving motor (either induction or synchronous type) and an adjustable voltage d-c generator. Power from the d-c generator is fed into an adjustable speed motor generator set consisting of an adjustable speed d-c shunt motor driving the adjustable frequency alternator. An auxiliary exciter set is provided for control, consisting of an a-c driving motor, a constant potential d-c exciter to provide a regulated d-c control bus, a speed control amplidyne for exciting the d-c generator field, and a voltage control amplidyne for exciting the alternator field.

A frequency regulator acts on the fields of the speed control amplidyne The desired frequency is set on an adjusting rheostat. The actual frequency is measured by a tachometer generator which is coupled to the adjustable speed set. The tachometer output voltage is compared with the set reference in the regulator which regulates the d-c generator voltage so as to maintain constant alternator speed.

Although the equipment shown in Figure 5 makes use of generator voltage control only, leaving the d-c motor field excitation at a fixed value, it would be possible to extend the speed control range by motor field weakening. In such a case an additional amplidyne would be provided to furnish excitation to the d-c motor field. In the range of low speeds the regulator would maintain constant motor field and adjust the generator field, whereas in the range of high speeds the regulator would maintain maximum generator voltage and adjust the motor field.

Volts per cycle of the alternator is adjusted by the excitation of the alternator field. A volts per cycle regulator acts on the fields of the voltage control amplidyne. The desired volts per cycle is set on an adjustable reactor. The alternator voltage is measured by a potential transformer and compared in the regulator with the established volts per cycle reference, so that the regulator adjusts the amplidyne excitation to maintain the desired volts per cycle at the alternator terminals.

Frequency Regulator

Details of the frequency regulator are indicated in Figure 6. Field *F3-F4* of the speed control amplidyne is connected across the regulated d-c control bus in such a sense as to raise the d-c generator voltage. This boost field remains at constant strength. The buck field *F1-F2* opposes the boost field. The net difference between boost and buck field strength determines the output voltage of the amplidyne and thus the d-c generator field strength. Control is obtained by varying the strength of the buck field.

Two vacuum tubes control field *F1-F2*. Figure 6 shows only the principal tube circuits. Cathode heaters, screen grids,

suppressor grids, and grid bias networks have been omitted for the sake of simplicity. The desired frequency (or d-c motor speed) is set on the frequency adjusting rheostat, and a reference is established by the voltage between the negative bus and the slider of the rheostat. The voltage of the tachometer generator is loaded in a voltage divider the midpoint of which is connected to the slider of the frequency adjustment rheostat. The tachometer voltage is thus balanced against the reference voltage and a deviation of the system frequency from the set value initiates a corrective action.

When the tachometer voltage is low (which means frequency is lower than the setting calls for) the potential applied to the grid of tube *1* rises in a positive direction. Tube *1* passes more current, which lowers the potential applied to the grid of tube *2*. Thus, tube *2* passes less current and reduces the excitation of field *F1-F2*. This increases the net excitation of the amplidyne and the d-c generator voltage rises until the frequency reaches the set value. Conversely, when the frequency rises above the set value, tube *1* is turned off, tube *2* is turned on, and the amplidyne net excitation is reduced to lower the d-c generator voltage.

An antihunt feature is provided by a potential transformer connected to the armature terminals of the d-c generator. When the generator voltage undergoes a change, a voltage is induced in the potential transformer, which is proportional to the rate of change of generator voltage. The potential transformer voltage is added to the frequency control signal in such a sense as to oppose the change in generator voltage.

If the frequency adjusting rheostat is turned suddenly up or down, the resultant rapid acceleration or deceleration may cause excessive current to flow in the armature of the d-c machine. On many installations a current limit control feature is added. The voltage drop across the commutating fields of the d-c generator and motor is a measure of the armature current. This drop is applied to the grid control of tube *2* in such a manner that during acceleration it decreases the amplidyne excitation, and during deceleration it increases it so that the armature current is limited to a value which can be commutated safely.

Volts Per Cycle Regulator

Figure 7 shows the details of the volts per cycle regulator. Figure 7*A* is an elementary diagram of the regulating circuits acting on the fields of the voltage control amplidyne. The voltage of the alternator, appearing across the secondary winding of the potential transformer is rectified and impressed on amplidyne field *F3-F4*. The same voltage is also impressed on field *F1-F2*, but with opposite polarity. An adjustable reactor, the coil of which is wound as a toroid with a sliding contact to tap off different numbers of turns, is connected in series with the *F1-F2* field circuits. This reactor is saturable so that the current flowing through *F1-F2* is not proportional to alternator voltage. This reactor is set by the operator and determines the desired alternator voltage. Capacitors *2C* and *3C* introduce phase shifts to compensate for the resistance of the reactor and the rectifier and to maintain volts per cycle at very low frequencies.

Amplidyne field *F7-F8* serves a dual purpose. Through a resistor it is connected to the regulated d-c control bus so that a fixed amount of flux is contributed by that field. It is also connected to the amplidyne terminals through capacitor *1C* and acts as an antihunt field whenever the amplidyne voltage undergoes a change.

For an explanation of the regulator performance refer to Figure 7*B*. The alternator voltage is plotted versus magnetomotive force of the amplidyne which can be expressed as the ampere-turns of the amplidyne fields contributing to the net excitation of the amplidyne. Curve *a* is the saturation curve of the alternator expressed in terms of volts versus amplidyne magnetomotive force for a certain frequency. Line *b* is the fixed magnetomotive force established by field *F7-F8*, which is independent of alternator voltage. Line *c* represents the excitation contributed by field *F3-F4* which changes in proportion to alternator voltage. Curve *d* is the magnetomotive force supplied by field *F1-F2*. With low alternator voltage, the magnetomotive force changes in proportion to the voltage, but with higher voltage the reactor saturates and the magnetomotive force increases much faster than the voltage. Curve *e* is the net magnetomotive force of the amplidyne, that is the difference between line *c* and curve *d*. Point *x*, marking the intersection of curves and *e* is the operating point of the alternator.

When the frequency is changed, for instance halved, the saturation curve of the alternator changes to a'. The magnetomotive force of fields *F3-F4* and *F7-F8* does not change and line *c* stays as is. Curved *d*, however, changes to curve d' so that at halved frequency the net magnetomotive force of the amplidyne becomes curve e', and x' is the new operating point of the alternator. It will be noted that the voltage at x' is one half the voltage at x, thus volts per cycle are the same for both operating conditions.

By proper selection of the components of the amplidyne field circuits, it is possible to maintain volts per cycle within narrow limits over a wide range in frequency and load.

Induction Frequency Converters

An induction frequency converter is built like a wound rotor induction motor. If a fixed frequency is applied to the primary winding and the rotor is at standstill, the frequency appearing at the secondary terminals is equal to the primary frequency. However, if the rotor is driven in the same direction or in

Figure 3. Two 375-horsepower rotation motors for testing contraturning propellers, mounted on torque stand for calibrating

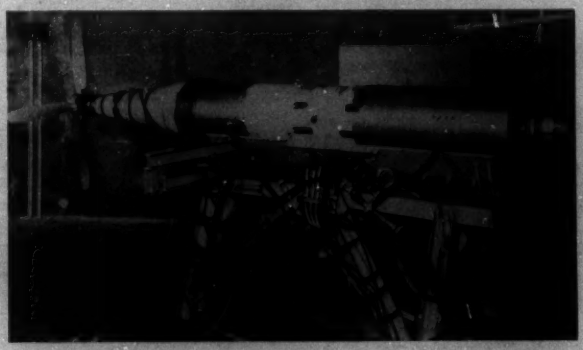

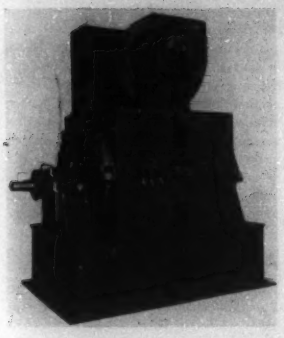

Figure 4. A 3,000-horsepower squirrel-cage induction motor for testing gas turbines, rated 3,600 rpm at 120 cycles

where

f_1 = primary frequency in cycles per second
f_2 = secondary frequency in cycles per second
n = converter speed in revolutions per minute
n_s = synchronous converter speed in revolutions per minute
= $120 \times f_1$/number of poles

The plus sign is used when converter rotation is opposite to flux rotation, and the minus sign is used when converter rotation is the same as flux rotation.

The output voltage of the converter is determined by the primary voltage and the secondary frequency. If there were no drops and no losses in the converter, the secondary voltage would be equal to the primary voltage multiplied by the ratio of secondary to primary frequency. Actually, this ratio is not accurately maintained. However, by using an adjustable voltage power source for the converter primary, the secondary voltage can be adjusted and regulated.

Frequency Converter Sets

A practical system of adjustable frequency control by using a frequency converter is illustrated in Figure 9. It resembles the system of Figure 5. An alternator is added to the constant speed motor generator set, which supplies primary frequency excitation to the converter. To prevent drifts in primary frequency on account of load changes, the constant speed motor generator set should be driven by a synchronous motor. The adjustable speed set consists of the d-c motor and the frequency converter. The circuit breaker for protecting the converter preferably is placed in the line be-

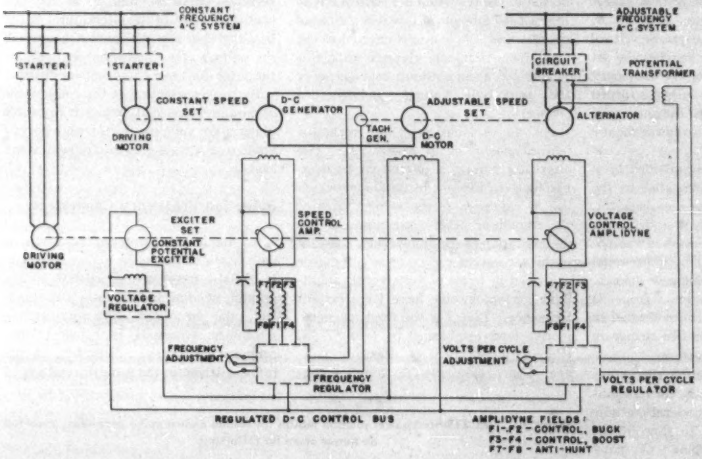

Figure 5. Adjustable frequency control system with adjustable speed alternator

the opposite direction of the rotating flux, the secondary frequency is lower or higher than the primary frequency. From a theoretical point of view it is immaterial whether the primary winding of the converter is on the stator or the rotor. For reasons of machine design, large converters usually are built with the primary winding on the rotor and the secondary winding on the stator.

The relationship between converter speed and secondary frequency is illustrated in Figure 8. The secondary frequency, expressed in terms of the primary frequency is

$$f_2 = f_1\left(1 \pm \frac{n}{n_s}\right)$$

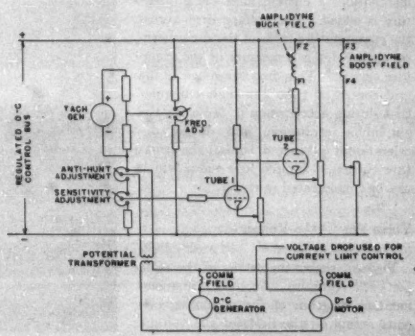

Figure 6. Frequency regulator

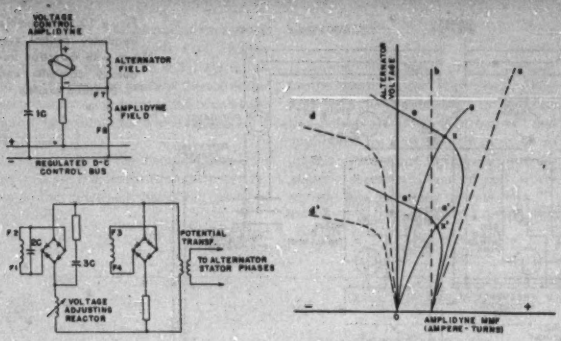

Figure 7 (above). Volts per cycle regulator

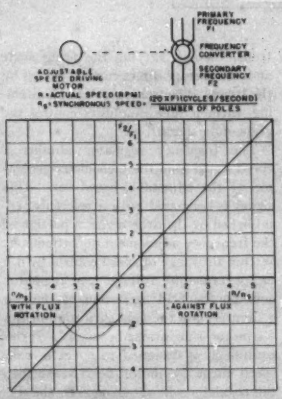

Figure 8 (above). Secondary frequency versus speed of induction frequency converter

tween alternator and converter where standard low frequency devices can be employed to de-energize the high-frequency secondary circuit.

Frequency control is obtained by controlling the field of the d-c generator which in turn controls the speed of the d-c motor. A frequency regulator as shown in Figure 6 controls the field excitation of the speed control amplidyne which excites the generator field. The speed signal is obtained from a tachometer generator coupled to the adjustable speed set. To make the speed signal proportional to secondary frequency, a small auxiliary tachometer set is provided, consisting of a small synchronous motor driving a tachometer generator at constant speed. This auxiliary tachometer generator is connected in series with the tachometer generator of the adjustable speed set. At standstill of the d-c motor the speed signal causes amplidyne fields *F1-F2* and *F3-F4* to be balanced. Within the frequency range between zero and primary frequency, the voltages of the two tachometer generators subtract and amplidyne field *F1-F2* becomes stronger than *F3-F4*, the net excitation causing d-c motor rotation in the negative direction, until synchronous speed or zero secondary frequency is reached. Within the frequency range above primary frequency, the tachometer generator voltages are additive. Amplidyne field *F1-F2* becomes weaker than *F3-F4* and the d-c motor rotates in the positive direction until its rated speed and maximum secondary frequency is reached.

It is undesirable to operate the adjustable frequency system at exactly primary frequency, that is to say, with the frequency converter at standstill, as this would cause burning of the converter slip rings. For this reason the regulator is so adjusted that it cannot be set at exactly zero d-c motor speed, but that the minimum speed setting will result in the d-c motor turning at a few revolutions per minute.

Adjustable frequency voltage is controlled by a volts per cycle regulator as shown in Figure 7. This regulator acts on the fields of the voltage control amplidyne which excites the field of the alternator. The voltage signal is obtained from a potential transformer connected across one phase of the frequency converter secondary. Thus the field excita-

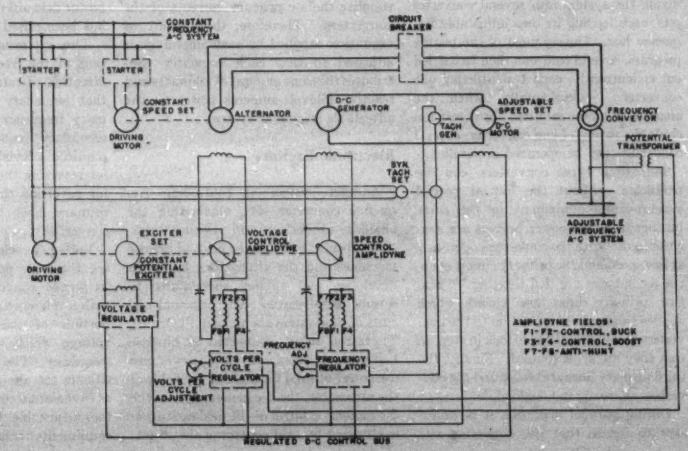

Figure 9. Adjustable frequency control system with induction frequency converter

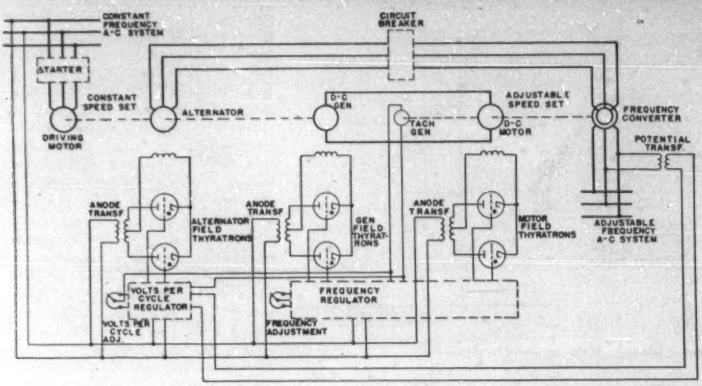

Figure 10. Adjustable frequency control system with induction frequency converter and thyratron exciters

tion of the alternator and consequently the alternator voltage is adjusted so as to maintain constant volts per cycle on the adjustable frequency system.

The choice of frequency converters versus synchronous alternators is determined somewhat by the range in adjustable frequency and the economics in manufacturing the rotating machines. Advantages of induction frequency converters are their high overload capacity, stability, and the ease with which several converters may be operated in parallel. When establishing the required capacity of a testing equipment the few tests must be considered which require the full system capacity. During most tests only a portion of the available capacity may be needed. It is then advantageous to subdivide the system into several converter sets, each feeding its own adjustable frequency bus. During most of the testing program, several tests can then be carried out concurrently, each test utilizing one converter. Occasionally, when the amount of power required for a test exceeds the rating of one converter, several converters can be operated in parallel.

Induction type converters can be paralleled without the aid of special synchronizing equipment in the same manner in which power Selsyns are synchronized. With the converters operating at low speed and the primary circuit open, the secondaries are tied together. Then, two primary lines are closed which applies single phase excitation to the converters and causes them to lock in step, so that they are synchronized. Finally, the third primary lines are closed and the converters are ready to take load.

During parallel operation it is necessary to insure that the converter sets share their load. The frequency and volts per cycle regulators are paralleled, and connections are so arranged that all regulators respond to the frequency and volts per cycle adjustments of one set which acts as the master. The drops across the commutating fields of the d-c generators and motors, which are a measure of loop circuit currents and consequently the shaft torques of the adjustable speed sets, are compared and any differential is fed into the frequency regulators so as to equalize the d-c loop circuit currents. The primary currents of the converters, which are a measure of the reactive power contributed by each converter to the secondary power system, are compared and any differential is fed into the volts per cycle regulators so as to equalize the a-c primary currents of the converters. Therefore, the amount of excitation supplied by each amplidyne is adjusted so that each converter contributes the same amount of kilowatts and reactive kilovolt-amperes power to the adjustable frequency system.

Electronic Exciters

Another system of controlling frequency converter sets, eliminating the auxiliary exciter sets and utilizing thyratron tubes for exciting the fields of the d-c machines and the alternators, has been developed and applied successfully to several installations. The principal circuits of this system are given in Figure 10. Thyratron tubes, connected as biphase half-wave rectifiers, convert a-c power into d-c power utilized for exciting the fields of the alternator, the d-c generator, and the d-c motor. Control of the field excitation is obtained by grid control of the thyratrons, thereby varying the firing angle and the average direct current passed by the tubes. Electronic regulators containing vacuum tube amplifiers control the grids of the thyratrons.

The frequency regulator obtains a speed signal from the tachometer generator of the adjustable speed set. This signal is compared with a reference, established by the drop across a portion of the frequency adjustment potentiometer. Within the range of speed control by d-c motor armature voltage, the regulator acts on the field excitation of the d-c generator, and the field excitation of the d-c motor is maintained constant. If the equipment is designed to cover a wide speed range by motor field weakening, the regulator will act to weaken the d-c motor field after the d-c generator voltage has been raised to its highest value.

The system as shown provides for rotation of the frequency converter in one direction of rotation only. This means that secondary frequencies above primary frequency only are available. If secondary frequencies down to zero are required, provision must be made either for reversing the frequency converter or for reversing the phase rotation of the primary lines between alternator and converter.

Volts per cycle is controlled by obtaining the volts per cycle signal from the frequency converter and comparing it with a reference which is obtained from a portion of the tachometer generator voltage which varies in proportion to frequency. The volts per cycle regulator adjusts the alternator field excitation so as to maintain constant volts per cycle on the adjustable frequency bus. When equipments are laid out to operate over a

wide frequency range and over a wide volts per cycle range, it may become necessary to provide for a voltage cutoff in the regulator to prevent the converter secondary voltage from rising beyond the maximum voltage for which the system is designed.

The details of the electronic regulator circuits are not described in the paper because they previously have been described elsewhere.[1]

Conclusions

Although this paper describes equipments which so far have found their principal field of application in the aviation industry, it is felt that they will find application, as time goes on, in other industrial fields where high speeds and adjustable speeds are wanted and where squirrel-cage induction motors offer advantages over other types of driving motors. The components described for controlling frequency and volts per cycle are suited for general applications wherever problems of speed control and voltage-control exist.

Reference

1. Electronic Control of Frequency Converter Sets for Testing Aircraft Models. G. W. Heumann, W. F. Strong. AIEE Transactions, volume 60, 1946, pages 981–9.

No Discussion

New Test Equipment and Testing Methods for Cable Carrier Systems

W. H. TIDD
ASSOCIATE AIEE

S. ROSEN
NONMEMBER AIEE

H. A. WENK
NONMEMBER AIEE

Synopsis: Three portable test sets developed for the improved cable carrier telephone system are described: A high sensitivity selective transmission measuring set covering 10 to 150 kc, a decade oscillator for frequencies from 2 to 79 kc, and a tube test set.

EARLY carrier systems having only a small number of channels were tested by taking the system out of service, in order to test amplifiers and other system components. Ordinarily, the test equipment did not require high sensitivity or selectivity. When the first cable carrier telephone system, known as *K1*,[1] was developed some steps were taken in the direction of testing in service, to avoid having to remove 12 communication channels from service. For this system large permanently mounted test equipment was provided.

With the advent of the improved cable carrier system, known as *K2* and described in a companion paper,[2] a new approach was made to the testing problem. The presence of large numbers of unattended repeater stations made it desirable to have small portable testing units which could be taken from place to place, thus avoiding expensive duplication. Accordingly, a complete new line of portable test equipment was developed, comprising a sensitive highly selective portable transmission measuring set, a portable decade oscillator, and a tube test set. With the first two of these it is possible to test 3-channel and 12-channel open-wire systems in addition to the *K1* and *K2* cable carrier systems. They largely replaced the test equipment previously used for *K1* systems. The portable sets are much smaller and cheaper than previous equipment, and fewer sets are needed. This paper describes these three units and outlines the testing methods for which they are used.

Paper 47-111, recommended by the AIEE committee on communication for presentation at the AIEE North Eastern District meeting, Worcester, Mass., April 23-25, 1947. Manuscript submitted November 14, 1946; made available for printing March 3, 1947.

W. H. TIDD, S. ROSEN, AND H. A. WENK all are with Bell Telephone Laboratories Inc., New York, N. Y.

Transmission Measuring Set

The main item of testing equipment provided for the maintenance of the cable carrier system is the *31*-type transmission measuring set by means of which the amplifiers and other system components can be tested in operation without affecting service. Briefly, the requirements for this set were that it should have a high input impedance for making bridging measurements, high sensitivity to permit measurements at both the input and output of the amplifiers, and extreme selectivity to enable the measurements of pilot frequencies and other test signals on the working system with adjacent communication channels busy. The set has a sensitivity of from 95 decibels below one milliwatt to 35 decibels above one milliwatt in 135-ohm circuits over a frequency band from 10 to 150 kc. This sensitivity is approximately equivalent to signals of seven microvolts to 20 volts. The set has an input impedance of 8,000 ohms which permits bridging measurements on the system with a negligible effect on through transmission. The nominal band width of the set is 50 cycles and the selectivity at 400 cycles away from midband is at least 32 decibels. At one kc and 10 kc from midband, the selectivity is appreciably better than 42 and 70 decibels respectively. Over the frequency band the sensitivity is uniform to within plus or minus 0.5 decibel. The set is operated from 115-volt alternating current and requires about 70 watts. The set is shown in Figure 1. The decibel meter and tuning arrangement are conspicuous.

A simplified circuit diagram of the *31*-type transmission measuring set is shown in Figure 2. The set is divided into two portions, called the selector and the detector. An input switch makes it possible to connect the input cord to either the detector portion of the set or the selector and detector portions in tandem. The input switch also has two other positions for special purposes. One of these connects a highly selective 49-kc crystal filter ahead of the selector part of this set to provide preselection for certain special tests. The other position is a 40-decibel voltage divider which may be connected ahead of the selector part of the set primarily for calibrating purposes. When the input switch is in the selector position, the input transformer which has a one-to-one ratio is terminated in a fixed step voltage divider having a total impedance of 8,000 ohms. This is the selector sensitivity control and is arranged in 10-decibel steps. A wide band stage precedes the modulator or first converter of the set which is a double-balanced modulator using a bridge arrangement of copper-oxide varistors. The primary purpose of this is to obtain some local oscillator balance. The modulator is followed by a crystal filter at 455 kc. This filter is required to obtain the extreme selectivity which is needed for system measurements. A two-stage intermediate frequency amplifier with double-tuned interstages follows the crystal filter.

The heterodyne type of set was selected so that the selectivity could be obtained at any point in the frequency band. The choice of 455 kc for the intermediate frequency was based on a study of spurious responses possible. It was determined that by using a frequency greater than three times the highest frequency of the signal band, spurious responses which involve higher orders of the oscillator frequency with the first order of the signal

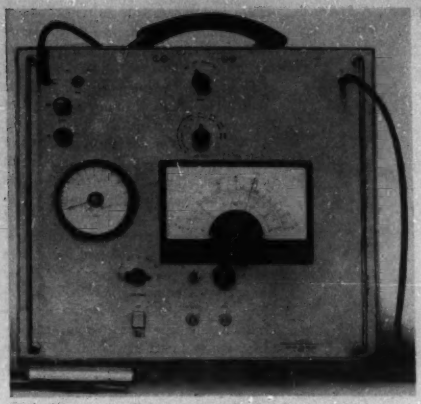

Figure 1. A *31B* transmission measuring set

frequency were eliminated. These responses are the most troublesome. Many of the higher order products up to the sixth order of the oscillator and signal frequencies are also avoided. Performance in this respect is considerably better than that for a system in which the intermediate frequency is located either below or just above the band of the set.

The oscillator for the converter or modulator is a simple coil feed-back type of oscillator with the frequency determining circuit in the screen grid circuit. The oscillator frequency range is 465 to 605 kc. The output is coupled by means of the electron stream to the plate circuit and is supplied to the modulator by means of a transformer.

The detector portion of the set is a three-stage amplifier with negative feedback. The output of this is connected to a half-wave diode rectifier. The negative feedback is sufficient to give the amplifier long time stability and also to improve the linear response of the output meter and rectifier circuit. The linear half-wave rectifier, or so-called averaging detector, was selected because of its superiority for measuring a signal in the presence of unwanted signals. An unwanted signal 13 decibels below the signal to be measured causes an error of only 0.1 decibel. For rms indicating devices the unwanted signal must be 16 decibels lower than the signal to be measured for the same error, and the level difference must be 39 decibels for a peak type rectifier. This discrimination against interference from unwanted signals eases the selectivity requirements for the rest of the set.

The detector portion of the set may be used separately for measuring signals over the frequency band from 1 to 150 kc where selectivity is not required. The sensitivity is from 25 decibels below one milliwatt to 35 decibels above one milliwatt. The stability with time of this section is plus or minus 0.1 decibel.

High Impedance Test Probe

A high impedance test probe has been designed as an accessory for the *31*-type set for making measurements of voltages within an amplifier of the system. The impedance is approximately 800,000 ohms and the effective shunt capacitance about nine micromicrofarads. The probe may be seen in Figure 1. The probe is essentially a 40-decibel pad which plugs into the input transformer in place of the normal input cord. The voltage divider consists of an 800,000-ohm resistance which in series with the 8,000-ohm input impedance of the set causes a 40-decibel loss. A small adjustable capacitance is connected across the 800,000-ohm resistor in order to equalize the transmission characteristic over the frequency band, to compensate for the capacitance of the cord.

Portable Oscillator

The *51A* oscillator is a direct reading decade oscillator covering the frequency band of 2 to 79 kc in 1-kc steps, making it useful for testing other carrier systems in addition to the *K1* and *K2* systems. An uncalibrated 1-kc continuous vernier control is included permitting the setting of any frequency between steps. In connection with the 2-kc step, the vernier control makes it possible to obtain frequencies down to 1 kc. It operates from a 115-volt a-c source. A panel view of the oscillator is shown in Figure 3.

The *51A* oscillator consists essentially of a Wien bridge circuit[3] for frequency determination, a 2-stage amplifier, and a cathode follower stage to provide a low impedance output (135 ohms). A simplified circuit is shown in Figure 4. One frequency determining arm of the bridge contains series resistance and capacitance, the other parallel resistance and capacitance. The two resistive arms of the bridge comprise a thermistor[4] and lamp. A simple compensated resistance interstage follows the first tube of the amplifier. This interstage is designed to compensate not only for the tube and circuit capacitance, but in addition, for the phase angle due to the frequency determining arms of the bridge circuit.

An output control voltage divider is connected across the plate of the second tube, providing the voltage to drive the

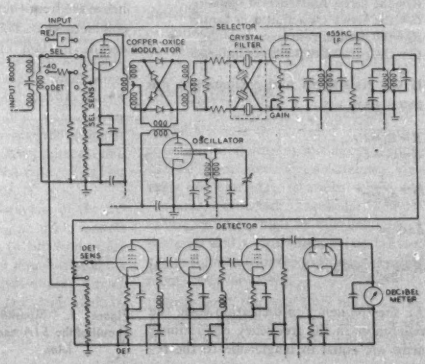

Figure 2. Simplified circuit of the *31A* and *B* transmission measuring sets

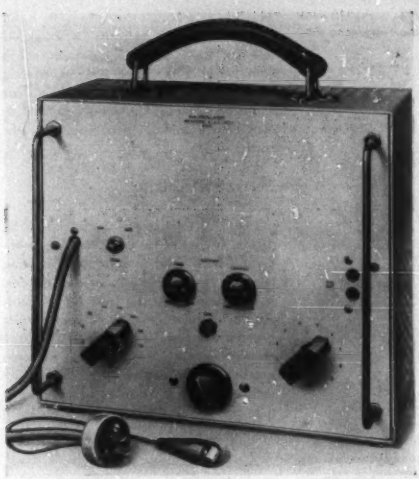

Figure 3. A 51A oscillator

output tube. The output transformer is connected in the cathode circuit of the power tube, to provide a 135-ohm balanced output impedance. This stage isolates the output circuit from the frequency determining circuits and provides power gain stabilized by negative feedback. The wave form is also improved by the negative feedback.

The operation of the Wien bridge oscillator will be outlined here only briefly. The general expression for the frequency of oscillation for this circuit is[3]

$$f_o = \frac{1}{2\pi\sqrt{R_1R_2C_1C_2}} \text{ cycles per second} \qquad (1)$$

when

R_1 = the series resistance in ohms
C_1 = the series capacitance in farads
R_2 = the parallel resistance in ohms
C_2 = the parallel capacitance in farads

If the resistances and capacitances are equal, as in the *51A* oscillator, then

$$R = R_1 = R_2$$
$$C = C_1 = C_2$$

$$f_o = \frac{1}{2\pi RC} \qquad (2)$$

and

$$R = \frac{1}{2\pi f_o C} = X_c \qquad (3)$$

At the frequency of oscillation then, the reactances in the frequency determining arms are equal in magnitude to the resistances. Also, the combined impedance of the shunt arm is equal to one-half that of the series arm. Thus, the voltages across bridge arms *AC* and *CB* are in phase and also in phase with the voltage applied to the bridge. The other two arms of the bridge are substantially resistive. The voltage across *DB* therefore will be in phase with the voltage across the bridge. Hence, if the voltage *DB* is less than *CB*, the voltage *CD* applied to the grid is in phase with the bridge voltage. If, in addition, the ratio of bridge voltage to the grid voltage is equal to the gain of the amplifier, the conditions for oscillation will be met.

In this oscillator, the capacitances of the series and parallel frequency determining arms have been made constant, hence the frequency is proportional to the conductance. This makes possible the decade method of frequency selection. There are two decade switches, one of which connects resistances in the series and shunt frequency determining arms of the bridge circuit for the 10-kc steps, the other connecting resistances for the 1-kc steps. The addition of any positions of these two switches make it possible to set frequencies in steps of one kc. A pair of variable resistances also connected in parallel with the decade switches permits continuous variation of frequency between the 1-kc frequency steps. It is, of course, possible to extend the decade system to smaller steps if desired. Resistors of 0.1 per cent accuracy are used in the frequency determining network. Trimming of the residual conductance inaccuracy and the stray circuit capacitances is accomplished with small variable condensers connected in each step of the shunt bridge arm.

In this type of oscillator, an adjustable resistor is usually provided in place of the thermistor in one of the resistance arms of the bridge. The setting of the resistor is determined by the characteristic of the particular lamp, requiring readjustment whenever the lamp is replaced. The resistor is adjusted to slightly more than twice the operating lamp resistance so that any increase in bridge voltage will cause the bridge to approach a balance due to the positive lamp characteristic and reduce the voltage supplied to the amplifier grid. This results in a highly stable output with changes in frequency or fluctuations in supply voltage. It was found that a thermistor[4] with a negative slope resistance characteristic when substituted for the adjustable resistor, would compensate automatically for the lamp characteristic. Since the amplitude of oscillation is controlled by the thermistor and lamp arms of the bridge, the tubes are permitted to operate over substantially linear portions of their characteristics. Also, the lamp and thermistor, being thermal devices, respond to changes

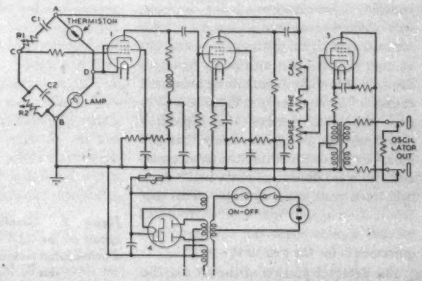

Figure 4. Simplified circuit of the 51A oscillator

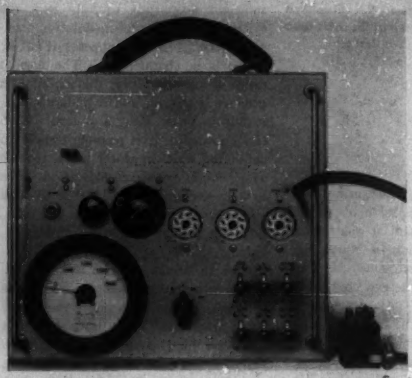

Figure 5. A *1AH* tube test set

in the effective value of applied voltage and not the instantaneous. This results in an output signal of good wave shape.

The frequency accuracy of the *51A* oscillator for any setting of the frequency switches is approximately 0.1 per cent. The oscillator is factory adjusted by means of the potentiometer designated *CAL*, to deliver a maximum of 16 decibels above 1 milliwatt into a 135-ohm load. The *COARSE* and *FINE* controls enable the output to be reduced to less than 75 decibels below one milliwatt. The oscillator output impedance is substantially 135 ohms throughout the frequency range and is independent of the setting of the output controls. The total power of any spurious frequencies including harmonics and power supply interference is at least 30 decibels below the fundamental and is substantially independent of the amplitude or frequency of the fundamental output signal. A ±5-volt variation of the a-c power supply voltage produces less than 0.1 decibel variation of the oscillator output. The frequency stability for a-c power supply voltage variations is of the order of 20 parts per million per volt.

The simplicity of operation and stability of output make this oscillator convenient for field testing and maintenance.

Tube Test Set

The *1AH* tube test set was specifically designed for testing the *373A* and *374A* filament type pentode vacuum tubes used respectively as voltage amplifier tubes and power output tubes in the amplifiers of the *K2* carrier telephone system. Since these tubes were a new development and were being applied to a new system, the opportunity was presented to develop new testing criteria and testing techniques which would not only determine the present condition of the tubes but also provide some better indication than had been available previously as to whether satisfactory performance would be obtained for at least the period of future operation until tests were again made. With this in mind the *1AH* tube test set has designed to measure the following tube characteristics:

1. Dynamic transconductance or G_M.
2. Peak plate current when the grid is driven to zero bias.
3. D-c plate current.
4. Filament activity—which is indicated by the change in the above characteristics when measured with the filament voltage reduced by ten per cent.
5. Grid current.
6. Maximum power output of the *374A* tube under amplifier load conditions.

The *1AH* tube test set is a portable device approximately 12 by 11 by 6 inches and weighing about 25 pounds. Three test sockets are provided to accommodate two *373A* tubes and one *374A* tube, the complement of a *K2* line amplifier. Power is supplied to the set by use of a permanently attached cord and plug which plugs into a standard amplifier power outlet provided on the amplifier bays. This power consists of regulated 60 volts at 60 cycles, 150 volts direct current, and grid voltage for the *374A* tube. The test set is shown in Figure 5.

The test set circuits consist of the circuits associated with the test sockets which allow the tubes to function under conditions very closely simulating those in the amplifier, a signal supply circuit obtained from from the regulated 60 volts 60 cycles, a peak reading vacuum tube voltmeter and various switching and control circuits required to make the various measurements. A simplified circuit diagram, Figure 6, shows the essential parts of the set, omitting other tube test sockets and switching.

The set is calibrated by applying a standard 60-cycle voltage from the signal supply circuit to the vacuum tube voltmeter and adjusting its sensitivity for a standard reading on the meter. Transconductance is measured by applying a known voltage from the signal circuit to the grid of the tube under test and measuring with the vacuum tube voltmeter the voltage developed across a known load resistance. To measure peak plate current, voltage which swings the grid to zero bias is applied to the grid by the signal circuit and the peak voltage developed across a known plate load resistance is indicated by the vacuum tube voltmeter. The true peak value is obtained by superimposing an indication of the d-c plate current on the indication for a peak a-c swing. The d-c plate current is measured by using the meter as a voltmeter across the known plate load with no input signal applied. By the use of a tap on the filament transformer, the filament voltage is reduced ten per cent and filament activity measurements are made. The vacuum tube voltmeter circuit is arranged with a calibrated input potentiometer so that the per cent change in transconductance during a filament activity test is indicated directly on the potentiometer dial.

Grid current is indicated by introducing a large resistance into the grid circuit and measuring the change in d-c plate current that results. To measure the maximum power capability of the *374A* tube, a load resistance is inserted in the plate circuit which causes the tube to operate on a dynamic load line whose value of plate current at zero bias grid swing corresponds to that obtained in the amplifier. The power output under this condition is indicated by the peak voltage developed across this load.

Testing Methods

The *K* system is provided with alarms to indicate abnormal operating conditions. Alarms from normally unattended stations are carried to stations where attendants are located. These alarms check failure of fuses, high or low voltages of batteries and a-c supplies, power failure, and automatic transfer to alternate equipment when provided.

In general, the only tests made on the *K* carrier system on a routine basis are tube tests and checks of the voltage of the

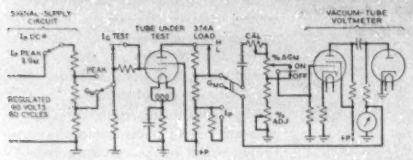

Figure 6. Simplified circuit of the *1AH* tube test set

grid bias batteries. Alternate sockets have been provided in the amplifiers so that a spare tube may be placed in parallel with a working tube, after which the working tube may be removed for test without interrupting service. The principal improvement in tube testing methods is that dynamic tube characteristics are measured rather than the d-c characteristics previously measured. Laboratory experience has indicated that dynamic characteristics are superior to d-c characteristics in indicating the condition of a tube and its probable future performance.

More elaborate tests are necessary when the system is reported in trouble. These tests include noise and modulation observations at the terminals and pilot level measurements and modulation tests at various repeaters of the system. The over-all voice-to-voice gain and noise tests made at the terminals give some information as to whether the system as a whole is in trouble or whether the trouble is limited to a single channel.

When a system appears to be in trouble, the first tests to locate the section in trouble are pilot level measurements. These may be made without disturbing transmission as mentioned previously by making bridging measurements with the *31*-type transmission measuring set. Measurements are usually made at attended stations first, and at unattended stations after the section in trouble has been located. Pilot levels may be sufficiently different from the expected levels or from the levels of adjacent normal systems to localize the trouble quite rapidly. However, there are some troubles of such a nature that the dynamic regulation is capable of pulling the pilot levels back into line in one or two repeaters thus precluding the location of trouble by pilot level observation at attended stations.

One type of trouble on the cable carrier systems is interchannel modulation. This occurs on multichannel systems due to non-linear distortion caused by an abnormal tube or circuit condition. The trouble manifests itself usually by the appearance of a characteristic type of noise in one or more channels of a system when one or more other channels are in use.

Measurements of modulation along a system suspected of having such a trouble are frequently useful in locating the amplifier at fault. The test is made by taking the top three channels out of service. Signals of 53 and 57 kc are applied to the line via the top two channels, and of sufficient magnitude to fully load the system. A third order modulation product, of the *2A–B* type, appears at 49 kc which is in channel ten. The normal range of magnitudes for this modulation product is known, and it adds approximately in phase along a system. With this knowledge, it is possible usually to determine which repeater has a trouble which causes excessive modulation. The 49 kc preselecting filter of the *31*-type transmission measuring set has been provided for making this specific measurement.

After an amplifier which is in trouble has been located, bridging tests may be made at selected points within the circuit of the amplifier. These tests are made using the high impedance test probe. Normal voltages with suitable tolerances have been determined for these test points and it is possible to track down the component or wiring trouble which is responsible. Also, comparison of voltages at any point in the suspected amplifier with those in a normal working amplifier may be made.

References

1. A Carrier System for Toll Cables, C. W. Green, E. I. Green. AIEE Transactions, volume 57, 1938, January section, pages 227–36; the *Bell System Technical Journal*, volume 17, January 1938, pages 80–105.

2. An Improved Cable Carrier System, H. S. Black, F. A. Brooks, A. J. Weir, I. G. Wilson. AIEE Transactions, volume 66, 1947, pages 741–46.

3. The Weim Bridge and Some of its Applications, J. S. Worthington. *Electronic Engineering*, volume 15, October 2, 1942, pages 214 and 216.

4. Properties and Uses of Thermistors—Thermally Sensitive Resistors, J. A. Becker, C. B. Green, G. L. Pearson. AIEE Transactions, volume 65, 1946, November section, pages 711–25; the *Bell System Technical Journal*, volume 26, January 1947, pages 170–212.

No Discussion

Transient Characteristics of Current Transformers During Faults—II

F. S. ROTHE
ASSOCIATE AIEE

C. CONCORDIA
FELLOW AIEE

Synopsis: The range of application of current transformers in bus differential protective systems is limited by saturation in the transformer cores under fault conditions, which may sometimes result in improper relay operations. It is shown that the addition of impedance in the relay circuit will reduce the relay current under fault conditions so as to increase the range of applications for which standard current transformers may be used.

SINCE part I of this paper was presented,[1] further work has been done in analyzing the transient behavior of current transformers under fault conditions. As before, the results have been obtained with the aid of a differential analyzer which permits an accurate representation of the non-linear effects of transformer saturation.[2,3,4]

This part of the paper presents the results of a study of the effects of mutual burden impedance on the differential current of transformers connected for bus differential protection. Several means have been suggested in the past to insure correct relay operation with this type of protection. One proposal is to use special current transformers such as linear couplers or air gap core transformers having a linear magnetization characteristic over the operating range.[5,6] However, it is the purpose of this paper to show what can be done using standard current transformers and explore the range of conditions over which they can be applied before it is necessary to resort to a special type of transformer. The effect of mutual burden impedance has been studied over a wide range of variables and data obtained in a general form, previous work having been limited to a study of particular transformers.[7,8] The concept of size constant developed in part I of the paper was used to make the results applicable over a considerable range of actual transformer ratings.

The variables considered were: magnitude of fault current, d-c time constant, number of transformers connected differentially, size constant, and the ratio of burden impedance to the current transformer secondary resistance. Both internal and external fault conditions were studied. The results were obtained from a differential analyzer in the form of a graph of differential current versus time. From the graph, the largest rms value of the differential current for a time interval of 1/60th of a second was calculated.

This one cycle rms differential current is probably a good measure of the performance of the instantaneous type of overcurrent relay and can be used to study the application of such a relay under the assumed conditions.

Summary and Conclusions

1. Data are presented showing the effect of mutual burden resistance on the differential current for an external or through fault whose current is 100 per cent offset and has a d-c time constant of 16 radians. The case of six similar transformers having size constants of 16,700 turns^2 inches/ohm was chosen as an example of the data obtained. The fault current was assumed to be equally divided on the other five transformers.

2. The effect of mutual burden resistance on the differential current for internal faults is also presented for the above conditions. The fault current was assumed to be equally divided among the six transformers.

From the data presented and from a large amount of unpublished data we can draw the following conclusions:

3. When through fault currents are large enough to cause appreciable differential error current to flow, the addition of mutual impedance will reduce the differential current. In order to reduce the rms one cycle error current to five per cent of the symmetrical rms value of fault current, the ratio of mutual resistance to transformer secondary resistance must be of the order of 15 to 1 for short time constants and 25 to 1 for time constants approaching 100 radians.

4. Under internal fault conditions the reduction in differential current from the addition of mutual impedance is not nearly as great as under external fault conditions. Consequently, there is a range of conditions over which the addition of mutual impedance will improve the performance of the relays considerably.

Analysis of Current Transformer Performance

External Faults

We shall assume $n+1$ identical transformers with their secondaries connected in parallel across a mutual impedance. Under the condition of a fault on one circuit we shall assume that the fault current divides equally among the remaining n circuits. Then we have

$$i_f' = n i_n' \tag{1}$$

where

i_f' = primary current in ampere-turns in faulted circuit

i_n' = primary current in ampere-turns in other transformers

In the secondary circuit

$$i_d = i_f - n i_n \tag{2}$$

Paper 47-107, recommended by the AIEE committee on protective devices for presentation at the AIEE North Eastern District meeting, Worcester, Mass., April 23-25, 1947. Manuscript submitted February 11, 1947; made available for printing March 7, 1947.

F. S. Rothe and C. Concordia are both with General Electric Company, Schenectady, N. Y.

The authors wish to acknowledge the able assistance in this investigation given by members of the General Electric Company's differential analyzer staff, consisting of A. C. Cook, L. W. Robbins, G. M. Miller, and J. R. Wilson. S. B. Crary, L. F. Kennedy, and A. J. McConnell of the company contributed many helpful suggestions and data on the project.

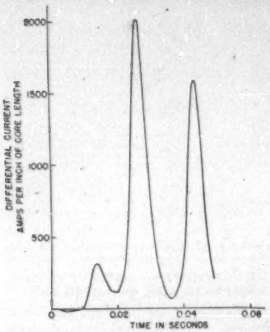

A. Ratio of mutual resistance to secondary resistance = 0

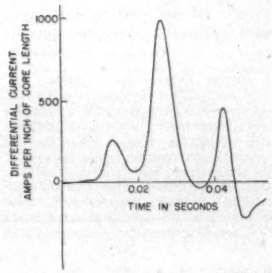

B. Ratio of mutual resistance to secondary resistance = 1

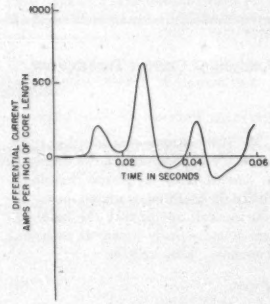

C. Ratio of mutual resistance to secondary resistance = 2

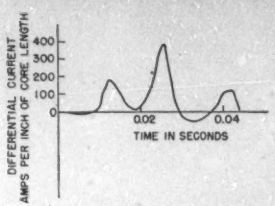

D. Ratio of mutual resistance to secondary resistance = 4

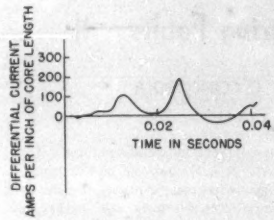

E. Ratio of mutual resistance to secondary resistance = 8

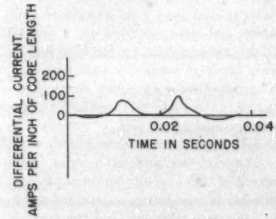

F. Ratio of mutual resistance to secondary resistance = 16

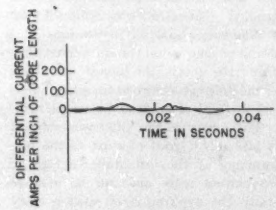

G. Ratio of mutual resistance to secondary resistance = 32

Figure 1. Differential current for an external fault

Symmetrical rms fault current = 990 ampere-turns per inch of core length

Size constant = 16,700 turns² inches/ohm — Fault current = fully offset

Time constant = 16 radians — Number of transformers = 1 versus 5

where

i_d = differential current in amperes in mutual circuit

i_f = secondary current in amperes in faulted circuit

i_n = secondary current in amperes in other transformers

The magnetomotive force in the transformer cores is given by

$$H_f = \frac{i_f' - Ni_f}{l} \tag{3}$$

and

$$H_n = \frac{i_n' - Ni_n}{l} \tag{4}$$

N = number of secondary turns of transformer

l = mean length of magnetic circuit of core in inches

Writing the voltage equations in the secondary of the faulted circuit and neglecting self-inductance in the secondary of the transformer,

$$\frac{d\beta_f}{dt} = ri_f + r_d i_d + L_d \frac{di_d}{dt} \tag{5}$$

Similarly the voltage equation in the secondaries of the remaining n transformers is,

$$10^{-8} NA \frac{d\beta_n}{dt} = ri_n - r_d i_d - L_d \frac{di_d}{dt} \tag{6}$$

A = cross sectional area of transformer core in square inches

β_f = flux density in core of faulted transformer in lines per square inch

β_n = flux density in core of the other transformers in lines per square inch

r = resistance in secondary of transformer in ohms

r_d = resistance in mutual circuit in ohms

L_d = inductance in mutual circuit in henrys

t = time in seconds

From equations 1 through 4 we get the differential ampere turns per inch,

$$\frac{Ni_d}{l} = nH_n - H_f \tag{7}$$

We shall replace t in our equations by θ as follows

$$\theta = 2\pi ft \tag{8}$$

f = frequency in cycles per second

Rewriting the two voltage equations and integrating we have,

$$\frac{2\pi 10^{-8} N^2 Af}{lr} \beta_f = \int \left(\frac{i_f'}{l} - H_f \right) d\theta + \frac{r_d}{r} \int (nH_n - H_f) d\theta + \frac{2\pi f L_d}{r} (nH_n - H_f) \tag{9}$$

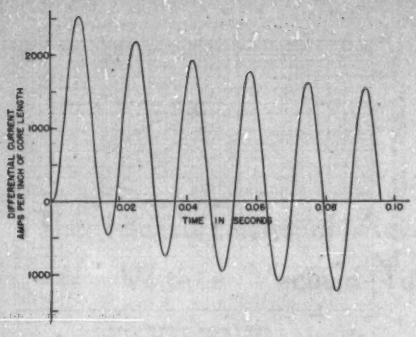

A. Ratio of mutual resistance to secondary resistance = 0

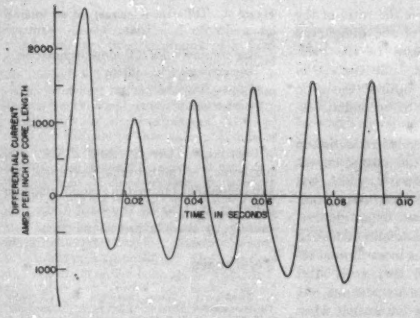

B. Ratio of mutual resistance to secondary resistance = 1

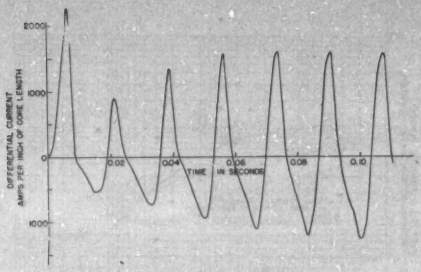

C. Ratio of mutual resistance to secondary resistance = 2

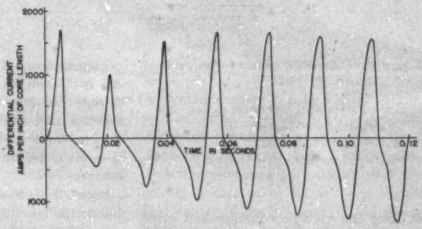

D. Ratio of mutual resistance to secondary resistance = 4

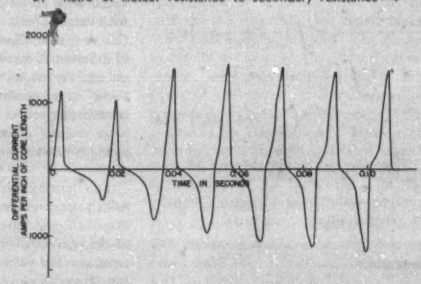

E. Ratio of mutual resistance to secondary resistance = 8

Figure 2. Differential current for an internal fault

Symmetrical rms fault current = 990 ampere-turns per inch of core length

Size constant = 16,700 turns² inches/ohm
Time constant = 16 radians
Fault current = fully offset
Number of transformers = 6

$$\frac{2\pi 10^{-8} N^2 A f}{lr}\beta_n = \int\left(\frac{i_f'}{nl} - H_n\right)d\theta - \frac{r_d}{r}\int(nH_n - H_f)d\theta - \frac{2\pi f L_d}{r}(nH_n - H_f) \quad (10)$$

We note that the coefficient of β_f and β_n is $2\pi f\ 10^{-8}\ C$, where C is the size constant defined in part I of the paper[1] as

$$C = \frac{N^2 A}{rl} \text{ turns}^2 \text{ inches/ohms} \quad (11)$$

The fault current i_f' was assumed to be of the form

$$i_f' = I_m[\cos\alpha\, e^{-\theta/T} - \cos(\theta+\alpha)] \quad (12)$$

I_m = peak value of symmetrical component of fault current in ampere turns
α determines the magnitude of initial offset and was assumed equal to 0 degrees for all cases
T = time constant of d-c component in radians

The remaining two relations needed to solve the problem were provided by the saturation curves,

$$\beta_n = f(H_n) \quad (13)$$

$$\beta_f = f(H_f) \quad (14)$$

Internal Faults

We shall assume $n+1$ identical transformers as in the case of the external faults and also shall assume that the total fault current divides equally among all of the transformers.

Then,

$$i_f' = (n+1)i_n' \quad (15)$$

and

$$i_d = (n+1)i_n \quad (16)$$

From equation 4 we get

$$\frac{Ni_d}{l} = \left(\frac{i_f'}{l} - (n+1)H_n\right) \quad (17)$$

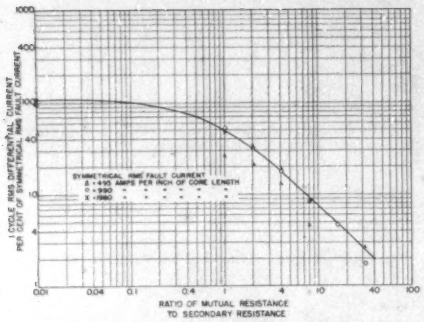

Figure 3. Differential current for an external fault

Size constant = 16,700 turns² inches/ohm
Time constant = 16 radians
Fault current = fully offset
Number of transformers = 1 versus 5

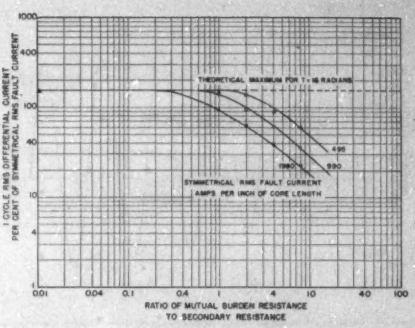

Figure 4. Differential current for an internal fault

Size constant = 16,700 turns² inches/ohm
Time constant = 16 radians
Fault current = fully offset
Number of transformers = 6

Writing the voltage equation and integrating we get,

$$\frac{2\pi 10^{-6} N^2 A f}{l r}\beta_n = \int\left(\frac{i_f'}{(n+1)l} - H_n\right)d\theta + \frac{r_d}{r}\int\left(\frac{i_f'}{l} - (n+1)H_n\right)d\theta + \frac{2\pi f L_d}{r}\left(\frac{i_f'}{l} - (n+1)H_n\right) \quad (18)$$

Equations 9 through 14 and 18 were set up and solved on the differential analyzer of the General Electric Company at Schenectady.

Results

The differential current through the mutual impedance is shown in Figures 1 and 2 for a fault current whose symmetrical rms value was 990 ampere-turns per inch of core length and whose d-c time constant was 16 radians. The transformer size constant was 16,700 turns² inches/ohm and there were six transformers in the differential connection.

Figure 1 shows the differential current under external fault conditions and Figure 2 shows this current under internal fault conditions.

Figures 3 and 4 show the ratio of the one cycle rms value of the differential current in ampere-turns to the symmetrical rms value of fault current in ampere turns plotted against the ratio of mutual resistance to secondary resistance.

Figure 1 shows a decided reduction in differential current as the mutual impedance is increased. Figure 2, which was taken with an internal fault, shows that with value of fault current of 990 ampere-turns per inch, there is a definite reduction in differential current as more mutual resistance is added and that even after steady state conditions are reached, the transformer cores are saturated when large values of mutual resistance are used, resulting in less differential current.

The data for Figures 3 and 4 were obtained from curves similar to those of Figures 1 and 2 by taking the rms value of the current over a time interval of 2π radians. For external faults the time interval was chosen to give the largest possible rms value of current. For internal faults, the particular time interval taken was from 0 to 2π radians. Figure 3 shows that as mutual resistance is added, the per cent differential current for any one value of mutual resistance tends to become independent of the value of fault current so that one curve can be drawn to fit a range of fault currents. This would not apply of course to those currents which would cause small differential currents with negligible mutual resistance in the circuit.

For relays having time delay, d-c, harmonic, or percentage restraints, results could be obtained in a similar fashion from an analysis of the basic data pertaining to these types of relays.

References

1. Transient Characteristics of Current Transformers During Faults, **C. Concordia, C. N. Weygandt, H. S. Shott.** AIEE Transactions, volume 61, 1942, pages 280–5.

2. A Differential Analyzer—A New Machine for Solving Differential Equations, **V. Bush.** *Journal of the Franklin Institute* (Philadelphia, Pa.), volume 212, October 1931, pages 447–88.

3. Differential Analyzer Eliminates Brain Fag, **Irven Travis.** *Machine Design* (Cleveland, Ohio), volume 7, July 1935, pages 15–18.

4. A New Differential Analyzer, **H. P. Kuehni, H. A. Peterson.** AIEE Transactions, volume 63, 1944, pages 221–8.

5. Linear Couplers for Bus Protection, **E. L. Harder, W. K. Sonnemann, E. H. Klemmer, E. C. Wentz.** AIEE Transactions, volume 61, 1942, pages 241–8.

6. New Current Transformer for Bus Differential Protection, **L. F. Kennedy, A. T. Sinks.** AIEE Transactions, volume 60, 1941, pages 1180–7.

7. Current Transformers and Relays for High-Speed Differential Protection, with Particular Reference to Offset Transient Currents, **E. C. Wentz, W. K. Sonnemann.** AIEE Transactions, volume 59, 1940, pages 481–8.

8. Considerations in Applying Ratio Differential Relays for Bus Protection, **R. M. Smith, W. K. Sonnemann, G. B. Dodds.** AIEE Transactions, volume 58, 1939, pages 243–52.

No Discussion

The Measurement of Acceleration With a Vacuum Tube

WALTER RAMBERG
NONMEMBER AIEE

Synopsis: Acceleration can be measured with a vacuum tube consisting of a fixed cathode and two plates, one on each side of the cathode. The plates are mounted elastically to deflect in response to acceleration normal to their plane. Displacement of a plate alters the electron current delivered from the cathode to that plate. A tube of this type is described which has a natural frequency of about 800 cycles per second, a flat response for sinusoidal accelerations up to 200 cycles per second, and a linear range of 150g. The output at accelerations of 10g is sufficient to drive a high frequency recording galvanometer directly, without the complications of an amplifier. The principal disadvantages of the tube are an unpredictable "zero drift" and a "zero shift," following impacts of very short duration.

THE vacuum tube acceleration pickup was developed for the Bureau of Aeronautics, Navy Department, at the National Bureau of Standards, with the co-operation of Sylvania Electric Products, Inc. The purpose of the development was to obtain a pickup with large output for recording accelerations on airplanes in flight. The large output was desired to obviate the necessity of an amplifier between the pickup and the recorder.

The measurement of acceleration on airplanes in flight requires linear response for frequencies up to 200 cycles per second and for accelerations up to 20g (20 times gravity). Furthermore, it requires that the pickup should retain its "zero" during a given flight maneuver, which might last several minutes, and that its performance should be unaffected by rough handling during installation and by high frequency vibration and impact present under flight conditions.

It will be shown that the vacuum tube acceleration pickup satisfies the first two of these requirements in its present stage of development, but that it fails to satisfy the last two. In spite of this failure to fulfill its original purpose, the pickup has certain attractive characteristics which have made it a useful tool in the laboratory.

Before proceeding to a description of the vacuum tube acceleration pickup, it should be emphasized that there is nothing new in the idea of utilizing the deflection of electrodes in a vacuum tube for the direct measurement of mechanical quantities. As early as 1936[1,2] Ross Gunn, of the Naval Research Laboratory, described a vacuum tube containing a twin diode, designed for measuring very small displacements. In 1937[3] E. D. McArthur described a diode which was developed at the General Electric Research Laboratories, also for measuring small displacements. In 1943[4] Jerome Rothstein proposed a microphonic electron tube for measuring small changes in pressure. Very recently[5] Harry Olsen described a vacuum tube phonograph pickup developed by the Radio Corporation of America Research Laboratories.

Construction

The principle of operation of the vacuum tube acceleration pickup and its construction is made clear by Figure 1.

The tube contains two elastically mounted plates P_1 and P_2 with a fixed cathode C between them. Acceleration in a direction normal to the plane of the plates (indicated by an arrow in Figure 1*a*) causes a displacement of the plates relative to the cathode. This increases the current between one plate and the cathode and decreases that between the other plate and the cathode. The change in current will be proportional to the component of acceleration normal to the plane of the plates for frequencies low compared to the natural frequency of the plates as an elastic body. It may be recorded with an electric bridge circuit. The use of symmetrically placed twin plates makes the output of the tube relatively insensitive to fluctuations in the total electron current from the cathode. The advantages of this arrangement already have been recognized and utilized by Gunn in his twin diode.[1,2]

The tube shown in Figure 1 is of a recent type, Sylvania type *SD 759*. It contains an indirectly heated cathode of rectangular section. The cathode is mounted rigidly in the two mica plates M. These, in turn, are built into a rigid box by the transverse bars B_1 to B_4. The

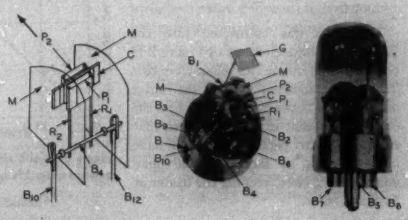

Figure 1. Arrangement of electrodes in tube

Paper 47-108, recommended by the AIEE committees on electronics and instruments and measurements for presentation at the AIEE North Eastern District meeting, Worcester, Mass., April 23-25, 1947. Manuscript submitted January 15, 1947; made available for printing March 11, 1947.

WALTER RAMBERG is with the National Bureau of Standards, United States Department of Commerce, Washington, D. C.

The author acknowledges the assistance of C. R. Smith and Paul Haas of Sylvania Electric Products, Inc., and of Samuel Levy and A. E. McPherson of the National Bureau of Standards.

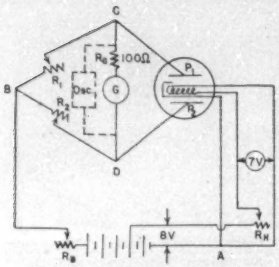

Figure 2. Wheatstone bridge circuit for measuring and recording output of tube

box is held in the base of the tube by the four vertical pins B_5 to B_8. The plates P_1 and P_2 are formed from thin sheet metal to reduce their heat capacity, and hence the warming up time of the electrodes. The plates are mounted on slender vertical rods R_1 to R_4 to give them the desired flexibility normal to their plane. The rods are welded to two of the transverse bars, B_3, B_4, holding the mica plates together. Electric connection is made to the vertical pins B_9 to B_{12} by connectors between ends of the transverse bars and the tops of the vertical pins.

The frequency range of the pickup may be controlled by the proper choice of diameters and length of the wires used in the supporting structure. In the pickup of type *SD 759* these were designed to give a fundamental frequency of about 750 cycles per second.

The sensitivity may be increased by decreasing the natural frequency or by decreasing the spacing between plates and cathode. This spacing is held at about 0.005 inch in the tubes of type *SD 759*.

The complete tube is shown in Figure 1*c*. It has a *T-9* glass envelope about 2 inches in length and a loctal base. The over-all dimensions of the tube can be estimated from the scale in Figure 1. The weight of the tube is about 0.06 pound.

Characteristics

The tube was connected into the Wheatstone bridge circuit of Figure 2 in order to determine its characteristics. This circuit applies 7 volts to the heater and 10 volts between each plate and the cathode. Recent experience shows that somewhat better performance might have been obtained by increasing the plate voltage to 12 volts, keeping the heater at 7 volts as before.

The procedure for determining the characteristics with the circuit of Figure 2 is described in reference 6. The following characteristics were found for 95 tubes of Sylvania type *SD 759* described in Figure 1.

The fundamental frequency of the plates was between 595 and 915 cycles per second. The average frequency was 847 cycles per second.

The plate to cathode resistances with 10 volts on the plate and 7 volts on the heater were from 88 to 314 ohms. The average value was 157 ohms. The ratio of the larger plate to cathode resistance to the smaller resistance was from 1.00 to 1.46. Deviations of the value of this ratio from unity may be taken as a measure of the electrical asymmetry of the electrodes in the tube.

The heater had a resistance of about 14 ohms at 7 volts. This leads to a total power consumption of about 7 watts in the Wheatstone bridge of Figure 2.

The sensitivity of the tube may be expressed in terms of a calibration factor K defined by

$$K = \frac{\Delta R}{R} \Big/ \frac{a}{g}$$

where

$$\frac{\Delta R}{R} = \frac{1}{2}\left(\frac{\Delta R_{P1}}{R_{P1}} + \frac{\Delta R_{P2}}{R_{P2}}\right)$$

which equals average change in unit plate to cathode resistance corresponding to an acceleration a in direction normal to the plates (R_{P1}, R_{P2} = plate to cathode resistance for two plates in tube).

The calibration factor K is obtained readily from the current output I_{2g} when the tube is connected into the bridge of Figure 2 and the acceleration normal to the plates is changed by 2g. Such a change in acceleration is produced easily

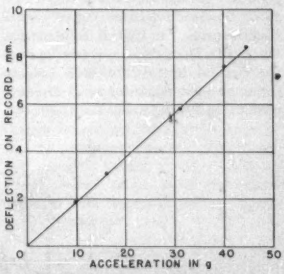

Figure 3. Calibration of tube 12 with type C galvanometer Heiland oscillograph *A401R-6*

Attenuation factor = 1/19

by turning the tube through 180 degrees in the earth's gravitational field. The calibration factor then is computed by substituting I_{2g} in the following equation, derived in the appendix of reference 6

$$K = \left(5 + \frac{R_{P1} + R_{P1}}{40}\right) I_{2g}$$

The calibration factors for the 95 tubes that were calibrated by this procedure ranged from 0.0029 to 0.0072. The average factor was $K = 0.0045$. These factors correspond to a current output of the order of 0.2 milliamperes per g when the tube is connected into the circuit of Figure 2. Recent tests have indicated that K can be increased about 40 per cent if the plate voltage is increased from 10 to 12 volts, keeping the heater voltage at its original value of 7 volts.

In calibrating tubes in this manner it is assumed that the calibration factor remains constant for the entire range of acceleration to be measured. This assumption has been checked for a number of tubes. Figure 3 shows the output of a tube, measured as deflection on an oscillograph record when the tube was connected into the circuit of Figure 2 with the oscillograph at G, and when it was subjected to a sinusoidal acceleration on a shaking table. The output is closely linear up to the highest acceleration applied, 45g. Recent tests of tubes subjected to centripetal acceleration on a spinnning table capable of applying steady acceleration up to 750g showed substantially linear output up to accelerations of 160g.

Tests on the spinning table provided a convenient means for measuring the maximum steady acceleration which can be sustained by the tubes without permanent damage. In tests of a few tubes it was found that the "zero shift in g"* exceeded 5 per cent of the maximum applied acceleration when this acceleration was greater than 160g. The source of the zero shift is now known; it probably is caused, at least in part, by excessive bending stresses in the slender rods supporting the plates. The output was nearly proportional to acceleration up to the point at which one of the plates made contact with the cathode. This occurred at an acceleration between 240g and 340g.

In using the tube, it is assumed that it does not respond to acceleration parallel to the plane of the plates. This assumption was verified approximately some time ago by tests of six tubes on a shaking table. Recently it has been checked more accurately for a tube subjected to centripetal acceleration on the spinning table.

* "Zero shift in g" was obtained by dividing the measured shift in unbalance current for 0g by the unbalance current $I_{2g}/2$ corresponding to 1g.

The output at an acceleration of 200g was equivalent to less than 10g for any direction of the acceleration in the plane of the plates.

Difficulty was experienced from the beginning with zero drift of the tubes. This zero drift shows itself by a gradual change in unbalance current when the tube is connected into the Wheatstone bridge of Figure 2 and is left there without any change in acceleration.

The drift was of an unpredictable nature. A drift of the order of plus or minus 1g in a few minutes remained even after special precautions were taken to shield the tube against temperature variations and to eliminate fluctuations in heater voltage and changes in contact resistance. The drift tends to decrease with the age of the tube. Twenty-nine tubes which had shown drifts greater than 1g in 15 minutes after a heating up period of 15 minutes showed a substantial improvement after being stored for six months. For 12 of the tubes the drift was between 0.2g and 1g and for the remaining 17 it was less than 0.2g.

Outside of the laboratory of the Bureau of Standards, considerable difficulty has been experienced with the tube because of its unusual sensitivity to impacts of very short duration, such as might be caused by sharply tapping the envelope of the tube. Such impacts may result in a large "zero shift," and even a change in calibration factor, if the impact is of sufficient intensity. A careful examination of the tube structure after impact showed that the zero shift was accompanied by bending of the rods supporting the plates. An explanation is suggested by a simple analysis of the plate considered as a mass mounted on a flexible cantilever beam which is brought to a sudden stop at the root. The analysis shows that dropping the tube on a rigid surface from a height of only one inch may produce stresses in the plate supports equal to those produced under a steady acceleration of 360g.

Figure 5 (above). Panel and recorder to balance bridges for three vacuum tube accelerometers

Figure 6 (right). Tube of Sylvania type 759A with connector tabs on plate and cathode pins

Method of Using Tube

Electric Circuit

An electric circuit for use with the tubes is shown in Figure 4. This differs from the simple Wheatstone bridge circuit of Figure 2 in having means for reducing the effects of changes in contact resistance in the plate circuit and in having an electric filter ahead of the recording galvanometer.

The effect of changes in contact resistance is reduced by adding two pairs of auxiliary 5-ohm resistances to form a Kelvin double bridge. The theory of the Kelvin double bridge[7] shows that the auxiliary resistances will be effective in eliminating differences in contact resistance at terminals *5, 8, 1, 4,* as long as the contact resistance is small compared to 5 ohms and as long as R_1, R_2, R_3, and R_4 are adjusted properly.

The low pass filter is inserted ahead of the galvanometer to eliminate oscillations at the natural frequency of the plates from the current passing through the recording galvanometer. Experience at the National Bureau of Standards indicates that filter *93051* built by the United Transformer Company is satisfactory for this purpose. The response curve for this filter is practically flat up to 300 cycles per second, and it cuts off sharply to a response of less than 1 per cent of that in the flat portion at 800 cycles per second. Insertion of the filter results in a 30 per cent loss of current sensitivity with a type *C* Heiland galvanometer (impedance 9 ohms, natural frequency 430 cycles per second). The filter weighs about 3 pounds.

In using the circuit of Figure 4, the resistance R_H is first adjusted to make the heater voltage across *AB* equal to 7 volts. The resistances R_1, R_2, R_3, R_4, then are adjusted to make the voltages across *AC, CE, AD, DF* equal to the desired plate voltage, for example, 10 volts. This balances the bridge approximately, so that the switches S_1 and S_2 can be closed.

Figure 5 shows the electric equipment used at the National Bureau of Standards for recording the output from three vacuum tube accelerometers. The equipment includes a panel *A* for each Kelvin double bridge with controls for adjusting the resistances R_H, R_1, R_2, R_3, R_4. A meter *B* can be switched into the bridge to measure the heater voltage and adjust the bridge voltages to the proper value. The leads from the filters are brought through switches *C* to the 6-element Heiland oscillograph *D*.

This circuit has been quite satisfactory as used at the Bureau of Standards.

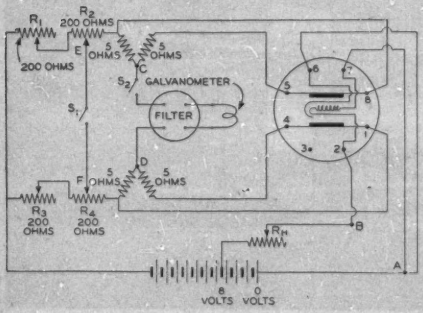

Figure 4. Electric circuit for use with tube, including Kelvin double bridge and filter

Figure 7 (left). Tube mounted in square edge clamp

Figure 8 (below). Tube mounted in ring clamp

With it, it has been possible to use ordinary loctal sockets for connecting the leads to the pins at the base of the tube. This facilitates the replacement of tubes and eliminates the need for soldering leads to the pins.

The effects of variations in contact resistance may be reduced also by using the most recent tubes, Sylvania type *SD 759A*. These tubes carry tabs welded to the plate pins and the cathode pin, as shown in Figure 6. The tabs are soldered to lugs on the underside of a Sylvania *6958* loctal socket. This avoids the danger of breaking the seal by overheating.

Attachment to Structure

Special care should be taken to clamp the tube to the structure in such a manner that it will experience the same acceleration as the structure. To accomplish this, the attachment must be rigid enough so that the fundamental frequency of the tube, when attached to a rigid structure, is high compared with the fundamental frequency of about 800 cycles per second of the plates in the tube. At the same time the clamping force must be distributed over the tube to prevent breaking the glass envelope during clamping.

A square clamp which satisfies both these conditions is shown in Figure 7. Detailed dimensions of this clamp are given in Figure 5 of reference 6. The load is distributed in this clamp by wrapping a layer or two of transparent cellulose tape on the metal sleeve of the tube before inserting it in the clamp.

Another clamp, used in recent tests at the Bureau of Standards, is shown in Figure 8. This clamp consists of a ring, 7/16-inch wide, to which a lug is silver-soldered to provide means for mounting on the structure whose acceleration is to be measured. The ring is cut from 1.25-inch brass tubing with a wall thickness of 0.032 inch. The lug terminates in a *10-32* screw for attachment to the structure. The vacuum tube is prepared for insertion in the clamp by filing off the index button projecting from the metal sleeve (Figure 1). It then is cemented in the ring with a paste of litharge and glycerine. A rigid attachment of the clamp and tube is obtained by drawing the face of the lug firmly against the structure. In some cases it is desirable to use a tapped hole in the structure. A spacer of the proper height then may be inserted between the lug and the structure to obtain proper orientation of the tube when tight.

Calibration

During the test it is desirable to calibrate the tube and its associated electric circuit by subjecting it to a known acceleration and recording the output.

If accelerations of not more than 10g are measured, the calibration is made conveniently by subjecting the tube to an acceleration 2g in the earth's gravitational field. For this purpose the plates are first placed horizontally with button *B*, Figure 1, at "9 o'clock," and the output is recorded. Then the tube is rotated about its horizontal axis to place the button at "3 o'clock," and the output is recorded again. Rotation through 180 degrees is particularly simple when the tube is held in the square edge clamp of Figure 7. Rotation with the clamp has the additional important advantage of preventing errors in indicated output caused by changes in physical contact between the tube and its surroundings.

In some cases a known change in acceleration is recorded as part of the test itself. This then may be used as a scale to convert displacement on the record into acceleration. Such a method is currently in use in drop tests of a model wing at the Bureau of Standards. Figure 9 shows five tubes mounted on the model wing and Figure 10 a record obtained from these tubes when the model was dropped for a 2-point landing. The model is released at time *A* (Figure 10), and it makes contact with the "landing field" at *B*. The steady acceleration changes from 1g prior to *A* to 0g throughout the interval of free fall between *A* and *B*. Superimposed on the steady accelerations are vibrations which are set up in the model by imperfect action of the release gear. In spite of these vibrations, it is possible to measure up the record under a microscope and to obtain from it a mean value for the deflection per g which can be duplicated in successive tests within a few per cent. By use of this value it is found in this drop that the maximum acceleration during the impact was 3.7g at the fuselage (record 3), 3.7g and 3.9g at the inboard engine masses (records 2 and 4), and 3.4g and 4.5g at the outboard engine masses (records 1 and 5).

In some applications in which the accelerations to be recorded are much larger than 2g it is necessary to calibrate with a larger output on the recording paper.

The larger output may be obtained either directly by imposing larger accelerations or indirectly by increasing the sensitivity (lowering the attenuation) for the calibration at 2g.

Figure 11 shows a portable calibrator developed for this purpose by Samuel Levy and A. E. McPherson of the Bureau of Standards. The calibrator is essentially a 3-mass system, consisting of a relatively heavy base M_1 and two relatively light masses M_2 and M_3. The light mass

Figure 9. Five tubes on model wing to measure accelerations during drop test

M_3 is supported flexibly from the base M_1, and the mass M_2 is supported flexibly from M_3. The vacuum tube acceleration pickups are clamped rigidly in the holes in mass M_2. They are subjected to a definite pulse of acceleration rising smoothly from zero when the mass M_3 is released suddenly from a deflected position. The direction of the acceleration is indicated by the arrow in Figure 11.

The masses M_1, M_2, and M_3 are connected by double flexure plates A and B. Double, rather than single, flexure plates are used, since they prevent rotation of the mass M_2, thereby subjecting all accelerometers on M_2 to the same pulse of acceleration. The position of M_3 relative to M_1 before release is controlled by the point of engagement of the pawl C with the 7-position ratchet D. The cable support E is provided to secure all except the last few inches of accelerometer cable to the heavy mass M_1. The whole calibrator is suspended on the wires F which provide an effective shock mount with negligible damping.

The mass M_3 is released by drawing the pawl C with the release wire G, which is guided to minimize its effect on the motion immediately after release.

A typical acceleration–time curve for the calibrator is shown in the insert in Figure 12. This curve was obtained with a vacuum tube acceleration pickup mounted in mass M_2. The vacuum tube previously had been calibrated on a sinusoidal shaking table vibrating at a known amplitude. The second peak of the acceleration–time curve (A, insert in Figure 12) is taken as the calibrating acceleration. The magnitude of the calibrating acceleration changes linearly with position of the engagement of pawl C (Figure 11) with the equally spaced teeth on ratchet D. The calibrating accelerations are plotted as points against released tooth in the main portion of Figure 12. It is seen that accelerations from about 1g to about 20g can be applied in six equal steps.

The sensitivity for calibration at 2g may be increased with the simple circuit of Figure 13. The figure also gives formulas for adjusting the resistances R_3 and R_4 to attenuate the signal through the galvanometer by a factor α without changing the impedance across the balance points CD of the Wheatstone bridge in Figure 2 or across the output of the filter in Figure 4.

For instance, we may want to increase the sensitivity by a factor of 10 in calibrating as compared with recording. This may be accomplished by choosing $\alpha = 1$ for calibrating and $\alpha = 0.1$ for recording. According to the formulas in Figure 13, this corresponds to $R_3 = 0$, $R_4 = \infty$ (open circuit) for calibrating and $R_3 = 0.9R_G$, $R_4 = R_G/g$ for recording.

Applications of Tube

Applications of the tube are limited by its peculiar advantages and disadvantages relative to other acceleration pickups. The advantages are a high output, high natural frequency, linearity up to large accelerations, and operation over a wide range of temperatures. The disadvantages are zero drift, zero shift under impact, warming-up time of about 15 minutes, high current consumption, and the need of a filter to remove natural frequency response.

The high output and high natural frequency of the vacuum tube make it possible to record rapidly changing accelerations without requiring an amplifier. This is an advantage in field tests where space and weight are at a premium. It also simplifies tests in the laboratory when amplifying channels are not readily available.

The linearity to large accelerations is advantageous in recording acceleration over a wide range and in making possible the filtering out of high frequency response to produce a record proportional to acceleration.

The tube will hold its calibration factor over a wide range of temperature, as it has its own heating element enclosed in a vacuum. This is an advantage for the measurement of rapidly changing accelerations under extreme conditions of temperature, as in a cold chamber.

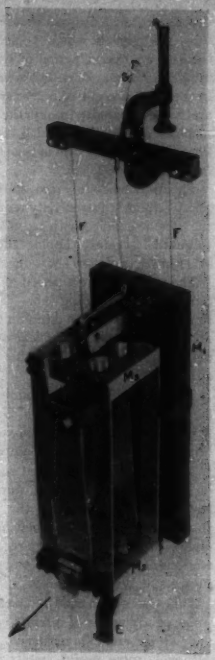

Figure 11 (above). Portable calibrator of "pulse" type for high frequency accelerometers

Figure 12 (below). Calibration of pulse type calibrator using vacuum tube accelerometer

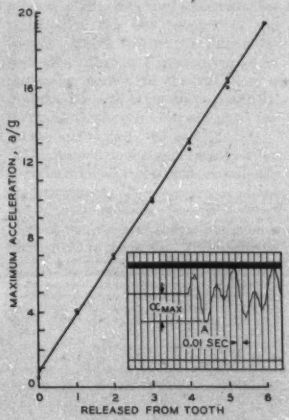

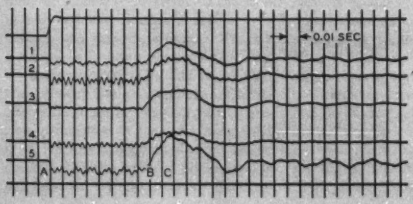

Figure 10 (left). Record of acceleration during drop test for tubes shown in Figure 9

The zero drift disqualifies the tubes in those field tests in which the acceleration is unknown over a period of time measured in minutes. Zero drift is not serious in the measurement of accelerations that are large compared to 1g, or in the measurement of accelerations which return to a known value in a period of time measured in seconds.

The possibility of zero shift and of abrupt change in sensitivity requires that the tube be handled with exceptional care to guard it against tapping and against other impacts of very short duration.

The tubes require a period of about 15 minutes for warming up. This may represent an excessive drain on the available power in certain applications, and it may introduce an undesirable delay in adjusting the equipment.

The filter represents an added item of expense and of weight which may be avoided in some cases by using pickups of other types with internal damping.

The tubes have been used successfully in recording accelerations during drop tests of model wings at the National Bureau of Standards. They have been used with varying success to record accelerations of "dummy pilots" and of human subjects at Wright Field.

Tubes have been tried out in the laboratories of a number of aircraft companies and of several Government agencies. Although some useful results were obtained in these laboratories, the general indication is that the tube in its present state of development is not suited for work in the field because of its sensitivity to tapping and other impacts. In addition some difficulties have been experienced because of breakage of the glass envelope in the clamp.

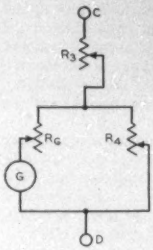

Figure 13. Circuit for changing sensitivity of tube without changing input impedance into recorder

a = attenuation

$R_3 = (1-a)R_G$

$R_1 = \frac{a}{1-a} R_G$

It appears from this that further development is needed to make the tube satisfactory instrument for general flight measurements. It was the general opinion that such a development should be undertaken because of the inherent potentialities of an acceleration pickup of the vacuum tube type.

Possible Improvements

It is of interest to consider possible ways that have been suggested for improving the performance of the vacuum tube acceleration pickup.

Sylvania Electric Products has suggested the possibility of replacing the indirectly heated cathode by a directly heated fine wire. This is a major change in design which would require considerable development. However, it might lead to all-around improvement by greatly reducing power consumption, reducing warming-up time, reducing the size with a resultant increase in frequency and in range, and decreasing zero drift.

The zero shift after impacts of very short duration appears to be due to excessive bending of the plate supports. This suggests the insertion of mechanical stops which would limit the displacement of the plates to a value obtained under steady accelerations of the order of 200g.

It has been suggested that replacement of the glass envelope by a metal envelope may reduce breakage during clamping.

References

1. Apparatus for the Detection of Displacements, **Ross Gunn.** United States Patent 2,155,420; reissued February 27, 1940, Re 21,372.

2. A Convenient Electrical Micrometer and Its Use in Mechanical Measurements, **Ross Gunn.** *Journal of Applied Mechanics*, American Society of Mechanical Engineers (New York, N. Y.), volume 7, number 2, June 1940, pages A49–A52.

3. Movable Anode Tubes, **E. D. McArthur.** *Electronics* (New York, N. Y.), volume 10, March 1937, pages 16–17.

4. Microphonic Electron Tube, **Jerome Rothstein.** United States Patent 2,389,935, November 27, 1945.

5. Mechano-Electronic Transducers, **Harry F. Olsen.** *Journal*, Acoustical Society of America (New York, N.Y.), volume 19, number 2, March 1947, pages 307–19.

6. Vacuum Tube Acceleration Pickup, **Walter Ramberg.** *Journal of Research*, National Bureau of Standards (Washington, D. C.), volume 37, number 6, December 1946, pages 391–8.

7. Electrical Measurements (book), **Frank A. Laws.** McGraw-Hill Book Company, Inc., New York, N. Y., 1917.

No Discussion

An Improved Cable Carrier System

H. S. BLACK
FELLOW AIEE

F. A. BROOKS
ASSOCIATE AIEE

A. J. WIER
ASSOCIATE AIEE

I. G. WILSON
NONMEMBER AIEE

Synopsis: A new 12-channel cable carrier system is described which is suitable for transcontinental communications. Important features are negative feed-back amplifiers of improved design, new arrangements for accurate equalization of the cable loss, and automatic thermistor regulators which continuously control the transmission of each system.

THE Bell System has used cable carrier systems for more than eight years. By this means, 12 1-way messages are transmitted simultaneously over a single 19-gauge cable pair. Two-way communication is afforded by the use of separate cables for the two directions of transmission. As many as 100 2-way 12-channel systems can be operated in the two cables. Due to their economy and superior transmission performance, these systems have been applied to a substantial portion of the important cable routes. Known as $K1$,[1] they provide 2,500,000 miles of long distance message circuits. More recently, a new and more economical system, known as $K2$, has been developed for this fast-growing network. Another 2,500,000 2-way message circuit miles are provided by $K2$ systems installed during the past three years.

General Description

To provide 12 satisfactory message circuits, a basic requirement imposed on the system is that the over-all transmission from the sending to the receiving end shall be only a few decibels and remain constant within very close limits. The $K2$ system is designed to be satisfactory over distances of 4,000 miles and more, with the necessary 240 or so tandem amplifiers and cable sections. At 60 kc the aggregate attenuation of the wires themselves in such a long cable path is about 16,000 decibels which in terms of power ratio is one followed by 1,600 zeros. Furthermore, in the transmission band from 12 to 60 kc this loss varies about 5,000 decibels with frequency. At each frequency, the cable loss must be balanced by an almost equal number of decibels of amplification so that the difference of these enormous quantities is a few decibels.[2] It is this difference, which must be stable and precisely controlled, that constitutes the over-all transmission of the system.

Although most of the cables are underground, the system also is used in aerial cables and both are exposed to substantial temperature changes during the year. Over a distance of 4,000 miles, the consequent variation in cable loss is upwards of 1,000 decibels. This must be compensated by an equal change in amplification under the control of a system of automatic regulation. Even though the variation in transmission caused by changes in cable temperature is much less than the fixed loss, the fact that the attenuation varies continuously in a complicated fashion makes the design of the automatic regulators a major problem. In the new system, regulation is accomplished with a minimum of apparatus and no moving parts by causing thermistors[3] to vary the gain of feed-back amplifiers. Because the output of each amplifier is individually regulated, errors in the outputs of the many amplifiers comprising a long system are not cumulative.

For transmission over a cable pair, the frequency allocation of the 12 telephone message channels is represented by the upper sidebands of 12 carrier frequencies, namely, 12, 16, 20 . . . . 52 and 56 kc. Since the lowest voice frequency transmitted over a channel is limited to frequencies above one to two hundred cycles and the highest a few hundred cycles below 4,000 cycles, "pilots" whose frequencies coincide with suppressed carriers and are 12, 28, and 56 kc can be located between channels and, as will be described, can be used to control regulators. A fourth pilot at 60 kc also lies outside the range of frequencies occupied by the channel side bands.

A simplified layout of a $K2$ system is shown in Figure 1. Matching the cable loss with gain to a high precision is accomplished with three kinds of amplifiers: "transmitting" (Figure 2), "line" (Figure 3) and "twist" (Figure 4). As the name implies, the transmitting amplifier occurs only at the sending end. Line amplifiers are by far the most numerous. Normally, they are spaced about 17 miles apart, although occasionally spans may be as short as 11 miles, and quite infrequently as long as 20 miles. At every fifth or sixth repeater station, if the cable is all aerial, and at longer intervals but not exceeding 15 stations if underground, a "twist amplifier" is used—so called because it also takes care of the variations in cable loss that are a function of both frequency and temperature. The three kinds of amplifiers are designed to complement each other in the over-all problem of compensating very precisely and yet automatically for the ever-changing cable loss.

Line amplifiers have three important functions. They provide the necessary high gain to make up for the loss of the preceding cable span; at an average temperature of the cable, they equalize for the variation of this loss between 12 and 60 kc; they regulate the gain automatically. Thereby they compensate for the major portion of the variation in transmission with temperature; namely, that portion which is independent of frequency and termed "flat gain".

This automatic flat-gain compensation is performed in a new and exceedingly simple manner. The amplifier is of the well known negative feed-back type.[4] Most of the power of the output tube is transmitted to the cable. The remainder

Paper 47-109, recommended by the AIEE committee on communication for presentation at the AIEE North Eastern District meeting, Worcester, Mass., April 23-25, 1947. Manuscript submitted November 13, 1946; made available for printing March 3, 1947.

H. S. Black is high frequency transmission engineer in the transmission development department of Bell Telephone Laboratories, Inc., New York, N. Y.; F. A. Brooks, A. J. Wier, and I. G. Wilson are members of the technical staff of Bell Telephone Laboratories.

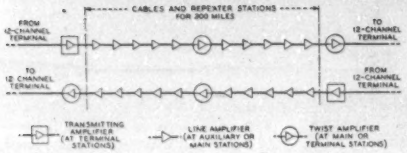

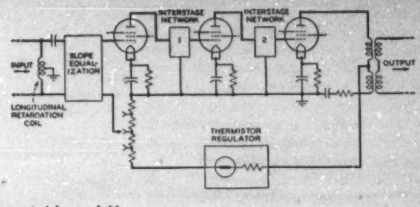

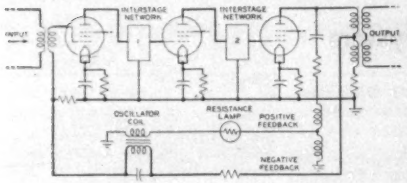

Figure 1 (above, left). Over-all layout of the *K*2 carrier-in-cable system showing three kinds of amplifiers

Figure 2 (left). Transmitting amplifier

Figure 3 (above, right). Line amplifier

flows through the feed-back circuit, in which is located a thermistor—a bead of temperature sensitive resistance material smaller than the head of an ordinary pin. Although this thermistor has considerable thermal lag so that it is slow to heat up and, hence, slow acting—nevertheless, it is so sensitive it responds to the weak currents in the feed-back path. Should the cable loss increase, for example, the thermistor resistance increases. This reduces the feedback and raises the gain of the amplifier. Thus, the thermistor maintains a constant rms value of currents at the output of the amplifier despite variations at the input. In this way, without any moving parts, changes in cable loss are compensated automatically.

To make such a scheme work, the transmitting amplifier must have some novel and interesting properties. In most systems, this amplifier merely raises the varying sideband or signal currents to a proper transmitting level. However, what each line amplifier needs is a constant value of input power, except as this changes due to variations in the loss of the preceding span. To accomplish this, the transmitting amplifier is made to oscillate at 60 kc, but in a peculiar manner. When no signal currents are present, it delivers a constant power to the cable, which holds the line amplifier thermistors at their proper resistance values. But when signal currents come on, the amplitude of the oscillations automatically decreases just the right amount so that the total rms output is constant. As a result, the gain of succeeding line amplifiers does not depend upon whether any of the 12 channels are busy.

This unusual operation of the transmitting amplifier is due to the simultaneous action of two feedbacks; one negative and one positive. The negative feedback path is quite orthodox and sets the amplifier gain at its required value. The positive path includes a thermistor, in this case a low-wattage resistance lamp, and an oscillator coil. Like other thermistor-controlled oscillators,[8] the oscillations increase in magnitude and heat the thermistor until its resistance is just the right value to make the loss of the positive feedback path equal to the gain of the amplifier. Although the tuned oscillator coil and positive feed-back limit the voltages fed back over this path to a narrow band of frequencies centered around 60 kc, the thermistor portion of this path is made equally responsive to all significant frequencies. Consequently, signal currents when present also flow through the thermistor and heat it. Because the resistance of the thermistor cannot change if the loss of the positive feedback path is to equal the gain of the amplifier, the oscillations, therefore, grow weaker until the rms or heating value of the signal currents plus oscillations becomes the same as that of the oscillations alone in the absence of signals. This automatically provides a nicety of control and insures constant rms output from the transmitting amplifier. The lamp has low thermal lag so that it substantially follows the signal variations.

Of the three types of amplifiers, the twist is the most complex. It not only does everything a line amplifier does but also compensates for variations in cable loss which are functions of frequency and temperature. Twist amplifiers are used only when these variations, which are small compared with the total, accumulate and necessitate their insertion. To control the gain of the twist amplifier, three weak sinusoidal waves having frequencies of 12, 28, and 56 kc are transmitted continuously to the line at constant magnitude. These "pilots" appear at the output of the twist amplifier, and are selected by narrow-band crystal filters and separately amplified. By suitable control circuits which change variable networks in the feed-back path, the gain of the amplifier at 12, 28 and 56 kc is set so that the output of each pilot is maintained quite constant. The 56-kc pilot controls a fast-acting flat-gain-regulator whose control element is a thermistor. Two variable equalizers controlled by the 12- and 28-kc pilots respectively are of the type described by H. W. Bode[4] in which the variable equalization is controlled by a single variable resistance. In the twist amplifiers, these variable resistances are thermistors.

Experience has shown that the *K*2 system based on this simple method of amplification, equalization, and regulation compensates accurately for the enormous and varying cable loss over distances of 4,000 miles and more.

Detailed Description

The publications previously referred to[1,2] together with other papers[7,5,9,10] present a comprehensive description of the *K*1 system. The discussion to follow is limited to additional important features of the *K*2 system.

Amplifiers

By relying on advanced techniques,[11,12] improved designs of negative feed-back amplifiers meet the extreme linearity and other exacting requirements imposed by amplifying 12 channels in a common amplifier and by operating many such amplifiers in tandem. The large amount of feedback necessary for this purpose is further increased because not only all of the automatic, but also a substantial part of the fixed gain adjustments are made by varying the loss of the feed-back path. Likewise, small low-figure-of-merit vacuum tubes having a reasonably long life and consuming a minimum of filament and plate power are used. Low figure of

merit tubes and high negative feedback over a broad band tend to be conflicting requirements.[11] Application of Nyquist's principle of conditional stability[12] (looped over amplifiers) as a practical means of solving this problem is one of the outstanding features of the $K2$ amplifiers.

The forward acting portion of each of the three amplifiers (Figures 2, 3, and 4) uses the same tubes and substantially the same parts. Each amplifier has two impedance-coupled stages followed by a power output stage. Although similar in many respects, the feed-back portions differ significantly because the function of each is markedly different. In each case, the maximum amplification without feedback is 115 decibels and the amount of negative feedback varies from about 40 to more than 60 decibels.

The good impedance match required between amplifier and cable is obtained by a simple hybrid coil feed-back connection at the output and by series feedback at the input. The low-side output impedance is controlled mainly by the impedance of the balancing network of the hybrid coil and is stabilized by the negative feedback action of the amplifier. At the input, the feedback reduces a substantial portion of the grid and transformer capacitances so that greater step-up can be used to override inherent tube noise and still obtain a satisfactory termination for the input equalizers.

Equalizers

Each line or twist amplifier provides basic equalization to compensate for the average characteristic at a predetermined temperature of the preceding section of cable. Additional slopes about this average allow spans of various lengths to be equalized. These characteristics are obtained essentially from the combination of the input transformer and equalizer. Elements are saved by using the distributed constants of the input transformer as part of the equalizer. Slopes equivalent to 13, 15, and 17.5 miles of cable are obtained merely by restrapping certain elements. With this feature, if it is found upon installation or subsequent line-up that a different slope is wanted, the change can be made readily. For the occasional 20-mile span, basic equalization is obtained by the use of an auxiliary equalizer to supplement the slope afforded by the 17.5-mile strapping.

With basic equalizers having so few parts, the over-all gain of the line and twist amplifiers (Figure 5) does not match the cable loss precisely. The differences are small and intentionally are given appropriate shapes which can be equalized readily and economically by a special deviation equalizer inserted at intervals of 5 to 8 repeater spans.

To aid in the reduction of unwanted noise and cross talk, all pairs in toll cables are highly balanced,[9] that is, each wire of a pair has a nearly like impedance to ground. An amplifier degrades these balances by only a trivial amount. Figure 3 illustrates how an unbalanced equalizer structure which saves elements is enabled to meet this high balance requirement simply by bridging a longitudinal retardation coil across the incoming pair and grounding the mid-point.

Regulators

As mentioned, each regulator measures its control signal and then makes an appropriate correction in the gain of the amplifier. A regulator following this principle is termed a "backward acting regulator." The fundamental concept of backward action as applied to a non-electrical regulator has been known for a long time. Likewise, it has long been a familiar experience in the operation of such regulators that, if the precision of control is made too exact, the system may hunt.

During the past 15 years, the technique of designing negative feed-back amplifiers has been developed to a high degree. The technique has been extended to cover a backward acting regulator by substituting the steady state envelope response of the loop path of the regulator, in place of the analogous steady state transmission response of the loop formed by the amplifier and feed-back path of a familiar feedback amplifier. This envelope response can be used either to apply Nyquist's criterion for stability to the backward acting regulator or to evaluate its transient behavior. These procedures were followed in the design of the $K2$ regulators. Figure 6 shows the steady state precision of control exercised by a line amplifier regulator.

In the $K2$ system there exists the additional problem of the stability of many regulators in tandem (Figure 7). Naturally, in a 4,000-mile system having more than 200 line amplifier regulators in tandem, this problem is complex.

Furthermore, in the case of the twist amplifier the gain is under the continuous control of three different regulators acting simultaneously. Here, not only does each regulator acting alone have to meet a tandem stability requirement, but, in addition, there is the more complicated question of their interaction, with the possibility that as many as 30 to 40 twist amplifiers may be operated in tandem.

The fast-acting 56-kc flat-gain regulator corrects for the imperfections of the line amplifier regulators inherent in the response characteristics shown by Figure 7. As mentioned, the 56-kc pilot is selected from the output by a crystal fil-

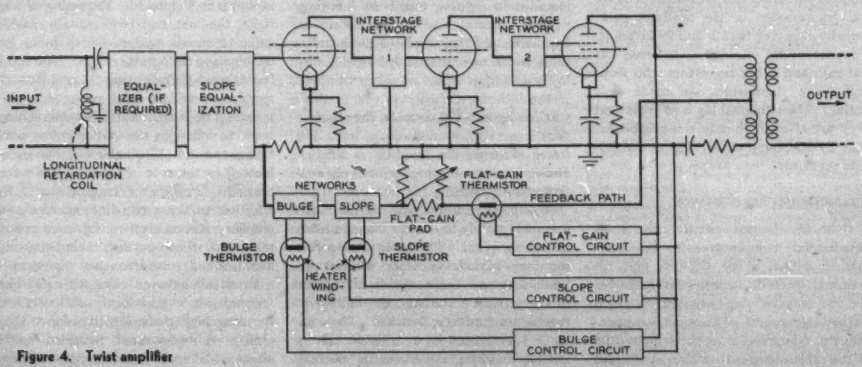

Figure 4. Twist amplifier

ter, amplified, rectified and used to control the output of an oscillator which supplies heater current to an indirectly heated thermistor.[3] This thermistor is in series with the feed-back path, but unlike a line amplifier regulator, is not heated appreciably by the signal currents. Figure 8 shows the typical steady state response and indicates the precision of control and operating range. Figure 9 shows the decibel response of these regulators as a function of time, to a sudden increase in input loss of one decibel.

The other two regulators used in a twist amplifier act similarly except that the resistance of each control thermistor (Figure 4) varies the loss characteristic of an equalizer located in the feed-back path. These equalizers are known as slope and bulge networks. The loss in the feed-back path, therefore, depends upon the combined loss of the flat-gain thermistor and these networks. It is necessary to select the pilot frequencies and network shapes so that the interactions are small.

For example, under the control of the 28-kc pilot, the convex or concave characteristics introduced by the bulge network produce their maximum change at 28 kc. At other frequencies, the loss variations are smaller. In particular, in the neighborhood of 12 kc, there is very little change in the attenuation of the bulge network as the resistance of its controlling thermistor changes. Similarly, although the characteristics of the slope network, which is controlled by the 12-kc pilot, change approximately linearly with frequency and pivot about a frequency in the neighborhood of 45 kc, the resulting variations in the loss of this network at 28-kc are sufficiently small so that interactions between regulators are minimized.

On the other hand, the 56-kc pilot controls the flat gain of the amplifier. Any changes in its control thermistor change the transmission of the feedback path, thereby changing the 12- and 28-kc pilots. To reduce the interaction between the flat-gain and other regulators, the slope and bulge thermistors are made slow acting. Their thermal lag is so great that they are affected to only a negligible extent by the rapid corrections of the flat-gain regulator.

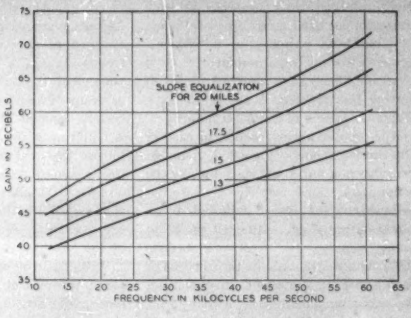

Figure 5. Typical gain-frequency characteristics of a line or twist amplifier

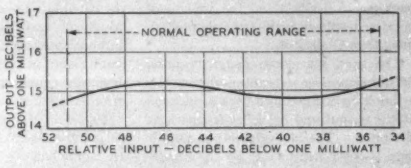

Figure 6. Typical steady state precision of control exercised by a line amplifier regulator

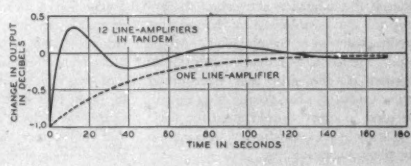

Figure 7. Decibel response of line amplifier regulators as a function of time to a sudden increase in input loss of one decibel

Transmission Performance

Over the longest circuits, the basic equalization compensates for the cable loss to within a few decibels and the terminals provide facilities for adjusting the transmission over individual channels to the value sought. The regulators maintain this transmission as the temperature of the cable changes to within about plus or minus one or two decibels. With the good transmission stability which these systems provide, they are used to carry the usual services encountered in the toll plant such as signaling, telephone messages, multichannel voice-frequency telegraph and high-quality program channels.

Equipment

In the larger centers, the equipment is installed in existing telephone buildings where systems may terminate. However, approximately two thirds of the installations are in new unattended single story brick buildings called auxiliary stations. If the ultimate capacity of one of these stations is 80 to 100 systems, the required floor space is about 600 square feet. For fewer systems, the building is smaller. Heating and ventilating facilities are controlled automatically.

About four times a year, routine visits are made mainly to test the vacuum tubes and power plant. This ability to operate for long periods of time without attendance is very important because some of the auxiliary stations are difficult to reach during adverse weather. The complete installation is so reliable that a trouble requiring attendance is unusual. However, if a major trouble occurs which might not be known at other stations, it is indicated in a controlling main station by an automatic system of alarms. Voice-frequency signaling and talking facilities provide the necessary maintenance communications between auxiliary and main stations.

A typical equipment arrangement for the east to west direction of transmission is shown in Figure 10. Beginning at the right, the first two bays contain sealed-cable terminals equipped with jacks for terminating the outside cables. The third bay is used for mounting the grid battery supply, alarm and other common equipment. The fourth and other succeeding bays, to follow as the station grows, contain amplifiers. A similar bay line-up is located to the rear of these bays for the opposite direction of transmission. In addition to these two lines of bays, an auxiliary station always contains a power plant and, when required, cable balancing facilities and voice-frequency repeaters.

Cross talk between office wiring at like transmission levels is kept sufficiently low by using high-grade low-impedance (135 ohms) rubber-covered shielded pairs about 3/8 inch in diameter. These

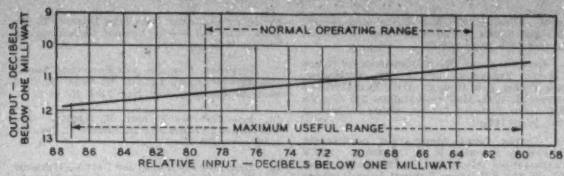

Figure 8 (above). Typical steady state response of the 56-kc flat-gain pilot-controlled regulator associated with a twist amplifier

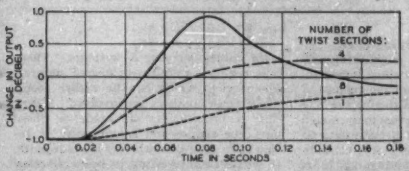

Figure 9 (left). Decibel response of 56-kc regulators as a function of time to a sudden increase in input loss of one decibel

Figure 10. Typical line of bays at a K2 auxiliary station

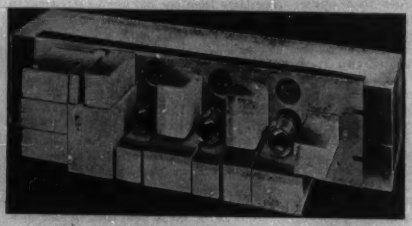

Figure 11. Front view of a line amplifier

hang loosely in the bay-cable duct and are laid on cable racks without sewing. Wiring carrying high-output power is separated from input wiring by segregating the outputs and inputs on the right and left sides respectively of the mounting bays. A cable duct type bay permits doing this in an efficient manner.

One of the difficult problems is to guarantee low cross talk between adjacent amplifier panels. For this purpose and to keep unwanted coupling within the amplifier to a sufficiently low value, direct wiring is used and all panels are flanged to overlap the can covers. On the line amplifier (Figure 11) nonmagnetic material for the panel and cover further helps to provide adequate shielding.

Since reduced maintenance is an important consideration, parallel sockets are used to simplify vacuum tube replacements. With this arrangement it is possible, because of the stabilizing effect of feedback, to replace tubes one at a time in a working system with no deleterious effects.

Three portable test sets[14] are provided for maintaining these systems. Simple activity checks made in a test set determine the condition of the tubes and whether they should be rejected. A transmission measuring set provides means for making accurate level measurements of the pilot frequencies on the high frequency line while a system is in service. This set, together with a high impedance probe, can be used for trouble shooting and measures the pilot currents on a bridging basis in the high impedance parts of the circuits. Stable frequencies from 12 to 60 kc for out-of-service tests are obtained from a test oscillator.

Uninterrupted service and infrequent maintenance necessitate continuous and dependable power supply sources. In main stations, regular 24-volt and 130-volt storage batteries are used in series for the plate supply. In auxiliary stations, a 152-volt battery is provided. The filaments are heated by regulated 60-vol 60-cycle alternating current fed to filament transformers located on each amplifier. In case of power failure, emergency power is obtained from the battery by means of an inverted converter. The converter starts automatically upon failure of outside power and before the filaments cool enough to affect appreciably the transmission performance of the feed-back amplifiers. During a protracted power failure, a portable engine driven generator is caused to charge the battery at an auxiliary station.

Conclusion

The development of the $K2$ system has provided improved performance at reduced cost, saved raw material, and aided in extending the carrier technique to a large fraction of old and new cable routes. By providing already about half of approximately 5,000,000 circuit miles of 2-way message facilities now furnished by K carrier, the $K2$ system represents an important step forward in making available, by the carrier-in-cable method, dependable long distance communications of high quality. This is a good example of the economies which can be effected by the application of research and development to a complex communication problem.

References

1. A Carrier System for Toll Cables, C. W. Green, E. I. Green. AIEE Transactions, volume 57, 1938, January section, pages 227–36; the *Bell System Technical Journal*, volume 17, January 1938, pages 80–105.

2. A Quarter Century of Transcontinental Telephony, Frank B. Jewett. Electrical Engineering, volume 59, January 1940, pages 3–11.

3. Properties and Uses of Thermistors—Thermally Sensitive Resistors, J. A. Becker, C. B. Green, G. L. Parsons. AIEE Transactions, volume 65, 1946, November section, pages 711–25; the *Bell System Technical Journal*, volume 26, January 1947, pages 170–212.

4. Stabilized Feedback Amplifiers, H. S. Black. AIEE Transactions, volume 53, 1934, January section, pages 114–20; the *Bell System Technical Journal*, volume 13, January 1934, pages 1–18.

5. The Bridge Stabilized Oscillator, **L. A. Meacham.** *Proceedings* of the Institute of Radio Engineers, volume 26, October 1938, pages 1278–94; the *Bell System Technical Journal*, volume 17, October 1938, pages 574–91.

6. Variable Equalizers, **H. W. Bode.** The *Bell System Technical Journal*, volume 17, April 1938, pages 229–44.

7. Cable Carrier Telephone Terminals, **R. W. Chestnut, L. M. Ilgenfritz, A. Kenner.** AIEE Transactions, volume 57, 1938, May section, pages 237–44; the *Bell System Technical Journal*, volume 17, January 1938, pages 106–24.

8. Crystal Channel Filters for the Cable Carrier System, **C. E. Lane.** AIEE Transactions, volume 57, 1938, May section, pages 245–49; the *Bell System Technical Journal*, volume 17, January 1938, pages 125–36.

9. Crosstalk and Noise Features of Cable Carrier Telephone System, **M. A. Weaver, R. S. Tucker, P. S. Darnell.** AIEE Transactions, volume 57, 1938, May section, pages 250–59; the *Bell System Technical Journal*, volume 17, January 1938, pages 137–61.

10. Copper Oxide Modulators in Carrier Telephone Systems, **R. S. Caruthers.** AIEE Transactions, volume 58, 1939, June section, pages 253–60; the *Bell System Technical Journal*, volume 18, April 1939, pages 315–37.

11. Relations Between Attenuation and Phase in Feedback Amplifier Design, **H. W. Bode.** The *Bell System Technical Journal*, volume 19, July 1940, pages 421–54.

12. Network Analysis and Feedback Amplifier Design (book), **Hendrik W. Bode.** D. Van Nostrand Company, Inc., New York, N. Y.

13. Regeneration Theory, **H. Nyquist.** The *Bell System Technical Journal*, volume 11, January 1932, pages 126–47.

14. New Test Equipment and Testing Methods for Cable Carrier Systems, **W. H. Tidd, S. Rosen, H. A. Wenk.** AIEE Transactions, volume 66, 1947, pages 726–30.

Discussion

J. P. Thurber (nonmember; New England Telephone and Telegraph Company, Boston, Mass.): I have followed with interest the paper which we have just heard on the *K-2* system.

The New England Telephone and Telegraph Company first turned to *K* operation on the Boston–Portland run in 1942, in which year three systems were installed for a total of about 360 system miles. By the end of 1947 it is estimated that there will be three routes on which both aerial and underground *K-1* and *K-2* operation will be used with a total of 20 systems operating over 2,200 system miles. These systems will give a total of 25,000 channel miles. In this connection it is interesting to note that if the circuits now using *K* had to be provided by cable there would be an increase of 300 million conductor feet in the New England Company copper requirements, or more than enough wire to circle the world twice with a single conductor.

The use of *K* systems thus has changed materially the method of engineering new plant on main toll routes since it has reduced the size of cables and the amount of loading on these routes. Although the *K-2* system has not been in service long enough for us to have very comprehensive data on its performance in this territory, all indications point to a material advantage in its use, particularly in changing the flat gain regulator from the old mechanical type to the new thermistor type. Again, due to the fact that there will be 12 circuits in service for each *K* carrier system and that the removal of any one system from service would put all 12 circuits out of order, it is believed that the use of parallel sockets will be an advantage in keeping systems in service during tube replacements.

It might be pointed out here that with the 60-volt a-c filament supply feature of the *K-2* system the associated 152-volt battery can be smaller than the similar battery used in the *K-1* system.

It is to be noted also that in the New England Telephone and Telegraph Company territory, or in one similar, it may be desirable to have taps introducing voice open wire or branch cable circuits into the main cables carrying *K* systems. These taps require carefully engineered suppression devices which can be rather costly where large numbers are involved. Every time rearrangements are made on these taps, the suppression layout must be reviewed to determine whether it is adequate. It would be interesting to know whether any development work is under way to reduce the need for these devices.

H. S. Black: The authors wish to thank J. P. Thurber for his comments on their paper. One of the principal requirements of any communication system is that the signal-to-noise ratio be satisfactory. In a practical systems layout, voice circuits are brought into the cable at various points along the route, and it is necessary to take special precautions to insure that these circuits are sufficiently free of high-frequency noise. With present available techniques, studies indicate that the use of the suppression devices referred to in Thurber's discussion represent the most economical method of mitigating noise from these sources.

The Transient-Energy Method of Calculating Stability

P. C. MAGNUSSON
MEMBER AIEE

Synopsis: The transient-energy method is a newly developed means of checking and quantitatively evaluating the transient stability of a system of three, or possibly more, synchronous machines. Each machine is represented by a constant-magnitude voltage behind a fixed reactance (usually the transient reactance) and all losses and nonsynchronous loads are assumed to be constant throughout the transient. The method is developed in this paper specifically for the 3-machine problem and is demonstrated in two examples. The potential energy required to displace the machine rotors from the relative positions which they would occupy in steady-state after-transient operation is the basic function utilized; it may be expressed as a scalar potential function of two rotor-difference angles. Two critical (zero-slope) points of the potential energy function are located graphically; those points are

1. The minimum, which is the locus of steady-state, after-transient operation.

2. The minimax, the rotor-difference-angle combination at which stability may be lost with the smallest amount of transient energy.

The potential energy of (2) with respect to (1) is computed and compared with the initial transient energy, calculated with respect to condition 1. If the allowable transient energy (former) exceeds the actual transient energy (latter), the system is stable.

THE TRANSIENT STABILITY of a system of three or more synchronous machines customarily has been determined by solving numerically the differential equations of the motion of the rotors.[1] For convenience this may be called the rotor-motion method. In this paper another attack, the transient-energy method, will be developed and demonstrated in the 3-machine problem.

The latter method answers the stability question without following the individual rotor movements from one instant to the next. In event the transient is compound, that is, consisting of two or more circuit changes initiated in quick succession, the transient-energy method is applicable only to the final transient. The rotor-motion method would be used for the time interval between the first and last circuit changes, an interval which is usually short compared with the duration of the complete transient.

In this treatment each machine will be represented by a constant-magnitude voltage behind the corresponding transient reactance, and the losses will be assumed constant. The latter may be regarded either as resistance shunts around the voltage sources just mentioned, or as constant torques which are combined with the external torques of the prime movers and loads. The angular differences between the voltage-behind-transient-reactance vectors and the positions of the respective field structures will be neglected, and the term "rotor position" considered synonymous with both.

The following steps are taken in applying the transient-energy method to a specific problem:

1. Determine the rotor-difference angles for steady-state operation of the system as it exists after the transient.

2. Determine that combination of rotor-difference angles at which stability can be lost, which can be attained from (1) with the smallest amount of transient energy.

3. Compute the potential energy of the latter rotor-difference-angle combination with respect to the former.

4. Determine the initial conditions (rotor-difference angles and rotor velocities relative to synchronous speed).

5. Compute the transient energy inherent in the initial conditions with respect to (1), and compare the result with that obtained in (3).

This is illustrated in the two examples in Appendix I.

A novel feature of the transient-energy method is that it provides a quantitative measure of the degree of stability or instability pertaining to a given set of parameters, which aids interpolation and the comparison of slightly differing systems.

Derivation of Transient-Energy Method

The equal-area method,[1,2] which readily may be applied to many 2-machine problems, makes a good starting point for the derivation of the multimachine transient-energy plan. Both are based on the principle of conservation of energy, and both apply the conservation principle to the energy which is available for transient relative motion of the rotors.

Equal-Area Solution of 2-Machine Problem

The circuit for a simple 2-machine problem is shown in Figure 1; the transient to be studied is that which results when circuit breaker A is opened. The lower half of Figure 2 shows the usual diagram for the equal-area solution.

Since the machines may have different numbers of poles, torques will be stated in terms of electrical rather than mechanical units, that is, torque is equal to power divided by synchronous angular velocity. Deviations from synchronous speed by the individual machines during the transient are neglected, hence the ratio between torque and power remains constant.

Let

$$T_1 = -[(e_1e_2)/(X_p\omega_s)] \sin (\delta_1 - \delta_2)$$
$$T_2 = -[(e_1e_2)/(X_p\omega_s)] \sin (\delta_2 - \delta_1)$$

Here T_1 and T_2 are the instantaneous torques during the transient exerted by the electric system on the rotors of machines 1 and 2, respectively, and e_1 and

Paper 47-90, recommended by the AIEE committees on electric machinery and power generation for presentation at the AIEE winter meeting, New York, N. Y., January 27-31, 1947. Manuscript submitted August 19, 1946; made available for printing December 23, 1946.

P. C. MAGNUSSON is assistant professor of electrical engineering, Oregon State College, Corvallis, Oreg. He was a member of the system engineering staff of Bonneville Power Administration, Portland, Oreg., at the time he prepared this paper.

e_2 are the voltages behind transient reactance. The "electrical speed" or synchronous angular velocity is ω_0, and δ_1 and δ_2 are the displacements (in electrical degrees) of the rotors of machines 1 and 2 from an arbitrary base which rotates at synchronous speed. Torques and rotor angles are considered positive when they are in the direction o rotation. The subscript F used in this paper indicates steady-state conditions after the transient.

From Figure 1

$$X_F = X'_{d1} + X_{12} + X_L + X_{13} + X'_{d2}$$

Let

$$T_{MF} = (e_1 e_2)/(X_F \omega_0)$$

and

$$\delta = \delta_1 - \delta_2$$

Then

$$T_1 = -T_{MF} \sin \delta \tag{1}$$

The prime mover torque T_{1t} impressed on the generator (machine 1) and the load torque T_{2t} on the motor (machine 2) will be equal and opposite to the torques T_1 and T_2 when the system is in steady-state operation. This sign convention is in accordance with the principle that the summation of the torques acting on a body is equal to zero.

$$\left.\begin{aligned} T_1 &= -T_1 \text{ when } \delta = \delta_F \\ T_{1t} &= T_{MF} \sin \delta_F \\ T_{2t} &= -T_{MF} \sin \delta_F \end{aligned}\right\} \tag{2}$$

The external torques T_{1t} and T_{2t} will be assumed constant throughout the transient The initial rotor-displacement angle δ_0 is determined by the external torques and the network before opening circuit breaker A, as follows:

$$T_{1t} = [(e_1 e_2)/(X_{0\omega_0})] \sin \delta_0$$
$$X_0 = X'_{d1} + X_{12} + (X_L/2) + X_{13} + X'_{d2}$$

In addition, let

δ_S = maximum value of δ attained during the transient

δ_L = maximum value of δ for which net torque tends to decrease angular displacement

Given δ_0, the equal-area criterion requires that δ_S be such that area *cde* (Figure 2) equals area *abc*. With δ'_0 as the initial angle, the system would be unstable, for area *cgh* is greater than area *cdfec*, which is the maximum available "restoring area."

The integral of a torque with respect to the angle through which it acts is the work done, or energy transferred, in the process. Thus the area *abc* represents the potential energy inherent in the initial displacement of δ from δ_F at the beginning of the transient. This potential energy has been tranformed into kinetic energy when δ equals δ_F, and is returned to the potential form while δ increases up to δ_S. Angle δ then will decrease back to δ_0, during which time the energy goes into the kinetic form again, and then back to potential. Since the idealized problem provides no damping for this motion, it will continue with this amplitude indefinitely.

Solution in Terms of Potential Energy Function

The integral of $-(T_1 + T_{1t})$ with respect to δ is the transient potential energy, and will be indicated by V. It is plotted as the upper curve in Figure 2. The potential energy at δ_F, the angle for steady-state operation after the transient, is taken as zero. The particular angle for which V is computed will be designated as δ_R in the following integration

$$V = -\int_{\delta_F}^{\delta_R} (T_1 + T_{1t}) d\delta \tag{3}$$

Equations 1 and 2 are substituted into equation 3.

$$\begin{aligned} V &= T_{MF} \int_{\delta_F}^{\delta_R} (\sin \delta - \sin \delta_F) d\delta \\ &= T_{MF} [\cos \delta_F - \cos \delta_R - (\delta_R - \delta_F) \times \sin \delta_F] \end{aligned} \tag{4}$$

The subscript R, used to denote the upper limit of integration, will be dropped hereafter.

The potential energies V_0 and V_S are equal; the system will be stable for any initial angle δ_0 for which V_0 is less than V_L. The potential energy function V is analyzed in some detail in Appendix III.

Extension to Three Machines

Derivation of Formula for Transient Potential Energy

The foregoing derivation of an expression for the potential energy V inherent in a rotor angle displacement other than the steady-state value may be extended readily to include three machines. Let the network which exists after the transient be reduced by means of standard transformations (Y-delta, delta-Y, and star-mesh) to the form of Figure 3, in which e_1, e_2, and e_3 are constant-magnitude voltages behind the transient reactances of the respective machines. In general, the network elements in the reduced circuit will include resistance as well as reactance, but usually the former will be small compared to the latter in those elements which link one voltage source with

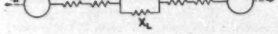

Figure 1 (above). One-line diagram for 2-machine problem

Figure 2 (below). Equal-area solution and transient-potential-energy function for 2-machine problem

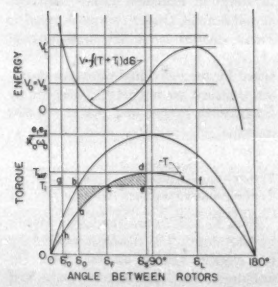

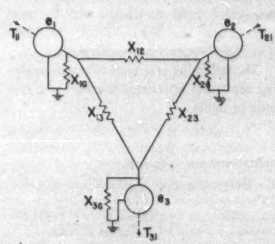

Figure 3. Reduced 1-line diagram for 3-machine problem

Figure 4. Critical points of function of two variables

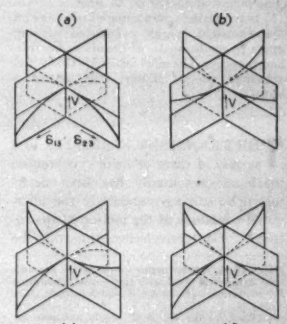

(a)—Maximum
(b)—Minimum
(c)—Minimax
(d)—Inflected surface with horizontal tangent plane

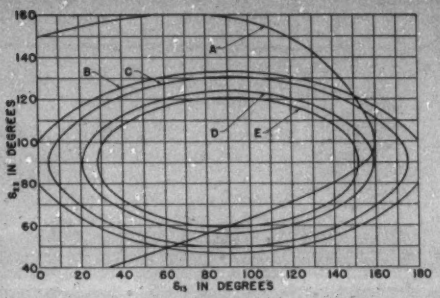

Figure 5. Loci of equations for critical points for examples *A* and *B*

See accompanying table

Reference Table for Figure 5

Curve	Locus of Equation	Input Powers in Per Unit P_1	P_3
A	15	0.50	
B	16	0.22	0.50
C	16	0.25	0.50
D	16	0.30	0.50
E	16	0.32	0.50

another. The oscillatory system may be made conservative, and thereby more readily subject to analysis, if the power consumed in the elements just mentioned is assumed to remain constant, at steady-state value, throughout the transient. The power consumed in those elements which shunt individual voltage sources will be constant, hence the entire power consumption of the static network under steady-state conditions may be computed, suitably apportioned among the synchronous machines, and the respective portion subtracted from the total power inpu of each generator, and added to the power output of each synchronous motor. The static network then, as far as intermachine power-flow relations are concerned, may be assumed (without great error) to consist of three pure reactances, X_{12}, X_{13} and X_{23}, as shown in Figure 3. The shunt reactances X_{1G}, X_{2G}, and X_{3G} have no effect on the machine torques.

The rotor angles, with respect to an arbitrary base which rotates at synchronous speed, may be taken as δ_1, δ_2, and δ_3.

Let

$$\left.\begin{aligned} T_{12M} &= (e_1e_2)/(X_{12}\omega_0) \\ T_{13M} &= (e_1e_3)/(X_{13}\omega_0) \\ T_{23M} &= (e_2e_3)/(X_{23}\omega_0) \end{aligned}\right\} \quad (5)$$

As in the 2-machine problem, the torques T_1 and so on will be regarded as the torques exerted on the rotors by the electric system.

Then

$$\left.\begin{aligned} -T_1 &= T_{12M}\sin(\delta_1-\delta_2) + T_{13M}\sin(\delta_1-\delta_3) \\ -T_2 &= -T_{12M}\sin(\delta_1-\delta_2) + T_{23M}\sin(\delta_2-\delta_3) \\ -T_3 &= -T_{13M}\sin(\delta_1-\delta_3) - T_{23M}\sin(\delta_2-\delta_3) \end{aligned}\right\} \quad (6)$$

The torques impressed by the prime movers or loads on the machines (after adjustment for proportionate share of loss in the static network) will be assumed constant, and will be indicated by T_{1t}, T_{2t}, and T_{3t}. These torques are equal and opposite to T_1, T_2, and T_3 during steady-state after-transient operation. The external torques are equal to the powers of the respective supplies or loads P_1, P_2, and P_3, divided by the synchronous angular velocity. The rotor angles corresponding to steady-state operation will be designated by δ_{1F}, δ_{2F}, and δ_{3F}.

Thus

$$\left.\begin{aligned} P_1/\omega_0 = T_{1t} &= T_{12M}\sin(\delta_{1F}-\delta_{2F}) + T_{13M}\sin(\delta_{1F}-\delta_{3F}) \\ P_2/\omega_0 = T_{2t} &= -T_{12M}\sin(\delta_{1F}-\delta_{2F}) + T_{23M}\sin(\delta_{2F}-\delta_{3F}) \\ P_3/\omega_0 = T_{3t} &= -T_{13M}\sin(\delta_{1F}-\delta_{3F}) - T_{23M}\sin(\delta_{2F}-\delta_{3F}) \end{aligned}\right\} \quad (7)$$

It is desired to find the potential energy, with respect to the steady-state condition, which the system has when the rotor angles have a different set of values δ_{1R}, δ_{2R}, and δ_{3R}. The net torques acting when the rotors are in other than steady-state relative positions are found by subtracting equations 7 from equations 6.

$$\left.\begin{aligned} -(T_1+T_{1t}) &= T_{12M}[\sin(\delta_1-\delta_2) - \sin(\delta_{1F}-\delta_{2F})] + T_{13M}[\sin(\delta_1-\delta_3) - \sin(\delta_{1F}-\delta_{3F})] \\ -(T_2+T_{2t}) &= -T_{12M}[\sin(\delta_1-\delta_2) - \sin(\delta_{1F}-\delta_{2F})] + T_{23M}\times[\sin(\delta_2-\delta_3) - \sin(\delta_{2F}-\delta_{3F})] \\ -(T_3+T_{3t}) &= -T_{13M}[\sin(\delta_1-\delta_3) - \sin(\delta_{1F}-\delta_{3F})] - T_{23M}[\sin(\delta_2-\delta_3) - \sin(\delta_{2F}-\delta_{3F})] \end{aligned}\right\} \quad (8)$$

The rotor of machine 1 will be displaced first, then that of machine 2, and finally that of machine 3.

$$V = -\int_{\delta_{1F}}^{\delta_{1R}} (T_1+T_{1t})d\delta_1 \quad (\text{with } \delta_2=\delta_{2F} \text{ and } \delta_3=\delta_{3F})$$
$$-\int_{\delta_{2F}}^{\delta_{2R}} (T_2+T_{2t})d\delta_2 \quad (\text{with } \delta_1=\delta_{1R} \text{ and } \delta_3=\delta_{3F})$$
$$-\int_{\delta_{3F}}^{\delta_{3R}} (T_3+T_{3t})d\delta_3 \quad (\text{with } \delta_1=\delta_{1R} \text{ and } \delta_2=\delta_{2R})$$

After integration, substitution of limits and collection of like terms, the following expression is obtained for V:

$$\begin{aligned} V = T_{12M}[&\cos(\delta_{1F}-\delta_{2F}) - \cos(\delta_{1R}-\delta_{2R}) - (\delta_{1R}-\delta_{1F}-\delta_{2R}+\delta_{2F})\times \\ &\sin(\delta_{1F}-\delta_{2F})] + T_{13M}[\cos(\delta_{1F}-\delta_{3F}) - \\ &\cos(\delta_{1R}-\delta_{3R}) - (\delta_{1R}-\delta_{1F}-\delta_{3R}+\delta_{3F})\times \\ &\sin(\delta_{1F}-\delta_{3F})] + T_{23M}[\cos(\delta_{2F}-\delta_{3F}) - \\ &\cos(\delta_{2R}-\delta_{3R}) - (\delta_{2R}-\delta_{2F}-\delta_{3R}+\delta_{3F})\times \\ &\sin(\delta_{2F}-\delta_{3F})] \end{aligned}$$

This may be simplified by means of the following substitutions:

$$\left.\begin{aligned} \delta_1-\delta_3 &= \delta_{13} \\ \delta_2-\delta_3 &= \delta_{23} \\ \delta_1-\delta_2 &= \delta_{13}-\delta_{23} \end{aligned}\right\} \quad (9)$$

The subscript R which was used to denote the upper limit of integration will be omitted henceforth.

$$\left.\begin{aligned} V = T_{12M}[&\cos(\delta_{12F}-\delta_{22F}) - \cos(\delta_{13}-\delta_{23}) - (\delta_{13}-\delta_{13F}-\delta_{23}+\delta_{23F})\sin(\delta_{13F}-\delta_{23F})] + \\ &T_{13M}[\cos\delta_{13F} - \cos\delta_{13} - (\delta_{13}-\delta_{13F})\times \sin\delta_{13F}] + T_{23M}[\cos\delta_{23F} - \\ &\cos\delta_{23}(\delta_{23}-\delta_{23F})\sin\delta_{23F}] \end{aligned}\right\} \quad (10)$$

The value of V is independent of the order in which the displacements in δ_1, δ_2, and δ_3 were made; the function V can be shown to be a scalar potential function of the two generalized co-ordinates δ_{13} and δ_{23} because the curl of the gradient of V vanishes identically.[2]

Nature of Potential Energy Function

Whereas in the 2-machine problem the transient potential energy V was a function of a single independent variable δ, and could be represented geometrically by a curve on a plane, in the 3-machine problem V is a function of the two independent variables δ_{13} and δ_{23}, and may be represented geometrically as a surface above a co-ordinate plane, on which the abscissas δ_{13} and δ_{23} are perpendicular to each other.

The critical points of the V surface, that is, those points at which the surface has zero slope, are of principal interest in this study. They may be located by means of the following necessary conditions:

$$\left.\begin{aligned} \partial V/\partial\delta_{13} &= 0 \\ \partial V/\partial\delta_{23} &= 0 \end{aligned}\right\} \quad (11)$$

Three types of critical point ordinarily may be expected in the function V for transient-stability studies

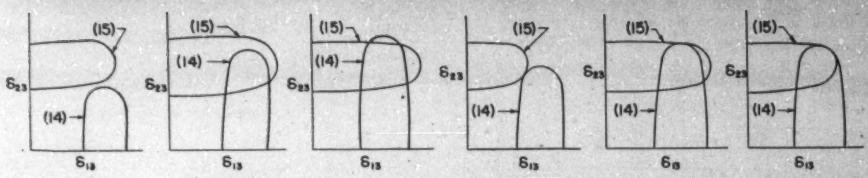

(a)—No real roots (b)—Two single real roots (c)—Four single real roots (d)—One double real root (e)—One double and two single real roots (f)—One triple and one single real root

Figure 6. Roots of equations 14 and 15 in terms of loci

1. Relative minima, at which V has a lower value than at any near-by point.
2. Relative maxima, at which V has a greater value than at any near-by point.
3. Minimaxs.

The surface surrounding a point of the last-named class resembles that of a saddle; if a small circle is drawn around it on the surface, the curve first will be below the critical point, then above it, again below it, and again above it, finally returning to the start below the critical point. In Figure 4, (*a*), (*b*), (*c*), and (*d*) illustrate a maximum, minimum, minimax, and an inflected surface with horizontal tangent plane, respectively. This last-named type of critical point may arise occasionally, but it is of only incidental importance in the application of the transient-energy method. The potential energy function is discussed further in Appendix III, with particular reference to the critical points.

Determination of Required Rotor-Difference Angles

The δ co-ordinates of a minimum and a minimax of the V surface are the rotor-difference angles required in items 1 and 2 of the summary of the transient-energy method given in the introduction. To locate the minimum and minimax, equation 10 is differentiated and substituted into equation 11, and the result simplified by substitution of equations 7.

$$\left.\begin{aligned} T_{13M}\sin(\delta_{13}-\delta_{23})+T_{13M}\sin\delta_{13}-T_{1i}=0\\ -T_{13M}\sin(\delta_{13}-\delta_{23})+T_{23M}\sin\delta_{23}-T_{2i}=0\end{aligned}\right\} \quad (12)$$

Equations 12 are equivalent to stating that the net torques at the machines are zero at angular displacements corresponding to the critical points of V. The number of parameters may be reduced, and equations 12 made dimensionless, by dividing each term by T_{13M}.

Let

$$\left.\begin{aligned} T_{1i}/T_{13M}&=k_1\\ T_{2i}/T_{13M}&=k_2\\ T_{13M}/T_{13M}&=k_3\\ T_{23M}/T_{13M}&=k_4\end{aligned}\right\} \quad (13)$$

Equations 12 then become

$$\sin(\delta_{13}-\delta_{23})+k_3\sin\delta_{13}-k_1=0 \quad (14)$$

$$-\sin(\delta_{13}-\delta_{23})+k_4\sin\delta_{23}-k_2=0 \quad (15)$$

The sum of these two equations is

$$k_3\sin\delta_{13}+k_4\sin\delta_{23}-k_1-k_2=0 \quad (16)$$

The critical points now are found readily by plotting the loci of any two of equations 14, 15, and 16; intersections are real roots of the equation set. For equation 14, choose values of δ_{13} and solve for δ_{23}; the reverse process should be used for equation 15. The solution of this set of equations is illustrated in Figure 5.

Zero, two, or four real roots may result from equations 14, 15, and 16, depending on the k parameters. Coincident real roots, which result when the loci of equations 14, 15, and 16 are tangent to on another at a point (see Figure 6*d*, *e*, and *f*) are discussed in Appendix III. In case there are no real roots (Figure 6*a*), the "after-transient" system is statically unstable under torques T_{1i} and T_{2i}.

With two real roots (Figure 6*b*), one proves to be a minimum, which is the point of steady-state operation, and the other, a minimax. When four roots are real (Figure 6*c*), one will be a minimum, one a maximum, and two will be minimaxs. It is the lower of the two minimaxs

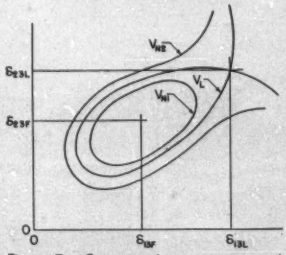

Figure 7 Contours of transient potential energy

which is of interest in transient stability; the selection is made by substituting the corresponding values of δ_{13} and δ_{23} into equation 10, the formula for V. The potential energy at the lower minimax (or at the minimax, if only one) will be designated as V_L.

For all values of V less than V_L, contours of constant V will be closed curves which encircle point δ_{13F}; δ_{23F} (see Figure 7). Contours of V slightly greater than V_L will not be closed; they partially will encircle δ_{13F}; δ_{23F}, approach closure near δ_{13L}; δ_{23L}, but then spread apart. The width of the "gap" near δ_{13L}; δ_{23L} increases as the value of V is increased.

Physical Interpretation of V Surface

If the total transient energy (kinetic plus potential) of the system is equal to some particular value V_N, and (as here assumed) the transient motion is undamped, the path of motion in terms of δ_{13} and δ_{23} eventually will come infinitesimally close to every point within the contour of V_N. This is known as quasi-ergodic motion;[3] it is to be expected rather than multiply-periodic motion because of the nonlinear torque-versus-angle function. A rigorous proof of this energy-transfer phenomenon will not be given here, but a familiar example, that of two pendulums suspended from a common cord (see Figure 8) will be pointed out as a rough analogy.

In this pendulum system, if pendulum A is started swinging while pendulum B is at rest, B will begin quickly to swing with increasing amplitude, while the amplitude of the motion of A decreases to zero. Then the process reverses, with the amplitude of A increasing back to its original amount, and that of B simultaneously decreasing back to zero. This process goes on indefinitely.

Thus, if the contour V_{N1} is closed (V_{N1} less than V_L) (see Figure 7) and the system is undamped, the rotors may be expected to oscillate with respect to one another with ever-varying amplitudes and rates. But the net torques will always be such as to tend to return the rotors to a steady-state rotor angle com-

bination corresponding to zero transient energy. Should the contour V_{N3} not be closed (V_{N3} greater than V_L), the torques at some time (possibly after several apparently stable oscillations) will tend to drive the rotors farther from the steady-state relation, and the rotor-difference angles relating one machine to the remaining two then will increase without limit, and stability will have been lost.

Initial Conditions

The remaining step is that of computing the initial transient energy, so that it may be compared with the V_L corresponding to the assumed load conditions. The initial transient energy includes both transient potential energy and transient kinetic energy; the latter is zero in case the rotors are not moving relative to synchronous speed at the start of the transient, (or start of the final transient, in the case of a compound transient).

Simple Transient

A simple transient will be defined as one in which all changes in the system parameters (network reactances or external torques or both) occur at the same instant. Then, if the system is not hunting at the moment before the transient, the initial transient kinetic energy is zero.

The initial rotor difference angles δ_{130} and δ_{230} may be found from the following equations:

$$\left.\begin{aligned} T_{1t} &= [(e_1e_3)/(X_{130}\omega_0)]\sin(\delta_{130}-\delta_{230}) + \\ &\quad [(e_1e_2)/(X_{120}\omega_0)]\sin\delta_{130} \\ T_{2t} &= -[(e_1e_3)/(X_{130}\omega_0)]\sin(\delta_{130}-\delta_{230}) + \\ &\quad [(e_2e_3)/(X_{230}\omega_0)]\sin\delta_{230} \end{aligned}\right\} \quad (17)$$

Here X_{130}, X_{120}, and X_{230} are the branch reactances of the equivalent delta network before the transient. It will be noted that these equations closely resemble equation 7; the method of solution is similar to that used for equations 14 and 15. Only the steady-state result (minimum) is of value.

The initial potential energy now may be found by substituting δ_{130} and δ_{230} for δ_{13} and δ_{23} in equation 10.

Compound Transient

A compound transient will be defined as one in which changes in the system parameters (network reactances or external torques or both) occur at two or more distinct times. An example of this situation is that which results when a fault is cleared a finite time after its occurrence by sequential opening of the two ends of the line involved. The transient-energy method is applied only to the "final transient", that is, the transient which takes place after the last change in system parameters. In the application of the transient-energy method, the "initial conditions" are those which prevail at the beginning of the final transient.

The procedure is first to calculate, by standard point-by-point methods, the motion of the machine rotors up to the time of the final change in the system parameters. This is illustrated in Appendix I*B*. Let δ_{13f} and δ_{23f} indicate the rotor displacement angles at this instant, and $\Delta\omega_{1f}$, $\Delta\omega_{2f}$, and $\Delta\omega_{3f}$ indicate the angular velocities of the rotors relative to synchronous speed in electrical radians per second. The transient kinetic energy ΔW which the system has gained up to that time is given by the following equation, which is derived in Appendix II.

$$\Delta W = (1/2)[I_1(\Delta\omega_{1f})^2 + I_2(\Delta\omega_{2f})^2 + I_3(\Delta\omega_{3f})^2] \quad (18)$$

Here I_1, I_2, and I_3 are the moments of inertia of the respective machines, in per unit torque seconds squared. They may be computed from the physical characteristics of the machines or estimated from the inertia energy quantity H as indicated in Appendix II, equations 22 and 19, respectively.

The initial transient potential energy is found by substituting δ_{13f} and δ_{23f} for δ_{13} and δ_{23} in equation 10.

More General Systems

Extension of the transient-energy method on a rigorous basis to systems of three or more machines linked with networks containing resistances does not appear feasible, although the equal-area method has been successfully applied to a 2-machine problem involving a general network.[1,4]

Theoretically the transient-energy method may be extended to an n-machine system linked with a purely reactive network. The labor involved in solving the equations for the critical points of the potential energy function increases rapidly with the number of machines, but a network calculating board could be used advantageously for that purpose. In addition, the increase in the number of independent variables increases the complexity of the possible configurations which the potential energy function might assume at each critical point, and this would call for careful investigation.

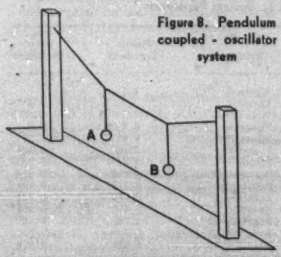

Figure 8. Pendulum coupled - oscillator system

Conclusions

In this paper the transient-energy method was developed for and applied to the 3-machine case. The method has been checked by comparison with results obtained by a standard point-by-point, rotor-motion solution (Appendix I*A*).

The margin by which the allowable transient energy exceeds the initial energy actually present, or vice versa, gives a quantitative basis or comparing various fault and load conditions. By interpolation of this margin of transient energy, limiting loadings readily may be found.

Appendix I. Illustrative Problems

Per unit quantities will be used throughout these examples, the circuits for which are given in Figure 9. When torque, power, and energy are expressed in terms of per unit, the following relationships are true:

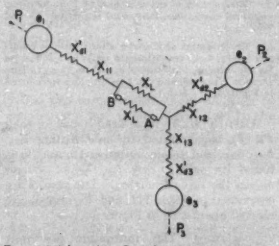

Figure 9 (above). One-line diagram for 3-machine problem

Figure 10 (below). Allowable and actual transient energies

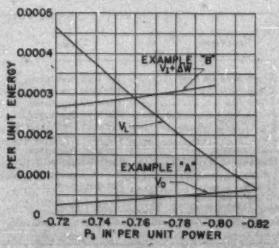

(Torque) = (power)/(synchronous angular velocity in electrical radians per second)

(Energy) = (torque) × (angle in electrical radians)

= (power) × (time in seconds)

The following quantities will be assumed in both problems:

Voltages behind transient reactance:

$e_1 = 1.2$ per unit voltage

$e_2 = 1.0$ per unit voltage

$e_3 = 0.9$ per unit voltage

Generator input power:

$P_2 = 0.5$ per unit power

The power P_1 supplied by generator 1 will be assumed equal to the motor load P_3 less P_2.

A. Power Limit With Simple Transient

Let the transient consist of opening circuit breaker A (Figure 9); find the heaviest motor load P_3 which the system can carry without losing synchronism during this transient.

Solution. The networks before and after the transient are reduced to the form shown in Figure 3. The system parameters are computed for both before and after-transient conditions from equations 5 and 13, and are listed in Table I.

For each assumed value of P_3 the following quantities are found:

1. The location of the minimum of V under before-transient conditions, (δ_{13B}; δ_{23B}) (equations 17).

2. The location of the minimum of V under after-transient conditions, (δ_{13F}; δ_{23F}) (equations 15 and 16).

3. The minimax of V under after-transient conditions (δ_{13L}; δ_{23L}) (equations 15 and 16). Schedules for the numerical solution of equations 15 and 16 are given in Table II, and the resulting loci are plotted in Figure 5.

After the six δ's have been found for each P_3, V_L is computed by substituting δ_{13L}, δ_{23L}, δ_{13F}, and δ_{23F} in equation 10, and V_0 is found by substituting δ_{130}, δ_{230}, δ_{13F}, and δ_{23F} in the same equation. The results are assembled in Table III, and V_L and V_0 are plotted against P_3 in Figure 10.

Conclusion. The maximum per unit load for P_3 for stable operation under this transient is 0.82.

Check by Rotor-Motion Method. This problem was also worked by the rotor-motion method, using method III (Dahl's classification[4]) for the point-by-point calculation, and using three different sets of inertia constants. With P_1 and P_3 taken as 0.32 and −0.82, respectively, the system failed to lose stability on the first swing, but when P_1 and P_3 were increased to 0.325 and −0.825, respectively (the initial operating angles were not adjusted for this change), stability was lost quickly. These results are consistent, to the accuracy of the numerical computations, with the transient energy solution.

B. Power Limit With Compound Transient

Let the system in Figure 9 be subjected to a 3-phase fault on the transmission-line side of circuit breaker A, and assume that 0.05 second later circuit breakers A and B open. Find the maximum motor load P_3 which the system can carry through this transient, with P_3 specified.

Solution. The data in Table I apply to this problem as well as to example A, and the values of δ existing before the fault are found in the same manner as in that problem. During a 3-phase fault at the specified location no power will be transmitted between any of the machines, hence the rotor accelerations prior to clearing will be directly proportional to the external torques T_{1t}, T_{2t} and T_{3t}. The equations during the 3-phase fault reduce to

$$I_1 d^2\delta_1/dt^2 = T_{1t}$$

$$I_2 d^2\delta_2/dt^2 = T_{2t}$$

$$I_3 d^2\delta_3/dt^2 = T_{3t}$$

The equations may be integrated directly. The angular velocities relative to synchronous speed at the start of the transient are assumed to be zero.

$$d\delta_1/dt = (T_{1t}/I_1)t$$

$$\delta_1 = (1/2)(T_{1t}/I_1)t^2 + \delta_{10}$$

$$t = 0.05 \text{ second}$$

In this example the moments of inertia will be estimated from the characteristic inertia quantity H (see equation 19, Appendix II).

It will be assumed that the rated kilovolt-amperes of each machine is equal to 1.3 times the kilowatt load on it. Values of H will be assumed as indicated in Table IV; the calculations of the angular velocities relative to synchronous speed and the rotor difference angles at the time of clearing (indicated by the subscript I) are summarized in the same table. The k's are the same as in example A, and the δ's for after-transient conditions are found as in that problem. The transient kinetic energy ΔW at the time of clearing is found by means of equation 18. The results of these computations are listed in Table V. V_L and $V_I + \Delta W$ are plotted against P_3 in Figure 10.

Conclusion. The maximum per unit load P_3 for which stability can be maintained through this transient is 0.758.

Table I. Examples A and B: System Parameters

Parameter	Units	Reference	Before Transient	After Transient
$X'_d + X_n + (X_L/2)$	Per unit reactance	Figure 9	1.3	
$X'_d + X_n + X_L$	Per unit reactance	Figure 9		2.3
$X'_d + X_n$	Per unit reactance	Figure 9	0.5	0.5
$X'_d + X_n$	Per unit reactance	Figure 9	0.6	0.6
X_{12}	Per unit reactance	Figure 3	2.88	4.72
X_{13}	Per unit reactance	Figure 3	3.46	5.66
X_{23}	Per unit reactance	Figure 3	1.33	1.23
$T_{13M\sin}$	Per unit power	Equation 5	0.416	0.254
$T_{13M\cos}$	Per unit power	Equation 5	0.312	0.191
$T_{23M\sin}$	Per unit power	Equation 5	0.675	0.731
k_1		Equation 13	$P_1/0.416$	$P_1/0.254$
k_2		Equation 13	1.202	1.969
k_3		Equation 13	0.750	0.751
k_4		Equation 13	1.622	2.878

Appendix II. Initial Kinetic Energy

The transient kinetic energy of the system will be defined as the total kinetic energy less the kinetic energy of steady-state operation.

Let

W = kinetic energy of steady-state operation

ΔW = transient kinetic energy

ω_0 = synchronous angular velocity in electrical radians per second

ω_1 = angular velocity of machine 1 during the transient, in electrical radians per second

I_1 = moment of inertia of machine 1, in per unit torque seconds squared

$$W = (1/2)(I_1\omega_0^2 + I_2\omega_0^2 + I_3\omega_0^2)$$

$$W + \Delta W = (1/2)(I_1\omega_1^2 + I_2\omega_2^2 + I_3\omega_3^2)$$

Let

$\omega_1 = \omega_0 + \Delta\omega_1$ and so forth

$$\begin{aligned}\Delta W = (1/2)(&I_1[(\omega_0 + \Delta\omega_1)^2 - \omega_0^2] + \\ &I_2[(\omega_0 + \Delta\omega_2)^2 - \omega_0^2] + \\ &I_3[(\omega_0 + \Delta\omega_3)^2 - \omega_0^2]) \\ = \omega_0(&I_1\Delta\omega_1 + I_2\Delta\omega_2 + I_3\Delta\omega_3) + \\ (1/2)&[I_1(\Delta\omega_1)^2 + I_2(\Delta\omega_2)^2 + I_3(\Delta\omega_3)^2]\end{aligned}$$

It is assumed that the external torques remain balanced; then the following is true because of the principle of conservation of angular momentum:

$$I_1\Delta\omega_1 + I_2\Delta\omega_2 + I_3\Delta\omega = 0$$

Hence

$$\Delta W = (1/2)[I_1(\Delta\omega_1)^2 + I_2(\Delta\omega_2)^2 + I_3(\Delta\omega_3)^2] \quad (18)$$

The inertia quantity H, which is the stored energy of rotation at synchronous speed per kilovolt-ampere of machine rating, has characteristic and fairly constant values for the various classes of machines;[1,5] it may be expressed in terms of the moment of inertia as follows:

$$HP_R = (1/2)I\omega_0^2 P_B \quad (19)$$

or

$$HP_R = (WR^2/2g)(2\pi n/60)^2(0.746/550) \quad (20)$$

Here

P_R = kilovolt-ampere rating of machine

P_B = kilowatt value of unit power

WR^2 = moment of inertia in pound-feet squared

g = acceleration of gravity

n = speed in revolutions per minute

Let

p = number of poles

Then

$$\omega_s = (2\pi n/60)(p/2) \tag{21}$$

The per unit moment of inertia may be found in terms of the ordinary dimensions by equating equation 19 to equation 20, and making use of equation 21.

$$IP_B = (WR^2/g)(0.746/550)(2/p)^2 \tag{22}$$

Appendix III. Potential Energy Function

Repetitive Character

The single-variable function V repeats itself, except for a constant, every 360 degrees. This constant may be evaluated readily by substitution in equation 4.

$$V(\delta+2\pi n) - V(\delta) = -2\pi n T_{MF} \sin \delta_F$$

Here n is any integer.

As a function of two independent variables, V likewise repeats itself, except for a constant, every 360 degrees in either variable. The constant pertaining to one variable differs, in general, from that pertaining to the other. Expressions for these constants may be derived from equation 10.

$$V(\delta_{13}+2\pi n; \delta_{23}) - V(\delta_{13}; \delta_{23}) = -2\pi n \times [T_{13M} \sin(\delta_{13F}-\delta_{23F}) + T_{13M} \sin \delta_{13F}]$$

$$V(\delta_{13}; \delta_{23}+2\pi n) - V(\delta_{13}; \delta_{23}) = -2\pi n \times [-T_{13M} \sin(\delta_{13F}-\delta_{23F}) + T_{23M} \sin \delta_{23F}]$$

Critical Points

The requirement that the first derivative or derivatives of a function equal zero is a necessary condition for the existence of a minimum or a maximum (or a minimax, in case of two independent variables) but it is not a sufficient condition. This situation will be investigated briefly by means of higher derivatives.

One Independent Variable

The function V has a relative minimum at δ_C if the following conditions are satisfied:

$$dV/d\delta = 0 \qquad \delta = \delta_C \tag{23}$$

$$d^2V/d\delta^2 > 0 \qquad \delta = \delta_C \tag{24}$$

If equation 23 is satisfied, but the inequality in equation 24 is reversed in sign, V has a relative maximum at δ_C.

In case equation 23 is satisfied, but the following conditions (equation 25) are fulfilled rather than equation 24, V has a point of inflection with horizontal tangent at δ_C.

$$\left.\begin{aligned} d^2V/d\delta^2 &= 0 \\ d^3V/d\delta^3 &\neq 0 \end{aligned}\right\} \tag{25}$$

The expression (equation 4) which was derived for V will be differentiated and substituted into equations 23, 24, and 25. As previously noted, the subscript R will be omitted.

$$V = T_{MF}[\cos \delta_F - \cos \delta - (\delta - \delta_F) \sin \delta_F] \tag{4}$$

$$dV/d\delta = T_{MF}(\sin \delta - \sin \delta_F) \tag{26}$$

$$d^2V/d\delta^2 = T_{MF} \cos \delta \tag{27}$$

$$d^3V/d\delta^3 = -T_{MF} \sin \delta \tag{28}$$

Substitution of equation 26 into equation 23 shows that the latter condition is satisfied for the following δ_C's:

$$\delta_C = \delta_F$$

$$\delta_C = 180° - \delta_F$$

If these values of δ_C now are substituted into equation 27, and that in turn into equation 24, the first proves to be a minimum, and the second, a maximum. Hence δ_L, the angle at which the net torque ceases to tend to reduce the angular displacement, is the second value of δ_C. Thus:

$$\delta_L = 180° - \delta_F$$

It will be seen that equations 23 and 25 can be satisfied simultaneously only if δ_F is equal to 90 degrees. This is the case if the system is operating at the steady-state power limit. It also can be seen by inspection of equations 26, 27, and 28 that the first, second, and third derivatives of V cannot all vanish simultaneously.

Two Independent Variables

A necessary condition for the existence of a critical point on the V surface was stated in equation 11, which is repeated here.

$$\begin{aligned} \partial V/\partial \delta_{13} &= 0 \\ \partial V/\partial \delta_{23} &= 0 \end{aligned} \tag{11}$$

As with the single variable function, the nature of V in the vicinity of a critical point may be investigated further by means of higher derivatives.[6] Let δ_{13C} and δ_{23C} indicate the co-ordinates of a critical point, and $\Delta\delta_{13}$ and $\Delta\delta_{23}$ denote small displacements from that point. Then V may be represented in the vicinity of δ_{13C}; δ_{23C} by the following Taylor's series (since, according to equation 11, the first derivatives of V are zero, they will be omitted).

$$\begin{aligned} V = V(\delta_{13C}; \delta_{23C}) &+ (A/2)(\Delta\delta_{13})^2 + \\ &C(\Delta\delta_{13})(\Delta\delta_{23}) + (B/2)(\Delta\delta_{23})^2 + \\ &(D/6)(\Delta\delta_{13})^3 + (E/2)(\Delta\delta_{13})^2(\Delta\delta_{23}) + \\ &(F/2)(\Delta\delta_{13})(\Delta\delta_{23})^2 + (G/6)(\Delta\delta_{23})^3 + \ldots \end{aligned} \tag{29}$$

Here

$$\left.\begin{aligned} A &= \partial^2V/\partial\delta_{13}^2 \\ B &= \partial^2V/\partial\delta_{23}^2 \\ C &= \partial^2V/\partial\delta_{13}\partial\delta_{23} \\ D &= \partial^3V/\partial\delta_{13}^3 \\ E &= \partial^3V/\partial\delta_{13}^2\partial\delta_{23} \\ F &= \partial^3V/\partial\delta_{13}\partial\delta_{23}^2 \\ G &= \partial^3V/\partial\delta_{23}^3 \end{aligned}\right\} \tag{30}$$

The following conditions, in addition to equation 11, are sufficient to identify the indicated types of critical points:

$$\left.\begin{aligned} AB > C^2 \quad A < 0 \quad &\text{Maximum} \\ AB > C^2 \quad A > 0 \quad &\text{Minimum} \end{aligned}\right\} \tag{31}$$

$$AB < C^2 \qquad \text{Minimax} \tag{32}$$

$$AB = C^2 \quad J \neq 0 \qquad \text{Inflected surface with horizontal tangent plane (discussed later in this section)} \tag{33}$$

Here

$$J = D + 3E(-A/C) + 3F(-A/C)^2 + G(-A/C)^3 \tag{34}$$

Let

$$AB = C^2 \qquad J = 0 \tag{35}$$

If the first of the conditions in equations 35 is true, the second is necessary, but not sufficient, for the existence of a maximum, and minimum, or a minimax. The fourth derivatives of V must be investigated in order to determine positively the character of a critical point which satisfies equations 35, but it may be inferred from physical considerations in the transient stability

Table II. Schedules for Solving Equations for Critical Points

(1)	(2)	(3)	(4)	(5)	(6)
Schedule for equation 15					
δ_{12}	sin (1)	(2) × k_1	(3) ÷ k_2	$\sin^{-1}$ (4)	(1) + (5) = δ_{12}
Schedule for equation 16					
δ_{12}	sin (1)	(k_1/k_2) × (2)	$[(k_1+k_2)/k_2]$ − (3)	$\sin^{-1}$ (4)	= δ_{12}

Table III. Example A: Summary of Calculated Data

	Reference		P_1 in Per Unit Power −0.72	−0.80	−0.82
P_1	Per unit power		0.72	0.80	0.82
k_1	(Before transient)	Table I	0.528	0.721	0.769
δ_{13}	Degrees	Equation 17	46.3	57.6	60.8
δ_{23}	Degrees	Equation 17	47.1	52.6	54.2
k_1	(After transient)	Table I	0.865	1.181	1.260
δ_{13F}	Degrees	Figure 5; equations 15 and 16	61.1	82.6	90.0
δ_{23F}	Degrees	Figure 5; equations 15 and 16	49.1	56.7	59.4
δ_{13L}	Degrees	Figure 5; equations 15 and 16	151.0	158.6	151.8
δ_{23L}	Degrees	Figure 5; equations 15 and 16	120.9	93.7	87.0
V_L	Per unit energy	Equation 10	4.632×10^{-4}	1.333×10^{-4}	0.700×10^{-4}
V_0	Per unit energy	Equation 10	0.257×10^{-4}	0.593×10^{-4}	0.668×10^{-4}
$V_L - V_0$	Per unit energy		4.375×10^{-4}	0.740×10^{-4}	0.032×10^{-4}

Table IV. Example B: Rotor Motions Before Clearing

Reference			Machine Number 1	2	3
H	Kw-sec per kva	(Assumed)	3	6	2
P_R	Per unit power	(Assumed)	$1.3P_1$	$1.3P_1$	$1.3P_1$
I	Per unit torque sec^2	Equation 19	$5.48\times10^{-5}P_1$	$10.96\times10^{-5}P_1$	$3.65\times10^{-5}P_1$
T_k	Per unit torque		$P_1/377$	$P_1/377$	$P_1/377$
$d^2\theta/dt^2$	Deg per sec^2	Appendix I B	2,770	1,385	−4,150
$\Delta\omega_1$	Deg per sec	Appendix I B	138.5	69.2	−207.5
δ_I	Deg	Appendix I B	$\delta_3+3.46$	$\delta_3+1.73$	$\delta_3-5.19$
δ_{11I}	Deg			$\delta_{13}+8.65$	
δ_{12I}	Deg			$\delta_{23}+6.92$	

Table V. Example B: Summary of Calculated Data

Reference			P_1 in Per Unit Power −0.72	−0.75	−0.80
P	Per unit power		0.22	0.25	0.30
k_1	(Before transient)	Table I	0.528	0.600	0.721
δ_{13B}	Degrees	Equation 17	46.3	50.3	57.6
δ_{13I}	Degrees	Table IV	55.0	59.0	66.3
δ_{13R}	Degrees	Equation 17	47.1	49.0	52.6
δ_{13I}	Degrees	Table IV	54.0	55.9	59.5
k_1	(After transient)	Table I	0.865	0.985	1.181
δ_{11F}	Degrees	Figure 5; equations 15 and 16	61.1	68.3	82.6
δ_{12F}	Degrees	Figure 5; equations 15 and 16	49.1	51.6	56.7
δ_{11L}	Degrees	Figure 5; equations 15 and 16	151.0	155.8	158.6
δ_{12L}	Degrees	Figure 5; equations 15 and 16	120.9	113.2	93.7
VL	Per unit energy	Equation 10	4.632×10^{-4}	3.277×10^{-4}	1.335×10^{-4}
VI	Per unit energy	Equation 10	0.183×10^{-4}	0.252×10^{-4}	0.413×10^{-4}
ΔW	Per unit energy	Equation 18	2.484×10^{-4}	2.600×10^{-4}	2.810×10^{-4}
$VI+\Delta W$	Per unit energy		2.667×10^{-4}	2.852×10^{-4}	3.223×10^{-4}
$VL-(VI+\Delta W)$	Per unit energy		1.965×10^{-4}	0.425×10^{-4}	-1.888×10^{-4}

problem that such a critical point is a minimax.

Conditions 31, 32, 33, and 35 may be checked by substitution in equation 29. Since the effects of small quantities of a given order are negligible compared to the effects of small quantities of a lower order, the derivatives of a given order affect the nature of V in the immediate vicinity of δ_{13C}; δ_{23C} only in those regions, if any, in which all resultant lower-order effects of lower derivatives vanish. For example, it may be seen by differentiation of equation 10 that, for the particular function V, the second partial derivatives A, B, and C in equation 29 will, under the condition of AB equals $(C)^2$, vanish along a line passing through the critical point with the direction $\Delta\delta_{23}/\Delta\delta_{13}$ equal to $(-A/C)$ or $(-C/B)$. In such a region, the third derivatives become significant, as indicated in equations 33 and 35.

No term is in common usage to describe the surface which is identified by equation 33; for convenience the name "inflected surface with horizontal tangent plane" has been adopted. Simple examples of this type of surface are given by the following functions:

$$Z_1 = X^2 + Y^2 \tag{36}$$

$$\begin{aligned} Z_2 &= -X^2 + Y^2 \\ Z_3 &= X^2 + Y^3 \end{aligned} \tag{37}$$

Critical points of Z_1, Z_2 and Z_3 exist at the origin; in the X plane the function Z_1 passes through a minimum, whereas in the Y plane, Z_1 has a point of inflection with horizontal tangent. The inflected surface with horizontal tangent plane sketched in Figure 4*d* is of the same type as Z_1. The principal planes of the function at the critical point, of course, need not be parallel to the abscissas' co-ordinate planes.

Function Z_2 passes through a maximum in X plane and has a point of inflection with horizontal tangent in the Y plane at the origin, while Z_3 has points of inflection with horizontal tangents in both planes at the origin. It will be noted that in the case of Z_3 all three second partial derivatives are zero at the critical point, a condition which, as may be seen by differentiation of equation 10, cannot arise in the function V.

Multiple Roots

The relation between the multiplicity of a root and the type of critical point which may be expected there will be considered next. Two general cases other than simple intersection of the loci of equations 14 and 15 are pertinent; in the first, illustrated in Figures 6*d* and 6*e*, the loci are tangent to each other at a common point but do not intersect there. This gives rise to a double root. The second case, illustrated in Figure 6*f*, is that in which the loci are tangent to each other and also intersect each other at the same point; then a triple root is present.

The loci will be tangent to each other if they have the same slope $(d\delta_{23}/d\delta_{13})$ at a common point; they cannot cross at the point of tangency if their curvatures $(d^2\delta_{23}/d\delta_{13}^2)$ differ. With a perfectly general function the loci may not cross at the point of tangency even if the curvatures are equal, but for the function V, equality of curvatures at the point of tangency may be assumed as sufficient to indicate crossing of the loci. The required derivatives may be obtained from equations 14 and 15 by implicit differentiation.[5] It will be recalled that equations 14 and 15 were obtained by differentiation of equation 10 and application of equation 11.

The condition of equal slopes of the loci reduces to

$$(-A/C) = (d\delta_{23}/d\delta_{13}) = (-C/B) \tag{38}$$

Equation 38 then simplifies to

$$AB = C^2 \tag{39}$$

The condition of equal curvatures of the loci reduces to

$$\begin{aligned} -[D+2E(-A/C)+F(-A/C)^2](1/C) &= \\ (d^2\delta_{23}/d\delta_{13}^2) &= \\ -[E+2F(-A/C)+G(-A/C)^2]\times & \\ (1/B) \end{aligned} \tag{40}$$

Equation 39 may be substituted into equation 40; the latter then reduces to

$$D+3E(-A/C)+3F(-A/C)^2+G(-A/C)^3=0 \tag{41}$$

Equations 39 and 41 now are compared with equations 33, 34, and 35, and the following conclusions may be drawn: if the loci of equations 14 and 15 are tangent at a common point, but do not intersect there, the function V will have an inflected surface with horizontal tangent plane there. If the loci of equations 14 and 15 are tangent at a common point and do cross each other there the function V will have a minimax there.

Practical Significance of Multiple-Root Critical Points

The situations illustrated in Figures 6*e* and 6*f* are of no unusual significance in transient-stability problems. In the first case the inflected surface, with horizontal tangent plane which exists at the point of tangency of the loci, is similar to Z_2 in equation 37 at the origin; it has a higher value of V than does the minimax, and the latter therefore governs the stability limit. In Figure 6*f* the minimax at the cross-over tangency of the loci is the same as one which arises from the simple intersection of loci, as far as application of the transient-energy method is concerned.

The inflected surface with horizontal tangent plane which is found in Figure 6*d*, which surface resembles Z_1 in equation 36 at the origin, is of considerable interest as a limiting case; it is a point of steady-state operation which has zero allowable transient energy. In short, it is a steady-state dynamic power limit.

References

1. Electric Power Circuits—Volume 2, Power System Stability, O. G. C. Dahl. McGraw-Hill Book Company, New York, N. Y., 1938, pages 391–412; 443–6; 622–5.

2. System Stability as a Design Problem, R. H. Park, E. H. Bancker. AIEE Transactions, volume 48, 1929, pages 170–94.

3. Introduction to Theoretical Physics (book), J. C. Slater, N. H. Frank. McGraw-Hill Book Company, New York, N. Y., 1933, pages 39–57; 79–81.

4. Stability of the General Two-Machine System, O. G. C. Dahl. Electrical Engineering (AIEE Transactions), volume 54, February 1935, pages 185–8.

5. First Report on Power System Stability, AIEE subcommittee on interconnection and stability factors. Electrical Engineering (AIEE Transactions), volume 56, February 1937, pages 261–82.
6. Advanced Calculus (book). F. S. Woods. Ginn and Company, New York, N. Y., 1934, pages 91–3; 116–17. (Other texts on advanced calculus also have pertinent discussions.)

Discussion

J. G. Holm (Gibbs and Hill, Inc., New York, N. Y.): The author's method of calculating transient stability is a new interpretation of the existing and widely used equal-area method. The new interpretation is quite complicated in the underlying theory and in its development. It is, in fact, more complicated than any already existing theory connected with the complex problem of system transient stability. The author, however, should be highly complimented for the conception and the clear and orderly exposition of the basic theory.

The application of the proposed method is illustrated on two examples in the advance copy. It is suggested that these be presented in a form less condensed and that the accompanying tables be expanded to include all the steps required by calculation, so that the method could be applied to an actual case without unnecessary difficulties.

The method proposed by the author apparently offers the same degree of accuracy as the equal-area method on which it is based. This is another compliment to the author. In other attributes—simplicity, rapidity in obtaining results, and ability to foresee them—this method does not seem to the writer to present advantages over the existing methods. Should the author feel to the contrary, it would be desirable that the advantages of this method be pointed out, so that a stimulus may be given to its practical application.

Edward W. Kimbark (Northwestern University, Evanston, Ill.): The author has stated fairly both the advantages and limitations of the transient-energy method of calculating stability. In the field where it is applicable (at present, to the final transient of three machines connected through a pure-reactance network) the extent of its use will depend largely upon the amount of labor required by this method in comparison to the amount required for computing swing curves. As the author has made check calculations by both methods, perhaps he can give us some information on the time required for each. Such data preferably should relate to a compound transient.

However, regardless of whether the new method ever will replace the old for everyday stability studies, it certainly provides stimulus for thought on the theory of transient stability. It raises a number of questions which cannot be investigated in the short time allowed for the preparation of a discussion. Perhaps the author can answer some of them.

Figure 2 of the paper shows a graph of the potential energy of a 2-machine system as a function of the angle between rotors. (As this curve results from the integration of the difference between a sine wave and a constant, it is the sum of a cosine wave and a sloping straight line.) If this curve is visualized as the profile of a roller-coaster track, the relative motion of the rotors can be imagined as the horizontal motion of a ball rolling on the track. Either the ball may be trapped in the valley, or it may have enough energy to carry it over the hump and then down with increasing speed through a series of ever-lower valleys. If trapped in the valley, it will eventually come to rest in the lowest spot, representing after-transient steady state.

Figure 7 of the paper is a contour map of the potential energy of a 3-machine system as a function of two of the three differences of rotor angles. (First question: Is there some way of showing all three angles, obviating the arbitrary choice of two? Triangular co-ordinates, which often are used to represent various mixtures of three constituents, come to mind.) The map portrays a surface having the shape of a bowl or depression surrounded by hills in which there is a notch, gap, or pass at elevation V_L. Again the relative motion of the rotors can be represented by a ball rolling on the surface. Either the ball may be trapped in the bowl, or it may escape thence. If the ball has enough energy it can even escape by crossing a high hill, but if it has less energy it can escape only through the notch.

Now here is the disturbing thing. The author assures us that any ball having energy exceeding V_L, no matter how slightly, eventually will find the gap and escape through it. It has been customary in transient-stability studies on multimachine systems to test stability by the first swing. If the machines furthest apart in angular position reach a maximum separation and then come toward one another, the system is judged stable. Seldom are the swing calculations carried out for many swings. Perhaps we have judged as stable systems which eventually would lose synchronism. This suggests the second question: If the transient energy slightly exceeds V_L, what is the probability of loss of synchronism on the first swing? The answer obviously depends on the initial point on the potential surface of Figure 7. Where is this point for the example of the paper? This matter of the number of swings before loss of synchronism appears to deserve further study.

Another point warranting further consideration than given in the paper is the possibility of including resistance in the network. As the author states, this has been accomplished for the 2-machine equal-area method. The surprising thing is that two machines connected through a network with resistance form a conservative system for transient energy. In other words, the resistance in the network does not cause damping of the swings. It appears reasonable that a similar conclusion might be reached for three or more machines.

Finally, further study should be given to the evaluation of the potential function of a multimachine system by use of the a-c calculating board.

P. C. Magnusson: Kimbark's first question suggests the use of nonorthogonal co-ordinates in which all three rotor-difference angles of the 3-machine problem would be shown. Such a co-ordinate set is sketched in Figure 1 of this discussion; this arrangement gives equal significance to all three angles instead of favoring two arbitrarily chosen independent angles. Contour plots in co-ordinates of this sort might better portray the transient-energy function than would orthogonal-co-ordinate plots such as Figure 7.

The probability of loss of synchronism on the first swing, when the actual transient energy slightly exceeds the allowable, is the subject of Kimbark's second question. A rigorous mathematical study of this problem, while doubtless very complex, would be highly desirable. Comparable solutions, made by the rotor-motion and transient-energy methods, indicate that a small amount of excess transient energy suffices to cause loss of synchronism on the first swing. It should be noted that the assumptions made in this method (constant generated voltages behind constant transient reactances, constant external torques, and so forth) would be but roughly true after the elapse of the time required for two or three complete swings.

As to the time and labor required for solving a problem by the transient-energy method as compared with the rotor-motion (step-by-step) method, a question which was raised by both Holm and Kimbark, the only observation that can be made at present is that the two methods are comparable. The excess (or deficit) of the actual transient energy over the allowable, or perhaps the ratio between those two quantities, might provide a good "common denominator" in terms of which the effects of load increments and relay and circuit breaker speeds could be systematically summarized and compared.

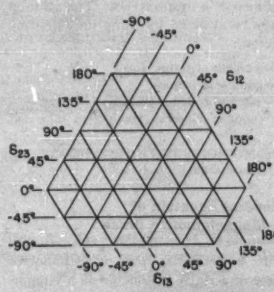

Figure 1. Nonorthogonal co-ordinates representing rotor-difference angles

$\delta_{12} = \delta_{13} + \delta_{23}$

The Magnetomotive Force of 2-Layer Windings of Rotating Machines

J. M. STEIN
Membership Application Pending

Synopsis: The development of general equations for the magnetomotive force of 2-layer windings depends upon the summation of the magnetomotive forces of the individual conductors in the slots. By the use of unique methods of summation, it is possible to derive equations for the winding factors of both integral and fractional slot windings without resorting to tabular or vector diagrams. The equations are developed for any phase angle and may be applied to 2-phase, 3-phase, 60- and 120-degree phase belts, or any other that represents a usable winding.

THE 2-LAYER winding consists of as many coils as there are slots in the stator, the front coils sides forming the bottom layer while the rear coil sides form the top layer. In dealing with the problem at hand, no reference will be made to the number of phases or the number of poles, as these are represented by the phase angle γ and the order of the harmonics n, respectively. The solution may be attained by using the following factors:

S = number of stator slots
g = number of groups
ϕ = pitch of coils in mechanical degrees
N = number of series conductors in a coil side
I = maximum current in any conductor
γ = phase angle

General Equation of Magnetomotive Force

If we consider the magnetomotive force of a single conductor on a circumferential air gap, we see that it is represented as in Figure 1, with a developed representation as in Figure 2. If the conductor position is defined by ψ mechanical degrees from a zero reference point, we may express its magnetomotive force by the equation:

$$\mathfrak{F} = \frac{i}{\pi}\sum_n \frac{1}{n} \sin n(\theta - \psi) \tag{1}$$

where θ is the angular measure around the air gap.

As there are N series conductors per coil side and there is one coil side per slot in each layer of the winding, we may write for the magnetomotive force of the top layer:

$$\mathfrak{F}_T = \frac{N}{\pi}\sum_{m=1}^{m=S} i_m \sum_n \frac{1}{n} \sin n\left(\theta - \frac{2\pi m}{S}\right) \tag{2}$$

and for the bottom layer

$$\mathfrak{F}_B = -\frac{N}{\pi}\sum_{m=1}^{m=S} i_m \sum_n \frac{1}{n} \sin n\left(\theta - \frac{2\pi m}{S} - \phi\right) \tag{3}$$

where i_m is the conductor current in the mth sloth of the top winding and, likewise, (in the opposite direction) the current in the other coil side.

The total magnetomotive force of the winding then is given by

$$\mathfrak{F} = \frac{N}{\pi}\sum_{m=1}^{m=S} i_m \sum_n \frac{1}{n}\left[\sin n\left(\theta - \frac{2\pi m}{S}\right) - \sin n\left(\theta - \frac{2\pi m}{S} - \phi\right)\right]$$
$$= \frac{2N}{\pi}\sum_{m=1}^{m=S} i_m \sum_n \frac{K_{pn}}{n} \times \cos n\left(\theta - \frac{2\pi m}{S} - \frac{\phi}{2}\right) \tag{4}$$

where K_{pn} is the pitch factor for the nth harmonic defined by

$$K_{pn} = \sin \frac{n\phi}{2} \tag{5}$$

Equation 4 represents the most general form of magnetomotive force, but has no practical value unless the summation over m is carried out.

Effect of Grouping

In equation 4, i_m is the current in the mth coil. If the coils are connected together to form g groups and the current in the cth group is i_c, we may write the sum $\sum_{m=1}^{m=S}$ as two sums as in equation 6:

$$\mathfrak{F} = \frac{2N}{\pi}\sum_n \frac{K_{pn}}{n}\sum_{c=1}^{c=g} i_c \sum_{m=1+(c-1)\frac{S}{g}}^{m=c\frac{S}{g}} \times \cos n\left(\theta - \frac{2\pi m}{S} - \frac{\phi}{2}\right) \tag{6}$$

Performing the summation over m, we have

$$\mathfrak{F} = \frac{2SN}{\pi g}\sum_n \frac{K_{pn}K_{dn}}{n}\sum_{c=1}^{c=g} i_c \times \cos n\left(\theta - \left[(2c-1)\frac{S}{g} + 1\right]\frac{\pi}{S} - \frac{\phi}{2}\right) \tag{7}$$

where K_{dn} is the distribution factor defined by

$$K_{dn} = \frac{g \sin \frac{\pi n}{g}}{S \sin \frac{\pi n}{S}} \tag{8}$$

We thus have arrived at the distribution factor without defining the nature of the current, that is, the phase angle γ. From this, we see that the magnitudes of the harmonics in the magnetomotive forces are independent of the phase γ and are defined completely by S, g, and ϕ. The introduction of the phase angle determines the existence of the various harmonics.

Effect of Phase Angle

The phase angle may be introduced by defining the group currents as in equation 9:

$$i_c = I \sin(\omega_{0t} - [c-1]\gamma) \tag{9}$$

Introducing this into equation 7 re-

Paper 47-100, recommended by the AIEE committee on electric machinery for presentation at the AIEE winter meeting, January 27–31, 1947. Manuscript submitted November 15, 1946; made available for printing December 26, 1946.

J. M. STEIN is with the Westinghouse Electric Corporation, Buffalo, N. Y.

sults in the magnetomotive force being completely defined by

$$\mathfrak{F}=\frac{SNI}{\pi}\sum_n\frac{K_{pn}K_{dn}}{n}\{K_{en}\sin(n[\theta-\alpha]+\omega_{0t}+\beta)-K_{fn}\sin(n[\theta-\alpha]-\omega_{0t}+\epsilon)\} \quad (10)$$

where K_{en} and K_{fn} are the existence factors of the positive and negative sequences magnetomotive forces respectively. They are defined by

$$K_{en}=\frac{\sin\frac{g}{2}\left(\frac{2\pi n}{g}-\gamma\right)}{g\sin\frac{1}{2}\left(\frac{2\pi n}{g}-\gamma\right)} \quad (11)$$

and

$$K_{fn}=\frac{\sin\frac{g}{2}\left(\frac{2\pi n}{g}+\gamma\right)}{g\sin\frac{1}{2}\left(\frac{2\pi n}{g}+\gamma\right)} \quad (12)$$

The angles, α, β, ϵ, are phase angles defining the relative position of the various harmonics and are defined by

$$\left.\begin{aligned}\alpha&=\frac{\pi}{S}+\frac{\pi}{g}+\frac{\phi}{2}\\ \beta&=\frac{g-1}{2}\left(\frac{2\pi n}{g}-\gamma\right)\\ \epsilon&=\frac{g-1}{2}\left(\frac{2\pi n}{g}+\gamma\right)\end{aligned}\right\} \quad (13)$$

The method of approach to equation 10 necessitated summation over a range of integral values and therefore can represent only integral slot windings.

It should be understood that $n=1$ corresponds to a 2-pole magnetomotive force, $n=2$ to a 4-pole magnetomotive force, and so on.

Subslots

In dealing with fractional slot windings we are confronted with a fractional value of the quotient S/g. We may surmount this difficulty by introducing the concept of subslots, which merely means dividing the angle between two slots into g groups, such that we may speak of having Sg subslots, which is divisible by the number of groups.

When this concept is introduced into the previous development, equation 4 becomes:

$$\mathfrak{F}=\frac{2N}{\pi}\sum_{k=1}^{k=Sg}i_k\sum_N\frac{K_{pn}}{n}\cos n\left(\theta-\frac{2\pi k}{Sg}-\frac{\phi}{2}\right) \quad (14)$$

This immediately would solve our problem, if we could express i_k in such a way that its value is zero for all values of k except $1, g+1, 2g+1, mg+1$. This can be effected by multiplying i_k by a factor n_k defined by

$$n_k=\frac{2}{\pi}\sum_{m=0}^{m=S-1}\int^{\pi}\sin k\alpha\sin(mg+1)\alpha d\alpha \quad (15)$$

The introduction of this factor gives an analytical expression for the magnetomotive force, but results in extremely complex summation or integration and cannot be used to derive the winding and existence factors.

If we permit all the i_k to be other than zero, we will derive a magnetomotive force which is not that of the actual fractional slot winding, but it is the sum of magnetomotive forces of the type sought. We will define this sum by $\mathfrak{F}'$ and write its equation:

$$\mathfrak{F}'=\frac{SgNI}{\pi}\sum_n\frac{K'_{pn}K'_{dn}}{n}$$

$$\left\{\begin{matrix}K'_{en}\\ -K_{fn}'\end{matrix}\right.\times\left.\begin{matrix}\sin(n[\theta-\alpha']-\omega_{0t}+\beta')\\ \sin(n[\theta-\alpha']-\omega_{0t}+\epsilon')\end{matrix}\right\} \quad (16)$$

where the primed factors are defined by:

$$\left.\begin{aligned}K'_{pn}&=K_{pn}\\ K'_{dn}&=\frac{g\sin\frac{\pi n}{g}}{Sg\sin\frac{\pi n}{Sg}}\\ K'_{en}&=K_{en}\\ K_{fn}'&=K_{fn}\\ \alpha'&=\frac{\pi}{Sg}+\frac{\pi}{g}+\frac{\phi}{2}\\ \beta'&=\beta\\ \epsilon'&=\epsilon\end{aligned}\right\} \quad (17)$$

If we define the magnetomotive force sought by equation 18, we may proceed to find its relation with equation 16:

$$\mathfrak{F}=\sum_n[A_n\sin(n[\theta-u]+\omega_{0t}+v)+B_n\sin(n[\theta-u]-\omega_{0t}+w)] \quad (18)$$

Superimposed Fractional Slot Windings

It can be shown, by superimposing fractional slot windings of the same grouping and displacing them from each other in a definite way, that the resultant magnetomotive force is the same as that expressed by equation 16. This is derived in Appendix I and results in the following relation:

$$\mathfrak{F}'=\sum_{m=0}^{m=\delta-1}\sum_{k=0}^{k=\frac{g}{\delta}-1}\mathfrak{F}\left(\theta-\frac{2\pi}{g}k-\frac{Z\pi}{gS}m,\ \omega_{0t}+k\gamma\right)$$
$$=\sum_n K_{pn}[A_nK_{An}\sin(n[\theta-u']+\omega_{0t}+v')+B_nK_{Bn}\sin(n[\theta-u']-\omega_{0t}+w')] \quad (19)$$

where

$$\left.\begin{aligned}K_{pn}&=\frac{\sin\frac{\delta\pi n}{gS}}{\sin\frac{\pi n}{gS}}\\ K_{An}&=\frac{\sin\frac{g}{2\delta}\left(\frac{2\pi n}{g}-\gamma\right)}{\sin\frac{1}{2}\left(\frac{2\pi n}{g}-\gamma\right)}\\ K_{Bn}&=\frac{\sin\frac{g}{2\delta}\left(\frac{2\pi n}{g}+\gamma\right)}{\sin\frac{1}{2}\left(\frac{2\pi n}{g}+\gamma\right)}\\ u'&=u+\left(\frac{g}{\delta}-1\right)\frac{\pi}{g}+(\delta-1)\frac{\pi}{gS}\\ v'&=v+\left(\frac{g}{\delta}-1\right)\frac{\gamma}{2}\\ w'&=w-\left(\frac{g}{\delta}-1\right)\frac{\gamma}{2}\end{aligned}\right\} \quad (20)$$

and δ is the greatest common divisor of S and g.

Magnetomotive Force of Fractional Slot Windings

Equating 16 and 19, we get

$$A_n=\frac{SgNI}{\pi}\frac{K'_{pn}K'_{dn}K'_{en}}{nK_{pn}K_{An}} \quad (21)$$

$$B_n=-\frac{SgNI}{\pi}\frac{K'_{pn}K'_{dn}K'_{fn}}{nK_{pn}K_{Bn}} \quad (22)$$

Figure 1. The magnetomotive force of a single conductor on a circumferential air gap

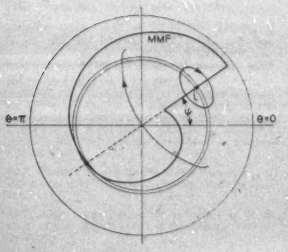

Figure 2. The magnetomotive force of a single conductor on a circumferential air gap as a linear development

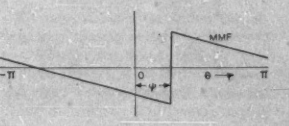

Combining these factors, we may write equation 18 as follows:

$$\mathfrak{F}=\frac{SNI}{\pi}\sum_{n}\frac{K_{pn}K_{dn}}{n}\{K_{en}\sin(n[\theta-u]+\omega_{0t}+v)-K_{fn}\sin(n[\theta-u]-\omega_{0t}+w)\} \quad (23)$$

in which the factors are defined by:

$$K_{pn}=\sin\frac{n\phi}{2}\ \text{(equation 5)}$$

$$K_{dn}=\frac{\delta\sin\dfrac{\pi n}{g}}{S\sin\dfrac{\delta\pi n}{gS}} \quad (24)$$

$$K_{en}=\frac{\sin\dfrac{g}{2}\left(\dfrac{2\pi n}{g}-\gamma\right)}{\delta\sin\dfrac{g}{2\delta}\left(\dfrac{2\pi n}{g}-\gamma\right)} \quad (25)$$

$$K_{fn}=\frac{\sin\dfrac{g}{2}\left(\dfrac{2\pi n}{g}+\gamma\right)}{\delta\sin\dfrac{g}{2\delta}\left(\dfrac{2\pi n}{g}+\gamma\right)} \quad (26)$$

These factors become identical with equations 8, 11, and 12 when $\delta=g$, which represents an integral slot winding. The form of equations 25 and 26 suggests the presence of subharmonics in some windings, which is known to be possible. The form of equation 23 includes the negative sequence, and the existence factor K_{fn} if not equal to zero for the fundamental indicates an unbalanced and impractical winding.

Conclusion

The foregoing analysis has resulted in simple expressions for the magnetomotive force of all types of 2-layer windings and should prove useful in developing expressions for magnitude of vibration, parasitic torque, and differential leakage.

Appendix I

The superimposing of a number of magnetomotive forces of a given type of fractional slot winding results in a magnetomotive force which defines an integral slot winding on a subslot basis. This may be illustrated by taking the simple case of $S=5$, $g=4$. The number of subslots is 20. Table I shows the layout of such a winding.

All four of these windings have the same 2-1-1-1 grouping, but are displaced successively by a complete group. Together all the subslots are carrying current and represent an integral slot winding. The total magnetomotive force of the four windings may be expressed by

Table I

Slot	1				2				3				4				5			
Subslot	1	2	3	4	5	6	7	8	9	10	11	12	13	14	15	16	17	18	19	20
Winding 1	•				•				•				•				•			
Winding 2		•				•				•				•				•		
Winding 3			•				•				•				•				•	
Winding 4				•				•				•				•				•
Group	1				2				3				4							

Table II

Slot	1				2				3				4				5				6			
Subslot	1	2	3	4	5	6	7	8	9	10	11	12	13	14	15	16	17	18	19	20	21	22	23	24
Wdg 1	•				•				•				•				•				•			
Wdg 2		•				•				•				•				•				•		
Wdg 3			•				•				•				•				•				•	
Wdg 4				•				•				•				•				•				•
Group	1				2				3				4				5				6			

Wdg = Winding

$$\mathfrak{F}'=\sum_{n}\sum_{k=0}^{k=1}A_n\sin\left(n\theta+\omega_{0t}-\frac{2\pi nk}{g}+k\gamma\right) \quad (27)$$

This is a case where S and g do not have a common denominator. To show the effect of a common division, we take the simple case of $S=6$, $g=4$, the number of subslots being 24. Table II shows the layout of such a winding.

All four of these windings have the same 2-1-2-1 grouping, but are displaced in two different manners, the first by groups and the second by subslots. The total magnetomotive force of the four windings may be expressed by

$$\mathfrak{F}'=\sum_{n}\sum_{m=0}^{m=1}\sum_{k=0}^{k=1}A_n\sin\left(n\theta+\omega_{0t}-\frac{2\pi nk}{g}+k\gamma-\frac{2\pi nm}{gS}\right) \quad (28)$$

By an extension of this reasoning, we may write for the general case:

$$\mathfrak{F}'=\sum_{n}\sum_{m=0}^{m=\delta-1}\sum_{k=0}^{k=\frac{g}{\delta}-1}A_n\sin\left(n\theta+\omega_{0t}-\frac{2\pi nk}{g}+k\gamma-\frac{2\pi nm}{gS}\right) \quad (29)$$

where S is the greatest common division of S and g.

Appendix II. Useful Summation Formulas

In the treatment of windings with distributed conductors, it is often necessary to find the sum of many terms involving the trigonometric functions. The prototype of these sums is

$$\sum_{n=a}^{n=b}e^{jn\xi}=\frac{\sin[b-a+1](\xi/2)}{\sin(\xi/2)}e^{j(b+a)(\xi/2)} \quad (30)$$

Resolving this expression into its real and imaginary parts, we have the two formulas:

$$\sum_{n=a}^{n=b}\cos n\xi=\frac{\sin[b-a+1](\xi/2)}{\sin(\xi/2)}\times\cos[b+a](\xi/2) \quad (31)$$

$$\sum_{n=a}^{n=b}\sin n\xi=\frac{\sin[b-a+1](\xi/2)}{\sin(\xi/2)}\times\sin[b+a](\xi/2) \quad (32)$$

If we include a constant displacement ϕ, two formulas result which are the basis of all the computation made in this paper:

$$\sum_{n=a}^{n=b}\cos(n\xi+\phi)=\frac{\sin[b-a+1](\xi/2)}{\sin(\xi/2)}\times\cos[(b+a)(\xi/2)+\phi] \quad (33)$$

$$\sum_{n=a}^{n=b}\sin(n\xi+\phi)=\frac{\sin[b-a+1](\xi/2)}{\sin(\xi/2)}\times\sin[(b+a)(\xi/2)+\phi] \quad (34)$$

No Discussion

Dynamic Brush Characteristics by the Dynamotor Method

C. J. HERMAN
ASSOCIATE AIEE

THE APPLICATION of carbon brushes to electric machines generally involves a long process of trial and error. Design and manufacturing variables in the machines combine with the relatively unknown performance characteristics of the brushes themselves to create most of the complex problems of brush application. To improve the accuracy and speed of brush application engineering, as needed during the second World War, it was necessary to determine the dynamic characteristics of the brushes more completely than had been done before.

A dynamotor test method was developed to measure "friction and contact drop versus brush face temperatures" accurately over wide ranges of operating conditions. Nearly three year's usage of data obtained by this method has shown that it provides dependable information for applying brushes to machines, and for analyzing many of the difficulties encountered. These data are especially useful in indicating where trouble may be experienced in the application of new brush materials.

When the characteristic data have been coupled with past experience, it has been possible to predict, with a fair degree of accuracy, which brushes will ride well over a broad range of operating conditions with several different types of brush holders. The contact drop characteristics have proved to match very closely those obtained on several different designs of good commutating machines. The indicated variations of contact drop with temperature have been used many times to explain reasonably changes in the operating characteristics of several types of machines which are sensitive to contact drop.

Paper 47-113, recommended by the AIEE committee on electric machinery for presentation at the AIEE summer general meeting, Montreal, Quebec, Canada, June 9–13, 1947. Manuscript submitted January 30, 1947; made available for printing April 2, 1947.

C. J. HERMAN is with the fractional horsepower division, General Electric Company, Fort Wayne, Ind.

The author acknowledges the assistance of W. R. Goss, and A. B. Ray, both of the General Electric Company.

Why Take Characteristics by the Dynamotor Method?

The purpose of this paper is to discuss the dynamotor method for measuring dynamic brush characteristics and to suggest that this technique represents a very useful advance in the search for better brush application data. Developed during the war to meet the needs for quick answers, the dynamotor method has given dependable brush application data on more than a hundred designs of small a-c and d-c machines, ranging from 6 watts to 4 horsepower, and from 1,725 to 15,000 rpm. The method has saved time, has permitted a broad range of applications with limited testing, and has seemed to give a new sense of direction to the problems of brush application and brushholder design.

Brush characteristics may be divided into two distinct categories:

1. Physical or static properties. Those of most general interest are: hardness, specific gravity, porosity, elasticity or resiliency, ratio of cross to direct resistance, specific resistance, transverse strength.

2. Dynamic characteristics. These properties of greatest interest to the motor designer include contact drop, friction, and riding ability.

Using dynamotor test apparatus, we easily can measure contact drop and frictional properties of the brush films laid down on specific metallic surfaces during actual or simulated operating condition.

The ability of the brush to ride well on collecting surfaces, when mounted in specific types of brushholders, is probably the most important and the least easily measured attribute. Riding ability appears to depend upon hardness and resiliency as well as the frictional characteristics of the brush. It has been possible to establish a useful series of empirical measurements of riding ability by use of a lightweight probe held in the hand with only the weight of the probe resting on the brush in the dynamotor.

Measurements of physical properties are extremely valuable to the brush manufacturer in controlling the uniformity of his product. The techniques for making these measurements have been well developed by the various manufacturers, and efforts toward standardized methods of measurement have advanced rapidly since the war. Although useful to the designer, these data often fail to help the application and design engineers predict how to apply the brush to the machine. There is a need for the better dynamic characteristics data which the dynamotor method provides.

Dynamic brush characteristics have been taken on 12 resin-bonded, 11 metal-graphite, 1 graphite, and 27 electrographitic grades covering a field of the widely used brushes from eight brush manufacturers. Several years operating experience have been obtained with 23 of these grades. Many peculiar problems of brush operation have been explained reasonably by observed peculiarities in the dynamic brush characteristics. It appears that considerable trial and error can be avoided if these characteristic data are used properly when the original brush application is made.

Why Consider Temperature the Most Significant Variable?

On many designs, the author has noticed large changes in the performance of machines, apparently caused by pronounced changes in the friction and contact drop characteristics of brush and commutator films. The general sense of

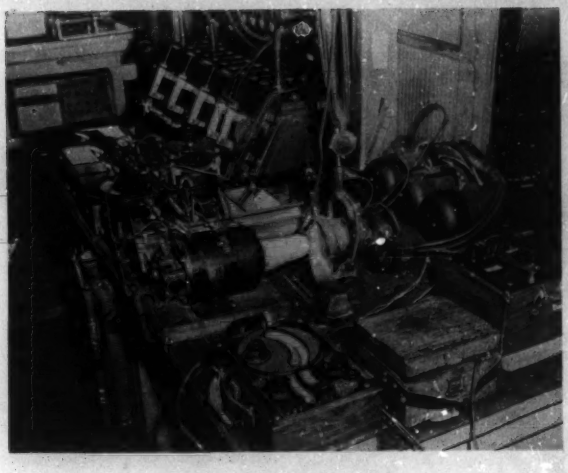

Figure 1. Brush testing dynamotor with auxiliary ventilation system and associated test equipment

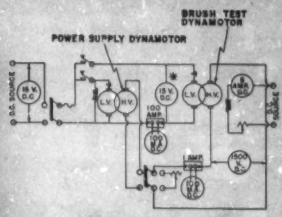

Figure 2. Circuit for determining dynamic brush characteristics

* Resistance of 1,000 ohms per volt, so that voltmeter will carry a minimum amount of current. The ventilation of the test dynamotor is obtained by use of a vacuum sweeper or similar blower operated from an adjustable voltage supply

these observations has pointed toward temperature of the brushes as the primary variable.

Whenever machines operated over wide ranges of temperature, two predominant difficulties were experienced with several grades of brushes on many different designs as follows:

1. Brushes would not ride well over the temperature range; as evidenced by chatter noise or marking on the brushes, or by measured vibration.

2. Brush and commutator films underwent large changes in contact drop; as evidenced by machine changes in output voltage, speed, commutation, stability, and other performance characteristics.

Several years of work were directed toward obtaining the best possible data concerning changes in friction, contact drop, and riding ability versus brush-face temperatures. The most useful curves were those taken with constant machine ventilation *using variable current density* to produce the desired brush face temperatures. The ventilation of the test apparatus was adjusted initially, so that average design practices were met as regards current densities over the 80 to 105 degrees centigrade usual temperature range of continuous-duty apparatus. Curves were extended rom zero to very high current densities to determine limiting conditions for safe operation of brushes well beyond conventional design practices.

Curves also were taken at *constant current density* using variable ventilation of the test apparatus to produce the desired brush face temperatures. The current density selected was usually the maximum suggested by the brush manufacturer or established by general design practice. The purpose of these curves was to help prove that temperature rather than current density was the primary variable affecting brush characteristics except for the very special conditions of

1. Zero current density.

2. Very high current densities of approximately 150 per cent or more of the normal brush rating.

Agreement of Typical Curves With Actual Experience on Machines

Case I. Medium commutating-ability electrographitic brush; grade *A;* both variable and constant current density; see Figure 4.

For this brush, contact drop and friction change sharply at 90 to 95 degrees centigrade as may be noted in curves for both variable and constant current density conditions. On a number of large industrial machines, it was necessary to increase the ventilation to hold brush temperatures below 90 degrees centigrade to obtain satisfactory performance.

Case II. High commutating-ability electrographitic brushes; grades *B* and *C;* variable current density; Figure 5. Grades *B* and *C;* constant current density; Figure 6.

These are two of the widely used brushes on large industrial apparatus, and they have been reported to have almost identical black band characteristics on large machines. The similarity of contact drop curves *B* and *C* suggests why this should be so, and also suggests that the commutating ability of a brush is governed primarily by its contact drop characteristics *over a wide range of temperatures* if it rides well throughout the range.

Grade *B* has been reported to give some riding trouble when lightly loaded. The characteristic curves show that this brush develops relatively high friction when at low temperatures and lightly loaded.

Case III. High-commutating ability electrographitic brush; grade *C;* variable current density; see Figure 7.

Figure 7 is a repeat of Figure 5, with grade *C* only, taken three weeks later and showing "hysteresis" effects of brush films when going through cycles of ascending and descending current densities.

Case IV. Resin-bonded graphite brush; grade *D;* variable current density; see Figure 8.

This was used on a machine very sensitive on commutation and on brush friction due to a particular type of brush mechanism. Curve *D* shows the grade as first used with very unsatisfactory results. Curve *DT* shows the greatly improved frictional and contact drop characteristics produced by an impregnation process over the usual 75 to 105 degree operating range. Brushes as per curve *DT* gave excellent riding and commutating performance on the application. The measured changes in dynamic characteristics indicate why the impregnated brush

was superior to the conventional material.

Case V. Metal graphite brushes, medium copper content; grades *E* and *F*; variable current density; see Figure 9. Grade *F*; constant current density; see Figure 10.

This was a case of very difficult commutation conditions, particularly on the severe overloads encountered on certain designs of low-voltage high-speed aircraft equipment.

The sharply rising contact drop characteristics of grade *F* and its higher drop at high temperatures suggest why it gave life of two to four times that of grade *E*.

Appendix I. Considerations Governing the Design of Suitable Test Apparatus

Brush characteristics data generally are taken on one of two basically different types of test equipment as follows:

1. Slip rings (using either d-c or a-c power).
2. Commutators (on commutating machines).

The complexities of brush behavior are such that neither type of test provides entirely adequate application data for the design engineer. If brush characteristics are to be taken by only one type of test, experience has indicated that the most generally applicable data are those obtained on a suitably designed commutating machine, rather than on slip rings. There is considerable data to show that brushes form films on rings very different from those on commutating machines. Therefore, to cover accurately both ring and commutator applications, brush characteristics should be taken on both types of apparatus.

The majority of brush applications involve the operation of brushes on commutators. It generally is believed that brush films are affected markedly by the short-circuit conditions of commutation. It does not appear practical to attempt to duplicate the effects of short-circuit conditions on slip ring or dummy commutator apparatus.

The basic design of test machine inherently should promote the best commutating conditions possible on d-c apparatus, so that the following requirements are met:

1. The commutating ability of the brush must not be an important factor in the successful operation of this apparatus. "Black," or non-sparking, commutation should prevail throughout the range of test conditions, even when the lowest-drop lowest-cross-resistance brushes commercially available are being tested.

2. There must be widely accepted design agreement that this type of apparatus does not involve controversial commutation conditions.

Many conventional 2-pole d-c-to-d-c radio dynamotors which operate on 14-to-28-volts input meet these requirements on the low voltage end of the machines. Therefore, it is proposed that brush characteristics data be taken on the low voltage end of dynamotors having the following general range of design features:

1. Speed between 5,000 and 10,000 rpm.
2. Commutator diameters.
(*a*). Low voltage is 1½ to 3 inches.
(*b*). High voltage is 2 to 3 inches.

3. Commutator materials: Silver-bearing lake copper is preferred because it is probably the most commonly used commutator bar material.

4. Winding: 2-pole, noninterpole, shunt or compound wound. Separate shunt excitation is desirable for test purposes.

5. Ventilation: Air flow past low voltage brushes and commutator should be approximately constant for all conditions of testing. It should be possible to secure the desired ranges of temperatures on the low voltage end by cooling the armature from the high voltage end. If used in altitude chamber tests, it must be highly ventilated by fan or other means; or, if nonventilated, commutators and brushes must be well exposed to the chamber air.

6. Ratio of transformation: This is not important for life tests, but for contact drop and friction measurements, the ratio of output to input voltage should be more than ten to one. Good results have been obtained between 40 and 80 to 1.

7. Type of brushholder: Radial cartridge type generally are used on this apparatus. They are suggested to be satisfactory for these tests, because most of the brush grades widely used on large and small machines will ride satisfactorily in these holders. Any holder which does not promote chatter of the grade to be tested may be used. It is recognized that all grades of brushes can not be used in only one type of holder.

8. Bearings and bearing loading: Use ball bearings, but apply finger-spring loading to eliminate radial looseness and thereby reduce dynamic commutator runout to the minimum.

9. Brush pressure: Initial pressure should fall within the 4 to 6 pounds per square inch widely used on small apparatus. It is suggested that 4.5 pounds initial and 3 pounds worn pressure be adopted for these tests. Characteristics may be taken at any other pressure desired, such as 2.5 often used on large apparatus.

Dynamotors similar to the 350-watt 14/-1,000- or 28/1,000-volt type widely used on *B17* and *B24* airplanes meet these requirements, except that the output winding preferably should be changed to 500 volts or less for safer and more reliable test conditions. Dynamotors appreciably smaller than the 350-watt types may not produce high enough brush temperatures and peripheral speeds to cause film breakdown of non-altitude-protected brushes.

Appendix II. General Test Procedure

The brushes to be tested are installed on the low voltage end of a test dynamotor. Contact drop and friction characteristics are taken by two methods over a brush temperature range of approximately 50 to 150 degrees centigrade.

1. Dynamotor ventilation is maintained constant, and the load (current-density) is varied to produce the desired brush-face temperatures.

2. Current density is maintained constant, and dynamotor ventilation is varied to produce the desired brush-face temperatures.

Before and after each test run, readings are then at zero current density (which is a particularly important test point). The zero density readings give valuable check results upon the accuracy of the test methods. They also provide excellent indications of the filming characteristics of the brush, and of the degree to which the brush face undergoes permanent change. Some brushes repeat filming characteristics very closely time after time—others change markedly after once being subjected to high temperatures and high current densities.

An endeavor has been made to establish an exact sequence of test conditions which

Figure 3. Typical test data

For each value of L_{LV}, all readings are recorded on horizontal lines

E_{HV}	I_{HV}	TWO 3 WINDING POWER IS APPLIED	E_{LV}	I_{LV}	I FIELD	RPM	BRUSH TEMP. °F/°C FROM FACE LV (°C)	BRUSH TEMP. °F/°C FROM FACE LX (°C)	TIME BRUSH CHANGES IN HOURS READING	DIFFERENCE BETWEEN TEMPERATURE HV WINDING	DIFFERENCE BETWEEN TEMPERATURE LX WINDING	POSITION OF LV BRUSHES	VENTILATION BLOWER SETTING	CHATTER RATING OF LX BRUSHES
264	290	LV	130	362	2.1	5000	106	110	4			IN	56	OK +
266	080	HV	104	0					1/60			IN		
266	.058	HV	0	0					1/60	644 (TAKEN WITH ARMATURE STOPPED)	.0091	OUT		

Figure 4 (below). Grade *A* brush material

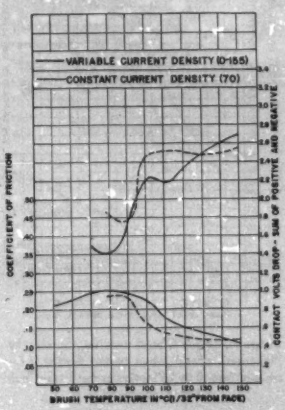

Figure 5 (below). Grades *B* and *C* brush materials

Variable density from 0 to 135 amperes per square inch

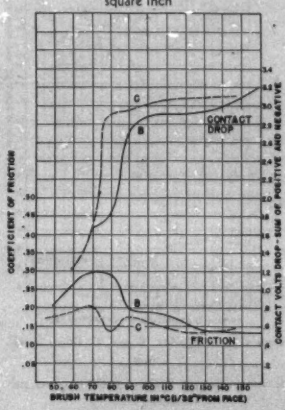

will simulate closely the ranges of conditions actually encountered on *good commutating machines*.

Exact Sequence of Test

VARIABLE CURRENT DENSITY—CONSTANT VENTILATION CONDITIONS FOR TEST DYNAMOTOR

Sand Low Voltage Brushes to Fit.

Clean the Low Voltage Commutator. Always begin test runs with a clean (film-free), true commutator surface.

Zero Current Density Point (Before the Brushes Ever Have Been Loaded). Drive from high voltage side. No load on low voltage side except voltmeter. Operate 15 to 25 hours before taking readings.

First Load Point. Drive from low voltage side. No load on high voltage side except voltmeter. Operate at least two hours (preferably three) before taking readings. This condition gives the lowest possible current density when driving from low voltage end, and usually results in about 70 degrees centigrade at the brush face.

Other "Increasing Current-Density" Load Points. Drive from low voltage side. Adjust resistance load on high voltage side for adequate load to cause the desired brush temperatures.

To progress from one load point to the next higher value, immediately increase the load to slightly less than the estimated value (from test experience). Check brush temperature at about 15-minute intervals. If temperature is approximately 3 to 5 degrees centigrade lower than the desired test value at end of 1/2 hour, slightly increase load.

It generally will take 3/4 to 1 hour for the brush temperature to level within 2 or 3 degrees centigrade of the desired test value. Then operate 1 to 3 additional hours at approximately equilibrium conditions before taking readings.

The preferred temperature steps in degrees centigrade: 80, 90, 100, 110, 125, 150.

Recheck of Zero Current-Density Point. If "decreasing current-density" load points are not desired, drive from high voltage side with no load on low voltage side except voltmeter for 15 to 25 hours before reading.

Alternate for the Preceding Step. If "decreasing current-density" load points are desired: Progress from one load point to the next lower value by immediately decreasing the load to slightly above the value previously determined during the "increasing current-density" test—for the desired test temperature. Check brush temperatures at about 15-minute intervals. If temperature is approximately 3 to 5 degrees centigrade high at end of 1/2 hour, slightly decrease the load. Then operate 1 to 3 hours more at approximately equilibrium temperatures before taking readings.

The preferred temperatures in degrees centigrade are (repeat 150 degrees centigrade again only if shutdown occurred after test for "increasing current-density" load points):

1. 125
2. 100
3. Approximately 70 (Drive from low voltage side, no load on high voltage).
4. Approximately 50 (Drive from high voltage side, no load on low voltage except voltmeter. Operate 15 to 25 hours before taking readings).

If overnight shutdown is necessary during this test, operate at the next desired brush temperature at least 3 hours before taking readings.

CONSTANT CURRENT DENSITY—VARIABLE VENTILATION CONDITIONS FOR TEST DYNAMOTOR (BUT APPROXIMATELY CONSTANT VENTILATION CONDITIONS AROUND THE LOW VOLTAGE BRUSHES)

Raise Low Voltage Brushes. Film on brush faces must not be touched or removed.

Clean the Low Voltage Commutator Only. Remove all film in brush track by sanding carefully with a U-shaped band of 4/0 or finer dry-type sandpaper. Drive from high voltage end at about 2,500 rpm for this sanding operation. Blow out all dust with clean air.

Zero Current Density Point. Lower low voltage brushes in place. Drive from high voltage side. No load on low voltage side except voltmeter. Operate 15 to 25 hours before taking readings.

Constant Current-Density Variable-Temperature Points. 1. Drive from low voltage side. Adjust resistance load on high voltage side to give the desired current-density on low voltage side. During the entire test run, make slight resistance adjustment as necessary to maintain *constant input current* on low voltage side.

2. First temperature point: Use all ventilation available to cool the armature from the high voltage end. Also direct a stream of clean air against the stator, but use a baffle to protect low voltage brushes from direct air blast.

Operate at least 3 hours before taking readings. This first temperature point usually will be from 85 to 90 degrees centigrade.

The preferred temperature steps in degrees centigrade are: 85 to 95, 100, 110, 125, 150.

To progress from one temperature point to the next higher value, reduce the ventilation as necessary. Operate 2 to 3 hours at approximately equilibrium conditions at each temperature point before taking readings.

Recheck of Zero Current Density Point. Drive from high voltage side. No load on low voltage side except voltmeter. Operate 15 to 25 hours before taking readings.

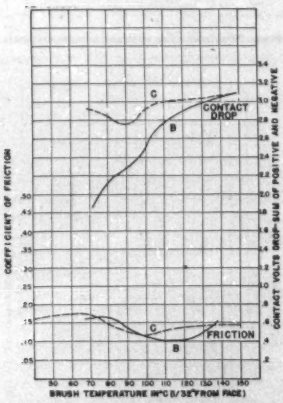

Figure 6. Grades *B* and *C* brush materials

Constant current density of 60 amperes per square inch

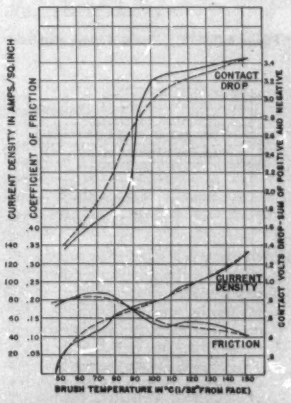

Figure 7. Grade *C* brush material, showing the "hysteresis effect" when current density is increased from 0 to 135 amperes per square inch and then decreased to 0

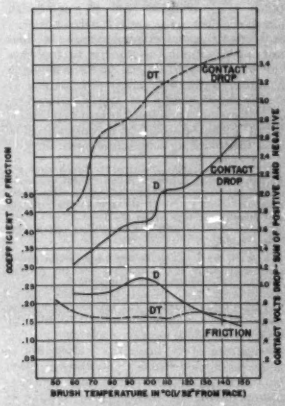

Figure 8. Grade *D* and *DT* (treated) brush material

Variable current density from 0 to 125 amperes per square inch

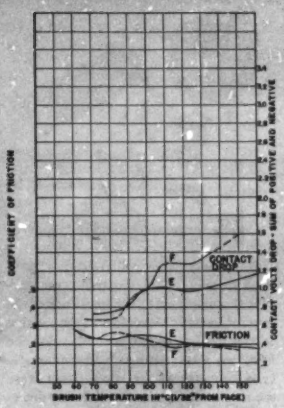

Figure 9. Grades *E* and *F* brush materials

Variable current density from 0 to approximately 200 amperes per square inch

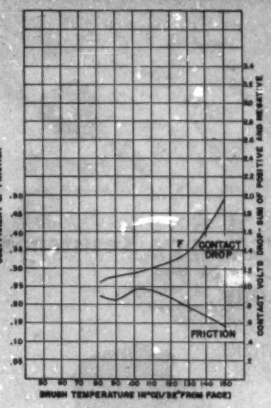

Figure 10. Grade *F* brush material

Constant current density of 100 amperes per square inch

General Test Conditions

1. To seat the low voltage brushes: Sand brushes to fit roughly the commutator using arbor and sandpaper. Drive dynamotor from high voltage end at about 2,500 rpm, clean low voltage commutator lightly with pumice stone to remove film, then install low voltage brushes and use additional pumice to seat brushes for 80 per cent or more face area. Clean the dynamotor thoroughly with air blast, and lightly wipe the commutator with a clean cloth.

Raise the low voltage brushes. Finally clean and polish commutator surface with a U-shaped piece of 4/0 or finer dry-type sandpaper.

Check spring pressures on brushes. Mark and maintain the rotational position of brush springs with respect to brushes.

2. On new armatures used for the first time, commutators should be diamond-turned (or equivalent) to give surfaces having a high quality of true eccentricity.

(*a*). Commutator eccentricity: With armature rotated on its own bearings, gauge runout should not exceed 0.0006 inch, and bar-to-bar offsets should not exceed 0.0001 inch.

(*b*). As a further check on eccentricity, a uniform brush film must extend completely across all bars peripherally, after the zero current density test runs.

3. Brush faces and commutator surfaces in the brush track must not be touched during the test runs.

4. Brushes must be seated 100 per cent before test readings are begun.

5. Test dynamotor must be supplied from an extremely high-quality stable d-c power source.

6. Use suitable power sources and double-throw switching arrangement, so that the power input can be switched very quickly to either the low voltage or high voltage sides of the dynamotor.

7. Use $4^1/_2$ pounds per square inch brush pressure, unless other pressures are wanted. Carefully check brush springs at beginning of tests and end of the last test run.

8. Maintain constant peripheral speed at all times. Keep speed within 5,000 rpm plus or minus 100 rpm by adjusting the input armature volts. Maintain constant shunt field current at all times equal to 2.10 amperes.

9. Precise readings of input volts and amperes, output volts and amperes, and low and high voltage armature resistances suitable for contact drop calculations are required. Sum of meter plus meter reading errors on low voltage voltmeter must not exceed plus or minus 0.05 volt.

Typical Calculation Formulas

Friction watts $= E_{HV}I_{HV}$ (with low voltage brushes in and $I_{LV}=0$) $- E_{HV}I_{HV}$ (with low voltage brushes out).

Brush contact drop (sum of plus and minus).

1. With Power Applied to the Low Voltage End.

Brush drop $= E_{LV} - (E_{LV}$ counter electromotive force $+ I_{LV}R_{LV})$

$$E_{LV} \text{ counter electromotive force} = \frac{E_{HV} + I_{HV}R_{HV} + HV \text{ brush drop}}{\text{ratio of } \frac{HV}{LV} \text{ armature winding turns}}$$

Normally "high voltage brush drop" may be disregarded, because it is too small (when compared with the high voltage output or input) to affect the calculated brush drop materially.

Then

$$E_{LV} \text{ counter electromotive force} = \frac{E_{HV} + I_{HV}R_{HV}}{\text{ratio of } \frac{HV}{LV} \text{ armature winding turns}}$$

2. With Power Applied to the High Voltage End. (I_{LV} = approximately 10 milliamperes taken by a 1,000 ohms/volt voltmeter)

Brush drop $=$ E_{LV} counter electromotive force $- E_{LV}$

$$E_{LV} \text{ counter electromotive force} = \frac{E_{HV} - I_{HV}R_{HV}}{\text{ratio of } \frac{HV}{LV} \text{ armature winding turns}}$$

No Discussion

Data on the High-Frequency Resistance of Coils

W. F. WITZIG
ASSOCIATE AIEE

Synopsis: The high frequency resistance of several coils was measured. An approximate method is derived to determine coil resistance for coils wound with flat strap. A short empirical method for obtaining coil resistance for coils wound with tubing also is shown. Factors affecting coil resistance are discussed.

SINCE the introduction of commercial induction and dielectric heating the coil components in high-power high-frequency equipment have been re-examined. The purpose of this examination was to reveal a simple method to determine the resistance of a coil at frequencies above power frequencies.

In the design of oscillators and induction heating coils the engineer must deal with high frequency resistance. Because of the power requirements the coils used in this application are made from copper tubing. The coils are generally air cored, having a pitch equal to about two tubing diameters. Coil lengths and diameters cover a large range. A few coils in the field just described were examined in the following investigation.

In this paper the resistance of coils wound with tubing is compared to the resistance of this tubing when it is straight and isolated. An empirical constant relating the two resistances is shown in the various figures for some common coil shapes. The resistance of a coil wound with flat strap is compared with an approximate formula for strap coils. With the aid of the figures the resistance of a coil similar to those tested can be approximated.

Paper 47-122, recommended by the AIEE committee on industrial power applications for presentation at the AIEE summer general meeting, Montreal, Quebec, Canada, June 9–13, 1947. Manuscript submitted November 13, 1946; made available for printing April 8, 1947.

W. F. Witzig is research engineer in the electrophysics department of the Westinghouse Electric Corporation, East Pittsburgh, Pa.

The author wishes to express his gratitude to R. M. Baker for many helpful discussions on this work. Part of this work was submitted to the graduate school of the University of Pittsburgh in partial fulfillment of the requirements for the degree of master of science in June 1944.

Description of Coils Tested

Table I gives a detailed description of the dimensions and geometry of the coils tested. All but two of the eight original coils were wound with 1/4-inch outside diameter commercial copper tubing. The nominal wall thickness of the 1/4-inch tubing was 0.035 inch. Exceptions to this were coils G and H. Coil G was made twice as big as coil F to test for similitude in the resistance measurements. In order to do this coil G was wound with 1/2-inch-outside-diameter commercial copper tubing with a nominal wall thickness of 0.049 inch. Coil H was wound with copper strap and had the same dimensions as coil A. With this arrangement tubing and strap could be compared as coil conductors. The copper strap used in coil H was 0.258 inch wide and 0.0625 inch thick and was cooled by 3/16-inch copper tubing soldered to its back. Figure 1A shows some of the coils tested.

Resistance Measurements

At the lower frequencies, below 15 kc, an inductor generator supplied sufficient power for measuring purposes.

Above 15 kc a Hartley type oscillator employing a type 889 water-cooled triode was the source of power. The oscillator was loaded by placing the coil under test in the ground side of the inductive branch of the oscillator tank circuit. With the available equipment, frequencies in the 40-to-500-kc range were obtained conveniently.

To calculate the coil resistance three measurements were required: the current through the coil, the frequency of the current, and the power lost in the coil due to the passage of the current. For the first two measurements a thermocouple type ammeter and a wave meter were used. Power lost in the coil was determined by the heating of water circulated inside the tubing of the coil. After thermal equilibrium of the water and coil was established, the temperature rise of the water and the rate of water flow were obtained. Temperatures were measured by mercury in glass thermometers and the rate of water flow by a calibrated Venturi section. The power input to the cooling water, W_T, can be found by using the formula

$$W_T = 4.19 \times V \times \Delta\theta \times h, \qquad (1)$$

where

W_T = power input to the water, watts
V = water flow, grams per second
$\Delta\theta$ = temperature rise of the cooling water, degrees centigrade
h = specific heat of water, one calorie per gram per degree centigrade

Because the coil would not always be at room temperature, a correction for the power lost to or absorbed from the room was made on the power input to the cooling water. With the corrected power loss due to the high frequency current, the total resistance of the coil, R_T, can be calculated by

$$R_T = \frac{W_c}{I^2} \qquad (2)$$

where

R_T = total resistance of the coil (including leads to coil proper), ohms
I = high frequency current in the coil, rms amperes
W_c = corrected power loss in coil due to high frequency current, watts

The actual coil resistance R_c can be found by subtracting the resistance of the coil leads from the total resistance. Since the leads were straight tubing, this calculation was made easily.

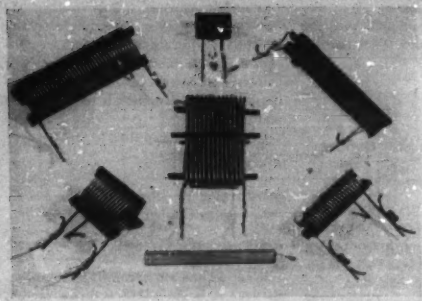

Figure 1A. Typical coils tested

Figure 1B (below, left). Schematic sketch of apparatus for measuring coil resistance

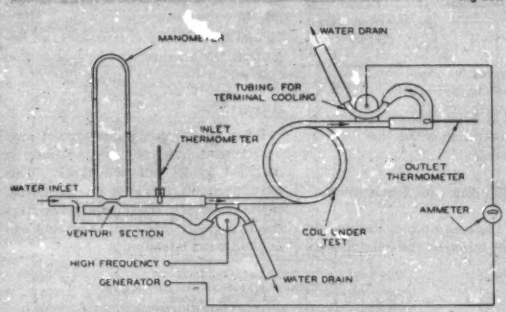

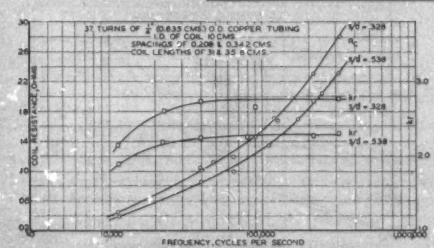

Figure 2. Coil resistance and ratio of coil resistance to tubing resistance of coil *A*

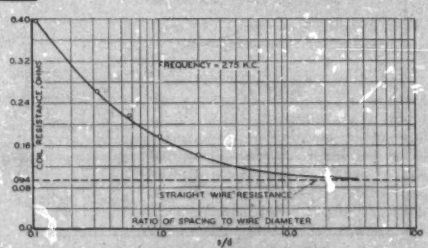

Figure 3. Coil resistance as a function of spacing, coil *A*

Figure 1*B* shows a schematic diagram of a coil undergoing resistance measurement. In this figure a method to prevent heat from flowing from the coil leads to the cooling water in the coil is shown. The method consisted of having a piece of tubing soldered at the coil connections and keeping the temperature of this tubing equal to that of the power measuring water alongside of it.

In order to make accurate resistance measurements the resonant frequency of the coil under test must be high compared to the frequency employed for the resistance measurement. Resonant frequencies of the coils were determined with the aid of a small tuned-plate tuned-grid oscillator. The coil under test for its resonant frequency was coupled loosely to the tank circuit of the oscillator. By varying the oscillator frequency a point of maximum voltage across the coil undergoing measurement could be found. The frequency at this point of maximum voltage was taken as the resonant frequency. All the eight coils were found to have a resonant frequency well above the frequencies employed to determine their resistance.

Determination of Straight Wire Resistance

The main purpose of this report is to compare tubular copper coil resistance with the resistance of the tubing when it is straight and isolated. To complete this comparison the following illustrates a procedure for resistance calculation of straight wires.

Resistance of straight, isolated, nonmagnetic, solid, round wire at high frequencies is a classical problem in many textbooks. The following equation has been derived by Warren,[1] Howe,[2] and others.

$$R_f = R_o\left(\pi r\sqrt{\frac{f}{\rho\times 10^9}}+0.25\right) \qquad (3)$$

where

R_f = resistance at high frequencies of straight isolated solid wire, ohms
R_o = d-c resistance of the wire, ohms
r = radius of the wire, centimeters
f = frequency, cycles per second
ρ = resistivity, ohm centimeters

Equation 3 reduces quite easily. For copper ($\rho = 1.7 \times 10^{-6}$ ohm centimeter) the high frequency resistance becomes

$$R_f = R_o(0.038d\sqrt{f}+0.25) \qquad (4)$$

where

d = outside diameter of the wire, centimeters

When the first term in the parentheses of equation 4 becomes much larger than 0.25, the resistance may be approximated by equation 5.

$$R_f = 0.038R_o d\sqrt{f} \qquad (5)$$

An experimental check on these resistance equations was made by the author. The resistance of coil *A* was found as a function of the coil length. This relationship is plotted in Figure 3. As the ratio of spacing between turns to tubing diameter s/d grows large (that is, as the tubing in the coil becomes straight), the coil resistance approaches the straight wire resistance.

These equations can be applied to tub-

ing which is straight, isolated, and round if the following condition is met. This condition requires that the depth of penetration of current must be less than the wall thickness. Depth of penetration of current (δ) is defined as the depth to which the total current in the conductor would have to flow uniformly to produce the power that is lost in the conductor. The following formula gives the depth of penetration in centimeters:

$$\delta = 5{,}030\sqrt{\frac{\rho}{\mu f}} \tag{6}$$

where

δ = depth of penetration of current, centimeters

μ = permeability of conductor (one for copper)

Equation 6 is graphed in Figure 12 for a few nonmagnetic metals. With the aid of equation 6 or Figure 12 the depth of penetration into the wall of the tubing can be found. If this is less than the wall thickness the resistance formulas can be used. However, the d-c resistance R_o must be calculated assuming the tubing solid.

Equation 6 also enables the calculation of resistance for flat, straight, isolated strap to be made. Assuming that the strap width is large compared with the thickness, the area through which current will flow is then

$$A_s = 2b\delta \tag{7}$$

where

A_s = current carrying area, centimeters squared

b = strap width, centimeters

The 2 in equation 7 results from the current flowing in both sides of the strap. Knowing the area the resistance of strap can be calculated by

$$R_s = \frac{\lambda}{A_s}\rho \tag{8}$$

where

R_s = resistance of the strap, ohms

λ = length of strap, centimeters

Equation 8 is applicable only when the depth of penetration is less than half the strap thickness.

Factors Affecting Coil Resistance

Knowing the resistance of the straight tubing wound into a coil, the coil resistance can be approximated. Coil resistance is found by multiplying the straight tubing resistance by an empirical resistance constant K_r. The constant K_r is the ratio of coil resistance to the resistance of the tubing in the coil, assuming it to be straight and isolated.

Coil resistance can then be written as

$$R_c = K_r R_f \tag{9}$$

Substituting into equation 4, the coil resistance is calculated by

$$R_c = K_r R_\rho (0.038d\sqrt{f} + 0.25) \tag{10}$$

With a method for calculating the coil resistance it is important to know factors affecting this resistance. Of these many factors that affect coil resistance, an important few are discussed here in outline fashion.

Resonance

When a coil is used at a frequency near its resonant frequency, its resistance is modified by its self-capacitance. This self-capacitance increases the circulating current flowing in the coil and hence gives rise to a greater coil loss. Apparent coil resistance can be shown as

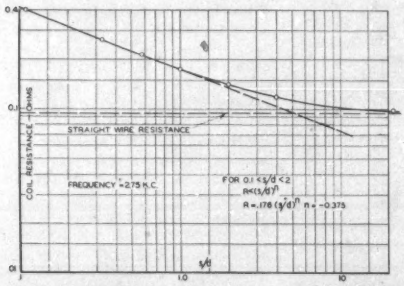

Figure 4. Log log plot of coil resistance as a function of the ratio of spacing between turns to tubing diameter

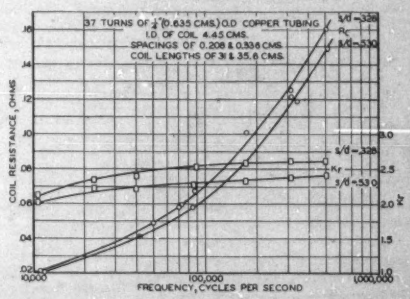

Figure 6 (above, right). Coil resistance and ratio of coil resistance to tubing resistance of coil C

Figure 7 (below). Coil resistance and ratio of coil resistance to tubing resistance of coil D

Figure 5. Coil resistance and ratio of coil resistance to tubing resistance of coil B

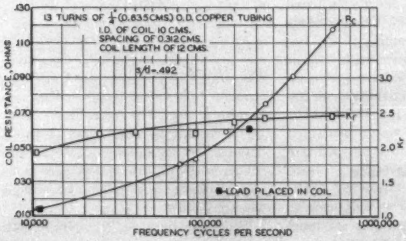

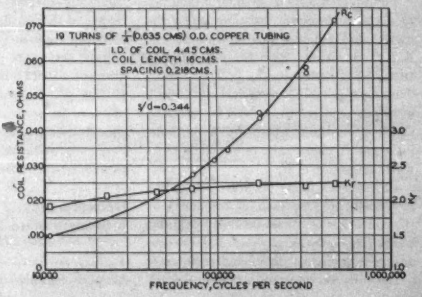

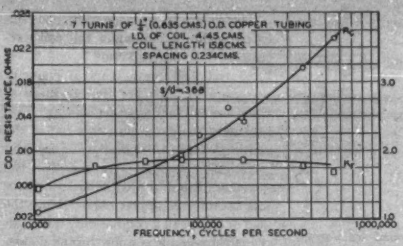

Figure 8. Coil resistance and ratio of coil resistance to tubing resistance of coil *E*

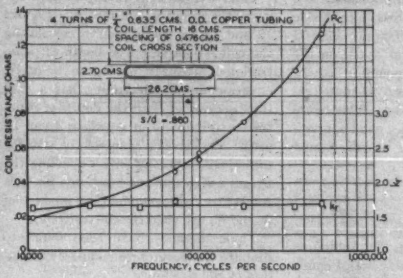

Figure 9. Coil resistance and ratio of coil resistance to tubing resistance of coil *F*

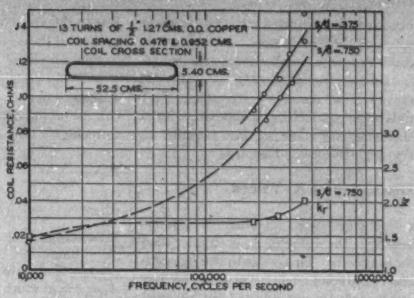

Figure 10 (above, right). Coil resistance and ratio of coil resistance to tubing resistance of coil *G*

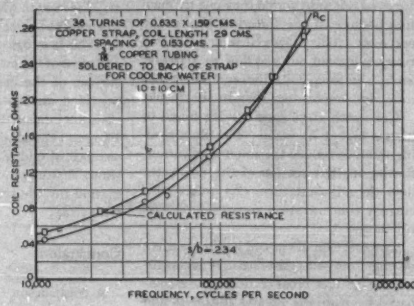

Figure 11. Comparison of calculated and observed resistance of flat strap coil *H*

$$R_c' = \frac{R_c}{(1-\omega^2 LC_o)^2} \tag{11}$$

where

R_c' = coil resistance including effect of self-capacitance, ohms
$\omega = 2\pi f$
L = coil inductance, henrys
C_o = self-capacitance of coil, farads

Equation 11 is not valid at the resonant frequency of the coil nor does it apply to coils that have a voltage induced in them when there is a capacitor in parallel.

To use equation 11 the distributed capacitance and the inductance of the coil must be known. The distributed capacitance of a coil as found by Mason[3] can be calculated by

$$C_o = 4.55\times10^{-14}\frac{l}{\log_e \frac{0.72l}{D}} \tag{12}$$

when

$l > D$

or

$$C_o = 1.43\times10^{-13}D \tag{13}$$

when

$l < D/2$

where

D = inside diameter of coil, centimeters
l = length of the coil, centimeters

Coil inductance can be measured or calculated from many formulas available in handbooks. With the inductance and self-capacitance known, equation 11 can be used to determine the effect of coil resonance.

Resistivity

The average resistivity of the coils tested was about 2.0×10^{-6} ohm centimeter at 15 degrees centigrade. Accuracy of resistivity values is not too important because the high frequency resistance varies only as the square root of the resistivity.

Coil Geometry

Size and shape of coils affect their high frequency resistance very broadly. A few aspects of coil geometry are discussed here in the limited field of the coils tested.

Spacing to Tubing Diameter Ratio

Increasing this radio produces a lower coil resistance as is illustrated in Figures 3 and 4. Figure 4 is the same plot as Figure 3 but on a log log plot. On the log log plot the coil resistance as a function of s/d is practically a straight line for small values of s/d. This means that the coil resistance is directly proportional to s/d raised to some power n. Tangent to the resistance curve is drawn a dotted line. The slope of this line is the power to which s/d must be raised and is equal to about -0.375. With other coils for which different values of s/d were available, the power n varied from -0.2 to -0.4.

Length to Diameter Ratio

An inspection of the figures reveals that this ratio has an effect other than just increased or decreased length. See Figures 6, 7, and 8. For coils having a constant pitch, cross section, and tubing size, the coil resistance is proportional to length when the l/D ratio is greater than three. When l/D is smaller than three the resistance seems to drop off faster than the length. This is an end effect proposition which is investigated further under discussion of K_r values.

Coil Cross Section

When conductors on opposite coil sides are brought close together, the current

becomes concentrated on the adjacent sides of the conductors. Since current must flow in a smaller area, the coil resistance is increased. In general, coil cross section remains a secondary effect unless the conductors on opposite sides of the same coil come as close together as two or three tubing diameters.

Discussion of K, Values

For short coils, all other dimensions constant, the value of K_r is smaller than for long coils. This is due to the phenomenon called end effect. Turns at the ends of the coil are not affected by adjacent turns on one side nor do they cut as much flux because of the spread of flux at the coil ends. This allows current in the end turns to spread out and flow in a greater area. In long coils the end effect has much less importance than in short coils.

Coils with close spacings are found to have a higher K_r value. The close spacing tends to reduce the amount of current flowing in that section of the conductor near the adjacent turn. As before, this current concentration increases the coil resistance.

Cross section of the coil had little effect on the observed resistance. A rectangular and circular cross section can be compared by studying Figures 9 and 10 and comparing them with the other figures. The K_r values appear to be lower for the rectangular cross section coils but this is due to the short length and not the cross section of these coils.

The empirical constant K_r can be avoided for coils wound with strap. Coil resistance in the case of strap conductors can be approximated by the following formula:

$$R_{cs} = \rho \frac{\lambda_c}{A_{cs}} \tag{14}$$

where

R_{cs} = resistance of coil wound with strap, ohms
λ_c = length of strap in coil, centimeters
A_{cs} = area in which the current flows, $b\delta$

A_{cs}, the area in which the current flows, is assumed to be one half of that in equation 7. This is a logical assumption since in a coil most of the current flows on the inside surface of the coil conductors. Coil H provided an experimental check on the resistance calculated by equation 14. In Figure 11 the measured and calculated resistance of coil H is shown. This figure shows that equation 14 is a good approximation for the resistance of coils wound with strap.

Conclusion

A comparison of strap and tubing as coil conductors can be made with Figures 2 and 11. In the frequency range covered the resistance of the two coils stayed fairly close together. Thus it appears that strap and tubing serve equally well as coil conductors.

The effect of a conducting body located within a coil upon the coil's resistance is shown in Figure 5, coil B. A brass rod 7.64 centimeters in diameter was used to duplicate the condition of using the coil for induction heating. Coil resistance observed with this rod in the coil is plotted in Figure 5 using the solid rectangular symbol. At the two frequencies, 10 and 180 kc, the coil resistance was not affected appreciably. Hence the load or charge in a coil has only a secondary effect when it is a few tubing diameters away from the coil conductors.

For coils wound with strap, equation 14 gives a good approximation of coil resistance providing the depth of penetration is less than half the strap thickness.

Coils wound with tubing require the use of the empirical constant K_r. Figures 12 and 13 are useful aids in calculating the coil resistance. The depth of penetration is obtained on Figure 12 or by equation 6. If the tubing has a wall thickness larger than the depth of penetration, Figure 13 or equation 4 can be used. This gives a value of the straight tubing resistance R_f. By inspecting the figures a K_r value can be chosen for coils similar to those tested. The product of R_f and K_r will yield the coil resistance.

These methods have been found to simplify the heretofore complex calculation of coil resistance.

List of Symbols

A_s = current carrying area of strap conductor, centimeters squared

Figure 12. Depth of penetration of current into a few metals

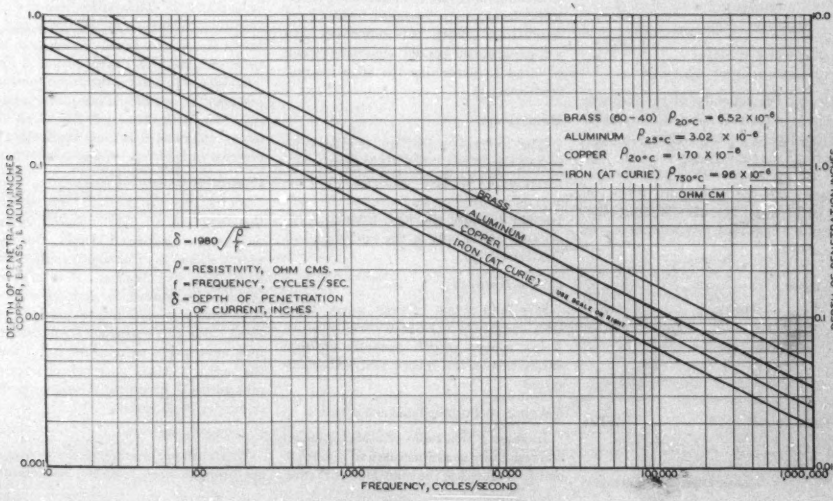

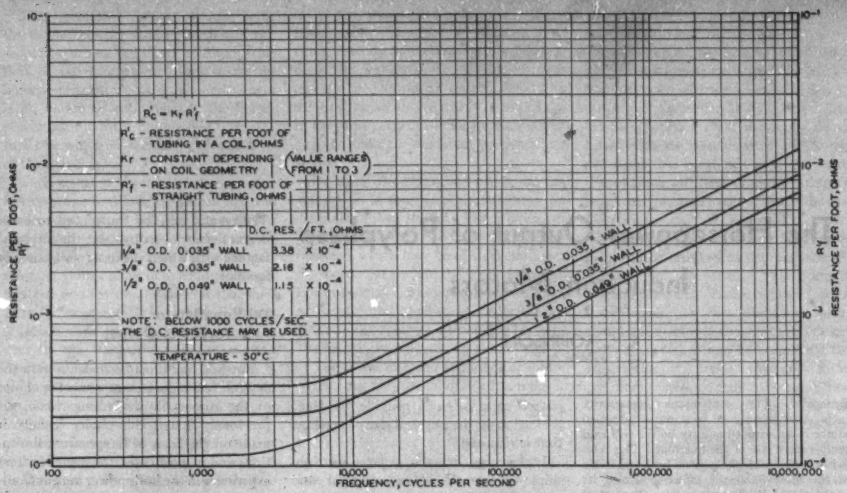

Figure 13. Resistance per foot of straight copper tubing as a function of frequency

Tubing assumed to be at a temperature of 50 degrees centigrade

A_{cs} = area in which current flows in a coil wound with strap, centimeters squared

b = strap width, centimeters

C_o = self-capacitance of coil, farads

δ = depth of penetration of current, centimeters or inches

d = outside diameter of the wire, centimeters

D = inside diameter of coil, centimeters

f = frequency, cycles per second

h_s = specific heat of water, one calorie per gram per degree centigrade

I = high frequency current in the coil, rms amperes

= ratio of coil resistance to the resistance of the tubing, assuming it to be straight and isolated

λ = length of strap, centimeters

λ_s = length of strap in coil, centimeters

L = coil inductance, henrys

l = length of coil, centimeters

μ = permeability of conductor

n = power that s/d is raised, to make it proportional to R_c

ρ = resistivity, ohm centimeter

r = radius of the wire, centimeters

R_c = coil resistance, ohms

R_c' = coil resistance per unit of tubing length, ohms per foot

Table I. Coil Specifications

Coil	D-C Resistance, Ohms	Weight, Lb	Cross Section	Inside Diam, Cm	Turns	Coil Length, Cm	Tubing Length, Cm	Tubing* Wall Thickness, In.	Resistivity, Ohm Cm, 25 C
A	0.0181	3.63	Circular	10	37	Varied	1,235	0.0335	2.12×10^{-6}
B	0.0068	1.31	Circular	10	13	12	435	0.0330	2.17
C	0.0095	1.81	Circular	4.45	37	Varied	591	0.0340	2.33
D	0.0045	0.97	Circular	4.45	19	16	304	0.0330	2.04
E	0.0018	0.41	Circular	4.45	7	5.8	112	0.0345	2.11
F	0.0108	2.28	Rectangular		14	16	728	0.0355	2.24
G	0.0060	14.57	Rectangular		13	Varied	1,430	0.053	1.90
H			Circular	10	36	29.4	1,164		
								Avg resistivity	2.13×10^{-6}

* Assuming 0.322 pound per cubic inch for copper.

R_c'' = coil resistance including effect of self-capacitance, ohms

R_{cs} = resistance of coil wound with strap, ohms

R_f = resistance at high frequencies of straight isolated solid wire, ohms

R_f' = resistance per unit of tubing length at high frequencies of straight isolated solid wire, ohms per foot

R_o = d-c resistance of solid wire, ohms

R_s = resistance of strap, ohms

R_T = total resistance of the coil (including leads to coil proper), ohms

s = spacing between turns of the coil, centimeters

$\Delta\theta$ = temperature rise of the cooling water in degrees centigrade

V = water flow, grams per second

$\omega = 2\pi f$

W_c = corrected power loss in coil due to high frequency currents

W_T = watts input to power measuring water

References

1. Mathematics Applied to Electrical Engineering (book), A. G. Warren. Chapman and Hall, Ltd., London, England, 1941. Page 248.

2. The High Frequency Resistance of Wires and Coils, G. W. Howe. *Journal* of the Institution of Electrical Engineers (London, England), volume 58, page 152.

3. Natural Frequency of Coils, R. C. Mason. Westinghouse Research Memo, Number *60-94290-10*, August 1943.

4. Theory and Calculation of Alternating Current Phenomena (book), C. P. Steinmetz. McGraw-Hill Book Company, New York, N. Y., 1916.

No Discussion

The Horsepower Output of Polyphase Induction Motors

R. C. ROBINSON
MEMBER AIEE

Synopsis: The continuous horsepower rating that is assigned to a given induction motor is determined mainly by the full load temperature rise of the machine. The temperature rise is dependent on both the losses in the motor and the effectiveness of its ventilation. While an accurate theoretical prediction of temperature rise is very difficult, a simple empirical method is presented here which gives good results over a wide range of motor sizes. The familiar D^2l equation for horsepower output is discussed from the point of view of temperature rise, and a new form of equation is suggested which takes into account both ventilation and motor losses. By relating the horsepower output directly to the major physical dimensions of the induction motor a consistent basis of design is established for machines of widely different sizes and speeds.

THE continuous horsepower output is only one of a number of operating characteristics that determine the suitability of an induction motor for a given application. The purchaser may place limits or guarantees on some or all of the following characteristics: starting torque, pull-up torque, pull-out torque, locked rotor inrush current, efficiency, and power factor at one half, three quarters, and full load and the temperature rise at the required horsepower output.

In the large majority of cases it is found that the desired operating characteristics as regards torques, inrush, efficiency, and power factor may be obtained by suitably proportioning the design constants within the motor. On the converse, the temperature rise and, therefore, the horsepower output in most cases provide the basic limitation on the physical size of machine that is required.

In bringing out the general relationships between horsepower output and physical size of motor the following specific results are obtained:

1. The variation of losses with motor size and speed is determined (see Table I).

2. The variation of ventilation with motor size and speed is determined (see equations 1 and 2).

3. Combining these two factors, a simple method is given for estimating the temperature rise of any given induction motor at any specific load (see equation 3).

4. Using the same two factors, a simple equation is given relating horsepower output for a constant temperature rise directly to the physical size and speed of the machine (see equations 4 and 5).

5. The problem of obtaining a theoretically correct method of predicting motor temperatures is discussed. The general line of attack is indicated but it is concluded that considerably more experimental work is needed before such a complete analysis can be made.

Incidental to the discussion of the five main points just listed the following useful information is obtained:

1. Application of the temperature prediction method to a specific motor will give a picture of the proportion of losses that will be dissipated by different parts of the machine.

2. Application of the method also will provide clues to possible improvements in the ventilation of a given machine and will indicate the probable maximum improvement that may be effected.

3. Certain basic reasons for various types of motor construction in different size ranges are indicated.

In all of the discussion that follows only standard open motors are considered. The results may be transposed to other degrees of enclosure by using the empirical factors with which the designer is already familiar.

Paper 47-123, recommended by the AIEE committee on electric machinery for presentation at the AIEE summer general meeting, Montreal, Quebec, Canada, June 9-13, 1947. Manuscript submitted November 7, 1946; made available for printing April 11, 1947.

R. C. ROBINSON is the assistant to the chief engineer of the Electric Specialty Company, Stamford Conn.

D^2l Equation for Horsepower Output

The first and most basic decision in the design of an induction motor is the choice of the major physical dimensions. As previously stated this choice usually is made on the basis of temperature limitations and in most cases it is guided by test experience in the horsepower output available from various standard frame sizes. However, when some distinctly new rating or size is under consideration, a preliminary choice of dimensions usually is made by extrapolation from previous tests, making use of the relation expressed in the D^2l equation.

This equation may be written in the following form:

$$\text{Horsepower output} = KD^2lnB_gA_{HP}$$

where

K is a numerical constant which equals 0.156×10^{-8} for the units given here.
D is the inside diameter of the stator punchings in inches.
l is the length of iron core in inches.
n is the speed in revolutions per minute.
B_g is the air gap flux density in kilolines per square inch.
A_{HP} is the stator ampere conductors per inch on an output basis.

Table I. Proportionalities Between the Components of Loss and the Major Design Constants

Stator and rotor slot	$I^2RaA_{in}^2laVA^2+D^4l^2n^2B_g^2$
Stator and rotor end	$I^2RaA_{in}^2DnaVA^2+D^3l^2nB_g^2$
Load loss	aVA
Fundamental iron loss in the stator teeth	$aD^2l^2B_g^2$
Fundamental iron loss in the stator core	$aD^2l^2n^2B_g^2$
No load high frequency loss in the stator and rotor iron	$aD^2l^2n^2B_g^2/g$
Friction and windage loss	aD^2ln^2

This equation is derived directly from the fundamental voltage equation of the induction motor and bears no direct relation to the temperature limitations on horsepower output. Consequently there is no reason to suppose that the horsepower output for a permissible temperature rise will vary directly with the D^2ln of the machine.

Consideration of practical designs over a wide range of diameters shows that the horsepower output will vary as a higher power than the square of the diameter. This is due largely to the fact that permissible values of ampere conductors per inch are less for small diameter machines than for large ones. The factors B_g and A_{NP} are sometimes spoken of as measures of the magnetic and the current loading respectively. While they are in a sense measures of the loading it would be incorrect to assume that keeping these values constant will assure the same temperature rise on different diameters or at different speeds.

The chief practical use of the D^2l equation is in extrapolation to obtain desired values of per unit torque and inrush rather than desired values of horsepower output. This is based on the fact that with constant magnetic permeances the per unit machine reactances will vary directly as the ratio of A_{NP} to B_g.

An equation for horsepower output based on temperature limitations must of necessity give consideration to the variation of losses and ventilation with changes in the design constants. These relations can only be approximate, but even as approximations, they have considerable value in setting forth average standards of performance.

Variation of Losses With Major Dimensions

An accurate calculation of the losses in a motor can be made only by considering all of the detail dimensions of the electrical parts. However, very useful relations may be obtained by considering only the variation in the losses with changes in the major dimensions. The minor dimensions are assumed to change in the same ratio as the major dimensions so as to make the machines geometrically similar.

By using the equations which are developed it is thus possible to obtain an estimate of the losses in a motor by extrapolation from the tested losses of another machine, which may be of a different size or speed. It should be kept in mind, however, that the equations are only approximate and apply only under the assumption of geometric similarity between the machines.

The power losses in an induction motor under load may be subdivided as follows:

1. Stator I^2R loss which may be further divided into the copper loss in the slot portion and the copper loss in the end turns.
2. Rotor I^2R loss which may be divided into copper loss in the slot portion and copper loss in the end rings or end turns.
3. Load losses which consist of eddy current losses in the stator copper and high frequency iron and copper losses due to the flow of load currents in the stator and rotor conductors.
4. No-load iron loss which consists of fundamental iron loss in the stator teeth and core and high frequency iron losses in the stator and rotor due to the slot ripples in the no-load air gap flux.
5. Friction and windage losses.

The first three groups are variable losses which change with the load on the motor, while the last two are constant losses which are substantially independent of the load.

The basic construction of a squirrel-cage induction motor may be represented as shown in Figure 1, and the major dimensions given the symbols D, l_s and g.

Let the volt-ampere input to the motor be represented by VA, the speed in revolutions per minute by n, the air gap flux density by B_g, the ampere conductors per inch on an input basis by A_{tm}, and the number of stator slots by Q.

To preserve geometric similarity between machines, consider that the outside diameter of the stator punchings, the inside diameter of the rotor punchings, and the depth of the stator and rotor slots all change in the same proportion as the stator bore diameter, D. Assume also that the ratio between the number of stator and rotor slots, the ratio of the slot width to the slot pitch, and the line frequency all remain constant.

Under these assumptions the various losses in a motor will vary with the major design constants approximately in the proportions shown in Table I.

The equation for the stator and rotor slot I^2R loss is derived on the assumption that the ratio of copper cross section to the slot cross section is constant. This will be approximately true except for very small diameter machines in which the slot insulation combined with the small size of wires will tend to make the space factor exceptionally poor. Since the slot I^2R varies as $A_{tm}{}^2l$ it is apparent that permissible values of ampere conductors per inch will be reduced as the machine diameters are decreased. This formula also indicates why small machines tend to have higher per unit resistance values than large machines and, since reactances vary as A_{tm}/B_g, it may be noted that the reduction in A_{tm} tends to produce lower per unit reactance values in small machines than in large ones. It is thus possible to use semiclosed or closed slots on small motors without obtaining excessively high values of per unit reactance.

The equation for end turn loss is derived on the basis that the copper cross section in the end turns bears a constant proportion to the copper cross section in the slots regardless of changes in speed or diameter.

The equation for no-load high frequency loss is derived from the relation that the no-load slot ripple is closely proportional to the expression $(K_{cs}-1)$, where K_{cs} is Carter's coefficient for the slots under consideration. This expression, in turn, is found to vary approximately as $\sqrt{b_s/g}$ in large machines with open slots and approximately as b_s/g in small machines with semiclosed slots, where b_s is the width of the slot opening at the air gap. The rapid decrease of this loss with diameter, together with the use of semiclosed slots on small motors, tends to make this component of loss almost negligible in small machines, whereas it is the predominant part of the no-load iron loss in large machines.

The manner in which the total motor losses will vary with the major design constants will depend on the proportions in which each component of loss is present. It is difficult to express this accurately in general terms. However, from test results it is found that the total full load loss, expressed as a percentage of the power output, varies approximately as $1/D^{0.5}n^{0.5}$ for large motors and approximately as $1/D^{0.5}n^{0.5}$ for small motors. Large motors are defined as those typically having open stator slots and radial vent ducts; small motors as those typically having semiclosed stator slots and no radial vent ducts.

Figure 1. Basic construction of radially ventilated induction motor

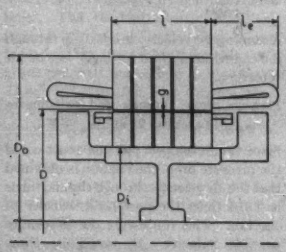

Variation of Ventilation With Major Dimensions

Air Velocities

Most of the heat in an open motor is dissipated by the forced circulation of cooling air over the coils and iron core. A small proportion of the heat is dissipated by radiation and static convection from the exterior surfaces of the machine but this part may be neglected for the purposes of this paper.

Most induction motors employ the radial system of ventilation in which fans on the rotor are used to circulate air over the end turns. Large motors generally have radial vent ducts in addition to the fans which allow additional cooling air to pass through the rotor and stator cores. Some small induction motors employ an axial system of ventilation while certain large high speed induction motors use various systems of combined axial and radial ventilation.

In the radial system of ventilation the rotor vent fingers may be considered as radial fans forcing air through the restriction imposed by the stator vent ducts. The radial ducts thus may be treated in a similar manner to the fans at the ends of the rotor core.

The relation between the volume of air being delivered and the developed pressure of a fan is given by the pressure–volume curve applying to the particular fan. Tests have been made on a number of centrifugal fans with various blade shapes and typical pressure–volume curves obtained.[1] Most induction motors use the radial blade type of fan due to the necessity of operating with either direction of rotation. The tests on two radial blade fans having different inside diameters but which were otherwise identical have been taken from C. J. Fechheimer's paper and are replotted in per unit terms as curves *A* and *B* of Figure 2. The test represented by curve *A* was taken on a fan having a ratio of inside to outside diameter of 83.3 per cent, while the test represented by curve *B* was taken on a fan having a ratio of inside to outside diameter of 66.7 per cent. Curve *C* of Figure 2 has been plotted for a ratio of diameters of 75 per cent and may be taken as approximately representative of the fans and vent ducts of a typical induction motor. All of these curves apply to radial fans without a diffuser. In one sense it might be expected that the stator vent ducts would act as radial diffusers for the rotor vent ducts and increase the available pressure. However, since the stator vent fingers are at a very unfavorable angle for diffusing action, it is unlikely that this effect is appreciable.

The pressure drop in forcing air through the stator vent ducts may be taken as about one velocity head. A velocity head in this case is defined as $(V_r/4{,}030)^2$ inches of water where V_r is the radial velocity of the air issuing from the rotor vent ducts expressed in feet per minute. On this basis, examination of curve *C* of Figure 2 shows that, provided the stator and rotor vent ducts are of the same width the radial velocity of the air on exit from the rotor ducts will be equal to 0.32 times the peripheral speed of the rotor. This is a very useful relationship since it then may be said that in general the average velocity of the air through the rotor and stator vent ducts is 0.32 times the peripheral velocity of the rotor and this velocity may be used to establish suitable thermal dissipation constants for the duct surfaces. It may be noted in passing that a considerable error in the assumption of one velocity head pressure drop through the stator will cause only a small change n the 0.32 value for the radial air velocity

Large induction motors with radial vent ducts normally are designed with stator and rotor vent ducts of the same width It is of considerable interest to note that an appreciable improvement in ventilation probably could be obtained by making the rotor vent ducts wider than the stator vent ducts. Considering a rotor vent duct as a radial fan, it is apparent that widening the duct would reduce the per unit air flow through it and thereby would raise its per unit developed pressure. The resultant higher pressure would increase the velocity of the air through the stator vent ducts and the heat dissipation from the stator duct surfaces would be improved correspondingly.

The velocity of the air on exit from the fans on the ends of the rotor is composed of two components. The first is a rotational component of velocity which, in the case of a radial blade type of fan, is equal to the peripheral speed of the rotor and the second is a radial component of velocity, dependent on the volume of air being delivered by the fan. This radial velocity cannot be stated accurately in general terms since it depends on the degree of restriction to air flow around the end windings. It may be noted on curve *C* of Figure 2 that the ratio of radial velocity to peripheral velocity of the fan may vary from zero when the air path is completely restricted up to 0.355 when the fan is operating "wide open," that is, with no restriction.

The radial velocity of air issuing from the fan, however, does not correspond to the air velocity around the end windings.

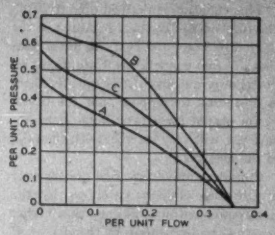

Figure 2. Pressure–volume curves of radial blade fans

A—Ratio of inside to outside diameter = 0.667
B—Ratio of inside to outside diameter = 0.833
C—Ratio of inside to outside diameter = 0.75

Per unit flow =

$$\frac{\text{volume—cubic feet per minute}}{(\text{outlet area—square feet}) \times (\text{peripheral velocity—feet per minute})} = \frac{\text{radial velocity}}{\text{peripheral velocity}}$$

Per unit pressure =

$$\frac{\text{developed pressure—inches of water}}{(\text{peripheral velocity—feet per minute}/4{,}030)^2}$$

As a matter of fact the velocity through the coils tends to vary in an inverse relationship to the radial velocity of flow from the fan When the fan is operating nearly "wide open" the radial velocity is relatively high but the air velocity through the end winding restriction is low since the developed pressure is very low. As the air flow path becomes progressively more restricted the volume of air and the radial velocity go down but since the developed pressure is increasing the air velocity through the end winding restriction will go up.

From curve *C* of Figure 2 there may be obtained general relations between the air velocity through the end turns and the peripheral speed of the fan. For the case where the air flow path is so restricted as to reduce the flow to almost zero:

Maximum developed pressure = 0.57 (peripheral velocity/4,030)^2 inches of water

Assuming 1.5 velocity heads drop through the end windings and letting V be the air velocity:

Pressure drop through end windings = $1.5(V/4{,}030)^2$ inches of water

Since the developed pressure must equal the pressure drop, the relation is obtained that the air velocity through the end turns is 0.615 times the peripheral velocity of the fan. This represents the maximum possible velocity. It would be theo-

Figure 3. Velocity distribution across the diameter of a round tube

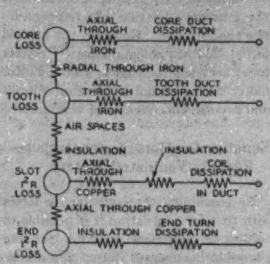

Figure 4. Typical thermal circuit of an induction motor stator

retically possible to reduce this velocity to zero by eliminating all restriction to air flow. However, in practice the end turns are sufficiently close to the fan to make it unlikely that this velocity will fall much below the radial velocity of flow from the fan or 0.355 times the peripheral velocity. The air velocity through the end windings thus will vary between the limits of 0.355 and 0.615 times the peripheral velocity of the fan.

Dissipation Coefficients

The phenomenon of heat dissipation from a plane surface to an air stream flowing over it is essentially one of thermal conduction through an air film.

Air flowing at high velocity through a round tube will have a velocity distribution across the cross section as shown in Figure 3. Near the walls of the tube the velocity distribution is linear and the flow is said to be "laminar" while near the center of the tube the air flow is turbulent. If the tube is maintained at a higher temperature than the air stream, heat will be transferred from the tube to the air by means of conduction through the laminar layer. The thermal resistivity of this laminar region will be the same as perfectly still air, that is, 1,600 degrees centigrade per watt per square inch per inch. Tests[2] indicate that the thermal resistivity of the turbulent region is only about 2.5 per cent of this value of 40 degrees centigrade per watt per square inch per inch.

The thickness of the laminar layer may be calculated by the formulas of hydraulics as follows:

For any cross-sectional shape of duct the hydraulic radius m = cross-sectional area in square feet ÷ "wetted" perimeter in feet

Diameter of equivalent round tube $D = 4m$ feet

Reynolds numer $R_e = DG/\mu$

in which G is the mass-velocity of flow expressed in pounds per hour per square feet, and μ is the viscosity of air expressed in pounds per hour per feet, which at normal machine operating temperatures is numerically equal to 0.046. When Reynold's number is less than 2 000, the flow will be laminar throughout the cross section of the duct, while at values of Reynold's number above 2,000 the flow will be partly turbulent as shown in Figure 3.

For a smooth duct and turbulent flow the friction factor $f = 0.3164 \div R_e^{0.25}$. This equation is also correct for rough tubes provided the thickness of the laminar layer is found to be greater than the maximum height of the surface irregularities.[3]

Thickness of the laminar layer $\delta = 32.8D \div R_e\sqrt{f}$ feet

It may be noted that the thickness of the laminar layer will vary inversely with the 0.875 power of the air velocity. Because the thermal resistance of the turbulent region is independent of air velocity the over-all dissipation coefficient will vary as some lower power of the velocity, which by test is found to be about the 0.8 power.

Once the thickness of the laminar layer has been determined it is then possible to calculate the thermal resistances of the laminar and turbulent regions and from their sum to determine the dissipation factor expressed in watts per degree centigrade per square inch.

This type of theoretical approach to heat dissipation is of particular value in giving a physical picture of the phenomenon and also in providing an adequate basis for the solution of unusual problems. For most practical cases, however, it is much simpler to use the following equation which is based on test results:[4]

Thermal dissipation $= 0.035(V/2{,}000)^{0.8}$ watts per degree centigrade per square inch

in which V is the air velocity in feet per minute.

It is important to note that this dissipation constant and that calculated by the theoretical method both apply to regions where the air flow has become stabilized; for example, near the middle of a long tube. At the inlet and outlet there will be additional turbulence which will increase very considerably the dissipation constant.

General Statement of the Temperature Problem

The maximum allowable temperature rise in a motor is determined by the rate of deterioration of the insulation that is used. Experience has shown that satisfactory life of class A insulation will be achieved if the temperature rise is limited to 40 degrees centigrade, measured by thermometer on the end turns or stator core, if the motor is operating in an ambient temperature of 40 degrees centigrade.

A motor which is carrying a constant load will reach its steady state temperature rise when the losses within the motor are being dissipated at the same rate as they are being produced. It is thus apparent that this continuous temperature rise is dependent on the magnitude of the losses and on the effectiveness of the dissipation or, in other words on the effectiveness of the ventilation. Because heat can be conducted from one part of the machine to another the temperature rise at individual points within the motor will be determined by the distribution of the losses, by the effectiveness of the ventilation throughout the machine, and by the thermal resistance to heat flow by conduction.[5]

It is theoretically possible to solve for the temperatures at various points within an induction motor stator by means of a thermal circuit such as shown in Figure 4. As a reasonable approximation the terminals may all be assumed to be at a temperature equal to the ave age temperature of the cooling air in passing through the stator. If the losse: are all expressed in watts and the thermal resistances in degrees centigrade per watt the thermal circuit may be solved either by "cut and try" or by superposition and the total temperature of each part of the stator will be obtained directly. Any desired degree of accuracy could be obtained with such a circuit by further subdivision of the losses and the heat flow paths.

While this circuit does not in itself appear too formidable there are great practical difficulties in making an analysis of this type. The greatest difficulty arises in attempting to evaluate the thermal resistance of the end turn dissipation. The pattern of the air flow over and through the end windings is extremely complicated making it difficult, if not impossible, to predict the air velocities over various surfaces of the winding. Dissipation constants are also not readily available for the cases in which components of the air velocity are perpendicular, rather than parallel, to the surface being cooled. Similar difficulties are encountered in analyzing the air flow and degree of turbulence in radial ducts and in assigning suitable dissipation constants to the iron and coil surfaces. A further, though less serious, difficulty is encountered in calculating the thermal resistance to heat flow between the copper in the slots and the

stator iron. This factor is quite largely dependent on the effectiveness of the varnish impregnation and is not known in advance with any degree of accuracy.

From the foregoing it is apparent that since so many of the critical elements in the circuit can only be approximated there is little value in attempting a solution as complicated as this. However, when more complete theoretical and experimental determinations of air flow and heat transfer constants have been made a thermal circuit of the type shown could be solved with a good degree of accuracy. The designer then would be able to make accurate temperature predictions without having to rely to such a great extent on previous test experience.

Equation of Temperature Rise

The difficulties inherent in making a scientific analysis of the temperature rise in an induction motor have been discussed previously. In view of these limitations it is logical that the method of analysis should be no more accurate than the data available. On this basis the method here presented is an empirical one based on a number of simplifying assumptions and is intended to cover average conditions rather than extremes of design.

It has been found that the temperature rise of an induction motor will be closely proportional to the total losses in the motor.[8] The total losses under any specified load may be obtained either by a detailed design, by the extrapolation method herein presented, or by an estimate of the operating efficiency.

Let the total estimated losses at the specified load be W watts.

Referring to Figure 1, let the peripheral velocity of the rotor be V_p feet per minute. Then, from the previous discussion of air velocities, the average velocity of the air through the rotor and stator vent ducts will be approximately $0.32V_p$ feet per minute. Due to the degree of turbulence in the vent ducts the thermal dissipation constant for a velocity of 2,000 feet per minute will be considerably higher than the value of 0.035 for stable air flow. It is found that a value of 0.050 used with the square root of the air velocity will give approximately correct results. The square root of the air velocity is used instead of the 0.8 power because part of the temperature drop occurs through the insulation and is unaffected by air velocity. The same air velocity and dissipation constant may also be used for the ends of the rotor and stator core.

Let the total area of the vent ducts and the ends of the core be A_{s+c}, in which $A_{s+c} = (\pi/4)(D_o^2 - D_s^2)\ (2n_v + 2)$ square inches, and n_v is the number of radial vent ducts.

On small machines having no vent ducts and no spider, n_v will be zero and D_s will be the shaft diameter.

The total dissipation from the vent ducts and core ends then will be

$$D_{s+c} = 0.050\sqrt{(0.32)(V_p)/2{,}000}\,(A_{s+c}) \text{ watts per degree centigrade} \quad (1)$$

The stator end windings may be considered as a cylindrical area A_w equal to $2\pi Dl_e$ square inches. Assuming that the fans have approximately the same diameter as the rotor, air will pass over this cylindrical area in a peripheral direction with a velocity of V_p feet per minute At the same time there will be a component of air velocity perpendicular to this area which, by reducing the thickness of the laminar boundary layer, will increase greatly the dissipation constant. It is found that a dissipation constant of $0.175\sqrt{V_p/2{,}000}$ watts per square inch per degree centigrade will approximately check tests.

The total dissipation from the end turns then will be

$$D_w = 0.175\sqrt{(V_p/2{,}000)}\,A_w \text{ watts per degree centigrade} \quad (2)$$

The total dissipation for the machine then will be $D_{s+c} + D_w$. Then

$$\text{Approximate temperature rise} = W/(D_{s+c} + D_w) \text{ degrees centigrade} \quad (3)$$

In spite of the broad assumptions involved in the derivation of this equation, it is found that the method gives reasonably good results over a range of sizes from the smallest motors to the largest. A number of factors are omitted, such as the velocity of air between the coils of the end winding and the thickness of the insulation, but the average effect of these items is included in the empirical dissipation factors. Effective shrouding of the end turns may decrease the temperature rise somewhat by raising the air velocity through the windings close to its maximum value of 0.615 times the peripheral velocity. On the converse high voltage insulation or recirculation of the air from the fans may increase the temperature rise considerably. However, the method as outlined will be approximately correct for either a squirrel-cage or a wound rotor motor having normal distribution of losses and average effectiveness of ventilation.

Equation for Horsepower Output—Radially Ventilated Motors

By combining the equation for losses with that for ventilation it is possible to obtain an empirical equation for the allowable horsepower output for a constant temperature rise.

The equation for temperature rise previously given is of the form

Temperature rise α total losses $\div$ (effective dissipating area) $\sqrt{\text{peripheral velocity}}$

This is equivalent to

Temperature rise α (per cent losses based on output) (horsepower output) $\div$ (effective dissipating area) $D^{0.5}n^{0.5}$.

Consequently, for a constant temperature rise

Horsepower output α (effective dissipating area) $D^{0.5}n^{0.5} \div$ (per cent losses based on output)

The effective dissipating area is a combination of the dissipating area of the end turns and the dissipating area of the vent ducts and end laminations. The end turn area is approximately proportional to D^2n while the vent duct area is approximately proportional to D^2l. It is found that large motors having one or more radial vent ducts typically will dissipate similar amounts of heat from the end windings and from the vent ducts. Con-

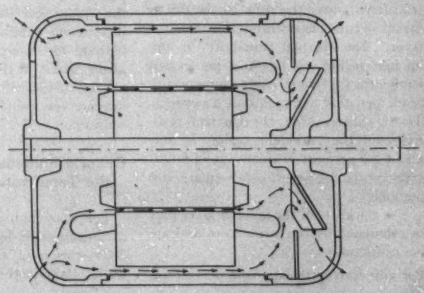

Figure 5. Axial ventilation of a small induction motor

sequently the total effective dissipating area will vary about as the expression $D^{2.5}n^{0.5}$.

By substitution in the output equation

$$\text{Horsepower output} \propto (D^{2.5}n^{0.5})(D^{0.5}n^{0.5}) \div \frac{1}{D^{0.5}n^{0.5}} = D^{2.5}n^{1.5}$$

Small machines having no radial vent ducts will dissipate almost all of their heat from the end turns. The effective dissipating area therefore will vary as D^2n.

By substitution in the output equation

$$\text{Horsepower output} \propto (D^2n)(D^{0.5}n^{0.5}) \div \frac{1}{D^{0.5}n^{0.5}} = D^{2.5}n^2$$

The two equations for horsepower output obtainable with a constant temperature rise are then

Large motors—open stator slots, radial vent ducts:

$$\text{Horsepower} \propto D^{2.5}n^{1.5} \quad (4)$$

Small motors—semiclosed stator slots, no radial vent ducts:

$$\text{Horsepower} \propto D^{2.5}n^2 \quad (5)$$

It is particularly interesting to note the rapid reduction of horsepower with a decrease in the diameter of small motors. In the very small sizes the reduction may be even more rapid due to the relatively large amount of space required for insulation in the stator slots.

In applying the equations to radially ventilated motors it should be borne in mind that they are based on many simplifying assumptions and represent only the general magnitude of changes in horsepower output with changes in the design constants. The equations, moreover, are not applicable to axially ventilated machines or to 2-pole motors, as both represent special cases.

Axial Ventilation

Many small induction motors are ventilated by means of a fan mounted at one end of the rotor which forces air axially through the machine. A typical scheme is shown in Figure 5.

The problem of axial ventilation is not as susceptible to generalized analysis as is radial ventilation. This is due to the fact that the ratio of the fan diameter to the rotor diameter may vary over a considerable range and also to the fact that the velocity of air over the back of the stator core may be varied over a wide range by changing the degree of restriction.

In designing a system of axial ventilation it is desirable to obtain a good compromise between the velocity of air through the machine and the total volume of air to be delivered. If the air flow path is restricted to a very small cross section the volume of air will be reduced but this reduction in volume will increase the developed pressure of the fan. With the higher developed pressure the velocity of the air through the machine will increase and the temperature rise of the machine parts above the average air temperature will be reduced. However, due to the reduced volume of air, the temperature rise of the air itself in passing through the motor will be increased, thus tending to raise the machine temperature. The best ventilation design will then be that in which the two effects are balanced in such a way as to give the lowest total temperature of the machine parts.

The temperature rise of the air in passing through the machine may be calculated from the volume of air and the otal losses of the motor as follows:

Air temperature rise = 1.8 (total motor losses in watts) ÷ (volume of air in cubic feet per minute) degrees centigrade

Axial ventilation has certain distinct advantages over the radial system of ventilation for motors of small diameter. In the first place, considerable flexibility may be obtained by increasing the fan diameter or its width and by suitably proportioning the restriction at the back of the stator core. Moreover, an axially ventilated motor dissipates a considerable proportion of its heat from the air gap surfaces and from the back of the stator core. The areas of these dissipating surfaces vary directly with the diameter of the machine while in a radially ventilated motor the areas of the dissipating surfaces vary as the square of the diameter. As the diameter is reduced, the effective dissipating area thus is decreased less rapidly with axial ventilation than with radial ventilation. Thus, a very small diameter motor with axial ventilation will be able to carry a greater load for a given temperature rise that an otherwise identical motor with radial ventilation.

Nomenclature

A_{HP} = stator ampere conductors per inch on an output basis

A_{in} = stator ampere conductors per inch on an input basis

A_{v+e} = total area of vent ducts and the ends of the core

A_w = cylindrical area of the end windings

B_g = maximum flux density in the air gap

b_s = width of slot opening at the air gap

D = inside diameter of the stator punchings

D_o = outside diameter of the stator punchings

D_i = inside diameter of the rotor punchings

D_{v+e} = total dissipation factor for vent ducts and ends of the core

D_w = total dissipation factor for the end turns

f = friction factor for turbulent flow

G = mass velocity of air

g = radial length of air gap

K_{cs} = Carter's coefficient for the slots

l = length of iron core

l_e = length of end turn extension

m = hydraulic radius

n = speed in revolutions per minute

n_v = number of radial vent ducts

Q = number of stator slots

R_e = Reynold's number

V = air velocity

V_r = radial velocity of air on exit from the rotor

V_p = peripheral velocity of the rotor

VA = volt-amperes input

W = total motor losses

δ = thickness of the laminar layer

μ = viscosity of air

References

1. Performance of Centrifugal Fans for Electrical Machinery, Carl J. Fechheimer. *Transactions* of the American Society of Mechanical Engineers (New York N. Y.), volume 46, 1924, pages 287–340.

2. Distribution of Velocity and Temperature Between Concentric Rotating Cylinders, G. I. Taylor. *Proceedings* of the Royal Society (London, England), volume 151, 1935, pages 494–512.

3. Evaluation of Boundary Roughness, Hunter Rouse. *Proceedings* of the Second Hydraulics Conference. University of Iowa Bulletin 27, 1943, pages 105–116.

4. Surface Heat Transfer in Electric Machines With Forced Air Flow, George E. Luke. AIEE Transactions, volume 45, 1926, pages 1036–47.

5. Longitudinal and Transverse Heat Flow in Slot-Wound Armature Coils, Carl J. Fechheimer. AIEE Transactions, volume 40, 1921, pages 589–645.

6. Steady Flow of Heat in Large Turbine-Generators, C. R. Soderberg. AIEE Transactions volume 50, 1931, pages 782–98.

7. The Cooling of Electric Machines, George E. Luke. AIEE Transactions, volume 42, 1923, pages 636–51.

8. Determination of Temperature Rise of Induction Motors, E. R. Summers. AIEE Transactions, volume 58, 1939, September section, pages 459–67.

9. Rating of General Purpose Induction Motors, P. L. Alger, T. C. Johnson. AIEE Transactions, volume 58, 1939, September section, pages 445–56.

No Discussion

The Maintenance of Hydroelectric Generating Units

A. S. ROBERTSON
MEMBER AIEE

R. O. STANDING
NONMEMBER AIEE

THE MAJOR hydroelectric development comprises many structures of various types and many components of mechanical and electric equipment. Its operation often involves complexities, while the problems it poses for a maintenance and repair staff vary from those of mere routine to those which demand a high degree of engineering skill combined with mechanical ingenuity and resourcefulness.

Throughout the systems of the Hydro-Electric Power Commission, 9 major hydroelectric stations are operated, together with 45 smaller plants, totaling in capacity over 1,500,000 kva. The oldest plants were designed and constructed at the turn of the century, while the latest plant was placed into service in September 1943.

From a fund of knowledge gained throughout this operating experience, a number of illustrations are presented herein, which it is hoped will prove of value to those whose duties include power plant electrical and mechanical maintenance.

One section is devoted to the practical aspects of operation of thrust bearings. Other sections are devoted to the description of a number of somewhat unusual maintenance and repair problems, the solutions to which involved the application of novel methods of electrical heating, drying-out processes, and electric welding.

The conclusions to be drawn from these illustrations indicate the necessity for thorough periodic overhauls of equipment, if trouble-free operation is to be obtained, and also indicate that even major repairs on large hydroelectric equipment can be undertaken at the site, using if necessary available tools and equipment improvised for the job.

It is the opinion of the Commission's operating staff that information obtained during the operation of electric generating and other equipment is vital to the improvement of the art of electrical design and should be made available to the designing engineer.

Drying-Out Large Horizontal Shaft Generators

The flooding of a major hydroelectric plant is an operating hazard with which few utilities have had to contend. Nevertheless, this particular fate has befallen the Ontario power plant of the Commission at Niagara Falls on two occasions.

This plant is located in the gorge of the Niagara River immediately below the Canadian Falls and on the shore of what is known as the Maid of the Mist Pool. When ice is running in the river, sufficient may be retained in this pool to give it an almost complete ice cover. Under certain circumstances, jams occur which can raise the level of the pool for short intervals many feet above normal.

Having knowledge of this phenomenon the original designers of the plant provided for an extreme high tailwater level approximately 30 feet above normal. Even this emergency provision was found to be inadequate when, in 1909, the tailwater rose sufficiently to flood completely the then existing powerhouse, in which six operating units, totaling 53,000 kw, were installed.

These units were horizontal-shaft open-frame units, their armatures having semi-closed slots with a chain winding design. Records indicate that attempts to dry out these generators were unsuccessful and that all subsequently were rewound.

Following this mishap, the design of the plant superstructure was changed, all window openings below the crane rails being closed to provide a water seal 10 feet above the previous maximum, or 40 feet above normal tailwater. This is the highest water level the plant can sustain without its stability being endangered.

Notwithstanding this precaution, a new high level was experienced in January 1938. An extremely rapid rise in tailwater brought a mixture of floe ice and water through the window openings in the south end of the powerhouse, depositing

Figure 1. Vacuum housing applied to horizontal shaft

Ontario power generating unit before erection of wooden insulating housing

Paper 47-120, recommended by the AIEE committee on power generation for presentation at the AIEE summer general meeting, Montreal, Quebec, Canada, June 9-13, 1947. Manuscript submitted November 27, 1946; made available for printing April 7, 1947.

A. S. Robertson is general superintendent of the Niagara Falls District, Hydro-Electric Power Commission of Ontario, Niagara Falls, Ontario, Canada, and R. O. Standing is mechanical engineer in the operating department of the Hydro-Electric Power Commission of Ontario, Toronto, Ontario, Canada.

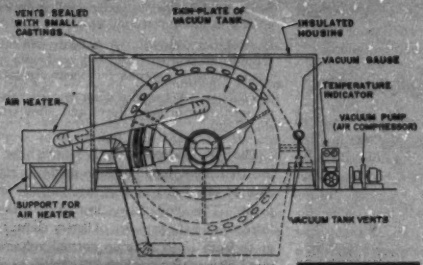

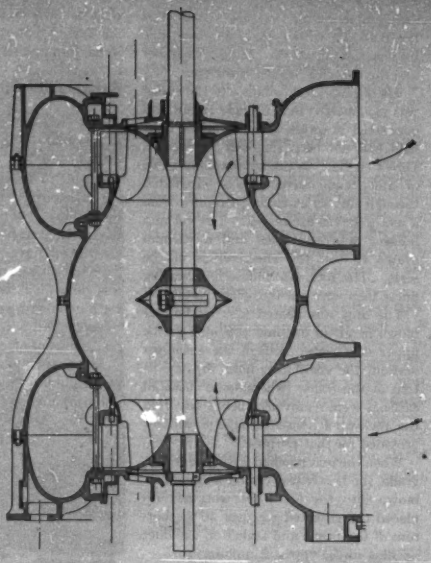

Figure 2 (above) Cross section illustrating over-all arrangement for vacuum drying of horizontal shaft generators

Figure 3 (left). Impregnated field coil arranged with clamping rod for baking operation

Figure 4 (right). Vertical section of vertical - shaft double-runner turbine units

Toronto power plant

nearly 100,000 tons of ice over and around units 1 to 6 and filling the remainder of the plant with water. The water drained from the plant naturally in the course of a few hours, but two weeks were required to remove the ice.

The drying out of the multitudinous pieces of auxiliary equipment provided many novel problems for the maintenance forces, but only the drying out of the 15 main generators will be discussed herein.

Preliminary steps were taken to dry out the eight more modern generators by the conventional circulation of short-circuit current plus forced heated air circulation. It was fortunate that the principal winter peak load season had passed, so that the loss of the 135,000-kw capacity would not affect seriously system operating conditions for some months, but it soon was found that conventional methods would not return these units to service for a very long period.

It was discovered accidentally that by heating the units to approximately 90 degrees centigrade for 24 hours and then rapidly cooling them to room temperature, the drying cycle was improved materially. This procedure therefore was adopted and the eight units returned to service progressively over a period of seven months. All have since operated successfully, with no failures attributed to the flooding.

The seven older units were recognized as a special problem, in view of the unsuccessful drying attempt after the earlier flood and because of the fact that they had been submerged in ice for nearly two weeks. Vacuum drying of electric equipment is a common place factory procedure and it was decided to attempt some modification of this practice on the generators in place.

Investigation indicated that it would be quite practical to arrange a housing around the frame of the horizontal shaft units which, combined with the frame, would provide a vacuum-proof arrangement (Figures 1 and 2). The stator first was moved over from its normal position to clear one of the main bearings and also to provide a working space in the pit below the unit. The end bel s were replaced with externally flanged support rings, to which were bolted internally supported skin plates of 1/2-inch steel, sealing the space between the support rings and the rotor shaft.

The internal support for these skin plates consisted of

1. Rings of 3/8-inch steel plate on each side centered by the fan casting and bearing against the rotor rim.
2. A row of 2-inch steel pipes placed between the spokes and extending from skin plate to skin plate.
3. Additional 3/8-inch rings bearing against each side of the rotor hub.

All ventilating openings in the armature frame were sealed with small castings, drawn down on square soft-rubber gaskets. One of these castings was tapped for a vacuum gauge and for two adjustable air-leak valves for controlling the vacuum. No machining of the large surfaces of the skin plates was attempted, it being found that a satisfactory seal could be obtained with 1/2-inch round rubber gasketing or 1/2-inch smooth or even corrugated garden hose, squeezed down to about 3/16 inch between rough flanges. The splits in the frame, joints between frame feet and sole plates, and miscellaneous other small leaks were sealed over with friction tape and painted with an insulating compound.

Ordinary station air compressors were used as vacuum pumps. The only special feature of the necessary piping system was the installation of a water-cooled condenser and trap in the line to the vacuum pump. This device served several useful purposes; it protected the pump against the entrance of any injurious foreign material, increased the pump capacity by removing the greater part of the water vapor, and gave an accurate indication of the completion of the process by the absence of condensate in the trap.

The following equipment was provided to heat the unit: a rock-wool-insulated wooden house to enclose the whole unit; an electric heater of 125-250-kw capac-

ity, complete with fan; also a branched heating duct with control dampers, one branch leading to the vacuum chamber and the other to the generator pit.

The 3-phase star winding of the stator was reconnected into a single circuit and connected in series with the field (if the field had not been removed for repair). Direct current, to the approximate value of full load current, was circulated through this series circuit, supplied from a motor-driven exciter set. The vacuum housing was assembled and a vacuum drawn to test the effectiveness of the seals. The rock-wool house and heating ducts then were put into place.

The unit was heated first by hot air blown in at an opening provided in the upper skin plate, through the generator and out the ventilating holes in the bottom of the frame (where some gasketed castings were removed), thence out from the rock-wool house through a window provided for that purpose.

When the unit reached 90 degrees centigrade, the heater was cut off and cold air blown into the pit while workmen replaced the gasketed castings at the bottom of the frame and sealed off the duct opening in the upper skin plate.

The air heater then was put on again and the current regulated in the windings to maintain the temperature of the upper coil ends at 90 degrees centigrade (the hottest coils in the machine). The pumps were started and the vacuum regulated by adjusting the leakage valves to give an increase in vacuum of one inch of mercury every 15 minutes, until a maximum vacuum of 26 inches was obtained, this to prevent the bursting of the coil insulation. The largest yield of water occurred at 16 inches of vacuum.

Five days were required to assemble, dry a unit, and dismantle the equipment. The fact that all units were similar made it quite convenient to move the equipment to each of the seven units in turn.

This method was applied successfully to the units which previously had been found impossible to dry by conventional methods, all being returned to service nine months after the flooding. All now have had over eight years' service without any failure that can be attributed to their immersion and drying-out procedure.

Bakelite Treatment of Field Coils

Much time could have been saved in drying out the machines by the hot air method if it had been possible to rotate the field. This could not be done, however, because the water-soaked fibrous insulation on the field coils had insufficient mechanical strength to withstand the centrifugal forces at normal speed. To prevent a recurrence of this difficulty it was decided in reinsulating the coils to use a nonhygroscopic material so that the repaired field coil would require little or no drying out after water immersion.

After experimenting with various materials it was decided to use Bakelite in the following forms:

1. *Bakelite TV-1112.* A bakelite compound used in this particular application as an impregnating material.

2. *Bakelite TC-6032.* A bakelite cement supplied in powder form and used with a special solvent to form a thin paste cement.

3. *Dilecto.* A bakelite impregnated fabric furnished in sheet form and standard thicknesses.

The coils were made ready for the bakelite treatment by first thoroughly being cleaned of all dirt and surface varnish or paint. The coil turn insulation was tested under the pressure of heavy clamps, up to from 15 to 20 times normal voltage using alternating current (25 cycles) as a test source. After testing, the necessary repairs to the insulation were made and the coil placed in first-class condition electrically.

The coil was then placed in a tank and impregnated under vacuum using bakelite *TV-1112* compound. It was found that this method gave complete impreg-

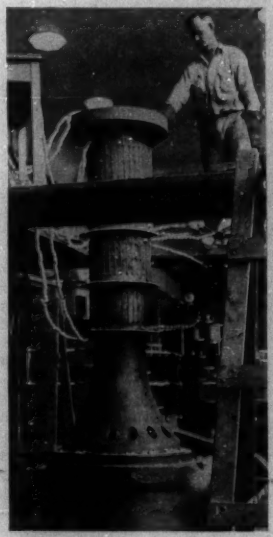

Figure 7 (above). General view of setup for removal of generator shaft by circulation of refrigerant in hollow shaft

Figure 8 (below). Stationary plate showing failure caused by fatigue of babbitt metal

Figure 6 (above). Welded section of turbine shaft arranged for heat treatment, insulation having been removed

Figure 5 (left). Typical shaft section of Toronto power plant units prior to commencement of welding operations

nation without applying pressure treatment. (See Figure 3.)

After impregnation the coil was placed in an oven and baked at 120 degrees centigrade for 18 hours. On completion of the baking all surplus varnish was removed and the coil prepared to receive the ground insulation. At this stage the coil was a solid mass, possessing high dielectric and mechanical strength.

Ground insulation consisting of three layers of 0.015-inch Dilecto cemented together was cemented under pressure to the inside of the coil, using bakelite cement (*TC-6032*). The complete coil then was baked at 120 degrees centigrade for 18 hours.

The coil was now ready to install on the field pole.

Assembly of Field Coil and Field Pole

In assembling the field coils on the field poles, it was decided to replace the original collars with Dilecto collars.

After the outer field pole collar and the coil were placed on the field pole, the coil was centered on the iron and parallel Dilecto wedges were inserted between the coil and the iron. These were cemented in position with Bakelite (*TV-1112*).

On completion of assembly, Bakelite *TC-6032*, thinned down, was applied to the outside of the coil with a brush and the whole assembly then was baked. Following the baking operation, the whole assembly, while still hot, was given a brush coat of Bakelite (*TV-1112*). On cooling, this gave the coil a smooth, durable, and easy-to-keep-clean surface.

Tests

It was found that field coils treated as described would withstand successfully voltages up to 7,000 volts; the limiting feature in all cases being the creepage distance around the edges of the field pole collars. However, normal requirements of field coils treated in this manner are that they stand a potential of 4,000 volts.

In order to form some opinion as to the success of the treatment in producing a coil that was waterproof, and to observe the effect of sudden temperature changes on the insulation, tests were made by plunging coils heated to 120 degrees centigrade into water at temperatures approaching freezing, and allowing them to stand for 24 hours. On removal and after wiping the coil off as would be done normally, inspection and tests indicated that no detrimental change was incurred by this severe treatment.

Some of these coils now have been in service for eight years, and inspection indicates no sign of change or deterioration in the insulation.

Figure 9. Illustration of fretting on mating surfaces of thrust collar and runner plate

Welding Cracked Turbine Shafts

Two of the original plants on the Canadian side of the river at Niagara Falls were designed with the turbines located in deep excavations approximately at tailwater level, shafts some 150 feet in length extending up to the generator rooms located at grade. The Toronto power plant, now owned by the Commission, has 11 such units with a total output rating of 105,000 kw.

Each unit has two turbine runners, one discharging upward and the other downward into a common draft tube, all then discharging into a tunnel emptying beneath the Canadian falls. The shafts carrying the runners are coupled together by means of a flanged coupling, located on the center line of the draft tube, this coupling being enclosed in a heavy streamlined shroud, split vertically and clamped into grooves in the upper and lower shafts. The two turbine guide bearings are approximately 22 feet apart. Figure 4 illustrates the arrangement.

Recently, and without previous warning, one shaft failed at the clamping groove above the shroud and the lower turbine runner with its shaft disappeared down the tailrace tunnel. Before inspection of the other units could be completed another unit failed in the same manner though the runner remained in the turbine.

Detailed inspection disclosed five other units with cracked shafts, four having cracks both above and below the coupling shroud. Preliminary information indicated that under wartime conditions, new shaft forgings could be obtained only after long delay and it therefore was decided to attempt the repair of the shafts by arc welding at the plant.

The turbine shafts are 14 inches outside diameter, having an internal bore of 8 inches. The clamping grooves were 10 inches wide, 3/8 inch deep, and originally were made without fillets. The most severe cracks extended over a considerable area from the clamping grooves, some extending through to the center bore. Minor cracks originated at the dowel holes drilled to support the coupling shroud.

Preparatory Steps

In preparing the shafts for repairs, it was decided to support them by means of an interna plug. A forged plug 24 inches was machined 0.004 inch over size and the internal bore of the shaft accurately machined to provide a parallel hole. The plug was also taper bored to ensure a reasonable degree of flexibility, a 2-inch wall (4-inch hole) being left n the center section spanning the breaks in the shaft, tapering to 1/2-inch wall (7-inch hole) at the outer extremities.

This insert was shrunk by dry ice and pressed inside the hollow shaft. In the case of the shaft that had parted in service, a step was left in the plug to act as a stop, in order to ensure the correct overall length. This step was machined off before welding operations were commenced.

The next step was to clean out the cracks preparatory to welding This frequently meant machining right through the original shaft. The clamping groove was widened considerably beyond its original width, generous fillets being provided. Figure 5 shows a shaft machined and ready for welding.

Welding Procedure

The original shafts contained approximately 40 points of carbon relatively poor welding material. Considerable study, therefore, was given the welding technique, the Commission's laboratory ultimately recommending that all welding

be carried out with welded sections at a temperature of 400 degrees Fahrenheit minimum, preferably 500 degrees Fahrenheit followed by heat treatment of 1,150 degrees Fahrenheit after the welding was completed.

Factory heat treating facilities being fully occupied with the demands of war, the field heating equipment was designed to provide for both the welding requirements and the later heat treatment. Electric heaters were constructed, consisting of number 9 iron wire wound on porcelain spools, the spools being supported on sheet iron arranged to form a belt around the section of the shaft to be heated. Four-inch-thick blankets of rock wool, held in place by wire netting, provided the necessary heat insulation.

To measure and regulate the shaft temperature, a specially calibrated millivolt meter connected to iron-constantan thermocouples was used, these couples being located on each side of the welded section.

The welding was done with the welded sections maintained over a temperature range of 500 to 700 degrees Fahrenheit, regulation being effected by resistor grids in series with the heating elements. In addition to the thermocouple temperature control, the welder was supplied with a 500 degree Fahrenheit Tempilstik as a standby. A welding rod was selected whose deposited properties would approximate the metal of the original shaft.

The shaft was placed on steel runners in a horizontal position so that it could be turned readily to distribute the welding in layers about its diameter. The first step was to tack weld the insert to the shaft, then welding circumferentially until the width of the V permitted longitudinal welding distributed to avoid bending stresses. Each weld required approximately 425 to 450 pounds of rod, the welding time approximating 200 continuous working hours per shaft.

Heat Treatment

The heat treatment was the most difficult part of the repair problem. It was specified by the laboratory that the heat treatment was to consist of raising the temperature of the welded section at a rate not exceeding 100 degrees Fahrenheit per hour to a maximum temperature of 1,150 degrees Fahrenheit, holding at this temperature for one hour per inch of thickness and cooling also at the rate of 100 degrees Fahrenheit per hour, the temperature of the cast-iron turbine hub located some five feet from the weld, not to exceed 400 degrees Fahrenheit at any time.

By supplementing the circular heaters used for the welding operation with a flat heater over the coupling end and changing from rock wool to 12 inches of glass wool, it was calculated the desired maximum temperature could be reached with a heater temperature of 1,400 degrees Fahrenheit. No difficulty was experienced in the operation of the heaters at this temperature, though, recognizing the short life that might be anticipated, the heating elements were replaced after treating each second shaft.

When heat treating the first shaft, a number of thermocouples were used to check the calculated temperature gradients and to secure a further check on the temperature of the turbine hub. For subsequent shafts two thermocouples were located inside the hollow shaft and a third between the heating element and the shaft.

At the commencement of stress relieving, all heaters were connected in series giving a power input of approximately 22 kw. Overnight operation in this position increased the shaft temperature to the neighborhood of 700 degrees Fahrenheit. The heaters then were reconnected in parallel, resulting in a power input at the higher temperature of approximately 36 kw and causing a further increase to the desired 1,150 degrees Fahrenheit in from five to six hours.

The disk type heater over the coupling end then was disconnected, causing the power input to drop to around 5 kw, approximately that required to maintain the heat treating temperature. Occasionally, it was necessary to control the circular heaters for more accurate conditions. If the upper thermocouples tended to read higher than the lower, a portion of the thermal insulation was removed to redistribute both the heat input and heat loss (see Figure 6).

Figure 10. Spring imprints on lower surface of stationary plate

From the outset, it appeared that a vertical position would be the most desirable for the stress relieving operation as this would remove the danger of sagging and creepage under the stress of high temperature.

However, it was thought that a horizontal setup could be arranged with less loss of time and one shaft was treated in this position by supporting it on brick piers. The stress in the high temperature region was reduced by supporting the coupling flange on a beam. One end of this beam was supported by a set of scales and the other on a screw jack. The upward thrust, required to reduce the bending movement to zero at the first inner pier, was calculated and the scale was set to balance at this load. During the heating and cooling period, the operator kept the screw jack adjusted so that the scale beam was in balance at all times. This was a troublesome procedure involving some risk and the remaining shafts were treated in a vertical position.

At the time of the first failure two new shaft forgings were ordered. However, the ten sections of shafts were repaired successfully and returned to service before these arrived. The portion of the upper shaft remaining after the first failure was also salvaged by obtaining a forging from which a new flange and stub end were turned. This shaft now is retained as a spare. Subsequent annual inspection of these arc-welded shafts appear to indicate the complete success of the operation, no incipient failures being evident to this date.

Removal of a Large Generator Shaft

In March 1937 an operator at the Commission's Queenston plant during the regular hourly inspection trip, noticed that the pilot exciter armature on one of the 55,000-kva vertical generators had developed a noticeable wobble.

The unit was shut down and investigation showed that a serious crack had developed in the main shaft at the circular keyway at the top of the thrust bearing collar. It was extremely fortunate that this crack was discovered before complete failure occurred, since this keyway supports the entire weight of the rotor and turbine and its failure undoubtedly would have wrecked the unit.

It was, therefore, necessary in order to effect repairs, to remove the shaft from

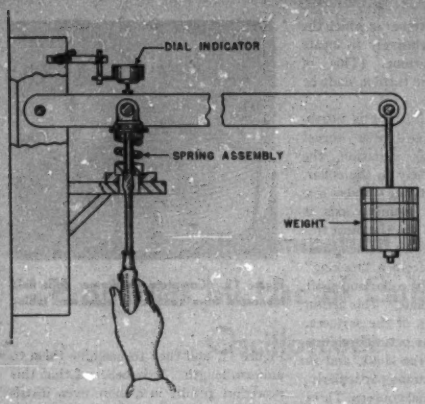

Figure 11. Fixture used for testing and preloading springs

the rotor. This shaft was 30 feet 3 inches long having an 8-inch hole through the center. There were three stepped fits each 12 inches long for the rotor spider, the largest being $32^1/_4$ inches in diameter. The spider was 5 feet long and was bored for a 0.0009-inch shrink fit. Allowing for certain eccentricity of the shaft it was estimated that a temperature differential between the shaft and spider hub of 50 degrees centigrade would be required in order to free the shaft. While it was known from previous experience that the spider could be removed by heating it to 300 degrees centigrade while passing water through the hollow shaft, this method required that the 16 field poles be removed.

Calculations therefore were made to determine whether the shaft could be removed without going to the considerable expense of removing the field poles. These calculations indicated that it was theoretically possible to remove the shaft by heating the spider to the maximum temperature allowed by the field coil insulation (85 degrees centigrade) and simultaneously passing a refrigerant cooled by carbon-dioxide ice through the hollow shaft. It was decided, therefore, to try this method.

The rotor and shaft were placed over a hatchway in the service generator floor of the plant which was specially braced to support this 307 ton weight. Two 75-ton hydraulic jacks actuated by a common pump were placed so that they could exert a downward thrust between the coupling and rotor to move the shaft out of the fits. The rotor was encased in a corrugated asbestos paper shroud and heated by several 10-kw heaters. The cooling unit, consisting of a hinged covered tank, $3^1/_2$ feet in diameter and 11 feet high equipped with strainers in the bottom, was connected to a 200-gallon-per-minute centrifugal pump. Rubber hose was used for connections from pump to shaft and from shaft to tank to allow the shaft to be moved clear of the fits without interrupting the cooling process. Shaft, tank, and piping were lagged as shown in Figure 7. A stove pipe vent was provided from the tank to the outside atmosphere to dispose of the large quantities of carbon dioxide gas. A 32-thermocouple system was installed to give temperature data on all the essential parts of the assembly.

It required five days to heat the rotor to the required 85 degrees centigrade, using an input of 55 kw. By this time, the spider had reached a temperature of 50 degrees centigrade and the shaft 28 degrees centigrade, giving a difference of 22 degrees centigrade between the shaft and spider. During this initial heating water was used to cool the shaft. Under this condition, a thrust of 200 tons did not move the shaft. We were optimistic, however, and had taken the precaution to sling the shaft from the crane hook.

The next step was to start the rapid cooling of the shaft. The water was removed from the cooling system and 300 gallons of alcohol were added to the cooling tank. Dry ice then was added slowly to the alcohol. This caused a violent liberation of gas. When this had subsided, the pump was started and dry ice was added in increasing quantities until there was approximately one ton of dry ice collected; this quantity was maintained in the tank until the shaft was released. This produced a temperature which approximated the minimum attainable temperature with dry ice and alcohol namely—72 degrees centigrade.

After about an hour, the jacks were observed to have lost their pressure, indicating that the shaft had moved. Jacking was started and because it met with diminishing resistance until the limit of the jack was reached the cooling was discontinued. Within an hour after the jack lost their pressure, the shaft was free and was lowered out of its fitted protions.

The heat transfer from the shaft to the alcoho proved to be below expectations due, no doubt, to the separation of bubbles of dissolved gas at the surface of the shaft. Doubtless a more rapid flow would have increased the heat transfer

Maintenance of Thrust Bearings

The thrust bearing, in large high-capacity water-wheel generators, constitutes one of the important components upon which continuous operation of the unit depends. These bearings, and those features of the unit assembly upon which their operation in turn depends, therefore, are given particular attention in tee maintenance routine

Two types of such bearings normally are supplied in Canada: the pivoted-shoe or Kingsbury bearing and the spring-supported bearing. A variation of the spring-supported type is supplied by some European manufacturers, in which the stationary plate is divided into sectors. In the Commission's operations extensive and quite satisfactory experience has been obtained with both types of bearings and no discussion of their relative merits is undertaken herein. All such bearings are located above the rotor, the alternative location below the rotor not having been adopted by the Commission to date, except in four 25,000-kva synchronous condensers where spherical-seated combined thrust and guide bearings of the Kingsbury type are used.

Operating Experience

The Commission has operated approximately 80 bearings of both types over periods of up to 25 years, 43 of which are loaded in excess of 240,000 pounds and 23 in excess of 800,000 pounds. A few of these bearings, including some of the largest size, have operated for 20 years and more without requiring replacements of any kind.

Of the 43 just mentioned, nine outright failures have occurred during this period. It is popularly thought that most bearing failures occur during the starting-up

period, but this has not been the Commission's experience. Eight of these failures occurred during normal service, the ninth being a bearing found to be irreparably damaged after the unit had been shut down because of evidence of bearing distress. This last case was attributed to fatigue failure of the babbitted surface and might be said to be the condition to which these bearings tend after prolonged service (Figure 8). One other failure was occasioned by loss of oil, three others by mechanical misalignment between halves of runner plates of the split type, and the remaining four by "wiping" of the babbitted surface, the causes of which were undetermined at the time.

Manufacturing and Installation Requirements

This generally excellent record has not been attained by installing bearings and then promptly forgetting them. Modern bearings will operate under conditions involving slight inaccuracies in assembly or alignment—in fact, successful operation under such conditions is not uncommon—but long-continued trouble-free service is attained only at the price of careful attention to

(*a*). Accurate design and painstaking manufacturing care.

(*b*). Correct procedure in the initial assembly and unit alignment.

(*c*). Maintenance of the original assembly and unit alignment conditions during operation.

All manufacturers agree as to the necessity for high-quality workmanship in the production of large thrust bearings, including close tolerances and finely finished rubbing surfaces. These standards are maintained strictly. Some disagreement occurs in one particular, the so-called "loose-fit" in the thrust collar, as is discussed later.

In the initial assembly of the bearing it is essential that the rubbing surfaces be dead level and exactly normal to the axis of the shaft. This requires careful positioning of the supporting bracket, by which the plane of the stationary surface is controlled, and of the thrust assembly in combination with the shaft of the unit.

Two factors tend to limit the attainment of desirable accuracy in the latter connection. One is the practice, sometimes adopted, of having the turbine, with its shaft, installed before generator erection is completed. In such cases the final alignment must be carried out with the turbine coupling as the principal center of reference. Our experience indicates that this procedure results in less accurate alignment than that in which the plumb line is used exclusively to locate the center of the turbine. (This, of course, requires that the turbine shaft be removed.)

The second limiting factor is attributed to the use of the "loose" thrust collar. Since, in this situation, the shaft may move relatively to the collar, establishment of the rubbing surfaces in a plane normal to the spinning axis is fraught with difficulty. In the most frequently encountered cases, bearing impairment has resulted from a "rocking" action set up between the collar and shaft and collar and runner plate. This action causes extensive pitting of the surfaces. Moreover, a loose collar permits relative vertical movement of the shaft, and in propeller wheel installations particularly, this is a matter of especial concern. Three cases of shaft fracture, all taking place in the circular key recess and all attributable in large part to fatigue, possibly combined with impact, serve to emphasize this point, and to furnish a further example of trouble arising from the use of the loose collar.

Maintenance Procedure

Bearing maintenance normally is carried out as part of the regular routine overhaul of the hydroelectric unit. Inspection has uncovered numerous cases in which bearing distress was present, although signs of this were manifest in only a few instances, as for example, by a rise in oil temperature. A number of such cases are recorded as "near" failures, the conditions disclosed on dismantling being such that continued operation would have resulted in eventual failure.

Maintenance procedure includes the complete dismantling, checking, and reassembly of the bearing itself and also the checking and readjustment of the unit alignment.

All parts of the bearing are cleaned meticulously and checked accurately for thickness, fit, and position. The thrust collar and shaft are examined for signs of "working" and the respective keyways checked for misalignment and inaccuracies in fitting. Defective parts, if any, are repaired or replaced.

Special attention is given the spring assemblies in modern spring-supported bearings, as it has become increasingly common to find the underside of the stationary plate marked by the springs in a manner suggesting wide variation in spring loading (Figure 10). The present practice is to check all springs individually, to preload them uniformly in the simple fixture shown diagrammatically in

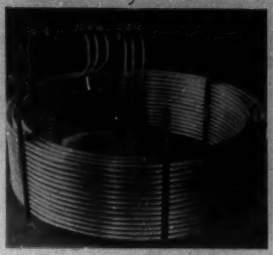

Figure 12. Complete transformer coils field fabricated from continuous aluminum tubing

Figure 11, and then to machine them to uniform length. It is believed that this procedure results in a more even distribution of stresses in the plate and a more accurate alignment of the shaft and plate under load, thereby reducing fatigue and wear of the rubbing surfaces.

Unit realignment is carried out with all rotating parts removed (including the turbine, if practicable), but with the guide bearings in place, if the bearing housings alone are not suitable. A plumb line is centered, usually in the generator upper guide bearing, and accurate measurements taken to the various bearing surfaces and turbine seals.

Properly interpreted, these measurements give a true picture of the state of the existing alignment. Correction of misalignment must necessarily be made on the generator since the turbine is fixed. It is important that bearing brackets be leveled precisely before adjustments are made. Following adjustments, any parts of the assembly moved must be redowelled in their new positions.

Reassembly commences with the placement of the rotating parts. The rotor is centered and supported on jacks; the the turbine runner on its seals. The thrust bearing is added, exercising extreme care. At this stage the rubbing surfaces are treated with a special lubricant such as Gredag *81½* or Oildag *100*.

If the thrust collar presents an interference fit, it is usual to warm it slowly and uniformly until it has expanded sufficiently to drop onto the shaft. The thrust key then is placed and the weight of the rotor transferred to the bearing.

No Discussion

Quantitative Determination of Magnetic Properties by Use of Cathode-Ray Oscilloscope

JOSEPH ZAMSKY
ASSOCIATE AIEE

Synopsis: This paper describes a means of producing the core loss loops of samples of magnetic strips on an oscilloscope screen and a method of obtaining the heat loss from the areas of these loops. The standard Epstein test for obtaining the core loss requires a correction for corner effects due to stacking of the laminations, whereas the method described here circumvents this problem by utilizing only the center portion of a relatively few short strips of the test material. Since quantitative measurements are made, circuit refinements, such as negligible phase shift couplings between amplifier stages and stabilized voltage supplies, are incorporated into the circuits.

FOR the study of low-loss high-permeability steel, having highly directional magnetic properties, it was desired to develop for the determination of these properties, a relatively fast method which would not require compensation for end effects as is necessary with the orthodox Epstein test of the American Society for Testing Materials.

Adler[1] has developed a method of obtaining the core loss curve of a punched washer sample on the screen of an oscilloscope. For studying oriented steel laminations, however, the use of a punched washer is not possible because direction of magnetization is of prime importance. Adler's method also requires the use of a phase shifting device which is not necessary in the apparatus described herein because of the high values of coupling capacitors and resistors used.

The equipment described here provides a method, not only for obtaining core loss and permeability, but also for obtaining retentivity and coercive force of the test specimen, as well as indicating the degree of saturation at a glance.

Magnetic Circuit

The magnetic circuit is indicated in Figure 1*A*. It consists of a yoke made of laminations stacked to give a cross section two by two inches. Four coils are placed on the yoke in such a manner that when they are energized the flux is directed through the test sample. The sample indicated in Figure 1 consists of 29 gauge strips 3 by 28 centimeters. Seven strips are placed on each side of a rectangular bakelite core and set in the magnetic circuit as in Figure 1*A*, with fiber spacers maintaining a nonmagnetic gap of about one-sixteenth inch at each end. The gap is included to prevent individual laminations from contacting the yoke and thereby carrying greater flux than those not making contact. The number of samples was chosen arbitrarily. It was desired to have a sufficient number to be able to obtain the average characteristics of a lot.

Two coils are used to pick up signal voltages for the electronic circuits supplying the vertical (flux density *B*) set of deflecting plates and the horizontal (magnetic intensity *H*) set of deflecting plates of the oscilloscope, respectively. (What is called magnetic intensity *H* in this paper contains both magnetization and eddy current components.)

The *B* coil is placed around the test samples equidistant from the ends. The flux linking this coil consists of that through the samples and that through the space containing the bakelite core. As the relative permeability of the laminations is of the order of several thousand, the flux in the enclosed space can be neglected without serious error. The voltage induced in the *B* coil is, therefore, directly proportional to the rate of change of flux, or rate of change of flux density, in the iron. This was found to be uniform over a length greater than that covered by the coil.

The *H* coil is placed in the space enclosed by the test samples, equidistant from the ends. A probe coil showed the flux to be uniform through a section greater than that covered by the *H* coil. Hence, the voltage induced in this coil is proportional to the rate of change of flux, or rate of change of flux density, in the space enclosed by the samples. Since

Figure 1. Magnetic circuit showing test samples in place

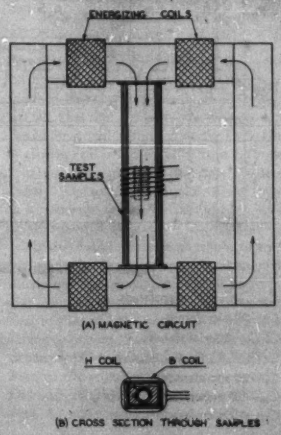

Paper 47-119, recommended by the AIEE committee on instruments and measurements for presentation at the AIEE summer general meeting, Montreal, Quebec, Canada, June 9–13, 1947. Manuscript submitted October 31, 1946; made available for printing April 14, 1947.

Joseph Zamsky is a research engineer in the engineering development division of Allis-Chalmers Manufacturing Company, Milwaukee, Wis.

The author wishes to acknowledge his appreciation for the assistance and advice of Walther Richter, J. R. Maklary, J. J. Borek, L. E. Royt, and R. D. Weinhold.

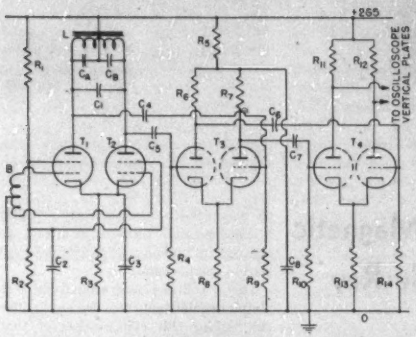

Figure 2. Wiring diagram of circuit supplying flux density deflection to cathode-ray oscilloscope

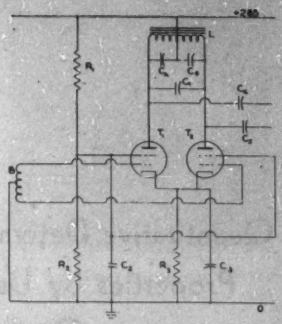

Figure 4. Wiring diagram of integrator circuit

C_A, C_B—10 microfarads
C_1—15 microfarads
C_2—20 microfarads
C_3—50 microfarads
C_4, C_5, C_6, C_7—1 microfarad
R_1—15,000 ohms
R_2—40,000 ohms
R_3, R_8—1,000 ohms
R_4, R_{10}, R_{14}—1 megohm
R_5—25,000 ohms
R_6, R_7—50,000 ohms
R_{11}, R_{12}—100,000 ohms
R_{13}—2,400 ohms
B—Flux density pickup coil
L—47-henry center tapped coil
T_1, T_2—6F6 tube
T_3, T_4—6SN7 tube

there is no magnetic material in this space, the voltage induced in the coil is also a measure of the rate of change of the magnetizing force, or rate of change of magnetic intensity, over the length covered by the coil.

The voltages, therefore, represent the rates of change of flux density and magnetic intensity over only the center portion of the samples and are not affected by end effects.

Since the voltages induced in the coils are proportional to the rates of change of flux density and magnetic intensity, it is necessary to integrate them to obtain voltages proportional to the flux density and magnetic intensity, respectively

Electronic Circuit

The electronic circuits for supplying the B signal and H signal to the deflection plates of the cathode-ray oscilloscope are shown in Figure 2 and Figure 3, respectively. The B circuit contains an integrator followed by two stages of amplification. The H circuit is the same except that two additional stages of amplification precede the integrator.

The amplifiers are standard push-pull

C_A, C_B—10 microfarads
C_1—15 microfarads
C_2—20 microfarads
C_3—50 microfarads
C_4, C_5—1 microfarad
R—15,000 ohms
R_2—40,000 ohms
R_3—1 000 ohms
B—Flux density pickup coil
L—47-henry center tapped coil
T_1, T_2—6F6 tube

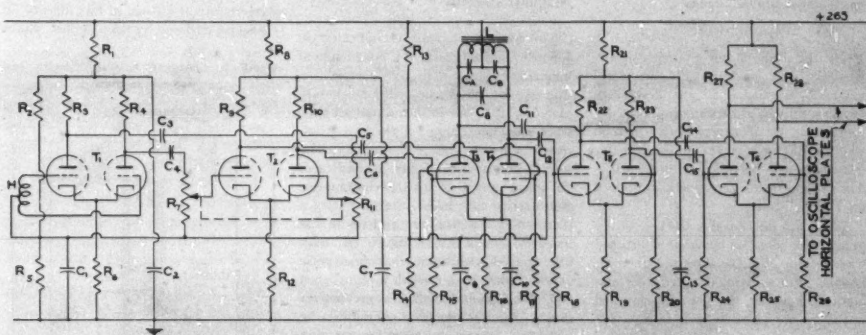

Figure 3. Wiring diagram of circuit supplying magnetic intensity deflection to cathode-ray oscilloscope

C_A, C_B, C_8—10 microfarads
C_1—60 microfarads
C_2, C_3—80 microfarads
$C_4, C_5, C_6, C_9, C_{11}, C_{12}, C_{14}, C_{15}$—1 microfarad
C_7—20 microfarads
C_{10}—50 microfarads
C_{13}—15 microfarads
R_1—30,000 ohms
R_2, R_3, R_4—20,000 ohms
R_5—10,000 ohms
R_6, R_9, R_{10}, R_{13}—15,000 ohms
R_{15}—7,500 ohms
R_{16}—40,000 ohms
$R_7, R_{11}, R_{14}, R_{17}, R_{18}, R_{20}, R_{24}, R_{25}$—1 megohm
R_{18}, R_{19}—1,000 ohms
R_{21}—25 000 ohms
R_{22}, R_{23}—50,000 ohms
R_{27}—2,400 ohms
R_{21}, R_{28}—100,000 ohms
H—Magnetic intensity pickup coil
L—47-henry center tapped coil
T_1, T_2, T_3, T_5—6SN7 tube
T_4, T_6—6F6 tube

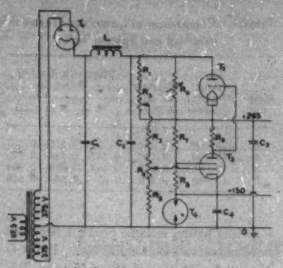

Figure 5. Regulated d-c power supply

C_1—8 microfarads	R_7—3,000 ohms
C_3, C_5—80 microfarads	R_8—7,500 ohms
C_4—20 microfarads	R_9—470,000 ohms
R_1—20,000 ohms	L—15-henry coil
R_2—1,000 ohms	T_1—5R4-GY tube
R_3, R_6—75,000 ohms	T_2—2A3 tube
R_4—20,000 ohms	T_3—6SJ7 tube
R_5—5,000 ohms	T_4—VR150 tube

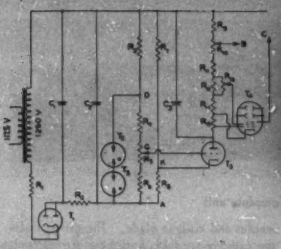

Figure 6. Cathode-ray oscilloscope regulated power supply

B connects to grid of vacuum tube voltmeter. C connects to the plus 150-volt tap of the power supply

C_1, C_2—2 microfarads	R_8—3,900 ohms
C_3—4 microfarads	R_{11}—153,000 ohm
R_1, R_{10}—3,000 ohms	R_{12}—51,000 ohm:
R_2—20,000 ohms	R_{13}—100,000 ohms
R_3—60,000 ohms	R_{14}—39,000 ohms
R_4—6,200 ohms	T_1—5R4-GY tube
R_5, R_{15}—25,000 ohms	T_2, T_3—991 tube
R_6—240,000 ohms	T_4—cathode-ray tube
R_7—234,000 ohms	T_5—6J5 tube
R_9—11,600 ohms	

Figure 7 (above). Core loss loop for peak flux density of 10,000 gausses

Figure 8 (below). Core loss loop for peak flux density of 15,000 gausses

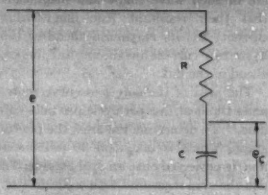

Figure 9 Basic integrating circuit

stages. The integrator stage alone is shown in Figure 4. Its principle of operation has been described by Clarke.[2] (See Appendix I.)

It was found necessary to include the capacitors C_A and C_B as shown. As the grids of the integrator tubes are coupled to the plates of the preceding tube in the H circuit, any sudden fluctuations in the supply voltage appear on the grids of the 6F6's with the same polarity, that is, as in-phase signals. Without C_A and C_B, those fluctuations are amplified so greatly that the grids of the final stage are either driven positive or to cause cutoff. By including capacitors C_A and C_B a low impedance path to ground is provided and the in-phase fluctuations, therefore, do not appear amplified on the grids of the tube following the integrator stage.

Capacitors and resistors of one microfarad and one megohm, respectively, are used for interstage coupling. At a frequency of 60 cycles per second the reactance of a 1-microfarad capacitor is 2,650 ohms. Combined with a resistance of one megohm, the phase angle is about 0.15 degree. The H circuit contains four such combinations, producing a total phase shift of about 0.6 degree. The harmonics are shifted even less. This amount of phase shift may be neglected.

The high value of the time constant of such large coupling capacitors and resistances necessitates the use of an extremely stable d-c power supply. Without such a supply, sudden fluctuations of the supply voltage are transmitted to the plates of the 6F6 tubes by the capacitors C_A and C_B and to the following tubes through the coupling network. The pattern on the oscilloscope screen jumps and then takes a long time before returning to its original position because of the large time constant. At times these kicks come often enough to keep the pattern "dancing" on the screen. The stabilized voltage supply used is shown in Figure 5. It is based on a circuit described in an article by Hunt and Hickman,[3] and provides a direct voltage of 265 volts, with sudden fluctuation less than two millivolts. (See Appendix II for discussion of operation.)

It was also found necessary to provide a regulated power supply for operating the cathode-ray oscilloscope. Without regulation, changes in supply voltage caused the size of the pattern on the screen to change. The circuit is shown in Figure 6 and is described in Appendix III.

The electronic circuit consists of push-pull stages to correct for nonlinearity of the tube characteristics and to provide symmetry of the pattern on the oscilloscope.

Determination of Loss From Curve

The H scale of the cathode-ray screen is calibrated by photographing the line which results when the H pickup coil is inserted in the known magnetic field of a cube-surface coil.[4] The B scale is obtained directly from the photograph of the core loss curve since the desired peak flux density is set by adjusting the value of the 60-cycle-per-second voltage applied to the energizing coils on the yoke. To set the flux density, the voltage induced in a coil wound directly over the B pickup coil is measured with a cathode ollower voltmeter[5] which reads average value The average value of this voltage is a measure of the peak flux density.[6] (See Appendix IV.)

Figures 7 and 8 are photographs of core loss curves of the same sample taken with maximum flux density of 10,000 and 15,000 gausses, respectively. It is noted that in Figure 7 the peak of the magnetic intensity occurs ahead of the peak of flux density. This is explained as follows. Assume the core loss curve axes represent flux and magnetizing current. If there were no eddy currents present, the core

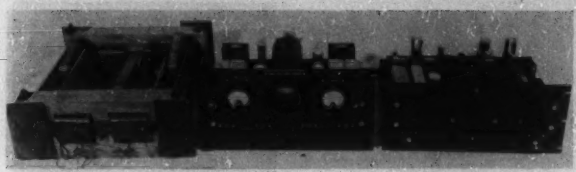

Figure 10. Complete unit

On left is shown the magnetic circuit with test samples and coils in place. The center assembly contains the amplifier and integrator stages, the cathode-ray tube, and the electronic voltmeter. The assembly on the right contains the power supplies

loss curve would be a true hysteresis loop and flux and current would reach their maximum values simultaneously. Since the flux lags the terminal voltage by 90 degrees, the peaks of the flux and hysteresis current would occur 90 degrees after that of the voltage. With eddy currents present, the magnetizing current now consists of a hysteresis current and an eddy current component. The eddy current is set up by the flux and is in phase with the terminal voltage. Hence, the eddy current reaches its maximum 90 degrees ahead of the hysteresis current maximum. At 10,000 gausses for the material tested, the two components of current are of such wave shape and magnitude that their resultant (the magnetizing current) has its maximum ahead of the hysteresis current maximum and, hence, ahead of the flux.

The area of the core loss curve represents the heat loss per cycle per unit volume.[7] To determine the area, the photograph, which is taken on 35 millimeter film, is projected onto an opal glass screen and the area measured with a planimeter. From the screen calibration and the density of the samples, the watt loss per pound is calculated.

Table I shows a comparison of results obtained by the electronic method with those from Epstein tests. Two different materials, listed here as A and B, were tested. The individual tests on each material were not made on the same pieces.

Appendix I. Operation of Integrator Circuit

The basic circuit for integrating a voltage is shown in Figure 9. It consists of a resistor R in series with a capacitor C whose reactance is negligible compared to the resistance of the resistor. If an alternating voltage is impressed as shown, the current that flows is then given by

$$i = e/R$$

and is in phase with the voltage e. The voltage appearing across the capacitor, is therefore

$$e_C = 1/C \int i\,dt = 1/RC \int e\,dt$$

Hence, the voltage appearing across the capacitor is proportional to the integral of the impressed voltage.

The equivalent circuit of the integrator stage shown in Figure 4 consists of a voltage source whose value is given by the value of the input voltage multiplied by the amplification factor of the tubes in series with the plate resistances of the tubes and the capacitor network of C_1, C_A, and C_B. The output voltage, which is that across the capacitor network, is proportional to the integral of the input voltage

Appendix II. Regulated Power Supply

The operating principle of the regulated power supply, shown in Figure 5, is the following: a portion of the variations of the load voltages and of the rectified voltage is applied to the grid of the *6SJ7* tube T_3, amplified, and applied to the grid of the *2A3* tube T_2 in series with the load. A rise in the load voltage raises the grid potential and therefore lowers the plate potential of the *6SJ7* tube an amplified amount. This lowers the grid potential of the *2A3* tube, resulting in a decrease of the current through the tube, which in turn lowers the load voltage.

Appendix III. Regulated Supply for Cathode-Ray Oscilloscope

In any tube, if the grid voltage changes a certain amount and the plate voltage changes μ (the amplification factor of the tube) times this amount but in an opposite direction, the plate current remains constant. This principle is employed in the regulated power supply shown in Figure 6.

Table I. Comparison of Losses by Electronic Method and Epstein Test

Material	Peak Flux Density, Gausses	Epstein Test, W Per Lb	Electronic Method, W Per Lb I	II	III
A	10,000	0.306	0.312	0.315	0.307
A	15,000	0.740	0.737	0.726	0.726
B	10,000	0.352	0.358	0.358	0.354
B	15,000	0.859	0.87	0.889	0.856

In this figure, assume point A becomes more negative by 21 millivolts. Point G (the grid potential of the *6J5* tube T_5), will also become 21 millivolts more negative since the *991* regulator tubes maintain point D at a constant potential difference with respect to point A. Point K (the cathode potential) will become

$$(21)(R_7)/(R_8+R_7) = (21)(234{,}000)/(11{,}600+234{,}000) = 20 \text{ millivolts}$$

more negative. The net result is that the voltage from plate to cathode has increased 20 millivolts while the voltage from grid to cathode has decreased 1 millivolt. Since this is a ratio of 20, which is the amplification factor of a *6J5* tube, the load current remains constant.

Appendix IV. Relation of Average Voltage Induced in a Coil to Peak Flux Linking Coil

The instantaneous value of the voltage induced in a coil is

$$e = N\,d\phi/dt$$

where

e = the instantaneous value of the voltage
N = the number of turns on the coil
ϕ = the flux linking the coil

Integrating the above equation over a half-period of the voltage wave

$$\int_{t_1}^{t_2} e\,dt = N \int_{-\phi_{maximum}}^{+\phi_{maximum}} d\phi = 2N\phi_{maximum}$$

but

$$e_{average} = \frac{\int_{t_1}^{t_2} e\,dt}{t_2 - t_1} = \frac{2N}{t_2 - t_1}\phi_{maximum}$$

where $t_2 - t_1$ is a half-period of the voltage wave.

References

1. B–H Curve Tracer for Lamination Samples, **Robert Adler.** *Electronics* (New York, N. Y.), volume 16, November 1943, pages 128–31, 314, 316–17.

2. Differentiating and Integrating Circuits, **James G. Clarke.** *Electronics* (New York, N. Y.), volume 17, November 1944, pages 138–42.

3. Electronic Voltage Stabilizers, F. V. Hunt, R. W. Hickman. *Review of Scientific Instruments* (New York, N. Y.), volume 10, January 1939 pages 6–21.

4. Cube Surface Coil for Producing a Uniform Magnetic Field. Sidney H. Rubens. *Review of Scientific Instruments* (New York, N. Y.), volume 16, September 1945, pages 243–5.

5. Cathode Follower Circuits, Walther Richter. *Electronics* (New York, N. Y.), volume 16, November 1943, pages 112–17, 312.

6. Magnetic Circuits and Transformers (book), Electrical Engineering Staff Massachusetts Institute of Technology. John Wiley and Sons, Inc. (New York). N. Y., 1943. Page 147.

7. Reference 6. Pages 125–8.

No Discussion

Dynamic Braking of Two D-C Series Motors

JOHN D. LEITCH
MEMBER AIEE

Synopsis: The problem of obtaining dynamic braking automatically in the event of power failure is discussed for 2-motor drives. Various methods of connecting the two motors are considered from the point of view of service requirements.

TWO identical d-c series motors frequently are used on a single drive because two smaller motors are more economical in cost and space and have a lower WR^2 than one larger motor.

The two motors may be connected permanently in series, in which case a single controller is obviously adequate, or they may be connected permanently in parallel requiring a duplex controller having separate reversing and accelerating contactors and separate resistors. Often double-pole contactors are used to insure simultaneous switching in the paralleled motor circuits.

It is desirable in certain important drives to provide automatic stopping in the event of power failure. This may be accomplished without magnetic brakes by using dynamic braking to decelerate the drive and inherent friction in the machine to bring it to rest.

Dynamic Braking in One Direction

Dynamic braking in only one direction requires a single pair of spring-closing contactors when the two motors are connected permanently in series as shown in Figure 1. The spring-closing contactors *FB1* and *FB2* close their contacts on power failure while all other contactors open. If motion is in the forward direction, a dynamic braking current will flow from *A1* at 1 through both fields without reversal back to armature *A2* at 3. Thus the current reverses in the armatures only, a sufficient condition for dynamic braking. In the reverse direction, dynamic braking is not provided by the circuit of Figure 1 since the current is reversed in both the fields and armatures. Obviously, if the two motors are connected in parallel, the circuit of Figure 1 would be duplicated with only one motor in each part.

Dynamic Braking in Both Directions (Single-Motor Methods)

A very simple method of obtaining dynamic braking in both directions on a 2-motor drive is that which provides dynamic braking by one motor in the forward direction and by the other in the reverse direction as shown in Figure 2 for two motors in parallel. On many machines adequate braking torque can be provided in this way with considerable saving in control equipment.

If the two motors are connected in series, it is necessary to use an additional contactor *S* to separate the two armatures during dynamic braking as shown in Figure 3.

In an earlier paper[1] methods of obtaining dynamic braking in both directions with a single series motor were discussed. Sometimes with 2-motor drives it is desirable, in emergency, to operate the machine with one motor and still obtain dynamic braking in both directions in the event of power failure. If, in addition, the motors must be connected in series during starting, and later in parallel to obtain higher speeds, dynamic braking must be provided regardless of whether the motors are in series or parallel at the instant of power failure. Such a controller requires means equivalent to those described for a single series motor for selecting the proper braking connections together with a system of disconnecting switches for operating the machine with either motor or both. The power circuit of a controller meeting these specifications is shown in Figure 4.

Each motor has associated with it four spring-closing contactors *FB1*, *FB2*, *RB1*, and *RB2*. Should power fail while the motors are rotating in the forward direction only the *FB* pair closes its contacts, while in the reverse direction only the *RB* pair closes. This may be accomplished by polarizing the spring-closing contactors as described in the case of a single series motor.[1]

Series and parallel operation is obtained by the series contactor *S* and the two parallel contactors *P1* and *P2* in the usual manner. Two 3-pole double-throw knife switches *K1* and *K2* permit disconnecting either motor from the system. With both knife switches in the up position, normal operation with two motors is obtained. With either of the

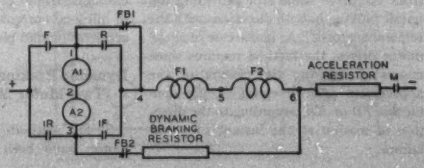

Figure 1. Braking in one direction

Paper 47-133, recommended by the AIEE committee on industrial control devices for presentation at the AIEE summer general meeting, Montreal, Quebec, Canada, June 9–13, 1947. Manuscript submitted March 27, 1947; made available for printing April 21, 1947.

John D. Leitch is chief engineer in The Electric Controller and Manufacturing Company, Cleveland, Ohio.

The author wishes to express his appreciation for the suggestions made by A. C. Dyer and L. D. Taylor, both of The Electric Controller and Manufacturing Company.

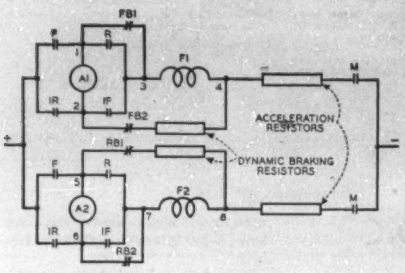

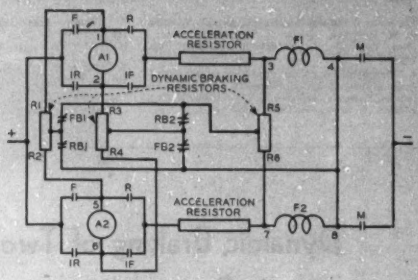

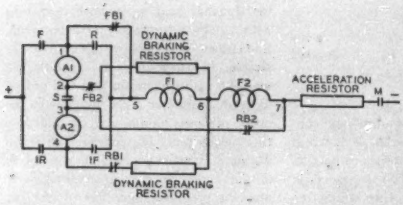

Figure 2 (left, above). Forward braking with one motor and reverse braking with the other

Motors in parallel

Figure 3 (left). Forward braking with one motor and reverse braking with the other

Motors in series

Figure 5. Bridging resistors, single motor method

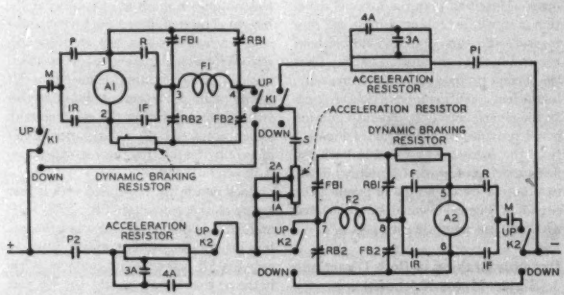

Figure 4. Braking in both directions, single motor method

two switches in the down position, the corresponding motor is disconnected.

If the two motors are connected in parallel only, it is possible to reduce the number of spring-closing contactors from eight to four by tying corresponding points on the two motors through bridging resistors as shown in Figure 5. Another advantage of this circuit is that it permits disconnecting either motor from the drive while still providing dynamic braking in both directions with the remaining motor. As in the case of single motor drives, the method requires some means of assuring the closure of the appropriate pair of spring-closing contactors *FB* or *RB*, according to the direction of motion at the instant of power failure.

There was some question as to the practicality of using bridging resistors since excessive circulating currents might be produced by any unbalance in the circuits and by small differences in the characteristics of the two motors. However, on test with two *MD408* motors, the bridging resistors could be reduced in ohmic value beyond that required for any practical application without producing circulating currents greater than ten per cent of full load current and then only during acceleration and plugging.

Dynamic Braking in Both Directions (Two-Motor Methods)

So far, methods applicable to a single motor have been applied to 2-motor drives. There are, however, a variety of 2-motor circuits which cannot be applied to a single motor but which are applicable to drives where the number of motors is a multiple of two. The main advantage of these circuits is that they require only four spring-closing contactors, all of which are permitted to close their contacts on power failure. This eliminates the need for control equipment which will hold one pair of spring-closing contactors open according to the direction of motion of the motors at the instant power fails. The 2-motor circuits, however, have the disadvantage that the drive cannot be driven in emergency by only one motor without loss of the dynamic braking feature.

Reversal by Reversing One Armature and One Field[1]

This circuit differs from all other circuits considered in this paper in that reversal is obtained by reversing the field of one motor and the armature of the other as shown in Figures 6 and 7. On power failure all four spring-closing contactors *DB1*, *DB2*, *DB3*, and *DB4* close their contacts to complete two separate dynamic braking loop circuits, in each of which the armature of one motor is connected in series with the field of the other. The direction of the dynamic braking currents in both loops is such that the fields are energized in their original direction while the armature currents are reversed. This occurs for both directions of motor rotation provided the motors are not being plugged when power fails.

Should power fail during plugging, the conditions are somewhat different. If the motors are running in the forward direction, the counter electromotive forces will be in directions 6–5 in *A2* and 2–1 in *A1*. On plugging, the current is reversed in the field *F1*, causing reversal of the counter electromotive force at armature *A1* to

direction 1–2 since the motor is still running in the forward direction. The counter electromotive force at armature *A2* remains in direction 6–5 since the field *F2* is not reversed. On power failure under these conditions, the currents in the two dynamic braking loops will be such as to reverse the fields of both motors. In other words, current will flow from *A1* at 2 through the field *F2* in direction 8–7 and from *A2* at 5 through the field *F1* in direction 3–4. If both motors were absolutely identical there would be a likelihood of losing both fields and the motors would drift to rest without producing dynamic braking. On test no such failure occurred. If it is assumed that one of the two motors dominates by having slightly higher counter electromotive force at a given speed, the behavior of the circuit is as follows. Assuming motor 1 to dominate, the field of motor 2 will be reversed before that of motor 1. This will cause immediate reversal of the counter electromotive force at *A2* to the direction 5–6 since the motors are still running in the forward direction. A current will then flow from 6 at *A2* through the field *F1* in direction 4–3 maintaining its "plugged" direction. Thus, instead of the conditions which hold for the forward direction of motion before plugging, the currents in the fields are reversed while the armature currents are in the same direction, a sufficient condition for dynamic braking with both motors. This applies to both Figures 6 and 7. In the latter figure, where the two motors are connected in series, it is necessary to add two contactors *S1* and *S2* for separation of the fields and armatures during dynamic braking.

Railway Method[3]

A well-known method of obtaining dynamic braking in both directions on 2-motor drives has been used for some years on d-c electric railway systems, particularly on streetcars. Because of the infrequent reversal of traction motors, it is customary to use double-throw knife switches in reversing the fields. The problem of plugging or rapid reversal is not a factor in the design of streetcar controllers.

Traction drives usually are accelerated by first connecting the motors in series and later in parallel. It is also desirable to provide numerous steps of service dynamic braking so that the motors can be decelerated at a controlled rate. A typical circuit providing these features is shown in Figure 8.

A 4-pole double-throw knife switch is shown for reversal of the fields. In accelerating, contactors *M1*, *M2*, *PS*, and *S* are closed, connecting the two motors in series. After acceleration has proceeded to a certain point, *S* opens and *P1* and *P2* close to connect the motors in parallel. On returning the master to the off point or coasting position, contactors *P1* and *P2* close or remain closed along with the dynamic braking contactor *DB*. Contactors *M* and *M1* drop out along with the accelerators.

If the knife switch never is reversed while the motors are rotating, the counter electromotive force always will be in the directions 2–1 at *A1* and 6–5 at *A2*. When the controller is connected in the coasting position, as shown in Figure 8, weak dynamic braking currents flow from 1 at *A1*, through resistor *R1-R2*, contactor *P1*, accelerating resistor, and field *F2* to 5 at *A2*, contactor *DB*, resistor *R4-R3* back to 2 at *A1*, and through a similar circuit starting from 5 at *A2* through *R4-R3*, field *F1*, and so on, back to 6 at *A2*. These currents maintain the fields energized in the proper direction and permit the rapid build-up of dynamic braking torque as the acceleration contactors *1A*, *2A*, and *3A* are closed in sequence, along with contactors *M2* and *PS*. In this way the retarding or decelerating torque can be varied as desired. On power failure, it is necessary only to establish the circuit of Figure 8 and to reduce the resistance of the dynamic braking circuits to a value giving the required torque.

Figure 6 (below, left). Reversal by reversing one armature and one field

Motors in parallel

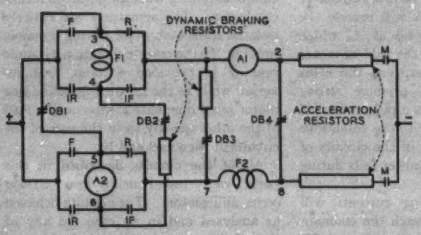

Figure 7 (bottom, left). Reversal by reversing one armature and one field

Motors in series

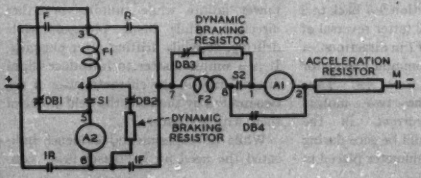

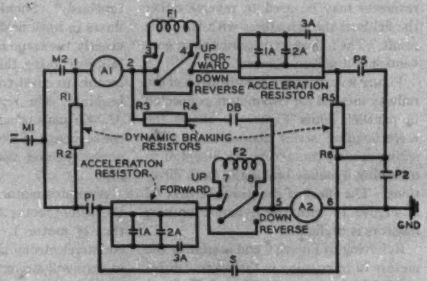

Figure 8 (right, above). Railway method

Series–parallel

Figure 9 (below). Modified railway method using common conductor

Motors in parallel

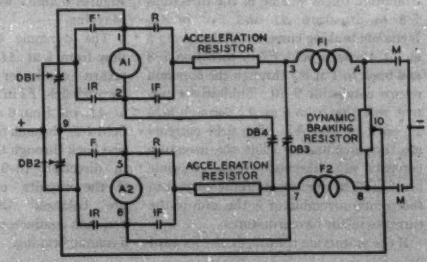

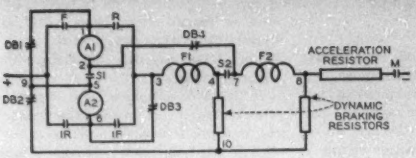

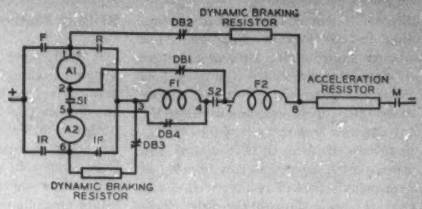

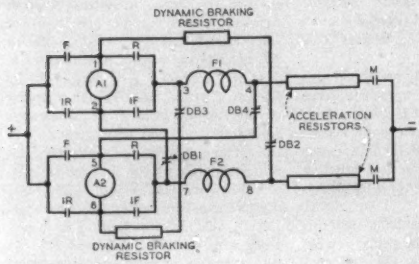

Figure 10 (above, left). Modified railway method using common conductor

Motors in series

Figure 11 (left). Modified railway method without common conductor

Motors in parallel

Figure 12 (above). Modified railway method without common conductor

Motors in series

Modifications of the Railway Method

Where frequent plugging and reversing operations are necessary, the use of reversing contactors is indicated. These reversers may be used to reverse either the fields or the armatures with the same result. The following diagrams show conventional armature reversal.

Figure 9 illustrates a modification of the railway method for two motors connected in parallel, while Figure 10 shows the corresponding series connection. Four spring-closing contactors are essential in obtaining dynamic braking in both directions. The effect of shunting the field *F2* in Figure 10 with the dynamic braking resistors is negligible.

Referring to Figure 9 and assuming the motors to be running in the reverse direction with contactors *R*, *1R*, and *M* closed at the instant of power failure, these contactors will open simultaneously with the closure of the four spring-closers *DB1*, *DB2*, *DB3*, and *DB4*. The counter electromotive forces will be in the directions 1–2 in armature *A1* and 5–6 in *A2*. Dynamic braking current will flow from 2 at *A1* through field *F2* in direction 7–8 and back to 1 at *A1* through the common return conductor 9–10. Similarly a current will flow from 6 at *A2* through field *F1* back to 5 at *A2*. The field currents are thus maintained while the armature currents are reversed giving dynamic braking. The dynamic braking current in the common conductor is the sum of the currents in the two armatures.

If the motors are rotating in the forward direction with contactors *F*, *1F*, and *M* closed, the counter electromotive forces will be in directions 2–1 in *A1* and 6–5 in *A2*. On power failure these counter electromotive forces would tend to reverse the currents in both fields simultaneously. Should it happen that the fluxes in both fields reach a zero value at exactly the same instant there is a possibility of losing the fields, permitting the motors to coast to rest without dynamic braking. On repeated tests with two *MD408* motors no such failure occurred, the sequence of events as determined by ammeters and voltmeters being as follows.

Assuming motor 1 to dominate motor 2, the field of motor 2 will be reversed before that of motor 1. This will reverse the counterelectromotive force at *A2* which in turn will strengthen the field of motor 1. As soon as this happens the fields rapidly build up to produce strong dynamic braking. This rapid reversal of only one field is similar to the conditions which hold in the case of the circuits of Figures 6 and 7 when power fails during plugging.

The dynamic braking currents will flow from 1 at *A1* through the common return conductor in direction 9–10, through field *F2* in direction 8–7 back to 2 at *A1*, and from 6 at *A2* (after reversal of field F2) through field *F1* in direction 3–4 and back through the common conductor in direction 10–9 to 5 at *A2*. Thus if the circuits of the two motors are balanced the current in the common conductor should be zero during dynamic braking. An ammeter placed in the common return circuit indicated a sudden rush of current of short duration as the fields collapsed, after which the current was practically zero. Removal of the common conductor did not alter the results in the forward direction. This means that after reversal of one field, the two motors are in series giving double the counter electromotive force but the same braking current since the amount of resistance in the circuit is double that for one motor

The behavior of the circuit of Figure 10 is essentially the same as that of Figure 9, the only important difference being the addition of two normally open contactors *S1* and *S2* for separation of the fields and armatures during dynamic braking.

Further modifications of the railway method are shown on Figures 11 and 12 for parallel and series connected motors, respectively. Comparing these circuits with those of Figures 9 and 10, the common tie between the fields has been eliminated along with the common return conductor. The armatures are entirely isolated from each other during dynamic braking. In the reverse direction dynamic braking is provided without field reversal, while in the forward direction one motor must dominate to reverse the field of the other quickly as in the case of the circuits of Figures 9 and 10.

All of the circuits described in this paper were tested using two *MD408* series mill motors. The circuits behaved as analysed and in no case did any of them fail to provide dynamic braking on power failure while running in either direction, while being plugged, while drifting, or while drifting after plugging. It is a simple matter to introduce slight dissimilarity in the characteristics of the two motors by shunting the field of one of them with a resistor.

While no experimental evidence indicated the need for a "teaser field" con-

nection during drifting, it is felt that in all circuits except that of Figure 8, such connection should be added as a means of assuring an appreciable counter electromotive force across each armature during drifting or coasting with the master on the off point.

Methods of providing graduated braking automatically in the event of power failure are described for a single motor elsewhere[1] and are equally applicable to 2-motor drives. Graduated service braking is provided easily by additional contactors for short-circuiting portions of the dynamic braking resistors as the motor decelerates.

References

1. Dynamic Braking of a Single D-C Series Motor, J. D. Leitch. AIEE Transactions, volume 66, 1947, pages 149–54.

2. Control of Electric Motors (book), P. B. Harwood. John Wiley and Sons, Inc., New York, N. Y. Second edition, pages 246–50.

3. Dynamic Braking With Traction Motors, L. G. Riley, G. M. Woods. AIEE Transactions, volume 64, 1945, July section, pages 517–19.

No Discussion

Modulation in Communication

F. A. COWAN
FELLOW AIEE

ANY signaling system requires some means for introducing a change in conditions at the sending end which may be recognized at the receiving end. The process by which the conditions are changed has come to be called modulation. There are many varieties of forms of change as well as a large number of conditions which are subject to change in response to the signals to be transmitted.

In early systems for communication at a distance the signal information might have been impressed upon a rising column of smoke, a light, a stone tablet, or a sheet of parchment. For modern communication wide use is made of systems in which the signals change the magnitude or condition of electric energy.

Starting with the electric telegraph a little more than a hundred years ago this medium of communication has grown steadily more important and more complex. To meet a variety of needs many systems of modulation have been developed and papers describing them in detail are available in the technical literature. Various aspects of the modulation processes have been analyzed carefully and presented and some of the earlier conceptions have acquired a classical textbook status. Recent trends have placed emphasis on modulation systems which more readily may be understood when viewed in a somewhat different manner. It is the purpose of this paper to present certain conceptions which may facilitate the understanding of the various systems of modulation and permit an improved perspective.

Paper 47-150, recommended by the AIEE committee on communication for presentation at the AIEE summer general meeting, Montreal, Quebec, Canada, June 9-13, 1947. Manuscript submitted March 26, 1947; made available for printing April 29, 1947.

F. A. COWAN is transmission engineer with the American Telephone and Telegraph Company, New York, N. Y.

Types of Modulation

Communication by electric means depends upon wave transmission. The information carried by a wave is determined by the manner in which the instantaneous wave magnitude varies with time. All modulation systems depend upon changing in some way this relationship between magnitude and time. The early telegraph and telephone systems employed a change of amplitude in response to the signals. While most of the present day systems also depend upon amplitude changes of some form there are also a large number of systems in which the amplitude of the waves is not changed and the intelligence is transmitted by changing the relative phase or time of occurrence of some periodic wave condition. Since the frequency of a wave is merely the rate at which a periodic wave recurs, a variation in the relative time of occurrence represents a change in frequency as well as phase.

Systems of modulation which employ amplitude changes may be designated broadly as "amplitude modulation" systems. Those employing changes in time of occurrence may be designated as "frequency modulation," "phase modulation," or "time modulation" systems.

Modulation to Change the Signal Medium

Translation of signals from one medium to another involves modifying conditions in the new medium in response to those existing in the originating medium. The electric signals produced for transmission from one point to another are converted from acoustic signals in the telephone, from mechanical signals in the telegraph and teletypewriter, and from light signals in television and telephotograph systems. At the receiving point another step of modulation or what is termed "demodulation" changes the signals back to the originating medium.

When, as is usually the case, the electric signals are produced by changing the magnitude of an otherwise unvarying quantity, such as might be produced by a direct current or voltage, the electric signal frequencies are the same as those in the originating medium. These frequencies are called "keying," "audio," and "video" frequencies for the telegraph, the telephone, and television, respectively. The term "base band frequencies" recently has come into use as a general term describing frequencies of this class.

When, however, the electrical quantities which are modified are changing periodically over a range of conditions, such as those produced by an alternating current, the signal frequencies resulting from the modulation are different from those in the originating medium and fall in the frequency range above and below the frequency of the unmodulated condition. The bands in which these frequencies fall are the well known "upper side band" and "lower side band" and the frequency around which the bands are disposed is the "carrier" frequency. Regardless of the method of modulation the side frequencies are displaced from the carrier by intervals equal to the signal frequencies or harmonics thereof.

The terms "modulation" and "carrier" came into general use when the first carrier and radiotelephone systems were being developed. The use of devices in which modulation changed the signal medium antedated the use of modulation to change signals from one location in the electrical frequency spectrum to another, and as a result is not generally thought of as modulation. Similarly, the idea of a direct current being a carrier current with zero frequency is encountered even less frequently. Although these conceptions are sometimes helpful in a broad over-all consideration, it is the present accepted practice to consider as "carrier systems" only those systems in which the frequency being modulated is other than zero. Those systems in which the carrier is effectively a direct

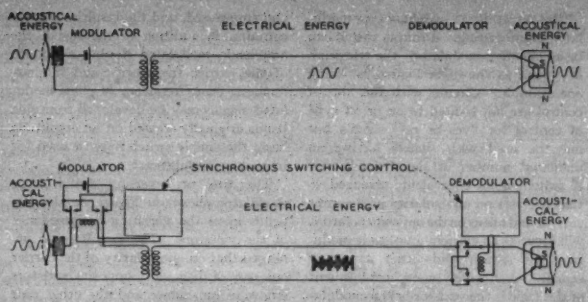

Figure 1. Possible telephone connections

Top—Voice frequency telephone circuit
Bottom—Carrier frequency telephone circuit

current are known as "direct current systems" in telegraph, as "voice" or "audio frequency systems" in telephony, and as "video systems" in television.

Modulation in the Telephone Transmitter and Receiver

In most telephone instruments the variation in resistance of the carbon granules in the transmitter in response to the impressed speech determines the value of a direct current. One arrangement used in supplying the current is indicated in Figure 1*a*. If this direct current were converted into an alternating current by the introduction of a pole changer in the manner shown in Figure 1*b*, the result of impressed speech would be amplitude modulation of this alternating current. The signal message then would be carried by the upper and lower side bands of the frequency produced by the pole changer.

In the usual telephone receiver a magnetic field produced by the signal currents interacts with the field of a permanent magnet to produce forces on the diaphragm which reproduce the speech. If the permanent magnet in the receiver were replaced by an electromagnet which was supplied with an appropriately phased alternating current of the same frequency as that supplied the transmitter by the pole changer, the receiver would reproduce the impressed speech from the signal side bands produced by modulation at the transmitter.

As an alternative to this arrangement it would be possible to introduce a pole changer at the receiving end, which would in effect rectify the a-c signal and then operate in the usual manner on the telephone receiver. It is this arrangement which is indicated schematically in Figure 1*b*. The difference between the telephone system employing voice frequency transmission and that employing transmission over an a-c carrier for a single channel is merely that of introducing the appropriately phased pole changers at each end of the circuit.

Types of Signals

The type of modulation employed frequently depends upon the nature of the signals it is desired to transmit. Signals introduced into a communication system may be divided into two broad classes: types with a limited number of conditions and types with an unlimited number of conditions.

The first category includes the 2-condition type of signals used in most telegraph and supervisory circuits. The 2-condition signals such as open or closed, marking or spacing, on or off, and positive or negative may be designated as "yes or no" signals. Special codes with more than two conditions are sometimes desirable. The synchronizing signals in television transmission with three amplitudes or conditions are an example. Two of the amplitudes correspond to each of the extreme picture conditions of black and white while the third is a higher amplitude.

The second category includes unaltered signals from a telephone, and those produced by scanning pictures for transmission over a telephotograph or television system. Here it is desirable to transmit a wide range of finely graduated tones or conditions. Since there is a limit to the extent to which fine gradations can be resolved or appreciated, it is possible to convert signals of the second category into signals of the first category.[1,2] In this alteration it is necessary to retain a sufficient number of gradations to insure acceptable reproduction at the receiving end.

Another characteristic of signals which is important is the rate at which the different conditions need to be transmitted. This rate of change of conditions may be relatively slow as in manual telegraph or exceedingly rapid as in the transmission of a television picture. The required rate of change determines the minimum frequency band width necessary for the signal transmission.[3] The width of the required signal band may be altered significantly by changes in the form of signals to be transmitted. For example, the 32 characters of a teletypewriter might be represented by 32 gradations in amplitude of a current, and only one of these gradations would need to be transmitted for each character. If, in order to differentiate with greater certainty between the different characters, it were found desirable to change to a 2-condition "yes or no" type of signal, a permutation code having five "yes or no" sequential conditions would be necessary in order to represent a total of 32 characters. Thus, in order to obtain greater certainty of correct recognition of conditions, the rate at which the different conditions must be transmitted has been increased fivefold, with a corresponding increase in the minimum band width required for the same speed of character transmission.

In the same way the representation of the gradations in amplitude of speech by a "yes or no" code, such as is used in pulse code or pulse counting systems requires a sevenfold increase in minimum signal band width where 128 gradations of amplitude are transmitted.[1,2]

Signals which have been resolved into the "yes or no" type with an accompanying change in the minimum band width required, do not necessarily represent the limiting extent to which signals can be changed in order to obtain greater certainty of correct reception. It is usually not necessary to make further changes in signal types but there may be instances where the adoption of more elaborate measures are desirable. Such a case is encountered in telegraph where there has been a practice of occasionally repeating messages.

Mechanism of Modulation

Any mechanism which will produce the desired changes in conditions in response to signals may be employed for modulation. The variable frequency oscillator used in transmission testing work fur-

nishes an example of two types of modulation by manual control. Frequency modulation may be accomplished by turning the frequency adjustment dial and amplitude modulation accomplished by turning the output or volume control dial.

So long as the signaling speeds are low, mechanically controlled switches, commutators, relays, potentiometers, and variable capacitors may be used satisfactorily. For higher signaling speeds variable impedance elements such as vacuum tubes, rectifiers, and varistors may be arranged to form networks which will accomplish the desired changes in response to the signals. Some of the instrumentalities used for modulation are shown in Figure 2. The changes introduced by the modulating circuits may be gradual over all or most of the range, or may be abrupt. An effective design is usually one in which the character of change is abrupt and approximates a switch.[4] In the analysis of such circuits it is often convenient to assume the elements to be replaced by equivalent switches capable of operation at the required speed.

Figure 2. Instrumentalities used for modulation

The versatility of switching type modulators is interesting. A simple switch can be an effective modulator—the telegraph key, such as shown in Figure 3*a*, being one example. Circuits with this abrupt control are not limited to on or off type of control for "yes or no" signals but may be used with signals having an unlimited number of signal conditions. A switch or its equivalent, arranged so that it closes on one polarity of a carrier current and opens on the opposite polarity, will serve as an efficient amplitude modulator for speech and other types of signals. One widely used arrangement of this type is the varistor bridge modulator shown on Figure 3*b*.[5] The switching action of the bridge-type modulator results from the variable impedance of the varistors forming the bridge. When the polarity of the carrier is in the direction in which the varistors conduct readily the current flow causes the effective impedance to drop to quite low values, thus effectively placing a low impedance across the circuit. When the polarity is in the opposite direction the impedance of the varistors is quite high, the impedance of the circuit is effectively high, and there is a negligible bridging effect which corresponds to the open condition of the switch. The signal in this case is alternately passed and suppressed, and the resulting output contains, in addition to the signal, the amplitude modulated double sidebands of the carrier frequencies and its harmonics. Since frequency or phase modulated signals may be developed from side bands originally created on an amplitude basis the simple switch may be used for frequency modulation.[6]

The ring or reversing switch type modulator shown in Figure 3*c* also depends upon the variation in impedance of the varistors. The circuit is so arranged that on one polarity of the carrier one pair of diagonally opposite varistors is low in impedance and the other pair is high. The reversal of this condition for the opposite polarity furnishes the effective reversal of the polarity for transmission through the modulator. This pole changing type of modulator has the advantage of placing the signal carrier and output terminals in a conjugate relationship, thus effectively limiting the output to the modulation products.

Two amplitude modulating switches arranged so that one switch is open while the other is closed, and vice versa, will permit signals from two separate channels to be connected to a line on a time division multiplex basis.[7,8] If the switches are

biased in such a manner that they are closed for a much shorter length of time than they are open, a number of such channels may be interleaved on a time division basis. The switching required for time division multiplex may be done with relays, mechanical commutators, special vacuum types with electric beam commutating, or with amplitude modulators employing varistors, crystals, or vacuum tubes to act as "gate" circuits under the control of switching currents.[9,10]

Two switches under the control of "yes or no" signals may develop frequency shift modulation if these switches were arranged so that under one condition of signal one frequency would be connected to the circuit, and under the other condition the other frequency would be connected.[11]

A switch, or a circuit equivalent to a switch, may be caused to generate pulses and, by proper control of the timing the various forms of pulse modulation may be generated. In pulse position modulation a pulse is generated once during each of a succession of fixed time intervals. The instant of generation within the interval is determined by the impressed signal. The usual arrangement is to have the operation retarded for one polarity and advanced for the other polarity of the signal, the degree of advancement or retardation being controlled by the amplitude of the signal.[12,13]

It is an interesting fact that the output of a pulse position modulator represents a frequency or phase modulation of the switching frequency.[14,15] The harmonics of this switching frequency which are generated by the abrupt switch operation also carry phase or frequency modulation so that still another means of deriving frequency modulated signals from a simple switching operation is available. The harmonics which are assumed to be used in this case would in other cases represent unwanted modulation products which readily may be removed by filters, since they fall well above the wanted band.

Modulation Products

Unwanted signal or modulation products in the modulator output are not objectionable as long as they can be removed by filters. However, in some cases the signal and carrier frequencies are so related that unwanted products may fall into the same band as the wanted products. Unwanted signal and carrier frequencies may be reduced greatly by the use of balanced ring type modulators, but this does not eliminate those modulation products associated with harmonics of the carrier. Since these arise from the abrupt switching action, removal would require that the switching operation be performed in such a manner that the current ratio corresponding to the transmission of the signal through the modulator would be a linear function of the instantaneous carrier magnitude.[16] Modulators of this type are difficult to achieve and for most situations would have no significant advantage. Such a modulator would be a so-called pure product modulator and the classical mathematical expressions for the product of the signal currents and a sine wave representing the carrier would be rigorously correct.

A rigorous mathematical analysis of the type of modulator with abrupt changes can be made by classical methods if the carrier is represented by a Fourier series determined by the current ratio of the signal transmission through the modulator as a function of time. This quantity, when combined with the signal currents on a product basis, will give the output currents.

Such an analysis will show that a signal introduced into a switching type modulator circuit, in which the switching is controlled by a carrier, will produce side band modulation products associated with the fundamental carrier frequency which are essentially the same as those which would result from a pure product modulator supplied with the same signal and a pure sine wave of the carrier frequency. A quite different result would be obtained if the signal and carrier were interchanged. This results from the unwanted harmonics occasioned by the abrupt changes falling well above the wanted products in the first case and falling within the wanted band in the second case.

Although it is convenient to think of the carrier being modulated by the signal the actual process by which this is accomplished is for the carrier to modulate the signal.

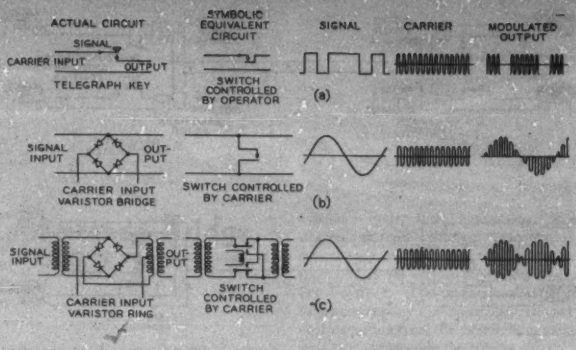

Figure 3. Illustrative modulation systems

Similarities Between Different Types of Modulation

The fact that the more important types of modulation can be produced by somewhat similar circuits indicates that the various types are related rather closely. There are certain other interesting relationships.

About 30 years ago Carson demonstrated that either of the two side bands resulting from the amplitude modulation of a carrier conveyed all of the information present in the signal, and that it should be sufficient to transmit only one of these side bands over the communication system.[17] This has resulted in the wide use of single side band transmission where two channels can be transmitted within the band which would be occupied by the double side band signal corresponding to one channel.[18,19] The manner in which such a 2-channel system could be set up is indicated schematically in Figure 4a. This type of multiplex operation commonly is called "frequency division."

Two channels also could be obtained by the time division method with amplitude modulation. The schematic arrangement for such a time division system is shown on Figure 4b. Used separately each of these time division channels is not different from a double side band amplitude modulation system with a carrier frequency determined by the switching rate. When they are combined for transmisson over the line, the frequencies of the two channels fall into the same band. They are so related, however, in phase that

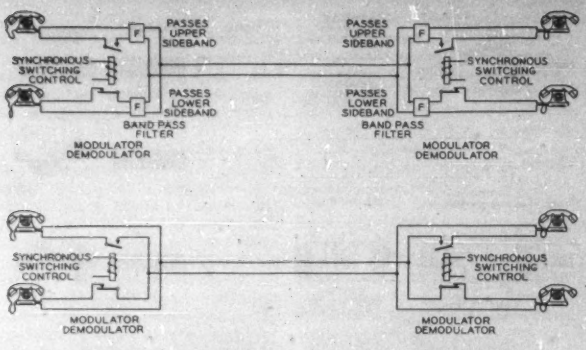

Figure 4. Comparison of 2-channel carrier systems

Top—Amplitude modulation—single side band frequency division transmission

Bottom—Amplitude modulation—time division transmission

they may be separated at the receiving end on a time division basis.

As is indicated on the chart, the elements of the two types of 2-channel systems may be identical except that in the frequency division case single side band filters are introduced to accomplish division by this means.

One factor which has occasioned the use in telephony of single side band systems in preference to time division amplitude modulating systems is the extreme precision in attenuation and phase response required in time division to keep interchannel cross talk at acceptable values. With "yes or no" telegraph type signals higher values of interchannel interference are permissible without serious reaction. Thus time division systems have been used widely in telegraphy. Time division is also coming into use in telephony when speech is converted to pulse position, pulse code, or similar signals.

Comparison of Modulation Systems

The determination of the desirable type of modulation or transmission system depends upon many interrelated factors which vary widely with the condition of application. Some of these are:

Length of system—more complex terminal or modulating system can be justified for long wire systems.

Relative availability of frequency space.

Variation of cost of transmission system with frequency band width.

Type of signals.

Ratio of minimum required frequency band to that practically necessary allowing for filters and frequency stability.

Desired fidelity or performance.

Nature of transmitting medium.

Each type of modulating system in general use has some feature which recommends its use under some conditions and not under others.

For most systems of modulation improved performance may be gained by utilizing a wider frequency band. This improvement generally is reduced when high values of noise or interference are present. With certain types of noise there is a tendency toward encountering this limitation more frequently as the frequency band is widened.

One outstanding exception to the rule of improvement accompanying increased band width is a single side band transmission system, when an improvement of about nine decibels with respect to a double side band amplitude modulated system may be obtained. This is about the same improvement as would be obtained by the use of frequency modulation employing $2^1/_2$ times the band width of a single side band system.

The qualifications which are necessary to accompany even these simple generalizations are an indication of the difficulty of attempting to determine the appropriate form of modulation for a given set of conditions without careful study.

References

1. Pulse Code Modulation, **H. S. Black, J. O. Edson.** AIEE Transactions, volume 66, 1947, pages 895–9.

2. Distortion in a Pulse Count Modulation (PCM) System, **A. G. Clavier, P. F. Panter, D. D. Grieg.** AIEE Transactions, volume 66, 1947, pages 989–1005.

3. Transmission of Information, **R. V. L. Hartley.** *Bell System Technical Journal* (New York, N. Y.), volume 7, July 1928.

4. Equivalent Modulator Circuits, **E. Peterson, L. W. Hussey.** *Bell System Technical Journal* (New York, N. Y.), volume 18, January 1939, pages 32–48.

5. Copper Oxide Modulators in Carrier Telephone Systems, **R. S. Caruthers.** *Bell System Technical Journal* (New York, N. Y.), volume 18, April 1939, pages 315–37.

6. A Method of Reducing Disturbances in Radio Signaling by a System of Frequency Modulation, **E. H. Armstrong.** *FM* (New York, N. Y.), volume 4, January 1944; August 1944.

7. Time Division Multiplex Systems, **W. R. Bennett.** *Bell System Technical Journal* (New York, N. Y.), volume 20, April 1941, pages 199–221.

8. Time Division Multiplex in Radio-Telegraph Practice, **J. L. Callahan, R. E. Mathes, A. Kahn.** *Proceedings* of the Institute of Radio Engineers (New York, N. Y.), volume 26, January 1938, pages 55–74.

9. Development of Silicon Crystal Rectifiers for Microwave Radar Receivers, **J. H. Scaff, R. S. Ohl.** *Bell System Technical Journal* (New York, N. Y.), volume 26, January 1947.

10. Thermistors, Their Characteristics and Uses, **G. L. Pearson.** *Bell Laboratories Record* (New York, N. Y.), volume 19, December 1940.

11. Frequency Shift Telegraphy—Radio and Wire Applications, **J. R. Davey, A. L. Matte.** AIEE Transactions, volume 66, 1947, pages 479–94.

12. A Multichannel Microwave Radio Relay System, **H. S. Black, J. W. Beyer, T. J. Grieser, F. A. Polkinghorn.** AIEE Transactions, volume 65, 1946, December section, pages 798–806.

13. Pulse Time Modulation, **E. M. Deloraine, E. Labin.** *Electrical Communication* (New York, N. Y.), volume 22, November 1944.

14. Spectrum Analysis of Pulse Modulated Waves, **J. C. Lozier.** *Bell System Technical Journal* (New York, N. Y.), volume 26, April 1947.

15. Distortion and Band Width Characteristics of Pulse Modulation, **H. L. Krauss, P. F. Ordung.** AIEE Transactions, volume 66, 1947, pages 984–8.

16. New Results in the Calculation of Modulation Products, **W. R. Bennett.** *Bell System Technical Journal* (New York, N. Y.), volume 12, April 1933, pages 228–43.

17. Notes on the Theory of Modulation, **J. R. Carson.** *Proceedings*, Institute of Radio Engineers (New York, N. Y.), volume 10, February 1922, pages 57–64.

18. Carrier Current Telephony and Telegraphy, **E. H. Colpitts, O. B. Blackwell.** AIEE Transactions, volume 40, 1921, pages 205–300.

19. Production of Single Sideband for Transatlantic Telephony, **R. A. Heising.** *Proceedings* of the Institute of Radio Engineers (New York, N. Y.), volume 13, June 1925.

No Discussion

A Self-Balancing Capacitance Bridge

A. H. FOLEY
ASSOCIATE AIEE

Synopsis: The combined advantages of the quick indicating capacitance meter and the precision capacitance bridge are obtained in a new form of self-balancing capacitance bridge. Features of the new instrument include per cent deviation indications, a wide capacitance range and an average balancing time of less than two seconds. A single scale, easily read and greatly expanded, serves for the entire range of the instrument and represents an improvement of some 3,000 per cent over conventional capacitance meters. The paper discusses the bridge network development, detector system requirements, and other design considerations.

IN QUALITY TESTING of mass produced electric components both speed and accuracy are prerequisites. Without these there can be neither good manufacturing economy nor adequate quality control. To provide the necessary test equipment for the manufacture of capacitors for applications critical as to capacitance, a self-balancing capacitance bridge, Figure 1, was designed having a range extending from 0.1 to 100 microfarads, an accuracy closely approaching one-tenth of one per cent over the entire range and an average balancing time of less than two seconds.

One of the most common instruments in general use for capacitance measurements is the capacitance meter. Such instruments are popular because their response is fast and because their indications are automatic, that is, balancing operations are not required to obtain capacitance indications. Capacitance meters, however, are at a disadvantage on three counts.

1. The over-all accuracy is limited; typical instruments may not provide an actual measurement accuracy as good as one per cent on the average.

2. A large number of instruments is required to cover a wide capacitance range. For example, for a range of from 0.1 to 100 microfarads at least six typical instruments will be required if an average accuracy approaching one per cent is to be obtained.

3. Where a number of instruments are used to cover the working capacitance range, interpretations must be made on several different types of scales.

Some of the disadvantages of the capacitance meter can be overcome by the use of a precision capacitance bridge. An accuracy of one-tenth of one per cent, or better, can be obtained along with an incremental or comparative accuracy of $^1/_{100}$ of one per cent, or possibly better. The capacitance bridge can cover an extremely wide capacitance range, a million to one or even more. The time consumed in balancing the precision bridge, however, makes it entirely impractical for factory use where speed is so essential.

The self-balancing capacitance bridge, Figure 1, provides the combined advantages of both the capacitance meter and the precision bridge. At the same time some additional advantages over either of these instruments is provided. Of particular importance is the feature of indicating the per cent deviation from the nominal capacitance, the nominal capacitance of the unit under test having been preset on appropriate direct reading dials. Another feature is the use of but a single scale for the entire capacitance range. A third improvement is the greatly expanded scale from which deviation readings are taken.

The decision to make the new instrument read per cent capacitance deviations was based on the almost universal practice of establishing capacitor acceptance limits on a percentage basis. In production testing, therefore, deviation readings permit a more direct classification of the capacitor under test. Operational procedure is extremely simple. The nominal capacitance of the group of units to be measured is set on direct reading dials. See Figure 1. The deviation dial then indicates, rapidly and accurately, the per cent deviation from this nominal for each unit as it is placed in the test jig.

Since the test results are expressed in terms of per cent deviation a single percentage scale serves for the entire range of the instrument. Some idea of the degree of expansion of this scale can be obtained from Figure 2. The scale covers a total range of 20 per cent (−10 per cent to +10 per cent) and actually exceeds 25 inches in length. This provides an improvement over typical capacitance meters of some 3,000 per cent. The probability of making an error in reading such a scale is reduced very materially, even with the greatly improved over-all instrument accuracy and when used for extended periods of time, as in production testing.

The Basic System

A schematic diagram of the self-balancing capacitance bridge is shown in Figure 3. The system, in its entirety, comprises a servomechanism.[1,2] The principle elements are

1. The bridge network, which supplies an error signal to
2. A detector amplifier system which, in turn, supplies power for operation of
3. A balancing motor. The balancing motor is coupled mechanically to the balancing resistance of the bridge thus closing the servomechanism loop.

When the bridge becomes unbalanced, as by the introduction of an unknown value of capacitance at C_x, the error signal, which is the bridge network output voltage, is amplified and causes the balancing motor to operate in a direction which, by virtue of operation of the balancing resistance, will bring about a balance of the bridge. Once balance has been achieved the error signal becomes zero with a resultant stoppage of the balancing motor. A suitably calibrated dial attached to the balancing resistance then

Paper 47-136, recommended by the AIEE committee on instruments and measurements for presentation at the AIEE summer general meeting, Montreal, Quebec, Canada, June 9–13, 1947. Manuscript submitted March 20, 1947; made available for printing April 24, 1947.

A. H. FOLEY is development engineer with the General Electric Company, Pittsfield, Mass.

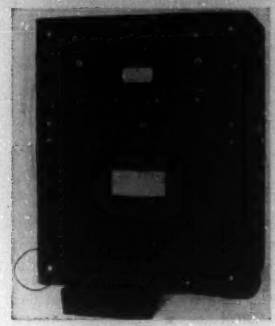

Figure 1. The self-balancing capacitance bridge and test jig

Nominal capacitance is set on the four decade dials and per cent deviations read from the large lower dial

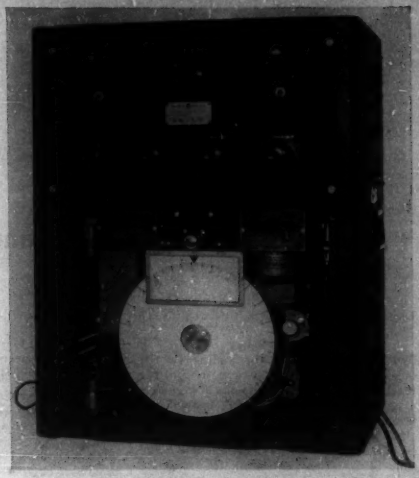

Figure 2. The deviation dial scale length exceeds 25 inches

indicates the capacitance of the unknown capacitor, C_x.

In the design of the self-balancing bridge described in this paper advantage has been taken of a commercially available amplifier and motor combination for a portion of the system. This combination is represented in Figure 3 as the power amplifier and balancing motor.

While the capacitance range is listed as extending from 0.1 to 100 microfarads, there is no fundamental difficulty in extending it in either direction from these limits. The per cent deviation limits also may be extended in either direction.

Development of the Bridge Network

The evolution of the principle bridge network for the self-balancing bridge is shown in Figure 4. In the adaptation of the circuit at (*a*) it is desirable to satisfy the following four conditions:

1. The nominal capacitance dials should read capacitance in microfarads directly.
2. The capacitance deviation dial should be direct reading in per cent deviation from the nominal capacitance.
3. The deviation dial scale should be linear.
4. The bridge voltage sensitivity should be constant over the entire bridge range.

The simplest form of capacitance bridge is shown in Figure 4*a*. It readily can be shown[2] that, at balance,

$$C_x = \frac{C_s R_1}{R_2} \tag{1}$$

where C_x is the capacitance of the unit under test, C_s is the capacitance of the bridge standard capacitor, and R_1 and R_2 are bridge arm resistances. From this equation it is seen that the capacitance of the unknown, C_x, is directly proportional to R_1. This immediately suggests the use of R_1 for setting the nominal capacitance, C_n. Any departure in the value of C_x from that of C_n would then have to be balanced by a corresponding adjustment of either C_s or R_2. For good circuit stability C_s should be reasonably large. Hence this element cannot be adjusted conveniently with sufficient smoothness. It is best therefore to fix C_s and make all adjustments in the resistance arms. The employment of R_2 for this purpose, however, leads to the use of either a tapered scale for deviation indications or a tapered rheostat if a linear scale is to be obtained. Neither of these is desirable. As will be seen later, a third objection to this assignment of controls to R_1 and R_2 is that the bridge voltage sensitivity would vary as a function of R_1 and hence would not satisfy condition 4 listed in the preceding paragraph.

The alternative arrangement is to employ R_2 for setting the nominal capacitance and make all deviation adjustments by varying R_1. At first this may appear to present some difficulties since R_2 must vary inversely with the nominal capacitance setting and, further, since it is proposed to make the nominal capacitance dials direct reading. This difficulty is overcome easily, however, by employing conductance type decade resistances for R_2. With conductance decades the resistance varies inversely with settings. Thus, with appropriate resistance values, the dials controlling R_2 easily can be calibrated to read the nominal capacitance directly. Table I shows typical resistance values for four conductance decades. By employing these singly and in appropriate parallel combinations, the conductance can be varied in ten uniform steps for each decade.

It is seldom necessary to allow for capacitance deviations of more than plus or minus ten per cent from the nominal. Hence the range through which R_1 must be adjustable is limited to a corresponding amount. This arm of the bridge therefore can be composed of two resistances, one fixed and the other variable, as shown in Figure 4*b*.

Referring again to equation 1 and Figure 4*a*, when the value of C_x is equal to that assigned to C_n equation 1 becomes

$$C_x = C_n = \frac{C_s R_1}{R_2} \tag{2}$$

When C_x and C_n are not equal

$$C_x = C_n + \frac{C_n \Delta C_x}{C_n} = C_n(1+\delta) \tag{3}$$

where ΔC_x is the difference between C_n and C_x and may be either positive or negative. $\delta = \Delta C_x / C_n$, the fractional deviation of C_x relative to the nominal capacitance C_n. C_x is now equivalent to C_n modified by the factor $(1 + \delta)$. Multiplying both sides of equation 2 by this factor

$$C_x = C_n(1+\delta) = \frac{C_s}{R_2} R_1(1+\delta) \tag{4}$$

Clearly the value of R_{11}, Figure 4*b*, will be that which achieves balance of the

Table I. Typical Resistance Values and Capacitance Calibrations for Each Step of Four Conductance Decades

Decade No.	Capacitance Calibration Per Decade Step, μf	Decade Resistor No.	Resistance, Ohms
		1	10.000
1	10.0	2	5.000
		3	3.333
		4	2.500
		1	100.00
2	1.0	2	50.00
		3	33.33
		4	25.00
		1	1,000.0
3	0.1	2	500.0
		3	333.3
		4	250.0
		1	10,000.0
4	0.01	2	5,000.0
		3	3,333.3
		4	2,500.0

bridge when δ corresponds to the lower deviation limit, R_{12} being zero. In other words, when the capacitance of C_x deviates to the lower limit, chosen by design, R_{12} is zero and R_{11} is the resistance required for balance. Under this condition

$$R_{11} = R_1(1+\delta_1) = \frac{R_3}{C_s} C_n(1+\delta_1) \qquad (5)$$

where δ_1 is the fractional deviation of C_x to reach the lower deviation limit and R_1 is, as before, the resistance required for balance when $C_x = C_n$.

Similarly, when C_x deviates to the upper design limit the total resistance in this arm of the bridge is

$$R_{11} + R_{12(max)} = R_1(1+\delta_2) = \frac{R_3}{C_s} C_n(1+\delta_2) \qquad (6)$$

δ_2 is the fractional deviation of C_x in deviating to the upper limit.

Subtracting equation 5 from equation 6 to obtain $R_{12(max)}$, the maximum resistance which must be provided for R_{12},

$$R_{12(max)} = \frac{R_3}{C_s} C_n(\delta_2 - \delta_1) \qquad (7)$$

remembering that δ_1 is negative if $C < C_n$. From equation 2 it is evident that since C_s has been fixed, the product C_nR_3 is a constant. Hence equation 7 can be rewritten

$$R_{12(max)} = K(\delta_2 - \delta_1) \qquad (8)$$

where $K = C_nR_3/C_s$. The dial attached to R_{12} therefore can be calibrated to read per cent deviation directly and, if R_{12} is a linear rheostat, the deviation dial scale will be linear. This satisfies condition 3 as outlined previously.

There remains but one further basic modification of the bridge network to adapt it to the self-balancing bridge in practical form. In practice, if the circuit of Figure 4*b* were to be used, the contact resistance of the slider on R_{12} would be included as a part of the resistance. In some designs R_{12} might be only a few ohms and this contact resistance, after a period of operation, might prove troublesome. To avoid this difficulty almost entirely the circuit of Figure 4*c* is employed. A resistance potentiometer is used in place of a rheostat, thereby placing the slider contact resistance in the detector circuit where, because of the relatively high impedance of the detector, it can have little or no effect. It will be noted that at times a portion of the resistance of the potentiometer will be included, as R_{13}, in series with the standard capacitor C_s. The effect of R_{13} is to increase the apparent dissipation factor of C_s. In practical designs this increase will be small and can have little or no effect on the accuracy of the capacitance measurements.[2] This point will be given further attention later.

The Shunted Potentiometer

Since in practice the resistance required for $R_{12(max)}$ may be only a few ohms, it may often be found that the incremental (turn to turn) resistance of a simple slide-wire potentiometer, as indicated in Figure 4*c*, is greater than can be tolerated for the degree of precision required in making the deviation calibrations. The use of a shunted potentiometer, Figure 4*d*, will provide a substantially smaller incremental resistance. This can best be illustrated by an example. Suppose $R_{12(max)}$ is 25 ohms and the total deviation range to be covered is 20 per cent. A typical 25-ohm slide wire may have but 250 turns of resistance wire. The per cent deviation corresponding to the incremental resistance of such a potentiometer will be 20 ÷ 250 = 0.08 per cent. For a calibration precision of 0.05 per cent or better this is clearly not fine enough.

With the use of a shunted potentiometer for this same example, a 1,000-ohm slide wire might be chosen. It would be shunted by a resistance, R_s, Figure 4*d*, to have a total value of 25 ohms. A typical 1,000-ohm slide wire may have 750 turns of resistance wire. The per cent deviation corresponding to the effective incremental resistance would be 20 ÷ 750 = 0.027 per cent, a figure which easily will permit a calibration precision of 0.05 per cent.

The equivalent resistance of that portion of the shunted potentiometer effective as R_{12} is

$$R_{12} = \frac{R_sR_{121}}{R_s + R_{121} + R_{131}} \qquad (9)$$

The value of R_{121} corresponding to any chosen value of R_{12} is

$$R_{121} = \frac{R_{12}R_p}{R_{12(max)}} \qquad (10)$$

where $R_p = R_{121} + R_{131}$, the total resistance of the slide-wire potentiometer, and $R_{12(max)} = R_{12} + R_{13}$. Both R_p and $R_{12(max)}$ are constant. Equations 9 and 10 hold only in cases where no current flows through the slider on the potentiometer element. When the bridge is at balance this condition is satisfied.

Bridge Voltage Sensitivity

Before a suitable detector system can be chosen for any bridge it is necessary to know something of the network voltage sensitivity characteristics. In the considerations to follow a detector of infinite

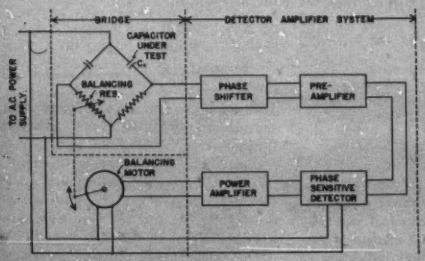

Figure 3 (left). Schematic diagram of the self-balancing capacitance bridge showing the complete servomechanism loop

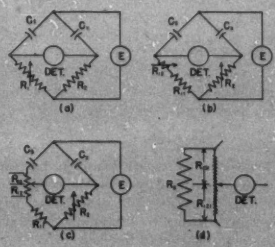

Figure 4 (right). Evolution of the bridge network

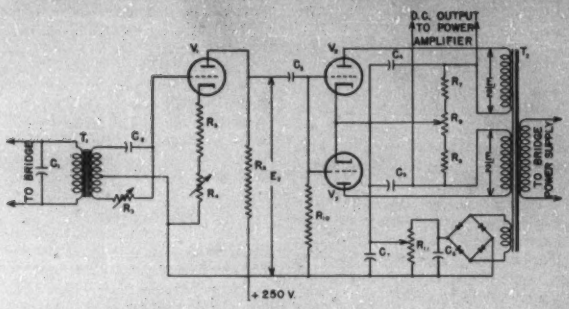

Figure 5. Schematic circuits of the phase shift network, the preamplifier, and the phase-sensitive detector

input impedance is assumed. This is permissible since the bridge feeds into an amplifier having an input impedance quite large compared to that of the bridge network, looking into the network at the detector terminals. This assumption will permit determination of the bridge voltage sensitivity on an open circuit basis.

In practice the ratio of the reactance of C_x to resistance R_3, Figure 4c, will be greater than 10 to 1. This is primarily for the purpose of keeping the resistance arms of the bridge at a comparatively low value, thereby stiffening the impedance as seen looking into the network at the detector terminals. This practice renders the network less susceptible to error as a result of any residual spurious currents which might flow in the bridge arms.

Suppose, for the moment, $C_x = C_n$. Since the reactance to resistance ratio is high the current which will flow through R_3 will be, very closely,

$$I_{r2} = \omega C_n E \tag{11}$$

where $\omega = 2\pi f$ and E is the voltage applied to the bridge. The voltage drop across R_2 then will be, very closely,

$$E_{r2} = \omega C_n E R_2 \tag{12}$$

If the bridge now is balanced by appropriate adjustments of R_{13}, the sum of the voltage drops across R_{11} and R_{12} will exactly equal E_{r2} and the voltage across the detector will be zero (except for a small quadrature voltage due to a possible difference between the phase angles of C_x and C_x.

Now suppose C_x is altered by the familiar factor $(1 + \delta)$. The voltage drop across R_2 is now, very closely,

$$E_{r2\delta} = \omega C_n (1+\delta) E R_2 \tag{13}$$

The voltage ΔE now appearing across the detector terminals will be the change in voltage across R_2. This change, or difference, is obtained by subtracting equation 12 from equation 13 to give, very closely,

$$\Delta E = E_{r2\delta} - E_{r2} = \omega C_n E R_2 \delta \tag{14}$$

As pointed out earlier in this paper the use of R_3 for setting C_n results in the product $C_n R_3$ being constant. Since the applied bridge voltage and frequency are constant, equation 14 can be rewritten

$$\Delta E = K_1 \delta \tag{15}$$

where $K_1 = \omega C_n E R_3$, the voltage drop across R_2 when $C_x = C_n$ as in equation 12. The sensitivity of the bridge, by using R_3 for setting the nominal capacitance, is therefore constant over the entire capacitance range and condition 4 in the section on bridge network development is satisfied.

Note, as a contrast, how the bridge sensitivity would vary if R_1 were chosen for setting the nominal capacitance. The voltage appearing across the detector terminals for a fractional deviation δ of C_x would be very closely

$$\Delta E = \omega C_x E R_1 \delta \tag{16}$$

In this case $\omega C_x E = K_2$, a constant, so that equation 16 becomes

$$\Delta E = K_2 R_1 \delta \tag{17}$$

The sensitivity therefore would vary directly with R_1. For a bridge covering a nominal capacitance range of, say, 0.1 to 100 microfarads, the sensitivity would vary 1,000 to 1 from one end of the range to the other. This is clearly a very undesirable condition. In orde for the detector to perform properly provision would have to be made for varying the response sensitivity as a function of R_1. Further, the detector would have to be unduly sensitive for small values of C_x.

The Detector System

The detector system for the self-balancing capacitance bridge differs from those employed with conventional manually balanced bridges in that instead of providing a visual or aural indication of bridge unbalance a motor is made to rotate. The direction of rotation is determined by the direction of bridge unbalance, that is, by whether C_x is greater or smaller than C_n. The motor, which is coupled mechanically to the bridge balancing resistance element, thus causes the bridge to become balanced without manual aid.

The detector system mu·t satisfy two principle requirements

1. Voltage sensitivity.
2. Phase selectivity.

Voltage sensitivity requirements are determined by the minimum fractional deviation δ of C_x relative to C_n to which it is required to have the bridge respond. The detector system therefore must have sensitivity enough to cause rotation of the balancing motor for this value of δ. For the bridge described in this paper δ is of the order of 0.0001.

Phase selectivity is required for two reasons

1. To cause the motor to operate in the proper direction for a given direction of bridge unbalance.
2. To prevent operation of the motor when a voltage due to a phase angle difference between capacitors C_x and C_x is impressed on the detector input.

Voltages due to the latter cause are essentially 90 degrees out of phase with those due to pure capacitance unbalances. The detector system characteristics must be such as to cause the balancing motor to respond to capacitance unbalance voltages and have no response, within limits, to voltages in quadrature. This latter requirement is included so that dissipation factors of the capacitors under test will have little or no effect upon the operation of the bridge.

As indicated in an earlier part of this paper, the detector system is divided into two parts

1. A preamplifier and phase-sensitive a-c to d-c detector.
2. A commercially available d-c responsive amplifier and motor combination.

A schematic diagram of the preamplifier and phase-sensitive detector is shown in Figure 5.

Transformer T_1 is employed to couple the bridge to the preamplifier. The secondary of T_1 is center tapped to accommodate the simple phase shift network containing C_1 and R_3.

The preamplifier consists of a single

triode stage employing a degree of negative feedback by omission of the by-pass capacitor across resistors R_4 and R_4. R_4 is adjustable to permit a limited control of the gain of the stage.

The phase-sensitive detector consists of triodes V_2 and V_3 and the associated capacitors and resistors. It will be noted that these two triodes have a-c plate excitation and that the circuit resembles that of a full wave rectifier. Bias for the two triodes is supplied by the copper oxide rectifier and resistance–capacitance filter network. The bias is adjusted so that the E_p–I_p characteristic of the triodes is essentially quadratic. Under this condition and, further, under the condition that a static balance of the circuit has been made by adjusting potentiometer R_9 so that the d-c output voltage is zero when the a-c signal is zero, an analysis of the circuit shows that the d-c output voltage, upon application of an a-c signal, is very closely

$$E_{d\text{-}c} = K_3 E_1 E_2 \cos \theta \qquad (18)$$

where E_1 is the a-c plate voltage, E_2 is the a-c signal voltage at the grids of V_2 and V_3, and θ is the phase angle between E_1 and E_2. K_3 is a constant determined by the various parameters of the detector circuit.

From equation 18 it is evident that the phase-sensitive detector is a form of electronic wattmeter. A reversal of E_2 with respect to E_1 causes a corresponding reversal of the d-c output voltage. If E_2 is 90 degrees out of phase with E_1, cos θ is zero and hence the d-c output voltage is zero.

Power for plate circuit operation of the phase-sensitive detector is taken from the same source which supplies the bridge network. This is indicated in Figure 3. It is therefore possible, by adjusting R_5, Figure 3, to shift the phase of the bridge output voltage so that the component due to capacitance unbalance is in phase with E_1 (or in phase opposition if the bridge is unbalanced in the opposite direction) at the grids of V_2 and V_3. Under this condition that component of the signal, at the same point in the circuit, due to a difference between the phase angles of C_t and C_s, the bridge standard capacitor, and the capacitor under test, respectively, is essentially 90 degrees out of phase with E_1 and hence will not alter the d-c output of the detector. While this 90-degree relationship is not strictly held over the bridge deviation range, the angular shift is small since a high ratio of reactance to resistance is employed in the bridge network. In practice a single adjustment of R_5 will hold for the entire range of the bridge. The bridge is therefore nonresponsive, within fairly broad limits, to variations in the dissipation factors of the capacitors under test.

Speed of Response

While the speed of response of the self-balancing capacitance bridge depends, to a considerable degree, on the response speed of the balancing motor, considerations for bridge network steady state conditions and servomechanism stability[1, 2] place practical limitations on the response time. In a typical case, however, it is easy to obtain travel of the deviation dial over the entire scale length in ten seconds. In normal use of the instrument it is seldom necessary for the dial to travel this far. The statistical distribution of capacitances in a group of capacitors having a given nominal capacitance usually is concentrated within a relatively narrow band. The average time required for balance is therefore but a fraction of the time required for full scale travel of the deviation dial. This is because, after each measurement, power is removed from the bridge network with the result that the deviation dial remains at the point of balance. The dial is therefore often near the point of balance for the succeeding measurement. In typical cases the average balance time is less than two seconds.

Accuracy

Unlike capacitance meters wherein accuracy is usually stated as some per cent of full scale deflection, the self-balancing capacitance bridge maintains a constant accuracy over its entire range. This is achieved primarily by adjusting all of the resistance elements in the conductance decades, on which the nominal capacitance is set, to the same degree of accuracy

The over-all accuracy of the instrument is, of course, determined by the accuracy with which each of the bridge network components can be determined and, indirectly, by the response sensitivity of the detector system. Resistance components can be adjusted to within a few hundredths of one per cent of the required values. The absolute value of the standard capacitor can be determined with an accuracy better than one tenth of one per cent. The detector system easily can be made to respond to unbalances in capacitance as small as 1/100 of one per cent. It is entirely practical, therefore, to obtain an over-all instrument accuracy closely approaching one tenth of one per cent.

Conclusions

The self-balancing capacitance bridge is particularly useful in checking large quantities of capacitors for applications where capacitances are critical, as in certain resonant circuits. Groups of capacitors which must be matched very closely are conveniently checked and assorted with the aid of the instrument. Matching to one tenth of one per cent is easy since the scale spread of the deviation dial and the instrument stability are great enough to permit taking readings with an accuracy of 0.05 per cent or better.

Since the instrument is direct reading and quite simple to operate skilled operators are not required. Hence, having high accuracy, a fast response, and a wide capacitance range, the self-balancing capacitance bridge is uniquely in a class by itself.

References

1. Fundamental Theory of Servomechanisms (book), L. A. MacColl. D. Van Nostrand Company, New York, N. Y., 1945.

2. Network Analysis and Feedback Amplifier Design (book), H. W. Bode. D. Van Nostrand Company, New York, N. Y., 1945.

3. Alternating Current Bridge Methods (book), B. Hague. Sir Isaac Pitman and Sons, Ltd., London, England, 1938.

No Discussion

Electronic Telemetering System

GEORGE E. FOSTER
ASSOCIATE AIEE

WILLIAM M. KIEFER
ASSOCIATE AIEE

IN 1938, the telemetering system used by the Commonwealth Edison Company to totalize and indicate system generation at the load dispatcher's office and station control rooms was becoming inadequate because of low accuracy and high maintenance costs. It was also desired to expand the system to include more stations. The system then in use was an impulse type telemeter with low pulsing rates, mechanical totalizers, and many relays. The impulse rate was made proportional to the load in kilowatts by originating the impulses from contacts on the shaft of a watt-hour meter operated by current addition of the several generator loads, and the selection of an average bus voltage for the potential coil. For operating the recorders, a current balance, with current impulses acting on one coil and current adjusted by the recorder in the other coil, was used.

A survey of existing telemetering systems was made to select the best possible replacement. Practically all systems investigated had as a disadvantage the requirement that the measured electrical quantity must be converted several times into other electrical or physical values in order to accomplish totalization and transmission of the measured quantities. Various conversion or transmission units might have to be connected in series, introducing electrical and mechanical lag and error into the readings. Adaptation of some of these systems to carrier current transmission results in relatively slow response. The basic principle of the original system which was to be replaced was reviewed and found to be desirable if the methods of impulse production, totalization, and conversion into an indicated reading were modernized.

Where kilowatts is the indication to be telemetered, the watt-hour meter is available as a highly accurate means of expressing the load value as an impulse rate. With this as a basic thought and with the experience obtained from the existing system, development began upon a telemetering system which started as an attempt to replace mechanical relays with electronic tubes but soon ventured into the realm of a completely electronic system.

An impulse telemetering system for kilowatts requires five basic elements

1. A converter of kilowatts to impulses.
2. An impulse totalizer.
3. A transmitter.
4. A receiver.
5. A converter and recording instrument for converting impulse rates into a reading.

Previously existing impulse systems used relays, impulse motors, and commutators to provide these means. An electronic system reduces the number of moving parts, friction, and inertia, and thus provides an excellent approach to an impulse system.

The block diagram of Figure 1 illustrates the arrangements of the various parts. The impulses are generated by photoelectric-tube pickups mounted in the generator watt-hour meters located in the stations. The output wave shape of the photoelectric tubes is formed and amplified by the amplifiers and applied to

Figure 1. Equipment at a generating station and the dispatcher's office

Arrows indicate path of load signals through elements of the system

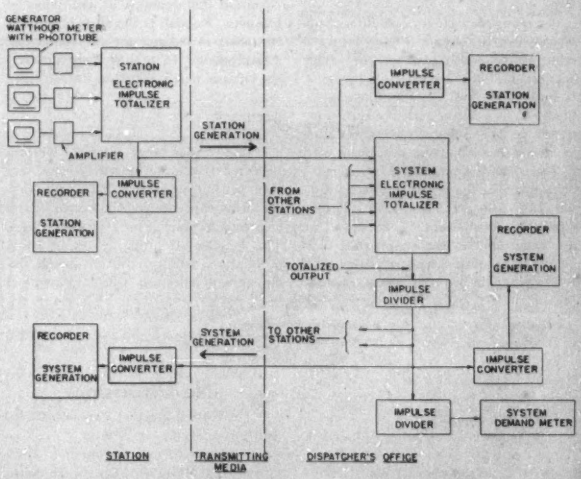

Paper 47-137, recommended by the AIEE committee on instruments and measurements for presentation at the AIEE summer general meeting, Montreal, Quebec, Canada, June 9-13, 1947. Manuscript submitted February 2, 1947; made available for printing April 24, 1947.

GEORGE E. FOSTER is chief engineer with the Foster Engineering Company, Chicago, Ill. WILLIAM M. KIEFER is assistant engineer in the testing department of the Commonwealth Edison Company, Chicago, Ill.

Figure 2. Photoelectric tube and lamp unit mounted above lower magnet in watt-hour meter. Amplifier for photoelectric tube is directly above meter

Figure 3 (rigth). Photoelectric tube and lamp unit removed from case

When in position, the watt-hour meter disk rotates at right angles to the partition between the lamps and photoelectric tube

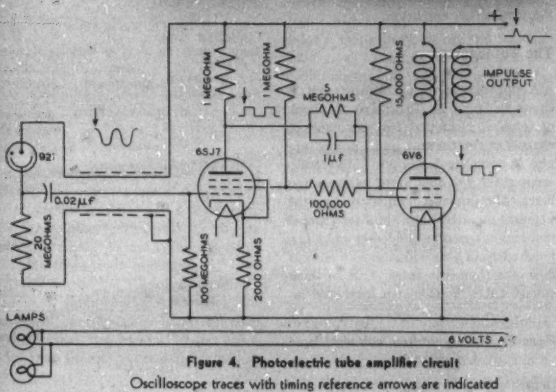

Figure 4. Photoelectric tube amplifier circuit

Oscilloscope traces with timing reference arrows are indicated

the impulse totalizers. The impulses arriving from the several generators located at the station are added by the totalizer. These totalized impulses are then applied to an impulse converter for controlling a typical 10-inch strip chart recorder. They are also applied to transmission media for transmission to the dispatcher's office.

At the dispatcher's office the impulses operate an impulse converter and recording instrument which duplicates the reading of the station generation. The impulses are also applied to the system totalizer for addition with the impulses from other stations to provide a rate of impulses proportional to the system total generation. The impulses from the system totalizer are divided by a factor of eight before further use. This is because the impulse rate had become high enough to cause possible interference in telephone circuits. After division, the impulses are applied to a converter which controls a recording instrument for providing the system total generation reading. The impulses also actuate an integrating-demand meter to provide a reading of the kilowatt-hours generated. They are also applied to transmission media for transmission to the various stations where they provide a reading of the system total generation on a recorder controlled by an impulse converter.

It will be noticed that an impulse once generated remains as an impulse throughout the totalization and transmission process. It is thus that the impulse telemetering system retains its high inherent accuracy.

The Photoelectric Tube Pickup and Amplifier

Figure 2 shows a photograph of the photoelectric tube unit mounted in the watt-hour meter, and, directly above, the amplifier mounted in a watt-hour meter case. An amplifier is used to permit mounting the totalizer at a convenient distance from the photoelectric tube. The optical system consists of placement of the light on one side of a partition and the photoelectric tube on the other side. The light passes from the lamp to the disk of the watt-hour meter and by reflection to the photoelectric tube. Low-reflection black lines painted on the disk cause the light to vary in intensity when the disc turns and this variation causes the current in the photoelectric tube to change. Figure 3 shows the photoelectric tube pickup removed from the case, showing the lamp, the photoelectric tube, the partition separating them, and the miscellaneous small capacitors and resistors.

The amplifier is mounted near the watt-hour meter as shown in Figure 2. Its function is to amplify the weak photoelectric tube currents and to provide peaked impulses in its output circuit whenever the photoelectric tube current passes a critical value. This occurs as each black line on the disk passes beneath the photoelectric tube. A simplified schematic diagram of the photoelectric tube and amplifier is shown in Figure 4. The amplifier must supply impulses of the same magnitude regardless of the im-

pulse rate, but must remain quiescent when the disk is stopped. At any given time only one of the two amplifier tubes is conducting and it requires a triggering impulse from the photoelectric tube to transfer conduction to the other tube. The current changes in the plate circuit of the second tube are always the same up to the maximum impulse rate, hence, the output impulses have the same shape and amplitude regardless of rate. The screen grids of the two tubes are coupled to provide feedback and insure rapid transfer of the conduction condition.

The Totalizer

A photograph of a totalizer unit is shown in Figure 5. It consists of a bank of totalizer elements (two per bank or chassis), a control unit, and a power supply. A complete description of the totalizer is much too lengthy to be presented here. The principle used is to store the impulses on arrival at a totalizer channel first as a charge on a condenser and a few hundredths of a second later as a current flow in a thyratron tube. One of these storage tubes is associated with each input channel and its conducting or nonconducting condition means that an impulse has or has not arrived at the particular channel. A "rotating electronic switch" removes any stored impulses one at a time. This is analagous to a continuously operating multicontact rotary switch that would test or "scan" each storage tube in turn to determine if an impulse had arrived there. If it contacted a conducting tube it would stop the conduction and originate an impulse in the totalizer output circuit. The time between successive scans of a storage tube must be shorter than the minimum time between the input impulses of that channel. Even though two or more impulses may arrive at the totalizer on several channels simultaneously the storage principle insures that all impulses are totalized and that none are lost or gained. Output circuits in the totalizer cause the

Figure 5. Impulse totalizer with eight input channels

Upper right column of eight tubes is the continuously scanning electronic switch. The third unit from the bottom contains totalizer control and output circuits

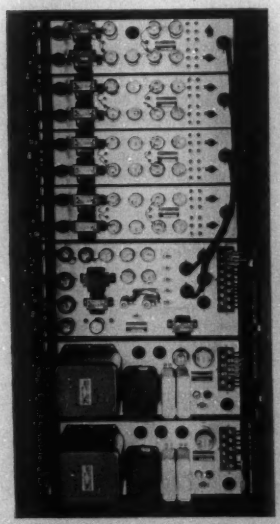

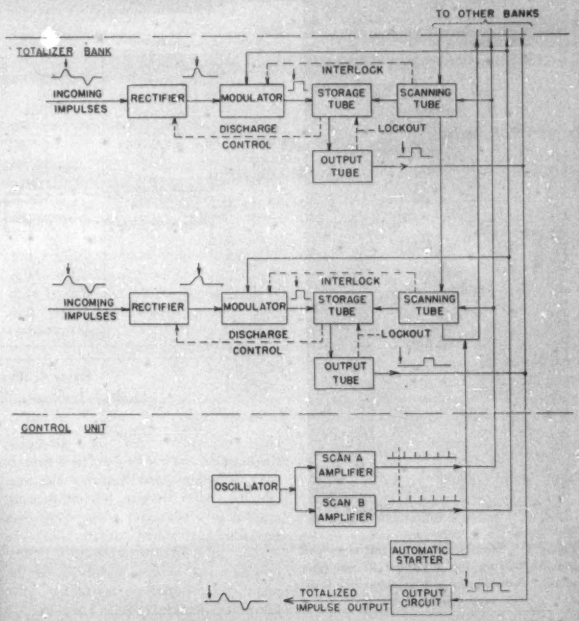

Figure 6 (above). A 2-element bank of a multichannel totalizer

Control and output circuits are shown at bottom. Oscilloscope traces with timing reference arrows are shown

Figure 7 (below). Impulse converter

Varying rate impulses are converted into electric effects measurable by the potentiometer-type recorder

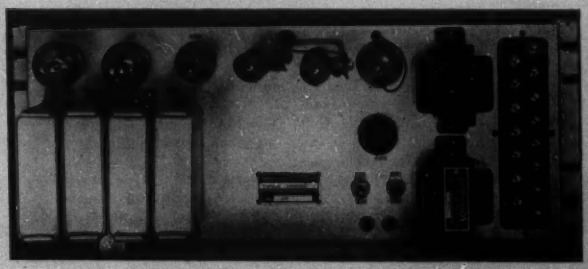

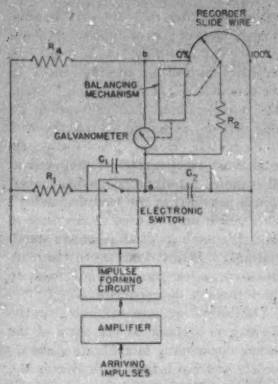

Figure 8. Converter and recorder circuits

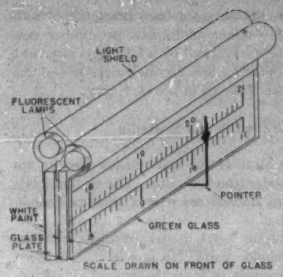

Figure 9. Detail of scale on double range meter

Edge-lighting the scale with fluorescent lamps provides reading ease

impulses to alternately reverse polarity and be of proper wave form for transmission over telephone lines.

It will be noted from this discussion that the outgoing impulses are not equally spaced in time. This occurs because impulses are arriving at the several input circuit of the totalizer in a random order. They, therefore, appear at the output in random order after a slight delay in the storage tube of the totalizer.

Figure 6 shows a block diagram of the totalizer. The control unit provides operating, starting, and output circuits. The totalizer banks each contain circuits for two input channels. The scanning tubes form the rotating electronic switch which serves to commutate the storage tubes. The passage of two simultaneously arriving impulses is shown by the wave shapes depicted. A totalizer control unit consists of an oscillator and associated amplifiers to govern the scanning speed of the electronic switch. Electrical interlocks were provided to eliminate undesirable interaction between the scanning and storage tubes, and to prevent each input impulse from providing more than one output impulse.

Impulse Converter and Recorder

The heart of the impulse-type telemeter is the conversion of impulses to a reading. This must be done as accurately as possible. Figure 7 shows the unit developed to operate in conjunction with the recorder. A simplified block and schematic diagram of this unit is shown in Figure 8.

The arriving impulses are passed through an amplifier, then a pulse forming circuit, and finally operate an electronic switch which consists of an argon-filled thyratron tube. Capacitor C_1 charges through resistor R_1 and is discharged by the thyratron into capacitor C_2. The potentiometer-type recorder consists of the usual galvanometer, slide wire, and balancing mechanism. If no impulses are arriving, the current in the galvanometer is such as to cause the balancing mechanism to move the slide wire contact to the point marked zero per cent, which then causes points a and b to be at the same potential and zero current flows in the galvanometer.

When impulses are arriving, the increased voltage developed across capacitor C_2 causes a current to flow through resistor R_2 and also through the galvanometer. The balancing mechanism operates and moves the slide wire contact until the galvanometer current is zero. To do this, the contact must move toward the 100-per-cent point. At balance the voltage across R_2 is equal to the voltage drop between zero per cent and the slide wire contact. The current through R_2 for any position of the slide wire contact is small compared to the normal slide wire current. The result is that, at balance with impulses arriving, the voltage on the capacitor C_2 is very nearly the same as the voltage for the no-impulse condition. This eliminates the effect of the charging curve of capacitor C_2 and a linear scale is provided on the recorder.

It will be noted that the circuit is a bridge and has the usual bridge stability. The meters may be calibrated by inserting a known impulse rate on the input of the impulse converter. Since the scales are linear, only one point needs to be calibrated. Once calibrated, the readings remain accurate for long periods and virtually independent of tube aging.

Most of the older impulse rate systems are subject to the defect of pulsation at the low end of the scale. The rate of impulses selected for this system is such that with damping adjusted no pulsation occurs even with readings of only one per cent of full scale, and yet the response is rapid. The recorders used balance every two seconds and the largest percentage of any sudden load change up to a maximum of about 1-inch pen travel will appear within that time. After 20 seconds the meter will have reached the final value. Any faster response results in too much fluctuation which conceals the trends which are desired by the operators. However, the impulse system makes possible an installation where meters of both slow response and fast response may be operated, since the impulses are available independent of any prior indicating systems.

Installation Features

Figure 1 is a block diagram of the essential units and connecting circuits making up the system. The impulse rate selected for the stations is one impulse per second per 10.8 megawatts. This is derived from the constants of the watt-hour meters and represents a value which permits a convenient number of lines to be painted on the watt-hour meter disks. In most cases it was possible to use the existing watt-hour meters.

Small stations were provided with recorders reading from 0 to 300 megawatts and large stations with recorders reading from 0 to 500 megawatts. Using the impulse constant it is seen that full scale represents an impulse rate of 27.8 impulses per second and 46.3 impulses per second respectively. Even on the 0 to 300 scale meter, 10 per cent of full scale gives 2.78 impulses per second. It is because of this relatively fast rate and the recorder time constant that no pulsation is noticeable in the reading. The upper limit is of the order of 2,000 impulses per second, determined primarily by the transmission media.

The system total impulse rate is divided by 8, hence, for the system total one impulse per second represents 86.4 megawatts. The system total recorder is calibrated from 0 to 2,100 megawatts, and full scale is produced by 24.3 impulses per second.

All of the system total recorders are provided with a scale changing arrangement. This effectively provides a chart 20 inches wide on 10-inch paper. Two

scales are provided, one from 0 to 1,100 megawatts and a second from 1,000 to 2,100 megawatts. A transfer region from 1,000 to 1,100 appears on both scales to prevent hunting. Limit switches operated by cams on the slide wire shaft operate a relay which switches the galvanometer circuit from one to the other of two slide wires mounted on the same shaft. Compensating resistors in series with the two slide wires were accurately calibrated initially to compensate for small differences in the resistances of the individual slide wires. A single control is provided to calibrate both scales simultaneously by the use of a variable resistor in series with the common current source for the slide wires.

An interesting point is the method used to indicate to the operators which of the two scales to read. This must be accurate and simple. Figure 9 shows a sketch of the system. Two standard fluorescent lamps are mounted so as to edge-light two strips of glass. The front one has a white background halfway down and the other a complete white background, but the upper half is behind the front glass and cannot be seen. The outer piece of glass is provided with figures and markings for the two scales, but only one scale is illuminated at any one time. A transparent green cover glass eliminates glare from the scale. The fluorescent lamps are switched by the relay which changes the scales. Light sprays from the lower edge of the glass and illuminates the strip chart. This double edge-lighted scale was developed by the lighting laboratory of the Commonwealth Edison Company. Figure 10 is a photograph of the recorders on which the scale lights may be seen. The upper right meter is the system total recorder and has the double scale. After the chart is removed from the instrument the times of transfer between scales appear with long horizontal lines across the chart. Transfers occur only twice in 24 hours and the chart time markings in conjunction with a knowledge of day and night loadings readily determine the scale to read.

At all stations indicating instruments for boiler rooms and supervision are provided. These are operated from the recorders by self-synchronous units or by a d-c current varied with an auxiliary slide wire in the recorder.

In some cases subtotals were desired, that is, partial totals as well as the complete total. An example is two stations that have both 25 cycle and 60 cycle generators. A total of the 25 cycle generation was desired in addition to the 25 cycle and 60 cycle total load. This was readily obtained from the totalizer with only minor additions. In another case the load carried by a large generator was desired for boiler room indication and this was obtained in the same way.

Transmission Systems

Most of the transmission circuits are 2-wire telephone lines. The system totals are transmitted over a simplex system, that is, between line and ground. The station total is transmitted over the metallic pair. No interference between channels or from the ground circuit occurs. Induction in the ground circuit causes no disturbance. The longest of these grounded circuits is about 50 miles. This is in contrast to most telemetering systems which are incapable of transmission on grounded circuits. The telephone lines need not be loaded.

Transmission over carrier channels is used for one station. This system has been described previously.[1] Basically, one impulse starts an oscillator, the next stops it. The stops and starts generate new impulses on reception. Frequency shift methods could also be used with equal ease.

Results Achieved

The complete system has been in operation more than five years. The accuracy goal has been achieved. The over-all error has not been more than about one-half per cent.

Recently a demand meter has been installed in the load dispatcher's office operating by means of a count-reducing circuit from the system total impulse rate. This integrated-demand meter checks the separate generator demand meter tapes from the individual stations to within one-half per cent and is available immediately at the end of the record day whereas the tapes require more than a day to collect and tabulate.

Since two or more recorders operate from each impulse rate, errors are observed soon after they appear. In addition, any loss or gain of impulses produces an irregular recording. As a result, the recorders furnish an accurate check on the operation of the telemetering system. The recorders hold their calibrations for long periods, exceeding six months with no observable change. Since the system total must be accurately reproduced at all stations, a calibration impulse generator is provided in the load dispatcher's office which may be used at any time to check the readings of all recorders simultaneously. If any doubt as to the readings occur, a test transmission is made to check possible discrepancies.

The calibrating generator also gives the dispatchers a check on the work of the testing department in calibrating the recorders and has helped in producing the confidence they have in the reliability of the system.

Maintenance costs on the system have been very low. Practically all troubles have been normal tube failures. Disconnecting switches are provided to remove sections in trouble from the rest of the system until they can be repaired. In most cases outages are repaired in less than an hour. A semiannual cleaning and tube checkup is given the equipment. Tubes which show no change from the previous check are left in operation. It has been found that tubes which have operated many thousands of hours are less likely to fail than some of those found in a complete new set of tubes. Some of the original tubes are still operating and have more than 50,000 hours of use. No other routine checks are made. It has been found more desirable to service only when trouble occurs.

Other Possibilities

Although it wasn't used, a circuit for subtraction was found feasible. This would permit subtraction of tie line loads or other similar loads if desired. Transmission of tie line loads is possible by polarizing the impulses. They could be

Figure 10. Station total and system total generation recorders

System total recorder on right is reading on the high range scale

added, subtracted, or indicated as required by the proper use of rectifiers.

This impulse system is used to telemeter and totalize megawatts. However, other quantities could be indicated in the same way. Functions which can be converted to impulse rates can be counted, totalized, and indicated by this method.

Conclusion

A telemetering system for transmission and totalization of megawatt readings which would have as slight an error as possible was desired. A system using impulses generated, totalized, and indicated by electronic methods was developed which has an error of less than one half per cent and is reliable and consistent.

Reference

1. Multichannel Carrier Current Facilities for a Power Line, P. N. Sandstrom, G. E. Foster. AIEE Transactions, volume 61, 1942, February section, pages 71–6.

No Discussion

The Design of New York Subway Motors for Dynamic Braking

B. A. WIDELL
MEMBER AIEE

THE MOTORS to be applied on modern cars for the New York, N. Y., subway system are truck mounted parallel to the axle and connected through a flexible coupling to a separate gear reduction unit. A similar application in service on the multisection cars of BMT Division having lighter weight per axle has demonstrated the following:

1. Advantage of less unsprung weight on axle.

2. Advantage of less shock on motor parts.

3. Quieter gearing and longer gear life have been obtained by the following means:

(*a*). Roller bearings on axle and pinion shaft to maintain gear center distance and small backlash on gears.

(*b*). Oiltight gear boxes providing adequate flow of oil on gear and bearings.

(*c*). Helical gear teeth.

4. Gearing stresses due to high braking torques at high speeds are within capacity of materials used.

5. Flexible couplings have proved practicable to handle motoring and braking torques with misalignments which occur between motor and gear reduction unit.

Each car will be equipped with four 100-horsepower 300–600-volt self-ventilated motors which will be similar but larger than the motors used on the President's Conference Committee cars. The motor is designed with armature windings having one turn per coil to obtain best commutating arrangement of conductors. The commutating duty is most severe when braking at high speeds and is kept within safe limits by using design constants which favor this condition. Above speeds of 42 miles per hour and developing maximum permissible braking effort, the motor, operating as a generator, is designed for a maximum output of 340-horsepower which is 3.4 times the 1-hour rating. As a result the motor is more conservative under motoring conditions of third rail surges and interruptions in power when crossing gaps than many of the older type of motors in service.

Commutators for these new motors are built and processed to narrow limits of eccentricity in order that brushes will ride the commutator satisfactorily at high peripheral speeds. The stresses in the commutator due to high speeds and heating are such as not to deform the commutator enough to produce detrimental sparking. The seasoning of the commutator is done after the armature has been completely wound and banded at a speed of 5,300 rpm or 20 per cent above the maximum permissible speed in service. At maximum armature speed of 4,420 rpm the peripheral speed of the commutator is 10,600 feet per minute as compared to 8,660 feet per minute for the President's Conference Committee motors at maximum speed of 4,800 rpm and 8,780 feet per minute for the *MS* train motors at maximum speed of 4,060 rpm.

The commutating pole pieces and frame are designed for low magnetic saturation of steel in order to avoid undercompensation at the maximum anticipated loading during period of high speed braking, to minimize sparking at the brushes as well as to maintain the maximum width of black band throughout the operating range as a motor. To accomplish this the commutating poles are wound with additional turns of overcompensation. Doing this also has a beneficial effect on motor commutation during transient surges which occur quite frequently on third rail systems.

The introduction of the truck mounted motor was responsible for the development of dynamic braking for the PCC cars and the modern subway cars, the reason being that the commutation problem is appreciably easier with the small high speed motor once the mechanical difficulties inherent with high speed operation have been overcome. Although considerable progress has been made in designing the commutating circuits of d-c series railway motors and better brushes

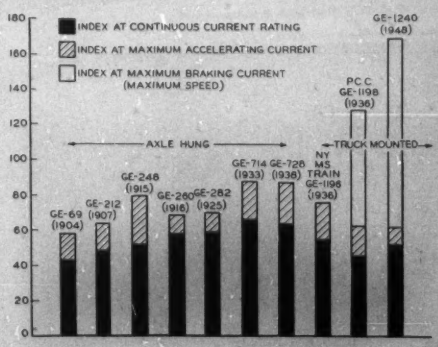

Figure 1. Index of reactance voltage for various types of General Electric motors in subway service

Solid section—Index at continuous current rating

Shaded section—Index at maximum accelerating current

Unshaded section—Index at maximum braking current (maximum speed)

Paper 47-154, recommended by the AIEE committee on land transportation for presentation at the AIEE summer general meeting, Montreal, Quebec, Canada, June 9–13, 1947. Manuscript submitted April 3, 1947; made available for printing April 30, 1947.

B. A. WIDELL is in the transportation motor engineering department of the General Electric Company, Erie, Pa.

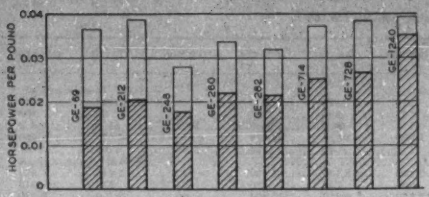

Figure 2. Horsepower per pound of total motor weight including accessories

Unshaded section 1-hour rating, shaded section continuous rating

have been developed to permit greater loading, there is a practicable limit on the reactance voltage which can be commutated. This limit is set by the permissible amount of commutator maintenance and brush life. The limit is well established in subway motors, some of which have been in operation over 40 years. The primary index of reactance voltage is the product of core length times amperes per circuit times turns per coil squared times coils in series times revolutions per minute times number of commutator segments. Motors having a relatively high index of reactance voltage may be considered as a better designed motor if of equal commutation performance.

In order to present a picture of the progress which has been made since 1904 when the first *GE-69* motor was placed in service in the New York subways, Figure 1 has been prepared showing the extent to which the index of reactance voltage has been increased at maximum braking current and maximum speed. It should be noted that both the *GE-1198* and *GE-1240* motors have appreciably lower reactance voltage index at the continuous current rating and maximum accelerating current than many of the older types of axle hung motors. This is in consequence of keeping the commutation within bounds at the maximum braking current at maximum speed. The average commutating duty probably will not be much more severe than on the older types of motors considering the fact that a majority of brake applications will be made at speeds less than maximum.

On motors with a high index of reactance voltage there may be some sparking at the brushes but this is detrimental only to the extent that the commutator etches or brushes have short life as a result. Of more consequence during braking at high speeds is the peak voltage between commutator bars, which, if permitted to rise high enough, the motor will flash and the braking effort be lost. The *GE-1240* motor in conjunction with the braking control will brake cars at a 3 mile-per-hour-per-second rate from a top speed of 42 miles per hour, without exceeding a conservative 40 peak volts per bar. If speed of braking begins over 43 miles per hour the field automatically is weakened to keep the peak volts per bar to a safe value, with the least loss of braking effort for a constant braking current. At maximum speed the braking effort, as a result, is reduced to 2,250 pounds per motor, which is sufficient to decelerate cars at 73 per cent of the 3-mile-per-hour-per-second maximum rate.

There are therefore many advantages to be gained by equipping subway cars with four truck mounted motors instead of two axle hung motors. The extent of operating advantages can be seen by reference to Table I which lists the ratings and performance of various equipment now operating in subway service and of the new truck mounted motors.

1. Maximum permissible car speed has been increased from 48 to 59 miles per hour.
2. Accelerating rates have been increased from 1 to 2.5 miles per hour per second.
3. Dynamic braking rate of 3 miles per hour per second has been added.
4. Weight of motors and accessories has been reduced from 12,400 pounds to 10,120 pounds per car.

Although the maximum weight handled by the new motors is about 30 per cent less than that of the original cars equipped with *GE-69* motors, the performance requirements have been increased and there is no appreciable change in the total 1-hour horsepower rating of motors per car. The continuous horsepower rating, however, is a considerably higher percentage of the 1-hour rating on the new motors than for any of the axle hung motors. This is a result of the new motor being built and rated according to allowable class *B* insulation temperature rises and also because of the relatively higher ventilation of motor.

The *GE-1240* motor horsepower ratings, one hour and continuous, per pound of weight of motor and accessories, are higher than any of the axle hung motors. The relative difference is shown on Figure

Figure 3. Pounds tractive effort per pound of motor weight at continuous rating geared to 60-mile-per-hour maximum speed

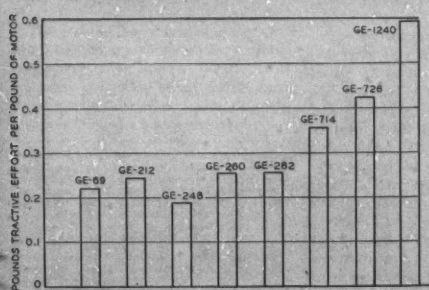

Figure 4. Characteristics of GE-1240 motor on 300 volts

Gear reduction 7.235 to 1; wheel diameter 32 1/8 inches

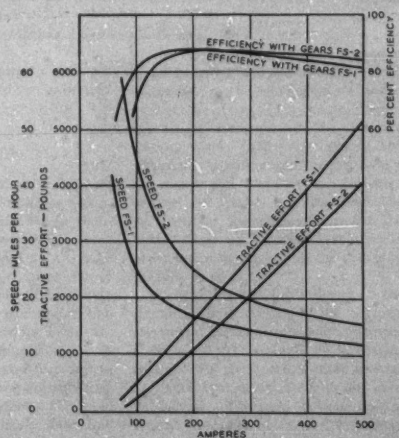

Table I. General Electric Subway Motors

	GE-69	GE-212	GE-248	GE-260	GE-282	GE-714	GE-728	GE-1196	GE-1240
Type of suspension	Axle hung							Truck mounted	
Started in service	1904	1907	1915	1916	1925	1933	1938	1936	1948
One-hr hp	225	235	160	195	200	190	210	60	100
Max permissible speed, mph	48.6	48.9	55.6	51.3	48.0	58.8	68.5	61.0	59.0
Max permissible speed, rpm	1,560	1,570	1,570	1,570	1,570	2,070	2,070	4,060	4,420
Accelerating rate, mphps	1.0	1.0	1.25	1.0	1.45	1.75	2.00	4.00	2.50
Braking rate, mphps, dynamic								(4.0*)	3.00
Weight of bare motor, lb	5,430	5,340	5,050	5,130	5,450	4,480	4,745	1,440	1,520
Weight of accessories, lb	770	710	670	620	790	620	675	670	910
Total weight, lb	6,200	6,050	5,720	5,750	6,240	5,420	5,100	2,110	2,530
Motors per car	2	2	2	2	**	2	2	**	4
Max tons per motor	41.4	41.4	43.2	40.0	36.7	31.2	34.3	10.7	14.6

* Eddy current brake. ** Articulated cars.

2 for several of the motors. In as much as the continuous rating represents the work a motor can do, a further comparison on Figure 3 is shown of the continuous tractive effort for minimum field strength with all motors geared to a maximum permissible speed of 60 miles per hour. These curves indicate that the continuous horsepower rating and the continuous tractive effort rating per pound of *GE-1240* motor and accessories are, respectively, 31 per cent and 40 per cent higher than for the *GE-728* axle hung subway motor which is the best previous design.

The *GE-1240* motor characteristics are shown on Figure 4 and are such that the new cars with four of these motors will have approximately the same speed–tractive effort characteristics as those of the present cars on the IND Division equipped with *GE-714* axle hung motors.

The change from a 2-motor axle-hung equipment to a 4-motor truck-mounted equipment was dictated largely by the necessity of providing sufficient rail adhesion to prevent wheel slippage for a maximum accelerating rate of 2.5 miles per hour per second and maximum braking rate of 3.0 miles per hour per second. The other advantages obtained by this change, better commutating motors, lighter weight motors, antifriction bearing motors and gear reduction units, more continuous capacity, and dynamic braking outweigh any objection to the greater number of units to maintain. The comparisons made between the new and older type of equipments show that a definite advance has been made in the direction of more capacity for less weight of motor equipment and that it has been made with improvements in commutation.

No Discussion

Electric Equipment for 2-for-1 Twister

E. C. GWALTNEY
NONMEMBER AIEE

H. J. BURNHAM
NONMEMBER AIEE

THE Saco-Lowell 2-for-1 twister is one of the most complete approaches to an all-electric machine ever attempted in the textile industry. This paper covers the problems encountered in electrifying the machine, means taken to overcome them, and the simplification of the electrical components of the machine.

Textile fibers are either natural or synthetic, and either type must be twisted into yarn before it can be woven into fabric. To put twist into a strand of fibers one element must revolve. This element is a spindle. In conventional twisting the yarn is either fed through a pair of rolls and twisted as it revolves around and is wound on a rotating package or the yarn is twisted as it is pulled from a rotating supply package and is wound on a take-up spool. Either way either the supply package or the take-up package must rotate on a spindle to get twist, obtaining one turn of twist for every revolution of the spindle. The amount of twist is measured in turns per inch and is the ratio of rotation of the spindle to linear speed of the yarn.

2-for-1 Principle

The possibilities of revolving the yarn being twisted around a stationary supply package and obtaining two turns of twist for every revolution of the spindle have been known for years. This principle involves holding a package stationary on a revolving spindle which carries a flyer operating at high speed as shown in Figure 1. One turn of twist is obtained between the stationary package and the rotating flyer, and a second turn is obtained between the flyer and the take-up spool which draws the yarn from the stationary package at a fixed linear speed. Up to the present time, this has never been done commercially except to a limited extent in Germany. By putting in two turns of twist for every revolution of the spindle we double the linear speed of the yarn and get double the production per spindle without increasing spindle speed.

Although it is planned ultimately to apply the 2-for-1 principle to all forms of twisting, its use at the present time is confined to the twisting of fine denier rayon and nylon. By this we mean the twisting of continuous filament yarns which go into the making of women's underwear, hosiery, dress goods, and the like requiring from 25 to 50 turns of twist per inch before they can be woven or knitted into fabric.

Conventional Machines

The conventional method of twisting this yarn is by what is known as an upstroke twister in which the supply package or spool of either one-half or one-pound capacity is revolved on a spindle at from 8,000 to 11,000 rpm. Power consumption is necessarily high because of revolving the supply package at high speed. Yarn tensions are far from constant because of a variation from top to bottom of supply spool and from full to empty spool. Tensions on this machine can vary over 100 per cent. It should be noted at this point that a reasonably constant tension is essential in making a high quality yarn. A large number of spindles per machine are driven by a single motor vertically mounted at one end of the machine using an endless belt.

The 2-for-1 Spindle

The 2-for-1 twister utilizes a stationary package and thus a substantial saving in power consumption results. Furthermore, power consumption is independent of whether the package is full or empty. Yarn tensions on the 2-for-1 twister are constant regardless of any variation in the supply package and can be held to plus or minus 5 per cent or closer.

The spindle unit is shown in Figure 1. The rotating spindle supports the package carrier on two ball bearings. These bearings allow the spindle to rotate within the stationary package carrier which is kept from revolving by two Alnico magnets in the bottom of the package carrier and two magnets mounted on the spindle support. There must be a free path for the yarn and flyer around the package carrier; hence the use of magnets to hold the carrier from revolving.

The yarn is pulled upward over the end of the supply package, down through the tension device, down through a hole in the center of the spindle, around a porcelain guide and out through a hole in the side of the spindle, thence to the eye of the flyer which rotates within the air gap of the magnets and up to the take-up spool, "ballooning" around the stationary package and carrier. Only the spindle and flyer revolve. One turn of twist per revolution is inserted in the yarn between the tension device and the flyer. A second turn per revolution is added between the end of the flyer and the take-up spool.

If one of the two top bearings on the spindle should ever fail, the package carrier and package would start revolving at the speed of the spindle due to bearing friction. As this speed is often as high as 12,000 rpm, some safety device must be utilized. The front bottom holding magnet is mounted in a "trap door"

Paper 47-35, recommended by the AIEE committee on industrial power applications for presentation at the AIEE North Eastern District meeting, Worcester, Mass., April 23-25, 1947. Manuscript submitted November 13, 1946, and originally presented at the AIEE winter meeting, New York, N. Y., January 27-31, 1947, as a miscellaneous paper; made available for printing March 12, 1947.

E. C. GWALTNEY is director of research, and H. J. BURNHAM is a test engineer; both of the Saco-Lowell Shops, Biddeford, Maine.

which swings open by gravity when this magnet is not held up by its matching magnet in the bottom of the package carrier. In addition to the force of gravity, the drop magnet in the trap door is given a definite push when like poles of the magnets pass by each other. A movement of only five degrees of the trap door releases a spring loaded brake which stops the spindle. Simultaneously, the driving force is removed from the spindle.

Drive Requirements for 2-for-1 Twister

The practical operation of the 2-for-1 twister requires that the spindles rotate at approximately 12,000 rpm, the yarn take-up be driven at various constant linear speeds, and that any given ratio between spindle speed and linear speed of yarn be maintained constant for all spindles during starting, running, and stopping of the machine. In addition to this, means must be provided for stopping individual spindles as well as for starting and stopping the entire machine.

The first attempts at the machine were along mechanical lines driving the spindles with an endless belt. Belt slippage and resultant twist variation, maintenance, power consumption, yarn cleanliness, and over-all flexibility were serious problems. The most serious was yarn cleanliness. Dirt and oil circulated by air currents created by the endless belt made black streaks in the yarn which would not come out in the finishing of the woven fabric.

Electrification

Complete electrification provides a satisfactory answer to these problems, and complete electrification in this case involves the use of individual spindle drive motors. Individual spindle drive has not heretofore had wide application in the textile industry except in rayon pot spinning and in certain related processes such as the fabric coating of rubber thread. The same advantages, however, which pertain to all forms of electric motor drives are apparent, namely: Reduction in mechanical complications, cleanliness, and efficiency of power transmission. High rotative speeds are readily obtained by the use of a-c motors supplied

Figure 1. Sketch of spindle unit showing use of magnets to hold supply package and passage of yarn

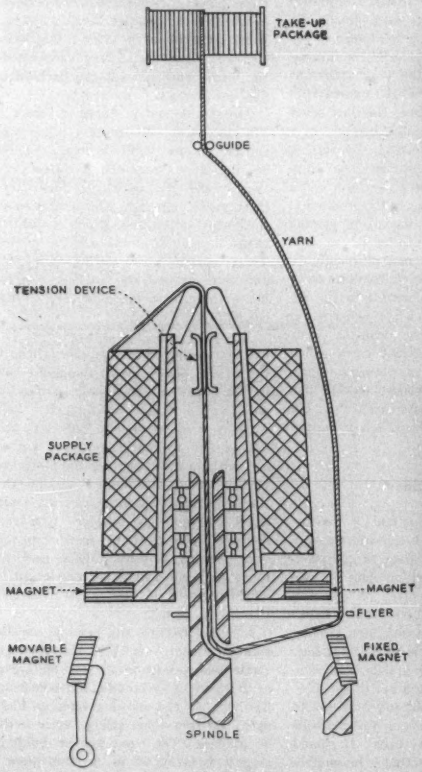

Figure 2. Close-up view of electric spindle assembly with "trap door" open

There are 72 of these units per machine

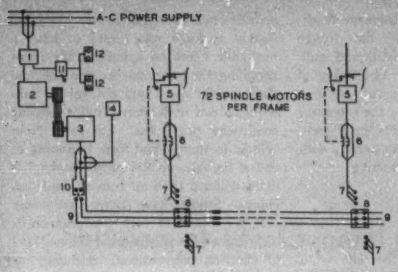

from power sources having frequencies higher than the conventional 60 cycles. This system results not only in simple inexpensive motors but also in a high degree of speed uniformity. It appears, also, that due to mechanical simplification which results, in many cases the advantages of individual motor drive may be realized without undue increase in over-all cost.

The advantages gained in electrification of the 2-for-1 twister are: reduction in power consumption, a more even twist because of constant ratio between spindle and take-up speeds, easier stopping of individual spindles, a simpler design, reduction in noise, and clean yarn. The last item is of utmost importance. Electrification of the machine has eliminated all possibility of any dirt or grease being thrown into the yarn from an endless belt.

Figure 3 (above). Electric equipment and connections for 2-for-1 twister

1. Magnetic switch (motor starter)
2. Induction motor, 5 horsepower, 1,800 rpm
3. Synchronous generator, 3 kw, 3,000 rpm, 60 volts, 3 phase, 200 cycles
4. Induction gear motor 1/6 horsepower, 63 rpm, 3 phase, 200 cycles
5. Spindle motor, 40 watts (input), 60 volts, 3 phase, 200 cycles
6. Motor switch (for automatic stop motion and individual operation)
7. Plug connector (polarized)
8. Double outlet (polarized)
9. 200-cycle bus
10. Phase reversing switch
11. Limit switch (safety switch on door)
12. Push button station, "Start—Stop" (One on either side of machine)

Figure 4. The head end with doors open to show take-up motor and gearing

Spindle Motors

Individual 2-pole 3-phase vertical induction motors rated 40 watts, 12,000 rpm, 60 volts, 200 cycles, are applied to the spindles. Motor shafts were extended upwards and become the spindles. Because of the synchronization required in spindle speeds and in ratio of spindle speeds to linear speed of yarn, the use of a-c motors, either synchronous or induction, was deemed essential. Induction motors were highly desirable because of reduced cost and better starting characteristics of individual spindles and were found to be adequate as far as constant speed is concerned, as the loading is constant, any variation due to variation in bearing friction having been found to be negligible because of the use of ball bearings. A 2-pole normally open switch actuated by the "trap door" allows stopping of individual spindles, as well as providing for disconnecting the power in case the door is opened by rotation of the package carrier. Figure 2 is a close-up view of an electric spindle assembly with the trap door open.

Motor-Generator Set

With spindle speeds up to 12,000 rpm and the use of a-c induction spindle motors, it became necessary to furnish a high-frequency power source. A motor generator set is built into each machine and spindle speed is adjusted by changing pulley ratio between motor and generator.

The motor generator set comprises a 3-kw 3,000-rpm 65-volt 3-phase 200-cycle generator and a 5-horsepower, 1,800-rpm 550-volt 3-phase 60-cycle driving motor.

Take-Up Drive

The take-up packages, (one for every spindle), are surface driven by cork covered drums on shafts running the length of the machine, one on each side. These shafts are driven by a gear motor rated 1/6 horsepower 60 volts, 3 phase, 200 cycles, 65 rpm output speed, powered from the same high-frequency source

which drives the spindles. This holds a constant ratio between spindle and take-up speeds assuring constant twist. Change gears are provided to alter take-up shaft speed to obtain desired twist.

Generator

A conventional generator would require a separate source of excitation and a means of maintaining this excitation during the coasting of the machine when stopping. Also, protection against power failures was needed as otherwise excitation would be lost entirely, with the spindles and take-up coasting to a stop independently of each other, resulting in a stretch of yarn with bad twist. The answer to this was a permanent-field generator. This generator uses standard stator windings with Alnico magnets built into the rotating field, the design of which is unique in a power generator.

By the use of the permanent field generator, we have not only taken care of power failures and machine stopping but have eliminated external auxiliary equipment for excitation. The extreme simplification resulting from the use of this generator can be seen in Figure 3.

The complete frame is started by pressing the start button at either push button station. The spindle motors and the take-up motor are connected to the generator. As the generator speed increases, the voltage and frequency increase at the same rate and the motor speeds (with allowance for slip) are synchronized with the generator and with each other. Similar synchronization takes place when the stop button is pressed and the system decelerates.

In bringing the spindles up from rest to operating speed, it has proven desirable to limit to some extent the acceleration rate. The result obtained from such limitation is reduction in maximum torque requirement in the spindle motors and a tendency to more uniform relation of speeds of spindle and take-up. To insure adequate break away torque, the driving motor for the generator is designed for approximately flat torque characteristics with standstill and pull-out values about equal. Limitation of acceleration is secured by the use of a small fly-wheel mounted on the generator shaft. This method results in a combination of good break-way torque with the desired limited rate of starting.

Complete Machine

The finished machine consists of a skeleton framework mounting 72 spindle assemblies, 36 on each side. The power for spindle motors is supplied from a bus bar assembly which is built into the beam supporting the spindles, and the cords of the spindle motors plug into it making it a simple matter to remove individual spindle assemblies for servicing without stopping the entire machine. A housing at one end of the machine contains the gear motor for driving the take-up and all necessary gearing as well as a cam motion to traverse the bars which guide the yarn onto the take-up spools. The housing also includes the magnetic switch for the main driving motor, two push button stations, one on each side of the machine, and a reversing switch for the spindle motors to produce the direction of twist required in the yarn being produced. The main driving motor and generator are mounted under the beam at the head end. It is so constructed that the application of power requires only the connecting of leads from the 3-phase mill power supply to the terminals of the across-the-line starter in the head end housing. Figure 5 shows the head end housing with doors open to show the gear motor for driving the take-up and the necessary gearing.

Test Results

Some very interesting facts came out of the innumerable power tests made on spindle motor requirements. Size of supply package was found to have a negligible effect on spindle-motor input revealing that the slip is constant and that spindle speed will not vary. Subsequent tests under actual mill operating conditions prove that the twist from spindle to spindle and from beginning to end of the take-up and supply package is more uniform than on conventional machines. Studies have shown that power cost per pound of yarn produced on 2-for-1 twisters is in the order of one-third of that on conventional machines. A higher quality yarn with less variation in twist and a tremendous reduction in number of fabrics rated as "seconds" because of oil and dirt are expected to offset the necessarily higher cost of the 2-for-1 twister as compared to the cost of conventional up-stroke twisters.

Future Possibilities

It is expected that 2-for-1 twisters will eventually replace all forms of twisting except on those yarns requiring an extremely low twist and that electrification of spindles on the present machine will point the way to future electrification in the textile industry.

There are over ten million spindles in the United States alone twisting the type of yarn to which the present 2-for-1 twister is suited. There is an ever increasing amount of rayon tire cord being used. The 2-for-1 principle is now being adapted to machine for the twisting of this cord. With this development, it will be possible to produce 20-pound cones of tire cord without a knot or splice in a 2-step operation and the power cost will be only a small fraction of that on present machines.

The 2-for-1 principle will also be readily adaptable to the so-called "Brownell" type of twisting which produces the highest quality of plied yarns known, and which has heretofore been handicapped by low speeds, high first cost, and expensive maintenance.

No Discussion

Solution of the General Voltage Regulator Problem by Electrical Analogy

E. L. HARDER
MEMBER AIEE

THE TRANSIENT performance of a generator voltage regulating system is the terminal voltage, as a function of time, following a voltage disturbance or following the sudden addition of load. The general quantitative solution to this problem is given for linear systems in terms of the parameters of the system. These are the time constants of the generator, exciters and damping transformers and the over-all voltage amplification. The data cover systems of up to three delays and were obtained by calculation and the use of the servo analyzer, an analogue type of computer for analyzing regulating systems. The paper reviews the problem, describes the servo analyzer method of solution, and gives the general solution, with interpretations.

Generator Voltage Regulating Systems

In this treatment, the generator voltage regulating system will be taken to include the generator, the exciter, the regulator, and any other elements entering into mathematical formulation of the regulating problem. There are proposals to term this an excitation system; however, it is believed advantageous here to term the over-all system a regulating system to identify it with the corresponding grouping of elements in other branches of engineering.

Two relatively simple generator voltage regulating systems are illustrated in Figures 9 and 2. Figure 1 illustrates a mechanical moving element called a Silverstat Regulator. If the generator terminal voltage drops, the spring moves the armature in a direction to close sequentially the silver contacts. This short-circuit resistance in the exciter field circuit and the consequent increase in field current restore the generator voltage to normal. The damping transformer feeds back a voltage proportional to the rate of change of exciter voltage to stabilize the system. The reference or pattern in this case is the constant spring force of the regulator, against which the voltage pull is balanced.

In Figure 2, there are no moving parts other than the rotating machines. The regulating element is a static network. The measuring circuit used is composed of a linear resistive branch and a nonlinear saturating reactor branch. At the normal voltage, both branches draw the same current. If the voltage is high, the saturating reactor current is greater than the resistor current, the excess flowing in the control field of the Rototrol exciter in a direction to lower the voltage. At low terminal voltage, the reverse takes place.

Both of these systems, and many others as well, may be represented by the generalized regulating system of Figure 3, or by modifications of it. This system is sufficiently general to include one or two exciters and one, two, or three damping transformers. Or it may represent one exciter plus delay in the regulator. It is to this idealized system that this paper primarily is directed.

The system of Figure 3 was studied by Hanna, Valentine, and Oplinger[1] who gave the differential equation for the terminal voltage, e_t, as follows:

$$e_t(1+pT_0)(1+pT_1)(1+pT_2) = -Ae_t[1+pt_1+pt_2(1+pT_2)+pt_1(1+pT_2)(1+pT_1)] \quad (1)$$

T_0, T_1, T_2 = the time constants of the three field circuits
t_1, t_2, t_3 = the time constants of the three damping transformer circuits
e_t = the generator terminal voltage
$p = d/dt$, the derivative with respect to time
A = the combined steady state voltage amplification around the circuit

Paper 47-110, recommended by the AIEE joint committee on servomechanisms for presentation at the AIEE North Eastern District meeting, Worcester, Mass., April 23-25, 1947, and the AIEE summer general meeting, Montreal, Quebec, Canada, June 9-13, 1947. Manuscript submitted November 13, 1946; made available for printing March 13, 1947.

E. L. Harder is consulting transmission engineer, Westinghouse Electric Corporation, East Pittsburgh, Pa.

The major portion of this paper is abstracted from a thesis, having the same title, submitted to the University of Pittsburgh in partial fulfillment of the requirements for the degree of doctor of philosophy, June 1946.

The author is indebted to H. S. Kirschbaum who constructed the pilot model and the first working model of the regulator analogue described in this paper, and to W. Carlson and J. Corbett for making some of the calculations for the curves.

Figure 1 (below). Essential components of a regulating system with direct acting regulator and self-excited exciter

Figure 2 (right). A voltage regulating system using a static measuring network

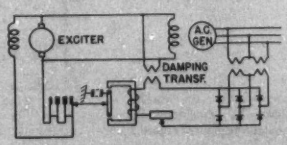

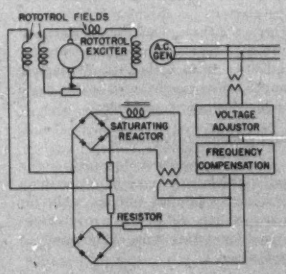

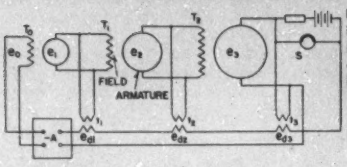

Figure 3 (left). An idealized regulating system having three delays and three damping transformers and having its amplification lumped at A

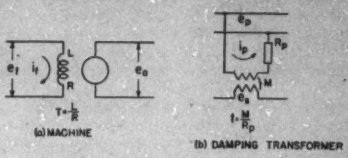

Figure 4 (right). Damping transformer

The damping transformer ideally provides across its secondary terminals a first derivative of the voltage supplied to its primary circuit. From Figure 1, the primary current is taken as:

$$i_p = \frac{e_p}{R_p} \tag{2}$$

This neglects the primary inductance of the damping transformer. Then,

$$e_s = Mpi_p = \frac{M}{R_p}pe_p = tpe_p \tag{3}$$

The damping transformer thus is defined by the time constant

$$t = \frac{M}{R_p} \tag{4}$$

The case of $t_n = T_{n-1}$, in which each damping transformer time constant is made equal to the preceding machine delay (time constant), results in a critically damped solution. It gives rise to the concept of each damping transformer "taking care of" the preceding machine time delay in respect to stability and damping. If critical damping be taken as 100 per cent, this concept provides a bench mark for stating the per cent damping used in each position.

By Routh's[4] criterion, if the determinantal equation corresponding to equation 1 be written as

$$p^3 + B_2p^2 + B_1p + B_0 = 0 \tag{5}$$

the regulating system will be stable, if

B_2, B_1, and B_0 are positive, and

$$B_2B_1 > B_0 \tag{6}$$

Stable operation, in general, is secured up to some value of amplification without the necessity of damping transformers, whereas, if the amplification is increased further, damping becomes necessary for stability. In fact, theoretically, infinite amplification can be used stably with proper damping transformers.

Some Unsolved Problems

The foregoing brief description of a few of the known concepts and criteria of voltage regulating systems, while far from complete, will serve as a rough background for stating some of the unsolved problems.

Though Routh's criterion defines the boundary limits of the stable operating region, it is sometimes necessary to know, not only that a system is stable, but also how quickly and how closely normal voltage will be restored following a disturbance. What amount and location of damping will result in the most rapid restoration of voltage to normal?

In a voltage-regulating system having time delays, the introduction of resistance in a stage reduces the time constant and also the amplification of that stage. How far is it efficient to go in this direction?

Damping transformers with or without primary delay may be introduced in any of several stages of a regulating system. There are stable and unstable combinations. The stable ones involve various degrees of damping, various speeds of recovery to normal voltage, and require greater or lesser amplitudes of linear variation in the devices involved. For example, the exciter may require a higher ceiling in one case than in another for the same over-all system performance. It is desirable, therefore, to determine the operation as a function of the damping transformers used, and to determine the optimum systems from the standpoint of

1. Minimum size and weight for a given performance.
2. Best performance for given rotating machines with static damping devices unrestricted.
3. Best performance with a single damping transformer.

This paper contributes primarily to two phases of the problem. First, the electrical analogy method is presented, proved, and its technique is worked out. Second, a linear-circuit solution by this method is given for the general case involving up to three delays and up to three damping transformers. By covering the full range of parameters, this solution includes inherently the solutions for simpler cases involving one or two delays and the use of one or two damping transformers.

Electrical Analogy Method

An electrical analogue for the regulating system of Figure 3 is shown in Figure 5. It consists of several delay circuits of adjustable resistance and capacitance which can be adjusted to have time constants, RC, proportional to the time constants, L/R, of the fields in the actual regulating system. The damping transformers are very similar to those used in the actual system, except that they are smaller and are made adjustable by taps on the primary winding and on the series resistors. Each stage is separated from the next by an electronic amplifier which draws so little energy from the resistance-capacitance circuit as to have negligible effect upon its operation at the frequencies involved. Each amplifier supplies power to the next resistance-capacitance stage as well as power to one damping transformer at a voltage proportional to the capacitor voltage of the preceding stage. The final amplifier, A, makes it possible to design the damping transformers to work into a high impedance input, which accounts for their small size.

The total voltage amplification of the analogue must be the same as the voltage amplification in the actual regulating system. However, it is not necessary that it

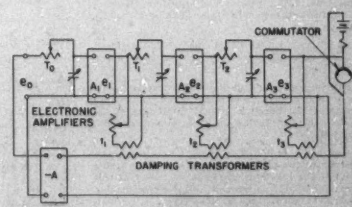

Figure 5. Analogue for regulating circuit of Figure 3

be distributed in the same manner so long as proper correction is made in the damping transformer time constants, as will be outlined in a subsequent section.

This analogy is an electrical analogy of an electric system. The great advantage of the analogy in this case lies in the ability to build the analogue practically in a readily adjusted laboratory model.

An alternative analogue, suggested by G. D. McCann, is shown in Figure 6. In this analogy the damping transformers have been replaced by common resistors in the preceding stages. This avoids parasitic oscillations which occur at certain frequencies with the damping transformers but requires isolation of the power supplies for the several amplifier stages.

Transient Calculating Laboratory

The regulating system analogue is incorporated with several other pieces of equipment to form a calculating laboratory for the solution of transient problems. It will clarify the discussion to point out the relationship of the several pieces of equipment in this laboratory.

Referring to Figure 7, the panel at the left is the regulating system analogy already mentioned. At the extreme right is a synchronously driven group of eight commutators operating at ten revolutions per second. Each commutator can be used to perform ten circuit opening and closing operations per second in the network, or analogue, which is set up for study. Usually, the time constants are so arranged that the transient practically is completed in about one half of this time, and the remaining one half of the time is used to permit or force the circuit to come to rest before being subjected to the same transient again. The transient voltage or current in any part of the circuit can be measured by one of the two oscillographs shown at the center of the main cabinet. As the transient is repeated, the transient voltage undergoing observation shows as a steady image on the oscillograph screen. It can be measured or recorded photographically. This method has been in use for some time for the study of transient voltages in electric power systems.[7]

The main cabinet in Figure 7, surrounding the two oscillographs, includes power sources, forcing functions, de-energizing resistors, and switches for connecting either the oscillographs or the commutators to any desired points of the network which has been set up. The central switching cabinet contains a large number of busses brought to terminals. Circuits to be analyzed and switched are connected to these terminals. The brushes on each of the commutators are connected to selector switches which can select these busses. The cathode-ray oscillographs also are brought to selector switches through which they can be connected to any of the busses. The brushes on each commutator are continuously adjustable throughout 360 degrees by means of cranks shown on the commutator assembly in Figure 7. Thus the period of closure of each commutator can be adjusted from zero to 180 degrees, while the phase of closure of one commutator with respect to another also can be varied throughout the full 360 degrees.

This equipment is sufficiently flexible to solve a large number of transient problems. To the busses of the central measuring cabinet can be brought not only the regulator analogy but also all manner of other circuits to solve various electrical and mechanical problems. For example, the panel in the background in

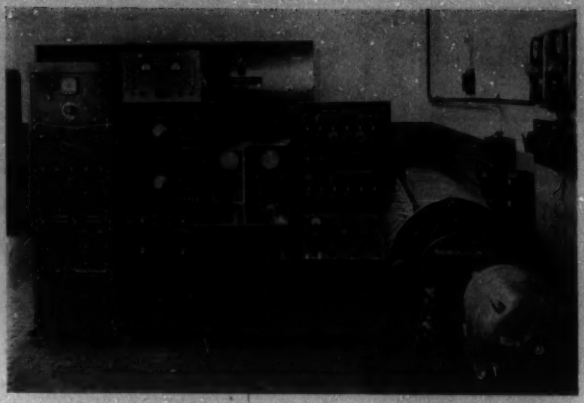

Figure 7. A front view of the calculating laboratory equipment

The recently incorporated regulating system analogy at the left includes variable resistance-capacitance circuits to represent time delays, adjustable damping transformers, and five stages of amplification

Figure 7 contains low loss inductances and capacitances for setting up analogues of mechanical systems.

Also, the a-c network calculator is located in an adjacent room and has connections directly to the transient calculator. The a-c network calculator is used ordinarily to solve steady state problems, or to make transient solutions by a series of steady-state step-by-step solutions. It contains several hundred circuits upon which entire power systems can be represented in miniature. The original combination used by Evans and Monteith[7] for studying power system transient voltages consisted of commutators, cathode-ray oscillograph, camera, and selector switches used in conjunction with the a-c calculating board circuits.

Servo Analyzer

The regulating system analogue used in conjunction with the commutators, power sources, and measuring equipment constitutes a servo analyzer. It is an analyzer of sufficient flexibility for studying the performance of many types of regulating systems. In the regulating system, Figure 3, and its analogue, Figure 5, for example, the recovery voltage following a sudden change in the reference voltage (change in the voltage-adjusting rheostat) may be determined by suddenly impressing a small d-c reference voltage by means of one of the commu-

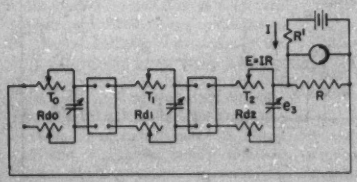

Figure 6. Alternate analogy using common resistors

(A) (B) (C) (D) (E)

Figure 8. Recovery voltage oscillations

A—Test

B—Calculation of 3-delay 3-damping-transformer case of the appendix

$A = 100$ $K = 4$

$T_0 + At_1 = 0.0765$

$T_1 = 0.263$

$t_2 = 0.096$

$t_3 = 0.232$

$k = 4$

C—Test: 2-delay double-damping case

$A = 100$

$T_0 + At_1 = 0$

$T_1 = 0.263$

$t_2 = 0.096$

$t_3 = 0.232$

D—Test showing change of reference voltage

E—Test showing sudden load of a machine

tators. The regulating system will act to raise the regulated voltage to the new reference voltage. The oscillation of the regulated terminal voltage as it approaches its new value is shown on the oscillograph screen and may be measured or photographed.

Analytical Proof of the Accuracy of the Analogue

In order to determine the accuracy of the analogue prior to its use in responsible engineering studies, several cases have been calculated analytically and compared with solutions obtained from the servo analyzer. McCann, Herwald, and Kirschbaum[6] already had shown good agreement for parts of the analogue involved in determining the response curves of simple error servomechanisms. However, several of the amplifying stages and damping transformers were not involved in their study, and also modifications had been made since that time.

Figures 8*A* and *B* show the comparison of calculated and servo analyzer solutions for the case of a 3-delay system with two damping transformers. The analytical solution is given in the appendix. The agreement between analytical solution and solution from the servo analyzer is entirely adequate for the general analysis of regulating systems contemplated. Agreement of either of these methods with actual machine performance is a matter of the refinement used in determining the constants and the extent of the effects of saturation not represented in the analogy or the calculation.

A calculation also was made for the case of a 2-delay double-damping system. In this case the calculated frequency and damping time constants were 0.43 cycle per unit and 0.577 per unit respectively compared with 0.45 cycle per unit and 0.53 per unit time constant obtained from the record reproduced in Figure 8*C*.

Boundary Conditions

In the general regulation study, it was found necessary to represent two types of boundary conditions in order to simulate voltage regulator action. These two conditions correspond with suddenly changing the reference voltage and with suddenly adding load to a generator. Figure 9*A* shows the method of representing a sudden change in reference voltage. When the commutator opens, the reference voltage E is applied, and the other conditions likewise are fulfilled, just as in an actual system.

Suddenly Applied Load. In the preceding case, the exciter voltages e_1 and e_2 were equal to the generator voltage, e_3, immediately after $t = 0$. In the case of inductive load suddenly applied to a generator, the transient drop in the terminal voltage is accompanied by a transient increase in field current (and field IR drop). The field IR drop after time = 0 is equal to the generator terminal voltage under the assumptions that the amplifications are external to the machines. However, the voltage e_3 at this instant is insufficient to support e_3, and e_3 starts with a downward slope.

From their values immediately after a load is added, the exciter voltages eventually will need to be increased an amount b to support the generator terminal voltage that exists right after $t = 0$; and increased a further amount, a, to restore normal voltage. The ratio $b/a = k$, varies from 1 to 4, depending on the type of generator and the amount of load added, as shown in Table I.[10]

For a sudden load that causes a transient voltage drop E, the boundary conditions are established properly if e_3 is an amount E below reference, and e_1 and e_2 are each an amount kE below e_3. This condition is established by the circuit of Figure 9*B* which, at the same time it establishes a reference voltage an amount E above e_3 (e_3 is 0), also adds a voltage, $-kE$ to e_1 and e_2. From this initial point, e_3 will have to rise an amount E, and e_1 and e_2 an amount $(1+k)E$, to reach the reference voltage. Actually, if the system is stable, they will settle at slightly below the reference, that is, at

$$e_1 = e_2 = e_3 = \frac{A}{A+1} E \tag{7}$$

It may be noted that the pilot exciter voltage starts up at the same rate, pe_1, whether the reference is changed suddenly

Figure 9. Simulation of boundary conditions

A—Sudden change of reference voltage

B—Analogue for suddenly applied load on a-c generator

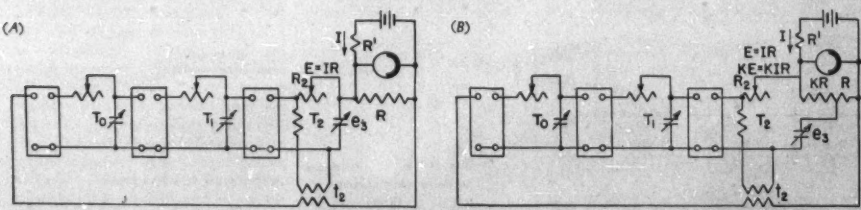

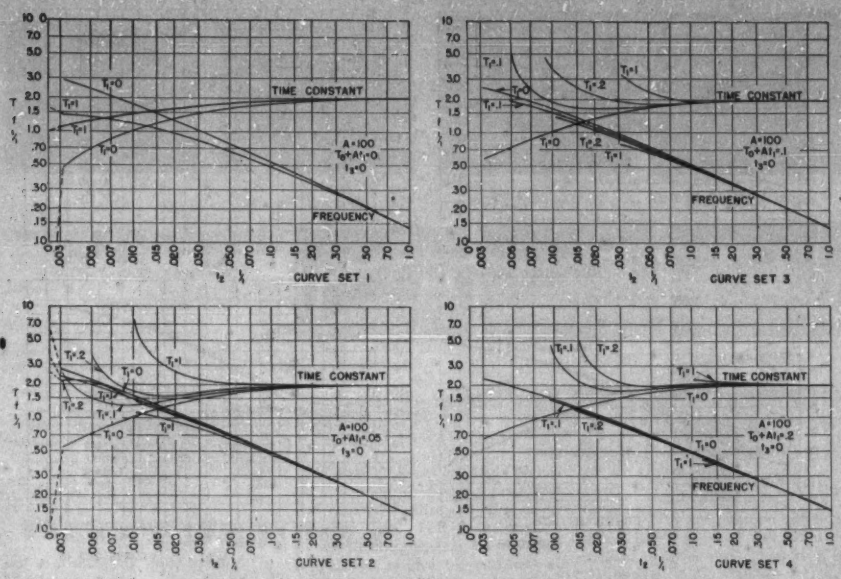

Figure 10. Performance of a 3-delay regulating system

$A = 100,\ t_3 = 0$

by an amount E or an added load causes a transient voltage drop, E. However, it has 2 to 5 (that is, $1 + k$) times as far to go to reach its final steady value in the latter case. As the main generator field current has about the same amount to change in either case, and the exciters are usually fast compared with the generator, this causes only a moderate over-all effect on e_3.

Cognizance must be taken of the fact that e_1 and e_2 now include the fixed shift voltage, $-kE$. However, as only the change in voltage after $t = 0$ is of interest, the fact that the constant portion, $-kE$, is not included in the oscillograph measurement of these quantities does not matter.

When the commutator is open, the voltage across the resistor connected to its brushes is fixed almost solely by the constant current power source, as this resistance is small, only a few hundred ohms, compared with the 25,000 ohms minimum in R_3, or with the 1-megohm damping transformer circuit. In Figure 8, D and E represent similar solutions taken under the two boundary conditions. It will be noted that the voltage time curve starts out horizontally in d, but with an initial downward slope in e. The former represents a change in reference with the regulator simply following up, whereas the second represents the sudden loading of a turbogenerator followed by regulator action restoring the voltage to normal.

The Quantitative Solution of the 3-Delay System

Useful data on the performance of voltage regulator systems obtained by the use of the new analyzer and by calculation are contained in this section. They include a graphical presentation of the performance of the general 3-delay 3-damping-transformer system of Figure 3. Contained in this solution are the special cases of one and two delays and of zero, one, and two damping transformers.

As performance indexes the following items are presented referring to the generator terminal voltage, e_3, as it oscillates about normal in recovering after a disturbance.

1. Time Constant in Per Unit, T. As the oscillation is primarily a single frequency phenomenon, its damping can be described in terms of the time constant, or time for the envelope of the oscillation to drop to 0.368 of its initial value. This time constant, like all other time constants of the system, is expressed in per unit of the main generator time constant, T_3. When the generator time constant is known for a particular system, the damping time constant, T, readily can be converted to seconds. In two time constants ($2T$) the oscillation decays to $0.368^2 = 0.135$ of its value at the beginning of the interval. In one half time constant ($0.5T$) it decays to

Table I

$k = b/a$ = Ratio of Initial Field Current Increase to Later Additional Increase When Load Is Added (Low Power Factor)

$$k = \frac{b}{a} = \frac{X_e}{X_d'}\,\frac{X_d - X_d'}{X_d + X_e}$$

	X_d	X_d'	X_e	b/a
2-pole turbogenerator	1.10	0.15	.2	4.08
			1	3.00
4-pole turbogenerator	1.10	0.23	.2	2.44
			1	1.81
Salient-pole generator	1.15	0.36	.2	1.40
			1	1.03
Synchronous condenser	1.80	0.40	.2	1.55
			1	1.25

X_e = reactance of load added
X_d' = generator transient reactance
X_d = generator synchronous reactance

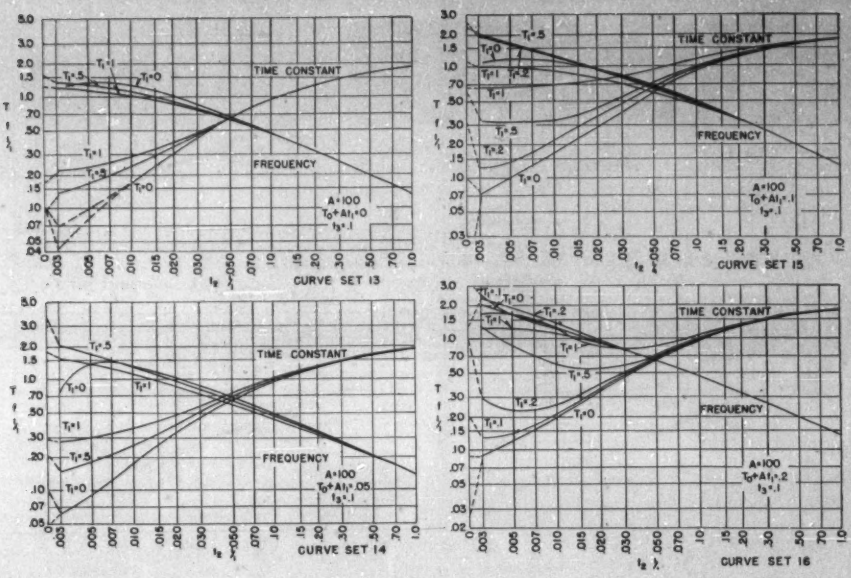

$0.368^{1/2} = 0.605$ of its initial value.

2. *Frequency in Cycles Per Unit, f.* As the unit of time is the generator time constant, T_2, the frequency is expressed as cycles in this time. The frequency and damping time constant together, largely determine the character of the oscillation. Termination of a frequency curve indicates that the phenomenon changes at that point to an exponential decay defined by its time constants, both of which are plotted.

Parameters of the System

The parameters of the generalized regulating system of Figure 3, namely, T_0, T_1, T_2, t_1, t_2, t_3, and A are seven in number. There would have been three more had not the amplifications of the three machines and the regulator already been lumped into a single amplification with appropriate corrections in the damping transformer time constants, t_1, t_2, and t_3. If only three numerical values of each of these seven parameters were considered, the total number of cases to be studied would be $3^7 = 2187$.

Figure 11. Performance of a 3-delay regulating system

$A = 100;\ t_3 = 0.1$

Actually, more than three values of most of the parameters would be needed. This illustrates the enormous value, in fact the outright necessity, of reducing the number of independent variables, if the job is to be handled at all in a reasonable time.

One possible reduction in the number of parameters is evident immediately upon inspection of differential equation 1 which can be written as follows:

Figure 12. Performance of a 3-delay regulating system

Set 6: $A = 200;\ t_3 = 0$
Set 10: $A = 50;\ t_3 = 0$

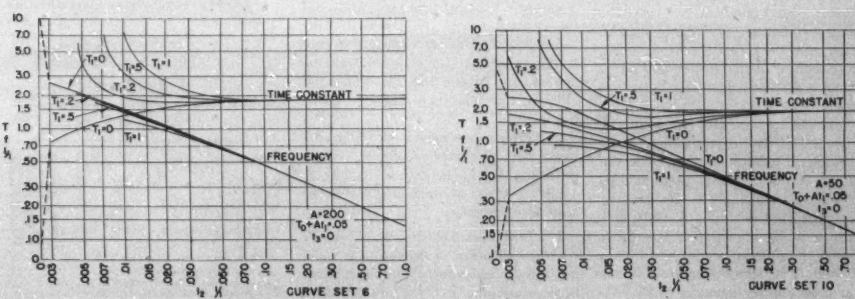

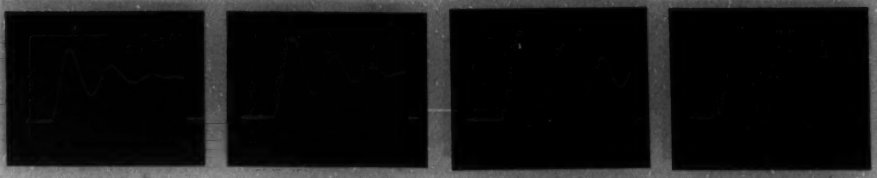

A—$T_0=0$ B—$T_0=0.017$ C—$T_0=0.042$ D—$T_0=0.084$

Figure 13. Effect of first stage time delay with no damping transformers

$A=100;\ T_1=0.21;\ t_1=t_2=t_3=0$

$$a_0(p^3+B_2p^2+B_1p+B_0)=0 \tag{8}$$

where

$$B_2=\frac{T_1+T_2}{T_1T_2}+\frac{T_1+At_2}{(T_0+At_1)T_1} \tag{9}$$

$$B_1=\frac{1}{T_1T_2}+\frac{(T_1+At_2)+(T_2+At_3)}{(T_0+At_1)T_1T_2} \tag{10}$$

$$B_0=\frac{1+A}{(T_0+At_1)T_1T_2} \tag{11}$$

As T_0 and At_1 always enter together as the function $(T_0 + At_1)$, this function can be treated as a single variable. In addition to reducing the number of variables to six, this result is important in itself. It shows that a first stage damping transformer, connected as indicated, has the same effect as lengthening the first stage delay which, as will be shown, makes the system less stable, other things being equal.

Also, as the study showed that a reduction of T_0 greatly improved the stability, the foregoing relationship suggested the possibility of securing stability, with the first damping transformer reversed to speed up the voltage rise instead of retarding it. The use of a negative value of t_1 has the same effect as reducing T_0. This must not be carried to the point of making $(T_1 + At_0)$ negative.

Previous investigators had pointed out that with each damping transformer time constant positive and equal to the preceding delay, critical damping occurred. Practical damping, therefore, had been viewed as involving positive time constants of one fifth to one tenth of the critical values. Thus the possibility of improvement in performance by negative damping in the first stage is in itself an important result of the study.

The Per Unit System

Use of the per unit system affords a further reduction of one parameter. The machine and damping transformer time constants all are expressed in per unit of one of them, usually of the generator time constant which is the longest. The times in the solution are likewise in per unit of this same time constant. The generator time constant then does not need to be varied in the solution to cover the full range of all parameters.

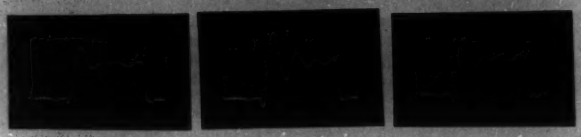

A—$T_0=0;\ t_1=0$ B—$T_0=0.084;\ t_1=0$ C—$T_0=0.084;\ At_1=-0.08$

Figure 14. Response is a function of T_0+At_1

First stage delay is canceled by reversed damping transformer

$T_1=0.29;\ t_2=0.012;\ t_3=0.27$

All in per unit of T_3

The number of variables now has been reduced to five. They are $(T_0 + At_1)/T_3$, T_1/T_3, t_2/T_3, t_3/T_3, and A. T_2/T_3 always will be one per unit and will not be varied. For convenience, the variables will be written $(T_0 + At_1)$, T_1, t_2, t_3, A, these being expressed in per unit of T_3. Thus, T_3 may be chosen any convenient value in the analogy, so long as the other time constants are the same per unit of T_3 in the analogy as in the actual system. The amplification, however, must be the same in the analogy as in the actual system.

Arrangement of the Data

The general data are arranged in the 24 curve sets indexed in Table II. Each curve set applies to particular values of A, $(T_0 + At_1)$, and t_3. In each set, curves are drawn for two or more values of T_1 between 0 and 1.0 as needed for interpolation. Each curve covers a range of t as abscissa from 0 to 1.0. The ordinates are damping time constant, T, and frequency, f, as outlined.

Data are given for three values of amplification, namely 50 100, and 200, with $t_2 = 0$, and for two values of t_3, namely, 0 and 0.1, with $A = 100$.

Interpretation

Certain points of interest may be noted concerning the curves, Figures 10 to 12.

Table II. Index to General Solution

For Each Curve, the Abscissa t_2 Is Varied From 0 to 1. In Each Set, Curves Are Drawn for $T_1=0$, $T_1=1$, and Intermediate Values. All Time Constants Are in Per Unit of T_3.

Curve Set	A	t_2	T_0+At_1	Figure	Curve Set	A	t_2	T_0+At_1	Figure
1	100	0	0	10	13	100	0.1	0	11
2	100	0	0.05	10	14	100	0.1	0.05	11
3	100	0	0.10	10	15	100	0.1	0.10	11
4	100	0	0.20	10	16	100	0.1	0.20	11
5	200	0	0	*	17	100	0.2	0	*
6	200	0	0.05	12	18	100	0.2	0.05	*
7	200	0	0.10	*	19	100	0.2	0.10	*
8	200	0	0.20	*	20	100	0.2	0.20	*
9	50	0	0	*	21	100	0.5	0	*
10	50	0	0.05	12	22	100	0.5	0.05	*
11	50	0	0.10	*	23	100	0.5	0.10	*
12	50	0	0.20	*	24	100	0.5	0.20	*

* These curve sets are available but were not included in paper. Curve sets 6 and 10 give a sufficient comparison of amplifications of 50 and 200 with 100. Curves 17 to 24 cover t_2 greater than 0.1 which does not appear necessary in view of the excellent performance with $t_2=0.1$.

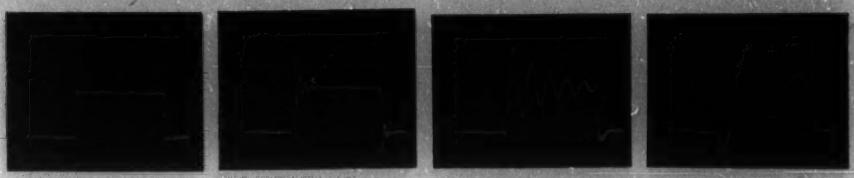

A—$T_1 = 0$ B—$T_1 = 0.05$ C—$T_1 = 0.53$ D—$T_1 = 3.73$

Figure 15. A 2-delay system is stable for all time constants

$T_0 = 0;\ t_1 = t_3 = t_4 = 0$
All in per unit of T_3

Set 1 represents a 2-delay system which is stable throughout. At $T_1 = 0$ it reduces to a 1-delay system. The exciter voltage damping transformer, t_2, is quite ineffective. It reduces the frequency of the oscillation but actually increases the time for the oscillation to die out. This would be tempered by saturation effects in an actual exciter. The high frequency implies a correspondingly high exciter ceiling.

As $T_0 + At_1 = 0$, the solution is a function of $T_1 + At_2$ instead of T_1 and t_2 separately. Note that the performance is the same for $T_1 = 1$, $t_2 = 0$ and for $T_1 = 0$, $t_2 = 0.01$, as $A = 100$.

Set 3 applies to a 3-delay system without generator damping transformer. It shows that t_2 is needed for stability and that there is an optimum point of damping for quick recovery. For $T_1 = 0$, the system is reduced to a 2-delay system.

Set 14 illustrates the benefits of a generator voltage damping transformer. With $t_2 = 0$, and $t_3 = 0.1$, it is well damped having a damping time constant of 0.1 to 0.2 per unit for practical exciter time constants. This is a small fraction of the shortest damping time constant that can be secured without the benefit of t_3, as can be seen by comparing with Figure 11.

With $t_3 = 0.1$ the 2-delay case, $T_1 = 0$ (set 14), is nonoscillatory below $t_2 = 0.003$. Consequently, the frequency curve stops at that point, while two time constants are shown below that point. Most of the recovery transient is associated with the larger of these two time constants.

Other Data

In addition to the general solution a number of exploratory cross sections have been taken to show variations of particular interest which would require comparing several curve sheets or to present performance data of a different nature. This additional information is outlined here.

Effect of First Stage Time Delay. In Figure 13 is shown the pronounced improvement in reducing the time delay of the first stage. Coupled with the differential equation, which showed that reversing the damping transformer connections (making t_1 negative) has the same effect as reducing T_0, this suggests the important possibility of improvement with negative damping in the first stage. This is one of the most important results of the study.

To demonstrate experimentally that the same effect as reducing T_0 could be secured by a reversed first stage damping transformer, the three oscillograms of Figure 14 were secured with identical settings of the analogue except for T_0 and t_1. In part *a*, T_0 and t_1 were both zero. In *b*, T_0 is 0.076 per unit, and $t_1 = 0$, while in part *c*, with T_0 still 0.076, t_1 has been increased until it neutralizes the effect of the first stage delay, T_0, almost completely.

A 2-Delay System Is Stable. This well-known fact is attested to by the oscillograms of Figure 15. With $T_0 = 0$ and no damping transformers in use, T_1 was varied over the extremely wide range of 0 to 3.73 per unit of the generator time constant, T_3.

Good Damping With Generator and Exciter Damping Transformers. The oscillogram of Figure 16*a* was taken with the analogue set up to represent a 3-delay system, $T_0 = 0.084$ per unit, and $T_1 = 0.29$ per unit. The generator and exciter damping transformers then were adjusted for optimum damping as judged visually with fast smooth recovery in mind. This resulted in $t_2 = 0.012$ and $t_3 = 0.12$.

Damping Transformer Adjustments. In the analogue the same damping transformer time constants can be secured with a transformer tap giving a higher mutual inductance and the use of a correspondingly increased primary resistance. This raises the primary inductance as the square of the increase in mutual, and hence increases the primary time constant. The use of two combinations giving the same mutual time constant, Figures 16*B* and *C*, shows that approximately the same solution is obtained in the two cases, although the primary time constant is four times as great in *B* as in *C*. However, the differences are appreciable, and in some other cases the effect was more than shown here. This effect, therefore, warrants further study.

Initial or Boundary Conditions (Figure 17). In general, two types of initial or boundary conditions have been used, representing respectively a sudden change in reference ($k = 0$), and the sudden application of load ($k = 1$ to 4). In Figure 17, k has been varied from 0 to 6, for a typical 2-delay system with an exciter time constant $T_1 = 0.29$ of T_3. This shows the initial downward trend

(A) (B) (C)

Figure 16

A—Shows good recovery obtained with $A = 100$; $T_0 = 0.084$; $T_1 = 0.29$; $t_1 = 0$; $t_2 = 0.012$; $t_3 = 0.12$

B and C—Show the same damping obtained with $t_3 = 0.03$ but with (b) 1:1 ratio and (c) 1:2 ratio damping transformer

$A = 100$; $T_0 = 0.084$; $T_1 = 0.29$; $t_2 = 0.012$; $t_1 = 0$

(A) (B) (C) (D) (E)

Figure 17. Effect of type of boundary condition

A—$k=0$ (change of reference voltage)
B—$k=2$ (salient-pole machine suddenly loaded)
C—$k=6$
D—$k=0$ (change of reference)
E—$k=4$ (turbogenerator suddenly loaded)
A, B, C—$A=100$, $T_0=0$, $T_1=0.29$, $t_2=0.02$, $t_3=0$
D, E—$A=100$, $T_0=0.14$, $T_1=0.29$, $t_2=0.02$, $t_3=0.01$

of generator terminal voltage and greater dip as k is increased.

Parts e and f of the same figure illustrate the same relations in a typical 3-delay system.

Refer to Table I to associate the initial or boundary conditions with machine types and loadings.

The Generator Voltage Damping Transformer. The effect of increasing t_3 in a typical 3-delay system is shown graphically in oscillograms a to f of Figure 18. This figure speaks for itself of the effectiveness of the generator voltage damping transformer. An exciter voltage damping transformer, $t_2 = 0.02$, was in use throughout this series of tests. The damping transformer overloads the third-delay stage, when $t_3 = 0.54$ and does not give a correct simulation.

Conclusions

The servo analyzer amply has demonstrated its value in providing the essential oscillographic data of Figures 13 to 18, which could not have been secured economically by test or calculation, and in checking and supplementing the calculated damping curves of Figures 10 to 12. Thus proved for the simple 3-delay system, it opens the way for obtaining general data on more complicated systems which could not be calculated. Even for the 3-delay system, it affords the most practical way of including initial conditions in a general study.

These curves show the performance of any 3-delay voltage regulating system. For example, consider a system consisting of a turbogenerator having a time constant of 5 seconds, an exciter of time constant 1 second, and a variable voltage pilot of time constant 0.5 second. Assume that the regulator is static or electronic and of substantially zero time constant and that the over-all voltage amplification of the system is 100. What recovery performance can be obtained with an exciter voltage damping transformer alone, or with a combination of generator and exciter voltage damping transformers?

In per unit of T_3 the time constants are: $T_1 = 1/5 = 0.2$, and $T_0 = 0.5/5 = 0.1$. Table II shows that with $A = 100$, $t_3 = 0$, $T_0 = 0.1$, curve set 3 applies. With $T_1 = 0.2$ and an exciter voltage damping transformer, optimum damping is secured with $t_2 = 0.04$, which results in a damping time constant $T = 1.8$ per unit or 9 seconds. Thus with the reference voltage suddenly changed 10 per cent, the terminal voltage is restored to within approximately 3.7 per cent of normal in 9 seconds and 1.4 per cent of normal in 18 seconds. For a sudden load causing a 10 per cent transient voltage drop, the time is a few tenths of a second longer. The frequency is about 0.75 cycle per unit (5 seconds) or 0.15 cycle per second.

If both generator- and exciter-voltage damping transformers are used, having $t_2 = 0.01$ and $t_3 = 0.1$, the damping time constant is 0.21 per unit or 1.05 seconds, compared with 18 seconds for the previous case. The frequency is 1.2 cycles per unit, or 0.24 cycle per second.

Damping Concepts

Several rather new concepts of damping have resulted from this study. It previously had been known that stability could be secured by making each damping transformer time constant equal to the previous machine delay. This was taken as a measure of complete damping with lesser amounts generally being used practically, even to the complete omission of one or two of the damping transformers. However, the analyzer studies have demonstrated that it is decidedly advantageous to reduce the first stage damping transformer. In fact, the system recovers more quickly with it reversed to assist rather than retard the first stage build up, so long as $T_0 + At_1$ is not made negative.

A generator voltage damping transformer is more effective than an exciter voltage damping transformer of the same time constant. When a system is stabilized by a generator voltage damping transformer, the reduction of the exciter voltage damping transformer time constant actually improves the recovery over

A—$t_3=0.01$ B—$t_3=0.02$ C—$t_3=0.05$ D—$t_3=0.10$

E—$t_3=0.18$

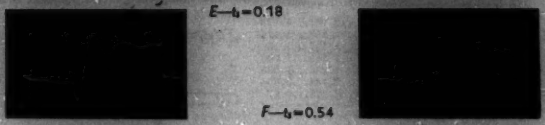

F—$t_3=0.54$

Figure 18. Effect of varying generator damping transformer

$A=100$, $T_0=0.14$, $T_1=0.29$, $t_2=0.02$, $k=4$
All time constants in per unit of T_3

a large part of the range. This transformer also might be reversed to advantage, although this was not tried.

A linear 3-delay system cannot be well damped by an exciter voltage damping transformer, t_3, alone. That is, it cannot be restored to normal in a small fraction of the generator time constant.

The exciter voltage damping transformer referred to here is one meeting practically the condition of no primary delay. If its primary time constant were made equal to that of the generator, it would become theoretically identical in action with the generator voltage damping transformer, t_3, of this study. While this is generally impractical with the usual generator time constants, it is in a direction worth investigating. Such an investigation was not within the scope of this study.

The studies indicate that in a typical 2-delay system, with a generator damping transformer, t_3, t_2 should be reduced to a low value, but not to zero for optimum results. (See $T_1 = 0$ in curve set 14.) The minimum damping time constant is 60 per cent of that for $t_2 = 0$.

Without damping transformers the addition of a small third time delay has a marked effect, even a small amount of added delay changing the system from quite stable to instable. However, when the system is well damped by t_3, variation of T_0 over the usual range has very little effect on the generator terminal voltage, e_3.

Possible Extensions

Throughout the study of the simple 3-delay system, it has been recognized that this is far from the most complicated of the systems in current or contemplated use. It is, however, an important class of systems, and it was believed necessary to work out the technique of the new analyzer with a system which could be checked frequently by mathematical analysis.

The greatest value of the analyzer for voltage regulation studies is visualized as being in the analysis of the more complicated systems which cannot be calculated economically. These include various regulating combinations and less simple exciters with coupled field circuits, and feedback or sustaining fields, and with the inclusion of saturation effects. Such studies should lead to improvements in designs and facility in the determination of the best system designs to meet any given requirements.

Table III. Calculation of Equation 21

Angle	t, Per Unit	e_3	Angle	t, Per Unit	e_3
0°	0	0	180°	1.164	1.125
15°	0.097	−0.29	210°	1.358	1.175
30°	0.194	−0.34	240°	1.552	1.15
60°	0.388	−0.17	270°	1.746	1.093
90°	0.582	+0.23	300°	1.940	1.035
120°	0.776	+0.65	330°	2.134	0.994
150°	0.970	+0.96	360°	2.328	0.97

These values are plotted in Figure 8.

Appendix. Analytical Solution of the 3-Delay 3-Damping-Transformer Case for Specific Boundary Conditions

In order to verify the accuracy of the servo-analyzer, the following analytical solution was made for a case that would bring into play all of the elements involved in any of the studies.

With reference to Figure 3 the solution for generator terminal voltage, e_3, as a function of time, is desired for the case of a suddenly applied load. The machine is assumed to be a 2-pole turbogenerator with an inductive load of approximately half of full load value, suddenly added. The assumed constants and the steps of solution follow.

Corrected Constants*

$A = 100$

$k = 4$

$T_0 + At_3 = 0.0765$

$T_1 = 0.263$

$T_2 = 1.0$

$t_2 = 0.096$

$t_3 = 0.232$

Boundary Conditions

The initial conditions corresponding to suddenly applied load are:

$$\text{Reference voltage} = E \text{ (a constant)} \quad (12)$$

$$e_1 = e_2 = -kE \quad (13)$$

$$e_3 = 0 \quad (14)$$

The reference voltage, E, will be taken as 1.0 following zero time.

The Determinantal Equation

When the constants are substituted in equations 8–11, the determinantal equation is the cubic equation,

$$p^3 + 495p^2 + 1{,}695p + 5{,}000 = 0$$

The roots of this equation are found to be:

$$p_1 = -491.59$$

$$p_2, p_3 = -1.71 \pm j2.74$$

The General Solution

The complete general solution is as follows:

$$e_3 = He^{-491.6t} + \epsilon^{-1.71t} \times (D \cos 2.74t + F \sin 2.74t) + \frac{A}{A+1} E \quad (15)$$

* Corrected for tube plate and load resistance and damping transformer primary resistance.

It is composed of a highly damped term having a time constant $1/491.6 = 0.00203$ per unit, and an oscillatory term having a frequency of $2.74/6.28 = 0.435$ cycle per unit, and a damping time constant of $1/1.71 = 0.585$ per unit.

Evaluation of Arbitrary Constants H, D, and F

$$e_2 = (1 + T_2 p) e_3$$

$$= -490.6He^{-491.6t} + \frac{A}{A+1} E + \epsilon^{-1.71t}(-0.71D + 2.74F) \cos 2.74t - (0.71F + 2.74D) \sin 2.74t \quad (16)$$

$$e_1 = (1 + T_1 p) e_2$$

$$= 63{,}109He^{-491.6t} + \frac{A}{A+1} E + \epsilon^{-1.71t}(-236D + 0.99F) \times \cos 2.74t - (2.36F + 0.99D) \sin 2.74t \quad (17)$$

At $t = 0$, $e_3 = 0$, and $e_2 = e_1 = -4$

$$e_2 = H + D + 0.99 = 0 \quad (18)$$

$$e_2 = -490.6H - 0.71D + 2.74F + 0.99 = -4 \quad (19)$$

$$e_1 = 63{,}109H - 2.36D + 0.99F + 0.99 = -4 \quad (20)$$

Solving equations 18–20 for the arbitrary constants, we obtain:

$H = 8.35 \times 10^{-5}$

$D = -0.99$

$F = -2.05$

The Resulting Solution for e_3 as a Function of t

$$e_3 = 8.35 \times 10^{-5} \epsilon^{-491.6t} + \epsilon^{-0.71t} \times (-0.99 \cos 2.74t - 2.05 \sin 2.74t) + 0.99 \quad (21)$$

References

1. Recent Developments in Generator Voltage Regulation, C. R. Hanna, K. A. Oplinger, C. E. Valentine. AIEE Transactions, volume 58, 1939, pages 838–44.

2. A Generator Voltage Regulator Without Moving Parts, C. P. West, I. D. Applegate. *Electric Journal*, April 1927, pages 181–3.

3. Design of Reactances and Transformers Which Carry Direct Current, C. R. Hanna. AIEE Transactions, volume 46, 1927, pages 155–8.

4. Regulation of A-C Generators With Suddenly Applied Loads, E. L. Harder, R. C. Cheek. AIEE Transactions, volume 63, 1944, June section pages 310–18.

5. Static Voltage Regulator for Rototrol Exciter, C. E. Valentine, E. L. Harder. AIEE Transactions, volume 64, 1945, August section, pages 601–6.

6. Electrical Analogy Methods Applied to Servomechanism Problems, G. D. McCann, S. W. Herwald, H. S. Kirshbaum. AIEE Transactions, volume 65, 1946, February section, pages 91–6.

7. System Recovery Voltage Determination by Analytical and A-C Calculating Board Methods, R. D. Evans, A. C. Monteith. AIEE Transactions, volume 56, 1937, June section, pages 695–705.

8. A New Device for the Solution of Transient Vibration Problems by the Method of Electrical-Mechanical Analogy, H. E. Criner, G. C. McCann, C. E. Warren. *Journal of Applied*

Mechanics (New York, N. Y.), volume 12, number 3, September 1945, page 135.

9. Transients in Linear Systems (book), M. F. Gardner, J. L. Barnes. John Wiley and Sons, Inc., New York, N. Y., 1942.

10. Solution of the General Voltage Regulator Problem by Electrical Analogy, E. L. Harder. University of Pittsburgh, Pittsburgh, Pa., 1946.

Discussion

C. Concordia (General Electric Company, Schenectady, N. Y.): We appreciate the great usefulness of the electric circuit method in the study of control systems and realize the practical impossibility of obtaining the numerous response curves by hand calculations. However, in view of Harder's conclusion that "The servo analyzer. . . . . affords the only practical way of including initial conditions in a general study," we feel obligated to mention that we have used the differential analyzer with considerable success for similar studies. In such studies we usually have considered specific cases including the effects of generator saturation, self-excitation, resistor steps, and so on, rather than a general linear case.

We have studied some linear cases, however. An example of some of the results of these studies is shown in Figure 1 of this discussion. This figure is presented since it illustrates an effect not specifically discussed in the paper, namely, the effect of variation in two of the factors comprising the over-all regulating-system amplification factor, keeping this over-all amplification factor constant. The factor a is proportional to the regulation amplification; b to the exciter amplification.

With regard to the use of general studies, we usually have found it desirable to make a detailed study of the case at hand, rather than depend on conclusions drawn from studies of idealized cases. An example of what we mean is given by Harder's conclusion that "A generator voltage damping transformer is more effective than an exciter voltage damping transformer of the same time constant." This conclusion, as he points out in the paper, depends upon his idealization of the stabilizer equation to the form of his equation 3

$$e_s = tpe_g$$

A more nearly correct expression, and one much more easily realized in practice, is of the form

$$e_s = \frac{abp}{bp+1} e_g$$

where b is the stabilizing transformer primary time constant. We do not believe that it is unreasonable to make the primary time constant b, equal to the generator field time constant T_k, in which case a stabilizing transformer supplied from the exciter voltage becomes equivalent to an idealized stabilizer supplied from the generator voltage.

We should like to ask what value of primary time constant was actually used in the electrical analogue.

We are completely in agreement with Harder that better performance usually can be attained by getting stabilizing signals from more than one place, and have made several installations of voltage regulators with such combinations of stabilizers.

E. L. Harder: Concordia has raised several questions regarding the use of the differential analyzer and the treatment of the problem. The reference to the analyzer being the only way to include initial conditions in a general study was meant to be in contrast to hand calculation methods rather than excluding the differential analyzer. This has been corrected in the published text. With the regulator problem set up in mathematical form and the differential equation known, a great deal of information about the performance can be obtained by analytical methods, particularly for systems of only three or four delays. From the roots of the determinantal equation one obtains the frequency and damping rates of transient oscillations. Also steady state frequency analysis is feasible for quite complicated systems. However, the point which was being stressed in the statement referred to is the inability to include initial boundary conditions by any but quite laborious methods of hand calculation. Thus, it is necessary to resort to a mechanical analyzer to obtain the solutions for specific boundary conditions for the large number of cases as needed in a general study.

Table for Figure 1. Effect of division of amplification between regulator and exciter

Curve	a	b
20	20	0.05
21	15	0.0667
22	10	0.1
12	8	0.125
1	5	0.2
13	2.5	0.4
14	1	1.0

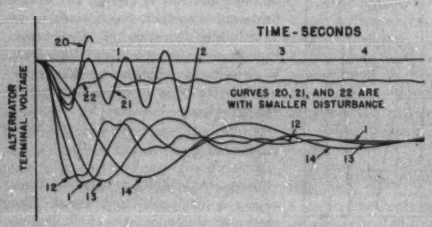

Figure 1. Voltage regulator response obtained on differential analyzer. See accompanying table

Insufficient information is given in connection with Figure 1 of Concordia's discussion to see why the solution should differ for the same over-all amplification but different distributions. The difference appears to be more than could be due simply to changed boundary conditions. In our general solution it was shown both theoretically and by tests that with all other parameters held constant, the solution did not change with variations in the distribution of the amplification around the closed loop. In the analogy studies, it was shown repeatedly that the location of the amplification was immaterial and it could be lumped at one point or distributed in any desired manner without affecting the solution. When feedbacks are used and the distribution of amplification is altered, it is necessary to change the feedback time constant in direct proportion to the change in amplification in that part of the loop reaching from primary winding to secondary winding of the feed-back device. This is necessary to keep the same effective feed-back time constant and hence the same differential equation. What we believe may have happened in the case shown by Concordia is that the distribution of amplification was made without the changes required to keep the feed-back time constant in the same relation to other delays and consequently the differential equation and the resulting solution was changed as shown in his figure.

This simply illustrates the important generalities obtained by defining all feed-back time constants on the basis of unit amplification from primary to secondary terminals. These data then can be interpreted in any actual system of that class, regardless of the distribution of the amplification.

In regard to the two equations given for damping transformer feed-back voltage, neither can be said to be more correct than the other. Both can be realized fully in practice, the first being a transformer in the field current proceeding a given voltage and the second being a transformer connected across a given voltage. Analogies were used representing both cases. It is believed that since the presence of primary time constants equal to the subsequent machine delay makes the performance equivalent to no primary time constant and the damping transformer connected one stage later, then the data presented in the paper covers the full situation. The performance as the primary time constant is varied from zero up to the machine delay is intermediate between the performance characteristics shown for the transformer in one position or in one stage later. It would hence be undesirable to increase the number of variables in the problem by introduction of primary delay as a separate variable since the effect can be determined from the data already presented.

A New Single-Side-Band Carrier System for Power Lines

B. E. LENEHAN
ASSOCIATE AIEE

Synopsis: A new method of single-side-band generation, working on the frequency-addition principle, is described. Apparatus consists of linear modulators combined with wide-range phase-splitting circuits to produce the signals.

THE USE of power-line conductors for communication has become quite common in the past ten years. Line fault protection and telemetering for load control have increased the demand for available frequencies so much that larger power systems are approaching a crowded condition in the available frequency space. At the present time, multiplex operation, by using various tone frequencies in the audible region, commonly is used to reduce the number of channels required.

The present range of frequencies in general use is from 50 to 150 kc, although some use has been made of frequencies from 40 to 300 kc. Extending the band of frequencies may not be a satisfactory solution in all cases. Losses in the power equipment connected to the lines and coupling difficulties limit the use of the lower frequencies. Radiation at the higher frequencies is appreciable, and the assignment of these frequencies to radio beacons for aircraft may prevent their use for power-line carrier over a large area. In some locations, widening the band may be practical, but a better solution is believed to be the use of the single-side-band system.[1] This system requires about half the frequency range per channel required by other systems.

When signals are to be transmitted at higher frequencies by power-line carrier or radio, some method of transferring the signals from their normal low frequencies to high frequencies at the sending end and back again at the receiving end is required. When the instantaneous value of the signal is transmitted by the rising and falling amplitude of the high frequency wave, the method is called amplitude modulation and is the most commonly used method. If the frequency is varied in similar manner, it is called frequency modulation. Another way to look at the problem is to resolve the signal wave into its component frequencies. When this is done, a voice signal may be found to have components from 150 to 3,000 cycles. When the signals are transferred to a higher frequency, the high frequency signal may be shown to consist of the normal frequency, a group of higher frequencies near by, called the upper side band, and a similar group of lower frequencies, called the lower side band. For amplitude modulation, there is one frequency in each band for each frequency in the signal. For frequency modulation there may be more than one. Each frequency component occurs at least twice, and this results in the signal occupying at least twice as much space in cycles as it did in its low-frequency state. The single-side-band system consists of transmitting only one group of these frequencies, each frequency being equal to the carrier frequency plus or minus the frequency of the signal component.

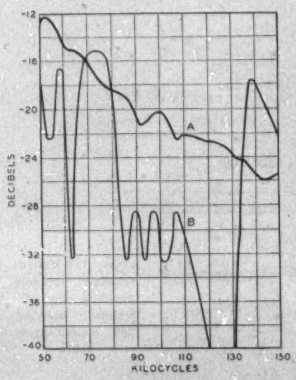

Figure 1. Typical power-line transmission characteristics

Application

Power-line carrier communication differs from other carrier signaling in using a channel designed for something quite different, carrying voltages of thousands of volts and currents of hundreds of amperes, which means that any impedances added to alter its characteristics will be of large physical size and corresponding cost. Also, the presence of other equipment must be tolerated. Figure 1 shows transmission curves at different frequencies for two lines. *A* is exceptionally good and *B* is exceptionally bad, as the result of several sections of different construction. A line such as *A* presents no problems, but line *B* has two wide channels and one narrow channel which might be used, and one of these is the second harmonic of another, which would be an undesirable allocation of frequencies. Equipment to be used on such lines must be continuously adjustable in frequency, which is the basis on which this system was developed.

Historical

There are two different methods of producing a single-side-band signal. The most used system consists of eliminating all components of the amplitude modulated signal, except the desired side band by using filter circuits. This system was

Paper 47-112, recommended by the AIEE joint subcommittee on power system applications of carrier current for presentation at the AIEE North Eastern District meeting, Worcester, Mass., April 23–25, 1947, and at the AIEE summer general meeting, Montreal, Quebec, Canada, June 9–13, 1947. Manuscript submitted November 20, 1945; made available for printing March 3, 1947.

B. E. LENEHAN is with the meter division of the Westinghouse Electric Corporation, Newark, N. J.

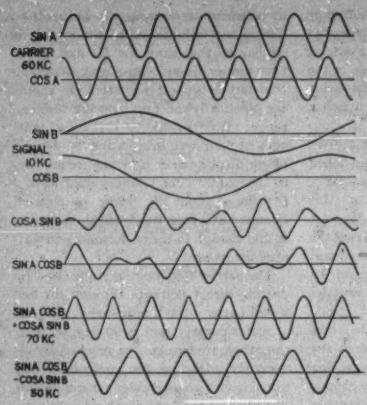

Figure 2. The frequency addition method

The first two lines represent carrier current; the next two, signal currents; the fifth and sixth, the two modulator outputs; and the seventh and eighth, the sum and difference frequencies

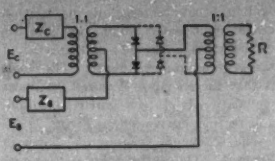

Figure 3. Schematic circuit of a copper-oxide ring modulator

described by John R. Carson, of the Bell System, about 1915.[3] Carson's patent shows tuned circuits instead of filters, probably because the filter circuit had not then been developed in the proper form. This type of system has been developed to a high degree and is used extensively by the telephone companies.[3,4] This type of system was not considered suitable for general power-line use because of the number of circuits to be retuned to change frequency and the difficulty of designing and building adjustable filters with the proper performance.

The other system consists of adding the carrier and signal frequencies together to produce the single-side-band frequencies. To do this requires polyphase sources of both frequencies, which is difficult to accomplish for a wide band of frequencies, such as the voice band. As any polyphase system can be changed to any other with transformers, a pair of voltages equal in magnitude and 90 degrees displaced in phase is required from every frequency component in the signal. A system of this type was invented in 1925 by R. V. L. Hartley in which this result was accomplished by using two multisection filters of different design.[5] Each filter section produces a phase change of 180 degrees as the frequency increases from the lower to upper edges of the band it passes. By making one filter with one more section and its pass band proportionally greater, the two outputs will be close to 90 degrees apart over a band of frequencies somewhat less than the band width of the narrower filter. The greater the ratio between the highest and lowest frequency, the more sections would be required. The patent estimates that "this probably would require filters having at least 20 sections" for the voice band. Such a complicated circuit would not be a practical solution. Later, an improved form of this circuit was used by Byrne as part of a polyphase broadcasting system.[6] By use of the later-developed phase correctors of the lattice type, the number of sections required was reduced greatly, but the system still required a large number of circuit elements. These methods have small magnitude errors, but large phase-angle errors. The method to be described in the paper uses a network of nine circuit elements to produce two currents very close to 90 degrees apart, with the main errors in the magnitude. Circuit theory indicates that only one of these conditions (90-degree phase or magnitude equality) can be met at a time over a range of frequency. Correct phase displacement was selected as the preferred condition, and a close approximation to equal amplitudes was secured.

The Modulating System

The amplitude of an a-c wave commonly is expressed as the sine of an angle proportional to time. Each low-frequency term must be added to or subtracted from the carrier-frequency term to produce the required single-side-band output. The trigonometric formula for the sine of the sum or difference of two angles is:

$$\sin(A \pm B) = \sin A \cos B \pm \cos A \sin B$$

As the cosine terms are 90 degrees out of phase from the sine terms, 2-phase currents of both carrier and signal frequencies are needed, and they must be multiplied together in pairs and added. This is shown graphically in Figure 2 and mathematically in Appendix I.

Two-phase currents of the signal and carrier frequencies are produced by phase-splitting circuits which produce 90-degree displaced outputs of closely equal magnitudes. These outputs are multiplied together by two copper-oxide modulators. Each of these consists of four rectifier disks connected in a ring, all facing the same way in series. This is shown in Figure 3. One current, the carrier, is larger than the other current, and its presence changes the resistance in the circuit of the other current. If the total signal circuit resistance is inversely proportional to the voltage output of the carrier phase-splitting circuit, the output current will be proportional to the desired product. This requires operating the modulator in a slightly different manner from previous practice, but the resulting signals are very free from undesired frequencies.[7,8] Each of the phase-shifting circuits is equivalent to a voltage with an impedance in series. This impedance is nearly all resistance, and the combination is shown in Figure 3.

Tracing through the signal current path, the circuit consists of the internal impedance of the phase shifter Z_s and the equivalent load resistance $R/4$ in series with a parallel circuit of the two halves of the carrier-frequency input transformer and the two rectifier disks shown in solid lines. These disks are in parallel for the signal and in series for the carrier input, but each circuit is independent and balanced against currents in the other, except for resistance changes in the rectifiers produced by the presence of the carrier current. When the carrier current changes polarity, the dotted disks come into service, and the connection to the output transformer is made to the other end, reversing the output polarity as it should. The resistance of the rectifier to the smaller signal current is, for the two parallel disks, one half the incremental resistance. For the larger carrier current, the resistance for the two disks in series is twice the usual resistance, $2e/i$. Operating conditions are chosen,

such that the total resistance in the signal circuit in inversely proportional to the carrier voltage E_c. The mathematics of this is given in Appendix II. The result is that the e-i curve required for linear modulation is closely similar to obtainable rectifier curves. (See Figure 7).

The schematic diagram is shown in Figure 4. The carrier phase splitter consists of a resistor, capacitor, and mutual inductor in series across the secondary of the input transformer. The voltage across the resistor appears in one branch of the output circuit, and the voltages across the capacitor and mutual inductor, connected to add, appear in the other. A change in frequency affects the voltages across the capacitor and mutual inductor in opposite directions, with the result that their sum varies only over a 25 per cent range for a 4-to-1 frequency range. The resistor branch has an inductor and capacitor added to the output side, and the inductor–capacitor branch has a resistor similarly added to make the internal impedances of the outputs equal at all frequencies. The voltages across the capacitor, inductor, and resistor at 80 kc, are in the ratio 1 to 1 to 2. Over the range of 50 to 150 kc, the currents in the two output branches will be balanced within 15 per cent and be 90 degrees apart. The actual outputs will be somewhat closer together, as some saturation will take place in the high voltage branch when the modulator is operating.

The signal phase splitter is similar in principle to the carrier phase splitter, but has an additional parallel resonant circuit added which increases the voltage in the resistor side by drawing out-of-phase current through the reactor and capacitor which are added to equalize the impedances. This voltage increases as the edges of the band are approached and improves the balance. The reactance introduced by the addition of this circuit is opposite in sign from the rest of the circuit and permits equalizing the output voltages at the edges of the band by varying the design proportions of the different elements. This circuit was designed for the operating range of 150 to 4,200 cycles and to provide at the same time the attenuation needed between the power level of the usual telephone line and the best operating level for the modulator. Figure 5 shows the performance obtained with the modulators replaced with 300-ohm resistors. At the low power levels used, the best measurement method available was the 3-voltage method which requires that the waves be sinusoidal to determine phase angles. The modultors are nonlinear resistors and so could not be used with this method. The performance is given in Figure 5 with ten volts applied to the phase-splitter input over a wide range of frequency. E_1 and E_2 are the two output voltages, and θ the angle between them. E_2 is repeated at 1/10 scale to permit the values at extreme frequencies to be plotted. The input admittance of the circuit is similar to the curve for E_2, and, when the proper input impedance-matching transformer is used, the outputs E_1 and E_2 are practically constant over the designed range. It is possible to have equal voltages at four frequencies and 90-degrees phase displacement at three frequencies in the band. The reactors used have a Q value of about 18. More complicated circuits have been tried, but do not seem to add enough to the performance to warrant their use.

The carrier frequency is suppressed by passing direct currents through the two signal paths. Each adjustment controls a carrier current that is 90 degrees from the other, so zero can be reached by alternately adjusting the controls similar to balancing an a-c bridge for magnitude and phase. Without these adjustments, the rectifiers normally will be balanced closely enough to reduce the carrier about 20 decibels below maximum signal. Adding these adjustments permitted −72 decibels to be obtained. The limitation was in the sensitivity of measurement. Balancing for the undesired side-band elimination is accomplished with the taps on the transformer secondary resistors. Figure 6 shows the modulation characteristic from line input to amplifier grid input. It is linear to the point where the output voltage is high enough to cause conduction to take place on one of the idle rectifier disks through the idle half of the output transformer winding. At this point, a limiting action takes place, and some distortion results. Distortion is low, even with overloading, but overloading produces some output in the undesired side band. The lowest harmonic appearing in the desired band is the fifth. Laboratory tests show less than four per cent distortion for the combined transmitter and receiver measured in the usual manner.

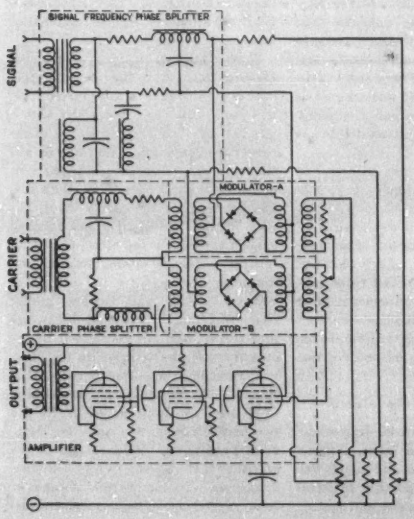

Figure 4 (left). Circuit arrangement of single - side - band transmitter

Figure 5 (below). Performance of signal-frequency phase splitter over an extended range of frequency

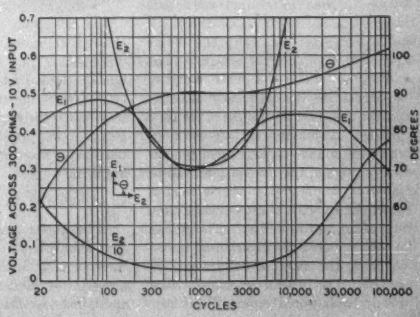

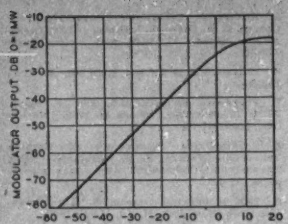

Figure 6. Modulator performance from signal input to amplifier input

This modulation arrangement is very versatile, as either or both side bands may be produced. The carrier can be added in phase with both side bands to produce amplitude modulation, or it may be added at 90-degrees phase to provide a form of phase modulation by superposing direct current on the signals in the same manner as the carrier is suppressed. Carrier with one side band also is obtained readily, which provides reduced channel width advantages with ability to be received on ordinary amplitude modulation equipment.

The oscillator in any single-side-band system is required to have better than ordinary frequency stability. The oscillator used has been described elsewhere.[9] It uses the transitron circuit and is temperature controlled to reduce drift with temperature changes. The circuit used is not sensitive to frequency changes resulting from tube characteristics of different tubes.

The receiving methods used are similar to those used for amplitude modulation. The carrier is added to the receiver output in a balanced demodulator stage, which also limits the signal output to prevent blasting during the time the automatic gain control is reducing gain. This arrangement is quite useful, if another transmitter is operated from the receiver, as overmodulation is prevented by the volume-compressing features of this arrangement.

This system normally would be used to transmit a voice band from 150 to 3,000 cycles for telephone or tone-telegraph operation. The performance of the modulator for frequencies above 3,000 cycles is still fairly good, the main result being a larger output of the undesired side band. As this undesired output is 6 to 12 kc removed from the desired band and 18 decibels lower in magnitude, a simple tuned circuit used in the transmitter can reduce the undesired output to a level where it would not be noticeable. The modulator thus can handle two channels if one first is converted to a single-side-band signal on 3-kc carrier upper side band, or 6-kc carrier lower side band; or the space above can be used for tone-telegraph control or telemetering signals.

Concerning the shift in frequency which takes place when sending and receiving oscillators are not at the same frequency, the question of its effect on the quality of transmission usually comes up. The ear perceives sound by a resonance indication, and the positions of the resonances along the frequency scale are shifted sideways a small amount. Music involves frequencies in definite ratios. Speech frequencies below about 800 cycles determine intelligibility. Since the frequency error is a greater percentage at low frequencies, one would expect the following conditions to be observed. Music sounds as if the instruments were out of tune when the difference is two to five cycles. Speech requires a 20-cycle difference before anything wrong is noticeable. If one were not making listening tests, or if one were not familiar with the speaker's voice, a difference of 50 cycles probably would be accepted without question. However, speech is still intelligible even at 200 cycles difference, but it sounds like a ventriloquist's efforts. Twenty cycles is considered a satisfactory limit, as music is not transmitted and most tone-signaling equipment requires channels wider than 40 cycles to transmit the telegraphic side bands. Twenty cycles is about one part in 5,000, which is within the possibilities of a well-designed oscillator.

Equipment operating on these principles has been designed and built. The standard 19-inch panel arrangement is used, permitting older type transmitters to be used as power amplifiers if conversion to single side band becomes necessary because of crowded frequency conditions. The general use of single-side-band transmission is almost equivalent to doubling the available frequency space, and additional advantages in noise reduction by greater equivalent power output also are realized.

Appendix I. Condition for Suppression of the Undesired Side Band

Let $S \sin At$ and $K_1S \sin (At+\theta)$ and $C \sin Bt$ and $K_2C \sin (Bt+\Phi)$ be the signal and carrier pairs of currents, θ and Φ being approximately 90 degrees.

The modulator output will be:

$$CS[\sin At \sin Bt + K_1K_2 \sin (At+\theta) \times \sin (Bt+\Phi)]$$

As $\sin X \sin Y = 1/2 \cos (X-Y) - 1/2 \cos (X+Y)$, the output can be written:

$$CS/2\{\cos (A-b)t - \cos (A+B)t + K_1K_2 \cos [(A-B)t+\Phi-\theta] - K_1K_2 \cos [(A+B)t+\Phi+\theta]\}$$

Combining the terms by vector addition gives the amplitude of the lower side-band term $(A-B)t$ as:

$$CS/2\sqrt{1+K_1^2K_2^2+2K_1K_2 \cos (\Phi-\theta)}.$$

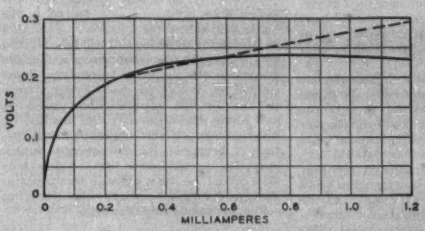

Figure 7. Comparison of required curve for linear modulation (solid) with possible rectifier curve (dashed)

Range up to 0.6 milliampere in practice

This is zero if $K_1K_2 = 1$ and $\Phi - \theta = 180$ degrees, or if $K_1K_2 = -1$ and $\theta = \Phi$.

Study of the vector relations shows that phase angle is of more importance than magnitude in securing good cancellation. The fact that the angles may be equal or supplementary to obtain cancellation permits residual phase errors to be minimized.

Appendix II. Conditions for Linear Modulation

Let

e_c = carrier voltage
r_c = internal resistance of carrier source
e_s = signal voltage
r_s = internal resistance of signal source
r_L = load resistance on transformer secondary
i_o = output current
e = voltage on rectifier disk
i = current in rectifier disk
K = a constant factor

$e_c = 2e + r_c i$.

$$e_s = i_s\left(r_s + \frac{r_L}{4} + \frac{de}{2di}\right)$$

For linear modulation

$$Ki_s = e_c e_s = (2e + r_c i)i_s\left(r_s + \frac{r_L}{4} + \frac{de}{2di}\right)$$

or

$$\frac{de}{di} = \frac{2K}{2e + r_c i} - 2\left(r_s + \frac{r_L}{4}\right)$$

The solution of this equation is

$$i = \frac{2e + r_c i}{r_c - 2r_s - \frac{r_L}{2}} - \frac{2K}{\left(r_c - 2r_s - \frac{r_L}{2}\right)^2} \log_e\left[1 + \frac{\left(r_c - 2r_s - \frac{r_L}{2}\right)(2e + r_c i)}{2K}\right]$$

This curve looks like an efficiency curve of a machine, and the portion below the maximum can be fitted quite well to a rectifier characteristic.

Figure 7 shows the curve for $r_s = r_c = 400$ ohms, $r_L = 300$ ohms, $K = 350$ in solid line, with the rectifier curve dotted.

References

1. A Comparison of the Amplitude-Modulation, Frequency-Modulation, and Single-Side-Band Systems for Power-Line Carrier Transmissions, R. C. Cheek. AIEE Transactions, volume 64, 1945, May section, pages 215–20.

2. United States Patent 1,499,382, John R. Carson.

3. Carrier Current Telephony and Telegraphy, E. H. Colpitts, O. B. Blackwell. AIEE Transactions, volume 40, 1921, pages 205–300.

4. A New Single-Channel Carrier Telephone System, H. J. Fisher, M. L. Almquist, R. H. Mills. AIEE Transactions, volume 57, 1938, January section, pages 25–33.

5. A Carrier Telephone System for Toll Cables, C. W. Green, E. I. Green. AIEE Transactions, volume 57, 1938, May section, pages 227–36.

6. United States Patent 1,666,206, R. V. L. Hartley.

7. Polyphase Broadcasting, John F. Byrne. AIEE Transactions, volume 58, 1939, July section, pages 347–50.

8. Copper-Oxide Modulators in Carrier Telephone Systems, R. S. Carruthers. AIEE Transactions, volume 58, 1939, June section, pages 253–9.

9. The Modulator Bridge, R. K. Hellman. *Electronics* (New York, N. Y.), March 1938.

10. Transitron Oscillator for High Stability, Werner Muller. *Electronic Industries* (New York, N. Y.), December 1945.

11. Single-Side-Band Generator, M. A. Honnell. *Electronics* (New York, N. Y.), November 1945.

12. A Simple Single-Side-Band Carrier System, R. C. Cheek. *Westinghouse Engineer* (Pittsburgh, Pa.), November 1945.

Discussion

R. W. Kenefake (General Electric Company, Syracuse, N. Y.): In the application of power-line carrier, it has been found very convenient to use equipment which is continuously adjustable in frequency. The system described by Lenehan, seems to have been developed from that viewpoint and, as it is described in his paper, it apparently enjoys that flexibility.

In describing a system for power-line communication, he has described the transmitter, but little information is given on the receiver. The characteristics of the receiver will largely determine the practical band width required per channel in the field.

In describing the transmitter, the suppressed single side band is reported to be 18 decibels down, above 3,000 cycles, and the logical question is, what degree of suppression is obtained below 3,000 cycles? The magnitude of the undesired side band is a potential barrier in attempting to double the number of carrier channels over a given frequency range.

The attenuation range of carrier equipment is as high as 50–80 decibels and, although the undesired side band may be down as much as 30 decibels, this side band would be strong when its transmitter is located near a receiver which is receiving a signal from a distant transmitter.

At the same time, the degree of suppression or selectivity of the receiver to interference on the undesired-side-band side, can prevent compressing the width of one channel. Single-side-band receivers are more susceptible than double-side-band receivers to interference on one side, because this interference is right in the audible range and not 4,000 to 6,000 cycles, as in double-side-band receivers, which is not reproduced very well by either a telephone handset or the human ear. Therefore, from the knowledge of the characteristics of his system, the author should be able to estimate what band width per channel will be required for the application of single side band to power lines.

Apparently, automatic volume control is obtained by automatic gain control in the audio portion of the receiver. This gain control in the receiving end will be activated by the strength of modulation as well as the power-line attenuation. Automatic volume control on double-side-band systems compensates for line attenuation changes only, and leaves speech levels to be handled by other means. If this single-side-band system is proposed for 2-frequency duplex operation it would seem that a hybrid balance would be very difficult to maintain. Perhaps the author can add some clarifying comments concerning that type.

B. E. Lenehan: The information given on the receiver was limited because it is very little different from previous receivers. A narrow channel receiver which is adjustable in frequency can be built on the superheterodyne principle, which will give the selectivity needed.

The undesired side band is present in all single-side-band systems to whatever degree the filters or other means may transmit it. This system gives 32 decibels or greater reduction before the transmitter tuned circuits are reached.

A carrier system having high attenuation, with a receiver and transmitter on adjacent channels, is often studied to determine application limits of particular equipment. However, nobody would ever so allocate frequencies if he could avoid it. A narrow channel system gives one more room to avoid such conditions.

It is true that a single-side-band receiver is more sensitive to interference on one side than on the other, and also true that a low-pass audio-frequency filter can make it very insensitive to interference on the other side. Changing sides is possible to clear up an interference condition on only one side. Also, interference on double-side-band systems is not limited to frequencies above 4,000 cycles, as the carrier transmitted will combine with the interference sidebands to demodulate the signal to audio frequency. This situation is almost exactly the same as on the "susceptible" side of the single-side-band receiver and is cured the same way by adequate receiver selectivity.

Automatic gain control can be applied anywhere to a single-side-band receiver, since each audio frequency is replaced by a single carrier frequency at the transmitter and a single intermediate frequency at the receiver. Actually, it is applied in the intermediate frequency stages and when gain limiting is needed to prevent singing or other difficulties, a low value of carrier can be transmitted to hold the gain from rising in the absence of received signal. This is accomplished by adjusting the carrier suppression circuits and would require a slightly wider band width. The 2-frequency duplex system does not seem to be a logical system to use when channel conditions are crowded, so hybrid coil balance conditions are not expected to be encountered too often; however, transmitting carrier in small amounts can limit the gain around the loop to values which will permit successful operation.

Proper allocation of channels should permit twice as many channels as a double-side-band system. I do not believe the limitations mentioned by Kenefake are any different from corresponding ones we now encounter on double-side-band systems.

Lightning Investigation on the 25-Kv System of the West Penn Power Company

WILLIAM C. BOWEN
MEMBER AIEE

EDWARD BECK
MEMBER AIEE

THE 25-kv system of the West Penn Power Company is practically an overhead network. It feeds 374 step-down substations supplying customers and distribution loads, and also serves directly a number of industrial customers. The system is located in regions where lightning storms are frequent and usually severe. Therefore, lightning is one of the principal hazards to continuity of service and protection of the substations is important. In order to obtain some knowledge of the demands made on the protective devices in the substations, the West Penn Power Company, with the co-operation of the Westinghouse Electric Corporation, in 1939 began an investigation of the discharge currents in the lightning arresters in certain of the 25-kv substations. The investigation ran continuously until the end of 1945. The substations studied were selected on the basis that they be within easy reach of the headquarters of the company and on past indications that lightning surges are likely to be frequent and severe at the locations, as shown by damaged substation apparatus or lightning arresters.

The purpose of the investigation has been to determine the frequency with which the arresters discharge and to obtain data on the character of the discharge currents. The recording instruments used were high- and slow-speed fulchronographs, surge crest ammeter links, magnetic surge front recorders, photographic surge current recorders, and paper disk indicators in which the discharge punctures a paper. These instruments have been described before the Institute.[1,2]

System Characteristics

The West Penn Power Company has five main generating stations with a total capacity of 560,000 kw. Power is fed into the 25-kv system at these generating stations and through a number of 132/25-kv step-down substations. In each of the source substations, the 25-kv windings of the transformers are Y connected with the neutral grounded through 18 ohms of resistance. The 25-kv substations under study receive their power from this system. In these stations the 25-kv windings of the transformers are delta connected. All of the substations under observation are dead-end stations of wood construction. They are equipped with transformers stepping down to distribution voltage, air break switches, fuses, and lightning arresters.

Typical 25-kv line construction is shown in Figures 1 and 2. Poles, crossarms, and crossarm braces are wood with 34.5-kv pin-type insulators on steel pins. Three standard 10-inch strain insulator disks are used when fastening to wood and four to steel. Guys are located so as to obtain the maximum flashover distance on wood consistent with mechanically strong design. Wood insulating members with flashover gaps are used in the guys so arranged that the over-all flashover value of the pole assembly is not reduced. Air break switches have wood insulating sections in their vertical operating pipes. The lines to each of the substations studied are highly exposed to lightning.

Substations Studied

Measuring equipment was installed in four 25-kv substations; Keystone Pipe Line, Ford Collieries Number 2, Ford Collieries Number 3, and Ligonier.

The Keystone Pipe Line substation is located at the end of a branch circuit 3.49 miles long. The contour is such that the line traverses rolling country with 60

Paper 47-114, recommended by the AIEE committees on protective devices and power transmission and distribution for presentation at the AIEE summer general meeting, Montreal, Quebec, Canada, June 9–13, 1947. Manuscript submitted November 8, 1946; made available for printing March 7, 1947.

WILLIAM C. BOWEN is assistant electrical engineer with the West Penn Power Company, Pittsburgh, Pa., and EDWARD BECK is manager of the lightning arrester section, protective devices engineering department, Westinghouse Electric Corporation, East Pittsburgh, Pa.

The authors wish to acknowledge the co-operation of those who assisted in the work of maintaining the equipment and collecting the data, and particularly the help of Doctor G. D. McCann who has been largely responsible for the instruments used and who co-operated in the co-ordination of the data.

Figure 1. Ford Collieries Number 2 substation and 25-kv line

Figure 2 (left). The 25-kv line adjacent to Ligonier substation

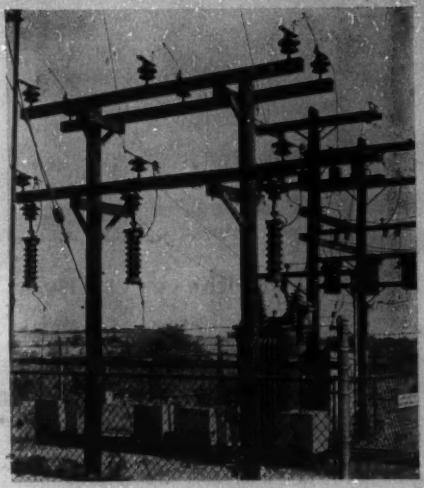

Figure 3 (right). Keystone Pipe Line substation showing fulchronographs, surge crest ammeter links, magnetic surge front recorder, and paper disk recorder

The photographic recorder is in back of the fulchronographs (left)

per cent of the line above the average elevation. This substation, Figure 3, is located on a hill at approximately the maximum elevation of the line. Until 1945 the principal load on this substation was a 600-horsepower 2,300-volt synchronous motor fed through a short underground cable from three 200-kva transformers in the substation. For some time, the motor operated without rotating machine protection, and during this period the motor winding failed. It was rewound and capacitors were installed on the machine bus. In the following year the motor failed again. It was rewound completely and lightning arresters were added at the capacitor bank to provide better machine protection. The motor has not been in service since December 1945, consequently, the capacity of the substation was reduced to one 3-phase 100-kva transformer shown in Figure 3.

The Ford Collieries Number 2 substation is located at the end of a branch circuit 1.2 miles long as shown in Figure 4. The line to this substation traverses a long valley and a long hill with the substation located approximately at the low point of the circuit. The substation and the line to it are shown in Figure 1. Ford Collieries Number 3 is located at the end of a branch circuit 2.3 miles long, Figure 4. The line to it traverses rolling country. Ford Collieries Number 2 has three 500-kva and Number 3 has three 667-kva transformers which supply 2,300-volt coal mine loads. Before the lightning investigations were started, there was a direct stroke of lightning to the 25-kv circuit at the fourth and fifth poles from the Ford Collieries Number 2 substation. Two out of three transformers approximately one year old were found with badly distorted and open-circuited coils. New transformers and modern arresters were installed and some time later a direct stroke occurred about one-half mile away resulting in an arrester failure at the substation. The transformers were detanked, examined, and found to be in good condition. A very high discharge current was indicated by a paper disk recorder connected in the common ground lead of the 3-phase arrester, the only measuring device installed at the time.

The Ligonier substation is located at the end of a 9.75-mile circuit, one of six circuits connected at the Latrobe 25-kv substation. Within six miles of Ligonier, the circuit rises approximately 1,000 feet and then drops 750 feet to the Ligonier substation. This substation has three 500-kva transformers supplying 4,800-volt distribution load. Before the lightning investigation was started and nine days after a bank of new transformers had been installed, one transformer failed during a storm No signs of a direct stroke could be found. Modern 20-kv line-type arresters were installed in 1943 and no troubles have been experienced since.

Recording Equipment

The installations of recording equipment in the several substations were generally the same. One is shown in Figure 3. A high speed fulchronograph and surge crest ammeter links were connected in the ground lead of each arrester pole of a 3-phase bank. A slow speed fulchronograph, surge crest ammeter links, surge front recorder, and paper disk recorder were connected in the common ground lead of each 3-phase arrester bank. The photographic recorders were in each arrester pole at two of the stations and in the common ground lead of the three poles in the third station. Three substations were equipped with all of these instruments. Data on the fourth station equipped only with the paper disk recorder also are used in this paper to amplify the information on the frequency of arrester discharges.

The substations and dates on which the observations were begun are listed in Table I.

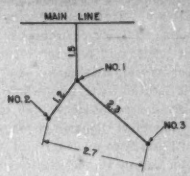

Table I

Name of Station	Year Begun	Arrester Years: Three Phase	Arrester Years: Single Phase
Keystone Pipe Line*	1939	7	21
Ford Collieries No. 2*	1940	6	18
Ligonier*	1941	5	15
Total arrester years studied		18	54
Ford Collieries No. 3†	1940	6	

* Photographic recorders were installed at these stations in 1943.

† Ford Collieries Number 3 had paper disk recorder only connected in the common ground lead of the 3-phase arrester bank.

The total number of 3-phase arrester years on which data were obtained with the paper disk recorder is 24. Data with the additional measuring apparatus were obtained on 18 3-phase or 54 single-phase arrester years. The data presented in this paper are in the form of statistical curves. Figure 5 is a plot of a typical fulchronograph record.

Frequency of Arrester Discharges

In Figure 6 are plotted the statistical data on arrester discharges as obtained in the stations studied. A considerably greater number of discharges were recorded by means of the paper disk indicator than by the fulchronograph indicating that there are numerous discharges of magnitude or duration, or both, below the sensitivity of the fulchronograph. Over the period of study, the average number of discharges in three phase arrester banks, recorded by the paper indicators, was between 5.6 and 6 from which it may be concluded that over a period of years the arrester banks in the four stations will discharge about the same number of times. In any one year, however, the number of discharges may vary from one to ten.

The fulchronograph data indicate fewer discharges and a greater variation in the average discharges per year, from 1.2 to 2.4, a ratio of 1 to 2. In any one year some arrester poles might not discharge any currents of magnitudes detectable by the fulchronograph as shown by curve 5 of Figure 6. Based on the fulchronograph data alone, the Keystone Pipe Line substation arresters discharged more often than the others. The average number of discharges per year through the Keystone Pipe Line arresters as measured by the fulchronograph was almost twice that at either Ford Collieries Number 2 or Ligonier.

During the investigation, 34 composite fulchronograph records were obtained. In 3 of these only one pole of the arrester discharged, in 6 cases two poles discharged, and in 25 all three poles discharged. In the case of the single pole discharges, the currents were low—200, 250, and 350 amperes.

An analysis of the discharges detected by the paper recorders in Ford Collieries Number 2 and Number 3 and of the dates on which they occurred indicates that of the total of 43 discharges recorded at the two stations, 25 occurred simultaneously as nearly as can be determined at both stations; 10 at Ford Collieries Number 2 only; and 8 at Ford Collieries Number 3 only. The simultaneous records obtained indicated in nearly all cases a relatively high current at one substation and a relatively low current at the other which

Figure 6 (below). Frequency of arrester discharges on several different bases

A—All discharges* as recorded in ground lead of 3-pole arrester bank (24 3-pole arrester years, 154 discharges)

Curve 1—Number of discharges in any one year

Curve 2—Average number of discharges per year for total period studied

B—Fulchronograph records† only, obtained in common ground lead of 3-pole arrester bank (18 3-pole arrester years, 34 records)

Curve 3—Number of records obtained in any one year

Curve 4—Average number of records per year for total period studied

C—Fulchronograph records† in individual arrester poles (54 arrester pole years, 90 records)

Curve 5—Number of records in any one year

Curve 6—Average number of records per year for total period studied

* All discharges include records obtained with the paper disk recorders, with fulchronographs and surge crest ammeters, and photographic current recorders. Where records were obtained on several instruments simultaneously, this is called a single discharge. Curves 1 and 2 cover four stations

† Records obtained with fulchronographs and surge crest ammeters only at three stations, Keystone Pipe Line, Ford Collieries Number 2, and Ligonier

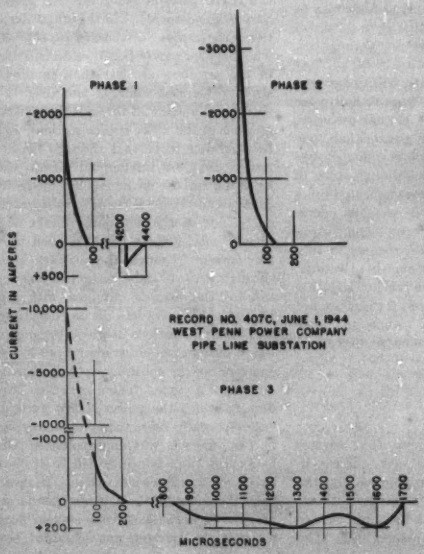

Figure 5 (left). Typical fulchronogram of lightning arrester discharge currents

Figure 7 (below). Statistical distribution of crest magnitudes of currents as recorded by fulchronograph and surge crest ammeter in individual arrester poles

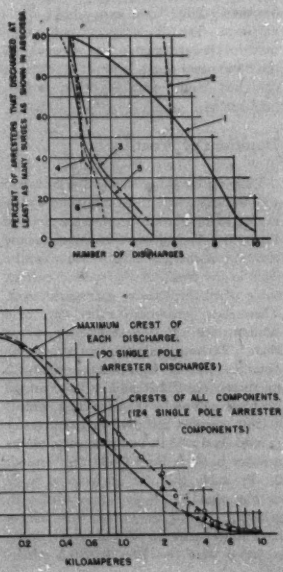

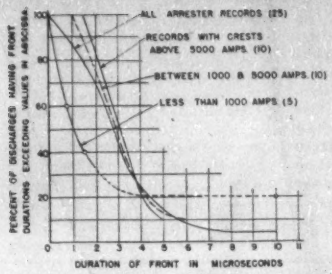

Figure 8. Distribution of the durations of the fronts of arrester discharge currents as measured by magnetic surge front recorder in common ground lead of a 3-pole arrester

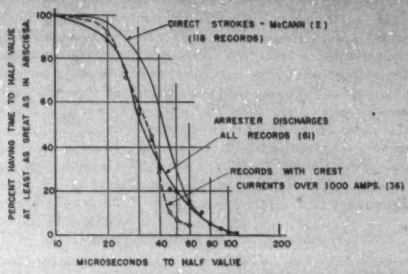

Figure 9. Times to half value of components of single pole arrester discharges as measured by fulchronograph

would be expected if the discharges were caused by the same disturbance.

The statistical distribution of the magnitudes of crest currents measured by the fulchronograph in each arrester pole is shown in Figure 7. The curve for maximum crests shows only the highest current in each complete or composite record, whether it has one or several components. The curve for all individual components is lower. The maximum currents measured in any arrester pole were two records of 10,000 amperes each. Fifty per cent of the components had crests above 550 amperes, and 2.5 per cent above 5,000 amperes. The discharge currents measured in the arresters under observation are lower than those in direct strokes[2] as also has been found in other investigations.

Durations of Fronts

Data on the durations of the fronts of the discharge currents as measured by the magnetic surge front recorder are given in Figure 8. The data indicate that the low current discharges have short fronts. This is the result of the sudden current surge when the arrester gap sparks over. These data corroborate other data of a similar nature.[3] For discharges of less than 1,000 amperes crest, one record was obtained with a front longer than 1.5 microseconds. This had a front of 10 microseconds and a negative crest current of 200 amperes recorded in the arrester ground lead and in one pole only of the arrester bank at Ford Collieries Number 2. Probably this was an induced surge or one that had been attenuated. In general, the higher current discharges have longer fronts. The shortest fronts recorded were two less than 0.5 microsecond with crests of 300 and 350 amperes. The steepest front measured was 1.5 microseconds for a current of 11,000 amperes recorded in the common ground lead, indicating an average rate of rise of current of some 7,340 amperes per microsecond. The highest crest current recorded in any of the poles of the arrester during this discharge was 7,900 amperes, indicating an average rate of rise in the individual arrester of 5,000 to 5,500 amperes per microsecond.

Times to Half Value

Figure 9 shows the data on the times to half value for each component discharge current recorded by the fulchronograph. One curve has been plotted for all records and one for those records with crests above 1,000 amperes only as these may be more significant. Similar data for direct strokes also are shown for comparison. The times to half value are less than those in direct stroke currents. Fifty per cent of the discharges had times to half value in excess of about 35 microseconds. None of the discharges greater than 1000 amperes had times to half value greater than 60 microseconds although some of the low current discharges indicated times to half value somewhat over 100 microseconds. It appears from a comparison with data obtained on arresters in substations on another system[4] that the times to half value recorded in this investigation are greater. The reasons for this are not known. They might reside in some differences in system construction or in locality.

Total Duration

The measured durations of the arrester discharge components are shown in Figure 10. The fulchronograph and the photographic recorder measurements are plotted separately, and the direct stroke data are shown for comparison. The photographic recorder data indicate longer durations than the fulchronograph because the photographic recorder is more sensitive. It will indicate low surge currents and also power follow current if present. The longest duration indicated by the fulchronograph was 2,000 microseconds and the longest by the photographic recorder was 22,900 microseconds, the equivalent of between two and three half cycles of 60-cycle current. Fifty per cent of the photographic recorder records had durations less than 3,000 microseconds, less than a quarter cycle of 60-cycle current. For the shorter durations, the arrester discharge and direct stroke data coincide. At the longer durations, the arrester discharges are shorter. This may be partly because the currents in the arresters are less than in direct strokes, because some of the long tail current is drained off through the neutral grounds at the 25-kv source stations, and because flow of current through the arresters may be interrupted before the lightning current in the line has died out. This is quite likely if the wave shape and magnitude of the lightning voltage and the 60-cycle voltage combine such that the current through the arrester goes through zero at some instant.[5] Inspection of the records obtained with the photographic recorders disclosed a large number of operations in which the power follow current was either absent or of very short duration, considerably less than a quarter of a cycle. There were four records on which the power follow current was apparently more than one half cycle: two in which it was approximately two half cycles, and two in which it was between two and three half cycles. In these cases the nature of the lightning discharge may have been such that current flow through the arrester was sustained be-

yond a half cycle or it may be due to restriking in the arresters.

Protection by Lightning Arresters

From the discharge currents recorded in the arresters, the magnitude of the voltage that would have appeared in the substation if no protection were present can be calculated. For the substations studied, a discharge current of 250 amperes through an arrester pole indicates a disturbance whose voltage, if uncontrolled, would have been 150 kv, the basic insulation level for 23-kv-class insulation. Any discharge current in excess of 250 amperes would indicate voltages that might be hazardous to the apparatus. It can be seen from Figure 7 that a considerable percentage of the discharges were greater than 250 amperes. An analysis of the 34 composite records obtained with the fulchronograph showed that in all but two cases there was a discharge in one or more arrester poles higher than 250 amperes. Thus, 32 of the indicated operations of an arrester in a substation were caused by disturbances that might have caused trouble. This involves 18 3-phase arrester or substation years or an average of 1.8 cases of trouble a year per substation. Some of these no doubt would have involved more than one phase, as indicated by the data of Figure 7.

Service Experience With Lightning Arresters

Previous to 1932 the West Penn Power Company had many 25-kv transformer failures every year, most of them occurring during lightning storms. Many failures were examined thoroughly and a study made of the age and insulation level not only of the transformers that failed but of others as well. At the same time a campaign was started of interconnecting all grounds and checking their resistances regularly. The characteristics of the various types of arresters used on the system also were given much consideration in the over-all study. As a result, it was decided to install 20-kv arresters on all the types of transformers that were failing and on all manufactured previous to 1920.

It was recognized that failures would occur on the 20-kv arresters because of the overvoltage that would be impressed on them when a ground occurred on the 25-kv system, but it was believed that it was better to lose an arrester occasionally than a transformer. Because of the possibility of having a 20-kv arrester fail during a storm, thus leaving a transformer without adequate protection, it was decided to install gaps on all transformer bushings.

When new line-type arresters with larger discharge capacity and improved characteristics became available in 1937 and 1938, these were applied on new installations and where better protection was needed. A study soon showed that the latest type 25-kv arresters would provide equivalent protection to the earlier 20-kv arresters and in some cases better protection so it was decided to use 25-kv arresters generally and 20-kv arresters only in very special cases on very old transformers.

A study was started to develop the failure rate on both the old and new 25-kv and 20-kv arresters and figures were set up on the basis of the number of arresters per 100 arrester years that were damaged by being demolished or otherwise becoming unfit for service. The first comparison made covering four years service of new and old arresters showed the rates given in Table II.

The present policy provides for general use of new 25-kv arresters and 20-kv arresters in special cases only. A check as of January 1, 1946, gives the following failure rate on the 100 arrester year basis

Table II

	Failures Per 100 Arrester Years	Number of Arrester Years
25-kv arresters		
Old types	6.25	2,533
New types	0.095	871
Old and new types	4.83	3,406
20-kv arresters		
Old types	8.44	963
New types	1.44	994
Old and new types	4.86	1,957
Total	4.83	5,363

for all new style arresters on the system covering a 6 to 7 year period.

25 kv—for 1,760 arrester years, 0.56 failure per 100 arrester years.

20 kv—for 1,602 arrester years, 1.6 failure per 100 arrester years.

From the standpoint of initial and replacement costs of arresters, the last figures for new arresters only indicate why 25-kv arresters should be used generally on the 25-kv system. At 132-kv stepdown stations the voltage may be as high as 26 kv which is a 30 per cent overvoltage on a 20-kv arrester. However, the 20-kv failure rate is not excessive when the advantages are considered of obtaining a lower level of protection where needed.

Since the adoption of the plan for using reduced voltage arresters where needed and the regular checking and reduction of substation ground resistances (75 per cent of all stations now have 7.5 ohms or less and practically all others have 10 ohms or less), transformers and other equipment failures have been reduced greatly. Old style arresters are being replaced as rapidly as can be justified economically.

Because of the extent of the system, the cost of replacing an arrester may be an appreciable part of the cost of the arrester itself, and with over 300 unattended substations it readily can be seen how important it is to make the proper application of modern arresters.

Conclusions

The maximum crest currents recorded in an arrester pole were two discharges of 10,000 amperes each. The highest average rate of rise of discharge current recorded in an arrester pole was 5,500 amperes per microsecond. Times to half value averaged 32 microseconds with a

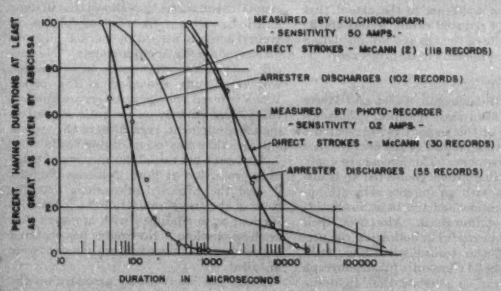

Figure 10. Total durations of individual components of arrester discharge records as measured by the fulchronograph and by the photographic recorder

maximum of 110 microseconds. The longest total duration was 22,900 microseconds. Fifty per cent of the discharges had durations less than 3,000 microseconds. Many operations were accompanied with power follow current of very short duration. However, in four cases the duration of the power follow exceeded one half cycle.

The same disturbance or storm will affect stations reasonably close to each other.

The composite fulchronograph records of 3-pole arrester discharges indicated that in 93 per cent of the cases voltages in excess of the 23-kv-class basic insulation level would have appeared in the substation if no lightning protection had been provided.

Service experience with modern lightning arresters indicates the importance of proper application. Arresters with ratings lower than the system voltages to which they might be exposed had higher failure rates. However, economics justify the use of reduced voltage rating arresters in special cases to provide maximum protection to old equipment, thereby reducing the risk of interrupting the service to important loads at the risk of an occasional arrester failure.

References

1. New Instruments for Recording Lightning Currents, C. F. Wagner, G. D. McCann. AIEE Transactions, volume 59, 1940, pages 1061–8.

2. The Measurement of Lightning Currents in Direct Strokes, G. D. McCann. AIEE Transactions, volume 63, 1944, pages 1157–64.

3. Field Investigation of the Characteristics of Lightning Current Discharged by Arresters, I. W. Gross, G. D. McCann, Edward Beck. AIEE Transactions, volume 61, 1942, May section, pages 266–71.

4. Field Investigation of Lightning Surges at Substations, I. W. Gross, G. D. McCann. AIEE Transactions, volume 66, 1947, pages 569–74

5. Discussion of reference 2, E. Beck. AIEE Transactions, volume 63, 1944, page 1370.

Discussion

Glen Appleman (Pennsylvania Power and Light Company, Allentown, Pa.): This paper is so well presented as to leave very few questions unanswered that might arise in connection with the stated purpose of the study as covered by the introduction.

It would be helpful to know whether the Ford Collieries Number 2 substation, at which two transformers approximately one year old failed, and the Ligonier substation at which one new transformer failed, had any kind of lightning protection at the time of these failures. It is clear that they were equipped with modern arresters soon after the failures.

One of the valuable contributions from this paper is in the paragraph which shows that 32 out of 34 recorded disturbances would have produced voltages high enough to be hazardous to the apparatus, if the arresters had not been in service. This feature probably has not been stressed as strongly as it should have been by protection engineers.

In the third paragraph under the heading of "Service Experience With Lightning Arresters" the statement is made "... so it was decided to use 25-kv arresters generally and 20-kv arresters only in very special cases on very old transformers." Under this same heading Table II shows 871 arrester years for *new* 25-kv arresters and 994 arrester years for *new* 20-kv arresters which would seem to indicate that there are more "very special cases on very old transformers" than general cases. The fifth paragraph also seems to indicate a great many special cases for the 6-to-7-year period, reported as of January 1, 1946, with 1,760 arrester years for 25 kv and 1,602 arrester years for 20 kv, "all new style arresters."

It seems that most operating companies would find much the same situation and it would be equally difficult to standardize on one arrester only, and at the same time obtain best protection to equipment, unless all are the lower voltage rated arresters. It seems quite possible that the improvements to grounding as discussed in the paper may reduce substantially the failure rate, especially on the lower voltage rated arresters and future performance show up more favorably for them.

It is assumed that these arresters are Westinghouse *LV* or *LVS* arresters; the impulse breakdown voltage based on a $1^1/_2$ x 40-microsecond wave is 68 kv for the 20-kv arrester and 84 kv for the 25-kv arrester and based on the AIEE standard 75 and 93 kv, respectively, which shows quite an advantage for the 20-kv arrester to protect the lower impulse level insulations. The 60-cycle rms breakdown values are 45 and 55 kv, respectively, which if corrected for the 25 per cent plus or minus tolerance still leaves values of 33.75 kv and 41.25 kv, respectively, for the 20-kv and 25-kv arresters. Even with 26 kv at step down feed in stations there would seem to be ample margin for using the 20-kv arrester at any station on the 25-kv system, even with a complete shift of ground potential from neutral to one of the phases.

H. W. Hartzell (The Commonwealth and Southern Corporation, Jackson, Mich.): The authors have presented an excellent technical paper which I believe should merit thoughtful consideration by every engineer who is interested in lightning protection of electric systems.

In connection with that part of the paper devoted to service experience with lightning arresters, it would be interesting to know what the experience indicated regarding the influence of X_0/X_1 and R_0/X_1 ratios on arrester failures. Also, are any limiting ratios of these sequence impedances observed by the application engineer when reduced-rated arresters are considered for application at a station to the extent that an arrester of reduced rating would not be applied in spite of the age and low insulation level of the equipment to be protected?

R. B. Reed (Shawinigan Water and Power Company, Montreal, Quebec, Canada): The authors of this paper have presented a very comforting picture of the effectiveness of modern arresters. This appears to apply particularly in stations connected to transmission lines with an impulse strength appreciably greater than the basic insulation level of the station itself. Moreover, their records may be useful in indicating the performance of the transmission line itself. The data from 34 composite fulchronograph records appear to indicate that lightning surge currents in excess of 350 amperes result in phase to phase flashes with their particular line construction. It may be of value in estimating line performance on similar systems if the authors would give some indication of

1. Whether the phase to phase flashovers occurred over insulators or in mid-span.

2. What percentage of the multiphase arrester discharges were accompanied by line outages.

3. The impulse flashover strength between phases on the line.

4. The impulse flashover strength to ground on the line.

William C. Bowen and **Edward Beck:** In reply to Reed's discussion, the critical impulse flashover from line to ground over the guyed poles is approximately 1,200 kv and between phase wires is approximately 700 kv. Regarding the probability of phase to phase flashovers and their correlation with the arrester discharges, considerable study was given this matter, but sufficient data were not available to warrant the drawing of definite conclusions. It appears that currents considerably in excess of 350 amperes would be required to produce sufficient voltage to cause phase to phase flashovers.

Referring to Hartzell's discussion, in view of the fact that the neutrals on the system are grounded through 18 ohms of resistance, it was recognized that during ground faults complete displacement of the neutrals is to be expected. In fact some general calculations have shown that in some locations voltages from sound phases to ground actually exceed the normal phase to phase voltage by small amounts. No specific calculations were made in connection with the study discussed in the paper. When reduced voltage arresters are applied, this is done entirely on the basis of protecting old equipment, regardless of the system voltages that may occur during faults.

Appleman has raised the question of lightning protection at Ford Collieries Number 2, and the Ligonier substations. At the time of the transformer failures, both substations were equipped with arresters that are now obsolete. No trouble has occurred in these stations since modern arresters were installed.

There are many 20-kv arresters on the

Table I. Arrester Performance Data

Arrester Rating, Kv	Arrester Years	Failures Per 100 Arrester Years
25	2,500	0.44
20	1,790	1.73

system as a result of the earlier policy. At the present time, no new 20-kv arresters are being purchased. The special cases now are taken care of by the relocation of such 20-kv arresters already on the system that are replaced by new 25-kv arresters. As a result, the ratio of 25-kv to 20-kv arresters is increasing. To bring the arrester performance data up-to-date, the figures of January 1, 1947 are shown in Table I of this discussion.

Comparison of these figures with those given in the paper for January 1, 1946, shows the trend.

In those substations where records of discharges were made, the arresters are Westinghouse. The tabulated data on service experience with arresters include not only Westinghouse but also those of other manufacture.

Appleman points out that the 60-cycle spa·k-over voltage of the 20-kv arresters is considerably in excess of the maximum system voltage that would appear across the arrester even with a complete shift of the neutral. Although this is a fact the 60-cycle spark-over is not a criterion of an arrester's ability to withstand system voltage, if it is discharged by a surge. This is determined by its rating which defines the maximum voltage of power frequency, applied across its line and ground terminals, against which the arrester can clear the power follow current and restore itself to an insulator following a discharge by lightning. In the case of the 20-kv arrester, this is 20 kv. The spark-over voltage is higher than the voltage which the arrester can interrupt successfully.

Lightning and 60-Cycle Power Tests on Wood-Pole Line Insulation

P. L. BELLASCHI
FELLOW AIEE

BECAUSE of the good impulse characteristics wood possesses, it now is utilized extensively and with specific intent as an economic means for providing the necessary impulse insulation strength required of present-day power transmission and distribution lines. Material progress has been made in this field in the course of the past ten years, as evidenced from technical contributions and the practical results achieved.[1–20]

Much has been accomplished in recent years, but certain fundamental data in regard to wood as an insulating material still are lacking or are not generally well known. It appears that further rationalization and progress in this important field require a more comprehensive knowledge of wood, not only from an impulse standpoint, but also in regard to its power-quenching ability and its properties with respect to leakage effects as well as to other significant characteristics that wood possesses. The need for more complete data on the performance of wood, in regard to both impulse and power-frequency operation, has been recognized for some time, and, in view of this, the results reported here should be timely and helpful. Because of the economic importance of wood, this contribution should serve to direct attention again to the possibilities of wood and to crystallize thought on the problems that merit further attention.

Impulse Strength of Wood-Pole Line Insulation

The first impulse tests on wood poles at the Sharon high-voltage laboratory were made in 1933 and are reported in Figure 1. Since that time similar investigations have been conducted on wood poles, wood crossarms, wood guy insulators, as well as on porcelain insulators in combination with wood. A 3-million-volt surge generator of high capacitance, 0.008 microfarad or better, was used throughout the tests. Unless otherwise indicated, the impulse voltage applied conformed to the standard $1^1/_2 \times 40$-microsecond wave. A summary of typical and significant tests appears in Table II. Figure 2 presents representative volt–time curves for a few of the wood-pole insulation structures studied.

Typical wood-pole line insulation tested is shown in Figures 10 and 11. Details of the wood structure, moisture content of wood, treatment, as well as other factors that may influence the impulse strength are summarized in Tables I and II. Pole 4, a 60-foot transmission line pole, was installed in the yard in 1931 and pole 5, a few years later. These and all the other poles, as well as the wood crossarms, were secured from a local utility, and are quite representative of line equipment actually used in service. In fact, some of the poles tested had seen service, but most of them were new. At the time of test, practically all of the poles were at least one or two years old and in some instances considerably more. Prior to the tests, poles 1 and 3 were outdoors lying on the ground throughout the winter and early spring and, no doubt, had a high moisture content. On the other hand, pole 2 was stored indoors in a warm, dry place and consequently was very dry at the time of test. The condition of the crossarms ranged from normal moisture content to a dry state. All the tests were conducted outdoors with the exception of the lightning-stroke tests.

Analysis of the foregoing data indicates that the impulse strength of wood is influenced primarily by three factors. They are

1. Length of the wood structure.
2. Duration of the impulse.
3. Moisture content in the wood.

Other factors are of secondary or little importance, and, in fact, these are not readily perceptible because of the inherently large variations in the strength of wood which may have a spread of ±15 per cent for any one group of tests (see Figure 1).

The data in Table II for the wood poles are plotted in Figure 3. The curves clearly show the relationship between length of wood structure and impulse strength. For instance, a cedar pole of normal moisture content has a strength of 100 kv per foot for a length of 12 feet and only 50 kv per foot for a 40-foot length. That is, the full wave strength of a 40-foot pole is 2,000 kv, whereas only 12 feet of the same pole will withstand 1,200 kv.

The second factor is apparent from a

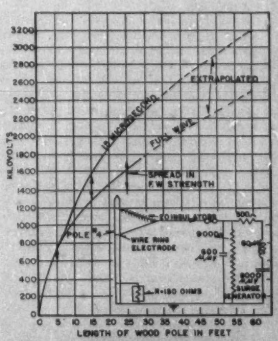

Figure 1. Impulse strength of transmission-line wood pole for various lengths of pole

Paper 47-115, recommended by the AIEE committee on power transmission and distribution for presentation at the AIEE summer general meeting, Montreal, Quebec, Canada, June 9–13, 1947. Manuscript submitted November 12, 1946; made available for printing April 2, 1947.

P. L. BELLASCHI is development engineer with the Westinghouse Electric Corporation, Sharon, Pa.

The author acknowledges the assistance of L. B. Rademacher also of the Westinghouse Corporation.

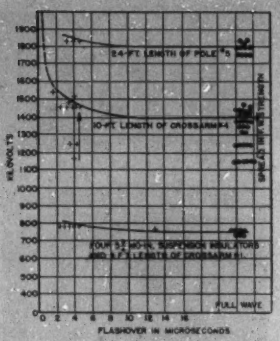

Figure 2. Volt–time characteristic of typical wood-pole line insulation structures

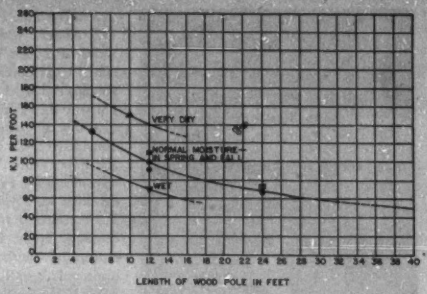

Figure 3. Impulse strength of wood poles as affected by moisture in wood

consideration of Figure 2 and the steep-front data in Table II. As shown in Figure 2, the volt–time characteristic of wood is practically flat from 40 to 2 microseconds. The data in Table II referred to Figure 2 indicate that for shorter impulses these characteristic curves rise very abruptly. At one half microsecond duration, which for the voltages considered here corresponds to a very steep-front impulse, the strength of wood for a 10-foot length of pole is 230 kv per foot, that is, more than twice the strength at 40 microseconds.

The third significant factor, which is the moisture content in the wood, is clearly brought out in Figure 3. Very dry wood may have an impulse strength 40 per cent higher than that of wood of normal moisture content (12 to 15 per cent). In fact, bone-dry wood may attain a strength comparable to the strength of air. However, when wood such as cedar or fir has been subjected to a wet season or to sustained rainy weather, it readily can suffer a reduction in strength of fully 30 per cent and possibly even more. When wood is dry, even a short sprinkle of rain will tend to lower the impulse strength or to introduce erratic behavior. This effect is indicated in the test data on a 10-foot crossarm reported in Figure 2 which were recorded on a dry crossarm during weather which was clear except for an occasional sprinkle. The low values apparently were the result of this condition. In general, more consistent results are obtained when wood is normally dry and in a state of moisture equilibrium with the atmosphere.

The following are some of the factors which appear to be of secondary importance. Age in itself does not seem to be a factor of importance in determining the impulse strength of wood. For instance, the 12-foot length of pole 4 which was tested in 1933 was retested in 1944 with practically identical results (Table II). From the data, we find that in general fir crossarms have a higher unit strength than cedar poles, but this is probably a result of the better over-all homogeneity of crossarms rather than the kind of wood. In connection with wet poles either alone or in combination with porcelain insulators, partial or incomplete breakdown could be observed in some of the tests. Most of the tests were made with positive polarity impulses, as the same or higher strength was expected from impulses of negative polarity. However, some of the check tests with negative impulses indicated perceptibly lower strength.

In comparing results it will be found that in general there is good agreement between the findings of this investigation and those given in references 11 and 13. This is particularly the case with reference to the impulse strength of insulators in combination with wood crossarms and also in regard to the effect of moisture on impulse flashover. For instance, the impulse strength of four suspension insulators and a 4-foot crossarm in Table II is 740 kv as compared with 770 kv from reference 11 for a similar insulation. From these and other investigations, ft often had been assumed, from tests usually limited to wood members not more than 8 or 10 feet, that the unit strength corresponding to these lengths would continue unchanged for greater lengths. This investigation actually shows that increasing the length of the wood member from 10 to 30 feet will result in a reduction of the unit strength from 110 kv per foot to nearly one half as much. On this point

Table I. Wood Poles, Wood Crossarms, and Other Line Insulation Structures Tested

Structure	Wood	Treatment	Moisture Content	Reference	Comments
Pole 1	Western red cedar	Butt creosoted	High content	Figure 10	Common distribution-line wood poles
Pole 2	Western red cedar	Butt creosoted	Very dry	Figure 10	
Pole 3	Western red cedar	Butt creosoted	High content	Figure 10	
Pole 4	Western red cedar	Butt creosoted	Normal exposure	Figures 10 and 11	Transmission-line 60-ft pole, 18-in. diam butt
Pole 5	Western red cedar	Butt creosoted	Normal exposure	Not shown	Distribution-line 45-ft pole, 14-in. diam butt
Crossarm 1	Douglas fir	Untreated	Normal exposure	Figures 10 and 11	Common distribution-line wood crossarms
Crossarm 2	Douglas fir	Untreated	Normal exposure	Figures 10 and 11	
Crossarm 3	Douglas fir	Untreated	Fairly dry	Figure 10	
Crossarm 4	Douglas fir	Untreated	Dry	Not shown	10-ft crossarm 3¼×4-in section
Crossarm and suspension insulators				Figures 10, 11 and 12	
Pole and apparatus insulators				Figures 13 and 14	
Wood-guy strain insulators	Apitong	Creosoted	Dry	Figure 7	8-ft wood guy with 42-in air gap
Approximately 100 poles	Cedar, pine, chestnut	With and without	Various	Figures 4 and 5	Poles used in lightning-stroke tests

(A) (B) (C)

Figure 4. Lightning-stroke flashover of wood poles in laboratory

and with respect to the rapid upturn of the impulse characteristic of wood below two microseconds, there is good agreement between reference 12 and the findings presented here.

Damaging Effects of Lightning and Protective Measures

Since the development of the lightning-stroke generator in 1935, nearly a hundred distribution wood poles have been tested. Most of these poles were western red cedar, and the remainder chestnut and pine. In this test, flashover of the pole is initiated by a very steep-front impulse rising at the rate of 3,000 to 4,000 kv per microsecond, followed in a matter of microseconds by a current discharge of lightning-stroke intensity and duration.[31] The current discharge attained amplitudes of 25,000 to 50,000 amperes and had a total duration of fully 100 microseconds. The character of these tests is illustrated in Figure 4.

About 20 per cent of the poles were damaged to the extent shown in Figure 5*B*, 15 per cent showed no damage of consequence (see Figure 5*A*), and the remainder were splintered to an amount not considered too serious. These percentages apply for a single discharge. Naturally, multiple discharges on the same pole usually accentuated the damage. Figure 6 shows typical damage to poles in service from actual lightning; this can be compared to damage produced in the laboratory. In addition to testing poles, a few crossarms in combination with poles also were tested. The damage to the crossarms was rather light; however the number of tests is not sufficient to draw a definite conclusion.

In the field, the probability that lightning currents discharging over poles may exceed 25,000 amperes is less than 50 per cent. Therefore, considering a rate of 50 strokes per annum per 100 miles of line, which is a reasonable figure for Pennsylvania and adjacent Central States for 33-kv and 66-kv lines completely unprotected, the laboratory tests indicate that less than a dozen poles in 100 miles of lines are likely to suffer damage to the extent shown in Figure 5*B*. Though the conditions for the laboratory tests differ somewhat from those in the field and field data on damage caused by lightning are limited, the foregoing estimate is surprisingly well borne out by actual cases of field experience (see reference 9).

The laboratory lightning tests further indicate that wood poles of high moisture content shatter with greater ease than dry poles. Apparently this has been the experience in the field too. It also was observed during the tests that the probability of the wood catching fire is remote, unless the wood is very dry and the stroke severe. The presence of a long-duration current component in the discharge, also referred to as "hot lightning," may well accentuate the probability of the wood catching fire.

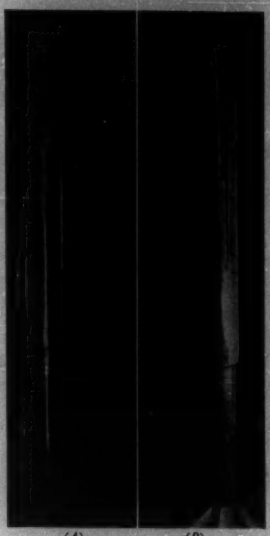

(A) (B)

Figure 5. Wood poles damaged by laboratory lightning

Table II. Typical Impulse Data of Wood-Pole Line Insulation

Insulation	Date of Test	Impulse	Flashover, Kv	Kv Per Foot	Condition of Wood	Weather
24 ft, pole 4	Nov 1933	1½×40 positive polarity	1,600	67	Normal exposure	Wet spell
12 ft, pole 4	Nov 1933	1½×40 positive polarity	1,130	94	Normal exposure	Wet spell
6 ft, pole 4	Nov 1933	1½×40 positive polarity	780	130	Normal exposure	Wet spell
12 ft, pole 4	May 1944	1½×40 positive polarity	1,200	100	Normal exposure	Fairly dry
24 ft, pole 5	May 1944	1½×40 positive polarity	1,800	75	Normal exposure	Fairly dry
12 ft, pole 5	May 1944	1½×40 positive polarity	1,300	108	Normal exposure	Fairly dry
10 ft, crossarm 4	May 1944	1½×40 positive polarity	1,400	140	Dry	Fairly dry with occasional sprinkle
10 ft, pole 2	April 1944	1½×40 positive polarity	1,500	150	Very dry	Fairly dry
12 ft, pole 3	April 1944	1½×40 positive polarity	700	70	Wet	Fairly dry
Four 5¾×10-in. suspension insulators plus 4 ft of crossarm 1	April 1944	1½×40 positive polarity	740		Normal exposure	Fairly dry
Two 14½×17-in. apparatus insulators plus 6 ft of pole 1	April 1944	1½×40 positive polarity	580		Wet	Fairly dry
8-ft wood-guy** insulator with 42-in. air gap	Nov 1938	3,500 kv/microsecond front, negative polarity*	1,800	250	Dry	Not exposed
10-ft wood pole	Dec 1935	3,000 to 4,000 kv/microsecond front, negative polarity*	2,300	230	Various	Not exposed

* Time to flashover approximately 0.5 microsecond.

** Effective length of wood, 7 foot.

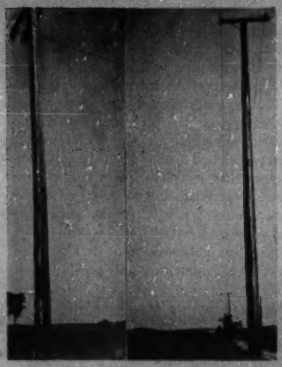

(A) (B)

Figure 6. Wood poles damaged by lightning in the field

Lightning-stroke tests also were made on wood-guy insulators in connection with application to wood-pole lines (see Tables I and II). Figure 7 illustrates one of these tests. In this insulator, the creepage distance of the wood is twice the air jump between the ends of the protective gap; the prongs are set at an angle of 30 degrees. Out of 15 lightning-stroke applications, 2 discharged over the wood. However, the amount of damage to the wood (apitong) was not considerable. Experience[7,9] indicates, and these tests confirm it, that for complete protection the horn gap on wood-guy insulators requires a setting of not more than 40 per cent of the wood insulation length and a clearance from horn tip to wood of about 20 per cent the wood insulation length.

Power-Quenching Characteristics of Wood-Pole Line Insulation

It had been suspected for some time that wood may possess deionizing or arc-quenching characteristics to some degree. The early impulse investigations gave evidence, and more recent tests clearly establish, that wood does possess this property to an appreciable measure. For example, as illustrated in the cathode-ray oscillograms of Figure 8, upon flashover or breakdown of the wood, residual voltages ranging from a few to 10 kv per foot may develop. An examination of the discharge and of its effect, such as shown in the examples of Figures 4 to 5, likewise point emphatically to the arc-quenching property of wood. There can be no question that, where the arc grazes the surface of the wood or is confined in the fibers, the normal deionizing action of the arc is intensified. It seems apparent that the underlying phenomena are complex and hardly conducive to engineering determination other than through actual testing and field experience.

In addition to utilizing wood for its good impulse strength, operators too, have been exploring its power-quenching properties. The field experience and observations reported in recent years in connection with wood-pole lines, either designed for or rehabilitated with these

Figure 7. Lightning-stroke flashover of wood-guy insulator in laboratory

objectives in view,[4,14–17] all lend encouraging support to the possibilities of wood in this direction. As the result, a demand for some fundamental studies on the power-quenching characteritics of wood developed, and, to this end, an investigation was undertaken at Sharon. The tests and results of this investigation are reviewed briefly and summarized here.

The circuit arrangement and method of test used are shown in Figure 9. Flashover of the insulation tested (A) was initiated by the surge generator previously described, much in the same manner as flashovers due to lightning occur in the field. Simultaneously, the insulation was excited at a 60-cycle voltage directly from a 2,500-kva $230/\sqrt{3}$ to 13.8-kv transformer (T_p) which in turn derived its power supply from a 2,000-kva generator (G) through a very low-impedance voltage regulating transformer (T_r) also of 2,000 kva. Most of the tests were made with this arrangement, though in a few of the tests the high-voltage transformer (T_p) was an 18,000 kva 100/13.2-kv transformer. The physical arrangement of the testing equipment and facilities, as well as the general outlay, are apparent from Figures 10 and 11. Typical tests on a wood crossarm in combination with four standard suspension insulators, resulting respectively in no power and power follow, are illustrated in Figures 11 and 12.

Other conditions of test were as follows. In the first place, provision was made to flash over the insulation under test at any point desired on the 60-cycle voltage wave. The magnetic oscillograms in Figure 15 illustrate this point, as well as indicating typical cases in which no power current (I_p) followed the impulse flash-

Figure 8. Residual voltages in wood-pole line insulation resulting from impulse flashover, as evidenced by cathode-ray oscillograms

over. Examples in which power followed are given in Figure 16. The magnetic oscillograms, in addition to recording the power currents and voltages involved, also provided pertinent data in respect to the characteristics of the power circuit. A point to note is that no power of any consequence was absorbed by the surge generator; a suitable air-blast multiple gap (PQ in Figure 9) was provided for

quenching power follow. Another point of interest is in connection with time of recovery of the power circuit. Oscillograms, as well as calculations, indicate that the time of recovery is not more than a few hundred microseconds. This value is comparable with rates of recovery usually encountered in service on transmission and distribution systems. Another condition of interest is that there were no limitations imposed on either the impulse voltages or the currents available. In fact, some of the currents used attained intensities approaching lightning-stroke currents.

A total of 117 impulse-power tests were applied to a 4-unit suspension insulator string in combination with various wood crossarms. The effective length of crossarm was varied from $2^1/_2$ to $7^1/_2$ feet. Table III summarizes the more pertinent data relating to these tests. An examination of these data will indicate that various factors determine whether 60-cycle power may or may not follow the impulse flashover over wood-pole line insulation. Practically, it is difficult to segregate from these data alone the individual contributing factors, but, as the total tests attain a reasonable number and do embrace in good measure the factors involved, statistically these data should suffice to draw a general curve or chart. And this has been done in Figure 17.

In Figure 17 the test data are reduced and expressed in per cent of power and no power follow, and plotted in terms of the 60-cycle voltage divided by total flashover length. This reference in kilovolt rms per inch not only is of interest practically speaking, but even more as it appears to embody fundamental significance. Figure 17 deserves careful study, and it should be considered that this is a chart of statistical character. A point of particular interest derived from this chart is that the probability of power following an impulse flashover—for the conditions of test as reported—diminishes to a vanishing point for an average operating stress of 0.5 kv rms per inch. That is, two inches per kilovolt for the discharge path over the wood crossarm, and the insulator string should limit to practically zero the probability of a power arc following impulse discharge. It can be observed from the chart that increasing the average operating stress to 2.9 kv rms per inch increases the probability of power follow to 50 per cent.

Similar tests were conducted on wood poles in combination with apparatus insulators, as illustrated in Figures 13 and 14. The results are summarized in Table IV, which comprises a total of 92 impulse-power tests. The behavior of pole 2 is particularly striking in that it shows a zero probability of power follow for a unit average stress as high as 2.6 kv rms per inch. This pole was very dry, which may account for this unusually good performance. Each time a test was made it was observed that a sliver of wood the entire length of the section tested would be removed, indicating apparently that the path of the discharge was under the surface of the wood throughout. In all other tests too, a good deal of slivering was observed as is evidenced in the photographs. That is, a discharge usually would gouge a sliver from the pole or crossarm, indicating deionizing action. With reference to poles 1 and 3, analysis of the data indicates that for these poles the average stress corresponding to zero probability of power follow is 0.5 kv rms per inch—a value identical with that for suspension insulators and crossarms. At 1.2 kv rms per inch, power invariably would follow. It is well to repeat that these poles had a high moisture content.

Deionization of Power Arc and Rapid Reclosure

Some tests were made in connection with the reclosure of the power circuit immediately following clearance of the fault. The mode of test is apparent from the circuit arrangement, Figure 9. Following the establishment of the power arc, in the manner previously described, the short circuit would be cleared, and then in a matter of 23 to 25 cycles the power voltage reapplied. Circuit breaker *B* was equipped for this clearing and re-

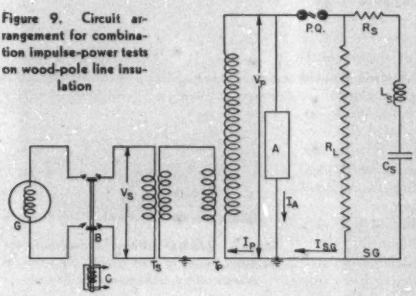

Figure 9. Circuit arrangement for combination impulse-power tests on wood-pole line insulation

G—2,000-kva generator
B—Circuit breaker
C—Tripout and reclosing device
T_P—2,500 kva, $230/\sqrt{3}$ to 13.8 kv, 17.8 per cent impedance transformer
T_S—Laboratory transformer for voltage adjustment: 2,000 kva, 1.1 per cent impedance
A—Insulation assembly tested
SG—Surge generator (circuit constants: C_S, L_S, R_S, R_L)
PQ—Power-quenching gap
V_S, I_P, I_{SG}—Power voltage and currents recorded at magnetic oscillograph

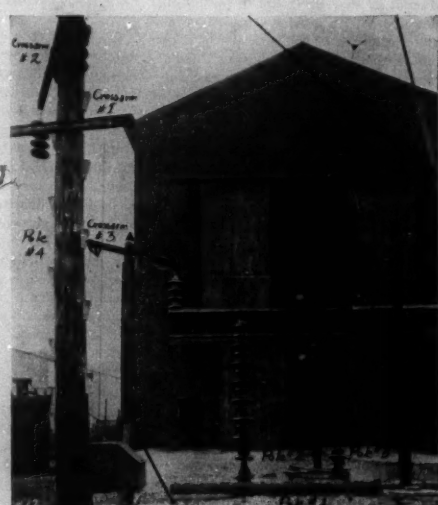

Figure 10. Typical wood-pole insulation structures tested (3-million-volt surge generator in background)

closure operation. The oscillograms of Figures 18 and 19 illustrate the sequence of events and also show, respectively, typical examples of successful reclosure of the power circuit and of restrike of the power arc. All these tests were conducted on six feet of pole 1 in combination with two apparatus-type insulators, the total path of surface discharge being slightly in excess of 100 inches. The test results are summarized in Table V.

These data show that at 92 kv, and for a time interval of 23 or 24 cycles following the clearance of the short circuit, the power circuit could be reclosed successfully each time. At a voltage 45 per cent higher (133 kv) the arc invariably would restrike. In these tests the average stress per unit length of discharge corresponding to successful reclosure is 0.92 kv rms per inch. As wood-line insulation, which is designed for zero-probability power follow, that is 0.5 kv rms per inch, would not approach a unit stress in excess of 0.92 kv rms per inch, a line so designed inherently has ample clearances from a consideration of reclosure.

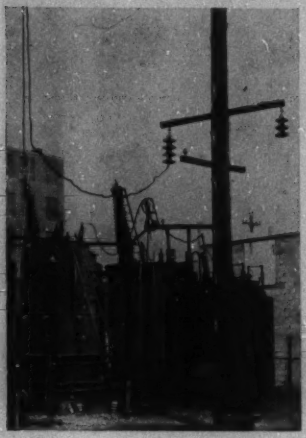

Figure 11 (left). Impulse-power test applied to suspension insulator string and wood crossarm

No power follow (note the impulse discharge over the insulators and wood crossarm)
Power voltage = 69 kv rms

Figure 12 (right). Impulse-power test applied to suspension insulator string and wood crossarm resulting in power follow

Power voltage = 100 kv rms

Table III. Combination Impulse-Power Tests on Four 5¾-by-10-Inch Suspension Insulators and Wood Crossarm

Test Group	Wood Crossarm	Positive Impulse Synchronized on 60-Cycle Voltage Wave at: Polarity	Point on Wave	60-Cycle Voltage Applied Kv-Rms	Number of Tests	With Power Follow	Without Power Follow	Comments*
1	Crossarm 1 4-ft length	Negative	55 deg before crest	69	3	None	3	One power follow occurred at 69 kv on preliminary tests. At 138 kv power-follow current attains a maximum of 70 amp rms. See Figure 16. Currents are proportional to voltage applied.
				92	5	1	4	
				115	6	None	6	
				138	7	4	3	
2	Crossarm 2 7½-ft length	Negative	55 deg before crest	138	1	None	1	
				115	1	None	1	
3	Crossarm 2 4-ft length	Negative	55 deg before crest	138	4	None	4	
		Negative	55 deg after crest	138	7	None	7	
4	Crossarm 2 2-ft length	Negative	55 deg after crest	138	6	2	4	Refer to Figures 10 and 15 for typical oscillograms of power follow and no power follow
				115	5	1	4	
				92	11	4	7	
		Positive	55 deg after crest	138	3	2	1	
		Negative	25 deg before crest	46	10	None	10	
				69	8	1	7	
				92	10	1	9	
				115	10	6	4	
				138	4	3	1	
5	Crossarm 3 4-ft length	Negative	25 deg before crest	69	5	4	1	
				46	6	None	6	
6	Crossarm 2 2½-ft length	Negative	25 deg before crest	69	1	None	1	View of actual tests are shown in Figures 11 and 12.
				92	1	None	1	
				100	2	1	1	

* Other conditions of tests:

1. Typical oscillograms of power follow are given in Figure 16. Currents are proportional to voltage applied.
2. In tests 1 to 5, power was supplied from a 2,500-kva high-voltage transformer. In test 6, power was supplied from an 18,000-kva transformer. See Figure 11.
3. For tests 1 to 4, the current of the impulse discharge is a 5-microsecond wave with superimposed damped oscillations, attaining a crest of 9,500 amp. For tests 5 and 6, the current discharge is a 50-microsecond duration, oscillatory wave, attaining a crest of fully 20,000 amp. In the first arrangement $C_1 = 0.008\mu f$ and $R_1 = 350$ ohms, and in the second $C_1 = 0.066\mu f$ and $R_1 = 0$. See Figure 9.
4. The atmospheric conditions during these tests were as follows: barometric pressure = 740 mm Hg; temperature 10 to 25 C; absolute humidity = 5 to 10 mm Hg; weather generally clear.

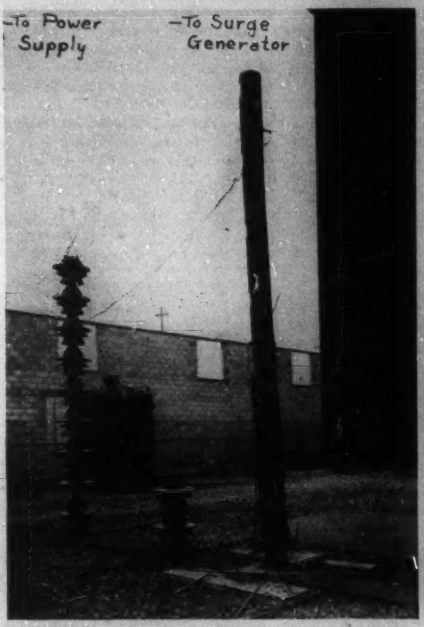

Figure 13. Impulse-power test applied to stack of two apparatus insulators in combination with wood-pole section

Power voltage = 69 kv rms

Figure 14. Impulse-power test applied to stack of two apparatus insulators in combination with wood-pole section resulting in power follow

Power voltage = 138 kv rms

In this investigation, circumstances and time did not permit exploring this field to the extent it really deserves. Though the tests made are not extensive enough to draw general conclusions, among other things they do point out a technique and method that can be followed to great advantage in future and more extensive research in this important field.

Leakage-Current Effects

The oscillograms of these investigations show that leakage currents invariably occurred when the wood was wet and when the primary (porcelain) insulation was proportioned inadequately with respect to the 60-cycle voltage applied. At no time were leakage currents observed when testing pole 2 and crossarms 1, 2, and 3 in combination with their respective porcelain insulators. As stated previously, all these wood members were in a dry state. Leakage currents were recorded frequently when testing poles 1 and 3, which were wet poles. Examples of these leakage effects are indicated in Figures 20, 21, and 22.

The oscillograms of Figure 20 were recorded when testing a 6-foot section of pole 1 (wet) in series with an air gap relatively short but spaced sufficiently to do more than withstand the 60-cycle voltage. Upon flashover of the pole and series air gap on the impulse and when power-follow current did not develop, a leakage current immediately would appear and would be sustained (see *C* of Figure 20). In these tests the first trace of leakage can be discerned on the oscillograms at 33 kv. As the 60-cycle voltage is increased, the leakage rises, but the rate is higher than proportional. For instance, at 54 kv the leakage current across the 6-foot section tested was 0.9 ampere, and at 122 kv it had gone up to 4.8 amperes. The corresponding resistances are 60,000 ohms and 25,000 ohms. As these currents were too feeble to operate the relays, this leakage effect continued unless the circuit was interrupted manually. None of the tests were continued more than 10 or 20 seconds, long enough, however, to develop incipient charring in spots (see Figure 13). In several instances considerable puffing out of the smoke from the pole, as well as concentrated burning in spots, could be observed, all giving the impression that the rate of damage must have been considerable. It stands to reason that even a leakage current of 0.9 ampere, developing 9 kv per foot length of pole, if sustained for any length of time, would result in serious damage to the pole. Also, it is well to point out that a leakage current of this magnitude definitely would constitute a shock hazard.

The oscillograms of Figures 21 and 22 correspond to tests made on 6-foot lengths of pole 1 (wet) and pole 3 (wet) respectively, each in series with a stack of two apparatus-type insulators. Oscillogram *A* of Figure 22 gives additional evidence of high sustained leakage currents, as previously observed. In oscillogram *B*, immediately upon impulse flashover of the

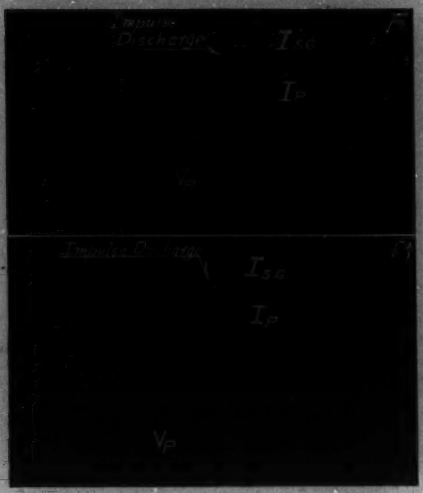

Figure 15. Synchronization of impulse flash-over with 60-cycle voltage

A preceding and *B* following crest of 60-cycle voltage

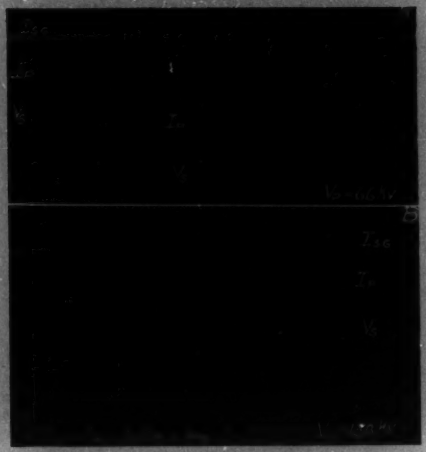

Figure 16. Typical oscillograms of power follow

insulator stack and pole, a high leakage current appears which develops quite rapidly into a short-circuit current. Similarly, in Figure 21 the short-circuit current really starts out as a heavy leakage rapidly deteriorating into a fault.

From the foregoing data and observations, as well as from recent studies conducted elsewhere[22, 23] there can be little doubt that the subject matter of leakage currents and the problems connected thereto have not been well understood and that additional studies in this field may well be pursued to advantage.

Discussion of Results—Their Practical Application

From an engineering standpoint, there is available now a good working knowledge in regard to the impulse characteristics of wood and also a reasonably good understanding of the performance of wood under lightning-stroke conditions. These developments naturally are the accumu-

Table IV. Combination Impulse-Power Tests on Two 14½-by-17-inch Apparatus Insulators and Wood Pole

Test Group	Wood Pole	Positive Impulse Synchronized on 60-Cycle Voltage Wave at: Polarity	Point on Wave	60-Cycle Voltage Applied Kv-Rms	Number of Tests	With Power Follow	Without Power Follow	Comments*
1	Pole 1, 6-ft length	Negative	55 deg before crest	67	10	None	10	At 138-kv power-follow current reaches maximum of 70 amp rms. Currents are proportional to voltage applied
				86 to 90	5	5	None	
				109	5	5	None	
				135	3	3	None	
2	Pole 2, 6-ft length	Negative	45 deg before crest	69	4	None	4	This pole had been stored in the laboratory and was very dry
				92	4	None	4	
				115	3	None	3	
				138	6	None	6	
	4-ft length			138	3	None	3	
	3-ft length			138	3	None	3	
	2-ft length			138	6	None	6	
	1-ft length			138	6	3	3	
3	Pole 3, 6-ft length	Negative	55 deg before crest	69	3	None	3	View of actual tests are shown in Figures 13 and 14
				92	3	2	1	
				115	3	3	None	
	12-ft length (4 insulators)			138	3	None	3	
4	Pole 3, 6-ft length	Negative	Near crest	46	2	None	2	
				69	9	1	8	
				92	5	5	None	
5	Pole 3, 6-ft length	Negative	Near crest	46	1	None	1	
				69	4	3	1	
				92	1	1	0	

* Other conditions of tests:

1. In tests 1 to 4 power was supplied from a 2,500-kva high-voltage transformer. In test 5, power was supplied from an 18,000-kva transformer.
2. For tests 1 to 3, $C_s = 0.008\mu f$ and $R_s = 500$ ohms. For tests 4 and 5, $C_s = 0.066\mu f$ and $R_s = 0$. See Table III for corresponding impulse currents.
3. See Table III for range of atmospheric conditions.

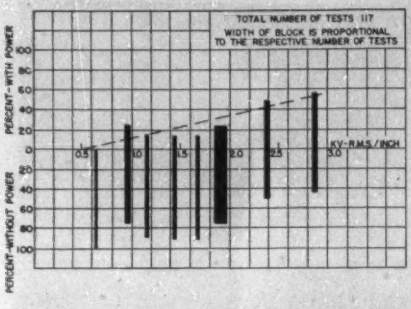

Figure 17. Per cent power follow versus average unit stress in kilovolts-rms per inch

Data apply to wood crossarm in combination with four suspension insulators

Table V. Data on Reclosure of Power Circuit Following Clearance of Fault Tests Made on Two 14¹/₂-by-17-In. Apparatus Insulators and 6 Foot of Pole 1

60-Cycle Voltage Kv-Rms	Reclosure Time*	Number of Tests	Successful Reclosures	Number of Restrikes
92	23¹/₂ cycles	5	5	None
109	24¹/₂ cycles	5	4	1
133	24¹/₂ cycles	3	None	3

* See Figures 18 and 19 for typical oscillograms and method of measuring reclosure time as used here.

lative result of other investigations, in addition to this contribution.

Likewise, the recent findings on the power-quenching characteristics of wood related in this paper and the corresponding field observations, as reported in references 14–18 and 20, all indicate that progress is being made in this direction too. The significance of the experimental results in Figure 17 may be visualized in part from a consideration of available field data. In this connection, for example, the field statistical data in references 14 and 15, relating to 33-kv wood-pole structures, specifically state that for insulation clearances (arc-over path), in which an average unit stress of 0.40 kv rms per inch is not exceeded, the annual rate of power-arc faults experienced practically reaches an asymptotic value. That is, a further decrease in average unit stress does not appreciably lower the power faults, whereas an increase in the stress to 1 kv rms per inch will more than quadruple the rate of power faults. In Figure 17, an average unit stress of 0.40 kv rms per inch lies in the zone of zero-probability power follow. The foregoing correlation is indicative of the fundamental character of the experimental data.

It stands to reason, however, that the experimental data on the power-quenching characteristics of wood cannot be projected directly into the application field without consideration being given to the additional influencing factors that are present in actual operation. Of particular importance is the total duration of the stroke discharge. Multiple and long-duration discharges naturally will accentuate the possibility of power follow. Other factors requiring attention are the effect of wind swinging conductors together or toward grounded objects, tree branches falling on the conductors, kites, and the like.

In applying the experimental data, consideration should be given to the relative frequency of flashover. For instance, an increase in the impulse level of a distribution line from 100 to 300 kv is likely to eliminate completely all flashovers originating from induced voltages and, to that extent, account for improved performance in addition to the betterment resulting from a threefold decrease in average unit stress. The foregoing facts illustrate the necessity of taking into consideration the essential factors of the practical problem, in applying the experimental data.

A criticism that might be raised against the experimental data in Figure 17, and the similar data for the poles, is that the power currents in these tests in no instance attained values above 100 amperes. In this connection, however, the point of fundamental considerations is that the phenomenon involved is one of probability of power follow resulting from impulse flashover. The amount of power current that actually may follow, once breakdown is established, does not appear to be a determining factor in affecting probability of power follow, provided the conditions of adequate surge current discharge and availability of power voltage are met. Therefore, similar results are expected from tests conducted entailing higher power-follow currents than were permitted by this investigation.

There can be no question of the desirability of further research and study, both in the field and in the laboratory, on the matter relating to the power-quenching characteristics of wood. In future studies of this character consideration should be given to multiple impulse discharges.

Likewise, the test results on the rate of deionization of power arcs, as well as the findings on leakage-current effects, all emphatically point to the need for additional work in this field. It would seem that the economic importance of wood as an insulator, and the means it provides for securing improved operating service, would well justify further studies. The results and methods presented here should indicate the direction in which future investigations may be approached.

Figure 18 (left). Oscillograms of power follow and successful reclosure

Figure 19. Oscillogram of power follow and restrike of arc

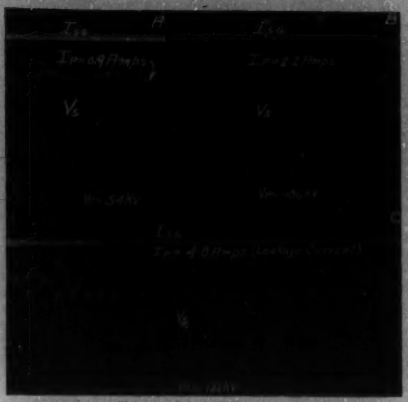

Figure 20. Typical oscillograms of sustained leakage currents

Figure 21 (above). Oscillogram of leakage current developing rapidly into power follow

Figure 22. Other typical oscillograms of leakage effects

Conclusions

1. The three predominant factors that determine the impulse strength of wood are: the length of wood; the duration of the impulse; and the moisture content in the wood.

2. The extent of shattering of wood poles and crossarms from lightning is limited. The amount of damage that may result can be estimated, and, if economically justified, means can be provided to reduce such damage.

3. Wood possesses distinct power-quenching characteristics which in a measure now are being utilized with intent by some operators. Experimental data presented in the paper indicate that for an average unit stress of 0.5 kv rms per inch the probability of power-follow is practically zero for single impulse discharge. However, the experimental findings cannot be projected directly into the application field without due consideration being given to the additional determining factors underlying service conditions.

4. Questions relating to the rate of deionization of the arc as well as the matter of leakage currents deserve further study. In this connection the paper presents methods of testing and technique that can be followed to advantage.

References

1. The Advantages and Limitations of Wood in Transmission Structures, A. O. Austin. International Conference on Large Electric High-Voltage Systems, Paris, France, 1927.

2. Impulse Insulation Characteristics of Wood-Pole Lines, H. L. Melvin. AIEE Transactions, volume 49, 1930, pages 21–7.

3. Transmission Research and Design With the Field as a Laboratory, F. E. Andrews, C. L. Stroup. AIEE Transactions, volume 49, 1930, pages 959–68.

4. Performance of Wood Insulation in Transmission Lines, F. E. Andrews. *Electrical World* (New York, N. Y.), April 25, 1931.

5. Lightning Investigation on a Wood-Pole Transmission Line, R. R. Pitman, J. J. Torok. AIEE Transactions, volume 50, 1931, pages 568–73.

6. Impulse and Dynamic Flashover Studies of 26-Kv Wood-Pole Transmission Construction, A. S. Brooks, R. N. Southgate, E. R. Whitehead. AIEE Transactions, 1933, volume 52, pages 494–501.

7. Operating Experience With Wood Utilized as Lightning Insulation, H. L. Melvin. AIEE Transactions, 1933, volume 52, pages 503–10.

8. Impulse Tests on Wood Line Materials, J. J. Torok, W. R. Ellis. *Electric Journal*, August 1938.

9. Damage to Wood Poles and Crossarms Caused by Lightning, Transmission and Distribution Committee Report. *Bulletin*, Edison Electric Institute (New York, N. Y.), February 1934.

10. Impulse Voltage Strength of Insulators and Materials, J. C. Dowel, C. M. Foust. *General Electric Review* (Schenectady, N. Y.), March 1937, page 141.

11. Lightning Strength of Wood in Power Transmission Structures, Philip Sporn, J. T. Lusignan. AIEE Transactions, volume 57, 1938, February section, pages 91–101; discussion pages 410–16.

12. Flashover Characteristics of Insulation, P. H. McAuley. *Electric Journal*, July 1938, page 273.

13. What Wood May Add to Primary Insulation for Withstanding Lightning, J. T. Lusignan, C. J. Miller. AIEE Transactions, volume 59, 1940, September section, pages 534–40; discussion pages 1177–80.

14. Minimum Insulation Level for Lightning Protection of Medium-Voltage Lines, H. N. Ekvall. AIEE Transactions, volume 60, 1941, March section, pages 128–32; discussion pages 719–22.

15. Lightning Performance of 13- and 33-Kv Wood-Pole Lines, H. N. Ekvall. Minutes, Transmission and Distribution Committee, Edison Electric Institute, New York, N. Y., 1945.

16. An Application to 69-Kv Wood-Pole Line Design, H. N. Ekvall, R. L. Catlett. Pennsylvania Electric Association, 1944.

17. Wood-Pole Line Protection Without Ground Wires, H. L. Rorden. *Electrical World* (New York, N. Y.), December 9, 1944, page 94.

18. Lightning Performance of Wood Lines Below 66 Kv, W. E. Gunlach. Minutes, Transmission and Distribution Committee, Edison Electric Institute, New York, N. Y., 1935.

19. Some Features of Wood H-Frame Design for High-Voltage Line Structures, W. C. Schmidt. *Bulletin* (New York, N. Y.), Edison Electric Institute, April 1943.

20. Lightning Investigations on 33-Kv Wood-Pole Lines, F. E. Andrews, G. D. McCann. AIEE Transactions, volume 64, 1945, November section, pages 768–76.

21. Laboratory Lightning—The Microsecond Switch, P. L. Bellaschi. *Electric Journal*, June 1936.

22. Burning of Wood Structures by Leakage Currents, P. M. Ross. AIEE Transactions, volume 66, 1947; pages 279–87.

23. Behavior of Red Fir Poles for 11-Kv Lines Under Electrical Stress Due to Insulator Failure, W. Letherwich. *Journal*, Institution of Electrical Engineers (London, England), August 1946, pages 387–93.

24. The Electrical Resistance of Wood Poles, P. B. Stewart. *Proceedings* American Wood Preservers Association (Washington, D. C.; Chicago, Ill.) 1936, page 353.

Discussion

E. C. Starr (Oregon State College, Corvallis, Oreg.): This paper provides a very agreeable answer to some of the wishful thinking many of us have been doing for a long time. It should now be possible to produce inexpensive wood-pole designs with the insu-

lation so co-ordinated as to obtain excellent lightning performance in regions of low to moderate storm frequency. Through the use of short-time and critical spark-over data already available for wood members, and the corona coupling factors reported by McCann[1], the structures, including flashover diverting members, can be so proportioned that a large majority of lightning flashovers will be confined to line-to-ground paths over wood. These paths can be made of sufficient length to give a low probability of power follow and subsequent line outage.

Figure 1 of this discussion as originally plotted was based upon meager data gleaned from long-arc tests and a number of investigations previously reported, and is now modified by a consideration of Bellaschi's results. An effort has been made to evaluate the average outage probability resulting from lightning spark-over as a function of total insulation expressed in terms of sparking distance. Six $5^3/_4$ by 10-inch suspension insulator units with a sparking distance of three feet constitute a part of the total insulation at each conductor support for the 115-kv class, and 12 units with a sparking distance of six feet were assumed to be used for the 230-kv class. These curves indicate that for an average ratio of outages to sparkovers of 50 per cent, the 115-kv line would require a total of 5.5 feet of line-to-ground insulation and 8.5 feet line to line. For the same outage ratio the 230-kv line would require 10.5 feet of line-to-ground insulation and 16.5 feet line to line. If the outage ratio is reduced to 10 per cent, the lengths of insulation required are 15 and 24 feet for the 115-kv class and 29 and 46 feet for the 230-kv class.

In calculating and plotting these curves approximate allowances were made for multiple and sustained-current strokes as well as for the relatively light strokes frequently encountered. Actually the sustained-current strokes are probably of little consequence when considerable lengths of wood are involved. This theory is advanced because the long-duration components are ordinarily so small that the conductor surge admittance, subjected to the residual voltages developed across the spark-over path, is more than adequate to drain these currents away

It must be remembered that these curves are intended to represent average conditions and that any one specific performance probably will deviate therefrom appreciably. Any comments by the author or other engineers and any data further modifying or confirming the curves will be greatly appreciated.

I should like to ask Bellaschi if the surge voltages applied during the combination impulse-power tests were of definite overvoltage magnitude or were just the critical values for the insulation involved. Is there any difference in the power-follow tendency if the initial spark-over results from the application of a surge of critical value or of high overvoltage?

Were any data obtained on the power-follow characteristics of porcelain insulators alone and air gaps alone? These data would assist in developing a more complete understanding of the subject.

There is a marked difference between the residual voltage shown in cathode-ray oscillograms *A* and *B* of Figure 8 of the paper. The former is for a pole of high moisture content and shows a residual voltage of 7.5 kv per foot. The latter is for a pole of normal moisture content and shows a residual voltage of only 3.33 kv per foot. Is this one of the idiosyncrasies of wood, or is there a logical explanation? What would be the residual voltages of similar lengths of air gap and of porcelain insulation?

This paper adds a very considerable amount to our knowledge of the performance of wood as supplementary lightning insulation. It encourages and lends confidence to the further use of wood, particularly in regions of moderate lightning exposure. As Bellaschi points out, there are, however, several important gaps yet to be filled. Among the further studies needed are

1. Additional tests on poles and crossarms of various lengths and of normal outdoor weather exposure to establish better average performance and to indicate normal limits (see Table II of the paper, test groups 4 and 5, and Table IV, test groups 1, 2, and 3).

2. The influence of number of porcelain insulator units on crossarm and pole performance.

3. The spark-over voltage and power-follow characteristics of crossarms with two strings of insulators representing line-to-line conditions.

4. Field studies employing structures with co-ordinated supplementary lightning insulation to establish more completely the approximate laws of performance.

5. Additional tests on high-grade wood members to determine the influence of cross-sectional area on power-follow characteristics. Some structural members, such as long guy insulators without gaps and flashover diverter elements, may be of small cross section and their performance should be determined. Perhaps Bellaschi can supply this information from data already available.

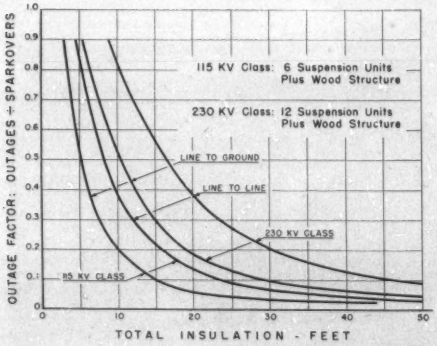

Figure 1. Approximate influence of total insulation strength on probability of outage following lightning spark-over

REFERENCE

1. THE EFFECT OF CORONA ON COUPLING FACTORS BETWEEN GROUND WIRES AND PHASE CONDUCTORS. G. D. McCANN. AIEE TRANSACTIONS, volume 62, 1943, pages 818–26.

R. W. Caswell and **F. E. Andrews** (Public Service Company of Northern Illinois, Chicago, Ill.): This paper covers a subject very pertinent with respect to design of medium-voltage wood pole lines. The factors influencing power follow now seem to be the most important missing link in the general problem of wood-pole-line lightning flashovers and this paper is an important addition to the knowledge of the subject. However, as indicated by the author, it is our opinion that considerably more work is necessary to provide a satisfactory quantitative basis for design. The author has dealt principally with the relationship of length of path over wood and voltage. The effect of factors other than these remain to be evaluated as influencing power follow.

For example, under "Power Quenching Characteristics of Wood-Pole Line Insulation," reference is made to the timing of the impulse and to the magnitude of the lightning stroke currents, but the effects of these variables are not discussed, presumably because the data obtained were not sufficient for drawing satisfactory conclusions. However, an inspection of Tables III and IV indicates that the timing of the impulse with respect to the power system wave has considerablebearing on the results. The number of cases with power follow is consistently greater for the impulse 25 degrees before crest in comparison with 55 degrees before crest. All of the tests reported by this paper are single impulse discharges and are not related to magnitude of lightning stroke current. The greater ionization resulting from higher lightning stroke currents and for multiple or long duration discharges undoubtedly will result in susceptability to power follow greater than for the single discharges of the value and type used in these tests.

From Figure 17 and the discussion pertaining thereto, it is considered that no power follow should occur with a voltage stress less than 0.5 kv per inch. This conclusion is quite contrary to our experience as reported in reference 20. In Table I of that paper, data are given on 33 kv line structures having a path of 110 inches over wood comprised of parts of both pole and crossarm. These data show that 14 per cent of the flashovers located by inspection in the field were accompanied by power follow. This is on the assumption that each structure where evidence of flashover was found was considered as only one case. From these data and from many other observations from high impulse level 33-kv lines, we know that power follow is not uncommon on structures of this type. These structures have a voltage stress of approximately 0.3 kv per inch of wood and our experience accordingly indicates that for satisfactory design the stress should be kept well

below this figure for avoidance of power follow. The differences between our field experience and the results of Bellaschi's laboratory work might be explained by other factors which were outside the scope of his data as presented, such as those already mentioned, voltage recovery characteristics, and amount of power follow current.

The records from photographic recorder installations described in reference 20 indicate a large number of multiple and prolonged lightning discharges. This points to the probability that the amount of ionization associated with lightning discharges of this type is an important factor influencing power follow.

The information shown in Figure 3 relative to decrease in impulse strength of wood in kilovolts per foot as the length of the section increases is of particular interest in the design of structures involving the longer wood sections. This point has not been shown so clearly in past data. More comprehensive test data to confirm the shape of the curves of Figure 3 would seem desirable.

Under "Leakage-Current Effects" it is stated that leakage currents invariably occurred with wet wood when the porcelain insulation was proportioned inadequately with respect to the 60-cycle voltage applied. It would be helpful if the author would give us information on the amount of porcelain used in these cases. If the amount of porcelain was comparable to what is used in normal practice, this point has considerable practical significance. Another question is whether the porcelain was wet or dry at the time of the tests.

In conclusion, we wish to reiterate our opinion that Bellaschi's work is an important contribution to a better understanding of power follow induced by lightning flashovers; and it is hoped that he and others will continue work along this line with the objective of obtaining additional data sufficiently comprehensive to provide a much more firm basis for design than now appears to exist.

H. N. Ekvall (Philadelphia Electric Company, Philadelphia, Pa.): This paper presents some very interesting laboratory results on the power-quenching characteristics of wood insulation which I would like to compare with field experience of the Philadelphia Electric Company.

The author concludes from Figure 17 that the probability of power current following an impulse flashover diminishes to a vanishing point for an average operating stress of 0.5 kv rms per inch or two inches per kilovolt expressed in terms of insulating flashover distance. This conclusion was based on single impulse discharges and on power follow currents no greater than 100 amperes.

Extensive field experience on the 33-kv wood-pole lines of the Philadelphia Electric Company indicated that when an operating stress of 0.5 kv rms per inch was reached, there was a leveling off effect in the rate of power arc faults and that further decreasing the unit stress, within practical 33-kv line design limits, did not lower the failure rate appreciably. At the point where leveling off began the rate was only 0.5 power-arc faults per 100 structures per year. It appeared that the vanishing point could not be reached without resorting to much longer flashover distances than obtained on our standard 33-kv wood-pole structures, using high ridge pin configuration with pin type insulators and 8-foot crossarms. With like size structures operating at 13 kv, the vanishing point appeared to have been reached with the elimination of wire "burndowns," but in this case the unit stress was 0.16 kv rms per inch or approximately six inches per kilovolt.

Therefore, under field conditions it appears more likely for the vanishing point to occur at a lower operating stress than the 0.5 kv rms per inch value found in the laboratory. One reason for this apparent discrepancy may be the presence of long-duration multiple strokes in the field whereas only single impulses were used in the laboratory. Another factor may be the difference in the recovery rates for fault currents of the order of 5,000 amperes in the field as compared to less than 100 amperes used in the laboratory.

J. T. Lusignan (Ohio Brass Company, Mansfield, Ohio): The information contained in Bellaschi's paper should prove very helpful to transmission engineers using wood to gain lightning insulation. Such information represents considerable laboratory work as it is not possible to draw worthwhile conclusions from wood studies with only a few tests. There is too much spread in the data points, the plus or minus 15 per cent figure which the author gives checking quite well with our findings obtained at the Barberton laboratory and given in his references 11 and 13.

We thoroughly concur as to the importance which moisture plays. I would like to emphasize that it is moisture *in* and not on the wood that controls. We determined this by splitting identical specimens and lacquering half of each one to exclude moisture. On subsequent wet tests, the flashover voltages were reduced the usual amount on the unlacquered specimens but scarcely affected on the lacquered ones. It was surprising to find how quickly rainwater penetrated wood specimens to affect flashover voltages. Our results (reference 13) showed that within a few minutes after the water was turned on the flashover values dropped and held at appreciably lower levels.

We found creosoting to have little effect on impulse flashovers either as to grade or quantity of oil used.

Partial breakdown of combined porcelain and wood insulation, noted by the author particularly on wet structures, checks with our findings. This behavior was readily discernible on oscillograph waves. It seems probable that the same thing occurs most of the time, even dry, with such different insulation members in series-parallel, such as wood, porcelain, and air. The voltages across each would depend on their relative impedances. The times of spark-over or puncture would depend on their individual volt–time curves. Accordingly, it seems reasonable that their breakdowns would not necessarily be simultaneous.

The author's laboratory studies of the effect of wood paths on power-follow currents are most interesting, particularly since they are apparently the first of their kind. I am wondering whether he found any measurable difference between the arc-quenching properties of woods that shattered easily and those that did not. What I have in mind is whether an arc forced to remain on the surface of a wood member would sustain better than one inside. In this connection, did the author find any difference in the quenching properties of creosote treatment of wood? If it could be determined that certain wood preservatives have a so-called deionizing effect possibly some future consideration could be given to that in addition to the preserving factor.

Paul M. Ross (Ohio Brass Company, Mansfield, Ohio): Bellaschi has made a worth while contribution by presenting pertinent and new information regarding the use of wood in transmission line structures.

Referring to the computation of the gradient data in Figure 17, were the 60-cycle test voltages divided by the total flashover length of the wood only or were they divided by the total of wood flashover length plus insulator flashover length? If the latter is the case, do your data permit identification of the arc quenching properties of the wood element separate from deionization occurring over the insulator path? Do your tests permit conclusions to be drawn regarding the length of a plain air gap that might be used to avoid power current follow after impulse flashover?

In Tables III and IV four points on the 60-cycle voltage wave were selected at which impulses were applied. How does the probability of power current follow vary as a function of the point of application of the impulse with respect to the voltage wave? During your research work for this paper did you find any indication that the probability of power currrent follow varies as a function of the magnitude of the lightning discharge current (assuming a fixed point on the voltage wave for impulse application)?

Regarding the leakage current effects reported, were the leakage currents initiated by impulse application to the air gap or insulator plus wood combination (Figures 20, 21, and 22)? If such was the case, was the impulse voltage of sufficient magnitude to cause flashover of both the insulation elements connected in series? Was there visible evidence of a low current arc across the air gap or insulator during these tests which would indicate that to be the path the leakage current followed in order to reach the wood element? The term "leakage currents," when used in relation to insulators, may refer to a current flow through surface contamination layers. These currents, even when the surface contamination layers are wet, are surge-like in nature, but rarely exceed a small fraction of the author's reported current magnitudes. Did the insulators used on these tests have clean surfaces?

H. L. Melvin (Ebasco Services, Inc., New York, N. Y.): After participation in some of the earlier laboratory and operating tests on wood, also combinations of wood, insulators, and air gaps (reported to the Institute in 1930 and 1933), it is gratifying to see the continued interest in this important investigation. The contribution made through the presentation by Bellaschi is very useful because data of greater accuracy and extended scope are made available for design purposes. It is believed that those of us who have employed wood construction extensively and utilized its impulse insulation characteristics will agree that actual operat-

ing experience confirms in large measure the results of these laboratory tests.

Only three suggestions or comments are offered, perhaps by way of emphasis to statements in the paper:

1. Test data from both the laboratory and field, as well as the wood itself, must be used intelligently if optimum operating and economic results are to be secured.

2. Possible damage to the wood, which would impair the mechanical security and life of the structures, must be taken fully into consideration in developing designs.

3. Selection and treatment of the wood, if necessary, for extending the life and retention of required factors of safety are important particularly for higher voltage lines.

P. L. Bellaschi: It is apparent from these discussions and from the paper that more work is necessary in this field. These are a few of the questions which require additional attention or on which more research is desired:

1. Effect of multiple and long-duration discharges on power follow.

2. Impulse and power-follow tests conducted on other insulation structures representative of practical design of low, medium, and high voltage wood-pole transmission lines.

3. Voltage recovery characteristics and amount of power follow.

4. Impulse current and voltage and mode of application.

5. Power follow as function of point of application of impulse with respect to 60-cycle wave.

6. Means for utilizing power-quenching characteristics of wood more effectively and to minimize damaging effects of lightning.

7. Relative deionizing action of insulators and air, alone and in combination with wood.

8. Mechanism of impulse breakdown of wood, alone and in combination with porcelain and air insulation.

9. Deionization of power arc and rapid reclosure corresponding to conditions of service.

10. Leakage effect in its various practical aspects.

11. Sundry others.

An answer in a practical sense is probably at hand to some of these questions but the fact remains that more comprehensive work need be done in this entire field to provide a much more firm basis for design. This further activity can be pursued to greatest advantage, to the industry at large, in three related areas

(*a*). Research and development in the laboratory.

(*b*). Investigation tests in the field.

(*c*.) Field studies on lightning and analysis of experience.

Heretofore our joint efforts have been limited to (*a*) and (*c*). Actual field tests would be very valuable in effectively integrating these two activities. A program of this character well planned and conducted certainly could be productive of very worthwhile and practical results. This would accelerate the answer to the various basic questions enumerated here. Such field tests naturally would require portable impulse-generator equipment amply proportioned to secure the practical and basic engineering results in view.

The field experiences on 33-kv wood-pole structures presented respectively by Caswell and Andrews and Ekvall when referred to a common basis appear to be in reasonably good agreement. In these field data, for a voltage stress of about 0.3 kv rms per inch approximately 14 per cent of the flashovers were accompanied by power follow. Accordingly, the chart in Figure 17, which holds for a single impulse discharge, is shifted to the left a corresponding amount when such factors as multiple and long-duration surges, amount of power-follow current, and voltage recovery characteristics as are encountered in the field become superimposed thereon.

In the tests impulse currents were as high as 20,000 amperes and durations greater than 50 microseconds (see Table III). In this respect as well as in the timing of the impulse with the 60-cycle voltage, more data appears desirable if quantitative conclusions are to be drawn. However, the total tests attained reasonable number, embracing the various factors sufficiently, to draw a statistical curve. In regard to the matter of leakage currents, invariably these occurred with wet poles in series with an air gap which was sufficient to more than withstand the 60-cycle voltage (Figure 20). Pole 3 (wet) when tested at 66 kv with a stack of two apparatus-type insulators likewise resulted in high sustained leakage currents. In this case the primary insulation appears inadequately proportioned. The writer well agrees with Caswell and Andrews that more comprehensive impulse data on wood-pole structures and lengths are desirable for design purposes.

The experiences at the Barberton and Sharon laboratories in regard to the impulse strength of insulators in combination with wood, the effect of moisture, partial breakdown, and similar factors, to which Lusignan refers, both run quite parallel to each other. The suggestion Lusignan advances in regard to possibly improving the power-quenching properties of wood by means of treatment did not receive specific consideration in these tests but is something worth considering. Too many variables were involved in these tests to draw clear-cut quantitative relationship between the degree of splintering experienced and the power-quenching ability of wood. In this connection I may say that we were surprised in the unusual good performance of pole 2. This pole was very dry. When testing this pole attention was given especially to the slivers removed. It was observed that each time a test was made a sliver the entire length of the section tested would be removed, indicating apparently that in this case the path of discharge was under the surface of the wood throughout.

The suggestions Melvin makes in regard to assessing intelligently the laboratory and field data when applying these to actual design, in designing for mechanical integrity of the wood structure even when this is subject to direct strokes, and prolonging its life by preserving it certainly are basic considerations. The pioneering engineering contributions Melvin has made in this field are worth restating here.

In his discussion Ross poses a series of questions. The data in Figure 17 are plotted in terms of the 60-cycle voltage divided by total flashover length. In this manner the power-quenching effects of the wood and of the insulator combined are taken into account together. Limited tests have been made on plain air gaps which indicate that about twice the distance is required to avoid power follow. As stated previously sufficient tests were made covering a sufficiently wide range of conditions in regard to surge current and timing of impulse with respect to the 60-cycle voltage wave to draw a statistical chart, but tests are hardly sufficient to segregate quantitatively the corresponding effects of each. The text will clarify the significance of and the conditions accompanying Figures 20, 21, and 22. Tests were made with both an air gap and insulators in series with the wood. The leakage current in the air gap and over the insulators definitely was visible in each test in the form of an arc. The insulators were maintained reasonably clean in these tests. Ross is quite right in stating that the term "leakage currents" needs better defining, for otherwise confusion very well can ensue in the use and significance of this term.

Starr raises some very interesting and pertinent questions which I shall endeavor to answer to the best of my abilities. In a territory where lightning is severe and where multiple and long-duration discharges are contributing factors to the operation of lines, the outage factors indicated in his curves lie probably too low. That is, under these conditions I would expect more frequent outages. For instance the field data on 33-kv wood-pole structures referred to previously indicate that for a voltage stress of about 0.3 kv rms per inch (wood) approximately 14 per cent of the flashovers were accompanied by power follow. The corresponding unit stress (wood plus insulators) in the curves for the path to ground is about 0.45 kv rms per inch for either 115 kv or 230 kv. In view of this it would seem that these curves might not be conservative for application in a severe lightning region such as Northern Illinois or Pennsylvania. However, in regions of low or moderate storm frequency and where conditions of multiple stroke may not be so preponderate it can well be that these curves are quite reasonable. In what direction they may be modified at a future date will depend on actual field observations and findings. I agree with Starr that the long-duration components may not be as important as they may seem, on account of the fact that these become absorbed by the line and can be diverted to ground through transformer windings on systems with the neutral grounded.

In the power-follow tests reported in the paper the impulse generator was set amply above the critical flashover voltage of the insulation structure tested so that invariably impulse flashover would result. As stated previously, limited tests were conducted on plain air gaps. These tests indicated that about twice the distances are required for plain air as for wood and insulator structures. No particular significance has been assigned to the residual voltages in Figure 8. In this connection it might be well to call attention again to the results observed from the tests on pole 2, which was very dry. The behavior of this pole was remarkable in that it showed a zero probability of power follow for a unit average stress as high as 2.6 kv rms per inch. Although the average results for either the poles or crossarms were substantially the same, a small cross-section member probably is likely to be less effective in quenching power follow than a large cross-section member. The wood itself can be a factor too. I certainly concur with Starr that more work can be done to advantage in this field.

Metering With Transformer-Loss Compensators

G. B. SCHLEICHER
MEMBER AIEE

Synopsis: Outstanding economies may be effected by metering high-voltage loads on the low-voltage side of the power transformers, and compensating the metering to include the transformer losses. The transformer-loss compensator is an accessory to the regular watt-hour meter on the low-voltage side and causes the meter to include the transformer losses in its registration. No changes are made in the meter itself, either structurally or in adjustments, it retains its integrity as a standard measuring instrument. The method is intended primarily for use on customers' installations where the contract provides for supplying and billing for energy and demand at distribution or transmission voltages. Based on established principles, the accuracy performance is equal to that of metering on the high-voltage side. Testing techniques have been developed and co-ordinated with meter testing practice, so that its routine application and maintenance can be done by metermen. This paper is the result of experience with compensating meters since 1932, and the more recent application of transformer-loss compensators. It is intended for electrical utility executives and engineers considering the possible advantages of the method for their systems and for guidance in co-ordinating the application of transformer-loss compensators with metering practice.

IN supplying industrial loads to the customers of electrical utilities, service often is furnished at distribution or transmission voltages. In such cases the customer either owns or rents the transformers which step down to the utilization voltage. Billing metering for installations of this kind ordinarily is placed on the high-voltage supply side, as the transformer losses are a part of the registration. Metering on the low-voltage side usually is less costly. It possesses the further advantages of simplifying the high-voltage construction with greater safety to men and equipment, and is protected entirely from lightning and surge disturbances on the high-voltage side.

The fundamental principles by which compensation for transformer losses is possible have been known to engineers for many years. Copper losses vary as the square of the current, and for practical purposes iron losses vary as the square of the voltage. Various networks have been designed by engineers to meet the metering requirements of specific installations, and the compensating meter was developed to make possible routine metering installations on the low-voltage side for utility customers supplied from high-voltage lines. The methods in use are:

1. Compensating metering,[1] in which a separate meter, connected to the low-voltage side, registers the transformer losses. Its registration is added to that of the regular watt-hour meter to obtain billing quantities as of the high-voltage side. The disadvantages of this method are that a special meter is necessary, the measurement of maximum demand is more complicated than with high-voltage metering, and special test equipment, normally not carried by meter testers, is required.

2. Line-drop compensators can be used to compensate the load watt-hour meter for copper losses,[2] but the commercial forms have the disadvantage of introducing relatively high burdens into the current transformer secondary circuits. This is not desirable on metering installations. Burdens have been reduced to some extent by omitting the reactance unit, which is not necessary where the desired measurement includes only power measurements.[1,2] The application of these devices generally requires special test equipment, and their periodic testing by conventional methods is outside of the scope of metermen.

3. The adjustments of the meters themselves can be used to approximate the losses.[3] The light-load adjustment of meters can be made to compensate for core losses quite closely, but as the full-load adjustment in principle raises or lowers the entire characteristic curve of the meter, its use for copper-loss compensation involves compromises in performance. In general, this method is suitable for billing only where the meters are known to operate within certain load ranges, or where the copper losses are relatively small.

4. The addition of calculated losses to load registration has been advocated,[4] and while feasible from an engineering point of view, this is practical only in special cases for utility billing of customers' loads. Loss factors may vary widely, not only between customers but also for the same customer from month to month. Data obtained by actual measurement with compensating meters on typical installations are included in Appendix III.

5. The transformer-loss compensator described in this paper has been designed to compensate for the transformer losses for the range of conditions that are characteristic of metering on the low-voltage side, where service is supplied at distribution or transmission voltages. No changes are made in the regular watt-hour meter, either in construction or in its method of adjustment; the burdens imposed on instrument transformers are sufficiently low to be acceptable for metering installations; and the measurement of demand as of the high-voltage side introduces no complications where a single transformer bank is installed. The methods of procedure that have been developed per-

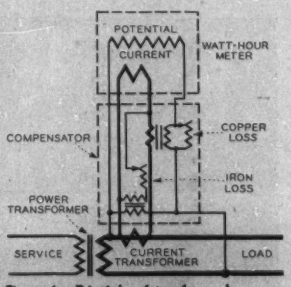

Figure 1. Principle of transformer-loss compensator

Paper 47-116, recommended by the AIEE committees on instruments and measurements and power transmission and distribution for presentation at the AIEE summer general meeting, Montreal, Quebec, Canada, June 9–13, 1947. Manuscript submitted March 29, 1946; made available for printing April 2, 1947.

G. B. SCHLEICHER is technical assistant in the meter division of the transmission and distribution department of the Philadelphia Electric Company, Philadelphia, Pa.

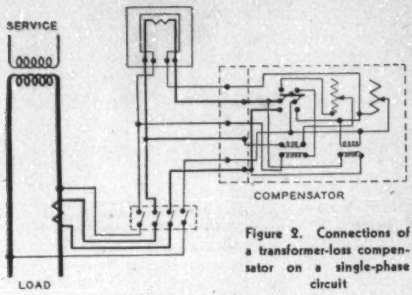

Figure 2. Connections of a transformer-loss compensator on a single-phase circuit

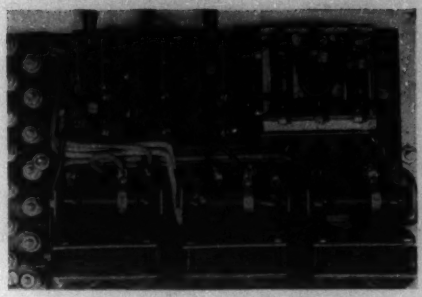

Figure 4. Three-element transformer-loss compensator

mit both the initial calibration and the routine maintenance of the installations to be done by metermen who are capable of handling the corresponding installations on the high-voltage side. These methods may be adapted to any system of meter testing practice.

Principle of Transformer-Loss Compensator

In the transformer-loss compensator, the line-drop compensator principle is used for adding the copper-loss increment to the registration of the load watt-hour meter. The burden imposed on the instrument transformers has been made sufficiently small to be acceptable for metering installations by designing the insulating transformer to step down rather than with the 1-to-1 ratio used in the commercial forms. The ratio of 5.0 to 0.5 amperes has been found to be satisfactory, but its exact value is unimportant when the method of adjustment described in this paper is used. Commercially, the copper-loss transformer is a 5-volt-ampere 1-volt 5-ampere to 10-volt 0.5-ampere unit of good phase-angle performance and is designed to be capable of carrying 100 per cent overload continuously. The 0.5-ampere side is connected to an adjustable resistor unit for which a value of 5 ohms has been found to meet the general range of requirements of commercial installations. For unusual conditions, higher or lower resistor values may be used. The difference of potential across the resistor is added to the secondary line voltage, and the combination is applied to the potential coil of the meter. As the voltage across the resistor is proportional to the current, the loss increment as registered by the watt-hour meter is proportional to the current squared.

For the measurement of the iron-loss increment the "dummy load" method is used.[4] A 7.5-volt-ampere 230/6-volt transformer is connected to the low-voltage supply, and the 6-volt side is connected in series with an adjustable resistor unit, so that a current equivalent to the iron loss is passed through the current coil of the meter. Ordinarily, a 250-ohm adjustable resistor gives sufficient range, but units of higher or lower values of resistance may be used if necessary to obtain the desired performance. For 115-volt circuits, the transformer has sufficient capacity to be operated at half voltage. The compensator, therefore, may be used either for 230-volt or 115-volt installations, or on the secondary of potential transformers. Figure 1 shows the principle of operation.

The assembly of transformers and resistors, together with a double-throw test switch and a terminal block, is intended as an accessory to the watt-hour meter, and its connections to a single-phase circuit on the low-voltage side of a transformer are shown in Figure 2. The test switch of the compensator in its normal position (up) connects the transformer-loss compensator into the circuit, and the transformer losses are included in the registration of the watt-hour meter. When the switch is in the test position (down), the transformer-loss compensator is inoperative, the meter is connected as a watt-hour meter, and may be subjected to all of the tests common to ordinary testing practice, including the test for creep. The compensator test switch is arranged so that the cover cannot be replaced while the switch is in the test position. The

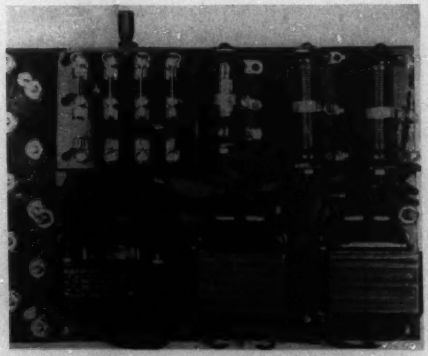

Figure 3. Two-element transformer-loss compensator

Figure 5. Internal connections of 2-element transformer-loss compensator

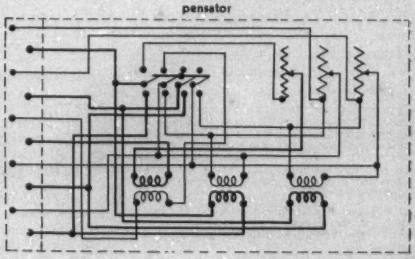

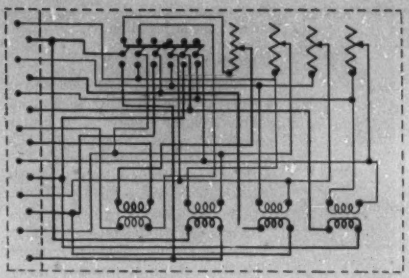

Figure 6 (left). Internal connections of 3-element transformer-loss compensator

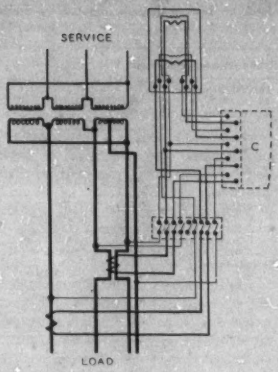

Figure 9 (right). Connections of 2-element transformer-loss compensator on 3-phase 4-wire delta circuits

connections are such that no changes are necessary in grounding practice of current transformer and potential transformer secondaries.

Polyphase Transformer-Loss Compensators

In the practical application of transformer-loss compensators there is little need for the single-phase device. Usually single-phase loads are supplied from low-voltage distribution circuits or networks and are metered and billed at the supply voltage. For polyphase circuits, duplicates of the single-phase unit may be used, but it is more practical to provide polyphase transformer-loss compensators. Two arrangements meet all requirements, one for use with 2-element meters, the other for 3-element meters.

For polyphase circuits it is practical to add the entire iron loss on one meter element, hence only one core-loss transformer is used in polyphase transformer-loss compensators. The 2-element form is shown in Figure 3, and the 3-element form in Figure 4. Their internal connections are shown in Figures 5 and 6 respectively. The connections of the compensator into various 2-element circuits are shown in Figures 7, 8, and 9, and for 3-element circuits in Figures 10 and 11.

In the interest of simplicity, potential transformers have not been shown in the various diagrams of connection. It is obvious, however, that, where potential transformers are used with metering on the low-voltage side, the voltage applied to the meter may be applied also to the potential element of the transformer-loss compensator. The compensator connections of Figure 7, shown with a power transformer bank connected in open delta, are applicable to any other transformer connection from which a 3-phase 3-wire supply may be obtained on the low-voltage side. In all cases the type of circuit on the low-voltage side determines the proper metering.

Practical Considerations

Installation

A transformer-loss compensator may be added to an existing installation which measures the entire output of a transformer bank on the low-voltage side. On installations of this type, however, there should be no means of disconnection between the low-voltage terminals of the transformer bank and the point where the meter potential transformers, or the meter potential circuits, are connected. This is necessary so that iron-loss registration may be obtained whenever the transformer bank is energized from the

Figure 7. Connections of 2-element transformer-loss compensator on 2-phase 3-wire, or on 3-phase 3-wire circuits

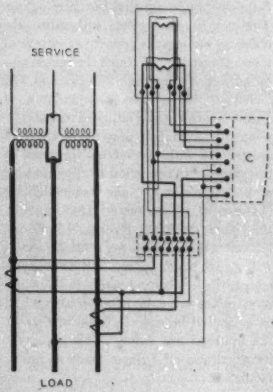

Figure 8. Connections of 2-element transformer-loss compensator on 2-phase 5-wire circuits

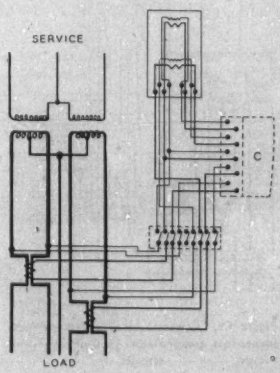

Figure 10. Connections of 3-element transformer-loss compensator on 3-phase 4-wire Y-connected circuits

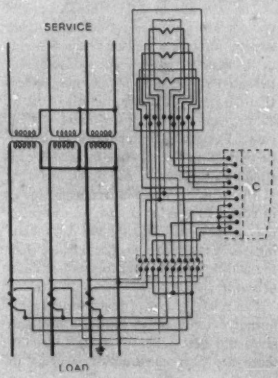

Table I. Tests of Burdens Imposed by Transformer-Loss Compensators on Instrument Transformer Secondaries

Compensator Adjustment						
Approximate Per Cent of Meter Rating	Resistor, Ohms	V	Amp	W	Va	Power Factor
Potential circuits						
0.5	122	115	0.0058	0.43	0.667	0.645
5.0	6.6	115	0.0177	1.85	2.035	0.900
0.5	126	120	0.00615	0.48	0.738	0.650
5.0	6.9	120	0.0185	2.12	2.220	0.964
0.5	146	230	0.0175	3.20	4.025	0.795
5.0	13.6	230	0.025	4.64	5.750	0.807
0.5	153	240	0.020	3.56	4.800	0.742
5.0	14.2	240	0.027	5.04	6.480	0.778
Current circuits						
0.5	1.0	0.340	5.0	1.69	1.70	0.995
1.25	2.5	0.414	5.0	2.06	2.07	0.995
2.5	5.0	0.525	5.0	2.60	2.625	0.990
3.75	7.5	0.651	5.0	3.22	3.255	0.989
5.00	10.0	0.768	5.0	3.76	3.840	0.979

high-voltage side, even though the load may be disconnected.

A simple form of meter panel construction provides a trough about three inches deep for enclosing the meter test switch and wiring. With this construction, the transformer-loss compensator needs no cover and may be mounted in the trough below the meter. Transformer-loss compensators have about the same dimensions as the various types of phasing transformers that are used to convert a watt-hour meter into a var-hour meter. Figures 12 and 13 show typical 2-element and 3-element meter panels with the cover of the trough removed to show the internal arrangement. Figure 14 shows the 3-element panel with the cover in place. In external appearance, the meter panel is entirely similar to that which would be provided for metering on the high-voltage side, or for low-voltage metering without compensation for transformer losses.

Economics

The economy of using transformer-loss compensators is greatest for the higher supply voltages. The cost of a 460-volt or 2,300-volt metering installation compensated to the 33-kv supply may be less than 30 per cent of the metering cost at 33 kv, thus saving approximately 70 per cent. For a 13.2-kv supply, savings may be only 20 per cent, while for a 2.3-kv installation metered at 230 volts, metering at the supply voltage is frequently lower in cost. In the latter case an exception may occur where existing 230-volt metering can be used with no other change than the addition of the transformer-loss compensator.

The relative cost of instrument transformer equipment at the two voltages gives the best index of costs. Usually there are also construction savings in metering at the lower voltages, both to the supply company and to the customer, and in some cases the space required for metering on the high-voltage side may be at a premium. Figure 15 shows the instrument transformer equipment on one of the older 33-kv installations. Figure 16 shows the metering transformers mounted in an outdoor cabinet for a comparable 33-kv installation metered at 460 volts. The same construction applies to 2.3-kv and 4.0-kv installations. Indoor installations at these voltages use an assembly of instrument transformers that may be mounted on the wall, in metal-clad switchgear, or on the ceiling as shown in Figure 17.

The economic advantage of low-voltage metering is reduced, and sometimes eliminated entirely, where more than one metering equipment on the low-voltage side is required in place of a single installation on the high-voltage side.

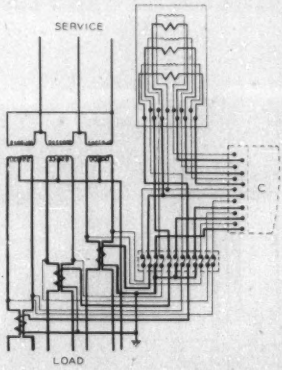

Figure 11. Connections of 3-element transformer-loss compensator on 6-phase 7-wire circuits

Burdens

When a transformer-loss compensator is connected into the meter circuits, an additional burden is placed on the instrument transformers. Table I gives test results of burden measurements. Potential burdens are given for 115 and 120 volts for two extreme conditions of adjustment, representing respectively iron losses equivalent to 0.5 per cent and 5.0 per cent of the meter rating. Current burdens are shown at five amperes for various adjustments for copper losses from 0.5 per cent to 5.0 per cent of the meter rating. The values given for 1.25 per cent of meter rating represent an average condition. With modern instrument transformers, the effect of adding these burdens will not require a retest of the instrument transformers.

Technical Considerations

The transformer-loss compensator becomes practical by co-ordinating its tests and adjustments with meter testing practice. Watt-hour meters connected to instrument transformers usually are tested at three loads, namely 0.5 and 5.0 amperes at power factor 1.0, and at 5.0 amperes at 0.5 lagging power factor. These are termed respectively light-load, heavy-load, and inductive-load tests. On polyphase meters, the final test is made usually with the current circuits of all elements in series and the potential circuits in parallel. This is known as the series test.

Losses in per cent of load are determined for the light-load and heavy-load test points, and the transformer-loss compensator is adjusted for these values. The compensator then will cause the meter to include the proper percentage of losses at any load to which the meter may be subjected in service. For example, the 2-element meter and compensator of Figure 7 is tested and adjusted on a single-phase test circuit at power factor 1.0, in accordance with the method outlined in this paper. In operation on 3-phase load at power factor 1.0, one meter element operates at power factor 0.866 lagging, the other at 0.866 leading. Full-load kilowatts then are 86.6 per cent of the kilowatt load under which the meter was tested, the loss compensation in kilowatts remains the same, and the *percentage* loss as measured becomes 1/0.866 of that at the full-load test value. This is correct for operation on 3-phase loads at power factor 1.0.

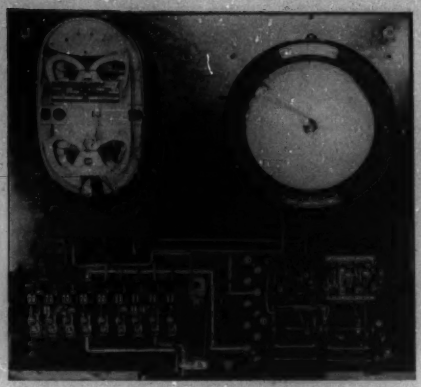

Figure 12. Typical 2-element meter panel with graphic demand meter and transformer-loss compensator (panel cover removed)

Loss Data

The method of calculation on which the calibration of transformer-loss compensators is based is similar to that developed for compensating metering.[1] The manufacturers of transformers, in general, make tests on each transformer rated 100 kva or over, and, for smaller ratings, tests are made on representative samples from production. The test data are obtained by furnishing the manufacturer with the transformer serial numbers and the voltage rating. For calibrating a transformer-loss compensator for use with a watt-hour meter, the following information is required:

1. Iron loss at rated voltage.
2. Copper loss at 75 degrees centigrade at rated full-load current.
3. Voltage taps provided in the high-voltage or low-voltage side.

If power factor tests are intended to be made on the low-voltage side, or if a watt-hour meter is to be calibrated, the following additional information is required:

4. Per cent exciting current at rated voltage.
5. Per cent impedance.

From the installation itself, information is obtained relative to the taps in use and the length, size, and material of the conductors from the low-voltage side of the transformer bank to the metering point. For most types of construction, the metering point is the point where the *potential transformers* (or the meter potential circuits) are connected to the circuit.

Determination of Compensator Settings

The iron and copper losses are calculated for full load on all elements of the meter at power factor 1.0, because this is the load at which the heavy load test of the meter is made. These losses are calculated in per cent of the kilowatt load at which the meter is tested. For a polyphase meter at the heavy load test point, this is the product of the number of elements of the meter and the kilovolt-ampere rating of each element. The per cent losses for any other test load may be calculated by proportion. While copper losses vary as the square of the load current, *per cent* copper loss varies *directly* with per cent load on the meter.[3] Similarly *per cent* iron loss varies *inversely* with per cent load on the meter. Therefore, it is simple to determine the per cent loss for any load. For meter test loads at power factors other than 1.0, it is necessary only to divide the per cent iron and per cent copper losses by the desired power factor. Details of the calculations for an actual installation are shown in Appendix I. Though only the three values determined in Appendix I are used for calibrating a transformer loss compensator, additional calculations were made to show more complete loss data for series tests on a 2-element meter. These loss characteristics are given in Table II, and shown graphically in curves *E* and *F* of Figure 18.

Accuracy Performance

Typical laboratory test results for a watt-hour meter and transformer-loss compensator combination, with the meter elements in series, are given in Table II and are shown graphically in curves *G* and *H* of Figure 18. Tests of the watt-hour meter without compensator are shown in Figure 19. It is interesting to note that the characteristics of the meter with compensator reflect, within the accuracy of the tests, the performance of the meter alone.

Tests in service on five actual installations showed the performance of the meters with loss compensators compared with the high-voltage billing meters to range from 99.84 per cent to 100.26 per cent, with an average of 100.08 per cent. This performance is well within the requirements of public utility commissions. The tests covered a period of 13 weeks, during which the total registration amounted to more than 2 million kilowatt-hours.

Conditions may arise where the iron loss alone is less than the starting load of the meter, or even the load under which the meter will continue rotating when the load is reduced. The same limitation applies to a watt-hour meter on the high-voltage side. The integration of iron loss alone is somewhat more accurate for meters with transformer-loss compensators than with actual measurement on the high-voltage side, because iron loss is added

Table II. Characteristics of Watt Losses and Typical Performance of a Watt-Hour Meter With Transformer-Loss Compensator

Meter Rating, Per Cent Kva	Copper Loss, Per Cent	Iron Loss, Per Cent	Total Loss, Per Cent	Registration, Per Cent		
				Desired	Actual	Error
Power factor = 1.00						
2	0.025	19.900	19.925	119.9	119.5	−0.4
5	0.062	7.960	8.022	108.0	107.9	−0.1
10	0.123	3.980	4.103	104.1	104.1	0
20	0.246	1.990	2.236	102.2	102.4	+0.2
50	0.616	0.796	1.412	101.4	101.9	+0.5
100	1.232	0.398	1.630	101.6	101.6	0
150	1.848	0.265	2.113	102.1	101.7	−0.4
Power factor—0.50 lagging						
2	0.049	39.800	39.849	139.8	138.9	−0.9
5	0.123	15.920	16.043	116.0	115.3	−0.7
10	0.246	7.960	8.206	108.2	107.7	−0.5
20	0.493	3.980	4.473	104.5	104.1	−0.4
50	1.232	1.592	2.824	102.8	102.7	−0.1
100	2.464	0.796	3.260	103.3	103.3	0
150	3.696	0.531	4.227	104.2	103.6	−0.6

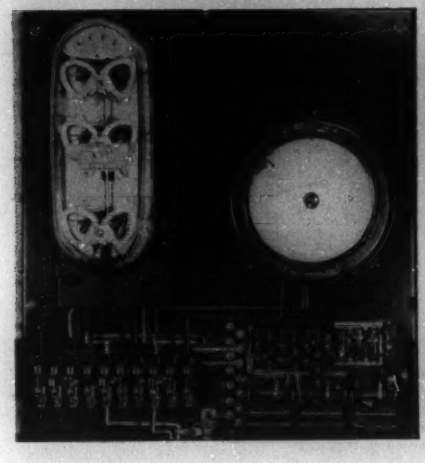

Figure 13. Typical 3-element meter panel with graphic demand meter and transformer-loss compensator (panel cover removed)

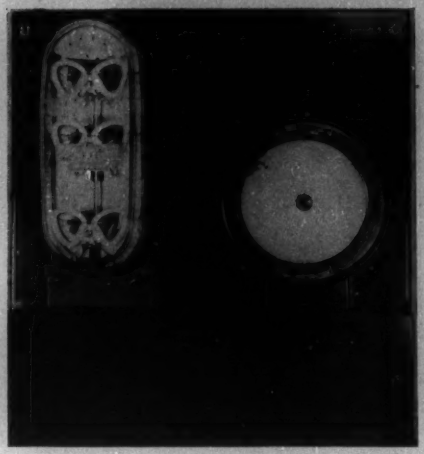

Figure 14. Typical 3-element meter panel with cover in place

at power factor 1.0 where the performance of meters is better than at the lower power factor of the iron loss itself.

Transformers With Taps

Transformers used on customer's services frequently are provided with full capacity taps to permit adjustments in the utilization voltage. Loss data supplied by manufacturers generally are based on the rated voltage, but sometimes on the full windings. Iron losses in watts measured at rated voltage are the same as those obtained when connection is made to a tap and its rated voltage is applied. For copper losses of transformers for the service under consideration, it is sufficiently close to consider that the losses are divided equally between the high-voltage and the low-voltage windings, and the size of conductors is the same throughout each of the windings. Taps on the high-voltage side are most common. With metering on the low-voltage side, if copper loss is given for rated voltage V_r and voltage tap V_t is used, the multiplier to be applied to copper loss at rated voltage

$$M_t = V_r/2V_t + 0.5 \qquad (1)$$

For taps on the low-voltage side, with metering also on the low-voltage side,

$$M_t = V_t/2V_r + (V_t/V_r)^2/2 \qquad (2)$$

Multipliers calculated in this way for the most common taps are given in Table III. The multipliers, where required, are incorporated in equations 4 and 23. Where taps are used on both windings, both multipliers are used.

In practical experience, it happens occasionally that the operating tap on a transformer is changed, or, when the metering equipment is to be calibrated, the tap to be used is not known. For the usual relations of losses, the effect of a change of plus or minus 10 per cent in tap voltage on a meter with loss compensator will be within plus or minus 0.1 per cent at power factor 1.0 and within plus or minus 0.2 per cent for power factor 0.5 As these deviations are well within the permissible test limits to which watt-hour meters can be adjusted, actual recalibration of the compensator is seldom necessary.

Automatic Tap Changers. Though these are not used ordinarily on the type of installations under consideration, they can be taken care of by basing the calibration on the median point, as deviations from it in both directions will tend to cancel. As their range is generally within plus or minus 10 per cent, the discussion of the preceding paragraph applies.

Effect of Transformer Connections

The connection of the power transformers may affect the calculation of copper losses for the determination of the meter setting points. For symmetrical connections, such as delta-delta, star-star, star-delta or delta-star, the losses furnished by manufacturers on the basis of single-phase tests apply directly.

Open-Delta Connections. For such connections, shown in Figure 7, it must be remembered that full-load losses occur when the kilovolt-ampere load on the bank is equal to 86.6 per cent of the sum of the individual ratings of the two transformers. For this connection, the value of the sum of the kilovolt-ampere ratings of the transformers is multiplied by 0.866 for use in equation 3.

Scott Connections. This is used commonly for transformation between 2-phase and 3-phase circuits. A number of methods of calculating the losses for these connections are available, but for application in determining compensator settings, the following simple procedure is useful.

The teaser transformer is connected on the 86.6 per cent tap. In accordance with Table III, the multiplier to be applied to copper loss will be 1.077 or 0.808,

Table III. Copper-Loss Multipliers for Common Transformer Taps With Low-Voltage Metering

Per Cent Tap	Tap on High-Voltage Winding	Tap on Low-Voltage Winding
86.6	1.077	0.808
90.0	1.056	0.855
92.5	1.041	0.890
95.0	1.026	0.926
97.5	1.013	0.963
100.0*	1.000*	1.000*
102.5	0.988	1.038
105.0	0.976	1.076
107.5	0.965	1.115
110.0	0.955	1.155

* Tap on which copper-loss data are based.

depending on whether the metering is on the 2-phase, or on the 3-phase side.

In the main transformer the angular relation between the currents in the two parts of the winding on the 3-phase side has an effect on copper loss. For metering on the 3-phase side, the copper loss multiplier is 0.875, and for metering on the 2-phase side the multiplier is 1.167. These multipliers are applied to equations 4 and 23.

Three-Phase 4-Wire-Delta Connection. With this a 2-element meter, as shown in Figure 9, combines two currents displaced by 120 degrees on the secondary of a double-primary current transformer. If meter tests are made on each element at line voltage, which is a common practice, percentage losses are determined as in Appendixes I and II. The percentage of copper loss as determined in equation 13 or 25 applies to the copper-loss adjustment for the meter element connected to the single-primary current transformer (the bottom element in Figure 9). For the top element, the multiplier of 1.155 is incorporated in equations 13 and 25. For operation in service, the registration of the loss increment then will be proportional to the load balance between the two meter elements.

Initial Calibration

The compensator settings having been determined as in Appendix I, the meter and compensator are connected for test. The watt-hour meter is adjusted in the usual way by placing the compensator test switch in the "test" position. When all tests on the meter are completed, the compensator test switch is opened, which places the copper-loss elements in circuit. The copper-loss resistors of the compensator are adjusted at the heavy load test point, so that the copper loss is added equally on all elements.* Then the compensator test switch is closed in the "normal" position which includes the iron-loss element in the circuit, and test connections are made for the series test. The iron-loss element is adjusted to the calculated light-load setting points. A final check should be made with compensator at heavy load and inductive load.

The operation of the compensator is automatic for changes in load power factor. It must be remembered, however, that any deviation in power factor from the nominal value of 0.5 lagging will result in differences from the desired performance. For inductive load tests, therefore, it is important that the test results be compared with desired values for the power factor at which the test is made.

* For 3-phase 4-wire-delta meters, see preceding paragraph.

Table IV. Interpretation of Service Test Results on Transformer-Loss Compensator Installations

Per Cent Registration			Conclusion	
With Compensator	Without Compensator	Difference	Whr Meter	Compensator
100.0	100.0	0	Perfect	Perfect
99.8	99.7	+0.1	Satisfactory	Satisfactory
100.3	100.3	0	Satisfactory	Perfect
99.6	99.7	−0.1	Adjust	Satisfactory
99.6	99.6	0	Adjust	Perfect
99.8	100.2	−0.4	Satisfactory	Adjust
100.0	100.4	−0.4	Adjust	Adjust

Figure 15. Instrument transformer equipment on a 33-kv metering installation

Service Tests

Tests in service follow the same principles. The "as found" accuracies with compensator *related to the percentages that the meter should read* are the accuracies of the combination. A test on the meter without compensator determines the need for adjustment, either of the meter or of the compensator. The compensator performance is indicated by the difference between the results of tests with and without compensator. Table IV shows the interpretation of typical test results. It is assumed that the permissible test limits are plus or minus 0.3 per cent.

If the compensator requires adjustment, errors on the heavy-load test are corrected with the copper-loss adjustments, those at light load with the iron-loss adjustment. If inductive load tests are desired in the field, it is important to establish and correct for the true power factor of the test load as discussed under "Initial Calibration." The phase-angle of loading devices, and possible variations in the 3-phase line voltages, all have an effect on the true power factor of the test load. However, it is not necessary to make inductive load tests in the field, as with a correctly designed compensator the heavy-load test gives a complete check of compensator performance.

Any method of meter testing may be used with transformer-loss compensators, but, as the total loss curves are not straight lines, the tests with and without compensator should be made at approximately the same test load, and as closely as practicable to the nominal values of test load. Where fixed phantom load devices are used, it is desirable to provide a separate tap in the heavy-load circuit, so that approximately the same current will be passed through the meter when the compensator is in circuit as when it is short-circuited for tests on the meter alone.

Power Factor Tests

In some utilities, power factor tests are made on customers' loads from time to time. When transformer-loss compensators are used for the watt-hour meter, such tests may be made on the low-voltage side and corrected to the point of supply by calculation. The procedure is the

Figure 16. Instrument transformer assembly installed outdoors on 460-volt metering installation (applicable also to 2.3-kv and 4.0-kv metering)

same as for compensating metering. This is described in Appendix *A* of reference 1.

Var-Hour Measurements With Transformer-Loss Compensators

In some utilities, var-hour meters are used for determining monthly average power factor, or with a demand meter controlled by the var-hour meter, power factor at the time of maximum demand. The most common type of var-hour meters used on polyphase circuits are watt-hour meters connected to autotransformers that provide a 90-degree phase displacement for the meter potential circuits. No actual installations of this type have been made with transformer-loss compensators, but from the results of tests the principle of the transformer-loss compensator may be applied also to var-hour meters of this type.

The percentage of var losses in transformers is much higher than the watt losses. The sample calculation in Appendix II gives values for setting points on the same service installation as in Appendix I. It was found that the iron-loss transformer of the compensator had sufficient capacity to take care of var loss and that its connection to the meter side of a standard autotransformer introduced no appreciable errors. For copper-loss compensation of vars, however, a larger transformer than that used with watt-hour meter compensators will be required. It is considered that a copper-loss transformer rated 20 volt-amperes, 4 volts, 5 amperes, to 20 volts 1 ampere may be expected to meet the requirements. Good phase-angle performance for this transformer is particularly important. Burdens for the var-hour compensator will be proportionately greater than those shown for the watt-hour compensator in Table I.

Tests were made to demonstrate the applications of the principle by using two 5/5-ampere current transformers in place of the regular copper-loss transformers. This improvised compensator was adjusted at 115 volts in accordance with the results of Appendix II, and comparative accuracy tests were made between two identical watt-hour meters, each connected to an autotransformer to measure var-hours. One meter was used as a standard, and the other, with compensator, was used to obtain the performance data in Table V. The tests were made at approximately 120 volts on a 3-phase 3-wire circuit, and the desired performance was calculated for each reading, in accordance with the principles outlined in this paper. The results are shown graphically in Figure 20.

In applying the loss compensator to var-hour meters, it should be remembered that the core loss of transformers in vars varies more nearly as the fourth power of the voltage,[1] rather than with the square of the voltage as in the transformer-loss compensator. Hence, for practical purposes, the most accurate performance for var-loss compensation will be obtained by adjusting the compensator at about the average operating voltage.

The fact that the test results in Table V and Figure 20 show the meter to be predominantly slow may be ascribed to the difference between the test voltage of

Figure 17. Instrument transformer assembly installed indoors on a 460-volt installation (applicable also to 2.3-kv and 4.0-kv installations)

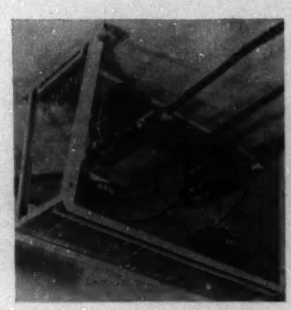

Table V. Characteristics of Var Losses and Performance of a 3-Phase 3-Wire Var-Hour Meter With Special Transformer-Loss Compensator

Var-Hour Meter Rating, Per Cent	Test Voltage	Copper Loss, Per Cent	Iron Loss, Per Cent	Total Loss, Per Cent	Registration, Per Cent: Desired	Actual	Error
Power factor = 0.0							
10	121.0	0.677	22.140	22.817	122.1	122.8	−0.7
25	120.7	1.603	8.856	10.549	110.5	110.1	−0.4
50	120.3	3.386	4.428	7.814	107.8	107.3	−0.5
100	120.2	6.771	2.214	8.985	109.0	108.9	−0.1
Power factor = 0.50 lagging							
10	121.5	0.782	25.570	26.352	126.4	125.6	−0.8
25	121.0	1.955	10.228	12.183	112.2	111.4	−0.8
50	120.8	3.909	5.114	9.023	109.0	108.8	−0.2
100	120.5	7.818	2.557	10.375	110.4	110.7	+0.3
Power factor = 0.866 lagging							
10	120.7	1.354	44.280	45.634	145.6	144.2	−1.4
25	120.5	3.386	17.712	21.098	121.1	120.3	−0.8
50	120.5	6.771	8.856	15.627	115.6	115.4	−0.2
100	120.3	13.542	4.428	17.970	118.0	118.2	+0.2

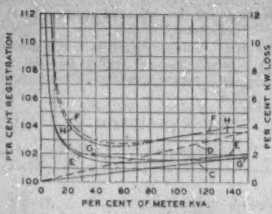

Figure 18. Loss characteristics and series test performance of a 2-element watt-hour meter with transformer-loss compensator on a 1,000-kva transformer bank

C—Per cent copper loss, power factor 1.0
D—Per cent copper loss, power factor 0.5 lagging
E—Per cent total loss, power factor 1.0 (desired performance, power factor 1.0)
F—Per cent total loss, power factor 0.5 lagging, (desired performance, power factor 0.5 lagging)
G—Actual performance, power factor 1.0
H—Actual performance, power factor 0.5 lagging

approximately 120 and the voltage of 115 at which the compensator was adjusted.

Other Applications

Though this paper deals largely with the routine application of compensators to utility metering installations on customers' loads, other application will be evident to engineers. For example, in statistical metering, losses of step-up and step-down transformer banks, together with line losses, may be included in a transformer-loss compensator to provide metering as of a remote point. Compensators may be connected to subtract losses if desired, hence they may be applied to metering in tie lines.

Conclusions

The application of transformer-loss compensators to metering on the low-voltage side, as compared with metering on the high-voltage side is advantageous

1. When the metering cost is appreciably lower than for metering on the high-voltage side.

2. For exposed locations on the system, where high-voltage instrument transformer equipment may be expected to be troublesome because of lightning or other disturbances.

3. When the limited available space makes the installation of high-voltage metering equipment difficult, hence more expensive.

4. When a customer with a rate for low-voltage service is changed to a high-voltage service rate.

The principle of the transformer-loss compensator can be applied to measuring var losses, but further development work on var-hour compensators is required.

Generally speaking, metering on the high-voltage side should be preferred

1. Where multiple compensator installations are necessary in place of one metering equipment on the high-voltage side.

2. Where a part of the load is used or distributed at the supply voltage (high-voltage metering is necessary in this case).

3. Where the cost of high-voltage metering is lower than a compensator installation.

Appendix I. Sample Calculation for Applying a Transformer-Loss Compensator to a Watt-Hour Meter

The application of a transformer-loss compensator to a watt-hour meter on a specific installation will clarify the procedure.

Table VI. Range of Monthly Measured Per Cent Losses in Kilowatt-Hours and at Time of Maximum Demand

Customer	Business Class	Months of Test	Transformer Capacity, Kva	Billing Power Factor	Range of Maximum Demand, Kw	Range of Monthly Per Cent Loss: Kwh	Range of Monthly Per Cent Loss: Max Demand, Kw
A	Abattoir	15	50	0.83	46–82	3.0–3.4	3.1–5.8
		22	112.5	0.83	50–76	2.6–3.8	2.8–3.8
B	Machine shop	31	75	0.67	53–76	2.4–6.4	0.8–4.6
C	Silk mill	4	50	0.68	82–88	4.3–4.6	3.8–4.5
		21	112.5	0.78	36–103	3.3–5.6	1.4–5.5
D	Street railway	24	300	0.62	64–170	3.1–5.0	2.0–4.8
E	Dairy	19	75	0.80	36–60	3.9–5.6	3.8–5.2
F	Steel mill	18	1,500	0.95	264–1,116	3.3–7.9	1.6–4.0
G	Steel mill	17	500		156–216	7.8–11.5	3.3–5.5
H	Steel mill	17	10,000	0.99	1,800–4,200	1.6–4.8	1.2–2.5
I	Penitentiary	15	1,000	1.00	176–408	2.9–32.9	1.7–3.5
J	Construction	14	300	0.81	40–207	2.6–13.8	1.6–4.3
K	Paper manufacturing	12	450	0.92	199–300	2.5–6.6	2.0–2.5
L	Hosiery mill	12	50	0.88	42–47	2.8–3.0	1.0–1.4
M	Pipe line	3	600		332–440	2.4–4.5	1.4–2.0

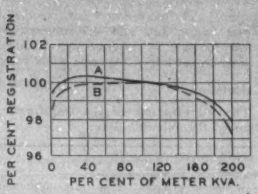

Figure 19. Accuracy characteristics of a modern watt-hour meter

A—Power factor 1.0
B—Power factor 0.5 lagging

Conditions Assumed

A 1,000-kva transformer bank, consisting of three 13,200/440-volt 333-kva transformers, is connected delta-delta. Metering at 440 volts will be by a 2-element instrument transformer-rated watt-hour meter connected to two 1,500/5-ampere current transformers and two 440/110-volt potential transformers. It is desired to compensate the watt-hour meter to read as of the 13,200-volt side of the power transformers, using a transformer-loss compensator.

A field inspection indicates that the connections from the low-voltage side of the transformers to the metering point consist of the following conductors

1. *Carrying phase current—each phase.* Three feet 500,000 circular mils copper conductor, and 8½ feet 1/4 by 4 inch copper bus.

2. *Carrying line current—each line.* Five feet 500,000 circular mils copper conductor (three in parallel) and 5½ feet 1/4 by 4 inch copper bus.

Standard meter testing practice provides for routine testing of polyphase meters with elements in series on the final test. Tests are made on meters at light load, heavy load, and inductive load, for which normal

Figure 20. Performance at lagging power factor of a 3-phase var-hour meter with transformer-loss compensator for a 1,000-kva transformer bank

L—Desired performance, power factor 0.0
M—Actual performance, power factor 0.0
N—Desired performance, power factor 0.5
O—Actual performance, power factor 0.5
P—Desired performance, power factor 0.866
Q—Actual performance, power factor 0.866

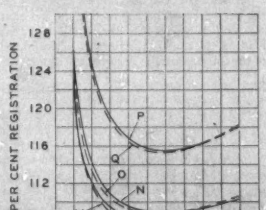

current values are 0.5 and 5.0 amperes at power factor 1.0, and 5.0 amperes at power factor 0.50 lagging. The nominal voltage on the low-voltage side is 460 volts.

Calculation

The manufacturer of the transformers supplied the following data:

Transformer Number	Transformer Kva Rating	Iron Loss at Rated Voltage, W	Copper Loss at Full Load, W	Per Cent Impedance	Per Cent Exciting Current
a	333	1,685	4,092	6.47	1.895
b	333	1,675	4,132	6.65	2.050
c	333	1,665	4,132	6.60	1.870
Total	999	5,025	12,356		

Line current on low-voltage side (full load on transformer bank)* $= 999 \times 1{,}000/440 \times \sqrt{3} = 1{,}310.9$ amperes (3)

Transformer copper loss at meter rating† $= (1{,}500/1{,}310.9)^2 \times 12{,}356 = 16{,}178$ watts (4)

Conductor copper loss (I^2R) at meter rating (resistance per 1,000 feet based on standard wire tables).

Carrying line current $1{,}500^2 \times 15 \times 0.00691/1{,}000 = 233$ watts (5)

$1{,}500^2 \times 16 \times 0.00815/1{,}000 = 293$ watts (6)

Carrying phase current $(1{,}500\sqrt{3})$. $866.1^2 \times 9 \times 0.02074/1{,}000 = 140$ watts (7)

$866.1^2 \times 26 \times 0.00815/1{,}000 = 159$ watts (8)

Total copper loss at meter rating $= 16{,}178 + 233 + 293 + 140 + 159 = 17{,}003$ watts (9)

Iron loss at standard voltage (460) $= (460/440)^2 \times 5{,}025 = 5{,}492$ watts (10)

Meter rating (for series test) $= 2EI \cos\theta = 2 \times 460 \times 1{,}500 \times 1.00 = 1{,}380{,}000$ watts (11)

At meter rating per cent iron loss $= 5{,}492 \times 100/1{,}380{,}000 = 0.398$ per cent (12)

Per cent copper loss $=$ ‡$17{,}003 \times 1{,}380{,}000 = 1.232$ per cent (13)

As per cent iron loss varies inversely as the per cent load on the meter, and per cent copper loss varies directly as the per cent load on the meter, the desired performance of the compensator is summarized as follows:

Test Load	Var-Hour Meter Accuracy Setting, Per Cent	Per Cent Loss: Iron	Per Cent Loss: Copper	Per Cent Loss: Total	Per Cent Desired Registration With Compensator
Light	100.0	3.98	0.123	4.103	104.1
Heavy	100.0	0.398	1.232	1.630	101.6
Inductive	100.0	0.796	2.484	3.260	103.3

This table is based on meter tests at power factor 1.00 at heavy load (100 per cent of meter rating) and at light load (10 per cent of meter rating). Inductive load tests are made at meter rating at lagging power factor 0.5.

When corrections for instrument transformer performance are used, the accuracy settings of the meter are entered under "Watt-hour Meter Accuracy Setting." These settings added to per cent total loss give the "Desired Registration With Compensator."

Appendix II. Calculations for Applying a Transformer-Loss Compensator to a Var-Hour Meter

The principle of the transformer-loss compensator can be applied to the usual forms of var-hour meters used on 3-phase circuits. These are watt-hour meters connected to autotransformers that produce the desired 90-degree phase displacement of the voltages applied to the potential coils of the meter.

In calculating the desired settings for the compensator, the per cent impedance and per cent exciting current obtained from the manufacturer of the transformers in Appendix I are used. The calculations are as follows:

Vars of Iron Loss

For transformer *a*

$va = 333{,}000 \times 0.01895 = 6{,}310$ (14)

$\cos\theta = 1{,}685/6{,}310 = 0.26703$
$\sin\theta = 0.9637$ (15)

$vars = 6{,}310 \times 0.9637 = 6{,}080$ (16)

In the same way vars of iron loss for transformer $b = 6{,}600$, and for transformer $c = 6{,}000$.

Total vars of iron loss at 440 volts $= 6{,}080 + 6{,}600 + 6{,}000 = 18{,}680$ (17)

At the standard meter voltage (460) total vars of iron loss $= (460/440)^4 \times 18{,}680 = 22{,}315$ (18)

Vars of Copper Loss

For transformer *a*

$va = 333{,}000 \times 0.0647 = 21{,}545$ (19)

$\cos\theta = 4{,}092/21{,}545 = 0.1899$
$\sin\theta = 0.982$ (20)

$vars = 21{,}545 \times 0.982 = 21{,}157$ (21)

In the same way, vars of copper loss for transformer $b = 21{,}746$, and for transformer $c = 21{,}591$.

Total vars of copper loss at full load on the transformers $= 21{,}157 + 21.746 + 21{,}591 = 64{,}494$ (22)

At the standard heavy load test point for the meter (1,500 amperes primary)

Total vars of copper loss† $= (1{,}500/1{,}310.9)^2 \times 64{,}494 = 84{,}443$ (23)

Meter rating (for series test) from formula $11 = 1{,}380{,}000$ vars

For tests at meter rating as a watt-hour meter, per cent vars of iron loss $= 22{,}315 \times 100/1{,}380{,}000 = 1.617$ (24)

per cent vars of copper loss‡ $= 84{,}443 \times 100/1{,}380{,}000 = 6.119$ (25)

The compensator settings are

Test Load	Var-Hour Meter Accuracy Setting, Per Cent	Per Cent Loss: Iron	Per Cent Loss: Copper	Per Cent Loss: Total	Per Cent Desired Registration With Compensator
Light	100.0	16.170	0.612	16.782	116.8
Heavy	100.0	1.617	6.119	7.736	107.7
Inductive	100.0	3.234	12.238	15.472	115.5

Appendix III. Test Data of Losses on Actual Installations

In considering methods of including measured transformer losses in billing metering, there appears to be a tendency for engineers to underestimate the magnitude of the losses in relation to the actual load. While transformer efficiencies are high, customer's installations are operated often under highly variable conditions. Transformers must be capable of carrying the maximum load, but in practice they will continue to be used even though load requirements are reduced greatly. Billing metering practices of utilities must be capable of meeting such variations with the same reliability as coaditions of heavy loads. The examples of today are plants with curtailed operations because of strikes; in other cases large transformers were installed for heavy war loads that may not be equalled for years in postwar production.

Table VI gives loss data in per cent of load for monthly kilowatt-hours and for 30-minute maximum demand of 13 customers, for which the losses were measured by compensating meters. Monthly losses varied from 1.6 per cent to 32.9 per cent. While the tests were made during the period from 1932 to 1935, customers *A* and *C* had increases in load that resulted in overloads and the installation of larger transformers; customers *B*, *E*, *F*, *K*, and *L* had maximum demands that required transformer banks of the rating actually installed, while customers *D*, *G*, *H*, *I*, *J*, and *M* could have carried their loads on smaller transformer banks during the entire period of the test. The results in general are quite typical of customers' installations, and it must be concluded that losses are sufficiently variable and important to be measured.

References

1. Compensating Metering in Theory and Practice, George B. Schleicher, AIEE Transactions, volume 52, 1933, pages 816–23; discussion, pages 829–31.

* For open-delta connections see text.
† For transformers with taps, see text.
‡ For 3-phase 4-wire-delta meters, see text.

2. Methods of Metering High-Voltage Circuits, L. J. Lunas. *Electric Journal*, April 1929, pages 180–1.

3. Adjusting Secondary Meters to Include High-Side Losses, Walter C. Wagner, George B. Schleicher. *Electrical World* (New York, N. Y.), February 25, 1933, pages 290–3.

4. Metering Power on the Low-Voltage Side, A. J. Petzinger, B. E. Lenehan. AIEE Transactions, volume 62, 1943, pages 159–63; discussion pages 406–10.

5. United States Patent 1,942,193, Oscar Reflas, Nicholas Szekely. January 2, 1933.

6. Compensating Metering Saves, Walter C. Wagner. *Electrical World* (New York, N. Y.), September 14, 1935, pages 35 and 84.

Discussion

Thomas J. Pearson, Jr. (Boston Edison Company, Boston, Mass.): The author's paper represents an excellent presentation of an advancement in the art of electric metering. It should be of value to utility companies who are utilizing methods of low voltage transformer loss measurement as well as to others who will recognize and adopt this type metering in the future. In the instances where compensated or compensating metering can be proved feasible, the several merits of the transformer loss compensator may warrant its use.

Mathematical Analysis of Transformer Loss Compensator

While the author has aptly described the principles of operation of the transformer loss compensator, it occurs to me that mathematical analysis of the method might be of interest to those reviewing the paper. Taking the simple case of the single phase compensator, as illustrated in Figure 1 of the paper, the vector diagram in Figure 1 of this discussion of currents and voltages may be drawn. In drawing the vector diagram, phase angles of the current transformer and the copper and iron loss transformers incorporated in the compensator are omitted in the interest of simplicity.

E_L = line voltage
I_L = line current
I_S = current transformer secondary current
A = current transformer ratio
R_3 = equivalent resistance of iron loss compensator circuit
E_L/R_3 = component of current proportional to line voltage (compensator current)
R_1 = equivalent resistance of copper loss compensator circuit
I_LR = component of voltage proportional to line current (compensator voltage)
E_M = total voltage applied to watt-hour meter potential coil
I_M = total current supplied to watt-hour meter current coil
θ = line power factor angle
θ_1 = power factor angle of current and voltage applied to watt-hour meter

An uncompensated watt-hour meter registers at a rate equal to the product of the line voltage, the line current, and the cosine of the phase angle or

$$E_LI_L \cos \theta$$

A compensated watt-hour meter registers at a rate equal to the sum of the products of the individual voltages and currents applied to the meter multiplied by the cosine of the respective phase angles or

$$E_MI_M \cos \theta_1$$

Accordingly

$$E_MI_M \cos \theta_1 = E_LI_L \cos \theta + I_L^2R_1 + E_L^2/R_3 + E_LI_L \cos \theta \times R_1/R_3 = \text{power} + \text{copper loss} + \text{iron loss} + \text{extra factor}$$

The so-called extra factor, $[E_LI_L\theta \cos (R_1 + R_3)]$, is a negligible quantity since $R_1 \approx 0.5$ ohm and $R_3 \approx 9{,}600$ ohms according to the values of resistance and transformer ratios indicated by the author under "Principles of Transformer-Loss Compensator." It should be further noted that while this extra factor occurs in the mathematical analysis of the compensator it actually is corrected for in the method used by the author in calibrating the compensator with the watt-hour meter.

Comparative Test of Transformer Loss Compensator With Compensating Meter

In order to determine the efficiency of the transformer loss compensator as a measuring device, a comparative test was made with a standard compensating meter under shop conditions. This test was made possible through the author's co-operative loan of an actual transformer loss compensator.

The meters used in this test are referred to as meters 1, 2, and 3 and are identified as follows:

Meter 1. Standard transformer rated watt-hour meter—$2^1/_2$ ampere, 120 volt, 3 wire, 2 element, 3 phase. Primary rating 1,500 ampere, 480 volt, 3 wire, 3 phase.

Meter 2. Same as meter 1, but used with transformer loss compensator.

Meter 3. Standard transformer rated compensating meter—$2^1/_2$ ampere, 120 volt, 3 wire, 3 element.

Each meter was calibrated carefully prior to making the comparative test. The compensating meter was calibrated for the same losses (actual losses of 1,000-kva transformer installed on system) as the transformer loss compensator.

In the comparative test a 120-volt 3-wire 3-phase service supplied test voltages and currents to the three meters which were connected in series. Y-connected balanced resistance loads were used.

In order to duplicate system load conditions, load curves were drawn for an actual installation and the duration of each value of load was determined. A fair duplication of actual load conditions was employed in the test although it was not feasible to follow the time schedule in every instance. One hundred per cent load was taken as $120 \times 5 \times \sqrt{3} = 1{,}040$ watts.

All accuracy figures in the test were obtained from actual registration figures. In order to eliminate errors due to difference in accuracy of meter 1 and 2, check runs were made at each load with the compensator cut out from the meter. A correction was then applied to the registration of meter 2 to compensate for any difference in accuracy.

The results of the comparative load test are listed in Table I of this discussion. They indicate that, with a unity power factor balanced load, no appreciable differences in registration were found in the two methods of low voltage transformer loss metering.

Additional tests were made with the same setup at 100 per cent load with unity power factor, 0 per cent load, and 100 per cent load with power factor 0.5 lagging. The results obtained are listed in Table II.

Under a condition of no load, the watt-hour meter (number 2) associated with the

Table I. Registration in Kilowatt-Hours

Per Cent Load	Meter 1	Meter 3	Meters 1+3	Meter 2	Per Cent Difference
5	1,271	54	1,325	1,326	+0.08
6	8,502	303	8,805	8,800	−0.06
7	2,702	82	2,784	2,789	+0.18
8	2,202	60	2,262	2,261	−0.05
9	4,440	110	4,550	4,550	0.00
10	11,022	252	11,274	11,279	+0.04
15	9,180	142	9,322	9,325	+0.03
20	10,328	128	10,456	10,456	0.00
25	7,986	85	8,071	8,061	−0.12
30	11,233	109	11,342	11,342	0.00
35	9,411	86	9,497	9,500	+0.03
45	21,832	191	22,023	22,003	−0.09
50	42,447	367	42,814	42,814	0.00
55	43,867	378	44,245	44,243	0.00
	186,423	2,347	188,770	188,749	−0.01

Table II. Comparison of Tests

Per Cent Load	Power Factor	Meter 1	Meter 3	Meters 1+3	Meter 2	Per Cent Difference
100	1.0	9,623	105	9,728	9,729	0.00
0		0	64	64	0	
100	0.5	9,367	214	9,581	9,537	−0.46

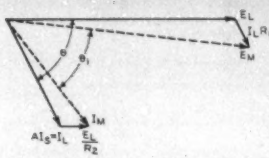

Figure 1. Vector diagram

transformer loss compensator failed to register the core loss. This failure is due to the fact that the transformer core loss was quite small, representing less than 0.2 per cent of the watt-hour meter rating. The compensating meter (number 3) is designed to measure such losses and did register the core loss.

When tested at 0.5 power factor, the watt-hour meter with compensator was found to have a relatively large error in terms of the losses being measured. The error is small, though, in terms of total load being measured.

Further test and analysis indicated that this low power factor error occurred in the measurement of copper loss and was caused by the potential coil currents of the meter flowing through the copper loss circuits of the compensator. The addition of suitably sized capacitors in parallel with the meter potential coils reduces this error to a negligible value.

Conclusions

The use of a transformer loss compensator in conjunction with a standard watt-hour meter appears to be an economical and efficient method for the secondary metering of power transformer input. It is compact, requires no special test equipment, and should be less expensive than the conventional compensating meter. It is not considered to be a superior substitute for primary metering in general, but rather an additional method of secondary metering to be considered in cases where such metering can be proved economically feasible.

W. M. Howe and **H. E. Trekell** (General Electric Company, West Lynn, Mass.): This paper describes an improvement over previous schemes of accomplishing the measurement of high voltage energy with metering equipment on the low-voltage side of power transformers. The introduction of the auxiliary transformers to furnish the iron loss compensation and the copper loss compensation makes possible the desirable decrease in burdens on the main instrument transformers. At the same time the auxiliary transformers and the impedances used allow the two compensators to be practically independent of each other. This results in simpler connections and convenient testing facility. The auxiliary equipment can be mounted in a self-contained compensator unit which in turn can be connected directly between the main instrument transformers and a standard watt-hour meter. The testing procedure is more straightforward and does not present hazards of error existing in previous schemes. This should result in a somewhat higher degree of accuracy.

The general advantages and disadvantages of the use of this type of metering over high-voltage metering have been discussed at considerable length in previous papers cited by the author and in discussions of these papers. In general, these advantages and disadvantages are not changed materially except in respect to lower burdens and improved installation and testing facility.

G. B. Schleicher: The discussions are appreciated. As pointed out by Howe and Trekell, the general advantages and disadvantages of the method described are the same as for the compensating meter (reference 1 of the paper). The transformer-loss compensator, and particularly the technique of its application, have been developed primarily to simplify installation and maintenance procedure.

The mathematical analysis by Pearson is useful to those who wish to review the fundamentals. In preparing the paper, the author has taken the position that the principles involved have been known in the art for many years (reference 2, 4, and 5 of the paper); but practical application has been limited to special situations, because each installation represented an individual engineering problem. One of the main reasons for the paper was the development of a technique for calibration and testing that could be applied by metermen with only general engineering supervision. Those interested in the theoretical aspects will be interested not only in the mathematical analysis in Pearson's discussion, but also in the appendix of reference 4 of the paper. This proves the correctness of copper-loss compensation by the line-drop compensator principle, using resistance only (reference 5 of the paper).

The comparative tests that are described are interesting. No comments are necessary for the tests at various loads at power factor 1.00. The over-all error value of −0.46 per cent at 0.5 power factor reported in the discussion compares with the author's value of 0 per cent in the next to the last line of Table II of the paper. The reason for the difference is in the phase angle performance of the copper-loss transformer. The ones used by the author were prewar transformers, and at the burden in use had a phase angle of +2 minutes. Later transformers, purchased during the war, had phase angles from +50 minutes to +60 minutes at the same burden. The tests reported in the discussion corroborate the importance of good phase-angle performance for the copper-loss transformers, and this has been indicated in the paper. It is anticipated that when commercial models of transformer-loss compensators become available, their performance will equal that of prewar units. The condition, when it exists, is evident from routine shop tests, in that a compensator properly adjusted at power factor 1.00 will show deviations from the desired value of performance in tests at 0.5 power factor, if the phase-angle error is appreciable. The correction of the error by connecting a capacitor across the meter potential circuits is feasible when the phase angle of the copper-loss transformer is positive. The capacitor in this case changes the power factor of the burden on the copper-loss transformer and furnishes a means for phase-angle correction. However, it appears more desirable to correct the error at its source, rather than to add corrective measures.

The tests at no load, which show that core loss alone when it is less than the starting load of the meter will not be registered, corroborate the author's findings. This is recognized in the paper under "Accuracy Performance." It should be remembered, however, that when the load is sufficient to start the meter, core loss is included in the registration. The same limitation of course applies to metering on the high-voltage side, and in this respect the compensating meter is superior.

The author agrees that the method described in the paper is not intended as a complete substitute for primary metering; it is offered as a companion method, of billing meter accuracy, and is intended for those cases where its use results in economies.

Performance of 161-Kv and 115-Kv Transmission Lines

K. E. HAPGOOD
FELLOW AIEE

C. P. ALMON, JR.
MEMBER AIEE

Synopsis: This paper presents engineering and lightning performance data on the Tennessee Valley Authority's 161-kv and 115-kv transmission lines. Normal maximum line loadings are tabulated, and certain transmission line operating practices are described.

THE Tennessee Valley Authority operates 2,195 miles of 161-kv lines and 795 miles of 115-kv lines in an area of approximately 80,000 square miles. The geographical area and the major 115-kv and 161-kv transmission lines are shown in Figure 1.

The 7-year period from August 16, 1939, to August 15, 1946, inclusive, has been chosen because the data are more complete than for prior years. The data are presented principally in tabular form and illustrations. Table I presents engineering and performance data for the 161-kv lines and Table II for the 115-kv lines. Figure 2 shows the configuration for steel tower lines and Figure 3 for wood pole lines.

The predominant type of construction for a given line is tabulated. Where the different types will be of interest, tabulations for more than one type of construction for a given line are shown. There are many cases of minor irregularities, such as a few spans of double-circuit construction in congested areas or the insertion of relatively short lengths of wood pole construction in a steel tower line to route the line around some war activity. These have no effect on the overall performance as the protection level of the particular line has been maintained.

Several short lines have been omitted because the performance of such lines does not reflect the true performance of a long line of the same construction. A comparison of the performance of references 21 and 37 of Table I will illustrate this.

All outages shown were caused by lightning as determined by oscillograph data and other available information. Lightning performance is given on the basis of outages per 100 miles per year. This provides a ready means of comparison of performance. Also, the average outages for the 7-year period are reduced to an isokeraunic level of 50 to provide a means of direct comparison.

Topographical and Other Characteristics

The terrain covered by the high-voltage transmission system varies from flat or rolling with sandy or clay soil in Mississippi and West Tennessee, to mountainous with rock formations in East Tennessee, Western North Carolina, and North Georgia. The greater portion of the area may be classed as rolling or hilly with clay soil prevailing.

The isokeraunic levels, Figure 1, vary from approximately 55 in the northern part of the area to approximately 65 in the southern part of the area in Mississippi. The 60 level is slightly below and more or less parallel to the southern boundary of Tennessee. Thunderstorms may be expected any month of the year. Based on 30 years of record,[1] one thunderstorm day in January and December, and 13 to 14 thunderstorm days in July may be expected.

The earth resistivity varies from three meter-ohms in the West Point, Miss., area, to 10,000 meter-ohms in the Blue Ridge, Hiwassee, and Fontana areas. The value which generally prevails is 600 to 700 meter-ohms.

Structural and Other Features

All the 161-kv and 115-kv lines constructed by the Authority are designed on the principle of the direct-stroke theory.

The majority of the 161-kv lines covered by this paper were constructed by the Authority. Generally, these are steel tower lines with two overhead ground wires. Steel grillages are considered a satisfactory means of grounding those structures erected on grillages. On structures requiring concrete footings, four ground rods are driven under each footing, bonded together and bonded to the reinforcing steel, and connected to the tower by two copper conductors.

Examination of old steel towers in the area indicates that galvanizing will last about 30 years, whereas wood poles deteriorate rapidly in this area of high precipitation and long hot summers. For these reasons, it is more economical to use steel towers for major lines.

Present designs using wood poles require full-length treatment of all poles, whether pine, fir, or cedar. Some of the early installations used butt-treated fir or cedar which proved unsatisfactory.

Wood pole construction is used on some 161-kv lines. Before the war, wood was used only when time was limited and construction could be expedited. Two overhead ground wires are used. The pole ground on each pole is connected to the overhead ground wire, bonded to the pole hardware, and stapled to a copper plate on the pole butt. A ground rod is driven in each pole hole with a sufficient length exposed to insure contact with the copper plate. The insulator hardware is not grounded. During the war, the copper plate on the pole butt was omitted as well as the ground rod in each hole and, instead, the ground wire was wrapped

Paper 47-117, recommended by the AIEE committees on power transmission and distribution and protective devices for presentation at the AIEE summer general meeting, Montreal, Quebec, Canada, June 9-13, 1947. Manuscript submitted November 18, 1946; made available for printing April 3, 1947.

K. E. HAPGOOD is chief, power engineering and design division, and C. P. ALMON, JR., is chief, power system operations division, both with Tennessee Valley Authority, Chattanooga, Tenn.

Table I. Lightning Performance and Design Features of 161-Kv Lines

REF	LINE DESIGNATION	DATE IN SERVICE	LENGTH IN MILES	CIRCUITS PER STRUCTURE	TOWER TYPE (FIG. NO.)	TOWER AVE. SPAN (FEET)	TOWER TOP COND. ABOVE GROUND (FT.)	INSULATORS NO. PER STRING SUSP./A.N.	INSULATORS SPACING (INCHES)	INSULATORS MIN. NO. EQUIV. WHITE SUSP. 5-3/4"	CONDUCTORS LINE SIZE (MCM)	CONDUCTORS LINE MATERIAL	CONDUCTORS GROUND WIRES NUMBER	CONDUCTORS GROUND WIRES SIZE (INCHES)	CONDUCTORS GROUND WIRES MATERIAL	WIRE SAG GND. WIRE AVE. SPAN (FEET)	WIRE SAG CONDUCTOR AVE. SPAN (FEET)
1	2	3	4	5	6	7	8	9	10	11	12	13	14	15	16	17	18
1	ALCOA-LOWNDALE-NORRIS	7-'37	43.3	1	2 A	1125	66	11/14	5-3/4	11	636	ACSR	2	7/16	Steel	36	38
2	CENTERVILLE-COLUMBIA	6-'38	25.6	1	3 C	855	50	10/10	5-3/4	10	397.5	ACSR	2	3/8	Steel	12.5	22
3	CENTERVILLE-WEST NASHVILLE (d)	1928	41.4	1	2 E	960	65	10/11	5-3/8	9.4	266.8	ACSR	1	3/8	Steel	30	35
4	CENTERVILLE-WILSON DAM	1-'50	68.8														
	DOUBLE CIRCUIT TOWERS (ONE CIRCUIT UP)	1-'50	15.9	1	2 C	885	65	10/11	5-3/8	9.4	266.8	ACSR	1	3/8	Steel	24	25
	SINGLE CIRCUIT TOWERS	1-'50	52.9	1	2 E	960	65	10/11	5-3/8	9.4	266.8	ACSR	1	3/8	Steel	30	34
5	CHEROKEE-DOUGLAS-ALCOA	4-'42	47.8	1	2 A	990	66	11/14	5-3/4	11	500	COPPER	2	3/8	Steel	30	37
6	CHEROKEE-NORRIS	4-'46	35.1	1	2 A	1090	66	11/14	5-3/4	11	636	ACSR	2	7/16	Steel	30	36
7	CHICKAMAUGA-WATTS BAR	2-'37	48.6	1	2 A	1150	66	11/14	5-3/4	11	636	ACSR	2	7/16	Steel	33	40
8	CLARKSVILLE-WEST NASHVILLE	9-'42	38.1	1	2 A	1050	71	11/14	5-3/4	11	636	ACSR	2	7/16	Steel	27	33
9	COLUMBIA-SOUTH NASHVILLE	2-'41	41.7	1	2 A	1080	66	11/14	5-3/4	11	636	ACSR	2	7/16	Steel	29	35
10	FONTANA-ALCOA	2-'42	27.7	1	2 A	1460	65	14/16	5-3/4	14	636	ACSR	2	7/16	Steel	53	64
11	FONTANA-SANFORTLAN	5-'42	3.8	1	3 C	590	38	11/14	5-3/4	11	636	ACSR	2	7/16	Steel	10	13
12	FORT LOUDOUN-ALCOA SW. STA.	8-'41	15.5	1	3 C	700	37	11/14	5-3/4	11	636	ACSR	2	7/16	Steel	11.5	14
13	GUNTERSVILLE-CHICKAMAUGA	12-'38	91.0	1	2 A	1100	66	11/14	5-3/4	11	636	ACSR	2	7/16	Steel	30	36
14	GUNTERSVILLE-HUNTSVILLE (e)	1-'43	24.0	1	3 C	500	38	11/14	5-3/4	11	300	COPPER	2	3/8	Steel	7.3	8.8
15	HIWASSEE-ALCOA SW. STA. (j)	6-'41	51.1	1	2 A	1060	66	11/14	5-3/4	11	636	ACSR	2	7/16	Steel	28	34
16	HIWASSEE-APALACHIA-CHICKAMAUGA (j)	5-'40	68.1	1	2 A	1400	66	11/14	5-3/4	11	636	ACSR	2	7/16	Steel	32	39
17	KARTUCKY DAM-CLARKSVILLE (f)	11-'44	70.8	1	3 C	620	38	11/14	5-3/4	11	636	ACSR	2	7/16	Steel	9.6	11.5
18	KARTUCKY DAM-MARTIN (g)	9-'41	60.6	1	3 C	520	38	11/14	5-3/4	11	300	COPPER	2	3/8	Steel	7.7	10.4
19	NORRIS-PINEVILLE	9-'41	50.9	1	3 C	600	38	11/14	5-3/4	11	300	COPPER	2	7/16	Steel	9.2	12.6
20	PICKWICK-NORTH MEMPHIS	6-'40	102.7	1	2 A	1050	66	11/14	5-3/4	11	636	ACSR	2	7/16	Steel	28	33
21	PICKWICK-SOUTH MEMPHIS	11-'37	103.5	1	2 A	750	63	16/19	5-3/4	16	636	ACSR	2	7/16	Steel	33	46
22	SOUTH MEMPHIS-NORTH MEMPHIS (h)	9-'40	8.7	1	2 B	650	72	11/14	5-3/4	11	397.5	ACSR	2	3/8	Steel	18	21
23	SOUTH NASHVILLE-LOUISVILLE #1	9-'42	177	2	2 B	1020	94	11/14	5-3/4	11	500	COPPER	2	7/16	Steel	26	38
	#2	9-'42															
24	SOUTH NASHVILLE-WEST NASHVILLE (i)	1929	14.5	1	2 C	660	76	11/14	5-3/4	11	266.8	ACSR	1	3/8	Cu.'weld	18	19
25	WATTS BAR-ALCOA SW. STA.	7-'38	45.4	1	2 A	1000	66	11/14	5-3/4	11	636	ACSR	2	7/16	Steel	30	35
26	WATTS BAR-FORT LOUDOUN	7-'41	34.4	1	3 C	600	37	11/14	5-3/4	11	636	ACSR	2	7/16	Steel	8.5	10.3
27	WATTS BAR-NORRIS	7-'36	64.3	1	2 A	1000	64	19/21	5-1/8	16.9	636	ACSR	2	7/16	Steel	29	39
28	WATTS BAR-SOUTH NASHVILLE	6-'41	127.9	1	3 C	600	38	11/14	5-3/4	11	477	ACSR	2	7/16	Steel	8.6	10.3
29	WHEELER-COLUMBIA #1	9-'36	65.5	1	2 A	1080	72	11/14	5-3/4	11	397.5	ACSR	2	7/16	Steel	39	43
30	WHEELER-COLUMBIA #2	3-'40	64.3	1	2 A	1070	72	11/14	5-3/4	11	397.5	ACSR	2	7/16	Steel	39	43
31	WHEELER-GUNTERSVILLE	12-'36	65.8	1	2 A	1120	66	11/14	5-3/4	11	636	ACSR	2	7/16	Steel	31	37
32	WHEELER-WATTS BAR	7-'36	161.5														
	WOOD SECTION		96.1	1	3 B	570	42	9/12	6.5/5.5	10.2	636	ACSR	2	3/8	Steel	6.7	11.0
	STEEL SECTION		65.4	1	2 A	980	64	19/21	5-1/8	16.9	636	ACSR	2	7/16	Steel	24	35
33	WILSON DAM-DECATUR-HUNTSVILLE (e)	5-'43	74.1	1	3 C	620	41	11/12	5-3/4	11	300	COPPER	2	1/2	Steel	12	19
34	WILSON DAM-PICKWICK #1	2-'35	44.8	1	3 D	710	37	11/13	5-3/4	11	397.5	ACSR	2	7/16	Steel	9.7	10.9
35	WILSON DAM-PICKWICK #2	1-'40	45.6	1	2 A	1080	63	16/19	5-3/4	16	636	ACSR	2	7/16	Steel	29	35
36	WILSON DAM-WHEELER #1	7-'36	15.5	1	2 A	990	64	19/21	5-1/8	16.9	636	ACSR	2	7/16	Steel	27	36
37	WILSON DAM-WHEELER #2	4-'40	15.4	1	2 A	990	64	16/19	5-3/4	16	636	ACSR	2	7/16	Steel	27	36

(a). Maximum angular swing producing minimum clearance to structure or ground.

(b). All counterpoise. These were installed as part of initial installation except for reference 3 (see note 4).

(c). At isokeraunic level of 50.

(d). Counterpoise completed September 24, 1943.

(e). Originally operated at 115 kv. See Table II, references 15, 16, and 18. Were converted to 161-kv operation on May 30, 1943.

Table II. Lightning Performance and Design Features of 115-Kv Lines

REF	LINE DESIGNATION	DATE IN SERVICE	LENGTH IN MILES	CIRCUITS PER STRUCTURE	TOWER TYPE (FIG. NO.)	TOWER AVE. SPAN (FEET)	TOWER TOP COND. ABOVE GROUND (FT.)	INSULATORS NO. PER STRING SUSP./A.N.	INSULATORS SPACING (INCHES)	INSULATORS MIN. NO. EQUIV. WHITE SUSP. 5-3/4"	CONDUCTORS LINE SIZE (MCM)	CONDUCTORS LINE MATERIAL	CONDUCTORS GND. WIRE NUMBER	CONDUCTORS GND. WIRE SIZE (INCHES)	CONDUCTORS GND. WIRE MATERIAL	WIRE SAG GND. WIRE AVE. SPAN (FEET)	WIRE SAG CONDUCTOR AVE. SPAN (FEET)
1	2	3	4	5	6	7	8	9	10	11	12	13	14	15	16	17	18
1	ARLINGTON-WATERVILLE (d)	1926	53.1	1	3 A	680	42	7/8	5-1/8	6.2	250	Copper	No	----	-----	----	19.5
2	ARLINGTON-MARYVILLE-OCOEE #1 (e)	1914	83.5	1	2 E	400	48	8/9	4-3/4	6.5	400	Alum.	1	3/8	Steel	4.4	9.0
3	BURNSVILLE-PUPKIN-WEST POINT	7-'39	90.7	1	3 C	560	40	7/9	5-3/4	7.0	4/0	ACSR	2	3/8	Steel	8.5	10.5
4	CHICKAMAUGA-CLEVELAND-OCOEE #1 (f)		29.7	1													
	CHICKAMAUGA-CLEVELAND SECT.	1926	25.7	1	3 A	480	38	8/8	4-3/4	6.6	3/0	Copper	No	----	-----	----	11
	CLEVELAND-OCOEE #1 SECT.	1913	14.0	2	2 C	585	66	8/9	4-3/4	6.6	2/0	Copper	1	1/4	Cu.Clad	14	15.6
5	CHICKAMAUGA-VALDEAU-HALES BAR		22.5	1													
	CHICKAMAUGA-VALDEAU SECT.	10-'41	6.1	1	3 C	550	38	7/9	5-3/4	7.0	4/0	Copper	2	3/8	Steel	8	12.6
	VALDEAU-HALES BAR SECT. (g)	1930	16.4	1	2 C	790	65	8/9	5-3/8	7.5	397.5	ACSR	1	3/8	Steel	20	21
6	GREAT FALLS-SO. NASHVILLE (h)	1913	76.8	1													
	GREAT FALLS-MURFREESBORO SECT.	1913	44.8	1	2 D	820	40	8/9	4-3/4	6.6	2/0	Copper	2	5/16	Steel	19	23
	MURFREESBORO-SO. NASHVILLE SECT.	1913	32.0	1	2 D	620	40	8/9	4-3/4	6.6	2/0	Copper	2	5/16	Steel	11	13.2
7	HALES BAR-GREAT FALLS-OCOEE #1-ENGLEVILLE (i)		199.1														
	HALES BAR-COLLEGE JCT. SECT.	1915	37.3	1	2 C	453	55	8/9	4-3/4	6.6	400	Alum.	1	3/8	Steel	7.6	9.1
	COLLEGE JCT.-GREAT FALLS SECT.	1913	31.8	1	2 D	665	40	8/9	4-3/4	6.6	2/0	Copper	2	5/16	Steel	12.5	15.0
	COLLEGE JCT.-CLEVELAND JCT. SECT.	1913	34.4	1	2 D	464	40	8/9	4-3/4	6.6	2/0	Copper	2	5/16	Steel	12.5	15.0
	FORT LOUDOUN-OCOEE #1 SECT. (j)	1913	68.7	1	2 E	510	48	8/9	4-3/4	6.6	4/0	Copper	1	3/8	Steel	7.4	10.4
	FORT LOUDOUN-WASHINGTON SECT.	1913	26.9	1	2 E	550	47	8/9	4-3/4	6.6	2/0	Copper	1	3/8	Steel	9.6	13.4
8	JACKSON-COVINGTON-RIPLEY-SO. MEMPHIS		112.1	1													
	JACKSON-COVINGTON SECT.	2-'40	48.1	1	3 C	560	44	7/9	5-3/4	7	4/0	ACSR	2	3/8	Steel	8.5	10.4
	RIPLEY-COVINGTON-MEMPHIS SECT.	1927	64.0	1	3 A	570	38	6/9	5-1/8	5.4	2/0	Copper	No	----	-----	----	10.6
9	JACKSON-MARTIN	2-'39	60.0	1	3 C	570	38	7/9	5-3/4	7	4/0	ACSR	2	3/8	Steel	8.8	10.8
10	NORRIS-COAL CREEK (k)	10-'41	4.4	1	2 E	525	36	8/12	4-3/4	6.6	2/0	Copper	1	3/8	Steel	7.9	13.0
11	NORRIS-WASHINGTON (l)	9-'38	27.6	1	3 D	700	32	7/9	5-3/4	7	397.5	ACSR	2	7/16	Steel	13.4	16.8
12	OCOEE #1-OCOEE #2 (m)	1915	7.5	1	2 C	673	66	8/9	4-3/4	6.6	2/0	Copper	1	5/16	Steel	18.5	20.5
13	PICKWICK-BURNSVILLE	2-'35	17.1	1	3 C	590	44	6/8	5-3/4	6	4/0	ACSR	2	3/8	Steel	9	11.4
14	PICKWICK-JACKSON	7-'36	52.4	1	3 C	540	44	7/9	5-3/4	7	4/0	ACSR	2	3/8	Steel	7.9	9.6
15	SO. HUNTSVILLE-DECATUR (n)	1925	21.2	1	3 C	520	28	8/12	5-3/4	8	300	Copper	2	1/2	Steel	7.4	8.9
16	SO. HUNTSVILLE-GUNTERSVILLE (n)	1920	21.0	1	3 C	630	34	7/8	4-3/4	5.8	1/0	ACSR	2	3/8	Steel	6.5	8.1
17	SO. NASHVILLE-SPRINGFIELD	10-'41	30.4	1	3 C	590	38	7/9	5-3/4	7	4/0	ACSR	2	3/8	Steel	9.5	11.6
18	WILSON DAM-DECATUR (n)	1925	49.4	1	3 C	670	28	8/12	5-3/4	8	300	Copper	2	1/2	Steel	12.0	14.9

(a). Maximum angular swing producing minimum clearance to structure or ground.

(b). Based on 1½ x 40 microsecond positive wave.

(c). At isokeraunic level of 50.

(d). Terminated at Douglas hydroelectric plant on June 30, 1945, leaving 31 miles in service between Douglas and Waterville. Remainder retired.

(e). Removed from service on December 3, 1944.

(f). Operated as two separate lines after December 19, 1943. Chickamauga-Cleveland section has steel crossarms.

(g). Installed two ground wires on top arm, two phase conductors on middle arm, or one phase conductor on bottom arm October 31, 1944. Original construction listed in table.

(h). After February 9, 1941, this line was operated as two separate sections.

(i). Prior to the retirement of College Junction-Cleveland Junction section on

Table I (continued). Lightning Performance and Design Features of 161-Kv Lines

Wire spacing at tower (feet - min.) Cond. Horiz.	Cond. Vert.	Gnd. wire Horiz.	Gnd. wire Vert.	Line clear. to struct. Inches	Cond. sag at 60°F/inches (a)	Maximum shielding angle (degrees)	Tower footing res. (ohms) Before aux. gnd. Max.	Min.	Ave.	After aux. gnd. Max.	Min.	Ave.	Auxiliary grounding	Ave. elevation above sea level	Insulator impulse flashover kv (b)	Isoceraunic level	Lightning outages: Outages per 100 miles per year 8-16-1939 to 8-15-1940	8-16-1940 to 8-15-1941	8-16-1941 to 8-15-1942	8-16-1942 to 8-15-1943	8-16-1943 to 8-15-1944	8-16-1944 to 8-15-1945	8-16-1945 to 8-15-1946	Ave. per 100 mi. per year: Actual	At 50 level (c)	Ref
19	20	21	22	23	24	25	26	27	28	29	30	31	32	33	34	35	36	37	38	39	40	41	42	43	44	45
21	--	33	21	75	52/48	12	96	5.5	30	--	--	--	No	1100	1020	55	0	2.94	2.31	4.62	2.31	0	0	1.74	1.58	1
16	--	16	11	56	50/42	55	--	--	--	--	--	--	No	750	940	55	7.82	0	0	3.91	0	0	3.91	2.23	2.04	2
22	14	--	9.2	69	35/66	59	131	1.9	28	52	1.9	25.0	26-STR.	750	890	55	4.96	11.40	16.28	9.13	9.13	15.98	11.40	11.40	10.35	3
																55	17.44	16.00	13.05	29.05	24.70	57.80	20.30	22.6	20.55	4
--	12.5	--	9.2	59	35/66	49	--	--	--	--	--	--	No	700	890											
22	14	--	9.2	69	35/66	59	--	--	--	--	--	--	No	750	890											
21	--	33	21	75	52/48	12	143	2.9	33	47	2.9	20	70-STR.	1100	1020	55			0	0	4.17	0	2.09	1.25	1.13	5
21	--	33	21	75	52/48	12	98	5.0	23	30	5.0	15.6	38-STR.	1100	1020	55							0	0	0	6
21	--	33	21	75	52/48	12	700	2.0	52.1	--	--	--	No	870	1020	60	4.12	4.12	0	6.17	2.06	0	8.24	3.53	2.94	7
21	--	33	21	75	52/48	12	68	1.0	12.0	--	--	--	No	650	1020	55							0	0	0	8
21	--	33	21	75	52/48	12	197	1.2	11.0	--	--	--	No	750	1020	55	4.96	0	2.4	0	0	0	0	1.21	1.10	9
25	--	24	22	94	52/55	11	260	3.0	70.7	30.8	3.0	21	75-STR.	1500	1280	55					0	0	3.6	1.20	1.09	10
17	--	17	13	72	47/42	30	--	--	--	--	--	--	No	1500	1020	55				0	0	0	26.3	6.58	5.98	11
17.5	--	17.5	14	72	47/42	50	176	4.0	74	--	--	--	No	1000	1020	55					0	0	0	0	0	12
21	--	33	21	75	52/48	12	285	2.3	59	--	--	--	No	850	1020	60	3.30	5.50	6.60	4.40	6.60	3.30	3.30	4.72	3.93	13
17	--	17	13	72	47/42	30	--	--	--	--	--	--	No	700	1020	60				0	0	0	0	0	0	14
21	--	33	21	75	52/48	12	410	1.6	52	348	1.6	55.3	143-STR.	1100	1020	55		21.0	1.95	1.95	1.95	0	1.95	4.11	3.74	15
21	--	33	21	75	52/48	12	150	0.8	172.3	50	0.8	19.0	198-STR.	1300	1020	60	32.8	4.63	4.63	8.89	1.46	0	2.89	7.04	5.85	16
17.5	--	17.5	13.6	72	47/42	30	290	1.5	38	--	--	--	No	550	1020	55							0	0	0	17
17	--	17	13	72	47/42	30	280	1.0	25	--	--	--	No	500	1020	55							0	0	0	18
17	--	17	13	72	47/42	30	--	--	--	--	--	--	No	1400	1020	55			2.08	1.96	3.92	1.96	1.96	2.21	2.01	19
21	--	33	21	75	52/48	12	195	0.7	22.0	--	--	--	No	500	1020	60	5.73	2.92	1.95	0.97	4.87	2.92	0	2.76	2.30	20
27	--	40	23	104	45/68	17	200	0.5	15.0	--	--	--	No	500	1440	60	0	0.97	0.97	0	0.97	0.97	0.97	0.69	0.58	21
27	15	17.5	15	71	45/48	9	--	--	--	--	--	--	No	280	1020	60		13.0	0	0	0	0	0	1.85	1.54	22
																				0.61	2.86	1.13	0.57	1.14	1.04	23
26	13.5	31	18	75	40/48	0	510	1.7	16	21.6	1.7	7.1	219-STR.	780	1020	55				0	2.26	1.13	0.57	0.99	0.90	
22	13.5	--	9.3	77	40/48	48	--	--	--	--	--	--	No	540	1020	55			35.40	0	21.0	0	0	8.05	7.32	24
21	--	33	21	75	52/48	12	560	3.0	44	--	--	--	No	1000	1020	55	4.41	11.01	4.41	6.61	2.20	2.20	2.20	4.72	4.29	25
17.5	--	17.5	14	72	47/42	50	360	1.6	94	--	--	--	No	1000	1020	55			0	0	0	6.45	0	2.15	1.95	26
27	--	40	24	110	45/68	17	128	2.0	42	--	--	--	No	960	1520	55	0	0	0	7.78	0	0	0	1.11	1.01	27
17.5	--	17.5	14	74	47/42	30	1580	1.8	130.0	--	--	--	No	1200	1020	55					18.18	0	1.56	6.58	5.07	28
21	--	33	21	76	52/48	11	105	2.8	30	--	--	--	No	880	1020	55	1.53	1.53	4.59	7.65	3.06	1.53	1.53	3.06	2.78	29
21	--	33	21	76	52/48	11	122	3.5	39	--	--	--	No	880	1020	55	3.73	3.10	1.55	4.65	4.65	1.55	7.75	3.85	3.50	30
21	--	33	21	75	52/48	12	208	1.7	48	--	--	--	No	760	1020	60	3.04	15.20	7.60	9.12	4.56	1.52	9.12	7.17	5.97	31
																60	0	1.24	4.33	0.62	2.48	1.86	0.62	1.59	1.32	32
16	--	60	13.6	70	41/42	45	2010	5.0	255	--	--	--	No	800	950											
27	--	40	24	110	45/68	17	2090	2.0	170	--	--	--	No	850	1520					12.62	4.05	5.39	1.35	5.86	4.89	33
17	--	17	10.5	75	28/42	33	--	--	--	--	--	--	No	700	1020	60										
17	--	29	13.6	72	47/42	10	1900	2.0	124	--	--	--	No	600	1020	60	6.55	4.46	0	0	0	0	4.46	2.21	1.84	34
27	--	40	23	104	45/68	17	1650	3.0	95	--	--	--	No	600	1440	60	0	2.19	2.19	0	2.19	0	2.19	0	1.25	1.04	35
27	--	40	24	110	45/68	17	125	1.5	28	--	--	--	No	630	1520	60	0	0	0	0	0	0	0	0	0	36
27	--	40	24	104	45/68	17	228	0.4	45	--	--	--	No	650	1440	60	0	0	0	0	0	0	0	0	0	37

(f). Operated temporarily at 115 kv from November 23, 1944, to September 16, 1945; thereafter at 161 kv.

(g). Operated temporarily at 115 kv from September 4, 1944 to September 17, 1945; thereafter at 161 kv.

(h). Originally 132-kv double circuit towers (steel). Converted to 161 kv by changing arms using two on one side of structure and one on the other.

(i). Changed operating voltage on November 1, 1944 from 115 kv to 161 kv.

(j). Operated first year without counterpoise.

Table II (continued). Lightning Performance and Design Features of 115 Kv Lines

Wire spacing at tower (feet - min.) Cond. Horiz.	Cond. Vert.	Gnd. wire Horiz.	Gnd. wire Vert.	Line clear. to str. Inches	Cond. sag at 60°F/inches (a)	Maximum shielding angle (degrees)	Tower footing res. (ohms) Max.	Min.	Ave.	Auxiliary grounding	Ave. elevation above sea level	Insulator impulse flashover kv (b)	Isoceraunic level	Lightning outages: Outages per 100 miles per year 8-16-1939 to 8-15-1940	8-16-1940 to 8-15-1941	8-16-1941 to 8-15-1942	8-16-1942 to 8-15-1943	8-16-1943 to 8-15-1944	8-16-1944 to 8-15-1945	8-16-1945 to 8-15-1946	Ave. per 100 mi. per year: Actual	At 50 level (c)	Ref
19	20	21	22	23	24	25	26	27	28	29	30	31	32	33	34	35	36	37	38	39	40	41	42
14	--	--	--	53	13/50	--	--	--	--	No	1400	630	55	30.21	20.8	35.95	41.60	37.8	34.09	25.8	32.31	29.40	1
13.6	5.7	--	6.9	46	17/32	48	--	--	--	No	900	680	55	4.72	10.62	28.40	36.25	44.18	15.71	--	18.89	16.61	2
12.5	--	13	9.2	50	60/26	30	1220	0.7	71	No	500	690	65	2.17	0	5.50	4.40	5.50	9.95	6.61	4.87	3.77	3
													60	9.55	33.40	19.10	19.10				20.29	16.90	4
13	--	--	--	46	55/42	--	--	--	--	No	870	680	60					33.1	31.1	7.78	23.33	19.40	
16.5	10	--	9.3	46	32/30	42	--	--	--	No	900	680	60					50.0	7.15	0	19.05	15.89	
																40.0	44.4	26.6	22.2	13.31	29.30	24.40	5
12.5	--	13	9.2	50	60/26	30	380	1	107	No	830	690	60								54.9	4.57	
--	11	--	9.7	56	47/32	50	390	2.1	93	No	1200	750	60	40.8	61.0						1.35	1.23	6
														1.35	1.35								
10.5	--	6	4.44	44	30/32	60	--	--	--	No	800	680	55		8.71	0	11.16	4.46	6.69	2.23	5.54	5.04	
10.5	--	6	4.44	44	30/32	60	--	--	--	No	700	680	55		9.38	0	0	0	6.25	6.25	3.54	3.31	
														5.02	8.02	10.04	6.02	2.51			6.32	5.28	7
--	10.5	--	7.48	47/32	52	--	--	--	--	No	850	680	60)					14.0	18.85	8.67	13.84	11.53	
10.5	--	6	4.44	46	30/32	60	--	--	--	No	850	680	60)										
10.5	--	6	4.44	44	30/32	60	--	--	--	No	850	680	60					39.8	13.1	18.92	23.94	21.75	
14	11	--	7.3	46	36/32	42	--	--	--	No	850	680	55					41.40	34.40	7.44	27.75	25.20	
18	11	--	7.3	46	45/48	50	--	--	--	No	900	680	55										
														10.38	15.92	11.51	15.92	23.10	28.35	16.82	17.46	15.85	8
12.5	--	13	9.2	50	60/26	30	--	--	--	No	400	690	55										
14.0	--	--	--	44	58/26	--	--	--	--	No	300	550	55										
12.5	--	13	9.2	50	60/26	30	330	1.3	48	No	400	690	55	0	1.66	0	1.66	1.66	3.33	1.66	1.62	1.29	9
19	12	--	7.3	46	45/32	49	--	--	--	No	1200	680	55						52.50	22.60	37.55	34.15	10
12.5	--	19	8.5	50	60/26	20	--	--	--	No	1100	690	55	0	3.92	0	3.92	0	7.84	10.86	3.70	3.34	11
16.5	10	--	9.3	46	50/32	42	--	--	--	No	1000	680	60	52.20	13.30	26.60	14.42				27.38	22.80	12
12.5	--	13	8.8	44	56/32	30	880	4.0	140	No	550	600	60	0	11.50	0	0	5.75	0	0	2.46	2.05	13
12.5	--	13	9.2	50	60/26	30	570	3.1	80	No	475	690	55	0	0	0	0	0	0	0	0	0	14
14	--	13.5	8.9	57	62/26	38	--	--	--	No	600	770	60	4.13	0	0					1.03	0.86	15
14	--	17.6	7.4	40	52/26	33	--	--	--	No	800	590	60	16.70	16.70	8.35					10.44	8.70	16
12.5	--	13	9.2	50	60/26	30	--	--	--	No	600	690	55			0	0	0	0	3.29	0.66	0.60	17
17	--	17.5	8.9	57	63/26	45	--	--	--	No	600	770	60	2.01	10.05	2.01	0				3.52	2.95	18

November 14, 1943, all lines operated as a unit. After that the lines operated as three separate lines, one Hales Bar-Great Falls, another Fort Loudoun-Ocoee 1, and a third Fort Loudoun-Washington (Knoxville).

(j). Includes 11.1 miles on double circuit towers with Cleveland-Ocoee 1 (reference 4). Original line was Ocoee 1-Knoxville, routed into Fort Loudoun October 10, 1943.

(k). Operated at 66 kv prior to October 1, 1944.

(l). Operated as Norris-Arlinton until November 5, 1944.

(m). Retired June 6, 1943; was on one side of double circuit towers, 66 kv on other side.

(n). Converted to 161 kv on May 30, 1943. See Table I, references 14 and 33.

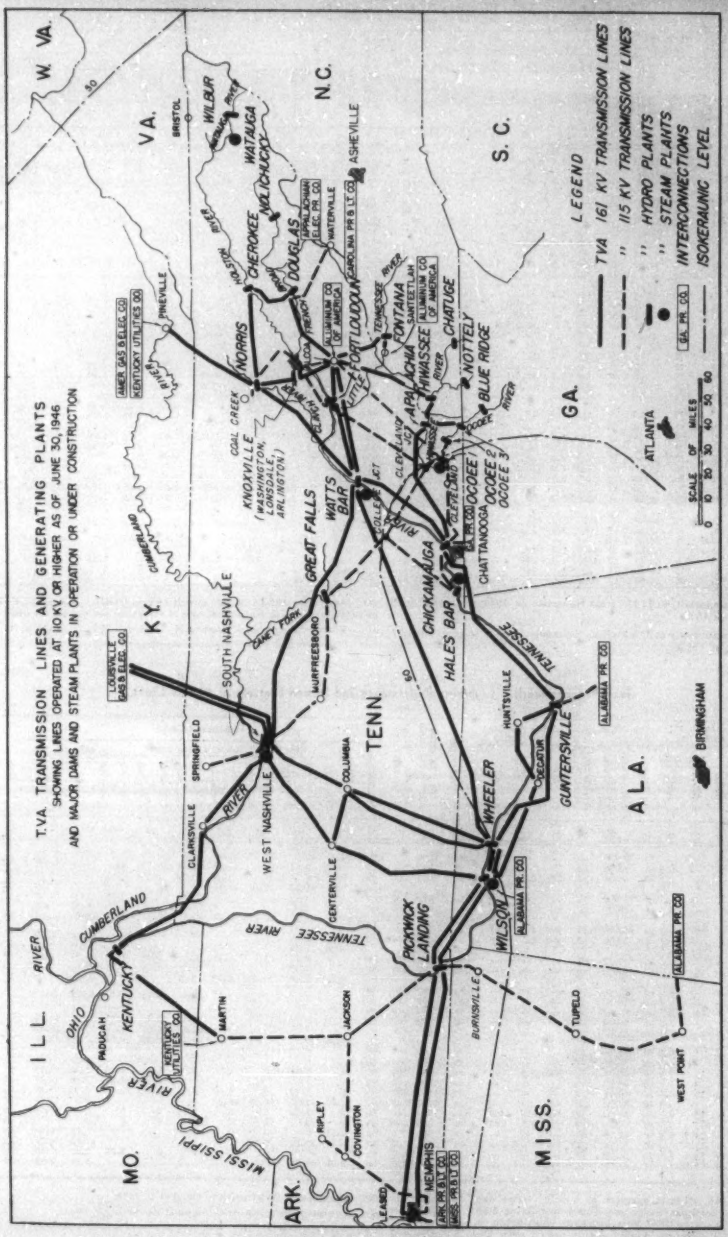

Figure 1. Tennessee Valley Authority transmission lines, showing isokeraunic levels

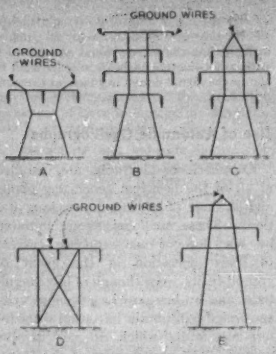

Figure 2. Types of steel construction

around the pole butt. The only exception to this type of construction is the Wheeler-Watts Bar line, reference 32. The wood pole section of this line, Figure 3*B* was constructed in order to obtain experience with this type of construction.

The 115-kv lines constructed by the Authority are of wood pole design with two overhead ground wires, pole grounds, and other features similar to the 161-kv design.

Counterpoise is installed by the Authority only where exceptionally good operation is necessary for system protection. Where two generating stations were connected to the system with only one line (item 5, Table I), this line was counterpoised to a 14,000,000-volt level. Generally, where a line forms part of a closed loop and the system is stable with a temporary fault on such line, rapid reclosing oil circuit breakers are used and the line is not counterpoised. Counterpoise is installed only when commensurate economies will be realized, and no

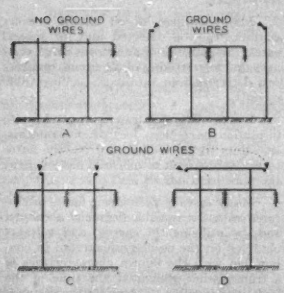

Figure 3. Types of wood pole construction

money is spent to get only a good line operating record. The benefits to the system are the main considerations.

Counterpoises are installed on nine 161-kv lines constructed by the Authority and one acquired 161-kv line. The protection level sought is from 10,000,000 to 14,000,000 volts, and the value is dependent upon various factors. In the case of the nine lines constructed by the Authority, the counterpoises were installed as a part of the original construction after initial tower-ground esistances were measured. The one acquired line on which a centerpoise was installed is the Centerville–West Nashville line (reference 3, Table I).

Where counterpoise has been installed a detailed study of the characteristics of each tower has been made, and installations have been made only on such towers and of such length as required to bring the protection level to the desired value. Generally, not more than 20 per cent of the towers in any line require counterpoise. Experience has proved to our satisfaction that the present designs based on the direct-stroke theory are conservative and that a steel tower line with an average resistance of 50 ohms or less will give good operation.

Counterpoises are not installed on 115-kv lines.

The 115-kv and 161-kv lightning arresters are located as nearly as practicable to the transformers in the generating plant and primary substations.

Ring gaps are installed, in general, on the high-voltage lines in the hydroelectric plant substations which have been built since 1939. These gaps are on one bus-supporting insulator of each phase at a convenient point between the line oil circuit breaker and the point where the line ties on to the substation structures. Gaps are not installed in the primary substations. The lines described in Tables I and II, with the exception of one 115-kv line, are not provided with gaps.

There are no sectionalizing air break switches except at substations, in the 115-kv or 161-kv lines which have been constructed since 1939. Some purchased lines were equipped with sectionalizing air break switches. In a few cases, the switches have been removed. There are a few installations of air break switches on short 115-kv tap lines. Standard insulation is used on these switches. The switch bases are connected to a ground field on the side of the structure opposite the operating handle. A ground plate, on which the operator stands, is connected to the operating pipe above the operating handle.

Transpositions have not been used in 161-kv and 115-kv lines constructed by the Authority, except one line; however, these were later removed because of flashovers resulting from improper clearances. On the Authority's system, there does not appear to be any condition requiring transposition.

The principal effect of the war period on line construction is that such material as was available was used. On some lines wood poles were used because they were available although steel towers would have been preferred. Likewise, conductor sizes were used which were different than normally would have been used. In one case, the South Nashville–Louisville double-circuit line, double-circuit steel towers were used although it would have been more desirable from the outage standpoint to have constructed two separate lines on separate rights-of-way.

Line Performance

As might be expected, the lightning record of the 161-kv lines is generally better than the 115-kv lines. The actual average outage per 100 miles per year for the 161-kv lines varies from zero to 22.6, with three-fourths of the lines having a value of less than four. Corresponding values for the 115-kv lines are zero to

Table III. Normal Maximum Loading of 161-Kv Lines

	Line Designation	Megawatts
1.	Alcoa—Lonsdale–Norris	150
2.	Centerville-Columbia	37
3.	Centerville-West Nashville	51
4.	Centerville-Wilson dam	80
5.	Cherokee-Douglas-Alcoa	153
6.	Cherokee-Norris	147
7.	Chickamauga-Watts Bar	130
8.	Clarksville-West Nashville	104
9.	Columbia-South Nashville	95
10.	Fontana-Alcoa	220
11.	Fontana-Santeetlah	105
12.	Fort Loudoun-Alcoa switching station	160
13.	Guntersville-Chickamauga	142
14.	Guntersville-Huntsville	100
15.	Hiwassee-Alcoa switching station	144
16.	Hiwassee-Apalachia-Chickamauga	160
17.	Kentucky-Clarksville	102
18.	Kentucky-Martin	72
19.	Norris-Pineville	137
20.	Pickwick-North Memphis	78
21.	Pickwick-South Memphis	70
22.	South Memphis-North Memphis	54
23.	South Nashville-Louisville { Line 1	75
	Line 2	75
24.	South Nashville-West Nashville	108
25.	Watts Bar-Alcoa switching station	170
26.	Watts Bar-Fort Loudoun	154
27.	Watts Bar-Norris	135
28.	Watts Bar-South Nashville	145
29.	Wheeler-Columbia number 1	115
30.	Wheeler-Columbia number 2	120
31.	Wheeler-Guntersville	105
32.	Wheeler-Watts Bar	120
33.	Wilson-Decatur-Huntsville	74
34.	Wilson-Pickwick number 1	67
35.	Wilson-Pickwick number 2	68
36.	Wilson-Wheeler number 1	100
37.	Wilson-Wheeler number 2	90

54.9, with over half of the lines having a value in excess of ten.

An interesting comparison of two lines in the same area which are almost of equal length is given in references 20 and 21 in Table I. Reference 20 is 161-kv design and reference 21 is 220-kv design, both operating at 161 kv. The average actual outages are 2.76 and 0.69, respectively. The performance of the double-circuit South Nashville–Louisville line (reference 23, Table I) is also of interest because of the relatively large number of 2-circuit outages.

The counterpoise was completed on the Centerville–West Nashville line on September 24, 1943 (reference 3, Table I). A comparison of the performance of this line with that of the Centerville–Wilson Dam line (reference 4, Table I) indicates an improvement in performance because of the counterpoise.

Lightning resulted in 687 outages on the 115-kv lines between August 16, 1939, and August 15, 1946. Of this total number of outages, 4.37 per cent resulted in damage sufficient to prevent the line from immediately being returned to service. Thus, 115-kv steel-tower lines had 7.17 per cent and the wood pole lines had 2.24 per cent permanent faults out of the total interruptions experienced on each type of construction.

The 161-kv lines experienced 399 outages from lightning, of which 1.755 per cent resulted in enough damage to prevent the line from being returned to service immediately. The steel tower lines had 1.44 per cent permanent faults, and the wood pole lines had no permanent faults out of the total number of interruptions experienced on each type of construction.

A combination wood and steel line had 11.11 per cent permanent faults. These faults were on the steel section of the line at a point where sufficient clearance was not allowed on the transposition tower. This difficulty has been corrected by the elimination of transpositions.

Line Loading

Three times each week, the power system dispatchers make a survey of the indicated amperes, kilowatts, reactive kilovolt-amperes and kilovolts which occur on the lines, transformers, generators, and synchronous condensers at the attended substations and generating plants. Tap positions on step-type and induction-type voltage regulators also are included in these readings, which are recorded in tabular form and are read on specified hours which represent minimum, average, and maximum hours of system load.

This survey supplies to the power system dispatchers a comprehensive picture of the operating data on the system and avoids the necessity for certain hourly log sheets.

Varied flows of water in the Tennessee River and its tributaries cause changes in the location of generation for hydroelectric energy in the network, and this results in a difficult problem of scheduling plant generation. This load survey, or its equivalent, is essential in the scheduling of both plant and interconnected transmission line loadings.

Table III shows normal maximum loading of the 161-kv lines as observed on the weekly survey and does not represent simultaneous maximum line loadings. Up to the present time, the full capability of certain individual lines has not been demonstrated because of the operation of the line in parallel with other lines, or with transformer banks, which keep the line from carrying higher normal maximum loads.

The 115-kv lines, in general, transmit quantities of power commensurate with their designed characteristics. Four of the 115-kv lines have transmitted normal maximum loads as follows:

Arlington–Waterville	66 megawatts
Norris–Washington	69 megawatts
Pickwick–Burnsville	50 megawatts
Pickwick–Jackson	54 megawatts

Signal Relays

Since line sectionalizing air break switches are not in every case available, signal relays which have a 90-to-425-ampere current range have been applied in order to locate faults and to minimize the patrolling time of the lines. The relay is a small device comprised of a magnetic circuit with a small hinged armature and glass reflector and a calibrated air gap suitable for changing the adjustment, thereby allowing the relay to operate at a prescribed current.

The relay is attached to the line conductor, and it will operate when current flows through the conductor to a line fault. By using several of the relays on the three phases at different places along a defective transmission line, the location of the fault can be readily determined.

Two methods of attacking the relays to the transmission line are found practicable.

1. By the permanent installation of a 6-foot hot-line stick to each of the relays (generally three to a set) so that the relay and stick may be hung directly on to the line and the armature reset with another hot-line stick.

2. By the use of a hot-line clamp attached to the side of the signal relay in such a fashion that the conventional ground stick with a hot-line clamp head may be used to clamp the signal relays in place on the conductor.

Use of Automatic Oscillographs

Automatic oscillographs are installed at all of the principal generating plants and at three of the larger switching stations. These oscillographs are initiated by the flow of zero-sequence current to start operation in the event of ground faults, even though of low magnitude, and by low positive-sequence voltage which will obtain initiation from interphase faults which do not involve ground. The performance of the transmission circuits mentioned herein were secured from automatic oscillograph records. In addition to this type of information, the automatic oscillographs are used.

(*a*). To secure performance records of protective relays applied to transmission lines.

(*b*). To verify the adjustment and performance of high-voltage oil circuit breakers.

(*c*). To secure information on the effective operation of the generator excitation system and the control voltage under abnormal conditions.

(*d*). To determine the location of permanent faults and weak points on the transmission lines.

A study of the oscillograms, from our viewpoint, has resulted in definite gains in performance and has served as a basis for improvement in facilities and equipment. Some salient points of such improvement are

1. The inadequacies of relays applied to long, heavily loaded transmission circuits and possible remedial changes in protective relays for such circuits were determined from automatic oscillographic records. This analysis effectively resulted in the development and application of the admittance type of transmission line relays on the Authority's system.

2. Maladjustment of oil circuit breaker contacts can be detected and, in several cases, the presence of dangerous surge voltages due to restriking of oil circuit breakers was detected from automatic oscillographic records.

3. Points of low clearances or inadequate insulation have been located on transmission lines by an indication from the automatic oscillograph of repeated flashovers at the same location.

4. Many cases of permanent faults are located with a reasonable degree of accuracy, and, by utilizing the current and voltages obtained on the oscillograph record in conjunction with the known characteristics of a transmission system at the time of the fault it is possible to compute the distance along the transmission line to the point of a

fault. This computation and approximate fault location frequently can be accomplished while the line maintenance personnel is being assembled for patrol and repair. Faults are usually found within three or four miles of the computed location. The maximum of error in location by computation is approximately seven miles.

5. Interesting and valuable information of the susceptibility of various lines to electric flashovers during lightning storms and the nature of such flashovers is determined from a study of the oscillographic records. From data collected and analyzed from February 1939 to August 1942, it has been deduced that 40 per cent of the faults appear to be single phase-to-ground faults. The remaining 60 per cent of the faults is approximately equally divided between faults which involve only two phase conductors and those which involve only three phase conductors for their inception. There are only a very few cases in which faults originate as single phase-to-ground faults and subsesequently involve additional phase conductors. Information of this type cannot be secured from relay targets. In fact, there are only a very few instances where all three phase targets have operated even on faults where oscillograph information indicates, conclusively, that the faults involved all three phase conductors from inception. Usually, on faults which involve two phase conductors, only one phase relay target was shown. The oscillograph analysis clearly indicates that the number of faults which involved all three phase conductors is much greater than the number expected based on previous information secured from relay targets and that the number of faults which involved only one phase conductor is much lower than was expected based on relay targets.

Relaying and Reclosing of Lines

The plan followed for the application of relays on the oil circuit breakers which control the 115-kv and 161-kv lines is to take advantage of any changes in relays or relay applications which will improve the performance of the lines as well as the system. Parallel with the improvement in relay schemes is the reduction in operating time and an increase in the interrupting rating of the oil circuit breakers.

The discussion in this section pertains to the relay and recloser scheme which is in operation as of August 15, 1946.

All of the 161-kv lines listed in Table I are equipped with some form of terminal comparison relays. Most of these lines employ 3-zone distance relays of either impedance, reactance, or admittance charactersitic to which terminal comparison is added to the second zone to permit instantaneous clearing for faults anywhere within the line. Two of the lines employ metallic circuits for terminal comparison; the remainder of the lines utilize carrier frequency superimposed upon the transmission circuit for that purpose. Six of the circuits employ single-zone impedance relays with carrier comparison for normal protection and with instantaneous and induction overcurrent relays for phase backup. Ten of the lines employ 3-zone admittance type relays or relays which utilize phase angle as well as the magnitude of voltage and current as a basis for determining the line distance to the point of fault. The remainder of the lines utilize 3-zone impedance or reactance relays. In all cases, ground relays consist of current polarized directional units with appropriate nondirectional residual ground units for high speed clearing of ground faults in conjunction with the terminal comparison carrier metallic circuit. Backup ground relays also are provided usually either for the current polarized directional units or for the potential polarized directional units.

Automatic reclosing with the oil circuit breakers is employed in some form on all of the 161-kv transmission lines. Immediate high speed reclosing at both terminals, with no check of voltage or synchronism, is employed on all circuits which utilize the admittance type relay units; the only limitation on this ultrahigh speed reclosing is that the breakers must be tripped through the carrier blocking channel or by zone one at both terminals in order to indicate that both line terminals were disconnected at substantially the same time. Also, instantaneous reclosing is prohibited if the protective relays indicate that tripping occurred due to excessive power swings rather than to an actual fault on the protected line. All of the 161-kv lines, including those equipped with ultrahigh speed reclosing, have facilities provided for reclosing into a dead line, closing on indication of synchronism, with the system at both ends of the affected line tied through another transmission circuit. At the substation ends of several of these transmission lines, facilities are provided for automatic closing of the oil circuit breaker onto a de-energized station bus when the line is energized from the generation end. Automatic synchronizing facilities are provided on several of the lines.

The 115-kv transmission lines listed in Table II are all equipped with distance relays of either the impedance or reactance characteristic. One of the lines also has carrier comparison applied to the distance relays. The ground relays employed usually consist of current-polarized directional ground relays. Frequently two in number, one is of the high-speed induction directional current-polarized type, and the other is either a standard-speed induction current polarized directional type or a potential polarized directional unit controlling a residual overcurrent element.

Reclosing features are provided on all of the 115-kv circuits which employ some form of check before closure. The checks employed are to ascertain dead line-dead bus, or that the parts of the system adjacent to both terminals of the affected line are in synchronism through other transmission circuits.

Summary

A definite decrease in lightning outages is obtained by the use of counterpoise. The record of the 161-kv lines is better than that of the 115-kv lines when considering lightning performance. The qualities of a line as related to design and operation must be considered on the basis of the individual line location and function.

Transmission line loads of 220, 170, and 145 megawatts have been transmitted, respectively, over distances of 27.7, 45.4, and 127.9 miles on the 161-kv class lines. The 115-kv class lines have transmitted 66 megawatts for a distance of 53 miles.

Proper application of protective relays and of oil circuit breakers is essential in obtaining the best over-all operation of a transmission line.

Material improvements in transmission line design and operation are made possible by the use of automatic oscillographs. Oscillograph records indicate 40 per cent of the faults caused by lightning of the 161-kv lines to be single phase-to-ground. The oscillograph affords a tool for locating a fault within a 4-mile range as observed from the records.

Observation of the operating record of steel tower transmission lines which have average ground resistance of 50 ohms or less indicates that there is little to be gained by installing counterpoise on such lines.

Reference

1. Electrical Transmission and Distribution Reference Book. Westinghouse Electric and Manufacturing Company, East Pittsburgh, Pa. First edition, 1942, page 306.

Discussion

E. W. Knapp (Shawinigan Water and Power Company, Montreal, Quebec, Canada): The authors have presented a very interesting and valuable paper. There are a number of points which have occurred to me,

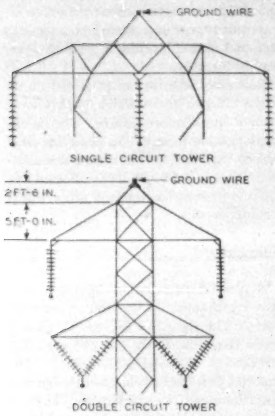

Figure 1. Original arrangement of ground wire

however, which might be clarified to advantage.

1. Is it the general practice to install short buried counterpoise wires radiating from individual towers?

2. Has continuous buried counterpoise been installed to any extent, and if so, approximately what is the relative per cent of lines equipped with short versus continuous counterpoise?

3. Is any distinction made between short and continuous counterpoise when applied to a transmission line constructed through territory of high resistance soil?

4. Is it customary to apply an automatic time interval reset feature to the automatic reclosing installations, and if so, is the reset feature limited in the number of successive reclosures?

J. D. Harper (Aluminum Company of America, Alcoa, Tenn.): The authors have presented a most interesting paper on transmission line performance. It is apparent that the Tennessee Valley Authority has done an excellent job of obtaining maximum performance from its lines. This experience will be of value to all concerned with transmission problems.

Early in 1928 there was a crystallization of the ideas concerning the use of the cathode ray oscillograph for field studies of lightning. The immediate result of this was the desire to establish lightning laboratories in the field.

The Aluminum Company of America, through its subsidiary, the Knoxville Power Company, afforded a transmission line of high insulation value and recognizing the importance of lightning investigation, joined the Westinghouse Electric and Manufacturing Company in a co-operative field research endeavor in 1928.

The determining factors governing the selection of East Tennessee were the great number and severity of thunderstorms, and the existence there of the most heavily insulated steel tower transmission line in operation in the Southeast at the time.

The transmission line consists of two circuits operated at 154,000 volts and extends from Alcoa, Tenn., to the Santeetlah power house in Western North Carolina, a distance of approximately 30 miles. A rugged country is traversed with several long river crossings, elevations ranging from around 700 feet at Alcoa to 2,600 feet in the mountainous sections.

This investigation indicated that low resistance tower footings and low resistance ground wires were desirable for decreasing flashovers.

Continuous progress has been made in the improvement of these lines since the investigation beginning in 1928.

1. The relaying has been modernized as the art of relaying progressed. The lines now are protected by high speed relays using carrier blocking.

2. Towers have been redesigned and two ground wires installed on all single circuit towers and the ground wire raised on the double circuit towers to comply with modern standards on double circuit towers. See Figures 1 and 2 of this discussion.

3. Some 130,000 linear feet of counterpoise has been installed on the 60.4 circuit miles of transmission line, which is around 12 equivalent miles, with two counterpoise cables or about 20 percent of the total circuit miles. Counterpoise has been installed on 120 towers or around 52 percent of the total number. It was necessary only to lower the resistance of the tower footings on certain sections of the line, therefore, all of the 120 towers are not tied together. The protective level is now 10 million volts. Calculations for this revision were made jointly by Tennessee Valley Authority and Aluminum Company of America. Computed probable outages per 100 miles per year is 0.94. Tower footing resistances were measured with the ground wires disconnected wherever possible and double the measured value was used where this was not possible. The counterpoise used was 5/16-inch galvanized steel strand buried to a depth of 18 inches. It was not possible to use conventional installation methods because of the rugged terrain and a special plow was made of a pavement ripper tooth fastened to a heavy tractor. Backfill was accomplished by running a 20-ton tractor back over the furrow. Hand digging was necessary in a few spots. The general layout of the counterpoise conforms to the same principles as applied on the lines whose performance is analyzed by the authors. See Figure 3 of this discussion for a typical counterpoise installation. In some cases the counterpoise was extended tower to tower. The length depended upon individual tower footing resistance.

4. All oil circuit breakers have been modernized from 1,500,000-kva interrupting capacity to 2,500,000-kva interrupting capacity with 8-cycle interrupting time.

5. Lightning arresters rated 161 kv have been installed or are planned at all line terminals.

6. Automatic reclosing has been installed at the Alcoa and Santeetlah ends of the line.

7. Automatic oscillographs are used to study line troubles.

These improvements as mentioned have been spread over the years from 1928 through 1945 and have cut down transmission outages from an average of around seven per year to two in 1944 and one in 1945 and none in 1946, and none to date.

Co-ordinated operation with the interconnected system has been much smoother due to the improved performance of our transmission lines.

S. B. Crary (General Electric Company, Schenectady, N. Y.): This paper has many points worthy of emphasis. Four of these are

1. Reduction in outages per 100 miles per year at the higher voltage levels.

2. Transmission line loadings appreciably higher than the surge impedance loading, even for line lengths up to and beyond 100 miles.

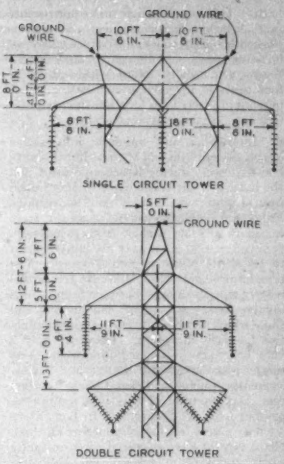

Figure 2. Present arrangement of ground wire

3. High percentage of multiphase faults.

4. Successful use of high-speed reclosing.

The authors' experience confirms the trend toward high circuit loadings as one of the most effective ways to reduce the cost of transmitting electric energy. High-speed reclosing, particularly for the interconnected type of system described, offers an effective means for obtaining reliability when carrying high circuit loadings. The high percentage of multiphase faults further substantiates, as has also been indicated on other high voltage systems, the desirability of 3-phase reclosing as contrasted with single-phase reclosing for the type of system described.

Single-phase reclosing, as is well known, has an important field of application for single-circuit lines and possibly double-circuit lines on the same tower with no other important parallel circuits, but sacrifices simplicity with little performance advantage for most of the circuits of a large interconnected system.

This paper points to the possibility of further reductions in line insulation, particularly at the higher voltage levels such as 230 kv and above. The use of lower levels of line insulation represents an important economical possibility now being given careful consideration. Outages due to lightning can be reduced in number by line shielding or made relatively inconsequential by rapid reclosing, depending upon the system under consideration. With lightning or outages produced by lightning better controlled the only other important source of overvoltage is the switching surge. Switching surges can also be controlled, to relatively unimportant values, by proper system grounding, use of circuit breakers with a minimum tendency to restrike, and the proper use and location of arresters. Arresters can be located on the line side of the circuit breaker, as well as at the terminals of the transformer, to afford

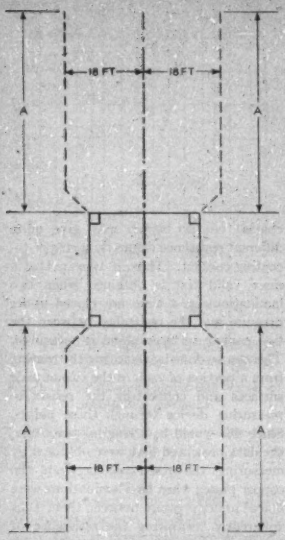

Figure 3. Typical counterpoise installation

Distance *A* depends on footing resistance of individual towers—100 feet minimum

lightning surge protection for the breaker and switching surge protection for the line.

Therefore, by an extension of the transmission design principles indicated in the paper by Hapgood and Almon, further important economies appear to be right at hand.

G. D. Floyd (Hydro-Electric Power Commission of Ontario, Toronto, Ontario, Canada): The statement in this paper regarding transpositions is very interesting. Transpositions, though well designed, are a point of weakness in a high voltage line, and it would be very desirable if they could be eliminated entirely. The Central Electricity Board, in Great Britain, has omitted transpositions on its 132-kv network, with, I believe, no adverse experience. It has, however, reversed the phases at substations, so as to obtain substantially balanced capacitances for the network. Could the authors state whether any like attempt was made to balance the capacitances in their circuits? Have any measurements been made to determine if operating telephone circuits were more noisy as a result of the unbalances? What was the effect, if any, on power line carrier circuits? What arrangements, if any, were made with communication interests to provide increased separation, or other remedial measures, as a result of the lack of transpositions in the power circuits?

K. E. Hapgood and **C. P. Almon, Jr.**: The authors appreciate the excellent discussions and questions by S. B. Crary, G. D. Floyd, J. D. Harper, and E. W. Knapp.

Crary mentions two important facts, namely, (1) in an interconnected type system, 3-phase high speed reclosing together with line shielding offer a means of improving reliability when transmission lines are operated at high circuit loadings; and (2) the possibility of reductions in the line insulation at voltage levels of 230 kv and above.

Floyd questions the effects of the omission of transpositions. No problems of unbalanced voltages nor harmful effects upon telephone circuits or power line carrier currents have occurred. Phases are not reversed at substations. In all cases, we furnish copies of location maps to all interested parties, such as telephone, telegraph and railroad companies, to check any possible difficulties. If it appears that difficulties might arise, a decision is reached among the parties as to corrective procedures. Such problems are anticipated as far as possible in the initial selection of the line location. As a result, the problems have been negligible and easily solved. All communication interests have been very cooperative.

Harper's discussion is of much interest, and confirms the beneficial results to be obtained from counterpoise. The benefits obtained from high speed reclosing and the use of automatic oscillographs for analysis of system performance parallels the Authority's experience.

Knapp has inquired as to the type of counterpoises used. Two general rules have been followed on installing counterpoises.

1. To install sufficient counterpoise at each structure to produce the desired protection level.

2. To install the counterpoise within the limits of the right-of-way.

In general, the counterpoise at each tower leg is relatively short and will parallel the transmission line. No distinction is made between a short and continuous counterpoise for the reason that the counterpoise is installed to provide the desired protection level. The experience so far is that there has been used a negligible amount of counterpoise connecting two or more structures.

Knapp also inquired as to the characteristics of the reclosing relay. This relay is a so-called "one-shot" reclosing relay. It has an adjustable time delay reset up to $1^1/_2$ minutes. In general, the $1^1/_2$ minute reset time is used. The timing motor circuit is initiated through an "*a*" switch on the breaker. The timing circuit is so arranged that the breaker must be closed for the full reset time interval for the relay to reset. If the breaker should open before the reset time has elapsed, the relay will require the full time interval to reset after the next closing of the breaker.

It is the belief of the authors that reliable system performance requires the proper use of line shielding, high speed reclosing, and adequate relaying in conjunction with one another rather than the use of any one of these by itself. Automatic oscillographs provided a very useful method of checking the performance of the various system components.

Interlaminar Eddy Current Loss in Laminated Cores

A. C. BEILER
ASSOCIATE AIEE

P. L. SCHMIDT
ASSOCIATE AIEE

Problem

INTERLAMINAR eddy current loss in cores of electromagnetic machines carrying a-c flux is a function of the reciprocal of the interlaminar resistance, the square of the lamination width, and the square of the magnetic flux density.[1] Since the core loss of iron varies approximately as the square of the induction, the interlaminar eddy current loss expressed as a percentage of the fundamental core loss is nearly independent of the flux density.

By applying this theory, it can be calculated that, for electrical grade steel (one per cent silicon), the loss due to interlaminar eddy currents will be approximately one per cent of the fundamental core loss if the interlaminar resistance is ten ohms centimeter squared per lamination for a punching six inches wide behind the slots when the laminations are short-circuited on the side away from the teeth, as is usual in rotating machinery. In cores, such as the usual transformer core, where the laminations are not short-circuited on one side, the required resistance for the same width of punchings is 2.5 ohms centimeter squared per lamination.

One per cent silicon steel sheet as received from the mill has an interlaminar resistance of the order of 0.05 ohm centimeter squared per lamination. To increase the surface resistance to a satisfactory value, the laminations sometimes are coated with an organic varnish or its equivalent or, in some cases, insulation is provided by oxidizing the laminations after punching.

Regardless of the treatment applied to produce more desirable surface resistance, it is found that the interlaminar resistance of pairs of punchings varies over a wide range of values. It is difficult to predict loss due to interlaminar currents in a complete machine because the theory is developed on the premise that the resistance between each pair of laminations is the same. A method of testing interlaminar resistance and of analyzing test results is desired which can be applied to predict accurately the loss resulting from interlaminar eddy currents in a core having a nonuniform interlaminar resistance.

Discussion of Methods of Testing and Analysis

Standard practice in measuring interlaminar resistance, according to the tentative American Society for Testing Materials method (*A 34-40-T*), is to place 40 Epstein strips between two copper plates backed with an insulating material, apply a predetermined pressure between the plates and measure the resistance across the stack. The interlaminar resistance in ohms centimeter squared per lamination is calculated by multiplying the value obtained by the area under pressure and dividing by the number of strips.

The following example shows how misleading such a procedure may be. Suppose a sample of 40 pieces has 38 contacts of low resistivity and one contact with a resistance of 400 ohms centimeter squared. Even if the value of the low resistance contacts approaches zero, the resistance across the stack will be more than 400 ohms centimeter squared and the interlaminar resistance will be calculated to be more than 10 ohms centimeter squared per lamination.

It may appear from this example that a reasonable test method would be to test one lamination at a time between two plates. This would disregard coating-to-coating contact which may give quite different resistance values than copper-to-coating contact. Thus, it appears that a more valid test is obtained when two laminations at a time are placed under pressure and the resistance between the two coated surfaces alone is measured. This can be done by removing the coating from a portion of each of the two outside surfaces and connecting the resistance measuring device through these points. Since this would be a lengthy procedure, the data presented here were obtained by measuring the resistance between the copper plates when two laminations were placed under pressure between them, thus apparently measuring the resistance of four surfaces.

In measuring the resistance across two contacting surfaces, the value obtained is the resistance of a number of parallel circuits made up from the alignment of low resistance spots on both surfaces. The high resistance spots have a negligible influence.

It has been found that for some types of surface treatment, notably those producing a thick coating, a high average resistance and a broad range of values, the copper-to-coating contact is of the same order of magnitude as coating-to-coating contact. For some other types of surface treatment the copper-to-coating contact is much lower than the coating-to-coating contact. This is generally true for coatings which are thin or surface treatments which may provide incomplete coverage. If there are a few low resistance points on each surface of the laminations, the probability of alignment of low resistance spots on adjacent treated surfaces is low, while, on the other hand, every low resistance spot on a treated surface makes contact with the copper plate, thus giving a low reading. Since it is impossible to tell what the copper-to-coating resistance may be

Paper 47-126, recommended by the AIEE committee on electric machinery for presentation at the AIEE summer general meeting, Montreal, Quebec, Canada, June 9–13, 1947. Manuscript submitted November 12, 1946; made available for printing April 14, 1947.

A. C. Beiler and P. L. Schmidt are engineers in the magnetic group of the materials engineering department of the Westinghouse Electric Corporation, East Pittsburgh, Pa.

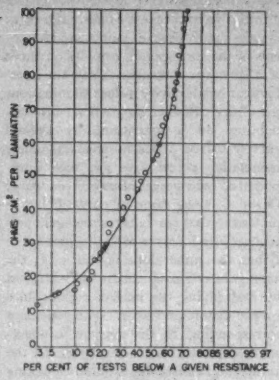

Figure 1. Arithmetic-probability curve of interlaminar resistance

Sample tested in 100 groups of two laminations each

without measuring it in each case, it is safe to consider the two pieces per test as two laminations in every case, since a correction for copper-to-coating contact would increase the value obtained.

Laminations rather than Epstein strips were used for the major portion of the tests on which this work is based in order to evaluate a surface treatment as an insulator of burr-ground areas or of two to three mil punching burrs as well as of the wide unbroken areas. It was assumed that this would give results representative of those to be expected from normal manufacturing procedures.

Obviously a test of only one group of two laminations could not represent adequately the resistance of a surface treatment and for this reason from 30 to 50 groups of two laminations each must be tested. The need for a method of analyzing results presents itself immediately.

An arithmetic mean of the 30 or 50 readings does not give a true picture because there are usually a few resistance values, both high and low, which seem inconsistent with the remainder of the data and because the resistance values are not repetitive, value for value, if the test is repeated.

Conclusions drawn from the data by examination of tables or graphs presenting all the data are based essentially on an arithmetic mean and were considered inadequate. However, a graphical study using points plotted for each resistance value indicated that the resistance values might fit a normal distribution curve.

To test this possibility, the resistance data were plotted on arithmetic-probability paper. This paper is designed in such a manner that a normal (symmetrical) distribution curve is transformed to a straight line if the percentage below a measured value is plotted against that measured value. Figure 1 shows a typical curve obtained by plotting cumulative per cent against resistance on arithmetic-probability paper and is plotted from data obtained from 100 tests (two pieces per test) of a single sample. Since the curve is not a straight line, it is evident that the distribution of the resistance values is not symmetrical but is skewed.

Since the curve in Figure 1 appears to

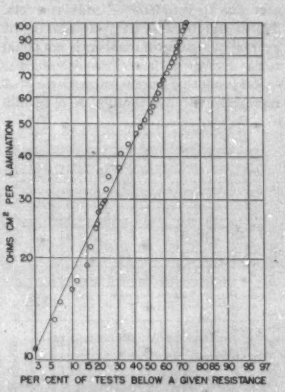

Figure 2. Logarithmic-probability curve of data from which Figure 1 was drawn

be exponential, logarithmic-probability paper seems more suitable. Figure 2 shows the same curve as a straight line on logarithmic-probability paper. While Figure 1 and Figure 2 are the result of 100 tests, it has been customary to facilitate testing by making 30 tests of a sample. It has been found that 30 tests of a sample will determine the distribution curve quite accurately although larger number of tests may give a set of points which will approximate a straight line more closely. However, in many cases the points from 30 tests lie in as straight a line as the points in Figure 2 which represents a good set of data.

It is apparent that there is a lower limit of resistance values dependent on the resistivity of the steel and, since there is no upper limit, a skewed distribution of some type is expected. Why the distribution of interlaminar resistance values is logarithmically skewed has not been determined but its existence has been verified by plotting curves from over 300 sets of data.

In order to show the significance of the slope and mean values of resistance distributions plotted on arithmetic-probability paper, three synthetic distributions are given in Figure 3. Curves *A* and *B* have the same median value and curve *C* has a higher median value. The slope of the curves is diminished progressively from *A* to *C*. The three cases shown in Figure 3, which are redrawn according to the usual method of plotting distribution curves (normalized to identical area), are identified by the same letters in Figure 4. The value at which a distribution curve (Figure 3) crosses the 50 per cent line is the arithmetic mean, the median value and the most probable value. It can be seen that a steep slope on arithmetic-probability paper signifies a broad distribution curve. As the arithmetic-probability curve approaches a horizontal slope, the distribution curve plotted in the usual manner becomes more sharply peaked.

In order to show the significance of slopes, median values and arithmetic mean values of resistance distributions plotted on logarithmic-probability paper, Figure 5 and Figure 6 are presented. The lines on Figures 5 are synthetic distributions typical of many we have observed. These curves are replotted in Figure 6 in the usual manner of plotting distributions and are designated by the same letters as in Figure 5. It can be seen from Figure 6 that all the curves are skewed toward low

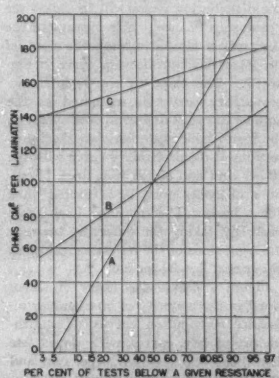

Figure 3. Synthetic arithmetic-probability curves

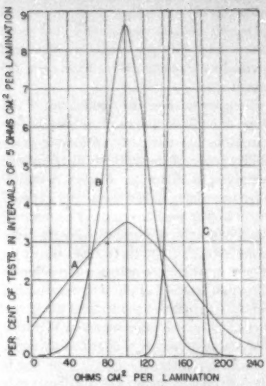

Figure 4. Normal distribution curves corresponding to arithmetic-probability curves of Figure 3

Peak of curve C is at 21 per cent

values. The value at which the logarithmic curve crosses the 50 per cent line is the median value, but because of asymmetry it differs from the corresponding point on an arithmetic-probability curve in that it is not the average value or the most probable value.

It can be seen that the distribution curve is peaked at a value below the median value and that the skewness, or shift of this peak from the median value, is proportional to the slope of the logarithmic-probability curve, increasing as the slope increases. The fraction by which the median value must be multiplied to obtain the value at the peak of the distribution curve will be called the "peak-shift" factor. This measure of the skewness is plotted against the slope of the logarithmic-probability curve in Figure 7. The slope of the logarithmic-probability curves is measured as the number of cycles or fractions of cycles on the logarithmic scale between the intersections of the probability curve with the 20 per cent and 80 per cent lines. Fractions of cycles must be measured on a linear basis. This may be done most easily by taking the difference between the logarithms of the resistance values at 80 per cent and 20 per cent.

Figure 7 covers the range of slopes found in the majority of interlaminar resistance distribution curves. Logarithmic-probability curves with slopes less than 0.25 cycle between 20 per cent and 80 per cent are nearly normal distributions and should be plotted on arithmetic-probability paper.

The arithmetic mean is above the median value for all cases on logarithmic-probability curves and the factor by which the median must be multiplied to obtain the arithmetic mean varies with the slope of the logarithmic-probability curve as shown in Figure 8. This factor will be called the distortion factor.

Application of the Method to Calculation of Interlaminar Eddy Current Loss in a Machine

Since the loss due to interlaminar eddy currents is a function of the reciprocal of the interlaminar resistance or of the interlaminar conductivity, it is not correct to use the average resistance value of the laminations to calculate the loss in the core due to interlaminar eddy currents. This is true because the reciprocal of the average of a group of numbers is not equal to the average of the reciprocals.

Referring to Figure 9, suppose curve *A* represents the distribution of a certain group of resistance test values. If a curve is drawn such that all points are reciprocals of the corresponding points on curve *A*, then curve *B* results. Thus, the interlaminar conductivity values (laminations per ohm centimeter squared) are also distributed on a logarithmically skewed curve. Curve *B* has no meaning unless cumulative percentages are now interpreted as percentages *above* a given value. Curve *C* is the same as curve *B* but is plotted so that percentages are again percentage *below* a given value. Since curve *C* has the same slope as curve *A*, the average interlaminar conductance is found by multiplying the median conductance by the distortion factor. The resistance corresponding to the average conductance, which will hereafter be called the antiaverage resistance, is found by taking the reciprocal of the average conductance. This is easily done by dividing the median resistance by the distortion factor.

Referring to specific values to illustrate this principle, the median resistance value from curve *A* (Figure 9) is 2.22 and the distortion factor from Figure 8 is 1.52. Multiplying these values gives an average resistance of 3.385. The median conductance is 0.450, and multiplying this by 1.52 gives an average conductance of 0.684. The reciprocal of the average conductance is found to be 1.46 which might also be called the antiaverage resistance. This same value is obtained more easily by dividing 2.22, the median resistance, by 1.52, the distortion factor.

A discussion of the interlaminar resistance required to obtain satisfactory machine performance is of interest. It has been stated previously that, if the resistances of all laminations are equal, a resistance of approximately ten ohms centimeter squared per lamination (Figure 10) is required to keep the loss due to interlaminar eddy currents at one per cent of the fundamental core loss of one per cent silicon steel for machines having a depth of core behind the slots of six inches

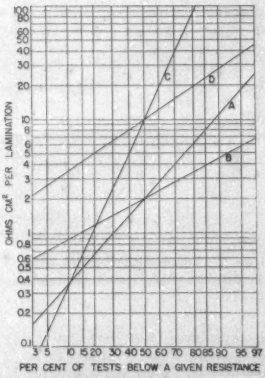

Figure 5 (above). Synthetic logarithmic-probability curves

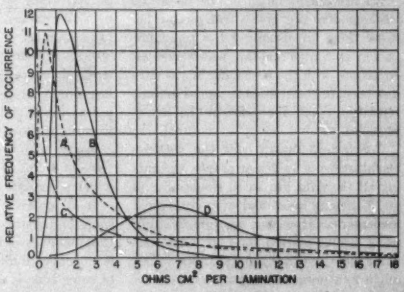

Figure 6. Skewed distribution curves corresponding to logarithmic-probability curves of Figure 5

Median values:
A and *B*—Two ohms centimeter squared per lamination
C and *D*—Ten ohms centimeter squared per lamination

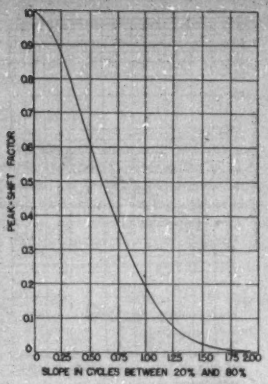

Figure 7. Peak-shift factor versus slope

(punchings short-circuited on a frame or shaft). A little thought will show that the eddy current loss of a core, which is made up of laminations which have nonuniform interlaminar resistance (conductance), is the same as the eddy current loss of a core which is made up of laminations whose interlaminar conductances are all equal to the average conductance in the nonuniform case. Thus, in a practical case where the interlaminar resistance of each of the laminations is different, the antiaverage resistance must be ten ohms centimeter squared per lamination to fulfill the aforementioned requirement.

The bulk of the tests on which this work is based were made at 50 pounds per square inch because of simplicity of operation of the available test device. Since actual machine pressures may be several times this value, a study of resistance variation with pressure has been made yielding the values given in Table I which applies to one type of surface treatment only. A large number of additional tests indicate a range of values from 0.24 to 0.57 for the ratio of median values of interlaminar resistance at 250 pounds per square inch to median values at 50 pounds per square inch obtained from the same samples. This range includes differences in types of surface treatments and probably is much narrower for any one type of insulation.

It is estimated that the average pressure in a machine does not exceed 150 pounds per square inch so it is conceivable that the loss in a machine due to circulating currents may be as much as two per cent of the rated iron loss if the antiaverage resistance, according to tests at 50 pounds per square inch, is ten ohms centimeter squared per lamination. If the actual pressure were 500 pounds per square inch, the loss due to circulating currents would increase to about four per cent of the fundamental iron loss.

If there is a spot in a machine where the loss is excessively high and the heat developed causes deterioration of the interlaminar resistance film on adjacent laminations, the fault becomes progressively worse and may cause the machine to fail. Therefore, in addition to knowing the antiaverage resistance, which determines the portion of core loss of the machine due to interlaminar circulating currents, it is most important to know that the poor end of the probability curve does not reach

Table I. Variation of Resistance With Pressure

Lb Per Sq In.	Ratio to Resistance at 50 Lb Per Sq In.
50	1.0
100	0.66
150	0.51
200	0.42
250	0.36
500	0.24
600	0.21
700	0.19

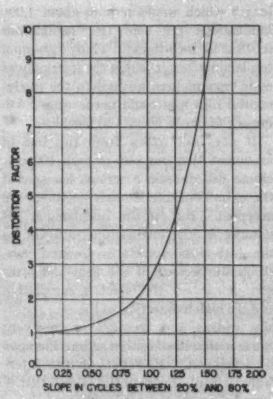

Figure 8. Distortion factor versus slope

values low enough to endanger the machine because of hot spots. In other words, one needs to know what percentage of resistance values may fall below a specified minimum value. This is a function of the slope, considering the median value to be constant. For example, in Figure 5, curve *B* represents a better condition than curve *A* even though the median values are the same because curve *B* has a smaller percentage of extremely low values.

The problem of possible hot spots in a core may be analyzed satisfactorily by obtaining answers to the following two questions:

1. What minimum resistance can be permitted in a specified small length of core?

2. How often will a low resistance group of laminations occur if ten per cent of the tests lie below the minimum resistance?

In answer to the first question, it seems safe to assume that for a short length of iron, say ten laminations (approximately one-fourth inch), double iron loss, or an interlaminar eddy current loss corresponding to 100 per cent in Figure 10, would be permissible. That would mean a resistance of 0.1 ohm centimeter squared per lamination would be permissible for ten per cent of the tests. This condition should be true at the pressures which may exist in a machine. If it is assumed that the pressure is 500 pounds per square inch and a ratio of 0.25 is used (approximate value from Table I), then the minimum resistance should be 0.4 ohm centimeter squared per lamination for not over ten per cent of laminations tested in groups of two at 50 pounds per square inch.

To answer the second question, it is necessary to estimate how often there will be ten consecutive laminations in a machine, each lamination having a resistance value of 0.4 ohm centimeter squared per lamination or less, if ten per

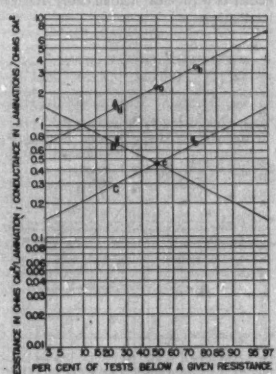

Figure 9. Relation of distributions of resistance and conductance

A—Interlaminar resistance
B and *C*—Interlaminar conductance
a—Median interlaminar resistance
b—Average interlaminar resistance
c—Median interlaminar conductance
d—Antiaverage interlaminar resistance
e—Average interlaminar conductance

cent of the laminations tested two at a time are below 0.4 ohm centimeter squared per lamination. According to probability theory, the probability of occurrence of simultaneous independent events is equal to the product of the individual probabilities. The applicability of this theory was verified experimentally by tests of the same set of laminations, two, four, and eight pieces at a time, 50 tests being made for the groups of two and four pieces, and 100 tests for the groups of eight pieces. These data are plotted in Figure 11 where the line for two pieces per test is drawn through the test points and the other two lines are calculated from it by applying this theory. It will be noted that the test points for four and eight pieces per test are in good agreement with the theoretical curves. Therefore, it is correct to extrapolate from tests involving groups of two or larger groups, provided that the insulation is of a type which provides about the same resistance in a copper-to-coating contact as in a coating-to-coating contact.

Now if ten per cent of the tests are below 0.4 ohm centimeter squared per lamination according to the distribution curve obtained from tests on two pieces at a time, this means that the probability of obtaining a test value of 0.4 ohm centimeter squared per lamination or less is 0.10. Then the chance of having ten such laminations (five groups of two) together is 0.10^{-5}, or once in every 100,000 laminations.

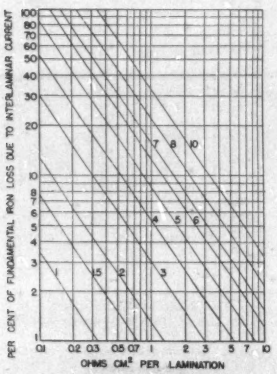

Figure 10. Interlaminar eddy current losses expressed as percentage of fundamental iron loss versus interlaminar resistance for 26 gauge one per cent silicon steel laminations short-circuited on the edge away from the slots

Curves are identified by the lamination width in inches

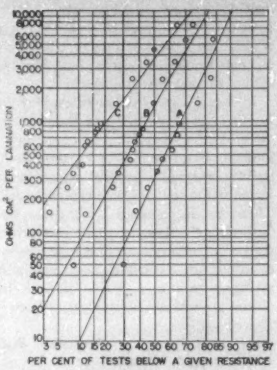

Figure 11. Logarithmic-probability curves for the same sample tested three ways

A—Two pieces per test (50 tests)
B—Four pieces per test (50 tests)
C—Eight pieces per test (100 tests)

For this size of lamination we have assumed (six inches wide behind the slots), 18 inches is a reasonable value for the core length which would require about 1,000 laminations per core (for laminations 0.018 of an inch thick). Thus, a group of ten laminations in which the interlaminar eddy current loss is equal to the fundamental iron loss could occur with a frequency of one in every 100 machines.

It does not follow from this line of argument that one out of each 100 machines will develop a serious hot spot if these limits of interlaminar resistance are accepted. But, if the interlaminar resistance of the laminations adjacent to the high loss section is lowered substantially because of the heat and pressure developed, the effect is cumulative and the high loss section of the core gradually widens and becomes progressively worse within itself until a serious hot spot is developed. However, if the interlaminar insulating material is such that it is not affected by a reasonable rise in temperature or pressure and if the insulation on the coils is unaffected, this cumulative increase of interlaminar loss will not occur and the limit that a maximum of ten per cent of the laminations may lie below 0.4 ohm centimeter squared per lamination is a conservative risk and is safely on the high side.

Reliability

This method of plotting logarithmic-probability curves of resistance values of punchings tested two at a time has

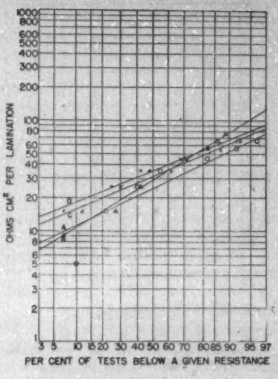

Figure 12. Reliability of test method

Each curve represents 30 tests on the same sample shuffled between the four groups of tests

A—○ C—×
B—△ D—●

proved reliable in that almost identical curves are obtained when the usual group of 30 tests is repeated on the same sample. This is illustrated by Figure 12 showing four curves obtained by testing the same sample four different times with thorough shuffling between each group of tests. The set of points from which curve A is drawn do not lie as near to a straight line as the other sets of points. However, when curve A is drawn so as to weight all points, it is in good agreement with the other curves.

It is apparent that the test method described here leads to more valid values of interlaminar resistance which are lower than would be obtained by the conventional methods. Further, properties of the logarithmic distribution have been recognized which lead to the use of a resistance value which is less than the median value for the purpose of calculating the interlaminar eddy current loss of a core. The use of the method of test and analysis described here increases the estimated core loss due to interlaminar eddy currents. Losses calculated in this way should be nearer the actual losses and, therefore, should be more reliable than estimates based on average interlaminar resistance value of larger samples. While an experience factor still would be necessary in the estimation of total core loss for a machine, the application of this method, plus the fundamental core loss (estimated from the product of the weight of laminations in the machine and the fundamental iron loss in watts per pound de-

termined by the Epstein test), should reduce the experience factor by accounting for part of the previously inexplainable loss.

Conclusion

Interlaminar resistance of punchings can be tested and evaluated so as to determine the probable performance in a finished machine by testing a set of laminations for interlaminar resistance in groups of two and treating the data statistically by plotting a logarithmic-probability curve. Two important facts can be obtained from the probability curve:

1. The resistance corresponding to the average conductance (antiaverage resistance) from which the core loss due to interlaminar currents can be calculated.

2. The percentage of laminations which lie below a minimum resistance at or above which resistance the danger from hot spots in a machine will be negligible.

Definite limits, which must be met in order that the losses due to interlaminar currents will be no more than one per cent of the total core loss, have been stated.

Reference

1. Interlaminar Resistance, James P. Barton. AIEE Transactions, volume 63, 1944, September section, pages 670–2.

Discussion

Guerney H. Cole (nonmember; The American Rolling Mill Company, Middletown, Ohio): In searching for the cause of excessive energy loss in the cores of electric equipment, it is frequently possible to eliminate from further consideration the interlaminar eddy current loss in a very simple way. In most 60-cycle machines, even of quite large size, the interlaminar loss will be negligible when the interlaminar resistivity of the magnetic core expressed in ohms centimeter squared per lamination is not less than the square of the core width expressed in inches. It is seldom necessary to have the resistivity so high as indicated by this simple relationship as it usually insures a margin of safety of several hundred per cent even when one side of the core is short-circuited and the resistivity measurements are made before one side of the core is short-circuited. This relationship is based upon the formula given later in this discussion and upon the well known transformer equation showing dependence of volts per turn upon frequency, induction, and area of core.

This simple relationship gives at least the order of magnitude of a safe value of resistivity. It is surprising how many engineers have little idea of the order of magnitude of interlaminar resistivity necessary for safe operation of their machines. This paper should stimulate interest in this subject. Furthermore, the paper presents many of the fine points of making and evaluating interlaminar resistance measurements of special value to those setting up acceptance test methods.

The interlaminar resistivity of some satisfactory cores will be found to be many thousands of times higher than that of other cores that result in no trouble. Sometimes this is due to the fact that the resistivity in both cases is adequate but in one case has a tremendous margin of safety. In other cases the rate of change of the total flux, or of the voltage per turn induced in the core, is so different as to permit a very widespread difference in interlaminar resistivity. Because of the wide range in requirements, the type of necessary surface treatment varies widely. This is illustrated by Figure 13. A laminated core built of pickled steel with no added precautions to prevent interlaminar loss may be adequate for a doorbell transformer inasmuch as the resistance of a cube one inch on a side would be 400 times as high as for solid steel. However, a resistivity thousands of times greater than that of a core made of pickled electrical steel laminations is required for power transformers or large rotating machines.

With no assumption other than that the flux density and the interlaminar resistivity are uniform (such as usually is approximately true when burrs have negligible effect) it can be shown that

$$P=(E/t)^2\times\frac{1}{12R}$$

where

P = interlamination loss in watts
E/t = number of volts per turn induced in any coils surrounding the magnetic core
R = resistance in ohms measured perpendicular to the plane of laminations

This loss will be four times as great if one side of the core is short-circuited. From this formula and design data it will be found that ten ohms centimeter squared per lamination is the proper value for the condition mentioned by the authors in the second paragraph of their paper.

In connection with the authors' discussion of the development of hot spots in cores, it may be of interest to point out that a method of insulating electrical sheet steel has been developed comparatively recently which greatly lessens the tendency of the insulation on the steel to disappear when excessive heat is developed in the core. This inorganic insulation for electrical steel, known as "Carlite" insulation, results from a chemical and thermal treatment of the surface rather than the application of a coating. The insulation resistivity will remain adequate even when the core is operated at a visible red temperature for many hours.

Although it is quite important to control interlaminar eddy current loss, few papers have been presented on this subject and hence the data and information given in this paper should be valuable both to design engineers and those responsible for insuring that electrical sheet steel is insulated adequately.

R. F. Franklin (General Electric Company, Schenectady, N. Y.): The authors of this paper have presented a very interesting analysis of a perplexing problem. The theoretical calculation of interlaminar eddy current loss in laminated cores has been presented ably in previous papers before the Institute but little attention has been given to adequate and practical methods of obtaining the essential factor of interlaminar resistance on which the calculation depends. This paper deals with this latter problem and the method of measurement and analysis of data presented should be helpful to a solution of this problem. A third and final step would be that of correlating the calculated interlaminar eddy current loss, using tested values of interlaminar resistance here presented, with actual test values as obtained in laminated cores. Because of the many factors present, this problem probably would involve the analysis of an extended number of tests by the probability method here used.

Another method of measuring the interlaminar resistance factor is described by the writer in a recent article.[1] This method, which is used by the General Electric Company for quality control of the application of enamel and oxides to laminations, has proved valuable because of its simplicity and convenience for mass production testing which is so important in assuring adequate interlaminar resistance. The method involves the use of a testing device which has ten separate insulated and spring mounted contacts, having a small resistance in series with each, which are applied to the surface of the insulated lamination under selected conditions of pressure, temperature, and voltage. A reading of the combined current through the ten contacts gives an indication of the magnitude of surface resistance. There is obtained, therefore, in one reading an average reading that would be obtained in taking ten separate contact measurements at different points on the surface. While interlaminar resistance is not measured directly, a theoretical relation exists between the instrument reading and surface reading which can be used for assuring adequate interlaminar resistance.

Reference

1. Measurement and Control of Interlaminar Resistance of Laminated Magnetic Cores, R. F. Franklin. *Bulletin* of the American Society for Testing Materials (Philadelphia, Pa.), January 1947, page 57.

A. C. Beiler and **P. L. Schmidt:** The authors agree with Franklin on the advisability of correlating the calculated interlaminar eddy current loss with actual test values on laminated cores. As he points out, it is necessary to apply statistical methods to such test values and large numbers of tests are involved.

Franklin makes reference to the test de-

vice which has been produced by the General Electric Company as described in his reference 1. The test device appears to be a practical one for evaluating various coatings which might be applied to steel sheets or to laminations. Because of the uniformity of the method in regard to test area, pressure, and the manner of making electric connection, the device should be an excellent one for shop control, or for development work in which relative resistance values of several types of insulation are desired. However, the authors feel it lacks several features which should be included in a device which is to provide data applicable to the calculation of interlaminar eddy current loss.

Coating to coating contact, a fundamental consideration in laminated cores, is ignored by the method used with Franklin's device. The importance of including such contact in resistance measurements and its effect on resistance values obtained are discussed in the body of the paper (see paragraphs 3, 4, and 5 under "Discussion of Methods of Testing and Analysis").

In the sixth paragraph under "Discussion of Methods of Testing and Analysis" the authors have discussed the necessity of including the effect of punching burrs on measurements of interlaminar resistance. This is another quality of all laminated cores which is not taken into account by the device developed by Franklin.

Still another feature which the authors feel needs improvement in his device is the relatively small total area under test. As the area under test is increased, the resistance will be reduced because the test value obtained varies inversely with the probability of alignment of low resistance spots or areas which are distributed over the entire lamination surface. Therefore, it is essential to test an area as large as possible, but such that a uniform pressure can be applied over the entire sample area. The best solution to the problem of test area is the use of an entire lamination whenever possible.

This problem appears to be one in which advantage has been gained through experimental attack along different lines by two groups working independently. A combination of the best features of both methods should lead to a more satisfactory test device than is now available. Such a device would incorporate Franklin's technique for making contact with the laminations and applying variable temperature and pressure, and would include other features such as contact of two lamination surfaces, the effect of punching burrs, and the greater reliability of larger test area.

Cole's discussion clearly brings out the fact that the interlaminar resistance required is determined by the application. This is influenced by three major factors, as follows:

1. Type of construction, that is, whether or not the laminations are short-circuited on one edge, or by through-bolts or rivets.

2. Type of operation, that is, intermittent or continuous and the allowable temperature rise in each case.

3. Lamination width, that is, the total flux enclosed in possible circuits through the laminations.

The last of these points is discussed in the body of the paper (paragraph 4 under "Application of the Method to Calculation of Interlaminar Eddy Current Loss in a Machine") and is illustrated in Figure 10.

Preliminary Report on Laboratory Aging Tests on Class *A* Insulation

AIEE TRANSFORMER SUBCOMMITTEE

Synopsis: The paper gives the results of a series of co-operative laboratory aging tests made on Manila paper in oil sealed in glass tubes. The aging temperatures were 100, 120, and 135 degrees centigrade. The changes in tensile strength, elongation, folding tests, oil color, and oil acidity are given in tabular form in Tables I, II, and III. The tensile strengths of the paper in per cent of initial versus time are plotted in Figures 1, 2, and 3. The 120- and 135-degree-centigrade tests are completed. The 100-degree tests are being continued.

THIS REPORT gives the results of aging tests conducted by the four co-operating laboratory groups located at Pittsfield, Mass., Sharon, Pa., Milwaukee, Wis., and Chicago, Ill.

The purpose of the tests was to determine whether the tensile strength of class *A* insulation (Manila paper) sealed in tubes with oil and protected from the air continues to decrease with time or whether the strength decreases to a certain percentage of its initial strength and then very little, if any, for long periods of time.

Tests were made at 100, 120, and 135 degrees centigrade. The 120- and 135-degree tests are completed. The 100-degree tests are still under way and will run for one or two more years.

Co-operating Organizations

The co-operating organizations were the General Electric Company, Westinghouse Electric Corporation, Allis-Chalmers Manufacturing Company, and The Armour Research Foundation of the Illinois Institute of Technology.

Description of Materials and Preparation of Test Samples

DESCRIPTION OF MATERIALS (Paper and Oil)

Manila Paper. Data on paper from Manning Paper Company:

Ash content, per cent	1.1
Alpha cellulose, per cent	88
pH of extract, per cent	7.6
Apparent density, gram per cubic centimeter	0.65
Porosity or air resistance, seconds	37
Carbon tetrachloride solubles, per cent	0.57

Transformer oil. Wemco *C* transformer oil.

PREPARATIONS OF TEST SAMPLES

Strips of Manila paper (0.0033 by 0.5 by 10 inches), formed into a $3^1/_2$-inch coil and tied with cotton string, were inserted into Pyrex test tubes, (25 by 200 millimeters). The tubes were constricted to a 1/4-inch neck 6 inches from the bottom. All test samples were vacuum dried and impregnated with Wemco *C* oil. Excess oil over 50 milliliters was removed from tubes. They were flushed with dry nitrogen and immediately sealed at room temperature and atmospheric pressure.

1. Amount of paper: 13 strips 0.0033 to 0.5 by 10 inches or 2.2 grams (dry weight) per tube.

2. Amount of oil: 50 milliliters oil (and paper) per tube.

3. Ratio paper to oil: 5 per cent paper, 95 per cent oil.

4. Gas space: 15 per cent nitrogen gas, 85 per cent oil (and paper).

5. Vacuum treatment: All test samples vacuum dried in one tank at 112 degrees centigrade for 24 hours of broken vacuum followed by 72 hours of fine vacuum (500 to 800 microns). Oil impregnated while hot. Soak under vacuum while cooling.

6. Drying of oil: Wemco *C* oil dried to 10 parts per million water content before impregnating by bubbling with dry nitrogen.

7. Water content tubes: 0.74 milligram per tube. Based on dry paper weight the water content of the paper would be 330 parts per million.

Information on Testing Methods of Each Laboratory Group

GENERAL ELECTRIC COMPANY

Tensile strength. Schopper tester, 125 millimeter gap. Samples tested immediately on breaking tube. Tested at 70 degrees Fahrenheit and 50 per cent

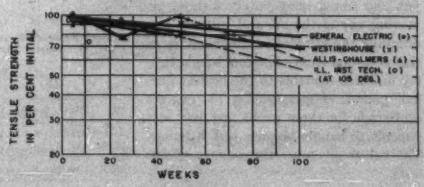

Figure 1. Aging of Manila paper at 100 degrees centigrade

Paper 47-127, recommended by the AIEE committee on electric machinery for presentation at the AIEE summer general meeting, Montreal, Quebec, Canada, June 9–13, 1947. Manuscript submitted March 25, 1947; made available for printing April 15, 1947.

Personnel of subcommittee on transformers: F. S. Brown, *chairman;* M. K. Brown, J. E. Clem, H. L. Davis, I. W. Cross, H. B. Keath, V. M. Montsinger, J. R. North, W. C. Sealey, F. L. Snyder, F. J. Vogel, C. F. Wagner, H. H. Wagner, E. R. Whitehead. **Members of working group:** V. M. Montsinger, *chairman;* P. L. Bellaschi, W. C. Sealey, and F. J. Vogel.

The subcommittee is indebted to the following men and organizations for assistance rendered:

The General Electric tests, under F. M. Clark's supervision, were conducted by S. W. Kernaghan.

The Westinghouse tests, under the supervision of Doctor C. F. Hill, were conducted by L. McCulloch.

The Allis-Chalmers tests were conducted by J. P. L. McCoy, W. H. Krause, and J. M. Doherty.

The Illinois Institute of Technology tests were made under the supervision of Professor F. J. Vogel, with the help of L. W. Matsch of the Armour Research Foundation in making the measurements.

The oil and paper were furnished by the Westinghouse Electric Corporation. The test samples were treated and sealed in the test tubes by the General Electric Company.

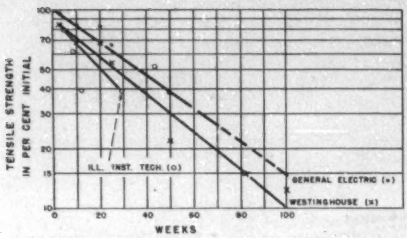

Figure 2(above). Aging of Manila paper at 120 degrees centigrade

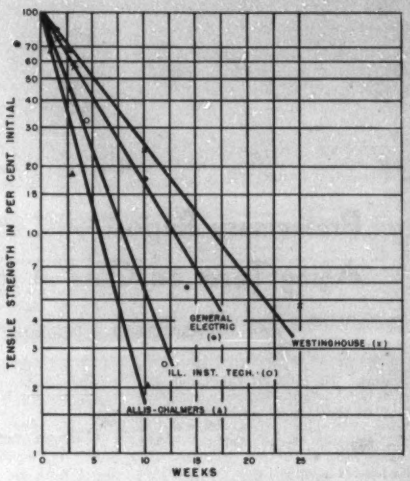

Figure 3. Aging of Manila paper at 135 degrees centigrade

relative humidity. Values given are the average of ten tests.

Folding test. Tinius Olsen folding endurance tester. One kilogram load. Records number of double 90-degree bends.

Oil color. American Society for Testing Materials units, by comparison with known oil standards.

Oil acidity. Solvent method, titrating with NaOH. Results calculated to milligrams KOH per gram.

Westinghouse Electric Corporation

Preparation of paper samples and tensile strength. All test strips were extracted with heptane and were conditioned for 24 hours at 65 per cent relative humidity and room temperature. Testing machines used were a Scott 0 to 50 pounds, a Schopper 0 to 10 pounds, and a Tinius Olson 0 to 10 pounds. Testing spacing was five inches. Tests were made according to ASTM *D202-43*. Values given are the average of five tests. Tensile strength is expressed in percentage of unimpregnated paper.

Oil color. ASTM units, by Union colorimeter.

Oil acidity. Titration by 0.02 normal KOH.

Allis-Chalmers Manufacturing Company

Method of testing for tensile strength. After the vials were broken, the paper and oil were transferred immediately to a clean dry jar with an airtight seal. The strips of paper were removed from the jars and tested immediately without removing any of the oil, and without conditioning the samples to the humidity of the room in a Henry L. Scott tensile testing machine readable to the nearest one-half pound. Paper held at 135 degrees centigrade for three weeks and over was difficult to handle because of brittleness. The values given are the average of five tests.

Oil acidity. Given in milligrams KOH per gram by titration.

Oil color. National Petroleum Association units.

Armour Research Foundation

Tensile strength. Tested with a Thwing-Albert tensile tester, with the pull adjusted to increase at four pounds per second. The results were expressed as pounds pull at failure. The test spacing was eight inches. Special care was used to cushion the pull at the clamps. Made immediately after sample had cooled and glass tube opened.

Table I. Summary of 100-Degree-Centigrade Aging Tests

Aging Time, Weeks	Tensile Strength: Lb Per In.$^2 \times 10^3$	Tensile Strength: Per Cent Initial	Elongation, Per Cent	Folding Test, Number, Double Folds	Oil Color, ASTM	Oil Acidity, Mg KOH Per G
General Electric Company						
0	14.1	100.0	1.3	90	1/1	0.005
5	13.9	98.7	1.1	74	1/1	0.004
25	13.5	95.8	0.8	53	1/1	0.003
50	11.7	83.0	0.6	16	1	0.007
100	12.6	89.4	0.4	7	1	0.025
Westinghouse Electric Corporation	Per Cent					
0	106	100.0	2.4		Less than 1	0.012
5	97	91.5	1.1		Less than 1	0.012
25	98	92.5	3.1		1	0.017
50	98	92.5			1	0.020
100	72	68.0				
Allis-Chalmers Manufacturing Company	Lb				National Petroleum Association	
0	22	100.0				
5	22	100.0			1.2	0.012
25	17	77.3			1.2	0.013
50	22	100.0				

Armour Research Foundation (aged at 105 C)

Tensile Strength: Lb	Tensile Strength: Per Cent Initial	Elongation: In. Per 8 In.	Elongation: Per Cent	Tear Tests: Force, G	Tear Tests: Per Cent Strength	Power Factor, Per Cent	Specific Inductive Capacity	Oil Acidity, Mg KOG Per G
0 23.2 (avg)	100.0	0.23	2.9	60	300			0.035
4.6 21.7 (avg)	93.6	0.11	1.4	33	55	0.9	2.16	0.05
8.66 21.1	91.0	0.11	1.4	35	58			0.052
12.0 17.1	73.7							
29.6 19.7	85.0	0.10	1.25	13	22			0.054
42.7 10.03	82.1	0.08	1.0			0.13	0.217	0.060

Tear test. Expressed as force in grams and tested with an Elmendorf tear tester.

Fold tests. Some tests were made with a Tinius Olsen fold tester, but because of the large variation was not considered as a satisfactory indication and the tests are not included in the results.

Oil acidity. Neutralization number obtained by ASTM procedure expressed in milligrams KOH per gram of oil.

Power factor. Oil from tubes tested at 100 degrees centigrade in a cell at 60 cycles.

Record of Temperatures

General Electric Company

The 100-degree-centigrade temperature was plus or minus 1.0 degree with no overheating.

The 120-degree-centigrade temperature was plus or minus 2.0 degrees averaging close to 120 degrees centigrade and twice the temperature was 124 degrees centigrade over night.

The 135-degrees-centigrade temperature was plus or minus 0.5 degree and was low at 129 degrees for two days.

Westinghouse Electric Corporation

The temperature of the three ovens did not exceed two degrees above the nominal values, and 80 or 90 per cent of the readings fell between the nominal temperatures and three degrees below. The average temperatures of the ovens from the 270 daily readings are 99.5, 119.4, and 134.4 degrees centigrade.

Allis-Chalmers Manufacturing Company

The oil samples were aged at 100 and 135 degrees centigrade in a Precision Scientific Company oven with temperature control resulting in a temperature variation of less than one degree.

Spread of Maximum and Minimum Values From Average Tensile Strength

General Electric Company

Above 38 per cent the initial strength of the variation was 6 to 14 per cent. Below 38 per cent the variation was from 24 to 70 per cent.

Westinghouse Electric Corporation

Above 40 per cent of initial strength the spread was from plus or minus 2.5 to plus or minus 7.5 per cent from average. Below 25 per cent the spread was from plus or minus 25 to plus or minus 50 per cent from average.

Table II. Summary of 120-Degree-Centigrade Aging Tests

Aging Time, Weeks	Tensile Strength: Lb Per In.^{2}×10^3	Tensile Strength: Per Cent Initial	Elongation, Per Cent	Folding Test, Number Double Folds	Oil Color, ASTM	Oil Acidity, Mg KOH Per G
General Electric Company (average of two separate tests)						
0	14.1	100.0	1.3	90	1/2	0.004
3	13.6	96.5	1.0	75	1/2	0.005
10	11.7	83.0	0.6	3	3/4	0.016
25	7.9	66.0	0.25	1	1	0.026
50	5.4	38.3	0.15	1/2	1	0.085
75	1.54	11.0	0	0	1	0.160
Westinghouse Electric Corporation	Per Cent					
0	106	100.0	2.4		Less than 1	0.012
3	89	83.9	2.1		1	0.017
10	72	67.9	1.5		1	0.012
25	57	53.7	1.0		1	0.012
50	23	21.7			1	0.02
82	16	15.1				
100	13	12.3				

Armour Research Foundation

	Tensile Strength: Lb	Tensile Strength: Per Cent Initial	Elongation: In. Per 8 In.	Elongation: Per Cent	Tear Tests: Force, G	Tear Tests: Per Cent Strength	Power Factor, Per Cent	Specific Inductive Capacity	Oil Acidity, Mg. KOH Per G
0	23.2 (avg)	100.0	0.23	2.9	60	100			0.035
4.6	20.6	88.8	0.09	1.1	27	45	0.11	2.17	0.056
8.6	16.3	70.3	0.09	1.1	21	35			0.057
12.0	9.1	39.2							
29.6	9.1	39.2	0.05	0.6	(0)	0	0.15	2.16	0.062
42.7	11.9	51.4	0.05	0.6	(0)	0	0.21	2.26	0.087

Table III. Summary of 135-Degree-Centigrade Tests

Aging Time, Weeks	Tensile Strength: Lb Per In.^{2}×10^3	Tensile Strength: Per Cent Initial	Elongation, Per Cent	Folding Test, Number Double Folds	Oil Color, ASTM	Oil Acidity, Mg KOH Per G
General Electric Company						
0	14.1	100.0	1.3	90	1/2	0.004
1	12.7	90.1	0.9	9	1/2	0.037
3	9.5	67.4	0.7	1	1/2	0.064
10	2.5	17.7	0	0	1	0.10
14	0.8	5.7	0	0	1 1/4	0.09
Westinghouse Electric Corporation	Per Cent					
0	106	100.0	2.4		Less than 1	0.012
1	89	84.0	1.3		1	0.012
3	66	62.2	1.0		1	0.017
10	25	23.6			1	0.023
25	5	4.7			1 1/2	0.058
50	0				Less than 2	0.100
Allis-Chalmers Manufacturing Company	Lb				National Petroleum Association	
0	22	100.0				
1	15	68.2			1.3	0.012
3	4	18.2			1.3	0.018
10	<1	(2.0)			1.5	0.040

Armour Research Foundation

	Tensile Strength: Lb	Tensile Strength: Per Cent Initial	Elongation: In. Per 8 In.	Elongation: Per Cent	Power Factor, Per Cent	Specific Inductive Capacity	Oil Acidity, Mg KOH Per G
0	23.2 (avg)	100.0	0.23	2.9			0.035
4.6	7.7	33.2	0.04	0.5	0.22	2.16	0.059
8.6	Brittle						0.071
12.0	0.6	2.6	0.002	0.025	0.37	2.16	0.129

Summary of Test Results

The results of the tests made at the four laboratories are given in Tables I–III. The per cent initial strength versus time data are plotted in Figures 1–3, respectively.

Discussion

Herman Halperin (Commonwealth Edison Company, Chicago, Ill.): In view of the sharp increases in recent years in the in-

stalled costs of electric equipment, it has become increasingly necessary to utilize the equipment as much as feasible. This means increasing the load capabilities up to temperature limits as far as available data indicate will be safe. Therefore, the data in this paper are of timely interest.

H. A. Adler of this office has found on analyzing data in the paper that the deterioration of the insulation follows a law expressed by the formula

$$d = 1 - (\epsilon^{-kt})$$

where

d = the per unit deterioration
t = time
k = constant

This means that the rate of deterioration at any given temperature is not a constant percentage of the original value, but rather that the rate of deterioration at any given time is a constant percentage of the remaining strength at that time. This would mean that the absolute values of deterioration per unit of time become smaller and smaller for long durations. From the available data it appears that the rate of deterioration as determined from tensile tests doubles for an increase in temperature of from 5 to 9 degrees centigrade.

It has been surprising to note that there is considerable difference in test results between the various laboratories in view of experience with oven-aging tests on cable insulation in Chicago, and earlier work at the Massachusetts Institute of Technology. Nevertheless, the data showing the highest rates of deterioration still indicate that it is safe, for example, to have occasional emergency operation at 135 degrees centigrade.

It is my understanding that all samples were prepared from the same material, by the same laboratory, and only the aging and the final tests were made by the various cooperating laboratories. The discrepancies in results may be due to differences in test methods between the various laboratories. It is noted that Westinghouse samples were tested after extraction of the compound which may account for some of the differences. However, apparently the other laboratories tested their samples in the impregnated condition.

The results of tearing tests and of folding during tests are of special interest. Both tests indicate much greater deterioration than the tensile tests. In service the insulation of transformer windings may be subjected to considerable distortion incidental to the great temperature changes to which the transformer may be subjected during operation. The temperature range between no load on winter days and heavy load may be as much as 125 degrees centigrade under normal operation and about 160 degrees, taking into account loading under emergency conditions. Considering the distortion to which the insulation may be subjected due to these temperature changes it seems to me that data on tearing strengths may be of more value than data on tensile strengths. This point is emphasized by the fact that the paper shows much greater deterioration in the folding endurance tests than have been shown in the tearing tests.

In connection with the over-all problem of safe temperatures, obviously more laboratory data such as shown in this fine paper will be welcome. In addition, utilities should find it useful to keep operating records on transformers that carry high loads during normal or emergency operation.

P. L. Bellaschi (Westinghouse Electric Corporation, Sharon, Pa.): The results of laboratory aging tests on insulation presented in this report should be of some help in clarifying understanding on this subject matter. For instance, these co-operative tests demonstrate that results are reproducible provided all conditions in method and test are the same. The differences in the results evidenced from Figures 1, 2, and 3 apparently may be due to some departure in the details among the four laboratory groups: in the preparation of the paper samples for tensile test, the testing, as well as such other factors as control and measurement of the temperature.

As stated in the report, these laboratory tests were made on Manila paper in oil in sealed glass tubes. One of the criticisms directed to this arrangement is that in a sealed test-tube arrangement such as this the decomposition products remain in continual contact with the paper, whereas in an actual transformer the decomposition products have ample opportunity of removal or escape from the paper proper and become absorbed elsewhere.

The effect of these decomposition products is well illustrated from tests made at the Westinghouse Research Laboratories which were conducted in the course of the co-operative tests presented in the report. In one series of tests, the volatile products of decomposition were removed from the test tube by means of a condenser, much in the same manner as volatile products are removed and condensed from any enclosed container. The results of these tests in which the volatile products are removed, show prolonged life of the Manila paper. Likewise, tests on Manila paper in oil in the presence of pressboard and other transformer insulating materials result in longer life of the Manila paper. This latter essentially is the method Sloat followed in his tests.

Many attempts have been made in the past to project the results of laboratory aging tests on insulation in terms of actual transformer operation in service, but invariably this approach has encountered serious difficulties. In this connection a statement appears in the introductory section of the present "Guides for Operation of Transformers" which because of its bearing on this subject is reproduced here[1]

> Practically all of the data in reference to the aging of insulation at different temperatures has been obtained in laboratory tests in which the decrease in mechanical strength has been measured. The relation between the life expectancy of insulation as indicated by laboratory tests and the actual life of a transformer is largely theoretical so that loading based on such information must be tempered by sound judgment based on experience.

With due cognizance to the place and significance fundamental research holds on the one hand and to the vital importance practical experience has on the other hand, there is an intermediate gap, however, that needs filling in this field of development. In recognition of this situation, life tests on 15 transformer models were initiated some four years ago at the Sharon transformer works. In these transformers all known methods of oil preservation are represented in the tank construction of the different units. The transformers are operated outdoors, subject to heavy load variations twice weekly, with top oil temperatures in the summer well up to 90 degrees centigrade for most of the transformers and as high as 100 degrees centigrade in one or two of the units. When completed we believe these life tests on actual transformer models will fill in an important gap that now exists between laboratory test-tube insulation tests on the one hand and practical experience on the other.

REFERENCE

1. GUIDES FOR OPERATION OF TRANSFORMERS, REGULATORS, AND REACTORS, AIEE Transformer Subcommittee. AIEE TRANSACTIONS, volume 64, 1945, November section, pages 797–805.

W. A. Del Mar (Phelps Dodge Copper Products Corporation, Yonkers, N. Y.): Bellaschi's tests of insulation in which he allowed the products of decomposition to escape and the comparison he made with tests in which the products of decomposition were retained in the test cell, remind me of tests made a few years ago by two cable manufacturers on a new synthetic oil which appeared to have promising qualities for cable insulation. The laboratory of one manufacturer made a point of allowing the products of decomposition to escape and came to the conclusion that the oil was exceedingly stable. The other manufacturer, realizing that the products of decomposition do not escape from a cable, made his tests in a closed cell and came to the opposite conclusion.

One explanation of this was that the harmful ingredient in the closed cell tests was chlorine from a catalyst used in processing the oil. I do not know whether that is the correct explanation, but it occurred to me that the presence of chlorine from bleach might be responsible for the committee's results with closed cells.

V. M. Montsinger: It is true, as pointed out by Bellaschi, that the conditions in a test tube do not represent the exact conditions in a transformer. It was agreed, however, by the working group of which he was a member, that for the purpose of these tests, namely, to see whether or not class *A* insulation ceases to deteriorate in mechanical strength when it reaches say 40 per cent of its initial value, the ratio of 5 per cent paper and 95 per cent oil plus 15 per cent gas space represented conditions in a sealed-type transformer, close enough for practical purposes.

If pressboard is an important factor it should have been added when the program was agreed upon. I do not believe that the addition of pressboard would have caused the curves to flatten out—that is, stop the continual decrease in tensile strength with time.

Unless Bellaschi can give some definite comparisons between life of insulations aged in tubes in which the volatile products of decomposition were (1) removed, and (2) were not removed, the tests apparently do not mean very much except perhaps to indicate that the unsealed (conservator) type has some advantage over the sealed type of transformer when subjected to short-time high temperatures.

In connection with Halperin's discussion, if the condition of insulation is judged by tearing tests (or folding tests) its life would be of the order of a year or so at a temperature of 100 degrees centigrade. We know that a transformer will last several times one or two years at 100 degrees centigrade. The life is probably too short even when judged by tensile strength but for the purpose of this study the tensile tests should be the best ones to use.

Halperin gives the equation which expresses the per unit of deterioration with time. It would be helpful if a simple equation could be derived factoring both time and temperature but it does not appear that this is possible.

G. H. Halsey of the transformer division has derived the following equation which fits approximately the General Electric 100- and 120-degree and Westinghouse 135-degree test lines. The equation is of the form

$$T_s = 100e^{-kt}$$

where

$$k = \frac{1}{1{,}000} e^{0.114T - 10.68}$$

T_s = per cent tensile strength
T = temperature, degrees centigrade
t = time, weeks

Rotating Stability Regulators for Synchronous Motor Drives

W. SCHAELCHLIN
MEMBER AIEE

IN transmitting power from a prime mover to a load by means of an a-c system consisting of either a synchronous or induction motor drive, it is necessary to provide sufficient torque margin so as to avoid pulling the machines out of step when subjecting them to momentary overloads.

Very often it is uneconomical to build all torque margin as inherent stability into the machines, that is, to make the continuous excitation high enough to take care of momentary overloads. It is obvious that such practice may result in motors and generators of excess capacity. Regulated stability, therefore, is being used more and more where possible, because it permits reducing the size of the machines as much as 20 to 30 per cent without danger of pulling out of step due to sudden load peaks. The advantage gained is particularly important in case of large machines where a reduction in size represents a real saving in weight and cost.

Regulated stability has been used successfully for several years and several papers[1,2] have been presented, giving a rather complete discussion of the various factors involved.

It is the purpose of this paper to describe the performance of the Rototrol stability regulator as applied to ship propulsion for tankers and troopships and which has proved equally successful for other drives, such as model motor drives associated with wind tunnels, steel mills, and hoists.

How Stability Control Functions

The performance of an a-c system can be illustrated by the well known vector diagrams of Figures 1 and 2 which represent the extreme cases of operating a synchronous motor from a generator of equal internal reactance X or taking power from an infinite bus. With the excitation held constant, the internal voltage vectors E_0 spread apart as the load increases until at a displacement of about 90 degrees the system becomes unstable and the motor pulls out of step.

Expressing this relation mathematically for round rotor machines and taking no account of losses, the energy transmitted by the system of Figure 1 is

$$\text{Kilowatts} = \frac{1.73}{1{,}000}\,\frac{E_0^2}{X}\,\sin\frac{\alpha}{2}\cos\frac{\alpha}{2} \qquad (1)$$

When operating the motor from an infinite bus as per Figure 2, the power transmitted is

$$\text{Kilowatts} = \frac{1.73}{1{,}000}\,\frac{E_0^2}{X}\,\sin\alpha \qquad (2)$$

In both cases the maximum power occurs at an angle of 90 degrees between the two internal voltages E_0 of Figure 1 or between the internal motor voltage E_0 and the line voltage E of Figure 2.

Regulating the steady-state stability of an a-c drive consists in automatically adjusting the excitation of the motor or generator as a function of load. Several methods are available to accomplish this. In some cases the volts or volts per cycle are held constant[3] while in other instances it is preferred to maintain constant steady-state stability as illustrated in Figure 3.

These curves illustrate the performance of a 5,400-kw turbine generator used for ship propulsion and show the line voltage and power output as a function of current. Assuming a desired steady-state stability with 10 per cent torque margin, for instance, the 90 per cent points of the various power curves are

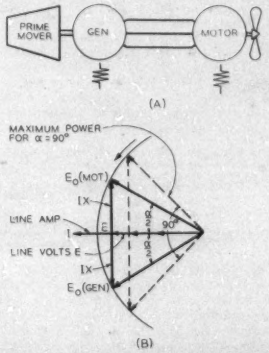

Figure 1. Typical vector diagram for synchronous motor propulsion drive with equal reactance in motor and generator

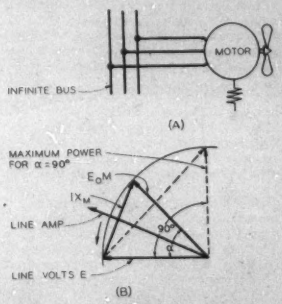

Figure 2. Typical vector diagram for synchronous motor connected across infinite bus

Paper 47-128, recommended by the AIEE committee on industrial control devices and marine transportation for presentation at the AIEE summer general meeting, Montreal, Quebec, Canada, June 9–13, 1947. Manuscript submitted April 26, 1946; made available for printing April 17, 1947.

W. SCHAELCHLIN is manager in the marine and general mill control engineering department of the Westinghouse Electric Corporation, East Pittsburgh, Pa.

The author wishes to acknowledge the contributions made by L. A. Kilgore and S. L. Lindbeck in working out the various solutions.

projected on their respective voltage curves as shown. The points thus obtained form a new curve that shows the voltage required for constant steady-state stability over the whole load range.

It is interesting that this regulated voltage curve is not flat but has a rising characteristic as the load increases. The lower end of the curve which applies to light loads usually is not extended below 50 per cent of normal and is made to follow the dashed line shown in Figure 3. This insures about unity power factor at no load and reduces the operating losses to a minimum. Little, if anything, would be gained by decreasing the excitation further.

For many applications the control of excitation is not critical at all as far as its relation to load is concerned. It is perfectly feasible, for instance, to increase the excitation much faster than shown in Figure 3, provided that the overload is of a transient nature only. By doing this the transient stability can be increased materially without complicating the control as will be discussed later.

Rototrol Stability Regulator

After having established the desired volt-ampere relation for maintaining proper torque margin, the information thus gained can be impressed as a suitable intelligence on a regulating device for the necessary amplification. Among the various means available for this purpose, the Rototrol has given excellent results because of its effectiveness and simplicity of operation.

The name Rototrol is derived from the words rotating and control and is applied to a d-c generator or exciter whose function it is to regulate the performance of an electric drive through automatic adjustment of the excitation of the generators and motors comprising the driving machinery. It is similar to any conventional exciter except that it is provided with various control fields and usually includes a self-energizing amplifying winding.

Figure 4*A* illustrates a typical application of a Rototrol stability regulator for variable-speed turbine-electric ship propulsion. It should be noted that the control field consists of three separate windings, *A*, *B*, and *D*. Two windings *A* and *B* measure current and volts per cycle, respectively, while the third winding *D* carries a fixed excitation. An additional self-energizing field *C* is connected in the Rototrol armature circuit and serves to amplify the intelligence fed into the control fields *A*, *B*, and *D*.

Figure 4*B* gives a typical picture of how a Rototrol functions. Its total voltage output *E* is produced by the ampere turns 0–2, of which only a small part 1–2 is supplied by the control windings. By varying the resistor *R*, it is possible to "tune" the armature circuit, that is, the self-energizing field *C* will supply all ampere turns to produce the voltage *E* and the line X_1 will fall together with the air gap line X_2. Maximum amplification is obtained under this condition.

With the fixed field *D* and the voltage winding *B* being of equal strength but of opposite polarity, it follows that the Rototrol would regulate for constant volts per cycle if the current coil *A* were omitted. The addition of the latter will produce a slope in the voltage curve such as is shown in Figure 3 or steeper if desired.

In determining the circuit constants of a Rototrol stability regulator, it is necessary to consider the amplification and speed of response required to insure a satisfactory transient stability of the combined equipment. Moreover, precautions

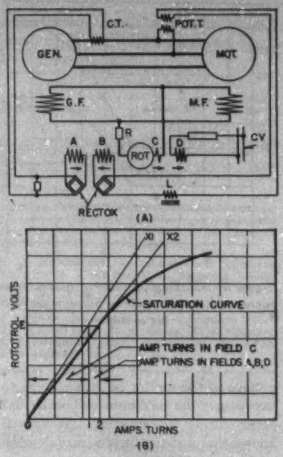

Figure 4. Rototrol stability regulator for ship propulsion

CV = constant voltage

have to be taken to avoid hunting, the danger of which increases with the degree of amplification required in the regulator.[4]

Calculations and actual operating data indicate that the scheme of stability control shown in Figure 4*A* is not critical and that it is possible to secure the proper speed of response without requiring high amplification and antihunting means that go with it. In this respect the current component of the Rototrol control field has a particularly beneficial influence. In case of a sudden load surge, it immediately provides full boosting of the excitation proportional to the load while the instantaneous drop in line voltage due to the transient reactance is relatively small. In most cases this reactance is only about one-third of the synchronous reactance so that for a given amplification the current component of the Rototrol control field is about three times as effective as the voltage component. In other words, the use of a current component permits a reduction of regulator amplification.

It is of course important that the time constant of the Rototrol exciter is relatively low as compared to that of the main machines. Moreover, it readily can be seen that the transient stability increases in almost direct proportion with the time constant of the generator and motor field which governs the delay of flux due to an increase of load.

In applying the stability control of Figure 4 to turbine-electric ship propul-

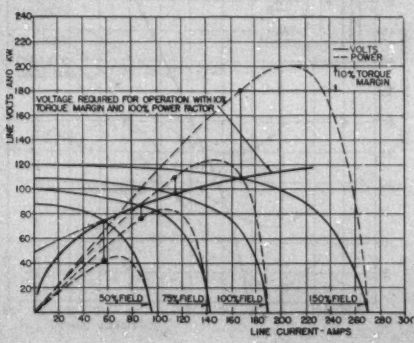

Figure 3. Performance curves for 5,400-kva turbine generator at 100 per cent power factor

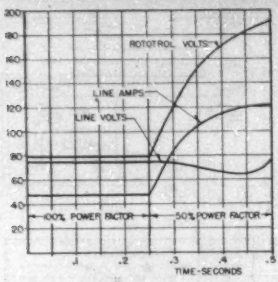

Figure 5. Oscillogram showing speed of response of Rototrol regulator during maneuvering of ship

sion, it is necessary that the ceiling voltage of the exciter be high enough to take care of the maximum load peaks that occur during maneuvering. It is well known that a steam turbine may develop as high as 300 per cent torque when suddenly applying full steam flow. Fortunately, however, the inertia of the turbine-generator set is high as compared to the WR^2 of the combined motor, propeller, and entrained water so that actual tests indicate a maximum torque of about 170 per cent only that has to be transmitted to the motor when accelerating a ship that is dead in the water. These load surges may occur rather suddenly, particularly during crash stops when the propeller load changes from a state of cavitation to an efficient slip stream of water around the wheel.

Figure 5 illustrates the transient condition for a 3,500-horsepower turbine-electric synchronous motor drive when changing from synchronous to induction motor operation during maneuvering of the ship. Even though the low power factor load as induction motor is heavily demagnetizing, the momentary line voltage dip does not exceed about 14 per cent.

Operation Beyond the Inherent Stability Point

Extensive tests have been made to investigate the various phases of stability control and to find out if and to what extent it is possible to operate a system with regulated stability beyond the inherent pull-out point.

One of the studies consisted of a test setup with two 130-kva synchronous machines coupled to d-c motors and generators as shown in Figure 6*A*. In order to find out the actual pull-out point with regulated stability, the line voltage was decreased while maintaining a constant load of 130 kw. Perfectly stable operation was obtained even though the voltage was reduced below the inherent pull-out point *B* of Figure 6*B* and the system became unstable only after the voltage was reduced to 1,650 volts or 70 per cent of the inherent pull-out voltage. Rough calculations indicate that the angle between the generator and motor voltage vectors was increased to about 130 degrees.

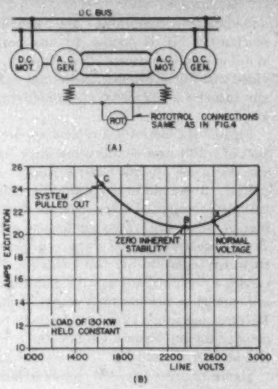

Figure 6. Operation with regulated stability beyond inherent pull-out point

For normal or steady-state operation, it is of course undesirable to operate below the inherent pull-out point since both the field and stator losses would increase unnecessarily. Nevertheless, it is interesting to know that the regulator will permit operation beyond the inherent pull-out which insures that much additional protection during transient conditions.

Stability Control of Constant Speed Synchronous Motors

There are many industrial applications of synchronous motor drives that can be provided with regulated stability in order to reduce their size and weight. Such motors are usually of the constant speed type and are connected to a constant voltage bus as shown in Figure 7.

A Rototrol exciter, either directly connected or separately driven, supplies the excitation for the motor. The control field consists of winding *A* and *B*, the ampere turns of which are suitably amplified by means of the self-energizing field *C*.

At no load the shunt field *B* only is supplying excitation. As the load increases the current field *A* becomes effective and increases the excitation to meet the higher torque demands. By properly porportioning the fields *A* and *B* it is possible so to design the slope of the excitation curve that the motor operates essentially with constant torque margin or constant power factor over the whole operating range.

When large loads are applied suddenly to a motor running at light load, the excitation characteristic may be selected on a basis of insuring high transient stability.

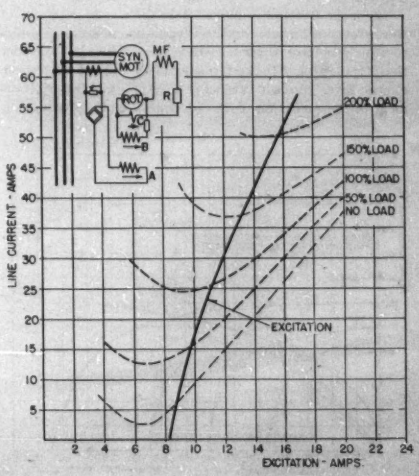

Figure 7. Typical Rototrol stability control for constant speed drive

Since the latter depends to a certain extent on the initial excitation, it may be desirable to operate with excitations greater than required to insure unity power factor below full load. The value of minimum excitation depends a great deal on the magnitude of the instantaneous load surge and the speed of response of the excitation system.

Various means are available for adjusting the excitation control to meet a given application requirement. They may consist in suitably proportioning the Rototrol control fields or in the use of saturable reactors that give a sharp break in the excitation characteristic. Sometimes the Rototrol fields are connected to maintain a definite power factor. Whatever control scheme is used, it should be borne in mind that the amplification required in the regulator depends a great deal on the quantity measured by it.

Conclusions

Test data as well as actual operating experience indicate that it is possible to design synchronous motor drives of variable and constant speed with low inherent torque margin and thereby gain a saving in weight and cost that is appreciable in many cases. Regulated stability is adequate to protect the motor against pull-out provided the time constant as well as the ceiling of the excitation system are selected to meet the load requirement.

The Rototrol stability regulator presents a simple means of accomplishing the desired results and the benefits derived from current compensation are particularly emphasized.

References

1. Synchronous Motors With Controlled Excitation for Suddenly Applied Loads, W. K. Boice, B. H. Caldwell, M. N. Halberg. AIEE Transactions, volume 62, 1943, March section, pages 113–19.

2. Steady-State Stability of Synchronous Machines as Affected by Voltage Regulator Characteristics, C. Concordia. AIEE Transactions, volume 63, 1944, page 215.

3. Static Voltage Regulators for Rototrol Exciter, E. L. Harder, C. E. Valentine. AIEE Transactions, volume 64, 1945, August section, pages 601–06.

4. Recent Developments in Generator Voltage Regulation. C. R. Hanna, K. A. Oplinger C. E. Valentine. AIEE Transactions, volume 58 1939, pages 838–44.

Discussion

A. Uno Lamm (Allmanna Svenska Elektriska Atkiebolaget, Ludvika, Sweden): The author mentioned that the magnetic amplifier or transductor might be used instead of the rotating regulator. We have found that the behavior of the transductor is very similar to that of the rotating d-c machine, and that also the mathematical treatment of both regulators in the dynamical case is the same. The speed of response of the transductor is fundamentally greater because of the absence of air gap in the magnetic circuit, with consequent absence of magnetic energy to store up and consume during regulation. There is, however, for the present an economic limit to the use of the transductor especially as the cost of the metallic rectifier, which is combined with the transductor, compares favorably with the rotating machine only below certain power rating, and this critical rating varies between about one-half and five kilowatts depending upon conditions.

W. Schaelchlin: Lamm's comment concerning the similarity of the rotating and transductor regulator is well taken in that both types are using the same fundamental circuits.

It is not quite clear, however, why the air gap of the rotating regulator should cause an increase in time constant, although it is admitted that the introduction of an air gap has a tendency to increase the input into the control windings. As we see it, the speed of response and the time constant depends a great deal on the amplification and the relative strength of the various windings. Moreover, it is also necessary to evaluate the armature speed of the rotating regulator in order to obtain a good comparison of the two types of regulators.

Operation of Power Line Carrier Channels

H. W. LENSNER
ASSOCIATE AIEE

POWER LINE CARRIER has become an accepted medium for the transmission of intelligence for high-speed relaying and several other functions between stations on a power system.[2,3] Because of its versatility, it has been applied extensively to transmission networks of all voltage classes and all degrees of complexity.[1] Its widespread use, however, has required a new line of thinking and appreciation of values by the power engineer who is accustomed to 60-cycle phenomena. Instead of megawatts and kilowatts, he will be dealing with watts and milliwatts. Where the power engineer has been accustomed to transmission efficiencies not far from 100 per cent, in carrier work he must expect efficiencies of one per cent down to 0.01 per cent or even less. Many applications of carrier to transmission lines uncover new problems which had not been encountered previously. Their correct solution results in a carrier channel of a dependability limited only by that of the power line itself. It is the purpose of this paper to describe the behavior of carrier frequencies on power systems, and to discuss some of the more common problems that arise in establishing a reliable carrier channel on a power line.

Differences Between Power and Carrier Frequencies

While the fundamental concepts of electric waves apply equally to power and carrier frequencies, the frequency difference of approximately 1,000 to 1 makes negligible at carrier frequencies many factors of prime importance at power frequencies and vice versa. Most transmission circuits are electrically short compared to the wave length of a 60-cycle wave, but at carrier frequencies with wave lengths as short as one mile the same circuits are electrically long in most cases.

Consider a typical overhead transmission line at power and carrier frequencies. Assuming a velocity of propagation equal to the speed of light, the wave length of a 60-cycle wave on such a line is about 3,100 miles. The voltage at the receiving end of a line one wave length long would be 360 degrees out of phase with that at the transmitting end. However, it is known that a maximum of power can be transmitted over a line when the receiving end voltage lags the generator voltage by 90 degrees. For this line, the theoretical power limit would restrict transmission to not more than a quarter wave length or 770 miles. On the same transmission line at a carrier frequency of 60 kc (60,000 cycles) the wave length would become approximately 3.1 miles. One fourth of this distance or a little over three quarters of a mile appears to be the maximum distance for efficient transmission of carrier. However, with carrier we are not so much concerned with transmission efficiency as with providing a voltage to energize a sensitive carrier receiver, and actually distances of several hundred miles are possible.

Relative Efficiencies

The foregoing discussion introduces another significant difference between power and carrier transmission, which is the relative efficiencies. The losses in any transmission circuit consist of series resistance and shunt leakage losses. On modern transmission lines the leakage losses are small, and the series losses are kept to a minimum by raising the voltage, thus decreasing the current required to transmit a given amount of power. Since most lines at power frequencies are electrically short, the impedance is determined primarily by the step-up and step-down transformers and the connected load at the receiving end.

With carrier transmission, however, the lines are electrically long and most of the power is absorbed in the line. Thus the receiving equipment has little effect on the transmitting end impedance. While the transmission efficiency at carrier frequencies may be determined quite easily for uniformly constructed 2-terminal lines,[1,4] the complexity of most transmission circuits is such that it is usually more practical to determine this efficiency by actual test. At first thought, it might seem that the very low efficiencies (in the order of one per cent) which are quite common, would be entirely unsatisfactory. However, it should be remembered that the energy losses of carrier transmission do not involve large amounts of power and modern carrier receivers operate on input power down to one milliwatt or even less.

As an aid in expressing transmission losses at carrier frequencies, the power engineer has borrowed a convenient unit from the communication field—the decibel. The decibel is nothing more than the logarithm of the ratio of two values of power, voltage, or current. Since the over-all efficiency of two or more circuit components in series is the product of the efficiencies expressed in per unit values, the total circuit loss in decibels can be determined easily by adding the decibel losses of all the components. The decibel can be defined in terms of the following equation:

$$\text{Decibels (db)} = 10 \log_{10} \frac{P_1}{P_2} = 10 \log_{10} \left(\frac{E_1}{E_2}\right)^2 = 20 \log_{10} \frac{E_1}{E_2}$$

Paper 47-142, recommended by the AIEE joint subcommittee on power system applications of carrier current for presentation at the AIEE summer general meeting, Montreal, Quebec, Canada, June 9-13, 1947. Manuscript submitted March 27, 1947; made available for printing April 25, 1947.

H. W. LENSNER is design engineer in the Westinghouse Electric Corporation, Newark, N. J.

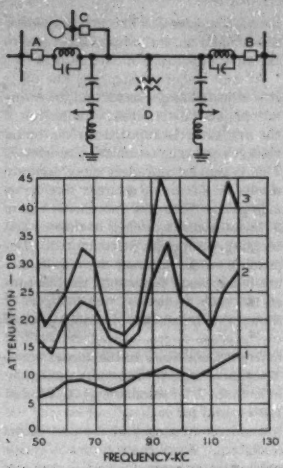

Figure 1. Typical power line for application of carrier, and frequency-attenuation curves under different line switching conditions

assuming that E_1 and E_2 are measured across circuits of the same impedance. In expressing the loss of a transmission circuit, P_1 and E_1 are input quantities, and P_2 and E_2 are the values measured at the receiving end.

Various power and voltage ratios and the corresponding decibels are shown in Table I.

Table I. Power, Voltage, and Decibel Relations

Power Ratio	Voltage Ratio	Decibels
1.26	1.12	1
2.0	1.41	3
4.0	2.0	6
10.0	3.16	10
100.0	10.0	20
1,000.0	31.6	30
10,000.0	100.0	40

In light of the table, consider a carrier channel with an attenuation of 30 decibels. If a carrier transmitter of P watts output will produce a satisfactory signal, doubling the transmitter output will allow satisfactory transmission through 33 decibels attenuation, and not through an additional 30 decibels, which would mean a total attenuation of 60 decibels. Commercial carrier equipment usually is rated in decibels range for a transmitter–receiver combination. If a transmitter of higher power is substituted, the increase in decibels operating range will be equal to the decibels increase in power output of the transmitter. The maximum decibels also can be increased by using a more sensitive receiver, but line noise limits the usable increase that can be obtained in this way. The more sensitive receiver will give satisfactory output in the absence of noise, but if the line noise is of the same magnitude as the desired signal, the added sensitivity is of no value. Under such a condition, a more powerful transmitter would be needed to give a satisfactory signal-to-noise ratio at the receiving point.

Characteristics of a Power System

The ideal carrier channel would be a single-circuit line connecting two power stations with no other lines to it at either station and with no taps on the line between the stations. Such a line, unfortunately, never is encountered in practice, but usually is complicated by the presence of parallel lines, taps, and other lines connected to the bus at the line terminals. The attenuation of a 2-wire uniform line increases approximately linearly with frequency, but on many actual lines the departure from linearity is very large. If there are one or more branch circuits, particularly circuits which are relatively short at carrier frequencies, the increase in attenuation is no longer proportional to the frequency, but may vary widely for a small change in frequency. In fact, a change of 5 per cent in the frequency may easily cause an increase or decrease of as much as 25 decibels in some circuits. If the power circuit is changed by system switching so that the branch circuits connected are changed, there may be equally great changes in attenuation. Therefore, it is desirable that the line be studied carefully in order to determine the most suitable frequency for operation of a carrier channel.

To determine a suitable frequency for a carrier channel on a line complicated with taps, it is often necessary to make a frequency-attenuation test of the line over the carrier-frequency band.[6] Such a curve for a typical line under various conditions is shown in Figure 1. The characteristic of the line AB with line traps at each end is shown in curve 1. The characteristic of the same line with tap C and its associated equipment in service is given in curve 2. The introduction of this circuit not only increases the average attenuation of the line AB, but also introduces irregularities caused by reflection and absorption effects. Thus between points five kilocycles apart there is as much as ten decibels difference in attenuation.

The characteristic of the same line section AB with both tap lines C and D is shown in curve 3. This curve shows not only an increase in the average attenuation because of the division of the carrier energy among the paths from A to B, C, and D, but also reflection effects that are so pronounced as to give a 20-decibel variation in attenuation over a 6-kc interval. Furthermore, there may be no similarity between the last two conditions. That is, the peaks and troughs in attenuation will not necessarily occur at the same frequencies. The peaks in attenuation are caused by reflection on the taps C and D at carrier frequencies for which the electrical lengths of the tap line are equal to an odd multiple of one-fourth wave length (1/4, 3/4, 5/4) at that particular frequency.[4] For this condition, the input

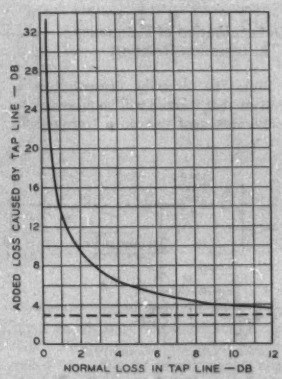

Figure 2. Additional reflection loss caused by tap line an odd quarter wave length long, plotted as a function of normal tap line loss

impedance of the taps may be very low (in the order of 10 ohms) compared to a normal line impedance of 500 ohms.[7] If it were possible to terminate the taps with their characteristic impedance (Z_0), then the input impedance of the taps would be essentially equal to Z_0 and the attendant increase in attenuation would be only a few decibels. As the length of the tap increases, the tap line attenuation reduces the severity of the reflection losses. This is shown in Figure 2 which is a curve of the added attenuation introduced by an odd-quarter-wave-length-long tap line as a function of its normal attenuation. If the normal attenuation is low, the reflection

loss will be very high. As the tap line attenuation increases, the reflection loss decreases, approaching a minimum of three decibels (half the power) for a tap with no appreciable reflection.

It is possible to minimize the effects of taps by inserting a line trap in the tap on the phase wire to which carrier is coupled (assuming phase-to-ground coupling). While this will not completely isolate the tap because of carrier energy which transfers to the other phase wires, it will reduce its influence to a negligible value. From an examination of the three curves of Figure 1, it may be possible to select a satisfactory operating frequency without using traps on the tap lines. For example, at 80 kc the attenuation varies only 10 decibels (from 8 to 18) for the three conditions, and the attenuation does not change too rapidly for a few kilocycles on either side of 80 kc. This would be a satisfactory operating condition for modern carrier receivers.

Determination of Frequency-Attenuation Relation

From the foregoing discussion, it is evident that it often will be necessary to make an actual test on a transmission system to determine suitable frequencies for carrier channels. This is particularly true if a single carrier circuit is to include two or more sections of a transmission line with their attendant busses, taps, transformers, and other circuit irregularities at carrier frequencies. While the frequencies for which a tap is an odd quarter wave length long can be calculated readily,[4] the actual frequency at which a tap line will present a low impedance is also dependent on the terminating impedance. This impedance is often a transformer bank whose characteristics at carrier frequencies effectively change the electrical length of the line. For this reason, it is generally not feasible to calculate the effect of taps. On a simple 2-terminal line section to be arranged for carrier relaying with line traps at both ends, the carrier frequency usually can be selected without tests on the line, since the power circuit will be nearly ideal for the application of carrier.

On complex networks the problem consists of making an actual test on the line by transmitting carrier from one terminal in steps of a few kilocycles, and measuring the strength of the received carrier at each frequency at the opposite end of the circuit over which a carrier channel is to be established. A suitable setup for making such a test is shown in Figure 3. Carrier is to be transmitted from station A to station B. Line traps are indicated as would be required for a relaying channel. If line traps are to be used, their impedance can be simulated reasonably by opening the circuit breaker behind them. A still better substitute, but less convenient, would be to open a disconnect switch on only the phase to which carrier is coupled. Voltmeters $V1$ and $V2$ are vacuum tube voltmeters suitable for carrier frequencies. Ammeter A is preferably a thermocouple instrument for measuring the radio-frequency current into the coupling capacitor. The power into the line thus can be determined from the $V1$ and A readings when the line tuner is adjusted to resonance. At the receiving terminal, however, the power is usually too low to use a voltmeter and an ammeter. Instead, the line tuner is disconnected from the carrier set and terminated in a noninductive resistor R, preferably equal to the characteristic impedance of the line. It usually will be sufficiently accurate to use a resistor value of 500 ohms for overhead lines and phase-to-ground coupling. If no line trap is to be used (as might be the case for a telemetering channel), the input impedance of the line at B may be far below 500 ohms because of the other lines connected to the bus at that station. It is desirable to know this value of impedance to aid in adjusting the line tuner, and it can be determined easily by transmitting any frequency from A which gives a satisfactory signal at B, then varying the value of R and determining the power dissipated in resistor R. This power will be a maximum when the value of R is equal to the input impedance of the line at B.

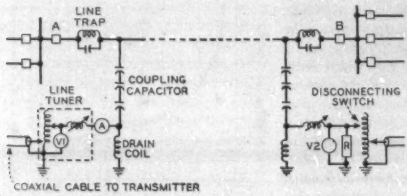

Figure 3. Setup for determining frequency-attenuation characteristic of a transmission line

At A, $P1 = V1 \times A$ watts

At B, $P2 = \frac{(V2)^2}{R}$ watts

Decibel loss $= 10 \log \frac{P1}{P2}$

At each frequency step, the line tuner A is adjusted to resonance and the transmitted power determined. Similarly at B the line tuner is adjusted for maximum voltage across the terminating resistor R. This is simpler and gives more accurate results than retuning a carrier receiver at each point. From the formulas in Figure 3 the total loss in decibels of the line and coupling equipment is computed. Depending on the accuracy desired, it may not be necessary to readjust the line tuners at each frequency step. Figure 4 shows the broadness of response of a typical phase-to-ground line tuner at three different frequencies in the carrier band. These curves were obtained by tuning the inductance L for resonance at 55, 75, and 120 kc, and for each setting varying the transmitter frequency above and below resonance. From these curves it is apparent that an error of not more than one or two decibels would be introduced by retuning the line tuner only a few times over the carrier band of 50 to 150 kc.

Figure 5 shows part of a power system provided with a carrier channel for telemetering and supervisory control. This particular system was not clean-cut for the application of carrier for three reasons: first, near the center of the line was a tap which extended two different distances in opposite directions from the line; second, there was a parallel path of a different length connecting the two stations; and third, at both line terminals there were numerous short lines connected to the station bus. Frequency-attenuation tests as previously described were made and the results also are shown in Figure 5. The curve clearly shows the effect of the tap at about 63 kc. From these curves, frequencies of 95 and 105 kc were selected, and proved satisfactory in subsequent operations. If a satisfactory frequency could not have been found for all operat-

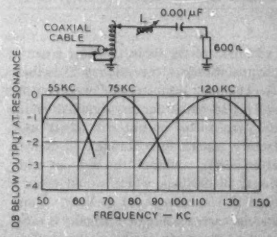

Figure 4. Response of phase-to-ground line tuner showing added loss caused by operation off resonance

ing conditions, a line trap could be inserted in the tap at X to isolate it sufficiently from the line to allow operation of the carrier equipment.

In many instances a less elaborate test is sufficient to select an operating frequency. At each frequency setting of the transmitter, the plate current of a simple biased-detector receiver, such as that used for carrier relaying (circuit in Figure 7), is read as an indication of signal strength. If the received signal is strong enough to saturate the receiver, the coupling can be reduced to operate on the linear slope of the detector characteristic. Of course, it is necessary to retune the receiver at each frequency. Such a test procedure will not give actual decibels loss over the carrier channel, but will give an indication of relative signal strength. This procedure is particularly useful if it is desired to explore a small part of the carrier band to determine if a given frequency is on a steep slope or at the valley of an attenuation curve. Results of such a test and the line on which the test was taken are shown in Figure 6. Frequencies of 85, 124, and 149.5 kc were already in use and from the curve, the obvious choice was 116 kc for a telemetering channel from station B to station D. Two years' operating experience at this frequency has confirmed the validity of the test.

Operating Practice

Manual Checks

After a satisfactory carrier channel has been established, periodic checks are necessary to insure continuity of service and foretell impending failure of the channel in many cases before it occurs so that corrective measures can be taken. One of the simplest tests is a manual check of carrier reception by station operators once an hour, once a shift, or any other desired interval. The operator at one station starts carrier, and the operator at the other end of the channel reads the biased detector plate current or any similar quantity to give an indication of reception. If the readings show a progressive decrease in value on successive checks, some impending trouble usually is indicated. Of course, it is necessary to correlate the readings obtained with other conditions such as weather, battery voltage, or system switching conditions, as will be explained subsequently.

A typical carrier receiver for relaying operates at plate current saturation for normal input signals, such as point $B1$ on the curve of Figure 7. For a wide variation in received signal ($B1$ to $B2$) there is little or no variation in detector plate current. To give a better indication of actual signal level, attenuation is introduced into the receiver input at point X in the circuit of Figure 7 to reduce the normal signal to the knee of the saturation curve of the receiver ($A1$ on the curve). Now, a reduction in received signal level from $B1$ to $B2$ will appear to the receiver as a reduction from $A1$ to $A2$, and the drop in detector plate current will indicate the change in signal strength. By taking two readings, one with the attenuator in and one with it out of circuit, a better idea can be obtained of the signal strength. Normally the attenuator is short-circuited through an auxiliary relay contact, and is inserted in the receiver input circuit only when checking reception. The use of this attenuator may be called accurately a "reserve signal" test. Since sleet is one of the chief reasons for reduction in received signals, the device is often called a "sleet detector."

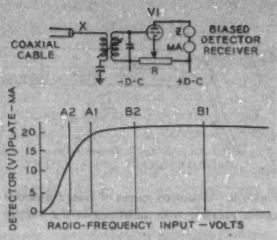

Figure 7. Circuit of biased-detector carrier receiver, and typical saturation curve

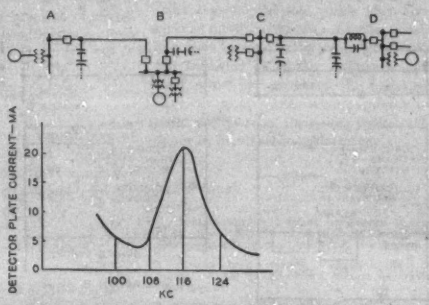

Figure 6. Transmission line response between stations B and D by plotting detector plate current against frequency

It might be well to point out a few factors other than weather conditions which will influence the readings obtained in the "sleet test." A change in battery voltage will affect the transmitted power and thus alter the received signal. Figure 8 shows a family of curves for a relay receiver operated at different supply voltages. From the curves it is seen that with a constant input signal such as point A, wide detector plate current variations can be expected with variation in d-c supply voltage. Changes in the system conditions (line switching) will alter the carrier attenuation as previously shown in Figures 1 and 5. As a result of these factors, a series of received signal readings must be analyzed care-

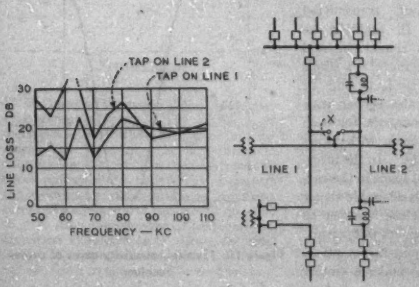

Figure 5. Power system for application of carrier telemetering and supervisory control channel, and frequency-attenuation curves for different line conditions

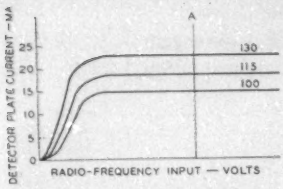

Figure 8. Saturation curves of biased-detector carrier receiver with variations in d-c supply

fully and correlated with other data to be interpreted properly.

Automatic Check-Back

A basic diagram of a completely automatic system for checking transmission and reception of carrier is shown in Figure 9. At station A, a timing motor $M1$ runs continuously, and transmits carrier for a few seconds at any desired interval such as one hour. Reception of the carrier signal at B picks up an alarm relay RA which seals in through contact $M1$ a timing relay M. This timing relay initiates transmission of carrier from B (through contact M) to send a "check-back" signal to A. Reception of carrier at A energizes an alarm relay RA which short-circuits the alarm bell. After a time interval sufficient for this to take place, a contact $M1B$ starts another timing relay $M2$ which closes a contact $M2$ in the alarm bell circuit. If carrier is being received, the alarm bell cannot ring as it is short-circuited by RA. After a few seconds $M1B$ opens and $M2$ resets, opening the alarm circuit. Then the $M2$ contact at station B opens, and M resets, stopping carrier from B. Relay $M1$ at A stops local carrier after a time interval sufficient for carrier from B to be received. Each time that carrier is received, a single-stroke bell is sounded. Failure of carrier at either A or B will interrupt the normal sequence and the alarm bell will seal in and ring continuously to call the operator's attention to the trouble.

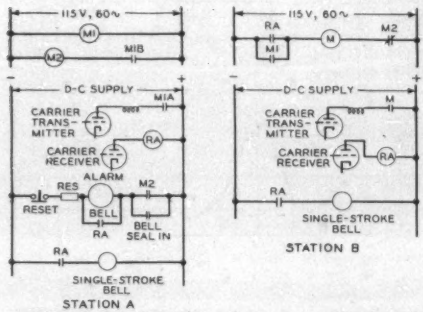

Figure 9. Circuits for automatic checking of carrier channel between two stations

Special Considerations

Two-Frequency Operation

For certain applications of carrier, 2-frequency operation is necessary; that is, the transmitters at the two ends of the line are tuned to different frequencies and the receivers are tuned to receive only the signal from the opposite end of the line. In this way it is possible to receive only the remote signal even though the local transmitter is operating. Such an arrangement is necessary where telemetering signals are transmitted in one direction over a carrier channel, and load control impulses are sent in the opposite direction. The simultaneous use of a carrier channel for telemetering and supervisory control is another instance where 2-frequency carrier operation is required to prevent interference between received telemetering signals and transmitted supervisory impulses. In addition at the terminal where both telemetering and supervisory impulses originate, if a single carrier transmitter is used, it will be necessary to modulate the carrier with two audio-frequency tones, one for each function, and separate them with filters at the other end of the line. In the interest of conserving channel space in the carrier frequency band, it is desirable to set the two frequencies as close together as the selectivity of the receivers will permit. With a given set of equipment it is unfortunately not possible to make a simple statement of minimum frequency separation which will apply in all cases. The attenuation of the carrier channel, the transmitter power, the type of transmission (continuous wave or modulated), and the permissible ratio between the wanted and unwanted signals are all factors which influence the minimum frequency separation. Briefly, the reason that no definite figure for channel separation can be given is the inherent shape of receiver selectivity curves.

Figure 10 shows a typical receiver selectivity curve. The abscissa scale is frequency, while the ordinate scale is decibels. The curve shows the rejection of a frequency other than f_r to which the receiver is tuned. Stated another way the curve shows the decibels increase in level above that of f_r in received signal at frequencies other than f_r which would be required to give the same receiver output as at f_r. For example, at frequency f' a signal 20 decibels above f_r in level would give the same receiver output as at f_r, similarly, 40 decibels for f'' and 60 decibels for f'''. Thus, a transmitter operating at f'' with a power output 20 decibels above the received signal would cause an unwanted signal in the receiver 20 decibels below the desired signal. However, if the incoming signal was so weak that the local transmitter output was 40 decibels above it, it would be necessary to operate at f''' to maintain a 20-decibel difference between the wanted and unwanted signals. This illustrates the relation between frequency separation, attenuation and the transmitter power. A statement of allowable frequency separation for given equipment which would be satisfactory under one set of conditions might not hold for a line of higher attenuation. For this reason no simple

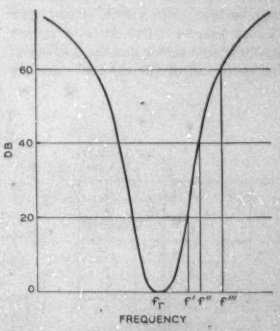

Figure 10. Typical selectivity curve of carrier receiver

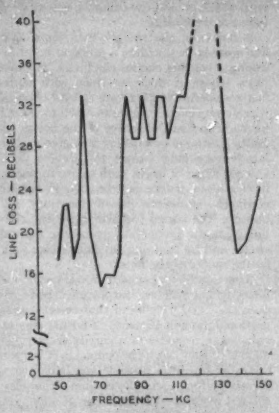

Figure 11. Frequency-attenuation curve of transmission line which includes several taps and a section of power cable

statement can be made to cover all cases.

As an aid in reducing allowable frequency separation, a parallel resonant trap circuit tuned to the local transmitter frequency can be inserted in the receiver input lead to greatly attenuate the unwanted signal. The frequency separation then is limited largely by the ability of the receiver to tune out the reactive component of the trap at the frequency of incoming signal.

Carrier on Power Cables

The application of carrier to power cables is fundamentally the same as for overhead lines. However, there are several new factors which must be taken into account. Perhaps the most important of these is the low characteristic impedance of a power cable, in the order of 25 ohms as compared with 500 ohms for an overhead line. A typical line tuner and coupling capacitor when tuned to resonance may have a resistive component of as much as 140 ohms.[3] This resistive component is in series with the power cable, and the transmitter output power is divided proportionally between the tuner and the cable. For the figures of 25 and 140 ohms, the coupling loss will be

$$10 \log_{10} \frac{25+140}{25} = 10 \log 6.6$$

$$= 8.2 \text{ decibels}$$

This value of coupling loss is considerably higher than the one decibel or so loss encountered in coupling to an overhead line.

Another important factor is the mismatch loss which occurs if the carrier circuit includes both an overhead line and a section of power cable. Because of the abrupt change in impedance and consequent improper termination, reflections occur at the junction. The reflection loss in decibels at the junction of circuit elements of different impedances is given by the formula

$$\text{Loss in decibels} = 20 \log_{10} \frac{Z_1+Z_2}{\sqrt{4Z_1Z_2}}$$

where Z_1 and Z_2 are the impedances of the two parts of the circuit. Applying this formula to cable and line impedances of 25 and 500 ohms, respectively, we obtain a mismatch loss of

$$20 \log_{10} \frac{500+25}{\sqrt{4\times500\times25}} = 7.5 \text{ decibels}$$

Thus, for a carrier circuit comprising both overhead line and cable, the coupling and mismatch losses alone add up to 16 decibels without taking into consideration the losses on the cable and the line proper.

A third important factor is whether the cable sheath is continuous or is separated into sections isolated with bonding transformers. If the latter is the case, the return path for the carrier energy cannot be through the sheath as the bonding transformers present a very high impedance and consequent attenuation to carrier frequencies. The earth is then the return path, and the carrier attenuation on a cable with bonding transformers is often so high as to preclude the use of conventional carrier equipment such as is used for relaying which will operate through a maximum loss of 30 decibels. A frequency-attenuation curve of a transmission circuit containing both cable and overhead line as well as several taps is shown in Figure 11.

Conclusions

A carrier channel will give dependable service if the equipment is installed, adjusted, and operated properly. Field tests to determine a satisfactory operating frequency are often necessary, particularly on complex power systems with parallel paths for the carrier energy and short taps on the line which may give serious reflection losses. As the power engineers become better acquainted with the behavior of carrier frequencies on their power systems, they will find that they can apply carrier advantageously to more and more of their lines with confidence in its ultimate performance.

References

1. Application of Carrier to Power Lines, F. M. Rives. AIEE Transactions, volume 62, 1943, pages 835–44.

2. Power-Line Carrier Channels, M. J. Brown. AIEE Transactions, volume 64, 1945, pages 246–51.

3. A Versatile Power-Line-Carrier System, H. W. Lensner, J. B. Singel. AIEE Transactions, volume 63, 1944, pages 129–33.

4. Communications Engineering (book), W. L. Everitt. McGraw-Hill Book Company, New York, N. Y.

5. Power Line Carrier, E. L. Harder. *Westinghouse Engineer* (Pittsburgh, Pa.), volume 4, July 1944, pages 98–104.

6. Adaptations of Power Systems for Carrier Installations, W. H. Blankmeyer. *Electrical World* (New York, N. Y.), March 2, 1946.

7. Measurement of Carrier Circuit Impedances, W. H. Blankmeyer. *Electrical World* (New York, N. Y.), August 3, 1946.

Discussion

W. E. Duncan (Tennessee Valley Authority, Chattanooga, Tenn.): The problem of determining just what line traps are required and when they can be omitted in transmission systems has been discussed in many papers, and I believe that Lensner's paper covers the major problems in making actual measurements of the lines in question so as to determine the carrier frequency attenuation characteristics. However, after such data have been secured, and it is determined that a frequency can be used without the aid of line traps, there is no assurance that the system operators will not upset the carrier channels during abnormal switching conditions, especially during bad weather.

Let us look at curves 1 and 3 in Figure 1 of this paper; this shows a difference of approximately ten decibels between different line conditions, and it can be seen that considerable differences in attenuation could occur when additional lines are connected or disconnected from the main line carrying the carrier frequency. The best possible way to overcome this erratic condition is to install line traps to isolate completely the carrier channel to start with. Under the foregoing condition, without the use of line traps in the trapped circuit, a transmitter power output of 100 watts will be required to produce the same results as would be achieved by the use of line traps and a 10-watt transmitter. This increase of power, of course, would give a possible interference to other channels. Therefore, the advantages of additional traps over higher transmitter power to obtain the same results would be lower interference to other carrier services, much more stable line conditions during weather changes, carrier frequencies restricted to specific areas, any frequency could be used rather than a selected few, the installation

could be engineered completely prior to the actual receipt of materials, construction could proceed without being held up by making a lot of time-consuming field tests to determine operating frequencies, and the shifting of frequencies would be permitted at any later date as the system may require. It is believed, in most cases, it would be found that the use of a few additional line traps would pay big dividends in carrier channel stabilization.

A. W. Walton (Oklahoma Gas and Electric Company, Oklahoma City, Okla.): The author has presented some important and interesting principles regarding the operation of power line carrier current channels. It is desirable to run tests to predetermine the optimum frequency, however, there are some factors that make this step impracticable. In a complex power transmission system, considerable carrier by-pass equipment may be necessary before any tests can be conducted. If the 50-to-150-kc carrier spectrum is well occupied the problem becomes more complex. We in the southwest area have found it necessary to use higher frequencies, repeaters, and line traps for telemeter channels.

If a carrier channel is to be reliable another factor must be considered. Lensner mentioned that line noise limits the usable increase obtained by using a more sensitive receiver. A high signal to noise ratio is desirable but very little has been said or published concerning this matter.

Receiver design and characteristics should be critically examined in this respect by those contemplating telemeter applications.

H. W. Lensner: The liberal use of line traps, particularly on an extensive power system with many carrier channels, is a desirable practice from the standpoints of choice of frequency and operation of the system. Where a large number of frequencies must be assigned with sufficient separation to avoid interference, the problem is simplified considerably if the transmission characteristics of the power lines need not be considered. This can be accomplished by completely isolating each carrier channel with line traps.

There are many instances, however, where frequency-attenuation tests are justified. In the example of Figure 5, practically all the high-voltage transmission circuits are shown. There was very little carrier on the system, so a wide choice of carrier frequencies was available. A few tests revealed suitable frequencies for a 2-frequency channel between stations. On similar systems which are not too complex, attenuation tests are worthwhile.

It has been the writer's experience that line noise is very seldom a problem in establishing a reliable carrier channel. In those cases where it does interfere with satisfactory operation, there are several ways of reducing its effect. First, an attempt should be made to find the source of the noise. A faulty insulator or bushing will give carrier interference long before the device fails. Certain types of loads, such as arc furnaces, have caused severe interference in carrier receivers. Judicious use of line traps will increase the signal-to-noise ratio by confining all the carrier energy to the desired circuit and by trapping out lines which may be the source of the noise.

Where audio tone modulation is used, tone filters in the receiver output effectively reduce the band width and thus reject a proportional amount of noise. Another way to reduce the response of a carrier receiver to noise is to slow down the operation of output relays as much as possible consistent with correct performance. By so doing, the relay will not respond to short pulses of noise, yet will operate on the desired signals of longer duration. A study of a noisy line to determine its cause plus the application of one or more of the remedial measures mentioned, will go a long way toward establishing a dependable channel.

Pulse Code Modulation

H. S. BLACK
FELLOW AIEE

J. O. EDSON
NONMEMBER AIEE

Synopsis: A radically new modulation technique for multichannel telephony has been developed which involves the conversion of speech waves into coded pulses. An 8-channel system embodying these principles was produced. The method appears to have exceptional possibilities from the standpoint of freedom from interference, but its full significance in connection with future radio and wire transmission may take some time to reveal.

THIS paper describes an 8-channel transmission system employing pulse code modulation (PCM) which was developed in portable form for field operation. Other work carried on simultaneously by W. M. Goodall, also of Bell Telephone Laboratories, resulted in the development of an experimental system using a different method of coding. A method for pulse code modulation is proposed in a United States patent issued to A. H. Reeves.[1]

In carrying out this new type of modulation, the speech wave applied to each channel is, in effect, transmitted sample by sample and each sample is represented by a multiunit code employing on-or-off pulses, hence the term PCM or pulse code modulation. Thus, code pulses carry the message in contrast to the continuous modulation of a carrier as in ordinary amplitude modulation, or to the timing or position of pulses as in a pulse position modulation[2] system.

The nearly instantaneous samples of the speech wave are taken at intervals sufficiently close together to permit the receiver to produce a faithful recreation of the original wave. The dependence merely on the presence or absence of pulses gives this new system a high degree of freedom from interference as compared with other types of modulation systems. The system also permits achieving regenerative repeating and thereby prevents noise from adding up from section to section in a long repeatered route.

The conversion of the voice wave into coded pulses involves two principles: sampling and quantizing.

Theory of Operation

Sampling Principle

The sampling principle states: if a signal is sampled instantaneously at regular intervals and at a rate slightly higher than twice the highest signal frequency, then the samples contain all of the information of the original signal. This means, if a non-periodic voice wave is plotted, it can be reproduced in all its detail from the values of a set of ordinates erected at equally spaced intervals provided the spacing of the sampling ordinates is less than half the period of the highest frequency component of the original wave. If a voice wave, for example, is passed through a low pass filter whose cutoff frequency is below 4,000 cycles, all of the information necessary for its distortionless reconstruction is contained in a set of very short samples of the voice wave taken at regular intervals at the rate of 8,000 per second. No intrinsic distortion is involved. This sampling principle was used in a previously described[2] microwave relay system using pulse position modulation.

Application of the sampling principle reduces the problem to one of sending a finite number of bits of information giving the magnitudes of the samples of the voice wave. However, this step alone does not permit translation to code because the possible magnitudes of these samples may and generally will occupy a continuous range of values. This difficulty is resolved by a second step, the application of the quantizing principle.

Quantizing Principle

If one experimenter were obtaining points on a curve and calling them to a second person for plotting on a graph, it would be necessary for them to agree upon the precision required. If they agreed to use two significant figures, for example, they might choose co-ordinate paper with 99 lines above and 99 lines below the axis. Each point then would be plotted on one of these lines. Those experienced in curve plotting would expect to obtain a good likeness to the original smooth curve in spite of the fact that only 199 possible discrete values of sample had been used. Were it desired to communicate this information, it is apparent that each discrete point could be represented by a code character composed of a sequence of on-or-off pulses.

The quantizing principle states: each of a set of small ranges into which a larger range may be divided is assigned a single discrete number. This number may be that corresponding to the mean of the range. In the example above, any value from -0.5 to $+0.5$ would be called zero, or the value between 94.5 and 95.5 would be called 95. It is quite apparent that some distortion or granularity is inherent in the application of the principle of quantization to samples of an electric signal carrying the information of the spoken word. The greater the size of the range assigned to a given character and the fewer characters used, the greater will be this granularity. The problem is to determine the smallest number of steps into which voice signals may be quantized without serious distortion, and what the size of each step should be.

Number and Size of Steps

The range of voltages covered by voice signals, from the peaks of a loud talker

Paper 47-131, recommended by the AIEE committee on communication for presentation at the AIEE summer general meeting, Montreal, Quebec, Canada, June 9–13, 1947. Manuscript submitted March 25, 1947; made available for printing April 21, 1947.

H. S. Black is high frequency transmission engineer, transmission development department and J. O. Edson is a member of the technical staff, Bell Telephone Laboratories, Inc., New York, N. Y.

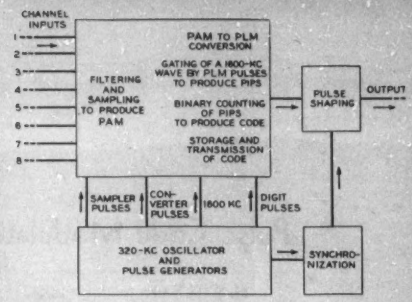

Figure 1 (left). One terminal of an 8-channel PCM system

Figure 2 (above). Functional diagram of PCM transmitter

to the weak passages of a weak talker, is of the order of a thousand to one. If the range of voltages assigned to each code character were small enough to keep the granularity within desired limits for the weaker passages, and if the range assigned to each character were the same, it would be necessary to assign several thousand characters to positive voltages and a like number to negative voltages, which would require approximately 8,000 different code characters. By making most of the steps vary logarithmically, nearly uniform percentage precision is obtained throughout the greater part of the range and far fewer steps are needed. It has been found by experience that 16 steps which vary logarithmically give quite intelligible speech; 32 give acceptable quality even if several such systems are connected in tandem; and the granularity introduced by a well designed system using 128 characters is little enough so that the reconstructed speech wave is reproduced to a high degree of fidelity as judged by experienced observers. With binary digits, the number of available characters is 2 raised to a power equal to the number of on-or-off pulses, called digits, comprising the code. Thus with four pulses, 16 characters are possible, with five pulses, 32 characters, and with seven, 128. Hence a 5-pulse code will give acceptable quality and a 7-pulse code gives very high quality.

To recapitulate, application of the sampling principle permits the reduction of a continuous signal to 8,000 discrete samples per second, and application of the quantizing principle, provided logarithmic steps are used, permits each sample to be represented with sufficient accuracy by a code character which uses one of the various combinations of five to seven on-or-off pulses.

PCM Time Division Systems

Pulse code modulation also permits multiplexing the channels by time division.[8] If the pulses are short, so that the five to seven on-or-off pulses comprising one character can be sent in a small fraction of the 125-microsecond interval between characters, the clear time may be occupied by code pulses from other voice channels thus permitting multiplex operation with many channels.

Figure 3. Block diagram of coder

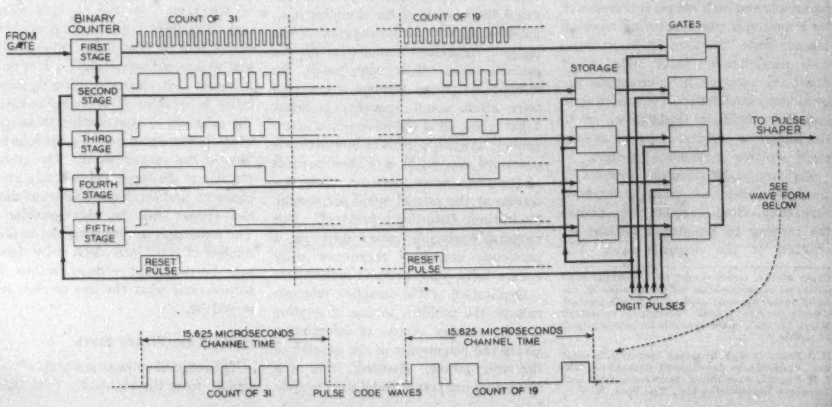

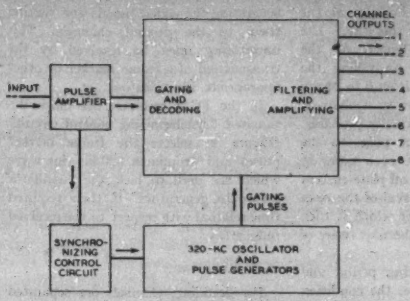

Figure 4 (above). Functional diagram of PCM receiver

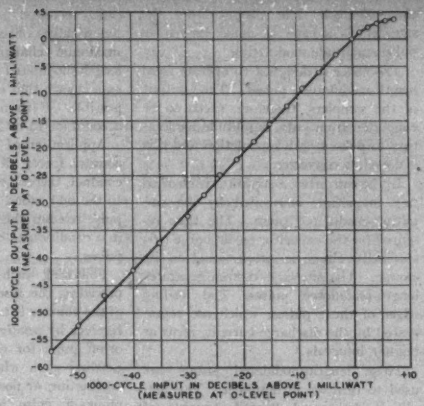

Figure 5 (below). Typical transmission-frequency characteristic

Figure 6 (right). Typical load performance

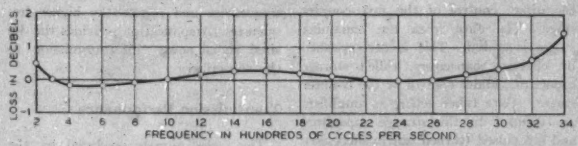

Speed of Operation

A single-channel PCM system carrying speech runs at 8,000 characters per second and the 8-channel system to be described runs 64,000 per second. The pulsing speed is $8{,}000 \times 8 \times 5$ which is 320,000 on-or-off pulses per second. It is apparent that high speed electronic devices must be used to attain such speeds of operation. A surprisingly large number of such electronic devices as well as many different methods of operation have been proposed.

Method of Operation

Outline of the Method

At the transmitting end, the method of operation depends on the use of a "binary counter"[4,5] to count the number of pulses passing through a "gate" which is opened for a length of time proportional to a speech sample.[1]

In the 8-channel PCM system (Figure 1) which uses conventional radio receiving tubes the following sequence of events, presently to be described in more detail, results in the automatic conversion of speech to code. Looking at the left of Figure 2, the voice signal of each channel first passes through a low-pass filter whose cutoff frequency is less than 4,000 cycles per second. Next the resulting signal is sampled at regular intervals 8,000 times a second. These samples (amplitude-modulated pulses) are converted to pulses of uniform amplitude and variable length. The length of each pulse is logarithmically related to the magnitude of the corresponding sample. These length-modulated pulses go to an amplifier and turn it on for intervals of time corresponding to the length of each pulse. This amplifier or gate passes a number of cycles of a frequency so chosen that the longest pulse passes 16 cycles more than the shortest. A binary counter counts the number of half cycles and its condition at the end of the count is utilized to produce the desired corresponding code characters.

Essentially, the function of the PCM receiver is to perform these operations in reverse although not necessarily by the same methods. The result is a copy of the original signals but at a later time. In a well designed system, the accuracy of copy depends chiefly upon the fineness of the steps used in quantizing the samples. During the intervals of time a channel is inactive, there need be no output or noise.

PCM Transmitter

In the PCM transmitter (Figure 2) the timing of all operations is fixed by a 320-kc crystal-controlled oscillator. In the diagram of Figure 2, this oscillator and a 5-stage and 8-stage ring counter[6] are included within the block designated "oscillator and pulse generators". The output of the oscillator is coupled to the 5-stage ring counter which divides the input frequency by five, producing in each stage of the counter 64,000 output pulses per second. Pulses in the output of a particular stage go to another ring counter which has eight stages and there produce pulses in each stage at the rate of eight thousand per second or every 125 microseconds. Each stage in the 8-stage ring counter produces pulses of $15^5/_8$ microseconds duration at 125 microsecond intervals and, at any instant, one and only one stage is producing a pulse.

Each voice signal passes through a low-pass filter to a sampler. Each sampler also receives pulses from a particular stage of the 8-stage ring counter. The sampler is designed to deliver pulses whose magnitude is determined by the voice signal and whose time of occurrence is coincident with that of the applied pulses from the ring counter. When a voice signal is applied to any channel input, corresponding positive or negative pulses (samples of the voice signal) appear in the time intervals assigned to

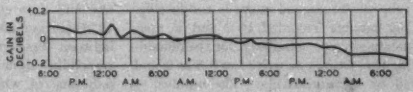

Figure 7. Transmission stability of 160-mile circuit

that channel. The output from the samplers is a type of signal known as pulse amplitude modulation.

The coder is designed to operate from length-modulated pulses. The output of the samplers, therefore, needs to be converted from pulse amplitude modulation to pulse length modulation and this is done in a converter.

In the converter, a capacitor is charged to a magnitude controlled by the amplitude-modulated pulse. The time required for the capacitor to discharge to a specified voltage is proportional to its charge. The discharge current generates length-modulated pulses. The leading edges of these pulses, which are represented by the discharge current, recur at regular intervals.

These length-modulated pulses are used to turn on an amplifier. This amplifier, designated "gate", consists of a twin tube whose grids are driven in push-pull by a 1,600-kc sine wave, obtained by generating the fifth harmonic of the 320-kc oscillations. The plates of the tubes are coupled to the first stage of the binary counter and deliver short pulses (pips) at a rate of 3,200,000 per second for the duration of each of the length-modulated pulses. These short pulses are counted.

Each stage of the 5-stage binary counter (Figure 3) consists of two tubes one of which may be called the odd tube and one the even tube. The circuit is designed so that when either tube conducts, the other does not. Thus, the application of a pulse causes a stage to reverse its position and assume the opposite state regardless of which state it was in. For example, if the even tube is conducting and the odd tube is not, the application of the next pulse causes the even tube to become nonconducting and the odd tube conducting. Coupling between stages is such that a pulse is applied to a succeeding stage only when the even tube of the previous stage is made to conduct. Knowledge of the condition of conduction of either of the tubes tells whether an even or odd number of pulses has been applied to that particular stage.

At the end of the counting interval, to discover how may pulses have been counted, it is sufficient to examine the odd tubes. If the odd tube of the first stage is found conducting, we write down 1 and if nonconducting, 0. If the odd tube of the second stage is conducting, the number recorded is 2 and if nonconducting, 0. Similarly, for the remaining three stages we write 4 or 0, 8 or 0, and 16 or 0, respectively. The number of pulses counted equals the sum of the five numbers obtained in this way. The maximum change in length of the length-modulated pulse controlling the gate is such that counts from 0 to 31 are possible. With no input to a channel, a count of 15 or 16 is equally probable.

Application of a reset pulse to the counter forces all of the even tubes to conduct, thereby cutting off plate current to the odd tubes. Removal of the reset pulse releases the counter which is then in a condition to count the next series of pulses.

Following each counting period and preceding the reset pulse, the condition of the counter is transmitted to the PCM receiver by sending in succession an on-or-off pulse for each counter stage depending upon whether the odd tube is conducting or non-conducting. The first on-or-off pulse is transmitted under the direct control of the first counter stage. The data from the remaining stages is stored. This is accomplished by charging capacitors, called storage capacitors, under control of the counter stages. Gate tubes acting as amplifiers are coupled to the storage capacitors and are pulsed (turned on) in successive intervals and do or do not deliver pulses as indicated by the condition of each counter stage.

As these pulses from the coder are not uniform in shape or duration, they are applied to a pulse shaper. This pulse shaper consists of a gate, opened or closed by the coder output, and fed by short pulses which recur uniformly at a 320-kc rate. By this means the coder pulses control the release to the line of pulses of uniform amplitude and duration.

In Figure 3 are shown idealized wave forms of the voltage as a function of time at the output of the various counter stages. Time advances from left to right as is conventional for oscillographic presentations.

Synchronization

In order that the eight channels may be separated, it is necessary that the receiver gates should receive pulses of exactly the right frequency and in the correct time relation. The transmitted signal contains a prominent 320-kc component which is selected by tuned amplifiers and limiters to produce a steady 320-kc wave. Suitable gate pulses are produced by dividing this frequency by five and then eight. After division by 40, there are 40 possible time relations between these gate pulses and the corresponding signals from the transmitter, only one of which results in correctly separating the coded signals and routing them to the desired channels. This uncertainty must be resolved by the transmission of a frame marker or other appropriate identification.

In the PCM receiver, the block designated "synchronizing control circuit" (Figure 4) selects the frame marker pulses and prominent 320-kc sine wave which are used to lock the "oscillator and pulse generators" in their required time relation with respect to the received pulse array.

PCM Receiver

For decoding, channels are separated by pulsed amplifiers serving as gates. As previously stated, the decoding process is functionally the reverse of the coding process and results in amplitude-modulated pulses. These are delivered to a low-pass filter which passes the voice frequencies and rejects the higher frequencies. Amplification provides the desired signal power for transmission to the subscriber.

Transmission Performance

The coded signals produced by the PCM transmitter can be transmitted by radio, coaxial cable, nonloaded cable pair, open-wire line or any other path suitable for transmitting 320,000 on-or-off pulses per second to the PCM receiver. The system has been operated successfully over a transmitting medium whose band width was limited to 420 kc.

Thus, in order to transmit the intelligence of each nearly 4,000-cycle message circuit, this particular PCM system uses a 52.5-kc band. This is appreciably more than the theoretical minimum for a single 5-digit PCM channel. Since a 4,000-cycle band is the theoretical minimum for transmitting 8,000 on-or-off pulses per second, and since each channel uses 8,000 5-pulse characters per second, 20 kc is the theoretical minimum band width for each PCM channel of this system. For comparison, a conventional single sideband carrier system uses a 4,000-cycle band for each message circuit.

The eight message circuits which each system provides give acceptable performance as indicated by the transmission-frequency and load performance characteristics of Figures 5 and 6. As might be expected, the transmission stability of each of the eight message circuits is outstanding. Figure 7 is a typical recording of the level of a 1000-cycle test tone received from one of the eight message channels and shows that the over-all variation in transmission is

less than 0.3 decibel. The 160-mile circuit referred to in Figure 7 was obtained by applying an 8-channel PCM system to a microwave radio-relay system having three repeaters.

Conclusion

With the good transmission performance which this type of system affords, the individual channels can be used to carry the usual message services including signaling and dialing. PCM appears to have exceptional possibilities from the standpoint of freedom from interference especially when applied to systems having many repeaters in tandem, but its full significance in connection with future radio and wire transmission may take some time to reveal.

References

1. United States Patent 2,272,070, **A. H. Reeves**, February 3, 1942, assigned to the International Standard Electric Corporation. Also French patent 852,183, October 23, 1939.

2. A Multichannel Microwave Radio Relay System, **H. S. Black, J. W. Beyer, T. J. Grieser, F. A. Polkinghorn.** AIEE Transactions, volume 65, 1946, December section, pages 798–806.

3. Time Division Multiplex Systems, **W. R. Bennett.** *The Bell System Technical Journal* (New York, N. Y.), volume 20, number 2, April 1941, pages 192–221.

4. Electrical Method of Counting, **C. E. Wynn-Williams.** *Reports on Progress in Physics* (London, England), volume 3, 1936, pages 239–61.

5. New Vacuum Tube Counting Circuits, **Herbert J. Reich.** *Review of Scientific Instruments* (New York, N. Y.), volume 9, July 1938, pages 222–3.

6. The Use of Thyratrons for High Speed Automatic Counting of Physical Phenomena, **C. E. Wynn-Williams.** *Proceedings* of the Royal Society of London (London, England), series A, volume 132, July 1931, pages 295–310.

Motor Control for Latest New York Transit System Subway Cars

L. G. RILEY
MEMBER AIEE

Synopsis: Early in 1948 the Board of Transportation of New York, N. Y., will place in service the first of several hundred new subway cars, marking the post-war revival of one of the oldest and best established branches of the electrical traction ndustry. Since the year 1900, more than 11,000 passenger cars have been built for the four large cities in the United States having rapid transit systems, a large percentage of which are still in service. An expansion program needs, therefore, to recognize and conform in general to established practices of operation, maintenance, and service conditions. This paper discusses the extent to which modern features of higher acceleration, dynamic braking, and smoother operation are being introduced without any major changes in the existing systems and operating methods.

THE 1948 traffic expansion program for the New York transit system subway divisions will include the construction of three sizes of passenger cars, all of which are to be supplied with identical motor and control equipments. Quadruple 100-horsepower high-speed motors will be used, each wound for 300 volts and permanently connected two in series. The maximum length of train will consist of 11 cars, all of which will be motorized and controlled from a single head-end operating station. A 32-volt battery and a motor generator charging set on each car will provide control voltage supply for all motor control and auxiliary equipment.

The control equipment will include electropneumatic unit switches and a cam controller similar to those now in successful operation in rapid transit service. The rate of acceleration is higher than on the present cars of the New York transit system. Dynamic braking will be included. These requirements necessitate the use of additional apparatus, compared to existing cars.

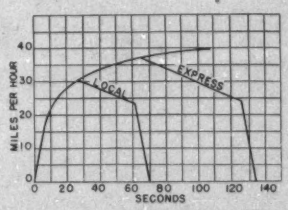

Figure 1. Speed–time curve during rush hour service

Weight of car = 77,000 pounds
Passenger load = 32,000 pounds
Four motors per car
Acceleration = 2.5 miles per hour per second
Braking = 3.0 miles per hour per second

Rush Hour Schedule

	Local	Express
Stops per mile	2.2	0.93
Length of stops, sec.	33.4	41.8
Speeds, mph	15.6	22.0

Series–parallel automatic acceleration will be provided at a rate of 2.5 miles per hour per second for each car, between the limits of the empty weight and the average rush hour load. Under average conditions, the motors will reach the full series connection at 6.5 miles per hour, parallel full field at 14.0 miles per hour, and parallel shunted field at 19.0 miles per hour.

Two important considerations have led to the adoption of dynamic braking as a supplement to the air brake system:

1. The additional safety to be derived from a dual brake system in the operation of long trains at close headways.
2. The elimination of a large percentage of the brake shoe dust which normally accumulates in the cars and subway structures.

The automatic dynamic brake will provide selective rates between 1.5 miles per hour per second and 3.0 miles per hour per second for seated loads, above which the air brakes will provide additional retardation up to 4.0 miles per hour per second total. Automatic blending of the two braking systems will be provided, both systems being controlled by a single brake lever. Full dynamic braking will be effective from 42 miles per hour to 10 miles per hour and will fade out at 5 miles per hour, being supplemented by the air brake for the final stop. Above 42 miles per hour, braking will be with shunted fields and at a reduced rate.

Figure 1 illustrates the speed–time operation of a train in typical express service.

Starting

As a means of improving schedule speeds, the acceleration rate will be considerably higher than that on existing New York transit system cars and will require a greater number of starting notches to produce smooth acceleration. The equipment will have eight notches in series, five notches in parallel, and five shunted field notches, making a total of eighteen. Four of the series notches will be used in building up to full rate. Notching increments in tractive effort will vary 10 per cent above and below the average. Electropneumatic switches will be used for all resistance and series–parallel switching, the rates being controlled by a current limit and automatic progression interlocking the switch units. All control circuits will operate from a 32-volt battery. Field shunting will be produced with a cam controller, electropneumatically operated. A fixed rate of 2.5 miles per hour per second will

Paper 47-148, recommended by the AIEE committee on land transportation for presentation at the AIEE summer general meeting, Montreal, Quebec, Canada, June 9–13, 1947. Manuscript submitted March 24, 1947; made available for printing April 29, 1947.

L. G. RILEY is in the transportation engineering department of Westinghouse Electric Corporation, East Pittsburgh, Pa.

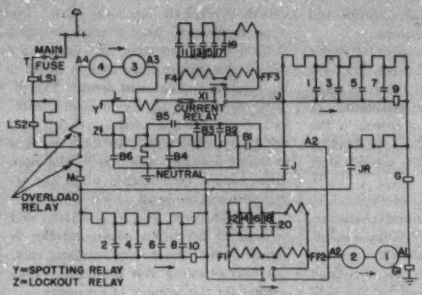

Figure 2 (above). Motor circuit schematic diagram. Power operation with motors in parallel

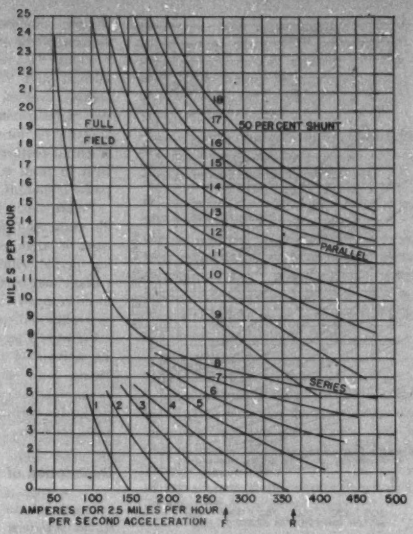

Figure 3 (right). Acceleration notching curve showing the 18 steps

be maintained at all times by means of a compounding coil on the current limit relay and a rheostat on the air brake variable load mechanism.

Three operating positions will be provided on the master controller: switching, series, and parallel shunted field. The first, or switching notch, will develop approximately 110 pounds per ton tractive effort. Transition from series to parallel will be by the bridging method, without loss of tractive effort.

Figure 2 indicates the disposition of the switch units in the motor circuits to complete the connections for parallel operation.

Figure 3 is a notching curve showing the uniform spacing of the eighteen starting notches.

Braking

All switching equipment provided for motor paralleling, resistor notching, and for field shunting will also be used for the regulation of dynamic braking, with the addition of sufficient resistors and switches to provide for high-speed brake applications. A total of 18 brake notches, including five field shunting points, will hold the notching increments to 10 percent above and below the average retardation effort.

In the power-off or coasting position, the brake circuits will be closed and at any speeds below 40 miles per hour, the field shunt notching will progress at a low braking current under the control of a "spotting" limit relay. The equipment is thus positioned in proportion to car speed and is prepared to respond promptly whenever a brake application is called for. Above 45 miles per hour, the initial brake current in the coasting position will develop a retardation effort sufficient to prevent the train from overspeeding on long down grades.

While the basic spotting system affects only the position of the field shunt controller, spotting may take place on any of the series resistor notches, depending on the shut-off speed and the length of the coasting period. In general, the spotting relay will select the proper notch, depending on the field strength required to get spotting current response. Two-way spotting on the field controller will insure proper positioning of equipment within one second after closing the coasting circuits. Brake response will be secured by building up field strength and one or two resistor notches, depending on the braking rate desired.

An electric top portion of the brake valve will close control circuits to set up dynamic brake and spotting connections, in the release position, with the power master controller in the off position. In the service positions, dynamic braking will be initiated and rate selection will be in proportion to straight air pressure on each car as determined by the position of the brake lever. For this purpose, a compounding coil on the limit relay will be energized in proportion to air pressure in an actuator attached to a rheostat.

Blending of the air brake system with the dynamic brake above the 3 miles per hour per second rate with seated load and below to 10 miles per hour will involve admission of sufficient air to make up the desired total above the dynamic brake effort being developed at any given time. The air brake system will include a lock-out magnet valve in the brake cylinder pipe,

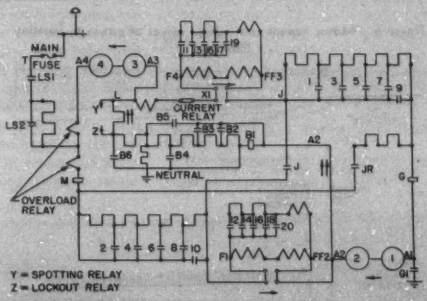

Figure 4. Motor circuit schematic diagram. Brake operation at 30 miles per hour

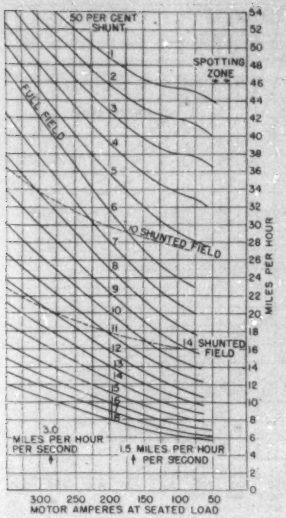

Figure 5. Brake notching curve showing the 18 steps

energized by dynamic current and adjusted to hold out the air except as required to make up the desired total braking effort.

From 10 to 5 miles per hour, while the dynamic brake is fading out, brake cylinder air will be admitted to produce the desired graduation for completing the stop. An emergency application of the air brakes from track trip, brake valve, or release of the controller handle will cut off power and nullify the dynamic brake.

Figure 4 is a corollary to the motor circuit diagram, Figure 2, showing the switching required to set up the loop circuits for dynamic braking.

Figure 5 is a notching curve similar to Figure 3, showing the disposition and spacing of the 18 braking steps.

Figure 6 is presented to show the motor current and voltage changes and the timing involved in the recapture of residual volts to start the circulation of spotting or initial braking current. The essential feature is to close the braking loop in from 0.10 to 0.20 second after power is shut off.

Figure 7 is a follow up of Figure 5 to illustrate the time and buildup characteristics of brake response following a coasting period, during which the spotting voltage and current have been regulated to correspond to car speed by the field controller and spotting relay.

Figure 8 is an enlargement of the braking portion of the speed–time curve of Figure 1 to show the build-up of the dynamic brake, and its blending with the air brake during the fade-out below 10 miles per hour.

Description of Apparatus

In general, the apparatus will be similar to the standard line of electropneumatic control equipments in regular use. There are now available numerous refinements and newly developed details which will increase the reliability and life of wearing parts and tend to reduce maintenance.

Master Controller

The master controller will consist of two drums, the reverse drum, and the main drum, assembled on concentric shafts. These drums will close the contacts necessary for the operation of the control circuits to the nine train line wires required for the simultaneous control of all power and braking functions on each car in the train. Three of these circuits must be energized to apply power, thus affording full protection against the loss of head-end control of power shut-off, due to any faulty crossing of train line circuits.

The operating shafts of the drums will extend through the top cover plate. The main handle will have a vertical spring motion which operates the emergency pilot valve and a rotary motion which is transmitted to the main drum. The reverse drum will be mechanically interlocked with the main drum so that it cannot be operated unless the main drum is in the off position. Conversely, the main drum cannot be operated when the reverse drum is in the off position.

In its location, handle positions, and method of operation, the controller is identical with those in all existing cars, thus perpetuating the established procedures for the training of operators.

In addition to the directional selective circuits, the reverse drum will include contacts for disconnecting the $B+$ supply to the main drum, and such other door and signal circuits as may be required. A starting relay, actuated by the closing of all doors will be included in the controller assembly.

Motor Disconnection Box

For ease in disconnecting the motors to remove the trucks, two 4-pole enclosed switches will be used. The switch box will be split in halves, one portion attached to the car body and the hinged cover portion connected to the flexible motor lead cables. By opening the box and separating the open hinge, the cover stays with the truck, and all leads are disconnected.

Main Fuse Box

Supplementing the third rail shoe fuses, there will be a main fuse of the copper ribbon type mounted in a suitable blowout and arc resisting box. The fuse element will be held with wedge clamps and released by insulated grips for easy replacement.

Main Knife Switch

A single-pole double-throw knife switch will be mounted in a sheet metal box with

Figure 6. Motor current and voltage curves of power to coasting transition

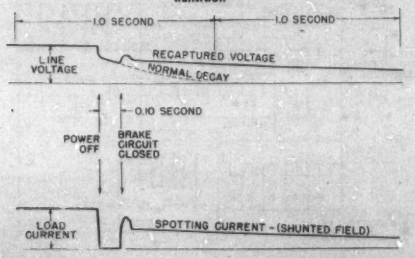

Figure 7. Motor current and voltage curves of coasting to brake transition

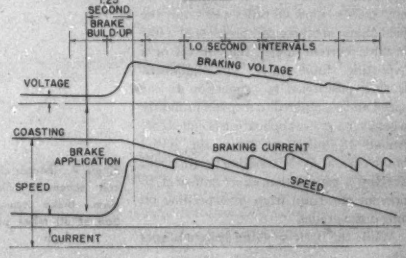

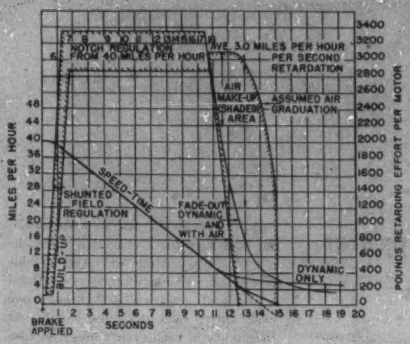

Figure 8. Speed–time retardation curve with combined air and dynamic brake

A 42.5-ton car (with seated load) from 40 miles per hour

insulated lining. In the open or test position, the motors and power circuits will be disconnected to permit inspection and control sequence testing, and the 600-volt auxiliaries will be connected to a bar plug attachment through an enclosed fuse.

Line Switch Box

Two heavy duty electropneumatic switch units will be supplied for power application and overload protection. An improved form of magnetic blowout and extended arc chutes will provide high interrupting capacity, together with long life of contact and arcing members. The units will be mounted in a sheet metal container having hinged side covers and felt dust guards.

A separate compartment on one end plate will house the relays with a hinged cover providing access to three sides of the relay panel. The relays will have supplemental dust protection.

Two overload relays will provide independent protection for each pair of motors. A line relay set to drop out at 400 volts will provide no-voltage release on rail gaps. A vent valve piped to the line switch cylinder will be opened by line relay and overload relay action to supplement the magnet valve exhaust and produce quick action in opening the line switches.

A low energy relay will be so connected and calibrated as to hold in from spotting or residual voltage until the speed drops to less than 5 miles per hour. Contacts on the relay close the unlock circuit to the doors when the relay drops out.

The magnetic valves used on the line switches, as well as those on the switches in the control box, will be a recently developed type with flat composition seats requiring no grinding. The shape and size permit a compact switch assembly and the valves will be detachable.

Control Box

All switching apparatus except that included in the line switch box will be assembled in a single container with covers on all sides for ready access to each item. The central compartment will include nine single-pole and six double-pole switches for completing the series–parallel, braking, and resistor switching circuits. These switch units will be of the same general design as the line switches, except that the arc chutes will not extend through the covers, and the size and capacity will be suitable for single motor circuits. Control circuit interlocks will be of the cam type, with silver contact elements.

One end container will enclose the air-operated reverser, having an all-metal drum and the current limit relay controlling the automatic switching progression for both power and brake load regulation. A second limit relay will control the positioning or spotting of the field shunting controller during coasting. The other end container will include the field controller for regulating the shunting of motor fields, during both power and brake operation. This controller will consist of a group of cam-operated switches, the cam shaft being operated by a rack and pinion actuated by a balanced-pressure air engine. Magnetic valves controlling the air engine will be of the same construction as those used on the unit switches.

Auxiliary relays will be mounted adjacent to the cam controller, supplementing the switch interlocking system in the transfer from power to brake operation. The relay panel will be provided with a supplemental dust-tight cover.

Inductive Shunts

The traction motor fields will be shunted to 50 per cent in the full speed running position. Inductive shunts will be used, combined with resistor tubes for the intermediate steps between full field and 50-per-cent shunted field.

Main Resistors

All starting and braking resistors will be of the wound-ribbon nonbreakable type, assembled in convenient sizes of frames, and proportioned for natural ventilation. Capacities will be such as to withstand the most severe duty cycles without injurious overheating.

Motor Generator Set

The unusually severe conditions imposed on the 600-volt–32-volt battery charging system by line surges and third-rail gaps require special provision in the starting and regulating equipment. Step starting, quick release on loss of power, and protection against motoring from the generator end will be provided.

Summary

Rapid transit service demands the ultimate in mechanical and electrical reliability for all elements of rolling stock design. Long life and economical maintenance follow as a matter of course. These factors have been given full consideration in the design and selection of a modern standard line of equipment for the New York subways.

References

1. Modern Car Equipment for New York City's Subway System, **B. F. Cordts.** AIEE Transactions, volume 66, 1947, pages 247–255.

2. Special 10-Car Train for New York City Transit System, **J. J. Sinclair.** AIEE Transactions, volume 66, 1947, pages 251–4.

3. Dynamic Braking With Traction Motors, **L. G. Riley, G. M. Woods.** AIEE Transactions, volume 65, 1945, August section, pages 517–19.

No Discussion

An Electronic Regenerative Repeater for Teletypewriter Signals

R. B. HEARN
NONMEMBER AIEE

THE important factor in teletypewriter signal transmission over circuits is the relative position on a time scale of the code pulses. If this timing is preserved, wide amplitude variations can be experienced without errors resulting. Correctly timed signal pulses at the transmitting end of a circuit are not necessarily properly timed at the receiving end, as the transmission path may shift the timing of some transitions with respect to others. However, if the signals are not too badly changed or distorted, it is possible to retime them at an intermediate point and send them on in their original form.

Many arrangements have been devised for automatically retiming and retransmitting teletypewriter signals. These arrangements are known as regenerative repeaters. A few of these have been designed to make use of electronic timing arrangements and the purpose of this paper is to describe such an electronic regenerative repeater, known as repeater *TG-29*, designed originally for use by the Armed Forces.

Theory

The usual start-stop teletypewriter code has seven time intervals for each character. In the arrangement discussed in this paper all of these intervals are of equal length in time with the exception of the last, or seventh, which is 1.42 units. The first interval or start pulse in the group of seven pulses required to transmit a teletypewriter character is always spacing, that is, some condition different from that existing when no messages are being sent. The next five pulses are selection pulses and may be any combination of marks or spaces. The seventh pulse is the stop pulse and is always marking. For best reception the various pulses as received should begin and end in their proper positions relative to the beginning of the start pulse and, although the receiving device is tolerant of a certain amount of time distortion, this may be exceeded on some circuits. A regenerative repeater inserted in the circuit before this limit is reached correctly interprets the distorted pulses and retimes them so that the signals retransmitted are substantially perfectly timed. The electronic regenerative repeater accomplishes this function. It employs a sine wave oscillator which begins to oscillate when the start transition of the teletypewriter code is received. This oscillator starts without a transient and oscillates through one cycle during each unit pulse length. At the middle of each cycle a short impulse generated under control of the oscillator determines the proper instant for transmitting a signal. The signal will be initiated by this impulse.

General Description

The regenerative unit is enclosed completely in a weatherproof wooden case with removable front and back and is shown closed for transportation in Figure 1.

The repeater may be connected to various line circuits such as neutral (open and close) telegraph circuits, 2-path polar telegraph circuits, or to a *BD-100* 10-line Army telegraph switchboard as a cord circuit. Except when used as a cord circuit repeater, the type of operation used on one side of the repeater is independent of the type used on the other side. The external circuit may be a simplexed field

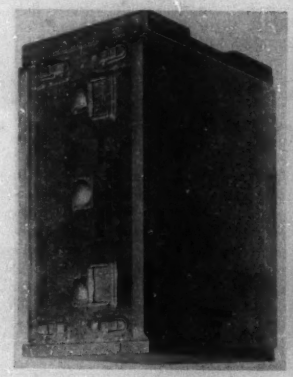

Figure 1. Repeater enclosed in wooden case ready for transportation

Weight 270 pounds

Figure 2. Front view of repeater with cover removed showing spare parts, repeater panel, and power supply

Paper 47-146, recommended by the AIEE committee on communication for presentation at the AIEE summer general meeting, Montreal, Quebec, Canada, June 9–13, 1947. Manuscript submitted November 14, 1946; made available for printing April 28, 1947.

R. B. HEARN is with the Bell Telephone Laboratories, Inc., New York, N. Y.

Figure 3 (above). Front view of repeater panel with lower compartment open for access to plug-in type polar relays

Weight 65 pounds

Figure 4 (below). Front view of repeater panel with upper compartment open for maintenance

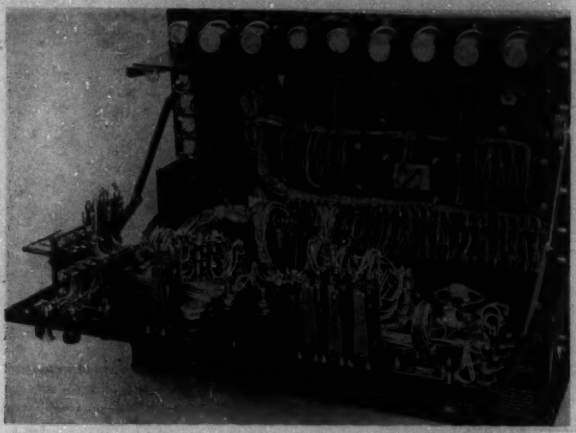

wire (up to 30 miles in length) terminated in another repeater *TG-29*, a *BE-77* type Army line terminating unit, or a line circuit of a *BD-100* switchboard, or it may be a local circuit connected to the local side of a d-c polarential line repeater or the local side of a voice frequency carrier terminal.

The cord circuit arrangement permits connection to two or more line circuits multiplied in the *BD-100* switchboard in such a manner that signals received by any line circuit are regenerated and retransmitted to each of the other line circuits in the multiple group. Such an arrangement is advantageous for connecting two long switchboard line circuits and for switchboard conference connections.

The necessity for providing for a wide range of applications necessarily has increased the complexity of the repeater circuit. For commercial use many of these applications would not be required.

Included with the repeater are a rectifier power unit for converting 115- or 230-volt 50–60-cycle a-c power supplied from an external source to plus and minus 115-volt d-c power for the operation of the repeater, and circuits for lining up the repeater and for adjusting polar relays. The power unit contains three regulated 115-volt d-c sources, a 6.3-volt supply for gas and vacuum tube heaters, and an autotransformer to supply 115 volts to a teletypewriter motor when the primary supply is 230 volts alternating current. One positive and one negative source of 115-volt d-c power are used in the operation of internal circuits. The third source of 115-volt direct current is negative and provides current for the external line circuits connected to the repeater when such a supply is needed.

Figure 2 shows the repeater with the front removed. The equipment is supported on an iron framework by means of shockproof mountings. It may be removed from the frame work and mounted on a standard 19-inch relay rack. As will be noted from Figure 2, binding posts are provided for line and ground connections, jacks for connecting a teletypewriter, a meter and switch for measuring voltages and currents for assistance in lining up the repeater and adjusting relays, together with such switches and rheostats as are needed for operation and adjustment of the repeater. The control panel mounted directly beneath the operating tubes is hinged for maintenance purposes and to gain access to a "speed" switch on the panel in the rear. This switch conditions the repeater for teletypewriter operation at either 368 or 404 operations per minute. Figures 3, 4, and 5 show the complete repeater unit without the power supply.

Operation

The functional diagram shown in Figure 6 indicates the major components of the repeater. Separate sending and receiving circuits are provided for each line. The receiving circuit for line *A* controls the bias and hold circuit for the receiving relay associated with line *B* and prepares the send relay associated with line *B* to be operated by the marking or spacing pulses from the electronic distributor. The receiving circuit also starts the electronic distributor at the beginning of each character. The receiving and sending relay circuits for neutral operation are shown in Figure 7.

A start pulse received from either line

operates a receiving relay which starts the character timer shown in Figure 8 and thereafter neither receiving relay can control the character timer for the duration of its timing period. The character timing is obtained from the $V2$ and $V3$ tubes and their associated resistances and capacitors. It is started by opening the plate circuit of gas tube $V2$. This causes an abrupt change in the potential on the cathode of the $V2$ tube from a slightly positive potential to 92 volts negative potential. The capacitor between the cathode and grid causes the grid to be about 60 volts negative with respect to the cathode at this time so that the closure of the plate circuit to positive battery will not cause the $V2$ tube to become conducting until the charge on the capacitor becomes approximately zero. A half pulse after the end of the fifth selection pulse, the character timer is ready to be restored. Re-establishment of current through the plate of $V2$ changes the voltage on the cathode to a slightly positive value which is applied to the grid of the $V3$ gas tube. The latter tube restores the charge on the capacitor between the grid and cathode of tube $V2$ and the character timer is then ready to time the next character.

The pulse timing oscillator and a pulse timing distribution circuit also are shown in Figure 8. The main elements of the oscillator circuit are the $L1$ coil with a tuning capacitor shunted across it and an amplifying tube $V4$. While tube $V2$ in the character timer is conducting, a positive potential is applied to the left-hand grid of tube $V4$. The path closed through the left-hand cathode and plate of tube $V4$ to the ungrounded side of the $L1$ coil will hold the circuit in a nonoscillating condition. While the $V2$ tube is nonconducting the left-hand grid of tube $V4$ is negative and the holding circuit path is blocked thus leaving the oscillator free to oscillate. The frequency of oscillation is determined by the inductance of coil $L1$ and the capacity of the capacitor shunted across it. It is approximately 46 cycles at 368 operations per minute, teletypewriter speed, and ten per cent higher at 404 operations per minute speed.

The $V5$ tube circuit receives a sine wave voltage which is inverted and repeated as impulses to the grids of the impulse distribution gas tubes $V6$, $V7$, $V8$, and $V9$. These grids normally are held at a negative potential by fixed potentiometer circuits. The impulses applied to these grids cause each of these tubes to become conducting when their plate circuits are closed to positive 115-volt potential. The constants in the regenerator circuit are arranged so that the first impulse for each character will occur one-half of a unit pulse length after the beginning of the start pulse is received and successive impulses will occur a unit pulse length apart. Typical wave shapes and time relations of pulses for one particular character are shown in Figure 9.

After receiving relay AR has opened its marking contact, thus starting the character timer, it will close its spacing contact, thus establishing a circuit through a winding of the A relay which will operate the A relay to spacing. When the A relay opens its marking contact, the biasing current in the receiving relay on the line B side, which was in a spacing direction, is reversed to provide a holding current through the 2–7 and 8–9 windings, and the marking current through the 2–7 winding and the spacing current through the 3–6 winding of the sending relay BS are interrupted. When the A relay closes its spacing contact, a circuit is closed from positive battery through the 8–9 winding of the BS relay to the plate of tube $V9$, a marking current is established through the 3–6 winding of the BS relay and the R relay (not shown) is operated to spacing. The R relay is controlled by currents through the $R36$, $R38$, $R35$, and $R37$ resistors. The $V9$ tube will become conducting on the first impulse and will cause a current to flow through the 8–9 winding of the BS relay which will be sufficient to overcome the marking current in the 3–6 winding and operate the BS relay to spacing.

The next marking pulse may occur on the first selection pulse or it may not occur until the stop pulse but when it is received, the AR relay will return to marking which will cause the A relay to do

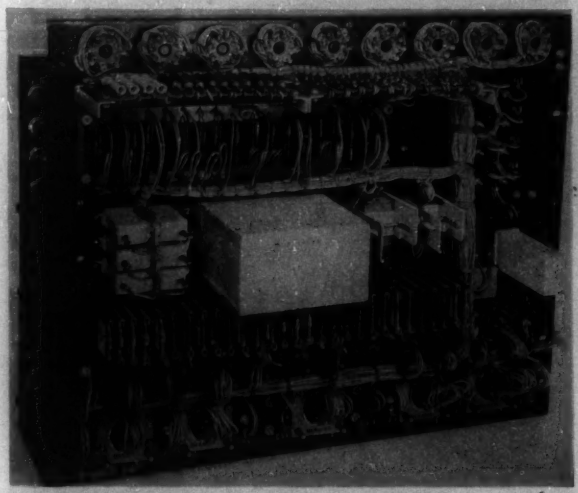

Figure 5 (above). Rearview of repeater panel Figure 6 (below). Functional block diagram

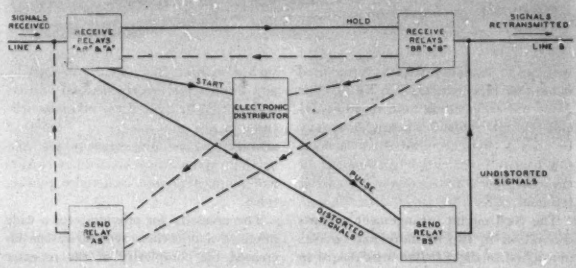

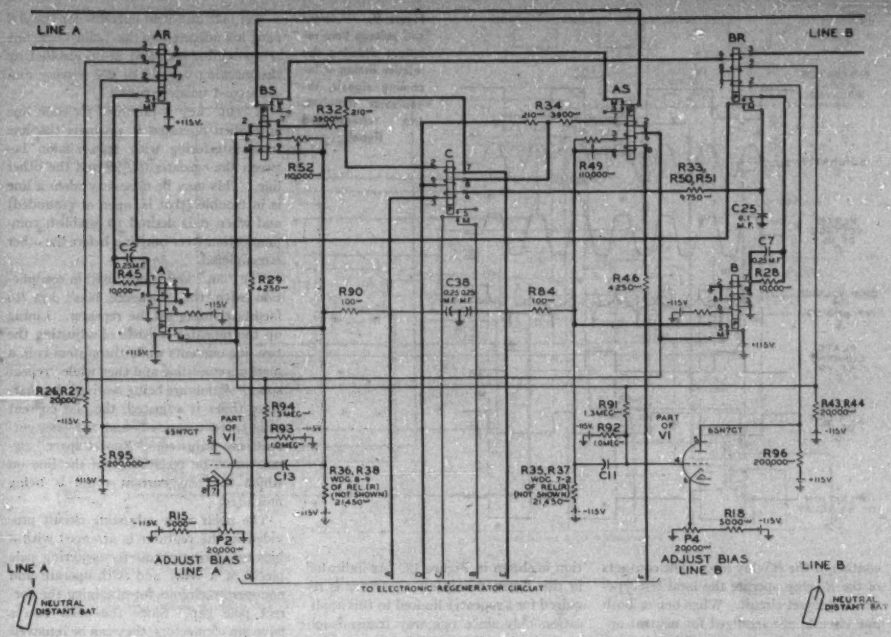

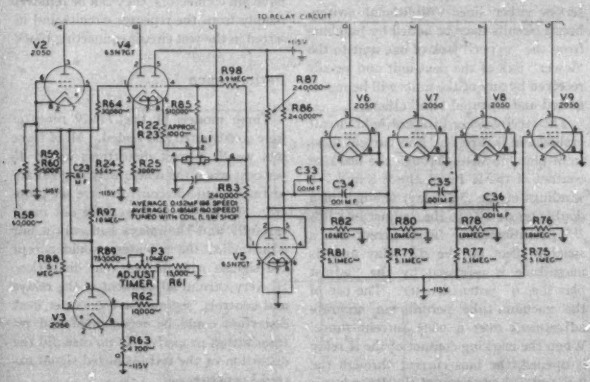

Figure 7 (above). Relay circuit arranged for neutral operation over lines having battery supplied at the distant end

Figure 8 (left). Electronic regenerator circuit started by the first pulse of a code and stopped after producing seven impulses

likewise. When the spacing contact of the *A* relay is opened, the spacing current through the 8–9 winding and the marking current through the 3–6 winding of the sending relay *BS* are interrupted, and the *R* relay is operated to marking. When the *A* relay closes its marking contact, a circuit is closed from positive battery through the 2–7 winding of the *BS* relay to the plate of tube *V7* and a spacing current is established through the 3–6 winding of the *BS* relay. The *V7* tube will become conducting on the first impulse after this circuit has been established and will cause a current to flow through the 2–7 winding of the *BS* relay which will be sufficient to overcome the spacing current in the 3–6 winding and operate the *BS* relay to marking.

Subsequent transitions will cause the same sequence of operation. After the fifth selection pulse, the character timer will be ready to stop the oscillator as soon as the elements of the circuit have been restored to marking by the stop pulse. Any transitions from marking to spacing or vice versa which are displaced with respect to the initial start pulse transition by 40 per cent or less can be received, regenerated, and retransmitted with substantially perfect timing by the method outlined here. This applies to displacements which occur at random (that is, some early and some late). An additional amount of systematic distortion such as bias may be handled in addition to the random distortion by adjusting the bias current of the receiving relay to remove the bias as it is received.

The *R* relay mentioned as being operated by the spacing contact of the *A* relay is arranged to operate from the spacing

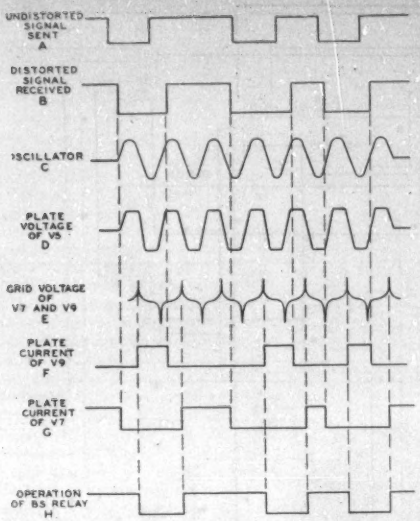

Figure 9. Current and voltage time relations showing the relative timing of incoming signals, regenerator impulses, and retransmitted signals

contact of the *B* relay also. The contacts of the *R* relay operate the local teletypewriter magnet circuit. When one or both line circuits are arranged for neutral operation the sending contacts of the teletypewriter are connected in series with one neutral line circuit. Regenerated signals are sent in one direction and nonregenerated signals in the other direction.

The sending contacts of the teletypewriter operate a local relay *S* which sends unregenerated polar signals in both directions when both lines are arranged for polar operation. The circuit for 2-path polar operation is shown in Figure 10. With 2-path polar operation, if relay *BS* or *AS* should fail to respond to the last marking pulse from line *A* or *B*, respectively, the repeater would remain inoperative in one direction unless some means were provided for operating relays *AS* and *BS* to marking. This condition is prevented by relay *C* which operates to spacing when current flow is through its 3–6 winding and one of the other windings. In operating to spacing, relay *C* opens the oscillator stop lead and thereby prevents the oscillator from being stopped by the character timer until relays *AS* and *BS* have both been operated to marking. Relay *C* acts in the same manner when neutral loops are used although it is not required to prevent a circuit tie-up.

When the *TG-29* repeater is connected to a *BD-100* switchboard, multiway regeneration is obtained. Such a connection is shown in Figure 12. As indicated in this figure, much less apparatus is required for a repeater limited to this application only since one way transmission serves either line. Additional switchboard circuits may be added by patching from the "upper" jack of one unit to the "lower" jack of the next unit and signals received by any of the units will be regenerated and repeated to all others.

The receive relay bias and hold circuit is shown in Figure 11. Bias current flows from plus 115 volts through the marking contact of the *A* relay, the 9–8 and 7–2 windings of the *BR* relay, one-half of a double triode *V*1, to the "adjust bias line *B*" potentiometer. This current has a spacing effect on the *BR* relay and its magnitude is adjusted by the "adjust bias line *B*" potentiometer. The use of the vacuum tube permits an accurate adjustment over a wide current range. When the marking contact of the *A* relay is opened, the bias current through the 9–8 and 7–2 windings of the *BR* relay is reversed and becomes a holding current. This path is traced from plus 115 volts through the *R*96 resistance, the relay windings, and the *R*43, *R*44 resistances to minus 115 volts. When the marking contact of the *A* relay is closed, the re-establishment of the spacing current in the windings of the *BR* relay is delayed until the charge on the *C*13 capacitor becomes sufficiently positive to permit current to flow in the *V*1 tube.

The bias and hold currents for the *AR* relay are adjusted by the "adjust bias line *A*" potentiometer and are controlled by the marking contact of the *B* relay and the second triode in tube *V*1.

A "cut" key is provided for each line and when operated it prevents the line from interfering with transmission between the repeater *TG-29* and the other line. This may be necessary when a line is in trouble (that is, open or grounded) and when it is desired to establish communication over one line before the other is completed.

The "cut" key is also used in conjunction with the "measure bias" key to facilitate lining up the repeater. Lining up the repeater consists of adjusting the two line currents while the system is in a marking condition and then while "repeat space" signals are being received the character timer is adjusted, the bias current ranges are measured, and the bias currents are adjusted. "Repeat space" signals must be received from the line on which the bias current range is being measured.

The polar relay adjusting circuit provided in the repeater is arranged with a bias measuring circuit for centering pole pieces of a relay and with operate and nonoperate circuits for obtaining the correct pole gap. Since the polar relays have pin connectors, they can be removed readily from the repeater circuits and inserted in the test circuit connecting block.

Performance

Three models of the *TG-29* repeater were constructed and tested. All of these sets would correct distortions up to 45 per cent when the relays were in good adjustment and the controls were set properly. When the settings were not made carefully and the relays had only a fair adjustment, the repeaters would accept the signals with 40 per cent distortion. By very careful adjustment of the relays and controls, signals having 48 per cent distortion could be regenerated and retransmitted properly. In no case did the distortion of the retransmitted signal exceed 5 per cent.

The repeater will retransmit a break signal satisfactorily.

The power supply is closely regulated so that the primary power may vary from 50 to 65 cycles and from 100 to 125 volts without interfering with the proper operation of the circuit.

Laboratory tests were made at 60-, 66-, and 100-word-per-minute speeds. The circuit is extremely stable at all speeds for long periods.

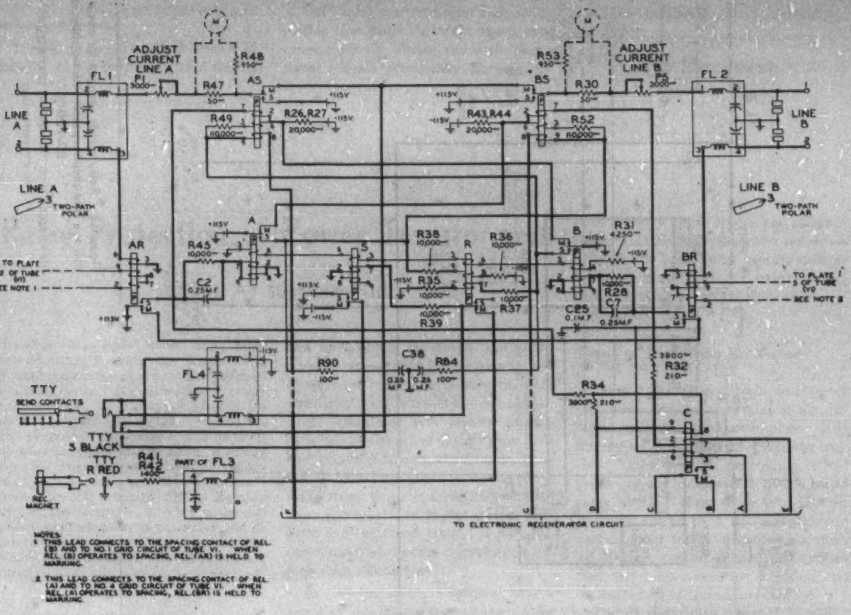

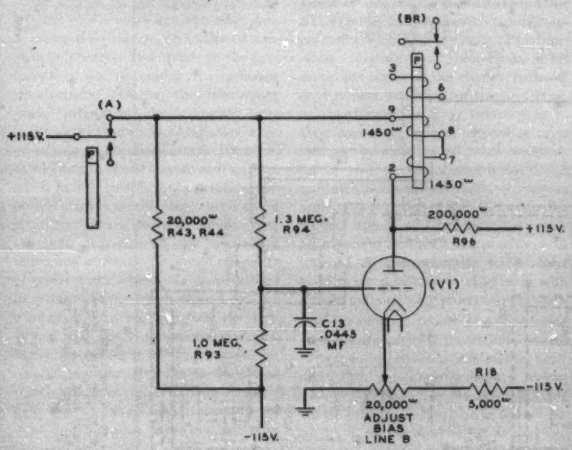

Figure 10 (above). Relay circuit arranged for 2-path polar operation

Figure 11 (left). Bias and holding circuit associated with receiving relay

Conclusion

The *TG-29* repeater was designed for portable use on whatever type of power supply was available. Thus the size and weight of the unit were greater than is necessary for central office use. The circuit also may be simplified for central office use as many of the options added for field use would not be required.

In spite of the satisfactory performance of the repeater, it was never put into production. This was largely due to the delay necessary to produce these repeaters whereas mechanical regenerative repeaters were already available.

The circuit components do not require close manufacturing tolerances. Compensation for variations in the tolerances of the components of the character timing circuit is made with the adjustable rheostat used for setting the speed. The oscillator circuit is tuned by adding small mica condensers in parallel to obtain an accurate tuning.

There are several advantages which will be gained by the use of the electronic device to replace a mechanical unit in obtaining regeneration. The most important of these are:

1. Freedom from the mechanical maintenance effort which is required to keep mechanical units in proper working order.
2. Freedom from lubrication difficulties at low temperatures.
3. Ability to operate at lower temperatures than is practical with mechanical units.
4. Stability of operation over long periods at high speed.

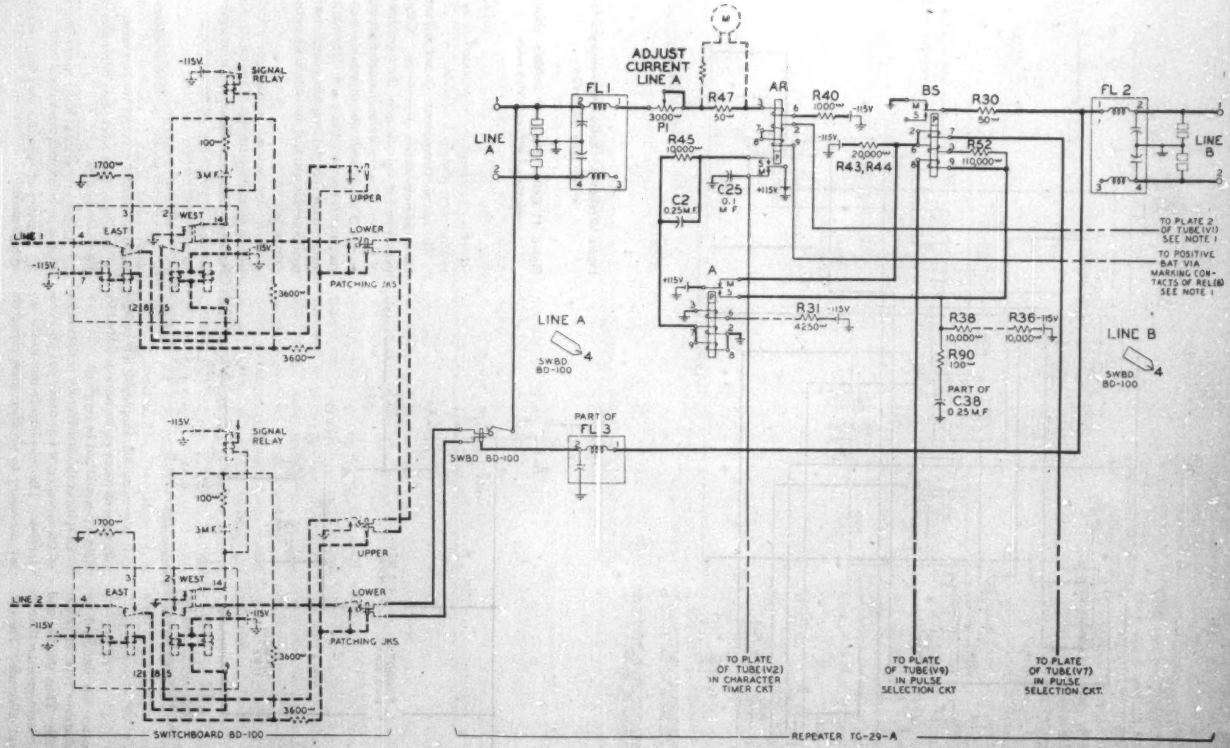

NOTES:
1. FOR THE CONDITION SHOWN, THE CURRENTS IN WINDINGS 2-7, 8-9 OF REL.(AR) HAVE A SPACING EFFECT ON THE REL. REL.(B) WHICH FURNISHES POSITIVE BAT. TO THESE WDGS WILL REMAIN ON MARKING BECAUSE BAT. IS NOT CONNECTED TO THE ARMATURE OF REL.(BR).

Figure 12. Relay circuit arranged for operation as a cord circuit repeater with switchboard BD-100

In this application the repeater provides multiway regeneration

5. It is readily adjusted for different operating speeds or codes

The ability to send a clean break is retained. This is very essential in the case of half duplex operation over long multisection circuits as the break signal may never reach the distant end if the break signal releases periodically allowing signals from the distant end to take control.

No Discussion

Relay Protection of Power Transformers

AIEE RELAY SUBCOMMITTEE

Synopsis: This report of the AIEE relay subcommittee presents the results of a 3-year investigation of present and preferred practices in the relay protection of power transformers. Consideration is given to the influence of advances in the protective art and progress in the design of and methods of operating power transformers. A survey covering experience with over 56 million kva of power transformers has been analyzed in the light of the characteristics of the relay devices now available, in order to develop criterions of adequacy of protection and its inherent limitations and to recommend desirable improvements in devices and methods.

FOURTEEN years ago, the relay subcommittee of the AIEE published a review of practices and trends in the protection of electric equipment, including transformers.[1] During the intervening years, interesting developments have taken place in the devices available for the protection of transformers. However, developments in the transformers themselves and in methods of operation employed to make maximum economic use of equipment[2] have brought about more stringent requirements for protective relays and devices. Improved reliability of power transformers has been utilized in system designs which depend on that reliability to achieve better electrical service with lower investment cost and relaying systems must not impair this reliability. The advances in the art of relays and devices have involved many disturbing compromises between the basic requirements of *service protection* and *limitation of equipment damage* because of magnetizing inrush current, and transformer ratio taps which limit the sensitivity of differential protection. These limitations have become increasingly felt as the art of system protection has progressed, and the standards of service have been raised. The increased magnetizing currents associated with the more general use of higher permeability irons and the trend toward higher concentrations of system short-circuit capacity are also factors.

In October 1944, Chairman W. A. Lewis of the relay subcommittee of the AIEE protective devices committee appointed a working group to study and correlate transformer protection. This group has reviewed the characteristics of devices now available for the protection of transformers, seeking evidence as to their adequacy, for the purpose of crystallizing information on what elements are in greatest need of improvement. A questionnaire was circulated to certain representative users of transformers in the United States and Canada, to determine both present and preferred practices. A total of 28 comprehensive replies have been received, covering experience with over 56 million kva of power transformers.

A preliminary report of the working group on transformer protection was sent to certain interested individuals in January 1946 and subsequently copies were distributed at a conference session on transformer protection held in New York, N. Y., at the January 1946 winter convention. A subsequent conference dealing with gas pressure and gas accumulator protection was held in Detroit, Mich., on June 27, 1946, at the AIEE summer convention, and a conference paper[19] presented at the January 1947 winter meeting developed additional information and discussion. The basis of this final report includes information developed through these conference sessions, and also certain data which were not available for the preliminary report, such as information on the co-ordination of thermal relay characteristics with short circuit protection.

Types of Protection Employed

Figure 1 illustrates the various types of protection now being employed for different sizes of power transformers. It is interesting that differential relaying continues to be the most generally accepted protection for transformers, over a broad range of size. However, a keen interest has been shown by a few companies in certain other forms of protection, such as pressure protection, thermal protection, and gas accumulator detection, and increasing use of these is anticipated.

The 28 companies reported 44 explosions or fires in the past five years. At least some of these transformers were protected by differential relays. Several cases were reported where partial winding faults were not cleared by the differential relays.

Differential Protection

The majority of differential relay installations protect a zone which includes the transformer high voltage and low voltage circuit breakers. Probably because of the increased reliability of power transformers, there is an increasing tendency to omit the transformer high voltage circuit breaker, securing differential protection by totalizing the currents in the high voltage line circuit breakers, and tripping these (as well as the low voltage circuit breaker) in case of a transformer fault. Thirteen of the companies are employing differential relaying with no local high voltage oil circuit breaker, using bushing current transformers in the power transformer to supply differential relays, and tripping the remote breaker, either through a pilot wire system or a carrier current transfer tripping scheme.[8] Eight of the companies report the use of a similar arrangement, except that local differential relays are used to close a

Paper 47-149, recommended by the AIEE committee on protective devices for presentation at the AIEE summer general meeting, Montreal, Quebec, Canada, June 9-13, 1947. Manuscript submitted April 10, 1947; made available for printing April 29, 1947.

Personnel of working group of the AIEE relay subcommittee of the AIEE committee on protective devices: W. R. Brownlee, *sponsor;* C. E. Asbury, E. T. B. Gross, E. L. Harder, L. F. Kennedy, W. A. Lewis, W. E. Marter, E. G. Ratz, J. J. Tesar, F. J. Vogel.

single-pole high-voltage grounding switch to cause opening of the remote high voltage circuit breakers.[4]

The relative sensitivity of differential protection may be expressed in per cent as the ratio of the pickup current of the relays to the full load current of the transformer bank. The reported sensitivity ranges from 30 per cent to 200 per cent, the average "typical" value being about 70 per cent. Certain installations of a generator and a transformer operating as a unit are reported with pickup currents as low as 11 per cent. Most of the companies reported relay speeds of about 0.1 second, although a few reported one-third to one-half second.

Limitations on Through Faults

It is indicated that the limitations in settings of differential relays brought about by through short circuits has been largely overcome, first by the use of ratio type differential relays, and especially by careful application of bushing current transformers and ratios for better performance.

Several methods of predetermining bushing current transformer performance have been presented in recent years.[6,8]

Limitations of Magnetizing Inrush Current

About three-fourths of the companies reported substantial difficulties with false tripping of differential relays on magnetizing inrush current. Some of those who reported no difficulties used relatively long relaying time (one-third to one-half second) or decreased sensitivity, or both. Other things being equal, the magnitude and duration of magnetizing inrush current has been shown to be influenced by

1. The ratio of the normal flux density to the saturation or maximum flux density of the iron.
2. The value and sign of the residual magnetism.
3. The total impedance of the circuit through which the current flows.
4. The point of the voltage wave at the moment of closing of the circuit.[7]

For any particular transformer, one important criterion of interference with sensitivity, other things being equal, may be taken as a function of the maximum short-circuit kilovolt-amperes at the bus from which the transformer is energized, divided by the kilovolt-ampere rating of the transformer. It has been shown[7] that the maximum inrush current (in per cent of rating) where this ratio is 50, is 3 times as great as the current associated with a ratio of 10. It is significant that in the most troublesome examples cited, the ratio of system short-circuit kilovolt-amperes to transformer bank capacity ranged from 15 to over 150, with a typical value of 70. The continued increase in the interrupting capacities of available circuit breakers and the resulting permissible greater concentration of system capacity indicate the growing importance of this factor.

The magnetizing inrush current problem is increased by the use of oriented iron with its higher normal flux densities and greater retentivity. The replies make little mention of the use of these units in the larger sizes. However, the design flux densities now permissible with modern low-loss silicon iron are substantially above those in common use 15 years ago.

Remedies Employed for Magnetizing Inrush Difficulties

One "solution" to the inrush current problem is equivalent to saying: "Just ignore it." That is, if the differential relays operate when the transformer bank is energized, the bank is then energized again, with the hope that the breaker will remain closed. Some feel that faults are more likely to occur when a bank is energized than at other times and that therefore this procedure is unsatisfactory. Also, the operating practices of many companies require leaving a transformer out of service until tested, when differential relays have operated, so as to minimize the possibility of serious explosions and fires when a defective transformer is re-energized.

Many replies indicated that increased pickup of the differential relays had been used. Considerable judgment must be exercised in such instances, since any increase in pickup will reduce at least proportionally the sensitivity for which differential protection has been provided. A few companies report the use of longer time settings.

Three companies reported the use of magnetizing inrush current "suppressors" which decrease the sensitivity for an adjustable time after a bank is energized, unless the voltage drops below a set value. Two other companies reported the use of harmonic restraint relays[8] and two others expressed plans for using either suppressors or harmonic restraint methods.

One company has developed a special relay which rectifies the offset current waves to desensitize the differential relays on inrush current.[9] Another device depends for its discrimination on the fact that the magnetizing inrush current is in effect a half-frequency wave.[10]

A number of companies use residual relays wherever an ungrounded winding of a transformer is connected to a grounded neutral system, and some report the additional use of differentially connected residual relays for the protection of grounded Y transformer windings. Another expedient which has been used to combat the magnetizing inrush problem is the provision of two current transformers per single-phase high-voltage winding for differential protection, similar to generator type, along with an over-all scheme of reduced sensitivity to clear faults outside of this zone. Increased sensitivity is gained in this case for ground faults only, since turn to turn faults produce no unbalance.

The number and variety of methods used to meet the magnetizing inrush situation without serious interference with the desired relay sensitivity, is an indication that this difficulty is quite general. There is need for improvement in differential schemes to provide increased sensitivity without incurring unnecessary tripping on energizing currents.

Fuse Protection

Many companies are using high voltage fuses with low voltage circuit breakers for protection against transformer faults.[11] This choice is an economic one, since in the smaller size of transformers, the cost of a high voltage circuit breaker may be a substantial portion of that of the transformer. Improvements in high voltage fuses and the increase in reliability of power transformers have influenced the trend away from providing high voltage oil circuit breakers for the smaller transformers. Application of fuses to the high voltage side of transformer banks requires careful analysis, since the fuse is a single pole device and individual phases can be cleared. Under certain conditions, it is possible for a phase-to-phase fault after blowing one high voltage fuse to be maintained through the load connected to the secondary of the bank. The impedance of the load may reduce the fault current to a value below the blowing point of the remaining fuses and the fault continues with no protection to clear it, resulting in burned-out transformer windings. Another condition which may cause difficulty is the separate fusing on the high voltage side of two banks which normally operate paralleled on both the high and low voltage sides. A fault occurring on the high voltage side of one bank blows the fuses on that bank only. The fault is again maintained and the application should be

checked to see that either the low voltage bank circuit breaker will trip or that the fuses on the second bank will clear the fault.

In most power transformer applications the high voltage fuses are needed to protect only those faults occurring in the transformer, or on the connections between the transformer and the low voltage circuit breaker. The increased size of fuses on distribution systems and resultant longer relay settings for distribution feeders sometimes give rise to a selectivity problem between the transformer fuses and the reclosing distribution breakers. More information on fuse operating characteristics as influenced by successive heating and cooling during typical reclosing cycles would be helpful.

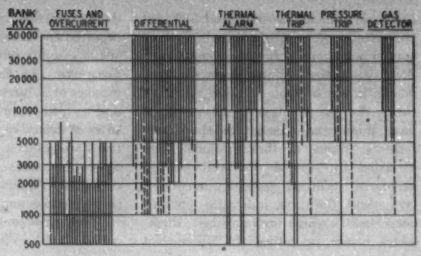

Figure. 1. Relay protection applications for various sizes of transformer banks

Each line represents one reporting company. Dotted lines represent tap changers only

Thermal Protection

Much progress has been made in studies of transformer loading involving hot spot temperatures as a function of time, both with no appreciable loss in transformer life, and with small emergency losses.[11] In order to make the most economic use of transformer capability, a method has been described for loading transformers by copper temperature,[12] using a bimetal element in the top of the transformer, heated from a current transformer. An ambient compensated time lag device has been offered for the purpose of duplicating the temperature-time capability of the transformer.[13]

A number of companies report the use of embedded temperature detectors. Recent transformer designs have avoided the use of such devices in the higher voltages, because of the difficulty of securing the desired high impulse level.

Most of the companies replying used the ordinary top oil type thermometers, which it is agreed are at best an approximation. About half of the companies make extensive use of hot-spot temperature devices for sounding alarms, and some are making increasing use of thermal relays for disconnecting transformers, even at attended stations. Two companies report several cases of faulty co-ordination between thermal type devices and feeder overcurrent relays, in that transformers have been disconnected incorrectly (and locked-out) during nearby short circuits. Investigation disclosed that some of these thermal devices had been designed to overprotect the transformer in the fault current range and hence would operate more quickly than the normal feeder protection. Fortunately, the shape of the time-current characteristics can be controlled by design within quite wide limits.

Co-ordination with overcurrent relay protection requires a rather substantial delay in operation of transformer thermal relays on short-circuit currents. Many distribution feeder circuits cannot employ instantaneous tripping devices because of the presence of nearby transformer banks with large fuses, and these feeder breakers are usually automatic reclosing for a total of four tripping operations. Also in many cases, the transformer will have a low voltage circuit breaker between its terminals and a bus from which circuit feeders are supplied, in which case complete co-ordination is required between the feeder breakers, the transformer breaker, and the transformer thermal relay, allowing ample margin for repeated operations, different initial top-oil temperatures, etc.

Therefore it is recommended that the short time characteristic of the transformer thermal devices be such that they will withstand without operating fault currents of at least the durations listed in the following table. These currents are assumed to be applied following full load operation and are on the basis of the self-cooled rating of the power transformer.

Fault Current Times Normal Load	Time in Sec (Minimum)
20	5
5	40

Below five times rated load the curve may blend into the thermal protective characteristic desired for the power transformer.

Pressure Protection

Considerable attention has been focused recently on the use of pressure relays to provide sensitive supplementary protection for power transformers. A simple type of device consists principally of a bellows, adjustable to operate when the tank pressure exceeds 5 to 15 pounds per square inch (depending on the relative position of the device on the transformer case). Another device is designed to operate on sudden changes in pressure, using a diaphragm with a small hole, sufficient to permit gradual changes in pressure to be equalized without operation. This element usually is furnished as part of a combination gas pressure and gas accumulator device. A third type of device consists of a combination unit mounted directly in the piping connection from the transformer to the conservator, the "pressure element" consisting of a float or vane which is pushed aside by a rush of oil through the connecting pipe.

The float or vane type of pressure device has found extensive applications in continental Europe[14,15] and Great Britain[16] as the principal protection for power transformers. A few of the perforated diaphragm units have been used in the United States,[17] although each company has installed only a small number of experimental units, and therefore little experience data is available. However, four of the larger users of transformers in Canada have made extensive applications of a perforated diaphragm type of unit and report very satisfactory results. Theory and limited available experience indicate that this pressure device may provide more sensitive protection than that usually obtained with differential relays.

More recent installations in the United States have been of the bellows type of relay. The operating speed is about one cycle at pressures 15 per cent or more above the setting. Five companies report using these on power transformers for increased sensitivity, three report their use for alarm only, and two report success with application to induction regulators which have no other *equipment* protection; (that is, the regulator is protected as part of distribution circuit). Successful installations are reported, even in the case of nonoiltight indoor units, where the pressure wave

has been sufficient to trip and lock out the circuit, preventing explosions which sometimes would occur on re-energizing. Also destructive failures have occurred where, in the opinion of those reporting them, the use of pressure relays might have minimized damage to the transformers. Some of these failures were preceded by several observed voltage surges or recorded ground currents of very short duration, indicating preliminary faults which extinguished themselves before operating the differential relays.

The working group that has prepared this paper believes that the use of pressure protection for power transformers offers much promise as supplementary protection with differential relays, for protection of smaller transformers together with overcurrent protection, and for difficult applications such as regulating transformers, feeder voltage regulators, rectifier transformers, and other special transformers.

Gas Accumulator and Gas Detector Devices

For many years the Buchholz type of gas accumulator fault detection[14] (combined with pressure protection) has found widespread use in continental Europe and in Great Britain.[15] Probably the rather extravagant claims made for this device as the sole protection for transformers, and the former royalty costs which were considered excessive[16] have been important factors in retarding applications in the United States. The device consists essentially of two float chambers connected in the piping from the transformer to the conservator so that any evolved gas will be trapped in the system. One float chamber collects gas bubbles given off gradually, and operates to sound an alarm. The float or vane in the other chamber is operated by a rush of oil through the piping to close a set of contacts which disconnect the transformer. Many examples have been cited of either core faults or partial winding faults which were detected by the gas accumulator system and severe damage thus prevented.

In Canada and in the United States, the diaphragm and float combination device has had moderate application. This device is designed for mounting directly on the transformer case, and contains a float chamber to sound an alarm on the accumulation of gases. Favorable experience is reported by four of the larger users of transformers in Canada, who have made extensive applications of the diaphragm–float combination relay. One reported the detection of several high resistance joints out of 40 transformers in ten years. Another cited detection of a number of failures of core bolt insulation, and a third reported discovery of seven cases of defective brazed joints out of 36 transformers in a period of slightly more than three years. All of these were detected and repairs made before the faults progressed beyond the incipient stage.

Those who prefer not to use gas accumulator relays usually cite as objections

1. That special transformer construction may be required.

2. That it is discouragingly expensive to untank and inspect a transformer after a relay indication, but before the fault has developed sufficiently that it can be found.

3. It is difficult to maintain the devices and to interpret their indications.

No special transformer construction was used in any of the reported Canadian installations, and methods used to interpret indications have been quite successful. Accumulated gas is tested for combustibility, and sometimes a chemical analysis is made. The color of the gas provides a quick indication. Considerable weight is given to the length of time between alarms, especially if the interval is decreasing. A Canadian manufacturer reported tests on a joint of 40 interlaced strands, one of which intentionally was made defective. Current was passed through the joint to complete failure, which occurred 12 weeks after the first gas alarm.

Available gas accumulator relays now are limited in application to conservator type transformers. An electrochemical device is available to detect incipient faults in askarel insulated transformers. Experimental installations have been made in Canada of a platinum wire type of device to detect combustible gases in small oil-insulated sealed-tank transformers.

It is believed that the value of gas accumulator relays for detecting incipient faults generally has been underestimated in the United States, and that with proper application and interpretation, their use with conservator type transformers may be worthy of more consideration. It is hoped that adequate methods will be developed for applying the gas detection principle to other types of transformers.

Conclusions and Recommendations

1. Differential protection is the generally accepted method of clearing transformer faults. This provides satisfactory speed of clearing, usually covers the entire zone between circuit breakers, and offers a fair degree of sensitivity.

(a). Incorrect tripping on magnetizing inrush current is a major problem, especially where the available short-circuit kilovolt-amperes on the bus to which the transformer is connected is large with respect to the transformer size. Trends toward higher design flux densities accentuate the problem.

(b). The use of either transferred tripping or a local line grounding switch to trip a remote circuit breaker offers attractive possibilities for providing differential protection to transformers without requiring separate high voltage circuit breakers.

(c). There is need for improvement in differential schemes to provide increased sensitivity without incurring unnecessary tripping on energizing currents.

2. Combinations of high voltage fuses and low voltage circuit breakers provide a reasonable compromise type of protection for the smaller sizes of power transformers. Problems of selectivity between these fuses and reclosing circuit breakers on feeders supplied from the transformer are complicated by the various reclosing cycles used. More information on the various heating and cooling time constants of different types of fuses would be helpful in developing better methods of predetermining fuse and breaker coordination.

3. The wider application of pressure protection offers considerable promise

(a). To provide supplemental protection with sensitivity greater than that usually obtained with conventional differential schemes alone.

(b). For protection along with overcurrent relays where it is not feasible to provide a satisfactory differential scheme.

(c). To solve inherently difficult applications, such as step regulators and rectifier transformers.

(d). For fast, low cost protection and reclosing lockout of feeder voltage regulators.

4. The value of gas accumulator relays for detecting incipient faults generally has been underestimated in the United States.

(a). Substantial experience in Canada has demonstrated the value of gas accumulator relays to detect conditions such as turn to turn faults, core insulation failures, and defective joints.

(b). Objections commonly raised to the gas accumulator method of detecting faults can be overcome largely by suitable application and proper interpretation of relay indications.

(c). The present commercially developed gas detector relays are limited in application to conservator type transformers. Experimental installations indicate that devices may be developed for extending gas detection principles to other types of transformers.

References

1. Recommended Practices for the Protection of Electrical Apparatus, **AIEE Relay Subcommittee.** AIEE Transactions, volume 52, 1933, pages 607–13.

2. Guides for Operation of Transformers, Regulators, and Reactors, **AIEE Transformer Subcommittee.** AIEE Transactions, volume 64, 1945, November section, pages 797–804.

3. Carrier Current Differential Protection for Transformer Banks, **T. A. Cramer.** AIEE Transactions, volume 62, 1943, August section, pages 545–8.

4. Grounding Switch Protects Transformer Installed Near Center of 50-Mile Line. *Electrical World* (New York, N. Y.), March 4, 1944, page 58.

5. A Simple Method for the Determination of Bushing-Current-Transformer Characteristics, **S. D. Moreton.** AIEE Transactions, volume 62, 1943, September section, pages 581–5.

6. Overcurrent Performance of Bushing-Type Current Transformers, **S. A. Bottomar,**

C. A. Woods, Jr. AIEE TRANSACTIONS volume 59, 1940, September section, pages 554–60.

7. TRANSFORMER MAGNETIZING INRUSH CURRENTS AND INFLUENCE ON SYSTEM OPERATION, L. F. Blume, G. Camilli, S. B. Farnham, H. A. Peterson. AIEE TRANSACTIONS, volume 62, 1944, pages 366–74.

8. HARMONIC-CURRENT-RESTRAINED RELAYS FOR DIFFERENTIAL PROTECTION, L. F. Kennedy, C. D. Hayward. AIEE TRANSACTIONS, volume 57, 1938, May section, pages 262–6.

9. RECTIFIER RELAY FOR TRANSFORMER PROTECTION, E. L. Michaelson. AIEE TRANSACTIONS volume 64, 1945, May section, pages 252–4.

10. ENHANCED TRANSFORMER PROTECTION THROUGH INRUSH-PROOF RATIO DIFFERENTIAL RELAYS, G. Bertula. *Brown Boveri Review* (Baden, Switzerland) volume 32, 1945, pages 129–33.

11. HIGH VOLTAGE FUSING OF TRANSFORMER BANKS, H. H. Marsh, Jr., G. B. Dodds. AIEE TRANSACTIONS, volume 61, 1942, July section, pages 533–5.

12. LOADING TRANSFORMER BY COPPER TEMPERATURE, H. V. Putman, W. M. Dann. AIEE TRANSACTIONS, volume 58, 1939, October section, pages 504–09.

13. THERMAL PROTECTION OF TRANSFORMERS UNDER OVERLOAD CONDITIONS, V. M. Montsinger, G. Camilli. AIEE TRANSACTIONS, volume 63, 1944, April section, pages 160–4.

14. BUCHHOLZ PROTECTION OF TRANSFORMERS, Professor H. Zipp. *Elektrizitätswirtschft* (Berlin, Germany), April 1927, (English translation).

15. OPERATING EXPERIENCE WITH THE BUCHHOLZ PROTECTIVE DEVICE FOR TRANSFORMERS, Bulletin by Buchholz, September 1930.

16. METROVICK BUCHHOLZ DEVICES FOR TRANSFORMER PROTECTION. Descriptive leaflet *342-3-1*, Metropolitan-Vickers Electrical Company, Ltd., Manchester, England.

17. HOW DO YOU FORESTALL FAULTS? Bulletin *A D451-6-34*, Walter Kidde and Company Bloomfield, N. J.

18. GAS PRESSURE RELAYS, R. A. Heatt. *Bulletin* of the Edison Electric Institute (New York, N. Y.), March 1938, pages 82–4.

19. SIMPLICITY IN TRANSFORMER PROTECTION, E. T. B. Gross. ELECTRICAL ENGINEERING, volume 66, June 1947, pages 564–9.

Discussion

E. L. Harder (Westinghouse Electric Corporation, East Pittsburgh, Pa.): This report represents the fulfillment of a very important part of the relay subcommittee program. It is the policy of the committee to review in turn the several important aspects of relay protection, that is, generator protection, transformer protection, line protection, and bus protection. This report is a thorough going examination of the transformer protection problem giving the present status of the art and delving quite thoroughly into each of the important phases. In the course of this delving, numerous problems arose and to most of these, solutions or tentative solutions have been agreed upon or proposed.

For example, consideration has been given to thermal protection of transformers and its co-ordination with protective relaying. At first it was thought that characteristic curves would be required on all thermal relays in order properly to co-ordinate them with protective relays. However, after study of the problem it was found that a single co-ordination characteristic could be established between all transformer thermal relays and all relay protection. This is a most important simplification as it provides a clear-cut division between the problems of transformer thermal protection, normally handled by transformer designers and users, and relay protection, normally handled by another group of engineers. The dividing line consists of a single operating time at five times normal and one at 20 times normal. All thermal relaying is to be slower and all protective relaying to be faster than these values. The exact values to be used are still subject to discussion. The value tentatively proposed in the report for five times normal of 40 seconds may be a little long. Our studies indicate that 30 seconds might be better from the standpoint of the transformer devices. However, there appears no doubt that the method will be workable, and that suitable values can be arrived at after study has been given both to the transformer and relay requirements. The tentative values proposed in the report represent the summary of replies from several relay users.

The report also very naturally has brought to light and crystallized a few problems which could not be resolved fully by the working group and which remain as a goal for solution by those interested in this problem. There are still rather wide differences of opinion on the use of gas accumulator and gas pressure relays. More work is needed on the practical sensitivity of the pressure type relay. There is little question of the sensitivity of the accumulator type, but in its present form it is believed non-applicable to transformers having a gas cushion above the oil. The agreement that differential and gas relays supplement in most cases rather than replace each other is quite notable.

There also remains the problem of determining fault current magnitudes for partial-winding faults and the consequent degree of protection afforded by differential relays.

In conclusion it is believed that this report and the attendant work and stimulus has been very beneficial to the industry and particularly to the engineers who have participated in the discussions and decisions. It is hoped that there will be further activity towards solving some of the currently unsolved problems so that by the time of the next report several years from now, the committee may be able to report satisfactory solutions to these problems also.

A. M. Doyle (Canadian General Electric Company, Toronto, Ontario, Canada): As the Canadian manufacturer of a gas detector relay described in the paper, we offer the following comments. Canadian operating experience using the relay has been discussed in another paper,[1] and therefore these comments will apply only to their general application.

Our company undertook the production of these devices at the request of the Shawinigan Water and Power Company and the Hydro Electric Power Commission of Ontario, and first shipments were made in 1939. The devices as produced were modifications of those formerly manufactured by the Walter Kidde company, from licenses under patents held by Max Buchholz.

Since that time some 600 relays have been applied in Canada to power transformers and regulating transformers in ratings from 667 kva to 50,000 kva. In some cases the relays were supplied as a part of new transformers; in others they were sold to other transformer manufacturers for incorporation in their products; and they also have been sold on a supply basis for application to existing transformers.

Originally, we were of the opinion that the device would only be expected to perform its function with sufficient sensitivity if extensive internal modifications were made to the transformer to ensure that any gas generated in it positively would be directed to the relay. Also, a number of false operations normally could be expected when a transformer is first put into service. For these reasons there was some hesitancy on our part towards the active promotion of this device. However, the operating experiences indicate that this attitude was too conservative and that more active promotion of the relay appears justified. This is particularly true in view of the successful performance of relays which have been applied to existing transformers where in many cases the only feasible location for the relay was on the manhole cover.

Our present practice in applying relays to new transformers is to locate the relay on the transformer cover near the wall of the tank, where it can be reached for servicing. Any reinforcing members on the underside of the transformer cover are made with slots to avoid the accumulation of gas pockets. Also, mounting flanges for bushings and relief vents are provided with an extension below the cover to prevent any gas creeping along the underside of the cover from entering these pockets.

It should, of course, be emphasized that at the present time the particular type of gas detector relay that is being manufactured in Canada is applicable only to transformers equipped with conservators. However, in Canada, the conservator is almost exclusively accepted as the desirable means of oil preservation.

REFERENCE

1. TYPICAL TRANSFORMER FAULTS AND GAS DETECTOR RELAY PROTECTION, J. T. Madill. AIEE TRANSACTIONS, volume 66, 1947, pages 1052–6.

Ben C. Hicks (Shawinigan Water and Power Company, Montreal, Quebec, Canada): The relay subcommittee is to be commended on its appraisal of the uses and limitations of the various forms of protection applied to power transformers. The information regarding trends and the recommendations for improvements are both interesting and valuable.

Regarding the remedies resorted to for overcoming difficulties with differential protections due to magnetizing inrush current when energizing transformers, it may be observed that none is entirely satisfactory. Concerning one of these remedies, namely, the desensitizing of the protection for an adjustable time when energizing the bank, it may be in order to remark that, although this method may have considerable value

when closing a switch to energize the bank, it would be ineffective when voltage is recovering following a nearby through fault; a condition under which magnetizing current also tends to flow.

Considering the difficulties inherent in securing a completely satisfactory differential protection, one is led to wonder whether any serious thought has been given to the possibility of devising something in the nature of a split phase protection for transformers. Any efforts in this direction would of course require the co-operation of the transformer designers but might be productive of something useful in the way of improved transformer protection.

F. L. Lawton (Aluminum Company of Canada, Ltd., Montreal, Quebec, Canada): The relay subcommittee has presented a very comprehensive analysis of present and preferred practices in the relay protection of power transformers.

It is interesting to note from the paper by John G. Noest[1] that "Buchholz relays were universally used on transformers with differential relays as back-up" and further "Buchholz relays were specified by the insurance underwriters."

Experience on the Saguenay system definitely has convinced us of the very real merit of the Canadian version of the Buchholz relay in picking up incipient troubles, such as defective core bolt and other core insulation, poorly brazed or poorly sweated joints in conductors, and many others. Our initial installation of 36 gas-detector relays on as many single-phase 13.2/154 kv 30,000-kva transformers has furnished conclusive proof of their effectiveness, fully substantiated by field installation of an additional 88 relays on transformers ranging from 18,750 to 30,000 kva.

The gas-detector relay, comprising a gas-accumulation element and a gas-pressure element, is the only device which will detect a slowly developing trouble in a transformer and give warning in ample time so that the transformer can be removed from service at the operator's convenience, untanked, and the evidence of the incipient fault found, so that remedial measures can be effected. Cost of repairs or alterations under such circumstances are far below the costs which would be incurred in event of a fully developed fault. It should be borne in mind that the differential protection can operate only after the transformer is in trouble, and after service interruption or inconvenience has been experienced.

After the gas-accumulation element has given warning of an incipient fault, it is possible to check the indication, on the site, by the use of a small portable device used in many industries for checking the inflammability of gases. We have confirmed some of our gas-detector relay indications in this manner and by later visual inspection, after untanking.

The device in question, one make of which is known as the "Vapotester", is an easily portable and rugged instrument for testing the inflammability of gas. Briefly, it consists of a Wheatstone bridge circuit in which two arms are composed of interchangeable platinum filaments. One filament is sealed in and the other so arranged that air or gas may be drawn over it. A combustible gas-air mixture will ignite on the surface of the exposed element, increase its resistance, and upset the balance of the bridge. The dial of the meter is calibrated in terms of percentage of the lower explosive limit. The instrument is extremely sensitive and in tests has proved very reliable.

REFERENCE

1. THE GERMAN ELECTRICAL UTILITY INDUSTRY DURING WORLD WAR II, John G. Noest. AIEE TRANSACTIONS, volume 66, 1947, pages 1037–51.

J. T. Madill (Aluminum Company of Canada, Ltd., Shipshaw, Quebec, Canada): Referring to gas accumulator and pressure protection of transformers it is gratifying to see the recommendations the committee has made. For the benefit of those who are doubtful, it may be stated definitely that on the Saguenay system, when any transformer is untanked, as a result of gas formation and gas tests with a device such as a "Vapotester", we are absolutely sure there is a fault in the transformer and that we can locate it. To date there is not sufficient experience available for the statement to be made that pressure protection will replace differential protection, and no one is making this claim. However, at the present time it would seem that pressure protection might make possible the consideration of larger or more extensive differential zones, since these should be called upon to operate very infrequently.

In the case of a transformer tripped by differential protection when being energized, the practice on the Saguenay system is to try it again. The winding and the oil temperature indicators show there is no high temperature, the gas detector relay shows there is no gas to explode and no pressure waves being set up, the ground relay shows no ground current. Therefore it is almost impossible for a real fault to be present.

In conclusion the committee is to be congratulated for their excellent report.

E. E. George (Ebasco Services, Inc., New York, N. Y.): The report presented by the relay subcommittee is very comprehensive and gives a well-balanced picture of present and preferred practices in transformer protection. One or two items are worthy of special comment. There is a statement that "the operating practices of many companies require leaving a transformer out of service until tested, when differential relays have operated, so as to minimize the possibility of serious explosions and fires when a defective transformer is re-energized." This practice suggests further uses for relays which indicate excessive temperature, sudden rise in oil pressure, or accumulation of gas. In cases where a transformer is needed to restore service, it is the practice of many operating companies to re-energize the transformer after differential operation if there is no evidence of trouble in the transformer itself. Heretofore such evidence generally has had to be obtained by external inspection. It is suggested that, if the transformer is equipped with relays which indicate sudden pressure rise or gradual accumulation of gas and if there is no indication from these relays and there is no indication of high top oil temperature, it should be reasonably safe to re-energize the transformer, since there is minimum possibility of fire or explosion. It is probable that there has seldom been an insulating oil fire where the top oil temperature previously has not reached at least 400 degrees Fahrenheit and it is likewise probable that there has seldom been a transformer explosion where there has not been a previous distillation of oil into gas over a period of time. The use of temperature, pressure, and gas relays therefore is suggested as a means of revising operating procedure to give maximum protection to both the equipment and the service.

It is very difficult to understand the reluctance of United States manufacturers to build or supply gas relays in this country. About ten years ago the writer attempted to purchase either Buchholz or Hackbridge relays from English manufacturers but was unable to do so because of the commercial restrictions of United States manufacturers. The relay subcommittee has done an excellent job in publicizing the successful experience of several of the large utilities in Canada with the Buchholz relay. If there is some reason why gas detector relays will not operate satisfactorily "south-of-the-border", perhaps the easiest way to convince the operating companies of this fact is for the manufacturers to let us try a few of these relays. The operating companies are very quick to interchange operating experience without any help from the manufacturers. If it should turn out that the gas relays are a satisfactory and generally needed means of supplementary protection, it will not take much effort to develop the United States market.

One further comment on the subcommittee report is submitted as a result of many questions asked about the meaning of the word "askarel" as used therein. Many operating and relay engineers who are not connected actively with transformer negotiations never have heard of this word which seems to refer to noninflammable insulating liquids such as "Pyranol" and "Inerteen."

Eric T. B. Gross (Illinois Institute of Technology, Chicago, Ill.): The report calls attention to the possibility of wider application of gas actuated relays (gas-accumulator and pressure relays) which have been applied quite successfully abroad, and more recently in Canada. Valuable information is contained in a paper on typical transformer faults and gas detector relay protection by J. T. Madill,[1] and additional Canadian experiences have been described by A. L. Hough.[2] Present applications of gas actuated relays were mainly on transformers with conservators, however, the same principles can be used for the development of relays for transformers with inert gas filling the space above oil level, or completely sealed.

REFERENCES

1. TYPICAL TRANSFORMER FAULTS AND GAS DETECTOR RELAY PROTECTION, J. T. Madill. AIEE TRANSACTIONS, volume 66, 1947, pages 1052–60.

2. GAS DETECTOR RELAYS, A. L. Hough. Reports for the 57th Annual Convention of the Canadian Electrical Association, Engineering Section, 1947, pages 56–69.

W. R. Brownlee: The relay subcommittee appreciates the confirming and supple-

mentary information provided by the discussers. It is especially gratifying to note an increasing awareness on the part of manufacturers and users of a number of protection problems, not yet completely solved, which have been emphasized by modern trends in the design, application, and operation of power transformers.

While this report concludes the special assignment of the working group, the relay subcommittee intends to maintain a continuing interest in the performance of present equipment, in the evolution of devices and methods for which improvement is indicated, and in new developments.

Electric Furnace Practice in Canada

J. L. BALLENY
MEMBER AIEE

HYDROELECTRIC developments in Canada have provided an abundance of low-cost electric power, which has encouraged the use of electricity for metallurgical operations, particularly those in which large amounts of power are consumed. In fact, today, other types of fuel are being replaced by electric heat where economy of operation is a major factor.

In the consideration of metallurgical installations which would be of interest to electrical engineers, a choice has been made of those electric furnaces or processes which are of large size or have unusual features, as well as others which are representative of electric furnace practice in Canada.

This paper therefore will describe several interesting installations, noting any special features in the usage or control of electric power, and quoting metallurgical results secured, which in some instances are not obtainable by other methods.

Steel Strip Annealing

In the manufacture of tin plate and black plate, coils of steel strip are passed through a cold reduction mill in which the thickness is reduced from 0.140 inch to as little as 0.008 inch. This severe cold working sets up very high stresses in the strip and modification of the structure of the metal is necessary before further satisfactory processing can be accomplished. This annealing can be performed by heating the strip to a temperature in excess of 1,200 degrees Fahrenheit; the higher the temperature, the shorter the time required at the elevated temperature for complete transformation.

Common practice has been to anneal such strip in coils in batch-type furnaces, but at the plant of Dominion Foundries and Steel Limited, Hamilton, a continuous-strip annealing furnace has been installed which for some applications produces a superior product and which in addition enables much quicker handling of special or emergency orders. Figure 1 shows a view of this furnace taken from the exit end. It is best described as a tower-type furnace and is the only one of its kind in Canada. Its size may be estimated by comparison with the workmen. It is 45 feet high by 10 feet wide by 50 feet long, this length including the loopers but not the coiling and uncoiling mechanisms.

Outline drawing, Figure 2, will enable the path of the strip to be followed from the uncoilers, through the welder, entry pinch rolls, entry looper, heating and cooling chambers, master pinch rolls, and delivery looper to the coiler. With eight strands in each looper, which is 40 feet high, the operators have a length of 300 feet or a time limit of approximately from one to two minutes in which to weld the strips together or to remove finished coil from coiler and start a new coil.

Speed of the strip may be varied from 60 to 400 feet per minute by Ward-Leonard control of the master pinch rolls at the exit end. Normal operation calls for a speed range between 150 and 300 feet per minute for strip thicknesses varying from 0.025 to 0.008 inch. The common width of strip is 32 inches. For simplification of operation of the furnace, temperature controls are set at a given value and the speed is the only variable which is regulated to give the metallurgical results desired.

Heating units in the four vertical chambers are divided into 28 60-kw single-phase circuits which are controlled in 11 separate zones by "on-off" contactor operation, actuated by temperature control instruments. The total connected heating load is 1,680 kw, being fed from a 2,000-kva transformer bank, equipped with taps to give furnace voltages between 195 and 242 volts.

Of the eight cooling towers, the first one is insulated to extend the hot zone and permit equalization of strip temperature and to control the initial cooling rate. The second tower is uninsulated, the third one is water-cooled, while the next four are water-cooled and also equipped with fans for agitation of furnace atmosphere past the water cooling coils to provide most effective cooling. The last tower is merely uninsulated, and bright strip leaves this tower at a temperature below 300 degrees Fahrenheit.

To prevent oxidation of the sheet or discoloration through oxidation, the furnace chambers, both for heating and cooling, are provided with a partially combusted gas atmosphere which is produced in one 4,000-cubic-feet-per-hour atmosphere-gas converter. This output gas is passed through a refrigerated cooler for removal of moisture to a low dew point before insertion into the furnace.

The user of this furnace reports that some metallurgical results have been secured which were unobtainable in batch-type furnaces. The fast anneal appears to give a product with very fine grain size, which is superior for some applications but not suitable for others, so that care is exercised in the use to which material is put following heat treatment by this method. The total power and heating

Paper 47-138, recommended by the AIEE committee on industrial power applications for presentation at the AIEE summer general meeting, Montreal, Quebec, Canada, June 9-13, 1947. Manuscript submitted April 7, 1947; made available for printing April 24, 1947.

J. L. BALLENY is with the Canadian General Electric Company, Ltd., Toronto, Ontario, Canada.

The following companies have contributed engineering data and photographs used in the preparation of this paper. Their co-operation is gratefully acknowledged by the author.
Aluminum Company of Canada Limited, Montreal, Quebec, Canada.
Auto Specialties Manufacturing Company (Canada) Limited, Windsor, Ontario, Canada.
Canadian General Electric Company Limited, Toronto, Ontario.
Dominion Foundries and Steel Limited, Hamilton, Ontario.
Fabralloy Canada Limited, Orillia, Ontario.
Ford Motor Company of Canada Limited, Windsor.
McKinnon Industries Limited, St. Catharines, Ontario.
Steel Company of Canada Limited, Hamilton.
Thompson Products Limited, St. Catharines.
Trauwood Engineering Company, Cleveland, Ohio.
Volta Manufacturing Company Limited, Welland, Ontario.

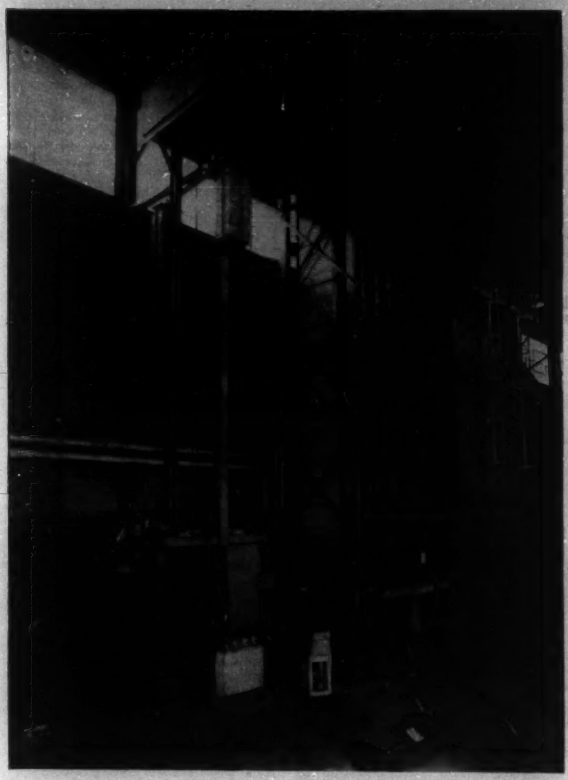

Figure 1. Continuous steel strip annealing furnace rated 1,680 kw, installed at Dominion Foundries and Steel Limited, Hamilton

View of furnace from outgoing end

consumption on typical runs has averaged as low as 175 kilowatt-hours per ton annea'ed.

Wire Patenting by Direct Resistance Heating

Medium or high carbon steel wire, following drawing operations, usually is "patented" to give the proper microstructure to enable further drawing or to make it satisfactory for general use. This process requires the wire to be heated uniformly to a temperature of 1,550 degrees Fahrenheit, followed by a lead quench or an air-cool.

At one plant of the Steel Company of Canada Limited in Hamilton, there is installed a continuous wire-patenting equipment utilizing the electric direct-resistance method for heating the wires. In this case heat is generated in the wires by passing through them a heavy current at low voltage. The temperature reached by the wires before being quenched is determined by the voltage applied, the distance between contact points, and the wire speed.

The sketch in Figure 3 illustrates, at the bottom, a side view of the major components of the equipment and above this view shows a partial schematic diagram of the voltage control devices. This equipment is built to handle 16 lines of wire in parallel, with a production capacity of 3,000 pounds of wire treated per hour. Normal run of wire is in sizes from 0.125-inch to 0.060-inch diameter and at speeds ranging from 75 to 150 feet per minute.

Power for heating is fed to the wires through a contact bath at the ingoing end and through the lead quench bath at the other end. The contact bath is insulated from ground amd maintained at a temperature of 1,000 degrees Fahrenheit by 129 kw of immersion type heating elements. This bath and contact mechanism are supported on a movable structure to regulate the distance the wires travel before entering the quench bath, which regulates the current flow.

While traveling between the two lead baths, the wires in parallel are the current conductors and become progressively hotter until the moment when they dip into the quench bath. It is interesting to watch this increasing temperature rise in the wires while they are merely passing through the air on suitably grooved heat-resisting separators.

The temperature of the lead quench bath is maintained at a value between 700 and 1,100 degrees Fahrenheit, depending upon the hardness and physical properties desired in the finished wire. This quench bath is equipped with 291 kw of immersion heaters to maintain its temperature, and also has a series of cooling tubes at the incoming end of the bath to carry away excess heat given up by the hot wires. Both heaters and the cooling are controlled automatically. It will be noted that the quench bath is considerably longer than the contact bath to ensure proper quenching of the wires.

The power supply for heating the wires

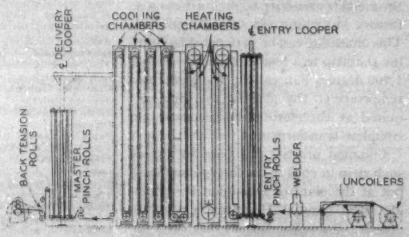

Figure 2. Schematic layout of continuous steel strip annealing furnace, indicating path of strip through furnace

is provided from a 400-kva single-phase transformer and voltage to the wires is controlled, within plus or minus one-half volt, through an induction voltage regulator actuated by a controlling voltmeter. Manual or automatic control is secured by manipulation of push buttons. The proper voltage to give required wire temperature first must be determined from optical pyrometer readings on the wires just before they enter the quench bath and tabulated for different wire sizes and speeds. Such voltages are of the order of 40 to 80 volts with transformer coils in parallel and 80 to 150 volts with coils in series. Currents vary from 7,500 down to 2,270 amperes on different taps.

The lead-patenting process produces wire with a denser grain structure which permits more cold working. It also enables higher tensile strength and fatigue properties to be developed in the finished wire. This method of resistance heating further assures a uniformly heated product so that duplication of results is simplified.

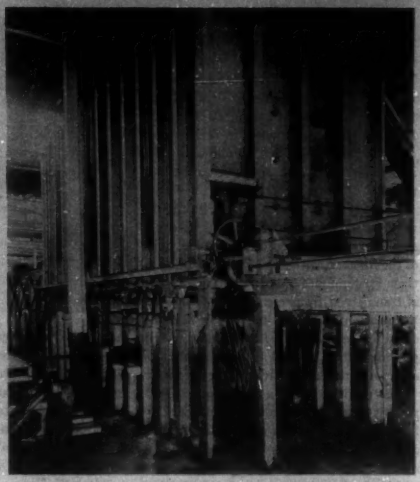

Figure 4. Elevator type aluminum heat-treating furnace, rated 760 kw, with quench tank below, installed at Aluminum Company of Canada Limited, Kingston

View shows load of sheets being raised into heating chamber

Heat Treatment of Aluminum Alloys

Installations of electric furnaces in the aluminum industry in Canada exceed 30,000 kw and various types of electric resistance furnaces are utilized in melting, holding, preheating, annealing, and heat treating of aluminum and its alloys. Figure 4 shows a general view of a typical furnace used for heat treating aluminum alloy sheets.

This may be described as a vertical-draft air heat treating furnace. It is box-shaped, post-supported over a quench tank, and equipped with a drying chamber, a trolley system for handling loads, and a horizontal door in the bottom. The various load-handling operations are performed hydraulically, being controlled by push buttons to provide either automatic sequence control or individual control of any operation.

Figure 3. Partial schematic diagram of continuous wire patenting furnace, installed at Steel Company of Canada Limited, Hamilton

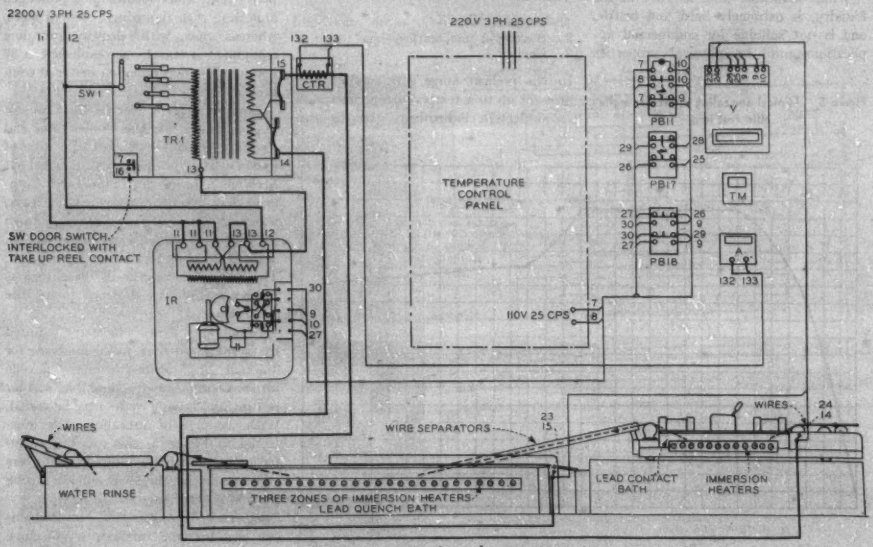

Furnace dimensions can accommodate a load of sheets up to 5,000 pounds, taking sheets 28 feet long by 6 feet wide. The load is raised into the furnace, heated to the desired temperature, and held at this temperature until assured of equalization, then fast-quenched into the water tank below the furnace. Following this, it is moved into the drying chamber for removal of water.

The electrical capacity is 760 kw, divided into four control zones. Heating elements are mounted on the inside walls of the furnace, with steel baffles in front of them for guidance of convected air. Heat is transferred from elements to the load by means of six axial-flow alloy fans located in the roof of the furnace, and which provide the high-speed air circulation necessary in aluminum heat treating furnaces.

This equipment has a capacity of 50,000 pounds of aluminum-alloy sheets per 24-hour day, heating to a maximum temperature of 1,020 degrees Fahrenheit and maintaining temperature uniformity within the furnace chamber to within plus or minus 5 degrees Fahrenheit of the control point. Such control is secured by potentiometer type controllers actuated from thermocouples located in the air stream

Short Cycle Annealing of Malleable Iron

White malleable iron, as cast in the foundry, is extremely hard and brittle, and is not suitable for commercial applications until its physical properties have been changed by annealing. This process precipitates the element carbon, which is in a combined state in the white iron, to a dispersed graphitic condition in the annealed state, and imparts to the metal strength, ductility, and the ability to take considerable distortions before rupture.

The ultimate use for the material determines the actual composition and the required heat treatment. The addition of silicon affects the heat treatment considerably; the higher the silicon content, the shorter will be the required annealing cycle. A typical cycle for malleable parts as used in the automotive industry is shown in the chart, Figure 5.

Three distinct stages may be noted. These are

1. Preheat.
2. Soaking at temperature.
3. Cooling.

In the preheat stage, the castings are brought up to a temperature in excess of 1,750 degrees Fahrenheit. During the soaking period they are held at this temperature for a sufficient time partially to alter the structure of the metal. Slow cooling through the critical range further alters the structure of the metal and it should be observed that the maximum rate of cooling through the critical range is 10 degrees Fahrenheit per hour.

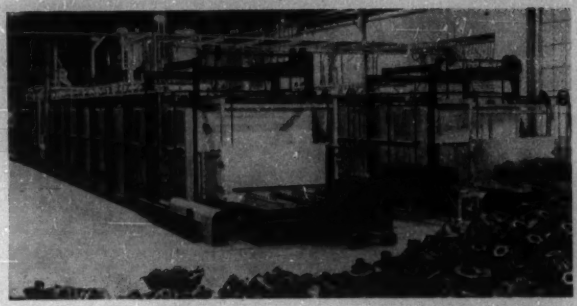

Figure 6. Pusher-type controlled-atmosphere malleable-iron-annealing furnaces, each rated 340 kw

Installed at McKinnon Industries Limited, St. Catharines

Prior to the adoption of electrometallurgy in the heat treating of malleable iron, the process was carried out in fuel-fired ovens, which resulted in a prolonged annealing cycle requiring 5 days or more, whereas now with electric annealing equipment it may be accomplished in 32 hours or less depending on material composition.

Continuous type electric furnaces are in general use for this application, and Figure 6 illustrates two out of a total of five pusher-type furnaces installed at McKinnon Industries Limited, St. Catharines. Castings are loaded on trays, which are pushed progressively through the heating chamber, fast cooling section, and slow cooling section to the exit end. The respective lengths of these various furnace sections are designed to suit the cycle required.

In jobbing plants which are required to produce different metal analyses for different applications, a more flexible furnace arrangement is desirable, so that heating and cooling cycles may be varied. With the type of annealing cycle illustrated in Figure 5, this can be accomplished by utilizing two furnace chambers and transferring the loads quickly during the fast cooling stage.

Figure 7 illustrates two double-chamber elevator-type furnaces which have

Figure 5. Typical annealing cycle for malleable cast iron

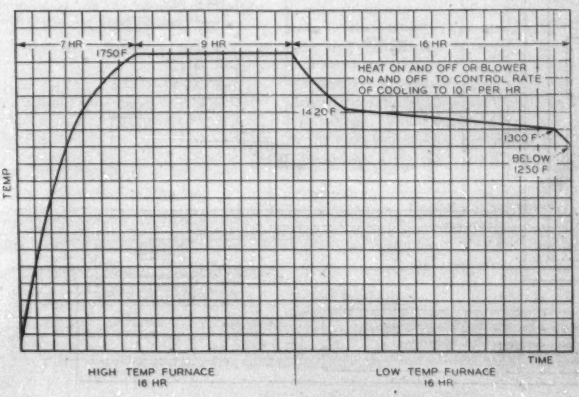

Figure 7. Double-chamber elevator-type malleable-iron-annealing furnaces, each rated 450 kw in high temperature chamber and 100 kw in low temperature chamber

Installed at Auto Specialties Manufacturing Company (Canada) Limited, Windsor

been installed at Auto Specialties Manufacturing Company, Ltd., Windsor. The high temperature chamber rated 450 kw takes the load of cold castings, heats them to 1,750 degrees Fahrenheit, and holds them at this temperature for the desired portion of the annealing cycle. In this chamber, also, the rich carbon content of the castings combines with the limited amount of air in the chamber to generate sufficient carbon monoxide (CO) atmosphere to protect the castings from scaling.

At the proper time the car is transferred quickly to the low-temperature chamber, which is then at a temperature of 1,200 degrees Fahrenheit or more, and in this chamber the cooling through the critical range (from 1,420 to 1,300 degrees Fahrenheit approximately) is controlled automatically by the use of heating units or of a blower which circulates air through cooling tubes. When the temperature has dropped below 1,250 degrees Fahrenheit the castings may be removed from the furnace and air-cooled.

This particular furnace accommodates a load 17 feet long by 4 feet wide by 3 feet high weighing 7 tons, and on the basis of 16 hours for heating and 16 hours for cooling, produces over 10 tons per 24-hour day from each pair of furnace chambers. The power consumption for a typical load will average 275 kilowatt-hours per ton.

Induction Heating for Forging and Hardening

The development of detachable drill bits has revolutionized the mining industry and millions of them per month must be forged and heat treated. In the forging operation the slugs are heated uniformly throughout, whereas in hardening the bits the hardness pattern required calls for a hard surface with a softer tough core.

Thompson Products Limited in St. Catharines have found that a 9,600-cycle induction heater can be utilized for both these processes, that is to heat up the slugs and bits prior to forging and hardening. Figure 8 shows such an equipment set up for heating bits prior to hardening

Figure 8. Three-station 9,600-cycle motor-generator-type induction heater rated 125 kw, installed at Thompson Products Limited, St. Catharines

Heated drill bits being removed from heater and inserted in quench bath

Figure 9. Elementary wiring diagram of 3-station induction heater

From Tocco manual of The Ohio Crankshaft Company, Cleveland, Ohio

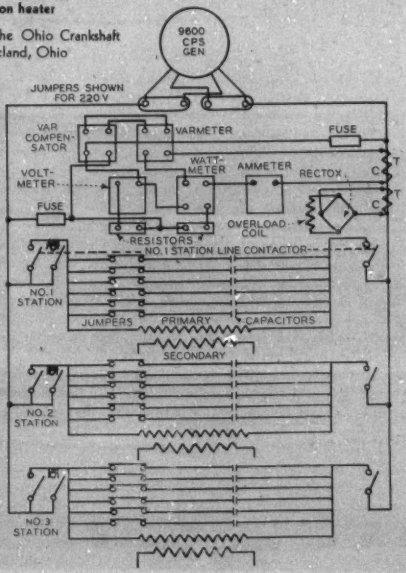

Figure 10. Work station for motor-generator-type induction heater, installed at Thompson Products Limited, St. Catharines

Heated slug being removed for forging into drill bit

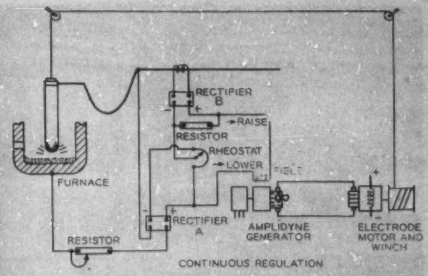

Figure 11 (above). Simplified circuit diagram of automatic electrode regulator, continuous type

From reference 1

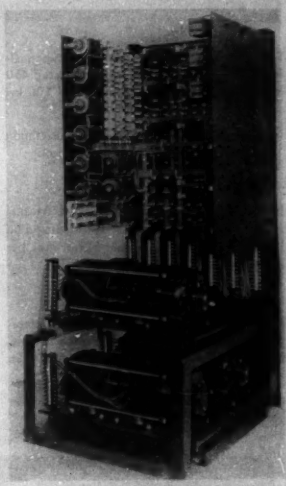

Figure 12 (right). Amplidyne - type electrode regulating controller installed on 3-phase 1,800 kva arc furnace at Ford Motor Company of Canada Limited, Windsor

and the sketch in Figure 9 shows the type of control which is involved in such a 3-station induction heater.

As illustrated in Figure 8, the bits are loaded into one end of a 2-inch-diameter quartz tube through which they are pushed by a reciprocating arm. The heating coil is of multiturn construction wrapped closely around 18 inches of the quartz tube. The next 22 inches of the tube are used for soaking the bits, during which time interval the temperature equalizes in the bit and as it is removed from the end of the tube it is at a uniform temperature of 1,500 degrees Fahrenheit.

Bits are removed individually from the tube by an operator and stood upright on a conveyor passing through a water bath with the cutting face immersed to a depth of only one-quarter inch, so as to control the hardness pattern. When putting bits through this heater at the rate of 20 per minute, each weighing an average of from 4 to 5 ounces, the power required is 40 kw.

As the hardening operation on these drill bits is the last operation performed on them, the equipment can be located at the end of the production line. The forging process, however, is accomplished in the early stages of manufacture in a part of the plant where smoke, heat, and dirt usually are prevalent. This type of induction heating equipment permits the location of the work station (illustrated in Figure 10) where desired and leaves the motor-generator equipment in a dust-free location. Power connection to the work station is made through special noninductive cables run through copper sheathed ducts to minimize losses.

The operation illustrated in Figure 10 is similar to that of heating prior to hardening. The slugs are fed intermittently through a tube and individually removed for transfer to the forging press. Since these slugs are of uniform cross section, they do not require additional time for temperature equalization but heat up uniformly in a tube 14 inches long which is surrounded by a multiturn coil. With a production of 11 slugs per minute, the power demand is 30 kw.

In this plant the use of induction heaters has replaced a standard type of heating furnace, since the operation is practically automatic and relative scale-free material is obtained. Water is circulated at a high rate of flow through the heating coils, and water output temperature is kept below a maximum of 75 degrees Fahrenheit.

The possibilities of automatic cycle control on this equipment by utilization of timers make for greater flexibility and their application to functions which cannot be duplicated by other means. At the present time these 3-station heaters cannot use all three stations simultaneously, but a type of amplidyne voltage maintenance control is being supplied to enable utilizing two or three work stations simultaneously for maximum operating efficiency.

Continuous Regulation of Electric Melting Furnaces

Electric arc melting furnaces are in general use throughout industry today and development work has been concentrated on improving their stability and reducing power surges. At the Ford Motor Company plant in Windsor an amplidyne control has been applied to one of the melting furnaces which has been

shown to give smooth performance under optimum operating conditions.

For best operation of an arc furnace, the regulator must utilize both arc voltage and arc current to control the electrode movement, which in turn varies the power input. Contact-making regulators have been built which operate on this combined principle, but the amplidyne method accomplishes the same functions in a smoother manner without utilizing any circuit-breaking devices.

The diagram illustrated in Figure 11 shows in simplified form how this type of control is applied to the furnace circuit. The output of the arc current transformer is rectified and passed through a resistor. The voltage across this resistor is then proportional to arc current. The reference voltage to balance against this current-produced voltage is set up from a rectifier across the arc voltage, which is reasonably constant during normal operation.

The net voltage unbalance between the two is applied to the amplidyne field, and the amplidyne output is applied to the armature of the electrode motors. High sensitivity results from the fact that a small voltage unbalance is arranged to excite the amplidyne to give full electrode motor torque. Any slight change in arc current thus promptly moves the electrodes, the amount of motion usually being small with overshooting practically eliminated.

Figure 12 illustrates the amplidyne control installed on one 1,800-kva furnace in Windsor which has demonstrated many inherent advantages in controlling a furnace for melting steel, cast iron, or alloy steel. It has been found most satisfactory when a suitable slag is maintained on top of the molten change.

Some of the advantages which have been reported from this installation may be mentioned briefly and can be observed in the operation of this equipment.

There is no hunting of electrodes. With the extreme speed of response, movement of the high-speed electrode motor shafts is normally only a fraction of a revolution at a time compared with several revolutions at a time observed on a similar furnace controlled by other means.

The power curve is smoother, since surges are minimized and operation maintained close to the optimum point, thus producing most efficient operation.

Lower maintenance is evident, since the operation of electrode motors is less frequent and much less violent; also, contactors or contact-making instruments have been eliminated. A further effect, not so evident, is that with no overshooting of electrodes, there is less electrode consumption.

Better quality low-carbon alloy steel has been produced since the reduction in electrode wastage has minimized carbon addition to the charge and enabled closer composition control.

Demonstrations of the operation of this amplidyne control equipment have shown to many furnace operators that these and other not so evident inherent advantages are being realized daily in this installation.

Alloy Steel Melting in Electric Arc Furnace

A typical installation of electric arc melting furnaces, utilized in the manufacture of alloy steels, is shown by Figure 13. These two furnaces are installed in the plant of Fahralloy Canada Limited, Orillia, one being rated 500 pounds per

Figure 13. Three-phase electric arc melting furnaces installed at Fahralloy Canada Limited, Orilla, rated 500 pounds and 1,500 pounds per hour, respectively

hour and the larger one 1,500 pounds per hour.

The 500-pound furnace is used exclusively for the production of heat-resisting alloys and stainless steels. The larger furnace is used principally for the production of mild and medium carbon steel castings, but its output can be varied to meet the occasional demand for castings in special types of steel, and for heat and corrosion-resisting castings of weights beyond the capacity of the small furnace. Typical analyses of alloy castings made in these furnaces are given in Table I.

All of the alloys produced are of the nickel-chrome series, having the remainder principally iron and with occasional additions of molybdenum or tungsten. The furnaces are acid lined and the melting practice consists of charging pure ferroalloys and low-carbon steel scrap, then melting and pouring as rapidly as possible. No refining process is required in the furnace as the charge is selected to give the correct analysis of alloy and carbon content.

Table I. Composition of Alloy Castings, Per Cent

	Chromium	Nickel	Molybdenum	Carbon
Heat resisting	18	36		0.35 to 0.45
	25	12		0.25 to 0.35
Corrosion resisting	24	15	3	0.20 maximum
	29	9		0.20 maximum

Monthly records of operation show that the average energy consumption when melting these alloys is in excess of 650 kilowatt-hours per ton. During the early stages of melting, before a steady arc is established, the demand fluctuates widely. However, when the melting process has steadied down, the demand stabilizes at approximately 350 kva for the 500-pound furnace and 750 kva for the larger furnace.

As new metallurgical processes develop, there is an ever increasing tendency to consider electric power as the sole source for heating—whether in the form of resistance, induction, or salt-bath furnaces—since it has been shown that time cycles may be shortened, automatic operation more readily applied, and more uniform results consistently secured.

Reference

1. The Three-Phase Arc Furnace Circuit, N. R. Stassel. *Electric Furnace Steel Proceedings* of the American Institute of Mining and Metallurgical Engineers (New York, N. Y.), volume 1, 1943, pages 30–42.

No Discussion

Trolley Coaches and PCC Street Cars Provide Successful City Transportation

W. J CLARDY
MEMBER AIEE

Synopsis: The importance of adequate city transportation is recognized. Successful handling of the rapidly increasing travel during the war as well as the subsequent high level of traffic that has been maintained proved difficult. Trolley coaches and Presidents' Conference Committee street cars were introduced in 1928 and 1936, respectively, and the total now exceeds 10,000. They established a high degree of availability and usefulness in meeting war demands and have a definite economic field of application for city transit ranging from 500 to 12,000 maximum passengers per hour in one direction. They use city streets efficiently and reduce traffic congestion. Operation is quiet, a feature which adds greatly to the comfort of the ride. The trolley coach has ample power for rapid accelerating at 3.5 miles per hour per second; it will run above 40 miles per hour, and normal stopping ability equals 3.5 miles per hour per second. The control provides quick, smooth starting and stopping. These performance details combine to produce schedule speeds of 12 to 15 miles per hour. Motor capacity of the PCC street car is liberal so as readily to permit 3.5 miles per hour per second starts. Car speeds exceed 40 miles per hour and service dynamic braking is at 3.15 miles per hour per second. The latter is supplemented by drum and track brakes. The 99-step control provides smooth starts and stops. These features combine to produce schedule speeds 25 per cent, or more, beyond those of old street cars. A conservative saving in operating expenses for the trolley coach is three cents per vehicle mile in comparison with the motor bus. PCC street cars effect savings in track and roadway maintenance, equipment maintenance, transportation costs, and accident expense when compared with old street cars while power costs tend to increase. However, the important factor in each case is the gain in revenue that these modern vehicles will produce in competition with other means of travel, as was demonstrated prior to the war. The economic advantages can be utilized in modernization programs and should be used more extensively.

Paper 47-147, recommended by the AIEE committee on land transportation for presentation at the AIEE summer general meeting, Montreal, Quebec, Canada, June 9–13, 1947. Manuscript submitted March 26, 1947; made available for printing April 29, 1947.

W. J. CLARDY is transportation engineer in the industry engineering department, Westinghouse Electric Corporation, East Pittsburgh, Pa.

Importance of City Transit

PEOPLE expect low cost and convenient means of travel between various sections of cities. Adequate transit establishes the required access of shopping and delivery districts, expands residential territory, and avoids the concentration of workers in homes near offices and factories. The growth of every large city depends on quick travel within the metropolitan area. The development and application of new vehicles must keep pace with this demand for utility in city transportation.

City Transit Problem Difficult

The rapid rise of transit traffic during 1941, 1942, and 1943 carried the level of travel up to 70 per cent more than that for the years 1936 through 1940. There was a further moderate increase in 1944 and the past two years have been close to 80 per cent ahead of the 1936–1940 average. The amount of business during 1946 was the equivalent of nine people being transported in comparison with each five for the 1936–1940 period.

The heavy demands placed on city transit systems, particularly in the war years, required both ingenuity and resourcefulness to meet service needs. The situation was further complicated by the existing inadequate supply of modern transit vehicles and the limitations placed on the production of new units. Inability to obtain sufficient maintenance personnel reduced the work which could be done to the minimum that would keep vehicles running. The objective was to provide a maximum amount of essential transportation with the least expenditure of materials and labor.

City transit systems gained a substantial number of passengers due to "necessity riding" created by wartime restrictions of automobile travel. The importance of retaining a major portion of these riders was appreciated and long before hostilities ended, means of providing service to accomplish this result were being studied. The problem was recognized as one of vital economic importance to the urban transit industry. It involved replacing all old vehicles with moderate types as rapidly as practicable. Fortunately, the use of public urban transit facilities has continued at a high rate since the end of the war for a much longer period than was anticipated. This has provided a greater opportunity for modernization before passengers change their riding habits.

Meeting City Transit Demands

The trolley coach and Presidents' Conference Committee street car have proved their usefulness and economic soundness for city transit service. The modern version of the former vehicle started its career in 1928 and the latter was first used in 1936. When the war began, trolley coaches and PCC street cars (in service and purchased) totaled 4,868. The limited procurements allowed during the principal war years—1942, 1943, and 1944—raised the total to 5,856 at the end of 1944, an increase of 21 per cent. Commitments were greater after termination of the European conflict and when all hostilities ceased, the total had gone up to 6,753. By the end of 1945, the total reached 7,762, and 1946 brought the

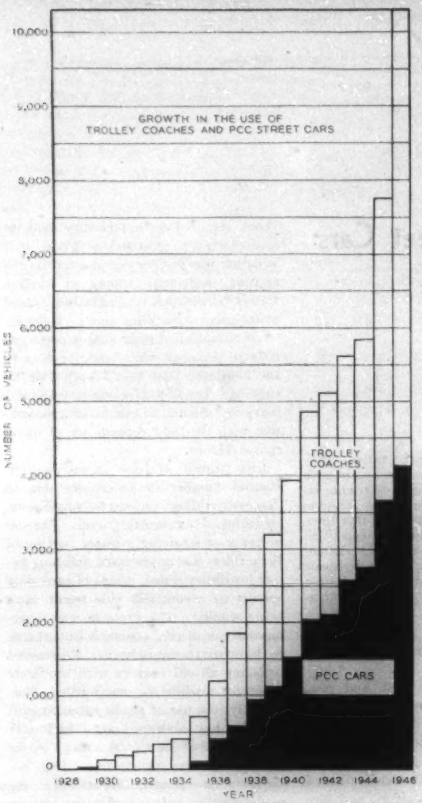

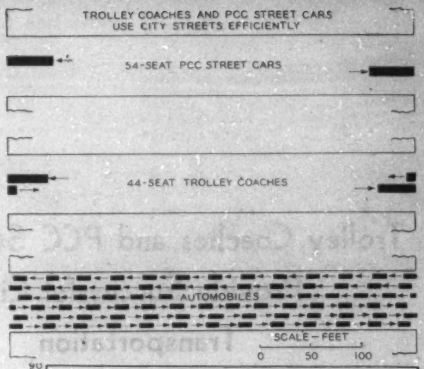

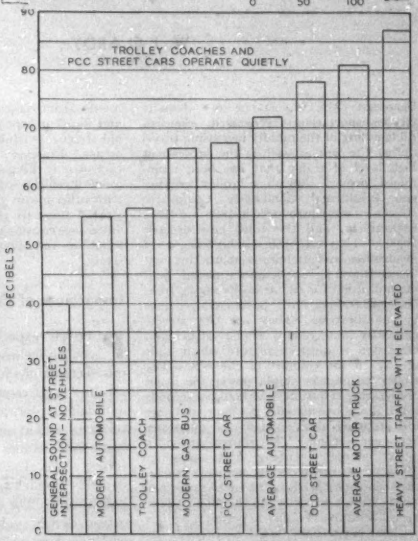

Figure 1 (left). Trolley coach operation started in 1928 and PCC street cars in 1936. The past two years, 1945 and 1946 show rapid expansion in the use of these vehicles

Figure 2 (top, right). Traffic delays caused by street congestion are a serious problem. Trolley coaches and PCC street cars require the least amount of street space for handling passengers. The chart shows actual space occupied for the same number of passengers

Figure 3 (above). A low noise level contributes substantially to passenger comfort. The trolley coach and PCC street car are both quiet operating vehicles

figure up to 10,274. Thus, 1945 and 1946 showed successive gains of practically one third for each year. The comparative figures are given in Table I. The increased "used trend" for the two vehicles is best illustrated by the chart in Figure 1.

Trolley coaches and PCC street cars have a wide range of economic usefulness in city transit service. The former can be applied for maximum hour travel as low as 500 passengers in one direction. It is the most efficient unit up to 2,500 passengers per maximum hour, and in many cases, is handling successfully much heavier traffic. The low point for the street car starts at 2,500 and goes up to 12,000 passengers per maximum hour in one direction. The latter figure represents 150 vehicles per hour on a 60-foot street—30-second headway—with loading equivalent to $1^1/_2$ times the seating capacity. This compares with possible peaks of 180 vehicles per hour and loadings equal to $2^1/_2$ times seating capacity. When travel exceeds 12,000 passengers per maximum hour for one direction, rapid transit trains are required.

Trolley coaches and PCC street cars established exceptional availability

Table I. Number of Vehicles

Date	Trolley Coaches	PCC Street Cars	Total
End of 1941	2,840	2,028	4,868
End of 1944	3,102	2,754	5,856
End of war	3,517	3,236	6,753
End of 1945	4,098	3,664	7,762
End of 1946	5,924	4,350	10,274

Figure 4. Trolley coach at the terminal of a heavily traveled city line

records during the war years when the sharply upward trend of transit traffic was in progress. Both vehicles were highly dependable under extremely adverse conditions. The long life of parts when renewal items were scarce and the minimum amount of attention needed from depleted maintenance personnel contributed substantially in providing essential transportation service. A 100 per per cent availability record often was attained and close approximation of this performance was a normal expectancy. The usefulness of these modern transit units was demonstrated and the reliability of the propulsion and control equipment was an important contributing factor.

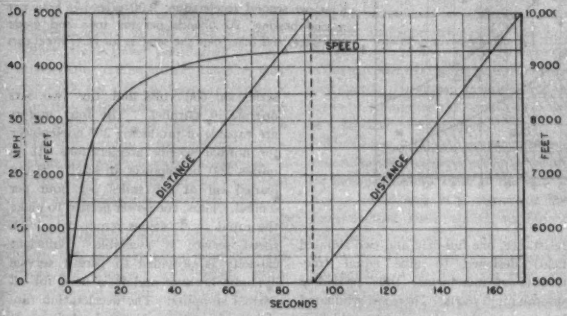

Figure 5 (below). Trolley coach speed time and distance–time curves

Trolley coaches start rapidly and operate up to speeds above 40 miles per hour. The curve is based on a 12-ton loaded coach, single 140-horsepower motor, 11.42 to 1 gear ratio, 43-inch rolling diameter tires, 550 volts, level roadway, train resistance from tests, and 3.5 miles per hour per second acceleration

Efficient Street Use and Quiet Operation

The limited capacity of city streets in metropolitan areas and the congestion caused by the automobile have made city dwellers realize more and more that street use is a civic problem. Large expenditures for widening, even where such measures are practicable, rarely prove to be a solution. Much can be gained by judicious allocation of existing street space. The elimination of parking and more general use of public transit vehicles are important factors.

The trolley coach and PCC street car are excellent units for transporting passengers over heavy thoroughfares. This is illustrated by Figure 2 which shows a street use comparison for 60-foot roadways. Two 54-seat PCC street cars in a 400-foot city block will transport 162 passengers (81 in each direction) when loaded on a basis of $1^1/_2$ times seating capacity. In the case of 44-seat trolley coaches, the equivalent of practically $2^1/_2$ of these vehicles would be needed in the same block. However, 81 automobiles would be required with an average of two passengers per car (checks show average loading to be 1.7 passengers per car).

Trolley coaches and PCC street cars

Figure 6 (below). The PCC street car is an efficient mass transportation vehicle for handling heavy city travel

Figure 7 (right). Smoothness in performance

Smooth operation is characteristic of the PCC street car. After the gradual build-up of acceleration, the rate is held constant until all resistance is cut out and the motor fields are shunted

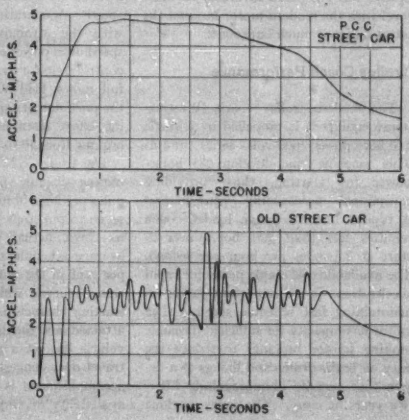

are among the quietest vehicles operating on city streets. The noise level of the former is practically the same as the modern automobile. This is illustrated by Figure 3 which compares various vehicles based on tests made in Cleveland and New York. The noise level of the trolley coach is far below the modern motor bus. The electric propulsion equipment is practically silent in its operation. There is no roar of an engine, vibration of the body, and rattle of exhaust. The extensive use of rubber in the construction of PCC street cars contributes substantially to its low noise level. Also, the vehicle has the advantage of quiet electric propulsion and the new "all electric" model eliminates brake rigging. As is shown by Figure 3, the PCC street car always has compared favorably in noise level with the modern motor bus and the latest design is much improved.

Trolley Coach Performance

The modern trolley coach (Westinghouse equipped) is propelled by a single 140-horsepower 600-volt series motor. This machine can develop 235 horsepower for starting, thus, providing exceptional accelerating performance. A typical 12-ton average loaded coach requires less than 200 horsepower to start at 3.5 miles per hour per second. The availability of ample power for rapid accelerations is an important factor in maintaining fast schedule speeds. The motor has capacity for sufficient dynamic braking (motor braking) to reduce the duty on brake drums and linings to a degree that permits obtaining long life—two years or more. The series machine has the inherent characteristic of rapidly increasing dynamic braking as speed goes up. When running down grade, and the electric brake is applied, the desired rate is obtained quickly. Braking effort can be held nearly constant over the entire speed range, thus maintaining a high average.

Westinghouse control apparatus, known as Electrocam, is an assembly of cam group and unit switches which have operating coils suitable for a 12-volt battery and generator power source. There are 15 accelerating steps (12 series resistance, one full field and two shunted field) designed to give equal tractive effort increments, thus providing smooth rapid starts. There is a graduated build-up to the selected rate which is maintained uniformly as the coach gains speed. Acceleration gradually decreases with the attainment of higher coach speed until power is cut off. There are 13 control steps for dynamic braking, all with full motor field strength. Here, again, the provision of equal increments of braking effort maintains a smooth rate of braking from 40 to 3 miles per hour.

The trolley coach is capable of maintaining schedule speeds of from 12 to 15 miles per hour in urban service with from seven to ten stops per mile. Tests made to check actual operation show that average schedule speeds are at least 80 per cent of the maximum. Figure 5 includes curves which depict the quick starting characteristics, the high speeds attained, and the distances covered. The vehicle has set a new standard for fast travel over congested city streets. This accomplishment is made possible by the availability of ample motor capacity to give rapid starts, a speed range that permits minimum running time with varying degrees of street congestion, rapid stops produced with combined dynamic and drum braking, and the ability to maneuver around slow moving vehicles and street obstructions.

PCC Street Car Performance

The propulsion equipment of the PCC street car consists of four 55-horsepower 300-volt series motors—220 horsepower per car. Two motors are connected in series on 600 volts and the two sets operate in parallel. The four motors are capable of producing 365 horsepower for normal service accelerations. It requires 300 horsepower to start a 21-ton loaded car at 3.5 miles per hour per second. Thus, the power needed to make the rapid accelerations required by high speed service is available. Sufficient capacity is provided to permit service dynamic braking and it is used for all normal stopping. The deceleration rate obtainable with a 21-ton loaded car is 3.15 miles per hour per second. The series motor gives a quick build-up of dynamic braking, provides simple braking connections, and facilitates equal division of braking duty among the four machines.

The control apparatus includes a line switch, a group of contactors for setting up the main circuits, and an accelerator for adjusting resistance when starting and stopping. The latter device, which is the most important item, has 99 steps for cutting resistance in and out of the motor circuits. During starting, the large number of notches results in such small tractive effort increments that acceleration remains practically constant after the selected rate is attained. The same situation exists during dynamic braking and the full rate is carried down to almost zero speed. Dynamic braking is supplemented by four shaft drum brakes and four track brakes. Drum braking and

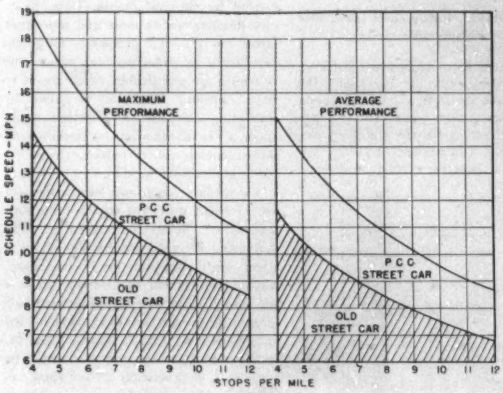

Figure 8. PCC street cars provide rapid travel

Schedule speeds are based on 21 tons loaded weight, four 55-horsepower motors per car, 7.17 to 1 gear ratio, 25-inch wheels, 550 volts, 3.5 miles per hour per second acceleration, 3.15 miles per hour per second braking, five pounds per ton grade resistance, Davis train resistance plus six pounds per ton for resilient wheels, and seven seconds average stop time. Old street cars are based on 23 tons loaded weight, four 40-horsepower motors per car, 15 to 58 gear ratio, 26-inch wheels, 1.75 miles per hour per second acceleration, 2.00 miles per hour per second braking, 20 pounds per ton train and grade resistance, and other data the same as for PCC street cars

track braking are used in emergency while the former completes the stop after dynamic braking fades out (about $1^1/_2$ miles per hour) and holds the car after it stops. Also, drum braking functions whenever the dynamic brake is inoperative. The control power for accelerating, braking, and all auxiliary circuits is supplied from a 32-volt storage battery so that the various devices can function even in case of a dewirement.

Smoothness in the performance of the PCC street car is an outstanding characteristic. This is illustrated by the curves which appear in Figure 7. One of the two curves included is applicable to an old type street car and shows the extreme variations in accelerating rate that are obtained. The other curve, taken on a PCC street car under the same conditions, demonstrates the smooth build-up of acceleration to the selected maximum. The rate is maintained until the notching is completed and the speed of the car begins to decrease.

The PCC street car can operate with schedule speeds 25 per cent, or more, higher than those maintained by old street cars. A comparison based on various stops per mile is shown in Figure 8. Curves are included for both maximum and average performance. The latter takes into account turns at street corners, delays at traffic signals, interference of street traffic, and other similar items that may affect schedules adversely. The improvements in schedule speeds result from the quick starting, high speed running, and rapid stopping characteristics that are obtained with ample motor capacity and smooth operating control.

Economic Considerations

The economic field of application of the trolley coach and PCC street car based on maximum hourly traffic has been mentioned. Trolley coaches will reduce operating expenses in comparison with motor busses because of savings in maintenance, power, and transportation costs. Fixed charges are affected by differences in investment and life of the equipment. A comparative analysis requires consideration of construction costs, investment in physical property, operating expenses, taxes, and renewals and replacements. Studies that have been made of proposed and existing trolley coach installations in many cities show that a saving of three cents per coach mile in operating expenses is a conservative estimate of the economy of the vehicle when compared with the motor bus.

PCC street car operating expenses are reduced in comparison with old street cars because of savings in track and roadway maintenance, equipment maintenance, transportation costs, and accident expense. Power costs are increased because of the operation of higher scheduled speeds. However, the important factor is to modernize the service so it will be attractive to passengers.

The necessity for retaining a high traffic volume on city transit systems is the urge for modernization. Prior to the war, the trolley coach and PCC street car both demonstrated their ability to increase revenues in competition with other means of travel. Trolley coaches produced improvements of 25 to 35 per cent while typical gains for PCC street cars ranged from 10 to 15 per cent. Thus, the two vehicles have proved their ability to attract passengers.

More Trolley Coaches and PCC Street Cars Needed

Trolley coaches and PCC street cars generally have been applied on city transit systems. These vehicles are the product of considerable engineering effort to provide a comfortable ride, improve performance, and increase operating efficiency. Results are creditable as a contribution to the betterment of city transit facilities and the new units will assist substantially in meeting the needs of modernization program. Action should be taken to expand the installations of these vehicles and thereby realize the benefits of the improvements in urban transit.

References

1. Results of Operation of PCC Cars in Pittsburgh, T. Fitzgerald. AIEE Transactions, volume 57, 1938, June section, pages 315–17.
2. Modern Motors Serve City Transit Systems, W. J. Clardy, C. A. Atwell. AIEE Transactions, volume 60, 1941, August section, pages 850–4.
3. Operating Results With PCC Cars, G. M. Woods. Electrical Engineering, volume 60, August 1941, pages 392–5.
4. PCC Car Operating Results in Pittsburgh, W. J. Clardy. AIEE Transactions, volume 61, 1942, April section, pages 214–17.
5. Some Recent Developments in the PCC Car, S. B. Cooper. AIEE Transactions, volume 66, 1947, pages 288–92.
6. Recent Developments in Track Brakes and Drum Brakes, S. J. Vouch. AIEE Transactions, volume 66, 1947, pages 302–4.
7. Route Cost Analysis and Selection of Transit Vehicles—Parts 1 and 2. American Transit Association (New York, N. Y.), November 1946 and March 1947.

No Discussion

Modern Railway Passenger-Car Auxiliary-Power Equipment

D. R. MacLEOD
MEMBER AIEE

JACK HAUSE
ASSOCIATE AIEE

THE purpose of this paper is to outline some of the principles which have governed the development of electric equipment for railroad passenger cars and to discuss some of the possible developments which may prove of advantage to the industry.

Immediately after the close of World War II the railroads began to order a large number of passenger cars in a determined effort to retain a large part of the passenger business which had come to them during the war years when the use of the private automobile was restricted severely. There are today approximately 3,000 cars on order for various railroads. This tremendous building program was foreseen during the war and insofar as was possible the engineers of the railroads and of the manufacturing companies planned for it. As might be expected, a large number of different ideas were given a quick trial and adopted by different railroads. All of these ideas had as their basis a very large increase in the amount of power which would be required for electric devices on the cars. Air conditioning, fluorescent lighting, and electromechanical water coolers were specified for almost all the cars. Air-conditioning equipment was specified with greater tonnage capacity available if it should be needed to take care of the increased quantities of fresh air which would be required to cope with the smoking problem in coaches. Some railroads have experimented with electrostatic-type air filters but as yet no widespread application of these devices has been made. The illumination in railway coaches has been raised at the reading level to from 18 to 24 foot-candles and in some cases higher levels have been used. One railroad which has ordered more than 400 cars since the end of the war has used 60-volt d-c fluorescent lighting, but the great majority of the other railroads have used 60-cycle a-c fluorescent lighting. Water coolers capable of cooling from 3 to 5 gallons per hour of water have been installed in practically all new coaches. Some sleeping cars have been equipped with individual tap water outlets in each compartment, roomette, or bedroom.

Some railroads have given consideration to small refrigerator units in each roomette for the storing of babies' milk bottles. A small auxiliary heater would be required to bring the milk to the required temperature for feeding. Electric blankets for sleeping cars and even for coaches have been given consideration and undoubtedly will be applied in the future. Public address systems have been supplied for coaches so that stations can be called over the loud speaker system and other important events announced. Some cars have been wired for the wire recorder. Equipment for radiobroadcast reception also can be installed if desired.

In keeping with their policy to provide the maximum degree of comfort and entertainment to their passengers, consistent with good economy, the railroads have been experimenting with the development of new types of dining cars. Electromechanical refrigeration soon will replace the old iceboxes in the kitchens. These new refrigerators will have different temperatures for the correct refrigeration of such diverse items as frozen foods, meats, fish, and beverages. The use of frozen foods in the kitchen will speed up the preparation of meals and reduce the number of men required in the kitchen. At least two railroads are experimenting with full scale electric cooking with the idea of reducing temperatures in the kitchen so that the kitchen crew can work in comfort. Other railroads have long used grill cars with small-scale electric cooking. Some railroads which have used garbage Disposalls in the past with a high degree of success will continue their use and others will adopt them. At least one railroad is trying out electric dishwashing with a view to further speeding up work in the kitchen. One railroad has equipped dining cars for the showing of motion pictures between meals, and other entertainment features undoubtedly will be added as they become available for use on railroad cars. The railroads contemplate equipping cars on feature trains with nurseries. These would be furnished with germicidal lamps, sun lamps, and other health preserving features to insure the comfort and sanitation of the younger travelers. Germicidal lamps also are being used in water coolers and other water outlets on the train.

All of these devices have called for increased generator capacities on cars. One all-electric diner which is now being built will have a total maximum generating capacity of 66 kw. Conventional dining cars are being equipped with generators having maximum kilowatt capacity of 50 kw. Coaches and sleeping cars are being equipped with generators having maximum capacities between 20 and 35 kw output. The great majority of cars that are being built today will be owned or controlled by the railroads in the East. Therefore, the great majority of new cars are being equipped with axle-driven generators. In the West where the railroads have to contend with long grades with limited horsepower locomotives, many have adopted engine-driven generators for lighting and engine-driven compressors for air conditioning. The majority of these have been of relatively low capacity in each unit and have used propane as the fuel. The trend ap-

Paper 47-153, recommended by the AIEE committee on land transportation for presentation at the AIEE summer general meeting, Montreal, Quebec, Canada, June 9–13, 1947. Manuscript submitted April 3, 1947; made available for printing April 30, 1947.

D. R. MacLeod is application engineer in the transportation department, and Jack Hause is in the transportation division of the General Electric Company, Erie, Pa.

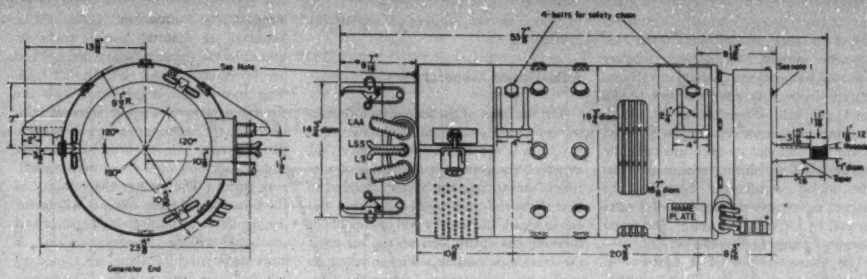

Figure 1. Outline drawing of type GMG-150 motor generator set

pears to be toward the use of a single engine-driven unit for the supply of electromechanical air conditioning, fluorescent lighting, and all other power services on the cars. These engines will probably be of the diesel type using standard diesel fuel as used for locomotives and will probably drive 3-phase, 60-cycle alternators at 1,800 rpm. Even on these cars equipped with engine-driven alternators, batteries will be required for emergency lighting and for supplying power in terminals or other locations where the engines cannot be run either for reasons of economy or because of noise or fumes.

Cars equipped with axle-driven generators have been equipped with batteries ranging from 1,200 ampere-hour capacity for 32 volts to 600 ampere hours for 64-volt and 114-volt d-c systems. A large number of these cars have been supplied with means for converting direct current to alternating current for use by fluorescent lights and fan motors. In some cases this a-c supply has been of extremely small capacity as required for electric razors. The great majority of the new axle generators are equipped with a-c motors so that they can be plugged in, in yards and terminals, for the supply of power while the car is not in motion and for battery charging after the battery has been run down. These a-c motors are all 220-volt 3-phase 60-cycle, as this has been very well standardized by the railroads for use in their terminals. Many of the axle-driven generators are driven by a Spicer drive. The Spicer drive consists of a gear unit mounted on the axle of the car, a propeller shaft, and a clutch. Power is transmitted from the axle through the axle mounting to the gear unit and through the propeller shaft to the clutch and generator. The gear unit consists of a hypoid gear mounted on a quill which rotates on antifriction bearings. The gear drives a hypoid pinion which also is mounted on antifriction bearings. The clutch is a safety device consisting of a single-plate friction clutch with the capacity controlled by spring pressure. In case of very heavy overload on the generator, the clutch slips at the friction surfaces, generating heat in the safety plate which in turn is transferred to the safety plugs causing these to melt and allow the safety plate to move out of engagement with the friction facings. This type of drive has been used very successfully for a number of years for generators before the advent of the motor generator sets which are now in common use. When a motor generator set is used for the axle generator an automatic clutch is used in place of the simple safety clutch. This clutch engages and releases automatically. It engages when the drive shaft from the axle of the car is rotating at approximately 280 rpm, thus permitting the motoring of the generator by means of the a-c motor mounted on the same shaft.

There are in use on railroad passenger cars today, 32-volt d-c, 64-volt d-c, and 114-volt d-c batteries with the corresponding charging voltages. There are also 220-volt 3-phase 60-cycle, 110-volt 3-phase 60-cycle, 110-volt single-phase 60-cycle, and variable-voltage, variable-frequency systems with a nominal frequency of 60 cycles. Since it appeared impossible for the railroads to standardize on any one voltage or system of power supply, it became necessary for the electrical manufacturers to design their equipment with the objective of using the greatest number of parts common to all units of a given line to keep manufacturing costs and the number of renewal parts within reason. A good example of this thought of standardization is described later in connection with the axle-driven generators developed by the company with which the writers are associated. When the electrical loads on passenger cars were small there was no compelling reason to depart from the 32-volt d-c system which, by 1930, had become standard on almost all railroad cars. With the growth of load which accompanied the introduction of air conditioning, the heavy currents which had to be handled and the large cables required to transmit these heavy currents with low voltage drop caused a number of railroads to investigate the possibilities of higher voltage systems. One big drawback to higher voltage systems was the increased hazard of grounds due to leakage over battery terminals. Consideration also had to be given to the requirements of some types of cars so that in case of failure of the lighting system on one car, the circuits could be plugged through to an adjacent car. This factor plus the leakage problem and the development of a 64-volt d-c fluorescent lamp led to the adoption of 64 volts direct current (nominal) by some railroads. Other railroads decided to go all the way in the direction of using d-c motors designed for voltages that were standard in industry. They also decided that the increased efficiency of the higher voltage justified any increased hazard due to leakage. There also appears to be some saving in weight with a 114-volt (nominal) d-c system, as compared with the same kilowatt-hour capacity at a lower voltage. None of the arguments appears to be conclusive to the writers of this paper, and it is hoped that the railroads eventually will standardize on one direct voltage for all new cars.

Batteries

There are two types of batteries in general use on railway passenger cars. These are the lead-acid type battery[1] and the nickel-iron-alkaline type. The lead acid type uses 16 cells for the nominal 32-volt d-c system, 32 cells for the nominal 64-volt d-c system, and 57 cells for the nominal 114-volt d-c system. The nickel-iron-alkaline type uses 25 cells for

the 32-volt system, 50 cells for the 64-volt d-c system, and 90 cells for the 114-volt d-c system. In railway practice lead-acid batteries are charged at voltages ranging from 2.25 volts per cell to 2.5 volts per cell. Some railroads use a charging voltage of 2.35 volts per cell during the summer months and raise the charging voltage during winter months. The nickel-iron-alkaline batteries are charged at voltages ranging from 1.6 volts per cell to 1.8 volts per cell. The usual charging voltage is 1.7 volts per cell.

The characteristics of a battery on charge consist of a family of curves with a rising characteristic when plotted with charging current as the abscissa, charging voltage as the ordinate, and per cent charged as the parameter for the family of curves. This family of curves is affected by the temperature of the battery and its age. Some railroads using lead-acid batteries have applied temperature-responsive relays in the battery boxes to adjust the charging voltage in response to battery temperature. This is done toward assuring a more nearly correct amount of charge. When the battery becomes fully charged, the excess current not required for converting the active material decomposes the water of the electrolyte and oxygen which are released as bubbles of gas. Some railroads have adopted the device of lowering the charging voltage slightly when the charging current falls below a certain value. The temperature-compensating relay accomplishes the same purpose and is a more correct indication of the charging voltage to use.

Other things being equal, a battery having high rates of charge and discharge will have a shorter life or require more maintenance than one having lower rates of charge and discharge. In the application of axle-driven generators, therefore, on passenger cars, the objective should be to keep the rates of charge and discharge as low as possible. The criterion of ampere-hours into the battery and ampere-hours out of the battery therefore is used to determine the correct application of axle-driven generators as discussed in the section on axle-driven generators.

Axle-Driven Generators

The function of the axle-driven generator is to supply the load on the car while the train is moving at speeds above that at which the generator is capable of cutting in and to keep the battery charged so that when the train speed falls below the cut-in speed, the battery will be capable of carrying the entire load on the car until the train can resume a higher speed or until it reaches a terminal where the axle-driven motor generator may be plugged in, or the batteries put on d-c charging if a straight axle driven generator is used on the car. The drive may be provided with a number of different gear ratios so that the same generator operating within its permissible speed range may be used for high speed trains operating as high as 120 miles per hour or on slower-speed trains which may only have a maximum speed of 80 miles per hour. Intermediate ratios are also available. Some railroads have profiles on which they run at speeds in excess of 100 miles per hour in some sections and at speeds which may fall as low as 20 miles per hour in going over heavy grades. If these grades were of sufficient length to require a prolonged drain on the battery a generator with a wide speed range from the no load cut-in speed to maximum permissible operating speed is required. Considerable freedom of selection exists within a given size of generator. It is always possible to exchange volts for amperes by using a different number of turns in the armature coils. There is also freedom in selection of the size of the field, depending upon the range of excitation which will be required to cover the given operating conditions. At the high-speed end of the operating range of the generator, the designer must provide a shaft of adequate dimensions so that the critical speed is at a safe distance above the maximum permissible operating speed. The generator must also commutate satisfactorily the maximum load at the maximum speed when the exciting field strength is at a minimum. Care must be taken to see that the ampere turns required by the field at the maximum speed are lower at no load than at full load. This means that a generator with the greater number of ampere turns in relation to the armature-reaction ampere turns over the pole face is considered more stable than one with fewer exciting ampere turns. The greater the stability of the generator, the less likely it will be for the regulator to hunt at high speeds and the better will be the commutation. A more stable machine, therefore, should result in lower maintenance. The degree of stability that is built into a machine is determined by the judgment of the individual designer in relation with the accumulated experience of similar designs. Since most railroads have some margin above their maximum operating speed, the stability of the generator becomes of particular importance at speeds below approximately 90 per cent of maximum permissible speed. However, the regulator designer must take the maximum stability into account in designing his regulators to prevent hunting at the maximum permissible speed.

At the lower end of the speed range the designer is faced with the problem of field heating because the field amperes are a maximum at the cut-in speed. If a low cut-in speed is required in relation to the maximum permissible speed for a given

Figure 2 (left). Type GMG-150, a-c d-c motor generator set

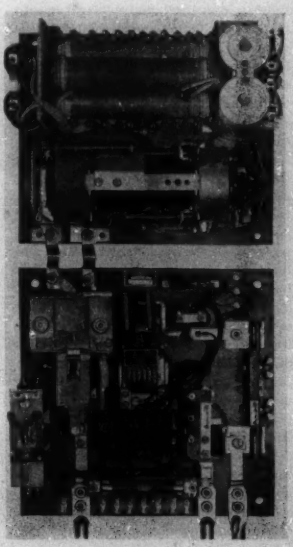

Figure 3 (right). Assembly of voltage control relay panel (upper) and (lower) generator control panel

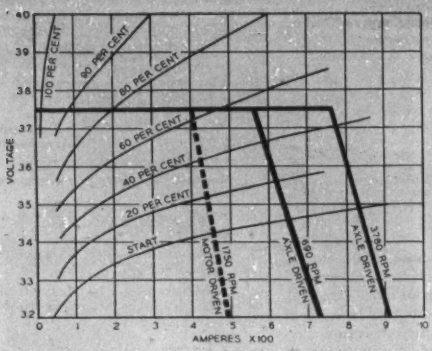

Figure 4. Charging characteristics, lead-acid batteries, 20–25-kw motor generator

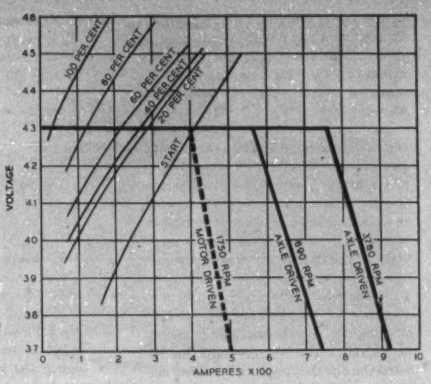

Figure 5. Charging characteristics, nickel-iron-alkaline battery 20–25-kw motor generator

field structure, the designer may use a greater number of turns per coil on the armature. This gives him more volts for a given excitation but reduces the section of his copper for a given slot dimension. Thus a 64-volt (nominal) d-c generator with exactly the same physical dimensions and field copper may be designed with three turns per coil or with four turns per coil. The no-load cut-in speed at 85 per cent of normal voltage of the 4-turn machine might be 520 rpm with a maximum permissible speed of 3,780 rpm while the 3-turn machine would have a no-load cut-in speed at 85 per cent of normal voltage of 690 rpm. However, the kilowatt capacity of the 4-turn machine would be less than 75 per cent of that of the 3-turn machine. There is some loss in capacity due to the poorer copper space factor with four turns as compared with three turns. The full load speed is the significant speed and these also will be proportional to the number of turns. Full-load speed is defined by the American Association of Railroads specifications in the following manner:

The generator with covers arranged as in summer service shall be capable of delivering for three hours for enclosed and five hours for ventilated machines at the output side of the generator regulator at all speeds above 1.25 times minimum full load speed:

1. Rated current at rated voltage without exceeding specified temperature rises.

2. Rated current at all voltages between 20 per cent above and 20 per cent below rated voltage without injurious heating.

The motor generator sets for 32-, 64-, and 114-volt d-c batteries, manufactured by the company with which the writers are associated, all have the same outline dimensions and approximately the same weight (see Figures 1 and 2). They are 2-bearing machines for suspension by bonded rubber resilient mountings beneath the car body. The machines are self-ventilated with fan mounted on the armature shaft. Baffle type air cleaning is provided in the air entrance passages at both a-c and d-c ends of the machine. Many of the parts such as brush holders, are interchangeable on the four different machines. Table I gives some of the pertinent data for these motor generator sets.

The control system for these motor generator sets consists of a voltage control relay panel, generator control panel (see Figure 3), and a 3-pole cross-the-line a-c motor starter.

The voltage-control panel incorporates a contact-making, electromagnetically controlled relay with both voltage and current elements. The voltage element acts to maintain constant direct voltage output from the d-c generator from full-load cut-in speed to the current-limit cut-in value of amperes load. At the point where current-limit cut-in value is reached the current element acts on the voltage-control relay to reduce the d-c generator voltage while permitting the load current to increase. The slope of this voltage curve at the full-load cut-in speed is approximately 25 per cent increase in amperes for approximately 15 per cent reduction in voltage. The point where current-limit cut-in is reached increases in amperes load as the speed of the generator increases, thus taking advantage of the increased rating of the self-ventilated machine at the higher speeds.

The 32-volt 20–25-kw motor generator battery charging characteristic when operated with voltage control relay is shown in Figures 4 and 5.

The generator control panel mounts the reverse-current relay, the line contactor, the load-limit shunt and relay, and main fuse or overload relay. A voltage element is included with the reverse-current relay as a differential element to pick up the generator contactor when the generator voltage exceeds battery voltage by approximately two volts. The generator contactor is opened again by the reverse-current element of the same relay with a reverse load-current of approximately seven amperes. The load limit shunt and relay act to change the current limit cut-in value to hold 15.5-kw output of the d-c generator at 1,750 rpm when operating from 220-volt 3-phase 60-cycle wayside

Table I. Data for Motor Generator Sets

Nominal d-c battery voltage, v	32	64	64	114
Regulated d-c charging voltage, v	37.5	75	75	134
Kw	20–25	20–25	30–35	25–30
Maximum output (lead battery), kw	28.5	29	40	33.5
No load (85 per cent normal volts) cut-in speed, rpm	520	520	690	590
Full load (100 per cent volts) speed, rpm	690	690	915	780
Maximum speed, rpm	3780	3780	3780	2470
A-c motor, hp	25	25	25	25
D-c output on a-c wayside power, kw	15.5	15.5	15.5	15.5

plug-in power from the 25-horsepower induction motor. A relay is included to prevent load being applied to the motor generator set until it comes up to normal operating speed when operating from wayside power.

The motor generator has an armature reversing switch mounted on the commutator end of the set. The initial revolution of the motor generator operates this armature-reversing switch to correct generator polarity for the direction of train travel. The generator builds up its terminal voltage as a self-excited machine.

In applying these axle-driven motor generator sets for a particular run it is necessary to consider not only the kilowatt rating but also the minimum full-load speed. The best generator for the job is the one that results in the least ampere-hour discharge from the battery. Certain railroads have long runs involving mountain grades where speeds average 18 to 25 miles per hour and also relatively long restricted speed approaches to route terminals. In these cases low cut-in speed is more important than having a high kilowatt output from the generator. However, other railroads have runs where almost all of the traveling is done at relatively high speeds in which case a high kilowatt rating is more important than low cut-in speed.

As an example of this, an application study was made of a run from Washington, D. C., to St. Louis, Mo., using the actual speed–distance curves and converting them into speed–time curves for calculating the ampere-hour charge and discharge duty on the battery. The results of the computations are given in Table II.

Table II. Calculation of Charge and Discharge Duty on Battery

	A	B
Generator capacity, kw	20–25	30–35
Full load cut-in speed, rpm	690	915
Amp-hr charge	2,117	3,820
Amp-hr discharge	696	1,057
Amp-hr charge × 0.7	1,482	2,680

Calculations from speed–time curves based on 17.8 kw, constant load 235 amperes at 75 volts charging and constant load 235 amperes at 64 volts discharging.

These data indicate that generator *A* will give a more satisfactory operation because of lighter-load duty on the battery even though the kilowatt rating of the generator is lower. This advantage of low cut-in speed of course becomes less important as the percentage of operation becomes predominately high speed.

A-C Power Supply

The railroads long have realized the advantages of induction motors for use on passenger cars instead of commutator motors. This advantage of a-c power has been brought more forcefully to their attention in recent years by other innovations such as fluorescent lighting, electric razors, radios, public address systems, and sound motion pictures.

This requirement for a-c power has led the railroads into many different methods of obtaining it, such as

(*a*). Head-end power cars with engine-driven alternators and distribution lines to feed a-c power back through the train.

(*b*). Engine-driven alternators mounted on individual cars.

(*c*). Motor-alternator sets driven by d-c motor from the battery.

(*d*). Vibrating-reed inverters operating from the battery.

(*e*). Amplidyne-booster inverters, or simple inverted-synchronous converters operating from the battery circuit.

Head-End Power

An ideal system of power supply for the electric loads on railroad passenger cars consists of a large engine-driven generator power plant consisting of two or more units at the head end of a train. The operating disadvantages are principally those associated with an interchange of cars between different railroads and between different trains on the same rail-

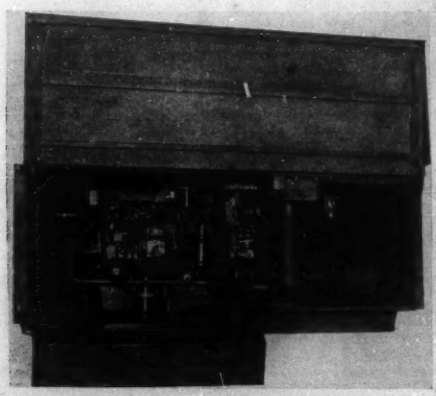

Figure 6. Diesel-engine-driven 25-kw alternator power unit for undercar mounting; cover open, engine alternator in undercar position

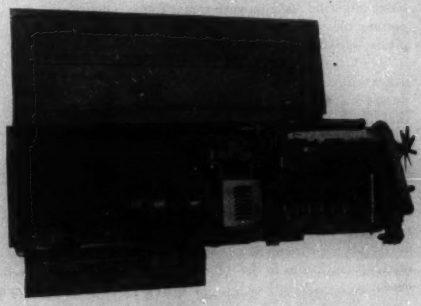

Figure 7. Diesel-engine-driven 25-kw alternator power unit for undercar mounting; cover open, engine alternator swung out 180 degrees

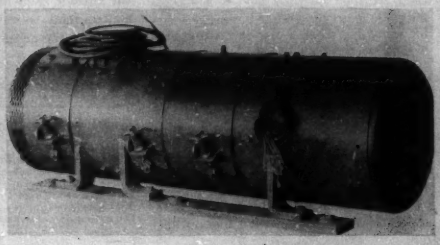

Figure 8 (below, right). Type 5LY153 amplidyne-booster inverter for supplying 60-cycle 3-phase power for railroad passenger cars

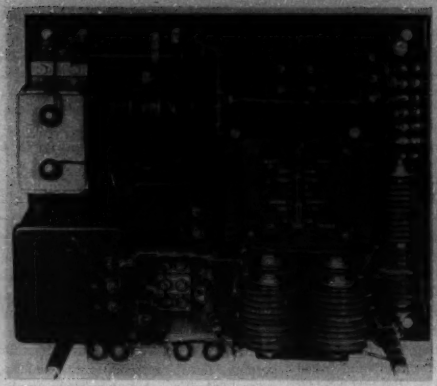

Figure 9. Voltage-regulator panel 3G-NA13 for use with amplidyne-booster inverter

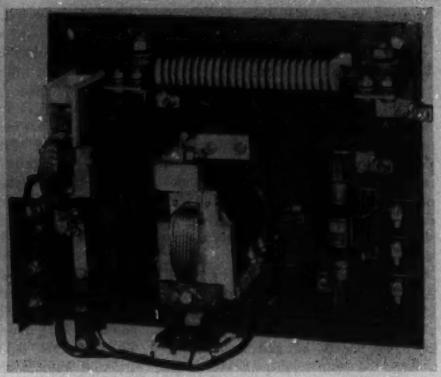

Figure 10. D-c starting panel, type 17FM-63 for amplidyne-booster inverter

road. The advantages and disadvantages of this system have been discussed thoroughly by J. D. Loftis.[2]

Engine-Driven Generators for Car-Mounting

Most railroads require that any passenger car be capable of carrying its air-conditioning load for at least two hours independent of any outside power source. Even where a-c plug-in power is available in yards and terminals there are other conditions which require a relatively large battery. These batteries must be charged at a relatively high rate, while the car is running, putting a heavy drag on the locomotive. For example, a 20-car train may require as much as 800 horsepower from the locomotive for the electric power taken by a car. This is an appreciable percentage of the locomotive rating for normal operation. On some railroads the variation in the number of cars that have to be hauled by the same locomotive in different trains may be so great that no credit can be given to a self-contained power plant for the saving in locomotive horsepower. However, where trains of the same length are hauled by the same locomotives day after day the saving in locomotive horsepower can be credited to the self-contained power plant. In this case an engine-driven power plant on each passenger car with a relatively small battery for starting the engine and for emergency incandescent lighting will be more economical than an axle-driven generator and large storage battery. The problem of noise, exhaust fumes, and maintenance must be evaluated and these considerations may outweigh first cost advantages of the individual power plant.

A number of railroads have used two propane engines on each car for driving air-conditioning compressors directly and a small d-c generator for the lighting, auxiliaries, and charging a small battery.

In recent years Diesel fuel has become available on a number of railroads and railroad shops have become proficient in maintaining this type of engine. The advantages of a-c power for motors and fluorescent lighting have turned the attention of several railroads to Diesel-engine-driven power plants that can be mounted under a car. Several manufacturers are developing Diesel-engine-driven a-c power plants for undercar mounting. Some consideration also is being given to engine-driven d-c generators. Advances made during the last war in the design and building of reliable small engines and also advances made in the electrical field in design and construction of a-c generators and the voltage-control components have made this possible. Figure 6 and 7 show a 25-kw a-c 230-volt 3-phase 60-cycle power plant for undercar mounting. Much attention has been given to accessibility of the power unit for maintenance.

There are several problems associated with the use of small engine-driven alternators on cars. First and foremost is the need for clean air for the engine intake. If the air is taken from under the car the filters are bulky and will require frequent cleaning. If taken from inside the car a location must be found where the noise will not be objectionable. Since fluorescent lighting usually will be operated on the same bus as the air-conditioning compressor motors the response of the engine governor and the speed of the voltage regulator must be given careful consideration. Most small engines usually are supplied with mechanical governors which have relatively slow response to suddenly applied loads. On the converse, the mechanical governor is less likely to hunt if the engine-driven generators are to be operated in parallel. It is desirable to use unloading valves on the compressor to reduce the high torque of the compressor when the start is made from an unfavorable position of the piston. A high speed regulator is needed to reduce lamp flicker of fluorescent lights due to the high starting current of induction motors.

Motor Alternators

Self-regulating motor alternators use static devices and auxiliary fields to control alternating voltage and frequency. Resistors that change their value with voltage are used to modify the field of the d-c motor in response to load and a differential field excited by rectified a-c load current is used to compensate for changes in speed due to load. The d-c motor current is fed into the a-c field to compensate for impedance drop with load. Since the a-c amperes depend on the kilowatts of the load and its power factor and the d-c motor amperes depend upon kilowatts load and applied direct voltage, it can be seen that this system gives only approximate control of voltage and frequency under varying load conditions. It is used where a-c motors are not started from the

same bus that supplies fluorescent lighting.

Vibrating-Reed Inverters

These devices are used where small a-c power outputs are required as for razor outlets on Pullman cars and coaches that do not have other sources of alternating current. They have proved economical on applications where intermittent service is required. The modern type is designed[3] for ease in replacing parts that are subject to wear.

Amplidyne-Booster Inverters

The only practical method that has been developed of getting constant-voltage constant-frequency a-c power from the axle of a car is to generate direct current by means of an axle-driven generator and then convert to alternating current. This double conversion means a serious loss in power and, therefore, it is important to use as efficient a conversion unit as possible. With existing air-conditioning systems the advantage of driving the air-conditioning compressor with an a-c motor has not justified the conversion of all the d-c power to a-c power.

The nearest combination to the all a-c power car would be a car with a-c power for motors, fluorescent lighting, radio and public address systems, and electric razor outlets, except the air-conditioning compressor motor and emergency lighting. This a-c power can be supplied by one machine if that machine has voltage characteristics that will allow a 1-horsepower induction motor to be started on the same a-c power supply bus as the fluorescent lights. This has been done by supplying 5-kw 6.25-kva amplidyne-booster inverters. The principal electric loads on the car, except the 15-horsepower air-conditioning compressor motor which is fed directly from the d-c bus, are carried by the amplidyne booster inverter. In the case of one railroad, this includes a 1-horsepower 3-phase 60-cycle condenser fan motor, a 1-horsepower 3-phase 60-cycle evaporator fan motor, two single-phase 1/3-horsepower exhaust fan motors, all fluorescent lighting, a single-phase drinking water cooler motor, and other small a-c loads.

The amplidyne-booster inverter supplies substantially constant 230-volt 3-phase 60-cycle power within the operating range of the axle-driven generator and storage battery. The equipment consists of an inverted converter in series with an amplidyne mounted on the same armature shaft and in the same frame, a static voltage regulator of the saturable-reactor type, and a step-type d-c motor-starting panel. Figure 8, 9, and 10 show pictures of the equipment. The amplidyne bucks or boosts the direct voltage from a medium value to maintain substantially constant alternating voltage at the slip rings of the inverter. The frequency variation is between 58 and 62 cycles with d-c battery voltages of 105 volts to 160 volts for 114-volt battery and corresponding direct voltages for a 64-volt battery. The control field of the amplidyne requires an output of approximately one watt from the static regulator and the response is practically instantaneous with suddenly applied loads.[4]

The curves of Figure 11 shows the d-c kilowatt input versus a-c output at 80 per cent power factor of typical 6.25-kva and 8-kva a-c amplidyne-booster inverters when operating on the battery. The efficiency will be higher at higher voltages. The 6.25-kva machine is used on sleepers, parlor cars, and coaches. The 8-kva machine is for application on diners where additional a-c power is required for food storage locker refrigeration.

D-C to D-C Booster

The development of fluorescent lights suitable for use on 60 volts direct current led to some demands for a booster that would step up power from a variable-voltage nominal 32-volt circuit to 60 volts direct current. An ordinary motor-driven series booster can be used for this purpose,[5] but the response is slow and the control is bulky. A motor-driven amplidyne has been used to maintain 60 volts direct current for fluorescent lights. The field of the amplidyne requires very little power and it was, therefore, possible to control the field directly by means of a glow tube. This scheme could be used in place of the inefficient lamp regulator for 60-volt fluorescent lamps operating on 64-volt batteries. The higher cost of the equipment has been a factor in preventing any but a few experimental installations from being made.

Variable-Voltage Variable-Frequency Inverter

This system may be used where relatively small motors are to be started from the a-c bus while fluorescent lamps are in operation or where larger motors do not have to be started while fluorescent lamps are in operation. This method of supplying power for railroad passenger cars was suggested by M. A. Edwards of the consulting engineering laboratory of the company with which the writers are associated. It has been in successful opera-

Figure 11. Input–output curves, 6.25-kva and 8-kva amplidyne-booster inverters

96–160 volts direct current, 230 volts 0.8 power factor alternating current curves calculated at 115-volt d-c input

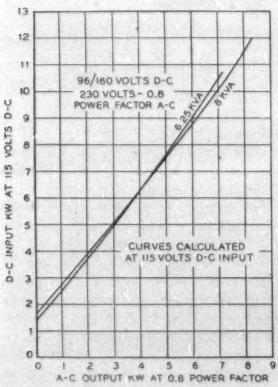

Figure 12. Variation of lamp current with voltage and frequency

72T8 Slimline *F* lamps with reactance ballast (choke coil only of catalogue *59G513* ballast)

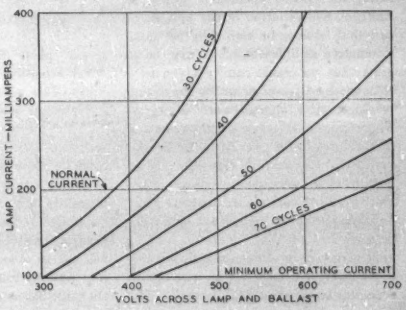

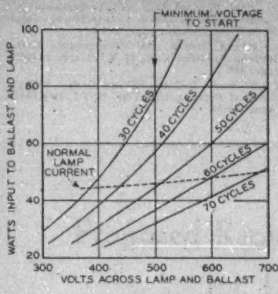

Figure 13. Losses in 72T8 Slimline F lamp with reactance ballast

Choke coil only of catalogue 396513

tion on a Pennsylvania Railroad car since early in 1945 supplying power to fluorescent lighting only.

The current taken by an air cored reactance will remain constant if the voltage is decreased as the frequency of the power supply is decreased to maintain a constant volts per cycle. A fluorescent lamp using an inductive ballast will take approximately the same current at different frequencies if the constant-volts-per-cycle relationship is maintained. Figure 12 shows the variation of the current taken by a 72-inch *T8* type *F* fluorescent lamp with an inductive ballast in series with the lamp as the voltages and frequencies are varied. The lamp current at 600 volts, 60 cycles, is 0.200 ampere while at 400 volts, 40 cycles, the lamp current is 0.160 ampere. An alternator with fixed excitation driven by a d-c motor from a variable-voltage power supply therefore could operate over a wide range in speed within a somewhat less than proportional change in lamp intensity. The lamps may not start at 400 volts; in general the 72-inch lamp requires more than 500 volts to start the arc. Once the arc is started the lamp will continue to function until the lamp current is reduced appreciably below 100 milliamperes but for satisfactory operation should not operate below 100 milliamperes. Lower voltages are required to start the shorter lamps. For example, the 42-inch *T8* requires about 400 volts to start and may start at lower voltages under favorable conditions.

Since the alternating voltage of an inverted direct synchronous converter (inverter) varies in proportion to the direct voltage input and since the speed of a shunt-excited inverter is a direct function of the applied direct voltage, a simple inverter may be used to supply power for fluorescent lighting from the variable direct voltage on railway passenger cars. The designer of the inverter can design for approximately constant volts per cycle in order to keep the lamp current reasonably constant for a wide variation in voltage. It will be noted from Figure 13 that the watts input will remain approximately constant if the lamp current is kept constant as the voltage and frequency are varied. If the voltage is reduced faster than the frequency the lamp intensity is reduced and the watts input to the lamp and its ballast is reduced. For example, the power input at 600 volts, 60 cycles, is 48 watts; at 350 volts, 30 cycles, the power input is 37 watts; but at 400 volts, 50 cycles, the power input is 31 watts. Where small batteries are used or when prolonged periods of running on the battery are necessary, it is desirable to design the inverter so that the alternating voltage falls off more rapidly than the frequency to reduce the lamp load when the charging generators are not operating.

Fluorescent lamps when operated on alternating current have a nonuniform light output caused by the cyclic variations in current. This effect, known as stroboscopic, becomes more noticeable as the frequency is decreased. With electric discharge lamps there is little energy stored to maintain the light during the zero current part of the cycle as is the case with filament lamps. Thus the light output goes nearly to zero each half cycle when the current passes through zero in the fluorescent lamps, although the fluorescent powders (except blue) do phosphoresce to some extent. If lamps are connected alternately on each of the three phases of a 3-phase system the stroboscopic effect is greatly minimized since two of the lamps will have current when the third lamp is out. Thus, if the lamps are so arranged that the area to be lighted receives light from lamps on each phase, the stroboscopic effect ordinarily is not noticed. Similar results can be obtained through the use of a Tulamp auxiliary which operates two lamps 90 degrees out of phase.

However, this type of auxiliary is not satisfactory on a variable-voltage variable-frequency system because of a capacitor which is in series with one of the lamps. Therefore, with this system it is recommended that three phases be used to overcome the stroboscopic effect.

The charging current taken by a capacitor varies directly as both the voltage and the frequency. If the lagging current taken by an inductive ballast be corrected by means of a capacitor across the line to give unity power factor at 60 cycles, the resultant current taken by the lamp ballast and capacitor will lag more and more as the d-c battery voltage falls. This fact can be used to give some control of the voltage–frequency relationship corresponding to different direct voltages.

The synchronous speed of an induction motor varies directly with the frequency. A low-slip, 3-phase, induction motor operating from a constant-voltage variable-frequency source will deliver torques at per-unit slips approximately proportional to the frequency for a wide range in frequency. For all practical purposes, therefore, the speed of the motor will be directly proportional to the frequency. The rotor loss is, therefore, practically proportional to the horsepower output for a wide range in frequency. The torque of an induction motor varies as the square of the voltage so that if the voltage is reduced to 58 per cent of the normal the maximum torque becomes equal to the normal torque at normal voltage and normal frequency (60 cycles).

The cubic feet per minute delivered by a fan varies directly as the speed and the static pressure varies as the square of the cubic feet per minute. The total air horsepower, therefore, may be assumed to vary approximately as the cube of the speed. If the frequency applied to the induction motor is lowered from 60 cycles to 45 cycles, the motor will run at approximately 75 per cent of normal 60-cycle speed and the fan will require only 56 per cent of normal torque, or 42 per cent of normal 60-cycle horsepower. The voltage could be reduced as much as 50 per cent without exceeding the pull-out torque on 45 cycles. The maximum torque at 45 cycles is greater than the maximum torque at 60 cycles because of the lower reactance on the lower frequency.

The operation of evaporator fans on the variable-voltage variable-frequency system has the advantage of reducing the fan load when the battery is not being charged. It also reduces the noise level of the fans at a time when the masking effect of train noise is absent. The make-up air taken into the car is reduced and the total load on the air-conditioning system is reduced, giving further reduction of the electrical load on the battery. The evaporator fans should run continuously to provide air circulation as long as the car is in use so that the fluorescent lights will not be affected by frequent starting of the motors. The condenser fan motor should not be run on the variable-frequency supply because it will start frequently. A separate inverter would be required for any motors that draw rela-

tively high starting current and have to start frequently on the same bus as fluorescent lights. The amplidyne-booster inverter is used in this case to provide the high speed regulating effect of the amplidyne.

References

1. Storage Battery Charging, **J. Lester Woodbridge.** AIEE Transactions, volume 54, 1935, pages 516–25.

2. The Case for Head End Train Power, **J. D. Loftis.** *Railway Age* (New York, N. Y.), February 1, 1947, pages 265–9.

3. New Type of D-C to A-C Vibrator Inverter, **O. Kiltie.** AIEE Transactions, volume 59, 1940, April section, pages 245–8.

4. Power System for Pennsylvania Cars. *Railway Age* (New York, N. Y.), March 1, 1947, pages 456–7.

5. 60 Volts D-C on 30-Volt Cars. *Railway Electrical Engineer* (New York, N. Y.), July 1941, pages 146–51.

No Discussion

Proposed Rapid Transit System for Toronto

W. E. P. DUNCAN
NONMEMBER AIEE

IN January 1946 the citizens of Toronto by an overwhelming majority voted in favor of a proposal for the construction of a rapid transit system in Toronto as presented to the City Council by the Toronto Transportation Commission.

Population

The population of metropolitan Toronto is now well over 940,000 and is growing steadily. The City of Toronto itself contains about three quarters of this metropolitan population and occupies an area of 35 square miles.

The city is in the form of an inverted T with a width along the lake front of about 11 miles, an average depth of about $3^1/_2$ miles, and a depth along the leg of the T of about 7 miles. In the leg of the T there is a community of over 80,000 people who are served by only one continuous north and south street.

The business district is concentrated in a comparatively small central area and is surrounded by a semicircle of residential communities which extend well out into the surrounding municipalities. There are no diagonal streets and the topographical conditions force traffic into a few main north and south and east and west thoroughfares, all of which have to accommodate public transportation facilities as well as other street traffic. Approximately 50 per cent of all transit passengers in Toronto have to make a transfer to another vehicle to reach their destination. There have been practically no annexations to the city in the last 30 years and with the exception of University Avenue, there have been no major improvements in traffic arteries in the central downtown area in the same period.

The increase in the volume of traffic during the last three decades has been spectacular, and downtown traffic movements have increased almost five times. There are few if any places on the American continent where rush hour congestion equals that on Yonge Street, the main north and south artery in Toronto, where the rush hour speed of traffic averages about six miles per hour in the downtown section.

Toronto Transportation Commission

The local transportation facilities are provided by the Toronto Transportation Commission. This is a civic commission consisting of three commissioners appointed for a term of three years by the City Council, to which the city has handed over all its powers, rights, authorities, and privileges for the construction, maintenance, operation, control, and management of its transit facilities. It now operates in Toronto surface street railways, busses, and trolley coaches on a universal fare system of $6^1/_4$ cents with free transfer. It also operates similar services under agreement with nine municipalities on separate fare systems.

By means of its subsidiary company, Gray Coach Lines, it operates interurban service on the highways, westerly 120 miles to Buffalo, northerly 200 miles to North Bay, and easterly 35 miles to Oshawa. It also operates a fleet of ferry boats for the city between Toronto and Toronto Island.

The commission is an entirely separate corporation receiving no assistance of any kind from taxation and it is compelled by its act of incorporation to fix such tolls and fares as to make all transportation facilities under its control and management self-sustaining. It has been able to do this since its incorporation in 1921 in spite of increasing cost of labor and material, without increasing its fare system. It has established a reserve for rehabilitation and deferred equipment renewals of approximately $20,000,000, and this is the foundation on which it proposes to base its rapid transit system.

Rapid Transit Proposal

As a partial solution of Toronto's growing traffic problem, the Toronto Transportation Commission advocates the separation of public transportation from other traffic on two major routes (see Figure 1) by the construction of

(*a*). One north and south subway under and near Yonge Street, extending from the Union Station on Front Street to the corner of Eglinton Avenue and Yonge Street.

(*b*). One east and west subway under and in the vicinity of Queen Street, extending from Trinity Park in the west to just east of Broadview Avenue in the east.

Estimates of probable traffic in the Yonge Street and Queen Street subways indicate a total one way movement during the maximum period of about 15,000 passengers per hour on the Yonge Street subway and from 8,000 to 9,000 passengers per hour on the Queen Street subway.

The estimated peak traffic on Yonge Street is greater than a surface transportation system can handle on one route, and is heavier even than the maximum outbound hourly movements in the street car subway system in Boston, Mass. For this reason the Yonge Street line has been designed for full rapid transit operation utilizing special rapid transit trains.

The Queen Street line for the present would be operated by the surface type of street car, but the structure would be designed to accommodate the larger type of

Paper 47-155, recommended by the AIEE committee on land transportation for presentation at the AIEE summer general meeting, Montreal, Quebec, Canada, June 9–13, 1947. Manuscript submitted March 31, 1947; made available for printing May 2, 1947.

W. E. P. DUNCAN is chief engineer in the Toronto Transportation Commission, Toronto, Ontario, Canada.

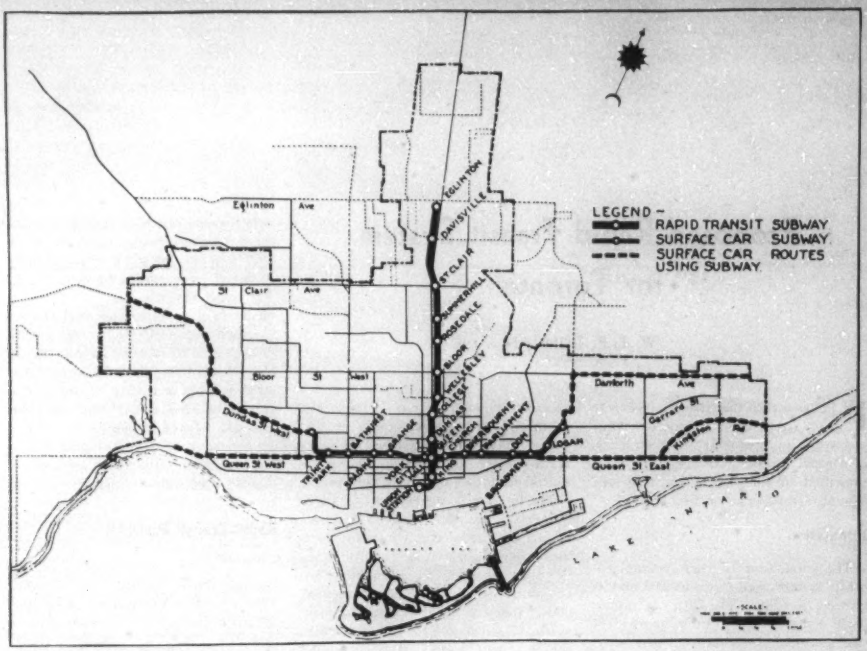

Figure 1. Rapid transit for Toronto

Route map

rapid transit cars as a later development.

Yonge Street Subway

Plans and specifications for the Yonge Street subway are now well advanced. The final route for this subway is shown on Figure 2, and is as follows:

From Union Station in subway under Front Street and under Yonge Street to Carlton Street; then swinging eastward on to a private right of way about 150 feet east of Yonge Street and continuing northward in subway to a point north of Davenport Road; then emerging to an open cut on private right of way through Rosedale; thence in subway under the Canadian Pacific Railroad at North Toronto Station; in open cut to St. Clair Avenue; in subway from St. Clair Avenue to Heath Street swinging across under Yonge Street to the west side emerging in open cut north of the old Belt Line Railway and continuing on the west side of Yonge Street to Berwick Avenue with an underground terminal between Berwick Avenue and Eglinton Avenue.

The subway structure in general will be kept as close to the surface as possible, consistent with the provision of necessary coverage for water pipes and other utilities below the street level. The minimum depth between the surface and the top of the subway structure will be approximately six feet.

The total length of the Yonge Street subway will be 4.56 miles of which 3.20 miles will be in subway construction and 1.36 miles in open cut.

The subway will be designed to operate a maximum of 30 10-car trains with a passenger capacity of about 40,000 in one direction per hour.

Cost

The cost of the Yonge Street subway is estimated as follows:

Rapid transit structures	$19,835,000.00
Fixed subway equipment	4,805,000.00
Off street rights of way	4,210,000.00
Total	$28,850,000.00

This does not include the cost of the rapid transit cars which will be approximately $5,000,000 more, replacing an equivalent number of obsolete street cars.

Design of the Structure

For the subway structure a 2-track box section has been adopted as shown in Figure 3. The typical subway section between stations has an over-all width of 32 feet 6 inches, an over-all depth of 18 feet 8 inches, and an inside width of 13 feet 6 inches for each track with a clearance over the top of rail of 13 feet.

At station sections, as shown on Figure 3, the subway structure is 52 feet 4 inches wide, and 19 feet 3 inches high, with a transverse clear span of 23 feet 5 inches between columns.

Where the depth of the subway permits, a mezzanine floor will be installed at the subway stations between the top of the subway structure and the street level, and fare collection and passenger control facilities will be concentrated on this floor (see Figure 4).

The open-cut sections, as shown on Figure 5, have been designed with two to one slopes. The typical section will have a width of 44 feet at the bottom of the slope and an over-all right-of-way width of 120 feet. To carry cross streets over the open cut a fixed frame steel bridge

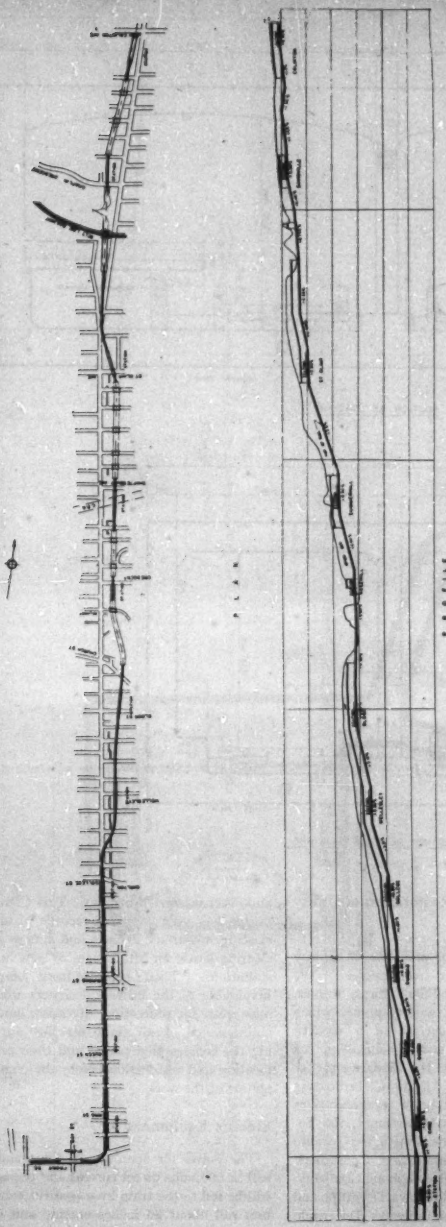

Figure 2. Yonge Street subway

General plan and profile

has been designed with a typical span of 48 feet 11 inches and a minimum vertical clearance above the top of rail of 13 feet.

Station platforms will be 500 feet long to provide for ultimate operation of trains of ten 45-foot cars. Platforms at all stations except terminals will be located at the side of the station and will be 12 feet wide. Stations will be located at all main intersections and there will be 12 stations on the Yonge Street subway. Plans for all the mezzanine stations include escalators as well as stairs for the convenience of passenger movement. Escalators also will be provided for passengers transferring between the Yonge Street subway and the Queen Street subway which intersect at the Queen Street station. The Queen subway will pass underneath the Yonge subway at this point.

Alignment and Gradient

In general the alignment has been laid out with long tangents and easy curves, the only curve of significant magnitude being the curve between Front Street and Yonge Street which has a radius of 400 feet. The maximum gradient, for short distances south of St. Clair Avenue and south of Davisville Avenue, respectively, is 3.5 per cent.

In determining the alignment it was found that if the subway had been continued north under Yonge Street the whole way, the gradients would have been much more severe or the subway would have been much deeper at intermediate stations with consequent inconvenience and delay to passengers. The increased cost of such an alignment would have been in the neighborhood of $6,000,000.

In view of the fact that the remainder of the Toronto system will continue to be serviced by surface vehicles and that passengers will have to transfer at all main intersections, it is essential that the subway should be close to the surface.

Method of Construction

The soils to be encountered in Toronto are favorable to subway construction and the excavation generally will be through top soil, sandy clay, tough blue clay, and sand and gravel. A short section at the south end will be founded on Dundas shale.

The method of construction proposed is by cut and cover on the subway section and by open cut on the remainder.

It is proposed on the subway section to drive heavy rolled steel sections on both

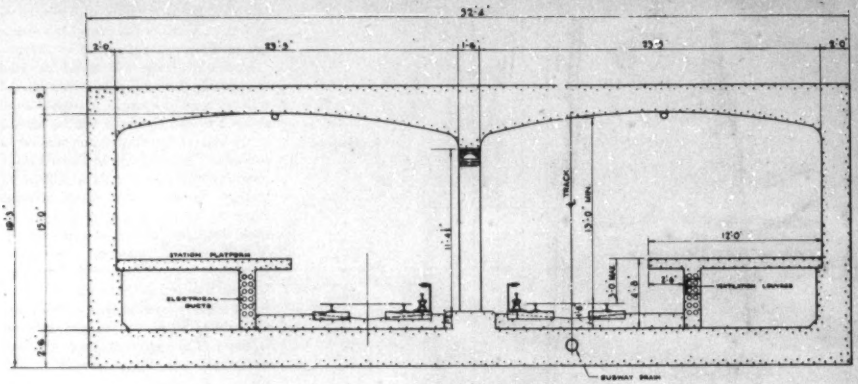

SECTION AT STATION

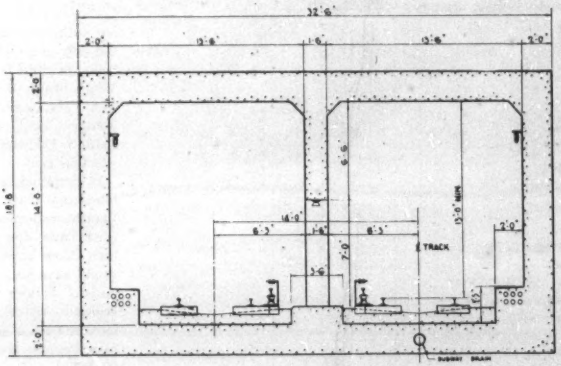

SECTION BETWEEN STATIONS

Figure 3. Typical cross sections of subway

sides of the line of excavation and install wood lagging to support lateral side pressure. Steel beams then will be installed to span the subway excavation and on these there will be constructed a temporary wooden street surface to carry all normal traffic. Construction work then will proceed under this.

All utility pipes and cables will be suspended from the temporary steel structure during the construction period except gas mains which will be removed from the excavation and relaid along the side of the street or otherwise provided for.

Protection and Restoration of Utility Services

One of the major problems of subway construction is the maintenance of the utility pipes, conduits, ducts, cables, splicing chambers, and manholes which lie beneath the surface of a modern street. Planning in this connection has been facilitated by the existence in Toronto of a Public Utility Co-ordinating Committee consisting of representatives of the City Works Department, the Toronto Hydro-Electric System, the Toronto Transportation Commission, Consumers' Gas Company, Bell Telephone Company, Canadian Pacific Railways Telegraph and Canadian National Railways Telegraph, and other interested utilities. This Committee has very complete records of all existing subsurface utilities and acts as a clearing house for all changes or new installations. Their records have been invaluable to the subway designers who must plan for protection, diversion, and maintenance of all these services during the construction period and their relocation and restoration before the completion of the work.

Electric Equipment

The power for operation of the trains will be 600 volts direct current and power will be fed to the train by a positive contact rail about 20 inches outside and 6

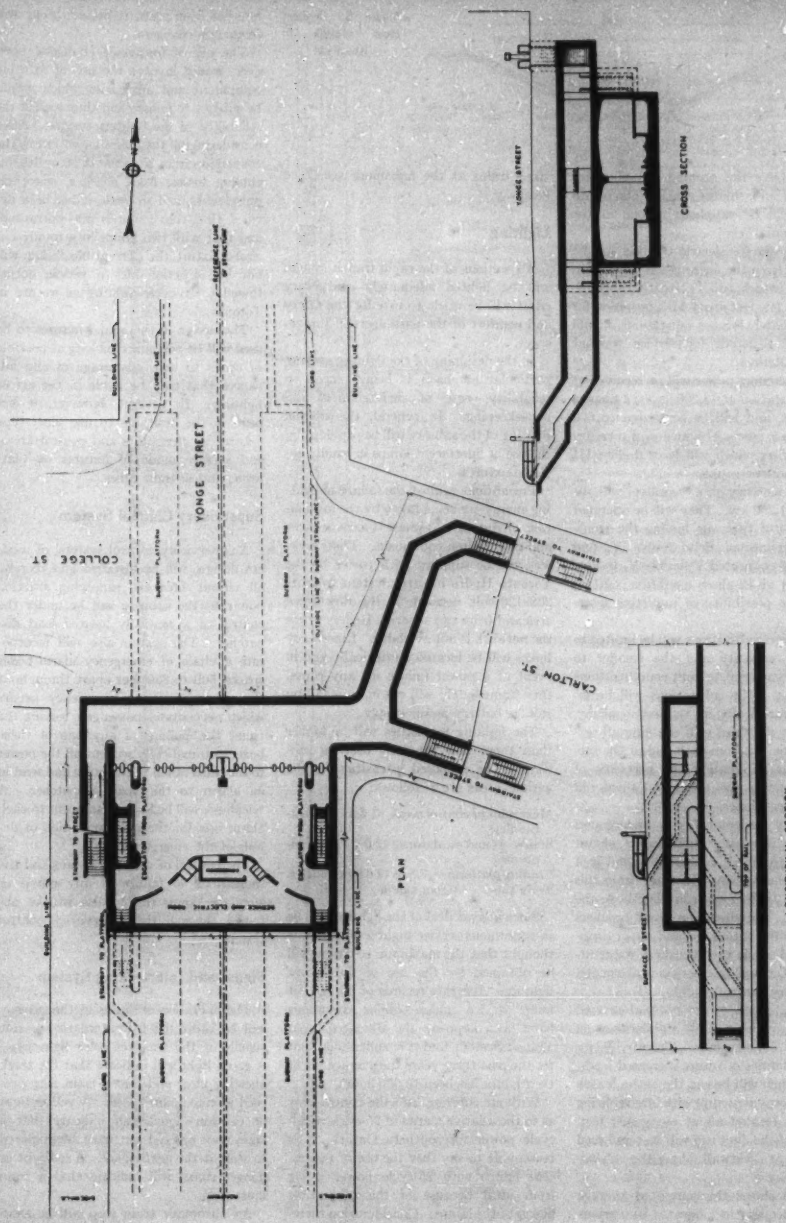

Figure 4. Typical station layout

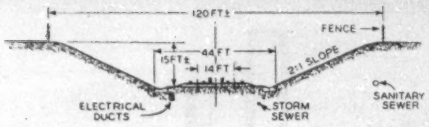

Figure 5. Typical cross section in open cut

inches above the running rail and protected by an insulator guard. The return circuit will be supplied by one of the running rails.

The power for electric traction will be supplied from the commission's own substations, which will be located approximately 6,500 feet apart with provision for intermediately located substations, should increased demands for service warrant the installation.

The incoming power will be received at each substation at 13,200 volts, 3 phases, 25 cycles, and will be converted to 600 volts direct current by means of mercury arc rectifiers which will have a class III railway service rating.

Each mercury arc rectifier will be rated at 1,250 kw. They will be operated in groups of two, one having the transformer connected delta-double Y, and one being connected Y-double Y, to give the effect of 12-phase operation, cutting down the possibility of inductive interference.

The larger substations will be limited to 5,000-kw capacity and the smaller to 2,500-kw capacity, to limit concentrations of current. The substations will be located strategically at the sectionalizing points on the third rail, enabling all sections to be fed from each end of the section, thus eliminating the necessity of supplementing the 140-pound third rail with feeder copper.

The d-c feeders will run undergound from the d-c substation feeder circuit breakers to circuit breakers located in a room in the subway structure; from this point the feeders will run directly to the third rail. The substation circuit breakers will be fully automatic and supervisory controlled, while the "breaker" room circuit breakers will be emergency alarm and supervisory controlled only.

It is intended to use nonlead-covered cable throughout and standardize on 1,500,000 circular mils. To provide for the possibilities of future increased loads, a duct bench will be run the entire length of the subway structure with large splicing chambers located about every 400 feet. The top of the duct run will be reinforced and used as a catwalk along the subway right of way.

Table I shows the computed average running demand in kilowatts for various sized trains at the maximum scheduled headway.

Lighting

All sections of the rapid transit system will be lighted adequately and every effort will be made to care for the safety and comfort of the passengers in this respect.

In the designing of the lighting system, particular emphasis is being placed on reliability, ease of maintenance, and housekeeping. In general, the normal lighting of the subway will be provided by the use of fluorescent lamps in totally enclosed fixtures.

Precautions against the failure of lighting energy are being taken by the installation of duplicate 3-phase 4-wire services and distribution equipment. These services will be supplied with power by the Toronto Hydro-Electric System from its 208–120-volt network in the downtown area and from two separate feeders where the network is not available. Emergency lights will be located strategically and in event of a power failure for any cause, they immediately will cut in on stand-by storage battery power supply.

The lighting intensities will be higher than those now generally used in subways. The proposed intensities for the various areas are as follows:

Mezzanine or control areas—7.5 to 12.0 foot-candles.
Stairways and escalators—10.0 to 12.0 foot-candles.
Loading platforms—7.5 to 12.0 foot-candles.
Train tubes—1.0 foot-candle.

Since a great deal of the lighting will be in continuous service night and day, it is thought that the maximum economy will be obtained by the use of fluorescent lighting. Accurate records of fluorescent lamp service under similar conditions have been kept by the Chicago Rapid Transit System, and it is understood that for the past three years the average life of their lamps has been 10,000 hours.

Without entering into the controversy as to the relative merits of 25-cycle or 60-cycle power for southern Ontario, it is reasonable to say that the use of fluorescent lamps with 25-cycle power is far from ideal because of the perceptible flicker of the lamps. Consideration therefore has been given to providing our own frequency changers.

The use of frequency changers, however, would involve the use of rotating equipment and auxiliaries which would be subject to failure and thus reduce the reliability of the lighting service. After considering all the factors involved in the conversion from 25 cycles to 60 cycles, including losses, fixed charges, space requirements, and so forth, it has been decided that conversion is not warranted, and that with two lamps in a totally enclosed fixture the perceptible flicker will not be objectionable to people accustomed to 25-cycle lighting as we are in Toronto.

The design of the actual fixtures to be used will be postponed as long as possible in order to take advantage of any advances that may be made in the art of lighting. In general, however, it appears to be desirable to use flush type fixtures in mezzanine and control areas, and surface mounted fixtures on platforms and in train tubes.

Supervisory Control System

A supervisory control system, of modern design, will be installed and thereby all circuit breakers supplying traction power to the subway will be under the control of a centrally located load dispatcher. This system also will incorporate a chain of emergency alarm boxes spaced 500 to 800 feet apart throughout the subway. If an emergency occurs which necessitates passengers leaving the train, the pulling of any one of these boxes automatically will cut off the power to the third rail in that section and send in an alarm to the load dispatcher. A telephone will be located adjacent to each alarm box for the communication of details of the emergency.

The control of ventilating fans and the indications of failure of any pump or auxiliary power supply also will be obtained through the supervisory control system.

Signal and Interlocking System

The operation of trains in the subway will be protected by automatic wayside signals of the 3-aspect color light type. A green light will indicate that the track ahead is clear and that a train may proceed at maximum speed. A yellow light or caution signal will indicate that a train may proceed but must be prepared to stop at the next signal. A red light or danger signal will indicate that a train must stop.

An automatic train stop will be asso-

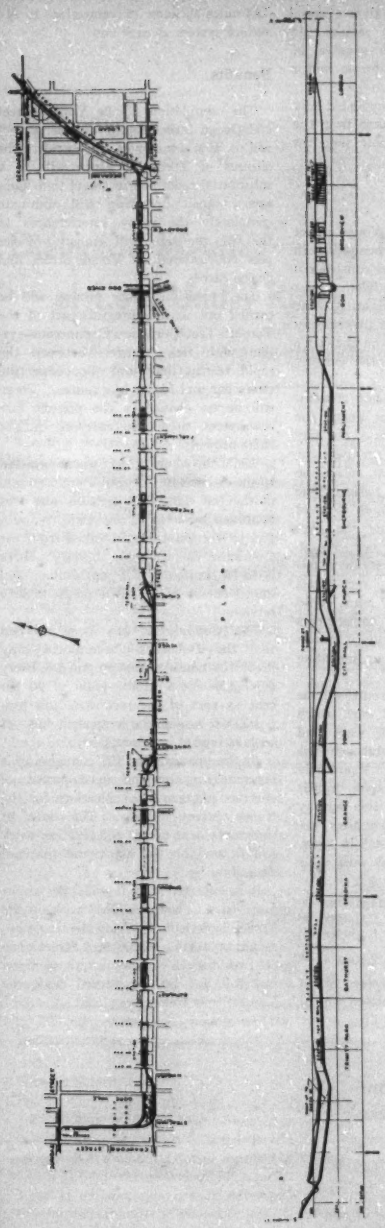

Figure 6. Queen Street subway

General plan and profile

Table I. Power Demand in Kilowatts

Cars in Train	Three 2-Car Units	Four 2-Car Units	Five 2-Car Units
Headway, sec	120	120	120
Richmond	2,640	3,525	4,430
Bloor	2,320	3,190	3,990
St. Clair	2,195	3,055	3,800
Eglinton	1,095	1,485	1,850
Total	8,250	11,255	14,070

ciated with each signal and will enforce obedience to the "stop" indication. This device, which will be located between the rails, consists of a lever which is held in the clear position when the signal is green or yellow. When the signal is red, this lever is raised to a position where it will engage a trip arm on the train which will cut off the power and apply the brakes.

The signals will be spaced one track block apart. The length of the track block will be determined from the emergency braking distance of the train at the maximum speed at which it is expected to run.

At crossovers and other special work, the operation of the switch points will be interlocked with the signals and train stops to absolutely prevent two trains from coming together.

Rolling Stock

The Yonge Street subway operation will be carried out by means of the most modern subway equipment and the design of the car is now being undertaken by the commission's own engineers in conjunction with the manufacturers.

Because of local conditions the proposed design will differ somewhat from conventional subway car design. There are no existing rapid transit services in Toronto. Therefore, there are no restrictions on the design of the proposed car to meet fixed platform and coupler heights, as would be the case if the new cars were to operate in conjunction with old cars.

The anticipated operating schedule for the Yonge Street subway will require accelerating and braking rates that cannot be obtained with the conventional electric equipment and the standard type of car. However, the desired performance rates can be obtained with PCC car equipment as already developed. It is planned, therefore, to use PCC car truck and electric apparatus, to avoid the very extensive development, and delay, which would be involved in producing and testing new heavy weight electric equipment.

Noise reduction in the proposed subway has been given careful study. This is an

important consideration, because subway operation tends to magnify car noises. Experience in Toronto with PCC cars, which use a considerable amount of rubber to reduce noise, indicates that using this type of equipment will help in reducing noise in the subway to a minimum.

Maintenance of the proposed subway cars will be greatly simplified by using PCC car equipment. There are already in operation, or on order, 390 PCC cars in Toronto, with maintenance facilities available to handle 1,500 cars. It will be unnecessary, therefore, to set up any new or extensive facilities for maintenance of the rapid transit equipment.

The design of the car proposed to meet these conditions will consist of two bodies, each 45 feet long and 10 feet wide, semi-permanently coupled together. Each body will be carried on two standard PCC car trucks and equipped with PCC car electric apparatus. The body construction will be of lightweight design, using high strength alloys where necessary. It is estimated that a 2-car unit will weigh not more than 75,000 pounds light and equipped for service, which is well within the capacity of the existing PCC car truck.

Each of the 2-car units will be arranged with a cab at the outer end to permit double-end operation. The interior will be arranged to provide as many seats as possible, consistent with allowing free movement of passengers through the car, and during loading and unloading.

Following the latest practice in New York, N.Y., and London, England, subways there will be an unusually high ratio of door area to body length, three doors being provided in each side of each body 45 feet long.

The electric equipment will be essentially the PCC car type with certain modifications to meet subway operation. It is not considered necessary to provide an infinite number of accelerating and braking rates, as for surface car operation, three rates only being proposed. This will simplify the control equipment for multiple-unit operation considerably.

It is planned to operate trains up to five 2-car units in length, and any lesser number as may be required to meet service conditions. This will require the electric equipment to be capable of operating ten sets of quadruple motor equipments in multiple.

The 2-car units will be uncoupled only when the cars are being taken from the subway to the central repair shop for heavy overhaul.

Queen Street Subway

After completion of the Yonge Street subway it is proposed as a second step in the rapid transit project to construct a subway from east to west under or near Queen Street, as shown in Figure 6. The exact design and location of this subway will depend to some extent on the city's plans for improvement of the existing Queen Street.

However, the present plan contemplates subway construction under the street in the central section of the city with open-cut sections on private right of way to the east and west. The line will extend from Trinity Park in the west to Carlaw Avenue and Gerrard Street in the east, crossing the Don River on a high level bridge.

It is estimated that the present maximum traffic on the Queen Street route, about 9,000 passengers per hour, could be carried satisfactorily by surface cars operating through the subway at speeds of about 15 miles per hour including stops.

Initially, therefore, this route will be operated by surface street cars which will extend east, northeast, west, and northwest beyond its portals on the existing surface system. Eventually when traffic justifies it rapid transit equipment will be used in this subway also, and the subway structures are being designed with this end in view.

The estimated cost of this work is as follows:

Structures	$11,800,000.00
Fixed equipment	2,300,000.00
Off street rights of way	5,200,000.00
Total	$19,300,000.00

The total length of the Queen Street route as at present contemplated will be 4.54 miles between its connections to the surface system at each end.

Benefits

The completion of the Yonge Street and Queen Street Rapid Transit project will provide a major improvement to the citizens of Toronto. There will be a substantial reduction in travel time since rapid transit operation will eliminate completely the many interferences to the free movement of transit vehicles now encountered on Yonge Street and Queen Street.

The operation of the subway will be carried out as an integral part of the Toronto Transportation Commission system with free transfers between the rapid transit lines and the connecting street car and feeder bus routes. There will be no change in the present fare consequent upon the carrying out of these projects.

While the whole project was submitted to the citizens of Toronto by referendum at the last municipal election, and was approved by a ten to one majority, subject to a grant being obtained from the Dominion Government, the city's share is to be limited to the replacement and improvement of its own public utility services.

The Commission has been advised that the Dominion Government may favorably consider the proposed subway as eligible for a timing grant of 20 per cent as part of the reconstruction proposal, but no definite agreement has yet been arrived at in this respect.

At the present time the commission is concentrating on the development of contract plans and specifications for the Yonge Street subway. The date of commencement of the construction work will depend on the labor and material situation.

It is expected that it will take about four years to complete this work on the Yonge Street subway from the time construction starts. The Queen Street project will take a similar length of time, but will not be commenced until the Yonge Street line is completed.

No Discussion

Dielectric Heating—The Measurement of Loss Under Rising Temperature

J. B. WHITEHEAD
FELLOW AIEE

THE heating of dielectrics under alternating electric stress has been recognized since the early days of high voltage power transmission. With increasing values of voltage and frequency, the losses in insulators have assumed great importance, and have placed a premium on the development of low loss insulating materials. On the other hand, in relatively poor insulators the losses may be so great, and the heating so rapid, that this method of heating has replaced, with advantage, steam and other agents for many industrial heating processes on composite materials having moderate insulating characteristics.

The engineering of dielectric heating for large industrial processes is not yet clearly developed. The losses are apparently the result of dielectric absorption, or interfacial polarization, and are greatest somewhere within the frequency range 1 to 100 megacycles. So far, however, knowledge of the changes in value of the electric constants of the material being heated, over the range of temperature of the process, is wanting. In most cases a rapid heating cycle is desirable and rates of temperature rise of 60 degrees Fahrenheit per minute, or higher are common. Moreover, it often happens that it is not possible to interrupt the heating cycle without impairing the efficiency of the curing process and the quality of the resulting product.

The Problem

Consequently, the problem presented is that of the measurement of the dielectric properties of a material during a period in which its temperature is changing rapidly. Most of the methods already developed for the measurement of dielectric loss at, say, ten megacycles and upward, are substitution methods, involve two or more settings (see American Society for Testing Materials designation *D150-44T*—for example, ASTM shunted susceptance variation method), and voltage gradients so low that no appreciable change in temperature resulting from dielectric loss occurs during the measurement. Such methods, therefore, are not suitable for the problem before us. Calorimetric methods for the measurement of power loss usually involve a hot steady state and the measurement of temperature gradients in the ambient medium.[1] Such methods are either time consuming or involve elaborate protection of the ambient field in which the temperature gradients are measured. However, if the volume of the dielectric is fairly large and the duration of the heating cycle several minutes, it should be possible, by means of a proper selection and location of d-c electric heaters, either to duplicate in another sample the a-c heating curve, or to derive it in a point-by-point method of equivalent thermal input. This is a substitution method therefore; and while not in the "precision" class, it nevertheless

Paper 47-158, recommended by the AIEE committee on industrial power applications for presentation at the AIEE summer general meeting, Montreal, Quebec, Canada, June 9-13, 1947. Manuscript submitted January 6, 1947; made available for printing May 5, 1947.

J. B. Whitehead is professor of electrical engineering, The Johns Hopkins University, Baltimore, Md.

The author acknowledges the support of the Armstrong Cork Company, Lancaster, Pa., at whose request the work was done; the co-operation of Doctor G. W. Scott, Jr.; and the assistance of Doctor C. Frank Miller, Doctor F. G. Whelan, W. Rueggeberg, and C. B. Boenning in the experimental work.

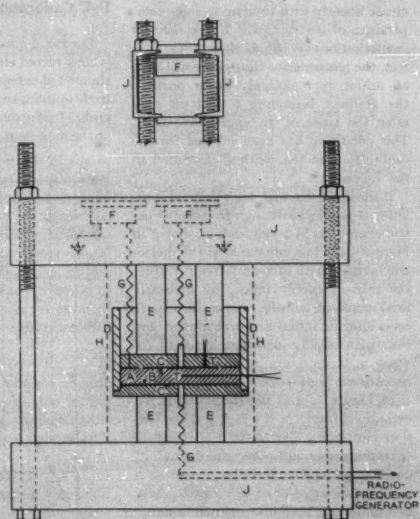

Figure 1. Test cell

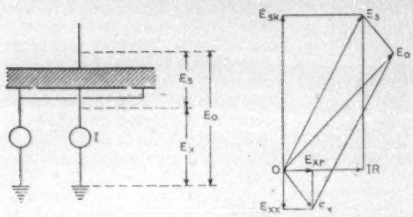

Figure 2. High-frequency measurement

$$E_{xk} = \sqrt{E_o^2 - (IR + E_{xr})^2} + E_{xr}$$

$$E_s = \sqrt{E_{xk}^2 + IR^2}$$

$$IR = \frac{\text{heating watts}}{I}$$

$$\text{Power factor} = \frac{IR}{E_s}$$

$$K = \frac{I}{E_{xk}} \times \text{constant}$$

has yielded a very satisfactory degree of accuracy.

The Method

If a mass of dielectric material is completely insulated thermally, and if its thermal properties do not change with rising temperature, then when it is supplied with thermal energy uniformly, and at a constant rate, its temperature will increase linearly with time up to some temperature of destruction. If the thermal insulation is very good, though not perfect, the temperature-time curve will have an initial approximately linear portion, the gradient beginning to fall off only after the lapse of an appreciable time. This condition has been utilized for d-c calibrations in the method described in the following.

If the dielectric with high thermal insulation is supplied with high-frequency electric energy, as in a cell such as shown in Figure 1, the loss constants of the dielectric increase with increasing temperature, the rate of energy input (by dielectric loss) increases, and the temperature curve soon loses its initial linear character, and rises with rapidly increasing gradient toward a temperature of combustion or breakdown (see Figure 4).

In Figure 1, *A* is the dielectric of flat cylindrical form; *B*, the high and low tension electrodes, the latter consisting of central member and outer guard ring; *C*, backing plates of "Formica"; and *D* a surrounding cylinder of "Transite"; these two materials have low thermal conductivities and high tensile strength. The whole measuring cell is mounted on steatite pillars *E*, and within an outer steel framework *J* equipped for applying pressure to the sample *A*. Radio-frequency thermoammeters *F* read the currents from main and guard electrodes to ground. Temperatures are read by the thermocouples *T*. *H* is an electrostatic screen surrounding the cell.

The simple electric connections are shown in Figure 2, together with the vector diagram of voltages. The diagram also includes the vectors for the small inductive impedance of the ammeter and connection to ground. Voltage across the sample is read on a vacuum tube voltmeter. Thus current and voltage are read directly, and if the total heating watts are obtained by d-c calibration, the *IR* component in the vector diagram is known, and *K*, cos θ, tan δ, and other quantities are derived at once.

D-C Calibration

For the d-c calibration a duplicate cell is constructed identical in all respects with the a-c cell except that, instead of the electrode system, two, three, or more heating grids of thin sheet nichrome are inserted at the outer surfaces of the dielectric, and at times within its mass. The a-c electrodes are of the same material as the heaters, and the amount and location of all materials in the a-c and d-c cells is very closely the same. In calibrating, the d-c cell filled with an equal amount of dielectric replaces the a-c cell in the cell mounting, and a constant value of continuous current is applied to the heating circuit. Internal temperatures again are read with the needle thermocouple. After about one minute the temperature throughout the mass of the specimen becomes approximately uniform and increases linearly with time as shown in Figure 3 (for several values of heating current). The linear relation continues for five, six, or more minutes when the curve begins to fall off as the cell begins to lose heat. Each of these curves in its linear portion represents a uniform rise of temperature—time gradient of so many degrees rise per minute, corresponding to a uniform supply of energy in watts resulting from the constant heating current. The family of heating curves may be combined in one curve showing heating watts as function of rate of rise of temperature, also shown in Figure 3. It will be noted that this curve is also a straight line up to 50 or 60 degrees Fahrenheit per minute; it passes through or near to a zero point of no energy and no temperature rise; and beyond 60 degrees per minute turns upward slightly, as the cell begins to lose heat at large values of d-c energy input.

Experimental Results

Figure 4 shows the average location of the heating curves of two variations of the same material, each mixed with a binder, put under pressure in the cell of Figure 1, and heated by applying electric stress of 0.8 volt per mil at ten megacycles. The

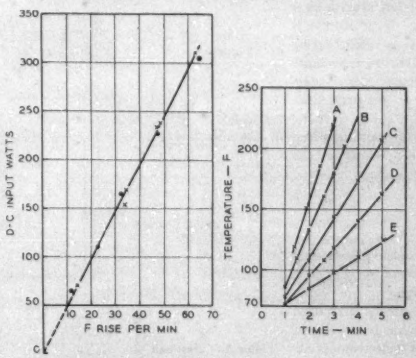

Figure 3. D-c calibration curves

A—307.5 watts, 64.6 degrees Fahrenheit per minute

B—228.7 watts, 47.7 degrees Fahrenheit per minute

C—166.1 watts, 32.3 degrees Fahrenheit per minute

D—110 watts, 22.8 degrees Fahrenheit per minute

E—64.5 watts, 11.88 degrees Fahrenheit per minute

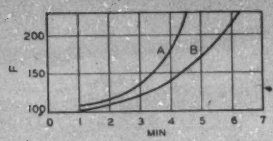

Figure 4. Temperature–time curves

400 volts, 10 megacycles

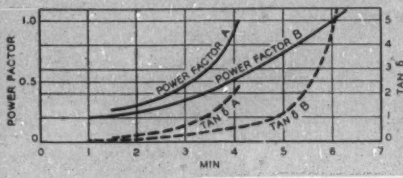

Figure 5. Power factor and tan δ

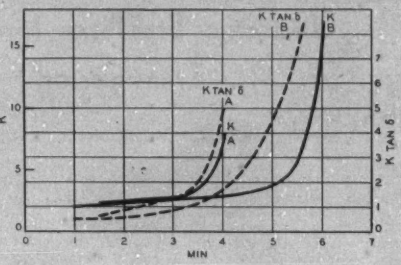

Figure 6 (right). *K* and *K* tan δ

rate of heating is controlled readily by varying the applied voltage. Temperature, current, and voltage can be read at one-half minute intervals. A tangent to the heating curve at any point gives the rate of temperature rise at that point. The corresponding rate of energy input, that is, watts, may be taken from the d-c calibration curve. If R is the effective resistance of dielectric heating, then the d-c watt input may be written as I^2R, in which I is the measured high-frequency current corresponding to the point in question of the heating curve. The vector IR of Figure 2 is now known and all quantities readily computed. Values for the two materials in question, of power factor, dielectric constant, tan δ, and loss factor are plotted in curves of Figures 5 and 6.

Accuracy

As to accuracy, the instruments used ensure precision measurements within say one per cent or two per cent. More important, however, are variables resulting from the rapid changes of temperature in the upper range, and the time interval necessary to adjust the thermopotentiometer; and from inherent variations of the material under test from one sample to another. The latter is reflected at once in the initial value of the high-frequency current, which may vary by as much as five to ten per cent in successive otherwise identical samples. For samples showing the same value of starting current, the heating curves repeat quite closely. An example for three specimens is shown in Figure 7.

The method is the more accurate the longer the heating cycle and the better the thermal insulation of the a-c and d-c cells. For a long cycle a differential thermocouple circuit between the a-c and d-c cells in simultaneous excitation should be possible, allowing continuous adjustment of direct current to balance the a-c input. For short cycles this is not possible for the direction of heat flow in the two samples is not the same, and a definite time interval is necessary for the equalization of temperature throughout the d-c specimen. This is, in fact, a chief limitation of the method. The a-c energy is developed uniformly throughout the sample, the direct current is applied by heater grids. However, this difference may be reduced by subdivision of the sample, increasing the number of grids, and by other methods. In the 3- to 6-minute cycles described, satisfactory uniformity of temperature in both a-c and d-c samples is reached after one minute.

Discussion

The chief advantage of the method, as here described, is the simplicity of the linear d-c calibration shown in Figure 3. This, in turn, results from the relatively good thermal insulation, and the relatively low curing temperature of the materials, that is, less than 250 degrees Fahrenheit. For higher temperatures, thermal insulation is more difficult, linear d-c heating curves become shorter, and further subdivision of sample and heaters must be introduced. Best of all corrective measures is a longer heating cycle.

From Figure 4 it will be seen that power factor and loss factor increase rapidly with increasing temperature, the former reaching nearly the value "unity" at the end of the cycle (225 degrees Fahrenheit); beyond this point the material begins to burn. The dielectric constant also increases; less rapidly during the early stages, and more rapidly, in fact towards an infinite value, as the power factor approaches unity.

Two pictures of the mechanism of dielectric heating present themselves. First, interfacial polarization: The conductivities of internal conducting paths of limited length increase rapidly with increasing temperature, causing greater resistance losses under the rapid reversals of the absorption component of the charging current, thereby resulting in increasing values of power and dissipation factors. As a second cause, molecular polarization. This, in general, would give the same type of behavior as interfacial polarization, although not coincident therewith over a range of frequency. The question of their relative importance can be answered best by measurements over a range of frequency. Studies in this direction are under way.

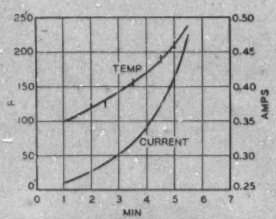

Figure 7. Material *A*

Current and temperature versus time

References

1. Calorimetric Measurement of Dielectric Losses in Solids, H. H. Race, S. C. Leonard. Electrical Engineering (AIEE Transactions), volume 55, 1936, December section, pages 1347–56.

2. Principles of High-Frequency Heating, L. Hartshorn. *Chemistry and Industry*, number 37, September 8, 1944, pages 322–5.

No Discussion

Electronic Stabilizer for Power Transmission

ERNST F. W. ALEXANDERSON
FELLOW AIEE

DAVID C. PRINCE
FELLOW AIEE

Synopsis: Voltage regulation of an alternator historically has depended upon variation of the field current, and high-speed regulators have been developed in order to improve synchronous stability. This paper describes a voltage control brought about by varying the output current. A reactive load is connected to the generator terminals. This load is varied electronically in such a way as to maintain the desired voltage and line current. Whereas regulation by field control is limited by the long time constant of the field winding, the electronic stabilizer acts upon the transient reactance and therefore it has the fast response needed to regulate the terminal voltage. The paper describes a new method for increasing the stability limits by supplementing present known methods and extending the limits of a-c power transmission. The electronic stabilizer is intended to take care of certain regulating functions which cannot be performed by a field regulator. The use of the two in combination, therefore, can be expected to yield still further improvement. No attempt has been made to compare this method with other methods of compensating the line and it is intended that these methods may be used in combination. Tests of a model equipment are described. A rough comparison has been made between this system and the use of series capacitors. Using present costs and parameters, the cost of the series capacitors was somewhat less. Further cost changes may alter this comparison, or there may be cases where series capacitors are not acceptable.

THE LIMITATIONS of conventional synchronous power transmission are well known. It has been pointed out that most long distance transmission lines operate at a load corresponding to surge impedance.[1,2] This is the loading where the inductance and capacity of the line neutralize each other so that the voltage remains constant throughout the line. Voltage regulation of an alternator historically has depended upon variation of the field current, and high-speed regulators have been developed in order to improve synchronous stability. This paper describes a voltage control brought about by varying the output current. A reactive load is connected to the generator terminals. This load is varied electronically in such a way as to maintain the desired voltage and line current. Whereas regulation by field control is limited by the long time constant of the field winding, the electronic stabilizer acts upon the transient reactance and therefore it has the fast response needed to increase the stability of long transmission lines.

In its function it is analogous to a synchronous condenser because it is used to regulate the voltage at the point where it is connected by drawing a controllable current from the line.

Analysis

With fixed excitation the conditions for stability limit are shown in Figure 1. As the load motor (or equivalent) pole axis lags behind the generator pole axis by the angle θ, the vector difference E_D of effective voltages follows a circular locus. The current follows a similar locus. Neglecting circuit resistance, the current I has the greatest projection on the voltage E_g when $\theta=90$ degrees. For any greater angular lag, the restoring torque as measured by $E_gI\cos\theta/2$ is less and the load falls out of step.

Corresponding to this condition, the difference voltage may be considered as divided into fractions, 0–1 the drop corresponding to the generator armature reaction, 1–2 the drop across the generator transient impedance, 2–3 line drop, 3–4 load transient impedance, 4–5 load armature reaction. Quantities E_2 and E_5 are the voltages actually seen by voltage measuring devices at the machine terminals. For short lines E_3 and E_5 are approximately 0.7 times E_g and E_L. The validity of the diagram presumes no correction in excitation during a transient variation in θ. For the diagram ideal round rotor machines are assumed.

If excitation response is fast enough to hold E_1 and E_4 constant during a transient, then the stability diagram takes the form of Figure 2. The angle θ at pull out is now greater than 90 degrees but the angle θ_1 between the maintained voltages

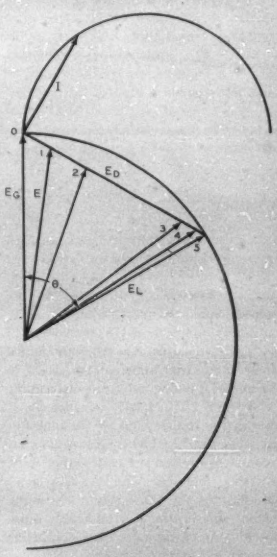

Figure 1. Fixed excitation

Paper 47-162, recommended by the AIEE committees on electronics and power transmission and distribution for presentation at the AIEE summer general meeting, Montreal, Quebec, Canada, June 9–13, 1947. Manuscript submitted March 24, 1947; made available for printing May 15, 1947.

ERNST F. W. ALEXANDERSON is consulting engineer and DAVID C. PRINCE is vice-president in charge of electrical engineering department, General Electric Company, Schenectady, N. Y.

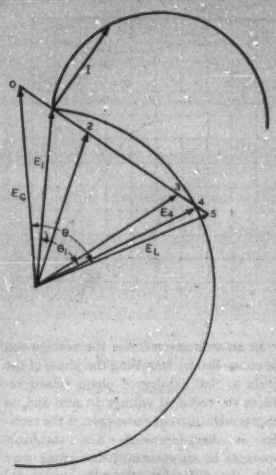

Figure 2. Regulated excitation

is 90 degrees. Quantities E_3 and E_4 have now considerably greater numerical values, but these are not real voltages. They are the voltages that would exist at no load with the same excitation and with no saturation. The demagnetizing effect of the load current results in only the voltages E_1 and E_4 actually being induced. Under transient conditions the inductance coupling between field and armature tends to maintain these generated voltages and so the regulator must be only fast enough to support currents already set up by transient currents.

Following this reasoning one step farther, if we can maintain the magnitudes of E_3 and E_4, the stability diagram becomes Figure 3. The stability limit now corresponds to the angle $\theta_2 = 90$ degrees. The generated voltages E_1 and E_4 exist but the difference between them and terminal voltage is absorbed as drop in the machine's transient reactances.

In the past, efforts have been made to introduce a corresponding change in the generated voltage E_1 and E_4 by an increase in field current, but such a change takes place so slowly that very little improvement in stability has been realized above that corresponding to holding E_1 and E_4 constant. The proposed system of control consists of carrying continuously a dummy inductive load on the generators so that the field strength needed to meet the transient already is established. It is the function of the electronic stabilizer to check the current flow in the dummy load so that the higher voltage inherent in the generator is impressed on the line terminals without any delay.

Without the stabilizer, the system would fall out of step when the angle of E_1 and E_4 exceeds the critical angle because an increase of phase angle would reduce the voltage so that the torque reaction of the generator shaft would be reduced and the change would become accumulative. With the stabilizer the opposite happens. A swing toward larger phase angle causes the electronic control to reduce the wattless dummy load so that the voltage increases. This, in its turn, causes the torque reaction on the shaft to increase so as to restore the normal phase angle. An artificial synchronizing force thus is introduced which, added to the natural synchronism force, makes it possible to carry higher load.

Test Equipment

Figure 4 represents the model test setup used for studying this method of operation. It consists of a generator, a motor, an artificial transmission line, and an electronic stabilizer. The latter is a short-circuited phase controlled rectifier combined with current limiting reactors. The grids are controlled from current transformers in the line conductors at the generating end.

The vector diagram, Figure 5, shows the relationship of currents and voltages of the line, the generator, the stabilizer, and the motor. The line has an electrical length of 630 miles equivalent to 67 electrical degrees at 55 cycles. It can be operated reliably at a phase displacement of 60 degrees between terminals. At this load the current is leading at both ends. If there is a swing of phase angle due to a shock on the system, the power flow will increase with increasing phase angle and thus reacts as a synchronizing force. In ordinary synchronous operation, the synchronizing force is produced by an increase of current. In this case, however, the current is nearly constant because the line resonance gives it an effect approaching infinite impedance. A synchronizing force, however, is produced for two other reasons: the line current which at normal load was leading swings into phase; and the electronic stabilizer draws less current so that the voltage increases. The practical conclusion is that a long line should be operated a little below surge impedance load. Further refinements of control may make the margin negligible, but the results obtained by the sample equipments are in themselves very encouraging.

The use of the electronic stabilizer can be approached from two points of view. One is as an adjunct to a conventional system with natural stability in order to increase the effective stability and to carry more power. The other is to use the stabilizer as a necessary part of a long transmission line system which has low natural stability but is designed to depend upon the electronic stabilizer for its operativeness. The latter point of view is the more interesting. Our model test equipment was set up to explore this case; and, therefore, an artificial transmission line built with an electrical length of 630 miles. The tests were made at 55 cycles because of the speed of motors that were

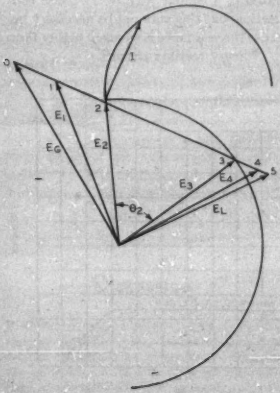

Figure 3 (left). Regulated terminal voltage

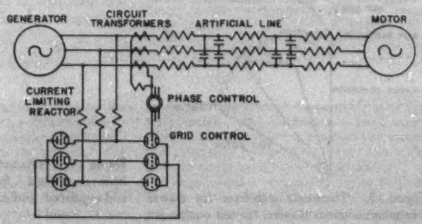

Figure 4 (right). Electronic stabilizer for power transmission test equipment

readily available, but it may be said that this choice of frequency has the advantage of being close to both of the important frequencies of 50 and 60 cycles. A generator of 5-kva rating was operated with a line loading of 6 kw, whereas an alternator of a 15-kva rating was used to represent a large receiving system with other sources of power.

The following are the constants of the test equipment which was operated at 250 volts:

Artificial line

Three coils with a total inductance of 0.037 henry.

50 microfarads in delta between coils 1 and 2.

50 microfarads in delta between coils 2 and 3.

Generator

Synchronous impedance 12.5 ohm.
Transient impedance 1.4 ohm.

Motor

Synchronous impedance 2.5 ohm.
Transient impedance 0.6 ohm.

Stabilizer

Reactor in series with stabilizer 0.024 henry. The tube equipment connected through a step-up transformer of two-to-one ratio.

Figure 6 shows the characteristics of the generator with stabilizer at varying loads. In this case the excitation is fixed and the phase control of the grids is fixed except for the automatic action of the current transformer. It should be noted that the stabilizer maintains substantially constant terminal voltage but that the voltage rises at high load when the grid control becomes effective. The fact that the voltage rises instead of drops, as it would without the stabilizer, gives the system an artificial synchronizing force.

Figure 7 shows the same characteristics with regulation applied to the generator field and the phase control of the grids. The grids are regulated so as to maintain constant terminal voltage up to full load, after which the voltage is allowed to rise at overloads. The field is regulated so as to maintain constant current in the stabilizer.

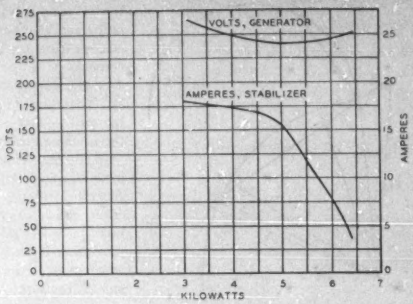

Figure 6. Characteristics—fixed field and fixed grid control

Synchronization

The artificial synchronizing force differs in its action from the natural synchronizing force. The oscillogram, Figure 8, shows the process of synchronization. When the line switches are closed, the system synchronizes promptly with a current swing which only slightly exceeds the normal. It was observed that before synchronization the generator was running four per cent faster than the motor. During the process of pulling into step, the stabilizer acts as a commutator increasing the power flow when it is in the right direction and decreasing it when it is in the wrong direction. The oscillogram, Figure 9, shows currents and voltages of full load operation.

Grid Control

For those who are not familiar with power electronic devices, an explanation may be in order to show how the grid control serves to regulate the current in the wattless dummy load.

In an ordinary rectifier the voltage can be controlled by retarding the phase of the grids so that 90-degree phase retard reduces the rectified voltage to zero and no appreciable current flows even if the rectifier is short-circuited. The stabilizer operates in substantially the same way with the difference that the usual reactance in series with the d-c terminals is eliminated in order to speed up the action. On the converse, the reactance in series with the a-c terminals is greater than the usual one so that the maximum current that can flow is limited to a moderate overload.

Wave Shape

The oscillograms show a harmonic distortion of the current flowing through the stabilizer. The harmonics are mostly the 5th and 7th because a 6-tube circuit was used. In practice, the tubes will be used in groups of 12 and so connected that these harmonics are eliminated. The 11th and 13th harmonics may be eliminated in a similar way by 24-phase connection, but this may not be necessary because the reactance is so much higher than in ordinary rectifier circuits.

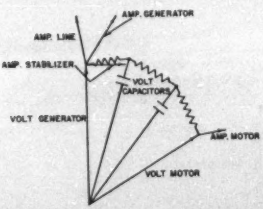

Figure 5. Electronic stabilizer for power transmission vector diagram for test equipment

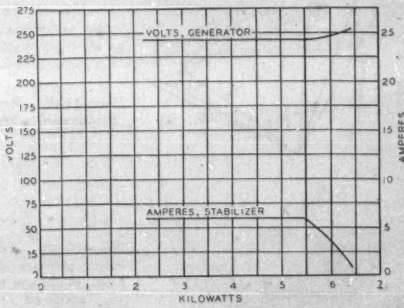

Figure 7. Characteristics—regulated field and regulated grid control

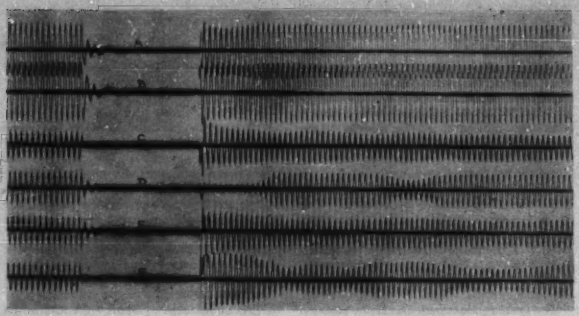

Figure 8 (above). Oscillogram showing synchronization

A—Volts generator
B—Volts receiver
C—Amperes receiver
D—Amperes stabilizer
E—Amperes line
F—Amperes generator

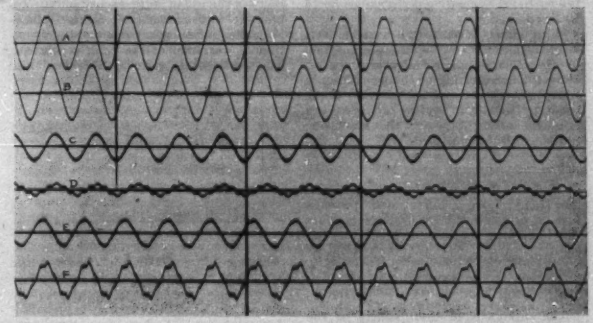

Figure 9 (below). Oscillogram of full load operation

A—Volts generator
B—Volts receiver
C—Amperes receiver
D—Amperes stabilizer
E—Amperes line
F—Amperes generator

Size of Stabilizer

A question that must be answered is what is the proportion between the kilovolt-amperes of the stabilizer and the kilowatts of the transmission line. Our tests indicate that the kilovolt-amperes of the stabilizer need not be more than 50 per cent. The model system can be operated with 25 per cent kilovolt-amperes, but the higher ratio has greater margin of safety. The following analysis may explain these findings.

Due to the interaction of inductance and capacitance of a long line, the current in the transmitting end follows the voltage in the receiving end by phase as well as amplitude. Therefore, if there is a swing of phase angle of plus or minus 15 degrees between the transmitted voltage and the received voltage, we can expect the transmitted current to swing plus or minus 15 degrees relative to the transmitter voltage. The normal current is of substantially unity power factor, and the phase swing of the current can be represented by the addition of a wattless dummy load swinging plus or minus 25 per cent of full load current. This wattless component is absorbed by the stabilizer. But we must do more than compensate for the phase variation of the current. We must overdo the compensation so as to create an artificial synchronizing force. We therefore may regulate the system so that 15-degree phase displacement causes the flow of a 50 per cent wattless current.

Conclusion

This paper has been presented in order to suggest a new approach to an old problem—the extension of electric power transmission. It is less radical than d-c transmission. The electronic equipment may be of a type with which we have many years experience in the Carnegie Illinois frequency changer. No pretense is made of treating this subject exhaustively or to make economic or technical comparisons with other known methods of extending a-c transmission. Those other methods are specifically intermediate synchronous condenser stations and series capacitors. When to these we add the electronic stabilizer, we have three methods which all differ in principle but, nevertheless, may be used in combination. Whether the new method will compete economically in operating characteristics with other methods is for the future to determine.

References

1. Transmission-Line Electric Loadings, S. B. Crary. AIEE Transactions, volume 63, 1944, pages 1198–1204.

2. Stability Limitations of Long-Distance A-C Power-Transmission Systems, Edith Clarke, S. B. Crary. AIEE Transactions, volume 60, 1941, pages 1051–9; discussion, pages 1299–1303.

Discussion

E. C. Starr (Oregon State College, Corvallis, Oreg.): The electronic stabilizer proposed by the authors is an interesting device for the improvement of long-distance transmission performance. The general long-distance problem rapidly is assuming greater importance as large low-cost generating plants are developed and industrial and metropolitan loads grow progressively heavier. The economic phase of the problem is always of uppermost importance, and technical improvements must meet the final cost test. In this case, from a superficial study, it appears that the present cost aspects may be unfavorable. The authors and their associates are in a position to examine this angle critically on a comparative basis, and such a study would be of value to the industry.

The proposal is technically sound in that it adds to the shunt-reactor loading scheme a highly refined control system. It permits

the generators and synchronous condensers to operate normally under saturated conditions with high air gap or induced voltages. Low terminal reactances thus are provided, and the ability to restore terminal voltages following a disturbance is practically instantaneous. The "infinite bus" condition is thereby more nearly approached. The possible high cost of the reactor control equipment is the only questionable item.

This proposal again brings up the possibility of employing shunt reactors with a switching scheme to drop them when the terminal voltages begin to fall and the system begins to swing apart. They then could be reclosed on the system after the swing had reversed and the voltages had been restored by fast regulator action. In this case, low-voltage reclosing circuit breakers and bank switching of the reactors would replace the electronic equipment and its finely graduated, fast control. The cost probably would be less, but the operating performance would be less desirable.

With either scheme, the system costs would be increased by the large reactors and by the reduced power factor or increased kilovolt-ampere rating of the generators in addition to the control equipment. If the resulting increase in system capability can bear the added expense, the stabilizing equipment will be justified.

C. H. Willis (Princeton University, Princeton, N. J.): Long distance power transmission on conventional a-c systems presents two important problems or aspects as follows:

1. The problem of reflection.
2. The problem of stability.

The authors have dwelt largely on the problem of stability and have shown that the limits of power transfer can be raised by the use of the electronic stabilizer. It should be emphasized also that a reactive load at the line terminal will modify the reflection coefficient and may be employed to prevent dangerous voltages. The operation of the line with a reactive termination readily may be understood by considering the voltage curve of a lossless line terminated in

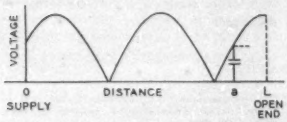

Figure 1

an open circuit which is shown in Figure 1 of this discussion. There will be a voltage maximum at the open termination when the line is supplied from the distant end. If, however, the line be terminated in a capacitive reactance this reactance is equivalent to an extension of the line and the voltage maximum will occur at the end of this equivalent extension, and therefore the voltage at the actual end of the line will not be a maximum. This condition is represented by point *a* on Figure 1.

This affect may be illustrated further by considering a 620-mile 60-cycle or 1/5-wavelength line. When operated as an open line with an impressed voltage of 110 kv at the generator end the open end voltage would be 356 kv as shown in Figure 2. If, however, this line be terminated with a suitable capacitive reactance, the operation may be modified as shown in Figure 3 where there is a voltage minimum at the middle of the line and the receiving and sending end voltages are identical. The line may be terminated so that the voltage is a minimum at the center whenever the terminal load differs from the characteristic impedance. This operation necessitates a variable reactance at the receiving termination which is capacitive in character and continuously adjustable as the watt load increases from zero up to the load corresponding to characteristic impedance termination.

The synchronous condenser is one solution for this variable capacitor. Another possibility is the use of static capacitors in combination with an electronic reactor (phase-controlled tubes) to provide rapid and continuous variation of the reactive current. This continuously variable "stabilizer" also

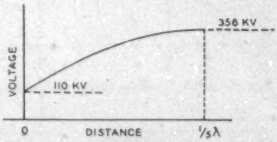

Figure 2

may be employed as an exciter for an induction generator and when so employed provides another avenue of attack on the problem of stability. The advantages of an induction generator were recognized fully by Steinmetz but the excitation for this machine has presented a serious problem. The Scherbius exciter is not particularly attractive and when a synchronous condenser is employed the advantages of the asynchronous generator are forfeited. No other alternatives have been commercially available until recently. The perfection of power factor correction capacitors and the successful use of electronic tubes in power equipment provide the new means of exciting the induction generator.

The stabilizer which consists of a fixed capacitor and an electronically variable inductor makes it possible to reconsider the induction generator for long distance power transmission. This machine in combination with an electronically controlled reactor appears to provide a possible solution for a-c power transmission over distances approaching a half wave length or 1,550 miles at 60 cycles.

The economic aspects of this solution using an induction generator must be compared with other methods of solving this problem to determine the most promising approach to long distance power transmission. It should be observed, however, that the tubes handle the power only once in this application and not twice as in d-c transmission or frequency conversion. This makes the use of tubes for controlling reactive current more favorable economically.

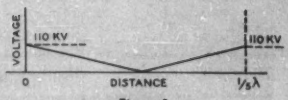

Figure 3

Alexander Dovjikov (Bonneville Power Administration, Portland, Oreg.): For the Northwest and northern California, the problem of increasing stability of the interconnected systems and thereby making the transmission of power over distances of the order of 500 miles more economical is of particular and pressing interest. It is not a problem of future planning but of today's design of the major parts of such transmission.

The component systems—the Columbia River system of the Bonneville Power Administration interconnected with other systems of the Northwest and the Shasta development on the Sacramento River—being mostly hydro systems and built in combination with large irrigation projects represent a very favorable set of conditions for economy by correlated operation of two large watersheds with a favorable diversity of run off, diversity of irrigation load maximums, and one system providing water storage space for the other.

Due to the distance of this proposed a-c transmission the considerations of stability would keep the loading of a conventionally designed line too far below its economic loading. To make such long and therefore costly lines economically justifiable, measures must be taken to increase the loading even above its surge impedance load. Whether the reactance of such a long line should be reduced by series-capacitor compensation, or whether synchronous condensers of proper characteristics should be installed at intermediate sectionalizing substations, the problem of excitation for synchronous machines is still one of most importance. Although there is no particular difficulty in overcoming the effect of armature reaction, the conventional methods of high-speed excitation, whether by a rotating d-c exciter with high-speed response or an electronic exciter, are too slow to overcome the transient reactance voltage drop during the swings. The authors therefore propose to establish, even for normal operating conditions, increased excitation and an internal voltage of a magnitude which will be necessary during transient disturbances. In order to obtain rated terminal voltage during normal operating conditions, the synchronous machine is loaded with regulated shunt reactors. Similar ideas of using shunt reactors on generator terminals (or step-up transformers operating at flux densities considerably above normal and drawing large magnetizing current) have been suggested previously. The novelty of this proposal is the smooth and fast control of current through such reactors by means of grid-controlled mercury-arc rectifiers between phases of the reactors. As the grid control requires a very small amount of power, very large currents through the rectifiers and therefore through the reactors may be controlled by instantaneous static voltage regulators, such as a static impedance voltage regulator or by a regulator

based on the phase angle of the current as is proposed by authors of the paper. The last type of regulator is not described sufficiently in the paper, and we assume that the authors' idea is to regulate in accordance with phase angle between voltages at the sending and the receiving ends of the system—an idea which in a different and more complicated form has been advocated for some time by Brown-Boveri Company of Switzerland. Although the Brown-Boveri Company idea employs the comparison of actual voltages at both ends of the system (as well as time rate of change of this phase angle), Messrs. Alexanderson and Prince state that the phase angle between current and sending-end voltage should be satisfactory for the purpose, and in this way considerably simplify the arrangement.

With all the engineering attractiveness of the scheme proposed by the authors of the paper, and although the authors state ". . . no attempt has been made to compare this method with other methods," we cannot get away from economic considerations—is it the most economic way to increase the stability of the system? The authors, being connected with a large manufacturing company, could give the comparative cost in the most authoritative way, and we hope that they eventually will do so. It seems, however, that the expected increase in cost will be quite considerable. If we assume, as the authors do, that the reactors may be about 50 per cent of the kilovolt-amperes of the generators, the scheme increases the rated capacity of the generator that otherwise would operate, let us say, at unity power factor, to 112 per cent, and changes the generator power factor from unity to 0.9. Both of these factors increase the cost of the generator. To this must be added the considerable cost of reactors and of controlling mercury-arc rectifiers—and to be effective they, must be, as the authors state, about 50 per cent of the generator capacity. This economic problem is particularly important because the authors state that with the proposed method of stabilization, "The practical conclusion is that a long line should be operated a little below surge impedance load." We doubt that such solution of long-distance transmission could stand the economic test. There are other ways of increasing stability besides that described by the authors, as for example, electronic exciters on generators of moderate reactance, decrease of line reactance by means of series static capacitors, and these, or their combination, are just as valid from the stability point of view, and would permit transmission of amounts of power greater than the surge impedance loading of the circuit. The decision, therefore, will be made on the basis of comparative cost of transmission per unit of transmitted power. We are looking forward to such economic clarification of the proposed schemes.

J. G. Holm (Gibbs and Hill, Inc., New York, N. Y.) and **A. M. Taylor** (Economic Transmissions, Ltd., Birmingham, England): There has been for quite some time a need for a new device, or a new method, for improving stability of transmission lines, particularly under transient conditions. The device proposed by the authors is new in that rectifiers are used for control of the reactive load connected to the generator terminals. The method, however, of connecting such a load seems to be similar to that involved when shunt reactors are placed on the generator bus. The latter method has been analyzed by one of the discussers.[1] It has been shown that the reactor increases the total system transfer reactance, increases the excitation voltage, and lowers the power factor on the generator. The increase in the total system transfer reactance lowers the system stability limit, while the increase in the excitation voltage raises it. When the latter factor predominates the system stability limit will increase. Since, however, the power factor of the generator is lowered, the installed kilovolt-ampere capacity of generators must be greater when reactors are used than it otherwise would be. The improvement in stability limits obtained varies with the size of the reactor. The benefit obtained, however, is not sufficiently high, when all costs are considered, to render the method very attractive. It, therefore, has not been used frequently, although such reactors have been installed both here and abroad.

It may be that the electronic stabilizer has some additional advantages not pointed out sufficiently clearly in the paper, or that we have misunderstood some of the statements made by the authors, for one must say that some very pertinent data cannot be found in the paper. It is not stated, for example, what is the nominal voltage of the line, its rating, and the amount of power transmitted. Still from the data given it seems fairly certain that with the electronic stabilizer at the sending end the generator kilovolt-amperes will have to be increased appreciably.

We would like to ask whether or not sudden momentary load increases at the receiving end have been considered, and if so, whether or not the electronic stabilizer can manage a 20- to 40-per-cent increment of power thrown on the system when it carries its full load, reachings its maximum value in about one cycle. Unless the stabilizer can prevent the system from falling apart under these conditions it could not fulfill the purpose implied in its name. It does not seem to us that placing the electronic stabilizer at the receiving end also, that is, at both system ends, will help the line. Even though an electronic stabilizer will strengthen the field of the generators at the receiving end, under a momentary load increment of from 20 to 30 per cent the generators will have to decelerate because the steam valves will not have had time to open and meet the sudden increment of load. Therefore, the necessary driving torque would not be forthcoming. It seems to us, therefore, that an electronic stabilizer will be helpful when placed at the sending end only. But even then other means will have to be employed if it is expected to raise appreciably the system stability limit, especially on a 630-mile long line studied by the authors. Since it is our understanding that properly functioning series capacitors are not yet available for the higher voltages, intermediate synchronous condensers would have to be installed in at least two places.

There seems to be, however, a different method for stabilizing a transmission line. If there is a deceleration at the receiving end resulting from a sudden increment of load, from whatever cause it might come, the only way to stop deceleration is either to have the sending-end generators to provide a sudden voltage boost, transmitting momentarily additional accelerating power, or to have at the receiving end an arrangement by which the load increment could be met locally. During the last few years we collaborated on this general problem. A new method—the Taylor stabilizer—was developed. Patents for it have been applied for in England, the United States, Canada, and some other countries.

The Taylor stabilizer is a synchronous machine having certain characteristics which are easy to incorporate in the design. It is connected to the receiving end of the system through a special circuit. The rating of the machine is some 15 to 20 per cent of the rating of the receiving-end rotating machinery. When a load increment equal to 20 to 30 per cent of the system normal load is applied suddenly, the stabilizer circuit operates instantly. A required additional quadrature and in-phase voltage boost immediately is introduced into the line. Thus extra power is provided for receiver acceleration. The stabilizer supplies the additional load momentarily, grabbing the increment of current. Thus it is not necessary to transmit the extra power from the sending end, and the system while under a shock stabilizes with normal current passing over the line. This is maintained until the momentary load increment is over or the fault cleared. The power factor at the sending end remains unaffected, so that there is not any need for the sending generators to have a greater kilovolt-ampere rating.

On shorter lines the Taylor stabilizer may be placed at the receiving end only. In lines of over 500 miles additional complete stabilizers, with their circuits and boosting arrangements, are placed at intermediate points. These stabilizers supply the boosts required only by the line section between the stabilizer intermediate stations. The kilovolt-ampere rating of their synchronous machines is considerably smaller than that of the receiver-end stabilizer. As the length of the line is increased the number of the intermediate stabilizer stations is increased. The power factor at the sending end remains at unity, and power is transmitted without increasing the sending-end voltage which remains at a constant potential. The stabilizer scheme works like a very large relay and is instantaneous and automatic in its action. Thus power may be transmitted over distances exceeding anything heretofore contemplated.

The Taylor stabilizer may be used on short lines or in power plants where sudden heavy load changes occur similar to rolling-mill loads. On long transmission lines it helps to transmit power without loss of stability and it increases the limit of power that may be transmitted. The cost of this stabilizer is moderate; in the long lines it is appreciably less expensive than series-capacitor compensation, at an estimated cost of $10 per capacitor kilovolt-ampere.

At this time laboratory tests are being arranged for in England. Whether or not studies on artificial systems will come entirely up to expectations is impossible to say today. At any rate, theoretical studies, on paper, show this method to be promising, sufficiently so as to warrant laboratory tests and expenditures involved. Since much is yet to be done and the apparatus is not yet fully developed, only an outline of the prin-

ciple of the new stabilizer is given in this discussion, and cautiously so, without any claim that it is a solution to the difficult problem of system stability.

It might be that, when successfully developed, it would prove advantageous to apply the Taylor stabilizer jointly with other methods, of which one perhaps could be to have the electronic stabilizer at the sending end and the Taylor stabilizer at the receiving end of the system. It is too early to pass on this at the present time.

Reference

1. Stability Study of A-C Power Transmission Systems, John Grzybowski Holm. AIEE Transactions, volume 61, 1942, pages 893–905.

A. Uno Lamm (Allmanna Svenska Elektriska Aktiebolaget, Ludvika, Sweden): It should be quite clear that in Sweden there has been no doubt about the technical possibility to solve all our problems of power transmission according to the a-c system. However, our investigations have shown that the yearly costs of the line, including the losses, are so much lower with direct current that the use of such current must be considered seriously. Herlitz has shown that the yearly cost for the line itself is 31 per cent less with direct current as compared with alternating current, the same amount of power and most economical voltage being assumed in both cases. A rough estimation of the additional cost of the terminal stations in the case of direct current shows that the economic superiority of direct current should begin at transmission distances of about 300 to 350 miles.

These calculations, however, are based upon the assumption that the a-c line can be loaded up to the economical optimum, that is, that the stability does not limit the load. This condition is not fulfilled when the transmission distance is greater, and the economic superiority of direct current over alternating current grows, therefore, very steeply with increased distance.

In Sweden, where in the future about 2,000,000 kw have to be transmitted over distances of from 600 to 900 miles, as Borgquist has shown, such large amounts can be saved by the use of direct current that it seems quite unjustifiable not to spend the necessary money to develop the d-c system.

The authors have shown that electronic equipment also can be used to increase the possible load of a long a-c line towards the economical optimum, which appears to be a very interesting alternative solution to the problem of reducing transmission costs. The 31 per cent saving in total line cost with the use of direct current will still be true, of course, and when comparing the terminal stations we now also have to consider certain electronic equipment in the a-c case, possibly including also high voltage transformers for the stabilizer in a mid-point station. This means that the additional costs of terminal stations (including mid-point stations in the a-c case) will not be so unfavorable to the d-c system as before.

There is another interesting aspect of the electronic stabilizer. It gives the possibility of trying out high-voltage mercury-arc rectifiers on a big scale on existing or planned a-c transmissions. Thus experience can be gained for such electronic equipment without economic sacrifice, which experience later can be applied also to electronic rectifiers for d-c transmission.

The Swedish trial plant for d-c transmission which has been built by the State Power Board and ASEA in co-operation, is intended for 90,000-volt 6,500-kw direct current. It will comprise two series-connected rectifiers in each terminal station, but is now, in the first stage, operating with only one rectifier in each station and thus with half voltage and power. The line length is about 40 miles. The rectifiers are in full-wave connection using single-anode pool-cathode tubes. It is expected that the next big trial step will be of the order of magnitude of 100,000 kw at 250 kv using a fourth wire on an existing 3-phase line, and the overhead ground wires as a return for the direct current. Even if such trial plants must involve a considerable economic sacrifice, it seems to be the most direct way of arriving at the big economic saving for long transmission lines which are offered by the d-c system, if the technical problems can be solved.

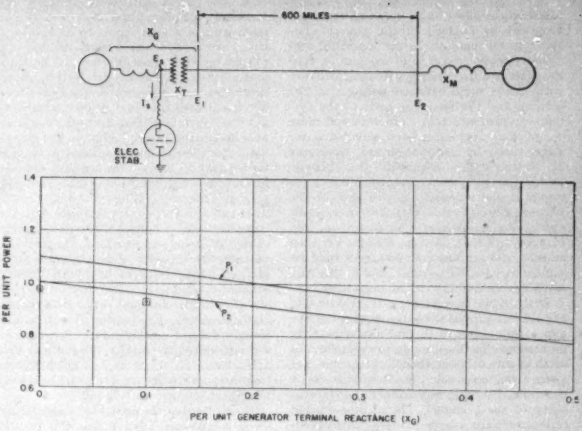

Figure 4. Effect of generator terminal reactance X_G on steady state stability limit of 600 mile line*

$X_M = 0.25$
$X_T = 0.10$
$X_G = 0.40$
$I_s = 0.25$
$x = 0.8$ ohm per mile
$E_1 = E_2 = 1.0$
$r = 0.08$ ohm per mile
$b = 5.2 \times 10^{-6}$ mho per mile
$y_s = \Delta I_s / \Delta E_s$ or $\Delta I_s / \Delta E$

⊙ = electronic stabilizer regulating high-voltage transformer terminal, $y_s = 10$
⊡ = electronic stabilizer regulating generator terminal, $y_s = 10$

* All quantities except when otherwise designated are on a kilovolt-ampere and kilowatt base of 2.5 (kv)².

S. B. Crary (General Electric Company, Schenectady, N. Y.): An electronic stabilizer for power transmission presents an interesting possibility for increasing the power limits of long-distance power transmission worthy of careful consideration. Functionally, the electronic stabilizer provides a mean by which a relatively large decrease in reactive current may be made at a point where it is located on the system for a relatively small drop in voltage. The electronic stabilizer must be located at a point in the system where there exists or is made available an excess above normal of reactive (overexcited) kilovars. This makes it possible, as the authors have pointed out, for the electronic stabilizer to reduce in effect the terminal generator or terminal system reactance. Thus, the electronic stabilizer provides a method for obtaining a relatively small effective terminal reactance for a relatively small steady state or continuous current. This is making fullest use of the electronic valve principle. The practicability of the use of such a principle for power transmission depends, however, entirely upon its economical justification. The following will attempt to show some of the relative advantages and disadvantages of such a scheme.

Figure 4 of this discussion shows the effect on the steady state stability limit of decreasing the terminal generator reactance for a typical 600-mile straightaway transmission line. As is now well recognized, by the use of a properly co-ordinated excitation system, the steady state stability limit is determined essentially by the transient reactance of the generator. Accordingly, in Figure 4, for a typical case where the per unit generator transient plus transformer reactance = 0.40, the received steady state power limit can be increased from 0.82 to 1.0 per unit if it were possible to, in effect, reduce to zero the total generator terminal reactance. By the use of an electronic stabilizer, it should be possible to obtain almost this increase in power limit as shown on Figure 4 of this discussion, provided the electronic stabilizer is capable of holding the high-voltage terminal voltage by main-

taining a low admittance ($y_s = \Delta I_s/\Delta E_s$), where ΔI_s is the change in stabilizer reactive current for a change of high-voltage terminal voltage ΔE_s. As shown on Figure 4 of this discussion, a control admittance of $y_s = 10$ would result in practically obtaining the theoretical value equivalent to zero generator terminal impedance (X_g).

This increase in steady state limits can be compared with other methods of line compensation of long distance power transmission systems. As is also well known, it is possible to use either series capacitors or special intermediate synchronous condensers along the line to increase the possible loading in order to maintain economical values of rated load for the longer distances. Such compensation equipment costs in the neighborhood of $10 per rated capacitor kilovolt-ampere for series capacitor compensation and special intermediate condensers are economically competitive.

For the simple straightaway 600-mile-line case of Figure 4 of this discussion, 30 per cent line compensation of the line reactance by series capacitors would result in the same increase in steady state stability limit as may be realized by an electronic stabilizer holding the generator high voltage. The 30-per-cent line compensation at $10 a kilovolt-ampere of a 600-mile 60-cycle line which has a surge impedance of 400 ohms and a reactance of 0.8 ohm per mile will cost $3.60 per transmitted kilowatt, when the rated load is the surge impedance loading. This is the amount available to pay competitively for the electronic stabilizer and a larger generator in order to carry the reactive current required by the stabilizer.

For this simple case of steady state stability the electronic stabilizer meets with very difficult competition by the known methods of line compensation. Actually for a 600-mile line some margin would be required in the steady state stability limit so that some form of line compensation probably would be required, even if the electronic stabilizer was used, so as to be able to transmit the unit or surge impedance power shown.

Most transmission systems are not of the simple type indicated in Figure 4, but constitute parallel circuits so designed and arranged that a fault may occur on any one line section or on the connected systems without loss of synchronism. In other words, the system must be able to withstand transient shocks and must have the requisite transient stability. Studies of such systems indicate that the transient stability limits are, in general, less than the corresponding steady state power limits, either before or after the loss of the faulted line section. For the case of transient stability, the electronic stabilizer is less effective than it is for steady state as it is able during the important first swing only to reduce suddenly to zero the reactive kilovolt-amperes that it was drawing initially. Therefore, its contribution is to increase somewhat the initial voltage behind transient reactance and possibly to decrease slightly the initial operating angle. However, line compensation methods effectively increase the transient power limits as well as the steady state. The series capacitors can contribute as much as four times their rated kilovolt-amperes during the transient swing and the current output of the intermediate synchronous condensers is increased greatly during the transient condition.

Some consideration has been given to placing the electronic stabilizer along an uncompensated line, but this presupposes that the line is loaded at impractically low or uneconomical loadings at less than the surge impedance loading. Such low loadings would be necessary so that the line can furnish the required reactive current or excitation for the electronic stabilizer.

Based on such analyses, it can be concluded that the electronic stabilizer's field of application would be for a single circuit transmission system where the steady state stability limit, with the system in normal operation, is the determining limit and when there exists a prejudice against the use of line compensating means. Both of these conditions are not likely to occur simultaneously as the single circuit line can be compensated easily by standard methods of series capacitor compensation as it presents no serious or new problems for this simple type of single circuit application.

H. C. Steiner (General Electric Company, Schenectady, N. Y.): The authors have presented a new and very interesting approach to the stability problem in long distance a-c transmission, and I would like to comment on the proposal from the tube standpoint. Frequently new applications of electronic tubes involve both the development of a tube and an estimate based on engineering judgment as to its performance. In the proposed application we are fortunate in being able to evaluate these factors of performance from actual experience.

At the Edgar Thompson plant of the Carnegie-Illinois Steel Corporation there is installed a 20,000-kw electronic power converter for exchange of power between their 25- and 60-cycle systems. For control purposes the 20,000-kw capacity is divided into two units of 10,000 kw each. Each unit uses 12 pentode ignitron tubes for rectification and 12 for inversion; or 48 tubes in all. In operation alternating current is first converted to direct current and then inverted to the frequency of the system requiring additional power. The nonsynchronous d-c link in this case is only a few feet in length. It operates at a potential in the order of 15,000 volts. The first unit was installed in December 1943 and the second in February 1944. Figure 5 of this discussion shows a general view of the installation. Performance in terms of tube life is shown in Figures 6 and 7. The upper curve in Figure 6 shows the average life of the original tubes now in service and the lower curve the average life of all tubes in service. Figure 7 shows the replacement history. All tube removals are shown regardless of whether the cause was a tube problem or an equipment adjustment or operation problem. The curve shows clearly the initial problems encountered and the improvement that may be expected with these problems removed.

The pentode ignitron tubes used are designed for operation at potentials of 20 kv peak inverse and forward and with a current rating of 150 amperes (average) continuous, 200 for two hours, and 300 for one minute. Six such tubes connected to the generator terminals as the authors have shown would control 7,500 kva, on the basis of the con-

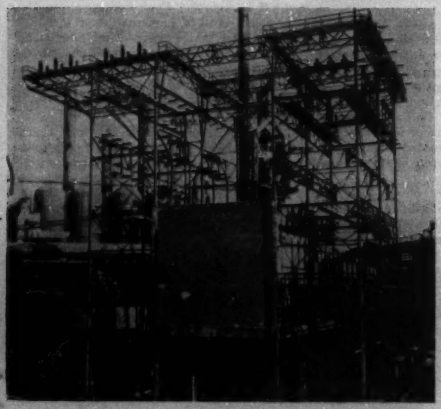

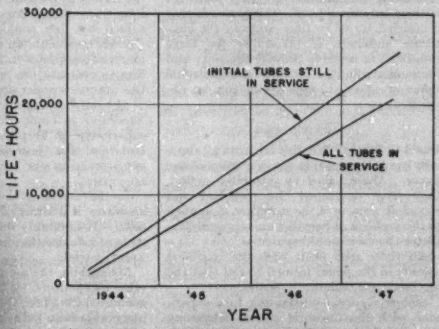

Figure 5 (left). View showing installation of the Carnegie-Illinois Steel Corporation 20,000-kw electronic power converter

Figure 6 (above). Pentode ignitron tube life at the Carnegie-Illinois 20,000-kw electronic power converter

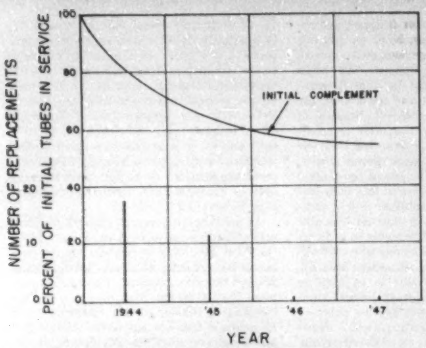

Figure 7. Chronological record showing pentode ignitron tube replacements and number of the initially installed tubes still in service

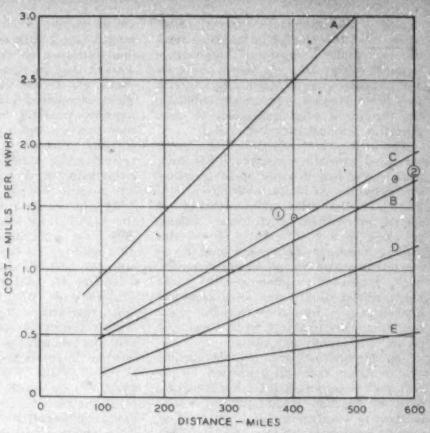

Figure 8. Cost of transmission of energy

A-c transmission—partially compensated line two circuits

①—Actual cost of transporting coal by rail and barge from West Virginia points to New York, N. Y.

②—Actual cost of transporting coal by rail and barge to Boston, Mass.

A—A-c transmission, 50 per cent load factor

B—A-c transmission, 100 per cent load factor

C—Cost of transporting coal by rail

D—Cost of transporting natural gas by 24-inch pipe line

E—Cost of transporting oil by pipe line

tinuous average current rating, or 10,000 kva if the 2-hour rating were considered because of the relatively low duty required at maximum load conditions. The conditions that occur during commutation are a good measure of tube duty. This duty depends on magnitude of the current commutated and the initial inverse voltage that occurs at the end of commutation. In the usual rectifier both factors tend to increase with increasing load, but in the proposed circuit, the voltage factor becomes zero at full-load current and a maximum at zero-load current. The duty therefore should be more favorable than that encountered in rectifier service.

In the electronic stabilizer there is a single conversion of current. Because of this and in view of the favorable duty the 48 tubes in the 20,000-kw frequency changer would have a capacity of 80,000 kva in the electronic stabilizer. Such a unit would be capable of controlling a transmission line of 160,000-kw capacity on the basis of the 2-to-1 ratio of generating to stabilizer capacity that the authors have considered. It is probable that a multiplicity of rectifier units in the electronic stabilizer is preferable for large capacities in order to provide diversity and harmonic reduction but if larger electronic tubes are needed, such tubes can be developed.

David C. Prince: We wish to thank all those who have taken part in the discussion of our paper. Almost as if by concerted action, they have developed the technical and economic aspects of the stabilizer as applied to the problem of long distance transmission better than we could have done it.

All those who dealt with the technical aspects of the paper seemed to feel that the proposals are technically sound.

Steiner reported satisfactory tube experience with the Carnegie Illinois frequency changer which establishes the tube part of the electronic stabilizer on known ground

As Willis has pointed out, the combination of the electronic stabilizer and a static capacitor can be used instead of the usual synchronous condenser. It also would provide substantially instantaneous voltage control for asynchronous generators, although it is itself asynchronous.

Holm and Taylor may have missed the point that the wattless kilovolt-ampere drain of the reactors is cut off by the electronic regulator during such times as pull-out is threatened. We know both from theory and test that the regulator will do its work at either end of a line or distributed at intervals along a line. The applicability of the device is not related to any particular line loading such as surge impedance loading.

If this discussion is representative, one may judge that the electronic stabilizer should be sound technically.

It is interesting to learn from Dovjikov's comments that there is an immediate need for means to increase the stability limit of long transmission lines, such as can be obtained by line compensation. I believe Crary's comments on this paper will be of material assistance to Dovjikov in enabling him to evaluate the probable economics of this approach under present conditions.

The outstanding questions are economic. According to Lamm, a d-c line itself has a superiority of 31 per cent for long lines. However, that theoretical advantage is not yet a practical one because of the terminal apparatus.

In the matter of cost of the electronic stabilizer, it is always difficult to get general costs. It is doubly difficult to get general costs of a device that has not yet been given a service trial.

Meanwhile, the a-c transmission line has other competitors. Where electric energy is generated from fuel, the generation can take place anywhere between the source of fuel and the distribution center. Figure 8 of this discussion shows the comparative costs of transmitting electric energy as such or as fuel by rail or pipe line. These data are confired generally by similar data presented by E. E. George.[1] From this, it appears that if power is to be generated from fuel, it is difficult for the a-c transmission line to compete with straight transportation of the fuel. As the amount of power to be transmitted and the load factor are increased, the relative position of the transmission line is improved.

The electronic stabilizer—which is the subject of this paper—represents one effort to increase the transmittible power with a view to making electric transmission competitive. We shall do well to press the development of any available expedient in this direction, if we hope to maintain our favorite medium in a competitive position.

Reference

1. Discussion by E. E. George of Economics of Long Distance A-C Power Transmission, S. B. Crary, I. B. Johnson. AIEE Transactions, volume 66, 1947, pages 1092–1102.

The Analysis and an Optimum Synthesis of Linear Servomechanisms

DONALD HERR
MEMBER AIEE

IRVING GERST
NONMEMBER AIEE

Synopsis: The concepts of minimum band width and nonminimum band width servomechanisms are introduced. Minimum band width servomechanisms are dealt with in this paper. A systematized approach to the synthesis of such servomechanisms is outlined and the method applied and detailed results obtained for one practical class of such servomechanisms. The technique enables the stability requirements and the accuracy requirements to be considered separately in succession. An engineering criterion of servomechanism stability is enunciated. The critical design parameters and performance characteristics, including amplitude and phase margins, are tabulated for a practical class of minimum band width servomechanisms over the range of degree of stability of engineering interest. The corresponding build-up times, damping factors, and natural frequencies also are tabulated. Extensions of the viewpoint and method described are outlined.

THE current literature is replete with numerous examples and types of servomechanisms. The methods of treatment thereof include the steady-state response method, the linear differential equation approach, a hybridization of these two methods of analysis and design, or the empirical method involving free use of physical concepts such as "velocity damping", "acceleration feed back", and "integral-derivative control."[1–16, 20]

It is the purpose of this paper to attempt a further contribution to this rich background in the art along the lines of a generalized approach to the servomechanism design problem, where possible. To do so, it is believed necessary that the basis for such an approach be stated clearly at the outset.

It is believed that the first item to be recognized is that it is the "loop-transfer function", or "loop-gain function", which uniquely defines all of the properties of the linear servomechanism and that for each such loop-gain function there is an infinite variety of physical embodiments of servomechanisms having this loop-gain function. Hence, the first point in the organized approach proposed herein is the categorization of linear servomechanisms according to the mathematical form of the loop-gain function, not according to a particular physical configuration which has that loop-gain function.

The second item in the organized approach proposed herein arises from the engineering nature of most all servomechanism design problems, namely, that most frequently certain determining elements of the servomechanism, physically and mathematically, are fixed from the outset and literally "handed to" the servomechanism engineer as invariants in the servomechanism design problem. For example, a relatively large and expensive prime mover, hitherto operating as the power amplifier driving the member to be controlled on an open-loop basis, becomes a fixed element of the servomechanism in controlling the motion of the driven member on a closed-loop basis. This is equivalent to saying that, in our servomechanism design, a certain portion of the loop-transfer function is itself invariant and this fixed portion of the loop-transfer function corresponds to the fixed physical elements of the servomechanism.

A third item to be recognized in the formulation of our organized approach arises from the fixed nature of the "driven member" or element which is to be controlled. This also makes its own invariant contribution to the over-all loop-transfer function of the servomechanism to be synthesized.

A fourth item to be recognized in this formulation is the fact that, whereas our servomechanism may possess many internal feed-back loops, each with or without its own distinctive transfer function in the feed-back path, it is assumed that the basic problem is that of having the driven member correspond in its motion as closely as possible, within the prescribed bounds of stability and accuracy, with the input signal (mechanical, electrical, or otherwise) as a function of time.

A fifth item entering into our formulation arises from viewing the servomechanism as being substantially a low-pass filter. The meaning of the words "optimum synthesis" in the present formulation of the problem is the design of that class of servomechanisms having the least band width consistent with the prescribed stability and accuracy characteristics. In other words, synthesis on the minimum pass-band basis insures that energy transmission through the servomechanism for control of the driven member is confined to that least band of controlling signal frequencies requisite for accurate and stable control, on the one hand, and automatically eliminates from consideration those customarily encountered system noises outside the required pass band. This, from experience, is known to be a practical and fortuitous basis of design in many cases.

The sixth item in the formulation of the problem, based on all of the foregoing, is the choice of that mathematically simplest class of loop-transfer function which, if designed into the servomechanism, will make available the simplest form that the servomechanism can take in fulfilling the performance requirements.

The seventh and last point then amounts to merely a description of the method as follows. We recognize that

Paper 47-165, recommended by the AIEE joint subcommittee on servomechanisms for presentation at the AIEE summer general meeting, Montreal, Quebec, Canada, June 9–13, 1947. Manuscript submitted April 2, 1947; made available for printing May 5, 1947.

DONALD HERR is assistant to vice-president in charge of engineering and IRVING GERST is a research mathematician in the Control Instrument Company, Inc., Brooklyn, N. Y.

The authors gratefully acknowledge the assistance of Doctor Leroy A. MacColl, Bell Telephone Laboratories, Inc., New York, N. Y. and J. L. Bower, formerly with the Control Instrument Company, Brooklyn, N. Y.

the idealized loop-transfer function (a complex function of frequency) is a rational function, consisting of a ratio of two polynomials in the frequency. The degree of the numerator and denominator polynomials establishes the degree of mathematical complexity. We choose a simple class of idealized loop-transfer function which enables us to fulfill the accuracy and stability requirements of most present-day servomechanism design problems. We investigate all the properties of such loop-transfer functions, in which the parameters have been so adjusted that they correspond to minimum band width servomechanisms. We characterize the degree of stability (assuming the basic requirements for stability, at all, first have been satisfied) by the maximum value of the steady-state system response function. In a sense, this measures the greatest proximity of the loop-transfer function to the Nyquist point on a steady-state zero-to-infinite-frequency response basis. We further characterize the steady-state accuracy of response by the value of the constant multiplier of the loop-transfer function which, at the determining frequency or frequencies, maintains the ratio of the error in the output of the servomechanism to the amplitude of the input to the servomechanism, at that frequency or frequencies, less than the prescribed value or values. The method of synthesis then becomes that of deciding upon the degree of stability desired, the nature of stability desired (conditional or absolute), the choice of the corresponding loop-transfer function in normalized form, the introduction of the appropriate constant multiplier corresponding to prescribed steady-state accuracy requirements, and finally, the eliciting of the critical frequency parameters for use in design. This, then, results in the complete statement of the idealized loop-transfer function necessary to meet the stated requirements on a minimum bandwidth basis. From this idealized loop-transfer function must first be removed the transfer functions of the fixed elements in the servomechanism loop. The residual transfer function is that transfer function which must be synthesized into the servomechanism loop. In some cases this can be done exactly, in others this reduces fundamentally to an approximation problem. Having synthesized the residual transfer function into physical components, the loop connection of all the components results in physical achievement of that loop-transfer function which meets (approximately or exactly) the stated requirements.

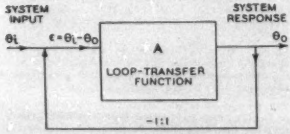

Figure 1. Fundamental system

It is the purpose of this paper to present the results of the foregoing method with one class of idealized loop-transfer functions. While other classes of functions of lesser and greater mathematical complexity may be shown to be required in some servomechanism design problems, the class dealt with herein has been of great utility and broad scope.

The Idealized Loop-Transfer Function, A, and System-Response Function, M

Basically, we need consider only the configuration in Figure 1. The box labeled $\boldsymbol{A}$ in Figure 1, contains all of the physical components of the system including the signal receiver, the controlling network, the prime-mover, and the driven member. The box labeled $\boldsymbol{A}$ may contain a variety and number of internal feed-back paths. It is assumed that the major closure of the servomechanism loop is accomplished through the -1 to 1 feed-back connection between output θ_o and the input θ_i. Hence, the true input to the box labeled $\boldsymbol{A}$ is ϵ, the instantaneous difference between the input function and the output response, namely

$$\epsilon=\theta_i-\theta_o \tag{1}$$

We denote by the same letter $\boldsymbol{A}$ the complex loop-transfer function of the box labeled $\boldsymbol{A}$. This we call the steady-state loop-transfer function. Hence

$$\theta_o=\boldsymbol{A}\epsilon \tag{2}$$

$$\theta_i=\epsilon(1+\boldsymbol{A}) \tag{3}$$

The steady-state system response function, $\boldsymbol{M}$, expressing the ratio of output response to input function is given by

$$\boldsymbol{M}=\frac{\theta_o}{\theta_i}=\frac{\boldsymbol{A}}{1+\boldsymbol{A}}=M\underline{/\varphi} \tag{4}$$

We arbitrarily choose, but for physically valid reasons, a most useful class of loop-transfer functions given by

$$\boldsymbol{A}=\frac{K}{(j\omega)^p}\frac{\left(1+j\frac{\omega}{\omega_1}\right)^s}{\left(1+j\frac{\omega}{\omega_2}\right)^t}=A\underline{/\theta} \tag{5}$$

where r, s, and t form the following combinations:

Case	r	s	t	Increasing Frequency A Behavior
I	3	2	1	$1/f^2:1/f:1/f^3$
II	2	1	1	$1/f^2:1/f:1/f^3$
III	3	2	2	$1/f^2:1/f:1/f^3$
IV	2	1	2	$1/f^2:1/f:1/f^3$

Hence, ω_1 and ω_2 (where $\omega_1<\omega_2$) are seen to be, respectively, the "transition frequencies" located approximately at the points where the loop-gain function enters upon and emerges from a behavior on a frequency basis like $1/f$. They are sometimes called the "knee" or "corner" frequencies. For ease in mathematical manipulation the loop-transfer function given by equation 5 is normalized to

$$\boldsymbol{A}=\frac{1}{x^r}\frac{(1+ax)^s}{(1+bx)^t} \tag{6}$$

by the substitutions

$$\left.\begin{aligned} x&=\frac{j\omega}{\sqrt[r]{K}}\\ a&=\frac{\sqrt[r]{K}}{\omega_1}\\ b&=\frac{\sqrt[r]{K}}{\omega_2}\end{aligned}\right\} \tag{7}$$

All "normalized frequencies" x have their corresponding "real frequencies" $\omega=2\pi f$. By a^r we denote the reciprocal of a, and by b^r we denote the reciprocal of b.

The following additional nomenclature is used:

In the loop-transfer function A:

x_c is the cut-off in the loop-transfer function, $A(x_c)=1$.

x_N is the frequency of cross-over in the loop-transfer function, $\theta(x_N)=\pi$.

A_N is the amplitude margin in the loop-transfer function, $A(x_N)=A_N$.

$\pi-|\theta_c|$ is the phase margin of the loop-transfer function, $\theta(x_c)=\theta_c$.

In the system-response function M:

$M(x_m)=M_{max}$

$M(x_u)=1 \qquad (x_u\neq 0)$

$\varphi(x_m)=\varphi_m$

$\varphi(x_u)=\varphi_u$

Figures 2 to 9, inclusive, illustrate the behavior of these functions, and of the corresponding Nyquist diagrams, for each of the case functions specified.

System Stability Considerations

The proximity of approach of the loop-gain function to the Nyquist point, $-1+j0$, in the $\boldsymbol{A}$-plane is well known to be a measure of degree of stability. Refer-

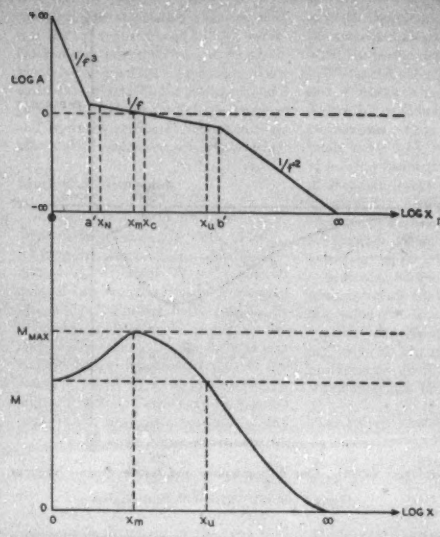

Figure 2 (left). Case I loop-transfer and system-response functions

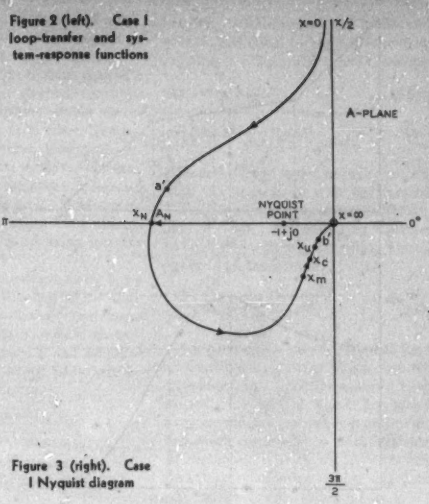

Figure 3 (right). Case I Nyquist diagram

ence to Figure 10 demonstrates that this is almost equivalent to the determination of the maximum value which the system-response function attains as the frequency varies from zero to infinity. Hence, in this paper, we use M_{max} as this measure of degree of stability. The range of practical interest in the values of M_{max} is from the theoretically perfect value of unity to about 1.5, and, hence, is the range dealt with in this paper.

The original Nyquist criterion of stability,[17] and the one which must be resorted to *in toto* in all questionable cases, involves the question of the number of net encirclements which the plot of the loop-transfer function makes about the Nyquist point as the frequency varies from minus infinity through zero to plus infinity and then back to minus infinity along a semicircular contour of infinite radius in the complex frequency plane. For example, case III behavior of the loop-transfer function as the frequency variable proceeds along the contour shown in Figure 11, is that shown in Figure 12. For stability, according to the simplest form of the Nyquist criterion, zero net encirclements of the Nyquist point occur. Needless to say, such detailed consideration of a mathematical nature is sometimes considerable inconvenience to the engineer. Hence, for the use of servomechanism engineers, the simpler practical criterion of stability for the class of loop-transfer functions treated herein is simply that the Nyquist point must always be "seen" to the left when progressing along the loop-gain function characteristic in the direction of increasing frequency. It is obvious that the ability to "see" the Nyquist point to the left is not altered fundamentally by the occurrence of miscellaneous loops in the loop-gain function in the neighborhood of the origin of the A-plane or elsewhere in regions essentially remote from the Nyquist point.

Provided the Nyquist criterion of stability, succinctly just stated, is satisfied first, then the indicated value of M_{max} is a true measure of the degree of such stability.

The foregoing assumes that when the box labeled A in Figure 1 contains minor feed-back loops the box labeled A itself represents a stable structure.[18–21]

An alternate approach to the stability question is that utilizing the Routh criterion which really amounts to the determination of the negativeness of the real parts of the roots of the system-determinantal equation. In investigating the detailed nature of the transient response, these roots always must be obtained, but the degree of stability is obtainable directly by use of the Nyquist criterion without first eliciting the roots of the system-determinantal equation. However, these criteria are merely two directly related different aspects of the stability problem. Their close interdependence will be evident in the typical results which follow.

System Accuracy Considerations

In the present status of the art of servomechanisms, accuracy requirements often are expressed in one of two ways, or a combination of both. One way involves what substantially might be called "steady-state accuracy". A type of such is the steady-state response of the servomechanism to an impressed sinusoid of relatively low frequency. For the high-performance systems treated herein, the frequencies at which such accuracy requirements are specified are so low that $A >> 1$. Hence, at such accuracy-determining frequencies, equation 3 is, almost exactly,

$$\frac{\theta_i}{\epsilon} \approx A \tag{3a}$$

Denote by ω_e that accuracy-determining frequency for which the accuracy requirement is most stringent and by A_e the requisite loop gain to fulfill that accuracy requirement. Then, assuming that ω_e is less than ω_1, equation 5 yields

$$\frac{\theta_i}{\epsilon} \approx \frac{K}{(j\omega_e)^r} \approx A_e \tag{8}$$

Hence, the constant multiplier K in equation 5, for a fixed error-frequency ω_e is directly proportional to the stringency of such accuracy requirement. In other words, as the accuracy requirement increases, the requisite gain level of the system must increase correspondingly.

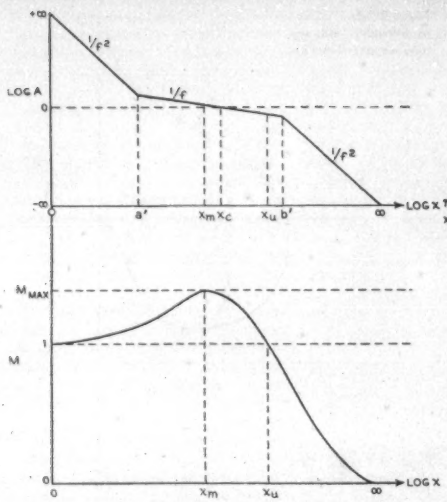

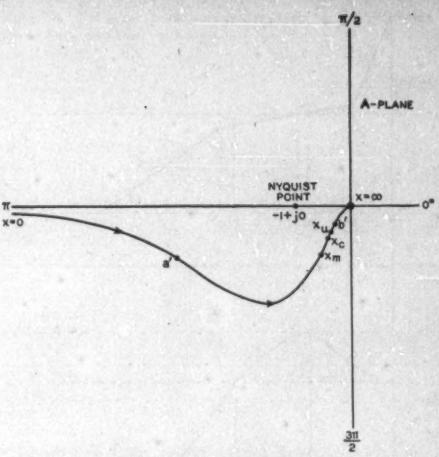

Figure 4 (left). Case II loop-transfer and system-response functions

Figure 5 (above). Case II Nyquist diagram

For a fixed accuracy requirement, the gain level, or accuracy-factor K, is directly proportional to the r'th power of the accuracy-determining frequency, ω_s. The gain level, or accuracy-factor, for an odd-type loop-gain function (case I or case III), is in a ratio of ω_s to the K factor of an even-type loop-gain function (case II or case IV), for the same accuracy requirement at the same frequency, ω_s. The same x values of normalized frequency ($x=\omega/\sqrt[r]{K}$) correspond to real frequencies in the ratio of the sixth root of A_s for the case II and IV functions as compared to the case I and III functions.

Another type of the steady-state accuracy of the servomechanism is that corresponding to input functions of the constant displacement, velocity, and acceleration, and higher-order derivative, types. These already have been dealt with sufficiently in the literature. Suffice it to say that systems corresponding to the case II and IV functions have zero static error and zero constant-velocity error, whereas systems corresponding to the case I and III functions have zero static error, zero velocity error, and zero constant-acceleration error. Servomechanisms of the type with loop-transfer functions having only a first order pole at the origin ($\omega=0$) fulfill only the zero static error condition.

The other type of accuracy by which servomechanisms often are characterized is the so-called "transient accuracy." This basically involves consideration of the nature of the response of the servomechanism to a step-function of unity (on a normalized basis). One feature characterizing "transient accuracy" is the "time-of-build-up" which we simply define as the time required for the output response to go from approximately 1/10 final unit value to 9/10 final unit value, in response to the applied unit step-function. The second feature characterizing transient accuracy is the amplitude of "overshoot", when existent, this being defined as the amount in excess of unity experienced as initial output response to applied unit step-function input. The third feature often associated with transient accuracy is the total time required for the normalized output response, to applied unit step-function input, to achieve a prescribed proximity to unity, never thereafter deviating from unity by more than that prescribed amount. Because, however, of the interdependence of the third characteristic upon the first two, the first two characteristics are employed most commonly.

As will appear subsequently, the steady-state accuracy and the transient accuracy are wholly interdependent and fixed for systems having the same loop-gain function and degree of stability.

Minimum-Band-Width Considerations

Two major considerations enter into the choice of the minimum-band-width type of servomechanism singled out for treatment. The first is that of minimizing the transmission of noise in the unnecessary portion of the signal spectrum through and beyond the system. The second minimum-band-width consideration arises from the fact that the fixed elements in many practical servomechanisms are essentially very low-pass transducers whose frequency-response characteristics generally can only be varied, or their band width extended, with great difficulty. Minimum-band-width servomechanisms meeting the prescribed stability and accuracy requirements utilize such servomechanism elements in the most effective manner possible. Viewed from another standpoint, servomechanism synthesis on the minimum-band-width basis establishes just what stability and accuracy requirements it is possible to meet with the fixed elements at hand. In some cases, it may be used to demonstrate that it is not possible to control, on a closed-loop basis, the response of the invariant driven member through the fixed prime mover with the degree of accuracy and stability desired. Considered from still another viewpoint, it may be absolutely necessary to use a nonminimum-band-width servomechanism, at some sacrifice in noise suppression, in order to satisfy the prescribed stability and accuracy requirements. In any case, for sheerly pragmatic reasons, and in the absence of being able to formulate any more cogent basis for these considerations at the pres-

cut time, the stipulation that we shall consider minimum-band-width servomechanisms, plus the choice of loop-gain functions of practical importance, yields useful design data, on the one hand, and a greater insight into the interdependency and contrary attributes of servomechanism stability and accuracy, on the other.

Method of Analysis

In equations 4 and 5, for a given K or accuracy-factor value, the value of M_{max}, its frequency location ω_m, and the frequency ω_u, at which $M = 1$, are all uniquely and simultaneously determined by ω_1 and ω_2. Further, both ω_m and ω_u lie between ω_1 and ω_2 in the increasing frequency sequence ω_1, ω_m, ω_u, ω_2. In normalized terms, equations 4 and 6, the values of M_{max}, x_m, x_u, all are determined uniquely and simultaneously by a and b (and, hence, by their reciprocals, a' and b'). On an increasing x basis, the sequence is a', x_m, x_u, b'.

Since a' and b' (ω_1 and ω_2) bracket x_m and x_u (ω_m and ω_u), we define minimum-band-width servomechanisms (having loop-transfer functions of the type used herein) as those servomechanisms having the degree of stability characterized by M_{max} and the degree of accuracy characterized by K, for which b' (ω_2) is a minimum. For each b' (ω_2) value there is a corresponding unique a' (ω_1) value. The reciprocal pair, a and b, and K specify completely the idealized loop-transfer function, equations 5 and 6, around which the servomechanism is to be designed to fulfill the performance requirements.

We restrict ourselves to those pairs of a and b values which characterize (conditionally or absolutely) stable servomechanisms. Case II is the only absolutely stable type in that the systems corresponding thereto are stable for all values of loop-gain level; the other three cases are all of the conditionally stable type in that the systems corresponding thereto are stable or unstable depending upon the loop-gain level.

Beginning with equations 4 and 6, we form first of all, the function M the absolute value of the complex system-response function, $\boldsymbol{M}$. However, instead of dealing with M, the analysis and synthesis problems are more easily dealt with by considering the function

$$C(x,a,b) \equiv \frac{1}{M^2} - 1 \equiv \frac{f(x,a,b)}{g(x,a)} \tag{9}$$

where f and g denote functions of the variables indicated. We may write

$$g(x,a) \cdot C(x,a,b) \equiv f(x,a,b) \tag{10}$$

At the point x_m at which $M > 1$ is a maximum and $C(x,a,b)$ a minimum* we have

$$g(x_m,a) \cdot C(x_m,a,b) = f(x_m,a,b) \tag{11}$$

and

$$\left[\frac{\partial}{\partial x} g(x,a) \cdot C(x,a,b) = \frac{\partial}{\partial x} f(x,a,b)\right]_{x=x_m} \tag{12}$$

* In each case, there is one and just one such value for a given a and b.

Let M_{max} be assigned a fixed value and set $C(x_m,a,b)$ equal to the corresponding constant, C. Equations 11 and 12 become

$$Cg(x_m,a) = f(x_m,a,b) \tag{13}$$

$$\left[C\frac{\partial}{\partial x} g(x,a) = \frac{\partial}{\partial x} f(x,a,b)\right]_{x=x_m} \tag{14}$$

Equations 13 and 14 define b as a function of a. In accordance with our method just outlined, we now maximize b (minimize $b' \sim \omega_2$). Differentiating equation 13 implicitly with respect to a, and using equation 14, there results

$$C\frac{\partial}{\partial a} g(x_m,a) = \frac{\partial}{\partial a} f(x_m,a,b) \tag{15}$$

The three equations 13, 14 and 15 form a simultaneous system which can be solved for x_m,a,b. Solutions are restricted to positive values of x_m,a,b, for which $b<a$, for which b is actually a maximum, and which correspond to stable systems. In the appendix is shown for each case the (b,a) relationship which must be satisfied for system stability.

In cases II and IV, the exact solution, utilizing equations 13, 14, and 15, is employed. We use case IV as an example of the method. Since $r = 2$, $s = 1$, and $t = 2$,

$$f(x,a,b) = b^4x^2 + 2b^3x^4 + x^4(1 + 2b^2 - 4ab) - 2x^2 \tag{16a}$$

$$g(x,a) = 1 + a^2x^2 \tag{16b}$$

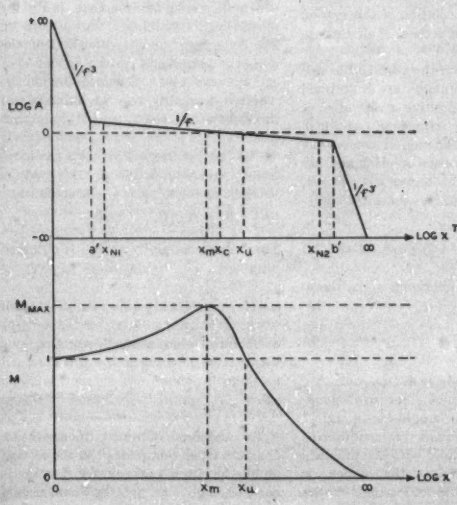

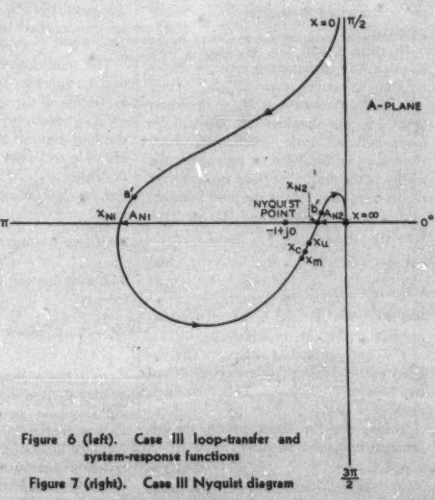

Figure 6 (left). Case III loop-transfer and system-response functions

Figure 7 (right). Case III Nyquist diagram

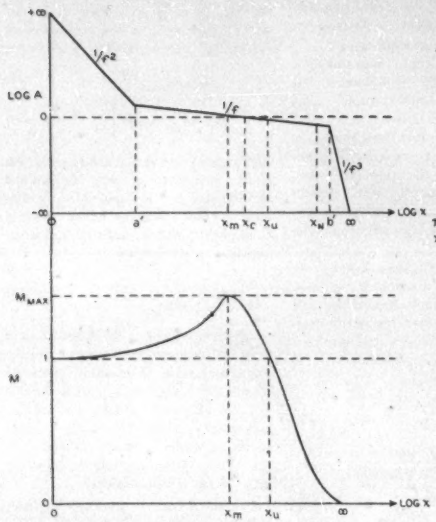

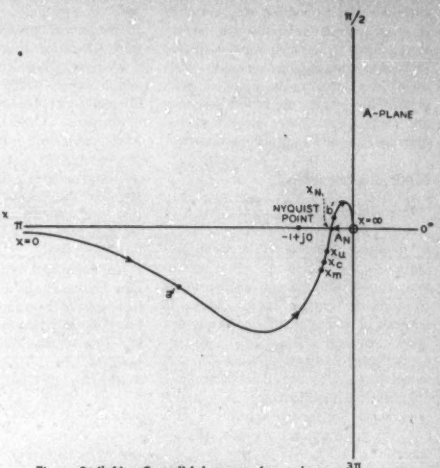

Figure 8 (left). Case IV loop-transfer and system-response functions

Figure 9 (right). Case IV Nyquist diagram

The simultaneous system corresponding to equations 13, 14, and 15 is

$$b^4x_m^8+2b^2x_m^6+x_m^4(1+2b^2-4ab)-2x_m^2 = C(1+a^2x_m^2) \quad (17)$$

$$4b^4x_m^6+6b^2x_m^4+2x_m^2(1+2b^2-4ab)-2 = a^2C \quad (18)$$

$$aC=-2bx_m^2 \quad (19)$$

The results of the solution of this system are summarized in section D of the appendix.[23]

In cases I and III, an approximate solution, having maximum error of 4.4 per cent in the extreme case ($M_{max}=1.5$) and considerably less error as M_{max} decreases from 1.5, was employed to lighten the computational work. Such approximation was possible, without decreasing the utility of the results for these two cases by recognizing that, in the range of interest, $a^2x^2>>1$. For cases I and III, we have exactly

$$g(x,a)=(1+a^2x^2)^2 \quad (20a)$$

$$f(x,a,b)=x^4f_1(x,a,b) \quad (20b)$$

We use $g_1=a^4$ instead of g, and $f_1(x,a,b)$ instead of $f(x,a,b)$, in equations 13, 14, and 15 and proceed as before. The validity of the approximation may be checked by Newton's method. This has been done.

Taking case I as an example of the approximate method, we have

$$f(x,a,b)=x^4[b^2x^4+(1-2a^2b)x^2+2(b-2a)] \quad (21a)$$

$$g(x,a)=(1+a^2x^2)^2 \quad (21b)$$

Substituting g_1 and f_1, in place of g and f in equations 13, 14, and 15, there results the following system of equations:

$$b^2x_m^4+(1-2a^2b)\cdot x_m^2+2(b-2a)=a^4C \quad (22)$$

$$2b^2x_m^3+(1-2a^2b)=0 \quad (23)$$

$$abx_m^2+1=-a^2C \quad (24)$$

The results of the solution of this system are summarized in section A of the appendix.[23]

The conditions on the permissible values of a and b for stability are established in terms of the positive real value of $x=x_N$ ("cross-over frequency") at which the loop-transfer function $\boldsymbol{A}$ crosses the negative real-axis of the $\boldsymbol{A}$-plane and has the value A_N. This occurs when $|\theta|=\pi$. For the class of functions considered herein

$$\theta=(4-r)\frac{\pi}{2}+s\tan^{-1}(ax)-t\tan^{-1}(bx) \quad (25)$$

The equation for obtaining x_N is, therefore,

$$(r-2)\frac{\pi}{2}=s\tan^{-1}(ax_N)-t\tan^{-1}(bx_N) \quad (26)$$

Case I has a single real cross-over frequency x_N at which A_N, the corresponding loop-gain or "amplitude margin", must be greater than unity for (conditional) stability in accordance with the practical criterion enunciated in the section on "System Stability Considerations." See Figure 3. Case II possesses no real cross-over frequency for all $b<a(\omega_1<\omega_2)$, and, hence, is absolutely stable. See Figure 5. Case III has two real cross-over frequencies, x_{N1} and x_{N2}, and for (conditional) stability the corresponding loop-gain values must satisfy the conditions $A_{N1}>1$ and $A_{N2}<1$. See Figure 7. Case IV has a single real cross-over frequency at which A_N must be less than unity for (conditional) stability. See Figure 9. The foregoing conditions establish the uniquely permissible paired values of a and b in each case. See appendix for the required inequality between a and b, and the expressions for x_N and A_N, in each case.

The "cut-off frequency" x_c in the loop-transfer function, defined by $A(x_c)=1$, is obtained as the solution to the equation

$$x_c^r(1+b^2x_c^2)^{t/2}=(1+a^2x_c^2)^{s/2} \quad (27)$$

The "phase-margin", $\pi-|\theta_c|$, is obtained from

$$\theta_c=(4-r)\frac{\pi}{2}+s\tan^{-1}(ax_c)-t\tan^{-1}(bx_c) \quad (28)$$

The unit-response band width x_u, the value of $x\neq 0$ for which $M=1$, is obtained as the solution of

$$f(x_u,a,b)=0 \quad (29)$$

The method of obtaining the remaining characteristics summarized in the section on the idealized loop-transfer function is considered obvious, and the literal results

of all the foregoing for this class of loop-gain function are listed in the appendix.

Summary of Results

Servomechanisms of interest and utility in most present-day applications are characterized by M_{max} values in the neighborhood of 1.3. Accordingly, the foregoing analytical results have been employed in computing the pertinent system data for design use and performance analysis, for values of M_{max} from 1.01 to 1.5 in discrete steps. The corresponding information for intermediate values of M_{max} may be obtained easily by interpolation.

In Table I are shown tabulated as a function of M_{max} the characteristic data for the normalized steady-state loop-transfer and system-response functions, using the nomenclature of the section on loop-transfer and system-response functions. In Table II are tabulated first the roots of the normalized system-determinantal equations, $1+A=0$, and second, the normalized build-up time and percentage overshoot of output response to an impressed unit step-function input, with the system starting from "rest" conditions. Both the normalized roots and the normalized build-up times are tabulated for the same discrete values of M_{max} as are the data in Table I. All "normalized frequencies" (x values, a' and b') and "normalized roots" must be multiplied by $\sqrt{K}$ to obtain physically real frequencies ($\omega=2\pi f$) and damping factors. "Normalized build-up times" must be divided by the same factor to obtain physical build-up times in seconds. Finally, it is noted that the "normalized roots", given specific initial conditions, enable one to calculate the residues and the complete transient response of the corresponding systems.[22] The various phase-angles are given in actual degrees and the amplitude margins are listed in actual decibels, and may be used directly for comparison purposes.

Note that $r=3$ for cases I and III (odd), and that $r=2$ for cases II and IV (even).

A Typical Example

Suppose it be desired to design a servomechanism of the minimum-band-width type described herein. Suppose further that the servomechanism be of the conditionally stable type with a degree of stability characterized by an M_{max} value of 1.3. Suppose finally that the response displacement error is to be 3 minutes or less for a sinusoidal input signal having a frequency of 1/9 cycle per second and an amplitude of 25 degrees.

First

$$\left.\begin{aligned} A_e &= \frac{25\times 60}{3} = 500 \\ \omega_e &= \frac{2\pi}{9} = 0.698 \end{aligned}\right\} \quad (30a)$$

Let us introduce a 2-to-1 margin of safety in meeting the accuracy requirements by using an A_e value of 1,000. Then

$$\left.\begin{aligned} K_{odd} &= A_e\omega_e^2 = 340 \\ K_{even} &= A_e\omega_e^2 = 487 \end{aligned}\right\} \quad (30b)$$

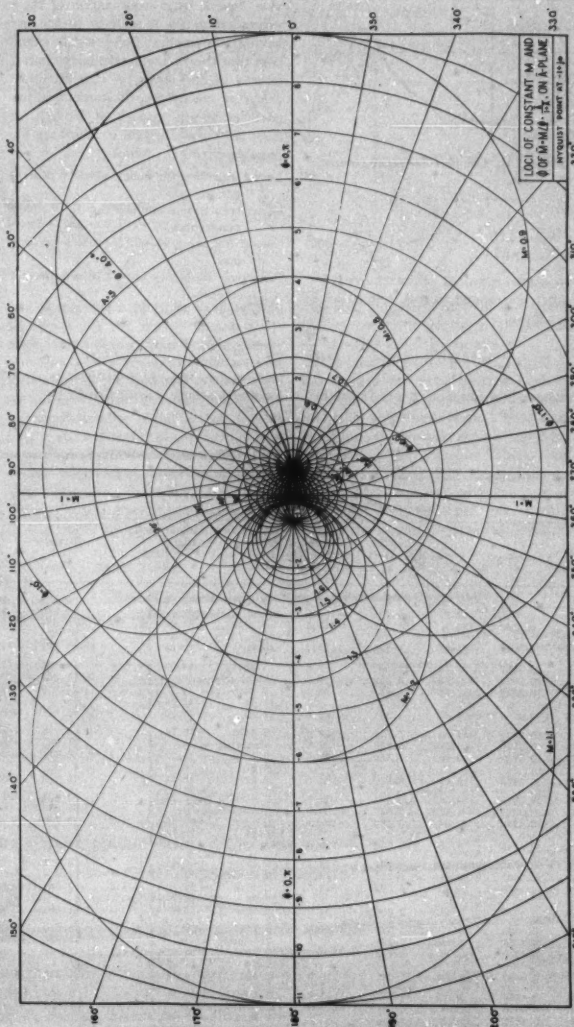

Figure 10. Interdependence of loop-transfer and system-response functions

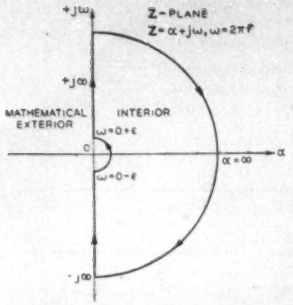

Figure 11. Complex frequency contour

and

$$\left.\begin{aligned} \sqrt[3]{K_{odd}} &= 6.98 \\ \sqrt[3]{K_{even}} &= 22.1 \end{aligned}\right\} \qquad (30c)$$

The same x values of normalized frequency correspond to real frequencies in the ratio of

$$\frac{\omega_{even}}{\omega_{odd}} = (A_s)^{1/3} = (1{,}000)^{1/3} = 3.16 \qquad (30d)$$

for the even A functions (cases II and IV) as compared to the odd A functions (cases I and III).

For the $M_{max} = 1.3$ stability requirements specified it is possible to go directly to Tables I and II for the normalized parameter values, roots, and build-up time of the minimum-band-width servomechanism. Among all four cases available, case I, upon examination of the x values tabulated, is seen to be the one having the smallest band width. Suppose that this be the determining characteristic in our choice of case function. Then, by multiplying all normalized frequencies by the cube root of K_{odd}, or 6.98, the physically real ω values are obtainable directly as follows:

Lower transition frequency $\omega_1 = 2.96$ radians per second

Upper transition frequency $\omega_2 = 51.7$ radians per second

Cut-off frequency $\omega_c = 32.8$ radians per second

Cross-over frequency $\omega_N = 3.16$ radians per second

Frequency of M_{max}, $\omega_m = 25.7$ radians per second

Frequency of M unity, $\omega_u = 43.7$ radians per second

Phase margin $180 - |\theta_c| = 46.6$ degrees

Amplitude margin $A_N = 26.6$ decibels

Phase of M at ω_m, $\varphi_m = -46.2$ degrees

Phase of M at ω_u, $\varphi_u = -95.0$ degrees

The resulting idealized loop-transfer function is given by

$$A = \frac{340}{(j\omega)^3} \frac{\left(1 + j\dfrac{\omega}{2.93}\right)^2}{\left(1 + j\dfrac{\omega}{51.7}\right)} \qquad (31)$$

It is this loop-gain function which must be synthesized as closely as possible into the servomechanism in order to satisfy the foregoing stability and accuracy requirements. Viewed from another standpoint, the transfer functions of the fixed elements (such as the prime-mover and driven element) first must be removed from the idealized loop-transfer function given in equation 31, and the resulting residual transfer function must be synthesized into the other elements in the servomechanism loop. In most practical cases the synthesis of the residual transfer function is an approximation problem. Viewed from still another standpoint, the transition frequencies ω_1 and ω_2 are those around which the servomechanism must be designed with the gain level so adjusted that

Table I. Minimum-Band-Width Servo Parameters

Loop-Transfer Function: A								System-Response Function: $M = \frac{A}{1+A}$						
Case	$a' \propto \omega_1$ a'	$b' \propto \omega_2$ b'	Cut-Off $A(x_c) = 1$ x_c	Phase Margin $180° - \lvert\theta_c\rvert$ θ_c, Deg	Cross-Over $\theta(x_N) = \pi$ x_N	Amplitude Margin $A_N = A(x_N)$ A_N, DB	M_{max}	$M(x_m) = M_{max}$ x_m	$\varphi(x_m) = \varphi_m$ φ_m, Deg	$M(x_u) = 1$ x_u	$\varphi(x_u) = \varphi_u$ φ_u, Deg	$a = 1/a'$ a	$b = 1/b'$ b
I	0.1696	68.49	31.57	−115.4	0.1701	+52.20		5.869	−10.6	19.14	−33.2	5.895	0.01460
II	0.09921	19.65	9.139	−115.5	Absolutely stable			1.989	−11.5	5.768	−34.7	10.08	0.05090
III	0.1707	136.1	33.32	−117.1	0.1716	+51.80	1.01	5.921	−9.95	22.38	−39.1	5.859	0.007347
					135.4	−17.88							
IV	0.09970	39.98	9.583	−117.4	39.89	−17.94		1.995	−11.5	6.603	−39.6	10.09	0.02501
I	0.2807	23.57	11.49	−118.8	0.2841	+38.92		4.612	−21.7	10.46	−53.4	3.562	0.04242
II	0.2078	8.787	4.322	−119.0	Absolutely stable			1.983	−24.7	4.079	−55.6	4.812	0.1138
III	0.2832	47.71	11.75	−120.4	0.2865	+38.70	1.05	4.579	−21.6	12.28	−63.2	3.531	0.02096
					47.15	17.56							
IV	0.2129	17.87	4.381	−120.0	17.85	−17.42		1.986	−25.0	4.608	−63.1	4.696	0.05537
I	0.3399	14.96	7.714	−123.0	0.3479	+33.74		4.213	−30.0	8.486	−68.5	2.942	0.06684
II	0.2740	6.094	3.236	−122.8	Absolutely stable			1.965	−33.8	3.611	−70.0	3.650	0.1641
III	0.3469	30.70	7.820	−123.6	0.3549	+33.22	1.1	4.114	−29.7	9.576	−78.0	2.883	0.03257
					30.01	−16.98							
IV	0.2879	12.61	3.270	−124.0	12.32	−16.82		1.949	−34.2	4.014	−78.8	3.474	0.07933
I	0.3979	9.569	5.501	−128.2	0.4156	+29.28		3.828	−40.0	6.957	−82.3	2.513	0.1045
II	0.3399	4.175	2.537	−128.9	Absolutely stable			1.938	−44.7	3.236	−87.6	2.942	0.2395
III	0.4132	20.09	5.480	−129.1	0.4314	+28.30	1.2	3.736	−40.4	7.735	−97.2	2.420	0.04978
					19.24	−15.98							
IV	0.3743	8.961	2.506	−129.8	8.578	−15.77		1.912	−46.1	3.512	−97.8	2.672	0.1116
I	0.4252	7.402	4.701	−133.4	0.4519	+26.55		3.681	−46.2	6.227	−95.0	2.352	0.1351
II	0.3687	3.310	2.267	−133.7	Absolutely stable			1.914	−51.8	3.056	−99.2	2.712	0.3021
III	0.4498	15.90	4.603	−133.5	0.4776	+25.80	1.3	3.554	−47.4	6.921	−110.0	2.223	0.06289
					14.98	−15.16							
IV	0.4248	7.402	2.200	−134.2	6.920	−14.86		1.884	−54.0	3.257	−109.6	2.354	0.1351
I	0.4386	6.177	4.308	−136.5	0.4735	+26.17		3.610	−51.8	5.884	−103.5	2.280	0.1619
II	0.3804	2.789	2.124	−137.5	Absolutely stable			1.894	−56.9	2.946	−107.9	2.629	0.3588
III	0.4730	13.60	4.143	−136.9	0.5105	+24.02	1.4	3.445	−52.8	6.444	−119.4	2.114	0.07355
					12.60	−14.42							
IV	0.4583	6.373	2.032	−138.0	5.952	−14.12		1.846	−60.0	3.099	−120.3	2.182	0.1569
I	0.4444	5.388	4.083	−140.6	0.4864	+25.58		3.569	−55.6	5.738	−111.3	2.250	0.1856
II	0.3828	2.431	2.037	−140.6	Absolutely stable			1.878	−60.8	2.868	−114.6	2.612	0.4114
III	0.4855	12.11	3.864	−140.1	0.5359	+22.90	1.5	3.372	−60.0	6.132	−127.5	2.047	0.08256
					11.04	−13.61							
IV	0.4808	5.760	1.932	−141.1	5.257	−13.28		1.825	−64.6	2.984	−127.8	2.080	0.1736

the loop gain at a frequency of 1/9 cycle per second is 1,000.

Although tachimetric and other rotating electric equipment, in conjunction with simple configurations of static elements (coils, capacitors, and resistors, with or without amplifiers), at present commonly are employed in solving this synthesis problem either exactly or approximately, more elegant and often more economical solutions are available by synthesizing the residual transfer function into static networks entirely. This newer technique is largely mathematical and uses the fundamental tools of the networks synthesis specialist.

Reference to Table II gives the roots of the system-determinantal equation, $1 + A = 0$, which roots, when multiplied through by the factor 6.98, yield the physical zeros of the system for calculating transient response for any given initial conditions and input.

The last columns in Table II show that this servomechanism, if exactly synthesized, possesses a build-up time of 0.035 second and 28.7 per cent overshoot in response to a step-function starting from "rest" conditions. In some applications this is a sufficiently rapid transient response; in others, a more rapid build-up time may be necessary. However, the $1/\omega^2$ behavior for frequencies close to zero frequency is a condition only approximately obtained by most servomechanisms. The behavior of the physically realizable servomechanism for frequencies close to zero will generally be of the order of $1/\omega$.

The data contained in Tables I and II will be of qualitative value even in those cases where the behavior in the loop-gain function at frequencies close to zero is different from $1/\omega^2$ or $1/\omega^3$, provided that at some very low frequency, and above, the loop-gain function behavior assumes the nature of the class function treated herein. In those cases for which the foregoing conditions are satisfied, the Nyquist diagram will differ from those shown in Figures 3, 5, 7, and 9 for only very low frequencies, the essential conditions for stability in each case remaining unchanged.

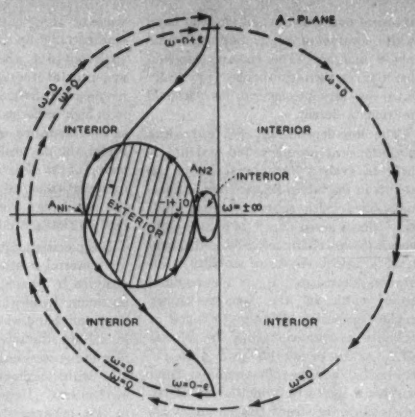

Figure 12. Complete Nyquist diagram (case III)

Conclusion

In addition to the design usefulness of the particular data tabulated herein, it is hoped that the underlying viewpoint and method proposed and employed in this paper also may serve to stimulate further investigation along these lines, if only for the pragmatic reasons listed in the beginning. The specific class of generalized loop-transfer function dealt with is obviously only one in the sequence of increasingly complex loop-transfer functions possible of practical consideration, starting from the simplest. Others may see fit to complement the foregoing results by the presentation of similar data regarding the other classes of loop-gain functions of practical use in servomechanisms.

The engineering criterion of linear servomechanism stability enunciated under "System Stability Considerations" is applicable to these other classes of loop-gain functions as well as to those treated herein having a second or third order pole at the origin ($\omega = 0$).

The data tabulated in the tables for the four generalized cases make available a wide range of high-performance servomechanism characteristics. They make it possible to choose in advance that particular loop-gain function which meets the particular system design requirements, for example, conditional or absolute stability, degree of stability, steady-state accuracy, transient accuracy,

Table II. Roots, Build-up Time, and Percentage Overshoot

M_{max}	Case	$x_{1,2}$	x_3	x_4	x_5	Build-up Time	Percentage Overshoot
1.01	I	$-34.07 \pm 34.60j$	-0.1589	-0.1825		0.043	5.3
	II	$-9.775 \pm 10.03j$	-0.1002			0.148	5.2
	III	$-39.24 \pm 41.41j$	-0.1598	-0.1842	-193.4	0.042	5.5
	IV	$-11.52 \pm 12.18j$	-0.1001	-56.82		0.130	5.0
1.05	I	$-11.49 \pm 12.39j$	-0.2463	-0.3349		0.141	9.9
	II	$-4.285 \pm 4.697j$	-0.2174			0.305	9.7
	III	$-13.39 \pm 14.78j$	-0.2483	-0.3586	-68.05	0.102	9.9
	IV	$-5.079 \pm 5.564j$	-0.2233	-25.74		0.268	10.0
1.1	I	$-7.126 \pm 8.271j$	-0.2879	-0.4365		0.167	14.8
	II	$-2.898 \pm 3.481j$	-0.2970			0.365	14.5
	III	$-8.356 \pm 9.646j$	-0.2925	-0.4501	-43.94	0.147	14.7
	IV	$-3.403 \pm 4.038j$	-0.3150	-18.09		0.345	15.0
1.2	I	$-4.342 \pm 5.807j$	-0.3254	-0.5594		0.222	22.3
	II	$-1.895 \pm 2.689j$	-0.3857			0.470	22.0
	III	$-5.128 \pm 6.570j$	-0.3346	-0.5991	-28.99	0.200	23.0
	IV	$-2.255 \pm 2.999j$	-0.4397	-12.97		0.423	23.5
1.3	I	$-3.216 \pm 4.920j$	-0.3420	-0.6272		0.248	28.7
	II	$-1.441 \pm 2.381j$	-0.4272			0.525	28.0
	III	$-3.815 \pm 5.394j$	-0.3563	-0.7034	-23.11	0.226	30.0
	IV	$-1.744 \pm 2.570j$	-0.5264	-10.79		0.485	30.0
1.4	I	$-2.583 \pm 4.470j$	-0.3530	-0.6696		0.265	33.4
	II	$-1.173 \pm 2.217j$	-0.4432			0.545	32.8
	III	$-3.078 \pm 4.771j$	-0.3696	-0.7804	-19.80	0.238	35.0
	IV	$-1.392 \pm 2.327j$	-0.5894	-9.373		0.520	35.0
1.5	I	$-2.180 \pm 4.220j$	-0.3540	-0.6750		0.273	37.7
	II	$-0.9933 \pm 2.117j$	-0.4445			0.560	37.0
	III	$-2.583 \pm 4.449j$	-0.3767	-0.8238	-17.85	0.265	38.7
	IV	$-1.182 \pm 2.179j$	-0.6336	-8.524		0.531	40.0

transient overshoot, actual physical band width, location of M_{max}, amplitude, and phase margins. The chosen loop-gain function is then synthesized physically into the servomechanism, as outlined previously herein.

The interdependency of steady-state and transient accuracy and stability is believed evident by examination of the results in the tables for the class of minimum-band-width servomechanism studied. For a given degree of steady-state accuracy, as characterized by the gain level K as the degree of stability is increased (decreasing M_{max}) the required band width of the servomechanism rapidly increases. For a given degree of stability, as characterized by the value of M_{max} as the degree of steady-state accuracy is increased the required band width also increases. For a given degree of stability, the steady-state accuracy increases directly as the gain level K; the transient accuracy (measured as the reciprocal of the build-up time of response to a step function) increases directly as the r'th root of the gain level K. For a fixed gain level K the steady-state accuracy remains fixed and the transient accuracy increases, but not linearly, as the degree of stability increases. As the normalized and the actual physical band width increase, the build-up time decreases and the transient accuracy increases.

The results in Table II demonstrate that the percentage overshoot in the transient response to a step function is practically the same for all four cases considered, for a specified degree of stability or M_{max} value. The percentage overshoot is approximately the same, whether there is a second or a third order pole at the origin ($\omega=0$), and correlates directly with the steady-state M_{max} value. For example, all four cases have approximately 30 per cent transient overshoot for $M_{max}=1.3$.

The results in Table II also demonstrate that the normalized build-up time time is determined largely by the behavior of the loop-gain function at $\omega=0$. For example, both odd (I and III) cases have approximately the same normalized build-up time for a particular value of M_{max}; both even (II and IV) cases have approximately the same normalized build-up time for a particular value of M_{max}. The ratio in the normalized build-up times between the odd and even cases, for a particular value of M_{max}, varies from roughly 1 to 2 for $M_{max}=1.5$, to roughly 1 to 3 for $M_{max}=1.01$. The ratio in the actual build-up times in seconds between the odd and even cases, for a particular value of M_{max}, is this ratio in the normalized build-up times multiplied by the sixth root of A_s, the absolute value of the loop-gain at the steady-state accuracy-requirement frequency, ω_s. Hence, for most high-performance ($100 \leqq A_s \leqq 1{,}000$) servomechanisms of the type described herein, the physical build-up time in seconds is of the same order for all four cases, for a particular value of M_{max}, and, like the percentage overshoot, correlates directly with the steady-state M_{max} value.

It is possible clearly to draw the foregoing powerful conclusions from the cases analyzed by having initially imposed the minimum band-width condition. Nonminimum band-width servomechanisms, in certain instances, possibly may be found to possess characteristics not available with minimum-band-width servomechanisms. Here, however, the connection between steady-state and transient accuracy and stability does not appear to be quite so clear nor so definite as the foregoing treatment makes possible for generalized minimum band-width servomechanisms. Further, until all the properties of generalized minimum band-width servomechanisms, characterized by increasingly complex loop-gain functions, have been elicited and made available to the profession, by methods similar to those employed herein, it appears that the use of a nonminimum-band-width servomechansim will continue, in each case, to be a matter requiring individual treatment. It may well be that our increased understanding of minimum-band width servomechanisms subsequently will make the analysis and synthesis problems of nonminimum-band-width servomechanisms more tractable.

Appendix

A. Case I—Theoretical Summary (Approximate Solution)

$$A=\frac{K}{(j\omega)^2}\frac{\left(1+j\frac{\omega}{\omega_1}\right)^2}{\left(1+j\frac{\omega}{\omega_2}\right)}$$

$$=\frac{1}{x^2}\frac{(1+ax)^2}{(1+bx)}$$

$$=A\angle\theta$$

$$A=\frac{1}{x^2}\frac{(1+a^2x^2)}{\sqrt{1+b^2x^2}}$$

$$\theta=-\frac{3\pi}{2}+2\tan^{-1}ax-\tan^{-1}bx$$

$$M=M\angle\phi$$

$$=\frac{A}{1+A}$$

$$\phi=2\tan^{-1}ax-\tan^{-1}\frac{[-x^2+2ax]}{[bx^4-a^2x^2+1]}$$

$$M=\frac{1+a^2x^2}{\sqrt{b^2x^6+(1-2a^2b)x^4+(2b-4a)x^2+(1+a^2x^2)^2}}$$

$$a=\frac{1}{a'}=\frac{\sqrt[3]{K}}{\omega_1}=\sqrt[3]{\frac{1}{q}\left(\frac{1}{v_r}-1\right)}$$

$$b=\frac{1}{b'}=\frac{\sqrt[3]{K}}{\omega_2}=\frac{a}{2(a^2q+1)}$$

where

$$q=1/M^2_{max}$$

and v_r is the single positive real root <1 of

$$v^3-4v^2+4v+(q-1)=0$$

$$x_m=\sqrt{\frac{2a^2b-1}{2b^2}}$$

$$x_u=\sqrt{x_m^2+\sqrt{x_m^4+\frac{4a-2b}{b^2}}}$$

$$x_N=\sqrt{\frac{1}{a^2-2ab}}$$

$$A_N=\frac{2a}{x_N^2}$$

$$x_c=\sqrt{y_r}$$

where y_r is the single positive real root of

$$b^2y^4+y^3-a^4y^2-2a^2y-1=0$$

$$x=jx$$

$$x=\frac{\omega}{\sqrt[3]{K}}$$

For conditional stability

$$b<\frac{a}{2}-\frac{1}{4a^2}$$

B. Case II—Theoretical Summary (Exact Solution)

$$A=\frac{K}{(j\omega)^2}\frac{\left(1+j\frac{\omega}{\omega_1}\right)}{\left(1+j\frac{\omega}{\omega_2}\right)}$$

$$=\frac{1}{x^2}\frac{(1+ax)}{(1+bx)}$$

$$=A\angle\theta$$

$$A=\frac{1}{x^2}\sqrt{\frac{1+a^2x^2}{1+b^2x^2}}$$

$$\phi=-\pi+\tan^{-1}ax-\tan^{-1}bx$$

$$M=M\angle\phi$$

$$=\frac{A}{1+A}$$

$$\phi=\tan^{-1}ax-\tan^{-1}\frac{[-bx^2+ax]}{[-x^2+1]}$$

$$M=\frac{\sqrt{1+a^2x^2}}{\sqrt{b^2x^6+(1-2ab)x^4-2x^2+(1+a^2x^2)}}$$

$$a=\frac{1}{a'}$$

$$=\frac{\sqrt{K}}{\omega_1}$$

$$=\sqrt{\frac{2}{3C(C+1)}[-1-\sqrt{4+3C}]}$$

$$b=\frac{1}{b'}=\frac{\sqrt{K}}{\omega_2}=\frac{a^2q+2a}{2}$$

where

$$C=-1+1/M_{\max}^2$$

and

$$q=C^2+C$$

$$x_m=\sqrt{-\frac{aC}{b}}$$

$$x_u=\sqrt{\frac{2ab-1+\sqrt{(2ab-1)^2+8b^2}}{2b^2}}$$

$$x_c=\sqrt{y_r}$$

where y_r is the single positive real root of

$$b^2y^3+y^2-a^2y-1=0$$

$$x=jx$$

$$x'=\frac{\omega}{\sqrt{K}}$$

Absolute stability for all $a>b$.

C. Case III—Theoretical Summary (Approximate Solution)

$$A=\frac{K}{(j\omega)^2}\frac{\left(1+j\frac{\omega}{\omega_2}\right)^2}{\left(1+j\frac{\omega}{\omega_1}\right)^2}$$

$$=\frac{1}{x^2}\frac{(1+ax)^2}{(1+bx)^2}$$

$$=A\angle\theta$$

$$A=\frac{1}{x^2}\frac{(1+a^2x^2)}{(1+b^2x^2)}$$

$$\theta=-\frac{3\pi}{2}+2\tan^{-1}ax-2\tan^{-1}bx$$

$$M=M\angle\phi$$

$$=\frac{A}{1+A}$$

$$\phi=2\tan^{-1}ax-\tan^{-1}\frac{[b^2x^3-x^2+2ax]}{[2bx^4-a^2x^3+1]}$$

$$M=\frac{1+a^2x^2}{\sqrt{b^4x^{10}+2b^2x^6+(1+4ab^3-4a^2b)x^6+(4b-4a)x^4+(1+a^2x^2)^2}}$$

$$a=\frac{1}{a_1}=\frac{\sqrt[3]{K}}{\omega_1}$$

$$=\sqrt[3]{\frac{(v_r-2)z_r-v_r}{Cv_r}}$$

$$b=\frac{1}{b'}=\frac{\sqrt[3]{K}}{\omega_2}=az_r$$

where $0<z_r<0.172$ and z_r is a derived function corresponding thereto.

$$x_m=\frac{\sqrt{z_r}}{b}$$

$$x_u=\sqrt{y_r}$$

where y_r is the single positive real root of

$$b^4y^3+2b^3y^2+(1+4ab^3-4a^2b)y-4(a-b)=0$$

x_c is the single positive real root of

$$b^2x_c^6+x_c^3-a^2x_c^2-1=0$$

$$x_{N1,2}^2=\frac{a^2+b^2-4ab\pm\sqrt{(a^2+b^2-4ab)^2-4a^2b^2}}{2a^2b^2}$$

$$A_{N1,2}=\frac{1}{x_{N1,2}^2}\frac{(1+a^2x_{N1,2}^2)}{(1+b^2x_{N1,2}^2)}$$

$$x_{N1}=\frac{1}{abx_{NT}}$$

$$x=jx$$

$$x'=\frac{\omega}{\sqrt[3]{K}}$$

For conditional stability $A_{N1}>1>A_{N2}$.

D. Case IV—Theoretical Summary (Exact Solution)

$$A=\frac{K}{(j\omega)^2}\frac{\left(1+j\frac{\omega}{\omega_1}\right)}{\left(1+j\frac{\omega}{\omega_2}\right)^3}=\frac{1}{x^2}\frac{(1+ax)}{(1+bx)^3}=A\angle\theta$$

$$A=\frac{1}{x^2}\frac{\sqrt{1+a^2x^2}}{(1+b^2x^2)}$$

$$\theta=-\pi+\tan^{-1}ax-2\tan^{-1}bx$$

$$M=M\angle\phi$$

$$=\frac{A}{1+A}$$

$$\phi=\tan^{-1}ax-\tan^{-1}\frac{[-2bx^3+ax]}{[b^2x^4-x^2+1]}$$

$$M=\frac{\sqrt{1+a^2x^2}}{\sqrt{b^4x^8+2b^2x^6+(1+2b^3-4ab)x^4-2x^2+(1+a^2x^2)}}$$

$$a=\frac{1}{a'}=\frac{\sqrt{K}}{\omega_1}=2\sqrt{-\frac{v_r}{C}}$$

$$b=\frac{1}{b'}=\frac{\sqrt{K}}{\omega_2}=\frac{2a(a^2q+4)}{a^4C^2+16}$$

where

$$C=-1+1/M_{\max}^2$$

$$q=C^2+C$$

and v is the positive real root, less than $-1/C$, of the equation

$$v^4+(1+2/C)v^3+\frac{1}{4}(1+4/C)v^2-\frac{v}{2C}-\frac{1}{4C}=0$$

$$x_m=\sqrt{-\frac{aC}{2b}}$$

$$x_N^2=\frac{a-2b}{ab^2}$$

$$A_N=\frac{a^2b}{2(a-2b)}$$

$$x_u=\sqrt{z_r}$$

Table III. Amplitude Margin and Corresponding System Response

System Response M	Amplitude Margin A_N: Arithmetic Ratio $A_{N\pi L}$	Arithmetic Ratio $A_{N\pi S}$	Logarithmic Ratio $A_{N\pi L}$ in Db	Logarithmic Ratio $A_{N\pi S}$ in Db
1.5	3.00	0.600	+ 9.55	−4.45
1.4	3.50	0.583	+10.88	−4.08
1.3	4.33	0.565	+12.67	−4.96
1.2	6.00	0.546	+15.55	−5.27
1.1	11.00	0.524	+20.80	−5.62
1.05	21.00	0.513	+26.45	−5.79
1.01	101.00	0.502	+40.10	−5.99
1.00	$+\infty$	0.500	$+\infty$	−6.03

M	A_0	$A_{N\pi}$	A_0 in "Db"	$A_{N\pi}$ in Db
0.9	9.00	0.473	+19.08	−6.51
0.8	4.00	0.444	+12.04	−7.04
0.7	2.33	0.413	+ 7.28	−7.70
0.6	1.50	0.375	+ 3.52	−8.54
0.5	1.00	0.333	0	−9.55
0.4	0.667	0.286	− 3.52	−10.87
0.3	0.428	0.231	− 7.28	−12.73
0.2	0.250	0.167	−12.04	−15.57
0.1	0.111	0.0909	−19.08	−20.82
0	0	0	$-\infty$	$-\infty$

Subscript π denotes cross-over in left-half A plane. Subscript L denotes larger value of $A_{N\pi}$ for $M>1$.
Subscript 0 denotes cross-over in right-half A plane. Subscript S denotes smaller value of $A_{N\pi}$ for $M>1$.
All A_N ratios refer to Nyquist point, $-1+j0$.
A_0 not existent with A function class treated herein. (As referred to unit circle.)

where z_r is the single positive real root of

$$b^4z^3+2b^2z^2+(1+2b^2-4ab)z-2=0$$

$$x_c=\sqrt{y_r}$$

where y_r is the single positive real root of

$$b^4y^4+2b^2y^3+y^2-a^2y-1=0$$

$$s=jx$$

$$x=\frac{\omega}{\sqrt[3]{K}}$$

For conditional stability

$$b<\frac{2a}{4+a^2}$$

Amplitude margin and corresponding system response are given in Table III.

References

1. Directional Stability of Automatically Steered Bodies, **N. Minorsky.** *Journal*, American Society of Naval Engineers (Washington, D. C.), volume 34, 1922, pages 280–309.

2. Automatic Steering Tests, **N. Minorsky.** *Journal*, American Society of Naval Engineers (Washington, D. C.), volume 42, 1930, pages 285–310.

3. Theory of Servomechanisms, **H. L. Hazen.** *Journal*, Franklin Institute (Philadelphia, Pa.), volume 218, 1934, pages 279–331.

4. Design and Test of a High-Performance Servomechanism, **H. L. Hazen.** *Journal*, Franklin Institute (Philadelphia, Pa.), volume 218, 1934, pages 543–80.

5. The Analysis and Synthesis of Linear Servomechanisms (book), **A. C. Hall.** Technology Press, Massachusetts Institute of Technology, May 1943.

6. The Analysis and Design of Servomechanisms, **H. Harris.** Fire Control Committee (Section *D*-2), National Defense Research Council, Office of Scientific Research and Development, Washington, D. C., Number 454, 1942.

7. Considerations in Servomechanism Design, **S. W. Herwald.** AIEE Transactions, volume 63, 1944, December section, pages 871–6.

8. Linear Servo Theory, **Robert E. Graham.** *Bell System Technical Journal* (New York, N. Y.), October 1946, pages 616–51.

9. The Application of Lead Networks and Sinusoidal Analysis to Automatic Control Systems, **G. J. Schwartz.** AIEE Transactions, volume 66, 1947, pages 69–77.

10. A Comparison of Two Basic Servomechanism Types, **Herbert Harris.** AIEE Transactions, volume 66, 1947, pages 83–93.

11. Dimensionless Analysis of Servomechanisms by Electrical Analogy—II, **G. D. McCann, S. W. Herwald.** AIEE Transactions, volume 66, 1947, pages 111–18.

12. Forms and Principles of Servomechanisms, **S. W. Herwald.** *Westinghouse Engineer*, September 1946, pages 149–54.

13. Theory of Servo Systems, With Particular Reference to Stabilization, **A. L. Whiteley.** *Journal*, Institution of Electrical Engineers (London, England), part 2, August 1946, pages 353–72.

14. Theory of Linear Servomechanisms, **Richard Latter.** Naval Research Laboratory, Washington, D. C. Released by the Office of Technical Services, United States Department of Commerce, Washington, D. C., *PB 23123*.

15. Frequency Response of Automatic Control Systems, **Herbert Harris.** AIEE Transactions, volume 65, 1946, pages 539–46.

16. Dynamic Behavior and Design of Servomechanisms, **G. S. Brown, A. C. Hall.** *Transactions*, American Society of Mechanical Engineers, volume 65, July 1945, pages 503–24.

17. Regeneration Theory, **H. Nyquist.** *Bell System Technical Journal* (New York, N. Y.), volume 11, 1932, pages 126–47.

18. Stabilized Feed-back Amplifiers, **H. S. Black.** *Bell System Technical Journal* (New York, N. Y.), volume 13, 1934, pages 1–18.

19. Regeneration, Theory and Experiment, **E. Peterson, J. G. Kreer, L. A. Ware.** *Proceedings*, Institute of Radio Engineers (New York, N. Y.), volume 22, 1934, page 1191.

20. Fundamental Theory of Servomechanisms (book), **L. A. MacColl.** D. Van Nostrand and Company, New York, N. Y., 1945.

21. Network Analysis and Feed-back Amplifier Design (book), **H. W. Bode.** D. Van Nostrand and Company, New York, N. Y., 1945.

22. Transients in Linear Systems (book), **M. F. Gardner, J. L. Barnes.** John Wiley and Sons, New York, N. Y., 1942.

23. Theory of Equations, Volumes I and II, **Burnside, Panton.** Longmans, Green and Company, New York, N. Y., 1928.

No Discussion

Selective Tripping of Low-Voltage Air Circuit Breakers

WILLIAM DEANS
FELLOW AIEE

Synopsis: Selective or sequential tripping in low-voltage air circuit breaker application provides for removal from the system of a faulted part only, leaving the rest of the system in operation. Present standard circuit breakers generally are not suitable. Solution of the problem is through direct-acting series tripping means with distinct current–time characteristics in ranges of overcurrent and fault current, with minimum time to complete interruption the objective. This subjects the circuit breaker to the very severe duty of having to carry short-circuit currents for appreciable times, whereas standard circuit breakers have been designed to open instantaneously. Modified standard circuit breakers may be applied to selective tripping, with limitations of application based upon (1) rated interrupting capacity and (2) series trip coil rating. As tests show that modified standard circuit breakers will carry short-circuit current for necessary times, they also may be applied with relay schemes requiring delayed tripping. In systems using cascade or backup arrangements of circuit breakers, little is gained by selective tripping. It is recommended that for a particular installation choice be made between selective tripping and cascade arrangement, according to relative importance of advantages of each.

ENERGY flows at utilization voltage through two or more circuit breakers in series, in the usual low voltage distribution system. In such a system with sequential or selective tripping, circuit breakers are set to trip in predetermined sequence, so that the one closest to the fault of those directly involved is the only one opened. The remainder of the system is left in operation. Complete sequential or selective tripping on a system requires that the predetermined sequence be effective not only throughout the range of overcurrent but also through the range of fault current to interrupting rating of the circuit breaker.

Necessary sequence is by timing, separately, in overcurrent and in fault-current ranges. Circuit breakers having tripping characteristics required for sequential or selective tripping in the range of overcurrent alone are common. Sequential or selective operation in the ranges of both overcurrent and fault current is new. Suitable current–time tripping devices are required, and it is necessary to study behavior of circuit breakers carrying current of interrupting rating for an appreciable time.

Selective Tripping Device Requirements

Present standard low voltage air circuit breakers have dual overcurrent tripping means. Inverse time characteristic is effective for current between 1 and 12 times overcurrent setting, and, at 12 times, tripping is instantaneous. That is, inverse time overcurrent is provided, but at 12 times the setting, the circuit breaker is tripped instantaneously. Such tripping characteristics are proper because overloads for permissible times are allowed, and protection of feeder circuits is excellent. Two or more such circuit breakers in series may be set to trip selectively on overcurrent. But, if the current is equal to or greater than the instantaneous trip value, all circuit breakers may trip. Severe short circuit may shut down large sections of the system or perhaps the whole system. Current at or above the instantaneous trip calibration trips all circuit breakers through which it flows.

Direct-acting series overcurrent tripping devices are used on low voltage air circuit breakers, except for the higher a-c ratings. In fact, there also, tripping is substantially the same, the distinction being that in large a-c circuit breakers, the tripping means is fed through a current transformer. Direct-acting series devices are possible because the circuit voltage is low. They are desirable because of simplicity, ruggedness, low cost, small space, easy maintenance, high operating speed.

The tripping device for selective tripping is a direct-acting series device for the same reasons. A series coil excites an electromagnet, the armature of which moves at a calibrated current but is restrained by two timing devices mechanically in parallel. At and above a predetermined critical value of current, one restraining means is ineffective. The net result is a device which provides long time delay for current between 1 and 12 times the current at which it is set, and very short time delay for current in the range from 12 times normal to interrupting rating. The circuit is protected the same as with present standard circuit breakers, and in addition, system operation is improved.

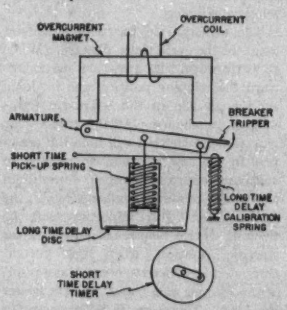

Figure 1. Scheme of operation of tripping device

Paper 47-118, recommended by the AIEE committee on protective devices for presentation at the AIEE summer general meeting, Montreal, Quebec, Canada, June 9–13, 1947. Manuscript submitted November 13, 1946; made available for printing April 3, 1947.

WILLIAM DEANS is chief engineer for the I-T-E Circuit Breaker Company, Philadelphia, Pa.

The author acknowledges the assistance of his colleagues J. D. Wood, F. J. Pokorny, C. J. Ridgley, C. J. Varrick, and R. B. Smith and his former colleague H. C. Graves, Jr.

In the range of fault current, time that current is allowed to flow must be just long enough to give opportunity for tripping the circuit breaker next in sequence in direction of energy flow. This time must be very short to prevent damage to conductors or apparatus and to minimize stress. It is measured in cycles, so the apparatus is called the "cycle timer."

Selective Tripping Device

A tripping device for selective tripping is shown schematically in Figure 1. Implied in the figure is the fact that the long-time timer is a dash pot or adhesive disk device. Design is not limited to these forms; for instance, the thermal-magnetic principle can be applied. So far, a successful purely mechanical timer has not been found for this application.

The armature of the series-excited electromagnet starts to move at the calibrated current and drives both timers in parallel when the current is between 100 and 1,200 per cent of setting. The drive of the long-time timer is through a preset calibrated spring; the drive of the cycle-timer is direct. The spring is preset and calibrated so that for current above 1,200 per cent it deflects. The long-time timer thus is eliminated as a restraint at a definite current; at higher current, the armature is restrained by the cycle timer only.

Accurate measurement of time for these very short intervals is obtained by a mechanical escapement. Precision is realized by accuracy of manufacture based upon design which uses maximum practical motion of escapement, and the device is enclosed completely to prevent foreign material from interfering with its performance. It is adjustable in the field over a range of approximately 5 to 20 cycles. A differential setting between circuit breakers of five cycles is sufficient for selective tripping.

The armature of the tripping device actuates the cycle timer directly. While so performing, the armature moves toward the tripping position and in doing so, the air gap in the tripping electromagnet is reduced. At the reduced air gap, the current that will hold the armature in the new position, or cause it to continue toward tripping, is lower than that which produces similar effects in the first position. It is important that the tripping device return to its normal or starting position when the current through it is reduced to normal, as a result of the opening of a circuit breaker nearer the load. Therefore, it is necessary in driving the timer for the maximum required interval, that the motion of the armature be small. It is necessary that at the end of this action the air gap be great enough, so that the armature will not be held in its new position or carried toward tripping by the new, lower current that flows when a circuit breaker nearer to the load opens. The motion of the armature should be limited to the practical minimum for maximum interval measured by the timer.

At the same time, the cycle timer must be capable of being set for accurate performance. Timing is by inertia of an oscillating member, actuated by a toothed wheel. Intervals measured are multiples of the time corresponding to the action of one tooth. With a small number of teeth in the toothed wheel, settings will be relatively rough; successive settings will differ by amounts fixed by the action of one large tooth. For fineness of setting, many teeth should actuate the oscillating member during the interval measured. The distance the driving armature moves must be small for reasons given. These opposing requirements are satisfied through the use of a gear train between driving armature and toothed wheel, so that motion of the toothed wheel is a multiplication of the motion of the driving armature. At the end of the measured interval, the restraint of the cycle timer is removed automatically from the tripping armature. The armature is then quite free to move, and tripping of the circuit breaker is positive.

The cycle timer is supported in a substantial housing and is completely enclosed. The mechanism is protected against dirt and accidental rough handling. The main driving shaft extends through a sealing bearing in the housing and is actuated by the armature through a lever and link outside. The housing serves also as the support for the cycle timer in the tripping device assembly. Adjustment of the cycle-timer is accomplished by rotating the housing to required position, and it is clamped there.

Advantage of Separate Timing in the Two Current Ranges

First attempts to solve the problem of selective tripping were based on extending the long-time timer action beyond the 12 times normal current limit. The instantaneous trip was set at 20 to 25 times. When the instantaneous trip is set at 12 times, the performance is indicated in Figure 2, by the curve *ABFC*. When the instantaneous trip is set at 20 times, performance is shown by curve *ABDGE*. That performance is unacceptable. It is objectionable as to circuit protection, because very high current is permitted for time measured in seconds. It is objectionable as to design in that great difficulty is experienced in arranging for repetitive current–time performance with required precision.

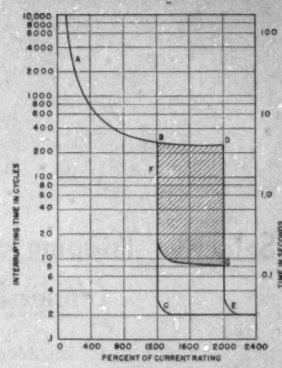

Figure 2. Comparison of performance—dual overcurrent versus selective tripping

To prevent damage to apparatus involved from high current, it is necessary that the current be interrupted as speedily as possible. The basis of discrimination in selective tripping is comparative time of opening the several circuit breakers involved, so each such time must be the practical minimum. These times must be measured in cycles, rather than in seconds. The cycletimer, therefore, was introduced, and with it, the performance is as shown in Figure 2 by curve *ABFGE*. By the cycle timer, conditions represented in shaded area of Figure 2 were removed from device operation and added to safety of apparatus, so to speak. The cycle timer limits the time of flow of high currents to a matter of cycles. Because the cycle timer, responsive directly to current, in turn acts directly upon the circuit breaker, a fast device in itself, the requirement that it quickly interrupt fault current is satisfied.

Inverse Time Versus Definite Time for Cycle Timer

Fixing specifications for cycle timer performance included consideration, of whether it should have definite time–current or inverse time–current characteristics. Inverse time–current was chosen. Explanation will be upon the basis of a typical system of three stages of circuit breakers. Main circuit breaker *1* feeds a bus; from that bus several circuits are fed, each through a circuit breaker, *2*, and

each circuit breaker *2* serves several circuits, each protected by a circuit breaker, *3*. Loads include motors, and it is well known that motors contribute current to the fault, because they effectively become generators driven by their inertia. For a fault on the load side of circuit breaker *3*, more such motor current flows through that circuit breaker *3* than through circuit breaker *2*. This is so because motor current through *3* is the total from all the motors on the system (except those on the particular faulted circuit, of course), whereas motor current through affected circuit breaker *2* is from some of the motors of the system, namely, those on circuits fed from the bus which feeds circuit breaker *2*. The component of fault current coming from the main power source is the same for each of the circuit breakers involved. Therefore, for a fault on the load side of a circuit breaker *3*, the total current through that circuit breaker, *3* is greater than the total current through its *2* circuit breaker, and that, in turn, is greater than the total current through *1*. Timers with definite time characteristics all will perform as though the same current flowed through all. Timers with inverse time characteristics will perform individually, according to magnitudes of respective currents, and with higher current, action is quicker. With inverse-time characteristics, therefore, the performance of the whole selective system is altered automatically in the desirable direction. The circuit breaker that should open is made to do so more quickly. In addition, because current through circuit breaker *3*, is greater than that through *2*, *3* automatically is speeded up relative to *2*. In effect, the interval between scheduled openings of *3* and *2* has been increased automatically, and happily by decreasing time for response by *3*. Inverse-time characteristic cycle-timers, therefore, improve performance of selective tripping systems. The fault-current is interrupted more quickly, and the reliability of the system is improved. The adjustment of the system is made coarser by the automatic increase in intervals between scheduled openings of successive circuit breakers.

Severe Conditions Imposed on Circuit Breaker

Delayed opening at short-circuit current imposes very severe duty on the circuit breaker. To produce smaller circuit breakers, of lower cost, tendency in design has been toward lighter parts and higher opening speeds. The designer has relied upon limiting the duration of short-circuit current in producing smaller circuit breakers capable of interrupting enormous current. Duration of the fault with standard circuit breakers is as low as 1/2 to $1^1/_2$ cycles for small circuit breakers to 4 or 6 cycles for larger ones. Many standard low voltage circuit breakers have inherent instantaneous trips. There was some question, therefore, whether standard circuit breakers could be modified to meet the severe requirements of selective tripping.

Tests on Circuit Breakers Carrying Short-Circuit Current

Tests were performed to determine whether standard circuit breakers could be modified so that they would carry full short-circuit current for the necessary times, without excessive damage to themselves and without impairing rated interrupting capacity. A time of 30 cycles was chosen for tests. This is somewhat greater than the maximum timing required and provided by the cycle timer. The tests were carried on in accordance with standard procedure. A circuit was set up to give current not less than the standard interrupting rating for each circuit breaker tested. This calibrated circuit did not include the circuit breaker. The circuit breaker then was inserted. The tests included an *O* operation followed by a *CO*. The circuit breaker under test opened the circuit at the end of the 30 cycles. In all tests, contact welding, action of contacts, action of circuit breaker as a whole, and interruption were considered matters of particular importance. The circuit breaker in each case was mounted in a steel enclosure of standard size and design for it. All tests were three phase.

The results of the tests are summarized in Table I. A typical oscillogram is shown in Figure 4. Circuit breakers with higher ratings of series trip coils in each interrupting capacity rating performed quite satisfactorily in all respects, but it was established that there is a limitation based on the rating of the series trip coil.

Application Limited by Trip Coil Rating

Low voltage air circuit breakers are available in standard ratings (interrupting capacity and continuous current) shown in Table II. Lower continuous current ratings involve series trip coils, which compared with those for higher continuous ratings, are of greater number of turns of smaller cross section conductor. Smaller continuous current rating trip coils, therefore, have lower thermal capacity and mechanical strength. The higher impedance of the lower rated coils does not reduce the current sufficiently to balance fully the lower thermal capacity and mechanical strength. Therefore, smaller continuous rating trip coils are unable to stand the same current for 30

Table I. Typical Data From Short-Time Rating Tests

Circuit Breaker		Description of Test			Current Through Circuit Breaker		
Interrupting Rating, rms Amp	Coil Rating, Rms Amp	Type of Operation	Average Current at 1/2 Cycle, Rms Amp	Duration in Cycles	Inrush (Average), Rms Amp	At Tenth Cycle, Rms Amp	Remarks
15,000	225	O	18,000	20	20,000	12,500	Operation satisfactory
15,000	225	CO	18,000	35	22,000	12,500	Operation satisfactory
15,000	225	O	18,000	52	20,500	12,500	Circuit breaker welded then opened
15,000	60	O	18,000	37	17,500	12,000	Series coil burned open
25,000	600	O	24,000	30	27,000	20,000	Operation satisfactory
25,000	600	CO	24,000	30	23,000	19,500	Operation satisfactory
25,000	600	CO	18,000	13	27,000	14,500	Circuit breaker failed to close and contacts were destroyed; voltage on control was abnormally low
25,000	600	CO	18,000	10	24,000	12,500	Circuit breaker closed and latched control voltage normal. Operation satisfactory
50,000	1,600	CO	35,000	18	42,000		Operation satisfactory
50,000	1,600	O	50,000	29	45,000	42,000	Operation satisfactory
75,000	2,000	O	79,600	24	93,400	60,000	Operation satisfactory

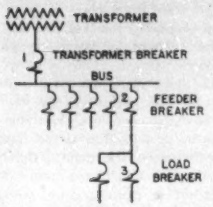

Figure 3A. Typical low voltage distribution system

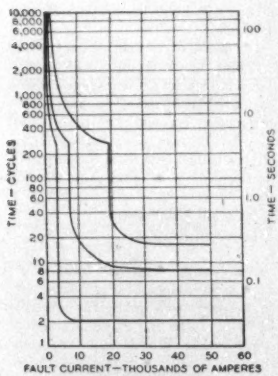

Figure 3B. Family of curves for selective tripping in typical system

cycles as those of higher rating. Early in the tests, some of the smaller trip coils failed in less than 30 cycles. Further tests made on a variety of ratings showed that, in general, the series trip coil may be used safely for 30 cycles in a circuit where the current measured in the standard way (circuit breaker short-circuited) is not greater than 100 times the continuous rating of the coil. When a coil smaller than the minimum is required, it is necessary to derate the circuit breaker 30-cycle rating to 100 times the continuous rating of the trip coil. Thus the minimum trip coil rating that can be used in a 15,000-ampere circuit is 150 amperes.

Conclusions From Tests

Modified standard circuit breakers will carry safely short-circuit current corresponding to their interrupting rating for 30 cycles, except in the lower continuous current ratings. In those cases, the series trip coil is the limitation. In general, the 30-cycle rating may be given as 100 times the continuous rating of the series trip coil. In all cases, the circuit breaker interrupted the current satisfactorily.

Performance of System With Selective Tripping

Performance of circuit breakers with dual overcurrent and with selective tripping are compared in Figure 2. A typical low voltage distribution system is shown in Figure 3*A*, and the related family of circuit breaker performance curves for selective tripping are given in Figure 3*B*. In the usual system, the maximum time to be measured by the cycle timer is 20 cycles. The last circuit breaker in selective tripping succession, that is, the one nearest the load need not have a cycle timer. There is no circuit breaker beyond it with which it can race in opening. Therefore, it has instantaneous trip instead of cycle timer, so that it is really dual overcurrent. Its time–current characteristics in the range of overcurrent must be in proper relation with those of predecessors in the succession.

All circuit breakers used in the system illustrated have standard rated interrupting capacity equal to at least 1.25 times estimated symmetrical short-circuit current. Additionally, even though that condition is satisfied, application must be examined further, because application is limited by 30-cycle current rating of the series trip coil. Suppose, for instance, circuit breaker *1* of Figures 3*A* and 3*B* is 1,600-ampere continuous rating; circuit breaker *2* is 400 ampere, and *3* is 300 ampere; all have standard (instantaneous trip) interrupting rating of 50,000 amperes. Where there is small impedance between stages, as in assembled switchgear, such a succession of circuit breakers would be applicable for a required (computed) interrupting capacity not greater than 30,000 amperes. The limit, 30,000 amperes, is set because of limitations of series trip coil rating (300 amperes) and is computed as 100 times that rating.

Closing Against Fault Current

Circuit breakers commonly remain closed, carrying current for long periods, so that usually a fault develops while they are closed, and they are required to open the fault from closed position. It is not impossible, however, that a fault is set up from some cause while a circuit breaker is open, so that the next time it is closed, it is closed against the fault. This operation is severe on the circuit breaker under any circumstances, but especially so in a selective tripping system. A circuit breaker of today's standard construction, closed against a fault, will trip free and open instantaneously. It is not imperative that the closing operation be brought completely to the fully latched position. A circuit breaker applied in selective tripping is not tripped instantaneously; it is expected to carry the short-circuit current for its time interval. Should it be incompletely closed while that current flows through it, it probably will suffer great damage. In selective tripping, therefore, the circuit breaker must close, latch, and remain closed satisfactorily throughout its scheduled time.

Tests showed that standard circuit breakers of 15,000- and 25,000-amperes rated interrupting capacity do close satisfactorily against short-circuit current with normal control voltage. Those of 50,000-amperes interrupting rating and larger generally do not, and special oversize closing mechanisms are required. Circuit breakers for selective tripping generally require more powerful closing mechanisms than present standard circuit breakers.

Relay Tripping

For most applications, series tripping devices will be found quite adequate, and they have the advantage of lower cost and space economy over relays. There may be conditions where relay tripping is deemed preferable. The question whether it might be applied to low voltage air circuit breakers has been much discussed. Opposition is based on emphasis upon instantaneous tripping on fault current in present standard designs. Especially where instantaneous trip is built into the circuit breaker, it is difficult, if not impossible, to arrange for proper functioning in delayed tripping systems under all conditions up to full rated short-circuit current.

The modified circuit breakers discussed here as being applicable to selective tripping will close against short-circuit current, carry that current for 30 cycles, and interrupt the current. They, therefore, may be used with relay tripping, provided the 30-cycle period i not exceeded. Because there is no series trip coil in these applications, that limitation does not exist.

Total time is the sum of relay time, shunt trip time, and time for circuit breaker to open fully. It is this total time for the circuit breaker the opening of which is delayed longest which must not exceed the 30 cycles. A shunt trip takes some time to operate, and its operation is part of the circuit breaker opening process. Therefore, it is to be included as

part of the scheduled interval between successive circuit breakers. Direct-acting selective tripping devices are designed so that they will reset if the fault is removed (for instance, by opening of a circuit breaker nearer the fault) before the expiration of the time they are set to measure. It can not be arranged to recall a shunt trip, once it has started, except by opening its coil circuit very soon after it is closed. So it is possible the chances for false tripping may be greater with relay tripping than with direct-acting series selective tripping, unless individual scheduled times are set properly.

Cascaded Circuit Breakers

To reduce the first cost of switching and protective equipment, the backup or cascade arrangement of low voltage air circuit breakers sometimes is used. In this arrangement, the circuit breaker nearest the source of power has fully the interrupting capacity for the circuit, but the circuit breakers in the next two stages are applied at twice and three times their rated interrupting capacities, respectively. To protect the circuit breakers thus used beyond their rating, the circuit breakers in the series are tripped instantaneously as the short-circuit current approaches interrupting rating of the overloaded members. Short-circuit current of such magnitude, therefore, causes two circuit breakers to open, or all three, if the fault is severe. The smaller circuit breakers are backed up by those of higher interrupting ratings, and their very life depends upon the backup circuit breakers opening simultaneously with them. Obviously, too, in order to be effective, the backup circuit breaker must be tripped instantaneously, and all circuit breakers involved must open in proper co-ordination. Should the backup circuit breaker be retarded in opening, as by selective tripping devices, the small circuit breakers of the system then are called upon to try to interrupt current in excess of their atings, and they may be damaged badly. As many circuit breakers must open, the feeds to many loads are interrupted.

Full advantages of selective tripping,

Table II. Ratings of Standard Circuit Breakers

Rated Interrupting Capacity	Rated Continuous Current	Ratio Interrupting Rating Continuous Current Rating
15,000....	25 to 225.....	600 to 66.7
25,000....	50 to 600.....	500 to 41.6
50,000....	200 to 1,600.....	250 to 31.2
75,000....	2,000 to 3,000.....	37.5 to 25.0
100,000....	4,000 to 6,000.....	25 to 16.6

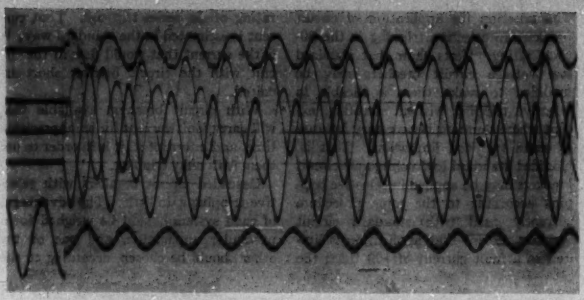

Figure 4. Typical oscillogram of tests

Test on 2,000-ampere circuit breaker

	Current in Amperes, Rms			
	Phase A	Phase B	Phase C	Average
Inrush.....	102,000	69,700	108,500	93,400
At one half cycle.	91,000	60,300	87,500	79,600

therefore, can not be realized in the cascade arrangement. Combination of overcurrent trip, providing long-time overload, with short-time delay fault current trip plus instantaneous trip, has been applied in a few cases of cascaded circuit breakers. The instantaneous trip was set at 80 per cent of the rated interrupting capacity of the next smaller circuit breaker in series. Above this current, selective tripping is impossible. Little is gained, therefore, toward continuity of service by the added complication of selective tripping with circuit breakers in cascade.

Figure 5 shows the performances of three stages (the maximum allowable) of circuit breakers in cascade, and the same circuit breakers with selective tripping. The curve *AB* is the same for both; it shows performance of the circuit breaker nearest the load. Performance of the circuit breaker next nearer the power source is shown (1) for cascade arrangement by curve *CD* and (2) for selective tripping by *CD′*. Performance of the circuit breaker nearest the power source i shown (1) for cascade arrangement by curve *EF* and (2) for selective tripping by curve *EF′*. In a comparison of performance in the two cases, the advantage of selective tripping over cascade arrangement is represented by the shaded area.

Instantaneous trips are necessary on the backup circuit breakers in cascade, and because of it selective tripping on high fault currents can not be had. It would be good judgment in general, therefore, to confine selective tripping to noncascaded circuit breakers. Where the benefits of selective tripping are wanted, all the circuit breakers must be of full interrupting rating; none should be applied beyond its interrupting rating.

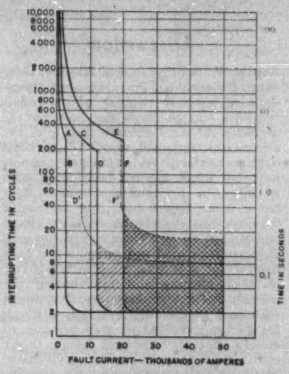

Figure 5. Comparison of performance—cascade arrangement versus selective tripping

Conclusions

Selective or sequential tripping of low voltage air circuit breakers is desirable. With it, only a faulted part of a system is removed, and the rest of the system continues in operation.

Selective tripping is accomplished through a special direct-acting series tripping device on the circuit breaker, which provides long-time delay on overcurrent and very short-time delay on fault-current. The several circuit breakers in series are set so that they will respond to overcurrent and to fault current in proper sequence.

Delaying the opening o a low voltage air circuit breaker while it is carrying fault current is somewhat revolutionary. Design has been upon the basis of quickest possible opening of fault current.

The criterion for application of circuit breakers in selective tripping is the 30-cycle rating. Tests show that standard low voltage circuit breakers may be modified to make them applicable in selective tripping without derating, except where derating is necessary because of series trip coil limitation. That is, modified standard low voltage air circuit breakers may be applied in selective tripping according to the same procedure currently used with standard circuit breakers, except that application is limited to a fault current of 100 times the rating of the series trip coil. That current is estimated in the standard way; it is the current that would flow in the circuit with the circuit breaker short-circuited.

With circuit breakers available that will carry fault current for an appreciable time, and interrupt it, it is in order to use them with relay tripping.

Cascaded circuit breakers with selective tripping gain little. The advantages of each system should be weighed for a particular application, and one or the other should be chosen, according to the immediate importance of respective advantages.

References

1. Protection of Low Voltage Circuits by Air Circuit Breakers in Cascade Arrangement, C. H. Black, A. E. Anderson. AIEE Transactions, volume 60, 1941, pages 1151–60.

2. Improved Selective Tripping of Low Voltage Air Circuit Breakers, Charles P. West. AIEE Transactions, volume 63, 1944, August section, pages 608–10.

3. Fault Protection on Shipboard A-C Power Distribution Systems, H. G. Rickover, P. N. Ross. AIEE Transactions, volume 63, 1944, pages 1109–20.

Discussion

Robert W. Smith (General Electric Company, Philadelphia, Pa.): In most discussions of selective tripping of air circuit breakers, the emphasis has been on the necessity for more accurate timing of the overcurrent tripping devices. Deans points out another factor which is equally important, but which has not been emphasized so much in previous discussions. This factor is the requirement that air circuit breakers must be capable of being closed and latched on high short circuit currents, of remaining closed and carrying this high current for a specific time interval, and of then opening and interrupting the current. Present breakers were not designed with such severe duty in mind, although Deans has indicated it was possible to modify some of the present designs to get satisfactory performance on such duty. It may be that satisfactory performance was obtained, but the data presented in Table I and Figure 4 of the paper are inadequate to prove such performance. For example, Table I indicates that the test illustrated by Figure 4 had a duration of 24 cycles, yet Figure 4 shows only 13 cycles of this test and further, it does not show the interruption of the circuit at the end of the test. Also the contact welding indicated on test 3 and the magnitude of the currents at the end of the current-carrying period should be more thoroughly discussed. In any event I agree with Deans as to the importance of a high close-and-latch rating and a high 30 cycle rating. Certainly in any new circuit breaker designs, such ratings should be just as much a requirement as the providing of accurate short-time tripping devices.

H. L. Rawlins (Westinghouse Electric Corporation, East Pittsburgh, Pa.): Deans has outlined the reasons for selective tripping of breakers and has excellently described some of the factors involved in the selective operation of low voltage breakers.

We have also been working on this problem and agree with most of Deans' conclusions. As might be expected, we disagree with others. We agree that selective operation of low voltage breakers is desirable. In fact, it should have been done long ago. We agree that the short time delay used to obtain selective operation should have an inverse characteristic since advantage can be taken of the difference in breaker ratings to provide greater differences in time between steps of selectivity to increase the reliability of timing or to provide a shorter over-all time at the higher fault currents. Both of these are desirable.

We also agree that low voltage breakers should have a short time (or 30-cycle) rating equal to the interrupting rating up to 50,000 amperes. To close and latch in on currents of 50,000 amperes and above requires stronger and more expensive closing mechanisms which are not required. An application study has indicated that short time ratings above 50,000 amperes are not required provided that higher rated breakers have a short time rating of 50,000 amperes and can provide short time delay up to that curren with instantaneous tripping at higher currents.

We differ somewhat from the author in that we feel a cascaded system can be improved through the use of selective tripping. Although a cascaded system is definitely inferior to a full capacity system, we can see no reason for not taking advantage of selectivity on such a system. The very fact that a cascaded system works at all indicates that selectivity would be beneficial.

Since both the liquid film delay and the mechanical delay have definite limitations, we feel that their combination will be unsatisfactory. We have supplied this combination but are discarding it in favor of sealed units having positive fluid displacement.

William Deans: A great many tests were made in investigating this subject. The data presented are intended merely to be typical—to be illustrative of the nature of the investigation. Conclusions drawn in the paper are based upon the complete data.

There is no doubt that selective tripping may be applied with circuit breakers in cascade, and to some advantage. It is clear, though, that full advantage of selective tripping may be had only when all circuit breakers have full interrupting capacity required.

Silicone Insulation as Applied to Naval Electric Power Equipment

H. P. WALKER
NONMEMBER AIEE

Synopsis: The general problem of shipboard electric equipment is reviewed in relation to the use of silicone insulation as a possible means of providing smaller lighter weight equipment. Silicone compounds are discussed giving physical and chemical properties which are of interest to the Navy. Laminated and molded insulation is discussed giving the development problems involved as well as showing present test data.

THE Bureau of Ships, United States Navy Department, is very much interested in obtaining light weight, small size, and more reliable electric equipment for shipboard use.

Until the coming of silicones, a new class of high polymeric materials,[1] the maximum operating temperature of electric equipment was 125 degrees centigrade. This temperature is the total winding or coil temperature measured by the rise in resistance method and all coil temperatures mentioned hereafter will be those measured by the rise in resistance method. The 125-degree-centigrade value is the maximum operating temperature for class *B* insulated equipment, where the insulation consists of inorganic materials such as woven glass cloth, tape and cordage, mica, and asbestos bound together by an organic varnish. The inorganic materials will withstand higher operating temperatures, but temperatures over 125 degrees centigrade will soon damage the organic varnish. Once the varnish or binder is damaged, the electric equipment soon fails electrically since the ever-present vibration, abrasion, and moisture cause loss of dielectric strength of the insulation, and short circuits and burn-outs occur.

In many types of electric equipment, such as motors, generators, and transformers, the 125-degree-centigrade temperature limits any further reduction in size or weight of the equipment. The bottleneck is the heat endurance of the insulating varnish.

When preliminary laboratory tests indicated that the silicone insulating varnishes had more heat endurance than organic insulating varnishes, the Bureau of Ships became extremely interested.

The assistance of a group of manufacturers was requested by the bureau to set up a test program. This group consisted of representatives of three motor manufacturers (Westinghouse Electric Corporation, General Electric Company, Reliance Electric and Engineering Company); two silicone manufacturers (General Electric Company, and Dow Corning Corporation); and the Bureau of Ships. A testing program was formulated, consisting of four parts

1. Laboratory tests on basic materials.
2. Simulated service tests on special motors.
3. Simulated service tests on electric equipment designed "from-the-iron-up" to take full advantage of the heat endurance of silicone products.
4. Installation of silicone designed equipment for actual shipboard operation.

Silicone electrical insulating varnishes are one form of the many types of silicone products. Other types of interest in the electric equipment field consist of

1. Silicone resins for building laminated and molded thermosetting materials.
2. Silicone resins for high temperature paints.
3. Silicone lubricants for bearings.
4. Silicone rubber for gaskets.

Paper 47-132, recommended by the AIEE committee on electric machinery for presentation at the AIEE summer general meeting, Montreal, Quebec, Canada, June 9-13, 1947. Manuscript submitted March 31, 1947; made available for printing April 21, 1947.

H. P. WALKER is an electrical engineer in the electrical department of the Bureau of Ships, United States Navy Department, Washington, D. C.

Silicone Varnish

The Westinghouse Electric Corporation and Dow Corning Corporation have done a large share of the work on thermal testing of silicone varnishes.[2, 3] This thermal testing is being done on three silicone varnishes

DC-990A
DC-993
DC-996

At the present time laboratory tests on basic materials and simulated service tests on special motors are being conducted. The laboratory tests consist of flexibility tests after heat aging, cold checking, dielectric strength (both dry and wet), insulation resistance, abrasion, and so forth.

Flexibility tests made on varnish films baked on aluminum panels indicate that the life obtained at 225 degrees centigrade is 1,750 hours; that is, before the film cracks when bent over a 1/8-inch mandrel. When compared to similar tests on organic varnishes, this gives silicone varnishes a margin of about 100 degrees centigrade

The next phase of the test program was to use silicone varnish on an actual motor. Westinghouse built a standard commercial motor using glass covered wire, glass and mica tape, and *DC-990A* silicone varnish. This motor was operated for 3,800 hours at 240 degrees centigrade when bearing failure occurred. The insulation was still in good condition. From this preliminary test, it was estimated that the ultimate life of the insulation would be about 5,000 hours at 240 degrees centigrade. This life was so extraordinary that an extensive program was undertaken by Dow Corning and Westinghouse under the sponsorship of the Bureau of Ships.

Westinghouse built a number of special motors for test purposes. These motors were 10-horsepower 440-volt 3-phase 60-cycle sizes. The windings consisted of glass covered wire, glass and mica tape,

and *DC-993* impregnating varnish. The *DC-993* was an improvement over *DC-990A*. Because bearing failure had occurred on the previous motor, special precautions were taken to keep the bearing temperatures below 100 degrees centigrade, even though the motor winding temperature was well over 300 degrees centigrade. Using the special motor design, the heat stability of the insulation could be tested without running into bearing trouble.

A test procedure was set up so as to approximate actual shipboard operation. It was agreed to run the motors at high temperatures followed by humidification. In such a cycle the heat run produces actual aging or deterioration of the insulation while the humidification serves as an indicator of weakness that may be developed from the heat. Since frequent testing of the insulation was desirable, it was decided that 25 of these heating-humidification cycles would be attempted during the estimated life of the insulation. At that time no definite data were available for estimating life of a silicone insulated motor. However, from the results of the flexibility tests, it was felt that a life rule of 8- to 12-degree-centigrade rise would halve the life. A curve was established based on the tests on the first motor tested (5,000 hours at 240 degrees centigrade) which, when extrapolated back to a proposed operating temperature of, say, 175 degrees centigrade, would give a life of about 50 years.

Motors were run at temperatures of 200, 240, 280, 300, and 310 degrees centigrade to check these life line values and establish more complete data. Cycling tests were made and only actual running time of the motor was considered. The latest data available on this test were reported as of August 1, 1946, and are shown in Table I. It is interesting to note that this test started several years ago and is still in progress. As can be seen from Table I, the *DC-993* motor that failed at 310 degrees centigrade would give satisfactory performance for 400 years at a winding temperature of 190 degrees centigrade (hot spot temperature 205 degrees centigrade), or about 800 years at 180 degrees centigrade (hot spot temperature 195 degrees centigrade). From all data available to date, it is considered that a total hot spot temperature of 200 degrees centigrade maximum may be a satisfactory tentative limit for Navy rotating equipment utilizing this type of silicone resin, provided the bearing problem can be solved. Other engineers[3] have recommended that the limiting hot spot temperature for silicone insulation be set at 175 degrees centigrade. This temperature limit appears conservative. In line with obtaining more data on the thermal aging of the newer silicone resin *DC-996*, the Bureau of Ships has contracted with Dow Corning to run tests on a group of Navy-type motors presently being rewound with *DC-996* at the Philadelphia Naval Shipyard, Philadelphia, Pa. These tests will be made using the same procedures as listed here for the *DC-993* motors.

Table I. Silicone-Insulated-Motor Tests

Material	Temperature, C	Cycles	Hours	Years at 160 C*	Remarks
DC-993	310	46	5,131	3,395	Failed on 47th cycle
DC-993	300	44	5,402	2,040	Still running
DC-993	280	35	6,600	773	Still running
DC-993	240	1	189	2	Recently started
DC-993	240	1	221	2	Recently started
Class *B* and *DC-996*	275	35	1,280	111	Original class *A*
Class *B*	275	33	1,056	92	Failed on 33d cycle
Class *B*	200	40	3,760	4	Failed on 40th cycle

* Extrapolated on basis of 10-degree rise in operating temperature reducing life by 1/2.

Tests on a d-c subway traction motor insulated with *DC-990A*[4] were discontinued after operating 1,675 hours at 285 degrees centigrade (hot spot temperature 300 degrees centigrade) without failure, and the motor was replaced with another traction motor wound with *DC-993* silicone varnish. Tests are now starting on this motor.

Another set of tests,[5] made on a group of motor controller contactor coils of the solenoid type, revealed that when the coils were operated at 275-degree-centigrade temperatures, the resistance of the coils increased from about 1.5 per cent at 7,000 hours to 8 per cent at 12,000 hours. This indicated that at temperatures around 275–300 degrees centigrade the copper wire oxidizes, and the diameter of the wire is reduced, so that the resistance of the wire is increased. This oxidizing of the copper wire can be discouraged by plating the wire with cadmium.

The Kuhlman Electric Company, under contract to the bureau, has designed, constructed, and tested silicone-insulated single-phase 440/117 dry-type power distribution transformers. The transformers are 3 kva and 25 kva rated at 150-degree-centigrade temperature rise, and are lighter and more compact than any transformers of equivalent output previously used by the bureau. The coils are insulated with glass-served silicone-bonded wire (*DC-993*) and impregnated with silicone varnish. Silicone varnished glass cloth is used as layer insulation. Silicone glass laminated insulation is used for coil bracing. Because of the high operating temperature, lead wire is insulated with silicone rubber. The enclosing case is painted with silicone paint.

The weight and size information on these transformers is shown in Table II.

The electrical characteristics of these transformers indicate that the regulation at 100-per-cent power factor for the 3-kva unit is 2.93 per cent, and for the 25-kva unit, 2.19 per cent. At 80-per-cent power factor, the regulation for the 3-kva unit was 3.68 per cent and for the 25-kva unit, 2.10 per cent.

The temperature rise data indicated that temperatures of 106 degrees centigrade and 110 degrees centigrade were obtained in the voltage coils. In order to fully utilize the 150-degree-centigrade temperature limit, further studies are being made to determine how the regulation values and losses can be adjusted without affecting the over-all performance of the electric power system.

Laminated Insulation

One of the most diversified insulation products is probably laminated sheets, rods, tubes, and special shapes. This material is used in practically every electric device and in sheet thicknesses from a few mils to several inches. From the early electrical installations using electrical slate for panels, the Navy has progressed through ebony asbestos, paper and fabric reinforced phenolic insulation, and glass cloth base melamine material; and, at present, the Bureau of Ships is investigating glass cloth and silicone resin combinations.

Working with General Electric Company and Dow Corning Corporation as resin suppliers, and with Owens-Corning Fiberglas Corporation, Gustin-Bacon Manufacturing Company, and Glass Fibers, Inc., as glass products suppliers, the bureau is carrying out a large program of development work on laminates with such laminators as Formica Insulation

Table II. Weight and Size of Transformers Tested

	Navy Class B Specified Limit	Kuhlman	Per Cent Saving
3 kva weight, lb	70	45	36
volume, cu in.	1,020	777	24
25 kva weight, lb	295	215	27
volume, cu in.	5,750	3,600	37

Company, General Electric Company,[6] National Vulcanized Fibre Company, Mica Insulator Company, Taylor Fibre Company, and Continental Diamond Fibre Company. The development covers detail investigations of the following nature:

1. What sizing, if any, should be used on glass cloth.

2. Continuous versus staple fiber glass filaments.

3. Type of weave to give maximum properties.

4. Woven versus non-woven glass materials.

5. Thermosetting properties of silicone resin.

6. Improvement of silicone resin for mechanical strength.

The desired properties of a fire and arc resistant laminated material are shown in Table III, along with the best obtainable properties from a study of the various manufacturers' test data. Preliminary applications of this material have been made in various types of Naval electric equipment with excellent results, especially where heat resistance is of prime importance.

As can be seen from this data, not all of the desired properties have been achieved as yet, nor have all the properties been available in a single combination of glass and resin. However, it is evident that the trend is toward the desired properties. The development work to date has indicated the following consideration in producing a satisfactory material:

1. Starch and oil sizings on the glass cloth are deleterious and must be removed before any resin treatment is made.

2. Heat cleaning has a tendency to weaken the glass.

3. Chemical cleaning reduces the tensile strength of the glass.

4. Water soluble sizings are satisfactory.

5. Silicone oils as sizings adversely affect the mechanical properties.

6. Silicone "elastomers" are satisfactory as sizings.

7. Silicone resin should have high solids content.

8. After-baking treatment of laminate should start at relatively low temperature to prevent blistering.

As a matter of interest, an acid resistant silicone-glass laminate has been developed which is ten times less soluble than hard rubber when tested in battery acid. It is contemplated using this material for walking flats in submarine battery compartments if all the desired properties are achieved. Also, rods, tubes, and special shapes have been produced from both the chemical and electrical grades of silicone laminate.

Table III. Properties of Laminated Glass-Silicone Insulating Material

Properties	Navy Desires	Manufacturers' Data
Mechanical properties		
Flexural strength, condition *A**, 1/2-in., psi		
Flatwise, lengthwise	22,000	18,000
Crosswise	17,000	20,000
Edgewise, lengthwise	22,000	16,500
Crosswise	17,000	16,700
Tensile strength, condition *A**, psi		
Lengthwise	18,000	17,700
Crosswise	12,000	7,730
Compressive strength, condition *A**, psi		
Flatwise	30,000	38,000
Edgewise, lengthwise	10,000	11,900
Crosswise	10,000	10,200
Izod impact strength, condition *A**, ft-lb per in. of notch		
Flatwise, lengthwise	16	17.0
Crosswise	16	11.6
Edgewise, lengthwise	16	7.0
Crosswise	16	4.8
Bonding strength, condition *A**, lb		
Lengthwise	1,200	860
Crosswise	1,200	860
Water absorption, condition *D** 24 hr at 25 C, per cent 1/8 in. thick	0.50	0.40
Electrical properties		
Dielectric strength, condition *A**		
Perpendicular, step by step, v per mil	275	295
Short time, v per mil	275	315
Parallel, step by step, kv	50	41
Short time, kv	50	69
Dielectric losses		
1 megacycle, condition *A**		
Power factor, per cent	0.10	0.14
Dielectric constant	3.50	4.25
Loss factor, per cent	0.40	0.60
1 megacycle, condition *D** 24 hr at 25 C		
Power factor, per cent	1.00	0.81
Dielectric constant	4.00	4.57
Loss factor, per cent	4.50	3.90
30 megacycles, condition *A**		
Power factor, per cent	2.00	0.25
Dielectric constant	4.00	4.19
Loss factor, per cent	8.00	1.05
30 megacycles, condition *D** 24 hr at 24 C		
Power factor, per cent	4.00	0.80
Dielectric constant	4.00	4.29
Loss factor, per cent	16.00	3.43
Insulation resistance, megohms		
Condition *A**	125,000	200,000
Condition *D** 96 hr at 50 C	1	264
Condition *D** 96 hr at 30 C and 90 per cent relative humidity	1,000	
Arc resistance, condition *A**, sec	300	265

* For complete specifications see *J A N P-13*, Plastic Materials Laminated Thermosetting Sheets and Plates United States Government Printing Office, Washington, D. C., September 1944.

Molded Insulation

The development of a satisfactory fire and arc resistant molded silicone-glass material has likewise been accompanied by a lot of problems, due, no doubt, to the newness of the silicones and the lack of experience in their use, which can only be gained by such developments discussed herein.

As with the laminates, the material suppliers are Dow Corning Corporation; General Electric Company; Owens-Corning Fiberglas; and Glass Fibers, Inc. Watertown Manufacturing Company is also developing resin formulations using Dow Corning material. Molders include such organizations as General Electric Company; Watertown Manufacturing Company; Chicago Molded Products Corporation; Cutler-Hammer, Inc.; Arrow, Hart, and Hegeman Electric Company; and Formica Insulation Company. The developments cover detail investigations of the following nature:

1. What sizing, if any, should be used on glass filaments.

2. What length and diameter glass gives optimum mechanical strength.

3. What catalyst concentrations should be used.

4. Effect of addition of inert fillers on properties.

5. Use of present available molds.

6. Hot ejection from the molds.

7. After-baking cycle to prevent blistering.

8. General moldability and wear.

The desired properties of a relatively high impact grade of molded glass-silicone

Table IV. Properties of Molded Glass-Silicone Insulating Material

Properties	Navy Desires	Manufacturers' Data
Mechanical properties		
Izod impact		
Ft-lb	1.20	0.81
Ft-lb per in. of notch	2.40	1.62
Ft-lb per in. sq	15.00	10.12
Flexural strength, psi	9,000	6,515
Tensile strength, psi	5,000	2,666
Compressive strength, psi	20,000	10,588
Shrinkage, mils per in.	8.0	1.39
Specific gravity	1.60–1.70	1.70
Water absorption, 47 hr, per cent	1.5	0.60
Ash, per cent	85.00	86.00
Heat distortion, mils at C	5.0/250–300	3.0/–300
Electrical properties		
Dielectric strength, step by step, 100 C	150	156
Dielectric loss, 25 C		
1 megacycle dry		
Power factor, per cent		0.14
72 hr wet		
Power factor, per cent	0.10	9.92
Dielectric constant	3.5	4.56
Loss factor, per cent	0.40	45.12
Volume resistivity, megohms per cm cube	20×10^3	8.78×10^3
Arc resistance, sec	300	263

material are shown in Table IV along with the best obtainable data from a study of the various molders' data.

As can be seen from the data in Table IV, there is still quite a bit of development to be done to produce a moldable material having the desired characteristics. However, it is believed that the properties can be achieved, and satisfactory parts can be molded. The following considerations must be taken into account in producing a high impact grade of material:

1. Unsized or silicone-sized (*DC-2103*) glass should be used.

2. Fiber length should be between 3/4 and $1^1/_2$ inches.

3. Resin should have high solids content.

4. Mixing machinery should be of a type which will not tear the glass fibers.

5. Milled glass fibers are not satisfactory—random chopped fibers are satisfactory.

6. Molding compound should be heated to drive off volatiles before molding.

7. After-bake should be started at relatively low temperatures to prevent blistering of part.

Conclusions

The Bureau of Ships has undertaken a program for the development of silicone materials as well as developing specific types of equipment designed to utilize silicone insulation in its varied forms. Such electric equipment as generators, motors, controllers, transformers, circuit breakers, switches, meters, bus transfer equipment, and welders have been included in this program. Some of the problems yet to be worked out are as follows:

1. Toxic effects of products of decomposition, if any, of silicone materials used for motor insulation.

2. Cause and correction of commutating difficulties and excessive brush wear on silicone insulated d-c motors and generators of the enclosed type using air recirculation.

3. Development of a satisfactory silicone enamel for magnet wire, which will not crack or peel and which will not be soluble in impregnating varnish.

4. Variation in arc resistance of molded and laminated material and variation in test methods.

5. Improvement in fire resistant characteristics.

It is considered that by completing the total program for developing fire and arc resistant insulating materials, the Bureau can provide more reliable, lighter, and smaller electric equipment for shipboard installations. It is believed that many of the problems which are solved under this program will aid commercial utilization of better insulating materials, thereby helping to reduce the present high cost of silicone and glass products through wide spread usage and volume production.

References

1. Silicones, a New Class of Polymers, S. L. Bass, J. F. Hyde, E. C. Britton, R. R. McGregor. *Modern Plastics* (New York, N. Y.), volume 21, 1944, page 124.

2. Silicone Insulation Proved by Test, T. A. Kauppi, George Grant, G. L. Moses, R. F. Horrell. *Westinghouse Engineering* (Pittsburgh, Pa.), September 1945, page 135.

3. The Application of Silicone Resins to Insulation for Electric Machinery, J. DeKlop, L. R. Hill, G. L. Moses. AIEE Transactions, volume 64, 1945, March section, pages 94–8.

4. Investigation of Silicone Insulation on High-Temperature Railway Motor, George Grant III, T. A. Kauppi, Graham Lee Moses. AIEE Transactions, volume 66, 1947, pages 305–11.

5. Silicone-Resin-Treated Magnet Coils, Graham Lee Moses, Julius J. Torok. AIEE Transactions, volume 65, 1946, July section, pages 412–16.

6. Silicone Resin Bonded Glass Laminates, L. V. Larsen, J. J. Whelton, J. J. Pyle. *Modern Plastics* (New York, N. Y.), volume 23, March 1946, page 160.

Discussion

George Grant (Dow Corning Corporation, Midland, Mich.): Walker has done a very nice job of summarizing what has been done and what is being done by and in behalf of the Bureau of Ships.

He has tabulated data on some eight motors under thermal aging tests. At the present time this testing program is well into its third year and data recently obtained from failures that occurred since this paper was prepared, when completely analyzed, will yield several interesting observations and conclusions. Failures on four silicone insulated units and two class *B* units have taken place. The class *B* unit that failed after 1,000 hours of running at 275 degrees centigrade was entirely destroyed insofar as insulation is concerned. Had there been any vibration, it would have failed much sooner. In comparison, a silicone insulated unit after operating the same length of time at the same temperature appears to be as good as new.

In another instance, a class *B* unit failed after 3,700 hours at 200 degrees centigrade while a silicone unit failed after a somewhat longer time at 300 degrees centigrade. At failure these two units are considered to be in a comparable state of deterioration.

From these tests, it is safe to say that under comparable conditions, where reliability and continued performance are of paramount importance, a silicone insulated unit will outlast a class *B* unit by a factor of at least 10.

Where reduction in weight is of paramount importance, the design can be safely altered until a temperature 100 degrees centigrade above class *B* ratings is obtained, and life equal to that of class *B* may be expected. Considerations other than the thermal endurance of the insulation, however, may make it desirable to use something less than the full 100-degree-centigrade advantage silicone insulation has over class *B* insulation. In that case, additional life as well as reduced weight will be obtained.

Previous recommendations to the AIEE

have suggested 160 degrees centigrade by resistance as a preliminary standard for silicone insulation. The Bureau of Ships, according to this paper, is considering approximately 185 degrees centigrade. These are 40 and 65 degrees centigrade above present class *B* standards. It is clear that both of these temperatures are very conservative when compared to the 220 degrees centigrade indicated by the motor tests.

Walker mentions a bearing problem about which it might be well to say a word here. Until the coming of silicones, there was a top limit of 100 degrees centigrade on ball bearings lubricated with petroleum grease. Now, by using silicone grease, it is safe to go to 125 degrees centigrade in practically all machines of current design. Further, to attain such a bearing temperature in such machines, a minimum winding temperature of approximately 200 degrees centigrade by resistance is required. This exceeds the winding temperatures presently considered.

If winding temperatures of 225 degrees centigrade are considered in order to take full advantage of the thermal stability of the silicone insulation, a maximum bearing temperature of 140 degrees centigrade may be encountered. In such a case, trouble due primarily to mechanical design and bearing metallurgy, is likely to result. This problem is now under intensive investigation by several manufacturers and the Navy.

With the information now on hand, two distinct observations seem to be warranted. A motor of current design, insulated and lubricated with silicones, may be expected to

1. Operate with no attention for at least 10 times as long as a class *B* unit under the same conditions.

2. Be continuously overloaded to a winding temperature of 200 degrees centigrade with a life at least equal to and probably longer than that of a class *B* unit.

Graham Lee Moses (Westinghouse Electric Corporation, East Pittsburgh, Pa.): Walker's paper presents an excellent picture of the current status of silicone insulation, especially as adapted to Naval electric equipment. As indicated by the author, the general development of materials has progressed rapidly; and for many applications, there are suitable high temperature insulation combinations.

The tests referred to demonstrate that the thermal stability of silicone insulation is of a higher order of magnitude than that of conventional class *B* insulations. This has given impetus to the current activity of the Institute in recognizing silicone insulating materials as class *H* insulation with higher permissible operating temperatures.

The next step in the development and application of silicone insulated apparatus should consist of broader usage of such equipment in applications where the characteristics of silicone insulation appear to be needed and applicable. Additional experience is desirable on broader use of these new materials to permit economic evaluation of this development.

Little information has been published on the fire resistant properties of silicone insulation but considerable data have been accumulated. This indicates that silicone resins in combination with fiber glass, mica and asbestos can be processed to produce a highly fire resistant composite insulation.

Walker's paper indicates that great progress has been made in the field of silicone insulation and at the same time presents a challenge to solve the further problems which still remain. It is recognized that many of these problems must be attacked aggressively and ultimately solved to permit application on all types of apparatus. However, there are many applications on which silicone insulation can be applied where currently available materials are suitable. In such cases, field experience should be obtained in parallel with additional development work.

R. L. Webb (Consolidated Edison Company of New York, Inc., New York, N. Y.): Walker is congratulated on having presented an interesting discussion of the Navy's interest in silicones, both early in their development during the war period and in their present stage of manufacture.

The data presented in Table III of the paper, giving the characteristics which the Bureau of Ships would like to see in these materials, is also valuable information. I am sure the Navy has other interesting information to give us, on their experience with silicones, and it is hoped that the bureau will see fit to prepare another paper for a future meeting giving actual experience data with silicones used on board ship.

It was interesting to note that the Navy's experience leads the author to conclude that a hot spot temperature of 200 degrees centigrade would be satisfactory for silicones in rotating machine windings provided the bearing problem can be solved. The AIEE recently has adopted a hot spot temperature recommendation for silicones of 180 degrees centigrade. This recommendation will appear in the new revised issue of AIEE Standard 1, which was completed recently by co-ordinating committee number 4 of the Standards Committee. We are pleased to see a limit for hot spot temperature established at this time since it will place manufacturing designs and proposals on a common basis, as well as provide a conservative limit of temperature to which these materials may be worked.

The copper oxidation, to which the author referred when speaking of a solenoid coil which was operated at 275 degrees centigrade, is most interesting indeed. It would be of further interest if we knew why the rate of oxidation was relatively small during the first 7,000 hours of operation and several times as much during the last 5,000 hours. Since silicone is fairly free of porosity, it would appear that the insulation had developed cracks which would permit the air to come in contact with the copper following the first few thousand hours of operation. If this is a condition which may be expected at temperatures as high or higher than 275 degrees centigrade, then it would appear that plating of the copper or some other protective method, not affected by the high temperature, will be necessary where silicone materials are worked to such limits in special applications.

The use of high temperature insulations in machine windings requires special consideration to the complete design of the equipment both electrical and mechanical. In this connection, I would like to ask Walker a question about the iron core of rotating machines and of other equipment where laminated steel is subjected to the high temperatures permitted where silicones are used. Are the insulating varnishes, used to insulate the steel laminations, attacked by the high temperature to the extent that special varnishes, such as silicones or other high temperature coatings or insulations, have to be used to prevent short-circuiting of the steel sheets?

William A. Del Mar (Phelps Dodge Copper Products Corporation, Yonkers, N. Y.): What was the thickness of insulation used in making the dielectric strength tests recorded in Tables III and IV?

Were any dielectric strength tests made on the aged samples? If so, how did this property hold up, compared to its initial value, before aging?

R. G. Lorraine (General Electric Company, Schenectady, N. Y.): This paper presents much new and interesting material. A comparison of the General Electric Company's experience[1,2] resulting from having built and tested a wide variety of types and sizes of silicone insulated equipment, much of it in connection with the Navy's development program, shows general agreement with the evidence and conclusions presented in this paper.

Supplementing the discussion in the paper, our tests have indicated at least two additional factors which may be important in determining the temperature limits suitable for silicone insulation.

1. The mechanical properties of silicone materials change with temperature and in certain cases may limit the hot spot temperature below the temperature required for chemical stability of the material.

2. In some situations, the presence of ionizable contaminants makes it possible for the contaminant solution to enter more rapidly surface discontinuities of the insulation, resulting from heat aging, which may produce failure of the insulation. In the absence of ionizable contaminants, for example, water alone tends to stand in fine droplets on the surface of the silicone insulation without entering the discontinuities.

It is well to emphasize that design factors may also influence the maximum temperature which may be realized regardless of the temperature stability of the insulation. In this category, the author points out the bearing temperature limitation and in connection with transformers, the voltage regulation and loss limitations. A phenomenon called, "temperature creep" aggravates this situation. Operation of copper at high temperature increases its resistance, because of its positive resistance temperature coefficient, hence the copper loss which in turn further increases the temperature. It is important that temperature creep be taken into account in design to avoid failure from this cause when abnormal operating conditions are encountered.

From the economic standpoint, operating temperature of high-temperature insulation is frequently limited in continuously loaded apparatus by the poor efficiency which results from relatively greater losses brought about by working the apparatus harder in attempting to take advantage of the inherent higher operating temperature limit permitted with silicone insulation. In effect, the chief advantage generally of a

Table I. Silicone Insulated Versus Class *A* and Class *B* Insulated Transformers

Ratings: 3 Kva, 450/117 Volts, 60 Cycles, 150 C Rise; 25 Kva, 450/117 Volts, 60 Cycles, 150 C Rise

Kva	Weight, Lb			Per Cent Weight Saved		Volume, Cu In.			Per Cent Volume Saved	
	Class A	Class B (Navy Specifications)	Silicone Insulation	Over Class A	Over Class B	Class A	Class B (Navy Specifications)	Silicone Insulation	Over Class A	Over Class B
2 (steel case)	92	70	45	51	36	2,200	1,020	777	65	24
3 (magnesium case)			39.0	57.5	44	2,200	1,020	777	65	24
25 (steel case)	420	295	215	49	27	5,162	5,750	3,600	30	37
25 (magnesium case)			197	53	33	5,162	5,750	3,600	30	37

high-temperature insulation, such as silicone, is to reduce insulation operating temperature from a prime factor in the design considerations to a less important consideration among the many factors involved.

REFERENCES

1. SILICONE INSULATION, C. E. Kilbourne. *Machine Design* (Cleveland, Ohio), August 1946, pages 109–13.

2. SILICONE RESIN BONDED LAMINATES, L. V. Larson, J. J. Whilton, J. J. Pyle. *Modern Plastics* (New York, N. Y.), March 1946, pages 160–62.

M. L. Manning (Kuhlman Electric Company, Bay City, Mich.): This paper, which reviews the activity of the Bureau of Ships in promoting development work for the production of lighter weight shipboard electric equipment by use of silicone insulation, is timely. Use of silicone insulation in electric equipment opens new pathways and a new era in design.

From the standpoint of a manufacturer of silicone insulated transformers mentioned, I should like to discuss the paper. During the past year the Kuhlman Electric Company designed and manufactured for the bureau 3- and 25-kva 450/117 volts silicone-insulated distribution transformers with pressed steel and magnesium cases and a 150-kva 3-phase-to-2-phase, 450/30– 16 volts resistance furnace transformer. All designs resulted in approximately one third volume and weight reduction over existing Navy Department specifications for class *B* insulated units.

It is interesting to review the volume and weight reduction in 3- and 25-kva dry-type transformers accomplished in the past decade by use of better grade core steels and insulation. Comparative figures for class *A*, class *B*, and silicone insulated transformers are found in Table I of this discussion. For 3- and 25-kva designs the weight reduction for silicone insulated units is 50 per cent compared with class *A* insulated designs. Electrical characteristics of class *B* and silicone insulated transformers of these ratings are shown in Table I of this discussion.

The paramount issue for consideration in using silicone insulation in transformers has been the question of losses and regulation at high temperatures. By proper design balance, losses need not be out of step with those prescribed. Regulation, at operating temperatures for the transformers considered in the paper, was practically in agreement with Navy Department specifications for class *B* designs.

Weight reduction by use of magnesium cases for transformers offers possibilities. A transformer case constructed of magnesium weighs approximately 40 per cent as much as a case made from pressed steel. Shock tests prescribed by the Navy Department must be withstood.

The advantages of the use of silicone in-

Table I (continued). Silicone Insulated Versus Class *A* and Class *B* Insulated Transformers

Ratings: 3 Kva, 450/117 Volts, 60 Cycles, 150 C Rise; 25 Kva, 450/117 Volts, 60 Cycles, 150 C Rise

Electrical Characteristics											
Temperature		Losses, watts				Per Cent Regulation					
		Core		Total		100 Per Cent Power Factor			80 Per Cent Power Factor		
Rise, C											
Class B	Silicone Insulation	Class B Specifications	Silicone Insulation	Class B Specifications (80 C Rise)	Silicone Insulation (116 C Rise)	Class B Specifications (80 C Rise)	Silicone Insulation (116 C Rise) 50 C Ambient Temperature		Class B Specifications (80 C Rise)	Silicone Insulation (116 C Rise) 50 C Ambient Temperature	
80	116	41	36	105	126	2.6	3.21		4.3	4.09	
80	116	41	36	105	126	2.6	3.21		4.3	4.09	
					(120 C Rise)		(120 C Rise)			(120 C Rise)	
80	120	170	144	565	710	1.8	2.19		3.8	2.10	
80	120	170	144	565	710	1.8	2.19		3.8	2.10	

sulation for transformers can be summarized as follows:

1. Organic bonds, impregnants, and surface treatment used in class *B* insulation have limited temperature range. Silicone materials containing inorganic components permit continuous temperatures of 250 degrees centigrade.

2. Life of insulation under high thermal conditions has been a determining factor in transformer design. Recent use of silicone insulations in low voltage distribution transformers promises to be a solution. Silicone insulated transformers have operated continuously at 300 degrees centigrade without signs of deterioration. Overloads are permissible.

3. It must be recognized that a transformer offers more difficult voltage problems than those for motor applications. In a transformer insulation structure, materials having different properties must be used to withstand voltage and temperature conditions.

4. Development work described is a step in the direction of building dry type transformers having less weight and volume and greater overload capacity for low voltage distribution circuits. For supplying power to machine tools and related loads, the silicone insulated transformer offers great promise. Overload capacity can be provided without adding additional kilovolt-amperes in transformer ratings.

5. Further studies of the effect of transformer losses and how to proportion them, should be made on electric power systems.

H. P. Walker: R. L. Webb has asked if special varnishes are needed to protect the steel laminations used in core construction where the design is contemplated for high temperature operation. For any high temperature electric equipment where steel laminations are used a satisfactory high temperature insulating medium must be used to prevent short circuiting of the steel sheets. Water-glass (sodium silicate) and silicone varnish have been used successfully on Navy type machines.

W. M. Del Mar has asked what thickness of insulation was used in making the dielectric strength tests recorded in Tables III and IV. Dielectric strength tests were made on material 1/8 inch thick. In regard to reduction in dielectric strength on thermal aging, tests on silicone-glass laminates showed values of 200 volts per mil at temperatures of 200 degrees centigrade, while melamine-glass laminates tested 120 volts per mil and phenolic-glass laminates tested 60 volts per mil.

G. L. Moses has stressed the need for service experience in parallel with development work. The bureau has in effect at the present time many contracts to build electric equipment for actual shipboard installation and trial. This equipment is being designed for high temperature operation and consists of turbogenerators, Diesel generators, welders, motors, motor generator sets, and various types of control equipment. Service tests on this equipment should permit an economic evaluation of the development of silicone electrical insulation as well as provide a basis for more accurate specification requirements.

Distortion and Band-Width Characteristics of Pulse Modulation

H. L. KRAUSS
ASSOCIATE AIEE

P. F. ORDUNG
ASSOCIATE AIEE

Synopsis: Various types of pulse amplitude and pulse time modulated waves have been analyzed by a novel method to determine their exact frequency spectra. Using these results the inherent distortion produced when the audio signal is recovered with a low-pass filter is calculated. The minimum allowable ratio of pulse repetition frequency to maximum audio frequency is expressed in terms of the distortion and the percentage modulation. The form of the result is shown to be common to all types of pulse time modulation. The effects of pulse width, pulse shape, and percentage modulation on the required bandwidth are also discussed.

THE use of repeated pulses of short duration for the transmission of information has increased considerably in the past few years, primarily because a high ratio of peak to average power output is desirable at the transmitter in order to make efficient use of present-day microwave tubes. To transmit information some type of modulation must be applied to the pulse wave. Modulation is defined as the process whereby the amplitude or some other characteristic of a wave is varied as a function of the instantaneous value of another wave. Basically, pulse modulation is a process of double modulation. In one form, some geometric characteristic (such as the length, amplitude, or position of successive pulses) of a repeated pulse wave is varied as a function of the modulating wave. The modulated pulse wave is used in turn to 100-per-cent amplitude modulate a high frequency carrier. In another form, a uniform repeated pulse wave is used to sample a high frequency carrier which has already been amplitude or frequency modulated. The samples, which correspond to the duration of the pulses, are transmitted at the pulse repetition rate. This paper is concerned with the first type mentioned, in which the primary modulation is performed on the pulse wave itself.

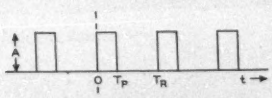

Figure 1. Unmodulated pulse wave

A mathematical method which gives an exact solution for the spectra of various types of modulated pulse waves is given. The results are used to indicate relations between parameters such as pulse length, average repetition rate, maximum allowable time or phase-shift of the pulse, and others, with respect to their effect on distortion and band width.

Definition of Terms

Standard terminology for describing the various types of modulation which may be impressed on a pulse wave has not been adopted. In this paper the following definitions are used.

PULSE AMPLITUDE MODULATION OR PAM

Type A—The instantaneous amplitude of each pulse is related linearly to the modulating signal at that instant. The amplitude varies *during* the pulse and the pulse-tops are shaped like sections of the modulating wave.

Type B—Each pulse has constant amplitude (rectangular pulse) but the amplitude of successive pulses is related linearly to the instantaneous value of the modulating signal at some reference point on the pulse (such as the leading edge, center, or trailing edge).

PULSE TIME MODULATION OR PTM

In pulse time modulation the values of instantaneous samples of the modulating wave are caused to vary the time of occurrence of some characteristic of a pulse carrier. This includes pulse position and pulse length modulation.

Type A—Pulse Length Modulation or PLM

Type $A1$—The leading edges of the pulses remain fixed in their unmodulated positions. The trailing edges have a time displacement proportional to the amplitude of the modulating signal at the instant of the trailing edge.

Type $A2$. The trailing edges of the pulses remain fixed in their unmodulated positions. The leading edges have a time displacement proportional to the amplitude of the modulating signal at the instant of the leading edge.

Type $A3$. Leading and trailing edges have opposite time displacements from their unmodulated positions. These time displacements are proportional, respectively, to the amplitude of the modulating signal at the leading and trailing edges.

Type B—Pulse Position Modulation or PPM

In this type the leading edges of the pulses have a time displacement proportional to the amplitude of the modulating signal at the instant of the leading edge. The trailing edges are generated automatically in such a way that the pulse length remains constant.

Symbols

$\frac{\omega_R}{2\pi} = f_R$ = mean pulse repetition frequency

$\frac{\omega_A}{2\pi} = f_A$ = frequency of the audio modulating signal

$T_R = \frac{1}{f_R}$ = repetition period of unmodulated pulse wave

$T_A = \frac{1}{f_A}$ = period of the modulating signal

T_P = length of an unmodulated pulse

$f_P = \frac{1}{2T_P}$ = pulse-length frequency

A = amplitude of unmodulated pulses

t = time in seconds

k = order of a harmonic of ω_R

Paper 47-166, recommended by the AIEE committee on communication for presentation at the AIEE summer general meeting, Montreal, Quebec, Canada, June 9–13, 1947. Manuscript submitted March 20, 1947; made available for printing May 5, 1947.

H. L. KRAUSS is assistant professor and P. F. ORDUNG is an instructor in electrical engineering at the school of engineering, Yale University, New Haven, Conn.

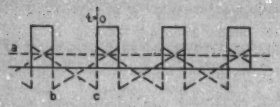

Figure 2. Method of synthesizing pulse wave

$$\text{D-c term } a=\frac{AT_P}{T_R}$$

$$\text{Sawtooth } b=\frac{A}{\pi}\sum_{k=1}^{\infty}\frac{-1}{k}\sin k\omega_R(t-T_P)$$

$$\text{Sawtooth } c=\frac{A}{\pi}\sum_{k=1}^{\infty}\frac{1}{k}\sin k\omega_R t$$

n = order of a harmonic of ω_A
m = modulation factor
X = modulation parameter in pulse time modulation
C = error term necessary to correct wave shape of synthesized pulse wave

Method of Mathematical Analysis

To ascertain mathematically the distortion and band-width characteristics of a particular kind of pulse modulation, the time function which represents it must be known. The starting point in synthesis of this time function is the Fourier series which represents the unmodulated wave shown in Figure 1. For the reference $t=0$ located at the leading edge of a pulse the series is

$$f(t)=A\frac{T_P}{T_R}+\frac{A}{\pi}\sum_{k=1}^{\infty}\frac{1}{k}\sin 2\pi k\frac{T_P}{T_R}\cos k\omega_R t+\frac{A}{\pi}\sum_{k=1}^{\infty}\frac{1}{k}\left(1-\cos 2\pi k\frac{T_P}{T_R}\right)\sin k\omega_R t \quad (1)$$

When a modulating signal is applied, thus varying some characteristic of the pulse wave, the coefficients of the Fourier series which represents the wave must be obtained by integrating over the time interval in which the resulting wave is repetitive, and this interval may be very large. This process of integration for a modulated wave is very laborious, for the integration must be performed over a large number of pulses. Furthermore, the proper application of the modulating function in order to obtain the correct expressions in the case of length and position modulation is very difficult.

Most of the aforementioned difficulties can be avoided by recognizing that the time function representing a particular kind of pulse modulation must meet the dual requirements of having its discontinuities (leading and trailing edges of the pulses) occur at the instants of time required by the particular law of modulation, and of describing the desired pulse shape. Neither of these parameters can be ascertained readily from equation 1. By a trigonometric manipulation, equation 1 is rearranged into the following form from which the location of the discontinuities and the pulse shape may be discerned easily.

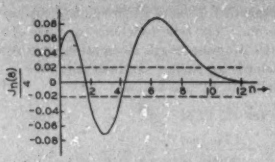

Figure 3. $\frac{J_n(2X)}{X}$ versus n, with $X=4$

For all $n>9.6$, $\left|\frac{J_n(8)}{4}\right|<0.02$

$$f(t)=A\frac{T_P}{T_R}+\frac{A}{\pi}\underbrace{\sum_{k=1}^{\infty}\frac{1}{k}\sin k\omega_R t}_{y_1}+\frac{A}{\pi}\underbrace{\sum_{k=1}^{\infty}-\frac{1}{k}\sin k\omega_R(t-T_P)}_{y_2} \quad (2)$$

Each of the series in equation 2 is the Fourier representation of a sawtooth wave.[1] Figure 2 illustrates how these sawtooth functions and the constant term add to give the pulse wave of Figure 1. The representation of the pulse wave by two sawtooth waves is useful in that it simplifies the location of the pulse edges, and allows each of these edges to be operated upon independently as will be shown later.

The first series in equation 2 has discontinuities at

$$\omega_R t=2m\pi$$

where

$$m=-\infty,\ldots-1,0,1,\ldots\infty \quad (3)$$

and the second series at

$$\omega_R(t-T_P)=2m\pi$$

where

$$m=-\infty,\ldots-1,0,1,\ldots\infty \quad (4)$$

In the pulse-length and pulse-position modulation processes to be considered, the positions of the discontinuities of either or both of the sawtooth components become time-variable functions. This is accomplished mathematically by replacing the t in equation 2 by the $\phi(t)$ that expresses the particular law of modulation. This distorts the wave shape with the result that the pulse tops and intervening spaces are not of constant amplitude.

The wave-shape error may be corrected by adding to the function a term which will compensate for the amplitude distortion but not affect the discontinuities. To compute the correction term the wave-shape error in equation 2 when t is replaced by $\phi(t)$ must be determined. This is accomplished by noting that the instantaneous amplitudes (y_1 and y_2) of the two sawtooth terms may be expressed as

$$y_1=\frac{A}{2\pi}[\pi-\omega_R t] \text{ for } 0<t<T_R \quad (5)$$

and

$$y_2=\frac{-A}{2\pi}[\pi-\omega_R(t-T_P)] \text{ for } T_P<t<T_R+$$

respectively. As time increases, the values of y_1 and y_2 pass through discontinuities which are expressed in equations 5 and 6 by the addition of constant terms. These constants do not affect the wave-shape error, but merely give the amplitudes of the leading and trailing edges, respectively, of the pulses. Between pulses, the amplitude of the complete wave equals zero, thus

$$C+y_1+y_2+A\frac{T_P}{T_R}=0 \quad (7)$$

The correct function is obtained by adding C to the function obtained by replacing t by $\phi(t)$ in equation 2. An example of this procedure for synthesis of pulse-length modulation is given in the appendix.

To synthesize the function for pulse amplitude modulation the locations of the discontinuities are not affected. However, the amplitude constant A becomes a function of time which describes the particular law of modulation. Otherwise, the process is identical to that previously described.

Pulse Amplitude Modulation

Type A PAM

The time function which represents type A pulse amplitude modulation when the modulating wave has the equation

$$e=E\sin\omega_A t$$

is

$$f(t)=A\frac{T_P}{T_R}+\frac{mAT_P}{T_R}\sin\omega_A t+\frac{A}{\pi}\sum_{k=1}^{\infty}\frac{1}{k}(1+m\sin\omega_A t)\sin k\omega_R t-\frac{A}{\pi}\sum_{k=1}^{\infty}\frac{1}{k}(1+m\sin\omega_A t)\sin k\omega_R\times(t-T_P) \quad (8)$$

The terms of the form

$$\frac{A}{2\pi}(1+m \sin \omega_A t) \sin k\omega_R t$$

in this series are identified readily as amplitude modulated waves in which the carriers have frequencies kf_R and amplitudes $A/(\pi k)$, each carrier being modulated by a wave of frequency f_A. Equation 8 therefore represents a d-c term, an audio-frequency term, and the series of amplitude modulated waves just discussed. No harmonics of the audio frequency are present.

In a receiver the audio term may be recovered from the pulse wave by a low-pass filter. To prevent interference between the frequency components ($f_R - f_A$) and f_A in the filtering process, the repetition frequency should be made 2.5 to 3 times the highest audio frequency to be used.

The choice of the pulse length T_P has no effect on side-band interference with the audio frequencies, but it does affect the amplitude of the audio component which may be recovered from the wave. The band width of the pulse wave also is determined by T_P as will be discussed later. In particular applications, T_P must be evaluated in terms of the characteristics of the tubes used and the permissible band width of the system.

Type B PAM

The time function for type B pulse amplitude modulation with the modulating wave used in the foregoing is

$$\begin{aligned} f(t) = {} & \frac{AT_P}{T_R} + \frac{mA}{\omega_A T_R}[\sin \omega_A T_P \sin \omega_A t - \\ & (1-\cos \omega_A T_P) \cos \omega_A t] + \\ & \frac{A}{2\pi}\sum_{k=1}^{\infty}\left\{\frac{2}{k}[\sin k\omega_R T_P \cos k\omega_R t + \right. \\ & (1-\cos k\omega_R T_P) \sin k\omega_R t] + \\ & \frac{\pm m}{k \pm \frac{T_A}{T_R}}[\sin k\omega_R T_P \sin (k\omega_R \pm \omega_A)t - \\ & \left. (1-\cos k\omega_R T_P) \cos (k\omega_R \pm \omega_A)t]\right\} \quad (9) \end{aligned}$$

Comments given for type A apply to type B also.

Pulse Length Modulation

In each of the types of pulse length modulation a pulse-edge is shifted from its unmodulated position by an amount proportional to the amplitude of the modulating wave at the instant of occurrence of the respective pulse-edge. In Appendix I the time function for type $A1$ pulse length modulation, with a modulating wave $e = E \sin \omega_A t$, is developed and expanded to show the frequency components. The time functions for types $A2$ and $A3$ pulse length modulation were obtained by similar methods and the results are given as follows.

Type $A1$ PLM

$$\begin{aligned} f(t) = {} & \frac{AT_P}{T_R} + \frac{mAT_P}{T_R} \sin \omega_A t + \\ & \frac{A}{\pi}\sum_{k=1}^{\infty}\frac{1}{k} \sin k\omega_R t - \\ & \frac{A}{\pi}\sum_{k=1}^{\infty}\frac{1}{k} \sin k\omega_R (t - T_P - \\ & mT_P \sin \omega_A t) \quad (10) \end{aligned}$$

where m can have a maximum value of 1.0.

Type $A2$ PLM

$$\begin{aligned} f(t) = {} & \frac{AT_P}{T_R} + \frac{mAT_P}{T_R} \sin \omega_A t + \\ & \frac{A}{\pi}\sum_{k=1}^{\infty}\frac{1}{k} \sin k\omega_R (t + mT_P \sin \omega_A t) - \\ & \frac{A}{\pi}\sum_{k=1}^{\infty}\frac{1}{k} \sin k\omega_R (t - T_P) \quad (11) \end{aligned}$$

where m can have a maximum value of 1.0.

Type $A3$ PLM

$$\begin{aligned} f(t) = {} & \frac{AT_P}{T_R} + \frac{2mAT_P}{T_R} \sin \omega_A t + \\ & \frac{A}{\pi}\sum_{k=1}^{\infty}\frac{1}{k} \sin k\omega_R (t + mT_P \sin \omega_A t) - \\ & \frac{A}{\pi}\sum_{k=1}^{\infty}\frac{1}{k} \sin k\omega_R (t - T_P - mT_P \times \\ & \sin \omega_A t) \quad (12) \end{aligned}$$

where m can have a maximum value of 0.5.

With the maximum values of m specified in the foregoing sections, the pulse length will vary from 0 to $2T_P$ during a modulation cycle. Each of these time functions contains a d-c term, an audio frequency term, and terms of frequency-modulated waves in which the carriers are the pulse repetition frequency and its harmonics. There are no harmonics of the audio frequency present in these functions. Thus the audio signal may be recovered from the pulse wave by means of a low-pass filter. As before, the lower side bands of f_R and its harmonics must not extend into the audio frequency band. This requirement may impose more severe limitations than in the case of pulse amplitude modulation, because the frequency-modulated terms may have several side frequencies due to each audio frequency. In Appendix I the lower side-band terms for type $A1$ pulse length modulation are developed. The terms for types $A2$ and $A3$ may be obtained by similar methods, and the results are given as follows.

Type $A1$ PLM

$$e_{SB} = -\frac{A}{\pi k} J_n(k\omega_R m T_P) \times \sin [k\omega_R (t - T_P) - n\omega_A t] \quad (13)$$

Type $A2$ PLM

$$e_{SB} = (-1)^n \frac{A}{\pi k} J_n(k\omega_R m T_P) \times \sin (k\omega_R - n\omega_A)t \quad (14)$$

Type $A3$ PLM

$$\begin{aligned} e_{SB} = {} & -\frac{A}{\pi k} J_n(k\omega_R m T_P) \times \\ & \sin [k\omega_R (t - T_P) - n\omega_A t] - \\ & (-1)^n \sin (k\omega_R - n\omega_A)t \quad (15) \end{aligned}$$

where in each of these expressions, $k = 1, 2, \ldots \infty$, and $n = 1, 2, \ldots \infty$.

The lower side frequencies of importance are those which may overlap into the audio band, that is, those for which $kf_R - nf_A \leq f_A$. For these side-band frequencies, the ratio of the side band to audio frequency voltage for all three types is of the same form

$$\frac{E_{SB}}{E_A} = \left|\frac{J_n(2X)}{X}\right| \quad (16)$$

where

$$X = k\frac{\pi m T_P}{T_R}$$

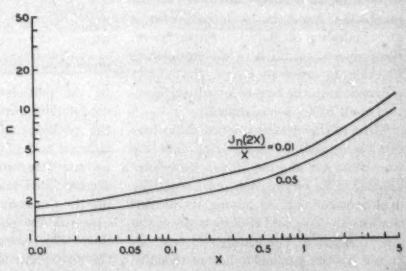

Figure 4. The number n of side frequencies with amplitudes that exceed one per cent of five per cent of the audio signal are plotted versus the modulation parameter X

Using the limiting values for m given with equations 10, 11, and 12, and letting $T_P/T_R=1/2$ (its greatest permissible value with m maximum), X will have a corresponding maximum value for each k used. Since the ratio $f_R/f_{A\max}$ determines the side-band interference with the audio frequency, $X_{\max}$ is defined in terms of the repetition frequency, $k=1$, for each of the modulation types. Substituting these values into the expression for X gives $X_{\max}=\pi/2$ for types $A1$ and $A2$ pulse length modulation and $X_{\max}=\pi/4$ for type $A3$.

In practice X may be used to determine the minimum allowable ratio f_R/f_A for a given value of E_{SB}/E_A. For $E_{SB}/E_A=0.01$ and $X=\pi/4$, f_R/f_A must be greater than 5.3 as shown in Appendix II.

Pulse Position Modulation

When the modulating wave has the form $e=E \sin \omega_A t$, the time function which represents the wave defined previously as type B pulse position modulation is

$$f(t)=\frac{AT_P}{T_R}+\frac{mAT_P}{T_R}\{\sin \omega_A t-\sin \omega_A(t-T_P)\}+\frac{A}{\pi}\sum_{k=1}^{\infty}\frac{1}{k}\times \sin k\omega_R(t+mT_P \sin \omega_A t)-\frac{A}{\pi}\sum_{k=1}^{\infty}\frac{1}{k}\sin k\omega_R[(t-T_P+mT_P\times \sin \omega_A(t-T_P)] \quad (17)$$

where m is defined as the modulation factor proportional to the amplitude of the modulating signal. This time function is similar to those for pulse length modulation, except that m may be greater than unity in this case. The limiting value of m occurs when the instantaneous pulse repetition period $T_R(t)$ becomes equal to T_P. As in pulse length modulation, the side frequencies which may cause distortion are those which lie in the audio band. The amplitude of these side frequencies is

$$e_{SB}=(-1)^n\frac{A}{\pi k}J_n(k\omega_R mT_P)\times [\sin (k\omega_R-n\omega_A)t-\sin (k\omega_R-n\omega_A)\times (t-T_P)] \quad (18)$$

When $kf_R-nf_A=f_A$, this expression is given approximately by

$$e_{SB}\approx(-1)^n\frac{A}{\pi k}J_n\left(\frac{2\pi kmT_P}{T_R}\right)\omega_A T_P \cos \omega_A t \quad (19)$$

From equation 17, if $\omega_A T_P<0.17$, which usually is satisfied, the audio voltage is

$$e_A\approx\frac{\omega_A T_P{}^2 mA}{T_R}\cos \omega_A t \quad (20)$$

The ratio of side-band to audio voltage is

$$\frac{E_{SB}}{E_A}=\left|\frac{J_n(2X)}{X}\right| \quad (21)$$

for

$$X=\frac{\pi kmT_P}{T_R}$$

which is the same form previously obtained in pulse length modulation. As in pulse length modulation, a given X and E_{SB}/E_A establishes the minimum permissible f_R/f_A.

Band Width

Only the band width of the pulse wave will be treated here, since the results of amplitude or angular modulation of a high-frequency carrier are well known in terms of the frequencies contained in the modulating signal. The factors which determine the band width required for the pulse wave are the side bands due to modulation and the allowable distortion in pulse shape at the receiver. The shape of the pulse after demodulation from the high frequency carrier in the receiver must be sufficiently close to the ideal rectangular shape to permit the receiver circuits to determine the exact pulse height in the case of amplitude modulation, and to determine the exact time of the leading or trailing edges or both in the case of pulse time modulation or in multiplexing systems.

A perfectly rectangular pulse would require an infinite band width as may be seen from equation 1. However, if the allowable distortion in pulse shape may be specified in terms of an arbitrary value of rise time for the leading edge, a finite band width results.[3] For a rise time equal to 0.1 T_P the band width required is

$$BW=\frac{10}{2T_P} \quad (22)$$

But $1/2T_P$ is the fundamental frequency contained in a square wave having $T_P=$ the time of a half cycle. Letting

$$f_P=\frac{1}{2T_P} \quad (23)$$

the band width given in equation 22 must be $10 f_P$ for the specified rise time. If the pulse definition requirements are as stringent as this, the side bands due to modulation generally will have a negligible effect on band width since $f_P \gg f_R$. Thus the minimum value of T_P, or the shortest interval between pulses if this is less than the minimum T_P, determines the band width. This is an important design consideration in pulse time modulation systems.

Conclusions

In both types of pulse amplitude modulation, distortion in the audio signal recovered from the pulse wave is caused by side bands of the amplitude modulated components in the wave that have frequencies within the audio band. To prevent this, the minimum ratio $f_R/f_{A\max}$ is slightly greater than 2, and for ease of filtering probably should be 2.5 or 3.

In pulse time modulation the interval occupied by the modulated pulse in all systems is the same per cent of a repetition period for a common value of X, the modulation parameter. The value of X determines the ratio $f_R/f_{A\max}$ when the distortion arising from the side-band terms having frequencies within the audio band is limited to a given value. For very small modulation parameters, the ratio f_R/f_A must be slightly greater than 2, probably 2.5 or 3 for ease of filtering. Larger modulation parameters require correspondingly larger separations, as may be seen from Figure 4.

In pulse length modulation and in pulse amplitude modulation the amplitude of the audio term varies directly as the percentage modulation and is independent of the audio frequency (with the restriction in type B pulse amplitude modulation that $T_P \ll T_A$). In pulse position modulation the amplitude of the audio term is directly proportional to the audio frequency and to the percentage modulation. Either in producing the pulse position modulation or in its recovery, a de-emphasis circuit must be employed to make the recovered signal independent of the audio frequency. In all of these types, no second harmonics of the audio frequency occur in the wave.

The band width required is shown to be determined by the length of the shortest pulse. Conversely, in a given system the permissible band width serves as a limit for the length of the shortest pulse. This factor serves to limit the maximum percentage modulation that may be employed in all forms of pulse time modulation. When the band width of the receiver is exceeded, distortion results because of the inability of the receiver to distinguish individual pulses.

Appendix I. Type A1 Pulse Length Modulation

In this type of modulation, the position of the trailing edge of the pulse is determined by the modulating wave such that the width of the pulse is directly proportional to the value of the modulating wave

at the instant of generation of the trailing edge. By definition, T_P as expressed in equation 2 is replaced by the $T_P(t)$ which expresses the law of modulation. For this type of modulation, equation 2 becomes

$$f(t)=\frac{AT_P(t)}{T_R}+\frac{A}{\pi}\sum_{k=1}^{\infty}\frac{1}{k}\sin k\omega_R t-\frac{A}{\pi}\sum_{k=1}^{\infty}\frac{1}{k}\sin k\omega_R(t-T_P(t)) \quad (24)$$

wherein $T_P(t)$ is linearly related to the amplitude of the audio voltage at the discrete instants of time when

$$\omega_R[t-T_P(t)]=2\pi r \quad (25)$$

where r is any integer.

For a modulating wave of the form $e=E\sin\omega_A t$, the pulse length function which satisfies the desired law of modulation is

$$T_P(t)=T_P(1+m\sin\omega_A t) \quad (26)$$

Here m is defined as the percentage modulation effected by the modulating wave and T_P is the length of the unmodulated pulse. The time function which satisfies the modulation law requirements concerning the wave shape and the location of the discontinuities is obtained by adding a wave shape correction term C to the function resulting from substitution of equation 25 into equation 23. The desired function is therefore

$$f(t)=\frac{AT_P}{T_R}+\frac{mAT_P}{T_R}\sin\omega_A t+\frac{A}{\pi}\sum_{k=1}^{\infty}\frac{1}{k}\sin k\omega_R t-\frac{A}{\pi}\sum_{k=1}^{\infty}\frac{1}{k}\times\sin k\omega_R(t-T_P-mT_P\sin\omega_A t)+C \quad (27)$$

Following the method outlined in the mathematical analysis section, the correction term is obtained by summing the amplitudes of the terms in equation 27 for the region between pulses as follows:

$$0=C+\frac{AT_P}{T_R}+\frac{mAT_P}{T_R}\sin\omega_A t+\frac{A}{2\pi}(\pi-\omega_R t)-\frac{A}{2\pi}(\pi-\omega_R t+\omega_R T_P+\omega_R mT_P\times\sin\omega_A t) \quad (28)$$

Solving for C in equation 28 gives

$$C=0$$

Therefore the time function for pulse length modulation with the trailing edge modulated and the leading edge fixed is

$$f(t)=\frac{AT_P}{T_R}+\frac{mAT_P}{T_R}\sin\omega_A t+\frac{A}{\pi}\sum_{k=1}^{\infty}\frac{1}{k}\times\sin k\omega_R t-\frac{A}{\pi}\sum_{k=1}^{\infty}\frac{1}{k}\sin k\omega_R\times[t-T_P(1+m\sin\omega_A t)] \quad (29)$$

The time function in the second series can be translated into a series of sinusoidal terms if the term

$$\sin k\omega_R[t-T_P(1+m\sin\omega_A t)]$$

is recognized as representing a frequency modulated wave having a carrier frequency of $k\omega_R$, a modulating wave of frequency ω_A and a modulation index of $mk\omega_R T_P$. Using the following Fourier-Bessel identity:[3]

$$\sin(x+\beta\sin y)\equiv J_0(\beta)\sin x+\sum_{n=1}^{\infty}J_n(\beta)[\sin(x+ny)+(-1)^n\times\sin(x-ny)] \quad (30)$$

equation 29 is rewritten in such form that all terms are simple sinusoids as follows:

$$f(t)=\frac{AT_P}{T_R}+\frac{mAT_P}{T_R}\sin\omega_A t+\frac{A}{\pi}\sum_{k=1}^{\infty}\frac{1}{k}\times\sin k\omega_R t-\frac{A}{\pi}\sum_{k=1}^{\infty}\frac{1}{k}\{J_0(k\omega_R mT_P)\times\sin k\omega_R(t-T_P)+\sum_{n=1}^{\infty}J_n(k\omega_R T_P m)[\sin(k\omega_R(t-T_P)-n\omega_A t)+(-1)^n\sin(k\omega_R(t-T_P)+n\omega_A t)]\} \quad (31)$$

Appendix II

In the various types of pulse time modulation the function

$$\left|\frac{J_n(2X)}{X}\right|=\frac{E_{SB}}{E_A}$$

appears as the ratio of the lower-side-band terms of ω_R and its harmonics to the audio term (see equations 16 and 21). This function may be used to determine the minimum allowable ratio of ω_R to the maximum ω_A to make the side-band term which falls in the audio range less than a given percentage of the audio signal. When $J_n(2X)/X$ is plotted versus n for some arbitrarily assigned value of X a curve which oscillates about zero results as shown in Figure 3.[4] If a particular value for $|J_n(2X)/X|$ is specified as shown by the dotted lines in Figure 3, the largest value of n which will give this magnitude may be determined from the curve. Similar results may be obtained for other values of X. Figure 4 shows how this largest value of n varies as a function of X for $|J_n(2X)/X|=0.01$ and 0.05.

The factor X contains the product $(m\times k)$. The factor n is the order of the side frequency around ω_R and its harmonics (see equations 13 and 19). Assuming that values have been assigned for m, k, and the maximum allowable E_{SB}/E_A, the corresponding value of n may be found from a curve such as those in Figure 4. When

$$kf_R=(n+1)f_A$$

the side frequency which causes distortion is equal to f_A. Choosing $k=1$ and using the maximum audio frequency, the pulse repetition frequency must be

$$f_R\geqq(n+1)f_{A\max} \quad (32)$$

where the proper value of n is obtained from Figure 4. Once f_R has been chosen on this basis, values of $f_A<f_{A\max}$ will satisfy the criterion of equation 32. Similarly, if the harmonics of f_R are considered, X will increase proportionally with k, but the limiting value of n obtained from Figure 4 always will be such that the lower side band of kf_R will have components of negligible amplitude in the audio range.

As an example, consider type $A1$ pulse length modulation. The maximum value of X was given as $\pi/2$ for this type. If E_{SB}/E_A is to be limited to 0.01, the corresponding value of n from Figure 4 is 5.9. Thus the minimum allowable $f_R/f_A=n+1=6.9$. In practical systems the value of m probably would not exceed 0.5 in order to limit the band width to a reasonable value. This would limit X to $\pi/4$, giving $f_R/f_A>5.3$.

References

1. Radio Engineer's Handbook (book), F. E. Terman. McGraw-Hill Book Company, Inc., New York, N. Y., 1943, pages 20–2.

2. Communication Networks (volume 2), E. A. Guillemin. John Wiley and Sons, New York, N. Y., 1935, page 479.

3. Frequency Modulation (book), A. Hund. McGraw-Hill Book Company, Inc., New York, N. Y., 1942, page 350.

4. Tables of Functions (book), E. Jahnke, F. Emde. Dover Publications, New York, N. Y., fourth edition, 1945, page 126.

No Discussion

Distortion in a Pulse Count Modulation System

A. G. CLAVIER
NONMEMBER AIEE

P. F. PANTER
NONMEMBER AIEE

D. D. GRIEG
ASSOCIATE AIEE

Synopsis: In the further development of pulse time multiplex systems the form of modulation known as pulse count modulation[1,2] has been studied both theoretically and experimentally. This paper reviews briefly the principles of pulse communication and its extension to pulse count modulation (PCM). Unlike the conventional types of modulation, PCM is represented by a discrete scanning of the amplitude of the modulating signal rather than a continuous amplitude scanning, in addition to the discrete scanning in time which is common to the other forms of pulse modulation. The discrete nature of such a system introduces a type of distortion which is a function of the number of amplitude levels used. The relation between the numbers of levels and this type of distortion has been investigated and is discussed. Several types of signals are analyzed mathematically; namely, a single-frequency signal, a 2-frequency signal, and finally a continuous band of frequencies. In connection with the multifrequency case, the application of the Fourier transform to pulse amplitude modulation and its extension to PCM is introduced. In addition, the cross talk introduced in different channels of the modulating frequency is shown graphically for several amplitude levels.

THE methods of transmitting intelligence by means of short bursts or pulses of energy have shown increasing application within recent years. Such applications have included radio relay systems, telephone multiplex, telemetering, and multiplex broadcasting, all of which have been described in the technical literature.[3-7] Pulse modulation exhibits many important characteristics which makes the method particularly applicable to communication transmission systems. One of the fundamental properties is the ease of transmitting more than one intelligence signal through multiplexing by means of time division. With this method the increments of each modulating signal are interleaved in time sequence and since only one increment is transmitted at any one instant of time nonlinearities in the transmission system do not introduce interchannel cross talk products such as would be obtained in the more conventional frequency division multiplex. Another characteristic is the noise reducing properties obtained as a function of the transmission band width utilized. A third factor obtained with pulse systems utilizing constant amplitude pulses is the corresponding constant amplitude transmission characteristic which permits the system to be independent of fading and other transmission vagaries. A further important property is the flexibility of the pulse function which allows the various transmission constants to be interchanged, that is, band width for signal-to-noise ratio, distortion and cross talk for band width, number of channels for signal-to-noise ratio or band width and other combinations, thus permitting a system design directly suited to the specific application.

Since pulses are characterized by the several parameters of amplitude, timing, duration, frequency, build-up time, decay time, and pulse shape, a large number of modulation methods involving these characteristics singly or in combination may be envisaged. For example, the amplitude may be modulated resulting in pulse amplitude modulation. Alternatively, the width or duration of the pulses can be made to vary in accordance with the modulating signal resulting in pulse width modulation. In this case a variation of the average power similar to amplitude modulation is obtained, but with constant amplitude pulses which permits the advantages of limiters and clippers to be obtained in the system. Instead of varying the individual pulse characteristic, the time between pulses or with reference to a marker pulse can be varied resulting in what has been called pulse time modulation. It should be noted that pulse time modulation can be derived from pulse width modulation by utilizing the leading or trailing edge of the width modulated pulses. In this manner the noise reduction advantages gained by the use of limiters are obtained, but at the same time a considerable reduction of power for the same peak power realized. The repetition frequency of the pulses may be modulated similarly to conventional frequency modulation giving rise to pulse frequency modulation. For both pulse frequency modulation and pulse time modulation the average power is essentially constant, with the deviation in frequency and time, respectively, being proportional to the amplitude of the modulating signal and the rate of change of these quantities a function of the modulating frequency. Figure 1 illustrates the fundamental characteristics of these several methods of modulation. The additional pulse characteristics may of course be varied, such as the pulse shape, and also combinations utilized; for example, time modulation together with amplitude modulation of the pulse series.

It should be pointed out here that the discussion has been limited to the so-called video or d-c pulses without regard to the specific method of radio frequency transmission. It is obvious that any of the well-known methods of modulation of the radio-frequency carrier may be utilized such as amplitude, frequency, or phase keying, in addition to the modulation of the pulse sub-carrier.

Paper 47-152, recommended by the AIEE committee on communication for presentation at the AIEE summer general meeting, Montreal, Quebec, Canada, June 9–13, 1947. Manuscript submitted March 14, 1947; made available for printing April 29, 1947.

A. G. CLAVIER is assistant director of research, P. F. PANTER is group leader of the theoretical group of the communications division, and D. D. GRIEG is head of the communications division, Federal Telephone and Radio Laboratories, New York, N. Y.

Acknowledgment is made to Doctor L. Goldstein for participation in early discussions and H. Anderson for aid in the more tedious numerical computations.

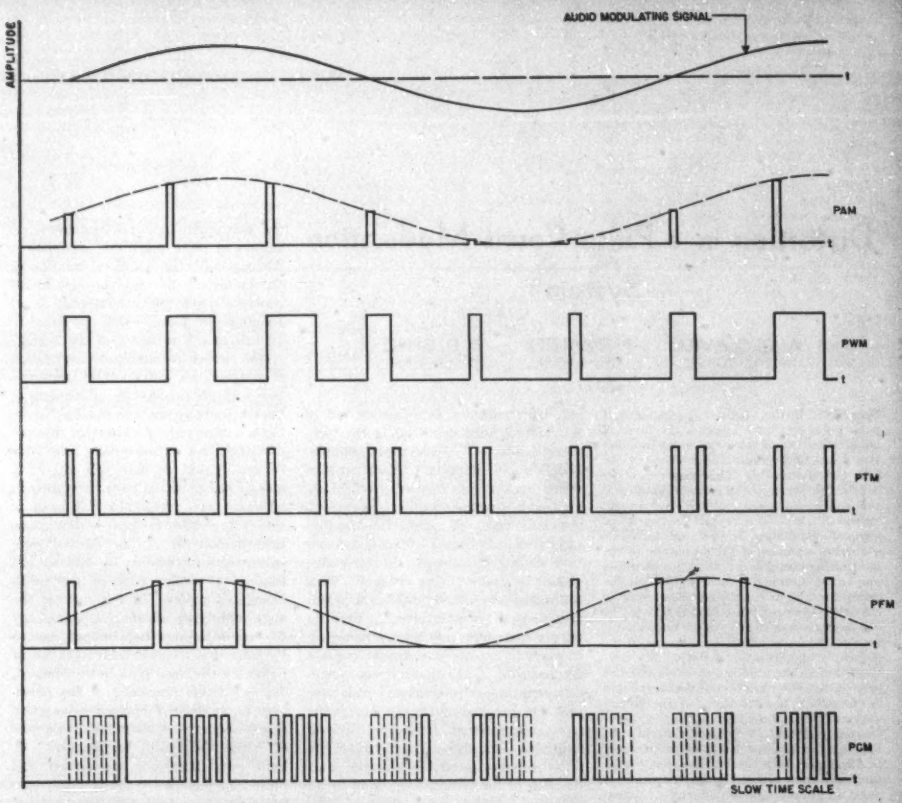

Figure 1. Pulse modulation methods

In all the systems described it has been implied that for a period corresponding to several modulating cycles, values of the instantaneous samples of the modulating wave encompass all possible amplitudes of the signal transmitted. In the case of pulse amplitude modulation the pulses assume all values of amplitude corresponding to the modulation signal function. A similar situation is true for the other methods of modulation with the continuous equivalent of pulse width, pulse displacement, and pulse frequency. However, a second class of modulating methods complementary to these previous methods can be derived in which only selected amplitude values are transmitted, i.e., a double system of discreteness is utilized involving both amplitude sampling as well as time sampling. In this the amplitude range is divided into a number of discrete levels. If the instantaneous amplitude of the signal to be transmitted falls between two levels, either the lower or upper level only is transmitted depending upon the level which is closest. Figure 2 illustrates this process as applied to a single sine wave.

Since only a finite number of levels is involved it is possible to transmit the information by a coded pulse system similar to the standard printing telegraph system.[1-2] A transmission system of this type has been termed PCM. Thus, for example, if a modulating signal is divided into a total of 31 levels a five unit binary numdering system may be used for identifying each of the discrete amplitudes. In this example all numbers from 0 to 31 would be transmitted in terms of zero and unity, or absence and presence of pulse respectively. Zero (0) is transmitted as 00000, one is transmitted as 00001, two is transmitted as 00010, three is transmitted as 00011, four is transmitted as 00100, and so forth.

It is apparent that with this transmission system the many advantages that are obtained with teletype could likewise be extended to voice transmission. For example, cross talk introduced through carry-over from one pulse to the adjacent pulse is minimized since only the presence or absence of a pulse characterizes the intelligence. A similar situation is true with reference to noise introduced into the system. In order to deteriorate transmission, noise pulses must occur with the proper am-

Table I. Per Cent Distortion in a PCM System for Different Levels

N, Number of Levels Per Half Cycle	A_1, Amplitude of First Harmonic, Per Cent of A	D, Per Cent of Distortion = $\frac{1}{\sqrt{6}N} \times 100$
5	100.97	7.55 ... 8.16
10	100.34	3.80 ... 4.09
20	100.12	2.00 ... 2.04
50	100.03	.81 ... .816

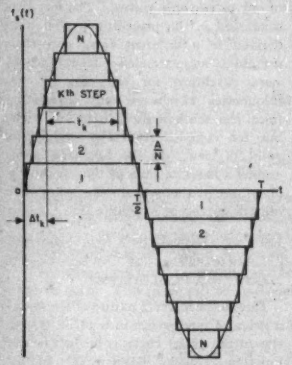

Figure 2. Step representation of a sine function

plitude and at the proper time and phase in order to introduce a spurious pulse or suppress an existing one. Since the probability of noise occurring under these conditions is relatively small the system permits a large signal-to-noise improvement factor to be obtained. A further advantage of pulse count modulation is that the transmission band width may be made relatively small to the extent of producing considerable carry-over from one pulse to the next without affecting the transmitting capabilities.

With a pulse system involving the single discreteness of time sampling only,

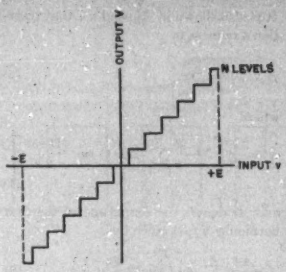

Figure 3. Transfer function characteristic in PCM

a minimum of modulation distortion occurs provided sufficient samples in time are taken to properly delineate the modulating signal. For pulse amplitude modulation the minimum ratio of pulse sampling frequency to the modulating frequency bandwidth is two to one. With PCM a similar relation holds insofar as spurious frequency distortion is concerned, however, since only an approximation in amplitude of the modulating signal is produced it is obvious that a price must be paid in terms of non-linear distortion for the teletype advantages gained. An increase in the number

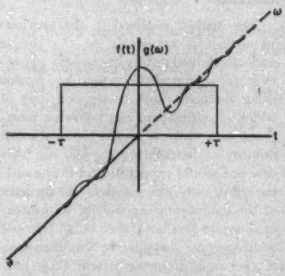

Figure 4. Fourier transform pair

of levels utilized decreases this distortion, but the number of pulses required is increased and hence the band width necessary to accommodate the system is increased accordingly. The degree of distortion with a system of this type thus determines to a large extent the transmission characteristics.

A study has been made of the relationship between the number of levels and the resulting distortion as well as the relation between the cross-talk and this distortion in a PCM system. The purpose of the present paper is to indicate the several aspects of these characteristics resulting from the study, as well as the special methods of analysis which were found necessary to solve the problem, and which are applicable to similar problems of this type.

PCM Applied to a Signal Consisting of One Sine Wave

General

It is well known that when an infinite train of square topped pulses are used in pulse amplitude modulation to scan a sine wave, the output spectrum does not contain any harmonics of the modulating frequency.[8] However, in a PCM system, due to the discrete nature of the sampling process, it is to be expected that harmonic distortion would be produced dependent on the number of amplitude levels used in the transmission of the intelligence. In the limit, when the number of amplitude levels is greatly increased, a PCM system will convert to the equivalent of a pulse amplitude modulation system with no harmonic distortion in the output.

In order to calculate the distortion introduced in the system when PCM is applied to a sine wave, one can replace the signal with a step function consisting of $2N$ levels of equal height as shown in Figure 2. In this representation, the system will recognize amplitudes to the nearest half level. Obviously applying pulse amplitude modulation to

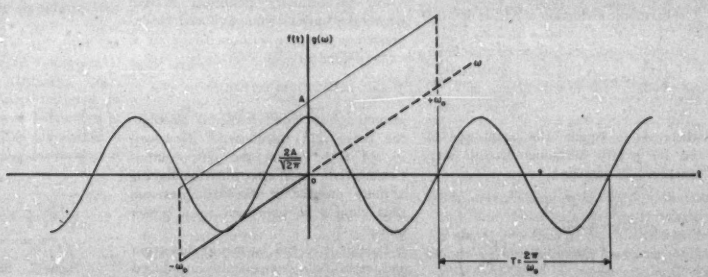

Figure 5. Fourier transform of a cosine function

such a step function is equivalent to applying PCM to a sine wave, for the modulated pulses carring the intelligence will be identical for two cases and thus the harmonic distortion of such a step function must equal the distortion introduced in the process of PCM.

Calculation of Harmonic Distortion of the Step Function

Consider a sine wave $f(t) = A \sin \omega t$ to be replaced by a step function $f_s(t)$ as shown in Figure 2. This step function may be considered as a superposition of N pairs of rectangular steps per cycle of the same period T equal to that of the fundamental sine wave, of the same height A/N and of different width t_k such that

$$t_k = \frac{T}{2} - \frac{2}{\omega} \sin^{-1} \frac{2k-1}{2N} \tag{1}$$

It is shown in Appendix I that the kth rectangular step pair may be represented by the Fourier series

$$\sigma_k(t) = \sum_{\nu=0}^{\infty} \frac{4A}{\pi N(2\nu+1)} \times \cos\left[(2\nu+1) \sin^{-1} \frac{2k-1}{2N}\right] \times \sin (2\nu+1)\omega t \tag{2}$$

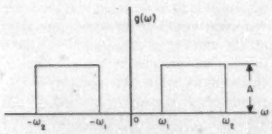

Figure 6. Frequency spectrum of modulating signal

only odd harmonics being present and

$$f_s(t) = \sum_{k=1}^{N} \sum_{\nu=0}^{\infty} \frac{4A}{\pi N(2\nu+1)} \times \cos\left[(2\nu+1) \sin^{-1} \frac{2k-1}{2N}\right] \times \sin (2\nu+1)\omega t \tag{3}$$

The harmonic distortion of $f_s(t)$ is defined by

$$D = \frac{\sqrt{\sum_{\nu=1}^{\infty} (A_{2\nu+1})^2}}{A_1} \tag{4}$$

where $A_{2\nu+1}$ equals the amplitude of the $(2\nu + 1)$th harmonic of the step function $f_s(t)$ namely

$$A_{2\nu+1} = \frac{4A}{\pi N(2\nu+1)} \sum_{k=1}^{N} \times \cos\left[(2\nu+1) \sin^{-1} \frac{2k-1}{N}\right] \tag{5}$$

It is also shown in Appendix I that equation 4 reduces to

$$D = \frac{\sqrt{\bar{A}^2 - A_1^2}}{A_1} \tag{6}$$

where

$$\bar{A}^2 = \frac{2A^2}{N^2}\left[N^2 - \frac{2}{\pi} \sum_{k=1}^{N} (2k-1) \sin^{-1} \frac{2k-1}{2N}\right] \tag{7}$$

and A_1 equals the amplitude of the first harmonic of $f_s(t)$ given by

$$A_1 = \frac{4A}{\pi N} \sum_{k=1}^{N} \cos\left(\sin^{-1} \frac{2k-1}{2N}\right) \tag{8}$$

Numerical Results

No closed form was found for the distortion formula given by equation 6. However, this formula is useful for numerical calculations and the results are tabulated in Table I.

It is seen that the distortion components are always odd harmonics of the fundamental. Also from Table I for N large the distortion D approaches $1/\sqrt{6}N$ which is a very interesting limit of equation 6 and which remains to be proved mathematically.

PCM Applied to a Signal of Two Sine Waves

General

The method outlined in the previous paragraph is applicable to the simple case of one modulating frequency. However for composite modulating signals other methods must be devised, one of which is outlined in the following paragraph and which is applicable to a small number of modulating signals. In this case one would expect to find in the output, not only the original frequencies of the modulating signal, but also intermodulation products, that is, all possible additive and subtractive combinations of the input frequencies and their harmonics.

For an ordinary nonlinear system where the output voltage V can be expressed as a power series of the input v, namely

$$V = av + bv^2 + \ldots$$

attempts have been made to calculate the cross talk introduced.[9] However, in a PCM system the output–input characteristic is a step function having a finite number of discontinuities and thus cannot be expressed in a power series

To calculate the harmonic distortion and cross talk components introduced the output V is expressed as a Fourier series of the input v within the operating range of the modulating signal. Expressing v as a function of time namely

$$v = \sum_{k=1}^{n} E_k \sin \omega_k t$$

the output signal V is thus given as a function of time which is then analyzed into its frequency components. This method was applied to a signal consisting of one or two sine waves. The formulas developed in the preceding section were derived in a different form and their usefulness was extended. New relations were developed for the case of two frequencies which are very interesting from the mathematical point of view, but too complex from the engineering point of view. In the following paragraphs a short résumé of this method is given, the mathematical steps being more fully dealt with in Appendix II.

Fourier Analysis of a Step Function Characteristic of Output Versus Input in a PCM System

Due to the discrete nature of the transmission of intelligence in a PCM system the output–input curve is in the form of function as shown in Figure 3. In this representation the system is assumed to recognize amplitude levels to the nearest half level, similar to Figure 2. Actually Figure 3 is derived from Figure 2 by eliminating the time variable.

The output V may be expressed as a Fourier series of the input v in the range

$$-E \leqq V \leqq E$$

$$V = \sum_{n=1}^{\infty} B_n \sin \frac{n\pi v}{E} \tag{9}$$

where

$$B_n = \frac{2E}{\pi n N}\left[\frac{\sin \pi n}{2 \sin \frac{\pi n}{2N}} + N(-1)^{n-1}\right] \tag{10}$$

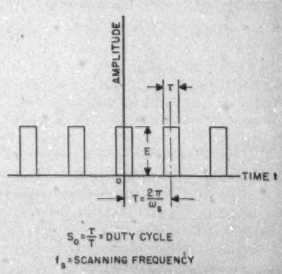

Figure 7. Series of scanning pulses

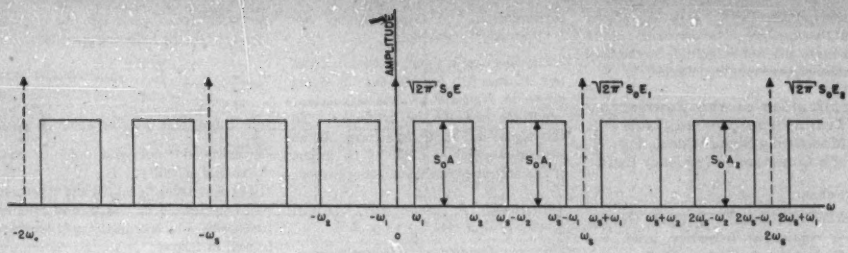

Figure 8. Frequency spectrum of "exact scanning" process

therefore

$$V=\frac{2E}{\pi N}\sum_{n=1}^{\infty}\left\{\frac{1}{n}\left[\frac{\sin \pi n}{2\sin\frac{\pi n}{2N}}+N(-1)^{n-1}\right]\times \sin\frac{n\pi v}{E}\right\} \quad (11)$$

In equation 11 v must be expressed as a function of time making sure that v is always within the range considered, and by analyzing the output V, the different components of the output may be determined. Two cases will be analyzed here

$v=E\sin\omega t$

$v=\frac{E}{2}(\sin\omega_1 t+\sin\omega_2 t)$

Input Signal Consisting of a Sine Wave $v=E\sin\omega t$

Equation 11 becomes

$$V=\frac{2E}{\pi N}\sum_{n=1}^{\infty}\left\{\frac{1}{n}\left[\frac{\sin \pi n}{2\sin\frac{\pi n}{2N}}+N(-1)^{n-1}\right]\times \sin(\pi n\sin\omega t)\right\}$$

$$V=\frac{4E}{\pi N}\left[N\sum_{n=1}^{\infty}\frac{(-1)^{n-1}}{n}+\sum_{n=1}^{\infty}{}_{2n}\frac{\sin \pi n}{2\sin\frac{\pi n}{2N}}\right]\times \sum_{\nu=0}^{\infty}J_{2\nu+1}(\pi n)\sin(2\nu+1)\omega t \quad (12)$$

where $J_{2\nu+1}$ represent the Bessel function of the order $(2\nu+1)$.

From equation 12 it is seen that the output V consists of the fundamental frequency plus odd harmonics only, a result which has been outlined in "Calculation of Harmonic Distortion of the Step Function." The amplitude of the fundamental frequency in the output A_1 reduces to

$$A_1=E\left[1-\frac{2}{\pi N}\sum_{l=1}^{\infty}\frac{(-1)^{l-1}}{l}J_1(2\pi lN)\right]$$
$$=\frac{4E}{\pi N}\sum_{k=1}^{N}\cos\left(\sin^{-1}\frac{2k-1}{2N}\right) \quad (13)$$

and the amplitude of the $(2\nu+1)$th harmonic becomes

$$A_{2\nu+1}=-\frac{2E}{\pi N}\sum_{l=1}^{\infty}\frac{(-1)^{l-1}}{l}J_{2\nu+1}(2\pi lN)$$
$$=\frac{4E}{\pi N(2\nu+1)}\sum_{k=1}^{N}\cos\left[(2\nu+1)\sin^{-1}\frac{2k-1}{2N}\right] \quad (14)$$

The last two equations are identical with equations 5 and 8.

By using the asymptotic expansion for $J_1(2\pi lN)$ equation 13 may be expressed in a closed form, namely

$$A_1\approx E\left[1+\frac{\sqrt{2}}{\pi^3N^{3/2}}\sum_{l=1}^{\infty}\frac{(-1)^{l-1}}{l^{3/2}}\right]$$
$$=E\left[1+\frac{0.1096}{N^{3/2}}\right] \quad (15)$$

The values computed for A_1 for different levels N are compared with those of Table I and are shown in Table II.

An approximate expression for $A_{2\nu+1}$ was also found.

$$A_{2\nu+1}\approx\frac{(-1)^{\nu}\sqrt{2}E}{\pi^3N^{3/2}}\left[0.7650-\frac{0.8670[4(2\nu+1)^2-1^2]}{16\pi N}-\frac{0.9278[4(2\nu+1)^2-1^2]\times[4(2\nu+1)^2-3^2]}{512\pi^3N^2}\right] \quad (16)$$

As an example consider $N=5$, $\nu=1$

$$A_3=\frac{\sqrt{2}E}{\pi^3 5^{3/2}}[0.7650-0.1207-0.0069]$$
$$=-0.818 \text{ per cent of } E$$

Using the exact formula 5

$$A_3=\frac{4E}{3.5.\pi}\sum_{k=1}^{5}\cos\left[3\left(\sin^{-1}\frac{2k-1}{10}\right)\right]$$
$$=-.818 \text{ per cent of } E$$

One must realize that the labor involved in the calculation of $A_{2\nu+1}$ is very great when using the exact formula of equation 5, especially when N is large. It should be observed, however, that for large N only two terms of equation 16 will suffice.

Input Signal Consisting of Two Sine Waves $V=\frac{E}{2}(\sin\omega_1 t+\sin\omega_2 t)$

The method used in the preceding section may be extended to two frequencies. Equation 11 reduces to:

$$V=\frac{E}{2}(\sin\omega_1 t+\sin\omega_2 t)-\frac{2E}{\pi N}\sum_{l=1}^{\infty}\frac{(-1)^{l-1}}{l}\times\left\{J_0(\pi lN)\left[\sum_{\nu=0}^{\infty}J_{2\nu+1}(\pi lN)\times\sin(2\nu+1)\omega_1 t+\sum_{\rho=0}^{\infty}J_{2\rho+1}(\pi lN)\times\sin(2\rho+1)\omega_2 t\right]+2\sum_{\rho=0}^{\infty}\sum_{\lambda=1}^{\infty}J_{2\rho+1}(\pi lN)\times\sin(2\nu+1)\omega_1 t\times\cos 2\lambda\omega_2 t+2\sum_{\rho=0}^{\infty}\sum_{\eta=1}^{\infty}J_{2\rho+1}(\pi lN)\times J_{2\eta}(\pi lN)\times\sin(2\rho+1)\omega_2 t\times\cos 2\eta\omega_1 t\right\} \quad (17)$$

The amplitudes of the odd harmonics of the two input frequencies ω_1 and ω_2 are given by

$$A'_{2\nu+1}=-\frac{2E}{\pi N}\sum_{l=1}^{\infty}\frac{(-1)^{l-1}}{l}J_0(\pi lN)\times J_{2\nu+1}(\pi lN) \quad (\text{where } \nu\geq 1) \quad (18)$$

The similarity between this result and equation 14 in the case of one frequency is interesting.

The amplitudes of the cross products are given by

$$A_{(2\nu+1)\omega_1\pm 2\lambda\omega_2}=-\frac{2E}{\pi N}\sum_{l=1}^{\infty}\frac{(-1)^{l-1}}{l}\times J_{2\nu+1}(\pi lN)J_{2\lambda}(\pi lN) \quad (19)$$

Approximate expressions for equations 18 and 19 are found in Appendix II, where it is also shown that in the case of two frequencies the harmonic components are greatly reduced in comparison with the

single frequency case. It is also shown that the cross-products components are of the same order of magnitude as the harmonics of the input frequencies.

Application of the Fourier Transformation to PAM Modulating Signal Consisting of a Continuous Frequency Band

General

When the modulating signal consists of a continuous frequency band, the method outlined previously fails due to the complexity of the mathematics encountered. However, such an analysis can be made by the use of Fourier transforms at first applied to pulse amplitude modulation and then extended to PCM.

The results obtained in pulse amplitude modulation when the modulating signal consists of a sine wave are generalized for a complex modulating signal in the following analysis. The components of the output spectrum and the frequency response are thus extended to a case which clearly corresponds to a practical communication problem, where the modulating signal is, or can be constituted by all frequencies in the modulating band simultaneously.

The usefulness of Fourier transforms with their extensive and flex ble properties will be shown still more clearly in the paragraph dealing with the computation of crosstalk introduced in a PCM system, due to the process of quantization

Introduction to the Theory of "Fourier Transforms"

Consider first a signal given as a function of time $f(t)$, for instance the signal shown in Figure 4 to have a constant amplitude from $t=-\tau$ to $t=+\tau$. To this signal a Fourier transform can be associated which is obtained by means of the following mathematical operation:

$$T_t^{\omega} f(t) = \frac{1}{\sqrt{2\pi}} \int_{-\infty}^{+\infty} f(t) e^{-j\omega t} dt \qquad (20)$$

This is a function of ω namely, $g(\omega)$, which for the particular signal considered is readily found to be

$$g(\omega) = \frac{2A\tau}{\sqrt{2\pi}} \cdot \frac{\sin \omega\tau}{\omega\tau} \qquad (21)$$

The function also shown in Figure 4, but in a plane perpendicular to the t plane, is usually denominated the frequency spectrum of $f(t)$, for reasons which will appear more clearly later on.

It can be shown that all functions $f(t)$ such that the integral $\int_{-\infty}^{+\infty} |f(t)| dt$ exists are transformable by the previous mechanism into spectra $g(\omega)$ without ambiguity.

When $g(\omega)$ has been found it can be conversely transformed into the original signal $f(t)$ by the following operation:

$$T_{\omega}^{t} g(\omega) = \frac{1}{\sqrt{2\pi}} \int_{-\infty}^{+\infty} g(\omega) e^{+j\omega t} d\omega \qquad (22)$$

and all functions $g(\omega)$ for which $\int_{-\infty}^{+\infty} |g(\omega)| d\omega$ exists do not give rise to any theoretical difficulty.

The associated signal $f(t)$ and spectrum $g(\omega)$ constitute a regular pair of Fourier transforms, which property may be symbolized as follows:

$$\left.\begin{aligned} T_{\omega}^{t} T_t^{\omega} f(t) &= f(t) \\ T_t^{\omega} T_{\omega}^{t} g(\omega) &= g(\omega) \end{aligned}\right\} \qquad (23)$$

The value of the Fourier transformation comes from the fact that many problems can be solved by one of the following methods:

1. Starting from the signal, the spectrum is found. This spectrum is submitted to a modification resulting from the operation of a piece of apparatus, a filter for instance. The modified spectrum is then reconverted to the signal–time plane of co-ordinates.

2. Inversely, starting from the spectrum, the signal is found. This signal is modified by the operation which is considered. The modified signal is then reconverted to the spectrum–frequency plane of co-ordinates.

In the first instance the shape of the modified signal is compared with the original signal to see how far it is distorted; in the second instance the modified spectrum is compared to the original one, to investigate how much frequency distortion, or nonlinear distortion or cross talk has been introduced by the process under examination. This second method has been rarely used so far, though it is easily seen that, when the mathematical difficulties are not insuperable, it should prove to be a powerful instrument for the analysis of a number of problems with which the communication engineer is confronted.

General Properties of the Fourier Transforms

In order to facilitate the understanding of the following paragraphs, and to give an idea of the remarkable flexibility of the Fourier transformation, the follow-

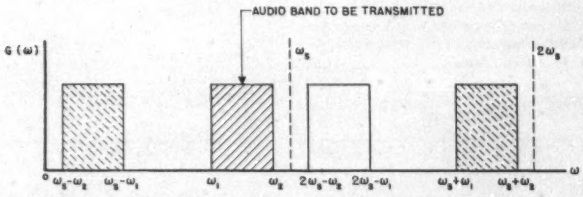

Figure 9. Sideband distribution ($\omega_2 < \omega_S < 2\omega_1$)

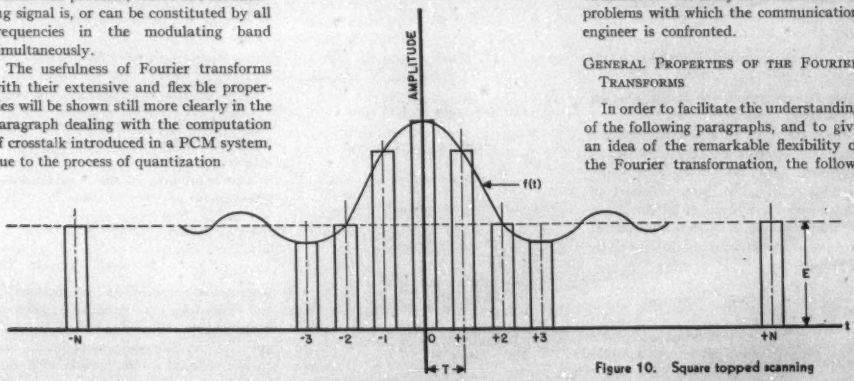

Figure 10. Square topped scanning

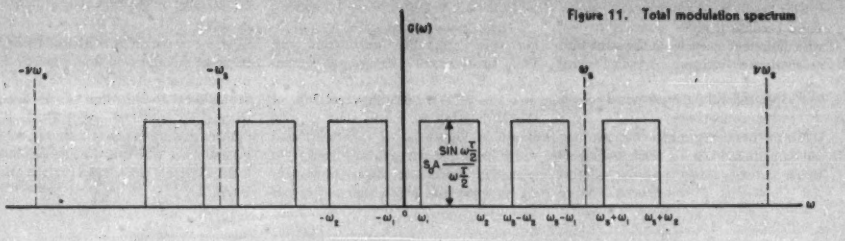

Figure 11. Total modulation spectrum

ing tabulation been prepared, in which the essential properties of the Fourier transformation are listed.

1. Definitions and Notations.

$$\left.\begin{aligned} T_t^\omega f(t) &= g(\omega) = \frac{1}{\sqrt{2\pi}}\int_{-\infty}^{+\infty} f(t)\epsilon^{-j\omega t}dt \\ T_\omega^t g(\omega) &= f(t) = \frac{1}{\sqrt{2\pi}}\int_{-\infty}^{+\infty} g(\omega)\epsilon^{+j\omega t}d\omega \end{aligned}\right\} \quad (24)$$

2. Change of Sign of the Variable.

$$\left.\begin{aligned} T_t^\omega f(-t) &= g(-\omega) \\ T_\omega^t g(-\omega) &= f(-t) \end{aligned}\right\} \quad (25)$$

3. Translation of the Variable.

$$\left.\begin{aligned} T_t^\omega f(t-t_0) &= \epsilon^{-j\omega t_0}g(\omega) \\ T_\omega^t g(\omega-\omega_0) &= \epsilon^{j\omega_0 t}f(t) \end{aligned}\right\} \quad (26)$$

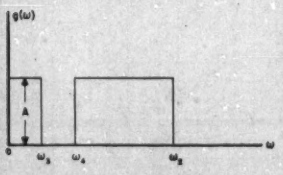

Figure 12. Frequency spectrum of modulating signal, one channel unoccupied

4. Interchange of Function.

$$\left.\begin{aligned} T_t^\omega g(t) &= f(-\omega) \\ T_\omega^t f(\omega) &= g(-t) \end{aligned}\right\} \quad (27)$$

5. Multiplication of Functions.

$$\left.\begin{aligned} T_t^\omega f_1 f_2 &= \frac{1}{\sqrt{2\pi}}\int_{-\infty}^{+\infty} g_1(-x)g_2(\omega+x)dx \\ T_\omega^t g_1 g_2 &= \frac{1}{\sqrt{2\pi}}\int_{-\infty}^{+\infty} f_1(x)f_2(t-x)dx \end{aligned}\right\} \quad (28)$$

6. Differentiation and Integration With Respect to the Variable.

$$\left.\begin{aligned} T_t^\omega \frac{df}{dt} &= j\omega g(\omega) \\ T_\omega^t \frac{dg}{j\,d\omega} &= -t\times f(t) \end{aligned}\right\} \quad (29)$$

$$\left.\begin{aligned} T_t^\omega \int_{-\infty}^{t} f(t)\,dt &= \frac{1}{j\omega}g(\omega) \\ T_\omega^t\, j\int_{-\infty}^{\omega} g(\omega)d\omega &= -\frac{1}{t}\times f(t) \end{aligned}\right\} \quad (30)$$

From these fundamental properties, a number of others can be derived, such as:

7. Computation of the Sine and Cosine Fourier Integrals.

$$\left.\begin{aligned} \frac{1}{\sqrt{2\pi}}\int_{-\infty}^{+\infty} f(t)\cos\omega t\,dt &= \frac{1}{2}\times[g(\omega)+g(-\omega)] \\ \frac{1}{\sqrt{2\pi}}\int_{-\infty}^{+\infty} f(t)\sin\omega t\,dt &= j\cdot\frac{1}{2}\times[g(\omega)-g(-\omega)] \end{aligned}\right\} \quad (31)$$

8. Energy Integrals.

$$\int_{-\infty}^{+\infty} f(t)^2dt = \int_{-\infty}^{+\infty} g(\omega)^2d\omega \quad (32)$$

The usefulness of Fourier transforms can however be still further increased when they are extended to include some important, though essentially singular functions. This will be explained in the following fundamental case.

Consider the signal $f(t)$ shown in Figure 4. Let the domain of time during which $f(t)$ exists decrease and at the same time the amplitude increase so that $\int_{-\infty}^{+\infty} f(t)\,dt$ remains constant. For the particular signal of Figure 4, this means that $2A\tau$ will remain constant. However small τ may be, the signal has a well defined transform. When τ approaches zero, the limit constitutes an essentially singular function of time, which is zero for all values of time, except for $t=0$ for which, though the amplitude becomes infinite, the limit of the area covered remains finite. This is the "impulse function." It can be conventionally written $2A\tau\delta_0(t)$. The symbol $\delta_0(t)$ is equal to zero for all values of t except $t=0$, for which it is equal to $+1$.

Let it now be tentatively written that:

$$T_t^\omega 2A\tau\delta_0(t) = \lim_{\substack{\tau\to 0 \\ A\tau\text{—constant}}} \frac{2A\tau}{\sqrt{2\pi}}\times\frac{\sin\omega\tau}{\omega\tau} = \frac{2A\tau}{\sqrt{2\pi}}$$

that is to say

$$T_t^\omega \delta_0(t) = \frac{1}{\sqrt{2\pi}} \quad (33)$$

It will be necessary to show that this is consistent with

$$T_\omega^t \frac{1}{\sqrt{2\pi}} = \delta_0(t)$$

To do this, it is only necessary to consider 1 as the limit of $\epsilon^{-\alpha|\omega|}$ for $\alpha+\nu\epsilon$ approaching zero. It is found that

$$T_\omega^t \frac{\epsilon^{-\alpha|\omega|}}{\sqrt{2\pi}} = \frac{1}{\pi}\times\frac{\alpha}{\alpha^2+t^2}$$

Now

$$\int_{-\infty}^{+\infty}\frac{1}{\pi}\times\frac{\alpha\,dt}{\alpha^2+t^2} = 1$$

Let α approach zero. This limit is obviously $\delta_0(t)$. Thus $\delta_0(t)$and $\frac{1}{\sqrt{\omega 2}}$ can be considered as a pair of Fourier transforms. Applying general property 4 gives immediately

$$T_\omega^t \delta_0(\omega) = \frac{1}{\sqrt{2\pi}} \quad (34)$$

Property 3 gives

$$T_\omega^t \delta(\omega_0-\omega_0) = \frac{1}{\sqrt{2\pi}}\epsilon^{j\omega_0 t} \quad (35)$$

and consequently

$$T_\omega^t[\delta_0(\omega-\omega_0)+\delta_0(\omega+\omega_0)] = \frac{2}{\sqrt{2\pi}}\cos\omega_0 t \quad (36)$$

Table II. Amplitude of Fundamental Component of Output for Different Amplitude Levels

N, Number of Levels Per Half Cycle	A_1/E (Equation 8)	A_1/E (Equation 15)
5	1.0097	1.0098
10	1.0034	1.0035
20	1.0012	1.0012
50	1.0003	1.0003

This result is of fundamental importance because it gives a means to deal with discrete frequencies at the same time as continuous spectra. A cosine signal $\frac{2A}{\sqrt{2\pi}} \cos \omega_0 t$ will be represented in the spectrum–frequency plane by two impulse function $A\delta_0(\omega-\omega_0)$ and $A\delta_0(\omega+\omega_0)$ which is distinguished from the differential amplitudes of continuous spectra by means of the dotted lines. (Figure 5)

The method previously used for analyzing pulse amplitude modulation and PCM has consisted in studying the modulation of a series of pulses by a cosine wave. The corresponding spectrum of the modulating wave was thus the one shown in Figure 5. If a certain band width has to be covered, say from ω_1 to ω_2, and in case the modulation process includes operations which lead to possible interaction of the different frequencies involved, it becomes necessary to consider a number of simultaneous pairs of impulse functions in the plane. This computation generally leads to a lengthy arithmetical combination of the discrete frequencies involved from which it is difficult to deduce a clear statement of the general case, where all frequencies in the band width considered are present simultaneously.

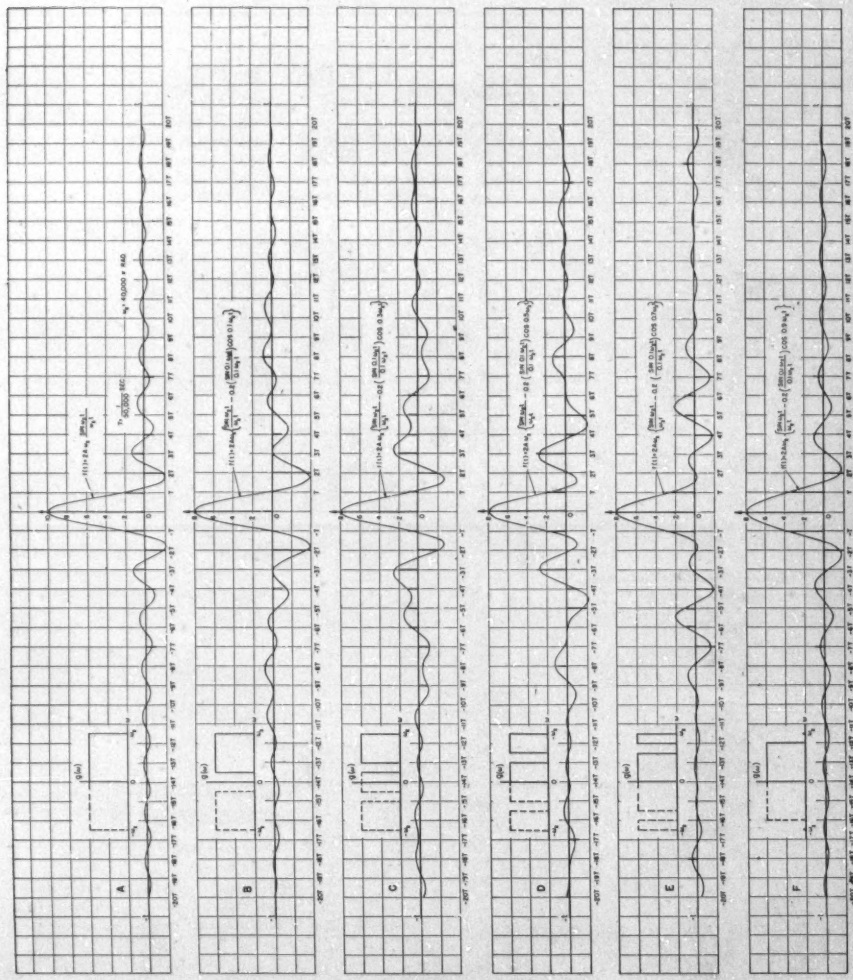

Figure 13. Time functions for various modulating signals

The Fourier transforms provide a powerful instrument in the treatment of such problems. For instance, the analysis of the operation of scanning and quantizing a number of cosine waves of equal amplitudes

$$A \cos \omega_1 t + A \cos \omega_2 t + \ldots\ldots + A \cos \omega_n t$$

all situated within a band $\omega_1 < \omega < \omega_2$ is replaced by the investigation of the signal corresponding to the spectrum given in Figure 6. Such a signal is readily found to be

$$f(t) = T^{-1}_{\omega} g(\omega) = \frac{2A\omega_2}{\sqrt{2\pi}} \left[\frac{\sin \omega_2 t}{\omega_2 t} - \frac{\omega_1}{\omega_2} \frac{\sin \omega_1 t}{\omega_1 t} \right] \quad (37)$$

Exact Scanning

By exact scanning a type of pulse modulation is meant in which the tops of the modulated pulses follow the modulating time function during the scanning interval.

Figure 6 gives the frequency spectrum of the composite modulating signal, the time function of which is given by equation 37.

Table III. Cross Talk in Unoccupied PCM Channels

Channel	Cross Talk, Per Cent
1	8.2
2	28.6
3	14.8
4	13.1
5	21.0

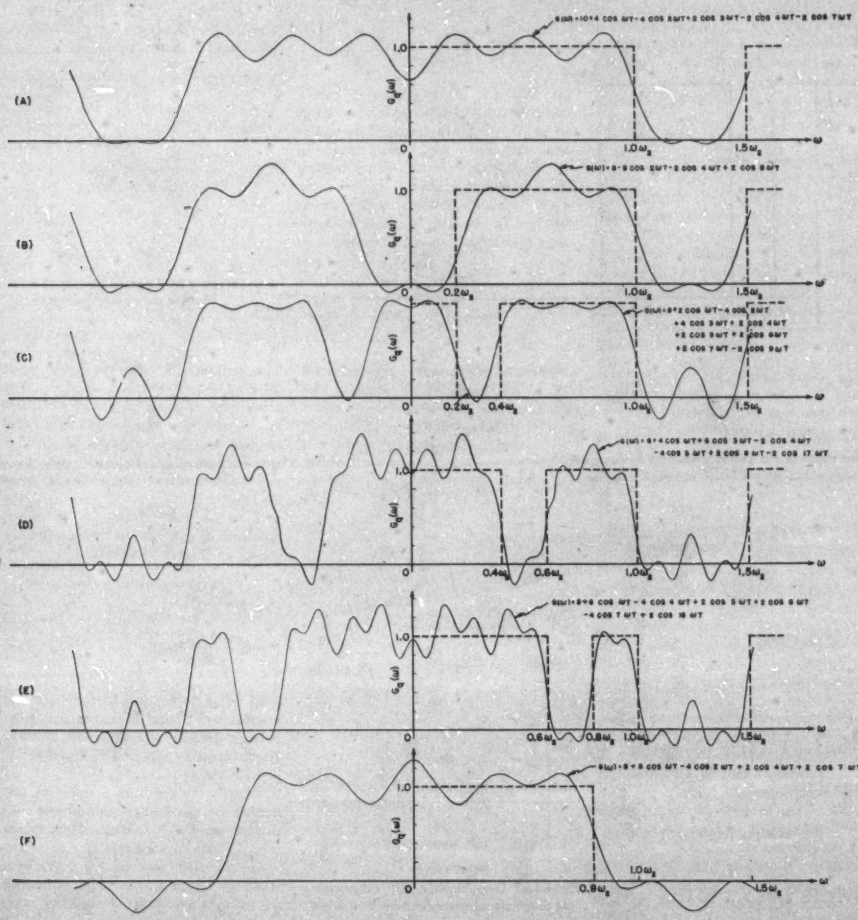

Figure 14. Effect of quantizing on modulating signal

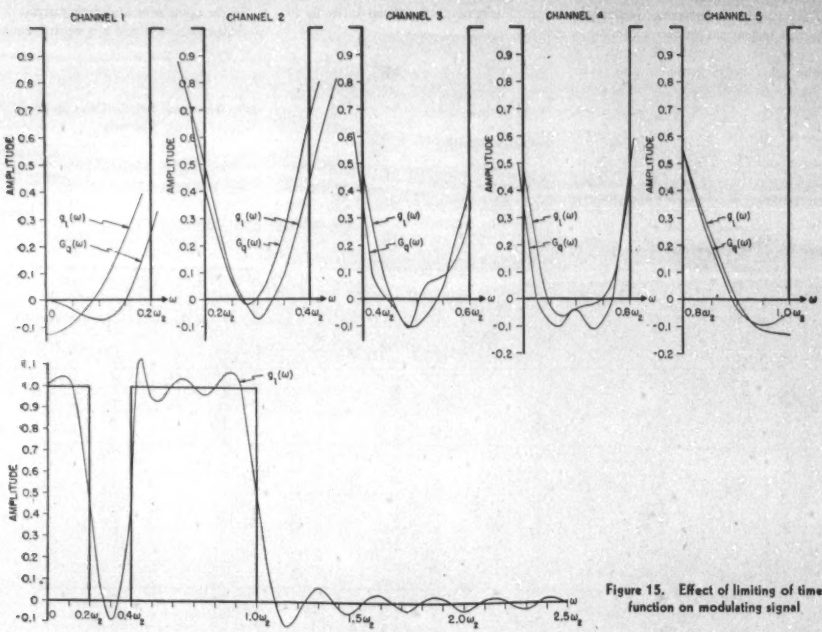

Figure 15. Effect of limiting of time function on modulating signal

The scanning pulses are represented in Figure 7. This is a periodic function which can also be represented by the Fourier series expansion

$$F(t)=S_0E\left[1+2\sum_{\nu=1}^{\infty}\frac{\sin\nu\pi S_0}{\nu\pi S_0}\cos\nu\omega_S t\right] \quad (38)$$

The corresponding frequency spectrum is immediately obtained (see equations 34 and 36)

$$G(\omega)=\mathfrak{T}_t^{\omega}F(t)$$

$$=\sqrt{2\pi}S_0E\left[\delta_0(\omega)+\sum_{\nu=1}^{\infty}\frac{\sin\nu\pi S_0}{\nu\pi S_0}\times\{\delta_0(\omega-\nu\omega_S)+\delta_0(\omega+\nu\omega_S)\}\right] \quad (39)$$

The exact scanning is equivalent to operating on $F(t)$ by $f(t)$ according to

$$F(t)\left\{1+\frac{1}{E}f(t)\right\}=\varphi(t) \quad (40)$$

So that the resulting frequency spectrum is

$$\mathfrak{T}_t^{\omega}\varphi(t)=\mathfrak{T}_t^{\omega}F(t)+\frac{1}{E}\mathfrak{T}_t^{\omega}F(t)\times f(t) \quad (41)$$

The first term represents the spectrum $G(\omega)$ of the unmodulated pulses. The second one is according to equation 28

$$\frac{1}{E}\mathfrak{T}_t^{\omega}F(t)\times f(t)=\frac{1}{E\sqrt{2\pi}}\times\int_{-\infty}^{+\infty}g(-x)\times G(\omega+x)dx \quad (42)$$

that is to say

$$\frac{1}{E}\mathfrak{T}_t^{\omega}F(t)\times f(t)=S_0\int_{-\infty}^{+\infty}g(-x)\left\{\delta_0(\omega+x)+\sum_{\nu=1}^{\infty}\frac{\sin\nu\pi S_0}{\nu\pi S_0}[\delta_0(\omega+x-\nu\omega_S)+\delta_0(\omega+x+\nu\omega_S)]\right\}dx \quad (43)$$

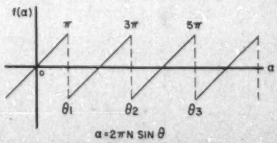

Figure 16. Discontinuities of $f(\alpha)$ corresponding to angular distances of steps from origin

The first term is equal to $g(-x)$ when $\omega+x=0$, that is it reproduces $g(\omega)$. Any other term is equal to $g(-x)$ when $x=\nu\omega_S-\omega$ and $x=-\nu\omega_S-\omega$ and it is equal to $g(\omega-\nu\omega_S)+g(\omega+\nu\omega_S)$; or as $g(-x)=g(x)$ it is equal to $g(\nu\omega_S-\omega)+g(\nu\omega_S+\omega)$.

For any term ω varying within the limits assigned to it by Figure 6, $-\omega_2<\omega<-\omega_1$ and $\omega_1<\omega<\omega_2$. Thus the frequency spectrum of $\varphi(t)$ can be represented as shown in Figure 8 where

$$A_\nu=A\frac{\sin\nu\pi S_0}{\nu\pi S_0}$$

$$E_\nu=E\frac{\sin\nu\pi S_0}{\nu\pi S_0} \quad (44)$$

In order to be able to filter out the original audio band from the first sideband, a sufficient condition (for an ideal filter) is readily apparent in Figure 8. It is: $\omega_S>2\omega_2$.

Actually this condition is sufficient, but not always necessary. Consider a continuous band of frequencies to be transmitted where $\omega_1\leqq\omega\leqq\omega_2$.

One can easily see from Fig. 9 that provided $\omega_2<2\omega_1$ the side band can be filtered out with the aid of a band pass filter when

the scanning frequency is such that $\omega_2 < \omega_s < 2\omega_1$.

Square Topped Scanning

Let the modulated pulse train be square topped, and let the amplitude of the pulses be modulated by the time function (t) (equation 37) derived above in such a manner that the value of $f(t)$ corresponding to the center of the pulse is effective in the modulation process.

The result of such a process is shown in Figure 10. The amplitude of the νth pulse can be written

$$E_\nu = E + f(t)\delta_0(t-\nu T) \tag{45}$$

Let $P^\tau(t-\nu T)$ be a function which takes the value one for all values of time such that $\nu T - \frac{\tau}{2} < t < \nu T + \frac{\tau}{2}$ and equals zero everywhere else. The function of time $\omega(t)$ corresponding to the modulated pulses can be written

$$\begin{aligned}\varphi(t) &= \sum_{\nu=-\infty}^{+\infty} E_\nu P_\tau(t-\nu T)\\ &= \sum_{\nu=-\infty}^{+\infty} EP_\tau(t-\nu T) + \\ &\quad \sum_{\nu=-\infty}^{+\infty} [f(t)\delta_0(t-\nu T)]P_\tau(t-\nu T)\end{aligned} \tag{46}$$

The problem consists in finding the spectrum of $\varphi(t)$

$$\begin{aligned}G(\omega) = \mathfrak{T}_t^\omega \varphi(t) &= \mathfrak{T}_t^\omega \sum_{\nu=-\infty}^{+\infty} EP_\tau(t-\nu T) + \\ &\quad \mathfrak{T}_t^\omega \sum_{\nu=-\infty}^{+\infty} [f(t)\delta_0(t-\nu T)]P_\tau(t-\nu T)\\ &= G_1(\omega) + G_2(\omega)\end{aligned} \tag{47}$$

The first part clearly reproduces the spectrum of the original unmodulated pulse. The second part is due to the modulation.

Take any term of this second part

$$\begin{aligned}\mathfrak{T}_t^\omega [f(t)\delta_0(t-\nu T)]P_\tau(t-\nu T)\\ &= [f(t)\delta_0(t-\nu T)]\mathfrak{T}_t^\omega P_\tau(t-\nu T)\\ &= [f(t)\delta_0(t-\nu T)]\epsilon^{-j\omega\nu T}\mathfrak{T}_t^\omega P_\tau(t)\end{aligned} \tag{48}$$

But

$$\mathfrak{T}_t^\omega P_\tau(t) = \frac{\tau}{\sqrt{2\pi}} \times \frac{\sin \omega \frac{\tau}{2}}{\omega \frac{\tau}{2}}$$

Each term is thus equal to

$$\frac{\tau}{\sqrt{2\pi}} \times \frac{\sin \omega \frac{\tau}{2}}{\omega \frac{\tau}{2}} [f(t)\epsilon^{-j\omega t}\delta_0(t-\nu T)] \tag{49}$$

The second part is thus:

$$G_2(\omega) = \frac{\tau}{\sqrt{2\pi}} \frac{\sin \omega \frac{\tau}{2}}{\omega \frac{\tau}{2}} \times \sum_{\nu=-\infty}^{+\infty} [f(t)\epsilon^{-j\omega t}\delta_0(t-\nu T)] \tag{50}$$

which can immediately be written

$$G_2(\omega) = \frac{2A\tau\omega_2}{2\pi} \frac{\sin \omega \frac{\tau}{2}}{\omega \frac{\tau}{2}} \times \left[1 - \frac{\omega_1}{\omega_2} + 2\sum_{\nu=1}^{\infty}\left(\frac{\sin \omega_2 \nu T}{\omega_2 \nu T} - \frac{\omega_1}{\omega_2} \times \frac{\sin \omega_1 \nu T}{\omega_1 \nu T}\right)\cos \omega \nu T\right] \tag{51}$$

The expression $G_2(\omega)$ contains the spectrum of the modulation energy which will be analyzed subsequently. This can be accomplished either by an operational method applied to equation 50, an approach which is elegant and concise and which will be carried out here, or by standard algebraic methods, as analyzed in Appendix III using the form of equation 51.

Consider the operation

$$\sum_{\nu=-\infty}^{+\infty} \delta_0(t-\nu T)$$

of equation 50. This may be considered as a periodic process of interval T and thus can be represented by a Fourier series operator. Symbolically this may be written as

$$\sum_{\nu=-\infty}^{+\infty} \delta_0(t-\nu T) = \sum_{\nu=-\infty}^{+\infty} [B\nu] \times [\epsilon^{j\nu\omega_s t}] \tag{52}$$

where

$$[B\nu] = \left[\frac{1}{T}\int_{-\infty}^{+\infty} \delta_0(t)\epsilon^{-j\nu\omega_s t}\, dt\right] = \left[\frac{1}{T}\int_{-\infty}^{+\infty} (1)\, dt\right]$$

Therefore

$$\sum_{\nu=-\infty}^{+\infty} \delta_0(t-\nu T) = \sum_{\nu=-\infty}^{+\infty} \times \left[\frac{1}{T}\int_{-\infty}^{+\infty} \epsilon^{j\nu\omega_s t}\, dt\right] \tag{53}$$

This means that for each term in equation 50 the operation

$$\frac{1}{T}\int_{-\infty}^{+\infty} (f(t)\epsilon^{j\nu\omega_s t}) \times \epsilon^{-j\omega t}\, dt = \frac{\sqrt{2\pi}}{T}\mathfrak{T}_t^\omega [f(t)\epsilon^{j\nu\omega_s t}] \tag{54}$$

is performed so that $G_2(\omega)$ becomes

$$\begin{aligned}G_2(\omega) &= \frac{\tau}{\sqrt{2\pi}} \times \frac{\sin \omega \frac{\tau}{2}}{\omega \frac{\tau}{2}} \times \frac{\sqrt{2\pi}}{T} \sum_{-\infty}^{+\infty} g(\omega - \nu\omega_s)\\ &= S_0 \frac{\sin \omega \frac{\tau}{2}}{\omega \frac{\tau}{2}} \sum_{-\infty}^{+\infty} g(\omega - \nu\omega_s)\end{aligned} \tag{55}$$

since

$$\mathfrak{T}_t^\omega f(t) = g(\omega)$$

Equation 55 contains, in a very compact form, all the information about the spectrum of the modulation energy, which is shown in Figure 11.

Note that output components are identical with those obtained for the simple case where pulse amplitude modulation is applied to a single sine wave.[8]

Conclusion

The preceding analysis shows that by the use of Fourier transforms it is possible to investigate the behavior of a band of modulating frequencies acting simultaneously in a given communication system. The generalization of the results obtained in the past for a small number of discrete modulating frequencies is accomplished with a surprising facility. This method of Fourier transforms will however reveal itself almost indispensable when the problem of PCM will be examined with a view to determine cross talk and distortion.

Application of Fourier Transforms to the Calculation of Cross Talk and Distortion in a PCM System

Introduction

It has been indicated previously that due to the discrete amplitude scanning, a PCM system will introduce cross talk. In practice, the total modulating frequency band $\omega_1 \leqq \omega \leqq \omega_2$ is divided into a number of channels, each channel carrying independent intelligence. Due to the cross talk introduced in any one of the channels, the problem reduces itself into calculating the energy appearing in a particular unoccupied channel in the band while the other channels are occupied. The concept of a time function, equation 56, being the Fourier transform of the modulating band of frequencies modulating an infinite train of pulses will be carried over to the analysis of PCM. However, the difference between the two processes of pulse amplitude modulation and PCM when applied to the time function $f(t)$ must be clearly understood. In

the case of pulse amplitude modulation $G_2(\omega)$, equation 51 is the total contribution to the spectrum of an infinite number of pulses to produce a spectrum containing the original audio band (without distortion) plus the side bands distributed about the harmonics of ω_s (see Figure 11). In PCM the modulated pulses are transmitted not with amplitudes proportional to $f(t)$ but with amplitudes equal to an integral number of amplitude levels, the nearest integral level to $f(t)$ being transmitted. In this case $G_2(\omega)$ will be modified by two causes: first, the fact that signals below a half a level are neglected thus rendering the number of modulated pulses finite, and second the process of quantization, that is the pulses transmitted are not truly proportional to $f(t)$ but are of integral value. The method of attack will be to reconstruct the new frequency spectrum $G_q(\omega)$ and to calculate the energy splashed over into the unoccupied channels in the process of PCM.

Calculation of Cross Talk in Individual Channels

Consider a modulating frequency band as shown in Figure 12. The transform of $g(\omega)$ is

$$f(t)=\frac{2A}{\sqrt{2\pi}}\int_0^\infty g(\omega)\cos\omega t\,dt$$
$$=\frac{2A}{\sqrt{2\pi}}\left[\frac{\sin\omega_2 t}{t}+\frac{\sin\omega_3 t}{t}-\frac{\sin\omega_4 t}{t}\right] \tag{56}$$

Let

$$\Delta\omega=\alpha\omega_2$$

where

$$0<\alpha<1$$

and

$$\omega_d=\frac{\omega_3+\omega_4}{2}$$
$$=\text{center frequency of channel under consideration}$$

Therefore

$$f(t)=\frac{2A\omega_2}{\sqrt{2\pi}}\left[\frac{\sin\omega_2 t}{\omega_2 t}-\alpha\left(\frac{\sin\frac{\Delta\omega\times t}{2}}{\frac{\Delta\omega\times t}{2}}\right)\cos\omega_d t\right] \tag{57}$$

It is important to note here that when α is very small, this time function will vary only slightly from the original one corresponding to a solid band 0–ω_2. As a result of this, the energy reflected in the narrow gap in the process of PCM will fill the gap completely, while in pulse amplitude modulation $g(\omega)$ is reproduced faithfully.

Returning to equation 57, the spectrum of the output in pulse amplitude modulation (see equation 51) would equal

$$G_2(\omega)=\frac{2A\tau\omega_2}{2\pi}\times\frac{\sin\frac{\omega\tau}{2}}{\omega\frac{\tau}{2}}\left\{(1-\alpha)+2\sum_{\nu=1}^{\infty}\times\left[\frac{\sin\omega_2\nu T}{\omega_2\nu T}-\alpha\left(\frac{\sin\frac{\Delta\omega\times\nu T}{2}}{\frac{\Delta\omega\times\nu T}{2}}\right)\times\cos\omega_d\nu T\right]\cos\nu T\omega\right\}$$
$$=A.S_0(2Tf_2)\frac{\sin\omega\frac{\tau}{2}}{\omega\frac{\tau}{2}}\left\{(1-\alpha)+2\sum_{\nu=1}^{\infty}\times\left[\frac{\sin\omega_2\nu T}{\omega_2\nu T}-\alpha\left(\frac{\sin\frac{\Delta\omega\times\nu T}{2}}{\frac{\Delta\omega\times\nu T}{2}}\right)\times\cos\omega_d\nu T\right]\cos\nu T\omega\right\} \tag{58}$$

In the process of quantization the number of contributing pulses becomes finite; the corresponding frequency spectrum

$$G_q(\omega)=(A.S_0)(2Tf_2)\frac{\sin\omega\frac{\tau}{2}}{\omega\frac{\tau}{2}}\times\left[(1-\alpha)+2\sum_{\nu=1}^{\nu=k}A_\nu\cos\nu T\omega\right] \tag{59}$$

where K equals the number of pulses contributing to the transmission of the intelligence and A_ν equals the quantized value of $f(\nu T)$.

For a given number of levels m corresponding to $f(0)$ one can determine K for a particular case and the corresponding amplitudes. This data will enable one to calculate the energy in any channel in the band under consideration.

Numerical Results

The method described is illustrated graphically in Figures 13 and 14. A frequency band of 0–20 kc with 4-kc channels and a scanning frequency of 50 kc are considered. Figure 13 illustrates the time functions corresponding to the different modulating signals, with the maximum amplitude of $f(t)$ in (A) corresponding to 10 levels, and the effect of quantization is clearly illustrated by the transmitted pulses. The corresponding frequency spectra $G_q(\omega)$(equation 59) were reconstructed in Figure 14 where the spectra corresponding to pulse amplitude modulation are also superimposed for comparison. The energy appearing in each unoccupied channel equals

$$\int_{\omega_2}^{\omega_4}G_q(\omega)^2d\omega\nu$$

and the cross talk equals the square root of the ratio of this energy to the normal energy per channel. The results are shown in Table III.

It is significant that the cross talk varies greatly from channel to channel. Of course the number of levels is rather small and it is impossible to arrive at definite conclusions as to the relation between cross talk and number of levels.

Cross Talk Resulting From Limiting of Function

Let us further investigate the effect upon the cross talk arising from the fact that $f(t)$ is not scanned from $-\infty$ to $+\infty$ but between the limits $-t_0\leqq t\leqq+t_0$. As explained in the introduction of this section in the PCM system amplitude levels smaller than half a level are neglected which results in scanning a limited time function $f_1(t)$. While the transform of $f(t)$, equation 56, equal $g(\omega)$ of Figure 12, the transform of $f_1(t)$ will produce a modified spectrum which will be denoted by $g_1(\omega)$ namely

$$\mathfrak{T}_t^\omega f(t)=g(\omega)$$
$$\mathfrak{T}_t^\omega f_1(t)=g_1(\omega)$$

Applying pulse amplitude modulation to such a frequency band, the output spectrum (see equation 55) equals

$$G_1(\omega)=S_0\frac{\sin\omega\frac{\tau}{2}}{\omega\frac{\tau}{2}}\sum_{\nu=-\infty}^{+\infty}g_1(\omega-\nu\omega_s) \tag{60}$$

In order to determine $G_1(\omega)$ the function $g_1(\omega)$ must be found which is the transform of $f_1(t)$.

$$\mathfrak{T}_t^\omega f_1(t)=\frac{A}{\pi}\int_{-t_0}^{+t_0}\left[\frac{\sin\omega_2 t}{t}+\frac{\sin\omega_3 t}{t}-\frac{\sin\omega_4 t}{t}\right]e^{-j\omega t}dt$$

Therefore

$$g_1(\omega)=g(\omega)-\frac{2}{\sqrt{2\pi}}\int^\infty f(t)\cos\omega t\,dt \tag{61}$$

where t_0 is greater than zero. Equation 61 contains the contribution to cross talk

due to limiting of $f(t)$ which is represented by the term

$$\frac{2}{\sqrt{2\pi}}\int_{t_0}^{\infty} f(t)\cos\omega t\,dt$$

Therefore

$$\frac{2}{\sqrt{2\pi}}\int_{t_0}^{\infty} f(t)\cos\omega t\,dt=\frac{2A}{\pi}\times\int_{t_0}^{\infty}\left(\frac{\sin\omega_2 t}{t}+\frac{\sin\omega_3 t}{t}-\frac{\sin\omega_4 t}{t}\right)\times\cos\omega t\,dt \quad (62)$$

or

$$g_1(\omega)=g(\omega)-\left\{\int_{t_0}^{\infty}\left[\frac{\sin(\omega_2+\omega)t}{t}+\frac{\sin(\omega_2-\omega)t}{t}\right]dt+\int_{t_0}^{\infty}\left[\frac{\sin(\omega_3+\omega)t}{t}+\frac{\sin(\omega_3-\omega)t}{t}\right]dt-\int_{t_0}^{\infty}\left[\frac{\sin(\omega_4+\omega)t}{t}+\frac{\sin(\omega_4-\omega)t}{t}\right]dt\right\}$$

$$=g(\omega)-I_1-I_2+I_3 \quad (63)$$

Where I_1, I_2, and I_3 vary through the different regions of ω_2 as shown subsequently

$O<\omega<\omega_2$.

$$I_1=\frac{A}{\pi}[\pi-S_i(\omega_2+\omega)t_0-S_i(\omega_2-\omega)t_0]$$

$$I_2=\frac{A}{\pi}[\pi-S_i(\omega_3+\omega)t_0-S_i(\omega_3-\omega)t_0]$$

$$I_3=\frac{A}{\pi}[\pi-S_i(\omega_4+\omega)t_0-S_i(\omega_4-\omega)t_0]$$

where $S_i(x)=\int_0^x\frac{\sin u}{u}du$

$\omega_2<\omega<\omega_4$.

$$I_1=\frac{A}{\pi}[\pi-S_i(\omega_2+\omega)t_0-S_i(\omega_2-\omega)t_0]$$

$$I_2=\frac{A}{\pi}[-S_i(\omega_3+\omega)t_0+S_i(\omega-\omega_3)t_0]$$

$$I_3=\frac{A}{\pi}[\pi-S_i(\omega_4+\omega)t_0-S_i(\omega_4-\omega)t_0]$$

$\omega_4<\omega<\omega_3$.

$$I_1=\frac{A}{\pi}[\pi-S_i(\omega_2+\omega)t_0-S_i(\omega_2-\omega)t_0]$$

$$I_2=\frac{A}{\pi}[-S_i(\omega_3+\omega)t_0+S_i(\omega-\omega_3)t_0]$$

$$I_3=\frac{A}{\pi}[-S_i(\omega_4+\omega)t_0+S_i(\omega-\omega_4)t_0]$$

$\omega_3<\omega<\infty$.

$$I_1=\frac{A}{\pi}[-S_i(\omega_2+\omega)t_0+S_i(\omega-\omega_2)t_0]$$

$$I_2=\frac{A}{\pi}[-S_i(\omega_3+\omega)t_0+S_i(\omega-\omega_3)t_0]$$

$$I_3=\frac{A}{\pi}[-S_i(\omega_4+\omega)t_0+S_i(\omega-\omega_4)t_0]$$

A plot of $g_1(\omega)$ for a particular case is shown in Figure 15 *F*. Note that $g_1(\omega)$ extends beyond ω_3.

During the process of pulse amplitude modulation, $g_1(\omega)$ will be reproduced without distortion at a reduced scale. However, the spectrum of $g_1(\omega_g-\omega)$ will overlap with the lowest audio band and thus introduce additional distortion in the gap which is clearly indicated in this figure.

Quantization of Limited Signal

The process of quantization may be expressed mathematically by modifying equation 46 as follows

$$\varphi_g(t)=\sum_{\nu=-\infty}^{+\infty}E_\nu[P_\tau(t-\nu T)+\xi_\tau(t-\nu T)] \quad (64)$$

where ξ_τ represents the quantization of the nearest level. Therefore

$$\varphi_g(t)=\sum_{\nu=-\infty}^{+\infty}E[P_\tau(t-\nu T)+\xi_\tau(t-\nu T)]+\sum_{-\infty}^{+\infty}[f_1(t)\times\delta_0(t-\nu T)]P_\tau(t-\nu T)+\sum_{-\infty}^{\infty}[f_1(t)\times\delta_0(t-\nu T)]\xi_\tau(t-\nu T)$$

By choosing the proper scale, the first term of $\varphi_g(t)$ may be adjusted to give zero. The second term equals

$$G_1(\omega)=S_0\frac{\sin\omega\frac{\tau}{2}}{\omega\frac{\tau}{2}}\sum_{\nu=-\infty}^{+\infty}g_1(\omega-\nu\omega_g)$$

which is equation (60), and the third term represents the contribution of quantization whose maximum effect seems to occur when $f_1(t)$ is distorted in the $+ve$ sense when $f_1(t)$ is $+ve$, and the $-ve$ sense when $f_1(t)$ is $-ve$. Also the maximum value of ξ_τ equals $1/2m$ times the maximum amplitude of $f(t)$, m being number of levels contained in this maximum amplitude, so that the complete distortion spectrum becomes

$$[G_1(\omega)]_m=\left(1+\frac{1}{2m}\right)S_0\frac{\sin\omega\frac{\tau}{2}}{\omega\frac{\tau}{2}}\times\sum_{\nu=-\infty}^{+\infty}g_1(\omega-\nu\omega_g) \quad (65)$$

The important conclusion to be drawn from equation 65 is that when m is large, the main contribution to cross talk arises from the limiting of the function $f(t)$ in the process of quantization.

In practice m is large and the problem is simplified greatly due to the fact that equation 63 may be used with some modification, since the main interest is in the channel $\omega_2<\omega<\omega_4$ only, where $g(\omega)=0$. The energy appearing in it will be due to I_1, I_2, and I_3 of equation 63 and proper consideration being given to the contribution of $g_1(\omega_g-\omega)$.

Figure 15 illustrates clearly that the main distortion is due to the limiting of the time function $f(t)$. The values of $G_g(\omega)$ of Figure 14 are superimposed here for comparison with $g_1(\omega)$. Where the distortion is small and the contribution of the factor $1/2m$ of equation 65 is comparable to it, the two curves vary. Hence, the following procedure may be outlined for the determination of the distortion in a particular channel:

1. Determine the time function $f(t)$ corresponding to the modulating signal (equation 56).
2. For a given number of levels m determine t_0 which represents the time of last significant pulse to be transmitted in the time function $f(t)$.
3. Calculate $g_1(\omega)$ (equation 63) from which the energy in the channel may be obtained.

Conclusion

An attempt has been made in the paper to analyze the distortion and cross talk arising in a PCM system. Solution of this problem was attempted in a number of ways. First an analysis along conventional lines has been made to PCM applied to a single sine wave and this analysis has been extended to cover the case of two sine waves and which is applicable to a small number of modulating signals. The method of the Fourier transform was then introduced in order to cope with the more formidable problem of analysis of PCM applied to a large number of modulating signals. With this tool it has been possible to satisfactorily solve the general case involving the cross talk introduced into any one channel when the modulating frequency band is divided into a number of intelligence-carrying channels. More important the Fourier transform method has proved to be of such convenience that it should serve as a useful adjunct to the radio engineer in the investigation of the behavior of a band of modulating frequencies acting simultaneously in a given communication system, as well as similar problems.

The results of these computations indicate that accepted standards of telephone transmission over wire and radio commercial systems can be obtained with a relatively small number of levels. Experimental work appears to confirm the order of magnitude of the distortion given in the attached Tables I and II.

Appendix I

With reference to Figure 2 for the Kth rectangular pair

$$\sigma_K(t) = \sum_{n=1}^{\infty} B_{nk} \sin (n\omega t)$$

where

$$B_{nk} = \frac{A}{N} \times \frac{\omega}{\pi} \int_{\Delta t_k}^{T/2 - \Delta t_k} \sin (n\omega t) dt$$

which reduces to

$$B_{nk} = \frac{4A}{\pi n N} \cos (n\omega \Delta t_k)$$

where n is odd and will be represented by $(2\nu + 1)$; but

$$\Delta t_k = \frac{1}{\omega} \sin^{-1} \frac{2k-1}{2N}$$

therefore

$$\sigma_k(t) = \sum_{\nu=0}^{\infty} \frac{4A}{\pi N(2\nu+1)} \times \cos \left[(2\nu+1) \sin^{-1} \frac{2k-1}{2N} \right] \sin (2\nu+1)\omega t$$

For N pair of rectangular pulses we obtain

$$f_S(t) = \sum_{k=1}^{N} \sigma_k(t)$$

resulting in equation 3. From the theory of harmonic analysis it follows that

$$\frac{2}{T} \int_0^T [f_S(t)]^2 dt = \sum_{\nu=0}^{\infty} (A_{2\nu+1})^2$$

From this, equation 4 reduces to

$$D = \frac{\sqrt{\frac{2}{T} \int_0^T [f_S(t)]^2 dt - A_1^2}}{A_1}$$

By direct manipulation it can be shown that

$$\frac{2}{T} \int_0^T f_S(t)]^2 dt = \bar{A}^2 \text{ of equation 7.}$$

Appendix II

With reference to Figure 3 and equation 9

$$B_n = \frac{2}{E} \int_0^E f(v) \sin \frac{n\pi v}{E} dv$$

$$= \frac{2}{E} \left[\sum_{k=1}^{N-1} \frac{kE}{N} \int_{(2k-1)E/2N}^{(2k+1)E/2N} \sin \frac{n\pi v}{E} dv + \int_{(2N-1)E/2N}^{E} \sin \frac{n\pi v}{E} dv \right]$$

$$= \frac{2E}{\pi n N} \left\{ \sum_{k=1}^{N-1} k \left[\cos (2k-1) \frac{\pi n}{2N} - \cos (2k+1) \frac{\pi n}{2N} \right] + N \left[\cos (2N-1) \times \frac{\pi n}{2N} - \cos \pi n \right] \right\}$$

$$= \frac{2E}{\pi n N} \left[\sum_{k=1}^{N} \cos (2k-1) \frac{\pi n}{2N} + N(-1)^{n-1} \right]$$

$$= \frac{2E}{\pi n N} \left[\frac{\sin \pi n}{2 \sin (\pi n/2N)} + N(-1)^{n-1} \right]$$

which is equation 10. Rewriting equation 12

$$V = \frac{4E}{\pi N} \left[N \sum_{n=1}^{\infty} \frac{(-1)^{n-1}}{n} J_1(n\pi) + \sum_{n=1}^{\infty} \frac{\sin \pi n}{2n \sin \pi n/2N} \right] \times \sum_{\nu=0}^{\infty} \times J_{2\nu+1}(\pi n) \sin (2\nu+1)\omega t \quad (12)$$

The fundamental is given by putting $\nu = 0$. Therefore

$$A_1 = \frac{4E}{\pi N} \left[N \sum_{n=1}^{\infty} \frac{(-1)^{n-1}}{n} J_1(n\pi) + \sum_{n=1}^{\infty} \frac{\sin \pi n}{2n \sin \pi n/2N} J_1(n\pi) \right] \quad (66)$$

The first part of equation 66 namely

$$\sum_{n=1}^{\infty} \frac{(-1)^{n-1}}{n} J_1(n\pi) = \frac{2}{\pi} \int_0^{\pi/2} \sin \theta \, d\theta \times \sum_{n=1}^{\infty} \frac{(-1)^{n-1}}{n} \sin (n\pi \sin \theta)$$

$$= \frac{2}{\pi} \cdot \frac{\pi}{2} \int_0^{\pi/2} \sin^2 \theta d\theta$$

$$= \frac{\pi}{4} \quad (67)$$

The second part of equation (66) gives

$$\sum_{n=1}^{\infty} \frac{\sin \pi n}{2n \sin (\pi n/2N)} J_1(n\pi)$$

which equals zero unless $n = 2\,Nl$, where l is any positive integer. Therefore

$$\sum_{n=1}^{\infty} \frac{\sin \pi n}{2n \sin \pi n/2N} J_1(n\pi)$$

$$= \sum_{l=1}^{\infty} \frac{\sin (2\pi lN)}{4lN \sin \pi l} J_1(2\pi lN)$$

$$= -\frac{1}{2} \sum_{l=1}^{\infty} \frac{(-1)^{l-1}}{l} J_1(2\pi lN)$$

$$= -\frac{1}{2} \cdot \frac{2}{\pi} \int_0^{\pi/2} \sin \theta d\theta \sum_{l=1}^{\infty} \frac{(-1)^{l-1}}{l} \times \sin (l \times 2\pi N \sin \theta)$$

To evaluate

$$\sum_{l=1}^{\infty} \frac{(-1)^{l-1}}{l} \sin (l \times 2\pi N \sin \theta)$$

note that

$$\sum_{l=1}^{\infty} \frac{(-1)^{l-1}}{l} \sin (l\alpha) = \frac{\alpha}{2}$$

where

$$-\pi < \alpha < \pi$$

But here the range of α is extended as shown in Figure 16.

where

$$\theta_1 = \sin^{-1} \frac{1}{2N}$$

$$\theta_2 = \sin^{-1} \frac{3}{2N}$$

$$\cdots$$

$$\theta_N = \sin^{-1} \frac{2N-1}{2N}$$

Notice that θ_K represents the angular distance of the kth step from the origin in the original sine wave. Therefore

$$\sum_{l=1}^{\infty} \frac{(-1)^{l-1}}{l} \sin (l\alpha) = \frac{\alpha}{2}$$

$$= \pi N \sin \theta (0 < \theta < \theta_1)$$

$$= \pi N \sin \theta - \pi (\theta_1 < \theta < \theta_2)$$

$$\cdots$$

$$= \pi N \sin \theta - \pi N (\theta_N < \theta < \pi/2)$$

so that the second part of equation 67 becomes equal to

$$-\frac{1}{\pi} \left\{ \pi N \left[\int_0^{\theta_1} \sin^2 \theta d\theta + \int_{\theta_1}^{\theta_2} \sin^2 \theta d\theta + \ldots \right] - \pi \left[1 \times \int_1^{\theta_2} \sin \theta d\theta + 2 \cdot \int_{\theta_2}^{\theta_3} \sin \theta d\theta + \ldots + N \int_{\theta_N}^{\pi/2} \sin \theta d\theta \right] \right\}$$

$$= -\frac{1}{\pi} \left[\pi N \int_0^{\pi/2} \sin^2 \theta d\theta + \pi (\cos \theta_2 - \cos \theta_1) + 2\pi (\cos \theta_3 - \cos \theta_2) + \ldots + (N-1)\pi (\cos \pi_N - \cos \theta_{N-1}) + \pi N \left(\cos \frac{\pi}{2} - \cos \theta_N \right) \right]$$

$$= -\frac{\pi N}{4} + \sum_{k=1}^{N} \cos \left(\sin^{-1} \frac{2k-1}{2N} \right)$$

Finally

$$A_1 = E \left[1 - \frac{2}{\pi N} \sum_{l=1}^{\infty} \frac{(-1)^{l-1}}{l} J_1(2\pi lN) \right]$$

$$= \frac{4E}{\pi N} \sum_{k=1}^{N} \cos \left(\sin^{-1} \frac{2k-1}{2N} \right) \quad (13)$$

Similarly it can be proved that

$$\sum_{n=1}^{\infty} \frac{(-1)^{n-1}}{n} J_{2\nu+1}(n\pi) = 0 \quad (68)$$

where ν is any positive integer and the amplitude of the $(2\nu+1)$th harmonic is given by

$$A_{2\nu+1} = \frac{2E}{\pi N} \sum_{l=1}^{\infty} \frac{(-1)^{l-1}}{l} J_{2\nu+1}(2\pi lN)$$

$$= \frac{4E}{\pi N(2\nu+1)} \sum_{k=1}^{N} \times \cos \left[(2\nu+1) \sin^{-1} \frac{2k-1}{2N} \right] \quad (14)$$

A_1 may be evaluated with the aid of the asymptotic expansion of $J_1(2\pi lN)$ for in practice N is large

$$J_1(2\pi Nl) \approx \left(\frac{2}{\pi(2\pi N)l}\right)^{1/2} \cos\left(2\pi Nl - \frac{3}{4}\pi\right)$$

$$= -\frac{1}{\pi\sqrt{2lN}}$$

Therefore

$$A_1 \approx E\left[1 + \frac{C\sqrt{2}}{\pi^2 N^{3/2}}\right]$$

where

$$C = \sum_{l=1}^{\infty} \frac{(-1)^{l-1}}{l^{1/2}}$$

$$= (1 - 2^{-1/2})\zeta\left(\frac{3}{2}\right)$$

$$= 0.2929 \times 2.612$$

$$= 0.7650$$

where

$$\zeta(s) = \sum_{n=1}^{\infty} \frac{1}{n^s}$$

the Riemann Zeta-Function. Finally A reduces to

$$A_1 = E\left[1 + \frac{0.1096}{N^{3/2}}\right] \tag{15}$$

In the case of a two frequency signal

$v = E/2(\sin \omega_1 t + \sin \omega_2 t)$

Therefore

$$V = \frac{4E}{\pi} \sum_{n=1}^{\infty} \frac{(-1)^{n-1}}{n} \Bigg\{ J_0\left(\frac{n\pi}{2}\right) \times \Bigg[\sum_{\nu=0}^{\infty} J_{2\nu+1}\left(\frac{n\pi}{2}\right) \sin(2\nu+1)\omega_1 t + \sum_{\rho=0}^{\infty} J_{2\rho+1}\left(\frac{n\pi}{2}\right) \sin(2\rho+1)\omega_2 t \Bigg] + 2\sum_{\nu=0}^{\infty}\sum_{\lambda=1}^{\infty} J_{2\nu+1}\left(\frac{n\pi}{2}\right) J_{2\lambda}\left(\frac{n\pi}{2}\right) \times \sin(2\nu+1)\omega_1 t \times \cos 2\lambda\omega_2 t + 2\sum_{\rho=0}^{\infty}\sum_{\eta=1}^{\infty} J_{2\rho+1}\left(\frac{n\pi}{2}\right) J_{2\eta}\left(\frac{n\pi}{2}\right) \times \sin(2\rho+1)\omega_2 t \times \cos 2\eta\omega_1 t \Bigg\} - \frac{2E}{\pi N} \sum_{l=1}^{\infty} \frac{(-1)^{l-1}}{l} \Bigg\{ J_0(\pi lN) \times \Bigg[\sum_{\nu=0}^{\infty} J_{2\nu+1}(\pi lN) \sin(2\nu+1)\omega_1 t + \sum_{\rho=0}^{\infty} J_{2\rho+1}(\pi lN) \sin(2\rho+1)\omega_2 t \Bigg] + 2\sum_{\nu=0}^{\infty}\sum_{\lambda=1}^{\infty} J_{2\nu+1}(\pi lN) J_{2\lambda}(\pi lN) \times \sin(2\nu+1)\omega_1 t \times \cos(2\lambda)\omega_2 t + 2\sum_{\rho=0}^{\infty}\sum_{\eta=1}^{\infty} J_{2\rho+1}(\pi lN) J_{2\eta}(\pi lN) \times \sin(2\rho+1)\omega_2 t \times \cos 2\eta\omega_1 t \Bigg\} \tag{69}$$

Now it will be proved that

$$\sum_{n=1}^{\infty} \frac{(-1)^{n-1}}{n} J_0\left(\frac{n\pi}{2}\right) J_1\left(\frac{n\pi}{2}\right) = \frac{\pi}{8}$$

and

$$\sum_{n=1}^{\infty} \frac{(-1)^{n-1}}{n} J_{2\nu+1}\left(\frac{n\pi}{2}\right) J_{2\lambda}\left(\frac{n\pi}{2}\right) = 0,$$

where ν is any positive integer and λ varies from zero to plus infinity in integral steps.

It is known that

$$J_\mu(x)\, J_\nu(x) = \frac{2}{\pi}\int_0^{\pi/2} J_{\mu+\nu}(2 \times \cos\theta) \times \cos(\mu-\nu)\theta d\theta$$

Therefore

$$\sum_{n=1}^{\infty} \frac{(-1)^{n-1}}{n} J_0\left(\frac{n\pi}{2}\right) J_1\left(\frac{n\pi}{2}\right) = \frac{2}{\pi}\int_0^{\pi/2} \cos\theta\, d\theta \sum_{n=1}^{\infty} \frac{(-1)^{n-1}}{n} \times J_1(n\pi\cos\theta)$$

Now

$$\sum_{n=1}^{\infty} \frac{(-1)^{n-1}}{n} J_1(n\pi\cos\theta) = \frac{2}{\pi}\int_0^{\pi/2} \sin\varphi\, d\varphi \sum_{n=1}^{\infty} \frac{(-1)^{n-1}}{n} \times \sin(\pi_n \cos\theta \sin\varphi)$$

put

$\alpha = \pi\cos\theta\sin\varphi$

Therefore

$$\sum_{n=1}^{\infty} \frac{(-1)^{n-1}}{n} \sin(n\alpha) = \frac{\alpha}{2} = \frac{\pi}{2}\cos\theta\sin\varphi$$

and

$$\sum_{n=1}^{\infty} \frac{(-1)^{n-1}}{n} J_1(n\pi\cos\theta) = \cos\theta \times \int_0^{\pi/2} \sin^2\varphi\, d\varphi = \frac{\pi}{4}\cos\theta$$

Finally

$$\sum_{n=1}^{\infty} \frac{(-1)^{n-1}}{n} J_0\left(\frac{n\pi}{2}\right) J_1\left(\frac{n\pi}{2}\right) = \frac{1}{2}\int_0^{\pi/2} \cos^2\theta\, d\theta = \pi/8 \tag{70}$$

Similarly it can be proved that

$$\sum_{n=1}^{\infty} \frac{(-1)^{n-1}}{n} J_{2\nu+1}\left(\frac{n\pi}{2}\right) J_{2\lambda}\left(\frac{n\pi}{2}\right) = 0 \tag{71}$$

Hence equation 69 reduces to

$$V = \frac{E}{2}(\sin\omega_1 t + \sin\omega_2 t) - \frac{2E}{\pi N} \times \sum_{l=1}^{\infty} \frac{(-1)^{l-1}}{l} \Bigg\{ J_0(\pi lN) \times \Bigg[\sum_{\nu=0}^{\infty} J_{2\nu+1}(\pi lN) \sin(2\nu+1)\omega_1 t + \sum_{\rho=0}^{\infty} J_{2\rho+1}(\pi lN) \sin(2\rho+1)\omega_2 t \Bigg] + 2\sum_{\nu=0}^{\infty}\sum_{\lambda=1}^{\infty} J_{2\nu+1}(\pi lN) \times J_{2\lambda}(\pi lN) \times \sin(2\nu+1)\omega_1 t \times \cos(2\lambda)\omega_2 t + 2\sum_{\rho=0}^{\infty}\sum_{\eta=1}^{\infty} J_{2\rho+1}(\pi lN) J_{2\eta}(\pi lN) \times \sin(2\rho+1)\omega_2 t \times \cos(2\eta)\omega_1 t \Bigg\}$$

The amplitudes of the $(2\nu+1)$th or $(2\rho+1)$th harmonic of ω_1 and ω_2 of the two input frequencies are

$$A'_{2\nu+1} = -\frac{2E}{\pi N} \sum_{l=1}^{\infty} \frac{(-1)^{l-1}}{l} J_0(\pi lN) \times J_{2\nu+1}(\pi lN) \tag{72}$$

where ν is greater than or equal to one.

In order to evaluate equation 72 the asymptotic expansion for $J_0(\pi lN)$ and $J_{2\nu+1}(\pi lN)$ must be found. The calculations are lengthy and only the result will be given here

$$J_1(\pi lN) J_{2\nu+1}(\pi lN) \doteq \frac{(-1)^{\nu+1}}{\pi^2 N} \times \frac{1}{l}\left\{1 - \frac{(2\nu+1)^2}{2\pi lN} + \frac{[4(2\nu+1)^2-1][11-4(2\nu+1)^2]-9}{128\pi^2 N^2 l^2} + \cdots\right\}$$

Finally this reduces to

$$A'_{2\nu+1} \approx \frac{(-1)^\nu \cdot 2E}{\pi^2 N^2} \left\{\frac{\pi}{12} - \frac{0.9015(2\nu+1)^2}{2\pi N} - \frac{7\pi^2[4(2\nu+1)^4 - 12(2\nu+1)^2 + 5]}{23{,}040 N^2} + \cdots\right\}$$

Notice that the harmonics produced in the case of a two frequency signal are much smaller than the harmonics of a one frequency signal. However, besides the harmonics, cross products appear whose amplitudes are given by

$$A_{(2\nu+1)\omega_1 \pm 2\lambda\omega_2} = -\frac{2E}{\pi N} \sum_{l=1}^{\infty} \frac{(-1)_{l-1}}{l} \times J_{2\nu+1}(\pi lN) J_{2\lambda}(\pi lN) \tag{73}$$

Again using the asymptotic expansion of $J_{2\nu+1}(\pi lN) \times J_{2\lambda}(\pi lN)$ the amplitudes are given by

$$A_{(2\nu+1)\omega_1 \pm \nu\lambda\omega_2} = \frac{(-1)^{\nu+\lambda} \cdot 2E}{\pi^2 N^2} \left\{\frac{\pi^2}{12} - \frac{0.9015[(2\nu+1)^2 - 4\lambda^2]}{2\pi N} + \cdots\right\} \tag{74}$$

Equation 74 shows that the amplitudes of the cross products are of the same order of magnitude as the harmonics.

Appendix III

The modulation spectrum $G_3(\omega)$, equation 51 may be analyzed as follows. Consider first the expression

$$G_3(\omega)=2\sum_{\nu=1}^{\infty}\left(\frac{\sin \nu\omega_2 T}{\nu\omega_2 T}-\frac{\omega_1}{\omega_2}\frac{\sin \nu\omega_1 T}{\nu\omega_1 T}\right)\cos \nu T\omega$$

$$=\frac{1}{\omega_2 T}\sum_{\nu=1}^{\infty}\times$$

$$\left[\frac{\sin \nu T(\omega_2+\omega)+\sin \nu T(\omega_2-\omega)}{\nu}-\frac{\sin \nu T(\omega_1+\omega)+\sin \nu T(\omega_1-\omega)}{\nu}\right] \quad (75)$$

$G_3(\omega)$ contains terms of the form $(\sin \nu\theta)/\nu$ and it is well known that

$$\sum_{\nu=1}^{\infty}\frac{\sin \nu\theta}{\nu}=\frac{1}{2}(\pi-\theta)$$

where

$$0<\theta<2\pi$$

In order to analyze the spectrum contribution of $G_3(\omega)$, the two cases examined previously for the relation of the scanning frequency to the frequency limits of the modulating signal which allow for filtering out of the signal in the output will now be considered.

I. $\omega_S>2\omega_2$. Consider again $G_3(\omega)$ Since

$$T\omega_S=2\pi f_S T$$
$$=2\pi$$

Therefore

$$2\omega_2 T<2\pi$$

In the summation of $G_3(\omega)$ several frequency regions will be examined.

1. $0<\omega<\omega_1$.

$$G_3(\omega)=\frac{1}{2\omega_2 T}[(\pi-T(\omega_2+\omega)+\pi-T(\omega_2-\omega))-(\pi-T(\omega_2+\omega)+\pi-T(\omega_1-\omega))]$$
$$=\frac{-T(\omega_2-\omega_1)}{\omega_2 T}$$

Therefore

$$G_3(\omega)=\frac{E\tau}{\sqrt{2}\pi}\cdot\frac{2A\omega_2}{\sqrt{2}\pi E}\cdot\frac{\sin \omega\tau/2}{\omega\tau/2}\left[\frac{(\omega_2-\omega_1)T}{\omega_2 T}-\frac{(\omega_2-\omega_1)T}{\omega_2 T}\right]=0$$

2. $\omega_1<\omega<\omega_2$.

$$G_3(\omega)=\frac{1}{2\omega_2 T}[(\pi-T(\omega_2+\omega)+\pi-T\times(\omega_2-\omega))-(\pi-T(\omega_1+\omega)-\pi+T\times(\omega-\omega_1))]$$
$$=\frac{1}{\omega_2 T}[\pi-T(\omega_2-\omega_1)] \quad (76)$$

Therefore

$$G_3(\omega)=S_p A\left(\frac{\sin \omega\tau/2}{\omega\tau/2}\right)$$

3. $\omega_2<\omega<(\omega_S-\omega_2)$.

$$G_3(\omega)=\frac{1}{2\omega_2 T}[(\pi-T(\omega_2+\omega)-\pi+T(\omega-\omega_2))-(\pi-T(\omega_1+\omega)-\pi+T(\omega-\omega_1))]$$
$$=-\frac{T(\omega_2-\omega_1)}{\omega_2 T}$$

Therefore

$$G_3(\omega)=0$$

Thus, so far the original band of frequencies $\omega_1<\omega<\omega_2$ has been recovered with the proper frequency response. It remains to investigate the behavior of $G_3(\omega)$ in the vicinity of $\nu\omega_S$, the νth harmonic of the scanning angular frequency.

Here again several frequency regions will be examined.

1. $[(\nu-1)\omega_S+\omega_2]<\omega<(\nu\omega_S-\omega_1)$.

To enable the use of equation 75, make the transformation

$$\bar{\omega}=\omega-(\nu-1)\omega_S$$

which is equivalent to shifting the ω origin to $(\nu-1)\omega_S$.

$$G_3(\omega)=\frac{1}{2\omega_2 T}\{[\pi-T(\omega_2+\bar{\omega})-\pi-T(\omega_2-\bar{\omega})]-[\pi-T(\omega_1+\bar{\omega})-\pi-T(\omega_1-\bar{\omega})]\}$$
$$=-\frac{T(\omega_2-\omega_1)}{\omega_2 T}$$

Therefore

$$G_3(\omega)=0$$

2. $(\nu\omega_S-\omega_2)<\omega<(\nu\omega_S-\omega_1)$. Here $T(\omega_2+\bar{\omega})>2\pi$

$$G_3(\omega)=\frac{1}{2\omega_2 T}\{[\pi-T(\omega_2+\bar{\omega})+2\pi-\pi-T(\omega_2-\bar{\omega})]-[\pi-T(\omega_1+\bar{\omega})-\pi-T(\omega_1-\bar{\omega})]\}$$
$$=\frac{1}{\omega_2 T}[\pi-T(\omega_2-\omega_1)]$$

Therefore

$$G_3(\omega)=S_p A\frac{\sin \omega\tau/2}{\omega\tau/2}$$

Similarly the side band to the right of $\nu\omega_S$ is derived. Actually by shifting the origin to $\nu\omega_S$, this frequency band becomes identical with the origin audio frequency band.

II. $\omega_2<\omega_S<2\omega_1$

With reference to Figure 9 several frequency regions will be discussed.

1. $0<\omega<(\omega_S-\omega_2)$. In this range $T(\omega_2+\omega)<T\omega_S=2\pi$

$$G_3(\omega)=\frac{1}{2\omega_2 T}[\pi-T(\omega_2+\omega)+\pi-T(\omega_2-\omega)-\pi+T(\omega_1+\omega)-\pi+T(\omega_2-\omega)]$$
$$=-\frac{T(\omega_2-\omega_1)}{\omega_2 T}$$

Therefore

$$G_3(\omega)=0$$

2. $(\omega_S-\omega_2)<\omega<(\omega_S-\omega_1)$. In this range $4\pi>T(\omega_2+\omega)>2\pi$. Therefore

$$G_3(\omega)=S_p A\frac{\sin \omega\tau/2}{\omega\tau/2}$$

Proceeding as before, it can easily be shown that $G_3(\omega)$ will contribute to the spectrum as shown in Figure 9 with an amplitude given by

$$S_p A\frac{\sin \omega\tau/2}{\omega\tau/2}$$

References

1. United States patent 2,272,070, **A. H. Reeves**, February 3, 1942, assigned to the International Standard Electric Corporation; also French patent 852,183, October 23, 1939.

2. Performance Characteristics of Various Carrier Telegraph Methods, **T. A. Jones, K. W. Pfleger**. *Bell System Technical Journal* (New York, N. Y.), July 1946, pages 483–531.

3. Multichannel Communication Systems, **F. F. Roberts, J. C. Simmonds**. *Wireless Engineer* (London, England), November 1945, pages 538–49.

4. Pulse Time Multiplex Radio Relay System, **D. D. Grieg, A. M. Levine**. *Electrical Communication* (New York, N. Y.), volume 23, number 2, 1946, pages 159–78.

5. A Multichannel Microwave Radio Relay System, **H. S. Black, J. W. Beyer, T. J. Grieser, F. A. Polkinghorn**. AIEE Transactions, volume 65, 1946, pages 798–806.

6. Electronic Commutation for Telemetering, **L. L. Rauch**. *Electronics* (New York, N. Y.), February 1947, pages 115–20.

7. Multiplex Broadcasting, **D. D. Grieg**. *Electrical Communication* (New York, N. Y.), volume 23, number 1, March 1946, pages 19–26.

8. Pulse Modulation, **R. S. Shepherd** (Letter to the Editor). *Wireless Engineer* (London, England), April 1946, pages 114–15.

9. Nonlinear Distortion in Transmission Systems, **R. A. Brockband, C. A. A. Wass**. *Journal of the Institution of Electrical Engineers* (London, England), March 1945, pages 45–56.

Discussion

A. G. Clavier, P. F. Panter, and D. D. Grieg: As a supplement to the paper the following discussion is aimed at clarifying some of the assumptions involved. This supplement resulted from comments made by P. R. Aigrain and discussions with the authors.

The pulse count modulation pulses can be considered as the sum of pulse amplitude modulation pulses (not quantized) and of "error pulses" representing the quantization to the nearest level. When fed in a low-pass filter, the pulse amplitude modulation pulses reproduce the undistorted signal. The error pulses, which are a function $\xi_\nu(t)$ of time, cause the distortion.

The calculation of the energy induced by a signal $\xi_\nu(t)$ in a frequency band ω_1 to ω_2 can be carried out, for example, by means of the following formulas. Let

$$\varphi(t) = \int_{-\infty}^{+\infty} \xi_\nu(\zeta)\xi_\nu(t+\zeta)d\zeta \tag{1}$$

Then

$$S(\omega) = \mathcal{T}_t^\omega \varphi(t) \tag{2}$$

is called the "energy spectrum" of $\xi_\nu(t)$ and the energy induced by $\xi_\nu(t)$ in the band ω_1 to ω_2 is

$$P = \frac{1}{\sqrt{2\pi}} \int_{\omega_1}^{\omega_2} S(\omega)d\omega \tag{3}$$

In the present case, $\xi_\nu(t)$ consists of pulses occurring at regular intervals so that $\xi_\nu(t) = 0$, except for $t = \nu T$ ($\nu = -2, -1, 0, 1, 2$, and so forth).

Consequently $\varphi(t)$ will also consist of pulses occurring at times $t = \nu T$, and the amplitude of these pulses will be given by

$$\varphi(\nu T) = \sum_{n=-\infty}^{+\infty} \xi_\nu(nT)\xi_\nu[(n+\nu)T] \tag{4}$$

That is, $\varphi(\nu T)$ will depend on the products two by two of the error pulses.

The input signal $f(t)$ can be split into two portions

1. One part for $t < -t_0$ and $t > t_0$, for which the successive maxima of the signal $f(t)$ are less than 1/2 level in absolute value. No PCM pulses are then transmitted. The error pulses, which then represent the time limiting of $f(t)$, are given by

$$\xi_\nu(\nu T) = f(\nu T)$$

$$\xi_\nu(t) = 0 \text{ when } t \neq \nu T$$

2. The second part for $-t_0 < t < t_0$ during which the maximum amplitudes of the signal exceed one level, so that the transmitted PCM pulses are not zero. $\xi_\nu(t)$ then depends on a very complex way on $f(t)$ and the relative position of $f(t)$ and the scanning pulses. But if the calculation strives only toward finding an average value of the distortion for all possible positions of the signal with respect to the scanning pulses, then it can be assumed, as a first approximation, that the amplitudes of the $\xi_\nu(t)$ pulses are distributed individually and collectively at random between minus one-half level and plus one-half level, that is, the probability that one of the error pulses, chosen at random, will have a value x between minus one-half and plus one-half level is the same for all x, independently of the value of the other error pulses.

$\varphi(\nu T)$ can then be considered as the sum of three terms

1. $\varphi_1(t)$ involving only the products of time limiting error pulses.

2. $\varphi_2(t)$ involving only the products of quantization error pulses.

3. $\varphi_3(t)$ involving the products of error pulses of the first two kinds.

Because of the assumption made in the preceding paragraph $\varphi_2(t)$ will, on the average, be zero. Taking now into account the second term, two cases will be considered:

$$\nu = 0,\ \varphi_2(0) = \sum_{-t_0}^{+t_0} \xi_\nu^2(t) \tag{6}$$

$\nu \neq 0$, $\varphi_2(\nu T)$ depends on the products two by two of different error pulses, which is zero on the average. Hence

$$\varphi_2(t) = 0$$

$$t \neq 0$$

The corresponding contribution to $S(\omega)$ is a constant $\frac{\varphi_2(0)}{\sqrt{2\pi}}$. As far as the first term is concerned, $\varphi_1(t)$ is simply the result of applying pulse amplitude modulation to the portion of the input signal which is not transmitted. The corresponding spectrum has already been calculated ("Cross Talk Resulting From Limiting of Function").

Thus a first result: the total distortion spectrum is the sum of a constant $\frac{\varphi_2(0)}{\sqrt{2\pi}}$ and of the distortion spectrum due to time limiting. This seems to differ from the results obtained previously, since it had been found that the distortion energy spectrum was zero at some frequencies, while the present study shows that it cannot be less than $\frac{\varphi_2(0)}{\sqrt{2\pi}}$. The reason is that the position of the signal $f(t)$ with respect to the scanning pulses was not chosen at random in the above paper, but rather one particular position had been assumed for the sake of convenience. The difference is, however, of no consequence.

The calculation can be carried a little further by evaluating $\varphi_2(0)$, and the average in frequency of $\mathcal{T}_t^\omega \varphi_1(t)$. The average value of ξ_ν^2 where ξ_ν can at random take any value between minus $a/2$ and plus $a/2$ ($a = 1$ level) is the average of

$$\xi_\nu^2 = \frac{a^2}{12}$$

Hence

$$\varphi_2(0) = \frac{t_0}{T}\frac{a^2}{6} \tag{7}$$

Concentrating now on $\varphi_1(\nu T)$ it is evident that

$$\varphi_1(-\nu T) = \varphi_1(\nu T)$$

Hence the corresponding spectrum consists of

1. A constant

$$\frac{\varphi_1(0)}{\sqrt{2\pi}} = \frac{2}{\sqrt{2\pi}T} \int_{-\infty}^{-t_0} f^2(t)\,dt \tag{8}$$

2. Terms of the form $\cos \rho\omega$, which are the transform of symmetrical pulse pairs. The average in frequency of these terms is obviously zero. Finally the average distortion, of cross talk in all channels, is given by

$$D^2 = \frac{\frac{t_0}{6}\frac{a^2}{6} + 2\int_{-\infty}^{-t_0} f^2(t)dt}{\int_{-\infty}^{+\infty} f^2(t)dt} \tag{9}$$

The maximum of the distortion could be much greater at some particular frequencies.

Equation 9 indicates how D varies with the number of levels N. Assuming that $f(t)$ vanishes at infinity as $\frac{1}{t^p}$, then

$$a \approx \frac{1}{N}$$

$$t_0 \approx N^{\frac{1}{p}}$$

$$t_0 a^2 \approx N^{-2+\frac{1}{p}}$$

$$\int_{-\infty}^{-t_0} f^2(t)\,dt \approx \int_{-\infty}^{-t_0} \frac{1}{t^{2p}}dt$$

$$\approx N^{-2+\frac{1}{p}}$$

Thus

$$D^2 \approx N^{-2+\frac{1}{p}}$$

$$D \approx \frac{1}{N^{1-\frac{1}{2p}}}$$

Hence depending on the signal input, D will decrease with N at least as quickly as $\frac{1}{N^{1/2}}$ (since $p \geqq 1$), at most as rapidly as $\frac{1}{N}$. This last condition holds only for the signals which are not subject to time limiting. For the case of the test signal used in the paper, the distortion varies as $\frac{1}{N^{1/3}}$. Equation 9 of the discussion shows, more precisely, that

$$D = \frac{1}{2\sqrt{N}}$$

For $N = 10$ and $D = 15.8$ per cent, an average of the distortion in each channel, as calculated in the paper, gives 17.2 per cent.

It thus appears that the intuitive feeling that the signal considered was a difficult test for the system is justified, since this signal is one of those for which the distortion diminishes the less rapidly. The choice of the hardest signal to transmit as a test may not be the most satisfactory one in theory. If a test signal could be found, for which the distortion would be correlated precisely with the performance of the system when transmitting speech, it would obviously be a better choice. Since no such signal, however, has yet been proposed, it is thought that the best test is still the most difficult one.

Hydroelectric Power Development in Quebec

F. L. LAWTON
MEMBER AIEE

THIS paper presents a comprehensive picture of hydroelectric power development, transmission, and power loads in the province of Quebec, Canada.

Quebec, with an area of almost 600,000 square miles, is the largest province in the Dominion of Canada. Second only to Ontario in population and industrial development, it has no known deposits of coal or oil. Quebec owes its rapid industrial growth to its great hydroelectric power systems developed by private enterprise, although the government has made an important contribution through the work of the Quebec Streams Commission in constructing some important storage reservoirs.

Quebec's unique power development, of which not a single kilowatt of steam power is comprised, has, as its most prominent characteristic, one of the greatest hydroelectric power pools in the world, the 4,000,000-horsepower Montreal–Shawinigan–Saguenay interconnected system. It is also noted for its great electric-steam-generator load. However, there are many other unusual features, such as the notable Beauharnois, Isle Maligne, and Shipshaw developments, the Montreal 120-kv cable, the 220-to-165-kv series transformers forming the essential tie between the Saguenay and Shawinigan systems.

Paper 47-124, recommended by the AIEE committee on power generation for presentation at the AIEE summer general meeting, Montreal, Quebec, Canada, June 9–13, 1947. Manuscript submitted March 13, 1947; made available for printing April 11, 1947.

F. L. LAWTON is assistant chief engineer of the general engineering department of the Aluminum Company of Canada, Ltd., Montreal, Quebec, Canada.

The author wishes to acknowledge data and assistance furnished by W. G. C. Gliddon of the Gatineau Power Company, W. R. Way of the Shawinigan Water and Power Company, H. W. Haberl of Quebec Hydro-Electric Commission, H. R. Fee of Aluminum Company of Canada, Ltd., and D. Anderson of Southern Canada Power Company, Ltd.

Physiography

Generally speaking, Quebec is not a region of high relief. Principal topographic divisions are

The Laurentian plateau.
The St. Lawrence lowlands.
The Appalachian region.

The Laurentian plateau comprises the whole northern portion of Quebec, north of the St. Lawrence and Ottawa rivers, more than 90 per cent of the province. It is an extensive plateau with an uneven, undulating surface, varying between 800 and 2,000 feet above sea level, with a few peaks approaching 3,000 feet. On the north, the Laurentian plateau extends to Hudson Bay and Hudson Strait. The southern edge of the plateau roughly approximates a line joining the cities of Hull, Quebec, and Quebec, Quebec, and constitutes the north shore of the St. Lawrence estuary. The southern edge of this Laurentian plateau is ordinarily an escarpment some 300 to 800 feet high. From the strait of Belle Isle, between Newfoundland and the mainland, to Quebec, the foot of the escarpment is marked by the St. Lawrence gulf or river. From Hull, the foot of the escarpment lies along the Ottawa river for a considerable distance.

The surface of the plateau has broad undulations and is cut by many streams, large and small, with numerous lakes and swamps. A striking feature of the region is the generally disorganized drainage, which is extremely intricate and characterized by a plenitude of lakes. Most rivers consist of a succession of attenuated lakes connected by short stretches of fast water in the restricted channels through the barriers impounding the lakes. Many lakes are quite large with very irregular shorelines.

The Laurentian plateau is drained towards the St. Lawrence by 13 rivers over 100 miles in length, the Ottawa River being 685 miles long. Three tributaries of the Saguenay and four of the Ottawa are over 100 miles long. Toward Hudson Bay, 14 rivers over 100 miles long, of which six are 250 miles or longer, drain the plateau. Three rivers over 350 miles long drain the northerly slope of the plateau towards Hudson strait. Near the headwaters of these three groups of rivers the relatively ill-defined drainage will permit extensive diversions of water from one watershed to another, a feature which will ultimately permit a significant addition to the economically utilizable water powers of the province.

The St. Lawrence lowlands comprise the V-shaped plain which lies south of the Laurentian plateau and extends on either side of the St. Lawrence from the region of Quebec to the western boundary of the province, with an arm running up the Ottawa to somewhat west of Hull. The lowlands vary between 100 and 500 feet in altitude, except for some scattered hills rising 500 to 1,000 feet above the plain, at Montreal, Quebec and eastward. The lowlands with an area of about 15,000 square miles, constitute the principal agricultural area of Quebec.

The Appalachian highlands comprise the hilly region lying south of the St. Lawrence lowlands, with an area somewhat less than 40,000 square miles. It is the most rugged area of the province, Mount Jacques Cartier in Gaspé having an altitude of 4,160 feet, and numerous others over 3,500 feet. To the south, near the international boundary, several peaks are over 3,000 feet high.

While numerous streams drain the St. Lawrence lowlands and the Appalachian highlands on the south band of the St. Lawrence, there are only three rivers of any great significance, the Chaudiere, the St. Francis, and the

Figure 1. Geographic distribution of water powers in Quebec

Richelieu, of which latter only 75 miles lies in Quebec.[1]

Precipitation

Average annual rainfall in Quebec is about 36 inches, including snow, but varies moderately with location and altitude. It increases somewhat from the southwesterly to the northeasterly portions of the province, and is generally greater at the higher altitudes where the rivers originate. Average snowfall is about 100 inches, equivalent to 10 inches of rainfall, but varies sharply.

Run-off averages about 50 per cent of precipitation but ranges from 35 to 40 per cent in dry years to 70 per cent in very wet years.

Rainfall, temperature and other useful meteorological data are obtained from some 100 stations distributed throughout the province, the majority of these stations being in charge of power, industrial, and pulp and paper companies. Observers, properly instructed in the necessary procedures, record the data and transmit it to the Quebec Streams Commission who work in close co-operation with the Meteorological service of Canada. Some stations transmit daily weather data to the regional office of the

meteorological service at Dorval, Quebec, which forms the basis for the daily weather forecasts.

Runoff

Average yearly runoff from Quebec rivers is about 1.6 cubic feet per second per square mile of drainage area. This value varies, as previously noted, the average runoff for the Saguenay river being 1.86 cubic feet per second per square mile. Ordinary maximum runoff usually occurs in the spring; on the larger rivers, it varies from 6 to 10 cubic feet per second per square mile; on the smaller streams it ranges from 20 to 25 cubic feet per second per square mile. Minimum runoff usually takes place in March and varies from 0.25 to 0.40 cubic feet per second per square mile of drainage basin, depending on the characteristics of the watershed.

Much higher flood runoff has been noted, as for instance in 1924. On the Ste. Anne de la Perade River, a drainage area of 672 square miles developed a discharge of 43,000 cubic feet per second or 64 cubic feet per second per square mile. On the Ste. Anne de Beaupre river, a drainage area of 400 square miles produced a discharge of 32,000 cubic feet per second, or 80 cubic feet per second per square mile. On the other hand, the 1,400-square-mile Lake Kenogami watershed has a runoff of 20 cubic feet per second per square mile.

Beginning in 1913, systematic flow measurements of the principal rivers have been made, the establishment, observation, and maintenance of gauges being largely a co-operative undertaking on the part of power utilities and pulp and paper companies on the one hand and the Quebec Streams Commission on the other hand. Since 1922, stream measurements have been carried out by the Dominion Water Power Branch, which works in close co-operation with the Commission, so that fully co-ordinated data on river flow are available to interested parties.[2]

Table I. Water Powers of the Province of Quebec; Ordinary 6-Month Flow, 80 Per Cent Efficiency

River or Watershed	Water Power Capacity, Hp
St. Lawrence (Ontario boundary to Montreal)	2,340,000
Ottawa	1,602,505
Saguenay	1,534,008
St. Lawrence tributaries, north shore	3,819,881
St. Lawrence tributaries, south shore	303,598
Total, St. Lawrence watershed	**9,599,992**
James Bay	2,445,287
Hudson Bay	500,669
Total, Hudson Bay watershed	**2,945,956**
Ungava	521,800
Chaleur Bay	4,534
St. John	267
Total, Province of Quebec	**13,072,549**

Water Powers

The water powers of Quebec, based on ordinary six months flow, and 80 per cent efficiency, total about 13,073,000 horsepower geographically distributed as shown by Figure 1. Table I is a tabulation of water powers available on each of the major watersheds.

Estimates of power on the basis of ordinary six months flow are made upon the assumption that it is good commercial practice to provide an installation of such capacity that continuous operation can be assured six months in the year, with the deficiency in output during the remainder of the year provided from storage, from interconnection with other plants on rivers of different regimen, or operating under different load conditions, or even parallel operation with fuel-burning power plants. Naturally, in evaluating the possibilities of any potential development, careful consideration must be given to all factors pertinent to the particular site or sites. An analysis of Canadian practice shows that, on the average, the usual water wheel installation has a capacity of 1.3 times that corresponding to the ordinary six months flow.[3]

In Quebec, principal reliance has been placed on storage for optimum development of power from a given site or sites on a specific river, with interconnection with other systems next in importance. There are no fuel-burning plants associated with Quebec's hydroelectric power systems.

Developed water powers, as at January 1, 1946, totalled 5,848,572 horsepower installed capacity, 57 per cent of the Canadian total and well over twice that for Ontario,[4] as indicated by Figure 2. This installed capacity is equivalent to 1,643 horsepower per 1,000 population. It is distributed as follows:

Central electric stations for general public service, central electric stations for pulp and paper industries, central electric stations for electrochemical, and electrometallurgical industries ..... 92.96 per cent

Other uses, such as direct-connected pulp grinders ..... 7.04 per cent.

Developed water powers in Quebec fall into several major groupings, as follows, aside from scattered plants some of which are of considerable size

Gatineau River.
Lievre River.
Ottawa River.
Saguenay River.
St. Lawrence River.
St. Maurice River.

Table II sets forth power developments on these rivers, the upper plant on a river being given first. It will be noted the total power development on these six power rivers is 5,388,423 horsepower, some 92.1 per cent of the total hydroelectric power development in Quebec.

Storage

Storage is essential to optimum development of practically all water powers in Quebec, with the exception of the St. Lawrence which is endowed with a remarkably uniform flow due to the great natural storage of the Great Lakes. Although the flow of Quebec rivers is

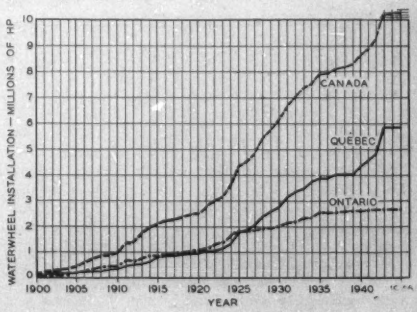

Figure 2. Installed water wheel capacity in Ontario, Quebec, and Canada

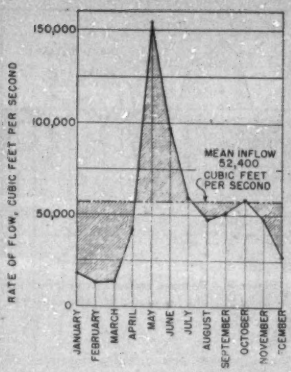

Figure 3. Average monthly inflow into Lake St. John for years 1913 through 1941

not flashy, it drops to a low value during the months of December to March or April and reaches flood stage during May and June. Occasionally, the discharge reaches a high value in October or November, following heavy fall rains.

The Saguenay River may be taken as a typical example. The natural flow ranges from a minimum low of 6,000 cubic feet per second to a maximum high of some 327,000 cubic feet per second.

Figure 3, which indicates the variation in average monthly flow, and Figure 4, showing the year-to-year variation in average flow, demonstrate the necessity for storage on the Saguenay. The average flow, as recorded over 34 years, is 52,600 cubic feet per second.

Storage in Lake St. John, developed by the construction of the first power plant on the Saguenay, provided a regulated flow of 28,000 cubic feet per second. This was increased to a minimum of 42,500 cubic feet per second, six years out of seven, by the construction of storage dams at Lake Manouan and Passe Dangereuse on the Peribonca River, with 78.5 and 183 billion cubic feet usable storage, respectively, as part of the Shipshaw power development, during World War II. Total storage of about 400 billion cubic feet in Lake St. John, Lake Manouan, and Passe Dangereuse reservoirs thus permits utilizing about 86 per cent of the average available water for firm power, as contrasted with about 15 per cent under natural conditions.

Major storage reservoirs, on the principal power rivers in Quebec, are located as in Figure 5. Some of the significant details appear in Table III.

Storage reservoirs in Quebec fall into three categories

1. Those built and operated by the Quebec Streams Commission.

2. Those built by power companies and operated by the Quebec Streams Commission.

3. Those built and operated by power companies.

In the case of storage reservoirs built and operated by the Commission, power companies benefiting from the additional flow provided must pay for such. The unit price is the same for all interests on the one river but varies from river to river. This unit price assessed by the Commission is based on the yearly amount needed to meet interest charges on invested capital, amortization charges on a term of years varying with type of dam or dams, and the cost of operation and maintenance, at a fixed value per horsepower-year.

While a number of storage dams have been built by the Quebec Streams Commission, and the capital cost paid by the Commission, some dams have been built at the request of power companies, under the supervision and control of the commission and at the expense of these companies. The benefiting companies, instead of having to reimburse the capital cost of the storage works by yearly installments covering the interest and sinking fund, undertook to pay at once the capital cost. The annual charges of the Commission are then limited to the cost of operation and maintenance of the dam, and a fixed amount to cover the privilege of flooding Crown lands when such are affected.[5]

Operating experience with large storage reservoirs located 150 to 200 miles or more from the power plant or plants at which the water is used shows very small losses of storage water in the form of ice,

Table II. Hydroelectric Generating Stations on Principal Power Rivers in Quebec

River	Station	Total Installed Waterwheel Capacity, Hp	Number of Units	Head, Ft	Type of Runner	Remarks
Gatineau	Paugan	238,000	7	132	Francis	Ultimate 476,000 hp, 25 cycles
	Chelsea	170,000	5	93	Francis	25 and 60 cycles
	Farmers	120,000	5	66	Francis	25 and 60 cycles
Lievre	High Falls	120,000	4	181	Francis	
	Electric Reduction Company	8,000		30		
	Buckingham	19,254		64		Partly direct-connected pulpwood grinders; partly hydroelectric
	Masson	136,000	4	194	Francis	25 cycles
Ottawa	Rapid 7	48,000	3	70	Francis	25 cycles
	Bryson	51,400	10	60		
	Chats Falls	224,000	8	38–58	Propellor	25 cycles, rated 28,000 hp at 53 ft
	Chaudiere Falls	107,419				Several developments
	Back River (Riviere des Prairies)	65,000	6	18–26	Propellor, manually adjustable blades	
Saguenay	Isle Maligne	540,000	12	110	Francis	
	Shipshaw number 1	300,000	4	155	Francis	Also known as Chute-a-Caron
	Shipshaw number 2	1,200,000	12	208	Francis	
St. Lawrence (in Quebec)	Cedar Rapids	206,400	18			
	St. Timothe	28,800	4			
	Beauharnois	675,600	13 at 53,000 hp			Six 25- and seven 60-cycle generators
			2 at 7,800 hp	80	Francis	2,000,000-hp ultimate
St. Maurice	Rapide Blanc	200,000	5	112	Francis	
	La Tuque	222,500	5	114	Francis	
	Grand 'Mere	201,000	9	80	Francis	
	Shawinigan Falls number 1		6			
	Shawinigan Falls number 2	280,000	8	145	Francis	
	Shawinigan Falls (Misc)	55,050		145	Francis	Horizontal d-c generators and pulp grinders
	La Gabelle	172,000		60	Propellor	

despite the rigorous winter conditions in the Quebec hinterland, where the temperature may drop below minus 40 degrees Fahrenheit for two or three day, and frequently falls below minus 30 degrees Fahrenheit for a week or so.

Development of Water Power

The early history of hydroelectric development in Quebec is characterized by the construction of isolated plants at favorable sites close to power markets or where markets could be developed. As markets expanded, what may be conveniently termed "river developments" came into being. These river developments entailed a fully co-ordinated program of construction for an entire river, embracing both power plants and storage.

Typical of these river developments are the Gatineau, Lievre, Saguenay and St. Maurice systems. The Ottawa and the St. Lawrence, while they will be fully exploited ultimately, do not present the same degree of co-ordination, due to the multiplicity of interests involved.

In the newer, relatively undeveloped areas of Quebec there are isolated plants, of best modern design, serving newsprint and mining industries. One such power development is that at Outardes Falls on the Outardes river, near tidewater on the north shore of the Gulf of St. Lawrence, which serves a large newsprint mill at Comeau Bay. The Outardes Falls plant contains two Francis-type water wheels developing 35,300 horsepower each at 208 feet normal net head.[6]

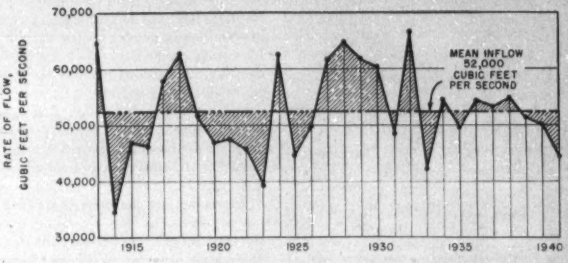

Figure 4. Average annual rate of inflow into Lake St. John for years 1913 through 1941

Gatineau River

The Gatineau River was unimproved until 1925, in which year a comprehensive scheme of power development embracing the Paugan, Chelsea, and Farmers plants was put in hand. The 2,181,000-acre-feet Lake Baskatong storage reservoir was completed in the spring of 1927, and was followed by the 1,033,000-acre-feet Lake Cabonga reservoir, tributary to the Baskatong reservoir, in 1929. These storages provide at Paugan a regulated flow of 10,000 cubic feet per second, as compared with 3,000 cubic feet per second average low water, and make economically feasible the co-ordinated development of 562,000 horsepower,[6] of which 528,000 horsepower is now installed.

Lievre River

Prior to 1928, the only power development on the Lievre River was at Buckingham. Water wheels with a capacity of about 6,600 horsepower, later increased by two 5,650 horsepower units, under a head of about 64 feet, drive direct-connected pulpwood grinders and provide electric power for the groundwood pulp mill of the James Maclaren Company, Ltd. Just above this plant is the 8,000-horsepower development of the Electric

Table III. Major Storage Reservoirs on Principal Power Rivers in Quebec

River	Storage Reservoir	Depth of Storage, Ft	Useful Storage Acre-Ft	Minimum Natural Flow, Cfs	Regulated Flow, Cfs	Maximum Natural Flow, Cfs	Watershed, Sq Miles: Above Control Point for Regulated Flow	Watershed, Sq Miles: For Minimum Natural Flow
Gatineau	Lake Cabonga		1,033,000					
	Lake Baskatong		2,181,000	3,000	10,000	75,000[a]		9,100[a]
Lievre	Mitchenamekus		450,600*					
			419,200†					
	Cedar Rapids		661,000*		4,000[b]		3,350[c]	2,890[d]
			560,000†					
Ottawa	Lake Dozois (under construction)		1,515,200					
	Rapid 7		390,300		5,600[e]			
	Lake Quinze-Expanse	11.5	992,000					
	Lake Timiskaming	11.0	826,500					
	Lake Kipawa	8.4	562,400	12,000	20,000[f]			
Saguenay	Lake Manouan	21.0	1,802,000					
	Passe Dangereuse	110.0	4,201,000					
	Lake St. John	12.0	3,180,000					
St. Lawrence (in Quebec)	Natural Great Lakes			16,000	241,000[g]	290,000[g]		275,000
St. Maurice	Gouin	45.0	6,440,000	5,800[h]	20,000[h]	172,000[h]		
	Manouane	10.0	567,000					
	Mattawin	60.0	776,000					

[a] At Paugan
[b] 97% of time
[c] High Falls
[d] Cedar Rapids
[e] At Rapid 7
[f] At Chaudiere Falls
[g] Average
[h] At Shawinigan

* Ultimate
† Present

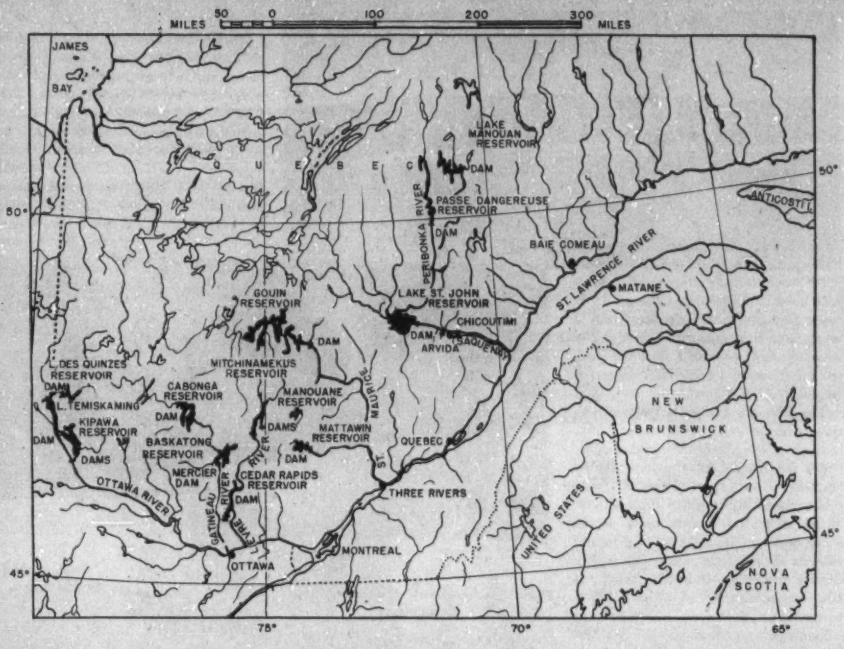

Figure 5. Major storage reservoirs on principal Quebec power rivers

Reduction Company with a head of about 30 feet.

In 1928, the James Maclaren Company put in hand the construction of a newsprint mill with a daily capacity of 250 tons, at Masson, Quebec. To meet the power requirements of this mill, the High falls power development (120,000 horsepower, 181 feet head) was begun in October 1928, by the Maclaren-Quebec Power Company, a subsidiary of James Maclaren Company. This plant went into service in August 1930. The Masson development was started in 1931 and put into operation in 1933. It has a capacity of 136,000 horsepower under 194 feet head. The plant is characterized by the 25-foot diameter tunnel well over a mile in length needed for concentration of head.

The Lievre, with a watershed of some 3,350 square miles above High Falls, could only sustain the High Falls and Masson plants by the provision of 560,000 acre-feet of storage in the Cedar Rapids reservoir, construction of which was commenced in October, 1928, and completed in June, 1930. This storage will provide a flow of 4,000 cubic feet per second or better at High Falls for 97 per cent of the time, with 5,000 cubic feet per second for more than 40 per cent of the time. The reservoir capacity will eventually be increased to 661,000 acre-feet.[7]

The Mitchenamekus reservoir in the upper basin of the Lievre river, was completed in 1942. With a useful storage of 419,200 acre-feet, which will ultimately be increased to some 450,600 acre-feet, the minimum regulated flow at Buckingham is increased by 700 cubic feet per second in normal years and by 400 cubic feet per second in dry years equivalent to a total of 36,400 horsepower for all existing power plants on the Lievre.

Ottawa River

The Ottawa River, over the greater part of its course, constitutes the interprovincial boundary between Ontario and Quebec and as such its water powers are divided between the two provinces. With an estimated capacity at ordinary six months flow and 80 per cent efficiency of some 1,310,510 horsepower, only about 401,000 horsepower capacity is as yet installed, of which about 239,800 horsepower is in Quebec. These figures do not include power on the Back River (Riviere des Praires), one of the mouths of the Ottawa, which lies entirely in Quebec, where the Montreal Island Power Company (now operated by Quebec Hydro-Electric Commission) has a 65,000-horsepower development. This plant operates under a head of 18 to 26 feet, and has an estimated continuous output of 40,000 horsepower.

Storage on the upper Ottawa river consists of the Lake Quinze-Expanse, Lake Timiskaming, and Lake Kipawa reservoirs, with a total capacity of some 2,380,900 acre-feet. These storages were originally constructed to facilitate navigation on the Ottawa, and increase the flow of the Ottawa at Chaudiere Falls from 12,000 cubic feet per second minimum under natural conditions to 20,000 cubic feet per second during low-water periods. Present storage of 390,300 acre-feet above Rapid 7 power plant and 1,515,200 acre-feet in the Lake Dozois storage reservoir, now under construction, will provide a regulated flow of about 5,600 cubic feet per second at the power plant instead of the existing 3,600 cubic feet per second.

In addition the Gatineau and Lievre river storages contribute to the low-water flow of the lower Ottawa river.

Saguenay River

The Saguenay hydroelectric power system consists of two separate power developments utilizing the full head available on the Saguenay River between Lake St. John and tidewater. With a useful storage capacity in Lake St. John and two headwater storages on the principal tributary of the lake, the Saguenay River watershed of some 30,000 square miles provides these power developments with a minimum regulated flow of 42,500 cubic feet per second six years out of seven, and an average minimum of 46,000 cubic feet per second, from the mean run-off of some 52,600 cubic feet per second.[8]

The first or up-river development is that of Saguenay Power Company, Ltd., located at Isle Maligne, about 9 miles below the Grand Discharge outlet of the Saguenay River from Lake St. John. When placed in service in 1925, with an initial eight units each rated 45,000 horsepower at 110 feet head, Isle Maligne was one of the largest single-stage hydroelectric power plants in the world. It now has a capacity of 540,000 horsepower.[9]

Figure 6 is an aerial view of Isle Maligne power plant.

The second or down-river power development, owned by Aluminum Company of Canada, Ltd., was constructed in two steps. Shipshaw number 1, sometimes called Chute-a-Caron, was placed in service in 1931. It has a capacity of 300,000 horsepower at 155 feet head, in four units.

One of the outstanding features of this plant was the use of a precast dam or obelisk, built on end and blasted into place to effect final closure of the cofferdam across the main river channel.[10]

Construction of the second stage Shipshaw number 2, began early in 1941. The first unit went into service November 23, 1942, and the twelfth and last on December 24, 1943. Taking its water from the same forebay as Shipshaw number 1, Shipshaw number 2 has a capacity of 1,200,000 horsepower at 208 feet head.

Probably the most outstanding feature of Shipshaw number 2 was the speed with which it was constructed and placed in service, at a time when Canadian manufacturing resources were geared to the production of war material for the United Nations. However, there are other outstanding features to which brief reference will be made later, such as the high water wheel efficiency, and welded scroll-cases.[11, 12]

Figure 7 is an aerial view of the complete Shipshaw power development while Figure 8 is an interior view of the generator room.

Canadian Pacific Air Lines Limited

Figure 6. Aerial view of Isle Maligne power development

Capacity is 540,000 horsepower at 110 feet head

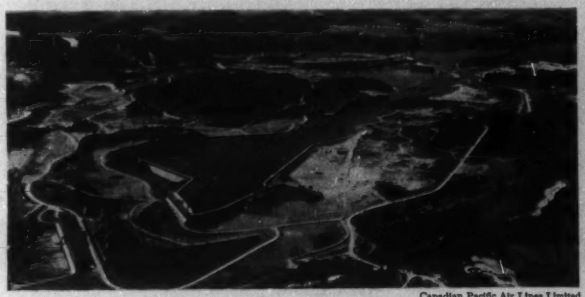

Canadian Pacific Air Lines Limited

Figure 7. Aerial view of Shipshaw power development

Shipshaw number 1 (Chute-a-Caron) seen in background has a capacity of 300,000 horsepower at 155 feet head. Shipshaw number 2 in left foreground has a capacity of 1,200,000 horsepower at 208 feet head

St. Maurice

The St. Maurice River which enters the St. Lawrence at Three Rivers, Quebec, has a drop between headwater and tidewater at the mouth of 1,325 feet, of which 1,125 feet is comprised in ten distinct falls and the remainder in various rapids. As it has a watershed of about 16,000 square miles, with a minimum natural flow of 5,800 cubic feet per second, a maximum discharge of 172,000 cubic feet per second, and a mean average flow of 25,600 cubic feet per second at Shawinigan Falls, it has great power possibilities.

The average annual run-off corresponds to about 22 inches of precipitation, some 61 per cent of the average annual precipitation of about 36 inches. Range is from a minimum annual precipitation of 26 inches to a maximum of 46 inches.

The initial power development on the St. Maurice was that at Shawinigan Falls, put under construction in 1900. By 1928, the plants at La Gabelle, Shawinigan, and Grand 'Mere utilized 285 feet of the total of 326 feet of head available on the lower St. Maurice. These are all operated by Shawinigan Water and Power Company. Figure 9 is an aerial view of the 172,000-horsepower 60-foot head La Gabelle plant.

The initial storage development on the St. Maurice river was constructed in 1908 on the tributary Manouane River. Its location relative to the power plants on the lower St. Maurice is shown by Figure 10, as are later storage reservoirs and power plants.[13]

Operation of this initial storage reservoir demonstrated that no appreciable loss of stored water, in the form of ice, occurred when impounded water in storage reservoirs more than 200 miles away from the power plant was released under the severe winter weather con-

ditions of the hinterland, even though the river characteristics are as favorable to the formation of frazil as the St. Maurice.

The Manouane storage was followed by the construction of the great Gouin reservoir by the Quebec Streams Commission in 1918. This storage reservoir, with a capacity of 6,440,000 acre-feet is one of the world's greatest. It provided a regulated flow of 16,000 cubic feet per second at Shawinigan Falls, almost three times the previously available flow of 5,800 cubic feet per second.

The Mattawin storage reservoir with a useful capacity of 757,600 acre-feet was constructed in 1931. Regulated flow of the St. Maurice at Shawinigan Falls is now 20,000 to 22,000 cubic feet per second, some 86 per cent of the mean average flow.

Canadian Pacific Air Lines Limited

Figure 9. La Gabelle power plant, with a capacity of 172,000 horsepower at 60 feet head

Figure 8. View of generator room in Shipshaw number 2 power plant

The Rapide Blanc power development on the upper St. Maurice, with a capacity of 200,000 horsepower at 112 feet head, was placed in service in 1934. Figure 11 is an aerial photograph of this plant, looking upstream. It was followed by the La Tuque plant of St. Maurice Power Corporation with a capacity of 222,500 horsepower at 114 feet head, a joint undertaking of Shawinigan Water and Power Company and Brown Corporation, the latter operating an extensive newsprint and pulp mill at La Tuque.[14]

The St. Maurice river thus presents, in somewhat less than 50 years, a coordinated river development, with an installed water wheel capacity of some 1,130,550 horsepower and a regulated flow of 3.5 times the minimum natural flow.

Beauharnois

Reference has already been made to two notable power developments in Quebec, those at Isle Maligne and Shipshaw. Another outstanding hydroelectric plant is that at Beauharnois, Quebec.

This development, located less than 25 miles from Montreal, when completed will have a capacity of 2,000,000 horsepower in one station, operated as a single unit. It will probably become and remain for a long time the largest hydroelectric station in the world, although it may be ultimately surpassed by the projected development in the Yangtze-Kiang gorge, in China.

The complete station, about 3,000 feet long, is supplied by a diversion canal about 15.5 miles long, taking water from Lake St. Francis on the St. Lawrence River, with the 3-part tailrace discharging into Lake St. Louis. The diversion canal is an integral unit of the projected St. Lawrence Seaway. Navigation locks will be constructed at the Lake St. Louis end of the canal. Control works at the head of Coteau Rapids regulate the flow and maintain the level of Lake St. Francis.

Between Lake St. Francis and Lake St. Louis there is a fall of 83 feet. Average mean flow of the St. Lawrence is 220,000 cubic feet per second, with maximum and minimum recorded flows of 318,000 and 160,000 cubic feet per second, respectively, in the past 85 years.

The canal is planned to carry the ultimate diverted flow of 220,000 cubic feet per second with a width of 3,000 feet.[15]

In addition to two 7,800-horsepower station service units, there are at present seven 53,000-horsepower 60-cycle units serving the Montreal load area and six 53,000-horsepower 25-cycle units tied in over 220-kv lines with the system of the Hydro-Electric Power Commission of Ontario. The eight 60-cycle unit is now being installed.

Figure 12 is a general view of the Beauharnois power development, constructed by the Beauharnois Light, Heat and Power Company and operated as a publicly-owned property by the Quebec Hydro-Electric Commission. Figure 13 is a general plan of the development.

Growth of Hydroelectric Power Development

The growth of water-power development in Quebec has been well maintained since the early days of the century when there were only a few scattered plants of small capacity. This trend is exemplified by Figure 14. Note also the improvement in load factor since 1900.

Loads

Aside from general industrial, commercial, and domestic load in the metropolitan Montreal area, Ottawa-Hull district, Quebec, Three Rivers, and a few other manufacturing communities, the extensive development of water power in Quebec shown by Figure 14 is attributable to the rise of newsprint and associated manufactures, and, in the Saguenay area, aluminum production

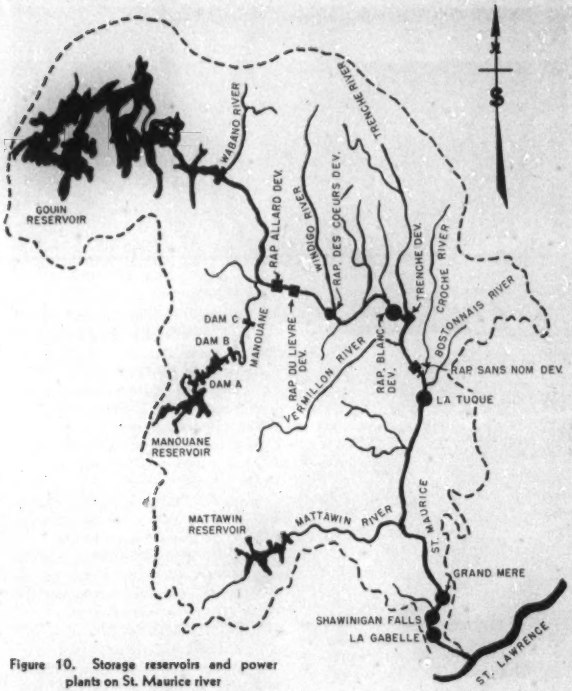

Figure 10. Storage reservoirs and power plants on St. Maurice river

■—Potential power development on upper St. Maurice

●—Power plant

as well. Expert of power to Ontario has also played a substantial part during the last quarter century.

The Gatineau Power Company system in Quebec, the backbone of which is constituted by the Gatineau river plants, supplies a very large newsprint and other wood-products load, in addition to which a very substantial block of 25-cycle power is transmitted at 220 kv to the Toronto, Ontario, area. The present system yearly peak demand is 445 megawatts. Installed electric-steam-generator capacity is 180 megawatts. The typical daily firm-power load characteristic is illustrated by Figure 15. Annual load factor is about 67 per cent.

The Lievre developments of the Maclaren-Quebec Power Company supply, for the greater part, the newsprint industry and export a large block of 25-cycle power at 220 kv to the Toronto area.

of Ontario, aside from a 60-cycle block fed through a frequency changer to their eastern Ontario system.

The Saguenay system load consists of aluminum-smelting and paper-mill loads and an excellent though relatively small general public service. The system primary load comprises a peak demand of 900 megawatts for aluminum production, 100 megawatts for pulp and paper, and a block of 75 megawatts transmitted to the Shawinigan system over tie *A*, a feature which will be discussed briefly later under the heading of "Interconnection." During World War II, approximately 83 per cent of the aluminum load was converted to direct-current power by mercury-type rectifiers and 10 per cent by synchronous converters. Daily system load factors are in the vicinity of 95 per cent.

During periods of high and normal river flow or when aluminum production is below full capacity, loads up to 375 megawatts are supplied to electric steam generators.[16]

In 1946, the gross generation on the Saguenay system was 8,665,167,000 kilowatt-hours, with a 60-minute peak of 1,233 megawatts.

The Shawinigan area, comprising the territory on both sides of the St. Lawrence river from Montreal to Murray Bay, some 80 miles below Quebec, is, as previously noted, the greater part of the St. Lawrence lowlands, lying between the Laurentian plateau and the Appalachian region. It is not only the principal agricultural area of Quebec but contains a wealth of diversified light and heavy industrial undertakings. This area is served mainly by the Shawinigan Water and Power Company, the Quebec Power Company, and the Southern Canada Power Company.

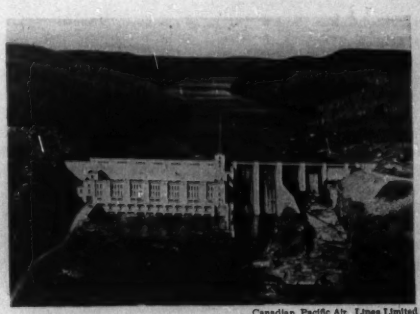

Figure 11. Aerial view of 200,000-horsepower 112-foot head Rapide Blanc power plant

Canadian Pacific Air Lines Limited

While most of the smaller water power plants on the Ottawa River furnish power for newsprint and associated manufactures, the Quinze and Rapid 7 power developments supply the mining districts near-by. The output of the 224,000 horsepower Chats Falls plant goes entirely to the 25-cycle Toronto system of the Hydro-Electric Power Commission

Figure 12. Beauharnois power station

The Shawinigan system firm load comprises paper mills, aluminum reduction and fabrication, carbide and carborundum manufacture, asbestos mines and mills, and a few specialty steel plants. Approximately 25 per cent of the load is distributed to urban and rural areas. System week-day load factors run about 92 per cent, with an annual load factor under prewar conditions of 71 per cent.

During flush-water periods, considerable secondary power is generated and purchased from interconnected power systems for use in electric steam generators supplying process steam to paper mills. As much as 500,000 horsepower peak of such secondary power has been sold to paper mills, thus replacing very substantial amounts of coal-produced steam.

Gross generation and purchased energy on the Shawinigan system in 1946 was 7,515,010,778 kilowatt-hours, with a maximum system load peak of 1098.6 megawatts on the combined 30-cycle and 60-cycle systems. Only a very limited part of the system is supplied at 30 cycles. Figure 16 shows typical summer and winter week-day prime load curves.

The Montreal area is supplied from the Beauharnois, Cedars Rapids, and St. Timothé plants on the St. Lawrence, the Back River plant on the Ottawa, and over four 110 kv lines from Shawinigan Falls, 90 miles away. The type of load is typical of any large metropolitan area, having a week-day load factor during winter of about 68 per cent. The prewar annual load factor was about 47.5 per cent. The annual peak occurs in November or December. The peak load tapers off noticeably during the summer. This characteristic is clearly shown by the typical summer and winter week-day firm load curves of Figure 17.[17]

During 1946, gross generation of the Montreal system of the Quebec Hydro-Electric Commission was 4,412,342,000 kilowatt-hours, purchased energy being 729,332,000 kilowatt-hours. System peak load was 809.54 megawatts.

Transmission Networks

As most power stations in Quebec are relatively remote from the load areas, quite extensive transmission networks are necessary for the transmission of power. Practically all lines are 220, 154, 110, or 60 kv. Overhead construction is usual, except in the Montreal area where 60 and 120 kv underground cables are used.

Steel towers are used for the 220-, 154-, and 110-kv lines. Wooden structures are used quite extensively for the 60 kv lines, although a considerable portion of the total circuit mileage is carried on steel towers or poles. Double-circuit construction is quite customary, except for the 220-kv lines and where limited load requirements obviate the necessity of the additional circuit.

In general, overhead lines are designed for 1/2-inch ice and 8-pounds-per-foot wind loading at 0 degrees Fahrenheit. Occasional bad sleet storms occur but

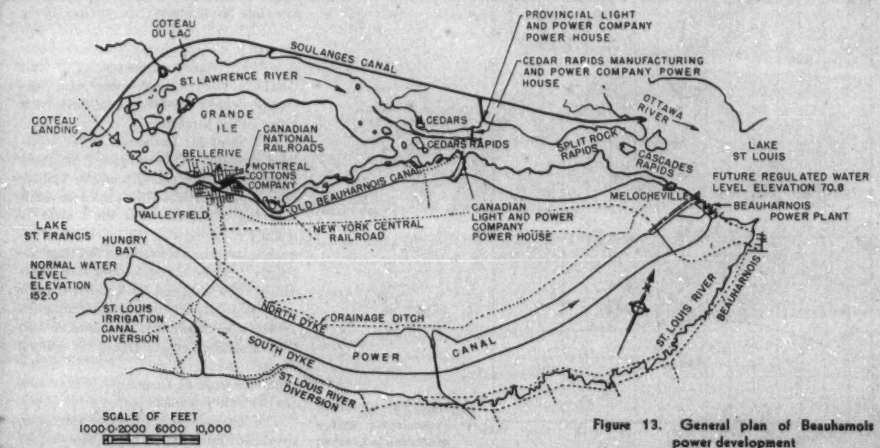

Figure 13. General plan of Beauharnois power development

are not frequent. Ground wires are usually provided, for shielding against direct strokes, and buried counterpoise is being more widely used, due to the high earth resistivity of much of the area traversed by overhead lines. This high resistivity arises from the rocky nature, exposed or covered by shallow overburden, of much of Quebec. This feature makes for relatively expensive and unsatisfactory counterpoise installations, inasmuch as the counterpoise conductors cannot be easily buried sufficiently deep to be free from disturbance.

However the frequency of lightning storms is moderate, ranging from about 17 per year in the Saguenay area to about 40 per year on the more exposed transmission links of the Shawinigan system.

By far the greater part of all transmission lines in Quebec have aluminum-cable steel-reinforced conductors, with armor rods on the newer circuits where the conductors are strung to the higher tensions. Compression-type joints are used almost universally.[18,19]

The most unusual overhead-line constructions in Quebec are the long St. Lawrence river crossings of the Shawinigan Water and Power Company and the Quebec Hydro-Electric Commission.

One of these crossings is that at Kanawake-LaSalle, Quebec, on the double-circuit 132 kv, 30-mile steel-tower transmission line on the south bank of the St. Lawrence river, which ties in Beauharnois and Cedars Rapids power plants with the Montreal system. The main span, which is 3,493 feet long, with a clearance of 86 feet above the water, is carried on 322.5 feet suspension towers. The adjacent 595.4 feet and 905.4 feet spans terminate on 90-feet high anchor towers.

The conductor used is 619,000-circular-mil aluminum-cable steel-reinforced, composed of 42 0.1214-inch aluminum strands and 19 0.1214-inch steel strands. It has a diameter of 1.093 inches and an ultimate strength of 46,800 pounds. Maximum tension is 23,400 pounds under 1/2-inch ice, 8-pound wind, at 0 degrees Fahrenheit. Two ground wires having the same characteristics as the line conductors are used. These ground wires, which are insulated, can be used in emergency for replacement of a defective phase conductor. The full details of how this crossing span was strung, despite the fast water, have been given in the literature.[20]

The Sorel–St. Lawrence River overhead crossing of Shawinigan Water and Power Company consists of two 110-kv circuits on towers 375 feet high, each weighing 234 tons. The main span is 3,950 feet long, and the back spans to anchor towers are each 1,740 feet in length. Three 1.5-inch plow-steel messenger cables, spaced 50 feet apart, each carry two 266,800-circular-mil aluminum cables, steel reinforced, 26 aluminum and 7 steel strands, which cables are spaced 10 feet apart. Nine 4.75-inch insulator units are used at suspension points and ten at strain positions.

The Three Rivers St. Lawrence river overhead crossing, of the Shawinigan

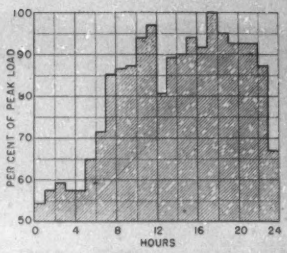

Figure 15. Typical daily firm power load curve of Gatineau Power Company

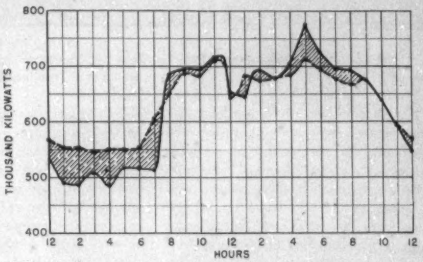

Figure 16. Typical week-day prime-load curves for Shawinigan Water and Power Company and St. Maurice Power Company combined

---- Typical summer week-day prime-load curve

—— Typical winter week-day prime-load curve

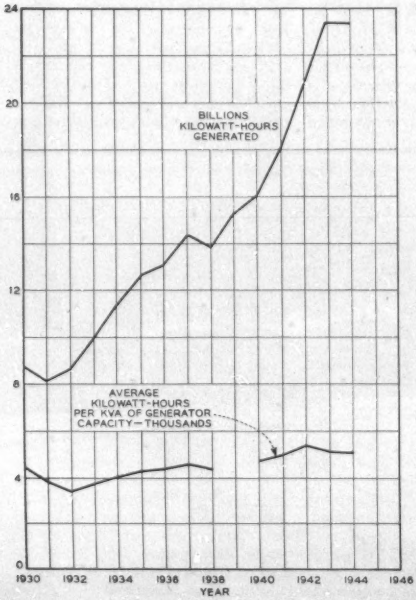

Figure 14. Growth of hydroelectric energy generation in Quebec

Water and Power Company, carries two 110 kv circuits (one presently operated at 60 kv) on towers 350 feet high, each weighing 178 tons. The main span is 4,801 feet, and the back spans are 560 and 981 feet in length. Three 1.375 inch plow-steel messenger cables, spaced 50 feet apart, each carry two power conductors separated 10 feet apart and supported at 13 points on the messenger. The conductors are 167,800-circular-mil diameter with six aluminum strands over one steel strand. Seven 4.75-inch insulators are used for suspension and eight for strain positions.

The Quebec St. Lawrence river overhead crossing of Shawinigan Water and Power Company, constructed for 110-kv service but presently operated at 60 kv, comprises two 200-foot towers carrying the main span of 3,415 feet. The back spans to the 83 feet high anchor towers are 1104.9 and 991.8 feet in length. The conductors have a horizontal configuration, being spaced 24 feet apart. Each conductor consists of 37 strands of extra-high-strength copperweld. There are two insulator strings per yoke, with seven 5.75-inch units per string, for suspension points, and three strings per yoke, each string with eight similar units, for strain positions.

Prior to World War II, the Montreal area was served by a 60-kv double-ring transmission network, mostly overhead construction but with important underground cable links. The close linking of the Montreal, Shawinigan, and Saguenay systems during the war, in order to utilize to the fullest possible extent all the energy resources of the combined systems for the production of aluminum, was, in part, accomplished by the installation by the Aluminum Company of Canada, of a 115-kv oil-filled underground cable about 34,600 feet long running through Atwater, Guy, and Terminal Stations 2 and 3. This cable operates in

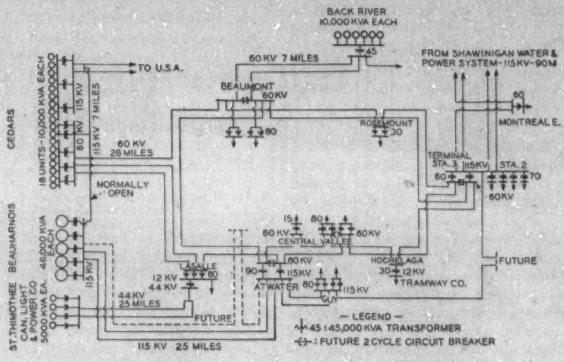

Figure 18 (above). Montreal system diagram

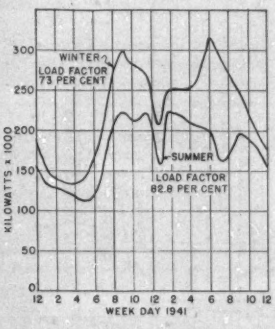

Figure 17. Typical 1941 summer and winter week-day firm-load curves, Montreal system

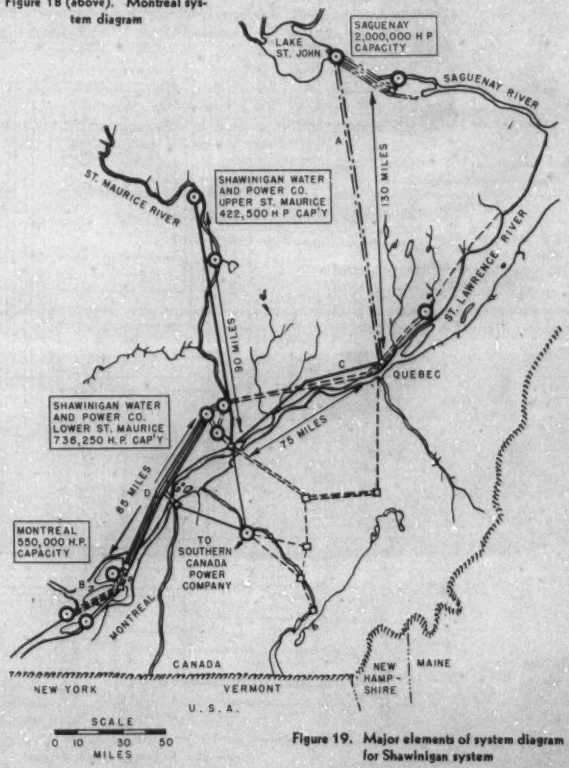

Figure 19. Major elements of system diagram for Shawinigan system

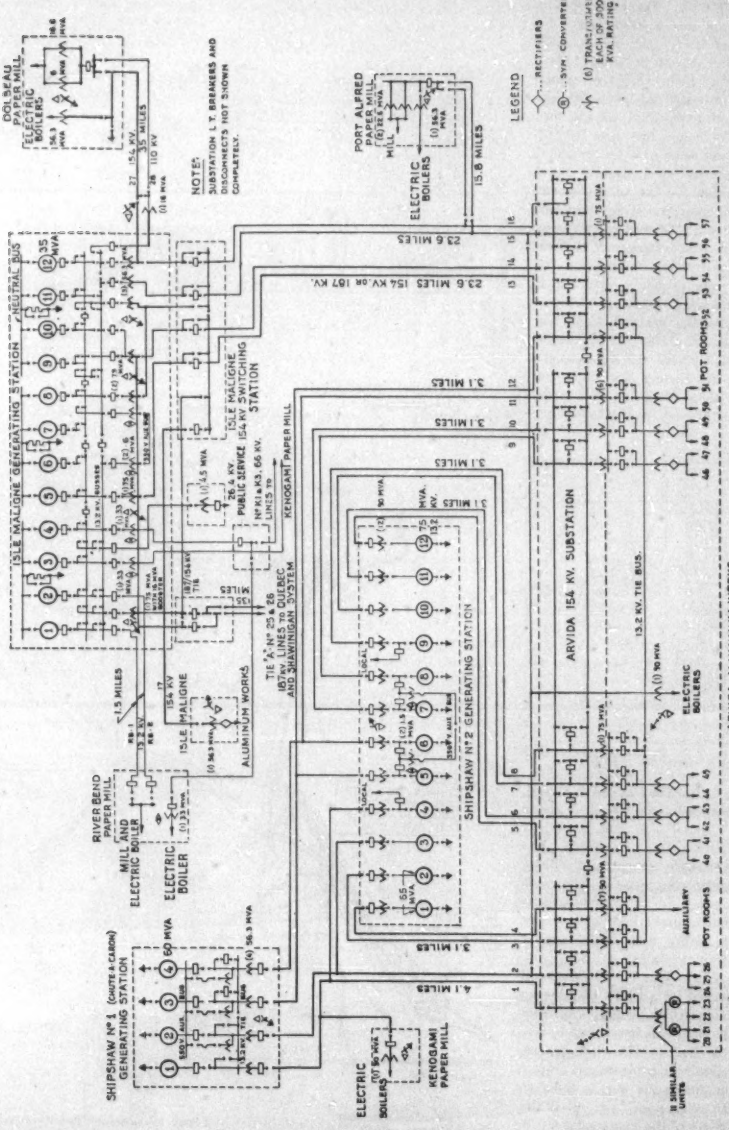

Figure 20. Saguenay system diagram

parallel with the 60-kv ring between Atwater substation and Beauharnois on the west, and Terminal Stations 2 and 3 and the Shawinigan system on the east. This 115-kv cable, installed between May 1940, and December 1941, eliminated the bottleneck, imposed by the Montreal 60-kv ring and load requirements, to maximum utilization of Beauharnois energy in the Saguenay area via the Shawinigan system.[17,21]

The system diagram of the Quebec Hydro-Electric Commission (now operating the Montreal Light, Heat and Power Consolidated) power network serving the Montreal area is shown by Figure 18. Major elements of the Shawinigan system are given in Figure 19. The power network of the Saguenay system is shown by Figure 20.

Major elements of the principal power system in Quebec which is not interconnected with the Montreal, Shawinigan and Saguenay systems is that of the Gatineau Company which is shown by Figure 21.

Interconnection

It has long been recognized by system engineers of Quebec power utilities that there are many advantages in interconnected operation with adjacent systems, such as

1. Better regulation of load, frequency, and voltage.
2. Optimum utilization of surplus energy.
3. Lower total reserve generating capacity requirements.
4. Full advantage can be taken of diversity in loads and hydraulic conditions.
5. Additional generating capacity can be added at the most economical location, considering the interconnected system as a whole, and to a lower total than if added to the component systems.
6. Equipment maintenance can be scheduled to better advantage.

The interconnected 60-cycle hydroelectric systems of the Saguenay Power Company, the Aluminum Company of Canada, The Shawinigan Water and Power Company, and Quebec Hydro-Electric Commission, with a combined capacity of some 4,000,000 horsepower, realize many of the advantages enumerated, so it will be of interest to examine the background of the interconnection in some detail.

The interconnected system comprises 16 major generating stations of 20,000 to 1,200,000 horsepower capacity, in addition to numerous smaller stations. About 3,700,000 horsepower of the connected total normally is operated in parallel.

Figure 19 also shows the major elements of the combined system. Relative inertia constants of the component systems are

Saguenay	56.3 per cent
Shawinigan	29.4 per cent
Montreal	14.3 per cent
Total	100.3

The Montreal system, as previously noted, is characterized by the relatively constant power-generating capability of the St. Lawrence power plants, which have no storage capacity, and the low-load-factor metropolitan load. (See Figure 17.) During prewar conditions the discrepancy between load requirements and generating capacity was equivalent to more than 100 megawatts at time of peak load, during the summer, while an additional 100 megawatts was available for about seven hours after midnight, each day. This discrepancy between available generation and load amounted to over 800,000,000 kilowatt-hours each year.

On the other hand, the Shawinigan system, with its large storages and regulating possibilities on the St. Maurice River, could convert a major portion of

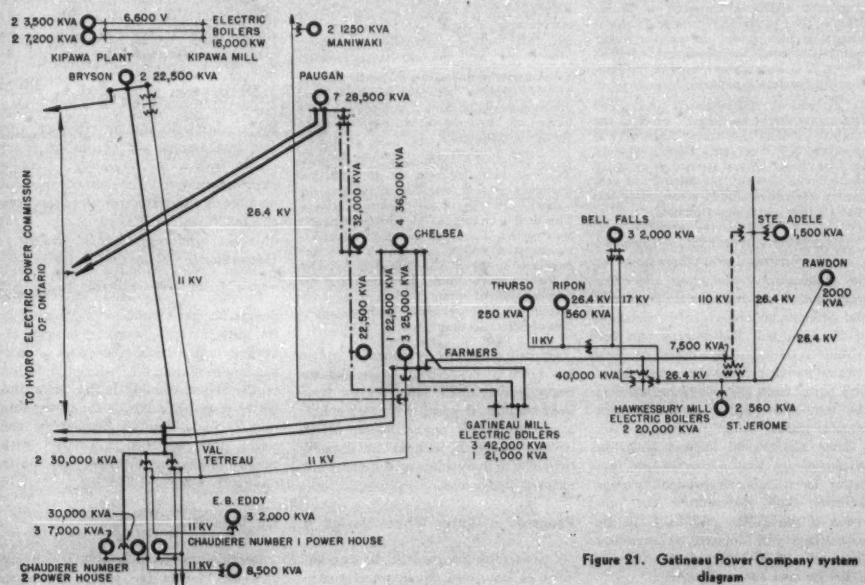

Figure 21. Gatineau Power Company system diagram

the available surplus energy into firm power. Also, there was a minimum of about 60 megawatts reserve generating capacity except during the two months' spring flood period. This reserve generating capacity could be utilized to convert daily or seasonal surplus energy of either the Montreal or Saguenay systems into firm power by storing the surplus energy in the form of water in the St. Maurice River storage reservoirs and returning it as firm power during the winter months to satisfy peak requirements. Additional generator capacity on the St. Maurice would, it was recognized, permit more complete utilization of available surplus energy.

In the Saguenay area, generator capacity normally available during the winter months could also be used in the conversion of surplus night energy of the Montreal system into firm power by storage in Lake St. John. Similarly surplus summer energy could be stored in the St. Maurice reservoirs and converted into winter firm power.

It was concluded that, for conditions prior to World War II

1. By suitably interconnecting the three systems to permit free interchange of power, energy, and reserve generating facilities; by utilizing the Shawinigan facilities to store off-peak energy from neighboring areas; and by the addition of some 125 megawatts additional capacity on the St. Maurice river to permit returning the stored energy as firm power during the winter months, it would be possible to convert almost all of the surplus energy of the combined system into firm power.

2. A total of 260 megawatts additional firm power might be gained, based on the combined system load factor under normal conditions of 74.6 per cent. Capital expenditure for the additional generating capacity and suitable tie lines, per kilowatt of firm power reclaimed, would be considerably less than for new power developments.

The outbreak of war in 1939 resulted in greatly increased firm-power loads or the production of aluminum and other war material, especially in the Saguenay and Shawinigan areas. Interconnection of the Montreal, Shawinigan, and Saguenay systems to the optimum, economical extent provided the maximum of firm power from the energy resources of the combined systems in the shortest possible time.

Some 825,000,000 kilowatt-hours of surplus energy were converted into firm power by utilizing Shawinigan storage facilities. This necessitated the provision of the 115-kv oil-filled cable tie across the city of Montreal, as previously discussed. This increased the transfer ability by over 100 megawatts.

Figure 22. Efficiency curves for outstanding North American water wheels

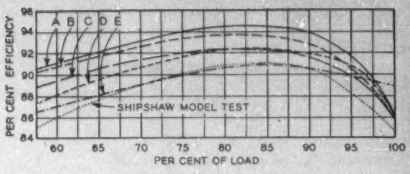

Curve	Unit	Hp Rating	Head, Ft	Specific Speed, Rpm
A	Shipshaw unit 9	105,200	208	52
B	Niagara unit 21	88,000	213.5	39
C	Grand Coulee unit L7	115,500	330	33
D	Osage unit 3	37,000	90	78
E	Boulder unit 5	125,000	520	21

To handle the increased flow of surplus energy from the Montreal area, store part of it, and transmit the remainder to the Saguenay system, it was necessary to

1. Provide additional transformers and voltage-regulating equipment at certain points on the Shawinigan system.

2. Provide an additional 182,400 acre-feet of storage on the St. Maurice river, equivalent to 16,000 horsepower-years.

3. Construct a 220-kv tie line between Quebec and Three Rivers, thus adequately interconnecting the Saguenay system with the Shawinigan and Montreal systems. This line was placed in service in December 1940.[17]

Some of the unusual features of the interconnected Montreal - Shawinigan-Saguenay system are

1. The long heavily-loaded tie lines.

2. The use of three 18,750-kva series transformers, having a transfer capacity of 75,000 kva each, between the 165-kv and 220-kv lines (Ties *A* and *C*, respectively, of Figure 19) at a cost of 57 per cent that of conventional 3-phase transformers or 81.5 per cent that of 75,000-kva autotransformers.

3. A variation in loading on tie *D*, the four 110-kv circuits between Montreal and Shawinigan Falls, from 120 megawatts delivered to Montreal to 130 megawatts fed back from Montreal.

4. A variation in loading on tie *A* between 285 megawatts fed into the tie from the Saguenay system and 204 megawatts delivered by the tie to the Saguenay system. This double-circuit 187-kv tie was originally constructed, it may be noted, to take a 75-megawatt block of firm power from the Saguenay system. The indicated variation in loading is, of course, infrequent and the transmission of power into the Saguenay system was a war measure, pending completion of Shipshaw number 2.[1]

Operation of the interconnected system has been very successful. Despite the heavy loading of the long ties, the transient stability is good, even with a line-to-ground fault on one of the two 187-kv circuits of tie *A*, cleared by 3-phase switching in five cycles and automatically reclosed in 20 cycles.

Progress in Water Wheel Design

Considerable progress in the development of improved water wheel runner designs has been effected by hydroelectric engineers in Quebec. Outstanding work in this connection has been done in the hydraulic testing laboratory of the Shawinigan Water and Power Company at Shawinigan Falls.[14]

The runners in the Shipshaw number 2 plant have developed the very high maximum efficiency of 94.5 per cent (Note Figure 22, comparing the performance of these units with other outstanding water wheels in North American installations.)[11]

The use of welding in the field assembly of the scroll-cases for the Shipshaw units proved most satisfactory, and no doubt contributed materially to the high efficiency obtained.

All the newer water wheels in Quebec have been made in cast steel, eliminating the tendency to fatigue cracking with cast iron designs and permitting easier repairs in the case of pitting. Definite improvements in repair methods used for maintenance of pitted runners have been effected.[22]

Generators

Progress in improved water wheel designs has been paralleled by progress in the direction of generator designs affording better cooling, superior stator-winding insulation life, reduced vibration of the stator winding in the slots and better assembly methods for stator core iron. Newer units, particularly the larger ones, are being provided with closed ventilating systems and water cooling.[22]

Ice Troubles

Despite low temperatures which are prevalent during the winter season in

Quebec, especially in the more remote areas, little trouble is experienced with ice. The reason for this is that hydraulic engineers early appreciated the necessity of

1. Limiting velocities of approach to racks and through head channels to such values that an ice cover would form early in the winter season and be maintained throughout the period of freezing temperatures.

2. Providing pondage of such extent and depth that rapids immediately above power plants would be eliminated.

3. Providing deep skimmer or curtain walls at intakes, so that sufficient heat insulation is provided between the metal of the intake racks in contact with water, and atmosphere, to prevent removal of the latent heat of freezing from the water passing the racks. If heat escapes at the racks, so-called "anchor ice" may form. If no heat escapes even thick "frazil ice" will pass without sticking, if not to excessive in volume.

In some cases, it has not proved practical to completely eliminate ice troubles, from both frazil and floe ice, notably at Cedar Rapids. At one or two other developments heated trash racks have proved to be the solution to ice troubles.

Where spillway and sluice gates must be operated during freezing weather, as at storage reservoirs, gain and skin heaters are employed to avoid damage to the gate seals, and provide easier operation. At some storage dams at relatively high altitudes, and in remote locations, steam boilers have been installed as a stand-by means of clearing ice from gates and, also, for removal of frozen spray from the deck. In general insulating covers are provided over gate wells or slots and other openings to conserve the stored heat of the water and minimize ice formation around the gates and lifting mechanisms.[9]

Operation

Notable strides have been made in Quebec in utilization of available energy resources to the optimum extent, by proper scheduling of water release from remote storage dams, where a delay of a few days before water is received at the plant of use must be taken into account. Use of available water so as to obtain maximum energy output is effected by proper division of load among units in accordance with output–discharge curves derived from efficiency tests by the Gibson and salt-velocity methods.[24] Responsibility for working out such optimum usage of water is placed with technically-qualified system operating engineers, who work in close conjunction with hydraulic and electrical engineers fully familiar with the characteristics of the units and the development as a whole.[25]

References

1. Geology of Quebec (volume II of a series), **John A. Dresser, T. C. Denis.** Quebec Bureau of Mines, Quebec, Quebec, Canada, 1944.

2. The Work of the Quebec Streams Commission, **O. O. Lefebvre,** *Transactions,* American Society of Civil Engineers (New York, N. Y.), volume 90, 1927, pages 867–82.

3. List of Water Powers in the Province of Quebec. A co-operative publication of the Dominion Water Power and Reclamation Service (Ottawa, Ontario, Canada), and The Quebec Streams Commission and The Hydraulic Service (Quebec, Quebec, Canada).

4. Water Power Resources of Canada. Dominion Water and Power Bureau (Ottawa, Ontario, Canada).

5. Storage Reservoirs in Canada, **O. O. Lefebvre.** *The Engineering Journal* (Montreal, Quebec, Canada), volume 13, 1930, pages 467–75.

6. The Outardes Falls Power Development, **H. G. Acres.** *The Engineering Journal* (Montreal, Quebec, Canada), volume 20, 1937, pages 757–67.

7. The Hydro-Electric Power Development at High Falls and Masson on the Lièvre River, **H. S. Ferguson.** *The Engineering Journal* (Montreal, Quebec, Canada), volume 15, 1932, pages 57–64. Discussion pages 308–10.

8. The Manouan and Passe Dangereuse Water Storage Developments, **F. L. Lawton.** *The Engineering Journal* (Montreal, Quebec, Canada), volume 27, 1944, pages 200–20.

9. Hydroelectric Development of the Saguenay River, **W. S. Lee.** AIEE Transactions, volume 44, 1925, pages 722–36.

10. Blasting a Precast Dam Into Place, **C. P. Dunn.** *Civil Engineering* (New York, N. Y.), volume 1, 1930, pages 159–64.

11. The Design of the Shipshaw Power Development, **H. G. Acres.** *The Engineering Journal* (Montreal, Quebec, Canada), volume 27, 1944, pages 221–33. Discussion, pages 449–58.

12. Electrical Equipment at Shipshaw, **R. A. H. Hayes.** *The Engineering Journal* (Montreal, Quebec, Canada), volume 27, 1944, pages 250–60.

13. Considerations Governing the Location of Hydro-Electric Developments on the Upper St. Maurice River, **C. R. Lindsay.** *The Engineering Journal* (Montreal, Quebec, Canada), volume 16, 1933, pages 293–300.

14. Construction of the Hydro-Electric Development at LaTuque, **J. A. McCory.** *The Engineering Journal* (Montreal, Quebec, Canada), volume 24, 1941, pages 54–63.

15. Beauharnois Development of the Soulanges Section of the St. Lawrence River **W. S. Lee.** AIEE Transactions, volume 52, 1933, pages 1056–63. Discussion, page 1066.

16. Canada's 2,000,000-Horsepower Hydro-electric Saguenay System Provides Unusually Reliable Service, **F. L. Lawton.** *Proceedings,* International Conference on Large Electric High Voltage Systems (Paris, France), 1947.

17. Power System Interconnection in Quebec, **W. R. Way.** AIEE Transactions, volume 61, 1942, pages 841–7.

18. Operating Experience With Steel-Tower Transmission Lines in the Saguenay District, **F. L. Lawton.** *The Engineering Journal* (Montreal, Quebec, Canada), volume 22, 1939, pages 257–63.

19. Earth's Crust Resistance and Lightning, **A. S. Runciman.** *The Engineering Journal* (Montreal, Quebec, Canada), volume 24, 1941, pages 170–6. Discussion, pages 177–9.

20. Crossing the St. Lawrence With Unstressed Cable Lengths, **W. A. Mace, J. E. Thicke.** AIEE Transactions, volume 55, 1936, pages 164–7.

21. Design, Manufacture, and Installation of 120-Kv Oil Filled Cables in Canada, **D. E. Farnham, O. W. Titus.** AIEE Transactions, volume 61, 1942, pages 881–8.

22. Stability Problems on Interconnected Power Systems in the Province of Quebec, Canada, **John Morse.** *Proceedings,* International Conference on Large Electric High Voltage Systems (Paris, France), 1947.

23. Improvements in Performance of Hydro-electric Generating Units on the 2,000,000-Horsepower Saguenay System, **F. L. Lawton,** AIEE Transactions, volume 65, 1946, pages 900–10. Discussion, page 1188.

24. Hydraulic Efficiency Tests on 43,000-Horsepower Unit by the Gibson Method and the Allen Method, **W. R. Way.** *The Engineering Journal* (Montreal, Quebec, Canada), volume 7, pages 625–33.

25. The Operation of a Hydro-Electric Power System—A Symposium, **C. R. Reid, W. R. Way, E. W. Knapp.** *The Engineering Journal* (Montreal, Quebec, Canada), volume 17, 1934, pages 266–76.

TVA Co-ordinated Communication System

T. DeWITT TALMAGE
MEMBER AIEE

Synopsis: This paper describes communication and control systems used by the Tennessee Valley Authority, principally to expedite the operation of its multiple-purpose dams, electric power generating stations, transmission lines, and substations. Seventy per cent of the 10,000-mile communication and control system is obtained by carrier channels superimposed upon power lines. This paper explains relationships which exist between carrier channels that are utilized for pilot relay, remote trip, telemeter, automatic load-frequency control, and telephone purposes. Close engineering co-ordination of 45 telephone switchboards, including 13 of the automatic type, and a variety of kinds of telephone circuits, totaling over 6,000 miles in length, permits the rapid handling of 2,500,000 telephone calls each year. The basic equipment used in establishing these circuits and their flexible interconnecting arrangements is standardized and the units are applicable to systems of any size.

THE Tennessee Valley Authority Act of May 18, 1933, required, among other things, that the Authority assume charge of certain properties located at Muscle Shoals, Ala. These properties included, in addition to Wilson Dam steam electric and hydroelectric generating stations, an automatic or dial telephone system that served the dam, locks, electric generating stations, switchyards warehouses, and other locations on Wilson Dam Reservation, including residences in several villages.

The construction stage of each additional multiple-purpose project authorized by Congress, required considerable communication service. Most of the telephone facilities devoted to construction activities were temporarily installed and later removed, but some of the telephone circuits were retained for operating the projects. Operating experience at Wilson Dam with the dial telephone system which included certain auxiliary services hereinafter described, used in conjunction with a manually-operated cordless or key-type telephone switchboard, was found to be satisfactory. Permanent telephone facilities for the majority of the new multiple-purpose dams followed the pattern worked out at Wilson Dam.[1]

Several acquisitions of power properties included a variety of communication facilities, chiefly of the open-wire type terminating in local-battery telephones and manual-type switchboards. These groups of telephone circuits were isolated from each other. It was necessary, therefore, early in the Authority's integration program, to connect these separated communication units and centralize their terminations so that a unified telephone system would be available for operating and maintaining the facilities which provide more than 13,000,000 acre-feet of water storage useful for flood control, a navigation channel 650 miles long, and a generating capacity of 2,500,000 kilowatts.

Development

In Tennessee, power-line carrier telephony was used first by others as early as 1923. The development of the present 3,263-mile carrier telephone system on the Authority's power lines started in 1937.[2] From time to time these carrier telephone channels were rerouted and extended to co-ordinate with the power system changes and additions. The Authority's power system on June 30, 1945, located in seven states, is shown in Figure 1. The system includes 6,078 miles of transmission lines, 279 substations, and 27 major generating stations that serve an 80,000-square mile area in which 600,000 customers buy power from 130 municipal and co-operative organizations.

The first installation of power-line carrier pilot relay protection on transmission lines in the Tennessee River Valley was made by the Authority in 1937.[3] This system has been extended until today it is used to protect 51 transmission lines.

Interconnections with large power systems, shown in Figure 1, and power interchange agreements with them, require close co-ordination of operation for mutual benefit. Direct telephone circuits between the majority of interconnecting system load dispatching offices have been established. The first such telephone circuit was in service between Wilson Dam and Gorgas steam electric generating station in 1933 when the Authority acquired Wilson Dam.

In addition, efficient control of power flows between systems required telemetering and automatic load-frequency control facilities. In some cases where only one metering or control function was required between two points, it was combined with the carrier pilot relay function. As the power systems grew and operating requirements became more rigid, separate power-line carrier channels were provided for telemeter and load-frequency control functions. The Authority placed its first carrier telemeter channel, of the multitone type, in operation in 1942, and its first master load-frequency control carrier channel, of the frequency-shift type, in service in 1944.

The Authority's telephone system, shown in Figure 2, is made up of 86 principal circuits serving 215 locations. These telephone facilities have been closely co-ordinated with the layout of the power system and include 22 telephone circuits established by carrier over power lines.

Paper 47-121, recommended by the AIEE joint subcommittee on power system applications of carrier current for presentation at the AIEE summer general meeting, Montreal, Quebec, Canada, June 9–13, 1947. Manuscript submitted November 4, 1946; made available for printing April 8, 1947.

T. DeWitt Talmage is communication and signal engineer in the department of power engineering and construction of the power engineering and design division of the Tennessee Valley Authority, Chattanooga, Tenn.

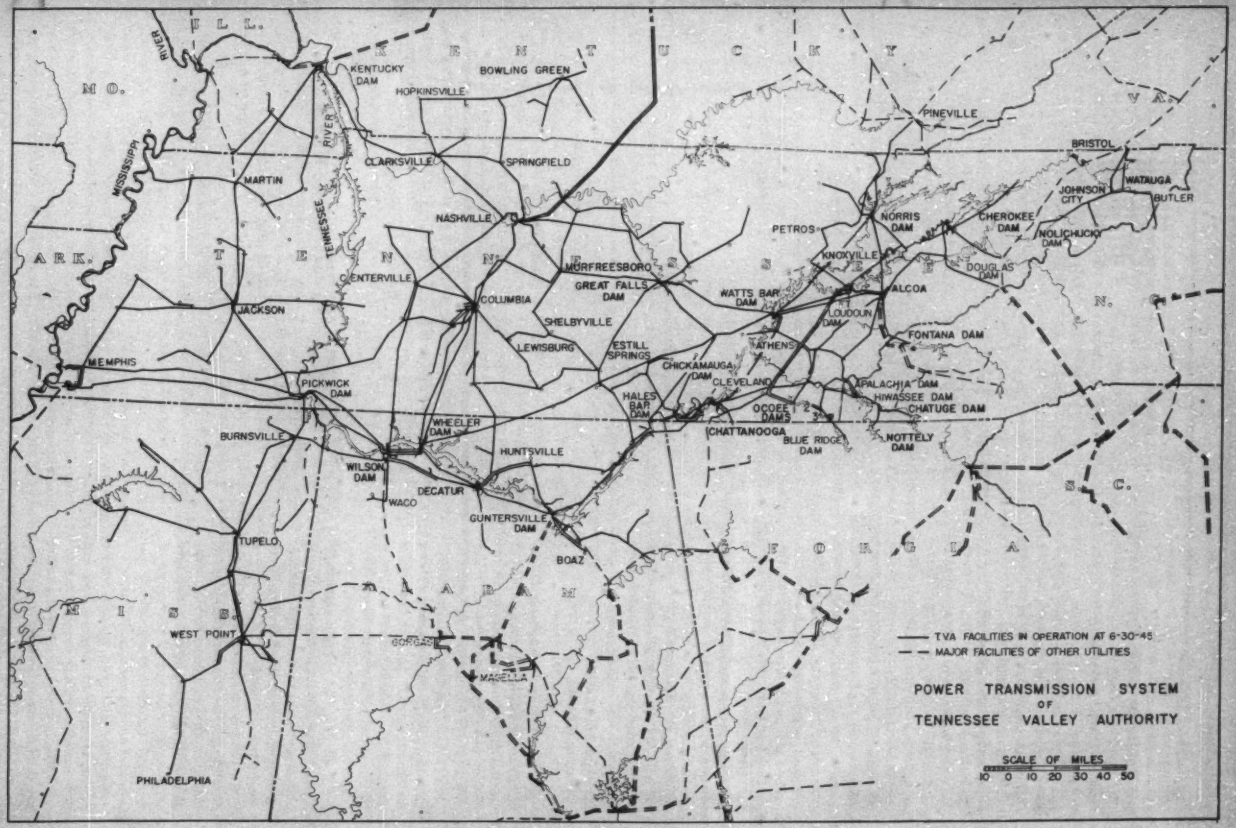

Figure 1. Power transmission system of Tennessee Valley Authority showing 6,078 miles of circuits

These carrier circuits, constituting one-half of the communication system mileage, are shown in more detail in Figure 3. This drawing is used, when the channels are colored for contrast in accordance with the list at the bottom of the figure, as a directory for this part of the communication system.

The designated stations in Figure 2 show the locations of attended stations and certain terminal points, the majority of which is equipped with telephone switching facilities. In the case of 13 hydroelectric generating stations, the manual-type telephone switchboards, labeled *TEL SWBD* in Figure 3, are the connecting links (*a*) between the intrasite dial telephone and the intersite telephone circuits, and (*b*) between intersite telephone circuits when it is necessary to extend telephone service from one area to another. The remaining 19 manual-type telephone switchboards serve the same purpose as *a* and *b*, except that since the intrasite telephone circuits at these locations are operated on a manual or non-dial basis, it is necessary that the additional function be performed of making connections manually between the intrasite telephones. Continuous telephone service is available since all manual-type switchboards are attended 24 hours a day.

Intrasite Automatic Communication

Thirteen automatic telephone switchboards and 900 dial telephones are used to provide quick communication to all important locations throughout 15 major electric generating stations. At both Wilson and Watts Bar Dams, the steam-electric and hydroelectric generating stations are jointly served by one automatic switchboard. Employees do not leave their assigned posts of duty to use these telephones. Jacks are provided in a number of places for the use of portable telephones. The convenient locations of telephones and jacks in a typical multiple-purpose project on the Tennessee River are shown in Figure 4.

The switchboards are arranged for two-digit operation and render full-automatic, individual-line telephone service complete with dial tone, revertive-ring tone and busy tone features. A photograph of a typical automatic telephone switchboard is shown on the left in Figure 5.

Duplicate sources of 20-cycle ringing power are supplied for each switchboard together with equipment for automatically changing from one source to another in case of failure of the first. A separate 24-cell 48-volt 120-ampere-hour telephone

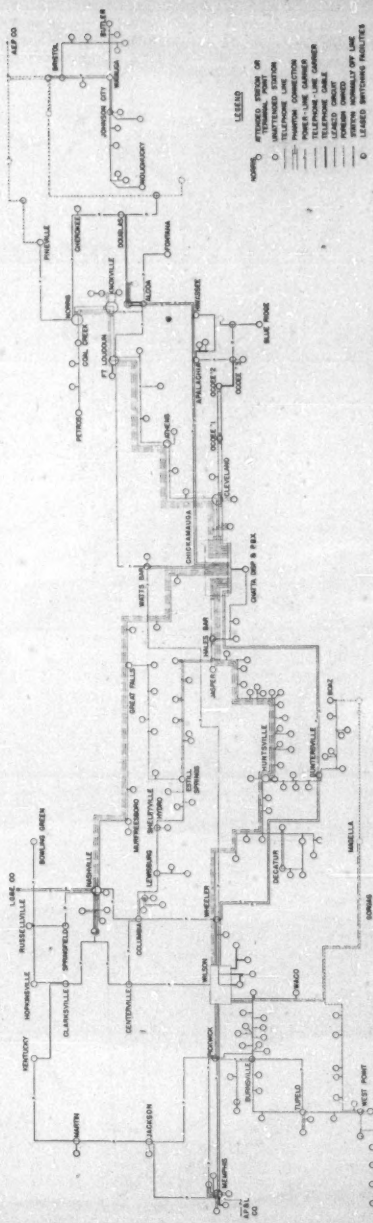

Figure 2. Single-line diagram of TVA telephone system

Eighty-six principal telephone circuits, totaling 6,000 miles in length, serve 215 locations

storage battery is provided with a 3-ampere copper-oxide charger. The charger is arranged to supply a continuous trickle charge to the battery and at the same time carry all of the normal load of the intrasite telephone system.

Code call service is an integral part of each automatic switchboard. This feature permits a dial telephone user to locate promptly, and to talk with personnel who cannot be reached on their regular telephones. In addition, general emergency, police, and fire alarm calls are included in the code call system. When these numbers are dialed they take precedence over any routine code call that may be in progress.

Conference telephone service is furnished by each automatic telephone switchboard. This feature provides for group discussions without personnel leaving their normal work-locations. By dialing an assigned number from any telephone it is possible to signal a maximum of six predetermined telephones simultaneously, which connects them to a common talking circuit.

Each automatic switchboard includes one right-of-way line from the main control room of the generating station which permits the control room operator to make calls to busy telephones so that in emergencies he has access to all telephones. When it is used, the control room operator may interrupt the existing conversation, or in the event he chooses to wait, a ringing signal is automatically sent to the called telephone as soon as the line becomes idle.

Most of the automatic switchboards are wired for direct-line telephone service for use between two points which call one another very frequently, such as the turbine operator and the control room operator. This feature provides very rapid communication since the lifting of the handset at either telephone automatically rings the bell at the other.

Each switchboard is equipped with a meter which records all originating calls. During the calendar year of 1945, 1,840,000 calls were handled by these 13 dial telephone installations.

Intrasite Manual Communication

By dialing *O* the control room is reached over one of several two-way trunk lines. These lines terminate on a 20-line size, cordless-type, turret-style, manual telephone switchboard located in the main control room as shown in Figure 6 which is typical of 13 such installations in generating stations. All relays and other apparatus associated with the cordless switchboard circuits are mounted on a rack in the telephone equipment room as shown in Figure 7, rack 3. The switchboard is equipped with two operator's telephone circuits which may be used simultaneously, and four universal-type connecting circuits. Visual and audible signals are provided for the operator's convenience. In addition to the duplicate sources of ringing power taken from the automatic telephone switchboard installation, the cordless switchboard is equipped with a hand-operated emergency ringing generator. An emergency source of battery supply is available at all manual switchboards.

The cordless switchboards provide terminations for the right-of-way line, previously described, the 2-way dial trunk lines, and the intersite lines which may be of the dial, common battery or magneto type. In addition there is provided a common battery line to the superintendent's office, a line to the microphone-speaker assembly adjacent to the main entrance door of the powerhouse, a key for actuating the electric release for the front door lock, jack circuits for the use of portable telephones at the main control benchboard, and in one case a key is provided for operating a small substation by remote control.

The main distributing frame, shown at the right in Figure 5, is of the conventional type used in small telephone central offices and includes standard telephone protectors. The distributing cables to each telephone, jack and code-call relay, and the cables leading out of the powerhouse terminate on the protectors. The automatic and mamual switchboard lines terminate on the opposite side of the frame. The terminals on the two sides of the frame are cross-connected by jumper wires.

Racks 4 and 5 in Figure 7 make up a combination testboard for rapidly locating trouble in the intersite telephone circuits terminating at Chickamauga Dam and the intrasite automatic and manual telephone lines at this point.

Manual telephone switchboards only are used to terminate both intrasite and intersite telephone lines in six additional generating stations.

Intersite Circuits

The majority of the Authority's 2,500 miles of open-wire and cable intersite telephone circuits are either jointly constructed on the same poles with power lines, mostly 44-kv and below, or built at the edge of power line rights-of-way. The remainder of the circuits are located on separate routes along highways and on pin space rented from commercial telephone and telegraph companies.

While the integration of acquired open-wire telephone lines required the extension of circuits to close gaps between isolated sections and the looping of other circuits in and out of near-by generating stations constructed by the Authority, the chief part of the communication unification program centered around Chattanooga, Tenn., where a general rearrangement and consolidation of facilities eliminated circuit bottlenecks, centralized terminations at Chickamauga Dam, and resulted in facilitating maintenance and interconnections of circuits in a more efficient manner.

Because of the acquisition of telephone properties from different companies, scarcity of certain materials during the war, and the fact that wire size on underbuilt pole lines is determined more by physical requirements than by telephone transmission loss limits, there are a number of different kinds and sizes of conductor used in the open-wire system. Some of the more common conductors are number *6* Copperweld, number *6* aluminum cable steel reinforced, and number *4* aluminum cable steel reinforced. Size *8A* Copperweld-copper has been used recently for circuits built under power lines, while number *8* and number *10* hard drawn copper are in general use on standard telephone pole lines.

There are 12 major telephone-type cables in use for control and communication purposes. The most recent cable installations are between Chickamauga Dam and the Chattanooga power building, Ocoee 2 powerhouse and the Ocoee 3 powerhouse, and Alcoa switching station and the Alcoa primary substation. These cables are similar in that they are all gas filled and the number *19* copper conductors are insulated by wrapped paper.

The Chickamauga Dam–Chattanooga power building cable is a standard installation of 51-pair lead-sheathed cable of both aerial and underground construction. Twenty-six of the cable pairs are loaded to reduce the transmission loss to about one-half of that of the nonloaded circuits.

The Ocoee 2–Ocoee 3 cable is of the trench-lay type, contains 51 pairs of conductors, and the lead sheath is protected with a spiral steel tape with a jute covering. This cable is buried at an average depth of two feet in the berm of the road between these two points and is used principally to operate Ocoee 3 hydroelectric generating station from Ocoee 2 powerhouse. As Figure 2 shows, there are sev

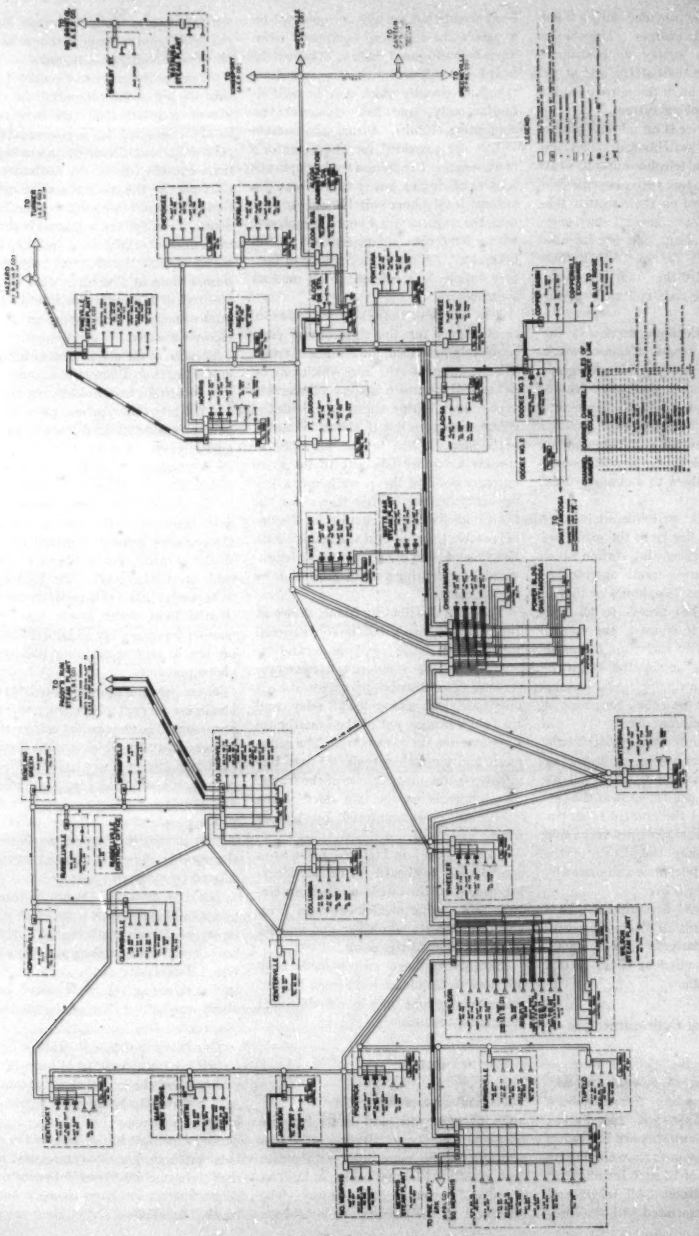

Figure 3. Power-line carrier telephone system

Showing 69 carrier sets connected to 26 telephone switchboards and 125 telephones. Twenty-two individual channels, totaling 3,263 miles in length, serve 53 key locations

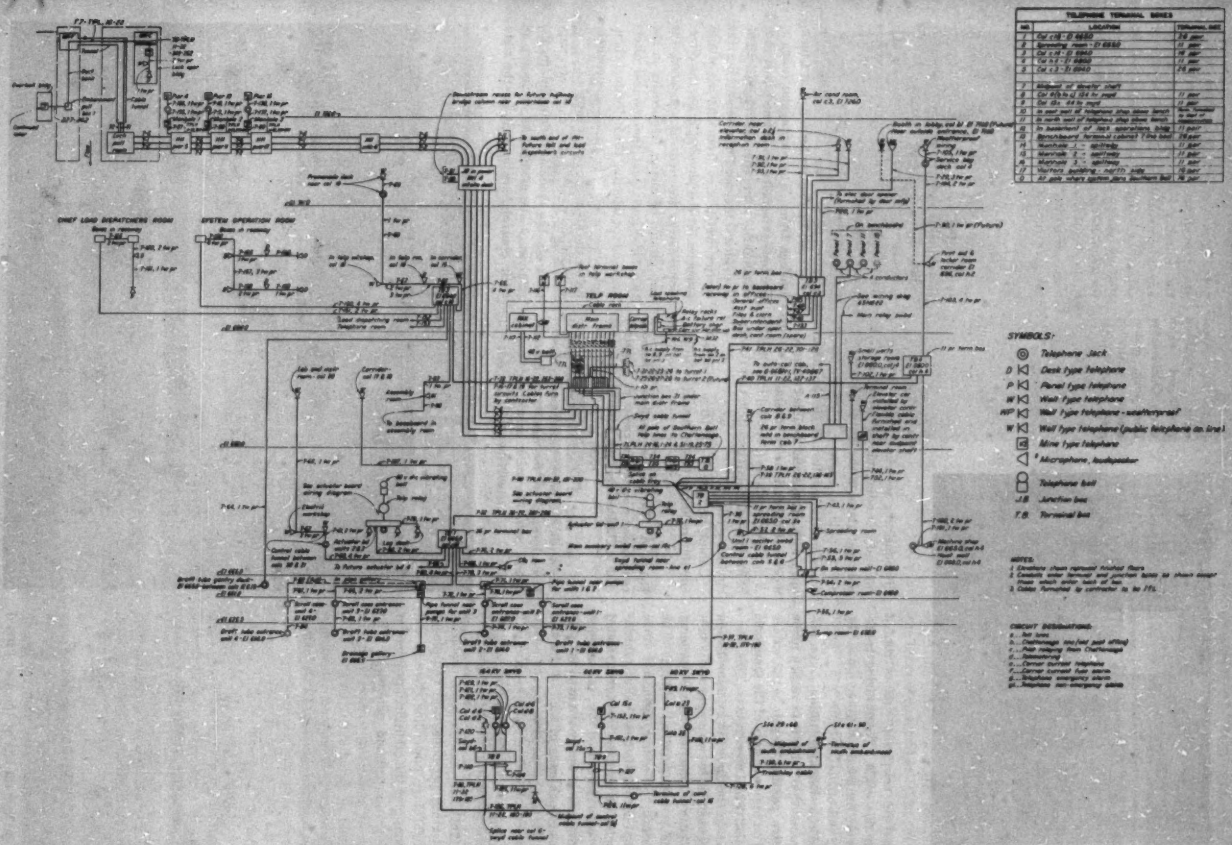

Figure 4. Single-line wiring diagram of typical intrasite automatic and manual telephone system

Showing distribution of telephones, jacks, and code-call signal devices

Figure 5. Automatic telephone switchboard which serves Chickamauga Dam, lock, hydroelectric generating plant, and switchyard

At right is a main distributing frame

eral intersite telephone circuits routed through this cable. Neutralizing transformers are installed for protection at the Ocoee 2 end only.[4]

The Alcoa switching station–Alcoa primary substation cable is in reality made up of two parallel 26-pair aerial cables erected on opposite sides of the same pole line on individual messengers. This twin-cable is near the three 154-kv transmission lines between these two points and is subject to heavy induction with consequent high induced longitudinal voltage. The lead sheath, of course, furnishes some shielding but to further increase this shielding number *00* hard-drawn bare stranded copper wire was used for messengers. Insulating transformers are used for protection at both ends of each of the two cables.

Protection

The Authority has the usual problems of protecting personnel and equipment from lightning, power-line crosses, and induction, plus the additional problem of rise of station ground potential. The number of power-line crosses and the magnitude of induction is greater than those experienced by commercial communication companies because of the extent and closeness of parallel construction between the telephone and power circuits. Even though the resistance of the ground at most stations is low, the maximum possible fault current is usually very high, resulting in an excessive rise of station ground potential.[5] It becomes necessary to insert in the telephone circuits either neutralizing[6] or insulating transformers to prevent this rise of ground potential from damaging equipment or injuring employees.

On open-wire telephone circuits, the protective transformers of either type are insured against damage from voltages in excess of their ratings by the use of fused disconnecting switches and short-circuiting and grounding relays,[7] installed on the pole just ahead of the transformers. Figure 8, pole *A*, shows typical insulating transformers installed at the junction of open-wire circuits and a cable entrance to a generating station or a substation. Pole *B* in Figure 8 shows a typical installation of fused disconnecting switches and short-circuiting relays.

Cables, because of the large number of circuits, require a larger structure to support the protective transformers, as well as to provide sufficient separation between the entrance cable which is at station ground potential and the main section of cable which is at a potential approaching that of remote ground. The equipment for maintaining gas pressure inside of the cable sheath is usually mounted on this same structure. A typical example of this construction is shown in Figure 9.

Telephone-Line Carrier System

Seven carrier telephone channels, totaling 900 miles in length, are superimposed upon four open-wire telephone circuits. Carrier equipment for one channel is rented.[8] The Authority's carrier equipment uses single side-band suppressed-carrier transmission and requires a frequency range of 4.3 to 28.5 kc.[9]

Figure 10 shows a front view of six telephone-line carrier terminals at Chickamauga Dam. The rectangular boxes at the top of the racks are the necessary line, directional, and channel filters. The line filters are used for separating the carrier frequencies from the voice frequencies on the physical line; the directional filters are used for separating the two groups of carrier frequencies in the two directions; and the channel filters are used for selecting the individual channel frequencies. The panels immediately below the filters are power supplies.

The large panels below the power supplies are the modulator-demodulator assemblies. The modulators, including all their controls, are located on the right

Figure 6. Twenty-line cordless telephone switchboard mounted in center of operator's desk in Chickamauga Dam powerhouse control room

At each side of telephone switchboard is annunciating-recording supervisory equipment. In background are the main control benchboard, main instrument board, and battery switchboards

Figure 7. Rack-mounted communication equipment in telephone room at Chickamauga Dam powerhouse

Racks 1 and 2, automatic telephone switchboard auxiliaries; rack 3, manual telephone switchboard relays and auxiliaries; racks 4 and 5, central telephone testboard; and rack 6, radio equipment

side of the modulator-demodulator panels, while the demodulators, including all their controls, are located on the left side of the same panels.

These six carrier channels connect Chickamauga Dam with Huntsville primary substation, Fort Loudoun Dam, Wilson Dam, and the Nashville, Tenn., area (three channels). As shown in Figure 2, all carrier channels are extended to the power building at Chattanooga, Tenn., by telephone-cable circuits. The three Nashville channels are superimposed upon one 150-mile telephone line which requires a carrier repeater at the mid-point. Two other carrier channels also utilize repeaters at intermediate points.

Figure 11 shows a side view of the 3-channel repeater located at Great Falls hydroelectric generating station. Panel 1 is the amplifier working in the Chickamauga–Nashville direction. Panel 2 includes control equipment for automatically connecting the repeater to an emergency power supply in case of failure of the normal 115-volt a-c source. Panel 3 contains the directional filters and a repeater-in-and-out switch. This switch by-passes the carrier frequencies around the directional amplifiers, and is useful when performing maintenance work. Panel 4 contains the power supply for both amplifiers, and operates from a 115-volt a-c source. Panel 5 contains the line filters and two filter-in-and-out switches. These switches are used for completely by-passing the carrier repeater when necessary for maintenance purposes. Panel 6 contains the amplifier working in the Nashville–Chickamauga direction.

The design of a carrier-frequency-type insulating transformer, having one-sixth the transmission loss at 30 kc that is encountered in the usual voice-frequency type transformer, has made it practical to use carrier circuits on exposed telephone lines. The wire telephone circuits are of the multiparty type and intermediate way stations were rearranged where necessary to reduce carrier frequency losses.

Figure 12 shows two carrier-type insulating transformers (item 1 and 2) mounted beside a standard voice-frequency type insulating transformer (item 3) along with line sectionalizing switches (item 4) at Great Falls carrier repeater location. The two carrier-type insulating transformers are in series with the Chickamauga–Nashville line, one on each side of the repeater. The voice-frequency insulating transformer is used in another telephone circuit terminating at this point. The knife switches are used for sectionalizing the physical telephone circuit in case of trouble on the Chickamauga–Nashville line.

The volume-level and quality of transmission of these seven telephone-line car-

Figure 8

Typical telephone cable terminal and protective transformer pole *A* used at junction of open-wire and cable telephone circuits serving electric power substations or generating stations. Protection on pole *B* consists of short-circuiting relays and fused disconnecting switches

Figure 9

Typical telephone cable protective structure serving 154-kv substations near Alcoa, Tenn., showing method of supporting telephone cables and terminals, protective transformers, and gas pressure equipment

rier channels are superior to those provided by the physical circuits over which they are routed. A general improvement of telephone service has resulted, therefore, between the points served by this equipment.

Power-Line Carrier Systems

The 220 power-line carrier sets establish 88 separate channels totaling 7,000 miles in length. Thirty-three of these carrier sets are owned by interconnecting power companies. About one-half of the Authority's transmission lines have carrier channels superimposed upon them. Thus, 2,500 miles of transmission line are used in furnishing 1,500 miles of carrier telemeter and load-frequency control channels, 2,500 miles of carrier pilot relay channels, and 3,263 miles of carrier telephone channels.

Some transmission lines have as many as six different frequencies operating over them. There are 13 carrier channels out of the total of 88 that require two frequencies each. Thus, 101 power-line carrier frequencies are used. Most of these frequencies are in the band of 50 to 150 kc. Careful planning has made possible the use of 20 frequencies two or more times each. This results in the use of only 63 different frequencies, a reduction of one-third from the number otherwise required. In one substation, 23 different carrier frequencies are in use.

In general, the two outside phase wires are used for communication channels while the middle phase wire is used with the ground as the return path for pilot relay and telemeter channels.[10] Coupling is made to the transmission line conductors on the line side of the oil circuit breaker disconnecting switch with the exception of the master load-frequency control channel, which, in the majority of cases, is coupled to all sections of the switchyard bus on a phase that corresponds to an outside line conductor.

Figure 11. Telephone-line carrier repeater at Great Falls hydroelectric generating station on the Chattanooga-Nashville telephone circuit

Panel 1, Chickamauga–Nashville amplifier; panel 2, emergency power supply control; panel 3, directional filter; panel 4, power supply; panel 5, line filter; panel 6, Nashville–Chickamauga amplifier

Figure 12

Two carrier-frequency (items 1 and 2) and one voice-frequency (item 3) insulating transformers. Item 4 is a telephone line sectionalizing switch panel

Figure 10. Five type *SC* and one type *H-1* (bottom of rack 2) telephone-line carrier telephone sets in telephone room at Chickamauga Dam powerhouse

Carrier Communication

Figure 3 shows the layout of 63 carrier telephone sets connected to 14 single-frequency multiparty telephone channels and 16 carrier telephone sets connected to 8 2-frequency telephone channels. Three-fourths of the power-line carrier telephone channel mileage is made up of single-frequency duplex-type sets.[11,12] Figure 13 is a photograph of five single-frequency duplex carrier telephone sets mounted in cabinets in the telephone room at Chickamauga Dam.

The majority of the single-frequency channels are equipped with selective ringing on a 3-digit dialing basis, to serve up

Figure 13. Five single-frequency duplex power-line carrier telephone sets on south side of Chickamauga Dam telephone room

These carrier sets are connected to 18 additional sets which establish 1,000 miles of telephone channels.

Figure 14. Front row of power-line carrier equipment racks in Alcoa 154-kv switching station telephone room

Rack 1, top, telemeter audio-tone receivers, bottom, multitone telemeter carrier receiver; rack 2, top, telemeter audio-tone transmitters, bottom, multitone telemeter carrier transmitter; rack 3, single-frequency duplex carrier telephone set; rack 4, a 2-frequency duplex carrier telephone set; rack 5, single-frequency duplex carrier telephone set; rack 6, miscellaneous panels

Figure 15. Seven power-line carrier sets mounted on racks on north side of Chickamauga Dam telephone room

Rack 1, top, master load-frequency control frequency-shift carrier transmitter, bottom, two telemeter frequency-shift carrier transmitters; rack 2, three telemeter carrier receivers; rack 3, a 2-frequency duplex carrier telephone set

to a maximum of six telephones at each location. This arrangement not only speeds up the use of the telephone channels by not requiring connections to be set up manually to these particular telephones, but it also reduces distractions in control rooms by eliminating signaling of unwanted telephones. Two single-frequency duplex carrier telephone sets are pictured on racks 3 and 5, Figure 14, in the telephone room at Alcoa switching station.

The 2-frequency duplex[11] carrier channels, constituting one-fourth of the carrier telephone system mileage, utilize magneto telephone circuits with code ringing. On channels of this type which make use of three of more different codes, selective ringing is secured, when required, by the use of unique code selector devices which respond to the reception of only the particular combination of short and long rings that have been assigned to each telephone.[13,14] Figure 14, rack 4, and Figure 15, rack 3, show photographs of 2-frequency carrier telephone sets. These two sets make up channel 11 included in Figures 2 and 3.

Both the single- and the 2-frequency carrier telephone sets use amplitude modulation with the exception of the 262-mile single-frequency channel 13, Figure 3, which employs frequency modulation of the one-to-one deviation ratio type.[11] This channel is now under construction.

Carrier Telemetering

The telemeter system brings to the system load dispatching office indications of the direction and amount of power flowing over intersystem tie lines, as well as the load being generated at certain stations. Twenty-five power-line carrier sets, consisting of 12 25-watt transmitters and 13 receivers, make up 12 telemeter channels. (One channel from South Nashville substation to Wilson Dam has a second receiver on it at Wheeler Dam.) In addition, six pilot relay carrier channels are jointly used for transmitting telemeter signals.

Three of the telemeter channels are of the carrier frequency-shift type and nine channels are of the multitone amplitude-modulated type. The frequency-shift channels transmit one indication per pair of closely-spaced frequencies. The multitone channels have a capacity of eight indications each which are obtained by the use of eight audio frequencies ranging from 485 to 3,000 cycles per second. Two types of telemeter impulses are used

1. Impulse duration.
2. Rate of impulse.

The majority of the system uses the impulse-duration method.

Racks 1 and 2 in Figure 14, and racks 1 (bottom) and 2, Figure 15, show installations of carrier telemeter equipment

Figure 16. Rear row of equipment racks in Alcoa 154-kv switching station telephone room

Racks 1 to 3, power-line pilot relay carrier sets; rack 4, main distributing frame; racks 5 to 7, manual telephone switchboard relays and auxiliaries

at Alcoa switching station and Chickamauga Dam, respectively.

Carrier Control

A master load-frequency control transmitter in the system load dispatching office at Chattanooga sends impulse-duration signals over a 7-mile telephone cable circuit to Chickamauga Dam where a 25-watt carrier frequency-shift transmitter is actuated. A pair of frequencies located at the low end of the carrier band is transmitted over the three 154-kv transmission lines radiating from Chickamauga Dam to seven receivers which automatically regulate the generation of power. The equipment at the top of rack 1, Figure 15, is the carrier frequency-shift transmitter in the telephone room at Chickamauga Dam.

The carrier frequency-shift equipment is not crystal controlled and requires spacing each pair of frequencies three-fourths of one per cent above and below the median frequency reference point. Now that crystals are more readily obtainable, it is planned to add crystal control to these carrier transmitters and receivers which will permit spacing each pair of frequencies as close together as 200 cycles per second. This will result in better operating characteristics as well as important conservation of the carrier frequency spectrum.

Carrier Pilot Relaying

Twenty-one transmission lines are protected by pilot relays that use telephone cable pairs as the pilot circuits. Forty-eight 154-kv and three 110-kv transmission lines are protected by pilot relays that use carrier pilot circuits routed over the transmission lines being protected. Six of these lines are intersystem tie lines. Two of the pilot relay carrier channels are 3-terminal installations while the remainder are 2-terminal installations. However, in two cases provisions are made to operate two adjacent 154-kv lines on a 3-terminal basis when required. In each case this necessitates that one pilot relay carrier set be arranged for two frequency operation.

In addition to the six pilot relay carrier channels that normally are used jointly for telemeter and pilot relay purposes, there are a number of other pilot channels equipped so that they may be used as auxiliary telemeter channels. Emergency telephone service is available over most of the pilot relay carrier channels. Remote oil circuit breakers are operated by audio-frequency signals sent over five pilot relay carrier channels, two of which are on intersystem tie lines. In all cases the pilot relays take precedence in the use of the pilot channels.

Racks 1, 2, and 3, Figure 16, show pilot relay carrier sets located in the telephone room at Alcoa switching station.

Figure 18. Three-position cordless telephone switchboard in Chattanooga load-dispatching office; telemeter and load-frequency control instruments on wall at right; and load dispatcher's board in background

Intersite Telephone Switchboards

Racks 4, 5, 6, and 7, Figure 16, show typical telephone terminal equipment associated with manual telephone switchboards used in 11 substations, principally for terminating intersite circuits. Figure 17 shows a key-type telephone switchboard which is typical of such installations in substations. Through the glass inspection-window in the left background of Figure 17 can be seen the front row of racks of carrier and telemeter equipment which is shown in more detail in Figure 14.

The 3-position key-type 50-line telephone switchboard in the Chattanooga load dispatching office is shown in Figure 18. A feature of this installation is the use of two telephone line terminations on each vertical mounting plate which results in substantially reducing the width of the switchboard. Each switchboard position has a separate panel at the right-hand end on which terminate the public telephone exchange lines and one out-dial line to the leased automatic branch exchange that serves the power building. Most of the telephone lines that appear on the dispatching telephone switchboard also appear on the leased 3-position manual switchboard located on another floor of the power building and used in connection with the Authority's general business.

All incoming telephone calls to the power building on circuits which serve both telephone switchboards are routed automatically to the proper switchboard in two different ways

1. The single-frequency duplex power-line carrier telephone sets incorporate a selective-ringing unit which provides separate extension lines for each switchboard.

Figure 17. Fifteen-line cordless telephone switchboard mounted on operator's control desk at Alcoa 154-kv switching station

Telephone equipment racks in telephone room seen through inspection window in background, are shown in greater detail in Figure 14

Figure 19. Communication equipment room associated with load-dispatching office pictured in Figure 18

Left to right, high-speed printer-telegraph transmitter and receiver, main distributing frame, telephone switchboard equipment racks, code selector panels, and telemeter equipment rack

2. The remainder of the circuits use code signaling and in these cases a pair of code selector devices have been added to each telephone circuit to differentiate between coded rings for the various points served by these multiparty lines. These code selector devices[13, 14] are shown on the right side of Figure 19.

Busy lamps are provided on each switchboard for speedy indications of circuits that are in use. This general arrangement relieves the power system dispatchers of all telephone operating duties that are not directly associated with their principal functions. Thus all of the Authority's offices in Chattanooga have a convenient means of making use of the telephone system shown in Figure 2.

A 2-position 30-line telephone switchboard is used in the load dispatching office at Wilson Dam.

Printer Telegraph

In the left foreground of Figure 19 is a 100-word-per-minute printer-telegraph transmitter and receiver which uses the electric typewriter as the basic unit. Similar equipment is located at Wilson Dam. For sending the printer-telegraph impulses from Wilson to Chattanooga, an audio tone on a direct carrier telemeter channel is used. A telephone-line carrier telephone channel is used for transmitting printer-telegraph impulses from Chattanooga to Wilson Dam at times when it is possible to take the channel out of telephone service. With two independent channels the printer-telegraph equipment can be operated in both directions simultaneously.

Radio Telemetering

The Authority maintains a system of rain and stream-flow gauges throughout the Tennessee River Valley, the readings of which are reported by telephone and telegraph to a central forecasting and control office. At isolated locations remote from means of communication, low-powered radio is used for transmitting rain and stream-flow data. These 39 unattended radio transmitters operate in the 2- to 3.5-megacycle band and have an output of 15 watts. By means of a timing device, a keyer, and a mechanical arrangement, the transmitter is turned on at timed intervals and transmits in simple code the transmitter identification and the hydrologic data.[16]

Two-Way Radiotelephony

The Authority has made use of two 50-watt portable radiotelephone sets which were designed for bridging gaps in telephone circuits during emergencies. The transmitter and receiver of one of these sets are shown on the lower half of rack 6 in Figure 7. These sets are of the amplitude-modulated type and operate on either of two frequencies in the range of 2 to 3.1 megacycles.[17]

An installation of one fixed radiotelephone station and four mobile stations, two of which are in boats, is being used in the western part of Tennessee for expediting the detection and suppression of forest fires. These equipments are of the five-to-one deviation ratio frequency-modulated type and operate in the upper part of the 30- to 42-megacycle band. Both the double-superheterodyne receivers and the 60-watt transmitters are crystal controlled.[18] The fixed station uses a half-wave vertically-polarized coaxial antenna which is supported by a 145-foot guyed steel tower, and the mobile units use quarter-wave whip antennas. The fixed station is normally operated by remote control over a telephone circuit from a point 3/4 of a mile away. Two-way contacts are held regularly with mobile units up to an air-line distance of approximately 50 miles from the fixed station.

A similar radio system is used in northern Alabama by the power operations department. This fixed station, which has its antenna located on top of a 164-foot water tank, is operated by remote control from either one of two points approximately two miles apart. Figure 20 shows one of these remote control units which performs the following functions:

1. Energizes the remotely located transmitter when it is desired to transmit.
2. Effects the circuit changes required for returning to the normal receiving condition at the end of each transmission.
3. Amplifies the voice signals both when transmitting and receiving to compensate for attenuation in the control circuit.
4. Monitors both the frequency and relative power output of the station transmitter.

This type of radio system assists in making maximum use of maintenance crews and materially speeds up maintenance work.

A few lightweight portable radiotelephone sets are being used by hydrographic surveying crews on the Tennessee River in ship-to-shore communication. Recently these same radio sets have been used to expedite barometric leveling work and triangulation surveys. This radio equipment was secured from army surplus stock. The operating frequency was necessarily changed to one assigned to the Authority. The use of these sets already has effected savings beyond their cost to the Authority.

Conclusion

As the communication and control systems outlined in this paper were developed during the past 12 years, each constituent part thereof was thoroughly tested for practicability. Operating experience indicates that a properly balanced combination of modern communication and signaling facilities used in conjunction with leased circuits and services can meet the exacting needs for constructing, maintaining, and operating a widespread flood control, navigation, and power project. Communication reliability is secured by using different types of facilities over different geographical

Figure 20. Equipment used for remotely controlling and monitoring very-high-frequency frequency-modulated fixed radio station for contacting mobile units

paths as shown in Figure 2. Direct communication circuits between key points furnish fast telephone service to important locations. That the types of standardized systems described herein meet basic requirements is attested by successful everyday operation, one example of which is the satisfactory handling of telephone calls at the rate of 2,500,000 messages a year.

References

1. TVA's Newest Dams Served by P-A-X's, **W. S. Cadwell.** *Automatic Electric Review* (Chicago, Ill.), volume 6, number 2, September, 1937, pages 17–19.

2. Carrier-Current Relaying and Communication on the TVA System, **M. Stephens Merritt, T. DeWitt Talmage.** Electrical Engineering, volume 61, number 11, November 1942, pages 561–72.

3. Carrier Current Solves TVA Relaying and Communication Problems, **M. Stephens Merritt, T. DeWitt Talmage.** *Electric Light and Power* (Chicago, Ill), volume 20, number 9, September 1942, pages 48–50, 52, 57.

4. Supervisory Control of 30,000-Kva Hydroelectric Plant, **C. W. Bohner, A. P. Marsza.** AIEE Transactions, volume 65, 1946, June section, pages 337–42.

5. Protection of Pilot-Wire Circuits, **E. L. Harder, M. A. Bostwick.** AIEE Transactions, volume 61, 1942, September section, pages 645–52.

6. Neutralizing Transformers, Engineering Report number 44, Joint Subcommittee on Development and Research, Edison Electric Institute and Bell Telephone System. *Publication H12*, Edison Electric Institute (New York, N. Y.), August 20, 1940.

7. Short-Circuiting Relay Protectors, Engineering Report number 41, Joint Subcommittee on Development and Research, Edison Electric Institute and Bell Telephone System. *Publication H17*, Edison Electric Institute (New York, N. Y.), August 22, 1938.

8. The Type-H Carrier Telephone System, **A. C. Dickieson.** *Bell Laboratories Record* (New York, N. Y.), volume 16, number 3, November 1937, pages 76–9.

9. Carrier Systems Used Widely by Pipe Lines, **L. E. Adler.** *Telephony* (Chicago, Ill.), volume 124, number 26, June 26, 1943, pages 16, 22, 24.

10. Application of Carrier to Power Lines, **F. M. Rives.** AIEE Transactions, volume 62, 1943, pages 835–44.

11. Standard Handbook for Electrical Engineers (book). McGraw-Hill Book Co., Inc., New York, N. Y., 7th edition, 1941. Section 24, Electronic Applications to Power Systems: Carrier Communication, page 2,181, paragraphs 92–4.

12. Electronic Switching Simplifies Power Line Communications, **J. D. Booth.** *Electronics*, volume 15, number 8, August 1942, pages 44–7.

13. Less Noise, Less Clanging on Dispatching Phones, **M. C. Westrate.** *Electrical World* (New York, N. Y.), volume 118, number 24, December 12, 1942, pages 56–7.

14. A New Ringing Selector, **R. A. Clark, Jr.** *Telephone Engineer* (Chicago, Ill.), volume 44, number 6, June 1940, page 30.

15. Frequency Modulation for Power-Line Carrier Current, **E. W. Kenefake.** AIEE Transactions, volume 62, 1943, October section, pages 616–20.

16. Transmit River Stages With Radio Gages, **Albert S. Fry.** *Electrical World* (New York, N. Y.), volume 114, number 16, October 19, 1940, pages 66–7, 117.

17. Bridging Breaks in Wire Circuits by Radio Telephone, **Austin Bailey.** *Bell Telephone Magazine* (New York, N. Y.), volume 21, number 4, November 1942, pages 228–40.

18. Two-Way Radio (book), **Commander Samuel Freedman, U. S. N. R.** Ziff-Davis Publishing Co., Chicago, Ill., 1946.

Discussion

E. W. Kenefake (General Electric Company, Syracuse, N. Y.): The author's paper is an excellent description of a complex and well planned communication system. It is obvious, from the subject matter covered, that this communication system has been developed from a thorough knowledge of the type of equipment that would render the service desired.

This system makes extensive use of power-line carrier communication, and it is interesting to note the large number of carrier channels in use on one power system. It is apparent that a well developed system of allocating frequencies is used in order to make maximum utilization of the frequency spectrum.

The number of carrier channels is mentioned in the author's paper and, based on the frequency spectrum used, the average system-wide channel spacing is only a little over one kilocycle. The subject of channel spacing and channel allocation alone would certainly be worthy of a separate paper. On such a large and comprehensive system there is certainly a wealth of information of this nature to draw upon. Also, the method of estimating channel spacing would be very interesting because too many users adhere strictly to the manufacturer's figure on channel spacing which is usually based on the worst possible operating conditions. These conditions are encountered only in a very few of the applications of carrier-current equipment.

The subject of telemetering was described only briefly and a subsequent paper on the application of and requirements for carrier equipment to handle telemetering and load control based on operating experience would be very useful to the industry.

The system described indicates that more or less standard power-line carrier equipment has been purchased and molded to the particular application intended. This shows that sound logic on economics has been used because it should give the lowest cost commensurate with good performance.

There are many other subjects in the paper that are merely touched upon briefly, which in themselves, would be quite worthy of a separate paper. I would urge that the author or some of his associates plan to follow through and cover some of these subjects in subsequent AIEE papers.

W. H. Blankmeyer (The Montana Power Company, Butte, Mont.): The communication network described by Talmage is probably the largest and most modern of any owned by a single power utility.

Planning and developing such an ideal and complete communication plant is an opportunity not enjoyed by many utility communications and electronics men. Especially outstanding is the practice of providing specific adequate space for proposed installation and maintenance of equipment.

It is interesting to note such extensive development toward a private system when many utilities are swinging toward complete leased facilities in the wire telephone field generally to eliminate investment, maintenance, and engineering costs involved through ownership.

Adequate communication in power systems, however it is provided, becomes increasingly important to maintain the extremely high standards of service demanded and deserved by customers.

In addition, with complete co-ordination through good communication, a widespread utility network becomes a closely knit efficient business institution where modern centralized streamlined methods become most effective. Such advantages may not be measurable directly in dollars but never-the-less are reflected in the over-all cost of operation.

The company with which the writer is associated found through a survey that supplying its own communication was best economically, functionally, and from the power service standpoint.

The system includes over 5,000 miles of physical telephone lines plus telephone line carrier, power line carrier, emergency radio, relaying, telemetering, load control, and many miscellaneous specialized electronic applications.

Operating in an area where distance between towns is much above average, this system has unique problems in signal attenuation and noise levels not encountered in short haul channels. Under such conditions special consideration must be given toward maintaining lowest possible attenuation to avoid, as far as possible, addition of special equipment and the attendant complications.

This company is associated with a group of ten other systems in a network called the Northwest Power Pool. Under guidance of a general co-ordinating committee the various carrier and electronic men meet regularly to discuss and rectify problems in carrier frequency allocation, interference between channels, and general application questions.

Such mutual agreement on frequencies to be used throughout the network has worked out with complete co-operation and satisfaction where much confusion might otherwise exist. Charts of existing carrier channels at various system voltages, distributed

to member companies, give further aid in planning new carrier applications.

Printer telegraph, a comparative newcomer to general use in power utility communication, will probably find rapidly growing popularity as should the still newer facsimile equipment now available.

Mario C. Charles (Tennessee Valley Authority, Chattanooga, Tenn.): The development of power line carrier current equipment has now reached the stage where the various manufacturers have standardized on equipment offered. However, the application is left to some extent to the individual user or purchaser. As carrier current equipment always involves two or more distant points or stations, it is necessary that the user adopt certain standards in applying the equipment. If this is not done, system co-ordination will not result and equipment operation will be hampered.

These standards are usually set up by the individual user as to meet his particular need or experiences. They change as the user acquires more experience in the use of the equipment. Since this paper deals with system co-ordination, it is in order to list some of the standards the authority has adopted in applying carrier pilot relaying. These general standards are listed and apply to substations and hydro plants

1. Wherever possible, the carrier pilot relay transmitter receiver set is mounted indoors in the telephone room. If no telephone room exists, it is located in the station control room.

2. If located in the telephone room, the carrier set is mounted on a standard telephone rack; if located in the control room, it is mounted on the wall in an indoor cabinet. The carrier set is never mounted as a part of the switchboard.

3. Carrier pilot relay channel with transfer trip (remote trip) is never used for telemetering or test telephone; however, the carrier set is equipped with test telephone facilities, but the power supply to the telephone equipment is not connected so as to make the equipment normally inoperative. This is contrary to some manufacturers' published data that carrier relay channels can be used jointly for pilot relaying, transfer trip, telephone, and telemetering purposes. Our experience shows that this is not practical. The multiuse of carrier relay channel decreases the reliability of the relay operation and makes it difficult to co-ordinate relay, telephone, and telemetering channels on a system such as the Authority has in use.

4. Carrier pilot relay channels without transfer trip are always equipped with test telephone and dual directional telemetering facilities.

5. Relay channels with telemetering are always equipped with 6-second time delay circuits so that they can be used with either impulse duration or base rate telemetering. The Authority has standardized on a circuit for this purpose which facilitates system co-ordination where two or more relay channels are electrically interconnected for telemetering purposes.

6. On telemetering, the Authority has adapted long impulses for impulse duration and high rate of impulses for base rate to designate power out of the station bus into the line or out of the Tennessee Valley Authority system.

7. On relay channels with transfer trip, the Authority has adapted a circuit for routine tests. This circuit is designed so as to give an over-all check on the performance of the transfer trip channel. It checks the performance of all the carrier equipment and relays up to but not including the operation of the oil circuit breaker. This circuit is equipped with a transfer switch with escutcheon plate marked "NORMAL" and "TEST." In the "TEST" position, a received transfer trip signal energizes and seals in a blue indicating light and energizes a single stroke, soft tone gong instead of operating the oil circuit breaker.

In our efforts to obtain a co-ordinated carrier system, these practices were evolved. They have now become standards which contribute to unified system co-ordination.

R. G. Obrecht (Tennessee Valley Authority, Chattanooga, Tenn.): Included in this paper is a description of the successful application of power-line carrier equipment made by the Tennessee Valley Authority for communication, telemetering, relaying, and remote control. It should be emphasized that because the Authority's high-voltage transmission system is one of the largest in the United States, the application of carrier presented some very interesting problems which were solved without the use of special equipment, the items required being procured as standard equipment from manufacturers.

The selection of the proper operating frequencies for the various channels was made relatively easy because extensive use has been made of carrier-frequency line traps. These traps limit the carrier frequencies to the desired circuits, thus creating as nearly as possible ideal conditions for carrier transmission by establishing carrier circuits free from taps and loops. The use of these traps in the carrier channels also allows transmission line switching to be carried out without adversely affecting the quality of carrier telephone service, unless the transmission lines to which the carrier is coupled are grounded, in which case the channel may be made inoperative if ground traps are not used.

The carrier frequency line traps used on this system are of two sizes, 400- and 800-ampere current carrying capacity. These traps are adaptable to any installation as they may be suspended either vertically or horizontally, or they may be mounted on pedestal-type insulators. When these traps are installed in suspension, the actual strain is kept less than 3,000 pounds although the ultimate tensile strength of the traps is in excess of 15,000 pounds. The weights of the 400- and 800-ampere traps are approximately 400 and 600 pounds respectively. The 400-ampere trap is designed to withstand 15,000 amperes symmetrical short circuit current and the 800-ampere trap 20,000 amperes. The carrier frequency impedance of these traps varies from approximately 8,000 ohms, when the trap is tuned to resonance at 50 kc, to 30,000 ohms when the trap is tuned to resonance at 150 kc. The impedances developed by these traps are sufficiently broad, in band width, and of sufficient magnitude to effectively isolate a broad-band channel which carries voice or audio-tone modulated signals, a band width of approximately 6 kc. All of the traps that are used on this system are capable of being tuned to block two frequencies, and in all cases where two frequencies are coupled to the individual phase wires they are double tuned. The tuning adjustment will remain constant over a period of years.

The carrier communication receivers are equipped with automatic volume control circuits which enable the carrier sets to operate successfully over extremely wide ranges of received carrier signal strength. This feature enables simultaneous party-line communication to be established between the several stations on a single-frequency channel and over transmission line-made up of steel reinforced aluminum conductors ranging in size from 00 to 636,000 circular mils or copper conductors ranging in size from 00 to 500,000 circular mils.

The use of carrier frequency line traps, automatic volume control circuit in the carrier receivers, and adequate power output from the transmitters has enabled long-haul power-line carrier communication channels to be established.

It should be pointed out that each of the 63 carrier telephone sets connected to the 14 single-frequency multiparty telephone channels makes use of a duplex control unit for automatically switching the set from transmitting condition to receiving condition or vice versa. This control unit automatically blocks the receiver and turns the transmitter on when the telephone transmitter is spoken into, it turns off the transmitter and unblocks the receiver when the telephone transmitter is no longer spoken into, and when a signal is received from a distant station it blocks the transmitter so that it cannot operate and then opens the receiver so that the received signals will pass through. All of this switching from receiving condition to transmitting condition or vice versa is accomplished within a half second so that in actual use this equipment performs in a manner similar to any telephone thus enabling anyone to make use of the communication channel and enabling these power-line carrier telephone channels to be interconnected with other telephone systems.

The carrier sets that are used for pilot relaying make use of very simple circuits for the transmitter and the receiver. By properly co-ordinating the control of these transmitter-receiver circuits with the transmission line relays, it has been possible to use these carrier sets for remotely controlling or transfer tripping oil circuit breakers, as well as performing the normal functions of the carrier channel for relaying. Audio tones are used for these additional functions. The opening of the remote breaker is accomplished by the transmittal of one frequency which is controlled either by the relays or manually while the closing is accomplished by transmitting a second frequency which is manually controlled.

Those pilot relay carrier sets that are jointly used for pilot relaying and telemetering transmit only one meter reading. Inasmuch as it is desired to transmit only one indication at a time with these sets, unmodulated carrier is employed thus allowing elementary carrier circuits to be used.

T. DeWitt Talmage: The discussions prepared by W. H. Blankmeyer, Mario C. Charles, E. W. Kenefake, and R. G. Obrecht indicate a good grasp of communication technique fundamentals as they apply to modern power industry practice. The important problem of choosing power-line carrier frequencies is mentioned by Blankmeyer, Kenefake, and Obrecht. In the beginning the frequency allocation problem was not too difficult, but the growth of the system complicated the factors to such an extent that considerable thought had to be given to the choice and spacing of frequencies.

The study of carrier frequency assignments has been expedited by the use of several flexible devices on which are recorded operating frequencies and which permit a convenient analysis of the available frequency spectrum. One of these ingenious

devices, developed by R. C. Gregg, takes the form of a series of disks, stacked one above the other, on a common center. Each rotatable disk is uniformally larger than the one above it, the largest disk being on the bottom. Each disk represents a substation having carrier facilities. A scale graduated in kilocycles appears along the edge of half the circumference of each disk and the occupied frequency band is colored according to the type of carrier service. A movable transparent arm with an engraved scale is pivoted in the center of this set of disks. By moving the disks, representing the stations to be studied, in such a position as to have their frequencies matched, and all others on the opposite side of the circle, the swinging arm is manipulated to various positions to permit rapid visualization of carrier frequency problems involving the selection of new or revisions of existing channels.

It is interesting to learn from Blankmeyer's discussion that the successful practices followed in his territory closely parallel those used in the southeastern part of the country in regard to holding periodic engineering meetings of interconnected power companies to co-ordinate the use of carrier frequencies between neighboring systems. Our experience with this co-operative effort has likewise proved very satisfactory.

The comments by Charles and Obrecht discuss, among other things, the joint use of power-line carrier channels. This is a very timely and interesting subject which unfortunately was not covered adequately because of limitations in permissible scope of any one Institute paper. The possibilities of joint use of carrier channels offer wide fields for further investigation.

The supplemental information furnished by all four discussers add some practical viewpoints which support the conclusions stated in the paper. The successful results obtained from the communication and control systems described are proof that these facilities adequately serve their indispensable functions. Moreover, experience indicates that these standard facilities can be placed in service most economically by including their design as an integral part of the original plans for power generating and transmission facilities, rather than an afterthought.

The German Electrical Utility Industry During World War II

JOHN G. NOEST
MEMBER AIEE

SINCE the late 1920's the German electrical utility industry has been in a state of steady progress in unification. Individual companies serving local areas became interconnected with each other and with the larger interstate companies. While the local companies were to a large extent privately or municipally owned, the larger interstate companies were generally co-owned by the German state. Also significant in this process of unification was the steady expansion of interconnection with industrial plants, whose business of generating electric power was in the nature of a by-product line. Another source of pressure toward unification was the promise of more economical overall operation by the combination of thermal plant capacity with the hydro storage plant capacity available in southern Germany and in Austria.

In 1935, by the promulgation of the energy economy law (Energie Wirkschafts Gesetz) the over-all control of the German electrical utility industry (as well as other industries producing energy as major product), was vested in the hands of the Minister of Economics. The Minister of Economics, through the Office for Energy (Amt Energy), acted to direct operating methods, to establish interconnections and to regulate the location and magnitude of new plant development.

When on September 1, 1939, Germany started the military phase of World War II by its invasion of Poland, the complete control of the German electrical utility industry passed into the hands of the National Load Dispatcher (Reichslastverteiler) by a sweeping executive order dated September 3, 1939. The National Load Dispatcher immediately subdivided Greater Germany (including by that time Austria and the Sudeten area, acquired from Czechoslovakia) into 12, and later 13 energy districts, each under the immediate supervison of a Distric Load Dispatcher (Bezirkslastverteiler) who, in turn, was in immediate control of all Local Load Dispatchers (Ortslastverteiler) within his district. The chain of authority was direct. The District Load Dispatcher was directly responsible to the National Load Dispatcher and the Local Load Dispatcher was directly responsible to the District Load Dispatcher.

Not only did the Energy Office take control of all operational functions, it also took control of all expansion by recommending to the Minister of Economics the degree of priority allocation for construction material and labor.

Thus, at the beginning of the war, the German electrical utility industry was not only completely unified and interconnected but the managerial functions of individual companies were in all important phases placed subservient to the Minister of Economics.

Capacity and Generation of the German Electrical Utility Industry

The assessment of capacity and generation of the German electrical utility industry is complicated; first, by the various geographical changes, such as the reannexation of the Saar area, and secondly, by the continual transfer of noninterconnected private plants to interconnected plants. Tables I, II, and III give a summary of data, which became available shortly after the end of the war, on capacity and generation. Table IV gives a comparison with data for the United States.

There are several significant facts discernible in Tables I to IV which require discussion. First of these is the rate of capacity increase.

In the years from 1937 to 1942 the capacity increase per year averaged 543 megawatts per year. This increase was not entirely due to new plant construction. The value of 543 megawatts per year included capacity gains due to acquisition of Austria and the Sudeten area as well as new plant construction. New plant construction alone is estimated at 400 megawatts per year which gave a capacity increase of approximately 4.38 per cent per year. The capacity increase from 1942 to 1943 was 800 megawatts or 6.75 per cent per year. This increase was the result of the accelerated completion of large water power projects in southern Germany and in western Austria, as well as the result of accelerated new construction, started with the beginning of the war, in new plants and existing plant expansion. Up to the middle of 1943, utility plant expansion enjoyed high priority. A large percentage of new development, either as new plants or as plant expansion, occurred in the newly developed central German industrial area, the development of which was greatly accelerated because of the realization that the principal industrial concentrations in the Northern Rhine–Ruhr area were dangerously exposed to aerial attack.

In 1941, it was realized by the ministry of economics that the German public utility industry was becoming overloaded and steps were taken toward the prompt construction of additional capacity in central Germany. Plans were made for the construction of ten identical plants, with equipment to be standardized, each of 300-megawatt capacity. These plans had high priority initially. It is surprising, therefore, that not a single plant of the ten projected ones was actually completed or even in partial operation, at the

Paper 47-135, recommended by the AIEE committee on power generation for presentation at the AIEE summer general meeting, Montreal, Quebec, Canada, June 9–13, 1947. Manuscript submitted March 24, 1947; made available for printing April 23, 1947.

JOHN G. NOEST is division engineer in the electrical engineering department of Consolidated Edison Company of New York, Inc., New York, N. Y.

Table I. Statistical Review of the German Electrical Public Utility Industry

	1937[1]	1942[1]	1943[1]	1944[1]	1945*[1]
Nominal capacity of generating facilities, megawatts	9,130	11,850	12,650	13,300	13,300
Capacity loss due to war actions, megawatts		0	370	2,060	3,110
Capacity loss due to unscheduled outages, megawatts		650	855	1,210	1,600
Available capacity (nameplate ratings), megawatts	9,130	11,200	11,425	10,030	8,590
Max demand (noncoincidental), megawatts	6,220	9,600	10,150	9,370	9,200
Peak curtailment, megawatts	0	375	610	1,780	3,100
Peak load (noncoincidental), megawatts	6,220	9,225	9,540	7,590	6,100
Peak curtailment, per cent of available capacity	0	3.45	5.35	17.75	36.1
Max demand,† per cent of available capacity	68.2	85.1	88.8	93.4	107.2
Generation of electrical utility plants, million kwhr	27,379	43,400	44,100	45,200	
Use factor of available capacity, per cent	34.2	44.1	54.4	51.4	
Load factor, per cent	50.2	53.5	52.9	68.0	

* For the month of January only.

† Maximum Demand = Peak Load Plus Curtailment.

end of the war. The reason for this situation was found in the increasing pressure upon the whole economic structure of Germany. The original high priority was lowered as time went on, and, in the later periods of the war, already installed equipment was cannibalized for replacement use in damaged older plants.

The capacity expansion between 1943 and 1944 was 650 megawatts, most of which also came from projects begun before 1942.

The growth of the maximum demand on plants reached a peak at the end of 1943 and then dropped off. The dropping off of maximum demand in 1944 was principally the result of destruction of consumer plant facilities. It reflects the intensification of mass bombing raids on cities and industrial areas. A measurable part, however, was due to the efforts of the National Load Dispatcher toward improvement of the load factor. To this end various steps were initiated. The appointment of energy conservation engineers for each larger industrial producer group resulted in many factories, still on a 6-day work week, shifting the day-off to weekdays. Other factories, not working on a 24 hour a day basis, arranged their shifts into the off-peak periods.

Beginning with 1942, the peak load was smaller than the maximum demand. The reason for this lay in the general application of load curtailment for consumers. The curtailment program was set up originally by the National Load Dispatcher to permit prompt load reduction in case of damage to utility plants by enemy action. It was designed to operate in ten steps with the tenth step calculated for a load reduction of 30 per cent. Curtailment was applied in two ways: continuous curtailment, based on kilowatt-hour consumption; and spot curtailment on maximum demand. The continuous curtailment on energy consumption was administered by the Ministry of Economy through the various industry groups, through which industries were allotted energy just as they were allotted raw materials. The curtailment of maximum demand, on the other hand, was administered by the National Load Dispatcher through the District and Local Load Dispatchers. The maximum demand curtailment list applied principally to large consumers, whom the District or Local Load Dispatcher could order, on instant notice, to drop load according to the prearranged steps. These plants were so chosen that an order to reduce load could be put into effect in two hours without resulting in spoilage of products. (Figure 1.)

Another, most significant effect of the war is visible in the values given for capacity loss due to unscheduled outages. This effect was laid, by all plant operators interviewed, upon the policy of deferring maintenance work: A policy adopted by the National Load Dispatcher on the premise of a short war. Deferring of maintenance created in time a large repair job in place of a promptly-attended-to small one. As the war progressed, the time required for major repair work increased in direct proportion to the overloading of the railroads and in direct proportion to the lack of experienced personnel in the factories of equipment manufacturers. At the end of 1942, nonscheduled outages amounted to 5.5 per cent of installed capacity. For 1943 the percentage had increased to 6.76 per cent, while for 1944 an increase to 9.1 per cent occurred. Only for the latter half of 1944 was this situation compounded by increasing difficulties in railroad transportation and by damage to equipment manufacturers' plants by aerial attacks. A bitter complaint in connection with this phase of experience was made against the authorities responsible for manpower allocation, because of their permitting indiscriminate absorption of key personnel into the armed forces, from power plants as well as from equipment manufacturers' plants.

Table IV, by giving comparative data for the electrical utility industry of the United States and Germany, shows an index to industrial potential, if consumption of electric energy can be taken as a measure of it, which should have given Germany cause for hesitation. The industrial potential of United States industry is thus shown to be approximately five times that of German industry. (Ratio 2 times ratio 3.) Although these ratios are based only on public utility capacity and generation statistics, and are therefore not all-inclusive, as they omit private plant values, they are significant and are of value for comparative purposes.

Generating Facilities

Tables II and III show that approximately 70 per cent of the total plant capacity existed in thermal plant capacity of which approximately 30 per cent used brown coal as fuel. While the hard coal burning plants were little different from similar plants in the United States, except for consistently smaller turbogenerator

Table II. Analysis of Generating Capacity and Generation of the German Electrical Utility Industry[1,2]

	1937				1944			
	Generation		Capacity		Generation		Capacity	
	Million Kwhr	Per Cent	Megawatts	Per Cent	Million Kwhr	Per Cent	Megawatts	Per Cent
Thermal plants using hard coal*	10.124	37.0	3,860	42.3	20.792	46.0	6,080	45.7
Thermal plants using brown coal†	11.382	41.6	2,810	30.8	14.916	33.0	4,420	33.2
Hydro plants	4.846	17.7	1,860	20.4	9.492	21.0	2,460	18.5
Miscellaneous	1.027	3.7	600	6.5	**	**	340	2.6
Totals	27.379	100.0	9,130	100	45.200	100	13,300	100

* Bituminous and anthracite.

† Lignite, peat, and so forth.

** Included in line 1.

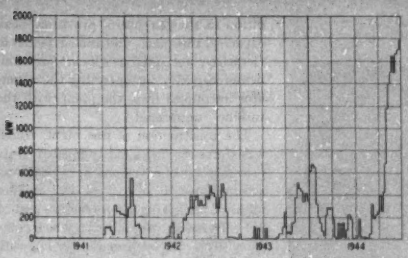

Figure 1. Peak load curtailment of the National Public Utility System

sets, the brown coal burning plants have no counterpart here. Initially these latter plants were only by-product plants in an industrial complex whose primary purpose was, in general, either the production of illuminating gas, brown coal briquettes for public sale, or chemical products in various combinations.[5] A typical complex of brown coal plants was invariably found assembled about an open pit brown coal mine, which mined brown coal in seams, varying in thickness from 3 to 50 feet under an overburden from a few feet to 30 feet in depth. Specialized machinery removed the overburden from above a brown coal seam and redeposited it in exhausted pit areas. The brown coal, having a heat content varying between 3,000 and 5,000 British thermal units per pound, and from 50- to 60-per-cent moisture, was stripped by mechanical shovels, scrapers or conveyors and loaded, either on standard railway cars, transport conveyors, or rope trolley systems for transportation to the nearby plants. In view of the low heat content of this coal, its transportation over any great distance is economically impossible. The cost of this coal, delivered to the generating plant, was given at 2.00 reichsmarks per metric ton, while the cost of bituminous coal of 14.400 British thermal units per pound was 14 reichsmarks per metric ton in the same area (Ruhr).*

A large portion of the brown coal was delivered to the briquetting plant where it was dried and compressed into briquettes, having a heat content of approximately 9,000 to 10,000 British thermal units per pound, with a moisture content of from 10 to 15 per cent. The briquettes were used in the manufacture of gas and coke and were sold to the public. The heat, required for drying of the brown coal, was obtained from back pressure turbines in the electric power plant. The electric power plant's purpose was, among others, the economical production of process steam used in briquette manufacture. To complete the utilization of the products of the brown coal pit, the electric plant's boilers were generally designed to burn brown coal, as mined, either on grates or in powdered form, with auxiliary burners for excess gas from the low temperature carbonization plant, for gas from which certain hydrocarbons had been removed, by the synthetic gasoline plant, or for burning of powdered coke from the illuminating gas plants. These brown coal burning thermal plants were invariably designed and operated as base load plants with load factors in the neighborhood of 90 per cent. Most of these plants operated with steam pressures up to 400 pounds per square inch, although a few had recently installed topping turbines and high pressure boilers, operating with pressures up to 1,600 pounds per square inch and steam temperatures near 1,000-degrees Fahrenheit. Topping turbine installations were more frequently found in hard coal burning plants. Turbogenerator sizes were usually found to be below 50,000 kw, although one plant of this type had two 100,000 kw units. Lyungstrom turbogenerator sets were frequently observed and these were invariably praised by the plant operators for their high efficiencies and low maintenance.

As practically all of the brown coal burning plants were located at the site of the brown coal pits, condenser circulating water had to be obtained by recooling in large cooling towers most of which were built of wood on steel frames (Figure 2), although the newer ones were built with concrete frames. These cooling towers were large structures. Typical dimensions and data are: base diameter 151 feet, height 188 feet, top diameter 80 feet, capacity 35,000 gallons per minute, 10-degree-centigrade cooling effect.

The hard coal burning plants visited showed little distinguishing features from similar plants in the United States, except perhaps, for certain boiler developments, a discussion of which is beyond the purpose of this paper.

A very noteworthy development, however, was found in hydroelectric plants. The German utility industry, aided by government subsidies, had invested heavily in hydro storage plants, both of natu-

Table III. Distribution of Plant Sizes[5]

Plant Size, Megawatts	Hard Coal	Brown Coal	Hydro	Misc	Total
Over 200	1	4	0	0	5
100–200	22	12	6	0	40
50–100	24	9	14	3	50
Total	47	25	20	3	95*

* The capacity of these 95 plants was 12,145 megawatts.

Table IV. Capacity and Generating Comparison Between the United States and the German Electrical Utility Industry

	United States 1937	United States 1944	Germany 1937	Germany 1944
Peak load, per cent of available capacity	68.2	82.5	68.2	75.5
Maximum demand, per cent of available capacity	68.2	82.5	68.2	93.4
Use factor in terms of available capacity, per cent	38.0	53.0	34.2	51.4
Available capacity per inhabitant, kw	0.274	0.372	0.116	0.123
Energy consumption per inhabitant per year, kwhr	911.0	1,720.0	347.6	554.2

		1937	1944
Ratio 1,	available capacity per inhabitant United States / available capacity per inhabitant Germany	2.36	3.02
Ratio 2,	kwhr per inhabitant per year, United States / kwhr per inhabitant per year, Germany	2.62	3.10
Ratio 3,	population, United States / population, Germany	1.83	1.68

* As conversion of German currency to United States currency by means of contemporary exchange rates would be grossly misleading, it is not attempted in this paper.

Figure 2. Bomb-blast damaged cooling towers at a brown coal plant

ral storage and of pumped storage type. Although exact statistics on this phase were not found, it is estimated that about one-half of the hydro plant capacity existed in such storage plants of which one-half again was either pure pumped storage or natural and pumped storage combinations. The description of a typical pumped storage plant can best be given in terms of the Koepchenwerk (Figure 3), located along the Ruhr River, some 15 miles east of Essen.

This hydro pumping plant contained three complete hydro turbine generator pump units and one hydro turbine generator unit for which the addition of a pump was in the project stage. Each turbine generator pump unit consisted of a horizontal shaft Francis turbine, a 32,000-kw 0.8-power-factor synchronous generator, and a 27,000-kw 2-stage centrifugal pump. A hydraulic-mechanical coupling connected the pump to the generator shaft. This coupling had a dual function: it was used to accelerate the pump to approximately 95 per cent of synchronous speed and then for final acceleration to synchronous speed used its plate type friction element, which, at synchronous speed, transmitted the required torque without slip. When the unit was used to pump, the turbine runner rotated with the generator and pump, while the turbine casing was unwatered. All controls required for a complete change-over from generation to pumping, and vice versa, were operated by an automatic sequence device, the operation of which was initiated by push button. The hydro turbine and pump operated with a head of from 517.5 to 582.5 feet. The upper reservoir was constructed by excavation of the top of a convenient hill to create an 18.5-acre reservoir, which, with a change of elevation of 65 feet stored 55 million cubic feet of water. This reservoir was connected to the generating station by means of penstocks 1,050 feet in length. The lower reservoir, known as the Hengsteysee, was created by the construction of a small concrete dam across the Ruhr River, which also furnished water to the Krupp factories in Essen.

Three pumps, operating at full capacity that is consuming 27,000 kw each, for ten hours were capable of filling the reservoir. This operation required 810,000 kilowatt-hours. The overall efficiency being 65%, a useful storage of energy equal to 525,000 kilowatt-hours was accomplished. This energy could be released by full capacity operation of all generators, giving 128,000 kw for approximately 4 hours. In addition to the purpose of providing peak capacity, this plant, and similar plants in Germany, were used as synchronous condenser capacity by operating the generator uncoupled from the pump with the turbine unwatered.

The construction of this plant, which was started in 1929 and completed to its present stage of development in 1932, was accomplished at a cost of 43.7 million reichsmarks, giving a construction cost of 341 reichmarks per kilowatt, which compares 500 to 520 reichsmarks per kilowatt for contemporary steam plants.

The Rheinische-Westphälische-Elektricitätswerke, Aktien Gesellschaftsystem, which supplied 23 per cent of German electric energy with a nominal capacity of 1,850,000 kw, owned approximately 300,000 kw of pumped and natural storage plant capacity, that is 16.2 per cent of its total capacity. By means of these plants, this system was able to operate its brown coal burning plants with a load factor of near 90 per cent. Figure 4 shows a typical load curve of this system.

Plant Equipment

German generating station equipment appeared little different from similar plant equipment in the United States. Generator sets were generally smaller, with ratings from 25 to 50 megawatts capacity appearing most frequently. The most modern plants used recently installed high pressure topping units for which a standard capacity of 25,000 kw was set up by governmental decree during the latter years of the war. Such generators were 3,000 rpm and generated voltages varied from 5,000 to 10,000 volts with the lower voltages in the majority. Invar-

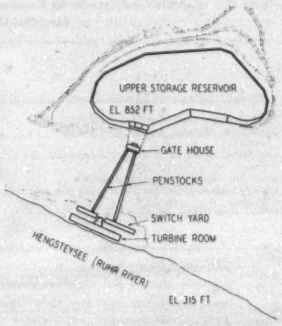

Figure 3. Plan of hydro pumping station (Koepchenwerk)

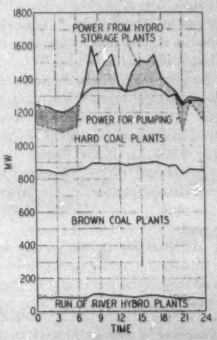

Figure 4. Typical daily load chart, Rheinische-Westphälische-Elektricitätswerke system

iably, the generators were operated ungrounded. Generators were usually designed for 0.8 power factor, although 0.75, 0.7, and 0.625 power factor generators were observed. Generators were designed for short circuit ratios between 0.5 and 0.7, the older units tending toward the higher short circuit ratios. Most units were provided with shaft exciters, and pilot exciters were practically absent. Considerable trouble was experienced with field winding distortion in the newer generators, particularly in the 3,000-rpm speeds. Automatic voltage regulation was general. No hydrogen cooled generators were found. Station auxiliaries were generally electrically driven except for boiler feed pumps, where duplex drives with motors and steam turbines were common. Electric precipitators were used universally even in plants located far from municipalities.

Auxiliary supply was obtained generally from house service transformers; in the newer plants, tertiary windings on 110-kv transformers, served the same purpose. A few installations of house generators driven by the main turbine shaft, were observed.

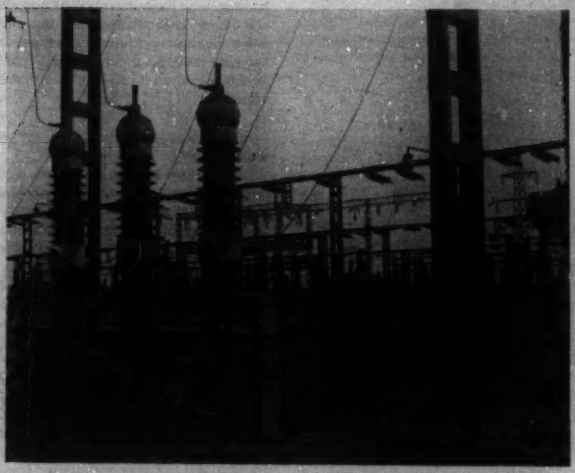

Figure 5 (above). Siemens-Schuckert 110-kv 1,500-megavolt-ampere expansion breaker

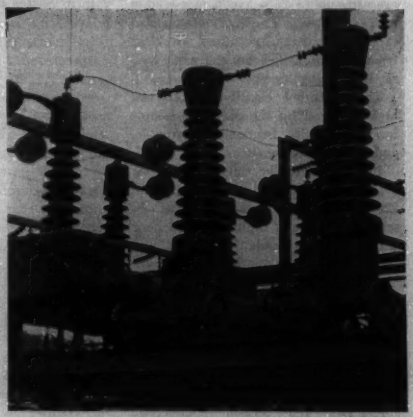

Figure 6. Allgemeine Elektricitäts Gesellschaft freistrahl breaker (extreme left) 110 kv, 1,500 mega-voltamperes, with current and potential transformers

Circuit Breakers

A distinct difference from the United States practice was observed in the almost total absence of oil circuit breakers. In newer stations, no switching was provided at generator voltage, except for auxiliary power; each generator being tied to the 110-kv bus by transformers with the switching on the high voltage side. In older stations, practically all generator voltage switching was done by means of air blast breakers, of which a great variety were seen. Phase isolation, either at generator voltage or at 110 kv was not observed anywhere. Wherever air circuit breakers were found, the air compressor installation was of the central type with the same air supply used for disconnecting switch operation, in which case pneumatical interlocking between circuit breaker and disconnecting switches was general. A few older installations of liquid circuit breakers[5,6] were noted and few installations of "oil-poor" circuit breakers were observed. The liquid used was a mixture of water and glycoll, known by the trade name of Expansine.

In the 110-kv class there were three principal types

1. Multibreak air blast.
2. Controlled expansion (Figure 5).
3. Free blast (*freistrahl*) types (Figure 6).

In the 220-kv class the two prevalent types were 1 and 2. A 400-kv installation project contemplated the use of two circuit breakers, either type 1 or 2 superimposed upon each other.

A most interesting type of circuit breaker design was observed in the *freistrahl* type, which was built for 110- and 220-kv circuit voltages, by the Allgemeine Elektricitäts Gesellschaft and Brown Boveri Company. This circuit breaker is an air blast breaker without any sort of interrupting chute whatever. Two contact arms, mounted on insulators, and capable of rotation either in a vertical or a horizontal plane, carry, surrounding a butt type contact, an annular air blast nozzle. When this circuit breaker is open, the two contact arms are separated by a free air space approximately 70 per cent of the ground clearance. To close the circuit breaker, the two contact arms are rotated to bring the two butt contacts together. The air blast begins when the contact

Figure 7. Tank bottom mounted bushings on a 60-megavolt-ampere portable transformer

separation approaches striking distance and stops when the contacts touch. On opening, the air blast starts immediately before the contacts begin to separate and it persists until slightly after the contacts have reached their open position. Air pressures up to 250 pounds per square inch are used. The arc interruption takes place in the unconfined air blast from both nozzles, hence the name *freistrahl*, meaning "free blast."

This *freistrahl* circuit breaker was highly praised by the operating people for its simplicity, freedom from trouble, and ease of maintenance.

In addition to the three types of air blast circuit breakers for the 110- and 220-kv circuit voltages, there was observed one type of multibreak, oil poor circuit breaker, made by Voight and Haeffner.[5]

In the circuit breaker types 1 and 2 and in the oil-poor high voltage circuit breakers, resistors were used to assist in the interruption of line charging current. These resistors were generally of relatively high ohmic value, approximately 2,500 ohms, and were built with water conductors and ceramic conductors. Considerable difficulty was experienced with these resistors and their development had, in the opinion of the operating people, not yet reached a satisfactory stage. The absence of such resistors in the *freistrahl* circuit breaker was one of the reasons for its preference.

In the medium voltage classes, the air blast circuit breakers were greatly preferred over oil-poor and water circuit breakers, and development work was practically confined to air blast types.

Circuit breakers were found with ratings up to 1,500 megavolt-amperes in the voltage classes up to 30 kv, and up to 2,500 megavolt-amperes in the 110- and 220-kv classes. Very little information was obtained on rates of recovery voltage rise but circuit arrangements were generally such that only relatively low recovery voltage rates could have existed. Facilities available for factory testing of circuit breakers were limited to about 600-megavolt-ampere capacity and field test records were found indicating that some tests had been made up to interrupting duties of 1,800 megavolt-amperes (calculated values).

Power Transformers

In the older generating stations and substations oil-immersed, water-cooled 3-phase transformers were frequently observed. The cooling arrangement was designed with the oil coolers submerged in a water tank so that the water level was well below the bottom of the transformer tank. This arrangement assured that no leak could result in the contamination of the transformer oil. Oil circulating pumps were provided.

Newer installations had forced-air forced-oil cooled transformers, which were standardized in the 30-, 60-, and 100-megavolt-ampere sizes. These standardized units were built integrally with 8- or 12-wheel railroad cars for instant portability. With this point in view, the high tension bushings were located near the

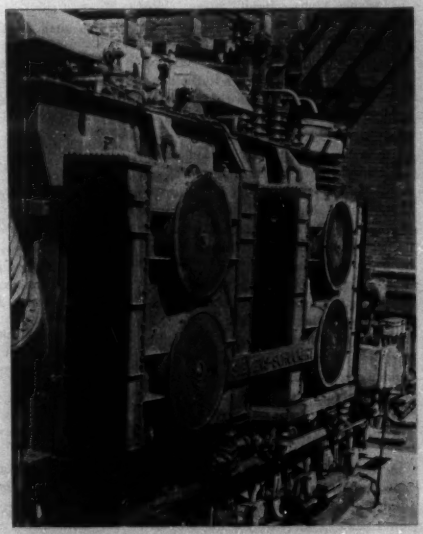

Figure 8. Forced-oil forced-air coolers on a 60-megavolt-ampere portable transformer

bottom of the tank, so that they could remain in place during transportation. (Figures 7 and 8.)

In the 220-to-110-kv ratings, the 220- and 110-kv windings were fully insulated and Y-connected for use with Petersen grounding devices. A 10-kv tertiary winding, delta connected, was used for harmonic suppression and for connection of shunt reactors. Tap changing under load was used where required, although this type of equipment was available only in the most recent designs. The high voltage windings were shielded and all high voltage bushings were gapped.

For connection between generator voltages and either 110 or 220 kv similar transformer designs were used, with the low voltage winding delta connected.

On observing the very high noise level on some of the latest transformers, it was found that in these designs very high flux densities, up to 14 kilogausses rms are used. This resulted not only in a high noise level, but also in high exciting current and high harmonic content. The high exciting current was not considered a disadvantage, since even at maximum load some shunt reactance was required. The high harmonic content did lead into some difficulties with telephone interference and with tuning of Petersen grounding devices. For control of this difficulty such high density transformers were dispersed.

Buchholz relays were universally used on transformers with differential relays as back-up. Buchholz relays were specified by the insurance underwriters. No Askarel transformers were found.

Transmission Facilities

The backbone of the German interconnected transmission system was a double-circuit 220-kv system in the shape of an inverted U (Figure 9). Starting in southwestern Germany, in the corner made by the borders of Switzerland and France, the western leg of the inverted U collected the power production of the run-of-river plants in the upper Rhine River as well as the power produced by the Schluchsee natural and pumped storage development. A branch at this point collected the generation from high-head developments in the Austrian province of Vorarlberg.

On the northward leg, this line, which for a large part of its run was paralleled by a third circuit, collected and supplied interconnected private and municipal plants. At Brauweiler, near Cologne, and at the Koepchenwerk, near Essen in the Ruhr area, both of which were principal switching points, a loop, consisting of a single circuit line, encircled the Ruhr–Rhineland industrial area. From the northernmost point of the loop a double circuit line extended eastward and interconnected via 110-kv circuits with the Berlin area.

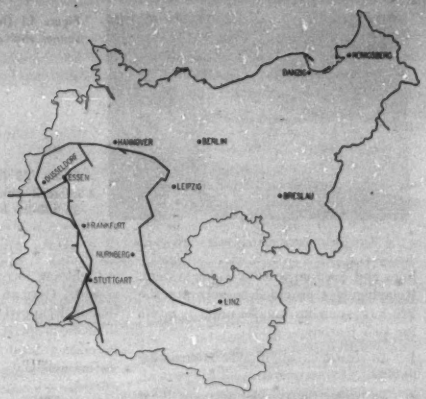

Figure 9. Map of the 220-kv transmission system in Germany

A principal interconnecting point was the Marke substation, near Leipzig. From this substation, the 220-kv system, again as a double circuit line, ran generally southward and terminated near Linz in Austria.

The transmission capacity of this system varied from point to point. It was variously stated to be between 300 and 400 megavolt-amperes for transmission between adjacent major interconnection centers. This 220-kv system was not, however, operated as one system. Instead, it was used for energy interchange between major interconnecting points, so that, in fact the German utility system was operated electrically in five to six independent, non-synchronized parts. Frequently it was found that a generating plant supplied a local area with several generating units, while other generating units were connected to the 220-kv system. The principal reason for not operating in a single system was the lack of means for controlling power flow. As, toward the end of the war, damage to generating plants mounted, attempts were made to operate large sections in synchronism, it was found that swings created by nonco-ordinated load changes often overloaded the lines to a point where they separated. The lack of phase angle regulating transformers prevented operating of closed loops.

While automatic frequency control equipment was available on some systems, with tie line bias control on still fewer systems, a co-ordinated system of automatic frequency and tie line control did not exist. The Rheinische-Westphälische-Elektricitätswerke system, which comprised the western leg of the inverted U, was operated completely with manual control of frequency and tie line loading.

An additional reason for operating in nonsynchronous parts was the grounding system, that is: resonant grounding by Petersen devices. For instance: The Rheinische-Westphälische-Elektricitätswerke 220-kv system had to be electrically separated at Brauweiler and at the Koepchenwerk so that the residual arc current for line-to-ground faults became low enough for self extinction of flashover arcs.

Grounding of the resonant type by means of Petersen grounding devices was used universally on the 220- and 110-kv

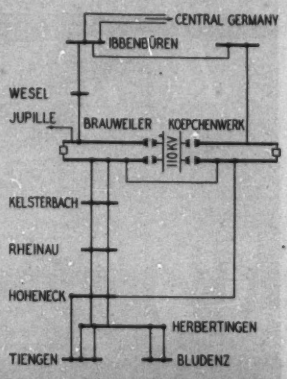

Figure 10. Schematic diagram of the 220-kv transmission system of the Rheinische-Westphälische-Elektricitätswerke

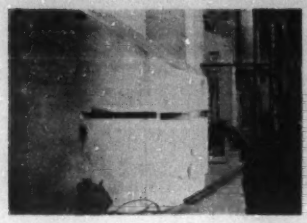

Figure 11 (left). Concrete personnel shelter in a turbine room

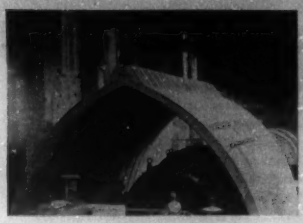

Figure 13 (right). Sectional reinforced concrete shelter for a 32,000-kw hydro turbogenerator set

lines and even on a 66-kv cable system. Relaying was provided to separate the 220-kv system into smaller units on faults for two reasons

1. To reduce circuit breaker interrupting duties.

2. To reduce the residual arc current on line to ground faults.

In some cases synchronism between parts was maintained by high impedance ties through the 110-kv system (Figure 10). Even though synchronism could thus be maintained through high impedance ties, a severe limitation of transmission capacity was imposed. These high impedance ties often separated because of instability. Although these limitations were of little consequence or inconvenience in normal times, when generating capacity was available all along the transmission lines, they imposed serious handicaps toward the end of the war, after large blocks of generating capacity had been disabled.

Carrier current was widely used for communication purposes and it was rarely used for relaying.

Lightning arresters were practically absent. German engineers explained, that with gapped transformers and line insulators, properly co-ordinated, and with Petersen grounding devices, lightning arresters were not worth the troubles they caused.

Distribution

Most of Germany was provided with a service voltage of 220/380 volts. Service was practically all radial, except in the largest cities, where low voltage network distribution was gaining favor. Network sections were kept small, that is, between 20 and 30 megavolt-amperes; although in the city of Berlin, sections as large as 70 megavolt-amperes existed. Network transformers were used in sizes from 160 to 250 kva with 6-kv primary feeders in the earlier installations and 30-kv feeders in the latest. The tendency was toward the higher primary voltage. Relatively high reactance transformers (7.5 per cent) were used and the total reactance from the substation bus was kept high, thus holding the short-circuit currents to low values but necessitating the frequent use of synchronous condensers and capacitors. The use of capacitors was gaining in the later years.

The network protectors were mostly pilot wire operated for opening on faults and by voltage relays or pilot wire for closing. Fuses of a special design, capable of interrupting 25,000 amperes at 400 volts, were used as back-up protection. Buchholz relays were universally used on distribution transformers for network use.

Figure 12. Damaged reinforced concrete shelter over exciter of a turbogenerator

Protective Measures Against War Damage

With the beginning of the war, plant managers were ordered to take measures for the protection of essential plant equipment and personnel. Personnel shelters were built in two types

1. For the protection of essential operating personnel at their posts.

2. Mass shelters for other plant personnel and office forces.

For essential plant personnel, individual shelters were provided (Figure 11). In some cases these were equipped with instruments for the supervision of most important plant functions, such as steam pressure, boiler feed water pressures, voltage, and frequency. In plants built during the war such shelters were integral with the turbine or generator foundations, smoke stack foundations, and so forth, elaborate instrumentation was provided, and remote controls were furnished.

For less essential plant personnel and office forces, mass shelters were provided under foundations and in the form of specially built cone shaped antiaircraft towers, built of concrete with 9-foot thick walls, up to six floors in height. In the base of such structures, emergency communication equipment, supervisory in

struments and controls were located. Such structures could not only accommodate the plant personnel not on duty, but also the families of all plant personnel as well.

For the protection of rotating machinery in the plant, various devices were employed. Most frequently observed were portable concrete structures, built in the cross-sectional shape of the letter A, reinforced and provided with lifting eyes for handling by means of cranes. These structures were eight feet high and approximately three feet wide, with interlocking joints to permit assembly into walls. These were found set up around generators, exciters, turbine valve gear, and turbine control boards. In addition, roofs were frequently found over turbogenerators made of concrete slabs supported on pipe frameworks (Figure 12). Semicircular reinforced concrete shields were also used, a pair of which formed a circular arc over a piece of equipment. These too were designed with interlocking joints so that a complete enclosure could be formed by the use of multiple units (Figure 13).

Operational measures were taken during air alarms, such as isolation and sectionalizing of steam pipes, boiler feed pipes, and circulating water piping. As the load dropped during an air attack, electrical machinery was quickly taken off and deenergized.

For large power transformers protective measures consisted of loose brick or cinder block walls, built to a height of one to two feet higher than the transformer tank. Earth embankments were thrown up between transformers to prevent spreading of oil fires, and fire fighting equipment was expanded and augmented.

All of these measures were highly effective against occasional low saturation raids. These measures were even effective with concentrated raids in that they limited the amount of damage. Only when highest concentration raids were made, were plants consistently shut down for prolonged periods (Figures 14 and 15).

One underground plant was found in Manheim, with a capacity of 30,000 kw obtained from a 1,620-pound-per-square-inch, 925-degree-Fahrenheit boiler and turbogenerator, of which the generator voltage was 22 kv. This plant was built in 1940. The whole plant, excluding coal handling, was built in a circular concrete caisson 100 feet in diameter, 75 feet deep, with 6-foot thick walls, and a 10-foot thick roof, the upper surface of which was 10 feet below grade. It was stated that the construction cost of this plant was practically the same as for a conventional type of plant. A heavy bomb hit, close by, severely damaged the turbine by earth shock.[2,5,6]

War Damage Experience

War damage experience can best be illustrated in terms of the experience of the Rheinische-Westphälische-Elektricitätswerke system, for which system a rather complete report is available.[7]

From the beginning of the war up to the spring of 1943, damage to the German electric utility plant was confined principally to line damage. This damage was from two sources

1. Falling antiaircraft shell splinters.
2. Trailing anchor cables from errant antiaircraft barrage balloons.

Particularly sensitive to falling antiaircraft shell splinters were the aluminum-steel core 110- and 220-kv conductors, strands of which were easily cut, and when cut, unravelled causing line-to-ground and line-to-line short circuits. Anchor cables of errant barrage balloons caused short circuits and even burn-off of conductors. Both types of damage were confined principally to areas of high industrial activity since these areas were also areas of dense antiaircraft defense.

From 1942 on, additional line damage occurred from aerial bombing because of direct blast damage of line structures, conductor damage by bomb splinters, and insulator damage due to direct and transmitted bomb blast effects. During 1942 there occurred on the Rheinische-Westphälische-Elektricitätswerke system 259 cases of line damage on 110- and 220-kv lines by war action, of which 49 cases were due to barrage balloons. In a single day 43 cases of line damage occurred.

Up to the end of 1942 no serious damage had been done to power plants, although a few isolated attacks by aircraft upon industrial plants resulted in minor damage to adjacent power plants. As a whole, up to the end of 1942, there had been no serious interference with the production and transmission of electric power.

With the beginning of 1943 came the beginning of concentrated air attacks against selected industrial plants, such as synthetic chemical plants for the production of motor fuel, rubber, and nitrogenous chemicals. With the beginning of 1943 also came the first concentrated area attacks upon whole cities. The stepping up of aerial attacks that year caused line

Figure 14. Bomb damage in turbine room
Ljungstrom turbogenerator in the background

damages to the amount of 197 cases for the first $3^1/_2$ months on the Rheinische-Westphälische-Elektricitätswerke system alone. In February 1943, an area attack upon the city of Cologne severed 43 110- and 220-kv lines, isolated the southern half of the Rheinische-Westphälische-Elektricitätswerke system from the northern half, and interrupted the connections between the 450,000-kw Goldenberg plant and the Brauweiler substation. The system lost 360,000 kw of generating capacity, which was made up by emergency transfer of 340,000 kw over undamaged 220-kv lines. This attack occurred on a Saturday; by Monday all essential lines had been repaired and restored to service.

Figure 15. Heavy bomb damage in a turbine room

Up to this time, all damage was easily and quickly repaired since the damage was practically confined to overhead lines.

March and May 1943 brought the first concentrated area attacks upon the Ruhr area and the city of Essen. These attacks created severe damage to underground distribution facilities, which from that time on could never be completely restored. The restoration efforts were directed principally to the re-establishing of service to industrial plants and other essential services, such as street car transportation systems and hospitals. As most of such essential consumers were radially fed, restoration was quickly accomplished. Repairs to the low voltage network were slow and difficult and finally after repeated attacks, were completely abandoned.

Up to that time the generating plants were loaded to capacity and the curtailment program was in effect to limit the demand over peak hours. The destruction of customers' industrial plants eased the load situation, so that the electric power plants were somewhat relieved.

In May 1943 came the celebrated attacks upon the Möhne and Eder dams. The loss of the Eder dam resulted in a capacity loss of 120 megawatts for 8 months because of damage of the hydro plants associated with this dam. As this development was a pumped storage plant, its loss was particularly severe. The loss of the Möhne dam, which had no hydroelectric plant directly associated with the dam, resulted in the loss of the Koepchenwerk pumping plant and a number of smaller plants along the Ruhr River by flooding, amounting to approximately 200 megawatts loss for four to six months.

From that time on, until May 1944, approximately 300 megawatts of the German utility system's capacity were unavailable because of war action (Figure 16).

From May 1944 on, sharply increased attacks resulted in rapidly increasing outages resulting from damage of plant facilities. Beginning with a capacity loss of 700 megawatts in May 1944, the capacity loss reached 1,900 megawatts by the end of October 1944. That date was the beginning of cessation of co-ordinated operation. Even up to that date, however, destruction of consumer plants kept apace so that the remaining plant capacity was able to supply the remaining demand with varying degrees of curtailment. After October 1944, one can no longer speak of a co-ordinated utility system. Conditions became rapidly chaotic. With the destruction of railroad communication, coal supply could no longer be maintained and restoration of damaged plants ceased.

Although official records stop with the end of October 1944, giving a total loss due to direct war action of approximately 1,900 megawatts, and although an official German statement gives the loss due to war action for January 1945 as 3,110 megawatts, the actual loss of capacity for the public utility system at the end of the war was probably between 5,000 and 6,000 megawatts, not counting as loss the unavailability of plants because of occupation.

Summary

1. Although the German electrical utility undertakings had facilities for nation-wide interconnections, and although they had a

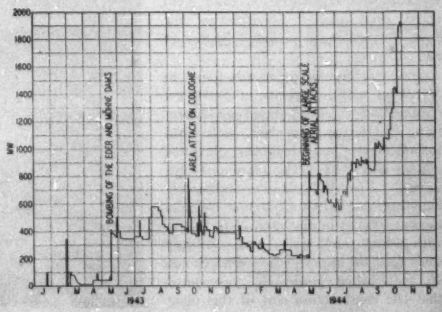

Figure 16. Capacity loss due to war action

well co-ordinated operating organization, the German electrical utilities did not succeed in nation-wide interconnected operation, mainly because of technical limitations.

2. Germany, like the United States, entered the period of World War II with identical percentages of spare capacity. Germany, unlike the United States, began to feel capacity shortages as early as 1940, which shortages became more pressing as the war progressed, while in the United States there was at no time during the war a shortage of capacity.

3. Except for the rapid development of air circuit breakers, development in design and construction of plant facilities progressed, in general, along similar lines as in the United States, although with somewhat less regard for reliability.

4. Although the German electrical utility industry was never a primary target for aerial assault, it suffered considerable damage principally through aerial warfare.

5. The collapse of the German electrical utility system was coincidental rather than contributory to the general industrial collapse of Germany toward the end of the war.

References

1. Statistches Yahrbuch für des Deutsche Reich (book). Germany Ministry Economy, Interior Department, Berlin, Germany, 1938.

2. United States Strategic Bombing Survey, Utilities Division Industry Report. United States Government Printing Office, Washington, D. C. August 10, 1945.

3. The German Wartime Electricity Supply. British Intelligence Objectives Subcommittee Report, H. Neubrunn. British Ministry of Economics, London, England. United States Government Printing Office, Washington, D. C.

4. The Electric Light and Power Industry in the United States. *Statistical Bulletin number 12*, Edison Electric Institute (New York, N. Y.) 1944.

5. The Power Industry of Germany; War Utilities Subcommittee Report, (volume 2), H. A. Bauman, W. W. Cerna, E. H. Horstman, H. J. Scholz, C. F. Wagner. Technical Industrial Intelligence Committee, Washington, D. C.

6. Few German Practices Found in Advance of American, H. J. Scholz, C. F. Wagner. *Electrical World* (New York, N. Y.), November 10, 1945.

7. United States Strategic Bombing Survey, Utilities Division Report Number 21. Electric Power. The RWE System of Western Germany. United States Government Printing Office, Washington, D. C.

8. The Power Industry of Germany; War Utilities Sub-Committee Report (volume 1), H. A. Bauman, W. W. Cerna, E. H. Horstman, H. J. Scholz, C. F. Wagner. Technical Industrial Intelligence Committee, Washington, D. C.

Discussion

C. W. Mayott (The Hartford Electric Light Company, Hartford, Conn.): This paper gives a most excellent presentation of the German electrical utility industry in a complete, concise, and understandable form by a man who is eminently fitted by training and first hand knowledge of all the facts as he presented them. Noest was one of the committee appointed by the Army to personally inspect and report on the German systems.

As shown in his paper, our industry in this country was considerably in advance of the German industry in many phases. In some they were our equal, and a few they surpassed us. It is to be noted that the total capacity of the German system was approximately one quarter that of the United States. In interconnections and co-ordinated operation, the German systems were materially behind this country. We have areas of much greater capacity than all the German systems operating in parallel continuously. We have other areas where this is done whenever there is any justification for doing so. In case of war such areas would be continuously in parallel. Our equipment for such operation is materially in advance of the Germans. Our trained personnel has the knowledge which the Germans had not acquired. In this country the industry effectively handled the operation of the interconnections with nominal advice from the Office of War Utilities which was manned by personnel from the utilities. Our line protection is basically different as they use the Petersen coil which has very little use here.

Noest reports that the German systems use much forced oil circulation in the transformers. This has been used in Hartford, Connecticut, for some 45 years although it has not had universal use in this country. The records show that the German load decreased almost as fast as the decrease in available capacity. As stated by Noest in the summary, the German electrical utility industry was never a primary target for aerial assault. If substations and power houses had been a primary target for aerial assault, the situation probably would have been vastly different. This must be given very careful consideration in future war planning.

In "Capacity and Generation of the German Electrical Utility Industry," he states that ten 300-megawatt plants were started in Germany in 1941 and that none were finished during the war. Efforts were made in this country to start a large hydro program during the war, a program which could not have been completed before the war ended and which would have caused material interference with the war effort. This was curtailed by the War Production Board and the Army and Navy Munitions Board. The load factor in this country was improved so that we obtained the equivalent of some 12,000,000 kw over and above the capacity on the basis of the prewar load factor. One big contrast was in the use of electric precipitators which were quite universally used in Germany as compared with our less general use in the United States. Part of the justification of this, was the war consciousness which made it desirable to keep down the telltale smoke columns as much as possible.

It is to be noted that Germany had a number of pump back stations. Some of these were of relatively large capacity, large enough to put the steam plants on a high load factor base operation. The only pump back station that I know of in this country is that belonging to The Connecticut Light and Power Company at New Milford, Conn., known as the Rocky River Plant with a capacity of some 25,000 kw.

George M. Tatum (Virginia Electric and Power Company, Richmond, Va.): I do not pretend to be an expert on this subject. Most of what I know about it, I have learned from Noest's paper. I will try to confine my discussion to planning our own electric systems to benefit from German experience.

Noest gives statistics on kilowatts and kilowatt-hours per inhabitant showing a three-to-one ratio for the United States to Germany. The area of the United States is, however, approximately 11 times that of Germany. Kilowatts per square mile is approximately 50 for Germany, 17 for the United States. Concentration of power in central and western Germany is probably of the same order as in the northeastern United States. The German experience therefore, should, teach us something of what may happen to the electrical utilities of North America in case of concentrated aerial attack.

We hope that there will be no more major wars, but leaving ourselves unprotected will not reduce the probability of an enemy attacking us. A major factor in our recent victory was the capacity of the North American countries to produce materials of all kinds. We must be prepared to produce even more if we are involved in another war and to produce with our countries under direct attack from which we were spared in 1941–45.

The most devastating weapon of World War II was not used against Germany. A single atomic bomb, effectively placed, would virtually destroy any North American city. If a city were destroyed, the extent of damage to its electric systems would be unimportant. Efforts are being made to develop international control of atomic energy and to outlaw its use in warfare. I do not believe that any nation would forego the use of atomic bombs and thereby lose a war which it could win by using them. On the other hand, the international commission would necessarily have broad powers of investigation and would notify the world if any nation started to produce the components of atomic weapons. Poison gas was not used in the recent conflict and I believe there is a basis for hope that atomic bombs will not be used in the next. In any case, we can learn nothing from the German experience about the effect of atomic bombing.

We can learn a great deal about the effect on an electric system of intensive bombing with ordinary high explosives and incendiaries and the general strain of total war over a long period of time.

Generation

We must give the Germans credit for ingenuity in utilizing very low grade fuel, but, thanks to our abundant natural resources, there is no need for us to follow their example. I note that the kilowatt-hours per kilowatt for the "brown coal" plants

dropped from 4,050 in 1937 to 3,380 in 1944 while energy per unit of capacity for other sources increased from 2,520 to 3,540. Whether this drop in load on the brown coal plants was due to war action, unscheduled outages or other causes is not indicated.

The German electrical industry apparently suffered much more severely than ours from unscheduled outages. We were sometimes unable to obtain materials for minor repairs, resulting in breakdowns and major repair jobs, but we did enjoy a high priority for materials and essential manpower and particularly for breakdown repairs so that unscheduled outages were usually of short duration. If there should be a tendency to lower these priorities in a future war, the German experience may provide a convincing argument against it.

In comparing our experience with Germany's, we should bear in mind that Germany was at war for two years longer than we were, suffered damage from enemy action and was operating under curtailment with resulting pressure to defer and reduce scheduled outages. I believe an important part of our defense system should be liberal reserve generating capacity. In 1946, the peak load on the electric systems of the United States was approximately 90 per cent of installed capacity. The ratio of capacity to load will probably continue critical through 1948 and capacity to provide normal reserves apparently cannot be installed before 1950. If we pull through this period without curtailment or extended interruptions of service, there may be a tendency to conclude that prewar reserves were much greater than necessary. It should not be forgotten that it was primarily because of these prewar reserves that electric power was never too little or too late. Also we should not overlook the fact that large amounts of materials, shop space, and manpower which might have been devoted to direct war production were expended on generating plants, both public and private, in those areas where reserves were a minimum.

It is interesting to note that the only underground power station in Germany was severely damaged by a near miss of a heavy bomb. Apparently, going underground is not the right answer.

Circuit Breakers

I have a great respect for outdoor oil circuit breakers. I believe that, in normal operation, the danger of a disastrous oil fire resulting from explosion of one of these breakers operated within its rating is negligible. I doubt that air circuit breakers for 115 kv and higher voltages will supplant oil breakers until it can be shown that, when produced in equal quantity, the over-all cost will be about the same for air as for oil breakers. Perhaps we should provide sumps with drains to carry the oil away in case of bursted tanks resulting from enemy attack.

It is almost universal practice in this country today to avoid use of electric equipment containing insulating oil inside of power stations. This should reduce fire hazard in case of bombing.

Transmission and Distribution

One outstanding difference between German and American transmission practice is the extensive use in Germany of resonant grounding. This type of grounding imposes limitations on interconnections, requires transpositions that are otherwise unnecessary, reduces flexibility of operation, imposes high dynamic voltage stresses on equipment, and requires reducing the margin of lightning arrester protection. Since most of the benefits obtained by this type of grounding are provided by high speed switching and reclosing without incurring any of these disadvantages, I doubt that the Petersen coil is practical for large transmission systems in this country. Resonant grounding must be particularly disadvantageous with abnormal system setups that must frequently occur when subject to enemy attack.

In Germany as in other countries subjected to heavy bombing, overhead lines suffered only minor damage which was quickly repaired. Underground distribution on the other hand was so severely damaged by earth shock that efforts to restore it were abandoned. It would be interesting to know whether all types of cables suffered equally; particularly if oil filled pipe cables were used and, if so, whether they were less subject to damage than other cables; also whether direct buried cables were damaged the same as cables in conduits. I wonder if the author has any additional information on this subject.

I believe there is a lesson for us in the relative immunity of the overhead lines to irreparable damage.

In many of our smaller cities there was, before the war constant and increasing pressure to force the electric lines underground. While the utility companies and the operators of municipal electric systems generally opposed this change, they were frequently forced to yield. I believe this opposition should be strengthened as a result of the war and every reasonable expedient should be tried to avoid major underground installations in these cities.

In our larger cities, distribution is generally overhead in residential areas, underground in heavy commercial areas and partly overhead, partly underground in industrial areas. The overhead lines in many cases can only be supplied through the underground system.

Perhaps overhead distribution could be designed to supply areas of heavy load concentration, but I doubt that it would have public acceptance. Our electric service has not yet been interrupted by bombing.

In some of our cities, overhead transmission lines are extensively used (Examples: Philadelphia and Pittsburgh). In other cities there are no overhead lines at all. Electric loads continue to grow and, in many cities, additional circuits are now needed to deliver power from generating stations to load centers. I suggest that, wherever possible, these circuits be run overhead and operate at the highest practical voltage. In many cases, overhead construction will cost more than underground because of routing difficulties and because phase shifters or series transformers and capacitors will be required to make the overhead lines carry the desired load where operated in parallel with cables. They may turn out to be lifesavers in restoring essential services in case of bombing.

Conclusion

I realize that engineers alone cannot build our electric systems for the next war. Cooperation of management and of public authorities is required. We can at least make an effort to obtain that co-operation.

I have premised this discussion on the assumption that we must prepare for another war at some future time, but that atomic bombs will not be used. If effective means to prevent atomic bombing are not devised, I know of nothing that we can do as electric utility engineers to reduce the catastrophe. Our greatest cities should be abandoned and their people dispersed through thinly settled areas. This would require so great a change in our civilization that I doubt if it can be done until after an atomic war. At that time the problem will at least be simplified, in a way, because our civilization will have been largely destroyed along with our cities and there will be few people left to disperse. Presumably, our enemies will have met with similar disaster. I feel that the efforts to control atomic energy must meet with success.

Robert Treat (General Electric Company, Schenectady, N. Y.): This paper contains much food for thought. One of many interesting subjects for speculation is suggested by studying Figure 1, then Figures 2, 12, 14, and 15, and finally Figure 16.

According to Figure 1, as early as the fall of 1941, the German electrical industry was unable to carry its peak load; during the winter of 1941–42 it was deficient by some 550,000 kw.

Figure 16 indicates that there was no substantial loss of generating capacity resulting from bombing until May of 1943 and, except for brief periods, the total capacity loss for all Germany amounted to only about 400,000 kw until May of 1944, after which the loss due to bombing grew rapidly.

I suppose it is natural for a person to feel that the industry with which he is associated and which therefore he knows best is the most important. A man in the ball-bearing industry would feel that the German war effort could have been vastly slowed down, if not stopped completely, by destroying their means of producing ball-bearings. Ditto synthetic gasoline; ditto synthetic rubber and other chemicals; ditto transportation, and other vital elements.

Therefore it is easy for one who has had a life-long intimate association with the public utility industry to convince himself that a policy of bombing German power plants just as early as it would have been possible to do so, and of continuing the bombing sufficiently to keep them out of operation would undoubtedly have so paralyzed German industry that their war machine would have broken down earlier than it did.

This matter is worthy of some thought by public utility men who are skeptical that the world has yet achieved permanent peace.

J. B. McClure (General Electric Company, Schenectady, N. Y.): In comparing our electrical industry with the European electrical industries, I fear we are prone to conclude that ours is generally superior. This interesting paper reveals that in some respects, at least, the German electrical industry was more progressive than ours.

Although they did not realize any benefits from it, the advantages of standardiza-

tion of power plant equipment were recognized about 1940. Our efforts along this line began in 1944, and partial results are being realized now on the larger rotating equipment. It is inferred from the paper that the German standardization program also included steam generating equipment, and I am wondering if this is correct.

Their newer generators have a short-circuit ratio of 0.5—even the older ones have a ratio as low as 0.7—and most of their generators were equipped with automatic voltage regulators. This is a goal that is being slowly approached in this country. Our preferred standard generators and industrial-size generators still have a short-circuit ratio as high as 0.8, and several metropolitan areas have not as yet applied automatic generator voltage regulators.

In contrast to this, however, much of their generation is designed for unusually low power factor. This is in line with the practice of supplying reactive power from the generating stations, not only for near-by metropolitan loads but also over transmission systems with consequent large transmission line voltage regulation. This difference in the design and operating practice on high-voltage systems is one of the major obstacles to the adoption of suitable international standards for high-voltage equipment.

Tables I and IV contain some very interesting information. If our construction program for 1947 continues at the present rate for the rest of the year, we will have increased our generating capacity by approximately 10 per cent, making use of our normal facilities and under peacetime conditions. In 1942, Germany increased its generating capacity by approximately 7 per cent, which appears to be an outstanding performance in the midst of a total war effort.

C. W. DeForest (Columbia Engineering Corporation, Cincinnati, Ohio): The writer was in England and Germany from March to July, 1945, as "London representative" of the Technical Industrial Intelligence Committee and organized the Public Utility Section of the Technical Industrial Intelligence Committee and later returned to Berlin, Germany, as Chief of Public Utilities for the United States from December 1945 to February 1947.

The following remarks represent the experience gained during these two periods of service.

The electric energy generating capacity in Germany treated in the paper includes only the public utility capacity connected to the "grid." The total capacity in Germany, including industrials, equivalent kilowatt capacity, totaled between 22 and 24 million kw. The equivalent kilowatt-hour production in 1943–44 was from 75 billion to 77 billion.

Of the total production, about 40 per cent was produced by industrials.

It was difficult to obtain accurate figures, even from the German central records office in Berlin, where we had assembled all records available, and had preserved the "nucleus" of the various German societies and groups operating Germany during the war.

The records and personnel were scattered in the United States, Russian, and British sectors and zones and many records had been destroyed or lost. However, the figures mentioned above give a fair approximation of the total capacities in Germany during the war.

A sizable proportion of the industrial capacity in industrials will not be useful in the post-war period, as much of it was in strictly war potential industries, which are completely restricted. Some are in plants which were destroyed and others in industrial plants given up for reparations.

In the assessment of electrical capacity for reparations by the quadripartite groups, the industrial capacities were included with the grid connected public utility plants to arrive at the total capacity.

The greater part of hydro capacity was located in the United States zone, French zone, and adjacent territory in Austria.

There was about 1,000,000 kw of installed hydro capacity in the United States zone proper. This included many small installations, low head plants, strung out along the rivers and controlled from one location. The firm hydro capacity in the United States zone during the six months of October to March was 350,000 kw based on 1943. If the year 1934 (a low year) had been taken as a basis, the capacity would have been approximately 250,000 kw. In addition to the hydro capacity in the United States zone of Germany proper, Germany had always controlled the hydro power from the Tyrol in Austria, from the Vorarlberg in Austria, and of course from the Schluchsee hydro development in the upper Rheinland or Palestine section, which is in the French zone.

The Vorarlberg hydro development of 280,000 kw, with an annual production of 540 million kilowatt-hours and with large storage capacity, made the full capacity available for peak load use, practically all the year.

This development was planned, financed and constructed entirely by the Germans under a treaty and contract made with the Sovereign Province of Vorarlberg in 1924.

The contract was for a period of 70 years, and was very favorable for the Province of Vorarlberg.

Now that Austria has been declared to be a liberated country, Austria claims ownership of the Vorarlberg, without compensation to Germany for the investment, and has been trying to negotiate with both France and Switzerland, for the sale of Vorarlberg power.

The United States zone of Germany has never been self-sufficient in electric power. During the high output months they have a surplus of hydro, which was transmitted to the west and north, but during the low hydro months, thermal generated power was transmitted to the United States zone from the Ruhr, or brown coal power was transmitted from the north (now the Russian zone).

As described in the subject paper, the German network consisted of two 230-kv circuits, in the shape of an inverted horseshoe, with the open ends resting in Eastern Bavaria and in Greater Hessen.

There are no transmission facilities to take hydro power from Bavaria directly across the United States zone to Wurttenburg Baden, Greater Hessen, and to the Ruhr. Likewise, thermal power from the Ruhr or Western Lands of the United States zone cannot be transmitted to Bavaria. The usefulness of the Eastern leg of the 230-kv network, has been destroyed by the Russians, as they have removed one 230-kv circuit from Helmstedt on one boundary of their zone, to Remptemdorf on the other boundary, together with all transformers and switching. In addition many other important transmission circuits in their zone, and transmitting equipment to Berlin, have been removed.

Before I left Berlin, authority had been secured to build a 230-kv transmission line between the East and West in the United States zone, thus closing the open portion of the horseshoe transmission system.

When this construction is completed, it will enable the United States and British zone to move surplus hydro power and thermal power where and when available and needed, thus making the greatest possible use of hydro power and conservation of coal.

Even though the 230-kv network was intact, the Russian zone, with its large brown coal generating capacity, would have no surplus power to send to the United States zone.

The quadripartite decision to limit the total electric capacity to 9 million kw, including public utility and industrial, was the result of a "poker game" decision, purely a compromise and not based on a factual economic study. Of the 9-million-kw total capacity to be left in Germany, the Russian zone was allotted 2,900,000 kw. They promptly stripped their zone to the allotted figure of 2,900,000 removing all of the newest and best facilities.

The 2,900,000 kw retained was made up of nameplate ratings, with the idea that by 1949 all equipment would be fully repaired and restored to full rated capacity. The result was that 1,400,000 kw was the maximum capacity obtainable during 1946 from the 2,900,000 kw left in the Russian zone and that for a short time only. Therefore the Russian zone is now a liability on the western zones so far as electric power is concerned.

The so-called "level of industry" and consequent electrical capacity, was arrived at too soon after the war. It was dictated more by emotion than by economic factual study and is now in process of being revised.

Germany as well as other countries of Europe is now right in the "lap" of the United States. Europe cannot be stabilized until Germany has become self-supporting and Germany will be a drain on the American taxpayer until she can earn her own way.

The only way Germany can become self-supporting and pay for her necessary imports of food and other raw materials is by exports. That means that Germany must sell in the world market, in competition with other countries, and to do so, must have the same efficient means of production as other countries, and that means electric power.

From my experience, I believe the Germans will co-operate, if we treat them properly. They must be encouraged. Human nature reacts the same the world over and you cannot regenerate a peoples unless they have something to live for.

We must realize that the present German generation was raised on Nazi propaganda. It is all they knew and any nation raised under the same conditions would react largely in the same manner.

The situation in Germany should be faced

realistically and the proper methods applied. If Germany is left a "cesspool of discontent" it will spread all over the world and fall directly under Russia's influence.

The recent report of ex-President Herbert Hoover is the first factual statement on Germany and existing conditions that I have seen coming from authoritative and high level sources. He has "hit the nail right on the head."

Eric T. B. Gross (Illinois Institute of Technology, Chicago, Ill): The author has given us very valuable information, not otherwise available, in the form of a digest and should be congratulated for his fine presentation. Limited space did not permit him to do more than mention some items, and I would like to ask a few questions.

The generally applied method for all schemes (unit connection or the parallel operation of generators on bus bars) was the grounding of generator neutrals through high resistances which lead to a single line to ground fault current of 5 amperes average. Very ingenious devices were in use to keep the fault current at approximately the same magnitude wherever the fault occurred, near the terminals or near the neutral-point of the generator. This type of neutral grounding (in use since 1928) was made by means of nonlinear resistances on the secondary of distribution transformers. Noest mentions in the chapter on equipment that the generators were operated ungrounded. It should be of interest to know why these changes were made, and if the reference made concerns unit operation only, or also generators which are synchronized on bus bars?

In contrast to the practice in our systems, voltage regulation of the large German 220-kv system was achieved mainly by shunt reactors (and not by synchronous condensers), and high exciting currents of transformers could be permitted. High saturation requires large fundamental frequency magnetizing currents and large higher harmonics of the 3rd, 5th, and 7th order. One German manufacturer (Allgemeine Elektricitäts Gesellschaft) developed transformers with auxiliary exciting windings on the split-yokes which provided the 5th and 7th internally so that the current taken from outside terminals was of sinusoidal wave shape. I am wondering if the author refers to this special construction, or the usual type of transformer produced by the other German manufacturers? Further, a mention of which part of Germany, which systems, and system voltages the report covers would provide helpful additional information.

It is well known that practically all systems in Germany, overhead and underground, 2 to 220-kv, are resonant grounded by means of ground fault neutralizers (Petersen coils) designed for continuous operation. Hence, ground faults are not short circuits and they are removed by manual breaker operation on the basis of the indications of sensitive ground relays at the various substations. Up to the beginning of the war there had not been found a limiting value for the self-extinction of the residual arc current in any system. Arcing ground faults in the 110-kv Bayernwerk comprising approximately 2,000 miles of interconnected lines, or in the 30-kv underground cable system of the city of Berlin with a residual arc current of 120 amperes (in-phase plus higher harmonics) were self-clearing. I am wondering if the separation of the 220-kv system (with an estimated in-phase residual arc current of 80 amperes) was really necessary to make arcing ground faults self-clearing? When the western part of the 220-kv system was designed (long before Hitler) it was decided to operate the two 220-kv circuits of this line in synchronism but electrically separated, and suction coils were installed in addition to Petersen coils to eliminate the capacitive (zero-sequence) coupling of the two circuits. The main idea was to prevent or reduce the number of consequent ground faults. The separation of some parts in the western and eastern sections of the 220-kv system in case of disturbances should be natural and in line with this principle. I am wondering if Noest knows of tests indicating that arcing grounds in the interconnected 220-kv systems were not self-clearing? The residual arc current as such gives no indication of self-clearing. Restriking of an arc to ground will be prevented if the recovery of the ionized arc space is quicker than the voltage return across the electrodes. Only high losses to ground of the system would influence this phenomenon, and it may be possible that corona losses in this large 220-kv system increased the in-phase component of the residual arc current so considerably that self-clearing was prevented.

I am wondering if the author would check my opinion that the breaker itself is shown on the extreme left of Figure 6, whereas the various pots in the front row and to the right are current and potential transformers of the "oil-poor" type which have been in use in Germany for the last 15–20 years.

J. G. Noest: C. W. Mayott's discussion brings up two pertinent points: one pertains to the operating procedures with which the German interconnected system was operated. The German utility operators and their system operators or load dispatchers were not only confounded by the existing technical limitations, some of which were described in the paper, but by political interference as well. Frequently the district of a load dispatcher was politically assigned to a District Leader (Gauleiter) whose influence was considerable. Cases were described, where the political district leader over-ruled the load dispatcher's assignment of curtailment. Moreover, favored industries were often exempted, through political pressure, from the general curtailment program. Such favored industries were those dominated by Goering and others, high in the ruling clique.

The other point raises the question of developmental superiority of the United States electrical utility industry versus that of Germany. Since economic conditions in the United States and in Germany are not comparable, the author can make only a general statement on this subject. In some lines German development was advanced, in others, it was behind that of the United States.

Mayott also mentions the use of forced oil cooled transformers. In the opinion of the author, the use of this type, particularly in triple rated transformers, is gaining in this country, because such equipment allows economic provision for second contingency operating problems.

G. M. Tatum's discussion gives his speculation on possible effects of war on the public utility industry in this country. In this country, with the public utility industry largely in private ownership, plant development is a matter of local economics. Each utility system develops its plants according to economic studies with the principal purpose of providing low cost electric energy with a satisfactory return on invested capital. Such utility companies cannot, on their own accord, incorporate in the design of utility plant provisions for defense in a future war. As long as regulating bodies can show only one aim in their policies, that is: A continual reduction of energy costs, which after all is the only way, under present conditions, that these regulating bodies can justify their existence to the public, so long can public utility companies design and develop plants only in accordance with such principles.

The planning of utility industry plant, as well as other industrial plant, with a view toward possible future war, is in the author's opinion, entirely neglected in the United States. No one at present knows what the cost of such planning might be; neither does any one know what design features should be incorporated in such planning. The author believes that here is a field in which some committee could do valuable public service.

Respecting Tatum's comments on deferred maintenance, the statistics given in the paper, do not tell the whole story, since these statistics only cover actual outages. There is a more insidious phase in this problem; for instance, plants were found which could not deliver rated capacity by various percentages, without actually having an outage in any equipment. The situation was this; here was one turbine with a row of blades missing, resulting in an increase in the water rate and thereby also in a reduction in capacity. There were boilers, in which a number of boiler tubes had been removed because it was impossible to obtain replacements. Elsewhere were pieces of apparatus in service with haywire repairs. All of these factors together reduced the peak of capacity considerably, while not disclosing their presence individually in any noticeable way. Such situations existed throughout the whole industry.

Robert Treat makes an interesting point, which illustrates the difficulties, with which the General Staff of the Armies is confronted, in choosing targets for attack. Generally, the situation is further confounded by the fact that, when such a choice must be made, there is always not enough war material and equipment on hand. The General Staff, therefore, must find its industrial target, on which, with the least amount of equipment, most over-all damage can be done.

C. W. DeForest's discussion adds to the paper by giving a continuation, as it were, to it. The recent presentation of the Marshall Plan is a confirmation of the validity of the comments made by this discusser.

In respect to McClure's remarks on standardization of equipment in Germany, the author would like to add that he was impressed by the degree of standardization achieved in the electrical utility industry in Germany. For instance, all bushings of the same voltage class and current ratings were

interchangeable, regardless of manufacture. Any one interested in the degree of standardization, which existed in Germany, need only look at a number of issues of the *Elektrotechnische Zeitschrift*.

E. T. B. Gross raises a number of questions in his discussion. The author wishes to point out that in a paper, such as the one presented here, it is necessary to make generalizations, which may not apply in all individual instances. In respect to the grounding of generators, the author did not consider a system to be effectively grounded, if it was grounded through potential transformers or small distribution transformers, only for the purpose of obtaining ground indication. Certainly such grounding did nothing to limit neutral to ground voltage on the system so that no advantage in insulation level could be taken. The above comments apply chiefly to generators, which were synchronized only through 110- or 220-kv busses. For generators, synchronized at generator voltage busses, all sort of variations of grounding procedure were observed.

In respect to Gross's comments on power transformers, manufactured by the Allgemeine Elektricitäts Gesellschaft in which special devices were employed for the suppression of harmonics, where high flux densities were used, the author can state only that such special devices were not mentioned by the German engineers, with whom such transformers were discussed. In respect to the questions raised by this discussor on the Petersen grounding of high voltage lines, it can be said that no particular difficulties were experienced with this type of grounding, until it was applied to the 220-kv system; only on this system was it necessary to limit the extent of metallically connected parts for the purpose of reducing residual arc current. The operators of the Rheinische-Westphälische-Elektricitätswerke system stated that they found it necessary to hold the residual arc current to values somewhat less than 30 amperes in order to assure self-extinction.

Doctor Gross's question in regard to Figure 6 is answered in the affirmative.

Typical Transformer Faults and Gas Detector Relay Protection

J. T. MADILL
ASSOCIATE AIEE

Synopsis: This paper describes a number of typical faults which have been experienced in large transformers on the Saguenay system. Cases are noted where gas detector relay protection would have obvious advantages. Some conclusions are noted regarding the value of this type of protection, based on faults selected from operating experience with 124 transformers over a period of about 26,200,000 kilovolt-ampere-years. Illustrations of incipient faults which have been detected by gas relays are included.

THE OBJECT of this paper is to present a description of several different types of transformer faults which have occurred on the Saguenay system. These transformer faults, it will be shown, are of the type which cannot be detected readily by ordinary relay protection, in the initial stages, but which are most readily detected very early in their development by gas detector relays. It is thought that this experience will illustrate some of the general types of transformer trouble found on one large Canadian power system, and it is hoped that it will illustrate some of the types of troubles which may be picked up by gas detector relays. These gas detector relays have been described before.[1] Briefly, they are usually mounted on, or adjacent to, the top of the transformer, and are connected by a pipe to either the transformer top, or to the connection to the conservator tank. They usually have two elements, the first, a float chamber for the accumulation of gas, operates an alarm, and the second, a diaphragm element, usually operates the trip circuits upon a sudden pressure rise.

All transformers referred to in this paper are single-phase 60-cycle conservator-type oil-insulated water-cooled units.

The following section will illustrate some typical faults.

Figure 1. New supporting structure and bus burns in an 18,750-kva transformer after failure of wooden support

Transformer Faults

Defective Insulating Structures

In a transformer of one manufacturer in use on the Saguenay system, the connections from the ends of the low voltage coils to just below the inner terminal of the bushings, are made with sections of 4- by 1/4-inch copper bus bar. This bus bar is supported by pieces of hardwood, some of which are $4^1/_2$ feet long, and all are about two by four inches in section.

These transformers are rated 56,250 kva for a bank of three single-phase units, 154,000 volts Y, 89,000 volts delta, 69,000 volts Y, and 44,000 volts delta to 13,200 or 6,600 volts delta.

It was necessary in one case, when reconnecting one transformer bank for use at different low and high voltages, to alter this bus work and the wooden supports in one phase. The transformer was placed in service with a low voltage of about 6,600.

This particular transformer operated on load at a substation as one phase of a 3-phase bank for a period of about eight days. On the eighth day the bank low-voltage circuit breaker opened automatically. It was observed that the explosion vent was bulged out considerably on this unit. The oil was lowered and an internal inspection showed that a short circuit had occurred between the copper bus bars leading up to the low voltage bushings. This short circuit had developed initially across the wooden support, as evidenced by the severe burning and charring of the wood between the vertical bus bars. This was a new piece of wood. The arc travelled down the bars and Figure 1 shows the result. The

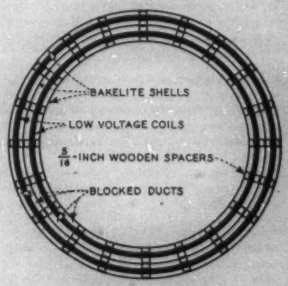

Figure 2. Section through low voltage winding of an 18,750-kva transformer indicating oil duct blockage

Paper 47-139, recommended by the AIEE committee on electric machinery for presentation at the AIEE summer general meeting, Montreal, Quebec, Canada, June 9–13, 1947. Manuscript submitted March 24, 1947; made available for printing April 25, 1947.

J. T. Madill is an electrical engineer with the Aluminum Company of Canada, Ltd., Shipshaw, Quebec, Canada.

Figure 3. Low voltage winding of 18,750-kva transformer showing insulation which blocked oil ducts

wooden support had been replaced by a micarta one when this picture was taken.

Here is evidence of a fault which developed over a period of eight days. During this period the voltage was constantly applied, but it was not until the leakage over the new wood had formed sufficient carbon to carry an arc that the short circuit developed. It is obvious that this type of slow failure of cellulose insulating material can be most readily detected by gas detector relays. It is only after the short circuit that ordinary protection can operate to isolate the transformer, and then the damage is done. This is only one case of failure of a supporting structure in a transformer, but it illustrates the principal. This is what would be expected, the leakage current either raises the temperature of the wood and effectively carries on a fractional distillation, with the carbon and heavier residues being left behind, and with the volatile fractions, which are highly combustible, being driven off, or due to minute local arcs on the surface of the wood, some of the oil is cracked. Hence the gas relay and a gas sampling "Vapotester" or some similar device, provide as adequate protection as can be obtained.

Defective Oil Circulation

Defective oil circulation, and the resultant damage to insulation and conductors due to excessive temperature, is illustrated by a condition found when one large power transformer was untanked for inspection, after about nine years of service.

Figure 2 shows a section through the low voltage coils. It was found that approximately 90 per cent of the oil duct clearance between the helices of the low voltage coils and the bakelite shells, was blocked due to lateral displacement of the cotton tape coil insulation. This bulging (see Figure 3) was caused by pressure exerted through wooden supporting blocks on the coil ends. The insulation was bulged sufficiently to be forced into contact with the bakelite shells, thus almost completely blocking the oil ducts. This stoppage of oil circulation prevented proper cooling of the copper which in turn, caused rapid deterioration of the insulation. The low voltage coil insulation was found to be in very bad condition. The cotton tape covering the coils was baked out from heat and was very dry and brittle. The fiber- and bakelite-impregnated paper insulation between strands in the individual turns of the winding was carbonized in places. In some spots the cotton tape was considerably carbonized.

It is definitely known that deterioration of cellulose insulation, under oil due to high temperatures, produces an inflam-

Figure 4. High voltage winding failure of a 25,000-kva transformer caused by a foreign body imbedded in the insulating cylinder

Figure 5. Damaged high voltage coils of 25,000-kva transformer caused by tap changer trouble

mable gas.[1] Therefore this condition would be picked up as soon as it begins to develop, with gas relay protection in service.

Foreign Bodies in Insulation

A 25,000-kva single-phase transformer was placed in service as one unit of a 3-phase 154,000-volt-Y- to 13,200-volt-delta-connected transformer bank at a generating station. After 9 months and 19 days a high voltage short-circuit developed which did considerable damage to one high voltage coil.

It was found upon dismantling the transformer that a piece of iron wire about six inches long had been left during manufacture, in the insulating barrier next to the high voltage coil and imbedded in the varnish. The high voltage winding was badly burned adjacent to the wire (see Figure 4).

Obviously the main flux linking the transformer windings, had by induction, raised the temperature of this foreign body to a high point, but despite this, a very long period was required for the trouble to develop sufficiently to cause a short circuit. Here again gas detector relays woud indicate the trouble long before it developed to the final state, as it has been shown that a hot metallic body under oil, produces gas continuously.[1]

Tap Changer Trouble

A 25,000-kva single-phase transformer, operating as one phase of a 3-phase 75,000-kva 154,000-volt-Y- to 13,200-volt-delta-connected bank, at a generating station, blew oil out of the explosion vent and produced a slight surge of the system. The bank was removed from service in a few minutes by the operator.

When untanked it was found that one leg of the double tap changer was badly damaged and that six of the coils on the high voltage winding of the corresponding leg were distorted, and showed signs of having carried a very heavy current. The copper of one coil was completely burned off. This is shown in Figure 5.

It was obvious that the trouble had originated in the tap changer from either a loose connection to the leads, a broken or loose connection inside, or poor contact between the movable fingers and the stationary rings. The tap changer is shown in Figure 6. The tap changer interior was completely charred by the arcing. Upon investigation of the coils and tap changer, the manufacturer agreed that the trouble started in the tap changer itself.

The tap setting had been changed on this bank 18 days before the explosion occurred, and the tap setting had not been changed for four years previous to this, when the bank first was placed in service.

This then, points to a condition which developed over a period of 18 days, again a logical condition to be detected by gas detector relays. It is true that a coil short-circuit may perhaps be picked up by differential protection. However in this particular type of trouble, the coil short-circuit was established only after the deterioration of the tap changer caused the formation of an arc, which short-circuited the turns.

Hot Spots

On a 75,000-kva, 3-phase, 154,000-volt-Y- to 13,200-volt-delta-connected bank at a substation, one of the three transformers blew oil out of the explosion vent. None of the ordinary relay protection operated. The high and low voltage circuit breakers were immediately opened by the operator.

When the transformer was untanked, the situation shown in Figure 7 was disintegrated. The arc apparently travelled to the left where another bad burn may be seen. If it is assumed that the trouble started as a turn-to-turn short circuit, it is difficult to explain why the taping around the series joint would have all been burned off, as this taping is very thick. Also, another point against this theory is that in the case of the coil above the one with the missing joint, the burning only progressed to the point where the heavy taping commenced. This is another case in which a hot insulated joint, over a period of time, deteriorated completely. This phenomenon has always been found to be accompanied by the formation of combustible gas.[1]

Figure 8. Main low voltage soldered joint of 25,000-kva transformer

covered. This photograph was taken after the tap changer was removed.

This trouble started in one of the series joints between the coils of the high voltage winding. It may be noted that these joints are rather heavily taped and that one of them is missing entirely. It would appear that the trouble was started by a hot spot in this joint which gradually carbonized the tape and the joint completely

Figure 7. Deteriorated series joint of high voltage winding of 25,000-kva transformer

Figure 6. Tap changer of 25,000-kva transformer after failure

Joint Soldering Failure

Several simultaneous phase-to-phase insulation failures occurred on the 13,200-volt ungrounded circuits served by one 75,000-kva, 154,000-volt-Y-to 13,200-volt-delta-connected transformer bank, located at one substation. After the trouble was cleared away an attempt was made to re-establish service. It was found that one 25,000-kva transformer of the three in the bank, was completely open-circuited on the 13,200-volt side.

The transformer was removed from service and untanked. The trouble started at a point where the coil conductors were soldered to the main low voltage lead, a flexible copper cable about 2 inches in diameter. The condition of this joint is shown in Figure 8. Apparently when the joint was originally made, the solder had not properly penetrated and a high resistance joint was the result. This transformer had been in service for at least 5 years, and presumably this condition took this period of time to develop to a total joint failure. As a point of interest, Figure 9, shows the same condition in a low voltage joint of a 6,000-kva 13,200-to-110,000-volt transformer.

It is now known that the material formed is a mixture of cuprous and cupric sulphide. As the affinity of copper for sulphur is very high, copper and sulphur readily react when heated, forming both sulphides. The product is black, or bluish-black, brittle, with a very high melting point, and an octahedral crystal structure.[5] It is also known that this type of failure gives off a combustible gas which can be readily detected early in the development of the trouble.

Figure 10. Short-circuited and burned high voltage coils of 25,000-kva transformer

Left coil is upside down

Figure 9. Main low voltage joint of 6,000-kva transformer

Internal Short Circuits

One 25,000-kva transformer of three similar ones in a 75,000-kva 154,000-volt-Y to 13,200-volt-delta connected transformer bank blew oil out of the explosion vent. Neither the high or low voltage circuit breakers were opened by any relay protection. The transformer was operating at slightly more than full load, and no switching operations had been carried on for some weeks previously.

When the transformer was untanked, the trouble was found on the high voltage winding of one leg, at a point about the center of the winding (from top to bottom and on the side of the winding opposite where the high voltage terminal leads were connected. It was evident that the trouble had started from a short-circuited turn, which had eventually burned itself clear, and had damaged three coils at the same time. This happened without any noticeable surge on the system. The coils which were removed are shown in Figure 10.

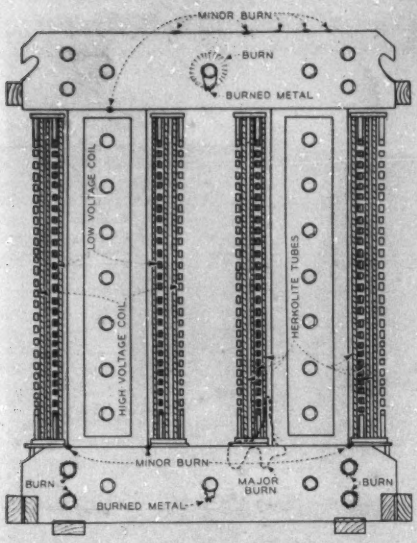

Figure 11. Location of core burns in 18,750-kva transformer

From this, and other data gathered from somewhat similar troubles, it has been concluded that failures of this type start to develop slowly and that the trouble develops more rapidly as it progresses. From this case, and from other evidence, it is thought that this type of failure might be picked up by a gas detector relay, before any explosion occurred. The high temperature of the copper, and the turn insulation at the point of failure will produce gas. However, it is admitted that, in certain cases, the element of time may not permit the operation of the alarm. In any case, the pressure element of such a relay would certainly operate on the final explosion caused by the arc.

Failure of Core Insulation

An explosion occurred in an 18,750-kva single-phase transformer which was operating with two similar ones in a 56,250-kva 154,000-volt-Y to 13,200-volt-delta connected three-phase bank. The explosion blew oil out of the explosion vent, but no relay operation occurred. The transformer bank was immediately de-energized by the substation operator.

Upon untanking it was found that the transformer low and high voltage windings were undamaged, but that very serious and extensive burning had occurred in the core iron and core bolts. These burned spots and areas are indicated in Figure 11. The major burn was located at the inside junction of one vertical leg and the bottom section of the core. This is shown in Figure 12, which is a view looking into the bottom of the window of the transformer. It was estimated that about 420 cubic inches of iron had been lost in this burn.

This transformer had been in service on the system for 12 years. The upper section of the core had been unstacked after 10 years of service, to permit work on the low voltage coils, but the legs and bottom section had never been touched. At the time the top section was reassembled, three of the top core bolts had been reinsulated, and an open-circuit test had been made, then, and again just 22 days before the failure. These indicated normal magnetizing current and a no-load loss only a few per cent higher than that measured in exactly similar transformers.

Here is a case of almost total destruction, and yet no ordinary relay operation occurred. The gas formation from such a breakdown will be considerable and would indicate long in advance, by its persistent reoccurrence and nature, that something is seriously amiss. Since ordinary transformer oil will begin to crack at a temperature of 600 degrees Fahrenheit,

Figure 12. Major burn located at bottom of window of 18,750-kva transformer

Figure 13. Remains of core bolt insulation and one lamination, showing heated area, from 18,750-kva transformer. Condition picked-up by gas detector relay

Figure 14. Main low voltage connection of 30,000-kva transformer

it is obvious that the typical cracking products of the lighter hydrocarbons and methane will be liberated long before the steel or iron is raised to the melting point, even by concentrated local heating. For detecting core trouble, nothing can even approximate the value of the gas detector relay. This was proved by recent experience with a 18,750-kva transformer similar to the one mentioned above, but equipped with a gas detector relay.

The relay indicated the presence of gas, which when tested proved to be highly combustible. The transformer was removed from service and untanked. It was found that the laminations of the top core yoke had become short-circuited around the center top core bolt. The core bolt insulating tube was burned from the outside toward the inside. The condition of this insulating tube and one lamination are shown in Figure 13. For comparison, a new insulating tube is also shown. The heated area on the lamination may be seen clearly.

Here is a direct comparison of the difference in damage with and without gas detector protection. The great contrast between Figures 12 and 13 may be very easily appreciated. There is no reason to doubt that Figure 13 would have been any different from Figure 12, had the gas detector relays not been in service.

Faulty Brazing

One 30,000-kva transformer of a 90,000-kva 3-phase 154,000-volt-Y to 13,200-volt-delta connected bank kept producing gas over a period of several weeks. This gas accumulated in the gas detector relay on the transformer and this was indicated on the station annunciator. This transformer had been in service for almost exactly two years at this time. A sample of the gas was collected and analyzed. The analysis is given in Table I. It shows that about 22 per cent was combustible. The bank was removed from service as soon as convenient, and this transformer was untanked.

The condition shown in Figure 14 was found. When the insulation, accumulated cuprous sulphide and carbon were removed, the remains of a main low voltage conductor joint, as shown in Fig. 15, were uncovered. This trouble definitely developed from faulty brazing of the original joint between the two low voltage coil ends. Since this, eight more similar cases have developed. These have all been detected by the gas detector relay, and using a gas analyzer known as the "Vapotester," the gas has been checked at the relay for combustibility. The relay location is shown in Fig. 16. This method is now proved beyond doubt to be completely reliable, simple, and very effective. Figure 14 may be compared with Figures 7, 8, and 9, in particular. While the actual difference in damage may not appear to be much less in the case of Figure 14, it must be remembered that this transformer was removed at a convenient time, after several gas warnings, while the other three referred to involved internal

Figure 15. Remains of brazed main low voltage joint of 30,000-kva transformer

Figure 16. Location of gas detector relay on top of 30,000-kva transformer

arcs, explosions and power interruptions. The damage caused by an explosion following an internal arc can be far more serious than the actual fault. The service interruption can also be very serious. Therefore, these facts must be kept in mind when comparing the damage found with and without gas relay protection. It is obvious that the gas detector relay is superior to any other protection for this type of trouble.

It has been shown here and elsewhere[1] that gas detector relays will operate on core trouble, with a great reduction in damage, and on any conductor trouble involving an increase in conductor temperature in the presence of ordinary insulating materials under oil, before the trouble produces an electrical break-down.

After about 6,000,000 kva-years of experience with gas detector relay protection, the organization with which the author is associated is now in the process of investing $26,000.00 to equip all 124 of its major power transformers, which are not so protected, with gas detector relays.

Conclusions

It is interesting to note, upon carefully examining all the records, that no transformer fault on the Saguenay System has failed to blow oil out of the explosion vent. In other words, whether the fault developed slowly or almost instantly, if it involved an electric breakdown, it produced a pressure rise. Therefore, it may be concluded that a gas detector relay having both an alarm element for gas accumulation, and a tripping element for a pressure rise, would have detected all faults on record. From some of the examples described previously, it may be concluded that in many cases, ordinary relay protection such as overcurrent, high-voltage and low-voltage neutral overcurrent, or even differential, will never operate until a fault has produced as complete destruction as it can, or this protection may never operate at all. This would seem to indicate quite a strong case for the application of gas detector relays on conservator type transformers, to protect against internal faults.

From the preceding section, it will be obvious that the following transformer troubles can be detected in their early stages by gas detector relays, and by these relays only:

1. Defective supporting and insulating structures.
2. Defective oil circulation and the resultant insulation damage due to excessive temperature.
3. Presence of certain foreign bodies inside of transformer coils or their electrical and magnetic fields.
4. Incipient tap changer trouble.
5. Improperly soldered series joints between coils.
6. Improperly soldered heavy main conductor joints, either high or low tension.
7. A short-circuited turn (this may be detected by differential protection).
8. Core troubles.
9. Improperly brazed heavy main low voltage conductor joints.

What is most important from all of the foregoing is this:

1. By detecting these troubles at an early stage, the equipment may be removed as soon as convenient, instead of being isolated automatically by the ordinary relay protection, after a more or less severe system fault with its attendant customer outage and system disturbance. This factor alone, though difficult to assess may be worth a great deal.
2. By detecting these troubles at an early stage, the cost of repairs is reduced to only a fraction of that otherwise encountered. Here is a direct saving of considerable magnitude. This saving alone is usually worth several times the cost of the gas detector protection.
3. By detecting troubles at an early stage, the possibility of finding the cause, and hence the prevention of the trouble, is infinitely greater. This in turn means that repair costs and outage time in the future will be reduced still further. This is a direct economic saving.

Table I. Analysis of Transformer Gas

Gas	Per Cent
CO_2	0.0
O_2	9.2
CO	0.0
H_2	6.2
Unsaturated hydrocarbons	3.5
CH_4	8.8
C_2H_6	3.6
N_2	68.4

This paper has been a brief attempt to present some actual experiences with failures in transformers, and to illustrate what types of trouble may be detected early in their development. It must not be inferred that the manufacturers' products are considered unusually defective. On the Saguenay system about 26,200,000 kva-years of transformer experience have been accumulated from 124 transformers of 18,750 kva or larger, (over 1,070 transformer years). The cases presented here are the exceptions, but they point the way to substantial reductions in repair costs in the future. It is with the thought that other users of large power transformers may wish to similarly benefit by the protection of gas detector relays, that this material is made available.

References

1. Report of Subcommittee on Gas Detector Relays, Canadian Electrical Association, Montreal, Quebec, Canada, Dec. 26, 1946.
2. A Comprehensive Treatise on Inorganic and Theoretical Chemistry, volume 3, J. W. Miller. Longmans and Company, London, England. Pages 210–14.

Discussion

D. B. Fleming (nonmember; The Hydro-Electric Power Commission of Ontario, Toronto, Ontario, Canada): This paper is a good attempt to exemplify the possible applications of the gas detector relay.

However, the advantages that might be obtained from the gas accumulating feature under "Internal Short Circuits," is open to question. If a transformer should have a between-turn weakness that would in the course of time result in a failure and gas is generated in the meantime, the relay would indicate trouble, but even if the transformer were removed from its tank the trouble would not be easy to locate while in the development stages. The speed of operation of the impulse pressure element after failure occurs would assure the clearing of the transformer from service in the minimum of time and thus limit the resulting damage to a minimum. If only a couple of coils were damaged, the cost of repairs would be very little more than if a defect were discovered in the initial stages. In either case, the transformer would have to be dismantled and the faulty coil replaced, the major cost being the dismantling of same and reassembling.

The Hydro-Electric Power Commission of Ontario has had similar experience and it may be of interest to note a few specific cases.

At one of the commission's generating stations there are in service three 24,000-kva banks of single-phase transformers rated 8,000 kva, 60 cycle, 110/12 kv which were built in 1919 and 1920.

The core bolt insulation was made of fiber sleeves and washers, and was impaired by the high temperatures developed in the core. Two transformers failed in a similar manner at different times after a number of years operation, as a direct result of the carbonizing of the core bolt insulation. The first indication of failure was the final col-

lapse of the transformers. The major portion of the core and one leg of the windings were ruined as the molten silicon steel burned through the cylinders and short-circuited the coils.

In view of these two failures all the transformers at this station were equipped with gas detector relays. Two relays have indicated gassing in their respective transformers since their installation. Their performance was watched closely for a few weeks and finally the transformers were dismantled. The core bolts were removed and reinsulated with high temperature-resisting insulation and the whole reassembled. The only evidence of trouble was the carbonized core bolt insulation and a couple of small burns on one core bolt. The cost of repairing one transformer following the original failure amounted to over $6,000, while the cost of replacing the core bolt insulation amounted to about $750 for each unit.

A 25,000-kva 25-cycle 220/110/13.2-kv 3-winding single-phase transformer equipped with a gas detector relay continued gassing at frequent intervals shortly after installation. Sample of the gas was collected and showed about 13 per cent combustible. During a light load period over a week end the oil was lowered in the transformer and the core insulation tested with a megohmmeter and a lamp bank. The core was constructed with two yokes, concentric and insulated from each other. The core bolts that were found grounded were removed and reinsulated without removing the core from the case. A ground between the two yokes was discovered and was burned clear with a heavy current. It has reoccurred on one or two occasions, evidenced by action of the gas relay, but provision is made in the ground connections whereby it is readily burned clear with a heavy current. Serious damage may have resulted to the core if not detected by the relay.

A failure occurred due to lightning on a similar transformer to the one cited previously and the instantaneous feature of the gas detector relay immediately cleared the unit.

The differential protection on the same transformer had only started to operate before the breakers cleared. The time of clearance is estimated as less than 1/4 second from the instance of failure. Although the bank was energized again after the first failure, the damage to the windings was limited to a relatively few coils including the static shield.

Two operations of the relay have occurred as a result of bushing failures where the latter were constructed with a hollow conductor and the pressure wave passed through this conductor to the relay.

The commission has over 200 transformers equipped with the gas detector relay and as a standard practice equips all 110-kv and higher voltage units with this means of protection.

E. G. Ratz (Canadian Westinghouse Company, Ltd., Hamilton, Ontario, Canada): Madill's paper brings out very forcibly the advantages of gas accumulating devices on transformers for the purpose of detecting incipient faults before they develop to the stage where they cause major breakdowns, interruptions, or damage, and this device is highly advantageous in that it gives an alarm and warning, without removing the transformer from service automatically, and permitting the utility to disconnect it when convenient.

While Madill's paper also describes a number of successful operations in which transformers have been cleared by means of the pressure element in case of faults therein, I do not agree with the inference that the pressure element can be used to replace the the differential protection which has been commonly used heretofore, although it may provide a valuable supplement thereto.

The pressure element would be operated as a result of major electric faults, and since such faults would disturb the differential protective zone it is obvious that the differential zone is nearer the source of the trouble although the pressure element may operate as a result thereof.

Generally, it seems desirable to have the protection for any device such that it detects the trouble as near the source as possible rather than operate upon the indirect consequences thereof, as the consequences can hardly have an accurate and uniform relation to the extent of the initial trouble.

The data available as to protective operations from pressure devices is relatively meager and covers a very short period of operating time compared to that covered by the regular electric differential protection. It seems to me that it would be hazardous to assume that pressure protection can be used in any manner to replace regular differential protection, as such must be based on the assumption that any fault which would operate differential protection will invariably operate the pressure element—and there is certainly insufficient data to substantiate this position.

Madill cites a number of cases of very successful pressure-element operations. I recently had occasion to examine a fault in a 30,000-kva transformer in which breakdown occurred across a barrier in the 60-kv winding, the normal voltage across the points of breakdown being approximately 8,000 volts. The breakdown was due to moisture caused by a slow leak in the cooling water system. The regular differential protection in this case cleared the transformer with practically no damage. The conductors at the points of fault were burned only so slightly that they could be returned to service practically as they were, and the insulation at the point of fault was very readily and inexpensively replaced. I mention this case as one in which the regular differential protection operated with a sensitivity and speed greater than that claimed for the pressure element.

F. L. Lawton (Aluminum Company of Canada, Ltd., Montreal, Quebec, Canada): The author has given an excellent review of faults experienced with large power transformers on one of the largest hydroelectric power systems in Canada, with particular reference to those types of faults which can be detected by the so-called gas detector relay, which is really a thoroughly-Canadian version of the Buchholz relay. The types of trouble discussed are probably indicative of experience on any large power system.

When the 1,200,000-horsepower Shipshaw development was built during the war, we decided that there was probably some merit to the gas detector relay but like many power systems in North America we had had no experience with them. These relays were installed on a group of 36 oil-insulated water-cooled single-phase 13,200/-154,000-volt 30,000-kva transformers of the core type. Since these transformers were placed in service, no fewer than nine incipient slowly-developing faults have been picked up successfully by the gas detector relay. Untanking and examination of the transformers after they had been removed from service, at convenient times, showed the incipient trouble causing the gas detector relay operation to be that indicated by the author in Figures 14 and 15—in other words, a poorly brazed joint in the connections between the low voltage windings. Aside from the untanking and repair of the defective joint, at a very moderate cost, it will be readily appreciated that the gas detector relays have done a 100-per-cent job, and saved several possibly major faults and certainly considerable service inconvenience.

As a result of the successful performance of this trial installation of gas detector relays, it was decided to equip all our major power transformers, involving a total of 124 single-phase units, rated 18,750 to 30,000 kva with gas detector relays. Since that time a number of other successful relay operations stemming from the same type of trouble have been recorded. We know that this is no fluke because examination of the transformers after they were untanked has revealed clearly the nature of the difficulties—all due to defective brazing of joints. There is no mystery about this particular fault and a thorough check with the manufacturer revealed that many, if not all, had been done by the same workman. However, the manufacturer has since instituted a much more thorough and effective inspection of such brazed joints.

Experience on our own system, as indicated by the author and by this discussion, and on two other major Canadian power systems, has shown that the gas detector relay, properly installed and maintained does a job that no other protective device can even approach. So far as relay protection is concerned, it can be said without fear of contradiction that the gas detector relay, which comprises a gas-accumulation element and a gas-pressure element, is the only device which will detect a slowly-developing trouble in a transformer and give warning in ample time so that the transformer can be removed from service at the operator's convenience, untanked, and the evidence of the slowly-developing fault found, so that it can be corrected.

As the author has pointed out, it is not only poor joints which can be picked up by gas detector relays but also many other types of faults.

It can also be said that the cost of gas detector relays is far below that of the differential protection ordinarily employed. It is predicted that we will see a rapid extension of usage of these relays.

Eric T. B. Gross (Illinois Institute of Technology, Chicago, Ill.): Madill has given us very valuable information concerning the effectiveness of gas and pressure actuated relays. His conclusions underline some of the recommendations contained in the report[1] of the Relay Subcommittee and we may expect a considerable increase in

the use of such relays in the United States too. As pointed out so clearly by Madill, the gas-element of the relay is of extreme importance; it gives a warning long before the fault can develop into serious trouble; therefore both the cost of and time required for the repair are considerably reduced.

The gas detector relays used in Canada are applied on transformers with conservators. In the United States attempts have been made to prevent aging of the oil by means of totally enclosing the transformer oil, and to substitute the conservator by a cushion of pure nitrogen. As yet, transformer designers in the various countries are not in agreement as to the necessity of such a drastic solution, and it is of interest that a recent investigation suggests that a more economical solution would be to add an inhibitor to the oil of transformers with conservators.[2]

Whatever the solution in the question of aging of oil may be, it should not be too difficult to develop a "gas-element" for transformers without a conservator. The problem amounts simply to the development of a device which gives an indication when the nitrogen space above the oil level inside the transformer tank is poisoned by some other gas. In addition to the gas-element, a pressure element is needed, but pressure relays have been developed and are available.

References

1. Relay Protection of Power Transformers, AIEE Committee Report. AIEE Transactions, volume 66, 1947, pages 911–7.

2. The Effect of Inhibitors on the Oxidation of Transformer Oil, H. Liander, G. Ericson. *Technical Achievements of Asea Research* (Allmanna Svenska Elektriska Aktiebolaget, Vasteras, Sweden), 1947, pages 174–86.

Ben C. Hicks (Shawinigan Water and Power Company, Montreal, Quebec, Canada): This paper is most timely and informative in view of the increasing interest being manifested in gas actuated relays as a means of securing improved protection for power transformers. It brings together much valuable information for those interested in the subject.

The paper provides a list of nine types of transformer troubles which can be detected in their early stages by gas detector relays, and by these relays only. I would point out that to this list might be added two more types of troubles, namely, defects in breathers, and defects in forced oil circulating systems.

It may be of interest to relate here our most recent experience with the Buchholz-type of gas actuated relay. It concerns a newly installed step voltage regulator which has a separate switch compartment for the tap changer built on to the side of the tank. In this switch compartment an insulating member of the mechanism, made of micarta, evidently developed a slow form of breakdown which resulted in the evolution of gas. Preliminary investigation suggests that this gas was eventually caused to explode when the tap changer operated, the explosion deforming the regulator tank inward and causing the pressure element of the gas detector relay, with which it was equipped, to operate and trip the circuit. Should this explanation be substantiated by the inspection which the regulator is now undergoing at the factory, it will add another to the growing list of types of faults to which the gas detector relay will respond.

W. R. Brownlee (The Commonwealth and Southern Corporation, Jackson, Mich.): The detailed case histories of transformer damage, the analyses of causes, and the influence of the sensitive detection of faults afforded by gas detector relays make a strong case for the application of these devices to conservator-type transformers.

The total number of faults (including incipient faults) of an internal nature mentioned by the author corresponds to an average of one fault per single-phase transformer in a period of about 50 years. However, the amount of major damage which the records show has been avoided (or can be avoided) for each transformer fault by means of gas detector relays makes their use attractive.

Especially where service protection as well as equipment protection is an important item, the use of differential protection which includes the entire zone between busses is highly desirable, regardless of the effectiveness of any purely internal protective scheme. That is, the pressure element of the relays described may be considered as supplemental protection to differential relays in the usual application rather than as a substitute for them.

It is recognized that pressure protection may be made quite sensitive and fast. It would be helpful if the author could furnish information on the approximate sensitiveness and speed of the differential relays which were used along with the pressure protection.

Questions have been raised concerning the difficulty of interpreting indications from gas detector relays. Have there been any instances in the applications described by the author where transformers have been untanked as a result of gas detector relay indications without finding any damage or fault indication?

J. T. Madill: I am indebted to the discussers for bringing out additional advantages and applications of the gas detector relay. In particular the practice on other large Canadian power systems is very illuminating. The cases described by Fleming and Hicks and the additional information submitted by Lawton clearly emphasizes the value of gas detector relay protection. The additional operating experience which they include contributes considerably to the value of the paper and should help to disperse the doubts that are entertained by some regarding this protection.

Fleming questions the advantage of gas detector protection in the case of turn-to-turn faults. Operating experience does not yet provide definite proof that the gas accumulation element will detect such a fault (there is no doubt that the pressure element detects the final break down of such faults.) However on the Saguenay system we have had two cases of transformer trouble in which it appears that the turn-to-turn break down developed slowly, and in which the incipient damage could have been detected had gas detector relays been available. The evidence is not clear and these were not described in the paper. In the future a definite answer may be forthcoming. The obvious advantage of detecting such trouble in advance is not so much the reduction of damage in this case, as it is the avoiding of an explosion, and the avoiding of any service interruption and system fault.

Ratz seems to read more into the paper regarding pressure protection than was intended. However the particular comments on operating experience made by Hicks and Fleming certainly illustrate the value of pressure protection. It must always be borne in mind that differential protection must sacrifice either or both sensitivity and speed to avoid trouble from the magnetizing inrush problem, whereas pressure protection is absolutely unaffected by this. As Lawton mentioned the considerable difference in cost between gas detector protection and differential protection is an important factor, particularly in the case of smaller sized units.

Brownlee arrives at a figure of one fault per single-phase transformer per 50 years. It might be mentioned that the paper did not attempt to describe all faults experienced, but rather to show the field of application of gas detector relays and to describe some general types of trouble, therefore this figure is not necessarily correct. On the basis of 124 transformers this figure would indicate an average of 2.5 faults per year, actually the transformer repairs are running considerably above this figure.

Regarding differential protection, at the Shipshaw station there is no low or high voltage bus and the transformer differential protection extends from the line side of the high voltage circuit breakers to the generator neutral leads. An inverse time overcurrent relay with an instantaneous trip attachment is used as the differential relay on each phase. The induction element is set to pick up with a differential current corresponding to 11 per cent of the bank full load phase current, and it has a time delay of 15 cycles at 5 times the pickup value. The instantaneous trip attachment is set to pick up at about 200 per cent of the bank rating.

Brownlee is concerned with false indications from gas detector relays. We have never experienced a false trip from a pressure element. To the best of our knowledge in no installation in Canada does the gas accumulation element trip any protective equipment, it only operates an alarm. The indications from the gas accumulation element must be interpreted by competent technical personnel. Using a device such as the "Vapotester" to check the gas combustability, and noting the past history of the transformer, and the rate at which accumulation alarms are coming, it is not difficult to decide on the correct course of action. When we untank a transformer on the basis of gas accumulation alarms we are absolutely convinced there is a fault in the transformer and that we can find it.

Automatic Operation of Electric Boilers

M. EATON
ASSOCIATE AIEE

ELECTRIC boilers were introduced in Canada after World War I for the purpose of utilizing surplus hydroelectric power. Since then about 200 units have been installed with an aggregate capacity of nearly 2,000,000 kw. There are a few installations in the United States aggregating about 100,000 kw. More than 80 per cent of these boilers are operated manually. Although satisfactory operation can be obtained with manual regulation, the need of precise automatic control has long been recognized.

Automatic process control and the design of control instruments are developed to such an extent that few continuous processes are now controlled manually. Many of them depend on automatic control. The electric boiler application has lagged behind mainly because instruments must be supplemented with specially arranged equipment as part of the controlling means.

A preceding paper[1] on this subject described methods for automatically regulating electric boilers of the electrode type applied to some of the early installations. These were designed before basic principles of automatic control were established and before satisfactory instruments were made for the application of these principles. As might be expected they have not proved to be entirely adequate.

Paper 47-129, recommended by the AIEE committee on industrial power applications for presentation at the AIEE summer general meeting, Montreal, Quebec, Canada, June 9–13. Manuscript submitted March 13, 1947; made available for printing April 17, 1947.

M. EATON is chief electrical engineer for Shawinigan Chemicals, Ltd., Shawinigan Falls, Quebec, Canada, and consultant on electric boilers for the Shawinigan Water and Power Company, Montreal, Quebec, Canada.

The author wishes to acknowledge information supplied by the Combustion Engineering Company, New York, N. Y.; the Dominion Engineering Company, Montreal, Quebec, Canada; the Canadian General Electric Company, Toronto, Ontario, Canada; and E. Leonard and Sons, London, Ontario, Canada, regarding installations of their electric boilers.

Following a brief discussion of the principles of automatic control, with reference to air-operated controllers, this paper reviews early methods for regulating electric boilers automatically, and describes later improvements based on fundamental principles.

Terminology

Although automatic control terms are fairly well established the literature[2–5] shows some difference in definition. The terms used in this discussion are defined as follows:

Automatic controller: an apparatus including measuring means, controlling means, and final control element for regulating the supply of a control agent to maintain within limits a controlled variable.

Measuring means: the elements which measure and communicate to the controlling means the magnitude of the controlled variable.

Controlling means: the elements actuating the final control element in response to the action of the measuring means.

Final control element: the part of an automatic controller that directly varies the supply of control agent.

Control agent: the supply medium for the energy or material required to maintain the value of the controlled variable.

Controlled variable: the quantity or condition of the controlled medium which is automatically controlled.

Controlled medium: the material in a process of which the controlled variable is the quantity or condition to be controlled.

Set point: the value of the controlled variable at which the controller is set.

Control point: the value of the controlled variable corresponding with the rate at which control agent is supplied.

Offset: the difference between the set point and the control point.

Two-position control: controller action having only two rates at which control agent is supplied.

Proportional control: controller action that maintains a linear relation between the position of the final control element and the deviation of the controlled variable from the set point.

Preset action: controller action that alters the position of the final control element an amount corresponding with the rate of change in the value of the controlled variable.

Reset action: controller action which increases the sensitivity of an automatic controller, following a change in control agent demand, for the purpose of overcoming offset.

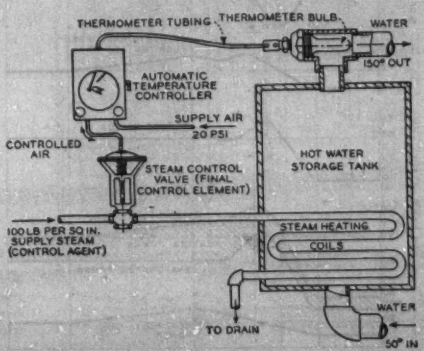

Figure 1. A typical temperature control process

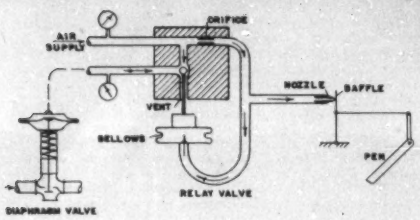

Figure 2. Schematic diagram of a controller mechanism with diaphragm valve

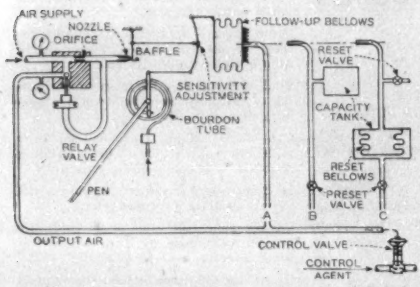

Figure 3. Schematic diagram

Showing alternatively the essential elements of

A—A proportional controller

B—A proportional controller with preset action

C—A proportional controller with preset and reset actions

Sensitivity: the ratio of the movement of the final control element to the corresponding magnitude of change in controlled variable.

Throttling range: the change in the controlled variable necessary to cause the final control element to move from one extreme to the other.

Floating control: controller action which varies the position of the final control element continuously, when the controlled variable deviates from the control point, and with no relation to the value of the variable other than direction. Floating control may be single-speed, multispeed, or proportional-speed.

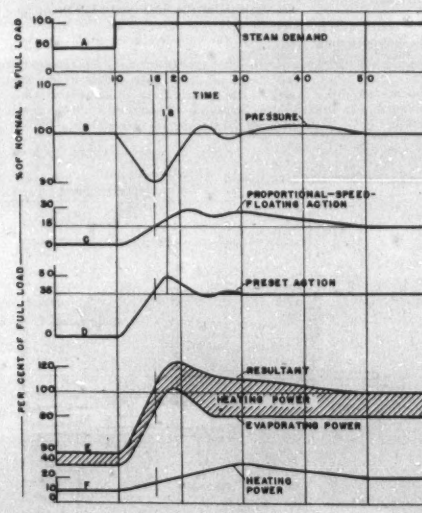

Figure 4. Graphical representation of controller actions

Proportional-speed-floating control: floating controller action that varies the position of the final control element at a rate proportional to the magnitude of deviation of the controlled variable from the control point.

Capacity lag: the lag between a change in the demand for control agent and consequent change in the magnitude of the controlled variable. It is directly proportional to the ratio of control agent storage to control agent demand.

Transition lag: the lag between a change in the flow of control agent and a corresponding change in the value of the controlled variable at the point of measurement.

Controller lag: the lag between a change in the magnitude of the controlled variable at the point of measurement and a corresponding change in the position of the final control element.

Choice of Control

The amount of stabilizing action required is proportional to $(A+B)/C$ where A, B and C are the transition, controller, and capacity lags respectively. The capacity lag is usually the determining factor. When the capacity lag is large compared with the other two a simple two position controller may be adequate.

Proportional control is satisfactory with moderate lags. If a low sensitivity adjustment is required for stable operation an objectionable amount of offset may result unless reset control action is provided. Proportional control plus reset is the equivalent of proportional-speed-floating control.

If the capacity lag is small compared with the other lags, and large changes in demand for control agent occur, proportional-speed-floating plus preset controller action is required.

Air-Operated Controllers

Figure 1 shows a typical temperature control process in which an air-operated controller is used to regulate the temperature of water taken from a hot water storage tank. The thermometer bulb, a Bourdon tube in the instrument, interconnecting tubing, and the liquid or gas they contain constitute the controller measuring means. The controlling means includes the elements which working together regulate the controller output air pressure and position the control valve accordingly. The valve is the final control element regulating the flow of control agent, which in this instance is steam. Steam is the medium of supply for the heat energy required to maintain the temperature (controlled variable) within limits.

The capacity lag is determined by the size of the hot water storage tank as compared with the demand for hot water. The transition lag includes the time it takes to transfer heat from the steam in the heating coils to the water, plus the time required for a change in temperature at the thermometer bulb resulting from a change in temperature at the heating coils. The controller lag is the time required to effect a change in the position (opening) of the control valve corresponding with a change in the temperature of the water at the thermometer bulb.

If the storage tank is quite large compared with the demand for hot water, two-position controller action is adequate. Moderate storage capacity requires proportional controller action for control stability, and if it is desired to maintain the control point close to the set point of 150°F. reset action is necessary. If the storage tank is small, with fluctuating demand, then proportional plus preset plus reset controller action is required.

Air-operated controllers supplied by the various instrument manufacturers differ considerably in design but all have much the same principle of operation.

Figure 2 shows diagrammatically the essential elements of a high sensitivity controller less the measuring means. Air from a constant pressure supply passes through an orifice and nozzle in series. The flow through the nozzle is restricted by a baffle which is positioned by the measuring means. The proximity of the baffle to the nozzle determines the back pressure and hence the position of the air relay valve, which in turn governs the output air pressure to the diaphragm valve. The set point adjustment determines the position of the baffle corresponding with the value of the controlled variable.

The diaphragm valve is shown to be normally closed (reverse acting). It is closed by spring pressure and opened by air pressure, the opening or position being determined by the relative spring pressure and controller output air pressure. Diaphragm valves may be either normally open (direct acting) or normally closed. The controller may also be direct acting (rising output air pressure with increasing value of the controlled variable) or reverse acting. A high sensitivity controller produces the effect of two-position, or on-and-off, controller action.

Figure 3, part *A* represents a proportional controller (direct acting). As the value of the controlled variable rises the pen turns in a clockwise direction and through interconnected linkages the lower end of the baffle is moved to the right.

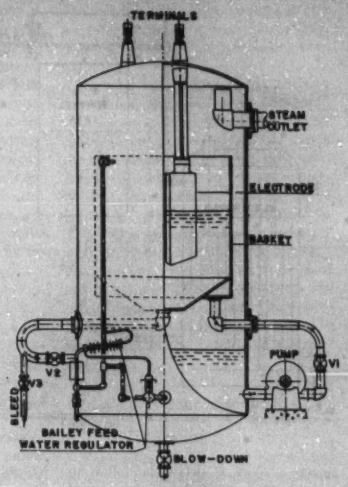

Figure 5. Sectional view of a Canadian General Electric boiler with control apparatus

This reduces resistance to air flow through the nozzle, thus decreasing the back pressure and causing the relay valve to increase its opening. Rising output air pressure decreases the opening of the direct-acting control valve. As the output air pressure rises, the follow-up bellows moves the top of the baffle to the left an amount, depending on the sensitivity adjustment. This action partly offsets the initial movement of the baffle away from the nozzle and has the effect of causing the control point to follow the controlled variable thus providing means for sensitivity adjustment.

The capacity tank and preset valve

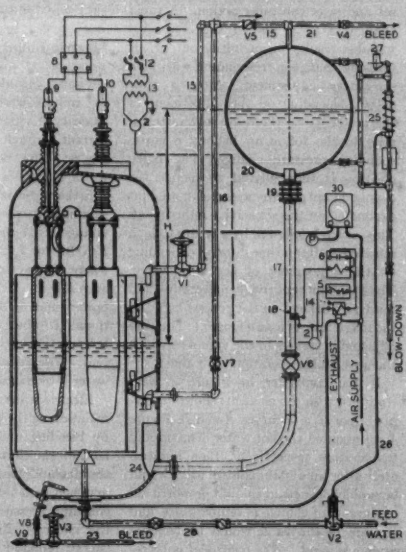

Figure 6. Sectional view of an electric boiler equipped with Eaton automatic control type WL

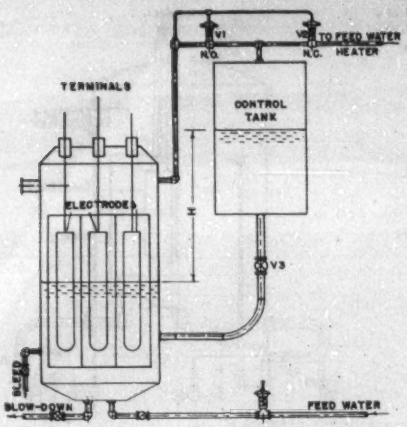

Figure 7. Schematic diagram of an electric boiler with control tank and control valves

shown as part *B* delay the follow-up action. The result is that in the event of a sudden change in the value of the controlled variable a large initial movement of the control valve occurs in the direction to correct it. This effect depends on the rate of change in the magnitude of the controlled variable regardless of its actual value.

Figure 3, part *C* shows the essential elements of a controller having both preset and reset controller action. A rapid change in the value of the controlled variable results in an initial output air pressure change corresponding with high sensitivity adjustment. After a time delay, depending on the adjustment of the preset valve, the reset bellows transmits to the follow-up bellows a corresponding pressure change. The baffle position is then altered to reduce the change in output air pressure an amount depending on the sensitivity adjustment. This action is followed by a return to high sensitivity after a time interval depending on the adjustment of the reset valve. The optimum sensitivity, preset rate, and reset rate depend on the process lags and the magnitude of load changes. They are adjusted in service to the values at which the most stable operation is obtained.

If the controller in Figure 1 were equipped with the elements shown in Figure 3, part *C* and curves *A* and *B*, Figure 4, represented the hot water demand and temperature respectively, then immediately after time 10 the control valve would be rapidly opened an amount proportional to the rate of change in temperature, and at time 18 the valve would be reclosed similar amount. The controller is thereby able to anticipate the change in demand for control agent and to pre-act in such a way as to minimize the magnitude and duration of the deviation. Proportional controller action brings the temperature back to the control point with minimum overshooting. Reset action follows and reduces offset by raising the sensitivity. The combined control effects result in the controlled variable being returned to the set point with minimum deviation and maximum control stability.

Electric Boiler Control

Figures 5 and 6 are sectional views of two well known electric boilers of the electrode type. Steam is raised by passing current through the water between electrodes. The power supplied $P=3I^2R$ watts where I is the 3-phase current and R is the water resistance to ground. Assuming unity power factor and the applied voltage E to be constant, and substituting $E/\sqrt{3}R$ for I, the power input $P=K/R$ where K is a constant. The water resistance R is inversely proportional, and the power input is therefore directly proportional, to the electrode immersion, the temperature of the water, and its salt content. The salt concentration increases as water is evaporated.

Electric boilers are usually regulated by maintaining the salt content within limits by bleeding and by varying the water level on the electrodes in accordance with the demand for steam. Power input is matched with steam demand to maintain constant pressure. The power input is the control agent supplying the heat energy required to generate steam, and the electrode immersion is the final control element.

The capacity lag is proportional to the steam storage capacity of the system under control. This depends on the amount of water at or near steam temperature and on the steam space. If the steam storage capacity is only that supplied by the electric boiler and steam mains, the capacity lag is small. The transition lag includes the time required to heat the feed water to steam temperature and to evaporate it. As the electrode immersion is the final control element the controller lag includes the time required to change the boiler water level. The transition and controller lags are therefore large compared with the capacity lag. An adverse temperature coefficient of resistance must also be considered. As the steam pressure and temperature rise the water resistance falls with increased power input and accelerated rise in pressure. Conversely as the steam pressure falls there is a reduction in power input when an increase is needed. For these reasons an electric boiler is difficult to regulate on fluctuating loads. Unless additional steam storage capacity is provided nothing less effective than the equivalent of proportional-speed-floating plus preset controller action will provide stable automatic control. This explains why early attempts to regulate electric boilers automatically were not entirely successful.

Cascade Inn Electric Boiler Control

The Cascade Inn boiler control was installed in 1929 and described in a previous paper.[1] It was applied to a 500-kw electric boiler used for supplying steam to the heating system and laundry.

The original means for varying the water level on the electrodes in response to the controlled pressure is shown diagrammatically in Figure 7. Two spring-loaded pressure reducing valves, one normally open and one normally closed, were connected, as shown, to control the transfer of water to and from the elevated control tank. The spring pressure of valve *1* was adjusted so that the valve closed at 40 pounds pressure and valve *2* was similarly adjusted to begin opening at 45 pounds steam pressure.

In operation valve *1* was normally open and the control tank empty. When the pressure rose to 40 pounds valve *1* closed and on further rise of pressure water was transferred from the boiler compressing and condensing steam in the control tank. The resulting drop in boiler water level and power input tended to restore normal

pressure. If this action were not sufficient the pressure continued to rise until valve 2 opened, discharging steam from the control tank and causing a further drop in boiler water level and power input. As the pressure fell, valves 1 and 2 resumed their normal positions and the water in the control tank returned to the boiler. The power input and pressure again rose and the cycle was repeated.

This controller action resulted in continuous cycling that was limited in magnitude by the adjustment of valve 3. The power and pressure oscillations were not very objectionable for a small boiler load and the performance would have been fairly satisfactory had it not been for maintenance troubles. Effective operation depended on valves 1 and 2 seating tightly, which required frequent valve grinding and packing gland adjustments.

If one of these valves, preferably valve 2, had been replaced with a manual valve it would not have been necessary that the other should be tight-seating. It could have been made to float in an intermediate position and the control performance would probably have been surprisingly good. Instead the pressure reducing valves were replaced with electrically-operated valves, responsive to pressure-actuated switches, and the key to stable automatic control was left lying by the wayside where it remained for more than a decade. There are two reasons for the length of this interval. The single control valve method involves a new principle of operation and it was a logical procedure to exhaust the possibilities of the original method before abandoning it to consider another. The other reason is that the boiler was not free to be taken out of service for an appreciable length of time in order that extensive changes might be made in the installation. The next step in the development was left for a subsequent installation. If more adequate facilities for experimental work had been available the years might have been reduced to months depending on the availability of the necessary control apparatus. Lack of experimental equipment operating under service conditions handicaps instrument manufacturer engineers and for this reason industrial engineers are usually in a better position to determine the most effective instrumentation for industrial processes.

Conductivity Control

Following the Cascade Inn boiler control installation it was decided to apply automatic control to three 5,000-kw electric boilers used for process steam heating in a chemical plant.

An electric boiler may be regulated either by maintaining the salt content within limits and varying the water level, or by holding the water level constant and varying the salt content or conductivity. Partly because of lack of space for control tanks, and partly because of instability in the operation of the Cascade Inn boiler control, it was decided to apply conductivity control to these 5,000-kw boilers.

A complete description of this control is included in the previous paper.[1] In this instance the boiler water conductivity is the final control element. Controlling means is provided whereby the conductivity is increased by adding salt solution (soda ash) and decreased by bleeding. The salt solution control apparatus, by being made partly responsive to steam flow, anticipates the demand for salt solution and the bleed valve operates in two stages. The result is something a little more effective than 2-speed-floating control.

Fourteen installations of conductivity control were installed between 1930 and 1934 for electric boilers having an aggregate capacity of 148,000 kw. Although the operation is much improved, as compared with manual control, some independent steam storage capacity is required for stable operation on fluctuating loads. There is also appreciable maintenance work necessary to keep the equipment in good working order, and an objectional loss in boiler efficiency results when frequent bleeding to drop load is necessary. Because of these defects it was decided to develop further the water-level type control.

Water-Level Control of the Step Type

The original Cascade Inn control was revised in 1935 and applied to two electric boilers of 750- and 2,000-kw capacity. A cylindrical control tank was mounted horizontally in an elevated position. The feed water flow to the boiler was made responsive to the water level in the control tank and arranged so that the control tank was normally half full. The bleed control valve was made partly responsive to the boiler water level and partly responsive to the controlled pressure in such a way as to make the load current corresponding with the water level agree with a predetermined ratio. Electrically-operated valves, responsive to pressure switches, functioned to vary the water level on the electrodes in steps or fixed increments. This limited the range of oscillations which were at that time considered unavoidable.

A description of this control[8] was published in 1936. The performance was better than that of the Cascade Inn control but there was difficulty in maintaining adjustments. The electrically-operated valves were also a source of trouble because of operation at steam temperature.

Dominion Engineering Surge-Tank Control

The Dominion Engineering Company manufactures the electric boiler shown in Figure 6. As early as 1925 they made independent studies of means for automatically regulating these boilers and foresaw the possibility of obtaining effective control with controlling means including a separate control tank and two

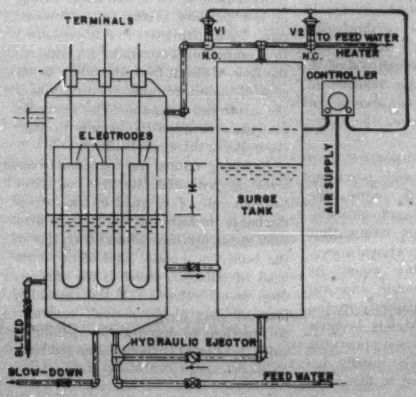

Figure 6. Schematic diagram of an electric boiler equipped with Dominion Engineering surge-tank control

control valves substantially as shown in Figure 7. Their first installation, however, was not made until 1932. The existing equipment and arrangement are as shown diagrammatically in Figure 8.

The control tank, or surge tank, is mounted vertically beside the boiler. The means for varying the boiler water level, in response to the controlled pressure, functions much the same as that of the Cascade Inn control, Figure 7, except that more modern control apparatus is used. The hydraulic ejector in the feed water line makes it possible to draw the surge tank water level down below that of the boiler, thus obtaining full use of the storage space. Feed water supply and bleeding to maintain the boiler water conductivity within limits are regulated manually.

The controller and valve *1* are reverse-acting and valve *2* is direct-acting. When the controlled pressure is below the set point, an amount depending on the controller sensitivity adjustment, the output air pressure reaches a value at which valve *1* is open and valve *2* is closed. This allows the surge tank steam pressure to rise, by passage of steam through valve *1* at boiler pressure, and water from the surge tank to be returned to the boiler by gravity or hydraulic ejector effect. The power input and steam pressure rise causing valve *1* to close and valve *2* to open. When the rate of discharge of steam through valve *2* exceeds the rate of passage through valve *1* the surge tank steam pressure begins to fall, thus causing water to be transferred from the boiler to the control tank. The power input and steam pressure fall again and the cycle is repeated.

For stable operation the surge tank steam pressure must be lower than that of the boiler by an amount equivalent to the head of water H plus the ejector effect E when the controlled pressure is on the control point. Neglecting pipe resistance to steam flow, this is the pressure drop across valve *1*. At the same instant the rates of steam flow through valves *1* and *2* must be equal and the controller output air pressure must be at an intermediate value. Even if $H + E$ were constant this condition would require a definite ratio of flow through the valves, corresponding with the pressure drop across each, which is hardly practicable. With $H + E$ variable the rates of steam flow through these valves remain in unstable equilibrium resulting in sustained oscillations of steam pressure and power input which may, however, be limited in magnitude by high sensitivity adjustment.

There is appreciable self-regulation. As the boiler pressure rises water is forced into the surge tank compressing the steam in it to boiler pressure and accelerating the rate at which steam is discharged through valve *2*. A drop in boiler pressure causes valve *2* to close and valve *1* to open. Water is then returned to the boiler because of excess surge tank steam pressure, which is partly dissipated by passage of steam through valve *1* to the boiler.

This self regulating effect, obtained with the use of a separate control vessel, was discovered by Bergeron, who was granted a patent on it in 1924. The equipment shown in Figure 6 employs the Bergeron effect to greater advantage in providing preset controller action.

The rate of change in boiler water level, controlled by the operation of valves *1* and *2*, is approximately proportional to the square of the deviation of the steam pressure from the control point. The controller action might therefore be described as variable-speed floating plus limited preset.

Three 8,000-kw electric boilers have been equipped with this type of control. Very little maintenance is required and the performance compares favorably with that of any control apparatus available at the time these installations were made.

Canadian General Electric Boiler Control

Figure 5 is a sectional view of a Canadian General Electric boiler equipped with automatic feed water regulation and means for manual control of the load.

The feed water regulator maintains the mean water level in the bottom of the boiler shell as indicated. Water is pumped from the bottom of the boiler to the electrode vessel, or basket, and returned by gravity through valve *2*. The opening of this valve remains in fixed adjustment and the opening of valve *1* is varied to regulate the water level on the electrodes.

By making valve *1* responsive to a proportional controller, and providing suitable means for bleed control, the steam pressure may be automatically regulated with controlling means that will function as a proportional-speed-floating controller. This would be adequate only with separate and appreciable steam storage capacity in the system under control. Mainly because of this limitation the control apparatus supplied with these boilers usually includes only what is shown in Figure 5. A few, however, have been equipped with complete automatic control.

Automatic Control of the Water-Level Type*

The Cascade Inn electric boiler was eventually released for experimental studies with the object of perfecting the water-level type of control.

The problem was not only to provide controlling means with nearly all the stabilizing features known to the art, but to do so with apparatus that is simple and reliable. Simplicity is necessary because some of the users do not have instrument men with sufficient skill to understand and maintain complicated control devices. Fortunately, in this application, simple apparatus provides effective control.

The control equipment shown in Figure 6 is the result of progressive development beginning with the original Cascade Inn control, which included means for limiting the rise in boiler water level similar to the existing means for obtaining water level limits. The feed water regulation and control tank arrangement differ little from those of the step-type control installed in 1935. The main feature is the means for automatically transferring water to and from the control tank in response to the operation of a single control valve.

Three variables, steam pressure, the rate of feed water flow, and the boiler water salt content are controlled independently but in such a way as to assist in maintaining control stability.

Pressure Control

Steam is bled through valve *4* from control tank *20* to a feed-water heater, or low pressure system, at a constant rate. A diaphragm valve *1*, responsive to a proportional controller *30*, regulates the flow of steam from the boiler to the control tank in response to variations in the controlled pressure. The controller pressure connection P is made with either the boiler or the steam header.

Assuming normal pressure and water levels as indicated, the flow of steam through valve *1* is equal to the rate of discherge through valve *4*. The control tank steam pressure is lower than that of the boiler an amount equivalent to the head of water H, which is the pressure drop across valve *1*. If the controlled pressure rises above normal, controller *30* functions to decrease the opening of valve *1*. Steam is then discharged from

* Patents pending.

the control tank faster than it is replaced resulting in transfer of water from the boiler to the control tank, decrease in power input and return to normal pressure. Valve increases its opening on falling pressure, allowing the control tank steam pressure to rise and water to be returned to the boiler by gravity, thus causing an increase in power input and return to normal pressure. This is proportional-speed-floating controller action.

The self-regulating effect, described with reference to Figure 8, is used to obtain effective preset controller action. The steam space in the control tank and valve *4*, Figure 6, serve the purpose of the capacity tank and preset valve, Figure 3, part *B*. Check valve *5* prevents boiler and control tank steam pressures being equalized by passage of steam through pipe *15* to the boiler.

Boiler Water Level Limits

If the boiler water level rises above the range indicated by *L*, access of steam to pipe *15* is cut off and water is transferred to the control tank by control action as previously described. If the level falls below *L*, steam rises through pipe *16*, by-passing valve *1*, and causing water to be returned from the control tank to the boiler. These water level limits are the extreme positions of the final control element.

The boiler load corresponding with the water level depends on the boiler water bleed control point.

Bleed Control

The bleed control apparatus includes transformer 13, current relay *6*, conductivity cell *18*, 3-way valve *14*, and bleed valve *3*. When the conductivity of the water in pipe *17* rises above the control point, as determined by the setting of relay *6*, the relay current reaches the value at which the contacts close to energize 3-way valve *14*, and to open the air-operated bleed valve *3*. As boiler water is bled off it is replaced by comparatively pure feed water thus reducing the salt content and conductivity to normal, at which relay *6* opens its contacts and valve *3* recloses.

The conductivity cell is located in pipe *17* in preference to the boiler shell because the passage of water through *17* washes the electrodes and a desirable timing effect is obtained. The water in the control tank is diluted with condensed steam resulting from contact with water slightly under steam temperature. For this reason the conductivity of the water in pipe *17* falls when water is being transferred to the boiler and rises when the water flows in the reverse direction, thereby tending to stop bleeding when the controller is functioning to increase the load and to bleed when it is necessary to drop load. This timing of bleed valve operation decreases controller lag.

The bleed control apparatus functions as a simple two-position controller, which is satisfactory because of large capacity lag in salt concentration. A constant bleed through valve *9* results in over-and-under, rather than on-and-off, controller action.

Feed Water Regulation

The control apparatus functions in such a way that all water admitted to the boiler, in excess of that required to maintain the operating water level, is transferred to the control tank which is maintained approximately half full, thus providing storage water for raising the level in the boiler and storage space for transfer of water from the boiler.

The generator assembly *25* of a Bailey thermo-hydraulic feed-water regulator is mounted vertically on the control tank as shown. The feed water flow to the boiler, through valve *2*, is responsive to the water level in the control tank.

An increase in steam demand results in falling steam pressure which is brought under control more rapidly if the rise in water level on the electrodes is effected entirely by transfer of water from the control tank. If this is partly accomplished by an accelerated rate of flow of feed water, additional heat energy is required to bring the feed water up to steam temperature. When water is transferred to the boiler to restore normal pressure the control tank water level falls and the resulting acceleration of feed water flow is delayed because of low sensitivity which results from mounting the generator tube vertically rather than in the inclined position as shown in Figure 5. The delayed response causes the acceleration of flow to have a stabilizing effect.

Controller Action

Figure 4 describes the controller action graphically. A sudden increase in steam demand occurs at time 10, as in curve *A*. The controlled pressure momentarily falls and is brought back to the control point, as in curve *B*. Curve *C* shows the increase in power input occasioned by proportional-speed-floating control alone, while curve *D* shows the load increase resulting from preset controller action. Curve *E* is the resultant of the two control effects. The feed water heating power is shown by curve *F* and the shaded area under curve *E*.

The power input at the instant the pressure is brought under control is as shown at time 16. An increase beyond this level is undesirable. Proportional-speed-floating controller action, curve *C*, continues to increase the power input until the control point is reached. Preset control action, curve *D*, is caused by momentary difference between control tank and boiler steam pressures. As the boiler pressure, curve *B*, falls water is transferred from the control tank to the boiler by excess control tank steam pressure with consequent rise in power input. When the pressure reaches its lowest value the control tank steam pressure has fallen to a value near that of the boiler pressure and at time 18 the boiler pressure begins to exceed the control tank steam pressure by an amount sufficient to cause transfer of water from the boiler to the control tank. The boiler water level therefore falls with resulting decrease in power input. Consequently when the pressure reaches the control point the power input, curve *D*, is lower than it was at time 16.

Curve *E* is the resultant of these controller actions. The shaded area shows that delaying the feed water regulator response retards the increase in heating power until the pressure is under control. Excess power that would otherwise cause overshooting is then absorbed in heating water for storage. The effect is to raise the capacity lag and thereby improve control stability.

The application of reset or preset action to controller *30* would serve no useful purpose. Reset is unnecessary because the controlling means is inherently a floating type, and preset action would increase the opening of valve *1* when check valve *5* is functioning to prevent flow of steam through it. A valve positioner, which is a device used to amplify the controller output air pressure for precise positioning of the diaphragm valve, may be used to advantage when low sensitivity adjustment is desirable.

Figure 9 is traced from charts showing the steam pressure and power input of an electric boiler supplying the steam required for a plant manufacturing roofing paper and operating steam-heated dryers. The drop in load at 2:30 a.m. is caused by a paper break.

Modifications

This control may be adapted to the following purposes:

1. To operate alternatively on pressure control and power input control.

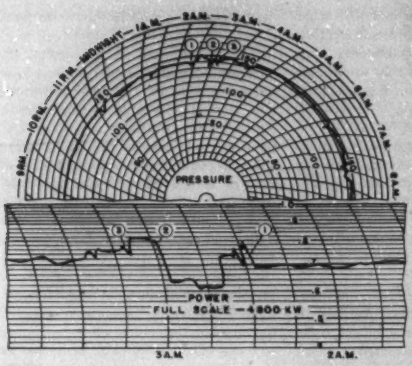

Figure 9 (above). Charts showing steam pressure and power input resulting from the automatic control of an electric boiler

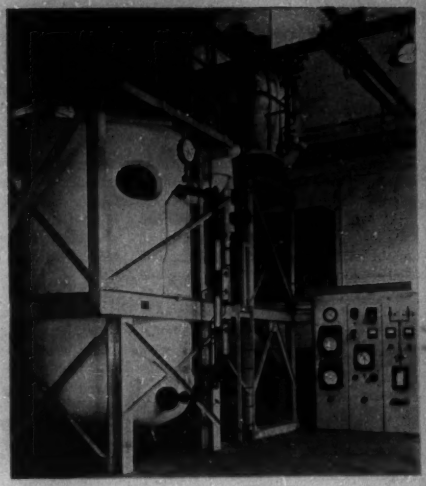

Figure 10 (right). A 20,000-kw electric boiler with equipment as shown in Figure 6

2. To maintain a constant demand on a system supplying both primary and secondary power.

3. To regulate electric boilers operating in parallel.

4. To control a 3-tank electric boiler which has the electrode pertaining to each phase mounted in a separate pressure vessel.

None of these modified controls has yet been installed.

Installations

Four installations of this control are in successful operation on boilers ranging in sizes from 500 to 20,000 kw and a fifth is being installed for a 37,500-kw boiler. The present installations provide stable and efficient operation of electric boilers supplying process steam in chemical plants and a paper mill. Charts such as those shown in Figure 9 indicate that precise control is obtained even with adverse load conditions.

References

1. Automatic Operation of Electric Boilers, **M. Eaton.** *Engineering Journal* (Montreal, Quebec, Canada), volume 16, May 1933, pages 201–9.

2. Teaching the Robot to Think Ahead, **Alan Osbourne.** *Chemical and Metallurgical Engineering* (New York, N. Y.), April 1931, pages 245–7.

3. Fundamental Principles of Automatic Control, **J. C. Peters, Theodore R. Olive.** *Chemical and Metallurgical Engineering* (New York, N. Y.), May 1943, pages 97–107.

4. Instruments and Process Control (book), **The New York State Vocational and Practical Arts Association.** Delmar Publishers Inc., Albany, N. Y.

5. Instructions A1000, Air Control Theory and the Free Vane Controller. The Bristol Company, Waterbury, Conn.

6. Automatic Control of Electric Boilers on Fluctuating Loads, **M. Eaton.** *Electrical News and Engineering* (Toronto, Ontario, Canada), volume 45, March 1946, pages 20–3.

Discussion

A. L. Stewart (Bailey Meter Company, Ltd., Montreal, Quebec, Canada): Eaton has given us a very complete and concise picture of the problems involved in automatic control of electric boilers. He can speak with considerable authority as he has had experience over a good many years with many types of boilers and with many types of control systems.

Eaton points out quite clearly the problems involved in control of these units because of the interrelated variables of temperature, salt content, electrode submergence, and steam pressure. In my opinion, he has stated the problem quite clearly and has indicated the proper approach toward solving the problem.

It is unfortunate that there is not more common agreement regarding automatic control terminology. We have been following the terminology selected by The American Society of Mechanical Engineers and published in *Mechanical Engineering* in February 1946, and we find Eaton's terminology at some variance from the ASME terms. The ASME definition of capacity and resistance in automatic control systems is not the same and is, in our opinion, somewhat better than usage applied by Eaton.

We cannot agree with Eaton's statement that proportional control plus reset is the equivalent of proportional speed floating control. While in its ultimate effect, this may be true, the floating action is a delayed action with the predominant action being the proportional position control. The proportional position control with reset is much more applicable to different types of control systems than the proportional speed floating action control.

The application of conductivity control to electric boilers is most interesting and we believe this is a very useful device in the operation of these boilers. It is entirely possible that the graduated type of conductivity control should replace the off-and-on type described by Eaton, where very large boilers are being considered.

The steam pressure and power input chart records of Figure 9 are very interesting. Since a record of steam flow from the boiler has not been included, it is assumed that the boiler from which these records were obtained was not equipped with a steam flow meter. While the steam flow record is of course not essential in demonstrating the effectiveness of the control system, in maintaining steam pressure constant with variable steam demand, since the steam output record closely parallels the power input record under normal conditions, it would be an interesting addition.

The control system illustrated in Figure 6 represents a very material advance in the art of controlling electric boilers. The layout and the equipment is simple and still all of the required functions for smooth control are present. In addition, a number of very desirable protective features are included. For the average small and medium size electric boiler, we feel that the control

equipment shown is entirely justified and that it can be operated with a minimum of maintenance difficulties. For very large units some refinement and additional control is probably needed and justifiable.

For instance, it is our feeling that worthwhile improvement in over-all control results could be achieved by utilizing our air-operated type of feedwater control in place of our thermo-hydraulic type illustrated in Figure 6. The single element air-operated level controller with reset action and wide range sensitivity adjustment should assist materially in establishing the rate of response best suited to the steam load and other local conditions encountered. Two-element air-operated control would be an additional refinement, providing opportunities for even greater improvement which would amply justify the slightly higher cost, especially on the larger boiler units. Steam output from the boiler and level of water in the storage tank would be the two controlling factors, and local plant conditions would establish which of these two factors should have precedence; the other serving as a readjusting feature.

In the matter of boiler and control tank design, presumably the volume of water between maximum and minimum levels in the control tank must bear a definite relation to the volume of water between the maximum and minimum levels in the boiler. It would be interesting to know what that proportion is.

It would also be interesting to know if any work has been done, and with what results, in establishing a relation between moisture content in the steam and boiler output or boiler water level.

F. L. Lawton (Aluminum Company of Canada, Ltd., Montreal, Quebec, Canada): The paper by Eaton is a masterly presentation of the present situation with regard to automatic control for electric boilers. The importance of such control will be recognized when it is realized that the installed capacity of electric boilers in Canada represents 2,000,000 kw, and that the total waterpower developed is about 10,312,000 horsepower. Most of this electric boiler load is located in Quebec, two of the major systems each carrying up to 375 megawatts of such load at times.

Automatic electric boiler control as applied in the early thirties was not too successful. It entailed automatic injection of soda-ash solution on a drop in pressure and automatic bleed on rise in pressure. Consequently, the bleed ran higher with automatic than with manual control, and the efficiency was somewhat lower—a very important factor, psychologically, when the cost of steam was measured by the kilowatt-hour meter. Actually, most of this apparent loss was recovered by passing the bleed through a heat exchanger in the feedwater circuit and to a flash tank, the flash steam going to the hot well.

Eventually the control was simplified so that it was automatic only on rise in pressure, providing a 2-stage bleed. It proved very effective, and resulted in superior over-all operation, as compared with straight manual control.

It may be of interest to note the automatic control cost only 7.6 per cent of the over-all cost from the step-down transformer terminals for an installation comprising two electric boilers with a total maximum capacity of 50,000 kw; this exclusive of building and feedwater pumps.

Fundamentally there appears to be no sound reason why even large electric boiler installations cannot be made completely automatic and provide lower cost steam. However, this is not yet practical because legislation in most areas requires certain steam-plant personnel to be on duty. Some plants, too, with a fairly steady steam demand find that manual control provides adequately uniform pressure. This is not, however, the case in paper mills, where most electric boilers are installed, as a broken sheet results in a sharp pressure rise.

The new water-level type control described by the author is a long stride forward in automatic control for electric boilers. If past operating experience is any criterion, it should meet a real need, for an efficient and reliable form of automatic electric boiler control.

E. W. Knapp (The Shawinigan Water and Power Company, Montreal, Quebec, Canada): One important consideration in power system operation is that of keeping voltage variations to a minimum.

In some cases a large boiler load may be connected to a low voltage bus supplying other loads. In these cases it is necessary to insure that the boiler does not create undue voltage disturbances, which would adversely affect the prime loads. This can usually be accomplished by careful manual operation. However, this requires constant vigilance on the part of the boiler operator and experience has indicated that even with the utmost care, manual operation is at times inadequate. Experience has also revealed that in certain functional operations, automatic control is more reliable than manual control. The automatic operation of an electric boiler is such a function. It is believed that Eaton has developed a scheme of automatic boiler control which is more reliable than manual control and which will prove more effective in keeping voltage variations to a minimum.

It is assumed that other features can be added to the automatic control under consideration, if future operating experience dictates the necessity. Eaton deserves much credit for the part which he has played in this development, and I am certain that if additional refinements became necessary in the future, that these will be developed with care and foresight.

C. R. Reid (formerly with Shawinigan Water and Power Company, Montreal, Quebec, Canada): This paper presents a masterly analysis of the factors involved in controlling the pressure on an electric boiler of the electrode type, with fluctuating steam output. The development of automatic control was begun some 25 years ago, shortly after the introduction of the Kaelin boiler. Eaton took an active interest in the matter at that time, and has since then developed a number of improved types of control. It appears that the type described in his paper is the ultimate step in development, as it is a highly successful controlling device, operates the boiler at maximum theoretical efficiency, and is devoid of components which are apt to get out of order.

As pointed out by the author, the adverse temperature coefficient of resistance of water causes the electric boiler to be inherently unstable in operation. A successful controlling device must act simultaneously with a variation from normal pressure and at a rate proportional to the amount of variation. At 150 pounds gauge pressure, the temperature of saturated steam and of the water in contact varies 1/2 degree Fahrenheit for each pound of change in pressure. The resistivity of water has been found to vary with temperature in accordance with the empirical formula

$$R = AT^{-B}$$

in which R is the resistance in ohms per inch cube, T the temperature in degrees centigrade, and A is a constant ranging in value from 30,000 to 120,000. The exponent of T is likewise a constant for a given sample but varies within rather narrow limits around a value of 0.75. When these curves are plotted on logarithmic paper, a straight line is obtained with slope determined by the value of B.

M. Eaton: The terminology referred to in Stewart's discussion is derived from the literature included in the references. The scope of the paper made it necessary to define terms with the fewest possible words and, although there is some disagreement with ASME definitions, control engineers are familiar with the terms as defined.

The importance of common usage of terms is exemplified in Stewart's reference to conductivity control, by which he means bleed control for the purpose of maintaining the conductivity of the boiler water within limits, and which is defined in this paper as a method of regulating electric boilers by varying the boiler water conductivity.

Stewart's suggested modifications in control apparatus for large installations are very interesting. As pointed out, the higher cost of an air-operated level controller, as compared with that of the thermo-hydraulic type, might be justified for large boilers.

The control tank dimensions are determined by the volume of the boiler between upper and lower water-level limits and on the extent of instantaneous load changes.

Lawton's discussion refers mainly to the earlier conductivity type of control. His cost figures would apply equally to the new water-level type control, the installed cost of which is approximately 5 per cent of the cost of the complete installation including power transformers.

As Knapp suggests, the instrumentation may be modified to obtain special control effects that would not be practicable with manual control.

Reid's equation for determining water resistance is not generally known. It has been proved experimentally and is found to be useful in the design of electric boilers.

The Application of Synchronous and Induction Motors to Chippers

R. R. BAKER
NONMEMBER AIEE

M. R. LORY
ASSOCIATE AIEE

Synopsis: Wood chippers require motors with special characteristics to operate under exacting conditions involving high peak loads, severe vibration, acceleration of high inertia, and exposure to dirt and moisture. Methods are given to select the most suitable size of chipper, to determine the proper rating and characteristics of a motor to drive it, to choose beetwen synchronous and induction motors, and to select the mechanical arrangement of the drive. The modifications in mechanical construction of the motors to enable them to withstand the severe operating conditions are described and illustrated. Desirable features to be included in the control are given.

Description of Chippers

THE chipper is one of the most important pieces of equipment used in the manufacture of chemical wood pulp. It cuts the barked logs into chips of suitable size to be chemically treated in the digesters. Chippers are built in a wide range of diameters to handle the various sizes of logs, which vary from 8 to 24 inches in diameter and are usually cut into 4- or 5-foot lengths in Canadian, Eastern, Southern, and Midwestern mills, but are handled in 30-foot lengths with diameters up to 42 inches or more in mills in the West.

In construction, a chipper consists of a heavy cast iron or steel disk, which has a number of slots in it. A knife is bolted in each slot with its cutting edge radial, and extending close to the outside of the disk. The disk is mounted on a shaft carried in two bearings. See Figure 1. The logs are fed through a spout that is inclined so that the knives cut across the grain at an angle of about 45 degrees. A heavy anvil at the lower end of the spout takes the shock of the cut. The knives are adjusted to produce chips which are five-eighths to seven-eighths inch long, measured parallel to the grain of the wood. As they are cut, the chips pass through the slots in the disk to the rear of the chipper, where they are broken up further by breaker bars attached to the rear face of the disk. As shown in Figure 2, a cover confines the flying chips, and they are discharged into a conveyor or blower system which takes them to the next step.

The capacity of a chipper is given in stacked cords per hour, and its capacity varies as the square of the diameter of the spout, and directly as the rpm and the number of knives. The diameter of the spout is usually from 20 per cent to 25 per cent of the diameter of the disk. The maximum stress in the disk from centrifugal force limits the maximum operating speed. Typical characteristics of a number of representative chippers are given in Table I. The figures are typical or average, and are not exact for any given design because the operating speed and spout diameter will vary a little for the same size of disk when built by different manufacturers. The formulas by which the values given in columns F to L of the table were calculated are given in Appendix I. The production and power values given in the table are for one knife, and must be multiplied by the number of knives used. The table is based on chips three-fourths inch long and on hemlock wood, which requires seven horsepower-hours per cord. The horsepower-hour requirement so for the species of wood are given in Table II. These values were obtained from numerous tests of chippers in normal production, and were checked by tests made under laboratory conditions.

Selecting a Chipper

The chipper size usually is selected so that all but the very largest logs will go into the spout without having to be split or sawed into cants. The chipper also must be designed so that it will maintain the required rate of production with a

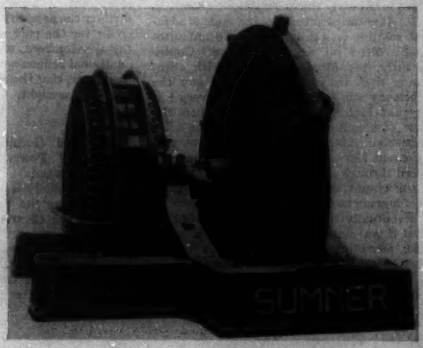

Figure 1. A 110-inch 4-knife chipper with cover removed to show construction of disk

Driven by overhung engine type synchronous motor

Paper 47-130, recommended by the AIEE committees on machine tools and material processing and fabrication for presentation at the AIEE summer general meeting, Montreal, Quebec, Canada, June 9-13, 1947. Manuscript submitted March 27, 1947; made available for printing April 17, 1947.

R. R. BAKER is with the Westinghouse Electric Corporation, East Pittsburgh, Pa., and M. R. LORY is in the transportation and generator engineering department of the Westinghouse Electric Corporation, East Pittsburgh, Pa.

run of average size logs. The log which gives the lowest production rate is one just over half of the spout diameter, as this is the smallest log that must be fed one at a time. The production rate of the chipper is ordinarily adjusted by choosing the proper number of knives, and chippers are built with 2, 3, 4, 6, 8, 10, or 12 knives to obtain the required production rate with the average size of log. It is possible to adjust the production by changing the speed, but this is not done often to any great extent as it is usually uneconomical to operate a chipper much below its maximum permissible speed.

As an example, assume that a chipper is required to produce 3/4-inch chips from hemlock logs which have a maximum diameter slightly less than 18 inches. From Table I, it is seen that an 88-inch chipper with an 18-inch spout is required, and this size has a permissible operating speed of 400 rpm. The following calculations are made for 4-knife and 8-knife designs, but the method can be used for any number of knives within the range of possible chipper design. The highest peak load comes on the motor when the largest or 18-inch-diameter log is being chipped, and the magnitude is obtained by multiplying the figure in column *J* of Table I by the number of knives, giving 736 horsepower for four knives and 1,472 horsepower for eight knives. The motor should have 250 per cent pull-out torque, for reasons given later, and the horsepower rating will be the figure in column *K* multiplied by the number of knives and increased to the next larger standard rating. In this case, the rating will be 300 horsepower for four knives and 600 horsepower for eight. With either number of knives, the log which will just load the motor to its rated horsepower will give maximum production. This optimum diameter is 11.4 inches, given in column *L*. All logs larger than this must be fed intermittently, as they will overheat the motor if fed end to end. The production capacity for various sizes of logs in stacked cords per hour will be as follows:

Table I. Characteristics of Typical Chippers

(A) Disk Diam (In.)	(B) Spout Diam (In.)	(C) Speed (Rpm) *	(D) WR² Disk (Lb-ft²)	(E) Stored Energy (Hp-sec)	(F) Cu In Per Full Cut †	(G) Energy Per Full Cut (Hp-sec) †‡	(H) Production Per Knife (Cords/hr) Peak †	(H) Production Per Knife (Cords/hr) Cont †**	(J) Power Per Knife Peak †‡	(K) Power Per Knife (Hp) Cont †‡**	(L) Optimum Log Diam (In.) †**
54	12	600	10,000	1,120	85	12.3	17.6	7.0	123	49	7.6
84	14	450	35,000	2,200	115	16.8	17.9	7.2	125	50	8.9
88	16	400	55,000	2,720	191	27.7	26.4	10.5	184	74	11.4
96	22	360	80,000	3,220	285	41.4	35.4	14.2	248	99	13.9
110	26	300	150,000	4,180	398	57.8	41.0	16.5	288	115	16.4
150	34	277	1,000,000	23,800	681	98.8	65.0	26.0	455	182	21.5
178	43	240	2,000,000	35,700	1,040	150.8	86.0	34.4	602	240	26.6

* Maximum permissible operating speed.
† Based on 3/4-inch long chips and diameter of log equal to spout diameter.
‡ Based on hemlock wood requiring 7 horsepower-hours per stacked cord.
** Based on motor with 250 per cent pull-out torque.

	4 Knives	8 Knives
Capacity with logs 11.4 inches in diameter (maximum without overheating motor)	42	84
Capacity with logs 9 inches in diameter (size log for lowest production)	26.2	52.4
Capacity with logs between 9 and 11.4 inches	Varies as square of diameter	
Capacity with logs between 11.4 and 18 inches	Slightly less than with 11.4-inch log	

The capacity with logs above the optimum diameter of 11.4 inches is limited by extra motor heating inherent in intermittent loads. From these figures for capacity it is possible to calculate the number of knives to use to obtain the desired production with the expected sizes of wood. In estimating the chipper capacity to suit the mill capacity, it is usual to allow two cords of wood for each ton of finished pulp. If the chipper is not operated during all shifts, its capacity must be increased accordingly, and it is desirable to have some excess capacity to allow for shutdown time to change knives and for other interruptions.

Figure 2. Chipper with cover in place

Note spout through which logs are fed

Determining the Motor Rating

In order to apply a motor to a chipper, it is necessary first to determine the maximum horsepower which the motor must develop. This maximum peak load occurs when the largest log is fed. For a log the size of the spout, the power required can be obtained from column *J* of Table I by multiplying by the number of knives. If conditions are not exactly as given in the table, the power can be adjusted to suit a different species of wood by applying the percentages given in Table II, and ratioed directly as the speed and as the square of the log diameter. The motor must be able to deliver the torque corresponding to this maximum horsepower. It is obviously possible to choose a number of combinations of rating and pull-out torque which will give the same maximum horsepower; but in general, it is most satisfactory and economical to use a motor with 250 per cent pull-out torque. With 250 per cent pull-out torque, the horsepower rating of the motor will be the maximum horsepower, as determined, for the largest log divided by 2.5, and the result adjusted to the next higher standard rating. If the power supply to the motor is such that the voltage drops when peak loads occur, the pull-out torque will be decreased when these dips occur, and the rating should be adjusted accordingly. Remember that the pull-out torque of a synchronous motor varies directly as the voltage, while the pull-out torque of an induction motor varies as the square of the voltage.

The motor horsepower rating ordinarily is based entirely on the maximum power required by the largest log. With 250 per cent pull-out torque motors which are

Table II. Energy Requirements of Chippers Cutting 3/4-Inch Chips from Various Species of Wood

Species of Wood	Horsepower-Hours Per Stocked Cord	Per Cent of Hemlock
Hemlock	7	100
Yellow Pine	6.1	87.1
Gum wood and poplar	10	142.8
Oak and other hard woods	12.3	175.7

recommended for most applications, the maximum continuous production rate is the value in column *I* of Table I multiplied by the number of knives. This rate is obtained with the optimum log size given in column *L*. If the average logs are larger than this optimum diameter, the capacity of the chipper must be reduced by intermittent feeding to avoid overheating the motor. If this reduction in rate of production does not permit the requirements of the mill to be met, the rating of the motor must be increased to obtain greater thermal capacity in the motor. If this is done, the pull-out torque in per cent can be reduced to maintain the same maximum horsepower. If a synchronous motor is used, the high pull-out torque required in a chipper motor will be obtained most economically by specifying an 80 per cent power factor motor.

Motor Starting Requirements

The chipper is started empty, and the motor needs to develop only sufficient starting torque to overcome the fricton of the bearings. Usually, 40 per cent torque is sufficient to start under the worst conditions which occur after an extended shut-down period in cold weather. If reduced-voltage starting is used, the full-voltage torque must be increased so that the required torque of 40 per cent is obtained at the reduced voltage. Once the motor starts to rotate, the torque drops to a very low value represented by the running friction of the bearings and the windage of the disk. In spite of the low torque requirements, it has been the practice in the past to specify 80 per cent pull-in torque or more for synchronous motors. Such high torque is not necessary for the motor to be able to pull the chipper into step, but it does insure a high average torque during acceleration and a reasonably short starting time. If a limited power system makes it desirable to hold the starting inrush of the motor to the lowest possible value, it may be better to allow a longer starting time to obtain the lower starting current which

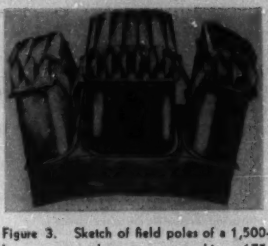

Figure 3. Sketch of field poles of a 1,500-horsepower synchronous motor to drive a 175-inch chipper

Note the heavy starting winding in the pole faces to accelerate the high inertia

the manufacturer can guarantee with 40 per cent or 50 per cent pull-in torque.

While accelerating the inertia of the chipper disk, an amount of heat is developed in the secondary or rotor windings which is equal to the stored kinetic energy of the rotating parts at full speed. In an induction motor with a wound rotor, this heat can be dissipated in an external resistor; but in squirrel-cage induction motors and synchronous motors, this heat must be absorbed by the motor rotor. The design of the starting winding becomes more difficult in the larger sizes. From column *E* of Table I, it is evident that the stored energy increases rapidly as the diameter of the disk increases, so that the ratio of the stored energy to the rated horsepower of the motor increases with disk diameter.

Figure 3 is a sketch of one pole of a 1,500-horsepower synchronous motor to drive a 175-inch chipper, and shows the special construction required to absorb the heat equal to the 37,500 horsepower-seconds stored in the chipper disk and motor rotor. The bars in the pole face are about four times normal size, and in this machine are made of monel, an alloy which maintains its high strength at elevated temperature. All bars are of the same material and are proportioned to come to approximately the same total temperature to prevent excessive stresses from unequal thermal expansion of the bars. A flexible joint in the short-circuiting end ring between each pole prevents thermal expansion of the ring from impressing extra stresses in a radial direction. When special designs similar to this one are used, synchronous motors can accelerate the inertia of the largest chippers without adverse effects. Synchronous motors are seldom belted to chippers except in the smallest sizes because a high speed motor for belted service is smaller physically than a direct-connected motor with its lower speed, and is less able to absorb the heat developed during acceleration.

Choosing the Type of Motor

The choice between an induction motor and a synchronous motor and the choice of the mechanical arrangement of the drive will depend on the size of the chipper. To drive the smallest chippers, up to about an 84-inch diameter, belted induction motors are most commonly used, although a few belted synchronous motors have been installed. Belting the motor permits it to operate at a speed considerably higher than the chipper speed, with some saving in cost. A high speed induction motor has better power factor and efficiency than a direct-connected motor. If the belted motor is put on a separate

Figure 4. Engine type synchronous motor mounted on chipper shaft with outboard bearing

Motor has wide collector rings to permit axial movement of the rotor to adjust the chipper

Figure 5. Squirrel-cage induction motor driving chipper through V belts

foundation from the chipper, it is protected to some extent from the vibration produced by the chipper, and standard mechanical construction can be used.

From 84-inch up to 110-inch chippers, either belted induction motors or engine type synchronous motors are used. Synchronous motors may be overhung on an extension of the chipper shaft, or an outboard bearing may be supplied as part of the chipper. See Figure 1 for an overhung motor and Figure 4 for a motor with an outboard bearing. By mounting the motor on the chipper shaft, considerable space is saved and belt maintenance is avoided. Unlike induction motors, synchronous motors have good efficiency at the low speeds required for direct-connected motors. Motors rated 80 per cent power factor will help to correct the average power factor of the mill. Some engine type motors are designed to permit a limited amount of axial movement of the rotor as required for the adjustment of some makes of chippers.

Synchronous motor drive has an advantage in that the production of chips holds up to a maximum because the speed remains constant, regardless of load. On the other hand, none of the stored energy in the chipper disk can be used to carry part of the peak loads. The high inertia does carry the motor through the very high momentary peaks that occur as each knife makes its cut. If column G of Table I is compared with column E, it is seen that the energy required for one full cut is never more than 1.4 per cent of the stored energy. The inertia smooths out the torque peaks so that the effect on the motor is about the same as if the actual torque is replaced by a constant torque equal to the average value of the actual torque. A synchronous motor must carry the entire load represented by the average torque required by the largest log. An engine type motor mounted on the chipper shaft must always be of special mechanical construction to withstand the severe vibration typical of this application.

Induction motors are also quite commonly used to drive 84- to 110-inch chippers. They are almost always belted to take advantage of the better performance of high speed motors. Standard mechanical construction is usually suitable for belted motors mounted on a separate foundation. Figure 5 is a typical installation. If an induction motor is used, it is possible to use some of the energy in the chipper disk to reduce the power peaks to be carried by the motor, and consequently reduce the maximum current drawn from the line. Appendix II gives a method by which the variation in speed, current, and power of an induction motor during a chipping cycle can be determined. Examples are given in this appendix of a synchronous motor, a normal-slip induction motor and a high-slip induction motor applied to the same chipper. The comparative characteristics of the three types are given in Table III.

Because of its reduced efficiency and lower rate of production, a high-slip motor should be used only in applications which have a power supply so limited that the higher kilowatt and kilovolt-ampere loads imposed by a synchronous motor or a normal-slip induction motor cannot be tolerated. It is not ordinarily possible to help the production rate of a chipper driven by a high-slip motor by using a belt ratio to give a higher speed at no load than is used with a normal-slip motor, as the chipper then will exceed its permissible speed at no load. A squirrel-cage motor can be built with high slip in small sizes, but above 150 horsepower, it is difficult to dissipate the rotor losses if the slip required is more than three or four per cent. If higher slip is required, it is necessary to use a wound-rotor motor with a permanent external resistor inserted in the rotor circuit.

Very large chippers with disk diameters above 110 inches to 175 inches usually are driven by synchronous motors coupled through flexible couplings. These large chippers are suitable for the large logs found in the Northwest, which are handled in lengths of 30 feet or more. A log 30-feet long has a volume equal to 480 full cuts with 3/4-inch chips. A 42-inch log which could be fed to a 175-inch chipper requires 150.8 horsepower-seconds per full cut, (from column G of Table I), or 72,400 horsepower-seconds are required to chip the log. The stored energy of the disk given in column E is only 35,700 horsepower-seconds, so it is evident that the inertia will not carry the load, and the motor must carry the peak load before the end of the log is reached, even if a high-slip induction motor were used. A synchronous motor will carry the peak load with less current at better power factor than an induction motor, so it is favored for this application.

Mechanical Features of Synchronous Motors

When one of the chipper knives enters the log, a shock is imposed on the disk and the anvil and transmitted to the shaft and foundation. Some of the resulting vibration is transferred unavoidably to the motor. Engine type motors which have their rotors mounted directly on the chipper shaft and their stators mounted on the base of the chipper are subjected to a large portion of the vibration. Even motors coupled through flexible couplings are subjected to severe vibration and must be made much stronger than for normal applications, and consequently cost more than standard motors.

To withstand the vibration, special

Table III. Motor Performance for 88-Inch, 4-Knife Chipper Hemlock Logs 18 Inches in Diameter, 4 Feet Long

	Motor A*	Motor B†	Motor C‡
Time to chip one log, sec	2.4	3.34	4.7
Maximum power drawn from line, hp	790	750	580
Maximum current drawn from line (based on 2,300 volts), amp	164	186	138
Efficiency at peak load, per cent	93	87	73
Approximate average efficiency, per cent	93	89	79

* Motor A—300-horsepower 2,300-volt synchronous motor with 250 per cent pull-out torque.

† Motor B—Similar to A except squirrel-cage induction motor with 2 per cent full-load slip.

‡ Motor C—300-horsepower wound-rotor motor with 10 per cent full-load slip, 200 per cent pull-out torque.

construction is used which can be seen in the cut-away view of a large synchronous motor of Figure 6. In the stator, the main frame rings are made thicker and larger in diameter than standard. A heavy cover plate is welded to them and is extended to the ends of the feet, both above and below the base. Additional bracing members also are used to stiffen the frame against axial movement, and a large number of heavy bolts are used to fasten the frame to the bedplate. The rotor is of equally strong construction, with a heavy, one-piece, forged steel spider being shown in the picture. This construction often is used for motors rated 1,000 horsepower and larger, although cast steel or fabricated steel spiders are adequate for the service. In the smaller sizes, the spider usually is fabricated of heavy steel plate, with the rim, hub, and web being made thicker than normal, and with additional bracing members added to strengthen the structure against axial forces.

Coupled motors are made with very heavy bedplates, and at least twice as many foundation bolts of increased size are used as in standard machines. Motors can be supplied with either sleeve bearings or antifriction bearings. Sleeve bearings can be replaced without disassembling the motor, can be rebabitted by the user, and have less loss during normal operation than antifriction bearings, although they require more starting torque. The chippers usually use antifriction bearings which must be very large to support the weight of the disk. If specified, motor bearings which are interchangeable with the chipper bearings can be supplied at an increase in cost.

With each knife cut, a torsional shock is imposed on the rotating parts. The torsional system formed by the chipper disk, the motor rotor and the connecting shaft should be checked to make sure that it is not resonant at one of the imposed frequencies. The knives are not necessarily uniform, and this can give impressed frequencies lower than the principal knife frequency which, in cycles per minute, is the rpm multiplied by the number of knives. One dull knife will impose a force once a revolution to give the lowest possible frequency. The torsional system actually will have two critical frequencies because the electrical forces between the rotor and stator of the motor act like a spring, giving rise to a natural frequency much lower than the one with a node in the connecting shaft. In most applications, this lower critical frequency will be safely below the lowest forced frequency produced by one dull knife.

Other adverse conditions to which motors driving chippers are subjected are excessive moisture and the fine sawdust which escapes from the chipper housing and is carried into the motor. Some operators use enclosed motors and ventilate them with clean air. This protects the motor, but requires duct work and a motor-driven fan to circulate the ventilating air. If the motors are not completely enclosed to exclude the dirt entirely, it is usually better to make them as open as possible so that the dirt can be cleaned out more easily. End bells to provide mechanical protection to the windings should be made of steel straps which do not trap the dirt and permit it to be blown out easily. Some makes of chippers require special protecting covers for engine type driving motors mounted very close to the chipper housing.

The motor windings must have the best possible insulation and treatments to withstand dirt and moisture. The stator windings must be braced more securely than usually is done for full-voltage starting, as the coils must be held securely against the stresses imposed by heavy starting duty and loads that fluctuate widely and often approach the pull-out point.

Control Requirements

The requirements for the control for a chipper motor are relatively simple, as the only operating functions required are to start and stop the motor, and to provide adequate protection against abnormal conditions. In stopping the motor, it is frequently considered desirable to provide dynamic braking to reduce the stopping time. Without dynamic braking, the stopping time is long because of the high inertia of the disk. Dynamic braking reduces the outage time required to change knives, which may have to be done as often as every four hours to maintain productive capacity and chip quality.

Enclosed control is recommended for chipper installations. It must provide adequate overload protection and still permit uninterrupted operation within the thermal capacity of the motor when it is subjected to intermittent peak loads. In addition to overload protection, controls for synchronous motors must provide protection against pulling out of step. Pull-out protection usually disconnects the motor from the power supply, if the peak load torques exceed the maximum torque of the motor and pull it out of synchronism. The motor cannot be resynchronized until the chipper has been unloaded. When short logs are being fed, it is possible to interlock the motor control with the log feed, and automatically unload the chipper when the motor pulls out of step by stopping the feed. The inertia of the disk will finish chipping the log that is already in the machine. Under these conditions, the control can be arranged to remove the field current and initiate the starting cycle after the motor pulls out, which will cause the motor to accelerate and synchronize again without a shutdown. A damper winding protective relay is another desirable feature to include in the control for synchronous motors. This relay is responsive to conditions which cause excessive heating of the pole-face starting winding, such as failure to start, and will trip the motor off the line before serious damage is done.

Wound-rotor motors applied to chippers require special starting resistors with

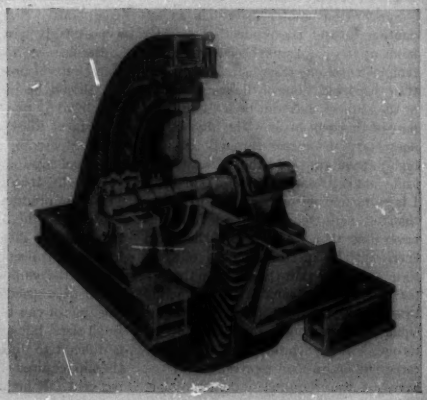

Figure 6. Cut-away view of a 1,500-horsepower synchronous motor to drive a 175-inch chipper

Note forged steel spider, heavy frame, large shaft, and rigid construction throughout

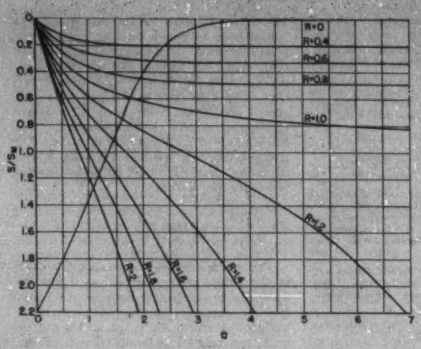

Figure 7. Curves of speed variation of an induction motor with load suddenly applied

S_m = slip at maximum torque
R = ratio of applied torque to pull-out torque
Q = proportional to time
See Appendix II for explanation

high thermal capacity. If permanent resistors are used to increase the full-load-slip, they must be specified for continuous duty. The secondary control for a wound rotor induction motor may be either manually operated or magnetically operated depending on the size of the motor and the equipment layout. Automatic control is recommended for the primary circuit of all types of motors, with electrically operated main circuit switches and a control station located at a convenient point.

The capacity of the mill power distribution system will determine whether full-voltage starting can be used, or if reduced-voltage starting is required for either synchronous or squirrel-cage induction motors. If reduced-voltage starting is used, the starting torque must be specified high enough so that the actual torque at the starting voltage will not be less than about 40 per cent to give some margin above the static friction. With very limited systems which require the starting kilovolt-amperes to be held to a minimum, a wound-rotor induction motor should be applied.

In controls for synchronous motors, it is possible to provide automatic means to adjust the field current to suit the load. By the use of this feature, the peak load that the motor will carry can be increased by at least 25 per cent. When low starting current is wanted, a smaller motor with lower starting kilovolt-amperes can sometimes be used, and the required peak torque obtained by automatically increasing the field current during the peak loads.

All controls must have the interrupting capacity to open the maximum fault currents at the motor leads. Normal interrupting capacity of standard industrial control is ten times the motor rating, but higher interrupting capacity can be provided to meet the actual circuit conditions. Interrupting capacities up to 50,000 kva at either 2,300 or 4,160 volts can be furnished in standard industrial controls which use circuit breakers. These interrupting capacities can be increased to 150,000 kva at 2,300 volts or 250,000 kva at 4,160 volts by using current limiting fuses and contactors. For still higher interrupting capacities, heavy duty switchgear can be supplied to interrupt 500,000 kva at any voltage which may be used in pulp and paper mills.

Conclusion

Chipper drive is one of the most exacting applications to which motors are applied. The size of the motor is determined primarily by the high peak loads which occur intermittently when large logs are fed. Motors for this application must be made mechanically stronger than standard to withstand the shock loads and vibration imposed by the chipper. By using modern motors and control, designed and built to suit this application, operators are assured of many years of trouble-free service.

Appendix I

A stacked cord of round wood occupies 128 cubic feet of space, of which the solid wood occupies $\pi/4$ times the total volume, giving 100.5 cubic feet or 173,720 cubic inches of solid wood per stacked cord. If D is the diameter of the log in inches, and the chips are three-fourths inch long, measured along the grain, the volume in cubic inches of one full cut across the log is given by

$$V=\frac{3}{4}\times\frac{\pi}{4}\times D^2=0.589\ D^2 \qquad (1)$$

E, the energy in horsepower-seconds required for one full cut across a log of diameter D is the horsepower-seconds required to chip one cord multiplied by the ratio of the volume of a full cut to the total cubic inches in a cord. If W is the horsepower-hours required to chip one cord from Table II

$$E=\frac{3{,}600\ W\ 0.589\ D^2}{173{,}720}=0.0122\ W\ D^2 \qquad (2)$$

The values for V for the largest size of log with a diameter equal to the spout diameter are given in column F of Table I. The corresponding values of E for hemlock wood are given in column G.

Each knife makes one cut per revolution, and the volume of each cut is given by equation 1. The cords per hour chipped by one knife will be the revolutions per hour, or 60(rpm), multiplied by the volume of one full cut and divided by the cubic inches of solid wood in one cord, which gives $2.035\ D^2$

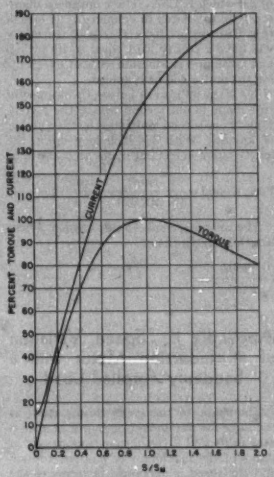

Figure 8. Curves of current and torque plotted against the ratio of actual slip to the slip at pull-out

Torque is expressed in per cent of pull-out torque. Current is in per cent of the real current at pull-out
See Appendix II

(rpm) 10^{-4}. The cords per hour per knife for the maximum size of log are given in column H of Table I. To obtain the actual peak rate of production, multiply by the number of knives. The power required per knife is the number of cords per hour per knife as given, multiplied by W, the horsepower-hours per cord

$$P=2.035\ W\ D^2\ (\text{rpm})\ 10^{-4} \qquad (3)$$

Values of P for hemlock wood are given in column J of Table I. To obtain the total power required, the values in this column must be multiplied by the number of knives. The values given in column J are for the

speed given in column C. If the chipper is operated at any other speed, the power must be ratioed directly as the speed.

In Table I, it has been assumed that the motors have 250 per cent pull-out torque. If the horsepower rating of the motor is chosen so that at the pull-out point it will carry the load imposed by the maximum size of log, the continuous rating will be the maximum power divided by 2.5. The continuous power rating for one knife is thus the value in column J divided by 2.5, and is tabulated in column K. The rate of production is proportional to the power, so the continuous rate is the peak rate divided by 2.5, and is given in column I. Both the horsepower required and the rate of production are proportional to the square of the diameter of the log. Therefore, the diameter of a log which will require rated power from the motor equals the maximum diameter of log divided by the square root of 2.5 which is 1.57. These optimum diameters are tabulated in column L. If logs of this diameter are fed end to end, the motor will have a steady load equal to its rating, and maximum production without overheating the motor will be obtained.

If k is the number of knives, the number of cuts made in one second will be the revolutions in one second multiplied by the number of knives. With 3/4-inch long chips, the length of log in feet cut in one second will be

$$\text{Feet/second} = \frac{3k\ (\text{rpm})}{4\times 12\times 60} = \frac{k\ (\text{rpm})}{960}$$

The time in seconds to chip one log, whose length in feet is L, is

$$t = \frac{960L}{k\ (\text{rpm})} \tag{4}$$

Appendix II. Speed Variation of an Induction Motor with a Suddenly Applied Load

The shape of the speed–torque curve is the same for any induction motor at speeds near full speed if the torque is expressed in terms of the maximum or pull-out torque, and the speed is expressed in terms of the slip at which pull-out occurs. This fact is used to determine the curves of Figure 7 from which the variation in speed of any induction motor can be found when a sudden load of constant torque is applied. Although the curves are based on a constant applied load torque, they are accurate when used for a motor driving a chipper, because the high inertia of the chipper disk smooths out the torque peaks which occur as each knife makes a cut. The effect on the motor is the same as if the actual torque had been replaced by a constant torque equal to the average torque required by the chipper. The derivation of these curves is beyond the scope of this paper, but instructions for using them are given with some illustrative examples.

In order to use the curves, it is necessary to know the full load slip, S_m, the pull-out torque of the motor, and the stored energy of the rotating parts. Then proceed as follows:

1. Determine rated torque in per cent of pull-out torque. This is 10,000 divided by the pull-out torque in per cent.

2. Read S/S_m from the torque curve of Figure 8 for the preceding torque.

3. Determine S_m, the slip at pull-out. S_m is the full load slip divided by the value of S/S_m from step 2.

4. Find the maximum power required by the log from equation 3 or column J of Table I. Multiply by the number of knives and ratio to the *full load* speed of the motor.

5. Determine R.

$$R = \frac{\text{Maximum power from step 4}}{\text{Rated horsepower} \times \text{per cent pull-out torque}/100}$$

6. Assume either an initial value of slip or an initial value of torque when the log is fed. In either case, determine S/S_m for the initial condition, using torque curve of Figure 8 if initial value of torque is assumed, or dividing by S_m from step 3 if an initial value of slip is assumed.

7. Using this initial value of S/S_m and R from step 6, read the initial value of Q from the proper curve of Figure 7. Interpolate between curves for intermediate values of R.

8. Assume an average value of slip and determine the corresponding average speed.

9. Determine the time required to chip one log from equation 4 of Appendix I, using the average speed from step 8.

10. Calculate H_m. H_m is obtained by multiplying the stored energy in horsepower-seconds by the speed at full load in per cent, and dividing this quantity by the rated horsepower multiplied by the pull-out torque in per cent.

11. Calculate the relation between Q and time in seconds. $Q = \dfrac{t}{2H_m S_m/100}$ if S_m is in per cent.

12. Find Q corresponding to the time to chip one log from step 9.

13. Add this value of Q to the initial value found in step 7 to obtain the final value of Q.

14. Read the final value of S/S_m from proper curve of Figure 7, interpolating if necessary for intermediate values of R.

15. Determine the final value of slip by multiplying the value of S/S_m from step 14 by S_m from step 3.

16. Compare the initial and final values of slip with the average value assumed in step 8. If the assumed value was wrong, make a new assumption and repeat steps 8 to 16.

17. On current curve of Figure 8, read current for final value of S/S_m from step 14.

18. Similarly, read the current for the full-load value of S/S_m found in step 2.

19. The maximum current drawn from the line is approximately the full-load current multiplied by the ratio of the current from step 17 to that from step 18.

20. On torque curve of Figure 8, read torque for final value of S/S_m found in step 14.

21. Maximum power drawn from the line is approximately the input at full load multiplied by the ratio of the torque from step 20 to the torque from step 1.

22. On curve for $R = 0$ of Figure 7, read Q for the initial and final values of S/S_m from steps 6 and 14, and take the difference.

23. Convert this to seconds by the relation of step 11. This is the recovery time for the motor to reach the initial conditions again after chipping a log.

24. Total time to chip one log is the time from step 9 plus the time from step 23.

The use of the curves will be illustrated by two examples.

Example 1

A 300-horsepower squirrel-cage induction motor with normal slip is belted to the 4-knife, 88-inch chipper considered under "Selecting a Chipper." The motor has 250 per cent pull-out torque and the slip at full load is 2 per cent. The stored energy from column E of Table I will be increased 10 per cent to allow for the motor and the belt sheaves to give a total of 2,990 horsepower seconds. Full-load torque is 40 per cent of pull-out torque, and for this value, we read 0.21 for S/S_m. S_m is then 2 per cent divided by 0.21 or 9.5 per cent. All speeds should be referred to the chipper speed, rather than the motor speed. The full-load speed is 98 per cent of 400 or 392 rpm. Using this speed in equation 3, the maximum power is found to be 723 horsepower for four knives.

$$R = \frac{723}{300\times 2.5} = 0.965$$

This value does not correspond to any of the values on the curve, so it will be necessary to interpolate between $R=1$ and $R=0.8$. Assume that the motor is carrying half load when the log is fed, or the torque is 20 per cent of pull-out torque. From Figure 8, S/S_m is 0.1 for this initial condition, and the initial slip is 0.1×9.5 per cent or 0.95 per cent. From the curves of Figure 7, the initial value of Q is 0.12. If we assume that the average slip is 4 per cent and the average speed is 96 per cent, from equation 4, the time to chip a 4-foot log will be 2.5 seconds.

$$H_m = \frac{2{,}990\times 98}{300\times 250} = 3.9$$

$$Q = \frac{t}{2\times 3.9\times 0.095} = 1.35t$$

Then for 2.5 seconds, Q is 3.38, and when the initial value of 0.12 is added to this, the final value of Q of 3.5 is obtained. From Figure 7, the corresponding value of S/S_m is 0.69. The final value of slip is 0.69×9.5 or 6.55 per cent. Since the initial slip was 0.95 per cent, the average between the initial and final values is 3.75 per cent. This value does not differ much from the 4 per cent originally assumed, so the determination will not be repeated with a more accurate value. The current for the final value of S/S_m is 123 per cent and for the full load value is 46 per cent, giving a maximum current of 268 per cent of full load current or approximately 186 amperes. The torque corresponding to S/S_m of 0.69 is 0.93 giving a total power drawn from the line of 750 horsepower for a motor with 93 per cent efficiency. The line currents are based on a 2,300 volt motor.

From the curve for $R=0$, Q is 2.8 for S/S_m equal to 0.1 and 1.67 for S/S_m equal to 0.69, giving a difference of 1.13, which gives 0.84 when converted to seconds. The total time of a chipping cycle with 18-inch-diameter logs, 4-feet log is 2.5 seconds to chip the log, and 0.84 seconds to recover the speed lost, or a total of 3.34 seconds.

Of course, since the maximum torque required to chip the log is less than the pull-out torque of the motor, it would be possible to feed these maximum logs end to end, with an increase in the maximum current. From the torque curve of Figure 8, S/S_m for 96.5 per cent torque is 0.77, or the slip would be 0.77×9.5 per cent or 7.3 per cent, and the time to chip one log will be reduced to 2.59 seconds. The current for S/S_m of 0.77 is 132 per cent, an increase of 7 per cent which gives a maximum current of 199 amperes.

Example 2

For this example, let us consider a wound-rotor motor of the same characteristics as the squirrel-cage motor of example 3, except that it has a permanent resistance inserted in the secondary circuit to give the motor 10 per cent slip at full load. With this high slip, a portion of the load can be carried by the inertia, so a motor with only 200 per cent pull-out torque will be tried, instead of the 250 per cent required for the previous example. Then full-load torque is 50 per cent of pull-out torque, and for this value, S/S_m is 0.27 from Figure 8. S_m is then 10 per cent divided by 0.27 or 37 per cent. In calculating R and H_m, there is a question of the proper speed to use. Should 90 per cent, the value with the secondary resistor be used, or should the full-load speed of 98 per cent which the motor will have with the rings short-circuited be used? The proper speed to use is the one for which the torque guarantees were made. In this example, it is assumed that the motor was purchased as a normal machine with 2 per cent slip at full load, and the resistor added to increase the slip. Thus the pull-out torque is based on 98 per cent speed, and this should be used in calculating R and H_m.

$$R=\frac{723}{300\times 2}=1.204$$

Assume that the motor is carrying full load, or the slip is 10 per cent, when the log is fed. As determined, S/S_m is 0.27 for this condition, and the initial value of Q is 0.29 from Figure 7, using $R=1.2$. Assume that the average slip is 20 per cent or the average speed is 80 per cent. From equation 4, the time to chip a 4-foot log will be three seconds.

$$H_m=\frac{2{,}990\times 98}{300\times 2}=4.88$$

$$Q=\frac{t}{2\times 4.88\times 0.37}=0.277t$$

For three seconds, Q is 0.83, and when the initial value of 0.29 is added, the final value of 1.12 is obtained for Q. From Figure 7, the corresponding value S/S_m is 0.63, giving a final value of slip of 23.3 per cent. When this value is averaged with the initial slip of 10 per cent, the average slip is found to be 16.7 per cent, which differs from the 20 per cent assumed. If the assumed average speed is corrected to 83 per cent, the time to chip a log becomes 2.89 seconds, giving a value of Q of 0.8. When the initial value of 0.29 is added, a final value of 1.09 is obtained for Q. 0.62 is the corresponding value of S/S_m from the curve, or the final slip is 23 per cent, giving an average slip of 16.5 per cent which is close enough to the assumed value. Note that it is not rigorously correct to average the initial and final values to obtain the average speed, since the change in speed is not uniform; but it is accurate enough for our purpose. This is evident from the preceding, where it was found that a change from 80 per cent to 83 per cent in the average speed made only a minor difference in the result.

The current for S/S_m from Figure 8 is 114 per cent for the final value and 57 per cent for the full-load value, or the maximum current is 200 per cent of full-load current or 138 amperes for a 2,300 volt motor. The torque from Figure 8 is 90 per cent of pull-out torque, or the maximum power drawn from the line is 580 horsepower.

From the curve for $R=0$, for S/S_m equal to 0.27 and 0.62, Q is 2.25 and 1.75, giving a difference of 0.5. The corresponding time for the motor to recover its speed is 1.81 seconds, and when this is added to the 2.89 seconds required to chip the log, a total time of 4.7 seconds is obtained for the cycle.

Example 3

For comparison, consider a synchronous motor to drive the same chipper as the previous examples. Since the speed remains constant at 400 rpm, the time required to chip a 4-foot log is 2.4 seconds. The motor must carry the full 736 horsepower required by the chipper at 400 rpm, and with a motor efficiency of 93 per cent, the power drawn from the line is 790 horsepower. The maximum current will be 218 per cent of full-load current, or 164 amperes for a 2,300 volt motor.

No Discussion

Some Fundamentals of a Theory of the Transductor or Magnetic Amplifier

A. UNO LAMM
ASSOCIATE AIEE

Synopsis: The old d-c presaturated reactor has experienced a revival with the appearance of the metallic rectifier. The combination of these two devices is studied with an idealized magnetization curve as a basis. Two typical connections are chosen as examples, namely one polyphase connection without self-excitation and one single-phase connection with self-excitation. The behavior is very similar to that of grid-controlled rectifiers. There is a marked difference as to the dynamic properties of the two connections. Much more rapid response is obtained at correct design than generally expected, making the application to quick-acting regulators often quite possible.

IN the last 15 years the d-c presaturated reactor, under the name of transductor,* has found wide application in Scandinavia in grid-control gear for mercury arc rectifiers, as a regulator for metal rectifiers, generators, and motors, as a transformer and amplifier for measurement purpose, as a voltage stabilizer for a-c networks, as a statical relay for flash-lighting, and as a sensitive amplifier for photoelectric cells and resistance thermometers. It has proved a useful tool for very accurate voltage and current control and has in many cases entered into successful competition with electronic regulators for similar purpose. It has the great advantage over the electronic tube of being mechanically as rigid as a transformer and having an almost unlimited life and constancy of its characteristics. A longstanding prejudice against the transductor in favor of the electron tube, owing to the former being an inductive device with a considerable time delay, has been diminished since a better knowledge of its characteristics has proved, both by theory and experience, that the inertia of a well-designed transductor may be very small. When used as a regulator for alternators, the time delay of the transductor can be almost entirely neglected.

The conventional design of a single phase transductor is shown in Figure 1*A*. On a three-leg core the a-c winding was applied on the outside legs and the d-c winding on the central leg or vice versa and the device was thus rendered symmetrical as regards the two a-c halfwaves. Much more pronounced properties can, however, be achieved by using two separate cores or *transductor elements* according to Figure 1*B*. The two elements can be built as ordinary single-phase transformers without air gap, and the d-c and a-c windings should be placed on the same leg with low magnetic leakage between them.

Figure 1

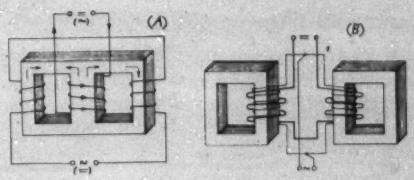

In most applications of the transductor its alternating current will be rectified, often in a metallic rectifier, and we shall therefore start at once by studying the combination transductor-rectifier.

Transductor Connections

In order to facilitate the reading of this paper some names will be given to the different modes of connection without any claim to consider this nomenclature as definite. The symbol of the transductor element is that of an ordinary single-phase transformer but also a simple symbol for the complete transductor should often be useful. Figure 2 shows the proposed Swedish standards for such symbols.

Figure 3 shows some connections of simple transductor-controlled rectifiers with separate a-c and d-c windings. In Figure 3*A* is a single-phase series-transductor; Figure 3*B* shows a single-phase parallel transductor; Figure 3*C*, a 3-phase transductor with a half wave rectifier; and Figure 3*D*, a 6-phase transductor with a full wave rectifier.

In the autotransductor connections of Figure 4 the alternating current and direct current flow through the same winding of the transductor elements. Such connections, of course, save a considerable amount of material. As will be shown later these connections have a fundamentally simpler action. Figures 4*A* and 4*B* are single-phase and Figure 4*C* is 6-phase. The latter connection is often called Nordfeldt-connection from its inventor, B. Nordfeldt. The six transductor windings A_1, A_2, A_3, B_1, B_2, and B_3 are arranged on separate cores.

The amplification of a transductor can be very much increased by self-excitation, that is, by letting the rectified output current pass through an excitation winding on the transductor itself. By proper choice of the number of turns of this winding, the self-excitation can be almost

Paper 47-141, recommended by the AIEE committee on industrial control devices for presentation at the AIEE summer general meeting, Montreal, Quebec, Canada, June 9-13, 1947. Manuscript submitted April 8, 1947; made available for printing April 25, 1947.

A. Uno Lamm is head of the general and rectifier departments of Allmanna Svenska Elektriska Aktiebolaget, Ludvika Works, Ludvika, Sweden.

* For convenience, the Scandinavian terms "transductor" and "transductor element" will be used in this paper.

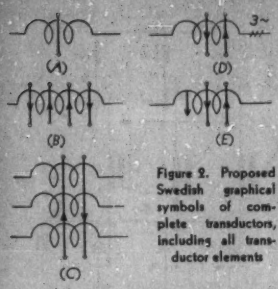

Figure 2. Proposed Swedish graphical symbols of complete transductors, including all transductor elements

The a-c windings are symbolized by a winding symbol and the control d-c windings by straight, crossing lines

A—general symbol

B—transductor with several control windings, the arrows indicating the relative winding direction

C—3-phase transductor

D—3-phase transductor in single-line diagrams

E—self-excited transductor, the arrow indicating the direction of the self-excitation relative to the other excitation windings

100 per cent, so that only a very small amount of additional excitation, positive or negative, has to be added to vary the impedance of the transductor from the highest to the lowest value. As high power amplifications as ten million times have been achieved in this way at an input power of 0.23 microwatt. The additional excitation will be called control current in the following but may also partly consist of a biasing excitation current. Self-excitation may be applied to all the connections shown in Figure 3 by connecting the d-c winding of the transductor in series with the rectifier output circuit and adding a control d-c winding to the transductor. Also the auto-transductor connections of Figure 4 may be used with self-excitation, the terminals of the transductor being fed from a current transformer in the a-c leads over a separate small rectifier.

The most interesting arrangements of an auto-transductor with self-excitation, however, are those shown in Figure 5. In each phase a transductor element and a rectifying element are series-connected. These connections are based upon the observation that in the conventional connections with 100 per cent self-excitation the resulting magnetisation ampere-turns of each core periodically varies between a very small negative or positive value and a great positive value. Rectifying elements inserted in such a way that they block the reverse current in the main winding of each transductor element will thus lend to the transductor the same character of self-excitation and sensitiveness to extra control excitation. Figure 5 gives some examples of this kind of self-excitation as applied to single-phase and polyphase transductors. The rectifying elements for the self-excitation may at the same time constitute the main rectifier, Figures 5*A*, 5*B*, and 5*C*, or there may be a separate rectifier as in the case of Figures 5*D* and 5*E*. If the rectifying elements are ideal, the self-excitation would be 100 per cent. With ordinary incomplete rectifiers a supplementary self-excitation may be arranged, for example by a few extra turns traversed by the d-c load current.

In this paper the problem of the behavior of the transductor will be approached from two different sides. On the one hand, the polyphase autoconnection without self-excitation will be examined from much the same viewpoints as an

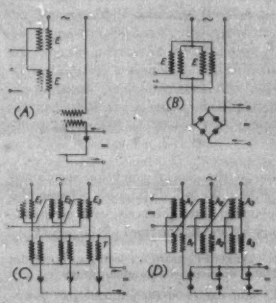

Figure 3

ordinary polyphase rectifier according to the theory of Dällenbach and Gerecke.[1] On the other hand, a self-excited single-phase transductor with a rectifying element in series with each transductor element will be analysed in a somewhat different way.

The traditional way of regarding the action of a transductor was the idea of varying the reactance of the a-c circuit by varying the permeability of the core material with the d-c pre-excitation. This picture does not, as will be shown below, very well describe the real performance of the transductor. In a fully utilized transductor the a-c flux density may vary during one a-c period from full saturation in one direction to a point near saturation in the opposite direction, and the permeability therefore varies within a great range during each period. In fact, the average flux density will not be determined by the d-c excitation but by the a-c voltage. We therefore are going to examine the transductor from another point of view, taking an idealized magnetization curve as a point of departure.

Definition of the Ideal Transductor and Some Fundamental Concepts

It is assumed that the transductor elements fulfill the following conditions:

1. The magnetization curve of the core is ideal, that is, the magnetization current is infinitely small up to the saturation value and increases very rapidly as the flux increases, after this value has been reached (Figure 6).
2. There is no magnetic leakage.
3. The windings have no ohmic resistance.

This means that as soon as a considerable resulting amount of ampere-turns exists the element will be fully saturated. In normal service of the transductor these resulting ampere-turns will always have a given direction, which we will call the positive direction, and the core will thus reach saturation only in one direction. When the ampere-turns change from a higher value down to zero the flux will attain the value of the bend point, which will be regarded as the zero point of flux. Lower values of flux can only be attained if the windings are made to absorb voltage. The deviation of the flux $\epsilon \cdot E_e$ from the bend point value is thus proportional to the voltage–time area, which the transductor element has absorbed since it prevailed at the bend point. We shall call this quantity $\epsilon \cdot E_e$ flux deviation.[7] The zero point of the magnetization curve is of no special significance in transductor theory. In normal service the flux deviation may rise to a maximum

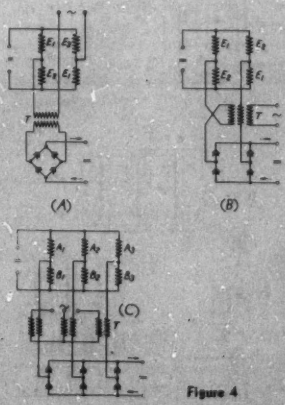

Figure 4

value represented by the distance between the positive and negative bend points. As long as the resulting number of ampere-turns is finite and positive, the flux deviation remains at zero and the windings cannot take up any voltage. If, however, positive voltage is applied to the element, the amount of ampere-turns immediately goes down to zero and the flux deviation begins to increase.

The Multiphase Autotransductor Connection (Nordfeldt Connection)

Figure 7 shows the Nordfeldt 6-phase connection of a transductor-controlled rectifier. This figure as well as the following reasoning may in part be readily generalized, so as to be rendered applicable to any even phase number. T_1, T_2, and T_3 are transformers. A sinusoidal 3-phase voltage is applied to their primary sides. The six rectifying elements are denoted by *1A*, *2A*, *3A*, *1B*, *2B*, and *3B* respectively. The direct current I_N supplied by the rectifier is consumed by the appliance *B*. The six transductor elements, each of which has a single winding, are denoted in an analogous way by *1A*, *2A*, *3A*, *1B*, *2B*, and *3B* respectively. The excitation current I_M is supplied to the conductor O_A and O_B by a source of direct current *K* whose voltage may be very low since the resistance of the windings is assumed to be very small.

To begin with, it is assumed that the transductor is excited to so high a degree, that is, I_M is so much larger than I_N that all the elements are fully saturated all the time and the rectifier operates as if the transductor were short-circuited. The current I_M is equally distributed on the three pairs of transductor elements so that each takes $I_M/3$ as an average value. The three a-c leads *M–T–N* of the rectifier each carry the current I_N during two 120 degree intervals and zero current during two 60-degree intervals of each period, just as an ordinary rectifier of this type. The current I_N is at the points *M* divided upon the two opposite elements, each taking the current $I_N/2$,† which is thus superimposed upon the forementioned current $I_M/3$, always adding to this current in one and subtracting from it in the opposite of two companion elements. As long as $I_M/3$ is equal to or greater than $I_N/2$, that is, I_M is equal to or greater than $3/2(I_N)$, the superposition principle holds good, but when I_M is reduced to a lower value the resulting current would tend to be negative in one of the two elements. This is impossible,

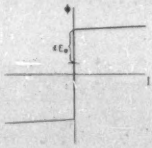

Figure 6

due to the general condition mentioned before. We will distinguish between the following three intervals, each constituting, all in all, one third of the period:

1. Current I_N in the a-c lead goes upwards: The *A*-element carries no current.
2. Current I_N in the a-c lead goes downwards: The *A*-element carries the current I_N.
3. Current I_N in the a-c lead is zero: The *A*-element carries a current, which we denote I_0.

Since the mean value for the whole period must be $I_M/3$, we have

$$\frac{0+I_o+I_N}{3}=\frac{I_M}{3}$$

$$I_0=I_M+I_N$$

So long as I_0 does not equal zero, the elements only carry no current during the time that the companion element is carrying current. O_A, O_B, M_1, M_2, and M_3 must then always have the same potential, since in that case both element in one of the three pairs of elements, and one of the elements belonging to the remaining two pairs, are always carrying current. None of the elements can therefore take up voltage but all elements remain continuously in a state of zero flux deviation, even when they do not carry any current.

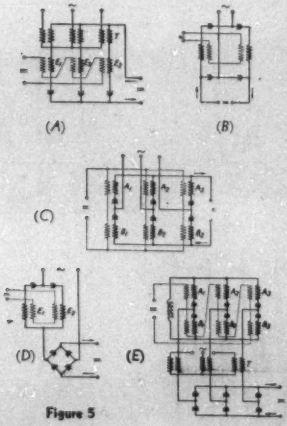

Figure 5

† The expression "degree of charge" also has been suggested. This wording is in fact preferred by the author as it so well pictures the purpose of the transductor element, alternatingly to accumulate and give off voltage-time amounts, and also is more flexible in using. In this paper, however, the expression flux deviation will be used, as being more rapidly grasped by those not familiar with the art.

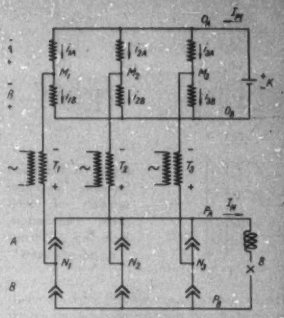

Figure 7

Consequently, in order that voltage absorption and reduction in rectifier voltage should take place, the condition I_M is equal to or greater than I_N must be fulfilled. However, I_M cannot be inferior to I_N because this would imply that the load current of the transductor elements could become negative. The current I_M is of course delivered by the source *K* which has to cover the d-c resistance loss in the transductor windings and therefore determines the value of I_M. Within the range where the transulator absorbs part of the 3-phase voltage, I_N must attain a value equal to I_M. The current of each transductor element will always follow exactly the same course as the corresponding rectifying element. The current of each transductor element periodically drops down to zero just as that of the rectifying element in spite of the fact that a constant d-c voltage is supplied to the excitation terminals O_A and O_B. If the output current I_M is not a smoothed direct current, the excitation current I_M will equal I_N also in respect of the wave form.

Voltage Conditions

Examination of the voltage conditions of the connection will start, with reference to Figure 8, from an instant when the elements *1A* and *3B* carry the current, phase T_1 of the feeding transformer having positive voltage and T_3 negative voltage. The flux of all transductor elements remains unchanged while the rectifier supplies the same voltage as in the absence of the transductor. When the

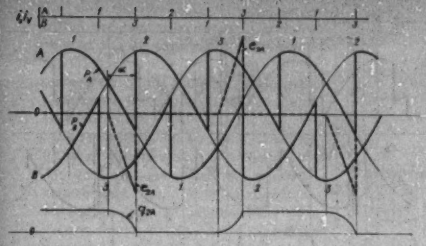

Figure 8

A—Voltage trace
B—Course of flux deviation q of element $2A$

moment comes at which N_2 becomes more positive than N_1, the current would be transferred from the rectifying element $1A$ to $2A$, if the transductor were not present, that is, if M_1 and M_2 had the same potential. Instead of this, M_2 becomes negative in relation to O_A and O_B, the transductor element $2A$, which has already obtained a certain amount of flux deviation (see the following discussion), is exposed to negative voltage and the transductor element $2B$ to positive voltage. Consequently, the flux deviation of $2A$ decreases and that of $2B$ increases. This implies, of course, that the element $2A$ takes up some amount of current, even though this current is infinitely small. The period which has now started will be called quasi-commutation. It is connected with a kind of overlapping between i_{1A} and i_{2A}, but the latter current remains infinitely small the whole time. Finally, however, the element $2A$ is getting saturated so that it loses the ability of absorbing more voltage. At that moment the rectifying element $2A$ takes up current, with the result that the whole current is transferred from the rectifying and transductor elements $1A$ to those of $2A$. This process is called real commutation. After this real commutation $2A$ and $3B$ are carrying the current.

Continue to follow the behaviour of the transductor element $2A$, as it may be concluded from the symmetry that all other elements pass through the same course of events. During the next commutation period $3B$ leaves the current to $1B$ as usual. This takes place in an analogous way involving a period of quasi-commutation and a period of real commutation. During the following period of commutation $2A$ hands over the current to $3A$ in a corresponding manner. When the latter period of commutation is completed, the element $2A$ does not carry any current, but it is still in the condition of zero flux deviation. During the interval following this, when the elements $3A$ and $1B$ are carrying current, while both $2A$ and $2B$ carry very nearly no current, the potential of M_2 is the same as that of O_A and O_B. Consequently the elements $2A$ and $2B$ do not carry any voltage and remain in an unchanged condition of flux deviation. At the next period of commutation the current is transferred from $1B$ to $2B$. During the quasi-commutation M_2 is positive in relation to O_A–O_B, so that the flux deviation of element $2B$ decreases, while that of element $2A$ increases. When the element $2B$ is saturated quasi-commutation is superseded by real commutation, and the increase of flux deviation of $2A$ is therefore completed. Afterwards the element maintains this flux unchanged until the element itself passes through a period of quasi-commutation and again loses its flux deviation.

We have thus found that a transductor element obtains its flux deviation when the opposite element passes through a period of quasi-commutation, loses it while the element itself passes through a period of quasi-commutation, and its flux remains unchanged in the meantime.

Figure 8 shows the oscillographic traces of the voltages and marks (top of the figure) the intervals of time during which the rectifying elements and the transductor elements are carrying current. The sine waves *1*, *2*, and *3* represent the voltages across T_1, T_2, and T_3, respectively. The upper thick contour line represents the voltage of the conductor P_A with the potential of O_A–O_B as the zero line, while the lower thick line in the same way represents the voltage of the conductor P_B. Consequently, the difference between these voltages represents the output direct voltage across the load B. The voltage e_{2A} across the transductor element $2A$ is represented by a dash-line. Figure *8B* shows the variations in the amount of flux deviation q of the same element.

It follows from Figure 8 that the transductor exerts the same influence on the rectifier voltage as the grid-control of mercury arc rectifiers. Accordingly, we speak here of an angle of retardation α analogous to that of grid-controlled rectifiers.

Since the transductor elements act to a certain degree as rectifying elements, it may be of interest to imagine for a moment that they are replaced by the latter. It follows that a transductor of this kind acts like a grid-controlled short-circuited rectifier whose rectifying elements replace the transductor elements in the circuit. The fact that the transductor alone still cannot be used as a rectifier or inverter, but can only operate as a short-circuited converter is, of course, bound up with the circumstance that a transductor element must always absorb the same voltage–time area for each polarity of voltage.

The rectifier equipped with transductor control, as described in the previous paragraph, possesses an interesting property, namely, that each of its rectifying elements gives off its current during the real commutation entirely, irrespective of the fact that it is a rectifying element. Even if the conductivity of the rectifying element in the reverse direction were good, its current would decrease to zero, but would not become negative because the companion of the outgoing transductor element is charged and therefore not able to absorb current at once. Advantage has been taken of this property for a type of moving contact rectifiers, or with the object of reducing the need of absolute accuracy of the contact opening.

The voltage–time area needed by each transductor element, that is, the area corresponding to the maximum flux deviation, is equal to that voltage–time area which is subtracted from the output direct voltage D between P_A and P_B because of the operation of the element. If the amount by which the voltage on the d-c side is reduced by regulation is ΔD volts, the transductor absorbs an alternating voltage, referred to the fundamental frequency, whose mean value is $2\,\Delta D$, where p is the total phase number. The total transformer rating of the p transductor elements, referred to the fundamental frequency, will be

$$\frac{\pi}{2\sqrt{p}} \times \Delta D \times I$$

or in the case of $p=6$

$$\frac{\pi}{2\sqrt{6}} \times \Delta D \times I = 0.64 \times \Delta D \times I$$

taking into account the fact that we have in this case only one winding in contradistinction from the two windings of a transformer. It might be interesting to note that in the case of $p=\infty$ the total transductor rating will be zero.

It has been assumed, however, that two opposite transductor elements do not

take up any voltage in the intervals when they carry no load current. This assumption does not quite agree with the real conditions. Even if the current of a transductor element, which is not saturated, is very low according to the idealized conditions, there might be a considerable percentage difference between the little currents of the two elements. This difference current must escape through the M-point of the pair of elements and pass through the corresponding a-c lead, transformer winding, and rectifying element. This means that after the completion of real commutation the transformer voltage will be applied to the two elements in the out-going phase. The same voltage is applied to both elements but with opposite polarity. The small current and the voltage prevail up to the time point where both elements have attained the same flux deviation and therefore the same small magnetization current. The phenomenon has therefore been denoted process of equalization.

Figure 9 shows the voltage conditions when considering the process of equalization. The new process means that the voltage–time area induced in each element will be doubled as compared with the above case, that is, the transductor rating will be doubled for the same regulation capacity. This is valid up to a control angle of 41 degrees, 24 minutes ($\rho=6$). When the control angle is increased further, the interval of quasi-commutation and that of equalization begin to coincide. The increase in voltage stress upon the transductor, due to the process of equalization, is then reduced.

The process of equalization is of quite obvious importance for the dimensioning of transductors of this kind. It is, however, to a certain extent suppressed by the hysteresis of the core material and it can also be neutralized by artificial means.

This whole chain of reasoning holds good up to a control angle of $\alpha=60$ degrees, that is a direct voltage reduction of 50 per cent.

It is obvious that the voltage–current characteristic of a rectifier controlled by an idealized transductor of this kind will be such that the voltage remains constant at the full value up to a load current equal to the excitation current of the transductor and thereafter steeply drops, keeping the current constant at that value. The latter range, where the rectifier output current is kept constant, is that where the transductor really comes into operation. If the control current I_M of the transductor is varied, the output current also varies and always equals the control current, irrespective of the variation of primary voltage and d-c load resistance. This so called current-transformer characteristic is typical of well-designed transductors and is also of great importance where self-excitation is used, to make it effective within a large range of regulation.

The constant current regulation of the simple transductor-controlled rectifier is also made extensive use of for battery charging, as in electric vehicles.

The deviations of the real transductor from the idealized case appear in the first instance in the fact that the two branches of the magnetization curve are not perpendicular to each other but that both have a certain slope. The leakage reactance of the winding can be represented by an increased slope of the magnetization curve within the saturation range. This slope, on the other hand, will have that effect upon the mode of action of the transductor that the real commutation does not take place momentarily but has a certain duration. In the course of the rectifier output voltage, the interval of real commutation will appear quite in the same way as the well-known interval of overlap in ordinary polyphase rectifiers. Figure 10 shows the voltage trace of this case and also the voltage e_{2A} absorbed by one of the transductor elements. The line i_{2A} represents the current in the same element.

The slope of the magnetization curve within the nonsaturated range will be of less significance but has a certain influence upon the current i_{2A} shown in the figure.

The effect upon the output voltage–current characteristic of the rectifier will be a certain slope of the upper branch of the characteristic due to the mentioned overlap, on one hand, and reduced steepness of the voltage drop, when the current tends to pass through the value of the excitation current, on the other hand. The shape of the entire voltage–current characteristic of the rectifier can be calculated readily from the data of the magnetization curve, but the demonstration of this calculation will extend beyond the scope of this treatise.

Figure 11 shows some oscillograms taken at actual tests of the connection studied. The transductor elements were built as ring cores of the mu-metal-type iron-nickel alloy. Figure 11A shows a case of light load and low reduction of d-c voltage by transductor control and is to be compared with the theoretical picture of Figure 9. The intervals of equalization and quasi-commutation are seen clearly in the course of the element voltage e_{2A}. A small oscillation just after the end of the former interval is due to winding capacity. The oscillogram of Figure 11B is taken at higher load, where the effect of

Figure 10. Phase retardation angle α, overlap angle u, current in element 2A i_{2A}

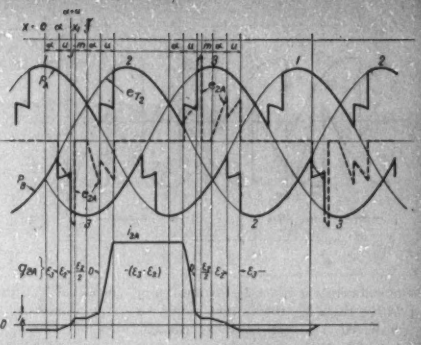

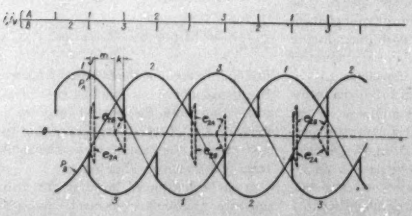

Figure 9

the slope of the magnetization curve within the saturation range is considerable, so that the duration of the real commutation is visible. It appears in the oscillogram of the voltages in quite the same as the interval of overlap in a mercury arc rectifier.

The measurements represent, of course, a case of a particularly good transductor. But with far more primitive, commercial transductors, too, the phenomena described are so well pronounced that a theory fundamentally based upon the concept of an idealized transductor has proved to be justified.

Other polyphase connections can be investigated in the same manner as the Nordfeldt connection. The 6-phase 2-winding transductor, according to Figure 3*D*, has thus been investigated by the described method and proves to bring about regulation of the d-c output voltage in fundamentally the same way as the Nordfeldt connection. The total transformer rating of the transductor will, however, in this case be more than three times that of the former connection.

The Single-Phase Transductor With Self-Excitation Rectifying Elements Directly in Series With Each Transductor Element

This type of connection, illustrated in Figures 5*B* and 5*D*, is chosen as a second example, partly because it has a great practical interest, and partly because its theoretical behavior to a certain extent is contrasted with that of the Nordfeldt connection.

The simple series-connection of a transductor element, a rectifying element, and a low resistance, according to Figure 12, will first be studied. A sinusoidal alternating voltage is impressed upon the circuit. The transductor element is pre-excited by the small control current I_S, which is smoothed by a large reactor L. The magnetization curve of the transductor core is in this case only so far idealized that the upper branch is considered horizontal and the bend point sharp, while the slope within the non-saturated range may be finite. The voltage course is described with reference to Figure 12*C*. The sine wave represents the primary a-c voltage, while the thick contour line will represent the voltage across the load resistance R and therefore also the current in the circuit. Before the point 0 the primary voltage was negative and therefore absorbed as reverse voltage of the rectifying element, the current being zero. The current I_S of the control winding,

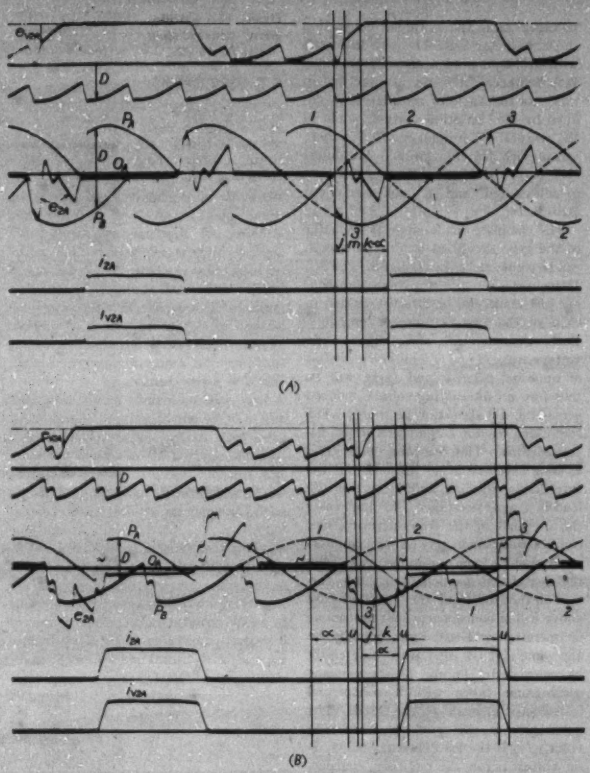

Figure 11. Oscillograms, corresponding to Figures 9 and 10

A—Light load *B*—Heavy load
e_{gA} = voltage and i_{gA} = current of rectifying element 2*A*
D_{d-c} = output voltage
e_{2A} = voltage and i_{2A} = current of the transductor element 2*A*

which may be negative or positive and is indicated in Figure 12*B*, is thus the only magnetization current of the transductor element and therefore also determines its flux deviation. During the interval $0-\alpha_0$ the transductor element absorbs the voltage, the flux deviation decreases and a small increasing positive magnetization current passes through the circuit. This gives rise to a slight voltage drop in R. At point α_0, however, the flux deviation has reached zero, that, is the saturation point is attained. The transductor element then ceases to absorb voltage and the whole voltage is applied upon the resistance. After the point π, where the voltage reverses, the transductor element can again absorb the voltage, now with increasing flux deviation. The current through the circuit is still maintained in the positive direction but at the low value of the unsaturated element, and at point $\alpha_0{}^1$ the current has dropped to zero, and during the remaining part of the negative interval the voltage is applied as reverse voltage over the rectifying element. After the point 2π the course is repeated in the same manner. The two voltage–time areas M and O are absorbed by the transductor element and are equal, while the area N represents the output voltage applied to the load R.

By varying the control current I_S we can vary the angle α_0 and the output

voltage. As in the Nordfeldt connection the transductor control is quite analogous with grid-control of a mercury arc tube. It is, however, interesting to note that in this case the angle of retardation is defined by the excitation current, while in the case of the Nordfeldt connection there was no such definite relation. The difference is typical of the difference between a self-excited and a non-self-excited transductor.

The complete single-phase transductor of the type described in this paragraph can be connected as in Figures 5*B* and 5*D*. If the load is resistive, the chain of reasoning just made can be directly applied to each of the two transductor elements. Each element will absorb the same voltage areas *M* and *O* simultaneously but of opposite polarity and there will be therefore no alternating voltage induced across the d-c excitation terminals. The smoothing reactor *L* can therefore be dispensed with. This reasoning holds good as long as there is no resistance in the transductor winding and as long as the load is a pure resistance. In most cases the d-c load of the transductor-rectifier combination is inductive or has a counter-electromotive force and in that case, as in the case of real magnetization curve, certain deviations from the idealized case above will of course occur, but that mode of operation will still fundamentally be the same and the deviations may easily be calculated. Figure 13 shows some oscillograms taken with a commercial transductor element of this kind. The quantity e is the primary alternating voltage, i_A is the load current, and e_V is the voltage across the rectifying element. The figure shows three cases with different amounts of phase control.

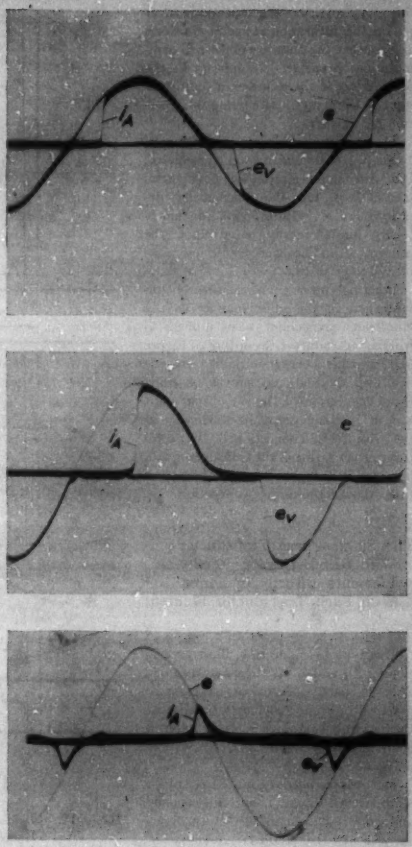

Figure 13. Oscillogram, corresponding to Figure 12

e = a-c primary voltage
i_A = load current
e_V = voltage over rectifying element

A practical characteristic of a commercial transductor amplifier of this kind is shown in Figure 14, the transductor built with ring cores of silicon-steel transformer sheets. The abscissa represents the current through the control winding, which had a resistance of 240 ohm, while the ordinate represents the output direct current, which passed through a load resistance of 65 ohms. It can be seen that between the points P_1 and P_2 an output variation from 0.65 to 16 watts has been obtained by an input variation of $\Delta i = 0.2$ milliampere or 10 μw, calculated as $(\Delta i)^2 \times 240$, that is, a power amplification of about 10^6. On the transductor elements there is still space enough for two more control windings of this rating. A stable primary voltage of 100 volts is assumed; if the primary voltage is not constant, a somewhat lower amplification must be expected.

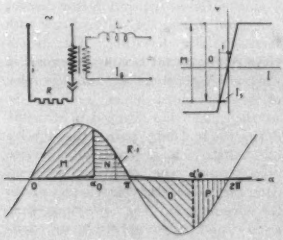

Figure 12

A—Circuit diagram
B—Idealized magnetization curve
C—Voltage and current trace

Dynamic Conditions

The currents on the output and control sides of a nonself-excited transductor follow each other momentarily. If the voltage across the control terminals is suddenly changed, however, the ultimate current values are only reached with a certain delay.

In "The Multiphase Autotransductor Connection" it was found that the voltage–time area absorbed by each transductor element during one period is in a fixed relation to the output voltage of the rectifier. The average flux and its deviation from the saturation point therefore also has a fixed relation to this quantity. It should be especially observed that the average flux is thus not primarily related

to the control direct current. Now every change of average flux in the transductor elements, which will always have the same direction in all elements in relation to the control d-c terminals, will induce a voltage in the d-c winding. Seen from the other side, a voltage applied to the d-c terminals will provoke such a change. Within reasonably small control intervals the flux deviation is proportional to the output direct voltage D. If D_M is the control voltage we therefore have

$$\frac{dD}{dt} = c \times D_M$$

where c is a constant.

For the Nordfeldt connection a special calculation, for which there is no space here, has given $c = 3f$, where f is the a-c frequency. This formula means that if a certain voltage—exceeding the resistance drop in the winding—is applied to the control terminals, the output direct voltage is changed by a certain time rate. The time delay of a certain regulation process is therefore fundamentally not dependent upon the characteristics of the transductor, but upon the character of the load. If, for instance, the load is a pure counter-electromotive force so that the quantity D is kept constant, the current can be changed without inertia. If, on the other hand, the load is a resistance, it will delay the establishment of a new state of equilibrium, as in that case a change of output voltage must be achieved in order to obtain a change of current. Even if the foregoing formula has, of course, a rigorous validity only for the ideal transductor controlling an ideal rectifier, it is, with reasonable approximation, applicable to most practical cases of nonself-excited transductors.

The dynamical problem of the self-excited transductor is most conveniently approached in a somewhat different way. The single-phase transductor with a rectifying element in series with each transductor element is, again, chosen as an example. (Compare Figure 5*B* or Figure 5*D* with Figure 12.)

It was found in "The Single-Phase Transductor With Self-Excitation Rectifying Elements Directly in Series With Each Transductor Element" for that connection that the maximum flux deviation was solely determined by the amount of control current. Also, the voltage absorbed by the transductor and the output direct voltage are therefore defined by the control current, independently of the momentary value of the load impedance. The output voltage will immediately follow a change of the control current. But such a change will be accompanied by a variation of average flux. This will induce a voltage in the control winding, tending to delay the change of control current. The action is similar to that of an ordinary reactor, and a time constant $T = L/R$ can be defined where R is the resistance of the control winding and L has a simple relation to the slope of the magnetization curve within the non-saturated range. With this type of transductor, the time constant is thus primarily attributed to the transductor itself and comparatively independent of the load circuit.

These fundamental conditions are typical of all transductors with 100-per-cent self-excitation and are very similar to those of a separately excited d-c generator. Generally the relation between speed of regulation and amplification factor is much higher for the transductor than for the machine. It may be still increased by the use of higher a-c frequency.

Conclusions

The transductor, treated from an idealized viewpoint, acts more as a switching than an inductive device, with pronounced similarity to the grid-controlled rectifier. Characteristics not very far from that of the idealized case, and easy to calculate from that case, can be obtained with commercial transductors, built up from a number of single-phase transformer cores equal to the number of phases. Very high power amplification

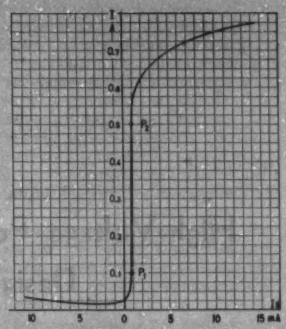

Figure 14. Measured characteristic of single-phase ring-core transductor

and good utilization of the material make the properly designed transductor a useful tool in regulators of a great variety. The dynamic properties of a given transductor and application can be precalculated in a comparatively simple way, which is valuable in the design of stable regulators.

References

1. Die Strom-und Spannungsverhältnisse des Grossgleichrichters, W. Düllenbach, E. Gerecke. *Archiv für Elektrotechnik* (Berlin, Germany), volume 14, 1924, pages 171–248.

2. Theory of D-C Excited Iron-Core Reactors and Regulators, A. Boyajian. AIEE Transactions, volume 43, 1924, pages 919–36, discussion pages 940–6.

3. Reactance Amplifiers, A. S. Fitzgerald. *Electronics* (New York, N. Y.), volume 10, 1937, pages 28–30; *Electrical World* (New York), volume 107, 1939, number 19, page 83.

4. The Transductor and Its Applications, A. U. Lamm. *Journal*, Allmanna Svenska Elektriska Aktiebolaget (Vaesteraas, Sweden), volume 16, 1939, pages 66–80.

5. The Transductor, D-C Pre-Saturated Reactor, with Special Reference to Transductor-Control of Rectifiers (book), U. Lamm. Esselte Aktiebolag, Stockholm, Sweden.

6. The Design of Transductor-Circuits (in Swedish), S. E. Hedström, U. H. Krabbe. *Asea's Tidning* (Vaesteraas, Sweden), 1944, pages 146–61.

7. The Transductor in the Measuring Technique (in Swedish), S. E. Hedström. *Teknisk Tidskrift* (Stockholm, Sweden), 1945, pages 517–23.

8. The Transductor Principle and Applications (in Swedish), U. H. Krabbe. *Asea's Tidning* (Vaesteraas, Sweden), 1946, pages 47–59.

No Discussion

High-Voltage Power-Transformer Design—II

M. B. MALLETT
MEMBER AIEE

Synopsis: The previous part of this paper covered the initial development and application of the distributed concentric type of power transformer design. This type of design is chiefly suited for the larger sizes of power transformers in voltage classes of 138 kv and up. This part deals further with the distributed concentric type transformer. Principal points covered are

1. Commercial impulse voltage testing is discussed. Impulse distribution tests made at low voltage have been adopted as standard commercial tests for distributed concentric type transformers. These tests determine the distribution of impulse voltage in the transformer winding for any specified shape of applied wave. Typical distribution tests are reported as taken on a commercial transformer.

2. A new form of insulating cylinder has been developed for application in the major insulation structure. The cylinder wall is unique in that it is porous and contains no bonding agent. This results in improved characteristics as compared to conventional type composition cylinders. The porous cylinder is made by a novel process which is illustrated and described.

3. Application of the basic design has been extended now to include transformers in the 138-kv, 161-kv, and 230-kv voltage classes. A particularly large transformer, weighing 250 tons complete, has been manufactured. Shipment was made to the Pacific Coast with the transformer proper assembled. The shipping clearance problem was met with a novel tank construction which is illustrated and described.

4. Field experience is reported with transformers subjected to short circuit while in service, and also with a transformer involved in a railway wreck during transportation.

IN THE WINTER of 1942–43 three 90,000-kva banks of single-phase distributed-concentric-type transformers were installed at the famous war-built Shipshaw powerhouse in upper Quebec, Canada. Each bank steps up the output of one generator to the transmission voltage of 154 kv.

The initial development of the distributed concentric type of transformer design, and its application to the Shipshaw transformers, were covered in 1943 by an Institute paper.[1] The basic design is also covered and described in British patent number 581506.

This type of design is suited chiefly for the larger sizes of power transformers in voltage classes of 138 kv and up. Essentially the design comprises a series of cylindrical high-voltage coils which are distributed concentrically between a cylindrical shield and the low voltage winding. See Figure 1.

Since 1943 further development and application of the basic design have been carried out. This further work, together with field experience on the Shipshaw transformers, forms the basis of the present paper.

Commercial Impulse Voltage Testing

Full voltage impulse testing of commercial transformers is a controversial and complex subject. The following analytical points are submitted on this widely debated subject.

1. The specific subject of commercial impulse voltage testing is often confused with the general subject of impulse voltage research and experimentation. In the transformer shop, the primary function of commercial testing is to *prove* the product to the greatest degree practical; the primary function of impulse voltage research is to *improve* the product to the greatest degree practical. These fundamental concepts must be kept in mind. Under present circumstances the desirability of full voltage impulse testing of commercial transformers is questioned. The desirability to the transformer manufacturer of a continuous impulse voltage research program, together with full voltage laboratory facilities, is not questioned.

2. Full voltage tests may cause incipient failures which cannot be detected by any of the standard American Standards Association methods.[2] An additional method has been proposed involving pictures of the neutral impulse current.[3] At the present time there is no positive assurance that this new method is infallible. The importance of detecting failure in commercial testing is paramount. Any testing procedure of commercial transformers which may result in undetected damage is difficult, if not impossible, to justify. This inescapable point has been raised many times. It must be faced squarely. Of secondary importance is the fact that full voltage commercial testing, conducted in accordance with present methods, is complicated and of the nature of a highly specialized laboratory procedure. Such testing does not lend itself readily to routine production work. Undue expense and loss of time are incurred.

3. It is no doubt safe to say that most of the high voltage power transformers, as now installed in any particular country throughout the world, have not been impulse tested. Also, that high voltage power transformers have a remarkably good over-all service record in any particular country, including South Africa where lightning conditions in general are more severe than in North America. Viewed in proper perspective then, it would seem that the question of commercial impulse testing is actually not as critical as we often are led to believe. However, most operators on this continent are concerned deeply over the hazard of lightning failure. Also, many operators believe that the low frequency test alone does not prove the high voltage transformer to a sufficient degree in respect to service voltage conditions.

Careful consideration of these points has led to adoption for the present of the following procedure in respect to distributed concentric type transformers.

1. Impulse voltage distribution tests are made on the high voltage windings of all commercial transformers for which such tests are specified by the purchaser. These tests are made at low voltage (about one kilovolt). They determine the distribution of impulse voltage in the winding for any specified shape of applied wave. In contract tenders, the distribution of impulse voltage in the high voltage winding, corresponding to a stated shape of applied wave, is specified to the purchaser by actual figures. Thus, the degree of control of impulse voltage distribution is predefined. When the machine is assembled the distribution of voltage is measured and the results compared with the specified maximum values in the contract.

Paper 47-144, recommended by the AIEE committee on electric machinery for presentation at the AIEE summer general meeting, Montreal, Quebec, Canada, June 9–13, 1947. Manuscript submitted March 5, 1947; made available for printing April 28, 1947.

M. B. MALLETT is transformer engineer in the English Electric Company of Canada, Ltd., St. Catherines, Ontario, Canada.

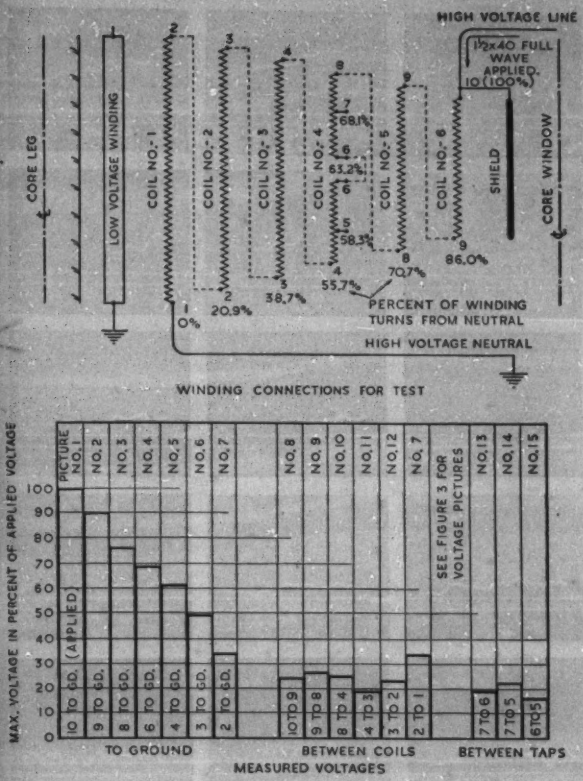

Figure 1. Measured distribution of impulse voltage in a 230-kv winding

2. No full voltage impulse tests are made on commercial transformers.

3. A continuous impulse voltage research program is carried on in order that the basic design can be improved continuously. All testing in connection with this program is carried out on experimental structures. The program includes low voltage distribution testing, as carried out on commercial machines. These tests provide basic stress data. The program also includes full voltage testing to destruction of complete winding structures as well as component parts thereof. These tests provide basic insulation strength data.

Insulation testing of a transformer winding can be considered as a demonstration that the strength of each part is sufficient to withstand the stress imposed thereon with specified voltage conditions held at the winding terminals. The low frequency test checks the strength versus stress relationship for each part under low frequency conditions, that is, with uniform voltage distribution. The impulse distribution test checks the stress only, as imposed on the parts under impulse voltage conditions, that is, with nonuniform voltage distribution. However, by demonstrating the actual distribution of impulse voltage, the distribution test considerably increases the significance of the low frequency test.

The more closely the distribution of impulse voltage approaches uniformity, the more nearly the low frequency test becomes a valid means of judging the impulse voltage strength.[3] Tests demonstrate that, for all practical purposes, the impulse distribution in the distributed concentric winding does not deviate unduly from uniformity. Thus the low frequency test becomes a criterion of impulse voltage strength to a considerable degree. While the combination of distribution test and low frequency test does not prove directly the impulse strength, it does provide the purchaser with considerably more evidence and data than the low frequency test alone.

As contrasted to commercial full voltage testing, the commercial distribution test completely eliminates the serious hazard of undetected damage. Also, the distribution test is inherently a simple and practical test which lends itself readily to routine production work. Such testing can be conducted quickly and at reasonable expense.

The testing procedure as just outlined steers a middle course between the extremes of no commercial impulse testing and full voltage commercial impulse testing. The procedure has been adopted for the present as a practical compromise which best meets the conflicting factors as they now exist.

Figure 1 shows the results of a distribution test as taken on a commercial distributed concentric type transformer. The measured voltages were scaled from the oscillograms shown in Figure 2.

In practice it is only necessary to take a relatively small number of measurements in order to establish the ruling stress picture in the distributed concentric winding structure. Typical measurements ordinarily required are as tabulated in Figure 1, excepting that voltages involving tap leads are included only for one tap connection. The measurements shown determine ruling stresses to ground, between coils, and between taps. Excepting for tap portions, all ruling stresses for this type of winding structure ordinarily are located at or near the coil ends. See discussion of voltage distribution in part I of this paper.

The ruling stresses between turns are substantially less than five per cent of applied voltage. It is not practical to measure such small voltages and therefore turn voltages are not included in Figure 1. If desired, however, turn to turn taps can be built into a critical portion of the winding, such as adjacent to the line. While it is not practical to scale these turn voltages on the oscillograms, the pictures will demonstrate that the maximum amplitudes are less than five per cent.

Figure 3 was taken when the test actually was being conducted. The permanent winding connections are not completed and all coil ends and tap leads are available for testing. The test is made conveniently with the transformer

on the shop floor and out of oil, the stress distribution with air immersion being substantially the same as that with oil immersion.

Equipment used for the test includes a low voltage impulse generator, cathode ray oscillograph, wave meter, and camera. The generator is arranged to discharge repetitively. By repetitive sweeps the oscillograph records the voltage–time picture as a standing image on a fluorescent screen. Thus photographic records can be made quickly and conveniently with an ordinary camera.

In commercial testing, photographs are taken of the applied wave and of all the measured voltages. A permanent commercial test record is made up which includes data as shown in Figure 1, together with prints of all the films as shown in Figure 2.

Porous Insulating Cylinders

Insulating cylinders are a vital part of the core type transformer. In the distributed concentric structure, a number of spaced concentric cylinders function dielectrically as the primary solid component of the major insulation. At the same time the cylinders function mechanically as a supporting frame work for the entire high voltage winding and shield structure. Thus the dielectric and mechanical characteristics of these cylinders are of first importance.

Conventional insulating cylinders, as heretofore used in power transformers, are of composition type. They comprise wound paper strip plus a binder such as shellac or bakelite. The wall structure is impregnated completely with the binder. Such a cylinder structure has the following limitations:

1. Thin fissures are commonly present in the wall structure. These may develop during manufacture of the cylinder or subsequently, and are difficult to detect. Since impregnation with the binder makes the cylinder wall impermeable, it is ordinarily impossible to fill these fissures with the transformer immersing oil. Accordingly, composition cylinders containing fissures present a serious breakdown hazard, particularly under conditions of high axial stress.

2. As compared to plain unimpregnated fibrous material, the presence of the binder tends to reduce the axial creepage strength along the cylinder. Also, the binder promotes tracking under conditions of excessive stress.

3. Composition cylinders are brittle. They tend to crack when subjected to deformation or a sharp blow.

A new type of insulating cylinder has been developed in which these deficiencies are eliminated. The cylinder structure comprises a dense felted mat of interlocked cellulose fibers, and contains no cement or bonding agent of any kind. Because of their nature the cylinders have been called "fiberlock" cylinders.

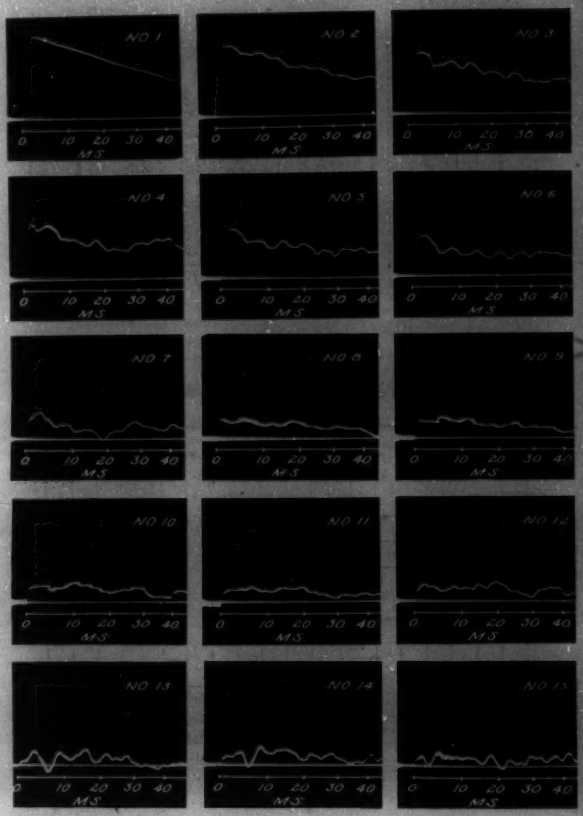

Figure 2. Typical oscillograms included in commercial test report

Since the wall structure contains no binder it is porous. Any fissures which may exist are filled readily with the transformer oil and the hazard of breakdown caused by sealed-in voids is eliminated. Also, the fiberlock cylinder possesses superior creepage and antitracking characteristics. Mechanically the cylinder wall is a unitary and homogeneous structure which is hard, strong, and tough. At the same time the cylinder is not brittle.

In the manufacture of fiberlock cylinders, wet fibrous stock is first built up on a mandrel. The raw material is brought in from a board-making mill. It comprises felted rolls or sheets of rag fibers which have been maintained in the original wet state as first taken from the pulp solution.

The wet stock then is kneaded and compacted by the unique method illustrated in Figure 4. In this method an endless steel cable loop is wrapped spirally about the cylinder, the cable being held in tension by an overhead traveling air cylinder. The mandrel is then revolved, with the result that the cable helix travels laterally by screw action across the cylinder surface. Pressures up to 1,000 pounds per square inch thus are applied progressively and repetitively to the entire fibrous mass. This simple method

effectively works the wet material into a unitary mat having a high degree of compactness.

Finally the remaining water is extracted from the structure by the application of heat and vacuum. This produces a further increase in density, due to the powerful natural shrinkage action of the now compact and unitary fibrous mat about the supporting mandrel. The density of the finished dry cylinder thus produced exceeds 1.1 grams per cubic centimeter.

Changes in dimension of the finished cylinder due to reabsorption of moisture are relatively small. Moisture reabsorption and dimensional changes are eliminated, however, by impregnating the cylinder with hot paraffin when it is dry and still on the mandrel. When the transformer is oil immersed, the paraffin is leached out of the cylinder structure and is replaced by the transformer oil. The small percentage of wax thus added to the oil volume of the transformer does not affect materially any of the characteristics of the oil.

In general the electrical and mechanical characteristics of the fiberlock cylinder are similar to those of calendered rag stock pressboard—a material universally considered as one of the best transformer insulations available.

Fiberlock cylinders have been applied over the past three years to more than a million kilovolt-amperes of transformers.

Figure 4. Processing fibrous insulating cylinders

A typical application is illustrated in Figure 5.

Application of Design

Since completion of the 154-kv Shipshaw transformers in 1943, application of the basic design has been widened to include transformers in the 138-kv and 230-kv voltage classes. The 138-kv transformers were all single-phase units with typical power transformer ratings.

A particularly large 230-kv transformer of the distributed concentric type has been manufactured and shipped to the Pacific Coast. A sister unit is now under construction in the shop. The transformer is three phase and is for tying a 230-kv transmission circuit, tapped off the Bonneville system, with the 69-kv primary distribution system of the British Columbia Electric Railway Company. The chief function of the tie is to provide 2-way stand-by service between the two systems.

An on-load tap gear is connected directly in the 230-kv winding to provide tie-in flexibility. In addition, a third winding of the transformer provides for synchronous condenser regulation at the tie point.

The machine has an equivalent physical capacity of 50,000 kva and weighs 250 tons complete. It has banked radiators and occupies a floor space of 34 by 29 feet.

Shipment was made with the transformer assembled, including core and coils, tank proper in one piece, tank cover proper, and on-load tap gear. Thus maximum protection of the transformer was assured, together with minimum installation work.

Shipment of so large a transformer in this manner was made possible by a unique tank construction. All three shipping dimensions—height, length, and width—required special consideration.

The problem of shipping height was met by a novel well type of tank construction. See Figure 6. In this construction the core and coils are slung between the side walls of a well at the bottom of the tank. The core and coils rest directly on the bed plate of the well and the lower end of the core is only one inch above the car loading platform. The sub-base structure, required for horizontal transfer of jacking force, is built around the well and made integral with the side and end walls of the well. Thus, the shipping height is reduced by an amount approximately equal to the

Figure 3. Conducting a commercial distribution test

Figure 5 (left). "Fiberlock" cylinder foundation for paper shield structure

Figure 6. Well-type tank construction

depth of sub-base structure, as compared to conventional construction where the sub-base is underneath the core.

The available length of car loading platform imposed another problem. This was met by extending the tank cantilever fashion up over the car deck. See Figure 7. This extension supports the tap gear and houses the tap gear reactor.

In order to meet the limiting shipping width it was necessary to detach the side-wall reinforcing beams required for vacuum oil filling. These beams were then bolted on at the site. See vertical rows of bolt holes, Figure 7.

Structural Stability

Many breakdowns of power transformers are due to mechanical failure of the winding under conditions of short circuit. Also, the winding structure must be of rugged construction to withstand transportation shocks.

The importance of structural stability was stressed in part I of this paper. Also, the specific means provided to ensure stability in the distributed concentric winding structure were described. The following experience in the field tends to confirm the design in this respect:

1. Distributed concentric transformers at the Shipshaw powerhouse were subjected to short circuit in July of 1943. The fault was a 3-phase arc on the generator side of the transformer bank. Power was fed to the fault through the transformers from the high voltage system. Duration of the fault was estimated at 10 cycles and the voltage maintained on the high voltage terminals of the transformers calculated at 73 per cent of normal. After the fault was cleared the transformers were put back in service and have been operating satisfactorily ever since.

2. In February of 1943 one of the Shipshaw transformers was involved in a railway wreck. According to a written report from an eye witness, the transformer was being moved down grade on a rail spur by means of a switching locomotive coupled to the transformer car. Because of ice on the rails the locomotive was unable to hold back the transformer car, with the result that it ran away over one-eighth mile of rough track, attaining an estimated speed of 40 miles per hour at the end of the spur. The spur ended at a rock dump where a flat car was standing. The locomotive, which was ahead of the transformer car, threw the parked flat car to one side and climbed the rock pile. The transformer car left the track completely and stove in the tender of the locomotive. The transformer was returned to the shop and completely disassembled. No parts were misplaced and no parts were damaged. The machine was then reassembled, retested, and reshipped. It has been in service ever since.

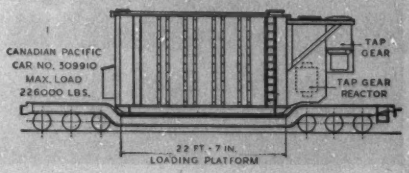

Figure 7. Cantilever tank construction

Summary

1. Impulse distribution tests made at low voltage have been adopted as standard commercial tests for distributed concentric type power transformers. These tests determine the distribution of impulse voltage in the transformer winding for any specified shape of applied wave.

2. A new type of insulating cylinder has been developed for application in the major insulation structure of the distributed concentric type transformer. The cylinder wall is porous and contains no bonding agent. This results in improved characteristics as compared to conventional type composition cylinders. This type of cylinder has been applied to more than 1,000,000 kva of transformers.

3. Application of the distributed concentric type design has been extended to now include transformers in the 138-kv, 161-kv, and 230-kv voltage classes. A particularly large 230-kv transformer has been manufactured. The machine weighs 250 tons complete and occupies a floor space of 34 by 29 feet.

4. Mechanical stability of the power transformer winding structure is of paramount importance. Field experience during the past four years indicates that the distributed concentric winding structure is of rugged and stable construction.

References

1. High-Voltage Power-Transformer Design, M. B. Mallett. AIEE Transactions, volume 62, 1943, August section, pages 526–31.

2. Progress in Impulse Testing of Transformers, J. H. Hagenguth. AIEE Transactions, volume 63, 1944, pages 999–1003.

3. Lightning Studies of Transformers by the Cathode Ray Oscillograph, F. F. Brand, K. K. Palueff. AIEE Transactions, volume 48, 1929, pages 998–1008.

Discussion

F. L. Lawton (Aluminum Company of Canada, Ltd., Montreal, Quebec, Canada): The author has presented a refreshingly candid analysis of commercial impulse-voltage testing. The combination of the usual low-frequency voltage tests with low-voltage impulse voltage distribution tests on commercial transformers plus a continuous impulse voltage research program on experimental structures is basically sound. There appears to be little sound justification for expensive full-voltage impulse tests on commercial units, with acceptance by the purchaser of undetectable damage which may lead to failure in service.

The distributed concentric type of design results in a structurally rugged transformer. However, there is one question which comes to the fore with this particular design, as inferred indirectly by the author in discussing the inherent weaknesses of insulating cylinders of the composition type, and the use of the new "fiberlock" design. This question is: What is the likelihood of the formation of chains of minute particles of water between coils of the concentric high-voltage windings, under certain conditions? Would the porous fiberlock cylinders be as effective as cylinders of the composition type?

The reference to formation of chains of minute particles of water in insulating oils is to a phenomenon observed in circuit breaker oil containing some moisture. Under certain temperature conditions, widely dispersed water molecules appear to coalesce into visible drops and move in such a fashion between electrodes with a high potential difference that the chain of droplets constitutes a breakdown path, with breakdown likely to occur at relatively low voltage.

J. T. Madill (Aluminum Company of Canada, Ltd., Shipshaw, Quebec, Canada): In regard to the nine 30,000-kva distributed concentric coil type power transformers at Shipshaw it can be reported that they all are operating very satisfactorily with almost no maintenance. In the case of one of these transformers installed as one phase of a 3-phase bank with two conventional transformers as the other two phases, the winding and coil temperatures seem to indicate that there is less difference between the winding and oil temperature for this type of transformer than for the conventional ones. The difference between the types seems to be about 10 degrees centigrade, probably indicating slightly better oil circulation in the distributed concentric coil type.

The fiberlock insulation is an interesting development and we would be very much interested in some figures showing the mechanical strength of this insulation compared to the conventional types now used.

G. D. Floyd (Hydro-Electric Power Commission of Ontario, Toronto, Ontario, Canada): The author proposes use of a voltage distribution impulse test in place of the presently accepted impulse test to prove the impulse strength of transformer insulation. This test, which is at best a compromise, would have its chief value as a design test, for improvement in the design of the insulation structure. As an acceptance test, it proves nothing except the distribution of the impulse voltage through the winding at a number of selected points. To be an acceptance test in the strict sense of the word, the adequacy of the insulation to withstand the stress also should be proved. There is always the possibility that the points selected for measurement of distribution may not include the place where the ratio of impulse insulation strength to impulse test voltage is the least. Impulse failures in transformer insulation often occur in unexpected places, and the unexpected place is the one most likely to be overlooked in the voltage distribution test. To make this type of test the basis for acceptance as to impulse strength is questionable, although it is recognized that information of considerable value to the designer can be obtained in this way.

M. B. Mallett: The author wishes to thank contributors of discussion for their interest and comments.

It is particularly gratifying to hear of the good service which the nine 30,000-kva distributed concentric type transformers are giving at Shipshaw, as reported by Madill. He asks for figures showing the relative mechanical strength of fiberlock cylinders as compared to conventional composition type cylinders. It is hardly feasible to answer this request, in that both the compression strength and tensile strength of composition materials vary widely (as much as three to one), depending on the type of bonding agent used and the processing method involved. In general, fiberlock cylinders have mechanical characteristics closely approaching those of calendered rag stock pressboard. As is well known, such material is exceedingly tough and nonbrittle, as contrasted to the marked brittleness of composition cylinders. In this regard we have experienced considerable trouble in the past with composition cylinders breaking as a result of severe transportation shocks.

Floyd stresses that the impulse voltage distribution test does not prove the impulse voltage strength of the transformer and is therefore limited in value as an acceptance test. The author agrees entirely with this conclusion. As specifically stated in the paper, the impulse distribution test in combination with the low frequency test is a compromise procedure and does not directly prove the transformer impulse strength.

Floyd states, however, that the full voltage impulse testing of commercial transformers is an accepted test. To this the author takes exception. Full voltage impulse testing of commercial transformers never has been accepted at all by the electrical industry in Canada and only to a limited extent in the United States. The question as to whether such tests should become routine standard tests in the industry has been debated many times before the Institute over the past ten years. The question has never been settled and such testing has never been generally accepted by the industry. This nonacceptance results directly from the inescapable point that to date no positive and infallible means has been devised which will detect damage from incipient impulse voltage failure.

Because full voltage impulse testing of commercial transformers has not been accepted generally by the industry, it would seem that the procedure proposed by the author, specifically the combination of low frequency test and impulse distribution test, should be compared to the existing practice of making the low frequency test only. Certainly any compromise procedure which provides any information whatsoever in respect to the impulse voltage strength of the transformer, is an addition and an improvement over providing the purchaser with no impulse test data at all.

Lawton's comments in respect to commercial impulse voltage testing are particularly significant, since the company with which he is associated has an unusually large number of high voltage power transformers on the system.

Lawton has raised the point as to whether

the porous fiberlock cylinder is effective in preventing lining up of minute water particles. The density of the cylinder is such that it certainly should preclude the continuous line-up of water particles from coil to coil, and effectively function as a solid barrier the same as conventional type composition cylinders. It seems to the author that this point has been confirmed over a period of many years by the use of pressboard casings between tank and coil structure, the use of pressboard collars for the end insulation structure of the transformer, and the use of pressboard collars between sections of disk coils. Calendered pressboard stock as thus used for many years is porous and practically identical physically with the newly developed fiberlock cylinder.

Economics of Long-Distance A-C Power Transmission

S. B. CRARY
FELLOW AIEE

I. B. JOHNSON
MEMBER AIEE

THIS paper summarizes the results of economic studies of a-c power transmission for distances from 100 to 600 miles. Particular emphasis is placed on the economics of higher voltages. Conclusions have been drawn as to the effect of voltage, distance, and loading. Several papers have been presented dealing with the technical problems[1–4] involved in transmitting power long distances, whereas comparatively few have dealt with the economic problem.[5–9] This is quite understandable. The economic problem depends to a considerable extent upon conditions surrounding the particular case under consideration, and in time may be altered by new developments and change in costs.

However, in view of the widespread attention now being given to longer distance and higher voltage transmission and the comparisons currently being made with other methods of transporting energy, it is considered worthwhile to show for assumed costs and conditions some of the important economic factors and the conclusions resulting therefrom.

The costs used in this study are believed to be representative although they are necessarily averaged values. In this paper, the costs correspond to averages considered to be representative in 1945, and no attempt has been made to adjust them for recent changes. The higher voltage levels selected for parameters, 360 and 450 kv, are not necessarily standard voltages, as this study was made before standardization of the higher voltage steps has been realized.

Several of the important possible variations in cost were carefully studied and considered in order to test the validity of the conclusions which were being drawn during the course of the study. The effect of these variations have tempered the conclusions, which are presented here. Therefore, the results of this study as summarized in the conclusions are believed to give a fair appraisal of the present economic problem.

Conclusions

Based on the results of this study, the following conclusions have been drawn:

1. The cost of a-c energy transmission given by Figure 1 may be attained by rational transmission system design for power transfers of 200,000 to 350,000 kw per circuit, for a load factor of 50 per cent and an annual charge on investment of 11.5 per cent. Higher load factors or lower annual charges will reduce the transmission costs. As energy transmission costs are chiefly those of investment, the cost is almost inversely proportional to the load factor and almost directly proportional to the annual charge.

2. Line compensation by either series capacitors or special intermediate synchronous condensers becomes desirable for straightaway transmission distances exceeding 200 to 300 miles. Below these distances, line compensation does not appear to be justified.

3. The 287-kv voltage level is about the most economical for power transfers of 200,000 kw per circuit for straightaway distances of 300 miles and for higher loadings at shorter distances up to 350,000 kw per circuit for 100 miles.

4. The 360-kv voltage level is about the most economic voltage for distances in the range from 300 to 600 miles when line compensation is used for power transfers of 300,000 to 350,000 kw per circuit.

5. The difference in energy transmission costs for any two voltage levels near the optimum is relatively small even for the same power transfer and becomes practically inconsequential when the optimum economic loadings for each of the voltages are used.

6. The terminal transformer costs approach that of the transmission line when the line length is in the range of 100 miles.

7. Transformer costs limit the use of higher voltages than 360 to 400 kv for the shorter distances whereas for the longer distances up to 600 miles circuit breaker costs also limit the use of higher voltages when intermediate stations are used.

8. Operation of high-voltage systems with grounded neutrals materially reduces the transmission costs by allowing for the use of the next lower level of transformer insulation as well as reducing the transmission line costs.

9. The lower resistance conductors result in generally lower transmission costs over a greater range of loads even for load factors as low as 50 per cent. Also, since the larger

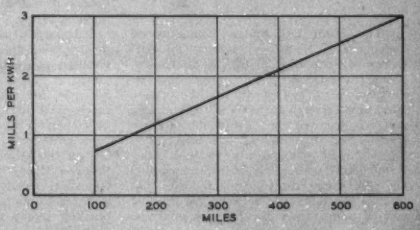

Figure 1. Cost of electric energy transmission at 50 per cent load factor based on 11.5 per cent annual charge on investment

At 200,000 to 350,000 kilowatts per circuit. Other conditions and assumptions given in paper

Paper 47-163, recommended by the AIEE committee on power transmission and distribution for presentation at the AIEE summer general meeting, Montreal, Quebec, Canada, June 9–13, 1947. Manuscript submitted March 26, 1947; made available for printing May 7, 1947.

S. B. CRARY and I. B. JOHNSON are both with the central station engineering divisions, General Electric Company, Schenectady, N. Y.

The authors wish to acknowledge the assistance given to them by Mrs. Doris Stupp and Miss Doris Bryant for making the calculations.

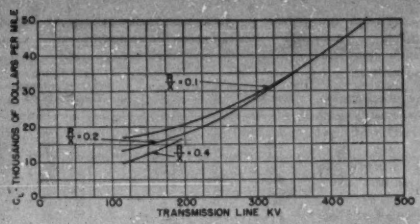

Figure 2. Line cost per mile versus transmission line kilovolts

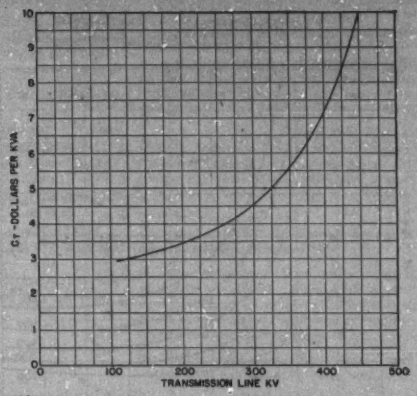

Figure 3. Average of sending and receiving transformer installed costs per kilovolt-ampere versus transmission line kilovolts

High-voltage windings Y-connected and grounded. Less than normal reactance for higher voltage levels (360 and 450 kv)

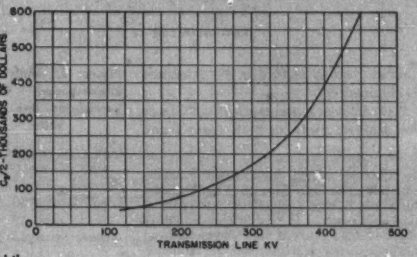

Figure 4. Circuit breaker installed position cost versus transmission line kilovolts

Multiply by two to obtain total installed station cost per circuit

conductors have a greater emergency loading, they will be preferred generally.

10. The most economic kilowatt loading varies from 60 per cent above the surge impedance loading at 100 miles (uncompensated line) to about the surge impedance loading 2.5 (kv)^2 for a distance of 600 miles (compensated line). See Table I for representative surge impedance loadings.

11. Hydroelectric generators and their step-up transformers delivering power to long-distance transmission systems justifiably can be built with lower-than-normal reactance.

12. Multiple transmission lines with more or less parallel rights-of-way used for firm power supply can justify economically intermediate switching stations located about every 100 miles.

13. Electric energy transmission at high load factors in substantial amounts, of the order of 200,000 to 350,000 kw per circuit, making full use of present-day knowledge and equipment becomes more competitive than formerly with other methods of transporting energy and can be expected to be accorded a correspondingly renewed interest.

14. Systems are now entering a stage in their development where added generating capacity will be located at relatively greater distances from the utilization areas. The economics of power transmission therefore will be in the direction to encourage the development of large generating stations for connection to well-integrated systems so that the transmission may be accomplished at high circuit loadings and load factors.

Analysis

This analysis is in three parts

I. Two hundred to 600 mile transmission. Line loading based on steady state power limits with 25 per cent margin with systems having typical terminal impedances.

II. One hundred mile transmission. Line loading based on most economic loading independent of stability.

III. Two hundred mile transmission. Line loading based on transmission of 1,000,000 kw dependent on transient stability limits.

Although the problem is approached in these three different ways the results are consistent between themselves such

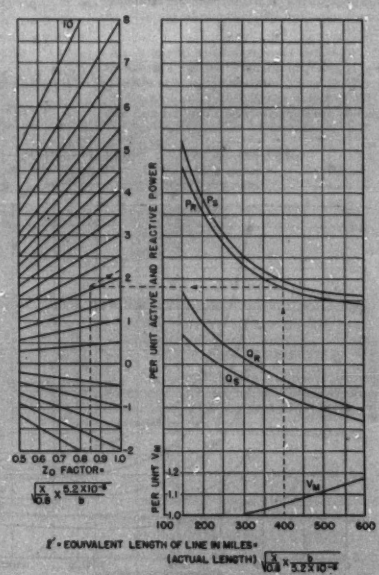

Figure 5. Steady state stability curves (from reference 2)

$E_s = E_R = 1.0$

$r/x = 0.1$

Base kilovolt-amperes = base kilowatts = (kilovolts)^2. Line with synchronous terminal equipment. Generator plus transformer impedance = 40 per cent on kilovolt-amperes at sending end of line. Receiving end impedance (including transformer) = 25 per cent on kilovolt-amperes at receiving end of line. 25 per cent steady state stability margin based on receiver power (P_R). P and Q are active and reactive power, respectively, in per unit of (kilovolts)^2, the subscripts S and R indicating sending and receiving ends of the line, respectively. V_M is maximum voltage along the line under load. x = positive phase sequence reactance ohms per phase per mile. b = positive phase sequence capacitive susceptance, mhos per mile. Effect of line compensation obtained by assuming infinite distribution and modifying x and b according to degree of series or shunt compensation

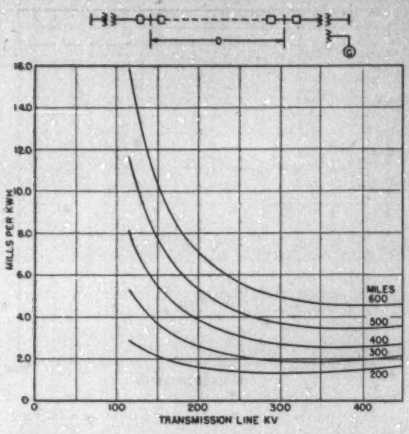

Figure 6. Mills per kilowatt-hour versus transmission line kilovolts

No line compensation.
No intermediate stations
Load factor = 50 per cent
Annual charge = 11.5 per cent
$x = 0.8$ ohm per mile
$b = 5.2 \times 10^{-6}$ mho per mile
Conductor resistance = 0.08 ohm per mile

Table I. Surge Impedance Loadings per Circuit of Typical Transmission Lines*

Line Kv	$2.5\ (Kv)^2$ Surge Impedance Loading (Kw)
115	33,000
138	47,600
161	65,000
194	96,000
230	132,000
287	206,000
360	324,000
450	505,000

* Surge impedance taken equal to 400 ohms per phase to neutral resulting in surge impedance loading in kilowatts = $2.5(kv)^2$.

that an over-all picture of the economics is obtained.

The following assumptions and basis for analysis apply to both parts I and II of this study:

1. Cost per mile of single circuit transmission line given by Figure 2. Only the cost for a line having a conductor resistance of 0.08 ohm per mile is used in part I. Other studies indicate that at high load factors and loadings such a conductor is in the economic range even for the lower voltages (110 to 230 kv).

2. Cost per kilovolt-ampere of transformers is given in Figure 3 as the average of receiving-and sending-end transformer costs. This includes installation costs and corresponds approximately to a sending-end low voltage of 13.8 kv and a 3-winding transformer (primary, secondary, and tertiary) as the receiving-end transformer. The high-voltage windings of the transformers are Y-connected and effectively solidly grounded. The 450-kv transformer costs have been increased to allow for the use of transformers of 60 per cent of normal leakage reactance and the 360-kv transformer costs have been increased to allow for the use of transformers with 80 per cent of normal leakage reactance. It is to be noted that whereas the cost data are given here by a smooth curve, actual costs would tend to be higher than this curve at points intermediate between those representing standard voltage levels.

3. Installed circuit breaker position costs versus transmission line kilovolts are given in Figure 4. These figures, when multiplied by two, give the installed station cost per station per single transmission line circuit. This curve also was obtained by drawing a smooth curve through average repre-

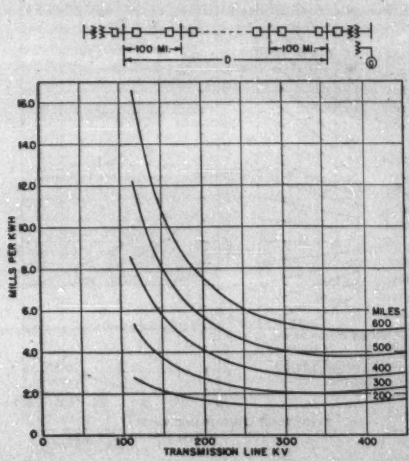

Figure 8. Mills per kilowatt-hour versus transmission line kilovolts

Line compensation = 50 per cent
No intermediate stations
Load factor = 50 per cent
Annual charge = 11.5 per cent
$x = 0.8$ ohm per mile
$b = 5.2 \times 10^{-6}$ mho per mile
Conductor resistance = 0.08 ohm per mile

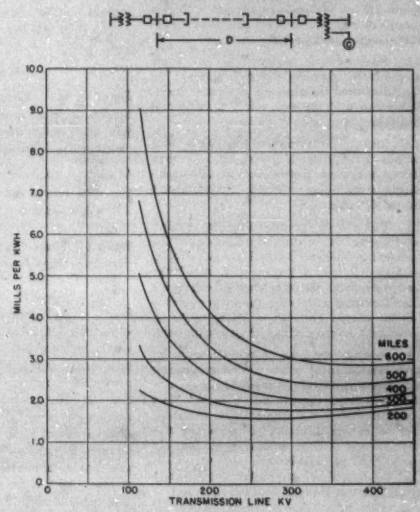

Figure 7. Mills per kilowatt-hour versus transmission line kilovolts

No line compensation.
Intermediate stations every 100 miles
Load factor = 50 per cent
Annual charge = 11.5 per cent
$x = 0.8$ ohm per mile
$b = 5.2 \times 10^{-6}$ mho per mile
Conductor resistance = 0.08 ohm per mile

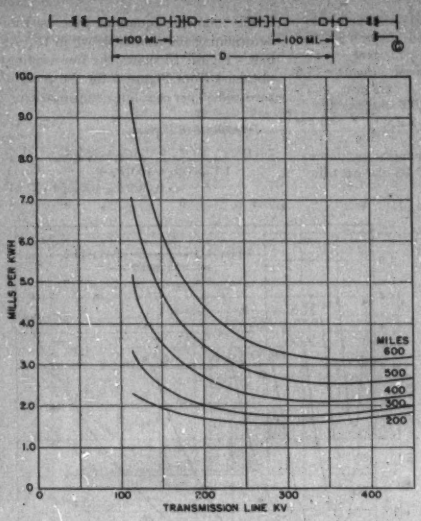

Figure 9. Mills per kilowatt-hour versus transmission line kilovolts

Line compensation = 50 per cent
Intermediate stations every 100 miles
Load factor = 50 per cent
Annual charge = 11.5 per cent
$x = 0.8$ ohm per mile
$b = 5.2 \times 10^{-6}$ mho per mile
Conductor resistance = 0.08 ohm per mile

sentative costs at the standard and assumed standard voltage levels.

4. Synchronous condensers were taken as six dollars per kilovolt-ampere installed at a kilovolt-ampere rating 15 per cent above the receiving-end transmission line kilovar requirements for correction to unity power factor of the receiver power at the receiving-end high-tension terminal. No additional transformer cost for this synchronous condenser capacity was assumed since the receiving-end transformer tertiary would in general have sufficient capacity for the reactive kilovolt-ampere requirements at or near the most economical transmission line loading.

5. The cost of line compensation was assumed to be ten dollars per kilovolt-ampere for series capacitor compensation. This figure includes the necessary protective equipment and insulation above ground. An alternative method of compensation is to use special intermediate synchronous condensers[1] which can be expected to be competitive with series capacitors.

6. A load factor of 50 per cent was assumed. Increased load factors will reduce the energy charge for transmission as the energy charge is almost inversely proportional to the load factor.

7. The transmission line power losses were evaluated at 4 mills per kilowatt hour with annual equivalent hours of 3,300.

8. The transformer losses were evaluated at 4 mills per kilowatt hour, 4,380 annual equivalent hours, and 0.6 per cent losses of total kilovolt-ampere of sending- and receiving-end transformer capacity.

9. Synchronous condenser losses were evaluated at 4 mills per kilowatt hour, 6,580 equivalent hours, and 1.7 per cent losses on their kilovolt-ampere rating.

10. The capacity charge for the transmission line plus transformer power losses was assumed as $100 per kilowatt.

11. The annual charges for interest, depreciation, taxes, and maintenance were assumed to be 11.5 per cent of the total investment cost.

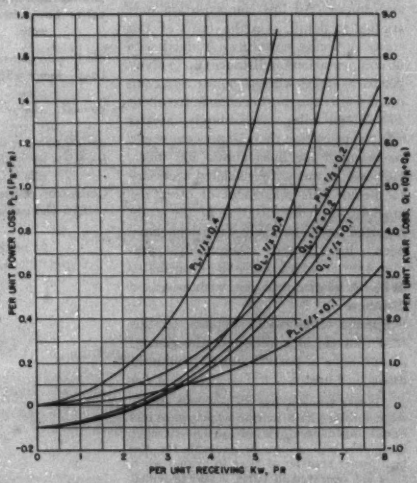

Figure 11. Real and reactive power loss with change in conductor resistance and loading for 100-mile line, equal sending- and receiving-end voltages (from reference 12)

$x = 0.8$ ohm per mile
$b = 5.2 \times 10^{-6}$ mho per mile
No load losses neglected

Figure 10. Ratio of received power to surge impedance loading

$[P_R/2.5\ (\text{kilovolts})^2]$ versus transmission miles

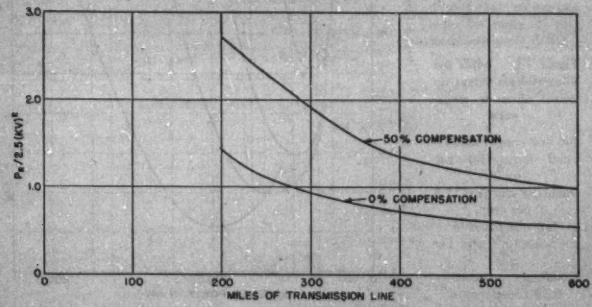

I. Two Hundred to 600 Miles

The stability limitations are more important for the longer distances. As a basis for the economic study of transmission in the range of 200 to 600 miles the power transfer was taken equal to that which has an adequate steady state sta-

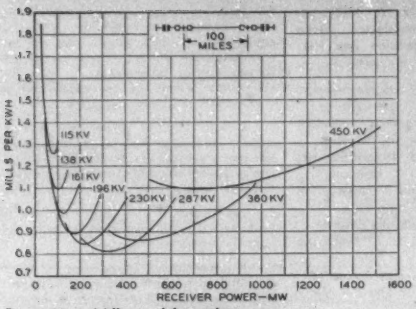

Figure 12. Mills per kilowatt-hour versus receiver power in megawatts

No line compensation
Load factor = 50 per cent
Annual charge = 11.5 per cent
$x = 0.8$ ohm per mile
$b = 5.2 \times 10^{-6}$ mho per mile
Conductor resistance = 0.08 ohm per mile

bility margin with representative terminal impedances. No line compensation and 50 per cent line compensation were studied in detail. On the basis of this study optimum costs are obtained with no compensation for distances up to about 200 to 300 miles whereas 50 per cent compensation is the most economic for about 400 to 500 miles. Accordingly, greater line compensation than 50 per cent would be required for lines above 500 miles. However, it was not considered necessary to include this refinement of other degrees of line compensation in the study reported here, as such variations have been investigated thoroughly previously[2,9–11] which show the desirability of increased compensation with increased distance.

Specific assumptions applied to this case (part I) in addition to the general assumptions of parts I and II previously mentioned are:

1. Power transfer has 25 per cent steady state stability limit margin with typical terminal impedances (Figure 5 from reference 2). This will allow, in general, for the firm power transfer of lines so loaded when they are operated in parallel and provided with intermediate stations.
2. Intermediate switching stations were assumed to be located at every 100 miles so as to provide 100-mile line sections for switching. Also for comparison, the transmission costs were calculated, assuming no intermediate switching stations except those at the sending- and receiving-end terminals.

Somewhat lower transmission costs would have been obtained by assuming a smaller steady state margin corresponding to that of a single-circuit line without intermediate switching stations delivering power to a system with reserve system capacity sufficient to allow for a line outage in case of a fault. A reduction in energy transmission costs of about 10 per cent may be possible under such conditions for the longer lines.

The following equations were used for determining the results shown in Figures 6–9. Figure 10 shows the line loadings obtained from Figure 5 for the cases of zero and 50 per cent line compensation.

Investment in Dollars.

$$I = D \times C_L + (K_R + K_S)C_T + SC_S + 1.15 \times 6Q_R + 100[P_L + 0.006(K_R + K_S)] + C_g \quad (1)$$

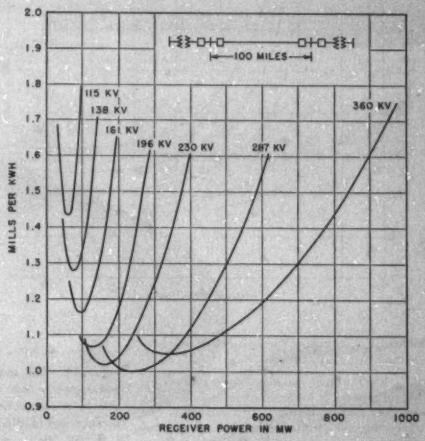

Figure 13. Mills per kilowatt-hour versus receiver power in megawatts

No line compensation
Load factor = 50 per cent
Annual charge = 11.5 per cent
$x = 0.8$ ohm per mile
$b = 5.2 \times 10^{-6}$ mho per mile
Conductor resistance = 0.16 ohm per mile

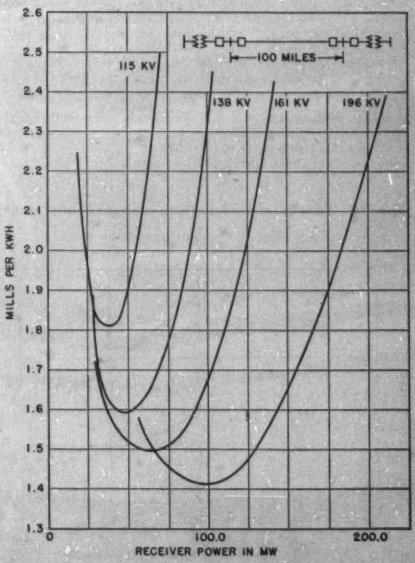

Figure 14. Mills per kilowatt-hour versus receiver power in megawatts

No line compensation
Load factor = 50 per cent
Annual charge = 11.5 per cent
$x = 0.8$ ohm per mile
$b = 5.2 \times 10^{-6}$ mho per mile
Conductor resistance = 0.32 ohm per mile

Table II. Circuit Parameters of 200-Mile Transmission System

System Voltage Kv	x_1 Ohms Per Phase Per Mile	r_1 Ohms Per Phase Per Mile	y_1 Mhos Per Phase Per Mile $\times 10^{-6}$	X_1 Ohms Per Phase	R_1 Ohms Per Phase	$Y_0/2$ Mhos Per Phase $\times 10^{-6}$	Base Voltage Kv	Per Unit Values Base Kva = 1,000,000 X_1	R_1	$Y_0/2$	X'_d	X_t	X_R	Inertia Constant H	Critical Switch Time Sec
230	0.754	0.12	5.45	147	22.7	0.543	230	2.78	0.428	0.029	0.50 0.30 0.20	0.10	0.20	3.5	0.068
287	0.754	0.12	5.47	147	22.7	0.547	287	1.79	0.276	0.045	0.30 0.20	0.13	0.20 0.30	3.5 5.0	0.068 0.100
360	0.75	0.12	5.41	148	22.7	0.541	360	1.14	0.175	0.071	0.30 0.20	0.15	0.20	3.5	0.068

$R_F = 0.008$ per unit on 1,000,000 kva. (Assumed value of resistance between voltage behind transient reactance and fault point at receiving bus during fault period.)

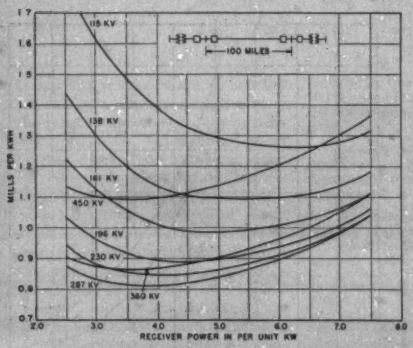

Figure 15. Mills per kilowatt-hour versus receiver power in per unit kilowatts

Unit kilowatt = (kilovolts)^2
No line compensation
Load factor = 50 per cent
Annual charge = 11.5 per cent
$x = 0.8$ ohm per mile
$b = 5.2 \times 10^{-6}$ mho per mile
Conductor resistance = 0.08 ohm per mile

Annual Charge in Dollars Per Year.

$$A = aI + 3{,}300 \times 0.004\, P_L + 1.15 \times 0.017 \times 6{,}580 \times 0.004 Q_R + 0.006 \times 4{,}380 \times 0.004\, (K_R + K_S) \quad (2)$$

Energy Cost in Mills Per Kilowatt-Hour.

$$T = \frac{1{,}000A}{0.5 \times 8{,}760 \times P_R}$$

where

I = total investment
D = distance in miles
C_L = cost of line per mile (Figure 2)
C_T = installed transformer cost (Figure 3)
C_S = installed station cost per circuit (Figure 4)
C_c = cost of series capacitor compensation

$$= \frac{0.008\, R_c D}{(\text{kv})^2} \left(\frac{K_S + K_R}{2} \right)^2$$

K_R = receiving-end transformer kilovolt-amperes $= \sqrt{(P_R)^2 + (Q_R)^2}$
K_S = sending-end transformer kilovolt-amperes $= \sqrt{(P_S)^2 + (Q_S)^2}$
S = number of switching stations
= 2 for no intermediate stations
$= \left(\frac{D}{100} + 1 \right)$ for intermediate stations every 100 miles
Q_R = receiving-end reactive kilovolt-amperes (Figure 5)
Q_S = sending-end reactive kilovolt-amperes (Figure 5)
P_R = receiving-end kilowatts (Figure 5)
P_L = power losses in kilowatts $= P_S - P_R$
R_c = ratio of compensated length to total length of line
Q_L = transmission line reactive kilovolt-ampere losses $= Q_S + Q_R$
A = annual cost in dollars
a = per unit annual charge of total investment
T = cost of energy transmission in mills per kilowatt-hours

II. One Hundred Miles

Whereas stability is the chief limitation of the loading of the circuit for the longer distance, the most economic loading for 100-mile transmission will depend more upon the I^2R and I^2X losses. Because of this difference in limitations, the loading of the 100-mile transmission was varied to find the most economical point rather than assuming the loading to be determined primarily by the stability power limit. Also, for this reason, it was unnecessary to include the effect of line compensation. Two circuit breaker positions per transmission circuit were assumed at both the sending and receiving ends with no intermediate stations. Otherwise, for this case, the same general assumptions

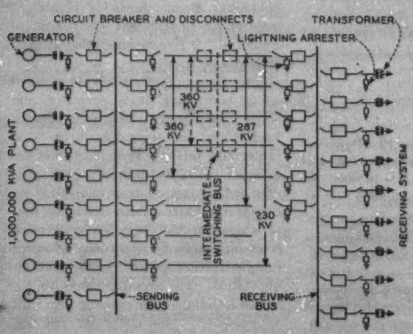

Figure 16. Schematic arrangement of equipment for study of the transmission of 1,000,000 kw a distance of 200 miles

Figure 17. Equivalent diagram of system of Figure 16 for transient stability study

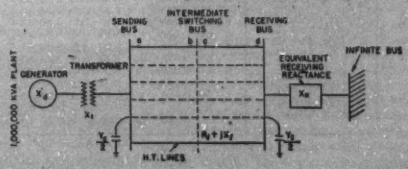

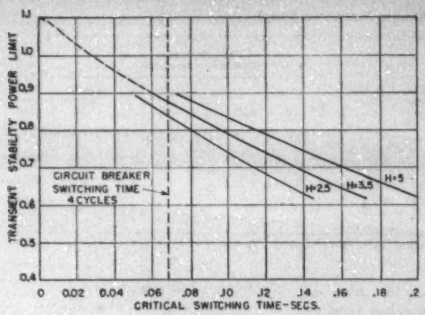

Figure 18. Transient stability power limit versus critical switching time

1,000,000-kva plant
287 kv—6 lines
$x_d' = 0.30$ per unit
$x_t = 0.13$ per unit
$x_R = 0.30$ per unit
H = generator inertia constant in kilowatt-seconds per kilovolt-ampere
Base kilovolt-amperes = base kilowatts = 10^6

and conditions previously described were used.

The equations used for this part of the analysis are the same as those used for part I, except in equation 1 the receiving-end and sending-end kilovars were taken as equal to half the total line kilovar loss or $Q_R = Q_S = Q_L/2$. Figure 11 (from reference 12) gives the real and reactive power losses directly for a given receiver power for typical 100-mile transmission lines.

Figures 12, 13, and 14 show the transmission line energy cost based on these conditions for variations in received power for $r/x = 0.1$, 0.2, and 0.4 respectively. Figure 15 is for the same conditions as Figure 12 except the ordinate is in terms of (kilovolt)^2 instead of megawatts. As shown for this distance (100 miles), the optimum cost points occur at loadings appreciably above the surge impedance loading of 2.5(kv)^2.

III. Two Hundred Miles

This part summarizes the results of a study to determine some of the basic system design factors which would give optimum performance for the transmission of 1,000,000 kw a distance of 200 miles.

The transient stability limits were assumed to be the determining limitation for the transmission of power a distance of 200 miles. A transient stability study was made to determine the number of transmission line circuits required for the transmission line voltages of 230, 287, and 360 kv for the system of Figure 16. The equivalent circuit shown in Figure 17 was set up to represent the system of Figure 16. It is to be noted that all generators and transformers at the hydroelectric plant or sending bus are grouped as an equivalent single generator and single transformer. The transformers, loads, lines, and generators in the load center and interconnecting network are assumed to be distributed over a wide area and are lumped as an equivalent receiving reactance at the receiving bus. It is assumed that the receiving network is of such capacity as to have in effect infinite inertia compared to the generating station. The circuit breakers are assumed to have 3-cycle opening time plus approximately one cycle for relaying

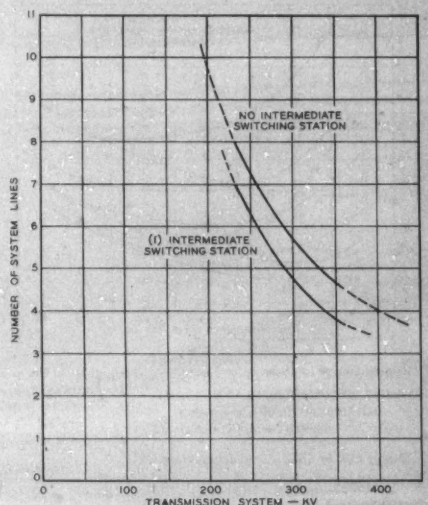

Figure 20. System stability requirements, number of lines versus system voltage

1,000,000-kva plant
200 miles transmission distance
Power at receiving bus = 970,000 kw approximately

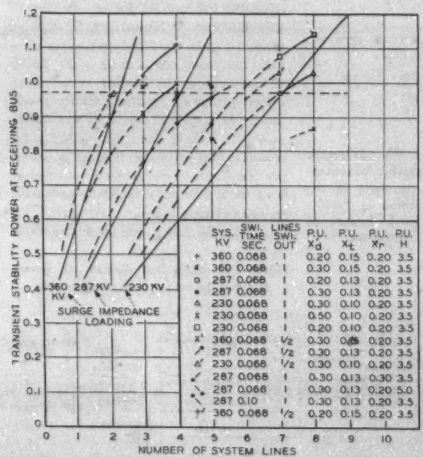

	SYS. KV	SWI. TIME SEC.	LINES SWI. OUT	P.U. X_d	P.U. X_t	P.U. X_R	P.U. H
+	360	0.068	1	0.20	0.15	0.20	3.5
x	360	0.068	1	0.30	0.15	0.20	3.5
o	287	0.068	1	0.20	0.13	0.20	3.5
•	287	0.068	1	0.30	0.13	0.20	3.5
△	230	0.068	1	0.30	0.10	0.20	3.5
x	230	0.068	1	0.50	0.10	0.20	3.5
□	230	0.068	1	0.20	0.10	0.20	3.5
x'	360	0.068	1/2	0.30	0.15	0.20	3.5
↗	287	0.068	1/2	0.30	0.13	0.20	3.5
△'	230	0.068	1/2	0.30	0.10	0.20	3.5
↙	287	0.068	1	0.30	0.13	0.30	3.5
⁂	287	0.068	1	0.30	0.13	0.20	5.0
↖	287	0.10	1	0.30	0.13	0.20	3.5
†'	360	0.068	1/2	0.20	0.15	0.20	3.5

Figure 19. Power received versus number of lines for transient stability

1,000,000-kva plant
Base kilovolt-amperes = base kilowatts = 10^6
Initial sending bus voltage = 1.0 per unit
Initial receiving bus voltage = 0.957 per unit

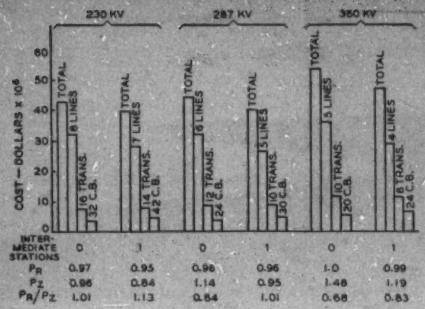

Figure 21. Installed cost of transmission systems

x_R = 0.20 per unit
P_R = per unit transient stability received power limit
x_d' = 0.30 per unit
H = 3.5 per unit
P_Z = per unit surge impedance loading
Base kilovolt-ampere = base kilowatt = 10^6

time. High-voltage bussing rather than low-voltage bussing was used, because of the greater stability and operating flexibility. No bus sectionalizing circuit breakers were included in the cost analysis, however, a circuit breaker was included for each generator and transformer. Accordingly, the number of circuit breakers used in an actual case may be more or less than the number assumed in this study. Bus reactors to reduce short-circuit currents were not used because modern circuit breakers of 5,000,000 kva interrupting capacity can be expected to satisfy the short-circuit kilovolt-ampere requirements of this system. The system disturbance for determining the transient stability power limit was taken as a 3-phase fault occurring in front of one of the line circuit breakers at the sending bus and the subsequent switching out of the faulted line section a–d or a–b of Figure 17.

In Table II are recorded the circuit constants. Where more than one value is given, calculations were made for the variation in parameters indicated.

Figure 18 is a typical transient stability power limit versus critical switching time curve that is obtained. Figure 19 was derived from numerous curves similar to Figure 18. Included in Figure 19 are curves of the approximate surge impedance or unity power factor loading of the lines at the various voltage levels based on the receiving bus voltage.

The results of Figure 19 indicate

1. That 5 lines at 360 kv, 6 lines at 287 kv, and 8 lines at 230 kv will be required with four cycles fault clearing and with generators having a transient reactance of 30 per cent and an inertia constant of 3.5 kw seconds per kilovolt-ampere.

2. That increasing the inertia constant from 3.5 to 5 or 43 per cent produces an increase of transient stability power of about 3 per cent.

3. That decreasing the generator transient reactance from 30 per cent to 20 per cent increases the transient stability power about 10 per cent and permits the elimination of one transmission line for all three voltage levels.

4. That increasing the equivalent receiving reactance from 20 per cent to 30 per cent decreases the transient stability power about 10 per cent.

5. That increasing the switching time or duration of the fault from 0.068 second to 0.1 second or 47 per cent decreases the transient stability power about 12 per cent.

6. That using an intermediate switching station such that one-half of a line is switched out instead of one line, increases the power limit by 8 per cent and allows the elimination of one line for all three voltage levels.

7. That eight lines operating at 230 kv with a generator transient reactance of 30 per cent have a transient stability power limit when switching out one line equal to the surge impedance loading of all of the lines; similarly, for five lines operating at 287 kv with a generator transient reactance of 20 per cent.

Figure 20 was obtained for a power received of approximately 970,000 kw showing the number of lines required with no intermediate switching stations, and the number of lines required with one intermediate switching station as a function of system voltage. The three system voltages chosen lie on the knee of each curve, indicating that they are in the region of the most economic cost for transmission.

An installed cost comparison of transmission systems with and without intermediate stations is shown in Figure 21 with generators of $X_d' = 30$ per cent and $H = 3.5$ kw seconds per kilovolt-ampere and with a receiving system reactance of 0.20. Transmission line, installed transformer, and installed circuit breaker costs correspond closely to that given by Figures 2, 3, and 4.

A cost comparison of systems using different generator transient reactances indicate that 20 per cent rather than 30 per cent is fully justified economically. The lower generator reactance system requires one less transmission line than the system using the higher value of generator reactance ($X_d' = 0.30$).

Although this analysis was made on a somewhat different basis than that of parts I and II, it indicates not much difference in transmission cost for the three voltages of 230, 287, and 360 kv with a slightly lower cost for 287 kv.

References

1. Long-Distance Power Transmission as Influenced by Excitation Systems, C. Concordia, S. B. Crary, F. J. Maginniss. AIEE Transactions, volume 65, 1946, pages 974–87.

2. Stability Limitations of Long-Distance A-C Power Transmission Systems, Edith Clarke, S. B. Crary. AIEE Transactions, volume 60, 1941, pages 1051–6.

3. Static Stability Limits and the Intermediate Condenser Station, C. F. Wagner, R. D. Evans. AIEE Transactions, volume 47, 1928, pages 94–123.

4. Bibliography of First Report of Power System Stability AIEE Subcommittee on Interconnection and Stability Factors. Electrical Engineering (AIEE Transactions), volume 56, 1937, February section, pages 280–2.

5. The Maximum Distance to Which Power Can Be Economically Transmitted, R. D. Mershon. AIEE Transactions, volume 23, 1904, pages 759–61.

6. High-Voltage, Long-Distance Transmission, F. Bussmann. Siemens-Schuckert, Allegemeine Gesellschaft, Berlin, Germany, September 1945. Translated by Alexander Dovjikov, United State Department of Interior, Bonneville Power Administration, Portland, Oreg.

7. Power System Stability, Steady State Stability, volume 1, S. B. Crary. John Wiley and Sons, Inc., New York, N. Y., 1945. Chapter 10, "Straightaway Transmission Line Comparative Economic Study," pages 151–73.

8. Problems of 220-Kv Power Transmission, A. E. Silver. AIEE Transactions, volume 38, 1919, pages 1037–1100.

9. Characteristics of a 400-Mile 230-Kv Series-Capacitor-Compensated Transmission System, E. V. Hoard. AIEE Transactions, volume 65, 1946, pages 1102–14.

10. Series Capacitors for Transmission Circuits, E. C. Starr, R. D. Evans. AIEE Transactions, volume 61, 1942, pages 963–73.

11. Steady-State and Transient Stability Analysis of Series Capacitors in Long Transmission Lines, J. W. Butler, J. E. Paul, T. W. Schroeder. AIEE Transactions, volume 62, 1943, February section, pages 58–65.

12. Transmission-Line Electric Loadings, S. B. Crary. AIEE Transactions, volume 63, 1944, pages 1198–1204.

Discussion

E. C. Starr (Oregon State College, Corvallis, Oreg.): The studies of transmission economics by Crary and Johnson will be welcomed by engineers confronted with the various problems of long-distance power transmission. We have made similar studies in connection with the engineering work of the Bonneville Power Administration, and our results, taking into account differences in certain design factors and in energy and investment costs, are in good general

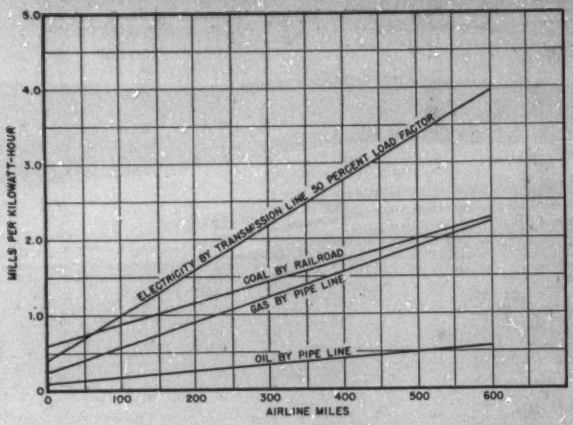

Figure 1

agreement with those presented in this paper.

The curves of Figures 6 to 9 and 12 to 15 of the paper are particularly significant. They emphasize the improved economies possible in very long distance transmission through the use of series capacitors, the importance of adequate loading of high voltage circuits, and the advantages to be gained by employing low resistance conductors. The first two points were also stressed in a paper before the Institute in 1942 by Evans and Starr (reference 10 of this paper).

It is important to note that for long-distance straightaway transmission of large blocks of power the best economies are effected by employing voltages between 230 and 360 kv. It is shown also that the loads of maximum economy vary practically as the square of the line voltage, and that reduced loadings result in rapidly increasing costs. Long lines are seldom built without intermediate loads or interconnections, and in these cases, because of transformation and switching costs, the most economical voltage is near the lower limit of the range given.

From the 230-kv and the 360-kv curves of Figure 19 of the paper, it can be shown that for the system of fixed load network and generation shown in Figure 16 of the paper, the transmission stability limit varies as the voltage raised to the 1.4–1.5 power when the factors not influenced by voltage remain constant. It is interesting to compare this relationship with the familiar square law which obtains when the terminals are changed in size (constant per unit reactance on own base) in direct proportion to the fundamental capacity of the line.

The paper could be clarified and its usefulness extended by the addition of several minor items including the answers to questions as follows:

1. What are the assumed right-of-way costs in Figure 2? Our current design estimates for average construction indicate a substantially greater cost increase for voltages above 230 kv than shown in this figure.

2. In Figure 5, what is the basis for assuming a receiving system impedance of 25 per cent based on kilovolt-amperes at the receiving end of the line? Have tests been made to indicate that metropolitan loads, including the high voltage transformers and low voltage circuits, have impedances of that order of magnitude?

3. In Figures 6 through 9, what is the line loading? Is it the stability limit on a single-circuit basis for the voltage indicated? It would be of considerable interest to repeat Figures 8 and 9 for higher degrees of line compensation, for example 65 and 80 per cent.

4. In Figure 10 is the received power equal to the line stability limit?

5. In Figures 12 through 15 the stability limits should be indicated for each voltage. Additional curves might well be included for the higher voltages and the lower resistance conductors for lines of greater length. The 360-kv caption in Figure 15 apparently should be directed to the third curve from the bottom in the region of 4.0 per unit power.

6. In Figures 18 and 19 what is the transmission distance?

7. It would be of considerable value to repeat Figures 20 and 21 for a longer transmission distance including series compensation.

This paper, combined with reports of previous technical studies, helps very materially to clarify the over-all long distance transmission problem. Large blocks of power generated at convenient low-cost locations can be transmitted economically over long distances to serve remote load centers. The long range program of general industrial development should be carried out with these thoughts in mind.

R. E. Pierce and **E. E. George** (Ebasco Services, Inc., New York, N. Y.): In conclusion 13, Crary and Johnson state that the cost of high load factor, high voltage, heavy duty transmission under present-day conditions is more competitive than formerly with other methods of transporting energy. This is probably the most vital conclusion in their paper and should be examined carefully. Ordinarily, one thinks of hauling coal by rail and transmitting power electrically as the most typical competitive methods. However, this is only a small part of the picture. In a number of economic and financial studies for oil refining companies, chemical companies, power companies and transportation systems, various methods of transporting energy have been studied and compared including:

1. Hauling coal by rail.
2. Hauling coal by ship.
3. Hauling gas by pipe line.
4. Hauling oil by pipe line.
5. Hauling oil by rail.
6. Hauling oil by tanker.
7. Hauling electricity by transmission line.

In comparisons of various methods of transporting energy annual load factor is a basic factor, because fixed charges are greater than operating expenses, except possibly in the case of rail hauls. In the use of published tariffs of common carriers, the actual annual load factor is unknown, but is assumed to have little effect on unit costs in this discussion.

Ordinary fuel oil for power plant use is too viscous for long haul by pipe line, and therefore generally is secured from terminal refineries. In many pipe lines, crude oil and

Figure 2

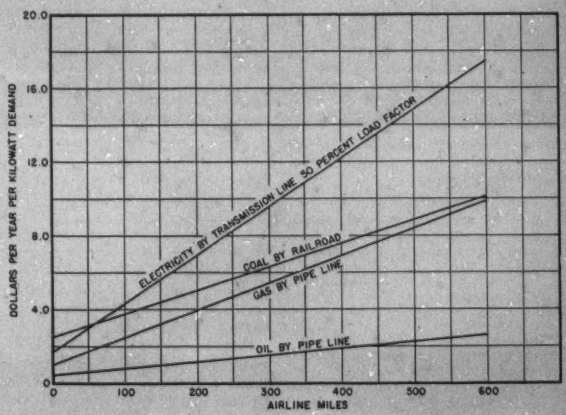

lighter refinery products are handled interchangeably.

The handling of oil by rail in tank cars is somewhat of a retail operation as compared with pipe line delivery. It is generally limited to points where there are no pipe lines and where there is insufficient traffic to justify a pipe line.

The hauling of oil by tanker is much cheaper than other means but is limited by geography to river and coastal terminals. Probably the best summary of costs of transporting oil is that given by Joseph E. Pogue:[1]

"Because of automatic loading and bulk, the oil tanker represents the ultimate in transportation efficiency, exceeding that of the pipe line. Comparative costs per ton-mile are approximately 8.3 mills by rail, 3.2 mills by pipe line, and 1.25 mills by tank vessel. In consequence the tanker competes with the pipe line and diverts as much traffic as the geographic pattern permits."

It should be noted that the cost of transmitting energy by gas pipe line is several times as high as the cost of transmitting energy by oil pipe line.

Comparisons between coal, gas, oil, and electric transmission may be made by using conventional conversion factors and efficiencies. The following approximations permit easy comparison.

1 barrel of oil = 6,250,000 Btu.
1,000 cubic feet of gas = 1,000,000 Btu.
1 ton of coal = 25,000,000 Btu.
1 kilowatt hour = 12,500 Btu (modern steam plant).

Figure 1 shows costs for transporting energy by various means with mills per kilowatt-hour plotted against airline miles. To obtain the costs in cents per million Btu, multiply the mills per kilowatt-hour by eight.

All data for transportation of fuel are average commercial rates. The electric transmission costs are for 50-per-cent load factor and include fixed charges, losses, operation, and maintenance. The electrical costs are 35 per cent higher than those in Figure 1 in the paper, to reflect the increase in price level from 1945 to April 1947.

Although Figure 1 is based on estimated averages, it answers in part the basic question as to how far bulk power can be transmitted economically. At 50-per-cent load factor, the high voltage transmission line and the coal car are generally competitive up to about 150 miles.

The situation for base load plants is more competitive. Load factors of 90 per cent or more are involved. Transmission line costs are almost exactly inversely proportional to load factor, however, the costs of pipe line transportation possibly also should be modified to reflect higher load factor.

At 90-per-cent load factor (base load operation) electric transmission may well be as cheap as coal or gas for any distance.

Regardless of load factor, the electric transmission line cannot compete with the oil pipe line, much less with the oil tanker.

This paper should help in fundamental planning of power systems with due regard for economics as well as for electrical science.

All figures for electric transmission in this discussion assume optimum loads and voltages for various distances (200,000 kw or more on long hauls).

Figure 2 is the same as Figure 1 except that total costs are shown on a capacity basis instead of an energy basis, thus facilitating comparisons with hydro power.

One outstanding effect of such simple and tangible expressions for transmission cost is to prove that so-called "cheap power" is not cheap if it has to be transmitted electrically to a distant market. The slope of the electrical transmission cost lines in Figures 1 and 2 gives directly the difference in cost of transmission for different distances, and is approximately 0.60 mills per kilowatt-hour per 100 miles or $2.63 per kilowatt per year per 100 miles, both for 50 per cent load factor. At lower load factors these unit cost differentials per 100 miles would be even greater. It is readily apparent, therefore, that with the investment cost of a hydro plant generally greater than for a similar size steam plant, hydro power would be more costly than steam power by the time it was delivered a few hundred miles away. In areas of low fuel cost, hydro power transmitted even shorter distances would be more expensive than steam power.

REFERENCE

1. ECONOMICS OF THE PETROLEUM INDUSTRY, Joseph E. Pogue. Privately printed, New York, N. Y., 1932.

David C. Prince (General Electric Company, Schenectady, N. Y.): Crary and Johnson are to be congratulated for their courage in presenting such an excellent economic picture showing where alternating current transmission now stands. There are so many variables in any such analysis that a realistic generalization is very difficult to make. Nevertheless, without such a generalization, we cannot see where we are going. Crary and Johnson have made that generalization; and, if one may judge by the discussion at this meeting, the validity of their generalization has not been questioned.

E. E. George, in his discussion, has made another valuable contribution in that he shows how the high voltage a-c transmission line compares economically with such alternative forms of transporting power as coal by rail, oil and gas by pipe. I have had an opportunity to check George's findings and presented a chart similar to his in connection with the closure of a paper by Doctor E. F. W. Alexanderson and myself.[1]

From all these data it appears that at the present state of the art the favorite medium of the electrical engineer—the high voltage transmission line—appears at a disadvantage where it is in competition with the transportation of power from fuels. This is certainly a challenge to us as engineers, both in the manufacturing and operating fields.

As the art advances, we should be able to improve our economic position in two ways:

1. A reduction in the cost of present components.
2. An increase in the amount of power which we are able to transmit over a given line.

We have for years sought to reduce the cost of our components. Therefore, this is no new thought. Increasing the power that can be transmitted over a given line should be a joint project of the manufacturer and operating engineer.

Higher speed circuit breakers, higher speed reclosing circuit breakers, more effective voltage regulators, and different methods of line compensation are all in this direction.

Also, we may have gone too far in the spread between overvoltage limits and operating voltage. Any increase in the ratio of operating voltage to maximum surge voltage increases the power per dollar as the square.

Might it not be worthwhile to have the appropriate committees of the Institute explore the possibilities in that direction?

REFERENCE

1. ELECTRONIC STABILIZER FOR POWER TRANSMISSION, Ernst F. W. Alexanderson, David C. Prince. AIEE TRANSACTIONS, volume 66, 1947, pages 950–8.

W. R. Brownlee (The Commonwealth and Southern Corporation, Jackson, Mich.): The value of the curves of transmission costs as a function of voltage, distance, and load is materially enhanced by the comprehensive list of unit costs, annual charges, and energy costs on which these curves are based.

It is noted that intermediate switching stations appear economically desirable whenever the transmission distance exceeds 100 miles. In populated areas, intermediate switching stations may be economically desirable for shorter distances, since these may be used to serve increasing intermediate loads as well as to strengthen the transmission capability. That is, transmission lines which are constructed originally as "long lines" may become "short lines" in the course of a few years.

The work of the authors naturally is concentrated on the use of bulk transmission of power from a low-cost to a high-cost area. Substantial amounts of transmission have been built between areas of similar generating costs to make feasible the co-ordinated maintenance schedules of major generating units. The resulting increase in permissible size of such units for a given system may provide a worthwhile reduction in generating investment. Such lines may be most economical at a lower voltage or even with a smaller conductor size than would be indicated for continuous bulk transmission.

It is believed that conclusion 14, "Systems are now entering a stage in their development where added generating capacity will be located at relatively greater distances from the utilization area," should be limited to areas where fuel is relatively inaccessible. Based on the investment and energy figures given by the authors as representative of steam plants and on corresponding figures for firm hydro generation, it appears that the higher capital cost of the latter, together with the cost of transmission, may make it uneconomical for distances of the order of 200 to 300 miles.

S. B. Crary and I. B. Johnson: The discussers have all added very materially to a clearer understanding of the factors involved in the economics of long-distance a-c power transmission. The discussion by R. E. Pierce and E. E. George is a very valuable extension as it compares the relative cost of transmitting energy by different methods. The factors which they present must necessarily be taken into consideration in a rational economic evaluation of electric power transmission. It is well to emphasize, as they have indicated in their concluding paragraph, that the transmission of energy is only one of the major economic considerations. It is also essential that transmission be correlated with the cost of generation and

also the cost of the high-voltage subtransmission to obtain the over-all cost of bringing power into a given area.

It was the objective of our paper to show the important factors which affect long-distance power transmission. It should be understood that the transmission costs must be correlated with the other system economics to obtain the best over-all result. As was pointed out by Pierce and George, and also by D. C. Prince, the cost of transporting energy by pipeline, either gas or oil, may be lower per airline mile than transportation of electrical energy or coal. However, the airline miles for each method may be necessarily different and the cost of the basic fuel may constitute such important factors as to change radically a conclusion based only on a comparison such as is indicated by the illustrative charts of Pierce and George. Pierce and George have commented in regard to our conclusion that transmisson under present day conditions "is more competitive than formerly with other methods of transporting energy." We believe that two important reasons why this conclusion is justified are the increased reliability of transmission as well as the continuing growth of electrical systems. These now make possible the building and operation of heavily loaded transmission circuits carrying 200,000 or 300,000 kw per circuit. Also, there is a continuing trend to use reduced insulation particularly at the higher voltages and this may be considered to be another important factor in reducing transmission costs. Another factor of importance is the use of larger unit transformer capacities.

We are in substantial agreement with the comments of Brownlee. Brownlee and also Starr point out that the use of intermediate switching stations and transformers to serve intermediate areas will result in lower voltages as being more economic than when no intermediate loads exist. This is true of course and is a factor which should be taken into account when considering the ultimate development of an area. Brownlee is also correct that there may exist other situations which justify lower voltages and smaller conductor sizes than that indicated for long-distance high load-factor power transmission. However, it should be recognized that these two requirements result in different system design patterns and that it is generally uneconomical to superimpose upon a low-load-factor transmission system the requirement for continuous bulk transfer. For many systems it may become necessary to depart from the design pattern which was adequate for the past conditions but which is totally inadequate for the future. Brownlee in referring to conclusion 14 concludes that the figures given in our paper indicate to him that it may be uneconomical to transfer power for distances of the order of 200 to 300 miles. The question whether conclusion 14 is correct depends upon whether or not the 200 to 300 miles mentioned by Brownlee is an extension of the distances previously considered as the economic limit. We believe that for some systems a distance of 200 to 300 miles for the transfer of bulk power represents a considerable advance beyond the previous requirements placed on those systems.

Prince makes a plea for the further study of insulation co-ordination, a subject which has been and is being given active study by many groups of engineers.

We are in substantial agreement with the comments of Starr and are particularly pleased to have his comments because of his active work in this field. Starr has asked several questions which we will try to answer. He points out that from Figure 19 of the paper "the transmission stability varies as a voltage ratio to the 1.4–1.5 power when the factors not influenced by voltage remain constant." Our studies have shown that when stability is an important limitation the use of transformers and generators of less than normal reactance is justified. It can be shown, for example, that a 20-percent reduction of transformer reactance can be obtained at about the same cost as would be required for line compensation to effect the same increase in power limit. It can be shown that it is economical to reduce the terminal equipment reactance so as to maintain about a square law relation between power and voltage particularly for the longer distances.

Starr asks in regard to right-of-way costs. Our costs necessarily represent only averages with no attempt at separating the elements of cost. It is a relatively simple matter to show the effect of change in one of the cost factors for the analysis given in our paper. We have found that the general nature of our conclusions is not changed by a fairly substantial change in the relative cost curves with increasing voltage. To us, this is one of the encouraging features of this type of study.

Starr asks in regard to using a receiving system impedance of 25 per cent. This value was selected partially on the basis that the equivalent impedance for the receiving system, in general, would have a lower impedance than the generating station. This comes about because of the diversity of the load area capacity between loads, synchronous condensers, and generating capacity. The use of such a value should not in any way preclude the use of a better receiving system representation for any actual case. It should be evident also that the value at the receiving end impedance can be changed over a rather wide range without changing the results materially.

Starr asks in regard to the line loading for Figures 6 through 9. This is shown on Figure 10 of the paper, and is a loading corresponding to that having a 25 per cent steady state stability limit for the voltage indicated. Cases of higher line compensation have been studied and these additional analyses have indicated that the optimum compensation on the basis of the assumptions of our paper is about 70 to 75 per cent for the 600-mile line.

For Figures 12 through 15, the stability limits for the 100-mile case are not considered to be the prime limitation, but rather, as explained in the paper, the limitation would be determined by the losses. We did not include curves for conductor resistances less than 0.08 ohm per mile because of the difficulty of obtaining reasonably accurate transmission line cost data for these lines using larger conductors. Starr is correct that additional curves might be included for higher voltages and greater lengths although we are inclined to believe that distances from 300 to 600 miles represent the next important step for long-distance power transmission and that to consider longer distances at this time is to project ourselves a little further than is probably necessary. However, reasonably accurate estimates of power transmission cost at this distance can be made. Figures 18 and 19 are for the 200-mile line case of Figure 16.

Starr's last question suggests the preparation of additional curves. We agree that such additional curves would be of considerable value and we have made several such extensions of the work presented in this paper.

We are pleased that there is unanimity of opinion as to the economic goals to be sought such as increased power circuit loading, lower cost transmission lines, and terminal equipment. We hope this will encourage others to present their work so that a better understanding may be obtained of this important problem.

Control of Slip-Ring Motors by Means of Unbalanced Primary Voltages

N. L. SCHMITZ
ASSOCIATE AIEE

HOISTS, DRAWBENCHES, and other similar machines can in many cases be operated simply and economically by means of a single slip-ring motor. The speed–torque characteristics required by the above applications can be obtained by applying unbalanced primary voltages to the stator and connecting capacitance, inductance, and resistance in series with the secondary circuit.

This paper presents a method of obtaining suitable speed–torque characteristics and describes the application of these characteristics to hoists and drawbenches. The behavior of an induction motor with secondary capacitance is analyzed by developing a more general equivalent circuit and correlating the primary current locus to the conventional circle diagram.

It will be shown that landing speeds[1] as low as 18 per cent of synchronous speed can be obtained with full load on a hoist. This is accomplished with less than 150 per cent current in any stator winding through the use of secondary capacitors. It is also shown that even without the capacitors and with only a single phase autotransformer in addition to the other standard devices associated with slip-ring motor control, the following features can be obtained:

1. Landing speeds as low as 50 per cent with less than 250 per cent current when lowering full load.

2. Slow braking speeds without danger of accidentally hoisting an empty hook.

3. No-load speeds at any point between standstill and synchronous speed.

4. Kickoff or motoring torques from 50 to 150 per cent for no-load speeds from 40 to 100 per cent.

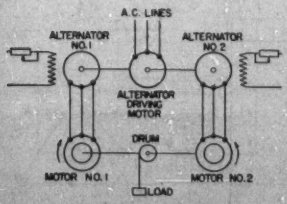

Figure 1. Two slip ring motors with oppositely rotating stator fields, coupled to a common shaft

Methods of Operating Hoists and Drawbenches

The use of slip-ring motors in hoists and drawbenches is not new. The use of this type motor has in the past, however, imposed serious limitations upon the operation of hoists. These limitations arose from the inability of the control scheme to provide one or more of the necessary features of satisfactory operation.

D-c motors can be made to provide these features through the use of either an adjustable voltage control scheme or an armature shunt scheme with a constant potential system. A-c motors have been used to obtain similar features by means of auxiliary machines as in a Kramer or Scherbius[2] drive. Another type of a-c drive employs two slip-ring motors connected so that their torques oppose each other in such a manner as to permit stable operation at speeds less than 100 per cent. All of these schemes present problems regarding either power supply, cost, size of equipment, or complication of control. The latter method, however, suggests a means whereby the previously outlined features may be obtained with only one slip-ring motor.

It has been shown[3] that the operation of an induction motor with unbalanced primary voltages is equivalent to that of two identical motors operating on balanced voltages and so connected that their torques oppose each other. The use of a single motor with unbalanced voltages applied in a definite, predetermined manner will yield characteristics similar to those of the two motor combination. Many types of unbalanced voltage schemes have been investigated. Among these are

1. Direct current from a constant potential source applied, simultaneously with balanced or unbalanced primary voltages, to the motor primary.

2. Scheme 1 with direct current from a pilot generator whose voltage varies as a function of motor speed.

3. Scheme 1 or 2 except with direct current applied to the motor secondary.

4. Tapped primary windings to permit an unbalanced primary flux in connection with balanced or unbalanced voltages.

5. Variable impedance connected in series with one or more motor primary windings to one or more supply lines.

6. Resistance, capacitance, and inductance connected, either singly or combined, in series with one or more primary windings to one or more supply lines.

7. Grid controlled rectifier tubes connected back-to-back and in series with the primary circuit.

8. Unbalanced primary voltages obtained from a single autotransformer and applied directly to the motor primary.

9. Scheme (h) with capacitance and/or inductance in addition to resistance in the secondary circuit.

All of these methods have been investigated analytically and experimentally. The last four schemes have found com-

Paper 47-134, recommended by the AIEE committee on industrial control devices for presentation at the AIEE summer general meeting, Montreal, Quebec, Canada, June 9–13, 1947. Manuscript submitted March 28, 1947; made available for printing April 23, 1947.

N. L. Schmitz is in the development department of Cutler-Hammer, Inc., Milwaukee, Wis.

This paper is based upon development work done at Cutler-Hammer by Eric Pell and the author under the direction of E. W. Seeger. The author gratefully acknowledges the assistance of Professor G. F. Tracy in supplementing and preparing this work for presentation as a thesis leading to the master of science degree at the University of Wisconsin, Madison, Wis.

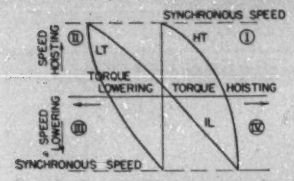

Figure 2. Speed torque curves resulting from motors connected as shown in Figure 1

LT—Lowering torque resulting from negative sequence voltage

HT—Hoisting torque resulting from positive sequence voltage

1*L*—Net torque obtained as the algebraic sum of *HT* and *LT*

mercial applications. Because of the large number of hoists and drawbenches now using the autotransformer, scheme 8, this scheme and its generalization in scheme 9 will be described and analyzed.

Description of Operation

Figure 1 shows two alternators, 1 and 2, connected to motors 1 and 2 so that the motor torques oppose each other. These alternators are shown only to aid in the discussion. In the actual control they are replaced by a single autotransformer suitably tapped for obtaining unbalanced voltages, and only one motor is used. Motors 1 and 2 are connected to the same shaft so that their net torque 1*L* in Figure 2 is the algebraic sum of their component torques, hoisting torque *HT* and lowering torque *LT*.

Since both positive and negative speed and torque quantities are used in this discussion, it is necessary to consider all four quadrants of the co-ordinate system. Quadrant I represents positive speeds and positive torques. This indicates motor action or hoisting speed and torque. Quadrant IV represents negative or downward speed and positive or upward torque. This indicates braking action as in lowering a load. Quadrant III represents negative speed and torque, indicating motor action tending to lower the hook. Quadrant II indicates braking action in a direction opposite to Quadrant IV.

Increasing the field strength of one of the alternators will raise its voltage and increase the torque of its motor in proportion to the square of the voltage. In this manner, *HT* is made greater than *LT* and consequently 1*L* intersects the horizontal axis to indicate a stalled torque in the hoisting direction. This characteristic is similar to the one used for first point lowering in the unbalanced primary type of hoist control. As long as the stalled torque is kept less than the torque required to overcome the friction of the hoist, there is no possibility of an empty hook being hoisted on the first point lowering.

Thus we see that by increasing or decreasing the voltages applied to motor 1 or motor 2 (Figure 1), it is possible to change the position of the net torque curve 1*L* (Figure 2) to obtain various speeds. This is further illustrated in Figure 3 which shows two of the many possible variations. A slow lowering speed with a light hook is obtained as shown by the solid lines. This is done by increasing *LT* (Figure 2) so that in Figure 3 its magnitude is slightly greater than that of *HT*, thus resulting in *LT*2, *HT*2, and 2*L*. The lowering speed may be increased further by reducing the magnitude of the *HT*2 torques and increasing the *LT*2 magnitudes as shown by the dotted lines *HT*3, *LT*3, and 3*L*.

Although two alternators, two motors, and a d-c field supply have been used to illustrate the theory, the same results can be obtained by substituting only one slip ring motor and a single-phase autotransformer for this combination of equipment. This may be done in two steps

1. Eliminate one motor. Connect the windings of the alternators in tandem so that their two balanced polyphase voltage systems of opposite phase sequence are combined. From the method of symmetrical components it can be shown that this will result in a system of unbalanced voltages. If this unbalanced voltage system is applied to the remaining motor, its behavior can be analyzed by considering each set of voltages as acting independently to obtain the previously discussed *HT* and *LT* torque components. Since the components are the same, the net torque characteristic will also be the same as with two motors.

2. After eliminating one motor, substitute an autotransformer for the alternators and

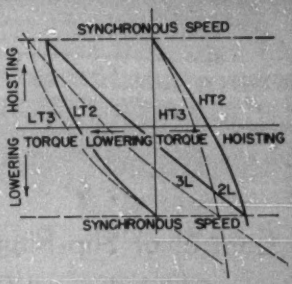

Figure 3. Changes in net torque characteristic effected by changing the magnitudes of the positive and negative sequence voltages

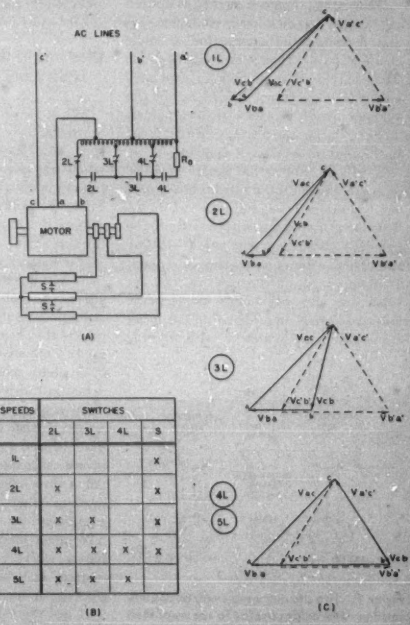

Figure 4. Autotransformer used in obtaining the required magnitudes of positive and negative sequence voltages

A—Connection diagram

B—Switching sequence for autotransformer connections

C—Vector relations among unbalanced voltages

SPEEDS	SWITCHES			
	2L	3L	4L	S
1L				X
2L	X			X
3L	X	X		X
4L	X	X	X	X
5L	X	X	X	

(B)

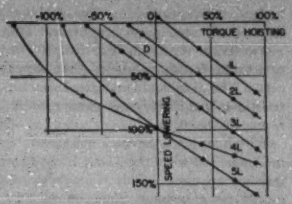

Figure 5. Speed–torque characteristics, lowering of an a-c hoist control with connections as shown in Figure 4

Characteristic *D*, used with drawbenches, provides 40 per cent hook-on speed

their driving motor. A system of unbalanced voltages having positive and negative sequence components of the same magnitude as the two alternator voltages can be obtained with a polyphase supply and a suitably tapped autotransformer. The connections used to accomplish this are shown in Figure 4*A*.

Figure 4*A* shows the contactors used in selecting the lowering speeds of a standard type of hoist control. Hoisting operation is conventional and speed control in this direction is accomplished by commutating steps of secondary resistance. In the lowering direction, the contactors are operated in accordance with the tabulation shown in Figure 4*B*. The speed–torque characteristics obtained in this manner are shown in Figure 5. In addition to hoist characteristics, Figure 5 also shows a dotted characteristic *D* which is suitable for operating drawbenches. In drawing tubes this characteristic provides a no-load or hook-on speed of about 40 per cent of the drawing speed in order to prevent pulloffs and breakage of the tubes or rods. By means of a limit switch or load relay, acceleration is initiated when the carriage is pulled away from the die block. At the end of the draw, slowdown is initiated with the motor exerting a braking torque to decelerate the chain and then a motoring torque to drive the chain at the slow hook-on speed. A selection of transformer taps is usually provided so that hook-on speeds may be changed to accommodate different types of work.

Figure 4*C* shows the vector relations among the motor primary voltages for speeds 1*L*, 2*L*, and 3*L*. The vector diagram for speed 1*L* shows a condition approaching single-phase operation with two motor leads connected together. If this condition were realized, the positive and negative sequence voltages would be equal. The displacement of point *b* from point *a* by an amount equal to the magnitude of voltage V_{bn} makes the positive or hoisting sequence voltage slightly larger than the negative sequence voltage and results in sequence *a-b-c* at the motor terminals. The component torques obtained under this condition are the same as those shown in Figure 2. This displacement of point *b* provides about 10 per cent slower full load landing speed than is obtainable with equal sequence voltages (single-phase). Displacing point *b* more than the amount shown in the diagram usually results in the motor's overcoming the static friction of the hoist under light hook conditions. This causes the hook to hoist slowly on point 1*L*.

The vector relations for point 2*L* show point *b* to have been displaced in a direction opposite to that for point 1*L*. This results in sequence *c-b-a* at the motor terminals, indicating a greater negative or lowering sequence voltage. The component torques for points 2*L* and 3*L* are the same as those shown in Figure 3.

The vector relations for points 4*L* and 5*L* show the voltages obtained from the transformer which differ in this case from the voltages at the motor terminals by an amount equal to the voltage drop in the primary resistor R_b. This resistor functions to limit the torque at standstill (kickoff torque) to less than 150 per cent, thus reducing the shock to the hoist mechanism in starting to lower the hook. This method of limiting the torque avoids the need for commutating the secondary resistance in accelerating downward, and thus permits a more simple control scheme. An exact method of analyzing the 4*L* and 5*L* speed torque characteristics has been developed, but it is not considered in this paper. Braking torques in the normal range of operation can be predetermined within 5 per cent by considering the motor voltages to be the same as those obtained directly from the transformer. Standstill torque can be predetermined accurately by solving for the

Figure 6. Capacitor in secondary circuit of slip ring motor with balanced primary voltages

A—Connection diagram
B—Speed–torque characteristics
2*H*–5*L*—Characteristics with capacitor
6*H*–3*H*, 6*L*—Characteristics without capacitor (switch *A* closed)
T—Countertorque lowering characteristic without capacitor

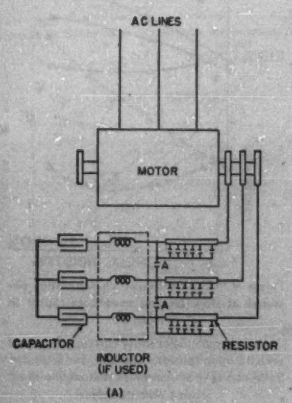

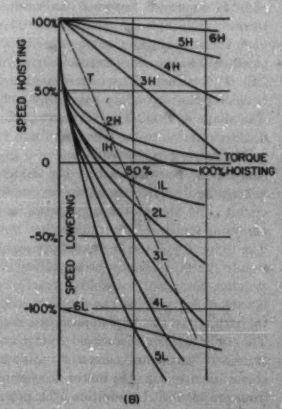

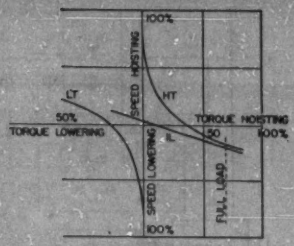

Figure 7. Slow landing speeds for a wide range of load

Capacitor and inductor in series with secondary circuit. Unbalanced voltages applied to motor primary
LT—Lowering torque resulting from negative sequence voltage
HT—Hoisting torque resulting from positive sequence voltage
1*L*—Net torque obtained as the algebraic sum of *HT* and *LT*

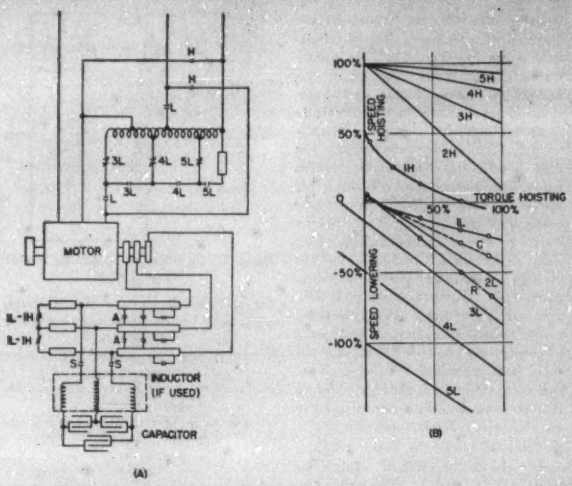

Figure 8. Hoist control with secondary capacitance and unbalanced primary voltages

A—Connection diagram
B—Speed–torque characteristics *R*, 2*H*–5*H*, 3*L*–5*L*—Secondary resistance only
C—Secondary resistance and capacitance
1*H*, 1*L*, 2*L*—Secondary resistance, capacitance, and inductance

motor voltages and then applying a method which will be described later in connection with the 1*L*, 2*L*, and 3*L* characteristics.

The full load braking torque required of the motor is about 70 per cent of the torque required to hoist full load. This difference is due to the friction of the hoist. At 70-per-cent torque in Figure 5 it is seen that the landing speed is 50 per cent. At less than full load the landing speeds are correspondingly less. Attempting to decrease the full load landing speed to less than 50 per cent by either decreasing the secondary resistance or increasing the primary voltages usually results in overheating the motor. This limitation occurs with the transformer type of control using only secondary resistors.

Secondary Capacitance and Inductance

In a high-speed hoist, a wider speed range is often necessary in order to provide a safe landing speed. This wider range can be obtained by using capacitance in addition to resistance in the secondary circuit, or by using a combination of resistance, capacitance, and inductance. In fact, full load lowering speeds as low as 18 per cent can be reached. Speed–torque characteristics obtained with capacitance in the secondary circuit differ from those obtained with resistance alone. Figure 6 shows this type of characteristic as obtained on balanced voltages. The characteristics obtained with the capacitor are numbered from 2*H* to 5*L*. These characteristics do not represent the final form of the speed–torque curves which are used. They could be employed, however, in a countertorque-type of hoist controller. They have the advantage of smaller speed variation with load as compared to characteristic *T* obtained with conventional controllers using secondary resistance only. The shape of the 2*H* to 5*L* curves has a definite relation to the secondary current.

The current in the secondary of a slip-ring motor is determined by the induced voltage and impedance of the secondary circuit. As the motor approaches synchronous speed, its slip approaches zero. The induced voltage decreases in proportion to the slip. When the secondary impedance consists of capacitive reactance, it various inversely as the slip, increasing to infinity as the slip approaches zero. The combination of decreased voltage and increased impedance causes a rapid decrease in current as the motor accelerates from standstill. In addition, the power factor is low and leading because of the high capacitive reactance. The combination of low secondary current and low power factor results in less than 10 per cent torque for slip values less than 50 per cent. The disadvantage of these characteristics is that there is still an appreciable torque at standstill.

With light load, the hook will therefore move upward when the 1*L* to 5*L* characteristics are used. This is common to most types of countertorque control.

The hoisting of a light hook on points 1*L* to 5*L* can be prevented by using unbalanced primary voltages. Figure 7 shows the component torque characteristics *HT* and *LT* resulting from the positive and negative sequence components of the unbalanced primary voltages. Addition of these components results in a 1*L* speed–torque characteristic which possesses advantages of slow landing speed, simplicity of control, and stator currents of less than 150 per cent.

Connections for a hoist control using secondary capacitance are shown in Figure 8*A*. Unbalanced primary voltages are obtained as previously described in explaining Figure 4*A*. The secondary circuit includes a capacitor which can be connected in series with the secondary circuit for speed points 1*H*, 1*L*, and 2*L*. Using the capacitor only, full load landing speeds as low as 30 per cent are obtain-

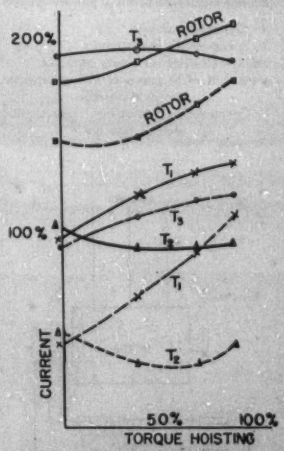

Figure 9. Current–torque characteristics obtained at slow landing speeds as shown in Figure 8

Dotted characteristics show currents associated with 1*L* using resistor, capacitor, and inductor. Solid curves show currents associated with 1*L* using resistor only

able. The use of inductance in series with the secondary capacitor permits a further reduction in speed. With this combination, speeds as low as 18 per cent are obtainable for lowering full load. The continuous kilovolt-ampere rating of the capacitor needed for 30- and 18-per-cent speeds is about 20 per cent of the rated kilovolt-ampere input of the hoist motor.

Speed–torque characteristics are shown in Figure 8*B*. Curves as obtained with resistance alone and curves with resistance and capacitance in series are shown for comparison. In point 2*L*, a resistor is connected in parallel with the inductor and capacitor so as to reduce their effect.

With unbalanced primary voltages applied to its stator, the rotor current of an induction motor contains two different frequency components at any condition other than standstill or synchronous speed. One frequency component results from the positive or hoisting sequence stator voltages and the other from the negative or lowering sequence stator voltages. At 20-per-cent lowering speed, a 60-cycle motor has a 72-cycle rotor current component due to the hoisting sequence voltages and a 48-cycle rotor current component due to the lowering sequence voltages. In order to obtain the maximum net hoisting or braking torque at a given slow lowering speed, it is desirable to have the hoisting sequence rotor currents large and at a high power factor. This increases the hoisting torque component *HT* in Figure 7. It is also desirable to reduce the lowering torque component *LT* in Figure 7 by minimizing the lowering sequence currents and having their power factor low. This is accomplished by inserting inductance in series with the secondary capacitors so as to approach resonance at 72 cycles. The impedance to 72-cycle current will then be less than the impedance to 48 cycle current by an amount depending upon the sharpness of resonance.

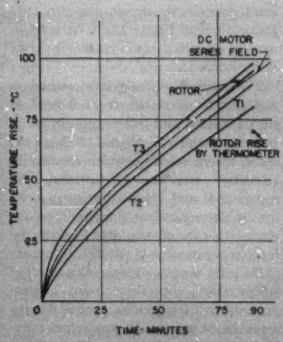

Figure 10. Temperature rises of a-c and d-c cargo winch motors operated on identical loads and duty cycles

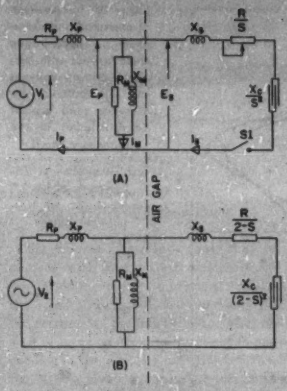

Figure 11. Equivalent circuits for calculating the performance of a slip-ring motor operating on unbalanced primary voltages

A—Positive sequence circuit
B—Negative sequence circuit

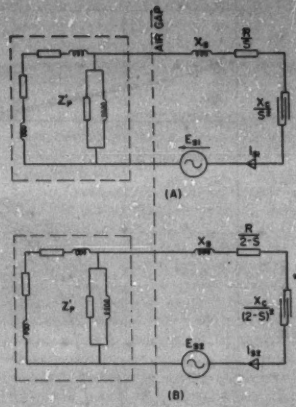

Figure 12. Simplification of circuits shown in Figure 11

Full load landing speeds less than 18 per cent can be obtained by increasing the sharpness of resonance and by causing resonance to occur at speeds less than 25 per cent, but this usually requires a larger capacitor and inductor. It also reduces the braking torque available with the 1*L* characteristic between speeds of 50 and 100 per cent. In applying the characteristic to hoists, the constants of the secondary circuit are selected so that the braking torque at all speeds is always greater than 150 per cent of the required full load braking torque. This is done to avoid the possibility of a slow rate of deceleration from 150- to 50-per-cent speed. In addition, the control scheme is arranged so as to insure deceleration on points 3*L* and 2*L* before transferring to 1*L*.

Motor Currents at Slow Landing Speeds

This scheme in lowering full load requires less than 150 per cent current in the most heavily loaded stator winding. As shown by Figure 9, the current in motor winding T_3 is 120 per cent at a full load torque of 70 per cent. The remainder of the dotted curves show currents in other motor windings. It is significant that the T_1 current approaches that in T_3, indicating a condition favorable for minimum heating in the hottest winding. The rotor current at full load is shown to be 170 per cent. Heating of the rotor is not necessarily a limiting factor since its temperature rise as shown in Figure 10 is less than that of stator phase T_3.

Even with an unbalanced primary type control employing resistance only in the secondary circuit, the currents in the motor windings are within 200 to 250 per cent of normal. This is shown by the solid curves in Figure 9. If necessary, the T_3 current can be decreased by changing the phase relation between positive and negative sequence currents until the T_1 and T_3 currents are equal. This involves no change in the speed–torque characteristics. The magnitudes of the positive and negative sequence voltage systems remain the same, but their phase relation to each other is altered. This requires an additional single phase autotransformer. Since no particular difficulty with heating has been encountered in the large number of hoists and drawbenches now controlled by means of unbalanced primary voltages, it is not considered advisable to sacrifice simplicity and economy by using more than one autotransformer.

Heating of the Motor Windings

Any consideration of heating involves not only the current in the motor but also the duty cycle upon which the motor

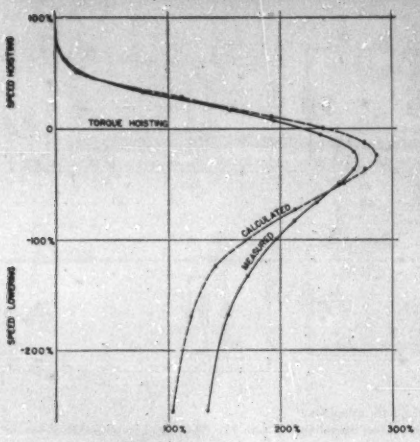

Figure 13. Comparison of measured and calculated speed–torque characteristics with balanced primary voltages and with resistance, inductance, and capacitance included in the secondary circuit

Test data taken at 75-per-cent voltage
Results shown for 100-per-cent voltage

operates. The currents encountered with the unbalanced primary type of hoist and drawbench control are no greater than those common in d-c hoist motors. These currents reach 200 to 250 per cent of normal. The satisfactory service records of such motors has shown that heating is not excessive.

The reason that the d-c and a-c hoist and drawbench motors do not overheat is that the duty cycle is intermittent in all cases. The most severe duty cycle included in ASA specifications is 15 seconds on out of 45 seconds. Even with a more severe duty cycle, undue heating is not like y because

1. Coils adjacent to the hot winding are cooler, facilitating heat transfer;

2. The temperature equalizes rapidly when hoisting with balanced currents and also when the motor is at rest.

Figure 10 shows this to have proved true in tests as well as in theory.

In obtaining the temperature curves shown in Figure 10, two similar cargo winch drives were tested. One employed a 50-horsepower 440-volt 60-cycle 575-rpm totally enclosed slip-ring motor. This motor was used in the unbalanced primary control scheme shown in Figure 8. The other employed a 50-horsepower 230-volt, 600-rpm totally enclosed d-c motor. This motor was used in a constant potential d-c cargo winch control scheme. These motors were mounted in turn on a standard cargo winch arranged to hoist and lower full load. The duty cycle used was a standard United States Maritime Commission cycle of 17 seconds hoist, 17 seconds lower, and 20 seconds off. The temperature rises indicated on Figure 10 were obtained by means of resistance measurements with a Kelvin double bridge. In the a-c test, auxiliary slip rings were used to bring out potential leads from the rotor winding to the Kelvin bridge. This allowed resistance measurements during each 20 second off period without opening the motor housing. Twenty thermocouples were also placed at various points on the windings and core of each motor. These all indicated temperature rises less than the temperature rise by the resistance method. As shown by Figure 10, the highest temperature rise of the a-c motor is for all practical purposes the same as that of the d-c motor. Temperatures of the armature, interpole, and shunt field windings of the d-c motor were comparable to those of the less heavily loaded a-c motor windings.

Although the a-c scheme employed secondary capacitors, no appreciable difference from the above results would be likely to occur in substituting an a-c scheme employing secondary resistance only. The reason for this is the short time that the slow speed is used in relation to the entire cycle of operation. Also, with a somewhat higher landing speed, the 1*L* characteristic with resistance only would be in operation for shorter periods of time for the same distance traveled.

Calculation of Currents and Torques

The mathematical analysis of the unbalanced primary type of control scheme is based upon the method of symmetrical components applied to the equivalent circuit of the induction motor. The application of this method to induction motors has been capably explained elsewhere.[3,4] This method involves the resolution of a given set of unbalanced 3-phase voltages into two sets of balanced voltages, the phase sequence of the first set being opposite to that of the second. The behavior of the motor is analyzed by considering the effect of applying each set separately and then combining the results. The analysis in each case is made by means of the appropriate equivalent circuit. The two equivalent circuits are shown in Figure 11. Circuit *A* is used in calculating positive sequence currents and torques, and circuit *B* is used in calculating the corresponding negative sequence quantities. The only difference in the two circuits is in the terms containing slip, *S*. This difference can be explained by an illustration: with the motor turning against the direction of the positive sequence stator field at 40-per-cent speed, the frequency of the positive sequence rotor current is equal to the slip, *S*, or 140 per cent. At the same time, the frequency of the negative sequence rotor current due to the oppositely-rotating negative sequence stator field is equal to $2-S$ or 60 per cent. Hence $2-S$ in the negative sequence circuit replaces *S*.

Except for the terms representing secondary capacitive reactance, the circuits of Figure 11 are identical to the conventional equivalent circuit in which internal and external secondary resistance are included in one term, *R*. The more general circuit containing secondary capacitance is developed in Appendix I.

Where a large number of torque calculations are to be performed, it is convenient to simplify the circuits of Figure 11 to obtain those of Figure 12. The development of simplified, series circuits is shown in Appendix II.

The accuracy of the above methods is indicated by the close agreement between the calculated and test results shown in Figures 13 and 14. Figure 13 shows the speed–torque relations which result with secondary resistance, inductance, and capacitance and balanced primary voltages. The equivalent circuits do not include either the effect of iron losses in the rotor or the increase in effective resistance of the rotor winding at high values of slip.[5] Above 200% slip, these losses become large enough to cause an appreciable increase in the measured torque values, causing them to exceed the calculated values.

Figure 14 shows current loci corresponding to the speed–torque curves of

Figure 13. The loci calculated from the equivalent circuit of Figure 12*A* are compared to test results. Slip values for the various operating points are indicated by the percentage figures on each curve.

The current loci with secondary capacitance may be obtained in a manner similar to that used in constructing the conventional circle diagram of an induction motor. The circle diagram of an induction motor represents the current locus obtained when a variable resistance is connected in series with a fixed reactance.[6] The diameter of the circle is perpendicular to the reference voltage E_S and its magnitude is equal to E_S/X. The operating point on this conventional circle diagram for any given slip, S_0, can be located by means of a conventional slip scale. Another means of locating the operating point is to construct a circle with its diameter coincident with E_S and equal in magnitude to $E_S/(R_P'+R/S_0)$. This circle represents the current locus obtained with fixed resistance and variable reactance. The only condition satisfying both loci occurs at their intersection, the operating point. By constructing a series of constant resistance loci, a series of operating points for various values of slip may be located, and performance curves for the induction motor can be plotted.

A similar procedure may be followed for obtaining a series of operating points in the case of an induction motor operating with secondary capacitance. The only difference in the two procedures is that occasioned by the term X_C/S^3. This shows that the reactance of the motor changes as a function of slip, and thus requires a different diameter, constant reactance circle for each value of slip. The diameter equals $E_S/(X-X_C/S^3)$. If a series of constant resistance and constant reactance circles are drawn for a number of values of slip, their intersections can be used to determine the current locus of the motor currents obtained with secondary capacitance. The method can be extended to include loci corresponding to torque lines and output lines in the circle diagram, but torque and output may be more directly obtained from the equivalent circuit.

Although there are more convenient ways of determining motor currents, this method is useful in visualizing the behavior of the induction motor when operating with secondary capacitance. At large values of slip the diameters of the constant-R and constant-X circles are large. As slip decreases, the constant-R circles become smaller. The constant-X circles increase in diameter until resonance is reached, at which point the diameter is infinite, and the locus becomes a vertical line. Further reductions in slip result in successively smaller circles of constant R. The constant-X circles become capacitive current loci and their diameters also decrease. At zero slip, or synchronous speed, the diameters are zero as would be expected since secondary current is also zero for this condition.

Design of Controllers Using Secondary Resistance Only

The above illustrations show that by starting with a given set of circuit elements and a given set of primary voltages the speed and current characteristics can be accurately predetermined. The design of a controller usually involves proceeding in the opposite direction by starting with a given set of speed–torque requirements and certain current limitations. With this information it is necessary to determine the circuit elements and voltages which will provide the desired characteristics. Assuming that the designer desires the slowest practical landing speed, the magnitudes of V_1 and V_2 are made as large as possible without exceeding the maximum permissible flux density in the motor. The ratio V_1/V_2 is made as large as possible without exceeding the maximum of 10-per-cent hoisting torque allowable at standstill. The phase angle between V_1 and V_2 is fixed by the type of transformer connection used to obtain the unbalanced voltages. Adding the V_1 and V_2 sequence voltage systems at the prescribed phase angle then determines the voltages applied to the motor terminals. More frequently the last step is accomplished by assuming a certain transformer connection and then analyzing the unbalanced voltages thus obtained to ascertain how closely they approximate the required V_1 and V_2.

It has been found that a positive sequence voltage V_1 of 68 per cent of rated motor voltage and a negative sequence voltage V_2 of 64 per cent will meet the above limitations. This is illustrated by Figure 15 which shows that *HT* and *LT* characteristics corresponding to these voltages produce the desired 10-per-cent standstill torque in their combined 1*L* speed–torque curve. When V_1 and V_2 are known, a value of R may be assumed, and the *HT* and *LT* speed–torque characteristics can be calculated. Experience with a large number of hoist and drawbench applications indicates that R should equal approximately 50 per cent of the

Figure 14. Current loci for characteristics shown in Figure 13 compared to circle diagram

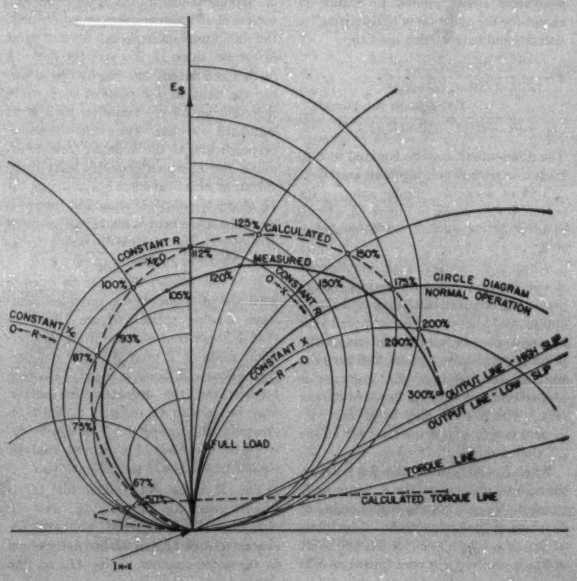

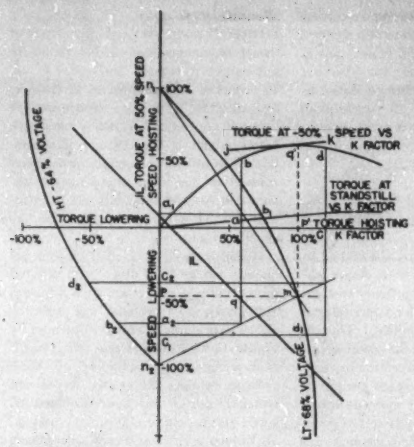

Figure 15. Graphic construction for determining optimum secondary R with scheme using unbalanced primary voltages and secondary resistance only

rated secondary E/I of the slip-ring motor. Starting with this value of R, it is possible to apply a correction factor, K, which will determine an accurate, optimum value of R to permit the slowest landing speed.

R may be determined by partially differentiating the expression for net torque with respect to R. In an approximate equivalent circuit similar to Figure 11 except for the omission of magnetizing resistance and magnetizing reactance

$$T=\frac{V_1^2R/S}{(R_P+R/S)^2+(X_P+X_S)^2}-\frac{V_2^2R/(2-S)}{[R_P+R/(2-S)]^2+(X_P+X_S)^2} \qquad (1)$$

The differentiation when equated to zero leads to a sixth degree algebraic equation.

A more workable, graphic solution for optimum R is shown in Figure 15. Optimum R is determined by the relation R/K.

When it is recalled that doubling R, $K=50$ per cent will cause torques which previously occurred at 150-per-cent slip to appear at 75-per-cent slip, it is seen that line m–n may be used to determine the positive sequence torque at 150 per cent slip for any value of K. Point m is located on line p–q at a K factor of 100 per cent. The K scale may be of any convenient length, and m need not fall on the LT characteristic.

When $K=60$ per cent, line q–b is drawn through 60 per cent on the K factor scale which in this case has the same number of divisions as the torque scale. The intersection of q–b with m–n_1 locates the point at which positive sequence torque a_1–b_1 is measured. Similarly, the negative sequence torque a_2–b_2 is measured at the intersection of q–b with m–n_2. The difference between a_1–b_1 and a_2–b_2 determines the $1L$ torque a–b for $K=60$ per cent. By performing a series of constructions, a curve representing torque variation with respect to K may be determined. The maximum value of this curve indicates the K, and consequently the R for maximum torque at 150 per cent slip, or, conversely, the minimum landing speed for any value of torque, since $1L$ is a straight line. A further refinement may be had by drawing the tangent j–k parallel to a curve representing torque variation with K at standstill. A line from the tangency, perpendicular to the K factor scale determines the K which provides least speed variation with load when operating on the $1L$ characteristic. If standstill torque is less than 10 per cent, a further adjustment of sequence voltages can be made to reduce the landing speed.

It is not always desirable to operate with the R value which provides minimum landing speed. Figure 15 shows that a 20-per-cent increase from the optimum value of R produces only a 5-per-cent increase in landing speed. In some applications, the reduction in current may be enough to warrant a slight increase in landing speed. This can be decided on the basis of a current analysis similar to the above torque analysis.

The R value determined for $1L$ is usually used for the $2L$, $3L$, and $4L$ characteristics. Sequence voltages for characteristics $2L$ and $3L$ are determined in the same manner as for $1L$, on the basis of saturation and the ratio V_1/V_2 required to provide a given no-load or full-load speed. Secondary resistance for point $5L$ is determined on the basis of the highest desired full-load lowering speed.

Design of Controllers Using Secondary Capacitance

Circuit constants for $1L$ characteristics employing secondary capacitance are based upon considerations other than minimum landing speed. In explaining operation with secondary capacitance and inductance, it was indicated that full load landing speeds of less than 18 per cent can be had by using large amounts of inductive and capacitive reactance. In this manner, resonance can be made sharp enough to exclude all but the smallest amount of negative sequence torque at any lowering speed. Therefore, a graphic analysis similar to that with resistance only does not apply. The problem can be attacked by analyzing the positive sequence characteristic to determine maximum torque with respect to R, S, X, and X_c individually when all quantities other than the one under consideration are held constant. This has been done as shown in Appendix III.

The $1L$ characteristic with capacitance may, of course, be analysed by starting with various assumed circuit constants and solving the equivalent circuits as outlined under "Calculation of Currents and Torques."

Conclusions

Controlling a slip-ring motor by adjusting the degree of unbalance of its primary voltages affords a simple and reliable means of obtaining characteristics which would otherwise require the use of more complicated equipment. The characteristics can be predetermined accurately by means of calculations based upon the equivalent circuit of the induction motor.

The scope of this paper includes only the main circuit elements and the characteristics of the unbalanced primary type of slip-ring motor control. Other interesting features related to this type of control but not covered in this paper include an off-point dynamic braking relay for the reduction of brake wear and a load relay for automatic transfer to a high speed winding where a 2-speed motor is used for fast handling of a light hook. Any or all of these features can be used in combination with the characteristics which have been described to permit a-c operation of many types of hoists, drawbenches, and similar machines.

Appendix I

Determination of Secondary Impedance in the Equivalent Circuit of a Slip-Ring Motor Having Capacitance in Series With the Secondary Circuit

The following analysis considers a motor with a 1-to-1 ratio of transformation. If a ratio other than unity is used, currents, voltages, and impedances must be adjusted accordingly.

Referring to Figure 11*A* it is seen that

$$Z_S = E_S / I_S \tag{2}$$

Where all quantities are considered at primary frequency

At slip frequency

$$E_S' = SE_S \tag{3}$$

Where secondary voltage is considered at secondary frequency

And since I_S is the same whether considered at primary or secondary frequency

$$Z_S' = SE_S / I_S \tag{4}$$

From equations 2 and 4

$$Z_S = Z_S' / S \tag{5}$$

When X_L and X_C are measured at primary frequency

$$Z_S' = R + j(SX_S - X_C/S) \tag{6}$$

From equations 5 and 6

$$Z_S = \frac{R}{S} + j\ \ X_S - \frac{X_C}{S^2}\Big) \tag{7}$$

Equation 6 leads to the equivalent circuits shown in Figure 11.

Appendix II

Simplification of Exact Equivalent Circuit to Facilitate Torque Calculations and to Permit Further Analysis With a Simple Series Circuit

The exact equivalent circuit may, through the use of Thevenin's Theorem, be reduced to a simple series circuit without impairing the accuracy of calculated results.

Referring to Figure 11*A* it is seen that with switch *S*1 open and with V_1 impressed upon the motor primary winding, E_S may be readily calculated. This voltage is a constant for a given motor and primary impressed voltage, and is independent of secondary resistance, inductance, and capacitance. With switch *S*1 closed, current I_{S1} results in the secondary circuit.

Replacing voltage source V_1 with its equivalent-impedance and impressing the previously calculated E_S across switch *S*1 results in the same current I_{S1} through the secondary circuit, as shown in Figure 12*A*

$$I_{S1}^2 = \frac{E_{S1}^2}{(R_P'+R/S)^2 + (X - X_C/S^2)^2} \tag{8}$$

$$T_4 = I_{S1}^2 (R/S) \text{ synchronous watts} \tag{9}$$

$$T_1 = 7.04 I_{S1}^2 R/SN \text{ pound-feet} \tag{10}$$

By analogy, T_3 may be calculated from the circuit shown in Figure 12*B*

$$T_3 = 7.04 I_{S2}^2 R/(2-S)N \text{ pound-feet} \tag{11}$$

Using the foregoing method, the calculation of a series of speed–torque points for a given sequence involves only one calculation of E_{S1} and one calculation of Z_P'. In calculating Z_P', the impedance of the voltage source is usually negligible and only the motor impedances are involved. The secondary resistance and capacitive reactance are calculated for each assumed value of slip, and the series circuit is solved for torque in terms of power dissipated in the secondary resistance.

This method has particular merit where speed, torque, and secondary current are the only quantities to be calculated. When primary current is desired, the labor involved is about the same as that required by the conventional circuit.

Appendix III

Determination of Secondary Resistance, Inductance, Capacitance, and Slip for Maximum Torque With Balanced Voltages

Maximum torque with *R*, *X*, X_C, and *S* considered individually may be determined by partially differentiating the expression for torque with respect to the quantity under consideration, all other quantities being held constant.

Referring to Figure 12, the magnitude of the secondary current may be determined from equations 8 and 9.

$$T = \frac{E_S^2 \dfrac{R}{S}}{(R_P'+R/S)^2 + (X - X_C/S^2)^2} \tag{12}$$

Maximum Torque With Respect to Slip

Differentiating with respect to *S* and equating to zero, the slip at which maximum torque occurs for a given *R*, *X*, X_C, and primary resistance may be determined.

$$\frac{\partial T}{\partial S} = 0 = \frac{E_S^2 R}{[(R_P'+R/S)^2 + (X - X_C/S^2)^2]^2} \times \frac{\left[\begin{array}{l}(R_P'+R/S)^2 + (X - X_C/S^2)^2 - \\ \quad -S^2 \\ (-2R/S^2)(R_P'+R/S) + \\ \quad (4X_C/S^3)(X - X_C/S^2)\end{array}\right]}{S} \tag{13}$$

Since only positive, finite values of slip are under consideration, and since $S \neq 0$, it follows that the last factor must vanish, thus leading to the relation

$$0 = -\frac{R_P'^2}{S^2} - \frac{2RR_P'}{S^3} - \frac{R^2}{S^4} - \frac{X^2}{S^2} + \frac{2XX_C}{S^4} - \frac{X_C^2}{S^6} + \frac{2RR_P'}{S^3} + \frac{2R^2}{S^4} - \frac{4XX_C}{S^4} + \frac{4X_C^2}{S^6} \tag{14}$$

Simplifying the above expression

$$0 = (R_P'^2 + X^2)S^4 + (2XX_C - R^2)S^2 - 3X_C^2 \tag{15}$$

Solving for S^2

$$S^2 = \frac{R^2 - 2XX_C \pm \sqrt{R^4 - 4R^2XX_C + 4X^2X_C^2 + 12X_C^2(R_P'^2 + X^2)}}{2(R_P'^2 + X^2)} \tag{16}$$

If $X_C = 0$ the above expression can be reduced to the conventional relation for determining the slip which results in maximum torque in an induction motor.

$$S^2 = \frac{R^2}{R_P'^2 + X^2} \tag{17}$$

For maximum power transfer with $X_C = 0$, the load resistance must equal the source impedance.[7] This condition is met as shown in equation 18.

$$R/S = \sqrt{R_P'^2 + X^2} \tag{18}$$

Maximum Torque With Respect to Resistance

The secondary resistance for which maximum torque results may be determined by differentiating with respect to *R* and equating to zero.

$$\frac{\partial T}{\partial R} = 0 = \frac{E_S^2/S}{[(R_P'+R/S)^2 + (X - X_C/S^2)^2]^2} \times \left[(R_P'+R/S)^2 + (X - X_C/S^2)^2 - \frac{2R}{S}(R_P'+R/S)\right] \tag{19}$$

Since only positive values of *R* are under consideration, it follows that the last factor in the above expression must vanish.

$$0 = R_P'^2 + \frac{2RR_P'}{S} + \frac{R^2}{S^2} + X^2 - \frac{2XX_C}{S^2} + \frac{X_C^2}{S^4} - \frac{2RR_P'}{S} - \frac{2R^2}{S^2} \tag{20}$$

Simplifying equation 20

$$\frac{R^2}{S^2} = R_P'^2 + X^2 - \frac{2XX_C}{S^2} + \frac{X_C^2}{S^4} \tag{21}$$

Solving for R^2

$$R^2 = S^2 R_P'^2 + S^2(X - X_C/S^2)^2 \tag{22}$$

For maximum power transfer, the load impedance must equal the source impedance. This condition is satisfied as shown by the following relation which is obtained from equation 22:

$$R/S = \sqrt{R_P'^2 + (X - X_C/S^2)^2} \tag{23}$$

Maximum Torque With Respect to Inductive and Capacitive Reactance

The total inductive reactance for which maximum torque occurs can be obtained by differentiating with respect to *X* and equating to zero.

$$\frac{\partial T}{\partial X} = 0 = \frac{(2E_S^2 R/S)(X_C/S^2 - X)}{[(R_P'+R/S)^2 + (X - X_C/S^2)^2]^2} \tag{24}$$

Since all quantities in equation 24 are positive and finite, the last term in the numerator must vanish, and

$$X = X_C/S^2 \tag{25}$$

A partial differentiation similar to the foregoing may be performed with respect to X_C to obtain the same result as that shown by equation 25.

$$\frac{\partial T}{\partial X_C}=0=\frac{(2E_S^2R/S^2)(X-X_C/S^2)}{[(R_P'+R/S)^2+(X-X_C/S^2)^2]^2} \tag{26}$$

Equation 25 may also be obtained by eliminating R and R_P' between equations 15 and 21.

Maximum Torque With Respect to X, X_C, S, and R Considered Simultaneously

In order to obtain the greatest possible torque, at some slip, S, it is necessary to simultaneously satisfy equations 22 and 25. Equation 25 can be satisfied by selecting the ratio.

$$X_C/X=S^2 \tag{27}$$

The magnitudes of X and X_C determine the sharpness of resonance. When this ratio is applied to equation 22, the last term vanishes and

$$R=SR_P' \tag{28}$$

Since the resistances of the primary and secondary windings of an induction motor are approximately equal, this relation represents a condition obtainable only at slip values greater than unity.

Equations 27 and 28 involve series resonance, and since the resistances are low, a reduction in impressed voltage is necessary to limit the current in the motor.

Appendix IV

Symbols

V_1 = positive sequence voltage at motor primary terminals (phase to neutral)

V_2 = negative sequence voltage at motor primary terminals (phase to neutral)

T_1 = torque in synchronous watts resulting from positive sequence voltages (per phase)

T_2 = torque in synchronous watts resulting from negative sequence voltages (per phase)

T = net torque in synchronous watts resulting from positive and negative sequence voltages in combination (per phase)

Z_1 = impedance to positive sequence current (per phase, assuming star-connected motor)

Z_2 = impedance to negative sequence current (per phase, assuming star connected motor)

R_P = resistance of motor primary winding (per phase, assuming star connected motor)

R_S = resistance of motor secondary winding (per phase, assuming star connected motor, referred to primary)

R = total resistance in motor secondary circuit (per phase, referred to primary)

X = total inductive reactance of the motor primary and secondary circuit in the simplified equivalent circuit of Figure 12 $X=X_P'$+internal and external inductive reactance of the motor secondary circuit.

X_C = external capacitive reactance when connected in series with the motor secondary circuit (measured at primary frequency)

S = per unit slip

X_P = inductive reactance of motor primary winding

X = inductive reactance of motor secondary winding (measured at primary frequency)

E_P = primary induced voltage

E_S = secondary induced voltage (referred to primary frequency)

E_S' = secondary induced voltage measured at secondary frequency

Z_S = total impedance of secondary circuit, referred to primary

Z_S' = total impedance of secondary circuit at secondary frequency

W_S = watts dissipated in secondary circuit (per phase)

N = synchronous speed of motor in revolutions per minute

Z_P' = total impedance of primary circuit viewed from the secondary circuit with motor primary terminals either short circuited or connected together through an impedance equal to that of the voltage source

R_P' = resistive component of Z_P'

X_P' = reactive component of Z_P'

Quantities related to the positive sequence circuit are denoted by a subscript 1. Quantities related to the negative sequence circuit are denoted by a subscript 2. All symbols refer to a motor having a 1-to-1 ratio of transformation.

References

1. Electric Cargo Winch Speeds, **F. V. Smith**, *Marine Engineering and Shipping Review* (New York, N. Y.), October 1939, pages 484–85.

2. Control of Electric Motors (book), **P. B. Harwood**. Wiley and Sons, New York, N. Y., 1944. Pages 330–47.

3. Symmetrical Components (book), **C. F. Wagner, R. D. Evans**. McGraw-Hill Book Company, New York, N. Y., 1933. Page 345.

4. Method of Symmetrical Co-ordinates Applied to the Solution of Polyphase Networks, **C. L. Fortescue**. AIEE Transactions, volume 37, 1918, pages 1027–1115.

5. Induction Motor Characteristics at High Slip, **Theodore H. Morgan, William E. Brown, Arthur J. Schumer**. AIEE Transactions, volume 59, 1940, August section, pages 464–8.

6. Alternating Current Circuits (book), **K. Y. Tang**. International Textbook Company, Scranton, Pa., 1940. Pages 161, 277, 192.

7. Communication Engineering (book), **W. L. Everitt**. McGraw-Hill Book Company, New York, N. Y., 1937. Pages 48–51.

8. Alternating Current Machines (book), **A. F. Puchstein, T. C. Lloyd**. Wiley and Sons, New York, N. Y., 1942. Page 250.

Discussion

L. F. Stauder (University of Notre Dame, South Bend, Ind.): After hearing N. L. Schmitz's excellent paper on this subject at the 1946 AIEE Great Lakes District meeting, its content as of that time was introduced into a course in symmetrical components given to some of the seniors at the University of Notre Dame last fall. From test data we evaluated the circuit constants listed in Figure 11 of the present paper and used them with several unbalanced primary voltages to anticipate line currents, torque, power input, and efficiency. The actual electrodynamometer test data checked very well with that calculated using the method of symmetrical components and the equivalent circuit. The addition of the content of Appendix II and Figure 12 which aptly apply Thevenins Theorem will make possible considerable saving in time consuming calculations of torque. No inductance was added to the secondary, no attempt was made to maximize torque as outlined in Appendix III of the present paper. Tests were run also at half voltage (balanced) at 300 rpm intervals of speed from 100 per cent plus to 100 per cent minus and performance checked with that anticipated from equivalent circuit calculations.

The students were interested and duly impressed by the scheme of speed control and the check obtained between calculations and test data. One of them, Myles E. Wood, used it as the subject of a paper which won him the right to present it in the District Branch paper competition where it received honorable mention.

This limited experience as a teacher of the subject, indicates to me that apart from the obvious practical application value of the scheme, N. L. Schmitz's paper is an excellent academic vehicle to illustrate the merits of the method of symmetrical components. A disadvantage of using the example of the squirrel cage motor operating to and beyond full load torque is that the calculated magnitude of the negative sequence torque is so small, say 2 per cent of positive sequence torque, even at considerable unbalanced primary voltage that the student is not instinctively sold on the need and virtue of the method. Likewise, when static impedances are used, other methods of solving balanced circuits often are shorter and equally good.

Seldom does a single application in 3-phase give the opportunity to apply so effectively theorems like Thevenin's, maximum power (torque), and circle diagrams in array such as in Figures 14 and 15. As only the usual laboratory apparatus and moderate time are required to obtain confirming test data, the scheme and the content of the comprehensive paper could well be incorporated in courses in motor control, advanced a-c machinery and especially in courses in symmetrical components.

John F. H. Douglas (Marquette University, Milwaukee, Wis.): The discussion on Appendix II of Schmitz's paper, indicates a considerable contribution to more rapid calculations for slip-ring motors. We wonder if the method would facilitate the calculations of concatenated motors.

In Figure 6 of the paper one useful combination of capacitors is shown with desir-

able torque characteristics shown in Figure 8 when supplied with unbalanced voltage. "Methods of Operating Hoists and Drawbenches," part 9 appears to contemplate other combinations of *R*, *L*, and *C*. While, undoubtedly, this matter has been given attention, and no useful combination yet found, there is room for further improvement and additional reports will be awaited with interest.

The author does not emphasize the fact that the effect of increasing capacity would raise the resonant point in Figure 13 to a positive speed, however, when counter torque diagrams are drawn for this case in the manner of his Figure 7, undesirable characteristics are obtained. Is the author ready to announce any successful use of capacitors in the motoring quadrant?

John D. Leitch (The Electric Controller and Manufacturing Company, Cleveland, Ohio): A very comprehensive and interesting paper has been presented by Schmitz. The mathematical treatment of the induction motor operating with balanced voltages and with capacitive reactance in the secondary is of great assistance in explaining the reduction in motor heating and the higher torque at lower speed when the motor primary is unbalanced. Schmitz's results are in complete agreement with the work we have done on this subject.

Schmitz shows how to determine the size of the capacitor in microfarads for lowering with an unbalanced primary and states that the continuous kilovolt-amperes of the capacitor is about 20 per cent of the rated kilovolt-amperes of the motor. Since the capacitor is connected in series in a circuit in which voltage, current, and frequency are varying concurrently, I would like to ask how this kilovolt-ampere rating is determined and the basis of giving the capacitor a continuous rating.

The use of an inductance in addition to a capacitor sharpens the peak of the speed–torque curve and reduces the speed at which maximum torque occurs for a capacitor of a given size. Is it not true that adding an accurately known inductance in the secondary permits the control designer to neglect the actual reactance of the motor or at least allows a less accurate approximation of its value?

Carl J. Fechheimer (consulting engineer, Milwaukee, Wis.): Considering that many years have been spent by engineers in endeavoring to obtain a satisfactory a-c motor for cranes, and hoists, and that it was believed that only with complications or with a-c commutator motors could desirable speed–torque characteristics be secured, it may now be regarded as an achievement that such are obtainable with a simple slip-ring induction motor operating on various degrees of unbalance, and with predetermined values of secondary impedances.

In the usual 3-phase motor with a moderate unbalance in primary voltages, there is generally a considerable unbalance in currents, but not a large diminution in torques. Yet for small torques, according to Schmitz's Figure 9, the maximum phase current is about 190 per cent, and the minimum 90 per cent, with the secondary external impedance consisting only of resistors; by the introduction of properly chosen resistors, capacitors, and inductances the currents in all phases was decreased appreciably further. It is gratifying to note that temperature rises have not been injurious. If glass and silicone insulation are employed, breakdowns will probably not occur, even in extreme cases.

I ask the author

1. Has it been found necessary to apply a larger frame size than would be employed for balanced conditions, and if so, about how much larger?

2. Have the suppliers of power, or others, objected to the unbalance in currents and voltages occasioned by such applications?

N. L. Schmitz: The author is in entire accord with Professor Stauder as to the possibilities of the unbalanced primary type control as an academic vehicle for the teaching of symmetrical components.

This application has also been used as an illustration and as a subject for problems by Professor G. F. Tracy in a course in symmetrical components given at the University of Wisconsin and by Professor Douglas in advanced courses in rotating machinery given at Marquette University. The author has, from his own experience, found the unbalanced primary type of control quite generally useful in the teaching of a-c circuits, control, and laboratory courses.

Although Fortescue's original paper gives full emphasis to the application of symmetrical components in analyzing the behavior of rotating machinery, the use of this valuable engineering tool in this manner appears to have been curtailed by a lack of suitable problems. After several years of relatively little use in this field compared to its application with static impedances in power system short circuit analysis, the method of symmetrical components now finds everyday application in the design of a-c hoist and drawbench controls. It is gratifying to note that our educational institutions are keeping abreast of these advances.

Douglas' suggestion as to the use of Thevenin's Theorem in calculating the performance of concatenated motors will probably lead to a simplification of calculations for applications of this type. Other combinations of secondary resistance, inductance, and capacitance have been investigated in addition to the series resonant circuit analysed in the paper. These circuits have parallel branches which cause parallel resonance so as to minimize undesirable currents and torques at certain frequencies. The advantages gained are less speed variation with changes in load, and slightly reduced currents. These advantages appear to be more than offset by the increased cost due to the additional circuit elements which are required. Capacitors have been successfully used in the motoring quadrant. When used in this manner they provide a speed–torque characteristic similar to that obtainable at slow speed with a d-c series motor. This type of characteristic is shown by curves 1*H* and 2*H* in Figure 6*B* and curve 1*H* in Figure 8*B*.

Leitch raises a question which has a close parallel in the development of the capacitor-start and capacitor-run fractional horsepower motors. These motors originally required capacitors having a greater kva rating than is now necessary in the light of more complete knowledge of duty cycles and characteristics of capacitors. It is expected that similar improvements will be made in the case of the secondary capacitors in the unbalanced primary type of control.

Present engineering practice is to determine the size of the secondary capacitor on the basis of the required capacitive reactance, peak voltage rating, and maximum allowable heat dissipation in the capacitor. The peak voltage at any given speed can be determined by calculating the positive sequence secondary current as outlined in Appendix II. When multiplied by the capacitive reactance at the given speed, the rms and peak voltages due to positive sequence current can be obtained. A similar procedure is used to determine the negative sequence peak voltage. The arithmetic sum of the two peak voltages thus determined yields the peak voltage across the capacitor. The analysis with respect to heating may be approached in a similar manner, although in intermittent duty applications such as hoists, it has not appeared as a limiting factor.

The comment with respect to additional inductance sharpening the resonant peak and reducing the speed at which maximum torque occurs is correct. The inductance of the motor, however, is seldom less than 25 per cent of the total inductance needed, and can therefore be neither neglected nor too roughly approximated.

Fechheimer effectively summarizes the accomplishments of the unbalanced primary type of a-c hoist control. He also raises several points which should be emphasized in closing.

1. The frame sizes of hoist motors are determined by the requirement of adequate pull-out torque for safety in hoisting. When determined in this manner, the motors are adequate for all hoisting and lowering operations in the usual type of unbalanced-primary hoist-control application. As in all types of a-c and d-c schemes, when an unusually long, slow speed lowering operation is required, additional consideration is needed.

2. Power systems which are adequate for industries requiring hoists and drawbenches have, to the author's knowledge, experienced no difficulty with regard to the unbalanced currents which comprise only a small part of the system capacity.

3. Although the usual 3-phase squirrel cage motor exhibits undesirable characteristics when subjected to even moderate voltage unbalance, these characteristics as such are not a part of the unbalanced primary type of hoist and drawbench control using a slip-ring motor. The addition of secondary resistance permits us to reduce the undesirable, negative sequence current and to emphasize the negative sequence torque so as to produce a total speed–torque characteristic which can be easily controlled by adjusting the voltages applied to the motor primary.

A Simplified Double-Film Klydonograph With an Improved Coupling Method

J. H. WAGHORNE
NONMEMBER AIEE

Synopsis: Two improvements in klydonograph surge recording are described. The first is a simplified double electrode recording unit in which a rubber band is used to hold the unit together and make it light-tight and weather-proof. The second is a coupling unit used for high voltage lines and equipment which greatly facilitates the use of the klydonographs by connecting them on the line side of the capacitance voltage divider.

SINCE J. F. Peters[1] first published his description of a klydonograph in 1924 using Lichtenberg figures to record surge voltages on photographic film, several improvements in this method of surge recording have appeared. The recording of both a positive and negative figure regardless of the actual surge polarity by using a double film unit[2] considerably improved the ease of interpretation of the figures. There have since been many variations of these original units using either stationary or clock-driven film.

Similarly there have been many methods of coupling to high voltage lines and equipment in order to supply a reduced voltage to the recording units.[2–4] These capacitance voltage dividers have used various arrangements of rings, bars and insulator strings as capacitors. However they all have been large, more or less permanent installations, and frequently coupled in some degree to other phases or circuits as well as the one desired.

This paper describes a simplified double recording unit using stationary film and a simplified coupling method that allows installation almost anywhere at any time.

Recording Unit

A diagram of the recording unit is shown in Figure 1 and a photograph showing the parts and their arrangement in Figure 2. The construction is symmetrical except that the one bakelite cap is black and the other brown and the threads on the black end are different from those on the brown so that the unit cannot be installed backward. Each unit carries a serial number engraved on the black end and on both sides of the bakelite disk. A *B* is also engraved on the bottom or black side of the disc and a *T* on the top or brown side. The engraving on the disk is filled with a radium compound so that the films are automatically numbered by an exposure of anywhere from one day to two months.

There is no physically grounded plane used in conjunction with the electrode carrying the surge. However, since the unit is electrically symmetrical and shielded by the conducting layer on the bakelite caps, a neutral plane is established through the center of the unit at a voltage midway between that appearing at the terminals. Thus, the recording is similar to that in a unit with a ground plane except that twice the voltage is required to produce the same size figures.

The direct calibration of this unit is shown for both positive and negative figures using a $1^1/_2$x40 microsecond wave in Figure 3.

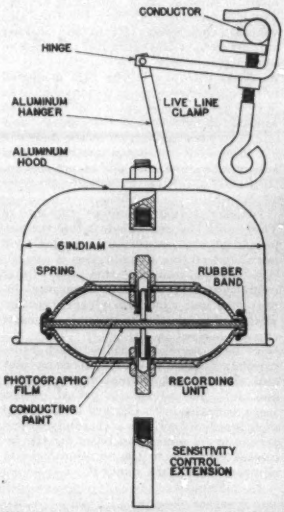

Figure 1. Construction details of the klydonograph recording unit, coupling unit, and sensitivity control

Figure 2. Exploded view of a recording unit showing relative location of the two $3^1/_2$-inch square commercial orthochromatic films and assembled recording and coupling units ready to attach to the live line

Paper 47-151, recommended by the AIEE committee on instruments and measurements for presentation at the AIEE summer general meeting, Montreal, Quebec, Canada, June 9–13, 1947. Manuscript submitted March 26, 1947; made available for printing April 29, 1947.

J. H. WAGHORNE is assistant research engineer with The Hydro-Electric Power Commission of Ontario, Toronto, Ontario, Canada.

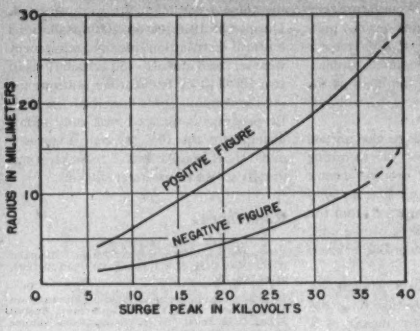

Figure 3. Direct calibration of the recording unit using a $1^1/_{15}$x40 microsecond surge

Broken line indicates range of film tracking

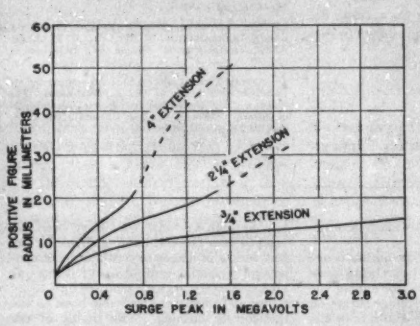

Figure 4. Calibration of combined recording and coupling units for three different length calibration extensions

Broken line indicates film tracking

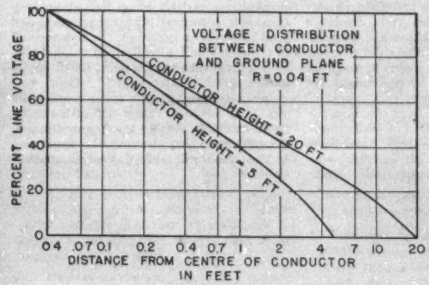

Figure 5. Potential distribution between a conductor and ground plane

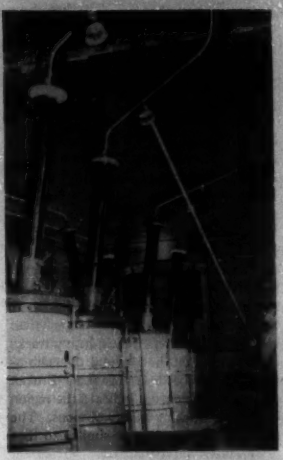

Figure 6. Servicing klydonographs at an indoor transformer station

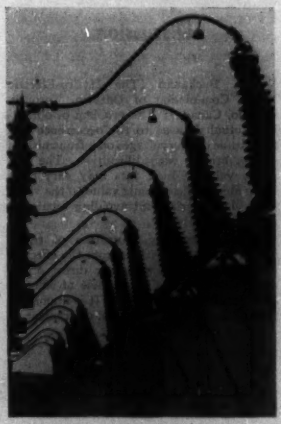

Figure 7 (right). Klydonographs installed on 220-kv circuit breaker leads at an outdoor station

Coupling Unit

The normal coupling to high voltage lines and equipment with the recording unit at the grounded end has required a small electrostatic capacitance from the unit to the line compared to the capacitance from the live terminal of the unit to ground. The coupling described here reverses this condition by connecting the unit on the line side of the capacitance divider.

The voltage distribution in the neighborhood of a conductor is relatively independent of the location of the ground plane or grounded objects for spacings greater than about five feet. The fraction of line voltage at a point x feet above a ground plane and below a conductor of a radius R feet and height h feet is given by

$$V_x/V_L = [\log (2h-x)/x]/\log 2h/R$$

For a conductor of radius 0.04 foot (1-inch diameter) the voltage distribution is shown in Figure 5 for values of h equal to 20 and 5 feet. For the space involving the klydonograph the ratio of the voltage at a given point for h equal 5 feet to that for the same point with h equal 20 feet is 1.27. The klydonograph hood will disturb the distribution near the conductor but not appreciably at distances greater than five feet. Its main function is to control the effective pickup distance of the bottom of the recording unit from the conductor.

This means that the calibration is practically independent of location so long as the klydonograph is five feet or more from

grounded equipment. This has been checked in the laboratories on both alternating voltages and surges.

A diagram of the coupling unit is shown in Figure 1 and it is also shown in the photograph of Figure 2. In use, a recording unit is screwed up into the coupling unit hood with the black side down and a sensitivity-control extension screwed on to the bottom of the recording unit. Different size extensions are used to couple to equipment or lines at different voltages. Figure 4 shows the calibrations for the recording and coupling units combined using three different sizes of sensitivity-control extensions. A $1^1/_2$x40 microsecond wave was used for these calibrations. For figures larger than about 22 millimeters radius, heavy tracks are produced on the film and the calibration possibly becomes unstable. Broken portions of the curves indicate the region where this tracking is very obvious. The accuracy of recording is similar to that of previous klydonographs—errors of single readings up to about 25 per cent.

The concave downward curvature seen in the three curves of Figure 4 is not present in the calibration curve of the recording unit alone shown in Figure 3. Ionization around the edge of the hood at the higher voltages might be a possible explanation for this difference.

If it is desired to reduce the normal alternating voltage across the recording unit so that it does not produce a dark spot on the film, a resistance of from 20 to 100 megohms can be connected from the hood to the bottom of the recording unit. This will not affect the recording of steep wave front surges.

These klydonographs are installed and removed from the high voltage lines and equipment while alive by means of a treated wooden stick with a head designed to operate the clamp shown in Figure 1.

Application

During the 1945 lightning season, 40 installations on 2,300-volt rural lines using these recording units were serviced. During the 1946 season, 400 installations on rural distribution lines and equipment were serviced and also 450 installations in two 220/110 kv transformer stations using the coupling units described. A similar program is planned with only minor changes for the 1947 season. Figures 6 and 7 show installations of these klydonographs at two transformer stations.

References

1. The Klydonograph, J. F. Peters. *Electrical World* (New York, N. Y.), volume 83, April 19, 1924, pages 769–73.

2. The Measurement of Surge Voltages on Transmission Lines Due to Lightning, Everett S. Lee, C. M. Foust. AIEE Transactions, volume 46, 1927, pages 339–56.

3. The Klydonograph and Its Application to Surge Investigation, J. H. Cox, J. W. Legg. AIEE Transactions, volume 44, 1925, pages 857–70.

4. Applied Science From the Viewpoint of an Electrical Engineer, W. B. Buchanan. *The Bulletin*, The Hydro-Electric Power Commission of Ontario (Toronto, Ontario, Canada), July 1938, volume 25, pages 236–46.

Discussion

W. B. Buchanan (The Hydro-Electric Power Commission of Ontario, Toronto, Ontario, Canada): The problem of obtaining factual data as to the occurrence and magnitude of overvoltages on a transmission system bristles with difficulties. The economic value of such data may vary from being merely of academic value to the value of service security and avoiding repairs to expensive equipment.

A study covering protection of transformer and other stations from the effect of atmospheric lightning, either direct or induced strokes, requires the use of suitable recorders in large numbers. It is important that such devices be reliable, convenient to install and collect and give as much information as possible.

The device described by the author is one result of rather extensive studies being made on the general problem of determining the nature and source of overvoltage surges on a system, their distribution and rate of dissipation or attenuation. The operating engineer is not completely satisfied to know that an overvoltage sufficient to result in failure of important insulation has occurred but also wants to know where did it come from, how often might he expect it, and if of severe magnitude what means might be adopted for protection therefrom.

Much information has been obtained relating to natural lightning. Practical experience has indicated that there have been cases also where very high voltages were induced in the electric system itself. Voltages as high as 4,000 volts have been developed on a 110-volt lighting circuit by the fast action of a mercury switch on disconnecting a special type of load. Surges as high as 50,000 volts were reported on a 13-kv feeder and these were traceable back to the transformer bushing. The timing of the latter surges coincided with opening a breaker on overload which fed a large arc-furnace transformer. Other surges detected tend to throw suspicion on the balance-coil of tap-changing mechanisms as being a possible source when tap-changing under heavy load.

Investigations of such types require devices very compact in construction due to the space available usually being very limited. We anticipate that the device as developed by the author will find many useful applications.

Factors in the Economic Supply of Energy in Hydroelectric Systems

A. H. FRAMPTON
FELLOW AIEE

G. D. FLOYD
MEMBER AIEE

ECONOMIC SUPPLY in the electric power system must be considered both from the viewpoint of peak (or power) supply and from that of energy supply. In systems having predominantly thermal-electric generation, these two viewpoints will be closely related, but in systems having predominantly hydroelectric generation, the generating costs per peak kilowatt or per kilowatt-hour may vary independently. For this reason the economics of hydro generation may differ from those of thermal generation.

It is the object of this paper to review those factors which affect the economics of energy generation (as distinct from peak generation) in the system deriving its supply predominantly from hydroelectric sources. It will discuss

1. Factors in the designs including storage problems, efficiency of plant arrangement, unit efficiency, and combination with existing sources.

2. Factors in operation, including operation of units in a single plant and also of units in plants operating in parallel and the effect of load and frequency control and of maintenance schedules.

3. Factors in the load, including seasonal variations, type of customer contract, load building, and secondary energy generation.

Its conclusions will indicate that numerous factors in planning, design, and operation must be considered to utilize most effectively available hydraulic resources. Certain of these factors, discussed only briefly herein, have been the subject of earlier papers but are worthy of further detailed treatment, bringing up-to-date cost and other considerations into proper perspective. It is hoped that this review will stimulate the presentation of such additional material.

Paper 47-168, recommended by the AIEE committee on power generation for presentation at the AIEE summer general meeting, Montreal, Quebec, Canada, June 9–13, 1947. Manuscript submitted March 26, 1947; made available for printing May 2, 1947.

A. H. Frampton is director of engineering and G. D. Floyd is in the planning section of the electrical engineering department of The Hydro-Electric Power Commission of Ontario, Toronto, Ontario, Canada.

General

The objective of the modern electrical utility is to deliver electric power and energy to its ultimate consumers at minimum cost consistent with sound engineering practice and standards. The attainment of this objective is a responsibility shared by the planning, designing, and operating divisions of the utility, properly correlated in their respective endeavors.

In the utility predominantly supplied from thermal-electric generation, certain factors will vary from those encountered in the utility whose power resources include substantial proportions of hydroelectric generation. For example, the location of the thermal station may be controlled within limits, to secure optimum transmission and distribution costs. Such plants may be designed for operation at specific load factors, but their actual operating load factors (either daily or seasonal) may be adjusted to suit either varying load conditions or changing system arrangements. The generating efficiency is largely determined by design factors and the operating costs include the major item of fuel consumption.

Thermal plant efficiencies were improved materially in the period between 1910 and 1935, with a much slower rate of improvement since. Over-all system efficiencies therefore are attained by controlling the operation of the available plants, in general by operating new and higher efficiency plants on base load and the older, less efficient plants as peak or standby resources, or more specifically by some application of the principle of incremental loading.

In systems which include major proportions of hydroelectric generation, over-all system efficiency is not attained simply. Hydro plant locations are essentially uncontrollable and their capital cost governs the unit output cost, operating expenditures being but a small component. The economic operating load factor must be determined at the outset, based on anticipated future load and capacity requirements. A subsequent revision in the predetermined operating requirements (unless provided for in the original design) may be difficult and perhaps impossible.

Plant outputs are subject to some extent to the vagaries of nature, stream flow conditions varying with precipitation. This factor in design is one which appears susceptible of more accurate analysis than is usual, using the methods of the theory of probability. This phase is not referred to in detail herein, but is worthy of detailed treatment at some future time.

Finally, hydroelectric plant efficiencies are difficult to estimate accurately in the design stages. Extensive field testing is required,[1] after the plant is placed into operation, to establish these data, but their establishment is important to the attainment of optimum economy. Each principal unit should be tested and its actual efficiency curves calculated, so that the system supervisor may operate the various facilities with the assurance of his colleague in the thermal system.

Factors in the Design

The basic possibilities of the hydroelectric plant site, as a source of power and energy, are determined by the natural conditions existing at the site and in the watershed above the site. The extent to which these basic possibilities can be

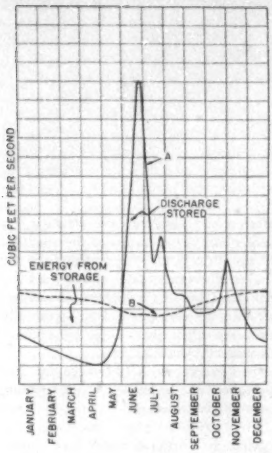

Figure 1. Annual discharge curves for an assumed case

A—Uncontrolled
B—Controlled to exactly meet system energy demand

developed and utilized becomes a series of economic problems.

This discussion is concerned with those economic problems which affect the energy generation, and these may be discussed under the three headings.

Control of Stream Flow

The natural uncontrolled flow in most rivers of North America varies from brief periods of extremely high flow (as during the spring freshet) to usually longer periods of low flow during the fall or winter. Such variation may be of the order of 200 to 1. Outstanding exceptions are found in the Niagara and St. Lawrence Rivers draining the Great Lakes basin.

In virtually no case will this natural variation coincide with system load variations, so that some degree of flow control is essential in all cases. The first problem facing the hydraulic designer, therefore, is to determine the economic extent to which the total flow may be controlled by storage, thus transferring the available energy resources from their natural periods to those coinciding with the load demand.

In a typical river of the North American continent the natural discharge curve would approximate that shown in curve *A* of Figure 1. The ultimate desirable curve might look like *B* in the same figure. Some curve intermediate between these two usually is found to be the economic limit.

Detailed contour and other surveys, exploratory drilling to determine foundation conditions, space available to accommodate the various structures, accessibility to transportation will have indicated the desirable plant location. A preliminary layout of the structures will have established the general arrangement of the project and the approximate head which can be developed.

Coincident with this work, the storage possibilities above the main dam will have been investigated. The flood lines will have been determined and the possibility of storage dams in the main or tributary rivers developed. In certain cases, the rights of other riparian owners in the river will have been canvassed, insofar as they may place limitations on the new project. Other plants under company ownership may exist on the river, which may benefit by the new development or also impose limitations.

With these respective limitations in mind, the hydraulic designer commences to develop alternative steps in the control of the natural flow. Each step towards complete control will require increased storage areas and therefore greater capital investment. Estimates of the total costs at each step permit the establishment of the incremental cost of the greater energy generation effected. Such process, it will be noted, is likely to involve the law of diminishing returns, in that the greater the storage area provided, the higher the cost and the lower the probable return per unit investment.

In the simplest case, additional storage will be provided by increasing the height of the main dam. Storage so obtained has the dual advantage of being usable at the higher gross head, thus increasing both the peak and energy capacity. In other cases, storage may be obtained at points distant from the plant, perhaps on tributary streams. Such storage areas provide control only and their value is appraised in terms of the additional primary energy thus obtained.

Less extensive (pondage) areas close to the plant, preferably in the forebay itself, will have marked advantages in the day-to-day operation of the plant, permitting the daily load variations to be followed without corresponding regulation of the main river.

Combined with the storage studies will be those concerning the installation of equipment at the generating station. Each increment of storage capacity will permit either the operation of the planned capacity at higher average load factors or the installation of greater capacity to operate at the same load factor. These studies will involve, not only the cost of equipment at the plant, but also the facilities required to deliver the plant output to the utilization centers.

The ultimate objective of these combined studies will be to determine that plan of development which delivers to the load the maximum of power and energy consistent with the limitations imposed by the controlling factors. The controlling factors may be alternative sites for development, competing energy sources (such as fuel-burning plants at the load centers) or the rates at which certain classes of service are rendered—this latter item being most important if surplus or secondary energy markets are available. Figure 2 illustrates, for a hypothetical case, the results of such a study, including increased storage costs with increased plant and transmission facilities.

Figure 3 is a similar hypothetical illustration for the run-of-river plant. In such cases, an installation based on the minimum flow would operate contimu-

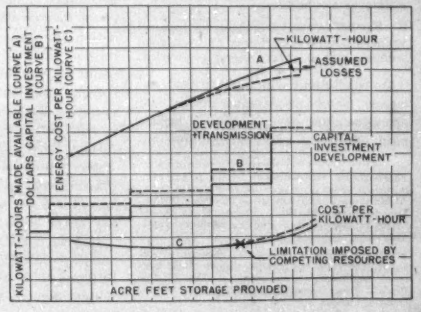

Figure 2. Assumed case of providing additional water storage

Illustrating effect on
A—Energy made available
B—Capital investment
C—Average cost of the energy

ously; each new unit would operate for progressively shorter intervals in the natural flow cycle until the point is reached where a further additional unit would not normally operate for sufficient time to justify its installation.

In summary, therefore, optimum energy generation costs, insofar as they may be determined at this stage in the planning studies, will be attained only if painstaking efforts are made to determine the limits of the possibilities presented and to fit each alternative to the load demand curve and to the competing sources of generation. Each hydroelectric site will present its own problems and its own specific solutions. Imagination and sound economic thinking will be demanded of the planning and designing engineers, whose work need not suffer from lack of variety.

Efficiency of Water Passages and Turbine Unit

Each cubic foot of water in the plant forebay represents potential energy, but the proportion of this energy actually delivered will depend on the over-all plant efficiency. Again economics will have a marked bearing on establishing those plant arrangements which result in maximum efficiency consistent with return on the capital investment.

If the powerhouse forms part of the main dam, that is where long intake water passages are absent, the efficiency factors become those of the turbine water passages only. If long intake canals, tunnels or pipe lines are required, the determination of the area of these passages requires the balancing of costs and financial return.

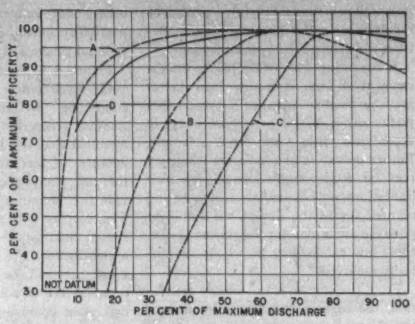

Figure 4. Typical relative efficiency curves for various turbines

A—Impulse
B—Reaction
C—Fixed blade propeller
D—Adjustable blade propeller

The larger the intake area, the lower will be the hydraulic losses and hence the greater the net delivery. These same considerations enter the tailrace design, as loss of head in both cases reduces the net head available at the turbine.

In these studies the plant capacity and its operating load factor must be considered, in that a smaller plant capacity, operating at high load factors, reduces the maximum flow and hence the area of the intake and tailrace passages. Conversely, increasing the plant capacity for lower load factor operation, increases the maximum flow at peak output, indicating larger water passages. Step-by-step comparison of alternatives again will be required.

The efficiency of the turbine and its associated passages is usually a problem which the utility designer transfers to the manufacturer, except to the extent that a selection is possible from among alternative types.

In any given case, the utility designer will be faced with the selection of that turbine type best suited to the particular site conditions. Basic types include the impulse (Pelton), reaction (Francis), fixed-blade propeller, and adjustable-blade propeller (Kaplan), each having characteristics adapted to specific head and flow conditions. Typical efficiency curves for each type are illustrated in Figure 4.

Omitting the infrequent high-head plant (above 800 feet), for which the impulse or Pelton wheel is adopted, the Francis type is best suited to medium head installations (60 to 800 feet). However, the particular runner design chosen will depend on the designed operating conditions. If the plant is to operate at high load factors, or if it contains sufficient units that the number operating can be adjusted as the total plant load varies, so that each is loaded to near full capacity, then even a sharply peaked curve, having maximum efficiency near full load, may be most suitable. If, on the other hand, the unit loading is likely to vary considerably as for example, if the station is to be used for frequency control—a curve having a much broader peak, even though slightly lower maximum value, may result in higher long-term efficiency.

The fixed-blade propeller unit is best suited to the low heads (below 70 feet), in plants where the operating head and unit loadings vary over relatively narrow limits. If the operating head is subject to wide seasonal variations, or if the units are to be operated at widely varying loads, detailed study of the improved long-term efficiency, compared to the added revenue secured, may indicate the desirability of the more expensive Kaplan installation.

In this selection of efficiency characteristics the hydroelectric plant designer is presented with yet another opportunity to attain optimum generation costs.

Combination of the New Plant With Those Existing

In visualizing the design specifications for any new plant, a full appreciation of the system into which the new plant is to be fitted is essential. For example, the new plant may be on the same river with other plants, its output may have to be transmitted long distances, it may be required to supply some specific component in the load curve (either base power or peak) or it may be required to operate in parallel with either existing or

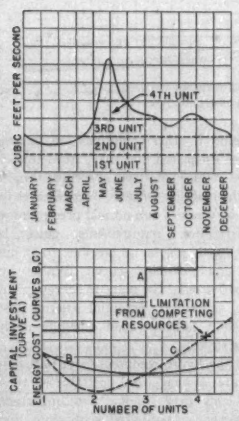

Figure 3. Assumed case of increasing number of units to utilize a specified river discharge

Illustrating effect on
A—Capital investment
B—Average cost of the energy
C—Incremental cost of the energy

proposed new thermal plants. Each such requirement will bear on the characteristics which affect the over-all economy.

If operating with other plants on the same river, the operating load factor may be fixed in advance if these other plants either deliver or require water in accordance with some fixed schedule. Future operation at maximum efficiency may be detrimentally affected by such limitations, unless correctly evaluated and allowed for in the design. If sufficient pondage can be developed between plants, these limitations may be wholly or partially removed.

From the standpoint of energy generation, the higher the average loading of the transmission system the lower will be the cost per unit transmitted. Where energy cost only governs, distant plants normally may be expected to be high load factor plants, their output being combined with other lower load factor plants close to the load centers. Figure 5 illustrates the approximate variation of energy cost with load factor, for a plant involving 240-mile transmission.

Fitting a new hydroelectric plant into the progressive requirements of estimated future system load curves is a study involving detailed consideration of all factors previously discussed and could be made the subject of a separate paper. Some sites lend themselves economically only to limited high load-factor development and would be fitted into the system when the need for such supply was indicated. Others may be susceptible to a wide range of development and economic factors would need to be nicely balanced before the optimum intermediate and ultimate design arrangements could be selected. Again others may indicate an economic peak possibility, even in competition with thermal generation.

Figure 6 illustrates one approximate study made to determine the economy of combining hydraulic resources with thermal generation at the load. It was assumed that the hydraulic plant could operate to medium load factors, the thermal plant operating only to provide the minimum peak energy demand. The surplus hydraulic energy was assumed sold in secondary markets at approximately the cost of fuel replacement. It will be noted that energy economy is indicated so long as the thermal plant operating load factor is held below approximately 35 per cent (fuel cost $7.00 per ton).

Specific further problems would be introduced if considering the question of system reserve or stand-by capacity.

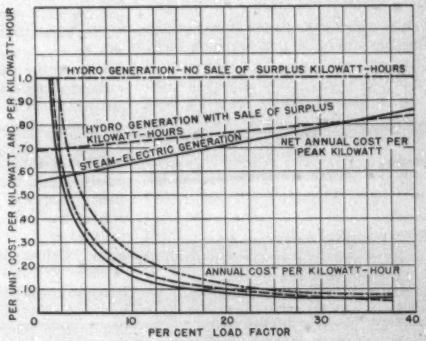

Figure 6. Assumed economic comparison of low load-factor hydraulic and peak load steam plants

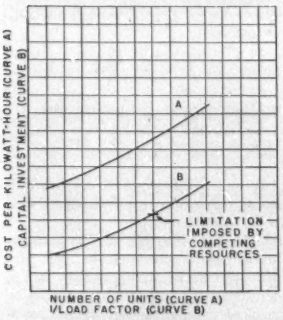

Figure 5. Variation of capital investment and energy cost with plant load factor and number of units installed

Such capacity might be economical in the hydro plant (as discussed later) or might be in thermal plants built or extended for this service.

Factors in Plant and System Operation

The attainment of economic energy generation in the operation and maintenance of the hydroelectric system is largely a matter of recognizing, and being governed by, those factors upon which the original plant and system design was based. Broadly speaking, the problems narrow down to so utilizing the available water (which represents potential energy) that maximum efficiency is realized, measured in terms of the revenue secured from the electric energy delivered to available markets. Five principal points may be discussed.

Operation of the Storage Resources

Water storage represents the stockpile of energy. Unlike the thermal plant coal pile, storage can be filled only at specific intervals. Once used, water reserves cannot be replaced until the next natural period, but if not used, their natural replacement is of necessity wasted.

These facts indicate the desirability of planning the annual use of storage, based on estimates of the precipitation and of load demand. Estimates of precipitation are difficult to make, because of the uncertainty of weather conditions, but such practices as snow surveys, determination of run-off are of material assistance.

When the hydro plant forms part of a dual purpose development, complicating factors arise. Flood control necessitates the maximum drainage of storage areas prior to the flood conditions and may result in inefficient utilization if other conditions fail to meet those estimated and may, from time to time, reduce long-term efficiences because of the inability to carry over reserves for use in years of sub-normal precipitation.

Irrigation requirements must be scheduled, insofar as possible, to fit into the load demand curve. Water bypassed around the plant to serve agriculture represents potential energy lost, which a different load schedule might have saved.

If the hydro resources form part only of the system total, certain of these problems may become less important. However, co-ordinated scheduling may permit reducing the total system capacity, by reducing the thermal plant capacity required as reserve against failure to realize, at key load seasons, the full weight of the hydro capacity.

Figure 7 is included as indicating

typical annual use of one storage basin in the Commission's systems. It will be noted that, being only one of several storage areas, its use in any one year may vary due to load conditions or the operation of other resources. In each year, its operation is scheduled with full consideration of all conditions affecting the ultimate system economy.

Operation of the Individual Plant

Operation of the individual plant for maximum efficiency, in its simplest form is a matter of arranging that those units on load at any time are just sufficient that all operate at or near their maximum individual efficiencies. It is a simple matter, when all units are duplicates, to prepare a plant curve indicating the number of units which should be operating at any load level assigned by the system despatcher. If certain units have different characteristics, the problem is less simple but not difficult.

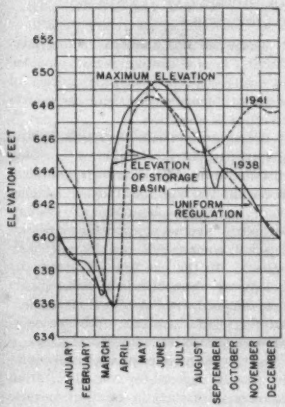

Figure 7. Typical annual utilization of hydraulic storage basin

Approximate limits in a typical case are indicated in the following: one plant in the systems of the Commission includes eight 23,500-kva fixed-blade propellor-type units and normally operates at approximately 50 per cent daily load factor. Energy generation throughout the average winter day equals 1,560,000 kwh. Assuming the same flow conditions, but assuming only six units operating at their point of maximum efficiency for 12 hours per day, the calculated plant output is 1,575,000 kilowatt-hours. Conversely, if four units were operated at an equal part load throughout the 24 hours, the plant generation is calculated as 1,155,000 kilowatt-hours. The minor loss of energy with scheduled operation, as compared to the material loss with prolonged operation at part gate, is evident.

Figure 8. Illustrating a maintenance schedule adjusted to conform with system energy demand

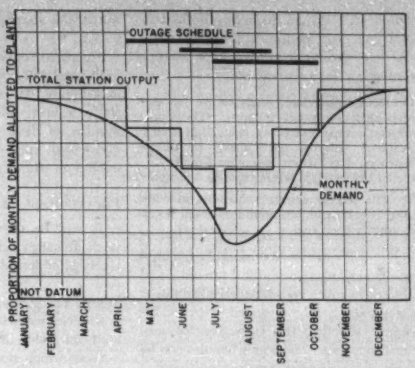

Part load operation is frequently necessary for system kilovar or voltage control, in plants where provision is not made for operation of the turbine free of the tailwater. Tailwater depressing may be a dividend-paying investment and is being included in many modern plant designs.

Operation of a Group of Plants

The hydroelectric system which includes several plants operating in parallel becomes a more complicated problem of the same type as the individual plant. Two cases may be discussed briefly.

If the plants are all on the same river, scheduling of the water resources probably involves only one storage system. The problem then is to pass the water down-river and through the individual plants at optimum efficiency. Various schedules of plant loading may be devised which transfer the daily loading from plant to plant as the water progresses downstream. Pondage between plants assists in this scheduling, otherwise the load factor of the various plants must be carefully adjusted to avoid wastage.

Additional complications are introduced when plants are located on different rivers, each of which has its own storage and flow problems. No set rules can be laid down in such cases except perhaps to state that control should be centralized in the power supervisor's office. Continuous knowledge of the draw-down from the various storages, plant outputs, tie line loadings, system load characteristics, and so forth plus an intimate knowledge of the general system behavior, enables the alert trained supervisory staff, assisted by the planning staff with its technical data, to attain a high standard of proficiency in operating even extremely complicated systems.

Effect of Load and Frequency Control

Automatic control applied to hydroelectric stations is becoming of increasing importance. Load control, in its various forms, may assist materially in maintaining efficient operation of the individual plant. Automatic holding to prearranged load schedules results in higher efficiency than hand operation. Starting and stopping of units can be arranged to suit availability of water in isolated plants. Control of forebay level permits a plant to be operated closer to the loadings dictated by the most efficient operating head (forebay level).

However, automatic frequency control tends to reduce plant efficiency, to the extent that units must be operated at loadings other than "best gate" in order to maintain the frequency regulation margin. Tie-line load control will operate similarly. In both cases, such control is best applied in the plant that operates at the lower load factors, rather than on the base load plant where water not otherwise used might be wasted.

Maintenance Schedules

Like the operation of storage reservoirs, plant maintenance should be scheduled to fit the river flow and load demands. Routine over haul of hydroelectric units need not be an annual affair (perhaps once in three to five years), but in a

complicated system, including both base load and peak plants, a definite outage schedule promotes efficiency of energy generation, for two reasons.

1. Routine overhaul tends to prevent unscheduled emergency outages. The Commission's experience has been that many incipient failures, particularly in thrust bearings, have been discovered and corrected before major unit damage occurred.[2]

2. The outage can be scheduled at such time as results in minimum loss of efficiency in system operation.

Figure 8 illustrates the monthly demand on a typical plant containing ten units and illustrates how a maintenance schedule for three units can be arranged, without adversely affecting the operation of any remaining unit. Similar schedules can be devised to suit most system conditions.

Factors in the Load

Unless a system supplies substantially electrochemical or other loads of very high load factor, consumer demands will vary during the day and also from season to season. These variations, particularly the seasonal variations, will be more pronounced the greater the difference between average summer and winter temperatures.

In the northern United States and Canada, typical daily load curves will approximate those of Figure 9, being typical summer and winter load curves for the principal system of the Commission. In the "between seasons" the curve tends towards the shape of the next following season.

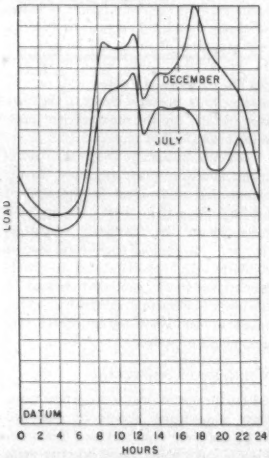

Figure 9. Weekday load curves for typical system

Figure 10, curve A is a plotting of the individual daily peaks in the same system and Figure 10, curve B a summary of these figures, plotted to indicate the number of days per year in which the daily peak exceeded percentages of the maximum winter peak.

Provision of Peak Reserve Capacity

It will be noted that the maximum peak demands occur during only a relatively brief period and therefore represent only a very small proportion of the total annual energy consumption.

Reserve capacity in any system normally provides against two contingencies —those which result in the loss of peak generating capacity (or the ability to supply peak demands) and those which involve loss of energy production. In the hydroelectric system, emergency outage of a generating unit reduces the system peak capacity but not necessarily its energy capacity.

For example, a given hydro plant may include six units, normally arranged to operate at a daily load factor of 60 per cent. Loss of one unit would still permit the generation of full energy, at a load factor of 72 per cent and loss of even two units need not reduce the daily energy output, as the plant might still operate at a load factor of 90 per cent.

To provide against loss of peak capacity, spare generating units may be installed in selected plants. In the event of a unit outage, either under emergencies or for routine overhaul, the spare unit may then operate in the place of that removed from service. Installation of such a unit, for this purpose, normally would be relatively inexpensive (involving only additional building space and the unit itself) and its additional operating expense virtually nil. Nevertheless its installation would permit the following energy economies:

1. All units may continue to operate as previously, at maximum efficiencies (within the requirements of the load) and without disturbance to the planned flow of water in the river.

2. By-passing of water around the plant, with consequent loss of energy production, may be avoided.

In the alternative, advantage may be taken of the load characteristics in the form of contract granted certain types of consumers. Electrochemical and electrometallurgical customers, and others in whose processes cost of electric power is an important component, may be interested in a form of contract which reduces these costs to the mutual benefit of the consumer and the utility. Such a form of contract would permit the utility to interrupt all or part of the power supply, for stated intervals during the load season in which peak reserve is most desirable.

Such an arrangement would reduce the generating plant investment (by saving the spare unit installation), system peak reserve being obtained in the right to interrupt interruptible customers during peak emergency periods. The cost of peak reserve would be that loss of annual revenue involved in the difference between firm and interruptible power rates. This arrangement has the disadvantage that, during unit outages, the plant may have to operate at other than best efficiency in order to maintain full energy output.

Development of "Off-Peak" Consumption

Somewhat of a corollary to the interruptible form of contract is that provided by water-heating and other forms of consumer demand that lend themselves to off-peak operation.

It frequently occurs that hydroelectric plants, particularly those involving long-distance transmission, are operated economically at high load factors—higher than normally obtaining in systems including average proportions of industrial, commercial, and domestic consumers. In the one field of system development, these high load factor plants are combined with lower load factor fuel-burning plants to secure optimum overall energy costs.

In the alternative, promotional activity may be directed towards the creation of off-peak markets in an effort to raise the average consumption per kilowatt of installed capacity more nearly to equal the capability of the generating resources. Domestic and commercial water heating is one fruitful field for this latter development. Many control schemes are available to effect off-peak operation, and the revenue per kilowatt-hour ample to justify the distribution costs involved.

Similar forms of load are found in other consumer brackets—infrared drying, annealing and curing operations—operations which normally can be carried out during the night hours. The transfer of this energy over system interconnections and its sale to adjoining utilities may be another outlet.

The combination of such off-peak or load building markets with the normal markets, increases the gross revenue per kilowatt installed and therefore

represents an increase in over-all system economy.

Sale of Surplus or Secondary Energy

The designed capacity and operating characteristics of the hydroelectric plant necessarily must be based on the long-term conditions of water supply. If the system has entirely hydro supply, conservative designing will be based on flow conditions in effect a large proportion of the total time; if combining hydro with steam, higher, and therefore less dependable, flow conditions may be assumed.

However, in either case, there will be seasons of the year and also full years in the long-term precipitation cycle, when stream flows will exceed those required to meet the plant design factors. Furthermore, with system load characteristics such as illustrated above, there will be times in the years of even normal flow when the full peak and energy capacity of the plant is not required for the firm system demands. The surplus or secondary energy available under such circumstances may be utilized to reduce average firm generating costs in the system.

If the system combines water with steam, or is interconnected with systems having thermal plants, these energy surpluses naturally may be used to reduce fuel consumption, providing only that system facilities are available by which they can be delivered to utilization centers.

In the all-hydro system, or that providing only limited replacement of fuel, an outlet for such capacity is frequently found in special forms of surplus at-will or secondary power contracts.

In Canada, the electric steam generator or electric boiler has provided a convenient and economic outlet for these energy surpluses, which otherwise would be unusable, in paper mills and other plants having much larger steam demands than that proportionate to their electric power demands. The installed cost of electric boilers is low (approximately $1,000 to $1,300 per thousand pounds per hour of steam generated, including 110-kv transformation) and can be installed economically as an adjunct of the fuel-fired boiler plant even when the seasonal supply is a fraction only of the total year.

The revenue secured per kilowatt-hour normally is based on the replacement value of the coal or other fuel. Where coal costs approximate $6.00 per ton, and assuming a fuel-fired efficiency of 85 per cent and an electric boiler efficiency of 94 per cent, the replacement value will approximate 0.085 cent per kilowatt-hour. The actual sales price per kilowatt-hour would depend on the subdivision of this replacement value between the utility and the customer.

Nevertheless this revenue, while seemingly low, is found-money and represents a credit that tends to reduce the net generating cost of the firm power demand.

Figure 10. Annual variation in daily peak loads

A—In sequence
B—As percentages of the yearly maximum peak

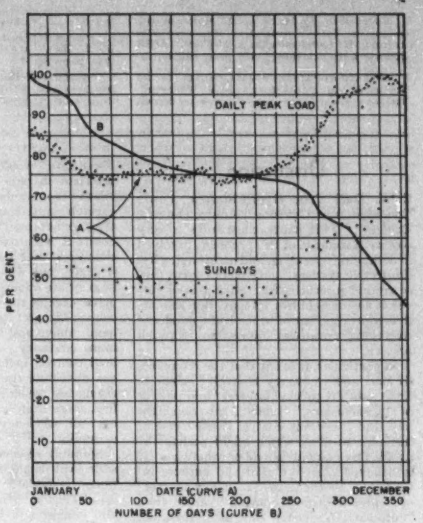

Conclusions

1. The economics of energy generation in the typical hydroelectric plant will be affected by the following design factors:

(*a*). In the predominantly hydroelectric system, by the extent to which the full stream flow can be controlled by storage works and thus adjusted to meet the demands of the load. The extent of this control will depend on the availability of storage sites and on other owners on the same stream in which further riparian rights are vested.

(*b*). In the predominantly thermal-electric system, controlled stream flow may be less important and hydro plant operation may more nearly approach run-of-river characteristics. The capacity installed (and hence the energy generation) in this case will be controlled by increment costs at the load, relative to competing thermal costs.

(*c*). In the individual plant, by the efficiency attained in the water passages and turbine unit and, in a combination of plants on the same river, by the extent to which the individual plant characteristics are adjusted so that all plants may operate as a single unit.

2. The economics of energy generation also will be affected by the following operating factors:

(*a*). By the planning of load schedules for individual plants such that units may operate at the highest practical over-all efficiency and similarly, in a group of plants, so that each plant may be accorded load schedules adjusted to most effectively meet unit efficiencies and available water storage resources.

(*b*). By the scheduling of unit outages for maintenance so as to permit adjustment of plant outputs to the reduced capacity available.

(*c*). Automatic frequency control may tend to reduce the efficiency of energy generation.

3. Economic energy utilization may be affected favorably by forms of power contract which recognize inherent characteristics in hydroelectric development.

(*a*). The interruptible form of contract provides a means of establishing reserve capacity against emergencies which reduce peak generation but not energy generation, alternative to the installation of spare peak generating capacity.

(*b*). Water heating, and other forms of load lending themselves to off-peak operation, have a particular advantage in hydro systems where the load factor of generating resources exceeds that of the normal consumer demands.

(*c*). Surplus or secondary energy available seasonally, or during periods of above-normal stream flow, can be sold providing satisfactory markets are available, thus reducing firm power costs. Such markets are usually where fuel consumption can be replaced, either within the system, in interconnected systems, or in customers' plants where electric boilers form an economic component in operation.

References

1. Technique of Electrical and Hydraulic Testing of Hydroelectric Units, G. D. Floyd, J. J. Traill. AIEE Transactions, volume 65, 1946, pages 163–9; discussion, page 493.

2. The Maintenance of Hydroelectric Generating Units, A. S. Robertson, R. O. Standing. AIEE Transactions, volume 66, 1947, pages 776–82.

3. Conditions Controlling the Economic Selection of Prime Movers, B. G. A. Skrotzki. AIEE Transactions, volume 63, 1944, pages 1099–1108.

4. Electrical Design of the Tennessee Valley Authority Hydroelectric Stations, R. A. Hopkins. AIEE Transactions, volume 64, 1945, pages 778–86.

5. Electrical and Mechanical Design of the Tennessee Valley Authority Hydroelectric Stations, H. J. Petersen, R. A. Hopkins. AIEE Transactions, volume 65, 1946, pages 920–31.

6. Operation of Multipurpose Projects of the Tennessee Valley Authority, S. M. Woodward. *Mid-West Power Conference Proceedings*, Illinois Institute of Technology, (Chicago, Ill.), 1941.

7. Power System Interconnection in Quebec, W. R. Way. AIEE Transactions, volume 61, 1942, pages 841–7.

8. System Voltage Programs Release Capacity Margins, A. E. Silver. *Electrical World* (New York, N. Y.) October 2, 1943, pages 62–4.

9. Use of Automatic Control to Increase Plant Capacity, H. H. Gorrie. *Mid-West Power Conference Proceedings*, Illinois Institute of Technology (Chicago, Ill.), 1943, pages 90–6.

10. Control of Load, Frequency, and Time of Interconnected Systems, C. K. Duff. AIEE Transactions, volume 64, 1945, pages 778–86.

Discussion

C. K. Duff (The Hydro-Electric Power Commission of Ontario, Toronto, Ontario, Canada): This paper constitutes a very concise statement of the problems involved in designing, operating, and maintaining hydroelectric systems, and covers a great deal of ground in small space. Such a brief survey of a wide field has its uses, but also its disadvantages, one of which is the danger of conveying erroneous impressions through brevity.

In particular, it is felt that the references to load and frequency control, "Effect of Load and Frequency Control" and part 2c of "Conclusions," imply that *automatic* load and frequency control is the cause of inefficient loading which might perhaps be avoided by manual control or otherwise. It is believed therefore that the authors intended to use the term "frequency control" or "close frequency control," rather than "automatic frequency control." Even so, the onus seems to be placed upon a secondary agency rather than upon the principal cause of inefficient loading, namely fluctuations in customer demand, which necessitate changes in load of generators on the system.

The term "load control," as used in the first part of "Effect of Load and Frequency Control" is very broad but does not include tie-line load control referred to in the second paragraph of that section. With the modern trend toward more extensive interconnection of power systems, tie-line load control becomes the major problem, with frequency control a minor responsibility since it is usually shared by all the interconnected systems. Load control of a tie line is directed towards maintaining scheduled loads up to the maximum capacity of the tie. This requires supplementary control of generator output, just as for frequency control. Only automatic control can accomplish this effectively on ties between large systems because of the rapidity and frequency of load swings which cannot be followed manually. The type of regulator commonly used has elements responsive to both frequency and tie-line load, so the control is briefly called frequency-load control, or simply load control, when the context makes the meaning clear.

As the authors indicate, tie-line load control has the same effect on the generators of a local system as frequency control would have on the same system when isolated from its neighbors. In either case the regulating plant or plants must take care of the load swings caused by variations in customer demand in the local system.

The authors give as the reason for operating generators at other than "best gate" the necessity of maintaining a frequency-regulating margin. It should be pointed out that the most efficient gate is generally somewhat below full load of the unit, so that a sufficient number of generators, all operating at "best gate" would, in the aggregate, have sufficient margin of capacity or "spinning reserve" for regulation. It is only when the variable system demand is imposed upon these generators that they depart from the point of maximum efficiency. For small changes of unit loading the loss of efficiency is slight, but when the system swings are large or are imposed upon a relatively small percentage of the connected generating capacity, the unit loads fluctuate over a wide band, above and below the point of maximum efficiency. Automatic frequency or load control, including unit load dividers, can distribute the load changes among the regulating generators, whether many or few, more uniformly, thus securing better over-all efficiency than can be attained manually.

Spinning reserve sufficient to cover possible load demands always must be maintained, especially on isolated systems responsible for their own frequency control and aiming at a high standard of service. When the margin of spinning reserve is limited due to heavy demand, or when available water must be either used or spilled, automatic frequency control equipment will maintain acceptable frequency up to higher values of unit loading than can be accomplished manually, because of the prompt, proportional and continuous action of automatic control. This reduces wastage of water and minimizes the ratio of installed capacity to permissible peak load.

Because fluctuating loads must be accepted, while at the same time satisfactory frequency service must be maintained, it is a question of how to regulate with maximum efficiency under the conditions imposed. A regulating plant having low or medium load factor and broad efficiency curves (as the authors state), also having ample generating capacity and adequate forebay storage, will give most favorable results. As between manual and automatic control, for a given grade of service, the use of automatic control, properly applied, always contributes to the more efficient utilization of water and of prime mover capacity.

Basically, the cause of inefficient loading is variable demand, not the means which are employed to offset or minimize the undesirable effects of variable demand.

F. L. Lawton (Aluminum Company of Canada, Ltd., Montreal, Quebec, Canada): The authors have given a thoroughly integrated analysis of those factors which must be kept always to the fore in the planning, design, and operation of power systems wherein hydroelectric plants constitute the major energy sources. Not only is the paper thoroughly readable but it points the way to more of those papers which can best serve a great portion of AIEE membership.

In discussing operation of storage resources, the authors drew attention to the necessity of planning the annual use of storage. As a general working basis, it can be said that stored water should not be held over to the next water year unless that year is foreseen to be a year of low run-off. Application of this basic principle entails being able to predict well in advance of the event

1. The end of the drawdown period, or the date on which new water is obtained in adequate volume to carry system requirements and refill storages—that is, the freshet period.

2. The volume of run-off during the high-flow period.

3. Load demands.

4. Occurrence of years of subnormal run-off.

There is still very little sound data the hydroelectric system-operating engineer can use as a basis for forecasting the beginning date of the freshet period. Snow surveys are helpful in forecasting the volume of run-off during the high-flow period, but there are many other complicating factors, such as precipitation immediately preceding the freshet period and general meteorological conditions during this period. Correlation of run-off with the sunspot cycle on a long term basis is helpful but our present knowledge of the relationship is scanty.

This discussion, it is hoped, will serve as a plea and encouragement for presentation before the Institute of more papers dealing with these important factors, so necessary for optimum usage of our energy resources.

The authors have drawn attention to the necessity of plant efficiency tests after a hydroelectric power development is constructed. It is submitted that, in plants where water wheel pitting is an important factor, with subsequent repairs by welding, efficiency tests should be made after a period of years, depending on the severity of pitting. Index tests, as developed by Forrest Nagler, are useful and simple to carry out.

W. L. Maney (General Electric Company, Schenectady, N. Y.): Frampton and Floyd have stated as a conclusion in this paper, "Automatic frequency control may tend to reduce the efficiency of energy generation."

While this may be true of a casual application, frequency control in one form or another has come to be a requirement of system operation and it seems pertinent to examine the possibilities of improved operation resulting from a comprehensive application.

Either of two procedures may be followed in controlling system speed, the first being the use of a single machine or station for regulating, while the second is the use of a multiplicity of units, or in the limit, all units for regulating.

The first procedure appears advantageous when controlling speed manually as it places the responsibility for the proper maintenance of speed upon a single operator, and in doing so, probably tends to minimize tie-line load changes between stations.

Moreover, this procedure admits of the use of a supplementary flat frequency control device, as for example, a frequency meter with contacts to adjust speed on the controlled unit in accordance with system demands. Also, this procedure admits of base load operation of the more efficient units of the system as these units can be set to operate at fixed load. It is, however, open to question if this procedure is advantageous as it is detrimental to system efficiency since obviously the controlling unit or station must operate over a relatively wide range in load, depending upon system load changes, and therefore much of the time will be operating at points other than its maximum efficiency point.

The execution of the second procedure, namely, multiple station control, is evidently somewhat more difficult, but if the execution can be carried out, it will result in maximum over-all system efficiency. Thus, by distributing the load changes among all the machines in the system in proportion to their ratings, which is substantially what will occur if all machines are controlling speed, the load change on any one unit will be small and consequently all units will be able to operate at or near their points of maximum efficiency. Admittedly occasions will exist when machines should be operated nonregulating as for instance full gate during flood stage. Also it is recognized that operation within the desired load range will require starting and stopping units as system load changes over the 24-hour period. However, this procedure should not interfere with such objectives as control of forebay level mentioned by the authors since, in this case, the requirement is to maintain an average flow over a period of time, which simply means that the average loading of the machines at a forebay level control station shall be such as to permit the stipulated flow of water, and this will not interfere with their ability to contribute to frequency regulation. Figure 4 of the authors' paper shows that the efficiency of a unit is high over a fairly wide range of load.

It is possible that the reason the second procedure has infrequently been used is the lack of realization that control equipment is available which will permit such operation. Such equipment has been referred to by Crary and McClure.[1] This equipment is completely automatic in its operation and by measuring time error assigns to any controlled unit its proportional share of any load change in the system. The most recent discussion of multiple station control is contained in a paper by Robert Brandt.[2] This paper describes the principle of supplementary basic frequency control with tie-line bias, thereby permitting distributed automatic control and simultaneously satisfying tie-line requirements.

It is believed that the concept of allocating the control of frequency to a multiplicity of stations merits further consideration.

REFERENCES

1. SUPPLEMENTARY CONTROL OF PRIME-MOVER SPEED GOVERNORS, S. B. Crary, J. B. McClure. AIEE TRANSACTIONS, volume 61, 1942, April section, pages 9–13.

2. THEORETICAL APPROACH TO SPEED AND TIE LINE CONTROL, Robert Brandt. AIEE TRANSACTIONS, volume 66, 1947, pages 24–30.

J. T. Madill (Aluminum Company of Canada, Ltd., Shipshaw, Quebec, Canada): Under factors concerned with the design of hydroelectric systems, it would seem that water diversion from one river or drainage system to another should be included. The Hydro-Electric Power Commission of Ontario has built and operates at least two of these diversions and these have been described in the technical literature. For a given expenditure, a diversion may show a considerably higher return both directly to the power system and indirectly through other economic benefits than other possible alternatives such as increased storage.

Referring to operation, one factor which would be of great importance to a predominately hydroelectric system is the development of long range weather forecasting. A plea in this connection was made at the 1947 AIEE winter meeting and this is reiterated here. Such forecasting would be of inestimable aid in the operation of hydroelectric systems.

It is interesting to note that the authors have stressed the importance of secondary and dump energy. On an all-hydro system or an all-hydro interconnection this secondary energy is of great economic importance in the operation of the system.

The authors are to be congratulated on the scope and coverage of this paper.

A. H. Frampton and **G. D. Floyd:** The authors realized when preparing this paper, that it would be possible only to make very brief reference to any of the factors involved and stated at the beginning, that the paper was only a review. We are grateful, therefore, for the very clear exposition of the important factor of frequency and load control given by Duff and Maney. This factor until recently, has not received the attention it merits. Duff has stated that our reference to automatic frequency and load control implied that these were the cause of inefficient loading. The paper states that automatic holding to prearranged schedules results in higher efficiency than hand operation, and that automatic frequency control tends to reduce plant efficiency only to the extent that this control causes the units to be operated at other than best gate. We agree with Duff that if proper application of frequency control is made, and if the same grade of service is to prevail for both, then there can be no difference between automatic and manual control. It is the casual application referred to by Maney, which should be examined carefully for possible loss of energy supply, either potential or actual. Among a number of points mentioned by Lawton, that of efficiency tests after turbine runner maintenance was one not discussed directly in our paper. A periodic check of over-all efficiency, especially in the larger hydroelectric plants, would seem to be well worth the trouble and expense. Too often, even if efficiency tests are made initially, no further attention is given to this, with the result that a lowering of efficiency and loss of revenue occurs that might have been corrected in its early stages. Madill noted the omission as a factor, of water diversion from one drainage area into another. This may be, of course, a very tangible method of economically increasing the energy made available on the watershed having power developments, either actual or proposed. Both short and long range weather forecasting have improved, and there is closer co-operation between our meteorological services and operating organizations, so that the former better appreciate what information is valuable to the operating man, and the latter is better able to use the information made available. It is expected, therefore, that the use of meteorological data will become more widespread as an aid in system operation.

The Application of Heterodyne Modulation to Wide-Band Frequency-Modulated Television Relays

WILSON P. BOOTHROYD
NONMEMBER AIEE

IN late 1944 it became evident that there was an immediate need for superior methods for the radio relaying of television or other wide band signals over considerable distances. In order that equipment could be designed and placed in operation as early as possible, an investigation of possible methods of distortionless remodulation and reamplification was started and is still continuing. The theoretical study has not been limited by any practical considerations, such as the nonavailability of components; but it was a premise to the accompanying development work that the equipment would be built around components then available and known to be reliable. The success of the development work, which has resulted in the construction of usable equipment, seems to point out that even our presently available tools have not been exploited fully, either for present day applications or for their value in checking the conclusions of theoretical studies.

To meet the requirements that the relay system be capable of handling, with excellent fidelity, the signal frequency range from 30 cycles to five megacycles and that the signal to noise ratio after multiple relaying be superior to commercial television broadcast standards, a relatively high-powered wide-band frequency-modulated system of radio relaying using a heterodyne method of remodulation was developed.

Figure 1 is a simplified typical block diagram of a possible system assembly. In terms of television relaying the transmitting terminal might be either a remote pickup equipment, a studio transmitter equipment, or the sending end terminal of a relay chain. The repeater is primarily for the retransmission of signals from the sending end terminal, although it may readily be used for the demodulation of incoming signals as well as for the introduction of new outgoing signals. The receiving terminal is, of course, a received signal demodulator.

The scope of this paper will not permit a full discussion of all the components of the complete system, or of the numerous advantages of wide band frequency modulation for transmission of composite video signals.[1] However, the following paragraphs will indicate the method of operation.

The transmitting terminal receives signal information in the form of a composite television or other video signal which, after a single stage of amplification, is translated in the deviator unit into a frequency modulated carrier in the 115-megacycle region. Figure 2 is a specific plot of the d-c carrier swing for the maximum peak to peak video input voltage. The figure also shows the band width allowed for first order side bands occurring at the limits of the picture signal voltage. The frequencies noted are typical and show a d-c mean carrier swing of 12 megacycles with the negative peak of the video signal (that is, the synchronizing pulse of a television signal) established by levelers and automatic frequency control at 107 megacycles. The frequency modulated carrier thus generated is amplified by a wide band power amplifier having an amplitude response which has a relative response greater than eight-tenths of maximum from 105 to 125 megacycles and a phase response with a maximum

Figure 1. Relay system block diagram

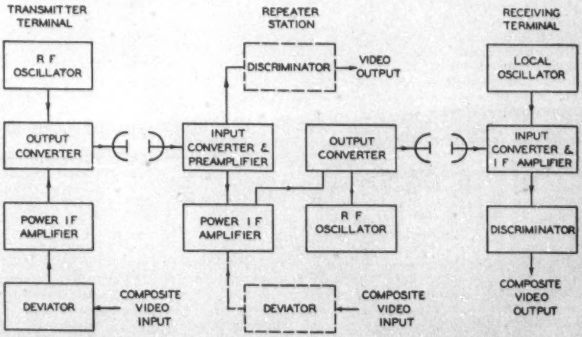

Paper 47-171, recommended by the AIEE committee on communication for presentation at the AIEE summer general meeting, Montreal, Quebec, Canada, June 9–13, 1947. Manuscript submitted March 26, 1947; made available for printing May 2, 1947.

WILSON P. BOOTHROYD is a project engineer in the research division of the Philco Corporation, Philadelphia, Pa.

The author acknowledges the most valuable contributions made to the work here described by William E. Bradley and other associates in the Philco research division.

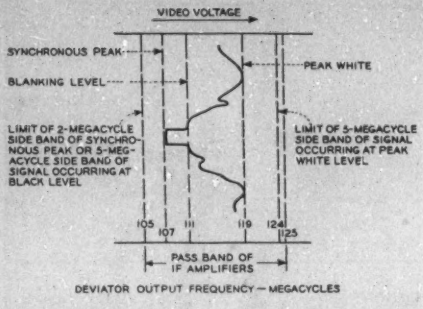

Figure 2. Deviator characteristics

departure from linearity of less than five degrees.

This frequency-modulated intermediate-frequency amplifier output signal and a signal of equal amplitude from a radio frequency power oscillator are applied to an output converter from which the sum frequency signal is applied to a transmitting antenna. This output converter is the principal component of the system and we will consider it in detail later. Throughout the transmitting terminal equipment, and its counterpart in a relay station, care must be taken to cause all undesired signal outputs from all converters to fall outside the normal signal frequency band so as to be adequately attenuated to prevent beat interference.

The receiving terminal is an essentially standard superheterodyne receiver, having an intermediate-frequency amplifier which has a 20-megacycle pass band in the 75-megacycle region and a wide band high level discriminator capable of delivering the full amplitude of video signal to a video output stage suitable for driving the 75-ohm output cable and termination.

An automatic frequency control system is used to control the local oscillator frequency so as to establish the signal corresponding to the peak of the synchronizing pulse at a constant intermediate frequency when television signals are being relayed.

In the presence of strong adjacent channel or intermediate-frequency signals at the receiver antenna, some form of radio frequency preselection may be required. Tuned stub lines have been used for this, or radio-frequency selector cavities may be inserted in the antenna lead.

The repeater station is a combination of receiver and transmitter in which the receiver 75-megacycle intermediate-frequency signal is converted to a 115-megacycle signal for additional amplification and for the remodulation of another radio-frequency carrier. A deviator unit may be switched into the circuit, if the repeater is to be used also for the initiation of programs. A multichain radio relay system would include as many repeaters as the geographical location of the terminals might require.

Many factors influenced the choice of the relay system described. First, relaying is accomplished by a heterodyne system of amplification in which complete demodulation to the original video signal or other amplitude-modulated signals is entirely avoided. By providing intermediate-frequency amplifiers and radio frequency components of adequate performance, the reamplification of a signal is accomplished easily and all critical adjustments heretofore required are eliminated. Operation of radio relays without an operator thus has come nearer reality. Second, the use of a frequency modulated carrier considerably relieves the amplitude linearity requirements of all amplifiers, since amplitude limiters may be used at each relay station; and only the phase-frequency response (which is not a function of tube characteristics) need be designed for extreme linearity. An excellent phase response is not particularly difficult to obtain in multistage amplifiers, even in excess of the bandwidths noted, when modern calculating techniques are employed. Thus multiple relaying without signal degradation due to poor amplifier fidelity can be accomplished. Third, the use of wide band frequency modulation with a peak to peak carrier swing of 12 megacycles results in noise reduction in excess of six decibels after demodulation compared to an amplitude modulated system. This factor places the system within the power and sensitivity limits of available components for the 1,350-megacycle frequency band. Table I shows, in summary, the measured values for one installation. The values given are conservative and can be obtained reliably by good engineering practice. Signal to noise ratios of 50 decibels are obtainable even with portable equipment and additional 10 decibels or more may be obtained by properly installed fixed equipment.

The relay equipment required the solution of many design problems, including the construction of a deviator unit of excellent linearity, the design of wide-band intermediate-frequency amplifiers and discriminators, and the design of a high level microwave converter stage suitable for use as the final stage of the transmitter. The solution of the latter problem is most interesting and may well find numerous associated applications.

From the foregoing description of the system, it is clear that the microwave converter stage should be designed to receive two input signals having a large frequency difference and to have an output signal which is the sum or difference frequency signal of the two input signals. Power output should be as great as possible in the desired frequency band, yet all other products of the input signals must be suppressed adequately.

Theoretical considerations indicate several converter arrangements which may be considered. Figure 3 shows a fixed

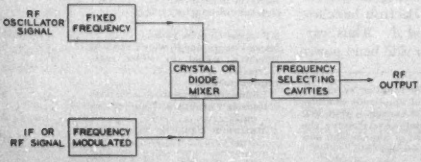

Figure 3 (left). Mixer type heterodyne modulator

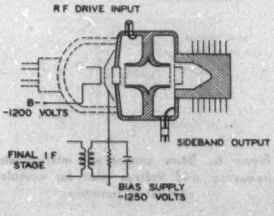

Figure 4 (right). Class C heterodyne modulator

frequency radio-frequency oscillator whose output is mixed with a frequency modulated intermediate-frequency signal in a crystal or diode mixer with undesired output suppressed by frequency selective cavities in the output lead. Such a system, considered at this time, has the advantage that almost any desired output frequency could be generated. For example, a 1,300-megacycle signal could be obtained from the beat of 3,000 and 4,300-megacycle oscillators. The obvious disadvantages, along with others, are the high cost of generating radio frequency power at these frequencies and the lack of commercially available and tested mixer crystals or tubes capable of handling the desired power levels. Figure 4 shows a more promising possibility. In this case, a microwave amplifier designed for high power output, for example a multicavity klystron, is caused to operate as a class C amplifier with the electron beam being gated by a frequency-modulated intermediate-frequency signal. The final cavity may be tuned to the upper or lower side band of these signals. In this case the klystron is serving as a nonlinear amplifier-mixer. This arrangement, capable of many specific forms, can be designed for any frequency for which tubes are available and has the great advantage that little intermediate-frequency signal drive power is required, since it controls only an electron beam from which

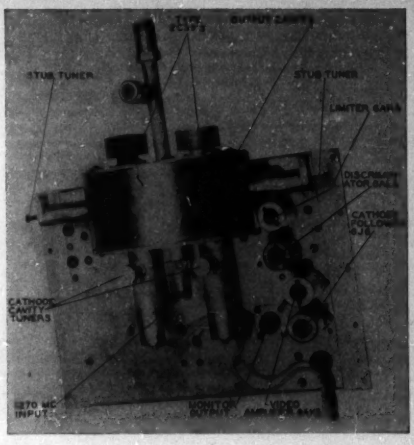

Figure 7. A 1,350-megacycle heterodyne modulator assembly

the output power is derived. To increase the efficiency of direct modulation methods of this type, and to prevent the generation of undesired side bands, the arrangement of Figure 5 is interesting. Here a multiple cavity klystron is driven by radio-frequency drive applied to the buncher cavity, and intermediate-frequency drive applied between cathode and buncher cavity. The intermediate-frequency drive (added to the cathode potential) serves to vary the electron velocity at the bunched cavity grids and through the cavity drift space. The intermediate-frequency modulation therefore serves to modulate the spacing of the bunches and the degree of bunching and phase modulates the radio-frequency carrier. Phase modulation of 1.86 radians will produce maximum energy in the first side, and this energy can be converted to useful output by tuning the output cavity to this side band frequency. Figure 6 is a representative plot of electron beam current density versus time at the output cavity grids through the interval of one intermediate-frequency cycle. An investigation of the mathematical expression describing the energy transfer from the electron beam to the catcher cavity ($W = \int ei\,dt$), shows that the upper side band power is present during the periods of close spacing of the electron bunches, approximately the period A. Thus, carrier frequency and lower side band power may be eliminated by cutting off the electron beam, except for that portion of the intermediate-frequency drive cycle which produces desired side band energy. This can be achieved by applying intermediate-frequency drive to the control grid through a phase shifting network to produce the grid–cathode voltage as sketched in Figure 7, which permits beam current only during the peak of the intermediate-frequency cycle.* A converter of this type has the material advantages of more nearly complete carrier suppression with single side band output, lower tube duty cycle with consequent higher efficiency and increased peak beam current possibilities. To date, the lack of suitable microwave tubes of proved reliability

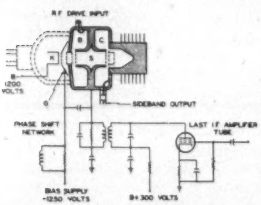

Figure 5. Complex heterodyne modulator

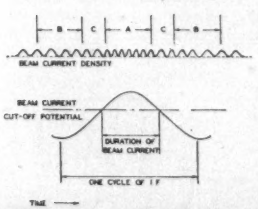

Figure 6. Beam current and intermediate-frequency grid voltage plot for complex modulator assembly

* This concept may be more familiar to circuit engineers as the application of amplitude modulation to a frequency-modulated carrier so that side bands due to amplitude modulation reinforce the frequency-modulated side band of similar sign and reduce the side band if opposite sign.

Table I. System Performance

	Db	Db
Transmitter power (20 watts)	+ 13	
Space loss (31 miles, 8-foot reflectors with 65 per cent efficiency, 1,355 megacycles)	− 70	
Transmission line loss (150 feet of flexible coaxial line 7/8 inch outside diameter)	− 8	
Received signal level		−65
Crystal conversion loss		−10
(This figure is six db below minimum due to the band width and impedances of crystal circuits)		
Receiver noise level	−125	
Crystal noise factor	+ 6	
	−119	−75
RF signal to noise ratio		+44
Improvement due to wide band FM		+ 6
Effective signal to noise ratio (rms)		+50
Improvements:		
Elimination of coaxial cable lines		+ 8
Redesign of crystal coupling circuits		+ 3
Maximum signal to noise ratio (rms)		+61

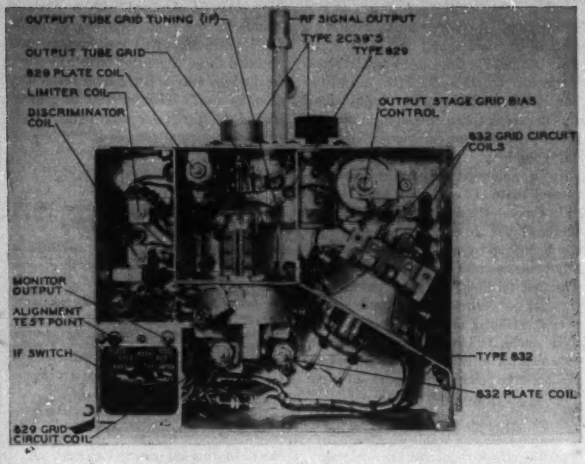

Figure 8. Intermediate-frequency driver stages for 1,350-megacycle modulator

tunable to authorized frequency bands has prevented the construction of a relay using this attractive modulation method. However, tubes designed for class *C* amplitude modulation or for phase modulation as described may be made available soon.

As an immediately available solution for verifying theoretical conclusions and providing improved program service, a converter using triode tubes appeared best and the following design was developed. To serve as the output stage of the transmitter, the converter was designed for high level operation to provide maximum output of the sum frequency, that is, the upper side band, of the two input voltages. For a definite total magnitude of input drive, maximum power in the side band is obtained in this type of modulator with approximately equal drive from each of the input signals. The general theory of this type of frequency conversion and its many variations is well known.[2–4] However, it is not so well known that when the converter is operated at high level class *C*, its efficiency may be made equal to that of a conventional class *C* amplifier. In the particular unit to be described a pair of type *2C39* tubes were used in the converter. In one case, the carrier frequency was approximately 1,235 megacycles and the modulating signal was frequency modulated in the band 107 to 124 megacycles. Figure 7 shows the converter assembly mounted on a chassis with a part of the intermediate-frequency amplifier; and Figure 8 shows the underside of the same chassis showing the final intermediate-frequency amplifier stage; and Figure 9 is a diagrammatic cut-away section of the converter assembly.

The assembly may be considered to comprise a cathode cavity and a plate cavity separated by the grid plane, Figure 10. The cathode cavity is reactively loaded by the approximately quarter wave transmission lines, by means of which the filament connections are made, so as to be resonant to the frequency of the radio-frequency drive Thus, with cathode cavity signal applied by magnetic coupling, the grids are driven push-pull at the radio-frequency frequency. Modulating signal drive is applied to the grids in parallel by a connector extending into the cavity along an equipotential line of the cavity electric field. The plate cavity is excited in the same mode as the cathode cavity and output signal is derived by magnetic coupling. Of course, precautions must be taken to insure equal drive to both tubes and equal output loading. The grid plane has a direct current return to ground by way of the intermediate frequency drive circuit and grid resistor, and a radio frequency return by way of the pair of quarter wave grid support transmission lines which are tuned to the center of the output frequency band. In this construction, the band width of the output cavity when lightly coupled to a load is about 15 megacycles and tests show that this is somewhat the result of the plate cavity being loaded by feedback to the cathode cavity due to imperfect radio-frequency grounding of the grid plane. A different design with special attention to this feature will, no doubt, permit a reduction of this band width with consequently greater power output, should a narrow band width be desired for other applications. For the relay here described a band width of more than 20 megacycles is desired and accordingly the output transmission line is coupled closely to the output cavity to produce additional loading. Spurious frequency outputs from the transmitter are about 40 decibels below signal level at the transmitter output terminal and are depressed further by a frequency selective antenna or by separate radio-frequency filter cavities in the antenna lead as required.

Specifically a pair of *2C39* triodes oper-

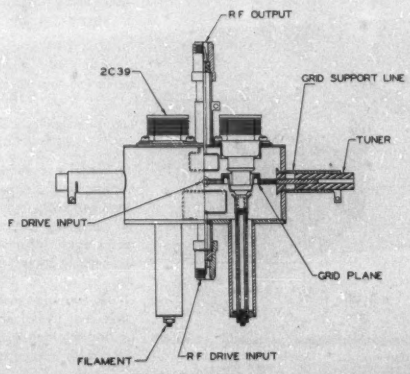

Figure 9. Diagrammatic drawing of 1,350-megacycle modulator assembly

ate well with 700 volts plate voltage and total grid drive to produce 40 volts of self-bias at 40 milliamperes of total grid current. The plate current is about 60 milliamperes per tube. Such operation will give greater than 25 watts of output signal into a 50 ohm load at 20-megacycle output band width. This corresponds to a plate circuit efficiency of 30 per cent. These operating conditions are well within the plate dissipation ratings of the tubes, but increasing the plate input without additional grid drive does not increase materially the power output. In turn, the grid drive is limited by the safe peak grid current. Temporary tube failure results from excessive grid current due to the expansion of the grid structure. Tubes of various manufacture vary greatly in their safe grid current rating. Tests to date seem to show that normal tube life can be expected when operated in the described manner. One design precaution may be interesting. A class *C* amplifier output is rich in harmonics, and a spurious signal may be found in the output due to higher harmonics (such as the 11th or 12th) of the intermediate-frequency input signal unless care is taken to maintain an optimum plate current conduction angle[5] so as to obtain a maximum of power output with a minimum of intermediate-frequency harmonic output.

In general, the component stability and design balance of equipment usually can be judged by the number of operating adjustments which normally are required. The first terminal equipment of this design has been operating now for field tests over a period of months without adjustment since its initial installation. The only control intended for the operator's use are the power switch and an input level (gain) control so that normal deviation may be obtained with a plus or minus 25 per cent video signal input level tolerance. This performance has satisfied those connected with this work of the feasibility of heterodyne remodulation for radio relay systems in general and of this particular wide band television relay.

References

1. UHF Television Relay System, **W. P. Boothroyd.** *Electronics* (New York, N. Y.), March 1947, pages 86–97.

2. Linear Detection of Heterodyne Signals, **F. E. Terman.** *Electronics* (New York, N. Y.), November 1930, pages 386–7.

3. Modulation and Heterodyne, **W. Jackson,** *Wireless Engineer* (London, England), volume 8, 1931, pages 425–6.

4. Frequency Analysis of the Heterodyne Envelope, **F. M. Colebrook,** *Wireless Engineer* (London, England), volume 9, 1932, pages 195–201.

5. Harmonic Analysis of Overbiased Amplifiers, **U. R. Furst,** *Electronics* (New York, N. Y.), March 1944, pages 143–4.

No Discussion

Applications of the Electrodynamic Instrument Mechanism

A. J. CORSON
MEMBER AIEE

N. P. MILLAR
ASSOCIATE AIEE

AN ELECTRODYNAMIC INSTRUMENT is, by definition,[1] an instrument which depends for its operation on the reaction between the current in one or more moving coils and the current in one or more fixed coils. In its elementary form as shown in Figure 1, the resultant torque is expressed by the relationship[2]

$$\tau = i_a i_f dm/d\alpha \tag{1}$$

where

τ = instantaneous torque in dyne-centimeters
i_a = instantaneous current in the moving coil in amperes
i_f = instantaneous current in fixed coil in amperes
$dm/d\alpha$ = change of mutual inductance of coil system with respect to change in angular deflection

As applied to the measurement of active or reactive power, the load current or a definite fraction of it is passed through the fixed coils, a second current derived from the in-phase or quadrature potential is passed through the moving coils, the electrodynamic torque is balanced by a spiral control spring and equation 1 becomes

$$\alpha = \boldsymbol{KI} \cdot \boldsymbol{V} dm/d\alpha \tag{2}$$

where $\boldsymbol{V}$ and $\boldsymbol{I}$ represent sinusoidal potential and current, the frequency of which is high with respect to the damped period of the moving system and α is the resultant angle of deflection of this system. The angular rate of change of the mutual inductance is determined by the geometry of the system. The coil proportions are not infrequently selected to obtain a constant value of $dm/d\alpha$, which by reference to equation 2, is shown to produce a uniformly distributed scale. This instrument, therefore, may be calibrated in terms of active or reactive power, when the appropriate potential circuit impedor is applied for each of these measurements. This briefly summarizes the application of the electrodynamic system to its principal measurement function.

Generalized Measurement Circuit

The application of this mechanism, omitting control spring torque, to such measurements as frequency, temperature, and pressure is based on the current–torque relationship expressed in equation 1 but on a different method of relating these currents to the quantity under measurement. The basic circuit, Figure 2, consists of

1. An impedor or bridge Z_b, which contains the primary detector[3] of the quantity under measurement.

2. The electrodynamic mechanism, or end device, as previously described.

The effective value of Z_b, as it influences the instrument indication is a unique function of the quantity under measurement. The instrument is energized by an a-c source of sinusoidal wave form. The moving system is free of mechanical torques such as those due to control springs or lack of perfect balance. To illustrate briefly the principle of operation, the following analysis will be limited to derivation of a qualitative relationship between pointer deflection and quantity under measurement. Using instantaneous values, the field current is

$$i_f = I_f \sin \omega t \tag{3}$$

Assume a moving coil current due to the sum of the induced voltage in the moving coil and that derived from the primary detector, of the form

$$i_a = F_1(m,x) \sin \omega t + F_2(m,x) \cos \omega t \tag{4}$$

where $F_1(m,x)$ and $F_2(m,x)$ are functions of the deflection or mutual inductance m the quantity being measured x and independent of time. Equation 4 can be written

$$i_a = I_f Z_x \sin (\omega t + \theta), \tag{5}$$

where

θ = phase angle between I_f and i_a
$= \tan^{-1} F_2/F_1$

$$F_1(m,x) = Z_x \cos \theta \tag{6}$$

$$F_2(m,x) = Z_x \sin \theta \tag{7}$$

and

$$Z_x = \sqrt{F_1^2 + F_2^2}. \tag{8}$$

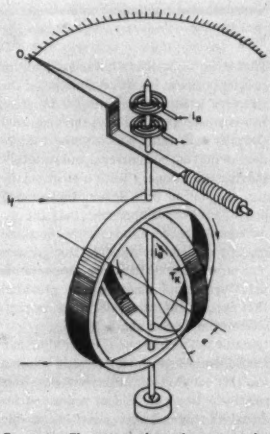

Figure 1. Elementary electrodynamic mechanism

Paper 47-169, recommended by the AIEE committee on instruments and measurements for presentation at the AIEE summer general meeting, Montreal, Quebec, Canada, June 9–13, 1947. Manuscript submitted March 31, 1947; made available for printing May 2, 1947.

A. J. CORSON is instrument engineer and N. P. MILLAR is design engineer, General Electric Company, Lynn, Mass.

The authors are indebted to their fellow workers T. A. Rich, who suggested this method of measurement, and V. L. Weaver and S. C. Haley, who cooperated in the development of these instruments.

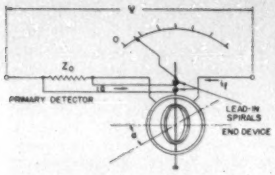

Figure 2. Elementary measuring circuit using electrodynamic mechanism

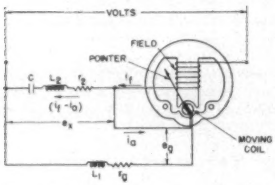

Figure 3. Diagram of frequency measurement system

The average torque of the electrodynamic system (where $dm/d\alpha = k$) is

$$T_K = k\frac{1}{T}\int^{T} i_a i_f dt \tag{9}$$

Substituting equations 3 and 5 in equation 9, integrating and equating to zero (the necessary condition for steady state indication) there results

$$Z_x \cos\theta = 0 \tag{10}$$

or from equation 6

$$F_1(m,x) = 0 \tag{11}$$

Equation 11 now can be solved for m in terms of some function of x

$$m = f(x) \tag{12}$$

Hence the value of mutual inductance, or pointer position, is a direct function of the quantity under measurement. In other words, a change in value of the measured quantity will cause an in-phase component of moving coil current, and resultant moving coil torque. With correct polarities this torque will deflect the moving coil to a new position such that the induced voltage will eliminate this in-phase current component and restore balance. The arrangement therefore represents a valid system of measurement provided that appropriate values of torque, responsiveness, and other characteristics are obtainable. The iron cored electrodynamic mechanism shown in Figure 3 is suitable for this method of measurement, since relatively large and linear values of induced moving coil voltage are obtainable at power frequencies. While this measurement system can be applied to any one of a large number of physical quantities, this paper will limit itself to measurements of (*a*) frequency and (*b*) temperature. In these cases, the mutual inductance function is related to the independent variable, or quantity to be measured, neglecting the iron losses in the field circuit; also extraneous moving system torques.

Application to the Measurement of Frequency

Consider a frequency measuring device represented schematically as shown in Figure 3 where

r_2, L_2, C = impedance of control circuit or frequency sensitive circuit containing resistance, inductance, and capacitance

r_0, L_1 = total resistance and inductance of armature and series load

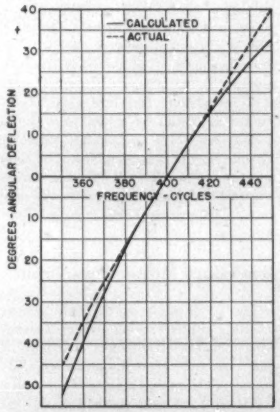

Figure 4. Comparison of the calculated and experimental frequency–deflection curves

i_f, i_a = instantaneous currents in the field and in the armature

e_0 = armature induced voltage

e_x = control voltage or voltage across the control impedance

Now it is assumed that the instantaneous field current is

$$i_f = I_f \sin \omega t \tag{13}$$

where I_f is the peak value of the field current and $\omega = 2\pi f$, f = frequency. Then it can be shown that the instantaneous armature current becomes (see Appendix I)

$$i_a = \frac{I_f}{R}\left(\frac{Z_y}{Z_L^2}\right)\cos(\omega t - \theta) \tag{14}$$

where

Z_L = armature loop circuit impedance

R = armature loop circuit resistance

Z_y = impedance function involving the circuit constants and the mutual inductance

θ = phase angle between the field and armature currents

When these instantaneous currents are substituted in the instantaneous torque equation 9 and utilizing the condition $dm/d\alpha = k$, and finally integrating the torque equation over a complete period, the average torque is found to be

$$T_K = \frac{kI_f^2}{2RZ_L^2} Z_y \sin\theta \tag{15}$$

At equilibrium the average torque T_K must equal zero Hence

$$Z_y \sin\theta = 0 \tag{16}$$

From equation 16 the mutual inductance m in terms of the radian frequency becomes

$$m = \left[1 - \left(\frac{\omega_0}{\omega}\right)^2\right]\left[\frac{1}{\omega^2 C} - \frac{\omega^2 r_2 RLC^2}{(\omega_0^2 LC - 1)(\omega^2 LC - 1)}\right] \tag{17}$$

where ω_0 is the radian frequency at which $m = 0$.

Figure 4 shows a comparison of the calculated and actual deflection–frequency characteristics. In the plotting of this curve equation 17 was modified to plot the angular deflection α instead of the mutual inductance m, and so chosen that negative values of deflection correspond to counterclockwise movement of the pointer with respect to the mid-scale reference frequency. For the particular comparison shown the frequency range was 350 to 450 cycles with 400 cycles as the

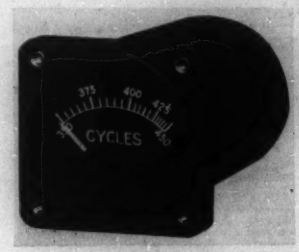

Figure 5. A 2½-inch 90-degree-scale 350–450-cycle small panel frequency meter

At 120 volts, 400 cycles, the input is 3.0 volt-amperes. The accuracy is two per cent of normal frequency with a responsiveness of 1.0 second and equivalent factor of merit of 1.0

reference frequency. It will be recalled that the reference frequency in equation 17 was made to correspond to zero mutual inductance. Hence the mid-scale position of 400 cycles is also the position of zero deflection or zero mutual inductance in this application. There is fairly good agreement between the two curves. Figure 5 shows the physical instrument and its associated scale distribution.

Application to the Measurement of Temperature

Again consider a temperature measuring system which utilizes the mutual inductance principle together with a resistance bridge network having in one arm of the bridge a temperature sensitive resistance as a primary detector of temperature. Such a system can be represented schematically as shown in Figure 6.

r_g, L_1 = resistance and inductance of armature and series load
r_1, r_2, r_3, r_4 = bridge resistances
r_t = temperature sensitive resistance
i_a = instantaneous armature current
i = instantaneous primary field current
i_f = instantaneous secondary field current
e_g = armature induced voltage
e_x = bridge voltage

An analysis of this circuit follows the same procedure as outlined in the preceding section on the frequency measuring device. If we assume a sinusoidal current in the field primary, then the current in the secondary also will be sinusoidal. Hence

$$i = I \sin \omega t \tag{18}$$

and

$$i_f = nI \sin \omega t \tag{19}$$

where n is the ratio of primary turns to secondary turns on the field or

$$n = i_f / i \tag{20}$$

By solving the differential equation for the armature current (see Appendix II)

$$i_a = \frac{IZ_t}{\omega^2 R_0^2 L_1^2 + (r_g R_0 - R_1)^2} \sin(\omega t - \theta) \tag{21}$$

Z_t = impedance which is a function of the circuit constants and the mutual inductance
θ = phase angle between i_a and i

R_0 and R_1 are defined in Appendix II.

Now the instantaneous product of i_a and i will give the instantaneous torque which, if integrated over a complete period, will become the average torque over that period.

$$T_K = \frac{kI^2}{2[\omega^2 R_0^2 L_1^2 + (r_g R_0 - R_1)^2]} Z_t \cos\theta \tag{22}$$

Again for equilibrium the average torque must be zero, therefore

$$Z_t \cos\theta = 0 \tag{23}$$

This expression then contains the mutual inductance as a function of the temperature sensitive resistance r_t. But r_t can be represented as a function of temperature as follows:

$$r_t = r_{t0}[1 + \alpha_1(T_1 - T_0) + \beta_1(T_1 - T_0)^2 + \ldots] \tag{24}$$

where

T_1 = temperature to be measured
r_{t0}, T_0 = resistance at temperature T_0
α_1, β_1 = temperature coefficients of resistance

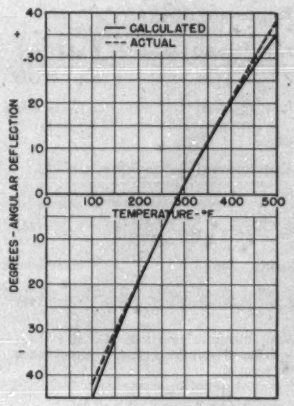

Figure 7 (above). Comparison of the calculated and experimental temperature – deflection curves

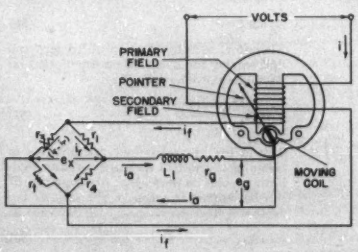

Figure 6. Diagram of temperature measurement system

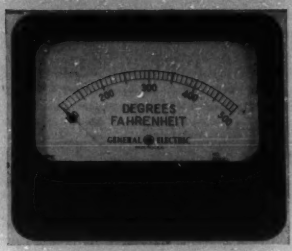

Figure 8. A 4½-inch 90-degree-scale small panel temperature meter

Energized at 120 volts, 60 cycles, the input is 7.7 volt-amperes. The scale range is 100–500 degrees Fahrenheit. Characteristics depend on the primary detector used

For most cases where the temperature range is not too great the variation of resistance with temperature will be essentially linear, in which case equation 24 reduces to

$$r_t = r_{t0}[1 + \alpha_1(T_1 - T_0)] \tag{25}$$

With this simplification the solution of equation 23 for the mutual inductance m in terms of the temperature T_1 reduces to

$$m = \frac{n r_{t0} \alpha_1 (T_1 - T_0)}{\omega^2 L_1} \times \left\{ \frac{\alpha_1(T_1 - T_0)(r_g - 2r_{t0}) + 4(r_g - r_{t0})}{[\alpha_1(T_1 - T_0) + 4]^2} \right\} \tag{28}$$

Figure 7 compares the calculated and experimental deflection–temperature characteristics. Likewise, in the plotting of this curve, equation 28 was modified to use the angular deflection instead of mutual inductance, for direct comparison with the practical working instrument. Good agreement exists between the actual and calculated scale distributions. Figure 8 shows the instrument with its corresponding scale calibrated for a temperature range of 100 to 500 degrees Fahrenheit.

Conclusion

The electrodynamic mechanism is, without special modification other than windings, adaptable to a variety of measurements. This adaptation consists of application, to the moving coil circuit, of an appropriate voltage—derived from the field current and the quantity to be measured. This voltage causes the establishment of definite values of induced voltage in the moving coil corresponding to definite angular positions thereof. The system is adapted to wide frequency ranges but iron clad mechanisms are preferred at

power frequencies to obtain good torque and operating characteristics. These characteristics, including scale distribution, are calculable by methods outlined herein. Neglect of effects of iron losses and extraneous torques on the moving system cause only secondary discrepancies between computed and experimental results.

Appendix I

Frequency Measuring System—Derivation of the Equation Between Mutual Inductance and Frequency

Refer to the circuit diagram, Figure 3. Let

$$i_f = I_f \sin \omega t \tag{29}$$

and

$$e_g = m di_f/dt = \omega m I_f \cos \omega t \tag{30}$$

where m is the mutual inductance between the field and armature coils. The voltage drops around the armature loop circuit are

$$L_1 di_a/dt + i_a r_g + e_g = e_x \tag{31}$$

also

$$e_x = (i_f - i_a) r_2 + L_2 (di_f/dt - di_a/dt) + \frac{1}{C}\int (i_f - i_a) dt \tag{32}$$

By substituting equations 29, 30, and 32 in equation 31 and remembering that

$i_a = dq/dt$

q = capacitor charge

$$\frac{1}{C}\int i_a dt = q/C$$

$$\frac{1}{C}\int i_f dt = -I_f/\omega C \times \cos \omega t$$

and

$$di_f/dt = \omega I_f \cos \omega t$$

the differential equation becomes after collecting terms

$$(L_1 + L_2)\frac{di_a}{dt} + (r_g + r_2) i_a + q/C = r_2 I_f \sin \omega t + I_f \times \left[\omega(L_2 - m) - \frac{1}{\omega C}\cos \omega t\right] \tag{33}$$

Let

$$L = (L_1 + L_2) \tag{34}$$

$$R = (r_g + r_2) \tag{35}$$

and differentiate equation 33.

The differential equation in i_a is

$$L\frac{d^2 i_a}{dt^2} + R\frac{di_a}{dt} + \frac{i_a}{C} = \omega I_f \times \left\{r_2 \cos \omega t - \left[\omega(L_2 - m) - \frac{1}{\omega C}\right] \sin \omega t\right\} \tag{36}$$

To solve equation 36 assume that the current takes the form

$$i_a = F_1(m,\omega) \sin \omega t + F_2(m,\omega) \cos \omega t \tag{37}$$

where $F_1(m,\omega)$ and $F_2(m,\omega)$ are functions of the mutual inductance and radian frequency.

Substitute equation 37 into 36 and, after collecting terms in $\sin \omega t$ and $\cos \omega t$, the equation becomes

$$\left\{-F_1\omega^2 L - F_2\omega R + \frac{F_1}{C} + \omega I_f \times \left[\omega(L_2 - m) - \frac{1}{\omega C}\right]\right\} \sin \omega t + \left\{-F_2\omega^2 L + F_1\omega R + \frac{F_2}{C} - \omega r_2 I_f\right\} \times \cos \omega t = 0 \tag{38}$$

For this equation to become zero, the coefficients of $\sin \omega t$ and $\cos \omega t$ must be zero thus giving two equations in F_1 and F_2 which can be solved simultaneously and substituted back in equation 37.

The simultaneous equations are

$$F_1\left(\omega L - \frac{1}{\omega C}\right) + F_2 R = I_f\left[\omega(L_2 - m) - \frac{1}{\omega C}\right] \tag{39}$$

and

$$F_1 R - F_2\left(\omega L - \frac{1}{\omega C}\right) = r_2 I_f \tag{40}$$

The solution of these for F_1 and F_2 yields

$$F_1 = \frac{I_f}{RZ_L^2}\left[r_2 Z_L^2 + r_g\left(\omega L - \frac{1}{\omega C}\right)\left(\omega L_x - \frac{1}{\omega C}\right)\right] \tag{41}$$

$$F_2 = \frac{I_f r_g}{Z_L^2}\left(\omega L_x - \frac{1}{\omega C}\right) \tag{42}$$

where

Z_L = armature loop impedance

or

$$Z_L = \sqrt{R^2 + \left(\omega L - \frac{1}{\omega C}\right)^2} \tag{43}$$

and

$$L_x = \frac{1}{r_g}[r_g(L_2 - m) - r_2(L_1 + m)] \tag{44}$$

Now substitute equations 41 and 42 into equation 37 and the armature current takes the form of

$$i_a = \frac{I_f}{RZ_L^2}\left\{\left[r_2 Z_L^2 + r_g\left(\omega L - \frac{1}{\omega C}\right) \times \left(\omega L_x - \frac{1}{\omega C}\right)\right] \sin \omega t + r_g R\left(\omega L_x - \frac{1}{\omega C}\right) \cos \omega t\right\} \tag{45}$$

Let

$$Z_y \sin \theta = r_2 Z_L^2 + r_g\left(\omega L - \frac{1}{\omega C}\right)\left(\omega L_x - \frac{1}{\omega C}\right) \tag{46}$$

and

$$Z_y \cos \theta = r_g R\left(\omega L_x - \frac{1}{\omega C}\right) \tag{47}$$

Therefore equation 45 or the instantaneous armature current becomes

$$i_a = \frac{I_f}{R}\left(\frac{Z_y}{Z_L^2}\right) \cos(\omega t - \theta) \tag{48}$$

where θ is the phase angle between i_a and i_f with value

$$\tan \theta = \frac{r_2 Z_L^2 + r_g\left(\omega L - \frac{1}{\omega C}\right)\left(\omega L_x - \frac{1}{\omega C}\right)}{r_g R\left(\omega L_x - \frac{1}{\omega C}\right)} \tag{49}$$

also

$$Z_y = \sqrt{r_g^2 R^2\left(\omega L_x - \frac{1}{\omega C}\right)^2 + \left[r_2 Z_L^2 + r_g\left(\omega L - \frac{1}{\omega C}\right)\left(\omega L_x - \frac{1}{\omega C}\right)\right]^2} \tag{50}$$

Now, if we assume an iron-cored dynamometer system is used in which the air gap flux is essentially constant over the range of deflection experienced, then the change of mutual inductance with respect to a change in angular deflection becomes a constant or

$$\frac{dm}{d\alpha} = k \tag{51}$$

Therefore the instantaneous torque developed between two coils in such a system can be expressed

$$\tau = k i_f i_a \tag{52}$$

and the average torque over one complete period is

$$T_K = \frac{k}{T}\int_0^T i_f i_a dt \tag{53}$$

where

$T = 2\pi/f$

By substituting equations 29 and 48 into equation 53 the torque expression becomes

$$T_K = \frac{k I_f^2}{R}\left(\frac{Z_y}{Z_L^2}\right)\frac{1}{T}\int_0^T \sin \omega t \cos(\omega t - \theta) dt \tag{54}$$

Upon integration the average torque over a period is

$$T_K = \frac{k I_f^2}{2RZ_L^2}(Z_y \sin \theta) \tag{55}$$

At equilibrium the average torque must be zero, hence

$$Z_y \sin \theta = 0 \tag{56}$$

Therefore, setting equation 46 to zero and first solving for L_x and then the mutual inductance m, we have finally

$$m = \frac{(\omega^2 L_2 C - 1)}{\omega^2 C} + \frac{r_2 RC}{(\omega^2 LC - 1)} \tag{57}$$

This is the mutual inductance function in terms of the radian frequency at any equilibrium point on the scale. Also equation 57 can be written in terms of the angular deflection α since upon integrating equation 51

$$m = k\alpha \tag{58}$$

In general it is convenient to express the equilibrium equation in such a manner that the value of m or the deflection is zero at a given reference frequency.

When $m = 0$ let

$$\omega = \omega_0 \tag{59}$$

Substitute this boundary condition into equation 57 and after solving for L_2, substituting back into equation 57, and rearranging terms, the final equilibrium equation takes the following form:

$$m = \left[1 - \left(\frac{\omega_0}{\omega}\right)^2\right]\left[\frac{1}{\omega_0^2 C} - \frac{\omega^2 r_3 RLC^2}{(\omega_0^2 LC - 1)(\omega^2 LC - 1)}\right] \tag{60}$$

Appendix II

Temperature Measuring System—Derivation of the Equation Between Mutual Inductance and Temperature

Refer to the circuit diagram, Figure 6. Let

$$i = I \sin \omega t \tag{61}$$

$$e_g = m\frac{di}{dt} = \omega m I \cos \omega t \tag{62}$$

$$i_f = ni \tag{63}$$

where n is the ratio of primary turns to secondary turns on the field, and m again is the mutual inductance.

From equations 61 and 63

$$i_f = nI \sin \omega t \tag{64}$$

The voltage drops around the armature loop circuit are

$$L_1 \frac{di_a}{dt} + i_a r_g + e_g = e_x \tag{65}$$

Now for simplicity of calculations assume that

$$r_1 = r_2 = r_4 = r \tag{66}$$

in the bridge circuit. It will be recognized that if these branch resistances were not equal, a balance still could be established and a final derivation attained however complex it might be. With this simplifying assumption the voltage drops around the bridge are

$$(3r + r_t)i_r = i_a(r_t + r) + i_f(r_t + r) \tag{67}$$

from which

$$i_r = \frac{(r_t + r)(i_a + i_f)}{(3r + r_t)} \tag{68}$$

where r_t is the temperature sensitive resistor. Also

$$e_x = 2ri_r - i_f r \tag{69}$$

By substituting equation 68 in equation 69

$$e_x = \frac{2r(r_t + r)i_a + r(r_t - r)i_f}{(3r + r_t)} \tag{70}$$

Now substitute equation 64 in equation 70 and equation 70 in equation 65 and collect terms. Hence

$$R_0 L_1 \frac{di_a}{dt} + i_a(r_g R_0 - R_1) = nR_3 I \sin \omega t - \omega m R_0 I \cos \omega t \tag{71}$$

where

$$R_0 = (3r + r_g) \tag{72}$$

$$R_1 = 2r(r_t + r) \tag{73}$$

$$R_3 = r(r_t - r) \tag{74}$$

This is the differential equation for the instantaneous value of armature current. To solve this equation assume

$$i_a = F_1(m, r_t) \sin \omega t + F_2(m, r_t) \cos \omega t \tag{75}$$

where $F_1(m, r_t)$ and $F_2(m, r_t)$ are functions of the mutual inductance and temperature sensitive resistance. By substituting equation 75 in equation 71 and collecting terms in $\sin \omega t$ and $\cos \omega t$

$$[-\omega R_0 L_1 F_2 + (r_g R_0 - R_1)F_1 - nR_3 I] \sin \omega t + [\omega R_0 L_1 F_1 + (r_g R_0 - R_1)F_2 + \omega m R_0 I] \cos \omega t = 0 \tag{76}$$

For this equation to be zero the coefficients must be zero, or

$$(r_g R_0 - R_1)F_1 - \omega R_0 L_1 F_2 = nR_3 I \tag{77}$$

$$\omega R_0 L_1 F_1 + (r_g R_0 - R_1)F_2 = -\omega m R_0 I \tag{78}$$

The solution of this simultaneous equation for F_1 and F_2 yields

$$F_1 = I\left[\frac{nR_3(r_g R_0 - R_1) - \omega^2 R_0^2 L_1 m}{\omega^2 R_0^2 L_1^2 + (r_g R_0 - R_1)^2}\right] \tag{79}$$

$$F_2 = -\omega R_0 I\left[\frac{m(r_g R_0 - R_1) + nR_3 L_1}{\omega^2 R_0^2 L_1^2 + (r_g R_0 - R_1)^2}\right] \tag{80}$$

which when substituted back into equation 75 gives for the instantaneous armature current

$$i_a = I\left\{\frac{[nR_3(r_g R_0 - R_1) - \omega^2 R_0^2 L_1 m] \sin \omega t - \omega R_0[m(r_g R_0 - R_1) + nR_3 L_1] \cos \omega t}{\omega^2 R_0^2 L_1^2 + (r_g R_0 - R_1)^2}\right\} \tag{81}$$

Let

$$Z_t \cos \theta = [nR_3(r_g R_0 - R_1) - \omega^2 R_0^2 L_1 m] \tag{82}$$

$$Z_t \sin \theta = \omega R_0[m(r_g R_0 - R_1) + nR_3 L_1] \tag{83}$$

then

$$i_a = \frac{IZ_t}{\omega^2 R_0^2 L_1^2 + (r_g R_0 - R_1)^2} \sin(\omega t - \theta) \tag{84}$$

where

$$\tan \theta = \frac{\omega R_0[m(r_g R_0 - R_1) + nR_3 L_1]}{[nR_3(r_g R_0 - R_1) - \omega^2 R_0^2 L_1 m]} \tag{85}$$

and Z_t is defined by combining equations 82 and 83.

Following the same procedure with respect to torque as was outlined in Appendix I, the average torque over a complete period is

$$T_K = \frac{kI^2}{2[\omega^2 R_0^2 L_1^2 + (r_g R_0 - R_1)^2]}(Z_t \cos \theta) \tag{86}$$

For $T_K = 0$

$$Z_t \cos \theta = 0 \tag{87}$$

From equation 82 set equal to zero in accordance with equation 87 and when the expressions for R_0, R_1, and R_3 have been substituted back into the equation, the mutual inductance function is related to r_t as follows:

$$m = \frac{nr(r_t - r)}{\omega^2 L_1}\left[\frac{r_t(r_g - 2r) + r(3r_g - 2r)}{(r_t + 3r)^2}\right] \tag{88}$$

Now apply the condition, when $m = 0$,

$$r_t = r_{t0} \tag{89}$$

where r_{t0} is a reference resistance value at reference temperature T_0. For this condition

$$r_{t0} = r \tag{90}$$

which when substituted back into equation 88 gives

$$m = \frac{nr_{t0}(r_t - r_{t0})}{\omega^2 L_1} \times \left[\frac{r_t(r_g - 2r_{t0}) + r_{t0}(3r_g - 2r_{t0})}{(r_t + 3r_{t0})^2}\right] \tag{91}$$

Now if it is assumed that for reasonably short ranges of temperature variation, the change of resistance with change in temperature is linear, then

$$r_t = r_{t0}[1 + \alpha_1(T_1 - T_0)] \tag{92}$$

where

α_1 = temperature coefficient of resistance
T_1 = the temperature to be measured
and T_0 is the reference temperature.

When equation 92 is substituted into equation 91, the equilibrium equation for the mutual inductance in terms of the temperature to be measured reduces to the final form

$$m = \frac{nr_{t0}\alpha_1(T_1 - T_0)}{\omega^2 L_1} \times \left\{\frac{\alpha_1(T_1 - T_0)(r_g - 2r_{t0}) + 4(r_g - r_{t0})}{[\alpha_1(T_1 - T_0) + 4]^2}\right\} \tag{93}$$

Likewise, as was shown in Appendix I, equation 93 also can be expressed in terms of the angular deflection in accordance with equation 58.

Appendix III. Symbols

C = capacitance, farads
e_g = instantaneous induced voltage in moving coil
e_x = instantaneous control voltage
f = frequency, cycles per second
F_1, F_2 = functions of mutual inductance and independent measurable variable. (See Appendixes I and II for values of these functions.)
i = instantaneous primary field current, amperes
i_f = instantaneous secondary field current, or in some cases just field current, amperes
i_a = instantaneous armature field current, amperes
I = peak primary field current, amperes
I_f = peak secondary field current or field current, amperes

i_r = instantaneous current in arm of bridge current, amperes
k = constant in torque equation
K = constant in torque equation
L_1, L_2 = self-inductance of armature circuit; control circuit; henrys
$L = (L_1 + L_2)$
$L_x = 1/r_g[r_g(L_2 - m) - r_2(L_1 + m)]$
m = mutual inductance of coil system, henrys
n = ratio of primary to secondary field turns
q = capacitor charge
r_1, r_3, r_4 = resistance in bridge arms, ohms
r_t = temperature sensitive resistor, ohms
r_g = resistance of armature circuit, ohms
r_{t0} = reference resistance value of r_t at reference temperature
$r = r_1 = r_3 = r_4$
r_2 = resistance of control circuit
$R = (r_g + r_2)$
$R_0 = (3r + r_t)$
$R_1 = 2r(r_t + r)$
$R_2 = r(r_t - r)$
t = time, seconds
$T = 2\pi/\omega$
T_1 = temperature
T_0 = reference temperature
T_K = average torque over a period
V = volts
$Z_L = \sqrt{R^2 + (\omega L - 1/\omega C)^2}$
Z_x = generalized impedance containing the mutual inductance and measurable variables
Z_y—See Appendix I, equation 50
Z_t—See Appendix II, equations 82 and 83
α = angular deflection—usually measured from the position of zero mutual inductance
α_1 = first temperature coefficient of resistance
β_1 = second temperature coefficient of resistance
θ = phase angle between the field current and armature current
τ = instantaneous torque
$\omega = 2\pi f$—radian frequency, cycles per second

References

1. Definitions of Electrical Terms, American Standards Association, New York, N. Y., ASA Standard *C-42*. 1941, paragraph 30.20.200.

2. Principles of Electricity (book), L. Page, N. I. Adams. Pages 364–71.

3. Functional Analysis of Measurements, I. F. Kinnard. AIEE Transactions, volume 65, 1946, pages 987–95.

No Discussion

The Probable Breakdown Voltage of Paper Dielectric Capacitors

HAMILTON BROOKS
MEMBER AIEE

Synopsis: The frequency of occurrence of defects in electrical insulation can be shown to follow the Poisson law of probability. One of the more important defects in thin paper insulation is conducting particles. In this paper expressions are derived for the probable breakdown voltage as a function of conducting particle occurrence. It is shown by statistical evidence that large conducting particles exist in the insulating paper and bridge one or more layers of paper in the finished capacitor through chance reorientation caused by manufacturing processes and operation. The degree and frequency of reorientation of particles with a typical grade of paper is determined experimentally, and the probable insulation thickness and consequent voltage strength of various size capacitors is calculated. A method of determining the optimum voltage strength of this insulation is illustrated. It is concluded that conducting particles are a predominant factor in determining the voltage strength of present day capacitors and that one of the greatest opportunities for improvement lies in the reduction of the conducting particle content in the paper.

THROUGHOUT the past 25 years, power capacitors and capacitors for many other low frequency and direct current applications have made use of a working dielectric composed of layers of thin paper impregnated with an insulating liquid. The progress in capacitor manufacture has been governed to a large extent by improvements in thin paper manufacture. One important improvement has been in the reduction in the number of conducting particles in the paper. The existence of these conducting particles is more important in capacitors than in other uses of insulation because of the extremely large areas involved in a single unit and the correspondingly greater probability of their presence reducing the effective insulation at some point.

In the early days of paper dielectric capacitor manufacture, progress by the paper mills in reducing the conducting particle count was quite rapid. This made it possible to increase the working area of dielectric in a single capacitor and to design economical capacitors for the lower utilization voltages, such as 460 and 575 volts. Further improvement eventually made it practical to build large 230 volt capacitors where the area is very great and the total dielectric thickness very small.

With the most modern product of the paper makers skill, however, these large low voltage capacitors remain difficult to build and even with closely controlled conditions are manufactured with relatively high scrap. It commonly has been assumed that factory test failures and many service failures are due simply to the alignment of conducting particles in two or more sheets of the paper. The better performance with increasing number of sheets has likewise been attributed to the less frequent occurrence of alignments. A simple mathematical analysis, however, shows that the frequency of short circuits on test and the decreasing dielectric strength with decreasing insulation thickness and increasing area cannot be accounted for satisfactorily by an alignment theory.

Another way that variations in dielectric strength and occasional short circuits may be explained is through the chance reorientation of large conducting particles. If it is assumed that such reorientation takes place so that particles extend into and through adjacent sheets, and if the proper laws of chance are applied, the dielectric strength of a capacitor ceases to be an irratic and unpredictable quantity. The purpose of this paper is to show that this is the case. When sufficient data on the paper are available and when the necessary design factors are known, remarkably accurate predictions can be made with respect to dielectric strength and factory rejects. Furthermore, a basis is established whereby field performance can be anticipated assuming, of course, that the capacitors are normal in other respects.

Conducting Particles in the Paper

Modern capacitor paper is made almost exclusively of wood. This must be reduced to very small pieces by mechanical means and then digested by cooking. The resulting pulp is passed through beaters which further reduce and separate the fibers by mechanical action. In all of these operations, a certain amount of contamination is incurred in the form of slivers of metal, carbon, and scale. These vary in size from microscopic particles up to bodies capable of puncturing layers of paper several thousandths of an inch thick. The shapes are naturally irregular and occur as slivers or needles, crystalline clusters, grains, and so on. Most of these particles are separated from the pulp by centrifugal processes just prior to forming the sheet of paper, but the small amount remaining is sufficient to be a predominant factor in determining the dielectric strength of low voltage capacitors.

The frequency of occurrence of conducting particles in domestic papers manufactured to generally accepted specifications for capacitor tissue appears to be quite stable. In fact, records of conducting particle count show very little change since the adoption of thin kraft papers in 1934. Figure 1 shows the average frequency of occurrence of particles in sheets of various thicknesses which are of sufficient size to short-circuit a single

Paper 47-164, recommended by the AIEE committees on basic sciences and power transmission and distribution for presentation at the AIEE summer general meeting, Montreal, Quebec, Canada, June 9–13, 1947. Manuscript submitted April 7, 1947; made available for printing May 2, 1947.

HAMILTON BROOKS is a design engineer with the Westinghouse Electric Corporation, East Pittsburgh, Pa.

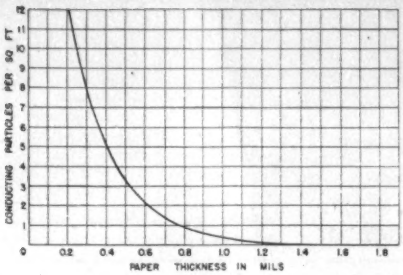

Figure 1. The average number of conducting particles in paper which are large enough to register as short circuits by the standard conducting particle test

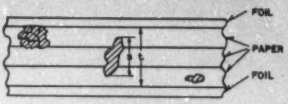

Figure 2. A cross section showing some possible occurrences of conducting particles in the paper dielectric of a capacitor

sheet of paper. This data was obtained by passing a metal roller over a sheet of paper and counting the number of clicks heard in a telephone connected between the roller and a metal plate beneath the sheet. Particles smaller than the thickness of the sheet of paper are not detected. Also, particles just large enough to extend through the sheet are not distinguished from particles much larger than the thickness of the paper.

One of the final operations in the paper mill is calendering. In this, the sheet of paper is passed between smooth rolls and subjected to an ironing action. On passing between the calender rolls, large conducting particles are either crushed and broken into smaller bits or they are compressed into the body of the sheet with their long axis tending to parallel it. Whether the particles are crushed or whether they are simply buried in the paper has an important bearing on the subsequent breakdown characteristics of the capacitor into which the paper is wound. If the particles are crushed so that their maximum size is no greater than that of the paper thickness, their effect on the insulation thickness of the capacitor can be minimized by lamination or multiple layers of paper, and the effective thickness of insulation thus obtained may be counted on being just the thickness of one sheet of paper less than the total. If, however, many large particles are only buried so that they later may be reoriented, they may then puncture several layers of paper and lamination cannot be depended on to insure uniformity. This is illustrated in Figure 2.

It seems conclusive that such reorientation takes place and to such a degree that it determines to a large extent the strength of the finished capacitor. The forces causing displacement of a particle from its original position can occur in many ways. It has been observed that the mere act of rewinding the paper into smaller rolls after slitting increases the conducting particle count materially, and this seems most certainly due to the appearance of particles that were previously buried. Other opportunities for reorientation are present in winding the capacitor and the handling during assembly, not to mention the possible forces due to swelling and contracting paper fibers in drying and impregnation or even to changing humidity before the capacitor is in manufacture.

The Mathematical Probability of Conducting Particle Occurrence

Let the occurrence of conducting particles be considered a problem in probability. The occurrence of a conducting particle in the insulation of a capacitor may be called an event s. This event may be a particle of microscopic size or it may be a particle of such size and position as to completely short circuit all the layers of paper separating the two foil electrodes. Since the concern is primarily with the extent to which the insulating layers are bridged by a particle, it must be distinguished between these events. This may be done by breaking up the event s into subevents, one for each degree of bridging and the subevents designated as s_1, s_2, $s_3 \ldots s_i \ldots s_j$. If these are written in order of decreasing size, s_1 may stand for a complete short circuit between the two foils and s_j for the occurrence of some infinitely small particle at the other extreme.

Now the size or degree to which the particle bridges the insulation is, of course, a continuous variable which may take on an infinite number of values between the short circuit conditions s_1 and the extreme of smallness s_j. To avoid difficulty and for practical reasons, let the events be grouped into some finite number of class intervals of convenient range so that if s_1 is the occurrence of a particle of any size large enough to cause a short circuit, s_2 might be, for example, any particle that short circuits 90 to 100 per cent of the space between the foils, s_3 a bridging of 80 to 90 per cent, and so on. With this understanding, some finite value may be assigned for the probability of occurrence of each one of these events. These probabilities may be denoted by p_1, p_2, $p_3 \ldots p_i \ldots p_j$, corresponding to their respective events.

If the event s_1, a short-circuiting particle, occurs in a capacitor, all the other events s_2, $s_3 \ldots s_i \ldots s_j$, being some degree less than a short circuit, are of no consequence. The capacitor insulation is punctured completely and any partial bridging has no significance. Calling the probability of obtaining a short circuit P_1, it is obvious that it has the same value as

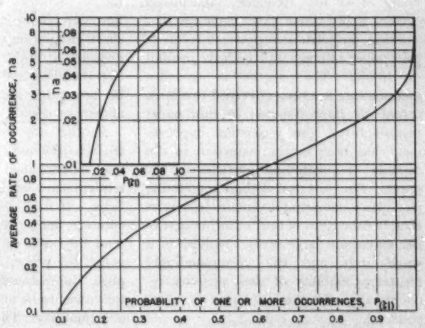

Figure 3. Summation of the Poisson distribution given by $P_{\geq 1} = 1 - \epsilon^{-na}$ which gives the probability of one or more occurrences of an event when na is its average rate of occurrence

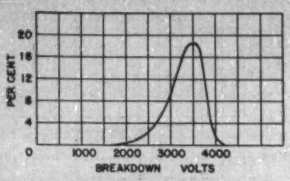

Figure 4. A typical frequency distribution curve of capacitor breakdown voltage

Figure 6. Histogram for the breakdown voltages of Table II

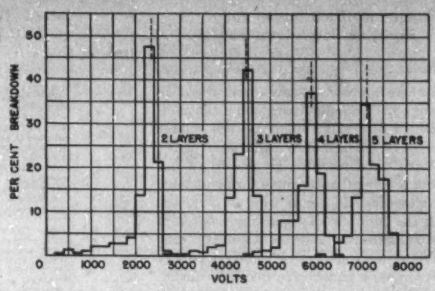

the probability of occurrence of the short-circuiting particle s_1 or

$$P_1 = p_1$$

In the event that particle s_1, or a short circuit, does not occur then s_2 is the significant occurrence to the exclusion of all the rest because it establishes the minimum insulating space between the foils and determines the voltage strength of the capacitor. The probability that s_2 will occur has been given as p_2. The probability that s_1 will not occur being complementary to the probability of occurrence is

$$q_1 = 1 - p_1$$

The probability P_2, associated with the significant occurrence of s_2 is therefore the product of the probabilities of the occurrence of the two independent events s_2 and $\bar{s}_1$($\bar{s}_1$ standing for the nonoccurrence of s_1) or

$$P_2 = p_2 \times q_1$$

In a similar manner, the probability of the significant occurrence of s_3 is the product of the probabilities of three independent events s_3, s_1 and $\bar{s}_2$ or

$$P_3 = p_3 \times q_1 \times q_2$$

and in general the probability that any

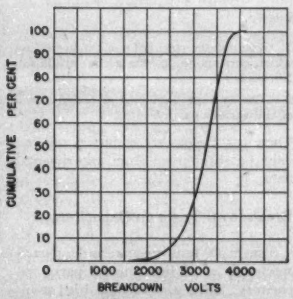

Figure 5. The same data as for Figure 3 shown as a cumulative frequency distribution

particle s_i is the largest that occurs and therefore determines the insulation thickness is

$$P_i = p_i \times q_1 \times q_2 \times q_3 \ldots \times q_{i-1}$$

So far the effect of conducting particles has been considered only from the standpoint of the occurrence or nonoccurrence of various sizes and the consequent degree of bridging the insulating layers. Actually, the event of a short circuit s_i may occur at several points in a capacitor. In fact, if the capacitor is large enough and the insulation thin enough, it may be more likely to have two short circuits than one. It makes no difference, of course, in the dielectric strength of the capacitor if a short circuit or a partial short circuit, as the case may be, occurs at one point or at several points. The probabilities, however, of just one occurrence and of one or more occurrences are considerably different.

A set of events may be said to be distributed "individually at random" throughout an interval provided each event of the set is placed at random independently of all the rest. A set of events may be said to be distributed "collectively at random" throughout an interval, provided the probability of any subinterval containing c events is independent of the number of events in any other subinterval not wholly or partly included in it. Under these conditions, it can be shown[1] that the probability of just c occurrences in any interval n is given by the Poisson distribution function

$$P_{c,n} = \frac{(na)^c \epsilon^{-na}}{c!}$$

where na is the expected or average number of occurrences in that interval. The occurrence of conducting particles certainly satisfies these conditions of randomness so it is concluded that the frequency of occurrence must follow the Poisson law.

Now it has been pointed out that only two eventualities need be considered. These are

1. The probability that the number of occurrences is one or more, or c is equal to or greater than one.
2. The probability that the number of occurrences is zero, or c is equal to zero.

Fortunately, the Poisson law reduces to a very simple equation for c is equal to zero, and for this case may be written

$$P_{0,n} = \epsilon^{-na}$$

Also, the events "no occurrence" and "one or more occurrences" being mutually exclusive, which is to say that one or the other must take place, the probability for c being equal to or greater than one must be one minus the probability of c being equal to zero or

$$P_{\geq 1,n} = 1 - P_{0,n} = 1 - \epsilon^{-na}$$

The way that $P_{\geq 1}$ varies with na is shown by Figure 3. It is thus evident that any general equation for the significant occurrence of a conducting particle must take into account the interval under consideration, or more specifically, the area of paper in the capacitor as this governs the values of p and q. It is convenient to refer the expectation na to some unit base so a is defined as the average frequency of occurrence in the capacitor of a particular size conducting particle, s_i in one square inch of paper; and n is the total number of square inches of paper between the electrodes. Then if the symbol p is redefined to mean the probability of occurrence of one or more particles, it becomes the $P_{\geq 1,n}$ of the Poisson formula. Likewise, q is equivalent to $P_{0,n}$. Substituting these symbols gives

$$p = 1 - \epsilon^{-na}$$
$$q = \epsilon^{-na}$$
$$P_i = p_i \times q_1 \times q_2 \times q_3 \ldots \times q_{i-1}$$

These are the equations for the occurrence of conducting particles in a capacitor.

Frequency Distribution and Probable Breakdown Voltage

If voltage is applied individually to a sample lot of capacitors and raised in steps until failure occurs, and if the number or percentage failing at each voltage step is grouped into class intervals or "cells" and recorded graphically, a frequency distribution curve for breakdown voltage such as Figure 4 will be obtained. If the entire lot of capacitors was tested simultaneously and the total per cent failure after successive voltage increases recorded, a cumulative frequency distribution such as Figure 5 would be obtained. Now each of these voltage failures has taken place at a point in the insulation where some defect has made it weaker than at any other. If there were a means whereby the cause of this first failure might be removed and the capacitor retested, a new failure would be expected at some higher voltage. If such a process could be repeated indefinitely, there should come a time when all defects are removed, and the breakdown strength becomes a constant determined only by some quality characteristic of the dielectric.

Should it happen that these defects which determine the various breakdown voltages are predominantly due to variations in true insulation thickness caused by partial bridging of conducting particles, the probability of breakdown should take the same form as found for the probability of conducting particle occurrence. To reconcile the two, it is only necessary to determine the particle size or degree of bridging in terms of the voltage strength of the insulation which remains unbridged. To illustrate, Figure 2 shows a cross section of capacitor dielectric which is partially bridged by a conducting particle, s being the length of the path normal to the layers of paper or the extent of the bridging and t the total distance by which the foils are separated. The true thickness of insulation is clearly the difference between the two or

$$t' = t - s$$

The breakdown strength of this section of dielectric is then some voltage corresponding to t' rather than the foil separation t, and this may be expressed as the function

$$v = F(t - s)$$

For a particular design of capacitor, the value of t for practical purposes may be regarded as constant. There is then a certain value of t' corresponding to each value of s, and as this requires the probability of t' to be the same as the probability of s, the probability of v, under the conditions assumed, can be no different. In other words, the probability of a capacitor failing at v_i is

$$P_i = p_i \times q_1 \times q_2 \times q_3 \ldots \times q_{i-1}$$

where

$$v_i = F(t - s_i)$$

If the percentages in the frequency distribution curve Figure 4 have been determined by a sufficient number of tests, their values expressed as fractions may be considered equivalent to the probabilities of occurrence of the respective failure voltages. This, however, is the probability P_i. It follows then that the frequency distribution is simply the successive values taken on by P as s is considered over the increments represented by s_1 to s_i or for

$$v_1 = F(t - s_1),\ P_1 = p_1$$
$$v_2 = F(t - s_2),\ P_2 = p_2 \times q_1$$
$$v_3 = F(t - s_3),\ P_3 = p_3 \times q_1 \times q_2$$
$$v_i = F(t - s_i),\ P_i = p_i \times q_1 \times q_2 \times q_3 \ldots \times q_{i-1}$$

Likewise, the cumulative frequency distribution being the summation of the successive percentages may be written, for

$$v_1 = F(t - s_1),\ \Sigma P = P_1$$
$$v_2 = F(t - s_2),\ \Sigma P = P_1 + P_2$$
$$v_3 = F(t - s_3),\ \Sigma P = P_1 + {}_2 + P_3$$
$$v_i = F(t - s_i),\ \Sigma P = {}_1 + P_2 + P_3 \ldots + P_i$$

The symbols and equations that have been developed are tabulated in Table I for reference. With these relations, it should be possible to calculate a frequency distribution for capacitor breakdown voltage provided two things are known.

1. The voltage strength v of the insulation which corresponds to the actual insulation thickness t'.

2. The average frequency of occurrence a of the various particle sizes.

These two factors are empirical and can only be determined from experimental data.

Table I. Nomenclature

Symbol	Definition
s	The event of a conducting particle occurring in the paper dielectric of a capacitor. When distinguished as to size, it is one of the series of events $s_1, s_2 \ldots s_i \ldots s_l$. Also, the thickness of insulation in mils which is short circuited by the conducting particle
n	The number of square inches of paper between the foil electrodes of a capacitor; which is the product of the area of the two foils, and the number of layers of paper between them
a	The expectation or average frequency of occurrence *in a capacitor* of a particular size conducting particle in particles per square inch
t	The average spacing in mils between foils in a capacitor, or the total paper thickness times a space factor
t'	The actual insulation thickness in mils remaining when a conducting particle partially short circuits the insulation. $t' = t - s$
v	The breakdown voltage of the insulation thickness t'
p	The probability of occurrence in a capacitor of one or more conducting particles of a particular size s. $p = 1 - e^{-na}$
q	The probability of the nonoccurrence in a capacitor of a conducting particle of a particular size s. $q = 1 - p = e^{-na}$
P	The probability of the significant occurrence of a conducting particle in a capacitor, or the probability that a particular size particle occurs at least once and is the largest particle that does occur. $P_i = p_i \times q_1 \times q_2 \ldots \times q_{i-1}$. Also, the probability that a capacitor will fail at voltage v_i, where v_i is the insulation strength of the thickness t' corresponding to a conducting particle size s_i
$\sum_{n=1}^{i} P$	The probability that a capacitor will fail at a voltage v_i or less. $\sum_{n=1} P = P_1 + P_2 \ldots + P_i$

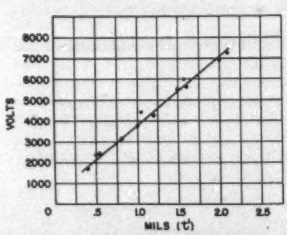

Figure 7. The rms breakdown voltage of oil impregnated paper at small spacings when free from major imperfections

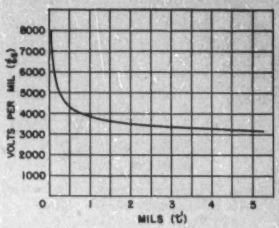

Figure 8. The rms breakdown voltage gradient corresponding to Figure 7

Fitted to the formula $g_s = g(1 + b/\sqrt{t'})$ where $g = 2{,}600$ and $b = 0.46$

Breakdown Tests on Capacitors

Some 6,000 tests are on record for small specimens of oil-impregnated paper capacitors. These were vacuum dried at approximately 125 degrees centigrade, and while heated and under vacuum, the pa-

Table II. RMS 60-Cycle Breakdown Data for Oil-Impregnated Paper Between Aluminum Foil Electrodes

Electrode Area 16.9 Sq In.

Two Layers			Three Layers			Four Layers			Five Layers		
	Failures			Failures			Failures			Failures	
Voltage Range	Number	Per Cent	Voltage Range	Number	Per Cent	Voltage Range	Number	Per Cent	Voltage Range	Number	Per Cent
0– 200	0	0	2,001–2,200	0	0	3,201–3,400	0	0	5,801–6,000	0	0
201– 400	1	0.4	2,201–2,400	1	0.4	3,401–3,600	2	0.8	6,001–6,200	1	0.4
401– 600	3	1.2	2,401–2,600	0	0	3,601–3,800	0	0	6,201–6,400	0	0
601– 800	1	0.4	2,601–2,800	1	0.4	3,801–4,000	2	0.8	6,401–6,600	8	3.2
801–1,000	2	0.8	2,801–3,000	1	0.4	4,001–4,200	2	0.8	6,601–6,800	12	4.8
1,001–1,200	5	2.0	3,001–3,200	1	0.4	4,201–4,400	0	0	68,01–7,000	33	13.2
1,201–1,400	5	2.0	3,201–3,400	2	0.8	4,401–4,600	1	0.4	7,001–7,200	87	34.8
1,401–1,600	7	2.8	3,401–3,600	2	0.8	4,601–4,800	2	0.8	7,201–7,400	52	20.8
1,601–1,800	7	2.8	3,601–3,800	5	2.0	4,801–5,000	3	1.2	7,401–7,600	44	17.6
1,801–2,000	10	4.0	3,801–4,000	6	2.4	5,001–5,200	5	2.0	7,601–7,800	13	5.2
2,001–2,200	34	13.6	4,001–4,200	33	13.2	5,201–5,400	20	8.0	7,801–8,000	0	0
2,201–2,400	119	47.6	4,201–4,400	58	23.2	5,401–5,600	20	8.0			
2,401–2,600	53	21.2	4,401–4,600	106	42.4	5,601–5,800	40	16.0			
2,601–2,800	3	1.2	4,601–4,800	34	13.6	5,801–6,000	93	37.2			
2,801–3,000	0	0	4,801–5,000	0	0	6,001–6,200	47	18.8			
						6,201–6,400	12	4.8			
						6,401–6,600	1	0.4			
						6,601–6,800	0	0			
Total	250	100.0		250	100.0		250	100.0		250	100.0

per was impregnated with a good grade of insulating oil. The specimens were tested by applying a low 60-cycle voltage and raising it continuously at the rate of 400 or 500 volts per second until failure occurred. Each specimen had an area of 16.9 square inches between aluminum foils, and the tests covered dielectrics of two, three, four, and five layers of paper.

The data from one series of 1,000 tests are shown in grouped frequency form in Table II. The paper used in this series was a super-calendered kraft with an average thickness of 0.525 mil, density of 1.029, and 3.7 conducting particles per square foot (American Society for Testing Materials Specification *D 202*). Figure 6 gives the results charted as a histogram in 200-volt cells.

True Voltage Stress at Failure

It has been pointed out that relative frequencies such as shown in Figure 6, when derived from a large number of tests, may be considered to represent the probabilities of occurrence of events. Figure 6, being based on 250 tests for each set of specimens, may be considered then as a fair approximation of the probabilities of failure in each of the cells or voltage ranges shown.

From this point of view, it is obvious that the voltage range or cell in each histogram which has the highest percentage of breakdowns is also the most probable breakdown voltage of the specimen, and following out previous reasoning this should correspond to a conducting particle size which has the greatest probability of significant occurrence. Now, the paper area in these specimens is such that a short circuiting particle may be expected on the average, from one to two times in each. These short circuiting particles are predominantly 0.5 mil, or slightly larger in size. Smaller particles occur more frequently, but they have no significance when occurring simultaneously with the 0.5 mil particle; and effectively, larger particles occur with such a smaller order of probability, depending as they do on chance reorientation that it must be concluded that the most probable breakdown voltage of these specimens is the result of the occurrence of a 0.5-mil particle. In other words, the most probable event in *this size* capacitor is that just one sheet of paper is short circuited and the remaining sheet or sheets constitute the insulation.

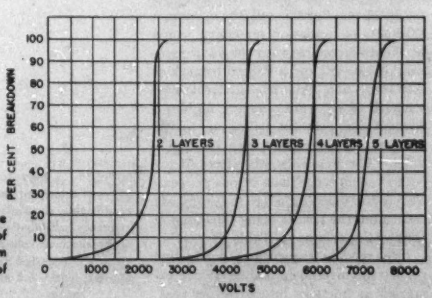

Figure 9. Cumulative frequency distribution of breakdown voltage from the smoothed data of Table II

One of the two empirical relations needed to apply the formula for mathematical probability of breakdown voltage is the dielectric strength of various thicknesses of capacitor insulation when free from defects. This relation might be obtained by testing a large number of samples of impregnated paper with electrodes so small that their chance of including defects within their area is negligible. This, however, is exactly the condition obtained by testing an area where a conducting particle short circuits just one sheet of paper. The conducting particle then constitutes one of the electrodes between which the insulation failure occurs and this electrode area is so small that the breakdown voltage should show little influence from defects in the other sheets of paper. The most probable breakdown voltage as indicated in Figure 6 therefore should give a reliable measure of the ideal strength of impregnated paper if the thickness of one sheet of paper is subtracted from the total dielectric thickness.

Figure 7 shows the most frequent breakdown voltage from a number of sets of tests plotted against mils insulation thickness, the thickness being one less than the total number of sheets of paper or

$$t' = t - s$$

as previously given, s being in this case an effective particle size equal to the thickness of one sheet of paper.

It has been found[3] that the breakdown gradient of composite dielectrics such as impregnated paper appears to follow an empirical formula of the form

$$g_0 = g\left(1 + b/\sqrt{t'}\right)$$

where g is the breakdown volts per mil at relatively large spacings, t' is the insulation thickness of the sample, and b is a constant. Fitting this formula to Figure

7, a value of 2,600 volts per mil is obtained for g and 0.46 as the value of the constant b or

$$g_s = 2{,}600(1+0.46/\sqrt{t'})$$

Figure 8 gives the curve of breakdown volts per mil calculated from this formula. The breakdown voltage for a thickness t' of oil-impregnated paper may now be determined. It is simply

$$v = 2{,}600t'(1+0.46/\sqrt{t'})$$

This is the first of the two empirical relations needed.

The Expectation of Conducting Particle Occurrence

The breakdown strength relation of Figure 7 makes it possible to translate the frequency distribution of breakdown voltage into a distribution of particle sizes since each value of breakdown voltage has been shown to correspond to a particular thickness of insulation of ideal quality with the remaining space between the foils taken up by a conducting particle. Figure 6, however, is constructed with uniform steps of voltage and as the concern is fundamentally with conducting particle size, it is desirable to convert this data into uniform steps of particle size. To accomplish this, the frequency distribution is redrawn to show the cumulative frequency of occurrence, Figure 9.

The analysis then proceeds as follows: a cell value, or particle size range, of 0.1 mil is chosen and considering first the two layer capacitor, it is obvious that any particle between 1.0 to 1.1 mil effective size would leave 0.05 mil of insulation as a maximum. Figure 7 shows 0.05 mil of ideal insulation to breakdown at 400 to 500 volts and referring to Figure 9, it is found that one per cent of the specimens fail between zero and 450 volts. The frequency of occurrence of particles of 1.0 mil and over must therefore be one per cent. Next, a particle size of 0.9 to 1.0 mil is taken. For this cell, the maximum thickness of insulation remaining would be the difference between the foil separation of 1.05-mil and a 0.9-mil particle or 0.15 mil, and this has a breakdown strength of 850 volts. Figure 9 gives a total of two per cent failing up to 850 volts or one per cent between 450 to 850 volts. The frequency, therefore, of the 0.9 to 1.0 mil range must be one per cent. This is continued for a 0.8- to 0.9-mil cell and so on, the results being tabulated in the first five columns of Table III.

If the relative frequencies of conducting particle occurrence in Table III are expressed as fractions instead of per cent, an estimated value of the probability of their significant occurrence is obtained. This is the probability

$$P_i = p_i \times q_1 \times q_2 \ldots \times q_{i-1}$$

From this the probability of one or more occurrences and the probability of no occurrences may be determined readily. With reference to Table III, the probability p of the occurrence of one or more particles 1.0 mil or larger must be the same as the probability of their significant occurrence P since any particle in this range causes a short circuit or at most a breakdown at 450 volts. There is tabulated, therefore, in Table III, columns 6 and 7, values for p and q derived as follows:

For the short-circuited condition

$$p_1 = P_1 = 0.01$$
$$q_1 = 1 - 0.01 = 0.99$$

For the 0.9- to 1.0-mil cell the probabilities are

$$p_2 = \frac{P_2}{q_1} = \frac{0.01}{0.99} = 0.0101$$
$$q_2 = 0.9899$$

And for the 0.8- to 0.9-mil cell the probabilities are

$$p_3 = \frac{P_3}{q_1 \times q_2} = \frac{0.02}{0.99 \times 0.9899} = 0.0204$$
$$q_3 = 0.9796$$

And so on for the complete distribution.

Since the probability p is a Poisson distribution function, its value in each case is determined by the expectation or average frequency of the conducting particle occurrence. That is to say, if given a value for p, the corresponding average number of occurrences in the specimens may be obtained from the solution of the Poisson equation in the form

$$p = 1 - \epsilon^{-na}$$

The values of na for each value of p may be obtained from Figure 3. Finally, the expectation for one square inch of paper is obtained by dividing na by the number of square inches of paper in the test specimen, and these are tabulated in column 9.

This average rate of occurrence a is the other of the two empirical relations that were required to calculate the probability of capacitor failure. Experimental values obtained as in Table III are plotted on the curve Figure 10. It will be noted that

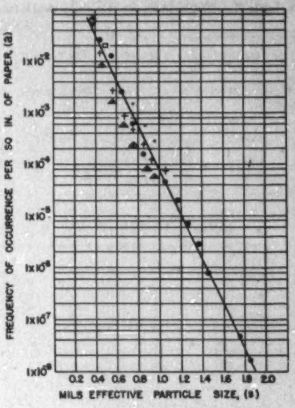

Figure 10. The average frequency of occurrence of conducting particles in a capacitor for class intervals of 0.1-mil effective size

The nominal paper thickness is 0.5 mil

□—From standard paper test
•—From 2 layer sample of 33.8 square inches
△—From 3 layer sample of 40.7 square inches
+—From 4 layer sample of 57.6 square inches
⊙—From 5 layer sample of 84.5 square inches
⊕—From 3 layer sample of 7.0×10^4 square inches
●—From 3 layer sample of 8.4×10^2 square inches

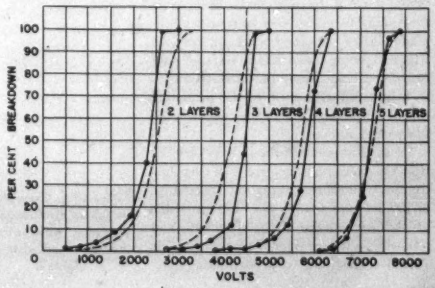

Figure 11. Comparison between calculated and experimental cumulative frequency distributions of breakdown voltage for oil impregnated capacitors with 0.5-mil paper

Table III. Calculation of Conducting Particle Occurence

s	t′	v	Σf (Per Cent)	f (Per Cent)	p	q	na	a
(Two layers of paper, n = 33.8 sq in., t = 1.05 mils)								
Over 1.0	0.05	450	1	1	0.01	0.99	0.01	
1.0–0.9	0.15	850	2	1	0.0101	0.9899	0.01	3.0×10^{-4}
0.9–0.8	0.25	1,200	4	2	0.0204	0.9796	0.02	5.9×10^{-4}
0.8–0.7	0.35	1,600	8.5	4.5	0.047	0.953	0.049	1.5×10^{-3}
0.7–0.6	0.45	1,950	16	7.5	0.082	0.918	0.085	2.5×10^{-3}
0.6–0.5	0.55	2,300	40	24	0.286	0.714	0.33	9.8×10^{-3}
0.5–0.4	0.65	2,650	99	59	0.984	0.016	4.2	1.2×10^{-1}
0.4–0.3	0.75	3,000	100	1	0.99+			
(Three layers of paper, n = 50.7 sq in., t = 1.58 mils)								
Over 1.0	0.58	2,400	0.5	0.5	0.005	0.995	0.005	
1.0–0.9	0.68	2,750	0.8	0.3	0.00302	0.997	0.003	5.9×10^{-5}
0.9–0.8	0.78	3,100	1.2	0.4	0.00404	0.996	0.004	7.9×10^{-5}
0.8–0.7	0.88	3,400	2.3	1.1	0.0111	0.9889	0.011	2.2×10^{-4}
0.7–0.6	0.98	3,750	5.0	2.7	0.0277	0.9723	0.028	5.5×10^{-4}
0.6–0.5	1.08	4,050	12.0	7.0	0.0738	0.9262	0.076	1.5×10^{-3}
0.5–0.4	1.18	4,400	44	32	0.365	0.635	0.45	8.9×10^{-3}
0.4–0.3	1.28	4,700	98	54	0.968	0.032	3.5	6.9×10^{-2}
(Four layers of paper, n = 67.6 sq in., t = 2.1 mils)								
Over 1.1	1.0	3,800	0.7	0.7	0.007	0.993	0.007	
1.1–1.0	1.1	4,150	1.2	0.5	0.00504	0.995	0.005	7.4×10^{-5}
1.0–0.9	1.2	4,450	2.0	0.8	0.0081	0.9919	0.008	1.2×10^{-4}
0.9–0.8	1.3	4,750	3.4	1.4	0.0143	0.9857	0.014	2.1×10^{-4}
0.8–0.7	1.4	5,100	6.5	3.1	0.032	0.968	0.033	4.9×10^{-4}
0.7–0.6	1.5	5,400	12.5	6.0	0.064	0.936	0.066	9.8×10^{-4}
0.6–0.5	1.6	5,700	27	14.5	0.165	0.835	0.18	2.7×10^{-4}
0.5–0.4	1.7	6,000	73	46	0.63	0.37	1.0	1.5×10^{-3}
0.4–0.3	1.8	6,350	99.6	26.6	0.982	0.018	4.0	5.9×10^{-3}
0.3–0.2	1.9	6,650	100	0.4	0.99+			
(Five layers of paper, n = 84.5 sq in., t = 2.63 mils)								
Over 0.9	1.73	6,100	0.3	0.3	0.003	0.997	0.003	
0.9–0.8	1.83	6,400	1.5	1.2	0.012	0.988	0.012	1.4×10^{-4}
0.8–0.7	1.93	6,700	6.5	5.0	0.0508	0.9492	0.053	6.3×10^{-4}
0.7–0.6	2.03	7,050	25	18.5	0.198	0.802	0.22	2.6×10^{-3}
0.6–0.5	2.13	7,350	74	49	0.655	0.345	1.07	1.3×10^{-2}
0.5–0.4	2.23	7,650	97	23	0.892	0.108	2.2	2.6×10^{-2}
0.4–0.3	2.33	7,900	100	3	0.99+			

points from other data are also located on Figure 10, and their correlation with the data from Table III is particularly significant. The point which is marked "Paper Test Point" is simply the frequency of occurrence of particles between 0.4 mil and 0.5 mil calculated from Figure 1 and is based, therefore, on direct counting of short circuiting particles. The other points are from production records of commercial capacitors which were analyzed in the manner described for the test specimens.

The principal value of the breakdown tests on the specimen capacitors lies in the relations that can be derived from the data rather than their statistical accuracy. For example, in evaluating a factor such as the expectation a, 250 tests on small specimen capacitors made under the somewhat artificial conditions of the laboratory certainly do not carry the weight of thousands of tests on very much larger capacitors culled from production records although the latter may be valueless in establishing trends or statistical laws. For this reason, in drawing the curve on Figure 10 much less weight is given to the experimental points than to the relatively few derived from the production records, and the lone "Paper Test Point." The curve is fitted largely to these points and has the equation.

$$a = 1.5e^{-10t'}$$

It must be regarded as a very satisfactory confirmation to find that points from these various sources cluster so closely around a single line.

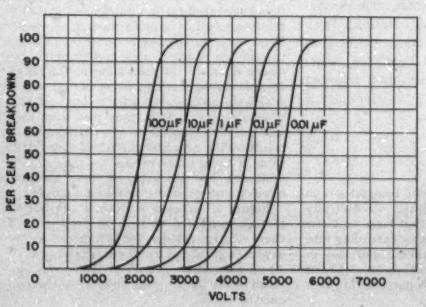

Figure 12. Calculated cumulative frequency distribution of breakdown voltage for a range of capacitor sizes, all with three layers of 0.5-mil oil impregnated paper

Calculation of Probable Breakdown Voltage

It is now possible to calculate the probable breakdown voltage of any oil-impregnated capacitor made with 0.5-mil kraft paper. The computation is simply a reversal of the steps followed in analyzing the breakdown data to determine the expectation of particle size occurrence. Before starting such a computation, the value of the average foil spacing t must be determined very carefully. The thickness of a sample capacitor may be measured and divided by the numbers of layers of paper and foil less the foil thickness or a value for t may be assigned as a design constant, consisting of the total nominal thickness of the paper layers times a space factor. An average value for space factor is 1.25. Next, a maximum conducting particle size must be chosen, and this should be such that p lies between 0.001 to 0.01. A trial or two may be necessary to establish this. Cell values of 0.1 mil spread are then set up starting with the maximum particle size and corresponding values for a, na, p, q, P, and ΣP are then tabulated. Finally, the true insulation thickness t' and its breakdown voltage is listed. A sample tabulation for a 1.0-microfarad capacitor is given in Table IV. Figure 11 shows how breakdown voltages calculated from the adjusted curve of Figure 10 compared with the experimental data of Table II. It will be observed that the greatest deviation between the test points and the calculated points is less than 10 per cent in voltage. Since the curve on Figure 10 was adjusted to represent the best values found in a large number of tests or that occur in the long run, the calculated distributions of Figure 11 may be considered as more dependable values over the long run than the test values from the relatively few specimens.

Discussion of Results

The relations between conducting particles and dielectric strength developed in this analysis provide a mathematical

Table IV. Calculation of Breakdown Voltage Distribution

Capacity 1.0 Microfarad; Mineral Oil Impregnated; Three Layers of 0.5-Mil Paper; Foil Separation = 1.9 Mils; Area of Paper (n) = 6,250 Square Inches

a	a	na	p	q	P	ΣP	t'	v
1.5–1.4	9×10^{-2}	0.0056	0.006	0.994	0.006	0.006	0.5	2,150
1.4–1.3	2.2×10^{-2}	0.0137	0.014	0.986	0.014	0.020	0.6	2,450
1.3–1.2	5.6×10^{-2}	0.035	0.034	0.966	0.0335	0.0535	0.7	2,800
1.2–1.1	1.6×10^{-1}	0.10	0.095	0.905	0.090	0.1435	0.8	3,100
1.1–1.0	4.7×10^{-1}	0.29	0.255	0.745	0.218	0.3615	0.9	3,450
1.0–0.9	1.2×10^{-1}	0.75	0.53	0.470	0.338	0.6995	1.0	3,750
0.9–0.8	3.3×10^{-1}	2.06	0.87	0.130	0.260	0.9595	1.1	4,100
0.8–0.7	1.0×10^{-2}	6.25	0.998	0.002	0.030	0.9984	1.2	4,400

method of evaluating the effect of area, number of layers, and the quality of the paper on voltage strength of the capacitor. In addition, the better understanding of how failure comes about because of conducting particles points the way to improvements to reduce their influence.

Figure 12 illustrates one of the valuable results of this method of calculating probable breakdown strength. Here is shown distribution curves of breakdown voltage for a series of capacitors ranging from 0.01 microfarad in size up to 100 microfarads but all having the same insulation of three layers of 0.5-mil paper. It has long been recognized that strength goes down with increasing size of capacitor, but there has been no mathematical means of correctly predicting this decrease. Derating, therefore, for loss of strength due to increasing size has been a matter of expensive and time-consuming tests or else the designers intuition. Figure 12 shows this decrease on a logical and mathematical basis.

The concept of reorientation of large particles removes the necessity of trying to explain short circuits in two and three layer capacitors by particles lining up, a possibility that is so remote as to be unimportant. To illustrate, suppose a sheet of paper containing a short circuiting particle were magnified 1,200 times. The conducting particle would occupy about the area of a tin cup and if it were considered as hidden in the area of a 10-acre field, this would be equivalent to three conducting particles per square foot that indicate short circuits on the paper test. The chance of two particles lining up is represented by the chance of tossing a marble into the 10-acre field and having it drop into the tin cup. The probability is about one in 5,000,000. To get three particles to line up, two marbles in succession must find the cup.

Another fallacy is the feeling that the strength of the insulation can be approximated by discounting one sheet of paper since one sheet is sure to be short-circuited. It is true that this is the most probable condition for some area of paper, but it has been shown that this is just about the area represented by the tests in Table II or an impractically small capacitor. In a 0.1-microfarad capacitor it is most likely that two sheets out of three will be short-circuited, and a 100-microfarad capacitor is saved from puncture of three sheets largely by the oil films arising from a large space factor.

Nothing has been said thus far regarding the effect of lamination or number of sheets of paper. Considering the sides of the paper facing the electrodes, it is apparent that there may be a difference in the opportunity for reorientation of a particle if it lies in a two layer capacitor rather than in one of three or four layers. If the particle lies near the surface next to the foil, its maximum size would be limited by the surface of the foil whereas if it were contained between two layers of paper, it might not be so restricted. This seems to be borne out in the characteristics of relatively large two sheet capacitors where the occurrence of large particles appears less than normal. The breakdown strength becomes unpredictable in this case, however, for another reason. If the probability is high that the insulation will be completely short-circuited, there will be many cases where the insulation remaining between the conducting particle and the foils is only a microscopic oil film, and the determination of insulation strength from Figure 7 is no longer valid. In the case of capacitors of three layers or more, any restriction to reorientation imposed by the foil appears of little consequence and may be neglected.

Conclusions

1. The statistical evidence brought out in this analysis is explained satisfactorily only by the assumption that large particles are capable of puncturing or extending into and through adjacent sheets and can in themselves produce breakdown without necessarily lining up with particles in other sheets of paper.

2. It appears possible for large conducting particles to become reoriented and therefore harmful by flexing of the sheet such as occurs in winding.

3. The data on conducting particles in a representative sample of paper by the electric roller test may be considered as measuring an important quality, even though this test does not measure particles buried in the paper.

4. The effects of reducing the thickness of single sheets and increasing the number of layers can now be evaluated in terms of capacitor designs and field performance as affected by local defects can be calculated more accurately than in the past.

5. The advantage of further reductions in the conducting particles in capacitor paper can now be directly evaluated, and the overall economics of designs using superior papers can be studied without the necessity of accumulating field experience over a long period.

References

1. Probability and Its Engineering Uses (book), T. C. Fry. D. Van Nostrand Company, Inc., New York, N. Y., 1928. Page 227.

2. Dielectric Phenomena in High Voltage Engineering (book), F. W. Peek, Jr. McGraw-Hill Book Company, Inc., New York, N. Y., 1929. Page 239.

Discussion

J. D. Stacy (General Electric Company, Pittsfield, Mass.): This paper gives an interesting analysis of the effect of conducting particles in capacitor paper on breakdown strength of capacitor dielectrics. It has long been recognized that the frequency of occurrence of conducting particles in an area of capacitor paper has an important bearing on dielectric design and, because of this, co-operative development between capacitor manufacturers and the paper mills has been carried on to secure lower particle count. This has resulted in reduction during the past 25 years from about 200 particles per square foot to 1 particle per square foot in 0.0005-inch paper. With the present low particle count it is my opinion that a region of diminishing return has been reached in development of further particle reduction in relation to other imperfections in the paper sheet such as thickness variation between increments of sheet area and channels between fibers in the formation of the sheet. It appears to me that some of the effects which the author attributes to reorientation of conducting particles may well have been due to such imperfections. Although the result on the capacitor dielectric may be the same if these other causes are present, the approach by the paper manufacturer to develop improvement would be different.

Figure 12 gives, I believe, a pessimistic picture compared to tests of capacitors of these relative ratings, for instance, I would expect to get about 8 per cent breakdowns on 10-microfarad capacitors at 2,500 volts instead of the 22 per cent shown by the calculated curve.

J. B. Whitehead (The Johns Hopkins University, Baltimore, Md.): Several years ago we conducted at The Johns Hopkins University a series of tests of the breakdown strength of impregnated paper. The capacitor was cylindrical, 1-inch inside diameter, and the dielectric 15 layers of paper, 4 mils thick, assembled and impregnated as in underground power cables. The method of test was to apply a relatively high voltage and to observe on a suitable recorder the rectified high frequency component of the current through the insulation to ground. If the insulation is not overstressed no high frequency component appears; when overstress begins this component appears and increases steadily and more or less rapidly, depending on the applied voltage, until complete failure occurs. Interruption of the circuit permits examination of the specimen at any stage of the breakdown and it is found that almost invariably this begins as a small black channel through one or two paper tapes.

It is obvious that in our tests minute metal particles play no part in the breakdown; the paper is too thick and there are too many layers. It is equally obvious that in the Brooks' test no account is taken of the time element of the applied stress in its influence on the stability of the impregnated insulation. There are thus two possible types of breakdown of impregnated paper and so a question arises as to whether the Brooks tests give a complete picture of probable behavior under the conditions of service.

Hazards of Static Electricity in Hospital Operating Rooms

HORATIO B. WILLIAMS
MEMBER AIEE

THE USE of ether as a general anesthetic dates from 1846. For over a half century after its introduction it continued to be administered by the same crude method which Morton employed in his original demonstration. In the early years of the twentieth century the giving of anesthetics began to be developed as a specialty, and the method of administering ether was greatly improved. Apparatus was developed for mixing ether vapor with oxygen in definite proportions and later other substances having anesthetic properties were investigated, notably ethylene and cyclopropane gases. These gases were found to offer many advantages over ether. Cyclopropane in particular seems to be in many respects the best general anesthetic available at present.

Although ether vapor mixed in proper proportions with air is highly explosive, fatal explosions of it were almost unknown in the early years. One instance of fatality occurred when bleeding in a throat operation led the operator inadvertently to use a cautery. With the use of pure oxygen as a diluent and with the use of rubber bags and tubing, explosions occurred more frequently, though in comparison with the total number of anesthesias the incidence was small. Even when care was taken to avoid open flames, cauteries, and electric arcs, accidents still occurred. Eventually these were traced to occurrence of sparks due to discharge of static charges, either in the immediate neighborhood of the patient's face, or within the apparatus itself. When ether vapor is used, the propagation of an explosion can be stopped by metal gauze as in the Davy lamp. In cyclopropane and ethylene the velocity of the explosion wave is so great that this device is ineffective.

The obvious procedure to diminish this risk seemed to be the keeping of all personnel and equipment at ground potential. This requires limitation of the use of nonconductors in the operating room to bare essentials. Floors should be of conductive material in connection with ground, and personnel should wear shoes with conductive soles. All furniture should be of metal in conductive connection with the floor and the anesthesia apparatus itself should be made entirely of conductive material. In 1940 highly conductive rubber, loaded with carbon black, became available and its use for flooring and shoe soles offered a partial solution to the problem. The anesthesia machine has as essential components a face mask, either of metal edged with rubber, or entirely of rubber. Two long flexible tubes connect the face mask to the machine, and there is also a rubber bag from which the patient breathes the mixture. Loading the rubber of the bag and tubes with sufficient carbon black to make it highly conductive throughout results in a product so stiff as to be useless. Attempts to get sufficient conductivity by coating these parts with a thin conductive layer have been partly successful, but the conductive layer loses its conductivity rather soon and daily testing is necessary. This is at present the weakest part of the system.

Rubber flooring is satisfactory, though somewhat expensive. During the war it was not available. Conductive linoleum has been developed. While its resistance as measured with low voltage is too high, it is satisfactorily low when the impressed voltage is 100 volts or more; and this is sufficient. Both have been used for several years at the Presbyterian Hospital in New York.

Floors of terrazzo, commonly used in operating rooms, often have a conductivity when measured to ground from a conductive contact such as the sole of a shoe of conductive rubber, of the order of one reciprocal megohm. At first it was considered that such floors might be safe. It was found that in very dry weather when the relative humidity falls as low as 10 per cent such floors develop a high surface resistance and are unsafe. Tile floors are good insulators. The thin line of cement between tiles is conductive when damp, and such floors can be made conductive by mopping with 4 per cent calcium chloride solution; but in dry winter weather this becomes ineffective. High resistance may develop within half an hour after mopping. In air-conditioned operating rooms where a high relative humidity is maintained, such treatment of a tile floor may be employed as an emergency measure; but is not recommended as standard procedure, since safety then depends on technic, and it is safer if it can be made to depend on construction.

At one time it was thought that humidification of a room would prevent accumulation of static charges. In the dry-cleaning industry this had proved effective. A fatal explosion occurred in Boston, Mass., which was investigated by J. W. Horton.* This operating room was air-conditioned and kept at a relative humidity of 65 per cent. Doctor Horton found that the carbon dioxide was being completely removed by the air-conditioning process; and with air free of carbon dioxide, no conductivity was conferred on insulators by humidification. Later investigation indicates that the conditions in such a room actually favor accumulation of charge.

It has been difficult to appraise information which has been received from vari-

Paper 47-170, recommended by the AIEE committee on safety for presentation at the AIEE summer general meeting, Montreal, Quebec, Canada, June 9–13, 1947. Manuscript submitted April 28, 1947; made available for printing May 5, 1947.

HORATIO B. WILLIAMS, professor emeritus of Columbia University, is a consulting engineer with the Cambridge Instrument Company, Inc., New York, N. Y.

* Oral communication to the writer.

ous sources regarding the incidence of explosions under varying conditions. One hospital in the Adirondacks had an operating room floored with waxed linoleum, an excellent generator of charge by friction. Cyclopropane anesthesia was employed in this room in severe cold and dry weather for several years without a single mishap. There are many other reports showing no accidents, though cyclopropane has been used regularly without special precaution.

An explosion occurred in April 1940 in New York, N. Y. The floor was terrazzo. The resistance from an area of 25 square centimeters to ground was about one megohm. The anesthetist wore shoes of ordinary rubber. These had a resistance of over 1,000 megohms. Under these circumstances, a larger charge could have accumulated than would have been possible had the floor been of insulating material. If dependence is to be placed on grounding, there must be no breaks in technic. Accumulating experience indicates that safety is secured by the grounding technic, if it is carefully and completely carried out; but otherwise it actually may be safer to work on an insulating floor. Small sparks then probably will be of frequent occurrence, but with energy below the critical value which will initiate an explosion. This seems to be an unnecessary risk, but the risk of carelessness when grounding is attempted may be even greater.

It appeared desirable to determine the minimum energy required to explode a stoichiometric mixture of cyclopropane and oxygen. The capacity of the human body when insulated and near a large grounded conductor is of the order of 200 micromicrofarads. A variable air capacitor of range 40 to 250 micromicrofarads was calibrated and used as indicated in Figure 1. The capacitance of the electrostatic voltmeter varied with the deflection but it was so small as to be negligible. The switch was a well insulated type made by Leeds and Northrup for capacitance measurements. To avoid dissipation of energy by a spark when the switch was thrown, the capacitor was charged to a voltage below the spark-over voltage. After throwing the switch the capacitance was diminished until, as the voltage rose, spark-over occurred. The deflection of the voltmeter then fell to half value.

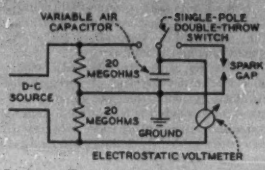

Figure 1. Test circuit to determine minimum energy required to explode mixtures of gases

The adjustable spark gap was placed in the gas mixture which was contained in a thin rubber bag. With a gap of 0.002 inch spark-over occurred regularly at 450 volts. The energy was 2×10^{-5} joule. When the gap was reduced to 0.0015 inch, spark-over occurred at 375 volts. The energy was 10^{-5} joule. With the longer gap and greater energy every spark produced an explosion. With the short gap and half the energy no explosion occurred. Since cyclopropane diffuses through rubber rather rapidly, it is necessary to work rapidly; and when no explosion occurs, it must be proved by subsequent test that the mixture remained explosive. After passing the weaker sparks without explosion, the energy was increased by giving the capacitor a higher charge; and the explosion then occurred even with the short gap. The sparks which cause explosion when passed in air are nearly inaudible and can be seen only in a darkened room. It may be of interest to mention by way of comparison that to operate an ordinary 3-volt flashlight for one second requires an energy of one joule.

How low must the resistance to ground be in order to prevent sparking voltages? Horton* found that with the human body insulated except for a ground connection through a resistance of one megohm, a foot rubbed on linoleum produced no sparks as indicated by an antenna and amplifier connected to a loud speaker. Increasing the resistance to 10 megohms resulted in some sparks and further increase to 20 megohms gave a continuous shower of sparks. One reciprocal megohm seems a reasonable minimum conductivity. Too great conductivity should be avoided because of the danger of electric shock from low voltage power appliances.

* Oral communication to the writer.

Discussion

Wills Maclachlin (Toronto, Ontario, Canada): The Institute is fortunate in having a man such as Doctor Williams, an outstanding member of the medical profession as well as an outstanding electrical engineer, present a paper on this subject.

The explosions in hospital operating rooms are not frequent, but the result is usually disastrous. Doctor Williams has ably presented the problem. The solution is a difficult one in that small charges of static electricity created from the soles of shoes rubbing on floor, blankets being pulled over one another, or the placing on the face or the taking off the face, of a face mask, is sufficient to cause an explosion. To develop satisfactory short-circuiting and grounding apparatus on movable pieces of equipment in the hands of lay people, as far as electric equipment is concerned, is a most difficult problem. Possibly the solution may lie in working out the best possible techniques and drilling the operating room staff in absolute conformity to these techniques. This, of course, presupposes that everything possible has been done in the preparation of the floor of the operating room and the larger pieces of equipment; but so many smaller pieces of equipment of a movable character are used, that strict practice must be drilled into the operating room staff.

May I again repeat that the Institute is fortunate in having an eminent scientist of Doctor Williams' caliber present such a clear paper on this important subject?

W. C. Wagner (Philadelphia Electric Company, Philadelphia, Pa.): The hazards due to discharges of static electricity are serious and are not confined to hospital operating rooms. Industry as a whole is making individual efforts to combat this by the inclusion of safeguarding provisions in the several safety codes concerned with hazardous locations; such as those where ignitable vapors, dust, and gases are present.

However, certain safeguards in themselves may increase possible hazards under certain conditions, and the precautions as indicated by Doctor Williams should be given serious consideration by all interests affected.

A National Fire Protection Association pamphlet[1] recently revised, covers the subject of such hazards and means for their reduction, including methods to meet them. Instruments are described for detecting, measuring, and recording electrostatic conditions. This is also an outstanding contribution to the general subject, in another field.

From the character of the two presentations, and others appearing from time to time in the technical press, it is clearly evident that there has been no definite concerted and comprehensive effort to deal with the fundamentals underlying this problem as a whole, to evaluate more definitely the conditions, and to provide, as a result of investigations and tests, sound engineering bases for safety provisions to be formulated by those branches of the industry concerned with the prevention of fire, explosion, and accident prevention from this cause.

New processes and new materials, some

involving the actual use of electrostatic discharges, are entering the fields of science and industry. We are now advised that not only friction, but the making or breaking of contacts of dissimilar materials, are sources of electrostatic potential. The writer is convinced that the general fundamentals underlying this problem should be developed comprehensively and adequately by our Institute.

It represents both a responsibility and an opportunity to serve industry by including the entire field of electrical static discharge phenomena met in industry.

The writer, with a background of experience in the development of national electrical safety codes, therefore cannot recommend too strongly the formation of a special committee, representing those substantially concerned, to deal with the fundamentals of this project and to develop the essential general engineering principles for the guidance of those concerned with the preparation and revisions of related safety rules and procedures.

Reference

1. Static Electricity (pamphlet). National Fire Protection Association, Boston, Mass., 1947.

An Improved Overcurrent Tripping Device for Low-Voltage Circuit Breakers

H. L. RAWLINS
MEMBER AIEE

JEROME SANDIN
MEMBER AIEE

Synopsis: The necessity for greater service continuity on low voltage systems has focused attention on the limitations of present delayed overcurrent tripping devices and created a demand for their improvement. This paper reviews the limitations of present devices and states the requirements for delayed overcurrent trips. A new device meeting all of the requirements is described and its characteristics shown. The new device is universal in its application in that the same elements provide for circuit breaker selectivity up to the highest values of fault current and yet give correct timing to permit motor starting. Tests are described which show the adequacy of the new device for its intended service as well as indicating an unusual degree of reliability.

THE tripping requirements for low voltage circuit breakers have been satisfied until recently by a self-contained series device that provided sufficient delay on overcurrent tripping for the immediate load at hand and which became instantaneous at rather low values of fault current. This characteristic was sufficient to provide for some circuit breaker selectivity on the lower values of fault current. Where complete circuit breaker selectivity has been required, it was accomplished through relays in the same manner as with high voltage circuit breakers. With increased concentrations of power, the necessity for selective tripping of low voltage circuit breakers throughout a greater range of fault currents has become apparent. It is also recognized that relays and accompanying current transformers are undesirable in most installations from the standpoint of complexity and cost.

The selective tripping of these circuit breakers can be accomplished by the addition of definite short time delay tripping devices that are effective throughout the required range of fault currents. This has been done in some instances and complete selectivity has been accomplished. The accomplishment of selectivity in these instances has required considerable engineering study and skill and it has become evident that an improved type of delayed trip is needed to simplify the application of low voltage circuit breakers.

Review of Delay Elements Used on Overcurrent Trips

The reliability and usefulness of a delayed overcurrent trip depends mainly upon the characteristics of the delay element. The delay elements in general use at the present time are:

1. *Liquid Film Delay.* In this device, the delay is obtained by the adhesion of liquid to two co-operating surfaces. This has been by far the most popular type of delay device since it is relatively simple in construction, the only requirement being two carefully finished surfaces. It has, however, certain limitations as follows:

(*a*). Inaccurate timing.

(*b*). Inability to operate with suitable delay on high values of fault current.

(*c*). Failure to provide any delay whatsoever when grit or dirt gets between the co-operating surfaces.

(*d*). The liquid is exposed to the atmosphere where it may become dirty, sludged by oxidation, or gummed by evaporation.

2. *Thermal Delay.* Since the liquid film type of delay did not provide reliable timing at the longer time necessary to start certain motors, thermal trip devices have been developed which are responsive to heating elements. The thermal trip device is simple on the smaller circuit breakers of relatively low interrupting ability, such as moulded case breakers, since the heating element may be connected directly in the circuit without fear of damage. For use on higher interrupting ability breakers, the heating elements usually are connected in the circuit by transformer action which, due to saturation, protects the heating elements on high values of fault current. Since the temperature rise of thermal elements must be held within reason, time values and pickup values are affected by ambient temperatures. It is necessary, therefore, either to compensate the bimetal element with a second bimetal element for ambient temperature or to provide a magnetic source of energy for tripping the circuit breaker which is released by bimetal movement but which is inoperative below fixed current values. The use of the magnetic means with bimetal operating latch is the usual method provided since the bimetal element does not provide enough force for circuit breaker tripping on the larger ratings. The limitations of the thermal trip device are

(*a*). It cannot be used to provide delay at high values of fault current.

(*b*). It is relatively complicated when used on higher rated circuit breakers.

(*c*). It is not suitable for use on higher rated d-c circuit breakers.

3. *Dashpot Delay.* Dashpot delay involves the actual displacement of liquid by a piston in a cylinder and, although not in general use at present for low voltage circuit breaker tripping devices, it is used for obtaining delayed tripping with transformer trip devices on higher voltage circuit breakers. These devices will provide sufficient time delay for motor starting purposes and are also capable of providing the delay required for higher values of fault current. The defects of the conventional dashpot arrangement are that dirt or foreign material may enter the liquid and cause sticking of the piston. Also, the piston may stick because of sludging or gumming of the dashpot oil. A tripping device involving a moving core in a completely sealed dashpot and a differential flux arrangement operative to trip the circuit breaker after a predetermined travel of the core is used on certain types of small moulded-case circuit

Paper 47-145, recommended by the AIEE committee on protective devices for presentation at the AIEE summer general meeting, Montreal, Quebec, Canada, June 9–13, 1947. Manuscript submitted March 25, 1947; made available for printing April 28, 1947.

H. L. RAWLINS is manager of the protective devices engineering department and JEROME SANDIN is senior design engineer with the Westinghouse Electric Corporation, East Pittsburgh, Pa.

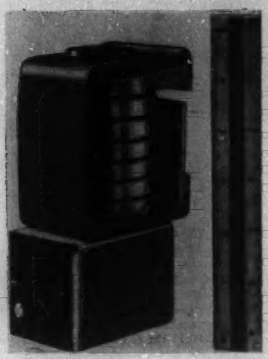

Figure 1. New trip unit, 225-ampere rating

breakers. This device avoids the troubles due to dirt or deterioration in the liquid but is not suitable for obtaining delays at even moderate values of overcurrent due to instantaneous action of the external armature.

4. *Mechanical Delay.* Mechanical delays involving escapement mechanisms, air vanes, or inertia devices connected through gearing to series magnets have been in common use in foreign countries but have not been used in the United States until recently where they have been used in simple form for obtaining the short time delays necessary for circuit breaker selectivity. A device of this type to provide delay sufficient for motor starting is essentially a clockwork mechanism which, during system faults, may be subjected to high forces. In the quantities involved in low voltage circuit breaker manufacture, these devices are not suitable for American manufacturing. Their maintenance also requires an unusual degree of skill which is not generally available. For the relatively short times involved in circuit breaker selectivity, a mechanical inertia device may be made in a simpler form so as to be suitable for normal American manufacture and maintenance. Such devices have been used either by themselves or in conjunction with other devices to provide circuit breaker tripping characteristics suitable for selectivity on high currents. The limitations of mechanical delay devices are

(a). They require very accurate workmanship and are, therefore, subject to variations in manufacture.

(b). An appreciable part of the driving effort is used to overcome friction, and they are, therefore, subject to variations in pickup and may become inoperative under adverse conditions of corrosion.

In order to obtain long time delay to permit motor starting and short time delay for selectivity, it has been necessary to use the mechanical delay device in conjunction with one of the other delay means. This results in a complicated structure where the chances of trouble are multiplied.

Requirements for Delayed Tripping Devices

The problems involved are not those of application, but concern the design of the devices for obtaining delay. The requirements for satisfactory tripping devices are few, but they all should be fulfilled by a single device. The requirements are

1. Sufficient delay must be provided throughout the range of motor starting currents to permit starting of motors having the highest values of locked rotor currents.

2. Above locked rotor currents, the device should be capable of providing the shortest permissible delay necessary for selectivity.

3. In order to provide the maximum possible protection to associated equipment and to other circuit breakers when connected in cascade, the device should be capable of tripping instantaneously at any fault current up to the short time rating of the circuit breaker.

4. There should be a wide range of pickup adjustment on the delay element.

5. The device should be suitable for both a-c and d-c circuit breakers.

6. The trip unit should be easily removable and interchangeable to facilitate changes in circuit breaker ratings and characteristics.

7. The device should be reliable and maintain its reliability without maintenance under all types of service conditions.

Up to the present time, these requirements have not been met by a single type of device. The requirements for the relatively long time delay for motor starting and short time delay for selectivity have involved two entirely different devices based on different operating principles.

An analysis of the existing elements together with the requirements for overcurrent tripping devices indicated that the ideal timing device should

1. Provide delay by the positive displacement of a fluid.
2. Be hermetically sealed.

The first attempts to accomplish this involved bellows operated sealed units, but further development revealed a simple and improved method that has resulted in an entirely new type of delayed overcurrent trip.

The New Overcurrent Tripping Device

The device incorporating all of the required features is shown in Figure 1. This unit is arranged to be readily removable so that interchangeability of trip units having various ratings and characteristics can be obtained. The unit shown has a 225-ampere coil rating and is suitable for both 225- and 600-ampere frame size circuit breakers. For a clear understanding of the theory and operation of this new device, reference should be made to Figure 2 which shows a sectional view of the new unit in the normal position. The elements of this trip unit are

1. The magnetic frame.

2. The series coil.

3. The sealed timing element incorporating upper and lower cores suitably restrained by a reset spring, the timing stem which determines the time characteristics, and the controlling fluid.

4. The instantaneous armature which provides instantaneous tripping above prescribed currents independent of any action within the sealed unit.

5. Calibration details for setting the minimum pickup of the unit.

Pickup occurs when the attraction of the cores exceeds the restraining force exerted by the weight of the sealed unit and the calibration spring. Delay is obtained by positive displacement of the fluid which is forced through the space between the upper core and the timing stem. The timing stem is the only variable in the sealed unit, and its diameter determines the size of annular orifice and, therefore, the time characteristics.

In operation, the upper core is held stationary by the attraction of its upper surface to the annular edge of the magnetic frame while the attraction between the upper core and the lower core raises all parts of the sealed unit except the upper core. This action, shown in Figure 3, raises the trip bar to unlatch the circuit breaker. The anchoring of the

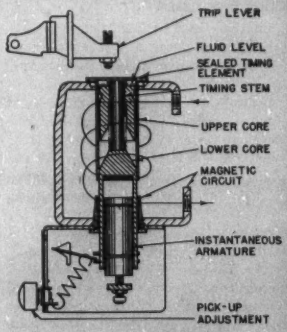

Figure 2. Sectional view of new unit in normal position

sealed upper core in space relative to the stationary frame while it is subjected to very strong force and with surrounding parts in motion was the major problem in this development, and its solution made possible the new tripping device. Successful operation requires that the force of attraction of the upper core to the magnetic frame exceed all forces restraining the movement of the sealed unit. These forces are the trip load required to unlatch the circuit breaker, the weight of the moving elements, the pull of the calibration spring in its maximum position, and the inertia forces of the moving masses. Strong upward pull on the upper core is obtained by increasing the flux density on the top surface of the core through suitable shaping of magnetic parts, the use of a small air gap, and through the use of tapered conical surfaces between the upper and lower cores. This permits an increased amount of flux to flow through the upper and lower cores which, although not adding appreciably to the pull between them, does increase the flux density between the upper core and the magnetic frame. The calibration or settings for minimum pickup is obtained by applying a suitable restraining force on the moving element. The toggle arrangement used to apply spring load to the moving element permits wide variations in pickup settings.

The instantaneous armature provides for instantaneous tripping of the circuit breaker irrespective of any action within the sealed timing element. On currents above the prescribed value, the instantaneous armature is picked up by the flux inside of the lower core, after it has saturated, and bodily raises the whole sealed element. This action, shown, in Figure 4, can be obtained for any value of current from 5 to 100 times coil rating by adjusting the position or by varying the cross-sectional area of the instantaneous armature. Since this armature is within the field of a solenoid, it will have a force exerted on it dependent upon the series current through the coil. This permits pickup adjustments for the instantaneous armature at all values of current. This would not be the case if it were a clapper type of armature where saturation would limit the forces at higher currents.

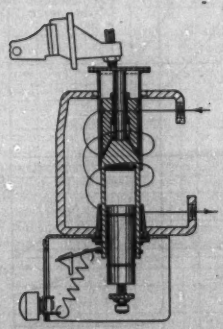

Figure 3. Position of parts when tripping with time delay

Since fluid pressure in the sealed chamber is dependent upon the series current, it is possible to provide long time delays for currents up to predetermined values and, by the operation of a by-pass relief valve, to provide short time delay for higher currents. This by-pass valve may be incorporated in the timing stem as shown in Figure 5. The stem with the valve as shown in part *B* merely is substituted for the simple stem shown in part *A*. The operation of the by-pass valve is simple in that above a certain pressure the valve spring is compressed, permitting the fluid to flow through a much larger orifice than the annular orifice on the outside of the timing stem which provides for long time delay.

The reset spring serves to position the upper core in the normal position and to reset the core after its movement during overcurrent conditions. The resulting delay on resetting makes the trip unit historic, that is, it remembers previous electrical history of the circuit in which it is connected. The only advantage of the thermal trip over previous devices providing the same delay is that the thermal device is historic due to its storage of heat. This new device may be given a better or worse memory than a thermal trip by making the reset spring weak or strong.

The fluid used to obtain timing is an important factor in this new trip unit. Silicone fluid is used because of its stability at higher temperatures and its smaller changes in viscosity with varying ambient temperatures. A fluid of high viscosity is used since it permits more clearance of moving parts and larger orifices which result in smaller changes in characteristics with manufacturing variations. The tube and top disk are made of nonmagnetic stainless steel because of its high resistivity, sturdiness, and resistance to corrosion. The cores are made of special silicon steel to reduce eddy currents and losses on alternating currents. On sealing, moisture and oxygen are removed from the fluid and internal parts by heat and vacuum treatment which insures freedom from corrosion for the sealed parts. The final sealing of the timing element is performed very effectively by projection welding the disk to the flanged top of the tube. This operation, performed in a fraction of a second, in no way injures the liquid or internal parts.

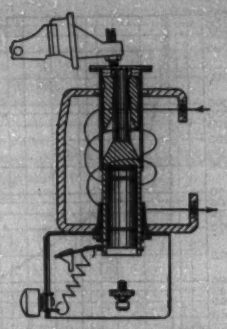

Figure 4. Position of parts when tripping through instantaneous armature

Characteristics

Tests on the new trip unit have revealed that any desired time–current characteristic can be obtained by varying the timing stem. A discussion of characteristics, therefore, does not consist

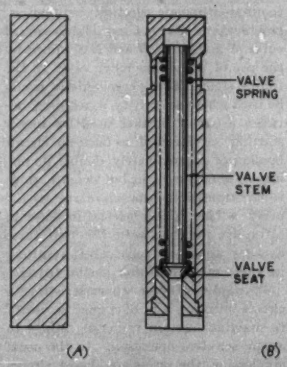

Figure 5. Timing stems used to obtain different timing characteristics

A—Simple stem for single delay curve
B—By-pass stem for obtaining combined long and short time delay

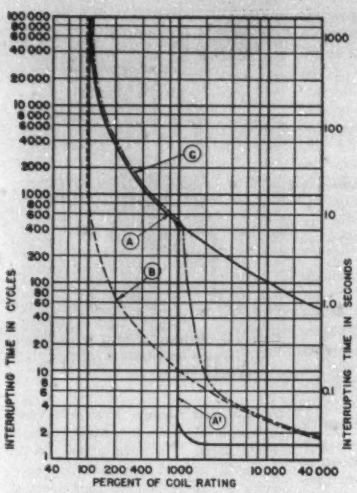

Figure 6. Typical time–current characteristic curves of new tripping device

of presenting some fixed curves but is a question of "what will you have." Figure 6 shows three time curves that can be obtained through the use of three different timing stems and represent desirable characteristics. Curve *A* provides sufficient delay for motor starting with the instantaneous trip operating at *A'* to provide rapid clearing of all fault currents above locked rotor values. Curve *B* provides a short time delay for all values of fault current and can be used to obtain complete selectivity between circuit breakers. Curve *C* is a combination of curve *A* and curve *B* and is obtained by the use of a by-pass relief valve in the timing stem. This characteristic would be used where selectivity is required between a circuit breaker used for motor starting service and a back-up circuit breaker of approximately double its rating. There is a slight but definite slope to the transition from one curve to the other. This is due to the increase in attractive force between the two cores as they approach each other, resulting in valve operation after partial travel.

In applying these characteristics to circuit breakers, it is, of course, necessary to maintain certain ratios of ratings to assure selective operation. In the usual application, the ratios are almost always more than sufficient due to other factors. Figure 7 shows the curves for a typical selectivity application using the three characteristics previously described. Here a 100-ampere-load circuit breaker is provided with long time delay and instantaneous trip to permit motor starting. A 400-ampere feeder circuit breaker is equipped with both long time and short time delay to obtain complete selectivity with the motor starting load circuit breaker. A 1,600-ampere transformer circuit breaker supplying power to the system is set to pickup at 3,000 amperes and is equipped with short time delay only since that will provide for selectivity with the 400-ampere feeder circuit breaker and all other feeder circuit breakers. If the transformer can deliver more than 25,000 amperes and the interrupting rating of the load and feeder circuit breakers is 25,000 amperes, the system should be operated with combined cascade and selectivity by providing the feeder and transformer circuit breakers with instantaneous trip armatures set at 20,000 amperes as indicated by the dotted line at *D*. Such an arrangement would result in getting all that is possible out of the circuit breakers and the system.

One of the outstanding characteristics of the new device is the combination of long time delay to permit motor starting with a wide range of pickup adjustment that permits it to be applied universally for either motor service or for general load service. The short time delay and combined short and long delay characteristics would be used in selectivity applications and therefore, would be on back-up circuit breakers.

Tests

The design, the adaptability, the characteristics, and the accuracy of pickup and timing of this new overcurrent tripping device have been verified by thousands of tests over a $2^1/_2$-

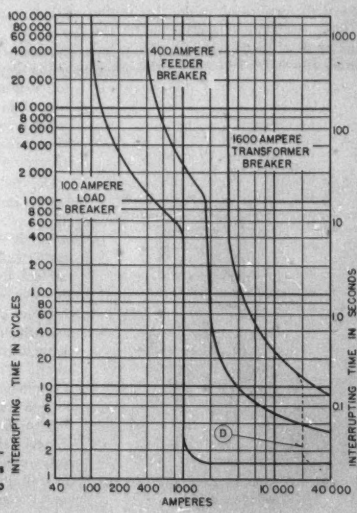

Figure 7. Time–current characteristics of circuit breakers equipped with new type trip units for selective operation

year period. Tests on fluids of various viscosities in structures having different orifices have shown that any desired time characteristic may be obtained. Pickup tests from 80 to 200 per cent of coil rating in the same unit show that such a unit may be used either to provide for motor starting or for miscellaneous applications, thereby replacing both the old type thermal-magnetic and the so-called "dual-magnetic" with one universal overcurrent trip unit. Timing, selectivity, and instantaneous armature pickup tests on currents up to 100 times coil rating have proved the ability of this device to provide for selective tripping of circuit breakers on all reasonable applications of selective tripping and combined selective tripping and cascade.

The sturdiness of the new trip unit has been verified by its ability to withstand short-circuit currents up to 500 times the coil rating. It has also been verified by the ability of the sealed unit to withstand severe shock tests.

The ability of the sealed unit with its silicone fluid to maintain its characteristics throughout a long life is indicated by the operation of six units for over six months at a temperature of 150 degrees centigrade with no change in characteristics. Some of these units after being sealed for over $1^1/_2$ years were dismantled, and all of the parts were found to be bright and clean. Several units have had over 1,000 overcurrent operations without change in characteristics and without noticeable wear.

Tests show that the device will operate at all temperatures from −40 to 100 degrees centigrade. For the range of temperatures from 10 to 55 degrees centigrade which represents the usual condition for low circuit voltage breakers, the change in time is only 34 per cent of the change occurring on devices using petroleum oils. For wider ranges of temperatures, the per cent improvement is much greater.

It is believed that these tests, when considered with the proved reliability of other hermetically sealed devices such as solder sealed capacitors and treated and sealed transformers, prove the complete adequacy of the new tripping device for the service intended.

Conclusions

Demands for greater continuity of service on low voltage systems have focused attention on the weaknesses of present overcurrent tripping devices. A new overcurrent tripping device has been developed in which the timing characteristics are obtained by the positive displacement of fluid in a hermetically sealed chamber. The universal characteristics of the new device permit the replacement of both the old thermal-magnetic and dual-magnetic with one universal type of trip unit which is equally applicable to a-c or d-c circuit breakers. The positive displacement of fluid provides accurate timing for all values of fault current, thereby permitting the selective tripping of circuit breakers to localize all faults. The use of magnetic cores within the series coil provides inverse timing and also permits accurate pickup settings for the instantaneous trip at all values of fault current. This arrangement permits selectivity up to the interrupting ability of the smaller circuit breakers and cascade or instantaneous back-up protection at higher fault currents. This new tool will provide the application engineer with a means for solving the various problems connected with low voltage systems.

The use of a sealed timing element with simple action assures an unusual degree of reliability with minimum maintenance.

References

1. Improved Selective Tripping of Low-Voltage Air Circuit Breakers, Charles P. West. AIEE Transactions, volume 63, 1944, August section, pages 608–10.

2. Fault Protection on Shipboard A-C Power Distribution Systems, H. G. Rickover, P. N. Ross. AIEE Transactions, volume 63, 1944, pages 1109–20.

3. Protection of Low-Voltage Circuits by Air Circuit Breakers in Cascade Arrangement, C. H. Black, A. E. Anderson. AIEE Transactions, volume 60, 1941, pages 1151–60.

Discussion

Robert W. Smith (General Electric Company, Philadelphia, Pa.): Relative simplicity of the new overcurrent tripping device described in this paper, together with its reported consistency of calibration are, without question, very desirable features. However, the construction of the device is such that there is an inherent relation between the various components and it would seem that any change in one of the calibration settings must necessarily also change the other calibration settings. For example, if the pickup adjustment of the long time element is raised by increasing the tension of the calibration spring, which can be done in the field, such a change will also raise the pickup value of the short time element and the selective tripping co-ordination between circuit breakers may be spoiled. Also, the effect of the short time element on the long time characteristic for current values approaching the pickup setting of the short time element can be appreciable, as well as the effect of the instantaneous element on the short time characteristic for current values approaching the pickup setting of the instantaneous element.

For these reasons, the advantage gained in simplicity by the use of a single element for obtaining combined functions, may be more than offset by the disadvantages of application, together with the difficulties which must inherently be encountered in the original factory adjustment of calibrations which are interdependent.

H. L. Rawlins and **Jerome Sandin:** The effect of the change of one calibration setting on the pickup of another setting is of vital importance in the application of these devices to co-ordinated systems. Therefore, the questions raised by Smith are ones that were considered carefully in the development of this trip unit.

There is no measurable change in the pickup of the short time element due to a change in setting of the long time element, say from 80 to 200 per cent coil rating, when the short time pickup is approximately 1,000 per cent coil rating. If the short time pickup is approximately 500 per cent of coil rating, the change in this pickup will be slight. Tests have shown it to be much less than the normal variation expected between units and not enough to effect the selective tripping of circuit breakers.

The short-time element does not affect the long time characteristics as it approaches the short-time pickup setting. The curves in the paper were determined by tests and show the sharp break at the pickup of the short time delay. Also, the instantaneous element does not affect the short time characteristic as it approaches the pickup setting of the instantaneous element. Although a curve of short time delay with instantaneous tripping is not shown, the action is the same as with long time delay and instantaneous which is shown. No effect should be expected since a different armature is used to obtain instantaneous tripping.

Galloping Conductors and a Method for Studying Them

E. L. TORNQUIST
MEMBER AIEE

C. BECKER
NONMEMBER AIEE

Synopsis: This paper presents results of a study of the large amplitude oscillations of aerial conductors called galloping. The work was undertaken in an attempt to evaluate the possibility of mitigating the damage caused by these disturbances. A full scale experimental line is described which is so constructed that, without ice formation, it will gallop typically and vigorously under ordinary wind conditions, thus allowing study of various means of mitigation. Data on the behavior of this line are presented.

It is hoped that this paper will stimulate further study on this important problem and thus hasten the development of a practical solution.

IN THE OPERATION of an overhead electric transmission and distribution system, galloping of conductors often results in considerable damage to the line and overhead structures. Violence of the galloping is often sufficient to cause contact between conductors with resultant tripping out of the line. This phenomenon is most common during periods of glaze formation, and in a general storm may constitute a serious threat to continuity of service. Because of its seriousness this problem has prompted much study and research by the industry in the hope of finding a practical solution.

The company with which the authors are associated was confronted in 1944 with the problem of revising one of its major transmission lines so that it would be less susceptible to outages caused by galloping. It was decided to review the literature and to determine whether a program should be instituted to investigate further the possibility of a practical means of mitigation. The initial study indicated the need for a full scale experimental line which would gallop in ordinary winds thus permitting evaluation of any proposed mitigating devices. Such a line was designed and built, and galloping resulted.

Although galloping is known to take place under widely different conditions, the literature and many private reports indicate that in most of the cases affecting operation of power lines, glaze or snow was present on the conductors. In many of these incidents the glaze, at its thickest point, was approximately one-quarter of an inch or more thick, but in other cases, on conductors as large as one inch or so in diameter, it was only of the order of one-sixteenth of an inch, or even less. However, there are reports of instances of galloping where no glaze or snow was present. Here the conductors ranged in size from number 4 (0.204-inch diameter) bare solid copper wire to lead-sheathed telephone cables, 2.5 inches in diameter.

It can be seen from these examples of galloping that the effect is produced under a variety of conditions. All forms, however, may be found to be susceptible to alleviation by the same means.

Galloping caused by corona or other electric effects[1] can be dismissed as harmless and of very rare occurrence.

It is not the purpose of this paper to discuss fully the various explanations of galloping and the associated aerodynamic theory. However, it is thought that some brief discussion will make clear the reasoning leading up to the experimental procedure used and will provide a common basis for discussion.

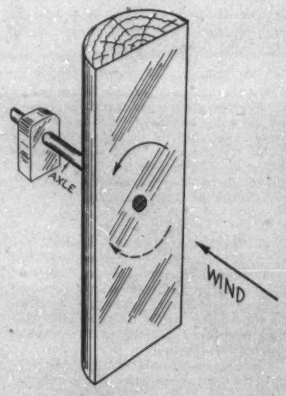

Figure 1. The half-round bar on an axle as mounted by Lanchester

It continues to rotate in either direction when once started

Aerodynamic Theory

The behavior of a fluid such as air, as it passes over solids of various cross sections has been studied for many years. That a rotating sphere in an air stream experiences a sidewise force, in addition to that exerted parallel to the flow, was known to Newton in 1672.[2] Magnus performed the first laboratory experiments involving this phenomenon, and these were reported in 1853.[2] The curved path sometimes followed by golf balls and baseballs, and the "drift" of projectiles, are examples of the "Magnus effect."

It is possible that the experiments of Magnus led to the discovery by an unidentified individual of a case of "autorotation." This was reported by Lanchester in 1908.[3] If a half-round bar of wood is mounted on an axle through its center and placed normal to an air stream directed at its flat face, it will continue to rotate in either direction when once

Paper 47-143, recommended by the AIEE committee on power transmission and distribution for presentation at the AIEE summer general meeting, Montreal, Quebec, Canada, June 9-13, 1947. Manuscript submitted March 27, 1947; made available for printing April 25, 1947.

E. L. TORNQUIST is engineer of tests and research and C. BECKER is chief chemist with the Public Service Company of Northern Illinois, Chicago, Ill.

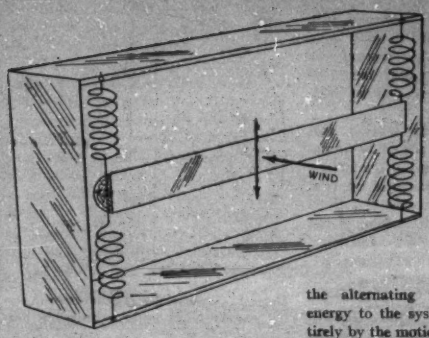

Figure 2. This simplified form of Den Hartog's apparatus was the type used to test various sections for stability

For maximum effect the frame must be weighted or fastened to a firm table. The half-round bar suspended on springs oscillates in a vertical plane

started (Figure 1). Again, as in the case of a rotating sphere or cylinder a sidewise force is experienced. With the half-round bar this force is in the same direction as that of the force producing the initial starting motion and, if the axle friction is not too great, is sufficient to cause continuous rotation. This behavior may also be exhibited by square, rectangular, triangular, circular-segment, and certain more complex cross sections. The wind must be directed at the flat face.

The autorotation phenomenon is a vital factor in the dangerous "tail spin" of the airplane.[4]

In 1919 Glauert[5] reported his work on autorotation of airfoils. He presented a theory in mathematical terms which states that the region of autorotation is determined by the condition that,

$$\frac{dC_L}{d\alpha}+C_D<0 \qquad (1)$$

where C_L and C_D are the coefficients of aerodynamic lift and drag, and α is the angle of incidence of the wind. These values are determined readily by tests on a static model in a wind tunnel. This criterion was of value in the development of the airplane.

Sometime after publication of Glauert's work it was found that if a cross section susceptible of autorotation were suspended with elastic restraint in an air stream it would oscillate spontaneously and continuously. This motion is called "reversible autorotation."[6] A small random disturbance, such as a gust of wind, is sufficient to initiate the oscillation. During each cycle there is a small energy input from the wind. These successive reinforcements steadily increase the amplitude which reaches a maximum when the energy input by the wind is just dissipated by damping. Reversible autorotation is a "self-induced" form of vibration. This is an oscillation in which the alternating forces furnishing the energy to the system are controlled entirely by the motion of the body. When the motion stops, the alternating force disappears.[7] A self-induced vibration may also be considered as a free vibration whose amplitude is increased by "negative damping."

"Rotary instability," for the purpose of this discussion, will be the term used to designate that aerodynamic instability, defined by the Glauert criterion,[1] which renders a cross section susceptible of autorotation and, of course, of reversible autorotation.

One other type of aerodynamic behavior will be mentioned here. When a fluid, such as air, passes over an obstacle of blunt cross section, for example a cable, eddies or vortices may be alternately generated and shed at the lee of the two sides of the obstacle, forming a double-row trail of vortices downstream. This was first studied experimentally by Benard in 1908 and explained by von Karman in 1911.[8] The trail is called a "Karman vortex-street." The alternating eddy formation produces an alternating force on the obstacle in a direction at right angles to the air flow. This is the cause of the high-frequency low-amplitude vibrations of transmission line conductors which induce fatigue. Vibrations induced by Karman vortices may be called "wind-eddy" vibrations.

Davison and Den Hartog Theories

Davison,[9] in 1930, presented the results of his important pioneer work on galloping. He suggests that galloping is the result of the aerodynamic lift produced by the reaction of wind and glaze, and a periodic twisting of the conductor which controls the application of the lifting force. Den Hartog[10] followed in 1932 with a theory which does not require a twisting of the conductor about its axis. Den Hartog explains that galloping is the result of glaze formation which, with the conductor, has a cross section capable of causing a certain type of aerodynamic instability. This is the rotary instability defined by Glauert's criterion,[1] which results in reversible autorotation (oscillation) when the airfoil is suspended elastically.

Den Hartog used two sets of opposing vertical coil springs attached to a heavy steel frame to suspend elastically Lanchester's half-round bar. The steel frame was mounted on springs. When placed before a desk fan, the bar oscillated transversely with an amplitude of two diameters. This performance was cited as supporting the theory.

During the past 20 years a number of explanations have been advanced to account for galloping. References to most of these are given in Davison's paper.[9] Others are given herein.[10–13]

After a study had been made of these theories it appeared that they might account for many of the cases of galloping, but not for all. (See the Appendix.)

Tests With Oscillating Models

In order to design an experimental line that would gallop, a series of tests was undertaken. The first of these was Den Hartog's experiment mentioned above. The simplified apparatus shown in Figure 2 was used, since with it much greater

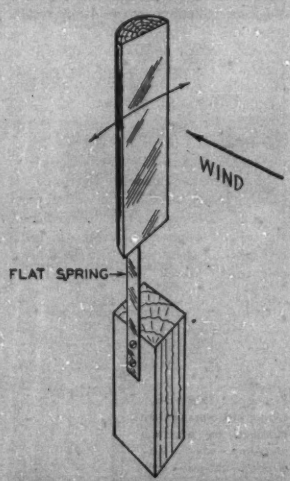

Figure 3. Vertical cantilever suspension of the half-round bar which was used to obtain low-frequency oscillations in the order of 20 cycles per minute

The model oscillates transversely to the wind

oscillation amplitudes could be obtained. Ordinary steel coil springs were mounted in a simple frame which, for stability, was either weighted or fastened to a firm table. With the half-round bar the desk fan had to be run slowly to prevent the model from striking the frame which was 15 inches in height. The frequency was 220 cycles per minute.

A model suspended in this manner was found to have excessive torsional flexibility about its longitudinal axis and about a vertical axis passing through its center of length. Also, the frequency was high as compared with the 15 to 30 cycles per minute noted on most galloping suspension-insulator transmission lines. With this apparatus the frequency cannot be reduced materially without a still further increase in flexibility. Consequently, two other vibrating systems were tried. One apparatus consisted of a half-round bar fastened to a length of flat steel spring, mounted as a vertical cantilever as shown in Figure 3. Suitable choice of spring and other dimensions resulted in frequencies of 25 cycles per minute and less. The model oscillated through angles exceeding 150 degrees. Another apparatus consisted of a four or five foot length of rubber tubing with a coil spring at each end, suspended between supports. Attached to the tubing was a strip of modeling clay with the cross section shown in Figure 4. Vigorous galloping in two loops results when this is subjected to a suitable air stream, but the apparatus is difficult to control. The springs supply the requisite elasticity. In a transmission line the conductors furnish the elasticity, since they are, of course, in a state of elastic suspension as a result of elastic stretch or deformation, caused by their weight.

Tests were next made to determine the relative rotary instability of various cross sections. Because of its convenience, the type of suspension shown in Figure 2 was used for these tests. At the time of this work, March 1944, a "standard" wind tunnel was not available and, with reluctance, it was decided to resort to an improvised tunnel. This was of the open-circuit open-jet type, 20 inches by 20 inches. The turbulence was not measured.

About 30 models, representing cross sections of various shapes, glaze formations, and actual sections of conductors, were tested in an apparatus of the type shown in Figure 2. Lengths of 7 to 38 inches were used, the latter being placed centrally in front of the jet. Diameters or breadths ranged from 0.25 to 2.5 inches, weights from 0.1 to 4.0 pounds, and oscillation frequencies from 130 to 350 cycles per minute. Several surface finishes were tried. End attachments on the models permitted them to be rotated about the longitudinal axis for the purpose of varying the vertical angle of presentation. The frame supporting the springs was pivoted to permit changing the angle between the longitudinal axis of the model and the horizontal wind. Wind velocities ranged from 1.0 to 28 miles per hour.

The instability of the models was judged by the amplitude of vertical oscillation and the degree of "flutter" (torsional oscillation about the longitudinal axis of the model).

Peculiar results were obtained when some of the models were tested with their longitudinal axis at an angle other than 90 degrees to the horizontal wind. The results obtained with these oblique winds are discussed in the Appendix.

Conclusions in Tests With Oscillating Models

These tests indicate that a suspended conductor, to which is attached a wooden airfoil of proper cross section and dimension, should gallop under suitable wind conditions. An airfoil of half-round section was selected as the suitable one for use on the proposed line. A rectangular cross section, applied in the vertical position, probably would cause galloping with winds on either side of the line, but it is materially less unstable than the half-round cross section.

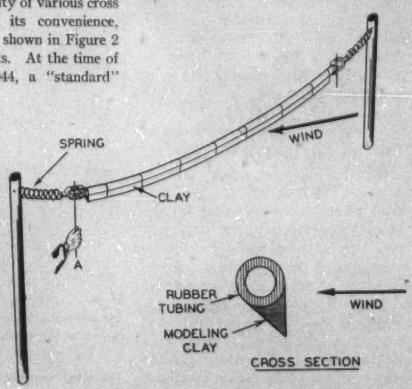

Figure 4. This rubber tubing with cross section modified by attached modeling clay, suspended between coil springs, gallops vigorously in two loops

Polarizing device at *A* may be needed to prevent twisting of the flexible tubing

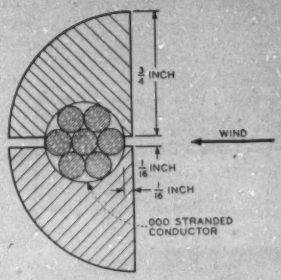

Figure 5. Cross section of conductor and airfoil assembly used on the experimental line

First Experimental Line

As an intermediate step, a 250-foot single-span experimental line was built. The conductor was number 000 stranded copper. It was "dead-ended" on two 30-foot wood poles. End clamps were provided with means for sag adjustment. Airfoils, of half-round cross section, were made from 3/4-inch white pine quarter-rounds 30 inches long, grooved and varnished. They were fastened to the conductor by means of three ties of 0.054-inch diameter soft steel wire (Figure 5). A space of three-sixteenths of an inch was allowed between successive pairs of airfoils. The flat face was vertical. The groove was placed as close to the flat face as possible, one-sixteenth of an inch. Unit weight of the airfoils was 0.132 pound per foot and of the coated conductor, 0.65 pound per foot. Direction of the line was 10 degrees east of north.

Pertinent data taken on this line are shown in Table I.

During the 40 days that this span was in place the largest amplitude recorded was 2.5 feet. This was during a two-loop gallop. Most of the observations were made using a sag of 6.13 feet. The smallest sag was 2.33 feet. The highest wind velocity recorded during a test was 13 miles per hour. At times, wind velocities of one mile per hour produced

amplitudes of one to two inches. Winds between 20 and 60 degrees to the line gave rise to the larger amplitudes. No galloping or other oscillatory motion was observed when the winds were between 80 and 90 degrees to the line. When the line was given a forced start, at various resonant frequencies, the gallop was not sustained in winds of this direction which occurred on four different days and had a velocity range of approximately four to nine miles per hour. Winds directed at the curved side of the airfoils caused no noticeable oscillation.

During galloping, the flat face of the airfoil followed the same vertical, slightly curved path in both the upward and downward stroke, except that under some conditions of violent galloping the airfoils and conductor were twisted rapidly and at random about their longitudinal axis. The timing and nature of the motion was such that it is not believed that it contributes to the aerodynamic instability of the system. This motion had a very slight tendency to change the position of the airfoils on the conductor. An elliptical path was never observed nor was a gallop with one loop (fundamental mode). When the conductor was forced by hand into a 1-loop gallop at the natural frequency, the motion was soon dissipated and changed into two loops. Most of the galloping occurred with two loops and with a stationary node at the center of the span. Galloping with six loops took place frequently. Four loops were seldom observed and three, five, or seven loops were never seen. Upon one occasion the conductor was forced by hand into three loops. This motion continued for 10 minutes and then gradually changed to a 2-loop position. The largest number of loops observed was 10 or 12.

Winds greater in velocity than four or five miles per hour produced only the 2-loop gallop. No gustiness determinations were made, but from the "feel" of the wind, together with velocity and amplitude observations, it was apparent that wind gusts had a marked effect in reducing amplitude. In "steady wind" the amplitude increased with the velocity. Wind angles as small as two or three degrees engendered, at times, several inches of amplitude.

Oscillation frequencies observed on this line checked fairly well with those calculated from the measured sag by combining the equation for vibrating strings and the standard parabolic line-design equation for the deflection of a suspended cable (Figure 6). Similar agreement is found in natural galloping, that is, that occurring in the field.

The galloping obtained with this single span experimental line compared well enough with that observed in the field to justify the construction of a multiple-span suspension-insulator line.

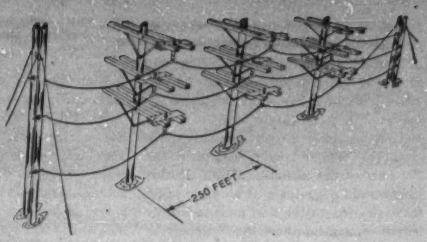

Figure 7. Second experimental line

Four spans; three conductors; simulated suspension-type "insulators"; wooden airfoils. (Not to scale)

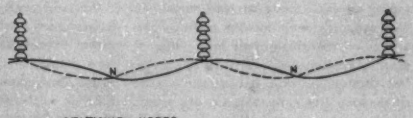

Figure 8. Galloping of type 1, two loops with the node stationary. Insulators do not swing. Adjacent spans often are not in synchronism

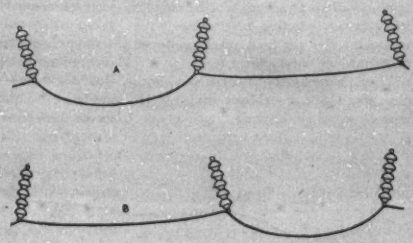

Figure 9. Galloping of type 2, one loop with adjacent spans exactly 180 degrees out of phase

Insulator swing exaggerated in the drawing. *A* and *B* show the extremes of a cycle

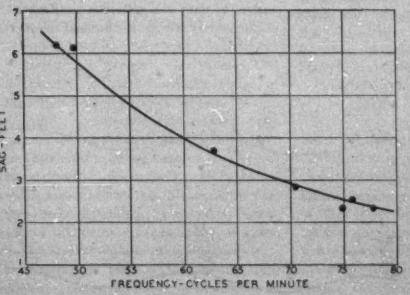

Figure 6. Relation of frequency and sag

The points are the frequencies of the 2-loop gallop as observed on the single-span experimental line. The solid curve represents the values calculated from the relation

$$\text{Sag in feet} = \frac{1.006}{[\text{Frequency in cycles per second}]^2}$$

Second Experimental Line

It was decided to make this a 4-span 3-conductor, suspension-insulator line (Figure 7). No change was made in the airfoil design. This line consisted of 250-foot spans of number 000 stranded copper conductor dead-ended on the end poles. The top conductor was dead-ended on a separate pole. At intermediate poles conductors were suspended from wood cross-arms by free-swinging steel bars 12 inches in length. The conductors were in vertical arrangement with four-foot separation, the center one offset 11 inches; the bottom conductor was 12 feet above the ground at mid-span. The

sag was 5.25 feet. Steel bars were used in place of insulators to permit application of certain test attachments. The sag was not altered during these tests. Direction of the line was east—west for operation with northerly winds.

This line galloped readily with practically all oblique winds directed at the flat side of the airfoils. Winds at this location did not remain at an angle of 80 to 90 degrees to the line for a sufficient length of time to allow the observers to decide whether these winds caused galloping or not. However, such winds on four separate days did not produce galloping of the single-span line. The 4-span line often galloped with one loop, but this motion was never seen on the single-span line. In no case did winds directed at the curved side of the airfoils cause noticeable oscillation.

Winds down to an angle of 20 degrees still were very effective. Velocities of five to seven miles per hour often produced amplitudes of one to three feet.

Three characteristic types of galloping, data for which are shown in Table II, were observed as follows:

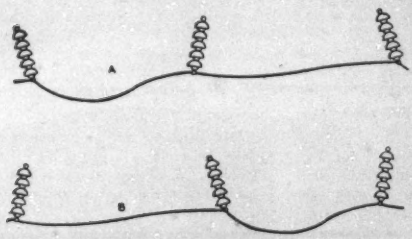

Figure 10. Galloping of type 3, two loops with the node moving up and down at the frequency of the 1-loop gallop

Insulator swing exaggerated in the drawing. *A* and *B* show the configuration at the extremes of the 1-loop cycle

1. Two loops, with the node stationary (Figure 8). The adjacent spans often were not in synchronism. The "insulator string" motion was an oscillation of approximately 0.20 inch amplitude in each direction, with a frequency twice that of the conductor loops.

2. One loop, with adjacent spans exactly 180 degrees out of phase (Figure 9). The "insulator strings" swing towards the falling span and away from the rising span. The frequency was one-half that of the 2-loop gallop. In one test, marked "Type 2A" in Table II, the three conductors were interconnected at the one-third point of the span with a piece of cord pulled taut. All three conductors galloped in the 1-loop mode, in exact unison, and with an amplitude of 7.6 feet. The "insulator strings" swung approximately three inches in each direction. There was a great deal of twisting and swaying of the crossarms and poles.

3. Two loops, with the node moving up and down at the frequency of the 1-loop gallop (Figure 10). This is the 2-loop state superimposed on the 1-loop condition. The "insulator strings" behaved as they did with the 1-loop gallop. The amplitudes were similar to those given for types 1 and 2 in Table II.

With types 1 and 3 the oscillation, particularly near the supports, sometimes developed an additional violent, snake-like or sinuous motion in a vertical plane. This behavior, as well as that of the three types described, have been observed on actual lines and in motion pictures. Galloping of the sort shown in Figure 11 is believed to take place in the field, but was not observed on this test line.

At times, with natural galloping, insulator strings are said to jump up and down, even to the extent of causing the line to trip out by contacting the crossarm. No jumping of the insulators was noticed on this line. However, since the steel bar simulating the insulator string permitted a vertical motion of only 0.75 inch, jumping at this point might have taken place without being observed.

Calculated frequency of oscillation checked the observed values more closely than did those of the single span reported in Figure 6. More accurate sag measurements were possible with the 4-span line.

The first visible motion of the conductor as it builds up to galloping appears to take two different forms

1. The conductor is observed to quiver "suddenly" over part or all of the span with, say, 0.1-inch amplitude and loop lengths of perhaps 10 to 20 feet. This motion increases and develops into the 1- or 2-loop gallop.

2. The conductor motion seems to develop directly into the 1- or 2-loop gallop.

It is certain that the former pattern took place; the occurrence of the latter is somewhat doubtful and requires further observation.

Traveling disturbances or waves, which can be seen clearly as they reach the supports and are reflected, are observed on the experimental line and in natural galloping. They are not seen until the galloping is well under way. At times they are not visible, particularly in the 1-loop gallop, which often is so smooth and steady throughout the line that it is difficult to think of it in terms of a wave. Rather, the aspect of the entire system of insulators and line is that of a giant swing or pendulum. Its behavior follows the mathematics of vibrating strings.

No typical configurations have been seen by the authors in natural galloping which were not also experienced on the test line with the exception of the elliptical path of the conductor sometimes found in natural galloping. The authors have observed two parallel transmission lines of 500-foot span, one having 300,000- the other 750,000-circular-mil copper conductors. There was approximately 0.20 inch of glaze on the windward side. It could not be determined whether the glaze extended to the top side. Smaller conductors, which were accessible, had glaze only on the side (windward). This glaze was somewhat mushroom shaped. Its vertical face was blunt and slightly larger in diameter than the conductor. While galloping violently with amplitudes up to 16 feet, the 300,000-circular-mil line was observed to oscillate in a single vertical plane with no visible deviation, while the conductors in the 750,000-circular-mil line often described an elliptical path, perhaps one to two feet in horizontal width. A motion picture record was obtained showing this difference in behavior. It is essential to stand practically under the line in order to determine the path of a galloping conductor.

One very rough mechanical measure-

Figure 11. Galloping in two loops with adjacent spans in phase

Insulator swing exaggerated in the drawing. This motion was not observed on the test line, but is thought to exist in the field. *A* and *B* show the configuration at the extremes of the insulator swing cycle

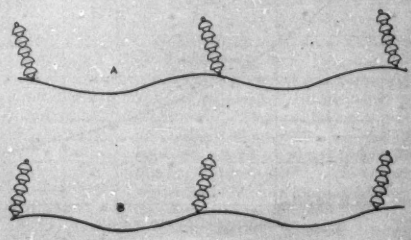

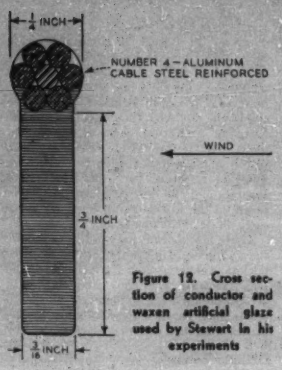

Figure 12. Cross section of conductor and waxen artificial glaze used by Stewart in his experiments

Length of glaze varied from 1.5 to 3 times the diameter of the conductor. Conductors were numbers 4, 6, and 10 solid bare copper wire. The wind which produced galloping was in the opposite direction from that existing during the formation of glaze

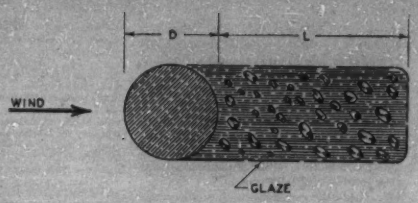

Figure 13. Cross section showing glaze observed on lines galloping during the storm of January 16, 1943

ment of the power required to sustain a forced resonant 1-loop gallop of 2.0-foot amplitude, in four spans of one coated conductor, gave a value in the order of five watts. The test was made in a 1-mile-per-hour wind blowing parallel to the line. Amplitude–time measurements of the building up of the gallop from rest have not yet been made, nor have similar measurements been made of the deceleration of coated and uncoated conductors from forced large-amplitude resonant oscillations in still air.

There may be material differences in the damping characteristics of this test line and in those of an actual line as normally constructed. For example, the wooden airfoils may increase the effective interstrand friction far above normal. However, this will be more or less offset by the greater effectiveness of these half-round airfoils as compared with most, if not all, glaze formations experienced in the field. It is not believed that these factors will cause serious interference with the purposes for which the line was built.

Remedial Measures

Baker and Mikina[14] have presented calculations of displacement type dampers intended for transmission lines. Undoubtedly a mathematical study of remedial measures should be undertaken.

Some experimental work has been started on methods of mitigation, but is not reported in detail because it is as yet inconclusive. Apparently all types of galloping observed on the experimental line can be significantly reduced by damping or interference applied at points ten feet or less from the conductor clamp.

One simple method which was tried appears to be effective with the multiple-loop gallop, but not with the 1-loop. It is not known whether this method or one of similar principle can be made effective for the latter condition.

With suspension-type insulators the 1-loop gallop appears to be more difficult to control, in general, than the multiple-loop. On one 880-foot span transmission line having a sag of 31 feet, it was found that of five traceable contacts between conductors, the results of galloping, all took place near the quarter point in the span. This indicates that the line in each instance galloped in two loops, although the 1-loop gallop may also have been present in a combination similar to that shown in Figure 10. Contrariwise, of five traceable contacts in a 500-foot span 16-foot sag transmission line all were found close to mid-span. If the absence of the 1-loop gallop were found to be characteristic of lines of certain designs and span lengths, the problem could be somewhat simplified, because of the apparent lesser difficulty with which the multiple-loop gallop is suppressed.

Conclusions

An experimental line has been constructed which will gallop typically and vigorously in ordinary winds of seven to ten miles per hour and higher velocity. It is the opinion of the authors, based upon their various observations, that the oscillations produced in an experimental line of the type described closely simulate natural galloping and can be used for the study of remedial measures, even though natural galloping may sometimes be caused by aerodynamic mechanisms different from that which is active in the case of the half-round cross section.

In the event that a damper or other remedial measure is developed, which is effective on the experimental line, it may be necessary to test it further on a section of actual transmission line equipped with suitable airfoils.

The practical solution of the galloping problem is not yet in sight and probably a large amount of work remains to be done, but the hope of finding an answer is sufficient to justify further work and to encourage others to study the problem.

Appendix

Gaps in the Theories of Galloping

Theories requiring a periodic twisting or torsional oscillation of the glaze-coated conductor about its longitudinal axis will explain satisfactorily certain cases of galloping, but observations by the authors suggest that only a few of the cases of galloping fall into this classification.

Stewart[13] conducted an interesting experiment in which an airfoil of wax, of the cross-section and dimensions shown in Figure 12, was attached to a 104-foot span of number 4 aluminum cable steel reinforced (0.25-inch diameter) cable. This span developed a single-loop rotary motion similar to that which results when two children swing a long skipping rope. A point at the center of the span described a vertical ellipse whose axes were two feet by three feet in a 35-mile-per-hour wind blowing at an angle of 90 degrees with the span. The wax and the cable, at mid-span, twisted or rotated periodically through 180 degrees and acted both as a sail

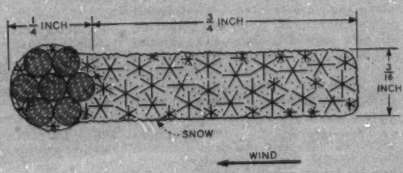

Figure 14. Cross section showing snow formation observed by Stewart on galloping conductors

and as an airplane wing. The minimum wind velocity which produced the skipping-rope motion was 25 miles per hour, directed at an angle of 90 degrees with the span.

Some explanations depend upon a gusty, oblique wind, as follows. Each gust exerts a force on the conductor as it travels along the line. If the interval between gusts coincides with one of the lower natural periods of the conductor, reinforcement will take place and eventually produce galloping. One would expect gusts of such uniform frequency and with the requisite period, to be of rare occurrence in natural wind.

Den Hartog's theory, previously described, may account for those cases of galloping in which the cross section of the glazed conductor fulfills Glauert's criterion for rotary instability.

In the opinion of the authors, there is some question whether any of the theories as proposed offer a thoroughly convincing explanation of the galloping which occurs under the following conditions:

1. No glaze or snow on conductors (stranded or round).

2. Glaze very thin in relation to the conductor diameter, for example, 1/16-inch thick glaze on one-inch diameter conductor.

3. Conditions observed by one of the authors and an associate during a case of galloping over a 5-hour period on January 16, 1945. The glaze of rectangular cross section was attached to numbers 4, 6, and 10 bare solid copper conductors in a position within two or three degrees of the horizontal (Figure 13). Length of the glaze cross section was 1.5 to 3 times the diameter of the conductor. Sides of the rectangle were as flat and parallel as the eye could detect, the corners slightly rounded. The glaze was so precise in form that it appeared to have been machined. Glaze was broken from galloping wires for inspection, some of which could be approached to within three feet. Glaze of the same shape and in the same relative position was observed on fence wires. Galloping was in two or more loops in a vertical plane with varying amounts of elliptical motion. On all conductors, save one slack wire, the glaze remained close to a horizontal position throughout the cycle, that is, there was no coupled motion. This means that there was no torsional oscillation associated with the gallop. The glaze was on the lee side during galloping. Wind of little gustiness and at a velocity of five to nine miles per hour was directed at an angle of 30 degrees to 50 degrees to the line.

4. Stewart[13] reports galloping of a conductor, 0.25 inch in diameter, bearing a snow formation of rectangular cross section, three-sixteenths of an inch by three-fourths of an inch attached in a nearly horizontal position as in Figure 14. He does not state whether torsional oscillation occurred. Wind velocity and direction is not given. The galloping continued for one day.

Wind-Eddy Effects

It has been known for at least a decade that wind eddies are capable of sustaining vibrations of an elastically suspended body at frequencies far different from the wind-eddy frequency for the body at rest. The authors have seen no data on the maximum extent of this effect. If with a given conductor the wind-eddy frequency should be altered sufficiently to sustain oscillations of a frequency equal to that of, say, the characteristic 2-loop gallop at resonance, then it may be that galloping could result. The work of Farquharson[18] suggests a possible mechanism for production of the initial excitation. In a study of suspension bridge models he proposes that wind eddies may induce a small amplitude, subharmonic oscillation. As the wind velocity increases, however, the section begins to assume control of the flow with the result that the subharmonic excitation yields slowly to harmonic excitation with the vorticity completely in phase with the motion. Richardson,[16] in reference to suspension bridges, suggests periodic "starting" vortices superposed on the Karman trail tendency as the early phase of the oscillation.

These mechanisms may aid in explaining the galloping of glaze-free, large diameter telephone cables (about 2.5 inches in diameter). Because wind-eddy frequency is inversely proportional to diameter, these proposals may not be as fruitful when applied to cables one-half inch or so in diameter.

Oblique Winds

Forms such as the cylinder are considered to be stable except for wind-eddy vibrations. However, as noted in a case above, conductors, unglazed and of circular cross section, are known to gallop at times.

Wind tunnel tests, under static conditions, of cylinders, stranded wires, and streamlined sections placed in an oblique wind indicate only a reduction in drag.[17,18] In some of the present tests, however, on oscillating models suspended in an apparatus of the type in Figure 2, it was noted that peculiar behaviors resulted when the long axis of the model was placed at an oblique angle with the horizontal wind. Models such as the cylinder, and those of certain smooth elongated cross sections mounted with the major axis of the section "along" the wind, became unstable and oscillated in winds of 15 to 28 miles per hour velocity. With the wind normal to the long axis of the model, only the typical wind-eddy oscillations occurred and these only in winds up to five miles per hour velocity. The half-round section, which was stable under certain conditions of a perpendicular wind, oscillated when the wind angle became oblique. The ends of the models were faired. Using a model 38

Table I. Data Taken on the Single-Span Line

Sag, Ft	Tension, Lb*	Amplitude, Ft	Number of Loops	Frequency, Cycles Per Min	Wind: Velocity, MPH	Wind: Direction, Deg†	Temp, F
6.13	829	2.5	2	50	7	50–60	40
6.13	829	2.5	2	50	13	20–30	
2.33	2,180	1.5	2	75	8.5	15–30	55
6.13	829	1/12–1/6	2 or 4		1	35–50	

* Angle formed by wind and line.
† Calculated value.

Table II. Data Taken on the 4-Span 3-Conductor Line

Type of Galloping	Loops	Node	Adjacent Spans	Sag, Ft	Tension, Lb*	Total Amplitude Ft	Frequency Cycles Per Min	Wind: Velocity, Mph	Wind: Direction, Deg†	Wind: Temp, F	Vertical Motion of Conductor: At	Rise: Ft	Rise: Per Cent‡	Fall: Ft	Fall: Per Cent‡	Insulator Swing In.
1	2	Stationery	Often not in synchronism	5.2	970	2.7	53.2	7–12	40–90	68	1/4-point	1.85	69	0.85	31	0.4
2	1	None	180 deg out of phase	5.2	970	4	26.6	10–11	50–80	68	Mid-point	2.4	60	1.6	40	3–4
2A	1	None	180 deg out of phase (3 conductors in unison) **	5.2 (at 68 F)	970	7.6	26.8	10–12	45–60	59	Mid-point	4.5	59	3.1	41	6

* Calculated for 68 degrees Fahrenheit.

† The angle formed by the wind and line.

‡ Per cent of the total amplitude that the conductor rose or fell from the normal position.

** The three conductors were interconnected at the 1/3-point with a cord pulled taut.

inches in length, placed centrally in front of the wind tunnel jet (20 inches wide), did not change the results. No definite conclusions have been drawn from these rough, preliminary tests. It is planned to make a further investigation, with more appropriate apparatus, of these effects.

Calculation of the Reynolds number for the test conditions employed, indicates that the instabilities observed probably could not be associated with the large and sudden change in drag coefficient which occurs in the critical region of Reynolds number.

The experiments by Relf and Powell[17,18] show that a model of nonstreamlined section suffers a large reduction in drag when the angle of the wind to which it is exposed becomes oblique. Figure 2 in Davison's paper[8] shows a condition under which the $\frac{dC_L}{d\alpha}$ term of Glauert's criterion[1] may be negative for a conductor very lightly, and only partially, glazed. These facts suggest that under certain conditions a conductor with such a section may be susceptible of autorotation.

It would be wise, perhaps, to investigate the possibility that the apparently unexplained cases of galloping mentioned above may be found to be associated with wind-eddies, the effects of an oblique wind, or a combination of the two.

References

1. Discussions by C. B. Basinger, E. W. Dillard. AIEE Transactions, volume 51, December 1932, pages 1078–83.

2. Modern Developments in Fluid Mechanics (volume 1), S. Goldstein, Editor. Oxford University Press, Oxford, England, 1938. Footnote, page 83.

3. Aerodynamics (book), F. W. Lanchester. London, 1908. Pages 42–5.

4. Wind Tunnel Tests on Autorotation and the Flat Spin, M. Knight. *National Advisory Council for Aeronautics Report 273* (Washington, D. C.), 1927, pages 343–58.

5. The Rotation of an Aerofoil About a Fixed Axis, H. Glauert. *Advisory Committee for Aeronautics Reports and Memoranda* (London, England), number 595, March 1919, 6 pages.

6. A Study of Wing Flutter, R. M. Bear. *National Advisory Council for Aeronautics Report 285* (Washington, D. C.), part I, 1928, pages 111–20.

7. Mechanical Vibration (second edition), J. P. Den Hartog. McGraw-Hill Book Company, New York, N. Y., 1940. Page 324.

8. Applied Hydro- and Aeromechanics (book), L. Prandtl, O. G. Tietjens. McGraw-Hill Book Company, New York, N. Y., 1934. Page 131.

9. Dancing Conductors, A. E. Davison. AIEE Transactions, volume 49, October 1930, pages 1444–9.

10. Transmission Line Vibration Due to Sleet, J. P. Den Hartog. AIEE Transactions, volume 51, December 1932, pages 1074–6. Discussion page 1086.

11. Mechanical Vibrations in Transmission Lines, C. D. Niven. *Canadian Journal of Research* (Ottawa, Ontario, Canada), volume 7, 1932, pages 95–102.

12. Some Features of Atmospheric Eddies With Applications to the Vibrations of Transmission Lines, W. E. K. Middleton. *Canadian Journal of Research* (Ottawa, Ontario, Canada), volume 8, number 2, February 1933, pages 105–10.

13. Vibration of Overhead Line Conductors, E. W. W. Double, W. D. Tuck. *Journal*, Institute Electrical Engineers (London, England), volume 86, January–June, 1940, pages 129–60.

14. The Calculation of Dampers for Systems Subject to Self-Induced Vibrations, J. G. Baker, S. J. Mikina. *Journal of Applied Mechanics* (New York, N. Y.), volume 3, December 1936, pages A121–6.

15. Experimental Study of Dancing Cables, D. C. Stewart. AIEE Transactions, volume 56, pages 759–60.

16. Discussions by E. A. Richardson, F. B. Farquharson of Rigidity and Aerodynamic Stability of Suspension Bridges, D. B. Steinman. *Proceedings*, American Society Civil Engineers (New York, N. Y.), volume 110, 1945, pages 476–85, 492–501.

17. Tests on Smooth and Stranded Wires Inclined to the Wind, E. F. Relf, C. H. Powell. *Advisory Committee for Aeronautics Reports and Memoranda* (London, England), new series, number 307, January 1917, pages 8–12.

18. The Resistance of Inclined Struts, C. H. Powell. *Advisory Committee for Aeronautics Reports and Memoranda* (London, England), number 599, March 1919. Pages 1–4.

Discussion

Gordon B. Tebo (The Hydro-Electric Power Commission of Ontario, Toronto, Ontario, Canada): The authors are to be congratulated upon having produced vigorous galloping on full-size test spans, representing 33-kv transmission lines. It may be objected that the simulated ice section is quite unlike actual ice formations, but the fact that it does produce galloping outweighs this objection.

Since galloping occurs on the authors' test spans frequently and under diverse wind conditions, the ice section chosen probably represents an extreme case of aerodynamic instability, and remedial measures found effective will probably be adequate for similar spans with sleet load. Caution is required, however, to avoid condemning remedial measures on these test spans which might be adequate for actual sleet-loaded spans.

In considering remedial measures, facts gained in studying suppression of aeolian vibrations may be useful. Dampers are frequently designed to withstand severe vibration and dissipate considerable energy, yet in actual operation effective dampers may not be required to do so. By preventing synchronization of the small wind-imparted disturbances the dampers may avoid rather than absorb vibration. In the case of galloping, also, it would be desirable to prevent cumulative input rather than merely to limit the amplitude.

A conductor has within itself the ability to dissipate energy by interstrand friction. By utilizing the torsional spring constant of the conductor, the attachment of an eccentric mass is all that is needed to form an effective damper. The designs of torsional damper found effective for aeolian vibration at frequencies as low as 3 cycles per second might be capable of extension to the lower frequencies found in galloping.

The authors' measurement of 5 watts to sustain 1-loop galloping on four 250-foot spans at 2-foot amplitude and frequency of 0.45 cycles per second appears high compared with power measurements made by a method[1] developed by Doctor Carroll of Stanford University. A value obtained in a 167-foot span of 477,000-circular-mil aluminum cable steel reinforced (Hawk), with knife-edge end supports at 1.5-inch total amplitude and a frequency of 4.6 cycles per second showed an input of 0.04 watt. Results through a range of frequencies of 4 to 20 cycles per second and amplitudes of 0.1 to 1.5 inches showed that the power varied as not more than the square of the amplitude and not less than the cube of the frequency. Applying these limiting relations to the authors' galloping conditions, power required should be not more than

$$0.04\times\frac{1{,}000}{167}\times\left(\frac{24^2}{1.5}\right)\times\left(\frac{0.45^3}{4.6}\right)=0.058\text{ watt}$$

While this is a rather extreme extrapolation of test results, it probably indicates that a large part of the 5 watts measured by the authors is dissipated in end supports and suspensions rather than in windage and interstrand friction distributed through the length of the conductor.

In considering system security the importance of 110- and 220-kv lines suggests an early extension of the authors' method to spans of 600 to 1,000 feet. This will be a large undertaking an the initial choice of an ice-section is important. An unsuccessful attempt has already been made in which a single 750-foot span of 477,000-circular-mil aluminum cable steel reinforced on steel towers was fitted with V-shaped wooden sections quite similar to the authors' section in Figure 4. No galloping resulted although vigorous aeolian vibration was observed. On the other hand a mushroom-shaped snow load on the top of a 1,000-foot test span of 605,000-circular mil aluminum cable steel reinforced did produce galloping during the few hours the snow lasted.

The authors' successful work has provided justification for the renewal of such experiments on long-span construction.

Reference

1. Laboratory Studies of Conductor Vibration, Joseph S. Carroll. AIEE Transactions, volume 55, 1936, May section, pages 543–7.

W. B. Buchanan (The Hydro-Electric Power Commission of Ontario, Toronto, Ontario, Canada): The authors have given a very interesting account of their studies and, in general, these tend to indicate that the problem of galloping and mitigation of hazards therefrom is very complex.

In the writer's opinion, some of the reactions observed on a full size line can be explained only by the application of the traveling wave theory. For example, galloping is substantially in a vertical plane on suspension construction while on pin-type it may develop large horizontal components. The reflection factor for vertical waves at supports is quite high and for horizontal components on pin-type construction, while the latter on suspension units are free to pass down the line indefinitely.

The authors note that remedial measures which appear to be effective on the multiple-loop per span condition are not with the 2-loop. Since such motion can be set up by a series of opposing tugs at the opposite ends of a span a quite different mechanical treatment might be required for its elimination.

Long insulator strings, for example, eight units or more, can oscillate under such conditions and absorb a substantial amount of energy.

Little is reported which gives any quantitative values of the energy input in terms of the energy stored in the conductor at its maximum amplitude of motion. If the problem is to be solved on anything more than a cut-and-try basis, some scheme will be necessary to introduce usable quantitive values. The writer has proposed a method of analysis which, stated briefly, is the application of the theory of damping, positive for losses, negative for energy input minus losses, and by decrement or attenuation curves with respect to time or space. Graphic records of oscillations on lines of long spans (for example 1,000 feet) and large conductors (477,000-circular-mil aluminum cable steel reinforced and up) indicate that in some cases they build up very slowly as though there were very little surplus of energy input over losses; in other cases they build up more rapidly. It seems logical to conclude that the mild palliative treatment which might be quite satisfactory in the first case would not necessarily be sufficient in the latter case.

Having this point of view in mind it would be of general interest to learn from the authors what they might say as to the rate of building up of the galloping phenomena for each type of construction, for example conductor size, weight, tension, and span length under the various tests. Corresponding data from field experience on lines in operation could be of considerable value in studies which aim to solve these problems on a quantitive basis.

A brief discussion of the significance of such data and a method of interpreting the same to give practical results may be of interest and value.

It appears to agree with the facts and will probably be generally accepted that various causes may contribute to initiating a mechanical surge on a line conductor, for example gusts of wind or dropping of ice load. Thereafter in order to build up the amplitude of the loop or loops within a given span there must be a net resultant of all forces acting on the span substantially in phase with the motion of the conductor at any time and place. It appears to be impossible to do more than conjecture as to all possible causes of such forces much less estimate their magnitude, timing and distribution. A cue, however, as to the general virulence in any installation may be obtained by noting the rate of rise of amplitude of any given type of motion during successive cycles as a percentage of the energy existing in the wave at the commencement of each cycle.

The growth then may be represented as following the law governing compounding of interest where a given principal sum P with an annual rate of increment x attains a value of s at the end of a period of n years (cycles), or

$$s = P(1+x)^n$$

A perspective in quantitive terms of the amount of damping required to prevent the build-up of any type of wave may be obtained by noting certain facts which have been observed.

The time (t) required for a wave to travel back and forth in a span between point of reflection is $2l/v$ (where l is the length of the span and v the velocity of the wave) and equals $\sqrt{T/m}$ (T being the tension of the conductor and m the mass per unit length).

For a 500-foot span, this may be approximately 2 seconds. It is reported that some appreciable time period is necessary (up to a minute) for the waves to build up to the larger amplitudes and this would require approximately 30 cycles.

Suppose now a conductor be given an initial impact resulting in a wave of 8 inches amplitude and thirty cycles later it attains an amplitude of 8 feet or twelve times its initial value. Then by the formula

$$s = 12P$$
$$= P(1+x)^{30}$$

$$30 \log (1+x)$$
$$= \log 12$$
$$= 1.07918$$

$$\log (1+x)$$
$$= 0.035973$$

$$1+x$$
$$= 1.0863$$

$$x = 0.086$$

Thus far in the argument no restrictions have been made as to wave-length, whether two foot or two hundred, or whether the wave be approximately sinusoidal or contains a number of higher harmonics. The resultant accumulated energy per cycle need not exceed nine per cent to build up such waves to 12 times the initial value.

The increments of energy involved in the build-up of what is known as galloping conductors must be much more erratic and variable than in the case of aeolian vibrations. Nevertheless if it requires appreciable time, of the order of one minute, to attain hazardous amplitudes it should be possible to avoid this by introducing a loss of ten per cent in each and every cycle of wave-travel.

Just how such loss can be introduced is another branch of the problem and while important it is beyond the scope of the present discussion.

References

1. Vibration Analysis—Transmission Line Conductors, W. B. Buchanan. AIEE Transactions, volume 53, 1934, November section, pages 1478–85.

2. Cable and Damper Vibration Studies, L. A. Pipes. AIEE Transactions, volume 55, 1936, June section, pages 600–14. Discussions, pages 1147–50.

A. S. Runciman (Shawinigan Water and Power Company, Montreal, Quebec, Canada): The Shawinigan Water and Power Company constructed a galloping span model consisting of three 166-foot spans of 7-strand 000 aluminum cable.

The airfoil was simulated using 3/4-inch quarter-round wood of face. This quarter-round was machined to fit the conductor at what would be the center of a complete circle of quarter-round pieces, two of which were applied, making a half circle. The wood pieces were 30 inches long and bound by wire to the conductor. The result was that, the wood airfoil, a half-circle, did not balance on the conductor, but tended to roll, thus making a spiral airfoil which rolled toward the center of the span from one end and back to vertical at the other end.

The model would not gallop under any wind condition. After observing the Chicago Model recently, corrections were made to the airfoil so that the wood balanced, maintaining a flat face toward the wind. This work completed, the model galloped with approximately 2-foot amplitude.

The above leads to a suggestion for experiment—an attachment might be mounted at the insulator with counter-balancing weights so that normally, the conductor remains higher than the attachment point but as a load of ice accumulates, the conductor would twist between the fixed support and the rolling support, thus forming a spiral airfoil such as we had before correctly balancing the wood on the conductor. Details of this conductor rolling device may be worked out by some mechanically minded engineer.

G. W. Stickley (Aluminum Company of America, New Kensington, Pa.): The study of dancing conductors reported in this paper is very interesting and certainly contributes much to a better understanding of the phenomenon and to its solution.

In this connection it is of interest to report several experiences that the Aluminum Company of America has had at their test spans located at Massena, N. Y. These spans are used primarily for studying resonant vibration, but on several occasions, dancing has been observed.

The first occurrence was in a 1,000-foot suspension span of 795,000-circular-mil aluminum cable steel reinforced when covered with sleet. The cable moved in two rather distinct loops with an amplitude estimated at 10 to 20 feet.

At the other times that dancing was observed, sleet was not present but the test cables were somewhat irregular in section. In a certain test two cables, each 397,500-circular-mil aluminum cable steel reinforced, were to be strung at the same sag in a 1,000-foot suspension span with the two cables side by side. The cables were taped together at intervals. It was impractical, however, to obtain exactly the same sags, but the difference was less than one cable diameter. Dancing of these dual cables occurred several times. In one case there were four loops and an amplitude of 18 inches, with a frequency of about 0.9 cycle per second. In later experiments these two cables were twisted together, but dancing of the twisted pair was never observed.

A third occurrence of this dancing phenomenon was observed in a 400-foot span of a special small cable having a "cloverleaf" cross-section. This cable sometimes fluttered. It was evident that the fluttering was a form of the dancing phenomenon, and was not resonant vibration.

F. P. Kaspar (Oklahoma Gas and Electric Company, Oklahoma City, Okla.): The authors of this paper are to be commended for their efforts in furthering a better understanding of the phenomena of "galloping conductors." The Oklahoma Gas and Electric Company transmission and distribution system has been subjected to several severe cases of galloping conductors in years

past and the subject is of particular interest to engineers of this company.

Damping Devices

Consideration has been given to the use of damping devices but no experiments have been made. During glaze storms in 1938 it was necessary to use hand lines and hot sticks to tie the conductors to fence posts to prevent the "galloping" from taking the line out of service. This tying down of the conductors was necessary in the transposition crossover spans of an H-frame line. (Although galloping occurred in other spans, no damage was incurred because of the flat configuration of the conductors.) It was noticed that very little pull on the hand lines was necessary to keep the conductors from galloping. This suggests that the use of a dampener or spreader device at the center of the span might be of value. It would be interesting to know if such a device has ever been used.

It is doubtful if a friction damper can be devised which can be placed near the hanger to eliminate galloping of the conductors. Too many variables are present which may cause galloping, most of which are not yet thoroughly understood. The damper, to be effective, would have to dissipate the energy at the very beginning of the motion. The formation of an ice load on the damper itself may also enter into the problem.

It has been the policy of the Oklahoma Gas and Electric Company to accept the fact that galloping conductors will occur under certain conditions of ice loading and wind and to design transmission lines to withstand them as far as economic considerations justify.

Conditions Causing Galloping Conductors

A very brief review of factors causing galloping conductors on the Oklahoma Gas and Electric system may be of interest here. Practically all of the winds that occur during glaze or sleet storms in this territory are from the northwest to north. This means that galloping occurs only on east and west lines, and on cross-country lines running northeast and southwest. Only one instance of a north and south line galloping has been recorded. This was in 1937 and was caused from a west by northwest wind at a velocity of three to five miles an hour. Most galloping on this system has occurred at wind velocities of 15 to 30 miles an hour although galloping has been observed at velocities as high as 50 miles an hour and as low as 3 to 5 miles an hour. Winds of 5 to 30 miles an hour are quite prevalent in Oklahoma during the winter and early spring months.

Glaze formations usually begin when a light mist, sleet, snow or rain is falling and the temperature falls below 32 degrees Fahrenheit. Most heavy formations have occurred at temperatures of 28 to 30 degrees Fahrenheit.

Conclusions

Observations of several instances of galloping conductors have led to the following conclusions as regards galloping conductors on the Oklahoma Gas and Electric system:

1. The galloping is in an elliptical motion and only 1-loop galloping is prevalent.

2. Galloping in north and south sections of existing lines occur so seldom that it is considered uneconomical to rebuild such lines.

3. Short spans of a given conductor are more susceptible to galloping than are long spans.

4. Conductors having a high ratio of diameter to weight are more susceptible to galloping than those with a lower ratio of diameter to weight.

5. Violent and prolonged galloping does damage to hangers and conductors, particularly if the conductors were weakened by burns or bad splices.

6. The H-frame type of construction (with sufficient vertical and horizontal offset clearances between the conductors and the shield wire to provide a 30-degree shielding angle at the pole, and with increased clearances at midspan to prevent midspan flashovers) is the best and most economical design to combat galloping conductors.

7. Where necessary to use single pole suspension lines (in towns or where rights-of-way difficulties are encountered), consideration should be given to the following:

(a). The use of a longer bottom arm to provide a horizontal offset between the upper and lower conductors on the same side of the pole.

(b). The vertical clearance between the conductors and between the conductors and shield wire. The Oklahoma Gas and Electric Company's practice is to provide a minimum spacing between arms (on east and west sections of line subject to galloping) of 125 per cent of the loaded sag plus six inches. This method of determining the spacing was advanced by Davison in a letter to this company.

(c). Placing the top and bottom conductors on the windward side of the pole to gain advantage in those cases in which the elliptical motion is at an angle to the vertical.

8. A flexible trunnion-type shield wire clamp assembly is of value in reducing cable damage at the shield wire clamp during galloping.

9. The wrapping of the conductor at points of rigid support (pin-type lines and neutral brackets) prolongs the life of the conductor on rural lines during galloping. This was determined by setting up a testing device in which the weighted conductor after being strung to normal tension, was vibrated eccentrically by a mechanical device to simulate a galloping motion. Wrapping the conductors with 0.05" copper ribbon at the point of support prolonged the life of copperweld conductors 500 per cent and copper conductor 50 to 100 per cent. A special tool has been devised for wrapping this ribbon around the conductor.

E. L. Tornquist and **C. Becker:** The inquiry made by Kaspar as to the use of spreader devices between conductors is best answered by referring to the experiment mentioned in the paper in which a cord was tied from one to the other of the three conductors on the experimental line. The result was that all three conductors continued to gallop, but in unison and with an amplitude of eight feet. Interconnecting the conductors of a transmission line probably would prevent contact between phases, but might allow excessive forces to be exerted on the supports. We have performed no experiments with spreader devices between conductors in a horizontal configuration, but in the light of work done by others it would seem that this scheme is worthy of investigation.

Kaspar also inquires as to the use of a damper device between conductors. We have considered several devices of this type, but have made no experiments. This scheme might be feasible if the problem of insulation can be overcome.

Doubt is expressed by Kaspar that a damper can be devised for placement near the hanger for the mitigation of galloping, since "too many variables are present which may cause galloping, most of which are not yet thoroughly understood." Our investigation leads us to believe that all forms of galloping can be suppressed effectively by the use of a suitable damper near the supports. This is possible because any disturbance or motion of the conductor which may take place out in the span necessarily is transmitted in both directions towards the supports as a traveling wave. If this traveling disturbance is dissipated or damped sufficiently at the supports, then the energy recovered in the span will not be enough to produce a large amplitude vibration. If the gallop has the typical configuration between supports of say, two loops or more, then a damper near the support is also effective, since the dissipation of the kinetic energy of the moving conductor near the support affects the entire wave. In the case of the 1-loop gallop, experiment has shown that a damper can affect two motions near the support, namely, the insulator swing and the motion of the conductor. The limitation of these motions with a damper suppresses the 1-loop gallop and also other forms of galloping. Devising such dampers which would be practical is quite another matter and remains to be accomplished. However, it should be remembered that this approach to the problem of mitigation is only one of several.

Kaspar states that the damper to be effective would have to dissipate the energy at the very beginning of the motion. Thus far, our experience with dampers on the experimental line does not indicate that such is the case.

The special cases of galloping cited by Stickley are very interesting. The dual cables which galloped when a slight difference in sag existed, but which appeared to be stable when they were twisted, brings to mind the following case:[1] a twisted pair of one copper wire and one steel wire when exposed to a wind running parallel to the line was found to develop an oscillating rotary motion about the longitudinal axis. This motion resulted in early failure of the wires.

We agree with Buchanan that the multiple-loop and the one-loop gallop present different problems with respect to damping. Some dampers are effective on both forms, while others appear to be effective only on the multiple-loop form of galloping. Aerodynamically these two forms are a product of the same phenomenon, but mechanically they are different. Buchanan notes that long insulator strings when oscillating can absorb a substantial amount of energy due to this swinging motion. However, this dissipation of energy does not seem to be great enough since it does not prevent the 1-loop gallop.

In answer to Buchanan's questions the paper states that we have not yet made amplitude–time measurements of the acceleration and deceleration of the airfoil-coated conductor. Consideration should be given to the possibilities of determining the decrement for a conductor on an actual transmission line by forcing it mechanically into resonant one and two-loop galloping of an amplitude similar to that observed with natural galloping. Acceleration data for natural galloping are scarce and are very difficult to obtain. We are hopeful that wind tunnel experiments will be conducted in the near future to determine the energy input obtainable with different cross sections, frequencies, amplitudes, and so forth.

We agree with Buchanan that quantita-

tive data will be necessary if the damping problem is to be solved on anything more than a cut-and-try basis.

Tebo suggests that because of the abnormal instability of the half round cross section, actually workable dampers might appear to be inadequate when tested on the experimental line. This point is well taken. However, we believe that the studies mentioned in the foregoing paragraphs may prove useful in deciding the course to be followed in this respect. Moreover, should it become desirable to make the galloping less violent on an experimental line a lower amplitude could be obtained by turning a sufficient percentage of the airfoil sections through 90 degrees or 180 degrees on the conductor.

We have felt for some time that the torsional damper developed by Tebo and Buchanan in their work on aeolian vibrations offers possibilities for adaptation to galloping and it is hoped that they will investigate these possibilities in the near future.

Tebo's extrapolated figure of 0.058 watt power input necessary to sustain galloping probably cannot be applied to the case of forced galloping of the experimental line described in the paper. His calculation is based on Carroll's data for conductors with knife-edge supports designed for low power loss. During galloping of the type described by us the crossarms and poles sway and twist; the insulator strings swing, and on unlubricated joints; and the conductor probably supplies an abnormal amount of interstrand friction as a result of the wired-on airfoil sections. It appears that Carroll attributes the power losses in his experiments very largely to "internal damping." This probably is not the case with natural galloping in the field.

Tebo mentions a V-shaped wooden section which failed to produce galloping on a single 750-foot span of 477,000-circular-mil aluminum cable steel reinforced. The V-shaped airfoil extended below the conductor about $1^3/_4$ times the conductor diameter and was attached with its major axis vertical. One important difference between this arrangement and that shown in Figure 4 in the paper is that the windward face of Tebo's airfoil is at an angle of perhaps 75 degrees or less with the wind, whereas in Figure 4 the angle is 90 degrees. In general, decreasing this angle lowers the instability. In addition, the V-shaped airfoil is long relative to the conductor diameter thus supplying a lever arm which in a wind might rotate the conductor on its axis. This would cause the airfoil to tend to align itself parallel to the wind and greatly reduce the aerodynamic instability of the type sought. This rotation occurred in Stewart's experiment, but in a high wind of 25 miles per hour or over a coupled motion resulted. This is described in the paper. With an appropriate cross section, coupling probably could occur at lower wind velocities. An icicle-type of ice loading often is not conducive to galloping. The mushroom-shaped snow load described by Tebo has a cross section commonly reported in cases of galloping.

An appropriate wind tunnel test is advisable for determining the characteristics of any proposed airfoil section intended to produce galloping.

The device described by Runciman is interesting and we hope that he will construct a model for experimental purposes.

An associate of the authors, H. E. Weaver, calls attention to the fact that an oblique wind blowing on a transmission line does not "see" the same cross section of glaze-coated conductor in the two halves of a span. The transition of cross section patterns occurs at midspan. Obviously, the aerodynamic reaction in the two halves of the span may be quite different. When there exist conditions favorable to galloping, this effect by its tendency to form a node at mid-span could direct the galloping into the 2-loop form which we believe to be the most common in the field.

Reference

1. Technical Note, *Scientific American* (New York, N. Y.), March 1944, page 129.

A Frequency Modulation Telegraph Terminal Without Relays

F. H. CUSACK
MEMBER AIEE

A. E. MICHON
MEMBER AIEE

Synopsis: Frequency-modulated carrier telegraph equipment provides advantages in transmission efficiency which have led to its extensive application. This paper describes a frequency-modulation telegraph terminal from which relays have been entirely eliminated so that the over-all circuit between ultimate operating positions is completely electronic. The circuits employed are described in detail, design considerations are discussed, and application information is given. The results of various performance tests also are included. In the development of this system, significant economies have been effected by reducing equipment complexity to a minimum, thereby saving space and simplifying maintenance.

DURING the past eight years the use of frequency-modulated carrier telegraph equipment has been extended in the Western Union system at a greatly accelerated pace until the channel mileage in service now runs into the hundreds of thousands. A paper[1] published in 1942 described the frequency-modulation channelizing equipment which is now in widespread use and discussed the advantages in transmission efficiency which it affords; namely, the singular ability of this system to tolerate large and rapid variations of received level, and its improved performance in the presence of noise. Since the frequency-modulation method was first introduced, there has been ample opportunity to compare its performance and continuity with that of the older method, amplitude modulation.[2] Experience has definitely established the superiority of the frequency modulation method, and as a result, all of the amplitude-modulation equipment has gradually been replaced. Meanwhile other workers in the field have published data confirming these conclusions[3,4] and frequency-modulation telegraphy has found many applications in wire-line and radio service.[5,6]

In the past, practically all of the frequency-modulation carrier telegraph channels in the Western Union system have been of the high-speed type, designed for 70-cycle signaling and employing a 300-cycle spacing. Channel terminals were provided with elaborate facilities for monitoring operation and were equipped to work with almost any type of telegraph circuit. This universal ability to serve was extremely useful when relatively small numbers were involved and circuit extensions to all manner of grounded and metallic facilities were required. However, with the advent of microwave radio relay systems and a vast expansion in the use of wire carrier to supplant d-c telegraphy, a new simplified carrier terminal became an economic necessity.

In the terminal described by this paper, the design has been limited intentionally to teleprinter and relatively slow-speed multiplex operation. Relays for transmitting and receiving have been entirely eliminated, and in their place, electronic devices have been used. All testing and regulating functions have been dissociated from the rack-mounted equipment and concentrated in a central test board. Individual monitoring equipment is not provided for each channel terminal, but rather in a ratio of one monitor set for every 18 channels. The channel terminal itself comprises only two units, one a panel mounting the sending and receiving filters, and the second a "transceiver" which, as the name implies, combines the transmitting and receiving functions. As a result of all these innovations, the cost of terminal construction has been materially reduced and equipment has been introduced which is more suitable for a telegraph system where carrier operation is the rule rather than the exception.

General Description

The new channel terminal has been designed for a maximum dot frequency of 35 cycles per second. This is sufficient for 2-channel multiplex working at the present speed of 66 words per minute and provides ample transmission margin for teleprinter signaling at 75 or even 100 words per minute. Frequency modulation of the transmitted carrier is accomplished by raising the channel frequency 35 cycles above its mid-channel value to send a spacing impulse and by depressing the frequency 35 cycles below its nominal value for marking. The individual chan-

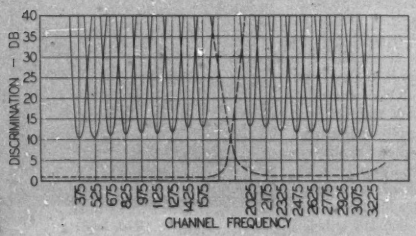

Figure 1. Channel layout

Paper 47-160, recommended by the AIEE committee on communication for presentation at the AIEE summer general meeting, Montreal, Quebec, Canada, June 9–13, 1947. Manuscript submitted March 26, 1947; made available for printing April 30, 1947.

F. H. Cusack and A. E. Michon are with The Western Union Telegraph Company, New York, N. Y.

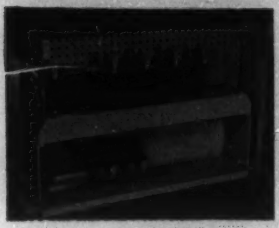

Figure 2. Filter panel

nels are given a band width of 80 cycles and are spaced at 150-cycle intervals in the spectrum.

These carrier telegraph terminals are furnished in nine different frequencies from 375 to 1,575 cycles. Two groups, or a total of 18 channels, can be operated over a voice frequency transmission band approximately 3,000 cycles wide. Figure 1 shows their relative positions in the spectrum and indicates the characteristics of the different receiving filters. One group of nine channels is transmitted directly while the second is modulated with a 3,600-cycle carrier to obtain channels from 2,025 to 3,225 cycles. Flexibility of "repeatering" is improved and warehousing is simplified to some extent by standardizing only nine different types instead of designing channels to fill the entire band.

Figures 2 and 3 show the sending-receiving filter panel and that of the transceiver, respectively. Together they occupy only $8^3/_4$ inches of space on a 19-inch rack. With a 10-foot ceiling height it is possible to locate eight terminals, complete with power supply, on each rack face as shown in Figure 4. In practice the 375-cycle channel is sometimes omitted because of band width limitations, so racks of eight channels are manufactured and shipped completely assembled and ready for installation. When used, the ninth channel is located elsewhere. Figure 5 shows the test board where the control panels and monitoring equipment are concentrated.

The essential elements of the terminal circuit are shown in the block diagram of Figure 6. The outgoing signals are transmitted by keying the sending leg to produce single-current telegraph impulses which in turn serve to switch a suitable reactance in the frequency-determining circuit of an oscillator. Electronic switching is employed, and the frequency is shifted abruptly between the spacing and marking conditions. The carrier next is amplified and padded to its proper level and then is transmitted through a band-pass filter to the sending bus. The incoming channel frequencies are selected from the receiving bus by a similar band-pass filter which is followed by an amplifier and limiter. The amplitude-limited signals are passed through a balanced linear discriminator and rectifier to obtain d-c telegraph signals. A low-pass filter removes the carrier and certain noise components after which a nonlinear d-c amplifier with a square wave output feeds single-current telegraph impulses to the receiving leg. By interconnecting the sending and receiving legs of two transceivers the equipment can be made to function as a repeater. An arrangement also is provided to permit half duplex operation using the same leg for sending and receiving.

Transmitting Circuit

In multichannel carrier telegraphy, considerations of spectrum economy make it essential that the transmitted band width be restricted to such frequencies as are required to minimize characteristic distortion. The transmission of higher order side bands is certain to produce excessive interchannel interference at the receiver unless spectrum space is wasted by locating the channels farther apart than would otherwise be necessary. There are two methods commonly used to restrict the transmitted band and both were employed in the equipment described by a previous paper.[1] A low-pass filter was interposed between the transmitting relay and the frequency-modulation oscillator causing the pulses to approach a sinusoidal wave shape during the transition periods. Since the oscillator was so arranged that its output frequency increased or decreased in proportion to the magnitude of the control current, the frequency variations occurred gradually and the transmitted carrier reached its steady-state marking or spacing frequency only for a portion of each pulse. In addition, a band-pass filter was connected between the oscillator output and the sending bus to insure suppression of the higher order side bands present to some extent even in sinusoidal frequency modulation.

The low-pass filtering method is not applied readily to a circuit from which the sending relay is omitted, and the frequency is modulated directly by line telegraph signals. The character of the d-c signals will be influenced somewhat by conditions on the leg circuit, particularly during periods of variable line insulation; and hence it becomes practically mandatory to use an abrupt frequency variation responsive to small changes in signal amplitude. Sufficient discrimination is then provided in the sending filter to suppress the resultant higher order side bands.

Figure 3. Transceiver

Figure 7 is a circuit diagram of the frequency-modulation oscillator. When the sending leg is open it draws no current except for possible leakage effects, and therefore the potential at point A is about 20 volts positive with respect to that at B. As a result the diode conducts and acts as an electronic switch to cut capacitance C_2 out of the tank circuit of the oscillator. The transmitted frequency now is determined by the values of L_1, L_2, and C_1 which are proportioned to produce the desired spacing frequency. As soon as the sending leg circuit is closed, a current flows which produces a drop of approximately 40 volts in resistor R_1 and causes the potential at A to become about 20 volts negative with respect to B. Consequently the diode becomes nonconducting and C_2 is switched into the tank circuit to lower the oscillator frequency. The value of C_2 is chosen so that the marking frequency is just 70 cycles below the spac-

Figure 4. Rack layout

Figure 5. Test board

ing frequency. It should be noted that the oscillator represents a low impedance termination regardless of whether the leg is opened or closed at the sending operating position. This reduces the effect of any induced interference on the line, while the fact that the termination is entirely resistive provides signals free from bias.

Figure 7. Transmitter circuit diagram

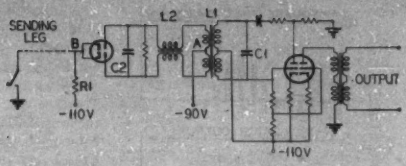

The resonant frequencies of the oscillator circuit are given by the following formulas:

$$f_z = \frac{1}{2\pi\sqrt{\frac{L_1 L_3}{L_1 + L_3} C_1}} \qquad (1)$$

$$f_m^2 = \frac{f_z^2 + f_x^2 \pm \sqrt{(f_z^2 + f_x^2)^2 - 4f_0^2 f_z^2}}{2} \qquad (2)$$

where

$$f_0 = \frac{1}{2\pi\sqrt{L_1 C_1}}$$

and

$$f_x = \frac{1}{2\pi\sqrt{L_3 C_3}}$$

It will be observed that equation 2 has two possible solutions indicating that the circuit has two natural periods of oscillation when C_3 is present. One of these is the desired marking frequency while the other is considerably higher depending upon the choice of values for the reactive elements. Conflict is avoided by making the resonant impedance at the higher frequency sufficiently low that a value of feedback which produces stable oscillation at the lower frequency is not enough to permit oscillation at the higher frequency. The rated output power of the oscillator and its associated amplifier is plus 10 decibels referred to one milliwatt.

When reactive circuit elements are switched electronically to produce direct frequency modulation, it is often difficult to obtain a satisfactory abrupt deviation. The sudden transition of the telegraph impulse induces a transient in the tuned circuit of the oscillator which can persist for the duration of the transition interval or even longer. This may cause considerable signal distortion. The problem was solved by using the balanced circuit configuration represented by the differential transformer, the split inductor L_3, and the twin diode of Figure 7. Switching transients are balanced out in the transformer secondary and thereby prevented from reaching the oscillator circuit.

Figure 8 shows the manner in which the oscillator frequency is varied by the control current in the leg circuit. The entire frequency swing occurs during the interval when the current ranges from 25 to 45 milliamperes. Since this current normally is adjusted to 70 milliamperes for marking, it is apparent that the proper deviation will be produced regardless of line variations within limits ordinarily encountered.

Figure 9 will serve to indicate the nature of the resulting frequency modulation. Figure 9*A* shows the side band amplitudes for square-wave modulation with a deviation ratio of unity.[7] Figure 9*B* shows the side band distribution measured at the output terminals of the oscil-

Figure 6. Block diagram of terminal

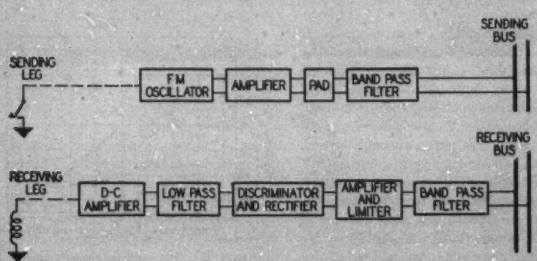

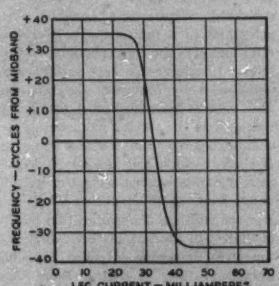

Figure 8. Transmitter frequency versus leg current

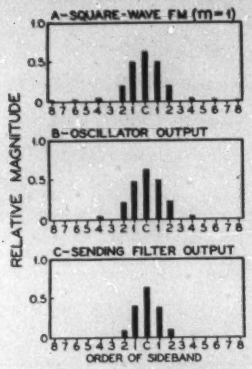

Figure 9. Side-band distribution diagrams

lator for the comparable condition, that is, when transmitting reversals at 35 cycles. The degree of agreement between the theoretical and measured values is sufficient to indicate that the frequency is being modulated very abruptly. Figure 9*C* shows the side bands remaining after the signals have passed through the band-pass filter to the sending bus. The carrier and first order side bands predominate and account for about 98 per cent of the transmitted power. The second order pair, which contain the remainder, fall between channels and are now so small that they are suppressed readily by the receiving filters.

Receiving Circuit

At the receiving terminal of a carrier telegraph system the band width assigned to a channel determines the permissible signaling speed as well as the amount of noise and interchannel interference experienced. Figure 10 shows the characteristics of a representative receiving filter and also the corresponding sending filter. Interference is kept within tolerable limits by providing the receiving filter with at least 30-decibel discrimination against the spacing frequency of the channel below or the marking frequency of the one above and at least 20-decibel discrimination against second order side bands from these channels. The overall band width of the sending and receiving filters in tandem has been made 2.3 times the maximum intended signaling frequency. This is slightly more than the theoretical minimum and has been found sufficient to permit operation without appreciable characteristic distortion.

Figure 11 is a schematic diagram of the receiver circuit. Incoming signals are amplified by the first section of twin triode V_1 and amplitude limited by the second section of this tube and by pentode V_2. The limiting action helps to reduce the fortuitous signal distortion caused by noise and renders the received signal immune to the influence of variations in received level. The output of the limiter is made constant for input levels between minus 50 and plus 10 decibels referred to one milliwatt.

Following the limiter is the familiar balanced discriminator represented by transformers T_1 and T_2, with their associated capacitances C_1 and C_2, and the twin diode V_3. The output voltage developed by one side of the diode has an amplitude–frequency characteristic whose slope is the opposite of that delivered by the other side. After these outputs are differentially combined the rectified signal voltage, as shown by Figure 12, is approximately linear for frequencies within the useful range and passes through zero at midband.

After filtering to remove the carrier, the rectified voltage is used to control the output pentode V_4. A plate current of 70 milliamperes flows in the receiving leg for a marking signal and is cut off for spacing. A control on the d-c grid bias is provided to permit adjustment of the operating point to secure unbiased signals. The nonlinear amplifier is made responsive to small changes in input and hence delivers a signal voltage approximating a square wave shape.

The low-pass filter inserted between the discriminator and the final amplifier is of interest because of the effect of this filtering on transmission. In addition to removing carrier, the low-pass filter also is useful in minimizing the effect of noise components whose frequencies lie outside the band assigned to the channel, and thus performs a function somewhat similar to that of the band-pass receiving filter. Consider, for example, any interference from an adjacent channel which succeeds in getting through the band-pass filter and into the receiver. The amount of frequency deviation imparted to the received signal by a given level of interference is proportional to its frequency separation from the signaling carrier. This results in the triangular noise spectrum obtained with a linear discriminator and may permit considerable fortuitous distortion to be produced by a relatively small amount of interference. However, it must be remembered that the deviation of the signal frequency is produced at a cyclic rate which also depends on the frequency separation between the interference and the carrier; and it is this rate of deviation which determines the frequency of the rectified interference. For a steady marking or spacing tone on the adjacent channel, the minimum possible frequency is 80 cycles. The interference component in the received signal will either range between 80 and 150 cycles or

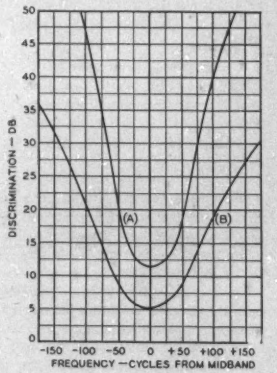

Figure 10. Filter characteristics

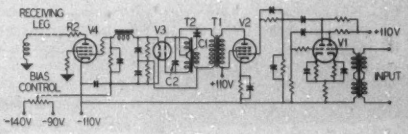

Figure 11. Receiver circuit diagram

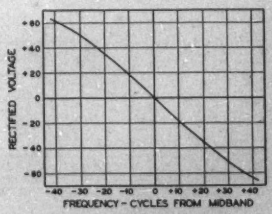

Figure 12. Discriminator characteristic

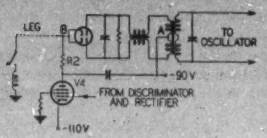

Figure 13. Half duplex circuit

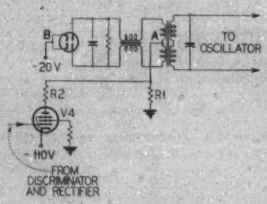

Figure 14. Repeater circuit

between 150 and 220 cycles. These frequencies are sufficiently far above the 35-cycle maximum signaling speed that the low-pass filter can be designed to reduce the interference and still not introduce characteristic distortion.

Half Duplex and Repeater Circuits

As mentioned previously, the channel terminals are not restricted to full duplex operation with separate leg circuits for the sending and receiving functions but also are equipped for two other methods of working. A 3-position switch on the face of the transceiver panel is provided for converting the circuit arrangement from duplex to half duplex or to repeater service.

With the half duplex arrangement shown in Figure 13, transmission is obtained in either direction but not in both directions simultaneously. Signals are transmitted by opening and closing the leg circuit to control the oscillator in exactly the same manner described for the duplex case. In fact the duplex and half duplex circuits are electrically equivalent just so long as a marking signal is being received to keep tube V_4 in a conducting condition. The method of receiving is also the same as that described previously. Single-current signals are supplied to the leg circuit by the plate current of tube V_4; and just so long as the leg is kept closed, the oscillator is effectively isolated from the circuit. When leg current is flowing for a marking signal, there is a drop of approximately 40 volts in tube V_4 and resistor R_2, so point A is about 20 volts negative with respect to B and the diode is nonconducting. When the leg current is cut off by V_4 for a spacing signal, point A is 90 volts negative with respect to B and the diode remains nonconducting. Thus the received signals can have no effect on the transmitting oscillator which continues to deliver a marking frequency.

In this way the system is used for transmission by either station provided the leg is kept closed at the distant station. One operator may then "break" the other by opening his leg circuit. If at that instant a marking signal is being received, this will transmit a spacing signal to stop the distant operator from sending. If the leg is opened at a time when a spacing signal is being received, there will be no polarizing potential applied to the diode of the sending oscillator. It so happens

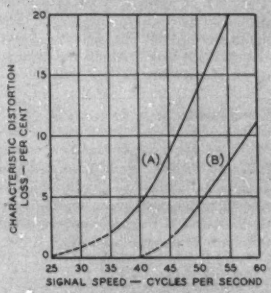

Figure 15. Characteristic distortion loss

A—With channel filters
B—Without channel filters

that the oscillator will transmit a marking frequency for this condition, but this is immaterial because the leg at the distant station is open. As soon as the leg circuit at either station is closed, a correct control of the transmission is once more established.

To repeat a channel from one carrier system to another, the sending and receiving legs of two transceivers are interconnected and the circuit arrangement is modified as shown in Figure 14. To repeat a marking signal, plate current from tube V_4 flows through resistor R_1 where it produces a drop of approximately 40 volts to make point A about 20 volts negative with respect to B. This makes the diode nonconducting and consequently the marking frequency is transmitted. When tube V_4 is cut off by a spacing signal, point A is 20 volts positive with respect to B and the diode becomes conducting to cause transmission of the spacing frequency.

Performance Data

The results of various tests of the overall performance of the new channel terminal are given in Figures 15 through 19.

Characteristic distortion loss varies somewhat from channel to channel because each of the nine terminals employs a different pair of band-pass filters with slightly different characteristics. The curve given in Figure 15 for distortion with channel filters represents the average obtained with all types. At the nominal maximum signal speed of 35 cycles the characteristic distortion loss is not more than 4 per cent on any channel. The effect of the low-pass filter which follows the discriminator in the receiver can be observed by removing the channel filters from the circuit. As shown by the second curve of Figure 15 characteristic distortion from this source is not appreciable until the signal speed reaches 45 cycles.

In Figure 16 the fortuitous signal distortion in milliseconds is plotted against the rms noise-to-signal ratio at the receiving bus. The channel was operated at signaling speeds between 30 and 35 cycles and was subjected to a disturbance consisting of random noise uniformly distributed over a band about 3,000 cycles wide. The noise-to-signal ratio at the output of the receiving filter was 17 decibels lower than the value at the re-

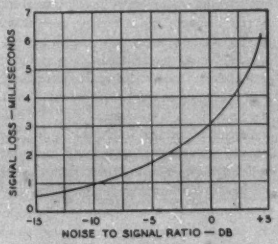

Figure 16. Effect of random noise

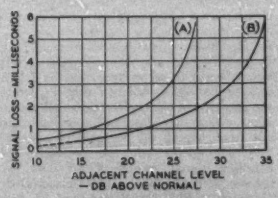

Figure 17. Effect of interchannel interference

A—Interference from channel above
B—Interference from channel below

ceiving bus. Except at the high noise levels where the curve is breaking sharply toward failure, the measurements of Figure 16 indicate a tolerance to noise in the neighborhood of eight to nine decibels

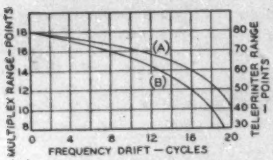

Figure 18. Effect of frequency drift

A—23-cycle teleprinter
B—35-cycle multiplex

greater than that obtainable on a comparable amplitude-modulated channel.

Figure 17 shows the effect of interchannel interference on the received telegraph signal. The distortion loss is not measurable with either of the adjacent channels working at its normal level and is small with levels 10 to 15 decibels higher than normal. Interchannel interference is not an important consideration under any conditions encountered in service.

It is recognized universally that frequency stability must be carefully maintained in a system operated by frequency modulation. Any drift in the received carrier frequencies creates an inequality between the spacing and marking signals delivered by a linear discriminator and thereby results in biased reception. From printing range measurements shown in Figure 18 it is concluded that the bias distortion is scarcely noticeable unless the frequency drift is permitted to exceed four or five cycles. This is a tolerance of about one part in 300 to 400, a degree of stability which is not difficult to exceed with simple circuit components. Channel oscillator frequencies are checked in a routine manner every three months and are readjusted easily whenever small errors develop. In the carrier systems over which the channels are operated, the drift due to variations in translating carrier frequency is not permitted to exceed one cycle.

Figure 19 shows printing ranges measured on a circuit consisting of many successive carrier systems operated in tandem. At the end of each section two transceivers were interconnected as a repeater so that the over-all circuit was entirely electronic. At the maximum speed a satisfactory operating range was obtained over a 6,500-mile circuit consisting of nine successive carrier sections. Therefore, it appears unlikely that all-carrier circuits within the geographical limitations of the United States will ever be sufficiently long to require regenerative repeaters anywhere in their makeup.

Conclusion

The development of this new carrier telegraph channel terminal has provided an improved type of equipment which already is finding widespread application in the Western Union system and is expected to appeal to many other users. A high grade of transmission efficiency has been achieved by taking full advantage of the superior performance obtainable through the use of frequency modulation. A method of operating d-c leg circuits electronically has been developed which is free from any abnormal effects caused by the presence of noise or leakage. This has made it possible to employ a system of direct transmission which avoids the use of relays anywhere in the over-all circuit between ultimate operating positions. Equipment complexity has been minimized, operating and maintenance procedure has been simplified, and savings in space have been effected by concentrating the supervisory functions in a central location and by reducing the types of leg operation. These features have resulted

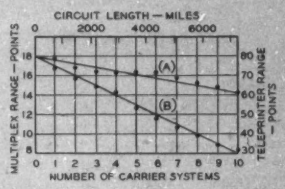

Figure 19. Printing range on multisection circuit

A—23-cycle teleprinter
B—35-cycle multiplex

in significant economies in initial expense and also in operating and maintenance costs.

References

1. Frequency-Modulated Carrier Telegraph System, **F. B. Bramhall, J. E. Boughtwood.** AIEE Transactions, volume 61, 1942, January section, pages 36–9.

2. High-Speed Voice Frequency Carrier Telegraph System, **F. B. Bramhall,** AIEE Transactions, volume 59, 1940, pages 873–9.

3. Performance Characteristics of Various Carrier Telegraph Methods, **T. A. Jones, K. W. Pfleger.** *Bell System Technical Journal* (New York, N. Y.), July 1946, pages 483–531.

4. Frequency Shift Telegraphy—Radio and Wire Applications, **J. R. Davey, A. L. Matte.** AIEE Transactions, volume 66, 1947, pages 879–93.

5. Observations and Comparison on Radio Telegraph Signaling by Frequency Shift and On-Off Keying, **H. O. Peterson, J. B. Atwood, H. E. Goldstine, G. E. Hansell, R. E. Schock.** *RCA Review* (New York, N. Y.), March 1946, pages 11–31.

6. A Microwave Relay Communication System, **G. G. Gerlach.** *RCA Review* (New York, N. Y.), December 1946, pages 576–600.

7. Frequency Modulation, **Balth van der Pol.** *Proceedings*, Institute of Radio Engineers (New York, N. Y.), volume 18, July 1930, pages 1194–1205.

Discussion

R. B. Steele (Canadian National Telegraphs, Toronto, Ontario, Canada): It is noted from the paper presented by F. H. Cusack and A. E. Michon that they rate the capacity of the channel terminal equipment which they describe at a maximum dot frequency of 35 per second, and yet they also point out the possibility of handling signal speeds of 45 dots per second without appreciable characteristic distortion. This signal speed of 45 dots per second is obtained, however, with the channel filters removed from the circuit. It appears reasonable, therefore, to assume that they recognize the idea generally accepted in connection with amplitude modulated carrier telegraph channels that the band width of channel filters determines the speed at which signals can be transmitted with a limited amount of distortion. From this deduction I conclude that the band filters used with their equipment determine the rated speed of transmission of 35 dots per second.

To pursue the subject of rated signal speed further, one may assume that the authors recognize a desirable ratio between frequency shift and dot speed, which in this case appears to be a ratio of 1. However, they suggest that the ratio is not critical and can be varied substantially, as in the handling of signals at the speed of 45 dots per second, without stated penalty so long as the filters will permit this. This question of the desirable ratio between frequency shift and signal dot speed may have been covered in an earlier paper listed in the references. I have not checked this point and would appreciate some discussion by the authors as to the possibility of increasing the speed rating of carrier telegraph channels provided by means of their equipment by the substitution of wider band filters but without any other change in the equipment.

R. B. Shanck (Bell Telephone Laboratories, Inc., New York, N. Y.): This paper pre-

sents in an interesting manner a description of a carrier telegraph system which differs mainly from older systems in that no mechanical relays are employed. It appears that this equipment will be found of much utility by the telegraph companies in providing good transmission circuits. The equipment described seems to be compactly and attractively arranged.

A few comments on certain specific points in the present paper may be of interest.

In the first paragraph it is stated that other workers in the field have published data confirming conclusions of this paper relative to the merits of frequency-modulation telegraphy. The data quoted in certain other papers (references 3 and 4 of this paper) are in somewhat different form from those herein; but, to the extent that the data are comparable, the conclusions of these other authors are not quite so favorable to frequency-modulation telegraph over amplitude modulation for wire lines, although large advantages have been demonstrated for frequency modulation in long distance radio telegraph transmission.

With regard to loop transmission, it is thought that with the arrangements described some difficulty may be experienced in breaking on half duplex circuits, except in cases where the transmission time of the telegraph circuit is comparatively small.

With reference to interchannel interference, the authors point out that the distortion produced by the presence of the adjacent channels is not measurable; and they conclude that such interference is not important under any conditions encountered in service. Although it is true that interchannel interference has, under normal conditions, but little effect on the signal distortion observed in short period measurements, it may reduce very materially the margin against the occasional bursts of fortuitous interference which are responsible for the sporadic errors which appear in practical layouts and whose frequency over a long period determines the operating qualities of a circuit.

It is stated in the paper that it appears unlikely that all-carrier circuits set up within the United States will ever be sufficiently long to require regenerative repeaters. In certain cases in furnishing extensive private wire networks it is impracticable to avoid association of d-c sections with carrier facilities to make up complete operating circuits. On long complicated networks of this type, regenerative repeaters have been found of great utility in improving reliability of service and reducing transmission maintenance costs. As an example of a very long and complicated private-line network on which 60 word per minute teletypewriter service is furnished by the Bell system, it may be of interest to note that one press association circuit comprises over 57,000 circuit miles serving more than 850 customer stations. This network includes 12 regenerative repeaters.

As an indication that the performance of a high-grade amplitude-modulation carrier telegraph system compares favorably with that of a frequency-modulation system, the results of an experiment made a few years ago over Bell system circuits between Oklahoma City, Okla., and Whitewater, Calif., might be cited. A carrier telephone circuit about 29,000 miles in length was first formed by connecting 12 type J channels in tandem; a 12-channel voice frequency telegraph system was connected to this circuit and the channels of this system were then connected in tandem forming a 12-section telegraph circuit about 345,000 miles in length. A short test message was sent by teletypewriter into one end of this circuit, and then the receiving end was connected quickly to the sending end through a regenerative repeater. This message then "circulated" around this circuit for one hour without error, traveling in this time the remarkable distance of about 380,000,000 miles or approximately two round trips from the earth to the sun.

F. H. Cusack and **A. E. Michon:** The point discussed by R. B. Steele is quite pertinent because there is an optimum ratio between frequency deviation and rated signal speed, and the choice of this ratio is just about the first decision which the designer of a frequency-modulation telegraph system has to make. On wire lines where frequency space must be used economically, it is reasonable to expect that frequency modulation should employ the spectrum every bit as efficiently as amplitude modulation. This is possible only if the deviation ratio is made unity or less than unity. The exact value is not critical; but ratios less than one are not attractive because reducing the shift does not permit any further reduction in the band width of the filters, but does make transmission more susceptible to noise and to frequency instability. For these reasons, it is customary to make the frequency deviation approximately equal to the maximum signal speed in systems operating over wire circuits.

To give a practical answer to Steele's question, it would be possible to increase the speed rating of the carrier telegraph channels slightly without any alteration of the equipment other than the substitution of wider band filters, but the permissible increase ordinarily would not be considered sufficient to justify the change. While designing the filters for a higher operating speed, it would be well worthwhile to change the transceiver tuning also and utilize the benefits of a greater frequency deviation.

The comments of R. B. Shanck cover a number of interesting points which deserve some further consideration. With regard to half duplex operation, circuits with time lags of 300 to 500 milliseconds have been tested and no difficulty has ever been experienced in transmitting a clean break.

The problem of interchannel interference does require special attention when designing filters for a multichannel system, because such interference is present continuously. As shown by Figure 17 of the paper, the filters reduce interference from the adjacent channels to a level at least 25 decibels below the value which is sufficient to cause printing errors. When added to a fortuitous disturbance where the distribution of peaks follows a normal-law probability relatiop, this small increment is of negligible importance.

A test of the type described by Shanck is indeed a tribute to the excellence of the carrier telephone and telegraph equipment involved. It demonstrates, as do the results in Figure 19, that a high-grade system can be expected to transmit teleprinter signals with excellent fidelity through as many as 12 carrier sections connected in tandem. Furthermore, the experiment was successful even though each carrier section was made extremely long and the signals traveled some 345,000 miles without benefit of a regenerative repeater. Of course, tests of this kind do not imply that regenerative repeaters are unnecessary when d-c telegraph sections are associated with carrier facilities.

As for the relative merits of frequency modulation when compared with amplitude modulation for telegraphy, it is true that the conclusions reached by the authors of references 3 and 4 do not agree thoroughly with the conclusions of the present paper, nor do they agree very well with each other. This will always be true as long as different workers attack this type of problem independently. Actually, all of the comparative results have been favorable to frequency modulation and the only difference of opinion seems to be in the conclusions which have been drawn as to the need for the improvement which frequency modulation affords.

It is generally agreed that properly designed amplitude-modulation and frequency modulation-systems will produce almost identical results when operating on an ideal transmission medium. The outstanding advantage attributed to the frequency-modulation method by all experimenters is its virtually complete immunity to level variations. While this characteristic and the greater tolerance to noise mean little to a user with quite stable circuits, they do make it possible for frequency-modulation systems to work through adverse conditions rendering amplitude-modulation channels temporarily inoperative. After years of operating experience in the Western Union system, it is this kind of performance which appeals to all who have followed the subject closely.

Performance Criteria of D-C Interrupters

E. W. BOEHNE
FELLOW AIEE

M. J. JANG
ASSOCIATE AIEE

Synopsis: A new approach to the analysis of the performance of d-c interrupters has been made in which the arc voltage of the interrupter is considered on an equal footing with the d-c generated voltage. The effect of variations in the circuit constants as well as circuit breaker speed and arc voltage wave shape and magnitude are evaluated on a quantitative basis. The equations and curves are presented on a per-unit basis which makes the work applicable to any d-c interruption problem. The work sheds light on design and application criteria of d-c interrupters. The presentation is arranged to be easily digested by the student of electrical engineering.

THE most successful of the d-c interrupters which are available today were developed by well-proved empirical methods employed in the creation of the great majority of our circuit interrupters. Following the creation of a successful d-c interrupter, little time was spent to rationalize the performance of an analytical basis. Instead the experience gained took record, and rightly so, in the form of the arrangement of conductors, contacts, coils, and arc chutes. The experience so collected has been retained and rationalized by many of our most renowned engineers of the circuit breaker art. The foundation of a new design usually was based upon this fund of accumulated knowledge. Extrapolation was enhanced by intuition and experience. The results were usually rapid and adequate. Much tribute should be paid to these pioneers in the art. The industry owes them much.[1,2]

Recently, however, analytical studies of the arcing period of a-c circuit interrupters have been simplified sufficiently as to influence our understanding of their performance.[5] It is the purpose of this paper to attempt the application of similar analytical methods to the performance of d-c circuits in order to evaluate, quantitatively, the essential circuital elements of d-c interruption. In making such a study the relative importance of the circuit constants in relation to the arc voltage of the interrupter will be emphasized. The advantages of rapidly inserting the arc voltage of the interrupter following the initiation of the short circuit will be weighed in relation to the time constant of the circuit. The essential criterion of the performance is assumed to be the arc energy liberated by the interrupter. This energy will be expressed quantitatively and its relation to the energy stored in the circuit inductance will be clearly shown.

There is little doubt that this empirical science, when reinforced with a simple, straightforward analytical treatment, should enhance the development and understanding of the performance of interrupters during the period of their creation (particularly by those less familiar with the fund of empirical data) and lead to a more accurate formulation of the rules relating to their proper application. Tests will always be required to prove the ability of any interrupter to do its job. Analysis of the oscillogram at this point can be of assistance as a record of the test performance and to reveal to the analyst why the performance was satisfactory or unsatisfactory. Extrapolation to new designs should become more scientific. Development time should be reduced to a minimum.

The principles discussed herein are applicable to any form of d-c interrupter. However, for illustrative purposes frequent reference will be made to circuit breakers.

The requirements of speed of operation of the d-c interrupter require the closest co-operation between the electrical and mechanical designer.[3,4] The tripping unit is usually a high speed so-called flux shifting latch, which operates in an overall time approuching 0.002 to 0.001 second. This releases a mechanism whose object is first to transfer the current from the primary contacts to the arcing contacts at the earliest possible moment. This act is the first prerequisite for developing the arc voltage of the interrupter so essential to interruption. Although the contacts have parted, valuable time might be lost with a contact and arc runner design which is sluggish in permitting the arc to transfer and move rapidly out into the interrupting chamber where the all important arc voltage is developed. It might be said that the first turning point in the interruption occurs when the arc voltage of the interrupter reaches the magnitude of the d-c circuit voltage. The first design objective of the interrupter should be focused upon bringing this equalization of voltages at the earliest possible moment following the beginning of the d-c short circuit. The efficiency

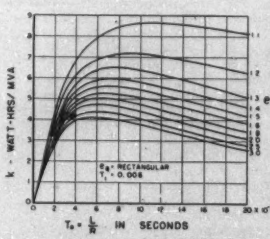

Figure 1. Relative energies liberated by a d-c interrupter which introduces a rectangular arc voltage 0.006 second following the inception of a short circuit

The magnitude of the arc voltage (e_a) is expressed in per unit of the direct voltage. The energy is expressed in watt-hours per megavolt-ampere. See Figure 10 for the geometry of this performance

Paper 47-173, recommended by the AIEE committee on protective devices for presentation at the AIEE summer general meeting, Montreal, Quebec, Canada, June 9–13, 1947. Manuscript submitted March 25, 1947; made available for printing May 2, 1947.

E. W. Boehne is associate professor, electrical engineering department, Massachusetts Institute of Technology, Cambridge, Mass.; M. J. Jang is in the switchgear division of the General Electric Company, Philadelphia, Pa.

of the interrupter then depends upon the ability of the interrupter to create a stable arc voltage in excess of the direct voltage of the system. The higher the arc voltage rises above the generated voltage, the more rapidly will the current decay and the lower the energy liberated. It is possible, however, to develop such high arc voltages as to be dangerous to the system insulation. One of the most efficient performances is obtained when the arc voltage rises to double the generated voltage and remains stable at this level until interruption. Under these conditions the rate of current decay is about the same as the initial rate of rise of short-circuit current. Although the arc energy is not a minimum under these conditions it is an excellent compromise with the magnitude of the voltage developed on the system insulation. These and other considerations now will be analyzed on a quantitative basis.

The Circuit Parameters

The circuit parameters, inductance and resistance, are of tremendous importance to the problem under consideration. These parameters will be assumed to be constant for any particular case. This assumption is justified for the modern high speed circuit breaker since currents are not permitted to rise high enough to saturate the machines which produce them.

The circuit resistance controls the magnitude of the available short-circuit current by the well-known relation

$$I_m = \frac{E}{R} \tag{1}$$

The circuit inductance L controls the initial rate of rise of short-circuit current in amperes per second by the relation

$$\left.\frac{di}{dt}\right|_{t=0} = \frac{E}{L} \tag{2}$$

These facts both stem from the general expression for the short-circuit current, namely,

$$i = \frac{E}{R}\left(1 - \epsilon^{-\frac{Rt}{L}}\right) \tag{3}$$

This is the well-known transient associated with the growth of current in the L, R, circuit. The rate of rise of current at the beginning of the short circuit (E/L) will be referred to frequently. It is an important quality of the d-c circuit and is expressed in amperes per second. This quantity will vary depending upon the type and size of the system, the type being the most important. In general, the rates of rise of

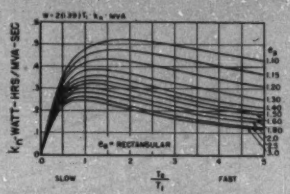

Figure 2. General energy coefficient for a d-c interrupter which develops a rectangular arc voltage following an interval of T_1 seconds from the inception of the short circuit

Note that the coefficient k_n must be multiplied by the time T_1 and the circuit megavolt-amperes to obtain the true energy in watt-hours

current (E/L) on railroad circuits are nominally between one and two million amperes per second. These circuits are hence highly inductive. On d-c industrial steel mill circuits the rate of rise is usually between 3 and 5 million amperes per second while in the electrochemical industry the rates of rise reach levels between 10 and 15 billion amperes per second. These circuits are the least inductive of all, except, for example, when the entire "pot line" of an aluminum plant is under consideration. This is a special case and is again a highly inductive low-rate-of-rise circuit. In general, circuits employing rectifiers are not as highly inductive as those which depend upon d-c machines for their current.

The circuit resistance also depends upon the type and size of the system, and particularly on the size. The maximum available amperes on any system may vary over a wide range. In general, the lower the inductance, the lower the resistance, and therefore the rectifier systems in the electrochemical industry are capable of producing extremely high available currents, 150,000 to 200,000 amperes not being unusual.

The Circuit Megavolt-amperes

In order to place the numerical considerations upon a per unit basis so that they may be applied to any system with equal ease, the short-circuit megavolt-amperes (MVA) will be used as the base of all energy considerations. The short-circuit megavolt-amperes is the product of the maximum available short circuit current and the direct voltage of the system, all divided by a million.

$$MVA = E_d \cdot I_m \cdot 10^{-6}$$
$$= \frac{E_d^2}{R} \cdot 10^{-6} \tag{4}$$

The megavolt-amperes is independent of the circuit inductance. On a large system operating at 750 volts the megavolt-amperes may be as high as 125 while on a relatively small 250-volt system the megavolt-amperes may be 10 or lower. The megavolt-amperes is important since it is the coefficient of the energy liberated in the system, in a manner about to be described.

The Circuit Time Constant

The time constant of the d-c circuit is the quotient L/R and will be known as T_0. It expresses the time in seconds required for the current to reach the E/R value *if* it continued in a straight line from any point on the current transient. A practical knowledge of the circuit permits the rapid approximations of this time constant without resorting to inductance calculations. This is possible since

$$T_0 = \frac{L}{R}$$
$$= \frac{\text{maximum available current}}{\text{rate of rise of current}}$$
$$= \frac{E}{R} \div \frac{E}{L} = T_0 \tag{5}$$

Hence a circuit capable of producing a maximum current of 120,000 amperes at an initial rate of rise of current of 8,000,000 amperes per second would have a time constant of 0.015 second. This circuit time constant is also a measure of the circuit energies as will be shown.

The Stored Energy in the System

The energy stored in the circuit inductance is important since this energy is the minimum energy which the circuit breaker must release in the act of interrupting.

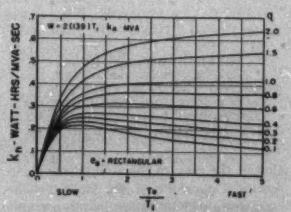

Figure 3. The general energy coefficient of Figure 2 re-expressed as a function of the per cent arcing time q as developed by a rectangular arc voltage e_a

See Figure 4 for the relation between the arc voltage and the arcing time q

The energy stored in the inductance of the system at any instant is equal to

$$W=\frac{1}{2}Li^2 \qquad (6)$$

where i is the current at the particular instant at which the energy is to be considered. The maximum energy that can be stored occurs when $i=I_m=E/R$. Under these conditions it readily can be shown that

$$W_m=\frac{1}{2}LI_m^2$$
$$=139\,L/R$$
$$=139T_0 \text{ watt-hours per megavolt-ampere} \qquad (7)$$

Note: $139=10^6/(2\times3{,}600)$

This reveals that the time constant T_0 is a measure of the maximum energy in the d-c system. The expression 139 T_0 will be found frequently in the energy relations and should be recognized as expressing the maximum stored energy of the system in watt-hours per megavolt-ampere. The energy coefficient will receive the designation k, such that the actual energy W becomes

$$W=k\cdot MVA \text{ watt-hours} \qquad (8)$$

Arc Energy Liberated by Circuit Interrupter

In Appendix I is derived the expression for the arc energy liberated by the circuit interrupter under the assumption that a trapezoidal arc voltage (e_B) is introduced at the instant (T_1) that the circuit current reaches a magnitude I_1; the trapezoidal arc voltage being so proportioned as to cause the current to decay linearly to zero from the value I_1 in an arcing time T_B. The total fault time hence would be T_1+T_B. Under these conditions (shown in Figure 9) the arc energy liberated is given by the expression

$$k=139T_0\left(\frac{I_1}{I_m}\right)^2\left\{1+q\left(\frac{I_m}{I_1}-\frac{2}{3}\right)\right\}$$
watt-hours per megavolt-ampere (9)

where

$$q=\left(\frac{T_B}{T_0}\right)$$

that is, the ratio of the arcing time T_B to the time constant of the circuit. The quantity q will be known as the per unit arcing time.

This exceedingly compact expression shows us much concerning the effect of circuit breaker speed and arcing time on the amount of energy liberated. Should $I_1=I_m$, that is, had the current attained its peak value, then the coefficient (139 T_0) represents the maximum energy of the system. Under these conditions the bracketed term reduces to "one plus one third the per unit arcing time," the latter being expressed in per unit of the time constant of the circuit.

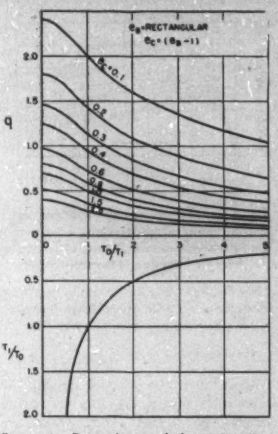

Figure 4. Dependence of the arcing time upon the magnitude of the rectangular arc voltage

The ratio of the arcing time T_B to the circuit time constant L/R or T_0 is termed q. Note that

$$\frac{T_1}{T_0}+q=\frac{T_1+T_B}{T_0}= \text{ per unit fault time}$$

Inspection will show that under all practical conditions the energy liberated by the circuit interrupter always will exceed the stored energy in the system at the instant the arc voltage is introduced. This fact is important and has a perfect mechanical analogy when applied to stopping an automobile.

Assume that a car of mass M traveling at velocity v is to be stopped. The stored energy in the car at this instant is $(1/2)Mv^2$. When the foot is removed from the accelerator, the clutch disengaged, the brakes applied, this energy will appear as heat in the brake (neglecting other friction). In this case the forward energy of the car is dissipated as heat in the brake. The true mechanical analogy of the d-c interrupter, however, is represented by the application of the brakes while the foot is still on the accelerator and the clutch engaged. Under these conditions the energy which appears as heat in the brakes is not only the stored energy of the moving vehicle but, in addition, the energy which is being supplied by the motor during the braking period. Fast stopping is indicated for minimum brake heating. Should the brake torque fail to overcome the driving torque then stopping would not occur and the brakes would burn up. Such occurs in the d-c interrupter when the arc voltage fails to exceed the d-c generated voltage. Under these conditions the current (analogous to velocity) hence is maintained at a level dictated by the difference between the two voltages and eventually will destroy the interrupter unless back-up protection is provided.

The absolute necessity of developing an arc voltage in the d-c interrupter which is in excess of the generated voltage explains why an oil circuit breaker is not a practical interrupter for d-c systems. This is true since the oil circuit breaker is inherently a low arc-voltage interrupter and except for only the very lowest voltage d-c circuits its application would be a dismal failure. The same is true of the air blast circuit breaker of conventional design. However, air circuit breakers of the magnetic type are most suitable for the interruption of d-c circuits because of their ability to develop high stable arc voltages. Their application is conditioned upon their speed of contact separation—an important factor in the determination of the circuit breaker liberated energy—as indicated by equation 9 and shown later in several practical cases.

Numerous other important cases are considered in the appendixes of this paper and equations given relating the

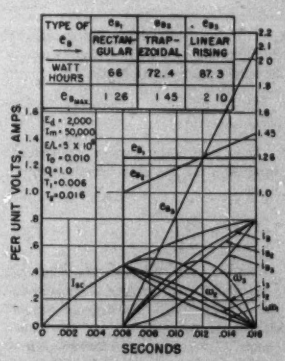

Figure 5. Comparison of the energies liberated, in a specific case, by the three typical arc voltage wave shapes of such magnitude as to permit interruption in 0.016 second following an arcing time of 0.010 second in each case

Table I. Performance Criteria

$E_d = 4{,}000$ Volts; E_B = Rectangular

E_B	I_M	$T_0 = L/R$	I_1, Amp $T_1 = 0.004$	I_1, Amp $T_1 = 0.006$	I_1, Amp $T_1 = 0.010$	T_2, Sec $T_1 = 0.004$	T_2, Sec $T_1 = 0.006$	T_2, Sec $T_1 = 0.010$	Watt-hours $T_1 = 0.004$	Watt-hours $T_1 = 0.006$	Watt-hours $T_1 = 0.010$	$E/L \times 10^{-4}$	$e_B = E_B/E_d$
4,500	100,000	0.050	7,600	11,250	18,100	0.0285	0.0395	0.0551	106	203	444	2	1.125
		0.020	18,100	25,800	39,300	0.0222	0.0288	0.0394	178	306	553	5	
		0.010	33,000	45,900	63,200	0.0172	0.0218	0.0286	206	332	514	10	
	60,000	0.030	7,380	10,880	16,900	0.025	0.033	0.046	96.7	160	314	2	
		0.012	16,900	23,600	34,000	0.018	0.024	0.031	126	199	320	5	
		0.006	29,000	37,900	48,700	0.0139	0.017	0.022	133	184	256	10	
	30,000	0.015	6,900	9,900	14,490	0.0188	0.0205	0.0279	58.5	96.6	166	2	
		0.006	14,460	18,980	24,360	0.0138	0.0172	0.0223	66.0	92.2	127	5	
		0.003	20,700	25,950	27,030	0.0098	0.0123	0.0165	55.9	69.0	76.5	10	
			T_2/T_1										
5,000	100,000	0.050	12.5	8.33	5.00	0.0171	0.0251	0.0375	69.4	136	317	2	1.25
		0.020	5.00	3.33	2.00	0.0150	0.0204	0.0292	123	228	440	5	
		0.010	2.5	1.67	1.00	0.0156	0.0202	0.0270	163	270	443	10	
	60,000	0.030	7.50	5.00	3.00	0.0163	0.0221	0.0328	58.7	114	256	2	
		0.012	3.00	2.00	1.20	0.0131	0.0174	0.0243	94.2	158	270	5	
		0.006	1.5	1.00	0.60	0.0105	0.0136	0.0187	110	159	224	10	
	30,000	0.015	3.75	2.50	1.50	0.0113	0.0154	0.0219	43.2	75.0	137	2	
		0.006	1.50	1.0	0.60	0.0105	0.0136	0.0187	54.0	79.0	112	5	
		0.003	0.75	0.50	0.30	0.0080	0.0105	0.0146	48.5	61.0	69.0	10	
			T_0/T_1										
6,000	100,000	0.050	0.08	0.12	0.20	0.0110	0.0165	0.0255	46.7	90.0	219	2	1.50
		0.020	0.20	0.30	0.50	0.0102	0.0143	0.0125	88.1	167	346	5	
		0.010	0.40	0.60	1.00	0.0091	0.0124	0.0183	129	217	370	10	
	60,000	0.030	0.133	0.20	0.333	0.0107	0.0153	0.0235	39.5	79.3	177	2	
		0.012	0.333	0.50	0.833	0.0094	0.0130	0.0191	70.7	125	225	5	
		0.006	0.667	1.00	1.677	0.0081	0.0109	0.0158	88.6	133	197	10	
	30,000	0.015	0.267	0.40	0.667	0.0081	0.0116	0.0172	30.7	57.6	111	2	
		0.006	0.667	1.0	1.667	0.0081	0.0109	0.0158	44.1	66.6	98.4	5	
		0.003	1.333	2.0	3.333	0.0067	0.0090	0.0131	42.1	55.0	60.3	10	

arc energy to the circuit constants. Some of the results of this study will be presented here in a few practical cases which will serve as examples of the type of information made available by this analytical study.

A Practical Case

One of the easiest and most practical arc voltages to consider is the flat top or rectangular arc voltage (Appendix II). It is recognized that the arc voltage seldom rises vertically to a fixed level and remains there without some fluctuations, however, actual d-c circuit breaker performance shows this condition to be closely approximated.[3,6] For all practical purposes, therefore, the assumption of such a rectangular wave shape is warranted to explore the effect of variations of other factors.

The arc energy liberated for the rectangular arc voltage is given by the equation

$$k = 2e_B\,(139T_0)\left\{\left(\frac{I_1}{I_m}\right) - (qe_c)\right\} \text{ watt-hours per megavolt-ampere} \quad (10)$$

where

e_B = magnitude of the rectangular arc voltage in per unit of the generated voltage $= E_B/E_d$

q = arcing time or duration of the rectangular arc voltage in per unit of the time constant of the circuit, T_0

$e_c = (e_B - 1)$ or the arc voltage in excess of generated voltage in per unit of the generated voltage

It is of interest to note that q, for the rectangular arc voltage, is given by the expression

$$q = -\log_e\left(\frac{e_c}{e_c + I_1/I_m}\right) \quad (11)$$

and

$$\frac{I_1}{I_m} = (1 - \epsilon^{-T_1/T_0}) \quad (12)$$

Armed with this information, it is practical to consider the relative energies that would be liberated by an interrupter (which produced this rectangular arc voltage) when the following four factors are varied over a reasonable range:

1. Circuit breaker speed, time to contact parting (variations in T_1).
2. Rate of rise of current (variations of L).
3. Maximum available current (variations of R).
4. Magnitude of the rectangular arc voltage (variation in E_B).

Allowing each of these quantities to take three separate values it follows that 3^4 or 81 solutions are indicated. These are tabulated in Table I for an assumed 4,000-volt d-c system in which these quantities take on the following numerical values:

1. Circuit breaker speed in seconds, beginning of arc voltage: (*a*) 0.004; (*b*) 0.006; (*c*) 0.010.
2. Rate of rise of current in amperes per microsecond $= E/L \times 10^{-4}$: (*a*) 2.0; (*b*) 5.0; (*c*) 10.0. (Multiply by a million to get amperes per second.)
3. Maximum available current I_m in amperes: (*a*) 100,000; (*b*) 60,000; (*c*) 30,000. Corresponding megavolt-ampere values for 4,000-volt system: (*a*) 400; (*b*) 240; (*c*) 120.
4. Magnitude of arc voltage E_B in volts: (*a*) 4,500; (*b*) 5,000; (*c*) 6,000.

Corresponding values of per unit arc voltage e_B, $e_B = E_B/E_d = E_B/4{,}000$: (*a*) 1.125; (*b*) 1.25; (*c*) 1.50.

Table I presents the three most important performance criteria, namely,

1. The current I_1 which, in the cases shown, is the peak current attained in the circuit.
2. The total fault time T_2 in seconds.
3. The arc energy in watt-hours.

Inasmuch as the value of I_1 is independent of the magnitude of the arc voltage (as long as it is in excess of the generated voltage) it follows that only 3^3 or 27 values of I_1 are shown; these appear at the top of the table under I_1.

A study of this table will reveal many

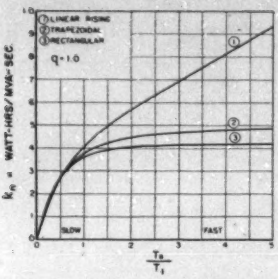

Figure 6. General energy characteristics of the three arc voltage wave shapes operating under conditions which permit the arcing time to be equal to the circuit time constant, q = 1.0

Note the superiority of the rectangular arc voltage

interesting features concerning the performance of the d-c interrupter in various types of circuits. These will be examined in detail.

The peak current in the circuit (I_1), as limited by the interrupter, is dependent upon the rate of rise of current, the interrupter speed, and the maximum value of the available current (I_m). The slow interrupter allows the highest peak current in each case. For high rates of rise of current, high speed interrupters are imperative.

The variations of liberated energy, however, are not as obvious as these variations of current. A few of these will be discussed from the table. When the arc voltage is only 12.5% in excess of the generated voltage ($e_B = 1.125$) the influence of the rate of rise of current is tremendous. For the fast interrupter ($T_1 = 0.004$ second) a change in the rate of rise from 2 to 10 million amperes per second increases the liberated energy from 106 to 206 watt-hours. For the interrupter whose operating time is 0.010 second instead of 0.004, these energy values rise respectively to 444 and 514 watt-hours. The merits of speed become obvious.

As a calibration of the type of audible report made by such an open type circuit breaker in releasing 514 watt-hours in 0.0186 second, it might be pointed out that the typical arc-back on a large 650-volt electrochemical system when cleared by a fast anode circuit breaker, releases between 80 and 90 watt-hours in about 0.008 second.[4] The 650-volt anode circuit breaker arc energy is approximated in Table I as the circuit breaker which develops an arc voltage of 6,000 volts ($e_B = 1.50$), 0.006 second after the contacts part, in a circuit which is capable of attaining 60,000 amperes at an initial rate of rise of 2,000,000 amperes per second.

A further study of Table I will reveal the merit of so proportioning the design of the arc chute so as to develop arc voltages well in excess of the generated voltage. Consider the circuit breaker whose speed is 0.006 second to the point of arc voltage insertion. When the arc voltage is only 12.5 per cent above the generated voltage ($e_B = 1.125$) the energies for rates of rise of 2, 5, and 10 amperes per microsecond are, respectively, 203, 306, and 332 watt-hours. However, when the arc voltage is increased to 50 per cent in excess of the generated voltage ($e_B = 1.50$) these same energies reduce to 57.6, 66.6 and 55 watt-hours. Note that in the latter case the highest energy is associated with the circuit having a rate of rise of 5 million amperes per second while in the former case the higher the rate of rise the higher the energy.

It is of further interest to observe that the slow circuit breaker ($t_1 = 0.010$) operating with an $e_B = 1.50$ has the highest energy liberated for the lowest rate of rise of current. When the arc voltage produced is only 12.5 per cent above the generated voltage, however, ($e_B = 1.125$) the relative order of liberated energy is reversed, the highest rates of rise producing the highest energy in spite of the reduction in arcing time. These numerical evaluations explain for the first time some of the empirical observations which have long been puzzling. A further study of this table will reveal other interesting trends which have a bearing upon the design and performance criteria of d-c interrupters.

General Characteristic Curves

Turning now from a description of a specific application as presented in Table I, it is proper that these results be made available in more general and useful form so that application may be made to any circuit. The next step in the evolution of these concepts is therefore presented in the form of curves shown in Figure 1. Here the circuit time constant ($T_0 = L/R$) is the abscissa of the curves which give the arc energy for various values of (e_B), the ratio of the magnitude of the rectangular arc voltage to the generated voltage. These curves are restricted to one particular circuit breaker time, namely, a T_1 of 0.006 second from fault initiation to the time of introducing the rectangular arc voltage. When applied

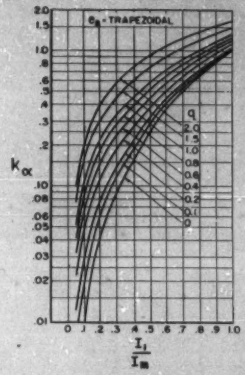

Figure 7. The dependence of the dimensionless energy coefficient k_{ax} upon the per unit arcing time q and the I_1/I_m ratio

The coefficient k_{ax} must be multiplied by $139L/R$ and by the circuit megavolt-amperes to obtain the true arc energy

for circuit breakers having this specific time the curves are quite general and cover as wide a range of circuit constants as desired. The general shape of these curves reveal that the higher the arc voltage the lower the energy and that for each particular arc voltage magnitude there exists a circuit time constant (T_0) which will give rise to the maximum energy per megavolt-ampere.

The restriction to one circuit breaker speed in Figure 1 is eliminated in the curves of Figure 2 by expressing the abscissa as a dimensionless ratio (T_0/T_1), namely, the ratio of the circuit time constant T_0 to the circuit breaker time T_1. The ordinate of the curves, however, does not express the arc energy directly but gives an arc energy coefficient k_a which is used in the equation

$$W = 278 T_1 \cdot k_a \cdot MVA \qquad (13)$$

where

k_a = a dimensionless coefficient obtained from the curves of Figures 2, 3, and 6

T_1 = the circuit breaker time from the initiation of the fault to the introduction of the rectangular arc voltage

$MVA = E_a \times I_m \times 10^{-6}$

W = arc energy in watt-hours

(Note $278 = 2 \times 139$)

Figure 2 teaches that it is desirable to make T_1 as low as possible. Also when high arc voltages are available the energy will be low, as previously indicated. In using the curves of Figure 2 it is to be re-

membered that not only does the value of T_1 control the magnitude of k_n but T_1 also appears as a coefficient of the arc energy (equation 13). It is of interest to observe that the arc energy is controlled primarily by the product $T_1 \cdot MVA$ which contains all the necessary dimensions of energy. The effect of the dimensionless constant k_n, as shown by the curves of Figure 2, plays a less important role and indicates

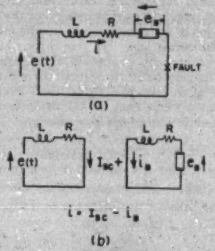

Figure 8. Circuits which show the method of applying the principle of superposition to solve for the net current by linear circuit methods although the characteristics of the interrupter are nonlinear

in particular the effect of the magnitude of the arc voltage upon the energy. Inspection will show that a circuit breaker time T_1 which is not in excess of one half of the circuit time constant T_0 is a particularly desirable goal provided the magnitude of the equivalent rectangular arc voltage is at least 50 per cent in excess of the generated voltage. When $T_0/T_1 = 0.5$ and $e_B = 1.50$ then, from Figure 2,

$$W = 84 \cdot T_1 \cdot MVA \qquad (14)$$

Now when $T_1 = 0.006$ second then the arc energy in watt-hours is about $0.50 \times MVA$. This value is strikingly close to the energy liberated each half cycle of arcing of a magnetic circuit breaker when clearing a 60-cycle circuit.[5] These relations provide a conservative basis for estimating the ability of a-c magnetic circuit breakers on d-c circuits, provided, of course, that the requirements of speed of operation (T_1) are fulfilled.

The cost of providing speed in a d-c circuit breaker and still meet all the other mechanical requirements is usually more costly than providing arc suppression and hence the present balance between mechanism and arc suppression characteristics to meet a given objective. Higher interrupting capacity at a given voltage might be accomplished, with present arc suppression characteristics, by increasing circuit breaker speed alone. Higher operating voltages, however, require arc suppression devices capable of producing proportionally higher arc voltage. This evolution, however, need not necessarily require larger circuit breakers. In fact, modern arc suppression devices in air are considerably smaller than those employed on early d-c circuit breakers in spite of the need for developing high arc voltages.[6]

The present need for releasing high values of energy during the interruption of high values of megavolt-ampere of d-c circuits explains why the arc chutes of these interrupters almost invariably are exposed to the atmosphere, totally enclosed structures being quite impractical or expensive. This situation likely will remain with us until some better method is found of absorbing the energy rather than expell it in disassociated gases. The principle of the current limiting fuse comes close to this ideal of noiseless, flameless energy absorption.[7]

Application to Oscillograph Measurements

Often it is necessary to determine the arc energy when both the circuit breaker mechanical time T_1 and the arcing time T_B are known or assumed. When the latter is expressed in per unit of the circuit time constant T_0 namely $q = T_B/T_0$, it follows that the arc energy can be determined for a rectangular arc voltage without immediate knowledge of its magnitude. This is possible through equations 11 and 12. Accordingly the curves of Figure 3 show the arc energy in a manner similar to Figure 2 except that the curves are for various per unit arcing times. The ordinate is again k_n and requires equation 13 to determine the true arc energy. These curves are particularly useful when determining the energy from an oscillogram in which the arc voltage or wattage traces are not available. The influence of the shape of the arc voltage upon these energy values will be discussed in the next section.

Arc Voltage Wave Shape

The three typical and practical arc voltage wave shapes treated in the appendixes of this paper are the trapezoidal, rectangular, and the triangular or linearly rising arc voltage. Energy equations for all three types have been derived and the first two discussed in the above text. It is of interest to compare the energy liberated by each of these three arc voltage wave shapes on the basis of a fixed arcing time. Figure 5 presents an analysis of a particular case of a circuit breaker capable of introducing its arc voltage in 0.006 second following the inception of a short-circuit current rising at a rate of 5 million amperes per second. The maximum available current is assumed to be 50,000 amperes in a 2,000 volt d-c circuit. All three arc voltage wave shapes will be so proportioned as to permit each interruption to take place following an arcing time of 0.010 second, that is a q of unity. The energy released in the three cases is respectively 66.0, 72.4, and 87.3 watt-hours, the rectangular or flat top arc voltage giving the lowest energy and the triangular or linearly rising arc voltage the highest. These voltages, their respective arc currents, and wattages are shown in Figure 5. These results are expressed in more general terms in Figure 6 where the arcing time T_B is at all times equal to the circuit time constant T_0, that is $q = 1.0$. The ordinate of Figure 6 is k_n as in Figures 2 and 3. The energy must be determined from equation 13.

The curves of Figure 6 are typical and demonstrate the merit of the rectangular arc voltage, particularly for the fast circuit breakers. The trapezoidal arc voltage, which permits a linear decay of current, is a close second in preference. The linearly rising arc voltage permits the current to increase higher than I_1 and adds measurably to the arc energy. Circuit breakers which are capable of transferring the arc rapidly to the arc suppression chamber and hence permit the arc voltage to rise as rapidly as possible to a magnitude in excess of the generated voltage, will be found superior to slower rises of arc voltage.

Blow out coils and the magnitude of the circuit current I_1 at the time of contact parting play an important part in determining the shape of the arc voltage. Numerous other design features, determined by empirical studies, enhance the speed of arc transfer. It follows that

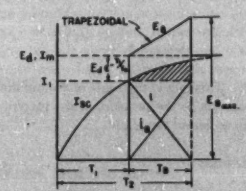

Figure 9. Circuit response in which the arc voltage E_B is introduced at time T_1 to cause a linear decay of current in a time T_B

Note that the arc voltage wave shape to produce this result is trapezoidal

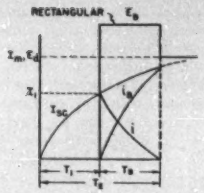

Figure 10. Circuit response in which a rectangular arc voltage E_B is introduced at time T_1 to cause the current to decay from I_1 to zero in a time T_B

Note that the current $i = I_{sc} - i_B$ where i_B is the current that would be produced by the arc voltage E_B acting alone in the circuit. See Figure 8

rapid arc transfer is essential to minimum contact burning. The absence of metal vapor, in turn, permits higher arc voltages to be developed.

The rectangular arc voltage not only produces the lowest arc energy of the three types discussed but also gives rise to the minimum peak value of arc voltage which in turn is impressed on the circuit insulation to ground. Malperformance of a d-c interrupter becomes critical when, during the arcing period the arc voltage falls below the generated voltage. When this occurs, the circuit current rises and usually causes a further decrease in arc voltage. Only under unusual conditions can interruption occur when this takes place.

From the foregoing treatment it is not to be inferred that any particular circuit breaker will develop the same arc voltage for any ratio and magnitude of circuit constants. Quite the contrary. The actual arc voltage is influenced by the magnitude of the circuit current and also dependent upon the past history of the liberated arc energy. However, with improvement in arc suppression devices the arc voltage wave shape and magnitude can be created and controlled for any particular circuit voltage application and made less dependent upon the old volt-ampere characteristic of an open arc in air. This fact is the basis of the circuital approach to the problem of d-c interruption as herein presented.

Summary

Three typical arc voltage wave shapes encountered in the performance of d-c interrupters have been compared, analytically, with respect to the arc energy liberated by the interrupter. The influence of circuit breaker speed in relation to the inductance and resistance parameters of the d-c circuit have been considered quantitatively and expressed as equations and presented in curves in such a way as to be applicable to a wide range of circuit constants. The use of the per unit system together with dimensionless ratios as abscissa and ordinate of the curves enhance their range and usefulness. The following major conclusions have been reached as a result of this analysis.

Conclusions

1. The arc voltage of the d-c interrupter is the most important characteristic relating its application to a specific d-c circuit.

(*a*). The magnitude of the arc voltage must exceed the generated voltage to achieve interruption; the higher the arc voltage the quicker the interruption and the lower energy expended. System insulation limits the advisable magnitude of the arc voltage.

(*b*). Arc voltages which rise rapidly and remain essentially stable at a fixed value, well in excess of the d-c generated voltage (commensurate with the system insulation), are superior to slowly rising arc voltage characteristics.

2. The early introduction of the arc voltage into the circuit following the initiation of a short circuit is a tremendous factor in limiting the amount of energy liberated by the interrupter.

(*a*). Quick parting of the circuit breaker contacts is the first prerequisite to accomplish this objective.

(*b*). Efficiently designed arc transfer means, employing blowout coils when needed, permitting the arc to be transferred rapidly to the arc suppression chamber, designed to develop the necessary arc voltage, is an essential factor in accomplishing this result.

3. The megavolt-amperes of the d-c short circuit, computed as the square of the generated voltage divided by the circuit resistance (and divided by a million) appears in all energy relations. This fact permits the curves and equations to be applied to any d-c system from a small battery circuit to a large steel mill interruption problem.

4. The influence of circuit inductance upon the performance of d-c interrupters is dependent upon the relative magnitude of other factors, as described hereinafter. This constitutes the essential contribution of the paper.

(*a*). Since the megavolt-amperes is independent of the circuit inductance it follows that for each circuit breaker time and arc voltage there exists a circuit inductance which gives rise to a maximum liberated energy. See Figures 2 and 3.

(*b*). Breakers which are fast usually will experience an increase in liberated energy as the circuit inductance is lowered. This fact is accentuated in high *MVA* circuits, low *R*.

(*c*). Slow circuit breakers (T_1/T_B) will experience a decrease in liberated energy as the circuit inductance is lowered. This factor is accentuated in low *MVA* circuits, high *R*. This follows due to the lower stored energy of the system, the essential contribution to the energy liberated by the switch.

(*d*). These considerations prove that the so-called rate of rise of current (E/L) as often referred to with respect to the interruption of d-c circuits is not a valid measure of the circuit severity. However, this rate of rise concept is important in estimating the magnitude of the circuit current at the time of contact parting (I_1) and hence becomes a *rough* measure of the severity of contact burning for a given design.

5. A new and more accurate severity standard for d-c circuits is needed which will include all the essential requirements of the breaker performance and represent a more accurate measure of the quality required of d-c interrupters to meet a specific time and current limiting specification.

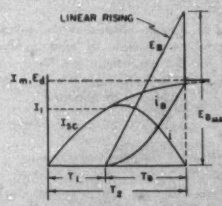

Figure 11. Circuit response in which a linearly rising arc voltage E_B is introduced at a time T_1 to cause the current to reach zero following an arcing time T_B

See Figure 8 for the method of solution

Nomenclature

E_d = magnitude of d-c bus voltage
E_B = arc voltage of the interrupter
e_B = per unit arc voltage of interrupter
= E_B/E_d
$e_c = (e_B - 1)$
= per unit arc voltage in excess of the d-c bus voltage
I_{SC} = short-circuit current
$I_m = E_d/R$ = maximum available short-circuit current
I_1 = circuit current at time T_1
i_B = current produced in the circuit by arc voltage acting alone
$i = (I_{SC} - i_B)$
= arc current
h = arc energy in watt-hours per megavolt-ampere

$k_a = \frac{k}{139T_0}$

= arc energy in per unit of the maximum stored energy in the circuit

$k_n = \frac{k}{E_d I_m T_1}$

= a useful energy coefficient

L = circuit inductance in henrys

MVA = megavolt-amperes available

$= E_d I_m \cdot 10^{-6}$

N = actual slope of linearly rising arc voltage

$n = \frac{N}{E_d/T_0}$

= per unit slope of linearly rising arc voltage

R = circuit resistance in ohms

T_1 = mechanical time of interrupter. Time from the beginning of the short-circuit current to the introduction of the arc voltage of the interrupter.

T_B = arcing time of the interrupter

T_3 = total fault duration

$T_0 = L/R$

= time constant of the circuit

$q = T_B/T_0$

= per unit arcing time

W = arc energy in watt-hours

W_0 = arc wattage in watts

W_m = maximum stored energy in the circuit

$= 139T_0$

Appendix I

Method of Analysis

The student of electrical engineering usually is well trained in determining the currents which flow when the proverbial switch S is closed to complete circuit containing an electromotive force E. The solution of this same circuit, however, when the switch S is opened usually presents problems of a more formidable nature. In this respect the student often finds himself in the same embarrassing position as the Sorcerer's Apprentice, who having spoken the magic words to start the flow of water from the broom handle is unable to stop the deluge.

The magic words for stopping the flow of electric current can be found in the principle of "superposition." This principle, in one of its simplest forms, states that the net current in a linear circuit is the algebraic sum of the currents produced by each of the electromotive forces acting separately. It is not appreciated generally, however, that the electromotive forces may be either source voltages or voltage drops in the circuit. When this method is used all other electromotive forces are short-circuited while the current due to each electromotive force is determined. When applied to a circuit interrupter this principle might be stated thus

The complete current through a switch is the algebraic sum of the currents produced by the source voltages when the switch is assumed closed and the current that would be produced in the circuit by the voltage drop of the switch acting alone (source voltages short-circuited).

The switch designer has under his control the voltage drop characteristic of the interrupter over a wide range of currents. From an analytical viewpoint this method is quite powerful inasmuch as many nonlinear circuits can be computed by straightforward linear theory. The circuit interrupter represents one of these nonlinear problems.

Derivation of Arc Energy Equations

Linear Current Decay

The general case of linear current decay is shown in Figure 9. At a time T_1 following the inception of a d-c short circuit the current is arrested and made to decay linearly from I_1 to zero in a time T_B. What energy is liberated? The first step in this solution is the determination of the voltage drop of the interrupter necessary to create the linear current decay.

Solution

The voltage drop of the interrupter necessary to level the short circuit at the magnitude I_1, that is, to cancel the shaded portion of the short-circuit current shown in Figure 9, is

$$-E_d e^{-\frac{RT_1}{L}} \tag{15}$$

This is a direct voltage whose magnitude is shown on the voltage scale of Figure 9.

The voltage drop of the interrupter necessary to create the linearly rising cancellation current i_B of Figure 9 naturally would be identical with the voltage produced in the L and R of the circuit when the linearly rising current $i_B = I_1 t/T_B$ is introduced. This current would generate in the circuit inductance a fixed voltage whose magnitude is

$$-\frac{I_1}{T_B}L \tag{16}$$

In the resistance of the circuit the current i_B would generate the voltage

$$-\frac{I_1 R}{T_B}t \tag{17}$$

It follows that the total voltage drop of the interrupter is the sum of equations 15, 16, and 17 or

$$E_B = -\left\{E_d e^{-\left(\frac{T_1}{T_0}\right)} + \frac{I_1 L}{T_B} + \frac{I_1 R t}{T_B}\right\} \tag{18}$$

This is the trapezoidal voltage drop shown in Figure 9 and would produce the linear decay of current desired.

The wattage W_0 is the product of the current and the drop in the interrupter

$$W_0 = E_B \cdot i \tag{19}$$

The current is given by the equation

$$i = I_1 - \left(\frac{I_1}{T_B}\right)t \tag{20}$$

The arc energy W is given by the integral

$$W = \int_1^{T_3} E_B \cdot i \cdot dt \tag{21}$$

Substituting and integrating there results

$$W = \left[\frac{I_1^2 L}{2} + \frac{I_1 R}{6}\left\{3I_m - 2I_1 T_B\right\}\right] \text{joules} \tag{22}$$

Dividing by the megavolt-amperes of the circuit and reducing to watt-hours per megavolt-ampere there results the energy coefficient k in watt-hours per megavolt-ampere

$$k = 139\left(\frac{I_1}{I_m}\right)^2\left\{\frac{L}{R} + \left[\left(\frac{I_m}{I_1}\right) - \frac{2}{3}\right]T_B\right\} \tag{23}$$

Now let the ratio of the interrupter arcing time T_B to the circuit time constant L/R be expressed as q, that is let

$$q = \frac{T_B}{L/R} = \frac{T_B}{T_0} \tag{24}$$

Then

$$k = 139\left(\frac{I_1}{I_m}\right)^2 T_0\left[1 + q\left\{\frac{I_m}{I_1} - \frac{2}{3}\right\}\right]$$

watt-hours per megavolt-ampere (25)

For the purpose of dimensionless plots, the factor k_a is defined as

$$k_a = \left(\frac{k}{139T_0}\right) = \left(\frac{I_1}{I_m}\right)^2\left[1 + q\left\{\frac{I_m}{I_1} - \frac{2}{3}\right\}\right] \tag{26}$$

Appendix II

The rectangular arc voltage case is shown in Figure 10. Here the arc current is the difference between portions of two exponential currents, one produced by the system voltage and the other produced T_1 seconds later by the rectangular arc voltage E_B. Current zero occurs when

$$\frac{E_d}{R}\left\{1 - e^{-\left(\frac{T_1 + T_B}{T_0}\right)}\right\} = \frac{E_B}{R}\left\{1 - e^{-\frac{T_B}{T_0}}\right\} \tag{27}$$

where $T_0 = L/R$.

Rearranging equation 27, there results

$$(E_B - E_d) = E_B e^{-\left(\frac{T_B}{T_0}\right)} - E_d e^{-\left(\frac{T_1}{T_0}\right)} \cdot e^{-\left(\frac{T_B}{T_0}\right)} \tag{28}$$

But since

$$e^{-\left(\frac{T_1}{T_0}\right)} = \left\{\frac{I_m - I_1}{I_m}\right\} \tag{29}$$

Then from equation 28

$$e^{-\left(\frac{T_B}{T_0}\right)} = \left\{\frac{E_B - E_d}{E_B - E_d\left(\frac{I_m - I_1}{I_m}\right)}\right\} = \left\{\frac{e_c}{e_c + \frac{I_1}{I_m}}\right\} \tag{30}$$

where

$$e_c = \left\{\frac{E_B - E_d}{E_d}\right\} \tag{31}$$

From equation 30 it follows that the arcing time T_B may be expressed

$$T_B = -T_0 \log_e \left\{\frac{e_c}{e_c + I_1/I_m}\right\} \tag{32}$$

or

$$q = -\log_e \left\{\frac{e_c}{e_c + I_1/I_m}\right\} \tag{33}$$

The arc energy is

$$W = E_B \int_{T_1}^{T_2} i \cdot dt \text{ joules} \tag{34}$$

Substituting

$$W = E_B \left[\frac{E_d}{R} \int_{T_1}^{T_1+T_B} \left(1 - \epsilon^{-t/T_0}\right) dt - \frac{E_B}{R} \int_0^{T_B} \left(1 - \epsilon^{-t/T_0}\right) dt \right] \tag{35}$$

Integrating and substituting

$$W = e_B \cdot E_d \cdot I_m \cdot T_0 \left[q(1 - e_B) + e_B(1 - \epsilon^{-q}) + \left(1 - \frac{I_1}{I_m}\right)(\epsilon^{-q} - 1) \right] \tag{36}$$

But

$$W = k \cdot MVA$$

when

$$MVA = E_d I_m 10^{-6}$$

Substituting and reducing

$$k = 2e_B(139T_0)\left(\frac{I_1}{I_m} - qe_c\right) \text{ watt-hours per megavolt-ampere} \tag{37}$$

The quantity $139T_0$ affords the dimensions to equation 37. A useful dimensionless relationship k_α then becomes:

$$k_\alpha = \frac{k}{139T_0} = 2e_B\left\{\frac{I_1}{I_m} - qe_c\right\} \tag{38}$$

Appendix III

At a time T_1 following the inception of a short circuit a linearly rising arc voltage, having a slope of N, is introduced. This voltage produces the backward moving current i_B. This is the current which would flow in the L, R circuit when a linearly rising voltage is applied. Using operational methods this current becomes

$$i_B = \frac{N}{R}\left[t - T_0\left(1 - \epsilon^{-\left(\frac{t}{T_0}\right)}\right)\right] \tag{39}$$

Now let the slope of the linearly rising arc voltage N be expressed in per unit of the circuit constants, namely, let

$$n = \frac{\text{slope of arc voltage}}{\text{unit slope}} = \frac{N}{E_d/T_0} \tag{40}$$

Therefore

$$N = nE_d/T_0 \tag{41}$$

and

$$e_B = \left(\frac{nE_d}{T_0}\right)t \tag{42}$$

Solving for the arc energy in a manner similar to that used in Appendixes I and II, there results

$$W = I_m \cdot E_d \cdot n \cdot T_0 \left[\frac{q^2}{2}\left(1 + n - \frac{2}{3}nq\right) + \left\{\epsilon^{-q}(q+1) - 1\right\}\left\{\epsilon^{-T_1/T_0} + n\right\}\right] \tag{43}$$

Now let

$$k_n = \left\{\frac{W}{I_m E_d T_1}\right\} \tag{44}$$

Hence k_n is a dimensionless quantity expressed from equation 43 as

$$k_n = \frac{nT_0}{T_1}\left[\frac{q^2}{2}\left(1 + n - \frac{2}{3}nq\right) + \left\{\epsilon^{-q}(q+1) - 1\right\}\left\{\epsilon^{-T_1/T_0} + n\right\}\right] \tag{45}$$

where

$$q = T_B/T_0$$

It follows that the energy may be expressed as

$$W = 278T_1 k_n \; MVA \text{ watt-hours} \tag{46}$$

The relation between n and q may be expressed as follows: At time T_2

$$i_B = I_{SC}$$

or

$$n\left[\frac{T_B}{T_0} - 1 + \epsilon^{-T_B/T_0}\right] = \left[1 - \epsilon^{-\left(\frac{T_1+T_B}{T_0}\right)}\right] \tag{47}$$

Therefore

$$n = \left\{\frac{1 - \epsilon^{-\left(\frac{T_1}{T_0}+q\right)}}{\epsilon^{-q} + q - 1}\right\} \tag{48}$$

Curve 1 on Figure 6 expresses the manner in which the arc energy varies for a linearly rising arc voltage which produces a current zero in an arcing time equal to the circuit time constant, that is, $q = 1.0$.

References

1. Air-Break Magnetic Blow-Outs for Contactors and Circuit Breakers Both A-C and D-C, **J. F. Tritle.** AIEE Transactions, volume 41, 1922, pages 262–70.

2. A New High-Speed Air Circuit Breaker, **A. O. Keep.** AIEE Transactions, volume 53, 1934, pages 322–6.

3. A New Multiple High-Speed Air Circuit Breaker for Mercury-Arc-Rectifier Anode Circuits and Its Relation to the Arc-Back Problem, **J. W. Seaman, L. W. Morton.** AIEE Transactions, volume 61, 1942, pages 788–96.

4. A Fast Circuit Breaker, **D. I. Bohn, O. Jensen.** AIEE Transactions, volume 61, 1942, pages 165–8.

5. The Geometry of Arc Interruption, **E. W. Boehne.** AIEE Transactions, volume 60, 1941, pages 524–32.

6. Anode Circuit Breaker Design and Performance Criteria, **E. W. Boehne, W. A. Atwood.** AIEE Transactions, volume 64, 1945, pages 337–45.

7. Performance Criteria for Current-Limiting Power Fuses—I, II, **C. L. Schuck, E. W. Boehne.** AIEE Transactions, volume 65, 1946, pages 1028–48. Discussion pages 1191–4.

Discussion

Harry Sohon (University of Pennsylvania, Philadelphia, Pa.): For a long time it was customary to decide that a circuit containing a nonlinear element was not susceptible to analytic investigation. Any attempted development therefore was based on empirical methods. The main weakness of empirical methods is that although they may show that a small deviation in any parameter leads to a poorer design, there is no guarantee that a large change in one or more parameters may lead to a much better design.

The arc in d-c interrupter is a nonlinear element. The authors have shown one way of making a comparatively simple analytic investigation of the interrupter circuit in spite of the presence of the arc. The type of study that is made does depend on the experimentally determined arc voltage. As long as a radical change in arc voltage does not result, this type of investigation is fairly simple and should prove very satisfactory. Of course it will be necessary to make models during an investigation of possible interrupter designs to be assured that the arc voltage is as assumed.

It will be interesting to see how the designers make use of the new concept. Theoretically it should be applicable to more than one nonlinear circuit element. If it is possible to estimate accurately the voltage across the nonlinear elements then each may be replaced by a generator developing the corresponding voltage and the resulting circuit becomes a linear circuit. The authors are to be commended for bringing this idea to the attention of the engineering profession.

Broken Conductor Effect on Sags in Suspension Spans

ALFIO BISSIRI
NONMEMBER AIEE

MAURICE LANDAU
NONMEMBER AIEE

Synposis: A method is explained of calculating and plotting tension–length curves for suspended conductors. Application of the tension–length curves to the determination of increased sags in suspension spans occurring when a conductor breaks and other transmission line problems are described and illustrated. Other than for the calculation of the tension–length curves, adequate accuracy is obtained using a 10-inch slide rule.

THE three Boulder transmission lines of the Department of Water and Power, City of Los Angeles, Calif., operate at 287.5 kv line voltage and are each approximately 266 miles in length. The spans are nominally 1,000 feet in length, but due to the topography vary widely in span length and difference in elevation of support. The suspension insulator assemblies are 12.58 feet from the point of support at the tower at which rotation in the direction of line may occur, and the point of support of the conductor.

The lines cross many other transmission lines of lower voltage, railroads, communication lines, and highways. In determining the height of each tower adjacent to these crossings, minimum allowable separations had to be maintained both under normal conditions and in the case of a break in a conductor in a span adjacent to such crossing. Calculations demonstrated that a clearance of 40 feet under normal conditions might decrease to 10 feet in the case of a break in the conductor in an adjacent span.

The method of calculation described in this paper was devised in order that every crossing involved be investigated and proper clearances maintained.

The problem, in general, is to determine the change occurring in a suspension span, or a series of suspension spans, from one condition of static equilibrium to another, which is caused by a variation in one or more of the factors that determine the equilibrium of the spans involved.

Static equilibrium requires that the vector sum of the forces at each point of support of the cable be equal to zero. In the absence of transverse wind load forces on the conductor, all of the forces are in the plane of the conductor. For equilibrium at each point of support of the conductor therefore

$$\Sigma H = 0$$
$$\Sigma V = 0$$

When a break occurs in a conductor adjacent to a suspension string of insulators, the insulators, being unrestrained, become part of the adjacent span, with the point of support at the top of the insulator string instead of the bottom. Effectively the length of the conductor in the span increases by the length of the insulator string, which in turn causes a drop in tension in the span and an increase in sag.

At the second string of suspension insulators beyond the point of the break, a difference in tension of the conductor occurs on either side of the second insulator string which tends to move the second string of insulators away from the break with a resulting decrease in tension in the second span. In progression the third and succeeding strings tend to move away from the point of the break.

At the second string of insulators, static equilibrium is reached when the tension in the first span plus the tension in the inclined second string is equal to the tension in the second span. In like manner in succeeding spans, equilibrium is had when the vector sum of the forces at the end of each succeeding string is equal to zero.

In calculating the resulting condition of static equilibrium, the elastic properties of wire must be taken into consideration due to the change in length of conductor occurring with a change in tension in the conductor.

Further, while the unstressed length of conductor remains constant, the span lengths and differences of elevation of the spans change as a result of the movement of the insulator strings.

From the preceding paragraphs it can be seen that calculations of the changes in static equilibrium of suspended spans resulting from a break in the conductor adjacent to a suspension string involve relationships between the following:

L = span length
D = difference in elevation
H = horizontal component of tension
S_u = unstressed length of conductor in span
E = modulus of elasticity of the conductor

Units and Notations

A = area or cross-section of conductor, square inches
$a = H/W$, feet
$a_{ss} = T_{ss}/W$, feet
β = horizontal displacement of the suspension clamp from the vertical point on the conductor, feet
D = vertical distance between supports, feet
D' = vertical distance between low points of adjacent spans, feet
d = horizontal displacement of end of insulator string, feet
E = modulus of elasticity, pounds per square inch
e = stretch of conductor from low point of span, to support, that is, $(s_u - s_l)$, feet
H = horizontal component of tension, pounds
h = vertical displacement of end of insulator string, feet
I = length of insulator string, feet
L = horizontal distance between supports, feet
L_s = straight line distance between supports, feet

Paper 47-175, recommended by the AIEE committee on power transmission and distribution for presentation at the AIEE Pacific general meeting, San Diego, Calif., August 26–29, 1947. Manuscript submitted May 26, 1947; made available for printing July 14, 1947.

ALFIO BISSIRI and MAURICE LANDAU are both with the Department of Water and Power, Los Angeles, Calif.

S = stressed length of conductor in span, feet

S_1, S_2 = length of cable supported by insulator string, feet

S_u = unstressed length of conductor in span, feet

$(S_u)_o$ = S_u for span with $D=0$, feet

s = length of arc from low point to any point, x, y, feet

s_1 = stressed length of conductor from low point of span to point of support, feet

s_u = unstressed length of conductor from low point of span to point of support, feet

T = tension at any point in conductor, pounds

T_{av} = effective or average tension of conductor, pounds

W = weight of conductor per unit length, pounds

X_E = distance to low point east of support, feet

X_W = distance to low point west of support, feet

x_1 = horizontal distance from low point of span to support, feet

x, y = co-ordinate of any point on the conductor, feet

y_1 = vertical distance from support to low point of span, feet

$\Delta = S_u - L$, feet

$\Delta_o = (S_u)_o - L$ that is, Δ for span with $D=0$, feet

Figure 1. Catenary, tension–length curves copper cable

$a = H/W$

H = horizontal tension, pounds

W = weight of conductor, pounds per foot

Δ_o = unstressed length of cable minus span lengths in feet for $D=0$

L = span lengths in feet

E = 16,500,000 pounds

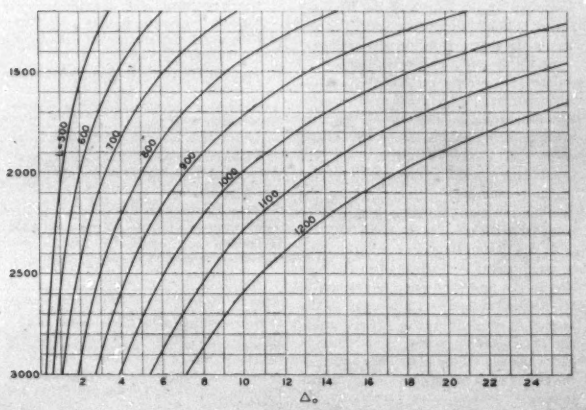

Figure 2. Diagrammatic presentation of suspension spans

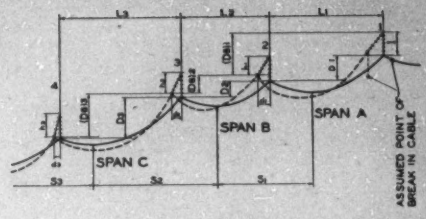

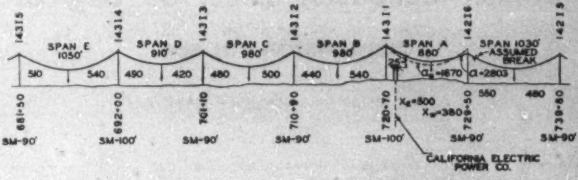

Figure 3. Portion of Boulder transmission line profile

Where D is small with respect to the span length, L, no accuracy is lost by assuming that the unstressed length, S_u, is equal to the sum of

1. The unstressed length for the same span length with $D=0$, and,
2. The difference of the straight line distance between the points of support of the conductor and the span length.

Expressed as an equation

$$S_u = (S_u)_o + \sqrt{L^2 + D^2} - L \tag{1}$$

$$= (S_u)_o + (L_c - L) \tag{2}$$

The equation of length of unstressed conductor in a level span is

$$(S_u)_o = \frac{s_{x_1}}{1 + a_{av}\dfrac{W}{AE}} \tag{3}$$

Where

$$s_1 = a\left(\sinh\frac{x_1}{a}\right) \tag{4}$$

$$a_{av} = \frac{1}{2}\left(y_1 + a + \frac{x_{1s}}{s_1}\right) \tag{5}$$

$$y_1 = a\left(\cosh\frac{x_1}{a} - 1\right) \tag{6}$$

$$a = \frac{H}{W} \tag{7}$$

$$x_1 = \frac{L}{2} \tag{8}$$

As stated previously, other than the introduction of the length of the insulator string into the span adjacent to the assumed break, the unstressed length of cable in each span remains constant. Changes in span length and difference in elevation of support occur due to the movement of the insulators.

By definition

$$\Delta_o = (S_u)_o - L \tag{9}$$

and

$$\Delta = (S) - L \tag{10}$$

Combining equations 9 and 10 with equation 2

$$\Delta = \Delta_o + (L_c - L) \tag{11}$$

It is thus apparent that the difference between the unstressed length of con-

CALCULATION FORM 1

TOWER DATA SHEET

TOWER NO.	TYPE	STATION	ELEV. BASE OF TOWER	ELEV. OF CONDUCTOR	SPAN	XW	XE	S	D	SPAN NO.
143 I 5	SM 90	681+50	1874.48	1951.75			510			
					1050				8.80	E
143 I 4	SM 100	692+00	1873.28	1960.55		540	490	1030		
					910				7.89	D
143 I 3	SM 90	701+10	1875.39	1952.66		420	480	900		
					980				1.50	C
143 I 2	SM 90	710+90	1876.89	1954.16		500	440	940		
					980				18.92	B
143 I 1	SM 100	720+70	1885.81	1973.08		540	500	1040		
					880				18.07	A
142 I 6	SM 90	729+50	1877.74	1955.01		380	550			X
					1030				4.59	
142 I 5	SM 90	739+80	1873.15	1950.42		480				

X = POINT OF ASSUMED BREAK

Figure 4. Calculation form 1 for data obtained from Figure 3

CALCULATION FORM 2

FOR DETERMINING THE VALUE OF "a" IN ANY SPAN, WHEN THE CONDUCTOR IN THE ADJOINING SPAN BREAKS

	SPAN NO. A TOWER NO. 143 I 1	SPAN NO. B TOWER NO. 143 I 2	SPAN NO. C TOWER NO. 143 I 3	SPAN NO. D TOWER NO. 143 I 4	SPAN NO. E TOWER NO. 143 I 5
(1) L	880	980	980	910	1050
(2) D	18.07	18.92	1.50	7.89	8.80
(3) a	2803	2803	2803	2803	2803
(4) (Lc − L)	0.19	0.18	0	0.04	0.04
(5) Δ_o	3.04	4.38	4.38	3.40	5.32
(6) Δ	3.23	4.56	4.38	3.44	5.36
(7) d	6.00	3.40	2.53	2.24	3.13
(8) h	11.00	12.1	12.3	12.4	
(9) (D) s	7.07	20.0	1.7	7.8	
(10) (Δ) s	9.81	7.16	5.25	3.73	4.87
(11) (Lc − L) s	0.03	0.21	0	0.04	0.04
(12) (Δ_o) s	9.78	6.95	5.25	3.69	4.83
(13) (R) s	1688	2302	2590	2792	2994
(14) S	1040	940	900	1030	
(15) $\frac{S}{2}$ (S+84.4)	614	288	202	202	

Figure 5. Calculation form 2, trial number 1

ductor and the straight line distance between supports changes with a change in static equilibrium.

Catenary Length Curves

Use of equation 3 directly in the solution of the change occurring in a series of suspension spans due to a break in conductors would require voluminous calculation. The calculations may be reduced by precalculating values of $(S_u)_o$ for various values of a and L.

In the solution of particular problems relative to change in static equilibrium, since Δ and Δ_o are the variables rather than (S_u) and $(S_u)_o$, and since Δ is a function of Δ_o the precalculated data may be in terms of Δ_o for various values of a and L, which are catenary length curves.

Referring to equation 3, it can be seen that the values of $(S_u)_o$ and thus Δ_o are functions of the elastic properties of the wire, expressed as W/AE.

Figure 1 consists of curves for various values of L, with Δ_o as abscissas and values of a as ordinates. The curves are for copper conductor with $W/(AE) = 0.2366 \times 10^{-6}$.

To plot the curves, points for each span length were calculated, values of a being assumed and the corresponding value of Δ_o calculated. The following is a typical calculation:

$$L = 1{,}000$$
$$a = 2{,}500$$
$$\frac{W}{AE} = 0.2366 \times 10^{-6}$$
$$x = \frac{L}{2} = 500$$
$$\frac{x}{a} = \frac{500}{2{,}500} = 0.20$$
$$\cosh\frac{x}{a} - 1 = 0.02007$$
$$\sinh\frac{x}{a} = 0.20134$$
$$y = a\cosh\frac{x}{a} - 1 = 50.175$$
$$s = a\sinh\frac{x}{a} = 503.35$$
$$a_{ns} = \frac{1}{2}\left(y + a + \frac{xa}{s}\right) = 2{,}516.77$$
$$(S_u)_o = \frac{2s}{1 + a_{ns}\dfrac{(W)}{(AE)}} = \frac{2 \times 503.35}{1 + 2{,}516.77 \times 0.2366 \times 10^{-6}} = 1{,}006.10$$
$$\Delta_o = (S_u)_o - L = 1{,}006.10 - 1{,}000 = 6.10$$

Enough points are calculated, for each span, to draw the curves using values of a from 1,200 to 3,000 and the spans from 500 feet to 1,200 feet in 100-foot intervals.

Description of Method of Determining Sags Under Broken Conductor Conditions

Figure 2 is a diagramatic sketch of a series of suspension spans. The position of the insulator strings and conductor before a break occurs is shown in solid lines. The position of the insulator strings and conductor after a break occurs is shown in dotted lines. Referring to Figure 2

Assume a series of spans $A, B, C \ldots$ of span length $L_1, L_2, L_3 \ldots$, supported by suspension insulators $1, 2, 3, 4 \ldots$, each of length I, with differences of elevation $D_1, D_2, D_3 \ldots$. The subscript B denotes values existing with a conductor broken.

A break at X causes the insulator string 1 to swing over and assume a dead-end position. Insulator 2 swings over an amount d_1.

We then have a new span length of $(L_1 + d_1)$, for span A, with a difference in elevation $(D_B)_1 = (D_1 + h_1)$. The length of conductor in the span before the break was $(L_1 + \Delta_1)$. After the break the insulator string 1 becomes part of the span so that the unstressed length of conductor in the span becomes $(L_1 + \Delta_1 + I)$.

The insulator string 2 not being vertical, it will have a horizontal component of tension. The value of H_B for span B will equal the value of H_B for span A, plus the horizontal component of tension in insulator 2; in other words,

$$(H)_B(\text{span } B) = (H)_B(\text{span A}) + \frac{d_1}{h_1}\left(S_1 + \frac{\text{weight of insulator string}}{2W}\right)W$$

Where

$$(H)_B = \text{horizontal component of tension} = a_B W$$

and also assuming the center of gravity of the insulator string at the center of the string.

In like manner insulator string 3 moves away from the break a distance d_2. The unstressed length of conductor of span B remains $(L_2 + \Delta_2)$ but the span length decreases and becomes $(L_2 + d_2 - d_1)$.

Similar to the condition at insulator 2 preceding,

$$(H)_B(\text{span } C) = (H)_B(\text{span } B) + \frac{d_2}{h_2}\left(S_2 + \frac{\text{weight of insulator string}}{2W}\right)W$$

Proceeding away from the point of break, successive insulators will approach the vertical and thus the value of $(H)_B$ will approach the initial value of H.

If a value of d_1 is assumed, the horizontal tension $(H)_B$ for span A for such assumed value of d_1 may be determined by use of the catenary length curves (Figure 1.) These curves being plotted in terms of a, it is necessary to use the relationship: $H = aW$.

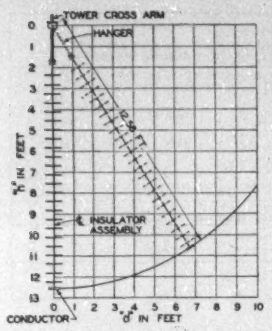

Figure 6. Swing diagram for insulator string assembly

$(H)_B$ for span B then can be calculated as indicated.

Using the catenary length curves, the increased amount of cable necessary to lower the horizontal tension in span B from H to $(H)_B$ may be noted. Since the actual amount of conductor in the span is constant, this increased conductor necessary may be accounted for only by a decrease in span length. Thus the value d_2 is equal to d_1 minus the excess conductor required to lower the tension in span B from H to $(H)_B$.

In a similar manner $(H)_B$ for successive spans may be determined. If the assumed value of (d_1) is correct, $(H)_B$ for successive spans away from the break will approach H as the limit.

By trial of various values of d_1 the correct value of d_1 may be obtained and thus the value of a for the broken conductor span.

Having the value of a for the span A in question, the position taken by the conductor under this condition can be plotted and thus the broken conductor clearances may be measured.

Solution of a Typical Broken Conductor Problem

Figure 3 is a portion of the profile of the Boulder transmission line in the vicinity of the Mojave River, east of Victorville, Calif. At this point the Boulder transmission line crosses a transmission line of the California Electric Power Company. The problem is to determine the clearance of the Boulder transmission line over California Electric Power Company's line if a conductor were to break in span *14215–14216*.

To aid in this and similar problems, two form sheets were devised, form 1, Figure 4, and form 2, Figure 6. Figure 4 is for tabulating the span data while Figure 5 is a calculation form. Solution of this and similar problems require ready means of determining the horizontal and vertical displacement of the conduct or at its point of support, due to swing of the insulator string. Figure 6 is an insulator swing chart for the suspension insulator strings of the Boulder transmission line and provides a graphical means of obtaining the vertical displacements of the end of the insulator string corresponding to horizontal displacements.

Tne first step in the solution of the problem is to tabulate the span data of Figure 3 on form 1.

1. Tower number.
2. Type and height of tower.
3. Station of tower.
4. Elevation of base of tower.
5. Elevation of conductor.
6. Span length.
7. X_W (X–West) = horizontal distance from tower to low point of span west of the tower.
8. X_E (X–East) = same as 7 except east of the tower.
9. $S = X_E + X_W$.
10. D = difference in elevation.
11. Span numbers: Designated A, B, C, and so forth.

The normal horizontal tension of the Boulder line is 4,400 pounds; the weight per foot of conductor is 1.57 pounds; the length of insulator string from the point of support of the string, 0.15 foot below the tower arm, to the conductor is 12.58 feet

$$a = \frac{H}{W} = \frac{4{,}400}{1.57} = 2{,}803$$

The weight of a suspension insulator string is 265 pounds.

Using calculation form 2, Figure 5, values corresponding to items 1 through 6 are tabulated for spans A, B, C, and so forth, as follows:

1. Span length—from tabulation Figure 4.
2. D = difference in elevation—from tabulation Figure 4.
3. a = 2,803—as noted previously.
4. $(L_e - L)\sqrt{L^2 + D^2} - L$.
5. Δ_e—from catenary length curves Figure 1.
6. Δ—item 4 plus item 5.

Values of Δ_e correspond to the particular values of span length L and a, and are obtained from the catenary length curves Figure 1.

Calculation of the value

$$L_e - L = \sqrt{L^2 + D^2} - L$$

can be facilitated by use of the following equation:

$$L_e - L = \frac{D^2}{2L + (L_e - L)}$$

Accurate calculation of $(L_e - L)$ may be made on a slide rule using the method of successive approximations.

Insulator swing chart, Figure 6, shows the relationship between the vertical distance from the point of support of the insulator string to the conductor at the point where it is attached to the insulator string, this distance being designated h, and the horizontal displacement of the point of support of the conductor from a vertical line running through the point of support of the insulator string, this distance being designated d; thus, where the insulator string hangs vertically, h = 12.58 feet and d = 0.

The foregoing items 1 through 6 relate to the spans under normal unbroken conductor conditions. In the following,

CALCULATION FORM 2

FOR DETERMINING THE VALUE OF "a" IN ANY SPAN, WHEN THE CONDUCTOR IN THE ADJOINING SPAN BREAKS

	SPAN NO. A TOWER NO. 143 I 1	SPAN NO. B TOWER NO. 143 I 2	SPAN NO. C TOWER NO. 143 I 3	SPAN NO. D TOWER NO. 143 I 4	SPAN NO. E TOWER NO. 143 I 5
(1) L	880	980	980	910	1050
(2) D	18.07	18.92	1.50	7.69	8.80
(3) a	2803	2803	2803	2803	2803
(4) (Lc−L)	0.19	0.18	0	0.04	0.04
(5) Δ_e	3.04	4.38	4.38	3.40	5.52
(6) Δ	3.23	4.56	4.38	3.44	5.56
(7) d	5.7	2.65	1.03	0.06	−1.38
(8) h	11.20	12.3	12.5	12.6	
(9) (D) a	6.87	20.0	1.7	7.8	
(10) (Δ) a	10.11	7.61	6.0	4.41	6.98
(11) (Lc−L) a	0.03	0.21	0	0.04	0.04
(12) (Δ_e) a	10.08	7.4	6.0	4.37	6.94
(13) (a) a	1680	2232	2453	2534	2539
(14) S	1040	940	900	1030	
(15) ℄ (S+84.4)	572	221	81	5	

Figure 7. Calculation form 2, trial number 2

where a subscript B is used as $(a)_B$, and so forth, the value is one existing with the assumed broken conductor.

Continuing on form 2, Figure 5

A value d is assumed arbitrarily; in this case d is assumed equal to 6 feet. Then for column (span A—tower *141S1*)

7. $d=6.00$—assumed value of "d".

8. $h=11.00$—h corresponding to $d=6$ feet—from Figure 6.

9. $(D)_B=7.07-(2)-(8)$.

10. $(\Delta)_B=9.81-(6)+12.58$ (length of insulator string)—(7).

11. $(L_c-L)_B=0.03-L_c-L=\sqrt{880^2+7.07^2}-880$.

12. $(\Delta_o)_B=9.78-(10)-(11)$.

13. $(a)_B=1,688$—From Figure 1 for $(\Delta_o)_B=9.78$ span $=880$.

14. $S=1,040$—from Figure 4.

15. $\frac{d}{h}(S+84.4)=614-\frac{6}{11}\times(1,040+84.4)=614;\ \frac{265}{2\times1.57}=84.4$.

For column (span B—tower *143I2*)

9. $(D)_B=20.0-h$ for tower *143I2* will be about 12.1 which gives the value of 20.0.

13. $(a)_B=2,302-(13)+(15)$ column (span A—*143I1*).

12. $(\Delta_o)_B=6.95$—from Figure 1 for span $=980$ and $(a)_B=2,303$.

11. $(L_c-L)_B=0.21$—span $=980$ and $(D)_B=20.0$; $L_c-L=0.21$.

10. $(\Delta)B=7.16-(11)+(12)$.

7. $d=3.40-(7)$ column (span A—tower *143I1*) minus (10) plus (6) that is, $6.00-(7.16-4.56)$.

8. $h=12.1$
14. $S=940$
15. $\frac{d}{h}(s+84.4)=288$

Values obtained in similar manner as values for column (span A—tower *143I1*).

For columns (span C — tower *143I3*) and (span D — tower *143I4*,) proceed in the same manner as column (span B — tower *143I2*.)

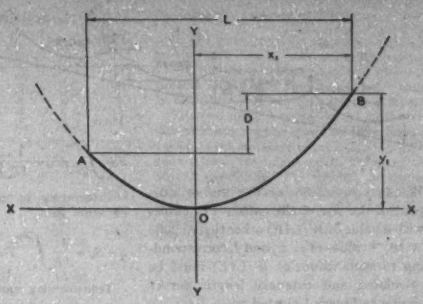

Figure 9. Typical catenary curve

It will be observed that with the assumption of $d = 6$ feet that (a_B) for succeeding spans increased beyond $a = 2,803$, and also that values of d in succeeding spans do not approach zero. If the assumed value of d had been correct (a_B) for succeeding spans would have approached 2,803 as a limit and the value of d for succeeding spans approached zero as a limit. Therefore, since (a_B) increased beyond $a = 2,803$, for succeeding spans the assumed value of $d = 6$ is too great.

A second trial is made arbitrarily assuming $d = 5.7$, at tower *143I1*, and the calculations are shown on Figure 7. With this assumption (a_B) approaches a limit less than 2,803 and the value of d for succeeding spans passes beyond zero and takes on negative values. Thus $d = 5.7$ is less than the correct value of d at tower *143I1*.

For a third trial a value of $d = 5.8$ is assumed and calculations are shown on Figure 8. In this case the limit of (a_B) while less than 2,803 is greater than in the case of assumed $d = 5.7$. The values of d for succeeding spans approach a limit closer to zero than in the case of the assumed value of $d = 5.7$.

Comparing the values of (a_B) for the span adjacent to the break, from the preceding three calculations it is evident that the correct value lies between 1,668 and 1,688, the value of 1,668 being closer to the correct value than 1,688.

The accuracy required does not justify further refinements in calculation. Within the degree of accuracy required, we may take $(a_B) \approx 1,670$.

With the value of $(a_B) = 1,670$ a catenary is plotted in span A on Figure 3, from which point-to-point distances may be measured and the broken conductor clearance of the Boulder transmission line over the California Electric Power Company line is found to be 25 feet.

Thus, in this problem the clearance of the conductor, above ground, before the break is 45 feet and after the break the clearance to ground is reduced to 29 feet. The clearance between the Boulder transmission line conductor and that of the California Electric Power Company before the break is 35 feet while after the break it is reduced to 25 feet.

This problem was recalculated assuming an insulator string length of 6 feet for a 132-kv line rather than the 12.58 feet for the 287.5-kv line. All other conditions were the same. The resulting broken conductor value of $(a)_B$ is 2,010, for the span adjacent to the assumed break. With the clearance of the conductor above ground before the break of 45 feet it becomes 40 feet after the break. The clearance between the Boulder line conductor and that of the California Electric Power Company before the break of 35 feet is reduced to 30 feet.

The longer the suspension insulator string is used, the greater the increase in sag under broken conductor condition.

Generally the higher the initial tension and the shorter the spans involved, the greater will be the increase in sag under broken conductor condition.

Figure 1, herein, is applicable to problems of any cable with characteristics of

CALCULATION FORM 2

FOR DETERMINING THE VALUE OF "a" IN ANY SPAN WHEN THE CONDUCTOR IN THE ADJOINING SPAN BREAKS

	SPAN NO. A TOWER NO. 143 I 1	SPAN NO. B TOWER NO. 143 I 2	SPAN NO. C TOWER NO. 143 I 3	SPAN NO. D TOWER NO. 143 I 4	SPAN NO. E TOWER NO. 143 I 5
(1) L	880	980	980	910	1050
(2) D	18.07	18.92	1.50	7.89	8.80
(3) a	2803	2803	2803	2803	2803
(4) (Lc-L)	0.19	0.18	0	0.04	0.04
(5) Δ_o	3.04	4.38	4.38	3.40	5.52
(6) Δ	3.23	4.56	4.38	3.44	5.56
(7) d	5.8	2.95	1.60	1.02	0.14
(8) h	11.1	12.2	12.4	12.5	
(9) (D) B	6.97	20.0	1.7	7.8	
(10) (Δ) B	10.01	7.41	5.73	4.02	6.44
(11) (Lc-L) B	0.03	0.21	0	0.04	0.04
(12) (Δ_o) B	9.98	7.20	5.73	3.98	6.40
(13) (A) B	1668	2254	2505	2629	2716
(14) S	1040	940	900	1030	
(15) $\frac{d}{h}$ (S+84.4)	588	249	124	87	

Figure 8. Calculation form 2, trial number 3

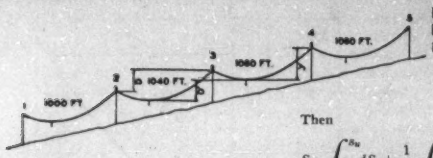

Figure 10. Portion of Boulder transmission line in the mountain section

$W/(AE) = 0.2366 \times 10,^{-6}$ and is indepent of the size of the cable. For cables with a value of $W/(AE)$ other than $0.2366 \times 10,^{-6}$ values of a, Δ_s and L corresponding to such values of $W/(AE)$ must be calculated and catenary length curves similar to Figure 1 plotted.

For the purpose of determining the probable magnitude of the increase in sag due to a broken wire and whether the accurate calculations should be made, the assumption may be made that with the span length unchanged, the unstressed length of cable, in the span adjacent to the break, will be increased by an amount equal to 1/2 to 2/3 of the insulator string length. The value of a_B, for the assumption, can be had by adding the increase in cable length to the value of Δ_o, of the span adjacent to the break, for the initial value of a and determining the value of a_B from the catenary length curve corresponding to this increased value of Δ_o. The increased sag corresponding to this value of a_B then may be obtained from the profile, and the magnitude of the sag increase will determine whether a detailed calculation is justified.

Appendix I. Derivation of Formulas

Let the conductor be represented by the curve A–B, Figure 9.

The fundamental formulas of the catenary referred to the point where it has a horizontal tangent are

$$y = a\left(\cosh\frac{x}{a} - 1\right) \tag{12}$$

$$s = a\left(\sinh\frac{x}{a}\right) \tag{13}$$

The tension at any point on a suspended conductor is

$$T = Wy + H = W(y+a) \tag{14}$$

Derivation of a_{av} for a level span ($x_1 = \frac{L}{2}$, $D = 0$)

Divide the unstressed length of the conductor into elements ΔS_u. When the conductor is suspended the length of each element becomes

$$\Delta S = \Delta S_u \quad 1 + \frac{T}{AE} \tag{15}$$

Then

$$S = \int_0^{S_u} dS_u + \frac{1}{AE}\int_0^{S_u} T\, dS_u \tag{16}$$

Integrating in part and transforming equation 16

$$S - S_u = \frac{1}{AE}\int_0^{S_u} T\, dS_u \tag{17}$$

Transforming equation 17

$$\frac{AE}{S_u} = \frac{\frac{1}{S_u}\int_0^{S_u} T\, dS_u}{s - S_u} \tag{18}$$

The effective (average) tension T_{av} is defined as that value of tension which satisfies Hookes Law, that is,

$$\frac{AE}{S_u} = \frac{T_{av}}{S - S_u} \tag{19}$$

Comparing equations 18 and 19

$$T_{av} = \frac{1}{S_u}\int_0^{S_u} T\, dSu \tag{20}$$

Equation 20 is very nearly equal to

$$T_{av} = \frac{1}{S}\int_0^{S} T\, dS \tag{21}$$

Since by definition $a_{av} = T_{av}/W$ and by reference to equation 14, equation 21 may be written

$$Wa_{av} = \frac{1}{S}\int_0^{S} W(y+a)\, dS \tag{22}$$

For a curve extending from co-ordinate points (0, 0), to (x_1, y_1), equation 22 may be written

$$a_{av} = \frac{1}{s_1}\int_0^{x_1} (y+a)\, dS \tag{23}$$

Differentiating equation 13

$$ds = \cosh\frac{x}{a} dx \tag{24}$$

Combining equations 12 and 24

$$y\, ds = a\left(\cosh\frac{x}{a} - 1\right)\cosh\frac{x}{a} dx \tag{25}$$

That is

$$y\, ds = a\left(\cosh^2\frac{x}{a} - \cosh\frac{x}{a}\right) dx \tag{26}$$

Equation 26 may be written

$$y\, ds = a^2 \cosh^2\frac{x}{a}\frac{dx}{a} - a^2\cosh\frac{x}{a}\frac{dx}{a} \tag{27}$$

Integrating equation 27

$$y\, ds = \left(\frac{a^2}{2}\sinh\frac{x}{a}\cosh\frac{x}{a} - \frac{x}{a} - a^2\sinh\frac{x}{a}\right. \tag{28}$$

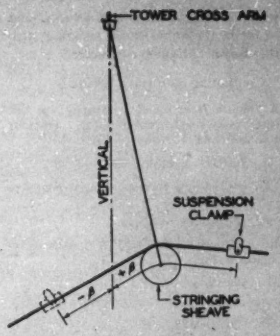

Figure 11. Diagram of insulator vertical alignment

Substituting equations 13 and 28 in equation 23

$$a_{av} = a + \frac{a^2}{a\sinh\frac{x_1}{a}}\left(\frac{1}{2}\sinh\frac{x_1}{a}\cosh\frac{x_1}{a} + \frac{x_1}{a} - \sinh\frac{x_1}{a}\right) \tag{29}$$

Simplifying equation 29

$$a_{av} = \frac{1}{2}\left(a\cosh\frac{x_1}{a} + \frac{x_1}{a\sinh\frac{x_1}{a}}\right) \tag{30}$$

Substituting equations 12 and 13 in equation 30

$$a_{av} = \frac{1}{2}\left(y_1 + a + \frac{x_1 a}{s_1}\right) \tag{31}$$

From the definition of e, E, a, and a_{av} as defined in the notation and units, we may write the following equations:

$$s_u = s_1 - e \tag{32}$$

$$e = \frac{T_{av}}{A}\left(\frac{s_u}{E}\right) \tag{33}$$

$$a = \frac{H}{W} \tag{34}$$

Table I. Calculations for Problem 1

		Span C 143I2–143I3	Span D 143I3–143I4
(1)	L	980	910
(2)	D	1.50	7.80
(3)	a	2,803	2,803
(4)	$L_c - L$	0	0.04
(5)	Δ_c	4.38	3.40
(6)	Δ	4.38	3.44
(1)	L	1,130	760
(2)	D	28.50	22.11
(3)	a	2,803	2,803
(4)	$L_c - L$	0.36	0.32
(5)	Δ_c	7.00	1.86
(6)	Δ	7.36	2.18

Table II. Calculation of Insulator Vertical Alignment Correction

Cable Data: W = 1.57 Pounds Per Foot, H = 4,400 Pounds, $a = H/W$ = 2,803

Tower	Span	D	y	d'	a	Δ_o	a'	Δ_o'	a''	Δ_o''	$(\Delta_o - \Delta_o'')$	Correction	Corrected $(\Delta_o - \Delta_o'')$	ϕ Feet
1			24											0
	1,000	+54	78		2,803	4.66	2,755	4.86	2,727	4.96	−0.30	0	−0.30	
2			30	+48										−0.30
	1,040	+54	78		2,803	5.31	2,803	5.31	2,777	5.42	−0.11	0	−0.11	
3			31	+47										−0.41
	1,060	+50	81		2,803	5.64	2,850	5.42	2,824	5.54	+0.10	−0.01	+0.09	
4			34	+47										−0.32
	1,060	+42	76		2,803	5.64	2,897	5.20	2,871	5.32	+0.32	0	+0.32	
5														0
Total			21.25			20.79			21.24		+0.01	0		

$$a_{ST} = \frac{T_{ST}}{W} \tag{35}$$

$$(S_u)_o = 2s_u \tag{36}$$

Combining equations 32, 34, and 36

$$s_u = s_1 - a_{ST} s_u \frac{W}{AE} \tag{37}$$

Simplifying equation 37

$$s_u = \frac{s_1}{1 + a_{ST}\dfrac{W}{AE}} \tag{38}$$

Combining equations 36 and 38

$$(S_u)_o = \frac{2s_1}{1 + a_{ST}\dfrac{W}{AE}} \tag{39}$$

Also by definition

$$\Delta_o = (S_u)_o - L \tag{40}$$

Derivation of $(L_c - L)$

$$L_c = L + (L_c - L) \tag{41}$$

Also

$$L_c^2 = L^2 + D^2 \tag{42}$$

Squaring equation 41

$$L_c^2 = L^2 + 2L(L_c - L) + (L_c - L)^2 \tag{43}$$

$$(L_c - L) = \frac{D^2}{2L + (L_c - L)} \tag{44}$$

Appendix II. Illustrative Problems

There are problems other than the broken conductor problem, to which the methods described in this paper are applicable. The catenary length curves described originally were devised for the solution of "broken conductor problems." These curves have been found useful in the solution of many other problems where a change occurs from one known state of equilibrium to another.

One application has occurred where it has been necessary to raise towers or move towers because of development of highways, roads, and other public works. Calculations of increases or decreases in the length of conductors required to maintain proper tensions and clearances where necessary. Use of catenary length curves, such as those illustrated in Figure 1, have aided materially in such calculations as shown in problem 1.

Another application arises in stringing of conductors. In stringing conductors on a series of suspension spans through sheaves, the tension on either side of each sheave is equal. Where the spans vary materially in length or difference in elevation, the horizontal components of tension in the several spans will vary with a consequent inclination of the suspension insulators. Good design dictates that under normal temperatures the horizontal tensions in a series of suspension spans be equal and the suspension strings be vertical. The catenary length curves are useful in calculating the necessary movement of the suspension clamps along the conductor to attain this condition. Problem 2 is a typical calculation.

In making the connections of the dead-end clamp to the cross arm, during the stringing operation, a certain amount of overtravel is required in order to set the coupling pin in place. The catenary length curves give a visual means of determining the increase in tension in the span occurring under such conditions. In short spans with high tensions, this overtravel may be limited by the lack of slack in the span and if the cross arm is not flexible and allowed to move, the connection will have to be done at the cross arm by installing the dead-end insulators and connecting the conductor to the strain clamp in the air.

Sagging conductors is in reality a means of measuring the conductors. Where changes must be made in a line which is in service, the time may be limited during which the line can be taken out of such service in order to make necessary changes. Precalculating the length of conductors required, actually measuring the conductors, and placing the clamps on the conductors in advance, in many cases, materially shortens the time required to make line changes. Catenary length curves may be used to advantage in the calculations required.

Problem 1

In the series of spans shown in Figure 3, tower *14313* is to be moved 150 feet toward *14314* and the tower raised 80 feet above its present elevation. How much cable must be added to maintain the existing tension?

The two spans involved in the solution of this problem are the spans on either side of tower *14313*, namely, spans C and D. The calculations are tabulated in Table I. As stated previously, the normal horizontal tension in this series of spans is 4,400 pounds and the weight per foot of cable is 1.57 pounds.

Therefore

$$a = \frac{H}{W} = \frac{4{,}400}{1.57} = 2{,}803$$

For span C before the tower is moved and raised

$L = 980$

$D = 1.50$

and

$a = 2{,}803$

then

$$L_c - L = \frac{1.50^2}{2 \times 980 + (L_c - L)} = 0+$$

$\Delta o = 4.38$ feet

The value is obtained from the catenary length curves, Figure 1, and corresponds to

$L = 980$, $a = 2{,}803$

$\Delta = 4.38$ feet

$$\Delta = \Delta_o + (L_c - L) = 4.38 + 0$$

For span C after the tower is moved and raised

$L = 1{,}130$

$D = 28.50$

and

$a = 2{,}803$

then

$L_c - L = 0.36$

$\Delta_o = 7.00$

and

$\Delta = 7.36$

The two conditions for span D are calculated in a similar manner

$\Delta = 3.44$ before the tower is moved and $\Delta = 2.18$ after the tower is moved.

The sum of the Δ's for spans C and D before the tower is moved is

$4.38 + 3.44 = 7.82$ feet

The sum of the Δ's after the tower is moved is

$7.36 + 2.18 = 9.54$ feet

The additional conductor required is the difference between

9.54 and 7.82 and equals 1.72 feet

Problem 2

Figure 10 is the profile of a series of four suspension spans between dead-ends. Under stringing conditions, while the conductor is in sheaves, the sheaves will be inclined from the vertical. The problem is to calculate the points at which the suspension clamps should be placed on the conductor so that the insulators will remain vertical.

Figure 11 is a diagram of a conductor supported by a sheave, the sheave being inclined from the vertical. In order that the insulators remain vertical, the suspension clamp is set a distance β on the conductor from the vertical point directly below the tower cross arm.

Calculations of the values β for the spans of Figure 10 are shown in tabular form on Table II.

In sequential order the tabular calculations, Table II, are prepared as follows:

1. The differences of elevation of Support D, sag y, and differences of elevation of low point of adjacent spans D' are measured from the profile, Figure 10.

2. With the insulators clipped in, and vertical the value of a for each span will be 2,803.

3. Δ_o for each span with $a = 2{,}803$ is obtained from the catenary length curves.

4. When the conductor is in sheaves the value of a in adjacent spans will differ by the amount D'.

For the purpose of calculation, the value of a' for one of the spans is assumed arbitrarily to be 2,803. The corresponding values of a' for the other spans are obtained by applying the values of D'. For these values of a' and the respective span length, values Δ_o' are obtained from the catenary length curves.

In the problem the sum of the values of Δ_o is 21.25 feet and the sum of the values of Δ_o' is 20.79 feet, the difference being 0.46 feet.

Apportioning this difference in the Δ_o' for the first span

$$0.46 \times \frac{4.86}{20.79} = 1.10 \text{ feet}$$

Adding 0.10 feet to Δ_o' for the first span $\Delta_o'' = 4.96$.

From the catenary length curves a for the first span is found to be 2,727. Applying the values of D' we obtain the corresponding values of Δ_o'' for the succeeding spans. The sum of the values of Δ_o'' is 21.24 feet, which differs from the sum of the values of Δ_o by 0.01 foot.

The operation $(\Delta_o - \Delta_o'')$ then is performed. The difference of -0.01 foot is added to the span with the largest $\Delta o''$. The sum of the corrected $(\Delta_o - \Delta_o'')$ is then zero. The first and last towers being dead-ends, the β correction is zero at these towers. Adding the values of corrected $(\Delta_o - \Delta_o'')$ consecutively the "correction β" is obtained, the sign designating the direction in which the conductor clamp is to be moved.

References

1. Mississippi River Crossing of Crystal City Transmission Line. H. W. Eales, E. Kittinger. AIEE Journal, volume 44, October 1925, pages 1106–16.

2. Transmission Line Catenary Calculations, D. O. Ehrenburg. Electrical Engineering (AIEE Transactions), volume 54, July 1935, pages 719–28.

3. Unbalanced Conductor Tensions—Tests to Show Their Effect in a Long-Span Transmission Line, E. S. Healy, A. J. Wright. AIEE Transactions, volume 45, 1926, pages 1064–70.

No Discussion

Capacitance Fuel Gauges

N. C. CLARK
NONMEMBER AIEE

M. H. ADOLPHE
MEMBER AIEE

PREVIOUS to the development of capacitance-type fuel gauges, the quantity of gasoline in airplane fuel cells was measured volumetrically. This is misleading when the fuel temperature changes, since the energy provided by the fuel depends directly on its mass rather than on its volume. A capacitance type fuel gauge consists primarily of a stationary electric capacitor partially immersed in the fuel, a remote indicating capacitance meter, and the necessary associated equipment, and has potentialities for considerably better accuracy than the float type gauge in common use.

The popular conception of the savings in fuel load (and available increase in payload) which accrue by making a fuel gauge exceptionally accurate, is erroneous. There are, however, other reasons for requiring an accurate fuel gauge, particularly in increasing the safety of long range flight by a more precise determination of fuel remaining. Some flight personnel indicate a need for accuracy better than one per cent.

An analysis of fuel temperature effect shows that a negative error of four per cent or more is expected as a result of temperature variation of the fuel from minus 65 degrees Fahrenheit to plus 110 degrees Fahrenheit. It is possible to use temperature compensated fuel tank units to reduce this error to about plus or minus two per cent throughout all variations of fuel level.

The five models of capacitance type gauges described in this paper differ only in the methods used to measure and remotely indicate the capacitance of the tank unit. Their errors, as found in laboratory tests, are shown in Table I. Attention is called to the fact that these errors are characteristic of the particular models tested; in contrast to the temperature error previously mentioned, they are not inherent in this type of fuel gauge.

Mass–Energy Relationship

The potentially available thermal energy of a fuel such as gasoline is a constant value per pound of fuel regardless of temperature. This means that the energy per gallon varies directly with the mass per gallon as the temperature changes. For the typical aircraft gasoline considered in this paper,[1] the specific gravity, and therefore the energy per gallon of fuel, is less by ten per cent at plus 110 degrees Fahrenheit than its value at minus 65 degrees Fahrenheit. For this reason established practice[2] requires the use of temperature correction on all volumetric fuel measurements for accurate engine performance calculations.

One of the most important advantages of the capacitance method of fuel quantity measurement is the fact that its quantity indications are more nearly proportional to the mass than to the volume of the fuel. A further advantage, gained by the detail design of the fuel measuring capacitors, or tank units, is a theoretically negligible error due to limited variations in the flight attitude, regardless of the shape of the tanks used. This is accomplished by using several tank units in each cell, and by so proportioning and positioning them that their combined capacitance is substantially constant for a given fuel quantity regardless of the attitude of the airplane.

Fuel Temperature Errors

A capacitance type fuel gauge is basically a remote indicating meter which continuously measures the capacitance of the tank unit. This capacitance depends upon the length of the tank unit probe, the fraction of the latter that is immersed in fuel, and the dielectric constant of the fuel. As the temperature of the fuel increases, the volume and depth of fuel increase and the dielectric constant decreases. For fuels commonly used in aircraft these variations are not exactly inverse, so that, unless a compensating device is added, the capacitance of the tank unit varies slightly with fuel temperature.

Linearity of indicator readings, end effects, and sensitivity do not enter into the problem; the first two affect only the scale distribution, and the third factor determines the relative ease of reading small increments of fuel change at different levels. Errors due to other variables such as abnormal voltage or frequency of the power supply, variations in "dry" capacitance of the tank unit with temperature due to dimensional changes, and variation in response of the electronic units and indicators with changes in ambient temperature due to the use of uncompensated resistors and condensers and so forth, in the circuit, can be omitted from this discussion since their effects are directly additive anyway.

The variations in gasoline volume and dielectric constant with temperature are, however, in an approximately inverse relationship with each other. Figure 1 shows the relative magnitudes of these changes produced by a temperature rise from minus 65 degrees Fahrenheit to plus 110 degrees Fahrenheit.

Because the temperature variation of density does not equal that of dielectric constant, the application of this method of fuel measurement includes a temperature error[3] which, incidentally, is relatively large compared to other inaccuracies inherent in this type of apparatus. This error depends on fuel quantity as well as temperature, because the increase in wetted probe area with temperature expansion of the fuel volume is compensated for partially by the decrease in dry probe area remaining. The extent of this compensation depends on the relative

Paper 47-176, recommended by the AIEE committee on instruments and measurements for presentation at the AIEE Pacific general meeting, San Diego, Calif., August 26–29, 1947. Manuscript submitted May 22, 1947; made available for printing July 11, 1947.

M. H. Adolphe is electrical flight test engineer and N. C. Clark is electrical research engineer for the Lockheed Aircraft Corporation, Burbank, Calif.

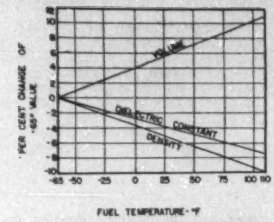

Figure 1. Temperature variations of physical constants of typical aircraft fuel

Figure 2. Tank unit error, or change in capacitance, produced by fuel temperature rise from minus 65 degrees Fahrenheit to plus 110 degrees Fahrenheit. The error is expressed as a percentage of the normal increase in capacitance caused by adding fuel at minus 65 degrees Fahrenheit to the empty tank

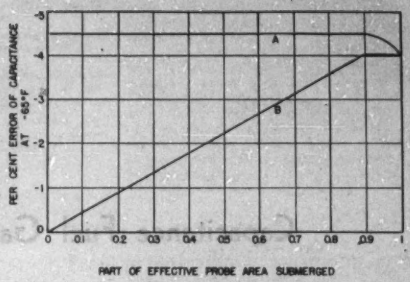

A—Error in terms of the quantity of fuel actually in the tank

B—Error in terms of full tank quantity

amounts of wetted and dry probe areas.

Disregarding errors produced by the instrument equipment, the indicator will respond to changes in capacitance of the tank unit, and can be read as mass of fuel according to its calibration. Variations in capacitance resulting from fuel temperature changes will be interpreted therefore as corresponding variations in fuel mass.

The capacitance measured at any fuel level is given by the relation

$$C_T = a[K_T \cdot A_T + (A - A_T)] + c \qquad (1)$$

where

C_T = measured capacitance at temperature T

a = constant of proportionality

K_T = dielectric constant of fuel at temperature T

A_T = wetted probe area at temperature T, and can be any function of tank volume, usually linear

A = total probe area wetted at full tank level

c = total lumped capacitance resulting from end connections, cables, and all other incidental equipment.

c is not necessarily constant, but its variation is not a function of fuel conditions.

The error in capacitance as a percentage of the change in capacitance from zero level to the fuel level considered is

$$\text{Per cent } \Delta c = \frac{(C_{T_2} - C_{T_1})(100)}{C_{T_1} - a \cdot A} \qquad (2)$$

The error in capacitance as a percentage of the change in capacitance from zero to full tank level is

$$\text{Per cent } \Delta c = \frac{(C_{T_2} - C_{T_1})(100)}{a(K_{T_1} \cdot A) - a \cdot A} \qquad (3)$$

Equations 2 and 3 are important in indicating that the fuel temperature error is independent of the surplus capacitance added to the tank unit by equipment and connections. This is important in allowing the design of the capacitance measuring circuit and equipment to develop unencumbered by restrictions as to the capacitance of interconnecting leads, in so far as temperature effects are concerned.

Calculations based on equations 2 and 3 are plotted in Figure 2 assuming that wetted probe area is directly proportional to fuel mass. From these curves, three important observations are made.

1. The fuel temperature error is almost a constant percentage of the indicated reading.

2. The fuel temperature error does not exceed approximately 4.1 per cent of full scale indications.

3. The fuel temperature error is negative, rather than positive, as might be erroneously inferred from the data in Figure 1.

The first of the above observations suggests that one easily remembered correction factor can be applied to adjust fuel mass readings for variations in fuel temperature. The second observation suggests the use of a temperature compensated fuel tank probe or circuit element of such a nature as to remove completely all fuel temperature errors at the half tank or other preselected level. This then would reduce the fuel temperature error to plus or minus two per cent of full scale as a maximum for the temperature variation considered herein. Graphically, this would shift curve *B* of Figure 2 to intersect the zero ordinate at the half probe area point. Attention is directed to the fact that the temperature error is directly proportional to the difference between the temperature for which there is no error and the temperature at which the reading is being taken.

These observations, of course, do not apply to the general case where wetted probe area is a nonlinear function of fuel mass. In such circumstances, the fuel temperature errors can be calculated using equations 2 and 3, and the wetted probe area versus fuel mass function.

Long Range Flight Planning

It is maintained by some authorities[4] that the most important single factor in calculating aircraft performance for long range flight is the mileage realized per gallon of fuel consumed. The prime purpose of all long range flight planning is to promote efficiency in this respect.

For the purposes of this investigation into the necessary requirements of a capacitance fuel gauge, a brief consideration of long range flight planning is illustrative of the extent to which such planning is dependent on fuel gauge accuracy. Long range flight planning consists of calculating the optimum altitude, course, engine power, engine speed, required fuel load, and air speed for the proposed flight on the basis of the known engine and flight characteristics of an airplane, projected meteorological data, the flight course data, and the passenger and cargo loading. This is done for one of three conditions, which are

1. Constant engine horsepower.
2. Constant indicated air speed.
3. Maximum range.

These calculated data of airplane operating conditions are used in both tabulated and graphical form by the flight engineer as a plan to which engine controls are set and maintained, and as a continual check against actual performance by plotting the operational data from the flight log on the flight graph. This continuous graphical check on actual against calculated performance is used

1. To insure proper balance between payload and fuel load.

2. To give flight personnel a continuous means of checking actual flight performance.

3. To increase operational safety by considering beforehand the flight plan changes required by engine failure or other emergency.

Because of the nature of this flight graph, and the uses to which it is put, it is gen-

Table I. Errors in Per Cent of Full Dial

Variable		Gauge A Fuel Level 1/4	Gauge A F	Gauge B 1/4	Gauge B F	Gauge C 1/4	Gauge C F	Gauge D 1/4	Gauge D F	Gauge E 1/4	Gauge E F	Gauge F 1/4	Gauge F F
Voltage 105–130 a-c 18–28 d-c		0.0	0.5	0.0	0.0	3.5	0.5	2.0	0.5	0.0	0.0	2.5	1.2
Temperature equipment (less tank unit)	K	−1.0	−1.0	−0.5	−0.5	0.0	0.0	+0.4	+0.4	+8.3	+8.3		
	N	−0.6	−0.6	−0.3	−0.3	0.0	0.0	+0.2	+0.2	+5.2	+5.2		
	J	+0.4	+0.4	+0.2	+0.2	0.0	0.0	−0.2	−0.2	−3.1	−3.1		
Temperature, dry tank unit	K	+0.6	+0.6	+1.3	+1.3	+0.7	+0.7	X	X	+29.0	+29.0	0.0	0.0
	N	+0.3	+0.3	+0.7	+0.7	+0.4	+0.4	X	X	Y	Y	0.0	0.0
	J	−0.3	−0.3	−0.7	−0.7	−0.4	−0.4	X	X	Y	Y	0.0	0.0
Fuel temperature	K	+0.9[C]	−2.0[C]	−1.1	−4.0	−1.1	−4.0	−1.1	−4.0	−1.1	−4.0	+2.8	+11.1
	N	+0.5[C]	−1.0[C]	−0.8	−2.0	−0.6	−2.0	−0.6	−2.0	−0.6	−2.0	+1.4	+5.6
	J	−0.5[C]	+1.0[C]	+0.6	+2.0	+0.6	+2.0	+0.6	+2.0	+0.6	+2.0	−1.4	−5.6
Total error	K	+0.5	−2.9	−0.3	−3.2	−3.9	−3.8	−2.7[Z]	−4.1[Z]	+36.0	+33.0	+5.3	+12.3
	N	+0.2	−1.8	−0.2	−1.6	−3.7	−2.1	−2.4[Z]	−2.3[Z]	Y	Y	+3.9	+6.8
	J	−0.4	+1.6	+0.1	+1.5	+3.7	+2.1	+2.4[Z]	+2.3[Z]	Y	Y	−3.9	−6.8

K—Calibrated at −65, fuel at +110, and readings taken at +165 degrees Fahrenheit.
N—Calibrated at +22, fuel at +110, and readings taken at +165 degrees Fahrenheit.
J—Calibrated at +22, fuel at −65, and readings taken at −65 degrees Fahrenheit.
N and *J*—Calculated from *K*, assuming linearity.
There was no error due to frequency fluctuations in these gauges.

C—Compensated unit.
X—Not measurable. Tank unit built as part of fuel cell.
Y—Error too large to permit linear interpolation.
Z—Neglecting any possible dry tank unit temperature effect

erally referred to as a "Howgozit" chart. The typical form of such a chart is shown in Figure 3. These curves are a plot of calculated performance data showing the fuel remaining at any point of the flight, and in particular, indicating the point beyond which no return to the take-off location can be made safely.

Included in the fuel load allowances are generally four fuel reserves as shown in Figure 3, indicated by the double-headed arrows. It is not within the scope of this paper to consider the detail computations[4] necessary to calculate the total fuel load; suffice it to say that all fuel reserves are added by rule-of-thumb, depending primarily on reliability of wind and weather forecasts, expected navigational accuracy, and availability of alternate routes and landing fields.

Nothing considered thus far indicates any opportunity for a more accurate fuel gauge to save in estimated fuel load in a long range flight plan. Fuel gauge accuracy is important in checking the readings of fuel flowmeters used to calculate the quantities of used and remaining fuel. However, when forced to place engines on cross-feed operation or other fuel flow condition not used normally, use of the flowmeters for this purpose is very impractical, if not impossible. Accurate fuel gauges in such a case would be welcome indeed, and if reliable enough, could remove the need for flowmeters almost entirely. But although safety of operation is increased with gauge accuracy, no direct saving of fuel load can be made because of it, based on the properly calculated flight graph.

However, some flight personnel indicate that a prevalent tendency exists in both commercial and military practice for the addition of an unrecorded extra fuel reserve, in excess of that authorized by the flight plan. This is brought about by two large doubts, the one concerning the validity of the flight plan when computed by others, the other concerning the accuracy of the measure of fuel load taken on board, this being quite common at remote airports which still use antiquated ground handling equipment. This extra fuel reserve of up to 200 gallons for a four-engine airplane sometimes is taken on board at a gross weight in excess of that allowed by authorities for the particular airplane, but apparently is condoned nonetheless. An accurate and reliable fuel gauge, independent of airplane attitude, ambient temperature, and fuel temperature would remove the doubt responsible for about half of this extra fuel reserve, and could eliminate perhaps up to 600 pounds of excessive weight, in an extreme case.

Over-All Fuel Gauge Requirements

The specific requirements for a capacitance fuel gauge are available in detail in specification form. However, the action of a fuel gauge includes the effects of installation design details and fuel ambient conditions as well as details of its own design.

Flight personnel indicate that the now prevalent type of float gauge is reliable to within 10 to 15 per cent, and that the immediate need is for a fuel gauge accurate to better than one per cent, and thoroughly reliable. Such a gauge must be compensated for temperature effects in the indicator and circuit components, and also for the capacitance error introduced into any capacitance fuel gauge measurement by temperature variation of the fuel. No fuel reading error should result from reasonably large changes in airplane attitude such as plus or minus 20 degrees in pitch. All calibrations should be made easily, and the empty and full adjustments should be independent of each other. The equipment components should be interchangeable with similar components, particularly vacuum tubes, without requiring recalibration. Normal variations in applied voltage and frequency should produce no errors. Installation and service of parts should be easy. The gauge should be capable of test in flight, and should "fail safe."

If the art develops a fuel gauge capable of providing better than two per cent accuracy, with commensurate dependability, the present practice of using one calibrated airplane installation for making instrument dials for successive production units no longer will suffice. As much as two per cent variation exists in fuel tank volume because of manufacturing tolerances and tank sealing methods. The ultimate in fuel gauges may require a tailor-made instrument scale for each airplane, based on its individual calibration.

Capacitance Measurement and Quantity Indication

The discussion which follows describes the methods used to measure the capacitance of the tank unit and to indicate this remotely, at the flight engineer's or pilot's station, in terms of fuel quantity. The equipment described was submitted by the manufacturers for test only; most of the models will be modified before production units are commercially available. The errors shown in Table I therefore may change, but the simplified circuits and basic methods of operation probably will remain substantially the same as shown here.

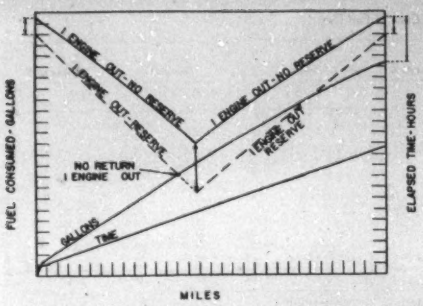

Figure 3. A simplified form of a long range flight graph

Gauge A

Description and Theory

This gauge consists of one or more tank units, an electronic unit and an indicator. The basic wiring and simplified circuit appear in Figure 4.

The tank unit consists of two concentric tubes which are insulated from each other and supported by a single suspension mounting head. The outer tube is grounded and serves as one plate of the capacitor and also as a shield for the inner tube which is the other plate. The tank unit is energized with approximately two volts at 490 kc. A feature of this gauge is the temperature compensation which is part of the tank unit and tends to correct for fuel temperature error.

The electronic unit contains a rectifier, a voltage regulator, a radio-frequency crystal-controlled oscillator, an amplifier, a special double-secondary transformer, and an output twin rectifier. The output of the amplifier, which is almost constant in both frequency and amplitude, is coupled through the primary, $L1$, of the special transformer, to the two secondaries, $L2$ and $L3$. The latter are tuned by their output circuits to lower natural frequencies than the primary $L1$ which is resonant with the amplifier. The windings and output loads are so adjusted that for empty tank condition the two secondaries link equal fluxes and pick up equal voltages, resulting in equal cathode drops in the twin rectifier and, therefore, in no current flow through the indicator.

The addition of fuel causes the capacitance of the tank unit to increase, decreasing the natural frequency of the $L3$ circuit. The latter is then further from resonance with the primary $L1$, and picks up less voltage, causing $L2$ to pick up more. The resonant frequency of the $L2$ circuit increases slightly, due to the reflected reactance of $L3$, further increasing the voltage picked up by $L2$. The rectified output voltage of $L2$ may triple, while that of $L3$ may decrease 30 to 40 per cent. The resultant differential voltage supplied to the indicator is more stable than would be obtained by tuning a simple resonant circuit, and the current is greater than would be afforded by a bridge network. Because of the stable oscillator and isolated output circuit, this gauge is free from errors due to fluctuation of voltage and frequency. This is an outstanding feature for this model of gauge.

The microammeter used as the indicator on the test equipment had 50 divisions on a 90-degree scale and was calibrated "off" and 0 to 100. A standard aircraft meter can be used on production models.

Installation and Adjustments

This gauge has four adjustments built into the electronic unit: "empty", "full", "calibration standard", and "amplifier output." The "full" adjustment is on the front of the case, the other three are inside. All adjustments are smooth in operation. The "full" adjustment has no appreciable effect on the "empty" adjustment, though the "empty" adjustment affects "empty" and "full" about the same extent. The "calibration standard" button substitutes, in place of the tank unit and cable, an adjustable condenser which is set during initial calibration to equal the terminal capacitance of the empty tank unit plus the coaxial cable connecting the latter to the electronic unit. This gauge is the only one submitted for test which was equipped with a satisfactory means for checking the calibration in flight.

There is no provision for damping on the experimental model, but it will be provided in the tank unit on the production model. The warm up period is less than 15 seconds. In case of power or tube failure the indicator will go off scale at the empty end, which is a desirable condition.

Only one tube in the gauge is sensitive to normal tube replacement, the diode rectifier or output tube. This is due to differences in the tube characteristics between the two diodes. Correction in calibration when this tube is replaced is accomplished by the use of a standard calibration push button provided within this instrument.

In the experimental model, the crystal holder was located between two vacuum tubes, spaced so that the heat from the tubes caused the crystal holder to warp after operation over a long period of time The manufacturer is changing th s on subsequent models. This was the only trouble experienced during a total of 280 hours of operation.

The amplifier may be removed from the case for service by disconnecting three cable plugs and releasing two fasteners

Bench testing of this gauge requires a 115-volt power supply at either 60 or 400 cycles, a 100-microampere ammeter, an electronic unit, and a tank unit or adjustable condenser.

Gauge B

Description and Theory

This gauge consists of one or more tank units, an electronic unit, and an indicator. The basic wiring and simplified circuit appear in Figure 5.

The tank unit consists of three concentric aluminum tubes insulated from each other and supported by a single suspension mounting head. The outer tube is grounded, and gives both mechanical and electrical protection to the other two. The inner tubes form the main capacitor and are energized with 65 volts at 400 cycles. The transformer supplying this voltage has high impedance, and feeds

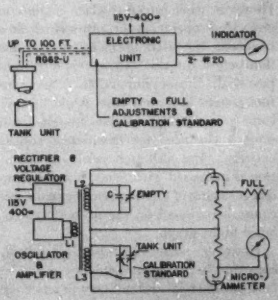

Figure 4. Gauge A basic wiring and simplified circuit

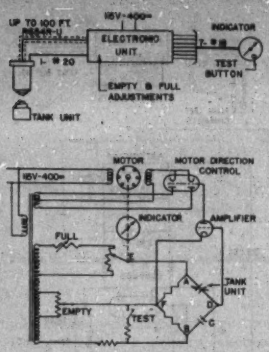

Figure 5. Gauge B basic wiring and simplified circuit

through a 500-ohm series resistor, so that very little energy is available at the tank unit on short circuit.

The electronic unit contains a 400-cycle transformer, a rectifier for electron tube plate supply, part of the bridge circuit, a dual output rectifier tube, and all of the adjustments. Voltage is supplied to corners *A* and *B* of the bridge, Figure 5. The potential of point *F* is fixed, but that of point *D* depends upon the relative capacitances of the tank unit and the fixed capacitor *C*, and also on the potential of point *A*, and therefore on the position of the rebalancing potentiometer arm *E*. As the capacitance of the tank unit increases, due to the addition of fuel, the potential of *D* increases relative to *F*. This causes the amplifier to apply alternating grid voltage to the motor direction control (dual rectifier) tube in such a phase position as to rotate the motor in the direction that moves the potentiometer balance arm so that points *F* and *D* are at the same potential, at which condition the motor stops. The indicator needle moves with the balance arm. When the fuel quantity decreases, the voltage *FD* is in the opposite phase position from the condition just described. This supplies opposite phase current to the second phase-winding of the motor and moves the balance arm and the indicator pointer the other way.

In this type of circuit the electron tubes are used only to amplify the bridge unbalance and pass motor current. Therefore, reasonable variations in tube characteristics have no effect upon the balance position, accuracy, or calibration.

The indicator contains the potentiometer, the dial indicator, the two-phase geared motor which drives them, and a test button. Depressing the button unbalances the bridge, causing the pointer to move downscale if the gauge is working properly. When the button is released, the pointer moves back to its correct position. The dial has 300 divisions in 300 degrees, and is calibrated from 0 to 300.

Installation and Adjustments

This gauge has two adjustments, "full" and "empty", located under the cover plate of the rear section of the electronic unit. They interlock to the extent that it becomes difficult to make fine adjustments at either end of the scale. The "empty" adjustment shifts both ends of the scale simultaneously, and adjustment to less than one division is difficult. Adjustments can be made only with the fuel cells correspondingly full or empty, and therefore, cannot be made in flight.

Damping of the gauge for rapid attitude changes is accomplished by the fixed speed of the indicator motor. The warm up period is of the order of ten seconds. In case of gauge failure for any reason, the indicator will remain at the position of indication at the time of failure. No trouble was encountered in 280 hours of operation.

The front section of the electronic unit can be removed by releasing two thumb locks, exposing the tubes for service. The entire chassis may be released from the base by other thumb locks, but eleven nuts and washers must be removed to release it from the connecting cables.

Bench testing of this gauge requires a 115-volt, 400-cycle power supply, an indicator, an electronic unit, a tank unit or adjustable capacitor, and a special set of connecting cables.

Gauge C

Description and Theory

This gauge consists of one or more tank units, a power unit, a junction box, and an indicator. The basic wiring and simplified circuit are shown in Figure 6. The manufacturer proposes to combine the tank unit and junction box in future models.

The tank unit consists of two concentric tubes insulated from each other and supported by a single suspension mounting head. The outer tube is grounded and serves as one plate of the capacitor, and also as a shield for the inner one which is the other plate. The tank unit is energized with about 40 volts at a preset frequency between 5 and 20 kc. Coaxial cable is required between the tank unit and the junction box; the length should not exceed six feet and the capacitance should be less than the total empty capacitance of the one or more tank units fed by the cable.

The junction box contains two transformers, two selenium rectifiers, and a fixed capacitor. The power unit contains the oscillator and a single stage of amplification. It delivers a signal of fixed frequency and constant voltage to the junction box, which senses the fuel quantity by response of the tank units and thereby controls the indicator reading.

The principle of operation is to measure the tank unit capacitance by comparing the current passed by it with the constant current drawn by a parallel circuit with fixed capacitance *C*. The two currents are transformed, rectified, and applied to the coils of a ratiometer. Since the two parallel circuits are fed by a common voltage source, the instrument is reasonably independent of variations in voltage and frequency or of tube replacement. It depends, however, on the use of matched selenium rectifiers in the junction box, items which other manufacturers have not been able to procure. The equipment tested had a dual type indicator. Each scale had 50 divisions in a 90-degree arc, calibrated 0 to 100.

Installation and Adjustments

This gauge has two adjustments, "full" and "empty", which are smooth in operation and have a two per cent interlocking effect. They are located on the rear of the indicator, which simplifies calibration since one operator can both make the adjustments and watch the effect on the indicator reading. This is an outstanding feature of this gauge. Adjustments can be made only with the fuel cells correspondingly full or empty, and therefore, cannot be made in flight.

Damping is accomplished by restrict-

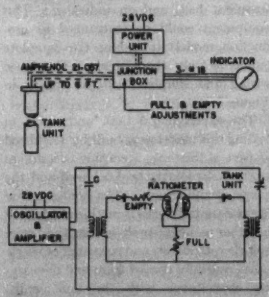

Figure 6. Gauge C basic wiring and simplified circuit

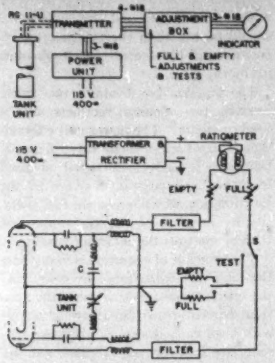

Figure 7. Gauge D basic wiring and simplified circuit

ing the rate of fuel passage into and out of the tank unit. The warm up period is about 15 seconds. In case of power or tube failure, the indicator will go off scale at the empty end, which is a desirable condition. No trouble was encountered in 280 hours o˚ operation.

The power unit may be removed for servicing by disconnecting one cable plug from the rear, and taking out four sheet metal screws from the front panel. No change in calibration is required when vacuum tubes are replaced.

Bench testing of this gauge requires a 24-volt d-c supply, a ratiometer, a power unit, a junction box, and a tank unit or adjustable condenser.

Gauge D

Description of Equipment and Method of Operation

This gauge consists of one or more tank units, a power unit, a transmitter, an adjustment box, and an indicator. This equipment could be rearranged in production models to reduce the complete gauge to only three items. The basic wiring and simplified circuit appear in Figure 7.

The experimental tank units used in testing this model were built by Lockheed as part of the tank, according to a design worked out jointly by Lockheed and the gauge manufacturer. The configuration of these units differed from those furnished by other manufacturers in that they were of larger diameter, and consisted of single tubes carefully spaced from and developing capacitance with the tank walls. In order to obtain sufficient capacitance, one tube was installed near each corner and the four connected in parallel. The response of this type of tank unit is greater near full and empty fuel levels than at intermediate points because of the end capacitance effect. The total capacitance change ratio obtained was about 1.4, whereas tank units using two concentric tubes as plates of the capacitor will produce a change ratio of approximately 2.0. A 50-volt 200-kc potential was applied to these units using coaxial connecting cable type *RG11-U*, which in the tested equipment could not exceed one foot in length. The tank units for the production model will probably use two concentric tubes supported by a single mounting head, and will be connected to the transmitter by a cable of much greater permissible length.

The "power unit" consists of a transformer, a selenium rectifier, and a filter condenser. It supplied direct current to the indicator and oscillators, and 400-cycle power to the heaters of the oscillator cathodes.

The "transmitter" contains two double triodes operating in parallel as two tuned-grid oscillators. One pair of grids is tuned by a fixed capacitor *C*, the other by the tank units. The plate current for each pair of plates is supplied through a coil of the ratiometer, acting as an indicator, and through the adjustable resistors in the adjustment box. As the fuel level in the tank unit changes, one oscillator changes its tuning, resulting in a change in the d-c plate current coming through the corresponding coil of the indicator, while the other oscillator and indicator-coil current remain unchanged. The indicator used in the tests had 25 divisions on a 270-degree antiparallax scale, calibrated from 0 to 500.

Installation and Adjustments

This gauge has adjustments for "empty", "full", and "calibration standard". The "empty" adjustment changes the indicator from 0 to 40 per cent of full dial with fuel at zero level. The "full" adjustment causes a change of 8 per cent of full dial at the empty end of the scale, which complicates calibration. Calibration adjustments can be made only with the fuel cells correspondingly full or empty, and therefore, cannot be made in flight. When the test switch *S1* is used, the "full" circuit of the indicator is disconnected from the oscillator and connected to a d-c supply pre-adjusted, according to the position of switch *S2*, to the full or empty values that normally would be expected from the oscillator. This permits checking the indicator and part of the transmitter unit, but does not provide any test of the tank unit or coaxial cable, and therefore, disqualifies this circuit as a calibrating adjustment. The "calibration standard" will be changed for the production models. The resistor circuit will be omitted, and a condenser will be provided that can be adjusted to the empty capacitance of the combined tank unit and coaxial cable. This will permit making flight adjustments at the zero end of the scale.

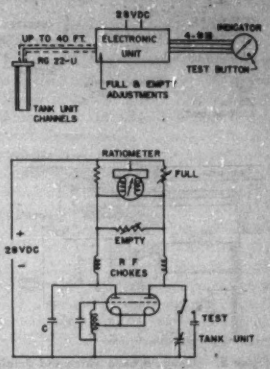

Figure 8. Gauge E basic wiring and simplified circuit

There is no provision for damping on the model tested. The warm up period is approximately 15 seconds. In case of power or tube failure the indicator will go off scale at the zero end, which is a desirable condition.

Seven new stock tubes were used to determine the sensitivity to normal tube replacements. Various combinations of these tubes produced a maximum error of two per cent of full scale.

The power unit, transmitter or adjustment box may be removed by disconnecting two, three, or two plugs respectively, and removal of four machine screws in each case.

Bench testing of this gauge requires a 115-volt 400-cycle power supply, a power unit, a transmitter, an adjustment box, a ratiometer as an indicator, a tank unit or adjustable capacitor, and a set of cables with terminal connectors.

Gauge E

Description of Equipment and Method of Operation

This gauge consists of one or more tank units, an electronic unit, and an indicator. The basic wiring and simplified circuit appears in Figure 8. The particular

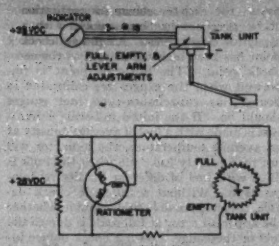

Figure 9. Gauge F basic wiring and simplified circuit

model tested was a 2-channel device, consisting of twin tank units, two electronic units in one case, and a dual indicator.

Each tank unit consists of two concentric tubes insulated from each other and supported by a single suspension mounting head. The outer tube is grounded and serves as one plate of the capacitor, and also as a shield for the inner one which is the other plate and is energized with less than one volt at 160 kc. The tank units used in this test were shorter and of smaller diameter than standard fuel cell units because they had been designed for a specific oil tank installation. A third tube or plate will be included in the production model tank unit, for use in the water detection circuit, described later.

The electronic unit contains the "full" and "empty" adjustments, several circuit components, and a dual triode vacuum tube. The two grids are connected in parallel and drive both halves of the tube as an oscillator at a fixed radio frequency determined by the coil and capacitor contained in the unit. Each plate is connected through a radio frequency choke and a coil of the ratiometer to the 28-volt d-c supply; and is loaded (that is, connected to the supply negative) by a capacitor. The capacitor for one plate is fixed; the other one is the tank unit. For the full tank condition the two plate circuits are adjusted to draw equal currents, and the ratiometer used as an indicator takes a corresponding position. When the fuel level decreases, less charge is stored per cycle by the reduced capacitance of the tank unit; and, for a fixed frequency, less d-c charging current flows to that branch of the circuit. Since the other plate is operating with the same voltage, frequency and capacitance as in the full condition, it draws the same d-c plate current. Thus the indicator coil currents are in a different ratio and the pointer takes a new position. Variations in line voltage are applied equally to both plate circuits.

The indicator on the test equipment was a dual meter with 60 divisions on each 90-degree scale. A test button was provided but was not used.

Installation and Adjustments

The equipment tested has two adjustments, "full" and "empty", located on the electronic unit. They interlock to the extent of 25 per cent of full scale range, making adjustment and calibration difficult. The removal of the case of the electronic unit causes a calibration shift of two per cent of full scale. Both adjusting screws are live parts to the extent of the input voltage to ground; an insulated screwdriver is required in making adjustments.

A button is provided on the indicator for test and water detection. The third plate of the tank unit, previously described, affords the necessary pickup for the water detection circuit. Pressing the button actuates a relay in the electronic unit, changing the tank unit connection. If water is not present, the indicator pointer will register a definite reading, marked with a green line on the dial. If water is present on the third plate, the indicator will swing off scale. Adjustments for calibration can be made only with the fuel cells correspondingly full or empty, and therefore, cannot be made in flight.

Damping is accomplished by restricting the rate of fuel passage into and out of the tank unit. If a channel type of tank unit were used, no damping would be provided. In case of power or tube failure, the indicator will go off scale at the empty end, which is a desirable condition. Variations in tube characteristics may cause a calibration shift by tube replacement of as much as 62.5 per cent of full scale. This gauge may drift for 65 minutes before becoming stable.

Following the preliminary tests reported herein, this gauge was returned to the manufacturer, at his request, for further development.

Gauge F

Description of Equipment and Principle of Operation

This gauge consists of one or two tank units and an indicator. The basic wiring and simplified circuit appears in Figure 9. This gauge is a mechanical float device included for comparison. It responds to the physical level of the liquid in the fuel cell, and is equipped with a resistance bridge network which controls a ratiometer as an indicator.

The tank unit consists of a sealed cork float, a pivoted arm, and a mounting head containing an electrical resistor network. The potentiometers comprising the resistor network are linked mechanically through metal bellows to the float arm. The indicator of the model tested had 60 divisions on a 270-degree scale, and was calibrated from 0 to 60. Installations in which one indication is controlled by two tank units require six number 18 unshielded wires between the tank units, and a 4-coil ratiometer as an indicator.

As the float position follows changes in fuel level, the potentiometer arm moves to change the ratio of currents sent through the coils of the ratiometer, giving an indication of fuel depth.

Since there are no electronic tubes used, there is no warm up period and no change in calibration due to replacements. There is no provision for damping, nor for adjusting the relationship of indicator motion to float motion to permit using a uniform scale for odd-shaped tanks.

The response of this type of gauge to changes in attitude of the airplane depends upon the shape of the fuel cells and also on the exact position of the tank unit. The tank unit requires vibration to minimize the effect of friction in the bearings, and, in some models, in sliding parts of the linkage. This is worse when calibrating the gauges, or in taking readings without the engines running, and results in a slight lag or sluggishness of the indicator Tests indicate that in new equipment the errors due to lack of vibration may be as much as 6.7 per cent of full dial due to tank unit friction.

Installation and Adjustments

This gauge has adjustments for "full", "empty" and "resistor arm travel", all located within the head of the tank unit. The full and empty adjustments are smooth to operate and have no appreciable interlocking effect. The resistor arm travel adjustment is a means of obtaining exactly full range on the indicator as the float moves through its full travel. It requires a special hole in the fuel cell because the float must be moved to its extreme positions in making the adjustment. Scale range corresponding to half of the float diameter is lost at each end of the dial. In case of power failure the gauge goes off scale at the zero end, which is a desirable condition.

Some care is needed in handling the tank units during installation or overhauling because of the length of the float arms and the relatively delicate bearings and mechanical linkage.

Bench testing requires a 28-volt d-c supply, a tank unit, and an indicator.

General Comment

Aircraft fuel gauges are being improved by continuous research and development. The test results reported herein therefore should be appraised as indicating only the present condition of equipment design.

References

1. Some Characteristics of Aircraft Engine Fuels; Their Influence On Capacitor Type Tank Gauges. Office of Scientific Research and Development, National Defense Research Committee, Division 17. Report Number 4016, June 30, 1944, 48 pages.

2. Fuel Quantity Measurement Problems, **Snyder**. *Aeronautical Engineering Review* (New York, N. Y.), volume 4, October 1945, pages 13–19.

3. Potentialities of a Capacitance Measurement Method for Fuel Quantity Gauges in Aircraft, **Savage, Pearson**. *Aeronautical Engineering Review* (New York, N. Y.), volume 4, April 1945, pages 27–32.

4. Long Range Flight (book), **McIntosh**, McGraw-Hill Book Company, New York, N. Y., 1944, 173 pages.

Discussion

D. B. Pearson, General Electric Company, West Lynn, Mass.: The authors show that the errors in fuel quantity indication produced by changes in the dielectric constant of the fuel with temperature are negative, and suggest that compensation be incorporated in the tank probes. Tests have shown that tank probes alone have a positive temperature error that is caused primarily by changes with temperature of the dielectric constant of the insulating material used to separate the probes and is practically independent of dimensional changes with temperature in either the probes or the insulation. In general, the temperature error increases as the electrostatic field impressed on the insulator increases. By proper selection of insulating materials and suitable design, therefore, tank units could be built with the inherent temperature error that best compensates for the effects of temperature on the dielectric constant of the fuel.

It also was suggested in this paper that a correction factor might be applied to the indicator reading to correct for the temperature error of the fuel. The difficulties encountered in determining the temperature of the fuel, as well as temperature effects in the other circuit components, would appear to make this procedure somewhat hard to follow.

The description of the ideal fuel gauge given under "Over-All Fuel Gauge Requirements" indicates the need for a fuel-measurement system with errors less than one per cent of full scale. The capacitance fuel gauge can be designed and built to have this accuracy in the laboratory, but service requirements make this degree of accuracy difficult to obtain in aircraft installations. Correcting the temperature error of the fuel alone to within one per cent of full scale, particularly with irregularly shaped tanks where the wetted probe area is a nonlinear function of fuel mass, would be a very difficult task. The reduction of airplane attitude error to less than one per cent of full scale over a range of ±20 degrees in pitch would necessitate a large number of tank probes, particularly for odd-shaped fuel cells. This would increase unduly the weight and complexity of the system. It is believed, however, that the capacitance gauge is an improvement over the float-actuated instrument and is a step towards the ultimate ideal fuel-quantity gauge.

The comparisons given of the capacitance fuel gauges tested describe some of the characteristics of each gauge. Since these tests were made, several changes have been planned for gauge *D*. As stated in this paper, the resistor scheme for calibration check purposes has been replaced with a capacitor check device. A full-scale check point has been included as well as the zero-check point. The full-scale point is important when the gauges are calibrated in pounds, as capacitance-type fuel gauges should be. If the initial full-scale calibration is made with a fuel of average density at an average temperature, the indicator will not read exactly full scale when the tank is filled with fuel of different density or temperature. Without a full-scale check device, it is not possible to determine whether the apparent error at full scale is due to the fuel or the gauge. With a check device including both empty and full scale substitute capacitors, and operated by a double-throw switch on the indicator panel, both end-scale points can be checked at any time, regardless of the quantity, type, or temperature of the fuel.

The full-scale adjustment has been redesigned, and now produces negligible effect on the zero point. The empty adjustment does affect full scale, but since the zero adjustment normally is made first, this condition should not cause serious difficulty.

The tank units now consist of concentric cylinders with a minimum spacing of one-eighth inch. The holes through which the fuel gains access to the capacitor are made small enough to provide suitable damping in the tank probes. Sufficient coaxial cable may be used to connect the tank units together and to the transmitter unit.

The small change in indication obtained when the vacuum tubes were replaced does not appear to be very serious, when the normal life of present-day tubes is considered. Tubes are expected to last at least 1,000 hours, so replacement should not be necessary between the normal overhaul periods of the aircraft. However, if a new tube should be needed, the readily accessible adjustments and check device makes any necessary recalibration a simple process that is possible even during flight.

Automatic Temperature Control for Transport Airplanes

R. E. HEDGES
ASSOCIATE AIEE

THE *DC-6* air conditioning system to be described in this paper represents one of the latest developments for obtaining maximum comfort to the passengers and the crew of transport airplanes. The operation of this system is fully automatic and requires no attention after an initial setting prior to flight. The cabin pressurizing system utilizes two engine-driven superchargers, each capable of supplying 550 cubic feet per minute (30.6 pounds per minute) of fresh air to the cabin at 70 degrees Fahrenheit and a cabin altitude of 8,000 feet when the airplane is flying at an altitude of 20,000 feet. With 55 occupants, the cabin ventilating rate will be 20 cubic feet per minute of fresh air per person and a complete change of air in the cabin every three minutes. The cabin temperature control system conditions all air prior to its entering the cabin, and a control is provided so that the cabin attendant may select a cabin temperature within the limits of 65 degrees Fahrenheit and 85 degrees Fahrenheit.

Before explaining the operation of the cabin temperature control system, a brief description of the cabin pressure system is in order to better understand how the complete air conditioning system functions.

Cabin Pressure System

Air enters the system through intake scoops located in each wing and, after being supercharged, flows through ducts to the temperature conditioning equipment. (Refer to Figures 1 and 2.) The conditioned air flows through cabin floor ducts and wall ducts to outlets spaced at intervals along each side of the cabin. Exhaust ducts pass the spent air from the cabin to the lower fuselage compartment, and it is released from the fuselage through a cabin pressure control valve. Pressurization is maintained and controlled by throttling the discharge of air through this valve. Regulation of the valve is accomplished by an electronic control system consisting of a cabin pressure regulator, a cabin pressure limit control, and an amplifier. Inside the control instruments, a system of pressure sensitive capsules actuate mechanical linkages which in turn make and break electric contacts in accordance with pressure requirements. The resulting signal currents are fed to the amplifier unit, which then closes one of two relays and causes a motor to actuate the pressure control valve for increasing or decreasing the rate of air flow from the fuselage.

The cabin pressure regulator incorporates two selector knobs by which the operator may set the altitude at which he desires cabin pressurizing to begin on ascent or stop on descent, and the flight altitude for the particular route. No further adjustment will be required during the flight. The cabin pressure rate of change will be proportional to the outside air pressure rate of change for all altitudes up to the selected flight altitude and will vary in accordance with the following ratio:

$$\text{Ratio} = \frac{\text{cabin altitude} - \text{start pressurizing altitude}}{\text{flight altitude} - \text{start pressurizing altitude}}$$

The ratio will vary in accordance with the selector knob settings. At altitudes above the selected flight altitude, the cabin will fly at altitudes which maintain a maximum pressure differential of 4.16 pounds per square inch between the cabin and outside air until an altitude of 25,000 feet is reached. Above 25,000 feet, the differential will be slightly lower due to the limiting of the constant compression ratio on the superchargers.

The cabin rate limit control indicator incorporates two selector knobs so that the operator may set the desired maximum rate of cabin ascent and descent in feet per minute. If a change in flight plan is made which requires changing the pressure regulator adjustments, the resulting rate of change of cabin pressure will not exceed the limits set into the rate limit control indicator. The instrument may be used as a pressure regulator, if desired, by moving the indicator hands together to whatever rate of pressure change is desired. In this event, the cabin pressure will change at the rate indicated, rather than at a rate proportional to the outside air pressure rate of change, as is the case when the cabin pressure regulator is the controlling instrument.

The cabin pressure limit control functions as an override on both of the aforementioned instruments for providing a safety factor and for preventing overcompression beyond the maximum allowable differential pressure for the cabin and supercharger compression ratio limits.

Cabin Temperature Control System

Heat of compression of the supercharged air provides the basic heat requirement for the cabin. Cabin temperatures between 65 degrees Fahrenheit and 85 degrees Fahrenheit are obtained by either cooling or heating the supercharged air. This is accomplished by dividing the air ducting into three paths. The first path is through an aftercooler and to an expansion turbine to provide cold air; the second path is through the aftercooler only to provide moderately cool air; and the third path is through a surface com-

Paper 47-179, recommended by the AIEE committee on air transportation for presentation at the AIEE Pacific general meeting, San Diego, Calif., August 26–29, 1947. Manuscript submitted May 26, 1947; made available for printing July 10, 1947.

R. E. Hedges is with the engineering department of the Douglas Aircraft Company, Inc., Santa Monica, Calif.

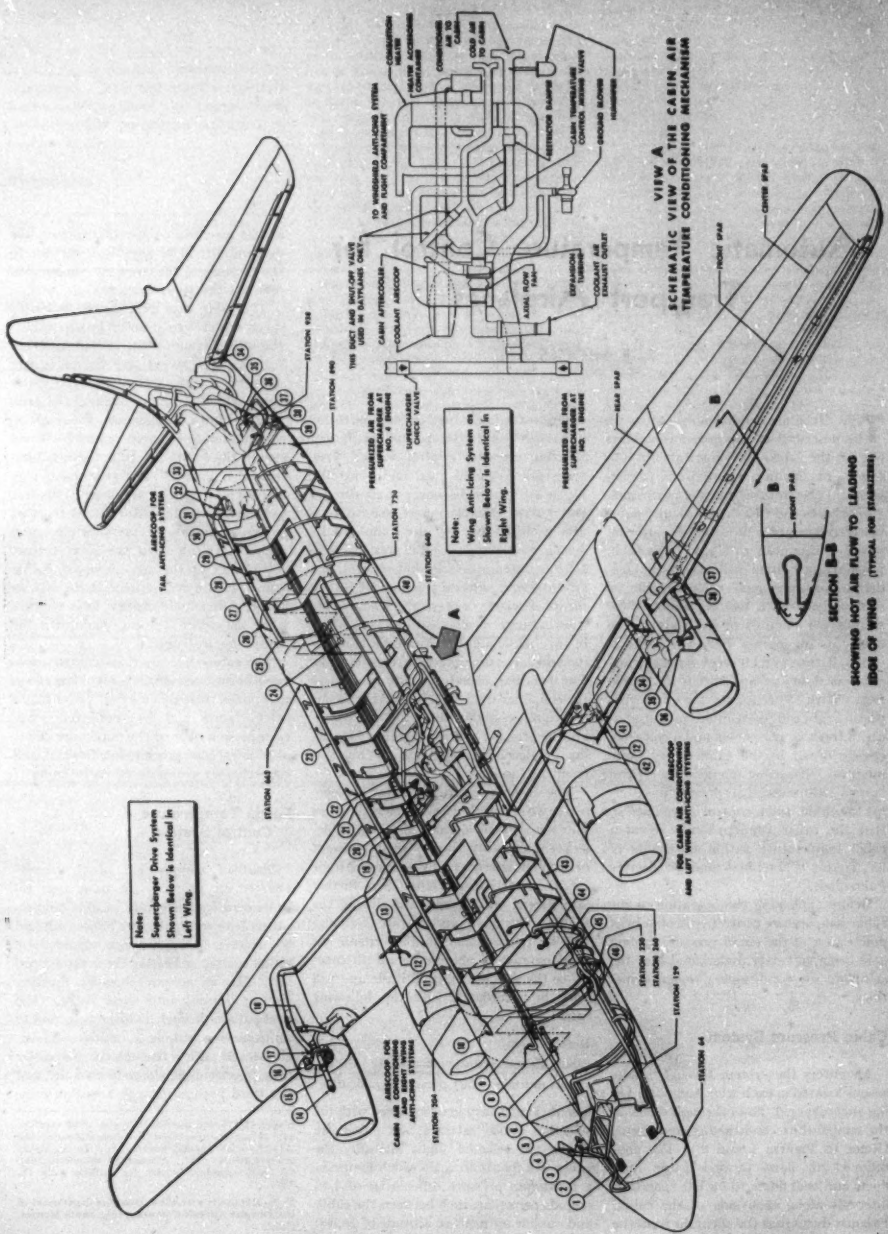
VIEW A
SCHEMATIC VIEW OF THE CABIN AIR TEMPERATURE CONDITIONING MECHANISM
SECTION B-B
SHOWING HOT AIR FLOW TO LEADING EDGE OF WING (TYPICAL FOR STABILIZERS)
Note:
Wing Anti-Icing System as Shown Below is Identical in Right Wing.
Note:
Supercharger Drive System Shown Below is Identical in Left Wing.
TAIL ANTI-ICING SYSTEM
STATION 930
STATION 890
STATION 770
STATION 640
STATION 445
STATION 304
STATION 220
STATION 244
STATION 139
STATION 64
CENTER SPAR
FRONT SPAR
REAR SPAR
RIGHT SPAR
A
B
B
TO WINGFIELD ANTI-ICING SYSTEM AND FIRST COMPARTMENT
COMBUSTION HEATER
HEATER ACCESSORIES CONTAINER
CONDITIONED AIR TO CABIN
TO D.C. AIR CONDITIONER
RESTRICTOR DAMPER
CABIN TEMPERATURE CONTROL BYPASS VALVE
GROUND BLOWER HOUSING
EXPANSION CHAMBER
COOLANT AIR EXHAUST OUTLET
AXIAL FLOW FAN
COOLANT AIRSCOOP
CABIN AFTERCOOLER
TWIN DUCT AND SHUT-OFF VALVE USED IN BATTLEARD CIRCUIT
PRESSURIZED AIR FROM SUPERCHARGER AT NO. 4 ENGINE
SUPERCHARGER CHECK VALVE
PRESSURIZED AIR FROM SUPERCHARGER AT NO. 1 ENGINE
AIRSCOOP FOR CABIN AIR CONDITIONING AND SHUT-OFF VALVE ANTI-ICING SYSTEMS
AIRSCOOP FOR CABIN AIR CONDITIONING AND LEFT WING ANTI-ICING SYSTEMS

Figure 1. DC-6 heating and pressurizing system

1. Pilots' foot warmer
2. Pilots' cold air ventilator
3. Emergency pressure relief valve control
4. Upper instrument panel (right section) Cabin pressure automatic controls
5. Upper instrument panel (left section) Heater, controls, windshield and surface anti-icing controls
6. Heater fire protection control panel Flight compartment temperature control
7. Smoke detector. Lower forward cargo compartment
8. Forward lounge conditioned air inlet
9. Windshield anti-icing control valve
10. Forward lounge cold air ventilator
11. Smoke detector. Fuselage accessories compartment
12. Heater fuel shut-off (and drain) valve
13. Wing and tail anti-icing heater fuel pump
14. Supercharger drive shaft
15. Supercharger planetary gear box
16. Supercharger airflow control regulator
17. Supercharger assembly
18. Supercharger bypass check valve
19. Cabin pressure control valve and diffuser duct
20. Cabin pressure automatic emergency relief valve
21. Cabin pressure emergency relief valve
22. Exhaust air blower
23. Forward cold air distribution duct. Main cabin
24. Smoke detector. Lower aft cargo compartment
25. Aft cold air distribution duct. Main cabin
26. Upper berth cold air ventilator
27. Upper berth conditioned air inlet
28. Lower berth and main cabin cold air ventilator
29. Lower berth and main cabin conditioned air inlet
30. Aft toilet
31. Thermistor and cabin air temperature indicator thermocouple
32. Aft lounge cold air ventilators
33. Vacuum relief valve (on pressure dome)
34. Ground blower
35. Combustion air check valve
36. Heater accessories container
37. Combustion heater
38. Heater exhaust outlet
39. Aft lounge conditioned air inlet
40. Cabin attendant's temperature control panel
41. Cabin heater fuel pump
42. Heater solenoid-operated selector valve
43. Main cabin exhaust air outlet
44. Toilet compartment cold air ventilator
45. Forward toilet
46. Flight compartment mixing valve

bustion type heater to provide warm air. (Refer to Figure 3.) The heater operates only when the temperature of the supercharged air is not sufficiently high to maintain the cabin temperature at a desired level. A portion of the cold air flows directly to individually controllable cabin outlets for each passenger.

Figure 2. Cabin air circulation

The heart of the system is a mixing valve by which the preceding three portions of conditioned air are blended into a single air stream having the desired temperature. The valve has three inlets and one outlet port. When the valve is in its extreme counterclockwise position, port 1 is fully open and only cold air from expansion turbine passes to the cabin. As the valve rotates clockwise, port 1 gradually closes while port 2 opens to mix the warmer aftercooler air with the cold air from port 1. Continued clockwise rotation of the valve, when only port 2 is fully open, causes a flap in the aftercooler coolant air discharge duct to gradually close, thereby decreasing the effectiveness of the aftercooler which reduces the cooling effect on the supercharged air. Further clockwise valve rotation gradually closes port 2 and opens port 3 to mix the warm supercharged air with the aftercooler air. Finally, only port 3 is open and the mixing valve approaches its extreme clockwise position. If still more heat is required, a limit switch at the extreme position stops valve rotation and starts the clockwise rotation of a program motor, which drives a rheostat that controls the rate at which the surface combustion type heater will cycle on and off to provide hotter air through port 3, as required.

Automatic Control Circuit

Automatic control of cabin temperature is accomplished by means of a temperature sensitive bridge circuit that senses and anticipates varying temperature conditions within the cabin and air ducts and causes a motor actuator to position the mixing valve accordingly for changing the temperature of air supplied to the cabin. A second bridge circuit causes heater cycling when required at a rate determined by the position of a rheostat driven by the program motor. The cabin attendant sets one calibrated rheostat to the desired cabin temperature, and without further attention, the bridge circuits react to position the mixing valve or cycle the heater for maintaining the cabin at the selected temperature. The functioning of the circuits will be described individually in the following paragraphs.

Figure 4 is a schematic diagram of the temperature control bridge circuit. The main cabin temperature control permits the attendant's selection of a desired cabin temperature between 65 degrees Fahrenheit and 85 degrees Fahrenheit, by adjusting a variable resistor in one leg of the bridge. A sensitive micropositioner relay detects the unbalance and operates to start mixing valve actuator rotation for repositioning the valve. As the valve rotates (and alters the mixed air proportions), a follow-up rheostat geared to the actuator rotates and rebalances the bridge circuit as the proper valve position is reached. The micropositioner sensitivity is high and operates on as little as 0.12 volt unbalance in either direction. The polarity of unbalance determines whether power will be applied for clockwise or counterclockwise valve rotation.

The cabin thermistor, consisting of a pair of highly temperature sensitive resis-

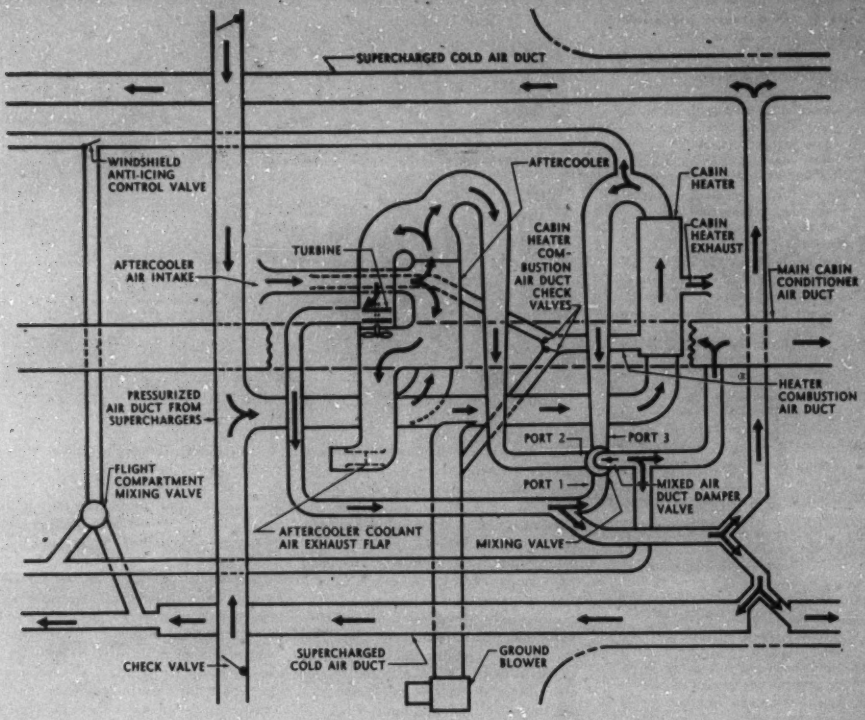

Figure 3. Cabin air temperature conditioning mechanism

tors having an average negative coefficient of −4 ohms per plus or minus one degree Fahrenheit, detects intracabin temperature variations, and inserts the proper unbalance to the bridge circuit when required to reposition the valve and thereby maintain the selected cabin temperature.

A temperature sensitive outside resetting element in one of the ram air ducts detects variations in outside air temperature being supplied to the system. By anticipating these changes, it provides an unbalance in the bridge to compensate for them. If the outside air temperature goes down suddenly, the circuit will react to reposition the valve and supply more heat to the cooler air. Similarly, an increase in outside air temperature will cause less heating of the air being supplied to the cabin.

The high-low limit resistors, located in the output duct of the mixing valve, anticipate changes in mixed air temperature and begin to rebalance the bridge circuit before the cabin thermistor detects the change. By so doing, it corrects the mixing valve position and reduces any surge of hot or cold air to the cabin. If the cabin thermistor had to act alone in this capacity, the cabin air temperature would hunt between wide limits before the thermistor could react due to the time lag involved. The high-low limit resistors, anticipating action, due to their quick and early response, smooth out the temperature changes which are passed on to the cabin.

The final item of the bridge circuit is another follow-up rheostat, the purpose of which is to extend the effective range of the mixing valve. When the valve is at its full clockwise position, power circuits are transferred from the valve actuator motor to the program motor so that demands for more heat will cause it to rotate its gear train clockwise. This follow-up rheostat performs the same balancing action on the bridge circuit as the rheostat within the mixing valve actuator performs. A second rheostat on the gear train is connected to the heater control bridge circuit, and it causes an electrical unbalance of the circuit to a degree depending upon the amount of heat required.

The heater control bridge circuit shown schematically in Figure 5, when unbalanced by the position of the rheostat geared to the program motor, causes a micropositioner relay to close and thereby energize the surface combustion type heater. The temperature sensitive heater discharge elements in the hot air duct measure the increase in hot air temperature and turn off the heater by rebalancing the bridge circuit when the proper degree of heat has been reached. This

cycle repeats at a rate determined by the degree of unbalance produced by the control rheostat position and required to maintain an elevated air temperature. If little heat is required, the heater "on" period will be short and the "off" period relatively long. If a lot of heat is required, the "on" period will lengthen and the "off" period shorten correspondingly.

The heater unit serves the dual purpose of not only supplying heat to the cabin, but also supplying heat for windshield anti-icing purposes. When the pilot turns on the windshield anti-icer switch, a relay connects a fixed resistor into the heater control bridge circuit in place of the rheostat. This causes the heater to cycle at a predetermined rate for supplying heat to the windshields through a duct located at the heater output. Back pressure to force the hot air through the duct is created by a restrictor damper positioned to 45 degrees in the mixing valve duct. As long as windshield anti-icing is required, the cabin temperature control bridge has no control over heater operation. However, heater operation does not affect the cabin temperature in this event because the sensing elements will reposition the mixing valve for supplying more cool air to maintain a constant temperature air to the cabin.

Additional System Features

The foregoing paragraphs have explained the operation of the major control features of the *DC-6* cabin pressure and temperature control systems. To complete the picture, however, a few additional features of the system should be mentioned although the length of this paper does not permit a detailed explanation of their operation.

The pilot is provided with a rheostat by which he may adjust cockpit temperature to make it colder or warmer than the cabin as desired. A follow-up type bridge circuit positions a smaller mixing valve for adding warmer or cooler air to that being supplied by the cabin system.

In both the pressure and temperature control circuits, manual push button controls are provided for operating the system in case of malfunctioning of the automatic system. When access doors are opened to expose these manual controls, the automatic control circuits are disengaged. The cabin attendant's manual controls consist of two push buttons, one for increasing cabin temperature and one for decreasing it. The push buttons apply power to rotate the mixing valve actuator. The co-pilot's manual controls consist of two push buttons, one for increasing cabin pressure and one for decreasing it. The push buttons apply power to open or close the pressure control valve.

A ground blower motor is provided to supply cabin ventilating air while the airplane is on the ground. Its operation is also automatic. Interlocked relay circuits determine when the blower should operate, since it depends on whether or not the plane is airborne, whether or not at least two engines are running above a certain speed, whether or not an external power source is connected to the plane, and other deciding factors.

A humidifier unit is provided so that

Figure 4. Cabin heating and ventilating control bridge

Schematic wiring diagram

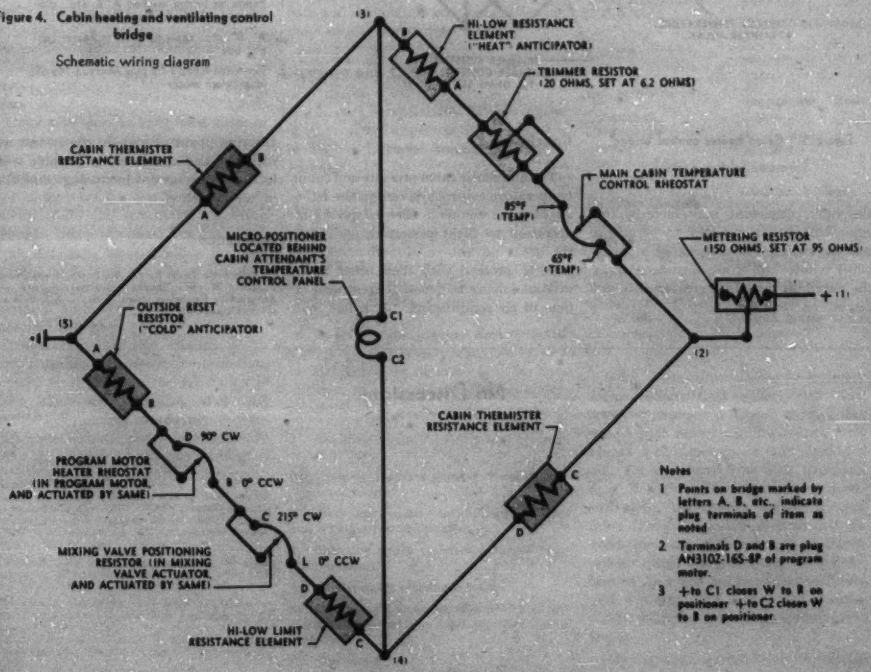

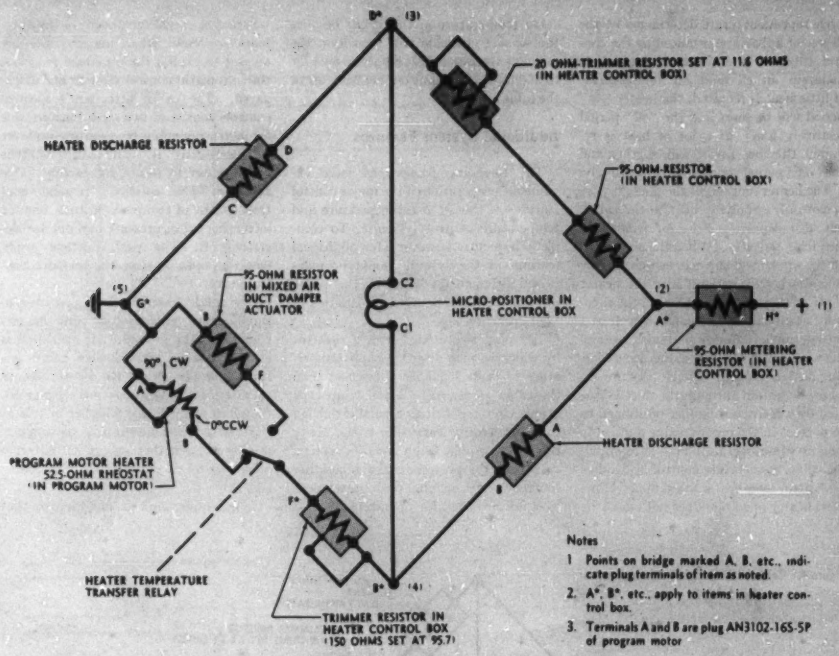

Figure 5. Cabin heater control bridge

Schematic wiring diagram

the cabin attendant may increase the cabin humidity, if required, by turning a selector switch. It consists of a water boiler whose vapors are introduced into the mixed air duct to a greater or lesser degree, as required.

Conclusion

The automatic cabin pressure and cabin temperature control systems on the *DC-6* airplane are unique in their simplicity of operation by flight personnel, and have the great advantage of permitting the crew to proceed with their other tasks without having to devote a great deal of time to air conditioning. It is felt that the time spent in making the system as foolproof and automatic as possible will lead the way toward increasing comforts in air travel.

Reference

1. Mock Up Tests Prove Air Conditioning for Planes, W. W. Thayer. *Journal*, Society of Automotive Engineers (New York, N. Y.), February 1947, page 84.

No Discussion

Tests and Developments in Connection With Hot-Line Insulator Washing

G. LESLIE HILL
ASSOCIATE AIEE

CONTAMINATED and dirty insulators are a source of considerable maintenance expense, trouble, and annoyance to electrical power utilities. This is especially true in certain geographical and industrial areas that have a wet and a dry season each year, or in areas where there is a considerable period of time between rains. The insulators become dirty and contaminated during the dry period and when a fog or light rain dampens the insulators, the leakage current becomes excessive, causing pole top fires or flashovers.

Large expenditures have been made in the past for cleaning insulators by wiping them by hand. This is a slow, tedious, and very expensive process requiring, in most cases, that the line be taken out of service while the insulators are being cleaned. It is also a hazardous method as there is always the possibility that the lineman will climb a pole or structure supporting one energized line and one de-energized line and start cleaning the energized insulators

The Pacific Gas and Electric Company's department of electric operation, decided to investigate the feasibility of more efficient, economical, and safe methods of cleaning insulators. A committee was formed; and it was decided to carry on experiments in the washing of energized insulators with a high pressure stream of water, and to make a study of equipment and apparatus so that standardization for the whole system could be accomplished.

It was the part of the writer, on this committee, to carry out the experimental work; and this paper is a compilation of data and information accumulated during these tests and experiments.

Purpose and Outline of the Work

The work was primarily for the purpose of carrying out a systematic investigation of hot-line insulator washing and determining

1. The feasibility of cleaning energized insulators with a high pressure water stream.
2. To obtain information that could be used as a guide for the maintenance men in the field.
3. To test various nozzles so that an efficient nozzle could be obtained.

The information and test data obtained during the work is segregated and divided in the following sections for the convenience of anyone interested in a particular phase of the work.

1. Cleaning insulators with a high pressure water stream.
2. Leakage current passing through the stream of water.
3. Tests on various manufactured nozzles and on experimental nozzles.
4. Effect of water resistivity during insulator washing.
5. A new water resistance tester.
6. Operating economics effected by cleaning insulators with a high pressure water stream.
7. Summary.

Experiments on Cleaning Insulators with a High Pressure Stream of Water

These tests were made to determine the effectiveness of cleaning contaminated energized insulators with a high pressure stream of water. For this purpose a number of contaminated insulators were removed from power lines in various localities over the Pacific Gas and Electric system.

The following list gives the localities from which contaminated insulators were obtained, all of them in northern California.

Coast Valleys Division

King City
Soledad
Salinas

San Jose Division

Davenport
Permanente Cement (near San Jose)
Redwood City

East Bay Division

West Vaca (near Newark)
Concord area
Berkeley
West Oakland
Richmond industrial area
Livermore
Emeryville

North Bay Division

San Rafael
Petaluma
Napa

Sacramento Division

Sacramento
Rio Vista
Dixon

Stockton Division

Jackson, Calaveras cement plant
Stockton

San Joaquin Power Division

San Luis Obispo
Santa Maria
Lompoc

Some of the insulators had the ordinary accumulation of dust and dirt; and others, removed from a railroad right-of-way near an oil refinery in Richmond, were coated with a mixture of dust, soot, and oil. Those removed from West Vaca lines near Newark were coated with calcium carbonate, magnesium carbonate, and other foreign materials such as salt deposits carried in the air from evaporating ponds. Other insulators were coated with cement dust and ordinary dust and grit, and deposits from smoke and furnace fumes that are prevalent in industrial areas.

The tests and experiments performed on

Paper 47-180, recommended by the AIEE committee on power transmission and distribution for presentation at the AIEE Pacific general meeting, San Diego, Calif., August 26–29, 1947. Manuscript submitted June 16, 1947; made available for printing July 17, 1947.

G. LESLIE HILL is assistant engineer in the engineering department's bureau of tests, Pacific Gas and Electric Company, San Francisco, Calif.

The author gratefully acknowledges the co-operation of his associates in this work, especially C. M. Buck for his recording and preparation of test data, and the mechanical staff of Emeryville shops, Pacific Gas and Electric Company, San Francisco, Calif.

Table I. Contaminated Insulators Washed with Line Potential Applied

3,000 Kva Available if Flashover Occurred

Test	Type of Insulator	Catalogue Rating, Kv Dry	Catalogue Rating, Kv Wet	Kind of Contamination	Voltage Applied to Ground, Kv	Water Pounds Per Square Inch Nozzle	Water Resistance	Water Orifice Size, In.	Results
1	Pin type used on 12-kv lines	110	80	Dirt and oil from oil refinery area	7.0	550	1,800	1/4	Cleaned 80 per cent. No flashover
2				Dirt and dust from heat insulation Factory area	7.0	550	1,800	1/4	Cleaned 95 per cent. No flashover
3 and 4	Pin type used on 12-kv lines	110	75	Dirt and dust from agricultural fields—sandy loam soil	7.0	550	1,800	1/4	Cleaned 100 per cent. No flashover
5	Insulators on 12-kv pole top disconnect switch	95	65	Dirt and dust from agricultural fields—sandy loam soil	7.0	550	1,800	1/4	Cleaned 100 per cent. No flashover
6	Line post type used on 12-kv lines	125	100	Dirt, dust and oil near railroad track in industrial area	7.0	550	1,800	1/4	Cleaned 90 per cent. Considerable arcing, did not flashover
7	3-shed pin type used on 66-kv lines	170	135	Bad deposit of cement dust—set on insulator by fog and rain	39	550	1,800	3/16	Could not wash cement off. All insulators flashed over
8									
9									
10	3-shed pin type used on 66-kv lines	170	135	Dirt and dust from agricultural field	39	400	2,100	5/16	Cleaned 100 per cent. No flashovers
11									
12									
13	3-shed pin type used on 66-kv lines	170	135	Dirt and dust from agricultural field	39	400	2,100	5/16	One shell punctured and flashed over—old insulator
14	4-shed pin type used on 60-kv lines	180	140	Dirt and dust from agricultural field	39	400	2,100	5/16	Cleaned 100 per cent. No flashovers
15	Line post type used on 66-kv lines	175	150	Dirt and dust and deposit—from paint factory and industrial area	39	400	1,700	5/16	Cleaned 95 per cent. No flashover—high leakage current over insulator—200 ma when water applied
16	5 10-inch suspension used on 66-kv line	320	245	Dirt and dust and deposit from industrial area	39	550	1,800	1/4	Cleaned 95 per cent. No flashover
17	4 10-inch suspension used on 66-kv line	265	200	Dirt and dust and deposit from industrial area	39	550	1,800	1/4	Cleaned 95 per cent. No flashover
18	5 10-inch suspension used on 66-kv lines	320	245	Calcium carbonate–magnesium carbonate dirt and dust and salt deposit. Very bad	39	550	1,800	1/4	Cleaned about 70 per cent Did not flashover but heavy leakage current
19	4 10-inch suspension used on 66-kv lines	265	200	Calcium carbonate–magnesium carbonate dirt and dust and salt deposit. Very bad	39	550	1,800	1/4	Cleaned about 70 per cent. Flashed over

these insulators were divided into three parts

1. Washing the insulators with a constant line potential applied.

2. Washing the insulators to determine the increase in wet flashover.

3. Washing the insulators to determine the effectiveness of an abrasive in the stream of water.

Test 1

These tests were made at the power testing plant of the bureau of tests in Emeryville, Calif. A 3-phase 12-kv grounded Y line was the power supply. The power was limited to 3,000 kva by suitable reactors in case of a flashover. The tests made at 7 kv were line to ground and the tests at 38 kv were made on the

Table II. Contaminated Insulators Washed to Determine Increase in Wet Flashover Voltage

Water Resistance 1,800 Ohms Per Inch Cube

Type of Insulator	Kind of Contamination	Insulator Number	Flashover in Fog Before Cleaning, Kv	Per Cent of Flashover of Clean Insulator	Flashover in Fog After Cleaning, Kv	Per Cent of Flashover of Clean Insulator	Per Cent of Contamination Removed
10-inch suspension. Catalogue rating: dry, 80 kv; wet, 50 kv. 9 in string: dry, 535 kv; wet, 430 kv	Usual dust, grit, soot in industrial areas near oil refinery. Flashed over in service on 110 kv. Y ground line. Very bad	1	27	60	36	80	Not recorded
		2	34	75	42	93	Not recorded
		3	30	67	45	100	Not recorded
		4	29	64	38	84	Not recorded
		5	27	60	36	80	Not recorded
		6	28	62	38	84	Not recorded
		7	24	53	42	93	Not recorded
		8	36	80	42	93	Not recorded
		9	20	44	36	80	Not recorded
		9 insulators in string	170	50	Did not flash over at 260 kv	?	
12-inch special suspension. Catalogue rating: dry, 95 kv; wet, 60 kv. 11 in string: dry, 650 kv; wet, 465 kv	Calcium carbonate, magnesium carbonate, and dirt. Very bad	11 insulators in string Flashed over in service	130	31	236	56	50
Pin type used on 12-kv lines. Catalogue rating: dry, 90 kv; wet, 50 kv	Dust and dirt and dehydrated alfalfa dust caused pole top fires	1, 2, 3	27 (av of 3)	54	50	100	95
5 10-inch suspension. Catalogue rating: dry, 320 kv; wet, 245 kv	Heavy dark dust from agricultural area	5 in string	117	60	195	100	95

high voltage side of a 3,000-kva 36,000-to-6,600-volt bank of transformers.

About 50 tests were performed, and the washing followed the same procedure as field practice. The stream of water was played on the insulators at about the same angle as it would be from the ladder on the washing truck. The suspension-type insulators were cleaned in a string as suspended on the line except that the tension was applied with a set of blocks.

Representative data obtained are shown in Table I.

Summarizing the power tests, the ordinary dirt and dust was removed easily; but the cement dust, calcium and magnesium carbonate, soot and oil combinations, and bad industrial contamination could be removed only with varying degrees of success.

There were no flashovers while washing any of the contaminated insulators used on the 12-kv lines during the tests. There were no flashovers on the insulators used on the 66-kv lines which had only the ordinary dirt and dust contamination. All the insulators, with the exception of a string of 5-10-inch suspensions, that had a bad accumulation of cement dust, calcium and magnesium carbonate, and so forth flashed over during the washing tests. One 4-shed pin-type insulator, used on 66-kv lines, punctured during the washing tests. This was an old insulator; it had been in service a long time; and it is considered it would have failed in service during the first rainstorm.

Test 2

Table II gives representative data on the increase in flashover value that may be expected after washing dirty and contaminated insulators with a high pressure stream of water.

The flashover tests were made with a 2,500-to-250,000-volt 250-kva potential transformer with a suitable regulator and reactor limiting the power to 1,250 kva at 250 kv.

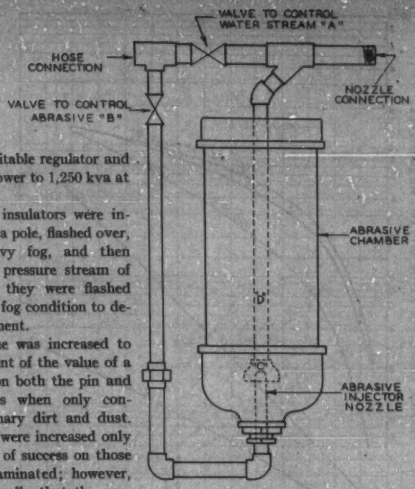

Figure 1. Abrasive injector used in insulator cleaning with high pressure stream of water

The contaminated insulators were installed as received on a pole, flashed over, in an artificial heavy fog, and then cleaned with a high pressure stream of water; after which, they were flashed again under a similar fog condition to determine the improvement.

The flashover value was increased to practically 100 per cent of the value of a new clean insulator on both the pin and the suspension types when only contaminated with ordinary dirt and dust. The flashover values were increased only with varying degrees of success on those insulators badly contaminated; however, it was conceded generally that the contamination had been removed sufficiently so that the insulators could have remained in service. Referring to the table, one string of 9 10-inch suspension insulators was increased from 170 kv to above 260 kv. Another string of 11 12-inch suspension insulators was increased from 130 kv to 236 kv. Both of these strings had flashed over in service on 110-kv lines.

Test 3

Experiments were made on the removal of the cement dust, calcium carbonate, and the combination of soot and oil, by injecting an abrasive into the water stream. Representative test data are shown in Table III. The four pin type insulators used on 12-kv lines, and the string of nine 10-inch suspension insulators coated with calcium carbonate and magnesium carbonate were washed using an abrasive in the water stream. The percentage of the contamination removed from the insulators varied from 60 to 85 per cent depending on the length of time the water stream was played on the insulators. The water stream was played on each pin type insulator for less than 30 seconds and on the strings of nine 10-inch suspension units for about 1 to 1½ minutes.

In the case of the string of nine 10-inch suspension type insulators, shown in Table III, the flashover voltage was increased from 82 kv to over 270 kv (highest attainable from the potential transformer at the laboratory) by cleaning from 75 to 85 per cent of the surface.

Table III. Contaminated Insulators Washed to Determine Increase in Flashover Voltage Abrasive Used in Water Stream

Water—1,800 Ohms Per Inch Cube

Type of Insulator	Kind of Contamination	Insulator Number	Flashover in Fog Before Cleaning, Kv	Per Cent of Flashover of Clean Insulator	Flashover in Fog After Cleaning, Kv	Per Cent of Flashover of Clean Insulator	Per Cent of Contamination Removed
10-inch suspension from 110-kv line. Catalogue rating (each): dry, 80 kv; wet, 50 kv. 9 in string: dry, 535 kv; wet, 430 kv	Calcium carbonate and magnesium carbonate and dirt, 2 months accumulation. Very bad	1	16	36	40	99	85
		2	8	18	32	71	85
		3	8.5	19	30	67	85
		4	5	11	34	75	85
		5	6	13	32	71	85
		6	5	11	26	58	75
		7	11	24	28	62	75
		8	8	18	28	62	75
		9	7.5	17	36	80	85
		9 insulators in string	82	24	Did not flashover at 260 kv		
Pin type used on 12-kv lines. Catalogue rating: dry, 140 kv; wet, 80 kv	Calcium carbonate and magnesium carbonate and dirt. Very bad	1	28	41	56	83	75
		2	32	47	52	77	70
		3	24	35	63	93	65
		4	49	72	60	89	60

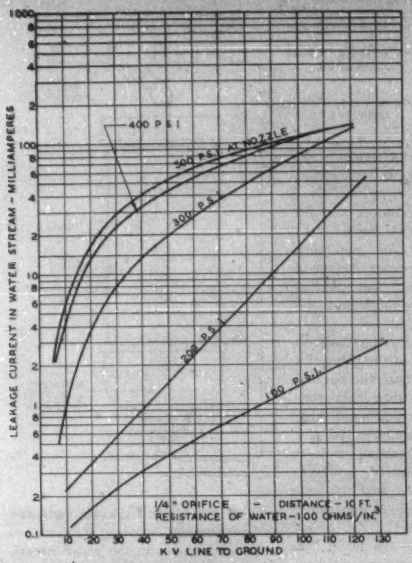

Figure 2. Leakage current through a stream of water at 10 feet for 100, 1,000, and 3,000 ohm water and various pressures

Figure 2 C (right)

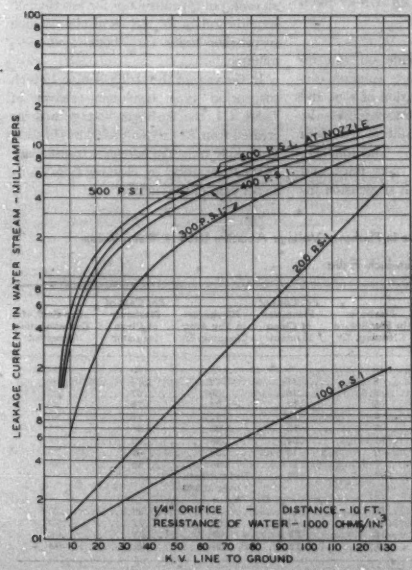

Figure 2 B

Figure 2 A

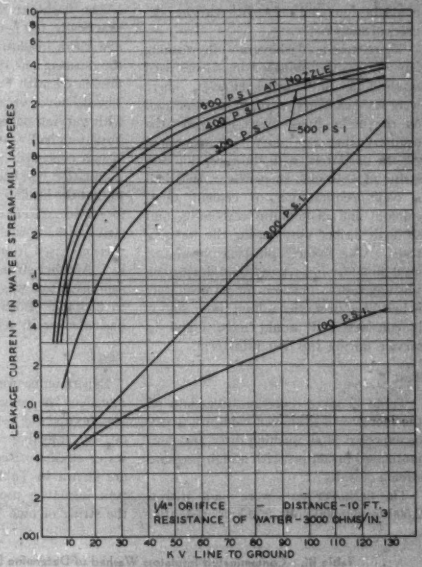

When using an abrasive in the water stream, it is necessary to keep the stream in motion at all times; for if it is allowed to play on an insulator in one spot for more than a few seconds, it will destroy the glaze.

The abrasive used in these tests was ground Monterey sand. Marble dust was tried but did not remove a sufficient amount of the contamination and packed in the injector.

The experimental injector used for the abrasive is shown in Figure 1. The abrasive is injected into the water stream by opening valve *B* which by-passes some of the water through the orifice at *C*. The velocity of the water through the orifice forces the abrasive into tube *D* and thus into the water stream. Larger quantities of the abrasive material can be forced in the water stream by closing valve *A* slightly which increases the differential pressure across the injector. A larger and more practical injector for use in the field could be made if found necessary.

The abrasive injector has not been tried out in the field and the test results are preliminary to a more thorough investigation. It has been demonstrated that a more thorough cleaning job may be accomplished with an abrasive in the stream of water on badly contaminated insulators.

It was found that the flashover voltage can be increased considerably if the contaminations which are hard to remove are broken up into smaller areas so that they do not present a continuous path over the insulator surface on which an arc can start. A good example is the case of the string of 11 special 12-inch suspension type insulators shown in Table II. These insulators had only 50 per cent of the surface cleaned yet the flashover voltage was nearly doubled.

Leakage Current Passing Through the Water Stream

Since the beginning of the electric power business it has been taught and instilled into the personnel in the power business never to come in contact with an energized power line even if the contact be no more positive than a stream of water. Because of this education for safety, playing a stream of water on a power line or washing energized insulators with a stream of water practically was unheard of until a few years ago.

The first tests conducted by the pacific Gas and Electric Company to determine the leakage current in a water stream were made in May 1941. This information was desired as it was intended to

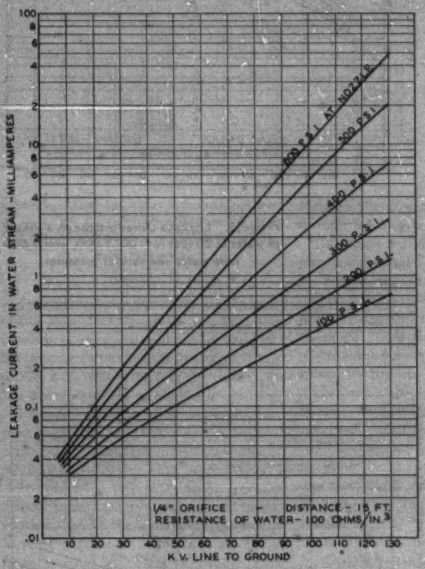

Figure 3 B

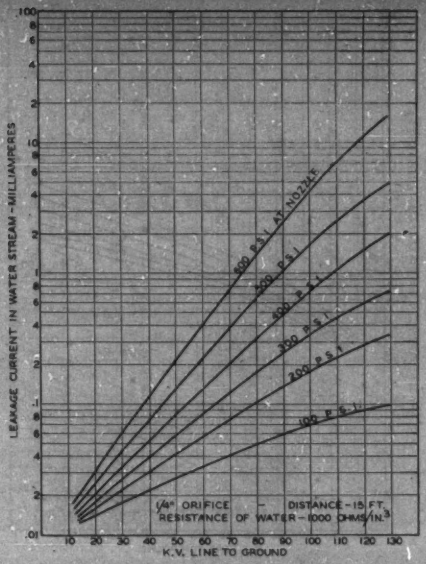

Figure 3 A (left)

Figure 3. Leakage currents through a stream of water at 15 feet for 100, 1,000, and 3,000 ohm water and various pressures

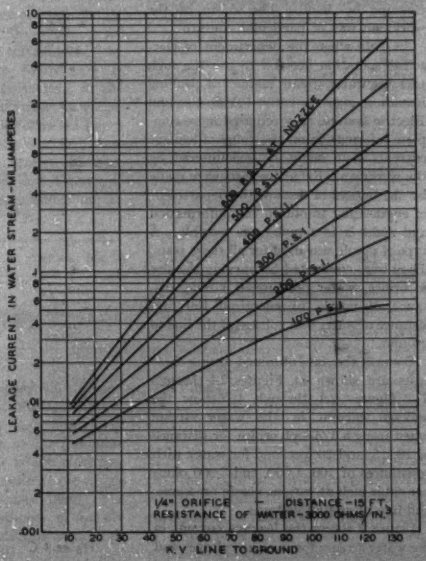

Figure 3 C

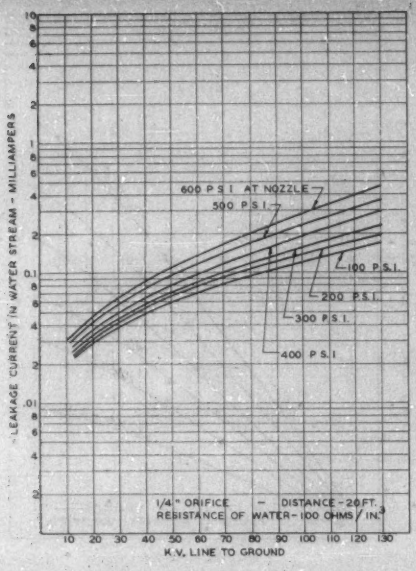

Figure 4 *A*

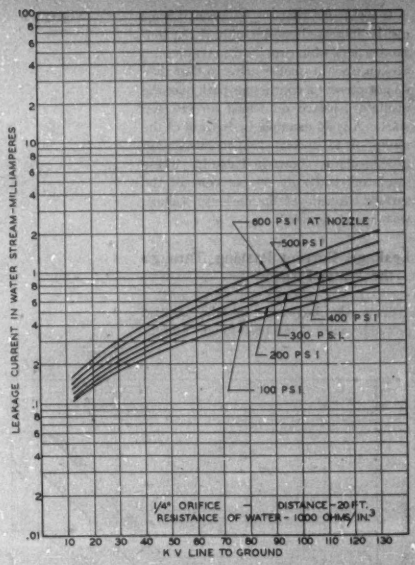

Figure 4 *B*

Figure 4. Leakage currents through a stream of water at 20 feet for 100, 1,000, and 3,000 ohm water and various pressures

clean energized insulators by washing with a stream of tap water in some locations where it was very difficult to de-energize the line or bus for wiping and cleaning by hand. The safety of the workman was of particular concern.

In 1944 when the department of electrical operation decided to use the high pressure water stream method of cleaning insulators over the entire Pacific Gas and Electric system, they required more complete information on the value of leakage currents that might be encountered by the workman. Extensive tests were made by the bureau of tests of the department of engineering to obtain this information and make it as complete as possible. A type *A* nozzle was used for all these tests. They were conducted by varying the size of orifice, water pressure at nozzle, distance of nozzle to energized line, resistance of water and voltage of the line to ground.

Some of the data obtained during these tests are shown in Figures 2*A* through 7. Figures 2*A* through 4*C* show the leakage current in the water stream when using a 1/4-inch orifice for distance of 10, 15, and 20 feet, and for water with resistances of 100, 1,000, and 3,000 ohms per cubic inch at various nozzle pressures, and line-to-ground voltages.

Figure 5 shows the leakage current in the water stream for various voltages and

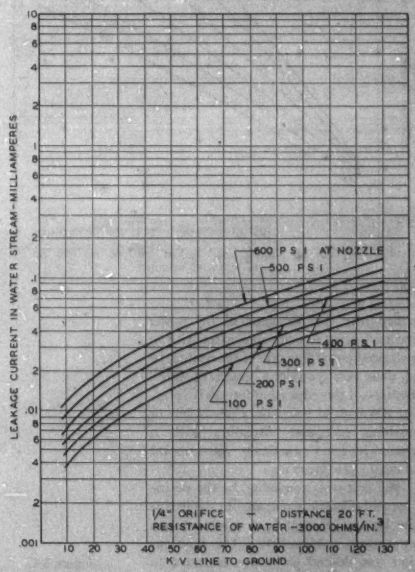

Figure 4 *C*

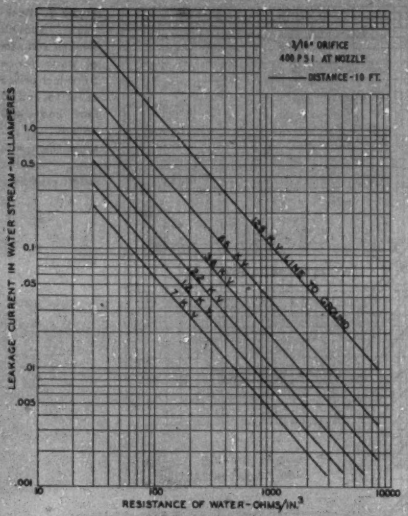

Figure 5. Leakage currents through a stream of water for a 3/16-inch orifice at 10 feet and 400 pounds per square inch with variable water resistance

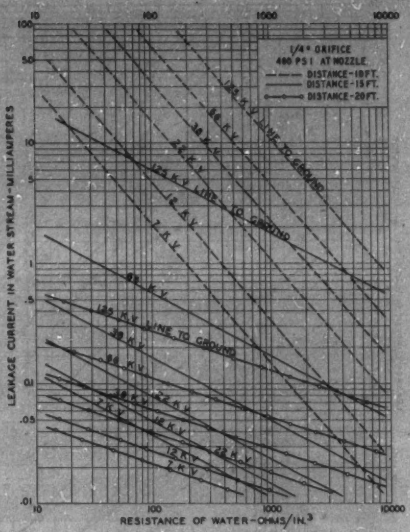

Figure 6. Leakage currents through a stream of water for a 1/4-inch orifice at 10, 15, and 20 feet and 400 pounds per square inch with variable water resistance

water resistances when using a 3/16-inch orifice at a distance of 10 feet with 400 pounds per square inch at the nozzle. For distances greater than 10 feet when using a 3/16-inch orifice the leakage current in the water stream is negligible.

Figures 6 and 7 show the same information when using a 1/4-inch or a 5/16-inch orifice except that the data for distances of 15 feet and 20 feet have been added.

It was observed that above certain critical pressures the stream would break into a spray and the leakage current would increase a relatively small amount for a large increase in nozzle pressure. This will be noted especially in the curves for short distances, such as 10 feet, and pressures of 400, 500, and 600 pounds per square inch at the nozzle.

The effect of water resistivity on the leakage current became less for a given voltage as the distance increased. This will be noted by referring to the curves in Figures 6 and 7. If the test setup had been carried out to 25 feet, 30 feet, and beyond, the curves would have become very nearly parallel to the abscissa. This would indicate that if the stream is broken up entirely into a spray, the current is carried from one drop of water to another as an electric charge, and not through the stream as a solid fluid conductor.

Grounded shielding was used over the nozzle and metal hose fitting for all setups to reduce the currents flowing in the circuit due to induced voltage. Corrections were made for these currents so that consistent data could be obtained for plotting the curves. In certain setups the induced currents were comparable or higher than the leakage current in the stream of water, but in all cases they were practically negligible insofar as the safety of the workman is concerned. The following gives the maximum currents obtained, due to induced voltages, at a distance of 10 feet from the hot terminal to the nozzle:

Voltage to Ground, Kv	Current, Ma
12	0.0045
20	0.012
40	0.030
70	0.045
125	0.065

To illustrate the use of the curves, assume that approximately 1.0 milliampere is the maximum leakage current that will be allowed to pass through the water stream, and assume the minimum resistance of the water is 500 ohms per cubic inch and the pressure at the nozzle is 400 pounds per square inch. The minimum working distances to be observed under these conditions would then be as shown in Table IV.

Table IV. Minimum Working Distances, Feet

Line Voltages, Kv—Grounded Y	1/16-In. Nozzle (See Figure 5)	1/8-In. Nozzle (See Figure 6)	5/16-In. Nozzle (See Figure 7)
12/7	6	9	12
23/12	7	10	14
44/25	8	11	15
66/38	9	12	16
110/66	10	13	17
220/127	12	16	20

One milliampere was selected for the reference current, as tests which have been conducted[1] indicate that the average man barely will feel one milliampere of current. This was verified by the writer while washing energized insulators. The length of the stream of water was shortened gradually by walking toward the "hot" line until a perceptible current was felt and the reading noted on a milliammeter.

The writer considers that it is very unlikely that any workman will get nearer than these minimum distances given while washing energized lines. The preceding paragraphs are based upon observations of insulator washing crews and from personal experience. If a workman should

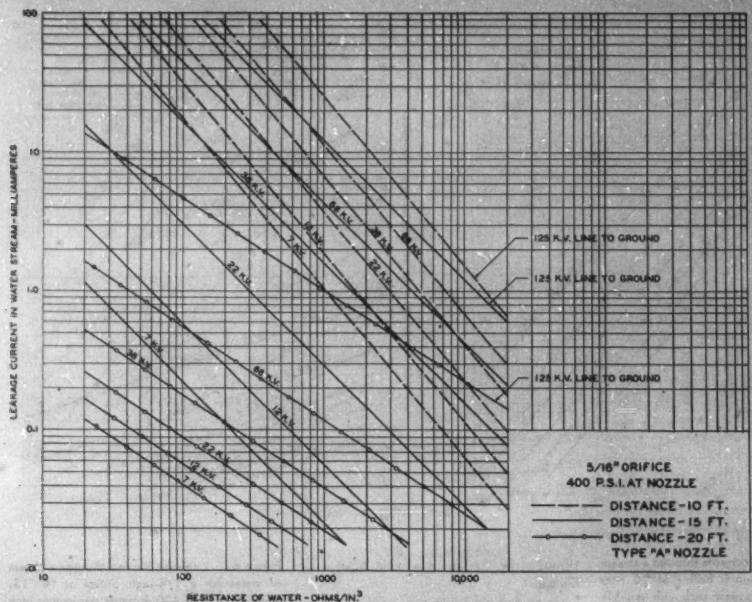

Figure 7. Leakage currents through a stream of water for a 5/16-inch orifice at 10, 15, and 20 feet and 400 pounds per square inch with water variable water resistance

inadvertently turn the stream of water on a hot line that was too close, and the current obtained was above the "let go"[1] value of 10 to 15 milliamperes, he automatically would break the continuity of the circuit by his muscular reaction moving the nozzle.

Tests on Various Manufactured Nozzles and on Experimental Nozzles

A 3-stage reciprocating pump having a capacity of 55 gallons per minute at 800 pounds per square inch was acquired when the insulator washing experiments were started. About 12 nozzles of various designs were obtained from manufacturers of fire fighting and tree spraying equipment and some from the testing plant fire apparatus.

The tests were conducted by setting up a board scaled in feet as the background, and taking pictures of the stream of water against this background for comparative observation. It was recognized at the start of the tests that visual observation and memory were entirely unsatisfactory as a basis of comparison. All the photographs were taken with the same exposure (one second) and on the same type of photographic film.

The photographs of the streams from some of the typical nozzles are shown to give a general idea of the results obtained from the various manufactured nozzles; see following table for identification.

Manufacturer	Diagram	Photograph
A	Figure 8*A*	Figure 9*A*
B	(Returned before dimensions recorded)	Figure 9*B*
C	Figure 8*B*	Figure 9*C*
D	Figure 8*C*	Figure 9*D*

None of the manufactured nozzles tested was found suitable for insulator washing as they evidently were designed for fire fighting or tree spraying equipment. The stream from the nozzle of manufacturer *A* shown as Figure 9*A*, was the most satisfactory of any tested. It was originally an adjustable nozzle used in tree spraying. The adjustable interior parts were removed and the housing and orifice used for insulator washing. The stream from the nozzle of manufacturer *B*, shown as Figure 9*B*, was the most unsatisfactory of any tested; it could almost be classed as a fog nozzle.

All the manufactured nozzles tested were made of a soft metal such as brass or bronze and some had cadmium or chromium plating on the interior. Visual

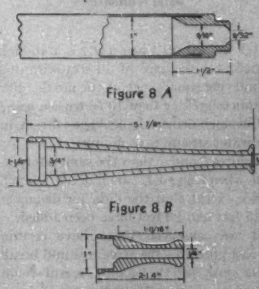

Figure 8. Drawings of representative manufactured nozzles tested

inspection of the various orifices showed that none had the polish necessary to create a satisfactory stream for insulator washing.

The ideal nozzle for insulator washing is one that projects a solid or compact stream of water for as great a distance as possible from the nozzle without breaking into a spray. The stream of water should strike the insulator with sufficient force to wash off the contamination. To give the stream sufficient energy to do this, the pressure at the nozzle should be of the

Figure 9A

Figure 9B

Figure 9C

Figure 9D

Figure 9. Streams of water obtained from representative manufactured nozzles tested

Figure 10A

Figure 10B

Figure 10. Streams of water obtained from the type *A* nozzle with and without straightening tubes

Figure 11A

Figure 11B

Figure 11. Streams of water obtained from the type *B* nozzle with and without straightening tubes

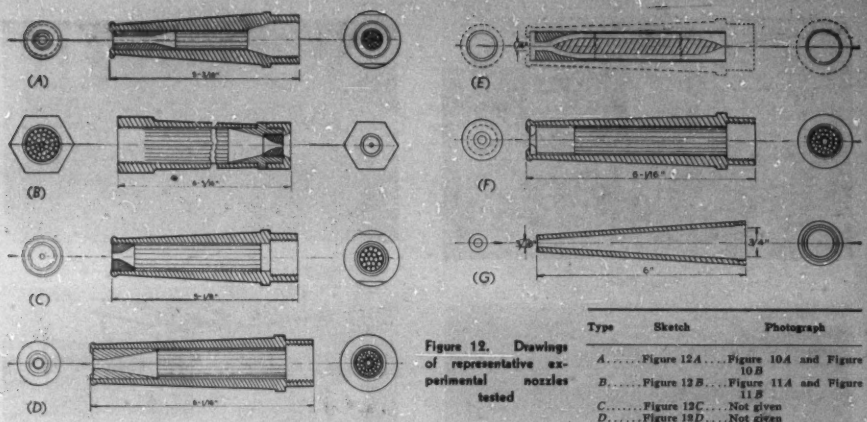

Figure 12. Drawings of representative experimental nozzles tested

Type	Sketch	Photograph
A	Figure 12*A*	Figure 10*A* and Figure 10*B*
B	Figure 12*B*	Figure 11*A* and Figure 11*B*
C	Figure 12*C*	Not given
D	Figure 12*D*	Not given
E	Figure 12*E*	Not given
F	Figure 12*F*	Not given
G	Figure 12*G*	Not given

order of 400 to 500 pounds per square inch or higher. The volume of water used should be a minimum so that a maximum number of insulators can be washed per tank of water. To conserve on water and still have enough energy in the water stream to do the work, the orifice should be as small as practical and still throw sufficient water for the washing job.

With this objective in view a study was then made to determine what data was available on nozzle design from the experiments of others.[2–7]

Due to lack of time our search may not have been complete but the most interesting and thorough data found were the experiments made on fire nozzles[2] by John R. Freeman, in the year 1888–89 for the Associated Factory Mutual Insurance Company.

A good fire nozzle was developed from these experiments. The final design suggested by Freeman, as the standard nozzle, has been in use up to the present with little or no change.

This design of nozzle was not suitable for insulator washing, as the water did not remain in a solid or compact stream for a sufficient distance from the nozzle to strike the insulator with enough force to remove the contamination. The nozzle was designed for maximum pressures of the order of 150 pounds per square inch and at higher pressures tended to spray.

The study indicated that there was very little information available for the design of a special insulator washing nozzle, so it was developed by experiment, utilizing some of the information obtained as a guide.

Several experimental nozzles were designed, built, and tested, and the following table gives the type, diagram number, and corresponding photograph of the stream of water obtained if one is appended.

Figure 13. Variation of water resistance with temperature

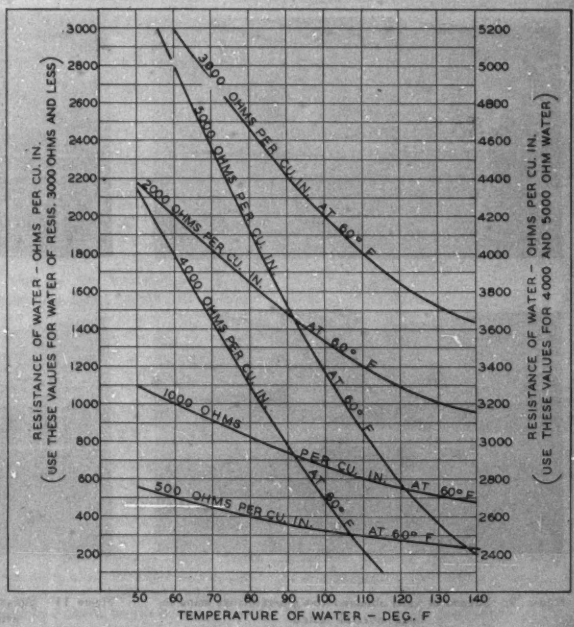

Referring to the sketches, one of the nozzles (Figure 12*G*) is a plain tapered tube, and one (Figure 12*E*) has a center member similar to a parabolic pointed needle in a parabolic shaped orifice. All of the other experimental nozzles have

Figure 14. Water resistance measuring instrument, front view. Lucite receptacle at right for water sample

a center cluster of small brass tubes used as straightening devices to take the turbulence out of the water as the orifice is approached.

All of the orifices in the nozzles were polished highly before testing, and observations made before and after polishing proved the importance of this operation in the shop.

It was found early in the tests that the straightening tubes improved the water stream in any design in which they were used. Reference to the views of the type *A* and *B* nozzle (Figures 10*A*, 10*B*, 11*A*, and 11*B*) show the improvement when the straightening tubes are used.

It was found also, early in the field experience and verified by tests, that the abrasive effect of foreign particles in some of the water used made it necessary for frequent polishing. In some locations a plain tapered orifice shown as Figure 8*B* and Figure 12*G*, that was made out of soft brass, would have to be polished at the end of each day of washing.

The orifices of the type *A*, *D*, *E*, and *F* nozzles (Figures 12*A*, *D*, *E*, and *F*) were made of stainless steel and polished. The orifices of the types *B* and *C* nozzles (Figures 12*B* and *C*) were cemented tungsten carbide wire drawing dies and also polished. These nozzles were used for one full insulator washing season and all had approximately the same service. They were returned then for visual inspection to determine the abrasive effect of sediment in the water. It was found that both types showed a slight amount of wear and after polishing could be used for another full season.

The reports of the men in the field and the measured diameter (from the pictures) of the compact part of the stream for a given distance from the nozzle was used as a basis for rating the nozzles. This gave the relative rating of the nozzles for washing insulators as seen in Table V. For comparison the relative rating of the manufactured nozzles are given also.

Figure 15. Interior view of water resistance measuring instrument

At the present time the Pacific Gas and Electric Company is equipping all the insulator washing trucks with the type *A* nozzles having orifices of various sizes to meet different washing conditions. The orifice is made of stainless steel. Tool steel also was tried but rusting would require frequent repolishing.

Table V. Relative Rating of Nozzles

500 Pounds Per Square Inch at Nozzle

Type of Nozzle	Reference Drawing	Diam. of Solid Water Stream 15 Feet From Nozzle, In.	Distance from Nozzle at Which Stream Shows Evidence of Spray, Feet	Relative Nozzle Rating for Washing Insulators, Per Cent
Type *A*	Figure 12*A*	1.84	4	100
Type *B*	Figure 12*B*	2.75	2	70
Type *C*	Figure 12*C*	2.75	2	70
Type *D*	Figure 12*D*	2.2	2½	80
Type *E*	Figure 12*E*	3.6	1	55
Type *F*	Figure 12*F*	3.0	2	65
Type *G*	Figure 12*G*	3.8	1	50
Manufacturer *A*	Figure 8*A*	3.3	1½	60
Manufacturer *B*	No drawing	No solid stream	0 (at nozzle)	20
Manufacturer *C*	Figure 8*B*	3.85	1	50
Manufacturer *D*	Figure 8*C*	3.85	1	50

Table VI. Minimum Usable Water Resistance

Insulator Type	Catalogue Ratings, Kv Wet	Catalogue Ratings, Kv Dry	Service Line to Line Kv	Test Kv, Line to Ground	Minimum Resistance of Water Before Flashover, Ohms Per In.	Recommended Minimum for Use in Field Ohms Per In.
Three part, pin type	125	170	66	38	600	900
Four part, pin type	140	180	66	38	320	475
Pin type	70	110	12	6.9	175	250
10-inch suspension type, four in string	200	265	66	38	150	225
10-inch suspension type, nine in string	430	535	110	69	200	300
Two large pedestal type in stack	290	330	110	69	300	450
Line post type	150	175	66	38	880	1,350

Effect of the Resistance of Water Used for Washing Energized Insulators

The conductivity of the water used for cleaning insulators with a high pressure stream is very important. If a water used has a resistance which is too low, it will cause a flashover of the insulator being cleaned. The resistance of water also varies with temperature; that is, as the temperature of the water increases, its resistance decreases.

In order to determine the minimum resistance of the water that can be used safely, a number of tests were made by washing energized insulators using waters of various conductivities.

Several representative types of insulators were used for these tests, and the tests were made using the approximate line to ground voltage of the circuit on which the insulators are normally used.

The test procedure was to reduce the resistance of the washing water, by the addition of sodium chloride, to a value low enough to cause a flashover of the insulator under test. Table VI gives the minimum resistance of water that can be used on various types of energized insulators that are clean and the recom-

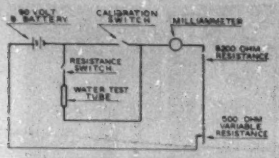

Figure 16. Wiring diagram of water resistance measuring instrument

mended minimum that should be used in the field making allowances for dirty insulators.

As more experience is obtained in the field the recommended minimum values of water resistance of Table VI may be revised.

Because of the fact that the resistance of water changes with temperature, it is very necessary to measure its resistance periodically, especially when it has been standing in a tank in the hot sun. The variations in water resistance with temperature are shown in Figure 13.

As an illustration, assume that 3-part pin-type insulators are being washed in a 66-kv line during a hot day. The resistance of the washing water used measured 1,000 ohms per cubic inch at 60 degrees Fahrenheit when taken from the main or well. During lunch hour the tank of water was left standing in the hot sun and its temperature increased to 80 degrees Fahrenheit. Referring to Figure 13, its temperature, if measured, now would be only 820 ohms per cubic inch instead of 1,000 showing that cognizance should be taken, by the washing crew, of this lower resistance. Several instances have occurred in the field where flash-

Table VII. Power Loss

Type of Insulator	Line Voltage, Kv	Voltage Applied Line to Ground, Kv	Power Loss, Watts—Heavy Fog Dirty	Clean
Pin type	12	6.9	9.0	2.5
Pin type	12	6.9	22.0	15.0
Pin type	12	6.0	51.0	9.7
Line post type	66	38.0	330.0	113.0
5 10-in. suspension	66	38.0	304.0	148.0
3-part pin type	66	38.0	506.0	194.0
4-part pin type	66	38.0	292.0	69.0
9 10-in. suspension	110	63.0	274.0	180.0
14 10-in. suspension	220	125.0	542.0	288.0

Figure 17. *A* (left) and *B* (right). Typical washing equipment used by the Pacific Gas and Electric Company

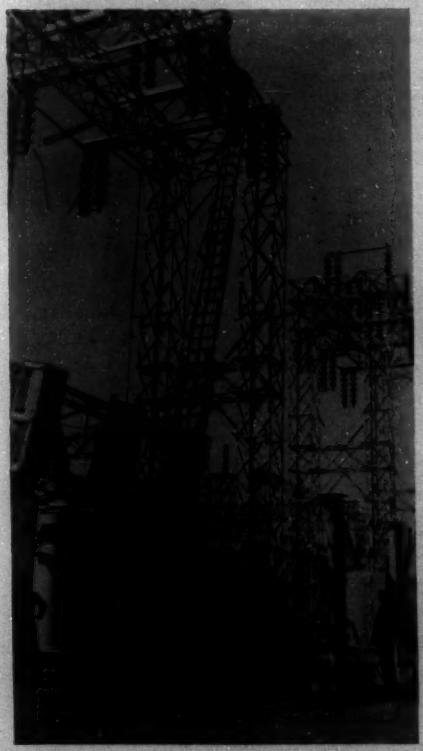

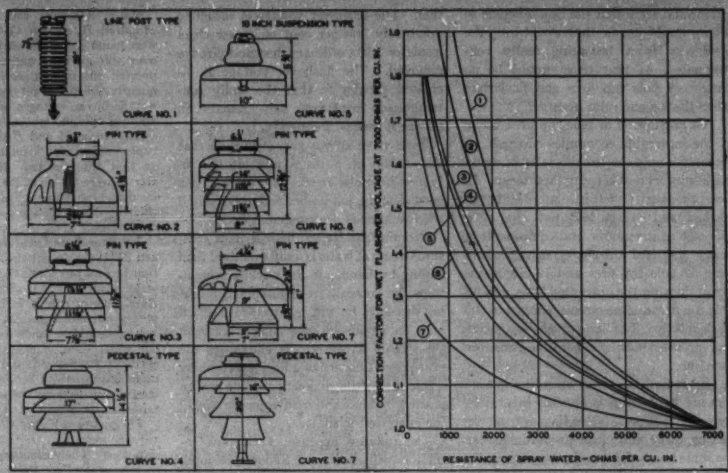

Figure 15. Correction factors for wet flashover voltage at 7,000 ohms per cubic inch for various water resistances and types of insulator

overs have been traced directly to the use of water of too low resistance.

Water Resistance Tester

An instrument to measure the resistance of the water is required, as it is very important that the washing crews know the resistance of the water before using it to clean energized insulators.

Inquiries indicated that there were no instruments available on the market which were simple to use and would show the resistance of the water directly without intermediate calculations. To meet this requirement water resistance testers were designed and built[8] at the bureau of tests of the Pacific Gas and Electric Company.

The instrument is designed on the same principal as the ohmmeter but uses a higher voltage to reduce errors due to polarization. The instrument is scaled to read the resistance of the water sample directly in ohms per inch cubed. A photograph of the water resistance tester is shown in Figures 14 and 15, and a schematic wiring diagram of the circuit of the instrument is shown in Figure 16.

To measure the resistance of water, a sample is placed in the water test tube which is shown below the calibration adjuster in Figure 14. The zero of the instrument then is adjusted by depressing the calibration switch and turning the calibration and adjuster until the instrument reads zero. The resistance switch then is pressed, and the instrument will read the resistance of the water being tested directly in ohms per inch cubed.

One of these instruments is supplied on each washing truck so that the crew always can measure the resistance of the water in order to be sure that its resistance is above the minimum allowed before using it for cleaning energized insulators.

Measurements to date show resistances of the water used in the various territories served by the Pacific Gas and Electric Company varied from 180 to 10,000 ohms per cubic inch. It is possible a wider range of resistance may be found. The aforementioned values show how important it is to check the water in use.

Operating Economics Effected by Washing With a High Pressure Stream of Water

There recently has been a symposium composed of contributions from power companies (including the Pacific Gas and Electric Company) on the subject of cleaning energized and unenergized insulators by various methods. These contributions were published[9] in a booklet and have been of considerable assistance in carrying out these tests and developments.

It was noted that the question of determining the washing schedule was an important one brought out by several of the contributors. This is a very difficult question to answer as it depends on so many factors, such as

1. Kind of contamination.
2. Seasonal weather conditions.
3. Type of insulators and so forth.

One method used by the Pacific Gas and Electric Company to determine the washing schedule was to hang several pilot insulators in the areas and bring insulators in for periodical wet flashover tests. The washing schedule then is set up which gives a flashover with a safety factor above line to ground potential.

Table VIII. Cost Comparison

Report	Voltage of Line, Kv	Equipment Washed	Number of Insulators Washed	Total Costs: High Pressure Water	Total Costs: Other Methods	Savings
A	12 and 66	19 small substations	?	$190.00	$2,062.00	$1,872.00
B	12 and 66	12 small substations	?	229.00	777.00	548.00
C	12 and 66	9 substations 5 66-kv lines	?	1,057.00	4,840.00	3,783.00
D	12, 66, and 110	4 substations 4 lines	?	711.00	3,365.00	2,654.00
E	12, 22, and 66	2,246 poles	17,441	2,825.00	8,505.00	5,680.00
F	12, 70, and 110	260 poles	5,796	375.00	1,665.00	1,290.00
G	12, 22, and 66	6,387 poles	53,000	7,538.00	Estimated 2 to 3 times washing	Estimated ⅓ to ⅔ of wiping

It would seem that the best schedule to set up would be one that would keep the insulators from becoming badly contaminated, so that there would be no danger of pole top fires and flashovers when the fog and rains occurred.

The prevention of pole top fires is one of the intangible economies effected. A recent example showed the value of washing insulators and keeping them clean. In a certain district some insulators had been washed and others had not, due to a shortage of manpower and equipment; a heavy fog and drizzle occurred; there were 57 pole top fires and 12 circuit interruptions on the unwashed lines, and no pole top fires and no circuit outages on the washed lines. The line voltage, insulators and circuit conditions were the same for each line.

The saving in power when line insulators are kept clean is another intangible economy effected. Readings of power loss on dirty and clean insulators under the same heavy fog conditions were made. Table VII gives some of the results obtained.

A very tangible economy may be found when a comparison is made between the cost of cleaning insulators by the high pressure water stream method and the dry wiping method. Table VII shows some costs taken at random from reports of various divisions.

Photographs of the typical washing equipment used by the Pacific Gas and Electric Company are shown as Figures 17*A* and *B*. As a general rule the pumps have a capacity of 55 gallons per minute at 800 pounds per square inch.

Summary

The tests definitely have shown and subsequent field experience have demonstrated that the high pressure water stream method of cleaning insulators is both practical and more economical than other methods used. It presents one of the best opportunities for the reduction of the maintenance cost on transmission and distribution lines.

A high pressure compact and solid water stream will remove practically 100 per cent of ordinary dust and dirt and from 50 to 85 per cent of bad contamination. The flashover voltage is raised to practically 100 per cent of a new clean insulator when ordinary dust and dirt are removed. The flashover voltage is increased enough so that the badly contaminated insulators may remain in service if washed frequently.

Tests have shown very definitely that the stream of water should hit the insulator before it breaks into a spray if a good cleaning job is obtained, especially if the insulator is contaminated badly.

Cleaning insulators with a high pressure stream of water is a safer method than wiping by hand. If the workman maintains the generally recognized safe working distance, he will not receive a shock or a dangerous leakage current through the stream of water. It eliminates the ever present hazard of a lineman climbing a pole supporting an energized line and an unenergized line and inadvertently wiping the energized insulators.

The reduced expense of cleaning insulators will allow more frequent cleaning and will eliminate to a very great extent pole top fires.

Cleaning the insulators with a high pressure stream of water instead of climbing poles and wiping by hand reduces to a minimum a very obnoxious job insofar as the workman is concerned, which in turn aids employee-management relationship.

A set of well built and highly polished nozzles of various sizes is essential for a successful insulator washing program. Although relatively an inexpensive part of the apparatus, it is very important; and further work should be done to improve the nozzles at the higher pressures.

Appendix

Correction Factors for Wet Flashover Voltage at 7,000 Ohms Per Cubic Inch for Various Water Resistances and Types of Insulators

During the experimental work on washing energized insulators it was brought to our attention, by analysis of test data, that two insulators of different designs, having the same wet flashover value when using 7,000-ohm water, would have entirely different wet flashover values with a water having some other value of resistance.

When reference was made to AIEE Standard 41, section 41–600 (1930) curves were found giving the variation of wet flashover voltage with water resistance. It is pointed out in this section that it is frequently difficult to get consistent results for wet flashover voltages when the tests are made in different laboratories.

The curves *A* and *B* shown are only for typical suspension insulators manufactured at that time in two different countries. Curves were not given for various designs of insulators, so it may be assumed that it was thought the correction factors would apply to all types.

The later Standard 41*A* (1941) and Standard 29 (1941) do not show curves of correction factors but state the resistance of the water shall be 7,000 ohms per inch cube. As a general rule it is not convenient to obtain water of a specific resistance so correction should be made for the resistance of the water used, if results of a reasonable accuracy are desired, and if it is desired to make a comparison between various manufacturers catalogue values and data obtained in the field.

The curves of Figure 18 were obtained for various insulators and various water resistances. The correction factors are given to correct for wet flashover at the AIEE standard of 7,000 ohms per inch cube. These curves are given for the information and convenience of anyone desiring to use them while performing wet flashover tests on the types of insulators shown.

The wet flashover tests were made according to the AIEE Standards. The under surfaces of the insulators were wetted thoroughly before the voltage was applied, but an appreciable variation in wet flashover voltage was experienced as it was difficult to keep all physical variables constant.

References

1. Electric Shock. **Charles F. Dalziel, J. B. Lagen, J. L. Thurston.** AIEE Transactions, volume 60, 1941, pages 1073–8.

2. Experiments Relating to the Hydraulics of Fire Streams. **John R. Freeman.** *Transactions*, American Society of Civil Engineers (New York, N. Y.), volume 21, 1889.

3. Hydraulics. **Hughes, Safford.**

4. Hydraulics. **Mansfield Merriman.**

5. **Crosby, Fisk, Forster.** *Handbook of Fire Protection*, National Fire Protection Association, Boston, Mass.

6. Hydraulics (book). **H. P. Hammond.** International Text Book Company.

7. Characteristics of Fire Jets. **J. S. Blair.** Institution of Civil Engineers (London, England), volume 16, 1941.

8. Wash, Water Tests Prevents Flashovers. **G. L. Hill.** *Electrical World* (New York, N. Y.), May 24, 1947.

9. Methods Employed in Cleaning Insulators. *O. B. Hi-Tension News*, Ohio Brass Company, Mansfield, Ohio. Issue of August 1944 to February 1945.

No Discussion

Submarine Detection by Sonar

A. C. KELLER
NONMEMBER AIEE

SONAR, the only effective method of detecting completely submerged submarines was a major factor in the defeat of the *U*-boat and the winning of the Battle of the Atlantic. A majority of the 996 enemy submarines sunk during World War II was detected and located by sonar. The word sonar is formed from the phrase SOund Navigation And Ranging and applies broadly to under water sound devices for listening, echo ranging, and locating obstacles.

The *QJA* sonar system, one of those which got into active service during World War II, is described here. This equipment was designed by Bell Telephone Laboratories and manufactured by the Western Electric Company. It consists of electronic control and indicating equipment (Figure 1) associated with a retracting mechanism (Figure 2) which houses the transducer (Figure 3) (supersonic transmitter-receiver) inside of the streamlined dome (Figure 4) designed to reduce turbulence at ship operating speeds. The transducer makes use of *ADP* (ammonium dihydrogen phosphate) synthetic piezoelectric crystals which are capable of handling high power at high efficiency.

For echo ranging, a short pulse of supersonic sound usually about 25 kc is transmitted into the water by the transducer as a highly directional beam. Immediately after a short pulse of sound is transmitted, the electric system is transferred to a receiving condition and the transducer then acts as a hydrophone to pick up supersonic signals, in particular, a reflected portion of the outgoing signal from an enemy submarine as indicated in Figure 5. The received energy is amplified and converted into both visual and audible indications. The time required for the pulse to travel to the submarine and return is a measure of the range. The target range is indicated automatically by two types of visual indicators. One of these shows the range on a calibrated circular scale as a flash of light. The other is a cathode ray oscilloscope on which the range is indicated by the distance a spot has moved from its starting point. The oscilloscope is part of a *BDI* (bearing deviation indicator) unit and also shows, by a suitable deflection of the spot, whether the target is to the right or left of the transducer bearing.

In addition to echo ranging, the equipment is also used for sound listening to provide means for determining the bearing of any source of noise or signals within the frequency range of the equipment. A trained operator, by listening, can estimate the type, size and speed of the sound source. Used for telegraph communication under water, the equipment permits communication with near-by vessels provided with suitable equipment.

As shown in Figure 6, the electronic, control, and indicating equipments are mounted on or near the bridge and the retracting mechanism containing the transducer and dome is mounted in a sound room below decks.

The major units contained in the control rack of Figure 1 are as follows:

1. Receiver and driver oscillator.
2. Driver amplifier.
3. Indicator and control unit.
4. Bearing deviation indicator.
5. Training control amplifier.

In addition to these, directly associated with the control rack are a loudspeaker, a head telephone set, a hand telegraph key, and a push-button switch for the raising or lowering of the dome containing the transducer.

Some of the principal features of the *QJA* equipment are as follows:

1. Unicontrol of frequency of transmitted signal and receiver tuning.
2. *TVG* feature (time variation of gain control).
3. *ADP* crystal transducer with broad band feature.
4. A sound transparent stainless steel dome.
5. Sweep frequency signaling pulse as well as constant frequency pulse.
6. Sealed plug-in type relays for controlling transmitted pulse and switching to receiving condition.
7. Commutator-type transmitter for training control of transducer.
8. Beat frequency control of received audio signal.
9. Audio band width selectivity.
10. *MTB* (maintenance of true bearing).
11. Optional hand wheel or push button control of transducer bearing.
12. Elimination of limit controls on transducer bearing mechanism by use of a rotary contactor.

Theory of Operation

The theory of operation of the *QJA* equipment is shown in schematic form in Figures 7 and 8. These schematic drawings are single line type in order to represent the transmission path and so simplify the diagrams.

Figure 7 shows a schematic diagram of the frequencies employed in the transmitting circuit during the generation and sending of a pulse into the water without the use of the so-called sweep frequency feature.

A frequency of 150 kc is generated by tube *V*-110 and is amplified by tube *V*-109. Relay *K*-101 in the receiver and driver oscillator unit and relay *K*-2901 in the bearing deviation indicator unit are

Paper 47-182, recommended by the AIEE committee on communication for presentation at the AIEE Pacific general meeting, San Diego, Calif., August 26–29, 1947. Manuscript submitted June 18, 1947; made available for printing July 11, 1947.

A. C. Keller is switching apparatus engineer at the Bell Telephone Laboratories, Inc., New York, N. Y.

In addition to the co-operation of the large number of Bell Telephone Laboratories personnel who were engaged in the development, design, and preparation for manufacture of Navy sonar equipment, the author wishes to express appreciation for the fine co-operation received from other groups, particularly from members of the Bureau of Ships of the United States Navy Department, the Naval Research Laboratory, the National Defense Research Committee, and the Western Electric Company for the production of sonar equipment.

operated momentarily to transmit the pulse. The relays are under control of the keying mechanism in the indicator and control unit (not shown in Figure 7). The amplified 150 kc is impressed on the varistor modulator *CR*-101. Tube *V*-107 is a variable frequency oscillator which generates any frequency from 160 to 180 kc. The variable capacitor for controlling the frequency of oscillation is ganged with another variable capacitor in the tuned input circuit of the receiver which has a tuning range from 10 to 30 kc. The circuit is so arranged that tube *V*-107 oscillates at a frequency which is always 150 kc higher than the input tuning. The tuning dial is scaled to correspond with the input tuning, that is, 10 to 30 kc. Accordingly, for a given setting of the tuning dial, tube *V*-107 oscillates at a frequency which is 150 kc higher than the dial setting. For example, if the tuning dial is set at 24 kc, tube *V*-107 will be tuned to oscillate at 174 kc. The output of the oscillator tube *V*-107 is amplified by tube *V*-108 and is impressed on the varistor modulator *CR*-101.

The varistor modulator *CR*-101 modulates the two frequencies impressed upon it, namely 150 kc, and for the example chosen 174 kc, and produces the difference frequency 24 kc. It should be noted that the output of the modulator *CR*-101 has the same frequency as the setting of the tuning dial.

The output frequency of the varistor modulator which is a short pulse, in this case of 24 kc, is amplified by the driver amplifier and is then transmitted to the transducer.

Figure 8 shows a schematic diagram of the frequencies employed in the receiving circuit during the reception of an echo with the sweep frequency control in the "off" position. Again assuming that the echo which strikes the two halves of the transducer is a frequency of 24 kc, the instrument transforms this sound wave into electric energy of the same frequency. The current generated flows to the *BDI* unit through the back contacts of relay *K*-2901 to the input modulator *CR*-2901. A 225-cycle-per-second frequency is also applied to the modulator which in effect connects the receiver input to either half of the transducer alternately at a 225-cycle rate. The modulator output then consists of the carrier frequency, 24 kc, and the two side bands 23.775 kc and 24.255 kc, all of which are applied to the input of the receiver and driver oscillator unit.

The input of the receiver is a tuned circuit which can be adjusted to any frequency from 10 to 30 kc under control of

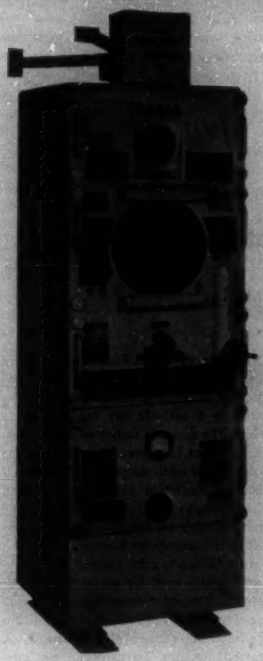

Figure 1. *QJA* control equipment rack

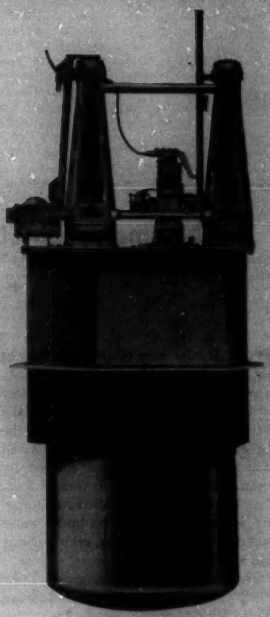

Figure 2. Retracting gear

the main tuning dial. With the tuning dial set at the same frequency as during the transmission of the pulse, in this case 24 kc, the received signal is modulated by the 225 cycles of the input modulator and the resulting frequencies are amplified by tube *V*-101 and then impressed on modulator tube *V*-102.

Tube *V*-107 is the same variable frequency oscillator used in the generation of the transmitted pulse and since the tuning dial has been assumed to be set at 24 kc, tube *V*-107 oscillates at a frequency of 174 kc, which is impressed on the modulator tube *V*-102. The modulator tube modulates the frequencies impressed upon it, namely, in this example 23.775, 24, 24.225, and 174 kc and produces the difference frequencies of 149.-775, 150 and 150.225 kc so that the output of the modulator tube will be near 150 kc for any setting of the tuning dial. These frequencies are amplified by tube *V*-103 and are impressed on tube *V*-104 which is a combined modulator and oscillator tube. One-half of the tube *V*-104 oscillates at a frequency between 150 and 151.6 kc as determined by the setting of the beat frequency oscillator which has a scale graduated from 0 to 1.6 kc. This oscillator generates a frequency which is 150 kc higher than the scale reading on the beat frequency dial. Accordingly, when this dial is set at 0.8 kc, the oscillator generates 150.8 kc. This frequency and the three frequencies received from tube *V*-103 are modulated in the other half of tube *V*-104 to produce the difference frequencies of 0.575, 0.800, and 1.025 kc. It will be noted that the scale on the beat frequency dial indicates the average output frequency of tube *V*-104.

The output of tube *V*-104 is connected to a band width switch which has three positions, namely, peak, band, and flat corresponding to about 100, 300, and 1,200 cycles, respectively. In any one of the switch positions, 800 cycles passes freely through the circuit.

For the example chosen, 575, 800, and 1,025 cycles are amplified by tube *V*-105 and are then transmitted to the *BDI* unit, to the phone jacks, and the loudspeaker. The *BDI* unit amplifies and then demodulates the three frequencies into a

225-cycle envelope which is compared to a reference 225 cycles supplied by the 225 cycle oscillator. This comparison is made in an amplitude and polarity sensitive conjugate rectifier, the output of which is a potential which is positive or negative depending on whether the transducer is trained to the left or right of the target. The spot on the cathode ray tube is deflected horizontally to the left or right depending on the polarity of the d-c output of the conjugate rectifier. A sweep circuit which moves the spot vertically at the same time indicates the approximate range of the target.

The 575-, 800-, and 1,025-cycle signal is also amplified by tube *V*-106 and is then connected to the neon lamp on the revolving disk in the indicator and control unit. This pulse of frequencies gives a short flash of the neon lamp. The position of the neon lamp at the instant of flash with respect to the fixed circular scale indicates the range in yards of the target which produced the echo.

A sweep frequency feature is provided in the equipment which is distinct in character and accordingly more easily identified under some conditions, especially for weak echos and in the presence of high noise levels. For this case, as shown in Figure 7, tube *V*-110 generates a frequency which begins at 150.4 kc when relays *K*-101 and *K*-2901 are operated and sweeps downward to 148.8 kc when the relays are released. Accordingly, the frequency of the pulse decreases 1,600 cycles during a period of about 150 milliseconds. In receiving a sweep frequency type signal, the tuning is broad enough to pass the sweep frequency which is a 1.6-kc band, 400 cycles below, to 1,200 cycles above the setting of the tuning dial.

As can be seen in Figure 8, the equipment is useful for listening for propellor and machinery noise generated by distant vessels. An experienced listener may be able to identify the type of vessel which creates the noise by its quality or character. When this feature is used, the pulse initiation circuit is disabled and the equipment is always in the listening position as in receiving echos during echo ranging. The strongest noise signal is generated when the transducer is aimed directly at the source of noise so that this bearing of the transducer shows the bearing of the source of noise but does not give an indication of the range. The equipment is responsive to frequencies in the 10 to 30-kc band and the strongest component in this band can be determined by sweeping the tuning dial through this range.

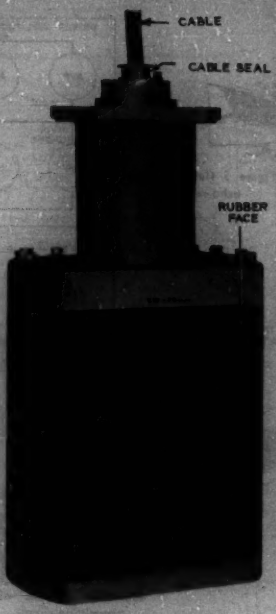

Figure 3. Transducer

Figure 4. Dome

Transducer

The transducer makes use of 45-degree *Z*-cut *ADP* synthetic piezoelectric crystals.[1] It is used for both transmitting and receiving and is highly efficient over a range of frequencies. When used in transmitting, it translates electric pulses into corresponding supersonic pulses into the water in a beam pattern with the highest intensity perpendicular to the crystal face shown in Figure 9. As a sound pickup device or hydrophone, it receives echos or reflections of the transmitted sound pulses and converts them to electric impulses for transmission to the receiver amplifier. The wide frequency range makes possible a choice of frequency which is not only useful in connection with simultaneous operation of equipment by several ships in the same area but also permits a degree of control over the directivity. The transducer is more directive at the higher frequencies, because of its larger size in terms of wavelength at those frequencies.

The design of the transducer determines in an important way the major characteristics of several of the other units of an echo ranging system. For example, the efficiency of the transducer in producing underwater sound of sufficient intensity determines the size of the power amplifier required. Also the frequency range of the transducer directly specifies one of the important characteristics of the receiver unit. The physical size and shape of the transducer also determine the size and weight of the streamlined dome and the associated retracting mechanism. For these reasons, considerable attention was given to the design of the transducer.

It was known that a beam width of about 20 degrees was required at points 10 decibels below maximum response in order to provide good operating characteristics. Calculations indicated that such a beam width could be obtained by a vibrating array of about 10 inches in diameter. This diameter was considerably smaller than transducers having similar directivity characteristics which were in use at the time transducers for the *QBF*[*] and *QJA* were being designed. Experimental work demonstrated the feasibility of obtaining these beam patterns with the small size in accordance with theory. Older designs which were examined, particularly of the magnetostriction type, required larger diameters for the same beam width because of the deflection characteristic of the diaphragm to which the actuating units were fastened. As a result of the diaphragm action, piston-like motion was not achieved so that the effective area was considerably less than

[*] The *QBF* equipment was designed prior to the *QJA* equipment and uses a similar transducer with 45-degree *Y*-cut Rochelle salt crystals.

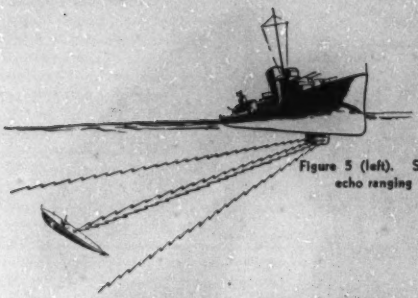

Figure 5 (left). Sonar echo ranging

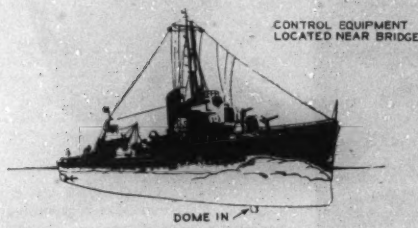

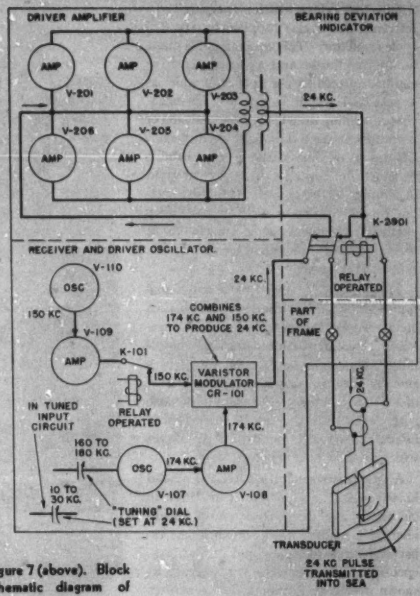

Figure 7 (above). Block schematic diagram of transmitting circuit

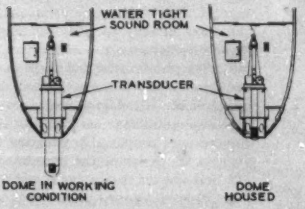

Figure 6. Outline of sonar equipment in ship

the real area of these earlier transducers.

As can be seen in Figure 9, the crystal array was provided with lobe suppression which is accomplished by grading the amplitude of motion of the crystals into two parts. The center and thinner crystals operate at an amplitude twice that of the outer crystals which are twice the thickness of the inner crystals. Electrically all of the crystals in each half of the transducer are connected in parallel so that the potential gradient across the thin crystals is twice that of the others. If all of the crystals were of the same size and therefore vibrated with the same amplitude to give a piston action over the entire crystal array, the first side lobes, as can be shown by calculation, are 13.5 decibels below the maximum response. In contrast, by grading the amplitude as shown in the array of Figure 9, the first side lobes can be suppressed to be better than 20 decibels below the main beam with only a slight increase in the width of the main lobe. The crystal array as shown in Figure 9 is about $10^1/_2$ inches on a side and gives the beam pattern shown in Figure 10.

The crystals are mounted in groups of about one inch square on one face of the steel base plate directly opposite steel resonators on the other face. These combinations provide efficient 1/2-wavelength units with a nodal point at the supporting base plate. The crystal groups are connected electrically into halves about a vertical line and each half is connected to the high side of a transformer; the low sides of the transformers provide impedance matches to the driver amplifier and receiver amplifier circuits. These transformers are mounted within the transducer case. The contacts between the crystals and their electrodes are gold to gold. Gold is evaporated on the crystals and gold plated metal foil is later attached to the prepared crystals. This combination provides very low interface electrical resistance and consequently minimizes heating at this point during the transmission of the high power outgoing pulse.

The crystal array and resonator plate assembly are supported in rubber mountings inside a steel case. A rubber closure essentially sound transparent is vulcanized to the steel case, forming the front face. The case is sealed by a rubber gasketed steel cover which also serves to house the matching transformers within the cylindrical section. A sound absorbent baffle consisting of alternate layers of 100-mesh wire cloth and expanded metal is fastened to the inside of the case directly back of the steel resonators. The function of this sound absorbent baffle is to attenuate signals through the back of the transducer and also to reduce reflections within the case. The transducer assembly is supported by a flange at the top of the cover casting which is attached to the vertical training shaft of the retracting gear. The transducer can be rotated within a cylindrical space 12 inches in diameter. The entire transducer weighs about 200 pounds.

The inside of the transducer is vacuum-filled with electrical grade castor oil from

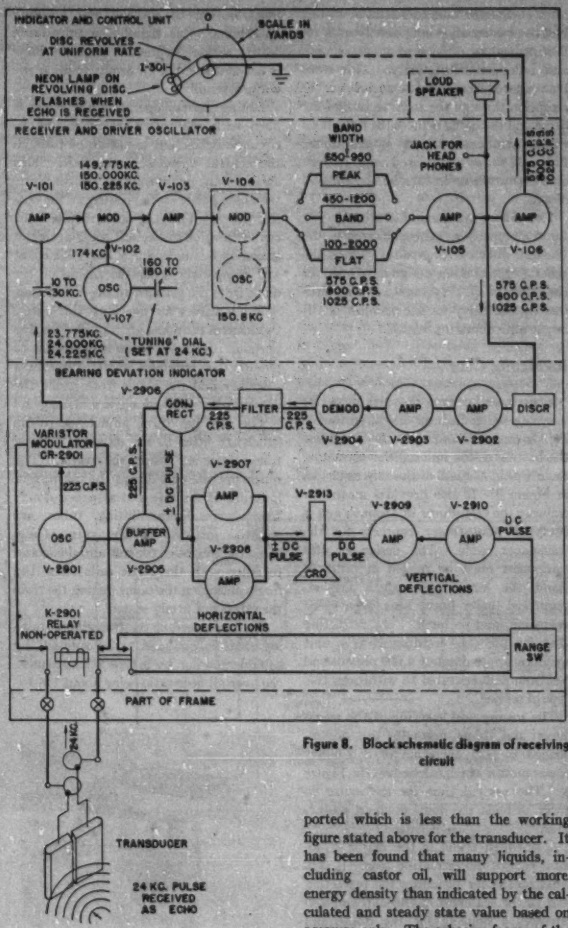

Figure 8. Block schematic diagram of receiving circuit

which air and water vapor have been removed by evacuation. The crystal array has an effective area of about 200 square centimeters so that with an electric power input of the order of 100 to 150 watts, it corresponds to at least 0.5 watt per square centimeter of crystal area. Because the conversion efficiency of the crystals is nearly perfect, most of this power is converted into acoustic energy. If the transducer is operated near the surface of the sea, which corresponds to atmospheric pressure, an energy density of one-third watt per square centimeter can be supported which is less than the working figure stated above for the transducer. It has been found that many liquids, including castor oil, will support more energy density than indicated by the calculated and steady state value based on pressure only. The cohesive forces of the liquid and the duration of the applied energy both have an effect on cavitation and therefore on energy density.

The earlier *QBF* system made use of a similar transducer using 45-degree *Y*-cut Rochelle salt crystals rather than 45-degree *Z*-cut *ADP* crystals. In this design it was found essential to provide thermistor protection for the transducer in order to avoid overheating of the crystals with subsequent electrical breakdown. In the *QBF* transducer design the thermistor was designed so that no appreciable reduction in output was observed for normal pulse lengths and pulse rates but prolonged application of power to the transducer automatically cut the input level. For prolonged application of full power to the Rochelle salt transducers, temperature of the crystals was found to rise and this in turn drove the water of crystallization of the Rochelle salt crystals to the crystal edges across which the operating voltage was applied. This marked reduction in leakage resistance causes a substantial increase in current with corresponding heating and melting and breakdown of the crystals under these conditions. In contrast to the Rochelle-salt design, the *ADP* crystal transducers will carry full power indefinitely without deterioration and without the protecting thermistor.

Streamlined Dome

Having determined that a satisfactory transducer could be designed rotatable in a cylindrical space 12 inches in diameter, it was then necessary to design a streamlined dome to surround the transducer, no wider than necessary, but sufficiently large to provide ample clearance for the rotating transducer. In co-operation with the United States Navy David Taylor Model Basin, a dome shape was worked out, of streamlined form, having a length of 50 inches and a maximum width of 16 inches, the maximum width being based on the transducer diameter together with suitable clearances, dome wall thickness, and so forth. The length-to-width ratio of the dome shape was selected to reduce self-noise and turbulence to a minimum at ship operating speeds. Figure 4 shows the dome which was designed for the *QBF* and the *QJA* systems. The body of the dome consists of a 1/8-inch stainless steel shell with straight vertical sides and the streamlined cross section. The front part of the lower portion of the dome is provided with a corrosion resistant steel window about 0.018 inch thick, reinforced internally by a stainless steel expanded metal web welded to the body of the dome and to the window at each intersection of expanded metal. The window is essentially sound transparent and permits transmission and reception of supersonic signals through an angle of about 135 degrees to the right and left of the major axis of the dome.

The development of this type of sound transparent window was the result of the investigation of many types of materials and constructions including plastics, impregnated wood, reinforced rubber. The window design, of thin stainless steel and expanded metal, causes less than a 1 decibel attenuation of the sound energy

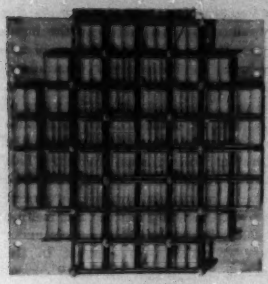

Figure 9. Crystal array

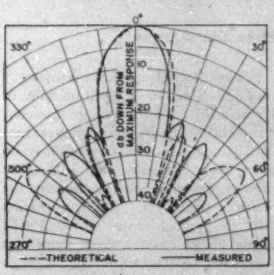

Figure 10. Transducer beam patterns

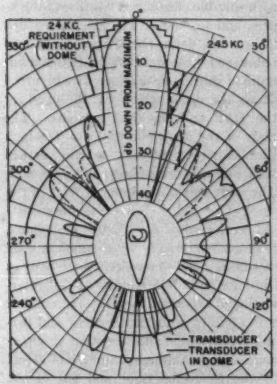

Figure 11. Transducer beam patterns with and without dome

over the frequency range of 10 to 30 kc of the equipment and also minimizes reflections inside the dome.

As can be seen from Figure 4, a stainless steel bulkhead is provided near the after end of the dome. Fastened to this bulkhead is an absorbing panel and a reflecting pad to provide sound absorption and reflection respectively. This combination reduces sound transmission or reception through the stern section of the dome and the baffle reduces the reflections within the forward part of the dome. Figure 11 shows a measured beam pattern of the transducer inside the streamlined dome.

The domes were manufactured by The Budd Company as subcontractors to the Western Electric Company. Later the general type of dome design developed for the *QBF* and *QJA* systems was standardized by the Navy for use on most of the larger antisubmarine vessels.

Retracting Gear

The retracting gear provides means for lowering the transducer and its surrounding streamlined dome into the sea below the bottom of the hull and for retracting them within the hull of the ship as shown in Figure 6. It also provides means for training the transducer in azimuth and is equipped with rotary contacts for the transducer cable. The design of this equipment must be rugged in order to stand the large forces which are encountered under heavy seas, high speed operation, and so forth. The retracting gear for the *QJA* equipment is a unit weighing approximately 4,000 pounds and has been demonstrated to withstand this type of service.

The raising and lowering of the transducer and dome normally are accomplished by the operation of a 2-horsepower motor which can be seen in Figure 2. The normal time for the motor to lower or hoist the dome is about 80 seconds.

A so-called trunk is the major structural part of the retracting gear. It provides means for fastening the retracting gear to the sea chest of the ship and also provides a housing for the dome and transducer when these are raised. It is fitted with tracks or guide rails for alignment during the raising and lowering operations. The trunk also provides a seating surface for the raft when the dome is lowered in order to firmly position the entire assembly.

During normal operation the dome is filled with sea water which is free to circulate in and out of the dome through the central opening in the raft. This arrangement provides "still" water inside the dome at the same pressure as the outside water. When the dome is raised, the central portion of the raft seats against a gasket on the underside of the trunk cover and completely seals the inside of the dome from the pressure of the outside sea. Suitable valves for checking the watertightness of the dome are provided for this purpose. In this position it is possible to remove the training shaft, transducer assembly and the water from inside the dome, provided the dome is undamaged.

The raft has three adjustable rollers which are fitted to run on three vertical tracks fastened inside the trunk. The rollers operate only during the raising and lowering of the raft and attached dome. Two perpendicular lifting tubes are securely fastened to the raft. These carry the weight of the raft and dome and together with the guide rails resist the forces acting on the dome during the time the raft is not firmly seated.

The upper end of the transducer training shaft is arranged to be rotated, by suitable gearing, by a type *7G* servo unit, the over-all gear ratio being about 118-to-

Figure 12. Rotary contactor

Figure 13. Receiver and driver oscillator

1. The *7G* servo unit is equipped with a mechanical damper to reduce hunting which takes place when a generator of this type is used as a driving motor.

A rotary contactor is mounted at the top of the transducer training shaft which provides quiet circuit connections between the rotating transducer and the stationary ship's cables and so permits training the transducer without limiting either the amount or direction of its rotation. Figure 12 shows the rotary contactor with the covers removed to show the arrangement of the six gold-to-gold slip ring type contacts and also the chamber for terminating the ship's cables. The lower portion of the contactor rotates with the transducer training shaft and the upper elongated portion is held against rotation by engaging a guide rail which is secured to the forward pillar of the retracting gear. This is necessary to accommodate raising and lowering of the transducer as can be seen in Figure 2. In addition to the *7G* servo unit, the retracting gear is also equipped with four spur gears for rotating a *5SCT* servo control generator and a *5G* servo generator. The *5G* servo generator transmits the transducer bearing indication to the transducer bearing arm in the indicator and control unit.

Receiver and Driver Oscillator

Figure 13 shows the receiver and driver oscillator unit shown in block schematic form in Figure 14. This unit generates a single frequency anywhere in the 10- to 30-kc range as required which is fed into an associated driver amplifier for driving the transducer. It is also equipped with a relay for switching from the receiving condition to the transmitting condition. The relay operates to feed the generated power into the driver amplifier and with the relay released, the receiver is in condition to receive signals from the transducer. These frequencies will be identical with the transmitted frequency in the 10- to 30-kc range with the exception of some frequency shift due to Doppler effects. These are caused by the relative motion of the ship and target. The received signals as just explained are amplified and converted to an intermediate frequency centered around 150 kc. After further amplification they are reduced to audible frequencies by a beat frequency converter. The audible frequencies are further amplified to operate a loud-speaker or a head telephone set, to furnish an input voltage for operation of the bearing deviation indicator unit, and to flash the range lamp in the indicator and control unit.

The receiver and driver oscillator unit contains its own power supply unit to provide the necessary voltages when the receiver is operated from 115 volts alternating current.

The receiver is provided with *TVG* (time variation of gain) adjustable by a dial on the front panel of the unit so that the effect of reverberation can be mini-

Figure 14. Block schematic diagram of receiver and driver oscillator

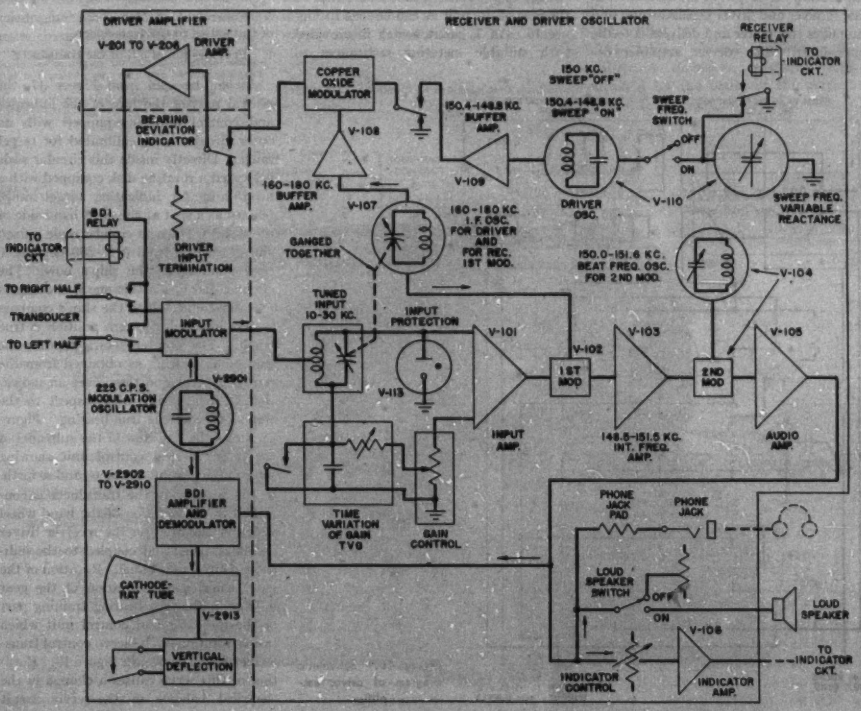

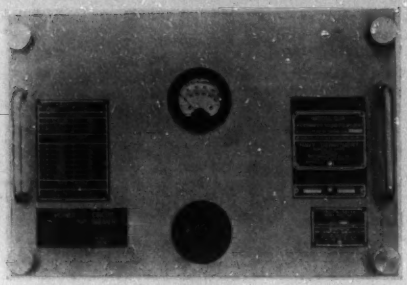

Figure 15. Driver amplifier

mized. *TVG* determines the rate at which the receiver gain is restored following the transmittal of an outgoing pulse.

Driver Amplifier

The driver amplifier supplies the signaling power to the two halves of the transducer connected in parallel during transmission of the outgoing pulse. It receives input from the output of the modulator in the receiver and driver oscillator unit and amplifies this power and delivers it to the transducer. The driver amplifier delivers about 100 to 150 watts to the transducer in the 24-kc region. The amplifier contains six type *807* tubes, three parallel sets of two in push-pull. The mode of operation of the amplifier is AB_2. The unit contains its own power supply and operates from 115 volts alternating current.

Provision is made to read potentials and currents for various parts of the circuit by means of a meter mounted on the face of the unit as can be seen in Figure 15. An 11-point switch is provided with suitable metering resistances to measure these quantities. Figure 16 is a schematic diagram of the amplifier portion of the driver amplifier unit. Shown also in the schematic is an inductance *L*-203 which serves as a shunt reactance to resonate the capacitance of the transducer and the output cable at about 24 kc and also serves as an autotransformer to match the impedance of the output circuit to that of the transducer. By this arrangement maximum transfer of power from the amplifier to the transducer is accomplished.

Indicator and Control Unit

Figure 17 shows the indicator and control unit which has the following general features and functions:

1. Shows the course of the ship.
2. Shows the bearing of the transducer with respect to the ship's bow and the true bearing.
3. Shows the range of the target when echo ranging.
4. Provides for training the transducer by means of a hand wheel or push buttons.
5. Controls the timing of the transmission of the pulses to the transducer.
6. Provides for *MTB* of the transducer.

As can be seen from Figure 17, the central part of the face of the indicator and control unit is equipped with an outer circular scale calibrated for target range. Directly inside this circular scale is located a rotating disk equipped with a neon lamp for indicating target range (shown as a spot at the right hand side of the scale). The next circular scale is fixed and graduated from 0 to 360 degrees, 0 corresponding to the ship's bow. The circular dial inside this one is a compass repeater connected to the ship's compass system in which the zero position is true north. The pointer shown repeats the transducer bearing as obtained from the retracting gear and thus gives an indication of the bearing with respect to the ship's bow and the true bearing. Figure 18 shows the top view of the subpanel of the indicator and control unit showing some of the gearing, contacts, and so forth.

The training of the transducer is controlled by the rotation of the hand wheel which is mounted on the receiver driver oscillator panel and coupled to the indicator control unit panel. Rotation of the hand wheel causes rotation of the gear linkage in the true bearing training part of the indicator and control unit which causes rotation of the servo control transformer *B*-305, shown in Figure 19. Rotation of this servo causes a change in the electrical balance in the servo circuit

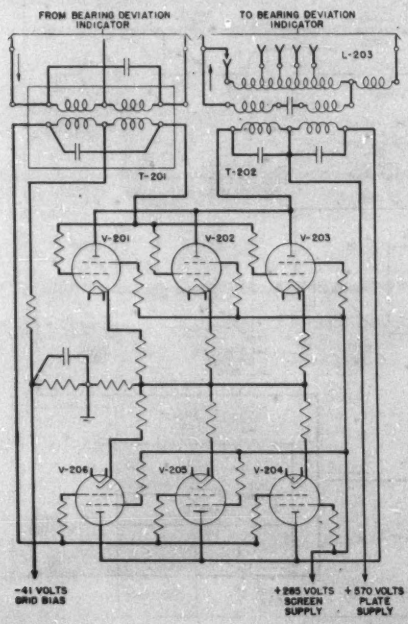

Figure 16. Schematic diagram of driver amplifier

Figure 17. Indicator and control unit

which causes a voltage to be applied to the input of the training control amplifier. This amplifier in turn then causes rotation of the armature of the induction motor *B*-306. As the motor rotates, a gear linkage associated with it causes rotation of the brushes of the commutator transmitter *T*-306*, thus repositioning the transducer. The rotation of the motor also feeds back through a gear linkage to reposition the servo control transformer to its original position, thus balancing the electric circuit and removing the voltage from the input of the training control amplifier. One turn of the hand wheel produces a change in transducer position of five degrees in azimuth. To obtain a large angular movement of the transducer quickly, two slewing buttons *K*-312 and *K*-313 are provided, one for each direction of rotation. Operation of either of these disconnects the training control amplifier output from the induction motor *B*-306 and connects one winding of this motor to a 30-volt power supply from transformer *T*-303, thus causing rotation of the armature of *B*-305 to reposition the transducer. At the same time that this voltage is applied to the motor, a locking magnet *K*-311 operates to lock the repeat back gear train, which is connected to the servo control transformer, to avoid rotation. Accordingly, rotation of the motor feeds through the differential gearing of the *MTB* unit and rotates the hand wheel and the transducer, the latter at approximately 4 rpm.

The *MTB* mechanism is associated with the training control amplifier and operates in the following manner. As can be seen in Figure 19, the 3-wire winding of the servo control transformer *B*-305 is connected to the ship gyro compass circuit. As the ship turns, the gyro repeater servomechanism *B*-301, of the indicator unit rotates, indicating the new position on the compass dial of the indicator. At the same time this introduces an electric change in the 3-wire winding of the servo control transformer which causes an induced current in the other winding of the servomechanism which is connected to the training control amplifier.

The training control amplifier is essentially a thyratron reversing relay controlled by the phase of the current supplied to its input by the servo control

* As shown in Figure 20, the commutator transmitter is a transformer with one bare winding on which three rotating brushes operate to pick up voltages corresponding to the mechanical angles between the brushes.

Figure 18. Subpanel of indicator and control unit

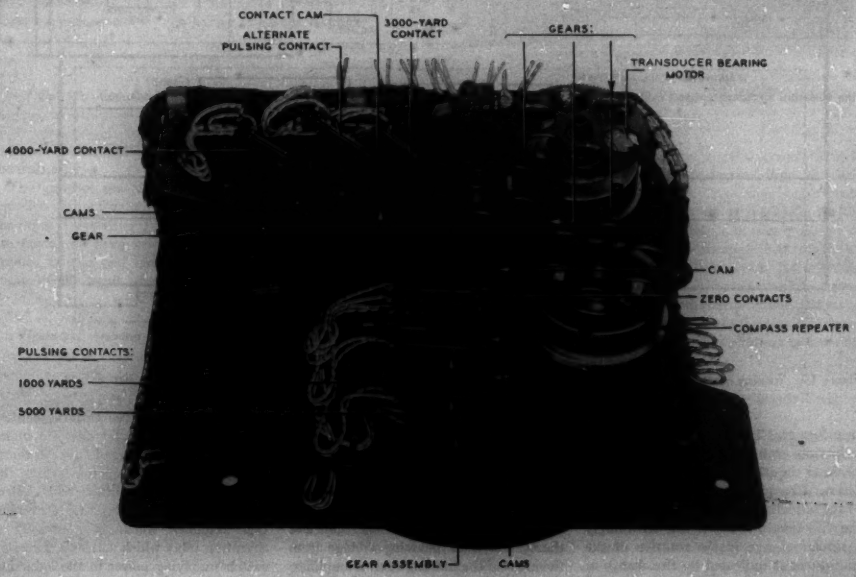

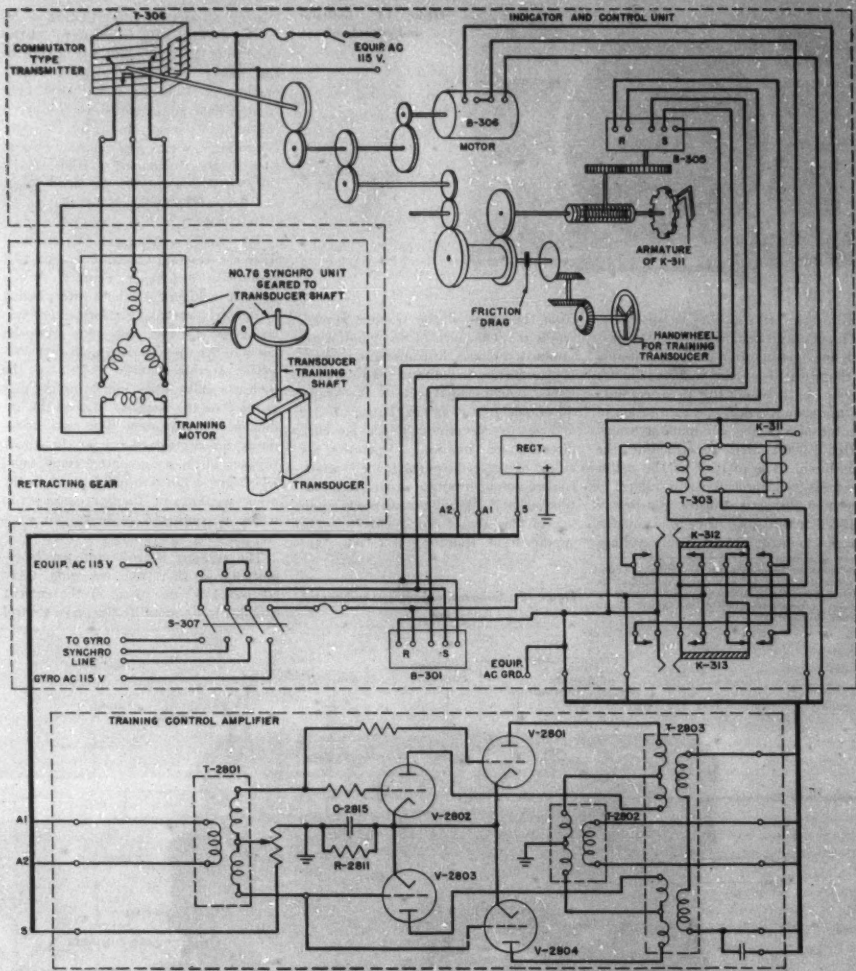

Figure 19. Training control system schematic

transformer. The amplifier supplies the induction motor *B*-306 voltage of one phase or the other depending on the input phase. Changing the phase of the voltage to the induction motor causes a change in the direction of rotation and accordingly a similar change in the rotation of the transducer as indicated by the change in the true bearing of the ship. As the induction motor rotates, repositioning the commutator transmitter *T*-306, to reposition the transducer, this motion is also transmitted through the gear linkage in the *MTB* unit and back to the armature of the servo control transformer *B*-305. This armature, in turn, is repositioned to give an electrical balance of the system thus removing voltage from the input of the training control amplifier.

Training Control Amplifier

Figure 21 shows the training control amplifier unit which provides for maintenance of true bearing of the transducer when used in conjunction with the apparatus in the indicator and control unit. Figure 22 is a schematic diagram of this amplifier which is essentially a thyratron relay which acts as a reversing switch supplying power to the induction

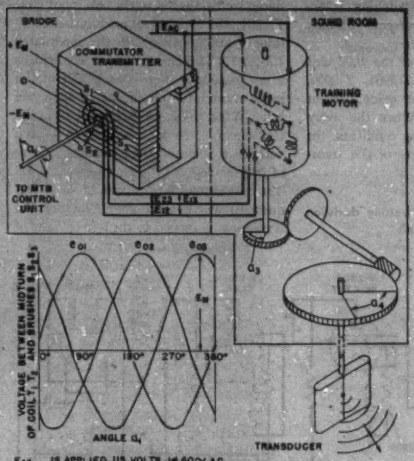

E_{AC} IS APPLIED 115 VOLTS, 1Φ, 60~ AC

α_1 IS THE MECHANICAL ANGLE BETWEEN BRUSH FOR S_1 AND A LINE PARALLEL WITH THE MIDTURN OF WINDING T_1 AND T_2 (α_1=120° FOR POSITION OF BRUSH S_1 AS SHOWN IN FIGURE.)

E_M IS THE MAXIMUM VOLTAGE FROM MIDTURN TO END TURN OF WINDING T_1, T_2.

e_{01}, e_{02}, e_{03} ARE THE VOLTAGES FROM MIDTURN OF WINDING T_1, T_2 TO BRUSHES S_1, S_2 AND S_3 RESPECTIVELY.

E_{12}, E_{23}, E_{31} ARE THE VOLTAGES BETWEEN LEADS $S_1 S_2, S_2 S_3$, AND $S_3 S_1$ RESPECTIVELY.

$\theta = \alpha_1 + 60°$

$e_{01} = E_M \sin(\alpha_1)$

$e_{02} = E_M \sin(\alpha_1 + 120°)$

$e_{03} = E_M \sin(\alpha_1 + 240°)$

$E_{12} = \sqrt{3} E_M \cos(\theta)$

$E_{23} = \sqrt{3} E_M \cos(\theta + 120°)$

$E_{31} = \sqrt{3} E_M \cos(\theta + 240°)$

$\alpha_2 = \alpha_3 = \alpha_1 = 118\ \alpha_4$ (APPROX.)

Figure 20. Commutator transmitter

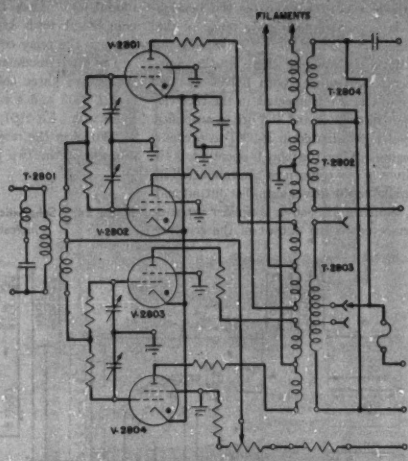

Figure 22. Schematic of training control amplifier

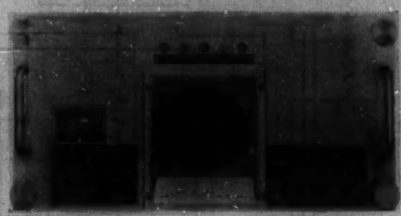

Figure 23. Bearing deviation indicator unit

motor *B*-306 located in the indicator and control unit.

The grids of the thyratron tubes are supplied with a low 60-cycle voltage from the input transformer *T*-2801. The tubes are prevented from firing by a d-c bias applied to the grid circuits. The constants of the input circuit are so chosen that the tubes fire with about 0.5-degree displacement from the balanced position of the servo control transformer *B*-305 of the indicator and control unit with an adjustment potentiometer provided to vary the sensitivity. The plate circuits of the thyratrons are supplied with about 225 volts at 60 cycles and with this circuit, the thyratrons are fired only when their grid and plate voltages are in phase, hence for one direction of displacement of the control transformer only two of the tubes *V*-2801 and *V*-2804 will fire and for the other direction of displacement which corresponds to a 180 degrees change in phase on the grid circuits, only the other two tubes will fire, namely, *V*-2802 and *V*-2803. Thus, the direction of rotation of the induction motor will change depending upon which of the tubes are fired.

Figure 21. Training control amplifier

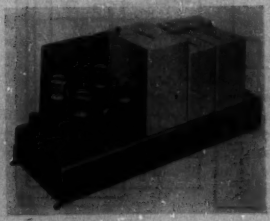

A resistance-capacitance network is connected in the cathode circuit of the thyratrons so that when the tubes are fired, an additional d-c bias appears on the grids of the tubes, causing them to cease firing when the control transformer is approximately 3 degrees from the balanced condition. Provision is also made to operate the training mechanism without the *MTB* feature in case of failure of the ship's gyro compass systems. For this condition, the compass dial is locked to a fixed position, gyro power is removed from the compass servo motor, the servo control transformer, and the training control amplifier, and equipment power substituted.

Bearing Deviation Indicator Unit

The bearing deviation indicator unit shown in Figure 23 and in schematic form in Figure 24 is equipped with a relay *K*-2901 for switching from the transmitting to the receiving condition. In the receiving condition the outputs of both halves of the transducer are modulated and fed to the receiving amplifier. A

cathode ray tube indicates the bearing deviation and approximate range of the target.

With the relay *K*-2901 in the non-operated position, both halves of the transducer are connected to the receiver input modulator and the driver amplifier input is terminated in *R*-2901 to prevent singing. When the relay is operated, both halves of the transducer are connected in parallel to the driver amplifier output and in sequence, the driver amplifier input is connected to the output of the receiver modulator. Thus the switching is accomplished with low currents flowing through the relay contacts.

The input modulator of the *BDI* unit consists of three coils, *T*-2901, *T*-2902, and *T*-2903 and a copper oxide varistor modulator *CR*-2901. When the relay *K*-2901 is in the receiving condition, the outputs of the two halves of the transducer are connected to the two input coils *T*-2901 and *T*-2902. A modulation oscillator *V*-2901 connects to the modulator *CR*-2901. This circuit alternately bridges a low impedance across each half of the input modulator circuit at a 225-cycle rate. When the signal frequency from the transducer is 24 kc, the output of the varistor modulator then consists mainly of frequencies 23.775, 24, and 24.225 kc. The magnitudes and phases of these frequencies will depend upon whether the transducer is turned to the left or right of

Figure 24. Schematic of bearing deviation indicator unit

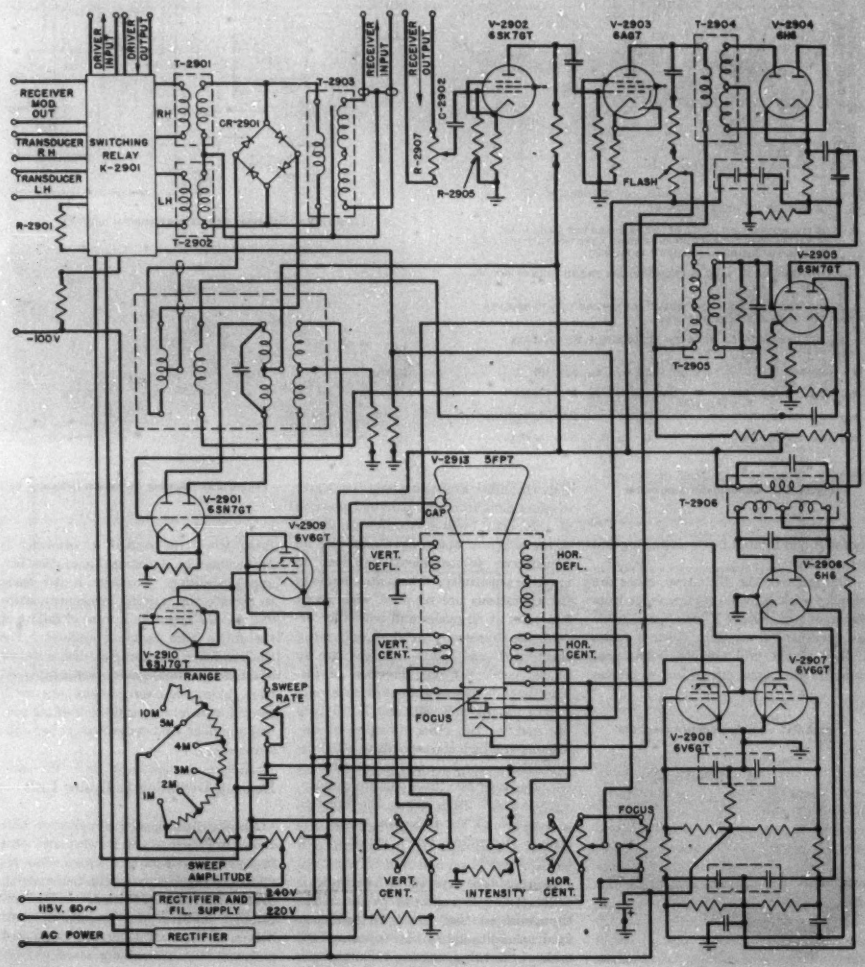

Figure 25 (left). Control equipment rack (units removed)

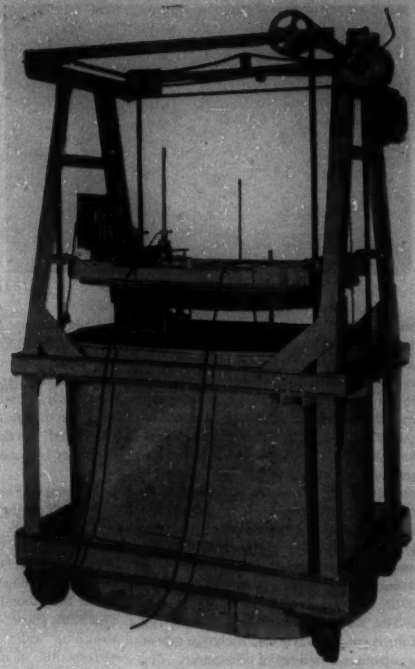

Figure 26 (right). Acoustic testing tank

the target. The output of the varistor modulator is fed into the modulator output coil *T*-2903 and in turn to the receiver.

The frequency of the modulation oscillator *V*-2901 is 225 cycles. One winding of the oscillator coil is connected directly to the modulator *CR*-2901. Another winding is connected to the grid of a buffer amplifier tube *V*-2905, the output of which is connected to a conjugate rectifier *V*-2906.

With the beat frequency oscillator set to give 800 cycles in the receiver output when the transducer is trained on a target, the output of the receiver consists of frequencies 575, 800, and 1,025 cycles whose phases and amplitudes depend upon the transducer output. The receiver output then is fed into the frequency discriminator circuit which converts the frequency modulated output of the receiver into an amplitude and phase modulated wave. This is accomplished by series condenser *C*-2902 and shunt resistance *R*-2905 which offers less attenuation to high frequencies than to low frequencies. A gain control potentiometer *R*-2907 changes the input level into amplifier tube *V*-2902. Hence adjustments can be made and deflections on the cathode ray tube due to noise can be properly suppressed.

The output of the frequency discriminator circuit is fed directly to the control grid of the input amplifier tube *V*-2902. The output of this tube is connected to *V*-2903 which is a voice frequency amplifier tube. The output of *V*-2903 is connected to the demodulator coil *T*-2904. The demodulator tube *V*-2904 is fed from coil *T*-2904 which delivers signal frequencies of 575, 800, and 1,025 cycles. The output of the demodulator tube is connected to a high pass filter consisting of a series capacity and a shunt resistance and a 225-cycle band pass filter *T*-2905. The amplitude of the 225-cycle output of the demodulator depends on the phases and amplitudes of the three frequencies from the receiver which in turn depend upon whether the transducer is trained to the left or right of the target. The demodulator circuit is also arranged with an electric gate circuit. A d-c bias is introduced in the midbranch of the demodulator circuit and is of such a magnitude as to prevent the normal voltages from noise alone from getting through to the output. The bias is of such a value that any signal voltage capable of making an indication will be allowed to pass to the output of the demodulator.

The output of filter *T*-2905 is connected to one of the input grids of tube *V*-2905 and the output of the corresponding plate is fed directly into the tuned coil *T*-2906. This coil is tuned by suitable condensers to the same frequency as the modulation or switching oscillator which is 225 cycles. The output coil *T*-2906 is connected to the anodes of the conjugate rectifier tube *V*-2906. The cathodes of the conjugate rectifier are connected to a low pass filter which in turn connect to the grids of d-c amplifier tubes *V*-2907 and *V*-2908. The modulation oscillator *V*-2901 delivers a 225-cycle reference voltage which is maintained

Figure 27 (left). Birchwood Lake test station

Figure 28. The *Elcovee*

substantially constant in phase and amplitude and is connected through the buffer amplifier to the midpoints of the balanced conjugate rectifier *V*-2906. Any change in the magnitude or polarity of the 225-cycle signal voltage across the balanced input will appear as a change in magnitude and polarity respectively of the d-c output of the conjugate rectifier. The d-c output of the conjugate rectifier is connected directly to the d-c amplifier tubes which amplify any d-c changes in their grid circuits. The outputs of the d-c amplifiers are connected to the horizontal deflection coil of the cathode ray tube *V*-2913.

The range sweep of the cathode ray tube is controlled by the discharge rate of a capacitor into a set of resistances. The intensity and focus of the spot on the cathode ray tube are adjustable by a potentiometer and rheostat, respectively. The spot is further adjustable by means of the vertical and horizontal centering potentiometers. Spot intensity also is increased when signals are received. With relay *K*-2901 operated, the output of *V*-2909 is large and flows through the vertical deflection coil. The current diminishes at a rate corresponding to a setting of the range sweep. The spot on the tube starts at the bottom and moves at a substantially constant rate towards the top of the screen depending upon the setting of a range control switch. The spot is deflected horizontally to the left or right depending upon the d-c output of the tubes *V*-2907 and *V*-2908 which in turn depend upon the 225-cycle signal output of *V*-2906. The *BDI* unit contains its own power supply and operates from 115 volts alternating current.

Control Equipment Rack

Figure 25 shows the control equipment rack, with the various units removed and the plug-in-type connectors. The units are in drawer form and plug into operating position when fully closed. For servicing, the drawer units may be removed from the rack and can be put in operating condition by means of a multiconductor patch cord. In this way, testing and servicing may be done conveniently.

Laboratory, Factory, and Field Testing

A special test tank commonly referred to as an artificial ocean because of its suppression of echo effects was developed for use in the laboratory and in the factory. This tank shown in Figure 26 has sound absorbing walls, top and bottom, and corresponds, in underwater sound work, to a highly damped room in air acoustics. It was used at the factory for checking every transducer manufactured for sensitivity, output, frequency characteristic, and beam pattern. Such factory tests established a new practice in production and made it possible to insure that the transducers delivered to the Navy were all within carefully specified limits of performance.

As in the work with telephone apparatus and systems, Bell Telephone Laboratories devoted a great deal of effort to the development of quantitative measurements and testing of sonar devices and systems including production control testing. In fact, Bell Telephone Laboratories' first underwater sound work which was undertaken just prior to World War II and later sponsored by the National Defense Research Committee, was the development of precise methods of measuring underwater sound. This effort provided groundwork for the standardization and improvement of Navy equipments and techniques in the field of underwater sound. As has also been found desirable in designing and manufacturing Bell System telephone equipment, which must give good service over long periods, field testing of sonar equipment in the development stage was stressed. To conduct suitable field studies, the laboratories established lake stations such as the one at Birchwood Lake, N. J., shown in Figure 27, as well as floating laboratories. The *Elcovee*, shown in Figure 28, was a floating laboratory on which all of the sonar systems and many of the sonar devices developed at Bell Telephone Laboratories were tested before they were submitted to the Navy, to insure meeting the rigorous requirements of the sea trials needed to anticipate combat duty. The *Elcovee* was used to take a variety of measurements including beam patterns, usually taken at anchor, and in addition complete operating systems were installed for measurement purposes and to study the action of the equipment with the boat under way. The *Elcovee* made it possible to work out the sonar operation and installation problems completely and to demonstrate operating systems to Navy personnel at an early date. The *Elcovee* was used to demonstrate the complete *QJA* and other sonar systems to the Navy before the start of Navy trials. By this arrangement the development work at the laboratories was expedited, changes in design largely were anticipated, and the Navy received better equipment at an earlier date.

Reference

1. The Elastic, Piezoelectric and Dielectric Constants of Potassium Dihydrogen Phosphate and Ammonium Dihydrogen Phosphate, W. P. Mason. *Physical Review* (New York N. Y.), volume 69, March 1 and 15, 1946, pages 174–193.

No Discussion

The Design and Performance of the Vertical Generator Thrust Bearings at the Bonneville Plant of the Corps of Engineers, War Department

F. M. LEWIS
MEMBER AIEE

T. W. GORDON
NONMEMBER AIEE

THE modern vertical thrust bearing is in many aspects the mechanical heart of nearly all large hydroelectric developments. Upon it may hinge the success or failure of the entire project. It supports the total weight of the rotating parts of the generator and turbine and also the hydraulic thrust load encountered in such installations. It permits the relative motion between these rotating parts and the stationary parts of the turbine and generator without which no electrical power could be produced. Its development has made possible the large vertical machines which are used to harness the rivers of America and the rest of the world to produce energy for the use of mankind.

The bearings in the generators at the Bonneville Plant of the Corps of Engineers typify one type of these large thrust bearings and their design and performance is of particular interest since they are, as far as is known to the authors, the largest waterwheel generator thrust bearings in the world. Not only are their dimensions remarkable, but also the loads which they carry. Each bearing supports a load equivalent to the total weight of a large sized destroyer, approximately 1,500 tons, 3,000,000 pounds! In both size and load carrying ability they exceed, by a considerable amount, any other waterwheel thrust bearings in the western hemisphere.

The Bonneville project, which was started in 1933, is one of a number of dam sites selected by the Corps of Engineers as part of a scheme for the development of the Columbia River. It is located at tidewater, forty-two miles east of Portland, Oreg. (Figure 1). As originally conceived the power plant was to house ten 48,000-kva 75-rpm vertical generators, each driven by a 60,000-horsepower Kaplan type hydraulic turbine. Two such units were placed in service in 1938. Two additional units were placed in service in 1940, with ratings increased to 60,000 kva at 75 rpm. These latter units were duplicated by two more units in 1941, and four more in 1943. The last of the ten units was placed in operation in December 1943.

The Construction of the Generators

The generators are of the vertical shaft hydraulic turbine driven type with direct connected main and pilot exciters mounted on top. Each is totally enclosed in a metal ventilating housing equipped with necessary duct work and coolers to make it a self-contained unit. The ten units in the completed power house are shown in Figure 2.

The pertinent interior details of the generator construction are shown in the cross section, Figure 3. From this cross section it may be seen that the shaft is held in alignment by guide bearings above and below the rotor. There is a third guide bearing at the lower end of the hydraulic turbine shaft. The main thrust bearing is located in a circular oil chamber on top of the lower bracket. Accessibility and general arrangement favored the use of external oil coolers and circulating pumps, piped to the oil chamber, which supply the bearing with a continual flow of cool oil. The lower bracket, on which the thrust bearing rests, and which transmits the load to the foundations, is fabricated from steel parts. It consists of eight equally spaced arms which are bolted and keyed to a central hub. Some concept of the size of the bracket and of the bearing chamber is conveyed by Figure 4 which shows a view of the inside of the generator pit.

The Thrust Bearings

The construction and operation of the thrust bearings must be considered in several stages, as the great increase in size of these bearings over the largest ones previously in existence introduced problems which had to be overcome. Consequently the bearings underwent a period of development. A general description of the conditions of operation and some details of construction will serve, however, to clarify the details dealt with later.

The bearings are designed for a load of 3,014,000 pounds, approximately 400 pounds per square inch, the weight of the revolving parts of the generator and turbine being about half this amount and the hydraulic thrust the other half. Although the normal speed of the unit is 75 rpm, the bearings and their lubricating systems are designed to operate under an overspeed, at runaway of the turbine, of 175 rpm. The shaft at the elevation of the thrust bearing is 43 inches in diameter which necessitated an inner bearing diameter of 50 inches. The outer bearing diameter is 112 inches.

Paper 47-184, recommended by the AIEE committees on electric machinery and power generation, and approved by the AIEE technical program committee for presentation at the AIEE Pacific general meeting, San Diego, Calif., August 26–29, 1947. Manuscript submitted April 23, 1947; made available for printing July, 1947.

F. M. Lewis is resident engineer, United States Engineers, War Department, Bonneville, Oreg., and T. W. Gordon is in the motor and generator engineering division of the General Electric Company, Schenectady, N. Y.

The authors gratefully acknowledge the assistance of J. F. Spease and C. R. Kilbourne in the preparation of this paper.

Figure 1 (left). A general view of the Bonneville project

Figure 2 (above). Interior view of Bonneville powerhouse

The bearing proper consists of a rotating plate, fastened to a combined thrust collar and rotor spider hub, as shown in Figure 3, which in turn is held to the shaft by a circular key; and stationary segmental babbitted shoes. The babbitted shoes possess some flexibility in themselves and in addition are supported by a large number of pre-compressed springs. These springs serve to equalize the load distribution among the shoes, preventing the development of high local pressures caused by disturbances in the machine alignment. The action of these springs, combined with the flexibility of the babbitted shoes aids in the formation and maintenance of an oil film when the rotor is in motion.

During rotation a film of oil, a few thousandths of an inch thick, is maintained between the stationary and running plates. This film is thick enough to prevent metallic contact of the surfaces and makes possible operation with an extremely low coefficient of friction. It is not sensitive to changes of speed or load, nor is it so delicate that small amounts of usually encountered fine impurities in the oil will disrupt it. When rotation is started boundary lubrication quickly becomes stable film lubrication, without aid from jacking the rotor or otherwise introducing oil between the surfaces. The machines at Bonneville are started and stopped at will with no concern for the bearings whether they be hot from previous running or cold from a prolonged shutdown.

The heat generated in the bearing is carried away by the oil which is circulated through the bearing within the oil chamber by centrifugal action. The oil leaving the bearing is then cooled by passing through an external water-cooled heat exchanger and is returned as cool oil to the bearing chamber.

The Initial Bearing Construction

The bearings for the first four units as originally constructed consisted of a 12-segment runner plate as shown in Figure 5. This type of construction with relatively small component parts to make up the runner plate offered ease in handling and assembling the bearing which was thought to be very desirable.

The stationary plate consisted of six babbitted shoes, as shown in Figure 6.

The initial runner segments of cast iron, had a chilled highly polished undersurface which was the moving surface of the bearing. The leading edges of each of the segments had a chamfered groove which, when the bearing was running, served as a passage for oil. The back surface of each segment had a T-shaped radial groove located on the radial centerline of the segment extending from the inner diameter outwards for approximately 3/4 of the distance across the segment. Also into the back surface of each segment were drilled two $2^1/_2$-inch dowel recesses for locating the segment in the bearing and several small tapped holes for handling the segment.

The bottom surface of the thrust collar was equipped with 12 radial, equally spaced, T-shaped keys which matched the dovetails in the backs of the segments. When assembling the bearing the runner segments were hung from these keys and slid radially inward to their proper position under the thrust collar. When two adjacent segments were in position there was approximately 1/16-inch clearance between them. Two dowels per segment were then dropped through matching clearance holes in the thrust collar into the recesses in the back of each segment, thus locking the segment against centrifugal force when in motion. The radial key locked the segment against circumferential displacement during starting.

Both the radial key in its keyway and the dowels in their dowel holes through the thrust collar had assembly clearances. The forces exerted on these segments during starting and running therefore acted to finally position the segments both circumferentially and radially, and the load on them was relied upon to hold the segments in position by friction once final seating had occurred. As the generators have only one direction of rotation, it appeared that once in final position these segments would remain there.

The stationary parts of these initial bearings are shown in Figure 6. The babbitted plate consists of six segments with a center groove dividing the surface of each and providing a duct through which oil flowed from the annular center opening outwards through the duct when the bearing was in motion. The babbitted plates were held against circumferential displacement during starting by

circular dowels at their inner periphery and by rectangular keys at their outer periphery, both of which were securely held by recesses in the base ring. Between the bottom of the babbitted plate and the base ring is the spring bed. This spring bed serves not only to support the babbitted plate and provide means of equalizing the load but also the openings between the springs and between the coils of the individual springs serve as passageways for the entrance of cool oil beneath the bearing. The large cooling surface provided by the bottom of the babbitted plate plus all the surface of the springs serves to conduct away a considerable portion of the heat generated at the rubbing surface and to transfer it to the oil.

The Final Bearing Construction

The bearings for the last six machines, and ultimately by replacements for all ten machines, differed from the initial bearings in several important respects.

Whereas the initial runners had twelve independent segments, loosely located by keys and dowels, the final runners were made in two pieces, for assembly purposes, and the halves keyed and bolted across the joints to prevent any movement of one half with respect to the other. One of the final runners, mounted on a special bearing finishing mill is shown in Figure 7. The holes in the side surfaces of the runner are the recesses for the joint bolts.

When installed in the machine the assembled runner is bolted against the thrust collar by $2^1/_2$-inch diameter bolts located in some of the same thrust collar holes formerly used for the segment locating dowels. Three of these holes in each half of the runner still contain dowels. Thus the final positioning of the new runner is determined by its assembly, with little opportunity left for adjustment or movement caused by the forces present when the machine is in motion.

A second difference between the two types of runners is obvious from a comparison of the figures. The first runners had 12 surface grooves, one per segment, and also a small opening between segments which extended up to the under surface of the thrust collar. The new runners have completely smooth surfaces, no grooves, and there is no space between the halves of the runner.

The babbitted plates in the final bearings consist of 12 separate shoes instead of 6 shoes with center oil grooves. The new shoes are essentially duplicates of the half old shoes and in fact some of the original shoes were parted along the center groove to make the new shoes. They are held in place against circumferential displacement during starting by the same dowels and keys as before with the addition of separating spacers between the shoes. See Figure 8.

Operation of the Bearings

Table I presents the log of the operation of the Bonneville station from June 6, 1938, to October 10, 1946, insofar as the performance of the bearings is concerned. Initial type babbitted plates and runners are designated by *I*, final types by *F*. Two experimental babbitted plates *E* and *Epb*, and one experimental runner, also indicated as *E*, were run.

Study of the table will reveal several divergences from the main theme of the initial and final type of bearings. Close

Figure 3. Cross-section view of one of the 60,000-kva vertical generators at the Bonneville power plant

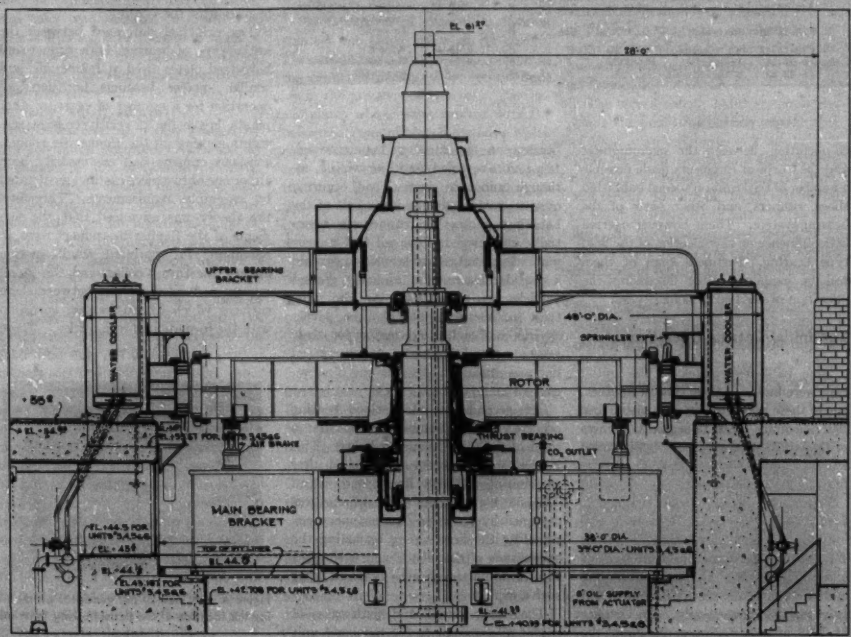

Table I. Log of Operation of Bonneville Bearings

Unit	Initial Date	Initial Event	Operating Hr	Type Babbitt Plate	Type Runner	Final Date	Final Event
1	7-18-38	To operation	1,157.51	I	I	10-31-38	Wipe 1
	11-8-38	Installed	735.76	I	I	2-27-39	Removed
	2-27-39	Installed	87.41	E	E	5-12-39	Removed
	5-13-39	Installed	3,980.55	I	I	3-4-40	Wipe 3
	3-9-40	Installed	3,850.53	I	I	9-14-40	Wipe 4
	9-15-40	Installed	3,031.50	I	I	1-20-41	Wipe 6
	1-21-41	Installed	1,654.00	I	I	4-2-41	Removed
	4-3-41	Installed	40,339.06	F	F	12-3-45	Routine inspection
	1-25-46	Returned		F	F		In service
2	6-6-38	To operation	1,535.88	I	I	11-14-38	Inspected
	11-23-38	Returned	1,965.55	I	I	7-15-39	Wipe 2
	7-24-39	Installed	3,219.08	I	I	3-13-40	Inspected
	3-15-40	Returned	1,939.17	I	I	7-26-40	Inspected
	7-28-40	Returned	3,945.50	I	I	1-3-41	Wipe 5
	1-4-41	Installed	597.30	I	I	1-30-41	Wipe 7
	2-1-41	Installed	42,155.06	E	F	12-17-45	Routine inspection
	2-12-46	Installed	2,609.73	F	F	6-1-46	Wipe 9
	6-29-46	Installed		F	F		In service
3	1-9-41	To operation	2,442.60	I	I	4-16-41	Removed
	4-17-41	Installed	38,733.52	E	E	10-18-45	Routine inspection (cracked babbitt)
	11-29-45	Installed	2,266.65	E	E	3-25-46	Inspected
	4-12-46	Installed		F	F		In service
4	12-23-40	To operation	2,399.10	I	I	4-9-41	Removed
	4-10-41	Installed	38,603.55	F	F	10-1-45	Routine inspection
	12-13-45	Returned		F	F		In service
5	9-5-41	To operation	37,711.03	F	F	1-27-46	Routine inspection
	3-5-46	Returned		F	F		In service
6	5-18-42	To operation	35,696.77	F	F	7-29-46	Routine inspection
	8-20-46	Returned		F	F		In service
7	1-4-43	To operation	29,171.61	F	F	9-23-46	Routine inspection
	10-5-46	Returned		F	F		In service
8	6-16-43	To operation	27,280.12	F	F	8-20-46	Routine inspection
	9-7-46	Returned		F	F		In service
9	9-15-43	To operation	18,340.77	Epb	F	11-9-45	Routine inspection
	11-12-45	Returned	7,746.85	Epb	F	10-6-46	Inspected while installing piezometers
	10-18-46	Returned		Epb	F		In service
10	12-15-43	To operation	6,432.74	F	F	9-13-44	Wipe 8
	9-21-44	Installed	16,568.75	F	F	9-9-46	Routine inspection
	9-20-46	Returned		F	F		In service

co-operation between the manufacturer and the Corps of Engineers made possible a number of trial runs on special babbitted shoes, runners, and other parts of the bearing system. These, however, exerted little influence on the selection of the final type bearing. Pertinent ones of them will be explained after discussing the operation of the two principal types.

The Initial Bearing Operation

Nine babbitted plates of the initial type were built. At one time or another, one of these plates was in each of the first four machines. Six 12-segment runners of the initial type were built. They also were at one time or another in one of the first four machines.

Preliminary testing began with unit 2 on March 9, 1938. This unit was followed by unit 1 on April 18, 1938. The bearings performed in a satisfactory manner and after routine checks the units were placed in service on June 6 and July 18, 1938 respectively. On October 31, 1938, after 1,157.5 operating hours, the bearing on the number 1 unit wiped. Inspection revealed that the wiping, although minor in degree, had occurred over approximately the inner half of the babbitted plate. The runner was essentially undamaged. The oil had a very murky appearance and seemed to contain a considerable amount of finely ground particles in suspension. At the time these particles were identified tentatively as iron oxides but no reason for their presence was advanced. Another bearing was installed and the machine returned to service.

The second case of a wiped bearing occurred on the number 2 unit after a total of 3,501.43 operating hours. This bearing was inspected and cleaned after the initial 1,535.88 hours and wiped 1,965.55 hours later. The wiping was attended by the same circumstances surrounding the first wiping, including the appearance of the oil. Figure 9 shows a typical babbitted shoe as removed after such a wiping.

The third, fourth, and sixth cases of wiping all occurred on the number 1 unit after respectively 3,980.55, 3,850.50, and 3,031.50 hours of operation and, like the first two cases, were surrounded by similar circumstances. Early in this chain of events the repetitive nature of the occurrence became evident and suspicion was directed towards the impurities obviously present in the oil. By this time these impurities had been identified positively as iron oxides. Confirmation of the fact that these impurities were the cause of the trouble was aided by plotting, against time, the degree of discoloration of samples of oil taken from time to time from the oil chamber. This established the fact that the wiping took place after a certain degree of discoloration had occurred and these time plots enabled the accurate prediction of the date when some of the later wipings would occur.

By this time the oil chamber and all of the associated lubricating system had been thoroughly cleaned a number of times and it seemed unreasonable to believe that the now identified iron oxide particles could owe their origin to improper cleaning of the oiling system. Other checks absolved the oil from any inherent tendencies in itself to promote the condition. Obviously, the origin of these particles was associated with the operation of the bearing.

The principal difference between the initial type of bearing, both runner and babbitted plates, used at Bonneville, and similar smaller bearings in successful operation for a number of years in other plants, lay in the 12 relatively loose segments making up the Bonneville runner. Previous runners had customarily been either one or two piece castings as dictated by assembly requirements. Therefore, the theory was advanced that the segments of the Bonneville runners were, in operation, in continual small motion against the thrust collar, and this small movement caused rubbing between these surfaces which led to fretting corrosion with the formation of iron oxides. These

Figure 4. A view of the generator pit showing the location of the thrust bearing in its oil chamber

Figure 5. Initial type 12-segment runner plate on a boring mill

Figure 7. Bonneville smooth runner being honed on special bearing finishing mill

Figure 6. Initial type 6-shoe babbitted plate

Figure 8. Bonneville 12-shoe babbitted plate being finished on special bearing mill

iron oxides escaped from the surfaces between the runner segments and the thrust collar and contaminated the oil. Deposits of iron oxide built up in local areas on the faces of the babbitted shoes, diminishing the running clearance between the shoes and the runners, and eventually wiping ensued.

One other case of wiping caused by oxide formation occurred. This was on the number 2 unit on January 4, 1941. This bearing was cleaned thoroughly after 3,219.08 and 1,939.17 hours of operation and wiped after an additional 3,945.50 hours. As the phenomenon was understood by this time the wiping was not a surprise.

Only one other wiping, in addition to the six cases discussed, occurred with the 12-segment runner. That occurred on unit 2 after only 597.3 hours of operation and was ascribed to foreign matter, other than iron oxide, which accidentally got loose in the oil bath. This bearing was removed and an experimental bearing formerly run in the number 1 unit installed. Parts of this experimental bearing were of a temporary nature and it was expected that the bearing soon would be replaced. However, due to wartime power demands, the bearing was not removed until December 1945 after 45,155.06 hours of operation. At this time the bearing was operating perfectly satisfactorily and was replaced only to make all bearings in the plant alike.

The Final Bearing Operation

The operation of the initial bearing pointed out three faults in its design. The major fault lay in the looseness of the runner segments. The second fault lay in the presence of grooves in the runner plates which when rotated over the babbitted shoes produced the force which caused the motion that created fretting corrosion. The third fault lay in the fact that the iron oxide escaped through the openings between the runner segments, from its generating surfaces downward to the babbitt surface.

A comparison of the initial and final bearing construction shows how these faults were overcome. The runner was made solid and bolted to the thrust collar. Grooves in the runner face were eliminated. Since there are no radial openings in the final runners, the former escape passages for the iron oxide have been eliminated. In addition to these changes in the runner, the babbitt plate also was changed although this babbitted plate change probably had no effect on the oxide problem.

A total of 13 sets of babbitted plates of the final type were made. Two of these were experimental plates, and several of the remaining 11 were converted from initial type plates by parting the initial shoe down the center groove. Twelve 2-segment runners were made. One of these, although of two segments, had grooves and was installed in unit 3 in April, 1941. It was regarded as an experimental runner and later was removed, leaving 11 2-segment smooth runners available. The final type bearing was installed in units 1, 2, and 4 by April of 1941 and was installed initially in the last six units.

With the installation of the final bearing, wiping due to oxide formation has ceased. As an example, with the initial type bearing unit 1 had four periods of operation averaging about 3,000 hours before wiping took place. The final type bearing was installed in this machine on April 3, 1941 and inspected in December, 1945, after 40,339.06 hours of operation. This was a routine inspection, not in any way influenced by the performance of the bearing, except perhaps on the score of curiosity. While there was evidence of comparatively small amounts of iron oxide on the usual surface where it had formed before, there was no evidence that the oil was contaminated so the babbitted plate and runner were returned to service. Similar records of 42,155.06, 38,733.52, 38,603.35, and so on, hours of operation prior to a routine inspection have been obtained on other units. It can be categorically stated that no case of wiping caused by iron oxide formation has occurred on the final type of bearing.

Figure 10 shows the excellent appearance of one of the babbitted plates removed for inspection after 38,603.35 hours of operation.

The record shows, however, two cases where the final type bearing wiped. One of these occurred on unit 2 on June 1, 1946, following several line disturbances, overspeed resulting from load rejection, and recent cleaning of the oil system, all of which possibly contributed to the wiping. At the time opinions varied as to whether this wiping was caused by foreign materials or by insufficient lubrication on the inner half of the bearing resulting from abnormal operating conditions and overspeed. The bearing was replaced and certain changes were made in the internal oil flow. These changes, and tests made to determine oil levels, are described later

Figure 9. Typical initial type babbitted shoe removed after wiping

in this paper. The other incident occurred on unit 10 on September 13, 1944. Prior to this failure the generator field had developed a ground. Examination of this bearing revealed quantities of foreign materials other than iron oxide and several small craters in the runner face. The bearing wiped on the outer half, while all other bearings which had wiped, wiped on the inner half of the bearing. The reason for this failure is a matter of conjecture as to whether it was the result of foreign materials or immediate local causes. All of these happenings are deemed independent of normal bearing performance and are regarded as due to the hazards of operation.

In addition to the events just described, an inspection of unit 3 in October, 1945, after 38,733.52 hours of operation, revealed cracked babbitt over a large part of the center area of the bearing. In operation this bearing showed no sign of distress or increase in plate temperatures. In fact, the operating plate temperatures were lower on this bearing than on most of the other bearings in the plant. This was the previously referred to experimental bearing with a grooved runner. The cracked babbitt plate was replaced with a plate of the same type and the bearing returned to operation. After 2,266.55 operating hours an inspection was made and babbitt cracking again was found. The experimental bearing then was replaced with one of the final type. The reason for babbitt cracking has not been ascertained definitely but it has been ascribed to extraneous causes which are not a logical part of the operating history of the station. Consequently, these incidents will not be considered further.

Additional Observations

Several experiments carried out in conjunction with the general program of investigation led to the results which are believed to be of interest although they do not affect the main sequence of events directly.

Lead Alloy Babbitted Plate

On October 1, 1943, the *Epb* (experimental plate) babbitted shoes were installed in unit 9. Tin base babbitt is normally used for thrust bearing plates and was used for all plates except this plate. Because of the tin restrictions which were necessary during the war and the then uncertainties as to whether or not tin could be obtained for making thrust bearing plates, this experimental plate was made with a lead-antimony-arsenic alloy. It was inspected after 18,340.71 hours of service and found to be in perfect condition. The bearing was inspected after 7,746.85 additional hours of operation during the installation of piezometer tubes to study the maintenance of internal oil levels. This inspection resulted in similar conclusions and the bearing was replaced without change. It is now in operation, a continuous record of nearly four years with every indication that this type of babbitt will perform satisfactorily. Figure 11 shows two segments of this plate after the last inspection.

Improved Oil Circulation

It has already been mentioned that the normal method of circulating oil in the entire oiling and cooling system consisted of supplying cool oil from the heat exchangers to the oil chamber, circulating that oil through the bearing by the centrifugal action of the bearing itself, and returning the warm oil to the heat exchangers. Within the oil chamber the cool oil passes through the spring bed to the center of the bearing, then exhausts through the grooves in the babbitted plate. Observations of the rate of flow of oil in this internal system led to the belief that if the cool oil were led directly to the central annular recess instead of entering through the spring bed by the pumping action of the bearing, more and cooler oil could be made to bathe the heat dissipating surfaces of the bearing. In a sense, the heat dissipating surfaces below the babbitted plate and those constituting the running surfaces could be put in parallel instead of in series with respect to the flow of cool oil. Also, since the flow of oil is positively outward through the bearing, any foreign particles tend to be flushed from the bearing surfaces.

With this thought in mind a cool oil distributing system consisting of a circular header, connected to the cool oil inlet pipe, and twelve radial outlet tubes was constructed. The circular header surrounded the bearing at about the elevation of the spring bed, and the radial outlet tubes projected into the center of the bearing through spaces in the spring bed immediately below the openings between the twelve babbitted shoes. Figure 12 shows this header in position around the spring bed. Figure 13 shows the assembled distribution system prior to installation, with oil flowing out of the twelve discharge tubes.

This distributing system was installed in unit 2 in June, 1946, and in unit 7 in October, 1946. Prior to installing these systems the operating temperatures of the bearing plates were 77 degrees centigrade for unit 2 and 86 degrees centigrade for unit 7. After the installation, the operating temperatures of the plates are 61 degrees centigrade and 60 degrees centigrade respectively. These temperatures are now lower than the corresponding temperatures in the remaining eight units. Under the same operating conditions the oil bath temperatures increased 2 degrees centigrade after the installation of the distributing system.

Maintenance of Oil Level

A series of experiments were made to determine whether or not the centrifugal pumping action of the bearing, with normal oil circulation, under usually encountered speeds, could pump more oil out of the central annular recess than could be replaced by flow through the spring beds, thus lowering the oil level at the center of the bearing and at other points radially outward in the bearing. Piezometer tubes, having their pressure

Figure 10 (left). Final type babbitted plate after 38,603.35 hours of operation

Figure 11. Lead alloy babbitted plate after 26,087.56 hours of operation

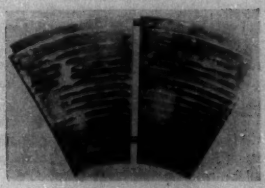

Figure 12. Oil chamber raised to show cool oil circulating header in position around the bearing

Table II. Increases in Static Oil Level as Affected by Speed

RPM	Head in Center Annular Opening, Inches Oil	Head 1/3 Radial Displacement from Center, Inches Oil	Head 2/3 Radial Displacement from Center, Inches Oil
0	0	0	0
40	1/2	13/16	15/16
60	1/2	7/8	15/16
75	1/2	15/16	15/16
90	7/16	15/16	15/16

Figure 13. Cool oil circulating system assembled on station floor

measuring heads located at the center of the bearing, one-third radially outward from the center, and two-thirds radially outward from the center were installed in two bearings in the spaces between the babbitted shoes. These tubes projected into the bearing much in the same manner as the tubes used for improved oil circulation. The machines were then run at various speeds from 40 to 90 rpm and the changes in oil head as recorded on the oil level indicating tubes attached to the piezometer tubes recorded. Table II shows the results of these measurements. The maximum change in level recorded is of the order of one-half to one inch. It is doubtful that a change of this magnitude has much significance since pulsations in the oil level in the indicator tubes were of the same order of magnitude. This pulsation probably was due to turbulence in the oil flow. Since the oil level above the babbitted plate is $6^1/_2$ inches the conclusion is drawn that no significant change in oil head occurs anywhere throughout the bearing at any speed up to that tested. Consequently the oil pumped out of the bearing is replaced completely by the flow through the spring bed.

Conclusion

In nine years of station operation, approximately 56 years of machine operation, there have been a total of nine cases of bearing wiping at Bonneville. Seven of these cases occurred on the initial type bearing. One wiped because of foreign material and the remaining six were caused by the formation of iron oxide, a condition which was eliminated early in 1941. There has been no recurrence of iron oxide wiping in the last 50 machine years of service. Two cases of wiping occurred on the final type bearing. Both of these are attributed to causes other than iron oxide. One is considered as no fault of the bearing and the other was surrounded by circumstances which make difficult the assignment of the wiping to any specific cause.

Since an average shutdown to replace a wiped bearing seldom exceeded two days, and was often less than this, the total outage time in comparison to the running time is exceedingly small. Six out of the ten machines never have had a bearing outage. Two of the remaining four had outages due to miscellaneous causes, and the other two units were the first two machines installed and went through their period of bearing development.

This paper has described the operating history of the initial and final types of bearings, used and in use at Bonneville. The operation of the first or initial type of bearing was not successful. The present or final type now in use has had approximately six station years of very successful operation. Recent inspections give every indication that this type of operation will continue. The experience gained on these bearings forms a foundation for the future, a future which the authors believe will bring corresponding progress in the building of even larger thrust bearings.

Reference

1. Modern Bearing Practice for Vertical Waterwheel Generators, C. M. Laffoon, R. A. Baudry, AIEE Transactions, volume 66, 1947, pages 363–9.

Discussion

S. J. Needs (nonmember; Kingsbury Machine Works, Inc., Philadelphia, Pa.): Publication of this paper makes available information long desired by the writer. Since shortly after the first machines at Bonneville went into operation there have been many rumors of thrust bearing trouble at that station. Like most rumors, these grew with time and distance until the picture became entirely distorted and most confusing. The authors' Table I clarifies the situation and shows exactly what happened since the first machine was started in 1938.

The authors have pointed out that the Bonneville thrust bearings are the largest in the world and also carry the greatest total thrust load. Carrying a load of 3,000,000 pounds is indeed no small accomplishment and represents a real stride forward. The unit load carried by the bearing, however, is only 400 pounds per square inch of bearing area and this accounts for its large dimensions. For purposes of comparison the heaviest total loads that Kingsbury-built bearings to date have been called upon to carry are 2,200,000 pounds. These loads are on the 94-inch diameter bearings at the Kentucky Dam of the Tennessee Valley Authority and the unit loading is 550 pounds per square inch. While the total load is not as great as at Bonneville, the unit load is higher resulting in a proportionately smaller bearing.

The flexible-plate, spring-supported thrust bearing used on vertical hydroelectric generators has been described by Linn and Sheppard[1] as consisting essentially of a "grooved rotating steel collar fastened rigidly to the shaft; a babbitt-faced stationary flexible steel plate with radial grooves, one of which is cut through the plate; and precompressed springs supporting the stationary plate."

The original Bonneville bearings apparently followed this description with the important difference that instead of one, six of the radial grooves were cut entirely through the flexible plate, thus changing the plate into six separate spring-supported segments or shoes. This was the first step towards the conventional pivoted-shoe design.

When the segmental collar or runner was found unworkable it was replaced by a grooveless runner having a continuous rubbing surface. This was the second step towards the pivoted-shoe design.

The radial grooves were then removed from the centers of the shoes by cutting them through, thus producing twelve shoes free from grooves. The grooveless shoe was the third step towards the pivoted-shoe design. Apparently the two latter steps made it possible for the bearings to operate

satisfactorily. Only removal of the springs and actual pivoting of the shoes remained to complete the transformation of the spring bearings. It might be pertinent to mention that an old United States patent, number 1,117,490, issued November 17, 1914, to Albert Kingsbury, covers the spring-supported, grooveless, segment-shaped thrust shoe.

The writer wonders if the above changes in the original design have resulted in a permanent cure of the early difficulties or will it be necessary to recondition the bearing surfaces from time to time.

The all-important subject of oil film thickness is mentioned but no indication is given of what the minimum film thickness might be. The subject of power loss is not discussed. Possibly the authors can throw some light on these interesting and important questions.

The paper properly points out that the thrust bearing is the mechanical heart of the vertical hydroelectric generator. There are hundreds of such bearings, large and small, in continuous successful service. Despite their importance, however, they seem to be taken for granted and seldom appear in the technical literature. The authors are to be congratulated on their important contribution which not only calls attention to a neglected subject, but gives reliable and accurate information regarding thrust bearing operation in one of the largest stations in the country.

REFERENCE

1. THRUST BEARINGS, F. C. Lins, R. Sheppard. American Society of Mechanical Engineers *Transactions* (New York, N. Y.), volume 60, 1938, pages 245–52.

J. F. Spease (General Electric Company, Portland, Oreg.): The authors have presented data on the design and performance of the Bonneville thrust bearings which I know is of great interest to all of us. Generators are being made bigger and of necessity thrust bearings are being made bigger to withstand these great weights and thrusts. Operating data and experience such as that given in this paper is very welcome to the design engineers of these large machines. During the preliminary design periods on the number 1 and number 2 generators at Bonneville a great deal of thought was given by the designers to the installation and maintenance of these machines. The experienced erectors were called in and the design, as to ease and speed of installation, was discussed with them.

A great deal of thought was given to the handling of guide bearings and thrust bearings both for installation and later maintenance.

The paper states that the loading on this thrust bearing was slightly over 3,000,000 pounds and that the thrust bearing was 112 inches in diameter. Upon designing this bearing it was found that the rotating plate weighed 12,000 pounds and that the stationary plate weighed 6,000 pounds. This is no small weight to handle in the space between the lower bearing bracket and the rotor.

A space of 42 inches, in which to work, was allowed between the rotor arms and the bearing bracket. A space of 20 inches was allowed between the bottom of the thrust bearing oil housing in its raised position and the main bearing bracket floor.

Keeping in mind this space, which is quite adequate, the designers cut the bearing into segments weighing a maximum of 1,000 pounds. That weight is much easier to handle and is of smaller dimension than if the plates had been cut in half, which would mean handling weights of 6,000 pounds.

The rotating segments were keyed to the rotor hub by inserted T-shaped keys. The segments slide into place on the keys, and are held in place by vertical pins against the centrifugal force. In order to handle these segments more easily, a circular track was built around the lower bearing bracket on which a 4-wheel car could be made to rotate around the shaft and bearings.

Segments of the bearing could be pulled out on this small transfer car, run around to the opening in the concrete foundation, and lowered by means of small chain hoists to the "37 floor". This would mean that all the work could be done in that space below the rotor and above the lower bearing bracket, and would not necessitate the removal of any of the generator air housing in order to lower a cable from the overhead cranes down between the rotor arms for handling the bearing segments.

This scheme of handling the bearing worked out very well and was used until the difficulties described in the paper arose. As operating experience was obtained, it was necessary to replace all of the 12 segment runners with a 2-piece runner and the original handling scheme could not be used except with the stationary plates.

As each section of the new runner weighs 6,000 pounds and must be moved from under the hub, one of the Army machinists at Bonneville designed a tricycle handling gear. This is a very ingenious device which allows the bearing to be pulled out on the rails without danger of damaging the bottom sliding surface of the bearing.

The points brought up in this discussion indicate the thought given to maintenance problems in the original and final design of these bearings. Events prove that perhaps originally too much emphasis was placed on maintenance but only experience could have verified this. Had the initial installation been as successful as the final one, the initial maintenance consideration would have been justified fully.

A. B. Lakey (nonmember, Kingsbury Machine Works, Inc., Philadelphia, Pa.): The authors are to be congratulated on their complete description and analysis of this great thrust bearing installation.

The following brief statement of the properties to be desired in the thrust bearing in a hydroelectric unit is inspired by the subject paper, and due to the present emphasis on hydro development, seems timely.

In any modern vertical hydroelectric unit, the thrust bearing is immersed in an oil bath, and the synchronous speed acting on the viscous lubricant generates enough oil pressure between the rubbing surfaces to support the imposed load either completely or nearly so.

An ideal bearing, when attained, will be 100 per cent available and reliable, giving service for indefinite periods without needing attention.

More particularly, the bearing and all its associated parts will withstand indefinitely the effects of any operating conditions, including the following:

1. Creeping at low speed due to gate leakage.
2. Slow starting.
3. Heavy or full loading at starting.
4. In fact, any kind of starting, stopping, or running.
5. Destructive friction, notably as limiting the life of the bearing surfaces.
6. Form changes in the foundations.

Further, an ideal bearing will

1. Increase generator output and therefore revenue from the unit by virtue of low running friction loss.
2. Minimize need for and use of auxiliary equipment, such as high pressure oil pumping and piping systems, whether their purpose be lubricating or jacking.
3. Avoid setting up mechanical vibrations, with their fatiguing effects in the bearing and elsewhere.

Finally, to eliminate fretting corrosion and other effects, an ideal bearing will have to be self-aligning under all working loads. The validity of this statement will be appreciated on consideration of any bearing of the opposite character; that is, one which is merely adjustable.

When out of adjustment and squareness it obviously will produce fluctuating, eccentric loads of greater or less magnitude in the stationary supports of the bearing, together with an equal and opposite set of loads in the fit between the thrust runner, thrust hub, keys and shaft. The first-named forces will subject the stationary parts mentioned to kneading, galling, and fretting action; the second set will similarly damage the revolving parts specified owing to the gyratory action present. We have assumed this bearing to be out of adjustment and squareness. This is the only safe hypothesis, as perfect squareness is rarely attained, and even the best adjustment eventually will be thrown out by subsidence or growth of foundations, or by earth movements.

Hence, any ideal bearing must be completely self-aligning.

Most of the ideals mentioned already are being realized in practice, and any problems in connection with the remainder seem in a fair way to solution.

C. L. Killgore (United States Bureau of Reclamation, Denver, Colo.): The authors have presented a very worthwhile paper on the design and performance of thrust bearings for large vertical hydroelectric generators. It is interesting to note that apparently all of the bearing failures at Bonneville occurred after the generating unit was in operation for some time. It has been our experience that most bearing failures occur during the starting up of the generating unit. After an oil film is established and the metal contact no longer exists between the thrust runner and stationary plate, the probability of a bearing failure is remote, occurring only through some operating condition such as interruption of cooling water supply or foreign material entering the bearing from any cause. Therefore, it is believed that the starting performance of a thrust bearing is one of its most important design characteristics. It is our opinion that a thrust bearing should be capable of starting up without lifting the rotating parts or in introducing oil between the thrust bearing surfaces

Nevertheless, we have found that such a procedure is desirable at one of our large installations and it would be interesting to have the comments of the authors on this practice. Two methods generally are used when starting up a generating unit. One method is to open the turbine gates slowly until the bearing breaks away. The other method is to open the turbine gates to approximately 0.2 gate opening to cause a quick break away of the bearing and then close the gates in order to reduce the speed. Apparently both methods are successful and it would be of interest to know which method is used at the Bonneville power plant.

It is noted that the Bonneville generators are of the overhung type with the thrust bearing located below the generator rotor. It has been our practice to use the more conventional type of construction where the thrust bearing is located above the rotor. No external oil piping or pumps are required and the cooling system is self contained in the thrust bearing oil reservoir. While the paper did not mention whether any trouble had been experienced with these additional auxiliaries, the need for this equipment to reduce the operating temperature of the bearing may be questionable. It is believed that the simplification in eliminating auxiliary equipment tends toward more reliable operation. An important feature of bearing design which was not covered in the paper is the type of protection which should be provided for large vertical generator thrust bearings. The recommendations of the authors would be of particular interest. Tests made at Bonneville to determine whether or not the centrifugal action of the bearing would cause a reduction in the oil level at the center of the bearing indicates the reduction in oil level is not significant, although, this has been a matter of concern to our operators in the past. It is believed that the experience gained with the Bonneville thrust bearing will result in advancement in the design of large thrust bearings and the authors are to be congratulated on their work.

F. M. Lewis and **T. W. Gordon:** The authors wish to express their appreciation for the interest exhibited in this paper and particularly to thank the discussers for their presentations. A few brief comments are offered on some of the points brought out in the written discussions.

Lakey has outlined very completely the required performance of the ideal bearing. Upon two of his points, however, we would like to comment. Point 6, about form changes in the foundation, is something an operator hopes will not happen and only makes the required corrections if and when it occurs. Point 1, about the friction losses in the bearing, is secondary to reliability from an operator's point of view.

Needs has also commented on bearing losses, suggesting the use of smaller bearings at higher unit loading, with pressures over 400 pounds per square inch. It might be stated that while higher pressures can be used, it is felt that since such large generating units are dependent upon the operation of these bearings, the manufacturer should be conservative in the unit pressures, that is, be liberal in the size of the thrust bearing. The largest loads to be carried are on generators at relatively low speed and, therefore, there is no great urge to use the smallest bearing possible in order to reduce friction loss. The few kilowatts saved in bearing loss that might be gained by using a smaller thrust bearing are usually of little concern in the overall efficiency of a hydroelectric unit in the power station.

Load conditions at Bonneville and in most other large stations are such that there is almost no opportunity to check closely on actual thrust bearing losses.

Killgore states that most of their bearing failures have occurred during starting. At Bonneville all failures except one occurred after many hours of continuous running. Each has been accompanied by a sudden rise in plate temperature without any preceding indication or warning. Starting and stopping may have been a contributory cause but there has been no means of determining this effect. Jacking of units, previous to starting, is not the practice at Bonneville. The units are started by slowly opening the gates to 0.2 or 0.3, depending upon head and the length of shutdown, and then returning the stop to the speed-no-load position after break-away.

The additional auxiliaries made necessary by the external cooler are not the most desirable arrangement. Although no trouble has been experienced with this equipment, the minimum of cooling equipment is preferable. The external coolers were installed in this plant, because of the restricted bearing space, to minimize the difficulties in assembly and removal.

The protective equipment consists of temperature detectors in six of the twelve babbitted plates, an indicating thermometer in one plate, and a shut-down temperature relay in one plate. The recording and indicating temperature indicators are equipped with alarm contacts. There is also a thermostat in the oil bath that keeps the circulatory oil pumps running until the oil bath drops to a predetermined temperature. It has been suggested that it would be well to omit these temperature indicators. In the opinion of the authors, two of the bearings would have continued in service except for these devices.

The authors are grateful to Spease for explaining further the reasons for the original design of the bonneville bearings.

Needs has raised the question as to whether or not the changes in the Bonneville bearings as described in the paper will be permanent. The authors believe that with no failures due to iron oxide since January 1941, it is reasonable to suppose that satisfactory operation will continue. The inspections made in 1945 and 1946 were more a matter of curiosity, based upon previous unfortunate experiences than on actual need for dismantling the bearings. The present plans are to inspect and clean these bearings every four years with the next inspection in 1949. At that time information will be gained on fretting corrosion, movement of parts, and the results of some minor mounting changes made in two units.

There is still a little fretting corrosion and iron oxide formation in these bearings. The amount of this formation is not considered serious or detrimental to operation. This leads to the conclusion that a high degree of accuracy and finish must be maintained in the manufacture of the bearing parts and that squareness and parallel surfaces are essential in all the component parts.

A New Grinding Circuit Feed Regulator

J. N. JONES
ASSOCIATE AIEE

WITH increased costs of production existing today, it is mandatory that manufacturing processes be made to function with the highest degree of efficiency practical. One method by which efficient operation is accomplished requires the use of machines controlled by regulators rather than by men. This does not necessarily mean the use of fewer employees, but it will increase production, lower costs, and make the operators' duties easier and simpler. The mining and milling industry is an attractive field for the application of regulators.

Because of the large tonnage milled in present day mine operations, cost factors that appear very small per ton assume important over-all proportions and demand careful consideration. The trend toward regulated control of grinding and classifying methods is evident in the large concentrators.

In these mills, the ore fed to the ball mills is a screened product from the crusher plant. This product will range in maximum coarseness from three-sixteenth to five-eighth of an inch. The ore is ground to a predetermined degree of fineness (established by laboratory tests) to free the sulfide copper grains from the gangue material. Attaining these results in ball mills requires control of water in the ball mill feed and in the classifier pool.

The hardness or grindability of the ore is another important factor. As the ore is mined from different parts of the ore body, the crusher product may vary several times during the day. The tonnage rates of the mills should be changed accordingly for most efficient operation.

These adjustments result in a uniform load of a coarse unfinished product, that is, the circulating load of sands being returned to the ball mill along with raw ore coming from the storage bins.

When the mills are operated under manual control, the adjustments are selected by the operator. If the ore changes are not watched closely, an appreciable amount of obtainable production will be lost when a change to soft ore occurs.

Continuous regulation of ore feed and water control will result in lower costs and higher over-all plant efficiency.

Application

Regulators for controlling the raw ore feed to ball mills have been in operation at the Castle Dome Copper Company mine[1] for the past 12 months with the first regulator operating since September 1945. It is one of the latest developments in the metallurgical field and has increased the mill's efficiency both as to tonnage and metallurgy. The regulator is simple, reliable, and inexpensive; automatically will change the rate of ore fed, to the grinding circuit as the grindability or coarseness of the ore changes; and also proportionately varies the amount of water added to the ball mill as the raw ore feed is varied. Varying the quantity of water proportionately with the ore feed promotes maintenance of constant density within the ball mill.

Milling practice at Castle Dome provides for concentration of ore in the following manner:

1. Crushing of run of mine ore until it will pass a 5/16- by 1-inch screen.
2. Grinding in grate-discharge ball mills which reduce the ore to about 12 per cent plus 48 mesh. Each grinding mill is operated in closed circuit with a rake-type classifier, the load and density in the circuit being regulated. (See Figure 1.)
3. Recovery of copper minerals and depression of iron sulfide by flotation.
4. Dewatering and filtering of final concentrates.

The original capacity of the $10^1/_2$- by 11-foot ball mill was 65 tons per hour, but this was increased to 70 and 75 tons per hour by the installation of grate discharges to replace the free discharge system originally used. Liner wear and ball replacement increased in direct proportion.

Raw ore is moved from the 14,500-ton storage bin to each ball mill by a conveyer belt driven by an adjustable speed d-c motor. This belt discharges onto a constant speed-belt which discharges into the ball mill. The constant speed belt moves over a scale which records the tonnage delivered to each mill. (See Figure 1.)

The regulator for the grinding circuit provides means to determine if a change in rate of feed is required, and how much it should be changed.

It is known that if the amount of ore being fed to the grinding circuit changes, if the friability of the ore or the coarseness of feed changes, the sand load of the classifier will change. Tests have shown that the load of the classifier driving motor changes appreciably with change in sand load, and this change in load is suited to supply the intelligence for regulating the grinding circuit.

Operation

Current relays are provided that are responsive to a change in load on the classifier motor. Action of these relays causes an increase or decrease in the amount of ore being fed to the mill by operating a motor-driven rheostat which changes the resistance in the shunt field circuit of the adjustable speed d-c motor driving the conveyor. The rheostat is a conventional type having 132 steps and provides an ore feed range of 20 tons per

Paper 47-181, recommended by the AIEE committee on mining, metal forming and rolling for presentation at the AIEE Pacific general meeting, San Diego, Calif., August 26-29, 1947. Manuscript submitted June 11, 1947; made available for printing July 14, 1947.

J. N. JONES is electrical service supervisor at Westinghouse Electric Corporation, Los Angeles, Calif.

The author specifically acknowledges his association with David Gray in the first installation of this regulator and the help of J. J. Luchessa, mechanical superintendent, Miami Copper Company, and R. L. Mountjoy, mill superintendent, Castle Dome Copper Company.

hour. The chutes opening onto the ore belts are adjusted to give a constant volume of ore per foot of belt so that the relationship between belt speed and tons per hour is fixed. Doubling the belt speed doubles the tons per hour delivered.

A timing device is provided that is adjusted to act at regularly repeated intervals permitting a change in rate of feed to occur when a change is required, so that small incremental changes are made rather than widely fluctuating ones. The time intervals between changes can be varied. The feed is not stopped and started, but the rate is changed in small, evenly spaced increments.

The motor-operated rheostat is mounted near a water valve which controls part of the water fed to the ball mill. The rheostat motor has a shaft extension which is connected by chain and sprocket to the water valve. A density controller is used to keep the density of the classifier pool constant by varying the water supply in this section. These two control valves are of the straight flow type, are motor-operated, and are provided with limit switches to prevent jamming the valves at either end of travel.

There are two chute-loaded conveyer belts for each ball mill, but only one belt is operated at one time to feed ore. A selector switch permits selection of manual operation or automatic control of either conveyer.

For operation of the regulator refer to Figure 2. Relay *CR8* stops the conveyer when changing from either manual or automatic operation and when changing the feed from one belt to the other.

The load on the classifier motor (25-cycle 3-phase 440-volt squirrel-cage induction motor) is measured through a 25-to-5 ampere current transformer, and the current of the secondary winding is rectified by means of full-wave dry-disk rectifiers. The secondary winding of the current transformer is short-circuited by the timing relay during the "off" period. The current relays *CR3* and *CR4*, type, are in the current transformer secondary circuit during the "on" period.

Relay *CR3* is adjusted to pick up at a lower current value than *CR4*. If the classifier load is low, neither *CR3* nor *CR4* pick up; when the load is as desired, *CR3* only closes its contacts; when the load is high, both *CR3* and *CR4* close their contacts..

Relays *CR5*, *CR6*, and *CR7* are a simple a-c, solenoid type of relay, and can be energized only during the "on" period of the timing relay. During the "on" period, *CR7* is always energized, but *CR5* is energized only when *CR3* contacts are closed, and *CR6* is energized only when *CR4* contacts are closed. The rheostat motor can be energized only during the "on" period when the *CR7* contacts are closed. The rheostat operating motor is a d-c series motor operating through a full-wave dry-disk rectifier and a small, dry-type transformer.

When the classifier load is low, *CR5* contacts remain closed permitting the rheostat motor to operate so as to insert resistance in the conveyer motor field circuit resulting in an increase in speed of the conveyer. When the classifier load is within the desired operating range, *CR5* contacts open holding the conveyer speed constant. When the classifier load is high, *CR5* contacts open and *CR6* contacts close reducing the speed of the conveyer belts.

Time delay in the grinding circuit (from the time a change in ore feed is made until there is a change in classifier load) is of the order of ten minutes. This process lag tends to cause the system to cycle over wide ranges with resultant overshooting of the classifier load and tonnage feed.

This feed regulator is a floating controller and employs a dead zone in order to prevent constant cycling. The dead zone is that region where slight changes in the classifier load do not result in any change in rate of feed. This zone is kept to that minimum which eliminates hunting. Figure 3 shows the rate of feed under actual conditions of manual operation, with the system hunting under regulator control

Figure 1 (below). Sketch of ball mill grinding circuit

Figure 2 (right). Schematic diagram of electric circuit of regulator

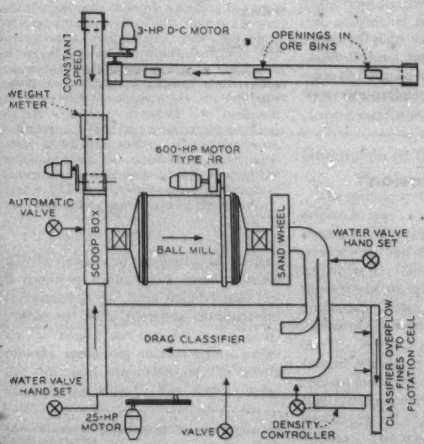

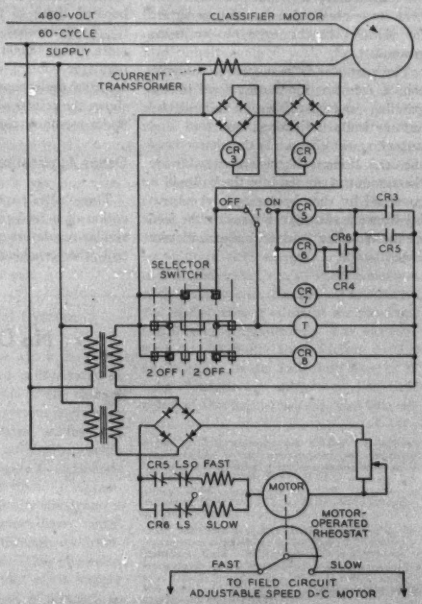

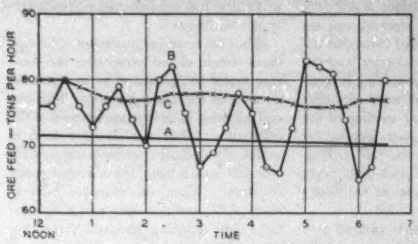

Figure 3. Mill operation tonnage charts

A—Hand control
B—Regulator hunting
C—Regulator

and with the system under control of the regulator properly adjusted.

The timing relay is adjusted at present to have an "on" period of one second and an "off" period of 30 seconds. The incremental load changes possible are one-quarter ton per hour each 31 seconds. The system is stable with this adjustment. Quick response was sacrificed to eliminate hunting, but the response retained is adequate for this particular application.

This regulator is of the type where the final position of the activating device bears no fixed relation to the value of the variable being controlled, and there is no characteristic droop or load error. The value of the classifier motor load does not have to remain at some point different from its original value in order to correct for changes in the type of ore being ground.

The purpose of the control is to maintain a constant circulating load in the grinding and classification circuit by automatically adjusting the feed and water to meet changes in the character of the ore. It is an electric system whereby the amount of ore fed into the ball mill is governed by the circulating load returning from the classifier, increasing the feed as the classifier load decreases and vice versa.

Gain

The importance of this control to an operation like Castle Dome becomes apparent when it is realized that no attempt is made to control the hardness and grindability of the ore mined and delivered to the concentrator for treatment. The ore is dumped into the coarse ore pocket as it best suits the mining operation. At times it may carry 1 per cent copper and at others 0.4 per cent. Moreover, on one day it may come from the eastern portion of the ore body where the ore is soft and the next from the western side where it is hard.

Since the regulator has been installed at Castle Dome, tonnage handled has been boosted three to five per cent. Latest figures show that the mill has handled more than 13,000 tons per day under regulator control while average tonnage is 12,000 under manual control. Figure 4 shows the results obtained with five units under regulator control.

Other Applications

Though this paper deals with the application of a feed regulator for ball mills, similar regulators can be adapted to control other crushing or grinding processes especially where a long time delay exists between the corrective step and the resultant change in the medium being controlled.

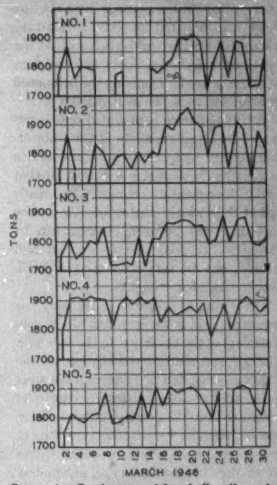

Figure 4. Production of five ball mills under regulator control

Average Values

Mill Number	Average Per Cent Grind +48 Mesh	Average Tons Per Day
1	11.2	1,731
2	12.2	1,791
3	11.3	1,795
4	10.5	1,855
5	11.7	1,795

Reference

1. Castle Dome—An Outgrowth of War. *Mining World* (Seattle, Wash.), October 1946, pages 40–7.

No Discussion

General Analysis of Speed Regulators Under Impact Loads

G. D. McCANN
MEMBER AIEE

W. O. OSBON
MEMBER AIEE

H. S. KIRSCHBAUM
ASSOCIATE AIEE

Synopsis: This paper presents the results of a generalized study that has been made on the transient speed response of basic forms of speed regulating systems to suddenly applied square wave load torques. The solutions were obtained on the transients analyzer and the electrical analogies for the systems are developed. The solutions are applicable to d-c motor drives with either variable armature voltage or motor field current control and two inherent time delays, one of which must be in the motor armature circuit. Stabilization is effected by means of an "anticipatory" RC circuit just following the error signal and an RC feed-back circuit just after the first inherent time delay. The type of system specifically illustrated in the paper is one with an electronic amplifier, Rototrol, and d-c generator that supplies the armature voltage. The study shows the effects of all system parameters, including a series self-energizing field that may be used with Rototrols to eliminate steady-state speed errors. It was found practical to define optimum forms for the response to impact loading in terms of crest transient speed dip, time to recover normal speed, and per cent system damping. A set of generalized dimensionless curves presents the performance of such regulating systems in terms of these characteristics, together with the anticipation and feed-back circuit constants required for optimum solutions. These curves cover the practical range of all parameters. The performance resulting from the operation of speed regulators over a range of speeds by changing the motor field current without readjustment of the antihunting parameters is discussed.

IN the design and application of modern precision rolling mill speed control equipment it has been found highly desirable to make complete transient response calculations and determine in detail the speed dip characteristics under the transient conditions of the billets entering the rolls.* For such systems it is a relatively simple matter to compute analytically the steady-state accuracy and to determine whether or not the system is stable. However a knowledge of the complete transient speed variation for a wide range of the controlling parameters is important in order to provide a design which yields the minimum impact speed drop and maximum rate of recovery to normal speed consistent with adequate damping, and which meets the required specifications regarding these quantities.

The transients analyzer[1-3] has been found admirably suited to this type of analysis since complete transient solutions and the effects of varying the controlling parameters can be obtained so rapidly. After studying and designing a number of steel mill regulating systems in this way it was considered desirable to make a general analysis of the basic systems used for steel mills over a comprehensive range of all important parameters. As the study was carried out the results were found applicable to an even greater range of speed regulator problems.

Description of Control System

The specific system for which the study originally was conducted is illustrated in Figure 1. The derivation of the characteristic equation of the system is given in Appendix I. The electrical analogy for this system as set up on the transients analyzer is shown in Figure 2. The derivation of the analogy is given in Appendix II. Figure 1 specifically illustrates a system with a d-c motor drive, speed control being effected through its armature voltage variation. The generator may supply all or only part of the supply voltage. The motor load is assumed to consist of a constant torque, a transient impact torque, and the motor and mill inertia. The inertia may include, in addition to that of the motor and rolls, a flywheel which sometimes is required to limit the crest impact speed drop. The generator is excited by a Rototrol which in turn is excited by an electronic amplifier. The control signal voltage is the difference between the tachometer voltage and the reference voltage E_ϕ. As shown in Appendix I, the series self-energizing field on the Rototrol, when properly tuned, reduces the steady-state speed error to zero. The regulator is stabilized with the anticipator circuit (R_a, C_a) and the feed-back circuit (R_f, C_f) from the generator field current. In such a system the steady-state speed can be changed by varying the regulator reference voltage E_ϕ. When the regulator has insufficient range to cover the entire speed range desired, it may be necessary throughout the upper part of the range to vary the motor field simultaneously with the reference voltage. If the generator is a booster in series with another supply voltage, speed changes over a wide range also can be made by simultaneous variation of the supply voltage and the reference voltage.

In the derivations of Appendix I it will be noted that inherent droop in motor speed is considered as due to IR drop alone. This assumes that the motor field strength remains constant for any particular value of field current. Actually the motor field strength may change somewhat with load, due to armature reaction and the demagnetizing effect of the armature turns being commutated. The justification for neglecting these factors in this analysis lies in the fact that changes in field strength are subject to the time delay of the field structure, and this de-

*See references 4–6 for impact drop analyses of unregulated motors.

Paper 47-186, recommended by the AIEE joint subcommittee on servomechanisms and approved by the AIEE technical program committee for presentation at the AIEE Pacific general meeting, San Diego, Calif., August 26–29, 1947. Manuscript submitted May 22, 1947; made available for printing July 18, 1947.

G. D. McCann is in the electrical engineering department of the California Institute of Technology, Pasadena, Calif.; W. O. Osbon is in the research laboratories of the Westinghouse Electric Corporation, East Pittsburgh, Pa.; H. S. Kirschbaum is in the electrical engineering department, Ohio State University, Columbus, Ohio.

lay is usually long compared to the time required to reach the maximum speed drop and recover to normal speed. Consequently, the field weakening effects exert but little influence on the important characteristics of the solutions as presented here.

As shown in Appendix I, the characteristic equation for this system (equation 14) represents to sufficient accuracy the performance of a speed regulator with a constant armature voltage source and with the regulating system controlling the motor field current. Also, as will be seen later, the solutions obtained for equation 14 are of even more general application.

System Parameters. In the presentation of solutions it is most convenient to specify them in dimensionless form as discussed in connection with equation 14*b*. Speed variations are thus expressed as the ratio of actual speed variation to the fractional speed dip D_0 of an uncontrolled motor, and time is expressed in units of the mechanical time constant T_0 instead of in seconds. D_0 and T_0 are both quantities that can be calculated quickly for a given system. As expressed in equations 14 and 14*b*, the parameters of actual regulators are simply the five time constants, the two dimensionless parameters A_1 and A_2, and the Rototrol self-energization factor K_r. These are all defined in the caption of Figure 1. The determination of these parameters for specific control systems will be illustrated later in connection with applications of the dimensionless solutions.

General Character of Speed Dip Solutions

In Figures 3 to 6 are shown typical speed dip solutions as obtained on the transients analyzer. In Figure 7 are presented the generalized dimensionless solutions. These are all solutions for which optimum values have been chosen for the R_fC_f feed-back time constant, feed-back ratio A_2, and anticipator time constant T_a. A fixed value of 3 was used for k over the entire range of solutions. These parameters are quantities that usually can be adjusted readily to any desired value as contrasted with the system time constants and parameter A_1. It thus was considered desirable to present in most cases only the solutions corresponding to the optimum values of these easily controlled quantities.

The solution of Figure 3*a* is typical of those determined as optimum with systems having series Rototrol fields. With reference to Figure 3*a* the characteristics considered important are the crest fractional speed dip D_1, the time to recovery of normal speed, and the system damping. It also was considered desirable to prevent any appreciable overspeed such as indicated by Figure 3*b*.

Effect of RC Feed-back Circuit. It was found that the *RC* feed-back circuit had a much more dominant effect on system damping than the "anticipatory" circuit. However, as will be discussed, this circuit has important effects on the solution for certain ranges of the basic parameters.

In the practical range of all parameters, there is only one dominant system frequency and all other roots of the solution correspond to very high damping. As is typical of *RC* feed-back stabilization, increasing the amount of feedback A_2 increases damping, but above some usually fairly critical value, it also rapidly increases the crest speed dip.

The magnitude of the feed-back circuit time constant T_f is also important as shown in Figure 3. Too large a value results in a longer time t_1 to recover to normal speed. Too small a value causes overshooting and impairs system damping. It was found that over the complete range of system time delays and amplification A_1, there exist well defined optimum values of T_f, A_2, and T_a for which an optimum combination of minimum speed dip and time to return to normal speed can be achieved with adequate damping.

Figure 1. Schematic diagram of basic speed regulated system

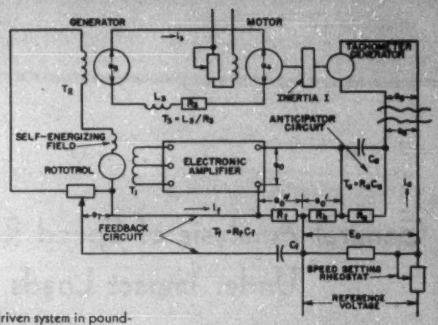

List of symbols:

= inertia of motor and driven system in pound-foot-seconds²

n = ratio of total system inertia to motor inertia

b = motor torque coefficient in foot-pounds per ampere

g = motor voltage coefficient in volts per radian per second

r_0 = motor-armature damping constant in foot-pounds per radian per second

$T_0 = I/r_0$ = mechanical time constant in seconds

T_1 = Rototrol field circuit time constant in seconds

T_2 = generator field circuit time constant in seconds

$T_3 = L_3/R_3$ = motor generator armature circuit time constant in seconds

$T_f = R_fC_f$ = feed-back circuit time constant in seconds

$T_a = R_aC_a$ = anticipator circuit time constant in seconds

$k = (R_a+R_b)/R_a$ = anticipator circuit ratio = 3 for all solutions

A_1 = over-all regulator system gain ($= e_3/e_4$ in steady-state with circuit break shown in Figure 1)

A_2 = gain around feed-back loop with $C_f = \infty$

K_a = over-all gain of amplifier, generator, and Rototrol without benefit of the Rototrol series field

K_1 = volts across R_b per radian per second in steady state

K_2 = voltage feed-back factor $= e_7/e_3$

K_r = fractional measure of degree of self-energization of Rototrol

M = applied impact load torque in foot-pounds

M_c = control torque developed by regulator in foot-pounds

ω = transient speed variation from reference value in radians per second

ω_0 = reference or normal speed in radians per second

ω_2 = steady-state speed drop with regulator in radians per second

ω_{s1} = steady-state speed drop for unregulated system in radians per second

s = no load speed in revolutions per second

$D = -\omega/\omega_0$ = fractional transient speed drop

$D_0 = -\omega_{s1}/\omega_0$ = fractional steady-state speed drop for unregulated system

$D_0 = M/6.28sr_0$

D_1 = maximum fractional transient speed drop

p = derivative operator d/dt

For application of full load torque:

$D_0 = (550 \times \text{rated motor horsepower})/(6.28s)^2r_0$

System characteristic equation:

$$-1-(1+T_0p+T_0T_3p^2)(D/D_0) = \frac{A_1(1+T_ap)(D/D_0)}{[1-K_r+(T_1+T_3)p+T_1T_3p^2](1+T_ap/k)} + \frac{A_2T_fp(1+T_0p+T_0T_3p^2)(D/D_0)}{[1-K_r+(T_1+T_3)p+T_1T_3p^2](1+T_fp)}$$

Effect of Rototrol Series Field. The effect of the Rototrol series field is shown by the solutions of Figure 4. The steady-state speed drop without it is calculated by equation 17b of Appendix I.

By comparing solutions both with and without the series field, it was found that over the complete range of the data presented here, the two conditions showed very little variation in crest speed dip (less than ten per cent). Also, the time to recover to normal speed for the case with the series field is practically the same as the time to reach the steady-state error without the series field. The same values of feed-back and anticipation constants apply to both cases and the damping usually is slightly higher without the series field. Thus the solutions presented in Figure 7 for a system with a series self-energizing field are applicable also to systems without this field.

Of some practical interest is the character of the generator field current as illustrated by the solution of Figure 4c. The steady-state current increase indicated by the solution is proportional to the amount of load thrown on the system. For all adequately damped solutions the transient peak generator field current (and thus also the generator voltage) is appreciably less than twice the change in steady-state value. Thus, in systems where boosters are used, since the steady-state voltage change must compensate only for the *IR* drop in the armature, boosters which are linear to a voltage equal to twice the rated-load *IR* drop of the associated motor will have sufficient range.

Effect of Anticipation Time Constant. It was found that for values of T_a/T_0 below 0.3 the optimum value of T_a is infinity for the complete practical range of the other time constants and A_1. This is equivalent to applying the tachometer differential voltage directly to the amplifier. For values of T_a/T_0 above 0.3 there are ranges where finite values of $T_a = T_2$ give somewhat better solutions as shown in Figure 7. Figures 5 and 6 show the effect of T_a in these two ranges.

Generalized Transient Solutions

The curves of Figure 7 present the results of the general study in a form which is suitable for the design of a wide range of speed regulating systems. The data specified in terms of three dimensionless parameters defined in Figure 1. These are T_3/T_0, T_2/T_0, and A_1. For each value of these parameters two sets of data are presented. One gives the optimum value of the R_fC_f feed-back constants in dimensionless form as T_f/T_0 and A_2, and also the optimum value of T_a. The other gives the basic performance characteristics for these parameters in terms of the crest transient speed dip D_1 and the time to recover normal speed t_1. These are plotted in the dimensionless form D_1/D_0 and t_1/T_0. For normal ratios of T_1 to T_3 and T_4 it was found that T_1 had but slight effect and this delay therefore was neglected in order to reduce the required amount of data. For most regulators T_1 will not exceed about ten per cent of T_3 and for such conditions its effect is negligible.

By referring to Figure 7, it will be seen that separate sets of curves are presented for each ratio of T_3/T_0 with the curves of each set plotted as a function of T_2/T_0. If it is desired to use the data for intervening values of T_2, interpolation methods are usually suitable. The variation of all solutions and optimum damping parameters are sufficiently uniform for this. If desired, the specific data can be replotted as a function of T_2. The range of T_3/T_0 covered is quite broad (0.001 to 3.0) so as to provide data not only for systems with light inertia loads but also for those with large flywheels increasing the system inertia by factors as large as 20. It is of course the small ratios of T_3/T_0 and T_2/T_0 that correspond to the large flywheel ratios, since T_0 varies directly as the inertia. For each ratio of T_3/T_0 the practical range of T_2 is covered. For ratios of T_2/T_0 up to 0.3 the best solutions were obtained with T_a equal to infinity which corresponds to applying the full error control signal to the system during the entire transient. With higher ratios of T_2/T_0 and T_3/T_0, regions were found where finite values of T_a give better results with different values of T_a applying to different regions. It was found, however, that the character of the solution with the exact optimum value of T_a was insignificantly better than could be obtained with T_a equal to T_2 as shown by the curves. This is of course under the conditions that for each value of T_a the optimum values of T_f and A_2 were used. Thus as can be seen from Figure 7*f*, in the region around $T_3/T_0 = 0.3$ an anticipation time constant of either infinity or a value equal to T_2 might be used. However, appreciably above $T_3/T_0 = 0.3$, a value of $T_a = T_2$ is to be preferred.

For T_3/T_0 below 0.3 it was possible to obtain rates of decay of oscillations higher than 95 per cent per cycle with no

Figure 2. Electrical analogy for system of Figure 1 as set up on the transient analyzer

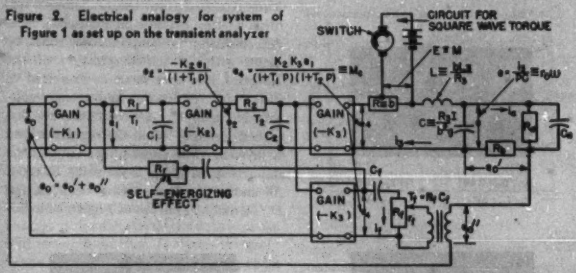

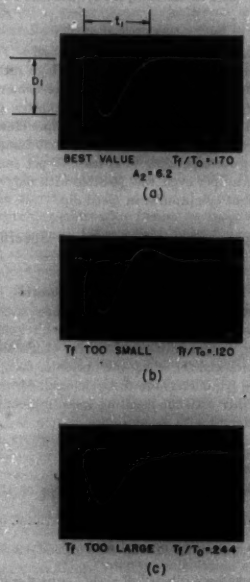

Figure 3. Typical transient impact speed dip solutions, showing effect of feed-back circuit time constant

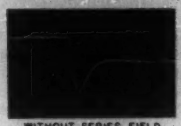

WITHOUT SERIES FIELD

(a)

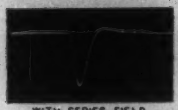

WITH SERIES FIELD

(b)

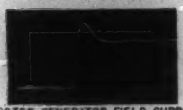

BOOSTER GENERATOR FIELD CURRENT

T_2/T_0=.10 T_3/T_0=.0125 A_1k=170

(c)

Figure 4. Impact speed dip solutions, showing effect of series Rototrol self-energizing field for correcting steady-state speed

appreciable sacrifice in D_1/D_0 and t_1/T_0. For higher ratios of T_3/T_0 such high rates of decay are either impossible to achieve or are obtainable only at the expense of an increase in the crest speed dip. However, it was found in all cases that damping corresponding to at least 70 per cent decay per cycle was possible with only a slight compromise in speed dip.

Application of Solutions to Specific Problems

As an illustration of the application of the curves in Figure 7 to a specific system, consider a variable voltage speed regulator system with the following characteristics and for which the optimum damping parameters are to be determined, together with the resulting speed dip characteristics for a sudden application of full load torque:

Motor

250 horsepower, 600 volts, 500 rpm, or 8.33 revolutions per second

Armature resistance = 0.120 ohm (total, including generator)

Armature $L_a/R_t = T_3 = 0.10$ second (total, including generator)

Armature rated full-load current = 350 amperes

Armature full load IR drop = 42 volts (total, including generator)

Other regulator constants

Total inertia $Wr^2/g = 300$ pound-foot-seconds^2

Generator field time constant $T_2 = 0.3$ second

System amplification $A_1 = 50$

The fractional unregulated speed drop is, from equation 18a,

$$D_0 = 42/600 = 0.07$$

The constant r_0 is given by equation 19

$$r_0 = \frac{M}{6.28\epsilon D_0} = \frac{550 \times \text{horsepower}}{(6.28\epsilon)^2 D_0}$$

$$= \frac{550 \times 250}{6.28^2 \times 8.33^2 \times 0.07}$$

$$= 720 \text{ pound-feet per radian per second}$$

$T_a = \infty$

D_1/D_0=.048 T_f/T_0=.135

t_1/T_0=.32 A_2=4.0

$T_a = T_2$

D_1/D_0=.077 T_f/T_0=.275

t_1/T_0=.50 A_2=6.40

Figure 5. Speed dip solutions, showing effect of anticipator time constant T_a in range where T_a equal to infinity gives best solutions

For these solutions $T_2/T_0 = T_3/T_0 = 0.03$; $A_1k = 75$

For reference to Figure 7

$T_2/T_0 = 0.3/0.417 = 0.720$

$T_3/T_0 = 0.10/0.417 = 0.240$

$A_1k = 3 \times 50 = 150$

Interpolation by direct ratio between the curves of Figures 7*e* and 7*f* gives the following data:

T_a = infinity

$T_f/T_0 = 0.46 + 0.7(0.83 - 0.46) = 0.72$

$A_2 = 21 + 0.7(41 - 21) = 35$

$D_1/D_0 = 0.13 + 0.7(0.21 - 0.13) = 0.186$

$t_1/T_0 = 0.83 + 0.7(1.7 - 0.83) = 1.44$

Thus the optimum stabilizing parameters are $A_2 = 35$, $T_f = 0.3$ second with no anticipation circuit and thus with an effective system amplification of 150 at all times. Upon sudden application of full load torque, the fractional speed dip D_1 is 0.0130 or 1.3 per cent of no-load speed, and the time t_1 to return to normal speed is 0.60 second.

System Amplification. The over-all system amplification A_1 can be computed from a knowledge of the individual amplification factors as given by the equations of Appendix I. It also may be determined for either a variable-voltage or variable-field-current controller by opening the regulator system at some convenient point such as the tachometer terminals, and computing or measuring the voltage change produced at the tachometer by unit change of voltage between the leads removed from the tachometer terminals. (See e_5 and e_6 in Figure 1.) The determination of amplification must be made with no self-energization of the Rototrol, and care must be exercized to insure that the loading and average voltages in the e_5 and e_6 circuits are not disturbed seriously when the regulator loop is broken. The effect of system gain on impact speed drop is of some interest. As shown by the spacing between the D_1/D_0 and t_1T_0 curves of Figure 7 for dif-

$T_a = \infty$

D_1/D_0=.165 T_f/T_0=.90

t_1/T_0=1.42 A_2=96

$T_a = T_2$

D_1/D_0=.117 T_f/T_0=.39

t_1/T_0=1.23 A_2=30

$T_a = T_0$

D_1/D_0=.156 T_f/T_0=.50

t_1/T_0=1.41 A_2=26

Figure 6. Solutions showing effect of anticipator time constant T_a in range where $T_a = T_3$ gives best solutions

For these solutions $T_3/T_0 = T_2/T_0 = 0.3$; $A_1k = 450$

ferent values of A_1k, the relative decrease in these quantities with increase in amplification decreases rapidly above a gain corresponding to A_1k equal to about 150. This effect is shown more clearly in Figure 8.

Operation of Steel Mill Speed Controllers Over a Range of Speeds

It is sometimes desired to operate variable voltage rolling mill equipment over a range of speeds by simultaneous adjustment of the motor field current and the reference voltage E_s (see Figure 1) without readjustment of the parameters of the damping circuits. This means that the damping constants can be set for optimum performance at only one speed. As can be seen from Appendix I, under this condition of operation, the motor constants b and g vary directly with field strength or inversely with motor speed. Thus the system amplification A_1 varies inversely with motor field strength or directly with the speed. Also, the constant r_0, being proportional to the product of b and g, varies directly as the square of the field strength so that T_0 varies inversely as the square of the field strength, or as the square of the speed.

Under this condition of operation it is important to know if satisfactory performance can be achieved with one setting of the stabilizing parameters and what their values should be. A study of such operation was made for a typical system with a range of conditions corresponding to a speed range by field weakening of four to one and a variation of system inertia of ten to one, corresponding to the addition of flywheels or load inertias of varying sizes. Some of the data obtained from this study are shown in Figures 9 to 11. The solutions of Figures 9 and 10 show the typical effects of varying speed without a corresponding change in stabilizing constants. One of the most important factors is the variation of system damping. Variation of field strength to either side of a point where adjustments are made for adequate damping results in a decrease in damping. The reduction of damping is usually more rapid in the direction of field current increase as shown by Figure 10. Also, the impairment of damping is greater for the lower values of T_0 corresponding to smaller added inertia. This effect is illustrated by Figure 9 for which the inertia ratio n is unity. For the specific system considered here, acceptable performance (as far as damping is concerned) for relatively high values of n, as illustrated in Figure 10, could be obtained by adjusting for optimum damping at the middle of the speed range. However, for $n=1$, illustrated in Figure 9, a slightly better setting was that made at the low end of the speed range. With low values of added inertia it was not possible to obtain adequate damping over the entire speed range without appreciable increase in the impact speed drop or time to recover normal speed. For the data shown in Figures 9 to 11, the stabilizing parameters were not set at exactly optimum values for the solutions shown, but in such a manner as to obtain a minimum of decrease in damping with speed change. Thus the solutions do not correspond to those of Figure 7. Figure 11 shows the variation in relative crest speed dip (D_1/D_0) with field setting and total system inertia.

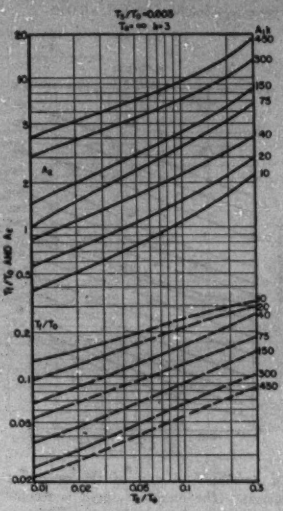

Figure 7b. Solutions for $T_s/T_0=0.003$

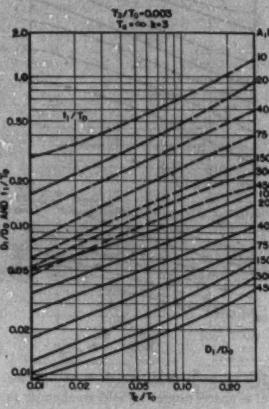

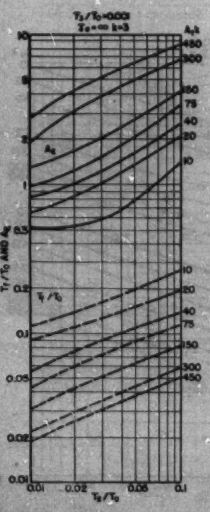

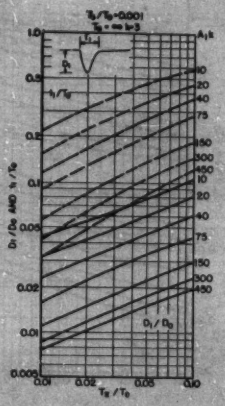

Figure 7. **Generalized solutions of optimum regulator damping parameters and resulting impact speed dip performance**

For definition of parameters, see Figure 1

Figure 7a. Solutions for $T_s/T_0=0.001$

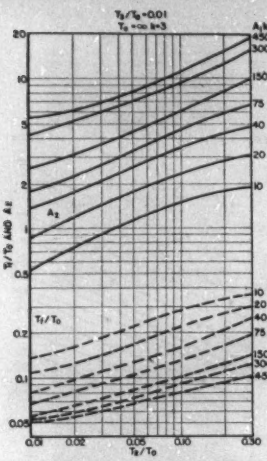

Figure 7c. Solutions for $T_3/T_0=0.010$

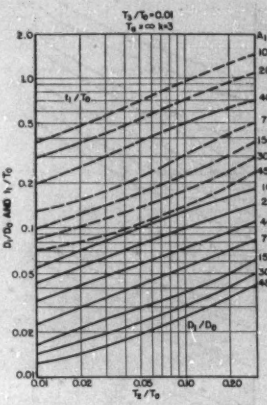

If a given system which is to operate over a speed range by field weakening is adjusted for the optimum antihunting parameters at any given speed in accordance with the data of Figure 7, considerably lower speed dips will be experienced than shown in Figure 11 for the range of T_3 below about 0.2. For speed variations not exceeding two to one, fairly good performance will be obtained for adjustment of constants of any of the operating speeds. The midpoint speed is recommended. It also was found satisfactory to use the data of Figure 7 in setting for speed change ratios up to four to one. For large relative values of the constant n (above 3 or 4) the adjustment is best made at the mid-point speed. For systems with ($n = 1$), the adjustment is probably best made at the lowest speed although good damping over a speed range as great as four cannot be expected with a single setting of the feed-back and anticipation feed-back parameters.

Conclusions

It has been found possible to present generalized transient response solutions for d-c motor speed regulators under impact load torques. The curves of Figure 7 give in dimensionless form the optimum values of the *RC* feed-back and anticipatory circuit constants for the practical range of system amplification and time delays, together with the resulting performance in terms of crest transient speed dip and time to recover to normal or steady-state speed. These solutions can be used not only for the design of systems to operate at a specific speed or over a range of speeds by armature voltage control, but also for most cases where systems operate over a range of speeds by motor field current variation.

Appendix I. Derivation of Control Equations for Basic Speed Regulators

The basic systems being considered are illustrated by Figure 1. The equations will be developed in terms of the deviations of the variables from their reference values at normal speed. The load on the motor is assumed to be the inertia load, the normal steady-state load torque, and the applied transient square wave torque.

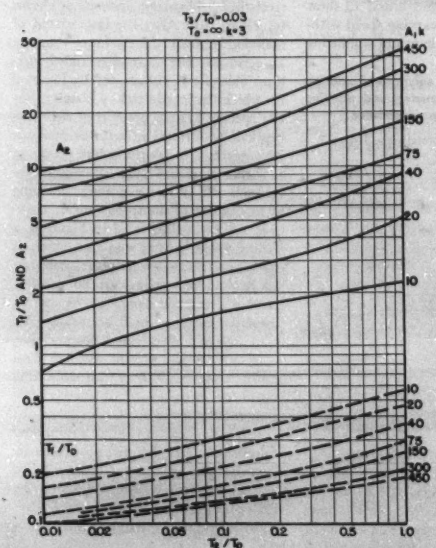

Figure 7d. Solutions for $T_3/T_0=0.03$

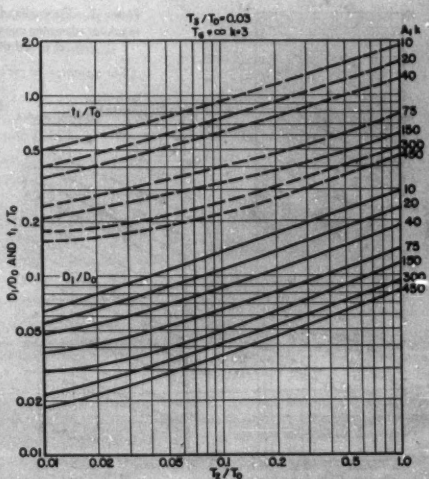

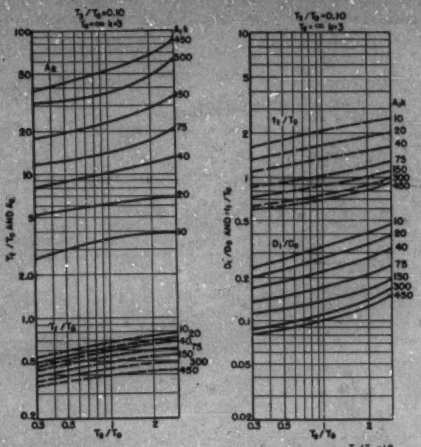

Figure 7e. Solutions for $T_3/T_0=0.10$

Regulation by Control of Armature Circuit Voltage. The additional torque developed by the motor when a speed change occurs is assumed proportional to the incremental armature current i_2. Thus the incremental torque equation has the conventional form

$$bi_2=Ip\omega+M \tag{1}$$

(See Figure 1 for definitions of symbols.)

The motor generator armature circuit voltage equation has the form

$$e_1=Ri_2+L_2pi_2+g\omega \tag{2}$$

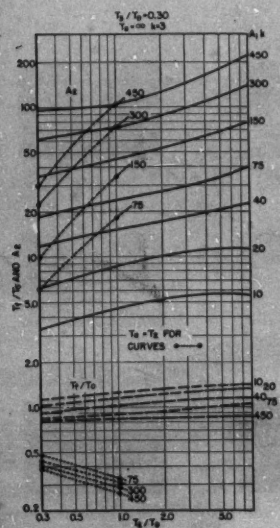

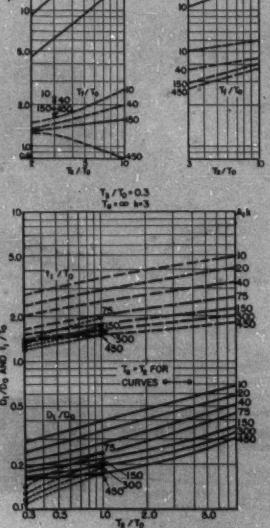

Figure 7g (below). Solutions for $T_3/T_0=1.0$ and 3.0

Equations 1 and 2 can be combined into a single mechanical torque equation in terms of ω as follows:

$$\frac{be_1}{R_2}=M_c=Ip\omega+\frac{L_2Ip^2\omega}{R_2}+\frac{bg}{R_2}\omega+M$$

reducing to

$$M_c=(1+T_2p)Ip\omega+r_0\omega+M \tag{3}$$

where M_c is defined as the control torque and

$$T_2=\frac{L_2}{R_2}$$

= armature circuit time constant

$$r_0=\frac{bg}{R_2}$$

= mechanical damping constant or torque per unit speed change.

Equation 3 can be rewritten as follows:

$$\frac{M_c}{r_0}=(1+T_2p)T_0p\omega+\omega+\frac{M}{r_0}$$

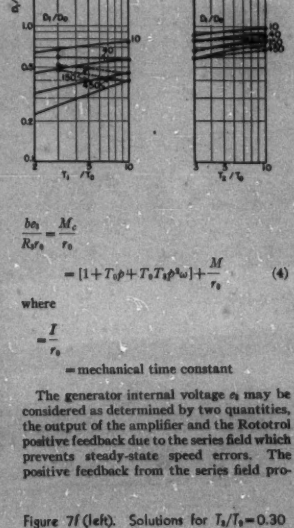

$$\frac{be_1}{R_2r_0}=\frac{M_c}{r_0}$$

$$=[1+T_0p+T_2T_0p^2\omega]+\frac{M}{r_0} \tag{4}$$

where

$$=\frac{I}{r_0}$$

= mechanical time constant

The generator internal voltage e_1 may be considered as determined by two quantities, the output of the amplifier and the Rototrol positive feedback due to the series field which prevents steady-state speed errors. The positive feedback from the series field pro-

Figure 7f (left). Solutions for $T_3/T_0=0.30$

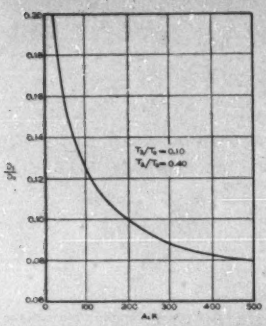

Figure 8. Effect of system gain on impact drop, all other factors remaining constant

duces a component of e_3 which may be expressed as

$$e'_3 = \frac{K_r e_3}{(1+T_1 p)(1+T_2 p)} \tag{5}$$

where K_r is the fractional measure of the degree of self-energization. When the Rototrol is completely self-energized or "tuned," $K_r = 1$ and when there is no positive feedback $K_r = 0$.

The output of the amplifier produces a second component

$$e''_3 = \frac{-K_6 e_0}{(1+T_1 p)(1+T_2 p)} \tag{6}$$

where K_6 is the over-all voltage gain of the amplifier, generator, and Rototrol without the latter's series field. Thus

$$e_3 = \frac{K_r e_3}{(1+T_1 p)(1+T_2 p)} - \frac{K_6 e_0}{(1+T_1 p)(1+T_2 p)}$$

or

$$e_3 = \frac{-K_6 e_0}{(1-K_r)+(T_1+T_2)p+T_1T_2p^2} \tag{7}$$

The amplifier input voltage e_3 contains two components e'_3 and e''_3. The first is due to the difference between the tachometer voltage and the reference voltage E_3 (modified by the R_aC_a circuit) and is thus a function of the velocity error ω. The second is from the R_fC_f feed-back circuit.

The first component is given by the equation

$$e'_3 = \frac{K_1(1+T_a p)\omega}{1+\frac{T_a}{k}p} \tag{8}$$

where

$$K_1 = \frac{R_b g_t}{R_a+R_b}$$

$$k = \frac{R_a+R_b}{R_b}$$

$$T_a = R_a C_a$$

By referring to Figure 1, equation 8 is derived as follows:

E_a = tachometer generator voltage $= g_t\omega$

$$g_t\omega = \left[R_b + \frac{R_a}{1+R_aC_ap}\right]i_a$$

where i_a is the incremental current.

$$i_a = \frac{g_t\omega(1+T_ap)}{(R_a+R_b)\left(1+\frac{R_b}{R_a+R_b}T_ap\right)}$$

Thus

$$e'_3 = R_b i_a = \frac{R_b g_t(1+T_ap)\omega}{(R_a+R_b)\left(1+\frac{T_a}{k}p\right)}$$

The second component of the amplifier input voltage is given by the equation

$$e''_3 = \frac{K_2 T_f p e_3}{(1+T_f p)} \tag{9}$$

where

$K_2 = e_f/e_3$; $T_f = R_fC_f$

This is derived as follows:

$$e_f = \left(R_f + \frac{1}{C_f p}\right)i_f$$

$$i_f = \frac{C_f p e_f}{(1+T_f p)}$$

$$e''_3 = R_f i_f = \frac{R_f C_f p e_f}{(1+T_f p)}$$

Since e_f is proportional to e_3, we have equation 9. Thus

$$e_3 = e'_3 + e''_3 = \frac{K_1(1+T_ap)\omega}{\left(1+\frac{T_a}{k}p\right)} + \frac{K_2T_fpe_3}{(1+T_fp)} \tag{10}$$

Substituting equation 10 in equation 7

$$e_3 = \frac{-K_6K_1(1+T_ap)\omega}{[(1-K_r)+(T_1+T_2)p+T_1T_2p^2]\left(1+\frac{T_a}{k}p\right)} + \frac{-K_6K_2T_fpe_3}{[(1-K_r)+(T_1+T_2)p+T_1T_2p^2](1+T_fp)} \tag{11}$$

Thus the term M_c/R_0 is given by the equation

$$\frac{M_c}{r} = \frac{be_3}{R_0r_0} = \frac{-\frac{K_6K_1}{g}(1+T_ap)\omega}{[(1-K_r)+(T_1+T_2)p+T_1T_2p^2]\left(1+\frac{T_a}{k}p\right)} \frac{K_6K_2T_fp\frac{M_c}{r_0}}{[(1-K_r)+(T_1+T_2)p+T_1T_2p^2](1+T_fp)} \tag{12}$$

since

$$g = \frac{r_0R_0}{b}$$

Substitution of the value of M_c/r_0 as given by equation 4 in equation 12 produces the complete differential equation defining the

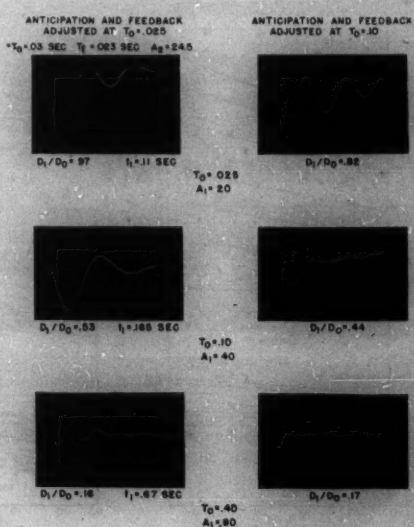

Figure 9. Illustrative speed dip solutions, showing relative performance for operation over a 4-to-1 speed range by changing motor field current but not readjusting stabilizing parameters

For these solutions n = (total Wr^2)/(motor Wr^2) = 1

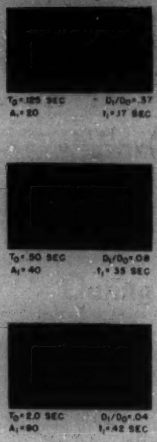

Figure 10. Illustrative speed dip solutions, showing relative performance for operation over a 4-to-1 speed range by changing motor field current but not readjusting stabilizing parameters

For these solutions $n=5$. Antihunt circuits adjusted at $T_0=0.50$ second $T_d=0.088$ second $T_f=0.10$ second $A_2=4.67$ $T_s=0.2$ $T_a=0.025$ $k=3$

system's speed variation under impact loads

$$-\frac{M}{r_0}-(1+T_0p+T_0T_2p^2)\omega=\frac{\left(\frac{K_0K_1}{g}\right)(1+T_ap)\omega}{[(1-K_r)+(T_1+T_2)p+T_1T_2p^2]\left(1+\frac{T_a}{k}p\right)}+\frac{(K_0K_2)T_fp(1+T_0p+T_0T_2p^2)\omega}{[(1-K_r)+(T_1+T_2)p+T_1T_2p^2](1+T_fp)} \tag{13}$$

or

$$-\frac{M}{r_0}-(1+T_0p+T_0T_2p^2)\omega=\frac{A_1(1+T_ap)\omega}{[(1-K_r)+(T_1+T_2)p+T_1T_2p^2]\left(1+\frac{T_a}{k}p\right)}+\frac{A_2T_fp(1+T_0p+T_0T_2p^2)\omega}{[(1-K_r)+(T_1+T_2)p+T_1T_2p^2](1+T_fp)} \tag{14}$$

where

$$A_1=\frac{K_0K_1}{g}$$

$$A_2=K_0K_2$$

Both A_1 and A_2 are dimensionless. If the Rototrol is tuned, the factor $(1-K_r)$ is zero.

Regulation by Control of Motor Field Current. For the case of motor field current control with constant armature circuit voltage, the Rototrol of Figure 1 supplies the motor field instead of the generator field. In this case the motor air gap flux, neglecting saturation, can be expressed as follows:

$$\phi=\frac{\phi_0}{i_{f0}}(i_0+i_f)$$

where

ϕ_0 = reference or steady-state field strength

i_{f0} = reference field current at reference velocity under steady-state conditions

i_f = transient field current variation

The motor voltage constant which is proportional to field flux can be written

$$k_f=\frac{g}{i_{f0}}(i_{f0}+i_f) \text{ volts per unit speed change}$$

Also the motor torque coefficient can be written

$$b_f=\frac{b}{i_{f0}}(i_{f0}+i_f)$$

Thus the *total* armature voltage equation and the motor torque equation can be written as follows:

Voltage equation

$$E_0=R_3(1+T_3p)(i_{a0}+i_a)+\frac{g}{i_{f0}}(i_{f0}+i_f)(\omega_0+\omega)$$

(E_0 in this equation is the fixed voltage applied to the motor.)

Torque equation

$$\frac{b}{i_{f0}}(i_{f0}+i_f)(i_{a0}+i_a)=Ip(\omega_0+\omega)+M_0+M$$

The transient portions of these equations are

$$0=R_3(1+T_3p)i_a+\frac{g}{i_{f0}}[i_{f0}\omega+i_{f0}\omega+i_f\omega] \tag{15}$$

$$\frac{b}{i_{f0}}[i_fi_{a0}+i_{f0}i_a+i_fi_a]=Ip\omega+M \tag{16}$$

In any practical speed controlling system the transient speed change will not be more than a few per cent of the reference speed; the field current variation i_f required for control will be a small fraction of the reference value i_{f0}. Neglecting the term containing $i_f\omega$ in equation 15 and the terms containing i_fi_{a0} and i_fi_a in equation 16 will result in an error not greater than approximately five per cent for most practical control systems, and the added complexity that results from including them thus is not justified. Equations 15 and 16 then become

$$-\frac{g\omega_0}{i_{f0}}i_f=R_3(1+T_3p)i_a+g\omega \tag{15a}$$

$$bi_a=Ip\omega+M \tag{16a}$$

Combining these as before gives

$$-\frac{\omega_0i_f}{i_{f0}}=M_e=(1+T_3p)Ip\omega+r\omega+M \tag{3a}$$

By comparing equations 3a and 3 it is apparent that equation 14 for the variable voltage system is also applicable, within the limitations of the approximations mentioned previously, when the control system supplies the variations in motor field current. In this case, however, T_3 in equation 14 is now the motor field time constant. Also, T_0 and possibly T_2 and A_1 vary with the speed setting so that appropriate values must be used at each point throughout the speed range.

Steady-State Speed Error With Regulator. In the stead-state condition $p=0$, and equation 14 becomes

$$-\frac{M}{r_0}(1-K_r)-\omega_s(1-K_r)=A_1\omega_s \tag{14a}$$

Solving equation 14a for the steady-state speed drop gives

$$\omega_s=-\frac{M(1-K_r)}{r_0(A_1+1-K_r)} \tag{17}$$

If the Rototrol is perfectly tuned, $K_r=1$, and

$$\omega_s=0 \tag{17a}$$

indicating perfect steady-state accuracy re-

Figure 11. Curves showing variation of crest speed dip as function of speed setting by field weakening and system inertia

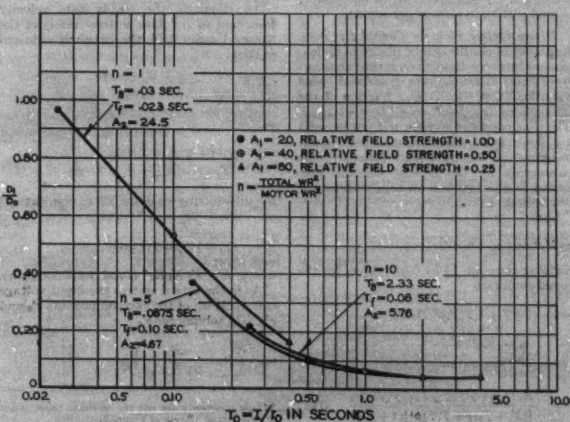

gardless of load or other system parameters.

If no self-energizing is used, $K_r=0$, and the stead-state speed error is

$$\omega_s=-\frac{M}{r_0(A_1+1)} \tag{17b}$$

Speed Drop of Unregulated Motor. For an unregulated motor, $A_1=0=K_r$ and thus according to equation 17, the steady-state speed drop is

$$\omega_{s1}=-M/r_0 \tag{18}$$

Comparison of equations 18 and 17*b* indicates that the effect of the regulator with $K_r=0$ is to reduce the steady-state error by the factor (A_1+1).

Equation 18 also can be obtained directly from equations 1 and 2. For an applied load and with constant steady-state armature voltage, equation 2 gives the following relation between the steady-state changes in armature current and speed:

$$0=R_3i_{s4}+g\omega_{s1}$$

or

$$\omega_{s1}=-R_3i_{s4}/g \tag{2a}$$

Equation 1 yields the current increase $i_{s4}=M/b$. Thus

$$\omega_{s1}=-MR_3/bg$$
$$=-M/r_0$$

which is the same as equation 18. At no load and neglecting losses

$$E=g\omega_0$$

where E is the normal armature voltage and ω_0 is the no-load speed. The fractional unregulated speed drop then can be defined as

$$D_0=-(\omega_{s1}/\omega_0)$$
$$=R_3i_{s4}/E$$
$$=\text{fractional resistance drop} \tag{18a}$$

Thus

$$r_0=M/D_0\omega_0=M/6.28sD_0 \tag{19}$$

where s is no-load speed in revolutions per second with ω_0 in radians per second.

Dimensionless Form for Control Equation. Equation 14 readily can be placed in dimensionless form by dividing each time constant by T_0 and expressing the fractional speed variation $(D=-\omega/\omega_0)$ as a fraction of the unregulated fractional drop $(D_0=-\omega_{s1}/\omega_0)$. The time constant division will not be written down as it simply complicates the appearance of the equation. However, the parameters for the general solutions presented in the text are all expressed in the dimensionless form.

Since

$$-M/r_0\omega_0=\omega_{s1}/\omega_0=D_0$$

dividing equation 14 by (ω_0D_0) gives for the tuned condition

$$-1-(1+T_0p+T_aT_0p^2)D/D_0$$
$$=\frac{A_1(1+T_ap)D/D_0}{(T_1+T_2)p+T_1T_2p^2]\left(1+\frac{T_a}{k}p\right)}+$$
$$\frac{A_2T_fp(1+T_0p+T_0T_2p^2)D/D_0}{[(T_1+T_2)p+T_1T_2p^2](1+T_fp)} \tag{14b}$$

The more general form for $K_r\neq0$ is given in the caption of Figure 1.

Appendix II. Derivation of Analogue for Speed Regulators

The control equation for the electric circuit of Figure 2 is completely analogous to that of the two types of speed controllers specified by equation 14. The output voltage of the final stage e_4 is analogous to the control torque M_c. The circuit formed by R, L, and C represents equation 3. This is shown as follows.

With reference to Figure 2

$$e_4=Ri_3+Lpi_3+i_3/pC+E \tag{20}$$

(The portion of resistor R which is shunted by the torque circuit is small compared to the total resistance so that the switching does not disturb the circuit appreciably.) If $i_3/pC\equiv r_0$ in the actual system, equation 20 becomes, when $Cr_0p\omega$ is substituted for i_3

$$e_4=RCr_0p\omega+Lr_0Cp^2\omega+r_0\omega+E \tag{21}$$

Thus if $e_4\equiv M_c$, $E\equiv M$, $R\equiv b$, $L\equiv bL_3/R_3$, $C\equiv K_3I/b^2g$, $RC\equiv T_0$, and $L_3/R_3\equiv T_3$, equation 21 becomes identical to equation 3.

By referring again to Figure 2

$$e_1=-K_1e_0+\frac{r_i}{R_r+r_i}(e_4)$$

where r_i is internal resistance of first stage output. (The capacitor in series with R_r is for blocking purposes only and is very large.)

$$e_4=\frac{K_2K_3e_1}{(1+T_1p)(1+T_3p)} \tag{22}$$

$$e_1=-K_1e_0+\frac{r_iK_2K_3e_1}{(R_r+r_i)(1+T_1p)(1+T_3p)}$$

$$\left[(1+T_1p)(1+T_3p)-\frac{r_iK_2K_3}{R_r+r_i}\right]e_1=$$
$$-K_1(1+T_1p)(1+T_3p)e_0$$

To eliminate the steady-state velocity error and to simulate perfect tuning of the Rototrol series field, the circuit is adjusted so that

$$\frac{r_iK_2K_3}{R_r+r_i}=1$$

Thus

$$e_1=-\frac{K_1(1+T_1p)(1+T_3p)e_0}{(T_1+T_3)p+T_1T_3p^2} \tag{23}$$

By substituting equation 23 in equation 22

$$e_4=-\frac{Ke_0}{(T_1+T_3)p+T_1T_3p^2}$$

where $K=K_1K_2K_3$* (total amplifier gain).

As in the actual system the input voltage e_0 is made up of the two components e'_0 and e''_0. In solving for e'_0

$$r_0\omega=\left(R_0+\frac{R_a}{1+R_aC_ap}\right)i_a$$

and as derived in the actual system

$$e'_0=(r_0\omega/k)\frac{(1+T_ap)}{\left(1+\frac{T_a}{k}p\right)} \tag{25}$$

In solving for e''_0

$$e_4\equiv M_c=\left(\frac{1}{pC_f}+R_f\right)i_f=\frac{1+T_fp}{pC_f}i_f$$

$$e''_0=r_fi_f=\frac{r_fC_fpM_c}{(1+T_fp)}$$

$$e''_0=\frac{A_2T_fpM_c}{K(1+T_fp)} \tag{26}$$

where

$$A_2=\frac{r_fK}{R_f}$$

is the gain around the feed-back loop for $C_f=\infty$ and

$$T_f=R_fC_f$$

Thus

$$e_0=e'_0+e''_0=\frac{r_0\omega(1+T_ap)}{k\left(1+\frac{T_a}{k}p\right)}-\frac{A_2T_fpM_c}{K(1+T_fp)} \tag{27}$$

By substituting equation 27 in equation 24

$$e_4\equiv M_c=$$
$$-\frac{Kr_0\omega(1+T_ap)}{k[(T_1+T_2)p+T_1T_2p^2]\left(1+\frac{T_a}{k}p\right)}-$$
$$\frac{KA_2T_fpM_c}{K[(T_1+T_2)p+T_1T_2p^2](1+T_fp)}$$

Dividing by r_0 and substituting the value of M_c/r_0 given by equation 4 gives the final performance equation for perfect tuning (equation 14 with $K_r=0$) when $A_1=K/k$.

*These constants are not the same as those given for the actual system of Figure 1.

References

1. Electrical Analogy Methods Applied to Servomechanism Problems, G. D. McCann, S. W. Herwald, H. S. Kirschbaum. AIEE Transactions, volume 65, 1946, March section, pages 91–6.

2. Dimensionless Analysis of Servomechanisms by Electrical Analogy, S. W. Herwald, G. D. McCann. AIEE Transactions, volume 65, 1946, October section, pages 636–9.

3. Dimensionless Analysis of Servomechanisms by Electrical Analogy, G. D. McCann, S. W. Herwald. AIEE Transactions, volume 66, 1947, pages 111–18.

4. Speed Regulation of Main Roll Drives, L. A. Umansky. *Proceedings*, Association of Iron and Steel Engineers (Pittsburgh, Pa.) 1947, pages 103–115.

5. Speed Transients of D-C Rolling Mill Motors, L. A. Umansky, T. M. Linville. Electrical Engineering (AIEE Transactions), volume 54, April 1935, pages 387–94.

6. An Extension of Impact Speed-Drop Analysis, F. E. Crever. AIEE Transactions, volume 66, 1947, pages 191–6.

No Discussion

Circuit-Breaker Current Measurements During Reignitions and Recovery

LAUREL J. LEWIS
ASSOCIATE AIEE

CONSIDERABLE attention has been given to the importance of transient recovery voltage across the terminals of a circuit breaker as a factor in arc extinction. Study of the voltage variation has been made using both analytical methods and direct measurement.[1,2] A knowledge of current variation during reignition and during final recovery is also necessary for full understanding of arc behavior. For one thing, a circuit containing a continually lengthening a-c arc, where current reverses each half-cycle and where the voltage across the arc space increases rapidly following each reversal, the amount of current flow is a measure of the arc conductivity during the critical period; the magnitude of the current during a short interval may serve to indicate how closely the circuit breaker comes to interrupting the circuit. Also of importance is the effect that the current has on the form of the recovery voltage; it is evident that arc conductivity introduces into the circuit a factor of variable resistance, which combined with the other circuit parameters and the generator voltages, determines the transient voltage across the arc space.

Few reports are available of current measurements in high-power a-c circuits during interruption tests, except for records made with the magnetic oscillograph. Such records have too low a recording speed and are so limited in sensitivity as to provide little precise data. A few high-speed measurements using the cathode-ray oscillograph have been made[3,4], but these have been generally of relatively low-current arcs in low-voltage circuits. It has not been demonstrated whether conditions in low-current arcs apply when the currents are large.

One of the principal problems of measuring the small currents of interest near the current-zero period is excluding the effects on the measuring apparatus of the large currents which exist each half-cycle at the crest of the current wave. If a shunt were placed in the test circuit large enough to obtain sufficient voltage for direct recording at the low point of the cycle, an excessive voltage would exist across it at other parts of the cycle, unless the voltage were limited by special means. One previously reported study[5] employed a nonlinear shunt, limiting the crest voltage to safe values; data from this study do not indicate progressive changes occurring during the arcing interval.

An investigation recently was undertaken to determine if current measurements of higher sensitivity could be made during each of the critical periods. Some new information on arc behavior has been obtained. In the following sections are indicated the techniques employed and the results achieved.

Methods of Test

Figure 1 shows the test circuit used in the investigation. Power was obtained from a 2,300-volt alternator, and short circuits, imposed from line to line across two phases, were interrupted by the test circuit breaker. A current limiting reactor limited the current available to approximately 1,600 amperes rms. Short circuits were initiated by a specially constructed synchronous closing switch which permitted control of the polarity of the voltage and of the point of the cycle at which short circuits were imposed, so as to give a symmetrical current wave. The test circuit breaker was one specially modified for the study, employing a single break under oil.

A shunt was placed in the test circuit to obtain a voltage for recording purposes, proportional to the current variation; a current transformer would not have been satisfactory for this purpose because of transient errors. A value of 0.01 ohm was selected as the resistance

Paper 47-185, recommended by the AIEE committee on protective devices and approved by the AIEE technical program committee for presentation at the AIEE Pacific general meeting, San Diego, Calif., August 26–29, 1947. Manuscript submitted June 9, 1947; made available for printing July 9, 1947.

LAUREL J. LEWIS is with the department of electrical engineering at the University of Washington, Seattle, Wash.

The material presented in this paper is abstracted from a dissertation presented for the degree of doctor of philosophy in electrical engineering at Stanford University. Acknowledgment is made to Doctor W. G. Hoover, of Stanford University, for his many valuable suggestions during progress of the investigation.

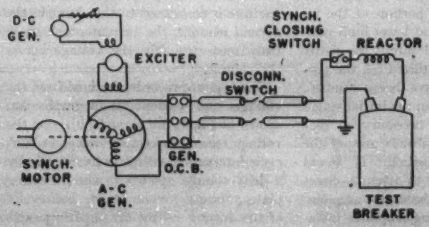

Figure 1 (left). Test circuit

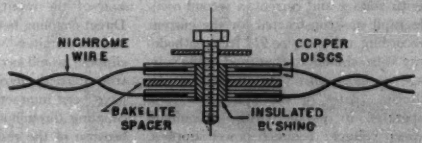

Figure 2. Current shunt

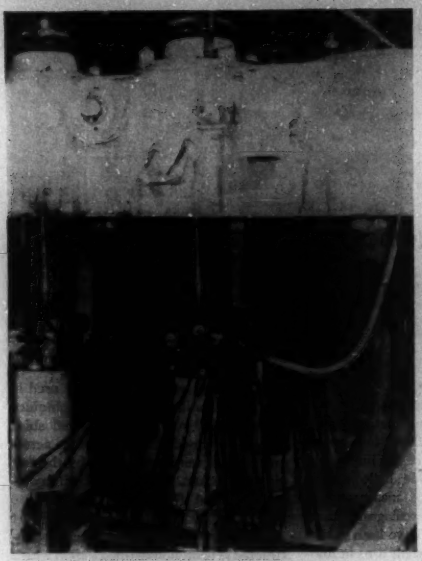

Figure 3 (left). Circuit breaker with tank lowered, showing shunt in place

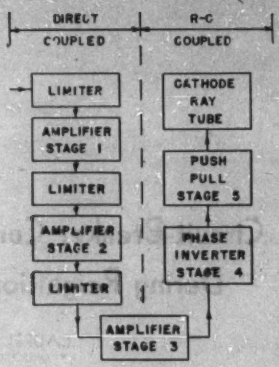

Figure 4. Block diagram of amplifier for current recording

of the shunt; a low value was chosen so that the test circuit would not be appreciably modified. This shunt, having the necessary resistance and thermal requirements, consisted of 30 pieces of number 18 nichrome wire, 19.8 inches in length, assembled between two terminal contacts, as shown in Figure 2. The location of the shunt in the circuit breaker is illustrated in Figure 3. The shunt was placed adjacent to the arcing contact, which is housed in an expulsion chamber. Current flow is through the entrance bushing, thence through the shunt, and to the arcing contact, with the normal current flow altered in the least possible manner. Individual wires of the shunt were twisted to minimize self-inductance and prevent coupling with adjacent magnetic fields.

Recording equipment utilized included a recovery-voltage oscillograph[6] for measuring the voltage across the arc space. This oscillograph has repetitive horizontal sweeps of short duration synchronized with the current zeros in the test circuit. To obtain simultaneous measurements of both voltage and current, a second oscillograph was constructed for the current recording, using a type *912* RCA cathode-ray tube, similar to that used in the voltage oscillograph. The horizontal deflecting plates of the two tubes were operated in parallel with a common sweep voltage; common power supplies, positioning, and focusing controls also were utilized.

It was desired initially to obtain full scale recording on the current oscillograph with the final one ampere of current in the test circuit, and this required an amplifier having an output of about 500 volts with the input of 0.01 volt obtained from the shunt. Design of a suitable amplifier constituted the basic problem of measurement. A block diagram of the amplifier employed is shown in Figure 4. This amplifier provides essentially linear amplification of small input signals; large signals are limited by diode clipper circuits so that overloading of the amplifier is prevented on the crests of the current wave. Limiting of the unwanted portion of the input signal was accomplished in three separate operations. After each limiting and subsequent amplification, the desired portion of the input signal occupied a larger portion of the region between upper and lower limit positions; and after final limiting the entire recording space was utilized for the portion of the input wave being studied. Direct coupling between the initial stages and the limiters was necessary so that clipping would occur always around the true current zero position. It would have been impractical to attempt direct coupling throughout the entire amplifier because of the resulting amplifier instability. Special attention was necessary even for two direct coupled stages, to minimize drift in the zero level which might have been interpreted as a change in signal magnitude. Each stage in the direct-coupled section employs two tubes operating in series in a balanced-bridge system across a power supply,[7] with the output voltage taken off between the tubes and the power-supply center tap. After limiting is completed, the modified signal, very nearly a square wave in form, is further amplified through conventional resistance-capacitance coupled stages; the final stage is in push-pull for symmetrical application of the signal to the vertical deflecting plates of the cathode-ray tube. The upper frequency limit of the amplifier exceeds 50,000 cycles.

Special attention was given to protecting the current measuring circuits from influence of the high voltage in the test circuit. The voltage across the shunt was applied directly, inside the circuit breaker, to a concentric line leading to the current oscillograph. Confirming tests demonstrated that with the inner conductor of the concentric line short-circuited to the shield, and both connected to one side of the shunt, no significant voltage was transmitted to the current oscillograph when current flowed in the test circuit. This assures that when the concentric line is connected to the shunt in the normal manner, the current oscillograph truly measures only the voltage across the shunt.

The types of records obtained from the voltage and current oscillographs are shown in Figure 5 (*A*) and (*B*). On the voltage record, successive sweeps at half-cycle intervals are displaced vertically by a drift voltage applied to the deflecting plates; traces for successive half-cycles of the current record are superimposed.

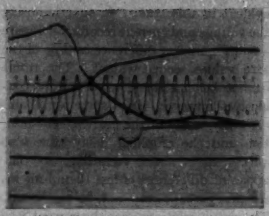

A. Oscillogram of arc voltage

Figure 5. Oscillograms of interruption by plain break at 1,340 volts and 780 amperes rms

200-kc timing wave

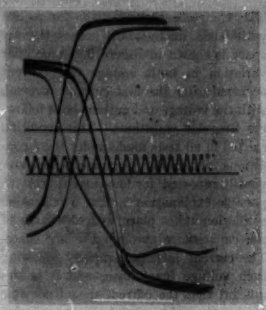

B. Oscillogram of arc current

The current magnitude exceeds the limit value during most of the cycle, except for the excursions through zero; thus the flat top portions of the current trace before and after the current passes through zero are not significant. An unusual feature of the current record is the displacement of the current zero positions in opposite directions on half-cycles of opposite polarity. Of the two zero lines shown, the upper one applies to the traces moving from the bottom to the top of the record. This is the same sort of displacement as occurs in amplification of a square wave by a resistance-capacitance coupled amplifier due to phase shift at low frequencies, and occurred here in the amplifier following final limiting. The variation in no way affects the recording accuracy, since the vertical displacement is negligible in the short time of the recording interval, but special methods were necessary to locate the zero positions for proper interpretation of results.

Test Results

Numerous tests were made to study the arc characteristics under different conditions, with both the expulsion chamber in operation and with its cover removed to give conditions of a plain break; variations were made in the generator voltage, in the polarity on the start of the short circuit, and in the amount of shunting capacitance across the circuit-breaker terminals.

A very noticeable difference has been observed in the form of the recovery voltage obtained on tests made under practically identical conditions, with special care taken to control the generator voltage, the point in the cycle for initiating the short circuit, and the circuit-breaker opening time. Such variations may be due to differences in internal arc conditions, possibly resulting from surface irregularities on the arc contacts, which cause changes in current density and electrode temperature. These variations make difficult the appraisal of changes in results due to differences in operating variables, except on a statistical basis. It seems rather surprising that little previous emphasis has been given to variations which can occur under the same test conditions; practically no published studies show records for more than one test taken under the same conditions. One might be led to conclude that an arc behaves in a well regulated manner, whereas no such regularity exists.

The form of the current variation occurring on successive half-cycles, in two tests with the plain break, is illustrated in Figure 6 (alternate half-cycles have been traced with reversed polarity so that the initial portions of the waves coincide). The current apparently experiences little deflection, in most cases, from its normal sine-wave slope until near the zero value, and the rate of increase following reversal becomes progressively smaller on successive half-cycles. On final recovery the current reaches a maximum and then returns to zero.

A modification was made in the recording procedure to obtain more detailed information on the course of the current after reversal a half-cycle prior to final recovery; this consisted of reducing the recording speed and the amplifier sensitivity. Results are shown in Figure 7. The current increased at a reduced rate until the end of the interval, when its slope again changed to correspond practically to that of the normal sine wave. A period of substantially zero current during the period preceding reignition, either before or after reversal, was not noted in any case. This is in contrast to previously reported results[4] on low-current arcs, where a reduced value of current was indicated for a considerable period, sometimes even with a glow condition preceding reversal. The difference in the two cases is possibly the result of the more rapid rate of change of current in high-current arcs and the fact that considerable time is required for thermal equilibrium to be established, so that not much change can occur in arc-space conductivity for high-current arcs, in the brief interval involved, except perhaps in the region near the electrodes.

The period following voltage reversal until the normal arc is re-established has sometimes been referred to as a "glow." More generally the glow is a low-current high-voltage discharge in contrast to the arc, where the current is high and the voltage low. It is to be noted that for the conditions in Figure 7 the magnitude of the voltage fits the glow classification but the current is much greater than that in the glow under equilibrium conditions. There is no doubt, however, that a change in the mechanism of conduction does occur at the end of the interval. These results illustrate the importance of time as well as of voltage magnitude in re-establishing the normal arc.

Accompanying the variations in recovery voltage occurring on practically identical tests was a corresponding variation in current during final recovery. The recovery voltage was inherently a double-frequency transient, due to the nature of the test circuit; the breaker capacitance and the current-limiting reactor were primarily responsible for a high-frequency oscillation, and the generator reactance

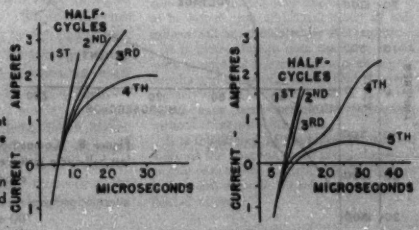

Figure 6. Current changes at successive half-cycles

Interruption by plain break at 1,340 volts and 780 amperes rms

and the capacitance of the generator and connecting cables were responsible for a lower frequency variation. Differences in the measured recovery voltage were manifest primarily by the amount of damping of the higher frequency component, which was sometimes eliminated entirely. In all cases where the highly oscillatory type of voltage transient was recorded for the unshunted arc, the residual current during final recovery was quite small and did not exceed 0.7 ampere at any time following reversal. In cases of high damping the current flow during final recovery sometimes reached values as high as 4.2 amperes. Figure 8 illustrates the variations occurring at the final half-cycle on three tests made under identical test conditions, in which the current and voltage are markedly different. From circuit considerations it is evident that a transient oscillation involving the current-limiting reactor and the breaker capacitance will be affected by a resistance in parallel with the capacitance; the arc conductivity provides such a resistance. When the resistance is below a definite critical value, the voltage transient is overdamped; for higher values of resistance the voltage transient is oscillatory. This would explain each type of voltage variation obtained, and would indicate that arc resistance was sometimes greater and sometimes less than this critical value.

Addition of considerable shunting capacitance across the circuit breaker terminals affected the characteristics in a number of ways. The most noticeable effect was a reduction in the frequency of the higher frequency component, an effect to be expected. Also it was noted in one test that the current exceeded 1.5 amperes during final recovery with voltage variation still of the oscillatory type; this illustrates that the critical resistance is lowered by addition of more capacitance, since such a large current would have resulted in extreme damping in the unshunted case. The complete characteristic for a test with 0.008 micro-farads across the arc space is shown in Figure 9. A peculiar variation in both voltage and current occurred after the first current reversal, with the voltage and current both following irregular variations. This condition existed in all tests made under these conditions. A similar phenomena was previously reported[3] for low-current arcs. A possible explanation is that a relaxation oscillation takes place with discharge of the capacitance through the arc space. The current increased rapidly following each voltage breakdown, and it is significant that the current magnitude was greater than the normal sine wave value after each increase. Without additional shunting capacitance (a minimum of about 300 micromicrofarads was provided by the bushings) such an oscillation sometimes occurred on the first reversal, but the frequency was so high that the oscillograph was unable to indicate it clearly and analysis was impossible. It is not clear why the phenomenon occurs only at the first half-cycle of arcing, but the length of the arc space may be a determining factor.

A question of considerable importance is whether or not the arc current and the voltage across the arc space both pass through zero at the same instant. Most investigators have assumed that they do, but there is no well established evidence to support such a conclusion. In fact, the redistribution of charge unevenly distributed in a gaseous region may induce a current flow in the metallic circuit connecting the electrodes without any actual transfer of charge between the electrodes and the gas space. Such a redistribution of charge is to be expected in an arc on reversal of voltage, when a new space charge must be created in front of the new cathode, so that a current flow might exist at the instant the voltage is zero. Some indication that the current and voltage zeros may not be coincident is evident in this study; in superimposing the voltage and current records for Figure 8 and Figure 9, a difference in time of the zero values seems evident. The result cannot be considered as definitely conclusive, however, since some small uncertainty exists in the current zero position and the amplifier delay time also affects the current recording, so that apparent differences of less than 5 microseconds perhaps may not be significant. The circuit relations near the current zero are of interest in this connection. In the unshunted case, the arc current and the current in the current-limiting reactor are essentially the same, and generally little deflection from the sine wave shape was evident up to the time of current zero. With a large shunting capacitance, a greater deflection from the sine wave shape was evident, and it is as though the increase of voltage across the large capacitance caused the capacitor to "rob" the arc of some of the reactor current. Since the rate of change of reactor current determines the recovery voltage, such an effect would delay the current zero relative to the voltage zero. If a purely resistive arc is assumed, it becomes necessary to account for the difference between current in the shunting capacitance and in the inductive reactance, when arc voltage is zero, as due to a current in the distributed capacitance across the reactor. It may be that the effect of this distributed capacitance has been given undue consideration.

Study of the results of changing polarity of the voltage on start of the arcing period has shown no significant effect. Comparisons of performance with the expulsion contacts and with the plain break indicated reduction in arcing time with the expulsion contact, but no difference

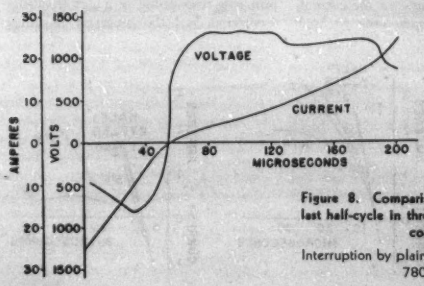

Figure 7 (left). Current and voltage variation at next to last half-cycle

Interruption by plain break at 1,340 volts and 780 amperes

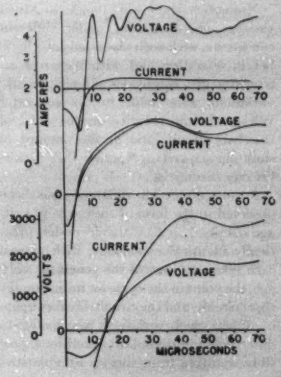

Figure 8. Comparison of characteristics on last half-cycle in three tests made under same conditions

Interruption by plain break at 1,340 volts and 780 amperes

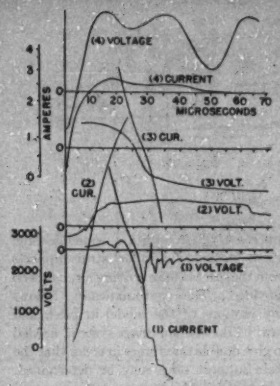

Figure 9 (left). Complete characteristics of arc shunted by 0.008 microfarad capacitance

Interruption by plain break at 1,340 volts and 780 amperes

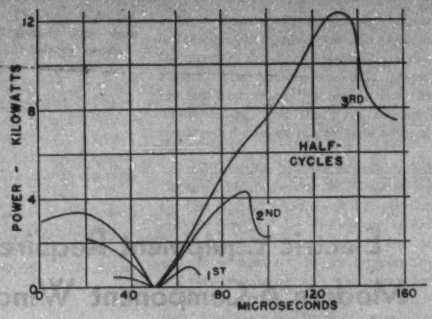

Figure 10. Power variations at successive half-cycles

Interruption by plain break at 1,340 volts and 780 amperes rms

in form of voltage or current. With the expulsion contact in operation with full generator voltage, the highly oscillatory type of recovery and low recovery current were evident more often than when operation was at half voltage and half current, but the over-damped type of voltage variation was still evident in some tests.

No completely satisfactory explanation of the reignition process has been formulated as yet. A widely held view is that the voltage breakdown strength of the arc space increases through recombination and diffusion of ions after the current reaches zero and that reignition occurs when the recovery voltage across the space builds up to a critical value. The data of Figure 7 permit an examination of such a theory. As indicated in this test, the normal arc was re-established, not at the time of the voltage maximum, but at a considerable later time, when the voltage was actually less and the time for removal of ions even greater. Significantly, the current increased throughout this entire interval, and there was no "breakdown" at all in the sense that there was a sudden increase in current. These data and other obtained under identical test conditions have been used to analyze the power relations. A comparison of three tests, all for next to the last current zero period, showed practically the same rate of power input to the arc space, and this in spite of differences in voltage and current in the separate tests. An example of the power input at successive half-cycles in one test is shown in Figure 10. The power reached a maximum value of the order of twice that existing at beginning of the normal arc, just before final breakdown. It may be that a minimum energy is required to maintain the cumulative ionization process in the normal arc and that the deficiency of energy supplied in the initial part of the reignition period must be replenished by a higher energy input to the latter part of the period before the arc economy can again reach a balance. A longer time seems to be required to replenish the loss in a long arc, in spite of a higher rate of energy increase, because the losses occur at a much higher rate with a long positive column. With such an emphasis on the power relationships affecting recovery, less emphasis needs be given to the rate of rise of recovery voltage; the average voltage throughout the critical period would seem to be more significant than the maximum value occurring during the interval.

Conclusions

The practicability of current measurement, demonstrated by experiment, has a greater significance than that of any specific findings made in this study; extension of the technique may make available more fundamental knowledge of arc behavior. The present study indicates that the current during recovery may have a pronounced effect on the recovery voltage; in the present study, the effect of the current was such that in a period followed by reignition, at no time did the recovery voltage reach a value equal to the generator voltage. Whether the current has as much effect in high-power tests at high voltage, on modern high-speed circuit-breakers, still remains an open question. Survey of the techniques employed indicates that similar measurements could be extended to much higher values of test circuit current. A most promising possibility is that measurements of current during recovery might provide a criterion for judging when a circuit breaker is approaching the limit of its interrupting capacity.

References

1. System Recovery Voltage Determination by Analytical and A-C Calculating Board Methods, **R. D. Evans, A. C. Monteith.** Electrical Engineering (AIEE Transactions), volume 56, June 1937, pages 695–705.

2. Arc Extinction Phenomena in High Voltage Circuit Breakers, **R. C. Van Sickle, W. E. Berkey.** AIEE Transactions, volume 52, 1933, pages 850–7.

3. Reignition of Metallic A-C Arcs in Air, **S. S. Attwood, W. C. Dow, W. Krausnick.** AIEE Transactions, volume 50, 1931, pages 854–70.

4. Ein Beitrag Zum Verhalten Kurzer Wechselstromlichtbogen Waehrend des Stromnulldurchganges, **M. Steenbeck.** *Zeitschrift für Physik* (Berlin, Germany), volume 65, 1930, page 68.

5. Special Tests on Impulse Circuit Breakers, **W. F. Skeats.** Electrical Engineering (AIEE Transactions), volume 55, June 1936, pages 710–17.

6. An Oscillograph for Recording Transient Recovery Voltages, **W. G. Hoover.** AIEE Transactions, volume 65, 1946, pages 1086–91.

7. Survey of D-C Amplifiers, **M. Artzt.** *Electronics* (New York, N. Y.), August 1945, pages 112–18.

Discussion

W. G. Hoover (Stanford University, Stanford University, Calif.): The investigation described indicates considerable progress in the quantitative determination of one of the often discussed but little measured phenomena in electric power engineering. It is to be hoped that additional study of this subject will be stimulated by this paper.

It is interesting to note that this is one more example of the usefulness of electronic circuits and equipment in the field of power engineering. The measurements reported would have been practically impossible without these valuable tools.

It is the interest of the power engineer to welcome the progress of the art of electronic measurement and control and to extract from it full value in the advance of his own field of interest.

Electric Equipment Required in a Modern 6-Component Wind-Tunnel Model Suspension System

H. ORVILLE COX
ASSOCIATE AIEE

THE variable density wind tunnels recently completed at the Cornell Aeronautical Laboratory (formerly Curtiss Wright Corporation Airplane Division Research Laboratory) at Buffalo, N. Y., and the Southern California Co-operative Wind Tunnel at Pasadena, Calif., provide two of the most modern and versatile aerodynamic testing facilities. Their versatility permits testing at air pressures above as well as below atmospheric pressure giving increased Reynolds numbers or greatly increased air velocities, respectively. An increased Reynolds number means that the effects on a small scale model would be equal to those of the full scale plane. Under the rarified atmospheric conditions of approximately one-fourth of an atmosphere absolute pressure, it has been possible to obtain air speeds which closely approach the speed of sound in these tunnels, and yet tunnel drive horsepower installed for each has a nominal continuous rating of 10,250 horsepower. To retain the value of the tunnels' operating possibilities, it became a prime consideration that the design and construction of the model handling and force measurement equipment be such that a minimum of time would be lost in rigging, making adjustments, and instrumenting the models used in the test section.

This requirement, that the model be handled, positioned, and controlled on the balance system installation as quickly and efficiently as possible resulted in the system's mechanical equipment being much more complex than is to be found in balance systems of earlier tunnels.

The "metrical" or force measuring elements, always the fundamenta parts of any balance system, are incorporated in "model suspension system," a term given to the model handling facilities in these tunnels. It is this "model suspension system" which will be discussed. The electrical control problems, the way the components are motorized, one of the instrumentation problems, and some of the interesting electrical construction details are to be considered.

Development of the Balance System

In early tunnels the balance system consisted only of the basic metrical system, that is the elements needed to take the actual force measurements. Such a system usually was made up of wire suspensions with some type of winch that was able to change the model in angle of pitch. This required a fractional horsepower motor, probably a reversible universal type motor, which would operate the pitch changing apparatus through a remote control station. It was normal procedure during a test to remount a model on its side in a system which could change angle of pitch only. This effectively made the system usable for changing angle of yaw, but as mentioned required a rerigging operation on the model. Pitch may be defined as rotation about a lateral axis whereas yaw is rotation of a model about a vertical axis.

Many improvements have been made on this elementary balance system, until now we have it incorporated in a modern suspension system that is capable of moving the model in both angle of pitch and of yaw and can do the same simultaneously if necessary. In addition, windshielding, which protects the model strut supports from the forces of the moving air, has been provided. This automatically follows any motions of the model in pitch and yaw. Likewise, an image system, needed to give double tare forces in order that the main support tares may be determined, is included. This system also is powered by automatic following drives.

The major supporting members have been assembled on "cart" structures which allow the model to be placed into the tunnel test section or rolled out of it in a matter of a few minutes. The carts have been motorized with electric transfer motors and an elevating motor is provided on each to raise and lower the entire cart and model when positioning it properly in the test section. Actually three carts are available at each tunnel allowing the rigging work to progress on three different models simultaneously. This preparation of the models for the tunnel tests can be handled outside the tunnel proper and does not tie up the operation of the tunnel at any time.

The Six Components

Before considering the electric equipment and the control problems found in the balance system we are concerned with, it might be well to brief a rather simple six component balance system. The six components the "aerodynamicist" is interested in when taking force measurements on a tunnel model in its various attitudes of angle of attack and yaw

Paper 47-205, recommended by the AIEE committee on air transportation and approved by the AIEE technical program committee for presentation at the AIEE Pacific general meeting, San Diego, Calif., August 26-29, 1947. Manuscript submitted March 17, 1947; made available for printing July 2, 1947.

H. ORVILLE COX is electrical engineer, Bechtel Corporation, Los Angeles, Calif., and was formerly with Cornell Aeronautical Laboratory and the Southern California Co-operative Wind Tunnel design group at California Institute of Technology.

The author wishes to acknowledge the technical abilities of Doctors A. L. Klein and E. E. Sechler and of P. V. H. Serrell, L. G. Fenner, K. P. Gow, and J. B. Taylor, who, under the direction of Doctor Clark B. Millikan at the California Institute of Technology, were responsible for a major part of the design of the special electric equipment discussed in this paper.

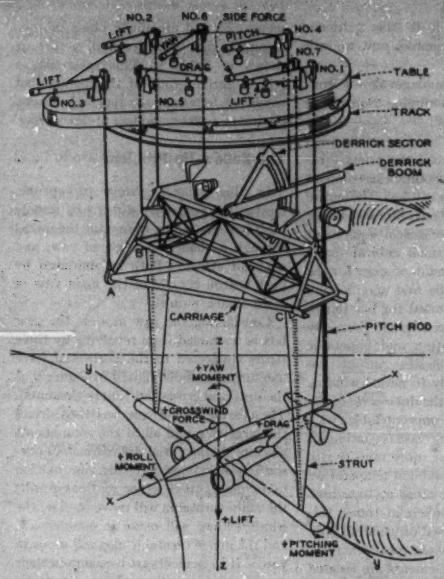

Figure 1. A 6-component strut type balance system

easily can be pointed out. The equations for these components in terms of the balance reaction read on ordinary beam balances can also be set down. The system in Figure 1 is a 6-component strut type balance system. The balance room is located directly above the tunnel test section and the model is attached to the strut trunnion in an inverted position. This is customary practice where the model is supported on a balance system that is located above the tunnel test section. The tunnel air flow is from left to right and in a direction parallel to the xx axis when the model is in a position of zero yaw. The six components are these: the lift force shown along the zz axis, the drag force along the xx axis, the crosswind force along the yy axis, a pitching moment resulting about the yy axis, a yawing moment resulting about the zz axis, and a rolling moment about the xx axis. These components are equated to the beam balance air load reactions, the F's, as follows:

$$\text{Lift} = F_1 + F_2 + F_3 + F_4$$
$$\text{Drag} = F_5$$
$$\text{Crosswind} = F_7$$
$$\text{Pitching moment} = K_1F_3 - K_2F_4 - K_3F_4$$
$$\text{Yawing moment} = K_2F_6$$
$$\text{Rolling moment} = K_3(F_6 - F_5) - K_4F_7$$

The constants K_1, K_2, and K_3 are the lever arm distances that apply because of the physical structure of this system.

The Modern Suspension System

To continue now and consider the system, as installed at the Cornell tunnel, at first it may seem rather complex. However, the system is definitely similar to that just mentioned, and this should be evident if a few points are remembered.

1. The tubular structure assembly of the simple system now has become heavy structural members.

2. The balance system is located below the working section and the model appears upright.

3. The actual forces and moments are impressed on nine Tate-Emery capsules which convert these to hydraulic pressures and transmit them to the control room where they are totalized into the six components and read directly on six 20-inch dials.[1-3]

However, additions have been made; the windshielding system and image system are now an integral part of the suspension system. It is here that our job of automatic control presents itself. In this system the synchronized or following motions of the windshielding and the image system do not require mechanical linkages that must be separated at the time force measurements are taken. All of the components of the system are kept in their proper relative positions through the means of the control system to be discussed. The balance elements proper are free from grounding action with the windshielding, and the force measurements can be taken at any time without fear of errors.

An innovation in these tunnels is that the entire balance system is housed within the tunnel shell. As a result it is a system entirely free of the ground or tunnel foundations. With the tunnel free to expand or contract due to temperature and pressure changes and free to considerable motion due to the design of its structural supports, a problem was presented of maintaining an absolute level condition in the balance system by some mechanical means. This is a requirement that must be met to prohibit errors in measurements due to inter-reaction of different forces caused by the tilting. Electrical instrumentation such as the "tiltmeter" was devised to check the amount of "out of level." Control of electric jacking motors installed inside the tunnel below the balance system on two of the three corners allowed any tilt to be corrected.

Another problem was presented in that all the control and instrumentation connections had to pass through the steel tunnel shell and be pressure tight against the varying pressure conditions inside the tunnel. These connections were located primarily in one spot known as the "sump." This area was designed specially to handle the pressure fitting connections and greatly simplified the connection problem.

Functions of Windshields and Image System

The windshielding allows the trunnion or strut type of model attachment to present the lowest tare drag possible. Normally the drag of the model support ends and the small length of tail strut exposed may be less than 20 per cent of the net minimum drag of the model.

The image system, consisting of actual images in shape of the windshields around the main model supports and tail strut, permits the proper configurations of model attachments to be set up so that the attachment tares may be determined. This is done by mounting the dummy struts on the wing of the model with dummy windshielding identical to the main windshielding surrounding them and comparing set-up measurements with and without these. Actually in some cases measurements must be taken under four different configurations before the results

wanted can be calculated. The purpose of this work is twofold

1. The true airflow inclination past the model is determined.

2. The true drag coefficient of the model in its normal position without the effect of the supporting struts is determined.

Such measurements must be made for the same attitudes of the mode' as those at which the tests are made that are to be corrected, and likewise at the same air speeds.

Motor Drives

The complete suspension system assemblage is shown in elevation in Figure 2. The primary structural elements of the system that must be considered while discussing the mechanical motions to be handled electrically are the base frame, the large ring with the yaw box assembly attached, the moment table, and the crossbeam with the attack mechanism (tail boom). These make up the metrical system. In addition there are the windshielding structures and the image system.

With reference to Figure 2, seven of the motor drives are pointed out: at *A* the image system angle of attack drive motor, at *D* the adjusting motor for one of the static moment compensator counterweights and at *E* the drive motor to handle the main strut rotation Then we find at *F* the angle of attack motor for driving the tail boom (this is the element to which the model tail strut is attached). At *G* is one of the two jacking motors for maintaining absolute level of the base frame and as a result the entire metrical system above it. At *H* is the yaw drive motor which will yaw the large ring and the metrical structure above it. At *J* there is a vertical drive motor for the tail strut windshielding and at *K* the fore and aft drive motor for the same tail strut windshielding. At *L* is the 2-dimensional "reluctance" control unit we will discuss later.

Actually the assemblage shown contains 16 motor drives ranging from 1/2 to 20 horsepower.

The motors used in connection with this equipment first had the primary requirement that they should be as compact in physical size as possible. The entire balance system represents an exceedingly large amount of mechanical equipment forced into a rather small cubical space. This left only a minimum of space for the motors and set up the first specification that the motors be rated for one-fourth hour at 55 degrees centigrade rise. By using class *B* insulation and bimetallic disks as protective devices, cut-out protection is limited only to actual winding temperature. Since the duty cycle of the motors is somewhat unpredictable, with the exception that in no case is continuous operation expected for more than five to ten minutes, and the ambient temperature may vary over a wide range up to as high as 125 degrees Fahrenheit at times, this type of protection based on winding temperature seemed to be the most practical. The bimetallic disk elements are located at the end of the stator windings, one in each of the two phase windings. On overheating in either phase winding the motor contactor in the remote unit-design control center switchboard is opened.

In order to obtain the accurate positioning required on the system nearly all motors were equipped with motor mounted magnetic brakes.

The general specifications covering other details were that the motors should be induction motors of the high torque type, totally enclosed with ball bearings, and for 110- or 220-volt 60-cycle 2-phase power. One exception was the cart moving motors which already have been mentioned and are single phase motors. Complete characteristics of all motors are shown in Table I. This table lists a representative group of the motors that would be found on the metrical system, the image system, and one of the "carts."

The Follow-Up Problem

In this balance system two prime-motions are controlled directly by remote push buttons; those of moving the model through a change of angle of yaw, and angle of attack. Both are initiated by push-button control of the main yaw or main attack motors.

Considering the yaw motion, the gear box is restrained from revolving by three struts connected to the horizontal force measuring capsules (noted in Figure 2 as the drag and crosswind Emery elements). The gearing in the yaw box then drives the large ring and all of the components assembled above it at approximately one-sixth rpm in yaw. If this yaw motion takes place, three other motions result: the main turntable will move in yaw, the windshielding will move in counteryaw, and the image turntable also will move in yaw. If all elements are to maintain their proper yaw position three automatic follow-up motor drives are required.

However, let us pass over the problem of changing angle of yaw and consider a change in angle of attack. This change likewise requires three automatic follow-up motor drives and will be quite suitable for discussing the control problem involved. If the tail boom is moved, causing it to swing through a certain angular arc, three other drives automatically must make their components follow.

1. A drive which moves the tail windshielding along a horizontal guide (this effectively increases or decreases the horizontal distance between the main windshields and the tail-strut windshield).

Table I. Motor Characteristics

Motor	Rating, Hp	Line Amp Starting	Line Amp No Load	Line Amp Full Load	Power Factor, Per Cent Starting	Power Factor, Per Cent Full Load	WR,² Motor Rotor	Starting Torque, Lb-Ft	Brake Torque Lb-Ft
(110 v, 2 phase)									
Main attack	1	24	4.6	7.4	65	65	0.25 lb-ft²	13.9	10
Main yaw	1	22	2.9	6.6	70	78	0.25 lb-ft²	9.25	3
Image attack	1	24	4.6	7.4	65	65	0.25 lb-ft²	13.9	10
Image yaw	3	64	8.7	14.6	65	80	0.40 lb-ft²	27.0	10
Strut rotation	3/4	21.8	3.8	5.0	65	70	0.25 lb-ft²	10.5	3
Windshield turntable	3	64	8.7	14.6	65	80	0.40 lb-ft²	27.0	10
Tail windshield, fore and aft	3/4	19.8	2.0	4.4	68	79	0.25 lb-ft²	7.0	3
Tail windshield, vertical	3	64	8.7	14.6	65	80	0.40 lb-ft²	27.0	10
Counterweights	1/2	26		3.6			8.0 lb-in²		
Base leveling	1	36		4.8			22.5 lb-in²		
Tail windshield trim	1/4	14.4		2.0					
(220 v, 2 phase)									
Cart jacking	20	200	14.2	47.3	70	85	5.3 lb-ft²	176	25
(220 v, 1 phase)									
Cart transfer	1/2	43	7.2				20 lb-in²		

2. A second drive which moves the tail windshielding along a vertical guide, maintaining the portion of the strut exposed to the wind stream as a constant, regardless of the angle of attack.

3. A third drive that must move the image system dummy tail-strut windshield through a corresponding angle of attack.

The Follow-Up Power and Control

As already stated, three drives must operate and follow automatically when the main attack motor is controlled by push button. The circuit for the basic power distribution and the related control elements is shown in the schematic diagram of Figure 4.

All drive motor power is provided by a 40-kva Scott-connected transformer bank. The primary windings are supplied by 440-volt 3-phase 60-cycle power.

This is transformed so that two 2-phase bus groups are supplied, one at 180 volts, and the other at 120 volts. Each of the bus groups has voltages available in the relative phasing of 0, 90, and 180 degrees when any one bus is used with the neutral bus. The power at 180 volts is fed to the reactor units through the interlocked control contactors. The reactor unit voltage output is controlled by the tube unit, and the follow-up motor drive is powered by this output.

A reactor unit actually contains three controllable saturable reactors. The reactor in the third phase which is 180 degrees out of phase with the first provides a voltage output instead of the first phase when the reverse direction of rota-

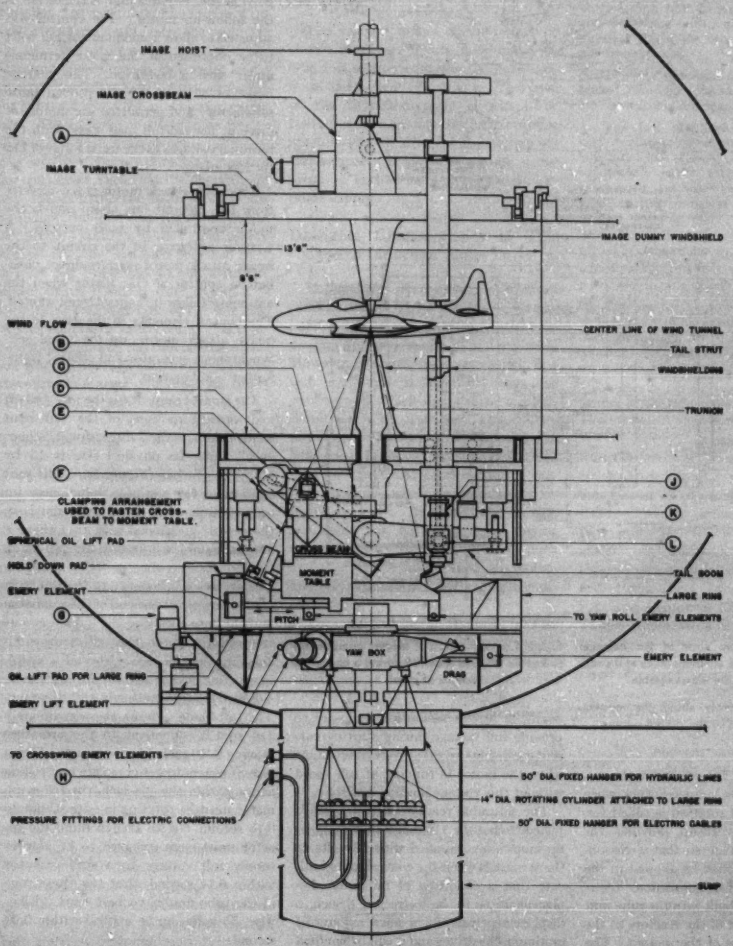

Figure 2. Section of wind tunnel balance system showing elevation view of units

A—Image system angle of attack drive motor
B—Strut rotation worm gear drive
C—Torque tube for revolving static moment compensator counterweight guides
D—Static moment compensator counterweight and adjusting motor
E—Strut rotation drive motor
F—Angle of attack motor for driving tailboom
G—One of jacking motors for leveling large ring
H—Yaw drive motor
J—Vertical drive motor for tail strut wind-shielding
K—Fore and aft drive motor for tail strut wind-shielding
L—Two-dimensional "reluctance" control unit

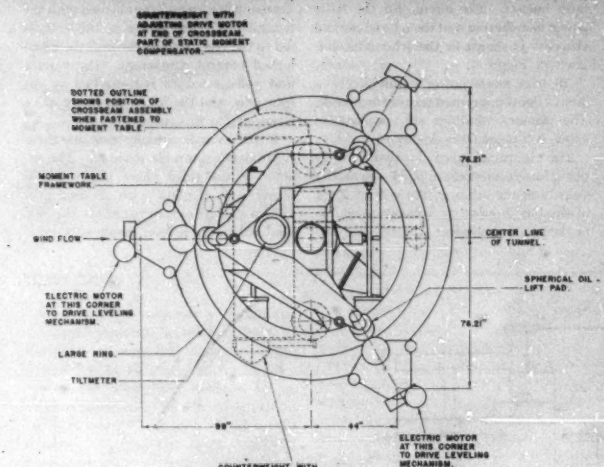

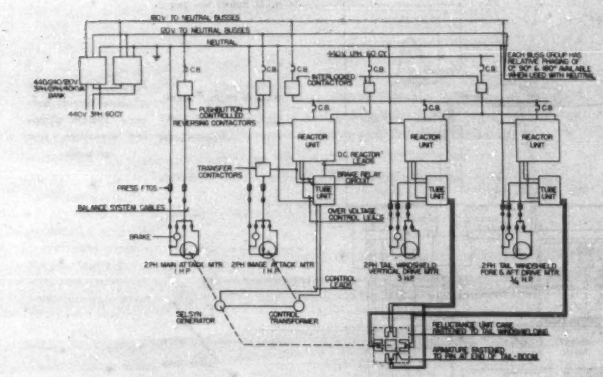

Figure 3 (top). Plan view of the balance system fixed metrical elements taken at the top surface of the moment table

The crossbeam assembly above the moment table is indicated by the dotted outline

Figure 4. Connection of electric components to handle motions required during a change in angle of attack

tion is required. The reactor in the second phase provides voltage output when either direction of rotation is called for. The 180-volt bus group provides the necessary overvoltage so that a reasonable voltage drop may be allowed in the reactors during a loaded condition. Overvoltage control is built into the tube unit to limit the output of the reactors to the full voltage ratings of the motors. The degree of reactor saturation necessary to provide full voltage during starting current conditions would provide overvoltage when the motor is running at full speed without this voltage limiting control.

The saturable reactor control was adjusted so that the 110-volt 2-phase follow-up motors are supplied with 80 volts at the terminals when the control units indicate that a condition of minimum displacement is to be corrected. Such a displacement calls for a small amount of motion in the drives and it can be handled at a reduced torque, the required accelerating rate of the drive being considerably less than normal under this condition. This voltage as set is the minimum at which proper operation of the magnetic brake is maintained and the starting torque is sufficient to meet the mechanical system's requirements. With displacements smaller than this minimum the terminal voltage on the motors is kept below 10 volts at all times. When the control unit indicates a large displacement between elements has resulted it effectively is calling for the highest speed possible and requires high acceleration in the follow-up motor. The control was adjusted to allow a maximum of 140 volts to be impressed at the motor terminals under such a condition. This voltage range of 80 to 140 volts proved quite satisfactory and permitted the motors to drive at normal full load speed with the terminal voltages in the usual range of 110 to 120 volts.

The main attack motor is fed directly from the 120-volt bus group and is the motor controlled by push buttons. A transfer contactor in the circuit to the image attack motor permits direct push-button control of this motor when the automatic follow-up control is not wanted. The control elements in the case of the image attack motor are the usual self-synchronous generator and control transformer combination.

The control element for the fore and aft and vertical motions of the tail strut windshielding is the 2-dimensional "reluctance" unit. Its physical size is 13 by 13 by $2^1/_2$ inches (Figure 5). This unit consists of two variable inductances for each motion. A 4 sided armature is in the center, positioned such that there is approximately a 3/16-inch air gap on all the inductances when perfectly centered. The armature is fastened to the tail strut connecting pin at the end of the tail boom and the case enclosing the inductances is fastened rigidly to the tail strut windshielding assemblage. Normal controlling action will result within as little as 1/8-inch relative motion in any direction. The tail boom moving at approximately 1/6 rpm is equivalent to the armature moving 8/10 inch in one second. Therefore, if we are to get complete controlling action within the 1/8 inch, the follow-up motor must be rotating in approximately 0.16 second. With this in mind the reactor units were designed to be able to supply full voltage to a stalled motor within 0.14 second after the thyratrons in the tube unit have been fired. Likewise, 75 volts can be applied within 0.09 second.

Figure 5. The "reluctance" control units and armatures

The 2-dimensional control unit and armature are at the left, the yaw control and the armature at the right

Figure 6 includes a schematic sketch of a similar yaw control unit and some of the safety features built into the unit are shown. In case of undue time lag in the action of the follow-up motors or an excessive mechanical drag the armature may drive against the inductance assembly. The inductance assembly is free to slide and operate limit switches behind it. The limit switches are placed in series in a control circuit, such that the operation of any one will stop the main drive motor and allow the follow-up system to regain its proper position. Additional safety against jamming has been provided by a flexible pin connected to the armature center which normally rides free in a 1-inch-inside-diameter hole in the side case of the reluctance unit. On contact between this pin and the case all the drives are stopped through interlock relays and the operator is required to reset the relays before operation is resumed.

The Tube Units

The tube unit input circuit is shown in Figure 6. The output from the bridge circuit consisting of the two variable inductances and two resistors is placed on the input transformer primary winding. The vacuum tube acts as a phase discriminator and plate current flows in the proper side to give the right motor rotation. The plates are excited from 275-volt windings on the same transformer as is shown with the 20-volt and 60-volt windings. The tube plate circuit is completed back to the tube cathodes through a center-tapped antihunt inductance. Voltage resulting across the inductance provides grid control of power thyratrons. These are *FG105* thyratrons and they provide the current for the controlling 4-c windings of the saturable reactors.

The tube unit (Figure 7) makes use of five of the *FG105* thyratrons. It contains the amplification and phase detection unit for the control signal, an antihunt unit, the automatic voltage limiting circuit, and a motor brake control circuit.

Reactor Units

The reactor units, one of which is shown in Figure 8, are floor mounted. The top section contains the time constant and current adjusting resistors used in the thyratron plate circuits. The bottom section mounts the three saturable reactors and the thyratron plate supply transformer. This plate supply transformer is excited from a 440-volt single-phase supply.

Desirable Characteristics of This Type of Induction Motor Drive

In designing this system one might think that some of the standard industrial packaged drive units such as Mot-O-Trol or Thy-Mo-Trol might have been used. However, it must be remembered that this equipment is installed inside the wind tunnel which operates at variable density, ranging from four atmospheres down to one-fourth atmosphere and possibly less. Likewise, humidity conditions may be severe and condensation is possible at times when the pressure is relieved suddenly. As a result, the decision was made that no motor drives having commutators or slip rings would be used, and that all the motors should be standard polyphase totally enclosed ball-bearing motors.

The induction motor also was preferred due to the service problem involved. Many of the motors are buried in the mechanism in such a way that it would be impossible to give commutators and brushes the proper service.

The ball-bearing induction motor solves this problem since it has proved consistently that it can give many years of service with very little attention given to it.

The desirable features of the drive system can be summarized in the following:

1. The use of polyphase totally enclosed ball-bearing induction motors requires a minimum of service for long trouble-free operation.

2. The use of 4- and 6-pole speeds in connection with built-in gear reduction units and short time ratings allowed the over-all physical size of the drives to be kept to a minimum.

3. The gear reduction units and magnetic brakes can be purchased as standard mechanical modifications with each motor.

4. The fact that the motor, magnetic brake, and gear reduction unit are a factory fabricated unit allowed the complete drives to become easily interchangeable. The horsepower and speed ratings were chosen with this interchange of different drives in mind a desirable point from the maintenance standpoint.

5. The control units as built allowed the use of current carrying contacts in the tunnel proper to be kept at a minimum.

6. The reactor control allowed variable-voltage reversible-control of the 2-phase induction motors without any additional rotating equipment. In other words, true electronic control was possible.

7. A unit design was possible in the manufacture of the tube units and reactor units. This facilitated the manufacture of the units by subcontractors.

In the follow-up drives the horsepower ratings varied from 3/4 horsepower to 3 horsepower. Ten complete units, consisting of the co-ordinated reactor unit, tube unit, and follow-up drive motor were required and built for the respective balance system installations at the Cornell Aeronautical Laboratory and the Southern California Co-operative Wind Tunnel in operation at Pasadena.

Figure 6. Signal pickup circuits used with tube units

Follow-up system used for control of wind-shield turntable yawing Alternate circuit using Autosyn units for control of image system yawing

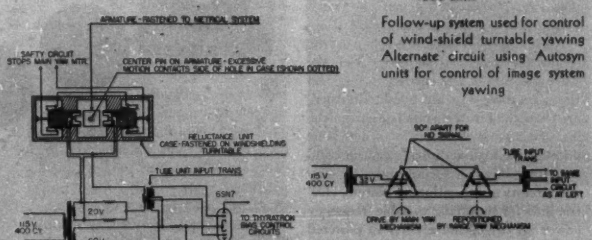

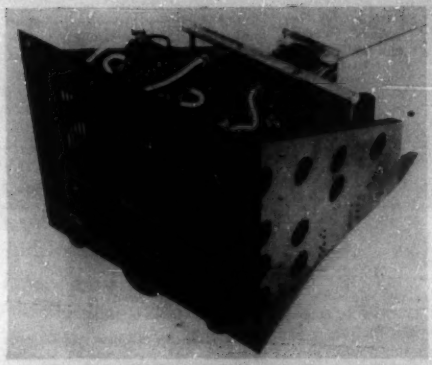

Figure 7. View of one of the tube units

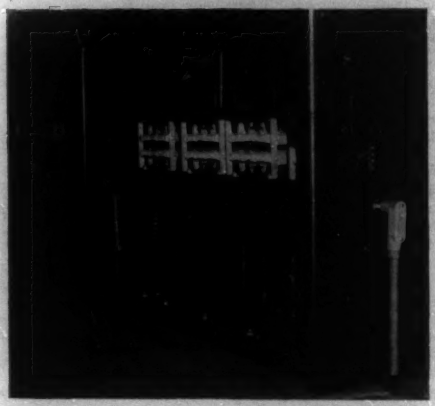

Figure 8. View of reactor units showing internal assembly of components

External Connections

When the balance system was described reference was made to the "sump." The purpose of this area is to handle all the external connections made to the metrical system and hold them properly positioned on an assemblage that will allow only a minimum of variable forces to be transmitted into the metrical system. These variable forces are caused by the varying strains on the cables resulting from the yawing action of the entire system. All the connections we are considering here are those that are a permanent part of the installation and they consist of hydraulic lines for the force indicating capsules and the oil lift bearings, electric lines for control circuits and positioning motors, electric lines for supplying variable frequency power up to 400 horsepower in powered models, and water lines for cooling the motors that are used on the powered models.

The "sump", noted in Figure 2, is a large cylindrical area directly below the metrical system housed in the decompression sphere of the tunnel and makes a projection on the bottom of the decompression sphere. Therefore, it is an area at the same pressure as that existing in the sphere and provides the necessary space above and below the yaw axis of the metrical system in which draping of electric cables and other lines can be handled properly.

The metrical system has been designed to permit operating angles of plus or minus 45 degrees when headed into the wind flow or it can be rotated 180 degrees and again operated through plus or minus 45 degrees in the new position. This last case would allow models such as tail first airplanes to be supported on this same system. As a result the cabling in the "sump" must be draped in such a way that a total yawing motion of 270 degrees is possible. The cables are first draped from the "inner" hanger (the 14-inch-diameter rotating cylinder) to the "intermediate" hanger (the 50-inch-diameter fixed hanger) with a sufficient loop to allow plus or minus 135 degrees of yaw motion. This loop is supported at the outer end on the intermediate hanger. This intermediate hanger maintains a fixed yaw position but still is supported from the metrical system, being fastened to the yaw gear box assembly. The second loop from this hanger to the fixed shell of the "sump" finally connects the cables to the outside or "ground" surface. In this way the first loop keeps the varying strains on the cables during yawing as an internal force between two parts of the metrical system, thus throwing no error into the force measurements. The outer loop as it is connected to the pressure

Figure 9. One of the electric pressure fittings shown disassembled

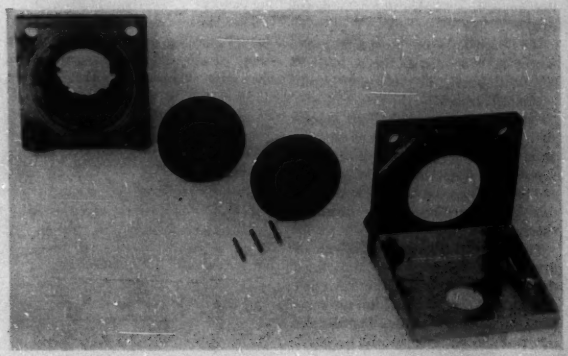

Figure 10. The control switchboard

fitting will interpose a force on the metric system due to its weight and the position at which it is connected on the intermediate hanger. However, it is an unvarying force since the cable maintains a fixed position at all times, and through initial adjustments of the distribution of the cables the forces can be made somewhat equal on all sides and a minimum constant force is left which can be subtracted initially from the force measurements as a constant.

The pressure fittings indicated in Figure 2 are necessary, the tunnel actually being a pressure vessel with steel walls varying from five-eighths to one inch thick. The fitting shown in Figure 9 provided a very effective unit for the electric connections. In most cases a cable of 19 number 12 American wire gauge or 31 number 16 American wire gauge conductors was handled in one fitting. The brass conductor pins were provided with a small shoulder midway between the ends. When a 1/32-inch neoprene disk with slightly undersized holes for the pins is clamped against this shoulder by means of the two bakelite disks a good permanent seal about the pins is maintained. The two disks are clamped tightly by the steel flanges and are capable of withstanding the maximum pressure of 51.7 pounds per square inch gauge that the tunnel is capable of holding. When the model-power 600-volt 3-phase variable-frequency lines had to be handled in the same fitting, only four conductor pins and proportionally larger spacing dimensions were used. Creepage dimensions on the faces of the disks were made exceptionally large to eliminate trouble due to condensation or moisture on the surface. This condensation is possible at the times when the pressure in the tunnel is released suddenly.

The Switchboard

The control switchboard (Figures 10 and 11) housing all motor control, the tube units, all interlocking relays, and a master interconnection section is located about 30 feet from the balance system "sump." This point locates it halfway between the tunnel working section and the main control room console.

The switchboard is of the back to back type with control sections on both sides. It is approximately 320 inches long, 108 inches high, and 24 inches deep. It is made up of 16 of the usual unit-design 20-inch sections. Among these are three sections used to house ten of the "tube units," and one section used as the master interconnection section. This last section contains sliding link type terminal strips. In it all interconnection between the interlocks in the control circuit are made. This allows all control device leads to be brought directly out of the sphere through portable cables in the "sump." A circuit after passing through the interconnection section is then carried back to the balance system in another portable cable if necessary. In this way interconnections are easily accessible outside the tunnel for testing.

Instrumentation Problems

In addition to the follow-up motor drive system we have discussed, instrumentation equipment had to be designed and incorporated as the construction of the balance equipment progressed.

One such item has been mentioned previously, the "tiltmeter", and presents an interesting application of an instrument quite similar to a torsion element seismic device.

The tunnel shell being free to move does not permit the base supports of the balance system to maintain a fixed position. Two jacking motors have been installed (as designated at *G* in Figure 2) that may be controlled by push buttons to tilt the balance system assemblage either in an upwind-downwind direction or in a crosswind direction. Likewise, the oil lift bearing surfaces between the large ring and moment table may not maintain equal and proper oil thicknesses and the moment table alone also may be displaced from an absolute level condition.

To detect the amount of tilt "tiltmeter" units were mounted in the main baseframe and likewise in the moment table. Through the proper instrumentation circuits it was then possible to give an operator the "out of level" information on microammeters at the control desk. He is able to correct the condition by the control of the jacking motors in the case of the main base frame. In the case of the moment table the flow of oil to the spherical oil pads can be regulated by the operator to increase or decrease the oil film thickness, thus restoring a level condition. The actual operating elements of the tiltmeters are copper disks with small out-of-balance weights supported on vertical 0.002-inch-diameter tungsten wires acting as the torsion restraining elements. The disk is placed in the air gap of a permanent magnet and a small 0.010-inch-thick concave aluminized mirror is fastened to the suspension wire. This mirror deflects a light beam as a twist is placed

Figure 11. The completed switchboard at the Southern California Co-operative Wind Tunnel showing the tube units in place at the near end

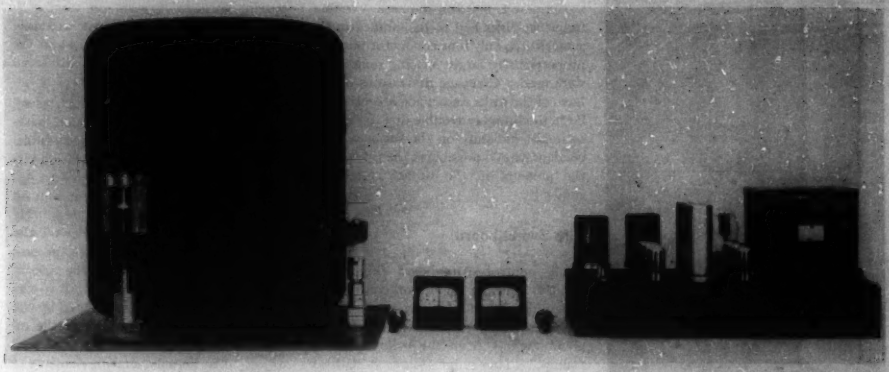

Figure 12. The tiltmeter, 2-channel amplifier and switchboard instruments used for reading the amount of tilt

in the suspension due to tilt of the instrument case. The sensitivity is such that as little as 1/200,000 radian of tilt can be detected. In Figure 12 the instrument (housed in an enclosing case that is absolutely dust tight and seals against moisture) is shown. Each of the instruments as built can detect tilt along two different axes, one represented by the upwind-downwind direction in the tunnel, and the other axis being across the tunnel at right angles with the first. Photoelectric pickups in the instrument are used with a 2-channel amplifier and the amount of tilt along the two axes is indicated to the operator on 15–0–15 range microammeters. The output of the photocells is in the order of one-fourth microampere and amplification is necessary to give suitable readings on the microammeters. With the use of two of these instruments in the balance system, the metrical system components can be maintained level within 1/100,000 radian at all times.

Conclusion

The description and discussion presented here covers the electrical installation in only one of the facilities that is required in a modern wind tunnel. It indicates that not all of the electrical problems evolve about the wind tunnel main drive unit and that many more applications of electric equipment, control, and instrumentation are required in a modern wind tunnel installation to make it an efficient and easily operable facility.

On equipment such as the balance system, which itself is a precision measuring device, it is evident that the most practical and simple solutions to the electrical problems must be sought out by the electrical engineer. In this way the electric equipment will require a minimum of attention. The operating personnel then is permitted to spend the major share of their time in maintaining high accuracy in the tunnel's aerodynamic test results.

References

1. New Features of Latest Wind Tunnels. *Aero Digest* (New York, N. Y.), part I, July 1945; part II, September 1945.

2. New Wind Tunnel Reaches Sonic-Speed Range, Clark B. Millikan. *Aviation* (New York, N. Y.), July 1945.

3. Co-operation in Research. *Aircraft Production* (London, England), volume 7, number 82, August 1945.

No Discussion

D-C Aircraft Generator Power Center

E. L. BOTTEMILLER
NONMEMBER AIEE

Synopsis: This paper covers the development of a co-ordinated d-c aircraft generator control and protective unit of the draw-out type. The scheme of operation of the unit is described briefly and the advantages of using such a co-ordinated control assembly are discussed.

THE aircraft generator power center consists of an assembly of a generator voltage regulator, generator control relay, reverse current circuit breaker, and circuit protective circuit breakers, into one draw-out unit which can be replaced by merely lifting a latch and withdrawing the unit, thus breaking all power and control circuits.

The purpose of this paper is three fold

1. To describe the design problems which were encountered during the development of the unit.

2. To discuss briefly the operation of the various devices.

3 To discuss the advantages of combining these various devices into a unit assembly.

Reason for Development

The aircraft generator power center was developed to meet a need in commercial aircraft for a centralized grouping of all control and protection for the aircraft generator. The assembly is built up on the draw-out principle in order to facilitate repair and maintenance of the various devices.

Previous to this time, these devices were usually individually mounted at various locations around the airplane and were wired together with a maze of cables and wire.

Paper 47-197, recommended by the AIEE committee on air transportation for presentation at the AIEE Pacific general meeting, San Diego, Calif., August 26-29, 1947. Manuscript submitted June 18, 1947; made available for printing July 14, 1947.

E. L. Bottemiller is associated with the General Electric Company, Schenectady, N. Y.

Development

Draw-Out Unit

All aircraft generators are provided with a voltage regulator and a generator control relay. In order to provide more complete generator protection and also to provide backup protection for the generator control relay, a reverse current circuit breaker is included. Small circuit protecting circuit breakers are included to protect the generator field circuit and the voltage lead which connects to the supervisory panel. These components are considered the very minimum that should be included to provide adequate generator control and protection.

These components are mounted on the back of a shallow pan of 1/8-inch thick magnesium alloy. (See Figure 1.)

The pan construction was used in order to provide rigidity and to allow utilization of the entire width of the base for mounting the devices. Also, the circuit breaker reset buttons, the voltage test plugs, and the withdrawal handle and latch are flush with the front of the mounting base. Since the power center will be located in an accessible place in the airplane, it is important that handles and buttons do not protrude to catch on the clothes of those who must maintain the equipment.

The voltage regulator which dissipates approximately 90 watts maximum power during operation was located at the top of the unit in order that its heat could be freely dissipated.

The original design enclosed the entire assembly in an aluminum cover but this was abandoned because of weight considerations. Since the components are individually enclosed, the only purpose the enclosure might serve would be to give mechanical protection to the devices during shipment or while in stock. A suitable shipping carton offers protection to the unit during storage or shipment.

Magnesium alloy brackets are included for mounting the sub base which supports the power and control disconnecting plugs and the reverse current circuit breaker. The weight of a complete draw-out unit is $14^1/_2$ pounds.

Framework

The framework (see Figure 5) is mounted in the airplane in such a location that the power cables and control leads can be brought to the rear of it and so that the draw-out unit can be withdrawn from the front. Approximately 8 inches of space is required in front of the framework to permit withdrawal of the unit. The framework is $10^1/_4$ inches deep, $12^3/_4$ inches wide, and 14 inches high.

The original framework was assembled of 1/8-inch thick and 1/2-inch wide aluminum alloy strip, but difficulty was encountered in spot welding the various 1/2-inch wide strips together. Three-quarter

Figure 1. Aircraft generator power center draw-out unit

Side view showing voltage regulator at top and generator relay at lower front

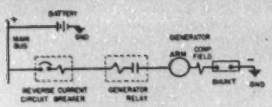

Figure 2. Elementary diagram of power circuit

Figure 3. Elementary power and control diagram for a d-c generator power center

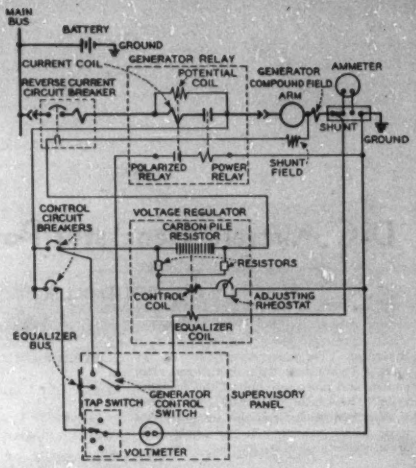

inch-width strips 1/8-inch thick were recommended if spot welding was to be used. Atomic hydrogen welding was tried but was found to be impractical as well as expensive.

With the co-operation of fabricators of magnesium alloy the use of angle and T extrusions was tried. The T and angles were hot formed into shape and riveted together with straps. Gussets were added to the corner bends to add rigidity.

The framework supports a base of insulating compound which supports the power and control male disconnecting plugs. A standard *AN* terminal block is used for the control terminals while the power studs are 1/2-inch (13 threads per inch) copper rod.

Power Disconnecting Plugs

A double-finger-type power disconnecting plug was developed for this application since no suitable aircraft-type disconnecting plug was available. The contact fingers are similar in design to those used on industrial draw-out-type equipment used on systems which may have as high as 50,000 kva capacity. The rating of a similar industrial type disconnecting plug used was 150 amperes. This rating was more than double for this application by adding silver plating to all of the parts and by operating at higher temperature rises.

Heat runs made on disconnecting plugs of bare copper at 400 amperes indicated a maximum temperature rise of 50 degrees centigrade at the hot spot, while tests made at 600 amperes indicated a maximum rise of approximately 64 degrees centigrade. The tests were made on the bare copper elements in order to check the rise under adverse conditions, that is, in case all of the silver plating should be worn off by frequent withdrawals of the plugs.

With 300 amperes passing through these disconnecting plugs the voltage drop is approximately 25 millivolts for each disconnecting plug.

The plug uses parallel current carrying members which tend to keep the contact resistance at a low value and which on high short-circuit currents attract each other and hence tend to maintain the circuit even under very high overload conditions. Contact pressures of from 15 to 20 pounds are used on the disconnecting plug contacts.

Reverse Current Circuit Breaker

The original design included a manual reset lever which would permit the resetting of the reverse current circuit breaker without removing the draw-out unit from the framework. However, this feature was changed after consultation with some of the aircraft manufacturers for reasons which will be explained later in "Operation of the Equipment."

The reverse current circuit breaker was removed from its aluminum alloy supporting base in order to conserve space and weight.

Voltage Regulator Mount

A new spring and rubber shock mount was developed for the voltage regulator since the conventional approved mount was too large and heavy.

The voltage regulator unit can be easily removed from the assembly by removing a locking clip to permit disconnecting the leads and by turning two locking lugs. The complete element can then be removed from the shock mounting support.

Operation of the Equipment

Voltage Regulator and Generator Control Relay

Figure 2 illustrates the basic power circuit for a single generator installation. The ammeter shunt is located in the negative side of the generator armature. Figure 3 shows the same circuit with the complete control circuits included.

Assume that the generator is not running, and that the battery is connected to the main bus. When the engine which drives the generator is started, the generator builds up voltage until its voltage is from 0.35 to 0.65 volt above the bus voltage, at which time the polarized relay of the generator control relay becomes energized and energizes the power relay of the generator control relay. When the power relay is closed, the generator armature current then flows toward the main bus and the battery. The closing of the generator control relay contacts short circuits the polarized relay shunt coil and leaves this relay subject to the positive or normal flow of current toward the main bus. The regulator senses the generated voltage and operates to increase and decrease pressure on the carbon pile and hence vary the generator field current to maintain a generated voltage of, say, 28.5 volts.

If the speed of the engine which drives the generator is reduced greatly, the generated voltage drops below the bus voltage and hence causes a reversal of the current which flows through the generator control relay contacts. When this current reaches a value of approximately 30 amperes, the polarized relay operates to de-energize the power contact of that device.

The voltage regulators are equipped with equalizer coils which are used only when the generators are operated in par-

allel. The purpose of these coils is to provide for proportioning the total load current among the several generators in proportion to the ratio of their individual rated capacities.

Adjustment of the system voltage and load which each generator assumes can be made by means of a rheostat which is accessible from the front of the draw-out unit.

Reverse Current Circuit Breaker

If a fault in the winding of the generator or in the cable between the generator and the power center occurs, a reverse current of large magnitude will flow. In order to quickly and safely interrupt this current a reverse current circuit breaker with an inverse time characteristic is included. It should be remembered that there are now two devices connected in series, both of which operate on reverse current. However, the reverse current circuit breaker is so constructed that it will trip first on any faults which exceed 500 amperes. There is an auxiliary contact on this reverse current circuit breaker which opens the generator field circuit when the breaker trips.

The tripping characteristic of this circuit breaker is shown in Figure 4. The drop out time of the generator relay is approximately 0.05 second and is practically independent of load current. Thus on currents below approximately 500 amperes the generator relay will disconnect the generator. When the generator recovers, the generator relay will attempt to place the generator back on the line in the normal manner.

However, if the reverse current is 500 amperes or more it will be caused by a fault and the generator field is opened and that generator is taken out of service. It is necessary to remove the draw-out panel from the framework in order to reset this reverse current circuit breaker. It is necessary that an inspection of the unit and of the cables from the generator to the unit be made and that the fault be remedied before the circuit breaker is reset and the draw-out panel is replaced.

Circuit Protective Circuit Breakers

All control circuits from the generator positive terminal on the generator load center to the supervisory center are protected with inverse time overcurrent circuit breakers. These circuit breakers protect the wiring to remote locations against short circuits. A 20-ampere continuously rated breaker is used in the generator field circuit while a 5-ampere continuously rated breaker is used in other circuits. These circuit breakers will trip in approximately 10 seconds at four times their rated current.

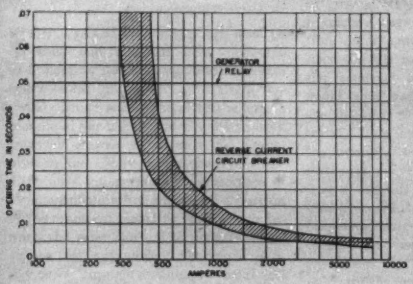

Figure 4. Time–current characteristic for a reverse current circuit breaker

Control and Power Disconnecting Plugs

The control and power disconnecting plugs are so arranged that the field circuit and the generator relay circuit are disconnected before the power circuit is broken if a draw-out unit is removed while the generator is under load. Therefore, the probability of having to interrupt power on the disconnecting plugs is small. This arrangement helps maintain these contacts in good condition.

Advantages of the Generator Power Center

Easily Installed. A complete installation of generator control and protective equipment consists of running one power cable and a shunt field lead from the generator to the back of the load center framework and a second power cable from the power center to the main bus. An additional equalizer lead is required if parallel operation of the generators is to be accomplished. Just before the engines are to be run up for preliminary checking the completely wired draw-out unit can be plugged into the framework. A bench adjustment and test of the complete draw-out unit can be made away from the airplane.

Easily Serviced; Units Interchangeable. The draw-out unit can be removed by raising the finger latch and pulling on the handle. Since the units are all fitted on one jig, they are all interchangeable, hence units can be stocked at various maintenance centers for quick replacement in case of trouble.

Circuits Are Simple; Maintenance Time Is Reduced. Conventional component devices and simple circuits are used, therefore, service men are familiar with them and should have no difficulty with maintenance. Simultaneous observation of the generator equipment for all generators simplifies trouble shooting and checking of continuity of circuits.

Parallel Operation Easily Accomplished. Since the units are mounted side by side in a framework, a 6-inch long piece of copper bus is all that is needed to provide parallel operation of two generators. The parallel bus can be fed to a number of individual feeder circuit breakers which can be located on top of the framework. Such arrangement allows the designer to plan a distribution system and a centralized main bus and power center. For a 4- or 6-generator airplane the units can be mounted side by side or one above the other in units of two equipments. In this manner paralleling of several generators is easily accomplished.

More Uniform Bus Voltage Maintained. Since the voltage regulators are located at

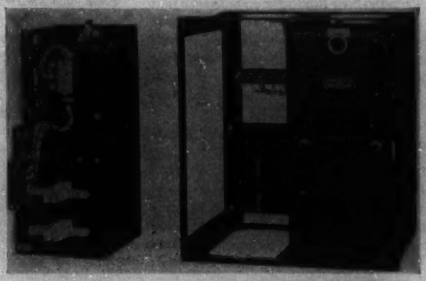

Figure 5. Two d-c aircraft generator power center draw-out panels and one 2-unit framework

One unit is withdrawn and turned to show power disconnecting plugs

the bus, the regulators will more uniformly maintain bus voltage since the voltage drops in the generator cables which vary as a function of load need not be considered. Since the generators are rated on the basis of a 30 volt d-c output, it is possible to reduce the size of cable from the generator to the load center and permit, say, a full 1.5-volt drop since the regulator operates to maintain the bus voltage at, say, 28.5 volts.

Provides Protection to the Generator. The use of the quick acting reverse current circuit breaker provides the generator with good fault protection in the case of a grounding of the generator winding or of its positive lead.

Unit Responsibility for Equipment. Since one manufacturer of necessity must assemble the equipment, he must take responsibility for the successful operation of the whole unit. Since the components are factory wired and tested, the chances of having to replace components is less than if each of the individual components were installed and wired in the airplane and then were tested.

Weight. A 2-unit generator power center completely wired and including a 2-section framework weighs 34 pounds. Magnesium alloy suitably pickled and finished with a baked crackle finish is used throughout in the construction.

Optional Features

The following optional features can be incorporated in a generator power center with a small increase in weight. These devices are not shown on the elementary power and control diagram.

Overvoltage Protection. A generator overvoltage relay to be added to the assembly has been developed.

Generator Thermal Overload Protection. The recent development of a generator temperature sensing element which rests against the generator commutating bus and hence "feels" its temperature permits the addition of generator thermal overload protection with a device which has no moving parts or contacts to be installed on the generator. The temperature sensing element has a negative temperature coefficient of resistance and when inserted in series with a small sensitive relay across a 28.5-volt d-c supply may be used to sound a warning or light a warning light.

Conclusion

There are a variety of opinions as to what constitutes adequate protection for an aircraft generating system and how and where the various devices should be located. This paper has illustrated one approach to the subject.

References

1. Electric-Circuit Fault-Protective Principles as Applied to D-C Aircraft Systems, **R. H. Kaufmann.** AIEE Transactions, volume 63, 1944, pages 333–44.

2. D-C Power Systems for Aircraft, **E. J. Finison, R. H. Kaufmann.** *General Electric Review* (Schenectady, N. Y.), September 1945, August 1946.

3. Paralleling and Regulation of 24–28-Volt D-C Generators in Multiengine Aircraft, **Arthur Siegal, Dennis G. Decourcey.** AIEE Transactions, volume 63, 1944, December section, pages 854–7.

No Discussion

Design and Application of Supersonic Flaw Detectors

DONALD C. ERDMAN
NONMEMBER AIEE

Synopsis: General parameters are given for the circuits that make up echo-type supersonic flaw detectors used in the location of defects in large metal forgings. Applications of such equipment are listed and a bibliography of pertinent articles is included

ECHO TECHNIQUES as are used in sonar and radar are also applicable to apparatus for locating hidden defects inside solid metal objects. High frequency sound waves traveling the length of a metal bar behave quite similarly to a transient electric signal in a long transmission line. Any abrupt changes in the distributed capacitance or inductance of the transmission line will cause a portion of the transient signal to reflect back toward the generator. The acoustic analogy is that any abrupt change in density or in Young's modulus in metal will cause a partial reflection of a pressure wave. Echoes are received readily from cracks, flakes, and holes. If working at sufficiently high frequencies, echoes can be detected from large grain boundaries.[1]

Method

A small quartz crystal is used as a transducer (Figure 1) to convert electric energy into pressure waves and vice versa; thus one crystal unit acts both as a loud speaker and a microphone. Extremely short blocks of radio frequency power are fed to the transducer. These pulses vary in commercial equipment, but in general, depending upon the carrier frequency, may be anything from a fraction of a microsecond up to several microseconds in length. Choice of carrier frequency depends upon the type of metal being inspected, the grain size, and the distance the supersonic beam must travel. For inspection of steel castings, frequencies as low as 500 kc are common. Fifteen megacycles is desirable for inspection of aircraft forgings and extrusions. Usual repetition rate of the pulses in low-frequency supersonic equipment is 60 cycles per second. Fifteen-megacycle equipment, with its shorter permissible pulse widths and more rapid attenuation of the pressure wave, can use repetition rates of 1,000 per second or higher.

Figure 2 illustrates how laboratory test equipment can be assembled for the inspection of small metal objects. The quartz crystal and casting are placed under water to allow the supersonic beam to be directed into fillets and curved surfaces. When large objects are being inspected, the surfaces are usually flat enough to allow the quartz crystal to be placed directly against the part. Oil or glycerine is used to insure good acoustic coupling with the part. An ultrasonic trainer *AN/APS-T3* contains most all of the equipment needed for an experimental flaw detector.[2]

A synchroscope can be used to combine the functions of the synchronizer and oscilloscope as illustrated in Figure 1. More elaborate oscilloscopes may be used for this purpose, providing they can be operated in single sweep fashion. A range mark generator built into either the synchroscope or oscilloscope is most desirable. When both small and large parts are being inspected, sweep rates taking from 100 to 1,000 microseconds to cross the screen are of great value.

Radio Frequency Pulse Generator

Many methods of producing short blocks of radio frequency power are available. Figure 3 shows the essential components of one generator. Although this unit is considerably more complex than thyratron ringer circuits, it has the advantage that continuous wave output is available for studies involving acoustic wave attenuation.[3] Characteristics desired of a radio frequency pulse generator are that it deliver to a coaxial line five to ten cycles of power, then wait until the next synchronizing signal arrives before sending out another wave train. The generator must present a fixed and, preferably, high impedance to the coaxial line so that returning echoes are not short-circuited by the generator. One of the difficult problems connected with genera-

Figure 1. Illustrating formation of supersonic echoes

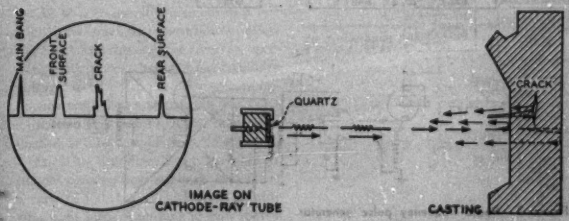

Paper 47-198, recommended by the AIEE committee on instruments and measurements and approved by the AIEE technical program committee for presentation at the AIEE Pacific general meeting, San Diego, Calif., August 26–29, 1947. Manuscript submitted June 17, 1947; made available for printing July 10, 1947.

DONALD C. ERDMAN is with Triplett and Barton, Inc., Burbank, Calif.

Valuable assistance was received from members of the Radiation Laboratory and the Research Construction Company of Cambridge, Mass., who counseled early phases of this work.

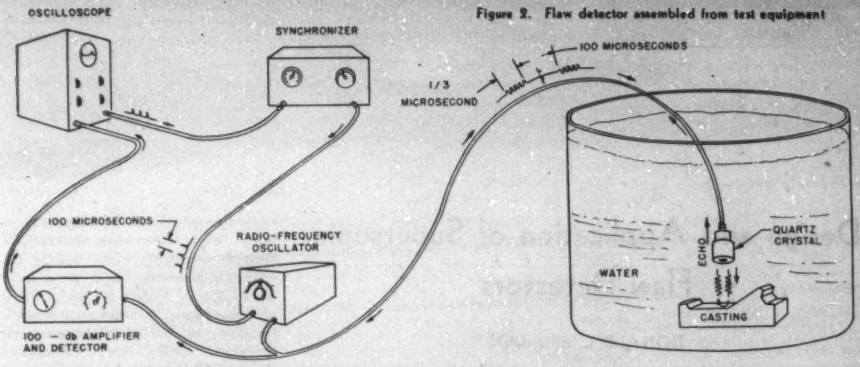

Figure 2. Flaw detector assembled from test equipment

tor design is one of obtaining a constant impedance match to the coaxial line although the generator is alternately off and on.[4] Since this is not accomplished readily, the compromise is to be certain that the other ends of any coaxial lines attached to the generator are terminated properly to prevent multiple reflections of the radio frequency pulse in the coaxial line.

A pulse one microsecond long, when converted into pressure waves, occupies one eighth of an inch in metal. When this is realized, the need for extremely short radio frequency pulses from the generator is apparent. Thus, if the quartz crystal is in contact with the surface of a metal bar, no echoes could be detected for at least the first one eighth inch because of the transmitter still being on. This dead time is one of the more serious problems connected with inspection by echo methods. Several other factors external to the radio frequency generator tend to lengthen the dead time. Any circuit with appreciable Q will tend to ring for a considerable time after being subjected to the several hundred volts from the radio frequency generator. A receiver adjusted to signals of the level of microvolts will overload and remain overloaded until the damped signal from the high Q circuit dies out; therefore it is good practice to reduce the Q of all inductances in a system to as low a value as is consistent with signal to noise ratio.

Quartz Crystal

Less easily dealt with, in the dragging out of the dead time, is ringing due to the mechanical Q of the quartz crystal. This ringing follows both the transmitted pressure wave and every strong reflection, which makes the detection of weak echoes near a strong echo quite difficult. The ideal solution to mechanical Q problems would be to sandwich the quartz crystal between two solid surfaces, one of which has high attenuation to the acoustic wave, and the other being the part inspected. These solid surfaces should have the same acoustic impedance as quartz. Unfortunately, available materials are a poor acoustic impedance match to quartz. In practice, one side of the quartz crystal usually is cemented to some absorbing material such as bakelite or Micarta, and the other side of the crystal is loaded acoustically by the oil or glycerine which is used to couple the crystal to the metal object being inspected. Much work has been done in the search for a practical liquid which will have an acoustic impedance value between quartz and steel. Mercury or mercury amalgams are quite effective where the chemical properties of mercury are not troublesome.[4] Other workers have had some slight success coating the crystal with thin films of plastic which act to transform acoustic impedance in much the same manner as a quarter-wave line impedance transformer changes electrical impedance. When chemically grown crystals such as "ADP" and "KDP" can be adapted for higher frequency operation, it is likely that they will have quite an advantage over quartz, because of their low inherent mechanical Q and their high electric activity.

Coaxial line termination at the crystal end is quite important to the gain of the apparatus. Crystals, such as are used in the *AN/APS-T3*, have an electrical impedance of around 15,000 ohms under normal operating conditions. A pie or L network usually is used near the crystal

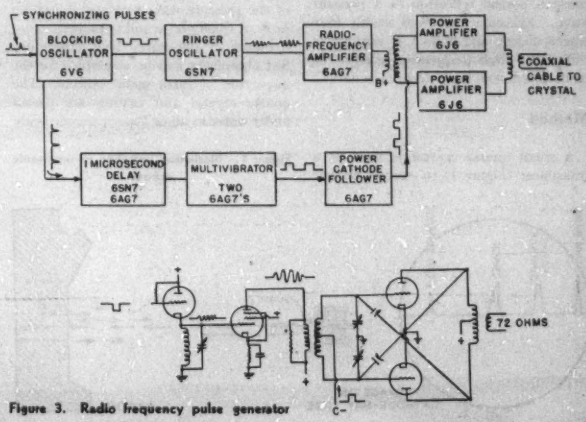

Figure 3. Radio frequency pulse generator

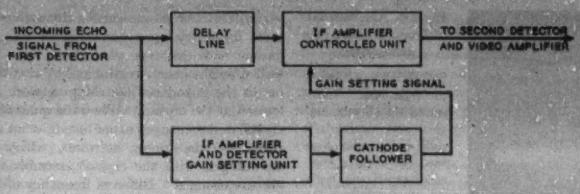

Figure 4. Block diagram of automatic gain setting circuit

to transform the 72-ohm line impedance to 15,000 ohms. A resistance from 5,000 to 20,000 ohms across the crystal will help to swamp out ringing caused by the inductance in the impedance matching network. Adjustment of the network for a maximum sensitivity to weak signals will not be the same as the adjustment for maximum discrimination between signals that occur close together. Contributing to this discrepancy are factors such as the constructive and destructive interference caused by acoustic echoes in the crystal holder.

Amplifier

An amplifier of at least 100-decibel gain is needed to bring the echo signals up to a level that can be handled by most synchroscopes. This amplifier should have a band width great enough to pass the shortest pulses used from the radio frequency pulse generator. If operating at a carrier frequency of 15 megacycles, the band width should be approximately 5 megacycles. All cathode by-pass capacitors and filter capacitors should be large enough so that during the time the generator is operating no change in potential will occur across the capacitors.

Radar systems use a transmit-receive tube which prevents the high power transmitted signal from being fed into the receiver. Such a tube is not applicable to low power circuits as are used in flaw detection. It is therefore necessary that the receiver be designed to take momentary inputs of several hundred volts and yet be able to amplify a signal of a few microvolts strength immediately afterward. A superheterodyne receiver, operating with lower than normal oscillator voltage, will feed to the intermediate frequency amplifiers a signal that has quite a definite maximum value; thus overloading of these amplifiers is reduced.

An echo amplifier must be able to handle signals whose strength varies over a ratio of 100 to 1. This would indicate that some form of automatic gain control is desirable. Several rapid automatic gain setting circuits have been tested. Such circuits have the disadvantage that the gain-establishing fed-back signal arrives too late to work on the signal that created it. Use of intermediate frequency amplifiers at 60 megacycles with 10 megacycle band width would reduce the "turn around" time to a more nearly usable value. To prevent the generation of transients in the intermediate frequency amplifier, the gain setting signal should be fed into a balanced stage. Figure 4 shows a quite promising system, although it is more complicated than would be commercially practical. In this system two amplifiers are used, one of which is used to set gain on the other. Signals to the controlled amplifier are delayed enough so that the gain setting amplifier has time to establish the amplification of the controlled amplifier before a large signal comes along. A delay of two microseconds is adequate and can be obtained by insertion of a multisection delay line or by using the delay in several hundred feet of coaxial cable. In experimental systems, the latter method is much the simpler since excess ringing, which would be a problem in a lumped constants delay line, is not encountered.

Design of the second detector and video amplifier circuits which follow the intermediate frequency amplifier should incorporate the following features:

1. Quick recovery to strong signals.
2. Ability to pass pulses one half microsecond long without deterioration of leading or trailing edges.
3. Freedom from ringing of the video peaking coils.
4. Sensitivity to weak signals.

These requirements are met in most radar receivers. A feature that has been incorporated in test sets where a spiral sweep is used in the indicator is to have a nonlinear resistive element across the input to the video amplifier. This helps prevent overloading the succeeding amplifiers on strong signals. Where greatest interpretability of the wave shape of the echoes is needed, a large oscilloscope and powerful video amplifier should be used so even the strongest signals can be shown without overloading the amplifier or without running off the screen. Fast time constant circuits as are used in radar must be used with caution in flaw detecting equipment, because of the dead time that follows long blocks of signals.

Indicator Characteristics

Indicators for use with supersonic flaw detection circuits should be chosen according to the type of inspection jobs most likely to be encountered. Large oscilloscopes are desirable in fixed location equipment since the operator can be further away from the screen and still get good visibility of the echo traces. Around the aircraft industry and oil distilleries, portability of the testing equipment is of paramount importance, hence the need for a small oscilloscope. When limited to a small oscilloscope, a circular or spiral sweep, rather than a single horizontal

Figure 5. Simplified circuit of portable flaw detector

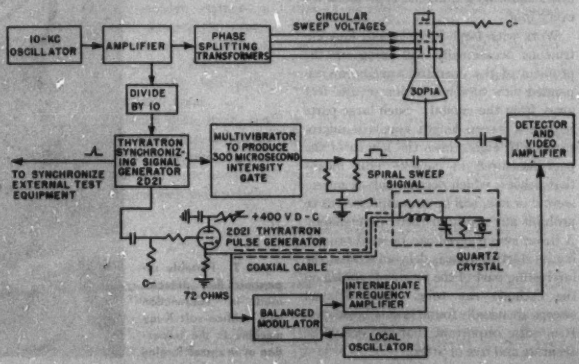

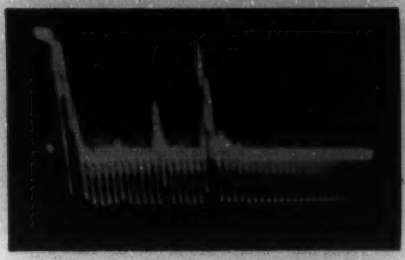

Figure 6. Oscilloscope pictures of test bar echo pattern

Signals reading from left to right are: Transmitted signal, echo signal from a number 70 drill hole, echo from rear side of part. Five-microsecond range marks are shown below the axis

trace, will allow the most echoes to be presented. An *SCR-718C* pulse-type radio altimeter contains the basic circuits needed in a circular sweep unit.[6]

Linearity of the sweep circuit is not as important as it might seem at first, providing range marks are available. The range marks let the operator know how far into the metal part a particular defect is located. If the range marks are adjusted to occur every eight microseconds, they will correspond to one mark per inch of steel. The range mark spacing should be adjustable so that compensation may be made for the different velocities of sound in various metals and plastics. Range marks may be applied to the Z axis, that is, they are caused to modulate the grid of the cathode ray tube. Other presentations of the marks are to have a square wave or a spike type deflection of the cathode ray trace. When inspecting large forgings the pressure wave often travels several feet before hitting a defect. If the range marks are set to occur once per inch, the operator has to count quite a number of marks in locating how far away the defect is. For this reason, it is desirable to have a double range mark system, one showing marks for each inch, and the other showing a different type mark for every foot.

Work with large forgings and long extrusions occasionally will bring up the problem of the operator wanting an expanded view of some section several feet away from the crystal. Such large parts require a sweep length equal in microseconds to eight times the length of the part measured in inches. This means that echoes, which occupy only a microsecond or less, will be so compressed as to prohibit any study of their wave shapes. A faster sweep speed can be used providing its starting time is delayed so that the interesting part of the forging is shown on the cathode ray tube. Such delayed sweeps are usually found in synchroscopes. It is quite important that the delays be accurate and free of jitter.

Commercial Design

In commercial design of a supersonic echo type flaw detector, as many of the afore-mentioned characteristics should be incorporated as is consistent with a practical instrument. Operating dials and controls should be kept to an absolute minimum. Several carrier frequencies are necessary, with switching from one frequency to another controlled by a single dial. Figure 5 gives a block diagram of a flaw detector designed for portability. This unit uses a 3-turn spiral sweep on the cathode ray tube. Each turn of the spiral represents one foot of steel, hence the unit is limited to forgings or extrusions less than three feet thick.

For reasons of simplicity and space saving, this unit incorporates a thyratron radio frequency generator. Carrier frequency with this type generator is controlled by the quartz crystal and by ringing in the impedance matching network located at the crystal. When the quartz crystal unit is changed to one of a different frequency, the tuning networks, which are integral with the crystal assembly, also are changed. Different frequency of operation requires only that the oscillator portion of the superheterodyne receiver be retuned. A 30-megacycle intermediate frequency amplifier is used. Band width is approximately 4 megacycles. In order that carrier frequencies of 1, 5, and 15 megacycles may be used, it is necessary to use a balanced modulator type of the first detector so that the local oscillator signal does not overload the intermediate frequency amplifier.

Regulated d-c power supplies are provided to make the apparatus relatively insensitive to line voltage changes. High voltage for the cathode ray tube is obtained from a transformer and rectifier operated from an 800-cycle power oscillator. This use of 800 cycles was necessitated by the desire to use the cathode ray indicator unit from the *SCR-718C* intact.

Three of the controls visible on the front panel of the apparatus are used only when it is desired to tie the unit in with an external synchroscope, or other test

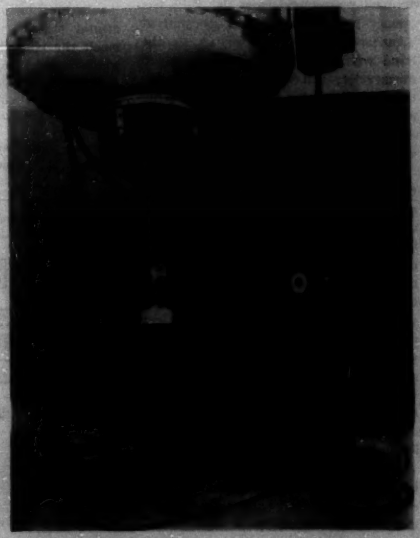

Figure 7. Portable supersonic flaw detector used in conjunction with million-volt X-ray machine in the inspection of an aircraft forging

equipment. Provision has been made for using two separate crystals, as in the British system for welding inspection.[6] It is sometimes desirable to couple to the test apparatus another unit such as a direct reading pulse position indicator, or a pulse strength measuring meter. These auxiliary units are useful when thickness measurements are made by noting the time elapsed between the transmitted supersonic pulse and the echo received from the far side of the object being measured.

Application

In the accompanying bibliography are listed many excellent papers on applications of the reflection type supersonic flaw detectors. The author's experience in the application of supersonic inspection has been limited to problems associated with the aircraft industry.[8] Chief interest in the new inspection tool has come about through the need for quality control on the forgings used in jet engines. Many of these parts are too thick to be successfully X-rayed, leaving no other method of internal inspection available. Supersonic inspection will detect tight cracks which are not likely found by X-ray methods, although X-ray has quite an advantage in being able to show defects in such a manner that the operator more easily can identify the type of defect. Interpretation of defects by supersonic echo techniques is still in its infancy. It is usually true that anything that will show a strong echo is serious inside highly stressed aircraft parts. Determination of size and location of a defect is accomplished quite accurately by scanning with the quartz crystal and noting the echo position relative to the range marks. There is no well defined limit to the thickness of a part that can be inspected by supersonic means providing the metal is homogeneous, and the proper frequency and power are used.

Some castings can be inspected providing they are not too porous. Magnesium castings are very transparent to 15-megacycle pressure waves. Defects common to magnesium castings, such as microshrinkage and channeling of porosity, throw strong and easily recognized echoes. Aluminum castings usually have too much gas porosity to allow good penetration of the supersonic pressure wave. If a low frequency is used, steel castings can be inspected. Forgings, extrusions, and wrought materials are penetrated most easily. Attenuation of the pressure wave in the materials is very much a function of their grain structure and hence of heat treatment. A change in attenuation of two to one occurs in *4130* alloy between the normalized state and the heat treated condition. Because of this sensitivity to grain size and grain boundary characteristics, most routine inspectiou is carried on at relatively low frequencies, such as two to five megacycles.

Sensitivity to defect is a function of the orientation of the defect to the supersonic beam direction. If the defect is normal to the beam, and if it intercepts between one and ten per cent of the beam area, it causes a detectable echo no matter how thin it is in the direction parallel to the beam. This is true because most defects are filled with gas or slag, which represents a tremendous change in Young's modulus as compared to the parent material. There is a definite relationship between the area of a defect that must be intercepted and the wave length of the supersonic pressure wave. Figure 6 shows a number 70 drill hole which easily can be shown through a foot of steel when testing at 15 megacycles. Yet, at 5 megacycles, this defect begins to get quite noticeably more difficult to show. Long cracks usually are found no matter which orientation they have relative to the beam, since the characteristic of most cracks is either to zigzag through metal, or to turn at one end or the other. Surface cracks can be located only if the beam is pointed normal to the crack.

Quite a number of interesting characteristics are being found in metal by other than direct echo techniques. If the gain of the amplifier is turned up to where multiple echoes are visible from the back side of a billet, one occasionally will note areas on the billet where the number of these reflections changes quite radically. Preliminary test on the metal where these changes in acoustic transmission occur indicate areas of considerably different grain structure. A sudden change in grain sometimes will disperse the supersonic beam, causing echoes from the back side of a part to disappear. Changing to a lower frequency usually will allow penetration through such areas.

More specific circuit data have not been included since there are numerous sources available for such information. Range mark circuits and their constants can be found associated with most articles on radar circuits.

Bibliography

1. Flaw Detecting Device and Measuring Instrument, **Floyd A. Firestone.** United States patent 2,280,226.

2. Ultrasonic Trainer Circuits, **Finn J. Larsen.** *Electronics* (New York, N. Y.), volume 19, June 1946, pages 127–9.

3. Supersonic Inspection Device, **Floyd A. Firestone.** United States patent 2,398,701.

4. Supersonic Fundamentals, **V. J. Young.** *Electronics* (New York, N. Y.), volume 17, March 1944, pages 122–5, 204–12.

5. Symposium on Supersonic Inspection Held By The Iron and Steel Institute, London, England. *The Welding Journal* (New York, N. Y.), volume 26, January 1947.

6. Pulse-Type Radio Altimeter, **Albert Goldman.** *Electronics* (New York, N. Y.), volume 19, June 1946, pages 116–19.

7. Refinements in Supersonic Reflectoscopy Polarized Sound, **Floyd A. Firestone, Julian R. Frederick.** *Journal*, Acoustical Society of America (New York, N. Y.), volume 18, July 1946, pages 200–11.

8. Inspection: Supersonic Inspection of Materials and Parts, **Donald Erdman.** *Journal*, Society of Automotive Engineers (New York, N. Y.), October 1946, page 74.

9. Method and Apparatus for Sounding and Locating Submarine Obstacles by Means of Ultra-Audible Waves, **Paul Langevin, Charles Louis Florisson.** United States patent 1,858,931.

10. Means for Indicating Flaws in Materials, **Sergey Sokoloff.** United States patent 2,164,125.

11. Method and Apparatus for Ultrasonic Testing, **Wilford E. Morris.** United States patent 2,378,237.

12. Ultrasonic Vibrations Reveal Hidden Flaws, **The Brush Development Company.** *Electronic Industries* (New York, N. Y.), volume 5, January 1946, pages 64–5, 164–6.

13. The Brush Hypersonic Analyzer. The Brush Development Company, Cleveland, Ohio.

14. Ultrasonic Measurement of Wall Thickness in Diesel Cylinder Liners, **Francis W. Struthers, Horace M. Trent.** *Journal*, Acoustical Society of America (New York, N. Y.), volume 19, March 1947, pages 368–71.

15. Velocity of Dilatation and Rayleigh Waves in Metal Bars, **J. Howard McMillen.** *Journal*, Acoustical Society of America (New York, N. Y.), volume 18, July 1946, pages 190–9.

16. The Supersonic Reflectoscope, an Instrument for Inspecting the Interior of Solid Parts by Means of Sound Waves, **Floyd A. Firestone.** *Journal*, Acoustical Society of America (New York, N. Y.), January 1946.

17. The Detection of Cracks in Steel by Means of Supersonic Waves, **Desch, Sproule, Dawson.** *Journal*, The Iron and Steel Institute (London, England), March 1946.

18. Supersonic Inspection of Aluminum Alloy (Editorial Citation to Aluminum Company of America). *Materials and Methods* (New York, N. Y.), volume 24, November 1946, pages 1172–3.

19. Supersonic Inspection of Materials, **H. R. Clauser.** *Materials and Methods* (New York, N. Y.), volume 24, pages 379–84.

20. Process Control Methods for Industrial Uses—Basic Transducer Systems for Conversion of Mechanical Effects Into Electronic Control Impulses, **Ralph R. Batcher.** *Electronic Industries* (New York, N. Y.), volume 3, May 1944, pages 112–14, 294.

21. Sheet Fractures Detected With Supersonics. *The Iron Age* (Philadelphia, Pa.), volume 153, June 8, 1944, pages 60–1.

22. Supersonic Testing in a Steel Plant, **J. V. Russell, H. E. Pullett.** *The Iron Age* (Philadelphia, Pa.), volume 157, January 31, 1946.

23. The Supersonic Reflectoscope for Interior Inspection, **Floyd A. Firestone.** *Metal Progress* (Cleveland, Ohio), volume 48, September 1945, pages 505–12.

24. The Supersonic Flaw Detector, **Eric N. Simons.** *Metal Progress* (Cleveland, Ohio), volume 48, September 1945, pages 513–16.

25. Supersonic Measurement of Metal Thickness, **Wesley S. Erwin.** *The Iron Age* (Philadelphia, Pa.), volume 154, November 9, 1944, pages 59–61.

26. Report of Meeting of National Electronics Conference. *The Iron Age* (Philadelphia, Pa.), volume 154, October 19, 1944, pages 116–18.

27. Ultrasonics—A New Metallurgical Tool. **C. M. Cosman.** *The Iron Age* (Philadelphia, Pa.), volume 147, May 15, 1941, pages 48–50.

28. Supersonic Flaw Detector. **Ralph B. De Lano, Jr.** *Electronics* (New York, N. Y.), volume 19, January 1946.

29. Some Results of Advances in Welding and Radiography on the Welding of Pressure Vessels. **O. R. Carpenter.** *The Welding Journal* (New York, N. Y.), volume 25, June 1946, pages 531–42.

30. Ultrasonics (book). **Ludwig Bergmann, H. Stafford Hatfield.** John Wiley and Sons, Inc., New York, N. Y., 1944.

31. Ultrasonic Generator. **Frederick W. Smith, Jr., Paul K. Stumpf.** *Electronics* (New York, N. Y.) volume 19, pages 116–19.

32. Curved Quartz Crystals as Supersonic Generators. **L. W. Labaw.** *Journal*, Acoustical Society of America (New York, N. Y.), volume 16, April 1945.

33. Supersonic Inspection Reveals Laminations and Deep-Seated Flaws. **Rupert LeGrand.** *American Machinist* (New York, N. Y.), May 23, 1946, pages 131–3.

34. Testing Materials for Internal Discontinuities With Supersonic Echoes. **J. W. Dice.** *Industrial Radiography*, spring 1947, pages 29–33.

No Discussion

Excitation Problems in Hydroelectric Generators Supplying Long Transmission Lines

C. L. KILLGORE
MEMBER AIEE

SUITABLE SITES for hydroelectric power developments usually are located at a considerable distance from the load center and, therefore, long transmission lines generally are associated with hydroelectric generators. This combination of long transmission lines and hydroelectric generators introduces problems in voltage regulation, overvoltage, and stability which can be solved by the proper application of modern excitation systems.

A long transmission line is in itself virtually a pure capacitive load which usually is more than balanced as the inductive load is picked up by the generating unit. However, a satisfactory excitation system must be capable of maintaining the voltage within specified limits when a hydroelectric generator is operating underexcited with a lightly loaded transmission line or overexcited with a fully loaded transmission line. Self-excitation must be protected against when a hydroelectric generator is charging a long transmission line. Dropping a heavy load at the receiving end and leaving an overexcited hydroelectric generator connected to a long transmission line may cause dangerous overvoltages. Overspeeding of a hydroelectric generating unit on rejection of load at the generating station also may cause dangerous overvoltages. In addition to providing a solution to the above problems, a satisfactory excitation system should be capable of increasing the stability limits of the transmission system and of preventing pull-out from insufficient excitation.

While these problems are not new, and have been solved to a certain extent, successfully in the past with presently available excitation systems, this paper first will review the principles and characteristics of these systems and the relative need for any particular characteristic, second, will attempt some evaluation of the practical importance of these characteristics, outlining desirable features which should be provided for excitation systems which are applied to hydroelectric generators that supply long transmission lines.

Excitation Systems Available

In accordance with present day practice, an excitation system for hydroelectric generators supplying long transmission lines consists essentially of a main and pilot exciter with an indirect-acting rheostatic-type voltage regulator for automatic excitation control of each generator.[1] The main exciter armature leads are connected directly to the collector rings from the field of the main hydroelectric generator without a main field circuit breaker or rheostat.

Control of the excitation is accomplished by means of a master element or regulator acting on a motor-operated rheostat in the field of the main exciter. High-speed contactors are provided to cut in or out the entire regulating resistance in the main exciter field and provision is made for automatic division of reactive power between any of the main hydroelectric generators which may be operating in parallel. Over-all performance of the excitation system depends on other factors such as the main generator characteristics and the transmission system.

Main Exciters

The main exciter consists of a separately excited shunt-wound d-c generator. A self-excited main exciter generally is not applicable to hydroelectric generators since its voltage is not stable and will drift with time[2] at light loads.

A main exciter kilowatt rating of 110 per cent of normal and a nominal collector-ring voltage of not more than 90 per cent of the exciter voltage rating are common practice. The nominal ceiling voltage should not be less than 120 per cent of the exciter voltage rating and ample margin usually is provided to take care of any possible reduction in speed or frequency which may occur during a severe system disturbance. An exciter speed-of-response of 0.5 as defined by the American Standards Association standards is considered standard equipment and is adequate for the average application although a speed-of-response of 1.0 may be desirable for certain more important installations.

It is common practice for the main exciter to be direct-connected to the shaft of the main hydroelectric generator. This arrangement has the advantage, especially for a remote hydroelectric installation, that no outside source of power is required to start the generating unit. Another important advantage of the shaft-driven exciter is that it is independent of disturbances on the system. Although the brushes must be changed with the main generator in service for continuous operation and any mechanical or commutation trouble will cause a shutdown of the main generator, experience has proved the reliability of slow-speed direct-connected shaft-driven main exciters for hydroelectric generators. A spare separate motor-driven main exciter

Paper 47-199, recommended by the AIEE committee on power generation and approved by the AIEE technical program committee for presentation at the AIEE Pacific general meeting, San Diego, Calif., August 26-29, 1947. Manuscript submitted June 25, 1947; made available for printing July 14, 1947.

C. L. KILLGORE is assistant to assistant chief engineer, electrical and mechanical, United States Bureau of Reclamation, Denver, Colo.

involves switching in the exciter armature circuit to the main generator collector rings and is difficult to justify. Spare exciters, therefore, usually are not provided. Some mention should be made of troubles which have been experienced with brushes and collector rings but these subjects are considered beyond the scope of this paper. The main exciters are of open-type construction and ventilation is not a problem.

Voltage Regulators

An indirect-acting exciter-field rheostatic-type voltage regulator usually is used with hydroelectric generators supplying long transmission lines. Excitation is controlled by automatic adjustment of the main exciter-field rheostat and by high-speed relays which cut in or out the entire regulating resistance in the exciter field. The main exciter-field rheostat is operated by a d-c motor and may be either a series or Wheatstone-bridge-type rheostat. These rheostats are of the face plate type which have proved to be simple, reliable, and able to withstand frequent operations successfully.

The master voltage-sensitive element is responsive to the average of all three voltages of the main synchronous generator. This is accomplished by either a polyphase torque motor whose torque is proportional to the average voltage or by a three-phase rectifier whose output voltage operates the regulator solenoid coil. These devices control a contact assembly which has two sets of contacts. One set operates the motor of the motor-operated main exciter-field rheostat for small changes in voltage and the other set of contacts operate the high-speed relays. These relays can apply maximum or minimum excitation in three cycles for large changes in voltage. Any value of excitation may be applied to the main-exciter field from maximum positive to slightly negative. Thus main synchronous generator field voltage can be reduced to approximately zero or it may be reversed slightly.

The sensitivity or nominal band of voltage regulation is plus or minus 0.5 per cent. The contacts for operating the high-speed relays usually are set to operate for a change in voltage of 5 per cent plus or minus. A voltage adjusting rheostat is furnished for changing the alternating voltage level to be held by the regulator over a range of 10 per cent above normal to 25 per cent below normal. This lower limit is required in order to permit synchronizing at the load end of the transmission line. In general, these rheostats are motor-operated so that they may be controlled from a central location. An inherent characteristic of this type of voltage regulator is the dead band in which no corrective action takes place. A lower limit of excitation is not available as part of the manufacturers' equipment and although some attempts have been made to add such a feature, they have not proved entirely satisfactory.

Pilot Exciters

The pilot exciter is a compound-wound self-excited d-c machine designed to hold essentially constant voltage for supplying excitation to the field of the main exciter. The pilot exciter is direct-connected to the shaft of the main hydroelectric generator. A manually operated pilot exciter field rheostat is provided to adjust the pilot exciter voltage for normal operation. It has been found in some installations that when the generating unit has been shutdown and is cold it is necessary to readjust the field rheostat when the normal operating temperature is reached.

Auxiliary equipment must be provided to protect against dangerously high pilot-exciter voltages which are produced during overspeed or runaway of the water wheel. This equipment usually consists of an overvoltage relay or an overspeed switch on the main shaft which operates to open the contacts on a normally closed high-speed auxiliary relay. This relay inserts a fixed block of resistance in series with the pilot-exciter field, thus reducing the voltage to a safe value during the abnormally high-speed conditions. This protection does not interfere with the voltage regulator which serves as an overvoltage protective device for the generator and main exciter.

However, a fixed resistor which will limit the pilot-exciter voltage adequately during runaway conditions generally is too high for overspeed conditions resulting from rejection of full load and will reduce the pilot-exciter voltage so far below normal that the main synchronous generator voltage cannot be maintained. This condition is important only when station-service power is being supplied from the main-generator bus and a direct-acting voltage regulator is used in the pilot-exciter field circuit to limit the overvoltages instead of a fixed block of resistance.

Some installations have been made which use the station battery instead of a pilot exciter as a source of constant voltage for supplying excitation to the field of the main exciter. This scheme appears to be quite successful and eliminates the mechanical disadvantages of a pilot excitor as well as the auxiliary overvoltage equipment, thus simplifying the excitation system.

Parallel Operation A-C Generators

The division of reactive current between a-c generators operating in parallel is controlled by the amount of excitation on each generator. An increase in excitation of one generator will increase the reactive current supplied by that generator, but it will not affect the bus voltage appreciably since the voltage regulator tends to hold a constant voltage regardless of the reactive current or power-factor of the a-c generator. It is necessary, therefore, to bias the voltage-sensitive element of the regulators with reactive current.

For example, if two identical a-c generators are operating in parallel with their voltage regulators sensitive only to voltage, the regulator with the higher setting would increase the excitation of its generator to the maximum limit and the regulator with the lower setting would decrease the excitation of its generator to the minimum limit which could result in pull-out of the generator with low excitation. The same conclusion would be reached with one generator under regulator control, and connected to a relatively large system such that the generator could not control the system voltage.

For a-c generators which are paralleled at the generator bus without reactance between them, cross-current compensating devices are provided to bias the regulators. However, if a unit-system design is used and the a-c generators are paralleled only on the high-voltage bus through their associated transformer banks, no auxiliary cross-current compensating devices are required. The overall effect of these methods is to make the voltage characteristics of each generator at the point at which they are paralleled "droop" with reactive current. The amount of "droop" necessary will depend on the sensitivity of the automatic control equipment.

Performance Requirements

The excitation system should be designed conservatively and should allow for the high currents which may flow in the excitation system during transient conditions and also for the high voltages associated with switching in the field discharge resistor during such transient conditions. Maximum reliability and dependability of service with a minimum of maintenance is essential. Actually the cost of the excitation system is a small part of the cost of any generating station,

but the cost of a failure of the excitation system could be relatively great.

The accuracy and sensitivity of an automatic excitation system, in accordance with industry standards, are understood to describe the ability of the control equipment to maintain voltage over the complete load range of the a-c generator when it is supplying an isolated load. Any equipment which is sensitive to load rather than voltage, such as devices required for parallel operation or for limiting excitation, is assumed to be inoperative. Although the performance requirements as given by this definition are inadequate and incomplete, the definition is important as it gives some of the information needed for proper application of automatic excitation systems.

Over-all performance requirements of an excitation system for hydroelectric generators supplying long transmission lines are summarized below

1. Improved system voltage regulation.
2. Increased system stability limits.
3. Controlled overvoltage on loss of load.
4. Stability during line charging.

Generator Characteristics

Certain characteristics of the main hydroelectric generator affect the over-all operation of the excitation system. These characteristics relate to the generator field current which actually determines the performance of the generator on the system, and include the power factor rating of the generator, its line-charging capacity, field-time constant, and field-heating limitations.

The transformation of mechanical energy from the shaft torque, produced by the water wheel, to electrical energy at the generator stator terminals is accomplished by the magnetic field or flux which crosses the air gap between the rotor and stator of the generator. This air-gap flux is determined primarily by field current. However, current flowing in the armature winding has a decided effect on the air-gap flux, and lagging current, which flows when the generator is short-circuited at its terminals or is supplying an inductive load, has a strong demagnetizing or weakening effect on the air-gap flux. Thus, the actual air-gap flux is the difference between that produced by the generator field current and the bucking effect of the armature demagnetizing current. The short-circuit ratio is an indication of the weakening effect of the armature demagnetizing current, and a generator which requires less field current to overcome the armature demagnetizing current has a higher short-circuit ratio and, in itself, is inherently more stable.

Power Factor

The stability of a generator supplying power to a system is a function of the load characteristics as well as of the generator characteristics. The power factor of the load which is being supplied by the generator determines how much field current is required to deliver the kilowatt load at the required voltage and frequency.

Hydroelectric generators supplying long transmission lines operate at approximately unity power factor and in general the generator power factor should be selected to correspond as nearly as possible to the expected system requirements. A generator with a low power factor rating but used at a high power factor is more unstable[3] than a generator of the same size and cost rated more nearly to the actual power factor of the load. This is evident, since operating at power factors higher than rated requires a field current lower than the rated value. Therefore, hydroelectric generators supplying long transmission lines usually should be rated at unity power factor.

Line-Charging Capacity

The line-charging capacity of a generator is defined as the kilovolt-ampere output at rated voltage when the excitation is reduced to zero. Hydroelectric generators with a short-circuit ratio of unity have a line-charging capacity of 80 per cent at rated voltage. An increase in short-circuit ratio increases the line-charging capacity in direct proportion.

A generator of the same size and cost rated at unity power factor inherently has a higher short-circuit ratio than a generator rated at a lower power factor. For example, generators of normal design but rated at different power factors have the following short-circuit ratios:

1.0 at 0.8 power factor
1.1 at 0.9 power factor
1.25 at 1.0 power factor

Line-charging requirements and stability limitations usually occur simultaneously and, therefore, the higher short-circuit-ratio unity-power-factor generator is a practical means of meeting both operating conditions.

Field-Heating Limitations

Experience has shown that some hydroelectric generators have overload capacity built into the armature winding, but that this same overload capacity is not built into the generator field winding. Operation of a generator either above its rated voltage or below its rated power factor in a lagging direction requires an increase in field current. A 4 per cent increase in field current means nearly an 8 per cent increase in field heating. Since in actual operation hydroelectric generators supplying long transmission lines usually operate at approximately 5 per cent above normal voltage and at approximately 0.97 per cent lagging power factor, the field winding should be of a liberal design. Normally, the excitation system has ample margin to operate at overload capacities.

Field Time Constant

The average value of the open-circuit transient time constant for a hydroelectric generator with amortisseur windings is approximately 6.6 seconds. Without them, the time constant is usually less and it may vary from 1.5 to 10.5 seconds.[4]

It is important to note that the time constant of the field circuit is scarcely subject to control[5,6] by the excitation system although schemes of superexcitation[7,8] have been investigated. The rate of variation of the flux in the generator field circuit and consequently of the flux in the armature depends on the applied maximum ceiling voltage of the main exciter and the speed with which this maximum voltage is obtained. However, since the time constant of the main exciter is always much smaller than that of the main generator field, the speed-of-response has a much smaller effect than the maximum ceiling voltage of the exciter.

Voltage Requirements and Performance

In the operation of long high-voltage transmission lines, it has been found desirable to set the voltage at the receiving end enough lower than the generator voltage, expressed in terms of the high-voltage system, to permit the generators to operate at unity or slightly lagging power factors for all loads. Ideally, this means that the line-charging current for light loadings should be furnished from the receiver end. However, this procedure is not always economical and the generators therefore should be capable of supplying the line-charging current at light loads without danger of pull-out. The excitation system should be capable of meeting the following voltage performance requirements.

System Voltage Level

The sending voltage for a normal 230-kv transmission system, in general, will

vary from approximately 230 to 240 kv. Since the higher voltage level is required most of the time, both the main generator and the excitation system should be capable of continuous operation at approximately 5 per cent above rated voltage. While fixed taps sometimes are provided on the high-voltage windings of the main step-up transformers, these taps are useful only to establish a fixed voltage level for the sending end of the transmission system. The large inherent regulation of long transmission lines can be accomplished best by means of the automatic excitation system. This method of control tends to improve the reliability of the main step-up transformers by eliminating taps in the high-voltage winding.

The division of reactive current between synchronous generators operating in parallel depends largely on the dead-band portion of the band of voltage regulation and also on the "droop" compensation. It is possible with the use of modern excitation systems to operate stably with small "droop" provided the dead band is small. The effect of "droop" compensation can be illustrated by two typical examples. The first is that of two identical generators paralleled at the generator bus with the automatic voltage regulators biased by means of cross-current compensators to have a "droop" of 4 per cent.

The second is that of a unit-system with two identical generators and their associated transformers paralleled on the high-voltage side. The inherent reactance of the transformers introduces a "droop" of 8 per cent. If the sensitivity of the voltage regulator control element is plus or minus 0.5 per cent for both cases, then the difference in reactive current for the generators with a "droop" of 4 per cent could be as much as 25 per cent while that for the generators with a "droop" of 8 per cent would not exceed 12.5 per cent. If we assume that the generators in both cases are carrying 80 per cent load in kilowatts, the total armature current of the two generators in the first case would be 94.2 and 84 per cent, a difference of 10 per cent which is fairly reasonable. In the second case, the total armature currents would be 84 and 81 per cent, a difference of only 3 per cent.

There is, of course, some voltage regulation with this application, and elimination of this regulation has been attempted by means of line-drop compensation. This device gives the voltage regulator a rising characteristic with load which in effect tends to compensate for the "droop" that has been introduced intentionally into the voltage regulator control circuit. Line-drop compensation, therefore, should not be used unless it is essential that some high voltage bus be held continuously at constant voltage and even then the application of line-drop compensation at the generating station should be reviewed carefully.

Actually the fundamental approach to the problem of better voltage control in the cases where that is necessary is to improve the sensitivity of the excitation system. Making the sensitivity plus or minus 0.25 per cent would allow operation with 2 per cent "droop" and allow the same division of reactive current between machines as was obtained with 4 per cent "droop" and a sensitivity of plus or minus 0.5 per cent.

Line Charging

The generators at a hydroelectric station should have sufficient line-charging capacity to build up voltage on the longest transmission line connected to that station for purposes of testing the line without becoming self-excited. Self-excitation is an unstable condition which would cause high and uncontrolled voltage on the generator and system being tested. However, if the capacitance load of the transmission line exceeds the line-charging capacity of one generator, additional generators can be paralleled[8] to provide sufficient capacity without a material reduction below the sum of their individual line-charging capacities. The excitation systems must, of course, be stable for this underexcited condition and should be capable of rapidly reducing the main generator field excitation to zero and preferably to a slightly negative value. A high-speed automatic excitation system will permit a salient-pole generator to be loaded purely capacitively up to the thermal limit of the generator.[9]

Rejection of Load and Overspeed

Rejection of load[10] on a hydroelectric generator by automatic operation of the protective relays or other means can cause dangerous overvoltages unless the automatic excitation system operates to protect against these overvoltages.

Either one of two conditions may occur. The load may be rejected at either the sending end or at the receiving end of the transmission line. It is evident that this sudden change of conditions from an inductive load which directly opposes the magnetic flux in the generator field to a pure capacitive load which directly aids the magnetic flux or to no-load could cause dangerous overvoltages. In addition to the above effect, the relative slow action of the governor on the wicket gates of the water wheel allows the generating unit to overspeed which adds to the rise in generator voltage. In order to control this overvoltage, the high-speed "lower" relay of an indirect-acting rheostatic-type voltage regulator operates to insert the entire regulating resistance in the exciter field. However, since this action reduces the main generator voltage to below normal, the high speed "raise" relay operates to increase the voltage again. Continued intermittent operation of both the "lower" and "raise" high-speed relays cause considerable oscillation of the generator voltage, but the net overall result is to hold the voltage within reasonable limits.

The condition of load rejection in which the transmission line stays connected to the generator could cause the highest overvoltages, especially at the receiving end since the no-load voltage rise of the transmission line itself must be considered. For a line 150 miles long the voltage rise would only be 5 per cent, but for a line 300 miles long, the voltage rise would be 22 per cent. Therefore, in order to prevent the possibility of the generator becoming self-excited and to provide back-up protection for the excitation system, it is common practice to provide an overvoltage relay which will disconnect the transmission line from the generator if there is an excessive rise in voltage at the sending end of the line.

Overvoltages

Although the reliability of indirect-acting rheostatic-type voltage regulators has been proven, the possibility of a failure should be considered since a number of contacts and relays are essential parts of such regulators. In case of a failure the equipment at the generating station and on the transmission system should be protected by "lightning arresters" which could be termed better voltage-limiting devices. When a salient-pole generator is supplying a highly capacitive load, there is the possibility of dangerous overvoltages occurring from resonance between the reactance of the generator and the load during unbalanced short-circuit conditions. The danger of these overvoltages can be eliminated by amortisseur windings[4,11] on the generator rotor.

Stability and Pull-out

That the steady-state stability limit[12] of a synchronous generator can be increased by a considerable amount by means of a properly designed excitation system is well known. This is evident since, if no change is made in the field excitation

short-circuit ratio and field excitation are practically the only generator characteristics[9] which determine the point of pull-out. A sudden load applied to a generator with low excitation and no voltage regulator may result in pull-out depending on the short-circuit ratio and load saturation. A generator with a higher short-circuit ratio and initial load saturation can pick up a larger load without loss of synchronism. However, short-circuit ratio is not a true criterion for the relative stability characteristics of generators operating with voltage regulators.[19] With the use of voltage regulators the factors which determine the stability characteristics under load are the synchronous and leakage reactance, the amount of load saturation, and the rate of change of saturation under load.

Voltage regulators can permit operation above the steady-state stability limit. This type of operation is known as dynamic stability[14,16] and is dependent entirely on the performance of the voltage regulator. Although power systems usually are not designed for this type of operation, it may be of considerable value during emergency conditions since it provides additional stability margins.

Speed of Response

Although the need for high speed of response in excitations systems is a relatively complicated subject, reviewing a few fundamentals will indicate what is required. With modern high-speed circuit-breakers and relays, there is little need for high-speed exciter response [16,17,18] since the fault is cleared so rapidly that the excitation system has little opportunity to function. It is known[19] that if stability can be maintained during the first swing, in general, it will be maintained during subsequent swings. However, since the generator field time constant is usually relatively long with respect to the time required for the first swing, any substantial improvement in stability would require a super-excitation system. The performance requirements which are of interest are

1. Voltage dip on sudden application of load.
2. Transient stability.

The initial voltage dip occurring on sudden application of load depends principally on the generator field current at the time of the load application regardless of the excitation system. The rate of voltage recovery, however, depends on the speed of exciter response.

The effect of the speed of exciter response on transient stability can be determined by referring to a particular example which shows a typical hydroelectric generating station supplying a large system over two transmission lines 140 miles long. A three-phase fault is applied to one line and cleared leaving a single circuit. The example shows the power that can be delivered through the three-phase fault and subsequent line clearing as a function of exciter response and switching time. Increasing the exciter response from 0.5, which has been commonly used, to 1.0 raises the power limit from 2 to 3 per cent while increasing the switching time from 0.10 to 0.05 second raises the power limit 10 per cent. Certainly transient stability is not improved materially by increasing exciter response.

Minimum Excitation Limit

The stability limit of an underexcited generator does not depend greatly upon the external system. It should be possible to insure sufficient excitation for a wide range of system conditions by means of a variable lower limit of excitation which is controlled by the water wheel wicket gate opening. Although relay protection[20] has been installed successfully which will trip a generator with inadequate excitation off the system before it pulls out-of-step, such protection generally is not applied to hydroelectric generators since damage[21] to the generator is not likely to occur unless out-of-step operation is prolonged.

Recent Development

A recently developed excitation system[1] which appears to have additional desirable characteristics for hydroelectric generators supplying long transmission lines consists of a "stabilized" self-excited main exciter and a static voltage regulator with a rotating amplifier. The term "stabilized" describes the fact that the design of the exciter intentionally controls saturation to give a positive crossing of the saturation curve with any field resistance line needed for the full range of operation.

The static voltage regulator controls the field of the rotating amplifier which is in series with the field of the main exciter and bucks or boosts the main exciter terminal voltage as required. Very little control power is required from the static voltage regulator to adjust the field of the rotating amplifier. This type of excitation system eliminates the dead band which is inherent with the indirect-acting rheostatic-type voltage regulator since the output of the static voltage regulator is varied continuously and practically instantaneously. A variable lower excitation limit can be applied to this type of excitation system successfully.

The rotating amplifier replaces a pilot exciter and is driven by an a-c motor from the station-service power system. Since the "stabilized" self-excited main exciter will provide excitation without any auxiliary equipment being in service this type of excitation system is applicable for remote hydroelectric installations where an outside source of power may not be available to start up the generating units.

Conclusions

1. System overvoltages resulting from rejection of load at the receiving end of a long transmission line and consequent overspeed of the hydroelectric generator can be controlled effectively by the excitation system and auxiliary devices.

2. In order to limit the overvoltage on shaft-driven pilot exciters during runaway of the water wheel generating-unit, additional protective equipment is required and elimination of the shaft-driven exciter is desirable.

3. A synchronous generator with a low power factor rating, but operated at a higher power factor, is more unstable than a generator rated more nearly to the power factor of the load. Hydroelectric generators supplying long transmission lines usually should be rated at unity power factor.

4. The line-charging capacity of a hydroelectric generator increases in direct proportion to an increase in short-circuit ratio and since a generator rated at unity power factor inherently has a higher short-circuit ratio than a generator of the same size and cost rated at a lower power factor, generators rated at unity power factor are a practical means to meet both line-charging and stability requirements for long transmission lines.

5. A modern high-speed automatic excitation system will permit a salient-pole generator to be stably loaded with a purely capacitive load up to the thermal limitation of the generator.

6. Since a hydroelectric generator supplying long transmission lines usually will operate at slightly above rated voltage and at approximately 0.97 per cent lagging power factor requiring increased field currents, the main generator field should be of a liberal design.

7. The reliability of slow-speed shaft-driven main exciters has been proved. The main exciter should be conservatively designed both as to normal current and voltage rating and transient operation. The nominal ceiling voltage should have ample margin to provide for possible reductions in speed during system disturbances.

8. Considerable gain in steady-state stability can be realized by means of a properly designed automatic excitation system and voltage regulators can permit operation above the steadp-state stability limit. Although operation at dynamic stability depends entirely on the voltage regulator, it may be of considerable value during emergency conditions since it provides additional stability margin.

9. With modern high-speed breakers and relays there is little need for high speed exciter response since the main generator field time constant is relatively long with respect to the time required for the first swing and any substantial improvement in stability would require a superexcitation system. An exciter speed-of-response of 0.5 is adequate for the average application although 1.0 may be desirable for certain more important installations.

10. Since the stability limit of an underexcited generator does not depend greatly on the external system, minimum excitation limits controlled by the water wheel wicket gate opening should be provided to insure adequate excitation for all system conditions. Relay protection which will trip a generator with inadequate excitation off the system has not been found necessary for hydroelectric generators.

11. A voltage regulator with high sensitivity will allow working with a voltage characteristic which has less "droop" than other excitation systems and, therefore, will afford better average system voltage for equally good division of reactive current for generators operating in parallel.

12. From the apparent superior performance and relative simplicity of the recently developed excitation system consisting of a "stabilized" self-excited main exciter and a static voltage regulator with a rotating amplifier it appears that this type of excitation system may become standard equipment for hydroelectric generators supplying long transmission lines.

References

1. Modern Excitation Systems for Large Synchronous Machines, **J. B. McClure, S. I. Whittlesey, M. E. Hartman.** AIEE Transactions, volume 65, 1946, pages 939–45.

2. Electric Power Circuits (volume 2), **O. G. C. Dahl.** McGraw-Hill Book Company, Inc., New York, N. Y.

3. Power System Stability (volume 1), **S. B. Crary.** John Wiley and Sons, Inc., New York, N. Y.

4. Electrical Transmission and Distribution Reference Book. Westinghouse Electric Corporation, Pittsburgh, Pa.

5. Alternator Exciter Systems, **R. David.** International Conference on Large High-Voltage Systems (CIGRE), Paris, 1946.

6. Stability Limits of Long Transmission Lines, **I. Herlitz.** International Conference on Large High-Voltage Systems (CIGRE), Paris, 1946.

7. Superexcitation, **D. M. Jones.** *General Electric Review* (Schenectady, N. Y.), December 1927.

8. Automatic Regulation of Synchronous Condensers Equipped with Superspeed Excitation, **L. W. Thompson, P. J. Walton.** AIEE Transactions, volume 49, 1930, pages 315–18.

9. Theory of Stability of Alternator Voltage Under Conditions of Capacitive Load. *The Brown Boveri Review* (Baden, Switzerland), August 1945, pages 251–63.

10. Overvoltage on Transmission Systems Caused by Dropping Load, **R. J. Burnham.** AIEE Transactions, volume 51, 1932, pages 105–12.

11. Effect of the Short-Circuit Ratio and Damper Windings on the Electrical and Mechanical Properties of Synchronous Machines. *The Brown Boveri Review* (Baden, Switzerland), December 1945, pages 445–50.

12. Steady State Stability of Synchronous Machines as Affected by Voltage Regulator Characteristics. **C. Concordia.** AIEE Transactions, volume 63, 1944, May section, pages 215–20.

13. Stability Characteristics of Turbine Generators, **C. Concordia, S. B. Crary, J. M. Lyons.** AIEE Transactions, volume 57, 1938, December section, pages 732–41.

14. Long-Distance Transmission of Energy and the Artificial Stabilization of Alternating Current Systems, **G. Darrieus.** International Conference on Large High-Voltage Systems (CIGRE), Paris, 1946.

15. Excitation Systems, **R. E. Doherty.** AIEE Transactions, volume 47, 1928, pages 944–56.

16. Quick Response Excitation, **W. A. Lewis.** *Electric Journal*, August 1934, pages 308–12.

17. Regulation of A-C Generators With Suddenly Applied Loads, **E. L. Harder, R. C. Cheek.** AIEE Transactions, volume 63, 1944, June section, pages 310–18.

18. Voltage Variation of Suddenly Loaded Generators, **H. C. Anderson, Jr.** *General Electric Review* (Schenectady, N. Y.), August 1945, pages 25–33.

19. Long-Distance Power Transmission as Influenced by Excitation Systems, **C. Concordia, S. B. Crary, F. J. Maginniss.** AIEE Transactions, volume 65, 1946, pages 974–87.

20. Interim Report on Application and Operation of Out-of-Step Protection, AIEE Relay Subcommittee. AIEE Transactions, volume 62, 1943, September section, pages 567–73.

21. Can Synchronous Generators Run Out-of-Step With the System?, **A. A. Johnson.** *Power* (New York, N. Y.), January 1947, pages 105–03.

Discussion

E. G. Olmstead (Department of Water and Power, Los Angeles, Calif.): Killgore is to be commended for his excellent summary of the excitation requirements of hydroelectric generators supplying long transmission lines.

These problems have been of importance to the Department of Water and Power, City of Los Angeles, Calif. The department's Boulder transmission system now consists of three 287.5-kv circuits from Hoover Dam to Los Angeles, with an average circuit length of 263.5 miles, with two intermediate switching stations. Thus it was necessary to give careful consideration to the line-charging capability of the generators. The generators at the power plant, with a guaranteed short-circuit ratio of 2.74, have ample line-charging capacity so that one generator can charge one complete circuit from Boulder to Los Angeles.

The department's proposed Owens River Gorge hydroelectric development, now in the design stage, is shown in Figure 1. Each plant will have one generator of about 37,500 kva. Thus it will be necessary to charge the 258.5-mile 230-kv transmission line with relatively small generator units. It is tentatively planned to use two generators operating in parallel to charge the line. The line charging requirement will be about 46,000 kva, or 23,000 kva per generator, at a generator voltage of approximately 70 per cent of rated voltage. Thus a short-circuit ratio of 1.80 would provide line charging capability somewhat greater than the line requirement.

During line charging, with normal voltage at the receiving end of the line, the generator field currents would be very small—approximately 15 per cent of the value corresponding to normal generator voltage at no load. However, satisfactory synchronizing power between generators would be available due to the magnetizing action of the leading armature current.

In order to avoid the possibility of overvoltages during line charging, it would seem desirable to synchronize the two generators, and then reduce their voltage to 15 per cent of normal, before closing the line breaker. However, the synchronizing power between the two generators would then be extremely small, in the order of 500 kilowatts. It is doubtful whether the two machines would remain in synchronism under this condition.

Consideration is being given to two alternatives to remedy this situation. The first alternative is to synchronize the two generators at reduced frequency, probably about 45 to 50 cycles, and at about 35 per cent of normal voltage. It is believed that the synchronizing power would be adequate at this voltage. Then at the reduced frequency the line circuit breaker would be closed, and since the line-charging current and the voltage rise between sending and receiving ends of the line would be less than at 60 cycles, the resulting voltage at the receiving end would be about normal. Then simultaneously frequency would be increased and generator field currents reduced until normal frequency is reached with normal voltage at the receiving end of the line. In the second alternative method the generators would be synchronized at about 35 per cent voltage, and put on voltage regulator control. The line circuit breaker then would be closed. It seems probable that voltage regulator action would prevent the receiving end voltage from rising much above normal. However, it is planned to make a further investigation of this method of line charging, including determination of the voltage-time curve for the period immediately following the closing of the line breaker.

R. B. Bodine (General Electric Company, Schenectady, N. Y.): The author has presented a good review of the problems associated with excitation of hydroelectric generators.

Of especial interest in the paper is the statement to the effect that exciters need not have a high rate of response if conventional generators, exciters, and high-speed circuit breakers and relays, which are practically standard equipment, are used. This follows from the fact, as Killgore indicates, that the longest time constant involved is that of the field circuit of the main generator. To make any appreciable gain in rate at which the field current of the main generator is controlled would require exciters having much higher ceiling voltages than are used at the present time. The possible gain in stability limit which may be made by use of such exciters, today, does not seem to warrant extra expenditure.

The voltage regulating equipments consisting of a static, impedance-type, voltage regulator and rotating amplifier to which Killgore calls attention have been in service on synchronous condensers and frequency-changers in the Pacific Coast area for some time. The voltage regulator in these applications employs a saturated reactor for voltage standard which permits elimination of all moving parts. Though development of this type of excitation system is not completed yet for use with hydroelectric generators, it is expected that such regulators will be available for this service in the near future.

Killgore's comments on power-factor rating of generators brings out a point which, I believe, should be emphasized. As is pointed out in the paper, in the average hydroelectric application, generators operate at about 0.97 power-factor overexcited. There has been a tendency to specify unity power-factor generators when connected to long transmission lines. The information given by the author, together with other information, leads me to believe that the generator power-factor, even for long distance transmission, should be not greater than 0.95 so as to be able to supply the reactive kilovolt-amperes necessary for high transmission circuit loadings.

J. H. Vivian (electrical and mechanical maintenance engineer, Southern California Edison Company, Los Angeles, Calif.): The author is to be congratulated for the preparation of this paper. Although a great deal of the material presented is not new and as the author stated, "The problems are not new and to a certain extent have been solved successfully in the past," there has been a need for a recapitulation of available material to aid engineers in keeping apace with modern design.

The paper has good continuity and should serve as a guide for junior engineers. The following comments are written to emphasize a few of the salient points which may be overlooked unless one is familiar with the subject:

1. It is only recently that the main exciter armature leads have been connected directly to the collector rings without a main field circuit breaker or rheostat. Many engineers are not in agreement with this practice, but the Southern California Edison Company has followed this practice for many years since its proposal by L. P. Hunt, now chief electrical engineer of our company.

2. The paragraphs on "Main Exciters," "Voltage Regulators," and "Pilot Exciters" are extremely interesting. The older units at hydro stations were not designed to operate with modern relay protection, and any constants of speed-of-response that approaches modern practice is merely coincidental. Yet, most of these units have been equipped with pilot exciters, modern regulators and perform excellently under all system conditions. When several generators are operated as a unit for load source, it has been found that the use of a direct-acting voltage regulator in the pilot-exciter field circuit not only limits overvoltages, but tends to aid in synchronizing the generators quickly. Also, all stationary coils of the main regulator are connected to a battery source, to eliminate changes in the coil constants and to prevent overvoltages.

3. The paragraph "Field Time Constant" is very appropriate. For instance, if load is rejected, the field current that was necessary to obtain normal voltage at a fixed load will be available instantly for obtaining some higher voltage at no load. If the generator is over-speeding, the condition is aggravated. As this phenomenon is inherently internal it is impossible to prevent high voltage by external regulation. However, quick response regulation greatly aids in lessening the duration of overvoltage.

4. We agree with the author in regard to the paragraph "System Voltage Level," wherein it is stated "This method of control. . . eliminates taps in the high voltage winding." It is the practice of engineers affiliated with the Edison Company to eliminate all high voltage taps on transformers at generating stations and receiving stations where automatic excitation systems are adequate to maintain the correct voltage level.

5. The paragraph "Overvoltages" is very interesting. Experience with "Lightning Arresters" as voltage-limiting devices is doubtful. Usually the arrester cannot meet the thermal demand of protecting power surges caused from switching. In several cases, arresters literally have blown up because of the large time constant present when high voltage switching occurs.

6. The Southern California Edison Company has several new voltage regulators in operation as described under "Recent Development." None of these are installed in hydroelectric stations and it is doubtful if they will be until further improvement is made. The difficulty is with the static voltage regulator operation during periods of overspeed on the generators. At the present time, several of the circuits are affected by a change in frequency, even though the rotating amplifier is driven from a separate source. The development has been splendid for synchronous condensers and steam units, and the industry will benefit when it is ready for use on hydroelectric generators as suggested by Killgore.

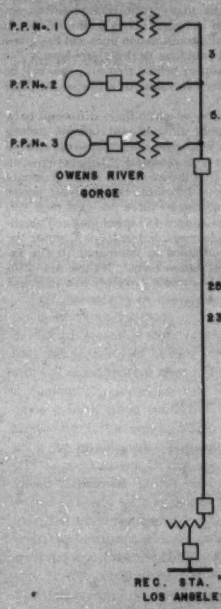

Figure 1. Tentative Owens Gorge transmission system

J. E. Barkle, Jr. (central station engineer, Westinghouse Electric Corporation, East Pittsburgh, Pa.): This paper is a very good example of the type of paper which assembles the pertinent information from a number of previously published papers and presents it in a clear and concise form. Details leading to certain conclusions have been omitted, but they can be found in the references easily. The paper does not include much in the way of new information, but the author has outlined the general practices followed by the Bureau of Reclamation and has provided the industry with a valuable source of information. In view of the rapid rate of development in the electrical industry at this time, more papers of this type would appear to be in order.

In the last paragraph under "Voltage Regulators" this statement is made: "A lower limit of excitation is not available as part of the manufacturer's equipment and although some attempts have been made to add such a feature, they have not proved entirely satisfactory." The author stresses the use of water wheel wicket-gate opening as a means of controlling a variable lower limit of excitation. A device known as a "watt-balance regulator" has been on the market for a number of years and provides a variable minimum excitation limit by balancing some power of the exciter voltage (usually exciter volts squared) against the watts output of the generator. If the voltage regulator should attempt to lower the excitation below that required for stability purposes, the watt-balance regulator will open both the "normal lower" and "quick lower" regulator control circuits, preventing further reduction of excitation. The watt-balance regulator functions to give the same results as the wicket-gate opening control but does so in a more straightforward manner. It has been used on both turbine-driven and slow-speed generators over a period of years and has proved very successful and superior to governor or wicket-gate opening control of minimum excitation.

With the advent of stabilized main exciters with rotating amplifiers as pilot exciters, a new type of variable minimum excitation limit control has been developed. It consists of a completely static network which functions in the same manner as the watt-balance regulator: that is, it balances the approximate square of the exciter volts against the generator watts output. The minimum limit is obtained by having the static network introduce a variable separate excitation into the rotating amplifier, thus maintaining a minimum exciter voltage dependent upon generator load.

Under the subject, "Recent Development," one type of excitation system utilizing a stabilized self-excited main exciter, a static voltage regulator and a rotating amplifier is described. For the sake of completeness a second system should be described. This excitation system uses a self-excited main exciter which is given positive stability for any condition of operation by the use of a small separately excited stabilizing field. By this means, a positive intersection of the saturation curve with any field resistance line is obtained as required by operating conditions over a range of operation equal to or greater than that obtained with present-day conventional excitation systems. The static voltage regulator controls the field of the rotating amplifier which, in turn, excites a separate field on the main exciter. This separately excited field aids or bucks the flux generated by the main exciter self-excited field to raise or lower the main exciter output voltage as required.

In the second conclusion, the author

states that elimination of shaft-driven exciters is desirable because additional protective equipment is required to limit overvoltages during runaway. Even in their most complicated forms, overvoltage protective equipments represent a very minor expense and elimination of the shaft-driven exciter with its many advantages cannot be justified. Earlier in the paper it was admitted that the shaft-driven exciter had an important advantage in that it is independent of system disturbances. Motor-driven exciters introduce a number of other possibilities of trouble which may be far more serious than overvoltages during runaway. Unless driven from a separate system, the motor-driven exciter does not answer the overvoltage problem because the motor speed and exciter voltage will increase with the system frequency much the same as a direct-connected exciter. Several cases of shutdown on hydroelectric systems could have been prevented if the exciters had been direct connected to the generator shaft. In order to be comparable in performance to direct-connected exciters, any excitation system using motor-driven exciters will be several times more expensive.

The third conclusion states that hydroelectric generators usually should be rated at unity power factor while the sixth conclusion states that they usually are operated at slightly above rated voltage and at approximately 97 per cent power factor. These conclusions appear to be contradictory. Purchasing a unity power factor machine for operation at 97 per cent power factor will not lead to a liberal design of generator field, but will be in the direction to overload the field, especially at slight overvoltage. Water wheel generator fields are designed to operate with a temperature rise of 60 degrees centigrade at generator rated load. A liberal design of field can be obtained by using a machine of lower power factor rating. The machine performance can be made approximately equal to that of a unity power factor generator by specifying the higher short-circuit ration. The machine will cost more, but it will meet the author's requirement of liberal field design.

B. V. Hoard (Bonneville Power Administration, Portland, Oreg.): The author has presented the many excitation problems encountered in hydroelectric generators which supply long transmission lines and has given practical solutions to these problems. For these reasons I believe that his paper will be of considerable value for reference on these problems.

One factor on which there still seems to be considerable difference of opinion among engineers is whether a high speed of response is necessary or desirable. Killgore cites an example that increasing the exciter response from 0.5 to 1.0 raises the transient power limit from two to three per cent over two transmission lines 140 miles long. This increase appears small, but let us examine the benefits obtained as compared to the increased excitation costs. If these were 230-kv lines, they would probably cost in excess of $6,000,000.00 and should transmit about 300,000 kw. A two per cent increase in transmission capability would be worth about $120,000.00 in transmission line investment, which, it is believed, is at least five times the additional cost of providing the higher speed of response; hence the higher response can be economically justified.

In conclusions three and six of the paper it is stated that hydro machines supplying long transmission lines usually should be rated at unity power factor; that usually the machine will operate at slightly above rated voltage and at approximately 97 per cent lagging power factor, both of which require increased field currents. Therefore, the field should be of liberal design. It is agreed that such operation using a unity power factor machine increases machine saturation and increases system stability, but care must be taken that the field design is quite liberal otherwise the combination of overvoltage and low power factor may produce overheating in the field. In recent discussions with manufacturer's representatives they have stated that they could design a better machine if actual operating power factor, for example, 97 to 95 per cent, is stated in the specifications rather than a unity power factor machine with field designed to operate continuously at 95 per cent power factor. However, it must be admitted that there appear to be many hydro generators rated at unity power factor which are operating a considerable portion of the time at 95 to 97 per cent lagging power factor in a very satisfactory manner.

Bearing Deviation Indicator for Sonar

O. H. SCHUCK
MEMBER AIEE

C. K. STEDMAN
NONMEMBER AIEE

J. L. HATHAWAY
NONMEMBER AIEE

A. N. BUTZ, JR.

Synopsis: This paper describes the bearing deviation indicator (BDI), a war development that greatly increased the effectiveness of sonar equipment in antisubmarine warfare. Limitations of sonar equipment without BDI are explained, the value of crossed-lobe techniques for improved bearing accuracy is discussed, and the value of simultaneous lobe comparison in underwater sound work is pointed out. Methods of meeting the over-all requirements are described, and examples are given of service equipment. Certain auxiliary features of these equipments—time-varied gain, reverberation-controlled gain, and own-Doppler nullification—are discussed, and mention is made of specialized test equipment.

DURING World War I, underwater listening equipment was used extensively for the detection of ships and submarines. By the use of directional arrays of microphones, the direction of a target could be determined quite accurately, while its range could be estimated roughly by the loudness and the quality of the sound. The military value of such equipment was demonstrated fully. However, more accurate range data were highly desirable, and submarines proceeding at very low speed made so little noise that they frequently were able to escape detection.

In order to eliminate these shortcomings, echo-ranging sound equipment was developed, and reached a high degree of perfection before World War II began. This equipment did not rely on sounds generated by the target vessel but radiated a short high-intensity sound pulse (or "ping") which was reflected from the target. The sound was emitted and received by transducer which produced a narrow sound beam, so that the bearing of the target was indicated with moderate accuracy by the direction of the transducer axis. Range was measured by timing the interval between transmission of the pulse and reception of the echo.

The application of the echo-ranging principle represented a major step forward in the development of underwater detection equipment, proved to be a satisfactory solution of the problem of measuring range. A typical echo ranging sonar recently was described in detail.[1]

As experience was obtained with experimental sound attacks on friendly submarines, however, it soon became evident that the accuracy of bearing information still left much to be desired. There were a number of reasons for this which became evident upon consideration of the trial-and-error process by which a bearing must be established. The sound beam was approximately 15 degrees wide between half-power points, and intensity varied so slowly with angle near the beam axis that when the operator attempted to train the beam to the direction of loudest received signal the angular discrimination was hardly better than 7 or 8 degrees. For that reason it was necessary to adopt a procedure which made use of the much more rapid variation of signal strength with angle on the sides of the beam pattern. The beam initially was aimed entirely off the target, and then rotated through small increments until a signal was first received on the edge of the beam. The mean of the two angles observed then was taken to be the bearing of the target. This procedure was referred to as the method of bow and stern "cut-ons."

It is apparent that by this method many pings were required to obtain a reliable bearing. The procedure took a considerable amount of time because the interval between successive pulses was several seconds (1.2 seconds for each thousand yards of range covered). In practice the operation was rendered even more difficult by large random variations in the intensity of successive echoes caused by interference among signals following different transmission paths. Furthermore, while the observations were being made, the bearing frequently changed quite rapidly because of the relative motion of the two vessels.

The combined effect of all these factors was sufficient to impair the usefulness of the sound equipment very seriously, so that considerable importance was attached to the development of means for obtaining improved bearing accuracy. The most obvious expedient was to use a sharper beam. However, this would have required either a larger transducer, which would be unwieldy, or a higher frequency of transmission which would result in a greater attenuation of sound in the water. Moreover, the use of a narrower beam increases the time required for the initial detection of a target because the surrounding ocean must be scanned in narrower angular increments.

Angular Discrimination by Lobe Comparison

Upon consideration of the cut-on procedure it is apparent that much of the

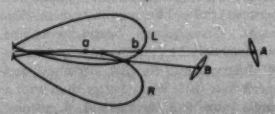

Figure 1. The overlapping directivity patterns established by two transducers whose acoustic axes diverge

Intersections at *a* and *b* show the relative signal strengths received on the *R* and *L* beams from a source at *A*

Paper 47-195, recommended by the AIEE committee on communication and approved by the AIEE technical program committee for presentation at the AIEE Pacific general meeting, San Diego, Calif., August 26–29, 1947. Manuscript submitted June 10, 1947; made available for printing July 18, 1947.

O. H. SCHUCK is in the research department of Minneapolis-Honeywell Regulator Company, Minneapolis, Minn.; C. K. STEDMAN is with Boeing Aircraft Company, Seattle, Wash.; J. L. HATHAWAY is with National Broadcasting Company, New York, N. Y.; A. N. BUTZ, JR., now is deceased.

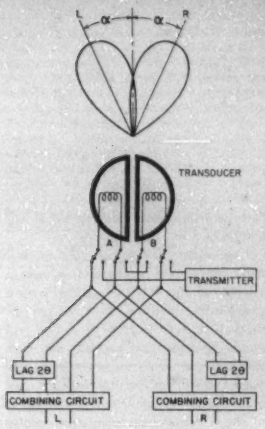

Figure 2 (left). The basic scheme for deriving two divergent receiving beams simultaneously from a single split transducer

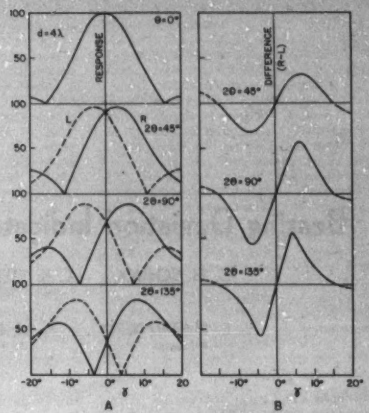

Figure 3

A. Right- and left-steered directivity patterns for different phase shifts in the lag line

B. Difference between signals received on right and left lobes, which may be used to indicate bearing deviation

difficulty results from time wasted swinging the beam to receive signals first on one side of the pattern and then on the other. This could be eliminated by providing two transducers with divergent beam patterns as shown by L and R in Figure 1. With this arrangement a single observation of the relative signal strengths on the two directivity lobes, as at a and b, will show the deviation of the target from the axis of symmetry. The two received signals might be distinguished from each other by time separation of the pulses or by the use of different frequencies. As a further improvement an instrument or cathode-ray tube could be used to indicate directly the difference between the two signals and so eliminate dependence on the human ear, which is notoriously a poor device for accurate comparison of sound intensities.

An experiment of this sort was first tried in 1941 using two transducers spaced about 12 feet apart. Unfortunately, the relative strengths of signals received on the two transducers proved to be subject to random variations of the same magnitude as those observed between successive pulses on a single transducer, presumably because of the difference in transmission paths. Consequently, bearings could be obtained only by averaging a large number of observations, so that accuracy and speed were little if any better than with a single beam and the method of cut-ons. Since the transducers were necessarily large compared with the wave length of the sound, it was not feasible to bring them closely enough into coincidence to realize identical sound paths. This system therefore was judged to be impractical unless means could be found for producing the two beams with a single transducer. This actually was accomplished a little later and constitutes the major advancement in technique which made possible the development of a practical bearing deviation indicator.

Simultaneous Lobe Comparison With Lag Lines

The method adopted is shown diagrammatically in Figure 2. The circular transducer is divided in half electrically along a vertical diameter. The two halves are connected together for transmission of a sound pulse, so that the normal directivity pattern is obtained. For reception, the electric signals from the two halves are supplied simultaneously to two directive networks connected in parallel. In each network the signals from the two halves are shifted in phase so that the directivity pattern is altered in the desired manner. When output A is lagged in phase with respect to output B by an angle 2θ, and the two signals subsequently are combined, the pattern has its axis shifted to the left by an angle

$$\alpha = 0.52 \frac{\lambda}{d} \theta \qquad (1)$$

where d is the diameter of the transducer diaphragm. In the same way a right-shifted pattern can be obtained by lagging B with respect to A. By this means the weakness of the system utilizing two separate transducers is overcome completely because the divergent lobes are produced simultaneously with a single transducer. It is also important to note that since both halves contribute equally to both patterns, the acoustical center of the transducer is identical for both the left and right channels and the full aperture of the transducer is utilized in each.

It can be shown that the directional pattern of a disk split along a diameter, measured in a plane perpendicular to that diameter, is given by

$$R(\gamma) = \frac{2}{\phi} [J_1(\phi) \cos \theta + S_1(\phi) \sin \theta] \qquad (2)$$

where

$$\phi = \frac{\pi d}{\lambda} \sin \gamma$$

2θ = relative phase shift of the halves
J_1 = first order Bessel function
S_1 = Struve function
d = disk diameter
λ = wave length
γ = angle measured from the axis of the disk

Patterns calculated from this equation for four different values of θ are shown in Figure 3*A*. It will be observed that shifting causes a distortion of the pattern, and in particular raises the level of the minor lobe on the side opposite that toward which the main lobe is shifted. A general study of the properties of segmented transducers, with phase shift between the segments, indicates that the pattern can be steered only through large angles, without distortion, if the segments are less than half a wave length wide. With the diametrically split sonar projector the segments are about two wave lengths wide and the pattern can be steered only a fraction of the width of the main lobe. However, this is quite sufficient for the purposes of a bearing deviation indicator.

The indicated bearing deviation, which

is measured by the difference in response from the left-shifted and right-shifted patterns, is shown in Figure 3*B*. These curves have been corrected to include the effect of the unshifted transmission pattern, and are therefore representative of actual echo-ranging conditions. Analysis of a more complete set of curves of this sort shows that increasing the phase shift 2θ has the following effects:

1. The sensitivity of the indication in the neighborhood of $\gamma=0$ is increased.
2. The angular range within which indications are proportional to γ decreases.
3. The angular range within which indications have the correct sense remains constant.
4. The ratio of the magnitude of the largest false indication to the magnitude of the true indication decreases.
5. Signal-to-noise ratio is impaired because the desired signals are received farther down on the pattern.
6. The magnitude of the maximum true indication (height of the first peak in Figure 3*B*) has a broad maximum at about $2\theta=120$ degrees. In practice 2θ does not appear to be particularly critical and a value of 75 to 90 degrees ordinarily is used.

Simultaneous Lobe Comparison by Sum and Difference

The simultaneous lobe comparison principle has been described so far with reference to a system based on the use of lag lines. This was the system most widely used in echo-ranging BDI equipment manufactured during the war. However, there are at least two alternative methods which have merit for particular applications. For purposes of comparison all three methods will be described with reference to a rectangular transducer, which lends itself to mathematical analysis more readily than a circular one. Figure 4*A* is a diagrammatic illustration of the lag-line system. A signal arriving at an angle γ produces output voltages V_1 and V_2, of equal amplitude but different phase in the two halves of the transducer. These are given by

$$\left.\begin{aligned} V_1 &= K\frac{\sin a}{a}\cos(\omega t+a) \\ V_2 &= K\frac{\sin a}{a}\cos(\omega t-a) \end{aligned}\right\} \quad (3)$$

where

$$a=\frac{\pi d \sin\gamma}{\lambda}$$

d = center-to-center spacing of segments
K = constant calibration factor

After the signals are passed through lead and lag networks and combined as shown, we have

$$\left.\begin{aligned} V_3 &= V_1\underline{/-\theta}+V_2\underline{/+\theta} \\ &= 2K\frac{\sin a}{a}\cos(a-\theta)\cos\omega t \\ V_4 &= V_1\underline{/+\theta}+V_2\underline{/-\theta} \\ &= 2K\frac{\sin a}{a}\cos(a+\theta)\cos\omega t \end{aligned}\right\} \quad (4)$$

If these voltages are plotted as functions of γ, it will be found that V_3 represents a right-shifted pattern and V_4 a left-shifted pattern similar to those plotted in Figure 3*A*.

Figure 4*B* is a diagrammatic illustration of a "sum-and-difference" system developed by Radio Corporation of America and designated the "vector bearing indicator." V_1 and V_2 are the output voltages of the two transducer halves as given in equation 3, while the sum-and-difference voltages are

$$\left.\begin{aligned} V_3 &= V_1+V_2 \\ &= 2K\frac{\sin a}{a}\cos a\cos\omega t \\ V_4 &= V_1-V_2 \\ &= 2K\frac{\sin a}{a}\sin a\sin\omega t \end{aligned}\right\} \quad (5)$$

These voltages are amplified and brought to the same phase by a 90-degree relative phase shift. The sum of the two resultant signals then is applied to one diode and the difference to another, giving

$$\left.\begin{aligned} V_5 &= G_s V_3\underline{/+45^\circ}+G_d V_4\underline{/-45^\circ} \\ &= 2K\sqrt{G_s^2+G_d^2}\,\frac{\sin a}{a}\times \\ &\quad \cos(a+\theta)\cos\left(\omega t+\frac{\pi}{4}\right) \\ V_6 &= G_s V_3\underline{/+45^\circ}-G_d V_4\underline{/-45^\circ} \\ &= 2K\sqrt{G_s^2+G_d^2}\,\frac{\sin a}{a}\times \\ &\quad \cos(a-\theta)\cos\left(\omega t+\frac{\pi}{4}\right) \end{aligned}\right\} \quad (6)$$

where

$$\tan\theta=\frac{G_d}{G_s}$$

Equations 6 are of the same form as equations 4 and, therefore, represent similar left-shifted and right-shifted patterns.

Figure 4*C* is a diagrammatic illustration of another sum-and-difference system developed by the Bell Telephone Laboratories and called the "phase-actuated locator." Voltages V_1 and V_2 are given by equations 3 as before. These voltages are amplified separately in matched amplifiers of gain G and shifted 90 degrees in relative phase. The sum is applied to one diode and the difference to another, giving

$$\left.\begin{aligned} V_7 &= 2GK\frac{\sin a}{a}\cos\left(a+\frac{4}{\pi}\right)\cos\left(\omega t-\frac{4}{\pi}\right) \\ V_8 &= -2GK\frac{\sin a}{a}\cos\left(a-\frac{4}{\pi}\right)\cos\left(\omega t-\frac{\pi}{4}\right) \end{aligned}\right\} \quad (7)$$

Again these equations are of the same form as equations 4, with the restriction that $\theta=\pi/4$, and correspondingly repre-

Figure 4

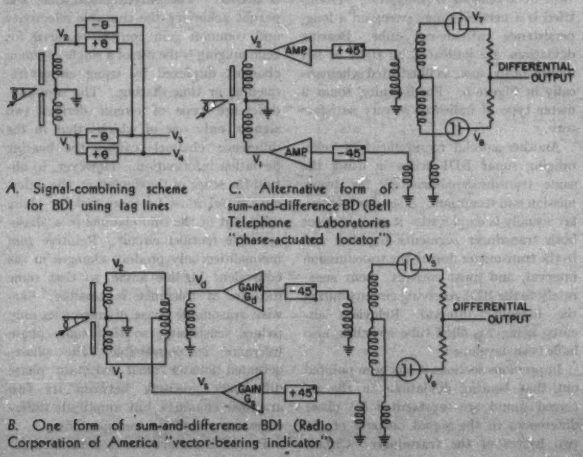

A. Signal-combining scheme for BDI using lag lines

C. Alternative form of sum-and-difference BD (Bell Telephone Laboratories "phase-actuated locator")

B. One form of sum-and-difference BDI (Radio Corporation of America "vector-bearing indicator")

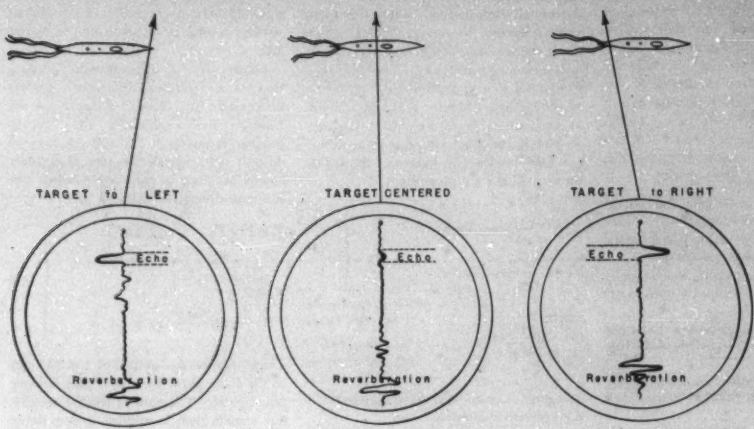

Figure 5. Diagrammatic representation of typical BDI traces

sent left-shifted and right-shifted receiving patterns.

The foregoing analysis shows that these three different systems of simultaneous lobe comparison are alike in principle to the extent that they all provide output voltages which are the same function of the angle of arrival of the sound signals. The relative merits of the three systems depend upon the special requirements of particular applications, and upon manufacturing and maintenance factors.

Receiver and Indicator Requirements

Although the development of BDI was called forth initially by its need in echo-ranging sonar, the feature of bearing deviation indication was recognized immediately as desirable in passive sonar systems that function by listening to the noise emitted by the target.[3] However, circuit performance requirements in the two cases differ considerably. For echo ranging, a narrow band width is necessary to give a good ratio of signal-to-own-ship's noise. Precise, sharp tuning accordingly must be possible and the gain should be increased gradually after emission of the ping to compensate for decreased echo-signal level with increasing range, and to avoid overloading the receiver and indicator by the reverberation from close by. Also, indicator response must be rapid to show the bearing deviation of a short echo. For noise listening, however, wide band width is desireable to average out the statistical fluctuations in noise, and precise tuning is not required. Gain need not be varied with time, but can be subject to manual or automatic volume control, and the indicator response should be slow enough to integrate fluctuations in the noise signal.

An indicator for echo-ranging sonar has the special requirement of allowing for correlation of the observed deviation indication with the audible sound produced by the received echo. A submarine echo often may be returned amidst other confusing sounds which arrive from random directions and produce their own bearing deviation indications. It has been found that simultaneous eye-ear indications are of great mutual assistance in identifying and following a target. Best of a number of indicating systems tried is a vertical range sweep on a long-persistence cathode-ray tube. Bearing deviations are indicated by right or left motion of the spot, as illustrated schematically in Figure 5. For listening sonar a meter type of indicator is very satisfactory.

Another special requirement of echo-ranging sonar BDI arises in using the same transducer alternately for transmission and reception. A send-receive relay usually is employed; it must connect both transducer segments together and to the transmitter during the transmission interval, and must connect them separately to the BDI receiving circuits during the listening interval. Relayless circuits, using gas-filled tube switches, also have been developed.

In previous sections it has been pointed out that bearing deviations in the received sound are represented by phase differences in the signal outputs of the two halves of the transducer. Circuit design problems revolve around the need for preserving these differences (either in the form of phase or amplitude) up to the point where the information they carry is changed into a form suitable for application to the indicator, despite requirements of tunability, wide changes in gain and allowance for tube replacement and line-voltage variations.

The lag-line type of circuit changes the phase differences immediately into amplitude differences, so that phase variations are thereafter unimportant, although the amplitude differences must be maintained exactly in relative magnitude. The signals are at a low level, so amplification is needed. The only method that will permit achieving the tuneable selectivity and common gain control required for echo ranging is the use of a single common channel, duplexed by using either frequency- or time-sharing. The sum-and-difference type of circuit derives two signals, only one of which—that in the difference channel—carries the bearing deviation information. However, to obtain the sense of the deviation, the difference signal must be compared for phase with that of the sum channel in a phase-sensitive rectifier circuit. Relative gain inequalities only produce changes in the equivalent lag-line angle, so that some measure of tolerance is possible; likewise, reasonable phase discrepancies only reduce sensitivity, so that some phase tolerance is permissible. The phase-actuated locator must maintain phase differences precisely between its two amplifier channels, but amplitude differences are relatively unimportant.

Provision for eye-ear co-ordination re-

quires that the signal from the whole projector be made available for the "audible" channel. In echo ranging, this output also is used for the range recorder and for auxiliary control functions described hereinafter. In the lag-line type a separate tuned amplifier channel must be provided for the listening channel; in the phase-actuated locator type the desired signal may be derived at the rectifier, while in the vector bearing indicator type it is already present in the sum channel. Choice among the various methods that may be used in realizing a bearing deviation indicator must be based on a careful study of the operating requirements, comparative ease of maintenance, and the other design details necessary to secure continued maximum performance under the severe requirements of naval service.

Historically, the immediate need during the early part of the war was for BDI equipment that could be added promptly to existing echo-ranging sonars already in fleet service. Such auxiliary equipment was developed at the Harvard Underwater Sound Laboratory, and models manufactured by the Astatic Corporation, Submarine Signal Company, David Bogen Company, and Radio Corporation of America saw service in quantity. New echo-ranging sonar equipments incorporating BDI as part of the original design were produced later by several manufacturers. The same progression from an accessory to an integral part of the design characterized the application of BDI to the listening sonars for submarine service developed by Columbia University's New London (Conn.) laboratory.

Since this paper is concerned primarily with the bearing deviation indicator itself, its purpose will best be served by describing two models of the auxiliary equipment designed for application to existing echo-ranging sonars. Both used the lag-line type of circuit; the first (X-3) accomplished single-channel amplification through 2-frequency duplexing, the second (X-4) through time-shared duplexing. Operating effectiveness of the two types was equal, but the X-4 model proved easier to build and maintain.

Practical BDI Circuits

Model X-3

Functional Characteristics. A general understanding of the electric circuits of the model X-3 BDI can be obtained by tracing signals with the help of the block diagram of Figure 6. In order to achieve maximum signal-to-noise ratio the electric signals from the two low-impedance projector halves are applied through tuned step-up input transformers to the grids of preamplifier tubes. The phase-shift network, or lag line, is connected transversely between the two preamplifier outputs, and converts the phase differences in the two input channels into amplitude differences at this point. Thus, the voltage appearing at one end of the lag line represents the combination of a direct signal from one half of the projector and a delayed signal from the other half, the combination having the directional characteristic of a receiving lobe steered a few degrees toward the delayed half of the projector. Conversely, the voltage appearing at the other end of the lag line has the delay introduced on the other side and so corre-

Figure 6. Block diagram of model X-3 BDI circuit

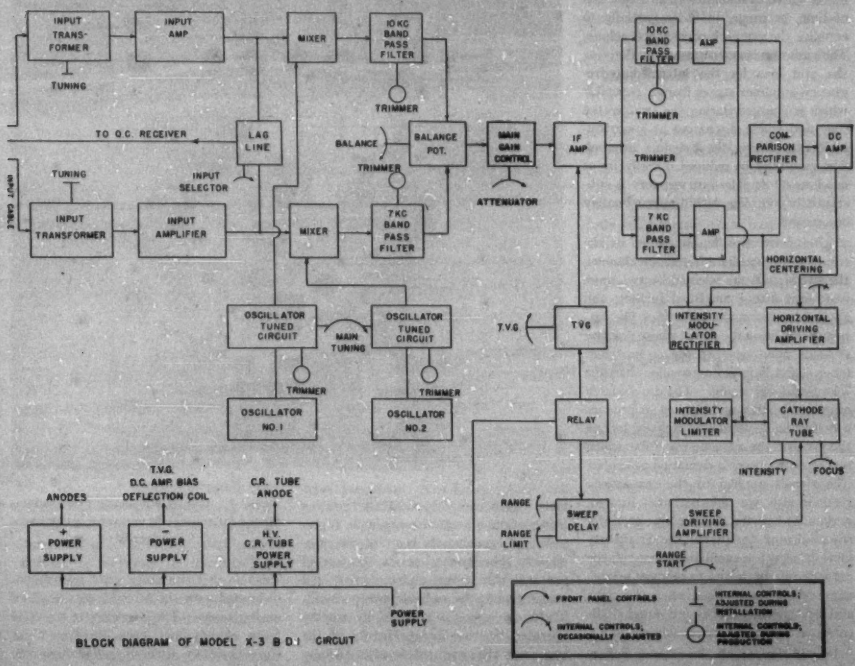

sponds to an oppositely steered receiving lobe. The signals at the ends of the lag line, which now correspond to right-steered and left-steered receiving lobes, are applied to two converter tubes where they are mixed with voltages from two local oscillators whose frequencies are such as to develop 10-kc and 7-kc intermediate-frequency signals for the right and left lobes, respectively. Band-pass filters reject other modulation frequencies and the 10-kc and 7-kc signals are combined in a common-channel intermediate-frequency amplifier.

All gain control is carried out in the common intermediate-frequency channel in order to preserve the amplitude ratio between the two intermediate-frequency signals which carry the bearing deviation information. A very wide range of gain variation must be provided, both to accommodate sonar installations having different acoustic output power and to handle the wide range of echo strength encountered from near and distant targets. In addition to a manual control, an automatic time-varied gain (TVG) circuit is provided. In this arrangement the gain of the intermediate-frequency amplifier is varied systematically as a function of time, or range, in order partially to equalize the strength of received echoes. The variation is accomplished by deriving the grid bias for the intermediate-frequency amplifier stages from a capacitor which is charged during the transmitted ping and which discharges at a controllable rate during the listening interval. The gain may be reduced initially by as much as 60 decibles but recovery is substantially complete within approximately one second.

After controlled amplification in the common intermediate-frequency channel, the two signals are selected by two more band-pass filters, amplified further, and applied to a comparison rectifier, the output of which is a d-c signal whose polarity depends upon whether the 10-kc (right lobe) signal is larger or smaller than the 7-kc (left lobe) signal. The d-c signal is amplified further and applied to produce a horizontal deflection to right or left on the face of the cathode-ray tube which serves as the bearing deviation indicator. The signals applied to the comparison rectifier also are differentiated, limited, and applied to the Z axis of the cathode-ray indicator to sustain the brightness of the trace for rapid deflection of the cathode-ray beam and to produce brightening of the beam trace when the right and left signal voltages are equal, indicating a "dead-on" target echo.

In addition to the horizontal deflections which carry the bearing deviation information, a vertical range scale is provided by sweeping the beam of the cathode-ray tube upward across the face of the indicator screen under control of a conventional type of linear sweep circuit. The range sweep is initiated by a relay operated by the keying circuits of the sonar set; the sweep rate is adjustable by steps so that the range scale may be coordinated with the interval between successive pings. The character of the BDI trace already has been illustrated for three positions of the target in Figure 5.

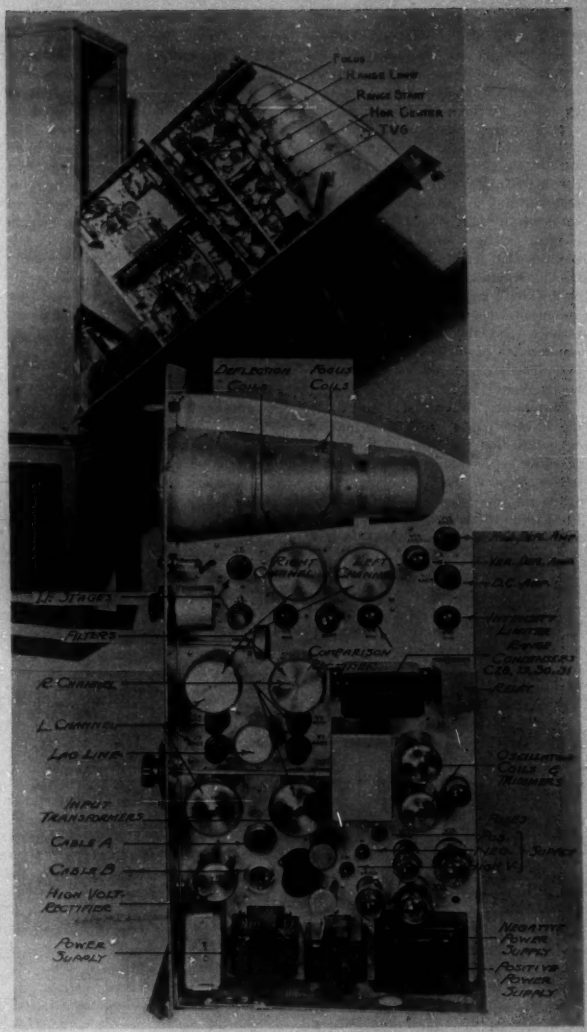

Figure 7. The edge-mounted BDI chassis is hinged for convenient access for maintenance and repair

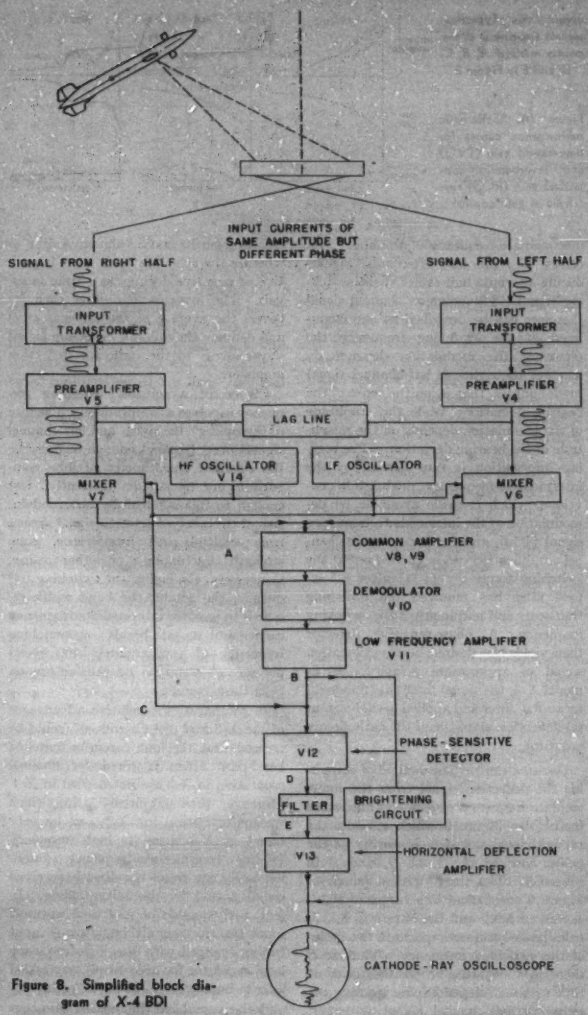

Figure 8. Simplified block diagram of *X*-4 BDI

As in the case of radar presentation these traces take on, under different echo-ranging conditions, a wide variety of characteristic forms which a well-trained operator soon learns to recognize and interpret.

Circuit Details. The lag line, which is connected transversely between the output terminals of the preamplifiers, comprises one full section of a simple constant-*k* low-pass filter. The desired phase shift of from 60 to 90 degrees is obtained if the cutoff frequency of the filter is approximately 1.6 times the lowest operating frequency. A voltage divider of sufficiently high resistance to have a negligible effect on the operation of the lag line is connected from the inductance mid-tap to ground in order to provide signals for the regular sound receiver of the sonar. Since the contributions from the two projector halves are delayed equally at this mid-terminal of the lag line, the signal behaves as though taken directly from both projector halves connected additively without provision for BDI. Thus, except for preselection by the tuned input transformers and some amplification, the operation of the sonar receiver, its audible output signals, and the receiver controls are unaffected by the addition of the bearing deviation indicator.

In order to achieve and maintain exact electrical balance, whereby signals from the direction of the projector axis produce no deflection, a "balance" control provides compensation for any inequality in gain between the 10-kc and 7-kc channels. It operates in conjunction with an "input selector" switch which, when thrown to the "balance" position, connects the two converter signal grids together and to the mid-tap of the lag line. With this connection, when the channels are balanced, there is no indicator deflection by incoming signals regardless of their amplitude or phase of arrival at the projector halves. Three other input selector switch positions provide for normal operation, for testing the right-sensitive channel by cutting off the left-sensitive, and for testing the left-sensitive channel by cutting off the right-sensitive.

The two local oscillators which heterodyne the echo signals to 10 and 7 kc operate above the signal frequency. They are of the modified Hartley type and their variable tuning capacitors are ganged and controlled by the calibrated "frequency control" on the front panel. Tracking of these oscillators must be adjusted carefully to maintain their frequency separation within 15 cycles per second of 3 kc over their entire tuning range.

The four band-pass filters employed in the *X*-3 unit use identical inductances for manufacturing economy. This requires different tuning capacitors and widely different circuit impedances in order to obtain substantially identical band-pass characteristics. Mica capacitors are mounted within the shield cans and exact final tuning is accomplished by means of ceramic trimmer capacitors. By means of these trimmers and a variable coupling adjustment, the band-pass filters are aligned individually for transmission identical within 0.1, 3, and 12 decibels for points respectively 300, 600 and 1,000 cycles per second on each side of the mid-frequency of the pass band.

At the output of the comparison rectifier there appear signal components of intermediate-frequency as well as transients accompanying the desired deflection

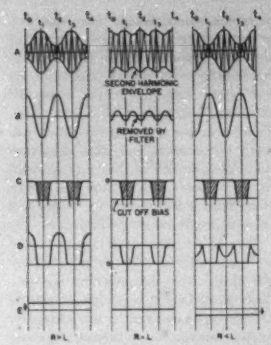

Figure 9 (left). Typical signals appearing at the points marked *A, B, C, D,* and *E* in Figure 8

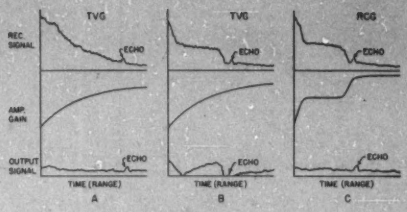

Figure 10. Schematic performance curves for time-varied gain (TVG) and reverberation-controlled gain (RCG) systems of gain control

signal. These high-frequency components are removed and the deflection pulse is "cleaned up" by a 2-section low-pass *R-C* filter. This filter is not critical but a time constant of 5 milliseconds for each section produces a suitable degree of pulse "tailoring."

The cathode-ray indicator is a 5-inch tube using magnetic focusing and magnetic deflection, and is operated at a second anode voltage of 3,400 volts. The compound *P7* phosphor provides a degree of persistence which is well adapted for the pulse recurrence rates used in echo ranging and which permits a comfortable degree of attention mobility on the part of the operator.

The model *X*-3 BDI is housed in a cabinet 33 inches high and 9 inches wide and all equipment is mounted on a single vertical chassis which is hinged at the bottom for convenient access to both sides. Figure 7 shows this arrangement, which was typical of BDI auxiliary units.

Model *X*-4

Functional Characteristics. The principle changes made in developing the *X*-4 BDI circuit are those associated with the use of time-shared duplexing for carrying the right- and left-steered channel signals through the common intermediate-frequency amplifier. Figure 8 is a simplified block diagram of the *X*-4 circuit which embodies these changes. As in the *X*-3 circuit, input transformers couple the transducer signals to preamplifiers and a phase-shifting lag line is connected transversely between the input circuits of the two channel mixer-switching tubes (*V*6 and *V*7). In these mixers a common high-frequency local oscillator generates the same intermediate frequency for each channel, but a low-frequency "switching" oscillator disables the two mixers alternately so that the common intermediate-frequency amplifier receives the right- and left-channel signals during alternate half-cycles of the switching signal. The common channel signal therefore can be described as one modulated at the switching frequency: the phase of the modulation depends on whether the right- or left-channel signal predominates, that is, on the sense of the bearing deviation; while the amplitude of the modulation depends on the magnitude of the bearing deviation. The bearing information is thus carried by the intermediate-frequency modulation envelope, which is made available by demodulation of the intermediate-frequency signal (*V*10), and further common-channel amplification can be carried out at the switching frequency (*V*11) after a low-pass filter has removed the switching transients and harmonics of the switching frequency. A phase-sensitive detector then yields the desired bearing deviation signal of appropriate polarity. As in model *X*-3, the signal finally is "tailored" by an *R-C* filter and applied to the horizontal deflection amplifier of the cathode-ray indicator.

Circuit Details. The method of extracting the deflection signal from the intermediate-frequency envelope is illustrated further by Figure 9 which exhibits the typical signal voltages appearing at the points marked *A*, *B*, *C*, *D*, and *E* in Figure 8. The three vertical panels of Figure 9 correspond to a target at right, center, or left; and the letters t_0, t_1, ... t_4 designate successive epochs in two cycles of the switching frequency. Thus at *B* there is a negative or positive peak at time t_1, t_3, ... depending on whether the right- or left-channel signal is larger. The phase sensitiveness of the detector (*V*12) is obtained by disabling it during alternate half cycles of the switching frequency. This is accomplished by introducing the signal shown at *C*, whose positive excursions are limited by a diode and whose negative swings are sufficient to carry *V*12 far beyond cutoff. As a result, *V*12 is responsive only during the epochs marked t_0, t_2, t_4, ... when its plate current, as shown at *D*, increases or decreases from its static value according to whether the signal envelope at *B* is positive or negative during these time intervals. The low-pass *R-C* filter then recovers the average of the currents at *D* and delivers the tailored deflection signal shown at *E* to the indicator deflection amplifier.

Choice of a suitable switching frequency involves a compromise. The rate of "sampling" the right- and left-channel signals must be rapid enough to preserve the essential simultaneity of lobe comparison or, to put it differently, fast enough to follow faithfully any modulation of the received acoustic signal arising from multiple-path interference, echo strength fluctuation, or other cause. Conversely, the higher the switching frequency, the greater the band width required to pass the intermediate-frequency carrier and its side bands. A switching frequency of approximately 400 cycles per second seems to be satisfactory on both these counts.

In comparing the relative advantages of the *X*-3 and *X*-4 circuits, it should be noticed that the four carefully matched band-pass filters required for channel separation in *X*-3 are not needed in *X*-4. Moreover, the input circuit tuning, which was quite critical for *X*-3, can be very broad in *X*-4 since its high frequency (60-kc) intermediate-frequency amplifier easily can reject the directly received signal passed by the mixer stages. In fact, early models of *X*-4 used untuned input transformers although low-*Q* input tuning (ganged with the high-frequency local oscillator for unicontrol) was added later to improve signal-to-noise ratio.

Both manual and time-varied gain controls are introduced in the common intermediate-frequency amplifier, as in the *X*-3 circuit. Other features of the *X*-4 and *X*-3 models, such as the range sweep, trace brightening, deflection amplifiers, and the cathode-ray indicator are also similar.

Various modifications of these circuits were introduced in different sonar equipments utilizing the *X*-4 time-sharing principle for BDI. Among these was the

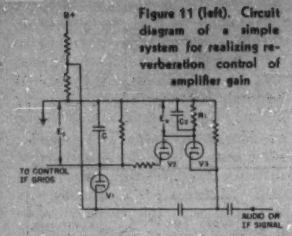

Figure 11 (left). Circuit diagram of a simple system for realizing reverberation control of amplifier gain

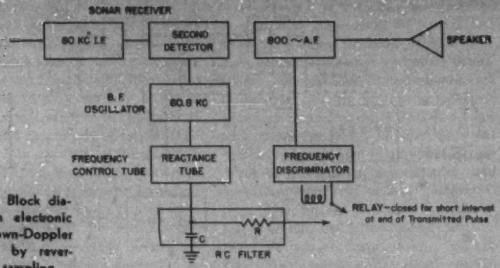

Figure 12. Block diagram of an electronic system for own-Doppler nullification by reverberation sampling

adoption of reverberation-controlled gain (RCG) instead of time-varied gain (TVG; see following paragraphs), and the use of improved phase-shift networks which reduced the variation of phase shift with frequency. This effect was accomplished by a combination of lag lines and lead lines arranged as shown schematically in Figure 4*A*.

Auxiliary Circuits for Sonar Equipment

In the course of development work devoted to BDI and other sonar equipment, several circuit arrangements were devised to produce useful improvements in the ratio of desired echo signals to undesired disturbances, and otherwise to assist the operator in perceiving and interpreting echo signals. These circuit modifications usually could be applied independently to sonar equipment already in service. Three typical examples, to be described, were designated as reverberation-controlled gain (RCG), own-Doppler nullification (ODN), and Doppler-controlled gain (DCG).

Reverberation-Controlled Gain

Time variation of gain was used in the *X*-3 and early *X*-4 BDI circuits to provide reduced amplifier gain during the period immediately following the ping, and thus to give protection against amplifier overload and to equalize variable echo strength. This feature quickly was recognized as being of such utility that it was adopted for the audible sound channel of standard sonar equipment even before BDI auxiliary units became available.

In spite of the value of time-varied gain for approximate equalization of echo strength, it was recognized that a single gain-recovery curve could not be ideal for all echo-ranging conditions. Even if a gain recovery curve of variable shape were provided the necessary complexity of adjustment would be too demanding on the operator and would offer too great a possibility of missing an echo through misadjustment. Automatic volume control (AVC) of the type used in most radio receivers was considered but it was not well adapted for use in the reception of pulses against a rapidly fluctuating background of reverberation and noise. Fortunately, a modification of automatic volume control, designated as reverberation-controlled gain, yielded a very satisfactory solution of this problem.

In order to contrast the behavior of reverberation-controlled gain with time-varied gain, the sketches of Figure 10*A* exhibit the performance of time-varied gain under idealized conditions. The received signals are indicated as dying away smoothly in a way that can be matched approximately by a complementary smooth increase of receiver gain, and the output signal is substantially uniform except for the received echo which stands out against the background at whatever range the echo occurs. However, the received signals seldom fall off in such a smooth manner. The greatest danger of missing or losing target contact occurs when the echo follows a hump in the reverberation decay curve, as shown in Figure 10*B*. A fixed gain-recovery curve of any shape sometimes may require the sacrifice of either earlier or later sensitivity, but even if the general trend of the decay curve is compensated, the echo still may be suppressed below the receiver threshold when it occurs just following an abrupt drop in reverberation. In the reverberation-controlled gain circuit the amplifier gain recovers very rapidly until the reverberation or noise output reaches a preset threshold level. The gain then is held at this level until the output drops below threshold, when gain restoration proceeds again. Thus the gain recovers just as rapidly as the decay of reverberation permits. However, no subsequent decreases in gain are possible after the initial gain reduction (in which respect reverberation-controlled gain differs from automatic volume control) so that blanking of a target echo following closely after a strong burst of reverberation is avoided. This action is illustrated in Figure 10*C*.

One type of circuit which is useful in achieving reverberation-controlled gain is shown schematically in Figure 11. Audio or intermediate-frequency signals appearing in the receiver during the transmitted ping are rectified in *V*1 and quickly charge the storage capacitor *C* so that a high negative voltage E_C is applied as bias to the controlled grids of the common-channel intermediate-frequency amplifier. Leakage into the receiver from the ping transmitter is usually sufficient to provide a large and relatively stable source for producing this initial reduction of amplifier gain. Discharge of the storage capacitor proceeds rapidly through the discharge control tube *V*2, which remains conducting as long as its anode is positive with respect to its cathode; however, the anode of *V*2 is biased by received reverberation or noise signals rectified by *V*3 and appearing across C_2 and E_R. When the amplifier gain has been restored to such a level that E_R is equal to E_C, the discharge rate of *C* drops abruptly and the gain remains substantially constant until the decay of the reverberation signal again brings E_R below E_C so that the discharge of *C* can proceed. Since *V*2 can conduct only in one direction, no recharging of *C* (with consequent gain reduction) can take place until receipt of a very large signal—sufficient to overcome the positive bias placed on *V*1 by the voltage divider from *B*+. Usually such a signal will not occur until the next transmitted ping.

Own-Doppler Nullification

As a result of the Doppler effect, all echo-ranging signals received from forward directions are increased in frequency by the motion of the echo-ranging vessel through the sound medium, while signals from behind are decreased in frequency. In general, when f is the transmitted frequency, V the ship's velocity, c the velocity of sound propagation in the medium,

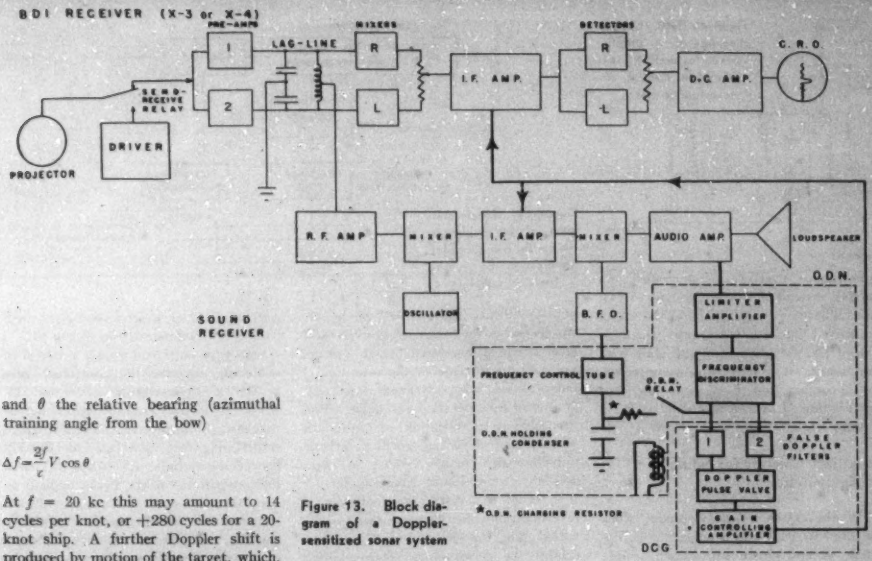

Figure 13. Block diagram of a Doppler-sensitized sonar system

and θ the relative bearing (azimuthal training angle from the bow)

$$\Delta f = \frac{2f}{c} V \cos\theta$$

At $f = 20$ kc this may amount to 14 cycles per knot, or $+280$ cycles for a 20-knot ship. A further Doppler shift is produced by motion of the target, which, if it is moving in the "line of sight," say, at 10 knots, can produce an additional shift of ± 140 cycles. To accommodate all possible conditions of relative motion the receiver therefore must have a pass band at least 900 cycles wide. Yet to receive a 33-millisecond pulse a pass band of only 30 cycles would be adequate! The consequent depreciation in signal-to-noise ratio is obvious.

Nothing can be done about motion of the target submarine—in fact, recognition of target Doppler effect is of great aid in estimating the course and the maneuvers of the submarine. Such recognition is accomplished by the sonar operator's noting whether the pitch of the heterodyned target echo is above or below the pitch of the prevailing reverberation, and estimating by how much. With the heterodyne beat note set at 800 cycles, a change of 14 cycles is marginally discernible. Better discrimination would be obtainable at 500 cycles, but then the variation due to own-Doppler effect could bring the echo pitch down into a frequency region where loudspeaker and hearing efficiency fall off. The obvious remedy is to remove the effect of own-Doppler effect, a process which became known as own-Doppler nullification (ODN). The pass band then could be narrowed to accommodate only target Doppler effect, and the pitch of the reverberation background would remain constant so that the sonar operator could judge more effectively changes of pitch in the target echo.

Two general methods for accomplishing own-Doppler nullification were developed. One was computed-correction own-Doppler nullification, and combined ship's speed V and relative bearing θ in an automatic computer to produce a compensating change in either the transmitted frequency or in the frequency of the receiver's first oscillator. Early experiments with a simple form of computed-correction demonstrated the value of own-Doppler nullification, but its application to the normal types of echo-ranging sonars involved equipment and installation difficulties. Accordingly, an all-electronic reverberation-controlled type was developed.

A functional block diagram of this circuit is shown in Figure 12. Immediately following the transmitted ping a relay closes for an interval of from 50 to 100 milliseconds, during which the near reverberation is sampled and the audio output frequency is returned to a standard reference value by a frequency discriminator-reactance tube feed-back circuit similar to that employed for automatic frequency control in radio receivers. When the sampling relay releases, a holding capacitor C preserves this corrected reference frequency during the remainder of the listening interval between pings. Thus, except for the short sampling period the frequency control circuit is disabled and the audible beat frequency output of the receiver can exhibit in a conventional manner the small frequency shifts characteristic of target Doppler effect even though the target speed along the line of sight is much less than that of the echo-ranging vessel.

The R-C filter shown in the own-Doppler-nullification block diagram is an important feature of the circuit. Its function is to establish the frequency correction on the basis of average reverberation received during the sampling interval so that a false Doppler effect is not established by a frequency fluctuation just before the sampling relay releases.

Specifications for the frequency discriminator differ materially from those imposed on discriminators for detecting frequency modulation of radio signals. A novel form of discriminator circuit exhibited the desirable properties of a very steep curve for small frequency deviations together with preservation of the sense of the correction signal for wide frequency deviations.

Doppler-Controlled Gain

Several functional by-products became available as a result of the stabilization of a reference frequency by own-Doppler nullification. Since echoes hav-

ing appreciable target Doppler shift often can be identified and target contact maintained even when such echoes are at the same or a lower level than the co-existing reverberation, it would be helpful to provide a selective increase of BDI deflection sensitivity when such signals are present.

Figure 13 shows the block diagram of a Doppler-sensitized sonar system. The top line can be recognized as a schematic representation of the model *X*-4 BDI, while the second line shows a separate listening amplifier system connected to the mid-tap of the lag line. The upper dashed box encloses the components which provide own-Doppler nullification, while the lower dashed box encloses the additional components required to provide Doppler control for the gain of both BDI and listening amplifiers. In the own-Doppler-nullification circuit the signal output of the frequency discriminator is applied for frequency control only during a brief sampling period; however, during the remainder of the listening interval between pings, the discriminator remains connected to the audio output of the listening channel so that signals carrying information about the deviation of the echo signal from the own-Doppler-nullification reference frequency are continuously available. By smoothing out these signals with *R-C* "false Doppler filters" any significant frequency departure in an echo will yield a control signal which can be applied as an auxiliary bias to the BDI and listening-channel intermediate-frequency amplifiers. Since the output of the frequency discriminator may be positive or negative according to the sense of the frequency deviation, an ingenious arrangement of diodes (the Doppler pulse valve) is required to deliver a positive signal for Doppler gain control for either sense of deviation.

The Doppler control signal connection to the listening channel intermediate-frequency amplifier is symbolic only. While the input to the frequency discriminator is protected by limiters it has been found better to omit Doppler enhancement in the amplifier chain supplying signals to the frequency discriminator circuit and to split off a separate audio amplifier chain for Doppler enhancement of audio signals and range recorder traces.

Of several other circuit modifications which were investigated, a few yielded promising results under controlled conditions but did not reach a suitably advanced state of development soon enough to be incorporated in service equipment. Among these the following deserve brief mention. A target-Doppler indicator was devised to make further use of the Doppler-controlled signals described before. In this arrangement an auxiliary cathode-ray tube had a horizontal range sweep, while the Doppler shift in received signals appeared as a vertical deflection giving visual indication to the operator of both sign and magnitude of target Doppler effect. In another modification, a very narrow-band elimination filter gave selective rejection of reverberation signals lying within a few cycles of the reference frequency established by own-Doppler nullification. By an ingenious arrangement, the same frequency-selective circuit components determined the own-Doppler nullification reference frequency and the center of the eliminated band so that these were held automatically in coincidence. In still another modification, the right–left deviation signals of the BDI were applied to motor control circuits which automatically trained the transducer toward the bearing of the target. This feature of automatic target training appeared likely to be of major importance but the relatively long time intervals elapsing between successive pings are not well adapted for smooth servo control of mechanical motion. Other sonar developments reduced the priority assigned to this study before it had reached the stage where the operator could be freed from excessive demands on monitoring of the automatic equipment.

Test Equipment and Training Aids

During field tests of BDI auxiliary equipment it became apparent that only transducers having directional patterns reasonably approximating the ideal would give satisfactory BDI operation. This led to the development of portable test equipment originally designated as the sound gear monitor. This device comprised a calibrated wide-range transducer with an associated oscillator, amplifier, and output meter, and made possible convenient measurement of directivity patterns and the relative efficiency of installed sonar systems both in transmission and reception. It was used around the world and contributed significantly to insuring initial and continued effectiveness of sonar equipment in service. A split-projector test unit made it possible to use the sound gear monitor to predetermine the suitability of transducers for BDI service in advance of installation. A BDI signal generator provided two outputs of adjustable phase relation to simulate signals from a split transducer for testing of BDI. A simpler phase-sensitivity test unit was provided as an auxiliary for the sound gear monitor so that BDI tests could be carried out more easily on installed equipment.

An artificial projector containing phase-shifting networks facilitated shore-based training in the use of the various test equipments. Adoption of BDI on a large scale posed problems of training great numbers of personnel in approved procedures of installation, maintenance, and operation. Matériel school instructors were given intensive laboratory courses; test material and other special instructional devices were worked up. Simulative BDI attachments for attack teacher equipment were devised for instruction of sonar operators and conning officers. Comprehensive investigations of operating accuracy were made and assistance was furnished to the Navy in establishing doctrine for most effective use of BDI. Thus the simple physical principle of looking, or rather listening, in two directions at once became a full-fledged military program.

Acknowledgements

The research studies and development work described in this paper represent the joint efforts of a large group, of which the principle members alone numbered more than thirty. It would be both impossible and misleading to tabulate in detail the specific contributions made by each individual. The authors present this report, therefore, simply as spokesmen for the entire group which was responsible for the Harvard Underwater Sound Laboratory program of sonar improvements.

As the program developed, other Office of Scientific Research and Development laboratories and various naval organizations became involved. Especially valuable assistance was rendered to the work at Harvard Underwater Sound Laboratory by officers of the Tenth Fleet, ASDev Lant, ComDesLant, and the personnel of the East and West Coast Sonar Schools, ASWIS (Boston, Mass.), COTCLant (Norfolk, Va.), SCTC (Miami, Fla.) and other ASW training activities.

References

1. Echo Ranging Sonar. *Electronics* (New York, N. Y.), August 1946, page 88.

2. Sonar for Submarines. *Electronics* (New York, N. Y.), April 1946, page 99. A description of a typical listening system without bearing deviation indicator.

No Discussion

Ground Power Supply for Modern Aircraft

T. B. OWEN
ASSOCIATE AIEE

J. A. MURRAY
ASSOCIATE AIEE

ALLEN ROSENSTEIN
ASSOCIATE AIEE

THE advent of the highly electrified commercial airplane since the war has posed many problems, both to the airline operator and to the airplane manufacturer. Not only has it been very difficult to obtain the necessary equipment, such as motors, relays, inverters, and generators, but it has been very difficult to obtain power supplies capable of carrying the airplane load continuously, principally because aircraft electrification has proceeded so rapidly that the necessary components have not been developed. To realize the magnitude of this problem, it is only necessary to think back to the time when the storage battery was considered as the primary power source of the airplane and the generators were used mainly to keep the batteries charged. The next step was in the direction of larger generators. The *DC-4* (commercial version of the *C-54*) was equipped with four 100-ampere 28-volt d-c generators and an 88-ampere-hour battery. Since the generators were installed on the basis that two could carry the entire load, it may be seen that generally the prewar airplane electrical load would be 200 amperes or less.

The problem of providing ground power supply for an airplane with a maximum load of 200 amperes is not particularly difficult. In an emergency, an ordinary battery cart may be used, particularly if the loads are monitored. Further, a small gasoline engine driving a 200-ampere 28-volt generator is entirely sufficient, as is a small rectifier cart taking power from available field a-c supply sources.

The modern commercial airplane, however, has a number of additional loads which require a different approach. A partial listing of these loads is given here; all may not be installed on one particular airplane, but a good proportion are.

1. Food warming and water heating devices.
2. Electrically heated windshields.
3. Landing flap actuators.
4. Cowl flap actuators.
5. Landing gear actuators.
6. Blowers for heat distribution or cabin cooling.
7. Cabin temperature and pressure control systems.
8. Propeller deicing.
9. Electric autopilots.
10. Scoop and carburetor anti-icing.
11. Emergency hydraulic pump.
12. "Fluxgate" or "gyrosyn" compass.
13. Fuel booster pumps.
14. Electric fuel quantity gauges.
15. Electric propeller control.
16. Humidifier heater.
17. Toilet flush pumps.
18. Fire and carbon-monoxide warning systems.
19. Electric razor power sources.
20. The 400-cycle 115-volt supply for radio compass, altimeter radar, and other instruments. (On aircraft with basic 28-volt d-c systems, the increase in these loads has necessitated a change from small to large inverters.)
21. Very heavy increases in lighting.
22. Refrigeration system for cabin ground cooling.

In the section following, the majority of the load figures given are taken from the personal experience of the authors but reference is made to airplanes that have types of equipment installed which make the ground loads much heavier.

Paper 47-202, recommended by the AIEE committee on air transportation and approved by the AIEE technical program committee for presentation at the AIEE Pacific general meeting, San Diego, Calif., August 26–29, 1947. Manuscript submitted June 11, 1947; made available for printing July 14, 1947.

T. B. Owen and J. A. Murray are with the Douglas Aircraft Company, Inc., Santa Monica, Calif.; Allen Rosenstein is with the University of California at Los Angeles, and is also consulting engineer for the Industrial Electronics and Transformer Company, Los Angeles.

Types of Aircraft Electrical Loads

With this as a basis, we may now start out to classify the various load conditions which may be obtained in an airplane on the ground. These are, generally,

1. Maintenance operations.
2. Passenger loading.
3. Engine starting and preflight.

These conditions will be discussed in that order.

Maintenance

Under this condition, every electric load in the airplane must be capable of being operated, not necessarily in the sequence that obtains when the airplane is in flight status, but in such sequence that maintenance personnel can check the operation of the equipment at their convenience. During such operations, the lighting system and at least a portion of the air conditioning system should be in service, as maintenance operations cannot be carried on properly under adverse temperature and ventilation conditions. With these loads, we can expect a minimum 200 amperes, with peaks going considerably above this.

In order to appreciate the fact that this estimate is not excessive, a brief résumé of the electric loads will be given in Table I. Under the heading of lighting, only those lights which are located in working compartments are listed for the day condition, with partial cabin lighting added for night conditions. Under motors, one 400-cycle inverter is considered as being on to supply power for the radio, instruments, or other a-c equipment, plus the ground blower for ventilation and some additional loading from various small actuators.

Table I. Twenty-Eight-Volt Aircraft System Loads in Amperes—Maintenance

	Day	Night
Lighting	35	95
Rotary equipment	140	140
Electronic and miscellaneous	30	30
Total	205	265

Only a small amount of load from the electronic devices is shown; this is mainly for filament heating of vacuum tubes.

On airplanes that use a refrigeration system for ground cooling of the cabin, very heavy additional loads may be encountered. These loads will run to 800 amperes or more steady state, with very severe starting loads. Further, where wing flaps, landing gear, and so on, are operated electrically, maintenance conditions may require that these units be operated, not necessarily simultaneously. The heaviest load here is the landing gear, where the steady state current may be 400 amperes or more. For some postwar aircraft the minimum maintenance ground power loading may run as high as 800 to 1,000 amperes.

Passenger Loading

Of all the operating conditions in which an airplane finds itself, the passenger loading one is the most critical. Nothing should be allowed to happen which will disturb the equilibrium of the passenger; his feelings during this period are probably the deciding factor as to whether or not he will use airplane travel in the future. He must enter an airplane that is comfortable and well lighted, and in which the temperature is neither excessively high or low. Therefore, the ground power supply equipment must be able to supply all lighting, heating, and refrigeration equipment, in addition to equipment essential to flight. These latter items must be put into operation at this point, both for warming up prior to use in flight and for checking the electric system of the airplane.

In addition, all lights in the cargo holds, wheel wells, and other maintenance points may be on for last minute checkups. The loads imposed by refrigeration equipment already have been noted, and if this equipment is installed the ground power supply must be capable of supplying it. This additional load is over 600 amperes for two compressors and 200 amperes for the condenser fan in one current model of airplane.

Table II. Twenty-Eight-Volt Aircraft System Loads in Amperes—Passenger Loading

	Day	Night
Lighting	90	160
Rotary equipment	190	190
Water and food warming	185	185
Electronic devices and miscellaneous	40	40
Total	505	575

It is entirely possible for the load under these conditions to be from 500 to 1,500 amperes. A brief résumé is given in Table II to show the character and magnitude of these loads on an airplane that is not completely electrified.

Engine Starting and Preflight

With passengers loaded, the doors may be closed, the engines started, and the airplane finally moved out on the flight ramp. The period between the time the doors are closed and the taxi run to the flight ramp begun is a time when very heavy and variable loads may be applied, and still the electric power system cannot be disturbed to the point of discomforting the passengers.

If the airplane is supercharged, that is, if the cabin is pressurized, the engines driving the supercharger are started first, bringing the pressure and temperature control system of the airplane into action. The loads here are relatively minor, consisting mainly of small actuators, relays, and electronic equipment. The temperature control system will already be in operation; however, the airfoil anti-icing and propeller anti-icing equipment well may be put into use. The loads for the latter equipment may be very heavy; not less than 200 amperes total.

If the propellers are electrically operated, pitch changes in this period may impose very severe loads, particularly if the propellers are reversed for test. The instantaneous current drain on the system by one manufacturer's equipment is well over 1,000 amperes, dropping to 400 amperes in one-tenth second.

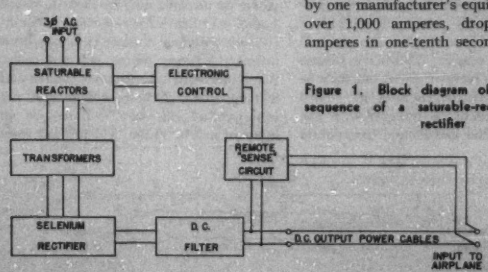

Figure 1. Block diagram of the electrical sequence of a saturable-reactor-controlled rectifier

Aircraft engine starting loads are very heavy, although the initial current drain is not nearly so severe with the direct-cranking starter as with the old inertia starter. Steady state current per starter is around 200 amperes, with a peak of 800 or more amperes.

Upon starting, the engines are run up, and in most cases the engine driven generators will come onto the line, operating in parallel with the ground power source. After warm-up, the engine speed may be reduced to a point where the generators will fall off the line. In any event, under ground operating conditions the generator cooling may be insufficient unless special ground cooling fans are installed, so that the generator cannot carry full capacity, and the ground power unit must be depended upon to carry the bulk of the load. This will be the case until the ground power supply is disconnected, and the airplane taxies out onto the flight ramp.

Under these final ground conditions, the ground power supply must be capable of supplying a minimum of 600 amperes continuously, and possibly up to 2,000 amperes. It must be emphasized here that if the ammeter of the power supply unit is watched, it rarely will go to the figures named, because the figures quoted here are possible maximums. However, a power supply designed for this load cannot be predicated on the lower figure, as the possible combination of loads that may occur is sure to overload the unit.

Character of Aircraft Electrical Loads

A large amount of the load on an airplane is purely resistive, such as lamps and heaters. For such loads, the change in current with change in voltage is linear, except in the case of lamps, where the lamp current at double voltage is about 1.6 times normal current.

The motor loads are mainly constant torque series motors, except for the fans, and the current remains relatively constant despite voltage changes. On series motors driving fans the line current will rise as the voltage rises, although not necessarily in a linear manner. Constant power loads, such as shunt motors driving fans and motor-alternators to supply 400 cycle current, tend to decrease in current as the voltage rises.

Most of the control systems in use in aircraft are independent of voltage changes, as they are ordinarily of the bridge type or the ratiometer type.

From the foregoing survey, it will be seen that voltage changes will be followed mainly by current changes, due to the

high lighting loads experienced. This may become critical if the voltage change is large and of any appreciable duration.

28-Volt D-C Regulation Requirements

The aircraft generating system ordinarily is adjusted to supply 28 plus or minus 0.25 volts on the bus, although the majority of the system components will work down to 18 volts with the exception of the motors which usually are rated down to 22 volts. The reason that a bus voltage of 28 volts was chosen is that the aircraft electric system is based on a 12-cell battery with a no-load fully charged voltage of 24 volts and a discharged voltage of 18 volts. The 4-volt differential is assurance that the battery is fully charged and ready for use in an emergency. A regulated bus voltage of 28 volts gives a load point voltage of 27 volts, assuming a 1-volt drop between the bus and the load.

The ground power supply should be regulated so as to supply this same voltage at the bus, regardless of load changes, and since there are rather long leads from the power supply to the airplane, the voltage at the power supply must be higher by the voltage drop in the supply leads. Means must be incorporated in the power supply device for measuring the voltage at or near the aircraft bus and regulating at that point; regulation at the power supply itself is useless, particularly where the loads are heavy and variable.

The ground power supply should be capable of voltage regulation that at least equals that of the airplane's electric system. That is, it should be capable of maintaining a voltage of 28 plus or minus 0.25 volts on the bus from light loads to full load conditions. The voltage dips and overshoots due to the application of heavy surge loads should be of very short duration. The overshoots particularly should be of low order and short duration, because of the possibility of burning out lamps and other equipment of this character.

Motor Ripple Requirements

The ordinary commercial motor is designed with wide margins on the magnetic circuit, but this is not true of the aircraft motor. Flux densities are high, and insulation is run at temperatures much higher than ordinary commercial practice. Nothing can be tolerated which will increase the heat generated in the motor. Ripple is particularly likely to be translated into heat when the iron is operated high upon the saturation curve, and a few per cent ripple may be the difference between successful operation and a burned out motor. Ripple, whether produced by the commutator action on a generator or the a-c ripple of a rectifier, should be held down to very low values, probably the maximum allowable should be five per cent at full load on the unit, with less than one per cent at light loads.

Radio Noise Requirements

A well designed aircraft electric system can tolerate a high level of radio influence voltage superimposed upon the bus without interfering with the operation of the radio equipment. This is done, of course, by proper filtering and shielding, and if the radio influence voltage (hereafter referred to as RIV) generators are located within the airplane the interference is generally very small. If, however, the RIV generator is located on an external unit connected to the airplane by cables, the ground return path of the RIV may be through the negative cable, the airplane fuselage, and through the airplane static ground device back to the generator. In extreme cases, where the power supply is the rectifier type fed from commercial primaries, the RIV generator may even be back in the hangar, so that the ground return path of the RIV is the whole area in which the airplane is located. The result is rather high field intensities which couple to the radio sets via the antenna.

The only practicable method of eliminating this RIV is by adequate filtering on the power supply device. This may be a very large problem in itself if the power device has to furnish currents in the order of 1,000 amperes. Filtering a circuit supplying this current is no mean task, requiring heavy duty elements. In any event, the ripple voltage should not exceed one per cent for a power supply designed to furnish power for radio checkouts, over this amount, the RIV may cause interference even in a well designed radio installation.

Polarity Reversal

Some means must be provided to prevent a reversal of polarity of the supply source if the airplane generators can feed back into the source. This is not a cause of concern on rectifier units, but may be serious on a motor generator set. Such protection should be integral with the supply unit, and also should incorporate provisions so that polarity reversal will not allow current to flow from the supply unit to the airplane.

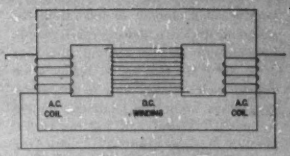

Figure 2. Saturable reactor windings

Paralleling With Aircraft Generators

Since the external power supply connects directly to the main bus, there is always the possibility that the ground power supply unit may be called upon to operate in parallel with the airplane's generators. This will always be so after the engines are started, because for several moments before the ground power unit is disconnected the airplane's generators and the ground power unit must operate in parallel. While at the moment no need exists for provisions for correct load division between the two sources, the regulation characteristics of the ground power unit must not be such as to cause hunting between the two sources on heavy applied loads. This means that in general the load regulation of the power supply unit should be better and firmer than the aircraft generators, which should not be too difficult at the low aircraft generator speeds that will obtain on ground conditions when the ground power supply unit is plugged in.

Portability

If the maximum use is to be obtained from the ground power unit, it should be capable of being used anywhere on the field; if necessary, being towed to the point of usage. In the case of a rectifier unit, this presupposes a power supply available at any location on the field where an airplane may be parked, which puts a very heavy load on the field facilities, since the power drain is so large that ordinary lighting wiring will not serve. A rectifier with a continuous capacity of 800 amperes at 28 volts, assuming 80 per cent over-all efficiency, will require an input of nearly 30 kw, which if fed from

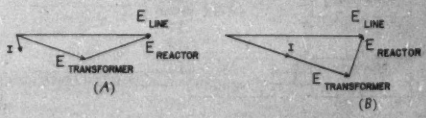

Figure 3. Vector diagrams of voltage controlled rectifier

commercial 440-volt 3-phase secondary windings will draw nearly 40 amperes per phase.

This phase of the problem will be dealt with more throughly in the next section of this paper.

Ground Power Supply for Aircraft

There are two general conditions that denote the status of any aircraft in service; ground operation and flight operation. An aircraft in flight condition is operating under its own power and both electric and hydraulic systems are supplied from the main power plants, or engines, through transducers. In flight the aircraft is under the control of the flight personnel and does not represent a direct problem to the ground personnel. However, mechanical, hydraulic, and electrical components in the airplane necessarily must be operated on the ground during loading, unloading, servicing, and maintenance when the aircraft's power plants are not operating. Any of these conditions constitute ground operations and an auxiliary source of power is needed to supply energy to these components. Since this discussion concerns only the electrical phase of the ground operation conditions, the term ground power supply will identify a source of electric power external to the airplane, as it is accepted universally in aircraft terminology. Also, since the rated bus voltage of commercial aircraft is 28 volts direct current, all ground power supply equipment described in this article is 28 volts direct current.

Types of Ground Power Supply

The two basic types of ground power supply are rotary equipment and static equipment. Rotating equipment consists of generators driven by several types of prime movers and static equipment refers to storage batteries and dry disk type rectifiers.

Rotating Equipment

Many types of rotary converters are in use at the present time and a description of these types is outlined in the following paragraphs.

Aircraft generators sometimes are used for ground power supply by driving the generator with V belts from a standard induction motor or gasoline engine. The belt drive is used to step up the generator speed above driving motor speed since aircraft generators are designed for operation at much higher speeds than standard 60 (or 50) cycle motor speeds. The type *0-1* aircraft generator is designed to deliver its full load rating of 100 amperes at a minimum speed of 2,500 rpm, as is the type *P-1*, which is rated at 200 amperes output. These two generators can be direct-connected to a standard 2-pole motor for constant speed operation at 3,600 rpm on 60-cycle systems. Aircraft type reverse current relays and voltage regulators are used for protective devices and control. The use of aircraft generators has not been very extensive because of cost and the problem of a special spline shaft coupling, together with a special bearing mount to prevent any radial loads from being imposed on the generator shaft, and a separate blower for adequate forced air cooling.

D-c arc welding generator sets also have been modified for use as ground power units by the use of standard aircraft regulators controlling the shunt field. Three-hundred-ampere arc welders require two regulators operating in parallel in order to handle the field current of the generator. Regulators of the older type, having a series of copper "fingers" for short-circuiting sections of a multitap resistor, proved better for this service than the carbon stack type. However, these modified arc welders were only a substitute device and were very troublesome in service. The cause of most of the trouble with these machines was frequent failure of the regulators to parallel satisfactorily, particularly on heavy load conditions, resulting in one of the regulators being forced to handle most of the field current and consequently failing because of this overload condition. As soon as one regulator failed the other one also would fail very shortly. In the modification of these welders, the lowest tap on the series (or cross) field is used, and large load currents cause an additional voltage drop due to the cross field effect on the armature reaction of the main field, causing the regulators to have more of a control problem. The only use of these modified arc welders has been as a last resort when better equipment is not available since an arc welder is designed basically as a constant current machine and even with the control modification its use as a constant potential machine has not been satisfactory.

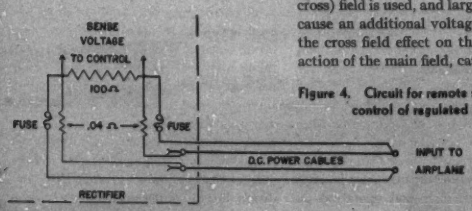

Figure 4. Circuit for remote sense voltage for control of regulated rectifier

The foregoing two types of rotary converters are not used very extensively in commercial practice but during the war were used by the armed services because of the shortage of adequate equipment. The latest designs in generators for use as 28-volt constant-potential machines tend toward more compact design by the use of higher grade steel in the magnetic circuits and welded frame construction. Some designers use the 2-bearing mounting where the prime mover and generator are supported only by the outer bearing point of each and are coupled rigidly together to eliminate the center bearing support. This method of construction is desirable only when the units are mounted on an adequate base and the mechanical coupling is of rugged design.

The exciter frame generally is mounted on the generator shaft end and coupled to the generator shaft by a standard flexible coupling in order to be easily removed for maintenance of the generator. Some generators are operated at high speeds—3,000 to 3,600 rpm—to achieve better cooling and thus be able to operate the armature windings at higher current densities. This is not a standard practice as the high speeds result in frequent bearing replacement and short brush life, together with excessive commutator wear. Recommended generator speeds for ground power service are from 1,400 to 1,800 rpm for the best compromise between effective cooling and mechanical life. Most generators are of the 4-pole type with interpoles for commutation, and straight shunt fields. The separately excited field in one design is operated at 125 volts in order to obtain a better amplification ratio and to keep the field current low, so that a single standard aircraft voltage regulator can be used. The exciter is a series generator with the voltage regulating resistance in series with the exciter and generator shunt field. This system results in very fast voltage recovery on load swings.

Another method used to limit the amount of field current through the voltage regulator is to connect an aircraft type voltage regulator in parallel with a fixed resistance in order to by-pass a portion of the field current around the regulator. This method is not desirable and reports from the field indicate unsatisfactory voltage regulation of this design.

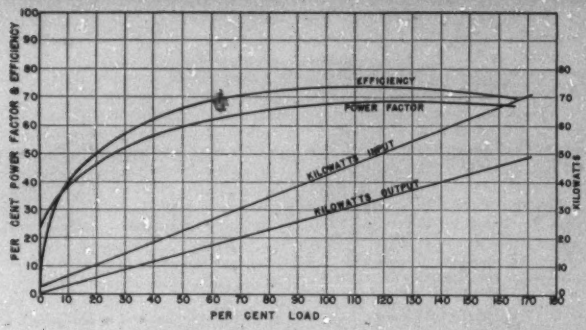

Figure 3. Performance curves of 1,000-ampere 28-volt d-c regulated rectifier

The output circuit should have a reverse current relay, overvoltage relay, and an undervoltage relay for protective devices.

General Comments on Rotary Converters

Compound generators are not desirable for ground power service because of the possibility of polarity reversal due to reverse current in the series field caused by the airplane generators feeding back. Normally the reverse current relay will clear the generator off the line but several cases have been reported where a relay failed to clear the generator and considerable damage was done to the airplane electric system.

Self-excited generators do not have as good voltage recovery characteristics as separately excited generators and are not recommended for ground power service. Until recently, generators for ground power service have not been made in ratings larger than 500 amperes. The problem of paralleling two generators for greater outputs involves the use of equalizing windings.

Commutation ripple, while not large in magnitude, causes radio interference and rotary converters require filters in the output to limit the RIV.

Portability

It is necessary to keep the voltage drop in the d-c leads to the airplane as low as possible and for this reason ground power units are mounted on a portable chassis and brought to the airplane. Unfortunately, very few airports have a-c power available on the flight ramps and it is necessary to use gasoline engines as prime movers for the ground power supply, which constitute a fire hazard to the airplane; especially so when the airplane is being supplied with gasoline at the loading ramp. For this reason, gasoline-engine-powered ground power units are located not less than 50 feet from the airplane which imposes a voltage drop problem in the long d-c cables necessary. The use of large cables in parallel (0000–0000 welding cable is standard) will keep the IR drop to a low value, but they are very cumbersome to handle.

Static Type of Ground Power Supply

The conventional lead-acid storage battery was the first—and simplest—type of ground power. Two 12-volt batteries were installed in a simple box cart and used for starting engines and for maintenance work. The growth of electric loads in the modern aircraft and the starting of large engines has outmoded the use of the battery alone. The next step was a small generator with batteries, but this too is now obsolete.

Dry disk metallic oxide rectifiers have been gaining in favor as a desirable ground power supply. Its advantages are quiet operation, long life, and especially the inherent high reverse resistance. Of the three commercial types of rectifiers namely, cuprous oxide, cupric sulphide-magnesium, and selenium, the selenium type has the most in its favor for ground power service—high inverse voltage and practically constant characteristics. Although the current density per plate is lower than the copper types, the additional size of the selenium stack over a comparable cupric sulphide type is compensated by the higher voltage rating per plate. The selenium rectifier is a comparative newcomer in the ground power field and rapidly is gaining over the other two types in the latest designs.

The voltage regulation of a simple rectifier system is poor, but this factor has not been important in ground operation on older styles of aircraft. However, it is very unsatisfactory for the latest type of commercial transports, because of the more critical components. The design of a voltage-regulated selenium-type portable rectifier is described later in this paper. Eight of these units are in actual service and reports indicate excellent performance, not only in servicing of commercial transport models, but in the starting of experimental engines where loads of 1,200 amperes at 28 volts are required for a period of 20 seconds. Performance curves of a 1,000-ampere 28-volt regulated selenium-type rectifier with resistive load are shown in Figure 5.

Ratings for Ground Power Supply Units

In determining the design rating of a ground power supply, the maximum ground operating load of the airplane must be considered. Even though this load rating may never be reached in service, the load factor nevertheless must be taken as 100 per cent. This is explained best by the fact that even though the airplane may represent an intermittent load condition, it is very possible that it may maintain its ground load condition much longer than expected and a power supply unit design based on 1/2-hour or even 1-hour rating will have a short life. The emphasis of consideration is not on the economics of the ground power supply design, but rather on the airplane. Where close to a million dollars investment in the airplane is compared to the investment in ground equipment and the possibility of loss of passenger confidence due to a failure of ground power, or even the worse condition of failure of an electrical component in the airplane due to faulty operation of the ground power supply, the major consideration must be on an adequate rating and design for all possible expected conditions. Also, the investment in ground equipment should be made with future requirements, so far as predictable, in mind.

Field Performance

Figure 6 is an oscillographic record of the control response time of a 1,000-ampere voltage-regulated portable ground power rectifier, and Figure 7 is the record taken with a 500-ampere gasoline engine-driven portable generator with a series exciter and mechanical aircraft-type voltage regulator. These oscillograms were made during maintenance operations on a new commercial transport aircraft and the current traces show an average load condition during ground operation. In both

cases, the load change was caused by turning on one of the 400-cycle 115-volt 3-phase inverters in the airplane. The response time of the rectifier-type ground power supply shows excellent control recovery.

Design of a Voltage Regulated Rectifier

General Requirements

The specifications for a modern ground power supply already have been outlined in the first part of this paper. Of these requirements, one of the obstacles to the use of rectifiers has been that of voltage regulation. Normal no-load to full-load voltage regulation for the average selenium rectifier is 10 per cent to 18 per cent. Much of this regulation occurs in the first 15 per cent of load. By use of bleeder loads, it is possible to reduce the regulation to approximately 8 per cent. However, this is rectifier regulation alone and does not take into account the drop in either the a-c lines to the rectifier or d-c lines from the rectifier to the airplane. Considering the fact that the rectifier often will be operated at the end of a long power line, the need for compensation of the a-c line drop becomes apparent. Even with short cables, currents of 1,000 to 1,500 amperes will give a 5 to 10 per cent voltage loss in the d-c leads from the rectifier to the plane. The over-all regulation of the unregulated rectifier easily becomes 20 per cent or more.

The addition of an electronic control to the rectifier produces a ground power supply with all of the desired regulation and operating flexibility. Variations in the a-c supply voltage can be corrected automatically, the inadequate natural regulation of the rectifier can be taken care of, and compensation for the drop in the d-c cables provided by this means. The electronic control also furnishes a means of fine adjustment of the rectifier output voltage.

Regulated Rectifier—Basic Elements and Design

The basic elements of a regulated rectifier (Figure 1) are saturable reactors, transformers, selenium rectifiers, d-c power filter, remote sense circuit, and the electronic control. A "sense" or control potential from the d-c output of the rectifier is fed through the remote "sense" circuit to the electronic control. In the control this "sense" voltage regulates the saturating current through the d-c coils of the saturable reactors. Thus the signal from the d-c output regulates the

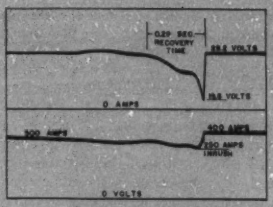

Figure 6. Oscillogram of regulated rectifier under actual service conditions

a-c drop across the reactors which in turn governs the voltage applied to the transformers and the rectifiers. Should an increase in load tend to cause a drop in the d-c output, the control saturates the reactors enough to raise the rectifier input voltage an amount sufficient to compensate for the load increase.

The basic design of a regulated rectifier begins at the d-c output and works back to the a-c input. Adding the voltage drops through the filter choke and d-c bus to the required maximum direct voltage output under full load gives the peak direct voltage to be supplied from the rectifying elements. Using this figure and computing the drop through the rectifier cells, the designer then has the maximum alternating voltage the transformers must supply the rectifiers. Since the voltage to the transformers is controlled by the reactors, the primary transformer voltage will be less than line voltage. The saturable reactors must have a minimum impedance at full load and a maximum at no load. The reactor construction and total control range will govern the saturating current required of the electronic control. Control sensitivity will be predicated upon the necessary over-all voltage regulation.

The design of the electronic control is straightforward. The "sense" voltage from the remote sense circuit is first "derippled" by a low pass filter with a very short time constant. It is then compared against the voltage developed across a potentiometer that in turn is connected across a constant standard voltage obtained from a gaseous voltage regulator tube. By adjusting the potentiometer, the rectifier output voltage may be set where desired. The difference between the "sense" potential and the potentiometer voltage is applied to the grid of a single-tube d-c amplifier. This amplifier, with a gain of approximately 250 to 1, is the heart of the control and governs the phase of the thyratrons' a-c grid voltage by means of an a-c phase shifting network. These thyratrons form a full wave adjustable rectifier to supply saturating direct current to the reactors.

Many methods of varying the alternating voltage supplied to the rectifiers were considered, among them being motor driven autotransformers, induction regulators, ignitrons, and saturable reactors. The response time of the induction regulator motor drive was considered to be too low. Ignitrons pose the problem of a cooling system—and with phase shift control would introduce more ripple into the d-c output. Saturable reactors seem the most economical solution, offering a simple, dependable, efficient system of voltage control.

To adjust the voltage to the 3-phase rectifiers, three reactors of the 3-legged type are used (Figure 2). The a-c coils of the outer legs are connected so that none of the a-c magnetic flux couples with the d-c coil on the center leg. However, the d-c flux of the saturating coil on the center leg flows out of the center leg to divide and flow through the outer legs, reducing their magnetic permeability. By careful design and with the two a-c coils of each reactor connected in series, the total time constant of the reactors can be reduced to less than one second.

Saturable reactors are quite efficient and yet a very wide range of control can be obtained. For example, a typical 1,000-ampere 30-kw regulated ground power supply is capable of continuous voltage adjustment from 25 volts to 30 volts. The output voltage is held within one per cent from no load to full load, and there is enough leeway left in the reactors to compensate for a 10-per-cent supply line fluctuation. This range of control is obtained with less than 350 watts of saturating power.

The no-load to full-load line demand characteristics of the rectifier and its transformers are rather convenient for operation with saturable reactors. At no load, the rectifier will demand from the line little more than the transformer excitation current. Since this excitation current is largely inductive, it will produce maximum voltage drop across the inductive reactors (Figure 3*A*). Under load, the transformer current is resistive which is fortunate, for to produce 95 per cent of the line voltage across the transformer, it is necessary to reduce the reactor drop to a vectorial quantity which is not 5 per cent, but approximately 30 per cent of the line voltage (Figure 3*B*).

Reactors must be designed between two limits. At full load the reactor impedance must be low enough to cause the reactor drop to be no greater than the vectorial difference between the minimum

line voltage that can be expected and the maximum required transformer voltage. For no load and a minimum d-c output voltage, the transformer excitation current through the unsaturated reactor must produce a drop equal to the vectorial difference between maximum possible line voltage and the minimum transformer input voltage.

Transformers, Rectifiers, D-C Filter

Because of the ripple requirements of the ground power supply, it is necessary to consider the over-all transformer, rectifier, and d-c filter design. In the larger units (1,000 amperes or more), the rectifier has been broken down into two sections, each with its own 3-phase transformer. The outputs are paralleled to give full rating. This arrangement reduces the size of the components and makes a compact assembly. Both transformers have primary and secondary windings connected in delta to give a 3-phase input to the rectifier. The rectifiers are assembled into a 3-phase full-wave bridge which will produce a ripple voltage that is 5 per cent of the d-c output and with six times the supply line frequency. Filtering, therefore, is necessary to reduce the ripple content of the d-c power to the 1 per cent or less required of ground power supplies.

Before using the 3-phase bridge with its 5 per cent total ripple, a 6-phase bridge giving a theoretical 1.4 per cent ripple content with a basic component of 12 times the supply line frequency was considered. Such an arrangement appears ideal at first glance, for not only is the ripple considerably lower, requiring less filtering, but also the ripple frequency is higher, making filtering still easier. However, experience has proved that 1.4 per cent ripple is obtained from the 6-phase bridge only under ideal conditions. It is quite common to find up to 3 per cent phase unbalance on 220- or 440-volt 3-phase supply lines. There is also the possibility of some small difference between phases in the resistances of the rectifier elements or some small phase unbalance in the output of the 6-phase transformer. The result is that while the higher frequency ripple components of a 6-phase bridge may be only 1.4 per cent, there is a possibility of a 60-cycle component of as high as 1 or 2 per cent caused by phase unbalance. As conservative design necessitated a filter capable of reducing a 3-per-cent phase unbalance to less than 1-per-cent rms ripple, there seemed to be no justification for using anything other than the simple 3-phase bridge. A check of the filter requirements shows that a filter large enough to reduce the 60-cycle phase unbalance will be more than ample for the 360-cycle ripple.

Filter design for a regulated rectifier presents the problem of obtaining sufficient attenuation of 50- or 60-cycle ripple voltages when carrying very heavy d-c currents with as low a direct voltage loss as possible. Although the electronic control will compensate for the d-c drop through the filter choke, this voltage drop does represent power loss and forces upon the saturable reactors a greater control range to maintain the output voltage. While inductance is obtained from additonal turns, additonal turns mean more d-c resistance. A compromise is necessary. A typical ground power supply filter choke will have a d-c drop of 1 volt when carrying 1,000 amperes. Since the resistance of the d-c load would be 0.28 ohm at 100 amperes, the inductance of the filter choke does not have to be much over 0.002 henry to obtain the required alternating voltage divison between the choke and the load. By using a choke with a nonlinear air gap, it is possible to obtain a "swinging" choke effect that will give the necessary filtering between approximately 100 amperes and full load without the use of filter capacitors.

Remote Sense Circuit

Even with large d-c cables, the ground power currents of 1,000 to 1,500 amperes probably will cause a loss of 1 or 2 volts in the cables from the ground power unit to the airplane. The electronic control of the rectifier automatically can correct for these drops if the controlling "sense" voltage is taken from the ground power plug at the airplane. To obtain this remote "sense" potential, a pair of small auxiliary leads must parallel the d-c power cables from the rectifier. Considering the hard usage ground power equipment normally experiences, these auxiliary leads could introduce the possibilities of equipment failure. For example, the auxiliary leads could be broken, short-circuited, or reversed. Any one of these conditions would feed a false signal back to the rectifier.

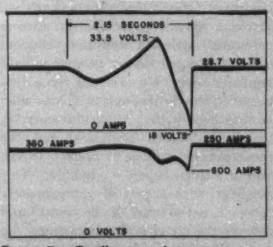

Figure 7. Oscillogram of generator power supply under actual operating conditions

The remote sense circuit (Figure 4) is a simple arrangement to eliminate these possibilities. The potential at the end of the d-c power cables is brought back by a pair of light auxiliary leads through 3-ampere fuses to the electronic control. A connection also is made from the d-c output terminal on the unit through small 0.4-ohm resistors to the electronic control. Thus, if the auxiliary leads should be disconnected or broken or be cross connected, causing the 3-ampere fuses to blow, the control still will receive a signal through the 0.4-ohm resistors.

Antihunt-Response Time

A glance at the block diagram (Figure 1) shows that the regulated rectifier circuit constitutes a positive feed-back system with the corresponding possibilities for hunting. Two major time constants are involved—that of the magnetic circuit and of the electronic control. Permanent stable operation can be achieved by adjusting the resistive values of either the magnetic circuit or the control.

The response time of the unit will be governed largely by the time constant (L/R) of the d-c saturating circuit of the reactors. Since the control cannot anticipate load changes, a variation in loading will cause an instantaneous change in output voltage. The control immediately tries to return the direct voltage to its original value by saturating or unsaturating the reactors. When the time constant is kept well under one second, load changes are hardly noticeable

Construction

Ground power supplies can be made either stationary or mobile. Mobile units are the more popular for present day flight operations. However, stationary supplies often are found in service hangars and if permanent "deplaning" positions are finally evolved along with a movement to eliminate service vehicles from the field, the stationary unit will be employed further. Remote "sensing" should be especially useful for the stationary supply.

The construction of a mobile 1,000-ampere regulated rectifier is shown in Figure 8. A 3-point type suspension is used with pneumatic tires. The mechanical assembly is dictated by the electrical sequence. The cart is headed by the three reactors which are followed by the two power transformers. The second-

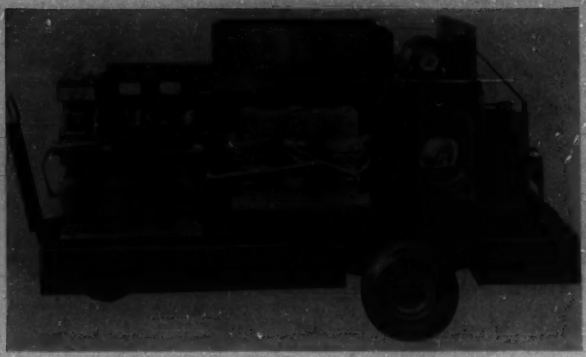

Figure 8. A 1,000-ampere voltage-regulated rectifier

aries of the transformers feed into the selenium rectifier assembled into an air duct in the center of the cart. Following the rectifiers are the centrifugal blowers which pull air through the bottom of the cart, up through the selenium cells to be exhausted to the rear. For compact design, two smaller blowers in tandem have been used instead of one large blower. The d-c filter choke is mounted on the end of the cart. D-c output terminals are mounted under the base plate where they are protected from accidental collisions and short-circuiting.

Performance

The operating record of regulated rectifiers has been very satisfactory. Maintenance has been negligible. The selenium rectifiers offer indefinite life, while conservative operation of the control vacuum tubes makes failures extremely rare. The ripple component of between one-half and one per cent allows interference-free operation of the most sensitive radio equipment. Voltage regulation is less than one per cent from no load to full load. Supply line fluctuations of up to ten per cent are compensated for. A 1,000-ampere unit has provided good regulation on loads up to 1,700 amperes.

Conclusions

The very large increase in electric loads on aircraft now in production and the definite trend toward still larger loads has made it necessary to review present ground power facilities.

The change to a-c systems in airplanes will be gradual with the result that d-c systems will continue to be used for some time. In view of this, larger d-c ground power capacity must be provided by some means. The method of doing this will be governed to a great extent by the conditions at the individual fields. Where adequate a-c power is available within reasonable distance of the field, the best long range solution appears to be the utilization of this power. The initial cost of providing proper a-c power on the flight ramp will be more than balanced by the flexibility, convenience, and lower operation and maintenance cost of units such as described in this paper.

References

1. Saturable Reactors for Automatic Control, W. D. Cockrell. *Electronic Industries* (New York, N. Y.), volume 5, 1946, pages 48–53.

2. Electronically Controlled Dry-Disk Rectifiers, A. Rosenstein, H. N. Barnett. AIEE Transactions, volume 63, 1944, January section, pages 21–3.

No Discussion

A Simple and Inexpensive Method for Accurately Measuring Steady-State and Transient High Voltages

H. L. LEVINTON
MEMBER AIEE

Synopsis: This paper presents a simple method for accurately measuring voltages present on high-voltage systems during both transient and steady-state conditions without modifying the conditions producing the voltage to be measured. An electronic amplifier having high input resistance and negligible circuit loading provides adequate current to operate magnetic oscillograph galvanometers (or meters and relays) in proportion to the input voltage obtained from capacitance voltage dividers. These may be transmission line switching-transient voltages, voltages across circuit breaker contacts, static capacitor transient voltages, or neutral displacement voltages. Frequencies ranging from direct current to a hundred or more kilocycles are within the capability of the device, although the actual value, determined by the indicating or recording instrument which it actuates, may be limited to a few thousand cycles. Limitations and problems encountered in the use of capacitance potential dividers are also briefly discussed.

THIS PAPER presents a solution to a problem which has vexed power system engineers for some time, namely, how to record accurately voltage on high-voltage systems during transient and steady-state conditions, particularly where the measuring device must not modify the conditions producing the voltages to be measured and which would be considerably less expensive than a conventional high-voltage transformer.

This solution to the high-voltage measurement problem resulted from difficulties which the Bonneville Power Administration encountered during 230-kv system tests several years ago, particularly during line-switching tests in which restriking occurred. Inaccurate and erratic results led to the development of the device covered by this paper which had as its immediate objective the accurate recording of transient and steady-state voltages by electromagnetic oscillographs within the accuracy of potential dividers and the recording ability of the oscillographs. The device itself, which for clarity will hereafter be termed an amplifier, can have almost unlimited frequency response range, the records obtained being limited by the frequency response characteristics of the oscillograph galvanometer or recording device. Even with conventional oscillograph galvanometers, results generally will be almost as useful and valid as those obtained with sealed-tube cathode-ray equipment during system tests because of the comparatively low rate of voltage change encountered as compared with impulse testing rates of voltage change.

Methods Used to Measure High Voltages

High voltages on electric power systems are measured most commonly by means of potential transformers, capacitance potential devices, and infrequently, voltage dividers.

1. Potential transformers give secondary voltages accurately proportional to the primary voltage over a wide variation of steady-state alternating voltage and are very appropriate for normal operating conditions. However, they are very expensive in the higher voltage ranges, and of greater technical importance; they may produce their own transients during rapid changes in applied voltage. These transients may so seriously distort the character and magnitude of the secondary voltage that it does not represent the applied primary voltage. Another limitation is that potential transformers cannot respond, except momentarily, to direct voltages which may be present, such as the trapped charge remaining on a transmission line following charging-current interruption; potential transformers also represent drain paths for such charge conditions.

2. Capacitance potential devices[1,2] are of a resonant character and being tuned to function over one narrow band of frequencies are by their very nature not appropriate for the measurement of the range of frequencies encountered during high-voltage system transients. Although inherently not very accurate, potential devices receive wide use where their limitations are not troublesome, such as in switchboard voltage indication, synchronizing service, and in some relay applications.

3. Voltage dividers for high-voltage measurement often have been considered as being more suited to laboratory use than field test use, probably because resistance dividers were considered. For high-voltage applications, resistance dividers are usually cumbersome and require great care to minimize capacitance effects where alternating currents are being measured. However, capacitance dividers are comparatively stable devices which, when noninductive and when having low leakage, are suitable for voltage measurement use over a wide range of frequencies including direct current. Voltage dividers are used with the amplifier device covered by this paper; capacitance dividers usually being employed for high voltages because of their more easy application, although either capacitance or resistance dividers may be used. Certain precautions which are believed necessary whenever capacitance dividers are used will be discussed later.

Figures 1 and 2 illustrate some of the points which have been discussed so far. Trace 3 of Figure 2 shows a record of a trapped charge remaining on a transmission line following the interruption of charging current without restrike; the trapped charge voltage corresponding to

Paper 47-203, recommended by the AIEE committees on instruments and measurements, and power transmission and distribution, and approved by the AIEE technical program committee for presentation at the AIEE Pacific general meeting, San Diego, Calif., August 26-29, 1947. Manuscript submitted June 26, 1947; made available for printing July 9, 1947.

H. L. LEVINTON is electrical engineer with the Bonneville Power Administration, Portland, Oreg.

The author wishes to acknowledge the helpful suggestions of A. Dovjikov (M '41) and R. C. Starr (M '29), and the valuable laboratory assistance of R. M. Holland and A. Kinyon (A '44).

Figure 1. Line switching test

Phase *A* voltage from three sources

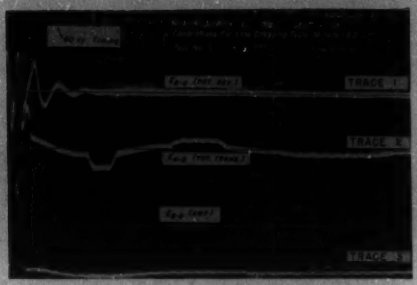

Figure 2. Line switching test showing trapped line charge on phase *B* (trace 3)

the 60-cycle instantaneous voltage at the moment of capacitive current zero, when interruption takes place. This record was made by an amplifier energized from a capacitive voltage divider. The slow decay of this record resulted from three causes

1. A high resistance across the grounded capacitance unit gave an RC time constant of approximately one second.
2. The 230-kv transmission line leakage.
3. Capacitance leakage which was negligible.

The slight low-frequency oscillation on the trapped voltage record was induced by another phase as will be explained later.

Trace 1 in Figure 2 shows the secondary voltage of a capacitance potential device connected simultaneously to the same phase as the amplifier of trace 3. Trace 2 shows the general form of the secondary voltage to be expected from a potential transformer when subjected to trapped line charges. The potential transformer was not connected to the same phase as the amplifier used for recording trace 3 because the potential transformer drains the line and modifies the test conditions. Not only does the potential transformer drain the line, but because of its inductance it produces line oscillation because of the interchange of energy between the line capacitance and the transformer inductance. This effect on the line is shown by trace 3 in Figure 1 where the low-frequency line voltage oscillation is shown clearly. This low-frequency oscillation also appears on the other phases to a slight extent by capacitance coupling between the line conductors as is shown in trace 3 in Figure 2. The three voltage traces of Figure 1 were obtained from three devices connected to the A-phase conductor. Trace 2 is the potential transformer secondary voltage for the line condition of trace 3; and trace 1 is a record of the output voltage of a capacitance potential device for the same line condition–three entirely different records of the same phase-to-ground voltage.

Summarizing, the true unidirectional voltage of the line following the interruption of charging current (trace 3, Figure 2) is modified by the presence of a potential transformer to a low-frequency oscillation voltage (trace 3, Figure 1) which the potential transformer reproduces as a distorted wave (trace 2 in Figures 1 and 2). The capacitance potential device output voltage records are also incorrect although very alike for both the unidirectional line voltage condition (trace 1, Figure 2) and for the low-frequency oscillatory line voltage condition (trace 1, Figure 1). Furthermore, although no oscillographic illustrations are given in this paper, shock excitation of potential transformers from restriking conditions or from the more rapid rates of recovery voltage rise following fault clearance may produce secondary voltage components of higher than 60-cycle frequency because of leakage inductance and distributed capacitance. These components may prove troublesome when investigating generator characteristics and line reflections.

Capacitance Potential Dividers

Capacitance potential dividers were chosen for use with the amplifier because of their convenience. Without any special installation, they are usually available in 230-kv switchyards in the form of bushing taps, carrier coupling capacitors, or even insulator units; when not otherwise available, special capacitance divider installations are installed easily.

All of these installations result in higher voltage between ground and the lowest voltage point on the divider than can be used conveniently, the voltage generally ranging from 3,000 to 30,000 volts. Therefore, it is necessary to place supplemental or auxiliary capacitance between ground and the tap point to lower the tap voltage to ground to a value ranging between a few volts and a few hundred volts, depending on the nature and purpose of the installation. Auxiliary capacitance values range from 10 or 20 microfarads when low tap-to-ground voltage is desired to 0.1 microfarad for higher values of tap-to-ground voltage. Exact values may be obtained from the equation

$$E_{T-G}=E_{HV-G}\times\left(\frac{C_{HV-T}}{C_{HV-T}+C_{T-G}}\right)$$

where E_{HV-G} is the capacitance divider voltage from the high-voltage point to ground, E_{T-G} is the divider voltage from the tap point to ground, C_{HV-T} is the divider capacitance from the high-voltage point to the tap point, and C_{T-G} is the divider capacitance from the tap to ground.

A few comments regarding the characteristics of the auxiliary capacitors are considered pertinent at this time because of inaccuracies which they can introduce. For high-voltage measurements the capacitance between the high voltage and tap points (C_{V-T}) is so much smaller than the tap-to-ground capacitance (C_{T-G}) that the variation of C_{T-G} over a fairly wide range will result in only second order variations in the current (I_c) through the divider, or I_c may be said to be determined by C_{HV-T}. Assuming that C_{HV-T} is a true capacitance and that its reactance decreases directly with frequency ($X_c=1/2\pi fC$), I_c will increase directly with frequency so long as the voltage magnitude remains constant. The tap-to-ground voltage (E_{T-G}), being the product of the current and the reactance of the tap-to-ground capacitor (I_cX_{cT-G}), will be pro-

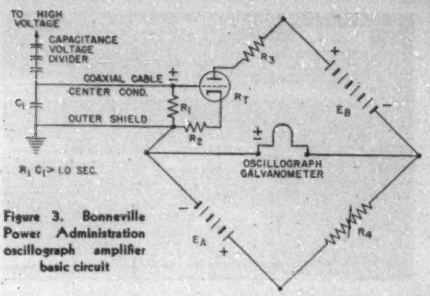

Figure 3. Bonneville Power Administration oscillograph amplifier basic circuit

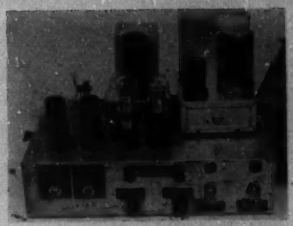

Figure 5 (right). Bonneville Power Administration oscillograph amplifier

Weather resisting cover open

portional to the high voltage only when X_{cT-G} decreases directly with frequency. However, if X_{cT-G} does not decrease directly with frequency for any reason, such as changing capacitance of the auxiliary capacitor with frequency, voltage proportionality will not be maintained.

Cylindrically wound foil capacitors are believed to display this nonlinear characteristic even when the ends of the foil turns are connected together because protective film cutouts connected across C_{T-G} set for 20 times E_{T-G} at 60 cycles have been punctured during rapid rates of voltage change on the system such as may occur with restriking or following a fault. These film-cutout punctures have not occurred when parallel plate capacitors such as mica capacitors have been used, or where the cylindrical foil capacitors have been shunted with mica capacitance to the point where the mica capacitor itself can hold the 60-cycle tap point voltage E_{T-G} to a value below the film-cutout puncture value. The explanation of this phenomenon, which the author regards as most likely correct, is that the self-inductance of the foil capacitors forces the large instantaneous current value occurring during rapid voltage change to the outer layers of the cylindrically wound capacitor, producing a "skin effect" which momentarily decreases the effective capacitance of the auxiliary capacitor, thereby raising its X_c, which in turn raises the tap point voltage E_{T-G} to a value sufficient to puncture the film cutout even though the high voltage does not rise above normal.

A similar effect, though to a lesser degree, may occur with parallel plate capacitors. This has not been investigated due to lack of necessary equipment; however, qualitative data indicate that the mica capacitors are reasonably free of the effect discussed. It is believed that those using cathode-ray equipment to record very high rates of voltage change by means of capacitor voltage dividers might well investigate the effects of this "skin-effect" phenomenon on voltage measurement accuracy.

Insofar as magnetic oscillography is concerned, the use of mica capacitors or mica capacitor shunting of foil capacitors is considered adequate because the effects discussed are far too rapid for the magnetic oscillograph to follow, and the mica capacitors are used merely to safeguard the capacitor installation and to prevent film-cutout puncture.

Returning to the problem of voltage measurement with capacitance potential dividers and assuming that suitable capacitors have been employed so that the tap voltage is proportional to the system high voltage, it is desired to record the system voltage on a magnetic oscillograph for co-ordination with other quantities simultaneously recorded or measured. Again certain precautions must be observed.

When constant voltage is applied to a capacitance voltage divider the current through the divider will vary with frequency since the reactance of a capacitor decreases with frequency. Consequently, measuring devices requiring current for their operation will be supplied with a current proportional both to voltage magnitude and frequency. Therefore such devices are considered unsuitable for voltage measurement.

Measuring devices requiring only voltage for their operation will respond only to voltage magnitude when connected across a section of a capacitance voltage divider because the voltage division ratio of a capacitance divider remains constant with frequency although the current through the divider varies with frequency. The presence of resistance in the measuring device will introduce both magnitude and angle errors in the voltage indications. Analysis of the vector diagram of the divider-measuring circuit shows that the indicated voltage magnitude will be

$$\frac{R}{\sqrt{R^2+X_c^2}}$$

of the true voltage of the divider.

Figure 4. Bonneville Power Administration oscillograph amplifier circuit diagram

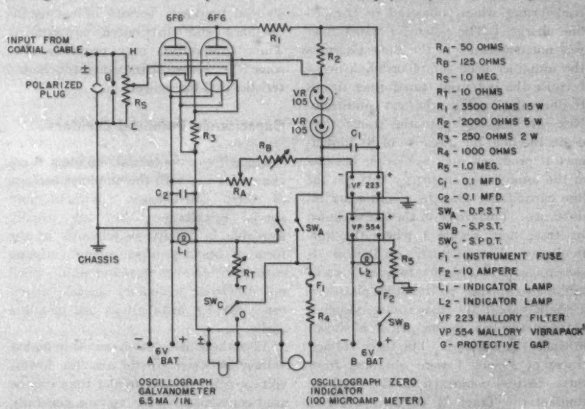

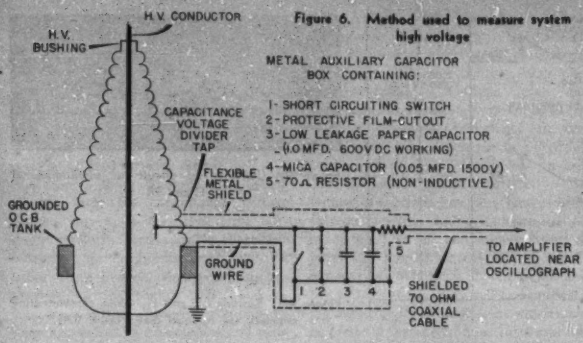

Figure 6. Method used to measure system high voltage

The angular displacement will be

$$\theta = \tan^{-1}\frac{X_c}{R}$$

where R is the resistance of the measuring device, X_c is the capacitive reactance of the divider section across which the measuring device is connected, and θ is the angle in degrees by which the indicated voltage leads the true voltage.

By making R very large compared to X_c for the lowest a-c frequency to be measured, voltage proportionality will be obtained with negligible error at the lowest a-c frequency to be measured and with decreasing error as the frequency becomes higher due to decreasing X_c. At the same time, if the RC of the circuit (R of the measuring device in ohms times the capacitance C of the capacitance divider section involved in farads) results in a time constant of a second or more, the rate of exponential decay of the voltage of the capacitor section will be slow enough to permit reasonably accurate determination of direct potentials which may be applied to the capacitance divider.

An example of the results to be expected is the use of a measuring device having a resistance R of 1,000,000 ohms which shunts a 1.0-microfarad capacitance divider section C having an X_c of 2,650 ohms at 60 cycles. The voltage indication will be

$$\frac{R}{\sqrt{R^2+X_c^2}}\text{ (true voltage)}$$

$$=\frac{1{,}000{,}000}{\sqrt{(10^6)^2+2{,}650^2}}\text{ (true voltage)}$$

or practically true voltage. The angle θ by which the indicated voltage leads the true voltage is

$$\tan^{-1}\frac{X_c}{R}=\tan^{-1}\frac{2{,}650}{1{,}000{,}000}=0.15\text{ degree}$$

which again cannot be distinguished on the usual oscillogram. The d-c time constant RC is

$$(1{,}000{,}000\text{ ohms})(1\times10^{-6}\text{ farad})=1.0\text{ second}$$

During the time corresponding to one cycle on a 60-cycle base (0.0167 second) a direct voltage will decay only about one percent of its original value.

Vacuum-tube circuits are readily adapted to the conditions indicated and provide a flexible means of meeting almost any desired operating condition. They are the basis of the Bonneville Power Administration amplifier, device. Before actually proceeding to a discussion of the amplifier it may be well to note that it is possible to meet the conditions without an amplifier if adequate capacitance, C_{HV-T}, is available between the high-voltage bus and the tap point to result in a fairly high voltage value across large auxiliary capacitors C_{T-G} between the tap and ground.[3] For these conditions sensitive galvanometers in series with moderately high values of resistance may be connected directly across the auxiliary capacitors for voltage measurement. This procedure often results in low deflection amplitudes, low-response frequency range (due to the use of very sensitive galvanometers), limited application because of the high value of C_{HV-T} required, and time constants so low that direct potential decay may be too rapid to permit accurate measurement across circuit breakers during opening operations.

The Amplifier

Any of a number of vacuum-tube circuits may be used for producing relatively large currents which are proportional to the voltage obtained from the capacitance dividers. These circuits may represent amplifiers, bridges, oscillators, modulators, cathode-followers, and so on as may be desired, providing they meet the requirement of operating over the necessary range of frequencies with adequate accuracy.

The Bonneville Power Administration device utilizes the amplifier-bridge type of circuit shown in Figure 3. This particular circuit, developed in January 1944, when materials were scarce, was designed to operate moderately sensitive magnetic oscillograph galvanometers from an amplifier made from available radio parts. A further requirement was that the amplifier could be operated from 6-volt storage batteries at locations where power sources including station batteries might be subject to transient voltage variations during staged tests. This form of amplifier is so simple and has given such good results that although a number of different designs have been considered, several duplicate amplifiers have been constructed for use during tests.

The bridge action of the circuit is shown in Figure 3. One arm of the bridge consisting of the tube cathod resistor R_3, the tube internal resistance R_T, the load resistor R_5, and the battery E_B; the second arm consists of resistance R_4 and battery E_A. With no signal on the tube grid, the current through the galvanometer from one arm is balanced by the current in the other arm through adjustment of resistor

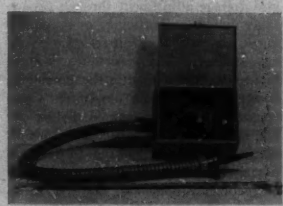

Figure 7. Auxiliary capacitance box and bushing tap fitting

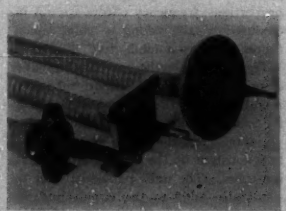

Figure 8. Three types of bushing tap fitting used with the capacitance voltage dividers

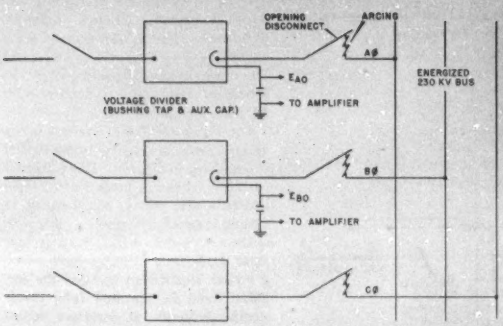

Figure 9A (left). Test circuit for oscillogram of Figure 9B

Figure 9B. Bushing E_{AO} and E_{BO} while disconnecting switches are opened (see Figure 9A)

R_4 until the galvanometer has zero deflection. The application of a voltage to the grid changes the tube resistance, unbalances the bridge, and deflects the galvanometer. Positive signal voltages decrease the tube internal resistance and negative signal voltages increase the tube internal resistance, thereby deflecting the galvanometer in opposite directions from its null or zero grid voltage position.

The tube also functions as an amplifier in that, while it produces an output current proportional to its grid signal voltage, it may be considered as amplifying the small signal current in its grid resistor R_1 circuit to a value sufficiently high to operate the galvanometer. The galvanometer deflection may be controlled by grid voltage adjustment through capacitance divider proportioning or by replacing R_1 with a grid circuit resistance voltage divider. The resistance voltage divider method is used in the Bonneville Power Administration amplifier. Compensation of the resistance divider for wiring and tube capacitance effects normally is not required due to the comparatively low frequency response limit of magnetic galvanometers; however, if frequencies above 10,000 cycles per second are to be recorded, this correction should be considered. Where deflection amplitude is adjusted by capacitance divider proportions, frequency effects are not introduced by the wiring or tube capacitances if R_1 is noninductive.

Figure 4 shows the complete amplifier circuit. Type *6F6* pentode tubes are used because of their comparative linearity and insensitiveness to plate voltage variation when the screen grid voltage is kept constant by the two *VR-105* regulating tubes. The unby-passed cathode resistor also adds to the circuit linearity through its degenerative feed-back action. Two *6F6* tubes in parallel provide a linear galvanometer current of 18 milliamperes direct current which is sufficient to give 5.5 inches peak-to-peak deflection to a galvanometer having a sensitivity of 6.5 milliamperes per inch. Larger tubes or more in parallel would require larger battery power sources and would decrease the general portability of the equipment. The sensitivity of the amplifier is approximately 1.6 galvanometer milliamperes per volt applied to the tube grids.

It should be noted that the vibrator voltage supply is insulated from the amplifier chassis except for the 1-megohm resistor. This is required to prevent vibrator "hash" from appearing in the oscillograph trace. A separate 6-volt storage battery (battery *B*) energizes the vibrator supply, also for "hash" suppression. The drain on this battery is approximately seven amperes with the vibrator supply adjusted for its maximum output voltage of about 325 volts under load. Another 6-volt storage battery (battery *A*) heats the *6F6* tubes and supplies balancing voltage for the second bridge arm. Separate sets of 6-volt batteries are required for each amplifier to eliminate vibrator "hash." Similar instantaneous polarities of the input and galvanometer circuits are indicated by the ± marks. Figure 5 shows a front view of an amplifier with its weather-protective cover open. Instruction notes covering the amplifier operation are given in the appendix.

Amplifier Uses and Results

Figure 6 is a sketch showing the method usually employed to connect the amplifier to a capacitance voltage divider. The auxiliary capacitors and other accessories used are housed in a metal weather protecting box. Various bushing tap fittings may be connected to the auxiliary capacitance boxes by means of conductors shielded from electrostatic fields by flexible metal tubing. Heavy ground wires are brazed to the two ends of the flexible tubing to overcome possible inductive effects due to the spiraled construction of the flexible tubing. The auxiliary capacitor box construction and three types of bushing tap fittings which are used are shown in Figures 7 and 8.

Coaxial-cable circuits between the auxiliary capacitor boxes and amplifiers are to be preferred since they minimize the possibility of electrostatic or electromagnetic effects. However, many suc-

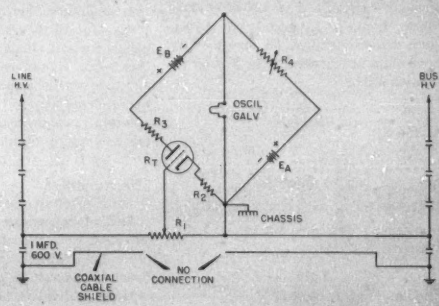

Figure 10. Measuring voltage across a circuit breaker

cessful tests have been made using spare control cable pairs in underground duct runs, only enough coaxial cable being used to run from the auxiliary capacitor boxes to the breaker control cabinet. Separate pairs of conductors were used for each voltage circuit with only one ground point (the respective auxiliary capacitor box) being used for each circuit.

Although Figure 6 employs a bushing tap to form the capacitance voltage divider, any capacitors that have adequate insulation and suitable characteristics, as previously discussed, may be used; these include carrier-coupling capacitors, static-capacitor units, and insulators. Where capacitor components have low values of capacitance and comparatively large area, such as insulator units, considerable care must be exercised in shielding the divider from other electrostatic fields in the vicinity.

An illustration of the results to be expected from amplifier-capacitance-voltage-divider combinations is given by Figures 9*A* and 9*B*. The rectangular voltage trace obtained during the disconnecting switch operation is due to the capacitance effect of the short section of bus and the oil circuit breaker bushing. As the switch first opens, the short bus and energized bus are at the same potential; the short bus having a d-c trapped charge corresponding to the crest voltage and the energized bus still varying sinusoidally. No current flows because at the instant of contact separation both bus sections have the same potential. A little later the energized bus voltage changes due to its 60-cycle sinusoidal periodicity to the point where the difference in potential between the busses is sufficient to arc over the switch gap or "restrike." The voltage of the short bus then changes with extreme rapidity, due to its low value of capacitance, to the bus voltage during a very brief flow of current of high initial magnitude. When the short bus reaches the voltage of the energized bus (neglecting high-frequency oscillations which may be present) the current flow ceases and the short bus again is left with a d-c charge until the bus voltage departs sufficiently to again break over the switch gap when the process is repeated. Since the disconnecting switch is being opened, the voltage necessary for its gap breakdown increases, as may be seen from the oscillogram of Figure 9*B*, until the gap gets long enough to withstand the voltage difference between the busses or double-crest voltage.

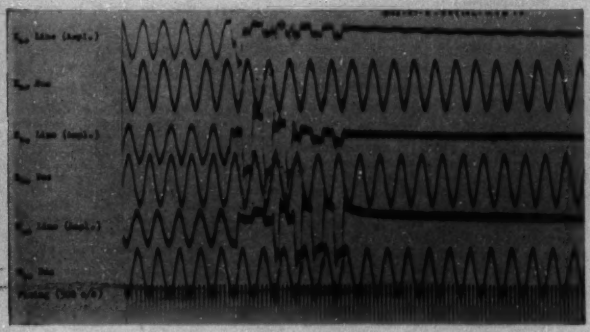

Figure 11. Line-voltage measurement with amplifiers during the interruption of line charging current of 71 miles of 230-kv transmission line with extensive circuit breaker restriking

The rapidity of decay of overvoltages produced by the restriking and the voltages induced in other phases by a restriking phase are of interest

Amplifiers are especially convenient for measuring the voltage across circuit breakers during fault current or line-charging current interruption.[4] In this service a capacitance voltage divider is connected to each side of the circuit breaker; these may be made with the circuit breaker bushing capacitances. Auxiliary capacitance values connected between the two tap points and ground should be adjusted so that both dividers will have the same tap voltage when the dividers are energized by the same high voltage. An amplifier connected between the tap points, as shown in Figure 10, will respond to the difference between the two voltages to ground. Due to the large tap-to-ground auxiliary capacitance and the low tap-to-ground voltage (usually ranging between 25 and 60 volts depending on the installation), no trouble should result from the amplifier chassis not being metallically grounded.

Another interesting use for the amplifier is the measurement of neutral-to-ground transient voltages on ungrounded systems or on equipment like ungrounded Y static capacitors. An amplifier connected to a capacitance divider between the neutral point and ground will give quite satisfactory performance without affecting the neutral circuit conditions. For this condition the capacitance divider should have as small an effective over-all capacitance value as possible; in no case should this effective value approach the neutral-to-ground capacitance of the circuit being measured. If no physical neutral exists, three additional matched capacitors forming an ungrounded Y connection to the test circuit can be used to form the neutral.

In all the previous discussion it has been assumed that some form of meter indication of the steady-state 60-cycle voltage is available as an oscillogram calibration reference. Where no calibration reference voltage is available, either the voltage division ratio or capacitance value ratio of the voltage divider is necessary. The deflection of the oscillograph galvanometer for a known low voltage applied to the amplifier tube grid circuit then can be correlated with the voltage divider ratio to give a calibration corresponding to the high-voltage system.

Appendix. Amplifier Operating Instruction Notes

Refer to Figure 4.

1. Adjust R_F to a value approximating the galvanometer circuit resistance and place switch *C* in its *T* position.

2. Turn the deflection control R_B to its *L* (zero) position.

3. Turn the zero adjusting control R_A to its mid-position.

4. Close switches *A* and *B* and allow at least five minutes warm-up time.

5. Inspect the two *VR-105* tubes; they should glow steadily. Fluttering indicates that battery *B* may not be charged, defective *VR-105* tubes, defective vibrator supply, or defective *6F6* tubes.

6. Adjust the zero adjusting control R_A and if necessary its series resistor R_B until the zero indicator (100-microampere meter) indicates zero.

7. Turn switch *C* to its zero position to

energize the oscillograph galvanometer. Readjust the zero adjusting control R_A as necessary to return the 100-microampere meter to zero.

8. Slowly turn the deflection control R_S toward its H (maximum) position until the desired oscillograph deflection is obtained.

9. Recheck the 100-microampere meter zero, adjusting the zero adjusting control R_A if necessary. The meter now should be removed from the circuit. The zero should be checked occasionally during a long test and following each time that the amplifier is re-energized after being turned off.

10. *Important.* Switch C should always be placed in its T position before the amplifier is turned on or off to prevent possible oscillograph galvanometer damage.

Figures 12 and 13 show two types of amplifiers which obviate the need of special balancing voltages. The static (zero signal) plate current is kept from the oscillograph galvanometer by balancing the plate current of one tube against the plate current of the other tube.

In Figure 12 the relative grid-cathode voltages of the two tubes are 180 degrees out of phase so the oscillograph galvanometer is subjected to a difference current whose magnitude is proportional to the voltage across capacitors C_1. Due to the series connection of these capacitors, their value is twice as large as in other forms of amplifiers without lowering the tap voltage. The RC time constant therefore is doubled which may be very advantageous for unidirectional voltage measurement.

The circuit of Figure 13 is fundamentally a dual amplifier in which the galvanometer responds to the difference between the voltages to the two grids; the same voltage on both grids results in zero deflection. If the grids are connected to the bushings on either side of a circuit breaker tank, the amplifier will respond to the voltage across the circuit breaker. De-energizing either grid causes the amplifier to respond to the line-to-ground voltage of the side of the circuit breaker energizing the other grid. A points X and Y additional galvanometers may be connected in the same manner as in the amplifier of Figure 4. If this is done, one amplifier can operate three oscillograph galvanometers for recording the line-side voltage, the bus-side voltage, and the voltage across the circuit breaker.

Any number of similar circuits or their combinations can be developed, each having features which may be advantageous to the user. In most circuits of these types, care must be taken to provide a sufficient number of adjustable circuit elements so that not only can the zero signal tube currents be balanced out to give zero galvanometer deflection, but the same value of high voltage should give the same galvanometer deflection irrespective of the capacitance-divider-tube combination to which it may be applied.

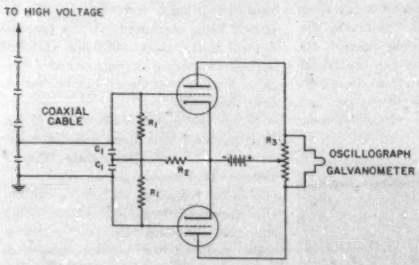

Figure 12. Amplifier basic circuit number 2

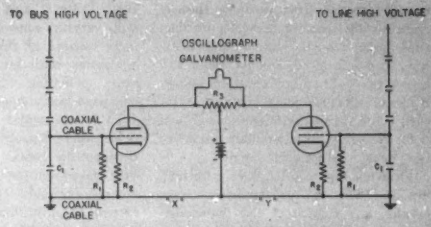

Figure 13. Amplifier basic circuit number 3

References

1. Application of Capacitance Potential Devices, J. E. Clem. AIEE Transactions, volume 58, 1939, January section, pages 1–10.

2. Transient and Steady-State Performance of Potential Devices, E. L. Harder, P. O. Langguth, C. A. Woods, Jr. AIEE Transactions, volume 59, 1940, February section, pages 91–102.

3. Resistors for 138-Kv Cable Switching, E. K. Sadler, T. M. Blakeslee. AIEE Transactions, volume 66, 1947, pages 39–50.

4. 4,370,000-Kva Short-Circuit Tests on Grand Coulee 230-Kv Bus, W. H. Clagett, W. M. Leeds. AIEE Transactions, volume 65, 1946, pages 729–35.

Discussion

C. J. Tirk (nonmember; Westinghouse Electric Corporation, East Pittsburgh, Pa.): The author of this paper is to be congratulated for his work which demonstrates that reliable transient voltage records can be obtained directly on magnetic oscillograms during high voltage switching operations, thus avoiding the necessity in many cases of a more expensive cathode-ray-oscillograph setup.

The usefulness of this method of amplifying the voltage available at the potential top of high-voltage circuit breaker bushings may be improved if an output at the oscillograph of 100 milliamperes or more can be obtained so that standard galvanometers with their higher frequency response may be used instead of sensitive or supersensitive elements. A standard galvanometer with a sensitivity of 150 milliamperes per inch has a flat response to as high as 3,000 cycles per second, dropping to 60 per cent at 5,000 cycles per second.

The author may be interested in a new d-c amplifier circuit which has proved very satisfactory for this type of recording. Special advantages in addition to the increased output include a very high input impedance of 10 megohms to increase the time constant of the capacitance potential divider circuit, and also an arrangement for two inputs when voltage is being measured for instance, directly across a circuit breaker.

The circuit is shown in Figure 1 of this discussion. Each of the vacuum tubes used is essentially two tubes in one envelope. The first *6SN7* is used as a cathode follower with a high input impedance but no amplification. The third stage likewise is used as a cathode follower with the oscillograph galvanometer connected across the cathodes. Thus all of the actual amplification is done in the second stage.

For convenience in field testing, all tubes are arranged to operate at the same plate voltage supply of 125 volts direct current, which is usually available from a station battery or generator. The filaments are operated from a standard 110-volt a-c source, while long-life dry batteries are used for the 135-volt d-c bias.

The frequency response for this amplifier is flat to 8,000 cycles per second with a rise of about ten per cent at 20,000 cycles per second. With 5 volts d-c input the output was linear over a range of -5 to $+5$ volts and -115 to $+115$ milliamperes. Magnetic oscillograph records of recovery voltage oscillations of 3,000 cycles per second during circuit breaker tests, using coaxial cable from a 115-kv bushing potential tap to the amplifier, showed excellent agreement with a cold cathode ray oscillograph connected

to a large capacitor divider on the same high voltage circuit.

Doctors W. M. Leeds and W. M. Brubaker provided helpful suggestions in connection with the design and application of this amplifier.

H. L. Levinton: The adoption of suggestions presented in my paper and corroboration of results obtainable by an oscillographer with Tirk's experience are indeed gratifying.

Tirk demonstrates the circuit simplicity obtainable for any specific need. His use of dual tubes results in equipment compactness and more balanced aging and thermal effects. The use of the station battery for plate voltage supply may introduce some error in results during field tests due to plate voltage changes during heavy battery discharge periods occurring with some circuit breaker operations. The use of alternating current for tube heating purposes also may affect results where tests modify the station a-c service. Improved results and greater simplicity should result from powering the entire device from alternating current using conventional plate supply rectifiers and filters. Supply power could be obtained from any auxiliary a-c source such as clock bus or carrier-current emergency supply equipment often included as station accessories. This arrangement also would eliminate the need of the bias supply battery.

In closing, I wish to stress that any number of simple circuits or circuit combinations may be developed for supplying measuring or control equipment with low voltages which accurately represent the steady-state and transient high voltages encountered on electric power systems.

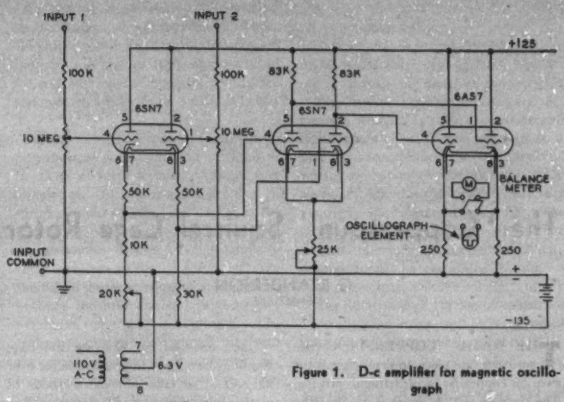

Figure 1. D-c amplifier for magnetic oscillograph

The "Copperspun" Squirrel Cage Rotor

G. R. ANDERSON
MEMBER AIEE

THE NAME "COPPERSPUN" describes a one-piece squirrel cage rotor cast of copper by a centrifugal process. The purpose of this paper is to describe briefly the method of fabrication and results obtained.

The original invention of the induction motor was a major factor in the early change from direct to alternating current. Since that time the squirrel cage type of induction motor has passed through a natural evolutionary development. This particularly applies to the design, construction, and manufacturing technique of the squirrel cage winding.

The squirrel cage is the simplest of all windings, yet it must carry many thousands of amperes at low voltage and must be rugged in construction for both mechanical and electrical reasons.

Many different types of rotor constructions have been used through the years; some of the earlier types were designed with rotor bars soldered to circular end rings. Some rotors were made with bars bent and riveted together on each end. One type of rotor was a modified cast en bloc design in which copper bars were inserted in the rotor slots and the end ring cast around the extension of each bar. Other types of rotors using copper or copper alloys employ rolled bars, brazed with bronze or silver, soldered to brass or copper end rings.

One-piece cast en bloc squirrel cage windings have been in production for over 25 years. Several different methods of casting one-piece rotors are in use, such as gravity casting, pressure casting of one form or another, and centrifugal casting. The majority of rotors built by these methods used aluminum or low temperature alloy metals. The use of copper and copper base alloys in the one-piece en bloc rotors has been produced successfully only in the last few years.

There is no question regarding the principle that the one-piece cast en bloc rotor is the ideal construction. Limitations in its use have been entirely because of materials or manufacturing processing problems.

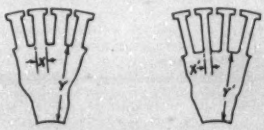

(A) **Figure 2** (B)

A. Punching for Copperspun rotors
B. Equivalent punching for cast aluminum rotors
The magnetic flux density at X is approximately 30 per cent lower than at X'
The magnetic flux density at Y is approximately 12 per cent lower than at Y'

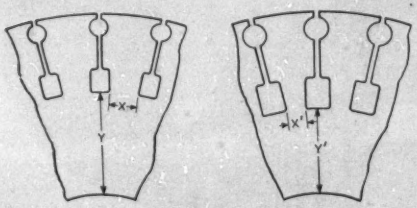

(A) **Figure 1** (B)

A. Typical double cage slot for Copperspun rotors
B. Equivalent double cage slot for cast aluminum rotors
The magnetic flux density at X is approximately 35 per cent lower than at X'
The magnetic flux density at Y is approximately 20 per cent lower than at Y'

Aluminum or white metal alloys have been used for one-piece squirrel cage windings with a variety of processing methods since the difficulties in manufacture were not unduly restrictive with low melting point metals. These processes, however, do not all produce the maximum in physical characteristics or electric conductivity.

Centrifugal casting is a preferred process from the standpoint of grain structure and casting porosity. This is verified by the improvements that have been made in centrifugal casting of iron and steel such as the brake drums for automobiles to obtain a tough long wearing structure. The successful centrifugal casting of high temperature metal such as copper or copper alloys has been the result of the solution of a number of manufacturing problems involving the following basic requirements:

1. The laminated cores must be stacked and held under pressure in order to produce satisfactory slot recesses for the squirrel cage winding.

2. Casting pressures must be sufficiently high to produce a dense nonporous structure of high conductivity and high strength. One of the advantages of centrifugal casting is the fact that pressure is controlled easily by adjustment of speed.

3. In the technique of casting, the copper must remain fluid a sufficient length of time to permit all recesses in the mold structure to be filled properly.

4. The design of the winding structure should be such that where change in section occurs, fillets should be used to avoid stress concentration.

5. There must be complete absence of fusion between copper and steel; otherwise there will be an alloying action between these elements that will cause a reduction of conductivity.

In actual practice, compression of rotor laminations during processing may be obtained by several methods. One method

Paper 47-206, recommended by the AIEE committee on electric machinery and approved by the AIEE technical program committee for presentation at the AIEE Middle Eastern District meeting, Dayton, Ohio, September 23-25, 1947. Manuscript submitted April 29, 1947; made available for printing August 7, 1947.

G. R. ANDERSON is director of engineering at Fairbanks, Morse and Company, Beloit, Wis.

Figure 3. A finished Copperspun rotor prior to assembly on shaft

in successful use employs air pressure against both ends of the assembled core, the pressure being maintained while the core is spun during casting. Another method employs centrifugal action to produce a positive pressure against the core during casting.

When centrifugal casting is used to obtain high density and ductile casting structures, the only limitation in the developed pressure is the maximum speed at which the structure can be rotated. In actual practice, copperspun rotors are produced with centrifugal casting speeds running as high as 4,000 rpm.

Maintenance of fluidity of metal for a sufficient length of time to fill completely all recesses in the rotor and mold structure is obtained by maintaining balanced temperatures between the various parts of the metal and mold structures. Molten copper at a given temperature requires a temperature relationship between the core and mold surfaces, in which the copper comes in contact, of a degree which will permit the copper to remain a fluid only for a sufficient length of time to fill completely all recesses in structure.

The use of high frequency induction furnaces for melting copper has been an excellent vehicle for the control of metal temperatures and maintenance of chemical purity. Automatic devices in general industry use provide satisfactory control for core and mold temperatures to create the necessary balance for successful casting.

The shrinkage allowances for cast copper, thermal expansion, and modulus of elasticity all favor the use of copper over aluminum. As a result the problem of shrinkage and stress concentricity in the 1-piece copper rotor is much less pronounced even though casting temperatures are practically doubled. Rotors should be designed with large fillet radii between the bars and end rings to give maximum ruggedness and strength. The high conductivity of the copper rotor with the resultant increase of magnetic sections gives greater freedom in the design and shape of the rotor slot.

The requirement for momentary fluidity in cast en bloc structures accentuates the possibility of fusion between steel and copper with the ultimate detriment to electrical characteristics of the copper windings. Thus, means must be provided for the prevention of fusion and pickup of chemical impurities. This is accomplished by sinterizing a silicate surface to the laminated core and by designing the molds with nonferrous surfaces that come in direct contact with the molten metal. This is particularly important where there is a flow of metal over the surface. The attainment in the control of fusion in the Copperspun rotor is evidenced by the fact that conductivity of the order of 90 per cent that of pure copper is obtained in the cast structure. This is nearly twice the conductivity of the purest aluminum.

High slip squirrel cage rotors, such as required for hoist and elevator motors, are fabricated the same as pure copper rotors, by the addition of alloying elements. Alloying is made in separate crucibles where quantity runs warrant or it may be accomplished for an individual casting operation by the addition of the necessary alloy agent prior to actually pouring. Experience has proved that the fabrication of a copper alloy rotor offers no particular complication and that conductivity can be controlled through a wide range with a single alloying agent.

The advantage in the use of copper for 1-piece squirrel cage rotors is apparent from the following metallurgical data:

Plus features in Copperspun rotor

Melting point of copper, degrees Fahrenheit 1,900–2,000
Melting point of aluminum, degrees Fahrenheit 1,100–1,200

Thermal conductivity of copper	100	Copper is twice as good a conductor of heat and electricity as aluminum
Thermal conductivity of aluminum*	52	
Electrical conductivity of copper	100	
Electrical conductivity of aluminum*	56 to 59	

Thermal expansion per degree centigrade:

Copper	0.000017	Note nearly 2-to-1 ratio for aluminum compared with steel with which it is combined in a rotor.
Aluminum	0.000024	
Steel	0.000013	

Modulus of elasticity (pounds per square inch):

Copper 16,000,000
Aluminum 10,000,000

*Expressed in per cent of same properties of copper.

Figure 5 (right). The copper squirrel cage winding disassembled from the magnetic core, illustrating absence of fusion

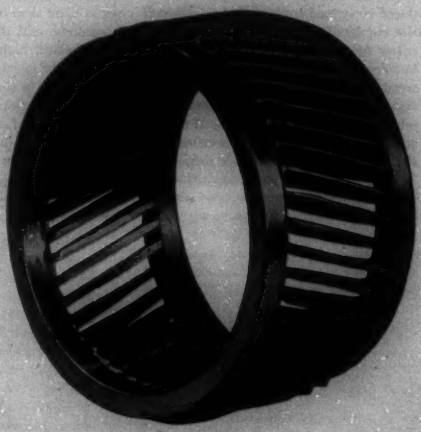

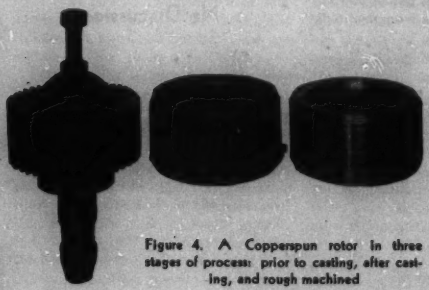

Figure 4. A Copperspun rotor in three stages of process: prior to casting, after casting, and rough machined

Strength of cast copper:

Tension.....22,000 to 25,000 pounds per square inch

Compression.....40,000 to 60,000 pounds per square inch

Strength of cast aluminum:

Tension.....12,000 to 15,000 pounds per square inch

Compression.....12,000 pounds per square inch

(From pages 559 and 560, "Standard Handbook for Electrical Engineers.")

The use of copper in 1-piece squirrel cage rotors not only provides a rotor of high mechanical strength but the high conductivity that is obtained permits the designer a greater freedom in choice of the electromagnetic circuit. Aluminum is not used in the stator because this would require slots nearly twice as large as those necessary for copper wire. By the same token, the slots and bars of the rotor can be considerably smaller with a resultant low magnetic density in the teeth and core of the rotor. This is more important in the design of Boucherot or double cage rotors. The high fluidity of copper permits a narrower neck in the slot between the outer and inner cages. This narrow neck in turn results in a reduction in the distance between the two cages; in other words, the lower cage can be brought nearer to the surface of the rotor. As a result of the reduction in slot space of the inner cage, it is possible to obtain improved speed–torque characteristics without the necessity of resorting to devices such as criss-crossed rotor slots. Figures 1 and 2 illustrate comparative slot sizes and shapes used for aluminum and copper rotors.

The high conductivity of the Copperspun rotor is also a factor in obtaining reduced stray load losses. The selection of slot combination is, of course, one of the major factors in control of stray losses, but since the use of high conductivity material permits a maximum freedom of design, the shape and number of slots can be selected to best advantage. Further, stray load losses due to surface currents in the squirrel cage winding are reduced in proportion to the increase in conductivity.

It is possible to design the mold and casting structure to provide fans cast integral with the rotor. This is a general practice with aluminum rotors. The Copperspun rotor, however, is equipped with separately mounted fans. This permits complete over-all machining of the rotor and provides improved means for checking the quality of production and improving the dynamic balance of the finished product.

The performance record of the Copperspun rotor has been proved in service of the severest nature. One particular example is its application to reversing duty where rotor troubles are largely predominant. The slightly higher weight of copper is more than offset by the increase in ruggedness and strength and the ability to withstand higher rotor temperatures. Further, the inertia of the rotor which is a major factor in the application of motors to reversing service is more dependent on the diameter of the rotor than on the weight since the inertia is proportioned to WR^2 which means that a reduction in diameter to obtain lower inertia is much more important than any slight reduction in weight.

Figure 6. Centrifugally casting a Copperspun rotor

The salient features of the Copperspun rotor can be summarized briefly as follows:

1. A high strength rotor with a dense and ductile 1-piece copper squirrel cage winding.
2. A rotor winding with a high melting point and no joints.
3. A rotor winding with low coefficient of expansion.
4. A rotor winding of high conductivity (90 per cent with nonalloyed copper).
5. A rotor winding of low porosity centrifugally cast.
6. A true running rotor, finished machined dynamically balanced.

No Discussion

Calculation of Slot Constants

A. F. PUCHSTEIN
MEMBER AIEE

Brief History

TOWARD the close of the last century the need arose to predict the regulation of alternators, the performance of induction motors, and the commutation of d-c machines. By 1900, two general approaches to the theory of the induction motor had appeared: the idea of leakage reactances due to Gisbert Kapp and C. P. Steinmetz; and the idea of leakage factors used by Andre Blondel, and Alexander Heyland about 1894. Blondel defined it as

$$\sigma = \frac{\text{magnetizing current}}{\text{magnetizing current} + \text{circle diameter}}$$

while Heyland defined it as

$$\sigma = \frac{\text{magnetizing current}}{\text{circle diameter}}$$

Because of this some care is necessary in applying them. Behrend gave his formula in 1896

$$\sigma = \frac{C\Delta}{\tau}$$

More elaborate forms were given by H. M. Hobart, H. Behn-Eschenburg, C. A. Adams, A. S. McAllister, R. M. Hellmund, F. M. Kierstead and others mostly by 1907. The concepts of slot, end-connection, zigzag and differential leakage all appeared by 1904 and are still in use.

Formulas for leakage reactance were given by Adams, Arnold, and La Cour, McAllister, I. E. Hansen, and others before 1909. Henri Boy de La Tour, for example, gave the present standard formula for the slot leakage in rectangular slots prior to 1906. An extensive study was published by Rezelman of Belgium at the time of World War I. P. L. Alger in 1928 gave what is probably the last American effort in wide use. Others since then have studied more special cases and done further work on differential leakage. Some rather comprehensive work was published by M. M. Liwschitz during the last few years. H. M. Norman in 1934 studied the effect of saturation in tooth tops, tooth tips and slot bridges.

Hobart, from measurements on models about 1904, established values for the leakage flux around the embedded and free lengths. These were 4 and 0.8 lines per ampere-conductor per centimeter, respectively, for a depth to width ratio of about 3.5. They were used for calculating alternator regulation and commutation in d-c machines. Arnold and La Cour in Germany gave formulas for the inductance of short-circuited coils in d-c machines at an early date, and C. C. Hawkins of England published an extensive serial in the *Electrical World* during 1903–04. The present paper focuses attention on slot leakage. The emphasis will be on induction motors.

Basic Assumptions

All formulas for the slot constant in current use are based on the assumption that the principle of superposition applies; that reluctance of iron is negligible; that conductors are very fine, in series, with zero skin effect; and that the slot leakage fluxes pass across the slot in parallel straight lines. The Field brothers, A. B. and M. B., in 1905 and 1906, R. E. Gilman in 1920, W. V. Lyon in 1921, Putman in 1927, and others gave formulas for the effective resistance and leakage reactance of various conductor arrangements when skin effect is present, all on the assumption that the slot leakage fluxes go straight across the slot. However, E. Roth in 1927, and B. L. Robertson and L. A. Terry in 1929, studied the problem with the aid of the La Place and Poisson partial differential equations of mathematical physics on the assumption of one and two solid conductors in a slot, with zero skin effect. This method shows that the leakage fluxes in general do not cross the slot in straight lines and that the conventional method gives results for rectangular slots which are about four per cent low with the proportions they used. No one seems to have applied this process to other slot or conductor shapes or when skin effect is present. Of course, at least for the smaller machines and for routine calculations on all sizes, such elaborate methods are too unwieldly. Adams in 1907, Alger in 1928, and Liwschitz in 1934 gave formulas for the slot factor in the case where the two layers in a rectangular slot carry currents which are not in phase, as in fractional pitch windings. The present paper gives the formulas for the slot constant on the conventional basis for most ordinary slot shapes. Those for elliptical, and rectangular or trapezoidal slots with one or both ends of semicircular shape seem to be new. All are based on the assumption of zero saturation, no skin effect, and that the leakage fluxes cross the slot in parallel straight lines.

Resulting Limitations

Because of the points indicated in the previous paragraph, the conventional method is incapable of giving perfect accuracy. Therefore, not too much should be expected from it. Only when circumstances demand, should specifications call for very close tolerances. When these are required the conventional method must be supplemented by experiment, the results of skin effect must be taken into account, or more precise methods of calculation used if and when these become available. However, because of its simplicity the conventional

Paper 47-208, recommended by the AIEE committee on rotating machinery and approved by the AIEE technical program committee for presentation at the AIEE Middle Eastern District meeting, Dayton, Ohio, September 23-25, 1947. Manuscript submitted May 23, 1947; made available for printing August 11, 1947.

A. F. PUCHSTEIN is consulting engineer with the Jeffrey Manufacturing Company, Columbus, Ohio.

method is extremely useful and has enjoyed wide use.

Example of the Integrations Used

To indicate the manner in which the formulas are obtained and to give some facility in their interpretation and use, the derivation for the case of a simple rectangular slot will be given in detail. For the other slot shapes and their various geometrical parts the process is similar, the principal difference being in the expressions for the permeance of the elementary leakage flux path, and the area in the slot below such path.

Referring to Figure 1*a*, with the previous assumptions, magnetomotive force acting at any point y in filled part

$$F = 0.4\pi In \times \text{area below path}$$
$$= 0.4\pi Inay$$
$$n = \text{turns per unit of slot area}$$

permeance of elementary path at any point y

$$d\mathcal{P} = \frac{\text{area}}{\text{length}}$$
$$= \frac{1 \times dy}{a}$$

elementary flux across slot at any point y

$$d\phi = Fd\mathcal{P}$$
$$= 0.4\pi Iny dy$$

turns interlinked with elementary flux at any point y

$$N = n \times \text{area below path}$$
$$= nay$$

interlinkages with elementary flux at y

$$= Nd\phi$$
$$= 0.4\pi In^2ay^2dy$$

or for the filled part of the slot

$$N\phi = 0.4\pi In^2a \int_0^{b_1} y^2dy$$
$$= 0.4\pi In^2a\frac{b^3}{3}$$

Next, replace n by N/ab then this becomes

$$(N\phi)_1 = 0.4\pi I \frac{N^2}{a^2b^2} a \frac{b^3}{3}$$
$$= 0.4\pi IN^2 \frac{b}{3a} \qquad (1)$$

This sets the pattern for the filled part, which will be followed throughout for the other slot shapes.

Similarly for the empty part b_1

$$\mathcal{F} = 0.4\pi Inab$$
$$\mathcal{P} = \frac{1 \times b}{a}$$
$$N = nab$$

$$N\phi = 0.4\pi In^2ab^2b_1$$
$$\phi = \mathcal{F}\mathcal{P}$$
$$= 0.4\pi Inbb_1$$

or replacing n by N/ab

$$(N\phi)_2 = 0.4\pi I \frac{N^2}{a^2b^2} \times ab^2b_1$$
$$= 0.4\pi IN^2 \times \frac{b}{a} \qquad (2)$$

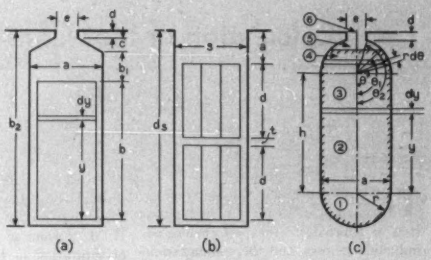

Figure 1. Rectangular slot shapes

(*a*). Partly closed slot
(*b*). Open slot
(*c*). Semicircular ends

This sets the pattern for the unfilled parts.

Noting that b_1 is the vertical height and a the width, by analogy we can write at once for the interlinkages of the tapered part

$$(N\phi)_3 \cong 0.4\pi IN^2 \times \frac{c}{\left(\frac{a+e}{2}\right)}$$
$$= 0.4\pi IN^2 \times \frac{2c}{a+e} \qquad (3)$$

though this is approximate. A more exact expression for the tapered part is given later.

And finally for the interlinkages due to the slot opening

$$(N\phi)_4 = 0.4\pi IN^2 \times \frac{d}{e} \qquad (4)$$

The interlinkages for the whole slot then equal the sum,

$$N\phi = 0.4\pi IN^2\left(\frac{b}{3a} + \frac{b_1}{a} + \frac{2c}{a+e} + \frac{d}{e}\right) \qquad (5)$$

The part in the parenthesis is called the slot constant and is designated by K_s. In the following work no separate symbol will be used when considering only the filled parts of a slot. In such cases the values for the unfilled parts must be added to get the value for the whole slot. For small air gaps, as in induction motors, the leakage flux from tooth top to tooth top around opening e is negligible, but for synchronous and d-c machines where large air gaps are used it is necessary to take it into account. Expressions for this have been given by Arnold, Lamme, Liwschitz, and others. (This is not the customary zigzag leakage flux of induction motor theory.)

Knowing the interlinkages per slot, the slot leakage inductance is

$$L_s = \frac{N\phi}{I \times 10^8} \text{ henrys per slot}$$

or for the phase as a whole

$$L_S = L_s \times \frac{\text{slots in series per phase}}{\text{branches in parallel per phase}} \qquad (6)$$

Outline of Usual Method for Calculating Leakage Reactance

If

L_E = leakage inductance per phase due to the end connections
L_{ZZ} = leakage inductance per phase due to the zigzag flux
L_D = leakage inductance per phase due to the differential flux

then the leakage reactance per phase for the stator is

$$x_1 = 2\pi f(L_{S1} + L_{E1} + L_{ZZ1} + L_D) \qquad (7)$$

A similar expression with $L_D = 0$ applies to the rotor. The leakage reactance X usually is taken as the sum $x_1 + x_2$ because we do not yet have precise methods of calculation.

The actual relation is less simple than this. Different writers treat the calculation of X in different ways. All calculate (in effect) L_{S1} and L_{S2} for stator and rotor respectively. Some calculate L_E separately for stator and rotor, others charge all of it to the stator. The same is true of L_{ZZ}. The differential leakage L_D practically always is charged to the stator. Only L_S is discussed in this paper. Nearly all writers ignore mutual inductance between phases, except when it takes place in the slots. This is generally permissible.

Effects of Tooth Saturation

Except for the work of Norman, so far as known, little precise information is available. He gave a method for calculating the ratios of zigzag and slot reactances when saturation is present to the values they have when saturation is absent. In locked rotor tests, some use voltages low enough so that the currents are not too much above rated. Liwschitz-Garik and Whipple on pages 213 and 214 of their volume 2 gave some data which indicates that the locked rotor impedance of a 600-horsepower 6-pole motor with squirrel-cage rotor is about 4.42 ohms to neutral at 500 line volts, and 3.71 at 1,500 volts, while values for a 75-horsepower 500-volt 106-ampere 10-pole 50-cycle motor were about 0.58 ohm per phase at 106 amperes on 107 volts, and 0.37 ohm at 770 amperes on 500 volts. Norman's example shows a locked current about 35 per cent higher than that indicated by the usual method. This was in a 7.5-horsepower 440-volt 1,800-rpm 60-cycle motor.

When Stator Slot Shapes Are Unequal

It occasionally happens that motors are built with slots of unequal shape and size. In such cases it is of assistance to have a way to obtain the resulting interlinkages in a more precise way than just estimating it. However, this is not to be despised.

The total interlinkages due to the slot leakage of a phase path are equal to

$$0.4\pi I \sum_{m=1}^{m} (N_m^2 K_{sm}) \tag{8}$$

From this the leakage reactance can be found as before.

Slot Constants for Various Slot Shapes

For Circular Slots

Figure 2 shows the slot constant represented by the filled and unfilled parts of circular slots, together with their sum, all plotted as functions of the angle θ_1. Curve A is for the filled part alone, for which

$$K_{s1} = \frac{r^4\left[\frac{\theta_1^3}{3}+\frac{\theta_1}{8}-\frac{\sin 2\theta_1}{4}+\frac{\theta_1\cos 2\theta_1}{2}-\frac{\sin 4\theta_1}{32}\right]}{2A_1^2} \tag{9}$$

where

$$A_1 = r^2\left(\theta_1 - \frac{\sin 2\theta_1}{2}\right)$$

= area in filled part of circle

For the unfilled part

$$K_{s2} = \frac{\theta_2 - \theta_1}{2} \tag{10}$$

If the slot is full, θ_1 and θ_2 both equal π and then $K_{s2}=0$. Curve B in figure 2 shows K_{s2} as a function of θ_1 if θ_2 is considered as equal to π. Curve C is the sum of curves A and B. To this must be added the part d/e for the tooth tips. The complete expression for the slot constant of the partly full slot then is

$$K_s = K_{s1} + K_{s2} + \frac{d}{e} \tag{11}$$

and for the full slot

$$K_s = \frac{\pi}{6} + \frac{1}{4\pi} + \frac{1}{10\pi} + d/e = 0.623 + \frac{d}{e} \tag{12}$$

When any of the slot constants, as K_{s1} or K_{s2}, say, are written without a prime mark, it means that the slot is empty in the sections above the one indicated by the subscript and that the value represented is that due to the leakage flux which crosses the wound section designated by the subscript (this part of the leakage flux interlinks with all conductors in sections below the one considered). When written with a prime mark, as K_{s1}' or K_{s2}', it means that some additional sections above it contain wire and that each of the primed values must be multiplied by a reduction factor before taking the sum to find the slot constant for the slot as a whole. The details for this are given at appropriate points.

Since the actual value of K_s is somewhat higher (assuming no saturation) than that given by the standard assumption of a straight path across the slot, some writers have replaced the 0.623 by 0.66 (Liwschitz) or by 2/3, so far as known, without explanation. In this and other cases where the walls are curved, one would expect this increase to be somewhat greater than the 1/0.96 suggested by Stevenson and Terry.

For Elliptical Slots

The values read from curves A, B, and C in Figure 2 apply if they are each multiplied by b/a, where b = half-diameter of ellipse at its vertical (usually the major) axis and a = that at its horizontal (usually the minor) axis. Then if the slot is partly full

$$K_s = \frac{b}{a}(K_{s1} + K_{s2}) + \frac{d}{e} \tag{13}$$

and if it is completely filled,

$$K_s = 0.623\frac{b}{a} + \frac{d}{e} \tag{14}$$

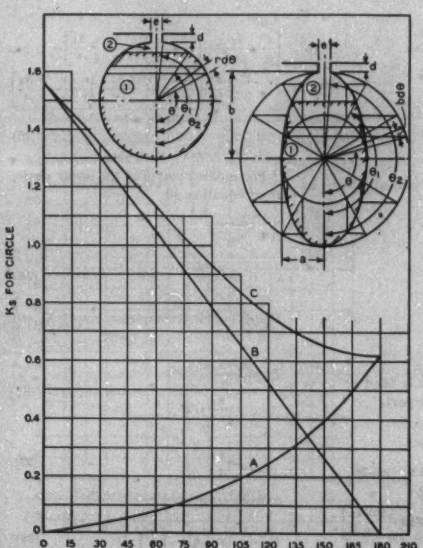

Figure 2. Circular and elliptical slot shapes

A—Slot constant for filled part
B—Slot constant for empty part
C—Sum of curves A and B
For the ellipse, multiply all values by b/a

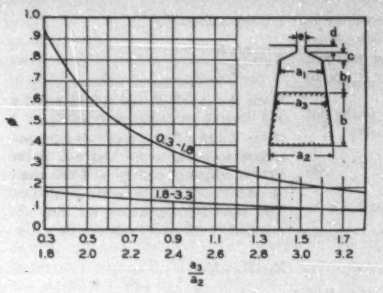

Figure 3. Curve for trapezoidal slots

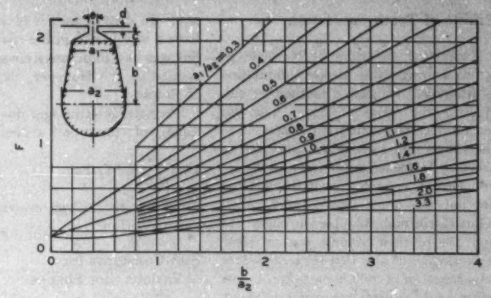

Figure 4. Curves for trapezoidal slots with semicircular bottom

The ellipse may be constructed graphically as shown, by making its horizontal width at any level equal to a/b times that of its major circle; by plotting it from its equation

$$\frac{x^2}{a^2}+\frac{y^2}{b^2}=1$$

or approximately by the method using arcs with two different radii. Still other methods are available.

For Rectangular Slots

The value of K_s most commonly used is that from equation 5

$$K_s=\frac{b}{3a}+\frac{b_1}{a}+\frac{2c}{e+a}+\frac{d}{e} \tag{15}$$

For the sloping parts, as the section of height c, it is more accurate when a is several times larger than e to take for the third term on the right in equation 15

$$\frac{2.30}{k}\log_{10}\frac{a}{e}$$

where

$$k=\frac{a-e}{c} \tag{16}$$

and similarly for the unfilled part b_1 when the taper is large.

If the upper part of the slot is an unfilled semicircle, the third term on the right in equation 15 has the value $\cong\pi/4$, from equation 10. Liwschitz writes for this term, in our notation,

$$\frac{1}{2}\sin^{-1}\sqrt{1-\left(\frac{e}{a}\right)^2} \tag{17}$$

For the slot in Figure 1*b*, Lamme gave in 1911

$$K_s=\frac{2.67d+4a+t}{4s} \tag{18}$$

If the bottom of the slot is circular, and it is filled with wire, K_s can be found from Figure 4, as

$$K_s=F+\frac{2c}{e+a}+\frac{d}{e}$$

Figure 4 was taken from a paper by P. H. Trickey and extrapolated slightly.

If the slot has semicircular ends as in Figure 1*c*, it is convenient to divide the total area into the six parts indicated by the numerals in the small circles. Here the spaces 5 and 6 may be empty; or also 3, 4, and 5 if the slot is filled only to level y. In the latter case 4 is considered as zero and the whole semicircle as space 5. This general idea is used also in other similar cases.

K_{s1}' is obtained from equation 9 or Figure 2.

$$K_{s2}=\frac{\frac{1}{3}a^2y^3+A_1ay^2+A_1^2y}{a(ay+A_1)^2} \tag{19}$$

where

$$A_1=\frac{1}{2}\pi r^2 \tag{20}$$

When the lower half circle is absent its area $A_1=0$ and then

$$K_{s2}=\frac{\frac{1}{3}a^2y^3}{a(ay)^2}=\frac{y}{3a} \tag{21}$$

For 3

$$K_{s3}=\frac{h-y}{a} \tag{22}$$

This is zero if the slot is filled up to or beyond the rectangular part.

For 4

$$K_{s4}=\frac{r^4\left[\frac{\theta^3}{3}+\frac{A_2}{r^2}\theta^2+\left(\frac{A_2^2}{r^4}+\frac{1}{8}\right)\theta-\frac{\sin 2\theta}{4}+\frac{\theta\cos 2\theta}{2}+\frac{A_2}{r^2}\cos 2\theta-\frac{\sin 4\theta}{2}\right]_{\theta_1}^{\theta_2}}{2(A_1+A_2+A_4)^2} \tag{23}$$

where

$\left[\ \right]_{\theta_1}^{\theta_2}$ means the value for $\theta=\theta_2$ minus the value for $\theta=\theta_1$

$\theta_1=\frac{\pi}{2}$ and $\theta_2=\pi$ or slightly less as indicated

A_1 = area of lower half circle $=\frac{1}{2}\pi r^2$

$A_2=ah$

A_4 = area of filled part 4

$$=\left[r^2\left(\theta-\frac{\sin 2\theta}{2}\right)\right]_{\theta_1}^{\theta_2} \tag{24}$$

If the slot, including the upper circle, is completely full, equation 23 becomes

$$K_{s4}=\frac{\left[\frac{\pi^3}{3}+\frac{A_2}{r^2}\pi^2+\left(\frac{A_2^2}{r^4}+\frac{1}{8}\right)\pi+\frac{\pi}{2}+\frac{1}{4}\frac{A_2}{r^2}\right]-\left[\frac{\pi^3}{24}+\frac{A_2}{r^2}\frac{\pi^2}{4}+\left(\frac{A_2^2}{r^4}+\frac{1}{8}\right)\frac{\pi}{2}-\frac{\pi}{2}-\frac{1}{4}\frac{A_2}{r^2}\right]}{2(ah+\pi r^2)^2} \tag{25}$$

with K_{s3} and K_{s5} both zero.

For unfilled part 5 of the upper circle, from equation 10,

$$K_{s5}=\frac{\theta_2-\theta_1}{2}$$

$$\cong\frac{\pi-\theta_1}{2} \tag{26}$$

If upper circle is completely empty $K_{s4}=0$ and then

$$K_{s5}=\frac{\theta_2-\pi/2}{2}$$

$$\cong\frac{\pi-\pi/2}{2}$$

$$=\frac{\pi}{4} \tag{27}$$

or from equation 17

$$K_{s5}=\frac{1}{2}\sin^{-1}\sqrt{1-\left(\frac{e}{a}\right)^2} \tag{28}$$

For part 6

$$K_{26}=\frac{d}{e}$$

Slot constant when slot is completely full

$$K_s=K_{21}'\left(\frac{A_1}{A_1+A_2+A_4}\right)^2+K_{22}'\left(\frac{A_1+A_2}{A_1+A_2+A_4}\right)^2+K_{24}+\frac{d}{e} \quad (29)$$

Where A_1 and A_4 each equal $(1/2)\pi r^2$, $A_2=ah$ with A_3 and A_5 both zero.

When spaces 1, 2, 3, and 4 are full with 5 empty

$$K_s=K_{21}'\left(\frac{A_1}{A_1+A_2+A_4}\right)^2+K_{22}'\left(\frac{A_1+A_2}{A_1+A_2+A_4}\right)^2+K_{24}+\frac{\theta_2-\theta_1}{2}+\frac{d}{e} \quad (30)$$

where A_1 and A_2 have the values under equation 29, and A_4 has the value from equation 24.

When spaces 1 and 2 only are filled, with 3, 4 and 5 empty, it is with $\theta_2\cong\pi$

$$K_s=K_{21}'\left(\frac{A_1}{A_1+A_2}\right)^2+K_{23}+\frac{h-y}{a}+\frac{\pi}{4}+\frac{d}{e} \quad (31)$$

where

$$A_1=\frac{1}{2}\pi r^2$$

and

$$A_2=ay$$

The presence of the lower circle has relatively little effect because $K_{21}'=0.142$, which is further reduced by the multiplier $[A_1/(A_1+A_2)]^2$.

Figure 5 gives values of K_s for both rectangular and trapezoidal slots with semicircular ends when completely full, omitting the part d/e, over a range of values for r_1/r_2 from 0.5 to 2 for four different slot depths chosen so that the distances between circle centers are, respectively, 1, 2, 3, and 4 times the diameter of the smaller circle. The curves were calculated with a 20-inch slide rule.

The reason for the presence of the area ratios, as say in equations 27, 28, 29, is that the derivations always assume the presence of a total of N conductors in the filled part considered and those below it. This is discussed further in the appendix.

For Trapezoidal Slots

We consider the several cases presented hereinafter. For Figures 6*a* and 6*b* (which include rectangular slots), the standard expression which includes partly full and full slots is

$$K_s=\phi\frac{b}{a_2}+\frac{2b_1}{a_1+a_2}+\frac{2c}{e+a_1}+\frac{d}{e} \quad (32)$$

where ϕ is read from the curve in Figure 3. Its value is given by

$$\phi=\frac{a_2}{(a_2+a_3)^2}\left\{\frac{3a_2+a_3}{4}+\frac{a_2^2}{(a_2-a_3)^3}\times\left[\frac{a_2^3-a_3^3}{2}+2a_2(a_2-a_3)+a_2^2\log_e\frac{a_2}{a_3}\right]\right\} \quad (33)$$

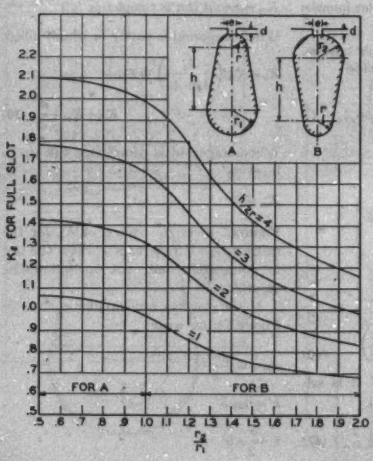

Figure 5. Curves for trapezoidal slots with semicircular top and bottom

This expression is the ratio of K_s for the filled part of a trapezoidal slot to b/a_2 for a rectangular slot. The general procedure is the same as outlined under "Example of the Integrations Used," with area

$$A=a_2y+\frac{1}{2}ky^2$$

and elementary permeance

$$d\mathcal{P}=\frac{dy}{a_2+ky}$$

for

$$k=\frac{a_1-a_2}{n}$$

It applies also if the top is displaced relatively to the bottom, though less accurately. A simple expression for ϕ can be obtained as follows.

In Figure 6*a*, let $k'=x/y=\tan\alpha$, and take y_1 equal to distance from apex to top of filled part

$$=\frac{a_1}{2\tan\alpha}$$

and

$$y_2=\frac{a_2}{2\tan\alpha}$$

Area in filled part

$$=A_2=k'(y_1^2-y_2^2)$$

and

$$K_{22}=\frac{0.25(y_1^4-y_2^4)-y_2^2(y_1^2-y_2^2)+y_2^4\log_e\frac{y_1}{y_2}}{2k'(y_1^2-y_2^2)} \quad (34)$$

when

$$\phi=\frac{K_{22}}{(h/a_2)}=K_{22}\times\frac{a_2}{y_1-y_2} \quad (35)$$

If the slot tapers in the opposite direction, Figure 6*b*, take

$$k'=\frac{x}{y}=\tan\alpha$$

with

$$y_1=\frac{a_2}{2\tan\alpha}$$

$$y_2=\frac{a_1}{2\tan\alpha}$$

area in filled part

$$A_2=k'(y_1^2-y_2^2) \quad (36)$$

$$K_{22}=\frac{0.25(y_1^4-y_2^4)-y_1^2(y_1^2-y_2^2)+y_1^4\log_e\frac{y_1}{y_2}}{2k'(y_1^2-y_2^2)} \quad (37)$$

and

$$\phi = \frac{K_{s3}}{\left(\frac{h}{a_2}\right)} = K_{s3} \times \frac{a_2}{y_1 - y_2} \tag{38}$$

If the slot has a semicircular end at the bottom as in Figure 6*c*, then

$$\theta_1 = \frac{\pi}{2} + \alpha$$

$$A_1 = r_1^2\left(\theta_1 - \frac{\sin 2\theta_1}{2}\right)$$

$$y_1' = y_1 - r_1 \sin \alpha$$

$$B = \frac{A_1}{k'} + y_1'^2$$

If slot is full to level y, K_{s1}' is read from curve in Figure 2 or from equation 9,

$$K_{s2}' = \frac{0.25(y_1'^4 - y^4) - B(y_1'^2 - y^2) + B^2 \log_e \frac{y_1'}{y}}{2k'(B - y^2)} \tag{39}$$

$$K_{s3} = \frac{y_1 - y_2'}{\left(\frac{a_1 + a_2}{2}\right)} \tag{40}$$

This is zero if slot is full to level y_2'.

$$K_{s4} \cong \frac{2c}{a_1 + e} \tag{41}$$

K_{s5} is not present.

$$K_{s6} = \frac{d}{e} \tag{42}$$

For the slot as a whole

$$K_s = K_{s1}'\left(\frac{A_1}{A_1 + A_2}\right)^2 + K_{s2} + K_{s3} + K_{s4} + K_{s6} \tag{43}$$

where $K_{s3} = 0$ if slot is full to level y_2'.

The sum of the first two terms

$$K_{s1}'\left(\frac{A_1}{A_1 + A_2}\right)^2 + K_{s2}$$

is equal to Trickey's F in his Figure 13.

If the slot has two semicircular ends as in Figure 7*a*, the areas,

$$A_1 = r_1^2\left(\theta_1 - \frac{\sin 2\theta_1}{2}\right)$$

$$A_2 = k'(y_1'^2 - y^2)$$

$$A_4 = \left[\theta_2 r_2^2\left(\theta - \frac{\sin 2\theta}{2}\right)\right]_{\theta_1}^{\theta_2}$$

$$\sin \alpha = \frac{r_1 - r_2}{h}$$

$$k' = \tan \alpha$$

$$\theta_2 = \frac{\pi}{2} + \alpha$$

and

$$B = \frac{A_1}{k'} + y_1'^2$$

K_{s1}' = value from Figure 2 or from equation 9

$$K_{s2}' = \frac{0.25(y_1'^4 - y^4) - B(y_1'^2 - y^2) + B^2 \log_e \frac{y_1'}{y}}{2k'(B - y^2)^2} \tag{44}$$

for

$$y \geqq y_1'$$

$$K_{s3} \cong \frac{y - y_1'}{\left(\frac{k'(y + y_1')}{2}\right)} \tag{45}$$

$$K_{s6} = \frac{d}{e}$$

When upper circle is full

$$K_{s5} = 0 \tag{48}$$

For the slot as a whole, when upper circle is partly or wholly filled,

$$K_{s3} = 0$$

and

$$K_s = K_{s1}'\left(\frac{A_1}{A_1 + A_2 + A_3 + A_4}\right)^2 + K_{s2}'\left(\frac{A_1 + A_2}{A_1 + A_2 + A_3 + A_4}\right)^2 + K_{s4} + K_{s6} + \frac{d}{e} \tag{49}$$

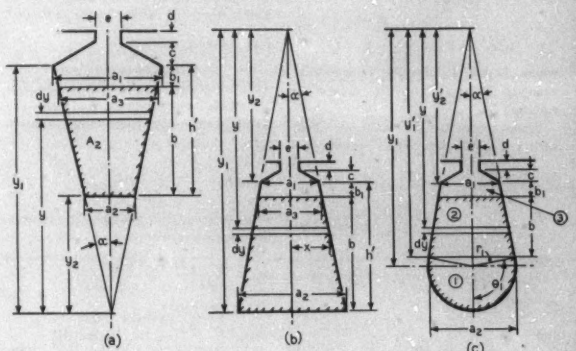

Figure 6. Quantities used in deriving formulas for trapezoidal slots

(*a*) and (*b*). For slots with straight bottoms.
(*c*). For slot with semicircular bottom

For 4 when filled, with $A = A_1 + A_2 - A_4'$ where

$$A_4' = r_2^2\left(\theta_1 - \frac{\sin 2\theta_1}{2}\right)$$

$$K_{s4} = \frac{\left[\frac{r_1\theta^2}{3} + \left(\frac{A^2}{r_2^4} + \frac{1}{8}\right)\theta + \frac{A}{r_2^2}\theta^2 - \frac{\sin 2\theta}{4} + \frac{\theta \cos 2\theta}{2} + \frac{A}{r_2^2}\frac{\cos 2\theta}{2} - \frac{\sin 4\theta}{32}\right]_{\theta_2}}{2\left(\theta_2 - \frac{\sin 2\theta_2}{2} + \frac{A}{r_2^2}\right)^2} \tag{46}$$

If part 4 is empty $K_{s4} = 0$. It is seldom necessary to calculate K_{s4}

$$K_{s4} = \frac{\theta_2 - \theta_1}{2} \cong \frac{\pi - \theta_1}{2} \tag{47}$$

K_{s5} = zero if slot is completely full

When trapezoid is partly or wholly filled

$$K_s = K_{s1}'\left(\frac{A_1}{A_1 + A_2}\right)^2 + K_{s2} + K_{s3} + K_{s6} + \frac{d}{e} \tag{50}$$

When trapezoid is completely full up to level y_2'

$$K_{s3} = 0$$

Figure 5 gives the values of K_s for the range $r_2/r_1 = 0.5$ up to 2.0 when the slot is completely full, not including the term d/e.

If the slot has semicircular ends as in Figure 7*b*, we write,

$$\sin \alpha = \frac{r_2 - r_1}{h}$$

$$k' = \tan \alpha$$

$$\theta_1 = \frac{\pi}{2} - \alpha$$

and the areas,

$$A_1 = r_1^2\left(\theta_1 - \frac{\sin 2\theta_1}{2}\right)$$

$$A_2 = k'(y^2 - y_1'^2)$$

$$A_4 = \int_{\theta_1}^{\theta_2} r_2^2\left(\theta - \frac{\sin 2\theta}{2}\right)$$

with

$$B = \frac{A_1}{k'} - y_1'^2.$$

K'_{s1} is read from Figure 2 or calculated from equation 9

$$K_{s1}' = \frac{0.25(y^4 - y_1'^4) + B(y^2 - y_1'^2) + B^2 \log_e \dfrac{y}{y_1'}}{2k'(B + y^2)^2} \tag{51}$$

If trapezoidal part is full, replace y by y_2'.

$$K_{s2} \cong \frac{y_2' - y}{\left(\dfrac{k'(y_2' + y)}{2}\right)}$$

more accurately

$$K_{s2} = \frac{1}{2k'} \log_e \frac{y_2'}{y} \tag{52}$$

K_{s4} from equation 23 or 46. Here part 4 will seldom be empty, but if so

$$K_{s4} = 0$$

$$K_{s3} = \frac{\theta_2 - \theta_1}{2} \cong \frac{\pi - \theta_1}{2} \tag{53}$$

K_{s5} = zero when upper circle is full

$$K_{s6} = \frac{d}{e} \tag{54}$$

For the slot as a whole, when upper circle is full or partly full,

$$K_{s1} = 0$$

and

$$K_s = K_{s1}'\left(\frac{A_1}{A_1 + A_2 + A_3 + A_4}\right)^2 + K_{s2}'\left(\frac{A_1 + A_2}{A_1 + A_2 + A_3 + A_4}\right)^2 + K_{s4}K_{s4} + \frac{d}{e} \tag{55}$$

When trapezoid is partly or wholly filled

$$K_s = K_{s1}'\left(\frac{A_1}{A_1 + A_2}\right)^2 + K_{s2} + K_{s3} + K_{s4} + \frac{d}{e} \tag{56}$$

When trapezoid is completely full up to level y_2', $K_{s2} = 0$ and K_{s4} is absent.

Appendix

The general procedure used in developing the principal formulas was outlined under "Example of the Integrations Used." It remains to give the expressions used to represent the elementary permeance and the area below an elementary flux leakage path for the less simple slot shapes, after which the integrations may be carried out in the regulation manner.

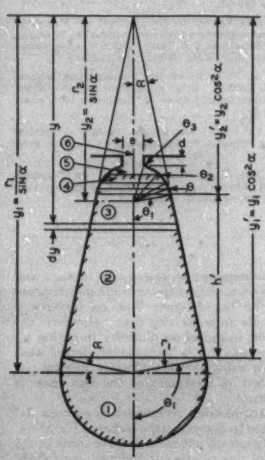

Figure 7. Quantities used in deriving formulas for trapezoidal slots with semicircular top and bottom

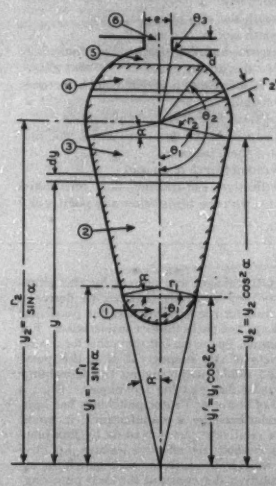

For the Circle

Length of elementary path $= 2r \sin\theta$
Width of elementary path $= rd\theta \times \sin\theta$
Permeance of elementary path $= d\mathcal{P} =$

$$\frac{1 \times rd\theta \times \sin\theta}{2r\sin\theta} = \frac{d\theta}{2}$$

Area below elementary path $= A$

$$= \int_0^\theta (2r\sin\theta) \times (rd\theta \times \sin\theta)$$
$$= \int_0^\theta 2r^2 \sin^2\theta d\theta$$
$$= r^2\left(\theta - \frac{\sin 2\theta}{2}\right)$$

In finding the interlinkages this is taken as a variable $A = f(\theta)$ for the filled part, and as a constant

$$A_1 = r^2\left(\theta_1 - \frac{\sin 2\theta_1}{2}\right)$$

for the unfilled part.

For the Ellipse

Length of elementary path $= 2a \sin\theta$
Width of elementary path $= bd\theta \times \sin\theta$
Permeance of elementary path $= d\mathcal{P} =$

$$\frac{1 \times bd\theta \times \sin\theta}{2a\sin\theta} = \frac{b}{a}\frac{d\theta}{2}$$

Area below elementary path $= A$

$$= \int_0^\theta (2a\sin\theta) \times (bd\theta \times \sin\theta)$$
$$= \int_0^\theta 2ab\sin^2\theta d\theta$$
$$= ab\left(\theta - \frac{\sin 2\theta}{2}\right)$$

This is equal to (a/b) times area in circle of radius b for same value of θ. As with the circle A is taken as variable, a function of θ, for the filled part; and as a constant

$$A_1 = ab\left(\theta_1 - \frac{\sin 2\theta_1}{2}\right)$$

for the unfilled part, when finding the interlinkages.

For the Trapezoid With Semicircular Ends

For the lower circle K_{s1}' is found in the same way as for the circle with

$$\alpha = \sin^{-1}\frac{r_1 - r_2}{h}$$

$$\theta_1 = \frac{\pi}{2} + \alpha$$

in Figure 7*a* or

$$\alpha = \sin^{-1}\frac{r_2 - r_1}{h}$$

$$\theta_1 = \frac{\pi}{2} - \alpha$$

in Figure 7*b*. K_{s1}' is zero if the lower circle is absent.

For the trapezoidal part two approaches are possible, to count the variable y from the apex, with the length of elementary leakage flux path equal to $2k'y$ where $k' = \tan\alpha$; or else to count y from the top or bottom of the trapezoidal part with the length of elemen-

tary leakage path expressed in the form $a+ky$. The first of these was chosen because it gives shorter expressions. For this, to find K_{m}

length of elementary path $=2k'y$

width of elementary path $=dy$

permeance of elementary path $=d\mathcal{P}=\dfrac{dy}{2k'y}$

area below elementary path $=A$

$$A_1+k'(y_1'^2-y^2)$$

in Figure 7*a* or

$$A=A_1+k'(y^2-y_1'^2)$$

in Figure 7*b* where

$$A_1=r_1^2\left(\theta_1-\frac{\sin 2\theta_1}{2}\right)$$

Here the area A is taken as a variable $=f(y)$ for the filled part 2; and as a constant with $y=b$ when finding K_{s1} and K_{s2} for the unfilled parts above 2.

For the Rectangle With One or Two Semicircular Ends

For the lower circle, K_{s1}' is found in the same way as for the circle, with $\theta_1=\pi/2$. K_{s1}' is zero if the lower circle is absent. For the rectangular part, to find K_{s1},

Length of elementary path $=a$

Width of elementary path $=dy$

Permeance of elementary path $=\dfrac{1\times dy}{a}$

Area below elementary path $A=A_1+ay$

where

$$A_1=\frac{1}{2}\pi r^2$$

Here the area A is taken as a variable $=f(y)$ for the filled part 2, and as a constant $A=A_1+ab$ for the unfilled part 3.

For the upper half circle to find K_{s4} of the filled part 4, the length, width, and permeance of the elementary path each are represented by the same expressions as for a circle, with the area below such path

$$A=A_1+A_2+\left[\frac{\theta_1}{\frac{\pi}{2}}r_2\left(\theta-\frac{\sin 2\theta}{2}\right)\right.$$

This is a function of θ. To find K_{s4}' of the unfilled part 5, the procedure is similar except that the area A containing wire

$$A=A_1+A_2+\left[\frac{\theta_1}{\frac{\pi}{2}}r^2\left(\theta-\frac{\sin 2\theta}{2}\right)\right.$$

is constant. This gives the value of K_{s4} in equation 29. If there is no upper half circle, values which fit the upper slot and tooth shape are substituted. See for example, equation 32. Of course, this slot shape is a special case, also, of the shapes in Figures 7*a* and 7*b*.

Slot Constant for Filled Part of a Slot

The constant will be determined for the condition when the slot constants for each of the filled sections are known. The reason for the use of the multipliers in equations 31, 32, 33, and so forth, is somewhat puzzling. In deriving the formula for each slot section, it was assumed that the number of turns N is both a variable and the value when the section considered (plus those below it) is full. For each such section the interlinkages are for the mth section

$$N_m\phi_m=0.4\pi I N_m^2 K_{sm}$$

If we next consider N as the total number of turns in the filled part of a slot, then for the mth section, the turns acting are

$$N_m=N\times\frac{\text{area of section considered, plus those below it}}{\text{area in all filled sections together}}$$

and therefore the total interlinkages

$$N\phi=0.4\pi I N^2[K_{s1}'(\ )^2+K_{s2}'(\ )^2+K_{s4}]$$

parentheses are interpreted as the area ratios shown in connection with the different cases considered.

Symbols

C = Behrend's constant $\cong 10$ to 15

L_t = slot-leakage inductance for one slot, in henrys

L_S = slot-leakage inductance for one phase, in henrys

Subscripts 1 and 2 are for stator and rotor, respectively.

m = mth slot of a phase-path belt

m = mth section of a slot

N = turns interlinked with the elementary flux at any point

It is sometimes a variable and sometimes a constant.

N_m = turns in mth slot of a phase belt

N_m = turns in the mth section of a slot and those below it

Δ = radial length of air gap

ϕ = effective slot-leakage flux interlinked with the turns below any point y or θ

ϕ = a coefficient from Figure 3

τ = pole pitch

References

1. The Induction Motor (second edition), **B. A. Behrend.** McGraw-Hill Book Company, New York, N. Y., 1921.

2. Magnetic Dispersion in Induction Motors, **H. Behn-Eschenburg,** *Journal,* Institution of Electrical Engineers (London, England), volume 32, pages 239–94.

3. The Leakage Reactance of Induction Motors, C. **A. Adams.** *Transactions,* International Electrical Congress, St. Louis, 1904, volume 1, page 706.

4. The Design of Induction Motors, **C. A. Adams.** AIEE Transactions, volume 24, 1905, pages 649–87.

5. Standard Handbook for Electrical Engineers (fourth, fifth, and sixth editions), section on a-c generators and motors, **C. A. Adams.** McGraw-Hill Book Company, New York, N. Y.

6. Magnetic Leakage of Induction Motors, **A. S. McAllister,** *Electrical World* (New York, N. Y.), January 26, 1907.

7. Leakage Coefficient of Induction Motors, **R. E. Hellmund.** *Electrical World* (New York, N. Y.), November 23, 1907.

8. Leakage Reactance of Induction Motors, **I. E. Hansen,** *Electrical World* (New York, N. Y.), March 30, 1907.

9. The Induction Motor (second edition), **H. B. De La Tour.** Translation by C. O. Mailloux, McGraw-Hill Book Company, New York, N. Y., 1906, pages 107–16.

10. The Calculation of the Armature Reactance of Synchronous Machines, **P. L. Alger.** AIEE Transactions, volume 47, 1928, pages 493–513.

11. Differential Leakage With Respect to the Fundamental Wave and to the Harmonics, **M. M. Liwschitz.** AIEE Transactions, volume 63, 1944, pages 1139–50.

12. Differential Leakage of a Fractional-Slot Winding, **M. M. Liwschitz,** AIEE Transactions, volume 65, 1946, May section, pages 314–20.

13. Induction Motor Locked Saturation Curves, **H. M. Norman,** Electrical Engineering (AIEE Transactions), volume 53, April 1934, pages 536–41.

14. Analytical Determination of Magnetic Fields. Simple Cases of Conductors in Slots, **B. L. Robertson, I. A. Terry.** AIEE Transactions, volume 48, October 1929, pages 1242–62.

15. An Analysis of the Shaded Pole Motor, **P. H. Trickey.** Electrical Engineering (AIEE Transactions), volume 55, September 1936, pages 1012–13.

16. Electric Machinery (book), **Liwschitz-Garik, Whipple,** D. Van Nostrand Company, New York, N. Y., 1946.

17. The Electrical Machines (in German), **M. M. Liwschitz, B. G. Teubner,** Leipzig and Berlin, 1934, volume 3, pages 55–6.

Discussion

L. A. Doggett (Pennsylvania State College, State College, Pa.): The train of thought among designers has been for many years something like this: they start with a leakage flux associated with a current and producing a quadrature voltage; they divide out the current and get a reactance; they divide out $2\pi f$ and get an inductance; they divide out $0.4\pi N^2$ and get a permeance, the permeance of the leakage path. Then after making a mental note to watch out for partial leakages and correct for this situation, they generally proceed to derive a formula for the permeance of the particular leakage flux paths under consideration. For example, Puchstein has done this for a wide variety of slot shapes. It is at this point that I would like to suggest the desirability of using flux plotting techniques. Once a line of stator and rotor punchings has been standardized by a manufacturer, it would be a relatively easy job to fix by flux plotting methods the effective leakage flux lines per ampere per inch for each punching, essentially a slot constant for each punching. The overhung slot, trapezoidal in shape and with rounded corners, presents quite a problem to the designer bent on deriving a formula to cover this case. However, designers have had no difficulty in setting up a formula for a rectangular shaped slot. When using the flux plotting method the method of treatment of the two cases is identical.

Flux plotting techniques have been described frequently in the technical literature. Designers do not seem to have made much use of flux plotting techniques, apparently preferring to rely on formulas. If some de-

signer should want to give flux plotting a try, I might suggest references 1 and 2 of this discussion.

REFERENCES

1. MATHEMATICAL AND PHYSICAL PRINCIPLES OF ENGINEERING ANALYSIS (book), Walter C. Johnson. McGraw-Hill Book Company, New York, N. Y. Pages 317–31, 335–6.

2. FUNDAMENTALS OF ELECTRICAL DESIGN (book), A. D. Moore. McGraw-Hill Book Company, New York, N. Y. Chapter 4 and following.

John F. H. Douglas (Marquette University, Milwaukee, Wis.): The author's formula is the one usually accepted. Slot permeances by this formula are too low. The method of integration presupposes flux paths equivalent to insulating partitions. These cramp the lines of force materially on the inside of slot openings, Lord Rayleigh[1] proved this fact. The term missing in the author's paper is given in my 1915 paper.[2] Using the notation in Puchstein's equation 5 we find we should add a term

$$N\phi_s = 0.4\pi I N^2[0.6 \log_{10}(a/e) - 2(c/a)(e/a)^2]$$

to agree with curves calculated in 1915 and verified with water-trough experiments.

The author's equation 12 is almost certainly low for a similar reason. The experimental arrangement I use for evaluating equivalent permeances in regions where there is curl has given excellent results. The setup for the round slot would be that shown in Figure 1 of this discussion. Electrodes are shown as heavy black dots or sheets. The boundary is wood, the conductor water, the source 1,000 cycles, 10 volts. The indicator is an oscilloscope, the potentiometer Leeds and Northrup decade boxes. The resistances R are radio resistances of 10,000 ohms each. Flux lines are traced by means of the probe and a pantograph (not shown). The theoretical reason for this experimental procedure is in the equation

$$\text{curl } H = \text{div } \phi$$

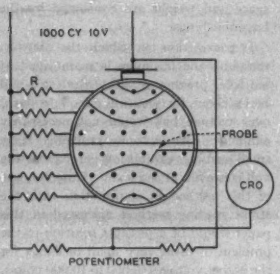

Figure 1

CRO = cathode-ray oscilloscope

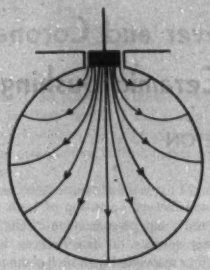

Figure 2

REFERENCES

1. THEORY OF SOUND (book), Lord Raleigh. Volume 2, section 305, page 175.

2. THE RELUCTANCE OF SOME IRREGULAR MAGNETIC FIELDS, John F. H. Douglas. AIEE TRANSACTIONS, volume 34, part 1, 1915, pages 1067–1125, figure 35, equations 55, 56.

A. F. Puchstein: Doggett raises some interesting points. The flux plotting technique deserves to be known to designers better than it is. To make it usable, for any flux path, it is necessary to evaluate its permeance, the area enclosed below it, the resulting interlinkages, and their sum for the entire area. By this means the slot constants for different slot shapes would have to be worked out and tabulated in advance of need. No one has done this. To determine them as needed requires too much time, and so the formulas for them have been preferred.

This work is an example of the very useful finite-difference or step-by-step methods of integration. These enable us to obtain reasonably accurate numerical results with less labor and often in cases where none at all can be obtained by formal integrations. Such methods deserve to be known more widely by engineers. It is surprising that while they date back to the days of Euler, they somehow have failed to get into courses on engineering mathematics. The advent of machine methods of calculation of course will make obsolete many present ones, but it always will be desirable to have at hand feasible alternates.

It would be nice if Doggett could have included a sample of his process and the results obtained.

In regard to the discussion by Douglas, it is true that the results for slot constants given by the standard approach tend to be too low for some slot shapes, as for example the circular slot, for which the standard value is 0.623. As pointed out in the paper, the figures 0.66 and 2/3 have been suggested by men of wide experience.

Referring to Figure 1a of my paper for a slot with the proportions

$e = 0.10$	$c = 0.15$	$b = 0.90$
$d = 0.05$	$b_1 = 0.30$	$b_2 = 1.50$

$K_s = 2.200$ from equation 15 or 2.303 if equation 16 is used. The correction suggested by Douglas would add 0.396, giving $K_s = 2.2000 + .396 = 2.596$, which is too high.

The test arrangement in his Figure 1 would seem to be incapable of giving correct results. With the electrode at the top, the lines of flow would be like those shown in Figure 2 of this discussion, from top to bottom instead of across the slot. It would have been well, too, if he had given some of the test figures. Finally, it is quite desirable when using expressions from classical vector analysis, as curl H = div ϕ, to give a brief interpretation in order to show the ideas involved, because most engineers are not trained in this field.

High Altitude Flashover and Corona Correction on Small Ceramic Bushings

W. W. PENDLETON
MEMBER AIEE

Synopsis: A marked improvement in corona starting voltage and flashover voltage for small ceramic bushings has been obtained by the use of semiconducting coatings. This is of special importance for airborne radio and radar equipment. The results cover both a-c and d-c behavior for several sizes of solder-seal bushings. A sensitive oscilloscopic method detects disturbances at voltage gradients where the ionization-by-collision process begins. These gradients, far below the visual corona points, are calculated from graphical maps of the dielectric fields associated with the bushings.

THE USE of modern radar equipment in aircraft has introduced high voltages which have resulted in corona and flashover problems. Freedom from corona as well as flashover is necessary for the satisfactory operation of both radar and radio equipment. One of the most serious sources of disturbances is the bushings associated with such components as transformers and capacitors. This problem is complicated further by the ever-present demand by aircraft design engineers for the lightest and most compact equipment.

There are a number of possible methods for improving the corona and flashover behavior of ceramic bushings. Some of these are

1. Design modifications of bushings.
2. Pressurization.
3. Shielding and air exclusion.
4. Grading of stress concentrations.

At sea level much can be done to improve the corona and flashover characteristics of bushings by changing their shapes and sizes. This involves either increasing the diameter to length ratio or designing the bushing so that the ceramic dielectric more nearly conforms with the electric field involved. Schwaiger[1] and Peek[2] have shown the effect of bushing shape on flashover behavior. The effect of increasing the diameter to length ratio will be discussed briefly in a later section of this paper. Both types of design changes give similar results and while they are quite effective at sea level, there is a sharp decline in flashover voltage as pressure is reduced until little improvement results in larger bushings.[3] Another objection to this method is that valuable space and weight are consumed by the larger bushings.

Pressurization, in which the air surrounding the bushings is maintained at sea level pressure at all altitudes, would be excellent for securing adequate flashover voltage but would not necessarily eliminate the corona problem, since small bushings exhibit low corona starting voltages even at sea level. However, use of this method in conjunction with the stress grading method discussed in this paper would be a possible solution to the problem of using very small bushings for the higher voltages (5,000 to 10,000 volts).

Shielding and air exclusion as is done in aircraft ignition systems would eliminate all corona and flashover problems at all altitudes since the radial field passes through only solid insulation. However, certain disadvantages such as additional cost, added weight, and associated com-

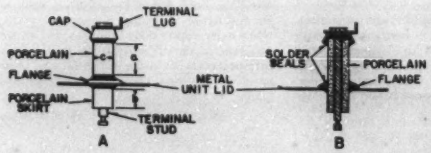

Figure 1. Westinghouse solder-seal bushing

A. External view
B. Cross-sectional view

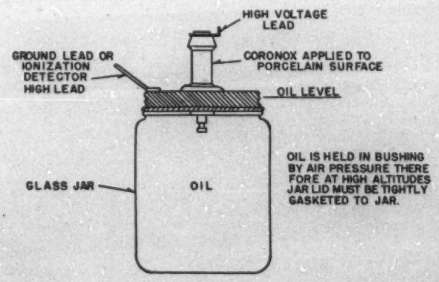

Figure 2. Test mounting of bushing

Paper 47-236, recommended by the AIEE air transportation, communication, and power transmission and distribution committees and approved by the AIEE technical program committee for presentation at the AIEE Middle Eastern District meeting, Dayton, Ohio, September 23–25, 1947. Manuscript submitted November 13, 1946; made available for printing August 7, 1947.

W. W. PENDLETON is research engineer, insulation department, Westinghouse Research Laboratories, East Pittsburgh, Pa.

The writer wishes to extend his thanks to Doctor C. F. Hill (F '39), manager, and Doctor L. J. Berberich (F '45), section manager, insulation department, Research Laboratories, for their many helpful suggestions and criticisms, and S. E. Brayshaw of the motor engineering department for his aid in conducting the tests; all of Westinghouse Electric Corporation, East Pittsburgh, Pa.

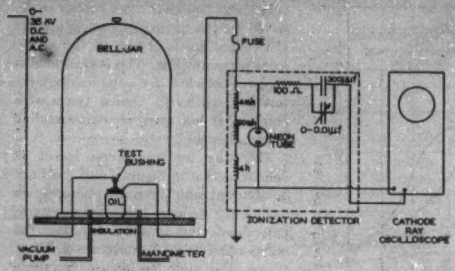

Figure 3. Corona detection equipment

plications might make this method impractical for use in commercial air-borne radar and radio installations.

The present paper is concerned primarily with the fourth method for improving corona and flashover voltages by a grading of the stress concentrations with a semiconducting coating applied to the external ceramic surface of the bushing. It was found that, by this method, very small bushings could be made essentially free from electrical disturbance up to flashover voltage for high altitudes and that the flashover itself could be raised appreciably. The initial electric disturbance was detected by a sensitive oscilloscope method which showed that this disturbance occurred at voltages far below the visual corona point. A further investigation, beyond the scope of the present paper, would be necessary to determine what level of disturbance can be tolerated in typical radar and radio installations.

Description of Test Specimen and Stress Grading Compound

A typical solder-seal bushing is shown in Figure 1*A*. The length *a* was varied from 0.25 inch to 1.25 inches, while diameter *c* was changed from 5/16 inch to 15/16 inch. Length *b* extends below the oil level in the apparatus to prevent internal flashover. A cross-sectional sketch of this bushing is shown in Figure 1*B*. In these bushings the zircon porcelain[4] is soldered to the flange and the cap by means of metallized bands on the ceramic.

The test specimen is shown in Figure 2. The bushing flange was soldered to the jar lid which was gasketed tightly to a 4-ounce jar filled with oil. Before testing, the specimens were inverted for a time to replace the air around the stud with oil. This test specimen simulates to a sufficient degree the actual apparatus.

The use of a semiconducting material to grade voltage stress concentrations in high voltage electric devices is not new. For example, certain types of line insulators long have been treated with bands of semiconducting glazes and the insulators so treated show considerable improvement in radio interference behavior.[5] This treatment is referred to as "radio interference protection" or simply "RIP." Also, in high voltage machines semiconducting coatings on the coil end-turns are used to reduce the stress concentrations at the coil surfaces as they merge from the slots.[6] An organic base semiconducting compound called "Coronox"[6] was developed for this application. This material consists essentially of an organic medium in which a semiconducting pigment is dispersed. The surface resistivity on application of the coating is controllable over a wide range by choice of the pigment used.

The ideal material for grading stresses in ceramic bushings is a semiconducting glaze such as is being used in line insulators. The existing glazes, however, are too low in resistivity for satisfactory performance on small ceramic bushings. Preliminary experiments indicated that complete coverage of the ceramic surface of the bushing with a coating having a resistivity of the order of thousands of megohms per square unit surface is necessary for optimum performance. Since controllable glazes in the high resistivity ranges have not yet been developed, use was made of the easily controllable organic base semiconducting compound. The compound is applied readily by a dipping procedure on completely assembled bushings. It dries to a tack-free condition in a few hours without requiring baking. The resistivity of the compound decreases with increasing temperature. While the resistivity changes by a factor of five from −55-degrees centigrade to 100-degrees centigrade, the required resistivity is not so critical that good performance cannot be obtained in this whole temperature range. The aging of the compound in this temperature range is quite small, the tendency being for the resistivity to decrease slowly when held at temperatures in the neighborhood of 100-degrees centigrade. A protective varnish coating usually is applied over the compound which not only improves the appearance but adds to the abrasion, fungus, and moisture resistance. Since the coating is organic, it is not recommended for direct exposure to weather.

Figure 4. Oscilloscope trace of corona discharge

Table I. Effect of "Coronox" on Corona Behavior

Voltage Type	Coating	Altitude	Diameter, In.	Bushing Length, In. 1/4	1/2	3/4	1	1 1/4
Alternating	Bare	Low	5/16	3,200	1,200	5,200	3,000	
	Coated	Low	5/16	14,200	13,400	13,400	11,800	
	Bare	High	5/16	1,200	1,800	2,200	1,600	
	Coated	High	5/16	3,000	4,500	5,600	6,200	
Direct	Bare	Low	5/16	5,300	4,800	3,000	2,700	
	Coated	Low	5/16	8,800	7,000	9,000	6,800	
	Bare	High	5/16	1,800	2,300	2,800	2,400	
	Coated	High	5/16	3,000	2,800	3,300	3,700	
Alternating	Bare	Low	7/16	5,200	7,000		6,400	10,600
	Coated	Low	7/16	9,900	14,800		14,400	13,400
	Bare	High	7/16	2,200	2,600		3,600	4,600
	Coated	High	7/16	3,100	4,400		4,200	4,600
Direct	Bare	Low	7/16	7,500	15,200		20,000	26,000
	Coated	Low	7/16	8,500	17,600		27,000	38,300
	Bare	High	7/16	1,600	2,500		2,300	3,500
	Coated	High	7/16	2,500	3,800		2,500	3,900

Sine wave peak alternating voltage (60 cycles per second). Negative direct voltage. Values obtained by ionization detector. Low altitude = sea level. High altitude = 50,000 feet.

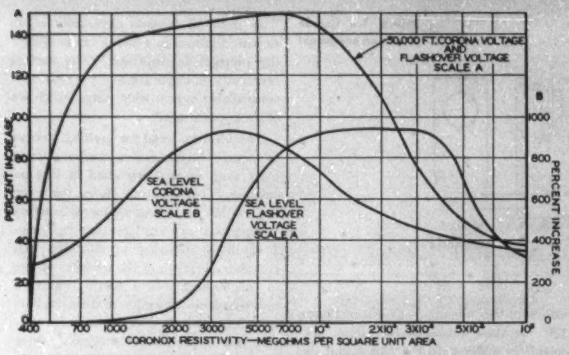

Figure 5. Effect of coronox resistivity on improvement to a-c corona and flashover voltages at sea level and 50,000 feet altitude for a 5/16-inch-diameter bushing having a 1/2-inch spacing

Corona Detection Equipment

To detect the high frequency discharges produced by corona, a modification of a Quinn[7] ionization circuit was employed. As shown in Figure 3, this consists of a number of air core inductances in series with the test bushing which allow power frequency currents to pass but block higher frequencies (especially above those of about 1 kc per second). Three inductances were used in order to cover the range of frequency from audio to radio bands. The high frequency currents were introduced to a cathode ray oscilloscope through a variable coupling capacitor. At the 300 micromicrofarad setting, which is the lowest capacitance, only the high frequency voltage appears on the screen. At higher coupling capacitances a 60-cycle sine wave with high frequency superimposed results. For corona point determinations, the lowest capacitance setting was used in order that the oscilloscope gain could be raised to a value of sensitivity of 0.1 volt per inch of deflection. At this sensitivity the a-c corona point could be determined to within about 200 volts. The d-c corona point was defined much less sharply, because of the intermittent nature of the discharges, and therefore could be determined to within only about 500 volts. A-c corona as detected by this device appears as a series of localized bursts of fuzz on the oscilloscope horizontal line. This is illustrated in Figure 4 which is for a typical bushing tested at sea level. Similar traces were obtained at low pressures corresponding to high altitudes.

The trace for d-c corona is not as definite as that in Figure 4 and could not be obtained with the usual photographic facilities. Besides being intermittent, unlocalized, and of short duration, the bursts of electrical disturbance on direct current were much less intense than those for alternating-current. The intensity of the direct-current traces approached those for alternating-current only as the visual corona point was reached at a much higher voltage than that when the first disturbance appeared on the oscilloscope screen.

Experimental Results

Visual corona tests in a darkened room revealed that the discharges first appeared at the junction of the metal flange and the ceramic insulator. This is not surprising since high stress concentrations are to be expected where the bushing passes through the metal flange. This region of the first appearance of corona remained fixed irrespective of the pressure down to the region of glow discharge with either alternating or direct voltages. Increasing the diameter of the bushing raised the voltage somewhat at which it appeared, but did not change the position. Increas-

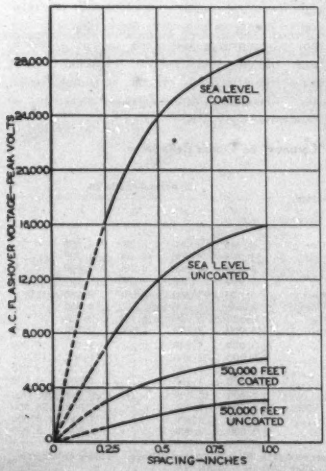

Figure 6 (left). A-c flashover voltage versus spacing

5/16-inch diameter

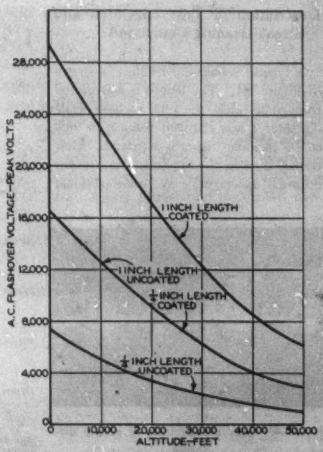

Figure 7 (right). A-c flashover voltage versus altitude

5/16-inch bushings

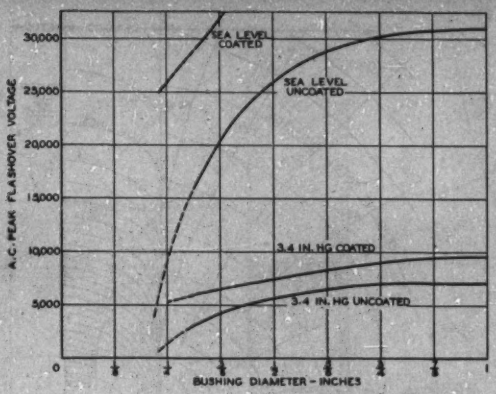

Figure 8 (above). Effect of bushing diameter on flashover voltage for 1-inch flashover distance

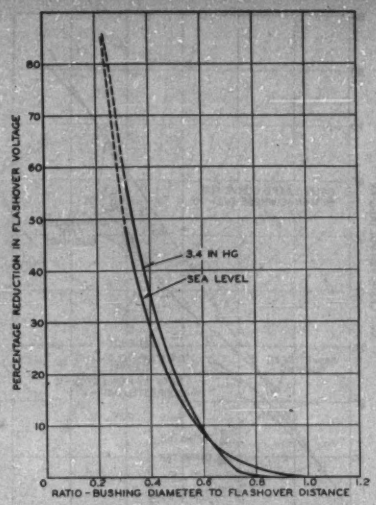

Figure 9. Percentage reduction in flashover voltage as a function of the ratio of bushing diameter to flashover distance

ing the length of the bushing had little or no effect on the voltage or the position where it first appeared. This is to be expected since increasing the length of the bushing does not change the field configuration at the flange.

One of the first problems was to determine the value of resistivity of the coating required for optimum performance of the bushing. It was obvious at the beginning that even though a low resistivity coating might give the desired grading, the resistivity should not be so low as to cause excessive current drain at operating voltages or excessive heating at any test voltage imposed on the apparatus. This was investigated experimentally by applying coatings of varying resistivities to the same bushing having a length of 1/2 inch and a diameter of 5/16 inch. The results of this work are shown in Figure 5 for both sea level and 50,000 feet altitude. The sea level data indicates that best results are obtained when the resistivity is in the range of from 5,000 to 50,000 megohms, while the high altitude data points to a range between 1,000 and 10,000 megohms. The best compromise value from the corona reduction standpoint for all altitudes between sea level and 50,000 feet, then, appears to be about 3,000 to 5,000 megohms per square unit area. While these values of resistivities do not contribute much to the flashover at sea level, they markedly do improve the flashover at high altitudes where it is much needed. The lowering of the curves at the low resistivities in Figure 5 is attributed to heating of the coating, while the lowering at high resistivities is ascribed to insufficient grading of the stress.

Using a semiconducting coating having a surface resistivity of approximately 3,000 megohms per square, a set of eight bushings was investigated for corona and flashover behavior, with and without semiconducting coatings on alternating current and negative direct current and at sea level and 3.4 inches of mercury. This latter pressure corresponds to the standard pressure at 50,000 feet altitude. Table I presents the values of corona voltage as observed with the ionization detector. As will be brought out in the discussion, these values are much below the visual corona points in every case. These values are quite conservative in that they are the lowest of five readings at each condition. It will be observed that some of these readings are erratic and not consistent. This must be expected since minor changes in the surface and shape at the flange produce major changes in the electrostatic field configuration. This fact made it necessary to show the effects of the semiconducting coatings on the same bushings that were tested before treatment.

Table II summarizes the readings in Table I by showing the average percentage increase in corona voltage for each test condition. In general, for alternating and direct current, there is more improvement for the 5/16 than the 7/16-inch-diameter bushings. This is true because of the greater field concentration existing in the smaller diameter bushings. In spite of the fact that high altitude d-c visual corona was eliminated entirely up to flashover voltage, only 40 per cent increase in corona point was recorded with the oscilloscope method. As will be seen later, this small increase in corona voltage is inconsistent with the rather large increase in high altitude d-c flashover voltage.

Table III is a summary for the average percentage flashover improvement on the same eight bushings as used in corona determinations. Just as with corona voltage, the semiconducting coating also raises the flashover voltage. At high altitudes adequate flashover voltage is very difficult to obtain.[3] Over 100 per cent increase in a-c flashover voltage and 70 per cent increase in d-c flashover voltage are obtained for the 5/16-inch-diameter bushings at high altitude.

Table II. Average Percentage Increase of Corona Voltage as Detected by the Oscilloscope Method

Voltage Type	Altitude	Bushing Diameter, In. 5/16	Bushing Diameter, In. 7/16
Alternating	Low	300	80
	High	200	30
Direct	Low	100	50
	High	40	30

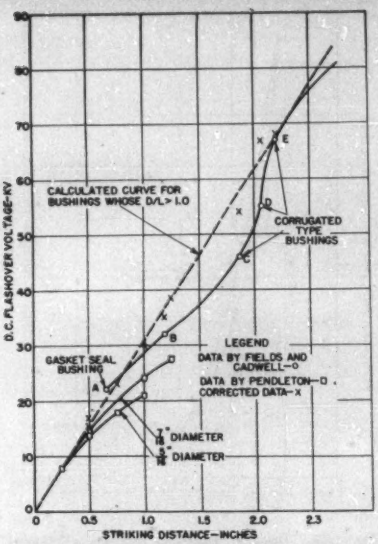

Figure 10. Reconciliation of d-c flashover data on bushings of various shapes and sizes

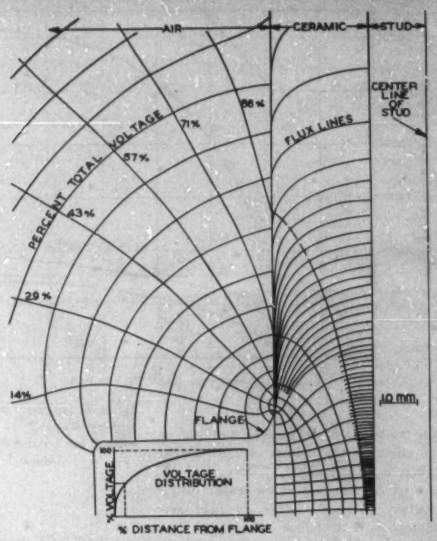

Figure 11. Electric field in vicinity of flange for uncoated bushing—one-half inch in length

The variation of a-c flashover voltage versus bushing length is shown in Figure 6 for the 5/16 inch-diameter bushings. It is seen that at 50,000 feet altitude a 1/4-inch treated bushing has the same flashover voltage as the 1-inch uncoated bushing. This is also true at sea level. In Figure 7 a similar comparison between these bushings is made on the basis of altitude. The middle curve serves both for the 1/4-inch coated bushing and for the 1-inch uncoated bushing. Assuming a 5,000-peak-volt maximum operating voltage, the coating allows the maximum altitude of the 1/4-inch bushing to be raised from 10,000 feet to 30,000 feet. For the 1-inch bushing length, this change is from 30,000 feet to more than 50,000 feet.

Table III. Percentage Increase of Flashover Voltage Average Values for Four Sizes of Bushings

Voltage Type	Altitude	Bushing Diameter, In. 5/16	Bushing Diameter, In. 7/16
Alternating	Low	90	40
	High	120	50
Direct	Low	20	20
	High	70	45

Tables IV and V give the voltages for essentially corona-free operation at 50,000 feet altitude, and altitudes for corona-free operation at 5,000 peak volts, respectively. Both uncoated and coated bushings are listed for comparison.

An investigation also was made to determine the relation between the diameter-to-length ratio and flashover. This was made on a series of bushings with constant lengths but with diameter ranging from 5/16 inch to 15/16 inch. Figure 8 shows the data taken at sea level and high altitude on these bushings which were both treated and untreated with semiconducting coating. These data are expressed in Figure 9 as a percentage reduction in flashover voltage versus diameter-to-length ratio (D/L) assuming that a constant flashover voltage is reached at values of D/L greater than unity.

The curves for both pressures are sufficiently close to be averaged as a single curve. This curve may be used to determine flashover values for bushings whose ratios of D/L are less than unity and provide a means for correlating the data taken on bushings of various shapes and sizes. Figure 10 shows such a correlation between d-c data taken on the eight bushings discussed previously and on larger bushings tested by Fields and Cadwell.[3] The "corrected" points may be connected by a straight line from the origin which represents the maximum which may be obtained by increasing the diameter-to-length ratio. The letters A to E in Figure 10 designate the bushings tested by Fields and Cadwell. A similar correlation for the a-c data can be made.

Electrostatic Field Configurations

To understand better the reason for the high stress concentration at the flange-to-ceramic junction and the effects of the semiconducting coating, two 3-dimensional field maps were prepared graphically for the untreated and treated cases. These maps were prepared by use of the method of 3-dimensional field plotting described by Leonard.[8]

Figure 11 shows the field plot for an untreated 5/16-inch diameter by 1/2-inch

Table IV. Voltages for Corona-Free Operation at 50,000 Feet for 5/16-Inch Diameter Bushings

Bushing Striking Distance, In.	Uncoated Peak Volts	Coated Peak Volts
0.25	1,000	2,500
0.50	1,500	3,500
0.75	2,000	4,500
1.00	2,500	5,000

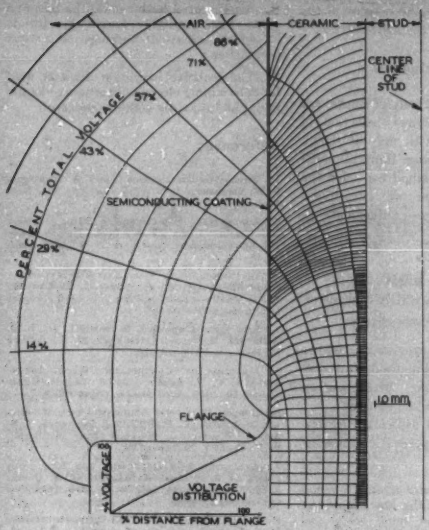

Figure 12. Electric field in vicinity of flange for coated bushing—one-half inch in length

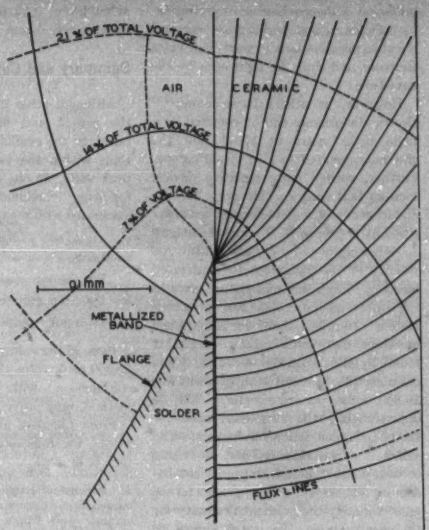

Figure 13. Greatly magnified view of dielectric field in vicinity of flange edge for untreated bushing

length bushing in the region of greatest stress, that is, at the junction of the flange and ceramic whose dielectric constant is 9. It is seen from this map and from the voltage distribution curve also shown in Figure 11, that the lower 7–8 per cent of the untreated bushing sustains 50 per cent of the total voltage. The major reasons for the great crowding of field lines at the junctions are

1. The high dielectric constant of the ceramic.

2. The sharpness and proximity of the metal seal.

3. Change of direction of the field from radial to tangential or longitudinal. This results in very high gradients at the junction even at voltages much below the flashover values. Thus, corona is initiated at this junction at very low over-all voltages.

Table V. Altitudes for Corona-Free Operation at 5,000 Peak Volts for 5/16-Inch Diameter Bushings

Bushing Striking Distance, In.	Corona-Free Maximum Altitude, Ft	
	Uncoated	Coated
0.25	10,000	30,000
0.50	20,000	40,000
0.75	25,000	45,000
1.00	30,000	50,000

The second graphical field map shown in Figure 12 is for the bushing treated with semiconducting coating. In contrast to that observed in Figure 11, the voltage distribution shown in Figure 12 is nearly linear. The voltage distribution was calculated from the following equation derived from standard transmission line formulas[9,10]

$$\frac{E}{E_g} = \frac{\sinh \beta x \cos \beta x + j \cosh \beta x \sin \beta x}{\sinh \beta l \cos \beta l + j \cosh \beta l \sin \beta l} \quad (1)$$

where

$$\beta = \left(\frac{1}{2}\,\omega r c\right)^{1/2} \quad (2)$$

and

E = voltage at any distance x from cap
E_g = total voltage
l = length between cap and flange
$\omega = 2\pi$ times frequency
r = resistance per unit length
c = capacitance per unit length

The voltage distribution shown in Figure 12 neglects

1. The distributed air capacitance to ground.

2. The change in phase angle along the line.

The error due to the former cannot be large since most of the system capacitance is in the high dielectric constant ceramic. The phase angle changes by only 30 degrees over the entire transmission line and this should not seriously distort the field plot, particularly in the vicinity of the flange where corona develops. These field plots present a fairly clear picture as to why the corona behavior of a treated bushing is much improved over an untreated bushing.

Discussion of Ionization Processes

Corona is the name usually given to a visual electric disturbance in which ions excited by high gradients emit light in returning to their stable energy levels. In nonuniform fields, air may be stressed over a definite distance called the "ionized layer" at or above 30,000 volts per centimeter, the gradient necessary for the complete breakdown of a uniform gap.[2] The thickness of this layer varies directly with the radius of curvature of the electrodes and inversely with the gas density. Loeb[11] has found that the gradient necessary for the start of visual corona is more than four times the 15,200 volts per centimeter necessary for the

initiation of the mechanism of ionization-by-collision. These gradients are necessary to cause negative ions to shed their extra electrons and emit the light seen by the naked eye.

However, as others have found,[12,13] electric disturbance can be detected by a radio noise meter at about half the gradients required to give visual corona. Further, with a more sensitive device, such as that used for this work, electric disturbance can be detected at even lower gradients. Figure 13 is a greatly magnified drawing of the dielectric field in the vicinity of the flange for the untreated bushing. From this plot the distance to the first equipotential line was estimated; knowing the over-all voltage at which electric disturbance began as found by the ionization detector, it was calculated that the initiating gradient was 16,800 volts per centimeter. This is approximately the threshold value for the collision ionization mechanism. The calculation was repeated for the visual corona point, the resulting gradient becoming 70,000 volts per centimeter or approximately the gradient necessary for the visual process. By use of Figure 12, the gradient for initial disturbance was calculated to be 15,800 volts per centimeter for the bushing coated with semiconducting material. Thus, it appears that the ionization detector is possibly twice as sensitive as the radio noise meter and detects the disturbance created at the very beginning of the ionization-by-collision process. As mentioned before, this disturbance may not be sufficient to distort radar signals and certainly will not impair radio reception. The difference between initial disturbance and visual corona at high altitude is much less than at sea level. This may be because of the increased thickness of the ionized layer.

Summary and Conclusions

Although other methods of improving the corona and flashover behavior of bushings are available, it may be shown that, within the voltage limit of 5,000 peak volts, no one method can offer the following combination of advantages associated with the stress grading method:

1. Allows the use of very small bushings, saving space and weight.
2. Entails only slight additional cost.
3. Does not require auxiliary equipment.
4. Does not require design changes.

Even in the voltage range from 5,000 to 10,000 peak volts, this method, if used in conjunction with the pressurization method, may prove to be practical.

From the data and associated experiments, the following general conclusions may be drawn:

1. Because of stress concentrations, visual corona first appears at the junction of the ceramic and flange on small solder-seal bushings.

2. Coating a small solder-seal bushing from cap to flange with a material having a surface resistivity of about 3,000 megohms per square unit area increases the high altitude a-c corona point by 200 per cent and raises flashover by 120 per cent.

3. The semiconducting coating eliminates d-c high altitude visual corona up to flashover which is raised by 70 per cent.

4. Sea level corona points are raised by 300 per cent for alternating current and by 100 per cent for direct current.

5. Small coated bushings can be made corona-free at 50,000 feet for voltages up to 5,000 peak volts.

6. Small coated bushings can be operated corona-free at roughly double the altitude at which uncoated bushings are about corona-free.

7. The sensitive ionization detector used for determining electric disturbance detects initial ionization-by-collision process.

References

1. Theory of Dielectrics (book), **A. Schwaiger, R. W. Sorensen.** John Wiley and Sons, Inc., New York, N. Y., 1932, pages 311–59.

2. Dielectric Phenomena in High Voltage Engineering (book), **F. W. Peek, Jr.** McGraw-Hill Book Company, New York, N. Y., 1929, pages 35, 48–108, 319.

3. Investigation of Porcelain Insulators at High Altitudes, **C. V. Fields, C. L. Cadwell.** AIEE Transactions, volume 65, 1946, October section, pages 656–60.

4. Low Loss Ceramics, **R. Russell, Jr., L. J. Berberich.** *Electronics* (New York, N. Y.), volume 17, 1944, pages 136–42, 338.

5. Methods of Controlling Radio Interference, **C. V. Aggers.** AIEE Transactions volume 59, 1940, April section, pages 193–9.

6. Corona Blackout Achieved in High Voltage Machines, **C. F. Hill, L. J. Berberich, J. S. Askey.** *Westinghouse Engineer* (East Pittsburgh, Pa.), volume 1, 1941, page 43.

7. A Method for Detecting the Ionization Point on Electrical Apparatus, **G. E. Quinn.** AIEE Transactions, volume 59, 1940, December section, pages 680–2.

8. Field Plotting in Non-Uniform Media, **M. G. Leonard.** *The Electric Journal*, volume 32, 1935, pages 31–3.

9. Alternating Current Circuits (book), **J. M. Bryant, J. A. Correll.** McGraw-Hill Book Company, New York, N. Y., 1925, page 331.

10. Principles of Electric Power Transmission (book), **L. F. Woodruff.** John Wiley and Sons, Inc., New York, N. Y., 1938, pages 105–18.

11. Fundamental Processes of Electrical Discharge in Gases (book), **L. B. Loeb.** John Wiley and Sons, Inc., New York, N. Y., 1939, pages 521–35.

12. Radio Influence Characteristics of Electrical Apparatus, **P. L. Bellaschi, C. V. Aggers.** AIEE Transactions, volume 57, 1938, November section, pages 626–33.

13. Instruments and Methods of Measuring Radio Noise, **C. V. Aggers, D. E. Foster, C. S. Young.** AIEE Transactions, volume 59, 1940, March section, pages 178–87.

No Discussion

The Air Gap Reactance of Polyphase Machines

P. L. ALGER
FELLOW AIEE

H. R. WEST
MEMBER AIEE

Synopsis: This paper presents some new formulas for the differential leakage reactance of distributed polyphase windings, such as those of induction motors and voltage regulators. Previous authors have used two distinct methods for evaluating the differential reactance, but the results obtained by these two methods have been inconsistent, particularly for open slot machines. The overlap method is based on calculating the average overlap of the teeth on the primary and secondary, and then calculating the leakage through the zig-zag flux path under the combined influence of the primary and secondary ampere turns. The "differential method" is that of calculating the leakage by taking the difference between the total flux produced by the primary or the secondary, and the fundamental sine wave of the flux. When the effects of flux fringing with open slots are included, the results obtained by the two methods are shown to be entirely consistent. The new formulas derived in this way are believed to be more general in application than any heretofore published. They show that the slot openings decrease the differential leakage reactance much more rapidly than they decrease the magnetizing reactance.

THE subject of "The Air Gap Reactance of Polyphase Machines" has been treated by several different investigators at different times during the last 50 years. Different formulas for calculating the zig-zag leakage of induction motors have been presented, some of which give considerably different results when applied to particular machines.

Paper 47-209, recommended by the AIEE committee on rotating machinery and approved by the AIEE technical program committee for presentation at the AIEE Middle Eastern District meeting, Dayton, Ohio, September 23-25, 1947. Manuscript submitted June 5, 1947; made available for printing August 21, 1947.

P. L. ALGER is staff assistant to the manager of engineering of the General Electric Company, Schenectady, N. Y. H. R. WEST is in the induction voltage regulator engineering division of the General Electric Company, Pittsfield, Mass.

One of the earliest investigators of this problem was C. A. Adams, who defined and described belt leakage reactance at the International Electrical Congress in St. Louis, Mo., in 1904,[1] and published a formula for the average zig-zag leakage permeance in the AIEE TRANSACTIONS[2] in the following year. This formula is

$$P_z = w(a_1 + a_2 - 1)^2/6g \tag{1}$$

Somewhat later, Arnold, in Germany, presented the formula

$$P_z = (s_2 - s_1)^2/6gw_2 \tag{2}$$

Although these two formulas appear to be quite different, they are identical for the particular case of equal numbers of rotor and stator teeth. The Arnold formula is a little more general, for it applies to a squirrel cage motor in which the rotor tooth may have any width between that of the stator slot opening and the stator slot pitch.

In 1921, L. H. A. Carr in England published a very short article[3] on the zig-zag leakage of induction motors in which he considered the air gap leakage flux as if it were produced by a solenoid whose turns threaded through the stator and rotor slots in such a way as to give exactly the same ampere conductors per slot as in the actual motor windings. He gave for the equivalent zig-zag leakage permeance per slot

$$P_z = \frac{l^2 - l_d^2}{6gw_1^2w_2} \tag{3}$$

where

$$l = \frac{l_1 + l_2}{2},$$

and

$$l_d = \frac{l_1 - l_2}{2}$$

This formula gives results different from those given by the Adams or Arnold formulas, except for the special case of equal numbers of rotor and stator slots and slot openings of negligible width. Within the limitations of the assumptions regarding the fringing flux, the formula applies generally to wound rotor polyphase induction motors having integral slot windings, and large numbers of slots per pole.

The derivation of each of the preceding formulas was based on analysis of the permeance and magnetomotive force variations of overlapping rotor and stator teeth. We, therefore, may speak of the general method as the tooth overlap method.

Several other investigators, whose work might be classified under the tooth overlap method have published papers on the subject, but these three formulas are representative.

Later investigators have treated the air gap leakage reactance on the basis of the difference between the total flux crossing the air gap and the useful flux. The method is, therefore, called the difference method, and the air gap leakage reactance is called the differential reactance. Using this method, one of the authors derived, and in 1928 published,[4] methods for calculating the belt and zig-zag components of the differential or air gap leakage reactance of polyphase machines. Curves were given for computing the belt leakage, and the following formula for the zig-zag reactance was given:

$$X_D = \frac{\pi^2 X_M}{12}\left[\frac{1}{s_1^2} + \frac{1}{s_2^2}\right] \tag{4}$$

where X_M is the magnetizing reactance and s_1 and s_2 are the numbers of primary and secondary slots per pole, respectively.

This applies to machines having negligibly small slot openings. Also, it applies specifically to wound rotor induction machines having many phases and one slot per pole per phase. For the aforementioned conditions and for the special case of equal numbers of rotor and stator slots, the preceding equation can be shown to be in perfect agreement with each of the formulas for zig-zag permeance

for stator slot as given by Adams, Arnold, and Carr.

In using the difference method, it generally has been assumed that the slot openings would be equally effective in reducing the exciting and zig-zag reactances. If this were true, equation 4 would be true for machines having open slots as well as for closed slots. Later it was found, however, that in cases where the slot openings were large, as is true of some induction regulators, this equation gives too high values. The authors were, therefore, led to study the effects of the slot openings on the air gap reactance, taking into account the fringing effects of open slots in different ways. In this study, the tooth overlap and difference methods both were used. The results and conclusions may be summarized very briefly as follows:

1. The tooth overlap methods and the difference method yield identical results for those cases where both can be used.

2. The slot openings have a much greater effect on the zig-zag leakage reactance than on the exciting reactance. Their effect, therefore, should not be neglected in the case of open slot machines.

3. The results of this paper indicate that the formula given in equation 4 should be modified as follows, to make it more generally applicable to open slot machines, and to include the effects of skewing.

$$X_D=\frac{\pi^2 X_M}{12}\left[\frac{(6k_1-1)F_{sc}+5\sigma^2}{5s_1^2}+\frac{6k_2-1}{5s_2^2}\right]+X_B \tag{5}$$

where F_{sc} is a factor normally equal to one, but less than one for squirrel cage windings with straight slots; σ is the ratio of angle of skew to one primary slot pitch; X_B is the belt leakage reactance; and k_1 and k_2 are the ratios of effective to maximum air gap length, due to the primary and secondary slot openings, respectively.

The Difference Method

In the paper of reference,[4] expressions were developed for the differential leakage reactance of distributed windings acting on a smooth periphery, with the magnetomotive force of each coil concentrated in a slot opening of negligible width. In this case, each individual coil produces a rectangular flux wave, and the total voltage induced in one phase is found by superposing the rectangles due to successive coils and phases. Limiting the present discussion to the case of a polyphase winding with one slot per pole per phase, s slots per pole, and 100 per cent pitch (as in the case of a squirrel cage), the self-reactance of a single phase will be taken as unity. This is represented by the voltage due to the rectangular wave of flux due to a single full pitch coil.

Figure 1

A. Flux produced by coil in end slots
B. Flux density at rotor surface, determined by density of lines at rotor surface in *A*
C. Assumed permeance as it appears at rotor surface

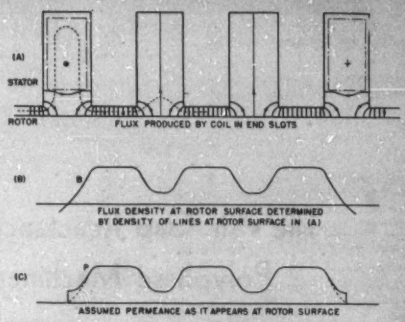

The linkages produced by phase B flux linking phase A, on this basis, are represented by a similar rectangle of height $\cos \pi/s$ times as great, and of width $s-2/s$ times as wide. The first factor takes account of the phase difference angle π/s between adjacent phases. The second factor allows for the fact that each coil spans $s-1$ teeth, carrying positive flux, and one tooth carrying negative flux, produced by an adjacent coil, giving a net span in common of $s-2$ teeth. The total linkages of one phase are represented therefore by the equation

$$\begin{aligned} L_t &= 1+\frac{s-2}{s}\cos\frac{\pi}{s}+\frac{s-4}{s}\cos\frac{2\pi}{s}+\ldots+\frac{2-s}{s}\cos\frac{(s-1)\pi}{s} \\ &= 1-\frac{2}{s}\left(\cos\frac{\pi}{s}+2\cos\frac{2\pi}{s}+3\cos\frac{3\pi}{s}+\ldots+(s-1)\cos\frac{(s-1)\pi}{s}\right) \\ &= \frac{1}{s}\csc^2\frac{\pi}{2s}* \end{aligned} \tag{6}$$

or approximately

$$L_t=\frac{4s}{\pi^2}\left(1+\frac{\pi^2}{12s^2}+\ldots\right) \tag{7}$$

The fundamental sine wave of the rectangular flux wave produced by a single phase has an area $8/\pi^2$ times that of the rectangle, (Figure 4*A*). The total sine wave linkages due to all the phases acting conjointly are $s/2$ times those of a single phase. Since the pitch and distribution factors of the one slot per pole per phase winding are unity, the fundamental sine wave linkages are equal to

$$L_s=\left(\frac{8}{\pi^2}\right)\left(\frac{s}{2}\right)=\frac{4s}{\pi^2} \tag{8}$$

*For derivation, see Appendix I.

Since only the fundamental flux wave can induce fundamental (or slip frequency) currents in the winding in the smooth rotor, L_s represents the useful flux; and, therefore, the per unit differential leakage reactance of the winding is, from equations 7 and 8

$$\begin{aligned} X_D &= \frac{L_t-L_s}{L_s} \\ &= \frac{\pi^2}{12s^2} \text{ approximately}\dagger \end{aligned} \tag{9}$$

This is the per unit differential reactance of the winding in question, with respect to the winding in the opposite member of the machine, assumed to be the rotor. The rotor will also have differential reactance with respect to the stator, its magnitude being determined by the number of the rotor slots. The total differential reactance of the machine then will be

$$X_D=\frac{\pi^2 X_M}{12}\left[\frac{1}{s_1^2}+\frac{1}{s_2^2}\right] \tag{10}$$

the belt leakage being zero in this case.

Before applying this method to the case of a machine having an open slot stator and a smooth rotor, we first should note the nature of the permeance and flux variations in the slots and air gap of typical machines. Figure 1*A* represents an extreme case of a relatively wide slot and a very large air gap.

The flux produced by one coil in the end slots is indicated in the flux plot, and from this plot we can determine approximately the curve of flux density at the rotor surface, which is shown in Figure 1*B*. For the space between but not including the end slots, this curve also represents the air gap permeance as seen at the rotor surface. With such a permeance distribution along the rotor surface, a current carrying coil concentrated in

†This was derived in reference 4.

points under the centers of the end slots and on the rotor surface would produce a flux distribution as indicated in Figure 1*C* which is identical with that of Figure 1*B* except for the end slots where there is a slight discontinuity instead of a gradual reversal of the flux density. Therefore, as far as flux distribution is concerned, we can assume with negligible error that the coils all are concentrated in the centers of the slots. This assumption also is justified as far as linkages are concerned, for nearly all of the flux which enters the slots enters the sides of the teeth without penetrating the conductors.

In Figures 2 and 3 are shown other extremes of slot and air gap proportions, with the corresponding permeance curves.

The greater we make the ratio of slot width to air gap length, the more nearly the permeance curve will approach that of

Figure 2

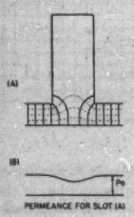

Figure 4*B*. The smaller we make the ratio of slot opening to gap length, the shallower the dips in the permeance curve, and the more rounded their shape.

Reactance of Open Slot Machines by the Difference Method

Formulas will be derived for the differential reactance of machines with open slot stators and closed slot rotors, having slot permeance characteristics of four different kinds.

Let us take, as our first case, *B*, that of an open slot stator with a closed slot rotor, where the air gap permeance is taken to be sinusoidal, as indicated in Figure 4*B*.

$$P_x = P_0 - P_1(1 + \cos 2s_1x) \tag{11}$$

The total linkages produced by a single stator coil are simply equal to k times the linkages in the closed slot case, where k is the ratio of average to maximum permeance along the air gap, or

$$k = \frac{P_0 - P_1}{P_0}$$

The same expressions for total self- and mutual-flux linkages as in the closed slot case are therefore, valid, if the values are multiplied throughout by the factor k. Therefore, for case *B*

$$L_t = \frac{4ks_1}{\pi^2}\left(1 + \frac{\pi^2}{12s_1^2} + \ldots\ldots\right) \tag{12}$$

The curve of flux density produced by a single turn is the same as that of the permeance, or

$$B_x = \frac{P_0 - P_1(1 + \cos 2s_1x)}{P_1} \tag{13}$$

The amplitude of the fundamental sine wave of this is

$$F_0 = \frac{2}{\pi}\int_0 B_x \sin x\, dx$$

$$= \frac{4}{\pi}\left[\frac{P_0 - P_1}{P_0} + \frac{P_1}{P_0}\,\frac{1}{(4s_1^2 - 1)}\right] \tag{14}$$

and the total flux of this fundamental component is

$$\varphi_f = \frac{8}{\pi}\left[\frac{P_0 - P_1}{P_0} + \frac{P_1}{P_0}\,\frac{1}{(4s_1^2 - 1)}\right]$$

$$= \frac{8}{\pi}\left[k + \frac{1-k}{4s_1^2 - 1}\right] \tag{15}$$

As in the closed slot case (case *A*), the per unit fundamental linkages are

$$L_0 = \frac{F_0 s_1}{2\pi},$$

so that

$$L_0 = \frac{4ks_1}{\pi^2}\left[1 + \frac{1-k}{k}\left(\frac{1}{4s_1^2 - 1}\right)\right] \tag{16}$$

The per unit differential reactance of the stator winding is then

$$\frac{L_t - L_0}{L_0} = \frac{\pi^2}{12s_1^2}\,\frac{(1-k)}{k(4s_1^2 - 1)} \tag{17}$$

To this, we must add the differential reactance of the rotor winding in order to obtain the total differential reactance of the machine.

The smooth core rotor is assumed to

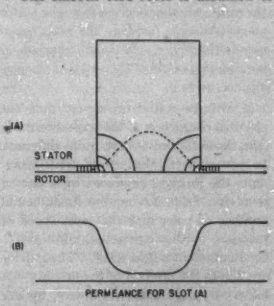

Figure 3

(Ordinates of curve *P* proportional to density of flux lines at rotor surface in *A*)

have s_2 slots per pole, and s_2 phases. The balanced s_2 phase currents produce a magnetomotive force wave which consists of a fundamental revolving at synchronous speed with respect to the stator, and of rotor slot harmonic magnetomotive forces which revolve at other speeds. Only the flux produced by the fundamental magnetomotive forces can induce line frequency voltages in the stator winding when the machine is running. If the rotor is turned very slowly, the average voltage induced in the stator winding is determined by the flux produced by the fundamental magnetomotive forces only. The fluxes produced by the harmonic magnetomotive forces of the rotor will induce line frequency voltages in the stator winding for different positions of the rotor; but, as the rotor is turned, these voltages will reverse with respect to that caused by the fundamental magnetomotive force, and their average will be zero.

The flux produced by the fundamental magnetomotive force wave of the rotor is not sinusoidal because it acts on a nonuniform permeance. Assuming balanced stator and rotor fundamental magnetomotive forces, the peak of the rotor fundamental magnetomotive force wave is $(4/\pi)(s_1/2) = 2s_1/\pi$ times the (unit) magnetomotive force of a single stator coil. The instantaneous flux density B_x at a point a distance x from one side of a reference stator coil is therefore

$$B_x = \frac{2s_1P_x}{\pi}\sin(x - wt + \theta)$$

where

$$P_x = P_0 - P_1(1 + \cos 2s_1x) \tag{11}$$

The instantaneous flux linking the reference stator coil is then

$$\varphi_1 = \frac{2s_1}{\pi}\int_0^\pi \sin(x - wt + \theta)\,[P_0 - P_1(1 + \cos 2s_1x)]\,dx$$

or

$$\varphi_1 = \frac{4s_1}{\pi}(P_0 - P_1)\cos(wt - \theta) - \frac{2s_1}{\pi}P_1\int_0 \sin(x - wt + \theta)\cos 2s_1x\,dx$$

The first term of this expression represents the flux that would link one stator coil if the permeance were uniform and of the value $P_0 - P_1$. The second term represents the difference in the linkages caused by the nonuniformity of the permeance.

Completing the integration, we get

$$\varphi_1 = \frac{4s_1P_0}{\pi}k\left[1 + \frac{1-k}{k(4s_1^2 - 1)}\right]\cos(-wt + \theta) \tag{18}$$

The (unit) flux produced by a single

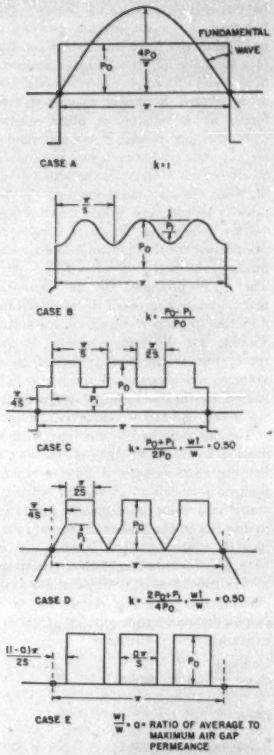

Figure 4. Flux wave due to a single full pitch coil

Case *A*. Closed slots. Permeance uniform
Case *B*. Open slots. Permeance sinusoidal. $P=P_0-P_1(1+\cos 2SX)$
Case *C*. Open slots. Permeance lower, but uniform across slot openings
Case *D*. Open slots. Permeance uniformly varying from slot edges to zero at slot centers
Case *E*. Open slots. Permeance concentrated in equivalent tooth width, with zero permeance in equivalent slot width
These diagrams show the flux wave form produced by a single full pitch coil, as it appears to a closed slot winding, or smooth pole face, on the opposite side of the air gap

Figure 5. Relative values of differential leakage reactance for open slot windings

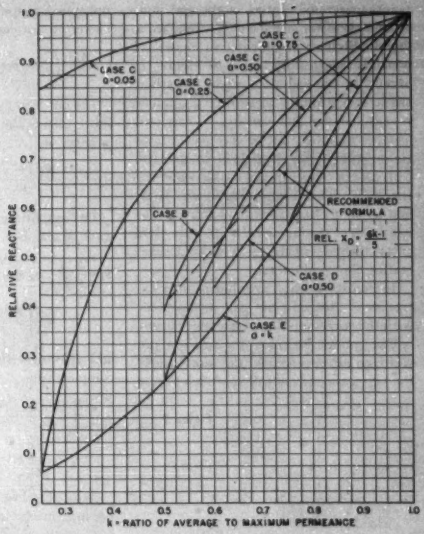

stator coil is πP_0, so that the per unit linkages produced by the fundamental rotor magnetomotive force are

$$L_{s_2}=\frac{4ks_1}{\pi^2}\left[1+\frac{1-k}{k(4s_1^2-1)}\right] \tag{19}$$

Comparing this with equation 16, we see that equal ampere turns in the stator and rotor windings will induce equal useful fluxes in the opposite members. Therefore, the quantity L_s corresponds exactly to mutual inductance in the case of two simple single-phase coupled circuits; and, therefore, the total per unit differential leakage is

$$X_D=\frac{L_{t_1}+L_{t_2}-2L_s}{L_s} \tag{20}$$

From the nature of the equations, it seems obvious that for any permeance characteristics which can be expressed by a Fourier series, the quantity L_s must be the same, whether derived from the stator magnetomotive force or the rotor magnetomotive force. In short, equation 20 is valid, regardless of the shape of the permeance wave.

It will be noted, however, that the physical characters of the second terms in equations 16 and 19 are quite different. In equation 16, the second term represents the linkages produced by a pair of revolving fields having the fundamental number of poles and the same speed of rotation, so they are actual additions to the fundamental field itself. These fields are due to the product of the primary slot harmonic magnetomotive forces, by the corresponding orders of harmonics in the permeance wave. However, the second term in equation 19 represents the linkages of two harmonic fields of the same numbers of poles and speeds of rotation as the primary slot harmonics, due to the product of the fundamental magnetomotive force wave of the secondary by the permeance harmonics of the primary. These harmonics induce fundamental frequency voltages in the primary and therefore form a part of the mutual flux.

Each rotor slot is assumed to carry s_1/s_2 times the current in each stator slot. The total linkage of one full pitch rotor coil, due to all of the rotor currents, is then

$$L_{t_2}=\frac{s_1}{s_2}\left[\frac{k}{s_2}\csc^2\frac{\pi}{2s_2}\right]$$
$$=\frac{4ks_1}{\pi^2}\left[1+\frac{\pi^2}{12s_2^2}+\dots\right] \tag{21}$$

in terms of the unit flux produced by the current in a single stator coil. From equations 12, 16, and 20, the total differential reactance is then

$$X_D=\frac{\pi^2X_M}{12}\left[\frac{1}{s_1^2}\left(\frac{\pi^2k+6k-6}{\pi^2k}\right)+\frac{1}{s_2^2}\right] \tag{22}$$

for case *B*.

Case *C*. Permeance as in Figure 4*C*

Here, as in case *A*, the value of L_{t_2} is the same as in the closed slot case except multiplied by k.

$$L_{t_2}=\frac{4ks_1}{\pi^2}\left[1+\frac{\pi^2}{12s_2^2}+\dots\right]$$

Table I. Values of Differential Leakage Reactance

Case	Permeance Wave	Per Unit X_D*	Range of k
A. Eq 9	Uniform	$\frac{\pi^2}{12s^2}$	1
B. Eq 22	Sinusoidal	$\frac{\pi^2}{12s^2}\left(\frac{(\pi^2+6)k-6}{k\pi^2}\right)$	1/2 to 1
C. Eq 26	Stepped, $a=0.25$	$\frac{\pi^2}{12s^2}\left(\frac{21k-5}{16k}\right)$	1/4 to 1
Eq 23	Stepped, $a=0.50$	$\frac{\pi^2}{12s^2}\left(\frac{7k-3}{4k}\right)$	1/2 to 1
Eq 26	Stepped, $a=0.75$	$\frac{\pi^2}{12s^2}\left(\frac{37k-21}{16k}\right)$	3/4 to 1
D. Eq 24	Tapered, $a=0.50$	$\frac{\pi^2}{12s^2}\left(\frac{22k-9}{16k}\right)$	1/2 to 3/4
E. Eq 25	Lumped	$\frac{\pi^2}{12s^2}(k^2)$	0 to 1

*These ratios are shown in Figure 5.

Also, as in case *A*

$$L_{t_2}=\frac{4ks_1}{\pi^3}\left[1+\frac{\pi^2}{12s_2^2}+\ldots\ldots\right]$$

As derived in Appendix II, by Fourier analysis of the case *C* diagram

$$L_s=\frac{4ks_1}{\pi^3}\left[1+\frac{\pi^2(1-k)}{32ks_1^2}+\ldots\ldots\right]$$

whence, from equations 12, 16, and 20

$$X_D=\frac{\pi^2X_M}{12}\left[\frac{1}{s_1^2}\left(\frac{7k-3}{4k}\right)+\frac{1}{s_2^2}\right] \tag{23}$$

Case *D*. Permeance as in Figure 4*D*

The formulas for L_{t_1} and L_{t_2} are the same as in cases *A* and *B*.

As derived in Appendix III

$$L_s=\frac{4ks}{\pi^3}\left[1+\frac{\pi^2(3-2k)}{128ks_1^2}+\ldots\ldots\right]$$

whence

$$X_D=\frac{\pi^2X_M}{12}\left[\frac{1}{s_1^2}\left(\frac{22k-9}{16k}\right)+\frac{1}{s_2^2}\right] \tag{24}$$

Case *E*. Permeance as in Figure 4*E*

By similar procedure

$$L_s=\frac{4ks_1}{\pi^3}\left(1+\frac{\pi^2}{24s_1^2}(1-k^2)\right)$$

and

$$X_D=\frac{\pi^2X_M}{12}\left[\frac{k^2}{s_1^2}+\frac{1}{s_2^2}\right] \tag{25}$$

The equation for L_s is derived in Appendix IV.

So far, the ratio of tooth width to slot pitch, w_t/w, has been taken equal to 0.50. The results for other values of w_t/w can be found by combining the results from equations 23 or 24 and 25. Considering Figure 4*C*, and letting $w_t/w = a$, the flux wave is made up of the sum of a uniform wave of height P_1, and an intermittent wave of height (P_0-P_1). The per unit linkages are, therefore,

$$L=\frac{P_1}{P_0}(L \text{ for case } A)+\frac{P_0-P_1}{P_0}\times$$

$$(L \text{ for case } E \text{ but putting } a \text{ for } k)$$

Hence, the differential leakage reactance is

$$X_D=\frac{\pi^2X_M}{12}\left[\frac{k+a(a+1)(k-1)}{ks_1^2}+\frac{1}{s_2^2}\right] \tag{26}$$

which reduces to equation 25 if $a = k$, and to equation 10 if $k = 1$.

The results are summarized in Table I, giving the factors by which the quantity $\pi^2/12s_1^2$ in the formula for the closed slot case must be multiplied to give the correct values for the different open slot cases. These factors are shown in Figure 5.

It is clear from this analysis that any opening of the slots, giving dips in the permeance wave, decreases the harmonic content of the total flux wave as compared with the fundamental sine wave for a winding embedded in the open slots; and therefore, decreases the per unit differential leakage reactance. Since in this analysis we have taken the number of phases equal to the number of slots, and the number of slots to be large, the lower order harmonics, or phase belt leakage fluxes, are eliminated, and the leakage flux is made up entirely of the tooth harmonic frequencies. The factors in Table I and Figure 5, therefore, do not apply to the formulas for belt leakage reactance.

Since, in practice, $w_t/w = a$, and k, are seldom less than 0.50 for rotating machines, the several curves of Figure 5 all can be represented to sufficient accuracy by the formula

$$\text{Reactance ratio}=\frac{6k-1}{5}\ \text{(approximately)} \tag{27}$$

whence we conclude that the differential leakage reactance of a slot embedded winding is

$$X_D=\frac{\pi^2X_M}{60}\left(\frac{6k-1}{s^2}\right) \tag{28}$$

where

X_M = magnetizing reactance, corresponding to fundamental sine wave of air gap flux.
s = number of slots per pole.
k = ratio of average to maximum air gap permeance, taking into account the slot openings on the winding side of the air gap only.

By this method, the slot openings on the other side of the air gap, if any, must be taken into account separately, as if each winding faced a smooth pole face. There are then two independent values, k_1 and k_2, corresponding to the primary and secondary slot numbers, s_1 and s_2, and the configurations of their openings. The over-all average air gap permeance is equal to k_1k_2, and this factor enters linearly in the calculation of the magnetizing reactance for the fundamental air gap flux, X_M.

The combined differential leakage reactance of two opposing slot embedded windings, with s_1 and s_2 slots per pole is therefore

$$\text{Total } X_D=\frac{\pi^2X_M}{60}\left(\frac{6k_1-1}{s_1^2}+\frac{6k_2-1}{s_2^2}\right) \tag{29}$$

The Average Overlap Method

It is well known that the slot reactance in ohms of a full pitch, one slot per pole per phase, winding is equal to

$$X_s=MP_s \text{ ohms} \tag{30}$$

where P_s is the slot permeance constant, or effective ratio of depth to width of slot, and M is a winding factor equal to*

$$\frac{8\pi^2fLqZ^2}{10^8ps}$$

f being the frequency, L the core length, q the number of phases, Z the number of series connected conductors per phase, p the number of poles, and s the slots per pole.

Also, the magnetizing reactance of such a winding is

$$X_M=\frac{DsMk}{\pi pg} \text{ ohms} \tag{31}$$

*Derived in reference 4.

where D = air gap diameter, k = ratio of effective to maximum air gap, and g = the maximum air gap length. Hence, the slot reactance may be expressed as a factor times X_M

$$X_s = \frac{\pi p g}{D s k} P_s X_M \tag{32}$$

The zig-zag leakage reactance then may be calculated by equation 32, if the effective, or average, permeance of the zig-zag flux path bridging one slot opening is known.

In the paper of reference 2, Carr derived the following formula for the effective zig-zag permeance per centimeter length of stator slot:

$$P_z = \frac{t^4 - t_d^4}{6 g w_1^2 w_2} \tag{33}$$

where

$$t = \frac{t_1 + t_2}{2} = \frac{a_1 w_1 + a_2 w_2}{2}$$

and

$$t_d = \frac{t_1 - t_2}{2} = \frac{a_1 w_1 - a_2 w_2}{2}$$

This equation was given by Carr for a particular range of relative slot and tooth proportions. As shown in Appendix V, the equation holds for any combination of stator and rotor slot and tooth widths, provided the numbers of slots per pole are not small.

Substituting for w_1 and w_2 their values $\pi D/ps_1$ and $\pi D/ps_2$ in equation 33, we get

$$p_z = \frac{a_1 a_2 s_1 \pi D}{12 g p} \left(\frac{a_1^2}{s_1^2} + \frac{a_2^2}{s_2^2} \right) \tag{34}$$

Putting p_z from equation 34 for p_s in equation 32, the zig-zag reactance is found to be

$$X_z = \frac{a_1 a_2 \pi^2 X_M}{12 k} \left(\frac{a_1^2}{s_1^2} + \frac{a_2^2}{s_2^2} \right) \tag{35}$$

The product $a_1\ a_2$, however, is merely the ratio of effective to total air gap length, which we have previously denoted by k. Hence

$$X_z = \frac{\pi^2 X_M}{12} \left(\frac{a_1^2}{s_1^2} + \frac{a_2^2}{s_2^2} \right) \tag{36}$$

This is the final expression for the zig-zag reactance of wound rotor machines calculated by the tooth overlap method. Comparing this with equation 25, we find that the overlap method gives a primary differential leakage identical with case E, Table I, varying in proportion to the square of a_1 or k_1.

Derivation of reactance formulas by the overlap method for types of permeance variation other than type E are considerably more difficult and laborious. The writers have applied the method to case C and to the special case of case D, in which $P_1 = P_0$, and have obtained identically the same formulas as have been obtained by the difference method.

Zig-Zag Reactance of Squirrel Cage Machines

The zig-zag reactance of a squirrel cage motor generally will be slightly less than that of the corresponding wound rotor motor. This is evident if we think of a squirrel cage winding as having been made by completely short-circuiting the end portions of a wound rotor winding. Short-circuiting any two points of a net work in general will reduce the reactance of the network.

The rule, which is stated in Appendix V, for determining the magnetic potential difference between rotor and stator teeth in wound rotor machines, does not hold true for squirrel cage motors because the rotor currents will vary from slot to slot in a more or less irregular manner. However, the average zig-zag permeance can be determined in a more direct manner if we consider the rotor teeth as being equivalent to isolated strips of steel separated from each other by an imaginary material of zero permeability. This procedure is perfectly legitimate; for, if the squirrel cage resistance is zero, no a-c flux can link any bar of the cage and, therefore, all flux which enters any tooth of the rotor from the stator must return to the stator from the same tooth.

In this way, a factor, F_{sc}, less than unity, may be derived, which should be multiplied into the expressions given in Table I, to obtain the net differential leakage reactance for a squirrel cage winding without skew. It is evident that the induced squirrel cage currents which cause this reduction in reactance set up revolving fields of their own, which link the stator winding, causing tooth frequency voltages to appear at the line terminals. These harmonics are the cause of the well-known effects of voltage ripples and increased stator iron losses, which occur when the squirrel cage has a much larger number of slots than the primary and is not skewed. If, as is usually the case, the slots are skewed approximately the width of one primary slot pitch, the value of F_{sc} becomes unity, since the primary slot harmonics then induce no net voltage and no circulating currents flow in the squirrel cage. It is hoped that these interesting relationships may be the subject of future papers before the Institute. They have been considered in a recent paper by J. H. Walker before The Institution of Electrical Engineers, London, England.[5]

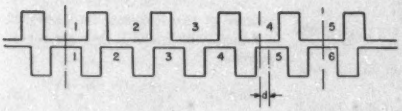

Figure 6

Extra Reactance Due to Skewed Slots

Thus far in the discussion we tacitly have assumed that the slots are not skewed. If the slots are skewed, the reactance is increased, because the phase angle of the voltage induced in the core length of a single secondary conductor varies through the angle α, making the net voltage proportional to the chord instead of the arc of the angle.

The ratio of mutual to total reactance of the primary is therefore, $(2/\alpha) \sin \alpha/2$, and the reactance due to skew is

$$X_{skew} = \frac{L_1 L_2 - M^2}{L_1} = \left(1 - \frac{4}{\alpha^2} \sin^2 \frac{\alpha}{2} \right) X_M,$$

giving the well-known formula

$$X_{skew} = \frac{\alpha^2 X_M}{12} = \frac{\pi^2 \sigma^2 X_M}{12 s_1^2} \text{ (approximately)}$$

where α = angle of skew in radians = $\pi\sigma/s_1$, where σ = angle of skew as a fraction of one stator slot pitch. Combining this with equation 28, and adding the term for belt leakage, we get for the total air gap reactance of a wound rotor induction motor

$$X_D = \frac{X_M}{6} \left[\frac{6k_1 - 1 + 5\sigma^2}{s_1^2} + \frac{6k_2 - 1}{s_2^2} \right] + X_B \tag{37}$$

and for a squirrel cage motor

$$X_D = \frac{X_M}{6} \left[\frac{(6k_1 - 1) F_{sc} 5\sigma^2}{s_1^2} + \frac{(6k_2 - 1)}{s_2^2} \right] \tag{38}$$

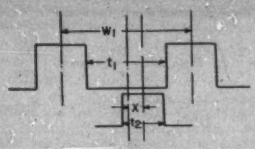

Figure 7

Summary

The formulas derived in this paper enable the differential leakage, or zig-zag, reactance of any motor or induction regulator to be calculated with good accuracy, whatever the width of slot openings and whatever the ratio of primary to secondary slots. The basic formula for the total differential leakage reactance is

$$X_D = \frac{\pi^2 X_M}{12}\left[\frac{(6k_1-1)F_{sc}+5\sigma^2}{5s_1^2}+\frac{6k_2-1}{5s_2^2}\right]+X_B \quad (5)$$

where

F_{sc} = a factor less than unity, expressing the effects of induced harmonic currents in a squirrel cage winding
= 1 for any wound rotor
= 1 for a squirrel cage winding with σ approximately equal to 1
σ = ratio of angle of skew to one primary slot pitch
X_M = primary magnetizing reactance
s_1, s_2 = primary and secondary numbers of slots per pole
X_B = belt leakage, due to magnetomotive force harmonics caused by phase belts and irregular windings, to be calculated as given in reference 4
= 0 for any squirrel cage winding

There still remains much more work to be done before fully adequate formulas for the reactance of all types of rotating machines are available. Two of the subjects not yet fully covered are the phenomena of induced squirrel cage currents, on which the value of F_{sc} in equation 39 depends, and the belt leakage reactance of irregular windings. Liwschitz[6,7] has treated both these topics; but has not considered the effects of alternative patterns for irregular winding distribution, nor has he given his results in the algebraic or per unit forms that are most convenient for calculations. The wide differences in viewpoints have prevented the authors from obtaining a clear comparison of the Liwschitz results for the effects of open slots on differential reactance with those of the present paper, so that more study should be given to this aspect of the subject. Kron[8] has given a general method for calculating the belt leakage of irregular windings, which could well be extended on the basis of the results in this paper. Finally, there is greatly needed a sound analytical treatment of the reactance of end windings, based on the geometry of the end structure, and giving formulas from which the end winding forces on short circuit can be derived. It is hoped that all these topics may be considered in future Institute papers.

Definitions of Symbols

Subscripts 1 and 2 refer to primary and secondary windings, respectively, unless indicated otherwise.

a = ratio of effective tooth width to slot pitch. In final reactance formulas, a is numerically equal to k
D = air gap diameter
E = energy
f = frequency
g = air gap length
k = ratio of average to maximum permeance along the air gap
L = length of core
L_q = linkages in a full pitch coil due to fundamental of the magnetomotive force wave of either member
L_t = linkages in a full pitch coil of rotor or stator due to all currents in the same member
M = winding factor
p = number of poles
P_0, P_1 = (Defined in Figure 4)
P_s = slot leakage permeance
P_z = zig-zag leakage permeance per slot
s = slots per pole
t = effective tooth width
w = slot pitch
X_B = belt leakage reactance
X_D = differential leakage reactance
X_z = zig-zag leakage reactance
X_s = slot leakage reactance
α = amount of skew in radians
σ = skew in terms of one stator slot pitch

Appendix I

Let

$$T = \sin\theta + \sin 2\theta + \sin 3\theta + \ldots + \sin(s-1)\theta \quad (39)$$

Then

$$\frac{dT}{d\theta} = \cos\theta + 2\cos 2\theta + 3\cos 3\theta + \ldots + (s-1)\cos(s-1)\theta \quad (40)$$

But

$$\sin\theta = -\frac{j(\epsilon^{j\theta}-\epsilon^{-j\theta})}{2}$$

so that

$$T = -\frac{j}{2}[\epsilon^{j\theta}+\epsilon^{2j\theta}+\ldots+\epsilon^{(s-1)\theta} - (\epsilon^{-j\theta}+\epsilon^{-2j\theta}+\ldots+\epsilon^{-(s-1)j\theta})] \quad (41)$$

Since

$$\sum_{n=1}^{n=(s-1)} r^n = \frac{r(r^{s-1}-1)}{r-1}$$

$$T = -\frac{j}{2}\left[\frac{\epsilon^{j\theta}(\epsilon^{(s-1)j\theta}-1)}{\epsilon^{j\theta}-1} - \frac{\epsilon^{j\theta}(\epsilon^{-(s-1)j\theta}-1)}{\epsilon^{j\theta}-1}\right]$$

$$= \frac{-j}{2(\epsilon^{j\theta}-1)}[\epsilon^{sj\theta}-\epsilon^{j\theta}+\epsilon^{-(s-1)j\theta}-1] \quad (42)$$

and

$$\frac{dT}{d\theta} = \frac{-\epsilon^{j\theta}}{2(\epsilon^{j\theta}-1)^2}[\epsilon^{sj\theta}-\epsilon^{j\theta}+\epsilon^{-(s-1)j\theta}-1] + \frac{1}{2(\epsilon^{j\theta}-1)}[s\epsilon^{sj\theta}-\epsilon^{j\theta}-(s-1)\epsilon^{-(s-1)j\theta}]$$

$$= \frac{1}{2\left(\epsilon^{\frac{j\theta}{2}}-\epsilon^{-\frac{j\theta}{2}}\right)^2}[\epsilon^{sj\theta}+\epsilon^{-sj\theta} - s(\epsilon^{sj\theta}+\epsilon^{-sj\theta}) - 2 + s(\epsilon^{(s-1)j\theta}+\epsilon^{-(s-1)j\theta})]$$

$$= \frac{1}{8\sin^2\frac{\theta}{2}}[2\cos s\theta - 2s\cos s\theta - 2 + 2s\cos(s-1)\theta] \quad (43)$$

If $s\theta = \pi$, this reduces to

$$\frac{dT}{d\theta} = \frac{-1}{4\sin^2\frac{\theta}{2}}[2-s+s\cos\theta]$$

$$= \frac{-1}{2\sin^2\frac{\theta}{2}} + \frac{s}{2} \quad (44)$$

Figure 8

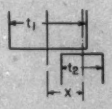

From equations 1 and 40

$$L_t = 1 - \frac{2}{s}\frac{dT}{d\theta} \quad (45)$$

Hence

$$L_t = \frac{1}{s}\csc^2\frac{\theta}{2} = \frac{1}{s}\csc^2\frac{\pi}{2s} \quad (46)$$

which verifies equations 6 and 40.

Appendix II

For case C

$$P = P_1\Big]_0^{\frac{\pi}{4s}} + P_0\Big]_{\frac{\pi}{4s}}^{\frac{3\pi}{4s}} + P_1\Big]_{\frac{3\pi}{4s}}^{\frac{5\pi}{4s}} + \ldots + P_0\Big]_{\frac{(4s-1)\pi}{4s}}^{\frac{(4s-1)\pi}{4s}} + P_1\Big]_{\frac{(4s-1)\pi}{4s}}^{\pi} \quad (47)$$

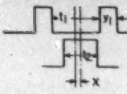

Figure 9

The fundamental sine wave of P is

$$F=\frac{2}{\pi}\int_0^{\pi} P\sin x\,dx=\frac{2P_1}{\pi}(-\cos x)\Big]_0^{\frac{\pi}{4s}}-\frac{2P_0}{\pi}(\cos x)\Big]_{\frac{\pi}{4s}}^{\frac{3\pi}{4s}}-\ldots \quad (48)$$

$$=\frac{2P_1}{\pi}\left[1-\cos\frac{\pi}{4s}+\cos\frac{3\pi}{4s}-\cos\frac{5\pi}{4s}+\ldots+\cos\frac{(4s-1)\pi}{4s}+1\right]+\frac{2P_0}{\pi}\left[\cos\frac{\pi}{4s}-\cos\frac{3\pi}{4s}+\cos\frac{5\pi}{4s}-\cos\frac{7\pi}{4s}+\ldots\right]$$

$$=\frac{2(P_0-P_1)}{\pi}\left[\cos\frac{\pi}{4s}-\cos\frac{3\pi}{4s}+\cos\frac{5\pi}{4s}-\cos\frac{7\pi}{4s}+\ldots+\cos\frac{(4s-1)\pi}{4s}-\cos\frac{(4s-3)\pi}{4s}\right]+\frac{4P_1}{\pi}$$

$$=\frac{4P_1}{\pi}+\frac{4(P_0-P_1)}{\pi}\sin\frac{\pi}{4s}\left[\sin\frac{\pi}{2s}+\sin\frac{3\pi}{2s}+\sin\frac{5\pi}{2s}+\ldots+\sin\frac{(2s-1)\pi}{2s}\right]$$

$$=\frac{4P_1}{\pi}+\frac{4(P_0-P_1)}{\pi}\sin\frac{\pi}{4s}\left[\frac{1}{\sin\frac{\pi}{2s}}\right]$$

$$=\frac{4P_1}{\pi}+\frac{2(P_0-P_1)}{\pi}\sec\frac{\pi}{4s} \quad (49)$$

The per unit fundamental linkages are

$$F\times\frac{s}{2}\times\frac{2}{\pi P_0}=\frac{Fs}{\pi P_0}$$

So

$$L_s=\frac{4s}{\pi^2}\left[\frac{P_1}{P_0}+\frac{(P_0-P_1)}{2P_0}\sec\frac{\pi}{4s}\right]$$

$$=\frac{4ks}{\pi^2}\left[1+\frac{\pi^2(1-k)}{32ks^2}\right]\text{ approximately} \quad (50)$$

Appendix III

For case D

$$P=\frac{4sP_1x}{\pi}\Big]_0^{\frac{\pi}{4s}}+P_0\Big]_{\frac{\pi}{4s}}^{\frac{3\pi}{4s}}+4P_1\Big]_{\frac{3\pi}{4s}}^{\frac{\pi}{s}}-4P_1sx\Big]_{\frac{3\pi}{4s}}^{\frac{\pi}{s}}+\frac{4sP_1x}{\pi}\Big]_{\frac{\pi}{s}}^{\frac{5\pi}{4s}}-4P_1\Big]_{\frac{\pi}{s}}^{\frac{5\pi}{4s}}+\ldots \quad (51)$$

The fundamental sine wave of P is

$$F=\frac{2}{\pi}\int_0^{\pi} P\sin x\,dx$$

$$=\frac{8sP_1}{\pi^2}(\sin x-x\cos x)\Big]_0^{\frac{\pi}{4s}}-\frac{2P_0}{\pi}(\cos x)\Big]_{\frac{\pi}{4s}}^{\frac{3\pi}{4s}}-\frac{8P_1}{\pi}(\cos x)\Big]_{\frac{3\pi}{4s}}^{\frac{\pi}{s}}-\frac{8P_1s}{\pi^2}(\sin x-x\cos x)\Big]_{\frac{3\pi}{4s}}^{\frac{\pi}{s}}+\frac{8P_1s}{\pi^2}(\sin x-x\cos x)\Big]_{\frac{\pi}{s}}^{\frac{5\pi}{4s}}+\frac{8P_1}{\pi}(\cos x)\Big]_{\frac{\pi}{s}}^{\frac{5\pi}{4s}}+\ldots=\frac{8sP_1}{\pi^2}\left[\sin\frac{\pi}{4s}-\sin\frac{\pi}{s}+\sin\frac{3\pi}{4s}+\sin\frac{5\pi}{4s}-\sin\frac{\pi}{s}+\ldots\right]+\frac{2(P_0-P_1)}{\pi}\left[\cos\frac{\pi}{4s}-\cos\frac{3\pi}{4s}+\cos\frac{5\pi}{4s}-\ldots\right]$$

$$=\frac{8sP_1}{\pi^2}\left(\sin\frac{\pi}{4s}+\sin\frac{3\pi}{4s}+\ldots\right)-\frac{16sP_1}{\pi^2}\left(\sin\frac{\pi}{s}+\sin\frac{2\pi}{s}+\ldots\right)+\frac{4(P_0-P_1)}{\pi}\sin\frac{\pi}{4s}\left(\sin\frac{\pi}{2s}+\sin\frac{3\pi}{2s}+\ldots\right)$$

$$=\frac{8sP_1}{\pi^2}\left[\frac{1}{\sin\frac{\pi}{4s}}-\frac{2\cos\frac{\pi}{2s}}{\sin\frac{\pi}{2s}}\right]+\frac{2(P_0-P_1)}{\pi}\sec\frac{\pi}{4s} \quad (52)$$

Figure 10

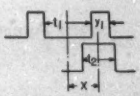

The total sine wave linkages for all phases are obtained by multiplying equation 52 by $s/\pi P_0$, as before, giving

$$L_s=\frac{4ks}{\pi^2}\left[1+\frac{\pi^2}{128ks^2}(3-2k)+\ldots\right]$$

Appendix IV

For case E

$$P=P_0\Big]_{\frac{(1-k)\pi}{2s}}^{\frac{(1+k)\pi}{2s}}+P_0\Big]_{\frac{(3-k)\pi}{2s}}^{\frac{(3+k)\pi}{4s}}+\ldots\ldots \quad (53)$$

The fundamental sine wave of P is

$$F=\frac{2}{\pi}\int_0^{\pi} P\sin x\,dx=\frac{2P_0}{\pi}(-\cos x)\Big]_{\frac{(1-k)\pi}{2s}}^{\frac{(1+k)\pi}{2s}}+\ldots\ldots$$

$$=\frac{2P_0}{\pi}\left(\cos\frac{(1-k)\pi}{2s}-\cos\frac{(1+k)\pi}{2s}+\cos\frac{(3-k)\pi}{2s}-\cos\frac{(3+k)\pi}{2s}+\ldots\right)$$

$$=\frac{4P_0}{\pi}\sin\frac{k\pi}{2s}\left(\sin\frac{\pi}{2s}+\sin\frac{3\pi}{2s}+\ldots+\sin\frac{(2s-1)\pi}{2s}\right)$$

$$=\frac{4P_0}{\pi}\sin\frac{k\pi}{2s}\csc\frac{\pi}{2s} \quad (54)$$

The per unit fundamental sine wave linkages are found by multiplying equation 53 by $s/\pi P_0$, giving

$$L_s=\frac{4s}{\pi^2}\sin\frac{k\pi}{2s}\csc\frac{\pi}{2s}$$

$$=\frac{4ks}{\pi^2}\left(1+\frac{\pi^2}{24s^2}(1-k^2)\right)\text{ approximately}$$

Appendix V

Consider a symmetrical polyphase machine having full pitch windings in both rotor and stator, the rotor position being such that its winding axes coincide with those of the stator. For this particular position the belt leakage is zero, and the total air gap leakage reactance is zig-zag leakage.

Figure 6 shows a stator and a rotor phase belt in the position for zero belt leakage as just stated. Equal ampere turns are assumed in rotor and stator. Between stator tooth 1 and rotor tooth 1 there will be no magnetomotive force drop, and we may take their common center line as a reference boundary. The magnetomotive force drop between any other two opposing rotor and stator teeth in the figure will then be proportional to the algebraic sum of all the ampere turns between the two teeth in question and the reference center line of the first teeth. For instance, between stator tooth 4 and rotor tooth 5, the magnetomotive force drop is

$$4\pi n_1 i_1\left[3-\frac{4w_2}{w_1}\right]$$

where

$n_1 i_1$ = ampere conductors per stator slot

and

$$\frac{w_2}{w_1}=\frac{\text{rotor slot pitch}}{\text{stator slot pitch}}$$

Now the distance between the center lines of stator tooth 4 and rotor tooth 5 is

$$d=(3w_1-4w_2)\text{ or }\left(3-\frac{4w_2}{w_1}\right)w_1$$

Substituting this in the expression for the magnetomotive force drop, we get

$$4\pi n_1 i_1 \frac{d}{w_1}$$

That is, the magnetic potential difference between any two teeth in the figure is equal to the magnetic potential difference per stator slot times the ratio of the distance between the two tooth center lines to one stator slot pitch.

Stated in another way, the magnetic potential difference between any two teeth in coaxial phase belts is equal to $4\pi ni$, where ni is the stator ampere turns per centimeter of air gap periphery.

This simple rule makes it possible to calculate the flux distribution as completely and accurately as our ability to allow properly for fringing will permit.

By making use of this simple rule, we can determine the flux density between any two opposing teeth, and hence the magnetic energy, and this in turn is a measure of the reactance. In the following, an expression is derived for the average energy per tooth for all relative positions of a pair of opposing rotor and stator teeth, throughout one slot pitch. This gives the average zig-zag reactance for the conditions stated and, therefore, also the average effective zig-zag leakage permeance per slot. Having a formula for effective zig-zag permeance for the particular conditions, we may assume reasonably that we can use this same value of permeance in calculating zig-zag reactance of fractional pitch windings.

For other noncoaxial positions of the rotor, belt leakage appears. This is superposed on the zig-zag leakage and may be accounted for accordingly.

An expression for the average energy per stator tooth can be obtained most easily by finding a formula for the average energy per slot of that member which has the narrower teeth, regardless of the slot pitch. By using this procedure we need study only two types of slot and tooth combinations

1. In which the narrower tooth is narrower than the slot in the opposite member.

2. In which the narrower tooth is wider than the slot in the opposite member.

This will cover all possible slot and tooth combinations.

In Figure 7 is represented a slot and tooth combination of the first type; that is, the rotor teeth are narrower than either the stator teeth or the stator slots.

As the rotor tooth moves through one stator slot pitch, there are three regions to be considered

1. Where the rotor tooth is entirely opposite the stator tooth.

2. Where the rotor tooth is partly opposite the stator tooth and partly opposite the stator slot.

3. Where the rotor tooth is entirely opposite the stator slot.

We must integrate through these regions separately in order to get the average energy.

TYPE 1

Region 1

$$0 \leq x \leq \frac{l_1 - l_2}{2} \quad \text{(Figure 7)}$$

Let the ampere turns per rotor slot be $n_2 i_2$. Then the potential difference between the two teeth is, according to the rule stated previously,

$$v = 4\pi n_2 i_2 \frac{x}{w_2} \tag{55}$$

The magnetic energy in the permeance P between the teeth is

$$E_a = \frac{Rv^2}{8\pi} = \frac{v^2 P}{8\pi} \tag{56}$$

Substituting for v and P their values of $4\pi n_2 i_2 x/2$ and l_2/g, we have

$$E_a = 2\pi (n_2 i_2)^2 \frac{x^3 l_2}{g w_2^2} \tag{57}$$

for the energy as a function of the rotor tooth position in region 1.

Region 2

$$\frac{l_1 - l_2}{2} \leq x \leq \frac{l_1 + l_2}{2} \quad \text{(Figure 8)}$$

In this region the rotor tooth is partly opposite the stator tooth and partly opposite the slot. The permeance is

$$P = \frac{1}{g}\left(\frac{l_1 + l_2}{2} - x\right) \tag{58}$$

so that the energy is

$$E_b = 2\pi (n_2 i_2)^2 \frac{x^2}{g w_2^2}\left(\frac{l_1 + l_2}{2} - x\right) \tag{59}$$

Region 3

$$\frac{l_1 + l_2}{2} \leq x \leq \frac{1}{2}$$

Here the rotor tooth is entirely opposite the stator slot, so that it carries no flux, and, therefore, $E_c = 0$.

The average energy of the rotor tooth flux through one stator slit pitch is

$$E_1 = \frac{1}{w_1/2}\left[\int_0^{\frac{l_1 - l_2}{2}} E_a dx + \int_{\frac{l_1 - l_2}{2}}^{\frac{l_1 + l_2}{2}} E_b dx + \int_{\frac{l_1 + l_2}{2}}^{\frac{w_1}{2}} E_c dx\right]$$

$$= \frac{\pi (n_2 i_2)^2}{6 g w_2^2 w_1} l_1 l_2 (l_1^2 + l_2^2) \tag{60}$$

The energy per stator tooth will be

$$E_t = \frac{w_1}{w_2} E_1 \tag{61}$$

and since $n_2 i_2 = n_1 i_1 w_2 / w_1$, the average energy per stator tooth is

$$E_t = \frac{4\pi (n_1 i_1)^2}{24 g w_1^2 w_2} l_1 l_2 (l_1^2 + l_2^2) \tag{62}$$

and therefore, the effective permeance per stator slot is, for type 1,

$$P_1 = \frac{l_1 l_2 (l_1^2 + l_2^2)}{12 g w_1^2 w_2} \tag{63}$$

TYPE 2 (FIGURE 9)

$$y_1 \leq l_2 \leq l_1$$

Region 1

$$0 \leq x \leq \frac{l_1 - l_2}{2}$$

This is the same as in type 1, region 1, and the equations are the same.

Region 2

$$\frac{l_1 - l_2}{2} \leq x \leq \frac{l_1 - l_2}{2} + y_1$$

The equations will be the same as for region 2, type 1.

Region 3

$$\frac{l_1 - l_2}{2} + y_1 \leq x \leq \frac{l_1 + y_1}{2} \quad \text{(Figure 10)}$$

In this region the rotor tooth covers the stator slot. There are two flux bands to consider. For the left hand band, the conditions are the same as for region 2, so that for this portion of the rotor tooth the energy is

$$E_{c1} = 2\pi (n_2 i_2)^2 \frac{x^2}{g w_2^2}\left(\frac{l_2 + l_1}{2} - x\right) \tag{64}$$

For the right hand band the potential difference is proportional to the distance from the center of the rotor tooth to the center of the right hand stator tooth.

$$v = 4\pi n i \frac{w_1 - x}{w_2} \tag{65}$$

and the permeance is

$$P = \frac{\frac{l_2 - l_1}{2} - y_1 + x}{g} \tag{66}$$

The energy in the right hand band is then

$$E_{c2} = 2\pi (n_2 i_2)^2 \frac{(w_1 - x)^2}{g w_2^2}\left(\frac{l_2 - l_1}{2} - y_1 + x\right) \tag{67}$$

The total energy of the flux entering or leaving the rotor tooth at any position is the sum of equation 64 and 67.

$$E_c = \frac{2\pi (n_2 i_2)^2}{g w_2^2}\left[x^2\left(\frac{l_2 + l_1}{2} - x\right) + (w_1 - x)^2\left(\frac{l_2 - l_1}{2} - y_1 + x\right)\right] \tag{68}$$

The average energy during a relative movement of one stator slot pitch is

$$E_2 = \frac{1}{w_1/2}\left[\int_0^{\frac{l_1 - l_2}{2} + y_1} E_a dx + \int_{\frac{l_1 - l_2}{2}}^{\frac{l_1 - l_2}{2}} E_b dx + \int_{\frac{l_1 - l_2}{2} + y_1}^{\frac{w_1}{2}} E_c dx\right]$$

$$= \frac{4\pi (n_2 i_2)^2}{g w_2^2 w_1} \frac{l_1 l_2}{24} (l_1^2 + l_2^2) \tag{69}$$

which is the same formula as the one which was obtained for type 1.

The expressions for the corresponding energy per stator tooth and the equivalent permeance are, of course, the same as in

type 1. From the fact that the expressions for the energy per tooth for stator and rotor are perfectly symmetrical, and also that they are the same for types 1 and 2 of slot combinations, it follows that the formula derived for the equivalent average permeance per stator slot in type 1 holds for any possible combination of slot and tooth widths, that is, the formula

$$P_1 = \frac{l_1 l_2}{12 g w_1 s_{w_2}} (l_1^2 + l_2^2) \qquad (70)$$

is perfectly general for full pitch wound rotor machines. This quantity when added to the slot permeance in the formula for slot reactance of the stator winding will give an additional reactance equal to the total zigzag reactance of the whole machine.

This formula approaches rigorous accuracy, for the stated conditions, as the numbers of slots per phase belt are made large and as the ratio s_1/s_2 is made to approach but not equal unity. It seems obvious that for all practical purposes this permeance might be used in all cases as an addition to the stator slot permeance to calculate the combined slot and zig-zag reactance, provided the number of slots per pole is fairly large. This seems quite true if the rotor and stator windings have equal pitches, and it seems fairly reasonable to use the formula in this way even in the case of a machine having unequal rotor and stator winding pitches.

References

1. The Leakage Reactance of Induction Motors, C. A. Adams. *Transactions*, International Electrical Congress (St. Louis, Mo.), volume 1, 1904, page 706.

2. Design of Induction Motors, C. A. Adams. AIEE Transactions, volume 24, 1905, pages 649–84.

3. Zig-Zag Leakage, L. H. A. Carr. *The Electrician* (London, England), volume 87, July 15, 1921, page 76.

4. The Calculation of the Armature Reactance of Synchronous Machines, P. L. Alger. AIEE Transactions, volume 47, 1928, pages 493–513.

5. Parasitic Losses in Synchronous-Machine Damper Windings, J. H. Walker. *Journal*, Institution of Electrical Engineers (London, England) volume 94, part 2, February 1947, page 13.

6. Differential Leakage with Respect to the Fundamental Wave and to the Harmonics, M. M. Liwschitz. AIEE Transactions, volume 63, 1944, October section, pages 1139–49. (See also the bibliography to this paper containing 42 publications on the subject.)

7. Differential Leakage With Respect to the Fundamental Wave and to the Harmonics, M. M. Liwschitz. AIEE Transactions, volume 65, 1946, May section, pages 314–20.

8. Tensor Analysis of Networks (book), Gabriel Kron. John Wiley and Sons, Inc., New York, N. Y., 1939. Chapter 12: *Reactance Calculation of Windings*, page 296.

9. Zig-Zag Leakage of Induction Motors, R. E. Hellmund. AIEE Transactions, volume 26, 1907, pages 1505–26.

10. Wechsel Stromtechnik (book), E. Arnold. Springer, Berlin, Germany, volume 5, part I, 1909, page 52.

11. A Study of the Induction Motor (book), F. T. Chapman. John Wiley and Sons, Inc., New York, N. Y., 1930.

12. Harmonic Theory of Noise in Induction Motors, W. J. Morrill. AIEE Transactions, volume 59, 1940, August section, pages 474–80.

Discussion

John F. H. Douglas (Marquette University, Milwaukee, Wis.): I wish to discuss formula 5 and in particular the term $(6k-1)/5$ which occurs therein. In so doing, I wish to cite Carter's first paper[1], Carter's second paper[2], and a master of science thesis "An Analysis of Zigzag Permeance in Induction Motors," by Kirkish, Marquette University, Milwaukee, Wis., April 1935.

Most engineers use the coefficients from Carter's second paper for leakage as well as magnetizing current calculations. This is erroneous, since with zigzag leakage one of the flux components passes from a tooth of one polarity to one of opposite polarity. The double fringe permeance in this case is 0.88 geometric unit smaller than in the other, where adjacent teeth have the same polarity. Kirkish made the correct use of these two permeances when slots are opposite teeth.

No one before has defined clearly the boundary between slot leakage and zigzag leakage. Kirkish did so by starting zigzag at the slot opening. Thus conventional values of zigzag are augmented by a term, which is considerable when slots are opposite. In this zone Kirkish used the Schwartz-Christoffel transformation with great care.

When zigzag permeance is plotted against the position of the rotor slot center by Kirkish result is like Figure 4*B*, of the paper. The ratios of average to maximum permeance are about 0.55 over quite a wide range of the ratios of slot width to gap.

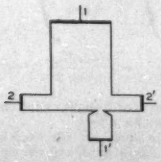

Figure 1. Kirkish's water trough

With regard to the chief conclusion of the paper, that slot openings reduce leakage faster than magnetising reactance, we cite the following figures from Kirkish's thesis.

We will use g in the same sense as in the paper, and define S_1 slot opening on the stator and S_2 as slot opening in the rotor. Then for the case where $S_1 = {}^1/_2 W_1$ and $W_1 = W_2$, Kirkish found values of zigzag permeance in excess of Adams' by the amounts in Table I.

Table I. Excess Value of Permeance, Per Cent

Values of S_1/S_2	S_1/g: 12	10	8	6
6	2.8	7.2	11.2	15.5
5	1.9	6.5	8.9	12.6
4	0.5	4.2	5.5	7.7

Perhaps Kirkish's greatest contribution is the one that may in the future lead to knowledge of current and flux ripples. Kirkish used a water trough shown in my Figure 1. This is a conjugate field, in which measured resistances give field permeances. With current supplied terminals 1-1', voltages 1-1' or 2-2' can be measured giving the permeance P_1 (including slot) and the mutual permeance P_{12}. With current supplied terminals 2-2', the permeances P_2 and P_{21} can be measured. Of course P_{12} checked P_{21} very closely. Kirkish's formula for zigzag permeance was

$$P_z = (P_1 - P_2) - (P_{12})(P_{21}) - (P_2)$$

This is the figure for the resistance of the trough with electrodes 2-2' short-circuited together. It is one of the consequences of Green's theorem, generally unnoticed, that it extends network theory to fields. I wish therefore to classify this equation (number 17 in the thesis) as a major contribution. The term P_z is the slot leakage.

References

1. *Journal*, Institution of Electrical Engineers, (London, England), volume 29, pages 925–33.

2. *Electrical World and Engineer*, (New York, N. Y.) volume 38, page 884.

M. M. Liwschitz (Polytechnic Institute of Brooklyn, Brooklyn, N. Y.): This paper is an important contribution to the field. In comparison with the paper published by Alger about 20 years ago, this paper takes into account two new factors, namely, the influence of slot openings, and the influence of skewing. However, the influence of the rotor currents on the leakage, as well as the leakage of the irregular, that is, fractional-slot windings, are not treated in this paper. The authors acknowledge that these topics are treated in my papers on differential leakage, published in the AIEE Transactions in 1944 and 1946. Yet, they attach to my papers two "buts." One "but" is that I have "not considered the effects of *alternative* patterns for irregular windings." I have treated in my paper the pattern for *maximum distribution factor* with respect to the main wave. This is the pattern which I and the Westinghouse designers normally use and the only one which is treated in detail in the literature. Occasionally, when a certain harmonic is to be avoided, we use another pattern, but only as an exception and, in my opinion, the layout of fractional-slot windings for maximum distribution factor is the right one. Furthermore, the different patterns yield values for the differential leakage which do not differ much from each other.

The other "but" is that I have not given my results "in the per unit form that is most convenient for calculations." There are some designers who use the output current as unit current, and others who use the input current as unit current, while some designers still calculate in ohms. In order to satisfy

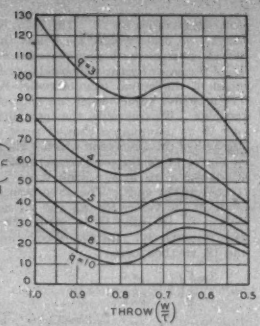

Figure 2. $\sum_{n\neq 1}\left(\frac{K_{dpn}}{n}\right)^2$ **for Integral-slot 3-phase 60-degree phase belt windings**

$q = Z$

$q=2$	W/τ	$\sum_{n\neq 1}\left(\frac{K_{dpn}}{n}\right)^2$
	1.0	265×10^{-4}
	0.833	205×10^{-4}
	0.667	199×10^{-4}

all of them, I have given my results in ohms. The designer can express my results in his units by dividing through by his unit impedance.

The authors write in the summary: "The wide differences in viewpoints have prevented the authors from obtaining a clear comparison of the Liwschitz's results for the effects of open slots on differential leakage with those of the present paper, so that more study should be given to this aspect of the subject." As a matter of fact, I do not see any difference in our general viewpoints. One of the mathematical expressions the authors used for the gap is the one I used to solve the problem of influence of slot-openings. However, there is a difference in the methods of attack of the whole problem and it is worth while to clarify this difference. The authors as well as I consider the difference between the real magnetomotive force wave and the main wave as the source of the differential leakage. The difference between both methods of attack is the following: The authors split the sum of all harmonics into two parts, the first part being the zigzag leakage, which comprises the harmonics of high order, and the second part, the belt leakage, which comprises the harmonics of lower order. I, on the other hand, consider each harmonic individually and add them up to a single sum. Alger and West solve the problem of the differential leakage in two steps. They first consider a winding, which has only slot harmonics, and then superimpose the influence of all other harmonics. My solution requires but one step.

The separation of the harmonics into two parts is justified for normal machines with a number of slots per pole per phase which is not too small by the facts that skew, slot-openings, and damping by the rotor influence the higher harmonics to a different degree than the lower harmonics. For this reason the division of the harmonics into two parts yields good practical results for normal machines.

However there is no real boundary between the harmonics of higher and lower order. The skew, for example, also influences the harmonics of low order, when the number of slots per pole per phase is small.

The method of individual treatment of the harmonics and of summing up their reactances, as used in my papers, is applicable to any number of slots per pole per phase and also to abnormal machines.

There is also another reason why I prefer the method of individual treatment of the harmonics.

Table II of this discussion shows the harmonic chart of a 3-phase 4-pole squirrel cage motor with 72 slots in the stator and 58 slots in the rotor. The harmonics are referred to a fundamental, the wave length of which is equal to the circumference of the armature.

Table II

Stator Harmonics n'	Rotor Harmonics $m' = K_2Q_2 + n'$: $K_2 = 0$	$K_1 = +1$	$K_2 = -1$	$K_3 = +2$	$K_4 = -2$
+2	+2	+60	−56	+118	−114
−10	−10	+48	−68	+106	−126
+14	+14	+72	−44	+130	−102
−22	−22	+36	−80	+94	−138
+26	+26	+84	−32	+142	−90
−34	−34	+24	−92	+82	−150
+38	+38	+96	−20	+154	−78
−46	−46	+12	−104	+70	−162
+50	+50	+108	−8	+166	−66
−58	−58	0	−116	+58	−174
+62	+62	+120	+4	+178	−54
−70	−70	−12	−128	+46	−186
+74	+74	+132	+16	+190	−42

□ = slot harmonic

The choice of such a fundamental has the advantage that no harmonics, the orders of which are equal to fractional numbers, appear in the chart. With this fundamental, the order of the main wave is $n' = 2$. The first column shows the stator harmonics. $n' = 10$ is the fifth harmonic of the stator, $n' = 14$ is the seventh, and so forth.

Each stator harmonic produces a series of rotor harmonics. These are the horizontal rows. The paper by the authors considers the stator harmonics, without taking into account the damping by the rotor, and considers only the *first* horizontal row of the rotor harmonics, that is, the differential leakage of the rotor with respect to the main wave only. The individual method of treatment of the harmonics leads automatically to the solution of the problem of the differential leakage of the rotor with respect to the stator harmonics. The knowledge of this leakage reactance is important, in order to calculate the dips in the torque–speed curve, the synchronous cusps, the dead points, the stray load losses, and the traveling forces which produce noise.

The designer of small motors circumvents most of these troubles by making different stators and rotors and trying out various slot combinations until the best is found. The designer of larger machines cannot afford to do this. He must watch the harmonics, and, not in lumps, but individually, since it is mostly one or, at the most, a few harmonics which produce the trouble.

The method used in my paper for the determination of the effect of slot openings on differential leakage corresponds to the general method of attack. After a mathematical expression for the gap has been introduced, the influence of this gap on the *individual* harmonics is investigated. It has been found that in integral slot windings one slot harmonic of a pair may be decreased by the slot opening, while the other slot harmonic of the pair is increased, resulting in a relatively small change of the leakage of the pair by the slot openings. This contradicts the results obtained by the authors which treat all higher harmonics as a unit. The problem is much more involved than the approximate formula given by the authors would indicate. The problem is similar to that encountered in the calculation of copper losses in a squirrel cage winding due to the harmonics. It has to consider the ratio between slot opening and slot pitch, the ratio between slot-opening and gap, and the signs of the distribution and pitch factors of the harmonics, as has been done in my paper.

There is another point to which the authors do not give enough attention. It is the assumption that the magnetomotive force has a stepped shape. It is shown in my paper that this assumption yields too high a value for the differential leakage.

Considering the differential leakage of the stator, the skew increases this leakage, the rotor currents decrease it, the slot openings decrease its harmonics of low order and may or may not decrease its slot harmonics, and, finally, the assumption of a stepped shape magnetomotive force leads to too high a value of this leakage. The taking into account of all these factors, complicates the calculation of the differential leakage. This complication is not justified, because the method of calculation of the end-winding leakage is inaccurate and also because the saturation of the leakage paths is still an unknown factor. For this reason I have proposed, in my previously mentioned papers, to use a simple approximate method of calculation of the differential leakage which disregards these factors with opposite influence.

For comparison, I have expressed my simplified formula in the authors' terms. Equations 1 and 2 show the comparison of both formulas.

$$X_D = \frac{\pi^2 X_M}{12}\left[\frac{(6k_1-1)F_{ac}+5\sigma^2}{5s_1^2}+\frac{6k_2-1}{5s_2^2}\right]+X_B \quad (1)$$

Table III

Three phases, 60 Cycles, $X_M = 1$

Hp	Poles	Eq 1	Eq 2		
3/4	6	0.0513	0.0575	Skewed	Semi-closed slots
1	4	0.0349	0.0372		
5	6	0.0580	0.0633		
7 1/2	4	0.0360	0.0388		
330	20	0.0135	0.0155	Not skewed	Open slots
800	8	0.083	0.0837		

$$X_D = \frac{\pi^2 X_M}{12}\left\{\frac{12}{\pi^2}\frac{1}{K_{dp1}^2}\sum_{n\neq 1}\left(\frac{K_{dpn}}{n}\right)^2 + K^2_{sk(n=1)}\frac{1}{s_2^2}\left[1+\left(\frac{S}{\tau_{s2}}\right)^2\right]\right\} \quad (2)$$

Equation 1 corresponds to equation 5 of the authors' paper. The first term of this equation is the differential leakage of the stator. The second term should take into account the damping by the rotor, but its magnitude is not given. The third term is the influence of skew; the fourth term is the differential leakage of the rotor, and the quantity X_B is the belt leakage. In wound rotor motors X_B consists of two terms, which are to be determined from curves.

In my formula, the first term is the differential leakage of the stator, the second term that of the rotor, and the third term takes into account the skew. The sum

$$\sum_{n\neq 1}\left(\frac{K_{dpn}}{n}\right)^2$$

is to be taken from the curves of Figure 2. K_{dpn} is the product of the distribution factor and pitch factor of the nth harmonic. n is the order of the harmonic with respect to the main wave. $K_{sk(n=1)}$ it is the skew factor for the fundamental wave which is in normal machines approximately equal to 1. S is the skew in units of the rotor slot pitch τ_{s2}. Figure 2 applies to integral-slot windings. The curves for fractional-slot windings are given in my paper.[1] My formula is at least as simple as that of the authors.

I have applied both formulas to several squirrel cage motors using in the authors, formula 1 for F_{s0}, that is, neglecting the damping by the rotor. X_M is assumed to be equal to 1. The calculated results are shown in Table III of this discussion. The authors' formula gives 10 to 15 per cent lower values for the differential leakage than my formula. I believe that the correction made by the authors for the slot-openings will yield values for the differential leakage which are too small.

I have used my formula[2] since approximately 1930.

My formula is an approximation. Sometime, when our knowledge about the end-winding leakage and about the saturation of the leakage paths will be larger than now, a more exact formula for the differential leakage will be necessary. All the elements necessary for such a formula are given in my papers.

I consider the method of treating each harmonic individually as being more promising for an exact formula than that of considering the harmonics to be lumped together.

References

1. Differential Leakage of a Fractional-Slot Winding, M. M. Liwschitz. AIEE Transactions, volume 65, 1946, May section, pages 314–20.

2. Electric Machinery (volume 2), M. M. Liwschitz. D. Van Nostrand Company, New York, N. Y., 1946.

P. L. Alger and H. R. West: We are in complete agreement with Douglas that it is important to use the Carter coefficient for teeth of opposite polarity, rather than the one for like polarity, when using the overlap method to determine zigzag leakage.

The thesis of Kirkish, to which Douglas referred, and which he since kindly has loaned us, represents the only case of which the authors know, in which an exact determination of zigzag permeance, based on actual, rather than approximate, flux distribution has been made. Since his results apply to squirrel cage motors and ours to wound rotor machines, a direct and accurate comparison cannot be made without going beyond the scope of our paper. In general, however, his results are in agreement with what we have found, which is that derivations or computations based on actual or closely approximate flux distributions give larger values for the reactance than those based on the assumption of lumped permeance as in our case E. Specifically, he finds the zigzag permeance to be from 2 to 17 per cent greater than given by Adams' formula (derived in his St. Louis Electrical Congress paper in 1904).

Table IV. Ratio of Additional Tooth Width Due to Fringing to the Air Gap

Slot/Tooth Equal to 1

Slot/Gap Ratio	End Slot Fringing	Carter Slot Fringing	Ratio
.5	2.47	1.61	0.65
10	3.33	2.50	0.75

Table V. Relative Reactance for Case B (Sinusoidal Variation)

Values of k	Sloping Ends Equation 3	Straight Ends Equation 22	Ratio
1	0.50	1.00	0.500
0.75	0.465	0.798	0.583
0.60	0.429	0.596	0.720
0.50	0.393	0.393	1.00

A. A. Bennett, in some unpublished work done in 1933, derived accurate formulas by the Schwarzian transformation method for the fringing into a slot between teeth of equal and opposite potential (the end slot of a single coil) and compared these with the usual Carter formulas for fringing between teeth of equal potential (the slots enclosed within a coil). For a particular case, the fringing coefficients are compared in Table IV.

These values verify the point mentioned by Liwschitz, that the assumption of a stepped shape for the end slot magnetomotive force yields too large a value for the differential leakage, since the actual flux falls to zero at the middle of this slot, as indicated by the dotted lines in Figure 1 C This point is well taken. In other words, our use of the assumed permeance characteristic of Figure 1 C of the paper for the sinusoidal case B, instead of the actual characteristic, Figure 1 B, may give values which are appreciably too high. We can make the correction for case B by assuming a characteristic as in Figure 3 of this discussion which is the same as Figure 1 C of the paper, except with the triangular areas a, b, c, and d. e, f, subtracted at the ends. The corrections to be made to the values for L_{t1} and L_s can be shown to be $(2k-1)/4s_1$ and $(2k-1)/2s_1$, respectively. Instead of equations 12 and 16, we then have

$$L_{t1} = \frac{4ks_1}{\pi^2}\left[\left(1+\frac{\pi^2}{12s_1^2}+\ldots\right) - \frac{3}{4}\left(\frac{2k-1}{k}\right)\frac{\pi^2}{12s_1^2}\right] \quad (1)$$

$$L_s = \frac{4ks_1}{\pi^2}\left[1+\frac{1-k}{k}\left(\frac{1}{4s^2-1}\right) - \left(\frac{2k-1}{8k}\right)\frac{\pi^2}{12s_1^2}\right] \quad (2)$$

Assuming that the value for L_{t1} is unchanged (equation 21), we get for the per unit differential reactance for case B

$$X_D = \frac{L_{t1}+L_s-2L_s}{L_s}, \text{ or}$$

$$X_D = \frac{\pi^2}{12}\left[\frac{1}{s_1^2}\left(\frac{1}{2k}-\frac{6(1-k)}{k\pi^2}+\frac{1}{s_2^2}\right)\right] \quad (3)$$

The corresponding expressions for the conditions of cases C and E, with the permeance tapered to zero at each end, are

$$L_{t1} = \frac{4ks_1}{\pi^2}\left(1+\frac{\pi^2}{12s_1^2}\left(\frac{3a-k}{2k}\right)\right) \quad (4)$$

$$L_s = \frac{4ks_1}{\pi^2}\left(1+\frac{\pi^2}{12s_1^2}\left(\frac{a}{k}-\frac{a^2+1}{2}\right)\right) \quad (5)$$

and

$$X_D = \frac{\pi^2}{12s_1^2}\left(a^2+\frac{1}{2}-\frac{a}{2k}\right)+\frac{\pi^2}{12s_2^2} \quad (6)$$

This last expression, 6, corresponds to equation 26 of the paper.

Substituting various values of k and a (noting that $k \geq a$), the corrected values of differential leakage due to the primary slots alone, are given in Tables V and VI in comparison with corresponding values taken from Figure 5 of the paper.

In all these equations, 1 through 6, the value of k is taken as the average over the maximum permeance for a central slot. When allowance is made for the tapered

Table VI. Relative Reactance for Cases C and E, Equations 26 and 6

Stepped Variation With Variable Tooth Width

Value of k	a=1			a=0.75			a=0.30			a=0.25		
	1*	2†	R‡	1*	2†	R‡	1*	2†	R‡	1*	2†	R‡
1.00	1.00	1.00	1.00	0.688	1.00	0.688	0.500	1.00	0.500	0.438	1.00	0.438
0.75				0.563	0.563	1.00	0.417	0.750	0.563	0.396	0.896	0.442
0.60							0.333	0.500	0.667	0.354	0.792	0.447
0.50	a=0						0.250	0.250	1.00	0.313	0.688	0.455
0.25										0.063	0.063	1.00
0.00	0.500	1.00	0.500									

* Sloping ends. † Straight ends. ‡ Ratio.

Table VII. Per Unit Reactances of Induction Regulators

Kva rating	950	1040	1730
X_M	1	1	1
X_{tot}	0.044	0.043	0.046
$X_{calculated}$			
$X_{coil\ end}$	0.0075	0.0116	0.0095
X_{slot}	0.0225	0.0187	0.027
$\frac{\pi^2}{12}\left[\frac{5k_1-1}{5r_1^2}+\frac{5k_2-1}{5r_2^2}\right]$	0.0165	0.0165	0.0080
Total	0.0465	0.0468	0.0454
$\frac{\pi^2}{12}\left[\frac{1}{r_1^2}+\frac{1}{r_2^2}\right]$	0.033	0.033	0.016

ends, the true ratio of actual to maximum permeance over the coil pitch is somewhat smaller than this value of k. This accounts for part of the discrepancy between the formulas for sloping and straight end permeance waves.

For large values of k (large air gaps) and small values of a (wide open slots), the indicated value of zigzag leakage is much smaller than that given by our recommended formula. However, under these conditions, the true fringing curve in the end slots lies well above the triangular shape used in these new calculations, so that the new values are undoubtedly on the low side. Also, as Douglas has mentioned, the lowered value may be offset in part by the leakage flux which curls over between two adjacent rotor tooth faces under a wide slot. As Liwschitz points out, the sloping end of the permeance curve is only one of several offsetting effects that should be taken into account.

So far as it goes, Table VI indicates that our final equation gives too high rather than too low results, contrary to the conclusion derived from the tabular comparison given by Liwschitz, and stated near the end of his discussion.

On the whole, therefore, we do not recommend any change in our final formula, equation 5.

One reason why we have chosen to calculate the zigzag leakage separately, and have disregarded the belt leakage in this paper, is that F_{zc} can be taken as nearly 1 for the former and as nearly zero for the latter, in the ordinary case of a squirrel cage rotor. This is true because it is customary to choose the secondary slot number and the skew so as to nearly eliminate induced secondary currents due to slot harmonics; while, on the other hand, the belt leakage voltages are quite effectively short circuited by the squirrel cage.

Probably the inclusion by Liwschitz of belt leakage harmonics, which we omit, is

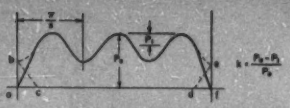

Figure 3. Sloping permeance distribution obtained by subtracting end triangles from sinusoidal distribution

the principal cause of the slightly higher reactance values he obtains. As he says, "We agree remarkably well on the subject as a whole. The differences between us arise from our deliberate choice of approximations, which seem to us to be convenient and to be justified by our experience."

The test values given in Table VII for three induction regulators having wide open slots in both rotor and stator show that our new formula, equation 5, checks the tests very well, whereas much too large values are calculated if the reduction in zigzag leakage due to slot openings is not taken into account.

In each of these machines, the rotor and stator winding pitches were the same, and the tests were made with the windings in coaxial positions, in which positions the belt leakage was zero.

A High Precision Dynamometer for Small Motor Measurements

J. E. DUFF
MEMBER AIEE

IN THE DESIGN and development of small shaded-pole induction motors a great many of the design constants must be chosen on an empirical rather than a mathematical basis. This is due to the complex mathematical relationships involved as well as the relatively large size of such indeterminant factors as bearing friction. A designer of small induction motors must therefore be guided in his work to a large extent by previous data gathered from tests of other small shaded pole motors. Unfortunately, however, since shaded pole motors are usually small in size and power output, the study and measurement of their characteristics must be made by equipment sensitive enough to measure to a reasonable degree of accuracy the factors involved.

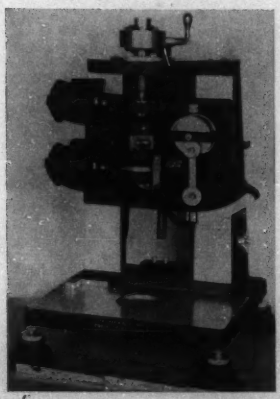

Figure 1. High precision dynamometer

Electrical measurements readily may be made to practically any degree of accuracy desired but mechanical measurements of torque have in the past been limited by the minimum torque sensitivity of conventional dynamometers of both the absorption and transmission types.

The dynamometer discussed in this paper therefore is one which has been designed primarily to minimize errors due to mechanical weaknesses rather than electrical ones and has been restricted in its design to a unit which is satisfactory only for motors having speeds less than 7,200 rpm and power outputs of less than 50 watts. The principles involved however could be readily applied to a larger design if such a unit were required but probably only at the expense of larger absolute error limits.

In general all dynamometers may be lumped into two classes: absorption and transmission. However because some of the measurements of the constants of an induction motor require that it be driven from an external source while torque measurements are being made, the absorption type was discarded. The absorption principle can be applied however if desirable in the measurement of motor output.

Among the various types of driving motors available for a small dynamometer of this sort the following may be listed:

1. Series motor—a-c or d-c.
2. Shunt motor—d-c only.
3. Induction motor.
4. Synchronous motor.

Both the series and shunt motor while having suitable characteristics as a dynamometer unit, among which may be listed their ease of control and wide speed range, suffer from the disadvantage of using brushes and a commutator. While it is quite true that any friction developed by the action of the brushes merely adds to the torque reaction of the unit while serving as a generator and disappears as a factor when it is used as a motor, the brush friction is not constant and may actually become so unstable in nature as to make consistent measurements impossible at very low torque values. These two types therefore may be discarded.

Both the induction and synchronous types have the restriction that in general they are relatively fixed speed devices. This is unfortunate since their lack of brushes would contribute materially to their stability. If however a source of variable frequency power is available then they become an ideal choice with the induction motor having the additional advantages of easy starting and reversible rotation.

As a dynamometer unit the induction motor has characteristics which satisfy very closely the requirements imposed. When used as a motor it has the important advantage of good speed regulation under load. This becomes important when it is necessary to measure the friction of small sleeve bearings. Such bearings under certain conditions of speed and lubrication may exhibit a negative speed–torque characteristic and when this happens, if the dynamometer drive has poor speed regulation under varying load it may become almost impossible to obtain accurate readings.

When used to absorb power from a motor under test the induction unit may be used in two different manners both of which have certain advantages. If direct current is applied to its stator winding the driven induction motor will absorb power in its rotor in the same way that an eddy current brake does. However as all the power absorbed must be dissipated in the rotor, its capacity necessarily is limited by its design. This difficulty may be

Paper 47-229, recommended by the AIEE committee on electric machinery for presentation at the AIEE Middle Eastern District meeting, Dayton, Ohio, September 23–25, 1947. Manuscript submitted April 7, 1947; made available for printing August 7, 1947.

J. E. Duff is in the engineering laboratories of The Hoover Company, North Canton, Ohio.

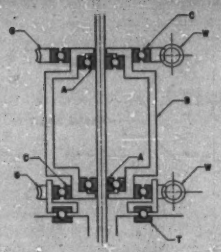

Figure 2. Dynamometer bearing and worm drive arrangement

Figure 3. Small output dynamometer use of scale and weights

Calculations
Horsepower = scale reading × multiplying factor × rpm × 10^{-5}
Watts output = horsepower × 746

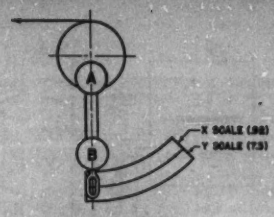

INDICATING SYSTEM

WEIGHT AND SCALE COMBINATIONS

OZ. WT. AT A	OZ. WT. AT B	USE SCALE	MULTIPLY SCALE BY	OZ. PULL AT 45° FROM VERTICAL	MAX. RANGE OF OUTPUT IN WATTS AT 3600 R.P.M.	1800 R.P.M.	900 R.P.M.
2.63	NONE	X	1	1.25	2.47	1.24	0.618
2.63	1.75	Y	1/2	5.0	9.90	4.90	2.45
2.63	4.09	Y	1	10.0	24.2	13.1	6.56
2.63	8.77	Y	2	20.0	39.2	19.6	9.80

overcome within limits, by using the unit as an induction generator.

Whether an induction machine operates as a motor or a generator depends entirely on the relative rotation of the armature as compared with that of its magnetic field. Below synchronous speed it will act as a motor, capable only of generating power; at synchronous speed it can neither generate nor absorb; and at speeds above synchronous it can act only as a generator pumping power out into the supply lines.

Therefore, at a fixed shaft speed, an induction unit as a dynamometer can be made to drive the motor under test at torques up to the maximum of the unit, absorb power from the motor up to the same limit, or generate or absorb power at any value between these two limits by doing nothing other than controlling the frequency of the power supplied to the dynamometer. This extreme flexibility of the induction type of dynamometer is unmatched in any other dynamometer type and together with its inherent stability and lack of brush friction make it ideal as a piece of laboratory equipment for highly accurate measurements of small shaded pole motors.

Definition of Requirements

Having established the type of dynamometer it is now necessary to set the desired limits of accuracy, speed and power handling capacity so that various design factors may be ascertained.

The question of speed range is a simple one since usually the 60 cycles per second performance of a 2-pole motor will give an upper limit of 3,600 rpm. However because of some special considerations the dynamometer herein described was designed with a maximum speed of 7,200 rpm. Power absorption capacity was to be at least 25 watts at 3,600 rpm. Twenty-five watts was somewhat greater than necessary for the motors to be tested but since power handling ability decreases with a reduction in speed it was felt desirable to have such an upper limit in order to still be able to handle 10 to 15 watts at 1,200 and 1,800 rpm. Torque sensitivity using the dynamometer as a generator was to be less than one per cent of the output of the motor under test. Inasmuch as this represents approximately 0.5 watt it does not, as will be shown later, represent much of a problem.

When the machine is used as a motor, to obtain various data from the small motor under test, the torque requirements become considerably more severe. Here again the speed requirements were the same (that is, 0 to 7,200 rpm) but the torques to be measured are now greatly reduced, since principally mechanical losses are being measured. Rather than set a maximum percentage of the torque to be measured as the upper limit of sensitivity it was decided to design for the best possible performance. As will be shown later the torque sensitivity is less than 0.02 watt or approximately 8×10^{-3} inch-ounce at 3,600 rpm for this particular dynamometer. This represents almost a ten-to-one increase in sensitivity over conventional dynamometers of this size and enables measurements of a high degree of accuracy to be made.

Description of Dynamometer

Figure 1 shows the complete dynamometer. The dynamometer is mounted on a vertical bed plate which can be adjusted by means of a screw drive to either a high or low position for connection to test motors which operate with either upward or downward vertically extended shafts. The main frame of the unit has four shock mounting feet to isolate vibration and each of the feet are adjustable in order to level the assembly. Leveling is indicated by the small dual spirit level mounted on the lower base plate of the frame. The frame itself consists of the lower base plate, two vertical machined ways, and an upper base plate. It was cast as a unit and carefully machined to preserve the proper relationships between finished surfaces. As may be seen in Figure 1, strength and rigidity have been emphasized in the construction of the frame to the point where flexure of the mounting plates or ways relative to each other is a negligible quantity. This is an important characteristic if accuracy is to be maintained.

The dynamometer bed plate is also of heavy construction and carries all active mechanical and electric components of the dynamometer. The dynamometer unit itself is mounted in cradles attached to the bed plate and moves up and down with the bed plate.

An important feature of the low power dynamometer and one which permits a high degree of precision in making torque measurements is the dynamometer trunnion bearing arrangement. This arrangement shown in Figure 2 functions as follows. In the past[1] in some large dynamometers, oscillation of the trunnion bearing outer races has been used to reduce the static or low speed rotary motion friction of the dynamometer trunnion bearings. This reduction in friction is accomplished by keeping the inner and outer races of the trunnion bearings moving at some velocity relatively high as compared with their normal motion in

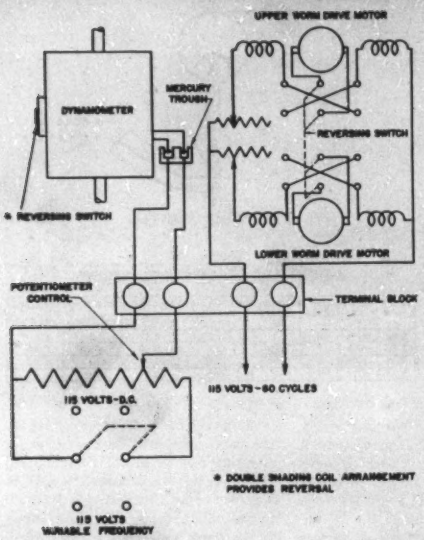

Figure 4 (left). Dynamometer electrical connections

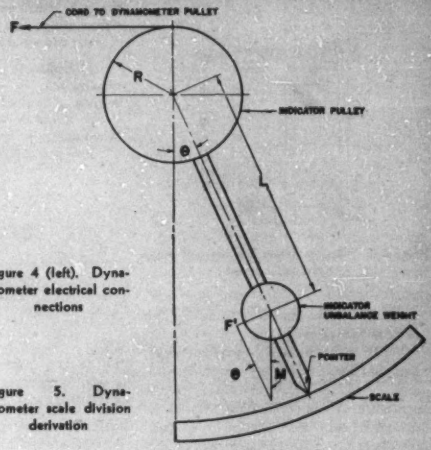

Figure 5. Dynamometer scale division derivation

following dynamometer torque changes. The dynamometer herein described goes one step farther and not only provides high relative motion of the trunnion bearing races but is also so arranged that the dynamic friction so introduced is in opposite directions for the upper and lower bearings.

Reference to Figure 2 shows that a total of five complete ball bearing assemblies is required. Bearings *A* are the shaft ball bearings of the dynamometer with ball races fixed both to the dynamometer shaft and body. The trunnion ball bearings *C* are similar to those of *A* except for their larger diameter. *C* bearings are fixed to the outer portion of the dynamometer body and the inner portion of a worm gear housing *G*. This housing, in turn, rotates in a sleeve guide and is driven by the worm *W* through small a-c series motors (these worm gear drive motors may be seen in Figure 1). The fifth ball bearing *T* is a thrust-type bearing and supports the entire dynamometer assembly *B*.

The whole bearing arrangement is accurately machined and aligned in order to keep the bearing friction to the least possible minimum. The two worm gears *G* are constructed of laminated phenolic material, as this was found necessary in order to reduce gear noise and vibration.

In operation, both the upper and lower worm wheels are driven in opposite directions at about 50 rpm through the 60-to-1 worm gear reduction drive. This bearing rotation (in opposite directions) tends to cancel out the static friction of the trunnion bearings and a more accurate reading of torque is secured. It should be emphasized that the use of these rotated trunnion bearings does not reduce any losses in the dynamometer bearings, it merely reduces the effect of the trunnion bearing position lagging behind the true torque value because of its static friction.

In order to compensate for any artificial torque introduced resulting from differences in drag of the two bearings, reversing means have been included as well as speed controls for the two worm-gear drive motors. The worm gear drive motors therefore may be reversed simultaneously and the speeds adjusted if a significant change of reading occurs. During test runs it has been found that these readings do not vary to any appreciable extent and that the torque indicator (described hereafter) swings very freely without the slightest tendency to stick or drag.

The worm drive motors are small fractional horsepower a-c series 115-volt motors and the couplings from motor to worm gear are specially constructed rubber shaft units in order to allow the necessary universal action and also to minimize the transmission of vibration.

Tests have shown that best results can be obtained with the trunnion motors operating at full voltage. Rheostats are connected in series with the motors to allow speed control and no other adjustments have been found necessary.

The indicator of the measuring device on the dynamometer is of the pendulum type and is shown in Figure 2. It is constructed with a large 3-inch pulley at the top and an indicating arm which supports the various weights needed for different scale ranges. The entire indicator is supported by two high precision pivot bearings which are accurately machined and aligned. The indicator also is provided with counterbalance weights so that under proper adjustment the pointer will not cause motion as a result of its own movements.

The indicating scale occupies a displacement of 45 degrees at approximately 6 inches from the pivot. Two scales are engraved on a stainless steel plate which is removable. The scale divisions are arbitrary units and when multiplied by revolutions per minute times 10^{-6} give horsepower output directly. Both scales are divided sinusoidally due to the fact that the top pulley is of constant diameter.

Since the indicating scales are sinusoidal in division and of the arbitrary calibration previously described, it was necessary to calculate their angular relationships accurately. The method for doing this is included in a brief appendix at the end of this paper.

Additional fixed weights may be added to the pointer to change the available

indicating range. A sketch of the indicator together with a table of weight and scale combinations is presented in Figure 3. Also shown is the maximum motor output in watts that may be measured at various shaft speeds and scale ranges.

Electrical Details

Little or no work of a complex nature was required in the electrical design of the dynamometer. The unit itself is a modified 4-pole shaded-pole General Electric Company type *KSP* induction motor. The only change required, other than the bearing modifications described, was the removal of the shading coils. The shading coils were then replaced by a pair of wound coils (one pair on each pole face) of ten turns of number 22 heavy "formex" insulated magnet wire. The corresponding coils on the four poles are connected in series and the two circuits brought to a single-pole double-throw switch mounted on the dynamometer body. By means of the switch therefore, one circuit of shading coils may be short-circuited to obtain rotation of the dynamometer (when used as a motor) in a given direction. To reverse it, it is only necessary to throw the short-circuiting switch to the other position.

The values of turns and wire size for the coils were determined by experimentation but were not found to be critical. The main polar windings are best left unmodified but if desired they may be readily replaced. Such a change would be desirable if for example the principal use of the dynamometer was to be at speeds of less than 1,000 rpm (requiring low applied frequency). This may be done by keeping the product of field turns and frequency constant and choosing a wire size such as will keep the current density constant.

Power is taken into the dynamometer by means of two fingers dipping into a double trough of curved shape which is filled with mercury. This trough cannot be seen in Figure 1 as it is mounted behind the dynamometer unit. Its end and terminals however are visible just to the left of the indicator system. The trough is milled from insulating material of a phenolic type and the two contacting fingers are made of a stainless steel to eliminate attack from the mercury. The two terminal screws seen in Figure 1 also serve as drain plugs for the mercury channels.

The two bearing drive motors are Bodine Electric Company type *C-3* 1/30-horsepower 115-volt 60-cycle models having a rated speed of 4,000 rpm. Here again however the units used are not critical so long as the bearing races are rotated at approximately 50 rpm. Smooth operation of the drive motors to reduce the effect of vibration is essential however.

Figure 4 is a schematic diagram of the wiring circuit of the dynamometer. It shows all the necessary electric components of the assembly with the exception of the source of variable frequency voltage. This may be obtained from either a variable speed motor generator set or an electronic source of the oscillator-power amplifier type. In order to avoid any difficulties due to possible wave form distortion, a variable frequency motor generator set is used at The Hoover Company. This unit is separately mounted in the laboratory with a frequency control rheostat brought to the dynamometer setup.

Performance

The performance of the dynamometer is excellent. When used as a generator to absorb power its sensitivity is well below the 1 per cent of total torque mentioned previously in this paper. Operation has been smooth and accurate at all times. Normally the loading is that of the induction generator type, however for tests of starting torque it is necessary to excite the fields with direct current and use it as an absorption dynamometer. Heating is not excessive under these conditions if tests are not too extended in time. The dynamometer is not designed for continuous use as an absorption unit however.

A small clamp has also been added to enable tests to be made of locked rotor torque. This clamp may be seen in Figure 1 directly below the dynamometer reversing switch. By the use of this clamp the dynamometer rotor and stator are locked together thus allowing the motor stalled rotor torque to be measured directly.

It is when used as a driving motor to measure bearing and windage losses that the full advantages of this dynamometer bearing arrangement appear. Even when using the lowest output scale, readings of torque may be repeated to within one scale division. At 3,600 rpm this represents only 0.03 watt output. An interesting comparison may be had by turning off the trunnion bearing drive motors when such tests are being made. Without power to the trunnion drive motors the dynamometer torque indicator may be moved up or down scale manually five or six divisions without sufficient torque being developed to overcome the static trunnion bearing friction and return the indicator to a true reading. With the bearing races being rotated however a displacement of less than one division will correct itself because of the torque unbalance.

Loads up to nearly 40 watts may be handled by the dynamometer operating either as a motor or a generator at 3,600 rpm and during some special test runs the performance was still satisfactory as an induction generator at 7,200 rpm at an output of 65 watts.

In conclusion it may be said that the combination of the induction generator type of dynamometer together with a variable frequency power source and oppositely rotated trunnion bearings makes a very satisfactory dynamometer for small shaded pole induction motor test work, yet with the exception of the precision machine tool work required its construction is not excessively difficult.

Appendix

Figure 5 is a diagrammatic sketch of the pointer details from which may be derived the equations pertaining to the scale calibration. As a starting point equation 1 is the fundamental expression for horsepower output as a function of speed and torque:

$$HP = \frac{2\pi SXF}{33{,}000 \times 16 \times 12} \qquad (1)$$

where

S = motor rpm
X = radius of dynamometer pulley plus the radius of the connecting string in inches
F = force on the connecting string in ounces

But

$$W = 746 \text{ horsepower} \qquad (2)$$

Where

W = watts output

Therefore

$$W = \frac{746 \times 2\pi SXF}{33{,}000 \times 16 \times 12} = 740 \times 10^{-6}\, SXF \qquad (3)$$

In Figure 5

$$F(R+r) = ML \sin\theta \qquad (4)$$

Where

R = radius of the indicator pulley
r = radius of the connecting string
M = unbalance weight of the indicator
L = radius of the unbalance M
θ = angle of the indicator deflection

Solving equation 4 for F and substituting in equation 3

$$W = \frac{740 \times 10^{-6}\, SXML \sin\theta}{R+r} \tag{5}$$

But all values except W, S, and $\sin\theta$ are constants and may be determined. Therefore

$$W = KS \sin\theta \tag{6}$$

Where

$$K = \frac{740 \times 10^{-6}\, XML}{R+r}$$

Therefore

$$\theta = \sin^{-1}(W/KS) \tag{7}$$

Or knowing the maximum watts output to be measured at a speed S the unbalance weight may be calculated for the maximum scale deflection (recommended limit 45 degrees). Then from equation 7 the scale may be divided into any number of divisions.

By this method it is possible to obtain a dynamometer scale such that the product of scale reading times speed times an arbitrary constant (10^{-6} for this dynamometer) will give the power output of the motor under test in either watts or horsepower.

Reference

1. Modern Equipment for the Precise Testing of Motors, **A. A. Emerling**. *General Electric Review* (Schenectady, N. Y.), volume 37, October 1934, pages 471–6.

Discussion

G. Mott, Jr. (Electrolux Corporation, Old Greenwich, Conn.): I should like to ask three questions

1. Do the trunnion bearings have a full complement of balls or do they have four balls apiece?
2. What lubrication is used for these bearings?
3. What form of coupling is used to the motor? Is it coupled by means of a spline or by a solidly attached coupling? I ask this question because the expansion of a rubber coupling under centrifugal action puts end thrust on the motor bearings.

J. E. Duff: In replying to these questions I should like to point out that the answers are merely the procedures found to be satisfactory at the Hoover Company and do not necessarily represent the only satisfactory solutions. This is particularly true of question number three.

1. The trunnion bearings are standard bearings in that a full complement of balls is used; they are, however, of the highest quality available commercially.

2. In lubricating the bearings a fine, light machine oil has been found to be most satisfactory. It should be well filtered to remove any foreign material and replaced regularly depending upon the amount of usage of the dynamometer.

3. A tubular rubber coupling is used in the dynamometer and has been found to be quite satisfactory as a coupling member. At the speeds and torques normally encountered the effect of centrifugal force plus axial shortening due to the torque transmitted has been found to be small if reasonably heavy walled tubing is used. If, however, it is necessary to make extremely critical tests these effects may be eliminated almost entirely by use of the following procedure:

With the motor under test operating on the dynamometer, adjust the spacing between the motor and the dynamometer to give the highest possible output (as indicated on the torque scale). Theoretically, if it can be assumed that the motor bearing losses are minimized by applying no end thrust, then this procedure will allow complete cancellation of end thrust merely by changing the spacing.

Reactances of Squirrel-Cage Induction Motors

T. C. LLOYD
MEMBER AIEE

VICTOR F. GIUSTI
ASSOCIATE AIEE

S. S. L. CHANG
STUDENT MEMBER AIEE

IN CALCULATING the reactances of induction motors, certain initial choices are made as to desirable procedures and methods. The material given here is based on these premises.

1. The fundamental calculations should be the same for either single phase or polyphase motors, modifying only the later steps in the process for the two types.

2. The calculations should be based on permeances of the magnetic paths, for ease in handling many calculations in the same laminations.

3. Only the slot, zigzag, and end connection permeances will be used in determining leakage reactance.

Slot Permeance

The permeance of a magnetic circuit depends upon the area divided by the length of path. For convenience, the constant 0.4π inherent with magnetic circuit calculations, will be absorbed with the permeance. Then in general, the permeance of a certain magnetic path will be defined as

$$P = 0.4\pi \times 2.54 \times \frac{\text{area in inches}}{\text{length in inches}}$$

This permeance expresses the lines per ampere per inch of conductor.

In dealing with slots, it is well known that every line of slot leakage flux does not link with every conductor, the linkages varying with the slot depth. In cases of straight, parallel sided slots, the effective linkages are only one-third of the product of slot flux and total conductors. It can be assumed that the effective area of the flux path is therefore only one-third of the actual area.

The permeance of the path of slot leakage flux is therefore, per inch of stack,

$$P = 3.19\left(\frac{{}^1/_3 b_c}{a_s}\right) \tag{1}$$

This expression now gives the effective lines per ampere per inch.

This assumes that only the air path offers effective reluctance in opposing the magnetomotive force, and that the laminations, no matter how highly saturated, are of zero reluctance.

The term in parenthesis used in equation 1 is called the "slot constant" and it expresses the effective linkages per inch of stack, per ampere. It can be calculated for all practical conditions of slot shape. Let it be denoted as K_s'. No values will be given here as they can be found readily in published form.

Going back to the fundamental expression for reactance ($X = 2\pi fL$) it follows that the inductance of the winding of any one slot per inch of stack is $\Phi_s c^2 10^{-8}$. Where

Φ_s = the lines per ampere per inch per conductor

c = the series conductors per slot

This assumes that all lines link all slot conductors.

Then for a total of S_1 slots, or S_1/n slots per n phase in the stator, the total inductance of the winding per phase per inch of stack is

$$\frac{S_1}{n}\Phi_s c^2 10^{-8} \tag{2}$$

If the total series conductors per phase are C, then

$$c = C\frac{n}{S_1} \tag{3}$$

and the inductance of the winding for all slots for L inches of stack becomes

$$LC^2\frac{n}{S_1}\Phi_s 10^{-8} \tag{4}$$

Then

$$X = 2\pi f C^2 n 10^{-8} L\frac{\Phi_s}{S_1} \tag{5}$$

Effective lines per ampere per inch have been given by equation 1 when the slot shape is considered through the slot constant. Then for L inches of stack,

$$X_1 = 2\pi f C^2 n 10^{-8}\left(\frac{3.19 L K_s'}{S_1}\right) \tag{6}$$

The preceding equation assumes that the conductors are all in series, carrying currents in the same phase relationship. If a double-layer winding of full pitch is used, the above formula is adequate. If short pitch windings are used, the current in coil side a *lags* that of b by θ degrees. Then the other side of b will be in a slot with conductors carrying current θ degrees *ahead* of the current in b. This means that the out-of-phase components of the voltages induced in the coils by leakage fluxes will cancel, but the in-phase components will be reduced. A correction, developed by Adams,[1,2] is used with equation 6. This can be read from his curves, or for pitches of not less than 50 per cent, the factor $(0.625p + 0.375)$ can be used instead. Here p is the pitch as decimal fraction. See Figure 1.

Rotor Slot Permeance

On the assumption that there are S_2 slots in the rotor, and that each bar per pole-pair represents a phase, the rotor is always made up of a winding of unity pitch and distribution factor.

Then to transfer a rotor value to stator terms, we can make use of the ratio of transformation

$$a^2 = \frac{n^2 C^2 K_w^2}{S_2^2} \tag{7}$$

Paper 47-212, recommended by the AIEE committee on rotating machinery and approved by the AIEE technical program committee for presentation at the AIEE Middle Eastern District meeting, Dayton, Ohio, September 23–25, 1947. Manuscript submitted June 19, 1947; made available for printing August 22, 1947.

T. C. Lloyd is chief engineer for Robbins and Myers Inc., Springfield, Ohio. Victor F. Giusti and S. S. L. Chang are also with Robbins and Myers Inc., Springfield, Ohio.

K_w = the winding factor (K_pK_d) for the stator

Following the procedure given for the stator slot leakage, the rotor slot leakage reactance is then, in stator terms; with $1/n$ of the total allotted to each stator phase

$$X_2 = 2\pi f C^2 n K_w^2 10^{-8}\left(\frac{3.19LK_s''}{S_2}\right) \quad (8)$$

wherein

K_s'' = the slot constant for the rotor slots

In this equation, note the absence of any winding factor for the rotor, based on the full pitch which follows from S_2/p rotor phases. Hence, no Adams pitch correction is needed for the rotor, but instead the winding factor of the stator squared is a fundamental part of the derivation. For convenience, it will be assumed that K_w^2 is equivalent to the Adams pitch correction. We then can combine the expressions for slot leakage reactance of both stator and rotor, into a final working formula

$$X_{slot} = 2\pi f C^2 n P_s 10^{-8} \quad (9)$$

$$P_s = L\left[3.60\left(\frac{K_s'}{s_1}+\frac{K_s''}{s_2}\right)\right](0.625p+0.375) \quad (10)$$

The so-called slot permeance, P_s, contains too many extraneous factors to be a true permeance to the purist. Furthermore, the theoretical constant 3.19, has been increased arbitrarily to 3.60 as an experience factor.

Summary

The previous material on slot leakage has been presented in some detail for several reasons. The actual derivation is very similar to that found in many texts, except that the transition to the final form as a function of permeances may prove complicated to the novice.

The addition of stator and rotor permeances, as used, is not strictly correct. It is of interest to note that the factor $(K_w)^2$ for the rotor is tacitly assumed to be equal to the pitch factor correction. This enables the permeance to be calculated as a constant of the lamination, regardless of winding factor, but should be an item for correction in extreme cases.

No derivation of slot constants nor tables of values are given here as they are available in the literature.

Zigzag Leakage

As will be pointed out in more detail later, practice varies in regard to the use of zigzag leakage. The method shown

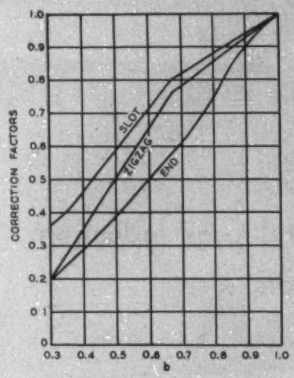

Figure 1. The Adams corrections for leakage reactance components as functions of pitch

here follows that of Adams[1,3] and it will need only the conversion from the original presentation, to the method of combined permeances, already covered in detail in the case of slot leakage.

The working formula for combined stator and rotor zigzag leakage reactance is

$$X_{zigzag} = 2\pi f C^2 n 10^{-8} P_{zz} \quad (11)$$

$$P_{zz} = \frac{8.5D}{(S_1)(S_2)\Delta}\left(\frac{T_e'+T_e''}{\lambda'+\lambda''}-0.5\right)^2 L \times (0.8p+0.2) \quad (12)$$

where

S_1 and S_2 = the number of primary and secondary slots, respectively
Δ = the actual radial air gap length in inches
λ' = the primary tooth pitch in inches
λ'' = the secondary tooth pitch in inches
T_e' = the corrected primary tooth face
T_e'' = the corrected secondary tooth face

In order to determine the effective tooth face due to fringing, Adams makes use of the term

$$f = 0.6 + 1.47 \log \frac{e}{2\Delta} \quad (13)$$

This is used when $e/2\Delta > 1$. When this ratio is equal to or less than unity, he recommends

$$f = 0.6 + \frac{e}{2\Delta} \quad (14)$$

In these equations f is the fringing band at each tooth side. Using these formulas the corrected tooth face becomes

$$T_e' = \text{actual tooth face} + 2\Delta f \quad (15)$$

A slightly modified method, put up in more convenient form, is shown in Table I. Note that e' or e'' are the respective primary or secondary slot openings.

End Connection Leakage. An empirical equation which has proved useful in practice, gives a simple expression for permeance of the leakage flux paths around stator and rotor windings.

$$P_e = \frac{\lambda}{p}K_e(1.25_p - 0.25) \quad (16)$$

where

λ = the pole pitch in inches
K_e = 0.45 for an end ring comparatively long in the axial dimension and extending considerably beyond the rotor core
= 0.65 for an end ring of comparatively great radial length

$$X_e = 2\pi f C^2 n P_e 10^{-8} \quad (17)$$

Total Leakage Reactance

For both stator and rotor, the total leakage reactance is

$$X = 2\pi f C^2 n P_L 10^{-8} \quad (18)$$

where

$$P_L = P_s + P_{zz} + P_e \quad (19)$$

Magnetizing Permeance

The magnetizing reactance is set up so that

$$X_m = 2\pi f C^2 n P_m 10^{-8} \quad (20)$$

$$P_m = \frac{0.32L\lambda K_w^2}{P\Delta K_1 S.F.} \quad (21)$$

and

λ = the pole pitch in inches

Table I. Effective Tooth Face From Fringing. Values of F

Effective Tooth Face T_e = Actual Face + F

Slot Opening e' or e''	Radial Gap-Length, Inches 0.010	0.015	0.020	0.025	0.030	0.040
0.04	0.021	0.024	0.026	0.027	0.028	0.029
0.05	0.023	0.028	0.031	0.032	0.033	0.035
0.06	0.026	0.031	0.035	0.037	0.039	0.041
0.07	0.028	0.034	0.038	0.041	0.043	0.046
0.08	0.030	0.036	0.041	0.045	0.048	0.051
0.09	0.031	0.039	0.044	0.049	0.053	0.057
0.10	0.032	0.041	0.047	0.052	0.056	0.062
0.11	0.034	0.043	0.049	0.055	0.059	0.066
0.12	0.035	0.044	0.052	0.058	0.062	0.070
0.13	0.036	0.046	0.054	0.060	0.065	0.073

K_1 = a factor greater than unity, expressing a correction for air gap length due to fringing. See equation 22.

$S.F.$ = the saturation factor, defined as total ampere-turns for complete magnetic circuit divided by ampere-turns for the corrected gap length.

To calculate K_1, use the corrected stator and rotor tooth faces as discussed under zigzag permeance.

$$K_1 = \frac{\lambda' \times \lambda''}{T_s' \times T_s''} \tag{22}$$

The preceding value of reactance is similar enough to the usual presentation as to need no derivation. In using the value which limits the no-load current, it is customary to deal with total reactance, defined as follows:

$$X_s = X_m + X_1 \cong 2\pi f C^2 n P_s 10^{-8} \tag{23}$$

wherein

$$P_s = \frac{0.32 L \lambda K_{ss}^2}{P \Delta K_1 S.F.} + \frac{P_L}{2} \tag{24}$$

Polyphase and Single Phase

In setting up the system of calculations described here, it was assumed that the values, once calculated for a lamination, would be useful for either polyphase or single phase motors. Actually a slight correction is required through the use of the pitch correction. All formulas previously given are applicable directly to polyphase calculations for double-layer windings. But single phase windings are assumed to be of the concentric type, and the last term in each component for leakage reactance, as given, corrects for pitch in the lap type winding. Therefore, these terms must be discarded. A new correction for distribution will be shown.

The previous equations involve n, the number of phases. In all single phase cases, n must be calculated as 2, including the use of X_s and X_m.

Single Phase Correction

Ideally, one over-all correction factor, as a function of winding factor, should be used for all components of leakage reactance. That is, for total leakage reactance

$$X(1\text{-}phase) = 2\pi f C^2 (n=2) K P_L 10^{-8} \tag{25}$$

where

K = a function of winding factor

The use of such a correction, assumes that the influence of winding factor is equally effective on slot, zigzag and end connection components.

The analysis of Appendix I, indicates a correction for slot and zigzag components, and a second correction for end connection components. However, one over-all correction factor, which tacitly assumes a division of the total reactance into definite components, has been found by long experience to be useful and reasonably accurate except on extreme values of K_{ss}. Figure 3 shows such a curve for K.

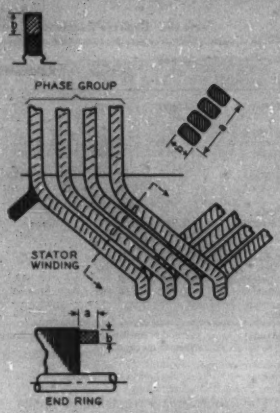

Figure 2. Diagrams illustrating the significance of the terms used by Arnold in calculating end leakage

Summary of Methods for Dealing with Single-Phase Values

$$X = 2\pi f C^2 (n=2) K P_L 10^{-8} \tag{26}$$

Read K from Figure 3.

$$P_s = L\left[3.60\left(\frac{K_s'}{S_1} + \frac{K_s''}{S_2}\right)\right] \tag{27}$$

$$P_{ss} = \frac{8.5D}{(S_1)(S_2)\Delta}\left(\frac{T_s' + T_s''}{\lambda' + \lambda''} - 0.5\right)^2 L \tag{28}$$

$$P_s = \frac{\lambda}{P} K_s \tag{29}$$

For greater accuracy, separate the corrections for winding factor

$$X = 2\pi f C^2 (n=2) P_L 10^{-8} \tag{30}$$

$$P_s = (27) \times K_{ss} \tag{31}$$

$$P_{ss} = (28) \times K_{ss} \tag{32}$$

Read K_{ss} from Figure 3.

$$P_s = (29) K_s' \tag{33}$$

Read K_s' from a calculated curve such as Figure 3.

For total permeance:

$$X_s = 2\pi f C^2 (n=2) P_s 10^{-8} \tag{34}$$

$$P_s = \frac{L\lambda \times 0.32}{P \Delta K_1 S.F.} + \frac{P_L}{2} \tag{35}$$

Comparison of Methods

It is of interest to note the treatment given leakage reactance by various writers. The equations they present are given in Appendix III and are taken as far as possible from the original presentation. (The presentation of Arnold was available only as notes.) This collection of formulas may prove useful, but in addition it has been regrouped into slot, zigzag, and end-connection components for comparison.

Slot Leakage

Table II shows the result of grouping all of the like factors and combinations of factors making up slot leakage into a constant K and comparing results. That is, K includes all terms which are found in each writer's analysis, such as number of turns, frequency, slot constant, the number of rotor and/or stator slots and the length of stack.

Comparison indicates that the values reduce to very much the same quantities, and that once the confusion of symbols is cleared away, writers agree on these calculations except for pitch corrections. The curve for this correction, used by Kuhlmann, is somewhat lower than that of Adams, while Gray's correction is entirely different. Arnold corrects only the stator slot leakage reactance.

Kuhlmann and Arnold follow theoretical considerations and consider the effect of pitch factor and distribution factor in reflecting rotor slot leakage to stator terms. Rotor coil and winding

Table II. Comparison of Slot Leakage Reactance Equations*

	Adams[1,2]	Kuhlmann[3]	Gray[4]	Arnold
Stator slot leakage	K (9.6)	K (9.57)	K (9.57)	K (9.57)
Pitch correction	(a)	(b)	$\cos^2\theta/2$	(a)
Rotor slot leakage	K_2(9.6)	$K_2$9.57$\left(\frac{f_2' f_w'}{f_s' f_w''}\right)^2$	K_2(9.57)	K_2 9.57$(f_2' f_w'')^2$
Pitch correction	(a)	(b)	$\cos^2\theta/2$	None

*(Like quantities grouped into a constant K are not to be confused with K used for single phase motors.)

(a). From curve, Figure 97, Section 7, Standard Handbook for Electrical Engineers Fifth Edition.

(b). From curve, Figure 143, Kuhlmann, Second Edition.

factors are considered unity for a squirrel cage. Punga and Raydt[6] present a slot leakage analysis identical with Arnold, with no correction for pitch.

Zigzag Leakage

The equations for zigzag leakage show a greater variety. The only two that are of comparable form are those presented by Adams and Gray. As before, by grouping all of the common factors into a constant K_3, we have the following comparative results.

$$\text{Adams zigzag:}\quad \left(2.66\frac{\lambda'+\lambda''}{S_1}\right)K_3$$

$$\text{Gray zigzag:}\quad \left[2.6\left(\frac{\lambda'}{s_1}+\frac{\lambda''}{s_2}\right)\right]K_3$$

where λ' and λ'' are tooth pitches of stator and rotor, respectively; and S_1 and S_2 are the number of stator and rotor slots, respectively.

It will be noted that the influence of the number of rotor slots appears in Adams' formula only due to the tooth pitch that results. In correcting for winding pitch, Adams uses the familiar curves of Figure 1; Gray uses the factor $\cos^3 \theta/2$.

Kuhlmann's zigzag reactance is a function of the number of poles, slots, and the magnetizing reactance. No direct correction for winding pitch is made as it is absorbed in the magnetizing terms.

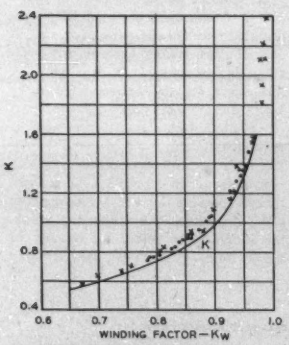

Figure 3. An over-all correction curve for concentric winding leakage reactance

Points shown are the theoretically correct values for correcting slot and zigzag components. The dots represent all cases of Appleman distribution; the crosses results from miscellaneous distributions. While the correction points for end leakage (K'_e) are not shown, in all cases they were from 0.11 to 0.15 less than the values of K_{ze}

Table III. Leakage Reactance of Sample Motor by Various Methods

	R. and M.	Adams	Kuhlmann	Gray	Arnold		Punga and Raydt
X Slot	1.400	1.233	1.180	1.238	Stator Rotor	0.845 0.335	1.178
Pitch Correction	0.863	0.860	0.835	0.884	0.86		None given
Final	1.21	1.06	0.985	0.194	1.06		1.178
X Zigzag	1.31	1.278	1.047	1.15	* 1.046 0.574	** 0.988 0.474	1.100
Pitch Correction	0.822	0.845	None given	0.884	0.845		None given
Final	1.08	1.08	1.047	1.018	1.460	1.309	1.100
X End	1.365	1.21	1.06	1.465	1.156		0.592
Pitch Correction	0.725	0.71	0.835	0.889	None given		None given
Final	0.99	0.861	0.880	1.295	1.156		0.592
X	3.28	3.001	2.920	3.407	3.676	3.525	2.870

*Arnold's exact method is multiplied by 2 as per Punga.
**Arnold's approximate method.

The doubly-linked reactance of Punga and Raydt is closely allied to the zigzag analysis of other writers, although yielding numerical calculations unusually low, and with no correction for pitch.

Arnold presents two forms of zigzag leakage equations. One is identified as an approximate method. The more accurate expression gives results which are about half of that expected, and the numerical work of Table III is multiplied by two in line with Punga and Raydt's comment on Arnold's error. The original form of the equations is given in the appendix. It appears that the correction is unnecessary with the approximate form.

End Leakage

End leakage reactance, due to those lines of flux which link only the stator end coils, and those lines which link only the rotor end ring, does not lend itself to simple analysis. For this reason, the experience of the individual author seems to play a major part in his choice of equation forms. Arnold's equations rely on the physical configuration of end coils and end rings, Figure 2, but give no pitch correction. Kuhlmann's equation includes the air gap diameter, but no direct account is taken of end coil or end ring shape. Adams and Gray rely on curves to supplement basically simple formulas.

Calculated Results

Using the individual formulas of Appendix III the 2 hp sample motor has been calculated by all methods discussed. Results are shown in Table III. To obtain these values, originally grouped terms have been divided to produce slot, zigzag and end components for ease in comparison. In addition, it has been necessary to convert the Punga and Raydt analysis from leakage flux in Maxwells to reactances.

Appendix I

Correction for Concentric Windings

In polyphase motors, the analysis of Adams indicates that the stator winding coil pitch influences each of the leakage components to a varying extent. The same factor applied to all leakage flux components would be ideal from the standpoint of calculation.

In the concentric type windings used in single phase motors, with various numbers of slots per pole, the effective leakage reactance varies as a function of the winding factor, K_w. The important question is whether or not each component of leakage flux varies as the same function of K_w.

For many years, the writers have used an over-all correction curve, multiplying the sum of the leakage permeances by a single correction depending upon K_w. This factor is shown as a curve in Figure 3. The source is unknown, and its accuracy will be investigated briefly here. To do so, we will consider the leakage flux consisting of two parts.

1. That portion which links the rotor only, giving rise to an inductance proportional to K_w.

2. That portion which links the stator only, giving rise to an inductance proportional to the concentration only, in case of slot and zigzag components, and proportional to the concentration times the pitch for end windings.

As will be shown, the resulting formulas give very good agreement with the over-all correction factor as used with well distributed windings. For more concentrated coils it gives higher values than used previously, in good agreement with experimental tests.

General Formulas

Let

$$F_r = \frac{\text{number of conductors in } r^{th} \text{ slot}}{\text{total conductors per pole per phase}} \quad (36)$$

K_{ze} = the correction for both slot and zigzag components

Table IV

(1) Slots M	(2) $0.045\ M$	(3) K_w Equation 39	(4) $\frac{K_w^2}{2}$	(5) (2) + (4)	(6) K_{ss}	(7) K end Equation 38
6	0.270	0.721	0.260	0.530	0.65	0.52
8	0.360	0.836	0.350	0.710	0.87	0.74
9	0.405	0.869	0.378	0.783	0.96	0.83
12	0.540	0.925	0.428	0.968	1.18	1.05
16	0.720	0.957	0.458	1.178	1.44	1.31
18	0.810	0.965	0.465	1.275	1.55	1.42

K_s' = the correction for end leakage

p = the pitch as a decimal fraction

Then

$$K_{ss}=\left[\frac{S_1}{4p}\sum_r (F_r)^2+\frac{K_w^2}{2}\right]1.22 \qquad (37)$$

and

$$K_s=\left[\frac{S_1}{4p}\sum_r (F_r^2\times p)+\frac{K_w^2}{2}\right]1.22 \qquad (38)$$

To apply these general formulas it is necessary to select individual cases. These are

(*a*). Windings distributed in the manner recommended by Appleman.

(*b*). Distribution based on coils of equal turns.

(*c*). Distribution based on coils of various miscellaneous percentages of turns.

Calculations

To illustrate the approach, the latter case mentioned will be calculated in detail.

Assume three coils per pole on a concentric winding, each pole having M slots. The number of turns in the outer and center coils is equal, and each is considered to be a 100 per cent coil. The inner coil has 50 per cent turns. The problem is to calculate the corrections K_{ss} and K_s'.

Coil Span	Per Cent Turns
M-1	100
M-3	100
M-5	50

$$K_w=\frac{2}{5}\cos\frac{90^\circ}{M}+\frac{2}{5}\cos\frac{270^\circ}{M}+\frac{1}{5}\cos\frac{450^\circ}{M} \qquad (39)$$

$$\frac{m}{4}\sum_r F_r^2=\frac{M}{4}\left[\left(\frac{1}{5}\right)^2 2+\left(\frac{1}{5}\right)^2 2+\left(\frac{1}{10}\right)^2 2\right] \text{ or } 0.045\cdot M$$

For various values of slots per pole M these formulas are evaluated in column 2 of Table IV.

$$\frac{M}{4}\sum_r F_r^2{}_p=\frac{M}{4}\left[\left(\frac{1}{5}\right)^2 2\times\frac{M-1}{M}+\left(\frac{1}{5}\right)^2\times 2\times\frac{M-3}{M}+\left(\frac{1}{10}\right)^2\times 2\times\frac{M-5}{M}\right]$$

These values of K_s' are shown in column 7.

Conclusions

The latter procedure shown has been used to investigate many cases and the points are plotted in Figure 3. It would appear that on the basis of the assumptions made, no single valued function of k_w is theoretically accurate as an over-all correction for all components of leakage reactance. However:

1. For $K_w < 0.92$, all different cases investigated show an agreement within 5 per cent. These values are higher slightly than the correction curve used, but inasmuch as the correction K_s' is always lower than K_{ss}, the over-all result is to bring the effective correction by rigorous analysis, reasonably close to the curve shown.

2. For $K_w > 0.92$, the values of K_{ss} for the same K_w but for different distributions, may differ by more than 10 per cent. Furthermore, a slight change in K_w (or error in calculating) causes a great change in K_{ss} and K_s'. Under these circumstances, for accurate work, cases of nearly concentrated coils should be calculated probably in detail rather than use the over-all correction.

Appendix II

Calculating the Sample Motor Reactance

Using the method outlined in this paper, the following significant terms are calculated.

Stator slot constant $K_s'=1.685$
Rotor slot constant $K_s''=0.947$
Stacking length used $L=3.00$ inches
Air gap length $\Delta=0.018$
Tooth pitch, stator $\lambda'=0.492$ inch
Tooth pitch, rotor $\lambda''=0.398$ inch
Stator-Tooth face, corrected $T_c'=0.420$ inch
Rotor-Tooth face, corrected $T_c''=0.372$ inch
Pole pitch used $\lambda=4.43$ inches
Ring constant $K_e=0.65$

From equation 10 the slot permeance, stator and rotor:

$P_s=0.74\times 0.863$ or 0.64

From equation 12 the zigzag permeance:

$P_{zz}=0.69\times 0.822$ or 0.57

From equation 16 the end connection permeance:

$P_e=0.723\times 0.725$ or 0.523

As the series conductors per phase are 408 for the 220 volt connection, it follows that

$X_s=1.21$ ohms
$X_{zz}=1.08$ ohms
$X_e=0.99$ ohm

Total leakage reactance = 3.28 ohms.

Magnetizing Reactance

The gap constant, allowing for fringing, is 1.255. Then from equation 21

$$P_m=\frac{0.32\times 3.0\times 4.43\times 0.815}{4\times 0.018\times 1.255\times 1.2} \text{ or } 32.0$$

$$P_p=P_m+\frac{P_L}{2} \text{ or } 33.03$$

$X_m=60.8$ and $X_p=62.8$

Appendix III

Leakage Reactance Equations

Some of the equations most commonly used for leakage reactance are presented in this appendix. They are listed as far as possible in the original authors' terms and new symbols are identified directly after each equation. A given symbol has a particular meaning in all the equations presented by one author, but the symbol may change meaning when used by another writer.

Leakage Reactance Equation for 3-Phase Squirrel-Cage Motors in Per Phase Terms

Adams[1,3]

Φ_{sl1} = slot leakage permeance of the stator slot

$$=\frac{3.2}{N_{spp}'}K_s' \qquad (40)$$

in which N_{spp}' is the number of slots per phase per pole in the stator, and K_s' is the stator slot constant.

Φ_{sl2} = slot leakage permeance of the rotor slot

$$=\frac{3.2}{N_{spp}''}K_s'' \qquad (41)$$

in which N_{spp}'' is the number of slots per phase per pole in the rotor, and K_s'' is the rotor slot constant.

Φ_{slot} = rotor and stator slot leakage permeance

$$=(\Phi_{sl1}+\Phi_{sl2})K_{ps} \qquad (42)$$

where

K_{ps} is the correction for winding pitch Figure 1.

Φ_{zz} = zigzag leakage permeance

$$=\frac{AT_1}{\delta N_{spp}'}K_{ps} \qquad (43)$$

$$A=2.13\left(\frac{a_1+a_2}{2}-1/2\right)^2 \qquad (43a)$$

in which a_1 is the stator tooth tip divided by the stator tooth pitch and a_2 is the rotor tooth tip divided by the rotor tooth pitch. Other symbols used are T_1 which is the average tooth pitch of rotor and stator, δ is the air gap, and k_{ps} is the correction for winding pitch Figure 1.

Φ_{ze} = end leakage permeance

$$=K_f K_3 \qquad (44)$$

where k_3 is the pole pitch in inches divided

by the length of stack, and k_f is taken from a curve Figure 1.

The total leakage permeance, $P_s = \Phi_{slot} + \Phi_{tb} + \Phi_{fb}$ (45)

and the total leakage reactance, X_s

$$X_s = 2\pi f 2pLN_{cpp}'^2 P_s 10^{-8} \quad (45a)$$

where

f = frequency

p = number of pairs of poles

N_{cpp}' = number of conductors per phase per pole

KUHLMANN[6]

X_{stator} = slot leakage reactance of the stator

$$= \frac{2.0 f l_g m N^2}{10^8 S_s} K_s' \quad (46)$$

in which l_g is the width of stack, k_s' is the slot constant of the stator, f is the frequency, m is the number of phases, N the total number of series conductors per phase, and S_s the number of stator slots.

X_{rotor} = slot leakage reactance of the rotor

$$= \frac{2.0 f l_g m N^2}{10^8 S_r} K_s'' \quad (47)$$

where the new symbols K_s'' and S_r are the slot constant and the number of slots in the rotor respectively,

$$X_{slot} = X_{stator} + X_{rotor}\left(\frac{f_c f_w}{f_{cr} f_{wr}}\right)^2 K_s \quad (48)$$

where f_w and f_c are the distribution factor and coil factor of the stator winding, respectively, and the addition of subscript r means rotor valves. The pitch factor, k_s may be taken from a curve.[5]

X_{zz} = zigzag reactance of the stator

$$= \frac{5}{6} X_m \left(\frac{P}{S_s}\right)^2 \quad (49)$$

in which X_m is the magnetizing reactance and p the number of poles.

X_{rz} = zigzag reactance of the rotor

$$= \frac{5}{6} X_m \left(\frac{p}{S_r}\right)^2 \quad (50)$$

X_z = total zigzag reactance

$$= X_{zz} + X_{rz} \quad (51)$$

X_e = end leakage reactance

$$= \frac{2 f m N^2 D K_e}{10^{12} p^2} \quad (52)$$

in which the new symbol, D, is the gap diameter.

GRAY[4]

$$X_{eg} = 2\pi f b_1 c_1 \left(\cos^2\frac{\Theta}{2}\right) p n_1 \left[\frac{\Phi_s L_e}{2n_1} + \left(\frac{\Phi_s+\Phi_e}{n_1} + \frac{\Phi_s+\Phi_e}{n_2}\right) L_g\right] 10^{-8} \quad (53)$$

where

f = frequency

b_1 = series conductors per slot

c_1 = number of slots per phase per pole in the stator

C_2 = Number of slots per phase per pole in the rotor

$\cos^2\frac{\Theta}{2}$ = pitch correction

Θ = angle in electrical degrees between the pitch used and full pitch

p = number of poles

n_1 = number of phases in the stator

n_2 = number of phases in the rotor

$\frac{\Phi_s L_e}{2n_1}$ = end leakage permeance and can be taken from a curve[3]

Φ_s = end leakage constant

L_e = length of end coils

for the quantity $\left(\frac{\Phi_s+\Phi_e}{n_1}\right)$ –

$$\Phi_s = \frac{0.26}{c_1}\frac{\lambda'}{\delta}\left(\frac{1}{C_1}+\frac{1}{C_2}-1\right)^2$$

$$\Phi_e = \frac{3.2}{c_1} \times \text{slot constant of stator}$$

where λ_1 is the stator tooth pitch, δ the air gap, and C_1 and C_2 are the Carter coefficients; that is

$$C_1 = \frac{\text{tooth pitch of the stator}}{\text{effective tooth face of the stator tooth}}$$

$$C_2 = \frac{\text{tooth pitch of the rotor}}{\text{effective tooth face of the rotor tooth}}$$

for the quantity $\frac{\Phi_s+\Phi_e}{n_2}$

$$\Phi_s = \frac{3.2}{c_2} \times \text{slot constant of rotor}$$

$$\Phi_s = \frac{0.26}{C_1}\frac{\lambda_2}{\delta}\left(\frac{1}{C_1}+\frac{1}{C_2}-1\right)^2$$

where λ_2 is the rotor tooth pitch and C_1 and C_2 are again Carter coefficients.

L_g = the gross length of the iron

Table V. The Coefficient of Doubly Linked Leakage[6]

Slots Per Pole in the Stator Rotor	Slip Ring Motor	Number of Stator Slots Smaller Than Rotor Slots	Number of Stator Slots Greater Than Number of Rotor Slots
6/9	0.0416	0.031	0.035
9/12	0.0227	0.016	0.0167
6/15	0.034	0.0193	0.026
9/15	0.020	0.0135	0.0153
12/15	0.0152	0.0096	0.0100
12/18	0.0138	0.008	0.0093
15/18	0.0115	0.006	0.0063

ARNOLD

X_1 = leakage reactance of the stator winding phase

$$= \left[\frac{2\pi f Z^2}{P q_s} L_g\right]\left(K_n\lambda_n + K_z\lambda_z + \frac{l_e}{L_c}\lambda_e\right)10^{-8} \quad (54)$$

where f is the frequency, Z the number of series conductors per phase in the stator, P is the number of poles, q_s is the number of slots under each pole containing series phase conductors in stator, L_c s the gross length of iron and

λ_n = slot leakage permeance of the stator slot

$$= 3.19 \times \text{slot constant} \quad (55)$$

λ_z = zigzag leakage permeance of the stator

Arnold gives two methods for calculating λ_z. In the approximate method

$$\lambda_z = 3.19\frac{l_f'' - e'}{6\Delta} \quad (56a)$$

in which l_f'' is the rotor tooth face, e' the slot opening in the stator and Δ is the air gap.

In the more accurate method, if $l_f'' \leq \lambda'$

$$\lambda_z = 3.19\frac{(l_f'' - e')^2}{6\Delta\lambda''} \quad (56b)$$

and if

$l_f'' > \lambda'$:

$$\lambda_z = 3.19\frac{(\lambda' - e')^2}{6\Delta\lambda''} \quad (56c)$$

where l_f' is the stator tooth face, e' is the stator slot opening, λ' is the tooth pitch of the stator and the double primes refer to corresponding rotor values.

λ_e = end leakage permeance of the stator

$$= 1.17\left(q_e \log_{10}\frac{1.5 l_e}{U_e}\right) \quad (57)$$

where q_e is the number of end connections in a phase group, l_e the length of one conductor, exclusive of its embedded length and

$U_e = 2(a+b)$

refer to Figure 2 for a and b. For K_n and K_z, the pitch correction factors for slot and zigzag, refer to Figure 1.

X_r = leakage reactance at the squirrel cage rotor in rotor terms.

$$= \frac{2\pi f}{p} L_c\left[\lambda_n + \lambda_z + \frac{1.84 D_r}{L_c N_2\left(\sin\frac{\pi P}{2N_2}\right)^2} \times \ldots \log_{10}\frac{2.4 D_r}{d+b}\right] \quad (58)$$

where

λ_n = slot leakage permeance of the rotor slot

$$= 3.19 \text{ rotor slot constant}$$

λ_z = zigzag permeance of the rotor (59)

Again two methods are available for calculating λ_z.

Approximately $\lambda_z = 3.19\frac{l_f' - e''}{6\Delta}$ (60a)

and, if $l_f' \leq \lambda''$

$$\lambda_z = 3.19\frac{(l_f' - e'')^2}{6\Delta\lambda'} \quad (60b)$$

and if $l_f' > \lambda''$

$$\lambda_z = 3.19\frac{(\lambda'' - e'')^2}{6\Delta\lambda'} \quad (60)$$

where the symbols are the same as those used for stator zigzag permeance. For the

end leakage permeance term, D_r is the mean diameter of the end ring, N_b is the number of rotor bars and for a and b, Figure 2.

X_l = total leakage reactance

$$= X_1 + \frac{4n_1(ZK_{ps}K_{ds})^2}{2n_b} PX_r \qquad (61)$$

in which n_1 is the number of stator phases, K_{ps} and K_{ds} are pitch factor and distribution factor of the stator winding respectively, Z is the number of series conductors per phase, and P the number of poles.

PUNGA AND RAYDT[6]

The stator slot leakage reactance is

$$X_{ss} = 2\pi f Z^2 q p \lambda_s' l 10^{-8} \qquad (62)$$

where f is the frequency, Z the number of conductors per slot, q is the number of slots under each pole containing series conductor per phase, p is the number of poles and λ_s' is the magnetic conductivity per inch of length of slot in the stator or 3.19 times the slot constant. The length of iron is l.

The rotor slot leakage in stator terms is

$$X_{rs} = 2\pi f Z^2 q p \lambda_s'' l 10^{-8} (K_{ps}K_{ds})^2 \qquad (63)$$

where the symbols refer to the stator except λ_s'' which is the magnetic conductivity per inch of length of the rotor slot, or 3.19 times the rotor slot constant. The symbols K_{ps} and K_{ds} are the winding pitch factor and distribution factor for the stator, respectively.

The stator end leakage is

$$X_{se} = 2\pi f Z^2 q^2 p \lambda_e' l_s' 10^{-8} \qquad (64)$$

where new quantities introduced are w_s', the smallest circumference of the cross section of the windings which belong together (see Arnold, U_e), and l_s the free length not in iron of a conductor to give

$$\lambda_e' = 1.17\left(\log_{10}\frac{l_s'}{w_s'} + 0.3\right)$$

The rotor end leakage in stator terms is

$$X_{re} = 2\pi f Z^2 q^2 p \lambda_e'' l_s'' 10^{-8} (K_{ps}K_{ds})^2 \qquad (65)$$

where λ_e'' is taken as 1.27 for squirrel cage and l_s'' is $\frac{\pi D_r}{p}$ and D_r is the mean diameter of the end ring.

The doubly linked leakage is

$$X_d = 2\pi f \frac{Z_{ep}}{2\sqrt{2}} \frac{\Phi\lambda_d}{I_{mag.}/S.F.} 10^{-8} \qquad (66)$$

where

Φ is the flux per pole

$$= \frac{E10^8}{4.2f\omega}$$

and E is the voltage per phase, and ω the number of turns per phase. $I_{mag.}$ is the magnetizing current, $S.F.$ is the saturation factor, and λ_d is the coefficient of doubly linked leakage, Table V.

References

1. FRACTIONAL PITCH WINDINGS FOR INDUCTION MOTORS, C. A. Adams, W. K. Cobart, A. E. Irving, Jr. AIEE TRANSACTIONS, volume 26, 1907, pages 1485–1503.

2. THE DESIGN OF INDUCTION MOTORS, C. A. Adams. AIEE TRANSACTIONS, volume 24, 1905, pages 649–87.

3. STANDARD HANDBOOK FOR ELECTRICAL ENGINEERS, C. A. Adams. McGraw-Hill Book Company, New York, N. Y. Fifth edition, Section 7.

4. ELECTRICAL MACHINE DESIGN (book), A. Gray. Second edition.

5. DESIGN OF ELECTRICAL APPARATUS (book), J. H. Kuhlmann. Second edition, page 219, Figure 143.

6. MODERN POLYPHASE INDUCTION MOTORS (book), F. Punga, O. Raydt. Translated by Hobart.

No Discussion

The Application of Surge Comparison Testing Equipment to Fractional Horsepower A-C Stator Windings

LLOYD W. BUCHANAN
ASSOCIATE AIEE

THE SURGE COMPARISON method of testing has been described by Foust and Rohats[1] and further developed by Moses and Harter[2] in preceding papers. This paper deals particularly with the testing of fractional horsepower stators. It makes an analysis of the voltage distribution in the winding and compares the effect of the surge voltage to a 60-cycle voltage. Previous studies have pertained mainly to the detection of short-circuited turns or wrong number of turns in 3-phase and large machines. These tests are combined here with others into a quick and accurate procedure to include additional information relative to quality and accuracy of winding; with these refinements, the surge comparison test lends itself readily to production testing of small motors.

Operation

The surge comparison tester is a means of applying voltage of two motor windings and comparing them to determine if there are any discrepancies or breakdown in insulation. A surge of steep wave front is applied to the two windings connected in series and the voltage wave across one of them is recorded on an oscilloscope. On each successive surge the two windings are interchanged. If the two windings are identical, the trace on the oscilloscope will be the same for each surge. If the windings are different, the traces will not coincide; and since the oscilloscope screen retains the trace for a short period, two images will appear. The surges are of very short duration, measured in a few microseconds, and applied 60 times each second. The energy supplied to the test windings is very low; consequently, the test voltage can be increased sufficiently to give a test of insulation without damaging the windings due to heating. The motor frames must be grounded; therefore, if the windings are connected according to Figure 1 the surge causes a voltage stress of insulation between turns coils, windings, and ground. A simplified circuit diagram of the surge comparison tester is shown in Figure 1. A motor which has been found to be correct and is retained for test purposes is referred to as the test standard and the motor being tested as the test motor. A charge is built up on capacitor *C1* by feeding the output of transformer *T2* through rectifier tube *G1*. The voltmeter *V* can be calibrated in surge voltage. The voltage surge is released by a grid-controlled gas tube *G2* and flows from point 2 of the winding to point 1. On the succeeding surge the synchronous switch has interchanged the connections and the surge flows from point 1 to point 2. On the first surge the oscilloscope indicates the voltage across winding 1, and on the second, across winding 2.

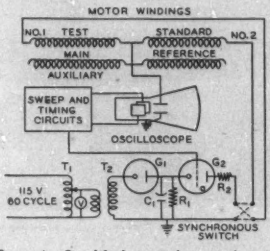

Figure 1. Simplified circuit diagram of surge comparison tests

T_1—Transformer
T_2—High voltage transformer
V—Voltmeter
C_1—High voltage capacitor
G_1—Rectifier tube
G_2—Grid-controlled gas tube
R_1—Grid-leak resistor
R_2—Current limiting resistor

Distribution of Voltage and Dielectric Stress of Insulation

The voltage curve at various points of a winding is plotted against time in Figure 2. A voltage surge of 2,000 volts was applied at point *A*, and point *J* was grounded.

The motor used for these tests was a 4-pole 60-cycle 115-volt fractional horsepower motor having 82 turns in each pole of the main winding, with three concentric coils per pole. These curves are similar to those recorded in previous papers on stresses resulting from surges in transformers and other electric machinery, and indicate that a distributed winding has little effect on the results from the surge. They also show that at one point the voltage slightly exceeds the applied voltage. Quite often, tests show the voltage at point *B* to be considerably higher than the applied surge for a portion of the time. Curve *K* gives the voltage at point *K* on the auxiliary winding when the main winding is being tested. Voltage between the main and auxiliary windings can be determined from this curve. These curves can be determined for any winding merely by connecting the lead from the oscilloscope to the various points in the winding, instead of connecting it to the point between the windings. The resulting traces can be either plotted or photo-

Paper 47-230, recommended by the AIEE committee on rotating machinery for presentation at the AIEE Middle Eastern District meeting, Dayton, Ohio, September 23–25, 1947. Manuscript submitted May 27, 1947; made available for printing September 2, 1947.

LLOYD W. BUCHANAN is design engineer for the Westinghouse Electric Corporation, Lima, Ohio.

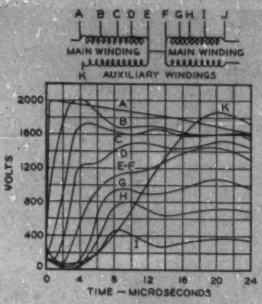

Figure 2. Voltage distribution at various points of a winding resulting from a surge voltage

graphed. Figure 3 is obtained by subtracting the voltage at one point of the winding from the adjacent point which has a higher voltage. It indicates the voltage across each pole. If a 2,000-volt surge test is applied to the motor of Figure 2 the voltage between adjacent conductors in a slot may be anywhere from the voltage per turn of four volts to the voltage per coil of about 200 volts. These peaks occur during the first five microseconds for the motor which has a terminal connected to the surge source. The voltage per coil in the motor which has a terminal connected to ground reached approximately 130 volts with a peak of much longer duration. Since the motor windings are interchanged during the test, both windings are subjected to these voltages.

Comparison of Breakdown of Insulation by Surge Voltage and 60-Cycle Voltage

The time duration of a voltage test is recognized by the National Electrical Manufacturers Association, and various curves have been recorded as to the effect of time on breaking down insulation. A test using a surge with a duration of its peak of the order of a few microseconds does not have the same effect on insulation as a 60-cycle wave having the same peak voltage. A record of averages of a number of tests on various insulation on a surge comparison test as compared to a 60-cycle test is shown in Table I.

It is necessary to use a surge voltage of approximately 1.7 times the rms or 1.2 times the peak 60-cycle voltage to obtain comparative results. As the conventional 60-cycle 30-second breakdown voltage of number 22 enamel covered wire is 88 per cent of its 1-second voltage, and the 30-second surge breakdown voltage is 97 per cent of its 1-second breakdown voltage, it is evident that the effect of time of test is less for the surge test than for the 60-cycle test. It may be deduced from this that the application of a high test voltage by means of a surge comparison tester does not damage a winding as much as a conventional test. The energy supplied by a surge comparison tester is very small, because a voltage is applied for only a small portion of each cycle. When a winding breaks down, there is little damage to adjacent conductors. As a result location of the fault is more difficult, but repair is considerably easier.

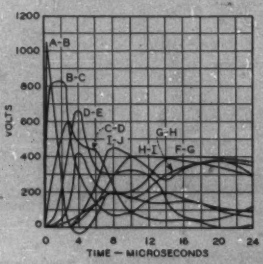

Figure 3. Voltage across each pole obtained from Figure 2

Test Methods

Some of the more common faults that occur in windings are short-circuited turns, wrong number of turns, grounded conductors, short circuited between main and auxiliary wings, reversed coils, and reversed rotation resulting from interchanging 2-colored or tagged leads when connecting them to the winding. For a large portion of single-phase fractional horsepower motors all of these checks can be made with a few simple tests on the surge comparison tester.

The surge comparison test is a means of comparing one winding to another. It is necessary to obtain a winding which has been completely checked to use as the test standard. This can be done by inspecting the first production winding by other means than the surge tester, or by retaining a stock of test standards. It is also possible to make a fairly complete test by comparing one-half of the motor winding against the other half. This is similar to the method of testing polyphase windings described in detail by Foust and Rohats,[1] whereby each phase is compared to another phase. If all phases are identical, the winding is correct, except for the possibility that the number of turns in all coils may be in error in the same amount.

The test described for Figure 1 will check for number of turns, short-circuited turns, short circuits between main and auxiliary windings, grounded conductors, and, in most cases, reversed coils. Motors having the wrong number of turns or a few short-circuited turns, will show two traces slightly apart as shown in Figure 4*B*, indicating that the winding being tested is slightly different from the standard. If two windings are compared and the traces coincide, shorting of one turn or decreasing the number of turns by one turn is easily detected. However, it is often difficult to segregate a 1-turn short circuit from allowable variations. Figure 4 shows the oscilloscope traces of a number of the more common faults.

In small motor windings, the relation of the various voltages in the winding remain constant. Therefore, the test voltage must be a compromise between several desired voltages. It is usually the voltage from winding to ground that

Figure 4. Oscilloscope traces for several common faults

A—Two windings identical—no fault
B—One turn short-circuited
C—Main winding grounded
D—Main winding short-circuited to auxiliary winding
E—Rotation correct and no reversed coils
F—Rotation reversed

limits the test voltage. The test voltage can be specified to give a check of insulation from winding to ground, which is roughly equivalent to the National Electrical Manufacturers Association ground test. It is often feasible to determine the test voltage to be applied by determining the surge voltage that will give a ground test equivalent to the National Electrical Manufacturers Association specifications. Ordinarily if this is done the turn-to-turn and main-to-auxiliary winding voltage is not excessive.

To have an effective ground test, the surge voltage should be about 1.7 times the present 1-second alternating voltage tests or about two times the 1-minute tests. Usually, this will give a turn-to-turn voltage consistent with reasonable turn-to-turn test voltages.

To check further for reversed coils and rotation, it is necessary to use a pickup coil located under each pole and to take a separate test with the pickup coil voltage fed to the oscilloscope. Location of the pickup coil with respect to the winding and the connections to the surge tester are shown in Figure 5. If the leads of the two stators to be compared are connected according to a prearranged code, either a reversed coil or reversed rotation will cause considerable divergence of the traces. Slight divergence can be neglected in this test, as location of the pickup coils is not necessarily accurate. The trace of this fault is shown in Figure 4*F*. Figure 6 shows a photograph of the tester with a test jig arranged to hold the stators during test and locate the pickup coils. The test jig also insures that the motor frames are grounded. Grounding of motor frames is necessary for the test and for the safety of the operator. The windings to be tested and type of test are selected by means of the push buttons and switches mounted on the panel of the tester. This eliminates the necessity of making different connections to the stator during tests.

Figure 6. Surge tester and test jig showing tester in production-line operation

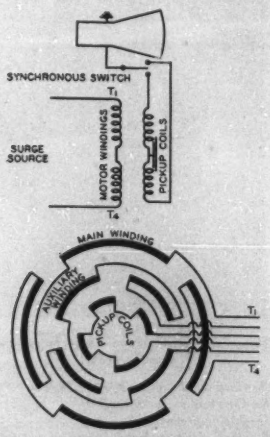

Figure 5. Location of pickup coils in relation to winding and method of connecting pickup coils for rotation check

Table I. Comparison of Breakdown Voltage Between Surge and 60-Cycle Test

Insulation	Time, Sec	Rms 60-Cycle Voltage	Surge Peak Voltage	Ratio
Enamel covered number 22 wire	1	3,330	5,540	1.66
Enamel covered number 22 wire	30	2,940	5,420	
Enamel covered number 19 wire	1	5,660	9,800	1.73
Cotton and enamel number 22 wire	1	4,460	8,040	1.80
0.010 thick rag paper		3,525	5,850	1.66
			Average	1.71

Summary

The surge comparison test can be adapted readily to testing fractional horsepower motors quickly and in large quantities. The effect of time duration of the test is minimized, and switching surges resulting from the testing apparatus are eliminated. The test applies a voltage stress to the winding, thereby showing any weaknesses. It detects short circuits, grounds, errors in turns, and errors in connections with a high degree of accuracy. Thus the surge comparison test is a valuable method of insuring a quality product with small expense and little interruption of production.

References

1. Insulation Testing of Electric Windings, C. M. Foust, H. Rohats. AIEE Transactions, volume 62, 1943, April section, pages 203–06.

2. Winding-Fault Detection and Location by Surge-Comparison Testing, G. L. Moses, Earl F. Harter. AIEE Transactions, volume 64, 1945, July section, 499–503.

No Discussion

Electric Drive for Aircraft

GEORGE C. CROM
NONMEMBER AIEE

Synopsis: The use of large amounts of power in aircraft becomes a power-handling problem; and electric transmission from the turbines mounted in the fuselage, to the propellers on the wings, has the same advantages as in handling very large amounts of power in industry. The advantages of electric power transmission are discussed, principally flexibility, reliability, ability to shut down prime movers, and lessened drag. Also the disadvantages—principally weight. An outline of an acceptable airplane and the calculation of fuel savings resulting from electric operation of a given flight plan are given, showing that it is possible to save enough fuel to cancel out the extra weight of the electric drive. Also, a discussion of weights of apparatus is given.

A Power-Handling Problem

When considering the design of very large high-speed propeller-driven aircraft from 250,000 pounds up to 500,000 pounds, the large output required of the power plant, 25,000 horsepower and up, introduces several problems which are largely functions of the physical bulk of the power plant.

The physical size of such power plants makes necessary the use of correspondingly large nacelles. There exists the possibility that, if the nacelles were reduced in size so their diameter was no greater than the depth of the wing, a significant increase in over-all aerodynamic efficiency of the aircraft could be obtained. Therefore, some method of removing the prime movers from the wings becomes attractive.

However, in large aircraft structures, wings and fuselage are flexible; and it is desirable to keep them flexible. It is difficult to transmit power mechanically any appreciable distance with flexible supports. In addition, the units of large turbine power plants should be operated somewhere near their lowest specific fuel consumption points; and with less than full load, it would be desirable to shut down some units so that the remaining units would be properly loaded. This is almost impossible to do with mechanical drives in aircraft. Clutches and flexible shafts or even hydraulic drives are heavy and hard to handle. Stopping engines and feathering the propellers directly connected to them is a rather unsatisfactory method of reducing power and is exceedingly dangerous under combat conditions, as it attracts the attention of enemy fighters.

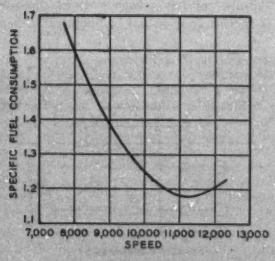

Figure 1. Fuel consumption taken from General Electric Company data on *I-40* engine

Turbine Power Plants

The development of gas turbine power plants with their light weight, high speed, and high efficiency, which are desirable in large aircraft power plants, has introduced additional problems.

The turbojet and turbopropeller engines operate at a minimum specific fuel consumption only over a limited speed range (Figure 1, which is taken from General Electric Company data on *I-40* engine). Normal rating of these engines as to speed and power usually is set near this point of minimum specific fuel consumption. Regarded in this light, turbines are constant speed devices and therefore are suitable for driving alternators.

Under usual operating conditions of bombers powered by reciprocating engines, the pilots make a given speed setting on the propeller governors and vary the speed of the aircraft by varying the output torque of the engine (and thus propeller thrust) through changes in manifold pressure. The range of allowable governor speed settings is rather wide; in the particular case of take-off, a significant increase in engine speed above normal rated is allowed for short periods of time.

In the case of direct-drive turbopropeller engines, rotational speed for cruising will be held within close limits to the point of minimum fuel consumption. No great increase in rotational speed, even momentarily as for control purposes, will be allowable due to structural considerations. The variation in propeller thrust will be accomplished by changes in blade pitch. Reduction gears will be needed to reduce the high turbine speed to the relatively slow rotational speed of large propellers.

The inertia of the turbine rotor at its high speed is higher than that of a reciprocating engine driving a propeller. When starting turbopropellers, the load on the starter is higher than on usual engines, as the compressor load has to be carried by the starter, and the firing speed is higher, and it takes more power to swing the propeller at this higher speed.

Electric Drive

It seems evident therefore that the propeller and the turbine should be separated and should be capable of being connected and disconnected from each other. Also

Paper 47-215, recommended by the AIEE committee on air transportation and approved by the AIEE technical program committee for presentation at the AIEE Middle Eastern District meeting, Dayton, Ohio, September 23–25, 1947. Manuscript submitted July 11, 1947; made available for printing August 19, 1947.

George C. Crom is with the Air Materiel Command at Wright Field, Dayton, Ohio.

Credit should be given to Colonel C. B. Reichert of Air Materiel Command, to Jack Cunningham and other engineers of Westinghouse Electric Corporation, and to Doctor Colson and other engineers of the General Electric Company for their assistance on this problem.

Table I. Calculation of Fuel Consumption for the Mechanical and the Electric Drives in the Case of the Projected Flight Plan

Flight Condition	Elapsed Time for Condition, Hr Start	Elapsed Time for Condition, Hr End	Duration of Condition, Hr	Number of Engines Operating	Total Engine Shaft Horsepower	Specific Fuel Consumption		Fuel Consumed During Period, Lb
A. Mechanical drive; efficiency of engine gearing 97 per cent								
Takeoff	0	1/12	1/12	4	22,000	0.65	1.00	1,225
Climb	1/12	1/2	5/12		13,000	0.61	1.08	4,410
Cruise	1/2	6	5 1/2		6,200	0.695	1.08	26,410
Target	6	8	2		9,500	0.55	1.08	11,610
Cruise	8	12	4		5,300	0.695	1.08	16,400
Cruise	12	15	3		4,800	0.755	1.08	12,080
Landing	15	16	1		3,000	1.62	1.00	5,410
							Total fuel consumed during flight	77,545
B. Electric drive; efficiency of motor gearing 97 per cent, of electric system 92 per cent								
Takeoff	0	1/12	1/12	10	22,000	0.65	1.00	1,335
Climb	1/12	1/2	5/12	6	13,000	0.57		4,150
Cruise	1/2	6	5 1/2	6	6,200	0.57		21,750
Target	6	8	2	10	9,500	0.55		11,690
Cruise	8	12	4	5	5,300	0.57		13,560
Cruise	12	15	3	5	4,800	0.55		8,900
Landing	15	16	1	3	3,000	1.62		5,440
							Total fuel consumed during flight	66,805

it would be desirable to be able to operate any or all propellers from any or all turbines. The only satisfactory method known at the present time to shift around large blocks of power between prime movers and loads is the electrical method which is in use throughout industry, giving neat, simple setups, reliability of operation, high efficiency, and complete flexibility. In this case, since alternators and motors would operate at constant speed, the pilot can control the power setting, which automatically would control the propeller pitch angle, by means of four levers (for a 4-propeller installation) or, possibly, by means of one composite lever.

The application of electric power transmission to aircraft is, however, difficult and beset with many limitations. The first, most important, and the hardest to design around is that of weight of the electric equipment used for transmission of power.

Alternating current is used almost exclusively in transferring power and the frequency commonly used in this country is 60 cycles. This is due to the ease of transmission, ability to transform, and to the reliability, ruggedness, and simplicity of the induction motor. In planning to adapt electric power transmission to aircraft, it becomes obvious that the induction motor should be used; but low frequencies are out of consideration as the equipment items become too heavy. Four hundred cycles or some frequency near it offers a maximum weight reduction and at the same time does not complicate apparatus design too much. The alternator design fits in well with the available gas turbine speeds of 8,000 to 12,000 revolutions per minute using four or six poles, letting the frequency be whatever is the result of the speed and pole choice.

A 6-pole induction motor seems to be the most practicable, giving some speed reduction with a 4-pole generator. The design of 8-pole induction motors is more difficult for 400 cycles, but can be used with good speed reduction but some increase in bulk and weight.

Propeller Motors

Ratings of induction motors to drive large propellers at slow speeds will be about 6,000 to 10,000 horsepower peak power for five minutes, based on four propellers per airplane and 250,000 to 500,000 pounds gross weight. The five minute rating is the usual take-off rating for maximum power. Diameters of such motors would be 28 to 34 inches, which can be buried in a wing or in a nacelle having a diameter equal to the wing depth. A block diagram of electric connections is shown in Figure 2.

Very careful estimation shows that the unit weight of motors of these types with proper allowance for forced cooling should be near 0.4 pound per horsepower, based on six poles. Similar estimation on alternators based on 4-pole direct-driven machines within the range of 3,000 to 5,000 horsepower peak rating should give a unit weight of 0.50 pound per horsepower.

Control wiring and miscellaneous should give 0.15 pound per horsepower. Total unit weight therefore is estimated as 1.05 pounds per horsepower, from the alternator shaft to the motor shaft. Gearing from the motor shaft to the propeller shaft is not included as similar gearing would have to be incorporated in a turbine propelled drive, assuming there is no change in speed between the two comparable cases.

Weight Discussion

The net weight of the electric transmission is large and its use can be justified only when there is a saving in weight due to the benefits of the system or other valid and useful features.

Due to the flexibility of the electric system the aircraft designer has more freedom as to placing of the propellers and their driving motors. There is no low frequency vibration due to the motor and usually a thin wing and nacelle can be used with the motors, with the turbines mounted in the fuselage and their exhaust carried outside to add some thrust. There will be a reduction of drag due to these facts which has been estimated by competent designers as having values of 8 to 12 per cent.

If the flight plan of the airplane includes large changes of power, such as extended cruise conditions at low power settings (see Figure 3), some turbine units can be shut down and the four propellers set for lower power sufficient to operate the remaining turboalternators at full load, thus reducing the specific fuel consumption when compared with four turbopropeller engines. The larger the number of turboalternators on the aircraft, the greater the savings, as the number of power steps available will be larger and those in use can be operated at full load.

Electric apparatus is limited in power output primarily in its ability to dissipate heat. It can stand severe overloads such as that required for take-off where the overload is necessary for only five minutes maximum. The continuous duty required will be that of the normal design of the electric motors, generators, and wiring. By reducing the generator and bus voltage for low power settings the four induction motors can be operated at near

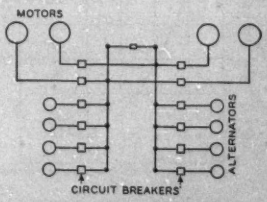

Figure 2. Block diagram of electric connections of motors to drive propellers

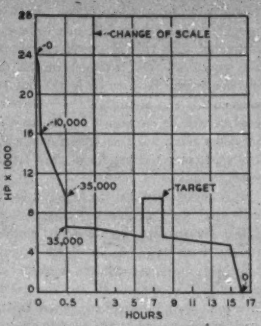

Figure 3. Flight plan worked out with aircraft laboratory, engineering division, Air Materiel Command

full load current and thus have better power factors than if they were operated at full voltage and smaller load currents. The copper losses would be unchanged, but iron losses would be reduced.

Aircraft Description

The following tenative description of an airplane that could be used for electric drive purposes was sent out to turbo-electric manufacturers in May 1945 and June 27, 1945:

(*a*). This is a high speed, (475–525 miles per hour) long range (6,500 miles) thin wing bomber to be driven by gas turbines located in the fuselage, giving approximately 80 per cent shaft horsepower and 20 per cent jet horsepower. Four propellers are to be located ahead of the wing and driven by induction motors. Total shaft horsepower 25,000 for take-off, five minute rating. Cruise at 60–70 per cent maximum power at 40,000 feet. Bomb load 20,000–40,000 pounds. Gross weight 200,000 pounds, or larger.

(*b*). Wings to have depth of 29 inches at deepest point, which is 100 inches from leading edge. Nacelles to have same depth as wing and to project forward 7–10 feet. Propellers not greater than 24 feet diameter.

(*c*). Turbines to drive 3-phase 400-cycle plus or minus 10 per cent alternators which will operate at constant speed at any frequency setting in that range, so they can be operated in parallel. Three-phase induction motors to be connected in parallel to bus. Voltage line to line not in excess of 2,000 volts. Motors and generators to be connected to bus by circuit breaker switches as needed so as to obtain maximum fuel economy. Pitch of propellers to control power delivered by motors and to include reverse pitch, all at constant speed.

(*d*). Cooling of motors and alternators to be by fan on the ground and by fan and ram in the air. Power sensing devices will have to be available to the pilot so that he may control properly the angle of propellers manually or automatically. Governors on turbines to control power as a function of speed or frequency. The relative speed of propeller blade angle change, power to motors and number of turboalternators operating is very important and is to be designed for best fuel economy, at all operating powers.

Weight Estimates

A flight plan, Figure 3, was worked out with aircraft laboratory, engineering division, Air Materiel Command. Computations based on this flight plan were made as described hereinafter and were distributed to those interested on October 19, 1945. These data are largely the work of engineers of the Westinghouse and General Electric companies.

Comparison of mechanical (four engines) and electric drive (ten engines) may be made as to weights of fuel consumed by each. The flight plan is taken as shown and power then is taken as shaft horsepower of turbine. Efficiency of electric drive is taken as 92 per cent. Increase of drag with mechanical system is taken as 8 per cent.

The calculations for the two types of drive are set forth in Table I. The formula relating fuel consumption to the other significant factors is as follows:

$$W = \frac{Ptsd}{E}$$

where

W = weight of fuel consumed in pounds
P = engine shaft horsepower
s = specific fuel consumption of engine in pounds per horsepower-hour
t = time in hours
d = drag factor, pure numeric
e = efficiency of engine reduction gearing combined, where applicable, with efficiency of electric system

The following comparison as to weight of fuel consumed then may be made:

Total fuel consumed, mechanical drive	77,545 pounds
Total fuel consumed, electric drive	66,825 pounds
Saving in fuel weight by use of electric drive	10,720 pounds

The weight of the engines and the electric equipment for the airplane described can be estimated on the basis of some data prepared by the Westinghouse company. The characteristics of a suitable turbine engine for this application are set forth in Table II.

The alternators proposed for this application would be rated at 2,000 kw, 88 per cent power factor, 1,300 volts, 12,000 rpm, and their weight has been estimated at 1,128 pounds each. The motors proposed would be rated at 6,400 horsepower at 1,300 volts and 80 per cent power factor; their weight is estimated at 2,300 pounds each. This aircraft would require ten of the engines, ten of the alternators, and four of the motors. In addition, there would be electric cables and control equipment having a total estimated weight of 3,060 pounds.

In summary, for the aircraft

Ten alternators at 1,128 pounds each	11,280 pounds
Four motors at 2,300 pounds each	9,200 pounds
Electric control equipment and cables	3,060 pounds
Total weight of electric system	23,540 pounds

If it can be assumed that the low mechanical-drive turbines would weigh the same as ten electric drive turbines of equal total power output, the following further weight comparison can be made

Total weight of electric equipment	23,540 pounds
Fuel saving by electric drive	10,720 pounds
Excess weight of electric scheme	12,820 pounds

It is possible that other savings can be made through improved design of the electric equipment after the first samples have been made, as up to the present time apparatus of this type has not been built. It is believed that the present design is conservative.

It is also possible that some savings may be made in gearing, as gearing in both cases was assumed to be the same; and the speed of motors was assumed to be the same as that of the generators. The combination of motor and gearing may have other values that result in lower weights.

It was assumed that the four mechanical-drive turbines would weigh as much as the ten turbines of equal total power in spite of the fact that the smaller turbines operate at high speeds and might have a lower total weight.

Reserve fuel weight for three hours also

Table II. Characteristics of a Turbine Engine Suitable for Use on an Electric Drive Aircraft

Normal power rating, sea level, shp	2,430
Military power rating, sea level, shp	3,300
Normal power rating, 35,000 ft altitude, shp	1,275
Normal power rating, 40,000 ft altitude, shp	1,010
Weight without accessories, lb	1,600
Weight complete, lb	1,750
Dimensions, inches:	
Length	120
Diameter	27
Diameter over accessories	36
Specific fuel consumption at 40,000 ft, 350 mph, including 20 per cent jet power (lb per hp-hr)	0.55

Shp = shaft horsepower

would reduce the excess weight of electric equipment; also the weight of fuel tanks would be less for the electric equipment as the total fuel is reduced.

Operation

The alternators as they are started would be synchronized manually or automatically and connected to the bus. Not having any load connected to them, the starting problem is simplified over that of the turbopropeller engine.

Probably it would be best to start the induction motors under reduced voltage and with a limited number of alternators connected to the bus. All four of the motors would be started one by one on, say, one or two alternators, with the propellers set at position of minimum thrust. After the propellers are rotating at normal speed, the remaining alternators can be synchronized and connected to the bus. Governors of each turbine can be interconnected by the flight engineer so that the turbines will respond to the demand for power at constant speed.

The power delivered by the propellers is determined principally by the pitch angle for a fixed speed, including reverse pitch, and the propellers would revolve at substantially constant speed at all times, as the speed is fixed by the turbine governor on the automatic control. As the pilot advances the power control lever, the motors will deliver more power and that power will be delivered by the turbogenerators, following standard power practice. Simultaneously, in accordance with signals received from power-sensing devices (electrical), the propeller blade pitch will increase to absorb this power and convert it to useful thrust.

Circuit breakers will have to be placed in between the bus and each motor and each generator and possibly in such position to sectionalize the bus, and will be operated by the flight engineer.

Circuit breaker weights will have to be reduced below weights used in 60-cycle practice and may have to be pressurized. A 3-phase 4-wire system, with the neutral grounded so that loss of one phase will not disable a motor propeller unit but only lower its rating, seems to be the best.

The details of the propeller and power control will have to be worked out. The necessity for brakes to stop rotation of a feathered propeller will have to be studied, as with no excitation of motor there is no retarding friction. Possibly, the excitation of one phase of the induction motor could be used as a brake. Rate of propeller pitch change will have to be coordinated with rate of power change of the governors and turbogenerators. A wattmeter will have to be in the line to each motor and an automatic or manual control will be necessary to change the propeller pitch angle in accordance with the wattmeter reading *for a given power setting*.

It is anticipated that the flight engineer will start turbogenerators, excite their fields, synchronize, set governor limits, remove from bus, and shut down generators in accordance with the schedule of power settings furnished by the pilot. The pilot would control the power delivered by adjustment of the electric power-sensing devices that, in turn, act on propeller blade angle.

Conclusion

In conclusion, the electric drive system can be used only on very heavy long range bombers having a wide power range in their operation. It is too heavy to be used on small aircraft, except where the flexibility resulting from its use can be shown to overcome the resulting weight increase.

No Discussion

A Capacitance-Type Fuel-Measurement System for Aircraft

D. B. PEARSON
ASSOCIATE AIEE

THE search for a fuel-measurement system more suitable for use on present-day and future aircraft than the conventional float-operated gauge has led to an investigation of the capacitance-type gauge. Several factors are responsible for this trend. In the first place, to eliminate the errors produced by changing fuels and by variations in ambient temperature, the energy content of fuel usually is determined in British thermal units per pound, rather than per gallon. Realization that the pound instead of the gallon is the more consistent unit for fuel-quantity measurements has made it essential for the search to center around systems that are sensitive to mass instead of to volume. Secondly, the desirability of reducing the errors in fuel-quantity indication caused by changes in airplane attitude, and the necessity for totalizing the contents of two or more fuel tanks on one indicator require that the fuel-measurement system be adaptable readily to totalized indication. The fact that the capacitance fuel gauge requires no moving parts, particularly in the fuel tank, is a feature that increases the reliability of this type of equipment. Of the fuel-measurement systems developed up to the present time, the capacitance type has proved to be the most satisfactory one that incorporates these and other desirable features.

Paper 47-216, recommended by the AIEE committees on air transportation, and instruments and measurements, and approved by the AIEE technical program committee for presentation at the AIEE Middle Eastern District meeting, Dayton, Ohio, September 29-26, 1947. Manuscript submitted June 19, 1947; made available for printing August 7, 1947.

D. B. Pearson is an engineer in the aeronautical instrument engineering division at the West Lynn Works, General Electric Company, West Lynn, Mass.

General Description of Capacitance Method of Fuel Measurement

The recently introduced method[1] for analyzing measurement equipment is useful in gaining an understanding of capacitance-type measurement systems. All systems of this type may be classified into the three functional groupings of components, as illustrated by Figure 1.

The primary detector is a varying-dielectric capacitor whose capacitance is a function of the quantity of fuel in the tank. Aircraft fuels in use at the present time have a dielectric constant of approximately two, while air, or fuel vapor, has a dielectric constant of one. As the amount of fuel is varied from maximum to zero, the capacitance of the primary detector changes by a ratio of about two to one.

The intermediate means, which involves the use of electronic tubes, is capable of sensing the change in electric capacitance of the primary detector and converting it into a variation in output current or voltage suitable for operating the end device. It must perform this function as accurately as possible under extreme conditions of temperature, altitude, humidity, and vibration, and over a broad range of supply voltage and frequency variations. The intermediate means may assume a variety of forms, and may include an electronic oscillator, amplifier, or a servosystem controlled by vacuum tubes.

The end device may be one of several types of indicators capable of giving visual indication of fuel quantity. An

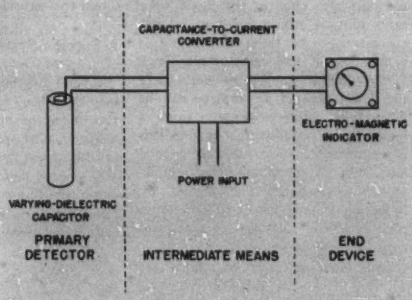

Figure 1. Functional analysis of general capacitance-type fuel-measurement system

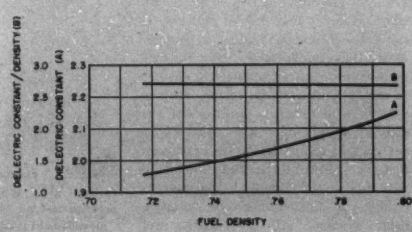

Figure 2. Characteristics of fuel

A—Dielectric constant versus density
B—Dielectric constant density versus density

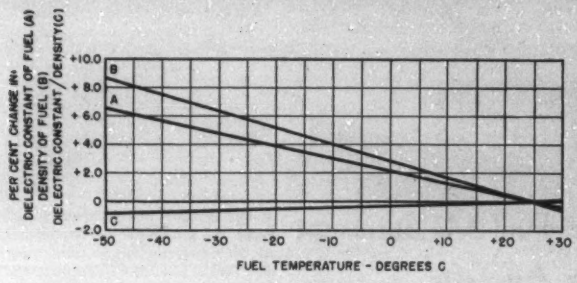

Figure 3. Characteristics of a typical aircraft fuel versus temperature

A—Dielectric constant
B—Density
C—Dielectric constant density

electromagnetic mechanism capable of driving a pointer over a scale is utilized in this device.

Inherent Characteristics of Capacitance-Type Fuel-Measurement Systems

The capacitance-type of fuel-measurement systems are mass-sensitive rather than volume-sensitive devices because the ratio of the dielectric constant to the density of the fuel remains nearly constant as shown by curve B, Figure 2.[2] When the fuel-quantity indication is obtained in gallons, the errors produced by changing fuel are in proportion to the difference in dielectric constant of the fuels used. When the temperature of the fuel varies, the density and dielectric constant also change, but again their ratio remains nearly constant. These characteristics are shown in Figure 3 as a function of fuel temperature for a typical aircraft-grade gasoline. Since the flying time of an airplane can be determined more accurately from a knowledge of pounds rather than gallons of fuel available, the capacitance method has a definite advantage over volume-measuring systems. The desired information is provided accurately for a wide variety of fuels and over a broad range of ambient temperature.

It is often necessary to totalize the outputs of several primary detectors. Limited instrument-panel space sometimes makes it desirable to indicate the contents of several tanks on one end device. To minimize the errors in fuel-quantity indication introduced by changes in airplane attitude, it usually is necessary to place primary detectors at two or more points in one fuel tank. Figure 4[3] shows the attitude errors obtained when first one and then three primary detectors were used in the same tank under similar conditions. Capacitance-type measurement systems are particularly well adapted to totalizing operations, as it is necessary only to connect in parallel the primary detectors whose capacitances are to be totalized, and to calibrate the measurement system properly.

When float-operated fuel-measurement systems are used, excessive oscillation of the pointer in the end device often is caused by sudden motions of the fuel in the tank. Properly designed primary detectors used with the capacitance-type system permit sufficient damping to be incorporated to reduce this pointer oscillation to a satisfactory minimum value.

A Specific System

Several different measurement systems may be utilized to obtain remote indication of fuel quantity by the capacitance method. The specific system described in this paper was chosen because it achieves the performance required without introducing undesirable features. Its functional parts are shown diagrammatically in Figure 5.

In this system the capacitance-to-current conversion is accomplished by an oscillator that is controlled by cylindrical capacitors in the fuel tank. The input to the oscillator is a direct current which varies with fuel quantity. A second oscillator also is used, whose input is a direct current that is independent of fuel quantity. Visual indication of fuel quantity is obtained with a conventional indicator which measures the ratio of these two direct currents.

To obtain proper input voltages for this measurement system, a suitable rectifier-transformer combination may be used when a 115-volt 400-cycle-per-second supply is available. For airplanes with a source of 28 volts direct current only, a conventional dynamotor may be utilized.

After several hundred hours of operation, or after the vacuum tubes have been replaced, it may be necessary to readjust the empty and full-scale points of the end device. An adjustment unit

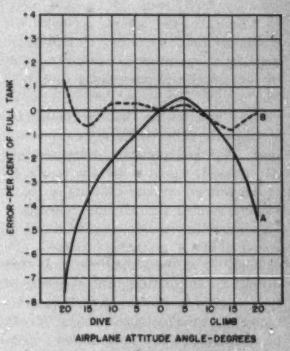

Figure 4. Airplane attitude error

A—One primary detector
B—Three primary detectors

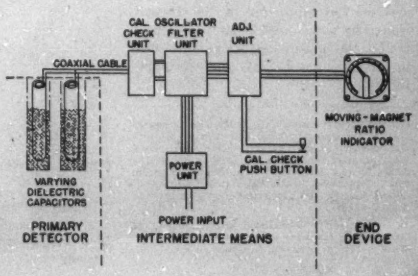

Figure 5. Functional analysis of a specific capacitance-type fuel-measurement system

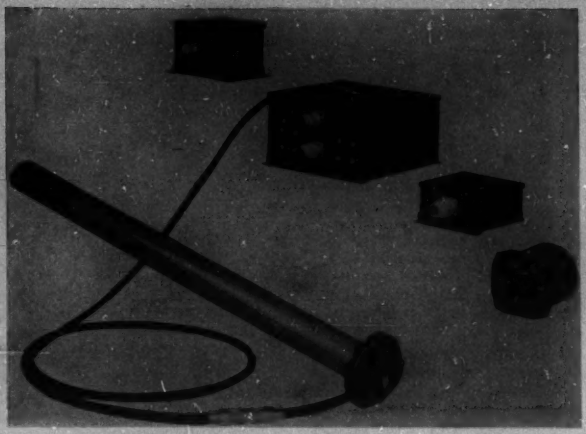

Figure 6. A complete set of capacitance type fuel-measurement equipment

is provided for this purpose. To permit an accuracy check of the measurement system at any time, in flight or on the ground, a calibration check unit may be included. These units are illustrated in Figure 6.

Operation of the Oscillator

The intermediate means, illustrated in Figure 7, consists of two tuned-plate tuned-grid oscillators, each of which has inductive coupling between the plate and grid coils. One oscillator operates at a fixed frequency, while the other oscillates at a variable frequency controlled by the capacitance of the primary detector. Two type *6J6* dual-triode vacuum tubes are used, with one triode of each tube in each oscillating circuit.

Referring to Figure 8, L_1 and C_3 form the resonant plate-circuit, while L_2 and the primary detector comprise the resonant grid-circuit for the variable-frequency oscillator. R_1 and C_1 provide self-biasing for the two grids. The resonant frequency of the tuned plate-circuit remains fixed, but the natural frequency of oscillation of the tuned grid-circuit depends on the capacitance of the primary detector which is a function of fuel quantity. Because the grid and plate-circuits are coupled, they must oscillate at the same frequency. With no fuel in the tank, the resonant frequencies of the two tuned-circuits are nearly equal, and the power required to maintain the oscillations is a minimum. As the tank is filled with fuel, the natural frequency of the grid circuit departs gradually from the resonant frequency of the plate circuit, and the power required to drive the oscillator increases. At a constant direct voltage, the direct current drawn by the oscillator is a measure of the power required to maintain the oscillations, and is a function of the quantity of fuel available.

Again referring to Figure 8, the resonant circuits of the second oscillator are comprised of L_3, C_2, L_4, and C_4, while grid biasing is obtained by R_2 and C_2. The operation of this oscillator is similar to the first, except both tuned circuits are independent of fuel quantity. The resultant frequency of oscillation and the power required to drive the oscillator remain constant for all values of fuel quantity. The variable direct current which is drawn by the first oscillator and which is a function of the fuel quantity, and the fixed direct current which is taken by the second oscillator comprise the two currents necessary for satisfactory operation of the moving-magnet ratio-type end device.

The dual oscillator circuit provides many advantages for this measurement system. The errors produced by vacuum-tube aging and replacement are within satisfactory limits, since any differences in tube characteristics produce similar changes in each oscillator circuit. Life tests have shown a maximum change of approximately two per cent of full scale indication after 1,000 hours of operation. Because each circuit is affected in a similar manner, the changes produced by variations in supply voltage, ambient temperature, and relative humidity are minimized.

Design Features

Each primary detector consists of two concentric aluminum cylinders sufficiently sturdy to withstand normal shipping, installation, and operation conditions without damage. A group of three primary detectors with their connecting cables is shown in Figure 9. Spacing between the cylinders is greater than $^1/_8$ inch, to prevent capillary action from holding either fuel or water between the cylinders. By varying the contours of the cylinders, or the spacing between them, the capacitance per inch of length

Figure 7. Oscillator-filter unit

of the primary detectors may be varied over a rather wide range. This feature permits the distribution of the indicator scale to be somewhat independent of the shape of the fuel tank, which is a characteristic necessary for satisfactory totalization. If greater readability of the end device is desired at one or more points on the dial, it can be obtained by properly adjusting the capacitance per inch of the primary detector.

For desirable indicator-scale distribution, as well as satisfying one of the conditions necessary for totalization of fuel quantities, the curve of primary-detector capacitance versus indicator-pointer travel should approach a straight line as closely as possible. This characteristic is necessary so that when totalizing is done, each micromicrofarad change always will produce, as nearly as possible, the same indicator pointer deflection. Figure 10 shows this relationship for the measurement system described in the paper.

Suitable damping is incorporated in the primary detectors by restricting the rate at which fuel may enter and leave the concentric cylinder capacitors. The holes through which the fuel flows are small enough to prevent sudden changes in fuel level within the capacitors, but are large enough to render unlikely the possibility of clogging by solid particles in the tank. This feature provides satisfactory indicator pointer operation in rough air.

To prevent the fuel-measurement system from producing interference in the radio equipment of the aircraft, suitable filters and shielding are used. The primary detectors, coaxial cables, and oscillator-filter units are shielded sufficiently well to prevent interference from direct radiation. The radio-frequency filter in the output leads of the oscillator unit prevents appreciable energy at radio frequencies from being conducted away from the unit.

Figure 9. Primary detectors with connecting coaxial cables

Best operation of this measurement system is obtained when the 115-volt 400-cycle-per-second power supply of the aircraft is utilized through the rectifier power unit. Absence of moving parts and reduced weight make this power unit more suitable than the d-c operated dynamotor. If 400-cycle-per-second power is not available, however, the fuel-measurement system can be operated satisfactorily from a dynamotor. Adequate radio-frequency shielding and filtering are incorporated in the dynamotor power unit.

The end device is a moving-magnet ratio-type indicator, utilizing a sturdy-moving-mechanism construction. The moving-magnet assembly has a travel of 100 mechanical degrees, while pointer travel of 300 degrees is obtained by a single set of gears similar to the type used successfully for many years in aircraft-engine tachometers. No hairsprings, sliding contacts, or electric connections to its moving-mechanism are used. A small control magnet provides off-scale indication at the zero end of the scale when no power is applied to the measurement system. Since the end device measures the ratio of the direct currents drawn by the oscillator unit, the indication is not dependent on the stability of instrument-type rectifiers. Errors in reading caused by parallax are eliminated by utilizing an anti-parallax scale, with the pointer and dial markings located in the same plane.

When compared with float-actuated fuel-gauges on a weight basis, capacitance-type fuel-measurement systems are at a disadvantage. A typical capacitance system weighs approximately $10^1/_4$ pounds as compared to $2^3/_4$ pounds for a float gauge. This disadvantage is partially offset when airplane-attitude-error correction or totalization of the contents of several fuel tanks are incorporated into the measurement system.

System Characteristics

It is necessary for the fuel-measurement system to produce fuel-quantity indication that is as accurate as possible under various extreme operating conditions. Considerable work has been done to reduce the humidity and temperature errors of the measurement system to suitable values. The insulators in the primary detectors, and the forms for the oscillator coils and grid-leak resistors in the intermediate means are made from one of the recently announced polyester resins that is highly resistant to moisture penetration. Additional surface protection against extremely humid conditions is obtained by an application of a moisture-repellent silicone on all surfaces where water might form a conducting path. After the oscillator coils and grid-leak resistors are wound, they are im-

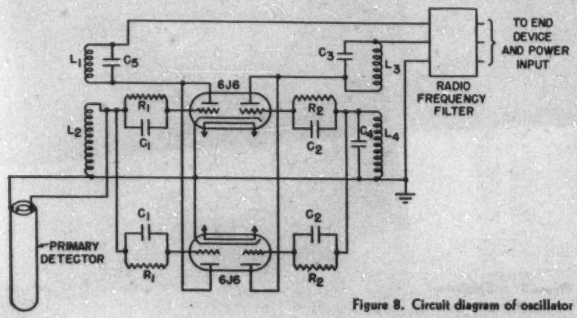

Figure 8. Circuit diagram of oscillator

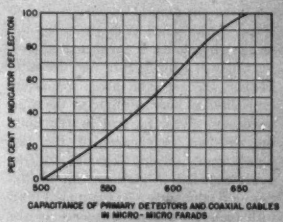

Figure 10. Characteristic distribution of measurement system

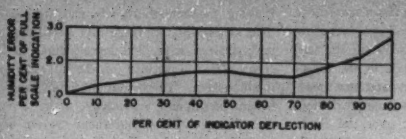

Figure 11. Typical errors in indication produced by two standard humidity cycles

pregnated with this newly-developed resin to form an assembly that is extremely resistant to moisture penetration. Figure 11 shows the errors produced by two humidity cycles such as are described by Army Air Forces specification 27558-*A*.

The temperature error in the primary detectors is reduced satisfactorily by choosing the proper insulating resin, and by suitable design of the unit. The effect of temperature changes on the dielectric constant of the new materials is minimized by reducing as much as possible the area of contact between the insulators and the concentric cylinders, and by maintaining large spacings between all metallic parts of opposite potential.

Temperature compensation has been incorporated in the oscillator-filter unit and in the end device. Resistors with a negative temperature coefficient of resistance are used in parallel with either a copper resistor or one whose resistance is unaffected substantially by temperature changes. Temperature characteristics are obtained that are approximately equal and opposite to those of the oscillator-filter unit and the end device. Typical temperature errors of the measurement system are shown in Figure 12, while characteristic voltage and frequency errors are shown in Figure 13. Tests in an altitude chamber show that no change in indication is produced by pressures similar to those that exist up to 40,000 feet above sea level.

It is desirable to have empty-and-full-scale adjustments for any fuel-measurement system readily accessible. The use of a separate adjustment unit permits its installation at any point in the airplane, making it possible for one operator to make the necessary adjustments. The full-scale-point adjustment has negligible effect on the zero point, so after the zero position has been adjusted to have no error, the full-scale point can be adjusted without need for rechecking the empty position.

To permit a check on the accuracy of the measurement system at any time, a calibration check device consisting of a capacitor and a relay may be used. When the relay is energized by closing a push-button switch at either the indicator or the adjustment unit, the primary detectors and coaxial cables are switched out of the circuit, and the capacitor is connected in their place. In this way, a predetermined point on the indicator scale may be checked at any time.

Power consumption of a characteristic capacitance-type gauge is about 18 watts, compared to 2 watts for a typical float-operated system. Most of the power in the former system is consumed in the heater circuit of the vacuum tubes.

Satisfactory flight tests of several hundred hours have been conducted. These tests include trans-Pacific and trans-Atlantic flights by commercial airlines, as well as several tests in the United States by the Army and Navy. These tests have been made under actual service conditions and the results indicate that the measurement system discussed in this paper is suitable for aircraft use.

Safety Features

Whenever any aircraft instrument is not functioning properly, a positive indication of trouble should be obtained. The most likely sources of difficulty in a measurement system of this kind are

1. Short circuit of the primary detector
2. Failure of a vacuum tube
3. Power failure

The likelihood of the primary detector becoming short-circuited by foreign material in the fuel tank is reduced by the large spacing between the cylinders. If a short circuit does occur at this point, the indicator pointer will move off-scale in the up-scale direction, indicating that this difficulty may exist. No permanent damage is caused and when the short circuit is removed, the measurement system will function normally again. Difficulty of this nature in one system will not affect the operation of other fuel-measurement systems in the airplane.

Should water accumulate between the cylinders of the primary detector, the indicator pointer will move off-scale at the up-scale end. The resistance of the water is low enough to cause the measurement system to act as though the primary detector were short-circuited directly. As in the case of a short circuit, no permanent damage is caused by the water, and when it is removed, the measurement system will function normally again.

Tests have shown that sufficient energy is not available at the primary detectors to cause an explosion in the fuel tank if a short circuit does occur at this point. The primary detector is connected in the

A—Equipment at −40 degrees centigrade
B—Equipment at +75 degrees centigrade

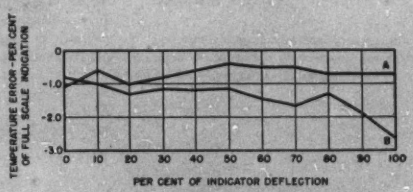

Figure 12. Typical temperature errors of fuel-measurement system, based on +25 degrees centigrade

A—105 volts, 400 cycles per second
B—120 volts, 400 cycles per second
C—115 volts, 360 cycles per second
D—115 volts, 440 cycles per second

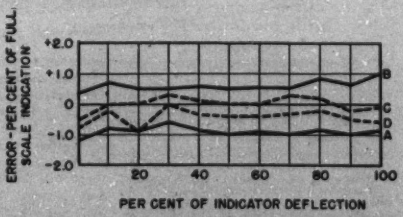

Figure 13. Typical voltage and frequency errors of fuel-measurement system, based on 115 volts, 400 cycles per second

low-energy grid-circuit, where the only power available is from the radio-frequency oscillator. If a short circuit in the primary detector occurs, the oscillations stop, and there is no energy available in the fuel tank.

To provide safe failure, the heaters of the two vacuum tubes are connected in series. If one heater burns out, both tubes are made inoperative, and the indicator pointer moves off-scale at the zero end. Also, if a power failure occurs, the pointer moves off-scale at the zero end.

With the push-button and calibration check device, the accuracy of the measurement system may be checked at any time. This feature, plus the automatic indication of primary detector short circuit, tube failure, and power failure already discussed, permits immediate detection of trouble in the measurement system.

Conclusion

Fuel-quantity measurement by a capacitance method has been discussed and compared to the float-actuated system. Several advantages of the capacitance method have been pointed out, including the absence of moving parts in the fuel tank and moving contacts in the measurement system. The capacitance measurement system is a mass-sensitive device, giving it an advantage over the float-operated gauge, since the present tendency is to require that the indication be in pounds. Because of these advantages, it is felt that the capacitance-type of fuel-measurement system will play an important role in this field in the future.

The specific fuel-measurement system that has been discussed incorporates several valuable features. The large spacing between the cylinders of the primary detectors add to the reliability of the system. Automatic and immediate indication of primary detector short-circuit, tube failure, and power failure, plus the convenient and instantaneous accuracy check, continuously provide information on the operation of the system. The reliability of indication is increased by the absence of instrument type rectifiers, indicator hair springs, sliding contacts in the measurement circuit, and electrical connections to the moving mechanism in the end device. The availability of large and small size end devices with 300-degree dials increases the versatility of the measurement system. These characteristics, and others mentioned previously, make the capacitance-type measurement system a superior means for obtaining remote indication of fuel quantity in aircraft which require a high degree of accuracy and dependability in performing this measurement.

References

1. Functional Analysis of Measurements, I. F. Kinnard. Electrical Engineering, volume 66, January 1947, pages 11–15.

2. Potentialities of a Capacitance Measurement Method for Fuel Quantity Gages in Aircraft, C. F. Savage, D. B. Pearson. *Aeronautical Engineering Review* (New York, N. Y.), April, 1945, pages 27–37.

3. Totalizing Contents of Aircraft Fuel Tanks, J. R. Macintyre. AIEE Transactions, volume 63, 1944, September section, pages 663–65.

No Discussion

A Design Method for Capacitor Start Motors

SHELDON S. L. CHANG
STUDENT MEMBER AIEE

IN THE DESIGN of capacitor-start induction-run motors, items of importance are the starting torque, starting current, voltage across the capacitor, the accelerating torque, and the amount of vibration before the switch operates. Formulas have been developed for the various values at starting, as well as capacitors needed for maximum starting torque; the circle diagrams can be drawn to show vector relationships, as well as the foregoing values. However, scarcely any work has been published towards predicting the accelerating characteristics.

In using such methods, it is tacitly understood that a starting winding has been assumed, and the problem then takes the form of calculating the starting characteristics. Unsatisfactory results requires redesign. An experienced designer usually has some idea about the maximum winding ratio that can be used without excessive vibration or too low accelerating torque before the switch operates. The ultimate result of the accelerating characteristics cannot be known until the motor actually is built.

It is the purpose of this paper to show a direct method of design for the starting characteristics reducing the number of items which can cause readjustment or redesign, and to give a limitation on the winding ratio that would not result in undesirable accelerating characteristics, considering the speed at which the switch operates.

The system set up here is based on curves which not only save time, once they are prepared, but offer the additional advantage of enabling the designer to observe trends in his choice of values. That is, operation near maximum points and the possible influence of changing certain parameters are observed readily when such curves are used.

The problem of selecting ratios of parameters to be plotted in the form of curve sheets is not a simple one. The parameters which affect the characteristics are

Main winding (assumed fixed)

Stator resistance and leakage reactance.
Rotor resistance and leakage reactance.
Leakage factor.

Starting winding (to be designed)

Stator resistance and leakage reactance.
Ratio of starting and main winding turns.
Value of capacitance.

It is believed that the combination of values which are used here in plotting these curves results in the minimum of preparation, with great flexibility in application.

The system to be followed throughout assumes that the capacitor is known. Any method which gives a capacity as a final result may yield values which are not commercially available, and hence require redesign. A part of the brevity of the method proposed here results from the assumption that the capacitor is known.

Curves for Starting Torque and Capacitor Voltage

The equations of starting torque and currents from which the curves are deduced are listed in the following:

$$T_{st} = 2aI_xI_yR_s \sin \theta_{xy} \text{ synchronous watts} \quad (1)$$

$$I_s(Z_s + Z_c) = V \quad (2)$$

$$I_mZ_m = V \quad (3)$$

The rotor currents and the stator currents are different due to the presence of the magnetizing admittance. However, in case the magnetizing reactance is very large as compared with the rotor resistance and leakage reactance, which is true as a rule, it can be shown readily that

$$I_x = \sqrt{K_r}I_r$$

$$I_y = \sqrt{K_r}I_m$$

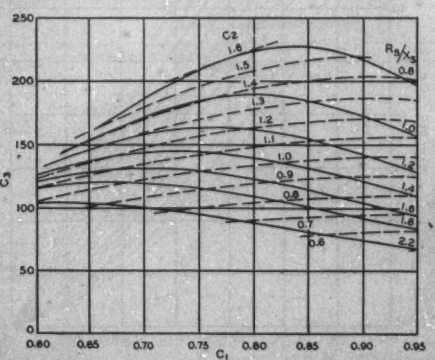

Figure 1. A typical sheet of curves showing the relations between the starting torque C_3, the capacitor voltage C_2, the winding ratio C_1, and the start winding copper area R_s/X_s for one value of R_m/X

$R_m/X_m = 0.8$

Paper 47-220, recommended by the AIEE rotating machinery committee and approved by the AIEE technical program committee for presentation at the AIEE Middle Eastern District meeting, Dayton, Ohio, September 23-25, 1947. Manuscript submitted June 23, 1947; made available for printing August 13, 1947.

SHELDON S. L. CHANG is with Robbins and Myers, Inc., Springfield, Ohio.

To the same degree of approximation

$$Z_s = (R_{1s} + a^2 K_r R_2 + j(X_s)$$

and

$$Z_m = (R_1 + k_r R_2 + jX)$$

It is always true when the motor is at standstill that

$$\theta_{zy} = \theta_{zm}$$

With this approximation introduced, equation 1 becomes

$$T_{st} = 2ak_r I_s I_m R_2 \sin \theta_{zm} \text{ synchronous watts}$$

$$= \frac{225.4}{\text{synchronous rpm}} \times ak_r I_s I_m R_2 \times \sin \theta_{zm} \text{ ounce feet} \quad (4)$$

The problem of plotting a set of universal curves is to chose a minimum number of parameters to express the important de-

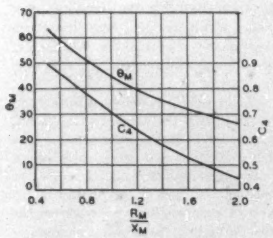

Figure 2. Curves for determination of the magnitude and angle of starting current in main winding

sign items. The significant parameters are

The lagging angle of the main winding current θ_m

The leading angle of the start winding current θ_s

The leading angle of the start winding impedance θ_z (without capacitor)

The three angles are related to the motor constants as

$$\tan \theta_m = \frac{X}{R_1 + k_r R_2} = \frac{X}{R_m} \quad (5)$$

$$\tan \theta_z = \frac{X_s}{R_{1s} + a^2 k_r R_2} = \frac{X_s}{R_z} \quad (6)$$

$$\tan \theta_s = \frac{X_c - X_s}{R_{1s} + a^2 k_r R_2} = \frac{X_c - X_s}{R_s} \quad (7)$$

Equation 7 can be solved for a universal turn ratio constant

$$C_1 = \sqrt{\frac{X_s}{X_c}} = \frac{1}{\sqrt{1 + \frac{R_s}{X_s} \tan \theta_s}} \quad (8)$$

The actual turn ratio constant a is related to C_1 by the following equation:

$$a = \sqrt{\frac{X_s}{X}} = \sqrt{\frac{X_c}{X}} \sqrt{\frac{X_s}{X_c}} = C_1 \sqrt{\frac{X_c}{X}} \quad (9)$$

Equation 9 assumes that the leakage factor of the main and start windings are the same. However, in case a very concentrated start winding is used, the start winding would have higher ratio of leakage to magnetizing reactances. In such cases, equation 9 should be modified by a constant multiplier.

Let C_3 be defined as the ratio of the voltage across the capacitor to the line voltage. Since this ratio is the same as the ratio of the reactance of the capacitor to the total start phase impedance, we have

$$C_3 = \frac{X_c}{R_z} \cos \theta_z \quad (10)$$

Eliminating X_c between equations 7 and 10

$$C_3 = \frac{R_s \tan \theta_s + X_s}{R_z \sec \theta_z}$$

$$= (\tan \theta_s + \tan \theta_z) \cos \theta_z \quad (11)$$

Substituting $C_1\sqrt{X_c/X}$, $C_3 (V/X_c)$, (V/X) $\sin \theta_m$ for A, I_s, I_m, respectively, in equation 4, the result is

$$T_{st} = \frac{225.4\, V^2 C_1 C_3 \sin \theta_m \sin \theta_{mz}}{\text{syn. } R.R.M. \times \sqrt{XX_c}} \cdot \frac{k_r R_2}{X} \text{ ounce feet} \quad (12)$$

Apparently T_{st} can be written as

$$T_{st} = \frac{C_5}{\text{synchronous rpm}} \cdot \frac{V^2}{\sqrt{XX_c}} \cdot \frac{k_r R_2}{X} \text{ ounce feet} \quad (13)$$

where

$$C_5 = 225.4\, C_1 C_3 \sin \theta_m \sin \theta_{mz} \quad (14)$$

It should be noted that C_1, C_3, and C_5 are functions of the three angles alone. The starting torque is expressed as the product of a unit multiplier and C_5.

The grouping of constants so far can be summarized in Table I. It should be noted that while the starting torque and voltage across the capacitor are functions of seven independent variables, their universal values C_5 and C_3 are functions of three parameters only. The two parameters R_m/X and R_s/X_s are fixed as soon as the rotor resistance and the copper areas per slot of the main and start windings are fixed. The other parameter C_1 takes care of the variation of the turn ratio. The reduction of the number of significant independent variables makes possible the preparation of curves.

Figure 1 shows the various possibilities of the curve method of design. Suppose after fixing the main winding, and rotor material, the designer finds that his R_m/X is 0.8 or very close to it. He then uses the curve sheet marked $R_m/X = 0.8$. Each solid line is a curve of starting torque plotted against turn ratio for a given amount of copper in the start winding. As the amount of copper increases R_s/X_s decreases and the starting torque is raised in general. The dotted lines are contours of equal voltage across capacitor, with the values of C_3 marked on each line. The chart not only enables the designer to choose a turn ratio to give highest starting torque for the capacitance and amount of copper he uses, but also enables him to

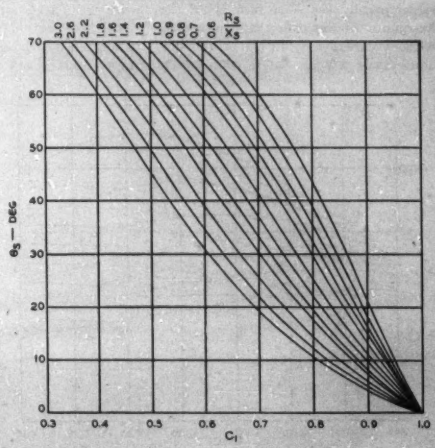

Figure 3. Curve for determination of the angle of the starting current in start winding

see the various possibilities of compromises, to determine what amount of copper he should use, and to select a point that gives reasonably high torque with low enough voltage across the capacitor. As most commercially available capacitors for capacitor start motors are rated at 115 volts, the values of C_3 are direct readings of the per cent of overload or underload as seen desirable for various purposes.

The chart also enables the designer to figure out how his starting torque is effected by the use of a range of capacitances for the same start winding. This is the actual situation as the commercially available capacitors are marked for a range of capacitances and that of a single capacitor may be anywhere in the range. The dependence of starting torque on capacitance for a given winding is not so obvious from the chart alone. Equation 13 shows that the starting torque is proportional to C_3 times the square root of the capacitance, while equation 8 shows that for a given winding C_1 is proportional to the square root of the capacitance. If for the range of C_1, corresponding to the variation of capacitance, C_3 decreases as C_1 increases in such a way that C_1C_3 is approximately constant, the designer is assured that the starting torques of his motors would be about the same though the capacitances used with the motors vary widely. An example of design using the charts is given later.

Equations 8, 11, and 14 are used to calculate the curves. θ_m is fixed by the value of R_m/X, θ_2 by R_s/X_s and a variety of values of θ_s is assumed for each curve. As both C_1 and C_2 are independent of θ_m, a chart of curves of C_2 plotted against C_1 with R_s/X_s as parameter is calculated once for all. The curves of C_3 plotted against C_1 have two parameters, R_m/X and R_s/X_s. Curves with the same R_m/X are grouped on the same chart. Then the contours of equal C_3 are located on each chart individually, as the values of R_s/X_s for a given C_3 and different values of C_1 can be read from the chart of C_2 plotted against C_1 with R_s/X_s as parameters.

The useful ranges of R_m/X and R_s/X_s are hard to determine. In general 16 charts covering a range of R_m/X from 0.5 to 2.0 in steps of 0.1 each should be adequate. The values of R_s/X_s for each chart should be in the range of R_m/X to $1.5 + R_m/X$. Any curve with R_s/X_s less than R_m/X is useless as it is scarcely necessary to use more copper in the start winding than that in the main winding. The range of C_1 is determined by the curves themselves. As all good designs should yield a starting torque not too far from the maximum value with given material used, the range of C_1 should include the peak of the curves and adjacent values.

Supplementary Curves for the Starting Currents

Although the C_1-C_T-C_4 curves described in the foregoing paragraphs will take care of the major part of the calculation, additional curve sheets are suggested as further aids in current calculations.

To determine the starting current in the main winding: The angle θ_m and a constant C_4 ($C_4 = \sin\theta_m$) are plotted as functions of R_m/X in Figure 2. The main winding current is

$$I_m = C_4 \frac{V}{X} \tag{15}$$

Direct reading of the start winding current phase angle: The magnitude of the start winding current can be calculated as V_s/X_s, but the phase angle is not yet known. Equation 7 can be rewritten into:

$$\tan\theta_s = \frac{1}{\frac{R_s}{X_s}}\left(\frac{X_c}{X_s} - 1\right) = \frac{\frac{1}{C_1^2} - 1}{\frac{R_s}{X_s}} \tag{16}$$

From equation 16, θ_s can be calculated as a function of C_1 with R_s/X_s as parameter. The result is plotted in Figure 3.

Calculation of Total Starting Current

With the foregoing component currents set up, the following procedure is the basis for determining the total starting current:

$$I_T = \sqrt{I_s^2 + I_m^2 + 2I_sI_m\cos\theta_{ms}}$$

$$= I_m\sqrt{1 + \left(\frac{I_s}{I_m}\right)^2 + 2\left(\frac{I_s}{I_m}\right)\cos\theta_{ms}} \tag{17}$$

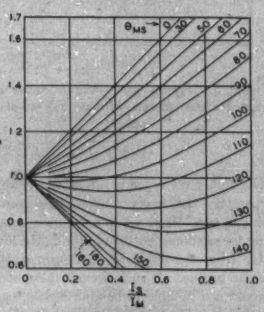

Figure 4. Curves for determination of the line current

A constant C_5 is defined as

$$C_5 = \frac{I_T}{I_m} = \sqrt{1 + \left(\frac{I_s}{I_m}\right)^2 + 2\left(\frac{I_s}{I_m}\right)\cos\theta_{ms}} \tag{18}$$

It is plotted as a function of I_s/I_m with θ_{ms} as parameter in Figure 4. Thus

$$I_T = I_m C_5$$

The auxiliary curves just mentioned are not necessary to the use of the fundamental C_1-C_T-C_4 curves for fixing the winding for a prescribed torque. Direct calculations can obviously be used in place of these C_4 and C_5 curves.

Limitation on Winding Ratio Due to Accelerating Characteristics

Figure 5 shows the general tendencies of the accelerating torque against speed. Curve *a* shows a case of very low winding

Table I. Grouping of Constants

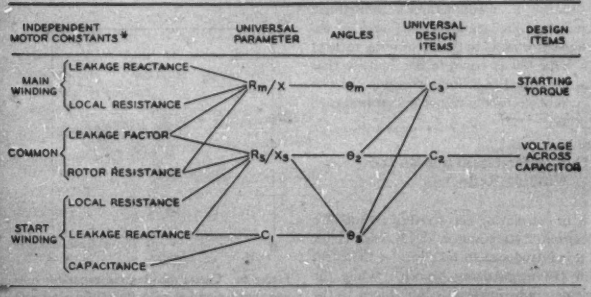

* Turn ratio is not an independent variable. It is fixed as soon as the leakage reactances of both windings are fixed.

ratio, the starting torque is low, but the motor is capable of producing high torque at higher speeds. Curve *b* shows a case of medium winding ratio. Curve *c* shows a case of high winding ratio. The accelerating torque drops rapidly as the motor gains speed. The dotted line shows the single phase torque.

It usually is considered satisfactory if, at the speed of switch operation, the split phase motor still has more torque than itself running single phase. Therefore, the maximum turn ratio that can be used depends on the point of switch operation.

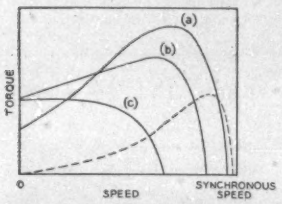

Figure 5. Typical speed–torque curves of capacitor start motors with various winding ratios

The higher the speed at which the switch operates, the lower the winding ratio should be. However, the switch operating speed should not be too far on the low side from the speed of maximum single phase torque. If such occurs, the motor would not be able to bring a heavy load to full speed, no matter what the starting torque is.

The voltage across the capacitor has a tendency as shown in Figure 6. Curve *a* shows a case of low winding ratio, curve *b* is for medium winding ratio, and curve *c* is for high winding ratio. It is essential to the longer service life of the capacitor that the switch should operate before the capacitor voltage reaches too high a value.

Besides insufficient accelerating torque and excessive voltage across the capacitor, the vibration of the motor is also an undesirable consequence of too high winding ratio. The computation of accelerating torque and voltage across the capacitor is complicated enough, the vibration of the motor depends not only on the electrical but also on the mechanical structure of the motor. It is, therefore, not practicable to fix the limit of winding ratio on an exact basis, though some sort of limit is necessary. A natural limitation is obtained from a study of the condition of operation of the motor.

At standstill the start winding current leads the main winding current by an angle of somewhere around 90 degrees. As the motor gains speed, the start winding current vector swings downward and the main winding current vector swings upward. In an adequately designed permanent capacitor motor the two current vectors never cross, and the start winding current always leads the main winding current. However, in a capacitor start motor, in which the start winding is cut off at running, high capacitance and high value of the universal winding ratio C_1 are desirable to produce high starting torque. As a result, the start winding current swings downward and finally ends in the fourth quadrant as the motor gains speed. At a certain speed, the start winding current and the main winding current become in phase, and the motor operates as a plain single phase motor. Above this speed, the start winding current lags the main winding current. It acts to reduce the torque instead of increasing it.

The speed at which the two current vectors are in phase is the proposed speed of switch operation, considering the following reasons:

1. At this speed, the motor operates as a plain single phase motor with an effective winding somewhere in between these two windings, carrying a current which is equal to $\sqrt{a^2I_s^2+I_m^2}$. Beyond this speed, the start winding acts only to reverse the motor and increase the watts.

2. The torque at this speed is higher but not too much higher than the single phase torque, with $a^2I_s^2R_2$ as a measure of the excess torque.

3. The amount of vibration of the motor at this speed is about the same with or without the start winding. Above this speed the vibration would be excessive with the start winding. The effect of the angle between the two current vectors upon the amount of vibration is given in reference 1.

4. The capacitor voltage, as a rule, begins to rise rapidly beyond this speed.

Usually a manufacturer's centrifugal switches are standardized, and a designer's work is to fix the winding ratio at a value less or equal to the limit, so that at the speed of switch operation the two current vectors have not yet crossed each other.

Curves for Limitation on the Winding Ratio

In calculating the starting torque of a capacitor start motor, the leakage factor k_r is introduced to take care of the effect of the magnetizing branch. While the same approximation is introduced to the equivalent circuit of a capacitor motor, the latter becomes that shown in Figure 7. It should be noted that such approximation holds only at high slip for motors of high magnetizing reactance, so that $R_2/(1-S)$ is small compared with the magnetizing reactance, being the ratio of the actual speed to the synchronous speed.

According to Figure 7, I_s' and I_m can be calculated from the following equations:

$$-\frac{jV}{a}=I_s'\left[\frac{R_c+R_{12}}{a^2}+\frac{k_rR_2}{1-S}-j\left(\frac{X_c}{a^2}-X\right)\right]+I_m\frac{Sk_rR_2}{1-S^2} \quad (20)$$

and

$$V=I_m\left[R_1+\frac{k_rR_2}{1-S}+jX\right]+I_s'\frac{Sk_rR_2}{1-S^2} \quad (21)$$

Since

$$I_s=\frac{jI_s'}{a}$$

the condition that I_m and I_s are in phase can be written as

$$I_m=\frac{iI_s'}{a}n \quad (22)$$

Where n is a real number. Substituting equation 22 into equations 20 and 21 we get

$$-\frac{jV}{a}=I_s'\left[\frac{R_c+R_{12}}{a^2}+\frac{k_rR_2}{1-S}-j\left(\frac{X_c}{a^2}-X\right)\right]+\frac{jI_s'}{a}n\frac{Sk_rR_2}{1-S^2} \quad (23)$$

and

$$V=\frac{jI_s'}{a}n\left[R_1+\frac{k_rR_2}{1-S}+jX\right]+\frac{Sk_rR_2}{1-S^2}I_s' \quad (24)$$

Eliminating V from equations 23 and 24, and equating the real and imaginary parts of the resultant equation, we get

$$a\left[\frac{R_c+R_{12}}{a^2}+\frac{k_rR_2}{1-S}\right]=\frac{n}{a}\left[R_1+\frac{k_rR_2}{1-S}\right] \quad (25)$$

$$a\left[\frac{X_c}{a^2}-X\right]-n\frac{Sk_rR_2}{1-S^2}=-\frac{n}{a}X+\frac{Sk_rR_2}{1-S^2} \quad (26)$$

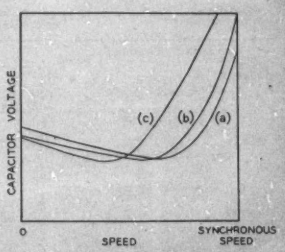

Figure 6. Curves showing the capacitor voltage versus speed of capacitor start motors with various winding ratios

In general R_1 is very small. R_{1s}/a^2 is equal to R_1 if the same amount of copper is used in the main and start windings. Though this is not true, it can be assumed that the difference $(R_c + R_{1s})/a^2 - R_1$ is very small as compared with $R_1 + k_r R_2/(1-S)$. Neglecting the former, equation 25 can be written as

$$a = \frac{n}{a}$$

or

$$n = a^2 \qquad (27)$$

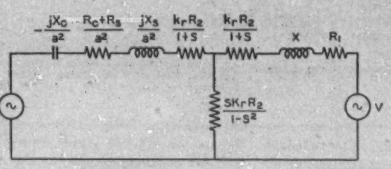

Figure 7. An approximate equivalent circuit of the capacitor start motor

Substituting equation 27 in equation 26 and simplifying the result

$$\frac{X_c}{a} = (1+a^2)\frac{Sk_rR_2}{1-S^2} \qquad (28)$$

The condition for the speed at which I_s and I_m are in phase is therefore

$$\frac{1-S^2}{S} = \frac{k_rR_2}{X_c}a(1+a^2) \qquad (29)$$

Equation 29 is plotted into curves as shown in Figure 8. For a designated speed of switch operation and knowing k_rR_2/X_c, the maximum winding ratio a can be read from Figure 8. If a winding ratio smaller than the maximum is used, the start winding current still is leading the main winding current at the speed of switch operation.

An Example of Design

The method described so far will be applied to the design of a 1/2-horsepower 115-volt 1,725-rpm 60-cycle capacitor start motor. A starting torque of 100 ounce feet is desired.

The following values concerning the main winding are known:

$X = 2.87 \qquad \frac{R_1}{X} = 0.272$

$k_r = 0.935 \qquad \frac{R_2}{X} = 0.61$

Then

$$\frac{R_m}{X} = \frac{R_1}{X} + k_r\frac{R_2}{X} = 0.835$$

Besides these given values, the available capacitors are rated at 115 volts allowing 20 per cent over rating. The switch operates at 1,400 rpm.

From the chart marked $R_m/X = 0.8$, the peak point of the curve for $R_s/X_s = 1.4$ gives a value of $C_3 = 1.15$. This is a proper point of operation because it utilizes the capacitor to 15 per cent over rating, which is about the highest within safety limits.

Assuming equal leakage factor

$$X_s = a^2X$$

and

$$\frac{R_{1s}}{X_s} = \frac{R_s}{X_s} - k_r\frac{R_2}{X} = 1.4 - 0.57 = 0.83$$

The amount of copper used in the start winding as compared to that of the main winding would be

$$\frac{\frac{R_1}{X}}{\frac{R_{1s}}{X_s}} = \frac{0.272}{0.83} = 0.328$$

or about a third of the amount of copper used in the main winding should be used in the start winding.

If the designer has a capacity in mind, he may calculate the necessary C_3 to give 100 ounce feet starting torque from equation 13. Then choose a point on the chart with higher C_3 than necessary, read C_1, and calculate the turn ratio. If he does not know what capacitance to use, he may determine it in the following way. The maximum C_3 on the curve marked $R_s/X_s = 1.4$ is 145. From equation 13, the maximum X_c should be

$$X_c = \left[\frac{145\times115^2}{1800\times\sqrt{2.87}\times100}\times.57\right]^2 = 12.83$$

corresponding to a capacitance of 206 microfarads. Then he finds from a list of available capacitors that the nearest higher capacity has a nominal value of 245 microfarads. This should be the capacitor used.

The peak point of C_3 occurs at $C_1 = 0.72$ approximately. The turn ratio should be

$$a = 0.72\times\sqrt{\frac{X_c}{X}} = 0.72\sqrt{\frac{10.8}{2.87}} = 1.40$$

To determine if a is within the permissible limit, calculate $k_rR_2/X_c = 0.152$, S at the switch operating point is $1{,}400 \div 1{,}800 = 0.78$. Then read from Figure 8 that the allowable winding ratio is 1.27. Therefore, a lower C_1 has to be used

$$C_1 = 0.72\times\frac{1.27}{1.40} = 0.653$$

The corresponding C_3 is 137, C_4 is 1.21

$$T_{st} = \frac{137\times115^2}{1800\times\sqrt{10.8\times2.87}}\times0.57 = 103 \text{ ounce feet}$$

The result is

Winding ratio $a = 1.27$

$\frac{R_{1s}}{X_s} = 0.83$ (fixes wire size)

Capacitor used = 245 microfarads

Capacitor voltage = 115×1.21 = 139 volts

Starting torque = 103 ounce feet

The leakage factors of the two windings are assumed to be equal. In case they are not, two constant multipliers should be used in the winding ratio and starting torque equations, while the general procedure remains the same.

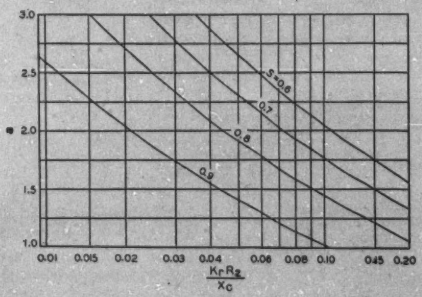

Figure 8. Curves showing the highest allowable winding ratio as a function of the speed of switch operation

Conclusion

In the foregoing material a system for designing capacitor start motors is described, in which the starting torque and capacitor voltage are used to determine the winding ratio, capacitance, and wire size. The use of curves allows the designer to observe the various trends and to pick up a favorable combination.

By limiting the winding ratio below a certain value it is possible to delay the speed at which the start winding current crosses the main winding current until the switch operates. By so doing, excessive vibration, watts, and insufficient accelerating torque can be avoided. The limit of the winding ratio is plotted against a combination of motor constants with the speed of switch operation as parameter.

List of Symbols

a = winding ratio
C_1 = winding ratio constant
C_2 = capacitor voltage constant
C_3 = torque constant
C_4 = main winding current constant
C_5 = line current constant
I_m = main winding current
I_s = start winding current
$I_s' = -jaI_s$
k_r = leakage factor $\left(=\frac{X_0-X}{X_0}\right)$
R_1 = main winding local resistance
R_2 = rotor resistance in main winding terms
R_{1s} = start winding local resistance
R_m = main winding apparent resistance
R_s = start winding apparent resistance
R_c = capacitor resistance
S = the ratio of actual speed to synchronous speed
T_{st} = starting torque
V_c = voltage across capacitor
V = line voltage
X_0 = main winding total reactance
X = main winding leakage reactance
X_s = capacitor winding leakage reactance
X_c = reactance of capacitor
Z_m = main winding apparent impedance
Z_s = start winding apparent impedance
Z_c = impedance of capacitor
θ_m = lagging angle of main winding current
θ_s = leading angle of start winding current
θ_{mt} = angle between the two currents $(=\theta_m+\theta_s)$
θ_2 = leading angle of start winding impedance

Reference

1. The Equivalent Circuit of the Capacitor Motor, Sheldon S. L. Chang. AIEE Transactions, volume 66, 1947, pages 631–40.

No Discussion

Aircraft Electric Power Protective Systems

B. O. AUSTIN
MEMBER AIEE

EVER-INCREASING demands on the electric power systems for aircraft have placed great emphasis on the need for soundly engineered protective equipment for systems using 28- and 120-volt direct current as well as those using 208-volt 400-cycle alternating current, or any modifications of these systems. The 28-volt d-c generator system had its beginning about 1941. High-voltage systems, both a-c and d-c, just now are coming into use. Those of us who were actively associated with the growth of the 28-volt d-c system have realized for some time that added protective equipment is vitally necessary. With the advent of higher voltage systems, either a-c or d-c protective features are even more important. In general, the same fundamental requirements apply to the development of protective equipment for the higher voltage systems. Voltage increase also means system capacity increase; this places still more emphasis on the need for protective equipment. Many of the needed protective devices have been developed and are in production. Further development is being accelerated to keep pace with the needs of the industry.

Analysis of Protective Requirements

There are many types of possible electrical faults or failures. The end result of most of them and the classification of their causes can be limited to a few basic fundamentals.

System engineering, apparatus design, application, installation, and maintenance are the basic steps which must be executed properly if the electric system on a given plane is to be successful and free of criticism. Failure to carry out diligently these requirements leads to equipment failures, faults, overheating, smoke, fires, explosions, panic, and loss of airplanes.

System engineering and the protection for that system against the common hazards are considered problems which must be treated simultaneously. In the analysis of the system development, consideration must be given to parallel operation, electrical faults, overvoltages, generator overtemperatures, positive opening through the use of dual contactors, and no-battery operation. All of these items are related directly or indirectly to system and apparatus protection.

Accurate Load Division

For the most part, paralleling of 30-volt generators has been accomplished by exciting the paralleling coil of the voltage regulator from a potential drop across a negative lead resistor or the drop across the series winding of the generator in combination with a potentiometer. Voltage drop across the negative lead resistor is exceptionally low and does not provide sufficient paralleling correction to the regulator coil. The use of much higher equalizer voltages, which are available from the series winding of the generator, is made practical by the use of a nonlinear ballast in series with the equalizer connections. Without this

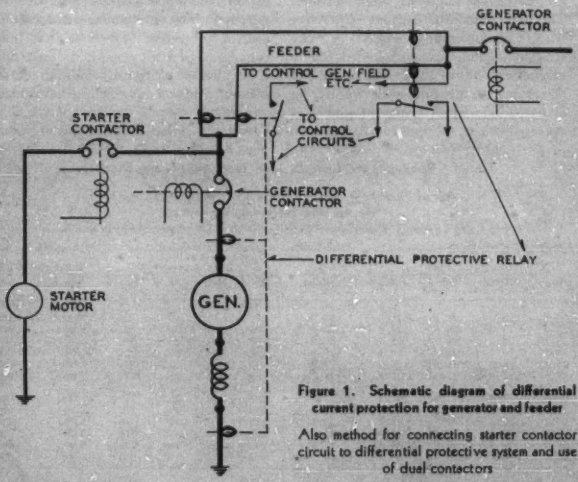

Figure 1. Schematic diagram of differential current protection for generator and feeder

Also method for connecting starter contactor circuit to differential protective system and use of dual contactors

Paper 47-222, recommended by the AIEE committee on air transportation and approved by the AIEE technical program committee for presentation at the AIEE Middle Eastern District meeting, Dayton, Ohio, September 23–25, 1947. Manuscript submitted July 7, 1947; made available for printing August 7, 1947.

B. O. Austin is the section manager for aviation control of the Westinghouse Electric Corporation, Lima, Ohio.

The author acknowledges the assistance in the development of the ideas presented in this paper of J. D. Miner, O. C. Walley, C. A. Stump, H. M. Rustebakke, and R. D. Jesses, all of the Westinghouse Electric Corporation, Lima, Ohio, and D. W. Exner, Boeing Aircraft Company, Seattle, Wash.

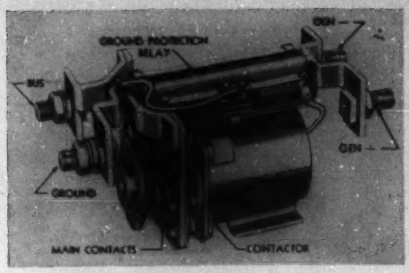

Figure 2 (left). Differential-current generator protective relay and contactor assembly

Mounted in nacelle when used

Figure 4 (right). Differential-current feeder-protective relay and contactor

Mounted in fuselage when used

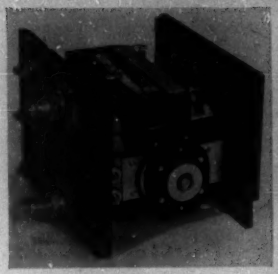

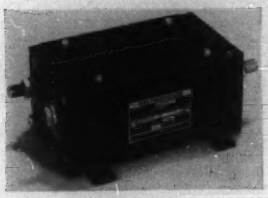

Figure 3. Differential-current generator and feeder-protective relay

Mounted in nacelle when used
Does not contain contactor

means an appreciable drop of the bus voltage will occur when the engine speeds are at wide differences. In this manner, high sensitivity for paralleling is obtained under normal operating conditions. This sensitivity falls off rapidly as the difference between engine speed increases, thus preventing serious drop in the system voltage.

Remarkably accurate paralleling obtained with this system is shown in the test-load division tables which are part of this paper. Mock-up and flight test results show very conclusively that with the use of this paralleling system it is practical to make all regulator adjustments and settings with the use of a standard test stand. Further adjustments of the regulator on board the plane are unnecessary. This is of considerable economic importance.

Electrical Fault Protection

Protection against battery drain and reverse-generator polarity have been in use for many years. These two features have worked reasonably well where low capacity and low voltage were involved. Systems with higher voltages and capacities have demonstrated that additional fault protection is a practical necessity. New provisions have been made for fault protection of the generator, generator leads, generator feeder, and prevention of sustained overvoltages which indirectly result in the protection of other equipment.

Differential-Current Fault Protection

Protection against fault currents of 100 amperes and greater in the d-c system is provided for by the use of the differential-current relay. Differential-current setting of 100 amperes is used with the present 300-ampere 30-volt generator system. Lower differential-current settings may be required and can be provided. The a-c system also uses differential-current protection and the current values in most cases are much lower than those used for the d-c system. The alternating voltages being much higher, the current consequently must be lower. The d-c differential-current protective relays fundamentally consist of two straight conductors surrounded by a magnetic circuit of the proper length and proportion to provide a device having actuated electrical contact which is operated when the current in the two conductors is unbalanced 100 amperes or more. These relays are located in the main power circuit so that they will function to eliminate the fault by interrupting the proper control circuit for the purpose. The outstanding advantage of such a protective system is that it is responsive to fault conditions only and is not affected by transient power requirements. Another very definite advantage, and perhaps equal to that of the first advantage, is that co-ordination of timing

Figure 5. Differential-current feeder-protective relay and dual contactors

Mounted in fuselage when used

Table I. Paralleling and Load Division Tests, 4-Generator Mock-up

Rpm of Number 4 Generator Varied From 3,000 to 9,000
Tested With Battery on the Bus
No Load Readings Were Taken With Generator Disconnected From the Bus

Generator Volts				Bus	Load Amperes				Generator RPM	
No. 1	No. 2	No. 3	No. 4	Volts	No. 1	No. 2	No. 3	No. 4	1–2–3	4
28.0	28.0	28.0	28.0	26.0	0	0	0	0	3,000	3,000
28.0	27.95	28.0	28.0	27.9	201	198	209	192	3,000	3,000
28.15	28.1	28.1	28.1	28.0	198	195	205	202	3,000	5,000
28.15	28.1	28.1	28.1	28.0	195	198	206	201	3,000	7,000
28.1	28.0	28.1	28.1	27.95	195	198	213	191	3,000	9,000
27.9	27.9	27.85	27.85	27.75	198	204	213	187	3,000	7,000
27.8	27.85	27.85	27.8	27.7	198	204	215	179	3,000	5,000
27.75	27.75	27.8	27.75	27.6	198	207	215	173	3,000	3,000
26.2	26.2	26.3	25.2	26.1	234	252	259	0	3,000	1,850
26.4	26.4	26.4	26.2	26.2	228	252	253	18	3,000	2,000
28.0	28.0	28.0	28.05	27.95	195	198	206	209	3,000	3,000
28.1	28.2	28.0	28.25	26.2	0	0	0	0	3,000	3,000

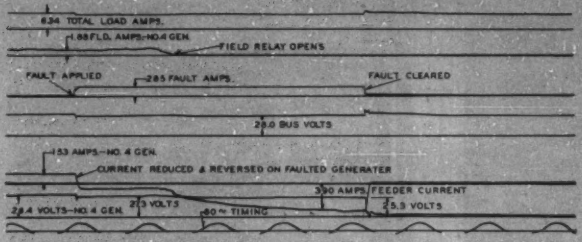

Figure 6. Oscillograph record showing operation of differential-current protection when feeder has been faulted in a 4-generator system

Four generators paralleled at 6,000 rpm; battery on line
Fault applied at fuselage end of number 4 generator feeder

with other apparatus such as the reverse-current cutout is not required. Also, environmental conditions are not critical with this type of apparatus. The method of procuring differential protection with the a-c system is slightly different than the method used in the d-c system. Instead of parallel conductors being in a common magnetic circuit, current transformers are used to surround the lead. An unbalanced current in the leads will cause voltage from the secondary of the transformers, thus operating the necessary control devices to clear the fault.

Effectiveness of the d-c differential-relay protective systems has been demonstrated on mock-up tests to be a very satisfactory arrangement. On a 4-generator mock-up, running at 6,000 rpm, a 237-ampere fault was applied at the number 4 generator *B* terminal. The field relay was opened by the action of the differential-protective relay in $2^1/_2$ thousandths of a second. Opening the field of the generator immediately eliminates the fault current from that generator. The main contactor coil also is opened at the same time by the field relay. Opening the main contactor immediately limits the current from the system to the fault. The oscillogram of this test indicated that 10 to 15 amperes flowed from the bus in the reverse direction through the generator feeder, while 237 amperes were flowing through the fault connection at the *B* terminal, proving that the faulted generator was supplying nearly all the fault current. The accompanying oscillogram, Figure 8, shows a fault at the fuselage end of the number 4 generator. Even in this case the reverse fault current is much less than the fault current supplied by the number 4 generator before the field relay opens the field of the generator. Some of the devices have been in actual flight tests, but no faults have occurred in flight to cause their operation. They have not produced any nuisance trips in the tests. Differential-current protection is trip free and reclosing of the contactor on a fault is prevented. Resetting closes only the field relay. If the fault still exists, the differential-current relay will trip the field relay before there is sufficient voltage to close the contactor through the polarized relay.

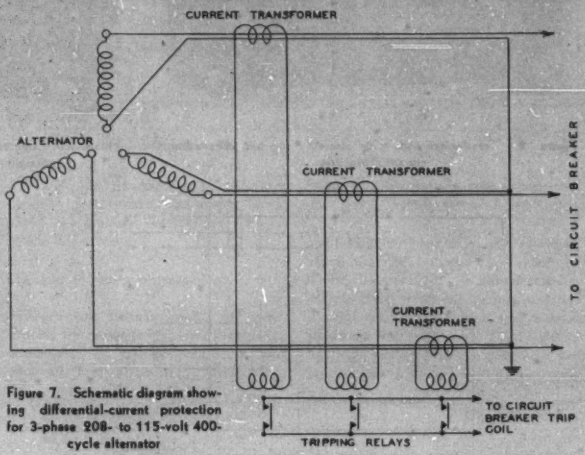

Figure 7. Schematic diagram showing differential-current protection for 3-phase 208- to 115-volt 400-cycle alternator

Table II. Paralleling and Load Division Tests, 4-Generator Mock-up

Two Regulators Set One Volt Low at No Load
RPM of Generators Varied
Tested With Battery on the Bus
No Load Readings Were Taken With Generator Disconnected From the Bus

Generator Volts				Bus	Load Amperes				Generator RPM,
No. 1	No. 2	No. 3	No. 4	Volts	No. 1	No. 2	No. 3	No. 4	1–2–3–4
28.5	27.5	27.5	28.5	25.4	0	0	0	0	3,000
27.8	27.75	27.8	27.8	27.75	225	180	197	207	3,000
28.2	28.15	28.2	28.2	28.05	228	189	186	210	4,000
28.1	28.05	28.0	28.05	27.95	222	192	183	209	5,000
28.15	28.15	28.1	28.0	28.0	222	195	180	207	6,000
28.1	28.05	28.1	28.1	28.0	222	198	174	204	7,000
27.85	27.8	27.8	27.8	27.7	216	198	192	198	6,000
27.7	27.7	27.65	27.7	27.6	210	192	186	197	5,000
27.5	27.45	27.45	27.5	27.4	216	186	187	197	4,000
27.0	27.0	27.0	27.0	26.9	195	192	183	198	3,000
28.4	27.5	27.2	28.5	26.2	0	0	0	0	3,000

Overvoltage

Overvoltage conditions may be a result of several types of faults. For example, broken regulator leads, shorted terminals or leads, or any type of fault which will increase the current in the field of the generator beyond the control of the regulator. Maximum allowable

Figure 8. Transformer and relay assembly for a-c differential current protection

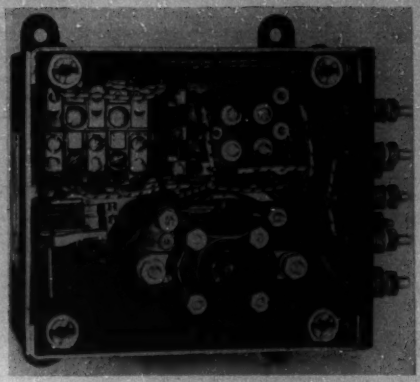

Figure 10. Contactor and relay assembly for differential-current protection for 3-phase window-heating alternator

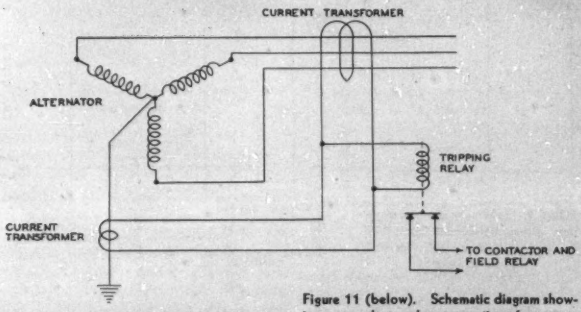

Figure 9. Schematic diagram showing differential-current protection for 3-phase window-heating alternator

Figure 11 (below). Schematic diagram showing over-voltage relay connections for proper selectivity of an overvoltage generator in a d-c system

continuous field current also can cause overvoltage under some conditions; for example, light-to-medium loads and normal-to-high generator speeds. In the past, this overvoltage was controlled to some degree by the generator being small and the batteries being of sufficient size to absorb most of the overvoltage. Modern wide-speed-range generators are capable of developing much more power at much higher voltages and are difficult to handle with apparatus designed for use with the smaller generators. Several near disasters have been reported; how many crashes have been caused by overvoltage never can be known. Overvoltage protection is a necessary operating requirement.

Overvoltage relays having an inverse time element seem to be the only acceptable device at this time. Circuit breakers and other forms of current-limiting devices have been suggested and are being used in the field lead to the generator in some systems for overvoltage protection. These devices are set at relatively high current values to prevent nuisance trips.

Oscillograph test records on four 300-ampere wide-speed generator mock-ups show that this type of circuit breaker offers very little protection. At a total load of 200 amperes on four generators, the number 3 generator regulator coil was open-circuited, the resulting field amperes of number 3 generator were 14. A circuit breaker in the field circuit must be set higher than the 14 amperes as this is a field current which easily can be reached under idling speeds and low-operating-

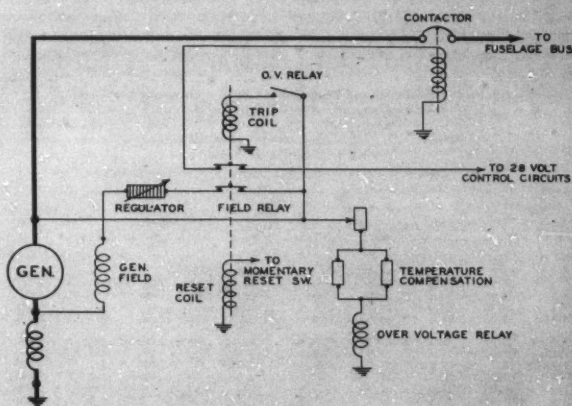

Figure 12. Inverse time element overvoltage relay

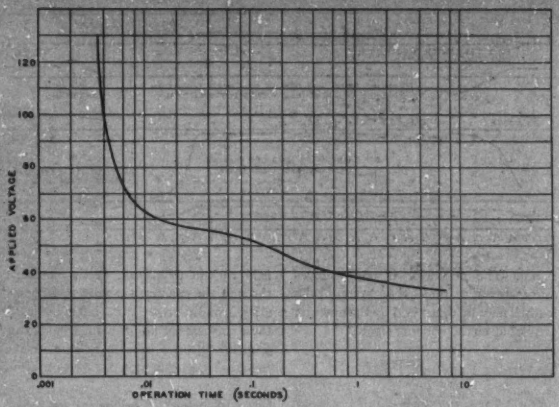

Figure 13. Overvoltage static voltage–time relay curve

temperature conditions. Therefore, the circuit breaker offers no protection in this case. The overvoltage in this case from the number 3 generator was 46. Overcurrent on the number 3 generator was 810 amperes. The overvoltage relay removed the number 3 generator from the system in one-third of a second. Without the overvoltage relay, the 810 amperes on the number 3 generator would have burned it up in a few minutes.

In a second test with a total load of 800 amperes on a 4-generator mock-up, the number 3 regulator was open-circuited. Field amperes rose to 11.4, which is less than normal when the generator is at low temperatures. This is much below the value at which a circuit breaker can be set and prevent nuisance trips. Overvoltage on number 3 generator was 36.3; number 3 generator amperes were 919. The overvoltage relay removed the number 3 generator from the system in three-quarters of a second. Without the overvoltage relay, the generator could be seriously damaged on take-off and burned out in a matter of a very few minutes. The oscillogram shown in Figure 18 is the test record.

In order to make the overvoltage relay select the proper generator, the operating coil of the relay must be connected so its operating voltage is taken near the generator terminals. Bus voltages are not increased by a fault condition causing a generator to have overvoltage nearly as much as the terminal voltage of the generator. In order for the overvoltage relay to properly select the generator whose voltage is excessive, its operating coil must be connected near the terminal volts of the generator. A schematic diagram accompanies this paper which shows satisfactory connections for the overvoltage relay.

Generator Overtemperatures

There are various causes for overheating the generator, many of which are eliminated by better paralleling and adequate fault protection. Overloading and insufficient ventilation are conditions which may be indicated by a thermal device incorporated in the generator. Such a device requires a current-sensitive heating coil, as well as a well-selected position in the generator. Such a device has been included in the generator and operates an indicating light as a warning

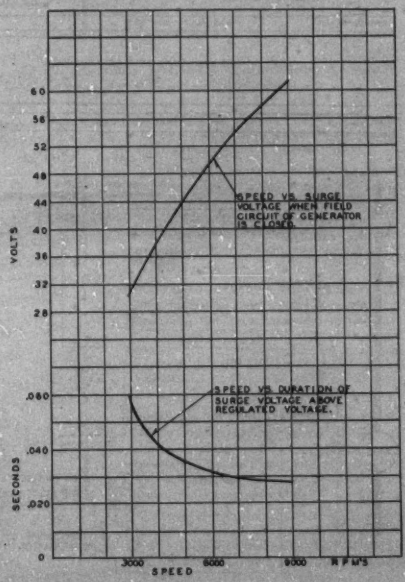

Figure 14. Curves showing the magnitude and duration of surge voltages above regulated voltage when the field of a 300-ampere generator is closed at speeds of 3,000 to 9,000 rpm

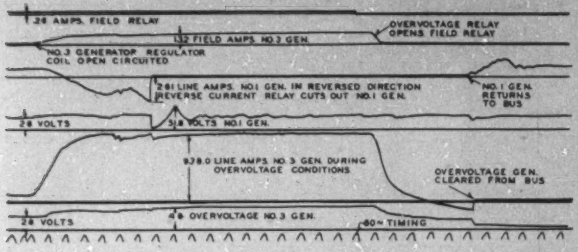

Figure 15 (left). Oscillograph test record showing the operation of the overvoltage relay at 400 amperes total system load using four generators

All generators paralleled, 9,000 rpm
Full field applied to number 3 generator

signal. The generator is not removed automatically from the system. Its loading may be controlled by the operator or pilot after the warning signal.

Generator Reversed Polarity

If the polarity of the generator becomes reversed, it is not available for use on the system. The polarity must be returned to a normal conditon by flashing the field before it can be used again. Numerous tests have shown that it is possible to reverse generators by interrupting the field current or passing reverse current through the generators under some operating conditions. It is believed that these reversals or failures of the generator to build up have been more in evidence than has been suspected. System tests have shown that a very small current through a high resistor from the main bus through the regulator and field guarantees against generator reversed polarity.

Figure 16 (below). Oscillograph test record showing the operation of the overvoltage relay at 800 amperes total system load using four generators

All generators paralleled, 9,000 rpm
Battery on line
Full field applied to number 3 generator

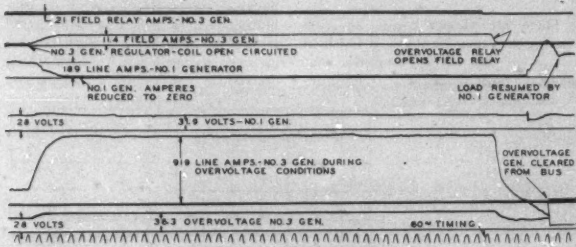

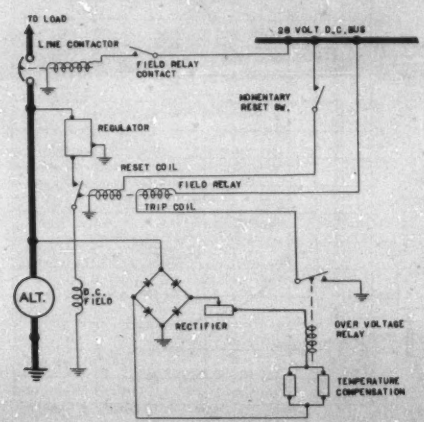

Figure 17. Schematic diagram showing overvoltage relay connection for overvoltage from an alternator

Generator Contactors

Generator contactors have been designed and are in use which are practically free from contact freezing. This development consists of using higher contact-operating force and inertia follow-up for the moving contact bar. Contact freezing is caused, in most cases, by rebounding of the contacts from the initial make, drawing an arc, which results in the softening of the contact material. This softening is often sufficient to cause welding or sticking together of the main contacts. High operating forces and the inertia follow-up prevents contact rebounding and therefore eliminates freezing or sticking together.

Dual Generator Contactors

Using two contactors whose main contacts are in series in the power circuit has been practiced many years in other forms of transportation. They provide safety, reliability, and continuity for the electric power system. Dual contactors whose main contacts operate independently, providing a total of four breaks, are very effective against a loss of either contact assembly or the generators from the system by backing each other up. It has been shown by system tests that single contactors with two breaks will not interrupt normal current under overvoltage conditions, which can be obtained from wide-speed-range generators. Serious fires, burns, and smoke are results. Dual contactors de-energized simultaneously will interrupt such current and voltages in very satisfactory manner. They are a practical necessity and are recommended strongly.

Operation Without a Battery

Some of the present protective schemes, which are self-clearing as a result of fault, operate from the battery voltage. However, by the use of the latch-type field relay, a system is available for operation without the use of a battery. The only

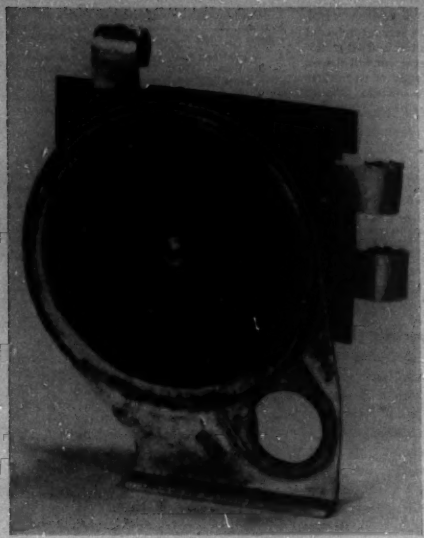

Figure 18. Thermostat which is located inside the generator for over-temperature light signal

Figure 19 (below). Main circuit schematic diagrams showing the location of differential-current protective devices for various degrees of protection

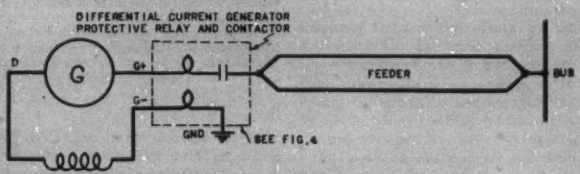

MAIN CIRCUIT SCHEMATIC GENERATOR PROTECTION ONLY

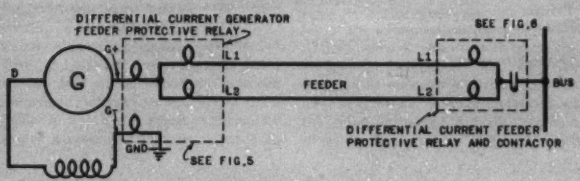

MAIN CIRCUIT SCHEMATIC GENERATOR AND FEEDER PROTECTION SINGLE CONTACTOR

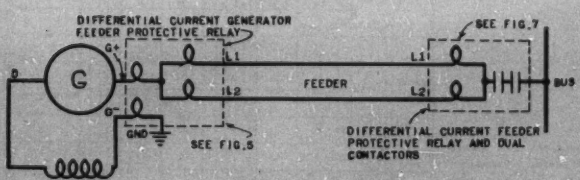

MAIN CIRCUIT SCHEMATIC GENERATOR AND FEEDER PROTECTION DUAL CONTACTORS

time the attention of the operator is required is when there is a fault. The latch-type relay then may be reset electrically if there is any energy on the bus; if not, it may be reset manually.

Concentrated Bus Versus Distributed Bus

A concentrated bus is one which is located in the fuselage at or near the wing center of the plane. Its length is generally less than two feet and consists of strap copper rigidly mounted. A distributed bus extends well out into the wings, also fore and aft in the fuselage.

A concentrated bus is preferable because it offers several distinct advantages over the distributed bus in the way of protection, voltage regulation, paralleling, and power availability to all load centers in the plane. Protection of the distributed bus requires sectionalizing which materially increases weight and apparatus. Voltage regulation and paralleling are difficult because of the bus voltage drops, and there is no common system voltage regulated point. A sectionalized bus generally feeds two or more load centers from each section. Fault at any one center cuts out all loads on that section. A rigid-concentrated bus properly installed avoids such hazards.

Conclusions

The following conclusions are reasonably self-evident:

1. Differential-current protective apparatus offers fault protection at low as well as high currents.

2. Differential-current protective apparatus requires no co-ordination with other devices in the power system, such as the reverse-current cut-out. The timing of each is independent of the other.

3. Differential-current protection responds to fault currents and nothing more.

4. The use of dual contactors for circuit interruption on over-voltage is a practical necessity and is recommended strongly. They lend reliability and continuity of the generator being on the system the maximum amount of time and avoid electrical fire hazards.

5. Single contactors have been designed within the last few years with freezing practically eliminated, as proved by test in service. However, this type of contactor, as a single unit, will not interrupt possible overvoltages that may be obtained from wide-speed-range generators.

6. Inverse-time-element overvoltage relays provide practical overvoltage protection. Fuses or circuit breakers in the field circuit are not adequate devices to cover the range of serious overvoltage conditions.

7. D-c systems having the required protective devices should be operative without the use of the battery.

8. The differential-current protective system is trip free and can be reset manually or remotely after a fault provided the fault is cleared.

9. Means should be provided for preventing reverse generator polarity, insuring greater continuity of the generator on the system.

10. Concentrated bus offers many advantages over the distributed type in the way of system protection and general operating performance.

11. Faults at the generator positive terminal or anywhere along the generator feeder can be high currents from the faulted generator and a very low reverse current drawn from the bus. The efficiency of the differential-current protective system is not affected by these fault conditions.

References

1. An Aircraft Differential-Voltage Cutout, O. C. Walley. AIEE Transactions, volume 63, 1944, September section, pages 632–4.

2. Pressure-Arc-Interruption Circuit Breakers for 400-Cycle Aircraft Electric Power System, B. O. Austin. Transactions, volume 65, 1946, February section, pages 58–63.

3. Control and Protection of Aircraft D-C Systems, B. O. Austin. AIEE Transactions, volume 65, 1946, November section, pages 741–5.

4. A 120-Volt D-C Aircraft Electric System, L. M. Cobb. AIEE Transactions, volume 63, 1944, pages 1327–34.

5. Paralleling and Regulation of 24–28-Volt D-C Generators in Multiengine Aircraft, Arthur Siegal, Dean's G. DeCourcey. AIEE Transactions, volume 63, 1944, November section, pages 854–7.

6. A-C and D-C Short-Circuit Tests on Aircraft Cables, J. C. Cunningham, W. M. Davidson. AIEE Transactions, volume 63, 1944, pages 961–9.

7. Electric-Circuit Burning Clear and Damage Phenomena on Aircraft Structures, C. M. Foust, J. G. Hutton. AIEE Transactions, volume 63, 1944, April section, pages 198–204.

No Discussion

Direct Coupled Oscillograph Amplifier

DEAN R. CHRISTIAN
ASSOCIATE AIEE

Synopsis: Progress in the field of direct-inking oscillographs has made the development of a d-c amplifier very desirable. This paper describes the circuits used to obtain the characteristics desired in a d-c amplifier when it is used with a direct-inking oscillograph. The combination of these circuits resulted in the development of a direct coupled amplifier which is operated entirely from an a-c source. The amplifier has a very low drift rate and, mechanically, is readily portable. The performance of the direct-inking oscillograph and d-c amplifier is illustrated with chart records showing recordings of d-c pulsations and sine waves. The treatment of the subject matter is concluded with a description of an industrial application in the use of the oscillograph with a d-c amplifier.

SINCE the direct coupled amplifier which is the subject of this paper was designed primarily to operate in conjunction with the Brush model *BL-201* direct-inking oscillograph, a short description of the latter will be given first. The active element of this device, the model *BL-902* Penmotor, consists of a coil of number 44 wire, of 1,450 ohms resistance, mounted in the field of an extremely powerful permanent magnet. A lightweight pen 3 inches in length is attached to the coil by means of a compliant member. Ink is fed through the pen by capillary action, making an instantaneous permanent record on a moving paper chart. The sensitivity of the Penmotor is such that 0.94 volt applied to the coil terminals results in one chart-millimeter displacement of the pen. The chart width is 50 millimeters, or ±25 millimeters from the center line. When fed from a low-impedance source the frequency response of the Penmotor is that given by the light solid line in Figure 1. By introducing the frequency compensation shown by the dotted line in the figure, the over-all response of the pen can be made equal to that shown by the heavy solid line in the figure. To obtain the damping necessary for the faithful reproduction of transients, it is necessary to drive the Penmotor from a low-impedance source of not more than a few hundred ohms.

Because the Penmotor will record any frequency from 120 cycles per second down to direct current, the full capabilities of the instrument never can be fully realized when it is used with a capacitance-coupled amplifier. The loss of the very low frequencies in these amplifiers have at times made the interpretation of the resulting record difficult. Such a record is illustrated in Figure 2 which shows the form of a d-c pulse of long duration recorded through a capacitance coupled amplifier. Due to *R-C* coupling networks in the amplifier circuit, a decay from the peak value recorded on the chart begins immediately even though the steady voltage is still applied. Removal of the direct voltage introduces a similar peak and decay in the opposite direction. Improvements in the low frequency response of capacitance-coupled amplifiers are limited by the practical size of the coupling capacitors and their leakage resistance, especially where a number of stages are needed.

In order to increase the sensitivity of the Penmotor, while at the same time taking full advantage of its ability to record d-c signals, a direct-coupled amplifier of the proper characteristics is absolutely necessary. There is, practically speaking, no limit to the sensitivity which would be desirable in a direct-coupled amplifier for this use. At the same time, it is generally true that the higher the input impedance of such an amplifier, the greater will be its usefulness. The problem therefore simply resolves itself into discovering what are the maximum values of both quantities obtainable in an amplifier designed for commercial production.

The basic problem encountered in any direct-coupled amplifier is "drift," a phenomenon which manifests itself as a slow random variation in the output of the amplifier even in the absence of any applied signal at the input. When a signal is applied to the input terminals this random variation is apparently superimposed on it. Drift behaves in many ways like a low-frequency variety of shot noise, in that its source is in the amplifier tubes themselves, and in that it

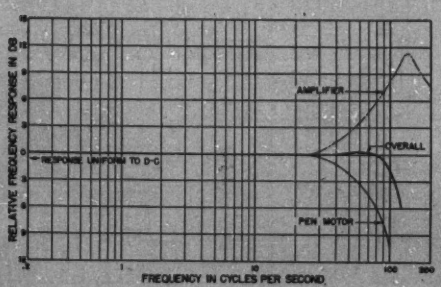

Figure 1. Average frequency response of Penmotor with and without frequency correction

Paper 47-226, recommended by the AIEE instruments and measurements committee and approved by the AIEE technical program committee for presentation at the AIEE Middle Eastern District meeting, Dayton, Ohio, September 23–25, 1947. Manuscript submitted June 23, 1947; made available for printing August 14, 1947.

DEAN R. CHRISTIAN is head of the instrument engineering department in The Brush Development Company, Cleveland, Ohio.

The author wishes to acknowledge the kind assistance of C. J. Wirkowski and L. E. Huldeman in the preparation of this paper.

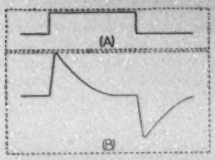

Figure 2. Comparison of wave form of a d-c pulse between the input and output of an a-c amplifier

is essentially random. It differs greatly from shot noise in its magnitude; however, where the shot noise in a good tube measured over the entire audio band from 20 cycles per second to 20 kc is normally equivalent to a signal of only a few microvolts applied to the control grid, the drift in the same tube, measured from zero to 20 cycles per second, in a period of 20 minutes, easily may exceed one volt.

Just as shot noise limits the magnitude of the audio signals which may be measured with a given tube, so does the drift limit the magnitude of the d-c signals which can be measured with a tube used as a direct-coupled amplifier. It is obviously not practicable to measure a signal of two or three millivolts when it apparently has mixed with it a random signal of the order of hundreds of millivolts. Consequently, the first problem in the design of any commercial direct-coupled amplifier is to determine the minimum drift rate which can be achieved and maintained in production. It is not sufficient to construct one amplifier which has a satisfactorily low drift rate; it is also necessary to know that the factors responsible for its performance are reproducible, and not merely, as is often the case, good luck.

Many factors result in drift in direct-coupled amplifiers. Foremost among these are changes in the plate and heater potentials of the low-level stages. Drift from this cause can be avoided, and the performance of such an amplifier greatly improved, by regulating the voltages applied to these stages. Even when this precaution is taken, however, it is commonly found that a considerable amount of drift remains, caused by random changes in the emission from the cathodes, and by temperature changes in the tubes, which has the same effect.

The only practical remedy which ever has been advanced to overcome this residual drift is to use balanced circuit arrangements employing nearly identical tubes, so arranged that the drift in one tube is cancelled by the drift in the other, but at the same time yielding an output signal when a signal is applied to the input. Many such circuits have been advanced, all having more or less merit, and all resulting in roughly comparable performance. Push-pull circuits are perhaps the classical example of such a circuit, but their usefulness is limited by the fact that they normally require that neither terminal of either the input or output be grounded.

Since in the vast majority of applications unbalanced operation is required the basic circuit shown in Figure 3 was chosen. Fundamentally, it is a bridge balanced circuit[1] in which all variables in the amplifying arm, including supply voltages and tube characteristics, are balanced against similar variables in a second arm of the bridge. In this type of circuit it is usual to make the cathode resistor of the tube V_1 variable to obtain a zero output with no input to the grid of V_1. In order that a more precise balance could be maintained, it was necessary to age the tubes and then select them as matched sets to obtain like characteristics. The improvement in performance which can be achieved by aging and matching tubes is apparent from the fact that a pair of unaged tubes, chosen at random, may show a drift rate of over 50 millivolts per hour in this circuit, whereas, by properly selecting aged tubes, the drift rate can be held at less than one millivolt per hour. An aging period of 1,000 hours at a plate current of about 50 microamperes is found to be necessary to assure relatively drift-free operation.

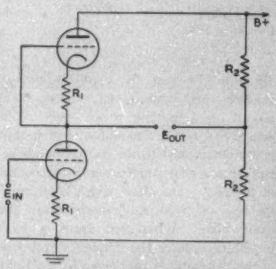

Figure 3. Basic bridge circuit

In the final circuit design of the d-c amplifier (see Figure 4) it was necessary to use two such series-balanced stages cascaded off the same B supply bleeder (see Figure 4C) in order to obtain an out-

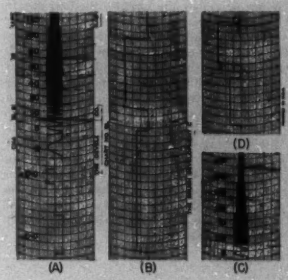

Figure 5. Frequency responses of d-c amplifier and magnetic Penmotor with resulting recordings of d-c pulsations

Figure 4. Schematic wiring diagram of d-c amplifier

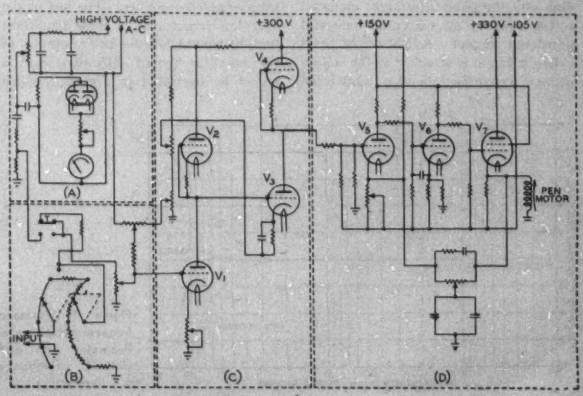

Figure 6. D-c amplifier

put level large in comparison with B supply voltage changes. This voltage change in the B supply is even smaller at the grid of V_8 due to the loss of the signal through the voltage divider network. The small voltage change at this grid is compensated by a similar change in another voltage divider network (originating also from the B supply) which places the cathode of V_8 at the correct potential with respect to ground for coupling.

Frequency Correction

The balanced stages are followed by three stages (see Figure 4*D*) containing degenerative feed back and a cathode follower circuit to work into the Penmotor impedance. In addition, the feed-back circuit provides high frequency compensation for the Penmotor. The frequency response of the Penmotor alone is essentially uniform from direct current to 30 cycles per second, falling thereafter to 120 cycles per second. The potentiometer and capacitor to ground in the frequency correction network tend to boost the high frequency end of the response. The capacitor by-passes the higher frequencies to ground, which results in less feed back at the cathode of V_8, which in turn increases the gain of the amplifier at these frequencies. Frequencies higher than 120 cycles per second may introduce undesirable effects in the Penmotor and in the output stage of the amplifier, such as heating of the Penmotor coil, and overloading of the output stage. The attenuation of the frequencies above 120 cycles per second is accomplished by a resistor and capacitor both in parallel with the potentiometer of the frequency correction network. The resistor and the capacitor tend to boost slightly the high frequency end up to 120 cycles per second and then rapidly attenuate frequencies above 120 cycles per second.

Calibration and Power Supply

A calibration circuit, shown in Figure 4*A*, is included in the amplifier so that the pen deflection of the oscillograph element can be correlated accurately to the input voltage. An alternating voltage, filtered to remove possible distorted wave form, is obtained from the high voltage winding of the power transformer and then applied to the calibrating circuit. The voltage then is measured in relation to the rectified direct current flowing through the *6H6* tube and meter. Filament power for the first two stages is obtained from a regulating transformer. The remaining filaments are operated from the filament winding of the power transformer. The B supply is regulated by means of voltage regulator tubes. The regulation of both supplies was incorporated into the amplifier circuit to obtain extreme precision of balance.

Characteristics

The normal sensitivity of the d-c amplifier used with the magnetic (Penmotor) recorder is one millivolt per one chart millimeter of displacement of the pen. Its frequency response is essentially uniform from direct current to 100 cycles per second. Figure 5*A* shows a characteristic frequency response of the d-c amplifier and Penmotor obtained with a normal adjustment of the high frequency compensation. With this compensation, d-c pulsations and square waves are charac-

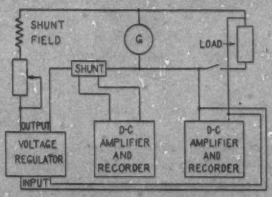

Figure 7. Diagram illustrating an application of the d-c amplifier and Penmotor in recording load characteristics of a d-c generator

Figure 8 (below). Chart record showing load characteristics of d-c generator

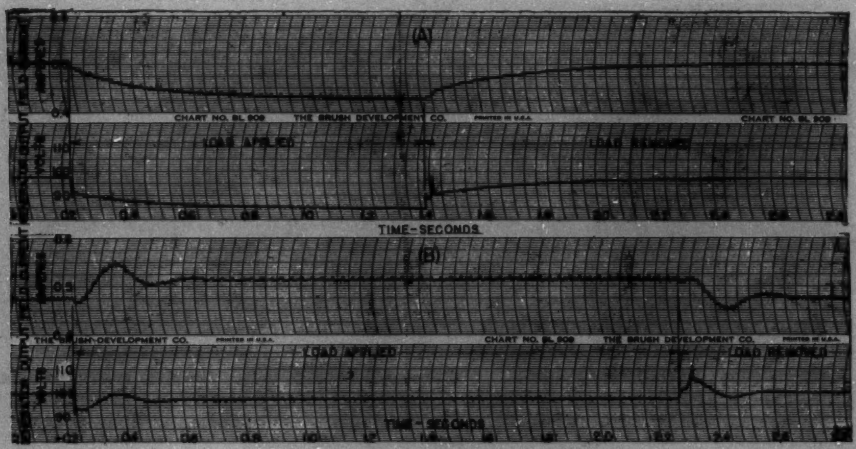

terized by a slight overshoot at the start of the pulse and at the return to zero. See Figure 5*B*. This overshoot can be eliminated by gradually reducing the amplitude of the high end of the frequency range of the amplifier and Penmotor.[3] This is accomplished by an adjustment of the high frequency compensation of the amplifier. See Figures 5*C* and 5*D*.

Line voltage variation from 110 to 130 volts does not affect the zero setting of the d-c amplifier. Its zero-signal drift in terms of pen displacement is not more than one chart millimeter per hour.

Application

The complete d-c amplifier, shown in Figure 6, is designed for use with the Penmotor to make permanent recordings of many types of phenomena heretofore measured with the aid of complicated intermediate equipment. A permanent recording of a transientory nature is exemplified in the following application. A load is supplied by a conventional d-c generator whose inherent load characteristic is a drop in output voltage from no load to full load. Two d-c amplifiers and their associated Penmotors were used to record this characteristic by recording simultaneously the field current and the output voltage of the generator system to regulate the output voltage. A schematic diagram of the setup and the resulting recording are shown in Figures 7 and 8*B*, respectively. From the record of Figure 8*B* and that of Figure 8*A* the effectiveness of the voltage regulator can be evaluated simply by determining the speed of the response of the regulator in hundredths of a second.

Studies of static or dynamic conditions, such as strain, displacement, pressure, light intensity, temperature, direct and alternating voltage or current, and many others are simplified by the use of these instruments.

References

1. Electrodynamic Direct-Inking Pen, H. B. Shaper. *Electronics* (New York, N. Y.), March 1946, pages 148–51.

2. Survey of D-C Amplifiers, M. Artzt. *Electronics* (New York, N. Y.), August 1945, pages 112–18.

3. Amplifier Testing, G. Swift. *Communications* (New York, N. Y.) February 1939, pages 23–6.

No Discussion

Using Air-borne Radar to Increase Airline Safety

R. W. AYER
NONMEMBER AIEE

MINOR but significant modifications to existing *X*-band air-borne radar types have made it practical for the pilot himself to use radar for avoiding collisions with terrain, for emergency negotiation of "letdowns" over terrain surrounded by hills, for avoidance of dangerous areas of precipitation (thunderstorms, freezing rain, hail, and snow) and its associated turbulence whether flying over land or water, and as weatherproof supplementary navigational aid where water–land or other "contrast" exists in the echoes.

Using the same modified *X*-band air-borne radar against ground responders ("racons" or "beacons"), a simplified navigation system has resulted which improves the precision of flying in areas of high traffic density, provides a simple means of making multidirectional low approaches to an airport under conditions of low visibility, and provides a weatherproof stand-by en route navigation system. The continuous information on ground speed provided by air-borne radar provides substantial economies in long hauls by permitting quick selection of the most favorable flight levels.

A procurement program for a suitable pilot-operated transport radar has been undertaken co-operatively by the Army, Navy, and an airline after one year of flight development and service test work by the airline. Nearly identical equipments will thus be supplied to National Air Transport Service, Air Transport Command, and those commercial airlines who wish to use radar.

Because air-borne radar indicates to the pilot immediately when it fails to operate or when it operates improperly, it is considered inherently a self-checking or "fail-safe" device. This feature greatly enhances its value.

A survey of the scheduled airline accidents over a period of five years indicates a preponderance of fatalities occurring in accidents in which the aircraft apparently flew into a hill, usually at night, and apparently without the pilot's being forewarned. Some 500 hours of flight and service test using air-borne radar indicates that if the past accident pattern continues to prevail, air-borne radar is capable of saving 50 per cent of these fatalities.

Air-borne Radar for Avoiding Terrain Collisions

During the fall of 1945, a group of airline flight engineering personnel took a cursory glance at two types of air-borne radar. The result was disappointment.

The *APS-10*, the first of those tested, was designed for the Air Transport Command toward the end of the war, and produced a cathode ray picture that was difficult and ambiguous of interpretation, particularly over land. *APS-4*, the second to be tested, because of its distorted cathode ray presentation, was even worse.

The winter of 1945–46 was witness to several horrible airline accidents which focused the attention again on some means of electronically "seeing" obstacles and avoiding them.

Working in close conjunction with an airline industry electronics laboratory, airline flight engineering personnel held conferences to decide what operating requirements were needed of an air-borne electronic device in order to provide a simple and easily interpretable cockpit presentation of collision information. The standard polar-plotted information available in the *APS-10* radar was selected, yet at the same time it was concluded that the radar itself must "look," if possible, only through a narrow horizontal slit essentially in the plane of flight, much as one would look through a slit in a parapet or tank.

From this it was decided to revert, as in the *APS-4*, to confining the energy of an all-around scanning radar such as the *APS-10* to as narrow a beam as practical, spilling a minimum amount of energy downward.

The result was a successful test flight on March 5, 1946, during which the engineering pilot flying under the hood, was able to pick his way through valleys in the Catskill region well below the levels of the peaks, using the radar as the sole means of navigation and avoidance of collision.

Figure 1 shows the radar display tube showing the terrain mapping that the narrow or pencil beam produces. With this type of cathode ray presentation one is flying up the picture, and the center circle is the point of zero range, or represents

Figure 1. Terrain mapping with "pencil" beam

A—Hudson River
B—Level terrain near Hudson River

Paper 47-233, recommended by the AIEE committees on air transportation and communication and approved by the AIEE technical program committee for presentation at the AIEE Middle Eastern District meeting, Dayton, Ohio, September 23–25, 1947. Manuscript submitted July 1, 1947; made available for printing August 29, 1947.

R. W. Ayer is assistant director of flight engineering for American Airlines, Inc., La Guardia Field, New York, N. Y.

Figure 2. Terrain mapping with energy spilled downward

A—Hudson River
B—Central Park on Manhattan Island
C—Queensboro Bridge spanning East River

Figure 3. Terrain mapping—"pencil" beam

A—Shadow merging with "safety" circle
B—Echoes from higher peaks beyond first ridge
C—Low level terrain on west bank of Hudson River

the airplane's position. The thin circles are range marks, in this case 2-mile marks. The aircraft is flying approximately 4 miles to the left of the Hudson River which shows on the radar "scope" as a jagged dark line. In the right forward sector the narrow pencil beam is picking up the level terrain near the Hudson River. Note in the left forward sector the echoes are stronger and that there is a deep shadow being cast by something approximately $8^1/_2$ miles range. Also, there are some shadows at 45 degrees to the left.

Perhaps the most significant fact of this type of radar presentation is the black area of no echo extending from the circle of zero range outward to the first echoes. This means simply that there is that much clear air space to fly through before there is any danger of collision; in this case almost 4 miles. This black area has been named the "safety circle," indicating to the pilot that he may proceed at his present level for the distance covered by the black area. The elimination of the energy that normally is spilled downward was not done on the radar used in Figure 2. Contrasting Figure 1 with Figure 2, it will be noted that in the latter, "the picture is painted" beginning immediately below the aircraft. Manhattan Island is shown clearly as a true map with the airplane directly over the Hudson River, Central Park dead ahead, and the East River with the 59th Street bridge just beyond. Yet it is quite obvious that there is no simple, easily interpreted collision information available in this picture.

In Figure 3 the airplane has moved from the position of Figure 1 about 4 miles on the same heading. Note that the deep shadow at 45 degrees to the left in Figure 1 has now merged in Figure 3 with the safety circle, indicating that it is a body of water. Dead ahead at a range of some 5 miles is a strong echo casting a deep shadow beyond it. The pencil beam of the radar picks up a few more echoes located in this shadow which are probably mountain peaks sticking up above the first one. At a glance the pilot can see that there is a terrain ahead of him with which he is likely to collide at a range of $4^1/_2$ miles, and to the right about 20 degrees is level terrain toward which he may turn with safety.

If he does turn, however, and the radar is installed as originally intended with no attempt to stabilize its axis of rotation with respect to the earth, the picture will look like Figure 4. Since the axis of the radar would tip with the airplane when it banks, the beam, as it passed through the left sector, would look directly down at the ground—conversely, up into the air n the right sector. Such a picture during a banked turn can be dangerous, so the transport radar is stabilized in roll, maintaining the plane of rotation of the pencil beam level with respect to the earth's surface. This stabilization is done with components of a standard automatic pilot and is done in such a way that no azimuth errors occur. As you will see later, any azimuth errors introduced by attempting to stabilize the radar through the tilt control of the dish would be detrimental, in fact dangerous, to the operation.

Figure 5 shows the "scope" taken with the aircraft about 2 miles closer to the hill in Figure 3. Now the pilot, keeping on his potential collision course, has pulled the nose of the airplane up to an attainable climb angle. He does this to determine if the radar beam will look over the hill with which he may collide. The picture shows that, although the echo from the level ground in the right quadrant has disappeared as a result of this maneuver, the hill echo now at $3^1/_2$ miles still is retained. Simply interpreted, this means that the pilot must turn away (can not climb over) to avoid the mountain.

Figure 6 shows the aircraft with the nose level again, still on the same heading, the safety circle badly distorted in the left forward sector, a strong echo at 2 miles with deep shadows beyond it, a collision imminent within 35 to 40 seconds. The significance of the safety circle perhaps can be seen most readily from this picture. Once the pilot learns to keep two or three miles of clear, black, air space out in front of him, he has a simple formula for avoiding terrain collisions and, perhaps even more important, taking the proper evasive action.

Figure 4. Distortion of radar cathode-ray picture caused by airplane turn with an unstabilized antenna

A—Ground painting
B—Radar beam scanning above ground level because of bank

Figure 5. Terrain mapping "pencil" beam continued

A—Terrain peak at or above extension of aircraft flight path

The evasive action is shown in Figure 7 in which the airplane was turned some 30 degrees to the right. Note that the hill is passing approximately 1 mile off to the left and the safety circle shows a little over 3 miles of clear air ahead and level ground beyond it.

In April 1946, the series of plan position indicator (PPI) pictures just shown was taken simultaneously with photographs out of the cockpit window. These were published within the airline industry at that time. Subsequently, further intensive flight research was undertaken to ascertain the extent to which this information could be used by the pilot, and also what other functions the radar could perform for the airline operator.

As an example of typical simultaneous photographs of the PPI "scope" and out the cockpit window, note that in Figure 8 the aircraft is being flown directly at the top of a portion of Mount Washington (actually a few feet above the top so that it can clear it after the picture was taken) and note the extreme arrestiveness of the radar display at this point with strong, bright echoes within a mile and a half and deep shadows being cast forward and beyond the first bright echo.

Figure 6. Hill echo infringes upon "safety" circle, warning of imminent collision

A—Echo from hill entering "safety" circle

Figure 7. Terrain collision avoided by means of effective evasive action

A—Clear path for three miles on course with level ground beyond

B—Peak now has passed to one mile to left of airplane

Figure 8. Comparison of "scope" picture and simultaneous photograph out of cockpit window as airplane approaches top of Mount Washington

To show the area photographed out of the cockpit window a V sector has been drawn on the PPI photograph

The normal mountainous terrain type of indication that would be seen by a pilot letting down, for instance, from Pittsburgh, Pa., into Washington, D. C., over the Allegheny ridges, is shown in Figure 9. In this case the safety circle is almost 6 miles, indicating adequate clearance and no need to consider evasive action for some time. If, however, evasive action were not taken and the letdown were continued directly toward the top of the hill, Figure 10 shows the type of collision indication that would confront the pilot just a few seconds before he hit the hill.

After several months of experimental flight on a *C-47* aircraft with the radar installation shown in Figure 11 (the "bug-eyes" on a radome are installed to give the antenna room to move sideways as it is stabilized), an installation of the same type of *APS-10* General Electric radar was made on a *DC-4* air freighter operating between Seattle, Wash., and Anchorage, Alaska. Figure 12 shows the nose type of radome employed. A great deal of research had to be undertaken to obtain a satisfactory radome for this installation, and as yet, although the transmissivity attained exceeds all other radomes, there are still spurious reflections of an annoying but not dangerous nature. This research activity is still under way to correct the faults of this radome. It is interesting to note that little change of the aerodynamic contour results from this radar installation even though the scan is 360 degrees and the antenna is stabilized for a total of 60 degrees in roll. The actual angle through which the antenna looks without encountering airplane structure is approximately 240 degrees.

Figure 13 shows the first officer's scope installation in this *DC-4* air freighter. An identical installation is made on the left hand side for the captain. The radar controls are located directly on the control console between the two automatic direction finders.

The six months of operation of this *DC-4* air freighter between Seattle and Anchorage resulted in a great deal of data being gathered, some of which has not been correlated. It was found that with the remarkably abundant land–water contrast available along the coast of Alaska a great deal of navigating could be done with the search phase of the radar, as well as to use it for avoiding mountain peaks, particularly during the letdown into Anchorage. The pilots found that they were able and willing to make blind letdowns with the radar alone, provided, in the event the radar failed, they had a predetermined heading on which to climb out safely. This phase of the collision prevention ability of the radar has yet to be exploited thoroughly. It is believed that only several years of actual line operation will disclose to what extent it can be used for the purpose of making an instrument letdown. Certainly it can be said at this time that it can be an *aid* to such a letdown but it does not seem right and proper to consider it as a primary means because of its possible failure.

A word about airplane-to-airplane collision prevention. The creation of the safety circle as described heretofore, now has made it possible, while scanning the ground, to have at the same time a modi-

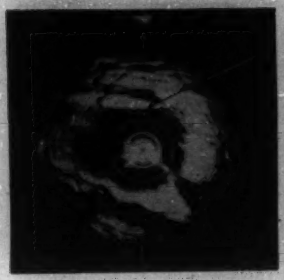

Figure 9 (left). "Let down" in mountainous region between Pittsburgh, Pa., and Washington, D. C.

A—Ridge below airplane level six miles ahead on course

Figure 11 (right). *APS-10* radar chin installation installed in experimental C-47

cum of protection against collision with aircraft flying level at or near the same level. This protection must be considered strictly as a "crutch," however, since the echo received from the aircraft is quite small and if missed for four or five scans, easily could travel through the full length of the normal sized safety circle before it would be seen. Furthermore, the airplane-to-airplane collision record shows that at least in the past there have been more collisions between climbing and descending aircraft than between aircraft flying level. Obviously the essentially horizontal scan with the pencil beam will not pick up such aircraft until they are much too close to be avoided. On the optimistic side, however, there are many cases when there is reason in the pilot's mind to doubt that he is being protected, when flying blind, against other aircraft flying on the same track and at the same level. Under these circumstances, the pilot can derive a certain amount of comfort from scanning horizontally with the radar to make sure that there are no aircraft at his level within approximately 5 miles, the measured maximum range of the *APS-10* radar on a tail-on small aircraft.

Figure 10. Comparison of radar "scope" picture and simultaneous photograph out cockpit window

A—Radar echo from Mount Washington touches zero range a few seconds before aircraft would hit it

Air-borne Radar for Avoidance of Dangerous Storms

Long before the airline investigation of radar began, it was recognized by both the Army and the Navy that air-borne radar had considerable usefulness for detecting storm areas, presumably by reflection from water droplets, and in particular, when flying over water because of the elimination of groundreturn. However, over land the assurance with which one would pick up the storm echo and distinguish it from the ground echo was very low because of the confusion between the two. The creation of the safety circle through the use of a pencil beam made it possible, when over land and scanning the ground, to see storm echoes that fell inside of the safety circle. Furthermore, by the simple expedient of raising the tilt of the beam so that the scan would be truly horizontal and would no longer see the ground, nothing but storm echoes would be seen.

The airline flight research program undertook to determine to what extent storm echoes could be seen, what droplet sizes could be seen and how far away, whether dangerous thunderstorm turbulence usually was associated with sufficient precipitation to show a radar echo, whether severe and dangerous icing conditions resulted from precipitation which would show a sufficient radar echo, and perhaps above all, to determine whether, when flying in areas of heavy precipitation, the radar would continue to provide terrain echoes from which collision warning information could safely be derived.

Many of these questions already have been settled at least on a research basis. They have yet to be settled once and for all as to whether the average line pilot in fact will use this ability of the radar.

Figure 14 shows several mild thunderstorms. The range of the radar is set such that the two small storms, showing up almost as specks, are approximately 8 and 12 miles away, respectively. It is significant that the storms in the right forward sector are seen one through the other. There is an echo within a few seconds of the point of zero range and, when the aircraft actually entered this echo, there was heavy rain and moderate turbulence. Note that the radar shows a channel of no precipitation slightly to the left of dead ahead which can be flown through. This actually was done and no heavy precipitation was encountered.

The echoes from behind are bounces of the radar pulses off of the nacelles and down to the ground as the radar looks aft.

Figure 15 is a more well developed thunderstorm with its characteristic "bay" or "cove" and its dumbell shape. In this particular case the pilot was able to see the thunderstorm visually and the time at which the radar echo coincided

Figure 12 (left). Nose radome housing *APS-10* radar in nose of *DC-4* air freighter

Figure 14 (right). Typical thunderstorm radar "scope" picture

A—Nearby moderate thunderstorms
B—Two small thunderstorms at greater range
C—Channel of no precipitation
D—Echoes from radar signal bouncing off engine nacelle

with the point of zero range, was coincident with the actual occurrence of heavy turbulence, rain, and hail.

Figure 16 is a typical PPI picture of a storm while the aircraft is in the middle of it. This storm was approximately 4 miles in diameter and was accompanied with the usual heavy turbulence, heavy rain, some hail, and violent up drafts.

Figure 17 shows a rain squall at 3 miles off to the right. Although this was not an icing condition, the photographs taken in heavy icing in the Alaskan area in many cases look almost exactly like Figure 17.

From the experimental flying and in particular from the *DC-4* service testing in the Alaskan area, it has been found that, in general, the density of the storm echo combined with a knowledge of the outside air temperature (anything below 31 degrees Fahrenheit) can give adequate warning of dangerous ice. It is perhaps fortunate that ice accretion which normally is not considered dangerous, frequently does not show as an echo at all or perhaps only as a little fuzz, whereas precipitation from which ice accretion will be rapid and heavy produces a very strong echo at a considerable range. It is believed that most, if not all, dangerous icing conditions can be avoided with an operable air-borne radar.

Likewise, dangerous hail which occurs in the Rocky Mountain and Allegheny areas during thunderstorms (sometimes with hail stones as big as baseballs) can be avoided with an operable air-borne radar.

In any flight research program on safety methods or devices, one of the earliest questions to be asked about the

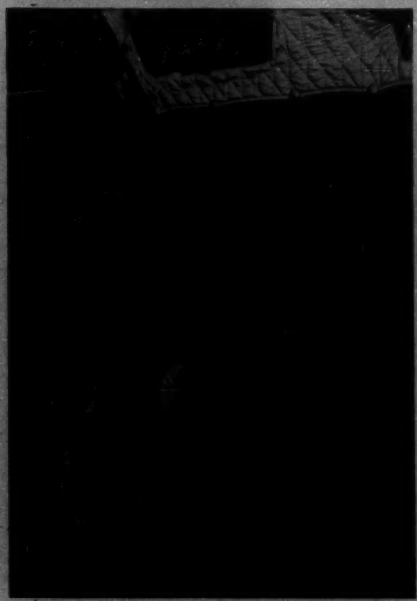

Figure 13 (left). First officer's radar "scope" installation *A* in the *DC-4* air freighter

Figure 15 (above, right). Characteristic picture of well developed thunderstorm

A—Typical thunderstorm with characteristic dumbbell shape
B—Ground clutter echoes showing with aircraft in nose down attitude

Figure 16 (right). Typical PPI picture of a thunderstorm while aircraft is in the middle of it

Figure 17. Rain squall three miles off to the right at *A*

equipment is whether its use will produce new and unexpected hazards. If, for instance, an air-borne radar leads a pilot into negotiations with mountain passes that otherwise he would avoid and then fails him when he gets into an area of precipitation, it might be safer to have no radar at all. Figure 18 is a PPI picture while flying in moderate-to-heavy rain and shows terrain echoes received clearly and distinctly through the rain. It has been determined that the range of the radar is reduced on the order of 10 per cent in the type of rain so far encountered. Admittedly torrential rain of high density with large droplet sizes and extending over a big area has not as yet been encountered during the tests.

An even greater potential hazard that might result from the use of the radar would be to mistake a hill echo for a storm echo and to attempt to fly through the echo. For several reasons this confusion to the extent of our present knowledge, does not appear to be likely, but as long as there remains any possibility of it, the rule must be to avoid flying through all echoes unless the pilot is absolutely positive that he cannot be below the level of any hills, or better still, cannot be in the vicinity of any hills. One reason that the confusion between terrain and storm echoes is not too likely arises from the fact that the average pilot is likely to scan above the horizon quite frequently whenever there is a possibility of any storms. The very act of scanning above the horizon (by definition until all ground echoes disappear) proves first, that it is safely above terrain, and second, that any echo that remains after having lost the terrain is likely to be a storm. This procedure is by no means infallible when flying below the level of hills in areas such as the Rocky Mountains. An infallible technique for distinguishing between hill and precipitation echoes in such areas is one of the items yet to be developed from this flight research.

The Malespina glacier in Alaska was found to give practically no echo at certain altitudes and ranges, appearing much as a lake. It can be concluded safely that smooth ice-covered areas cannot be relied upon to return an adequate collision echo. It is hoped that areas of this sort are of sufficient rarity that they will not constitute a serious hazard and can be treated as special cases. The question often has been asked whether snow-covered slopes would return an adequate echo. Certainly many mountains are snow-capped and it would be an unfortunate circumstance if the radar would fail to see them.

Figure 19 shows Mount Rainier on the PPI at approximately 5 miles range with a strong echo. Abundant evidence from other snow-capped peaks indicates that the chances are very good for an echo of some sort being returned.

Air-borne Radar as a Weatherproof Supplementary Navigational Aid

We have noted from the foregoing that *X*-band air-borne radar appears to "look" through fairly heavy precipitation. We know also that it looks through heavy snow and ice crystals. The service test of the radar has provided considerable evidence that St. Elmo's fire, northern lights, and severe snow static have no effect whatever upon the operation of the radar. These findings were to be expected from the characteristic of the frequency. It is comforting to know that when all other navigational facilities including very high frequency are inoperative, some navigational assurance can be obtained from the radar.

Air-borne Radar with X-Band Beacons

Much was learned during the war about the precision homing possibilities of a responder located on the ground replying to interrogations from an air-borne radar. The airline flight research has taken up where this left off and developed "beaconry" to a considerable extent.

Known, but perhaps not appreciated, were the possibilities of flying random tracks of the pilot's choosing over only two beacons located on the ground. Figure 20 shows the radar being flown between Philadelphia, Pa., and Floyd Bennett Field, New York, with the Floyd Bennett beacon lying almost dead ahead at a range of 58 miles and the Willow Grove (Philadelphia) beacon bearing 237 degrees at 22 miles. Note that the position of the aircraft is, from easy inspection of the radar "scope," 16 miles to the right of the line between the two beacons. There is no navigational device in operation today that will provide this kind of immediate and continuous position information to the pilot.

Figure 21 shows the aircraft being flown between the same two beacons, obviously intending to cross between the two, with its position 5 miles away from the centerline track between the two beacons. Again the easily digestible position information is present at all times.

Of equal significance to the track and position information provided by two beacons is the heading information which ordinarily is obtained from other instruments. Note in Figure 20 that the airplane is headed slightly to the right of the New York beacon, whereas in Figure 21 he is headed 58 degrees to the left of the New York beacon. Thus we have track, position, and heading information combined in easily digestible form in one instrument. This information has never been combined before and the present procedure without radar involves the scanning of several instruments to obtain it. It is apparent that enroute navigation with radar beacons is basically very easy and precise.

The same simplicity and reliability which makes en route navigation with radar beacons attractive, contributes mightily to the ability to navigate more precisely and hence more safely in congested areas of high traffic density. Recall, if you will, that present day navigation involves the mental digesting of information from several dials into a mental picture of position. When describing tor-

Figure 18. PPI picture with airplane flying in moderate to heavy rain shows terrain echoes through rain

tuous courses through congested areas with such an arrangement, even the experienced and skilled pilot is subject to becoming confused. This inevitably causes him to wander off the desired track, which either creates a potential collision hazard or requires such wide separations be held between airplanes that the traffic handling capacity of an area is reduced greatly.

In contrast, the radar navigation picture utilizing beacons is the simplest form of complete navigational information in existence today. With a picture of that type available to the pilot, it is practically impossible for him to become confused or build up mental pressure. There is no need for continuously double checking the indications from several instruments. The radar is inherently self-checking.

As an example of the almost fantastic precision available with even sparsely located radar beacons, flights were made every day for two weeks in July 1946, using a beacon located at Grumman on Long Island and one at Floyd Bennett airport. Idlewild airport lies between these two beacons. During the July flights, instrument let-downs were made at Idlewild, not at Floyd Bennett or Grumman, using only these two radar beacons, and the hooded pilot was able to "call" the instrument runway at Idlewild within two or three seconds in range, and to a lateral accuracy of one runway width to left or right. That this was not an isolated stunt was proved by "calling" many other locations on the terrain (such as a diving board on a lake in the Westchester area) located not closer than 10 miles from any radar beacon.

Such extreme simplicity of navigation with its self-checking quality should lend itself to instrument low approaches. Early in June of 1946, several beacon arrangements were tried near an airport and it was found possible to line up with the runway with reasonable accuracy, starting the landing approach out of a standard rate 180 degree turn, finishing the turn approximately 2 miles from the end of the runway. The precision of these approaches, however, was not quite enough to permit descending to much lower than 200 feet and in less than 1 mile visibility and still not have to make a drastic maneuver required prior to landing.

Figure 19. Mount Rainier at *A*, five miles at 60 degrees

Again, the research personnel, after many nights of failure and after trying many beacon arrangements, came up with an idea for a "magnifying glass" to improve the precision, during the last two or three miles, of the approach to the runway. Figure 22 shows the trick that was used to add this precision. It consisted of sending out one additional pulse from each beacon with a delay on each, adjusted so that the second pulses would lie very close to each other in range. Because the delayed pulses will always lie on a radial line from the center of the scope through the initial pulse, the two delayed pulses will show a greater off-course indication when such exists than will the two initial pulses, simply because they are farther out the radius.

An examination of each drawing in Figure 22 will make this clear. It is important to note the combined heading, track, and distance information inherent in this presentation.

The magnification of the angular displacement of the runway provided by the delayed pulses might appear at first to be misleading, but as they were flown day after day, it was realized that when looking from the radar picture out the window at the actual runway, the runway appeared to match the angle of the delayed pulses rather than the angle of the initial pulses. A little thought made it obvious why. The angle of the runway as seen out of the cockpit window also was exaggerated by the foreshortening effect of perspective.

This method of making low approaches to a landing runway under instrument conditions has several basic advantages, one of the most important of which is the fact that with readily available and easily moved facilities, multidirectional approaches can be made, whereas with our present system of making instrument low approaches, it is either very difficult or impossible to make a straight-in approach on more than one runway at a given airport. A good instrument approach becomes a very dangerous one whenever maneuvers have to be made underneath an overcast. Hence the need for straight-in approaches on all runways. During

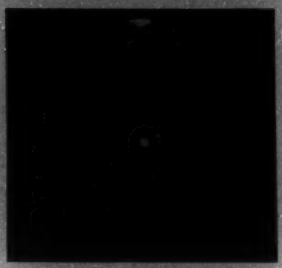

Figure 20. PPI beacon display

A—Radar beacon at Floyd Bennett Field
B—Willow Grove beacon (Philadelphia)

some of the late 1946 demonstrations of radar beacon low approaches at Denver, Colo., small portable beacons about the size of a suitcase were used. Frequently the beacons were run out to the ends of the runway in an automobile at the same time that the airplane was taxiing out to take off. Invariably by the time the airplane circled around and was ready to start an approach, the beacons would be set up, on the air, and ready to operate.

One other important feature of the radar beacon low approach method is that it is completely self-contained. It needs no cross-check device to make sure that it is functioning properly and not lying to the pilot. This cannot be said for any other device known or used today. On one evening during the July 1946 demonstrations in New York, 22 consecutive approaches were made at Grumman Field on a runway of moderate length with factory buildings on both sides. There were no other facilities available or used by which to double-check the radar operation. The approaches were made under actual conditions of a 200 foot ceiling and one-half mile visibility, at night and in rain. The average interval between the approaches was 4 minutes and 20 seconds. The pattern described by the airplane was very similar to that described by the average training airplane taking off and landing for practice in clear and unlimited weather, namely, a flat elipse with one leg on the runway.

There is, of course, at present no glide path or descent information available from the radar beacon method of low approach. Perhaps a glide path would be a convenience, but it does not appear to be a necessity largely because of the continuous distance information provided by the radar. Heretofore from our present facilities we have had only "check-

point" distance information, and of late a glide path. On such a system the glide path is quite necessary. But when we give the pilot continuous distance information, he can let down to safe altitudes at safe known distances from the runway with impunity. Actually the absence of the glide path eliminates one job that the pilot normally has to do, namely, to control the aircraft very precisely in pitch during the descent. In the case of the radar beacons, he can descend when and how he chooses, providing it is known to be safe.

Ground Speed Checks with Air-borne Radar

For the first time in the history of commercial aviation, we have in air-borne radar the means of continuously checking ground speed. For navigational purposes, this is an extremely vital piece of information. Few persons who have not had to navigate airplanes realize the vast difference in precision between navigating in the air and on land or sea. In the latter two cases, the dead-reckoning process is relatively simple and usually quite precise. But in the air, one has to cope with the unknown effect of cross, head, and tail winds. Unless very frequent position checks are available, neither the ground speed, nor the drift, and its affect on ground speed, is immediately apparent to the pilot. The result is that he may fly an hour or more at an unfavorable cruising altitude where there may be head winds; yet at some other altitude there may be more favorable winds.

With the radar, it is possible to pick out any handy target and measure the time that it takes to travel between, say two range marks on the radar "scope", and from this, immediately determining the ground speed and the drift. The process takes a little over two minutes. If not satisfied with the ground speed, the pilot may change altitude and, in the space of another two minutes, again check his ground speed. Frequently experience has indicated the possibility of picking the optimum altitude, not just the better altitude, within a space of 15 minutes, whereas with the present day facilities, the optimum altitude most likely never would have been found and the process of finding a better altitude would have taken perhaps hours.

The effect of this ability on the economy of airline operation can be very considerable. Although limited experience has been had up to the present time, the indications are that flight plans involving a 7-hour nonstop trip can be bettered by an average of 15 to 20 minutes, approximately a 5 per cent improvement in speed, which in turn shows up as a very considerable improvement in the economy of the operation.

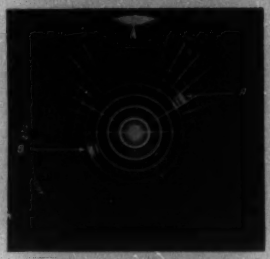

Figure 21. PPI beacon display

A—Floyd Bennett Field
B—Willow Grove beacon (Philadelphia)

A Joint Army-Navy-Airlines Procurement Program

Early in 1946, and after some of the basic advantages as well as the shortcomings of the *APS-10* radar were realized, a program was started by flight engineering personnel of American Airlines to establish operating requirements for a new transport radar. In the fall of 1946, these operating requirements had become sufficiently detailed to discuss with both the Navy and the Army. Several meetings were held from time to time and the outcome was a decision for a specification common to the civil, the military, and the naval requirements. Subsequently the Navy undertook to lead the procurement of a radar to these specifications. Considerable manufacturing talent has been called in upon occasion and at the present writing, suitable radars will be available to the commercial operators early in the spring of 1948.

The "Fail-Safe" Characteristics of Air-borne Radar

There is no one feature or characteristic of air-borne radar that can be considered more important and more likely to contribute to its universal adoption than its "fail-safe" or self-checking ability.

When reliance is put on an instrument or device to furnish information concerning the position or attitude of the aircraft, no possibility of that information being wrong can be tolerated unless the fact that the information is wrong is conveyed immediately to the pilot in easily recognizable terms.

For years our basic navigation device has been the aural radio range. The success of this device, in spite of all of its inadequacies, has been in large part due to the ability of the pilot continuously and automatically to check the fact that he is receiving the information from the correct station, and in fact is receiving the information.

The lack of success of many devices that do not have this automatic self-checking feature built in can be attributed usually to the fact. Many devices are not subject to being inherently self-checking. One of these is the standard meter indication by which we convey so much information to the pilot such as head temperatures, gyro compass heading information, and altitude. None of these indications is inherently self-checking, therefore the devices are duplicated where they are vital to the safety of flight. This provides an opportunity for the pilot to check one of the identical instruments against the other, and, when there is a discrepancy, he at least is informed that one of them is incorrect, thus will revert to some other source of information.

It is a most fortunate thing that the radar, partly because of its cathode ray type of presentation and the many interlocking circuits, is self-checking in nature, what we in the airline business like to call "closed circuit." Any failure of the radar so far experienced has resulted in either no indication on a PPI, or a completely nonunderstandable one. Many attempts have been made to "hash up" the radar information in an attempt to produce an unidentifiable lie. Only on one occasion has this been successful and this was chargeable in no way to the basic characteristics of radar.

The very fact that pulses are sent out by the radar and there is then a listening period during which time the echo is received, makes the radar basically closed-circuit and self-checking.

No greater compliment could be paid to any device upon which the pilot must rely for infallible information than to say that it is perfectly closed-circuit. It would be foolhardy to say that the radar were perfect in this regard, yet all data received to date indicates that it is.

The Effect of Air-borne Radar on the Accident Record

In order to evaluate the extent to which radar could help the airline industry achieve greater safety, it was obviously necessary to examine the accident record. Many factors came to light as a result of this examination, perhaps the most un-

Figure 22. Drawing showing radar cathode-ray display of two radar beacons with delayed pulses during turn in to runway

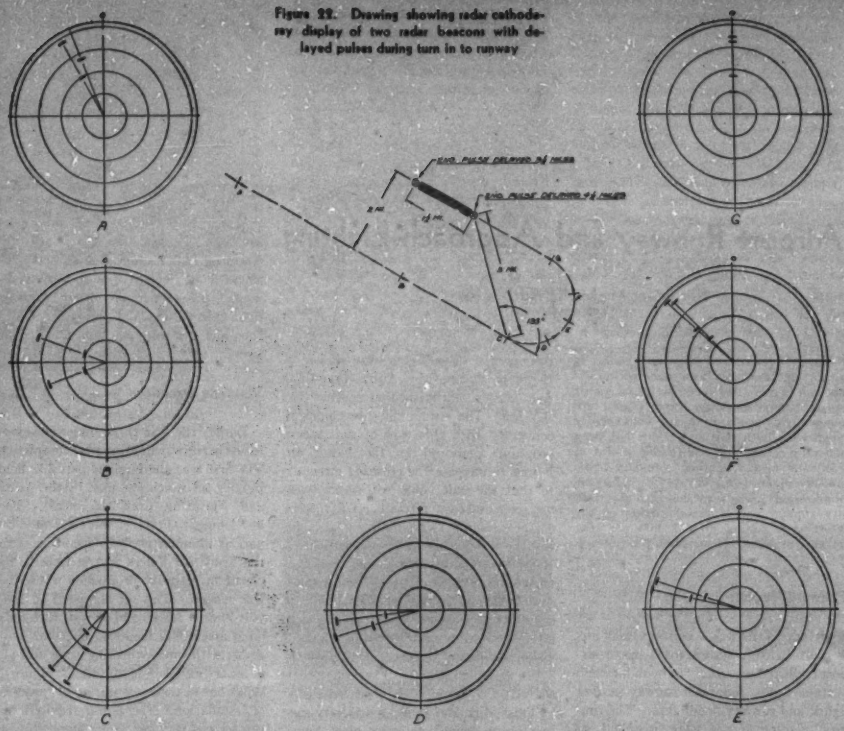

fortunate of which is that most any conclusions can be derived therefrom, depending upon the group of accidents that are studied and upon the assumptions made in the study.

In order to take the extremely conservative view, all accidents of the scheduled air carrier industry were chosen, omitting the nonscheduled and the military accidents as representing a phase of aviation in which the efforts taken to reduce the risk, and the means available to reduce risks, are not quite as great as in scheduled operations. The period taken was that from 1938 to 1945, during which it could be said safely that our navigational information remained approximately static, and during which there was no great influx of new personnel or new equipment.

Obviously out of all of the fatal accidents, many have been indeterminate in cause and many have been obviously a result of something entirely apart from inadequate navigational information. On the converse, there is a smaller group in which conjecture leaves one almost inevitably to conclude that severe turbulence or other dangerous weather was the contributory cause, although no proof is available.

Eliminating those upon which there can be any reasonable doubt and taking only those accidents in which it seems perfectly obvious that the pilot must have thought he was either in no danger of colliding with a hill or being destroyed by weather, we find that 11 out of the 31 fatal accidents during this period could have been prevented had there been an operable air-borne radar aboard. Of the 380 lives lost in these accidents, 160 could have been saved.

These conclusions are believed to be extremely conservative and it is believed that when the foreign operators, the nonscheduled operators, and the military transport operators are taken into account, the percentage of lives which probably could have been saved by air-borne radar will go from approximately 42 per cent in the foregoing study to approximately 70 per cent.

In conclusion, the round figure which is believed to be safe to assume in the event the accident record pattern remains about the same as it has in the past, is a 50 per cent improvement in respect of lives lost in air transportation if air-borne radar is installed and operating.

No Discussion

Airport Runway and Approach Lighting

G. M. KEVERN
ASSOCIATE AIEE

Synopsis: Rapid and extensive changes in airport lighting have been made within the last ten years. The necessity for providing elevated high intensity runway and approach lights as an aid during low visibility conditions, both day and night, has been generally recognized. With the advent of adequate runway lighting, boundary lights and floodlights (for runways) have become unnecessary. The provision of high intensity runway and approach lights of the latest type results in a 10,000 per cent increase in power consumption per runway.

Prewar Practice

PRIOR to the war a conventional airport lighting system for a major airport consisted essentially of boundary and obstacle lights, semiflush runway marker lights, and runway floodlights. The runway marker lights were installed at approximately 200-foot intervals along the edge of the runway pavement. They were placed in under ground cast iron bases, and the top of the light protruded not more than three inches above the pavement. These lights were similar to the type covered by Army-Navy-Civil Aeronautics Administration specification *AN-L-9*. The outstanding development connected with this type of unit was a program sponsored by the Army Air Forces to increase the crushing strength, so that the unit could withstand being run over by heavy aircraft. The success of the program is demonstrated by the fact the *AN-L-9* assemblies will withstand 100,000 pounds without damage, whereas most earlier types failed at 20,000 pounds. A comparison of the semiflush *AN-L-9* assembly with the elevated type *D-1* high intensity assembly is afforded by Figure 1 which is a view of the experimental installation at Arcata, Calif. It is evident that the *AN-L-9* assembly is obscured easily by grass, dirt, and snow, and is very susceptible to damage by snow plows, inasmuch as it is not high enough to be visible to snow plow operators.

Figure 1. Runway marker light installation, showing the high intensity type *D-1*, and the semiflush type *AN-L-9* lamp assemblies

The prewar semiflush runway marker lights almost invariably were connected in 6.6-ampere series circuits, with an individual circuit and moving-coil constant-current regulator for each runway. A 3-kw 230- or 2,300-volt regulator was the most common size. The control system was simple, consisting of a magnetic switch for each regulator, remotely controlled from the airport control tower. Prewar requirements were about 2 kw for a 6,000-foot runway, as either a 325-lumen series lamp or a 40-watt 115-volt lamp ordinarily was used. The 40-watt lamp was utilized wherever it was desired to use a series multiple transformer to isolate the lamp socket from the high-voltage series line. The use of a series circuit in lieu of a multiple distribution system results in an appreciable saving of copper, and elimination of serious voltage drop problems.

Except for a certain amount of developmental work carried on by the Army Air Forces and other agencies, high intensity approach lights were not used prior to the war. Several installations of neon approach lights were in use at various airports, but these were of value only during light fog or haze, and as an aid in distinguishing a runway from other long parallel rows of light.

Wartime Practices

During the war three major developments in runway lighting were completed. The first was the familiar portable field lighting set which was used by the Army and Navy all over the world. The development of this set was completed by various manufacturers co-operating with the Army Air Forces just in time to be placed in quantity production when the war started. This set consisted of 105-volt 10-watt (clear) and 25-watt (colored) lamp assemblies mounted on cones, together with interconnecting cable and all necessary auxiliary equipment. Figure 2 shows one of these sets during the process of installation. The power required by this set was very low, being supplied by a 115-volt 500-watt d-c power plant which was furnished with the set. A loop distribution system was utilized, using 2-conductor number 16 300-volt cable, with molded rubber plugs for all connections. The cable was laid on top of the ground, or buried a few inches. Extremely good results were obtained, as moisture caused less trouble than had been expected. The most serious trouble was caused by termites, which ate everything except the copper in the asphalt impregnated cables which were used when rubber was scarce.

The second major item to be developed was the elevated or "snow" runway marker lights. During the first part of the war, rapid expansion of flight operations began to be hindered by the fact that

Paper 47-235, recommended by the AIEE air transportation committee and approved by the AIEE technical program committee for presentation at the AIEE Middle Eastern District meeting, Dayton, Ohio, September 23-25, 1947. Manuscript submitted July 3, 1947; made available for printing August 8, 1947.

G. M. KEVERN is chief of the lighting unit, equipment laboratory, engineering division, Air Materiel Command, Wright Field, Dayton, Ohio.

Figure 2. Installation of a type *AN-S-2* portable field lighting set

semiflush marker lights were obscured easily by snow, dirt, and grass, and frequently were sheared off by snow plows. As the cone mounted portable lights were not subject to these defects, the logical step was to develop an elevated fixture which would be substituted for the semiflush unit. Figure 3 illustrates a fixture in accordance with Army-Navy-Civil Aeronautics Administration specification *AN-L-26*, which consists of a base plate for mounting on the same cast iron base as was used by the semiflush assemblies, an easily broken fiber mounting column, a cone for daytime marking, and a fixture utilizing a 40-watt 115-volt lamp and specially developed lenses. This assembly requires no more power than the semiflush units, but isolating transformers must be used. This fixture rises above the snow and, therefore, can be avoided by snow plow operators, produces a threefold improvement in useful light output, and was found to present no hazard to aircraft.

The third and most important development was the high intensity incandescent lamp assembly which is utilized for both runway and approach marking. This assembly, now known as the Army Air Forces type *D-1*, was the culmination of approximately 10 years of development by the manufacturers and the military services. This fixture, which is also mounted on standard *AN-L-9* bases, stands approximately 26 inches above runway pavement, and utilizes a specially developed 200-watt 6.6-ampere series lamp. The unit emits front and rear beams of approximately 40,000 candlepower (8,000 candlepower red) one degree wide and two degrees high, measured at a candlepower value equal to 50 per cent of the peak candlepower. Each unit is mounted upon a notched aluminum tube, which easily fractures when struck by an airplane or other vehicle.

Power supply and control methods for the type *D-1* installations were similar to those previously used, except that it was absolutely necessary to provide reduced brightness taps, to prevent blinding on clear dark nights. Resonant circuit constant current regulators having brightness taps of 100, 30, 10, 3, and 1 per cent were developed accordingly and used to the exclusion of moving coil regulators.[1] An average installation, consisting of a 6,000-foot runway and 2,400 feet of approach lights on one end, required approximately 20 kw, which was supplied by three 7.5-kw 2,300-volt 6.6/5.5/4.8/4.2/3.8-ampere regulators. The lamp assemblies were connected directly into the series circuit on overseas installations, while isolating transformers normally were used in domestic installations. One of the regulators normally was connected to runway selector relays to provide power for the conventional lighting circuits on other runways.

Figure 3. Elevated or "snow" runway marker light, type *AN-L-26*

Postwar Developments

The type *D-1* lamp assemblies, when installed along the edges of the runway, and in the standard 2,400-foot parallel row approach lighting system, gave excellent service both overseas and in the United States. The widespread use of this system resulted in substantial savings of life and property by making landing possible under weather conditions which would have been considered unflyable had the system not been available. As might have been expected, however, occasional unsuccessful attempts were made to utilize the system during visibility conditions worse than those for which the system was designed (one-quarter mile at night and one-half mile during daylight). During these lower visibilities, it was found that the electronic approach aids could not be flown with sufficient accuracy to insure that the airplane would come within the visual range of the extremely narrow beams of light emitted by the type *D-1* assemblies.[2] Development of wide beam units, therefore, was initiated by one manufacturer under a development contract from the Army Air Forces. A study revealed that sufficiently wide beams could be obtained for runway lighting without exceeding 200 watts, so no new power supply or control problems were introduced.

On the contrary, the same study revealed that the approach light wattage would have to be increased from 200 to 5,000, thus necessitating radical departures from previous power supply systems. The new system was installed by the Army Air Forces at the Landing Aids Experiment Station, Arcata, Calif., and proved quite successful by flight tests during heavy fogs. This system, therefore, is considered worth describing in detail.

The approach light, which is illustrated in Figure 4, consists of a 5-kw 115-volt 75-hour projection type lamp, a spherical reflector, an inner glass vertical condensing lens, an outer red plastic horizontal condensing lens, and a ventilating motor. It emits a beam having a peak candlepower of 25,000 (red), a width of 45 degrees, and a height of 35 degrees. Figures 5 and 6 are views of the experimental installation at Arcata showing how the approach lights were raised up to

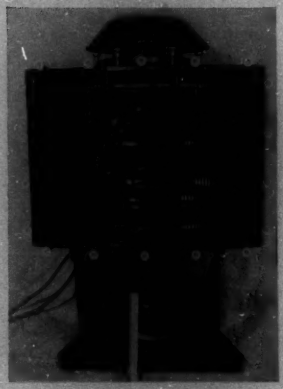

Figure 4. Approach light, 5,000 watts, 115 volts

runway level, above the low ground in the approach zone.

Both optical characteristics and location of these lamp assemblies were specifically designed to overcome the defects of previous systems.[2] Flight tests, although not yet complete, prove that the system is a substantial improvement over previous systems. Figure 7 is an aerial view, taken at dusk, which shows the complete runway and approach lighting system at Arcata.

The large amount of power required (180 kw) made the use of series circuits impracticable. Similarly, the distances involved, and the necessity for supplying exactly rated voltage at the lamp terminals, prohibited the use of a low voltage distribution system. A 3-phase 4-wire 2,400/4,160-volt distribution system, therefore, was selected. Protection was obtained by the use of a separate fuse for each line, on each side of the approach path, in lieu of a circuit breaker which would de-energize the entire system when trouble occurred. This system provides the following advantages:

1. Uses standard commercial equipment.

2. Tapped transformer for each light permits adjustment of the lamp voltage to within ± $1^1/_4$ per cent of rated voltage.

3. Each transformer has a secondary circuit breaker and a primary fuse. Trouble in any one light or transformer, is therefore, unlikely to have any effect upon the remainder of the system. Furthermore, the circuit breaker permits servicing of a lamp assembly without de-energizing the entire system.

4. Transformers are connected line to neutral, with every third transformer being connected to the same phase.

5. A maximum of reliability, therefore, is provided, as trouble in any one line will de-energize only every third light on one side. The lighting system will still be usable under all except the very worst visibility conditions.

Figure 7. View of the approach and runway lighting system, taken at dusk during a slight haze

Figure 6. Approach light and transformer installation

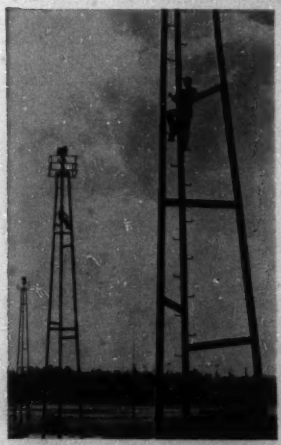

Figure 5. Approach light towers at the landing aids experiment station, Arcata, Calif.

Some method of brightness control for every high intensity approach lighting system is mandatory. Brightnesses of 100, 30, 10, 3, and 1 per cent eventually will be obtained on this system by means of a motor driven induction regulator. This regulator will be controlled from the airport control tower by the same type of 5-point selector switch as is now used to control resonant circuit regulators on conventional series circuits. In addition, the regulator automatically will compensate for variations in supply voltage. This regulator will be similar to standard commercial feeder voltage regulators, except that it will be wound for 1,380/-2,400-volt 4-wire primary, 75 per cent raise and lower.

Table I. Rheostat Settings

Brightness, Per Cent	Lamp Voltage	Generator Voltage, Line to Neutral
100	115	2,400
30	75	1,570
10	54	1,130
3	39	810
1	29	600

Unfortunately, considerable delay was encountered in delivery of the regulator, so brightness control now is being obtained by manually operated field rheostats on the 600-kw 2,400/4,160-volt Diesel generator which supplies power for the system. The settings required are tabulated in Table I.

Summary

It is evident that the art of airport lighting is in a state of rapid flux. Extensive changes have been made in the last few years, and many more changes may be expected within the next few years. Some of the most notable of the improvements already made can be summarized as follows:

1. The abandonment of boundary lights and runway floodlights in favor of adequate runway marker lights.

2. Recognition of the fact that high candlepowers are needed during low visibility conditions and that brightness levels as

low as one per cent are needed during clear dark nights.

3. Development of the necessary brightness control equipment.

4. Elevation of runway marker lights above grass, dirt, and snow.

5. Increase in runway lighting power requirements from 2 to 16 kw, for a 6,000-foot runway.

6. Increase in approach lighting requirements per approach zone from 0 or 1 kw for neon lights to 200 kw.

7. Recognition of the fact that low visibility landings cannot be made safely by electronic aids alone, but that high intensity approach and runway lights must be used to provide last minute visual contact.

In conclusion, it may be safely predicted that civilian airports gradually will be forced to recognize and make use of the foregoing improvements which are already in effect at most Army and Navy fields. In particular the following changes in civilian practice are expected:

1. Widespread use of elevated runway marker lights, as follows:

(a). Cone mounted 30- and 45-watt 6.6-ampere units as parts of series lighting sets for small airports.

(b). Conduit or cone supported 45-watt 6.6-ampere "snow" lights, mounted on conventional cast-iron bases, for noninstrument runways on commercial fields.

(c). High intensity 200-watt 6.6-ampere units mounted on grooved aluminum tubes fastened to conventional cast-iron bases, for all runways on which instrument landings will be made.

2. Use of series circuits, with an individual 6.6/6.6-ampere isolating transformer to feed each of the elevated runway lights.

3. Use of high intensity incandescent approach lighting systems in all approach zones in which instrument approaches will be made.

References

1. Resonant-Circuit Constant-Current Regulators, G. M. Kevern. AIEE Transactions, volume 64, 1945, pages 807–10.

2. Approach and Runway Lighting for Adverse Weather Conditions, G. M. Kevern. *Illuminating Engineering* (New York, N. Y.), June 1946, pages 455–73.

No Discussion

Control and Power Systems for Aircraft Window Deicing

C. L. MERSHON
ASSOCIATE AIEE

THE FORMATION of ice on the windshield of an airplane usually results in complete loss of vision within a very few seconds after icing conditions have been encountered. Although many methods for preventing the formation of ice have been used, nearly all have serious disadvantages. Numbers of airplanes, commercial and military, are equipped with provisions for deicing windows, which will serve for average flight conditions, but which are generally inadequate for severe icing conditions. In addition to the problem of window icing, the condition caused by the formation of fog or frost on the inboard side of the windows presents a hazard which is much more than an aggravating nuisance and can become as dangerous as icing.

A new type of heater formed by an electrically conductive film on the surface of the glass now promises to present an ideal solution to the problem of preventing icing and fogging of aircraft windows. The effectiveness of this new type of window depends to a great extent on the electric system used to control the operation of the heater. It is the purpose of this paper to consider the factors involved in the design of an effective electric system for this new method of window heating.

Methods of Heating Aircraft Windows

There are various means used to prevent icing and fogging of aircraft windows. The following are among those methods:

1. Hot air directed on the window or passed between a double section window composed of two plates with an air gap between.
2. Resistance wires imbedded in the plastic of a laminated vinyl-glass window.
3. Radiant heat (infrared) directed on the window.
4. Freezing-point depressants, such as alcohol, applied to the outside surface of the window.
5. Windshield wiper used in conjunction with a freezing-point depressant.

One of the most common means of preventing icing is hot air. A fairly successful system used on numerous commercial and military airplanes consists of two panels separated by an air space of approximately one-eighth inch. Hot air from combustion or exhaust heaters is passed through the air space between the two panels. The outer panel usually consists of a single plate of tempered glass. To improve strength and to provide additional insulation to reduce the quantity of heat dissipated into the cabin, the inner panel is laminated of one plate of glass and one sheet of vinyl plastic or one sheet of vinyl sandwiched between two plates of glass. The main disadvantage is the quantity of high temperature air which must pass through the air space in order to transmit enough heat to the outside surface of the glass to prevent icing under severe temperature conditions. There are the additional disadvantages of pilot discomfort from the radiated heat, and possible damage to the glass from stresses due to unequal heating.

Imbedded resistance wires in the window would seem to present an ideal solution to the window-heating problem. However, it is impracticable to imbed the wires in the glass, making it necessary for these heating elements to be located in the vinyl plastic of a laminated glass-vinyl panel. The deicing ability of such construction is limited by local overheating of the vinyl around the heater wires. Even though local heating is held within safe limits, some optical distortion results from the concentration of heat around the wires. In addition, there is the possibility of eye fatigue due to the closely spaced fine wires in the windshield.

In general, the other methods of window heating mentioned are more objectionable than the methods just described.

Figure 1. Two-position on–off window heating control circuit using a Wheatstone bridge and polarized relay

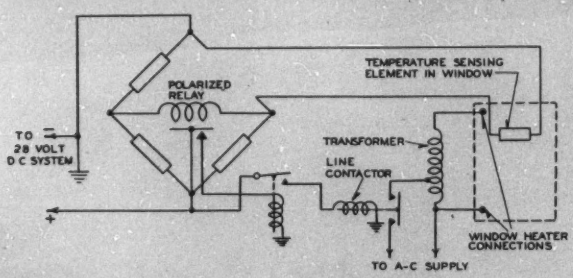

Paper 47-225, recommended by the AIEE air transportation committee and approved by the AIEE technical program committee for presentation at the AIEE Middle Eastern District meeting, Dayton, Ohio, September 23–25, 1947. Manuscript submitted July 9, 1947; made available for printing August 7, 1947.

C. L. MERSHON is design engineer, aviation engineering department, Westinghouse Electric Corporation, Lima, Ohio.

The author wishes to acknowledge the assistance of the Pittsburgh Plate Glass Company in the preparation of this paper.

Figure 2. On-off control box with cover removed showing polarized relay, bridge resistor, and control relay

Mounting feet are attached to the box by antishock mounts

Further discussions of these methods therefore will be omitted.

Windows Which Incorporate an Electrically Conductive Coating

Glass manufacturers have developed a transparent electrically conductive coating which can be applied to the surface of the glass to provide a heating element which promises to be superior to any method of heating windows now generally known.[1] A microscopically thin film of this material applied to the surface of the glass and processed at relatively high temperatures provides a durable electric conductor with a resistance of approximately 125 ohms per square area as measured across opposite edges of the glass. Electric power can be applied to the coated surface by means of bus bars which are formed by painting strips of silver paste lengthwise along the edges of the coating to form silver conductors. These silver conductors also are processed at relatively high temperatures. Fairly uniform heating of the entire area of the glass results from the dissipation of electric energy when current is passed through the coating. Heating is accomplished without distorting visibility and with small loss in direct light transmission. Reflectance is about ten per cent as compared to eight per cent for ordinary plate glass. An iridescent appearance occurs from reflected light. Reflections are minimized and light transmission is improved by laminating the coated glass with another plate of ordinary glass with an intermediate layer of vinyl plastic.

For a number of years laminated glass-vinyl window panels have been in general use on aircraft.[2,3] Impact-resistant panels of this type commonly are constructed of a layer of vinyl plastic one-eighth to one-fourth inch thick sandwiched between two tempered glass plates one-eighth to one-fourth inch thick. Such construction presents high strength against the impact of airborne objects such as birds or blunt heavy objects. Tests indicate that the impact strength drops off considerably when the temperature of the vinyl layer is below 70 degrees Fahrenheit and above 130 degrees Fahrenheit. However, the range of temperature at which maximum impact strength occurs varies with different types of vinyl plastics.

The laminated glass-vinyl window presents the ideal construction for the glass on which the conductive coating is applied. By applying the conductive film to the inner surface of the outside glass plate, mechanical protection and electrical insulation is provided for the coating. For optimum transfer of heat for deicing, it is desirable to have the coating on the outer surface of the outside plate. However, an exposed electric coating is not advisable from the standpoint of safety and durability. By locating the coating on the inner surface next to the vinyl layer, not only is the heat transmitted to the inside surface of the panel more satisfactorily for defogging, but the vinyl layer can be maintained within the temperature range at which maximum impact strength is realized.

Many military airplanes require bullet-resistant window panels. These panels are laminated with multiple layers of glass plate and vinyl plastic to thicknesses from one to five inches. Most of the vinyl layers are less than 1/16 inch thick. The temperature of the vinyl layers has little effect on the bullet-resistant characteristics of these panels. The conductive film for deicing is applied in the same manner as for the bird-resistant panels. Under most conditions of operation, the temperature gradient is such that for the thicker bullet-resistant panels little heat will reach the inner surface of the inside plate. For this reason, some panels are being equipped with a defogging heater coated on the inner surface of the glass plate on the cabin side of the panel. The problem of controlling such a heater is simple, since the power requirement is small and fairly constant. A manual on-off switch operated when desired by the pilot appears to be sufficient. For some applications, it may be necessary to provide a simple limit control to prevent the temperature from exceeding safe limits.

At the present time, the method of heating windows by use of an electrically conductive coating is relatively new. With present processes and techniques, it is difficult, if not impossible, to produce a uniform conducting coating on the surface of irregular-shaped windows. Most airplane windows are not simple rectangles, but involve trapezoidal areas and shapes with corners rounded to various radii. Theoretical considerations of the func-

Figure 3. Three-position control circuit which provides high power, low power, and off positions

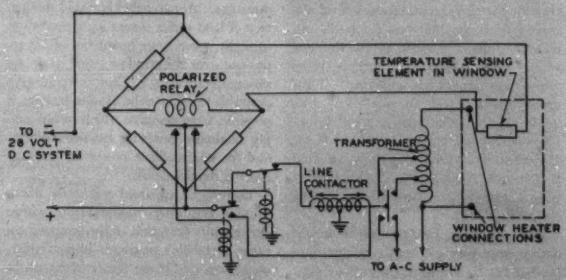

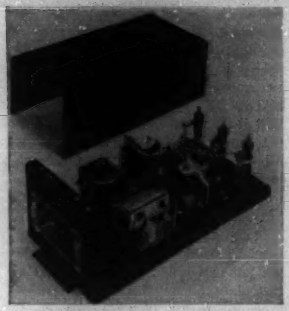

Figure 4. Three-position control box with cover removed showing bridge resistors, polarized relay, control relays, and transfer relay

tions of the conductive coating on irregular-shaped windows indicate that it is practically impossible to obtain uniform heating.[1] Thus, it can be seen that there is some possibility of overheating certain areas, even though the average temperature is relatively low. This condition is not considered as too serious. However, a more serious condition, which has been reduced in severity but has not been eliminated entirely, is the localized heating which occurs at the ends of the bus bars on curved end plates. Such a condition may result in bubbles in the plastic and fracture of the glass. The effect of this type of hot spot is minimized by locating the bus as near the edge of the glass as possible and by tapering the end of the bus.[1] Disregarding power and control effects, the possibility of damaging the window from localized heating depends on the pattern and location in the airplane as well as the surrounding air temperature and air movements across the surface of the panel. Laboratory tests indicate that the possibility of damaging the glass is reduced when air is flowing over the surface of the panel, even though the average temperature of the glass surface is the same for both conditions.[1] Thus, it would appear that one of the most dangerous conditions occurs when the airplane is standing on the ground under still air conditions. To avoid this condition, power could be applied only when the airplane is in flight. However, it is often absolutely essential that heat be applied to the windows before taking off to remove ice or frost to provide clear vision.

For certain applications where weight and temperature gradient considerations permit, the thickness of the outside plate of the window panel may be increased to 3/16 inch or greater. The thicker plate permits the glass to be tempered to a higher degree. The increased temper combined with the thicker glass results in greater resistance to fracture, and in some cases, almost entirely eliminates the danger of serious damage from stresses caused by localized overheating.

Power and Control Limitations

The power required for preventing icing varies considerably, depending upon the type of operations and the geographical location of such operations. Also, the window panel configuration, location, and angle with respect to the air stream have much bearing on the power requirement. Various power requirements ranging from 500 to 3,100 Btu per hour per square foot (147 to 910 watts per square foot) have been specified by aircraft builders and operators.

The maximum power is limited somewhat since the temperature gradient from the heater coating to the outside surface of the glass plate increases as the energy conducted through the plate increases, if all other conditions remain the same. In order to prevent excessive temperature gradients at high power inputs, the glass on which the conductive coating is located may be as thin as 7/64 inch. However, thicker glass is preferred when practicable to minimize waviness and provide higher strength.

Although there must be a large quantity of power available to combat extreme icing conditions, average operating conditions for most aircraft require much less than maximum power. Tests have indicated that hot spot conditions are more serious when energy is being applied to the windows at a high rate, such as 2,500 Btu per hour per square foot, than at a lower rate, when ambient temperature and air conditions are such that the heat is not dissipated rapidly from the windows, even though the energy is applied for a shorter duration. Apparently the rapid dissipation of heat under severe icing conditions in flight, when large quantities of air are passing over the window panel, prevents serious overheating. Thus, it would seem desirable to operate the window heaters, if possible, from a source which would supply maximum power for severe conditions and an intermediate power for average heating requirements.

There is no apparent reason for maintaining the vinyl temperature within closer limits than that of the temperature range over which maximum impact resistance is realized if the temperature gradient is such that the outside face of the panel remains above freezing temperature. Thus, in many cases it is only necessary for the control to hold the vinyl within a range of 70 to 130 degrees Fahrenheit. The range of temperature variation may be even greater for bullet-resistant panels since the temperature of the vinyl is not critical. However, it is desirable to hold the vinyl temperature as low as possible since higher temperatures tend to aggravate any localized overheating conditions.

Design Considerations for Temperature Control

The first consideration in the design of a temperature control is for reliability and safe operation of the window heater. The ideal control is one which will maintain the vinyl temperature within the range at which maximum impact strength occurs, and at the same time, prevent the application of high voltage to the window heater under conditions when a high rate of power input may result in damage to the window. A control that would sense all combinations of conditions would be too complicated to be practical. A simple approach to the problem is an on-off control, as shown in Figure 1, provided by a Wheatstone bridge and a polarized relay. Such a circuit will provide optimum reliability because it can be constructed with a minimum number of parts which are rugged and reliable. The operation of the on-off control is simple. The bridge is adjusted so as to balance at the desired window temperature. At all temperatures below the desired point, the bridge becomes unbalanced as a result of the change in resistance of the window temperature sensing element. The unbalance voltage output of the bridge actuates the polarized relay which energizes the control relay coil. The control relay causes power to be applied to the window by actuating the line contactor. When

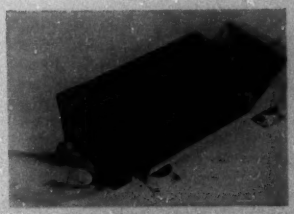

Figure 5. Control box shown in Figure 4 being removed from shock mounted rack

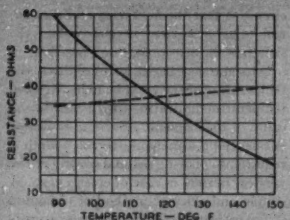

Figure 6. Curves indicating relative sensitivity of a nickel alloy wire temperature sensing element as compared with a metallic oxide element

Dashed line—Nickel alloy wire element
Solid line—Metallic oxide element

the temperature again approaches the desired value, the polarized relay is de-energized as the bridge becomes balanced, causing the power to be removed from the window. In this way, either maximum power is applied or power is disconnected entirely. The length of the on and off cycles is determined by the watts dissipated by the window. Although the on–off control provides a certain degree of satisfactory operation for many types of windows, it appears that for some panels, it is not desirable to apply power at a high rate for all conditions of operations. For this reason, a system with an intermediate power position seems to merit consideration. Such a control, as shown in Figure 3, provides an intermediate power position by using a 3-position polarized relay. Cycling under mild conditions occurs between the intermediate power position and the off position. Full power is applied to the windows only under severe icing conditions and when cold windows are initially energized. For mild conditions, when power is first applied, high voltage is applied for a relatively short time, but after once being energized, the sequence of cycling must pass through the intermediate power position so that the window is not "shocked" with high voltage from the off position. The 3-position scheme is favored for some applications at this time since it provides a more flexible control which can be easily adapted to a wide variety of systems. It is possible that additional experience with actual flight conditions will change the present picture entirely. If it is found that a 2-position control is adequate in applications where 3-position controls have been installed, the intermediate position of the control easily can be disconnected, thus providing a simple on–off control.

Figure 4 illustrates a 3-position control, complete with transfer facilities for shifting from the main to the alternate equipment, which is being used for commercial and military airplane window heating. The unit is designed to plug into a standard *JAN-C-172* shock-mounted base.

The necessity for applying heat to the windshield while the airplane is standing on the ground, when ice has formed obstructing the vision, has been discussed previously. If future tests and operating experience indicate that under certain conditions it may be unsafe to apply full voltage when the system is energized initially, it may be necessary to provide a timing device which will allow only an intermediate voltage to be applied to the windows for a period of time considered as safe. Such a device can be connected easily into the 3-position control circuit and could be incorporated in the operator's switch. In some cases, a switch operated by the landing gear to disconnect the high-power position of the control when the landing gear is down possibly would provide safe operation.

Window Temperature Sensing Elements

The temperature sensing element must sense the temperature of the vinyl as well as the temperature of the outside surface of the window panel. Since it is essential that the vinyl be held within a certain temperature range to prevent damage to the panel from overheating and to provide maximum strength for impact-resistant windows, the obvious location is in the vinyl plastic next to the heater film. In this location with 0.020 to 0.060 inch of vinyl separating the sensing element and the conductive coating, the element accurately senses the temperature of the vinyl and at the same time is near enough to the conductive film to provide rapid response to any tendency for localized overheating in the vicinity of the element.

Some factors that must be considered when selecting a temperature sensing element are sensitivity, reliability, size, transparency, and adaptability to simple control schemes. Four types of elements have been considered for temperature sensing

1. Thermocouple.
2. Thermostat.
3. Metallic oxide element.[5]
4. Wire element.

Thermocouples are eliminated immediately as satisfactory sensing elements because of the complex control which would be required. Thermostats which are rugged and reliable are not available in sizes small enough to be imbedded in the plastic of the window. Metallic oxide elements present the ideal units from the standpoint of sensitivity and adaptability. These elements are used in the form of disks ranging from one-eighth to three-fourths inch in diameter. Minimum thickness is about 0.050 inch. The faces of each disk are silvered presenting a convenient means for attaching leads. The main advantage is the high negative temperature coefficient of resistance. Tests have indicated that metallic oxide elements have excellent stability over long periods of time.[5] The main disadvantage results from the fact that during manufacture it is extremely difficult to hold the specific resistance within close limits. There may be as much as 20 per cent difference in resistance between units. Temperature sensing elements formed from fine wire of nickel or other metals or alloys which have high positive temperature coefficient of resistance are the most versatile. However, such elements are less sensitive than the metallic oxide elements and are therefore less desirable in many cases. Wire elements must be used from necessity in most bullet-resistant windows where the vinyl thickness is 0.060 inch or less. A satisfactory method of manufacturing such wire elements has been developed in which the fine wire is embedded in a small square of vinyl plastic. This unit after being laminated into a window panel presents little obstruction to vision.

Selection of a Power Supply

The size and configuration of most aircraft windows make the use of voltages of 300 and higher necessary in order to dissipate sufficient energy for satisfactory

Figure 7. Wire wound and metallic oxide temperature elements embedded in the vinyl layer of a laminated glass vinyl window

Figure 8. An 11-kva 3-phase 120/208-volt 400-to-800-cycle 4,000-to-8,000-rmp engine-driven aircraft alternator designed specifically for window heating service

window heating under all conditions. Logical sources of supply for such voltages are engine-driven alternators or inverters. In many cases of both new and old airplane designs, where the installation of the new window heating system is being considered, 120-volt 400-cycle inverters are available. In such cases, when the power capacity is adequate, the addition of transformers provides sufficiently high voltages for the window heaters. Generally, the most efficient operation can be obtained from engine-driven alternators. This is especially significant where a number of windows are to be heated, requiring large amounts of power. High voltage d-c machines are not favored because of difficulties encountered with commutation. In addition, by the use of transformers, alternating current provides a much more flexible system.

Aircraft engine-driven alternators can be provided with the high voltage output required for the window heaters. However, standard voltage machines of 120 volts or 208 volts output used in conjunction with transformers are preferred. Although, in some cases, the use of a transformer can be eliminated when using a high voltage machine, the hazard introduced by running high voltage leads from engine nacelles and the problem of providing high voltage switching and protective devices are objectionable.

Special Considerations

Because the function of the window heating system is of such a vital nature, it appears advisable to provide additional equipment for stand-by service in case of failure of the power system. Full advantage of the excess power capacity provided by stand-by equipment can be utilized for providing power to galleys, coffee makers, and other electric equipment which is not essential for the safe operation of the airplane. A complete system, including transfer facilities, is shown in Figure 10. Only one control unit is provided since the control components are such that there is little possibility of any failure during flight. The control panel, being of the plug-in type, may be replaced easily within a few seconds if satisfactory operation is in doubt. The transfer from one power system to the other is accomplished by a transfer relay within the control panel and transfer contactors, all actuated by the pilot's or operator's switch. The 3-position control in Figure 10 changes the operating point of the regulator to provide high and intermediate voltage positions. The control removes power from the system by opening the alternator field circuit.

A ground fault protection system is provided for the window heating system, as shown in Figure 11, to give complete protection against ground faults within the alternator or grounded cables from the engine nacelle to the contactors in the fuselage. The alternator neutral lead is passed through a ring-type current transformer at the ground point, and the 3-phase lines are passed through another ring-type current transformer at the contactor in the fuselage. The secondary windings of the two current transformers are connected in series and the operating coil of an a-c relay is connected across the transformer secondary loop circuit. Under normal conditions the balanced 3-phase load on the alternator does not induce any voltage in the secondary windings of the current transformer and therefore has no effect on the ground protection relays. Single-phase loads applied to the alternator result in equal voltages being induced in the secondaries of the current transformers, but these voltages are in series around the current transformer secondary loop, and therefore, the current in the two transformer secondary windings oppose each other and result in zero current. Any slight voltage which exists across the ground protection relay terminals, caused by unbalance in the resistance of the wiring, is far below the operating voltage of the relay. Yet, if a phase-to-ground fault occurs anywhere between the alternator neutral and the location of the line current transformer, it will cause the ground protection relay to trip as soon as the fault current exceeds the trip setting of the relays. A self-locking relay provides trip free operation by preventing reset until its coil is energized by throwing the operator's switch to the "off" or "reset" position. This relay sets up the circuit so that the field relay and the control relay coils are energized when the switch is thrown to the "on" position.

On some systems, it is desired that the temperature of the vinyl be indicated on a temperature indicating instrument in the cabin of the airplane. Such an indicator is essential if a manual override switch is required to provide manual control of the window heaters in case of emergency. A simple and efficient method of obtaining visual indication of window temperature is to connect a small milliammeter, calibrated in degrees of temperature, at the same points on the bridge circuit as the polarized relay in order to read bridge output current. With such a scheme, a switching arrangement disconnects the polarized relay and at the same time shifts the bridge balance in order to obtain zero bridge output current at the lowest reading on the meter dial. The indication must be only momentary since the control is inoperative when the polarized relay is disconnected.

Conclusions

Although the electrically conductive coating applied to the surface of the glass of an airplane window promises to be much more desirable than any previous means of window heating, difficulties sometimes are encountered under certain combinations of conditions, which possibly can cause damage to the window panel due to hot spots and resulting unequal stresses unless proper control is provided.

Although a simple on–off control is satisfactory for some types of windows, a 3-position temperature control scheme appears to minimize the possibility of damaging the windows by applying energy to the window heaters at a comparatively low rate under average con-

Figure 9. An 8-kva single-phase 120-volt 400-to-800-cycle 4,000-to-8,000-rpm engine-driven aircraft alternator which is being used as a power supply for window heating, radar, and radio applications

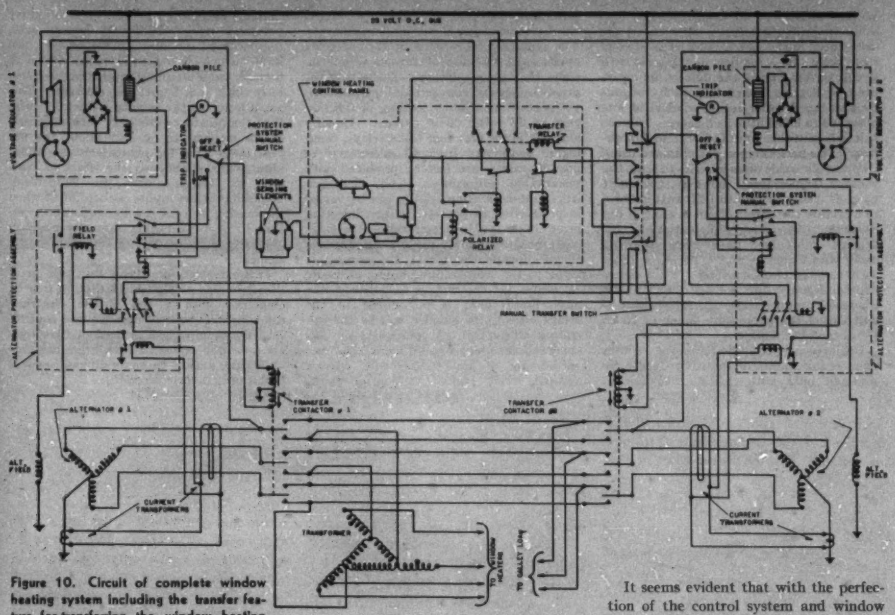

Figure 10. Circuit of complete window heating system including the transfer feature for transferring the window heating load from one alternator to the other

Provisions for connecting the idle stand-by equipment to nonessential loads are shown

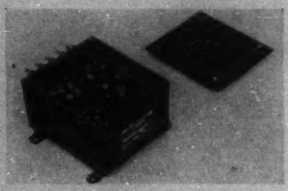

Figure 11. Ground fault protection control box with cover removed

Mounted within this box are the alternator field relay, a-c control relay, and two d-c control relays

ditions. Application of maximum power is limited to extreme temperature conditions and when power is first applied to cold windows. Operating experience may indicate that a simple timing device which can be incorporated in the starting switch is required to prevent the application of maximum power when the windows are cold.

Since the use of the electrically conductive coating for aircraft window heating is relatively new, the scope of laboratory and flight tests has been limited. At present, installations are being made on both commercial and military airplanes. Only after considerable operating experience has been accumulated on these installations, will sufficient data be available to determine the most effective method for controlling the window heaters.

It seems evident that with the perfection of the control system and window manufacturing techniques, which will come with time and operating experience, this type of window heating will provide a safe, efficient, and reliable method far superior to any previous system of heating aircraft windows.

References

1. Technical Glass Bulletin 15, Pittsburgh Plate Glass Company, Pittsburgh, Pa., July 1946.

2. New Windshield Developments, **A. L. Morse.** *Transactions*, Society of Automotive Engineers, New York, N. Y., 1943, pages 289–93.

3. An Aircraft Double Wind-Shield—Its Development and Use, **R. L. McBrien.** *Transactions*, Society of Automotive Engineers, New York, N. Y., 1943, pages 350–5.

4. Electrical Anti-Icing of Aircraft Windshields, **J. D. McCrumm.** AIEE Transactions, volume 65, 1946, December section, pages 786–91.

5. Properties and Uses of Thermistors—Thermally Sensitive Resistors, **J. A. Becker, C. B. Green, G. L. Pearson.** AIEE Transactions, volume 65, 1946, November section, pages 711–25.

Discussion

F. A. Glassow (Barber-Colman Company, Rockford, Ill.): The recommended system combines reliability and safe operation with simplicity and a minimum of weight. Although it is true that the use of electrically conductive coating for aircraft window heating is relatively new, several successful applications have been reported. The experience gained from these installations and the pooling of ideas made possible by meetings of this nature are contributing greatly to the improvement of safety in air travel.

Of particular interest in the control system is the polarized relay used in the temperature-sensitive Wheatstone bridge. Certainly the sensitivity of the system depends largely on the ability of the polarized relay to sense small unbalance of the bridge caused by slight resistance fluctuations occurring in only one leg of the bridge. The relay used in the circuit described by Mershon is operated with a power input of only 56 microwatts and with a voltage of 0.07 volt across its coil required to close the contacts.

Since the contacts open when the coil

voltage is reduced to approximately 0.05 volt, the bridge unbalance representing the differential of the system may be as little as 0.02 volt. In a similar installation with simple on-off control the differential measured in degrees Fahrenheit with thermocouples taped to an actual windshield was observed to be as little as 3 degrees Fahrenheit at a control point of 115-degrees Fahrenheit. This performance was obtained using two metallic oxide disks in series to sense the window temperature; however, the input to each disk was held to 1/20 watt in order to minimize the effects of self-heating of the elements. Operating differentials of 12-degrees Fahrenheit have been observed using wire elements and a polarized relay with comparable sensitivity. This differential, although broader, is adequate for windshield temperature control since it is well within the permissible range of 70 to 130 degrees Fahrenheit.

Until recently relay performance meeting these requirements of sensitivity could be obtained only with delicate instruments unsuitable for mobile installations where shock and vibration play a predominant role. The polarized relay used in these control applications combines electromagnetic principles in a unique fashion, eliminating the disadvantages of conventional instruments, yet permitting contact loading of 0.5 ampere at 28 volts, direct current. Equally amazing is the fact that these relays, ranging in sensitivity from 40 microwatts to greater values, are factory produced with remarkable uniformity. Coil characteristics and calibration readily can be varied in production to provide correct detection in a wide range of bridge circuits.

A consideration in the control systems which warrants discussion is the permissible input to the temperature sensing elements embedded in the window. Obviously, the more power that is introduced to the bridge circuit, the smaller will be the operating differential. Accompanied by this apparent advantage is an increase in the self-heating of the temperature sensing element which shifts the control point, making necessary the use of a sensitive polarized relay which will operate with minimum power input to the bridge. An input which has proved successful with metallic oxide elements approximately 0.050 inch thick is 1/8 watt per element. This small input to the sensing elements causes the temperature-resistance characteristic of the element to be only about ten per cent lower than the characteristic without input, thus minimizing the effect of variable air velocity over the windshield. Somewhat higher inputs can be allowed when the sensing element is a fine resistance wire since its heat dissipating surface is considerably greater than that of the metal oxide element.

It is extremely gratifying that this latest development in windshield deicing can be combined with a few simple electrical fundamentals to provide adequate control. Equally as important is the fact that variations of the same control system are providing the answer to many difficult control problems in modern aircraft.

Leakage Reactance of the Squirrel Cage Rotor With Respect to the Stator Harmonics and the Equivalent Circuit of the Induction Motor

M. M. LIWSCHITZ
MEMBER AIEE

THE leakage of the rotor is considered usually with respect to the main waves of stator and rotor. Since the rotor of a squirrel cage motor is induced not only by the main wave of the stator but also by the stator harmonics, the leakage of the rotor with respect to the harmonics is also of importance. Each stator harmonic produces a series of rotor harmonics one of which has the same number of poles as the stator harmonic producing it, and is at a standstill with respect to the stator harmonic producing it, independent of the rotor speed. This particular rotor harmonic together with the stator harmonic causing it produces a main "harmonic" flux, just as the main harmonic of the stator and the main harmonic of the rotor produce the main flux of the machine. The "harmonic" main flux and the currents induced in the rotor by it produce then an "induction motor" torque, exactly as the main wave and the currents of slip frequency induced by it in the rotor produce the main torque of the machine.

Leakage Reactance of the Squirrel Cage With Respect to the N'th Harmonic

As pointed out, only one of the series of rotor harmonics produced by a certain stator harmonic is at a standstill with respect to this stator harmonic at any rotor speed and causes a parasitic "induction motor" torque. All other rotor harmonics of the series add up to the differential leakage of the rotor with respect to the harmonic considered.

It can be shown[1] that the differential leakage reactance of the rotor with respect to the n' th harmonic is

$$X_{dn'}=\frac{1}{\pi^2}f_1Q_2\frac{\rho r l_e}{g k_c}k^2_{s\xi n'}10^{-7}\times \sum_{k_2\neq 0}\left(\frac{1}{k_2Q_2+n'}\right)^2 \text{ ohms per bar} \quad (1)$$

where

$$\sum_{k_2\neq 0}\left(\frac{1}{k_2Q_2+n'}\right)^2=\frac{1}{n'^2}\left(\frac{1}{\xi^2_{2n'}k^2_{s\xi n'}}-1\right) \quad (2)$$

$$\xi_{2n'}=\frac{\sin\frac{n'\pi}{Q_2}}{n'\pi/Q_2} \quad (3)$$

$$k_{s\xi n'}=\frac{\sin n'\frac{\pi}{Q_2}\frac{s}{\tau_{2s}}}{n'\frac{\pi}{Q_2}\frac{s}{\tau_{2s}}} \quad (4)$$

The slot leakage of the rotor with respect to the n' th harmonic can be calculated from the usual formulas taking into account the skin effect.

The slip of the rotor with respect to the n' th harmonic is

$$s_{n'}=1-\frac{n'}{p}(1-s) \quad (5)$$

where s is the slip of the rotor with respect to the main wave. Accordingly, the frequency of the rotor currents due to the n' th harmonic is

$$f_{2n'}=f_1\left[1-\frac{n'}{p}(1-s)\right] \quad (6)$$

and with this frequency the skin effect has to be determined.

For the end-winding leakage of the rotor with respect to the n' th harmonic, the empirical formula

$$X_{en'}=f_1\frac{Q_2}{m_1p}\left[0.67(L_B-L)+\frac{0.18}{0.36}\tau_p'\times \frac{\sin^2(\alpha_{n'}=p/2)}{\sin^2(\alpha_{n'}/2)}\right]10^{-7} \text{ ohm per bar} \quad (7)$$

can be used. The factor 0.18 has to be applied to machines with $p>1$, the factor 0.36 to machines with $p=1$. Further

$$\alpha_{n'}=\frac{2\pi}{Q_2}n' \quad (8)$$

The reduction factor of the rotor reactance and resistance to the stator is

$$(RF)_{n'}=\frac{4m_1[Nk_{dp\xi n'}]^2}{Q_2k^2_{s\xi n'}} \quad (9)$$

Calculation of the "Total" Induction Motor Torque

For the calculation of the total induction motor torque, that is, the torque produced by the fundamental wave *and* harmonics, the equivalent circuit can be used.

The n' th stator harmonic induces in the rotor bars a current I_{2n}' which referred to the stator is

$$I'_{2n'}=I_{2n'}\frac{m_2}{m_1}\frac{N_2k_{dp\xi n'}k_{s\xi n'}}{N_1k_{dp\xi n'}} \quad (10)$$

The voltage equation of the stator is

$$V_1=(r_1+jX_{1s\xi})I_1+jX_{m(n'=p)}\times [I_1+I'_{2(n'=p)}]+ j\sum_{n'\neq p}X_{mn'}(I_1+I'_{2n'}) \quad (11)$$

The second term represents the counter electromotive force due to the main flux ($n'=p$). The third term represents the voltage drops due to the resultant har-

Paper 47-210, recommended by the AIEE committee on rotating machinery and approved by the AIEE technical program committee for presentation at the AIEE Middle Eastern District meeting, Dayton, Ohio, September 23-25, 1947. Manuscript submitted July 14, 1947; made available for printing August 21, 1947.

M. M. LIWSCHITZ is a professor of electrical engineering at the Polytechnic Institute of Brooklyn, Brooklyn, N. Y., and a consulting engineer for the Westinghouse Electric Corporation.

monic fluxes. Since the third term already contains the harmonics, the leakage reactance of the first term must contain only the slot leakage and end-winding leakage.

The voltage equation of the rotor for the main flux is

$$0=\left[\frac{r_2'}{s}+jX'_{2(n'=p)}\right]I'_{2(n'=p)}+ jX_{m(n'=p)}[I_1+I'_{2(n'=p)}] \quad (12)$$

and that for the resultant n'th flux

$$0=\left(\frac{r_2'}{s_{n'}}+jX'_{2n'}\right)I'_{2n'}+ jX_{mn'}(I_1+I'_{2n'}) \quad (13)$$

It can be seen readily that the circuit of Figure 1 satisfies the voltage equation of the stator as well as the voltage equations of the rotor. The number of harmonic circuits to be taken depends on the number of harmonics to be considered. If, for example, for a 2-pole 3-phase skewed motor, the torques produced by 5th and 7th harmonics have to be determined, only 3 circuits corresponding to $n'=1$, $n'=5$, and $n'=7$, have to be considered. If the equivalent circuit of Figure 1 contains a small number of harmonic circuits, the leakage reactance of the stator harmonics not included in the equivalent circuit has to be added to X_{1sz}.

The equivalent circuit shown in Figure 1 has been used by E. Arnold in 1909[1], in order to explain the influence of the harmonics on the operation of the induction motor. However, E. Arnold does not give a derivation nor does he show how to calculate the leakage reactances of the squirrel cage with respect to the harmonics.

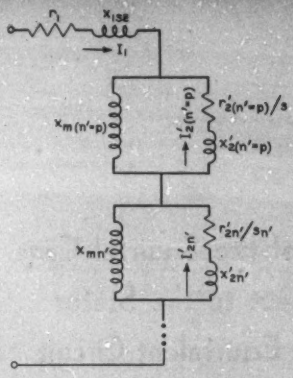

Figure 1. Equivalent circuit of the induction motor

It should be noted that the equivalent circuit Figure 1 does not give any information about the synchronous torque occurring in the induction motor. It shows only the asynchronous (induction motor) torques.

The main flux reactance for the main wave $X_{m(n'=p)}$, in equation 11 is

$$X_{m(n'=p)}=4.06m_1f_1[N_1k_{dp1(n'=p)}]^2\times \frac{\tau l_e}{pgk_ck_s}10^{-8} \text{ ohms per phase}$$

and the main flux reactance for the n'th harmonic, X_{mn}' is

$$X_{mn'}=X_{m(n'=p)}\left[\frac{k_{dp1n'}}{n'}\frac{p}{k_{dp1(n'=p)}}\right]^2\times \text{ohms per phase} \quad (14)$$

For the harmonics the saturation factor k_s can be assumed equal to 1.

List of Symbols

f_1 = line frequency
f_2 = frequency of the rotor currents
g = air gap
k_{dp} = distribution times pitch factor
k_{sk} = skew factor
k_c = Carter factor
k_2 = positive or negative interger including 0
k_s = saturation factor
l_e = effective core length
L = total core length
L_b = length of a rotor bar between end rings
m = number of phases
n' = order of the stator harmonic with respect to a fundamental whose wave length is equal to the circumference of the armature ($2p\tau$)
N = number of turns per phase
p = number of pole pairs
Q = number of slots
r = resistance
s = slip of the rotor with respect to the main wave
s_n' = slip of the rotor with respect to the n'th harmonic
s = skew (in inches)
X = leakage reactance
X_m = main flux reactance
α = angle between two rotor bars
τ = pole pitch
τ_p' = pole pitch in the middle of the end ring
τ_s = slot pitch

References

1. Differential Leakage with Respect to the Fundamental Wave and to the Harmonics, M. M. Liwschitz, AIEE Transactions, volume 63, 1944, pages 1139–49.

2. A-C Machines (book), E. Arnold, J. L. La Cour. Volume 5, part 1, 1909 Springer (in German).

No Discussion

Some Phases of Calculation of Leakage Reactance of Induction Motors

M. M. LIWSCHITZ
MEMBER AIEE

W. H. FORMHALS
MEMBER AIEE

THE object of this paper is to discuss some difficulties in the calculation of leakage reactance which make a theoretically accurate method of calculation tedious and therefore leads the designer to use a "practical" method of calculation corrected by constants gained from tests.

Four topics will be discussed

1. Influence of slot openings on the differential leakage
2. Influence of skewing on the differential leakage
3. Influence of saturation of leakage paths on slot and differential leakage
4. Influence of aluminum film on the rotor on leakage

Influence of Slot Openings on the Differential Leakage

The slot harmonics of first and higher orders constitute a large part of the differential leakage. Usually the assumption is made that the influence of the slot openings on the harmonics is the same as on the main wave, that is, that all harmonic fluxes are reduced by the slot openings in the ratio of one to the Carter factor. This is more or less correct for the harmonics of lower order but not for those of higher order.

In order to determine the influence of the slot openings on the harmonics of higher order, the gap permeance is assumed to be[1]

$$\left(\frac{1}{\varepsilon}\right)_{\text{eff}} = \frac{1}{\varepsilon}\left[1+\epsilon_1 \cos Q\frac{\pi}{p\tau}x + \epsilon_2 \cos 2Q\frac{\pi}{p\tau}x + \dots\right] \quad (1)$$

This presumes that the fundamental wave has two poles with a wave length equal to $2p\tau$ (for symbols see list of symbols).

With respect to the same fundamental wave, the n'th magnetomotive force harmonic is

$$f_{n'} = F_{n'} \sin\left(\omega t - n'\frac{\pi}{p\tau}x\right) \quad (2)$$

where

$$F_{n'} = \frac{\sqrt{2}}{\pi} mN \frac{k_{dpn'}}{n'} I \quad (3)$$

and, therefore, the n'th field harmonic

$$b_{n'} = \frac{3.19}{\varepsilon} F_{n'} \sin\left(\omega t - n'\frac{\pi}{p\tau}x\right) \times \left[1+\epsilon_1 \cos Q\frac{\pi}{p\tau}x + \epsilon_2 \cos 2Q\frac{\pi}{p\tau}x + \dots\right] \quad (4)$$

With the abbreviation

$$\frac{3.19}{\varepsilon} F_{n'} = A_{n'} \quad (5)$$

it follows from equation 4

$$b_{n'} = A_{n'} \sin\left(\omega t - n'\frac{\pi}{p\tau}x\right) + A_{n'} \sum_{c=1,2,3\dots} \frac{\epsilon_c}{2}\left\{\sin\left[\omega t + (cQ-n')\frac{\pi}{p\tau}x\right] + \sin\left[\omega t - (cQ+n')\frac{\pi}{p\tau}x\right]\right\} \quad (6)$$

Thus, due to the slot openings, the n'th magnetomotive force harmonic produces a series of pairs of traveling field waves. One wave of each pair travels in the direction of rotation, the other in opposite direction. Their respective velocities are

$$\frac{p}{cQ+n'}\frac{\tau}{\pi}\omega$$

and

$$\frac{p}{cQ-n'}\frac{\tau}{\pi}\omega$$

$$c = 1, 2, 3 \dots \quad (7)$$

These slot-openings waves may influence considerably those field harmonics with respect to which they are at standstill.

The n'th harmonic has the speed

$$V_{n'} = \frac{p}{n'}\frac{\tau}{\pi}\omega \quad (8)$$

Considering the orders of the slot harmonics

$$n'_{st} = \mp kQ + p \quad (9)$$

it follows that the slot-opening waves produced by the main wave ($n'=p$) are at standstill with respect to the slot harmonics and these are the only waves which are at standstill with respect to each other. It follows further from equations 7 and 9 that the slot-opening wave of the order $c=1$ is at standstill with respect to the slot harmonics of first order ($k=1$), that the slot-opening wave of the order $c=2$ is at standstill with respect to the slot harmonic of second order ($k=2$), and so on.

Usually the slot-opening waves of the orders $c=1$ and $c=2$ have to be taken into account. From equation 6

$$b_{po}' = A_{(n'=p)}\frac{\epsilon_c}{2}\sin\left[\omega t - (cQ+p) \times \frac{\pi}{p\tau}X - \Psi\right]\frac{I_m}{I_1} \quad (10)$$

and

$$b_{po}'' = A_{(n'=p)}\frac{\epsilon_c}{2}\sin\left[\omega t + (cQ-p) \times \frac{\pi}{p\tau}X + \Psi\right]\frac{I_m}{I_1} \quad (11)$$

where I_m is the magnetizing current. $A_{(n'=p)}$ is proportional to the primary current I_1. The factor I_m/I_1 takes into account the fact that the amplitudes of the slot-opening waves are proportional to the resultant main wave, that is, to the

Paper 47-211, recommended by the AIEE rotating machinery committee and approved by the AIEE technical program committee for presentation at the AIEE Middle Eastern District meeting, Dayton, Ohio, September 23-25, 1947. Manuscript submitted July 14, 1947; made available for printing August 29, 1947.

M. M. LIWSCHITZ is a professor of electrical engineering at the Polytechnic Institute of Brooklyn, Brooklyn, N. Y., and a consulting engineer to the Westinghouse Electric Corporation, and W. H. FORMHALS is with the Westinghouse Electric Corporation, Buffalo, N. Y.

main wave produced by the primary and secondary magnetomotive forces together (I_m). The angle Ψ has to be introduced because I_m is not in phase with I_1.

The slot harmonics are

$$b_{sl}' = A_{(n'=cQ+p)} \sin\left[\omega t - (cQ+p)\frac{\pi}{p\tau}X\right] \quad (12)$$

and

$$b_{sl}'' = A_{(n'=-cQ+p)} \sin\left[\omega t + (cQ-p)\times \frac{\pi}{p\tau}X\right] \quad (13)$$

The ratio between the amplitudes of two waves which travel in the direction of rotation is

$$r' = \frac{A_{(n'=p)}}{A_{(n'=cQ+p)}}\frac{I_m}{I_1}\frac{\epsilon_c}{2} = \left[\frac{k_{d(n'=p)}}{k_{d(n'=cQ+p)}}\right]\left[\frac{k_{p(n'=p)}}{k_{p(n'=cQ+p)}}\right]\times \frac{cQ+p}{p}\frac{I_m}{I_1}\frac{\epsilon_c}{2} \quad (14)$$

and the ratio between the amplitudes of two waves which travel opposite to the direction of rotation is

$$r'' = \frac{A_{(n'=p)}}{A_{(n'=-cQ+p)}}\frac{I_m}{I_1}\frac{\epsilon_c}{2} = \left[\frac{k_{d(n'=p)}}{k_{d(n'=-cQ+p)}}\right]\left[\frac{k_{p(n'=p)}}{k_{p(n'=-cQ+p)}}\right]\times \frac{cQ-p}{p}\frac{I_m}{I_1}\frac{\epsilon_c}{2} \quad (15)$$

The magnitude of ϵ_c depends upon the ratio of slot opening to slot pitch and upon the ratio of slot opening to air gap. For open slots, $\epsilon_1 = 0.5$ to 0.7 and ϵ_2 is negligible; for semi-open slots, $\epsilon_1 = 0.05$ to 0.25 and $\epsilon_2 = 0.05$ to 0.15.

The ratio of the distribution factors and pitch factors in the parentheses of equations 14 and 15 is equal to $+1$ or -1. The signs of these two ratios determine whether the slot-opening wave has the same sign as the corresponding slot harmonic thus increases the latter or has an opposite sign and decreases it.

The application of equations 14 and 15 to different machines shows that in certain cases one slot harmonic of the pair is increased by a certain amount and the other is decreased by approximately the same amount while in other cases both slot harmonics of the pair are decreased by approximately the same amount.

The magnitude of the differential (harmonic) leakage is determined by the influence of all harmonics. A practical method of calculation of the differential leakage can not consider each harmonic separately in the way just shown. If, in order to derive simple formulas for the differential leakage, it is assumed that the slot openings have the same influence on the harmonics of high and low order, inaccurate results may be obtained in certain cases.

Influence of Skewing on the Differential Leakage

The magnetic energy of the main wave and harmonics is practically the same whether the slots are skewed or not, that is, the coefficients of self inductance of stator and rotor windings are practically independent of skew. Skewing changes only the magnitude of the *main* wave of the rotor, since this wave depends upon the mutual position of the stator and rotor slots.

Skewing has the same effect as distributing a winding. The skew factor is a distribution factor and can be derived in the same manner as the distribution factor of any winding distributed in slots. However, distributing a stator winding reduces the harmonic leakage of this winding, while skewing increases the harmonic leakage of the rotor.

The total reactance of an integral-slot stator winding, that is, the reactance due to the main wave *and* harmonics, is[3]

$$X_{1t} = \frac{4}{\pi^2} m_1 f_1 N_1^2 \frac{p\tau l_e}{g k_c} 10^{-7}\left[\sum_{n'=1}^{n'=\infty}\left(\frac{k_{dpn'}}{n'}\right)^2\right] \text{ ohms per phase} \quad (16)$$

The reactance of the main wave ($n'=p$)

$$X_{1m} = \frac{4}{\pi^2} m_1 f_1 N_1^2 \frac{p\tau l_e}{g k_c} 10^{-7}\left[\frac{k_{dp(n'=p)}}{p}\right]^2 \text{ ohms per phase} \quad (17)$$

and, therefore, the reactance due to the harmonics, that is, the differential leakage reactance,

$$X_{1d} = X_{1t} - X_{1m} = \frac{4}{\pi^2} m_1 f_1 N_1^2 \frac{p\tau l_e}{g k_c} 10^{-7}\times \left[\sum_{n'=1}^{n'=\infty}\left(\frac{k_{dpn'}}{n'}\right)^2 - \left(\frac{k_{dp(n'=p)}}{p}\right)^2\right] \text{ ohms per phase} \quad (18)$$

Equations 16–18 do not take into account the saturation or the damping of the stator harmonics by the rotor harmonics. Each stator harmonic produces a series of rotor harmonics one of which has the same number of poles as the stator harmonic producing the series and is at standstill with respect to this stator harmonic, independently of the rotor speed. This particular rotor harmonic reduces the stator harmonic producing it, just as the main wave of the rotor opposes the main wave of the stator. The damping effect of the rotor with respect to the stator harmonics is greater the larger the number of slots in stator and rotor; it is also influenced by the chording. In a stator winding with two slots per pole per phase and a not too high number of rotor slots, the damping effect of the rotor on the stator harmonics can be neglected. In a two-pole winding with six slots per pole per phase and a coil span of 50 to 60 per cent, the reduction of the differential leakage reactance of the stator, as given by equation 18, is about 40 per cent.

However, this is true only for the non-skewed rotor. When the rotor is skewed, the interlinkage between the stator harmonics of the higher order and the rotor is reduced. Due to the poorer interlinkage, the rotor currents produced by the stator harmonics of higher order become smaller and their reaction upon the stator harmonics is also smaller. Thus, skewing increases the differential leakage of the stator. The increase is from 10 to 15 per cent as compared with the non-skewed rotor.

The influence of skewing on the differential leakage of the rotor is much larger than on that of the stator.

Since the rotor winding is always a polyphase winding, the results obtained for the polyphase stator winding also should be directly applicable to it, if the proper values for the number of phases, number of turns per phase, and so forth, are introduced in equations 16–18. However, this is true only with respect to equations 16 and 18 but not with respect to equation 17.

X_{1t} in equation 16 represents the reactance which corresponds to all fluxes in the air gap, that is, to the main wave and harmonics. It can be determined from the magnetic energy in the air gap due to the stator current. Since the magnetic energy practically is not influenced by skewing, equation 16 also applies to the rotor winding, phase belt as well as squirrel cage winding. The left part of equation 18 states that the differential leakage reactance is equal to the difference between the total reactance and the reactance due to the main wave. This is true for any winding and also applies to the rotor winding, whether the slots are skewed or not.

Equation 17 for the reactance of the main wave can not be applied to the rotor of a skewed machine, because skewing changes the interlinkage between the stator winding and the rotor winding. The change in interlinkage is given by the skew factor. Therefore, equation 17 is to be multiplied by $k^2_{sk(n'=p)}$ when applied to a skewed rotor. The skew factor has

to be introduced as a second distribution factor. Thus, the main wave reactance of the rotor winding, when the slots are skewed, is

$$X_{2m}=\frac{4}{\pi^2}m_2f_1N_2^2\frac{\tau l_g}{pgk_c}10^{-7}\times$$
$$[k^2_{dp(n'=p)}\,k^2_{sk(n'=p)}] \quad (17a)$$

$$k_{sk(n'=p)}=\frac{\sin\frac{\pi p}{Q_2}\frac{s}{\tau_{2s}}}{\frac{\pi p}{Q_2}\frac{s}{\tau_{2s}}} \quad (19)$$

Applying equation 17a to the squirrel cage rotor for which

$$m_2=Q_2 \quad N_2=\frac{1}{2} \quad k_{dp(n'=p)}=1$$

the main wave reactance of the squirrel cage winding, per bar, is

$$X_{2m}=\frac{1}{\pi^2}Q_2f_1\frac{\tau l_g}{pgk_c}10^{-7}\times k^2_{sk(n'=p)} \text{ ohms} \quad (20)$$

The currents of slip frequency produce in a squirrel cage winding the harmonics

$$m'=k_2Q_2+p \quad (21)$$

where k_2 is any positive or negative integer including 0. Further, for the squirrel cage winding, $k_{dpm'}=1$. Introducing the harmonics of the order m' and $k_{dpm'}=1$ in equation 16, the total reactance of the squirrel cage winding becomes

$$X_{2l}=\frac{1}{\pi^2}Q_2f_1\frac{\tau l_g}{pgk_c}\sum_{k_2=0}^{k_2=\infty}\left(\frac{1}{k_2\frac{Q_2}{p}+1}\right)^2 \text{ ohms} \quad (22)$$

According to equation 18, left part, the differential (harmonic) leakage reactance is obtained by subtracting the main wave reactance X_{2m} from the total reactance X_{2l}. Hence, the differential leakage reactance of a squirrel cage winding, per bar, when the slots are skewed is

$$X_{2d}=\frac{1}{\pi^2}Q_2f_1\frac{\tau l_g}{pgk_c}10^{-7}\times k^2_{sk(n'=p)}\times$$
$$\left[\frac{1}{k^2_{sk(n'=p)}}\sum_{k_2=0}^{k_2=\infty}\left(\frac{1}{k_2\frac{Q_2}{p}+1}\right)^2-1\right] \text{ ohms} \quad (23)$$

It can be shown that[2]

$$\sum_{k_2=0}^{k=\infty}\left(\frac{1}{k_2\frac{Q_2}{p}+1}\right)^2=\frac{1}{\xi^2_{(n'=p)}} \quad (24)$$

where

$$\xi_{(n'=p)}=\frac{\sin\frac{p\pi}{Q_2}}{\frac{p\pi}{Q_2}} \quad (25)$$

Inserting equation 24 in equation 23, the differential leakage of a squirrel cage winding, per bar, becomes

$$X_{2d}=\frac{1}{\pi^2}Q_2f_1\frac{\tau l_g}{pgk_c}10^{-7}\times k^2_{sk(n'=p)}\times$$
$$\left[\frac{1}{\xi^2_{(n'=p)}k^2_{sk(n'=p)}}-1\right] \text{ ohms} \quad (26)$$

Normally $\frac{Q_2}{p}\geq 10$ and $\frac{s}{\tau_{2s}}\leq 1.25$. With these values the angle $\frac{p\pi}{Q_2}$ and $\frac{p\pi}{Q_2}\frac{s}{\tau_{2s}}$ are relatively small and

$$\left(\frac{1}{\xi^2_{(n'=p)}k^2_{sk(n'=p)}}-1\right)\approx 3.3\left(\frac{p}{Q_2}\right)^2\times$$
$$\left[1+\left(\frac{s}{\tau_{2s}}\right)\right] \quad (27)$$

It is seen from this equation that skewing increases the differential leakage of the squirrel cage winding in the ratio of one to $\left[1+\left(\frac{s}{\tau_{2s}}\right)^2\right]$. A skew equal to one rotor slot pitch doubles the differential leakage of the squirrel cage winding.

However, these are theoretical values. The skewing is totally effective only when the rotor bars are insulated. The oxide film on the rotor bars does not represent a perfect insulation and the additional differential leakage in rotor and stator due to skewing will be smaller than that given by equation 27. The amount of additional leakage is different for die cast aluminum rotors and copper bar rotors and depends upon the manufacturing methods. The designer must resort to tests, in order to determine the percentage of the theoretical additional differential leakage due to skewing which he should use in his calculations.

Influence of Saturation of Leakage Paths on Slot and Differential Leakage

The calculation of leakage reactance usually is based on the assumption that the leakage paths are not saturated. The leakage reactance determined in this manner is divided then by a "saturation factor" which takes into account the saturation of the leakage paths at higher slips. For modern machines this factor lies between 1.15 and 1.3 or even higher and the designer must resort to tests in order to determine its magnitude, since no rational method for its calculation is known.

One is inclined to assume that the saturation of the leakage paths occurs in the tooth tips in a manner similar to that in the bridges of closed slots. This assumption leads to the conclusion that the saturation of the leakage paths should be larger in smaller machines with semi-

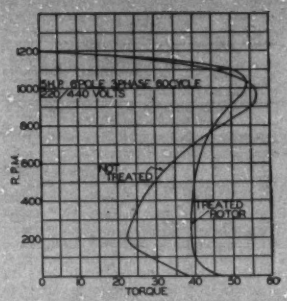

Figure 1. Influence of aluminum film on rotor surface on motor torque

closed slots in both machine parts than in larger machines having open slots in the stator. Experience shows that this is not the case and that the saturation of the leakage paths of a machine with open slots can be as high as that of a machine with semiclosed slots.

A large motor with open slots in the stator and with the following data will be considered as example:

800 horsepower, 8 poles, 3 phases, 60 cycles, 2,300 volts Y. Number of stator slots $Q_1=120$. Number of rotor slots (squirrel cage rotor) $Q_2=98$. Coil pitch of the stator winding = 80 per cent, that is, $k_p=0.951$. Corresponding to $q=\frac{120}{8\times 3}=5$ slots per pole per phase, $k_d=0.956$ and $k_{dp}=0.909$. Bore diameter $D=30.11$ inches, single gap $g=0.055$ inch. The slot width of the stator slot is approximately 50 per cent of the tooth pitch.

The per unit reactances of this motor calculated without taking into account any saturation of the leakage paths are

	Stator	Rotor
Slot+differential	0.0528	0.0605
End−winding	0.0345	0.0274
	0.0873	0.0879

The total leakage reactance is 0.1752. The output current is $I_{hp}=149.7$ amperes. Therefore, the calculated locked rotor current at full voltage, without saturation,

$$I_L=\frac{149.7}{.1752}=855 \text{ amperes}$$

The two lowest points of the tested locked rotor characteristic yield an average current, referred to full voltage, of 851 amperes. The locked-rotor current tested at full voltage is $I_{L(tst)}=1{,}200$ amp. The saturation factor is

$$k_{tst}=\frac{1{,}200}{851}=1.41$$

Table 1

Hp	Poles	Calculated Saturation Factor	Tested Saturation Factor
2	4	1.45	1.36
3	4	1.35	1.36
5	4	1.4	1.4
7½	4	1.49	1.45
7½	4	1.34	1.32
10	4	1.57	1.52
10	4	1.39	1.28
15	4	1.66	1.57
3	6	1.37	1.33
5	6	1.46	1.36
7½	6	1.29	1.21
10	6	1.4	1.29
50	6	1.14	1.125
½	8	1.36	1.22
15	8	1.12	1.09
500	8	1.16	1.135
800	8	1.41	1.41

and the saturated leakage reactance

$$X_{L(sat)} = \frac{0.1752}{1.41} = 0.1242 \text{ ohm per phase}$$

The decrease of the leakage reactance due to the saturation of the leakage paths is $0.1752 - 0.1242 = .051$ ohm per phase.

If the previously mentioned assumption is made that the saturation lies in the tooth tips, it would be concluded that in this machine with widely open slots in the stator the total decrease of the leakage reactance takes place in the rotor and that the saturated leakage reactance of the rotor is

$$X_{r(sat)} = 0.0879 - 0.051 = 0.0369 \text{ ohm per phase}$$

This corresponds to a reduction of 58 per cent in the total leakage reactance of the rotor and to a reduction of 84 per cent in the slot plus differential leakage reactance of the rotor.

From this the conclusion could be drawn that in machines with semi-closed slots in both machine parts, the saturation factor can be as high as 1.6. However, this is not the case and the saturation factor of machines with semi-closed slots in both machine parts is not higher than that of machines with open slots in the stator. This indicates that the saturation of the leakage paths lies not only in the tooth-tips but in the tooth body.

Experience shows that the magnitude of the saturation factor depends upon the number of slots, the dimensions of the teeth and the air gap. It is influenced little by the coil pitch. A larger number of stator and rotor slots reduces the saturation factor but increases the manufacturing costs and the stray load losses. The large influence of the number of slots indicates that the slot harmonics play a part in the saturation of the leakage paths. A method of calculation of the saturation factor, worked out on the basis of the harmonics of stator and rotor, gives satisfactory results, as shown by Table 1 in which calculated and tested values are compared. However, this method can not be considered as entirely satisfactory yet from a theoretical point of view and further work is required before it can be published.

Influence of the Aluminum Film on the Rotor on the Leakage Reactance

Many manufacturers die cast the rotor of the smaller motors with aluminum alloy. After the die casting the assembled rotor is machined to size. This process normally produces a film of aluminum on the surface of the rotor which is detrimental to the performance of the motor. The degree to which the film influences the performance depends upon such factors as continuity and thickness of the film. Figure 1 illustrates some effects of removing this film.

Since the removal of the film is an additional cost, the designer is reluctant to apply it on all motors. Therefore, an additional uncertainty is introduced into the calculation of the machine.

Conclusion

The topics discussed in the foregoing show that the present knowledge of the theory of electrical machines does not yield an exact method of calculation of the differential leakage and of the magnitude of the effect of saturation on the leakage reactances. Manufacturing methods introduce further uncertainties in the magnitude of the influence of skew and of aluminum film on the leakage reactances. These circumstances cause the designer to depend upon correction factors which are based on test on his particular machines. Thus not theory alone but theory in connection with experience enables the designer to adapt the electrical machine to all possible kinds of applications and to meet the guarantees fixed by standards or by the customer. The program which has been made in the development of the theory of electrical machinery during the past years indicates that in the near future more exact methods of the calculation will be available.

Nomenclature

A_n' = defined by equation 5
$b_{n'}$ = instantaneous value of n'th field harmonic
c = order of the slot-opening wave
f_1 = line frequency
$f_{n'}$ = magnetomotive force, instantaneous value
$F_{n'}$ = magnetomotive force, amplitude
g = air gap
I = current
I_m = magnetizing current
I_1 = primary current
$k_{dp} = k_d k_p$ = distribution factor × pitch factor
k_c = Carter factor
k_{sk} = skew factor
k = order of the slot harmonic
k_3 = positive or negative integer including 0
l_e = effective core length
m = number of phases
m' = order of rotor harmonic
n' = order of the stator harmonic with respect to a fundamental whose wave length is $2p\tau$
n_{s1}' = order of the slot harmonic of the stator
N = number of turns per phase
Q = number of slots
r' = ratio
s = skew (in inches)
t = time
ϵ_c = amplitude of the slot opening wave
τ = pole pitch
τ_s = slot pitch
$\omega = 2\pi f_1$
X = reactance
V = velocity

References

1. Differential Leakage of a Fractional-Slot Winding, M. M. Liwschitz. AIEE Transactions, volume 65, 1946, May section, pages 314–20.

2. Differential Leakage With Respect to the Fundamental Wave and to the Harmonics, M. M. Liwschitz. AIEE Transactions, volume 63, 1944, pages 1139–49.

Discussion

E. C. Barnes (The Reliance Electric and Engineering Company, Cleveland, Ohio): Both in the paper and in the existing literature, rotor skew is referred to and measured in terms of the slot pitch of either the stator or the rotor. While this approach is justified from the viewpoint of slot harmonics, there is evidence that from the standpoint of the fundamental wave, and lower order harmonics, skew should be measured in terms of pole pitch.

Several years ago, W. G. Hall made an experimental study* on the effects of skew

*"An Investigation of the Effect of Rotor Skew and Winding Pitch on Squirrel-Cage Induction Motor Speed-Torque Characteristics," W. G. Hall. A thesis submitted to Case Institute of Technology, September 1942.

on induction motor performance. In analysis of the experimental data, he found that when skew was considered as a function of the fundamental pole pitch, the results were much more consistent and meaningful than when skew was considered a function of slot pitch.

To investigate this further, I made a study of approximately 100 motor tests to determine the effect on skew on pull-out torque. This study embraced a wide range of motor sizes, skew, and numbers of poles; and again it pointed out the necessity for considering the skew in terms of pole pitch. This is particularly true when the skew is great.

I do not argue that skew never should be considered in terms of slot pitch because it is necessary in the study of higher harmonics, however, experimental data appears to indicate that for harmonics of the order five and lower, skew also should be measured in terms of pole pitch.

M. M. Liwschitz and **W. H. Formhals:** The skewing aims exclusively at the reduction of the influence of the stator slot harmonics upon the rotor. The wave length of these harmonics is approximately equal to a stator slot pitch and, therefore, the skew is most effective when it is approximately equal to this slot pitch. Since the magnitude of the skew is determined by the slot pitch, it seems logical to express the skew in slot pitches and not in pole pitches, that is, in lengths of the main wave which practically is not influenced by the skewing.

The skewing influences considerably the differential leakage of the rotor and stator. Since the differential leakage is approximately inversely proportional to the square of the number of slots and the number of slots depends upon the pole pitch, a certain relation exists between the skew, the pole pitch, and the differential leakage, and therefore, also between the skew, the pole pitch, and the pull-out torque. However, this relation is limited to a certain range of machines, and it will be different for small machines and large machines, for low voltage machines and high voltage machines, since size and voltage also influence the number of slots.

We do not see an advantage in expressing the skew in terms of a secondary quantity instead of the primary quantity which determines its magnitude, that is, of the slot pitch. Such a method of expression of the skew may lead to the result that inexperienced designers will miss the primary objective of skewing and will choose a wrong skew.

A Variable-Speed Constant-Frequency Generator

CARL S. ROYS
MEMBER AIEE

JOSEPH NADER
ASSOCIATE AIEE

MELVIN SPOTTS
NONMEMBER AIEE

Synopsis: Starting with the theory of operation of a-c commutator machines, it is shown how either a single or polyphase generator can be built whose frequency is controllable and essentially independent of speed and whose general characteristics are similar to those of a d-c generator. Among the principal topics discussed are

The generated voltage equation.
Compensating windings.
Commutation.
Self-excited operation.
Voltage regulation.
Parallel operation.
Motor operation.
Compounding.

THE PROBLEM of generating electric energy with a variable-speed prime mover as the driving device, is inherent to internal combustion vehicles such as busses, boats and aircraft, for example. Although direct current has been generally acceptable in the past, with the increased and more diversified loads being contemplated, many factors now favor alternating current for both generation and distribution. This requires the maintenance of essentially constant frequency over a range of speed variation which, in many instances, is of the order of magnitude of several hundred per cent.

The principal methods which have been proposed for accomplishing this are

1. Generation of direct current and subsequent inversion to alternating current by means of rotating machines.[1]

2. Generation of either direct current or varying frequency alternating current and inversion by means of electron tube apparatus.[2]

3. Variable-ratio-driven synchronous generators.[3]

4. Variable-speed constant-frequency generators, the subject of this paper.

Paper 47-217, recommended by the AIEE electric machinery committee and approved by the AIEE technical program committee for presentation at the AIEE Middle Eastern District meeting, Dayton, Ohio, September 23–25, 1947. Manuscript submitted July 8, 1947; made available for printing August 8, 1947.

CARL S. ROYS is professor, department of electrical engineering, Syracuse University, Syracuse, N. Y.; JOSEPH NADER is president and chief engineer and MELVIN SPOTTS is design engineer, Bicor, Inc., Chicago, Ill.

Theory of Operation

It should be recalled that, although the frequency of either a synchronous or induction generator is dependent upon speed, the frequency observed at the brushes of a commutator-type rotor is the same as the stator frequency. This is the principle utilized in a-c series motors,[4–6] variable-speed polyphase motors,[7,8] and the Hull generator.[9] It will serve also as the basis for the generator under consideration here.

There are several items which are unique in the a-c operation of commutator machines, which often affect both their design and performance. In general, such operation introduces problems whose solutions become more difficult with increased speed, voltage, and frequency. The more important of these are

1. An additional voltage in a coil undergoing commutation due to transformer action.

2. Lower efficiency than a d-c machine due to stator core losses and larger stray losses.

3. Low power factor field windings which require either a comparatively large amount of exciting voltamperes or the use of series capacitors.

4. Frequency stability and control in addition to voltage regulation.

Although these introduced serious limitations upon the ratings and design of the generators at first, they have been lifted as a result of a series of theoretical and experimental studies carried out by the authors. The present paper will be concerned chiefly with the theoretical aspects of the problem, experimental data being reserved for a later date.

Generative Voltage

If one assumes a sinusoidal time-variation in flux and neglects both tooth and commutator ripples, it can be shown in a manner similar to that followed in d-c machine theory that the instantaneous phase voltage which is generated between brushes, as a result of armature rotation, is given by*

$$e_{rn} = (\text{c.f.})(\text{p b.})\,\frac{pZN}{60\,mP}\,\Phi \sin \omega t \text{ volts} \qquad (1a)$$

It is seen from this that it is not necessary to maintain a sinusoidal flux distribution around the air gap in order to obtain a sinusoidal voltage. In order to minimize core losses, however, it is desirable to use a distributed set of field windings which will result in a close approximation to a sinusoidal flux distribution.

With the brushes on neutral, the effective value of single-phase voltage is

$$E_{r1} = 0.353(\text{c.f.})\,\frac{pZN}{60\,m}\,\Phi \text{ volts} \qquad (1b)$$

And for three phases

$$E_{r3} = 0.204(\text{c.f.})\,\frac{pZN}{60\,m}\,\Phi \text{ volts} \qquad (1c)$$

For the single-phase machine, equation 1*b* constitutes the entire generated voltage between brushes since, as for a repulsion motor, there is no induced voltage due to transformer action when the brushes are on neutral.

In the polyphase machine, coupling exists between each phase of the rotor and all of the windings in the other phases of the stator. This gives an extra set of rotor voltages which sometimes is considered as arising from a rotating field cutting the rotor at synchronous speed. The value of this voltage for an n-phase machine can be expressed as

$$E_{ts} = \frac{N_s}{N}\,E_{rn} \text{ volts} \qquad (1d)$$

* See Appendix III for list of symbols.

Hence, the total generated voltage in the rotor is

$$E_n = \frac{N_s - N}{N} E_{rn} \text{ volts} \tag{1e}$$

It is necessary to provide the stator with a set of compensating windings, which, when connected between the line and brush terminals of the polyphase machine, will nullify the effects of magnetic coupling between stator and rotor. Otherwise, there would be induction motor action between the two and, furthermore, the voltage of the machine would reduce to zero at synchronous speed.

Compensating Windings

Although compensating windings are used in both single and polyphase machines,[4-8,9] their effectiveness in neutralizing armature reaction in the latter has been restricted to balanced conditions. Inasmuch as large single-phase loads are being planned for aircraft, a set of compensating windings whose usefulness is independent of any normal or abnormal load conditions would be required. At the same time, they should neutralize the voltages induced in the armature by the stator field.

The arrangement of windings meeting both of these specifications is shown in Figure 1, the underlying development being given in Appendix I. As mentioned there, this is not the only arrangement possible. It has been selected because it results in a minimum amount of slot space required for the windings, it being $2/\sqrt{3}$ times that required for the armature coils, assuming a common current density.

Although windings for a 3-phase machine are shown, compensating windings having these properties can be designed for any number of phases, the number of possible solutions increasing with the number of phases. In general, compensating windings should be distributed uniformly for optimum performance and, when properly designed, will reduce the reactance of the combined, armature-compensating winding circuit to the so-called "zigzag value of reactance."[11] This is small in comparison with the synchronous reactance of an alternator.

Special Problems in Communication

In addition to the induced voltage resulting from the reversal of current through a coil while undergoing commutation, there is one due to transformer action. This was listed under "Theory of Operation." From ordinary transformer theory, the effective value of this voltage for a single-phase machine can be shown to be

$$E_{ct} = 2.22(\text{c.f.})fZ\Phi/b \text{ volts} \tag{2a}$$

$$= 1.11(\text{c.f.})pZN_s/60b\Phi \text{ volts} \tag{2b}$$

When compared with equation 1*b*, this gives

$$E_{ct}/E_{rt} = \frac{\pi m}{b}\left(\frac{N_s}{N}\right) \tag{2c}$$

In a polyphase machine, the voltage is equal to that due to a rotating field cutting the coil at slip-speed giving, for *n* phases,

$$E_{cn}/E_{rn} = \frac{\pi m P}{2(\text{p.b.})b} \cdot \frac{N_s - N}{N} \tag{2d}$$

This becomes, for three phases and a sinusoidal flux distribution,

$$E_{ct}/E_{rn} = \frac{\sqrt{3}\pi m}{b} \cdot \frac{N_s - N}{N} \tag{2e}$$

Since equations 2d and 2e reduce to zero at synchronous speed, from the standpoint of good commutation, it may be desirable to design the polyphase machine such that its synchronous and normal speeds are nearly equal.

Finally, since commutating fields are not effective over a wide range of speed variation, it is necessary to limit the total induced voltage in the short-circuited coil to a permissible value by means of the best combination of numbers of poles, commutator bars and turns per coil, type of armature winding, grade and thickness of brushes, and so on.

Self-Excited Operation

Single Phase

The schematic diagram for self-excited operation of the single-phase machine is given in Figure 2. The functions of the series capacitor in the shunt field circuit are

1. To prevent d-c build-up.
2. To control the frequency.
3. To minimize the volt-amperes required for excitation.

The approximate relations to be satisfied in order to obtain sustained self-excited operation are derived in Appendix II. They are

$$R_f + R_a + R_k = nX_{af} \tag{3a}$$

$$X_f - X_c = 0 \tag{3b}$$

$$f_0 = 1/\sqrt{LC} \tag{3c}$$

It is obvious from these equations that the machine continues to build up until the generated voltage and the a-c resistance drops are equal and the frequency is equal to the resonant frequency of the circuit.

It is shown also in Appendix II that the change in frequency under load conditions is given approximately by

$$\Delta f/f_0 = \frac{R_a + R_k}{2Z_1 Q_f} \sin\theta \tag{3d}$$

Three Phase

The schematic diagram for a 3-phase machine is given in Figure 1. Two important differences between that and

Figure 1. Schematic diagram of a 3-phase self-excited generator

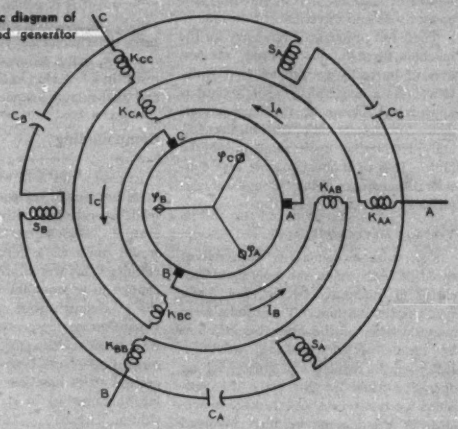

diagrams previously published are to be noted, as follows:

1. Series capacitors in the field circuits.
2. Type of compensating windings.

With regard to build-up, repeated experiments have shown that a small amount of either residual magnetism or initial excitation of any kind will start the process. Then for a given value of resistance and of capacitance in each circuit, the final, no-load steady-state condition consists of a balanced set of voltages of a given amplitude, frequency, and sequence, the last depending upon the connections and direction of rotation.

There is a pronounced tendency for the machine to maintain balanced voltages, even under badly unbalanced load conditions. As a single-phase short circuit is approached, however, it changes suddenly to single-phase operation, immediately recovering upon removal of the fault. It is of interest to note that considerable current will flow through a single-phase short circuit.

Voltage Regulation

The voltage regulation at constant speed of both single and polyphase machines is inherently better than for a synchronous machine. This results from neutralization of the armature reaction by means of compensating windings. However, the regulation is greater for a-c operation than for d-c, since the combined a-c resistances and leakage reactances of the various windings involved are greater than their d-c resistances.

Parallel Operation

Single and polyphase machines of this type will operate in parallel, either with other machines or with a line, in a satisfactory manner. When two or more machines are involved, their common frequency will be some kind of a mean of the frequencies of the individual machines when operating alone; when one is connected to a line of controlled frequency, it will be equal to the line frequency.

One feature worthy of note in connection with parallel operation consists of the lack of any need of synchronizing before making the final connection. Even for a 3-phase machine, before connecting it to the line, it is necessary only to obtain a reasonable approximation to the settings of the field resistors and capacitors, which, were the machine to build up, would give the correct conditions for synchronizing, that is, with the exceptions of speed and phase position which are important.

Motor Operation

Single and polyphase machines of this type will operate equally well as motors and generators, operation being similar to that of a d-c shunt generator. While operating as a motor, the resemblance to d-c operation persists in the starting and breakdown properties and in the speed regulation, provided that the field power factor is close to unity. Under this condition, the power factor of the armature circuit will be close to unity also.

Although it is known that power factor adjustment is possible over a restricted range, the practical limit of this has not been determined as yet. It is certain, however, that a reduced power factor will result in a lowering in the starting torque and load-carrying capacity of a motor.

Compounding

In case series field windings were used in either single or polyphase machines while operating as either motors or generators, the change in magnetization would result in a detuning of the field circuit. This would produce a frequency change in a generator or a reduction in the maximum torque of the motor, provided that no compensating arrangement were used. Although no machines with series fields have been built as yet, the general effect has been studied by shifting the brushes of straight shunt machines.

Appendix I. Three-Phase Compensating Field Windings

Referring to Figure 1, it follows from Kirchoff's laws that

$$(Z_{aa}+Z_{ba}+Z_{ca})I_a+(Z_{ab}+Z_{bb}+Z_{cb})I_b+(Z_{ac}+Z_{bc}+Z_{cc})I_c=E_a+E_b+E_c \quad (4a)$$

$$\left.\begin{aligned} I_A&=I_a-I_c\\ I_B&=I_b-I_a\\ I_C&=I_c-I_b \end{aligned}\right\} \quad (4b)$$

$$I_A+I_B+I_C=0 \quad (4c)$$

Assuming a symmetrical machine and that it is possible to devise a set of compensating field windings which will neutralize the armature reaction at all loads, the following relations hold:

$$Z_{aa}+Z_{ba}+Z_{ca}=Z_{ab}+Z_{bb}+Z_{cb}=Z_{ac}+Z_{bc}+Z_{cc} \quad (4d)$$

$$E_a+E_b+E_c=0 \quad (4e)$$

These lead to the added relation, when substituted into equation 4a,

$$I_a+I_b+I_c=0 \quad (4f)$$

Elimination of variables now gives, as one possible solution,

$$\left.\begin{aligned} I_a&=\frac{I_A-I_B}{3}\\ I_b&=\frac{I_B-I_C}{3}\\ I_c&=\frac{I_C-I_A}{3} \end{aligned}\right\} \quad (4g)$$

From these it follows that if compensating windings with one-third as many turns as there are turns per phase per pole on the armature are mounted and connected as shown in Figure 1, then the armature reaction will be counteracted under all load conditions.

Hence, the armature-compensating winding circuits will be noninductive, aside from leakage effects. Also, there will be no induced voltages between the line terminals of the machine due to transformer action with the shunt field windings.

Appendix II. Conditions for Self-Excited Operation

From Figure 2, the equations for the single-phase generator are

$$(Z_f+Z_a+Z_k-jX_c-2jX_{ka}-vX_{af})I_f+(Z_a+Z_k-2jX_{ka})I=0 \quad (5a)$$

$$-(Z_f-jX_c)I_f+Z_cI=0 \quad (5b)$$

The condition for sustained self-excited operation can be taken as that assumed for

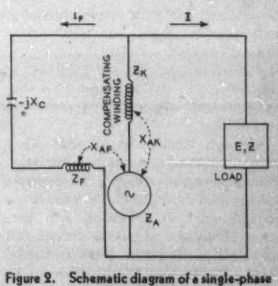

Figure 2. Schematic diagram of a single-phase self-excited generator

operation of a vacuum tube oscillator; that is

$$|Z|=0 \quad (5c)$$

This becomes for no-load conditions

$$Z_f+Z_a+Z_k-jX_c-2jX_{ka}-vX_{af}=0 \quad (5d)$$

Equating components

$$R_f+R_a+R_k=vX_{af} \quad (5e)$$

$$X_f+X_a+X_k-2X_{ka}=X_c \quad (5f)$$

Since

$$X_a+X_k-2X_{ka}<<X_f$$

for a properly designed compensating field, equation 5f becomes, approximately,

$$X_f=X_\epsilon \tag{5g}$$

or

$$\omega_0=1/\sqrt{LC} \tag{5h}$$

Under load conditions equation 5c becomes, after obvious substitutions,

$$\begin{vmatrix} R_f+R_a'-vX_{af}+j(X_f'+X_a') & R_a'+jX_a' \\ -(R_f+jX_f') & R_a'+jX_1 \end{vmatrix}=0 \tag{5i}$$

Equating components and solving

$$X_f'+X_a'=\frac{X_1R_a'R_f-X_a'Z_1^2}{Z_1^2+R_1R_a'+X_1X_a'} \tag{5j}$$

Assuming X_a' small gives, approximately,

$$X_f'=X_f-X_c=\frac{X_1R_a'R_f}{Z_1^2+R_1R_a'} \tag{5k}$$

Next, let

$$\omega=\frac{1+x}{\sqrt{LC}}=\omega_0(1+x) \tag{5l}$$

Substitution of equation 5l into equation 5k now gives

$$X_f-X_c=\omega_0(1+x)L_f=\frac{1}{\omega_0(1+x)c}\approx 2\omega_0L_fx \tag{5m}$$

Hence

$$x=\frac{\Delta\omega}{\omega_0}=\frac{\Delta f}{f_0}=\frac{X_1R_a'}{2Q_f(Z_1^2+R_1R_a')}<\frac{R_a'\sin\theta}{2Z_1Q_f} \tag{5n}$$

Appendix III. List of Symbols

p.b. = "phase belt factor"

$$=\frac{\int_{-\pi/p}^{\pi/p}B d\theta}{\int_{-\pi/l_1}^{\pi/l_1}B d\theta}$$

P = number of brush sets
= 2 for single-phase
= number of phases for $P \geq 3$

c.f. = chord, or winding pitch factor

p = number of poles

Z = number of armature conductors

m = number of parallel paths
= 1 for simplex wave and 2-pole lap windings

N = rotor speed in revolutions per minute

N_0 = speed of rotating field, or synchronous speed

Φ = maximum instantaneous value of flux per pole, in webers

$Z_{xy}=R_{xy}+jX_{xy}$, for x and $y=a$, b, and c, is the mutual impedance between phase windings of armature. In this

R_{xy} is the result of copper and stray core losses
X_{xy} is the result of leakage fluxes only

E_a, E_b, E_c = phase voltages caused by the rotating field

I_A, I_B, I_C = line currents

I_a, I_b, I_c = armature-phase currents

$Z_f=R_f+jX_f$ = equivalent impedance of a shunt field circuit

$Z_a=R_a+jX_a$ = phase impedance of the armature

$Z_k=R_k+jX_k$ = phase impedance of the compensating field

X_{ak} = mutual reactance between armature and compensating windings

X_{af} = mutual reactance between shunt field and armature

v = speed in terms of synchronous speed

f_0 = no-load frequency

Δf = change in frequency due to load

$Z_a'=Z_a+Z_k-2jX_{ak}$

$Z_f'=Z_f-jX_c$

$Z_1=R_1+jX_1$ = impedance of the load

$\sin\theta$ = load reactive factor

Q_f = quality factor of field windings

References

1. Aircraft Inverter Construction, C. T. Button. AIEE Transactions, volume 62, 1943, September section, pages 598–602.

2. Electronic Frequency Changers for Aircraft, O. E. Bowlus, P. T. Nims. Electrical Engineering, volume 66, May 1947, pages 463–6.

3. Constant-Speed Drives for Aircraft Alternators, C. J. Breitwieser. AIEE Transactions, volume 64, 1945, November section, pages 763–8.

4. Electrical Engineering Papers (book), B. G. Lamme. Pages 77–110.

5. Calculation of Electrical Apparatus (book), C. P. Steinmetz. Chapter 20.

6. Fundamentals of Alternating Current Machines (book), A. P. Sah. Chapter 23.

7. Alternating Current Machines (book), A. F. Puchstein, T. C. Lloyd. Chapter 30.

8. Application of Tensor Analysis to Rotating Electrical Machinery (book), Gabriel Kron. *General Electric Review*, Schenectady, N. Y. Page 52.

9. Low Frequency Self-Exciting Commutator Generator, J. L. Hull. AIEE Transactions, volume 52, 1933, pages 317–23.

10. Electrical Machine Design (book), Alexander Gray. Pages 361–87.

11. Universal Electric Motors, A. F. Puchstein, E. E. Kimberly. Engineering Experiment Station Bulletin 53. The Ohio State University.

Discussion

O. Krauer (General Aviation Equipment Company, Inc., New York, N. Y.): In his paper, Roys mentions the attractive possibility of operating a 3-phase unit near synchronous speed in direction of field rotation in order to avoid excessive bar-to-bar voltage in the commutation zone.

Roys also proves that the resultant voltage in the armature approaches zero as the armature is approaching synchronous speed in the direction of rotation. Figure 1 of this discussion indicates the vector conditions existing in this range. It appears that at synchronous speed all the energy is supplied by the compensating field winding and it is difficult to imagine stable operations in this region if the unit is self-excited and completely disconnected from any other sources of power. It would be greatly appreciated if Roys could elaborate on this point. Specifically, it would be very interesting to learn whether or not stable operation under these conditions at no load and under load actually was achieved.

Stable operation appears feasible above synchronous speed and through the entire range where the armature is rotating against field rotation. However, in this instance the bar-to-bar voltage in the commutating zone is large and limitations similar to those established for the single phase unit appear to exist.

Single-Phase Unit

In order to appreciate the governing factors, let us consider a single-phase generator. Figure 2 shows a d-c generator and it is assumed that its entire magnetic circuit is laminated. If this unit is operated on a-c excitation the relationship between field current and terminal voltage remains unaffected because the voltage induced by transformation is cancelled within the windings and only voltage due to rotation appears at the brushes. Assuming that the generator is built with a maximum practical number of bars, it follows that the entire design is determined by the desired output voltage and armature speed and is unaffected by the intended operating frequency. It is evident then that for a given maximum flux density in the air gap, the bar-to-bar voltage in the commutating zone is proportional to the frequency and the commutating difficulties mount in this proportion.

A single-phase generator intended for an output of approximately 3,000 volt-amperes was built and tested. The rated voltage is 115, the speed range between 2,500 and 8,000 rpm and the frequency approximately 400 cycles per second. The bar-to-bar voltage in the commutating zone is of the order of 20 volts. It was found that commutation was quite unacceptable. Tests over the entire frequency range from approximately 80 cycles to 400 showed a consistent deterioration with increase in frequency. The armature was rewound for approximately 20 volts, one turn per coil. In this instance the commutation was acceptable throughout the frequency range.

It was difficult to obtain good regulation under load. Evidently the leakage impedance of the armature is large enough to cause voltage collapse at approximately half load if operated at 400 cycles. The low voltage armature was tested in conjunction with a transformer so that the field winding was energized from 110 volts as before. It was found that the additional transformer leakage reactance prevented any operation under load.

No particular difficulty was experienced in obtaining self-excitation although occasionally it was necessary to "tease" the circuit by switching capacitors. The wave form was excellent except for commutating ripples which can be filtered out without much difficulty.

It was found that tuning for 400 cycles at low generator speeds was very much more difficult than at high speeds. This was attributed to the change in impedance of the

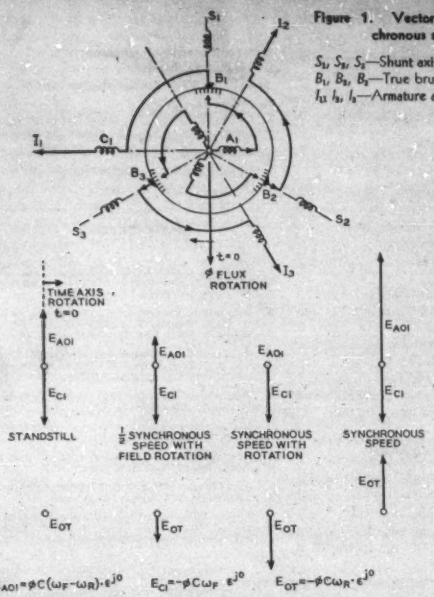

Figure 1. Vector conditions in synchronous speed range

S_1, S_2, S_3—Shunt axis
B_1, B_2, B_3—True brush axis
I_1, I_2, I_3—Armature and compensating axis

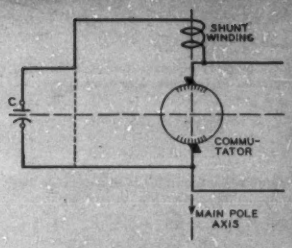

Figure 2. D-c generator

E_{a01}—Induced voltage in equivalent phase A_1 armature
E_{c1}—Induced voltage in compensating winding phase 1
ωF—Field rotation $= n\pi/30$
ωR—Armature rotation $= n\pi/30$

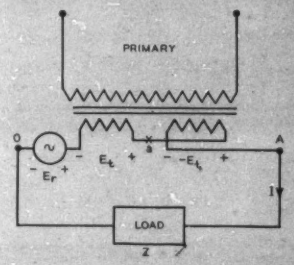

Figure 3. Analogous transformer-generator combination

shunt winding at different levels of the saturation curve.

I wish to summarize my viewpoints on the subject as follows:

1. Operation of single-phase units with bar-to-bar voltages in the commutating zone exceeding five volts is not practical at present and therefore low voltage armatures and step-up transformers appear to be required.

2. Impedance drops in armature interpole and compensating windings present great difficulties. They are of the order of 5 times IR drop.

3. The 3-phase unit appears to be subject to similar limitations due to apparent difficulties with operation near synchronous speed (in direction of rotation).

4. The generator appears quite feasible and practical for moderate frequencies such as 60 cycles but all difficulties mount at least in proportion to the operating frequencies.

Carl S. Roys: Referring to Krauer's remarks pertaining to the 3-phase machine, it has been operated as motor and generator over a wide range of load and speed conditions. These included self-excited generator operation at synchronous speed. Under no conditions were there any signs of either instability or power transfer due to transformer action. As stated in the paper, the armature terminal voltages became zero at no load and equal to the armature impedance drops at load, for synchronous speed operation.

As an aid to an understanding of the operation of the polyphase machine, consider the analogous transformer-generator combination shown in Figure 3 of this discussion. In this, the two secondary windings are connected in opposition. With the terminology used in the paper, the electromotive force equations are

$$(Z+Z_a')I = E_r + E_t - E_t \quad (1)$$

$$E_{a0} = E_r + E_t - (Z_a + Z_{ak})I \quad (2)$$

$$E_{A0} = E_r - Z_a'I = ZI \quad (3)$$

When $E_t = -E_t$, these become, respectively,

$$(Z+Z_a')I = E_r \quad (4)$$

$$E_{a0} = -(Z_a + Z_{ak})I \quad (5)$$

$$E_{A0} = E_r - Z_a'I = ZI \quad (6)$$

Thus, the only change is in the voltage E_{a0}.

Obviously there is no transfer of power in the system due to transformer action, the total complex power delivered being given by,

$$P = E_r I \quad (7)$$

Before closing this part of the discussion, it is the authors' belief that the popular conception that a "rotating field" actual rotates can lead to misleading results. It consists actually of a stationary distribution varying in a fashion such that the positions of crests and nodes progress around the air gap. In this regard, it is similar to the case of waves on deep water, in which the water rises and falls without longitudinal motion.

With this in mind, instead of assuming no voltages set up in the rotor conductors when moving at synchronous speed, it can be shown that the induced and generated voltages are equal and opposite. Hence, they cannot set up any current when acting alone. However, if an extra electromotive force is added, such as one which will neutralize the above induced voltages, for example, the instantaneous mechanical power will be proportional to the product of generated voltage due to rotation and conductor current, just as though the induced voltage were not present.

With reference to the questions regarding single-phase machines, the authors understood that the machine which he discussed was not provided with compensating windings. Under those circumstances satisfactory commutation could only be achieved under very restricted voltage and load conditions.

The Hysteresis Motor—Advances Which Permit Economical Fractional Horsepower Ratings

HERBERT C. ROTERS
MEMBER AIEE

Synopsis: The theory of the development of torque in a hysteresis motor is analyzed from both the hysteresis lag angle and total loop energy points of view. A new development, comprising the use of a closed slot stator in co-operation with a hysteresis rotor, which permits building hysteresis motors of high power output at high efficiency is explained qualitatively and supplemented by considerable quantitative experimental data. A new method of stator construction, permitting the use of closed slot stator laminations assembled on a mandrel with nonmagnetic bearing supporting spiders, wound externally in either a d-c type of armature winding machine or with form-wound coils, impregnated with a thermosetting resin and baked to form a unitary structure, is described. The electrical design of the machine is covered and quantitative data on both design details and operating characteristics are given on several models.

THE hysteresis motor, as a practical type of power motor, is virtually unknown. As a scientific curiosity and as an unloaded synchronous motor it has been known and used for many years. Almost all prior art applications have been confined to driving clocks or other timing instruments. The synchronous clock motor develops an inappreciable power output, of the order of from 5 to 10 milliwatts output. The input runs from 2 to 3 watts. The efficiency limits, therefore, range from a high of 0.5 per cent to a low of 0.16 per cent. A few larger hysteresis motors have been built but they do not appear to have assumed commercial importance. It is the purpose of this paper to describe changes in the art which have made practical synchronous motors of the hysteresis type of relatively large power outputs and high efficiency. Thus, some of the motors to be described are as large as one-seventh horsepower with an efficiency as high as 73 per cent. Developmental models have been built with an output of one-fourth horsepower and an efficiency of 80 per cent. The advances in the art primarily responsible for this improvement in hysteresis motors are

(*a*) The development of a method of eliminating spurious hysteresis loss in the rotor of the motor.

(*b*) The development of a method of reducing the exciting current.

The spurious hysteresis rotor loss, usually present in these machines, is produced by an undulation of the space distribution of the flux density of the rotor relative to the revolving field. This loss manifests itself as heat in the rotor, and in the usual prior art motor has been of the order of from one to three times the power output of the rotor. Inasmuch as this loss is due primarily to variations in magnitude and angular velocity of the revolving field, it can be eliminated by having an ideal revolving field. Such an ideal field can be produced only by a distributed winding in a stator having an infinite number of slots with an infinitesimal slot opening. Practically, a reasonably close approximation to the ideal can be produced by using a winding distributed in a finite number of slots, the openings of which are closed. Such a stator construction used with the right geometrical proportion of slots will reduce the spurious hysteresis loss to a negligible quantity.

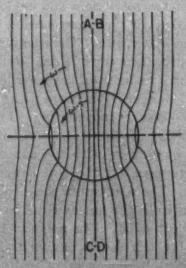

Figure 1. Iron rotor without hysteresis in magnetic field

The elimination of the spurious hysteresis or parasitic loss of the rotor has a secondary benefit which is not at first obvious. First, in prior art machines the attempt has been made to minimize this spurious loss by using a large air gap between the stator and the rotor, which of course, results in an excessive copper loss for excitation of the magnetic field. Reduction of the parasitic loss by the use of closed slots permits the use of a short air gap and so greatly reduces the copper loss.

The new permanent magnet materials available in recent years also have increased the available hysteresis energy per unit volume of material. While this factor enabled the reduction of the motors to a practical size, it had no effect on the unacceptably low efficiency inherent in this type of motor.

The sum net total effect of the elimination of parasitic rotor losses, reduction of copper loss, and the improvement in magnetic materials makes the hysteresis synchronous motor comparable in size and efficiency with the ordinary induction motor.

In certain applications when it is feasible momentarily to overexcite the

Paper 47-218, recommended by the AIEE electric machinery committee and approved by the AIEE technical program committee for presentation at the AIEE Middle Eastern District meeting, Dayton, Ohio, September 23-25, 1947. Manuscript submitted January 28, 1947; made available for printing August 7, 1947.

HERBERT C. ROTERS is consulting engineer, Fairchild Camera and Instrument Corporation, Jamaica, N. Y., and adjunct professor of electrical engineering, Stevens Institute of Technology, Hoboken, N. J.

rotor, it is possible to produce a state of permanent magnetization in the rotor such that the required exciting current is reduced greatly, resulting in a further diminution of the copper loss.

Another important feature of this type

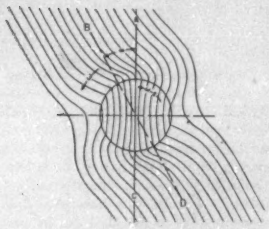

Figure 2. Iron rotor with hysteresis in magnetic field

of synchronous motor is the absence of transient oscillations of the rotor upon the removal or sudden application of load. Effective damping is produced by the hysteresis loss associated with the oscillation.

Theory of Operation

A. Qualitative

On the premise of an ideal magnetic field distribution it is a simple matter to calculate the performance of a cylindrical rotor up to the point of synchronism as the rotor goes through a normal magnetization cycle. As soon as synchronism has been reached the magnetic state of the rotor is unpredictable, being influenced by changes in mechanical load and variation or surges in line voltage. An ideal magnetic field distribution in a hysteresis motor is one that will cause no undulation of rotor flux density; that is, when slipping behind the revolving field the flux density at any point in the rotor must follow a major hysteresis loop continuously with no momentary recessions in flux density which would give rise to minor loops: likewise, when running at synchronism in a steady state, the flux density of any point in the rotor must remain constant. This condition will be realized if the vector distribution of magnetomotive force from the stator is absolutely invariant, revolving as a whole at constant angular velocity, and if, in addition, the rotor turns at constant angular velocity in synchronism with the field.

Assume in Figure 1 that we have a field as defined here revolving at an angular velocity ω, and a rotor within the field, which is slipping behind the field at S radians per sec.

If the rotor exhibited no hysteresis the magnetization of the rotor would be in phase with the magnetomotive force of the stator, and the magnetic axis A–C of the rotor would coincide with the axis B–D of the field, as illustrated, and there would be no torque on the rotor.

However, when hysteresis is present the magnetization of the rotor will lag behind the magnetizing force of the stator and the axis A–C defining the axis of magnetization in the rotor will lag behind the axis of the stator magnetomotive force B–D, by an angle α as shown in Figure 2. Assuming a sinusoidal field form, the torque on the rotor obviously will be proportional to the product of the fundamental component of the stator magnetomotive force by the fundamental component of the rotor flux and the sine of the angle of lag α.

Figure 3. Flux density and magnetic intensity relationships in a rotor of 17 per cent cobalt permanent magnet steel

B in kilomaxwells per square inch; H in ampere-turns per inch; $H_f' = 255$ ampere-turns per inch peak

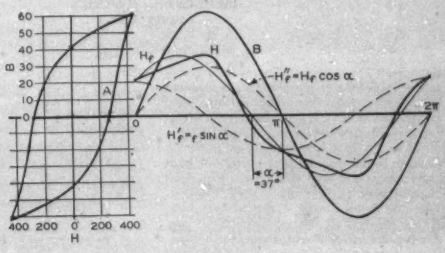

This condition is illustrated in Figure 3, which shows the hysteresis loop A for a permanent magnet steel rotor and the curve of instantaneous rotor magnetomotive force H derived from A for the sinusoidal rotor flux density wave B.

These curves as drawn show the relations in the rotor only and neglect the magnetomotive force consumed in the air gap and stator iron. The exciting magnetomotive force wave H can be resolved into two fundamental harmonic components: sinusoid H_f'' in phase with the flux density wave, representing the real magnetizing component, and sinusoid H_f' in quadrature with the flux density wave, representing the real power component. The resultant of these two components is H_f the fundamental harmonic component of H. The angle of lag between the flux density wave B and the fundamental component of stator magnetic intensity H_f is the angle α referred to in Figure 2.

The power converted from the electrical to the mechanical form per unit volume of rotor by virtue of hysteresis will be proportional to the following:

$$P \propto BH_f' \propto BH_f \sin \alpha$$

For the purpose of quantitative illustration the loop A of Figure 3 is an actual experimental loop obtained from a sample of 17 per cent cobalt permanent magnet steel (Simonds 81), and the magnetic intensity wave H has been derived from the loop A, and resolved into the harmonic components shown. The actual power converted by means of the hysteresis loop will be,

$$P = 4.44\, fB \frac{H_f \sin \alpha}{\sqrt{2}} \text{ watts per cubic inch}$$

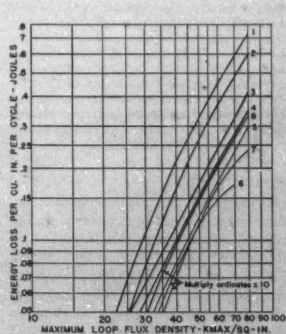

Figure 4. Hysteresis energy loss of commercial magnet materials

1—Seventeen per cent cobalt, Simonds 81
2—Same as 1, drawn at 300 degrees Fahrenheit
3—Three per cent cobalt, Simonds 83
4—Three and one half per cent chrome, Simonds 73
5—Same as 4, drawn at 300 degrees Fahrenheit
6—Alnico I, Simonds
7—Alnico II, Simonds
8—Alnico V, Simonds

where 4.44 fB represents the rms voltage per turn induced in the stator by the flux in one square inch of the rotor, and

$$\frac{H_f \sin \alpha}{\sqrt{2}}$$

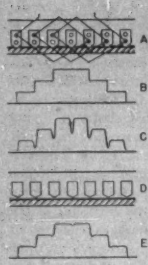

Figure 5. Open and closed slot magnetomotive force distribution

is the rms magnetomotive force per inch of rotor length in phase with the voltage induced in the stator. Assuming a frequency f of 60 cycles per second and using the numerical values shown on Figure 3, the following numerical result is obtained for this steel when operating at a maximum flux density of 62 kilomaxwells per square inch:

$$P = 4.44 \times 60 \times 62 \times 10^{-8} \times \frac{255}{\sqrt{2}}$$

$$= 29.8 \text{ watts per cubic inch}$$

The pattern of Figure 3 is correct only when the rotor is slipping or just has accelerated to incipient synchronism, and represents the magnetic conditions giving the maximum torque.

Disregarding any effects of eddy currents in the rotor this is the maximum torque which just can be brought into synchronism. When the rotor is slipping the axis of magnetization of the rotor will remain at a constant position with respect to the stator field, lagging by the angle α, but will be slipping with respect to the rotor; when synchronism has just been reached the rotor axis of magnetization will become stationary with respect to the rotor but will continue to lag the stator axis by α.

When the torque load is removed from the rotor the angle α will close and the rotor will advance in phase until the axis of rotor magnetization coincides with that of the stator where the mechanical torque is zero. If the rotor is advanced beyond this position by the application of a driving torque the machine, of course, will become a generator. It is obvious that during this process the component of voltage induced in the stator will shift its phase angle from a power absorbing component at full motor torque to a generating component when the rotor is driven.

However, whenever the rotor is allowed to change its phase, as for instance, from the full load position with a hysteresis lag angle of α to the no load position, the magnetization of the rotor will be changed. Thus, if it is loaded after having been allowed to run at no load, it will carry more load before it pulls out of synchronism than it previously was able just to synchronize. This is understandable because at no load the rotor axis of magnetization is oriented fully to that of the stator and hence is magnetized more fully than when slipping. It is for this reason that accurate quantitative results must be predicated upon a known state of magnetization. Such a state is most easily obtainable when the rotor is slipping.

B. Quantitative

The foregoing system of analysis is particularly useful for obtaining a qualitative picture of the mode of operation. While

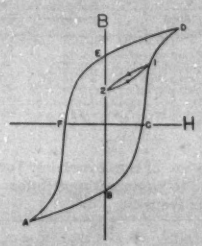

Figure 6. Major loop with parasitic minor loop

it can be used for quantitative calculations of rotor torque as has been illustrated, it is more convenient to use an energy method. Referring to Figure 2, as the rotor slips, the axis of rotor magnetization sweeps around the rotor, alternately subjecting each particle of the rotor to full magnetization first in one direction, and then in the other, at a periodicity corresponding to the slip.

The flux density–magnetic intensity relationship in each particle of rotor steel thus is described by a magnetic hysteresis loop, the various hysteresis loops for the various particles being identical except that they are displaced in phase corresponding to the electrical angular position of the particles. Each particle will go through a complete magnetic cycle for each pair of poles it slips by, and heat energy equal to area of the hysteresis loop for the particle will be released. As each particle of the rotor goes through the same maximum flux density, each will have the same loss and the total loss of the rotor per pair of poles slipped will be

$$W = V \int_{B=0}^{B=0} HdB \text{ joules}$$

where

$$\int_{B=0}^{B=0} HdB$$

is the area of the hysteresis loop in joules per cubic inch per cycle, and V is the volume of the rotor in cubic inches.

This energy loss in the rotor is transmitted from the stator through the agency of the magnetic field, as a torque times the speed of the field. The hysteresis power developed in the rotor will be

$$P = fV \int_{B=0}^{B=0} HdB \text{ watts}$$

and the torque developed will be

$$T = \frac{fV \int HdB}{2\pi n} \text{ joules per radian}$$

where n is the rotational speed of the stator field in revolutions per second, or converting to conventional units

$$T = \frac{fVW_h}{2\pi n} \times 8.86$$

$$= \frac{1.41\, fVW_h}{n} \text{ inch-pounds}$$

$$= \frac{22.6\, fVW_h}{n} \text{ inch-ounces}$$

where

W_h = area of hysteresis loop in joules per cubic inch per cycle
V = volume of rotor in cubic inches
n = rotational speed of stator field in revolutions per second

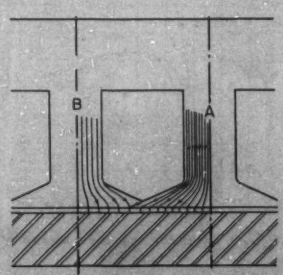

Figure 7. Distribution of flux in slot bridge

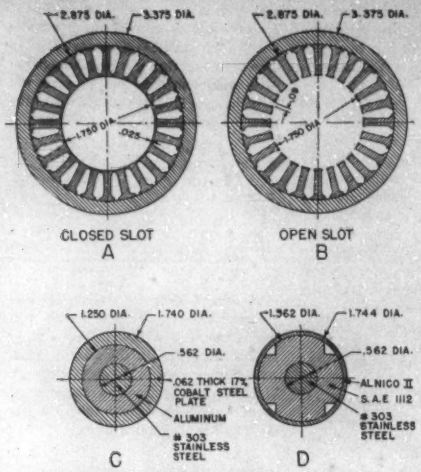

Figure 8. Stator and rotors used to measure benefits obtained by closed slot stator construction

Of this hysteresis power transmitted to the rotor, a portion, proportional to the slip, appears as heat in the rotor and the balance proportional to rotor speed appears as mechanical work at the shaft.

In Figure 4 there are given curves of W_h as a function of the maximum cyclic loop flux density Bm for various suitable permanent magnet materials.

From these data it may be seen that the power output that can be realized per cubic inch of steel is quite large. Thus, taking $Bm = 70$ kilomaxwells per square inch as a practical value for Bm, the following powers can be obtained per cubic inch of steel at 60 cycles per second, under ideal field conditions.

Table I

Steel	W_h, Joules Per Cu In. Per Cycle	P, Watts
3 1/2 per cent chromium	0.28	16.8
3 per cent cobalt	0.325	19.5
17 per cent cobalt	0.59	35.4
37 per cent cobalt	0.83	49.9
Alnico II	2.1	126
Alnico V	2.7	162

Deviation of Synchronizing Torque Due to Undulation of Rotor Flux Density

The potential outputs per cubic inch of rotor shown in Table I are predicated upon an ideal revolving field. The field form of an actual motor deviates from the ideal due to the following causes:

A. Slot Openings
B. Winding Distribution

A. Slot Openings

The most important factor in causing the synchronizing torque of a hysteresis motor to deviate from the ideal is the effect of open stator slots. These cause violent fluctuations in rotor flux density as the rotor passes from the short air gap under the solid tooth face to the relatively long and open gap under the slot opening. This results in the production of minor hysteresis loops superposed on the major loop. As these minor loops represent heat loss in the rotor, the energy for which is obtained as a mechanical drag on the rotor, they properly may be referred to as parasitic loops and the consequent loss as parasitic loss. This loss was previously so large in hysteresis motors that it presented a design limitation.

In Figure 5*A* there is shown a section of an open slot stator with the windings of one phase group. Figure 5*B* shows the wave form of magnetomotive force developed by the winding of Figure 5*A*. If the rotor has a very short air gap between it and the stator as shown in Figure 5*A*, the magnetomotive force available for the rotor directly under the teeth will be almost the same as that shown in Figure 5*B* because the reluctance drop in the air gap and stator yoke and teeth will be relatively small. However, between the teeth most of the magnetomotive force will be consumed in the reluctance of the long air path resulting in a reduction of the flux density on the surface of the rotor opposite the slots. This is illustrated in Figure 5*C*. Consequently, a drop in the rotor will experience a periodic diminution of flux density as it passes under the slot. This undulation in flux density is independent of any wave-form distortion introduced by the winding arrangement. Thus, referring to Figure 6, each point on the rotor will describe a minor loop similar to that shown by 1–2 as many times per cycle of the supply as there are teeth per pair of poles when the rotor is running synchronously.

The energy represented by these minor loops appears as heat in the rotor and reflects itself as a drag torque on the rotor. The maximum synchronous power that can be developed is proportional to the area of the major loop *ABCDEFA* of Figure 6. The power loss due to the slot openings will be proportional to the area of the average minor loop 1–2 multiplied

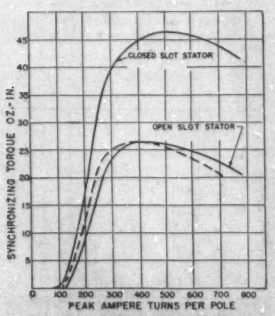

Figure 9. Synchronizing torque as affected by slot openings

Rotor of Figure 8C, 0.005 inch air gap; stators of Figure 8

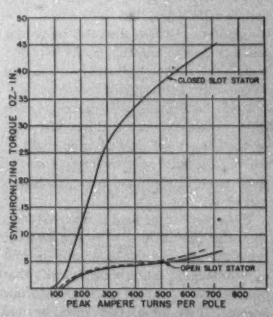

Figure 10. Synchronizing torque as affected by slot openings

Rotor of Figure 8D, 0.003-inch air gap; stators of Figure 8

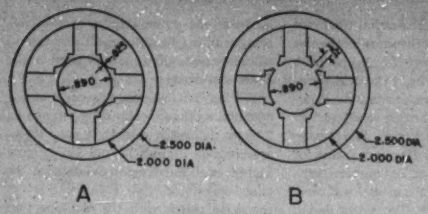

Figure 11. Four-slot stators used to show benefits obtained by closed slot construction

by the number of teeth per pair of poles. Without special precautions this loss is a major percentage of the power developed in the primary loop.

In some cases, where the slot openings are relatively wide and the air gap short, the minor loops can reach such proportions that their total area exceeds that of the major loop. When this occurs, the rotor will slip below synchronism. Equilibrium below synchronism is usually possible with a solid rotor due to the increase in torque produced by eddy currents in the rotor. Therefore, it has been the conventional practice deliberately to make the air gap between the stator and the rotor large so that the field between the slot openings is more uniform, thus minimizing the field distortion at the surface of the rotor to the extent where synchronous operation is possible. As stated before this practice requires increased magnetizing current and results in increased copper losses and reduced efficiency.

The parasitic hysteresis loss caused by open slots can be practically eliminated, or at least greatly minimized, if an unusual type of slot construction is resorted to. This consists of closing the slots as shown in Figure 5*D*. In conventional induction and synchronous motors, closed slots would be considered very detrimental to the characteristics because of the resulting reduction in power factor and output caused by shunting the flux away from the rotor. However, in the case of the hysteresis motor, closing the slots produces advantages which far outweigh the disadvantages just cited. Referring to Figure 5*E*, the effect of the closed slots will be to greatly reduce the dips in instantaneous rotor flux density in the intertooth space. The exact quantitative solution for the magnetic potentials along a closed slot would, of course, be very difficult to obtain as they will vary with the degree of saturation of the iron.

In Figure 7 let tooth *A* be at a higher potential than tooth *B*. Then, besides furnishing flux to the rotor, flux must flow from *A* to *B* through the slot bridge in order to establish a potential drop equal to the difference in potential between *A* and *B*. However, as the flux passing through the bridge is not sufficient to supply that required for the rotor under the adjacent tooth edge of *B*, some must be supplied direct from *B*. Hence, there will be a point on the tip of tooth *B* slightly left of the center of the slot bridge which will be at a potential slightly less than that at center of tooth *B*. The resulting wave-form pattern will be similar to that shown in Figure 5*E*, which pattern obviously will have less parasitic hysteresis loss due to minor loops than that of Figure 5*C* for open slots.

Because of the difficulty of quantitative deductions, the most direct data on the benefits of closed slots can be obtained by experiment. For this purpose two identical stators were prepared. The magnetic circuits of these stators are illustrated in Figure 8, *A* and *B*, and differ only in that one, Figure 8*B*, had the intertooth bridges milled away to make an open slot of conventional proportions. Both stators were wound the same; 2-phase 4-pole lap winding of two-thirds pitch with 75 turns of number 27 wire per coil. Two rotors of different types, illustrated in Figure 8, *C* and *D*, were tested in each stator.

In Figure 9 there is shown the synchronizing torque* developed by the rotor of Figure 8*C* in the stators of Figure 8, *A* and *B*, plotted as a function of the maximum ampere turns per pole. These data show that the closed slot stator develops about 75 per cent more torque in the higher operating range for the same ampere turns, and will develop a maximum synchronizing torque of 46.5 ounce-inches as compared to 26.5 ounce-inches for the open slot stator.

Part of the increase in torque is due to the fact that with bridged slot construc-

* By synchronizing torque is meant the torque the rotor can just pull into synchronism. It usually is checked by pulling the rotor slightly out of synchronism by momentarily adding load, as for instance, with a finger on the brake wheel and seeing if the applied load is pulled back into synchronism.

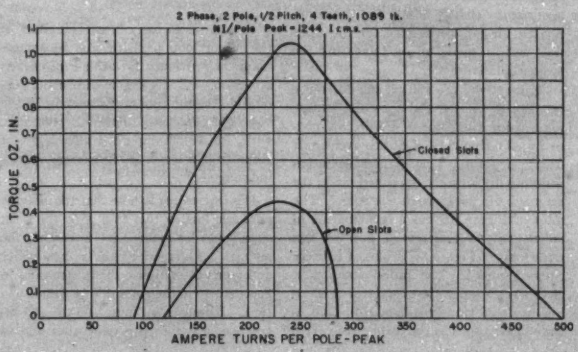

Figure 12. Synchronizing torque as affected by stator slot openings

Stators of Figure 11, 0.008-inch air gap

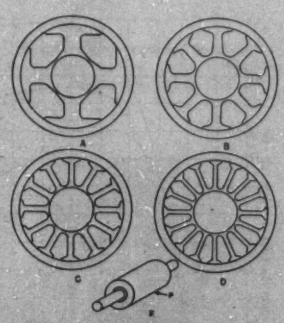

Figure 13. Stators and rotor used to measure the effect of the number of stator slots per pair of poles

P—Permanent magnet steel rotor

tion the same magnetomotive force produces a greater flux due to the lower reluctance of the air gap between the stator and rotor. However, the increase in torque due to this factor is a small part of the total improvement in synchronous torque.

Besides the increase of torque noted above a very significant difference in the operation of the two stators is the limit of synchronizing torque. The closed slot stator will develop a maximum torque of 46.5 ounce-inches at 500 ampere turns per pole. Increases in magnetomotive force above this value will cause the actual synchronizing torque to decrease. The open slot stator, however, will develop only 26.5 ounce-inches maximum at 400 ampere turns per pole and any further increase in magnetomotive force will decrease the torque. Obviously, this great increase in maximum synchronizing torque of 75 per cent can be attributed only to the beneficial effects of the closed slots, because any change in flux due to the decreased air-gap permeance for the open slots can be made up by increasing the magnetomotive force.

Figure 10 shows a still greater difference between the closed and open slot stators when using the rotor of Figure 8*D* consisting of a thin shell of Alnico over a soft steel cruciform. This greater deviation undoubtedly is due to the difference in the magnetic circuit through the rotor. The rotor of Figure 8*D* has a combination of radial and circumferential flow of flux while that of Figure 8*C* is almost entirely circumferential. The radial component of the field under the cruciform arms of Figure 8*D* obviously will be subjected to large fluctuations as the rotor passes from tooth to slot because the radial thickness of the Alnico is about the same as the slot width. The very short air gap of 0.003 inch also helps to intensify the field variations. For this particular rotor the maximum synchronizing torque developed in the closed slot stator was 43.5 ounce-inches as compared to 7.4 ounce inches for the open slot stator, at 720 ampere turns per pole, or an increase of 490 per cent. This is a case in which the motor design with open slots has caused the effect of the minor loop parasitic loss to assume major proportions. For this type of construction with any degree of practical excitation the limiting synchronizing torque was not reached. This characteristic with closed slots imparts a high degree of stability in a motor in the normal operating range.

It is interesting to note that the extreme parasitic loss in this case with the open slots could be reduced by increasing the air gap. A large air gap acts like a buffer and tends to minimize the fluctuations in flux density in the rotor due to slot distortion. However, an increased air gap introduces a higher gap reluctance and so increases the power required for excitation, resulting in an over-all decrease in efficiency and output as compared to the closed slot design.

Further data, showing the effect of slot openings on the synchronizing torque of a 2-phase 1/2-pitch 4-tooth 2-pole stator are given in Figures 11 and 12. Figure 11*A* gives all the dimensional data for the closed slot stator, while Figure 11*B* shows the same stator with the slot openings milled in. These stators are identical in all respects other than the slots. Figure 12 gives the synchronizing pull-in torque for each stator, as a function of the peak sinusoidal ampere turns per pole, when used with the same rotor. It will be observed that the addition of slots decreases the maximum synchronous torque that can be developed from 1.04 ounce-inches to 0.44 ounce-inch, a decrease of 58 per cent. Also the range of magnetomotive force over which synchronism can be maintained regardless of torque, varied from 498 to 93 peak ampere turns per pole for the unslotted stator, and from 288 to 168 for the slotted stator, a decrease of 58.4 per cent. The efficiency of the two stators also will be in about the same porportion.

Table II

Figure 8	Phases	Poles	Slots	Bore, In.	Slot Bridge Thickness, In.	Turns Per Coil	Coils in Series Per Phase	Coil Pitch	Avg Amp Turns Effective Over Pole Face Per Peak Amp
A	2	2	4	0.6196	0.0225	1,072	2	1/2	.648
B	2	2	8	0.6198	0.0240	432	4	3/4	.631
C	2	2	12	0.6220	0.0245	305	6	5/6	.592
D	2	2	16	0.6198	0.0215	242	8	5/8	.602

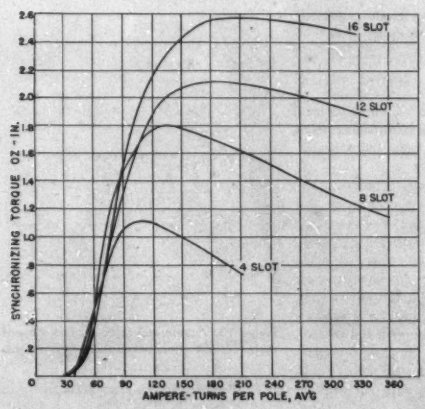

Figure 14. Synchronizing torque curves showing the effect of the number of slots per pair of poles

B. Number of Slots

The number of slots per pair of poles and the distribution of the coils in these slots determines the wave form of stator magnetomotive force. As the number of slots is increased the wave form is improved, approaching a sine wave more closely. However, as the wave advances it will undulate in magnitude, causing the magnetomotive force effective under a given region of the wave to vary up and down about an average value. The extent of these fluctuations will depend on the number of slots per pair of poles, decreasing as the number of slots increases. The actual variation in stator magnetomotive force for a 2-phase stator has been calculated from the instantaneous wave forms for a point on the rotor surface as it rotates synchronously with the field. This variation amounts to from 15 to 50

per cent of the average magnetomotive force for 12 and 4 slot stators, respectively. The actual flux density variation is reduced greatly below this figure when closed slots are used because the bridges between the teeth reduce the absolute magnitude of the variations.

A quantitative analysis of the effect of changing the number of stator slots would be very difficult, if not impossible, when closed slots are used. However, some conclusions can be drawn from carefully correlated experimental work. For this purpose a series of four stators, built to be identical, were prepared. These stators, illustrated in Figure 13, *A*, *B*, *C*, and *D*, have 4, 8, 12, and 16 slots, respectively. Their winding data are given in Table II.

Table III

No. of Slots	Max Synchronous Torque, Oz-In.	Average Ampere Turns Per Pole Effective	Relative Synchronous Torque, Per Cent	Relative Torque, Per Cent
4	1.12	110	100	43
8	1.81	134	161	70
12	2.12	183	180	82
16	2.59	193	231	100

Each one of these stators was tested on a balanced 2-phase power supply using the rotor illustrated in Figure 8*E*. This rotor is a plain annular ring of 17 per cent cobalt steel, 0.6104 inch outside diameter, 0.375-inch inside diameter, and 1 inch long.

In Figure 14 there are shown curves of synchronizing torque (as defined previously) plotted against the average stator magnetomotive force effective over the pole face.* An examination of these data gives the maximum values of synchronizing torque given in Table III.

Application of field strengths in excess of those shown in the table cause the synchronous torque to decrease as may be seen by reference to Figure 14. If a comparison is made at the ampere turns per pole (193) corresponding to maximum synchronizing torque for the 16-slot stator, we get Table IV.

Table IV

No. of Slots	Synchronous Torque, Oz-In.	Relative Torque, Per Cent
4	0.82	32
8	1.69	65
12	2.12	82
16	2.59	100

It is, therefore, quite advantageous to use the maximum possible distribution of the winding if one desires to develop the maximum possible power from a given rotor. A further study of Figure 14 shows that for low magnetizing forces all stators are equally good. Another interesting feature is that the rate at which the synchronizing torque drops off as the magnetizing force is increased after the maximum has been reached, is roughly inversely proportional to the number of slots. Thus, the torque of a 4-slot stator will fall off very rapidly if the magnetizing force is increased beyond that giving maximum synchronizing torque.

The explanation of these benefits derived by using a larger number of slots per pair of poles appears to be associated with the saturation of the slot bridges. Referring to the data of Table II, the comparison shown in Table V may be made.

Table V

No. of Slots	Conductors Per Slot	Relative Slot Amp-Turns for the Same Effective Magnetomotive Force Over Pole Face
4	2.144	413
8	864	170
12	610	128
16	484	100

These data show that the slot bridge of a 4-slot stator will reach saturation when the effective magnetomotive force over the pole face is only approximately 25 per cent of that required in a 16-slot stator to produce saturation. When the slot bridge saturates, it is essentially the same as having an open slot because the saturated bridge has a permeability only a few times that of air. Under these conditions excessive parasitic loss occurs at relatively low excitations. The use of a larger number of slots primarily enhances the effectiveness of the slot bridges because it places several of them in series, allowing them to perform their function of preventing pulsation in rotor flux density to much higher values of total pole magnetomotive force.

Practical Construction Embodying Closed Slots and Distributed Windings

A practical method of construction of a closed-slot distributively wound motor with a short air gap which retains all the advantages of the closed slots, together with ease of construction, is illustrated in the section drawing of Figure 15 and the photographs shown in Figure 16.

Figure 15 shows a cross section of the motor in which the various component parts are labelled. In Figure 16*A*, the various components which make up the stator are shown. The method of assembly and winding the stator is as follows: Two brass spiders with sufficient laminations to give the desired stack length are assembled on a mandrel as shown in *B*. The spiders and laminations are a reasonably close fit on the mandrel, the clearance between the diameters being between 0.0005 and 0.001 inch. The laminations preferably have been punched

Figure 15. Cross section of motor showing unitary structure and single concentricity bearing capsule alignment

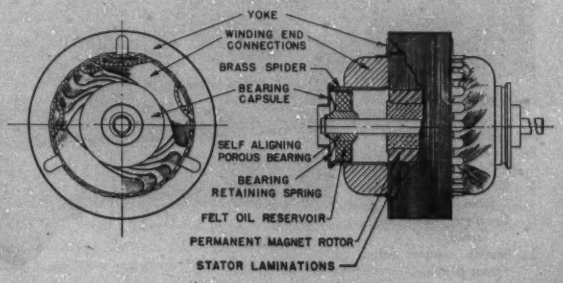

* The torque of a hysteresis rotor like that of Figure 13*E* is proportional to the maximum circumferential flux density, which in turn is merely proportional to the maximum rotor flux. Therefore, when plotting Figure 14 the average value of magnetomotive force over the pole face was used for the axis of abscissas because this number is proportional to the average value of maximum rotor flux density. The average value is used because the wave form instead of remaining exactly invariant as the field sweeps around the stator undulates. Hence, the average value would be proportional to the major hysteresis loop at which the rotor is working, while the undulations about this average value would represent the minor loops which are superimposed on the major loop. This average magnetomotive force was computed by finding the average of the instantaneous magnetomotive forces acting on each tooth of the pole face, averaged for different space positions of the field.

from a core plated stock and should be free of all oil or grease. The slots then are aligned if necessary and a suitable slot liner is placed in them. The mandrel assembly then is placed in an armature winding machine similar to those used for winding d-c armatures and wound with conventional lap coils, arranged in phase groups instead of being brought out individually as in d-c machines. If desired, the stack can be wound using preformed coils as shown in Figure 16*C*. After being wound the slots are sealed with wedges and the phase terminals brought out to lugs which may be located conveniently in the slot wedge as shown in Figure 16*D*. Following the winding process the wound stator with the mandrel in place is heated to 130 degrees centigrade for about one-half hour to drive out any moisture and then is immersed, while still hot, in a thermosetting synthetic resin for about one-half hour, allowing the resin thoroughly to impregnate the interstices between the wires and the laminations. The stack then is removed from the varnish and allowed to dry in air. Following this the stator with mandrel still in place is baked in an oven until the resin has been set. After cooling the stator is placed between centers in a grinder and the outside of the laminations are ground slightly so that the yoke rings may be assembled easily on the stator. After assembly of the yoke rings the entire assembly is again dipped in the resin and baked. This process converts the assembly into an integral mass. The mandrel now is pressed from the completed stack.

The completed stator assembly is shown in Figure 16*D*. In Figure 16*E* there is shown a standard type of capsule self-aligning sleeve bearing assembly, employing a porous bronze bearing surrounded by felt washers having a copious oil supply. Ball bearings also may be employed, in which case the ball bearing can be fitted into a housing which fits into the brass spider, or the outside diameter of the bearing may be chosen to fit directly into the brass spider.

Table VI

Grade of Steel	Rotor Power, W Per Cu In. at 60 CPS				Hm, Amp-Turn Per In.				Base Price, Cents Per Lb
	Bm = 50	Bm = 60	Bm = 70	Bm = 80	Bm = 50	Bm = 60	Bm = 70	Bm = 80	
3 1/2 per cent Chrome	9.1	13.0	17.1	21.0	178	218	283	420	12
3 1/2 per cent Chrome*	7.4	10.6	14.1	17.7	149	172	217	342	12
3 per cent cobalt	10.5	14.4	19.2	24.6	186	210	262	374	26
17 per cent cobalt	19.8	27.6	35.4	43.8	383	427	498	638	85
17 per cent cobalt*	15.7	22.0	28.8	36.0	301	327	368	455	85

Bm in Kilomaxwells per square inch.

* Drawn at 300 degrees Fahrenheit for 1 1/2 hour after hardening. Drawing at this temperature reduces the energy level approximately 20 per cent, but will give complete temperature stability up to 300 degrees Fahrenheit.

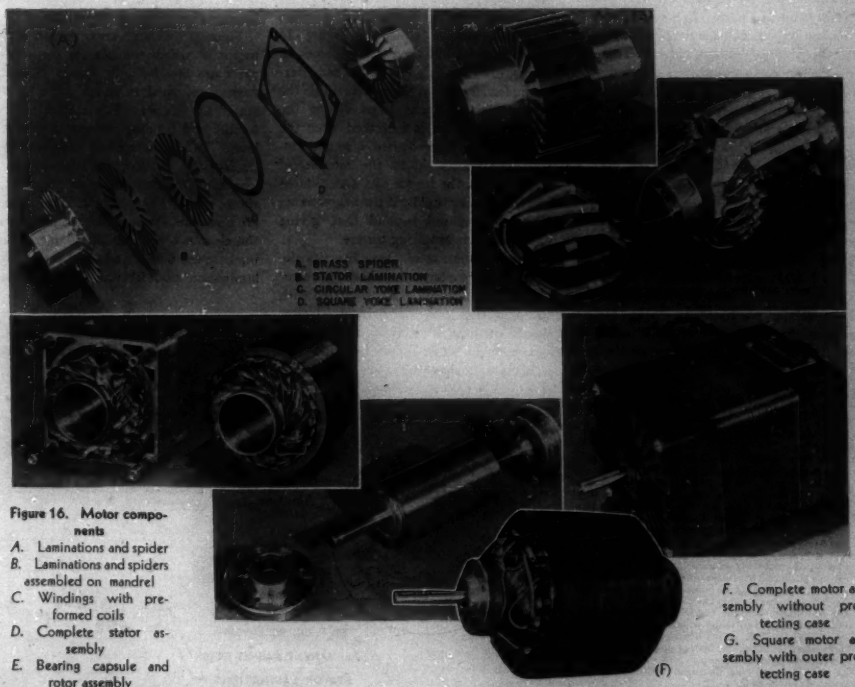

Figure 16. Motor components

A. Laminations and spider
B. Laminations and spiders assembled on mandrel
C. Windings with preformed coils
D. Complete stator assembly
E. Bearing capsule and rotor assembly
F. Complete motor assembly without protecting case
G. Square motor assembly with outer protecting case

Figure 17. Models of Table VII

Figure 19 (below). Unit 803 hysteresis motor load characteristics

Balanced 2-phase, 130 volts, 60 cycles, 1,800 rpm, 65 degrees centigrade rise full load

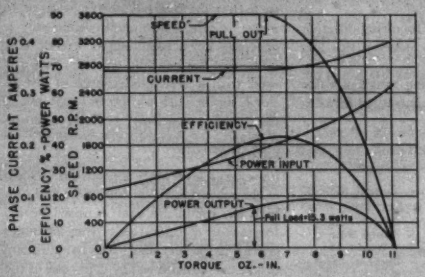

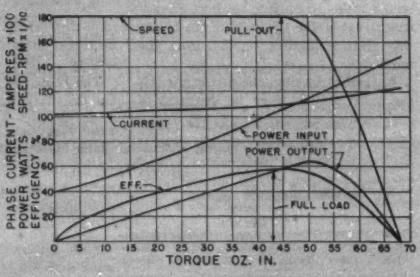

Figure 18. Unit 804 hysteresis motor. Load characteristics

Balanced 2-phase, 135 volts, 60 cycles, 3,600 rpm, 50 degrees centigrade rise full load

The rotor assembly also is shown in Figure 16*E* and generally consists of a hollow cylinder of permanent magnet steel supported by a nonferrous spider pressed on the motor shaft. For special synchronous effects the rotor can be modified. A salient pole construction will give a rotor which synchronizes at a fixed phase angle with reference to the supply.

The completely assembled motor is shown in Figure 16*F*, while the motor with an outer protecting case is shown in Figure 16*G*.*

The unique feature of the method of assembly described is that the stator is a unitary structure requiring no external frame for alignment, and the bore of stator and the bore of the brass spiders or bearing holders are aligned automatically to a high degree of concentricity without machining. This alignment is so good that the air gap on the production assembly for a 1.75 inch diameter rotor 3 inches long is only 0.008 inch. Preproduction models have been operated with a 0.003-inch air gap. The main feature of the alignment obtained by this method of construction is that it depends only upon one concentricity, that of the bearing, assuming, of course, that the rotor is concentric with its own shaft.

A short gap, which is commercially practical for the reasons described hereinbefore, is highly desirable from the performance standpoint as it reduces the required exciting current and hence the copper loss. However, this reduction in copper loss is only a net advantage if the reduction in air gap does not result in an increase in parasitic loss greater than the decrease in copper loss.† In the usual motor with open slots the economical minimum air gap is limited by parasitic losses. However, in the construction described with closed slots the parasitic losses are so reduced that the usual limitation in the length of air gap is manufacturing tolerance.

Electrical Design

The electrical design of a hysteresis stator of the type described is carried out in a manner exactly the same as for the stator of any polyphase synchronous or induction machine. As already indicated, where it is desired to operate at high power levels, special attention should be given to the wave form of stator magnetomotive force. To this end, within mechanical limits, the largest practical number of slots per pair of poles should be chosen.

* This particular construction is the development of Frank W. Stellwagen.

† See United States patent 2,328,743.

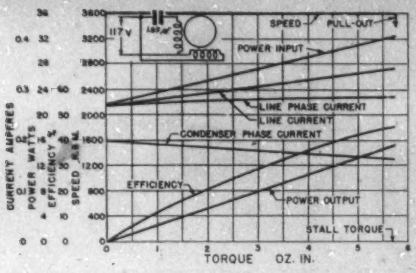

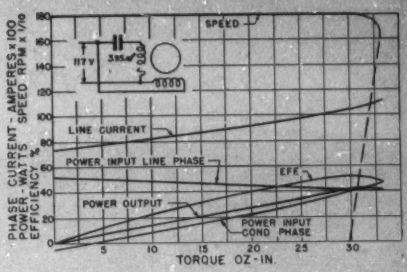

Short pitched coils are also advantageous as they help improve the wave form while at the same time increasing the ease of winding and decreasing the length of the end connections. The stator slots of course, should be closed to avoid losses due to parasitics. The minimum thickness of the bridge rings will be determined by mechanical considerations, while the circumferential length of this minimum section should be made as short as possible; that is, the thickness of the bridge ring should increase rapidly from the minimum.

Regarding the magnetic circuit, the stator tooth section must be designed to carry the rotor flux plus that of the bridge paths plus the usual leakage. The magnetomotive force that must be developed in the stator must be sufficient to send the flux through the rotor, across the rotor–stator air gap, through the teeth, across the stator tooth to the yoke ring air gap, and finally through the yoke ring. The copper of the stator must be sufficient to develop this magnetomotive force without exceeding a safe temperature rise.

The initial design of the machine commences with the choice of rotor material. This choice is almost entirely an economic question. Referring to Figure 4 it is seen that there are many materials available, all having different energy levels for the same flux density and requiring different magnetic intensities to develop this flux density.

Figure 20 (left). Unit 804 hysteresis motor load characteristics

Single phase, 117 volts, 60 cycles 3,600 rpm, 40 degrees centigrade rise full load

Figure 21 (right). Unit 803 hysteresis motor load characteristics

Single phase, 117 volts, 60 cycles, 1,800 rpm, 55 degrees centigrade rise full load

The economic working range of rotor flux density is from about 50 to 80 kilomaxwells per square inch, excluding the Alnicos.* Table VI gives a tabulation of the power which can be developed per cubic inch of rotor steel with an ideal field, for various flux densities in this range, together with the required magnetic intensity to excite the rotor and the base price of the steel.

The usual criterion in designing a hysteresis motor is to make the dimensions such that the over-all cost is least, or to make its size a minimum. Efficiency is generally not a requirement, except as it influences the heating, or if the motor is used with a restricted source of power. For a motor with an intermittent rating the greatest economy, both in size and material cost, results if the flux density is held high. The choice of a high versus low energy level steel depends on the cost of the rotor relative to the stator and how high the excitation can be raised during the period of operation. For machines operating for very short times a minimum of size can be achieved by using one of the higher energy level steels operating at a high density. However, as was pointed

Table VII. Typical Cylindrical Rotor Hysteresis Motor Data

General Design Data

		Stator			Rotor*				
Unit No.	Poles	Teeth	Min Slot Bridge thickness, In.	Outside Diameter, In.	Outside Diameter, In.	Length, In.	Air Gap, In.	Active Volume, Cu In.	Total Motor Weight, Lb Uncased	Total Motor Weight, Lb Cased
801	2	12	0.018	1.25	0.428	1.0	0.005	0.116	0.312	
802	2	12	0.025	1.78	0.613	1.0	0.006	0.205	0.61	
804	2	12	0.025	3.00	1.111	1.0	0.007	0.796	2.2	
803 *A*	4	24	0.025	4.00	1.734	2.31	0.008	2.63	6.8	9.5
803 *B*	2	24	0.025	4.50	1.734	2.31	0.008	4.42	9.5	
805	2	4	0.025	2.50	0.875	0.50	0.008	0.225	0.69	1.12

* Material—17 per cent cobalt, 300 degrees Fahrenheit draw, Simonds number 81.

* Owing to the high magnetic intensity required for magnetization, the Alnicos are more useful for special designs, such as the rotor of Figure 8*D*, where the soft steel spider produces a short radial path through the Alnico which is magnetized easily.

Table VIII. Typical Operating Characteristics on 60-Cycle Balanced 2-Phase Power

Hysteresis Motors of Table VII

	Input				Output						
Unit No.	Speed, Rpm	Phase Current, Amp	Phase Voltage, V	Phase Power, W	Syn.* Torque Oz In.	Power, W	Eff., Per Cent	Temp Rise Cont Uncased Deg C	Stall Torque Oz In.	Net Output Per Cu In. of Active Rotor, W Per Cu In.	Type Bearings
801	3,600	0.154	63	6.6	0.906	2.4	18.2	86†	0.906	20.6	Ball
802	3,600	0.121	117	7.9	1.94	5.15	32.0	48	2.125	25.1	Ball
804	3,600	0.416	144	24.3	7.55	20.1	41.4	58	11.1	25.3	Sleeve
803 *A*	1,800	1.065	130	49.7	43.1	57.4	57.8	65	68.4	21.8	Sleeve
803 *B*	3,600	1.90	117	80.2	40.4	107.3	73.1	65	100	24.2	Sleeve
805	3,600	0.186	97	7.7	1.0	2.64	17.1	36‡	1.125	11.7	Sleeve

‡ In case with fan. † Not recommended for continuous duty unless fan cooled.

* This is the torque the motor will pull into synchronism.

Table IX. Typical Operating Characteristics on 60-Cycle Single-Phase Power With Capacitor for Splitting Phase

Hysteresis Motors of Table VII

Unit No.	Speed, Rpm	Input Line Quantities: Current, Amp	Input Line Quantities: Voltage, V	Input Line Quantities: Power, W	Output: Syn.* Torque, Oz In.	Output: Power, W	Ref., Per Cent	Temp Rise Cont Uncased Deg C	Stall Torque, Oz In.	Net Output Per Cu In. of Active Rotor W Per Cu In.	Type Bearings	Capacitance, μf	Max Capacitor Voltage, V
801	3,600	0.152	117	17.7	.906	2.4	13.6	65†	.906	20.7	Sleeve	1.75	
802	3,600	0.130	117	13.8	1.69	4.5	32.4	50	1.77	22.0	Ball	1.58	
804	3,600	0.340	117	33.5	5.3	14.1	42.1	41	5.0	17.7	Sleeve	1.85	315
803A	1,800	1.02	117	81.5	30.6	40.7	50.0	39	28.3	15.5	Sleeve	3.55	363
803B	3,600	1.45	117	12.1	28.3	75.4	62.4	53	26.1	17.0	Sleeve	6.00	375
805	3,600	0.154	117	13.8	.90	2.40	17.4	30‡	0.75	10.7	Sleeve	0.55	300

‡ In case with fan. † Not recommended for continuous duty unless fan cooled.

*This is the torque the motor will pull into synchronism.

out in connection with Figure 14, operation at high excitation levels is only practical if the winding is well distributed in many slots.

Data on Preproduction Models

A. Normal Operation

Operating characteristics have been obtained on six different models, differing widely in size and output, but all built in accordance with the procedures outlined. Figure 17 shows five of these models in perspective so that an idea of their relative size may be obtained, while their principal data are tabulated in Table VII.

In Table VIII there are shown the maximum synchronizing characteristics of these machines when operated on a balanced 2-phase supply for the temperature rises indicated. The first five machines tabulated show an average output of 23.4 watts per cubic inch of rotor, which by reference to Table VI for 17 per cent cobalt steel drawn at 300 degrees Fahrenheit shows that the effective average rotor flux density is approximately 62 kilomaxwells per square inch. These machines can be operated economically at higher power levels than those shown in the table if means for cooling, such as a fan, is employed, or if they are operated intermittently. Figures 18 and 19 show the balanced 2-phase load characteristics for the unit *804* and the unit *803A* motors, respectively.

In Table IX data are given for the same machines wound for single-phase operation using a phase-splitting capacitor. Figures 20 and 21 show the single-phase load characteristics for the unit *804* and the unit *803A* motors, respectively.

B. Overexcited Operation

The largest element of power loss in the hysteresis motors described is the excitation copper loss. This loss can be decreased greatly if the motor is momentarily overexcited after synchronism is reached. Such overexcitation can be carried out by raising the voltage or current. Figures 22 and 23 give the load characteristics for the unit *804* and *803A* motors after being overexcited as noted. These operating characteristics may be compared directly with those of Figures 18 and 19, respectively, as both tests have been carried out at the same operating voltage on the same machines.

In Table X there is given a breakdown of the losses of these two motors with and without overexcitation. A study of these data shows that not only is the copper loss reduced but the pull-out torque is increased.

The benefits obtained from overmagnetization depend upon using the rotor in the same manner as an ordinary permanent magnet is used; that is, the rotor must supply magnetomotive force to its external magnetic circuit. Any condition of operation which tends to weaken the retained magnetism gradually will change the magnetic state of the rotor until it finally assumes those characteristics which it would have had if it had never been overmagnetized. Oscillation of the rotor produced by usual causes present in synchronous machines, or load surges, which momentarily change the phase position of the rotor, will cause such demagnetization. Hence, for stable operation in the overmagnetized state it is best

Table X. Comparison of Losses at the Pull-Out Point for Overexcited and Normally Excited Hysteresis Motors

Sleeve Bearings

	Unit 804 Excitation: Normal	Unit 804 Excitation: Over	Unit 803A Excitation: Normal	Unit 803A Excitation: Over
Overexcitation voltage, v		210		200
Operating voltage, v	135	135	130	130
Power input, w	38.4	37.7	99.4	117
Power output, w	16.5	20.1	57.4	85.0
Copper loss, w	18.0	13.0	32.5	22.3
Core and friction loss, w	3.9	4.6	9.5	9.7
Efficiency, per cent	43.0	53.5	57.8	72.6
Unit rotor output, per cu in	20.7	25.2	21.8	32.3

Figure 22 (left). Unit 804 hysteresis motor overmagnetized load characteristic

Same data as Figure 18 except momentarily magnetized at 210 volts. Running voltage 135 volts

Figure 23 (right). Unit 803 hysteresis motor overmagnetized load characteristic

Same data as Figure 19 except momentarily magnetized at 200 volts. Running voltage 130 volts

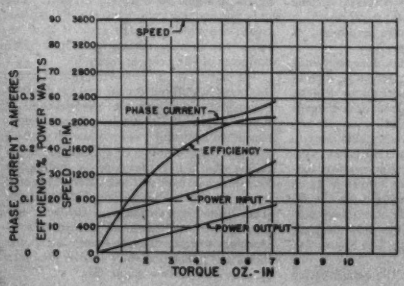

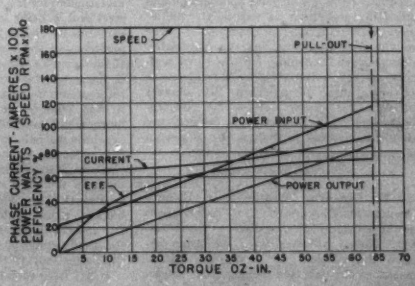

if the inertia of the load is low and if the machine is not operated too close to the pull-out point.

References

1. Theory and Calculations of Electrical Apparatus (book), C. P. Steinmetz. McGraw-Hill Book Company, New York, N. Y., 1917.

2. Theory of Hysteresis Motor Torque, B. E. Teare, Jr. AIEE Transactions, volume 59, 1940, pages 907–12.

Discussion

Benjamin Falk (Simonds Saw and Steel Company, Lockport, N. Y.): The author is to be congratulated, not only for the progress he has contributed to the development of economically rated hysteresis motors, but also for the lucidity of his presentation. This recent advance in design, no doubt has accounted for the present flurry of activity in the small motor field, particularly wherever low noise level or absolute synchronism is a prime requisite. Besides this net end result, it also has stimulated activity in the magnetic materials field.

As Roters pointed out, the stator for a hysteresis motor usually is designed to produce an exciting field that is substantially less than the accepted saturation value for the permanent magnet material in the rotor. Consequently, rotor calculations must be based on a flux density value measured at a peak magnetizing force comparable to the excitation produced by the stator. Up to the present time, however, the data on suitable magnetic materials have been concerned only with peak properties at saturation levels.

Due to the fact that magnetic properties are highly susceptible to variations in heat treating, I might mention that every metallurgical process concerned with the production of uniformly high quality rotors should be controlled rigidly. It is a well known fact that annealing any magnet steel for a machining operation results in a loss of available energy—that is, the lower the annealed hardness, the poorer the final properties. Too, the method of annealing to achieve a desired hardness can be varied, yet one procedure may yield a perfectly useless magnetic material.

In regard to hardening the machined rotor, the procedure should be chosen to achieve the maximum available energy from the steel. Every factor concerned with this process should be established carefully—the rate of heating, hardening temperature, soaking time at temperature, speed of quench, temperature and agitation of the quenchant, and subsequent aging.

The choice of aging procedure for the hardened rotor will depend upon design and operating conditions as well as the metallurgical characteristics of the material. Due to the fact that magnetic characteristics change after hardening, even at room temperature, it is well to stabilize the magnets at a temperature of at least 212 degrees Fahrenheit. Roters chose 300 degrees Fahrenheit. In general, this temperature should be at least as high as the maximum operating temperature of the motor.

B. E. Lenehan (Westinghouse Electric Corporation, Newark, N. J.): The hysteresis motor is essentially a machine of small output. Roters indicates how good design can raise the efficiency and output. Small machines are operated usually from single-phase supply and the very large number of small hysteresis motors used for clocks and timers are so operated. The capacitor type motor gives polyphase performance and is the preferred type wherever efficiency or output from a given size is important. Where output is small, single-phase shaded-pole types may be used, although starting torque will be 10 to 20 per cent of the same frame as a capacitor type and pull-in torque less than half as much.

When a hysteresis motor is operated on a single-phase field, there is, of course, no starting torque. The speed–torque curve shows very little torque until half speed is reached, when the torque rises to near the pull-in value, at which it remains until synchronism is reached. This condition is hard to analyze by methods used for single-phase induction motors, because the losses which are to be associated with each revolving field component in the rotor are not easy to determine. For a given magnetic material, the area of a displaced hysteresis loop is about the same for the same change in flux density B. However, the value which is common to the two field components is magnetizing force H. The result is that when the low frequency is near the crest value, the change in B resulting from the change in H at the higher frequency will be small as a result of saturation. The losses associated with the higher frequency will be reduced and so will the resultant negative torque. At half speed, the higher frequency is three times the lower and that is where the torque rises. The effect of an elliptical field is intermediate between the single-phase and polyphase types.

The ability of a hysteresis motor to pull a high inertia load into synchronism is one of its outstanding advantages over all other types.

C. H. Crouse (Robbins and Myers, Inc., Springfield, Ohio): Our experience with hysteresis motors has been with motors built in conventional construction, using standard stator laminations, bearing construction, and air gap lengths. A number of materials, laminated and solid, have been investigated for the rotor. A special chrome steel now is being used which represents a compromise choice from the standpoint of performance and economy.

While such a construction does not result in the same power output per cubic inch of rotor material as that described by Roters, it was possible to produce a hysteresis motor which resulted in starting torques and synchronous pull-out torques equivalent to the torques obtained in reluctance synchronous motors of the same horsepower output. In fact, the starting torque is much greater than the value realized by the reluctance motor of the same horsepower output and the hysteresis motor does not have the disadvantage of cogging (see Figure 1 of this discussion).

It has been found that the concentricity of the air gap is of major importance. Due to manufacturing variations, the hysteresis motor torques, especially the synchronous pull-out torque, will vary considerably with a very small percentage variation of air gap concentricity. Since the air gap used in our motor is approximately twice the air gap used by Roters and also since his percentage variation of concentricity due to manufacturing variations would be much greater than the value experienced in our motor, it would be interesting to know what Roters' experience has been in comparing air gap eccentricity to torque variation.

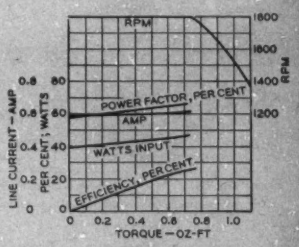

Figure 1. Performance curves

Frame SKH 85HOL, 1/100 horsepower, 115 volts, single phase, 60 cycles, 1,800 rpm, 50-degree-centigrade rise, permanent split capacitor

Torques in ounce-feet: full load, 0.466; synchronous pull out, 0.73; starting, 1.53; synchronous pull in, 0.71

Locked rotor amperes, 0.66

Herbert C. Roters: In reply to Crouse's comments I would like to state that in our experiments on hysteresis synchronous motors we have not observed that the synchronous pull-out torque varies with the concentricity of the air gap. Our method of construction is such that we never have experienced a change in concentricity sufficient to affect the results noticeably. The only concentricity affecting the air gap between the stator and the rotor is that between the bearing surface and the outside diameter of the bearing capsule.

We have found, however, that a great variation in pull-out torque will be obtained depending upon how the measurement is made. Thus, if the machine is allowed to run at no load and a torque load is applied gradually the pull-out torque will be much higher than if it is measured by finding the load which causes slip just after the motor has pulled in a slightly smaller load from just below synchronism. To get uniformity we have made all maximum synchronous torque measurements after the motor has pulled a slightly smaller load into synchronism from a slight slip.

Performance Calculations on Shaded Pole Motors

P. H. TRICKEY
FELLOW AIEE

IN 1936, the writer presented a paper[1] on "An Analysis of the Shaded Pole Motor," giving the fundamental circuit analysis, and deriving the equations for currents and torque at standstill condition. This paper extends that work, deriving equations for performance under running conditions, and presenting a calculation sheet or form for readily performing the mathematical operations.

Current Equations

Figure 1 shows the diagram of the typical shaded pole motor with four current circuits, primary, shading coil, and the two rotor phases. Writing the equation for each circuit consists of simply adding all the voltages induced or consumed in each circuit.

Harmonics are considered only so far as they increase the reactances.

It is assumed that the effective center of the shaded pole is 90 electrical degrees from the effective center of the main pole as shown in Figure 1.

Primary

$$I_1(r_1+jx_1')+j(I_1-I_{2m})X_{mm}+jI_1x_{bm}+jI_1x_{skm}+j(I_1-I_a)(x_{ska}+x_{ba}+x_{ba})+j(I_1-I_a-I_{2a})X_{ma}=E$$

Shaded Pole

$$I_a(r_a+jX_a)-j(I_1-I_a)(x_{ska}+x_{ba}+x_{ba})-j(I_1-I_a-I_{2a})X_{ma}=0$$

Rotor Main Phase

$$I_{2m}(r_{2m}+jx_{2m})-j(I_1-I_{2m})X_{mm}-S(I_1-I_a-I_{2a})X_{ma}+SI_{2a}x_{2a}=0$$

Rotor Shaded Pole Phase

$$I_{2a}(r_{2a}+jx_{2a})-j(I_1-I_a-I_{2a})X_{ma}+S(I_1-I_{2m})X_{mm}-SI_{2m}x_{2m}=0$$

For simplicity, the following definitions have been made

$$x_1=x_1'+x_{bm}+x_{skm}+x_{bm}$$
$$x_{a1}=x_{ba}+x_{ska}+x_{ba}$$
$$X_{m}=X_{mm}+x_{2m}$$
$$X_{a1}=X_{ma}+x_{2a}$$
$$r_2=r_{2m}=r_{2a}$$
$$i_m=E/X_{01}$$

By using these definitions, dividing both sides of the equations by X_{01}, and grouping in terms of the four currents, the following equations are obtained in form suitable for determinant solution.

$$\left[\frac{r_1}{X_{01}}+j\frac{x_1+X_{mm}+X_{ma}+x_{a1}}{X_{01}}\right]I_1+\left[-j\frac{x_{a1}+X_{ma}}{X_{01}}\right]I_a+\left[-j\frac{X_{mm}}{X_{01}}\right]I_{2m}+\left[-j\frac{X_{ma}}{X_{01}}\right]I_{2a}=\frac{E}{X_{01}}=i_m$$

$$\left[\frac{x_{a1}+X_{ma}}{X_{01}}\right]I_1+\left[j\frac{r_a}{X_{01}}-\frac{(X_a+x_{a1}+X_{ma})}{X_{01}}\right]\times I_a+[0]I_{2m}+\left[-\frac{X_{ma}}{X_{01}}\right]I_{2a}=0$$

$$\left[\frac{X_{mm}}{X_{01}}-jS\frac{X_{ma}}{X_{01}}\right]I_1+\left[jS\frac{X_{ma}}{X_{01}}\right]I_a+\left[j\frac{r_2}{X_{01}}-1\right]I_{2m}+\left[jS\frac{X_m}{X_{01}}\right]I_{2a}=0$$

$$\left[\frac{X_{ma}}{X_{01}}+jS\frac{X_{mm}}{X_{01}}\right]I_1+\left[-\frac{X_{ma}}{X_{01}}\right]I_a+\left[-jS\right]I_{2m}+\left[j\frac{r_2}{X_{01}}-\frac{X_m}{X_{01}}\right]I_{2a}=0$$

The solution of these equations in term of the currents is given in the appendix.

$$I_1=i_m\frac{N_{1h}+jN_{1r}}{U+jW}=i_m\frac{[B_7+(1-S^2)B_{12}]+j[B_{16}+(1-S^2)B_3]}{U+jW}$$

$$I_a=i_m\frac{N_{2h}+jN_{2r}}{U+jW}=i_m\frac{[B_1+SB_{16}+(1-S^2)B_{13}]+jB_{15}}{U+jW}$$

$$I_{2m}=i_m\frac{N_{3h}+jN_{3r}}{U+jW}=i_m\frac{[B_4+SB_7+(1-S^2)B_{11}]+j[B_{11}-SB_3+(1-S^2)B_6]}{U+jW}$$

$$I_{2a}=i_m\frac{N_{4h}+jN_{4r}}{U+jW}=i_m\frac{[B_3-SB_{11}-(1-S^2)B_2]+j[B_5+SB_2+(1-S^2)B_4]}{U+jW}$$

where

$$U=B_{14}+(1-S^2)B_{17}$$
$$W=B_{20}+(1-S^2)B_{18}$$
$$B_1=(r_2/X_{01})(r_2/X_{01})(x_{a1}+X_{ma})/X_{01}$$
$$B_2=(X_{ma}/X_{01})(X_a/X_{01})$$
$$B_3=(X_{ma}/X_{01})(X_a/X_{01})(r_2/X_{01})$$
$$B_4=(r_a/X_{01})(X_{ma}/X_{01})$$

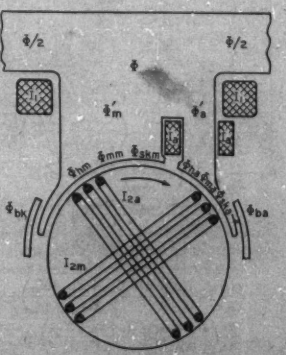

Figure 1. Diagram of poles and rotor circuits of shaded pole motor

Paper 47-219, recommended by the AIEE rotating machinery committee and approved by the AIEE technical program committee for presentation at the AIEE Middle Eastern District meeting, Dayton, Ohio, September 23–25, 1947. Manuscript submitted June 24, 1947; made available for printing August 18, 1947.

P. H. TRICKEY is chief engineer, Diehl Manufacturing Company, Somerville, N. J.

The author wishes to acknowledge the suggestions of A. R. Kelly regarding the arrangement of the current equations.

$$B_3=(r_a/X_{02})(X_{03}/X_{02})$$
$$B_4=(r_a/X_{02})(X_{03}/X_{02})(X_{mm}/X_{02})$$
$$B_5=(r_a/X_{02})(X_{ma}/X_{02})(r_2/X_{02})$$
$$B_9=(r_a/X_{02})(X_{mm}/X_{02})(r_2/X_{02})$$
$$B_{10}=(r_2/X_{02})(X_{mm}/X_{02})(X_{ma}/X_{02})$$
$$B_{11}=(r_2/X_{02})(X_{mm}/X_{02})(X_a+x_{a1}+X_{ma})/X_{02}$$
$$B_{12}=(X_{ma}/X_{02})^2-(X_{03}/X_{02})(x_{a1}+X_{ma})/X_{02}$$
$$B_{13}=(X_{ma}/X_{02})^2-(X_{03}/X_{02})(X_a+x_{a1}+X_{ma})/X_{02}$$
$$B_{14}=(X_{mm}/X_{02})[(X_{ma}/X_{02})^2-(X_{03}/X_{02})\times(X_a+x_{a1}+X_{ma})/X_{02}]$$
$$B_{15}=(r_2/X_{02})\{[1+(X_{03}/X_{02})][(x_{a1}+X_{ma})/X_{02}]-(X_{ma}/X_{02})^2\}$$
$$B_7=(r_2/X_{02})\{(r_2/X_{02})[(X_a+x_{a1}+X_{ma})/X_{02}]+(r_a/X_{02})[1+(X_{03}/X_{02})]\}$$
$$B_{16}=(r_2/X_{02})\{[1+(X_{03}/X_{02})][(X_a+x_{a1}+X_{ma})/X_{02}]-(X_{ma}/X_{02})^2-(r_a/X_{02})(r_2/X_{02})\}$$
$$B_{17}=(r_a/X_{02})\{(X_{ma}/X_{02})^2+(X_{mm}/X_{02})^2\times(X_{03}/X_{02})-(X_{03}/X_{02})[(x_1+X_{mm}+X_{ma}+x_{a1})/X_{02}]\}+(r_1/X_{02})\{(X_{ma}/X_{02})^2-(X_{03}/X_{02})][(X_a+x_{a1}+X_{ma})/X_{02}]\}$$

$$B_{18}=\frac{r_1}{X_{02}}\frac{r_a}{X_{02}}\frac{X_{03}}{X_{02}}+\frac{x_1+X_{mm}}{X_{02}}\left[\left(\frac{X_{ma}}{X_{02}}\right)^2-\frac{X_{03}}{X_{02}}\left(\frac{X_a+x_{a1}+X_{ma}}{X_{02}}\right)\right]+\left(\frac{X_{ma}}{X_{02}}\right)^3\times\frac{X_a}{X_{02}}-\left(\frac{X_{mm}}{X_{02}}\right)^2\left[\left(\frac{X_{ma}}{X_{02}}\right)^2-\frac{X_{03}}{X_{02}}\times\frac{(X_a+x_{a1}+X_{ma})}{X_{02}}\right]-\frac{X_a}{X_{02}}\frac{X_{03}}{X_{02}}\times\frac{(x_{a1}+X_{ma})}{X_{02}}$$

$$B_{19}=\frac{r_2}{X_{02}}\left\{\frac{r_1}{X_{02}}\left[\frac{r_2}{X_{02}}\left(\frac{X_a+x_{a1}+X_{ma}}{X_{02}}\right)+\frac{r_a}{X_{02}}\left(1+\frac{X_{03}}{X_{02}}\right)\right]+\left(\frac{X_a+x_{a1}+X_{ma}}{X_{02}}\right)\times\left(\frac{X_{mm}}{X_{02}}\right)^2+\frac{r_a}{X_{02}}\left(\frac{X_{ma}}{X_{02}}\right)^2+\left(\frac{x_{a1}+X_{ma}}{X_{02}}\right)\left(1+\frac{X_{03}}{X_{02}}\right)\left(\frac{x_{a1}+X_{ma}}{X_{02}}\right)+\frac{r_a}{X_{02}}\frac{r_2}{X_{02}}\frac{(x_1+X_{mm}+X_{ma}+x_{a1})}{X_{02}}-\left(\frac{x_1+X_{mm}}{X_{02}}\right)\left[\left(1+\frac{X_{03}}{X_{02}}\right)\times\left(\frac{X_a+x_a+X_{ma}}{X_{02}}\right)-\left(\frac{X_{ma}}{X_{02}}\right)^2\right]-\left(\frac{x_{a1}+X_{ma}}{X_{02}}\right)\left(1+\frac{X_{03}}{X_{02}}\right)\times\left(\frac{X_a+x_{a1}+X_{ma}}{X_{02}}\right)\right\}$$

$$B_{20}=\frac{r_2}{X_{02}}\left\{\frac{r_1}{X_{02}}\left[\left(1+\frac{X_{03}}{X_{02}}\right)\times\left(\frac{X_a+x_{a1}+X_{ma}}{X_{02}}\right)-\left(\frac{X_{ma}}{X_{02}}\right)^2-\frac{r_2}{X_{02}}\frac{r_a}{X_{02}}\right]+\frac{r_2}{X_{02}}\frac{X_a}{X_{02}}\left(\frac{x_{a1}+X_{ma}}{X_{02}}\right)+\frac{r_a}{X_{02}}\left(1+\frac{X_{03}}{X_{02}}\right)\left(\frac{x_1+X_{mm}+X_{ma}+x_{a1}}{X_{02}}\right)+\frac{r_2}{X_{02}}\left(\frac{x_1+X_{mm}}{X_{02}}\right)\left(\frac{X_a+x_{a1}+X_{ma}}{X_{02}}\right)-\frac{r_a}{X_{02}}\left[\left(\frac{X_{mm}}{X_{02}}\right)^2+\left(\frac{X_{ma}}{X_{02}}\right)^2\right]\right\}$$

Torque Equation

The torque equation given in the previous paper[1] applies equally well to the running condition.

$$T_{2s}=11.3p/f[X_{mm}(I_1-I_{2m})\ \text{conj}\ I_{2s}-X_{ma}\times(I_1-I_a-I_{2a})\ \text{conj}\ I_{2m}]\ \text{in ounce-inches}$$

Figure 2. Equivalent circuit of shaded pole motor

$r_m=E\div 60$ - cycle iron loss; $I_{Fe}=60$-cycle iron loss $\div E$

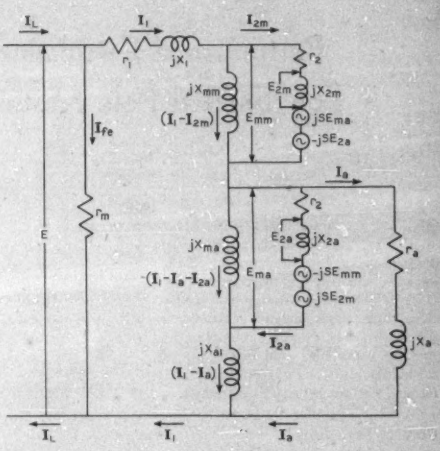

where real terms alone give average starting torque.

Breaking the current terms into their components and rearranging the coefficient, the torque becomes

$$T_{2s}=\frac{1{,}353}{syn}\frac{i_mE}{U_2+W_2}\left\{\frac{X_{mm}}{X_{02}}[(N_{1h}-N_{1h})N_{4h}+(N_{1s}-N_{3s})N_{4s}]-\frac{X_{ma}}{X_{02}}\times[(N_{1h}-N_{2h}-N_{4h})N_{1h}+(N_{1s}-N_{2s}-N_{4s})N_{1s}]\right\}\ \text{in ounce-inches}$$

Iron Loss and Friction

For the purpose of performance calculations, the friction, windage, and odd frequency iron losses are subtracted from the gross output. In order to keep the circuit equations from becoming any more involved and complicated, the fundamental frequency iron loss was neglected in the derivations. However, it must be accounted for, and is included in the losses when calculating the input. It is corrected for in the current by adding an in-phase component to the primary amperes.

Equivalent Circuit

While the foregoing equations are based on the diagram and circuits of Figure 1, the equivalent circuit as shown in Figure 2 is also helpful in understanding what is likely to take place when the constants are changed.

Calculation Sheet

Figures 3 and 4 show pages 1 and 2 of a calculation sheet or form which has been devised to simplify the numerical computations, and on which a typical 10-inch fan motor has been calculated as an example. The sheets have been arranged to give a minimum number of slide rule settings. All vector operations have been eliminated.

Items 93 to 101 have been added to page 2 simply as a check on the input calculations.

The heavy line on the left hand side indicates those items which are necessary if only current and watts versus speed are wanted. The heavy line on the right hand side indicates those items which are necessary to calculate the output from input minus losses. This short cut cannot be used for the standstill condition.

The friction, windage, and odd frequency iron loss should vary as a function of the speed. Usually it is sufficiently accurate to assume that these losses vary as the square of the speed.

In item 79 the primary copper loss is calculated using I_1, the primary current. It would be slightly more correct to use

1		r_1 hot	47.4	101		r_1/X_{02}	.1437	201		(109) (115)	.2975		
2		r_a hot	90.5	102		r_a/X_{02}	.274	202		(109) (117)	.310		
3		r_2 hot $(-r_{2m}-r_{2a})$	39.0	103		r_2/X_{02}	.1183	203		(109) (106)	.412		
4		X_{2m}	52.9	104		(103)^2	.014	204		(109) (126)	.883		
5		X_{mm}	277.0	105		X_{mm}/X_{02}	.840	205	B_1	(115) (104)	.00716		
6		X_{02} = (4) + (5)	329.9	106		(105)^2	.706	206		(115) (111)	.810		
7		X_{2a}	52.9	107		(108)^2	.178	207		(117) (111)	.843		
8		X_{ma}	139.0	108		X_{ma}/X_{02}	.422	208		(117) (106)	.376		
9		X_{03} = (7) + (8)	191.9	109		X_{03}/X_{02}	.582	209		(116) (107)	.0039		
10		X_{ha}	11.7	110		1	1.000	210	B_2	(116) (108)	.00924		
11		X_{ska}	5.8	111		(109) + (110)	1.582	211	B_3	(116) (108) (103)	.001093		
12		X_{ba}	12.0	112				212		(116) (115) (111)	.01771		
13		X_{01} = (10) to (12)	29.5	113				213		(116) (115) (109)	.0652		
14		(8) − (X_{ma})	139.0	114				214		(116) (115) (103)	.001324		
15		(13) + (14)	168.5	115		(15)/X_{02}	.511	215		(102) (111)	.434		
16		X_a	7.23	116		(16)/X_{02}	.0219	216		(102) (106)	.1934		
17		(15) + (16)	175.7	117		(17)/X_{02}	.532	217		(102) (107)	.0488		
18		X_1	20.6	118		E/X_{02} = I_m	.334	218		(216)+(217)	.2422		
19		X_{hm}	11.1	119		Fund Freq Iron Loss	2.000	219	B_4	(102) (108)	.1157		
20		X_{skm}	11.53	120		m Crc Iron Loss @ (1525) RPM	1.00	220	B_5	(102) (109)	.1593		
21		X_{bm}	12.0	121		F + W @ (1525) RPM	1.00	221	B_6	(220) (105)	.1339		
22		X_1 − (18) to (21)	55.23	122		m Crc F + W @ (1525) RPM	2.00	222		(220) (101)	.0229		
23		(5) − (X_{mm})	277.0	123				223		(103) (102)	.0324		
24		(22) + (23)	332.2	124		(24)/X_{02}	1.007	224		(103) (117)	.063		
25		(15)	168.5	125				225		(215)	.434		
26		(24) + (25)	500.7	126		(26)/X_{02}	1.517	226		(224)+(225)	.497		
								227	B_7	(103) (226)	.0588		
301		(107)	.1780	401		(107)	.178	228	B_8	(103) (219)	.0137		
302		(201)	.2975	402		(203)	.412	229	B_9	(103) (105) (102)	.02725		
303	B_{12}	(301) − (302)	−.1195	403		(401) + (402)	.590	230	B_{10}	(103) (105) (108)	.0420		
304		(107)	.1780	404		(204)	.883	231	B_{11}	(103) (105) (117)	.0529		
305		(202)	.310	405		(403) − (404)	−.293						
306	B_{13}	(304) − (305)	−.132	406		(102) (405)	−.0803	422		(101) (226)	−.0714		
307		(306) (124)	−.133	407		(310)	−.01897	423		(209)	.376		
308	B_{14}	(306) (105)	−.111	408	B_{17}	(406) + (407)	−.0333	424		(209)	.0039		
309		(306) (106)	−.0932	409		(309)	−.03320	425		(126) (223)	.0492		
310		(306) (101)	−.01897	410		(213)	.00652	426		(422) (425)	.5005		
311		(206)	.810	411		(409) + (410)	−.0867	427		(421)	.6877		
312		(107)	.178	412		(222)	.0229	428		(426) − (427)	−.1872		
313		(311) − (312)	.632	413		(209)	.0039	429	B_{19}	(103) (428)	−.0222		
314	B_{15}	(103) (313)	.0748	414		(412) + (413)	.0268	430		(101) (319)	−.0908		
315		(207)	.843	415		(307)	−.133	431		(126) (215)	.6580		
316		(107)	.178	416		(414) + (415)	−.1062	432		(124) (224)	.0634		
317		(315) − (316)	.6630	417		(411)	−.0867	433		(214)	.00132		
318		(223)	.0324	418	B_{18}	(416) − (417)	−.0195	434		(430) (433)	.8135		
319		(317) − (318)	.6326	419		(124) (317)	.670	435		(218)	.2422		
320	B_{16}	(103) (319)	.0749	420		(212)	.01771	436		(434) − (435)	.5713		
				421		(419) + (420)	.6877	437	B_{20}	(103) (436)	.0676		

Figure 3. Calculation sheet for shaded pole motor—page 1

I_L, the line current, containing the iron loss amperes. However, this would destroy the exact check between item 85 and item 99.

Since the impedances and losses used as a base for the calculation are subject to considerable error any way it was thought that the slight theoretical gain in accuracy was worth less than the numerical check on the input calculations. However, it is very simple to use item 20 instead of item 18 for primary copper loss calculation, if desired.

It is possible to use the method of the previous paper[1] as an independent check on the standstill condition, as the derivations have entirely different steps.

Symbols

In the previous paper[1] the symbols are defined and formulas are given for calculating the motor constants from motor

dimensions. Attention is called to an omission. On page 1014, C_4 should be

$$[1.332\alpha - \sin^2 \beta/2]/\sin^2 \beta/2$$

Conclusions

Formulas have been derived for the running performance of the shaded pole motor, and a calculation sheet devised for simplifying the numerical computations.

Appendix

Reference is made to Figure 1 and to the circuit equations given in the previous paper.[1]

Primary Winding

$$I_1(r_1+jx_1')+j(I_1-I_{2m})X_{mm}+jI_1\times(X_{atm}+X_{bm}+X_{bm})+j(I_1-I_a)\times(X_{ata}+X_{ba}+X_{ba})+j(I_1-I_a-I_{2a})\times X_{ma}=E$$

Shaded Pole Winding

$$I_a(r_a+jX_a)-j(I_1-I_a)(X_{ata}+X_{ba}+X_{ba})-j(I_1-I_a-I_{2a})X_{ma}=0$$

Rotor Main Phase

$$I_{2m}(r_{2m}+jX_{2m})-j(I_1-I_{2m})X_{mm}-S(I_1-I_a-I_{2a})X_{ma}+SI_{2a}X_{2a}=0$$

Figure 4. Calculation sheet for shaded pole motors—page 2

1	$i = .334\ S\frac{R.P.M.}{5x4}$	.975	.911	.847	.756	0	52	(13)	.0522	.0364	.0217	.0022	-.0732
2	S^2	.950	.830	.718	.571	0	53	(45)	-.0384	-.0361	-.0337	-.0303	.00496
3	$1-S^2$	.050	.170	.281	.429	1.00	54	(25)	.0422	.0252	.0092	-.0123	-.1123
4	(3) x B_{17}	-.00497	-.0169	-.0279	-.0427	-.0993	55	(53)+(54)	.0038	-.0109	-.0245	-.0426	-.1078
5	B_{19}	-.0222	-.0222	-.0222	-.0222	-.0222	56	(52)-(55)	.0484	.0473	.0462	.0448	.0346
6	U=(4)+(5)	-.02717	-.0391	-.0501	-.0649	-.1215	57	(56)x(33)	.00110	.000442	-.000187	-.000175	-.00250
7	(3) x B_{18}	-.0010	-.0033	-.0055	-.0084	-.0195	58	(16)	.0829	.1020	.1197	.1432	.2342
8	B_{20}	.0676	.0676	.0676	.0676	.0676	59	(49)	.0335	.0456	.0567	.0714	.1168
9	W=(7)+(8)	.0666	.0643	.0621	.0592	.0481	60	(26)	.0748	.0748	.0748	.0748	.0748
10	$\sqrt{U^2+W^2}$	.072	.0752	.0798	.0879	.1307	61	(59)+(60)	.1083	.1204	.1315	.1462	.1916
11	(3) x B_{13}	-.0066	-.0224	-.0371	-.0566	-.1320	62	(58)-(61)	-.0259	-.0189	-.0118	-.0030	+.0426
12	B_7	.0588	.0588	.0588	.0588	.0588	63	(62)x(38)	-.001174	-.00116	-.00093	-.000293	.00795
13	N_{1h}=(11)+(12)	.0522	.0364	.0217	.0022	-.0732	64	(57)	.00110	.000442	-.000187	-.000175	-.0029
14	(3) x B_5	.0080	.0271	.0448	.0683	.1593	65	(63)+(64)	-.000074	-.000178	-.001069	-.001178	.00506
15	B_{16}	.0749	.0749	.0749	.0749	.0749	66	(13)	.0522	.0364	.0217	.0022	-.0732
16	N_{1v}=(14)+(15)	.0829	.1020	.1197	.1432	.2342	67	(33)	.0227	.0094	-.0030	-.0195	-.0538
17	$\sqrt{(13)^2+(16)^2}$	.098	.1082	.1217	.1432	.2455	68	(66)-(67)	.0295	.0270	.0247	.0217	.0106
18	$1-i^m$ (17)/(10)	.455	.481	.510	.545	.627	69	(68)x(45)	-.001132	-.000975	-.000832	-.000658	+.000472
19	$I_{1v}=\sqrt{(18)^2-(96)^2}$	.3705	.374	.3855	.408	.487	70	(16)	.0829	.1020	.1197	.1432	.2342
20	$I_{1h}=\sqrt{(19)^2+(98)^2}$	.466	.492	.522	.558	.638	71	(38)	.0463	.0631	.0789	.0999	.1868
21	B_1	.00716	.00716	.00716	.00716	.00716	72	(70)-(71)	.0366	.0389	.0408	.0433	.0474
22	$S B_{10}$	.0410	.0383	.0356	.0318	0	73	(72)x(49)	.00123	.001775	.002315	.00309	.00553
23	(21)+(22)	.04816	.04546	.04276	.03896	.00716	74	(69)	-.001132	-.000975	-.000832	-.000658	.000472
24	(3) x B_{12}	-.0060	-.0203	-.0336	-.0513	-.1135	75	(73)+(74)	.000098	.000800	.001483	.002432	.005577
25	N_{2h}=(23)+(24)	.04216	.02516	.00916	-.01234	-.11234	76	$\left(\frac{X_{ata}+X_{ba}}{X_{ata}}\right)(75)/(10)^2$	.015790	.1189	.1957	.2698	.2745
26	N_{2v} = B_{15}	.0748	.0748	.0748	.0748	.0748	77	$\left(\frac{X_{ata}}{X_{ata}}\right)(65)/(10)^2$	-.00602	-.0535	-.0709	-.0643	.1250
27	$\sqrt{(25)^2+(26)^2}$	.0857	.0790	.0754	.0758	.1350	78	(76)-(77)	.02192	.1724	.2666	.3291	.1495
28	$I_2^{\prime}=i^m$ (27)/(10)	.338	.351	.3155	.288	.345	79	$I_1^2\ r_1$	9.80	11.0	12.35	14.1	18.65
29	B_9	.02725	.02725	.02725	.02725	.02725	80	$I_{1a}^2\ r_a$	14.35	11.2	9.00	7.5	10.80
30	$S B_3$	.00107	.00100	.00093	.00083	0	81	$I_{2m}^2\ r_2$	2.23	3.14	4.25	5.84	10.65
31	(29)+(30)	.02832	.02825	.02818	.02808	.02725	82	$I_{2a}^2\ r_2$	2.18	2.62	2.98	3.40	3.48
32	(3) x B_{14}	-.0056	-.0189	-.0312	-.0476	-.1110	83	(Fund. Fe Loss)	2.00	2.00	2.00	2.00	2.00
33	N_{3h}=(31)+(32)	.02272	.00935	-.00302	-.01952	-.08375	84	(78) Sin E	.786	5.78	8.31	9.16	0
34	B_{11}	.0529	.0529	.0529	.0529	.0529	85	Input (79)+(84)	31.35	35.74	38.89	42.00	45.53
35	(3) x B_8	.0067	.0227	.0376	.0574	.1339	86	Hi Cy Fe+F+W	2.65	2.31	2.00	1.59	0
36	(34)+(35)	.0596	.0756	.0905	.1103	.1868	87	Output (84)-(86)	-1.864	3.47	6.31	7.57	0
37	$S B_8$	.01335	.0125	.0116	.0104	0	88	Losses (85)-(87)	33.214	32.27	32.58	34.43	45.53
38	N_{3v}=(36)-(37)	.04625	.0631	.0789	.0999	.1868	89	R.P.M.=5x Sys.	1755	1640	1525	1360	0
39	$\sqrt{(33)^2+(38)^2}$	.0515	.0638	.0789	.1017	.2045	90	Tor.=1353 Output / R.P.M.	-1.40	2.86	5.60	7.53	4.13
40	$I_{3m}^{\prime}=i^m$(39)/(10)	.239	.2835	.330	.3865	.522	91	Eff.= Output / Input	0	9.7	16.23	18.0	0
41	(3) x B_2	.0005	.0016	.0026	.0040	.00924	92	P.F. = Input / E I_1	61.2	66.0	67.8	68.5	69.0
42	$S B_{11}$	.0516	.0482	.0448	.0400	0	93	(6) (13)/(10)^2	-.2735	-.252	-.171	-.0185	.521
43	B_8	.0137	.0137	.0137	.0137	.0137	94	(9) (16)/(10)^2	1.064	1.16	1.17	1.100	.660
44	(41)+(42)	.0521	.0498	.0474	.0440	.00924	95	(93)+(94)	.7905	.908	.999	1.0815	1.181
45	N_{4h}=(43)-(44)	-.0384	-.0361	-.0337	-.0303	+.00496	96	$I_{1h}=i^m$ (95)	.264	.303	.334	.362	.3945
46	(3) x B_4	.0058	.0137	.0325	.0497	.1157	97	$I_{1a}^{\prime}$ (83)/E	.0182	.018	.018	.018	.018
47	$S B_9$	.0266	.0248	.0231	.0206	0	98	I_{1a}=(96)+(97)	.282	.321	.352	.380	.4127
48	B_3	.00109	.00109	.00109	.00109	.00109	99	Input=I_{1a} E	31.0	35.30	38.70	41.8	46.5
49	N_{4v}=(46)+(47)x(48)	.0335	.0456	.0567	.0714	.11679	100	Losses = (79)+(83)+(84)	33.21	32.27	32.58	34.43	45.58
50	$\sqrt{(45)^2+(49)^2}$	.0510	.0582	.0660	.0775	.1168	101	Output=(99)-(100)	-2.21	3.03	6.12	7.37	—
51	$I_{2a}^{\prime}=i^m$(50)/(10)	.2365	.2585	.276	.2945	.2985		*If S=0, Torque = [illegible] (78) i_m E			6 Oz. In.		

FOR CALCULATION

Rotor Shaded Pole Phase

$$I_{2a}(r_{2a}+jX_{2a})-j(I_1-I_a-I_{2a})X_{ma}+S(I_1-I_{2m})X_{mm}-SI_{2m}X_{2m}=0$$

Let

$$X_1=X_1'+X_{s1m}+X_{h1m}+X_{2m}$$
$$X_{a1}=X_{s1a}+X_{h1}+X_{h2}$$
$$X_{m1}=X_{mm}+X_{2m}$$
$$X_{m2}=X_{ma}+X_{2a}$$
$$r_2=r_{2m}=r_{2a}$$
$$i_m=E/X_{m1}$$

Rearranging, dividing by X_{m1}, and multiplying the last three equations by j, puts the equations in a form suitable for determinant solution.

$$\left[\frac{r_1}{X_{m1}}+j\frac{(X_1+X_{mm}+X_{ma}+X_{a1})}{X_{m1}}\right]I_1+\left[-j\frac{(X_{a1}+X_{ma})}{X_{m1}}\right]I_a+\left[-j\frac{X_{mm}}{X_{m1}}\right]\times I_{2m}+\left[-j\frac{X_{ma}}{X_{m1}}\right]I_{2a}=\frac{E}{X_{m1}}=i_m$$

$$\left[\frac{X_{a1}+X_{ma}}{X_{m1}}\right]I_1+\left[j\frac{r_a}{X_{m1}}-\frac{(X_a+X_{a1}+X_{ma})}{X_{m1}}\right]\times I_a+[0]I_{2m}+\left[-\frac{X_{ma}}{X_{m1}}\right]I_{2a}=0$$

$$\left[\frac{X_{mm}}{X_{m1}}-jS\frac{X_{m2}}{X_{m1}}\right]I_1+\left[jS\frac{X_{ma}}{X_{m1}}\right]I_a+\left[j\frac{r_2}{X_{m1}}-1\right]I_{2m}+\left[jS\frac{X_{m1}}{X_{m1}}\right]I_{2a}=0$$

$$\frac{X_{ma}}{X_{m1}}+jS\frac{X_{mm}}{X_{m1}}\Big]I_1+\left[-\frac{X_{ma}}{X_{m1}}\right]I_a+[-jS]I_{2m}+\left[j\frac{r_2}{X_{m1}}-\frac{X_{m1}}{X_{m1}}\right]I_{2a}=0$$

$$a_1I_1+b_1I_a+c_1I_{2m}+d_1I_{2a}=k_1$$
$$a_2I_1+b_2I_a+c_2I_{2m}+d_2I_{2a}=k_2$$
$$a_3I_1+b_3I_a+c_3I_{2m}+d_3I_{2a}=k_3$$
$$a_4I_1+b_4I_a+c_4I_{2m}+d_4I_{2a}=k_4$$

where

$$a_1=\frac{r_1}{X_{m1}}+j\frac{(X_1+X_{mm}+X_{ma}+X_{a1})}{X_{m1}}$$

$$a_2=\frac{X_{a1}+X_{ma}}{X_{m1}}$$

$$a_3=\frac{X_{mm}}{X_{m1}}-jS\frac{X_{ma}}{X_{m1}}$$

$$a_4=\frac{X_{ma}}{X_{m1}}+jS\frac{X_{mm}}{X_{m1}}$$

$$b_1=-j\frac{(X_{a1}+X_{ma})}{X_{m1}}=-jd_2$$

$$b_2=-\frac{(X_a+X_{a1}+X_{ma})}{X_{m1}}+j\frac{r_a}{X_{m1}}$$

$$b_3=jS\frac{X_{ma}}{X_{m1}}$$

$$b_4=-\frac{X_{ma}}{X_{m1}}$$

$$c_1=-j\frac{X_{mm}}{X_{m1}}$$

$$c_2=0$$

$$c_3=-1+j\frac{r_2}{X_{m1}}$$

$$c_4=-jS$$

$$d_1=-j\frac{X_{ma}}{X_{m1}}=jb_4$$

$$d_2=-\frac{X_{ma}}{X_{m1}}=b_4$$

$$d_3=jS\frac{X_{m1}}{X_{m1}}$$

$$d_4=-\frac{X_{m1}}{X_{m1}}+j\frac{r_2}{X_{m1}}$$

$$k_1=\frac{E}{X_{m1}}=i_m$$

$$k_2=0$$
$$k_3=0$$
$$k_4=0$$

Determinant Solution

$$I_1=\frac{N_1'}{\Delta},\ I_a=\frac{N_2'}{\Delta},\ I_{2m}=\frac{N_3'}{\Delta},\ I_{2a}=\frac{N_4'}{\Delta}$$

where

$$\Delta=\begin{vmatrix} a_1 & b_1 & c_1 & d_1 \\ a_2 & b_2 & c_2 & d_2 \\ a_3 & b_3 & c_3 & d_3 \\ a_4 & b_4 & c_4 & d_4 \end{vmatrix}$$

$$N_1'=\begin{vmatrix} k_1 & b_1 & c_1 & d_1 \\ k_2 & b_2 & c_2 & d_2 \\ k_3 & b_3 & c_3 & d_3 \\ k_4 & b_4 & c_4 & d_4 \end{vmatrix}$$

$$N_2'=\begin{vmatrix} a_1 & k_1 & c_1 & d_1 \\ a_2 & k_2 & c_2 & d_2 \\ a_3 & k_3 & c_3 & d_3 \\ a_4 & k_4 & c_4 & d_4 \end{vmatrix}$$

$$N_3'=\begin{vmatrix} a_1 & b_1 & k_1 & d_1 \\ a_2 & b_2 & k_2 & d_2 \\ a_3 & b_3 & k_3 & d_3 \\ a_4 & b_4 & k_4 & d_4 \end{vmatrix}$$

$$N_4'=\begin{vmatrix} a_1 & b_1 & c_1 & k_1 \\ a_2 & b_2 & c_2 & k_2 \\ a_3 & b_3 & c_3 & k_3 \\ a_4 & b_4 & c_4 & k_4 \end{vmatrix}$$

Denominator Δ

$$\Delta=a_1\left\{b_2\left[\left(-1+j\frac{r_2}{X_{m1}}\right)\left(-\frac{X_{m1}}{X_{m1}}+j\frac{r_2}{X_{m1}}\right)-(-jS)\left(jS\frac{X_{m1}}{X_{m1}}\right)\right]-\left(jS\frac{X_{ma}}{X_{m1}}\right)\times\left[(0)(d_4)-(-jS)\left(-\frac{X_{ma}}{X_{m1}}\right)\right]+\left(-\frac{X_{ma}}{X_{m1}}\right)\left[(0)(d_4)-\left(-1+j\frac{r_2}{X_{m1}}\right)\times\left(-\frac{X_{ma}}{X_{m1}}\right)\right]\right\}-a_2\left\{b_2\left[\left(-1+j\frac{r_2}{X_{m1}}\right)\times\left(-\frac{X_{m1}}{X_{m1}}+j\frac{r_2}{X_{m1}}\right)-(-jS)\left(j\frac{X_{m1}}{X_{m1}}\right)\right]-\left(jS\frac{X_{ma}}{X_{m1}}\right)\left[\left(-j\frac{X_{mm}}{X_{m1}}\right)\left(-\frac{X_{m1}}{X_{m1}}+j\frac{r_2}{X_{m1}}\right)-(-jS)\left(-j\frac{X_{ma}}{X_{m1}}\right)\right]+\left(-\frac{X_{ma}}{X_{m1}}\right)\left[\left(-j\frac{X_{mm}}{X_{m1}}\right)\left(jS\frac{X_{m1}}{X_{m1}}\right)-\left(-1+j\frac{r_2}{X_{m1}}\right)\left(-j\frac{X_{ma}}{X_{m1}}\right)\right]\right\}+a_3\left\{b_2\left[(0)(d_4)-(-jS)\left(-\frac{X_{ma}}{X_{m1}}\right)\right]-b_3\left[\left(-j\frac{X_{mm}}{X_{m1}}\right)\left(-\frac{X_{m1}}{X_{m1}}+j\frac{r_2}{X_{m1}}\right)-(-jS)\left(-j\frac{X_{ma}}{X_{m1}}\right)\right]+\left(-\frac{X_{ma}}{X_{m1}}\right)\times\left[\left(-j\frac{X_{mm}}{X_{m1}}\right)\left(-\frac{X_{ma}}{X_{m1}}\right)-(0)(d_4)\right]\right\}-a_4\left\{b_2\left[(0)(d_4)-\left(-1+j\frac{r_2}{X_{m1}}\right)\times\left(-\frac{X_{ma}}{X_{m1}}\right)\right]-b_3\left[\left(-j\frac{X_{mm}}{X_{m1}}\right)\times\left(jS\frac{X_{m1}}{X_{m1}}\right)-\left(-1+j\frac{r_2}{X_{m1}}\right)\times\left(-j\frac{X_{ma}}{X_{m1}}\right)\right]+\left(jS\frac{X_{ma}}{X_{m1}}\right)\times\left[\left(-j\frac{X_{mm}}{X_{m1}}\right)\left(-\frac{X_{ma}}{X_{m1}}\right)-(0)(d_4)\right]\right\}$$

Completing the multiplication of the terms within the brackets give the following equation:

$$\Delta=a_1\left\{b_2\left[\frac{X_{m1}}{X_{m1}}-\frac{r_2}{X_{m1}}\frac{r_2}{X_{m1}}-S^2\frac{X_{m1}}{X_{m1}}-j\frac{r_2}{X_{m1}}-j\frac{r_2}{X_{m1}}\frac{X_{m1}}{X_{m1}}\right]-\left(jS\frac{X_{ma}}{X_{m1}}\right)\left(-jS\frac{X_{ma}}{X_{m1}}\right)+\left(-\frac{X_{ma}}{X_{m1}}\right)\left[-\frac{X_{ma}}{X_{m1}}+j\frac{r_2}{X_{m1}}\frac{X_{ma}}{X_{m1}}\right]\right\}-a_2\left\{b_2\left[\frac{X_{m1}}{X_{m1}}-S^2\frac{X_{m1}}{X_{m1}}-\frac{r_2}{X_{m1}}\frac{r_2}{X_{m1}}-j\frac{r_2}{X_{m1}}-j\frac{r_2}{X_{m1}}\frac{X_{m1}}{X_{m1}}\right]-\left(jS\frac{X_{ma}}{X_{m1}}\right)\times\left[j\frac{X_{mm}}{X_{m1}}\frac{X_{m1}}{X_{m1}}+\frac{r_2}{X_{m1}}\frac{X_{mm}}{X_{m1}}+S\frac{X_{ma}}{X_{m1}}\right]+\left(-\frac{X_{ma}}{X_{m1}}\right)\left[S\frac{X_{mm}}{X_{m1}}\frac{X_{m1}}{X_{m1}}-j\frac{X_{ma}}{X_{m1}}-\frac{r_2}{X_{m1}}\frac{X_{ma}}{X_{m1}}\right]\right\}+a_3\left\{b_2\left[-jS\frac{X_{ma}}{X_{m1}}\right]-b_3\left[j\frac{X_{mm}}{X_{m1}}\frac{X_{m1}}{X_{m1}}+\frac{X_{mm}}{X_{m1}}\frac{r_2}{X_{m1}}+S\frac{X_{ma}}{X_{m1}}\right]+\left(-\frac{X_{ma}}{X_{m1}}\right)\left[j\frac{X_{mm}}{X_{m1}}\frac{X_{ma}}{X_{m1}}\right]\right\}-a_4\left\{b_2\left[-\frac{X_{ma}}{X_{m1}}\left(1-j\frac{r_2}{X_{m1}}\right)\right]-b_3\left[S\frac{X_{mm}}{X_{m1}}\frac{X_{m1}}{X_{m1}}-j\frac{X_{ma}}{X_{m1}}-\frac{r_2}{X_{m1}}\frac{X_{ma}}{X_{m1}}\right]+\left(jS\frac{X_{ma}}{X_{m1}}\right)\left[j\frac{X_{mm}}{X_{m1}}\frac{X_{ma}}{X_{m1}}\right]\right\}$$

Writing in the b terms and multiplying through

$$\Delta=a_1\left\{\left[-\frac{(X_a+X_{a1}+X_{ma})}{X_{m1}}\right]\left[(1-S^2)\times\right.\right.$$

$$\frac{X_{02}}{X_{02}}-\left(\frac{r_2}{X_{02}}\right)^2\Bigg]+\frac{r_2}{X_{02}}\frac{r_a}{X_{02}}\left(1+\frac{X_{02}}{X_{02}}\right)+$$

$$(1-S^2)\left(\frac{X_{ma}}{X_{02}}\right)^2+j\frac{r_a}{X_{02}}\Bigg[(1-S^2)\times$$

$$\frac{X_{02}}{X_{02}}-\left(\frac{r_2}{X_{02}}\right)^2\Bigg]+j\frac{r_2}{X_{02}}\left(1+\frac{X_{02}}{X_{02}}\right)\times$$

$$\left[\frac{(X_a+X_{a1}+X_{ma})}{X_{02}}\right]-j\frac{r_2}{X_{02}}\times$$

$$\left(\frac{X_{ma}}{X_{02}}\right)^2\Bigg\}-a_2\Bigg\{-\frac{r_2}{X_{02}}\left(1+\frac{X_{02}}{X_{02}}\right)\times$$

$$\left(\frac{X_{a1}+X_{ma}}{X_{02}}\right)-j\left(\frac{X_{a1}+X_{ma}}{X_{02}}\right)\times$$

$$\left[(1-S^2)\frac{X_{02}}{X_{02}}-\left(\frac{r_2}{X_{02}}\right)^2\right]+$$

$$\frac{r_2}{X_{02}}\left(\frac{X_{ma}}{X_{02}}\right)^2+j\left(\frac{X_{ma}}{X_{02}}\right)^2-$$

$$j\left[S\frac{r_2}{X_{02}}\frac{X_{mm}}{X_{02}}\frac{X_{ma}}{X_{02}}+S^2\left(\frac{X_{ma}}{X_{02}}\right)^2\right]\Bigg\}+$$

$$a_3\Bigg\{\left[-S\frac{X_{ma}}{X_{02}}\frac{X_{a1}+X_{ma}}{X_{02}}\right]-$$

$$j\frac{X_{mm}}{X_{02}}\left(\frac{X_{ma}}{X_{02}}\right)^2+\left[\frac{(X_a+X_{a1}+X_{ma})}{X_{02}}\times\right.$$

$$\left.\left(\frac{X_{mm}}{X_{02}}\frac{r_2}{X_{02}}+S\frac{X_{ma}}{X_{02}}\right)\right]+\frac{r_a}{X_{02}}\frac{X_{mm}}{X_{02}}\frac{X_{02}}{X_{02}}-$$

$$j\frac{r_a}{X_{02}}\left[\frac{X_{mm}}{X_{02}}\frac{r_2}{X_{02}}+S\frac{X_{ma}}{X_{02}}\right]+$$

$$j\frac{X_{mm}}{X_{02}}\frac{X_{02}}{X_{02}}\frac{(X_a+X_{a1}+X_{ma})}{X_{02}}\Bigg\}-$$

$$a_4\Bigg\{\frac{r_2}{X_{02}}\frac{X_{ma}}{X_{02}}\frac{(X_{a1}+X_{ma})}{X_{02}}+$$

$$j\frac{X_{a1}+X_{ma}}{X_{02}}\frac{X_{ma}}{X_{02}}+\frac{(X_a+X_{a1}+X_{ma})}{X_{02}}\times$$

$$\left[S\frac{X_{mm}}{X_{02}}\frac{X_{02}}{X_{02}}-\frac{r_2}{X_{02}}\frac{X_{ma}}{X_{02}}\right]-\frac{r_a}{X_{02}}\frac{X_{ma}}{X_{02}}-$$

$$j\frac{r_a}{X_{02}}\left[S\frac{X_{mm}}{X_{02}}\frac{X_{02}}{X_{02}}-\frac{r_2}{X_{02}}\frac{X_{ma}}{X_{02}}\right]-$$

$$j\frac{X_{ma}}{X_{02}}\frac{(X_a+X_{a1}+X_{ma})}{X_{02}}-$$

$$S\frac{X_{mm}}{X_{02}}\left(\frac{X_{ma}}{X_{02}}\right)^2\Bigg\}$$

Grouping the real terms and the j terms

$$\Delta=a_1\Bigg\{\Bigg[(1-S^2)\left(\frac{X_{ma}}{X_{02}}\right)^2+\frac{r_2}{X_{02}}\frac{r_a}{X_{02}}\times$$

$$\left(1+\frac{X_{02}}{X_{02}}\right)+\left(\frac{r_2}{X_{02}}\right)^2\frac{X_a+X_{a1}+X_{ma}}{X_{02}}-$$

$$(1-S^2)\frac{X_{02}}{X_{02}}\frac{(X_a+X_{a1}+X_{ma})}{X_{02}}\Bigg]+$$

$$j\Bigg[\frac{r_a}{X_{02}}(1-S^2)\frac{X_{02}}{X_{02}}-\frac{r_a}{X_{02}}\left(\frac{r_2}{X_{02}}\right)^2-$$

$$\frac{r_2}{X_{02}}\left(\frac{X_{ma}}{X_{02}}\right)^2+\frac{r_2}{X_{02}}\left(1+\frac{X_{02}}{X_{02}}\right)\times$$

$$\left(\frac{X_a+X_{a1}+X_{ma}}{X_{02}}\right)\Bigg]\Bigg\}-$$

$$a_2\Bigg\{\left[\frac{r_2}{X_{02}}\left(\frac{X_{ma}}{X_{02}}\right)^2-\frac{r_2}{X_{02}}\left(1+\frac{X_{02}}{X_{02}}\right)\times\right.$$

$$\left.\left(\frac{X_{a1}+X_{ma}}{X_{02}}\right)\right]+j\Bigg[\left(\frac{X_{ma}}{X_{02}}\right)^2-$$

$$S\frac{r_2}{X_{02}}\frac{X_{mm}}{X_{02}}\frac{X_{ma}}{X_{02}}-S^2\left(\frac{X_{ma}}{X_{02}}\right)^2-$$

$$(1-S^2)\frac{X_{02}}{X_{02}}\left(\frac{X_{a1}+X_{ma}}{X_{02}}\right)+\left(\frac{r_2}{X_{02}}\right)^2\times$$

$$\left(\frac{X_{a1}+X_{ma}}{X_{02}}\right)\Bigg]\Bigg\}+a_3\Bigg\{\Bigg[\frac{r_a}{X_{02}}\times$$

$$\frac{X_{mm}}{X_{02}}\frac{X_{02}}{X_{02}}-S\frac{X_{ma}}{X_{02}}\left(\frac{X_{a1}+X_{ma}}{X_{02}}\right)+$$

$$S\frac{X_{ma}}{X_{02}}\left(\frac{X_a+X_{a1}+X_{ma}}{X_{02}}\right)+$$

$$\frac{r_2}{X_{02}}\frac{X_{mm}}{X_{02}}\left(\frac{X_a+X_{a1}+X_{ma}}{X_{02}}\right)\Bigg]+$$

$$j\Bigg[\frac{X_{mm}}{X_{02}}\frac{X_{02}}{X_{02}}\left(\frac{X_a+X_{a1}+X_{ma}}{X_{02}}\right)-$$

$$\frac{X_{mm}}{X_{02}}\left(\frac{X_{ma}}{X_{02}}\right)^2-\frac{r_a}{X_{02}}\frac{X_{mm}}{X_{02}}\frac{r_2}{X_{02}}-$$

$$\frac{r_a}{X_{02}}S\frac{X_{ma}}{X_{02}}\Bigg]\Bigg\}-a_4\Bigg\{\Bigg[\frac{r_2}{X_{02}}\frac{X_{ma}}{X_{02}}\times$$

$$\left(\frac{X_{a1}+X_{ma}}{X_{02}}\right)-\frac{r_a}{X_{02}}\frac{X_{ma}}{X_{02}}-S\frac{X_{mm}}{X_{02}}\times$$

$$\left(\frac{X_{ma}}{X_{02}}\right)^2+S\frac{X_{mm}}{X_{02}}\frac{X_{02}}{X_{02}}\times$$

$$\left(\frac{X_a+X_{a1}+X_{ma}}{X_{02}}\right)-\frac{r_2}{X_{02}}\frac{X_{ma}}{X_{02}}\times$$

$$\left(\frac{X_a+X_{a1}+X_{ma}}{X_{02}}\right)\Bigg]+$$

$$j\left[\frac{X_{ma}}{X_{02}}\left(\frac{X_{a1}+X_{ma}}{X_{02}}\right)-\frac{X_{ma}}{X_{02}}\times\right.$$

$$\left(\frac{X_a+X_{a1}+X_{ma}}{X_{02}}\right)+\frac{r_2}{X_{02}}\frac{r_a}{X_{02}}\frac{X_{ma}}{X_{02}}-$$

$$\left.S\frac{r_a}{X_{02}}\frac{X_{mm}}{X_{02}}\frac{X_{02}}{X_{02}}\right]\Bigg\}$$

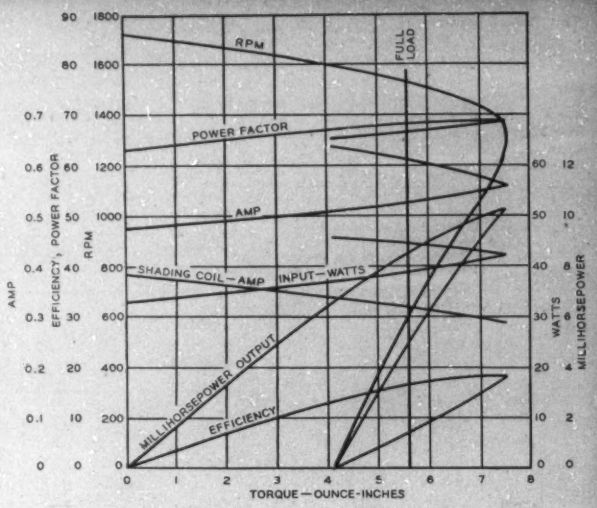

Figure 5. Calculated performance curves of a typical shaded-pole 10-inch fan motor

Writing in the a terms, multiplying through, subtracting, and combining the real and quadrature terms,

$$\Delta=\Bigg\{\frac{r_1}{X_{02}}\left[\frac{r_2}{X_{02}}\frac{r_a}{X_{02}}\left(1+\frac{X_{02}}{X_{02}}\right)+\left(\frac{r_2}{X_{02}}\right)^2\times\right.$$

$$\left.\left(\frac{X_a+X_{a1}+X_{ma}}{X_{02}}\right)\right]+\frac{r_2}{X_{02}}\times$$

$$\left(\frac{X_a+X_{a1}+X_{ma}}{X_{02}}\right)\left[\left(\frac{X_{mm}}{X_{02}}\right)^2+\right.$$

$$\left.\left(\frac{X_{ma}}{X_{02}}\right)^2\right]+\frac{r_2}{X_{02}}\left(\frac{X_{a1}+X_{ma}}{X_{02}}\right)\times$$

$$\Bigg[\left(1+\frac{X_{02}}{X_{02}}\right)\left(\frac{X_{a1}+X_{ma}}{X_{02}}\right)-$$

$$2\left(\frac{X_{ma}}{X_{02}}\right)^2\Bigg]+$$

$$\left(\frac{X_1+X_{mm}+X_{ma}+X_{a1}}{X_{02}}\right)\times$$

$$\Bigg[\frac{r_a}{X_{02}}\left(\frac{r_2}{X_{02}}\right)^2+\frac{r_2}{X_{02}}\left(\frac{X_{ma}}{X_{02}}\right)^2-\frac{r_2}{X_{02}}\times$$

$$\left(1+\frac{X_{02}}{X_{02}}\right)\left(\frac{X_a+X_{a1}+X_{ma}}{X_{02}}\right)\Bigg]+$$

$$(1-S^2)\Bigg[\frac{r_1}{X_{02}}\left(\frac{X_{ma}}{X_{02}}\right)^2-\frac{r_1}{X_{02}}\frac{X_{02}}{X_{02}}\times$$

$$\left(\frac{X_a+X_a+X_m}{X_{02}}\right)-\frac{r_a}{X_{02}}\frac{X_{02}}{X_{02}}\times$$

$$\left(\frac{X_1+X_{mm}+X_{ma}+X_{a1}}{X_{01}}\right)+\frac{r_a}{X_{01}}\times$$

$$\left(\frac{X_{mm}}{X_{01}}\right)^2\frac{X_{01}}{X_{01}}+\frac{r_a}{X_{01}}\left(\frac{X_{ma}}{X_{01}}\right)^2\Bigg]\Bigg\}+$$

$$j\left\{\frac{r_1}{X_{01}}\frac{r_1}{X_{01}}\left(1+\frac{X_{01}}{X_{01}}\right)\times\right.$$

$$\left(\frac{X_a+X_{a1}+X_{ma}}{X_{01}}\right)-\frac{r_1}{X_{01}}\left(\frac{r_2}{X_{01}}\right)^2\times$$

$$\frac{r_0}{X_{01}}-\frac{r_1}{X_{01}}\frac{r_2}{X_{01}}\left(\frac{X_{ma}}{X_{01}}\right)^2+$$

$$\left(\frac{X_1+X_{mm}+X_{ma}+X_{a1}}{X_{01}}\right)\times$$

$$\left[\frac{r_2}{X_{01}}\frac{r_a}{X_{01}}\left(1+\frac{X_{01}}{X_{01}}\right)+\left(\frac{r_2}{X_{01}}\right)^2\times\right.$$

$$\left.\left(\frac{X_a+X_{a1}+X_{ma}}{X_{01}}\right)\right]-\left(\frac{r_2}{X_{01}}\right)^2\times$$

$$\left(\frac{X_{a1}+X_{ma}}{X_{01}}\right)^2-\frac{r_2}{X_{01}}\frac{r_a}{X_{01}}\left[\left(\frac{X_{mm}}{X_{01}}\right)^2+\right.$$

$$\left.\left(\frac{X_{ma}}{X_{01}}\right)^2\right]+(1-S^2)\left[\frac{r_1}{X_{01}}\frac{r_a}{X_{01}}\frac{X_{01}}{X_{01}}+\right.$$

$$\frac{X_1+X_{mm}+X_{ma}+X_{a1}}{X_{01}}\left(\left(\frac{X_{ma}}{X_{01}}\right)^2-\right.$$

$$\left.\frac{X_{01}}{X_{01}}\left(\frac{X_a+X_{a1}+X_{ma}}{X_{01}}\right)\right)-2\left(\frac{X_{ma}}{X_{01}}\right)^2\times$$

$$\left(\frac{X_{a1}+X_{ma}}{X_{01}}\right)+\frac{X_{01}}{X_{01}}\left(\frac{X_{a1}+X_{ma}}{X_{01}}\right)^2+$$

$$\left(\frac{X_{mm}}{X_{01}}\right)^2\frac{X_{01}}{X_{01}}\left(\frac{X_a+X_{a1}+X_{ma}}{X_{01}}\right)-$$

$$\left(\frac{X_{mm}}{X_{01}}\right)^2\left(\frac{X_{ma}}{X_{01}}\right)^2+\left(\frac{X_{ma}}{X_{01}}\right)^2\times$$

$$\left.\left.\left(\frac{X_a+X_{a1}+X_{ma}}{X_{01}}\right)\right]\right\}$$

Rearranging the terms to facilitate numerical calculations

$$\Delta=\frac{r_2}{X_{01}}\left\{\frac{r_1}{X_{01}}\left[\frac{r_2}{X_{01}}\left(\frac{X_a+X_{a1}+X_{ma}}{X_{01}}\right)+\right.\right.$$

$$\left.\frac{r_a}{X_{01}}\left(1+\frac{X_{01}}{X_{01}}\right)\right]+\left(\frac{X_a+X_{a1}+X_{ma}}{X_{01}}\right)\times$$

$$\left(\frac{X_{mm}}{X_{01}}\right)^2+\frac{X_a}{X_{01}}\left(\frac{X_{ma}}{X_{01}}\right)^2+$$

$$\left(\frac{X_{a1}+X_{ma}}{X_{01}}\right)\left(1+\frac{X_{01}}{X_{01}}\right)\times$$

$$\left(\frac{X_{a1}+X_{ma}}{X_{01}}\right)+\frac{r_a}{X_{01}}\frac{r_2}{X_{01}}\times$$

$$\left(\frac{X_1+X_{mm}+X_{ma}+X_{a1}}{X_{01}}\right)-$$

$$\left(\frac{X_{a1}+X_{ma}}{X_{01}}\right)\left(1+\frac{X_{01}}{X_{01}}\right)\times$$

$$\left(\frac{X_a+X_{a1}+X_{ma}}{X_{01}}\right)-\left(\frac{X_1+X_{mm}}{X_{01}}\right)\times$$

$$\left[\left(1+\frac{X_{01}}{X_{01}}\right)\left(\frac{X_a+X_{a1}+X_{ma}}{X_{01}}\right)-\right.$$

$$\left.\left(\frac{X_{ma}}{X_{01}}\right)^2\right]\Bigg\}+(1-S^2)\left\{\frac{r_a}{X_{01}}\times\right.$$

$$\left[\left(\frac{X_{ma}}{X_{01}}\right)^2+\left(\frac{X_{mm}}{X_{01}}\right)^2\frac{X_{01}}{X_{01}}-\frac{X_{01}}{X_{01}}\times\right.$$

$$\left.\left(\frac{X_1+X_{mm}+X_{ma}+X_{a1}}{X_{01}}\right)\right]+$$

$$\frac{r_1}{X_{01}}\left[\left(\frac{X_{ma}}{X_{01}}\right)^2-\frac{X_{01}}{X_{01}}\times\right.$$

$$\left.\left.\left(\frac{X_a+X_{a1}+X_{ma}}{X_{01}}\right)\right]\right\}+j\frac{r_2}{X_{01}}\left\{\frac{r_1}{X_{01}}\times\right.$$

$$\left[\left(1+\frac{X_{01}}{X_{01}}\right)\left(\frac{X_a+X_{a1}+X_{ma}}{X_{01}}\right)-\right.$$

$$\left.\left(\frac{X_{ma}}{X_{01}}\right)^2-\frac{r_2}{X_{01}}\frac{r_a}{X_{01}}\right]+\frac{r_2}{X_{01}}\times$$

$$\left(\frac{X_1+X_{mm}}{X_{01}}\right)\left(\frac{X_a+X_{a1}+X_{ma}}{X_{01}}\right)+$$

$$\frac{r_a}{X_{01}}\left(1+\frac{X_{01}}{X_{01}}\right)\times$$

$$\left(\frac{X_1+X_{mm}+X_{ma}+X_{a1}}{X_{01}}\right)+\frac{r_2}{X_{01}}\frac{X_a}{X_{01}}\times$$

$$\left(\frac{X_{a1}+X_{ma}}{X_{01}}\right)-\frac{r_a}{X_{01}}\left[\left(\frac{X_{mm}}{X_{01}}\right)^2+\right.$$

$$\left.\left.\left(\frac{X_{ma}}{X_{01}}\right)^2\right]\right\}+j(1-S^2)\left\{\frac{r_1}{X_{01}}\frac{r_a}{X_{01}}\times\right.$$

$$\frac{X_{01}}{X_{01}}+\frac{X_1+X_{mm}}{X_{01}}\left[\left(\frac{X_{ma}}{X_{01}}\right)^2-\frac{X_{01}}{X_{01}}\times\right.$$

$$\left.\left(\frac{X_a+X_{a1}+X_{ma}}{X_{01}}\right)\right]+\left(\frac{X_{ma}}{X_{01}}\right)^2\frac{X_a}{X_{01}}-$$

$$\left(\frac{X_{mm}}{X_{01}}\right)^2\left[\left(\frac{X_{ma}}{X_{01}}\right)^2-\frac{X_{01}}{X_{01}}\times\right.$$

$$\left.\left.\left(\frac{X_a+X_{a1}+X_{ma}}{X_{01}}\right)\right]-\frac{X_a}{X_{01}}\frac{X_{01}}{X_{01}}\times\right.$$

$$\left.\left(\frac{X_{a1}+X_{ma}}{X_{01}}\right)\right\}$$

Assigning letters to the several groups of terms

$$\Delta=B_{19}+(1-S^2)B_{17}+j[B_{26}+(1-S^2)B_{18}]$$

$$\Delta=U+jW$$

NUMERATOR I,

$$N_1'=i_m\left\{b_1\left[\left(-1+j\frac{r_2}{X_{01}}\right)\left(-\frac{X_{01}}{X_{01}}+j\frac{r_2}{X_{01}}\right)-\right.\right.$$

$$\left.(-jS)\left(jS\frac{X_{01}}{X_{01}}\right)\right]-b_2\left[(0)(d_4)-\right.$$

$$\left.(-jS)\left(-\frac{X_{ma}}{X_{01}}\right)\right]+b_3\left[(0)(d_4)-\right.$$

$$\left.\left.\left(-1+j\frac{r_2}{X_{01}}\right)\left(-\frac{X_{ma}}{X_{01}}\right)\right]\right\}$$

$$N_1'=i_m\left\{b_2\left[\left(1-j\frac{r_2}{X_{01}}\right)\left(\frac{X_{01}}{X_{01}}-j\frac{r_2}{X_{01}}\right)-\right.\right.$$

$$\left.S\frac{X_{01}}{X_{01}}\right]-\left(jS\frac{X_{ma}}{X_{01}}\right)\left(-jS\frac{X_{ma}}{X_{01}}\right)+$$

$$\left(-\frac{X_{ma}}{X_{01}}\right)\left[\left(1-j\frac{r_2}{X_{01}}\right)\left(-\frac{X_{ma}}{X_{01}}\right)\right]\Bigg\}$$

$$N_1'=i_m\left\{\left[-\left(\frac{X_a+X_{a1}+X_{ma}}{X_{01}}\right)+j\frac{r_a}{X_{01}}\right]\times\right.$$

$$\left[(1-S^2)\frac{X_{01}}{X_{01}}-\left(\frac{r_2}{X_{01}}\right)^2-j\frac{r_2}{X_{01}}\times\right.$$

$$\left.\left(1+\frac{X_{01}}{X_{01}}\right)\right]+(1-S^2)\left(\frac{X_{ma}}{X_{01}}\right)^2-$$

$$\left.j\frac{r_2}{X_{01}}\left(\frac{X_{ma}}{X_{01}}\right)^3\right\}$$

Multiplying and separating the real and quadrature terms

$$N_1'=i_m\left\{\left[(1-S^2)\left(\frac{X_{ma}}{X_{01}}\right)^2+\frac{r_2}{X_{01}}\frac{r_a}{X_{01}}\times\right.\right.$$

$$\left(1+\frac{X_{01}}{X_{01}}\right)-(1-S^2)\frac{X_{01}}{X_{01}}\times$$

$$\left(\frac{X_a+X_{a1}+X_{ma}}{X_{01}}\right)+\left(\frac{r_2}{X_{01}}\right)^2\times$$

$$\left.\left(\frac{X_a+X_{a1}+X_{ma}}{X_{01}}\right)\right]+j\left[\frac{r_a}{X_{01}}\times\right.$$

$$(1-S^2)\frac{X_{01}}{X_{01}}-\frac{r_a}{X_{01}}\left(\frac{r_2}{X_{01}}\right)^2-$$

$$\left.\left.\frac{r_2}{X_{01}}\left(\frac{X_{ma}}{X_{01}}\right)^2+\frac{r_2}{X_{01}}\left(1+\frac{X_{01}}{X_{01}}\right)\times\right.$$

$$\left.\left.\left(\frac{X_a+X_{a1}+X_{ma}}{X_{01}}\right)\right]\right\}$$

Combining further those terms which are a function of $(1-S^2)$

$$N_1'=i_m\left\{\left[\frac{r_2}{X_{01}}\frac{r_a}{X_{01}}\left(1+\frac{X_{01}}{X_{01}}\right)+\left(\frac{r_2}{X_{01}}\right)^2\times\right.\right.$$

$$\left.\left(\frac{X_a+X_{a1}+X_{ma}}{X_{01}}\right)\right]+(1-S^2)\times$$

$$\left[\left(\frac{X_{ma}}{X_{01}}\right)^2-\frac{X_{01}}{X_{01}}\left(\frac{X_a+X_{a1}+X_{ma}}{X_{01}}\right)\right]+$$

$$j\left[\frac{r_2}{X_{01}}\left(1+\frac{X_{01}}{X_{01}}\right)\left(\frac{X_a+X_{a1}+X_{ma}}{X_{01}}\right)-\right.$$

$$\frac{r_a}{X_{01}}\left(\frac{r_2}{X_{01}}\right)^2-\frac{r_2}{X_{01}}\left(\frac{X_{ma}}{X_{01}}\right)^2+(1-S^2)\times$$

$$\left.\left.\left(\frac{r_a}{X_{01}}\frac{X_{01}}{X_{01}}\right)\right]\right\}$$

Assigning letters to the several groups of terms

$$N_1'=i_m\{B_7+(1-S^2)B_{13}+j[B_{15}+(1-S^2)B_{14}]\}=i_m[N_{1A}+jN_{1B}]$$

NUMERATOR I_2

$$N_2'=-i_m\left\{\left(\frac{X_{a1}+X_{ma}}{X_{01}}\right)\left[\left(-1+j\frac{r_2}{X_{01}}\right)\times\right.\right.$$

$$\left.\left(-\frac{X_{01}}{X_{01}}+\frac{r_2}{X_{01}}\right)-(-jS)\left(jS\frac{X_{01}}{X_{01}}\right)\right]-$$

$$\left(\frac{X_{mm}}{X_{01}}-jS\frac{X_{ma}}{X_{01}}\right)\left[(0)(d_4)-(-jS)\times\right.$$

$$\left.\left(-\frac{X_{ma}}{X_{01}}\right)\right]+\left(\frac{X_{ma}}{X_{01}}+jS\frac{X_{mm}}{X_{01}}\right)\times$$

$$\left.\left[(0)(d_4)-\left(-1+j\frac{r_2}{X_{01}}\right)\left(-\frac{X_{ma}}{X_{01}}\right)\right]\right\}$$

$$N_2'=-i_m\left\{\left(\frac{X_{a1}+X_{ma}}{X_{01}}\right)\left[(1-S^2)\frac{X_{01}}{X_{01}}-\right.\right.$$

$$\left(\frac{r_2}{X_{01}}\right)^2-j\frac{r_2}{X_{01}}\left(1+\frac{X_{01}}{X_{01}}\right)\Bigg]-\left(\frac{X_{mm}}{X_{01}}-\right.$$

$$jS\frac{X_{ma}}{X_{01}}\Bigg)\left[-jS\frac{X_{ma}}{X_{01}}\right]+\left(\frac{X_{ma}}{X_{01}}+\right.$$

$$\left.\left.jS\frac{X_{mm}}{X_{01}}\right)\left[1-j\frac{r_2}{X_{01}}\left(-\frac{X_{ma}}{X_{01}}\right)\right]\right\}$$

$$N_2'=-i_m\left\{\left(\frac{X_{a1}+X_{ma}}{X_{01}}\right)(1-S^2)\frac{X_{01}}{X_{01}}-\right.$$

$$\left(\frac{X_{a1}+X_{ma}}{X_{02}}\right)\left(\frac{r_2}{X_{02}}\right)^2-j\times$$

$$\left(\frac{X_{a1}+X_{ma}}{X_{02}}\right)\frac{r_2}{X_{02}}\left(1+\frac{X_{02}}{X_{02}}\right)+$$

$$jS\frac{X_{mm}}{X_{02}}\frac{X_{ma}}{X_{02}}+S^2\left(\frac{X_{ma}}{X_{02}}\right)^2-$$

$$\left(\frac{X_{ma}}{X_{02}}\right)^2-S\frac{r_2}{X_{02}}\frac{X_{mm}}{X_{02}}\frac{X_{ma}}{X_{02}}-$$

$$jS\frac{X_{mm}}{X_{02}}\frac{X_{ma}}{X_{02}}+j\frac{r_2}{X_{02}}\left(\frac{X_{ma}}{X_{02}}\right)^2\Bigg\}$$

$$N_2'=i_m\Bigg\{\left(\frac{r_2}{X_{02}}\right)^2\left(\frac{X_{a1}+X_{ma}}{X_{02}}\right)+S\Bigg[\frac{r_2}{X_{02}}\times$$

$$\frac{X_{mm}}{X_{02}}\frac{X_{ma}}{X_{02}}\Bigg]+(1-S^2)\Bigg[\left(\frac{X_{ma}}{X_{02}}\right)^2-$$

$$\frac{X_{02}}{X_{02}}\left(\frac{X_{a1}+X_{ma}}{X_{02}}\right)\Bigg]+j\frac{r_2}{X_{02}}\times$$

$$\Bigg[\left(1+\frac{X_{02}}{X_{02}}\right)\left(\frac{X_{a1}+X_{ma}}{X_{02}}\right)-\left(\frac{X_{ma}}{X_{02}}\right)^2\Bigg]\Bigg\}$$

Assigning letters to the several groups of terms

$$N_2'=i_m\{[B_1+SB_{13}+(1-S^2)B_{12}]+jB_{14}\}=i_m[N_{2h}+jN_{2v}]$$

NUMERATOR I_{2m}

$$N_3'=i_m\Bigg\{\left(\frac{X_{a1}+X_{ma}}{X_{02}}\right)\Bigg[\left(jS\frac{X_{ma}}{X_{02}}\right)\times$$

$$\left(-\frac{X_{02}}{X_{02}}+j\frac{r_2}{X_{02}}\right)-\left(-\frac{X_{ma}}{X_{02}}\times\right.$$

$$\left.jS\frac{X_{02}}{X_{02}}\right)\Bigg]-\left(\frac{X_{mm}}{X_{02}}-jS\frac{X_{ma}}{X_{02}}\right)\times$$

$$\Bigg[\left(-\frac{X_a+X_{a1}+X_{ma}}{X_{02}}+j\frac{r_a}{X_{02}}\right)\times$$

$$\left(-\frac{X_{02}}{X_{02}}+j\frac{r_2}{X_{02}}\right)-\left(-\frac{X_{ma}}{X_{02}}\times\right.$$

$$\left.-\frac{X_{ma}}{X_{02}}\right)\Bigg]+\left(\frac{X_{ma}}{X_{02}}+jS\frac{X_{mm}}{X_{02}}\right)\times$$

$$\Bigg[\left(-\frac{X_a+X_{a1}+X_{ma}}{X_{02}}+j\frac{r_a}{X_{02}}\right)\times$$

$$\left(jS\frac{X_{02}}{X_{02}}\right)\left(-\frac{X_{ma}}{X_{02}}\right)\Bigg]\Bigg\}$$

$$N_3'=i_m\Bigg\{\left(\frac{X_{a1}+X_{ma}}{X_{02}}\right)\Bigg[-jS\frac{X_{ma}}{X_{02}}\frac{X_{02}}{X_{02}}-$$

$$S\frac{r_2}{X_{02}}\frac{X_{ma}}{X_{02}}+jS\frac{X_{ma}}{X_{02}}\frac{X_{02}}{X_{02}}\Bigg]-\left(\frac{X_{mm}}{X_{02}}-\right.$$

$$jS\frac{X_{ma}}{X_{02}}\Bigg)\Bigg[\frac{X_{02}}{X_{02}}\frac{X_a+X_{a1}+X_{ma}}{X_{02}}-$$

$$j\frac{r_a}{X_{02}}\frac{X_{02}}{X_{02}}-j\frac{r_2}{X_{02}}\frac{X_a+X_{a1}+X_{ma}}{X_{02}}-$$

$$\frac{r_2}{X_{02}}\frac{r_a}{X_{02}}-\left(\frac{X_{ma}}{X_{02}}\right)^2\Bigg]+\left(\frac{X_{ma}}{X_{02}}+\right.$$

$$jS\frac{X_{mm}}{X_{02}}\Bigg)\Bigg[-jS\frac{X_{02}}{X_{02}}\frac{X_a+X_{a1}+X_{ma}}{X_{02}}-$$

$$S\frac{r_a}{X_{02}}\frac{X_{02}}{X_{02}}+jS\left(\frac{X_{ma}}{X_{02}}\right)^2\Bigg]\Bigg\}$$

$$N_3'=i_m\Bigg\{\frac{r_2}{X_{02}}\frac{r_a}{X_{02}}\frac{X_{mm}}{X_{02}}+S\Bigg[\frac{r_2}{X_{02}}\left(\frac{X_{ma}}{X_{02}}\right)\times$$

$$\left(\frac{X_a+X_{a1}+X_{ma}}{X_{02}}\right)-\frac{r_2}{X_{02}}\left(\frac{X_{ma}}{X_{02}}\right)\times$$

$$\left(\frac{X_{a1}+X_{ma}}{X_{02}}\right)\Bigg]+(1-S^2)\Bigg[\frac{X_{mm}}{X_{02}}\times$$

$$\left(\frac{X_{ma}}{X_{02}}\right)^2-\frac{X_{mm}}{X_{02}}\frac{X_{02}}{X_{02}}\times$$

$$\left(\frac{X_a+X_{a1}+X_{ma}}{X_{02}}\right)\Bigg]+j\Bigg[\frac{r_2}{X_{02}}\frac{X_{mm}}{X_{02}}\times$$

$$\left(\frac{X_a+X_{a1}+X_{ma}}{X_{02}}\right)-S\frac{r_2}{X_{02}}\frac{r_a}{X_{02}}\frac{X_{ma}}{X_{02}}+$$

$$(1-S^2)\left(\frac{r_a}{X_{02}}\frac{X_{mm}}{X_{02}}\frac{X_{02}}{X_{02}}\right)\Bigg]\Bigg\}$$

Assigning letters to the several groups of terms

$$N_3'=i_m\{[B_9+SB_{12}+(1-S^2)B_{14}]+j[B_{11}-SB_{13}+(1-S^2)B_6]\}=i_m[N_{3h}+jN_{3v}]$$

NUMERATOR I_{2a}

$$N_4'=-i_m\Bigg\{\left(\frac{X_{a1}+X_{ma}}{X_{02}}\right)\Bigg[\left(jS\frac{X_{ma}}{X_{02}}\right)(-jS)-$$

$$\left(-\frac{X_{ma}}{X_{02}}\right)\left(-1+j\frac{r_2}{X_{02}}\right)\Bigg]-\left(\frac{X_{mm}}{X_{02}}-\right.$$

$$jS\frac{X_{ma}}{X_{02}}\Bigg)\Bigg[\left(-\frac{X_a+X_{a1}+X_{ma}}{X_{02}}+\right.$$

$$\left.j\frac{r_a}{X_{02}}\right)(-jS)-(b_4)(0)\Bigg]+\left(\frac{X_{ma}}{X_{02}}+\right.$$

$$jS\frac{X_{mm}}{X_{02}}\Bigg)\Bigg[\left(-\frac{X_a+X_{a1}+X_{ma}}{X_{02}}+\right.$$

$$\left.j\frac{r_a}{X_{02}}\right)\left(-1+j\frac{r_2}{X_{02}}\right)-(b_5)(0)\Bigg]\Bigg\}$$

$$N_4'=-i_m\Bigg\{\left(\frac{X_{a1}+X_{ma}}{X_{02}}\right)\Bigg[S^2\frac{X_{ma}}{X_{02}}\frac{X_{ma}}{X_{02}}+$$

$$j\frac{r_2}{X_{02}}\frac{X_{ma}}{X_{02}}\Bigg]-\left(\frac{X_{mm}}{X_{02}}-jS\frac{X_{ma}}{X_{02}}\right)\times$$

$$\Bigg[jS\frac{X_a+X_{a1}+X_{ma}}{X_{02}}+S\frac{r_a}{X_{02}}\Bigg]+$$

$$\left(\frac{X_{ma}}{X_{02}}+jS\frac{X_{mm}}{X_{02}}\right)\Bigg[\frac{X_a+X_{a1}+X_{ma}}{X_{02}}-$$

$$j\frac{r_a}{X_{02}}-j\frac{r_2}{X_{02}}\frac{X_a+X_{a1}+X_{ma}}{X_{02}}-$$

$$\frac{r_2}{X_{02}}\frac{r_a}{X_{02}}\Bigg]\Bigg\}$$

$$N_4'=i_m\Bigg\{\frac{r_2}{X_{02}}\frac{r_a}{X_{02}}\frac{X_{ma}}{X_{02}}-S\Bigg[\frac{r_2}{X_{02}}\frac{X_{mm}}{X_{02}}\times$$

$$\left(\frac{X_a+X_{a1}+X_{ma}}{X_{02}}\right)\Bigg]-(1-S^2)\times$$

$$\Bigg[-\frac{X_{ma}}{X_{02}}\left(\frac{X_{a1}+X_{ma}}{X_{02}}\right)+\frac{X_{ma}}{X_{02}}\times$$

$$\left(\frac{X_a+X_{a1}+X_{ma}}{X_{02}}\right)\Bigg]+j\Bigg[\frac{r_2}{X_{02}}\frac{X_{ma}}{X_{02}}\times$$

$$\left(\frac{X_a+X_{a1}+X_{ma}}{X_{02}}\right)-\frac{r_2}{X_{02}}\frac{X_{ma}}{X_{02}}\times$$

$$\left(\frac{X_{a1}+X_{ma}}{X_{02}}\right)+S\left(\frac{r_2}{X_{02}}\frac{r_a}{X_{02}}\frac{X_{mm}}{X_{02}}\right)+$$

$$(1-S^2)\left(\frac{r_a}{X_{02}}\frac{X_{ma}}{X_{02}}\right)\Bigg]\Bigg\}$$

Assigning letters to the several groups of terms

$$N_4'=i_m\{[B_8-SB_{11}-(1-S^2)B_3]+j[B_3+SB_9+(1-S^2)B_4]\}=i_m[N_{4h}+jN_{4v}]$$

Reference

1. AN ANALYSIS OF THE SHADED POLE MOTOR, P. H. TRICKEY. ELECTRICAL ENGINEERING (AIEE TRANSACTIONS), volume 55, September 1936, pages 1007–14.

Discussion

H. B. Stone (Robbins and Myers, Inc., Springfield, Ohio): The author has contributed another needed milestone in the design of a shaded pole motor. The mathematics of the paper and its appendix are appalling and the average engineer would pass up the mathematical derivations and accept the final equations. In his first paper on shaded pole motors published in 1936, Trickey presented his method of obtaining the various reactance values used in both papers. Some of these calculations were far from clear, and I had the feeling that on some of them the author was not too confident as to their dependability.

A few of his statements should be questioned. He states that harmonics are considered only so far as they increase the reactances; my experience has been that some field designs can and do have very pronounced harmonics, especially the third, which must be considered. He also states it is assumed that the effective center of the shaded pole is 90 electrical degrees from the effective center of the main pole; that simplifies the problem and is a desideratum, but many times the angle is 60 to 75 electrical degrees.

Fundamentally, the shaded pole motor is the simplest of all single phase motors to build and the hardest to analyze from a mathematical standpoint. I wish the author had given an easy method of obtaining the maximum torque and idle amperes and watts, but with his present paper it should be possible to design this type motor and depend less on the "cut and try" method.

P. H. Trickey: Stone's comments are good and to the point. Much more work needs to be done on the formulas for the motor constants.

It is very likely that there may be considerable effect due to the harmonics in some designs. This particular design came fairly close to test results, but perhaps the constants were in error in a way to offset the harmonics.

While it is true the analysis of this paper is limited to cases where the main pole and the shaded pole are 90 degrees apart, the average design is closer to 90 degrees than would appear at first sight, when consideration is given to the magnetic wedges and fringing, and to the fact that it is electrical degrees that are involved, not mechanical. The case of any angle between poles should make a good subject for another paper.

Generating Reserve Capacity Determined by the Probability Method

GIUSEPPE CALABRESE
MEMBER AIEE

A FUNDAMENTAL PROBLEM in system planning is the correct determination of reserve capacity. Too low a value means excessive interruption, while too high a value results in excessive costs. The greater the uncertainty regarding the actual reliability of any installation the greater the investment wasted.

In the typical case of system generating capacity reserve, the problem not only concerns the risk of outage but also the economic balance between generator reserve and tie capacity in providing against local outage concentrations.

The complexity of the problem, in general, makes it difficult to find an answer to it by rules of thumb. The same complexity, on one side, and good engineering and sound economics, on the other, justify the use of methods of analysis permitting the systematic evaluations of all important factors involved. There are no exact methods available which permit the solution of reserve problems with the same exactness with which, say, circuit problems are solved by applying Ohm's law. However, a systematic attack of them can be made by a "judicious" application of the probability theory.

It is the purpose of this paper to describe this application, which resulted from a study, undertaken some ten years ago, for the purpose of rationalizing the reserve practice of the company with which the author is associated. More specifically, the application to the particular case of turbogenerator reserve will be referred to unless otherwise stated. Most of the conclusions, however, are general and may be extended to other cases.

The qualification "judicious" is essential because the results are subject to certain limitations which it is well to enumerate.

(*a*). It is assumed that forced outages of units are random events, independent from one another, governed by the same laws of chance governing the drawing of balls or the throwing of dice. A method will be given to check the general correctness of the assumed independence of forced outages of units.

(*b*). The probability theory aims only at foreseeing average performances. In the case under consideration, this means that the probability theory can predict only the average outage performance of a group of units during a long period of time.

(*c*). The basic information on which predictions for the future are made necessarily is obtained from previous experience of existing units. Some or all of these units may be of different design, or may have been operated under different operating conditions, or both, from those involved in the future.

With the approximation set by these limitations it will be shown that for a given system, or portion thereof, and for a given reserve value, probability calculations permit the prediction of

1. The fraction of time during which loss of load may be expected to occur during any future period.

2. The kilowatt-hour losses expected to result from forced outages.

The fraction of time as under (1) will be called the *loss of load duration* or the *loss of load probability*, and for convenience may be expressed in terms of "so many days upon which loss of load may be expected to occur during a given number of years," say 10 or 100. This number of days provides a first index for measuring and comparing service reliabilities.

Otherwise the energy losses as under (2) may be expressed in terms of so many kilowatt-hours per kilowatt of installed capacity, or of maximum load, per year or decade or century, thus obtaining two other indexes of service reliability.

It should be emphasized, however, that the calculated expected loss of load duration (whether expressed as a fraction of, or in number of days during a given period) and the calculated kilowatt-hour losses per kilowatt of installed capacity or of maximum load, refer to the long range prediction and cannot be expected to materialize year in and year out.

The choice of an appropriate level of service reliability, and thus of an appropriate reserve capacity, in any particular case, will be based on any one of these indexes or combinations thereof. Necessarily, this choice depends on personal judgment and is affected by local conditions.

Apart from the application of the probability theory to the determination of an appropriate absolute level of service reliability for a group of units connected to the same bus, there is another class of problem for the solution of which the probability theory seems especially well suited. This class of problems concerns the evaluation of the relative reliability of alternative plans. What is the reliability gained or lost by increasing or decreasing the reserve capacity of a group of units?—by changing the size and connections of ties?—by using a common header for a group of boilers? To the analysis of problems such as these, the probability theory is well adapted. It places, so to say, the alternative schemes in their proper relative positions from the standpoint of reliability.

Briefly, the method of reserve determination described in this paper proceeds from the assumption that forced outages of units are random events independent from one another and that

Paper 47-248, recommended by the AIEE power generation committee and approved by the AIEE technical program committee for presentation at the AIEE Midwest general meeting, Chicago, Ill., November 3–7, 1947. Manuscript submitted March 25, 1947; made available for printing September 18, 1947.

GIUSEPPE CALABRESE is assistant engineer, system engineering department, Consolidated Edison Company of New York, Inc., New York, N. Y.

The author wishes to express his thanks to K. F. Bellows (M'38) and P. Doane (A'26) for their cooperation and contributions in the preparation of this paper.

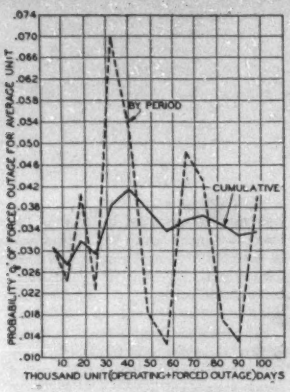

Figure 1. Graphical determination of the forced outage rate q

outage durations of units can be calculated by the well known binominal expansion. With this in mind, the paper includes the following major items:

1. Calculation of the average rate of forced outage of a group of units. This is the basic quantity of the method.

2. Probability calculations of various outage combinations. Binominal law.

3. Check of the independence of the individual outages. This check is necessary in order to establish the practical reasonableness of treating forced outages of units as random events obeying the laws of chance.

4. Probability of outages exceeding any given reserve. This is essential for the following three sections.

5. Effect of connections on the probability of outages.

6. Probability of loss of load.

7. Expected loss of kilowatt-hour output.

8. Effect of interconnections of stations on their reliability.

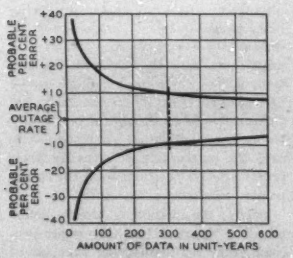

Figure 2. Probable error of average outage rate

1. Calculation of the Average Rate of Forced Outages of a Group of Units

Consider the performance of a single unit during a long past period T. During this period the unit has been in operation the time S_1 and out of service, due to forced outages of the unit itself, and not for causes external to the unit, the time O_1. The average outage rate of the unit is

$$q_1 = \frac{O_1}{S_1+O_1}$$

The sum S_1+O_1 is the demand time.* If the unit has been in demand during the whole period, and there have been no scheduled outages, S_1+O_1 is equal to T, otherwise S_1+O_1 is smaller than T. The outage and service times O_1 and S_1 may be expressed in hours or days. Though the use of hours seems entirely proper, days are used in this paper unless otherwise stated. A fraction of one day is called one day.

Practical problems involve a group of n units more or less similar among themselves or which may be subdivided into a small number of subgroups containing similar units.

If the n units of the group are, or are assumed to be, similar in design and operating conditions the outage rate of the individual average unit of the group is calculated with the formula

$$q = \frac{O_1+O_2+\ldots+O_k+\ldots+O_n}{(S_1+O_1)+(S_2+O_2)+\ldots+(S_k+O_k)+\ldots+(S_n+O_n)}$$

$$= \frac{O}{S+O} \qquad (1)$$

where O_k is the total forced outage time and S_k the total service time of the Kth unit. O is the total forced outage time and S the total service time of all units. The service rate p of the average unit is obtained in a similar manner. Evidently $p+q=$one.

With a given amount of the units past performance available a series of values of q are calculated by adding each year's forced outage and service times, respectively, to the cumulated forced outages and service times of the preceding years. If this leads to a stable value of q, that is, a value which changes little as $S+O$ increases, this value may be used to predict the expected future performance of the average unit. This is, this value of q may be taken as the average forced outage rate of all units, or simply the outage rate that may be expected to obtain during a sufficiently long period in the future, assuming that the units will be operating under the same conditions as in the past and that their performance will not be affected by aging. In this sense q may be called the expected forced outage duration or, more simply, the *outage duration* of the average unit during any future demand period, expressed as a fraction of the period.

The stable value of q may also be looked upon as representing the probability that any unit of the group will be out due to forced outages, or more simply the *outage probability*, during any future demand period.

More accurately the stable value of q should be corrected for the effect of future aging. This effect, if already present, may be detected by formal statistical methods or, graphically, by plotting the series of values of q obtained as previously stated.

Needless to emphasize that the outage probability q is the ratio between time out on forced outage and demand time and yields no information whatever relative to the duration of each outage.

The service rate, or service probability, or service duration, p of the units is obtained in a similar manner.

The outage rate q is the basic quantity on which depends the whole prediction of the future performance of a group of units. It is, therefore, essential that the value of q be stable and corrected for trends, due to aging or other causes. It is also necessary that its derivation from past records be checked for the assumed homogeneity of the group of units. To

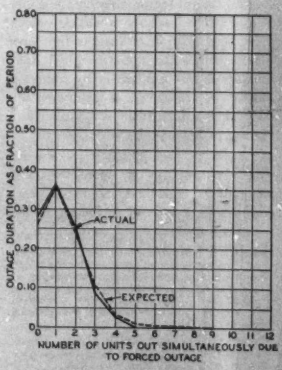

Figure 3. Actual versus expected experiences with simultaneous outages (44 units, 13 years, $q=0.03$)

* This definition of demand time as the sum of time in operation plus time out on forced outage will be adhered to in this paper.

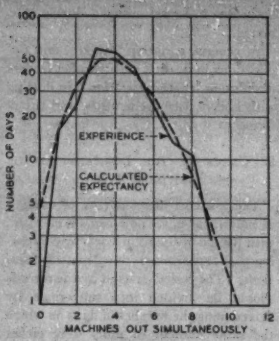

Figure 4. Actual versus expected experiences with simultaneous outages (309 units, one year $q = 0.0164$)

this end the group should be divided into subgroups according to some or all of the following characteristics: size, type, speed, age, demand factor, and pressure. A value of q should be obtained for each subgroup which should be tested for stability and trend as previously stated. How far this process of subgrouping should be carried depends on the amount of past information available. If there are no pronounced differences among the values and trends of the q's of the subgroups, one value of q may be used for the whole group, otherwise it may be necessary to consider two or more subgroups separately. Pioneering units as a rule form a class by themselves and need to be separated from the rest unless they are so diversified in size and location with respect to existing units that their effect may be neglected. Particular attention should be paid to the largest units because their outages are the most significant from the standpoint of reserve.

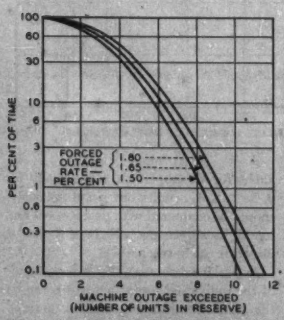

Figure 5. Effect of error in outage rate on calculated reserve (248 units)

Figure 1 illustrates the graphical method just described. The dotted curve gives the forced outage rate for each year. The solid curve gives the plot of the values of q obtained by adding the yearly forced outage days and the operating days of all units, respectively, to the corresponding cumulated values of the preceding years. Though the fluctuations of q decrease toward the end of the period it cannot be said definitely that a stable value has been attained. The data for this figure were obtained in the very early stage of this investigation, from the limited and, from the standpoint of this paper, incomplete records on outages of the Consolidated Edison Company. It was then impossible to segregate the real forced outages from outages which could have been postponed to week ends or even to the overhaul season. For this reason the forced outage rate $q = 0.03$ adopted at that time was high.

A further investigation of forced outages on several systems of boilers and steam turbogenerator units covering a period of six years resulted in the following outage rates:

Steam turbine generators

Below 1,000 pounds per square inch ..... 1.0 per cent
1,000 pounds per square inch and over ..... 1.9 per cent

Boilers

Below 1,000 pounds per square inch ..... 1.3 per cent
1,000 pounds per square inch and over ..... 2.1 per cent

The experience data available for the determination of q may be that of a relatively small number of units covering several years, or it may be that of a large number of units covering only a few years, say one or two. In the first case a plot such as shown in Figure 1 may be drawn to make a quick check of the stability of q. In the second case no such check can be made and recourse must be made to statistical methods in order to check the stability of q. This is illustrated in Figure 2 relative to 1-year experience with 303 units having a calculated averate outage of 1.98 per cent. Figure 2 gives the probable error of this average outage rate in function of the available data expressed in number of unit years.

If we have n units, having a forced outage rate q, what is the significance of q from the standpoint of future operation? Does it mean that during any future demand period D, in days, any given unit of the group will be out Dq days, or does it mean something else? It means that during the period D, the n units will be out on forced outage nDq unit-days with a probability approaching unity, that is certainty, as nD approaches infinity. This means that as the number n of units in the group increases the length of the period D necessary to attain a stable value of q, decreases and vice versa. At one extreme when the number of units n is very large, a number of them equal to nq is out continuously day in and day out; as one unit is restored to service another one goes out on forced outage so that the total number of units out is always the same with a probability approaching unity as the number of units n approaches infinity. At the other extreme with only a few units in the group, the probability is that it will take a large number of years before a stable value of q is reached. In subsequent years the same average outage rate may be expected to obtain during periods of the same duration with a probability approaching unity as the length of the period approaches infinity.

From the standpoint of reserve capacity the average outage rate need not be determined very accurately, the question then arises: how accurate does it need be? The effect of variations of q on reserve requirements will be analyzed in the following section.

Before closing this section, it seems appropriate to make a final remark regarding the calculation of the rate of outage of a unit composed of several elements connected in a series relation so that the outage of one element causes the whole

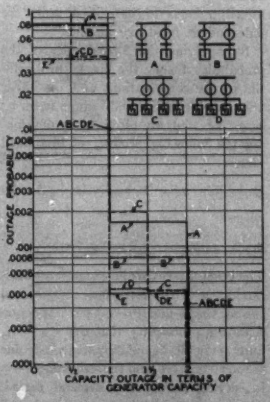

Figure 6. Effect of connections on reserve requirements

unit to be out. As an example, a turbogenerator outage may be caused by trouble in the boiler or boilers, or in the turbine or in the generator. In general a unit may be composed for several elements $a,b,c,d\ldots$ in series, having, respectively, the outage rates q_a, q_b, q_c, $q_d\ldots$ Each one of these outage rates is calculated considering only the outage caused by troubles in the particular element and not in the other elements. The corresponding service probabilities or durations are, respectively, $p_a = \text{one} - q_a$; $p_b = 1 - q_b$; $p_c = 1 - q_c$, and so forth. The quantity p_a is the probability or the expected total fraction of the time that the element a will be in service during any demand period. During the same fraction of time p_a it is expected that the element b will be in service the fraction p_b, so that the expected total fraction of time that both elements a and b will be in service during the whole demand periods is $p_a p_b$. By extending this reasoning to all the elements, the service probability p_1 of the units as a whole, that is the expected total fraction of time that all the elements will be in service, is $p_1 = p_a p_b p_c p_d\ldots$ The outage rate q_1 of the unit as a whole is thus $q_1 = 1 - p_1 = 1 - p_a p_b p_c p_d\ldots$

2. Outage Probability of Combinations of Units Connected in Parallel—Binominal Law

From the outage rate of individual units, calculated as described in the preceding section, the outage probabilities or outage durations of the combinations of a group of units connected in parallel, such as a group of boilers connected to the same header, now can be calculated, assuming, as previously stated, that forced outages of individual units are independent from one another.

By applying the formal rules of the probability theory the outage probabilities of the combinations of n dissimilar units having individual outage rates q_1, q_2, $q_3\ldots q_k\ldots q_n$ are obtained by developing the following product of binominal factors:

$$(p_1+q_1)(p_2+q_2)\ldots(p_k+q_k)\ldots(p_n+q_n) \qquad (2)$$

where

$p_1 = 1 - q_1$, $p_2 = (1 - q_2)$, and so forth

The general term of the expansion of this product is of the form $p_j p_l\ldots q_d q_f\ldots$ and contains mq's and $(n-m)$ p's. It represents the probability that the eth, $f^{th}\ldots$ units (m in all) be out simultaneously due to forced outages, and the remaining $n-m$ in service, during any demand period. The quantity m takes, successively, all $(n+1)$ values: 0, 1, 2...n and for each value of m there are $n!/[m!(n-m)!]$ terms in the expansion each corresponding to one combination of m units out of the total n.

If the n units of the group are, or are assumed to be, all similar, the same outage rate q is used for all of them. In this case the product of binominal factors (equation 2) degenerates into the following well known binominal formula:

$$(p+q)^n = p^n + np^{n-1}q + \frac{n!}{2!(n-2)!}p^{n-2}q^2 + \frac{n!}{m!(n-m)!}p^{n-mq^m} + \ldots q^n \qquad (3)$$

where $p = 1 - q$.

The general term

$$\frac{n!}{m!(n-m)!}p^{n-mq^m}$$

of the expansion gives the probability, or expected duration, of having m units, simultaneously, on forced outage and $n-m$ in service, during any demand period.

The probabilities, or durations, obtained from the two expansions (equation 2 or 3) are expressed as fractions; when multiplied by the length of any demand period in days they give the *expectancies* or the expected total number of days that m units will be out simultaneously due to forced outages, during that period.

In general, equation 2 should find applications in dealing with parallel feeders of different lengths, equation 3 in dealing with boilers, turbogenerators, and transformers.

3. Check of the Independence of the Individual Forced Outages

The assumed independence of outages of individual units now can be checked, with the aid of equation 2 or 3 by comparing past experience with calculated durations. The period covered by the records should be divided into subperiods by determining the number of days on which the same number of units were either operating or in a state of forced outage. For each period the expectancy of each combination of units should be calculated. The summations of the calculated expectancies for all subperiods, respectively for 0, 1, 2, 3, 4...units out simultaneously, should be compared with past records and found in agreement. Figures 3 and 4 illustrate such comparison.

As previously stated, this independence of the individual forced outages is one of the basic assumptions of the method. Figure 3 pertains to the experience with a group of about 44 units over a period of

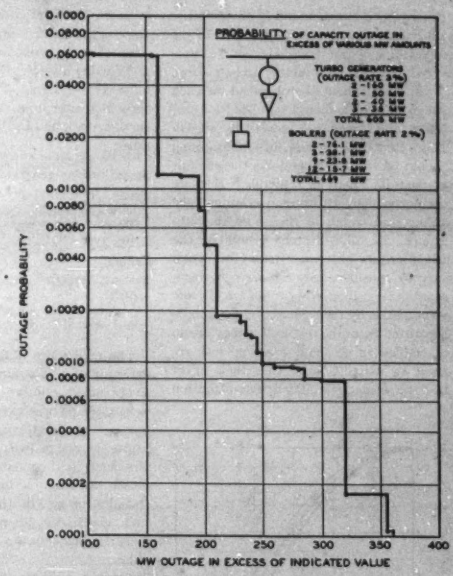

Figure 7. Example of outage probability curve

Table I. Probability in Millionths That Indicated Number of Units Would Be Out Simultaneously for Groups Having Given Number of Units When Outage Rate Is 0.02

Units Out	Number of Units in Group																
	1	2	3	4	5	6	7	8	9	10	11	12	13	14	15	16	18
0	980000	960400	941192	922369	903921	885842	868125	850763	833748	817073	800732	784717	768022	751642	735569	719799	689133
1	20000	39200	57624	75263	92157	108371	123918	138900	153377	167413	180978	193879	206227	217938	229043	239599	258133
2		400	1176	2580	3764	5354	7595	9921	12801	15314	18343	21371	24393	26841	32299	35175	41397
3			8	52	77	153	259	405	608	833	1125	1467	1863	2312	2826	3445	4425
4					1	3	8	11	16	24	36	54	75	113	173	234	382
5									1	1	1	2	4	5	8	11	22
6																1	1

Units Out	Number of Units in Group																
	20	22	24	25	30	35	40	45	50	75	100	120	140	160	180	200	210
0	667628	641170	615780	603465	545484	492513	445700	403100	364570	218765	132600	80850	49296	30070	18340	11182	6820
1	272140	281823	291070	295820	293970	285013	268437	248131	224867	131262	79572	48537	29603	18049	11000	6707	4088
2	52456	61247	70081	75622	86626	102791	124793	151974	179183	158062	95996	58511	35691	21768	13276	8095	4935
3	6468	8593	10996	12797	18225	29386	37828	46879	52746	66660	126114	122276	111188	92611	73604	55491	40642
4	565	814	1135	1384	2591	4650	7222	9421	12749	11583	25135	50828	72162	79735	82519	82819	81198
5	37	66	93	114	278	643	1050	1341	2296	2732	15482	35347	49734	66144	76661	80599	83484
6	2	3	6	8	25	64	125	210	326	418	3197	11471	23169	40206	54114	65380	77649
7					2	6	12	23	41	63	453	3139	7194	16944	26281	35082	41435
8							1	2	4	7	112	742	2534	5440	8754	13115	16986
9									1	1	17	155	867	2460	5010	10846	15382
10											2	29	158	790	2125	4728	8160
11											0	4	36	184	637	1654	3976
12												1	2	35	232	1273	2872
13													1	12	142	1000	2215
14														2	27	618	1627
15															26	373	1393
16															15	178	1162
17															7	76	1207
18															2	27	1063
19																10	1186
20																3	1165
21																1	1008
22																1	824
23																1	197
24																	81
25																	32
26																	12
27																	4
																	2
																	1

13 years. It represents one of the first checks made of the method, at the very beginning of this investigation, on the basis of an outage rate $q=0.03$, obtained from the analysis of the outage records of the Consolidated Edison system, previously referred to. Figure 4 pertains to 1-year experience with approximately 300 units.

Both Figures 3 and 4 verify the assumed independence of the individual unit forced outages.

4. Probability of Outages in Excess of Reserve

When the n units of a group are all of the same size C, the total capacity of any number m of them is mC. The outage probabilities of the various combinations of the units of the group can be calculated as described in section 2. The outage probability of a capacity larger than mC is obtained by adding successively the outage probability of the individual combinations from the one of maximum outage (all n units out) up to and including the $n!/[(m+1)!(n-m-1)!]$ ones of $(m+1)$ units out.

Tables I and II give the probabilities that, out of a group of n units, m be out on forced outage for values of q equal to 0.02 and 0.03, respectively, and for the various values of m and n. Thus if $q=0.03$ the outage probability of having more than two units out in a group of eight units is 0.00135.

It will be understood that this does not mean that the actual number of days on which more than two units will be out simultaneously during say a 2-year period will be exactly $0.00135\times730=1$ day. It means that $0.00135\times365=1/2$ day per year is the *average* rate which outages of more than two units would be expected to approach as the length of the period is increased. Actually, of course, such a condition may exist 10 days in one year and 5 in the next and not at all in the next 28 years. From the probability standpoint the chances are 135 in 100,000 that on any future day the condition will exist.

Table II. Probability in Millionths That Indicated Number of Units Would Be Out Simultaneously for Groups Having Given Number of Units When Outage Rate Is 0.03

Units Out	1	2	3	4	5	6	8	10	15	18	20	30	40	50	100
0	970000	940900	912673	885293	858733	832972	783745	737623	673027	631221	543774	401007	293712	218063	47832
1	30000	58200	84681	109521	134794	154572	195916	228069	276699	295777	336362	372069	384310	377218	317069
2		900	2619	5080	8214	11982	20931	31742	50216	65601	90850	144255	206829	255512	228152
3			27	106	254	492	1299	2612	8694	8523	18370	48164	66312	126342	227973
4					6	22	50	142	640	791	2411	10086	24727	49849	174826
5							1	3	25	34	299	1617	3506	15074	113502
6									1	3	18	219	994	5015	49610
7											1	22	159	980	22608
8												2	19	94	7402
9													2	14	2342
10														2	592
11															127
12															30
13															6
14															1
15															3

Table III. Array for Combining Outage Probabilities of Two Groups

$q = 0.03$

Units	Megawatts	Probability	Units	Megawatts	Probability	Units	Megawatts	Probability	Units	Megawatts	Probability	Units	Megawatts	Probability
			Three 22-Megawatt Unit Groups Separately											
Three 15-Megawatt Unit Groups			0	0	0.912673	1	22	0.084681	2	44	0.002619	3	66	0.000027
Separately			Combined Groups											
0	0	0.912673	0	0	0.832972	1	22	0.077286	2	44	0.002390	3	66	0.000025
1	15	0.084681	1	15	0.077286	2	37	0.007171	3	59	0.000222	4	81	0.000002
2	30	0.002619	2	30	0.002390	3	52	0.000222	4	74	0.000007	5	96	
3	45	0.000027	3	45	0.000025	4	67	0.000002	5	89		6	111	

We are now in a position to make a first check of the question previously raised regarding the accuracy of the average outage rate. The effect of variations of the average outage rate on the reserve required, for different values of outage durations, is illustrated in Figure 5 which gives the calculated reserve required by 248 units for different outage durations at three different outage rates, namely 1.80 per cent, 1.65 per cent, 1.50 per cent.

If the units of the group are similar but not all of the same size, it becomes necessary to calculate for each value of capacity rather than simply for number of units out. As an example, consider a group of three 15-megawatt and three 22-megawatt units. The outage probabilities for any number of 15-megawatt or 22-megawatt units may be calculated as previously shown. The probability of, say, one 15-megawatt and two 22-megawatt units out simultaneously, a total of 59 megawatts, is the product of the separate probabilities, namely, 0.08468 (one 15-megawatt unit out) by 0.002619 (two 22-megawatt units out). An array such as the one shown in Table III may be found useful. The process is completed by arranging the individual probabilities in order of capacity and cumulating the values as shown on Table IV.

From column 3 of Table IV the probabilities of outages exceeding any reserve value now may be determined for the case under consideration.

5. Effect of Connections on the Probability of Outages

Outage probabilites are affected by the manner in which the various elements of the equipment used for a given purpose are connected. Thus in the case of electric energy generation, outage probabilities are affected by the manner in which boilers, turbines, and generators are arranged. In calculating the reliability of the supply to a given load, the arrangement of the transmission and distribution equipment such as feeders and transformers must be considered in addition to the generating equipment. In the case of hydro plants the supply of water is in a series relation with the turbines. The procedure that may be followed in making calculations for such cases will be illustrated by a discussion of the case of steam electric generation mentioned before. In an arrangement commonly used all the boilers are connected to a common header which supplies all the turbines. This arrangement is more reliable than the one whereby each turbine has its own boiler and no common header is provided. That this is the case may be seen of course from the fact that if no common header is used, the loss of the boiler of one unit and the turbine or generator of another unit causes the loss of two units. If a common header is provided, under the same circumstances, only one unit would be lost. For the numerical evaluation of the increase in reliability due to the common header, the boilers are considered separately as a separate group and so are the turbogenerators. The outage rates of the individual boilers and turbogenerators are calculated as described in section 1. The outage probabilities for the various boiler and turbogenerator capacities are calculated as described in section 4. The outage probabilities of the station as a whole are calculated from these separate probabilities as shown in the following paragraphs.

For the sake of clarity three cases will be distinguished.

A. The total capacity of the boiler group equals the total capacity of the turbogenerator group. In this case a boiler outage of M_b kilowatts will cause a station outage of the same amount provided that any outage that may occur simultaneously in the turbogenerator group does not exceed M_b kilowatts. The corresponding station outage probability, or outage duration, is the product of the probability of losing M_b kilowatts in the boiler group by the probability of losing M_b kilowatts or less in the turbogenerator group. Vice versa, a turbogenerator outage of M_{tg} kilowatts will cause a station outage of M_{tg} kilowatts provided that any outage that may occur simultaneously in the boilergroup does not exceed M_{tg} kilowatts. The corresponding station outage probability is given by the product of the probability of losing M_{tg} kilowatts in the turbogenerator group by the probability of losing *less* than M_{tg} kilowatts in the boiler group.

The outage probabilities, or outage durations of the whole station for all kilowatt values, are obtained by giving to M_b and M_{tg} all values from zero to the maximum in the boiler group and in the turbogenerator group, respectively. The qualification "less than" in the case of station outages M_{tg} caused by turbogenerator outages M_{tg} is essential in order to avoid adding twice the terms relative to $M_b = M_{tg}$.

B. The total boiler capacity exceeds the total turbogenerator capacity by M kilowatts. In this case the first statement in the foregoing must be modified in the sense that a boiler outage M_b will cause a station outage of $M_b - M$ kilowatts, provided that any outage that may occur

Table IV. Summary of Probability of Outages for Groups of Three 15-Megawatt and Three 22-Megawatt Units

(1) Megawatts	(2) Probability of Outage Exactly Equal to Indicated Megawatts	(3) Probability of Outage Exceeding Indicated Megawatts
0	0.832972	0.167028
15	0.077286	0.089742
22	0.077286	0.012456
30	0.002390	0.010066
37	0.007171	0.002895
44	0.002390	0.000504
45	0.000025	0.000480
52	0.000222	0.000258
59	0.000222	0.000036
66	0.000025	0.000012
67	0.000002	0.000009
74	0.000007	0.000002
81	0.000002	
89		
96		
111		

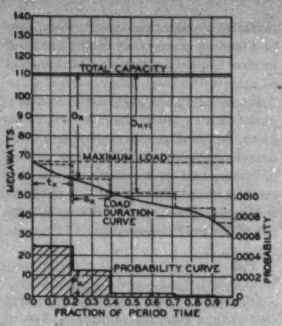

Figure 8. Calculation of the probability of loss of load

simultaneously in the turbogenerator group is equal to $(M_b - M)$ kilowatts or less. The product of the probability of losing M_b kilowatts in the boiler group by the probability of losing $(M_b - M)$ kilowatts or less in the turbogenerator group gives the probability of losing $(M_b - M)$ kilowatts in the station. The second statement as under *A* has to be modified in the sense that an outage of M_{tg} kilowatts in the turbogenerator group will cause a station outage of the same amount provided that any outage that may occur simultaneously in the boiler group is equal to $M + M_{tg}$ or less. Correspondingly the probability of losing M_{tg} kilowatts in the station is equal to the product of the probability of losing M_{tg} kilowatts in the turbogenerator group by the probability of *losing* less than $M + M_{tg}$ kilowatts in the boiler group. The qualification "less than" is necessary for the reason stated under *A*.

C. The total capacity of the turbogenerator group exceeds that of the boiler group by M_1 kilowatts. In this case a boiler outage of M_b kilowatts will cause a station outage of the same amount provided that any outage that may occur simultaneously in the turbogenerator group is equal to $M_1 + M_b$ or less. Correspondingly, the probability of losing M_b kilowatts in the station is equal to the product of the probability of losing M_b kilowatts in the boiler group by the probability of losing $(M_1 + M_b)$ kilowatts or less in the turbogenerator group. A turbogenerator outage of M_{tg} kilowatts will cause a station outage of $M_{tg} - M_1$ kilowatts provided that any outage that may occur simultaneously in the boiler group is equal to or less than $M_{tg} - M_1$. The corresponding outage duration of $(M_{tg} - M_1)$ kilowatts in the station is equal to the product of probability of losing M_{tg} kilowatts in the turbogenerator group by the probability of *losing less than* $(M_{tg} - M_1)$ kilowatts in the boiler group.

When $M_b - M$ or $M_{tg} - M_1$ are negative they should be replaced with zero. As an illustration, calculations were made for a group of two turbogenerator units with various boiler arrangements assuming, for the boilers and the turbogenerators, a forced outage rate $q = 0.02$. The arrangements considered were as follows:

A. Each unit is supplied by a single boiler of the same capacity as the turbogenerator. No common header is used for the boilers.

B. Two boilers are used as under *A*. The two boilers have a common header.

C. Each unit is supplied by two boilers. Each boiler has a capacity equal to one-half the capacity of the turbogenerator. No common header is used.

D. Four boilers are used as under *C*. The four boilers have a common header.

E. Same as under *D* assuming the boilers to be 100 per cent reliable.

The results of the calculations under case *D* are shown in Table V.

The outage probabilities under the various conditions *A*, *B*, *C*, *D*, and *E* are plotted in Figure 6. It is of interest to note that the curves for cases *D* and *E* are almost coincident, indicating that, under the proper circumstances when the number of boilers connected to a common header is large, the boiler outages may be neglected altogether. Figure 7 gives the outage probabilities for the Hell Gate station of the Consolidated Edison Company as calculated in the early stages of this investigation. With reference to this figure, it is of interest to note the large variation in the reliability gains for given increases in reserve at the various points. For instance, increasing the reserve of the

Table V

Capacity Out	Outage Probabilities: Specified Amount	Outage Probabilities: Specified Amount or Less
Boilers alone ($q = 0.02$)		
0	0.922368	0.922368
1/2	0.075295	0.997663
1	0.002305	0.999968
1 1/2	0.000031	0.999999
2	0.000001	1.000000
Turbogenerators alone ($q = 0.02$)		
0	0.9604	0.9604
1	0.0392	0.9996
2	0.0004	1.000

Station (boilers and turbogenerators together)

Capacity Out	Factors of Outage Probabilities: Boilers	Factors of Outage Probabilities: Turbogenerators	Outage Probabilities: Specified Capacity	Outage Probabilities: More Than Specified Capacity
0	0.922368	0.9604	0.885942	0.114158
1/2	0.075295	0.9604	0.072313	0.041845
1	0.002305	0.9604	0.041413	0.000432
	0.999968	0.0392		
1 1/2	0.000031	0.9996	0.000031	0.000401
2	0.000001	0.9996	0.000401	0.000000
	1.000000	0.0004		

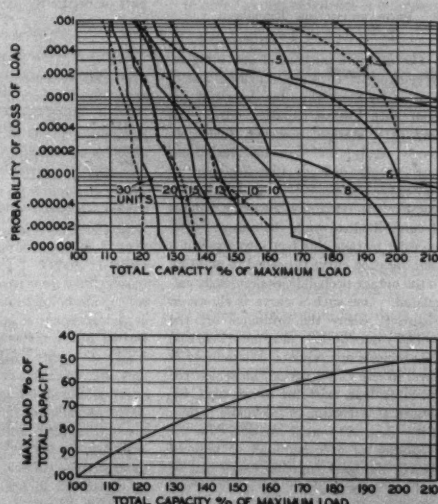

Figure 9. Probabilities of loss of load for groups of different number of units of the same size ($q = 0.03$ and $q = 0.02$), assuming the same load duration curve as in Figure 8

Solid lines = $q = 0.03$

Dashed lines = $q = 0.02$

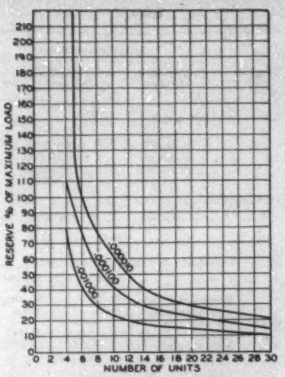

Figure 10. Effect of number of units on reserve requirements for three values of loss of load probability

From Figure 9

station from 200 megawatts to 210 megawatts decreases the outage probability from 0.0048 to 0.00185. However, further increasing the reserve from 210 to 230 megawatts decreases the outage probability from 0.00185 to 0.00175 only. In Figure 7 the probability curve is decidedly discontinuous. As the number of units increases this discontinuity decreases until, for very large systems, the probability curve is almost continuous.

6. Probability, or Expected Duration of Loss of Load

The ultimate purpose of providing reserve capacity is to guard against loss of load. The work thus far described has dealt with loss of capacity only. The load of a station, however, undergoes hourly, daily, and seasonal variations. Any capacity outages, therefore, may or may not result in loss of load depending on whether the remaining capacity suffices to carry the load while the outage exists. In order to take this fact into account a load duration curve is needed in addition to the outage probabilities previously calculated. One such a curve is shown in Figure 8, where the ordinates are the ranked values of daily maximum load and the abscissas are values of the number of days, in the entire period, on which the indicated load exists or is exceeded, expressed as a fraction of the entire period. If it is desired to make allowance for the possibility of carrying load at reduced voltage the load duration curve can be modified accordingly.

Each of the finite numbers of loss in capacity values $O_1, O_2, O_3, \ldots O_k, O_{k+1} \ldots$, obtainable with the various unit combinations, may be plotted down from the total capacity lines as shown by the horizontal dashed lines in Figure 8. Let Δ_k be the time interval between the intercepts on the load duration curve of the two successive capacity values O_k, O_{k+1}. For loads within the interval Δ_k, loss of load occurs whenever the capacity outage exceeds O_k. Let P_k be the outage probability of outages in excess of O_k. The product $P_k\Delta_k$ is the probability of loss of load, during the whole period, contributed by capacity outages exceeding O_k. Otherwise $P_k\Delta_k$ represents the total expected fraction of the whole period during which loss of load will occur, due to capacity outages in excess of O_k. In this sense, $P_k\Delta_k$ may be called the *loss of load duration* due to capacity outages exceeding O_k. In the same manner the probabilities $P_1\Delta_1$, $P_2\Delta_2 \ldots$ of loss of load due, respectively, to capacity outages exceeding O_1, O_2, $O_3 \ldots$ may be calculated. The Δ_k' between capacity values equal to, or smaller than, the peak time reserve are zero and so are the corresponding $P\Delta_k'$ probabilities The sum

$$P_e = P_1\Delta_1 + P_2\Delta_2 + \ldots + P_k\Delta_k + \ldots$$

gives the total probability of loss of load, or the expected loss of load duration, due to all capacity outages, during the whole period. By plotting the outage probabilities $P_1, P_2, \ldots P_k \ldots$ a probability step curve is obtained as shown in the lower part of Figure 8. Evidently P_e is equal to the area under this curve. The values of Figure 8 correspond to the group of units of Table IV assuming a peak load of 67 megawatts.

If the probability P_k varies continuously with O_k, as in the case of a hydro plant, or, for all practical purposes, in the case of a steam plant with a large number of boilers and turbogenerators, the step curve P_e shown in the lower part of Figure 8 becomes a continuous curve and the expression of P_e is equal to

$$\int_0^1 P_k dt$$

Otherwise, P_e may be calculated noting that with a capacity outage O_k, loss of load occurs during the time t_k when the load exceeds the available remaining capacity. If p_k is the probability of losing exactly the capacity O_k, the product $p_k t_k$ gives the probability of loss of load contributed by the capacity O_k outage. By considering all capacity values $O_1, O_2, \ldots O_k, \ldots$ a second expression may be written for the total probability of loss of load as follows:

$$P_e = p_1 t_1 + p_2 t_2 + p_3 t_3 + \ldots$$

As before the t's corresponding to capacity outages equal to or smaller than the peak time reserve are all zero and contribute nothing to the total probability of loss of load.

The numerical calculations for the example of Figure 8 are given in Table VI. The first method is used in the upper part and the second in the lower one. The

Table VI. Calculation of Probability of Loss of Load

Groups of Table IV With Reserve of 44 Megawatts

(1) Capacity Outage O_k	(2) t_k	(3) Interval of Time Δ_k	(4) Probability of Greater Outage, P_k	(5) Product of Column 3 × Column 4, $P_k\Delta_k$
44	0	0.018	0.000504	0.000009
45	0.018	0.192	0.000480	0.000092
52	0.210	0.185	0.000258	0.000048
59	0.395	0.318	0.000036	0.000011
66	0.713	0.003	0.000012	0.000000
67	0.716	0.196	0.000009	0.000002
74	0.912	0.088	0.000002	0.000000
81	1.000			
			Probability of loss of load	0.000162

(1) Capacity Outage O_k	(2) Number of Units Out	(3) t_k	(4) Probability of Specified Outage, p_k	(5) Product of Column 3 × Column 4, $p_k t_k$
44	2	0	0.002390	0.000000
45	3	0.018	0.000025	0.000000
52	3	0.210	0.000222	0.000047
59	3	0.395	0.000222	0.000088
66	3	0.713	0.000025	0.000018
67	4	0.716	0.000002	0.000001
74	4	0.912	0.000007	0.000006
81	4	1.000	0.000002	0.000002
			Probability of loss of load	0.000162

total probability of loss of load, with the assumed 44-megawatt reserve, is 0.00162. Calculations for other reserve values can be made in a similar manner.

In Figure 9, curves are given showing probabilities of loss of load as a function of total capacity in per cent of maximum load, and also as a function of maximum load in per cent of total capacity, for groups of different numbers of units of the same size, on the basis of a load duration curve of the same shape as that of Figure 8, and outage rates of $q=0.03$ and $q=0.02$, respectively.

From Figure 9, the curves of Figure 10 have been derived to illustrate the effect of the number of units, and thus of the unit size for a given load, on the reserve requirements, for three values of loss of load probability based on a forced outage rate $q=0.03$.

The product of the probability of loss of load P_e by the length D of the period, in days, gives the expected total number of days D_e on which load will be lost during the period under consideration.

Changes in conditions due to changes in the total capacity (as may be caused by overhaul) or to wide seasonal variations of the load duration curve may be taken into consideration by subdividing the year into periods $D_1, D_2, \ldots$. The probability of loss of load of each period is calculated as just described and the values $P_1', P_2', \ldots$ obtained. The expected loss of load days of the periods are, respectively, $P_1'D_1$, $P_2'D_2, \ldots$ and their sum $D_e = (P_1'D_1 + P_2'D_2 + \ldots)$ gives the expected total number of days of loss of load for the whole year. This of course does not mean that under the assumed conditions load will be lost D_e days year in and year out. It means that D_e is the per year average number of days on which loss of load is expected to occur over a reasonably large number of years. The reasonableness of this number of years should be determined on the basis of the number of unit demand days necessary to obtain a stable value of the forced outage rate.

A last remark in this section concerns the possibility of using the probability of capacity outage at peak time to determine the reserve requirements of a group of units instead of the more elaborate method of loss of load just described. The probability of capacity outage at peak time depends only on the number of units and the rate of outage q. The probability of loss of load depends on these two quantities and the load duration curve as well. It is then evident that there is no fixed ratio between the two probabilities. From a practical standpoint, however, particularly when dealing with a large number of units, preliminary calculations can be made on the basis of the probability of capacity outages at peak time and a final check made using the more accurate method of loss of load.

Calculations may be simplified by assuming that the load duration curve is a straight line or portion of straight lines. Strictly speaking this assumption is not correct; it is justified, however, by the very nature of the problem.

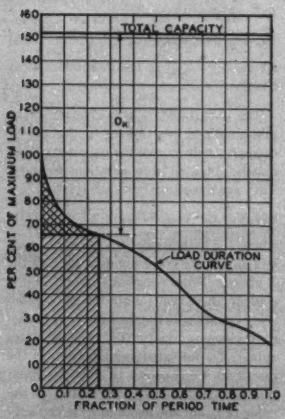

Figure 11. Calculation of expected loss of output for a capacity outage O_k

7. Probability of Loss of Kilowatt-Hour Output

Some writers on service reliability have considered that kilowatt-hour output or sales lost should be taken as the measure of service reliability. If this basis is to be used an assumption must be made as to the effect of a shortage of capacity. At one extreme, as for a single network, the entire load must be dropped. At the other extreme load may be dropped or added in such a way as to match exactly the available capacity. Figure 11 shows a load duration curve on an hourly basis. Under the second assumption above, the double-hatched area is proportional to the kilowatt-hours which would be lost as a result of a capacity outage O_k were it to last throughout the period. The sum of the single and of the double-hatched area is proportional to the kilowatt-hour loss under the first assumption above caused by the same outage O_k under the same conditions. In either case the product of the probability, p_k, of losing exactly the capacity O_k, by the kilowatt-hours represented by the relative area, gives the expected kilowatt-hour loss due to the particular outage. The summation of the expected kilowatt-hour losses of all capacity outages $O_1, O_2 \ldots O_k \ldots$ gives the expected total loss of kilowatt-hour output. The effect of operation at reduced voltage easily may be taken into consideration.

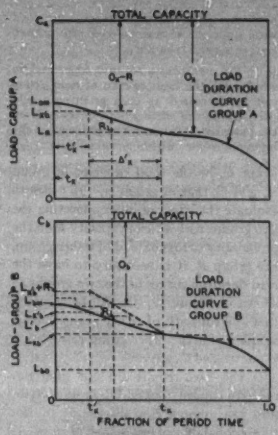

Figure 12. Calculation of the effect of interconnecting two groups of units on the loss of load probability of either

In order to obtain indexes of reliability this total loss of kilowatt-hour output may be expressed as

(*a*). "Expected loss of kilowatt-hour output per kilowatt of installed capacity," by dividing it by the total installed capacity in kilowatts.

or as

(*b*). "Expected loss of kilowatt-hour output per kilowatt of maximum load," by dividing it by the maximum load in kilowatts.

8. Effect of Interconnecting Groups of Units on Their Local Reserve Requirements

The preceding sections have dealt with the problem of determining the local reserve of a single group of units. In this section an analysis will be made of the effect of interconnecting a number of such single groups on their local reserve requirements.

The reserve requirements of two adjacent groups A and B can be fulfilled by either one of two alternative methods

(*a*). The two groups are isolated the one

from the other and each group is provided with sufficient reserve to give the desired level of service reliability.

(*b*). The two groups are interconnected, in which case the local reserve of each group can be decreased as each group can rely partially on the other group for its reserve; the more so the larger is the capacity of the interconnection, within certain limits.

Let C_a be the total capacity of group A, and C_b that of group B. In order to evaluate the effect of interconnecting the two groups with a tie of capacity R on the probability of loss of load of either group, say group A, it is necessary to have the load duration curves of the two groups as shown in Figure 12. It will be assumed that the capacity of either group will be available for the other group provided it is not needed locally.

If the two groups are not interconnected a capacity outage O_k, in A, contributes the amount $p_k t_k$ (Figure 8) to the total probability of loss of load of group A, as described in section 6. When the two groups are interconnected with a tie of capacity R, the same outage O_k will cause a loss of load the probability Q_k of which is composed of three parts calculated as follows:

1. In the first place, irrespective of what happens to group B and to the tie, a loss of load will certainly occur in A during the time t_k' that the load of this group exceeds C_a+R-O_k. Evidently t_k' is the abscissa of the intersection on the load duration curve of the capacity O_k-R measured down from C_a.

2. During the interval of time $\Delta_k'=t_k-t_k'$, group A will have to call upon group B for a transfer R_1, over the tie, varying from the maximum value R to zero. A loss of load will thus occur in group A, if simultaneously to the outage O_k in A, there occurs in B a capacity outage exceeding $O_b=C_b-(L'_b+R_1)$ irrespective of whether the tie is wholly or partially available or not. As seen from Figure 12, L_b' is the load of system B in the interval Δ_k'. The corresponding probability of loss of load in A is

$$p_k\int_{t_k'}^{t_k} P_b dt$$

where P_b is the probability of losing in group B a capacity exceeding O_b. With steam units, due to the discontinuous character of the capacities corresponding to the various unit combinations of the B group, this integral is actually equal to the sum of a few terms of the form $p_k P_b \Delta_t$ and thus easy to calculate.

3. During the interval Δ_k', even if the capacity outage in B is less than O_b, a loss of load occurs in A if, due to a tie outage, it should be impossible to effectuate the transfer R_1 from B to A. The corresponding probability of loss of load in group A is

$$p_k\int_{t_k'}^{t_k}(1-P_b)p_{r1}dt$$

in which p_{r1} is the probability of a tie capacity outage exceeding $(R-R_1)$, R being to total tie capacity. As before due to the discontinuous character of both tie and B capacities, this integral breaks up into the sum of a few terms of the form $p_k(1-P_b)p_{r1}\Delta_t$.

Thus the probability Q_k of loss of load is group A, with a capacity outage O_k in the same group, is

$$Q_k=p_k[t_k'+\int_{t_k'}^{t_k}\{P_b+(1-P_b)p_{r1}\}dt]$$
$$=p_k[t_k'+\sum\{P_b+(1-P_b)p_{r1}\}\Delta t]$$

Evidently

$$\Sigma\Delta_t=\Delta_k'$$

and

$$(P_b+(1-P_b)p_{r1})<1$$

for the different values of P_b and p_{r1} under Σ, so that

$$t_k'+\{P_b+(1-P_b)p_{r1}\}\Delta t<t_k$$

Q_k takes the place of $p_k t_k$ of section 6. Its value decreases from the maximum $P_k t_k$ to a minimum, as the tie capacity R increases from zero to a maximum value R_{k0} which, for the specified outage O_k, can be calculated as follows.

From Figure 12 it is evident that as far as the specified outage O_k is concerned, the tie capacity R used should satisfy the inequality

$$R\leqslant C_b-L_{k'b} \tag{5}$$

where $L_{k'b}$ is the B load corresponding to t_k'. This is because B has no capacity available to fulfill any transfer requirement not satisfying the inequality, equation 5. The maximum tie capacity R_{k0} giving the minimum value of Q_k also must satisfy the inequality.

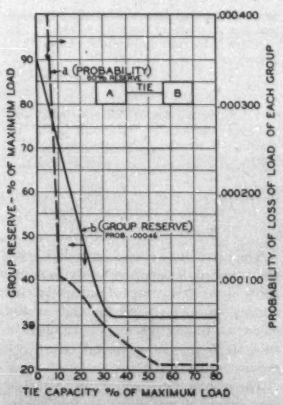

Figure 13. Illustration of the effect of tie capacity on the loss of load probability (curve a) and on the group reserve (curve b)

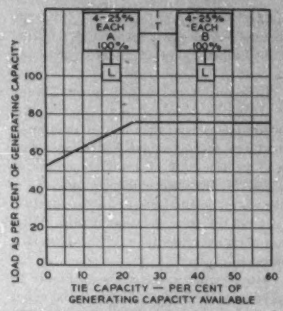

Figure 14. Effect of tie capacity on the load that can be carried by each one of two interconnected systems

From Figure 12 and the expression of Q_k it is seen that as R increases, t_k' and Q_k decrease. Evidently the minimum value that t_k' can attain is zero. Two cases are thus possible as R increases, starting from the zero value and t_k' decreases from the maximum value t_k:

(*a*). Before t_k' reaches the value zero, R becomes equal to $C_b-L_{k'b}$. In this case, the maximum tie capacity R_{k0} giving the minimum value of Q_k is

$$R_{k0}=C_b-L_{k'b} \tag{6a}$$

From this and Figure 12

$$O_k=C_a+C_b-(L_{k'a}+L_{k'b}) \tag{7a}$$

(*b*). The quantity t_k' becomes zero before R becomes equal to C_b and L_{kb}'. In this case the maximum value of tie capacity R_{k0} is that making $t_k'=$ zero.

From Figure 12

$$R_{k0}=L_{am}-L_a=O_k-(C_a-L_{am}) \tag{6b}$$

where (C_a-L_{am}) is the reserve at peak time.

The outages O_k, which give minimum probability of loss of load Q_k, for the tie capacity values making $t_k'=$ zero, thus may be obtained from equations 6*b* and 5. They are those satisfying the relation

$$O_k\leqslant C_b+C_a-(L_{am}+L_{bm}) \tag{7b}$$

where L_{am} is the peak load of the A group and L_{bm} is the corresponding load of the B group. From equations 7*a* and 7*b* it is evident, then, that for all outage O satisfying equation 7*b* the maximum tie capacity is given by equation 6*b*. For all larger outages O_k not satisfying equation 7*b* the maximum tie capacity is given by equation 6*a*. From equations 7*a* and 7*b* the value of t_k' for the maximum tie capacity R_{k0} may be obtained graphically by plotting a load duration curve sum of the two

load duration curves of Figure 12 and measuring O_k down from the (C_a+C_b) capacity line to this load duration curve. The abscissa of the intersection is the value of t_k' being sought.

As the value of the outage O_k increases, the maximum tie capacity R_{bo} increases also, being at the most equal to C_b-L_{bo}, where L_{bo} is the minimum load of group B. From a practical standpoint it will suffice to determine the tie capacity on the basis of the outages O_k giving the largest $p_k t_k$ products, as shown by inspection of calculations similar to those shown in the lower part of Table VI.

Calculations for the B group are carried in the same manner.

While in Figure 12 it has been assumed that the peaks of the two groups are coincident, this assumption is not necessary as any diversity between the two groups may be taken into consideration by drawing the B load duration curve in its proper relative position with respect to the A one.

By way of illustration Figure 13 shows two curves calculated for two identical groups of four units, serving identical loads, assuming all units of the same size. Curve a gives the variation of the probability of loss of load of either station in function of the tie capacity assuming a local reserve for each group equal to 80 per cent of the maximum load. In this case the values of R_{bo} for the various outages are

Outage	Tie Capacity	
$O_1 = 45 \ldots R_{10} = 0$		
$O_2 = 90 \ldots R_{20} = 10$		(From equations 7b and 6b)
$O_3 = 135 \ldots R_{30} = 55$		
$O_4 = 180 \ldots R_{40} = 90$		(From equations 7a and 7b)

Curve b gives the tie capacity necessary to obtain a probability of loss of load equal to 0.00046 with different local reserve capacities. Both curves a and b are based on an average outage rate $q=0.03$ and a load duration curve of the same shape as that shown in Figure 8.

From curve b it will be noted that the reduction in the reserve requirements of each system is approximately equal to the capacity of the tie so that the reserve requirements of the two systems considered together are reduced by twice the tie capacity. Of course this is true up to the maximum useful value of the capacity (30 per cent of maximum load) but not beyond this value. In Figure 14 curve b of Figure 13 has been redrawn to show the load L that can be carried as a percentage of the generating capacity available. Again it is noted that as the tie capacity increases from 0 to 24 per cent, the load that can be carried increases from 52 per cent to 76 per cent, that is, increases 24 per cent.

The method of analysis just discussed for the case of an interconnection between two groups of units may be extended to the case of a system of more than two groups. In general, it will be necessary to repeat the described calculations for each tie, or group of ties, and the two unit groups into which it divides the system. In order to simplify calculations it will be not only advisable but necessary to introduce some simplifications, the nature and extent of which must be judged by the case on hand.

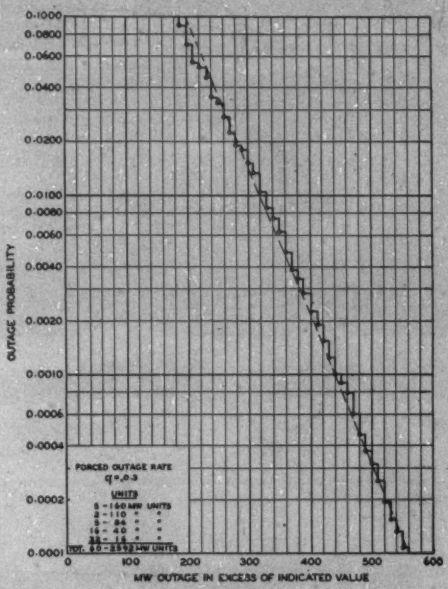

Figure 15. Exact and approximate probability curves for a large system

Approximate Method of Calculating the Probability of Loss of Load

The method of determining the loss of load probability outlined in section 6 requires long calculations. The very nature of the problem, justifies, in most cases time-saving simplifications. For this purpose it is proposed that, whenever possible, the following assumptions be made:

1. The probability P_k of capacity outages in excess of O_k, when plotted on semilog paper, is replaced by either a straight line or portions of straight lines.

2. The load duration curve also is replaced by a straight line, or portions of straight lines.

Strictly speaking, neither one of these two assumptions is correct. However, it is believed that in most cases both assumptions can be made without greatly sacrificing the practical correctness of the results.

By the first assumption the probability P_k of outages in excess of a capacity O_k can be expressed by an exponential (or portions of exponentials) of the form

$$P_k = A\epsilon^{-aM}$$

where A and a are two constants and M has been used in place of O_k.

By both assumptions, the step probability curve shown at the bottom of Figure 8 is replaced by a continuous curve (or portions of continuous curves) which is related to the maximum load L_m, the system capacity C, the reserve at peak time $R_0=C-L_m$, and the load factor l in per cent, by the relation

$$P_k = A\epsilon^{-a\left(1-\frac{100}{l}\right)L_m}$$

The probability P_e of loss of load becomes:

$$P_e = \int_0^{1.0} P_k dl = \frac{A\epsilon^{-aR_0}}{2a\left(1-\frac{l}{100}\right)L_m}\left\{1-\epsilon^{-2a\left(1-\frac{l}{100}\right)L_m}\right\}$$

which is easy to calculate.

The process is illustrated in Figure 15 relative to a large system with 60 units totaling 2,592 megawatts. In this figure the probability step curve, for all practical purposes and in the range of capacity outages shown, may be expressed by the equation

$$P_k = 5.3\epsilon^{-0.0192M}$$

By so doing the probability P_e of loss of load is given by

$$P_e = \frac{118.0\epsilon^{-0.0192R_0}}{\left(1-\frac{l}{100}\right)L_m}\left[1-\epsilon^{-0.0384\left(1-\frac{l}{100}\right)L_m}\right]$$

If the peak time reserve is 320 megawatts this becomes

$$P_e = \frac{0.0001315}{1-\frac{l}{100}}\left[1-\epsilon^{-94.7\left(1-\frac{l}{100}\right)}\right]$$

which for various values of l assumed the following values:

l, Per Cent	P_e
70	0.000435
90	0.001315
95	0.00265
100	0.01 (outage probability at peak time)

Conclusions

In concluding, it is believed that the method of probability should find a more extensive use than heretofore in the solution of reserve problems. In this respect it is hoped that the material presented in this paper may be of service to those engaged in the determination of system reserve.

As a large amount of past experience is required to make reliable predictions of the expected future performance of a particular group of units, it is hoped that the basic information collected under the auspices of the Edison Electric Institute soon will be made available.

The discussion of the preceding sections has been limited almost entirely to the case of generating unit reserve; it is evident, however, that the conclusions reached may be applied to a variety of other problems in the electrical field and in other fields.

References

1. Calcolo Delle Probabilità (book), Guido Castelnuovo. Nicola Zanichelli, editor, Bologna, Italy.

2. Introduction to Mathematical Probability (book), T. V. Uspensky. McGraw-Hill Book Company, Inc., New York, N. Y.

3. Probability Theory and Spare Equipment, S. A. Smith, Jr. *Bulletin*, Edison Electric Institute (New York, N. Y.), March 1934.

4. The Use of the Theory of Probability to Determine Spare Capacity, F. P. Benner. *General Electric Review* (Schenectady, N. Y.), July 1934.

5. The Probable Number of Steps Made by an Elevator, Bassett Jones. *General Electric Review* (Schenectady, N. Y.), August 1923.

No Discussion

Frequency Division Techniques for a Coaxial Cable Network

R. E. CRANE
MEMBER AIEE

J. T. DIXON
ASSOCIATE AIEE

G. H. HUBER
MEMBER AIEE

Synopsis: A description is given of developments employing frequency division techniques by which the telephone-message-carrying potentialities of the coaxial cable system are realized. By these methods 480 high quality telephone messages are prepared for transmission over the line and restored to original condition at main terminal points. At intermediate points appropriate groups of channels may be removed, inserted, bridged, or relocated in the frequency spectrum of the line.

THE coaxial cable system, known as type *L1*, is the latest of the Bell System's broad-band carrier systems to find large scale application in the nation's long distance communication network. The increase in message carrying capacity of this system over its predecessors is enormous. As designed at present, the *L1* system provides 480 long-haul message channels. By partially utilizing additional frequency space which is not satisfactory for long haul circuits, an extra 120 short-haul channels can be provided. A maximum circuit capacity of 600 1-way channels on a single coaxial circuit is possible as compared to 12 1-way channels per pair of wires obtained from earlier cable carrier systems.

The telephone message carrying potentiality of the coaxial cable has required the development of concentrations of terminal equipment to prepare the messages for transmission and to restore them to original condition at points where use can be made of large circuit groups. Another problem involved in utilizing the cable's potentiality is that of removing and inserting relatively small groups of circuits at many points between the principal message centers.

Examination of the map shown in Figure 1 will indicate the extent of the coaxial cable network which it is planned to establish within the near future. It can be appreciated that the hundreds of messages traveling the main highway of the coaxial cable at any point may have their origins and destinations at widely scattered towns and cities, some located on the coaxial cable itself and some at great distances from the cable. The coaxial highway is so broad and will accommodate so much message traffic that many new developments were required to provide the equivalent of entrances, separated lanes, traffic circles, exits, and connnecting approaches of appropriate size such as would be needed for efficient and reliable use of a vehicular superhighway.

Early developments looking toward wide-band usage of coaxial cables for telephone purposes have been described in previous papers.[1,2] The present paper indicates the form which these developments finally assumed when large scale production was undertaken.

As indicated by the title, the techniques employed for multichannel use of the coaxial line are of the general class known as frequency division. Each individual channel is assigned a particular frequency band for its journey over the cable and other messages assigned to other bands are not permitted to disturb the first band either by their method of entry into or exit from the cable or by their common use of the cable and repeaters.

The main telephone band of the *L1* system comprises line frequencies of 64 to 2,064 kc. Within this band, 480 single-side-band carrier-suppressed telephone channels are obtained. The voice frequency transmission band of each channel is 200–3,400 cycles. A line frequency space of 4 kc between carriers is allotted to each channel, irrespective of the channel location at line frequencies. The

Figure 1. Bell System coaxial cable program

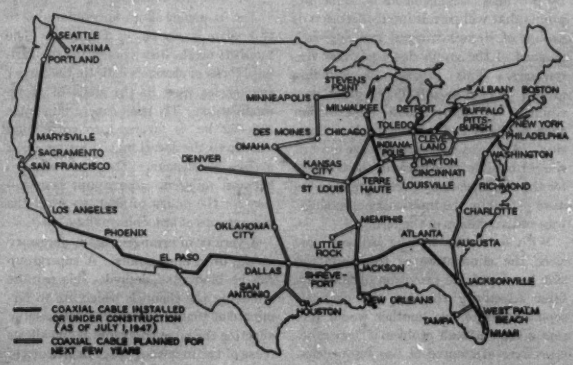

Paper 47-258, recommended by the AIEE communication committee and approved by the AIEE technical program committee for presentation at the AIEE Midwest general meeting, Chicago, Ill., November 3–7, 1947. Manuscript submitted August 18, 1947; made available for printing September 24, 1947.

R. E. Crane, J. T. Dixon, and G. H. Huber are members of the technical staff in the systems development department, Bell Telephone Laboratories, Inc., New York, N. Y.

accomplishment of this closely packed arrangement of channels throughout the whole usable frequency range presented a major technical problem. It is a result which appeared difficult to attain initially and is made possible by developments in the art of multichannel group modulation which were undertaken with this purpose in view.

The repeaters of the *L1* system transmit frequencies above 2,064 kc. It is in this range that additional short-haul telephone circuits will be obtained along the route. This paper, however, is concerned primarily with methods of providing the 480 long-haul circuits.

Design Objectives for Terminal and Intermediate Equipment

The general objective of the Bell System broad-band carrier development is to provide facilities giving satisfactory transmission and reliable service for telephone circuits up to 4,000 miles in length. These long circuits may be made up of a number of links, that is, of shorter circuits connected together. Some of the links may be channels on the coaxial system, some may be channels on other broad-band carrier systems,[2-6] and still others may be on voice frequency or other types of carrier facilities. In the future, large numbers of the circuits in the plant will involve links on coaxial facilities.

Some of the factors affecting the excellence of transmission of a carrier telephone channel depend primarily on the equipment individual to the channel. The variation of loss and envelope delay over the few thousand cycles of a channel band are examples. These, and the amount of the frequency shift of components of the speech, are controlled largely by the design of the terminal equipment.

Other factors affecting the excellence of transmission depend on the equipment used in common by a number of channels. Noise, interchannel interference, and variations of net loss with time are examples. These are controlled partly by the design of the terminal equipment and partly by the line repeaters and other parts of the system.

The amount of transmission distortion that can be permitted in the terminal equipment depends upon the amount of this equipment that will be included in a 4,000-mile circuit. This can be controlled to a certain extent in the design. For example, the band filters in the individual channels contribute most to distortion of the transmission-frequency characteristics of a channel. It is desirable for this reason, and also for reasons of economy, to keep the amount of this individual channel equipment to a minimum in setting up long circuits. This is accomplished by providing arrangements at branching points that will permit interconnection of groups of circuits without bringing each channel of the group down to voice frequencies. This process of handling groups of circuits introduces other possibilities of transmission imperfection such as noise and interchannel modulation. As it was desired to reserve most of the permissible allowance for these effects for the line repeaters, severe requirements were placed on the multichannel modulators and amplifiers in the terminal.

With only 4-kc spacing between carriers, the elimination of the unwanted side band and the provision of adequate filter selectivity to keep the channels separated from one another would present a very difficult problem if these processes were attempted at line frequencies. These functions accordingly are performed in a frequency range better adapted to a solution of the filter problem. The frequency range selected for this purpose is 60–108 kc where filters having low-loss piezoelectric crystal units can be constructed.

Terminal equipment for modulating and filtering a group of 12 channels in the 60–108-kc range was developed and has been used since 1937 on 12-channel type *J* and type *K* systems. The design of this 12-channel terminal equipment was made with a view to ultimate use on the coaxial system as well as on the types *J* and *K* system. Such use requires, of course, that the coaxial terminal include additional modulating equipment for transferring the channels from the 60–108-kc range to the coaxial line frequencies.

The required frequency translation is accomplished by two steps of group modulation. This has important advantages over the alternative of a single step of group modulation. It greatly eases the selectivity requirements on the filters needed in the group modulation steps, reduces the number of types of filters required, and provides the means for assembling the channels into larger groups to facilitate entry and exit of channels from the line at intermediate points.

Consideration of traffic requirements at intermediate points and relative complexity and cost of various terminal arrangements resulted in the conclusion that the original groups of 12 channels should be assembled into larger groups (supergroups) of 60 channels in the first step of group modulation. The second step of group modulation then assembles the supergroups of 60 channels to fill the entire frequency range of 2 megacycles. Thus, it is possible to effect entrance, exit, and transfer of circuits in blocks of 1, 12, 60, or 480 channels.

The frequency allocation conforming to this plan is shown in Figure 2. The numbers on the lines connecting the various blocks of channels indicate the carrier frequencies used in the steps of group modulation. The basic supergroup range 312–552 kc, is arranged to correspond exactly to the location of supergroup 2 at line frequencies. The space allowed between adjacent supergroups is necessary for the design of filters to select the supergroups at branching points.

A variety of arrangements is necessary at the branching points. A supergroup can be blocked if desired: this permits removing the channels which are to terminate at that point without appreciably affecting the other supergroups and allows reuse of the frequency space in sections of

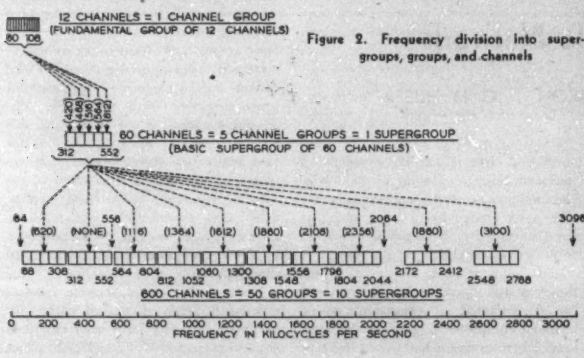

Figure 2. Frequency division into supergroups, groups, and channels

the cable beyond the branching point. A locked supergroup can be broken up into smaller groups of 12 channels; some of these can be reintroduced into the cable without reducing them to speech frequencies while others are terminated. Complete supergroups can be relocated in another position or transferred to another coaxial system without reducing them to speech frequencies. Groups of 12 channels can be separated from the coaxial cable and introduced into other systems without reduction to speech frequencies.

Since the channels are packed closely together, and the line frequencies are relatively high, a high accuracy is necessary in the carrier frequency generating equipment. The carrier frequencies are derived as harmonics of a very stable base frequency. Methods have been developed for controlling the base frequencies at a number of points from the base frequency at one point.

Modulators and Filters

The principal components employed in making a frequency division system are, of course, modulators and filters. Figure 3 indicates the arrangement employed in modulating and demodulating the 480 long-haul channels transmitted over the coaxial cable.

At the left, labeled channel equipment, are shown modulators, band filters, and amplifiers for 12 channels. This "channel bank" is the same as used for initial modulating steps in the types *J* and *K* systems[4,5,7] and has been described elsewhere. Only one bank is shown. Forty banks are required for a full-sized coaxial terminal. The filters in the channel bank, which are constructed primarily of piezoelectric elements, pass only the 12 wanted single side bands in the frequency range between 60 and 108 kc.

Each channel bank is connected to a group modulator as indicated in Figure 3 under group equipment. The purpose of the band elimination filter is to remove completely any residual carrier at 92 kc so that a signal of this frequency of constant magnitude may be introduced directly ahead of the group modulator. This will indicate the transmission condition of that group at any point where it is measured further along in the system. The band filters select a single side band of the modulation process. Since the lowest input frequency to a group modulator is 60 kc, adequate selectivity is obtained by filters constructed of inductor and capacitor elements.

The outputs of odd numbered and even numbered filters are multipled and the two sets are combined through a hybrid coil. The filters are designed with wide bands to minimize transmission distor-

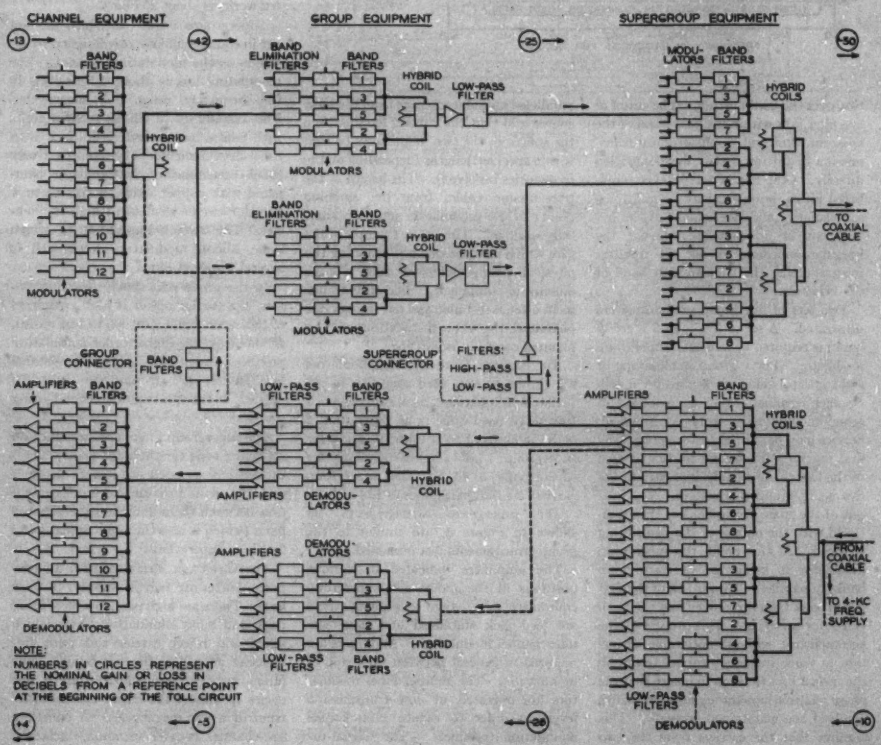

Figure 3. Schematic of terminal circuits

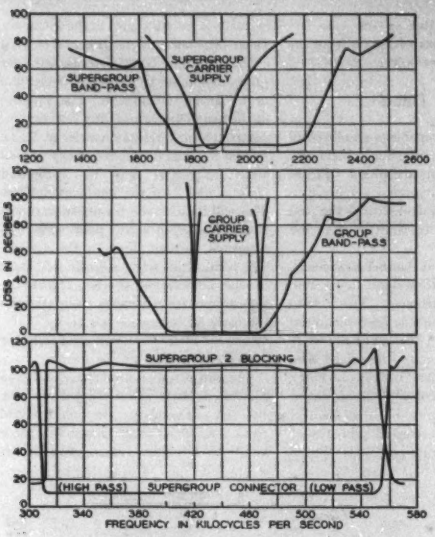

Figure 4. Loss characteristics of typical filters

tion over the used portion. The cutoff of one filter falls within the pass band of the adjacent filter and would produce transmission distortion if they were multipled directly. Odd numbered or even numbered filters, however, may be multipled satisfactorily and the balance of the hybrid coil is adequate to prevent the irregular impedance of one set of filters from affecting the transmission band of the other set.

Two sets of five group modulators are illustrated. A set of five (called a group bank) is required to feed each supergroup modulator. Forty group modulators, or eight group banks, are needed for a 480-channel terminal. Two spare banks of group modulators usually are supplied. Service may be shifted to a spare bank by first patching the second branch of each of the five channel banks into each of the five spare group modulators. The output of the spare group bank is then multipled with the output of the bank being replaced. At this point, the supergroup modulator is being fed by two group banks in parallel. The output of the first group bank then is removed and the bank is free for servicing. This process can be accomplished without noticeable distortion to voice frequency carrier telegraph channels if care is taken to insure that the phase relationships through the two banks involved are maintained properly. This requires that the carriers from the two paralleled modulators come from the same source and that the cabling lengths from the source to the two modulators be held within specified lengths (depending on the frequencies involved). The length of the transmission cables from the patching points to the modulators must be similarly specified. This is one example of the care which must be taken in planning the physical arrangements for such a large amount of equipment. Since this equipment often is installed and put into service piecemeal, the whole installation must be planned carefully in advance.

The carriers for the group modulators are chosen so that their used side bands (312 to 552 kc) are in an appropriate position to be used directly as supergroup 2 or be modulated to a lower position for supergroup 1 and higher positions for supergroups 3 to 8. The supergroup carriers are odd harmonics of 124 kc.

The supergroup arrangements, as shown in Figure 3, are similar to the group arrangements just discussed.

The amplifiers indicated in various positions in the group and supergroup equipment are 2-stage amplifiers; these are feed-back stabilized and have low interchannel modulation. Amplifiers are required in general between each step of modulation. The multichannel modulators are operated at low transmission levels in order to reduce interchannel modulation products. The signal-to-noise ratios would be degraded if two steps of modulation were attempted without intermediate amplification. The single channel modulators, however, are operated at a higher transmission level and no amplification is required between channel and group modulators.

All of the modulators and demodulators for the groups and supergroups (1 to 8) use copper oxide as the modulating element. The same units, in a ring circuit of four 3/16-inch-diameter disks, are used for all frequencies.[8] The modulating loss (signal input to single-side-band output) varies from about 5.5 decibels for the lowest frequency group modulator (420 kc) to 7.5 decibels for highest frequency supergroup modulator (2,356 kc). It is possible to use copper oxide at these frequencies, even with its relatively high shunt capacitance, by operating it in low impedance circuits and using series inductances to compensate for the capacitive reactance. The impedance into which the highest frequency supergroup modulator works is about 25 ohms.

Supergroups 9 and 10, which are not yet in commercial use, are designed to use silicon as the modulating element. The modulating loss is about 5.5 decibels in the frequency range 2–3 megacycles. The availability of silicon rectifier units with controlled characteristics is a wartime development. The comparatively small capacitance of these units, as compared with copper oxide, makes them a superior circuit element at high frequencies. The circuit impedance in which these silicon modulators work well is several hundred ohms.

In the group and supergroup modulators, the carrier power is high compared to the input signal (100,000 to 1 or more). In this way, the higher order modulation products, which could cause interchannel interference, are reduced at least 75 decibels below the wanted second order products.

The supergroup filters are inductor and capacitor type for the most part. Crystal sections are used in the supergroup 1 and 3 bands to provide sharp discrimination between them and the supergroup 2 band (which is also the input signal band for these supergroups).

The variety of filters used for all purposes, including carrier supply, is very large: There are high pass, low pass, band pass, and band elimination filters which select and reject carrier and pilot frequencies as well as the side bands. The filters vary in bandwidth from a few cycles to almost the entire coaxial spectrum of a few megacycles. A complete 480-channel coaxial terminal, including

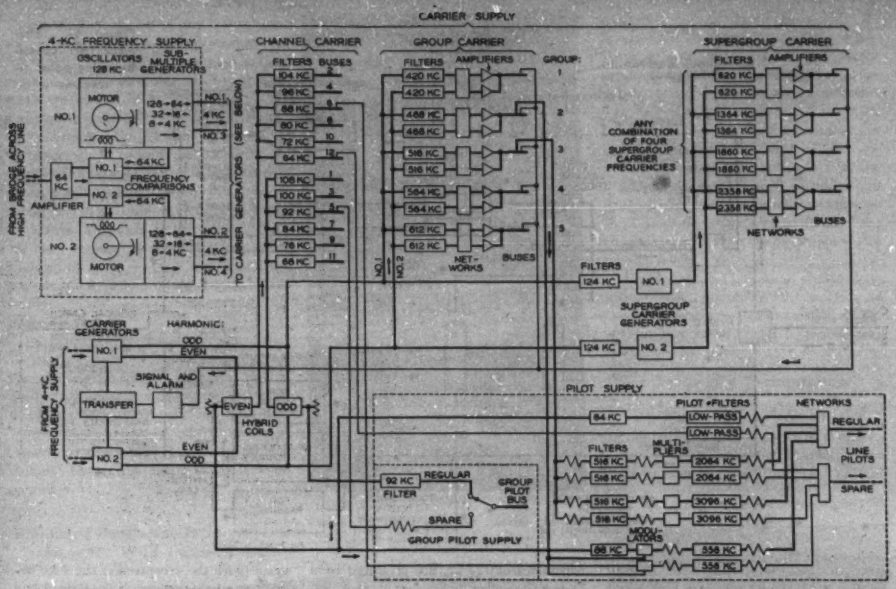

Figure 3. Schematic of carrier and pilot supply arrangements

the normally supplied spares, contains about 1,400 filters. Of these, 116 are used in the carrier supply. A total of 1,086 filters use piezoelectric plates.

Some typical characteristics of filters used in the terminals are shown in Figure 4.

Carrier and Pilot Supply

A high power carrier generating system operating from a single source is required to supply the large number of modulators used in a single carrier terminal. For a 480-channel terminal, there are 480 channel modulators and demodulators, 40 at each of 12 different carriers; 40 group modulators and demodulators, 8 at each of 5 different carriers; 7 supergroup modulators and demodulators, one at each of 7 different carriers (supergroup 2 requires no supergroup carrier). The derivation of all of these carriers from a single source is desirable. However, this imposes a requirement of extremely high reliability.

A problem of first importance in carrier supply design is the accuracy of the frequencies. There is both an absolute accuracy and a relative accuracy requirement.

Carrier frequencies and also pilot frequencies generated in the carrier supply system are selected for use by filters, some of which by the nature of their design are extremely narrow. One example is the pilot selecting filters which are located at repeaters throughout the length of the coaxial cable. The frequencies generated must remain within the passed band of these filters at all times. An absolute accuracy of the order of ± 10 parts per million is imposed from this consideration. The supply as finally built has an accuracy about $\pm$ 2 parts per million relative to standard frequency.

Carrier frequencies at two different terminals must maintain a relative accuracy with respect to each other such that frequencies delivered over any channel at the receiving end do not differ from the frequencies introduced at the transmitting end by more than a small amount. The amount necessary to secure satisfactory transmission depends upon the type of signal to be transmitted. High quality program signals impose a severe requirement. It is desirable that the difference should not exceed about 2 cycles per second for such service. Since there may be several links of program channels connected together, the permissible difference in each link is somewhat less than 1/2 cycle per second. To maintain $\pm$1/2 cycle frequency difference at 2 megacycles it is necessary that $\pm$2.5 parts per 10 million relative accuracy be secured.

The desired absolute accuracy is obtained by designing a crystal controlled oscillator at a favorable frequency (128 kc). The relative accuracy is achieved by designating the oscillator at one point as a master oscillator to control the frequency at other points.

The general arrangement of carrier and pilot supply equipment at a large office is illustrated in Figure 5. If the office is controlled by a distant terminal, a frequency of 64 kc, supplied over the coaxial cable, is selected by a narrow filter, amplified, and supplied to two frequency comparison circuits. Here a comparison is made between the incoming 64 kc and the 64 kc generator by the local circuits. These two frequencies are combined, split in phase, and applied to the grids of four rectifying tubes. The output of each of these tubes energizes one of the poles of a motor which moves a variable capacitor in the oscillator circuit, if the frequencies differ. If the local oscillator has a higher frequency than the reference frequency the motor revolves in a direction to lower the frequency, and vice versa. The motor moves as long as there is any difference in

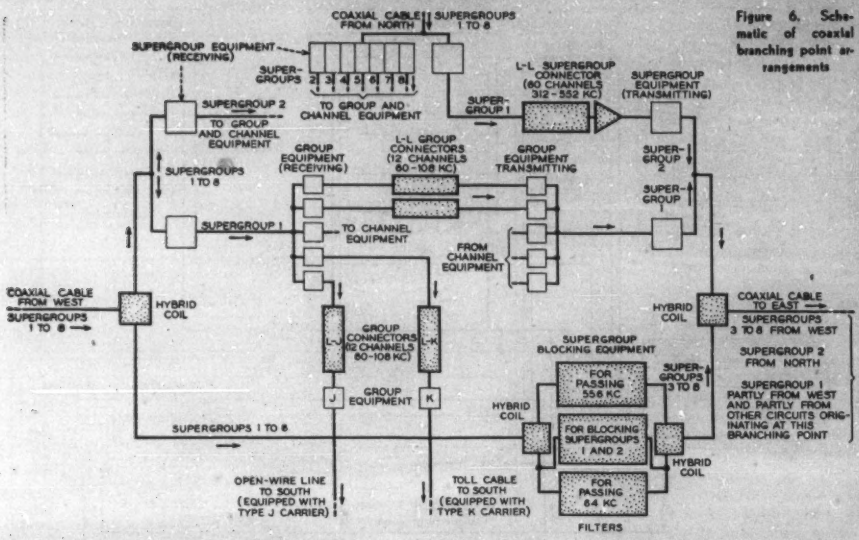

Figure 6. Schematic of coaxial branching point arrangements

frequency between the reference and local oscillator. If the incoming control should fail, the local oscillator continues to operate at its frequency at the time of failure.

A frequency of 128 kc was chosen for the local oscillator because good low-temperature-coefficient crystals are available at that frequency and because it can be subdivided in steps of 1/2 to obtain 4 kc, which is the basic frequency desired. The circuits for producing fractional frequencies have been described previously.[9]

Odd and even harmonics of 4 kc are produced in the carrier generator at sufficient amplitude to operate a number of channel modulators and demodulators connected directly to the channel carrier busses.

Odd harmonics of 4 kc up to 612 kc also are derived from the same generator but further amplification, as indicated in the diagram, is needed to supply the group carrier busses. It will be noted that the group carrier amplifiers are provided in duplicate. Both of them are normally energized from one or the other of the two group carrier filters. Failure of one amplifier or its removal for servicing does not reduce seriously the amount of group carrier available. Even a short circuit which might occur accidentally at the output of one amplifier will not reduce the group carrier to an unworkably low amount.

Supergroup carriers, which are odd harmonics of 124 kc, are produced by a carrier generator operating at that frequency (which is an odd harmonic of 4 kc). The supergroup carrier supply arrangements are, in general, similar to those of the groups except for the frequencies involved.

The carrier power available on channel busses is approximately 10 milliwatts, sufficient to operate about 10 channel modulators and demodulators. The group and supergroup busses have about 1 watt available which will supply 4 of these modulators and demodulators.

The amount of carrier supply equipment shown in the diagram provides for 120 channels in the channel carrier supply section, 240 channels (5 group frequencies, 4 modulators and demodulators per frequency) in the group section and 240 channels (4 supergroup frequencies, one modulator and demodulator per frequency) in the supergroup section. An additional 120 channels can be provided for in the channel section by connecting duplicate arrangements of the channel carrier filters and busses to the opposite sides of the odd and even hybrid coils where resistance terminations are shown in the diagram. These were omitted in the diagram for simplicity.

The amount of equipment just described provides carriers for one half of the 480 long-haul circuits on one coaxial. To take care of the additional 240 channels, the equipment shown on the diagram (with the exception of the 4-kc frequency supply section) is duplicated and connected as indicated to the frequency supply.

The arrangements for providing the pilot frequencies used to regulate the coaxial line are shown in the lower part of Figure 5. Four frequencies are used; 64, 556, 2,064, and 3,096 kc. Stability of frequency is obtained by deriving these frequencies from the same basic frequency source used for carriers. A high degree of stability of output in the 2,064 and 3,096 kc supplies was obtained by designing the multipliers (which convert 516 kc to these frequencies) to have a broad flat section in their input–output characteristic. A stable source of 64 kc, which is used both for line regulation and for synchronizing purposes, is obtained directly from the 4-kc harmonic generator. A stable source of 556 kc is produced by modulating 88 kc and 468 kc, both of which are obtained from the same harmonic generator.

The methods of insuring continuity of output are partially indicated on the diagram. All circuits involving an appreciable amount of apparatus are provided in duplicate. Normally only one of the carrier generators is functioning. The other is biased to an inoperative condition by potential supplied from the transfer circuit. All group and supergroup busses are monitored continuously by means of rectifiers which operate alarm relays.

The absence of carrier on any bus causes the alarm relay to release and produces a transfer from one carrier generator to the other. The second generator outputs reach the busses through different paths and carrier is restored. Other relays and lamps indicate the location of the disturbance which caused the transfer. A transfer from one generator to another ordinarily will produce a phase shift of considerable magnitude in the carriers. Therefore, a transfer is not made in the ordinary course of maintenance. All vacuum tubes (except in the carrier generators and frequency supply circuit) may be replaced without requiring a transfer of generators.

In addition to the circuit arrangements to insure reliability and continuity of operation, great care is exercised in the design of the components and in their mounting, accessibility and ruggedness to reduce the chance of individual component failure and the chance of causing a serious interruption during the process of servicing.

Figure 7. Rear view of coaxial terminal carrier and pilot supply equipment

Left to right: Two bays of supergroup carrier supply (for 480 channels); third bay, group carrier supply (for 240 channels); fifth bay, pilot and 4-kc frequency supply

Branching Points and Interconnection With Other Systems

A variety of arrangements is required at intermediate or branching points to provide the necessary flexibility in branching circuits off the main path economically. It was mentioned earlier that the frequency allocation of the system was chosen with these problems in mind. Space is left between supergroups to make possible the design of filters to block the transmission of some supergroups while permitting others to pass through a branching point. Filters have been designed for this purpose but not for all of the possible combinations. It is not likely that filters for a great many combinations will be required under arrangements to be used at branching points in the near future.

The diagram shown in Figure 6 illustrates some of the arrangements possible at a branching point. For simplicity only one direction of transmission is shown. Most of the supergroups arriving from the west cable are transmitted directly through the branching point to the east cable. Supergroups 1 and 2 are prevented from passing through the branching point by a high-pass filter which has a cutoff between supergroups 2 and 3. The 64-kc and 556-kc pilots from the west are transmitted to the east through narrow band-pass filters.

Supergroup 2 received from the west cable passes through the normal steps of supergroup, group, and channel demodulation, and provides 60 channels terminated at the branching point. Supergroup 1 received from the west cable passes through supergroup and group demodulation but as illustrated only one group passes through channel equipment for use at the branching point. The other four groups (12 channels each) are not demodulated further but pass through the branching point at 60–108 kc. Two of them are shown passing through *L-L* connectors to type *L* system group modulators which form part of supergroup 1 on the east cable. The other two pass through *L-K* and *L-J* connectors to group modulators of types *K* and *J* systems, respectively.

Another type of branching point connection illustrated is that of supergroup 1 from the north cable. This passes only through a supergroup demodulator. Since all 60 of these channels are assumed to be needed toward the east, the whole supergroup is passed through a supergroup connector at 312–552 kc and connected to supergroup 2 modulator of the east cable.

The various connectors referred to in the preceding paragraphs consist primarily of filters. The *L-L* connector is composed only of band filters since its function is to prevent portions of adjacent groups, which are not completely suppressed by the group band filters, from finding a path through the connector. The *L-J* and *L-K* connectors have both band filters and narrow band elimination filters. The band elimination filters remove residual carriers and pilots of the *J* and *K* systems. The *L-L* supergroup connector performs a function similar to the *L-L* group connector but an amplifier is required with it to secure proper transmission levels.

A more detailed picture of the arrangement of the connectors with relation to the other equipment is indicated on the general diagram of Figure 3.

Voice Frequency Terminations

Each channel of a coaxial system terminates as a 4-wire circuit at the jacks in the voice-frequency patching bay. The transmission levels at this point are the

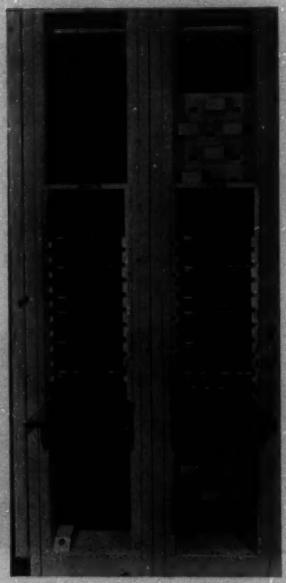

Figure 8. Transmitting and receiving high-frequency patch bays, each equipped with jacks for a 240-channel terminal

Coaxial jacks at left connect to supergroups; conventional jacks, (spaced to reduce coupling) connect to groups

same on all channels and also are identical with levels of channels on all other types of broad band facilities entering the office. Any type of equipment normally connected to a 4-wire voice-frequency circuit can be associated with the coaxial channels by cross connection to the jacks at the voice-frequency patching bay. Such equipment may include terminating sets for a 2-wire termination, 1,000-cycle signaling equipment, signaling equipment for toll line dialing, terminal echo suppressors, 4-wire switching pads, and voice-frequency telegraph terminals.

Figure 10. Group carrier supply distribution panel

Front view with cover removed. Distribution cables to modulators are connected to soldering terminals in center

Special Services

A telephone channel can be used for 18-channel voice-frequency carrier telegraph or for facsimile and picture transmission. As the channels are designed primarily for telephone service the transmission requirements have to be considered when other uses are made of the channels. In picture transmission, for example, equalizers must be provided for the delay distortion introduced by the band filters in the channel banks.

Program channels of various band widths can be obtained by merging the frequency space of several telephone channels. A single-side-band program terminal has been developed which uses the space of three message channels and provides an 8-kc program band and a control channel.

The coaxial system provides a flexible medium for realizing a variety of signal band widths for new services in the future.

Figure 9. Supergroup demodulator panel

Front view with cover removed

The broad band of the line is subdivided by the terminal equipment into supergroups of 240-kc band width and groups of 48-kc band width. Either of these bands can be used as a block or subdivided in any desired manner by the provision of appropriate terminal equipment. An example of this procedure, applied to the group, is the single-side-band program terminal referred to in the preceding paragraph.

Maintenance Features

Circuits which are carried in common along part of a coaxial route eventually may leave it and fan out over other routes to scattered points. Under these conditions, the removal of numbers of circuits from service for the purpose of terminal maintenance tests would be very difficult to effect. Consequently the coaxial system is arranged so that most routine maintenance tests and a certain amount of trouble testing can be made with the equipment in service. The vacuum tubes used in the various amplifiers of the coaxial terminal can be tested for filament activity without removing the amplifiers in service. Likewise, the arrangement of the jack terminations of the spare group and supergroup equipment is such that manual patches can be made from regular to spare without interrupting service even momentarily. As the channels may be used for other services than telephony, the design of the maintenance features and the plant operating routines take into account the requirements of these services so that all are safeguarded adequately.

Transmission testing and patching operations for equipment on the high-frequency side of the channel banks are concentrated at high-frequency patching bays. The voice-frequency terminations of the individual channels are concentrated in voice-frequency patching bays. Transmission tests on the channel banks group and supergroup equipment, and also certain tests in the coaxial line can be made from the high-frequency patching bay. Testing equipment covering the entire frequency range is provided.

Testing and patching is simplified by the standardization of transmission levels at the jacks of the high-frequency patching bay. The outputs of all channel banks have the same transmission level and the outputs of all group banks are the same.

Previous reference has been made to the arrangement whereby 92 kc is transmitted at low level over each group of the system. This tone is introduced as an aid to maintenance. A check on the over-all transmission of any group can be made at any time by observation of the level of the 92 kc at the receiving terminal.

The desired transmission levels at various points throughout the terminal are adjusted initially by means of pads in the various units of equipment and by the gain control potentiometers of the amplifiers. In general, subsequent service adjustments are confined to occasional changes of the gain control potenti-

ometers. The copper oxide units are sufficiently stable that no service adjustments for carrier leak balance are provided.

Photographs of Equipment

A few photographs are included to indicate the general appearance of the equipment. Figure 7 is a rear view of a row of bays containing terminal coaxial equipment. Only five bays are shown in the figure. A complete 480-channel terminal, with spare equipment as normally provided, would require 40 such bays. The types of equipment shown in the figure are, from left to right: two bays of supergroup carrier supply, group carrier supply, channel carrier supply, and pilot and frequency supply.

Figure 8 shows the high-frequency patching bays where access to group and supergroup circuits is provided.

Figure 9 shows a supergroup demodulator unit which is typical of the majority of terminal units.

In Figure 10 is illustrated the design of one of the carrier supply distributing units. Fiber guards are placed over all portions of the circuits where short circuits could cause failure of a number of channels. The accessible terminals, to which are connected cables running to modulators and demodulators, are protected by resistances against serious results of a short circuit.

Conclusion

The terminal equipment developed for the type *L1* system represents a practical solution of the problem of getting the most out of a coaxial line in terms of telephone message handling capacity. By use of frequency division and single-side-band transmission, only 4 kc of line frequency space needs to be allotted to each channel. A total of 480 channels thus is made available within a broad band of approximately 2 megacycles. The filter selectivities and carrier frequency stability requisite to this close packing of channels has been realized through developments in these fields, combined with the application of group modulation techniques. The methods used also meet the essential requirement of providing access to the broad band at intermediate points on the route so that groups of circuits may be added to or taken off the system as required by traffic conditions. It has proved practicable to meet the transmission and service requirements for long haul circuits. The methods described appear applicable to future coaxial systems having wider bands than 2 megacycles.

References

1. Systems for Wide Band Transmission Over Coaxial Lines, **Lloyd Espenschied, M. E. Strieby.** Electrical Engineering (AIEE Transactions), volume 53, October 1934, pages 1371–80.

2. A Million-Cycle Telephone System, **M. E. Strieby.** Electrical Engineering (AIEE Transactions), volume 56, January 1937, pages 4–7.

3. A Carrier Telephone System for Toll Cables, **C. W. Green, E. I. Green.** AIEE Transactions, volume 57, 1938, May section, pages 227–36.

4. Cable Carrier-Telephone Terminals, **R. W. Chesnut, L. M. Ilgenfritz, A. Kenner.** AIEE Transactions, volume 57, 1938, May section, pages 237–44.

5. A 12-Channel Carrier Telephone System for Open-Wire Lines, **B. W. Kendall, H. A. Affel.** AIEE Transactions, volume 58, 1939, July section, pages 351–60.

6. An Improved Cable Carrier System, **H. S. Black, F. A. Brooks, A. J. Wier, I. G. Wilson.** AIEE Transactions, volume 66, 1947, pages 741–6.

7. A New Crystal Channel Filter for Broad Band Carrier Systems, **E. S. Willis.** AIEE Transactions, volume 65, 1946, March section, pages 134–8.

8. Copper-Oxide Modulators in Carrier Telephone Systems, **R. S. Caruthers.** AIEE Transactions, volume 58, 1939, June section, pages 253–60.

9. Fractional-Frequency Generators Utilizing Regenerative Modulation, **R. L. Miller.** *Proceedings*, Institute of Radio Engineers (New York, N. Y.), volume 27, July 1939, pages 446–57

No Discussion

Impedance Relationships of the Adjustable-Speed A-C Brush-Shifting Motor

FRED BAUMANN
NONMEMBER AIEE

THE NEED for a dependable variable-speed a-c motor with shunt characteristics has led to the development and constant improvement of the polyphase brush-shifting motor (Schrage type). This type of machine has satisfied most effectively many of the a-c variable-speed applications. Although the adjustable-speed a-c brush-shifting motor has been the subject of several excellent papers in the technical literature, nevertheless, there is a need for a simplified procedure of calculating its performance.

The adjustable-speed a-c brush-shifting motor provides an ingenious method of obtaining adjustable speed with alternating current. Its speed is adjustable within a given range for various conditions of load, including no load. Unlike the wound rotor induction motor, the slip energy is converted to useful work instead of heat dissipated in the rotor and grids

It is the object of this paper to present a new and simple method of calculating the performance of the machine by the equivalent circuit method. Experience shows that the usual assumption of neglecting the reactance, which is mutual to the primary and commutated windings, may lead to considerable error. The following analysis will show the part which each of the mutual and leakage reactances play in determining the performance of the machine.

Paper 47-221, recommended by the AIEE rotating machinery committee and approved by the AIEE technical program committee for presentation at the AIEE Middle Eastern District meeting, Dayton, Ohio, September 23–25, 1947. Manuscript submitted July 2, 1947; made available for printing August 13, 1947.

FRED BAUMANN is in the induction motor engineering division, General Electric Company, Schenectady, N. Y.

The Machine Windings

The a-c brush-shifting motor (Figure 1) is essentially an induction motor with a primary winding in the rotor and a secondary winding in the stator. A third winding is placed in the rotor and connected to a commutator. A slip frequency voltage of adjustable magnitude and phase angle is taken from the commutator and applied to the secondary winding. At standstill the machine is simply a 3-winding transformer shown in Figure 2.

At standstill the equations for the terminal voltages of Figure 2*A* can be written as in the following forms.:

$$V_1 = Z_{11}I_1 + Z_{12}I_2 + Z_{13}I_3 \quad (1)$$

$$V_2 = Z_{12}I_1 + Z_{22}I_2 + Z_{23}I_3 \quad (2)$$

$$V_3 = Z_{13}I_1 + Z_{23}I_2 + Z_{33}I_3 \quad (3)$$

When the machine is running at a speed corresponding to a slip of S, the frequency remains constant in the primary and commutated windings but varies in proportion to the slip in the secondary winding. The reactance of the secondary winding will be proportional to the frequency and therefore the slip. Equations 1, 2, and 3 may be written to hold for any speed as follows:

$$V_1 = Z_{11}I_1 + Z_{12}I_2 + Z_{13}I_3 \quad (4)$$

$$V_2 = \bar{Z}_{12}I_1 + \bar{Z}_{22}I_2 + \bar{Z}_{23}I_3 \quad (5)$$

$$V_3 = Z_{13}I_1 + Z_{23}I_2 + Z_{33}I_3 \quad (6)$$

To complete the solution of equations 4, 5, and 6 it is necessary to find the relation between V_2 and V_3 and also between I_2 and I_3. The voltages V_1, V_2, and V_3 are voltage drops. The voltage drop V_2 must be equal to the voltage rise $-CV_3$ shifted at an angle α. The angle α is a function of brush position while C is a function of brush spacing and ratio of

Figure 1. Adjustable-speed a-c brush-shifting motor

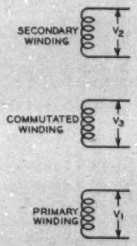

(A)

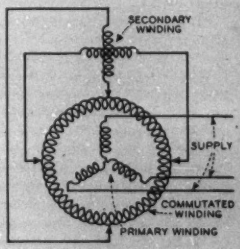

(B)

Figure 2. Connections

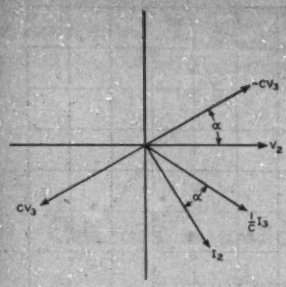

Figure 3. Vector relationships of currents and voltages in the secondary and commutated windings

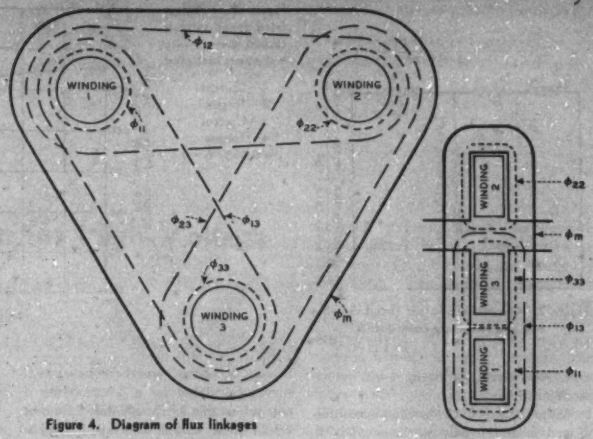

Figure 4. Diagram of flux linkages

commutated winding turns + secondary winding turns. Figure 3 shows the relation of these voltages and currents. It may be seen that the commutator acts as a frequency changer, phase shifter, and adjustable voltage source.

The relation of voltages and currents shown in Figure 3 is

$$V_3 = C\underline{/\alpha}\, V_2 = -\boldsymbol{T} V_2 \tag{7}$$

$$I_3 = C\underline{/-\alpha}\, I_2 = \boldsymbol{T}' I_2 \tag{8}$$

The solution of equations 1 through 7 yields the following two simultaneous equations:

$$V_1 = \boldsymbol{Z}_{11} I_1 + (\boldsymbol{Z}_{12} + \boldsymbol{T}'\boldsymbol{Z}_{13}) I_2 \tag{9}$$

$$0 = (\bar{\boldsymbol{Z}}_{12} + \boldsymbol{T}\boldsymbol{Z}_{13}) I_1 + (\bar{\boldsymbol{Z}}_{22} + \boldsymbol{T}'\bar{\boldsymbol{Z}}_{23} + \boldsymbol{T}\boldsymbol{Z}_{23} + \boldsymbol{T}\boldsymbol{T}'\boldsymbol{Z}_{33}) I_2 \tag{10}$$

Reactance Relations

It is necessary to examine the impedances shown in equations 9 and 10.

In a 3-winding machine the flux paths in general can be resolved into seven different paths as shown in Figure 4.

However, since windings 1 and 3 are placed in the same slots of the rotor, two of the fluxes (ϕ_{12} and ϕ_{23}) shown in Figure 4 can be eliminated. Figure 5 shows the flux paths which must be considered.

The presence of ϕ_{23} shown dotted in Figure 5 may seem out of keeping with the assumption of infinite permeability of the iron, but this component of flux is considered to correct for the difference in flux linkages between the flux produced by the current in winding 1 linking the conductors of winding 3 and the flux produced by the current in winding 1 linking the conductors of winding 1. This is usually a small loss (remembering that $\phi_{11} \cong X_1$, $\phi_{22} \cong X_2$, $\phi_{33} \cong X_3$, $\phi_{13} \cong X_1'$, $\phi_m \cong X_m$) the impedances of equations 9 and 10 may be written by inspection of Figure 5 as

$$\left.\begin{aligned}
\boldsymbol{Z}_{11} &= R_1 + j(X_1 + X' + X_m) \\
\boldsymbol{Z}_{12} &= jX_m \\
\boldsymbol{Z}_{13} &= j(X_m + X') \\
\bar{\boldsymbol{Z}}_{12} &= jSX_m \\
\bar{\boldsymbol{Z}}_{22} &= R_2 + jS(X_2 + X_m) \\
\boldsymbol{Z}_{23} &= jX_m \\
\bar{\boldsymbol{Z}}_{23} &= jSX_m \\
\boldsymbol{Z}_{33} &= R_3 + j(X' + X_3 + X_m)
\end{aligned}\right\} \tag{11}$$

Equations 9, 10, and 11 can be combined to yield the following equations:

$$V_1 = (R_1 + jX_1 + jX' + jX_m) I_1 + (jT'X' + (1+T')jX_m) I_2 \tag{12}$$

$$0 = \left(jX_m + \frac{\boldsymbol{T}}{1+\boldsymbol{T}} jX'\right) I_1 + \left[\frac{R_2 + \boldsymbol{T}\boldsymbol{T}' R_3}{S+\boldsymbol{T}} + \frac{jSX_2 + \boldsymbol{T}\boldsymbol{T}'(X' + X_3)}{S+\boldsymbol{T}} + jX_m(1+\boldsymbol{T}')\right] I_2 \tag{13}$$

Let us now arbitrarily substitute I_s for I_1 according to the following equation:

$$I_1 = (1+\boldsymbol{T}') I_s \tag{14}$$

Equations 12 and 13 then may be arranged as follows:

$$V_1 = (R_1 + jX_1 + jX' + jX_m)(1+\boldsymbol{T}') I_s \times ((1+\boldsymbol{T}')jX_m + \boldsymbol{T}'jX') I_2 \tag{15}$$

$$\left(0 = (1+\boldsymbol{T}')jXm + \boldsymbol{T}'jX' + \frac{\boldsymbol{T}-\boldsymbol{T}}{1+\boldsymbol{T}} jX'\right) I_s + \left(\frac{R_2 + \boldsymbol{T}\boldsymbol{T}' R_3}{S+\boldsymbol{T}} + \frac{jSX_2 + \boldsymbol{T}\boldsymbol{T}'(X' + X_3)}{S+\boldsymbol{T}}\right) + jX_m(1+\boldsymbol{T}')\Big) I_2 \tag{16}$$

With respect to the real and imaginary components of $\boldsymbol{T}$ and $\boldsymbol{T}'$

$$j\left(\frac{\boldsymbol{T}-\boldsymbol{T}'}{1+\boldsymbol{T}} X'\right) = \left(\frac{+2b}{1+a+jb}\right) X'$$

for the usual practical case where

$$|a| < 1$$
$$|b| << 1$$
$$\left|(1+\boldsymbol{T}')jX_m + \boldsymbol{T}'jX'\right| >> \left| j\frac{(\boldsymbol{T}-\boldsymbol{T}')}{1+\boldsymbol{T}} X'\right|$$

the term $j(\boldsymbol{T}-\boldsymbol{T}')X'/(1+\boldsymbol{T})$ is omitted and equations 15 and 16 can be rewritten as follows:

$$V_1 = [(R_1 + jX_1)(1+\boldsymbol{T}') + jX' + (1+\boldsymbol{T}')jX_m + \boldsymbol{T}'jX'] I_s + [(1+\boldsymbol{T}')jX_m + \boldsymbol{T}'.(jX')] I_2 \tag{17}$$

$$0 = [(1+\boldsymbol{T}')jX_m + \boldsymbol{T}'jX'] I_s + \left[\frac{R_2 + \boldsymbol{T}\boldsymbol{T}' R_3}{S+\boldsymbol{T}} + \frac{jSX_2 + \boldsymbol{T}\boldsymbol{T}' X_3 - S\boldsymbol{T}'X'}{S+\boldsymbol{T}} + j\boldsymbol{T}'X' + jX_m(1+\boldsymbol{T}')\right] I_2 \tag{18}$$

Equations 17 and 18 are of the form associated with a 2-winding transformer for an induction motor, where the mutual reactance is

$$j(1+\boldsymbol{T}')X_m + \boldsymbol{T}'jX'$$

The equivalent circuit of Figure 6, therefore, satisfies the above equations.

If $\boldsymbol{T}$ and $\boldsymbol{T}'$ are expressed in terms of their real and imaginary components the

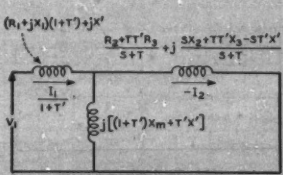

Figure 6. General equivalent circuit

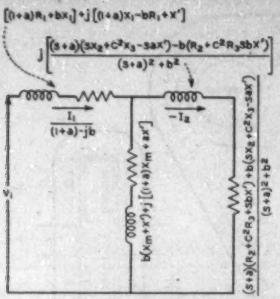

Figure 7. General equivalent circuit showing real and imaginary components

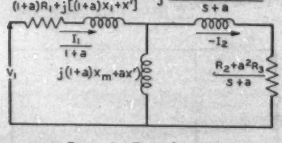

Figure 8. Equivalent circuit ($b=0$)

Figure 9. Calculated speed-torque-current curves with test points indicated

1—Current
2—Torque
3—Current
4—Torque
$a=0.555;\ b=0$

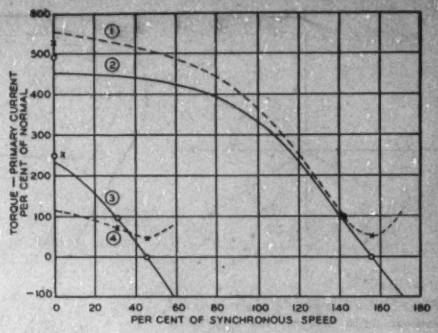

equivalent circuit of Figure 6 will reduce to that of Figure 7.

When the axis of the brushes is not displaced from the axis of the secondary, $b=0$. This condition results in the simplified equivalent circuit shown in Figure 8.

The similarity of the equivalent circuit of Figure 8 to the equivalent circuit of an induction motor is quite apparent. When $a=0$, it reduces exactly to the equivalent circuit of an induction motor. The no load slip will occur at $s=a$. If a is a positive number the no load slip will be above synchronous speed, and if a is negative the no load slip will be below synchronous speed.

The calculation of losses and torque follows the same pattern as is used in the calculation of an induction motor by equivalent circuit. The torque in synchronous watts is

$$T_s = R_s|I_s|^2\left(\frac{R_2+TT'R_3}{S+T} + \frac{jSX_3+TT'X_3-ST'X'}{S+T}\right) \quad (19)$$

Or if $b=0$

$$T_s = |I_s|^2\left(\frac{R_2+a^2R_3}{S+a}\right) \quad (20)$$

With the aid of the foregoing analysis, reasonable accuracy can be expected.

Figure 8 shows speed-torque-current-curves calculated for a 3-horsepower 4-pole adjustable a-c brush-shifting motor. While these curves are not typical of motors of larger sizes the test points show a good correlation with the calculated curves.

List of Symbols

V_1 = terminal voltage of primary winding
V_2 = terminal voltage in secondary winding referred to primary winding
V_3 = terminal voltage in commutated winding referred to primary winding
I_1 = current in primary winding
I_2 = current in secondary winding referred to primary winding
I_3 = current in commutated winding referred to primary winding
Z_{11} = total impedance of primary winding
Z_{12} = mutual impedance primary to secondary windings
Z_{13} = mutual impedance primary to commutated winding
Z_{22} = total impedance of secondary winding referred to primary winding at standstill
Z_{32} = mutual impedance of secondary to commutated winding in primary terms
Z_{33} = total impedance of commutated winding referred to primary winding
$\bar{Z}_{22}$ = total impedance of secondary winding referred to primary winding at primary voltage and at slip S
$\bar{Z}_{32}$ = mutual impedance of secondary to commutated winding in primary terms at slip frequency
$\bar{Z}_{12}$ = mutual impedance primary to secondary windings at slip frequency
$T = c/\alpha = jb$ = vector brush position
$T' = c/-\alpha = -jb$ = conjugate of T
a = per unit voltage applied to secondary winding from commutator
α = phase angle of V_3 with respect to V_2
s = per unit slip, $(1-S)$ per unit speed referred to synchronous speed as an induction motor
ϕ_{11} = total flux linking primary winding
ϕ_{12} = flux linking primary and secondary windings
ϕ_{13} = flux linking primary and commutated windings
ϕ_{22} = total flux linking secondary winding
ϕ_{23} = flux linking secondary and commutated windings
ϕ_{33} = total flux linking commutated winding
ϕ_m = flux linking all windings
R_1 = primary resistance
R_2 = secondary resistance referred to primary
R_3 = commutated winding resistance referred to the primary
X_1 = primary leakage reactance at primary frequency
X' = mutual leakage reactance of primary and commutated winding referred to primary at primary frequency
X_m = mutual reactance corresponding to ϕ_m referred to primary at primary frequency
X_2 = secondary leakage reactance referred to primary at primary frequency
X_3 = leakage reactance of commutated winding referred to primary at primary frequency

References

1. A Generalized Equivalent Circuit in the Theory of Polyphase Commutator Motors, W. B. Coulthard. AIEE Transactions, volume 60, 1941, pages 423–31.

2. Theory of the Brush-Shifting A-C Motor, A. G. Conrad, F. Zweig, J. G. Clark. Parts 1 and 2, AIEE Transactions, volume 60, 1941, August section, pages 829–36. Parts 3 and 4, volume 61, 1942, July section, pages 502–13.

3. The Equations and Circle Diagrams of the Schrage Motors, W. J. Gibbs. *Journal*, Institution of Electrical Engineers (London, England), December 1946.

4. Diagram of the Polyphase Commutator Motor Having A Shunt Characteristic Speed Regulation by Means of Brush Shifting, L. Schombourger. *Revue Générale de l'Electricité* (Paris, France), volume 31, May 21, 1932, pages 693–9.

No Discussion

Gaseous Insulation for High-Voltage Apparatus

G. CAMILLI
FELLOW AIEE

J. J. CHAPMAN
ASSOCIATE AIEE

Synopsis: A group of halogenated gaseous compounds have been investigated to determine their impulse ($1^1/_2$x40-microsecond wave) and 60-cycle strength in uniform and nonuniform fields at pressures of 1, 2, and 3 atmospheres. The scope of this investigation was confined to bare electrodes, and additional testing will be required to determine the behavior of these gases with various types of solid insulation. It has been found that sulphur hexafluoride (SF_6) possesses superior insulating properties for high-voltage apparatus, even at these relatively low pressures. Data obtained in an approximately uniform field indicate that at 30 pounds gauge pressure this gas approaches the impulse strength of oil. Therefore, certain classes of high-voltage apparatus advantageously may use this gas for their insulation, if other properties are adequate.

IN RECENT YEARS several papers have been presented before the Institute on the dielectric behavior of compressed gases. The fact that the dielectric strength of gases under certain special conditions can be superior to either liquid or solid insulating materials makes them very promising insulating media and has attracted the attention of many investigators.

Compressed air and nitrogen have been used in precision capacitors where low dielectric loss is essential, and compressed Freons have been used in X-ray transformers where reduced dimensions and noninflammability are of primary importance.[6] In general these apparatus have been operated indoors where the ambient temperature does not drop to a very low value. For outdoor equipment, a gas should be selected that will not require special heating auxiliaries to prevent condensation at low ambient temperatures. Another very important requirement is that the gas have sufficient impulse strength to protect the apparatus from failure due to a lightning stroke on the transmission lines to which it is connected.

Condensation of Gases

The outdoor problem of condensation at low ambient temperatures obtains a ready solution from the gas SF_6 and therefore will be discussed first. In Figure 1 the saturated vapor pressure curves of three gases (SF_6, Freon 22, and Freon 12) are shown. A gas cannot be operated at a pressure higher than its vapor pressure corresponding to the temperature under consideration. If the pressure were increased above the vapor pressure, the extra vapor probably would condense. The curves shown in Figure 1 indicate that sulphur hexafluoride can be operated at higher pressures than either Freon 12 or Freon 22. Let us assume for instance that a given apparatus is filled with Freon 22 at a gauge pressure of 150 pounds per square inch at a temperature of 40 degrees centigrade (point A). Also, impose the condition that the total quantity of gas in the system is unchanged. If the temperature of the vapor is lowered from its initial value at A, the pressure will drop to some value at B where saturation conditions take place. Over this interval (from A to B) the dielectric strength of the apparatus will remain virtually unchanged, because the pressure decreases as a perfect gas following the change in absolute temperature. However, any further decrease in temperature will re-

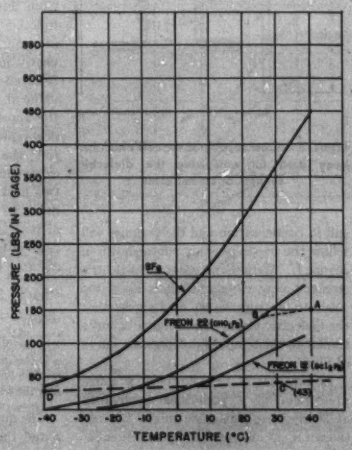

Figure 1. Saturated vapor pressure characteristics of sulphur hexafluoride, Freon 22, and Freon 12

Paper 47-240, recommended by the AIEE switchgear and transformer committees and approved by the AIEE technical program committee for presentation at the AIEE Midwest general meeting, Chicago, Ill., November 3–7, 1947. Manuscript submitted July 31, 1947; made available for printing September 25, 1947.

G. CAMILLI is research and development engineer and J. J. CHAPMAN is in the works laboratory both with General Electric Company, Pittsfield, Mass.

The authors wish to acknowledge the assistance of J. H. Hagenguth (M'39) and T. R. Walters (M'44) of the General Electric Company.

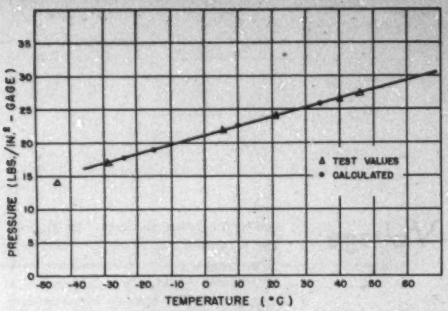

Figure 2. Relation between pressure and temperature in a constant volume of SF_6 gas

Comparison between calculated and tested values

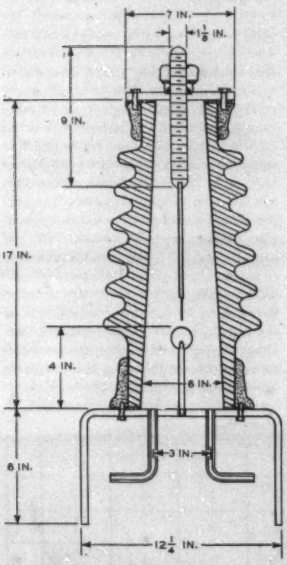

Figure 3. Cross section of the cell which has been used for comparing the dielectric strength of several gases

sult in condensation and the pressure will follow the vapor pressure curve shown in Figure 1. With many gases the dielectric strength very closely depends upon the absolute pressure, so we may expect that the dielectric strength will follow a curve similar to the temperature–pressure curve of Figure 1.

In the case of SF_6, however, a gauge pressure of only 43 pounds per square inch at 30 degrees centigrade might be considered a suitable operating condition because of the high dielectric strength of this gas. At a temperature of −40 degrees centigrade, the gauge pressure would be 30 pounds per square inch, having followed the path *CD* shown on Figure 1. In going from point *C* to point *D*, the SF_6 vapor pressure curve has not been intercepted, so no condensation will result. Figure 2 illustrates experimental proof that SF_6 behaves as a perfect gas over a wide region of practical application.

Basic Elementary Concepts Regarding the Breakdown of Gases[7]

The electron early was regarded as the initiating agent in the dielectric breakdown of gases. In traveling through a gas under the action of an accelerating field *F* it is able to create new electrons by disruption of gas molecules upon collision. If electrons be liberated from a plate in a rarefied gas, the current which they carry from this plate to one parallel to it is a function of the voltage. As the voltage increases, at first the current follows in a nearly linear fashion. Eventually, it is believed to reach a constant or saturation value at i_0. As higher fields are applied, the apparent saturation gives place to a new rapid increase of current with potential, the current eventually increasing exponentially in the form of a spark. At this field strength, the electrons are producing α new pairs of ions per centimeter of path due to collisions with the molecules of gas. The current increases with distance in gas according to law

$$i = i_{0\epsilon}^{\alpha x}$$

where

ϵ is the Naperian logarithm base.
α is the quantity just defined.
x is the length of path in centimeters.
i_0 is the initial current.

The quantity α is a function of pressure p and the field strength F. It depends upon the ability of the electron to pick up energy from the field and the probability of its ionization once it has the energy. If E_0 is the required energy to produce ionization, this condition takes place when the electron is accelerated over the mean free path distance λ_1 to such an extent that

$$Fe\lambda_1 = E_0$$

where e is the charge on the electron. The mean free path distance is a function of pressure, namely,

$$\lambda_1 = \lambda_0 \frac{p_2}{p_1}$$

If λ_1 is decreased by raising the pressure, F must be increased correspondingly in order to cause the same degree of ionization.

Paschen discovered his famous law in 1889, namely,

$$V_S = f(pd)$$

The sparking voltage is a function of the product of pressure and distance. This law also followed from theoretical extensions of Townsend's theory. We find experimental agreement with Paschen law for gases in uniform fields. As the pressure is decreased, the breakdown voltage decreases in a regular manner until the gas is quite rare and then the voltage rises again. The minimum breakdown voltage occurs at the "critical pressure." Even in this region the law has been proven valid experimentally.

If spark breakdown is dependent upon a local concentration of ions or influenced by the presence or deficiency of ions in any region, then for this electrode arrangement in gas, the law will not be obeyed.

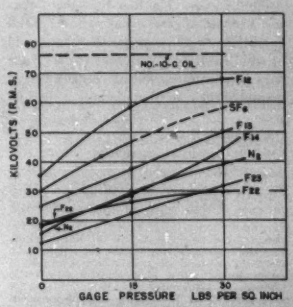

Figure 4. Sixty-cycle dielectric strength of gases and number 10-C oil tested between two 1-inch-diameter spheres spaced 1/4 inch and at gauge pressure up to 30 pounds per square inch

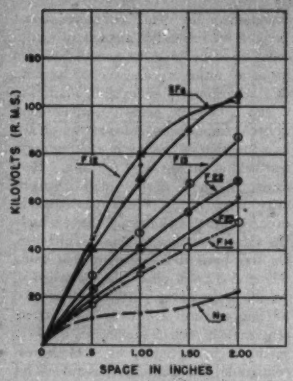

Figure 5. Sixty-cycle dielectric strength of gases tested between tungsten rod and 1-inch-diameter sphere at atmospheric pressure

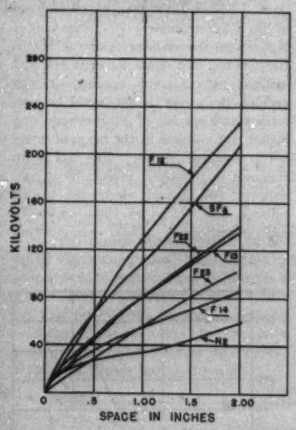

Figure 6. Negative impulse tests ($1^1/_2$x40-microsecond wave), at atmospheric pressure, of several gases tested between tungsten rod and 1-inch-diameter sphere

Therefore, with gases or electrode configurations, that make space charge concentrations possible before final breakdown, deviations from Paschen's law are to be expected.

In the original work, Townsend elaborated upon the collision process and introduced an ionization coefficient for positive ions causing further ionization by collision. From later experiments it appears that the positive ions do not cause significant ionization due to their collision with molecules. However, positive ion fields cause the creation of photons and attendant ionization. So the second Townsend coefficient for positive ions has a place in modern physics though quite different from the original intention.

Meek's theory of positive streamer propagation[7] suggests that the local field at the tip of the positive space charge left in the wake of an electron avalanche must be commensurate with the applied field for streamer propagation by photon processes. Since the shape and intensity of the streamer tip field are dependent upon the mobility and diffusion characteristics of the gas as well as the nature of the ions formed, it is not surprising that pressure changes in complex gases result in anomalous breakdown behavior.

Description of Apparatus and Method of Making Tests

A gas cell shown in Figure 3 was developed for the purpose of making high-voltage breakdown tests on the following gases:

N_2
F-12—($C F_2 Cl_2$)
F-13—($C F_3Cl$)
F-14—($C F_4$)
F-22—($C H Cl F_2$)
F-23—($C H F_3$)
SF_6

The bottom electrode was a 1-inch-diameter sphere at ground potential while the upper electrode was either a 1-inch-diameter sphere or a tungsten rod. The upper sphere was used for tests requiring a uniform field, while the rod provided an electrode for nonuniform gradients. This rod was 0.100-inch diameter and was rounded on the end to a 0.050-inch radius, thus providing a nonuniform field of known configuration. The separation of electrodes could be set accurately (within 0.0052 inch) without losing any gas pressure.

Since most of this test work was done during the war, halogenated gases were difficult to obtain and small volume testing became of paramount importance. About 5 liters of gas were required to fill the cell and tests could be run up to 350 kv impulse. In a few cases external flashover required that the cell be immersed in oil. After each gas was tested, the electrodes were polished and the inside porcelain wall was washed with soap and water and then with distilled water. Washing was quite necessary to remove the last traces of the halogenated gases so as not to interfere with ensuing tests. A vacuum drying procedure removed the last traces of moisture and then a blank test was run with N_2 before admitting a new gas for test. It was decided that the gases first should be evaluated according to dielectric strength as determined by tests in a uniform field. In the small volume used the most satisfactory uniform field possible was that provided by two spherical electrodes 1 inch in diameter, and spaced 0.25 inch apart. After some preliminary testing with N_2 at 30 pounds gauge pressure, it was found that positive and negative impulse breakdown values agreed within 10 to 15 percent. This at least indicated a moderate degree of symmetry of the electrodes and was accepted as the most ideal field possible in the small volume. It offered strikingly contrasting phenomena when compared to the tungsten rod–sphere type of configuration. This latter configuration was selected after preliminary investigation because "anomalous breakdown decrease with pressure" could then be demonstrated in a small volume of gas. Tests were made up to 2-inch spacing with this arrangement. Both types of electrodes were employed with impulse and 60-cycle voltage at 0, 15, and 30 pounds gauge pressure. The center line of the electrode system was approximately 3 inches from the porcelain wall. However, high-voltage testing within a confined space seldom yields results identical with testing in unlimited space. The 1-inch setting is considered the most reliable source of data with the nonuniform field arrangement and is therefore used as a point of comparison among the gases. The num-

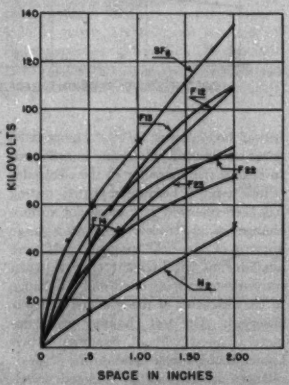

Figure 7. Positive impulse tests ($1^1/_2$x40-microsecond wave), at atmospheric pressure, of several gases tested between tungsten rod and 1-inch diameter sphere

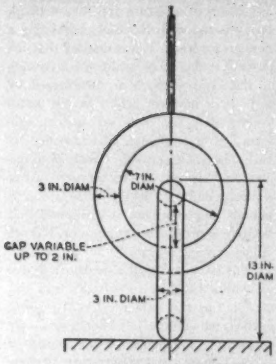

Figure 8. Test setup to obtain data at large gap spacings

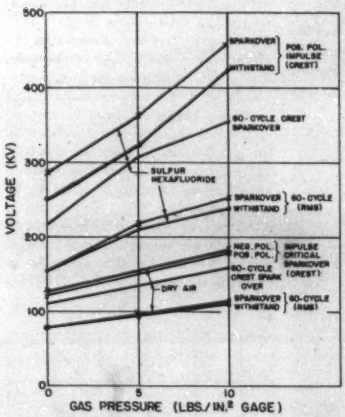

Figure 9. Impulse and 60-cycle spark-over and withstand voltages of SF_6 and air using 2-inch gap spacing in the test arrangement shown in Figure 8

ber of breakdowns for the halogenated gases was picked judiciously in order not to change the character of the electrodes before a refill, because repeated testing has been reported as a cause for surface change in electrodes.[2,3] Since a large number of identical tungsten rods were available to us, frequent change, when convenient, was exercised and no change in the character of the rounded end was observed. The test chamber was completely closed without windows. It is known that impulse breakdowns of air or nitrogen are affected by a closed vessel. In these tests this effect is shown by the fact that the impulse ratio for nitrogen is 2.8 instead of 1 as would be expected from tests in open air.

Each interruption planned or otherwise causing a change of gas meant the loss of a small volume even when it could be withdrawn into a liquefaction cylinder. Fortunately nitrogen is a common gas and was therefore ideal for the many blank tests that were necessary to check the cleanliness of the cell. The data (points) shown on the graphs represent an average of three trials. All of the Freon gases except F-14 invariably showed some carbon deposit when the cell was torn down preceding a refill; nitrogen and SF_6 showed no deposit.

A 500-kv Marx circuit was used for generating $1^1/_2$x40-microsecond impulse waves and breakdowns were observed with a cathode ray oscillograph. Fractional parts of the capacitor bank were used to facilitate tests in the lower voltage range. Sixty-cycle breakdowns were accomplished with a 50-kv and a 150-kv/300-kv cascade set. The wave form was close to sinusoidal, as indicated by rms and crest voltmeters.

Discussion of Test Results

In Figure 4 illustrating the 60-cycle breakdown in a uniform field, at zero pounds gauge pressure (1 atmosphere) the general superiority of the halogenated gases over nitrogen is illustrated, although at that particular pressure in the uniform field F-22 and F-14 are about the same value while F-23 is definitely lower than nitrogen. F-12 and SF_6 are definitely superior to N_2 and may be considered to have approximately the same respective margin over air. This is of some interest because an increasing amount of equipment rated up to 15 kv now depends on air as an insulating and cooling medium at 1 atmosphere pressure. In Figures 5, 6, and 7, 60-cycle, negative impulse, and positive impulse breakdowns are shown as a function of spacing in a nonuniform test field at atmospheric pressure. Here again, SF_6 and F-12 show marked superiority over nitrogen and consequently over air which is known to have closely the same breakdown values as nitrogen. On this basis it is apparent that using SF_6 or F-12 will allow the extension of gas-filled apparatus. SF_6 could be used for temperatures as low as −40 degrees centigrade in such an application but F-12 would begin to liquify at −20 degrees centigrade, thus limiting its usefulness for wide application. In Figures 5, 6, and 7 it is shown that in the nonuniform field at 1 atmosphere pressure SF_6 is 2.8 to 5 times as strong as N_2 depending upon the type of breakdown. In the uniform field data of Figure 4, the 60-cycle breakdown of SF_6 is approximately $1^1/_2$ times that of N_2. Since the uniform field was within the confines of a small porcelain cell and utilized only $^1/_4$-inch spacing, it was decided that some tests should be performed at a spacing of 2 inches requiring higher test voltages in the range of interest to design engineers. This test setup is shown in Figure 8: essentially it consists of two toroid electrodes looped through and placed at right angles to each other. Such a field configuration

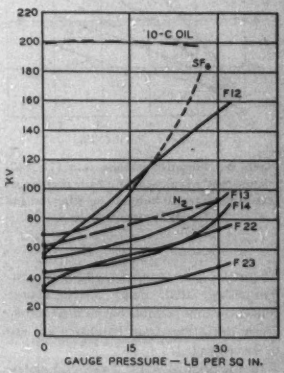

Figure 10. Impulse dielectric strength of gases

Test made between two 1-inch-diameter spheres spaced $^1/_4$ inch at gauge pressure up to 30 pounds per square inch

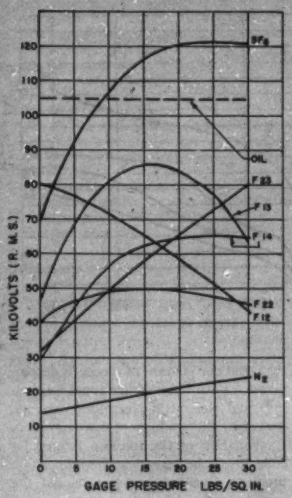

Figure 11. Sixty-cycle dielectric strength of gases

Tests made between tungsten rod and 1-inch diameter sphere spaced 1-inch. Values for number 10-C oil also are shown

would be practical in the design of some apparatus. SF_6 is compared with air in Figure 9 and at 1 atmosphere we see that it has 2.1 and 2.4 times the respective 60-cycle and impulse strength of air in the toroid electrode system. This test setup as indicated in Figure 8 was included in a rather large diameter porcelain shell. For this reason only the most promising halogenated gas (SF_6) was compared with air; this seemed advisable due to the scarcity of Freons during the war.

In Figures 5, 6, and 7, the advantages of SF_6 over nitrogen in a nonuniform field are very pronounced. In design of apparatus such a field is avoided wherever possible but sometimes only a compromise is possible. A distortion of the field always is associated with boundary surfaces between the gas and solid insulating barriers, wire insulation, and insulated supporting structures. An isolated winding or a bushing ground sleeve or tank part may provide the most sharply curved electrode so both polarities of impulse test are of importance in evaluating the performance of a gas in a nonuniform field. Positive impulse polarity applied to the electrodes of sharper profile renders lower breakdown values for gases than does the application of negative impulse polarity.

In the discussion of results thus far, the advantages over air or nitrogen at atmospheric pressure have been emphasized because this is a promising field of application. As the pressure is increased some of these gases show even more pronounced advantages over nitrogen. Therefore, another question is posed; are any of the gases suitable for replacing oil in some high-voltage apparatus?

In Figures 4, 10, 11, and 12 a comparison of the various gases is shown in a uniform field and in the nonuniform field up to 30 pounds gauge pressure. The insulation strength of oil is indicated by a horizontal line on each graph, because it is affected little by pressure. The comparison is made at 1-inch spacing in the case of the nonuniform field. This provided a high level of breakdown and was not near the 2-inch limit of the cell. In Figures 4 and 10, SF_6 and F-12 appear most hopeful in the comparison of the various gases with oil in a uniform field. However, in the nonuniform field data of Figures 11 and 12, F-12 suffers decreased strength with increase in pressure, both with 60-cycle and positive impulse voltages. Sulphur hexafluoride shows an increase in dielectric strength with pressure in Figures 4, 10, 11, and 12 and thereby at 30 pounds gauge pressure merits careful comparison with oil.

The results of a more detailed comparison between SF_6 and oil in a nonuniform field are shown in Figures 13, 14, and 15. The tungsten rod was varied in position up to a distance of 2 inches from the 1-inch diameter grounded sphere and the resulting breakdown values plotted on these graphs. The tests were made at 0, 15, and 30 pounds gauge pressure of SF_6; finally, the same tests were made with the electrodes immersed in oil. The positive impulse polarity applied to the tungsten rod is the criterion of the lowest impulse strength for SF_6; the polarity effect in the case of oil is negligible. Since either polarity is possible in field applications, the impulse strength of the gas and the liquid should be compared upon the basis of their individual low polarity values as shown in Table I (at 1-inch spacing). Table I is a comparison of data from Figures 4, 10, 13, 14, and 15.

In actual apparatus, neither the uniform field nor the severe nonuniform field will obtain; these conditions represent the extremes of the problem. Consequently SF_6 will not have the advantage of 115 per cent 60-cycle strength shown in one case, nor the disadvantage of only 73 per cent impulse strength of the nonuniform field used for these tests.

From the foregoing discussion, it appears possible that at a pressure of 30 pounds gauge the dielectric strength of SF_6 approaches that of oil. The deficiencies in dielectric strength of SF_6 are small enough that special considerations of

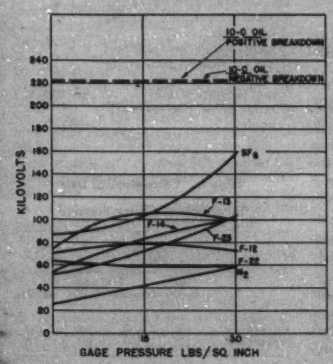

Figure 12 (left). Impulse dielectric strength of gases

Positive wave tests made between tungsten rod and 1-inch-diameter sphere spaced 1 inch. Positive and negative dielectric strength values of number 10-C oil are shown for comparison

Figure 13 (right). Sixty-cycle dielectric strength of SF_6 gas

Tests made between tungsten rod and 1-inch-diameter sphere (grounded). Dielectric strength of oil shown for comparison

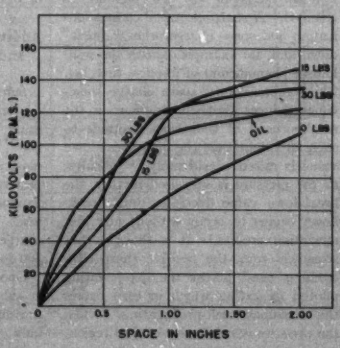

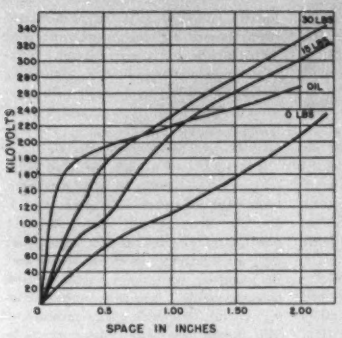

Figure 14 (left). Negative impulse dielectric strength of SF_6 gas

Tests made between tungsten rod and 1-inch-diameter sphere (grounded). Dielectric strength of oil shown for comparison

Figure 15 (right). Positive impulse dielectric strength of SF_6 gas

Tests made between tungsten rod and 1-inch-diameter sphere (grounded). Dielectric strength of oil shown for comparison

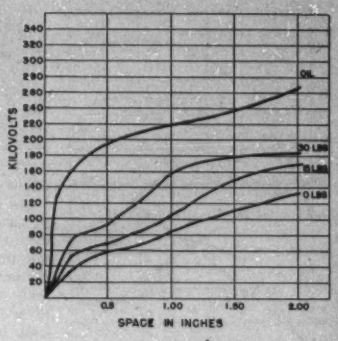

spacing and control of dielectric field may place it upon equal footing with oil in some high-voltage apparatus.

In Figures 11 and 12, which concern 60-cycle and positive impulse breakdown in the nonuniform field, it is noteworthy that some of the halogenated gases show a decrease in dielectric strength with increasing pressure. F-12, F-13, and F-22 do not exhibit a uniform rise in breakdown strength with increasing pressures; in fact, their breakdown strength levels off or decreases.

F-14, F-23, and SF_6 probably would exhibit "anomalous breakdown decrease with pressure" at pressures above the range investigated with the nonuniform field arrangement. This phenomenon has been previously reported for halogenated gases,[1,2] and also for nitrogen.[3] These investigations have supplied at least a qualitative picture for the departure from Paschen's law, and it may be invoked again to explain the present results.

With more complex gases, space charge and its attendant slow diffusion preclude uniform behavior as the pressure is changed. A sharp electrode creates ionization and space charge prior to breakdown and, for example, causes the well-known phenomenon of impulse time lag. This prebreakdown space charge sometimes reduces the field gradient in the neighborhood of the sharp electrode to such an extent that the final breakdown value is raised considerably.[2,3] Finally, as the pressure is increased further, the breakdown value decreases until breakdown begins to occur without any preionization process.[1] It is thought that streamers from the positive sharp electrode progress across the gap creating photon ionization which in turn makes the streamers self-propagating. When the pressure is below this critical region, preionization occurs first and the breakdown streamer has to break out through a cloud of space charge before it causes failure by propagating itself across the gap. As the pressure is increased, the diffusion of the ions of space charge is decreased, so that streamer propagation may start at the positive electrode before any extensive space charge cloud is formed. The streamer formation and propagation process is quite rapid and begins as soon as an ionizing positive potential is applied to the sharp electrode. Electrons are directed toward it; and upon acquiring sufficient energy from the electric field, these lead to an avalanche moving toward the positive electrode. A relatively slow-moving stream of positive ions are left in the wake, and until they diffuse throughout the volume they constitute an extension of the positive point. This filament extension propagates itself by causing photon ionization in the gas ahead and attracting new avalanches. With simple gases such as helium and hydrogen, diffusion is much greater so that such space charge anomalies are absent as a function of pressure.

Additional Characteristics of SF and Physical Data[5]

Sulphur hexafluoride is a colorless, odorless, tasteless, and noncombustible gas. The solid is a white crystalline mass; the gas is nontoxic. One of the most attractive features about its prospective application is that it is noninflammable and quite inert. It is stable when exposed to a silent electric discharge or when heated to approximately 500 degrees centigrade.

Good stability is shown when this gas is subjected to an arc at atmospheric pressure over a mercury surface in a glass bulb. After one hour of continuous arcing about one per cent of the gas is decomposed. Both the mercury (used for sealing) and the metal electrodes were attacked by the products of decomposition. Examination of the solution formed by collecting the gaseous decomposition products dissolved in water showed the presence of fluoride and sulphite ions.

Dry sulphur hexafluoride has no effect on ordinary metals (copper, steel, silicon steel, and aluminum). Tests were made at 110 degrees centrigrade with this gas at a pressure of 50 pounds per square inch. Examination of the gas at the end of a long aging period showed no evidence of decomposition. The metals had not changed either in appearance or weight.

Aging tests made at 100 degrees centigrade on kraft paper in the presence of sulphur hexafluoride show that at the end of the tests the reduction of the tensile strength is much less than when paper is aged in the presence of air.

Chemical formula	SF_6
Molecular weight	146.06
Gas density relative to air	5.106
Critical temperature, degrees centigrade	54
Weight, pounds per cubic foot (at 20 degrees centigrade and 760 millimeters)	0.406
Vapor pressure of liquid	See Figure 1
Melting point, degrees centigrade	−50.8

Table I. Comparison of Data

Thirty Pounds Gauge Pressure

	Uniform Field		Nonuniform Field	
	60 Cycles	Impulse	60 Cycles	Impulse
Oil, per cent	100	100	100	100
SF_6, per cent	75	100	115	73

Sublimation point, degrees centigrade.....−63.8
Coefficient of thermal expansion of liquid (average −20 degrees centigrade to −50 degrees centigrade) per 1 degree centigrade.....0.0029
Refractive index of vapor, n20/D, 760 millimeters.....1.000783
Heat conductivity at 25 degrees centigrade 7.1×10^{-5} calory per centimer per degree per second
Coefficient of viscosity at 25 degrees centigrade.....1.61×10^{-4}
Dielectric constant at 27.5 degrees centigrade.....1.00191

Summary

Compressed gases have been rather slow in finding applications in high-voltage apparatus, especially of the outdoor type. To compete with liquid insulation such apparatus had to be operated at relatively high pressures in order to have the dielectric strength of the former. However, the most serious drawback was the liquefaction that occurred at temperatures within the outdoor ambient range.

Sulphur hexafluoride is now available and surmounts these two difficulties. It also merits consideration because of the possibility of improving the design of air-filled apparatus at atmospheric pressure.

Impulse and 60-cycle breakdown tests performed on a group of halogenated compounds in uniform and nonuniform fields indicate that sulphur hexafluoride has superior qualities over the Freons. Thus, this gas increases in dielectric strength with pressure increase until it merits favorable comparison with oil at 30 pounds gauge pressure.

The more important advantages of gaseous insulation, as maintained by a pressure of SF_6, over liquid and solid insulation may be enumerated as follows:

1. By using sufficient pressure, the dielectric strength of some gases may rival that of mineral oil. SF_6 accomplishes this at a lower pressure than any other gas explored thus far.

2. Sulphur hexafluoride and other gases in general are not subject to permanent cumulative breakdown as is solid insulation.

3. Sulphur hexafluoride is stable at high temperatures. Most important is the fact that it is nonflammable.

4. Gases are generally self-healing after breakdown, except where a creepage path over solid insulation is involved. If decomposition of the gas results in a carbon deposit, a permanent type of defect remains. This does not apply to SF_6 because no carbon is contained in its molecular structure.

References

1. Effect of Pressure on Point-to-Point Plane Discharge in N_2, O_2, CO_2, SO_2, SF_6, CCl_2F_2, A, He, and H_2. H. C. Pollock, F. S. Cooper. *Physical Review*, (New York, N. Y.), volume 56, July 1939.

2. Breakdown Studies in Compressed Gases, Alvin H. Howell. AIEE Transactions, volume 58, 1939, May section, pages 193–204.

3. High-Pressure Gas as a Dielectric, Gordon C. Nonken. AIEE Transactions, volume 60, 1941, December section, pages 1017–20.

4. United States Patent 2,221,671. F. S. Cooper.

5. *Technical Data Sheet 352*. Hooker Electrochemical Company, Niagara Falls, N. Y.

6. Dielectric Strength of Insulating Materials, E. E. Charlton, F. S. Cooper. *General Electric Review*, (Schenectady, N. Y.), September 1937, page 438.

7. The Mechanism of the Electric Spark (book), Leonard B. Loeb, John M. Meek. Stanford University Press, Stanford University, Calif., 1941.

8. The Electric-Spark Discharge on Different Gases, T. E. Allibone, J. M. Meek. *Journal of Scientific Instruments*, (London, England), volume 21, 1944.

9. The Electric Strength of Air at High-Pressure—II, H. H. Skilling, W. C. Brenner, AIEE Transactions, volume 60, 1941, March section, pages 112–5.

Discussion

G. C. Nonken (General Electric Company, Pittsfield, Mass.): The work of the authors represents a valuable contribution in presenting the data on a wide variety of halogen gaseous compounds. The ideal physical and chemical characteristics of SF_6 combined with its high dielectric strength make it a very attractive gas for a high-voltage dielectric. For a score of years or more the chemists who were able to make fluorine made small flasks of SF_6 by direct reaction of sulfur with fluorine. They marveled at its remarkable physical and chemical stability, but found no practical use for it.

The curious phenomena of the decrease in breakdown strength of nonuniform field gaps with increasing gas pressure has been associated with the rate of diffusion of space charge of the positive ions. Since ion diffusion is inversely proportional to the square root of the molecular weight, it is of interest to plot the critical pressure at which the breakdown strength of these nonuniform field gaps start to drop off against the molecular weight of the gas. The data for this curve, Figure 1 of this discussion, were taken from the authors' Figure 11, from the authors' references 1 and 3, and from data by Goldman and Wul.[1]

It is seen that these data lay close to similar curves for all of the gases shown here except SF_6.

A familiar characteristic of sphere gaps, when used in open air and spaced apart up to a spacing of one fourth their diameter, is that they have a unity impulse ratio. The

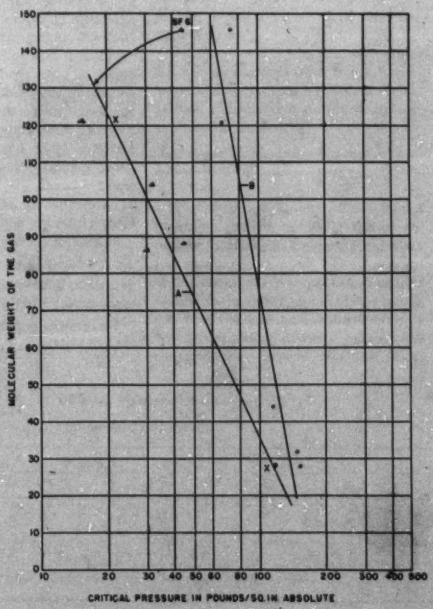

Figure 1. "Critical" pressure for nonuniform field gaps versus molecular weight of gas

Curve *A*—Alternating voltage applied
△—Camilli and Chapman
X—Nonken
⊙—Goldman and Wul
Curve *B*—Direct voltage applied
•—Pollock and Cooper

writers' work on high pressure gas dielectrics (reference 3 of the paper) shows a unity impulse ratio for nitrogen and other gases when tested between 6.25-centimeter spheres spaced 1 and 2 centimeters apart in a tank 4 feet in diameter, at pressures up to 200 pounds per square inch. However, the authors' Figures 4 and 10 show an impulse ratio of 2.7 for nitrogen at atmospheric pressure when tested between 1-inch spheres spaced one fourth inch apart. The impulse ratios of the other gases shown in these data are all greater than unity and vary between 1.3 and 1.7. The writer suggests that this impulse ratio greater than unity, particularly for nitrogen, may be due to the close proximity of the porcelain or other parts of the authors' test cell to the test gap.

Reference

1. Breakdown of Compressed Nitrogen in a Nonuniform Field—II, I. M. Gotéma, B. M. Wul. *Journal of Technical Physics* (USSR), volume 3, 1935, pages 16–27.

Calculating Probability of Generating Capacity Outages

W. J. LYMAN
FELLOW AIEE

THE SUBJECT of generating station capacity outages has been receiving an increasing amount of attention and the use of probability calculations to facilitate these studies has been gaining ground steadily. A practical method for evaluating outage probabilities is of considerable value, not only to aid in determining the proper amount of reserve capacity, but also in analyzing the effectiveness of interconnections, studying the effect of adding large generating units on reserve requirements, and miscellaneous problems of power station design and system operation.

A more extensive use of the probability theory for this purpose has been limited by the complex and time consuming calculations which are sometimes necessary. The binomial theorem and its application in this connection are fairly well known and when dealing with generating units of equal capacity, the calculations are relatively simple. However, very few systems have generators all of the same capacity, and the problem usually becomes quite involved.

The purpose of this paper is to present several methods which have been developed to obtain an approximate solution to complicated probability calculations. Such approximate methods are believed to be useful in the absence of an exact solution which would require much more time, particularly in view of the fact that such calculations do not involve exact data and are not expected to yield precise results. The basic data are equipment outage rates which obviously are based upon experience, which are different for different machines, and which vary widely from year to year. Even an exact determination of the probability of a certain capacity outage is, after all, only a statement of the limit which the average of future events will approach over a long period of time. The actual expectation for any one year, or even a period of five years, will vary considerably from the most probable mean value. Furthermore, whether the allowable probability for a certain occurrence should be 0.0005 or 0.00001 or some other value is largely a matter of judgment. Thus, methods which facilitate comparisons between various proposals and yield absolute values with reasonable accuracy have been found to be very useful. These approximate methods are intended to supplement rather than entirely replace the longer and more exact calculations.

This paper will describe the following devices which have been useful in making generator outage probability calculations:

1. A short-cut method applicable to a system with any number of generating units of different sizes.
2. Equivalent failure rates for different types of turbine and boiler layouts.
3. Method of combining two or more outage probability curves for different systems.
4. Effect on system outage probability curve of adding a generating unit.
5. Approximation with different equipment failure rates.

Hypothetical System

In the examples to follow, failure rates of 0.01, for both turbines and boilers, have been used since extensive industry-wide surveys, over several years, have shown performance to approximate these values for medium pressure plants. Caution should be exercised in using actual failure figures for any one system unless experience has involved enough machines over a long enough period to make the results statistically stable. This condition usually is not realized on a moderate sized system.

For purposes of illustration, a hypothetical system has been used which is patterned closely on unit sizes for a typical system. The boiler and turbine sizes are as shown in Table I.

Exact Method

Since there are 66 units, the binomial expansion[1] would be $(0.01+0.99)^{66}$ assuming that the failure rate for boilers and turbines is 1 per cent. The expansion of this binomial will show the probability of different numbers of units being out of service at the same time, but will not give the corresponding capacity outages because of the variation and unit sizes.

Table I. Number of Units

(B = Boilers; T = Turbines)

Unit Size, Megawatts	Plant A		Plant B		Plant C		Plant D		Total	
	B	T	B	T	B	T	B	T	B	T
10					26		12	2	38	2
20						2		3		5
30	2		6			3			8	5
40						3		1		4
60				3						3
70		1								1
									46	20

Paper 47-252, recommended by the AIEE power generation and system engineering committees and approved by the AIEE technical program committee for presentation at the AIEE Midwest general meeting, Chicago, Ill., November 3–7, 1947. Manuscript submitted August 18, 1947; made available for printing September 24, 1947.

W. J. LYMAN is engineering assistant to the manager in the planning and development department, Duquesne Light Company, Pittsburgh, Pa.

Table II. Outage Probabilities for Plant B

Six 30-Megawatt Boilers with Common Steam Header; Three 60-Megawatt Turbines

Megawatt Outage	No. of Units Out: Boilers	Turbines	Total	Probability of Each Combination	No. of Combinations**: Boilers	Turbines	Probability	Total Probability
0	0	0	0	0.913517247*	1	1	0.913517251	0.913517251
30	0	0	1	0.009227447	6	1	0.055364685	0.055364685
60	2	0	2	0.000093207	15	1	0.001398106	0.030800521
	2	1	3	0.000000941	15	3	0.000042345	
	1	1	2	0.000093207	6	3	0.001677727	
	0	1	1	0.009227447	1	3	0.027682343	
90	3	0	3	0.000000941	20	1	0.000018820	0.000019420
	3	1	4	0.000000010	20	3	0.000000600	
120	4	0	4	0.000000010	15	1	0.000000150	0.000297170
	4	1	5	$0.0^{10}/961$†	15	3	0.000000004	
	4	2	6	$0.0^{12}/970$	15	3	0	
	3	2	5	$0.0^{10}/961$	20	3	0.000000005	
	2	2	4	0.0000000010	15	3	0.000000450	
	1	2	3	0.000000941	6	3	0.000016938	
	0	2	2	0.000093207	1	3	0.000279622	
150	5	0	5	$0.0^{10}/961$	6	1	0.000000001	0.000000001
	5	1	6	$0.0^{12}/970$	6	3	0	
	5	2	7	$0.0^{14}/980$	6	3	0	
180	6	0	6	$0.0^{12}/970$	1	1	0	0.000000952
	6	1	7	$0.0^{14}/980$	1	3	0	
	6	2	8	$0.0^{16}/990$	1	3	0	
	6	3	9	$0.0^{17}/1$	1	1	0	
	5	3	8	$0.0^{16}/990$	6	1	0	
	4	3	7	$0.0^{14}/980$	15	1	0	
	3	3	6	$0.0^{12}/970$	20	1	0	
	2	3	5	$0.0^{10}/961$	15	1	0.000000001	
	1	3	4	0.000000010	6	1	0.000000010	
	0	3	3	0.000000941	1	1	0.000000941	
								1.000000000

* $P_0 = (0.99)^6$; $P_1 = (0.01)(0.99)^5$; $P_2 = (0.01)(0.99)^4$; and so forth.

**Combinations of two units out of six $= \frac{6!}{2!4!}$ or $\frac{6 \cdot 5}{1 \cdot 2}$; three units out of six $= \frac{6!}{3!3!}$ or $\frac{6 \cdot 5 \cdot 4}{1 \cdot 2 \cdot 3}$; two units out of three $= \frac{3!}{2!}$ or $\frac{3 \cdot 2}{1 \cdot 2}$

† $0.0^{10}/961 = 0.0000000000961$.

For example, three units out might result in capacity outages from 20 megawatts (two boilers and one turbine at plant *C* or *D*) to 190 megawatts for three large turbines. The outage probabilities, therefore, have to be worked out using the various combinations of unit sizes and also the fact that simultaneous boiler and turbine outages at the same plant do not add up (each plant has a common steam header). One straightforward method would be to determine the probabilities for each station separately and then combine them in groups of two. Table II illustrates how the outage probabilities can be computed for plant *B*. The other plants can be calculated in the same manner, plants *C* and *D* obviously being more complicated because of the greater number of units. Table III illustrates how plants *A* and *B* can be combined to get the over-all outage probabilities. This total then can be combined with plant *C* and the combination in turn combined with plant *D*. The result of this calculation is shown plotted as an outage probability curve on Figure 1 (curve *A*).

Strictly speaking this is a discontinuous curve. The only points which have actual significance are those at the calculated intervals. The points could be connected by a stepped curve wherein the length of each horizontal step would be the probability of having exactly that amount of capacity out of service. For practical purposes, however, it is usually more convenient to connect the points directly or to draw a smooth curve through them. This procedure is justified by the fact that capacities of the various units usually are rounded off to facilitate calculations with the result that capacity outages between the calculated points are possible. Furthermore, conditions frequently arise where unit capacities may be reduced by troubles such as induced draft fan outages or poor condenser vacuum, thus also giving capacity outages between the calculated points. In the following discussion outage probability curves usually will be plotted as smooth rather than stepped curves.

Short-Cut Method

A much quicker method has been developed whereby approximate outage

Table III. Combination of Outage Probabilities of Plants *A* and *B*

Megawatt Outage	0	30	60	70	90	100	120	130	150	160	180
Probability—Plant *B*	0.91352	0.05536	0.03080		0.000019		0.000297		0.000000		0.000001
Plant A											
Megawatts / Probability											
0 / 0.9703	0.88639	0.05372	0.02990	0.00000	0.000018		0.0002882		0	0	0.0000010
30 / 0.0196		0.01790*	0.00108		0.000603		0.0000004		0.0000058		
70 / 0.0101				0.00922		0.000559		0.000311		0.0000002	
Probability—Plants *A*—*B*	0.88639	0.07162	0.03098	0.00922	0.000621	0.000559	0.0002886	0.000311	0.0000058	0.0000002	0.0000010
Cumulative	1.00000	0.11361	0.04199	0.01101	0.001787	0.001166	0.000607	0.000318	0.0000070	0.0000012	0.0000010

*Product of 0.91352 for 0 megawatts at plant *B* and 0.0196 for 30 megawatts at plant *A*.

probability curves can be computed for any system no matter how many units, or how many different sizes of units are involved in a matter of one or two hours. This method is particularly useful for studies involving interconnected systems where the large number of units would make the exact solution tedious. It should be used cautiously, however, for determining small differences between different outage probability curves.

Referring again to the binomial expansion for the 66-unit system, each term gives the probability for a certain number of units being out of service. For example, the fourth term, which is

$$\frac{66\text{-}65\text{-}64\text{-}}{1\text{-}2\text{-}3}\,(0.01)^3(0.99)^{63}$$

shows probability of three units being out of service. The exponential portion of the term, which is equal to 0.00000053, gives the probability that any particular combination to three units is out of service. The coefficient, which is 45,750, gives the number of possible combinations of three units which can be made up from the 66 units. Obviously these groups of three units have widely varying total amounts of capacity and if we knew the proportion of these possible combinations which exceeded any given total, we quickly could determine the probability of exceeding that value of capacity outage with three units out of service. A similar calculation for 1, 2, 4, 5, and so on, units out simultaneously would give the overall probability of exceeding any given total outage.

At this point a statistical tool, namely, the normal distribution curve,[2] can be utilized to calculate the probability that any three units, for example, selected at random from the total of 66 units, will have a total capacity exceeding any given value. By calculating the mean and standard deviation of the unit sizes, a normal distribution curve is, in effect, fitted to the actual sizes. The standard deviation, or σ, is the "root-mean-square" value of the deviation of the individual points from the average or mean value of all the points. If a unit is selected at random from the group, the chance is presumably 50–50 that it will be above average size. Furthermore, the chance is 0.159 that it will exceed the mean by more than σ. The fact that the actual sizes do not fit exactly the normal curve is a source of error, but it has been found that unless they deviate considerably from the standard curve, the final error is relatively moderate. If the unit sizes do not fit a normal curve reasonably well, they should be divided into two groups as explained later.

Table IV. Probability That Total Capacity of n Units Taken at Random Will Exceed Any Given Value

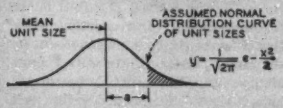

a	P_a	a	P_a
0	0.500	2.5	0.0062
0.1	0.460	2.6	0.00466
0.2	0.421	2.7	0.00347
0.3	0.382	2.8	0.00256
0.4	0.345	2.9	0.00187
0.5	0.309	3.0	0.00135
0.6	0.274	3.1	0.00097
0.7	0.242	3.2	0.00069
0.8	0.212	3.3	0.00048
0.9	0.184	3.4	0.000337
1.0	0.159	3.5	0.000233
1.1	0.136	3.6	0.000159
1.2	0.115	3.7	0.000108
1.3	0.0968	3.8	0.000072
1.4	0.0808	3.9	0.000048
1.5	0.0668	4.0	0.0000317
1.6	0.0548	4.1	0.0000207
1.7	0.0446	4.2	0.0000133
1.8	0.0359	4.3	0.0000085
1.9	0.0287	4.4	0.0000054
2.0	0.0227	4.5	0.0000034
2.1	0.0179	4.6	0.0000021
2.2	0.0139	4.7	0.00000130
2.3	0.0107	4.8	0.00000079
2.4	0.0082	4.9	0.00000048
		5.0	0.00000029

$$a = \left(\frac{C}{n} - M\right)\frac{\sqrt{n}}{\sigma}$$

where

n = number of units out of service
C = assumed value of capacity outage
M = average size of all units
σ = standard deviation of all units
P_a = probability that total capacity of units out of service will exceed C (column 12 in Table V)
= shaded area under curve beyond a divided by total area under curve

$$= \frac{1}{\sqrt{2\pi}}\int_a^\infty e^{-\frac{x^2}{2}}\,dx$$

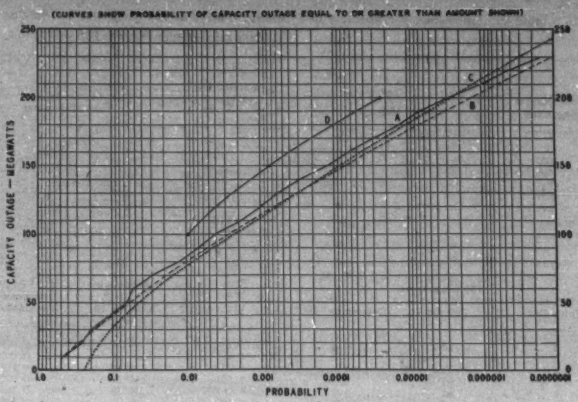

Figure 1. Outage probability curves

Illustration of accuracy achieved by the short-cut method

A—Curve calculated by exact method

B—Approximate curve calculated by short-cut method using all 66 boilers and turbines with a failure rate of 0.01

C—Approximate curve calculated by short-cut method using turbines only (20 units) with a failure rate of 0.011

D—Curve showing effect of adding an 80-megawatt turbine and boiler unit to curve *A*

Figure 2 shows the accumulated distribution curve for the 66 units together with the fitted normal distribution curve.[3] In this case the mean is 19.7 megawatts and the standard deviation, σ, is equal to 14.7 megawatts. A standard table[4] of normal distribution curve functions (given in abbreviated form on Table IV) shows the probability that any unit selected at random from this group will exceed a given value. For example, the table shows that the probability is 0.159 that the capacity would exceed the mean plus the standard deviation ($19.7+14.7=34.4$ megawatts).

When a group of two or more units is selected at random, it can be shown by statistical theory that the probability that the average value for the sample will exceed any given figure also may be determined from a normal probability curve for which the standard deviation is obtained by dividing the standard deviation of the original curve by the square root of the number of units in the sample. For example, with four units out of service σ would equal $14.7 \div \sqrt{4} = 7.35$. Thus, the probability[5] that the average of the four would exceed 34.4 (or that the total would exceed 137.6 megawatts) would be 0.0227

Table V. Calculation of Probability of a Capacity Outage of 150 Megawatts or More on 66-Unit System (Generators and Boilers)

Standard Deviation $= \sigma = \sqrt{215} = 14.7$

1 Unit Size, Megawatts	2 No. of Units	3 Column 1 × column 2, Megawatts	4 Deviation From Avg Size, Megawatts	5 (Dev.)²	6 Column 2 × column 5
10	40	400	−9.7	94.1	3764
20	5	100	−0.3	0.1	1
30	13	390	10.3	106.1	1379
40	4	160	20.3	412.1	1648
60	3	180	40.3	1624.1	4872
70	1	70	50.3	2530.1	2530
Total	66	1300			14194
Average		$M = 19.7$			215

7 n No. of Units Out	8 C/n 150 Megawatts ÷ Column 7	9 C/n − M Column 8 − 19.7	10 $\frac{\sigma}{\sqrt{n}}$ 14.7 ÷ √Column 7	11 a Column 9 ÷ Column 10	12 Pe from Column 11 and Table IV*	13 Pn (0.01 + 0.99)ⁿ	14 P Column 12 × Column 13
2	75	55.3	10.4	5.32	0.000000	0.113	0.0000003
3	50	30.3	8.5	3.57	0.000178	0.0243	0.0000040
4	37.5	17.8	7.35	2.42	0.00776	0.00386	0.0000300
5	30	10.3	6.58	1.57	0.0582	0.000484	0.0000282
6	25	5.3	6.00	0.88	0.1894	0.0000497	0.0000094
7	21.4	1.7	5.56	0.31	0.3785	0.00000430	0.0000016

Probability of outage of 150 megawatts or more = 0.0000735

$$* \frac{1}{\sqrt{2\pi}} \int_a^\infty e^{-\frac{x^2}{2}} dx$$

(from Table IV) since this value is σ above the mean.

Table V shows how this method may be used to compute the probability of having a capacity outage of 150 megawatts or more on the hypothetical system just described. The results of this calculation are shown in Figure 1 to compare with the exact probabilities determined from the long method. It can be seen that the error in the short-cut method is generally less than 8 megawatts, which is not over 6 per cent in the range of probabilities usually considered. Several other checks have been made by comparing the short-cut method with the much longer exact method for calculations of other large power systems and the errors in all other cases have been below 5 per cent. On one actual system of 60 units and over 2,000,000 kw, the error was between 4 and 5 per cent. In another actual system the error was found to be about 1 per cent.

There are two sources of error involved in the short-cut method. The first is the fact that unit sizes do not follow exactly the normal distribution curve. The second error is introduced when boilers and turbines both are considered, since the short-cut method does not recognize the overlapping of boiler and turbine outages within the same plant. These two errors ordinarily tend to offset each other. The overlap problem may be minimized by considering turbines only and using an equivalent failure rate to include the effect of boilers (described in a later section). This also reduces the "non-normal" error because the elimination of boilers, which are usually smaller in size than turbines, results in a more nearly normal distribution curve.

If the actual distributioh of unit sizes departs markedly from a normal curve, it is desirable to divide the units into two groups, separating the large from the small units, obtain an outage probability curve for each group, and combine the two curves by the method described in the following section. It frequently is found that a few of the large units account for the major portion of the outage probability. As an illustration, the four largest units in the 66-unit system described were found to account for more than half the probable outage. By calculating the

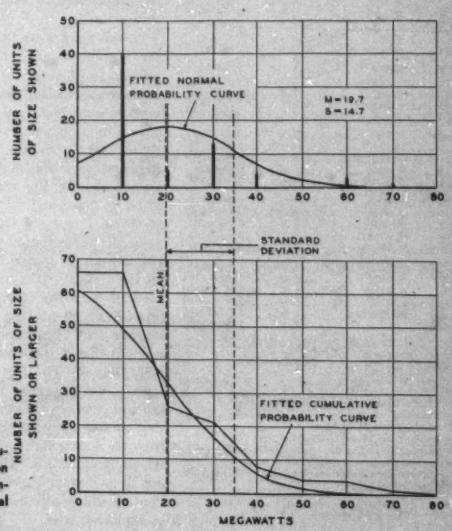

Figure 2. Distribution of unit sizes on 66-unit system compared with normal distribution curve

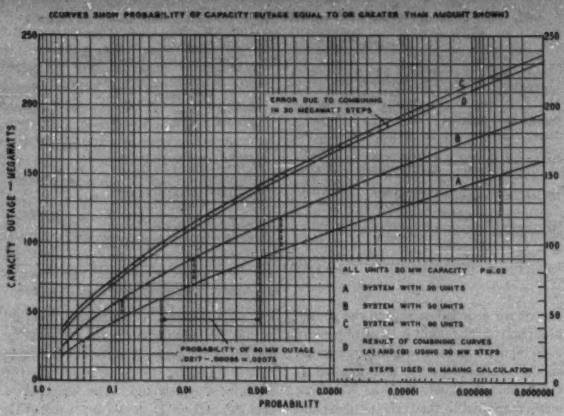

Figure 3. Combination of outage probability curves

Demonstrates accuracy of combining curves *A* and *B* by method shown on Table VI

exact curve for the four large units (a relatively short calculation), obtaining a curve for the remaining 62 units by the short-cut method, and combining the two curves, a result was secured which deviated less than 2 per cent from the results of the exact method and required only a fraction of the time. This modified short-cut method should be used unless the fit between unit sizes and the normal curve is better than that shown on Figure 2.

Combining Outage Probability Curves

It is sometimes desirable to combine the outage probability curves for two or more systems in order to determine the effect of interconnections on the over-all reserve requirements. It is a well known fact that as power systems are combined, the probability of having any given *percentage* capacity outage decreases; or conversely, for a given probability of outage, the percentage of total capacity is reduced. Where two such curves have been worked out by any suitable method, they can be combined quite readily by a step by step process. This is somewhat similar to the method shown on Table III for combining two power plants. Ordinarily the two curves to be combined will not have the same size steps, or there may be so many small steps that the calculations become very involved. Furthermore, the steps may be of different sizes, or the curve may have been prepared without using the step method. In any event, arbitrary steps of equal size can be selected and fitted under the curves. An example is shown on Figure 2 where the two outage probability curves *A* and *B* are combined to obtain curve *D*. This is seen to match quite closely curve *C*, the exact curve for the combined system. The probability of any step of capacity outage can be determined by subtracting the probabilities read from the original curve as illustrated on Figure 2. Table VI shows the calculations in this sample case.

The accuracy of the final result depends upon the number of steps into which the curves are divided. A larger number of steps increases the accuracy, but also increases the complexity of calculation. It has been found that if each curve is divided into 20 steps, the result will be within two or three per cent of the correct value. (The synthetic curve is usually on the low side.)

Equivalent Failure Rates

It is sometimes advantageous to calculate system outage probability rates using turbogenerator sizes only, together with a failure rate which will include the effect of boiler outages. The arrangement of turbines and boilers has a significant effect on outage probabilities. A hypothetical case has been worked out using 20 turbines of equal size with various boiler arrangements in order to illustrate this problem.

Figure 4 shows three typical boiler arrangements together with the outage probability curves. It also shows curves to match each of the three boiler arrangements secured by using different outage rates applied to the turbines only. This case has also been worked out on the basis of one per cent failure rates for both turbines and boilers.

Curves *A* and *B* show that the performance of a unit type station with boilers equal to the turbine sizes, and no steam headers, can be matched almost exactly by applying a failure rate of 2 per cent to the turbines only, that is,

$P = (0.02 + 0.98)^{20}$

Table VI. Combination of Two Outage Probability Curves Using 30-Megawatt Steps

Megawatt Outage	0	30	60	90	120	150	180	210	240
Probability—50-unit system	0.56	0.3616	0.0704	0.00752	0.000458	0.0000194	0.00000061		
30-Unit System									
Megawatts — Probability									
0 — 0.75	0.420	0.2712	0.0528	0.00564	0.000343	0.0000145	0.00000046		
30 — 0.2283		0.1278	0.0836	0.01607	0.001717	0.0001046	0.00000443	0.00000014	
60 — 0.0208			0.0116	0.00752	0.001464	0.0001564	0.00000952	0.00000040	0.000000013
90 — 0.000925				0.00052	0.000334	0.0000651	0.00000596	0.00000042	0.000000018
120 — 0.0000246					0.000014	0.0000089	0.00000173	0.00000019	0.000000011
150 — 0.00000043						0.0000002	0.00000016	0.00000003	0.000000003
Combined Outage Probability	0.4200	0.3990*	0.1470	0.02975	0.003872	0.0003493	0.00002335	0.00000118	0.000000045
Cumulative Probability	1.0000	0.5800	0.1810	0.0340	0.004248	0.0003738	0.00002448	0.00000123	0.000000045

*Probability of total outage of 30 megawatts = probability of 30-megawatts out on 50-unit system and none on 30-unit system (0.3616 × 0.75 = 0.2712) + 30 megawatts out on 30-unit system and none on 50-unit system (0.2283 × 0.56 = 0.1278).

The exact solution would be obtained with a failure rate of 1.99 per cent, that is,

$$P = (0.0199 + 0.9801)^{20}$$

Curve C shows the outage probabilities with boilers the same size as the turbines, but with steam headers, and assuming the units are divided into four plants or groups. The probabilities in this case are reduced below those in case A because some of the multiple outages involve boilers and turbines in the same plant wherein the loss in capacity is less than the combined capacity of boilers and turbines out of service. Curve D shows that this performance can be matched closely by applying a failure rate of 1.7 per cent to the 20 turbines alone.

Curve E illustrates the condition where boilers are one-half the size of turbines and the units again are divided into four plants using steam headers. Thus, there are five generators and ten boilers in each plant. Outage probabilities are reduced greatly compared with case C because of the larger number of smaller boilers.

Table VII. Effect of Adding 80-Megawatt Unit to 66-Unit System Shown on Figure 1

(Assume One Boiler—No Steam Header)

Outage After Addition	Capacity Out, Megawatts: 66-Unit System	Capacity Out, Megawatts: New Unit	Probability: 66-Unit System	Probability: New Unit	Probability: Product	Combined System
100 megawatts or more	100 or more	0	0.00414	×0.98	=0.00405	
	20 or more	80	0.272	×0.02	=0.00544	0.00949
150 megawatts or more	150 or more	0	0.000124	×0.98	=0.000122	
	70 or more	80	0.0301	×0.02	=0.000602	0.000724
200 megawatts or more	200 or more	0	0.0000028	×0.98	=0.0000027	
	120 or more	80	0.00100	×0.02	=0.0000200	0.0000227

the 1.1 per cent failure rate to the 20 turbines only. The result is shown by curve C on Figure 1 and it is seen that the exact curve, calculated by the long method, is approximated closely by the short-cut method applied to the turbines alone and using the equivalent failure rate.

It is interesting to note from this comparison that the unit-type installation requires about 30 megawatts more reserve in order to provide the same service reliability as would be required with boilers one-half the size of turbines and interconnected with steam headers. This difference, amounting to 3.75 per cent of the system capacity, should presumably be matched against the lower cost of the unit-type station.

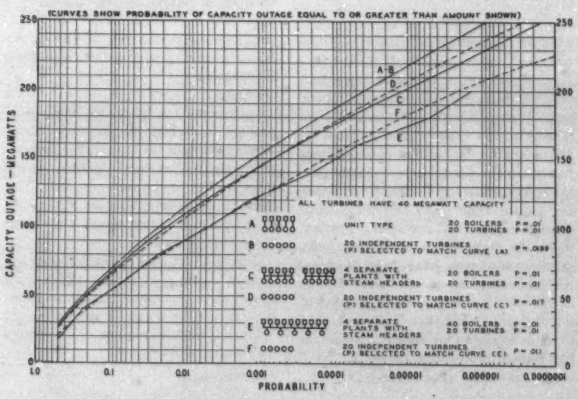

Figure 4. Effect of various boiler-turbine arrangements on outage probability

B, D, and *F* show equivalent failure rates to apply to turbines alone to include approximate effect of boiler outages

This condition is closely approximated by applying a failure rate of 1.1 per cent to the 20 generators disregarding the boilers. Inasmuch as the hypothetical 66-unit system, as described, has about twice as many boilers as turbines, and is made up of four power plants, the outage probability curve was calculated by applying

Effect of Adding a Unit

Plans to add a new generating unit, which possibly may be larger than any of the existing units, frequently raises the question as to the effect on reserve capacity requirements. Assuming that an outage probability curve for the existing system is available, it is usually a simple matter to adjust this curve to include the effect of the new unit. An example of this calculation is shown on Table VII, which shows the effect of adding an 80-megawatt generator and single boiler to the system shown on Figure 1.

This method is based on the fact that a capacity outage of C megawatts can occur in only two ways: a C-megawatt outage on the existing system with the new unit in service, or an outage of (C-80) megawatts on the existing system with the new unit out of service. The results are plotted as curve D on Figure 1 and the difference between this and curve A shows the effect of the new unit. In this case the capacity outage for a given probability is increased about 22 megawatts by the new unit. This may be interpreted in terms of the reserve policy of the company involved. Assuming that a minimum of 12 per cent of the installed capacity is maintained as reserve, this would mean that adding 80 megawatts of new capacity should increase the allowable system peak load by 88 per cent of 80 megawatts, or 70 megawatts (10 megawatts less than the capacity of the new unit). Since the outage probability has been increased 22 megawatts, the new unit must be discounted by 12 megawatts in evaluating the capacity gained. This, however, must be tied in with the capacity of available interconnections. If these are adequate to provide the additional 12 megawatts in an extreme emergency, the capacity discount, due to the large size of the new unit, could be disregarded.

Combining Different Failure Rates

It is sometimes necessary to recognize significant differences in the expected failure rates of different pieces of equipment. Moderate differences in past per-

formance probably do not warrant the use of a number of different rates in the probability calculations. Widely divergent experience, however, must be recognized. This can be done in using the binomial expansion by a method which permits using a uniform failure rate by varying the number of units in each group.

In the general binomial $P=(p+q)^n$ the quantity p is the outage rate or the probability that a unit will be out of service and q is the probability that the unit will be in service. For small values of p such as used in these calculations, it can be shown that the values of the first few terms in the expansion are determined principally by the product np. Thus, if a certain group of units in the problem have a failure rate double that of the rest of the units, this can be handled by using the same value of p but using twice the number of units.

This may be illustrated by comparing two cases

Case I. Ten units; failure rate 0.02; $np=0.2$

Case II. Twenty units; failure rate 0.01; $np=0.2$

Number of Units Out	Outage Probability: Case I—$(0.02+0.98)^{10}$	Outage Probability: Case II—$(0.01+0.99)^{20}$
0	0.817	0.8181
1	0.1667	0.1650
2	0.0153	0.0158
3	0.0008	0.00096

This approximation is sometimes useful with the short-cut method where a number of different types and sizes of turbines and boilers may be all grouped together in one binomial expansion.

References

1. Elementary Statistics and Applications (book). Smith, Duncan. McGraw-Hill Book Company, New York, N. Y., 1944. Pages 279–306.

2. Mathematical Analysis of Statistics (book). C. H. Forsyth. John Wiley and Sons, New York, N. Y., 1924. Pages 136–42.

3. Economic Statistics (book). Crum, Patton. A. W. Shaw Company. Page 198–201.

4. Tables of Probability Functions, Mathematical Tables Project, WPA, National Bureau of Standards, Washington, D. C. Table 1.

Discussion

E. S. Loane (nonmember) and **C. W. Watchorn** (both of Pennsylvania Water and Power Company, Baltimore, Md.): Lyman's suggested short-cut method interests us, because the longer method that we have used for developing the probability of availability of various amounts of capacity is rather time consuming.

The solid line curve (curve A) on Figure 1 of this discussion shows the probability of unavailability of various amounts of steam capacity for the Penn Water-Baltimore-Washington system obtained by a detailed method of computation, taking into account the manner in which the various turbines and boilers are interconnected, their location in various stations, and other factors. The dash line curve (curve B) shows these same data computed on the basis of a shorter method in which the interconnections between the various turbines and boilers on the actual system were disregarded. It was assumed in computing these data that the steam generating capacity was made up of combined boiler and turbine units of the same capacities as the various turbines on the interconnected system. The probability of unavailability of these combined boiler and turbine units was considered to be 2 per cent as compared with 1 per cent for the turbines and 1.24 per cent for the boilers, individually, as used in curve A. The work required in computing the data for curve B was reduced greatly as compared with that required to compute the data for curve A. The difference between the two probabilities of failure to carry the load, computed from curves A and B, is of no practical significance.

The circled dots on the diagram indicated by C thereon, were computed by the short-cut method suggested by Lyman. The computations were based, as in curve B, on combined boiler and turbine units of capacities equal to those of the actual turbines of the interconnected system and a 2 per cent probability of unavailability of such boiler and turbine units. The comparison between these data and those shown by curve B is very close and the differences are of no practical significance.

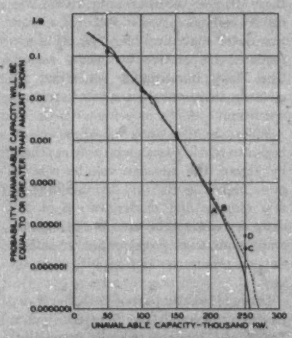

Figure 1. Comparison of the results obtained by different methods of computing the probability of unavailability of various amounts of system steam capacity

A—The exact method

B—The same general method as for curve A but assuming combined boiler and turbine units

C—The Lyman short-cut method applied to the assumptions for curve B

D—The Lyman short-cut method applied to the system boilers and turbines

The crosses on the diagram, indicated by D, also were computed by the short-cut methods. In this case, however, all the turbines on the interconnected system, together with all the boilers of capacity of 10,000 kw or greater, were considered to have an average probability of unavailability of 1.1 per cent. This comparison is still very close and would be improved with the use of an average probability of unavailability of 1.0 per cent instead of 1.1 per cent as used in the computations.

The computation of the data shown by the 5 circles and 5 crosses, together with the time required to understand the instructions for making these computations, required about 3 to $3^1/_2$ hours of our combined time. The possibility of obtaining satisfactory data on the probable availability of system capacity in such a short time is indicative of the real contribution made by Lyman's paper.

The data provided by this short-cut method are not in the exact form to be used in various subsequent calculations, such as the complete evaluation of the probability of failure to carry the load and the determination of the relative merits of various alternate capacity installations. Such computations are based on the probability of unavailability of various discreet amounts of capacity rather than the probability of unavailability of amounts of capacity greater than various specified amounts. The probability of availability of amounts of capacity within specified ranges can be read from curves drawn through the plotted points. Such differences need to be determined very carefully from a curve plotted on logarithmetic paper, otherwise too great differences may be pyramided in subsequent calculations.

The Application of Western Union Multiplex to Navy Radio

RAY HOOVER
MEMBER AIEE

Synopsis: At the beginning of and during the war with Japan, the wide expansion of operations in the Pacific Theater overtaxed the Navy's radio communications to a point where the need of additional communication channels became acute. The adaptation of a 4-channel Western Union type multiplex to a single-channel frequency-shift radio system appeared to be the most logical way to solve this problem quickly. Improvements in the radio and the use of the multiplex enabled the Navy to set up communication channels between the United States and all the principal naval bases in the Pacific. A 4-channel circuit was established between Washington, D. C., and Honolulu, T. H., and San Francisco, Calif., and Honolulu within approximately nine months after the beginning of initial tests. Other systems followed in close succession.

OF the many successful accomplishments of the United States Navy, the feat of providing adequate communication facilities for the conduct of a global war ranks high among those tasks acclaimed "well done." Just prior to Pearl Harbor, the problems confronting Naval Communications became more numerous due to rapidly increasing message load to far distant outposts for operational and administrative purposes, coupled with a growing usage of commercial cable and radio systems by other government agencies, notably the State and War Departments. At the time when most of the new Navy equipment was being allocated to the Atlantic area in support of our allies-to-be, there was available for Pacific coverage only one commercial submarine cable between the United States and the Philippine Islands with intermediate stations at Honolulu, Midway, and Guam, and a few Navy radio circuits which were single radiotelegraph channels operated manually or semiautomatically with tape transmitters and siphon recorders. Full automatic operation of these channels by teleprinters had not yet become fully practical.

With the beginning of hostilities after the Japanese attack on Pearl Harbor, these Pacific facilities immediately became overloaded, and it was only a short time later that the Philippine cable was rendered inoperative by enemy action. The Navy immediately set about increasing the number of radio circuits in operation.

When the allies took the offensive and began to regain bases previously captured by Japan, the message volume rose to even higher levels, and the building of new circuits and modernization of the older systems by the use of printing telegraph equipment could no longer satisfy the new requirements as rapidly as necessary.

During the early part of 1943, the Navy Department asked the Western Union Telegraph Company to assist in expanding message capacity and improving continuity of transmission over the existing Navy radio channels. Captain M. W. Arps, now retired, who was then officer in charge of the Cheltenham naval radio station, was assigned the duty of coordinating the planning and engineering of the project. The scope of the activity and the results achieved by the use of the Western Union multiplex on long Naval radio circuits are described in the following paragraphs.

The Radio Systems

The history of long-distance short-wave transmission shows that the most useful radio systems fall into two general classes of development. The first of these, intended for radiotelephony, comprise the single-side-band systems which conserve frequency spectrum and power to the highest degree. The most advanced design provides two telephone channels, one on either side of the carrier frequency, which is not transmitted. The systems of the other group comprising the second class of development are intended for radiotelegraphy, and were originally of the keyed continuous wave type. For many years semiautomatic tape sending and siphon recording on paper tape were used. To overcome the frequent loss of signal caused by selective fading of the single frequency, it became conventional to employ a frequency deviation of about 500 cycles in the carrier frequency in addition to the keying modulation. But when it became necessary to improve operation by connecting printing telegraph equipment to the terminals, it was found that the presence of echo signals and impulse noise made automatic operation impractical except on the very best circuits. Then followed a period during which terminal signal regeneration and antenna improvements, together with higher power, made possible the use of printers on a few of the better circuits. But these circuits were not dependable to the degree ordinarily experienced with ocean cable transmission. The invention of the error-proof printer, requiring seven instead of five code pulses per letter removed practically all of the remaining uncertainty,[1] but this required higher keying speeds for the same word speed, and rather complicated translation apparatus if transmission was to be integrated with systems employing 7-unit start-stop transmission, such as the teleprinter. Also, it should be remembered that space diversity reception was considered necessary to eliminate the effects of signal fading,

Paper 47-257, recommended by the AIEE communication committee and approved by the AIEE technical program committee for presentation at the AIEE Midwest general meeting, Chicago, Ill., November 3–7, 1947. Manuscript submitted September 18, 1947; made available for printing September 24, 1947.

RAY HOOVER is assistant to automatics research engineer, Western Union Telegraph Company, New York, N. Y.

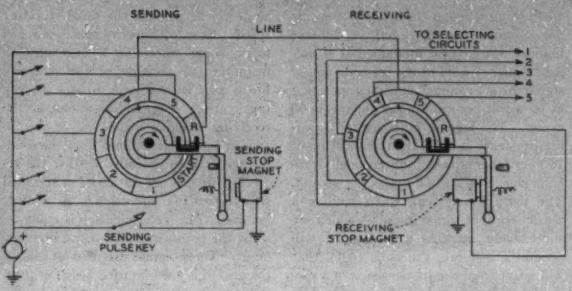

Figure 1. Elementary theory of a 7-unit start-stop telegraph system

which required such values of antenna separation that the system could only be used on fixed circuits, and was not suitable for transmission to air and surface ships of the Navy.

The remaining significant improvement applied to Navy radiotelegraph circuits during the first years of the war was frequency-shift keying. In this system, one frequency is employed for the marking pulses, and another frequency approximately 850 cycles removed is used for the spacing pulses. Frequency-shift keying had been used on wire circuits since 1938.[2] The carrier has substantially constant amplitude, but the instantaneous frequency may vary abruptly or gradually between the two limits. Hence it is a frequency modulation of the carrier frequency by a modulating wave which is obtained from the keying relay, but with a certain amount of shaping applied to the normally square signaling wave to reduce the band width required for transmission. This type of transmission is distinguished from 2-tone transmission in that a frequency-modulation detector and limiters are employed to convert the received signals into direct currents which operate the receiving relay.[3] The limiters act as fast automatic level controls which help overcome rapid fading, and without danger of raising the noise to the level of the signal, since the signal is transmitted constantly instead of intermittently. The system is relatively insensitive to impulse noise, and remains free of bias distortion resulting from rapid level changes. However, it requires approximately the same band width as the single-side-band telephone system previously mentioned, as contrasted with the narrow band originally needed for a continuous wave system.

It should be mentioned that the radiotelephone systems were multiplexed more easily, that is, made to carry several telegraph channels, by frequency division methods,[4] whereas the radiotelegraph circuits already consisted of single telegraph channels which could be multiplexed only by time division methods. The former system suffered the disadvantage that the available power of the transmitter had to be divided between several frequency bands, one for each telegraph channel, and the further disadvantage that two or more tone frequencies had to be used for each marking or spacing signal to avoid the effect of selective fading. Therefore, it was wise that the Navy decided to adopt frequency-shift keying which resulted in the best signal quality available, and then found a means to speed up the message flow over this system.

Initial Tests

When we first started work on the problem, a high-speed teleprinter which was under test in Western Union's New York laboratories was considered. It was thought that this machine would suffice for the interim of further research. One model geared to operate at 107 words per minute was dispatched to Cheltenham where it was placed under test. A distributor transmitter making use of a prepared tape was used to originate the signals, and circuits were set up on radio channels between Cheltenham and distant points such as Honolulu and Balboa, C.Z., where the signals were "repeatered" back to the printer. These tests were satisfactory, but since Western Union was not tooled for production of these printers, and only a few laboratory models were immediately available, it was necessary that we look for other ways for a final solution. Tests had already been started on the use of multiplex equipment and it developed that immediate delivery could be made if standard equipment could be used. A test using a standard Western Union 4-channel multiplex was made over a Navy radio circuit between Cheltenham and Honolulu with the signals repeatered back to Cheltenham from Honolulu, and while the actual printing test was of short duration, it was demonstrated that the use of the 4-channel multiplex was within the realm of possibilities. Further to test the system for printing margins, a circuit was set up from the New York laboratories over a wide-band-carrier channel to Washington and a Navy tone channel to Cheltenham, using the same radio system as previously used to and from Honolulu. The signals were retransmitted to New York over Navy tone and carrier channels. These tests enabled us to determine the weak points in the system. It also proved beyond all reasons for doubt that the application of multiplex to radio could become a reality with a minimum amount of effort. During these tests Naval observers were picking out flaws in the radio equipment, and as a result, they made recommendations on desirable changes in the standard Navy radio equipment. It also was suggested that consideration be given to the use of 7-unit start-stop teleprinters for recording the signals at the receiving side of the multiplex system instead of the conventional 5-unit multiplex printer. This would permit the extension or "repeatering" of a single channel into another radio link or to some remotely located outpost without the necessity of manual handling. It also was considered desirable to use a recently developed fork corrector instead of the conventional mechanical or motor type of corrector for maintaining the proper phase relation between the sending and receiving multiplex terminal sets. Both the Navy Department and Western Union set out to accomplish the changes agreed upon, and in April 1944 the first sets were installed in Washington and Honolulu. After the initial tests, that required less than a week, these two offices were interchanging messages at the rate of 60 words per minute per channel in each direction which is 240 words per minute over four multiplex channels working on a single Navy radio channel. Other installations followed in rapid succession. Practically all Naval bases of operation in the Pacific ultimately were equipped with this type of operation.

The Baudot and International Morse Codes

As a character of the Baudot code may have successive signal impulses of the opposite polarity, the maximum number

of cycles required to transmit the five impulses of a single character will be 2.5. All characters or functions of the Baudot code are transmitted in equal lengths of time, as distinguished from the International Morse code which requires differing lengths of time for the transmission of different characters. Operating speeds of telegraph circuits usually are stated in terms of words per minute transmitted, the average length of the word being assumed as five letters and a space. In the Baudot code, therefore, 30 signal impulses must be transmitted to convey any such word to the distant point. In the International Morse code varying numbers of such impulses are required, depending on the word considered. A dot requires the time of two impulses; a dash four; the interval between letters two; and between words two additional. It has been determined that a word representative of the average of 5-letter words is "Paris" and the time of 48 signal impulses is required to transmit it in Morse. The 4-channel multiplex system described in this paper and using Baudot code transmits 240 words per minute. From this ratio of length of codes, 30–48, it will be seen that the time length of the shortest signal impulse at this rate of transmission will be equivalent to the time length of the shortest signal impulse of the International Morse code when transmitted at the rate of 150 words per minute. Or if stated in another manner, the highest fundamental signaling frequency used in the transmission of signals by a 4-channel multiplex operating at 60 words per minute per channel is 60 cycles. The highest fundamental signaling frequency used in the transmission of 150 words per minute International Morse code signals is also 60 cycles per second. The multiplex system, when sending a steady train of signal impulses which are successively marking and spacing, will produce, therefore, the same signal that will result from the transmission of a succession of International Morse Code dots at the rate of 150 words per minute. The multiplex as applied to land line circuits[5] has been in use by Western Union since 1913.

Synchronization Between Receiving and Sending Terminals

It will be recalled that in order to maintain the brushes at the sending and receiving ends of the system in synchronism, and in phase with each other, each of the brush arms on the distributor is driven by an impulse motor, this motor being controlled by a tuning fork which is equipped with suitable contacts. When the system is first put into operation, both the sending and receiving tuning forks are set at as nearly as possible the same vibrating speed. Even with highly constant speed forks, some correction is necessary to maintain the position of the receiving brush arm with respect to the sending brush arm. A corrector system at the receiving terminal makes use of the incoming intelligence signal from the sending terminal to indicate whether the receiving brushes are advanced or retarded with respect to the position of the sending brushes. This determination is made by using the points at which signal reversals occur. These signals are used to control the grid of a vacuum tube which in turn, through its associated control circuits, varies the current through a damping coil applied to the tuning fork, either to slow down or speed up the vibrations of its tines.

Theory of the Multiplex as Applied to the Navy Radio Systems

To make the multiplex system applicable to the Navy's communications system, a start-stop 7-unit teleprinter was substituted for the conventional 5-unit multiplex printer. This substitution eliminated the necessity of manual retransmission from a multiplex radio circuit to a teleprinter radio circuit or a land line circuit. Because of the fundamental difference in operation of a multiplex

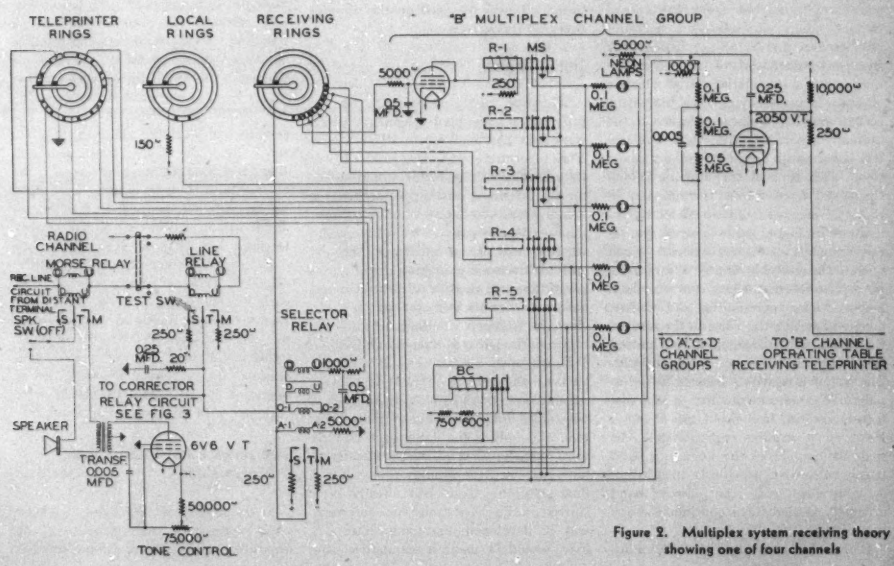

Figure 2. Multiplex system receiving theory showing one of four channels

system and a start-stop system, it was necessary to provide means on the receiving terminal distributor for converting the signals to the desired form. Figure 1 shows in theory a start-stop system. The distributors differ from those of a multiplex system in that the brush arms are driven by an electric motor through a friction clutch. Both brush arms are driven at a constant speed by synchronous or accurately governed motors. The receiving arm is slightly faster than the sending arm so the start signal at the sending distributor will cause the brushes to leave the rest segment on the receiving distributor at the proper time thereby maintaining the phase relation between the two stations. This system[5] commonly is called a start-stop 7-unit system, five units being used for transmitting intelligence, and the other two for synchronizing purposes. The segment positions on the receiving face plate are such that the brushes rotate simultaneously over similarly numbered segments at the two terminals. Each of the individual selecting circuits at the receiving terminals has a marking or spacing signal applied to it in accordance with the positions of the keys at the sending end. In the multiplex system it was not possible to initiate the start and rest pulses at the sending end, so to make it adaptable to the Navy's needs it was necessary that a storage means be provided at the receiving terminal in order that these two pulses could be inserted locally after the five intelligence pulses had been received.

Assuming that the signals originate in a transmitter at the sending end in the multiplex system, Figure 2 shows the receiving channel theory as finally developed for the Navy Department. Associated with each of the four receiving channels were five storage relays, five *6V6* vacuum tubes, five neon lamps, and a single *2050* vacuum tube. Common to all four multiplex channels were a polar line relay, a selector relay, and a second polar relay associated with a *6V6* tube and loud speaker. The polar line relay is used to receive the signals from the radio circuit. Applied to its spacing and marking contacts are positive and negative battery, respectively. This relay, as it operates, applies a signal to the corrector relay, Figure 3, and also to a coil of the selector relay, Figure 2. The ground connection through a capacitor and resistor to the line relay tongue merely acts as a spark protection circuit. The selector relay, which has three of its coils connected in series to the tongue of the line relay, together with the receiving rings or the distributor make up a terminal regeneration circuit. The purpose of this circuit is to regenerate the received signal which is finally applied to the grids of the selector tubes will be free of distortion. There is a limit, of course, to the distortion which may be present in the received signal and yet cause the selector relay to operate in accordance with the signal as transmitted. The terminal regeneration circuit does insure, however, that the grids of the selector tubes will have applied to them a definite solid signal, even though the received signal has been so distorted that it has failed to operate the line relay in accordance with the transmitted signal. As the receiving ring brushes pass over the segments associated with the *6V6* tubes connection is made from the tongue of the selector relay to the grid capacitor and grid of the *6V6* for that particular signal impulse. If the relay is in its marking position, the

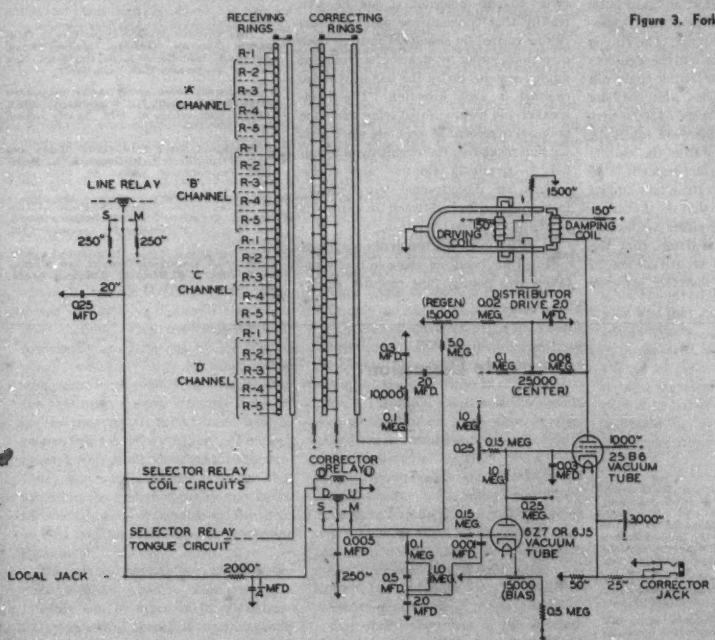

Figure 3. Fork corrector theory

capacitor will be charged negatively and the tube will be biased to cutoff. The neutral relay in the plate circuit therefore, will be de-energized. If the selector relay is in the spacing position, the capacitor will be charged positively and the tube will pass current. The neutral relay in the plate circuit then will become energized.

Summarizing this operation, the incoming signal operates the line relay which, in conjunction with the receiving rings, operates the selector relay. The selector relay in turn, through the receiving ring, controls the operation of the signal storage relays. During each complete revolution of the brushes, the incoming line signal is broken down into individual signal impulses for each of the four channels which then are set up in the storage relays. The channel relays are operated by the vacuum tubes. The multiplex signals now have been received and stored in the neutral relays and are ready to be sent to the teleprinter associated with the channel. The 5-unit code signals now must be converted into 7-unit code signals. This is done by controlling a thyratron tube from seven segments of a third ring on the receiving distributor. Two of these seven segments provide the start and stop pulse used in the code, while the other five provide the intelligence pulses. The ring is made up of 28 segments, and the segments are so located that their leading edges will be reached by the brushes, when they are rotating at the proper speed of 360 letters per minute, at 22-millisecond intervals, except that the interval from the leading edge of the following start segment is 35 milliseconds. The thyratron tube and its circuits are arranged so that the thyratron for the channel is made either conducting or nonconducting immediately that the brush reaches the segment, and the length of the segment is not, therefore, a factor in the operation of the circuit. The relationship between the segments of the receiving rings, teleprinter rings, and local rings is shown in Figure 2, together with the connections for the *B* channel. Channels *A*, *C*, and *D* are not shown. A functional representation of the teleprinter rings also is shown, that is, the effective length of each of the segments in operating the thyratron tube and thus the receiving printer is indicated.

The neutral relays associated with the channels previously described have two sets of contacts. One set is used to control the operation of the thyratron for the channel, in accordance with the incoming signal, and the other set is used in connection with a relay to cut off the transmission of blanks to the teleprinter when no intelligence is being transmitted over the channel. In order to prevent the transmission of these blanks to the receiving teleprinter, it is necessary to prevent the transmission of the start pulse following the reception of the blank, and this second set of contacts on the channel storage relays with their associated blank cutoff relay and circuits do this.

While the foregoing description outlines the transmission and reception of intelligence in one direction, it can be seen readily that transmission and reception can be carried on simultaneously in both directions, either by means of a grounded duplex system, or by the use of a radio channel in each direction. The loudspeaker and its associated relay and tube are used to receive Morse code when testing and regulating the circuit from terminal to terminal. Printers and transmitters are disconnected automatically from the four channels when the control is switched to Morse operation.

In addition to the terminal equipment outlined for handling message traffic between two points, tape repeater equipment was furnished that made it possible to join one or more channels of one radio multiplex link with another multiplex or radio system without the necessity of manual handling at the junction point of the different systems. Translation equipment also was designed and furnished so it was possible to use standard Navy start-stop cryptographic equipment for transmission to and reception from a multiplex channel.

Navy records show that it was not uncommon to maintain continuous 2-way transmission between Washington and Honolulu and between San Francisco and Guam over periods of 20 to 22 hours out of the day. This enabled them to handle 240 words per minute in each direction on a single radio channel, or four times the number of words possible with a single teleprinter channel. Equal records were established in other radio links where the multiplex system was used. When the war ended the Navy Department was called upon to handle many thousands of telegrams for the Navy personnel in addition to the heavy load imposed because of official Navy requirements.

References

1. Time Division Multiplex in Radio Telegraphic Practice, **Callahan, Mathes, Kahn.** *Proceedings*, Institute of Radio Engineers, New York, N. Y., January 1938, pages 55–75.

2. Frequency Modulated Carrier Telegraph System, **F. B. Bramhall, J. E. Boughwood.** AIEE Transactions, volume 61, 1942, January section, pages 36–9.

3. Frequency Shift Telegraphy—Radio and Wire Applications, **J. R. Davey, A. L. Matte.** AIEE Transactions, volume 66, 1947, pages 479–94.

4. Multi-channel Two-Tone Radio Telegraphy, **L. C. Roberts.** *Bell Laboratories Record*, New York, N. Y., volume 24, December 1946, pages 461–5.

5. Printing Telegraph Systems and Mechanisms (book), **H. H. Harrison.** Longmans Green, and Company, New York, N. Y.

No Discussion

Outage Expectancy as a Basis for Generator Reserve

HOWARD P. SEELYE
FELLOW AIEE

Synopsis: Probability calculations furnish a useful means whereby the average frequency and duration of generator outages on a power system, as shown by experience records may be converted into a consistent measure of the expectancy of multiple outages upon which the provision of reserves is based. This paper gives the mathematical development of relatively simple formulas for this purpose and methods of calculation and of exhibiting the results in tangible form. Use of these formulas does not require familiarity with technical probability mathematics.

THE element of chance plays an important part in the planning of adequate generating capacity for a power system. The peak load which has been carried is a certainty, but beyond that there must be capacity to care for future anticipated loads and for outages of equipment, both of which are uncertain. Past experience and good judgment are, of course, the basis upon which decisions to add capacity must be made, but the application of these to unknown conditions must include, either consciously or unconsciously, a sizing up of the chance which reasonably may be taken. The worst contingency which has happened in the past may be exceeded some time, or, on the contrary, it might have been so extreme that it is very unlikely to happen again. No matter what reasonable provision is made, a chance is taken that sometime the system capacity may be insufficient, due to a possible combination of load and forced outage of generating equipment.

The use of probability mathematics offers a means whereby some consistent measure can be taken of these chances. Many practical operating men no doubt feel that their experience is a sufficient guide and look at probability calculations as an academic mathematical exercise. It must be agreed that the reserves which have been provided on most systems in the past, when a free choice was allowed, have been quite adequate. With the increasing size of systems, the increasing cost of equipment, and the increasing scrutiny of cost of power, the possibility that the provisions made on this basis may be larger than actually necessary becomes of greater import. Every excess kilowatt of capacity represents a drain of something like $15 per year out of the net profits of operation. It would seem that any sound means of evaluating the chance being taken would help to keep the necessary reserve to a reasonable minimum, and is therefore a worth-while guide to economy.

The basis of probability studies is very simple. If something has happened only rarely in the past, it is likely to happen only rarely in the future. If the average frequency of its happening is known, that is, once a year or twice a year, it reasonably may be expected to happen about that often, on the average, in the future. If two things each happen infrequently on the average, the likelihood of their happening at the same time is still more remote. Probability mathematics merely uses these common sense ideas in algebraic form and combines them according to well established principles. Much of the apparent complication of the methods and formulas is due to the desire for accuracy in order to include all eventualities which might have an effect on the result. Approximations often may be made which are simpler and give a reasonably good answer, but the more complete methods are more dependable, if properly applied.

One of the objectives of the development described in this paper is to offer a method and formulas applicable to the study of generator outages which will be essentially accurate and yet will be very simple to use, even by one not familiar with technical probability mathematics. Another purpose is to exhibit the results by tangible conceptions which will be easy to grasp by those not accustomed to thinking of probability in terms of an abstract decimal.

Conceptions of Generator Reserve

There are, in general, three different conceptions of the purpose of reserve generating capacity. One is to provide for increase in load, particularly unexpected increases beyond that which reasonably can be foreseen. The second is to provide for taking equipment out for scheduled overhaul. The third is to provide for the loss of capacity due to forced outages of equipment. The first of these, unforeseen load, is subject to the same variables as those which govern the predicted load and should reasonably be included as a margin in load forecasts. The chance of an extreme unexpected load being coincident with an extreme outage of capacity is, however, a small one. In the second case, margin between load and generating capacity to allow scheduled maintenance frequently is provided, at least in part, by seasonal variation in load, and scheduled outages for this purpose also may be controlled to a considerable extent. The third class, forced outages, are, however, subject to the chance of failure of equipment. Such outages are uncontrollable but may be expected to follow in general the averages indicated by past experience. In this paper, generation reserve will be consid-

Paper 47-253, recommended by the AIEE power generation and system engineering committees and approved by the AIEE technical program committee for presentation at the AIEE Midwest general meeting, Chicago, Ill., November 3–7, 1947. Manuscript submitted July 31, 1947; made available for printing September 24, 1947.

HOWARD P. SEELYE is chief electrical engineer, engineering division, The Detroit Edison Company, Detroit, Mich.

The author gratefully acknowledges the valuable assistance of Edward M. Spencer in preparing the material for this paper.

ered from this standpoint only, that is, emergency reserve.

Basis of Probability Study

The study of probable generation outage for any individual system can be based best on the past records of the generators on that system if these cover a reasonably long period. Local practices in regard to design of plants, type of equipment used, and maintenance schedules can make appreciable difference in the frequency and duration of outages. Where adequate records are available, it is likely that the characteristic average frequency and duration of individual generator outages will be quite definitely indicated. Usually, however, sufficient reserve will be wanted for the less frequent occurrence of multiple outages of several generators at the same time. Such emergencies will probably not have happened often enough to indicate any dependable average frequency. By using the average characteristics of individual outages as a basic probability, however, the probability of simultaneous outages of two or more generators can be determined by calculation. Such a probability is a more reliable measure of the likelihood of the occurrence of these larger outages than is an average obtained from only a few actual cases. Also, by this means, the probability of extreme outages which never have been experienced can be indicated.

"Probability" is a measure of the chance of a certain event occurring by the ratio between the number of events that can occur in that certain way and the number of total possible events. For example, the probability of finding three generators out at any instant chosen at random may be obtained as a decimal, such as 0.002. This would indicate the proportion of total time which would be occupied by such outages. It is believed, however, that a clearer conception of the necessary reserve is obtained by the average frequency with which outages of various amounts might be expected to occur, that is once in 20 years or once in 30 years. This "expectancy" is the aspect which will be considered in this paper. It is obtained by the use of probabilities modified as will be illustrated later.

It should be understood clearly that the calculation of expectancy is in no sense a prediction any more than is the use of average frequency of past occurrences. Any conceivable outage may happen at any time, and, having happened, may happen again a short time later. The figures represent the *average* frequency with which such occurrences may be expected over a long period of time—a measure of the chance which is being taken that the reserve provided may at some time be inadequate.

Table I. Calculations for Combinations of Two Sizes of Machines

Order of j	Machine Combinations, Megawatts 30	50	Megawatts	n^j	E^j / n^j	E_j^2
1	1	0	30	2.0	4.3059×10^{-1}	0.86118
	0	1	50	5.4	4.3059×10^{-1}	2.32519
2	2	0	60	4.0	0.4478×10^{-2}	0.01791
	1	1	80	21.6	0.4478×10^{-2}	0.09672
	0	2	100	29.16	0.4478×10^{-2}	0.13058
3	3	0	90	8.0	0.02267×10^{-3}	0.00018
	2	1	110	64.8	0.02267×10^{-3}	0.00147
	1	2	130	175.0	0.02267×10^{-3}	0.00397
	0	3	150	157.0	0.02267×10^{-3}	0.00357
4	4	0	120	16.0	0.00076×10^{-4}	0.0000012
	3	1	140	172.8	0.00076×10^{-4}	0.000013
	2	2	160	699.8	0.00076×10^{-4}	0.000053
	1	3	180	1259.7	0.00076×10^{-4}	0.000096
	0	4	200	850.3	0.00076×10^{-4}	0.000065

Mathematical Development

The formulas shown later, as equations 3 and 4, may be used for studies of generator outage on any system without following through their mathematical development if their accuracy is accepted. Their development will be given in the following section.

As has been stated, the basic quantities used are the average frequency and duration of individual generator outages determined from past records. Assuming that these show no characteristic variation with size, make, or age of equipment, which is the case with the records used in this study, let

T = average period between occurrence of individual outages in terms of running time

$$= \frac{\text{total running time of generators on record}}{\text{total number of forced outages}}$$

d = average duration of outages, or repair time

$$= \frac{\text{total forced outage time for outages on record}}{\text{total number of forced outages}}$$

It is assumed that the number of outages for any generator is directly proportional to its exposure, that is to the time which it is run. This will differentiate between the probable outages for machines run a great deal and those run only occasionally. By estimating future proportion of running time, account can be taken of greater or less expected use of the equipment. If boiler outages reduce the generating capacity, they also must be included as outages of generation.

T is the average time which may be expected to elapse between outages for each generator. If this should be two years, for example, it means that on the average once in two years of running time each generator may be expected to be forced out of service. If there are ten generators, all running continuously, the expectation would be five outages per year. If they run only 60 per cent of the time, on the average, the expectation would be three outages for each calendar year.

The probability of outage for each generator expressed mathematically is $1/T$. T may be expressed in years (1/2), or in days (1/730), or in hours, or still smaller units, according to the use to be made of it, since once in two years is the same as once in 730 days. If the unit used is a day, the probability of a certain generator going out on some chosen day is $1/T$ (or one chance in 730 for the example given). It follows that the probability of its not going out on that day is $1-(1/T)$, or 729 chances out of 730. The complete probability, or all of the chances both of outage and of no outage, therefore may be expressed by the binomial

$$\left[\left(1-\frac{1}{T}\right)+\frac{1}{T}\right]$$

If there is more than one machine running, each possibility for outage or no outage for any of them may occur in combination with each possibility for all of the others. For two machines there are

$$\left(1-\frac{1}{T}\right)^2=\left(\frac{729}{730}\right)^2=\frac{531{,}441}{532{,}900}$$

chances of no outage

$$2\left(1-\frac{1}{T}\right)\frac{1}{T}=\frac{2\times 729}{(730)^2}=\frac{1{,}458}{532{,}900}$$

chances of a single outage

$$\left(\frac{1}{T}\right)^2=\frac{1}{(730)^2}=\frac{1}{532{,}900}$$

chances of a double outage

(Reduced to years, the last figure indicates that once in 1,460 years both generators might be expected to go out on the same day). If the process is extended to include n generators, it leads to the expansion of

$$\left[\left(1-\frac{1}{T}\right)+\frac{1}{T}\right]^n$$

to include all possible combinations of all n generators, each term of the expansion giving the probability of a specific number out together, that is 0, 1, 2, 3, and so forth.

Since an outage lasts for an appreciable length of time, if the average duration d is longer than the unit of time being used (one day, for example) additional outages of other generators may occur on any of the days of this outage, creating a multiple outage. Any possible combination of outage or no outage for the n generators on the first day may occur with any of the possible combinations on any of the succeeding days during d. This leads to the inclusion of d with n in the exponent of the binomial

$$\left[\left(1-\frac{1}{T}\right)+\frac{1}{T}\right]^{nd}=\left(1-\frac{1}{T}\right)^{nd}+nd\left(1-\frac{1}{T}\right)^{nd-1}\frac{1}{T}+\frac{nd(nd-1)}{2}\times\left(1-\frac{1}{T}\right)^{nd-2}\left(\frac{1}{T}\right)^2\ldots$$

Each term of this expansion represents the chance or the probability of a certain combination of generator outages being initiated during a period d. The first term is for 0 outage, the second for single outages, the third for double outages, and so forth. This may be generalized as follows:

j = the number of the term after the first (for which $j=0$)
= the number of generators out, or the order of the outage
P_j = the probability of an outage of order j
C_j^{nd} = the possible combinations of nd things taken j at a time

$$P_j=C_j^{nd}\left(1-\frac{1}{T}\right)^{nd-j}\left(\frac{1}{T}\right)^j=\frac{(nd)^j}{j!(nd-j)!}\left(1-\frac{1}{T}\right)^{nd-j}\left(\frac{1}{T}\right)^j=\frac{nd(nd-1)(nd-2)\ldots(nd-j+1)}{j(j-1)(j-2)\ldots1}\times\left(1-\frac{1}{T}\right)^{nd-j}\left(\frac{1}{T}\right)^j \quad (1)$$

T and d must be expressed in the same units, that is, days, hours, and so forth. If the unit used is very small, their values become very large. Practically, outages occurring within the same hour could be considered simultaneous and there would be no reason for using a smaller unit such as a minute. The whole value of the expression does not change greatly, as the unit is made smaller, since both the numerator and the denominator are increased. Any question of the proper unit can be removed, however, and the expression much simplified if it is evaluated as the limit when the unit used approaches 0.

$$nd(nd-1)(nd-2)\ldots(nd-j+1) \text{ approaches } (nd)^j$$

$$\left(1-\frac{1}{T}\right)^{nd-j} \text{ approaches } (0)^\infty$$

The latter term is indeterminate but can be evaluated by means of derivatives to give

$$\epsilon^{-\frac{nd}{T}}$$

where ϵ is the base of Naperian logarithms.

The limit for the general equation (1) as the unit approaches 0 is therefore

$$\Delta t\to 0,\ P_j=\frac{(nd)^j}{j!}\epsilon^{-\frac{nd}{T}}\left(\frac{1}{T}\right)^j=\left(\frac{nd}{T}\right)^j\frac{1}{j!}\epsilon^{-\frac{nd}{T}} \quad (2)$$

P_j is the probability that an outage of j machines will occur during a period d due to outages initiated during that period. If all outages are of the same duration d, it also represents the probability that there are j machines out at the end of any period d involving machines which have gone out during that period. Outages of the order of j may occur during the period d as a result of outages initiated during that period added to outages existing at the beginning of the period but initiated previously, but these previous outages will have elapsed before the end of d, if their duration is limited to that value. Since the period d was chosen at random, therefore, P_j represents the probability of finding j machines out at any random time. This also applies, in general, to outages of various durations if the average duration is d.

P_j does not represent the probability of all outages of order j occurring during a period d as has been explained. The expectancy of occurrance (or the average number per year) of all outages of order j is, therefore, not simply P_j divided by d, but must be obtained by further calculation.

An outage of the order j occurs by an individual outage being added to an existing outage of the order $j-1$. If the expected number of such occurrences per year is represented by E_j', and the expected total number of individual outages per year as determined by the average record is $1/T$ per machine or n/T for n machines, it follows that the probability that any individual outage chosen at random will be one which will create an outage of order j, by adding to existing outages, is $E_j'/(n/T)$.

This individual outage which creates the outage of order j must fall at a time when there is found an outage of the order $j-1$. The probability of this outage being found at any random time is shown by equation 2. Since the individual outage was chosen at random, the probability that it could be one creating an outage of order j is equal to the probability of finding an outage of order $j-1$ at the time

$$P_{j-1}=\frac{E_j'}{n/T}$$

If an "outage" is considered to refer to the whole group of individual outages, characterized by the largest number of machines out together at any time but including also the outages of lower order preceding and succeeding the time of that higher order, an outage thus created may be increased further by later outages to outages of higher orders than j, hence E_j' is really the expectancy of occurrence of outages of j *or more*, E_{j+}

Hence

$$P_{j-1}=\frac{E_{j+}}{n/T}$$

$$E_{j+}=\frac{n}{T}P_{j-1}=\frac{n}{T}\left(\frac{nd}{T}\right)^{j-1}\frac{1}{(j-1)!}\epsilon^{-\frac{nd}{T}}=\left(\frac{n}{T}\right)^j\frac{d^{j-1}}{(j-1)!}\epsilon^{-\frac{nd}{T}} \quad (3)$$

Table II. Calculations Arranged in Order of Megawatts

Megawatts	Of Event	Of Event or More	Equivalent Interval, Years	Expected Number in 100 Years
(More than		(Too small to be significant)		
4)	0.00000423			
200	0.000065	0.00007	14,150	
180	0.000096	0.00017	5,900	
160	0.000053	0.00022	4,550	
150	0.00357	0.00379	264	
140	0.000013	0.00380	263	
130	0.00397	0.00777	129	
120	0.0000012	0.00777	129	... 0.8
110	0.00147	0.00924	108	... 1
100	0.13058	0.13982	7.2	... 14
90	0.00018	0.14000	7.1	... 14
80	0.09672	0.23672	4.2	... 24
60	0.01791	0.25463	3.9	... 25
50	2.32519	2.57982	0.4	...258
30	0.86118	3.44100	0.3	...344

Since E_{j+} is the expectancy of occurrence of outages of the order of j or more and $E_{(j+1)+}$ the expectancy of outage of $j+1$ or more, it follows that the expectancy of occurrence of outages of order of j only is the difference between these quantities.

$$E_j = E_{j+} - E_{(j+1)+} = \left(\frac{n}{T}\right)^j \frac{d^{j-1}}{(j-1)!} \epsilon^{-\frac{nd}{T}} - \left(\frac{n}{T}\right)^{j+1} \frac{d^j}{j!} \epsilon^{-\frac{nd}{T}} = \left(\frac{n}{T}\right)^j \frac{d^{j-1}}{(j-1)!} \epsilon^{-\frac{nd}{T}} \left(1 - \frac{nd}{jT}\right) \quad (4)$$

Use of Formulas

The essential formulas are, therefore, as follows:

For the expectancy of outages of j *machines or more*

$$E_{j+} = \left(\frac{n}{T}\right)^j \frac{d^{j-1}}{(j-1)!} \epsilon^{-\frac{nd}{T}} \ldots \quad (3)$$

For the expectancy of outages of j *machines only*

$$E_j = \left(\frac{n}{T}\right)^j \frac{d^{j-1}}{(j-1)!} \epsilon^{-\frac{nd}{T}} \left(1 - \frac{nd}{jT}\right) \quad (4)$$

where

n = number of generators running
d = average duration of individual outages (in years)
T = average interval between individual outages (in years)
j = number of generators out at the same time
ϵ = base of Naperian logarithms, 2.7183

An outage refers to the whole group of individual outages characterized by j, the largest number of generators out together at any time during the continuous duration for the whole group.

Equations 3 and 4 are simple algebraic expressions whereby the expectancy, or the average number of occurrences per year which are likely to happen, for outages of the order j (equation 4) or of the order j *or more* (equation 3) may be obtained. The reciprocals of these quantities give the expected average period in years between such occurrences.

The reserve generating capacity which is provided will be used fully whenever an outage equal to it occurs. It will be sufficient, of course, to take care of all smaller outages. It will be used fully, but will be exceeded by greater outages. An adequate reserve, therefore, will be such that it will not be likely to be exceeded except at very long intervals, long enough to warrant taking a chance on this happening and dropping some load if it does. A reasonable interval might be once in 20 years, 30 years, or 50 years. The formulas allow the reserve corresponding to any chosen criterion to be obtained.

If all generators are of the same size and have the same characteristics in regard to running time, as well as frequency and duration of outages, equation 3 can be used directly to obtain the expectancy of outage of any number of them or more. Most systems, however, have a variety of generators and various practices in regard to operating them. By means of equation 4, this variety can be taken into account. In general, the method is to calculate the expectancy E_j for all possible combinations of machine outage for which the expectancies are large enough to be significant. If these then are listed in order of size (total capacity out) and the expectancies summed progressively, the expectancy for any specific amount or more will be obtained. The formula is based on n machines running continuously. To take account of different sizes and different running times, the machines may be grouped according to size and running time, and n becomes a polynomial of their sum.

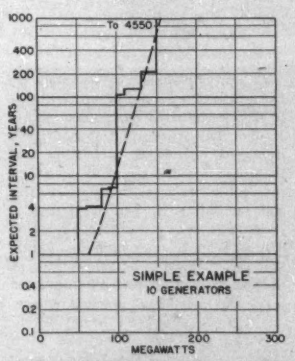

Figure 1. Simple example of variation of amount of outage with expected average interval between outages

System with six 50-megawatt and four 30-megawatt generators

The value of n equals $n_1a + n_2b + n_3c \ldots$ in which n_1a equals the number of machines of size a times their average use factor, n_2b the number of machines of size b times their use factor, and so forth. This polynomial should be used in the quantity $(n/T)^j$. The total n times average use factor may be used in $\epsilon^{-nd/T}$ and $[1 - nd/jT]$.

A simple numerical example will serve to illustrate the calculation with this formula.

Simple Example of Calculation

$$E_j = \left(\frac{n}{T}\right)^j \frac{d^{j-1}}{(j-1)!} \epsilon^{-\frac{nd}{T}} \left(1 - \frac{nd}{jT}\right)$$

Assume ten machines, six rated at 50 megawatts and four at 30 megawatts, with running times of 90 and 50 per cent, respectively, and an average running time of 74 per cent.

$n = 0.74 \times 10 = 7.4$
$T = 2$ (once in two years)
$d = 0.02$ (average duration of outage about one week)

$$\epsilon^{-\frac{nd}{T}} = \epsilon^{-\frac{7.4 \times 0.02}{2}} = \epsilon^{-0.074} = 0.93$$

$$\left(\frac{n}{T}\right)\epsilon^{-\frac{nd}{T}} = \frac{n}{2} \times 0.93 = 4.65\frac{n}{10}$$

$$\left(\frac{n}{T}\right)^2 d\, \epsilon^{-\frac{nd}{T}} = \frac{n^2}{4} \times 0.02 \times 0.93 = 0.456\left(\frac{n}{10}\right)^2$$

$$\left(\frac{n}{T}\right)^3 \frac{d^2}{2} \epsilon^{-\frac{nd}{T}} = \frac{n^3}{8} \times 0.0002 \times 0.93 = 0.02325\left(\frac{n}{10}\right)^3$$

$$\left(\frac{n}{T}\right)^4 \frac{d^3}{6} \epsilon^{-\frac{nd}{T}} = \frac{n^4}{16} \times 0.0000013 \times 0.93 = 0.000775\left(\frac{n}{10}\right)^4$$

j	$1 - \frac{nd}{jT}$	E_j
1	0.926	$4.3059\frac{n}{10}$
2	0.963	$0.4478\left(\frac{n}{10}\right)^2$
3	0.975	$0.02267\left(\frac{n}{10}\right)^3$
4	0.981	$0.00076\left(\frac{n}{10}\right)^4$

Since 0.00076 represents once in 1,300 years it is obviously unnecessary to proceed to higher orders.

To obtain combinations of the two sizes of machines (refer to Tables I and II)

$$n = (0.9 \times 6a + 0.5 \times 4b) = (5.4a + 2b)$$
$$n^2 = 29.16a^2 + 21.6ab + 4b^2 \ldots$$
$$n^3 = 157.5a^3 + 175.0a^2b + 64ab^2 + 8b^3$$
$$n^4 = 850.5a^4 + 1{,}259.7a^3b + 699.8a^2b^2 + 172.8ab^3 + 16b^4$$

The values from the tables may be plotted as shown in Figure 1. Figure 2 shows a plot for a more extensive system with more generators of greater variety.

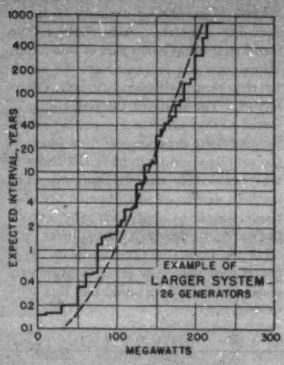

Figure 2. Example of variation of amount of outages for system of 26 generators of various sizes from 10 to 75 megawatts

Average size 47.2 megawatts

Significance of Charts

Such a chart indicates rather simply several significant facts. It shows, for example, the average frequency with which any given amount of reserve might be expected to be needed and to be exceeded. On Figure 2, for example, 150 megawatts will be used fully once in 13 years but will be exceeded only once in 29 years. The excess will be small, however, and 155 will be exceeded once in 35 years, 160 once in 43 years, and so forth. Conversely, if a criterion of once in 30 years is chosen, it appears that 155 megawatts is sufficient and 150 nearly so. If the criterion is once in 50 years, 160 is needed, if once in 100 years 185, and so forth. If, on the contrary, a reserve of only 100 is available, it may be expected to be exceeded once in two years.

It is interesting to note that the curve rises quite rapidly, the frequency being plotted to a logarithmic scale. This indicates that a more conservative criterion of frequency may be obtained by relatively small addition to the reserve but that large excess provision is likely never to be used. Conversely, frequent difficulty is to be expected if the reserve is much too small.

Simple Approximation

The broken curve on Figures 1 and 2 is plotted by use of equation 3 for E_{f+}, assuming n as the total number of machines of all sizes times average use factor of all of them. The capacity corresponding to each value of j is obtained by j times the average size of all generators. An example of the calculation may be shown by using some of the figures given in the example plotted in Figure 1.

$$E_{f+}=\left(\frac{n}{T}\right)^{j}\frac{d^{j-1}}{(j-1)!}\epsilon^{-\frac{nd}{T}} \qquad (3)$$

$$E_1=\frac{n}{T}\epsilon^{-\frac{nd}{T}}=4.65\frac{n}{10}=3.43$$

$$E_2=\left(\frac{n}{T}\right)^{2}d\epsilon^{-\frac{nd}{T}}=4.65\left(\frac{n}{10}\right)^{2}=0.253$$

$$E_3=\left(\frac{n}{T}\right)^{3}\frac{d^2}{2}\epsilon^{-\frac{nd}{T}}=0.02325\left(\frac{n}{10}\right)^{3}=0.00945$$

j	Interval	Kilowatts
1	0.29 years	42
2	3.95 years	84
3	106 years	126

This is a much simpler calculation than the one illustrated for equation 4 and will give results sufficiently accurate for the purpose with many systems, particularly if the sizes of generators are not too far apart. It must be used with some caution, however, with systems of extremes in sizes and a check against the longer method is advisable, if practicable, to determine its limitations. It is evident that this curve corresponds very closely with the step curve on Figure 2 in the range of frequencies most likely to be considered, but on Figure 1 the agreement is not so good. This method, however, will give an approximation of the result on most systems with much less calculation than the other method.

When this shorter method is found satisfactory, by choosing a definite criterion for frequency, such as once in 30 years, a useful curve such as Figure 3 can be obtained quite easily. In this case $E_{f+}=1/30=0.033$, and by use of equation 3, the corresponding value of j and hence of capacity ($j \times$ average size) for any number of generators n may be obtained. The relation between j and n is not simple but by calculating E_{f+} for successive values of j, such as 2, 3, and 4, the value of j may be interpolated for any desired value of E_{f+} by assuming the curve plotted on semilog paper is a straight line. For example, if j lies between 3 and 4, values of E_{f+} for $j=3$ and $j=4$ may be plotted and the value of j for $E_{f+}=0.033$ determined, or it may be calculated from the expression

$$j=3+\frac{\log D_f-\log D_3}{\log D_4-\log D_3}$$

where D is the interval in years corresponding to the j given as its subscript.

Such a curve as Figure 3 will show the increase in reserve necessary as generators are added to the system. It also shows the amounts of reserve required for systems of different sizes. The reduction in proportion of reserve as a system increases, or is combined with another system, is indicated. For example, for 10 generators, 130 is needed; for 20 generators, 165; for 30 generators, 190; and so forth. For actual systems, the variation in average size and other individual characteristics, of course, must be taken into account but the possible savings in reserve for large combined systems are evident.

Adaptations of Formulas

Although the formulas as given apply specifically to steam generation for which the outage in kilowatts is likely to be of prime importance and the duration less so, they may be adapted to cases in which the kilowatt-hour outage is of considerable interest, as is likely to be the case where hydro generation is involved. The average duration of an outage of j machines is inversely proportional to j, that is 1/2 as long for a double outage as the average for individual outages; 1/3 as long for triple, and so forth. The kilowatt-hours lost while j machines are out are therefore

$$\frac{d}{j}\times j\times \text{average size of generator}=d\times\text{average size}$$

If the kilowatt-hours involved in the whole outage, including the time $j-1$, $j-2$, and so forth, machines were out, are desired, it is

$$d\times j\times\text{average size of machine}$$

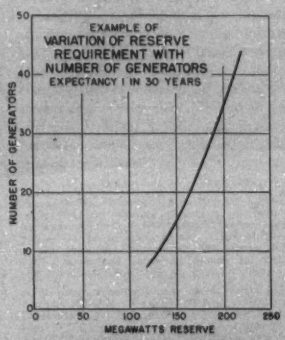

Figure 3. Example of variation of required reserve with number of generators on the system, assuming average size of generator constant

Outage expectancy once in 30 years

The scale for megawatts on the figure may be changed to megawatt-hours by this factor and the curves then will indicate the expectancy of loss of kilowatt-hours.

The formulas also assume the loss of capacity to be equally important at any time during the year. This may not be true, since loss at peak load time may be more important if there is ample drop in load at other times to allow for scheduled maintenance. However, if special provision of capacity is made to allow for maintenance, outage may be more important at off-peak seasons. In any case the chance of any occurrence during part of a year is proportionately less than during all of the year.

The methods shown here also may be used for showing the expectancy of outage in any plant or any part of the system. They may be applied to indicate the expected frequency of generator outage and some other contingencies, such as loss of important transmission lines, if the outage expectancy of the latter is known. There are other contingencies on a power system, the chance of which can be measured to advantage by the application of the general processes outlined in this paper.

Concluding Summary

There are, of course, many factors which enter into the actual decision on the amount of generating capacity to be installed on a system. Some of these were mentioned in the early part of this paper. Experience and judgment are the essential requirements in correlating all of these factors. The study of the probability of forced outage offers a systematic means for analyzing experience in this phase of the problem and in judging the order of what reasonably may be expected. The methods developed in this paper are relatively simple to apply, even by anyone not specially versed in the subject, and show the results in tangible form. It is hoped that they may serve to promote a wider understanding and use of this helpful tool.

No Discussion

Suddenly Applied Loads on a Variable-Ratio Frequency Changer

G. K. CARTER
MEMBER AIEE

F. J. MAGINNISS
ASSOCIATE AIEE

F. S. ROTHE
ASSOCIATE AIEE

THE OBJECT of this paper is to present the results of a differential analyzer study of the electrical performance of a variable-ratio frequency-changer set following the sudden application of load on the induction machine and including the case of sudden short circuit. This study was undertaken in order to provide information on the ability of such a set to maintain voltage, and on the manner of growth or decay of the load currents as determined by the magnitude and type (3-phase or single-phase) of the load impedance, by the operating slip, and by the operation of automatic controls.

The primary application of these results is as an aid in the selection of proper relaying equipment and settings and in the understanding of the performance of such relaying. The variable-ratio frequency-changer set differs from a synchronous-synchronous tie or from a conventional synchronous generator in that the induction machine is self-excited, that is, it derives its excitation from the output terminals. Thus, depending upon the severity of the disturbance or the magnitude of a suddenly applied load, voltage either will be sustained at a relatively large value or will collapse completely. A comparatively small increase in load thus may produce a major change in the resulting current at a critical value, and it becomes difficult to predict the exact course of the current at values near this point.

Conclusions

As a result of this study several conclusions regarding the ability of the induction machine of a variable-ratio frequency-changer set to maintain voltage when subjected to the sudden application of load have been drawn. These are

1. For the machine studied, the amount of load which can be carried without collapse of voltage is of the following order of magnitude:

Condition	Per Unit Load: Kva at Unit Voltage	Per Unit Load: Reactance on Loaded Phase
Three phase, 2.9 per cent slip, power-factor field resistor short-circuited	1.33	0.75
Three phase, 5.9 per cent slip, power-factor field resistor short-circuited	1.00	1.00
Three phase, 2.9 per cent slip, power-factor field resistor not short-circuited	<1.00	>1.00
Single phase, 2.9 per cent slip, power-factor field resistor short-circuited	2.00	0.25

2. The initial a-c decrement does not give a definite indication of whether or not voltage will be sustained.

3. While the d-c component has an exponential decay, the a-c component does not appear to exhibit definite exponential decay rates.

4. At lower slip, somewhat greater loads can be applied without causing the voltage to collapse.

5. Short-circuiting the power factor control field resistor at the instant of load application helps materially in sustaining the terminal voltage.

Assumptions

In reducing the transient equations to a form in which they are suitable for solution on the differential analyzer certain simplifying assumptions are made. These are

1. The speed of the set is held constant during any one run.

2. The set is initially operating at no load.

3. The output current used for excitation is negligible.

4. Resistance and inductance of the ohmic-drop exciter and its input transformer are negligible.

5. The load and power factor control field windings are coupled perfectly.

6. The effect of saturation is considered only in the main induction machine mutual flux path.

7. The power factors of the load, induction machine primary, and induction machine secondary circuits are equal.

8. The power factor control field resistor can be short-circuited at the instant of application of the load; all other control settings remain fixed.

Discussion of Results

The results of this study are summarized by a group of curves, such as Figure 2, which illustrate how the envelope of the a-c component of the load current varies with time following the sudden application of load. The set is assumed to have been running initially at no load.

In Figure 2, the load is shown in terms of the external reactance L_{ext} suddenly applied to the terminals of the induction machine for the 3-phase low-slip case with power-factor control field resistor short-circuited. This reactance varies from $L_{ext}=0$, the short-circuit case, to $L_{ext}=2.0$ in per unit. For $L_{ext}=0.5$ the a-c component of current is seen to be decaying continuously, while for $L_{ext}=1.0$ it is still growing after 0.35 second. For $L_{ext}=0.75$, however, the current settles down in about 0.1 second to a steady value. Based on 1.0 per unit terminal voltage, this limiting case corresponds to a kilovolt-ampere load of $1.0/0.75=1.33$ per unit, since the

Paper 47-259, recommended by the AIEE power generation and rotating machinery committees and approved by the AIEE technical program committee for presentation at the AIEE Midwest general meeting, Chicago, Ill., November 3–7, 1947. Manuscript submitted March 26, 1947; made available for printing September 23, 1947.

G. K. CARTER, formerly with central station engineering divisions, General Electric Company, Schenectady, N. Y., is with the engineering department of the University of Virginia, Charlottesville, Va.; F. J. MAGINNISS and F. S. ROTHE are with the central station engineering divisions, General Electric Company, Schenectady, N. Y.

The authors wish to acknowledge the suggestions and criticisms of C. Concordia (M '37) and the assistance of F. W. Baumann who supplied design data on the frequency changer, and of A. C. Cook who was in charge of differential analyzer operation.

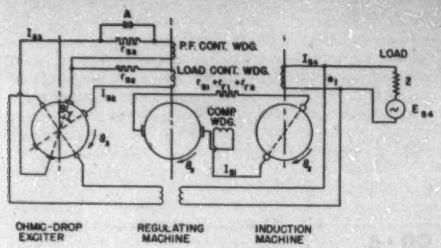

Figure 1. Schematic diagram of variable-ratio frequency changer, 25-cycle side

Table I. Values of RMS Terminal Voltage

L_{ext}	$I(t=0)$	$e_t(t=0)$	$I(t=0.3)$	$e_t(t=0.3)$
0	5.42	0		0
0.25	2.31	0.58	1.39	0.35
0.50	1.47	0.735	1.20	0.60
0.75	1.08	0.81	1.00	0.75
1.00	0.845	0.845	0.86	0.86
2.00	0.458	0.916	0.53	1.06

resistance component of the load impedance is so small as not to affect the current magnitudes appreciably. Actually the steady state terminal voltage is not unity but is $1.0 \times 0.75 = 0.75$ per unit.

Table I shows values of the rms terminal voltage initially (at $t=0$) and at $t=0.3$ second determined by multiplying the rms a-c component of current by the external impedance.

Both the cases $L_{ext}=1.0$ and $L_{ext}=2.0$ have initial voltage dips but recover. Thus the initial rate of decay gives little indication of whether or not voltage will be sustained.

Figures 4, 5, and 6 show actual instantaneous current versus time curves as drawn by the differential analyzer. They are for the short-circuit case and for the two cases surrounding the limiting case. Each of the figures consists of two curves marked phase *a* and phase *b*. These are the phase currents of the equivalent 2-phase machine used in the analysis, and initial values have been chosen such that in every case one phase current is symmetrical while the other is fully offset.

Figure 3 gives the d-c components of the currents whose a-c components are shown in Figure 1. All the curves are seen to be closely straight lines on semilog paper indicating an exponential rate of decay of the d-c component. No such regular decay is noted in the a-c components even in the cases in which the voltage collapsed.

Figure 7 is similar to Figures 2 and 3 for the case of suddenly applied single-phase load. This is likewise a low-slip case in which the power-factor control field is short-circuited upon application of load. Since one phase is still open-circuited and thus able to provide excitation after the load is applied, voltage is sustained even for $L_{ext}=0.25$. Again on the basis of unit terminal voltage, the load which may be applied without collapse is $1/2 \times 1/0.25 = 2.0$ per unit kva. The factor 1/2 is included since only one of the two phases is carrying current.

For this single-phase case both a-c and d-c components are shown on the same figure.

Figure 8 is the response curve corresponding to the short-circuit case of Figure 7, and Figure 9 that corresponding to $L_{ext}=0.375$. For each of these two cases, two runs each were made on the differential analyzer. For one of these, initial conditions were so chosen as to give a symmetrical current while for the other they were chosen to give a fully offset wave.

Figure 10 records two cases similar to two of those shown in Figures 2 and 3 except that the slip is twice as great as in the latter. Even for $L_{ext}=1.0$ the voltage is apparently collapsing. No case was taken in which voltage was sustained and it can be stated only that the limiting load is less than $1/1.0=1.0$ per unit.

In Figure 11 the same two loads as just stated are applied, this time to the low-slip 3-phase case but with the power factor control field not short-circuited at the time of load application. Here also the

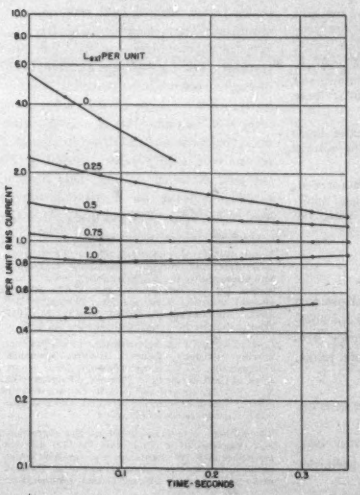

Figure 2 (left). Rms value of a-c component of load current versus time—effect of external reactance

Three-phase load current
No-load frequency = 25 cycles per second
Power-factor field short-circuited at $t=0$

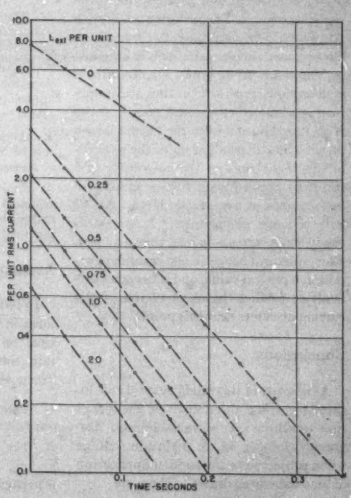

Figure 3 (right). D-c component of load current versus time

Three-phase load current
No-load frequency = 25 cycles per second
Power-factor field short-circuited at $t=0$

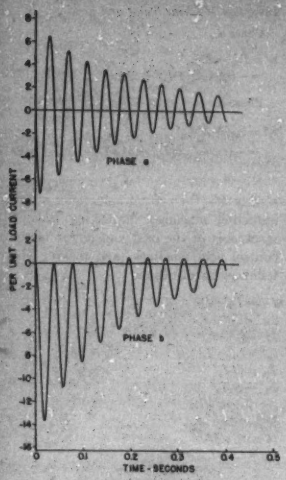

Figure 4 (left). Instantaneous values of load current in the two phases of the equivalent 2-phase machine

$L_{ext}=0$
Three-phase load current
No-load frequency = 25 cycles per second
Power-factor field short-circuited at $t=0$

Figure 5 (right). Instantaneous values of load current in the two phases of the equivalent two-phase machine

$L_{ext}=0.5$
Three-phase load current
No-load frequency = 25 cycles per second
Power-factor field short-circuited at $t=0$

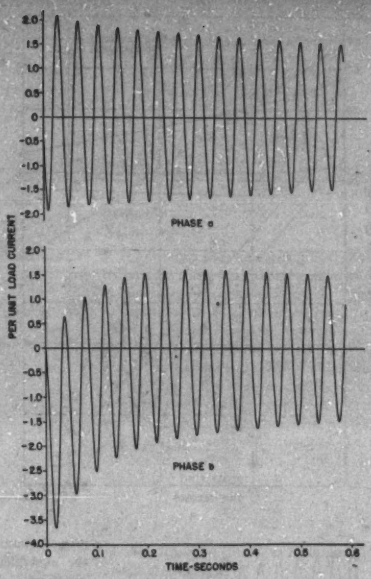

limiting load is less than 1.0 per unit. The effect of short-circuiting the power factor control field is seen to be considerable.

Description

The essential elements of the variable-ratio frequency-changer set considered in this paper and for which performance equations are derived in another paper[1] are shown schematically in Figure 1. The set contains also a synchronous machine (not shown in Figure 1) supplied in this case from a 60-cycle system and driving the ohmic-drop exciter, the regulating-exciting machine, and the induction machine all on the same shaft.

In normal operation the stator terminals of the induction machine are connected to the 25-cycle system and also to slip rings on the ohmic-drop exciter rotor. Slip-frequency voltages are taken as indicated in Figure 1 from two sets of brushes (at angles designated as β and γ in the performance equations) on the ohmic-drop exciter commutator to supply the power factor and load control fields of the regulating machine. The armature of the regulating machine supplies (through its commutator) slip-frequency current to the rotor of the induction machine. A more detailed description of a somewhat similar arrangement is given in reference 2.

It is not essential that the regulating machine be driven at the 60-cycle system speed, but the other two must be so driven. The variable-ratio frequency-changer set thus forms a link which may be used to transfer power between two systems which cannot be conveniently held always in synchronism. When, for example, the frequency of the 25-cycle system changes slightly, the slip frequency obtained from the ohmic-drop exciter inherently will change correspondingly, and the power and reactive output or input of the induction machine will deviate only moderately from the previous settings. In addition, automatic controls are provided which may shift the angles β and γ and the resistances in series with the power factor and load control field so as to bring the system back to the original load and power factor condition. The present paper is not concerned with this load-regulating feature, but only with the transient conditions which may arise following fault or sudden load changes. Reference 3 presents a general discussion of frequency changers in which the char-

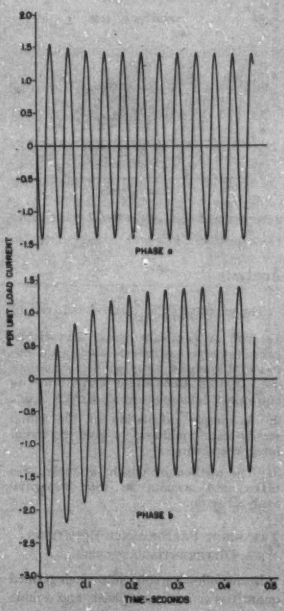

Figure 6. Instantaneous values of load current in the two phases of the equivalent 2-phase machine

$L_{ext}=0.75$
Three-phase load current
No-load frequency = 25 cycles per second
Power-factor field short-circuited at $t=0$

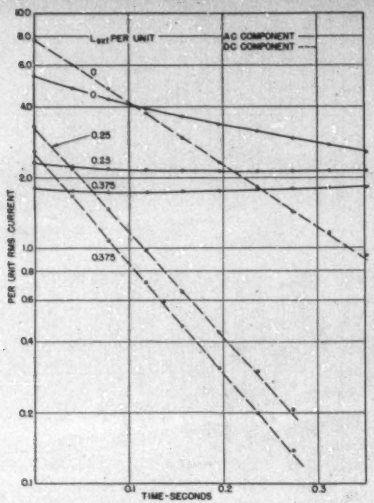

Figure 7. Rms value of a-c and d-c components of current versus time

Single-phase load current
No-load frequency = 25 cycles per second
Power-factor field short-circuited at $t=0$

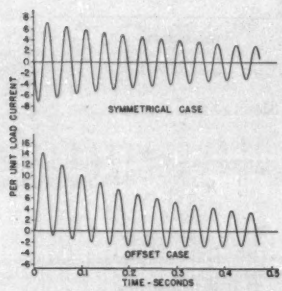

Figure 8 (left below). Instantaneous values of load current in the loaded phase versus time

$L_{ext}=0$ (loaded phase)
Single-phase load current
No-load frequency = 25 cycles per second
Power-factor field resistor short-circuited at $t=0$

acteristics of this, and several other types are described.

Analysis

The purpose of this analysis is to record

1. The transient equations of the variable-ratio frequency-changer as used in the differential analyzer setup. These equations are obtained from those derived for an equivalent 2-phase set by G. Kron.[1]

2. A sample calculation of the initial steady-state conditions to give the initial integrator settings.

3. The method by which saturation was taken into account in the differential analyzer setup.

Transient Performance Equations for Differential Analyzer

In the following equations single primed quantities refer to one phase, and double primed quantities to the other phase, of the equivalent 2-phase machine. The equations as derived in reference 1 are

Power Factor Control Field Winding

Phase *a*

$$0=(r_{s2}+L_{s2}p)I_{s2}'+L_{s2}p\theta_3 I_{s2}''+L_{sm2}pI_{s2}'+L_{sm2}p\theta_3 I_{s2}''+k_1(\cos\beta)e_t'+k_1(\sin\beta)e_t'' \quad (1)$$

Phase *b*

$$0=-L_{s2}p\theta_3 I_{s2}'+(r_{s2}+L_{s2}p)I_{s2}''-L_{sm2}p\theta_3 I_{s2}'+L_{sm2}pI_{s2}''-k_1(\sin\beta)e_t'+k_1(\cos\beta)e_t'' \quad (2)$$

Load Control Field Winding

Phase *a*

$$0=L_{sm2}pI_{s2}'+L_{sm2}p\theta_3 I_{s2}''+(r_{s2}+L_{s2}p)I_{s2}'+L_{s2}p\theta_3 I_{s2}''+k_2(\cos\beta-\cos\gamma)e_t'+k_2(\sin\beta-\sin\gamma)e_t'' \quad (3)$$

Phase *b*

$$0=-L_{sm2}p\theta_3 I_{s2}'+L_{sm2}pI_{s2}''-L_{s2}p\theta_3 I_{s2}'+(r_{s2}+L_{s2}p)I_{s2}''-k_2(\sin\beta-\sin\gamma)e_t'+k_2(\cos\beta-\cos\gamma)e_t'' \quad (4)$$

Regulating Machine Rotor and Induction Machine Rotor

Phase *a*

$$0=-M_1p\theta_3 I_{s2}'-M_1p\theta_3 I_{s2}''+[r_{s1}+r_{r1}+r_{r2}+(l_{s1}+l_{r1}+L_{r3})p]I_{s1}'+[l_{r1}p\theta_2+(l_{s1}+l_{r1}+L_{r3})p\theta_3]I_{s1}''-M_2pI_{s4}'-M_2p\theta_3 I_{s4}'' \quad (5)$$

Phase *b*

$$0=-M_1p\theta_3 I_{s2}''-M_1p\theta_3 I_{s2}''-[l_{r1}p\theta_2+(l_{s1}+l_{r1}+L_{r3})p\theta_3]I_{s1}'+[r_{s1}+r_{r1}+r_{r2}+(l_{s1}+l_{r1}+L_{r3})p]I_{s1}''+M_2p\theta_3 I_{s4}'-M_2pI_{s4}'' \quad (6)$$

Induction Machine Stator and Load

Phase *a*

$$e_t'=E_{s4}'+Z'I_{s4}'=-(r_{s4}+L_{s4}p)I_{s4}'+M_2pI_{s1}' \quad (7)$$

Phase *b*

$$e_t''=E_{s4}''+Z''I_{s4}''=-(r_{s4}+L_{s4}p)I_{s4}''+M_2pI_{s1}'' \quad (8)$$

Neglecting saturation everywhere except in M_2 (the mutual inductance of the induction machine), neglecting leakage reactances in the load and power factor control field windings, and making the following substitutions:

$I_M'=I_{s2}'+I_{s3}'$
$I_M''=I_{s2}''+I_{s3}''$
$I_g'=I_{s1}'-I_{s4}'$
$I_g''=I_{s1}''-I_{s4}''$
$\psi_g'=M_2I_g'$
$\psi_g''=M_2I_g''$
$r=r_{s1}+r_{r1}+r_{r2}$
$l=l_{s1}+l_{r1}+lL_{r3}$
$p\theta=p\theta_2=p\theta_3$
$L_{s2}=L_{s3}=L_{sm2}=M_1$

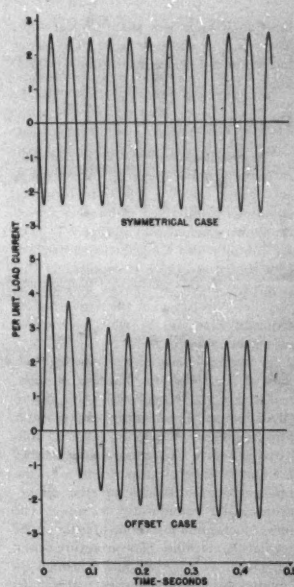

Figure 9. Instantaneous values of load current in the loaded phase versus time

$L_{ext}=0.375$ (loaded phase)
Single-phase load current
No-load frequency = 25 cycles per second
Power-factor field resistor short-circuited at $t=0$

the equations become

Phase a

$$0=r_{s1}I_{s1}'+M_1pI_M'+M_1p\theta I_M''+k_1(\cos\beta)e_t'+k_1(\sin\beta)e_t'' \quad (9)$$

Phase b

$$0=r_{s1}I_{s1}''-M_1p\theta I_M'+M_1pI_M''-k_1(\sin\beta)e_t'+k_1(\cos\beta)e_t'' \quad (10)$$

Phase a

$$0=-r_{s1}I_{s1}'+(r_{s1}+M_1p)I_M'+M_1p\theta I_M''+k_2(\cos\beta-\cos\gamma)e_t'+k_2(\sin\beta-\sin\gamma)e_t'' \quad (11)$$

Phase b

$$0=-r_{s1}I_{s1}''-M_1p\theta I_M'+(r_{s1}+M_1p)I_M''-k_2(\sin\beta-\sin\gamma)e_t'+k_2(\cos\beta-\cos\gamma)e_t'' \quad (12)$$

Phase a

$$0=-M_1p\theta I_M'+(r+lp)I_g'+p\psi_g'+(l_{r1}+l)p\theta I_g''+p\theta\psi_g''+(r+lp)I_{s1}'+(l_{r1}+l)p\theta I_{s1}'' \quad (13)$$

Phase b

$$0=-M_1p\theta I_M''-(l_{r1}+l)p\theta I_g'-p\theta\psi_g'+(r+lp)I_g''+p\psi_g''-(l_{r1}+l)p\theta I_{s1}'+(r+lp)I_{s1}'' \quad (14)$$

Phase a

$$e_t'=E_{s1}'+Z'I_{s1}'=-(r_{s1}+l_{s1}p)I_{s1}'+p\psi_g' \quad (15)$$

Phase b

$$e_t''=E_{s1}''+Z''I_{s1}''=-(r_{s1}+l_{s1}p)I_{s1}''+p\psi_g'' \quad (16)$$

If it is assumed that

$$E_{s1}=0$$

$$\frac{R}{L}=\frac{r_{s1}}{l_{s1}}=\frac{r}{l}=\delta$$

the currents I_{s1}' and I_{s1}'' are eliminated, and the equations written in the following integral form, which was that used on the analyzer:

$$I_{s1}'=\frac{1}{l_{s1}+L'}\psi_g'-\delta\int I_{s1}'dt \quad (17)$$

$$I_{s1}''=\frac{1}{l_{s1}+L''}\psi_g''-\delta\int I_{s1}''dt \quad (18)$$

$$\psi_g'=\frac{l_{s1}+L'}{l+l_{s1}+L'}[M_1p\theta\int I_M'dt-r\int I_g'dt-lI_g'-(l_{r1}+l)p\theta\{\int I_g''dt+\int I_{s1}''dt\}-p\theta\int\psi_g''dt] \quad (19)$$

$$\psi_g''=\frac{l_{s1}+L''}{l+l_{s1}+L''}[M_1p\theta\int I_M''dt+(l_{r1}+l)p\theta\{\int I_g'dt+\int I_{s1}'dt\}+p\theta\int\psi_g'dt-r\int I_g''dt-lI_g''] \quad (20)$$

$$I_g'=\frac{1}{M_2}\psi_g' \quad (21)$$

$$I_g''=\frac{1}{M_2}\psi_g'' \quad (22)$$

$$I_M'=\frac{r_{s1}}{(r_{s1}+r_{s2})M_1}\Bigg[-\left(1+\frac{r_{s1}}{r_{s2}}\right)\times M_1p\theta\int I_M''dt-r_{s1}\int I_M'dt-\left(\frac{r_{s1}}{r_{s2}}k_1\cos\beta+k_2\{\cos\beta-\cos\gamma\}\right)\times\frac{L'}{l_{s1}+L'}\psi_g'-\left(\frac{r_{s1}}{r_{s2}}k_1\sin\beta+k_2\times\{\sin\beta-\sin\gamma\}\right)\frac{L''}{l_{s1}+L''}\psi_g''\Bigg] \quad (23)$$

$$I_M''=\frac{r_{s1}}{(r_{s1}+r_{s2})M_1}\Bigg[\left(1+\frac{r_{s1}}{r_{s2}}\right)\times M_1p\theta\int I_M'dt-r_{s1}\int I_M''d\left(\frac{r_{s1}}{r_{s2}}k_1\sin\beta+k_2\{\sin\beta-\sin\gamma\}\right)\times\frac{L'}{l_{s1}+L'}\psi_g'-\left(\frac{r_{s1}}{r_{s2}}k_1\cos\beta+k_2\{\cos\beta-\cos\gamma\}\right)\frac{L''}{l_{s1}+L''}\psi_g''\Bigg] \quad (24)$$

Steady State No-Load Initial Conditions

The steady-state values required for the initial differential analyzer settings are for no load, normal voltage conditions. Then in equations 17–24 the load currents I_{s1}' and I_{s1}'' are zero, the load reactances L' and L'' are infinite, p is replaced by $j\omega_s$ and $p\theta$ by ω_r, where ω_s is the angular velocity of the stator voltage and ω_r is the rotor angular velocity. Moreover, since everything is balanced and symmetrical it will simplify matters if equations 17–24 are written in vector form. This is accomplished by letting:

$$\left.\begin{aligned} I&=I'+jI'' \\ \psi&=\psi'+j\psi'' \end{aligned}\right\} \quad (25)$$

Making these substitutions equations 19 and 20 are written

$$\psi_g(\omega_s-\omega_r)=-jM_1\omega_rI_M+[l_{r1}\omega_r-l(\omega_s-\omega_r)+jr]I_g \quad (26)$$

$$\psi_g=M_2I_g \quad (27)$$

Substituting equation 27 into equation 26

$$I_M=\frac{+jM_2(\omega_s-\omega_r)+[r+j(\omega_s\omega_r)l-j\omega_rl_{r1}]}{M_1\omega_r}I_g \quad (28)$$

All of the quantities on the right hand side of equation 28 are known. At least the magnitude of I_g (which is the same as I_{s1} at no load) is known to be the value necessary to give normal voltage on the saturation curve, namely, 190 amperes.

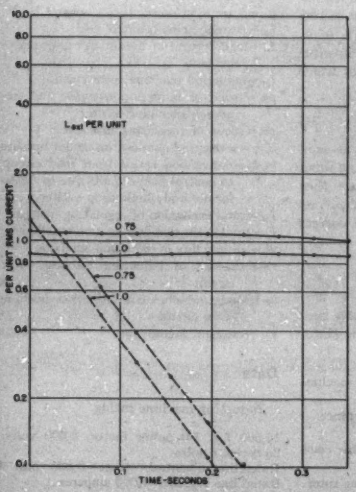

Figure 10 (left). Rms values of a-c and d-c components of current versus time

Three-phase load current
No-load frequency = 24.2 cycles per second (5.9 per cent slip)
Power-factor field short-circuited at $t=0$

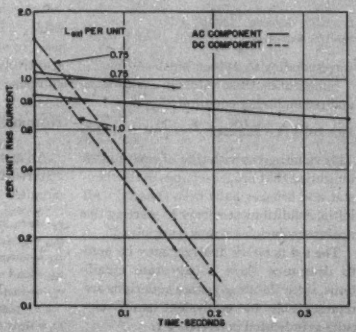

Figure 11. Rms values of a-c and d-c components of current versus time

Three-phase load current
No-load frequency = 25 cycles per second
Power-factor control field not short-circuited

The phase of I_g is given by $I_g'=0$ and $I_g''=190$, or $I_g=j\,190$. The other values necessary to determine I_M are (all quantities are referred to the induction machine stator)

$M_2=0.1278$ (normal voltage value) henry
$\omega_s=157.08$ radians per second
$\omega_r=161.56$ radians per second
$l_{r1}=0.0000566$ henry
$l=0.00218$ henry
$r=0.029$ ohm
$M_1\omega_r=1.115$ ohms

From these I_M is determined as

$$I_M=101+j4.9 \text{ amperes} \tag{29}$$

There remains another relationship connecting I_M and ψ_g (and consequently I_M and I_g), namely, that which may be obtained from equations 23 and 24. Here both r_{s2} and r_{s1} are determined by a single rheostat setting. The two brush angles β and γ then must be adjusted by a cam drive until the value of I_M obtained from equations 23 and 24 is the same as that given in equation 29. From equations 23 and 24 we have

$$I_M=\frac{r_{s2}}{(r_{s2}+r_{s1})M_1}\left\{\left[M_1\left(1+\frac{r_{s1}}{r_{s2}}\right)\frac{\omega_r}{\omega_s}+j\frac{r_{s1}}{\omega_s}\right]I_M-\left[\frac{r_{s1}}{r_{s2}}k_1\cos\beta+k_2(\cos\beta-\cos\gamma)\right]\psi_g+j\left[\frac{r_{s1}}{r_{s2}}k_1\sin\beta+k_2(\sin\beta-\sin\gamma)\right]\psi_g\right\} \tag{30}$$

where

$l_{s2}=0.0069$ henry
$k_1=-0.00463$
$k_2=-0.00514$

Choose

$r_{s1}=0.0551$ ohm
$r_{s2}=4.30$ ohms

corresponding to a given rheostat setting and

$\beta=123.1$ degrees
$\gamma=109.4$ degrees

corresponding to a given brush setting.

Substituting these values in equation 30 and remembering equation 27

$$I_M=101+j4.8 \text{ amperes} \tag{31}$$

This value agrees with that of equation 29 indicating that proper settings of the rheostat and brushes have been chosen. All initial conditions necessary to starting the analyzer solution are now determined.

The a-c network analyzer may be used to determine these steady-state conditions, since the steady-state equations are representable by equivalent static circuits as indicated in reference 1.

Figure 12. Magnetization curve for induction machine

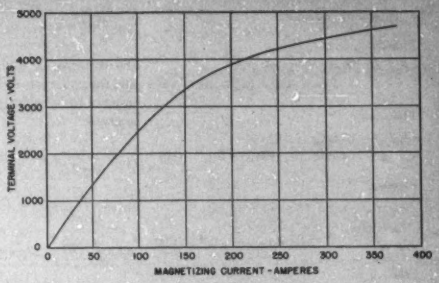

Differential Analyzer Representation of Saturation

In this study the currents I_g' and I_g'' were obtained from ψ_g' and ψ_g'' by means of the saturation curve, but in an apparently roundabout way. The known relationship is

$$\psi_g=M_2I_g \tag{32}$$

since the machine is a symmetrical one. In this study flux is known and current is to be determined from it. Moreover, it is required to find the two phase components of I_g. In this regard, likewise because of the symmetrical structure of the machine,

$$\left.\begin{aligned} I_g'&=\frac{1}{M_2}\psi_g' \\ I_g''&=\frac{1}{M_2}\psi_g'' \end{aligned}\right\} \tag{33}$$

However, M_2 is a function only of the absolute value of ψ_g. Therefore, it is first necessary to obtain this absolute value. On the differential analyzer, this involves using the vector table attachment which gives

$$|\psi_g|=\sqrt{\psi_g'^2+\psi_g''^2} \tag{34}$$

The quantity $1/M_2$ is plotted as ordinate against $|\psi_g|$ as abscissa on an input table. Two multiplier tables are then used to multiply $1/M_2$ by ψ_g' and ψ_g'', respectively, to give the required current components I_g' and I_g''.

Nomenclature

All quantities are assumed to have been referred to the induction machine stator circuit.

e_t = terminal voltage of induction machine
E_{s1} = system voltage
r_{s2} = power factor control field resistance
r_{s2} = load control field resistance
r_{s1} = resistance of regulating machine compensating field
r_{r1} = resistance of regulating machine rotor
r_{r2} = resistance of induction machine rotor
r_{s1} = resistance of induction machine stator
$Z=R+Lp$ = load or system impedance
L_{s2} = power-factor control field self-inductance
L_{2m2} = mutual inductance between power factor and load control fields
L_{s2} = load control field self-inductance
M_1 = mutual inductance between the control fields and the regulating machine rotor
l_{s1} = leakage inductance of regulating machine compensating field with respect to rotor
l_{r1} = leakage inductance of regulating machine rotor with respect to compensating field
L_{r2} = self-inductance of induction machine rotor
M_2 = mutual inductance between induction machine rotor and stator
L_{s1} = self-inductance of induction motor stator
l_{s1} = leakage inductance of induction motor stator
I_{s2} = current in power factor control field
I_{s2} = current in load control field
I_{s1} = load current or induction motor stator current
I_{r1} = induction machine rotor current
$p\theta_2$ = speed of induction machine and frequency-changing exciter
$p\theta_1$ = speed of regulating machine
β, γ = settings of ohmic-drop exciter brushes
k_1, k_2 = conversion ratios from load circuit to control field circuits due to transformer and ohmic drop exciter
I_M = total excitation of regulating machine
I_g = total excitation of induction machine
ψ_g = air-gap flux in induction machine
r = resistance of induction machine rotor circuit
l = leakage inductance of induction machine rotor circuit
δ = decrement factor

Data

Induction machine rating

12,500 kw, 1.0 power factor, 6,600 volts, 25 cycles, 6 poles
Rated line to neutral voltage = 3,820 volts
Rated line current = 1,093 amperes

Base impedance at 25 cycles = 3.48 ohms
Base inductance = 0.0222 henry

Synchronous machine rating

60 cycles, 14 poles, 514 rpm

Induction and regulating machine constants

$r_{s1} = 0.025$ ohm
$l_{s1} = 0.00188$ henry
$r = r_{s1} + r_{r1} + r_{r2} = 0.029$ ohm
$l = l_{s1} + l_{r1} + l_{r2} = 0.00218$ henry
$L_{r2} = L_{r2} = L_{sm2} = M_1 = 0.00690$ henry

$\delta = \frac{r}{l} = 13.30$ per second

$l_{r1} = 0.0000566$ henry
$k_1 = -0.00463$
$k_2 = -0.00514$
$p\theta = \omega_r = 161.56$ radians per second when synchronous machine frequency is 60 cycles

Initial rheostat and brush settings corresponding to no load conditions at the two frequencies considered are

25 cycles	24.2 cycles
Slip = −0.0286	Slip = −0.059
$r_{r2} = 0.0551$ ohm	$r_{r2} = 0.0551$ ohm
$r_{s2} = 4.30$ ohms	$r_{s2} = 4.30$ ohms
$\beta = 128.1$ degrees	$\beta = 164$ degrees
$\gamma = 109.4$ degrees	$\gamma = 112$ degrees

Appendix. Check Calculations

The initial value of the alternating current, either 3-phase or single-phase, can be approximated by

$$I_{\text{per unit}} \approx \frac{E_{ac}}{\omega(l + l_{s1} + L) I_{\text{base}}}$$

Values calculated in this way compare with the differential analyzer results as follows:

L (Per Unit)	I (Calculated)	I (Three Phase)	I (Single Phase)
0	5.48	5.42	5.42
0.25	2.315	2.328	2.32
0.375	1.796		1.800
0.5	1.469	1.468	
0.75	1.075	1.072	
1.0	0.847	0.846	
2.0	0.459	0.459	

The d-c decrement can be approximated by

$$\delta = \frac{r_{s1} + R}{l + l_{s1} + L}$$

which gives for the time to half of the initial value

$$t_{0.5} = \frac{\log_e 2}{\delta} = \frac{(l + l_{s1} + L) \log_e 2}{r_{s1} + R}$$

Calculated and analyzer values of time to half value compare as follows:

L (Per Unit)	t (Calculated)	t (Three Phase)	t (Single Phase)
0	0.1125	0.114	0.112
0.25	0.0674	0.068	0.066
0.375	0.0631		0.062
0.5	0.0607	0.062	
0.75	0.0582	0.058	
1.0	0.0569	0.056	
2.0	0.0546	0.054	

Both the initial values and the d-c decrements check as well as the curves can be read.

References

1. Tensorial Analysis and Equivalent Circuit of a Variable-Ratio Frequency-Changer, Gabriel Kron. AIEE Transactions, volume 66, 1947, pages 1503–6.

2. Application of Large Frequency Converters to Power Systems, E. J. Burnham. AIEE Transactions, volume 47, 1928, pages 1070–8.

3. Frequency Changers—Characteristics, Applications, and Economics, S. B. Crary, R. M. Easley. AIEE Transactions, volume 64, 1945, June section, pages 351–8.

No Discussion

Diffusion of Electric Current Into Rods, Tubes, and Flat Surfaces

K. W. MILLER
MEMBER AIEE

Synopsis: Electric current density penetrates or "soaks" into an electric conductor starting from the surface during current transients in a manner physically and mathematically analogous to thermal diffusion in transient heat flow. This useful concept is used to explain physically and evaluate numerically transient resistance and inductance of conductors subjected to rectangular current wave impulses.

DESPITE the large amount of mathematical work of many investigators, it seems that there is still something more to add on the subject of skin effect and transient resistance of conductors carrying nonconstant electric current, particularly from a physical or descriptive viewpoint.

Most of the published formulas for skin effect are for sinusoidal alternating currents, and the mathematics tend to obscure rather than clarify the actual physical behavior of current distribution and redistribution. In this discussion we will consider the application of an abrupt or rectangular (Heaviside unit function) constant current suddenly applied to a conductor. We first will anticipate in a qualitative way what happens, following later with mathematical results for isolated conductors having plane surfaces or cylindrically circular symmetry.

To some, the concept of "applying a current" (instead of a voltage) is not itself familiar. To those it may be helpful to conceive of a voltage applied to a circuit dominated by a pure resistance, large compared to the impedance of conductors which form the leads. The resulting current in the circuit may be considered, then, as "applied" to the leads, which are "conductors."

When electric current is caused suddenly to flow in a conductor, we find that the current flows for the first instant entirely on the surface of the conductor as would be expected. Then, and surprisingly slowly at that, the current density "diffuses" into the conductor, the direction of the "diffusion wave" of current penetration being transverse to the direction of flow of the electric current. The laws governing the penetration of current into the conductor (see equations 1 and 4) are mathematically identical with those for the temperature distribution in transient heat flow by thermal diffusion. In fact, for copper, the electrical diffusion constant is only about 11 times as fast as thermal diffusion. Numerically the coefficient of velocity of current penetration or diffusion for copper is

$$k = 11.6 \text{ centimeters per second}^{1/2}$$

The half-crest value wave front of current density will penetrate 1 centimeter into a copper conductor in about 1/75 second; approximately 1/21 second is required for 1-inch penetration, and so forth. The velocity of penetration of the wave front decreases inversely as the square root of time and the distance penetrated increases as the square root of time, that is, the "velocity" of current penetration or diffusion is not constant. However, it will be found that *velocity* of penetration is unaffected by geometrical configuration and is independent of whether the current diffusion is "parallel" penetrating from a plane surface, divergent spreading outward from an inside surface (say outward from the inner surface of a hollow tube), or convergent diffusing inward, say, from the surface of a solid rod conductor. In these various cases, only the crest value of diffusion wave (which crest remains fixed in place at the initiating surface, line, or point) has its rate of decay altered by the degree of geometrical convergence or divergence encountered by the advancing wave front of penetration.

As an instructive example let us consider an idealized electric circuit consisting of a thick tube of circular cross section enclosing a circular rod with mathematically infinitesimal insulation of "zero thickness" separating the concentric conductor pair, Figure 1. Let us short-circuit together one end of this concentric conductor pair and suddenly apply a constant voltage E to the other end of the conductor pair. At the first instant, current flow will be restricted to infinitesimally thin adjacent surfaces of the two conductors, schematically shown by + and − signs in Figure 1. There is, by hypothesis, no space for magnetic flux between the two conductors, and by well known electromagnetic laws no flux will be produced externally or internally to the double opposite pair of tubular equal current sheets on the adjacent faces of the conductors. Therefore, even in this circuit, which is "inductanceless" at zero time, the initial transient resistance is infinite due to zero thickness of current penetration and current must start at zero for any finite voltage application.

Nature usually finds a way to avoid infinities and abrupt energy discontinuities. Even if the inductance of a circuit due to flux outside of conductors is totally absent or cancelled, as in the foregoing example, yet a truly "impulsive response" is still impossible due indirectly to the process of creation of magnetic flux *within* the conductor. Resulting zero-time initial transient resistance is always infinite and, for any finite applied voltage, causes the current to build up from zero or alter in value smoothly and without discontinuity to the final state.

It must be noted that the (rapidly diminishing) transient resistance to a

Paper 47-266, recommended by the AIEE basic sciences committee and approved by the AIEE technical program committee for presentation at the AIEE Midwest general meeting, Chicago, Ill., November 3–7, 1947. Manuscript submitted August 22, 1947; made available for printing September 26, 1947.

K. W. Miller is assistant director, Armour Research Foundation, Chicago, Ill.

rectangular current wave application is infinite for only zero length of time—a mathematically indeterminate condition which can be resolved mathematically for the cases to be considered later. Actually, exactly perfect rectangular current application never can be realized experimentally but the mathematical convenience of considering the rectangular current wave or Heaviside unit function is justified as a very close approximation to some practical cases and is one very instructive from a physical viewpoint in understanding what actually goes on within the conductor.

Transient resistance is discussed by Steinmetz[1] with, however, little emphasis on the physical behavior of the current penetration process and mathematically, chiefly from the standpoint of "equivalent" depth of penetration. Steinmetz did not analyze mathematically the action in circular conductors. Besides the example of transient resistance in steel rails under moving electric locomotives given by Steinmetz, transient resistance of conductors may be an appreciable factor in many electrical engineering problems. For example, the current-time interruption characteristics of fuses may be explained or initially predetermined for very short time current impulses. Resistance of heavy conductor leads to electric welders on intermittent operating cycles involve transient resistance due to finite velocity of electric current diffusion. The resistance of internal surfaces of radar wave guides when subjected to pulses or high frequency "square wave" forms is still another field for application of the current diffusion concept. Transient resistance will afford a better understanding of the attenuation or rounding off of the wave front of a rectangular traveling wave, say, on a transmission line.

With these preliminary remarks we proceed to examine the phenomenon of current diffusion in more detail. If we set up the differential equation for skin effect in a cylindrical conductor having a circular cross section (see, for example, reference 2) but leave the time derivative $\partial i/\partial t$ general, *not* set equal to $j\omega$, we readily find

$$\frac{\partial^2 i}{\partial x^2}+\frac{1}{x}\frac{\partial i}{\partial x}=\frac{4\pi\mu}{\rho}\frac{\partial i}{\partial t} \tag{1}$$

where, in any consistent units,

i = current density at radial distance x
x = radial distance
t = time
μ, ρ = magnetic permeability and specific resistivity of conductor material (both assumed constant independent of i, x, and t) (equation 1 may be developed from the general wave equation, in cylindrical space co-ordinates for an isotropic medium where, since the medium is a conductor, say copper, having negligible voltage gradient within the metal, the displacement or capacity current term $\mu k\partial^2 i/\partial t^2$ is dropped from the right-hand side of the equation as a negligible quantity; see, for example, references 5 and 8).

If we set

$$\frac{4\pi\mu}{\rho}=\frac{1}{h^2} \tag{2}$$

in equation 1 where h is a constant, it will be recognized[3] as identical in mathematical form with that for 2-dimensional thermal diffusion for radial heat flow in a circularly symmetrical rod or tube. For thermal diffusion

$$h^2=k/(c\delta) \tag{3}$$

where k, c, and δ are, respectively, heat conductivity, specific heat, and density of the material all in consistent units. Values of h, both electrical and thermal, for three common materials are given in Table I in centimeters per square root-second units.

If we omit the $(1/x)(\partial i/\partial x)$ term on the left of equation 1, it reduces to the well known diffusion equation for parallel flow transverse to the plane surface of a semi-infinite solid, that is,

$$\frac{\partial^2 i}{\partial x^2}=\frac{1}{h^2}\frac{\partial i}{\partial t} \tag{4}$$

(which is equivalent to Steinmetz[1] equation 10).

The boundary conditions of present interest are simply that total current is zero until zero time, and constant, I, thereafter, that is, the integral of current density i over the total cross section available for current flow is constant. When this area is infinite (or may be considered as approximately so for short times when penetration depth is small compared to the conductor cross section), solutions[3] of equations 4 and 1 may be obtained by the Fourier transformation whence we obtain

$$i=2I\sqrt{\frac{\mu}{\rho t}}\,\epsilon^{-\mu\pi x^2/\rho t}=\frac{I}{h\sqrt{\pi t}}\epsilon^{-x^2/4h^2t} \tag{5}$$

for plane parallel flow from equation 4, and

$$i=I\,\frac{\mu}{\rho t}\epsilon^{-\mu\pi x^2/\rho t}=\frac{I}{4\pi h^2 t}\,\epsilon^{-x^2/4h^2t} \tag{6}$$

from equation 1. Equation 6 is for divergent diffusion of current density with total current, I, initially concentrated in an infinitesimal straight line filament in infinite material, that is, equivalent to initial current flow all concentrated along the axis of a solid cylinder of infinite radius.

The solution of equation 1 for constant total current (or heat) flow I starting to diffuse from the surface of a circular rod is

$$i=\frac{I}{\pi b^2}\left[1+\sum_{n=1}^{n=\infty}\frac{J_0(\mu_n x)}{J_0(\mu_n b)}\,\epsilon^{-h^2\mu_n^2 t}\right] \tag{7}$$

where

$$J_1(\mu_n b)=0 \tag{7a}$$

while the solution of equation 1 for constant total current starting to diffuse from the outer surface of a hollow tube is

$$i=\frac{I}{\pi(b^2-a^2)}+\sum_{n=1}^{n=\infty}A_n[J_0(\mu_n x)-C_nN_0(\mu_n x)]\epsilon^{-h^2\mu_n^2 t} \tag{8}$$

where

$$C_n=\frac{J_1(\mu_n a)}{N_1(\mu_n a)}=\frac{J_1(\mu_n b)}{N_1(\mu_n b)} \tag{8a}$$

$$A_n=\frac{I}{\pi}\left[\frac{Z_{01}(\mu_n b)}{b^2Z_{01}^2(\mu_n b)-a^2Z_{01}^2(\mu_n a)}\right] \tag{8b}$$

$$Z_{01}(\mu_n x)=J_0(\mu_n x)-\left(\frac{J_1(\mu_n x)}{N_1(\mu_n x)}\right)N_0(\mu_n x) \tag{8c}$$

In all equations 7 and 8, J and N are Bessel functions of first and second kinds, respectively, and of zero or first order according to subscript; b is the outer and a the inner radius (if any) of the circular conductor. Equations 7a and 8a deter-

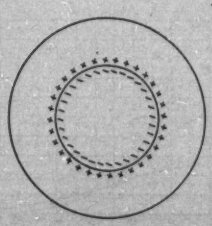

Figure 1. Transient current flow in adjacent surfaces of concentric rod—thick tube conductor pair

Table I

Material	Diffusion "Velocity" h, Cm Per Sec: Thermal	Electrical
Copper	1.06	11.6
Aluminum	0.91	14.5
Steel	0.41	1.9*

* Value of μ assumed constant at 1,000.

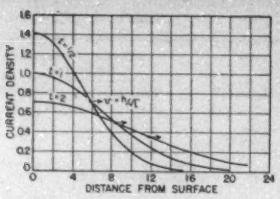

Figure 2. Parallel current penetration from plane surface

mine the roots μ_n and the latter equation the C_n ratios also. Equations 7, 8, and later dependent equations all are believed to be new. Their derivation is tedious and a bit tricky to avoid indeterminate values at time $t=0$ and will not be given here. Equation 8, and other equations to follow, for the hollow tube reduces to equation 7, and others, for the solid rod when $a \rightarrow 0$ as they should and all may be verified easily by appropriate differentiations and integrations.

In the equations already given and those to follow, it is highly convenient to take advantage of the well known principle of similitude and transform all equations into dimensionless form by making the substitutions

$$x = b\bar{x}$$
$$\bar{x} = x/b$$
$$t = \left(\frac{b}{h}\right)^2 \bar{t}$$
$$\bar{t} = \left(\frac{h}{b}\right)^2 t$$
$$\mu_n = \bar{\mu}_n/b$$
$$\bar{\mu}_n = b\mu_n \qquad (9)$$

The resulting equations become functions of pure numeric quantities $\bar{x}$, $\bar{t}$, and $\bar{\mu}_n$ only, which, except for a scale factor, are each directly proportional to distance, time, and roots, respectively. Final numerical results tabulated or plotted as curves in terms of these pure numeric variables easily may be reinterpreted in terms of actual dimensions and materials for any specific problem by reference to equations 9.

Equations 5 and 6, restated in terms of dimensionless variables, have been plotted in Figures 2 and 3 for three consecutive fixed instants of time in the ratio $\bar{t}=1/2$: 1:2. Figure 2 is for plane parallel diffusion, equation 5, and Figure 3 is for radially divergent diffusion from the axis of a cylinder of infinite radius, equation 6. In both cases, we note that the current density–penetration curves are always of the same shape (in fact, half of the hump of the normal error or probability curve) and differ for different instants of time only in vertical and horizontal scale. The wave front of current penetration typified by the point of half-amplitude for each curve (indicated by heavy dots) advances horizontally with a velocity proportional to $h/\sqrt{\bar{t}}$ and penetrates a distance d proportional to the square root of time, that is,

$$d \approx h\sqrt{\bar{t}} = 0.707 : 1 : 1.414$$

If we multiply the ordinates of the curves in Figure 2 by $\bar{x}$ and those of Figure 3 by $2\pi\bar{x}$ and integrate from $\bar{x}=0$ to $\bar{x}=\infty$, we find total current flow is constant in time. We note further that all curves have horizontal slope at the origins $\bar{x}=0$ and at $\bar{x}=\infty$ where they form long thin advance "toes" to the diffusion wave. (The infinite toes are the mathematical result of neglecting the negligible displacement current term in equation 1. These infinite toes are of trivial magnitude and, of course, physically impossible since they imply infinite velocity of propagation.)

The plane parallel diffusion case is one of practical importance in its own right (for example, surface of wave guides) and also useful later as a limiting initial approximation to more complicated cases. The case of divergent radial current diffusion from a line axis is admittedly highly artificial and has only qualitative significance for us. It shows that divergence or increase of area available to diffusion, as the wave front expands over ever greater circumferences, has no effect on either diffusion wave shape or velocity. Divergent flow merely causes the amplitude to "attenuate" faster to conserve the total current constant equal to I. Indeed, although meaningless in electric current diffusion analogy, in a similar manner it readily is shown that a fixed quantity of heat, diffusing radially outward in three dimensions with spherical symmetry from an initial instantaneous point source into a homogeneous infinite solid, produces a temperature distribution with profile shape and diffusion wave velocity exactly the same as given in Figures 2 and 3 for 1-dimensional diffusion with no divergence from a plane surface and for 2-dimensional divergent diffusion from a line filament, respectively. In other words, by mathematical analogy we conclude that convergent or divergent penetration of electric current density by diffusion into a conductor occurs at the same rate h regardless of conductor contour—even of compound surface curvature. Only the *time* rate of decrease of "amplitude" or current density values, particularly the maximum value at the surface, is affected.

Therefore, with convergent diffusion or penetration of current density radially inward from outer surfaces of cylindrical conductors, we correctly expect the wave shape and velocity $h/\sqrt{\bar{t}}$ of half-crest-value current density both to be unaffected *until* the advance toe on the wave front meets an internal tube radius or is "pinched out" at the central axis in a solid rod where circumference available to the advancing wave front shrinks to zero. In either such case, as time progresses, the current density piles up at such advance barrier and the current diffusion wave merges from a condition of an inwardly traveling wave into an intermediate leveling off process and final state of uniform current density (see Figure 4).

The thermal diffusion analogy is useful here. To a rod or tube of uniform (zero) initial temperature, a fixed finite quantity of heat Q is added to the outer cylindrical surface by exposing it to infinite temperature for zero time, after which it immediately is covered with a perfect heat insulator of zero thermal heat capacity and zero heat conductivity. The thermal diffusion temperature profiles would be identical as just described (and as shown in Figure 4) to those of current density when unit rectangular electric current suddenly is applied to the same conductor. Only the penetration velocity constant h is different. This thermal experiment is obviously difficult to perform! Likewise the mathematical solutions given by equations 7 and 8 for solid circular rods and tubes are very tedious to evaluate numerically for different radii for the intermediate times t of most interest because of slow convergence of the mathematical series requiring many terms which exceed the extent of tabulated values of the Bessel functions. Computing the several terms required even by asymptotic formulas[4] is very laborious. Figure 4 for the solid circular rod, equation 7, is a close approximation which illustrates the behavior, but should not be used for accu-

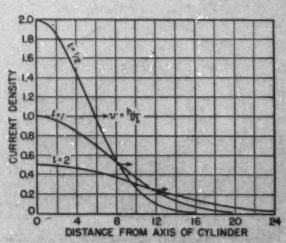

Figure 3. Divergent current penetration from line element

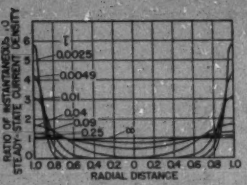

Figure 4. Transient current distribution in solid rod

rate numerical evaluation of losses or internal inductance for which more precise methods are available.

Thus, Figures 2, 3, and 4 represent the current density diffusion penetration curves for a rectangular electric current wave applied to conductors under three different geometric configurations, (1) parallel diffusion from the plane face of a flat surfaced conductor, (2) radially divergent diffusion from initial current concentration along a straight line filament, and (3) convergent diffusion radially inward from the surface of a circular rod, respectively. We pause again to recapitulate. What is it that "diffuses"? Initially, during the transient, it is not the electric current itself but, instead, the current density that diffuses. The electric current itself "propagates" in the direction of current flow with a true velocity $v = 1/\sqrt{\mu k}$ (or a more complicated expression for imperfect medium having resistance and leakage), μ and k being permeability and dielectric constant of the medium. Of present concern, the current density penetrates by "diffusion" from the conductor surface into the conductor section in a direction normal to the lines of electric current flow with a "velocity" $h/\sqrt{t}$ where h, given by equation 2, is a function of magnetic permeability and resistivity of the medium but is independent of its dielectric constant.

The diffusion constant h, about 11 centimeters per second$^{1/2}$, is also a measure of the velocity with which the electrons migrate or diffuse in the conductor. Just as in a gas, the velocity of propagation of sound vastly exceeds the velocity of gaseous diffusion, so in a metallic conductor the velocity of propagation of the wavefront of current vastly exceeds the electronic diffusion "velocity" $v = h/\sqrt{t}$. This diffusion starts as a sidewise penetration of current density from the conductor surface into its cross section, the entire subject of this paper, and continues (in time) as an axialwise or currentwise diffusion of electrons which form the electric current itself. This is the physical picture.

Because current density cannot migrate across a surface boundary into nonconducting surrounding medium, $\partial i/\partial x$ must be zero everywhere at the conductor surface. Therefore, at any finite instant of time, after the indeterminate initial zero time instant, the current density is constant or uniform at and in a direction normal to the conductor surface. Current density does not drop off exponentially with "depth of penetration" for a rectangular current wave. All the mathematical solutions and Figures 2, 3, and 4, given for special geometric configurations, comply with or yield this result.

One matter of prime interest in skin effect problems is the effective increase in resistance. The "a-c–d-c resistance ratio," or more properly here the "transient resistance" ratio for sudden application of constant current, is not a fixed quantity but varies with time after initiation of the rectangular current wave. Since the resistance ratio starts with an infinite and rapidly diminishing value, it is useful to define a cumulative time average ratio as well. Thus we define the quantities

$$W = \int_A i^2 \rho dA \tag{10}$$

$$W_{av} = \frac{1}{t}\int_0^t W dt \tag{11}$$

and the ratios

$$K = W/I^2R \tag{12}$$

$$K_{av} = W_{av}/I^2R \tag{13}$$

where

W = instantaneous value of resistance losses per unit length of conductor at time t
W_{av} = average value of resistance losses up to time t
A = conductor cross-section area
I = total current (constant after time $t=0$)
R = d-c resistance of conductor

Here K_{av} also may be considered as the ratio of total accumulated resistance losses to what the losses would have been for same time with uniform current distribution. We utilize, in addition, the transformations given by equations 9 to put all quantities in dimensionless ratio form. We consider now the special geometric configurations one at a time.

Squaring equation 5, introducing it into equation 10, and integrating x from 0 to ∞ yields W and then introducing W into equation 11 and integrating on t gives W_{av} for the case of plane parallel diffusion. We find

$$W = 2I_1^2\sqrt{\frac{\mu\rho}{2t}} \tag{14}$$

$$W_{av} = 4I_1^2\sqrt{\frac{\mu\rho}{2t}} \tag{15}$$

Because the distance co-ordinate x is infinite, these quantities have not been reduced to dimensionless ratio form. Here μ, ρ, and t are permeability, specific resistivity, and time in consistent units, and I_1 is current per unit length of perimeter of the conductor cross section. In this form equations 14 and 15 may be useful for use on wave guide surfaces and conductors of irregular cross section for conditions where $h\sqrt{t}$ is small compared to thickness and to surface curvature of the conductor under consideration.

From preceding remarks we see that for very short times the outer surface of a rod or tube of circular section may be considered as "plane" before penetration has proceeded very far. Thus, setting $I_1 = I/2\pi b$ in equations 14 and 15, and putting results in dimensionless form by equation 9, then equations 12 and 13 become approximately

$$K = (1/2\sqrt{2\pi t})(1-1/k^2),\ h\sqrt{t} < (b-a)/10 \tag{14a}$$

$$K_{av} = (1/\sqrt{2\pi t})(1-1/k^2),\ h\sqrt{t} < (b-a)/10 \tag{15a}$$

where $k = b/a$ = ratio of tube radii ($k = \infty$ for solid rod).

The accurate solution for loss ratio in solid circular conductors or rods is given by squaring equation 7 and substituting into equations 10 and 11. Here dA is $2\pi x dx$ and integration on x is from 0 to b. After putting all quantities in dimensionless form, we obtain

$$K = 1 + \sum_{n=1}^{n=\infty} e^{-\bar{\mu}_n \bar{t}} \tag{16}$$

$$K_{av} = 1 + \frac{1}{16\bar{t}} - \sum_{n=1}^{n=\infty} (e^{-\bar{\mu}_n \bar{t}})/(2\bar{\mu}_n \bar{t}) \tag{17}$$

Here μ_n are the roots of

$$J_1(\bar{\mu}_n) = 0 \tag{18}$$

and certain mathematical steps required in the summations are explained in the first part of the appendix. Equation 16 is plotted in Figure 5, and equation 17 is plotted as the top limiting curves in Figure 6.

The transient internal inductance of a solid rod to rectangular current application is given by the formula

$$L = \mu\left[\frac{1}{2} - 4\bar{t}\sum_{n=1}^{n=\infty} (e^{-\bar{\mu}_n \bar{t}})(2 - e^{-\bar{\mu}_n \bar{t}})/(\bar{\mu}_n \bar{t})\right] \tag{16a}$$

which also is plotted in Figure 5 (for $\mu = 1$). This is an instantaneous value; cumulative or average inductance is not here defined.

For hollow circular tubes the square of

equation 8 is substituted into equations 10 and 11. Again in equation 10, dA is $2\pi x dx$ and integration is now between limits a and b, the inner and outer tube radii. Integrations are straightforward but tedious. We find

$$K = 1 + \sum_{n=1}^{n=\infty} \left[\frac{(k^2-1)}{k^2 - \left(\frac{Z_0(\bar{\mu}_n)}{Z_0(\bar{\mu}_n k)} \right)^2} \right] e^{-\bar{\mu}_n^2 \tau_0 t} \quad (19)$$

$$K_{av} = 1 + \sum_{n=1}^{n=\infty} \left[\frac{(k^2-1)}{k^2 - \left(\frac{Z_0(\bar{\mu}_n)}{Z_0(\bar{\mu}_n k)} \right)^2} \right] \cdot \left[\frac{1 - e^{-\bar{\mu}_n^2 \tau_0 t}}{2\bar{\mu}_n^2 k^2 t} \right], \quad (20)$$

where as before $k = b/a$, other abbreviations are given by equations 8c and 9 to 13, and the roots $\bar{\mu}_n$ are determined from equation 8a which may be rewritten in dimensionless form as

$$J_1(\bar{\mu}_n k) N_1(\bar{\mu}_n) - J_1(\bar{\mu}_n) N_1(\bar{\mu}_n k) = 0 \quad (21)$$

The second and major portion of the appendix (starting with equation 26) discusses steps in evaluating equations 21, 20, and 19. The numerical work is quite tedious but, fortunately, once performed is final once and for all. (Only equation 20 was evaluated—Figure 6.) For short and intermediate times of prime interest, many terms of the series are required, just as many terms of a Fourier's sine or cosine series are required to fit accurately the sharp corners in a square or sawtooth wave form. For extremely short time the surface plane wave diffusion, equations 14a and 15a, and for very long time the d-c conditions, respectively, are asymptotically approached. For vanishingly small inner radius of hollow tube, the solid rod case applies; while for very thin tubes of "zero" wall thickness, the transient resistance ratio is unity from the start. Utilizing these limiting conditions, two intermediate cases of thick tubes with radii ratio $k = b/a = 3/1$ and $3/2$ were evaluated. Further curves with other k ratios were interpolated. The final results for average or cumulative transient resistance are plotted in Figure 6 which may be interpolated for any tube radii ratio from solid rod to very thin-walled tube and for any conductor material and h values.

As a numerical example of the use of Figures 5 and 6, suppose a constant current I suddenly is applied to a thick walled copper tube of 1/2-inch internal diameter and 3/2-inch external diameter. Transient and cumulative transient resistances and losses and inductance are desired, say, at time of 0.0001, 0.001, and 0.01 second. Here $k = 3/1 = 3$, $h = 11.6$ centimeters per second$^{1/2}$ for copper, $b = (2.54 \times 3/2)/2 = 1.905$ centimeters outer radius. Therefore, by equation 9, $l = (11.6/1.905)^2 \times 0.0001 = 0.0037$ and 10 and 100 times this at the three times desired. Entering Figures 5 and 6 with $k = 3$ and $l = 0.0037$, 0.037, and 0.37, we may prepare the following table:

Time t, Sec = 0.001	0.001	0.01
$\bar{t} = (h/b)^2 t$	0.0037	0.037	0.37
L, Figure 5	(0.08)	(0.23)	(0.49)
K, Figure 5	(3.6)	(1.37)	(1.00)
K_{av}, Figure 6	6.0	2.1	1.12

Strictly speaking, Figure 5 is for solid rods only but its use for hollow tubular conductors, particularly very thick walled ones and for very short times, is justified by considerations which were elaborated for Figure 4 and also by the close spacing and parallelism of the curves for $k = \infty$ and $k = 3$ in Figure 6. Therefore, the tabulated values, interpreted by means of equations 10 to 13, indicate that when this heavy tubular conductor is subjected to a rectangular current wave, the internal inductance L (which is zero at zero time) increases from about 1/6 final value at 1/10,000 second to nearly full value (1/2 in absolute units) after 1/100 second. The instantaneous transient resistance K, ratio, initially infinite, decreases from 3.6 times d-c resistance to normal in the same time interval, 1/10,000 to 1/100 second. The cumulative average or total resistance losses from zero time to the same time intervals are 6.0 and 1.12 times the d-c resistance values. Since the d-c values themselves easily are calculated by elementary methods, they will not be given here.

By returning to equations 7 and 8 and utilizing the Duhamel integral, it is possible to determine the current diffusion and transient resistance ratio for any current wave form whatever. In particular for sinusoidal current, one thus should obtain the known expressions for a-c skin effect in isolated rods and tubes previously obtained by other investigators by more direct methods. Since this would serve merely as a check on the present work and would be very tedious, it was not attempted. However, of much more practical interest, a continuous square wave-form current could be considered as an infinite sequence of consecutively superimposed, uniformly timed, alternately plus and minus Heaviside unit waves. The resulting current density and losses could be readily built up, then, from solutions herein derived for flat surfaces and circular tubes or rods. Lastly it should be mentioned that by minor modifications of boundary conditions the solutions could readily be obtained to electric current

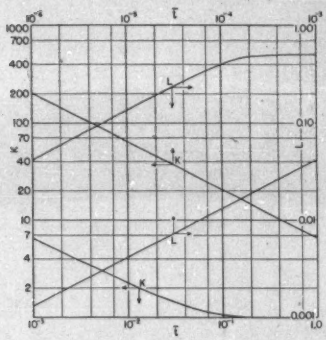

Figure 5 (left). K and L versus $\bar{t}$ for solid rods

Figure 6 (right). K_{av} versus $\bar{t}$ for rods and thick tubes

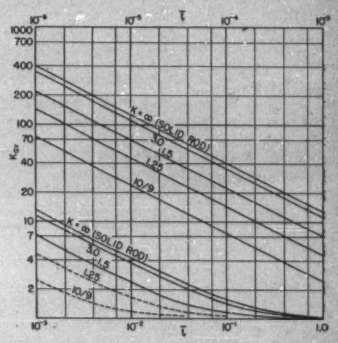

flow in concentric conductors, one side of the circuit or current flow starting to diffuse outward from the inner surface of the outer tubular conductor. There may be practical value in doing this for wave guides carrying high frequency square wave currents or current impulses.

However, the primary purpose of this paper has been to show that skin effect is due to a true diffusion type of penetration of current density as it "soaks" into the conductor starting from the surface. Since the analogy with heat diffusion and temperature is mathematically exact, then the greater general familiarity with heat flow concepts can be brought to bear for intuitive understanding and solution of the corresponding electrical transient resistance problems. The diffusion constant h, easily evaluated numerically, becomes then an immediate useful index or guide as to the velocity and depth of current penetration under any specified conditions regardless of conductor shape. Moreover, in some cases, difficult skin effect problems actually might be solved approximately experimentally by heat flow and temperature measurement in equivalent thermal circuits.

Appendix

In the derivation of equation 17 of the text, the lower integration limit $t=0$ results in the infinite summation of the reciprocal squares of all the roots of $J_1(\mu_n)$ each divided by $2l$ which latter may be factored out of the summation. This summation converges very slowly which is not true of the remaining summation in equation 17 which converges rapidly due to negative exponential factors. That the first summation reduces exactly to $1/(16l)$ may be demonstrated as follows.

Watson,[6] pages 498 and 15, gives the following two expressions for Bessel functions of order p:

$$J_p(z)=\frac{(z/2)^p}{\Gamma(p+1)}\prod_{n=1}^{n=\infty}[1-(z/\mu_n)^2] \tag{22a}$$

$$J_p(z)=\sum_{m=0}^{m=\infty}\frac{(-1)^m(z/2)^{p+2m}}{m!(p+m)!} \tag{22b}$$

Equating these two expressions, cancelling out common factors, then writing out the summation in explicit terms

$$\prod_{n=1}^{n=\infty}\left(1-\frac{z^2}{\mu_n^2}\right)=p!\sum_{m=0}^{m=\infty}\frac{(-1)^m(z/2)^{2m}}{m!(p+m)!}=\left\{1-\left[\frac{z^2}{2^2\cdot 1\cdot(p+1)}+\dots\right]\right\} \tag{23}$$

Taking logarithms of both sides and expanding

$$z^2\sum_{n=1}^{n=\infty}\frac{1}{\mu_n^2}+\dots=\left[\frac{z^2}{4(p+1)}\right]+\dots \tag{24}$$

In all these expansions we have discarded all terms in fourth and higher powers in z. Cancelling z^2 in equation 3, that is, equating coefficients for equal powers of z, and setting $p=1$ for the first order we find

$$\sum_{n=1}^{n=\infty}1/\mu_n^2=1/8 \tag{25}$$

from which the $1/16l$ term in equation 17 of the text follows at once.

Numerical evaluation of equations 19, 20, and 21, or of equations 8 to 8c of the text involves values of the Bessel functions far beyond tabulated values. Use was made of the semiconvergent expressions given by Jahnke and Emde,[4] page 203. Adhering to their notation, by multiplication, we readily establish, first, the identity

$$P_0(x)P_1(x)+Q_0(x)Q_1(x)=1 \tag{26}$$

If we set

$$Z_m(x)=J_0(x)-\left(\frac{J_1(x)}{N_1(x)}\right)N_0(x) \tag{27}$$

we also find by some trigonometric algebra and use of equation 26

$$Z_m(x)\approx-\sqrt{2/\pi x}/[P_1(x)\sin\phi_1+Q_1(x)\cos\phi_1] \tag{28}$$

where

$$P_1(x)=1+0.1171875/x^2-0.1441956/x^4+0.676593/x^6-\dots \tag{29}$$

$$Q_1(x)=0.375/x-0.10253906/x^3+0.2775764/x^5-1.993532/x^7+\dots \tag{30}$$

$$\phi_1=x-\frac{3}{4}\pi \tag{31}$$

Starting again with the asymptotic expressions for $J_p(x)$ and $N_p(x)$ given by Jahnke and Emde, page 203, again by the application of some trigonometric algebra, we find

$$\left(\frac{J_p(x)}{N_p(x)}\right)\approx-\tan\left[\phi_p+\tan^{-1}\left(\frac{Q_p(x)}{P_p(x)}\right)\right] \tag{32}$$

where

$$\phi_p=x-\left(p+\frac{1}{2}\right)\frac{\pi}{2} \tag{33}$$

Setting kx for x in equation 32 and equating yields

$$\frac{J_p(x)}{N_p(x)}=\frac{J_p(kx)}{N_p(kx)} \tag{34}$$

which, with $p=1$, is the desired root relation (equation 21) of the text. Substituting equations 32 and 33 into equation 34 then taking inverse tangent of both sides and recalling that $\tan^{-1}$ is a periodic function of period π we obtain

$$n\pi=(k-1)x+\tan^{-1}\left(\frac{Q_p(kx)}{P_p(kx)}\right)-\tan^{-1}\left(\frac{Q_p(x)}{P_p(x)}\right) \tag{35}$$

We may substitute the semiconvergent series for Q and P derived in equations 29 and 30 and expand $\tan^{-1}Q/P$ in series (or see Watson,[6] page 506) and for $p=0$ or 1, find

$$\tan^{-1}\left(\frac{Q_0(x)}{P_0(x)}\right)=-\frac{1}{(8x)}+\frac{100}{3(8x)^3}-\frac{34,336}{5(8x)^5}+\frac{24,046,912}{7(8x)^7}-\dots \tag{36}$$

$$\tan^{-1}\left(\frac{Q_1(x)}{P_1(x)}\right)=+\frac{3}{(8x)}-\frac{252}{3(8x)^3}+\frac{60,768}{5(8x)^5}-\frac{34,782,912}{7(8x)^7}+\dots \tag{37}$$

Equation 36 or 37 may be substituted into equation 35 and will yield a series of the type

$$y=ax+b/x+c/x^3+d/x^5+e/x^7+\dots \tag{38}$$

which may be inverted to yield

$$x=y/a+\beta/y+\gamma/y^3+\delta/y^5+\epsilon/y^7+\dots \tag{39}$$

where

$$\left.\begin{aligned}\beta&=-b\\ \gamma&=-a(b^2+ac)\\ \delta&=-a^2(2b^2+4abc+a^2d)\\ \epsilon&=-a^3(5b^4+15ab^2c+6a^2bd+3a^2c^2+a^3c)\end{aligned}\right\} \tag{40}$$

Utilizing these relationships, identifying coefficients a, b, c, . . . with their counterparts we may carry out the inversion and obtain, finally

$$x_m=\frac{n\pi}{(k-1)}-\left(\frac{k-1}{8k\pi n}\right)+\left(\frac{100(k^2+1)+76k}{3}\right)\left(\frac{k-1}{8k\pi n}\right)^3-\left(\frac{103,008(k^4+1)+87,008(k^3+k)+88,928k^2}{15}\right)\times\left(\frac{k-1}{8k\pi n}\right)^5+\dots \tag{41}$$

as the nth root of the zero order equation

$$J_0(x)N_0(kx)-J_0(kx)N_0(x)=0 \tag{42}$$

and

$$x_{1n}=\frac{n\pi}{(k-1)}+3\left(\frac{k-1}{8k\pi n}\right)-(84(k^2+1)+156k)\left(\frac{k-1}{8k\pi n}\right)^3+\left(\frac{60,768(k^4+1)+101,088(k^3+k)+118,368k^2}{5}\right)\times\left(\frac{k-1}{8k\pi n}\right)^5-\dots \tag{43}$$

as the nth root of the first order equation

$$J_1(x)N_1(kx)-J_1(kx)N_1(x)=0 \tag{44}$$

Equations 41 and 43, though only semiconvergent, are highly convergent for increasing n and for most ordinary (not too large) values of $k=b/a$. Often both will yield quite satisfactory numerical values even for the first root x_n when $n=1$. The relation, equation 41, is not required for our present purpose, but both root relationships (equations 42 and 44) frequently are encountered in hollow tube problems so the explicit solutions (equations 41 and 43) both are recorded here. (In review of this paper in manuscript, Professor Dwight

kindly pointed out that the equivalent of equations 41 and 43 may be found in reference 7. This reference is not generally readily accessible, nor the form of the equations there given as convenient for use as those given here.)

We have now all the mathematical apparatus we require. The equations involved in our problem include

$$Z_m(x) = J_0(x) - \left(\frac{J_1(x)}{N_1(x)}\right) N_0(x) \tag{45}$$

or its square, with argument (x_{1n}) or (kx_{1n}) where (x_{1n}) are the nth roots of equation 44. Values are required for argument greatly exceeding published tables of Bessel functions. It is possible to substitute equation 43 into equations 29, 30, and 31 and the results in turn into equation 28, but the algebraic result is very complicated and of no practical gain. It is best to proceed arithmetically in any particular numerical problem by first determining $k = b/a$ which reduces equation 43 to a numerical series in inverse power of n. This easily is evaluated for the first n values ($n = 1, 2, 3 \ldots n$) of the roots x_n. These enable the first n values of P_1, Q_1, and ϕ_1 of equations 29, 30, and 31 to be determined numerically for direct substitution into equation 28 with argument x_n or kx_n. All the series converge very rapidly with increasing n and the values for the first, second, and third roots are usually within the tabulated values of the Bessel functions, and so can be improved by interpolation and trial solution of equation 34 in such tables if required. The numerical work on which Figure 6 was plotted was so computed.

References

1. Transient Electric Phenomena and Oscillations (book), **C. P. Steinmetz.** McGraw Publishing Company, New York, N. Y., 1909, pages 379–86.

2. Electrical Coils and Conductors (book), **H. B. Dwight.** McGraw-Hill Publishing Company Inc., New York, N. Y., 1945, page 155.

3. The Mathematics of Physics and Chemistry (book), **Morgenau-Murphy.** D. Van Nostrand Company Inc., New York, N. Y., 1943, pages 234–5.

4. Tables of Functions (book), **Jahnke-Emde.** Teubner, revised edition, 1933, pages 203, 211, 213, 214, 228, 237, 260.

5. Electromagnetic Theory (book), **J. A. Stratton.** McGraw-Hill Publishing Company Inc., New York, N. Y., 1941, page 271.

6. Bessel Functions (book), **G. N. Watson.** MacMillan Company, New York, N. Y., revised edition, 1944, page 506.

7. On the Roots of the Bessel and Certain Related Functions, **James McMahon.** *Annals of Mathematics* (USA), volume 9, 1894, pages 23–30.

8. Radio Frequency Heating (book), **G. H. Brown, C. N. Hoyler, R. A. Bierwirth.** D. Van Nostrand Company Inc., New York, N. Y., 1947, pages 5, 17, chapters 1, 14.

No Discussion

Tensorial Analysis and Equivalent Circuit of a Variable-Ratio Frequency Changer

GABRIEL KRON
MEMBER AIEE

Synopsis: When two power systems with different frequencies are connected together through an asynchronous tie, the transient behavior of the tie under a sudden change of load on either side becomes of great importance. The paper derives by the tensorial method the steady-state equivalent circuit and the transient equations of a variable-ratio frequency-changer set consisting of an ohmic-drop exciter, regulating machine, and induction machine, when an unbalanced load is applied suddenly to the stator side of the induction machine. A companion paper by Carter, Maginniss, and Rothe gives the results of the solution of the equations by the a-c network analyzer and the differential analyzer.

The Tensorial Method of Attack

THE conventional method of analysis requires the visualization and understanding of the simultaneous relation of fluxes, magnetomotive forces, and voltages in every part of an interconnected structure. Such a study is bad enough for any one particular machine, as an a-c commutator machine, and it becomes an intolerable chore when several machines are interconnected. The presence of an unbalanced load merely supplies a legitimate excuse for the engineer for not undertaking the analysis.

The tensorial method of attack removes the necessity of keeping track of what goes on inside of each machine and reduces the study of a complex system of rotating machines to the study of a stationary network. (The latter may be viewed, however, not only from stationary, but also from moving reference axes, or from a combination of both types of frames.)

In the tensorial method of attack at first all interconnections between the component machines are removed. If the equations of the latter are not yet known then a further simplification is made by a return to a "primitive" machine, having neither brushes nor interconnections between its windings. The equations of the latter are assumed to be known (to be found in reference 1) and are used as the starting point in the analysis. The equations of the primitive machine itself have three basic forms (transformable into each other) depending on the reference frames assumed.

1. In the "first" primitive machine all axes are stationary in space (or all rotate with the same speed).

2. In the "second" primitive machine the stator axes rotate with a speed different from those on the rotor.

3. In the "polyphase" primitive machine only the forward rotating axes are kept and the backward axes are ignored.

On these primitive machines of reference 1 a salient pole is assumed on one member and asymmetrical windings on either the stator or the rotor. (When both members have asymmetrical windings the analysis requires time harmonics and the equations of the primitive machine assume more general forms, given in reference 2.)

Starting with the equations of a primitive machine for each of the component machines, the physical analysis merely consists of the establishment of a series of transformation matrices C, each showing a step in the interconnection of the windings into a machine and in the interconnection of the component machines into the resultant system. The final equations are found by a manipulation of matrices.

Although the analysis itself requires no visualization of any internal phenomena, the resultant equations (either after each step or in their final form) give a full, complete, and clear cut physical picture of what goes on inside of each machine. The torque on each machine, the effect of their saliency, asymmetry, and other factors all are incorporated in the component tensors in an unambiguous manner to be brought into the open whenever the need for them arises.

The Primitive System

The system to be analyzed is given in Figure 1 (only one of the two phases is shown). For analytical purposes it can be broken up into five parts (the "primitive" system) shown on Figure 2.

1. Ohmic drop exciter.
2. Regulating machine.
3. Induction motor.
4. Transformer.
5. Unbalanced load.

Because of the unbalanced load each phase equation will have to be established. However, all machines are symmetrical in structure and much labor may be saved in the analysis by assuming first a balanced load and setting up the equations of only one phase of a balanced 2-phase system. Afterward the number of equations will be doubled by a routine procedure and the unbalanced load added.

The logical reference frames to be assumed for the component parts *before* interconnection will be as follows.

1. Stationary frames in the ohmic drop exciter and the Scherbius machine.

2. Frames moving with the rotor in the induction motor.

Since the unbalanced load will require stationary frames in the induction-motor stator, the foregoing sets of frames will be modified after the interconnections have been made.

Each component part of the primitive system is itself rather complicated and it will be necessary to establish their equations by starting with still more primitive systems and building up gradually to the

Paper 47-260, recommended by the AIEE power generation and rotating machinery committees and approved by the AIEE technical program committee for presentation at the AIEE Midwest general meeting, Chicago, Ill., November 3–7, 1947. Manuscript submitted March 26, 1947; made available for printing September 23, 1947.

GABRIEL KRON is consulting engineer, General Electric Company, Schenectady, N. Y.

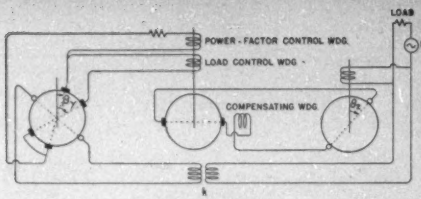

Figure 1 (left). The given system

Figure 3 (right). Development of the ohmic drop exciter

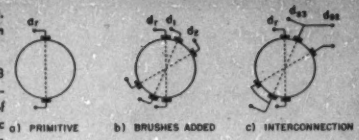

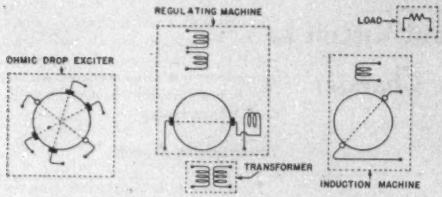

Figure 2 (left). The primitive system

Figure 4 (left). The regulating machine

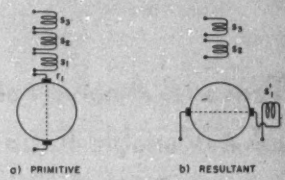

assumed component systems. Since only one phase of a polyphase system is considered, all primitive machines will be special cases of the so-called "polyphase primitive machine" (reference 1, page 179).

The Ohmic Drop Exciter

The fundamental frequency field impressed on the slip rings by the induction motor stator rotates in opposite direction to the exciter so that on the stationary brushes slip-frequency voltages are induced. These voltages are impressed on the stator of the regulating machine.

If the induction motor stator reference frame is assumed to rotate with its rotor then slip-frequency voltages appear on the stator. Similarly if the exciter slip rings are assumed to be stationary, the voltages impressed on it are also of slip frequency. Hence, the exciter may be looked upon as a phase shifter changing the voltage e_{s4} appearing across the stator of the induction motor into the voltages e_{s2} and e_{s3} appearing across the two control windings of the regulating machine. The matrix of transformation $\boldsymbol{C}$ changing e_{s3} may be established in four steps

1 The primitive machine representing the exciter consists of only one layer of winding on the rotor. Hence (Figure 3a) the matrix of transformation, changing the primitive polyphase machine with four windings into the exciter with one winding is

$$\boldsymbol{C}_1 = \begin{array}{c|c|} & d_r \\ \hline d_r & 1 \\ \hline \end{array} \qquad (1)$$

This axis may be looked upon as the axis of the slip rings expressed along a stationary frame.

2. The presence of the additional two sets of brushes at angles β and γ on the same layer of winding (Figure 3b) may be expressed by the transformation $\boldsymbol{i} = \boldsymbol{C}_2 \boldsymbol{i}'$ where

$$\boldsymbol{C}_2 = \begin{array}{c|c|c|c|} & d_r & d_1 & d_2 \\ \hline d_r & 1 & \epsilon^{j\beta} & \epsilon^{j\gamma} \\ \hline \end{array} \qquad (2)$$

3. The interconnection of the brushes (Figure 3c) may be expressed as $\boldsymbol{i} = \boldsymbol{C}_3 \boldsymbol{i}'$ where

$$\boldsymbol{C}_3 = \begin{array}{c|c|c|c|} & d_{s3} & d_{s2} & d_r \\ \hline d_r & & & 1 \\ \hline d_1 & 1 & 1 & \\ \hline d_2 & & -1 & \\ \hline \end{array} \qquad (3)$$

4. Hence the role of the exciter consists of the current transformation $\boldsymbol{i} = \boldsymbol{C}_4 \boldsymbol{i}'$

$$\boldsymbol{C}_4 = \boldsymbol{C}_1 \boldsymbol{C}_2 \boldsymbol{C}_3 = \begin{array}{c|c|c|c|} & d_{s3} & d_{s2} & d_r \\ \hline d_r & \epsilon^{j\beta} & \epsilon^{j\beta} - \epsilon^{j\gamma} & 1 \\ \hline \end{array} \qquad (4)$$

or of the voltage transformation $\boldsymbol{e}' = \boldsymbol{C}_4 \boldsymbol{e}$

$$\boldsymbol{C}_{44} = \begin{array}{c|c|} & d_r \\ \hline d_{s3} & \epsilon^{-j\beta} \\ \hline d_{s2} & \epsilon^{-j\beta} - \epsilon^{-j\gamma} \\ \hline d_r & 1 \\ \hline \end{array}$$

$$\begin{aligned} e_{s3} &= \epsilon^{-j\beta} e_{s4} \\ e_{s2} &= (\epsilon^{-j\beta} - \epsilon^{-j\gamma}) e_{s4} \\ e_{s4} &= e_{s4} \end{aligned} \qquad (5)$$

giving the voltages impressed on the control windings as a function of the voltage appearing across the stator of the induction motor. With the use of these voltage equations the exciter drops out of all future considerations. If the ratio of the transformer is k, then e_{s4} would be replaced by ke_{s4}.

The Regulating Machine

Its primitive (Figure 4a) consists of three stator and one rotor layer of winding. Its $\boldsymbol{Z}$ is

$$\boldsymbol{Z}_1 = \begin{array}{c|c|c|c|c|} & s_3 & s_2 & s_1 & r_1 \\ \hline s_3 & r_{s3} + L_{s3}p & L_{sm3}p & L_{sm1}p & M_1 p \\ \hline s_2 & L_{sm3}p & r_{s2} + L_{s2}p & L_{sm1}p & M_1 p \\ \hline s_1 & L_{sm1}p & L_{sm1}p & r_{s1} + L_{s1}p & M_1 p \\ \hline r_1 & M_1(p - j p\theta_1) & M_1(p - j p\theta_1) & M_1(p - j p\theta_1) & \begin{array}{c} r_{r1} + L_{r1} \\ (p - j p\theta_1) \end{array} \\ \hline \end{array} \qquad (6)$$

The matrix of transformation of the actual machine from Figure 4b, showing the rotation of a winding and of the brushes by 90 degrees and their interconnection, is

$$\boldsymbol{C} = \begin{array}{c|c|c|c|} & s_3 & s_2 & s_1 \\ \hline s_3 & 1 & & \\ \hline s_2 & & 1 & \\ \hline s_1 & & & -j \\ \hline r_1 & & & j \\ \hline \end{array} \qquad (7)$$

The resultant $\boldsymbol{Z}_1'$ is found by $\boldsymbol{C}_t^* \boldsymbol{Z}_1 \boldsymbol{C}$.

All constants are 1-turn quantities, hence the impressed voltages $\boldsymbol{e}$ will have to be changed by the turn-ratio matrix.

$$\boldsymbol{C}_{n1} = \begin{array}{c|c|c|c|c|} & s_3 & s_2 & s_1 & r_1 \\ \hline s_3 & n_{s3} & & & \\ \hline s_2 & & n_{s2} & & \\ \hline s_1 & & & n & \\ \hline r_1 & & & & n \\ \hline \end{array} \qquad (8)$$

The Induction Motor

The $\boldsymbol{Z}$ of its primitive is (Figure 5a)

$$\boldsymbol{Z}_2 = \boldsymbol{R}_2 + \boldsymbol{L}_2 p + \boldsymbol{G}_2 p\theta_2$$

$$\boldsymbol{Z}_2 = \begin{array}{c|c|c|} & s & r \\ \hline s & r_s + L_s p & Mp \\ \hline r & M(p - j p\theta_2) & r_r + L_r(p - j p\theta_2) \\ \hline \end{array} \qquad (9)$$

On both stator and rotor axes rotating with the rotor are introduced by

$$C = \begin{array}{c|c|c|} & s' & r' \\ \hline s' & e^{j\theta_2} & \\ \hline r' & & e^{j\theta_2} \\ \hline \end{array} \qquad (10)$$

Again as all constants are 1-turn quantities, the impressed voltages e are changed by the turn-ratio matrix

$$C = \begin{array}{c|c|c|} & s'' & r'' \\ \hline s'' & n_{s4} & \\ \hline r'' & & n_r \\ \hline \end{array} \qquad (11)$$

The resultant Z_s' is found by $C_t^* Z_s C + C_t^* L_s p C$.

The Resultant System

The two machines are interconnected by (Figure 6)

$$C = \begin{array}{c|c|c|c|c|} & s_2 & s_3 & s_1 & s \\ \hline s_2 & 1 & & & \\ \hline s_3 & & 1 & & \\ \hline s_1 & & & 1 & \\ \hline s & & & & 1 \\ \hline r & & & -1 & \\ \hline \end{array} \qquad (12)$$

Before interconnection the Z of the two machines is $Z_1' + Z_s'$ and after interconnection

$$Z'' = C_t(Z_1' + Z_s')C \qquad (13)$$

The transient impedance tensor of the polyphase system with a balanced load Z_L is then

$$Z'' = \begin{array}{c|c|c|c|c|} & s_2 & s_3 & s_1 & s_4 \\ \hline s_2 & r_{s2} + L_{s2}(p + jp\theta_2) & L_{sm2}(p + jp\theta_2) & & \\ \hline s_3 & L_{sm2}(p + jp\theta_2) & r_{s3} + L_{s3}(p + jp\theta_1) & & \\ \hline s_1 & -M_1 p\theta_1 & -M_1 p\theta_1 & r_{s1} + r_{r1} + r_{r2} + l_{r1} jp\theta_1 + (l_{s1} + l_{r1} + L_{r2})(p + jp\theta_2) & -M_2(p + jp\theta_2) \\ \hline s_4 & & & -M_2 p & r_{s4} + L_{s4} p + Z_L \\ \hline \end{array} \qquad (14)$$

The impressed voltage vector is

$$E = \begin{array}{c|c|c|c|} s_2 & s_3 & s_1 & s_4 \\ \hline kE_{s4}\frac{n_{s4}}{n_{s2}}\epsilon^{-i\beta} & kE_{s4}\frac{n_{s4}}{n_{s3}}(\epsilon^{-i\beta} - \epsilon^{-i\gamma}) & & E_{s4} \\ \hline \end{array} \qquad (15)$$

and the current vector is

$$I = \begin{array}{c|c|c|c|} s_2 & s_3 & s_1 & s_4 \\ \hline s^{i2} n_{s2} & s^{i3} n_{s3} & s^{i1} n_s & s^{i4} n_{s4} \\ \hline \end{array} \qquad (16)$$

where i and e represent actual machine quantities and I and E represent quantities reduced to one turn, such that

$$I = in \text{ and } E = \frac{e}{n} \qquad (17)$$

The transient equations of the polyphase system are then $E = Z''I$.

Two cases will be considered.

1. The steady-state equations without any outside load.

2. The transient equations with an unbalanced outside load.

Steady-State Equivalent Circuit

During steady state the frequency of currents in all axes is of slip frequency $s = 1 - v$. Hence in the transient polyphase Z all p become $js\omega$ and all $p\theta$ become $vs\omega$. If also the frequency tensor n is introduced changing all actual current in the windings to the same frequency

$$n = \begin{array}{c|c|c|c|c|} & s_2 & s_3 & s_1 & s_4 \\ \hline s_2 & 1/s & & & \\ \hline s_3 & & 1/s & & \\ \hline s_1 & & & 1/s & \\ \hline s_4 & & & & 1 \\ \hline \end{array} \qquad (18)$$

the resultant impedance tensor is

$$nZ'' = \begin{array}{c|c|c|c|c|} & s_2 & s_3 & s_1 & s_4 \\ \hline s_2 & \frac{r_{s2}}{s} + j & jX_{sm2} & & \\ \hline s_3 & jX_{sm2} & \frac{r_{s3}}{s} + jX_{s3} & & \\ \hline s_1 & -\frac{v}{s}X_{m1} & -\frac{v}{s}X_{m1} & \left(\frac{r_{s1}}{s} + jx_{s1}\right) + \left(\frac{r_{r2}}{s} + jX_{r2}\right) + \frac{r_{r1}}{s} + j\frac{(s-v)}{s}x_{r1} & -jX_{m3} \\ \hline s_4 & & & -jX_{m3} & r_{s4} + jX_{s4} \\ \hline \end{array} \qquad (19)$$

The equivalent circuit is shown in Figure 7. It automatically splits into two independent networks, the first one giving the voltage E generated in the rotor circuit of the regulator, the second giving the induction motor performance. As usual the torques on the individual machine are given by watt inputs into the rotor circuits.

$$\text{Torque}_1 = \text{real of } I^{i1} E_1^* s/v_1$$
$$\text{Torque}_2 = \text{real of } I^{i1} E_2^*$$

Effect of Unbalanced Load

In introducing an unbalanced load, several steps will be necessary to change the transient Z of equation 14.

1. Since the load is connected to the stationary stator axes of the induction motor, while the equations have been established for rotating axes, it will be necessary to change the latter. In order to avoid the appearance of expressions such as $\epsilon^{j\theta}$ in the new Z, *it will be advantageous to rotate all four axes of the system by the same angle* θ, with the matrix of transformation

$$C = \begin{array}{c|c|c|c|c|} & s_2' & s_3' & s_1' & s_4' \\ \hline s_2 & \epsilon^{-j\theta_2} & & & \\ \hline s_3 & & \epsilon^{-j\theta_3} & & \\ \hline s_1 & & & \epsilon^{-j\theta_1} & \\ \hline s_4 & & & & \epsilon^{-j\theta_4} \\ \hline \end{array} \qquad (20)$$

The effect of the C is to change all p in equation 14 to $p - jp\theta_2$. The steady-state equations (19) and the equivalent circuit of Figure 7 remain unchanged.

2. The complex quantities are changed to real quantities and the number of variables are doubled by the following transformations (reference 1, page 179).

(a). $i = i' + ji''$

(b). $e = e' + je''$

(c). $z = r + jx = \begin{array}{|c|c|} r & x \\ \hline -x & r \\ \end{array} \qquad (21)$

That is each element of the transient impedance matrix Z of equation 14 is replaced by four elements, thereby doubling its number of rows and columns. Now, for instance, e_{s1}' is the impressed voltage on one of the phases and e_{s1}'' is impressed on the other.

3. When an unbalanced load Z' and Z'' (where each $Z = R + Lp + 1/Cp$) is put in series with the stator of the induction motor (Figure 1) then the impressed voltage on axis s_1 is no longer E_{s1}' and E_{s1}'' as shown in equation 15 but E_α and E_β where

$$E_\alpha = E_{s1}' + I_{s1}' Z'$$
$$E_\beta = E_{s1}'' + I_{s1}'' Z''$$

and where now E_{s1} is the difference of potential appearing across the stator winding of the induction motor. On the other hand the voltages impressed across the two control windings s_2 and s_3 are still functions of E_{s1} as in equation 15.

It is possible to change E_{s1} in all compo-

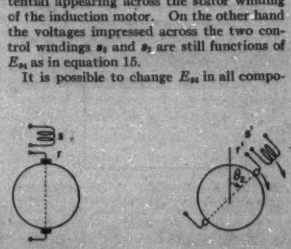

a) PRIMITIVE b) MOVING AXES

Figure 5. The induction machine

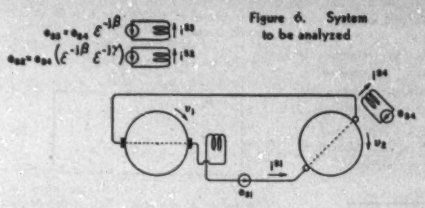

Figure 6. System to be analyzed

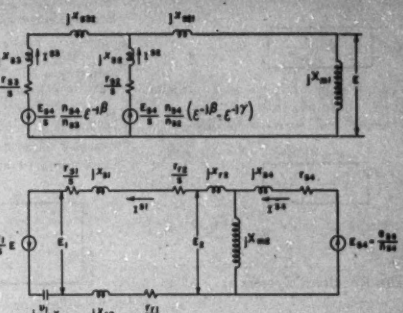

Figure 7 (right). Steady-state equivalent circuit

nents of the impressed voltage vector to E_α and E_β with the aid of equation 22. Its effect is to add additional terms to $\boldsymbol{Z}$ in the columns of I_{s1} and rows of s_2 and s_3.

Figure 8. Resultant transient equations

	s_2'	s_2''	s_2'	s_2''	s_1'	s_1''	s_4'	s_4''
$E=$	$k\frac{n_{s4}}{n_{s2}}\cdot(E_\alpha\cos\beta+E_\beta\sin\beta)$	$k\frac{n_{s4}}{n_{s2}}\cdot(-E_\alpha\sin\beta+E_\beta\cos\beta)$	$k\frac{n_{s4}}{n_{s2}}\cdot[E_\alpha(\cos\beta-\cos\gamma)+E_\beta(\sin\beta-\sin\gamma)]$	$k\frac{n_{s4}}{n_{s2}}\cdot[E_\alpha(\sin\gamma-\cos\beta)+E_\beta(\cos\beta-\cos\gamma)]$			E_α	E_β

$I=$	I_{s2}'	I_{s2}''	I_M'	I_M''	I_g'	ψ_g'	I_g''	ψ_g''	I_{s4}'	I_{s4}''
s_2'	r_{s2}		$L_{sm2}p$	$L_{sm2}p\theta_2$					$k\frac{n_{s4}}{n_{s2}}\cos\beta Z'$	$k\frac{n_{s4}}{n_{s2}}\sin\beta Z''$
s_2''		r_{s2}	$-L_{sm2}p\theta_2$	$L_{sm2}p$					$-k\frac{n_{s4}}{n_{s2}}\sin\beta Z'$	$k\frac{n_{s4}}{n_{s2}}\cos\beta Z''$
s_2'	$-r_{s2}$		$r_{s2}+L_{s2}p$	$L_{s2}p\theta_2$					$k\frac{n_{s4}}{n_{s2}}(\cos\beta-\cos\gamma)Z'$	$-k\frac{n_{s4}}{n_{s2}}(\sin\gamma-\sin\beta)Z''$
s_2''		$-r_{s2}$	$-L_{s2}p\theta_2$	$r_{s2}+L_{s2}p$					$k\frac{n_{s4}}{n_{s2}}(\sin\gamma-\sin\beta)Z'$	$k\frac{n_{s4}}{n_{s2}}(\cos\beta-\cos\gamma)Z''$
s_1'			$-M_1p\theta_1$		$r+lp$	p	$lp\theta_1+l_{r1}p\theta_1$	$p\theta_2$	$r+lp$	$lp\theta_2+l_{r1}p\theta_1$
s_1''				$-M_1p\theta_1$	$-lp\theta_2-l_{r1}p\theta_1$	$-p\theta_2$	$r+lp$	p	$-lp\theta_2-l_{r1}p\theta_1$	$r+lp$
s_4'						$-p$			$r_{s4}+l_{s4}+Z'$	
s_4''								$-p$		$r_{s4}+l_{s4}p+Z''$

Effect of Saturation

If saturation in the induction motor is considered, two additional steps may be made.

1. The rotor current I^{s1} may be replaced by the magnetizing current $I^g=I^{s1}-I^{r1}$ (since I^gM_2 represents the air-gap flux ψ_g) by the following transformation matrix:

$$C_1=\begin{array}{c|cccc} & g' & g'' & s_4' & s_4'' \\ \hline s_1' & 1 & & 1 & \\ s_1'' & & 1 & & 1 \\ s_4' & & & 1 & \\ s_4'' & & & & 1 \end{array} \qquad (23)$$

and find $\boldsymbol{E}=\boldsymbol{Z}\boldsymbol{I}=\boldsymbol{Z}\boldsymbol{C}_1\boldsymbol{I}'$. The impressed voltages $\boldsymbol{E}$ are not transformed.

2. An additional variable $\psi_g=MI_g$ may be introduced, representing the air-gap flux. Its effect is to add two additional columns to the $\boldsymbol{Z}$ matrix.

The equations may be simplified further by two steps.

3. I_{s1} is replaced by a new variable $I_M=I_{s1}+I_{s2}$ analogously to the previous step

$$C_2=\begin{array}{c|cccc} & g_2' & g_2'' & M' & M' \\ \hline s_2' & 1 & & & \\ s_2'' & & 1 & & \\ s_2' & -1 & & 1 & \\ s_2'' & & -1 & & 1 \end{array} \qquad (24)$$

4. The leakage reactances of the stator windings of the Scherbius machine are neglected, so that $L_{s2}=L_{s2}=L_{sm2}$.

The Transient Equations

The resultant transient equations $\boldsymbol{E}=\boldsymbol{Z}\boldsymbol{I}$ to be put on the differential analyzer are shown as Figure 8, where

$r=r_{s1}+r_{r1}+r_{r2}$

and

$l=l_{s1}+l_{r1}+l_{r2}$

$\psi_g'=I_g'M_2$

$\psi_g''=I_g''M_2$

References

1. A Short Course in Tensor Analysis for Electrical Engineers (book), Gabriel Kron. John Wiley and Sons, Inc., New York, N. Y.

2. Equivalent Circuit of the Rotating Primitive Machine With Asymmetrical Stator and Rotor, Gabriel Kron. AIEE Transactions, volume 66, 1947, pages 17–23.

3. Suddenly Applied Loads on a Variable-Ratio Frequency Changer, G. K. Carter, F. J. Maginniss, F. S. Rothe. AIEE Transactions, volume 66, 1947, pages 1489–95.

No Discussion

Two-Stage Rototrol for Low-Energy Regulating Systems

A. W. KIMBALL
ASSOCIATE AIEE

Synopsis: The fundamental principles of operation and application of Rototrols have been discussed in a number of papers and publications. These have dealt with a unit having only one stage of amplification of the control energy. Such machines have been applied widely during the last 15 years with excellent results. Recently a few applications have arisen in which the control energy available was too small to provide satisfactory regulation. The use of a second unit operating as a control energy amplifier was then needed. The development of the 2-stage Rototrol permits the use of only one machine in such applications. The simplest construction of this machine is a 4-pole design. It is a normal generator except for the field coils and armature connections. With such modifications this paper shows that the machine may be considered as three generators superimposed on one another. The output of only two of these is used in the machine under consideration. The analysis of operation and means of compensation for the resulting reactions are given. Tests of two designs show that high sensitivity and speed of response were obtained. It is concluded that the development of this machine provided a generating element for Rototrol systems which requires an extremely low value of control energy.

THE first installations using rotating machines to perform regulating or control functions were made by Westinghouse about 15 years ago. Some time later the generators of this type together with their associated circuits were called Rototrols. The name was coined using the first and last portions of the two words which described the system, namely, "rotating" and "control." Their performance was so satisfactory that their use now has expanded into nearly all industries employing electric machines.

In order to perform the function of regulating or controlling a system, it is necessary to measure the output obtained and compare this to some predetermined standard or pattern. The control means then must provide the necessary action to correct the output when any deviation from the pattern occurs. It also must remove any such action when the correct output is obtained. These intelligences are introduced into a Rototrol generator by means of windings on the field poles. When the comparison between the output and the pattern is made inside the machine separate windings are used for each intelligence. These are then called pilot and pattern fields, respectively. When the comparison is made external to the machine only one field then is required and it is called a control field. Thus, when the output does not match the pattern, a net excitation will exist which is used to initiate the required correction. Also, when the output is correct there is no net excitation resulting from the control energy and therefore no action is initiated.

The pilot and pattern intelligences provide a means of causing the Rototrol to change its output. However, since they neutralize each other when the correct output is obtained, some other means is needed to maintain the output at this value. This is accomplished by a self-energizing field. It may be of the shunt or series type or a combination of both. In any case, the self-energizing field is so designed and adjusted that it is of just sufficient strength to supply the excitation necessary to generate sufficient voltage to sustain itself. This can only be true over the range in which the saturation curve is essentially a straight line and operation of these machines therefore usually is limited to the air gap portion of the saturation curve.

The foregoing is a brief statement of the fundamental principles used in the usual design of Rototrols. Some systems require deviations from them to obtain particular characteristics. For instance, some applications may require a Rototrol output proportional to the control energy. In this case, only partial or no self-excitation might be used. A number of papers and publications have been presented discussing the fundamental principles of operation and application of this type of control.[1–7] In general, Rototrol generators of this type employ standard parts in all respects except the field coils and, in some cases, special materials or treatments in the poles and frames. This class of Rototrols has been used for a wide variety of applications with very satisfactory results.

Recently a few applications have arisen in which the control energy available was too small to utilize effectively in the standard industrial Rototrols and additional amplifying means were necessary. For some applications the most satisfactory solution has been to use electronic equipment to amplify the control energy and also provide regulating and antihunting features while the output of the electronic system provides the control input for the Rototrol. For certain other extreme applications two Rototrol units are operated in cascade forming a very simple and satisfactory solution. This paper describes a third method of handling regulating problems involving low control energy, namely, the design of a single 2-stage Rototrol which will give results similar to tandem or cascaded systems.

The simplest machine of this type, and therefore the one chosen for analysis, is a 4-pole design having a 4-pole multiple armature winding without equalizer connections. The stator is the same as that of a standard 4-pole generator except that no brush arm cross connections are used

Paper 47-262, recommended by the AIEE rotating machinery committee and approved by the AIEE technical program committee for presentation at the AIEE Midwest general meeting, Chicago, Ill., November 3–7, 1947. Manuscript submitted November 12, 1946; made available for printing September 25, 1947.

A. W. KIMBALL is an electrical engineer in the motor engineering department, Westinghouse Electric Corporation, Buffalo, N. Y.

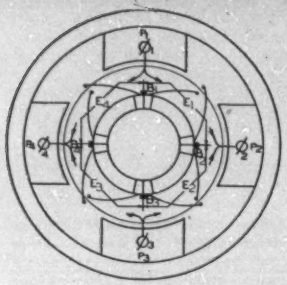

Figure 1. Fundamental electric and magnetic construction

and the field windings are connected in an unusual manner.

It is well known, and will be demonstrated, that if the main poles of a generator having a multiple wound armature have unequal field strengths then differences of potential are set up which cause currents to flow in the armature winding and balance the flux from all poles. Before equalizers were invented, the correcting currents flowed through the brushes and brush holder cross connections.

This condition is set up deliberately in the 2-stage Rototrol. The two north poles, P_1 and P_3 in Figure 1 for example, are unbalanced by the flow of current in the control coils which are on these poles only and so connected that one pole is increased and the other weakened. If brushes B_1 and B_3 were connected together heavy currents would start to flow from one brush to the other. In the 2-stage Rototrol we open this cross connection and this circulating current is made to flow through exciting windings on all main poles. These coils are deployed so as to build up the voltage of the generator in the usual manner and form the excitation circuit of the second stage. Since their function is to force the voltage to build up in the second stage we call them "forcing coils."

If nothing further were done the circulating current flowing through the armature and the forcing coils would produce a corrective magnetomotive force which would balance the excitation from the control coils. This is undesirable and consequently other windings called compensating and opposing windings are added to the machine. It should be understood that these windings play no functional part in this machine but are only corrective.

The compensating coils are located on the same axis as the armature magnetomotive force and carry the same current which sets it up. Since they oppose it they are truly compensating coils.

The opposition coils also are located on the axis of the magnetomotive force but they are excited by the current produced by it and its resulting flux. In this manner they tend to suppress the magnetomotive force, but cannot completely do so because their excitation is dependent upon the existence of it and its resulting flux.

It should be understood that the brush holder cross connection between B_1 and B_3 and that between B_2 and B_4 are connections between points of equal potential and are not short-circuiting connections. The mid points of these connections are used as the output terminals of the armature of the second stage. The main field coils of this stage whether shunt or series are connected in the normal fashion and the machine terminals connected to its load. This is, of course, the field of the machine which it is used to excite.

Fundamental Principle

It has been stated that if the poles of a generator, having a multiple wound armature, have unequal field strengths differences of potential are set up in the armature. This can be demonstrated by setting up the equations for the voltage generated.

Figure 1 illustrates a machine of this type. The armature conductors shown outside the armature circle represent the conductors in the top of the slots and those inside represent those in the bottom of the slots. In writing the equations for the voltage generated between the brushes, the polarity of the flux must be considered since conductors under a south pole will have a voltage generated in them opposite to that generated in the same conductors when under a north pole. Also, whether the particular conductors cutting this flux are top coil sides or bottom coil sides must be considered, because like voltages in one coil would oppose and result in no net voltage. For example, if two adjacent poles were both north and of equal strength then no net voltage would be generated in an armature coil whose sides lie under these poles even though a voltage would be generated in each coil side. If a constant K is used to represent the physical properties of the machine including the speed of rotation, then its sign can be changed when changing from a top to a bottom coil side. Thus if the sign of ϕ and K are both taken as positive when ϕ is north pole flux and conductors are top coil side, then we can write the following equations:

$$E_1=(+K)(+\phi_1)+(-K)(-\phi_2)$$
$$=+K(\phi_1+\phi_2)$$
$$E_2=(+K)(-\phi_2)+(-K)(+\phi_3)$$
$$=-K(\phi_2+\phi_3)$$
$$E_3=(+K)(+\phi_3)+(-K)(-\phi_4)$$
$$=+K(\phi_3+\phi_4)$$
$$E_4=(+K)(-\phi_4)+(-K)(+\phi_1)$$
$$=-K(\phi_4+\phi_1)$$

where

$$K=\frac{\text{rpm}\times\text{total armature conductors}\times\text{poles}}{\text{armature circuits}\times10^8\times60}$$

ϕ = flux in lines

The voltage existing between brushes B_1 and B_3 therefore becomes

$$E_1+E_3=K(\phi_1+\phi_2-\phi_3-\phi_4)$$
$$=K(\phi_1-\phi_3)$$

Also the voltage existing between brushes B_2 and B_4 becomes

$$E_2+E_4=K(-\phi_2-\phi_3+\phi_4+\phi_1)$$
$$=K(\phi_4-\phi_2)$$

Thus the voltage between brushes B_1 and B_3 is dependent on the strength of poles P_1 and P_3 only and not affected by poles P_2 and P_4. Likewise, the voltage between brushes B_2 and B_4 is dependent on the strength of poles P_2 and P_4 and not affected by poles P_1 and P_3. This characteristic therefore provides a means whereby two independent generators may be superimposed on the original one. These three generators are

1. Poles P_1 and P_3 and their brush arms B_1 and B_3.

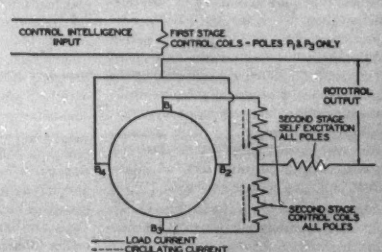

Figure 2. Fundamental circuit diagram

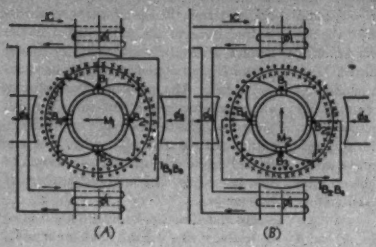

Figure 3. Distribution of current in armature coils

A—With current in brushes B_1B_3

B—With current in brushes B_2B_4

2. Poles P_2 and P_4 and their brush arms B_2 and B_4.

3. Poles P_1, P_3, P_5, and P_6 with brush arms B_1, B_2, B_3, and B_4.

Thus three stages of amplification could be obtained from one machine by properly exciting the first generator using its output to excite the second, which in turn excites the third.

Nearly all Rototrol systems operate on the tuned or balanced self-excited principle and the only function of the input intelligence is to control the output. The number of stages needed therefore depends on the amount of control energy available and the output required. Three stages are available in this unit if future applications should become such that additional amplification is needed. This discussion, however, is being limited to the 2-stage combination.

The fundamental windings used in such a design are illustrated diagrammatically in Figure 2. The control intelligence is used to excite coils on poles P_1 and P_3. These coils are so connected as to produce north-pole excitation on one pole and south-pole excitation on the other. The flux thus produced causes a voltage to be generated between brushes B_1 and B_3 which is used to excite coils on all four poles.

These are the control coils for the second or output stage of the Rototrol. They are divided into two sections, consisting of half the total turns on each pole in each section. The sections are then connected as shown, one half in series with brush B_1 and the other half in series with brush B_2. The common point of connection of these section forms one terminal for the output stage. The connection is made in this manner in order to neutralize any effect of the output current. That is, current flowing from B_1 to B_3 will make all these coils cumulative. However, load current flowing from both B_1 and B_3 and through the output circuit of the Rototrol will produce excitation on one section cumulative and in the other differential. Since each section consists of an equal number of turns on each pole the coils neutralize each other resulting in no net excitation. The second or output stage consisting of all poles and all brushes is self-excited in the normal manner. This diagram illustrates the series type of self-excitation although the shunt type can be used if desired. The output circuit and the self-excitation is so designed as to be self-sustaining in the usual manner. That is, since the operation of Rototrols usually is limited to the straight line or air gap portion of the saturation curve, the self-excitation is so designed that the line representing it is coincident with the air gap line. In this manner the Rototrol thus is made capable of supplying sufficient excitation to itself to maintain its output at any point on the straight portion of its saturation curve. The function of its control coils is thus limited to providing the means of causing the Rototrol to operate at a given output or to change from one condition of output to another as required in the operation of the system being controlled.

Armature Reactions

The flow of current in an armature winding produces a magnetomotive force, usually called the armature reaction. This machine also produces these forces in the normal manner when output current is drawn. However, an unusual armature reaction occurs when the load current is zero but internal circulating currents are flowing. If we excite the control coils and connect between brushes B_1 and B_3, leaving brushes B_2 and B_4 open, a current will flow through the armature and this connection. The distribution of this current in the armature is shown in Figure 3*A*. Only sufficient portions of the armature end turns are shown so that the winding can be traced. For analysis then, if the first stage control coils are excited by current I_c a flux is produced in poles P_1 and P_3. With clockwise rotation of the armature this produces a circulating current $I_{B_1B_3}$. This current flows in the top and bottom coil sides as shown by the arrow points and tails. Note that the current under P_1 is flowing into the figure and that under P_3 is flowing out of the figure in both the top and bottom coil sides. Also note that under poles P_2 and P_4, the current flow in the top coil sides is the opposite to that in the bottom coil sides. Thus the current flow in half of the armature winding is such as to produce a magnetomotive force in line with the axis of poles P_2 and P_4 and that in the remainder neutralizes itself.

The magnetomotive force thus produced is indicated as M_1 and it will result in a flux ϕ_2 in poles P_2 and P_4. A voltage then is generated between brushes B_2 and B_4. With these connected a current $I_{B_2B_4}$ then will circulate through the armature winding. Its distribution is shown in Figure 3*B*. Note that now the current under P_2 is flowing into the figure and that under P_4 is flowing out of the figure in both the top and bottom coil sides. Also note that under poles P_1 and P_3 the currents flow opposite each other in the top and bottom coil sides and thus neutralize. A magnetomotive force M_2 in line with the axis of poles P_1 and P_3 thus is produced which opposes the magnetomotive force of the control coils. Thus with

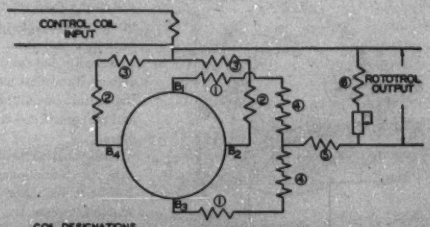

Figure 4. Diagram of coil connections

the brush arms cross connected in the normal manner and no provision made to oppose these reactions $I_{B_1B_3}$ and $I_{B_2B_4}$ would reach such values that M_2 would be less than the excitation of the control coils by just a sufficient amount to maintain the flow of currents $I_{B_1B_3}$ and $I_{B_2B_4}$. This would result in a very inefficient use of the control field energy.

Control of the Armature Reactions

Several means may be used to reduce the magnitude of M_2 and thus increase the output of the first stage. Some of these are as follows:

1. Resistance connected between B_2 and B_4. This is effective but results in an unnecessary loss of power in the output of the second stage of the Rototrol since it would have to carry its output current.

2. Opposition coils. These coils are mounted on poles P_2 and P_4 and are excited by current $I_{B_2B_4}$ such that their magnetomotive force opposes M_1. Such windings only partially can neutralize M_1 since it is the initial force which causes their exciting current $I_{B_2B_4}$ to flow. However, increasing the number of turns in these coils results in a decrease in the magnitude of M_1.

3. Compensating coils. Compensating coils of either the pole face type or concentrated pole type may be used. Those of the latter type are simpler and may be mounted on poles P_2 and P_4, carry current $I_{B_1B_3}$, and oppose M_1 or they may be mounted on poles P_1P_3, carry current $I_{B_2B_4}$, and oppose M_2. This type of correction is most efficient from the standpoint of coil space. It can be made practically 100 per cent effective.

Fundamental Circuit

Figure 4 is a diagram showing the connections of all coils which might be used in this type of machine. If a design using only oppositions as a means of controlling M_1 and M_2 is to be used, when coils 1 and 2 would be omitted. Likewise, if the design is to have compensation for M_2 only, then coils 1 and 3 would be omitted. Tests to date indicate that a design having approximately 90 per cent compensation for M_1 and M_2 in coils 1 and 2, respectively, and coils 3 opposing M_1 with approximately 65 per cent of the effective armature turns per pole give a minimum total coil space consistent with satisfactory operation.

Self-excitation of the series or shunt type may be used in the second stage, as stated previously. Sometimes both are used. This usually occurs when series excitation is preferred and the output current is high. Under these conditions the tuning resistor would be large and therefore undesirable. Slightly less than the full amount of series excitation required to produce a tuned output circuit therefore is used and a shunt field added. The remainder of the excitation needed is supplied by this field and all adjustments made with its rheostat.

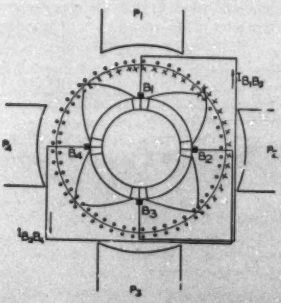

Figure 5. Armature current distribution with current in both armature circuits B_1 B_3 and B_2 B_4

Commutation

The method of analyzing the commutation of machines of this type differs from that in standard multiple wound generators because the current distribution in the armature and between the brush arms does not bear a fixed relation for all conditions of operation. That is, the currents in the armature and from the brush arms are practically balanced when the control coil excitation is zero. However, when the output current of the Rototrol is zero and the control coil is excited, a circulating current of perhaps as much as 25 to 50 per cent normal may be flowing in the B_1B_3 circuit and some other amount in the B_2B_4 circuits. For the purpose of the analysis, assume the currents in B_1B_3 and B_2B_4 circuits to be of the same magnitude and the load current zero. The resultant current distribution in the armature is then as shown in Figure 5. Thus the entire armature then produces a magnetomotive force in the axis located in the netural zones between poles P_1P_4 and poles P_2P_3 but none in the other two neutral zones. The problem then becomes one of producing commutating coils and their connections which will result in the correct polarities of poles and correct pole strengths to meet this condition as well as that occurring when only output current is flowing.

The diagrams shown in Figure 6 illustrate the system used. Each commutating pole has four coils mounted on it. The two shown next to the armature are duplicates and the two on the outside are also duplicates. The two pairs, however, do not have the same number of turns. The coils next to the armature have 150 per cent of the turns required to balance the normal armature reaction obtained with balanced output current plus the turns required to produce the commutating flux. The coils on the outside have 50 per cent of the turns required to balance the normal armature reaction obtained with balanced currents. The direction of flux produced in these coils by circulating currents only is shown in Figure 6*A*. Note that all coils are excited such that no net excitation exists in the zone between main poles P_1 and P_3 and in the opposite zone between P_2 and P_4 while all coils in the other two zones are such as to oppose the armature reactions as shown in Figure 5. The balanced or load current condition existing when the control flux is zero is shown in Figure 6*B*. In this case normal interpole strength and polarity is obtained since the outer coils oppose the inner coils in each case, thus producing the correct net turns needed to balance the armature reaction.

Figure 6. Commutating coil connections and directions of magnetomotive forces

A—With circulating current out B_2 and in B_1, also out B_4 in B_3 with 0 load current

B—Circulating current 0 and load current going in B_1 and B_3 and out B_2 and B_4

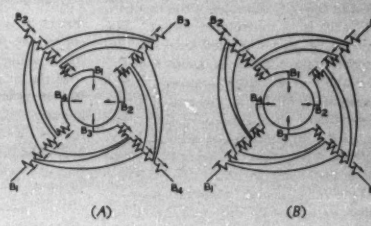

Performance

Two general designs of this class of machines were built to supply the excitation to and regulate the voltage of a 1,250-kw 3-phase 1,200-rpm a-c generator. One

of these had no M_1 or M_2 compensation coils, but reduced M_1 by opposition coils mounted on the poles P_3 and P_4. These coils had approximately 165 per cent of the effective armature turns. The other design had coils with turns for approximately 90 per cent compensation for M_1 and M_2 and approximately 60 per cent M_1 opposition. The turns required in the output of the first stage to control the second stage were much greater on the first design than on the second. The performance of both designs was satisfactory and practically identical. The Rototrol output required for proper performance of the system varied from 1.8 kw to 10.8 kw. This range was covered with a maximum steady state control coil input of 0.01 watt which was equivalent to a sensitivity of one-half of one per cent. The speed of response was such that, with a disturbance of 50 per cent rated load suddenly applied, the system returned to the specified limits of within ±3 per cent rated value in 0.4 to 0.5 second.

Another application of a similar design was used to reverse a 1,500-kw 675-volt d-c generator. In this case, the Rototrol reached its reversed ceiling voltage in 0.25 second, the main generator voltage reduced to zero in 0.44 second, built up to 90 per cent reversed voltage in 1 second, and reached full reversed voltage in 1.30 seconds. This operation was obtained without overshoot. A replot of an oscillogram of this operation is shown in Figure 7.

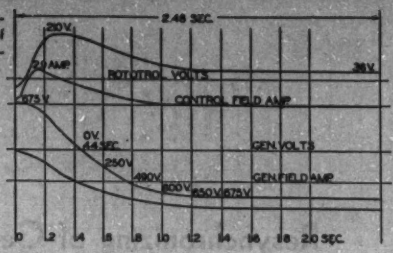

Figure 7. Transcribed oscillogram of reversal performance of 1,500-kw 675-volt d-c generator

Discussion

The 2-stage Rototrol of this type is structurally very similar to standard machines. Its armature core, commutator, brackets, brushes and brush rigging, poles, air gaps, and frame are of normal construction. When the values of control energy available are low, it is necessary to use special processes in the manufacture of the poles and frame to reduce the residual magnetism.

The use of laminated frames, where required, permits a higher speed of response.

The brush position is no more sensitive than on normal machines. A shift of one bar each side of neutral was made experimentally on a design having 35 slots and 105 commutator bars. This changed the tuning of the output circuit slightly but the commutation and performance was still satisfactory.

No application has been made to date using more than a 2-stage design. However, laboratory tests have been made with a 3-stage design in which the control energy is amplified twice before using it to control the output stage. This unit was not as inherently stable as the 2-stage unit, probably due to the high amplification and the time delay due to the additional stage.

Conclusion

This design of Rototrol provides a means of amplifying the control energy and thus permits the application of a single unit in systems having limited control energy. As much as three stages can be obtained from a 4-pole machine. More stages could be obtained by increasing the number of poles and providing the proper field winding.

The future of this type machine appears to be quite good as the existence of three generators in one set of parts will probably permit more items of intelligence to be introduced into a system with only one generator. Another future development may be the production of the Rototrol and main generator in d-c systems combined in one unit.

References

1. Rototrol—A Versatile Electrical Regulator, W. H. Formhals. *Westinghouse Engineer* (East Pittsburgh, Pa.), May 1942.

2. Electrical Drives for Wide Speed Ranges, G. A. Caldwell, W. H. Formhals. AIEE Transactions, volume 61, 1942, February section, pages 54–6.

3. Rototrol Provides Operating Advantages in the Pulp and Paper Industry, W. R. Harris. *Paper Trade Journal* (New York, N. Y.), November 26, 1942.

4. Rotating Regulator for Arc Furnaces, R. A. Gieselman, C. C. Levy, W. R. Harris. AIEE Transactions, volume 62, 1943, November section, pages 671–3.

5. Rototrol Application to Mine Hoists, J. G. Ivy. *Westinghouse Engineer* (East Pittsburgh, Pa.), July 1944.

6. Adjustable Voltage Skip Hoist Control, F. R. Burt. *Iron and Steel Engineer* (Pittsburgh, Pa.), August 1942.

7. Industrial Application of Rototrol Regulators, W. R. Harris, AIEE Transactions, volume 65, 1946, March section, pages 118–23.

No Discussion

Resynchronizing of Generators

C. CONCORDIA
FELLOW AIEE

M. TEMOSHOK
NONMEMBER AIEE

THE DESIGN of an electric power system ordinarily involves the determination of the power limits of stable generator operation both in the steady state and as affected by faults. In the usual stability study, the criterion of proper operation is that the generator shall not lose synchronism under the most severe fault that reasonably can be expected. Moreover, the generators, if possible, should be so chosen and so located that any one generator may be lost, if this becomes unavoidable, without an intolerable system disturbance. However, with almost all generators loaded to capacity, so that loss of a generator is to be avoided if at all possible, it becomes of interest to know whether a generator may not resynchronize spontaneously following a fault during which it has slipped one or more pole pairs, even though with the ordinary criterion it would be considered that the system is unstable and that the generator should be tripped off the line. Two questions are then to be answered: first, how large can the system impedance (that is, the impedance to a point of maintained voltage as viewed from the generator terminals) be for spontaneous resynchronization, and second, if synchronism is likely to be lost what is the best way in which to relay the machine?

A related problem is the loss of field excitation,[1,2] as may be caused either by field or exciter short circuit or by accidental opening of the field switch. If excitation cannot be re-established, there is of course no possibility of resynchronizing, so the machine should be tripped off the line as soon as feasible. It thus becomes of interest to determine the machine characteristics following loss of field with the object of obtaining the surest indication of when to trip the machine. In particular, use of a distance relay has been proposed and it therefore becomes necessary to determine the variation of equivalent generator impedance during these disturbances.

To determine the effects of the variables influencing the ability to resynchronize a generator after it has lost synchronism following a 3-phase short circuit, with subsequent clearing, is one purpose of this paper. A second purpose is to study the condition of generator loss of field under load.

Upon sustained short circuit or loss of load, a turbogenerator will increase its speed above synchronous to a slip contingent on the turbine speed governor characteristics. The rate of change of slip is determined by the initial loading, generator constants, inertia of the turbine-generator set, regulator response, and governor characteristics.

Loss of field with a generator under load and tied in with a system results in a speed increase of the set, depending on the initial loading, generator constants, and impedance of the system connected to the generator. The rate of change of slip for a given load depends upon the inertia of the turbine-generator set, regulator response, and governor characteristics.

Assumptions

1. The generator is a round-rotor machine with two amortisseur circuits in each axis, direct and quadrature, and with a field circuit in the direct axis for excitation. Mutual reactances between rotor circuits do not change with rotor position. The two amortisseur circuits in each axis have been chosen to represent as well as possible the solid-rotor eddy current characteristics of a typical turbogenerator.

2. Effects of saturation and hysteresis are neglected.

3. Voltage regulator and exciter time lags are assumed to be zero.

4. The generator terminals are connected to an equivalent system impedance which terminates in an infinite bus.

5. The system resistance is assumed to be one of two values, either 10 per cent or 15 per cent of the system reactance.

6. The system electrical time constant is assumed to be so much smaller than the generator time constants that on clearing of faults from the 3-phase short-circuit condition, the system currents instantaneously become equal to the generator armature currents.

7. All phase currents are assumed to be interrupted simultaneously on clearing of the three-phase fault.

Method of Solution

The General Electric Company differential analyzer was used for the study. It was possible to set up the machine equations and observe the stator currents and voltages, governor action, and field current. In addition the rotor position and rate of change in speed could be viewed. Voltage regulator action, rotor inertia, and speed governor time constant were varied. Effects on rotor acceleration of load torque, governor torque, and electrical torque could be viewed.

Output plots were made of direct- and quadrature-axis stator currents versus time; rotor angular displacement and rate of displacement versus time; and rate of displacement versus displacement. Readings were taken of field current to allow an accurate plot of field current versus time.

Conclusions

1. Resynchronization from the most unfavorable angle and with the maximum load considered is benefited largely by two factors

(a). Small system impedance after the generator is cleared.

(b). Small inertia of turbine-generator set.

2. Other factors favoring resynchronization to some degree are

(a). Voltage regulator action.

Paper 47-261, recommended by the AIEE power generation committee and approved by the AIEE technical program committee for presentation at the AIEE Midwest general meeting, Chicago, Ill., November 3–7, 1947. Manuscript submitted March 27, 1947; made available for printing October 1, 1947.

C. Concordia and M. Temoshok are in the central station engineering divisions, General Electric Company, Schenectady, N. Y.

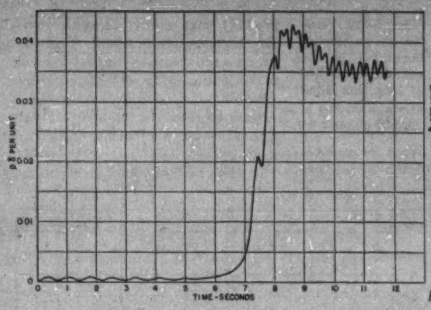

A $M=4{,}000$, $T_g=1/2$ second, $r_f=$ normal, $Z_s=0.030+j0.20$ per unit

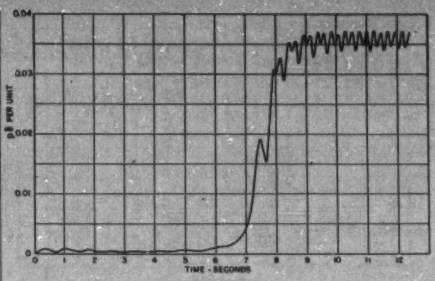

B. $M=4{,}000$, $T_g=1/8$ second, $r_f=$ normal, $Z_s=0.030+j0.20$ per unit

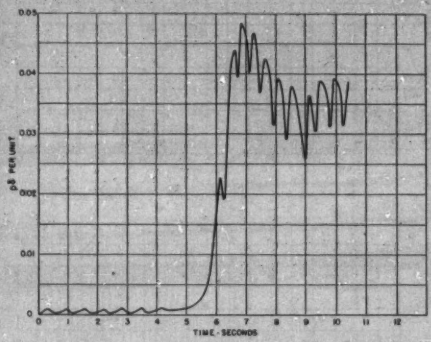

C. $M=2{,}667$, $T_g=1/2$ second, $r_f=$ normal, $Z_s=0.030+j0.20$ per unit

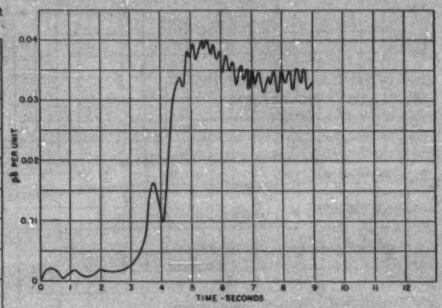

D. $M=4{,}000$, $T_g=1/2$ second, $r_f=2.5$ normal, $Z_s=0.030+j0.20$ per unit

(b). Large speed governor time constant.

(c). Small slip at time of fault clearing.

3. For a given system and load, resynchronization is determined principally by the machine angle at which fault clearing occurs.

4. The system reactance with which spontaneous resynchronization can occur varies from 10 per cent to 30 per cent, depending upon voltage regulator action, rotor inertia, and speed governor time lag. The results agree in order of magnitude with those presented in reference 6.

Figure 1. Effect of machine characteristics on generator slip following loss of field

Generator initially supplying 0.85 per unit load at 0.85 power factor

5. Voltage regulator action enabled resynchronizing on a system with impedance approximately 5 per cent (on the machine base) larger than with no regulator action.

6. Resynchronizing from 6.9 per cent slip after 1.5 seconds of fault application occurred with the same degree of ease as resynchronizing from 2.8 per cent slip after 0.5 second.

7. Out-of-step performance of a generator on loss of field can be predicted from the steady state slip–torque curve of the machine.

8. Distance relay settings can be determined for out-of-step operation due to loss of field and stator 3-phase short circuits, by viewing the equivalent generator impedance from the time of fault to the final conditions.

Discussion of Results

Loss of Field

With loss of field, resulting from short-circuiting across the generator slip rings

Figure 2. Effect of the initial load on the slip on loss of field with the generator having slip–torque relation illustrated by Figure 10

Machine characteristics: $M=4{,}000$, $T_g=1/2$ second, $Z_s=0.015+j0.10$ per unit

A. Initial load and torque = 0.85 per unit

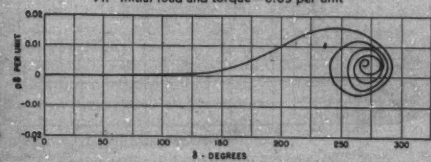

B. Initial load and torque = 1.00 per unit

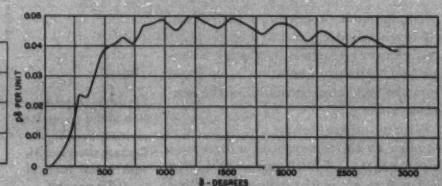

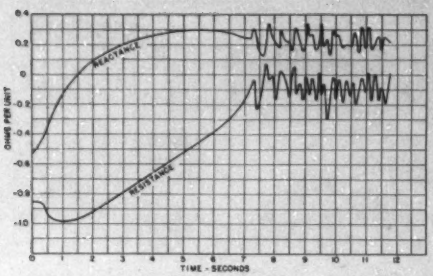

Figure 3(left). Variation of the terminal impedance of the generator with loss of field, with initial generator loading of 0.85 per unit

System impedance = 0.030+j0.20 per unit

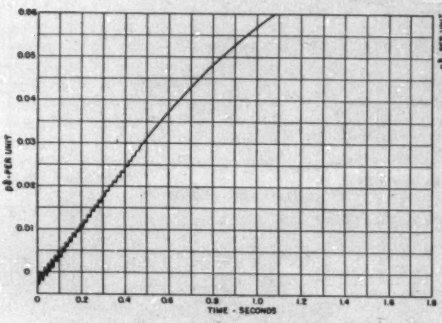

4A. $M=4{,}000$, $T_g=1.0$ second, regulator action

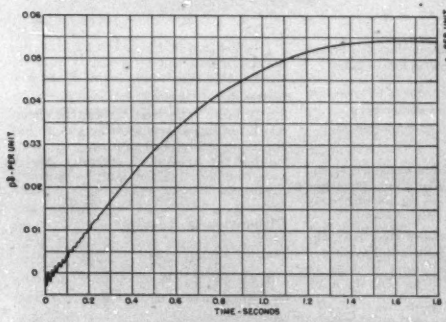

4B. $M=4{,}000$, $T_g=1/2$ second, regulator action

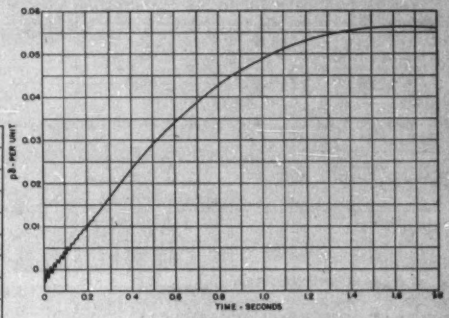

4C. $M=4{,}000$, $T_g=1/2$ second, no regulator action

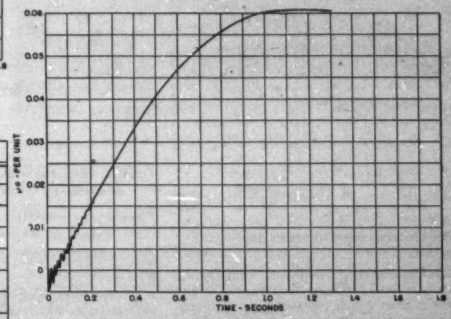

4D. $M=2{,}667$, $T_g=1/2$ second, regulator action

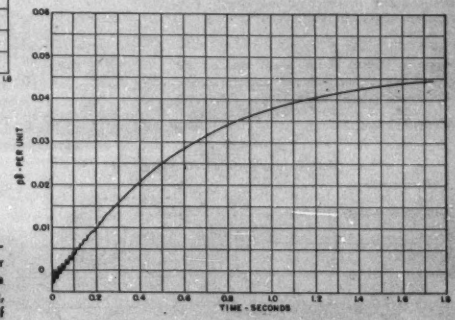

4E. $M=4{,}000$, $T_g=1/8$ second, regulator action

Figure 4. Acceleration of the generator after application of a 3-phase short circuit, with initial load of 0.85 per unit

or similar fault, a generator under load will reach a final slip dictated by the slip-torque curve of Figure 10, which is calculated on the basis of constant rotor speed from the generator constants of the generator under study.

With initial load torque of 0.85 per unit supplied by the generator to a system of impedance 0.015+j0.10 (per unit), loss of field will result in the generator settling to a very small positive slip with practically no change in load torque. Figure 2A indicates rotor advance through one pole and oscillation of the rotor about the second pole. The rotor angle constantly is increasing so that the third pole is slowly approached where a similar oscillation will occur.

To pass over the hump of the slip torque

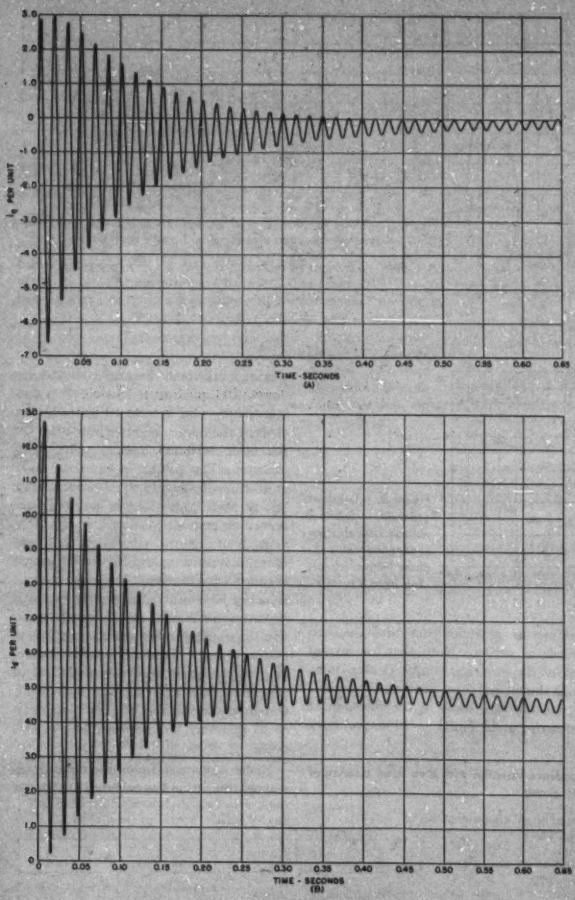

Figure 5. Short-circuit currents in direct and quadrature axes on application of 3-phase short-circuit fault with initial loading of 0.85 per unit

curve of Figure 10, the load torque was increased from 0.85 per unit to 1.0 per unit, the slip increased and the load torque supplied by the generator decreased to about one half of the initial value. Figure 2*B* illustrates the rotor slip versus time. The unsymmetrical variations are due to the natural frequency hunting of the set.

Comparison of Figures 2*A* and 2*B* shows that near the hump of the slip torque curve (Figure 10), a slight increase in load, keeping all other factors constant, can result in a change from a condition of close to normal operation to one of fairly large system disturbances.

The effects on rotor acceleration due to loss of field, set inertia, governor time constant, and field time constant are illustrated by Figure 1. An appreciable time of from five to seven seconds exists in each case before violent out-of-step phenomena occur.

The equivalent impedance of the generator on loss of field as viewed from the generator terminals is illustrated in Figure 3. With the aid of this information a distance type relay can be set to act on the faulted condition.

Three-Phase Short Circuit and Clearing of Fault

Since rotor angle at the time of fault clearing is one of the most important factors in resynchronizing, but is also the most difficult to control in practical operation, concentrated study was made with the rotor angle δ the most unfavorable, that is, 180 degrees or 360 degrees $\times$ $n+180$ degrees. This is the time the rotor is entering the motor region and is being given an additional acceleration.[3]

In most of the cases studied, the load and system impedance before the fault remained the same after clearing of the fault. If a system line was tripped during fault clearing the generator would be supplying a different power factor load to a new system. In a comparison of two generators clearing on a system of impedance $0.030+j0.20$ (per unit), one with a system impedance of zero before the fault, resynchronized; the other, which was feeding a system of $0.030+j0.20$ (per unit) impedance before the fault, did not resynchronize. Basically this difference in performance is produced by the difference in system voltage for the two cases compared, and this difference in system voltage in turn arises from the initial load power factor of 0.85 used in the study.

The governor setting was chosen to

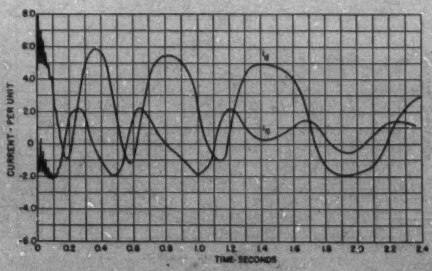

Figure 6. Direct- and quadrature-axes armature currents after clearing of 3-phase short-circuit fault, with generator initial loading of 0.85 per unit and stabilizing to a steady state load again of 0.85 per unit

Run 111

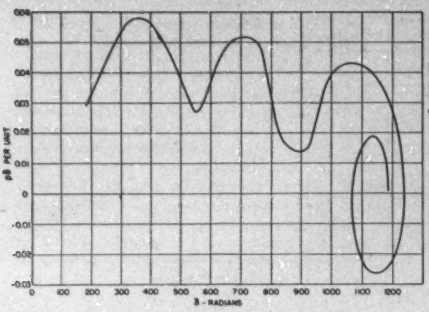

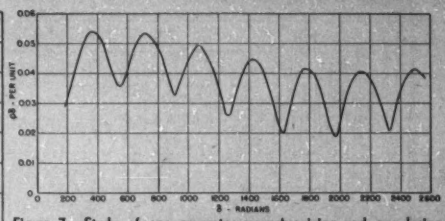

Figure 7. Study of one generator resynchronizing and one losing synchronism upon clearing of a 3-phase short circuit

A (left). Generator resynchronized when cleared on a system impedance of 0.015+*j*0.10 per unit, run 111

B (above). Generator lost synchronism when cleared on a system impedance of 0.030+*j*0.20 per unit, run 112

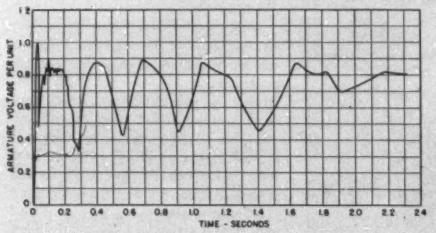

Figure 8. Transient generator terminal voltage after clearing a generator of a 3-phase short circuit and onto a system

give a 5.06 per cent slip for a change from 85 per cent load to no load. On a 3-phase short circuit the 5.06 per cent slip would be approached as generator losses are the only load. Figure 4 illustrates five cases of slip versus time, indicating the effect of set inertia, governor time constant, and regulator action. Note that for several cycles the electrical torque (losses) is so high that actual rotor deceleration occurs.

To illustrate some of the phenomena occurring under fault conditions and after clearing of the fault, Figure 5 indicates the direct- and quadrature-axis currents during a fault condition, and Figure 6, after clearing the fault. Figure 8 illustrates the generator terminal voltage after fault clearing. The voltage is less than unity at all times, and is slowly approaching its steady state value as the rotor is approaching a stable position.

Study of Figure 7*A* shows a typical case of resynchronizing, and Figure 7*B*, a case of loss of synchronism. Increase (positive slope) of $p\delta$ indicates the time the rotor is in the motor region, and decrease (negative slope) of $p\delta$ indicates time in the generator region. Transition from one region to the other occurs around time of zero slope, but the exact time may be affected by other factors. A complete cycle of $p\delta$ therefore indicates slipping of two poles.

Under the most favorable conditions, resynchronization has occurred at the first

Figure 9. The generator equivalent terminal impedance variation with time upon clearing of a 3-phase short circuit

A (below). Generator resynchronized when cleared on an equivalent system impedance of 0.015+*j*0.10, run 111

B (right). Generator lost synchronism when cleared on an equivalent system impedance of 0.030+*j*0.20, run 112

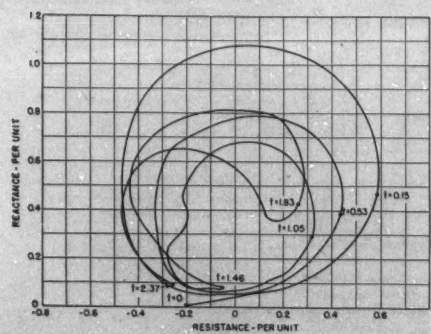

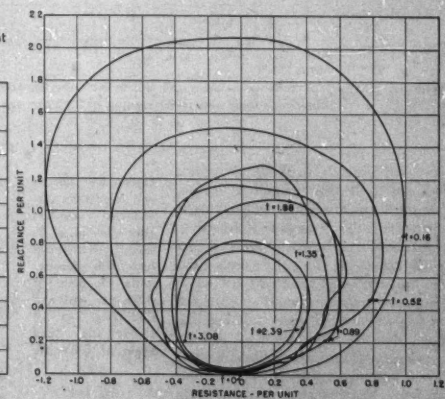

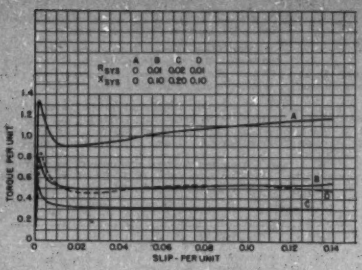

Figure 10. The slip-torque relationship of a solid-rotor generator with closed field as modified by the system impedance tied in with the generator

Curves *A, B, C*—Solid iron rotor
Curve *D*—Equivalent circuit of Appendix A

entrance to the generator region by the rotor. Under borderline conditions, the generator slipped 12 poles in one tested case before resynchronizing, and in a second case, 18 poles were slipped before the envelope of $p\delta$ versus time became positive in slope, the criterion for loss of synchronism.

A difficult problem presents itself in having relay action trip the generator when loss of synchronism will occur, but still not trip when synchronism will occur. As in the loss of field case, Figure 3, the equivalent generator impedance as viewed from the terminals is given by Figure 9. Figure 9*A* is a case of resynchronizing and is the same run as Figure 7*A*. Figure 9*B* is a case of loss of synchronism, and the same case as Figure 7*B*. Study of these figures leads to several possibilities of distance type relay settings.

Appendix I

The system diagram is shown in Figure 11*A*, and the equivalent 2-amortisseur winding circuit used is shown in Figure 11*B*. All values are in per unit.

The basic equations of Park[4,5] were used with modifications to adapt them to the differential analyzer.

$$\psi_d = r_a i_q + e\cos\delta - \psi_d p\delta - p\psi_q \tag{1}$$

$$\psi_q = -r_a i_d - e\sin\delta - \psi_q p\delta + p\psi_d \tag{2}$$

$$T_e = +\psi_d i_q - \psi_q i_d \tag{3}$$

$$\psi_d = G(p)E - x_d(p) i_d \tag{4}$$

$$\psi_q = -x_q(p) i_q \tag{5}$$

$$p\delta = \frac{1}{M}\int [-\psi_d i_q + \psi_q i_d + T]dt = \frac{1}{M}\left(-\int \psi_d i_q dt + \int \psi_q i_d dt + Td + a\delta + \int N dt\right) \tag{6}$$

$$i_q = -i_{1q} - i_{2q} - \frac{\psi_{aq}}{x_{aq}} \tag{7}$$

$$i_d = -i_{1d} - i_{2d} - i_{fd} - \frac{\psi_{ad}}{x_{ad}} \tag{8}$$

Figure 11. System diagram (*A*) and equivalent 2-amortisseur winding circuit (*B*)

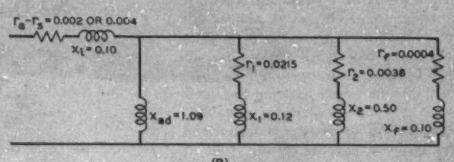

$$G(p)E = \frac{E}{\left(\frac{r_f}{p}+x\right)p} \Bigg/ \left(\frac{1}{x_{ad}} + \frac{1}{\frac{r_1}{p}+x_1} + \frac{1}{\frac{r_2}{p}+x_2} + \frac{1}{\frac{r_f}{p}+x_f}\right) \tag{9}$$

$$x_d(p) = x_1 + \frac{1}{\frac{1}{x_{ad}} + \frac{1}{\frac{r_1}{p}+x_1} + \frac{1}{\frac{r_2}{p}+x_2} + \frac{1}{\frac{r_f}{p}+x_f}} \tag{10}$$

$$x_q(p) = x_1 + \frac{1}{\frac{1}{x_{aq}} + \frac{1}{\frac{r_1}{p}+x_1} + \frac{1}{\frac{r_2}{p}+x_2}} \tag{11}$$

$$p\theta = 1 + p\delta \tag{12}$$

$$\psi_{aq} = \psi_q + x_1 i_q \tag{13}$$

$$\psi_{ad} = \psi_d + x_1 i_d \tag{14}$$

$$x_{aq} = x_{aq} \tag{15}$$

$$i_{1q} = \frac{p}{r_1 + px_1}\psi_{aq} \tag{16}$$

$$i_{2q} = \frac{p}{r_2 + px_2}\psi_{aq} \tag{17}$$

$$i_{1d} = \frac{p}{r_1 + px_1}\psi_{ad} \tag{18}$$

$$i_{2d} = \frac{p}{r_2 + px_2}\psi_{ad} \tag{19}$$

$$i_{fd} = \frac{p\psi_{ad} - E}{r_f + px_f} \tag{20}$$

$$T = T_0 + ap\delta + \frac{bp\delta}{pT_g + 1} T_0 + ap\delta + N \tag{21}$$

$$e_d = e\sin\delta \tag{22}$$

$$e_q = e\cos\delta \tag{23}$$

Appendix II. Nomenclature

x_{ad} = common mutual reactance for armature, armortisseur circuits, and field winding in direct axis

x_{aq} = common mutual reactance for armature and amortisseur circuits in quadrature axis

x_d = synchronous reactance in direct axis

x_q = synchronous reactance in quadrature axis

i_d = armature current in direct axis

i_q = armature current in quadrature axis

e_d = armature voltage in direct axis

e_q = armature voltage in quadrature axis

ψ_d = direct axis armature winding flux linkages

ψ_q = quadrature axis armature winding flux linkages

δ = angle between field excitation axis and armature voltage

$p\delta$ = generator slip

θ = angle between field pole axis and axis of phase *a*

$p\theta$ = rotor speed

M = turbine-generator set inertia coefficient

b = governor amplification factor = -16

a = slope of prime-mover torque–speed curve = $-T_0$

T_0 = initial per unit torque

T_g = governor time constant

i_{1q} = current in quadrature-axis amortisseur circuit 1

i_{2q} = current in quadrature-axis amortisseur circuit 2

i_{1d} = current in direct-axis amortisseur circuit 1

i_{2d} = current in direct-axis amortisseur circuit 2

i_{fd} = field current in excitation circuit direct axis

$G(p)$ = operator relating field voltage with armature current and linkages in the direct axis

$x_d(p)$ = operational impedance in the direct axis met by the current resulting from a change of terminal flux linkages in the direct axis

$N = bp\delta/(T_g p + 1)$, governor characteristic

ψ_{aq} = mutual flux linkages in the quadrature axis

ψ_{ad} = mutual flux linkages in the direct axis

r_a = armature resistance (total)

r_s = system resistance

x_s = system reactance

x_l = stator leakage reactance (total)

E = voltage across field terminals

$p = d/dt$

$Z_s = r_s + jx_s$ = equivalent system impedance as viewed from generator terminals

References

1. Re-establishing Excitation of a Loaded Alternator in Parallel With Others, D. D. Higgins, Earle Wild. AIEE Transactions, volume 50, 1931, pages 1194–8.

2. Loss-of-Field Protection for Generators, G. C. Crossman, H. F. Lindemuth, R. L. Webb. AIEE Transactions, volume 61, 1942, May section, pages 261–5.

3. Pull-In Characteristics of Synchronous Motors, D. R. Shoults, S. B. Crary, A. H. Lauder. Electrical Engineering (AIEE) Transactions, volume 54, December 1935, pages 1385–95.

4. The Operational Impedances of a Synchronous Machine, M. L. Waring, S. B. Crary. *General Electric Review* (Schenectady, N. Y.), volume 35, September 1932, pages 578–83.

5. Two-Reaction Theory of Synchronous Machines, R. H. Park. Part 1, AIEE Transactions, volume 48, 1929, pages 716–37; part 2, AIEE Transactions, volume 52, 1933, pages 352–4.

6. Synchronization of Machines in Disturbances of Stability, P. S. Shdanow. CIGRE (Paris, France), 1935, volume 1, paper 110.

No Discussion

Ignitor Characteristic and Circuit Calculations

D. E. MARSHALL
MEMBER AIEE

AN IGNITRON is a gas electronic tube whose cathode is a pool of liquid mercury. In operation, electrons are emitted from the mercury pool and move to the anode. Their motion constitutes an electric current. The action, however, is not self-starting. The conduction is started by means of a rod of material, called the ignitor, of resistivity high compared with the mercury, one end of which is submerged into the mercury pool.[1] When a current is passed through this rod, the arc will start at the junction of the mercury surface and the resistance rod. If such a tube is connected in series with a source of alternating voltage and a suitable impedance, the arc can be made to start whenever the anode is more than a few volts positive, and is extinguished automatically at the end of each positive half cycle. Therefore, control of the phase of starting of the arc is possible. The tube then has properties similar to those of a thyratron with the advantages of the high electron emission and long life properties of the mercury pool.

The current required to start the ignitor and the resistance of the ignitor must be known in order that circuits can be designed which will fire the ignitor reliably. In certain cases, such as resistance welding control, the load impedance is in series with the ignitor. The characteristic of the ignitor then limits the minimum loading which the tube will control satisfactorily. The firing current and voltage of an ignitor varies as a function of the constants of the circuit through which it is fired.

Problems exist in describing the characteristics of the ignitors of these tubes in such a manner that the data can be used in a practical way in estimating their performance under a particular set of circuit conditions. Of interest to the circuit designer are questions pertaining to the power required to drive the ignitor, the current and voltage rating of ignitor driving equipment, the energy expended, and other similar factors. These quantities may be calculated or estimated by the usual methods if the wave form, voltage and current of the ignitor firing pulse are known. The following material is intended to contribute to the solution of these problems.

Characteristics of Ignitors

The basic quantities involved in the description of the characteristics of an ignitor are shown in Figure 1. The volt-ampere characteristic of an ignitor as shown by an oscilloscope is shown in Figure 1a. The arrows indicate the direction of motion of the oscilloscope beam. The voltage across the ignitor increases with the current before the firing point is reached. This portion of the trace is usually quite linear for present commercial types of ignitors, as their thermal time constant is usually large compared with their cyclic conduction period and, therefore, their temperature and resistance remain very nearly constant over any one period. For the purposes of this paper, the ignitor resistance will be assumed constant over the firing period.

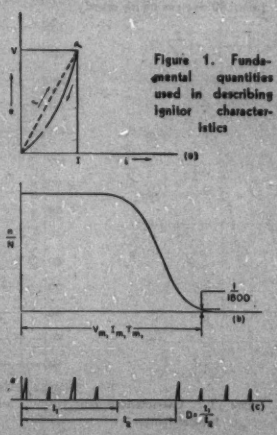

Figure 1. Fundamental quantities used in describing ignitor characteristics

The time of motion of the oscilloscope beam from point to point on the diagram can be measured by blanking the beam periodically, thus furnishing a time scale. The velocity of motion when the beam travels upward depends on the constants of the circuit furnishing power to the ignitor. On the downward sweep the path taken and the velocity of the spot depends on the speed of transference of the positive pole of the arc from the ignitor to the anode.

At some time during the upward travel of the oscilloscope beam, the ignitor will fire. The firing data are measured by observing the firing voltage V, firing current I, and the time T as shown on the diagram. The ratio of the firing voltage and current is the slope of the linear portion of the diagram or the ignitor resistance during one ignitor conduction period.

These quantities are not independent. The firing time and firing current are connected through the rate of rise of current in the ignitor circuit as determined by the circuit constants. The firing voltage and firing current are connected through the ignitor resistance which is mainly dependent on the ignitor temperature.

The measured value of the firing volt-

Paper 47-264, recommended by the AIEE electronics committee and approved by the AIEE technical program committee for presentation at the AIEE Midwest general meeting, Chicago, Ill., November 3-7, 1947. Manuscript submitted March 7, 1947; made available for printing September 29, 1947.

D. E. MARSHALL is section engineer, electronics engineering department, Westinghouse Electric Corporation, Bloomfield, N. J.

The author wishes to acknowledge the help and constructive criticism given by W. W. Rigrod in the preparation of this paper.

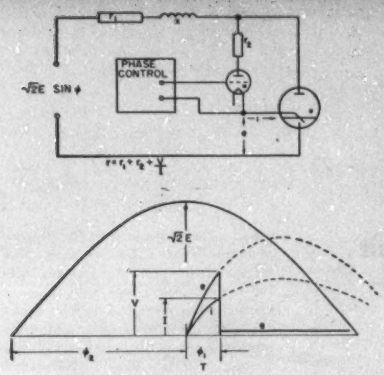

Figure 2. Ignitor wave forms in a-c circuit

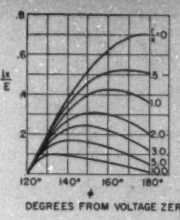

Figure 5. A-c wave forms, 120 degrees phase retard

have chosen to denote for testing purposes as the maximum firing voltage V_m that voltage on the diagram corresponding to a value of n/N of 1/1,800. Thus, roughly, the ignitor firing voltage is not to be higher than the value V_m more than one cycle in 30 seconds when operating on a 60-cycle system.

Although V_m so defined corresponds to an appreciable probability of misfiring, which would be too large for commercial operation, it approaches very closely the value of maximum voltage at which the probability of misfiring is negligible. For example, in order to reduce the probability of misfiring from 1/1,800 to 1/7,200,

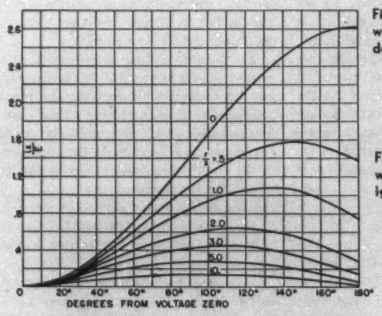

Figure 3 (left). A-c wave forms, zero degrees phase retard

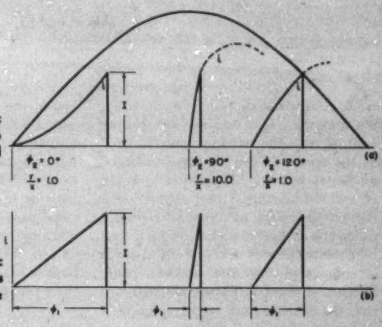

Figure 6 (right). A-c wave forms versus ignitor test wave forms

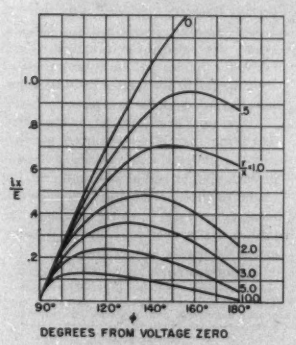

Figure 4 (left). A-c wave forms, 90 degrees phase retard

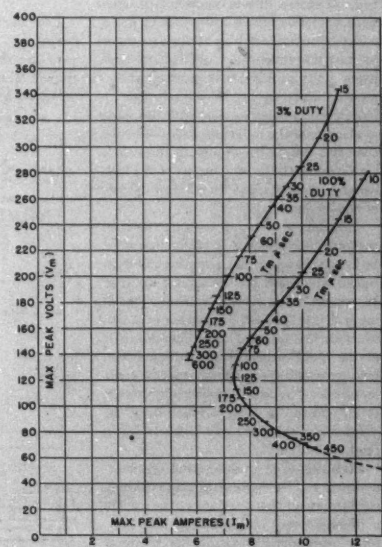

Figure 7. Characteristic of typical ignitor

age changes from cycle to cycle. Figure 1*b* illustrates this variability.[2] The ratio n/N represents the fraction of the large number of firing cycles observed in which the ignitor fired above a voltage V. We

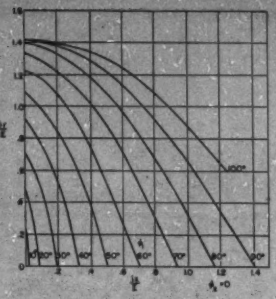

Figure 8. Volt-ampere a-c circuit characteristic

Phase retard zero degrees

the value of V_m for an ignitor normally measured at 90 volts would increase to 92 volts.

Because of the linearity of the volt-ampere characteristic, the ignitor current and firing time are also cyclically variable. The maximum firing current I_m and maximum firing time T_m corresponds to the maximum firing voltage.

The product of the duty D as illustrated in Figure 1*c*, the firing voltage, firing current, and the time indicated from zero to firing current determines the energy put into the ignitor before firing. This energy heats the ignitor and affects its resistance. In present commercial ignitors, the temperature coefficient of resistance is negative, and the ignitor resistance therefore decreases as the energy put into the ignitor increases.

The heating of the ignitor also is determined by a number of other factors, such as the magnitude of the current conducted by the ignitron in which they are used, the efficiency of cooling, and the speed of transfer of the arc to the anode. These factors are not inherent in the ignitor, and therefore are considered in this paper to be minimized.

Characteristics of Ignitor Circuits

In considering the operation of the ignitor, the circuit employed to fire it also must be considered, as the wave form of the prefiring current influences the ignitor characteristics through changes in the factors described above.

The circuit shown in Figure 2 is basic to a number of applications of ignitrons. For example, in the case of resistance welding the load circuit represents the welder transformer and the applied voltage is that of the a-c supply. In the case of anode-fired rectifier circuits, the load circuit represents the commutating reactance and the applied voltage represents the commutating voltage.

In terms of the quantities shown in Figure 2, and neglecting the thyratron tube voltage drop, the equation for the current wave form of this circuit can be written with the ratio of resistance to reactance (r/x) as a parameter as follows:

$$\frac{xi}{E} = \frac{\sqrt{2}}{\left(\frac{r}{x}\right)^2+1}\left[\left(\frac{r}{x}\sin\phi - \cos\phi\right) - \left(\frac{r}{x}\sin\phi_1 - \cos\phi_1\right)e^{\frac{-\pi}{180}\frac{r}{x}(\phi-\phi_1)}\right] \quad (1)$$

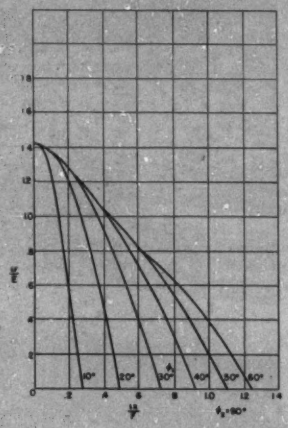

Figure 9 (above). Volt-ampere a-c circuit characteristic

Phase retard 90 degrees

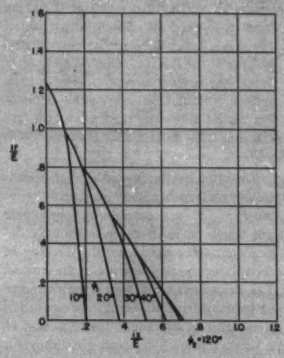

Figure 10 (right above). Volt-ampere a-c circuit characteristic

Phase retard 120 degrees

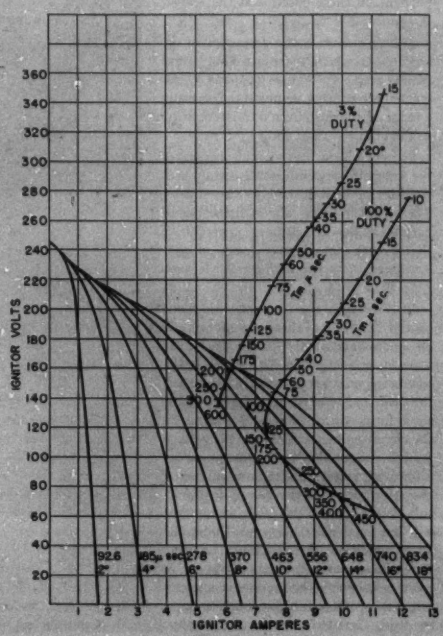

Figure 11. Combined ignitor and a-c circuit characteristic

$$\frac{ri}{E} = \left(\frac{xi}{E}\right)\left(\frac{r}{x}\right) \qquad (2)$$

The thyratron is fired at the angle ϕ_2, the current through the ignitor increases from zero following the wave form shown by the dotted curve marked i. The ignitor fires ϕ_1 degrees or T microseconds later at the value of current marked I. The voltage, since the ignitor resistance is constant, is of the same shape as the current and is shown marked e and at the firing point is marked V. The solid portion of the wave forms denotes the current and voltage of the ignitor. Immediately after firing, the ignitor current is zero and the ignitor voltage takes on a value dependent on its action as a probe in the arc stream. This voltage is of the order of 10 volts.

The circuit resistance used in the equation must include the resistance of the ignitor, which is constant over one cycle but which varies from cycle to cycle dependent on the motion of the mercury in the tube or the temperature of the ignitor. The calculated wave forms are therefore to be considered as being representative of conditions prevailing during period of a single cycle. They will go through a variation over a longer period of time dependent on these changes in the ignitor resistance.

The wave form is also a function of the angle ϕ_2 at which the controlling thyratron is fired. In Figures 3, 4, and 5, calculated wave forms are presented covering a range of r/x ratio from 0 to 10 for firing angles of $\phi_2 = 0°$, 90°, and 120°.

Figure 6a illustrates various portions of the foregoing data indicating certain possibilities of ignitor current wave forms. These vary from the almost linear rise of current at $\phi_2 = 120$ degrees, $r/x = 1.0$, to the extreme curved wave forms of $\phi_2 = 0$ degrees, $r/x = 1.0$, and $\phi_2 = 90$ degrees, $r/x = 10.0$.

In this paper, the assumption is made that at least two of these wave forms can be approximated by linear triangular wave forms as shown in Figure 6b. In the case of the wave form shown in the center, the justification of the use of a triangular wave form equivalent would depend on the circuit voltage. If the circuit voltage is high compared with the maximum ignitor firing voltage, the ignitor will fire on the rising portion of the curve. If the circuit voltage is not this high, the ignitor will fire on the flat portion. Under the latter condition, the variability of firing time will be relatively great. However, in most cases where this action is encountered, the voltage is high enough to cause the firing time to be small. An extreme case of such a wave form would be that of a rectangular wave form. The characteristic ignitor operation for this case has been considered by Dow and Powers,[4] and will not be treated further in this paper.

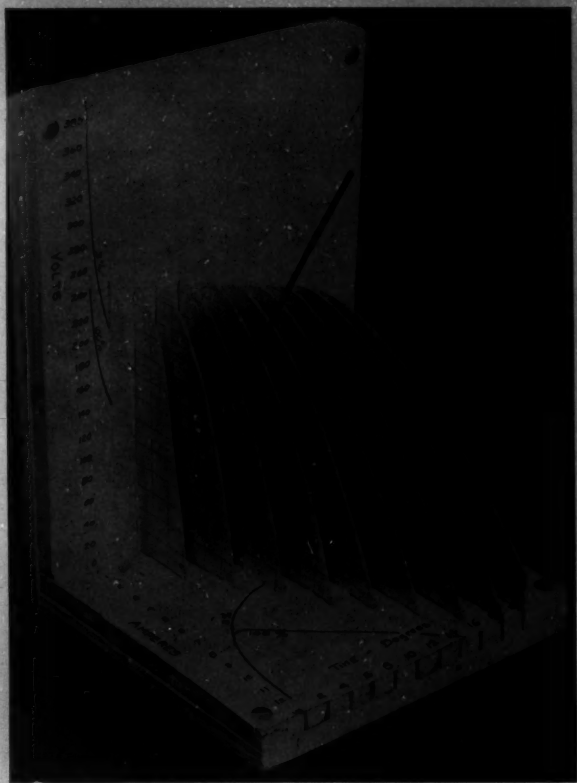

Figure 12. Three-dimensional model, quartering view

Characteristics of a Typical Ignitor

Data taken on a typical ignitor designed for intermittent duty such as resistance welding control are presented in Figure 7. On this one diagram, we have presented the effect on the ignitor characteristic of the four variables previously mentioned, namely, the maximum firing voltage, maximum firing current, circuit time, and duty. The last two are shown as parameters. The wave form used was triangular as described before. The test results were observed with an oscilloscope equipped with a time marker. The ignitor was fired at 60 cycles per second by power from a capacitor charged to a voltage considerably in excess of that required to fire the ignitor. The rate of rise of current was controlled by a variable reactor in series with the ignitor. The charge remaining on the capacitor at the firing time was shunted to the anode of the tube being tested when the ignitor fired.

The curve is the locus of the maximum firing voltages and currents obtained by varying the ignitor circuit inductance. The operation duty was held constant at the values shown for each curve. The figures on the curves are the maximum firing times T_m in microseconds.

The data are an average of a number of

tests. The minor curvatures shown may or may not be of significance. This particular ignitor remained at nearly constant resistance, 30 to 23.6 ohms, as the rate of rise of current was changed through the range shown when operating at the low duty of 3 per cent. The firing voltage correspondingly dropped from 350 to 135 volts, the change being most rapid at the shortest times.

At continuous duty or 100 per cent, the ignitor resistance was lower than at 3 per cent duty, due mainly to a decrease in firing voltage. It changed little until a firing time of 100 microseconds was reached. At longer firing times the maximum firing voltage decreased to 60 volts and the current increased to 12 amperes. The resistance decreased considerably, the over-all change being from 22.3 ohms to 6.4 ohms.

These data were taken under ideal conditions of operation. The average ignitron main anode current was low, thus minimizing motion of the mercury pool, and reducing heating of the ignitor by the arc. It is used here as being representative of the inherent characteristics of the ignitor as influenced by its own makeup independent of design factors of the tube in which it is used. For purposes of circuit design, it would be necessary to consider the foregoing factors. However, the same form of presentation of the data would be possible.

Volt-ampere Plot of Circuit Characteristics

The data in Figures 3, 4, and 5 may be plotted in another form as presented in Figures 8, 9, and 10. With values of ϕ_1 as parameters, the ratio of voltage across the total circuit resistance r to the circuit rms voltage ri/E as obtained from equation 2 is plotted as a function of the ratio xi/E.

These charts may be used as follows: Assume that a certain ignitor is known to fire at the values V_m and I_m, and that it is to be used in an a-c circuit fired at a retard angle of ϕ_2 degrees, having a reactance of x ohms and a resistance of r_1 ohms. The resistive voltage drop in the circuit at the firing point will be $V_m+I_m\times(r_1+r_2)$. The ratio of this quantity to the rms circuit voltage becomes (ri/E) and it, with the ratio $(xI_m)/E$, will define a point on the chart. This point will lie between curves having parameters ϕ_1 and ϕ_1'. The angular time from the initiation of the ignitor firing current until the ignitor fires will lie between these two parameters. Obviously, the charts can be extended to as small a difference in parameters as desired.

Figure 13. Three-dimensional model, side view

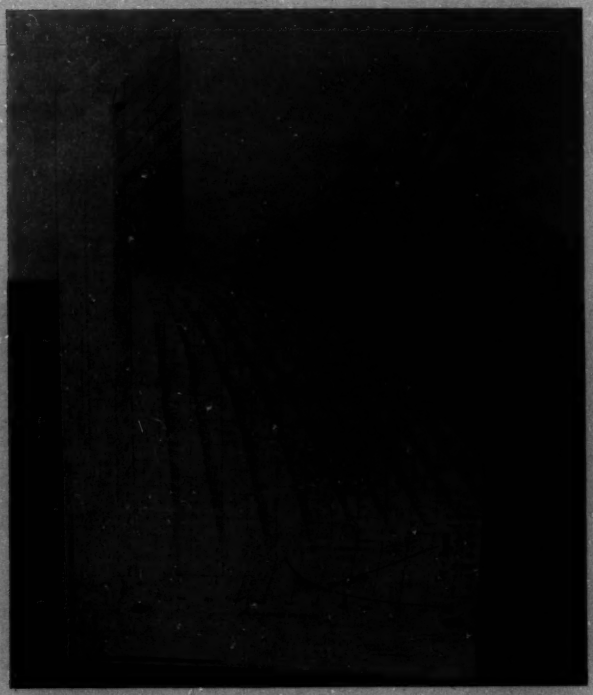

Combination of Circuit and Ignitor Volt-Ampere Plots

Because of the variable nature of the ignitor characteristics, the foregoing example is an academic one. A closer approach to the actual conditions can be realized by a superposition of the ignitor and circuit volt-ampere curves. When this is done, it may be possible to find an intersection between the two characteristics such that the circuit can supply the voltage and current required to fire the ignitor in that particular circuit. The mechanics of finding this intersection can be explained by an example.

In Figure 11, we have replotted the data from Figure 10 for the specific case of an a-c control circuit having the following data:

Load circuit current = 40 rms amperes
Supply voltage = 220 volts at 60 cycles per second
Angle ϕ_2 = 120 degrees
Ignitor series resistor = 1 ohm
Load circuit power factor = 25 per cent

A rough allowance for the voltage drop in the thyratron was made by calculating the data at 200 volts rms. The chart is drawn with an allowance for the voltage drop in the resistance external to the ignitor so that the vertical axis represents the voltage directly across the ignitor. The horizontal axis represents the current through the ignitor. The equivalent microsecond parameters are shown on the circuit curves. The ignitor data from Figure 7 are shown drawn on the same curve. Consider first the case for 3 per cent duty operation. The two families of curves cross each other at several points. However, only the intersection of curves whose time parameters are equal represents a true intersection where voltage, current, and time are the same for both circuit and ignitor. If such a point is found, these quantities can be picked from the chart. Obviously, unless a great

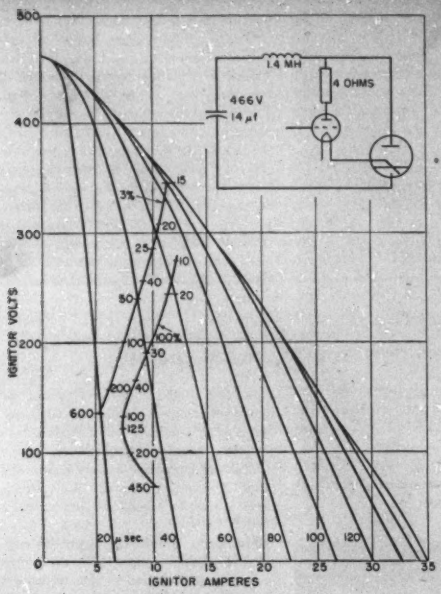

Figure 14. Combined Ignitor and capacitor circuit characteristic

many curves are drawn representing a fine gradiation in time variation, an approximate solution will be necessary. This may be done as follows

Starting at the high-voltage points of the ignitor characteristic, which correspond to low firing times, follow the curve in the direction of decreasing voltage and increasing firing time. When the circuit curves are reached, continue to descend the ignitor curve until the ignitor firing times at the intersections change from less than the circuit time to greater than the circuit time. The solution lies between these two intersections.

In this example, the solution lies near to 12 degrees delay. The ignitor maximum firing voltage would be about 138 volts and the current about 5.7 amperes.

Considering the 100 per cent duty operation, it is seen quickly that no solution is possible, as the longest time parameter on the ignitor curve is 450 microseconds and the shortest time parameter on the circuit curves where intersections occur is over 600 microseconds.

Since the method just described is actually a 2-dimensional method of solving a 3-dimensional equation, it was thought that a 3-dimensional model might make the situation more clear. Figure 12 shows a photograph of a 3-dimensional model of the foregoing example. The envelope of the cardboard contours defines a surface characteristic of the circuit. The black wire represents a space curve characteristic of the ignitor. The intersection of the ignitor space curve with the circuit surface can be seen plainly between 10 degrees and 12 degrees. The failure of the 100 per cent duty ignitor curve to intersect the circuit surface can be seen easily even though the space curve for ignitor at 100 per cent duty was not constructed, because its projection on the ampere-time plane does not intersect the projections of the circuit surface boundaries on the same plane. Figure 13 shows a view of the same model from the plane of projection used in the calculation.

For certain purposes, plots of ignitor–time curves or ignitor current–time curves with ignitor resistance parameters may be compared directly with the time wave forms of the circuit. This method of projection was used as it was thought to be the most interesting representation of the ignitor characteristics.

As an additional example, Figure 14 shows the superposition of circuit and ignitor curves using the characteristics of the ignitor just described in combination with a circuit firing the ignitor by a discharge from a capacitor. The circuit constants are shown in the diagram. In this case, the ignitor fires in about 40 microseconds at a maximum current of about 9 amperes for either value of duty. The maximum firing voltage varies with the duty, being 250 volts at 3 per cent and 180 volts at 100 per cent.

The foregoing method has been tested with good results in checking the operation of commercial ignitors over a considerable range of characteristics and in development work on experimental ignitors. It is adopted best to conditions where the available firing power is limited, but will be a guide to circuit design in all cases.

Appendix

Equation 1 in the text is derived in the form shown as follows. The differential equation for the current in the ignitor circuit of Figure 2 is

$$x\frac{di}{d\phi}+ri=\sqrt{2}E\sin\phi \qquad (3)$$

The well known solution is

$$i=\frac{\sqrt{2}E}{r^2+X^2}(r\sin\phi-x\cos\phi)+C_1\epsilon^{-\frac{r}{x}\phi} \qquad (4)$$

This can be written in terms of the ratio r/x

$$i=\frac{\sqrt{2}E}{x\left(\left(\frac{r}{x}\right)^2+1\right)}\times\left[\left(\frac{r}{x}\sin\phi-\cos\phi\right)+C_1\epsilon^{-\frac{r}{x}\phi}\right] \qquad (5)$$

If $i=0$ when $\phi=\phi_2$ and dividing by x/E

$$\frac{xi}{E}=\frac{\sqrt{2}E}{\left(\frac{r}{x}\right)^2+1}\left[\left(\frac{r}{x}\sin\phi-\cos\phi\right)-\left(\frac{r}{x}\sin\phi_2-\cos\phi_2\right)\epsilon^{-\frac{\pi}{180}\frac{r}{x}(\phi-\phi_2)}\right] \qquad (6)$$

The constant $\pi/180$ makes possible the direction substitution of angles in degrees.

References

1. A New Method for Initiating the Cathode of an Arc, J. Slepian, L. R. Ludwig. AIEE Transactions, volume 52, June 1933, pages 693–8.

2. Characteristics of Resistance Ignitors D. E. Marshall, W. W. Rigrod. *Electronics* (New York, N. Y.), volume 20, May 1947, pages 122–6.

3. Ignitor Characteristics, E. F. G. Arnott. *Journal of Applied Physics*, (New York, N. Y.), volume 12, number 9, September 1941, pages 660–9.

4. Firing Time of an Ignitor Type of Tube, W. G. Dow, W. H. Powers. AIEE Transactions, volume 54, 1935, September section, pages 942–7.

No Discussion

Present-Day Grounding Practices on Power Systems

Third AIEE Report on System Grounding

AN AIEE COMMITTEE REPORT

THE AIEE subject committee on present-day grounding practices has prepared this report on the grounding practices of power systems from replies to questionnaires submitted to those electrical utilities, both public and private, in the United States and Canada, having a generating capacity of more than 10,000 kw or having more than 10,000 customers.

The report covers separately grounding practices on generating stations and on transmission and distribution systems. The scope of this survey is indicated by:

Generating stations:

460 systems operating at 11 kv and above
33,752 megavolt-amperes in generating capacity
972 generating units

Transmission and distribution systems:

567 systems operating at 22 kv and above
119,081 miles of transmission and distribution circuits

These figures indicate that information was obtained on about three fourths of the facilities in the classes investigated.

Grounding methods are classified for generating stations according to the station layout, and for transmission and distribution systems according to the voltage class. Data are given as to size and number of systems, the ratio of phase-to-ground to 3-phase fault currents, and the sequence-impedance ratios. The principal characteristics of the grounding devices themselves are tabulated. The opinions of the utilities as to the importance of 16 different factors in the grounding problem as applied to their particular systems, as well as the assigned reasons for their specific practice, have been included. A particularly valuable part of the report reviews operating experiences including unsatisfactory operation, occurrence of double faults, and changes that have been made, are being made, or are contemplated. Trends in system grounding are discussed from current data and information from previous reports.

The body of this report is arranged in two parts: generating stations and transmission and distribution systems. An appendix provides a list of utilities that supplied data.

Paper 47-237, recommended by the AIEE protective devices committee and approved by the AIEE technical program committee for presentation at the AIEE Midwest general meeting, Chicago, Ill., November 3–7, 1947, and the winter general meeting, Pittsburgh, Pa., January 26–30, 1948. Manuscript submitted August 14, 1947; made available for printing September 8, 1947.

This report, which was prepared by the AIEE subject committee on present-day grounding practices and is sponsored by the AIEE committee on protective devices and its subcommittee on fault-limiting devices under the chairmanship of F. R. Longley, is the third report based by the AIEE upon replies to questionnaires distributed to the industry. The first report in this series was published in 1923[1] and the second in 1931.[2]

Personnel of AIEE Subject Committee on Present-Day Grounding Practices: R. D. Evans, *chairman*, Westinghouse Electric Corporation, East Pittsburgh, Pa.; A. A. Johnson, *vice-chairman*, Westinghouse Electric Corporation, East Pittsburgh, Pa.; J. E. Clem, General Electric Company, Schenectady, N. Y.; G. B. Dodds, Duquesne Light Company, Pittsburgh, Pa.; W. W. Eberhardt, Alabama Power Company, Birmingham; E. T. B. Gross, Illinois Institute of Technology, Chicago; F. A. Jeanne, Bell Telephone Laboratories, Inc., New York, N. Y.; B. W. Knapp, Shawinigan Water and Power Company, Montreal, Quebec, Canada; A. A. Kroneberg, Southern California Edison Company, Ltd., Los Angeles; W. W. Lewis, Union College, Schenectady, N. Y.; R. G. Norell, Sargent and Lundy, Engineers, Chicago, Ill.; H. P. St. Clair, American Gas and Electric Service Corporation, New York, N. Y.; W. T. Smith, Edison Electric Institute, New York, N. Y.; A. D. Caskey, member representing the committee on power generation, Public Service Company of Northern Illinois, Chicago; Edwin Hansson, member representing the committee on transmission and distribution, Pennsylvania Water and Power Company, Baltimore, Md.

The committee acknowledges the work of two former members, F. H. Hollister and H. E. Kent; also the many helpful suggestions of S. W. Hagerling and his assistance in tabulating the results of the questionnaire.

The comparative use of the various methods of grounding at generating stations is indicated by the following:

Grounding Method	Per Cent of Total Generating Capacity
Solidly grounded	25.7
Resistance grounded	39.4
Distribution transformer with secondary resistor grounded	1.4
Neutral reactor grounded	17.3
Grounding transformer grounded	2.3
Grounding transformer with neutral resistor grounded	4.6
Potential transformer grounded	7.9
Ground-fault neutraliser grounded	0.1
Ungrounded	1.3
Total	100.0

Grounding practices at generating stations are classified as to layout. The three layouts, with their relative usage, are listed as follows:

Layout	Per Cent of Total Generating Capacity
Unit system	39.4
Common generator bus *without* feeders at generated voltage	21.5
Common generator bus *with* feeders at generated voltage	39.1
Total	100.0

At generating stations with the unit system layout solid grounding is the predominating method, being used for slightly less than half of the generating capacity; while neutral-reactor grounding is second in importance, being used for about one fifth. For layouts involving a common generator bus *without* feeders at generated voltage, the principal method is neutral-resistor grounding, which is used on about half of the generating capacity; while neutral-reactor grounding is used on one fourth. For layouts with common generator bus and *with* feeders at generated voltage, neutral-resistor grounding is used on two thirds of the generating capacity. Mention should be made of the first reported application of a ground-

fault neutralizer to a generating system in the United States.

In the section on grounding practice on transmission and distribution systems, for the purpose of conciseness only the five principal grounding methods were considered; namely, solid grounding, resistance grounding, reactance grounding, ground-fault neutralizer, and ungrounded. As the presence of appreciable cable mileage in a system influences grounding practice, a division was made on the basis of those systems having more or less than ten per cent of the total mileage in cable.

The percentage breakdown by grounding methods of the 119,081 miles of transmission and distribution circuits is:

Grounding Method	Percentage of Total Mileage
Solidly grounded	77.9
Resistance-grounded	4.6
Reactance-grounded	6.4
Ground-fault neutralizer grounded	5.8
Ungrounded	4.3
Total	100.0

The foregoing figures show that the dominant grounding method for transmission and distribution circuits is solid grounding. For circuits with more than ten per cent of the mileage in cable, solid grounding predominates, and resistor grounding is the only other method used.

Detailed data on grounding practices are given in tabulations arranged by voltage class and grounding method which give per cent of systems, per cent of mileage, average mileage per class, and maximum mileage per class. The average length of transmission circuits per grounding point was found to be 63 miles.

The most significant indexes of system grounding are the sequence-impedance ratios, X_0/X_1, R_0/X_1, which are considered at length in this report. These impedance ratios determine the ratios of the phase-to-ground to 3-phase fault currents, and indicate the relative overvoltages on sound phases during fault conditions. Data on sequence-impedance ratios at grounding points are given for about three quarters of both the generating systems and the transmission and distribution systems. It is of considerable significance that about 20 per cent of generating systems and about 15 per cent of transmission and distribution systems that are solidly grounded, resistance-grounded, or reactance-grounded, have established limiting values for sequence-impedance ratios. It is also of interest that some utilities operating grounded generators or grounded transmission and distribution systems have established

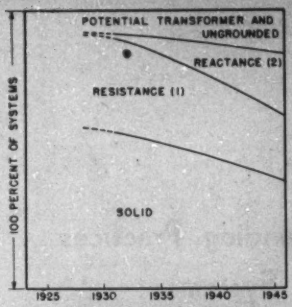

Figure 1. Relative use of grounding method on generators without feeders at generated voltage

1. Resistance includes neutral resistors, grounding transformers with resistors, and distribution transformers with secondary resistors

2. Reactance includes neutral reactors and grounding transformers

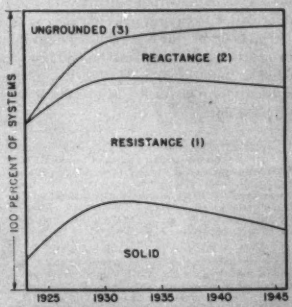

Figure 2. Relative use of grounding methods on generators with feeders at generated voltage

1. Resistance includes neutral resistors, grounding transformer with resistor, and distribution transformer with secondary resistor

2. Reactance includes neutral reactors, ground fault neutralizers, and grounding transformers

3. Ungrounded includes potential transformers

minimum values for the ratio of X_0/X_1 in order to limit ground-fault currents to the 3-phase fault values and thus reduce the mechanical stress in machines and avoid circuit breaker duties being increased beyond that required for 3-phase faults.

The most valuable and interesting parts of the report are those which summarize operating experiences. Of the 460 generating systems, 64 report unsatisfactory grounding experiences, 31 have experienced double faults, 86 have made changes of various kinds in grounding during the past 15 years, 35 are making or expect to make changes, and 40 see new trends in grounding practices. Of the 567 transmission and distribution systems, 63 report unsatisfactory grounding experiences, 53 have experienced double faults, 57 have made changes of various kinds in grounding during the past 15 years, 39 are making or expect to make changes, and 19 report new trends. These operating experiences are given in a number of tables which are supplemented by extensive notes. The operating troubles are difficult to summarize, but two types are outstanding; namely, excessive fault current with solidly-grounded generators and a large number of double faults on ungrounded or impedance-grounded transmission and distribution systems. Where available, information is given as to changes in practices that have been or will be made as a result of adverse operating experience.

One of the objectives of this survey of grounding practice was to obtain information on trends. The questionnaire inquired about new trends in grounding, but replies indicated only a trend away from ungrounded systems and were inconclusive in other respects. Certain trends, however, are indicated by using data from previous reports on grounding practices and data given in this report on operating experiences, length of time each system has been grounded in the present form, and the changes that have been made during the past 15 years. The trends are different for the different layouts of generating systems. Others are evident for transmission and distribution systems.

For generating systems *without* feeders at generated voltage, the trends are established without data from previous reports since this is the first report considering generating systems of this type. Data obtained in the 1947 report with corrections for changes during the last 15 years provide a basis for analyzing trends as shown in Figure 1. The curves show a decrease in both solid grounding and resistance grounding, and an important increase in reactance grounding. Potential transformer grounding, which as plotted includes a small percentage of ungrounded systems, show a small increase. Mention should be made of the introduction of a grounding method which uses a distribution transformer with secondary resistor.

For generating systems *with* feeders at generated voltage, the trends in grounding practices are shown in Figure 2. The points on these curves for 1923 and 1947

are plotted from the corresponding reports. The points for 1931, however, are based on the 1947 report corrected for changes in the last 15 years, as these figures are believed to be more suitable inasmuch as the data given in the 1931 report included some systems without generators. Figure 2 shows that between 1923 and 1931 there was a large increase in the use of solidly-grounded systems, but that there has been a slight decrease since that time. Resistance grounding decreased somewhat between 1923 and 1931, but has increased since that time and is the dominant method when viewed in terms of per cent of systems or in per cent of the total generating capacity. The use of reactance grounding began after the 1923 report, and made a further important increase between 1931 and 1947. The most significant change has been the reduction in the use of ungrounded systems.

For transmission and distribution systems, the trends in grounding are shown in Figure 3 which is plotted from data in the 1923, 1931, and 1947 reports. The data from the 1931 report, and data for practice at that time from the 1947 report, are in substantial agreement. Solid grounding was the dominant method used on transmission and distribution systems in 1923 and its use increased rapidly until 1931, but has made little relative change since that time. The use of resistance grounding on transmission and distribution systems was not large in 1923 and has decreased slowly since that time. Reactance grounding began after the 1923 report, and has made no noticeable increase since 1931. The use of the ground-fault neutralizer was starting in 1923, but its principal gain has been made since 1931.

Comparison of grounding practices in general suggests that the selection of the grounding method is a compromise between the conflicting merits of effective grounding and high-impedance grounding. This compromise especially is shown in the many reported instances of the difficulty of selecting or maintaining the optimum value of neutral resistance for systems with feeders at generated voltage. A number of these systems reported several progressive changes in the value of neutral resistance in an effort to both minimize double faults and avoid excessive ground-fault currents. Effective grounding minimizes the chance of double faults by reducing dynamic and transient voltages on sound phases during fault conditions, thus increasing the relative margin of apparatus and line insulation, and reducing permissible lightning arrester ratings. High impedance grounding reduces possible ground-fault currents and thereby reduces damage at the point of fault, limits mechanical stresses and reduces burning of iron in machines, and avoids circuit breaker duties being increased beyond that required for 3-phase faults. Operating experience presented indicates that on generating systems emphasis should be placed on reducing high ground-fault currents, while on transmission and distribution systems the emphasis should be put on reducing double faults. On transmission and distribution systems, double faults are reported for about four per cent of the solidly-grounded systems and for about one quarter of all ungrounded and high-impedance grounded systems. The data indicate that the occurrence of double faults is related to the type of grounding, being the least frequent on effectively-grounded systems, and the most frequent on high-impedance grounded systems of all types. However, that some of the reported double faults are undoubtedly the result of reduced insulation strength, as well as of excessive dynamic or transient voltages.

Special Definitions

The word "system" as used in this report includes lines and apparatus metallically connected by phase wires and operated at approximately the same voltage. Thus, two or more utilities, which are connected at the same voltage, are said to operate one transmission system. Circuits which are connected by means of transformers are considered as separate systems. The introduction of series reactors or regulators between parts of a system does not increase the number of systems. The terms used to describe the grounding method of power systems in this report are based on those in AIEE Standard 32, "Neutral Grounding Devices," issued May 1947.[3]

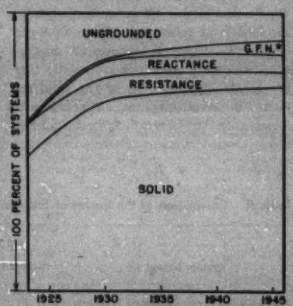

Figure 3. Relative use of grounding methods on transmission and distribution systems

* Ground fault neutralizer

Some systems reported use of combinations of two or more methods. Instead of making additional classifications, it seemed more practical to list such a system under one of the methods described.

Grounding-Method Terms Used in Connection With Generating Stations

Grounding method terms used in connection with generating stations are

1. Solid.
2. Neutral resistor.
3. Distribution transformer with secondary resistor.
4. Neutral reactor.
5. Grounding transformer.
6. Grounding transformer with neutral resistor.
7. Ground-fault neutralizer.
8. Potential transformer.
9. Ungrounded.

Compared with previous reports, this report introduces three additional grounding classifications: potential transformer, ground-fault neutralizer, and distribution transformer with secondary resistor. In preceding reports, potential transformers were not listed as a separate grounding classification. Previously, the ground-fault neutralizer had not been reported on a generating system, but one instance is reported now. The distribution transformer with secondary resistor is a grounding method[4, 5] which has appeared since the 1931 report. Instead of using a high-ohm neutral resistor directly in the ground path, a distribution transformer is connected between the generator neutral and ground with a suitable resistor in the transformer secondary.

Grounding-Method Terms Used in Connection With Transmission and Distribution Systems

Grounding method terms used in connection with transmission and distribution systems are

1. Solid grounding.
2. Resistance.
3. Reactance.
4. Ground-fault neutralizer.
5. Ungrounded.

In reducing the number of grounding methods to five, neutral resistors and grounding transformers with neutral resistor are classed under resistance grounding; similarly, neutral reactors and grounding transformers are classed under reactance grounding.

Part I. Grounding Practices at Generating Stations

This part of the report summarizes grounding practice at generating stations operating at 11 kv and above. The data are arranged according to three different station layouts.

1. *Unit System.* The unit system layout consists of a single generator supplying power to a step-up power transformer. The transformer may have a separate winding to receive the generator output, or it may be an autotransformer. In this type of system there are no power feeders at generated voltage, except possibly for station auxiliaries.

2. *Common Bus With No Feeders at Generated Voltage.* This type of system has two or more generators connected to the same bus which supply power to one or more step-up power transformers with no feeders at generated voltage, except possibly for station auxiliaries.

3. *Common Bus With Feeders at Generated Voltage.* As the title implies, this layout is for one or more generators on a common bus supplying power to feeders at generated voltage. In addition, step-up power transformers may or may not be in use.

The generating systems also are tabulated according to the nine grounding methods previously listed.

Present Grounding Practice

Grounding Methods for Different Station Layouts (Table I)

In Table I, under each of the three system layouts, a breakdown in per cent is given for each method of grounding by systems, by generator units, and by megavolt-amperes. In addition, the total number of systems, the total number of generator units, and the total megavolt-amperes are included so that actual values may be obtained by multiplying by the per cent.

Of the total 33,752 megavolt-amperes of generators reported, it is interesting to note that 45.4 per cent or 15,323 megavolt-amperes are on systems which are grounded through generator neutral resistors or devices introducing resistance in the ground path. Of generators supplying feeders at generated voltage, 69.7 per cent of the megavolt-amperes are on systems which are resistance-grounded; this represents 27.2 per cent of the total reported megavolt-amperes. It is interesting to note that generators, on a common bus without feeders at generated voltage, have about three times as many generators resistance-grounded as for the unit system.

There are 24.9 per cent or 242 generator units which are operating on solidly-grounded systems. An indication of the actual number of solidly-grounded generators on these solidly-grounded systems can be deduced as follows. The unit systems have 116 solidly-grounded generators, the common bus without feeders at generated voltage has at least one generator solidly grounded for each of the 13 systems, and the systems with common bus with feeders have at least 26 more solidly-grounded generator neutrals. This gives a minimum of 155 generators which are solidly grounded out of the total of 242 generators on such systems.

Neutral reactor grounding accounts for a total of 17.3 per cent megavolt-amperes; about one fifth being on systems with feeders at generated voltage. Potential transformer grounding represents 7.9 per cent of the total megavolt-amperes, most of which applies to generators without feeders at generated voltage.

A total of 972 generator units (11 kv and above) having an average rating of

Table I. Generator Grounding Methods for Different Station Layouts

Grounding Methods	Unit System No Feeders at Generated Voltage			Common Bus No Feeders at Generated Voltage			Common Bus With Feeders at Generated Voltage			All Layouts		
	Per Cent Systems	Per Cent Generator Units	Per Cent MVA	Per Cent Systems	Per Cent Generator Units	Per Cent MVA	Per Cent Systems	Per Cent Generator Units	Per Cent MVA	Per Cent Systems	Per Cent Generator Units	Per Cent MVA
Solidly grounded	45.3	45.3	45.9	16.0	13.4	8.5	21.1	19.7	14.8	33.7	24.9	25.7
Neutral resistor	13.3	13.3	15.5	44.5	37.0	44.5	46.3	51.2	60.6	27.6	37.8	39.4
Distribution transformer with secondary resistor	2.3	2.3	3.1	1.2	0.8	0.7				1.5	0.8	1.4
Neutral reactor	21.5	21.5	20.0	22.2	19.8	25.5	12.2	13.8	10.0	19.1	17.3	17.3
Grounding transformer	1.2	1.2	1.8	1.2	3.4	1.4	9.8	4.8	3.5	3.5	3.5	2.3
Grounding transformer with neutral resistor				1.2	4.2	4.9	4.9	8.0	9.1	1.5	4.9	4.6
Ground fault neutralizer							0.8	0.4	0.3	0.2	0.2	0.1
Potential transformer	15.6	15.6	13.3	8.7	13.4	10.1	1.6	0.8	1.2	10.7	7.8	7.9
Ungrounded	0.8	0.8	0.4	5.0	8.0	4.4	3.3	1.3	0.5	2.2	2.8	1.3
Total	100.0	100.0	100.0	100.0	100.0	100.0	100.0	100.0	100.0	100.0	100.0	100.0
Total number of systems	256			81			123			460		
Total number of generator units		256			238			478			972	
Total mva			13,289			7,260			13,203			33,752

Table II. Comparison of the Extent of Surveys of Generator Grounding (11 Kv and Above)

System Layout	1923 Report		1931 Report**		1947 Report	
	Systems	MVA	Systems	MVA	Systems	MVA
Supplying feeders at generated voltage	27	2,387	116	*	123	13,203
Supplying only step-up transformers	*		*	*	337	20,549
Total reported	27	2,387	116	*	460	33,752

* These types of data were not tabulated separately.

** Includes systems at 11 to 13.8 kv, with and without generators.

34,600 kva were reported in the survey. The average generator size for the unit system is 52,000 kva.

Comparison With Previous Surveys (Tables II and III)

Two previous grounding surveys have been made, one was reported in 1923 and one in 1931. Table II shows the extent of these previous surveys as compared with the present survey. The 1923 report had 27 systems supplying feeders at generated voltage. The 1931 report covered 116 systems, *with* or *without* generators, supplying feeders at 11.0 to 13.8 kv, and it is not possible to separate the systems with generators from the total. The present report covers 123 systems having generators with feeders and, in addition, it covers 337 systems where the generators supply step-up transformers without feeders at generated voltage.

Table III shows the only direct comparison which can be made for the three surveys. It applies only to generators *with* feeders at generated voltage and, as stated in the foregoing, the 1931 data are not applicable because a part of the 116 systems did not have directly-connected generators.

Using data obtained from the recent questionnaire, it has been possible to obtain figures for 1931 which the committee believes represent the 1931 generating systems with feeders; these figures have been included in Table III. One significant point from Table III is the decided decrease in the number of ungrounded or potential transformer grounded systems since 1923.

Table III. Comparison of Grounding Practices in the Three Surveys for Generators With Feeders at Generated Voltage

Grounding Method	1923 Report	1931 Report[d]	1947 Report: 1931[e]	1947 Report: 1947	1947 Report: 1947
	Per Cent of Systems	Per Cent of Systems	Per Cent of Systems	Per Cent of Systems	Per Cent of Generator MVA
Solidly grounded	11.1	34.5	31.7	21.1	14.8
Resistance grounded[a]	48.2	9.5	44.3	51.2	60.7
Reactance grounded[b]		12.0	14.0	22.0	13.5
Ground-fault neutralizer				0.8	0.3
Ungrounded[c]	40.7	44.0	10.0	4.9	1.7
Total	100.0	100.0	100.0	100.0	100.0
Total number of systems	27	116	79	123	
				Total MVA	12,203

(a). Resistance grounded includes systems with resistor connected to
1. Generator neutral.
2. Grounding transformer neutral.
3. Distribution transformer secondary.

(b). Reactance grounded includes systems with neutral reactor or grounding transformer.

(c). Ungrounded includes systems with no neutral devices or those connected to ground through potential transformers.

(d). Includes all systems at 11 to 13.8 kv, with and without generators.

(e). Deduced by the committee from 1947 data.

Sequence-Impedance and Fault-Current Ratios

The system characteristics that are affected by the grounding method may be expressed either in terms of the ratio of zero-sequence to positive-sequence impedances, or, less precisely, in terms of the ratio of phase-to-ground to 3-phase fault currents. These ratios are indicative not only of the ratio of phase-to-ground to 3-phase fault currents, but also of the magnitude of dynamic and transient voltages which may occur under unbalanced fault conditions. The importance of these sequence-impedance ratios was analyzed in the AIEE subcommittee report "Correlation of System Overvoltages and System-Grounding Impedances."[4] Accordingly, information on sequence-impedance ratios was requested, and as some utilities were presumed not to have these data available, the value of fault-current ratios also was requested. The practice of utilities in establishing limiting values for sequence-impedance ratios is tabulated, which presents additional evidence of their significance.

A synchronous generator normally is designed to withstand any currents that do not exceed the maximum phase current of a 3-phase short circuit at its terminals.[7] However, to limit winding currents to this value, for those faults involving ground a current limiting device usually is required in the neutral of those generators which are grounded. For a generator alone, the ratio of the phase-to-ground to the 3-phase short-circuits can be obtained from its sequence-impedance ratios. However, for interconnected machines, the over-all system sequence-impedance ratios are not sufficient to determine the individual generator phase currents under fault conditions.

Ratios of Phase-to-Ground Fault Currents to 3-Phase Fault Currents at Generator Terminals

Table IV is a summary of the ratios of phase-to-ground fault currents to 3-phase fault currents at generator terminals. The summary indicates that 81 generator systems have line-to-ground fault currents greater than the 3-phase fault currents. It also lists 155 solidly-grounded generator systems. Even though the reported fault current ratios range from 0.2 to 1.5 on these 155 solidly-grounded systems, it is possible, as pointed out in the foregoing, that the

Table IV. Ratios of Phase-to-Ground Fault Currents to 3-Phase Fault Currents at Generator Terminals

Grounding Method*	Number of Systems Replying: Generators Without Feeders at Generated Voltage: S	R	X	GT	GTR	Total	Generators With Feeders at Generated Voltage: S	R	X	GT	GTR	Total	Total All Layouts
Fault current ratios													
1.5–1.01	57		5			62	16	1	1	1		19	81
1.0–0.81	12		31			43	5		9			14	57
0.8–0.61	48	1	9			58	9		6	1		16	74
0.6–0.51	4	2	5			11	2		1			3	14
0.5–0.41			4			4	1		1			2	6
0.4–0.31	3					3		1		1		2	5
0.3–0.21	2	2	2			6	4	1	3	4		9	15
0.2–0.11	7	3				10		8		1	1	10	20
0.1 or less	45	2	2	1		50		48	4	4	5	61	111

* S = Solidly grounded
R = Neutral resistor
X = Neutral reactor
GT = Grounding transformer
GTR = Grounding transformer with neutral resistor

solidly-grounded generators will carry more current for a line-to-ground fault than for a 3-phase fault. The table also indicates there are 39 reactance-(reactor and grounding transformer) grounded systems plus 8 solidly-grounded systems which have line-to-ground fault currents of 0.6 or less of the 3-phase value. (The ratio of 0.6 on the average corresponds to an X_0/X_1 ratio of 3.0.) Excessive ground current may result in mechanical damage to generator windings, whereas too little ground current on reactance-grounded systems may result in excessive transient voltages.

Perhaps it should be pointed out that of the 155 solidly-grounded systems, 121 do not supply feeders at generated voltage. This indicates that machines whose terminals are not exposed directly to the hazards of distribution circuits are considered relatively safe from excessive short-circuit currents. However, faults at machine terminals are possible and so they should be given proper consideration.

Out of a total of 119 resistance-grounded generator systems, 93 allow 0.1 or less than 0.1 of the 3-phase fault current to flow for line-to-ground faults; a total of 15 allow 0.11 to 0.2 of 3-phase fault current; and the 11 others allow more. A total of seven grounding transformers with neutral resistors is listed, all of which limit the ground-fault currents to relatively small values.

Reported Sequence-Impedance Ratios at Generator Terminals

The sequence-impedance ratios R_0/X_1 and X_0/X_1 determined at the terminals of the equipment forming the grounding path are tabulated in Table V. A total of 151 solidly-grounded systems are reported of which 145 systems have an X_0/X_1 ratio of three or less. Where the X_0/X_1 ratio is greater than three, excessive transient voltages may be encountered. All of these solidly-grounded systems, however, probably have generator currents for line-to-ground faults in those generators which are solidly grounded, in excess of generator 3-phase fault currents. In some instances, as indicated in this report, these high currents in the generator windings are undesirable from a mechanical strength standpoint.[7]

For neutral reactor grounding, 41 systems have X_0/X_1 ratios of three or less. These ratios usually are considered satisfactory from a transient voltage standpoint. Where X_0/X_1 is greater than three, and there are 25 reactance-grounded systems listed in this class, excessive transient voltages may be encountered.

Resistance-grounded generator systems, of which 92 were reported, have R_0/X_1 ratios of 20 and up for 72 systems,

Table V. Reported Sequence-Impedance Ratios at Generator Terminals

	Number of Systems Replying								
	Generators Without Feeders at Generated Voltage				Generators With Feeders at Generated Voltage				Total All Layouts
Grounding Method*	R	GTR	Total		R	GTR	Total		
Sequence-Impedance Ratios	R_0/X_1								
0–1.0					1		1		1
1.1–2.0					1		1		1
2.1–3.0									
3.1–4.0	1		1						1
4.1–5.0									
5.1–10.0					3		3		3
10.1–20.0	12	1	13		2	4	6		19
20 and up	40		40		32	1[a]	33		73
Grounding Method*	S	X	GT	Total X_0/X_1	S	X	GT	Total	Total All Layouts
0–1.0	57	6		63	14	10	1	25	88
1.1–2.0	28	13		41	5	3		8	49
2.1–3.0	36	6		42	5	3	1	9	51
3.1–4.0	2	4		6	1	1		2	8
4.1–5.0	2	5		7					7
5.1–10.0		4		4	1	3	4	8	12
10.1–20.0		3	2	5		3	1	4	9
20 and up			2	2		2	4	6	8

*S = Solidly grounded
R = Neutral resistor
X = Neutral reactor
GT = Grounding transformer
GTR = Grounding transformer with neutral resistor
(a). For one system $R_0/X_1 = 56$ and $X_0/X_1 = -25$ because of cable sheath capacitance.

Table VI. Summary of Replies to Questions "Have Definite Sequence-Impedance Ratios for Grounding Been Established?" If so, "What Are the Ratios?"

	Number of Systems Reporting											
	Unit System				Common Bus				Common Bus			
	No Feeders at Generated Voltage				No Feeders at Generated Voltage				With Feeders at Generated Voltage			
Grounding Method	No	Yes	Systems With Ratio ϕ*	Systems With Other Ratios**	No	Yes	Systems With Ratio ϕ*	Systems With Other Ratios**	No	Yes	Systems With Ratio ϕ*	Systems With Other Ratios**
Solidly grounded	95	21	16	[a]	9	2	1	[b]	15	7	6	
Neutral resistor	28	1			23	9		[c]	42	10		[d]
Neutral reactor	10	12	8	[e]		3	6		6	4	3	
Grounding transformer	3				1				11			
Grounding transformer and neutral resistor					1				6			

* Ratio ϕ: "Effectively grounded" with $R_0/X_1<1$ and $X_0/X_1<3$ as defined in AIEE Standard 32-1.05, issued May 1947.[9]
** Other Ratios:
(a). Five systems $X_0/X_1>1$.
(b). One system $X_0/X_1>1$.
(c). One utility has made an effort to limit X_0/X_1 to values less than 10 to 1 or 20 to 1, depending upon relative value of capacitive reactances C_1 and C_0.[9]
(d). One system $R_0/X_1<10$; $X_0/X_1<1.7$.
(e). Two systems $R_0/X_1<1$; $X_0/X_1<3$.

ratios of 10.1 to 20 for 14 systems, and the remaining 6 were less than 10.1. Normally, such ratios of R_0/X_1 have been considered satisfactory from an overvoltage standpoint.[5]

Analysis of Tables IV and V leads to the same conclusion; a high ratio of X_0/X_1 for a reactance-grounded system means a low line-to-ground fault current as compared with the 3-phase fault current, and conversely. For most reactance-grounded systems where X_0 equals X_1, at the point of fault, the line-to-ground fault current is equal to the 3-phase fault current.

Established Sequence-Impedance Ratios

The questions "Have definite sequence-impedance ratios for grounding been established?" and, if so, "What are the ratios?" were asked in the questionnaire. The results are given in Table VI. A total of 321 systems answered the first question, 250 as "no" and 71 as "yes". Of the 71 systems, 50 gave the ratios and 39 of these are "effectively grounded" according to AIEE Standard 32[4] having $R_0/X_1 < 1$ and $X_0/X_1 < 3$.

In Table VI it should be pointed out that 30 of 149 solidly-grounded systems have established sequence-impedance ratios, whereas of a total of 151 solidly-grounded systems reported in Table V, 145 had X_0/X_1 ratios of three or less. It appears, therefore, that a large percentage of the solidly-grounded systems have sequence ratios in the "effectively grounded" class even though they are not considered in a premeditated fashion as being "established". For reactor grounding, about 57 per cent of the systems consider sequence ratios.

Time Ratings and Voltage Class of Reported-Neutral Grounding Devices

Time ratings on reported neutral-grounding devices as shown in Table VII vary over a wide range; in fact, from 1 second to continuous. The table includes 102 resistors. Time ratings for 80 of these vary from 1 second to 5 minutes; 53 of these had a time rating of 1 minute, and 8 had a time rating of 2 minutes. A total of 117 neutral reactors were reported which varied from 5 seconds to continuous, with 56 for 1 minute and 32 for 10 seconds. The other devices are so few in number they are not summarized here.

The voltage class of reported neutral grounding devices for generators is given in Table VIII. Of 88 neutral resistors reported, 49 have line-to-line volt-

Table VII. Time Ratings of Reported Neutral-Grounding Devices

Grounding Device and Time Rating	Number of Grounding Devices Reported: Unit System No Feeders At Generated Voltage	Common Bus No Feeders At Generated Voltage	Common Bus With Feeders At Generated Voltage
Neutral resistor			[a]
1 second		1	
30 seconds		1	3
37 seconds			1
40 seconds			1
45 seconds	1		2
1 minute	7	13	33
2 minutes	3	3	2
2.4 minutes	1		
3 minutes			4
5 minutes		1	3
Unreported	2	7	13
Distribution transformer with secondary resistor:			
Continuous	6	2	
Neutral reactor:			
5 seconds			1
10 seconds	28	2	3
1 minute	20	32	4
2 minutes	3		
5 minutes		1	
Extended time			9
Continuous	3		
Unreported	1		11
Grounding transformer:			
1 minute		1	6
Continuous			6
Unreported	3		2
Grounding transformer with neutral resistor			[b]
30 seconds			1
1 minute			1
2 minutes			2
5 minutes		1	
Unreported			1
Ground-fault neutralizer:			
Continuous			1

(a). First resistor burned out; rating was changed from 30 seconds to 120 seconds.
One system experienced trouble with a neutral resistor of 7.5 ohms and a second unit of 7.5 ohms was added in parallel.
One system has grounding transformer operated normally in parallel with generator grounded through neutral resistors.
Seven water boxes used as neutral resistors.
One system has neutral resistor which is by-passed 40 seconds at 1,200-ampere ground current. By-pass switch automatically opens when current falls to zero.

(b). On interconnected systems resistors are in each phase ahead of grounding transformer. Z_0 per phase is 49.3–j24.3 including 40-ohm external resistor in series with each phase.
The ground current normally is limited to approximately 1,700 amperes. Of this amount 400 amperes are supplied by a zigzag grounding transformer at one station, 800 amperes from another station, and 500 amperes from a third.
(Refer to AIEE Standard 32, "Neutral Grounding Devices," issued May 1947, for information on recommended time ratings.)

Table VIII. Reported Voltage Class of Neutral-Grounding Devices for Generators

Grounding Device and Voltage Classes	Unit System No Feeders At Generated Voltage	Common Bus No Feeders At Generated Voltage	Common Bus With Feeders At Generated Voltage
Neutral resistor			
Line-to-line	7	9	33
Line-to-neutral	4	7	23
25-kv	1	1	3[a]
Distribution transformer with secondary resistor			
Line-to-line	6	2	
Neutral reactor			
Line-to-line	26	11	16
Line-to-neutral	3		3
Grounding transformer			
Line-to-line		1	12
Grounding transformer with neutral resistor			
Transformer			
Line-to-line		1	6
Resistor			
Line-to-line			4
Line-to-neutral		1	2
Ground fault neutralizer			
Line-to-neutral			1

(a). Three resistors have line-to-neutral voltage rating but are mounted on insulators for line-to-line voltage.
(Refer to AIEE Standard 32, "Neutral Grounding Devices," issued May 1947, for information on recommended insulation class.)

age class, 34 have line-to-neutral voltage class, and 5 have special ratings. Of 59 neutral reactors, 53 have line-to-line voltage class and 3 have line-to-neutral voltage class. Of the remaining 36 miscellaneous devices, all except 4 have line-to-line voltage ratings; the 4 are rated line-to-neutral.

Factors Affecting Generator Grounding (Tables IX and X)

The questionnaire listed 16 factors which usually are considered as affecting grounding practice. The utilities were requested to check, for each grounding method, the factors considered as important, as well as those factors which were the final reason for the grounding method selected. The following table gives the final results without regard to type of system or the method of grounding.

Factors in System Grounding	Number of Replies: Important	Number of Replies: Reason for Practice
Relaying	286	50
Apparatus insulation	212	36
Damage at point of fault	203	32
Arcing grounds	192	21
Mechanical stress in equipment winding	146	25
Cable insulation	127	5
Operating procedure	105	3
Circuit breaker interrupting kilovolt-amperes	104	20
Double or consequent faults	103	3
Positive-sequence voltage during faults	95	10
Safety from voltage gradient consideration	94	2
Lightning protection	93	8
Equipment cost	89	1
Inductive co-ordination	52	9
Stability	20	4
Adaptability to interconnection	13	2

460 systems covered in report

It is noted that apparatus insulation, relaying, and damage at the point of fault stand out as being the most important, and these are also the highest rated as the reason for present practice. These factors give a general idea of the complexity of the grounding problem. Many utilities did not give reasons for present practice, presumably because no one factor could be assigned or because the answers were not available.

The factors rated as important for each type of system and for each grounding method are given in detail in Table IX. The interpretation of some of these important factors may be difficult. For example, under solid grounding, 29 systems stated that mechanical stress in equipment windings was important; nevertheless, these systems are solidly grounded and the answers may mean that mechanical stress was a point requiring investigation. Another example, under solid grounding, 21 systems stated that damage at the point of fault was important, but solid grounding usually will produce most damage at point of fault.

The summary of reported reasons for present generator grounding practice for each type of system and for each grounding method are given in detail in Table X. This table is very sketchy because the questions were not answered for more than half of the systems.

Time the Present Grounding Method Has Been Used

Table XI gives the length of time that the present grounding method has been used. This table gives the length of time in 5-year steps; namely, 0 to 5 years, 5 to 10 years, 10 to 15 years, and 15 years up for each type of system and each grounding method. These data are summarized for all types of systems and all grounding methods as follows:

0 to 5 years	94 systems
5 to 10 years	83 systems
10 to 15 years	47 systems
15 years up	179 systems
Total	403 systems

Of this total, 318 systems, or 79 per cent, still are operating with the same grounding method which was applied when the system was new. It is interesting to note from Table XIII that 86 changes in grounding practice have been made in the past 15 years; this number added to the 318 systems which have not been changed gives a total of 404 which compares well with the 403 systems noted.

It is surprising that 39 systems, involving at least 39 generators, have been solidly grounded within the past 10 years in view of ASA C-50 and its predecessors[7] which requires impedance in the neutral if the zero sequence impedance is less than the subtransient reactance.

Unsatisfactory Grounding Experience

The question "Has any grounding practice been unsatisfactory?" was answered by 448 systems and 64 answered "yes". A breakdown given in Table XII shows that 43 systems gave reasons which briefly are explained in footnotes. One definite conclusion which can be gleaned

Table IX. Summary of Reported Opinions on the Factors Affecting Generator Grounding Rated as Important

	Number of Systems Replying																										
	Solid			Resistor			DT & SR			Reactor			GT			GT & R			Gnd. Flt. N.			Pot. Tr.			Ungrounded		
Grounding Method Layout*	U	C	CF	U	C	CF	U	C	CF	U	C	CF	U	C	CF	U	C	CF	U	C	CF	U	C	CF	U	C	CF
(a). Apparatus insulation	85	8	15	25	16	12	3	1		22	4	7	3		2			1				5			1		2
(b). Cable insulation	43	5	11	14	13	17	3	1		5	1	5	2		1			3				2					1
(c). Mechanical stress in equipment windings	16	7	6	25	17	20	4			22	9	4	3		2	1	2					4			1	1	2
(d). Circuit breaker interrupting kilovolt-amperes	16	4	10	12	17	22				5	4	4	2		2			2				2			1		1
(e). Stability	3	2	3		3	9				1			3					2				2					1
(f). Positive-sequence voltage during faults	25	1	2	4	2	34	6	1		6	1	1	3		1	1	1				1	4					1
(g). Relaying	92	10	18	17	32	47	6	1		21	8	7	3	1	9		1	6				4			1		2
(h). Arcing grounds	59	7	11	15	24	34	6	1		11	5	4	2	1	7		1	3									1
(i). Double or consequent faults	31	2	6	11	18	16				4	4	2	2		4			3									
(j). Lightning protection	26	4	6	18	8	5				15		2	2		4			2									1
(k). Inductive co-ordination	31	2	4		1	3						5			3										1	1	1
(l). Adaptability to interconnection	2	1	4	2	1	1						1															1
(m). Operating procedure	10	3	4	14	13	17	1			2	1		3					3				1	27	3	2		1
(n). Equipment cost	17	4	5	16	11	11				15	3	1						3				1					1
(o). Safety from voltage gradient considerations	12	6	6	22	11	10	3	1		12	3		1		3							1	2				1
(p). Damage at point of fault	11	5	5	28	28	39	6	1		10	7	6	2		4		1	4				1	36	3	2	1	1	2
(q). Other considerations	[b]			[a]	[d]	[e]	[f]					[g]	[h]														[c]

*Layout: U = Unit system; no feeders at generated voltage.
C = Common bus; no feeders at generated voltage.
CF = Common bus; with feeders at generated voltage.
(See footnote to Table X)

Table X. Summary of Reported Reasons for Present Generator Grounding Practice

Ground Method Layout*	Number of Systems Replying																										
	Solid			Resistor			DT & SR			Reactor			GT			GT & R			Gnd. Flt. N.*			Pot. Tr.			Ungrounded		
	U	C	CF	U	C	CF	U	C	CF	U	C	CF	U	C	CF	U	C	CF	U	C	CF	U	C	CF	U	C	CF
(a). Apparatus insulation	34*		3	3	1	4							1														
(b). Cable insulation	1		1			3																					
(c). Mechanical stress in equipment windings	1			12	4	4							1	3													1
(d). Circuit breaker interrupting kva	3		2	3	5	2				3			1													1	
(e). Stability				1		2							1														
(f). Positive-sequence voltage during faults	16					1	1						1														
(g). Relaying	15	2	2	5	8	12	1						1	1	3												
(h). Arcing grounds	13	1	1		1	4	1																				
(i). Double or consequent faults		1				2																					
(j). Lightning protection	8																										
(k). Inductive co-ordination	5									2					2												
(l). Adaptability to interconnection	1		1																								
(m). Operating procedure																			1					2			
(n). Equipment cost																			1								
(o). Safety from voltage gradient considerations							1												1								
(p). Damage at point of fault	1			3	10	13				1			9											2			
(q). Other considerations	b		c	d	e	f				g			h												i		

*Layout:
U = Unit system; no feeders at generated voltage. C = Common bus; no feeders at generated voltage. CF = Common bus; with feeders at generated voltage.

(a). Seven systems grounded. Generator neutral as part of measures to protect from lightning surges from the high voltage side of the transformer.

(b). One system reports that manufacturer felt solid grounding of machine required.

(c). One system was solidly grounded to provide neutral for 4-wire 3-phase distribution system.

(d). Three systems—reduction of surges.

(e). Five systems—limit ground current.

(f). One system gave for use of neutral resistor reasons a, b, k, i, and n as compared with isolated neutral, and reasons c, f, h, and p as compared with solidly-grounded neutral.

(g). One system changed to reactor grounding in 1928 on basis of it being equal to resistor in effectiveness and less liable to burn out.

(h). One system—reduction of surges.

(i). One system operated ungrounded to reduce service interruptions from ground faults.

Table XI. Length of Time Present Grounding Method Has Been Used

Grounding Methods	Number of Systems Replying														
	When New			15 Years Up			10–15 Years			5–10 Years			0–5 Years		
	U	C	CF	U	C	CF	U	C	CF	U	C	CF	U	C	CF
Solidly grounded*	90	13	9	70	7	15	9		1	10	2	4	20	2	1
Neutral resistor	16	28	36	9	17	30	1	4	8	12	6	9	6	9	7
Distribution transformer with secondary resistor	2												6	1	
Neutral reactor	54	17	4			6	5		1	8	4	2	18	7	3
Ground fault neutralizer						1									1
Grounding transformer	3			4	1	4			1		1	5	2		2
Grounding transformer with neutral resistor		1	4		1	5						1			
Potential transformer	25	4	2	5	3	1	11	4		16		2	8		
Ungrounded	2	4	2	1	3	2			1			1	1		

U = Unit system—no feeders at generated voltage. C = Common bus—no feeders at generated voltage. CF = Common bus with feeders at generated voltage.

* It is interesting to note that a number of recently installed machines are solidly grounded in spite of ASA Standard C50 Paragraph 3.130 dated March 29, 1943, relative to limiting unbalanced-fault currents in generation by means of suitable neutral impedance.[1]

from these notes is that solid grounding gives too much fault current and, therefore, grounding devices to reduce this current are being applied.

In reviewing 43 cases, the question arises as to whether some of these unsatisfactory cases should be attributed to something other than the method of grounding. To clarify this would require analysis in detail of each unsatisfactory case. The following types of questions may be asked:

1. What is the condition of circuit and equipment insulation, particularly on systems which have substantially full displacement of the neutral on line-to-ground faults?

2. Is the relaying properly set to remove faulted circuits and equipment promptly and positively?

3. Are the double faults likely to have been caused by two lightning strokes occurring on two separate feeders at about the same time?

One system which is ungrounded has frequent insulation breakdowns and plans to ground distribution transformer neutrals. This method of grounding, under certain circumstances, may create danger of burning distribution transformers and may be difficult to relay satisfactorily.

Table XII also gives the answer to the question "Any trouble coincident with or consequent to ground faults elsewhere?" A total of 411 systems supplied answers to this question and 31 were "yes". It should be noted that of the 104 systems with feeders at generated voltage, there were 18 systems for which double faults were reported. Footnotes give some detail on 16 of the total of 31 cases reported.

Of the four ungrounded systems which reported double faults, three noted changes, one changed to solid grounding, one to resistance grounding, and one expects to ground the neutral of distribution transformers.

Five resistance-grounded systems report a number of double faults. Two of these changed to solid grounding but changed back to resistance because of excessive fault currents. One resistance-grounded system had a resistor flashover

on a line-to-ground fault, and another had a flashover in a cell after the failure of a breaker. Another system increased the ground-fault currents from 400 to about 1,700 amperes in several steps. On this system double or consequent faults still occur infrequently, lightning arresters have failed, and occasionally fuses have been blown on potential transformers connected line-to-ground.

Two systems with resistors in neutrals of grounding transformers indicated coincident faults. One system decreased the resistor from 15 to 5 ohms and has had no further trouble.

In spite of the larger number of systems reporting coincident faults elsewhere with resistance grounding, it appears that those systems operating ungrounded have more coincident faults. At least it can be said that ungrounded systems experiencing excessive coincident faults usually added some form of grounding device.

Changes in Grounding Practices in the Past 15 Years

Table XIII gives the number of systems reporting changes in practice in the past 15 years and the troubles with previous practices. Of a total of 429 systems, 86 indicated that changes had been made, and 63 gave some detail on the changes.

The footnotes of Table XIII show two trends, one that solid grounding is being replaced by some form of impedance grounding; and two, that ungrounded systems also are being replaced by some form of grounding. The changes, however, do not conform to a logical pattern. Of the 22 systems which abandoned solid grounding, four changed to reactors, five to grounding transformers, five to resistors, and eight to potential transformers. Of the ten ungrounded systems changed, one changed to solid, two changed to resistance, two to reactance, one to distribution transformer with secondary resistor, four to grounding transformers, and one to a ground-fault neutralizer. Three systems changed from reactance to resistance grounding. Nine systems changed from resistance to potential transformers. Most of the remaining changes concerned adjustment in resistor ohms or troubles associated with the grounding devices.

Changes Being Made in Grounding Practice

Table XIV gives the answers to the question "Any change in grounding practice being made?" Of 416 replies, 35 are "yes" and 28 gave explanations shown in the footnotes. The table indicates that a total of 19 systems have solid grounding

Table XII. Unsatisfactory Grounding Experience

Grounding Methods	Unit Systems No Feeders At Generated Voltage		Common Bus No Feeders At Generated Voltage		Common Bus With Feeders At Generated Voltage		Total All Layouts	
	No	Yes	No	Yes	No	Yes	No	Yes
Summary of replies to question, "Has Any Grounding Practice Been Unsatisfactory?"								
Solidly grounded	106	7[a,b]	13		20	16[c,d]	139	23
Neutral resistor	23	14[b,e]	32	12	42	2[f]	97	28
Distribution transformer with secondary resistor	6		1				7	
Neutral reactor	53	1[g]	18	3[h]	9	1[i]	80	5
Ground fault neutralizer					1		1	
Grounding transformer	3				3	1[j]	6	1
Grounding transformer with neutral resistor			1		4	2[k]	5	2
Potential transformer	31		7		2		40	
Ungrounded	2	1[l]	4		3	4[l,m]	9	5
Total all methods	234	23	76	15	84	26	354	64
Summary of replies to question, "Any trouble coincident with or consequent to ground faults elsewhere?"								
Solidly grounded	104	4[n]	10		21	3[d]	135	7
Neutral resistor	14	2[b]	32	4[e]	34	9[p]	80	15
Distribution transformer with secondary resistor	6		1				7	
Neutral reactor	54		18		10	[q]	82	
Ground fault neutralizer					1		1	
Grounding transformer	3		1		12	1[j]	16	1
Grounding transformer with neutral resistor			1		4	2[k]	5	2
Potential transformer	38	2	7		2		47	2
Ungrounded	1	1[l]	4		2	3[l,m]	7	4
Total all methods	220	9	74	4	86	18	380	31

(a). Two systems had too high ground current and changed from solid grounding to neutral resistor. One system reports ground current too large, disrupting house service.

(b). Two systems, initially resistance-grounded, experienced over a few years a number of multiple faults at the same or different locations as a result of a ground fault. Solid grounding was resorted to for a few months, but this resulted in extensive damage in underground cables at the fault location. The systems then were changed back to resistance-grounded.

(c). One system found operation unsatisfactory initially because of telephone interference, and later because of excessive stress in machine windings and conductor burning. Wave trap was installed in neutral of generator causing interference, and reactor was installed in the neutral of three other generators.
Two systems of 147 megawatts and 313 megawatts abandoned solid grounding in favor of resistor grounding in order to limit stress on equipment and to limit damage resulting from fault.
Interconnection with another system increased ground-fault currents with original solidly-grounded neutral on a single-phase frequency-changer set beyond maximum capacity of the machine winding.
One system with 12 generators now operates with one unit grounded through neutral resistor. This change was made because of unfavorable operating experience with only one generator solidly grounded.
One system found solid grounding gives too severe a burden on generator under line-to-ground faults.
Reactor to be installed in generator neutral.
One system found grounded Y autotransformer caused excessive ground currents in generator.
Five systems changed from solid grounding of generator to grounding transformer because of serious interference to communication systems.
One system experienced trouble with a neutral resistor of 7.5 ohms and a second unit of 7.5 ohms was added in parallel.

(d). One system experienced harmonics which produced telephone interference. Reactors at far end of system flash over occasionally which is attributed to coincident or consequent faults. Grounding transformer is being considered.
Two systems have neutral wave trap to minimize zero-sequence harmonics which caused telephone interference. One wave trap consists of one tuned element and one reactor in series for the higher harmonics. Flashovers were experienced as a result of lightning and surges making it necessary to install a by-passing resistor in parallel with the wave traps. This is done by a contactor which is operated from a gap which breaks down on overvoltage. The contactor drops out when the ground current disappears. In the other installation, three tuned wave traps are connected in series between generator neutral and ground. High transient voltage at the neutral of one generator connected to the bus and operated ungrounded was experienced, and this led to the installation of a lightning arrester between that machine neutral and ground.

(e). Two systems had resistors of an ohmic value which allowed a current in excess of resistor rating. Replaced with resistors of higher ohmic value.
Nine systems formerly operated with neutral resistors changed to potential transformer grounding to prevent burning of generator iron during generator faults.

(f). One system previously grounded through neutral resistor had bus fault which caused melting of resistor.

(g). One system views operation as doubtfully satisfactory because of appreciable damage resulting from failures to ground of generator cables.

(h). Two systems experienced double or consequent faults with an original installation of a 4-ohm neutral grounding reactor. Consequently reactor was replaced with a 4-ohm resistor.
One system formerly grounded through neutral reactor. Neutral bus failed with reactor in service. Neutral resistor installed in 1934. Reactor still available for emergency use.

(i). One system considers satisfactory operation questionable because appreciable damage has resulted from failures to ground of generator cables.

(j). Originally the 25-cycle system was operated at 6.6 kv ungrounded. The usual troubles inherent to an ungrounded system such as double faults and difficulty in locating faults were experienced. When the system was reconnected for 11.4-kv operation, two zigzag sets were installed to give approximately 400 amperes ground current. While faults then could be located more easily, double faults were still frequent, partially due to relaying and partially due to 6.6-kv cable on the system. As improved relaying was installed and as more stations were added to the system, the ground current was increased to 800 amperes, then to 1,200 amperes, and finally to the present value of 1,700 amperes. As operated now, all generating stations are assured of at least two or more ground sources.

(continued on page 1535)

Table XII (continued)

Double or consequent faults still occur infrequently on this system, particularly when the initial fault occurs on a tie feeder whose clearing time on a ground fault is 1.0 second or more. At such times lightning arrester failures on overhead lines have occurred and occasionally fuses have blown on potential transformers connected line-to-ground.

(k). One system previously used 15-ohm resistor in neutral of grounding transformer and experienced a considerable number of double cable failures. Resistor reduced to five ohms in 1929 and no double faults in cable encountered since.

(l). One system now solidly grounded experienced trouble when ungrounded from arcing grounds causing phase-to-phase faults or short-circuited turns resulting in excessive burning of windings and iron before breaker cleared.

(m). One system has a practice of 30 years standing of clearing faults manually. Insulation breakdowns are frequent. Plans to ground transformer neutrals on distribution system.
System was initially isolated neutral, but double-cable faults dictated change to grounded neutral.

(n). One system experienced a line-to-ground fault on one phase and failures of lightning arresters connected between other phases and ground at remote points.
One system experienced unsatisfactory operation because of aged insulation.

(o). One system suffered machine failure—lightning caused flashover in 132-kv line.
One system suffered flashover on grounding resistor.

(p). One system suffered flashover on an old bus in a concrete cell after failure of breaker in this structure.
One system experienced a few cable failures coincident with ground faults elsewhere. Resistors may be changed from 1.5 ohms to match cable on system.
One system has experienced apparatus failure coincident with ground faults elsewhere, an automatic oscillograph has been installed to facilitate further study of these conditions if they recur.

(q). One system states that coincident failures have not been proved.

Table XIII. Number of Systems Reporting Changes in Practice in Past 15 Years and the Troubles With Previous Practices

Present Grounding Methods	Unit Systems No Feeders At Generated Voltage		Common Bus No Feeders At Generated Voltage		Common Bus With Feeders At Generated Voltage		Total All Layouts	
	No	Yes	No	Yes	No	Yes	No	Yes
Solidly grounded	107	4[a]	13		21	4[b]	141	8
Neutral resistor	27	6[c]	24	12[d]	31	12[e]	82	30
Distribution transformer and secondary resistor	2	4[f]		1[g]			2	5
Neutral reactor	40	2[h]	14	1[i]	8	5[j]	71	8
Ground fault neutralizer						1[k]		1
Grounding transformer	3			1[l]	5	9[m]	8	10
Grounding transformer and neutral resistor			1		1	4[n]	2	4
Potential transformer	23	15[o]	4	3[p]	2		29	18
Ungrounded	2		4		2	2[q]	8	2
	213	31	60	18	70	37	343	86

(a). One system now solidly grounded experienced trouble when ungrounded from arcing grounds causing phase-to-phase faults or short-circuited turns resulting in excessive burning of windings and iron before breaker closed. One system installed neutral wave trap.

(b). One system operated two generators and one frequency changer set solidly grounded for over 15 years. About six years ago, two generators were added grounded through reactors.

(c). Two systems had resistors of too low current rating. Changed to resistor of higher ohmic value.
Two systems, initially resistance-grounded, experienced over a few years a number of multiple faults at the same or different locations as a result of a ground fault. Solid grounding was resorted to for a few months, but this resulted in extensive damage in underground cables at the fault location.

(d). One system formerly grounded through neutral reactor. Neutral bus failed with reactor in service. Neutral resistor installed in 1934. Reactor still available for emergency use.
Frames of grounding resistor to have better insulation.
Two systems experienced double or consequent faults with an original installation of a 4-ohm neutral grounding reactor. Consequently, reactor was replaced with a 4-ohm resistor.
Two systems had resistors of an ohmic value which allowed a current in excess of their rating. Replaced with resistors of higher ohmic value.

(e). Initial cast-iron resistor rated at 20 seconds was short-circuited by melting during a prolonged bus ground fault. The resistor was replaced by the present stainless steel design rated at five minutes. Improved bus differential relaying also has been added.
One system changed from ungrounded neutral to neutral resistor.
One system solidly grounded for more than 25 years added neutral resistor in 1945.
Two systems of 147 megawatts and 313 megawatts abandoned solid grounding in favor of resistor grounding in order to limit stress on equipment and to limit damage due to fault.
Interconnection with another system increased ground-fault currents with original solidly-grounded neutral on a single-phase frequency-changer set beyond maximum capacity of the machine winding.
System initially was isolated neutral, but double-cable faults dictated change to grounded neutral.
One system with 12 generators now operates with one unit grounded through neutral resistor. This change was made because of unfavorable operating experience with only one generator solidly grounded.
This station was placed in service in 1922. The turbogenerators were 6,900-volt, 3-phase, Y-connected. A 7-ohm (hot) 5.7-ohm (nominal) neutral grounding resistor was installed with circuit breakers so that any generator neutral could be connected to the grounding resistor bus. Only one generator was grounded at a time. In 1941, a 13,800-volt 3-phase Y-connected turbogenerator was added, and the 13,800-volt bus was connected to the 6,900-volt bus by two Y-connected 2:1 ratio autotransformers with delta tertiaries. The neutrals of the autotransformers were solidly grounded. A neutral grounding resistor also was provided for the 13,800-volt system. Consideration was given to arcing line-to-ground faults on the systems in the choice of the neutral grounding resistors. The 6,900-volt neutral grounding resistor was changed from 5.7 to 2.85 ohms. An 8.35-ohm resistor was chosen for the 13,800-volt system. A rough calculation indicated that such values would afford favorable ratios of X_0/X_1 and R_0/X_1. Since the calculations were made, several distribution autotransformers with solidly-grounded neutrals have been added. The resulting ratio of X_0/X_1 and R_0/X_1 appear to be less favorable.

(continued on page 1536)

which will be changed; 12 to reactors, 2 to a resistor, 1 to a grounding transformer, 1 to a potential transformer, and 3 unknown. The other changes do not follow a consistent pattern. One unit system now grounded through a reactor is considering a lower ohm reactor or a resistor, and another unit system grounded through a reactor is considering a distribution transformer with secondary resistor. A potential-transformer-grounded unit system also is considering the distribution transformer scheme. The remaining changes are all different; but in three instances, the changes are in the direction of reducing the impedance of the ground path.

Trends in Generator Grounding Practice

The question was asked "Any new trends in grounding practice?" That these replies were not conclusive is indicated by Table XV. Certain trends, however, are evident from the information in the report, particularly from the length of time each system has been grounded in its present form and the changes which have been made in the past 15 years. The trends are different for generator systems supplying step-up power transformers with no feeders and generator systems supplying feeders at generated voltage.

Trends on grounding methods since 1931 for generator systems *without* feeders at generated voltage are shown in Figure 1 and summarized as follows:

1. Solid grounding decreased from about 56 to about 38 per cent of the total systems of these types. Nine systems changed from solid to some other form of grounding.

2. Reactance grounding increased to about 20 per cent from about zero per cent. Three solidly-grounded systems changed to reactor grounding, three reactor-grounded systems changed to resistors, and three reactor-grounded systems changed to potential transformers.

3. Resistance grounding decreased from about 33 to 22 per cent. Nine resistor-grounded systems changed to potential transformers and three reactor-grounded systems changed to resistors. However, there recently has been a definite trend toward the use of a distribution transformer with secondary resistor in the generator neutral.

4. Potential-transformer grounding increased to about 15 per cent from about 7 per cent. Eighteen systems changed to potential transformers from some other form of grounding. Six of these potential transformers were provided with secondary resistors.

5. A trend is indicated to grounding devices which take a small current for line-to-

Table XIII (continued)

(*f*). One system changed from potential transformer grounding to distribution transformer and secondary resistor.

(*g*). One system changed from ungrounded to provide ground-fault indication and to improve machine protection.

(*h*). One system changed from solid grounding to reactor grounding to give mechanical protection for generators.

(*i*). One system with two generators was solidly grounded for 15 years before the reactor was installed.

(*j*). Two systems changed from solid to reactor grounding in order to limit ground-fault current.
One system changed from ungrounded in 1942.
One system of 115 megavolt-amperes and ten generating units, three of which were equipped with neutral reactors, were grounded with any one of the three units having neutral reactors. Two reactors are tuned as wave traps, but the third is not. These are by-passed with 10-ohm resistor during faults.

(*k*). Changed from isolated neutral to ground-fault neutralizer.

(*l*). One system installed grounding transformer banks for ground relay protection.

(*m*). One grounding transformer was replaced with larger size to obtain higher fault current and lower sequence ratio.
Two ungrounded systems added in transformer neutral grounds.
Five systems changed from solid grounding of generator to grounding transformer because of serious interference to communication systems.
One system grounded additional transformer neutrals to reduce the X_0/X_1 to less than five.
(See also footnote *j*, Table VI).

(*n*). One system previously grounded through neutral resistor had bus fault which caused melting of resistor.
One system previously used 15-ohm resistor neutral of grounding transformer and experienced a considerable number of double cable failures. Resistor reduced to five ohms in 1929 and no double faults in cable encountered since.
One system previously grounded through power bank.

(*o*). Nine systems formerly operated with neutral resistors changed to potential transformer grounding to prevent burning of generator iron during generator faults.
Six systems removed neutral reactors or solid-ground connections and applied potential transformers loaded with secondary resistors.

(*p*). Three systems changed from solid grounding.

(*q*). One system originally solidly grounded.
One system removed generator ground in order to reduce stress on generator winding.

Table XIV. Replies to Question "Any Change in Grounding Practice Being Made?"

Grounding Methods	Unit System No Feeders At Generated Voltage		Common Bus No Feeders At Generated Voltage		Common Bus With Feeders At Generated Voltage		Total All Layouts	
	No	Yes	No	Yes	No	Yes	No	Yes
Solidly grounded	100	14[a]	13	1[b]	21	4[c]	134	19
Neutral resistor	27		33	1[d]	44	6[e]	104	7
Distribution transformer with secondary resistor	6		1				7	
Neutral reactor	53	2[f]	17	1[g]	10	1[h]	80	4
Ground-fault neutralizer						1[i]		1
Grounding transformer	3		1		6	1[j]	10	1
Grounding transformer with neutral resistor			1		6		7	
Potential transformer	27	1[k]	4		2		33	1
Ungrounded	2		4			2[l]	6	2
Total	218	17	74	3	89	15	381	35

(*a*). Seven systems considering neutral reactors to limit mechanical stresses on generators.
One system—neutral reactor to be installed.
One system—reactors being considered.
Two systems considering change from solid grounding to resistor grounding.
One system considering change from solid grounding to potential transformer grounding.

(*b*). One system probably will install a neutral bus and one or two of seven machines will be grounded.

(*c*). One system found solid grounding gives too severe a burden on generator under line-to-ground faults. Reactor to be installed in generator neutral.
One system experienced harmonics which produced telephone interference. Reactors at far end of system flash over occasionally which is attributed to coincident or consequent faults. Grounding transformer is being considered.
One system considering change to neutral reactor to limit line-to-ground fault currents.
One system to minimize mechanical stresses in generators on ground faults will install neutral reactor in generator neutral with solid grounding of step-up transformers giving a lower ratio of single-phase to 3-phase fault currents.

(*d*). One system is adding arresters and capacitors on neutral connection.

(*e*). One system expects to reduce neutral resistor from four to two ohms in connection with other changes.

(*f*). One system is considering resistor or reactor of lower value.
One system is considering distribution transformer and secondary resistor.

(*g*). One system is considering low neutral impedance.

(*h*). One system considers establishing additional grounding points.

(*i*). Duplicate ground-fault neutralizer on order.

(*j*). One system changed from ungrounded to obtain relay and fuse protection. When additional generators are added, generator neutral-resistor will be installed to provide more ground fault current for better relay and fuse co-ordination.

(*k*). One system is considering change to distribution transformer and secondary resistance grounding.

(*l*). One system proposes to limit single-phase fault currents to 60 per cent of 3-phase value.
One system has practice of 30 years standing of clearing faults manually. Insulation breakdowns are frequent. Plans to ground transformer neutrals on distribution system.

ground faults such as potential transformers, potential transformers with secondary resistor, and distribution transformers with secondary resistor.

Trends on grounding methods since 1931 for generator systems *with* feeders at generated voltage are shown in Figure 2 and are summarized as follows:

1. Solid grounding decreased from about 32 to about 20 per cent for systems of this type. Ten systems changed from solid grounding to some other form.

2. Reactor grounding increased to about 12 per cent from about 5 per cent. Approximately 20 per cent of the new systems during the past five years were reactor grounded.

3. Grounding transformers increased to about ten per cent from about five per cent.

4. Resistance grounding increased to about 51 per cent from about 44 per cent. Six solidly-grounded systems changed to resistors and two systems changed from potential transformers to resistors. (Resistance grounding includes resistors and grounding transformers with neutral resistors.)

For all generator systems, regardless of the station layout, certain definite trends since 1931 can be obtained from the information in this report.

1. A definite decrease in the use of solid grounding.

2. A definite increase in the use of reactance grounding.

3. A definite decrease in the number of ungrounded systems.

4. A definite usage of sequence ratios in determining the adequacy of grounding methods. Seventy-two per cent of all systems reported sequence-impedance ratios, and of this number, 22 per cent had established definite ratios.

5. A trend toward less ground-fault current in order to reduce damage at point of fault.

(For Table XV, see page 1537)

Table XV. Summary of Replies to Question "Any New Trend in (Generator) Grounding Practice?"

Grounding Methods	Unit System No Feeders At Generated Voltage		Common Bus No Feeders At Generated Voltage		Common Bus With Feeders At Generated Voltage	
	No	Yes	No	Yes	No	Yes
Solidly grounded	105	5[a]	10		19	3[b]
Neutral resistor	26		33		44	7[c]
Distribution transformer with secondary resistor	2	4[d]	1			
Neutral reactor	51	2[e]	17		10	
Ground fault neutralizer					1	
Grounding transformer	3		1		7	
Grounding transformer with neutral resistor			1		6	
Potential transformer	17	17[f]	7			2[g]
Ungrounded	2		4		1	
Total	206	28	74	0	88	12

(*a*). One system considering change to resistor grounding.
One system will install a neutral reactor.
Three systems see trend to neutral devices which limit ground-fault currents to 3-phase fault current values.

(*b*). Three systems see trend to limit ground-fault currents to less than 3-phase fault current values.

(*c*). Resistor grounding for the purpose of limiting overvoltages.
Six systems see trend to limit ground current.

(*d*). Four systems see trend to distribution transformer and secondary resistor.

(*e*). One system sees trend to resistor grounding.
One system sees trend to reactor grounding for limitation of ground fault to 3-phase short-circuit current value.

(*f*). Seventeen systems indicate that they will consider distribution transformer and secondary resistor between generator neutral and ground for future installations.

(*g*). Two systems indicate that they will consider distribution transformer and secondary resistor between generator neutral and ground for future installations.

Part II. Grounding Practices on Transmission and Distribution Systems

This part of the report summarizes grounding practices on transmission and distribution systems at 22 kv and above. The practices are tabulated with respect to the five grounding methods as outlined: namely, solid grounding, resistance grounding, reactance grounding, ground-fault neutralizer, and ungrounded. Data on grounding practices also are classified with respect to eight voltage classes which have been selected so as to avoid divisions at the standard insulation classes or near the usual operating voltages. A further classification has been made with respect to the amount of system mileage in cable. Originally it had been intended to form three groups according to the ratio of cable mileage to the total mileage: namely, zero to two per cent, two to ten per cent, and ten per cent and above. However, there were few systems in the range between two and ten per cent. Accordingly, the classification adopted includes "aerial" systems with cable mileage less than ten per cent of the total, and "cable" systems with cable mileage greater than ten per cent of the total.

Grounding Method Summaries

The principal information in the replies to the questionnaires has been summarized in the tables which are included in this report. The discussion of various phases of grounding is arranged under paragraph headings with the principal supporting data identified by reference to the pertinent table.

Summary of Grounding Methods for All Systems

The over-all summary of grounding methods irrespective of voltage class and amount of cable is given in Table XVI. The table also includes the total mileage of the systems for each of the five grounding methods. From this table, it is apparent that solid grounding is the principal method in use, this method having about eight times the number of systems and about 11 times the mileage of any other grounding method. Also given in Table XVI are corresponding data selected from the 1923 and 1931 reports.

Summary of Grounding Methods by Voltage Classes (Tables XVIIA, XVIIB, XVIIC, and XVIID)

The principal methods of grounding have been tabulated with respect to voltage class, as it was thought by the committee that principal interest would center about the grounding practices that apply

Table XVI. Summary of the Three Surveys of Transmission and Distribution System Grounding

At 22 Kv and Above

Report Year	1923				1931*				1947			
	Systems		Miles of Circuit		Systems		Miles of Circuit		Systems		Miles of Circuit	
Grounding Method	Number	Per Cent	Number	Per Cent	Number	Per Cent	Number	Per Cent	Number	Per Cent	Number	Per Cent
Solidly grounded	34	48.6	13,855	64.0	115	73.7	34,980	79.4	419	73.9	92,848	77.9
Resistance grounded	8	11.4	2,626	12.1	13	8.3	4,493	10.2	32	5.6	5,456	4.6
Reactance or grounding transformer grounded	0	0	0	0	5	3.2	1,075	2.4	35	6.2	7,579	6.4
Ground-fault neutralizer	1	1.4	100	0.5	**	**	**	**	30	5.3	8,083	6.8
Ungrounded	27	38.6	5,068	23.4	23	14.8	3,524	8.0	51	9.0	5,115	4.3
Total	70	100.0	21,649	100.0	156	100.0	44,072	100.0	567	100.0	119,081	100.0

* This summary does not include systems at 22 kv as these data could not be separated from those for lower voltages in the 1931 report.

** Ground-fault neutralizers were included under reactance grounded in the 1931 report.

Table XVIIA. Grounding Method of Transmission and Distribution Systems Tabulated by Voltage Class

Report Year	Kv Class	Per Cent of Systems by Voltage Class: Solidly Grounded	Resistance Grounded	Reactance or Grounding Transformer	Ground-Fault Neutralizer	Ungrounded	Totals: Per Cent	Number of Systems
1923	22–30	31.6	21.1	0	0	47.3	100	19
	31–40	33.3	0	0	0	66.7	100	9
	41–60	58.3	0	0	8.3	33.4	100	12
	61–92	37.5	18.8	0	0	43.7	100	16
	93–130	90.0	10.0	0	0	0	100	10
	131–165	75.0	0	0	0	25.0	100	4
1931	23–33	57.2	20.4	2.0	*	20.4	100	49
	34–44	82.1	0	5.1	*	12.8	100	39
	45–66	70.3	5.4	2.7	*	21.6	100	37
	100–110	93.7	0	6.3	*	0	100	16
	120–132	100.0	0	0	*	0	100	8
	184–220	85.7	14.3	0	*	0	100	7
	Aerial Systems (Cable Less Than Ten Per Cent of the Total Mileage)							
1947	22–30	53.7	2.5	18.8	2.5	22.5	100	80
	31–40	59.0	2.4	8.7	13.4	16.5	100	127
	41–60	81.1	1.7	3.4	5.2	8.6	100	58
	61–92	80.0	10.0	2.0	2.0	6.0	100	100
	93–130	82.8	1.7	6.9	8.6	0	100	58
	131–165	93.7	0	2.1	2.1	2.1	100	48
	166–230	93.3	6.7	0	0	0	100	15
	231–Up	100.0	0	0	0	0	100	1
	Cable Systems (Cable More Than Ten Per Cent of the Total Mileage)							
1947	22–30	67.7	32.3	0	0	0	100	34
	31–40	97.4	2.6	0	0	0	100	38
	41–60	100.0	0	0	0	0	100	1
	61–92	60.0	40.0	0	0	0	100	5
	131–165	100.0	0	0	0	0	100	2

* Ground-fault neutralizers were included under reactance grounded in the 1931 report.

Table XVIIB. Grounding Method of Transmission and Distribution Systems Tabulated by Voltage Class

Report Year	Kv Class	Per Cent of Mileage in Voltage Class: Solidly Grounded	Resistance Grounded	Reactance or Grounding Transformer	Ground-Fault Neutralizer	Ungrounded	Totals: Per Cent	Mileage
1923	22–30	30.9	32.6	0	0	36.5	100	4,226
	31–40	58.2	0	0	0	41.8	100	1,357
	41–60	76.4	0	0	1.6	22.0	100	6,220
	61–92	55.2	13.1	0	0	31.7	100	3,392
	93–130	84.8	15.2	0	0	0	100	5,270
	131–165	56.4	0	0	0	43.6	100	1,184
1931	23–33	50.6	35.5	4.8	*	9.1	100	8,022
	34–44	94.9	0	1.4	*	3.7	100	4,556
	45–66	75.3	3.0	1.5	*	15.2	100	17,265
	100–110	95.9	0	4.1	*	0	100	9,075
	120–132	100.0	0	0	*	0	100	2,752
	184–220	89.4	10.6	0	*	0	100	2,402
	Aerial Systems (Cable Less Than Ten Per Cent of the Total Mileage)							
1947	22–30	60.0	1.4	15.7	6.3	16.6	100	8,039
	31–40	56.4	3.8	6.4	25.6	7.8	100	21,578
	41–60	73.9	1.7	8.1	4.8	11.5	100	12,419
	61–92	87.8	5.6	2.7	1.2	2.7	100	22,142
	93–130	86.4	4.4	5.2	4.0	0	100	35,887
	131–165	84.5	0	13.8	1.3	0.4	100	14,296
	166–230	95.7	4.3	0	0	0	100	5,868
	231–Up	100.0	0	0	0	0	100	799
	Cable Systems (Cable More Than Ten Per Cent of the Total Mileage)							
1947	22–30	73.6	26.4	0	0	0	100	5,726
	31–40	98.6	1.4	0	0	0	100	1,683
	41–60	100.0	0	0	0	0	100	43
	61–92	61.1	38.9	0	0	0	100	398
	131–165	100.0	0	0	0	0	100	211

* Ground-fault neutralizers were included under reactance grounded in the 1931 report.

Table XVIIC. Grounding Method of Transmission and Distribution Systems Tabulated by Voltage Class

Report Year	Kv Class	Average Mileage Per System*: Solidly Grounded	Resistance Grounded	Reactance or Grounding Transformer	Ground-Fault Neutralizer	Ungrounded
1923	22–30	218	345			171
	31–40	263				95
	41–60	679			100	342
	61–92	312	149			153
	93–130	496	802			
	131–165	222				518
1931	23–33	145	285	382	**	73
	34–44	135		33	**	34
	45–66	500	695	252	**	328
	100–110	530		375	**	
	120–132	344			**	
	184–220	358	254		**	
	Aerial Systems (Cable Less Than Ten Per Cent of the Total Mileage)					
1947	22–30	112	59	84	252	74
	31–40	162	271	125	324	80
	41–60	195	210	501	197	286
	61–92	243	124	303	128	101
	93–130	466	1,130	341	206	
	131–165	268		1,970	190	63
	166–230	401	252			
	231–Up	791				
	Cable Systems (Cable More Than Ten Per Cent of the Total Mileage)					
1947	22–30	183	138			
	31–40	45	24			
	41–60	43				
	61–92	81	73			
	131–165	106				

* Average mileage equals total mileage in class divided by number of systems in class.

** Ground-fault neutralizers were included under reactance grounded in the 1931 report.

to systems of the same or about the same voltage class. The data are arranged in two groups, "aerial" and "cable" systems, as defined previously. Data also have been included in Table XVII giving the corresponding information from the two earlier reports. The data in Table XVII have been arranged in four parts: Part *A*, in terms of per cent of the total number of systems; part *B*, in terms of per cent of the total mileage; part *C*, in terms of the average mileage per system; and part *D*, in terms of the maximum mileage per system.

On "cable" systems, solid grounding is predominant and resistance grounding is the only other method in use. On "aerial" systems, solid grounding is also predominant in all voltage classes, and especially in the highest voltage classes. Ungrounded and reactance-grounded systems are principally in the 22–30-kv and 31–40-kv classes. The ground-fault neutralizer is used mainly on the intermediate and lower voltage systems, and its mileage, while small in comparison with solid grounding, slightly exceeds that of any other grounding method.

The maximum system mileage for most voltage classes and for all classes above 60 kv occurs with solidly-grounded systems, and reaches a maximum of 2,835 miles for one 138-kv system. In the 31–40-kv class, the maximum system length is 1,427 miles which occurs with a ground-fault neutralizer system. It is worthy of note that the maximum mileage of ungrounded systems is low in comparison with other methods in almost every voltage class.

Average Circuit Mileage Per Grounding Point (Table XVIII)

The average mileage of transmission and distribution circuits per grounding point is about 63 miles for all voltage classes and for all grounding methods.

Sequence-Impedance and Fault-Current Ratios

The system characteristics that are affected by the grounding method may be expressed either in terms of the ratio of zero-sequence to positive-sequence impedances, or less precisely, in terms of the ratio of phase-to-ground to 3-phase fault currents. These ratios are indicative not only of the ratio of phase-to-ground to 3-phase fault currents, but also of the magnitude of dynamic and transient voltages which may occur under unbalanced fault conditions. The importance of these sequence-impedance ratios was analyzed in the AIEE subcommittee report "Corre-

lation of System Overvoltages and System-Grounding Impedances."[6] Accordingly, information on sequence-impedance ratios was requested, and as some utilities were presumed not to have these data available, the value of fault-current ratios also was requested. The practice of utilities in establishing limiting values for sequence-impedance ratios is tabulated, presenting additional evidence of their significance.

Sequence-Impedance Ratios Reported

The ratios of the zero-sequence impedances to the positive-sequence subtransient reactances, the ratios R_0/X_1 and X_0/X_1, as measured at the terminals of the equipment forming the grounding path, are tabulated in Table XIX. The ratio R_0/X_1 is tabulated for resistance-grounded systems only, while the ratio X_0/X_1 is tabulated for the solidly-grounded and reactance-grounded systems. In the case of reported resistance-grounded systems, the zero-sequence resistance is much higher than the zero-sequence reactance. The actual values of R_0/X_1 are distributed widely, both above and below the ratio of 20. These data show that 95 per cent of the reported ground points are "effectively grounded" as defined in AIEE Standard 32-105.[3] For those remaining locations not "effectively grounded" on solidly-grounded systems, and for most locations on resistance- or reactance-grounded systems, higher dynamic voltages will occur and higher transient voltages are possible.

Ratio of Phase-to-Ground Fault Currents to 3-Phase Fault Currents

The ratios of phase-to-ground fault currents to the 3-phase fault currents at the terminals of the equipment forming the grounding path are tabulated in Table XX. This table includes the results for only the solidly-grounded, resistance-grounded, and the reactance-grounded systems. These fault current ratios were obtained for about 74 per cent of all grounding points reported. For about 55 per cent of reported grounding points, the phase-to-ground fault currents are greater than the 3-phase fault currents. For these locations the circuit-breaker capacity usually is determined by the ground fault instead of 3-phase fault conditions. In general, the interpretation of Tables XIX and XX is the same. When resistance can be ignored, a fault-current ratio equal to or greater than 0.60 corresponds to a ratio of X_0/X_1 equal to or less than three which is an "effectively grounded" system.

Table XVIID. Grounding Method of Transmission and Distribution Systems Tabulated by Voltage Class

Report Year	Kv Class	Maximum Mileage of Systems: Solidly Grounded	Resistance Grounded	Reactance or Grounding Transformer	Ground-Fault Neutralizer	Ungrounded
1923	22–30	937	886			580
	31–40	657				185
	41–60	2,042			100	895
	61–92	910	200			355
	93–130	1,489	802			
	131–165	480				518
1931	23–33	2,064	1,358	382	*	228
	34–44	795		39	*	66
	45–66	1,556	1,131	253	*	1,345
	100–110	1,620		375	*	
	120–132	874			*	
	184–220	802	254		*	
Aerial Systems (Cable Less Than Ten Per Cent of the Total Mileage)						
1947	22–30	435	65	122	250	176
	31–40	774	469	700	1,427	306
	41–60	614	210	874	368	967
	61–92	1,160	186	365	232	170
	93–130	2,663	1,130	950	1,030	
	131–165	2,835		1,970	190	63
	166–230	1,300	252			
	231–Up	791				
Cable Systems (Cable More Than Ten Per Cent of the Total Mileage)						
1947	22–30	2,050	393			
	31–40	661	24			
	41–60	43				
	61–92	218	80			
	131–165	146				

* Ground-fault neutralizers were included under reactance grounded in the 1931 report.

Table XVIII. Average Number of Miles of Circuit Per Grounding Point

Kv Class	Solidly Grounded	Resistance Grounded	Reactance or Grounding Transformer	Ground-Fault Neutralizer	All Grounding Methods
Aerial Systems (Cable Less Than Ten Per Cent of the Total Mileage)					
22–30	62	59	45	72	58
31–40	47	271	66	221	65
41–60	69	210	125	197	76
61–92	57	73	151	85	59
93–130	65	283		147	67
131–165	50			95	50
166–230	117	126			117
231–Up	264				264
Cable Systems (Cable More Than Ten Per Cent of the Total Mileage)					
22–30	73	80			74
31–40	19	12			19
41–60	14				14
61–92	7	26			9
131–165	19				19
All classes	56	97	113	172	63

Establishing Sequence-Impedance Ratios of the System at Grounding Points (Table XXI)

The utilities were asked whether sequence-impedance ratios for the system had been established for faults at the terminal of the equipment forming the grounding path, and to state the ratio if one had been established. Sixty-nine systems reported having established sequence-impedance ratios. Thirty-seven of these, nearly all of which operate solidly-grounded systems, have established ratios of $R_0/X_1 < 1$ and $X_0/X_1 < 3$, which ratios define "effectively grounded" systems as described in AIEE Standard 32. These maximum values of the sequence-impedance ratios are established by the Standard for the purpose of limiting transient and dynamic voltages under ground-fault conditions.

For 16 systems a minimum value of the ratio of X_0/X_1 equal to one has been established. The reason as given in a number of instances for this practice is to limit ground-fault currents to values

Table XIX. Reported Sequence-Impedance Ratios at Terminals of Equipment Forming the Grounding Points

	Sequence-Impedance Ratios Reported																							
	Solidly Grounded								Resistance Grounded						Reactance Grounded				
Kv Class	22–30	31–40	41–60	61–92	93–130	131–165	166–230	231–Up	22–30	31–40	41–60	61–92	93–130	166–230	22–30	31–40	41–62	62–93	93–130
Impedance Ratios	$\frac{X_2}{X_1}$	$\frac{X_2}{X_1}$	$\frac{X_2}{X_1}$	$\frac{X_2}{X_1}$	$\frac{X_2}{X_1}$	$\frac{X_2}{X_1}$	$\frac{X_2}{X_1}$	$\frac{X_2}{X_1}$	$\frac{R_2}{X_1}$	$\frac{R_2}{X_1}$	$\frac{R_2}{X_1}$	$\frac{R_2}{X_1}$	$\frac{R_2}{X_1}$	$\frac{R_2}{X_1}$	$\frac{X_2}{X_1}$	$\frac{X_2}{X_1}$	$\frac{X_2}{X_1}$	$\frac{X_2}{X_1}$	$\frac{X_2}{X_1}$
0 to 1.0	87	130	46	183	135	106	42	3						1	2				
1.1 to 2.0	40	70	29	59	84	72	1		8					1	3	1	1		
2.1 to 3.0	10	59	4	18	7	39									3			1	3
3.1 to 4.0	4	2	2	1	6	3			2			1						2	3
4.1 to 5.0	1	2	3									5					1		
5.1 to 10.0	2	1	2									7			4	2		1	
10.1 to 20.0	2	1	3						1	1		1			6	6			
20.1 and up	2		1						10	4	1	9	1		2	5			

Figures are in number of ground points.

Table XX. Ratios of Phase-to-Ground Fault Currents to 3-Phase Fault Currents at Terminals of Equipment Forming Ground Path

	Current Ratios Reported																		
	Solidly Grounded								Resistance Grounded						Grounding Transformer and Reactance Grounded				
Kv Class	22–30	31–40	41–60	61–92	93–130	131–165	166–230	231–Up	22–30	31–40	41–60	61–92	93–130	166–230	22–30	31–40	41–60	61–92	93–130
Current Ratios																			
1.8 to 1.01	33	133	56	175	132	116	42	3				4			2				
1.0 to 0.81	40	112	25	93	81	70	8							1	3	1			
0.8 to 0.61	17	5	5	16	18	7	1							1			1	1	
0.6 to 0.51	26	2	2		3	5												2	1
0.5 to 0.41	1	2	2	1					8			1			1		1	1	1
0.4 to 0.31	3		1									2			2	4			
0.3 to 0.21	2	2	4		1				2			2			3	7			
0.2 to 0.11	4								3	2	1	7			5	4			1
Less than 0.1			1						8	3		7		1		1			

Figures are in number of ground points.

Table XXI. Replies to Question "Have Sequence-Impedance Ratios Been Established?"

	Solidly Grounded			Resistance Grounded			Reactance Grounded			Totals	
Voltage Class Kv	Do Endeavor to Limit R_2/X_1 and X_2/X_1 Ratios	Effectively Grounded $R_2/X_1<1$; $X_2/X_1<3$	Other Ratios*	Do Endeavor to Limit R_2/X_1 and X_2/X_1 Ratios	Effectively Grounded $R_2/X_1<1$; $X_2/X_1<3$	Other Ratios*	Do Endeavor to Limit R_2/X_1 and X_2/X_1 Ratios	Effectively Grounded $R_2/X_1<1$; $X_2/X_1<3$	Other Ratios*	Do Endeavor to Limit R_2/X_1 and X_2/X_1 Ratios	Effectively Grounded $R_2/X_1<1$; $X_2/X_1<3$
22– 30	21	17	3[a]				2	2		23	19
31– 40	16	8	7[a]							16	8
41– 60	3	1	2[a]							3	1
61– 92	7[d]	5	1[b]							7	5
93–130	7[d]	1	1[c]				2		2[e]	9	1
131–165	8	3	3[a]				1		1[e]	9	3
166–230	1[e]			1						2	
231 and up											
Total	63	35	17	1			5	2	3	69	37

Figures are number of systems
*(a). $X_2/X_1>1$.
(b). $X_2/X_1<5$.
(c). $X_2/X_1<1$.
(d). Several 110- and 66-kv systems report use of delta-star transformers in parallel with solidly-grounded star-delta transformers for control of X_2/X_1 ratio. Sequence ratios usually are not given.
(e). A 220-kv system reports the use of reactors in the neutrals of some of the transformers for control of fault currents. The transformers so grounded are operating in parallel with solidly grounded ones at the station, and are equipped with disconnects for solid grounding.

equal to or less than 3-phase fault current so as to avoid increased circuit-breaker duties.

Characteristics of Neutral Devices

Characteristics of Neutral Resistors (Table XXII)

A total of 68 neutral resistors is reported in use on transmission and distribution systems at 22 kv and above, these being principally in the 22–30-kv and 61–92-kv classes. Of the systems reporting data on the ratio of the voltage drop through resistors during a ground fault to the normal line-to-neutral voltage, 17 gave ratios of less than 0.10, and 35 gave ratios greater than 0.90. The insulation classes of neutral resistors are about evenly divided between line-to-line voltage and line-to-neutral voltage classes. The most common time rating is ten seconds; 31 are rated ten seconds or less; 25 are rated for more than ten seconds up to and including one minute; and 4 are rated for times longer than one minute. Six neutral-grounding resistors are water boxes. In one instance, the ohmic value of the neutral-grounding resistor was selected to give maximum braking effect under fault conditions on water wheel generators at the sending end of a 220-kv transmission system.

Table XXII. Characteristics of Neutral Resistors Used on Transmission and Distribution System

System Kv Class	Figures Represent Number of Devices					
	22–30	31–40	41–60	61–92	93–130	166–230
Total devices reported	24	7	1	30[a]	5[b]	1[c]
Ohmic drop/ V_{L-N} (per cent)						
0–10	10			7		
31–40						1
51–60				1		
81–90		2				
91–100	11	5	1	18		
Voltage class						
Line-to-line	7			12		
Line-to-neutral	14	7	1	3		
Below line-to-neutral				1[d]		1
Time rating						
8 seconds	10					
10 seconds	10			10		1
23 seconds	1					
30 seconds			1	8		
38 seconds	1					
1 minute	2	4		8		
2 minutes		3				
5 minutes				1		

(a). One device—home-made brine tank; four devices—water boxes.
(b). One device—water rheostat.
(c). Neutral grounding resistor selected for maximum breaking effect on generators during 220-kv unbalanced faults.
(d). Thirty-three kilovolt rating.

Characteristics of Neutral Reactors and Grounding Transformers (Table XXIII)

A total of 47 neutral reactors and grounding transformers is reported. Characteristic data were received for only a few of these.

Characteristics of Ground-Fault Neutralizers (Table XXIV)

Data are reported on 42 ground-fault neutralizers. The voltage class of these neutralizers is the minimum standard voltage class which is equal to or greater than the system line-to-neutral voltage. Table XXIV shows one unit with a one minute rating, 28 units with ten minute ratings, six with an "extended time" rating, and two with continuous ratings. AIEE Standard 32 has established ten minute ratings and "extended time" ratings and also the voltage class as previously stated for ground-fault neutralizers, which conforms with existing practice. Little information was given as to the procedure followed in the event of a sustained ground fault. However, the information indicates that the majority of systems employ devices which short-circuit the ground-fault neutralizer permitting ground relays to select the faulted feeder.

Grounding Factors

Opinions as to the Importance of Grounding Factors; Assigned Reasons for Present Practice (Tables XXV and XXVI)

The questionnaire submitted to the utilities listed 16 factors affecting the selection of the grounding method and asked for an indication of opinion as to the importance attached to these factors with reference to the system under consideration. Some replies listed many factors as important; others, only a few. Each of the 16 factors is rated as important for some solidly-grounded, ground-fault neutralizer, and reactance-grounded systems. A few factors were deemed unimportant on ungrounded systems.

The utilities also were asked to assign reasons for their current practice in terms of these 16 factors. Many utilities did not reply to this question, presumably because it was difficult to assign a particular reason for their practices. However, it is of some interest to list the 16 factors in system grounding and to give the number of replies for all methods of grounding and all voltage classes.

Factors in System Grounding	Number of Replies: Rated Important	Number of Replies: Assigned as Reason for Practice
Relaying	293	89
Apparatus insulation	239	62
Arcing grounds	223	48
Lightning protection	140	27
Equipment cost	133	35
Double or consequent faults	119	23
Adaptability to interconnection	87	25
Safety from voltage gradient considerations	85	10
Operating procedure	67	10
Inductive co-ordination	66	19
Positive-sequence voltage during faults	65	16
Damage at point of fault	65	
Cable insulation	61	21
Stability	59	8
Circuit breaker interrupting kilovolt-amperes	48	8
Mechanical stress in equipment windings	25	2
Total number of systems in report = 567		

Of these 16 factors, relaying, apparatus insulation, arcing grounds, lightning protection, equipment cost, and double or consequent faults are listed most frequently as important for each of the various grounding methods (except ungrounded systems).

The information contained in the foregoing tabulation and in the supporting Tables XXV and XXVI indicates clearly the complexity of the grounding

Table XXIII. Characteristics of Neutral Reactors and Grounding Transformers Used on Transmission and Distribution Systems

System Kv Class	Figures Represent Number of Devices					
	22–30	31–40	41–60	61–92	93–130	131–165
Total devices reported	16	15[a]	7	3	6[b]	[b]
Ohmic drop/ V_{L-N} (per cent)						
71–80				2		
91–100	2	4		1		
Voltage class						
Line-to-line	7	7		1	2	
Line-to-neutral	2					
Below line-to-neutral				2	2	
Time rating						
1 minute	4			3	1	
2 minutes		3				
10 minutes		4				
Continuous	2					

(a). One utility uses power transformers Y-connected on the 34-kv side instead of grounding transformers.

(b). Most of the devices in these voltage classes are on the systems of a utility which did not submit detailed information. One utility classed as reactance grounded has some transformers grounded through neutral reactors and the remainder either solidly grounded or ungrounded. Neutral reactors are used in locations of heavy power concentration to limit the short-circuit kilovolt-amperes of faults involving ground to values equal to or less than the 3-phase short-circuit kilovolt-amperes. In some locations, faults involving ground are limited by ungrounding the neutrals of one or more transformer banks with the others solidly grounded.

problem, the large number of important factors, and the wide variety of circumstances which influence the choice of grounding method in an individual case. While some factors such as relaying, apparatus insulation, arcing grounds, and equipment cost are always factors of importance, other factors, such as inductive co-ordination, are usually unimportant but may become the assigned reason for the practice in a particular case. It is evident from the replies that most of the factors are important, even though the method of grounding may be dictated by only one of the factors.

Review of Operating Experiences

Experience with Grounding Method

In Table XXVII are listed three questions and replies relating to operating experiences. In response to the first question, "Has any operating experience been unsatisfactory?", 424 systems replied, and 63 of these reported trouble. In response to the second question, "Any trouble coincident with ground faults elsewhere?", 53 systems out of 413 replying indicated that troubles of this kind had been experienced. Causes of unsatisfactory operation detailed in the notes include inductive co-ordination, excessive fault current, poor relaying, insufficient ground current, voltage dips and loss of synchronous motor loads, and difficulty of synchronizing the closing of by-pass switches of ground-fault neutralizers. In a number of instances, two or more types of trouble are reported for a single system.

It is evident from the foregoing that double faults (including coincident and consequent faults), being reported 53 times, are the principal cause of the unsatisfactory operating experiences reported. This is somewhat difficult to reconcile with the fact that double faults and arcing grounds were not listed as especially important among the grounding factors in Tables XXV or XXVI. It may be suggested that while most other grounding factors can be evaluated with fair precision, the magnitude of transient voltages and the probability of coincident faults easily are underestimated. It is of interest to note that on a basis of the ratio of those systems reporting double faults to the total number of systems covered in the report, about one fourth of the ground-fault neutralizer systems, ungrounded systems, and resistance-grounded systems reported double faults, whereas less than four per cent of solidly-grounded systems reported this trouble.

The third question, "Any grounding device been inadequate or caused trouble?" was intended to review performance of grounding devices in themselves. Eleven cases of inadequate or unsatisfactory grounding devices are reported. Of the specific troubles reported, three involved insufficient thermal capacity in the devices (one resistor, one reactor, and one grounding transformer).

Length of Time Grounding Method Has Been Used (Table XXVIII)

The utilities were asked to indicate the length of time that the present grounding method had been used, arranging their replies in five year intervals up to 15 years, and, in addition, to state whether the present method was applied when the system was new. Their replies are summarized in Table XXVIII.

Changes in Grounding Practices

In Table XXIX are listed the affirmative replies to three questions concerning changes in grounding practice, "Any changes in grounding practice during past 10–15 years?", "Any change in grounding practice being made?", and "Any new trend in grounding practice?" Of the

Table XXIV. Characteristics of Ground Fault Neutralizers Used on Transmission and Distribution Systems

	Figures Represent Number of Devices					
System Kv Class	22–30	31–40	41–60	61–92	93–130	131–165
Total devices reported	4	23[a]	3	3	7	2
Ohmic drop/ V_{L-N}						
71–80 per cent			1			
91–100 per cent	3	4				
Voltage class[b]						
Line to Neutral	3	16	3	3	7	2
Time rating						
One minute			1			
Ten minutes	3	13	2	3	6	2
Extended time		5			1	
Continuous		2				

(a). On one system, three power transformer banks are arranged for grounding and one zigzag grounding transformer is provided. Normally the grounding transformer neutral and two of the power transformer neutrals are connected to three separate ground fault neutralizers. All four neutrals are arranged to be shunted automatically to ground after a fault has existed for five seconds. The one ground fault neutralizer on a power transformer bank is solidly shunted to ground. The other two ground fault neutralizers and the one normally free neutral are shunted through 100-ohm reactors.

(b). Although 30 of these devices were reported to be line-to-line voltage, it is the understanding of the committee that all are line-to-neutral voltage class. Until recently, only the circuit voltage has been shown on the nameplate.

Table XXV. Factors in Transmission and Distribution System Grounding Practice Rated as Important

	Solidly Grounded	Resistance Grounded	Reactance or Grounding Transformer	Ground-Fault Neutralizer	Un-grounded	Total All Methods
(a). Apparatus insulation	214	3	12	3	7	239
(b). Cable insulation	58	1	1	1		61
(c). Mechanical stress in equipment windings	20	3	1	1		25
(d). Circuit breaker interrupting kilovolt-amperes	37	9	1	1		48
(e). Stability	50	4	2	3		59
(f). Positive-sequence voltage during faults	41	11	3	10		65
(g). Relaying	238	17	25	13	1	293
(h). Arcing grounds	166	11	24	20	2	223
(i). Double or consequent faults	96	9	9	4	1	119
(j). Lightning protection	115	3	8	13	1	140
(k). Inductive co-ordination	35	12	7	9	3	66
(l). Adaptability to interconnection	77	1	2	1	6	87
(m). Operating procedure	48	1	4	8	7	67
(n). Equipment cost	112	2	5	10	4	133
(o). Safety from voltage Gradient considerations	77		4	4		85
(p). Damage at point of fault	36	11	4	9	5	65
Number of systems in report	419	32	35	30	51	567

Figures represent number of systems replying affirmatively.

changes in grounding practices during the last 15 years, the following are reported:

Ten from ungrounded to solid grounding.

One from grounding transformer to solid grounding.

One from ground-fault neutralizer to solid grounding.

One from solid grounding to resistance grounding.

Five from solid grounding to ground-fault neutralizer.

One from solid grounding at the source to grounding on the distribution system.

One ground-fault neutralizer system divided.

Two decreased values of neutral resistance[a]

Of the changes being made or contemplated, the following are reported:

Two from solid grounding to ground-fault neutralizer.

One from solid grounding to reactor grounding.

Two from ungrounded to grounding transformer.

Table XXVI. Factors in Transmission and Distribution System Grounding Given as Reasons for Present Practice

	Solidly Grounded	Resistance Grounded	Reactance or Grounding Transformer	Ground-Fault Neutralizer	Ungrounded	Total All Method
(a). Apparatus insulation	50	3	1	1	7	62
(b). Cable insulation	21					21
(c). Mechanical stress in equipment windings	2					2
(d). Circuit breaker interrupting kilovolt-amperes	4	4				8
(e). Stability	4	3		1		8
(f). Positive-sequence voltage during faults	9	5	2			16
(g). Relaying	63	7	15	3	1	89
(h). Arcing grounds	36	4	8			48
(i). Double or consequent faults	17	1	4		1	23
(j). Lightning protection	18	3	4	2		27
(k). Inductive co-ordination	6	10	2	1		19
(l). Adaptability to interconnection	21			1	3	25
(m). Operating procedure	4		1	1	4	10
(n). Equipment cost	32	1	1		1	35
(o). Safety from voltage Gradient considerations	1					1
(p). Damage at point of fault	2	5			2	9
(q). Other considerations			[a]		[b,c]	
Number of systems in report	419	32	35	30	51	567

(a). To limit current in expulsion protector tubes.
(b). Expected line to ground faults to be self clearing.
(c). Excellent lightning performance.
Figures represent number of systems replying affirmatively

Table XXVII. Experience With Grounding Methods

All Figures in Number of Systems

Voltage Class Kv	1. Any grounding practice been unsatisfactory? Yes. Solid	Resistance	Reactance	Ground-Fault Neutralizer	Ungrounded	2. Any trouble coincident with ground faults elsewhere? Yes. Solid	Resistance	Reactance	Ground-Fault Neutralizer	Ungrounded	3. Any grounding device been inadequate or caused trouble? Yes. Resistance	Reactance	Ground-Fault Neutralizer
22-30		[e]		[m]	[p,q]	[w]	[e]		[C]	[p,F]	[J]	[K]	[m]
31-40	[a]		[f,h]	2	[r,s]	[x]		[g]	[D]	[r,G]		[h]	
41-60	[b,c]	[h]	[j]		[t]		[h]	[i]	1	[s,H]		1	
61-92	[g,d]	[j]		[u]	[v]	[y]	[j]		1	[u,I]	2		
93-130	[e]		2	[n]		[z]	1[A]						1
131-165	[f]					1			[E]				
166-230				[o]									
Total "yes's"	23	9	8	6	17	13	9	2	9	20	4	5	2
The above figures are totals of the positive answers. Below are shown the totals of the negative answers for comparison.													
Total "no's"	274	22	20	21	24	279	22	22	19	18	26	24	28

(a). One system has two solidly-grounded points and an additional point where the neutral of a 2,500-kva transformer bank is grounded through the 230-volt winding of a 5-kva 6.9-kv to 115/230 volt single-phase 25-cycle distribution transformer which has a 2,000-volt breakdown strength arc gap across the high winding, thus giving high normal, but low fault zero sequence impedance, necessary for inductive co-ordination as well as protection.

(b). One company states that two years experience with solid grounding on 46- and 60-kv systems allowed too many bad voltage dips and loss of synchronous motor load. A second grounding point is to be added to the 69-kv system.

(c). On one ground point in five on a system, inductive interference was unsatisfactory with a solid ground; distribution transformer was placed in neutral, to be cut out when ground current exceeds five amperes.

One ground-fault neutralizer system in the 41- to 60-kv class previously had grounded neutral but this was unsatisfactory on account of frequent tripouts during sandstorms.

(d). One station solidly grounded on 126-mile 66-kv system. One neutral grounded through fuse at customer station. Fused ground difficult to co-ordinate with instantaneous and inverse time relays. System not adequately grounded. Numerous equipment failures are result of line-to-ground faults. Opening of circuit breaker at grounded station and blowing of fuse at customer station leaves arcing ground on system. Studies under way on sufficient grounding, relaying, and faster circuit breaker operation. Trend to lower impedance grounding.

(e). Two systems in the 93- to 130-kv class were previously solidly grounded but this was unsatisfactory, so they changed to ground-fault neutralizer. One system in the 93- to 130-kv class changed from solid grounding to distribution transformer in the neutral on account of inductive interference.

(f). One utility, operating a very large system at 154 kv, originally grounded all transformers. Later, all, except one transformer bank at the main receiver station, were isolated from ground to reduce ground-fault current.

One utility operating a 154-kv system with all transformers solidly grounded reports that it considers X_1 too low at one large substation. It also reports that no change is being considered.

One system distribution transformer in neutral, is cut out when ground current exceeds five amperes to avoid inductive interference.

(g). One system with one third of its mileage cable reports 75-ohm resistance in neutral connection limit available relay current to such a low value that efficient ground relay operation was not obtained. With the high resistance the neutral shift during single-phase-to-ground fault conditions is excessive, quite frequently going outside of the delta. This resulted in excessively high voltage to ground on unfaulted phases and the consequent failures. Bus flashovers and cable failures have occurred coincident with or consequent to ground faults elsewhere in the network. Resistance in neutral will be lowered to 18.75 ohms or lower value if operating experience in other sections of the system with this value of resistance is satisfactory, and if approval of the telephone company for this procedure can be obtained. Resistance will be lowered to some value less than 18.75 ohms subject to same conditions.

(h). One system in the 41- to 60-kv class used solid grounding until 1930 when it changed to 150-ohm resistor which was changed back to solid grounding in 1944—because of bushing and lightning arrester failure when resistor was in service.

(continued on page 1545)

Table XXVII (continued)

(i). One system reports that prior to 1931 the 60-kv 25-cycle system, principally a radial system, was grounded through resistors whose combined ohmic value was approximately double the present value. These values of resistances proved inadequate because of the occurrence of multiple faults at the same or different locations, resulting from an initial ground fault. In 1931, the circuits were rearranged in the present form and additional grounds were added, both to reduce the system resistance and to facilitate relaying. This arrangement has reduced the occurrence of multiple faults, from an initial ground fault, to approximately two per year. It would be desirable to solidly ground this system if it were not for the close proximity of the 60-kv 25-cycle and 110-kv 60-cycle circuits, which affects the inductive co-ordination and relaying. Some studies now are being made to see if a further reduction in grounding resistance can be made from a relaying standpoint.

(j). One system reported excessive fault current. One utility reports, "We used to operate with delta-connected lines ungrounded and had trouble with transient overvoltages." This caused failure of some of our station equipment including arresters, bushings, and so forth. Also, we had trouble with relaying, selectivity, and clearing ground faults from lines. Grounding and ground relaying improved clearing time of some types of faults." All 132-, 69-, and 33-kv 60-cycle systems now are solidly grounded except one 33-kv system "where we got in trouble with harmonics generated by transformer bank. We used ground bank there." Grounding transformers also are used on the two 33-kv 25-cycle systems.

(k). One utility reports grounding transformer "Not entirely satisfactory. Insufficient ground current. One grounding transformer burned out."

(l). On one system, the grounding transformer is inadequate, flashovers occurred on system other than faulted portion.

(m). One system which changed from solid grounding has three ground-fault neutralizers operated in parallel and automatically shunted in five seconds. Type of construction is such that arc extinction by the ground-fault neutralizer has not been successful. The relaying of three parallel neutralizers is not successful. Many simultaneous faults have occurred. Plan to operate with a solid ground, except to obtain experimental data from time to time.

(n). One system had difficulty in simultaneous closing of by-pass switches.

(o). Arrester failures are reported on a 230-kv system because of switching surges.

(p). Two systems in the 23- to 30-kv class now ungrounded plan to ground their systems over a period of years. Both use automatic feeder reclosing. One company plans to ground through zigzag grounding transformers, the other plans to use star-delta grounding transformers. One company gives as the reason for the change a certain amount of trouble from flashovers and telephone interference. The other company stated the same reasons plus coincident faults and relaying.

One system in the 23- to 30-kv class, now reactance grounded, reports that it has been its practice to operate 26-kv feeders radially and ungrounded in order to improve continuity of service to its customers by permitting operation with one phase grounded. This method of operation has given some trouble from flashover on insulation and from telephone interference. Its present trend is to install zigzag grounding transformers and automatic feeder reclosing on existing feeders, whenever rehabilitation work is done at a substation.

One system in the 22- to 30-kv class, now reactance-grounded, reports a gradual change during past two years from an ungrounded—to lightly grounded—to solid grounding. Numerous instances of trouble on ungrounded and lightly grounded such as arrester failures, apparatus failures, multiple faults, and so forth. Replaced neutral resistors in some cases with reactors and finally short-circuited out the reactors. Trend is toward better grounding—always looking for ways to improve grounding.

(q). One system reported relaying not positive and arrester failures. The trend is to ground with grounding transformer.

One system in the 22- to 30-kv class was initially ungrounded but was changed to solidly grounded because of trouble with arcing grounds. A ground-fault neutralizer is on order and will be installed as soon as received.

(r). One system in the 31- to 40-kv class reports that before solid grounding many instances occurred of multiple faults, at the same or different locations, from an initial ground fault.

(s). One 31- to 40-kv-class system now solidly grounded was unsatisfactory when ungrounded.

On one system in the 31- to 40-kv class isolated neutral was unsatisfactory because of the number of interruptions—seven years ago tuned reactor installed—new device installed 1946—system divided for two devices.

(t). A 52-kv system 62 miles long reports change from ungrounded to solidly grounded ten years ago. Ungrounded system caused arcing grounds. Equipment failures and flashovers were result of ungrounded system.

A 55-kv delta system reports line-to-ground faults are difficult to locate and must be cleared manually. Faults frequently spread to other phase wires at remote points on the system, with occasional equipment damage. Insulation levels must be maintained high. Replacement of pin-type insulators with suspension type has improved operation and reduced pole top fires. Future plans include installation of zigzag grounding transformers of sufficient capacity to stabilize the neutral and to permit ground faults to be isolated by means of ground relays. Same comments apply to a 66-kv, a 45-kv, a 33-kv, and a 22.5-kv system, except that troubles are less marked on these smaller systems. Trend is toward a grounded system.

(u). One system in the 61- to 92-kv class had apparatus failures from consequent faults prior to installation of grounding bank with neutral resistor.

One utility, which has been operating its 63-kv system for more than 15 years with star-delta grounding transformers, originally operated with isolated neutral and ground selector. Its early experience of many coincident faults on different lines led to the present grounding scheme. Operation definitely was improved by the change in grounding practice.

(v). One solidly-grounded system in the 61- to 92-kv class was unsatisfactory when ungrounded.

(w). System converted from 7.5/15-kv 2-phase to 26-kv 3-phase. Terminal cable failures consequent to line-to-ground faults. System grounded at input stations. Proper apparatus and equipment grounding is under study. Soil conditions are such that Xe is probably in excess of 10,000 meter-ohms. Electrolytic arresters were replaced with spillgaps.

(x). One system had a failure of lightning arresters 30 miles from fault location and plans to establish additional ground points as opportunity presents itself.

One system reported that fuse holders and circuit breaker failed at same time at different locations.

One system reported that an airbreak switch failed at same time as line failed to ground at a different location.

(y). One 115-kv system with 458 miles of open-wire lines has been operated for 20 years with metallically separated lines and only one solidly-grounded transformer bank at the receiver station. Trouble frequently has been experienced from flashovers at the generating station when the grounded transformer bank was separated from a faulted line out of the generating station. It now is planned to ground all transformers at the generating station, but to maintain the metallic separation between lines.

One generator winding failure coincident with ground fault on 110-kv system.

A. One system reports trouble from coincident faults occasionally due to local conditions such as dirty or weak insulation.

B. One 33-kv system using a 22.6-ohm zigzag grounding transformer experienced a few failures of weak insulators during line-to-ground faults.

C. One system which changed from solidly-grounded neutral to ground-fault neutralizer in 1943 had occasional coincident insulator flashovers at different locations—not a serious problem.

D. Coincident failure from insulation reduced due to dirt conditions on one system.

One system which installed a ground-fault neutralizer to improve inductive co-ordination has had some trouble with old insulators flashing over.

On one system at 33-kv one type of new 37-kv lightning arresters has failed during ground fault causing change to 40-kv arresters.

One system reported some failures of weak insulation. Some additional difficulty with ground-fault relaying. Lost some defective bushings after ground-fault neutralizers were installed. Two bus flashovers under adverse weather simultaneous with line flashovers.

Fifty per cent of a system was solidly grounded before addition of ground-fault neutralizer. Multiple flashovers occurred when ground bank was temporarily out of service. Ground-fault neutralizers have been added. May install additional ground banks in future.

E. One system experienced bus insulator flashover coincident with line-to-ground fault 110 circuit miles distant.

F. Three 23-kv systems report equipment failures and replacing arresters with spillgaps. Considering installation of zigzag or grounded star-delta grounding transformers.

One system experienced frequent arrester failures resulting from multiple grounds and may install grounding bank in future.

G. One ungrounded system in the 31- to 40-kv class had trouble with multiple faults.

H. One system reports lightning arrester failures consequent to ground faults and is going to solid grounding to avoid the difficulty.

I. A 66-kv system, delta-connected for interconnection phasing, reports outages somewhat more frequent. Lightning arrester failures from remote ground faults.

J. One system reports that a circuit breaker failed to clear a ground fault, causing the grounding resistor to overheat severely and blowing out the windows in the resistor room. The resistor was not permanently damaged.

K. One system reported grounding device has insufficient thermal capacity.

One from ungrounded to solidly grounded.

One from ground-fault neutralizer to solid grounding.

In reply to the question on new trends, little information was given, perhaps because no trend, or rather no new trend, was apparent. Most of the replies appear to be restricted in their application to the system under consideration, and these do indicate a general trend toward better grounding.

Trends in Transmission and Distribution System Grounding Practices

One of the principal objectives of this report was to determine whether any new trends could be found in grounding practices. This question was included in the questionnaire, but the replies were not conclusive. Efforts also were made to determine trends by a comparison of corresponding data from the three surveys. Figure 3 and Tables XVI and XVII were prepared using these data. From Figure 3 and Table XVI, it is evident that solid grounding has been the dominant method since the 1923 report, that the important increase in the use of solid grounding was made between 1923 and 1931, and that little increase in relative use has occurred since that time. The use of resistance grounding has been on the decrease since the 1923 report, especially since 1931. The use of reactance

grounding was negligible in 1923, and then increased rapidly until the time of the 1931 report, with little relative change since then. The ground-fault neutralizer method was new in 1923; its use was not widespread in 1931 and was not separately listed in the 1931 report; however, this method has made important increases since that time. Undoubtedly the most significant change has been the continued decrease in use of ungrounded systems.

The trends in the various voltage classes can be analyzed by reference to Table XVII. For example, the most striking change is in the 22–30-kv class where it will be noted that a full 60 per cent now are grounded solidly whereas two thirds of the systems were ungrounded in 1923.

The trend in the average mileage of transmission and distribution systems is toward shorter lengths in the lower voltage classes and longer lengths in the higher ones. The maximum system mileage has increased, the highest value now reported being 2,835 miles for one 138-kv solidly-grounded system. Mention also should be made of the 1,427-mile ground-fault neutralizer system in the 31–40-kv class. For ungrounded and resistance-grounded systems, the change in maximum mileage with the years has been a decrease. For reactance-grounded and ground-fault neutralizer systems, the trend has been to increase the maximum mileage since the 1931 report.

Table XXVIII. Length of Time Present Grounding Scheme Has Been Used and Was Method Applied When Station or Grounding Device Was New

Voltage Classes Kv	Solid Grounding: Applied When New	Solid Grounding: 0–5 Years	Solid Grounding: 5.1–10 Years	Solid Grounding: 10.1–15 Years	Solid Grounding: 15.1 and Over	Resistance Grounding: Applied When New	Resistance Grounding: 0–5 Years	Resistance Grounding: 5.1–10 Years	Resistance Grounding: 10.1–15 Years	Resistance Grounding: 15.1 and Over	Reactance Grounding: Applied When New	Reactance Grounding: 0–5 Years	Reactance Grounding: 5.1–10 Years	Reactance Grounding: 10.1–15 Years	Reactance Grounding: 15.1 and Over	Ground-Fault Neutralizer: Applied When New	Ground-Fault Neutralizer: 0–5 Years	Ground-Fault Neutralizer: 5.1–10 Years	Ground-Fault Neutralizer: 10.1–15 Years	Ground-Fault Neutralizer: 15.1 and Over	Ungrounded: Applied When New	Ungrounded: 0–5 Years	Ungrounded: 5.1–10 Years	Ungrounded: 10.1–15 Years	Ungrounded: 15.1 and Over
22–30	41	7	5	15	19	10				6	10	3	2		9	1	1	1			11				12
31–40	37	12	13	8	17	2				2	3	3		6	1	4	1	10			13	1	2	4	8
41–60	24	2	2	2	20					1					2		1	2			5				5
61–92	66	4	9	10	43	5	1		1	7			1		1		1	1			5		1		4
93–130	41	2	9	2	28	1				1					4	3		2	3						
131–165	38	10	1	4	19										1	1			1		1				1
166–230	13	1	1	1	4	1				1															
231 and up	1			1																					
Total	261	38	40	43	150	19	1		1	18	13	6	3	6	18	9	6	17	1		35	1	3	4	28

Figures are in number of systems.

Table XXIX. Changes in Grounding Practice

(The Combination of a Numeral and a Letter in Parenthesis Represents the Number of Systems Which Follow the Practice Detailed in the Lettered Superscript Note)

Voltage Class Kv	Changed in Last 15 Years: Solid	Changed in Last 15 Years: Resistance	Changed in Last 15 Years: Reactance	Changed in Last 15 Years: Ground-Fault Neutralizer	Changed in Last 15 Years: Ungrounded	On Which Changes Are Being Made or Contemplated: Solid	On Which Changes Are Being Made or Contemplated: Resistance	On Which Changes Are Being Made or Contemplated: Reactance	On Which Changes Are Being Made or Contemplated: Ground-Fault Neutralizer	On Which Changes Are Being Made or Contemplated: Ungrounded	Reporting New Trends: Solid	Reporting New Trends: Resistance	Reporting New Trends: Reactance	Reporting New Trends: Ground-Fault Neutralizer	Reporting New Trends: Ungrounded
22–30	$5^{(a),(b)}$	$2^{(e)}$	3	$1^{(g)}$	2	$1^{(i)}$	7	$3^{(k)}$		4			$1^{(m)}$		$2^{(n)}$
31–40	$3^{(a)}$		$6^{(j)}$	$8^{(k)}$		3		2	3	$6^{(k)}$			$4^{(l),(m),(o)}$		4
41–60	$3^{(a)}$			$2^{(g)}$						1					2
61–92	$5^{(a),(c)}$	2	1	2		$1^{(i)}$	2					1			$1^{(r)}$
93–130	$4^{(b),(d)}$			$2^{(g)}$		3		2			3			$1^{(p)}$	
131–165	5					$1^{(k)}$									
166–230				$1^{(i)}$											
Total	25	4	10	16	2	9	9	7	3	11	3	1	5	1	9

Figures are in number of systems.

(a). Changed from ungrounded to solidly grounded.

(b). Changed from ungrounded delta to grounded Y at a higher voltage.

(c). Changed from grounding transformer to solidly grounded.

(d). Changed from solid grounding at the source to grounding out on distribution systems.

(e). Decreased value of neutral resistance.

(f). Changed from solid grounding to resistance grounding.

(g). Changed from solid grounding to ground-fault neutralizer.

(h). One ground-fault neutralizer system divided.

(i). The operation of a 220-kv 50-cycle ground-fault neutralizer system was discontinued after a few years of successful operation when the system was increased to two circuits tied metallically to a large system with solidly-grounded neutrals. One lightning arrester failure was experienced during the switching out of a faulted line section.

(j). Change to be made from solid grounding to a ground-fault neutralizer.

(k). A 132-kv system reports control of fault current distribution by opening (oil circuit breaker) the tertiary of 287.5/132-kv autotransformers. The growth of this system is expected to make necessary the installation of reactors in the neutrals of step-down transformers.

(l). Change to be made from radial ungrounded 26-kv feeders to grounding transformers.

(m). One system sees a trend on lower voltage systems from ungrounded to lightly-grounded to better-grounded systems.

(n). See trend to solidly-grounded system wherever practical.

(o). One system sees trend to replace delta-connected and grounding transformer banks with solidly-grounded neutral banks.

(p). One utility is considering adding open-ground wires and solidly grounding.

(q). One utility plans to ground system over a period of years.

(r). One utility states that future systems will be solidly or impedance grounded.

One important change during the last 15 years has been the increased importance attached to sequence-impedance ratios, which in response to the questionnaires were given for over 70 per cent of the grounding points. It is also significant that more than ten per cent of the systems have established definite sequence-impedance ratios.

A review of grounding practices on transmission and distribution systems indicates the following:

1. A continued dominance of solid grounding.

2. A trend away from ungrounded systems.

3. A trend away from the use of resistance-grounded systems.

4. A trend toward limiting ground-fault currents to the 3-phase fault current values or less.

5. A trend to greater use of ground-fault neutralizer systems.

References

1. Present Day Practices in Grounding of Transmission Systems. First Report of Subcommittee on Grounding of Protective Devices Committee (W. W. Woodruff, E. C. Stone). AIEE Transactions, volume 52, 1923, pages 446–64; AIEE *Journal*, volume 52, September 1923, pages 928–40.

2. Present Day Practice in Grounding of Transmission Systems, Second Report of Subject Committee on Grounding (C. A. Powel, chairman, interconnection subcommittee, power transmission and distribution committee). AIEE Transactions, volume 50, 1931, pages 892–900; Electrical Engineering, August 1931, volume 50, pages 638–41.

3. Neutral Grounding Devices. AIEE Standard 32, May 1947.

4. Grounding of Power-System Neutrals, S. B. Griscom. "Electrical Transmission and Distribution Reference Book," Central Station Engineers of the Westinghouse Electric and Manufacturing Company, chapter 17, pages 457–75.

5. Generator Grounded Through Transformer Primary; Resistor in Secondary, W. E. Marter, A. A. Johnson. *Electrical World* (New York, N. Y.), December 11, 1943, pages 2038–40.

6. Correlation of System Overvoltages and System-Grounding Impedances. AIEE Subcommittee Report (W. W. Lewis, chairman). AIEE Transactions, volume 62, 1943, January section, pages 17–24; discussion, page 383.

7. Rotating Electrical Machinery. Standard C50-1943, American Standards Association (New York, N. Y.), paragraph 3.130.

8. Effect of Restriking on Recovery Voltage, C. Concordia, W. F. Skeats. AIEE Transactions, volume 58, 1939, August section, pages 371–5.

9. Overvoltages on Transmission Lines Due to Ground Faults as Affected by Neutral Impedance. Engineering Report 30, Development and Research Joint Subcommittee of the Edison Electric Institute and the Bell Telephone System, volume 4, 1937, pages 105–37.

10. The Neutral Grounding Reactor, W. W. Lewis. AIEE Transactions, volume 42, 1923, pages 417–34; discussion, page 464.

11. The Peterson Coil, W. W. Lewis. *General Electric Review* (Schenectady, N. Y.), volume 38, 1935, page 197.

12. Grounding Principles and Practice—III: Generator Neutral Grounding Devices, A. A. Johnson. Electrical Engineering, volume 64, March 1945, pages 92–9.

Appendix. List of Co-operating Utilities

Power Companies

Alabama Power Company, Birmingham, Ala.

Albuquerque Gas and Electric Company, Albuquerque, N. Mex.

American Gas and Electric Service Company, New York, N. Y.

Appalachian Electric Power Company, Roanoke, Va.

Atlantic City Electric Company, Atlantic City, N. J.

Blackstone Valley Gas and Electric Company, Pawtucket, R. I.

Boston Edison Company, Boston, Mass.

Brockton Edison Company, Brockton, Mass.

Buffalo Niagara Electric Corporation, Buffalo, N. Y.

California Oregon Power Company, Medford, Oreg.

Cape and Vineyard Electric Company, Cambridge, Mass.

Carolina Power and Light Company, Raleigh, N. C.

Central Arizona Light and Power Company, Phoenix, Ariz.

Central Illinois Electric and Gas Company, Rockford, Ill.

Central New York Power Company, Syracuse, N. Y.

Central Ohio Light and Power Company, Findlay, Ohio

Central Power and Light Company, Corpus Christi, Tex.

Central States Electric Company, Cedar Rapids, Iowa

Cincinnati Gas and Electric Company, Cincinnati, Ohio

Cleveland Electric Illuminating Company, Cleveland, Ohio

Commonwealth Edison Company, Chicago, Ill.

Commonwealth and Southern Corporation, Jackson, Mich.

Connecticut Light and Power Company, Waterbury, Conn.

Consolidated Edison Company of New York, Inc., New York, N. Y.

Consolidated Gas, Electric Light, and Power Company of Baltimore, Baltimore, Md.

Dallas Power and Light Company, Dallas, Tex.

Dayton Power and Light Company, Dayton, Ohio

Delaware Power and Light Company, Wilmington, Del.

Detroit Edison Company, Detroit, Mich.

Duke Power Company, Charlotte, N. C.

Duquesne Light Company, Pittsburgh, Pa.

East Shore Public Service Company of Maryland, Salisbury, Md.

El Paso Electric Company, El Paso, Tex.

Empire District Electric Company, Joplin, Mo.

Georgia Power Company, Atlanta, Ga.

Gulf Power Company, Pensacola, Fla.

Gulf States Utility Company, Beaumont Tex.

Hartford Electric Light Company, Hartford, Conn.

Idaho Power Company, Boise, Idaho

Illinois Power Company, Decatur, Ill.

Illinois Northern Utilities Company, Dixon, Ill.

Indiana and Michigan Electric Company, South Bend, Ind.

Indiana Service Corporation, Fort Wayne, Ind.

Indianapolis Power and Light Company, Indianapolis, Ind.

Iowa Electric Company, Cedar Rapids, Iowa

Iowa Electric Light and Power Company, Cedar Rapids, Iowa

Iowa-Illinois Gas and Electric Company, Rock Island, Ill.

Iowa Power and Light Company, Des Moines, Iowa

Iowa Public Service Company, Sioux City, Iowa

Kansas Gas and Electric Company, Wichita, Kans.

Kentucky and West Virginia Power Company, Ashland, Ky.

Louisville Gas and Electric Company, Louisville, Ky.

Metropolitan Edison Company, Reading, Pa.

Minnesota Power and Light Company, Duluth, Minn.

Mississippi Power and Light Company, Jackson, Miss.

Missouri Power and Light Company, Jefferson City, Mo.

Missouri Public Service Corporation, Warrensburg, Mo.

Monongahela Power Company, Fairmont, W. Va.

Montana Power Company, Butte, Mont.

Mountain States Power Company, Albany, Oreg.

Montaup Electric Company, Fall River, Mass.

Nebraska Power Company, Omaha, Nebr.

New Bedford Gas and Electric Light Company, New Bedford, Mass.

New England Gas and Electric Association Service Corporation, Boston, Mass.

New England Public Service Company, Boston, Mass.

New Hampshire Gas and Electric Company, Portsmouth, N. H.

New Jersey Power and Light Company, Newark, N. J.

New Orleans Public Service Company, New Orleans, La.

New York Power and Light Company, Albany, N. Y.

New York State Electric and Gas Company, Binghamton, N. Y.

Northern Indiana Public Service Company, Hammond, Ind.

Northern States Power Company, Minneapolis, Minn.

Northwestern Electric Company, Portland, Oreg.

Northwestern Public Service Company, Huron, S. Dak.

Ohio Power Company, Canton, Ohio

Ohio Public Service Company, Elyria, Ohio

Pacific Power and Light Company, Portland, Oreg.

Pennsylvania Power and Light Company, Allentown, Pa.

Pennsylvania Water and Power Company, Baltimore, Md.

Philadelphia Electric Company, Philadelphia, Pa.

Plymouth County Electric Company, Plymouth, Mass.

Portland General Electric Company, Portland, Oreg.

Potomac Edison Company, Hagerstown, Md.

Potomac Electric Power Company, Washington, D. C.

Public Service Company of Colorado, Denver, Colo.

Public Service Company of Indiana, Indianapolis, Ind.

Public Service Company of Northern Illinois, Chicago, Ill.

Public Service Electric and Gas Company, Newark, N. J.

Puget Sound Power and Light Company, Seattle, Wash.

Safe Harbor Water Power Corporation, Baltimore, Md.

San Diego Gas and Electric Company, San Diego, Calif.

Southern California Edison Company, Los Angeles, Calif.

South Carolina Electric and Gas Company, Columbia, S. C.

Southern Colorado Power Company, Pueblo, Colo.

Southwestern Gas and Electric Company, Shreveport, La.

St. Joseph Light and Power Company, St. Joseph, Mo.

Toledo Edison Company, Toledo, Ohio

Tucson Gas, Electric Light and Power Company, Tucson, Ariz.

Union Electric Company of Missouri, St. Louis, Mo.

United Illuminating Company, New Haven, Conn.

Utah Power and Light Company, Salt Lake City, Utah

Virginia Electric and Power Company, Richmond, Va.

Washington Water Power Company, Spokane, Wash.

Western Massachusetts Electric Company, Springfield, Mass.

Western United Gas and Electric Company, Aurora, Ill.

Wisconsin Power and Light Company, Madison, Wis.

Municipal

Burbank Public Service Department, Burbank, Calif.

Detroit Public Lighting Commission, Detroit, Mich.

Eugene Water Board, Eugene, Oreg.

Glendale Public Service Department, Glendale, Calif.

Kansas City, Kansas, Board of Public Utilities, Kansas City, Kans.

Pasadena Muncipal Light and Power Department, Pasadena, Calif.

City and County of San Francisco, Public Utilities Commission, Hetch Hetchy Water Supply, Power and Utilities Engineering Bureau, San Francisco, Calif.

Seattle, Washington, Department of Lighting, Seattle, Wash.

Tacoma, Washington, Tacoma, Wash.

Los Angeles Department of Water and Power, Los Angeles, Calif.

City of Cleveland, Cleveland, Ohio

Power Districts and Authorities

Bonneville Power Administration, United States Department of Interior, Portland, Oreg.

Grand River Dam Authority, Vinita, Okla.

Imperial Irrigation District, Imperial, Calif.

Metropolitan Water District of Southern California, Los Angeles, Calif.

Nebraska Public Power System, Western Division, North Platee, Nebr.

Nebraska Public Power System, Eastern Division, Columbus, Nebr.

Tennessee Valley Authority, Chattanooga, Tenn.

Turlock Irrigation District, Turlock, Calif.

United States Bureau of Reclamation, Denver, Colo.

Parker Dam Power Project
Wyoming Interconnected System
Colorado–Wyoming Interconnected System
Colorado–Big Thompson Project
Shoshone Project
Boulder Canyon
Central Valley (Shasta)
Columbia Basin
Fort Peck Project
Rio Grande Project
Central Valley Project
Minidoka Project

War Department, United States Engineer Office, Fort Peck, Mont.

Fort Peck Dam Power Development

Utilities in Canada

City of Winnipeg Hydro-Electric System, Winnipeg, Manitoba

Hydro-Electric Power Commission of Ontario, Toronto, Ontario

Aluminum Company of Canada, Montreal, Quebec

Saguenay Power Company Limited, Ile Maligne, Quebec

Winnipeg Electric Company, Winnipeg, Manitoba

Shawinigan Water and Power Company, Montreal, Quebec

Quebec Hydro-Electric Commission, Montreal, Quebec

Discussion

W. R. Brownlee and **J. A. Elzi** (Commonwealth and Southern Corporation, Jackson, Mich.): It is believed that the reduction in equipment costs made feasible by effective grounding is of much greater importance than might be indicated by the data presented. This is especially true for transmission and distribution systems. In this connection, the statement that "High impedance grounding—avoids circuit breaker duties being increased beyond that required for 3-phase faults" may be subject to misinterpretation, since such duty increase is avoided if the zero sequence reactance at the point of fault is not less than the subtransient reactance, which obviously is not "high impedance" grounding.

It is believed also that the per cent of solidly grounded transmission and distribution systems very well might be somewhat higher than reported if it were not for the fact that where systems were designed originally with delta-delta transformers, solid grounding cannot be justified economically and grounding banks have been used.

Referring particularly to generator grounding, the objectives might be grouped as follows:

1. Minimizing the likelihood of faults through adequate surge protection.
2. Avoidance of double faults caused by arcing ground effects.
3. Prevention of mechanical damage to generator winding when ground faults occur at or near the terminals.
4. Limitation of damage to generator copper and especially iron when generator faults do occur.

As might be expected, certain of these objectives are conflicting. The report points out that some of those using solid grounding of generators are alert to mechanical stress considerations and calls attention to section 3.30 of ASA Standard *C50* which requires that short-circuit currents on any phase of a generator be limited to that of the 3-phase short-circuit current. However, the impulse strength of standard generator windings is presumed to be (ASA *C50*, section 2.124) no more than the crest value of the 60-cycle test wave, so that the application of generator arresters for adequate impulse protection requires an "effectively grounded" system. If both of these limitations are taken at face value, then the choice of generator grounding is indeed a narrow one.

The probability of double faults, especially those where a fault on insulators, cables, or bushings may result in a generator winding failure, may be reduced materially through relatively high resistance grounding, although evidence in the report indicates that still further improvement may be effected through solid or low reactance grounding. It is doubtful if there is any advantage from this standpoint of reducing grounding impedance below the "effectively grounded" value.

The increasing trend toward low reactance grounding of generators is probably influenced by the more recent installation of 3,600-rpm generators, in which the end turns of the wider coils are more difficult to brace and which are likely to have a zero-phase-sequence reactance of one-third to one-fifth of the subtransient reactance instead of about one-half of the subtransient reactance as is common with 1,800-rpm units. It is noteworthy that the addition of a neutral reactor sufficient to make the zero-phase-sequence reactance of the generator (and reactor) equal to the subtransient reactance of the generator will limit the cur-

rent in any generator winding to the three phase value regardless of the characteristics and magnitude of the connected system. That is, the specified current value will not be exceeded even if the generator should be connected to an infinite capacity delta system. In the popular "unit" system this usually will result in a ratio of *system* zero sequence reactance to *system* subtransient reactance of about two or slightly greater.

The committee's conclusion that "Operating experience presented indicates that on generator systems emphasis should be placed on reducing high ground fault current . . .," is open to some question. Objective 4 of this discussion, "limitation of damage," may be approached either by a reduction in fault current magnitude or by the rapid and positive disconnection of faults. It has been recognized that in the case of the conventional single winding generator the use of high neutral impedance may seriously interfere with the operation of differential relays for faults other than on the generator terminals. It seems significant that the consideration of "relaying" tops the list both in the number of users who feel its importance and the number of those giving it as a reason for the grounding practices employed. In view of the large majority of users having solid or low reactance grounded systems, it is safe to conclude that they also feel that a relatively heavy fault current cleared positively and rapidly will result in less damage than a reduced fault current cleared slowly or perhaps not at all.

M. M. Samuels (New York, N. Y.): The great diversity of grounding methods used on our power systems, from the generator to the meter and lighting fixture, as brought out by this comprehensive and elaborate committee report, is additional evidence, if any is needed, that we still know very little about grounds, that we are still unable to handle this specific feature of power system design with the same engineering competence and engineering certainty that we handle other parts of system design. We have direct grounds, resistance grounds, reactance grounds, and ground relays. Tests indicate that ground currents do not flow in the direction of the circuit but that voltage gradients are distributed almost uniformly in all directions from a ground conductor. This would seem to indicate a capacitance feature, and yet very little experimentation has been done with capacitor grounding. We know less about what goes on in the soil near a ground conductor than we do about what goes on in the clouds. An enormous amount of analytical study, testing, and operating experience is called for before we can handle grounding in a real engineering manner.

The report shows an enormous amount of work done by the committee and the contributing power systems. But after digging through the report, the numerous tables, and still more numerous voluminous footnotes, the question arises: So what? There is practically no answer. The design engineer who bases his engineering on statistical data relating to what other design engineers did, is not worth his salt. The fact that many systems, even the majority of systems, use a certain method or abandoned another method is no evidence that the first method is right and the second is wrong. Even a report that trouble was experienced when a certain method was used, is no evidence that the specific method is to be condemned in all cases or even in selected cases, as long as there is no report of a detailed investigation of the cause of the trouble in each individual case. The design engineer should not base his designs by merely concentrating on preventing something from happening that actually happened, because something that happened once or twice never may happen again but other things may happen. The design engineer must consider all things that possibly could happen in his specific case. The committee has done a pioneering job in establishing the various methods actually in use and classifying these methods systematically. Now it is suggested that the committee tackle the next step:

1. Exhaust all analytical procedure for each of the methods and present the analysis in a complete systematic form.
2. Establish all possible definite conclusions and recommendations based on the analysis.
3. Establish those conclusions which cannot be drawn from the analysis.
4. Establish all possible experience records in relation to item 3 and attempt to crystallize recommendations based on such experience.
5. Establish what cannot be determined without further tests and then proceed with those tests.

It is important that we guard ourselves against continuing the use of engineering methods merely for the reason that the method has been in common use. Some actual cases will serve the purpose of illustration. A number of years ago it was customary to install a set of choke coils in each circuit at each station. When a lightning arrester was ordered by catalogue number, a set of choke coils always was included even if they were not mentioned in the order. These coils were merely rated in amperes. For each ampere rating there was only one size without any consideration of the characteristics of the circuit. To the young engineer of today this would appear as sheer nonsense. It was only after some bad boys in the engineering profession who do a little original thinking now and then raised the question of the possibility of reflection that tests were made which showed that the coils are not only useless but may be harmful in some cases, because the tests showed in some cases higher voltages on the station side than on the line side. The practice of using such coils was dropped on short order everywhere. And yet, if an AIEE committee made a survey among power systems at that time the report would be that all power systems use choke coils.

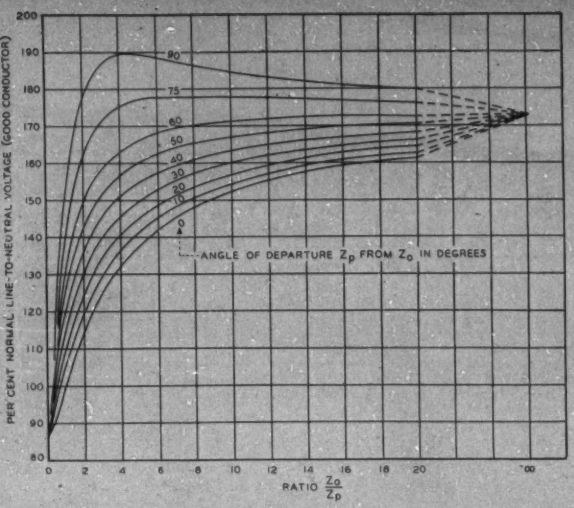

Figure 1. Voltage curves for one conductor to ground faults

Maximum good conductor voltage at point of fault for various ratios of Z_0 to Z_p and for various angles of departure of Z_p from Z_0. $Z_p = Z_n$

In the early days of outdoor substations it did not seem natural to place pin insulators with the axis in horizontal position. They were mounted at 45 degrees, with the resulting complications in disconnecting switch mechanisms and station design all around until one engineer started raising questions about wet flashover. Tests were made by all insulator manufacturers, which showed that the wet flashover of an insulator with the axis horizontal is never less than one with the axis vertical. The 45-degree mounting was established definitely as an unnecessary piece of nonsense, but, believe it or not, it is still in evidence here and there. Thus is the force of tradition. Let us beware of following general practice blindly.

V. J. Cisna (Tennessee Valley Authority, Chattanooga, Tenn.): I wish to protest against the continued practice of the protec-

tive devices committee in using X_0/X_1; R_0/X_1 ratios as the criteria for degree of neutral grounding. These ratios first were proposed by R. D. Evans and S. H. Wright in their paper "Power System Voltages and Currents Under Fault Conditions," presented in March 1931.[1] The curves presented in that paper have been reproduced in the books "Symmetrical Components" by Wagner and Evans and the "Westinghouse Electrical Transmission and Distribution Reference Book." A derived curve giving voltage rise on unfaulted conductors was used as Figure 2 in the protective devices committee's report[2] presented in January 1943.

The curves of Figure 2 of the correlation report and the various other curves were made assuming resistance in the positive and negative sequences to be negligible and, consequently, are not general, and have no application whatsoever on circuits having appreciable resistance. For example, assume a circuit in which $X_1 = X_2 = X_0 = R_1 = R_2 = R_0$. From Figure 2 of the correlation report it appears that an unfaulted phase to neutral voltage of approximately 130 per cent would exist during a single phase-to-ground fault whereas there would be no overvoltage at all. If $X_1 = X_2 = X_0$ and $R_1 = R_2 = R_0 = 3X_1$, the Figure 2 curves indicate an unfaulted phase voltage of approximately 167 per cent while, actually, there is again no overvoltage.

I believe that the committee should discard the X_0/X_1; R_0/X_1 ratios for determining overvoltages and for defining a solidly grounded neutral system. I also believe that a solidly grounded neutral system, or more properly, an effectively grounded neutral system, should be defined by the voltage rise on the good conductor or conductors during ground faults and that the protective devices committee should specify the permissible rise.

When the allowable voltage rise has been established, curves are useful in determining the voltage rise on unfaulted conductors and this writer has devised the curves of Figure 1 of this discussion for that purpose. The curves which are general for inductive circuits use impedance ratios and separate curves are drawn for various difference angles (angles of departure in Figure 1) between the positive and zero sequence impedance angles at the point of fault. If 135 per cent of rated system voltage is selected as the maximum allowable fault voltage, Z_0/Z_p ratios could be as much as 4.5/1. Approximately 135 per cent voltage is obtained from Figure 2 of the correlation report when $R_0/X_1 = 1$ and $X_0/X_1 = 3$ and this appears to be a very reasonable fault voltage to adopt as the standard for an "effectively grounded neutral system."

References

1. Some Effects of Unbalanced Faults, R. D. Evans, S. H. Wright. Electrical Engineering, volume 50, June 1931, 415-20.

2. Correlation of System Overvoltages and System-Grounding Impedance, AIEE Committee on Protective Devices. AIEE Transactions, volume 62, 1943, January section, pages 17-24.

W. W. Lewis (Union College, Schenectady, N. Y.): In V. J Cissna's discussion, he mentions a previous report presented in 1943. Cissna criticizes the previous report in that R_1 and R_2 (positive and negative sequence resistances) apparently have been ignored, thus giving higher calculated overvoltages due to line-to-ground faults than would be found if these resistances were present.

The values published in the 1943 report were intended to be conservative and to give outside limits of overvoltage resulting from line-to-ground faults. In those cases where R_1 and R_2 are appreciable, such as on distribution circuits with the fault remote from the station, then overvoltages on the unfaulted conductors would be reduced, and anyone who wished to do so could take advantage of this fact.

However, there still would be the possible condition of a fault near the station, and this would have to be reckoned with in determining whether or not the system were effectively grounded. Hence the conservative criterion still remains the one suggested in the 1943 report, that is, a system may be regarded as effectively grounded if the ratio X_0/X_1 does not exceed 3 and the ratio R_0/X_1 does not exceed 1, regardless of any values assigned to R_1 and R_2.

S. B. Crary (General Electric Company, Schenectady, N. Y.): The committee is to be complimented for compiling such a comprehensive summary. This report is well worthy of careful study.

Generator grounding practice is an important part of the problem of machine protection, which can be classified simply as follows:

I. Protection of Machine Against Failure

A. Transient overvoltage protection—accomplished most completely by modern surge voltage protective equipment at the terminals of the machine.

B. Overcurrent limitation for external faults—realized by using impedance in neutral. In case of reactance grounding by keeping X_0/X_1 equal to or greater than 1 for the machine branch of the circuit.

II. Protection of Machine Against Excessive Damage After Internal Failure

A. Accomplished *primarily* by accurate fault detection and prompt and reliable clearing of machine.

B. Accomplished *secondarily* by limitation of ground fault current to low values.

In order to obtain a high degree of protection *against failure* (item I) it may be necessary to sacrifice some protection *against damage after failure* (item II). For example, when relatively low reactance grounding is used a lower rated voltage protective means may be used whereas high current may be obtained if an internal fault does occur. It is evident therefore that the problem of grounding depends considerably upon the relative emphasis placed on protection of a machine *against failure* as compared with the protection of a machine *against damage after failure*. This relative emphasis may depend upon individual experience or even viewpoint and accounts for much of the divergence in practice. The trends shown in the report can be credited to a much better understanding of the problem based both on analysis and experience.

This report states that "Where X_0/X_1 is greater than 3, and there are 25 reactance-grounded systems listed in this class, excessive transient voltages may be encountered." This statement is somewhat misleading as ratios of X_0/X_1 in the range from 3 to 10 do not necessarily lead to excessive voltages. Excessively high voltages do not appear to occur until a value of X_0/X_1 higher than 10 is obtained. At these higher ratios, it has been shown in reference 8 of the report that transient overvoltages due to switching may become quite vicious, possibly sufficiently severe to damage protective equipment. Therefore, values of X_0/X_1 from 3 to 10 for reactance grounded systems can be expected to give satisfactory performance, although in this range it normally will be necessary to use a protective means having a voltage rating greater than that allowable when $X_0/X_1 > 3.0$.

Eric T. B. Gross (Illinois Institute of Technology, Chicago, Ill.): It was of great interest to me to listen to the discussion presented by M. M. Samuels, and I would agree with him that nobody should conclude from this report that certain grounding methods are being continued only because they have been in use for some time past. It is without doubt that a real engineer will not accept past practice blindly, and the introduction of "new" methods is proof of the fact that the majority of engineers does ask the question "Why and when do we ground systems at all, and what method is best in each particular case?"

The report shows the existence of certain sound trends as clearly indicated in Figures 1, 2, and 3. There is a trend away from solid generator grounding, as indicated in Figure 1; there is also a trend away from ungrounded transmission systems, and a remarkable increase in the number of resonant grounded[1] systems (*GFN* systems), as indicated in Figure 3.

It should be emphasized, however, that a study of the complete report which includes all the tables and the very important footnotes leaves the reader sometimes guessing (as happened also to some of the members of the subject committee when they tried to analyze the answers to the questionnaires), and one sometimes will conclude that an obsolete method may have been continued for lack of unsatisfactory experiences—if there were no primary disturbances to cause trouble, any grounding method becomes "satisfactory," as so well emphasized by Samuels.

The footnotes are an important part of the report. In many cases they provide the only means to a full understanding of the statistical data, or they help to correct a false impression which the statistical data alone may give. As an example, in Table XXVII, part 1, there are six cases of "unsatisfactory ground fault neutralizer practice" mentioned; however, footnotes (*n*) and (*o*) indicate troubles which have nothing to do with the operation of the ground fault neutralizer as such; footnote (*m*) is of a similar nature, at least it is not quite clear for what reason arc extinction should not be successful since the type of pole or tower construction has hardly any influence on the voltage across the path of arcing.[1] Therefore, if only the *GFN* practice as such were considered the number of unsatisfactory cases would be four or three instead of six, as given in the table.

Another point which deserves emphasis is the increased use of very high impedances (up to the impedance of a potential transformer) in the neutrals of generators, in particular those without feeders at generator

voltage. Tests have shown that there is a distinct advantage in the reduction of generator ground fault currents, in as much as burning damages are reduced considerably; in addition the sensitivity of a special ground relay scheme can be made considerably higher and also more reliable than the conventional differential protection would provide. Some engineers prefer solid or low reactance grounding of the generator neutral in order to make differential protection operate on ground faults as well as on faults between phases. An analysis of all the components of such a scheme reveals, however, that some of the conclusions reached are erroneous. An independent ground fault relaying scheme is in all cases reliable, much more sensitive, will cover grounds inside the generator winding and quite near its neutral point, and damage and repair will be reduced considerably if the ground fault current is reduced as much as possible. This seems to be one of the cases in which Samuels advice should be followed not to repeat previous practices. The reduction of otherwise high ground fault currents will be advantageous in many respects.

Reference

1. The Why and How of Resonant Neutral Grounding, Eric T. B. Gross. *Electric Light and Power*, volume 25, 1947, July and August.

A. A. Johnson: In replying to all of the discussions on this report, I would like to state first of all that the data represent the facts as obtained from the answers given in the questionnaires. The results or conclusions are not the opinions of the committee except where it is so indicated.

Brownlee and Elzi pointed out that the choice of generator grounding is very narrow if the generator must be effectively grounded because of the assumption that the impulse strength of the windings is not more than the crest of the test voltage. At present there are no standards covering impulse strength of generator windings. Experience has shown, however, that ungrounded or resistance grounded generators have been protected well by the use of special rotating machine lightning arresters and surge capacitors. In fact the report shows that 45.3 per cent of all generators are resistance grounded and 9.3 per cent are grounded through potential transformers, a ground fault neutralizer, or are ungrounded. The report certainly shows that most operating companies have no hesitation about using a grounding method which requires the application of line to line rated lightning arresters. In fact the trend is toward less effectively grounded generators systems where it is possible to do so.

Brownlee and Elzi also state that the conclusion "Operating experience presented indicates that on a generator system emphasis should be placed on reducing high ground fault currents . . ." is open to some question. Perhaps this conclusion is questionable, but nevertheless it represents the trend as obtained from the data. Certainly proper consideration should always be given to the speed of operation of relays and circuit breakers as the fast and proper operation of this equipment is very important. The method of grounding may or may not allow high speed operation of relays and circuit breakers as relay co-ordination and the type of intelligence used for relays will affect the speed with which action can be taken. All factors affecting the protection of a system must be considered when any method of grounding is applied.

I think that the discussion presented by W. W. Lewis answers in large part the questions raised in Cissna's discussion. I might add that the sequence ratios in the report were requested primarily to get a record of the practice with respect to transient voltages. Cissna's discussion refers largely to the dynamic displacement of the voltage during unbalanced faults to ground and not to the ratios as used with reference to transient voltages. As Lewis has pointed out, the ratios neglecting R_1 and R_2 give safe results for application work. Of course, where more accurate results are desired or where R_1 or R_2 are large with respect to other constants, the voltages should be calculated. A curve such as that shown by Cissna would be helpful.

Commenting on the discussion by M. M. Samuels, the protective devices committee and the fault limiting devices subcommittee have known for some time that a guide for the grounding of generator and transmission and distribution systems was desired. However, before such a guide could be prepared it was necessary to know the existing grounding practices. The present report gives the practices and work has been started on the preparation of guides for the grounding of generator systems and transmission and distribution systems. These guides cover the voltage classes covered in the paper.

The discussion by Gross re-emphasizes the need for a real study of the problems associated with the grounding of power systems. The report contains a number of inconsistencies with respect to grounding practices and, therefore, one cannot conclude from the data in the report what the proper grounding method should be. It is hoped that the guides on grounding of generator and transmission and distribution systems will be a step forward in outlining proper grounding procedures.

S. B. Crary's comments on the report summarized the problem of protecting generators and transmission and distribution systems very well. However, several points might be added to his discussion. Relative to the protection of machines against failure (part *A*) it is stated that the transient overvoltage protection is accomplished most completely by modern surge voltage protective equipment at the terminals of the machine. This is certainly true except that I believe the surge protective equipment should be looked upon as the last line of defense in the protection of a machine. Where possible the grounding method should be such that transient overvoltages are limited to such values that the surge protective equipment does not have to function. The grounding device should serve not only to limit possible fault currents involving ground, but it also should have such characteristics as to limit transient overvoltages to values less than the test voltages applied to the machine. Under part *B* of protection of machine against failure it is stated that for reactance grounding the ratio X_0/X_1 should be equal to or greater than one for the machine branch of the circuit. This will limit the value of current in the machine winding to a safe value, but a limitation should be placed on the maximum value of X_0/X_1 in order to protect machine windings against possible excessive transient overvoltage. Such a ratio has been established as X_0/X_1 equal to a maximum of three. Here again the X_0/X_1 ratio is established at such a level as to limit transient voltages to values below the protective level afforded by surge protection on the terminals of the machine.

Under part II of Crary's discussion, part *A* states that this can be accomplished "primarily" by accurate fault detection and prompt and reliable clearing of machine. I think that a limitation should be placed in this category also which states that X_0/X_1 ratio should be equal to or greater than one in order to protect the windings against mechanical damage.

Crary's discussion also states that for ratios of X_0/X_1 in the range of 3 to 10 do not necessarily lead to excessive voltages. It is further stated that excessively high voltages do not appear to occur until the value of X_0/X_1 higher than 10 is obtained. It is further stated that above a ratio of 10 transient overvoltages due to switching may become quite vicious. In view of these statements, therefore, it would appear that a ratio of X_0/X_1 of 3 to 10 might be questionable, particularly near the upper value of this range. It is believed, therefore, that a ratio of three is a safe conservative figure and should be used as a guide wherever possible.

I would like again to express the appreciation of the protective devices committee, the fault limiting devices subcommittee, and the working group for the co-operation received from the utilities in supplying answers to the questions in the questionnaire. Because of this co-operation the report was possible.

Switching High-Voltage Transmission Lines

I. B. JOHNSON
MEMBER AIEE

J. R. WILSON
NONMEMBER AIEE

IT is the purpose of this paper to present results and conclusions drawn from a study of switching surges including the effects of line voltage and length, lightning arrester, circuit breaker, and system characteristics. This information should be of value in the design of future high-voltage long-distance transmission systems.

An important element in the cost of high-voltage transmission systems is the level of insulation used in the transmission lines and terminal equipment. Rational reductions in insulation result in appreciable economic advantages.[1]

A primary requirement of insulation is the ability of the insulation to withstand transient overvoltages, particularly those caused by lightning. On lines, overhead ground wires and low tower footing resistance are used to assure that the impulse level ordinarily will not be exceeded by lightning surges,[2] whereas on terminal equipment, the use of properly located lightning arresters is considered essential.

Based on the experience of the higher voltage systems, outages due to lightning are not expected to increase with further increase in system voltage.[3] It is known, however, that the operation of lightning arresters in some systems is caused more frequently by switching surges than by lightning surges. Information, therefore, is desired on the severity of switching surges with regard to voltage magnitude and duration, and arrester discharge phenomena that could be experienced on a future transmission system of greater length and operating at higher voltage levels than the present-day maximum.

Nature of Problem

The condition most conducive to severe switching surges occurs when the arc is permitted to restrike across the parting contacts of a circuit breaker attempting to interrupt line charging current.[4] The time and number of restrikes are usually random in occurrence when the circuit breaker does not include effective arc-controlling means for the lower current values.

For convenience, the events associated with such restriking can be assumed to have four phases as follows:

I. The initial conditions of the line at the instant of the first current interruption.

II. The period between the first current interruption and the first restrike of the arc. Of interest in this period are (*a*) the rate of rise of voltage across the circuit breaker contacts, as determined by the variations in the voltage on the generator side of the circuit breaker and the variation in voltage on the line side, and (*b*), the rate of recovery of the dielectric strength of the circuit breaker. The variation in voltage on the line side will be determined by such factors as the redistribution of energy on the line, and the effect of connected apparatus such as a transformer (high or low side switching of line) or circuit breaker construction (absence or presence of shunting resistance across the parting contacts).

III. The period from the first restrike to the operation of the lightning arrester. The nature of the resulting switching surges is of interest during this interval.

IV. The period of lightning arrester operation. Of importance in this phase are the magnitude and duration of lightning arrester current and voltage insofar as a measure of duty and a measure of protection are obtained.

Assumptions

The analyses were made using a representation of the circuit in miniature.[5] The assumptions involved are these

1. The miniature system is representative of high-voltage systems having solidly grounded neutrals. In this study the line to line operating voltage is 360 kv.

2. The transmission system in miniature is shown schematically in Figures 1 and 2. In Figure 1 the sine wave generator represents a generating station providing excitation through the step-up supply transformers to line sections simulating various lengths of transmission line up to 400 miles in length. The transmission line is open-circuited at the receiving end. With switches 4, 5, and 6 open, switches 1, 2, and 3 representing circuit breakers simulate high-voltage switching of the line on the high side of the supply transformers. With switches 4, 5, and 6 closed, switches 1, 2, and 3 simulate low voltage switching of the line on the primary side of an autotransformer insofar as the effects of the magnetizing reactance of the grounded neutral line transformers are obtained on restriking phenomena between the

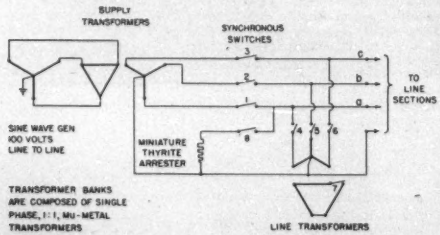

Figure 1. Simulated high and low voltage switching—connections for miniature system

With switches 4, 5, and 6 open high-voltage switching of line is simulated. With switches closed low-voltage switching of line is simulated

Paper 47-238, recommended by the AIEE committee on transmission and distribution and approved by the AIEE technical program committee for presentation at the AIEE Midwest general meeting, Chicago, Ill., November 3–7, 1947. Manuscript submitted, August 21, 1947; made available for printing October 1, 1947.

I. B. JOHNSON and J. R. WILSON are with the General Electric Company, Schenectady, N. Y.

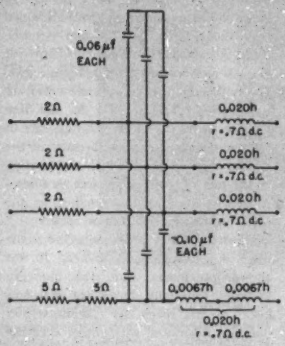

Figure 2. Miniature line section for ten miles of line

charged line and supply voltage, and on the trapped charge and surges of the line. The effects of leakage reactance were neglected. Switch 7 was used to determine the effect of an open or closed delta with the line transformers on the system for low-voltage switching. Switch 8 was used to close the lightning arrester circuit when switching surge voltages reached the value corresponding to the spark-over voltage of the gaps in the station-type lightning arresters. In Figure 2, a complete line section of the transient analyzer is shown. The values of line capacitance and inductance are equivalent approximately to 10 miles of high-voltage transmission line. By means of short-circuiting leads, the effect of some variations in line resistance and ground impedance can be observed.

3. The lightning arrester is simulated as described in Appendix I. The average breakdown voltage of the lightning arrester gaps is 2.4 times the normal crest line-to-neutral voltage and all gaps spark-over at this voltage.

4. In this study there is only one lightning arrester located at the sending end of the transmission line.

5. The transformers are represented in miniature as described in Appendix II. As indicated there, the miniature 2-winding transformers are equivalent in 3-phase kilovolt-ampere rating to the surge impedance loading of the lines at 360 kv. The transformers are nonresonating.

6. The restriking of the arc in the circuit breaker is accomplished by the opening and closing of mechanical switches (switches 1, 2, and 3 of Figure 1). All circuit interruptions are made at a normal or natural frequency current zero. The arc drop is zero. There is no shunting resistance across the interrupting contacts.

7. Unless mentioned otherwise, switching operations occur on one pole with the other two poles open.

8. The switching operation can be either of one of two types; namely, high-voltage switching between the high side of the transformer and the line, or low-voltage switching of the line on the low-voltage side of an autotransformer.

9. Lines to be switched are 100, 200, 300, or 400 miles in length.

Phase I. Initial Conditions

Interruption of 60-cycle charging current of a lumped capacitance at a current zero occurs with the voltage at crest, resulting in a storage of energy in the capacitor proportional to the square of this voltage. In the interruption of line charging current at a current zero, however, the line voltage is not necessarily at crest value and will depend upon the resistivity of the line and ground return and the length of line switched. Also, the magnitude of the voltage at the interrupter is not distributed uniformly along the line but varies as a consequence of the space phase displacement of the 60-cycle line-charging voltage along the length of the line and of the increase in voltage from the flow of the line charging current through the line inductance.

For a 400-mile line with $R_l/X_{ll}=0.13$, $R_0/X_{ll}=4.50$, $X_m/X_{ll}=4$, $X_{co}/X_{cl}=1.6$, zero value of the charging current lags the crest value of the voltage by the order of 30 degrees. For lines 100 to 400 miles in length with $R_l/X_{ll}=0.13$, $R_0/X_{ll}=0.13$, $X_m/X_{ll}=1$, $X_{co}/X_{cl}=1.6$, the instant of current zero at the interrupter is practically in phase with the crest of the voltage.

In Figure 3 the upper curve shows the energy trapped on the line in per unit of the energy trapped on the 100-mile line. The comparison was made by taking the energy as proportional to the squared value of the final steady-state uniform voltage—as recorded by an oscilloscope—existing on the miniature line after interruption of line charging current at a current zero. Practically, the 100-mile line is charged at a uniform voltage equal to the crest value at the interrupter. The curve holds, substantially, for lines with the range of parameters given in the preceding paragraph.

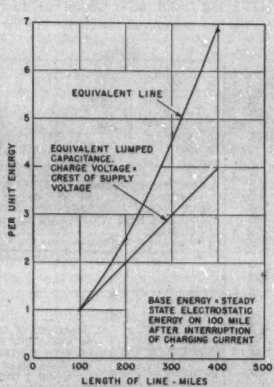

Figure 3. Initial energy trapped on line in per unit versus length of line opened on charging current

As a further comparison in Figure 3, the lower curve shows the per unit energy if each length of line were charged uniformly to the crest voltage at the circuit breaker. This curve is of interest in that it represents the energy stored on a lumped capacitance equivalent to a given length of line.

Phase II. Initial Recovery Voltages

Initial recovery voltages are discussed under two groups on the basis of (1) high voltage switching or (2) low voltage switching.

Group 1

Using the interrupting switch on the high-voltage side of the transformer between the transformer and the line, high-voltage switching is simulated. For no terminal equipment connected to the line, the voltage variations across the switch for a 100-mile line and a 400-mile line are shown in the two lower curves of Figure 4 as recorded by the cathode ray oscilloscope on the miniature system. Because of the initial nonuniform energy distribution of the longer line, greater average rate of voltage rise and greater peak recovery voltage are experienced.

These results show peak voltages of two or more times the normal crest line-to-neutral voltage across the interrupting switch occurring a half cycle after interruption, where time is measured from the crest of voltage wave at or in the immediate neighborhood of the current zero of interruption.

Group 2

Connecting a saturable reactor on the line side of the interrupting switch, low-voltage switching is simulated. For no other terminal equipment connected to the line, the voltage variations across the circuit breaker for 100- and 400-mile lines are shown in the upper two curves of Figure 4.

In Figure 5 are shown the maximum recovery voltage and the time to maximum voltage as functions of line length and various values of circuit parameters.

In oscillogram 189-11 of Figure 8 is shown the ferro-nonlinear oscillation in

the line voltage at the sending end for a 100-mile line.

On the basis of these results and numerous other observations, it is indicated

(*a*). That after a time delay of the order of a two or three thousand microseconds from the instant of interruption of charging current at a current zero the effect of the transformer saturating causes a sudden reversal of the recovery voltage.

(*b*). That the maximum recovery voltage across the interrupter during the first half cycle from the time of crest voltage at interruption will be of the order of normal line to neutral crest voltage or less.

(*c*). That the maximum recovery voltage across the interrupter during the interval between the first half cycle and the first cycle and a half from the time of crest voltage at interruption will be of the order of twice normal line-to-neutral crest voltage or less.

(*d*). That the results from traveling wave phenomena on equivalent lines and from circuit oscillation phenomena using lumped capacitance are in general agreement with regard to items (*a*), (*b*), and (*c*).

These indications hold with the delta opened or closed by switch 7 in Figure 1. They hold also with switches 5 and 6 closed connecting in the autotransformers on these phases with the delta opened or closed when energizing and switching on phase *a* only. The indications again are the same when energizing and switching all phases with phase *a* the last to clear and with an open or closed delta.

Phase III. Some Effects of Restriking

In the miniature system studied having no transformers or lightning arresters connected to the switched line, one restrike at the first peak recovery voltage across the switch resulted in the maximum

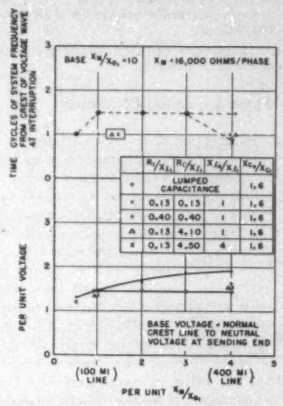

Figure 5. Maximum recovery voltage across circuit breaker on interruption of charging current and time to maximum voltage versus ratio of magnetizing reactance of transformer to positive sequence capacitive reactance of line—X_m/X_{c1}

line-to-ground voltages at the interrupting switch as shown in Figure 6 for single-phase or 3-phase switching and for various values of line constants. The restrike current was interrupted at the first subsequent zero of its natural frequency following initiation. These line voltages, it is seen, are of the order of $2^1/_2$ times normal, and if a lightning arrester were connected to the line, these voltages would cause its operation.

In Figure 7 are shown oscillograms 175-3, 180-7, and 180-14 for the variation in the line voltages at the circuit breaker resulting from one restrike with a lumped capacitance and with 100- and 400-mile lines. Oscillogram 184-9 in this figure for the 100-mile line on a different time scale shows the relatively slow time variation in voltages experienced. As the line lengths are increased the average rate of voltage change decreases, because of the greater time required for waves traveling at the rate of about 1,000 feet per microsecond to go from the sending to the receiving ends of the line and back.

When a transformer is connected to the line side of the circuit breaker, it was shown previously that the recovery voltages, especially during the first half cycle, do not reach the magnitude and duration associated with those occurring on lines alone. Consequently the probability of restriking and the magnitude of the restrike voltages should be lower. In Figure 6 are shown the range of maximum line to ground voltages as the result of one restrike observed for the 100- and 400-mile lines when these restrikes were initiated at maximum recovery voltage in the regions of 1, $1^1/_2$, or 2 cycles after interruption. The range of values are of the same order for both line lengths and are the results of single- and 3-pole switching for all the circuit conditions shown in this figure. The range of voltages is 60 per cent to 80 per cent of the order of voltages for the lines without the transformer and are below the lightning arrester spark-over voltage by about the same percentage margin.

Restriking in the period of the first half

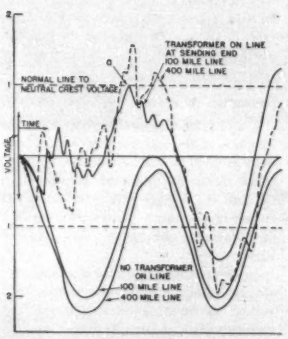

Figure 4. Recovery voltages across interrupting switch

Figure 6. Maximum line-to-neutral voltage at sending end from one restrike versus length of line switched

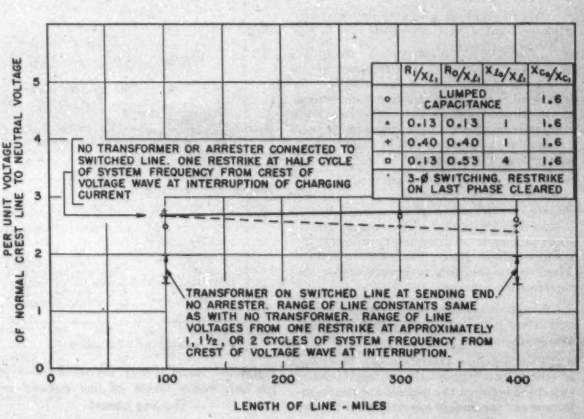

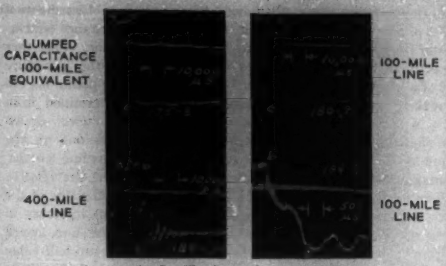

Figure 7. Variation in line voltage at circuit breaker for interruption of charging current at a, initiation of restrike at b, and interruption of restrike transient at c

Line—$R_l/X_{ll}=0.13$, $R_s/X_{ll}=0.13$, $X_{lt}/X_{ll}=1$, $X_{cs}/X_{cl}=1.6$

cycle after interruption did not produce any abnormal line voltages. Restriking in period during the second half cycle of interruption such as at point *a* of Figure 4 or of oscillogram 189-8 in Figure 8 for a 100-mile line resulted in the line voltage at the circuit breaker as shown in oscillogram 189-12 and in the recovery voltage of oscillogram 189-9, both oscillograms in Figure 8. The maximum line voltage following the restrike is about 1.63 times normal crest line to neutral as shown at *a* of oscillogram 189-12. It is to be noted also in oscillogram 189-12 that the effect of the transformer saturating causes several sudden reversals of the line voltage, the first occurring several thousand microseconds from the time of maximum line voltage caused by restriking.

For the effects of two restrikes—one at point *a* of oscillogram 189-8 and one at point *b* of oscillogram 189-9 of Figure 8—the recovery voltage, the line voltage at the sending end, the input line currents, and the line voltage at the receiving end are as shown in oscillogram 189-10, 189-13, 189-15, and 189-16 in Figure 8. At the sending end to the maximum voltage from restriking is the same as for one restrike only. At the receiving end the maximum voltage is caused by the first restrike and is of the order of 1.8 times normal line-to-neutral crest voltage at the sending end.

Although transformers connected to lines being switched lower the probability of obtaining abnormal line voltages, repeated restriking can build up voltages in excess of those required for lightning arrester operation, as shown in oscillogram 176-3 in Figure 9. This oscillogram is for the case of a lumped capacitance equivalent to 100 miles of line connected across the transformer. The first and second restrikes occur at points *a* and *b*, respectively. The maximum voltage following the second restrike is about 2.63 times normal line-to-neutral voltage.

Phase IV. Arrester Operation

The volt-time character of surges is a determining factor in transmission system insulation. To limit surges within prescribed limits, lightning arresters are used to provide a margin of protection of insulation on terminal equipment. It is of importance, therefore, to know the nature of the current discharges through a lightning arrester produced by switching surges and of the resulting voltage drops across the lightning arrester.

On the nature of discharges through a lightning arrester, Figure 10 shows the difference in the voltage variation across a lightning arrester between that from a line and that from a lumped capacitance equivalent to the line. The single-phase 200-mile artificial line shown in this figure was charged to a steady state voltage value of 2.4 times the normal crest line-to-ground voltage of the line and then discharged through the lightning arrester by closing switch *S*, and similarly for the lumped capacitance. The miniature lightning arrester characteristic is shown in Figure 11. As seen from Figures 10 and 11 there is a sudden drop to about 75 per cent of the spark-over voltage at the lightning arrester end of the line because of line regulation upon the flow of current through the line and lightning arrester. The voltage after spark-over remains constant for a period of 1,900 microseconds which corresponds approximately to the time required of a surge traveling at the rate of 1,000 feet per microsecond to go from one end of the 200-mile line and back. The other lower voltage steps of the line discharge are of similar duration. On the basis of a 360-kv lightning arrester having the same characteristics shown in Figure 11, the maximum discharge current from the line is of the order of 500 amperes. The second step of the discharge represents a current of 125 amperes. For the lumped capacitance, a smooth curve decay of voltage and current results, the initial current through the lightning arrester being much greater than for the line. Generally, it might be mentioned that the effects with lumped capacitance obtained here and in the foregoing phases of restriking are more representative of cable than line dropping.

Switching surges initiated by the restriking of the arc across the parting contacts of the interrupting switch result in line voltages at the lightning arrester as

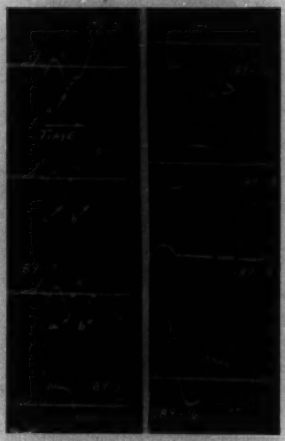

Figure 8. Low-voltage switching of 100-mile line

Oscillogram 189-8—Circuit breaker recovery voltage from line dropping
Oscillogram 189-9—Circuit breaker recovery voltage from line dropping with restrike at a
Oscillogram 189-10—Circuit breaker recovery voltage from line dropping with restrikes at a and b
Oscillogram 189-11—Line to ground voltage at sending end. Line dropped at a
Oscillogram 189-12—Line to ground voltage at sending end. Maximum voltage from restrike at a
Oscillogram 189-13—Line to ground voltage at sending end from line dropping and two restrikes
Oscillogram 189-15—Input current from line dropping and two restrikes
Oscillogram 189-16—Line to ground voltage at receiving end from line dropping and two restrikes at sending end

Line—$R_l/X_{ll}=0.13$, $R_s/X_{ll}=0.13$, $X_{lt}/X_{ll}=1$, $X_{cs}/X_{cl}=1.6$

Figure 9. Line to ground voltages for successive restriking with low-voltage switching

Capacitor equivalent to 100 miles of line connected across secondary winding of transformer. Circuit breaker on primary side of transformer

Oscillograms 176-3, 176-5—First restrike at *a*, second restrike at *b*

Oscillogram 176-5—Lightning arrester switched in at *c*, V_ϕ—normal crest line to neutral voltage

shown in oscillograms 183-3, 183-8, 184-3, and 184-5 in Figure 12*A* for lines of 400, 300, 200, and 100 miles, respectively. These oscillograms show a restrike starting at point *a* followed by switching in of the lightning arrester at point *b*. Oscillogram 184-7 in this figure is the voltage variation across a lumped capacitance and lightning arrester combination in which the capacitance is equivalent to 100 miles of line. The restrikes occurred a half cycle from the crest of the voltage at the time of current zero of interruption.

In Figure 12*B* are shown oscillograms 186-6, 187-2, and 187-3 of the line voltage at the lightning arrester for 400, 300, and 200 miles of line, respectively, with the restrikes occurring 1/3 of a cycle after the crest of the voltage at the time of current zero of interruption.

In Figure 12*C* are shown oscillograms 186-8, 187-6, 187-4, and 186-13 for the line voltages at the lightning arrester for 400, 300, 200, and 100 miles of line for the condition of two restrikes, one at point *a* and one at point *c*. These restrikes occur at 1/3 and 5/6 cycle from the crest of the voltage wave at the time of current zero of interruption. The lightning arrester was continuously in the circuit from the instant of the first spark-over of it by the first restrike.

A replot of oscillogram 187-2 is shown in Figure 13 together with the resulting lightning arrester current calculated from the curve of Figure 11.

In all of the oscillograms and curves of the foregoing based on the effects of restriking phenomena, the line constants in Figure 2 were arranged such that $R_l/X_{lt}=0.13$, $R_0/X_{lt}=0.13$, $X_m/X_{lt}=1$, and $X_{e0}/X_{e1}=1.6$. With these line constants representative discharge effects through the lightning arrester were obtained.

From the switching surge results based on restriking Figure 14 was drawn and shows the time after spark-over to half value of lightning arrester spark-over voltage as a function of the length of line switched. The curve was obtained with a circuit using lumped capacitance equivalent to various lengths of line. The other points indicated are for the miniature transmission system. The points for the miniature system were determined from an approximate mean curve drawn through the voltage variations on the oscillograms for the various line lengths. These results indicate that the relative duration of the time to half value of the *IR* lightning arrester drop increases in direct proportion with the line length switched and that the times to half value are of the order of 2,000 and 8,000 microseconds for the 100- and 400-mile lines, respectively.

In Figure 15 is shown the effective duration of current discharge through the lightning arrester as a function of the length of line switched. The duration is measured from the time of spark-over to the time of half value of the current. In Figure 16 are shown for this period the average current, and the ratio of the maximum current to the average current involved in the discharge. It is seen that a restrike initiated at 1/3 cycle from the crest of the voltage wave at interruption rather than at 1/2 cycle with maximum recovery across the interrupting switch causes a larger average current and a longer duration of current in the discharge upon switching the longer lines, whereas the converse is true for the shorter lines. This is to be expected from the fact that a restrike at a 1/2 cycle, for example, in dropping 400 miles of line (1/8 wave length) results in a component of the traveling surge being determined by that portion of the 60-cycle supply voltage between crest and zero, whereas restriking at 1/3 cycle results in this component being determined approximately by the central crest portion of the supply voltage. The maximum average currents to be expected

Figure 10 (below left). Discharge characteristics of lumped capacitance and line

Lightning arrester voltage versus duration of discharge

Figure 11 (below right). Effect of line regulation upon discharge of line through a lightning arrester

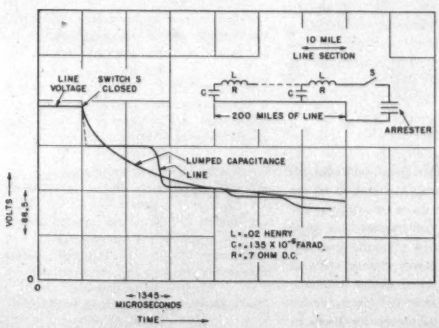

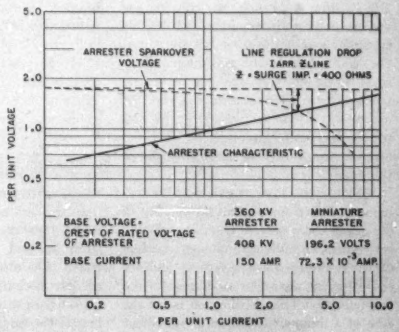

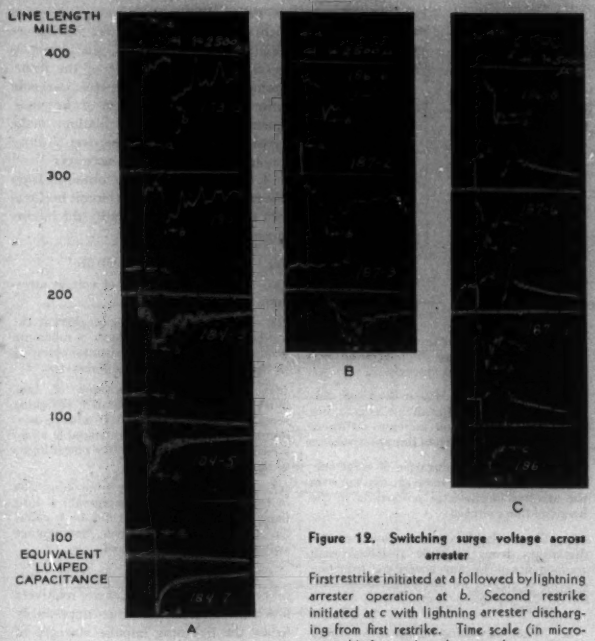

Figure 12. Switching surge voltage across arrester

First restrike initiated at a followed by lightning arrester operation at b. Second restrike initiated at c with lightning arrester discharging from first restrike. Time scale (in microseconds) for each column is shown in top oscillogram

Line—$R_1/X_{l1}=0.13$, $R_0/X_{l1}=0.13$, $X_{l0}/X_{l1}=1$, $X_{c0}/X_{c1}=1.6$

Restrikes measured from crest of voltage at interruption of charging current—*A*, one at 1/2 cycle; *B*, one at 1/3 cycle; *C*, one at 1/3 cycle and one at 5/6 cycle

from one restrike during the period to half value of lightning arrester current are of the order of 800 to 900 amperes for a 360-kv system and are independent of the line length considered; the crest currents are 1.4 times greater than the average values; the duration of the current increases with line length from about 700 microseconds for a 100-mile line to approximately 2,800 microseconds for a 400-mile line.

If two restrikes are initiated, the first at 1/3 cycle and the second at 5/6 cycle from the crest voltage at interruption, the voltage at the lightning arrester at the time of the second restrike as a function of line length is as shown in Figure 17. In per unit of normal line-to-neutral crest voltage, the recovery voltage across the circuit breaker at the time of the second restrike is somewhat less than two times for the 100-mile line and approaches three times for the 400-mile line. This is to be expected in as much as the time from the first restrike to spark-over plus the time of duration of maximum voltage associated with the effective duration of current through the lightning arrester increases approximately in proportion to the increase in the length of line switched. The probability, therefore, of multiple restriking producing multiple discharges increases with the length of the line switched.

For the effects of two restrikes in dropping a 300-mile line, the results are as shown in Figure 18. Here, as a measure of the effective duration of the current, of the time sequence of events, the curves are plotted as

$$\int_0^t I_{\text{arrester}}\,dt$$

versus time in microseconds. These curves indicate that with multiple restriking on the longer lines, multiple discharges of current can be expected of the same effective duration and magnitude as obtained from one restrike.

As to the effects of a transformer connected to the line, this is illustrated in oscillogram 176-5 of Figure 9 for a lumped capacitance equivalent to 100 miles of line. Because of existence of the ferro-

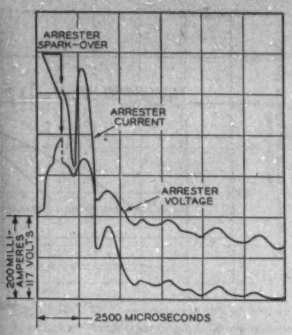

Figure 13. Lightning arrester current and voltage magnified and replotted from oscillogram 187-2

Line—$R_1/X_{l1}=0.13$, $R_0/X_{l1}=0.13$, $X_{l0}/X_{l1}=1$, $X_{c0}/X_{c1}=1.6$

One restrike 1/3 cycle from crest at voltage at interruption of charging current; 300-mile line

nonlinear oscillations during lightning arrester operation, interruption of discharge at the first or subsequent current zeros can occur.

An investigation of lightning discharges indicates that lightning arrester discharge currents have fewer components than found in direct strokes and are of lower crest magnitude with only 30 per cent exceeding 1,000 amperes. It also is indicated that the long-duration low-magnitude portions of direct strokes may be as high as 1,000 amperes with durations from 50 to 20,000 microseconds while lightning discharges through lightning arresters seldom last more than 300 microseconds.[8] In magnitude and duration, then, the current discharges that could be expected from switching surges

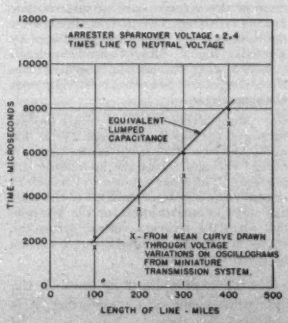

Figure 14. Time to half value of lightning arrester spark-over voltage versus length of line switched

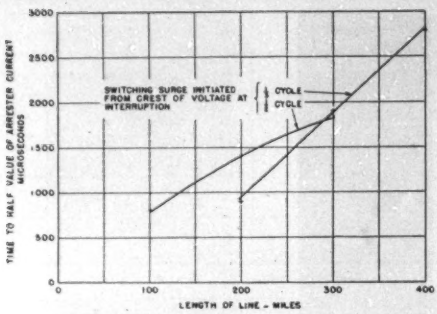

Figure 15. Effective duration of lightning arrester current discharge versus length of line switched

Line—$R_l/X_{l1}=0.13$, $R_a/X_{l1}=0.13$, $X_{la}/X_{l1}=1$, $X_{ca}/X_{cl}=1.6$

on long lines appear comparable to the long-duration low-magnitude portions measured in direct lightning strokes. And in terms of severity of discharge duty on lightning arresters, it appears, therefore, that the switching surge on long-distance high-voltage lines is of primary importance.

Summary and Conclusions

1. When switching surges are initiated by restriking upon dropping long lines on the high-voltage side of a transformer, it is indicated that

(*a*). On the basis of the systems studied, in which the maximum surge voltages of about 2.5 times line-to-neutral crest voltage were reached from one restrike, the time to lightning arrester spark-over voltage and the time to subsequent half value increase in proportion to the length of line switched. For the 100-mile line these times are of the order of 1,000 and 2,000 microseconds, respectively.

(*b*). Peak recovery voltages across the circuit breaker interrupting charging current without restriking reach two or more times the normal line-to-neutral crest voltage at a half cycle of system frequency from the crest of the voltage wave at interruption. During maximum current flow through the lightning arrester from a surge initiated by a restrike, higher voltages across the circuit breaker may be obtained, approaching three times normal line-to-neutral crest voltage on the longer lines.

(*c*). More severe switching surges are experienced for line lengths from 250 to 400 miles when restrikes occur before peak recovery voltages across the interrupter are reached. The range extends to 1/3 cycle of system frequency from the crest of the voltage wave at interruption for the 400-mile line when the recovery voltage across the circuit breaker has reached about 3/4 of the peak recovery voltage.

2. When dropping long lines on the high-voltage side of a transformer, it is indicated also, that

(*a*). The severity of switching surge discharges through an arrester is of equal if not of primary importance as compared with expected lightning surge discharges on well shielded and grounded systems.

(*b*). The maximum arrester discharge currents are comparable for all line lengths, but their effective duration increases in direct proportion to the length of line switched.

(*c*). On the basis of duration of surge current initiated by one restrike, the duty on the arrester increases in proportion to the length of line switched.

(*d*). The probability of multiple arrester discharges from multiple restrikes with components of the same severity as from one restrike is greater for the longer lines than for the shorter lines.

3. When switching on the low-voltage side of a transformer in comparison with switching on the high-voltage side, the recovery voltages across the interrupter as the result of ferro-nonlinear oscillations are reduced appreciably both in average rate of rise and magnitude. As a consequence the probability of restriking and of the resulting surge voltages reaching lightning arrester spark-over voltage are diminished greatly. If spark-over is reached, the initial effect of the transformer saturating in several thousand microseconds and the effect of the subsequent ferro-nonlinear oscillations make possible a reduction in the over-all duty imposed on the lightning arrester.

4. Switching surges as obtained from the restriking of the arc in circuit breakers can be reduced in severity by the following means:

(*a*). Grounding system neutrals.[7]

(*b*). Rational application of voltage arresters.

(*c*). Use of impulse circuit breakers of the stored energy type that have a minimum tendency to restrike[8] or resistance shunting of the contacts on the nonimpulse type.[4,9]

(*d*). Switching short sections of line. With lines operating in parallel, switching sections of line of about 100 miles is economically feasible and also desirable in increasing the transient stability power limits of the system.[1]

(*e*). Switching lines on the low-voltage side of the transformer. On sectionalized long lines, this, in general, will not be feasible. On cable circuits, however, low-voltage switching is entirely practical.

5. Lightning arrester discharge currents from switching surges are relatively low and result in *IR* drops appreciably below the lightning impulse strength of the insulation, which in this study was below the 60-cycle spark-over voltage of the lightning arrester. It appears that the switching surge is not a determining factor in the insulation requirements of lightning arrester protected systems.

6. Through the use of a representation

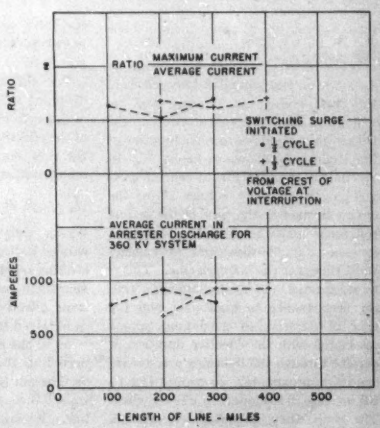

Figure 16. Lightning arrester discharge characteristics during period from time of spark-over to half value of lightning arrester current versus length of line switched

Line—$R_l/X_{l1}=0.13$, $R_a/X_{l1}=0.13$, $X_{la}/X_{l1}=1$, $X_{ca}/X_{cl}=1.6$

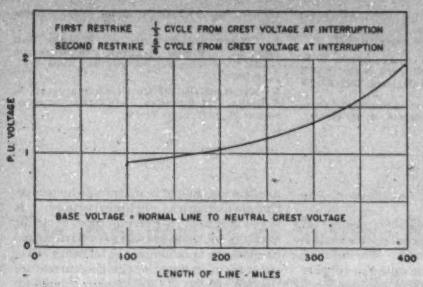

Figure 17 (above left). Lightning arrester voltage at time of second restrike versus length of line switched

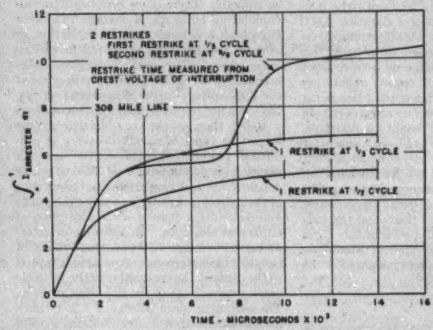

Figure 18. Lightning arrester discharge characteristics versus duration of discharge

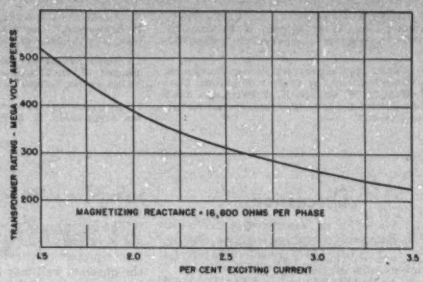

Figure 19. Kilovolt-ampere rating of 360-kv transformer bank represented in miniature system versus assumed exciting current

in miniature, an effective method has been demonstrated for the study of related phenomena involving voltage arresters and switching surges.

Appendix I. Lightning Arrester for Miniature System Study

For a solidly grounded neutral system in which the ratio of zero sequence reactance X_0 to positive sequence reactance X_1 lies between 0 and +3.0 for a ground fault at any location in the system, it is the practice to choose a lightning arrester with a maximum valve rating equal to 80 per cent of the normal line-to-line system voltage. Thus, for the system voltage of 360 kv being considered in this paper, an arrester rated at 288 kv rms (line to ground) could be used.

The minimum average voltage required to spark over a lightning arrester for a grounded neutral system is assumed equal to 2.4 times the crest value of the line-to-neutral voltage of the system, or for a 360-kv system,

$$\frac{360}{\sqrt{3}}\times 2.4\times 1.41 = 706 \text{ kv crest}$$

For the switching surge tests recorded in this paper, it is assumed that all of the gaps in each unit arrester of the stack spark over when the crest minimum spark-over voltage is reached.

Representation on the transient analyzer of the effects of transients in transmission lines and terminal equipment is accomplished by a reduction in the applied voltage with the equivalent circuit parameters held equal to those of the actual system. To get a lightning arrester for the miniature system with approximate characteristics to that of an actual lightning arrester for operation in a 360-kv system, the calculated value of resistance of the lightning arrester at the crest voltage rating is preserved; and the per cent variation in the current for a given voltage change across the lightning arrester must be the same in the miniature and actual systems. These requirements were met through the use of small thyrite disks. Through the proper selection and combination of several of these disks in series, the desired resistance at the crest voltage rating of the lightning arrester was obtained while the percentage variation in current as a function of voltage of these disks was approximately similar to the actual unit.

The choice of miniature system voltage level is limited to a line-to-ground voltage of 100 volts by the requirements of the transformer saturation characteristics. The crest of the rated voltage of the large lightning arrester units is 17 kv. The following equations then must be met:

$$\frac{24 \text{ units}\times 17 \text{ kv per unit}}{\dfrac{360}{\sqrt{3}}\times\sqrt{2}} = \frac{\text{miniature lightning arrester rated voltage}}{100\times\sqrt{2}}$$

$$\frac{24 \text{ units}\times 17 \text{ kv per unit}}{\text{Current at rated voltage}} = \frac{\text{miniature lightning arrester rated voltage}}{\text{miniature lightning arrester current at rated voltage}}$$

The linear curve in Figure 11 shows the volt-current characteristic of the miniature lightning arrester.

Appendix II. Transformer Representation in Miniature

The 2-winding transformers used in the miniature system were designed with saturation characteristics simulating modern large capacity transformers. The magnetizing reactance of these transformers is 16,600 ohms per phase at the normal operating voltage. Over-all, the transformers are considered to be qualitative approximations of high-voltage power transformers.

The kilovolt-ampere rating of the transformer bank represented in the miniature system is determined from the system voltage and the assumed exciting current. For example, if the system voltage is 360 kv and the exciting current is 2.5 per cent, the base ohms is 415 ohms (=2.5 per cent×16,600) and the transformer bank rating is 313,000 kva (=(360)²×1,000/415). In Figure 19 is shown the variation in transformer capacity as a function of the exciting current. The kilovolt-ampere capacity of the power transformers as represented in the miniature system appears to be of the order of the surge impedance loading and in the range of the economical loadings of the 360-kv line.[1]

References

1. Economics of Long-Distance A-C Power Transmission, S. B. Crary, I. B. Johnson. AIEE Transactions, volume 66, 1947, pages 1092–1102.

2. Co-ordination of Insulation and Spacing of Transmission Line Conductors, W. W. Lewis. AIEE Transactions, volume 65, 1946, October section, pages 600–3.

3. Performance of 161-Kv and 115-Kv Transmission Lines, K. E. Hapgood, C. P. Almon, Jr. AIEE Transactions, volume 66, 1947, pages 863–71.

4. Switching Overvoltage Hazard Eliminated in High-Voltage Oil Circuit Breakers, Lloyd F. Hunt, E. W. Boehne, H. A. Peterson. AIEE Transactions, volume 62, 1943, February section, pages 98–106.

5. An Electric Circuit Transient Analyzer, H. A. Peterson. *General Electric Review*, (Schenectady, N. Y.), volume 42, 1939, pages 394–400.

6. Field Investigations of Lightning, C. F. Wagner, G. D. McCann, Edward Beck. AIEE Transactions, volume 60, 1941, pages 1222–9.

7. System Overvoltages and Lightning Arrester Application, H. A. Peterson, E. M. Hunter. *Electric Light and Power*, (Chicago, Ill.), November 1941.

8. Circuit Breakers for the Boulder Dam Line, D. C. Prince. Electrical Engineering (AIEE Transactions), volume 54, April 1935, pages 366–72.

9. Resistors for 138-Kv Cable Switching, E. K. Sadler, T. M. Blakeslee. AIEE Transactions, volume 66, 1947, pages 39–50.

Discussion

P. L. Bellaschi (consulting engineer, Sharon, Pa.): This paper is of considerable interest for a number of reasons.

Perhaps the first dependable source of data on switching surges comes from the experience presented in an Institute paper in 1937[1] in which it was found that the setting of protective air gaps could be reduced to the equivalent of about 3 times the line-to-ground voltage for well grounded neutral systems without affecting the operation of the gap on switching surge operations. System overvoltages of this order were reported later[2] in an extensive investigation on the 12-kv Chicago system. From a critical survey of this general problem conducted over a period of ten years or more, which has been based on the foregoing experience and findings from here and abroad, I have come to the conclusion that on solidly grounded neutral system of the more recent design and of good behavior, system surges seldom if ever attain $3^1/_2$ times the line-to-ground voltage. A top figure of 3 times is a good figure to consider for insulation design purposes.

However, experience on isolated neutral systems definitely indicates the presence of system overvoltages attaining possibly 5 and 6 times. I am referring here to actual experience and to the more reliable data that have come available in recent years.

The data presented by Johnson and Wilson on high-voltage transmission lines pretty well substantiate the *3 times value* in regard to effectively grounded neutral systems. This paper I believe is an excellent contribution to the switching-surge problem as such, and is timely particularly in connection with the insulation problem in the field of extra high voltages. For it is clear that as we reduce the insulation more and more, switching surges assume increasingly greater importance and accordingly more dependable data become essential both in regard to the surge overvoltages developed and the strength of insulation to surges of this character.

The paper raises a number of points that are of interest from an insulation as well as from a protection standpoint. For instance, the question well may be raised as to what may happen to a lightning arrester when discharging a switching surge of some 900-ampere amplitude and of a duration 8,000 microseconds or more. Are lightning arresters of present-day design satisfactory for such service and can they be used to limit these surges in the same manner as they are applied to protect station apparatus against lightning surges? Here too actual tests on the equipment proper would be desirable. These tests would be of the same character as the switching-surge tests conducted a few years ago by the writer and Rademacher[3] on station and line insulation except that in the tests proposed on the lightning arresters both the voltage across them and the current discharged would be recorded. The duration of the surges applied should be commensurate to the values indicated in the more recent studies.

References

1. Application of Spill Gaps and Selection of Insulation Levels, H. L. Melvin, R. E. Pierce. Electrical Engineering (AIEE Transactions), volume 56, June 1937, pages 689–94.

2. Surges on Chicago 12-Kv System, F. O. Wollaston, H. J. Plumley. AIEE Transactions, volume 60, 1941, June section, pages 260–5.

3. Dielectric Strength of Station and Line Insulation to Switching Surges, P. L. Bellaschi, L. B. Rademacher. AIEE Transactions, volume 65, 1946, pages 1047–54.

I. B. Johnson and **J. R. Wilson**: From a review of the history of field tests and miniature system studies on overvoltages produced by faults and switching surges, it is indicated that voltages of sufficient severity to damage equipment are obtainable in systems wherein a process of cumulative restriking of an arc at successively higher voltages occurs, and wherein the surge voltages are not limited in magnitude by protective devices such as a lightning arrester. It is also indicated that certain types of circuit breakers which do not have effective means to eliminate or minimize the tendency to restrike when interrupting charging current are the only sources of this cumulative build up of voltage. There is no evidence that this cumulative build up of voltage can occur from fault arcs in air, in solid insulation, or under oil as has been suggested in various publications. The old scapegoat phenomena of the arcing ground as the cause of the high-voltage surges experienced on systems has not been verified experimentally.

Based, then, on the arc restriking process in certain types of circuit breakers as producing switching surges of the greatest severity, it is the intent of this paper to demonstrate and emphasize the importance of the lightning arrester as a switching surge voltage limiting device for the protection of apparatus and lines. In lightning-arrester-protected systems the maximum value of the switching surge voltage would be limited to the order of the crest value of the 60-cycle spark-over voltage of the lightning arrester. The switching surge voltage of 5 to 6 times normal for isolated neutral systems quoted by P. L. Bellaschi is representative on systems without lightning arrester protection and would be appreciably lower when limited by them. On solidly grounded systems ($X_0/X_1<3$), the switching surge spark-over voltage of lightning arresters is of the order of 2.4 times the line-to-neutral crest voltage. The value of 3 times normal given by Bellaschi is a little higher than should be expected with rational application of lightning arresters.

Past experience with lightning arrester discharge of switching surges initiated by certain types of circuit breakers on line dropping of long lines has given confidence that lightning arresters with sufficient discharge ability can be built provided the switching surges are minimized by circuit breakers with a minimum tendency to restrike.

The Application of Storage Batteries to the Control of Switchgear

E. A. HOXIE
ASSOCIATE AIEE

THE TOPIC of adequate control voltages for closing electrically operated circuit breakers now is receiving considerable attention from both manufacturers and users of switchgear.

This paper is written in order to present pertinent test data and to offer comments which may be of some assistance in the establishment of a standard practice covering the selection and operation of control batteries capable of meeting the requirements of modern switchgear.

Standard control voltages for closing and tripping electrically operated circuit breakers are defined in the National Electrical Manufacturers Association and the American Standards Association standards. These standards state that the operating voltage ranges of circuit breaker closing and tripping mechanisms, which nominally are rated at 125 volts direct current, are 90 to 130 volts for closing and 70 to 140 volts for tripping. Voltage limitations of indicating lamp assemblies, coils of relays, and control devices also limit the voltage of the control bus to a maximum of 140 volts.

However, it has been pointed out that in some cases the minimum voltage of 90 referred to in the NEMA and ASA standards is not sufficient to obtain proper operation under adverse operating conditions. In December 1943 a publication of a circuit breaker manufacturer stated that in order to realize published circuit breaker performance under maximum fault conditions, a control voltage of 112.5 volts at the closing mechanism terminals was necessary. This value of 112.5 volts is 90 per cent of the nominal 125-volt rating of the mechanism.

The AIEE Standard 19, dated June 1943, covering a-c power circuit breakers also contains a statement to the effect that the rated "making" current and the rated "latching" current of a circuit breaker is based on 90 per cent of rated control voltage being maintained at the closing mechanism of an electrically operated breaker which would be 112.5 volts for a nominally rated 125-volt control bus.

The American Standards for a-c power circuit breakers of the ASA, approved May 16, 1945, under the heading "Rated Making Current and Rated Latching Current" states

> The control voltage at the terminals of the closing mechanism, in the case of electrically operated breakers, is a factor in the determination of these values.

While the special requirements of electrically operated circuit breakers operating under conditions prevailing during a line fault have been pointed out as referred to in the three preceding paragraphs, the standard operating voltage range of 90 to 130 volts as defined by the NEMA and the ASA standards as yet has not been changed.

For many years control storage batteries have been selected on the basis of meeting the requirements of the 90- to 130-volt range at the mechanism, as given in the NEMA and ASA standards, and a maximum allowable control bus voltage of 140. The method used in determining the required capacity of the battery resulted in a battery of liberal size, but it is obvious that with few exceptions these batteries are not capable of providing 112.5 volts at the circuit breaker closing mechanism.

Determination of Required Battery Capacity

Before proceeding further with this discussion, a brief résumé of the factors involved in selecting a battery for a particular installation and the method of operation used may assist in a better understanding of the subject.

It has been accepted practice to select a battery in a given installation which is capable of delivering the maximum monetary current required for circuit-breaker operation, and, in addition, to supply the continuous load and the emergency lighting load for specified times, without the voltage at the battery terminals dropping below 1.75 volts per cell, or 105 volts for a 60-cell nominally rated 125-volt battery. Since there is a possibility that the various loads may be required simultaneously at the end of the discharge period, it is customary to evaluate the battery capacity required for each load singly and to add them together to obtain the total battery capacity. The maximum requirement from the battery occurs during an emergency caused by a failure of the normal power supply to the station lighting and the battery charging equipment, making it necessary for the battery to supply all of the load without assistance from the charging equipment.

On the basis of a minimum operating voltage of 90 and a minimum battery voltage of 105 it will be noted that a 15-volt differential has existed which has been available to counteract IR drop and to provide a factor of safety.

The required battery capacity has been determined on the basis of its furnishing the maximum momentary load for a period of one minute, notwithstanding the fact that this current is normally required for only a fraction of a second. The reason for this was that the voltage of the battery, when discharging at the 1-minute rate to 1.75 volts per cell, reaches a stabilized value after a few seconds, and drops very little, if any, for a minute or more.

It was known that the actual voltage

Paper 47-239, recommended by the AIEE switchgear committee and approved by the AIEE technical program committee for presentation at the AIEE Midwest general meeting, Chicago, Ill., November 3–7, 1947. Manuscript submitted July 24, 1947; made available for printing September 26, 1947.

E. A. Hoxie is electrical engineer, Electric Storage Battery Company, Philadelphia, Pa.

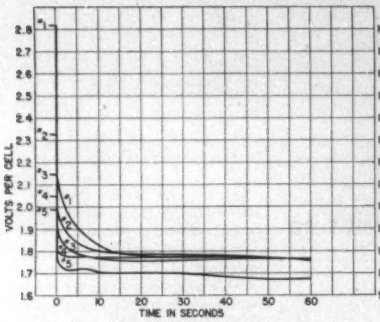

Figure 1. Approximate volt-time characteristics—type *EM-11* Exide chloride cell discharging at 240 to 252 amperes from various full charge voltages and from a 50 per cent discharged condition

Temperature, 77 degrees Fahrenheit; specific gravity, 1.210

Curves 1 to 4—Discharging at 250 amperes
Curve 5—Discharging at 240 amperes

Cell condition:

Curve 1—Fully charged and charging at 8-hour rate
Curve 2—Fully charged and charging at 2.33 volts per cell
Curve 3—Fully charged and floating at 2.15 volts per cell
Curve 4—Fully charged and on open circuit
Curve 5—Fifty per cent discharged and discharging at 12.5 amperes

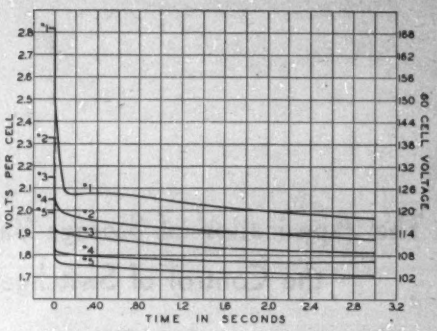

Figure 2. These curves depict the voltage for the first three seconds of the 1-minute period covered by Figure 1

from a fully charged battery during the short intervals of discharge required to close a circuit breaker (usually less than one second) was usually somewhat higher than 1.75 volts per cell. It also was known that the instantaneous discharge voltage was affected by the voltage existing at the battery terminals at the time of load application, but specific information under the conditions encountered in circuit breaker control service was not available. No attempt was made to take advantage of this momentary voltage in excess of 1.75 volts per cell, and any additional voltage obtained was considered as part of the factor of safety.

Method of Operation

The common method of operating these batteries has been to float them continuously by maintaining a voltage of 2.15 volts per cell or 129 volts for a 60-cell battery with occasional equalizing charges at a maximum voltage of 140 volts, or 2.33 volts per cell.

Another method frequently used automatically places the battery on charge once every hour at a rate which is usually between 20 and 50 per cent of the 8-hour discharge rate of the battery in amperes; the charge being terminated by a sensitive inverse temperature compensated voltage relay which operates when the charging voltage reaches 2.31 to 2.33 volts per cell or about 138 to 140 volts for 60 cells, at which point the battery is practically fully charged. Occasional equalizing charges are given at the same charging rate.

Both methods keep the battery at, or very near, the full charge point under normal operating conditions.

At this point it may be in order to state that this method of selecting battery capacity, and the method of operation described, has been in general use for 20 years or more, and, from a battery performance viewpoint, has been entirely satisfactory on the basis of a 90-volt minimum at the closing mechanism. In many installations where conditions have been favorable, the safety factor has been large, but in locations involving the closing of large circuit breakers where long runs of control cable exist between the battery and the farthest circuit breaker, satisfactory operation has been obtained which would not have been possible if a smaller battery had been used.

New Battery Data Required

Probably as a result of requests for higher control voltages the Electric Storage Battery Company has received several inquiries from manufacturers and from power companies during the last few years concerning the voltage of control batteries when discharging at high rates for short periods, such as are required for the closing of d-c operated circuit breakers.

Specific answers to many of these questions could not be given, as very little was known of the performance of a storage battery during the first fraction of a second at the current rates involved, particularly when the battery was influenced by floating or charging voltages at the instant of discharge.

It was evident that more detailed information pertaining to the actual instantaneous voltages obtainable from control storage batteries would assist considerably in arriving at a satisfactory solution.

The Electric Storage Battery Company, therefore, agreed to conduct a series of tests which were expected to provide the desired data.

The tests as laid out included discharges under the following conditions:

1. A fully charged battery being charged at various voltages.
2. A fully charged battery on open circuit.
3. A partially discharged battery discharging at a low rate.

Preliminary Tests—Noninductive Loads

In order to analyze battery performance, particularly during the first second of a discharge at a substantially constant rate, a series of tests were laid out in December 1943, in which a 4-cell *EM-11* battery was discharged at its 1-minute rate of 248 amperes to 1.75 volts per cell with the following conditions prevailing at the instant of load application:

1. A fully charged battery being charged at a rate equal to the 8-hour discharge rate in amperes.
2. A fully charged battery being charged at a constant voltage of 2.33 volts per cell.

3. A fully charged battery floating at 2.15 volts per cell.

4. A fully charged battery on open circuit.

5. A 50 per cent discharged battery discharging at a rate equal to 50 per cent of the 8-hour discharge rate in amperes.

In each case the condition as described was continued for a sufficient length of time to stabilize the charging current for conditions 1, 2, and 3, and the battery voltage previous to discharging for conditions 4 and 5.

With the exception of condition 1, the foregoing battery conditions previous to discharge are encountered or may be encountered in normal service. Condition 1 was included further to illustrate the momentary effect of an exceptionally high charging voltage existing at the battery terminals at the instant of load application.

With reference to condition 5, probably all control batteries will be called upon at some time during their life to operate while in a partially discharged condition, while at the same time furnishing some continuous current such as that required for indicating lamps or emergency lighting or both.

The battery was charged from a 115-volt d-c bus through resistors. The discharge currents indicated on the curves are the actual currents from the battery and do not include the small additional current furnished by the charging source.

A cathode ray oscilloscope was used to record the battery voltage. A noninductive fixed resistor was used as a battery load.

Figure 1 shows the average voltage per cell of the four cells as measured at the battery terminals when discharging at the 1-minute rate to 1.75 volts per cell for a period of one minute. The voltage during the first three seconds is amplified in Figure 2.

Analysis of Voltage Decline—Cells on Charge—Noninductive Load

A study of the shape of the voltage–time curve as the battery is discharged at a substantially constant current shows that the drop in voltage when the battery is reversed instantaneously from a charging to a discharging condition may be divided into four phases. These phases may be designated as follows:

(*a*). An instantaneous drop.

(*b*). A rapid drop.

(*c*). A less rapid drop.

(*d*). An almost imperceptible drop which may not exist in some cases.

By considering the curves on Figure 2 it will be observed that the instantaneous drop, (*a*), is increased when the charging voltage applied to the battery terminals is increased. This instantaneous drop is found to be 0.36 volt when the battery is being charged at the high charging voltage of 2.82 volts per cell, but is only 0.27 volt when the battery is being charged at 2.33 volts per cell, and 0.235 volt when trickle charged at 2.15 volts per cell.

Commenting further on this phase of voltage decline it appears that the instantaneous voltage drop in each case is mainly an *IR* drop in which *R* is the momentary internal resistance of the battery including the intercell connectors. (See section on "Internal Resistance".)

The second phase consisting of a rapid voltage drop which follows the instantaneous drop is defined very well on curve 1 of Figure 2 for the high charging voltage condition of 2.82 volts per cell. The amount of the drop is about 0.38 volt and the duration about 0.1 second. When the battery is being charged at a lower rate involving a charging voltage of 2.33 volts per cell, the amount and duration of this rapid drop is considerably less, being about 0.06 volt and 0.06 second. When the battery is being trickle charged at 2.15 volts per cell this phase of the voltage drop is scarcely noticeable, the amount indicated being about 0.015 volt and lasting for only about 0.02 second.

The next phase of the voltage drop for batteries on charge referred to as (*c*) "A less rapid drop," may be observed by consulting Figure 1. It will be noted that this phase represents a drop of about 0.29 volt for the battery being charged at 2.82 volts per cell, 0.21 volt for the battery being charged at 2.33 volts per cell, and 0.14 volt for the battery being trickle charged at 2.15 volts per cell. The duration of this portion of the voltage drop is about 15 seconds from the start of the discharge in each case, the battery reaching a comparatively stabilized value at this point.

The last phase [referred to as (*d*)] usually produces a slight falling off in voltage, but in many cases the voltage may remain practically flat or even increase somewhat for the balance of a 1-minute period. It will be noted that the trickle charged battery (curve 3 on Figure 1) had a slightly higher voltage at the end of a minute than it did at 20 seconds.

Analysis of Voltage Decline—Cells on Open Circuit or Partially Discharged—Noninductive Load

The decline in voltage as shown in curves 4 and 5 on Figure 1 and Figure 2 differ from curves 1, 2, and 3 in that the rapid drop, phase (*b*), does not exist.

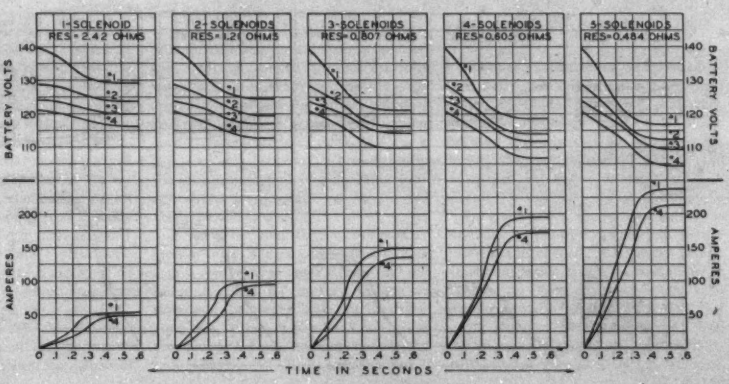

Figure 3. Approximate volt and current time characteristics—60-cell type EM-9 Exide chloride battery discharging into solenoids with plungers locked in

Temperature, 77 degrees Fahrenheit; specific gravity, 1.210

Battery condition:

Curve 1—Fully charged and charging at 140 volts

Curve 2—Fully charged and floating at 129 volts

Curve 3—Fully charged, open circuit

Curve 4—Fifty per cent discharged and discharging at 5 amperes

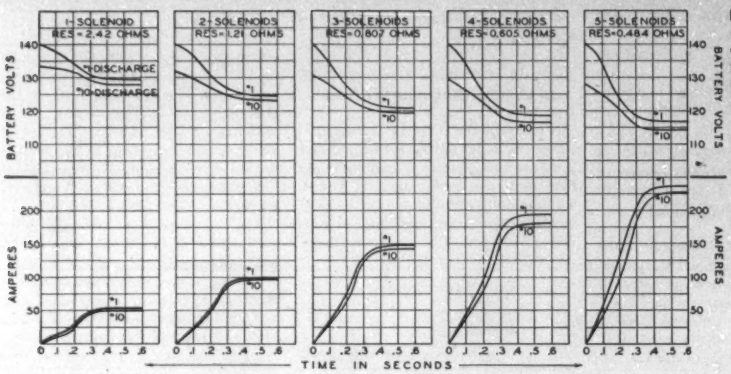

Figure 4. Approximate volt and current characteristics—60-cell type *EM-9* Exide chloride battery discharging into solenoids with plungers locked in

Temperature, 77 degrees Fahrenheit; specific gravity, 1.210
Comparison of first and tenth discharges
(20 seconds between each discharge)
Battery fully charged and charging at 140 volts

Therefore, under the condition of a fully charged battery discharged from an open circuit or a partially discharged battery that is discharging at a low rate, the voltage drop may be divided into three phases

(*e*). An instantaneous drop.

(*f*). A comparatively rapid drop.

(*g*). A gradual drop which in some cases may not exist, particularly with a fully charged battery.

The comparatively rapid drop following the instantaneous drop is indicated as lasting about three seconds and its value is less than the rapid drops following the instantaneous drops noted for batteries discharged from a charging condition. The last phase of the drop (*g*) in the case of the fully charged battery on open circuit (curve 4) is practically imperceptible, but curve 5 shows that the battery which was 50 per cent discharged dropped an additional 0.04 volt during this phase. The slight up-turn occurring in curve 5 at about 5 seconds is a characteristic that frequently is observed in battery discharges. Its cause is difficult to explain, and it is not always present.

Tests on a 60-Cell Battery Discharging Into Circuit Breaker Closing Solenoids

The tests described in which noninductive loads are used are useful in that they depict the actual battery performance when discharging at substantially constant currents without the complications encountered when discharging into inductive circuits.

Naturally, the delay in current build-up, due to the high inductance of a closing solenoid, has a considerable effect on the manner in which the battery voltage declines during a discharge.

The current build-up in a closing solenoid is a complicated procedure, the current value attained at any one instant being influenced by the inductance of the solenoid which is varied during the closing of the circuit breaker by the movement of the plunger. The current build-up also is varied to a small extent by the change in battery voltage as the value of the current is increased. It is also evident that different closing mechanisms or similar mechanisms attached to different types or capacities of circuit breakers will alter the current build-up in the solenoid. In order to obtain the exact conditions prevailing at a particular circuit breaker, it is necessary to obtain an individual oscillogram.

Realizing that the data obtained from the tests just described did not present a complete picture, the Electric Storage Battery Company arranged to run additional tests using a battery consisting of 60 cells, type *EM-9* battery with actual

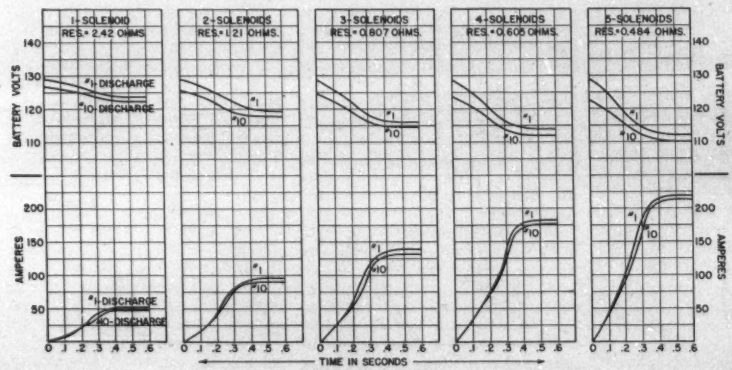

Figure 5. Approximate volt and current characteristics—60-cell type *EM-9* Exide chloride battery discharging into solenoids with plungers locked in

Temperature, 77 degrees Fahrenheit; specific gravity, 1.210
Comparison of first and tenth discharges
(20 seconds between each discharge)
Battery fully charged and floating at 129 volts

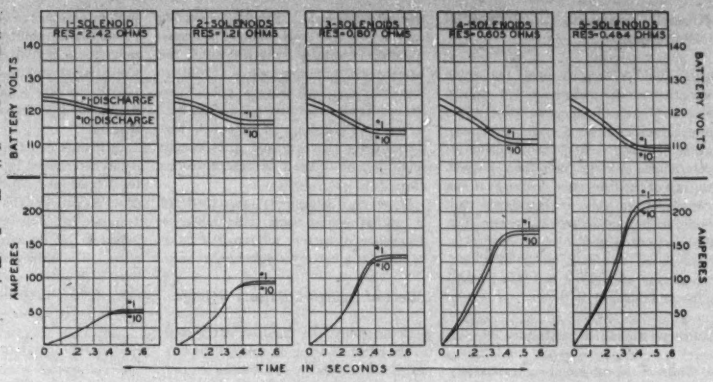

Figure 6. Approximate volt and current characteristics—60-cell type *EM-9* Exide chloride battery discharging into solenoids with plungers locked in

Temperature, 77 degrees Fahrenheit; specific gravity, 1.210
Comparison of first and tenth discharges
(20 seconds between each discharge)
Battery fully charged and at stabilized open-circuit voltage

operating conditions simulated by loading the battery on solenoids used in circuit breaker closing mechanisms. The *EM-9* battery is rated at 20 amperes for eight hours and 198 amperes for one minute to a final voltage of 1.75 volts per cell.

Five solenoids of the same size and type were loaned to the company by a circuit breaker manufacturer for these tests, each one having a d-c resistance of about 2.4 ohms. By connecting a single solenoid to the battery or paralleling groups of two, three, four, or five solenoids, battery loads were obtained which were approximately equal to 20, 40, 60, 80, and 100 per cent of the 1-minute rating of the battery to 1.75 volts per cell. To simplify the testing procedure the plungers were locked in a stationary position inside the solenoid coil. While the current build-up would not be the same as that obtained with a moving plunger actually closing a circuit breaker, it was considered to represent an acceptable compromise.

Since in actual practice it is often necessary to close several circuit breakers in rapid succession, it was agreed that the tests would include a series of discharges at each load. It was decided to repeat each discharge ten times with a period of 20 seconds intervening between each discharge. A time of 0.6 second was selected as representing the time that a typical solenoid may be connected to the control bus. An electronic relay combination and a solenoid control relay automatically to control the application of the load for a period of 0.6 second, with a period of 20 seconds intervening between discharges was used.

The results of the tests with the solenoid loads are shown on Figures 3 to 7, inclusive. Figure 3 shows the values of current and voltage obtained on the first of the ten discharges with the same battery conditions prevailing as for the tests employing noninductive loading resistors as depicted on Figure 1 and Figure 2.

The oscillograms indicate that there was no large instantaneous flow of current when the circuit was closed, and, therefore, the instantaneous voltage drop as noted in the previous tests was not present.

Figures 4 to 7, inclusive, show the variation in voltage from the first to the tenth discharge for the various conditions of the battery at the time of the discharge.

It will be noted that the voltage of the battery did not return to the original value of 140 or 129 at the beginning of the tenth discharge. In these tests the voltage at the start of each of the discharges was somewhat lower than that for the previous discharge, the decrements tending to decrease with succeeding discharges. The reason for this is twofold. In the first place, during each discharge the battery voltage is reduced and when an attempt is made immediately to restore the charging voltage to the previous value, a greater differential between the applied voltage and the battery counter-electromotive force causes the charging current to increase temporarily to a much higher value. Secondly, in the test setup the charging source had a drooping voltage characteristic and was of limited capacity.

It is evident that the voltage characteristic and capacity of the charging source will have some effect on the initial value of the battery voltage on repeated discharges from a charging condition, although the final voltage at the end of 0.6 second may be affected only slightly.

It will be noted that on Figures 4 to 7, inclusive, that the current in the solenoid builds up to a stabilized value which is a value equal to the applied voltage over the d-c resistance of the solenoid. However, in many cases the closing of a circuit breaker is completed before the current builds up to the value indicated by the applied voltage divided by the d-c resistance of the coil, with the result that the voltage of the battery at the opening of the solenoid control relay may be somewhat higher for solenoids having the same resistance as those used on these tests.

Figure 8 has been prepared from the same data used in constructing Figures 3 to 7. The curves on Figure 8 show the battery voltage when discharging into a solenoid load at various percentages of the 1-minute rate with the various voltages existing at the terminals of a fully charged battery and with the battery 50 per cent discharged and discharging at five amperes.

Intermittently Charged Batteries

When control batteries are operated by the intermittent charge method described under "Method of Operation" the voltage under discharge may be anywhere between the values shown on the curves for a charging voltage of 140 to the values shown for a battery on open circuit.

In some cases where the battery is discharged slightly between the hourly intermittent charges, the voltage will be somewhat lower than is indicated for a battery on open circuit. A few tests also were run on this 60-cell *EM-9* battery using the same timing relays and fixed noninductive resistors as loads. The results of these tests are shown on Figure 9.

Normal Variations in Individual Batteries

It should be kept in mind that some variation in the performance of storage batteries, even of the same make, type, and capacity, often is encountered, the cause of which is frequently difficult to determine. A variation in the voltage at the end of the 0.6-second discharge in the vicinity of two volts or thereabouts may occur in normal 60-cell batteries. The data presented in this report are taken from actual test data on an individual battery and should not be confused with published ratings.

Battery Internal Resistance

While on the subject of control battery characteristics it is not irrelevant to include a brief reference to the subject of internal resistance.

The Electric Storage Battery Company occasionally has received requests for internal resistance values pertaining to a particular cell or battery. In some cases, it was found that it was the intention of the person making the request to use this internal resistance value to calculate the initial voltage of the battery under load. Unfortunately, however, the internal resistance of the battery is not a fixed quantity, being affected by several factors such as temperature, state of charge, amount of discharge or charge current, previous history of the battery, and the age of the battery.

Considering the tests described in this report, the internal resistance of the battery used in these tests at that particular time is indicated by the instantaneous voltage drop shown on curves 4 and 5 on Figure 2. When the battery is charging, the instantaneous voltage drop shown on curves 1, 2, and 3 on Figure 2 indicates the drop in voltage occurring within the battery plus the difference in potential between the impressed charging voltage and the counterelectromotive force of the battery. This difference in potential, particularly for curves 2 and 3, is a very small portion of the total instantaneous drop.

However, it is desired to inject a word of caution against using these values or any values of battery internal resistance to estimate a battery voltage under load.

Effect of Aging on Battery Voltage

Occasionally, the question is raised as to the effect of aging on control bus batteries on their ability to meet the requirements of this service.

It is well known that in many services the capacity of a storage battery will tend to increase as it is worked until it reaches a maximum, and that later on in its life it gradually will fall off until the battery no longer is considered serviceable.

This is particularly true in service such as is encountered in electric trucks where the battery may be called upon to furnish a large portion of its available capacity nearly every day.

However, the degree of capacity build-up is not always uniform, and, in the case of a battery in control bus service where the battery is kept very close to the full charge point nearly all of the time, the tendency of the battery to build up additional ampere-hour capacity is much slower and may be less than is obtained from batteries operated in cycles of charge and discharge.

Another important fact is that in this service, there is more concern about the high rate discharge ability of the battery rather than its ability to furnish lower currents for a period of hours. In other words, what might be termed the ampere-second capacity is more important than its ampere-hour capacity at, say, the 8-hour rate.

In many cases, the ampere-hour capacity as determined by a test discharge at the 8-hour rate will not be an indication of its capacity at the 1-minute rate. Its 1-minute capacity is often more than is indicated by its capacity at lower currents. The ability of the battery to deliver high currents, such as its 1-minute rate, is best determined by a test discharge at that rate.

Such a test may be simplified by selecting several individual cells and observing the voltage of each cell about three seconds after load application. The actual voltage available for circuit breaker operating may be closely estimated by consulting the curve included in this paper corresponding to the conditions existing at the time of making the test.

Experience of the author has indicated that the voltage of a properly maintained control battery, discharging at its 1-minute rate to 1.75 volts per cell, usually will be maintained close to its rated value until it approaches the end of its useful life.

Allowable Voltage Drop

The allowable voltage drop is an important consideration which must be defined before the requirements of a battery power supply and the closing mechanisms can be specified. It appears probable, considering the elimination of several solenoid operated mechanisms requiring currents of 200 amperes and more, that

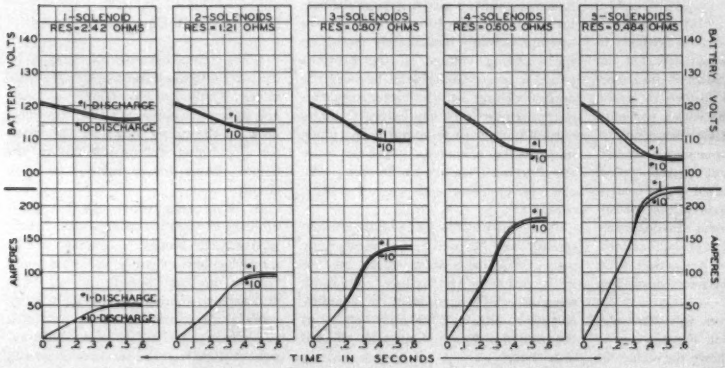

Figure 7. Approximate volt and current characteristics—60-cell type EM-9 Exide chloride battery discharging into solenoids with plungers locked in

Temperature, 77 degrees Fahrenheit; specific gravity, 1.210
Comparison of first and tenth discharges (20 seconds between each discharge)
Battery 50 per cent discharged and discharging at 5 amperes

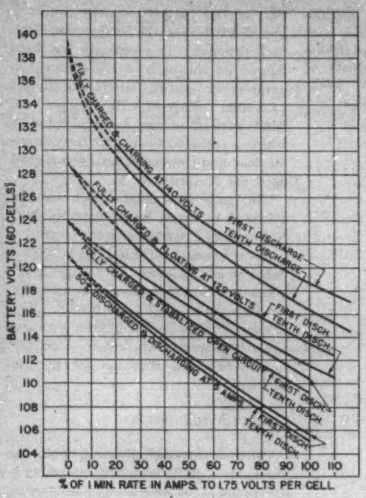

Figure 8. Approximate volt and current time characteristics—60-cell *EM-9* Exide chloride battery

Temperature, 77 degrees Fahrenheit; specific gravity, 1.210

Voltage and current at end of the first and tenth discharge of ten successive discharges of 0.6 second each with intervals of 20 seconds between discharges

Battery discharging into solenoids

the 15-volt differential between the minimum control bus voltage and the minimum allowable voltage at the mechanisms can be reduced materially.

Interpretation of Test Data

The problem under consideration may be defined as that of increasing the power supplied by the circuit breaker closing mechanism sufficiently to obtain full rated circuit breaker performance under all conditions of operation. This may be accomplished by increasing the flow of current through the solenoid coil by increasing the applied voltage, or possibly by changing the design of the mechanism.

A proper interpretation of the battery test data included in this paper indicates what may be expected from the control battery when considering means of meeting this demand for additional power.

While the cells used in the tests were of the Manchester-positive-plate box-negative-plate type of construction, it is believed that for practical purposes the performance may be considered typical of other types of batteries of comparable 1-minute capacity manufactured by the same company.

When these data are used to determine the recommended battery capacity for a practical application, it is suggested that the voltage values indicated on Figures 3 to 7, inclusive, which show the actual values observed in making the tests, be discounted somewhat, say, two volts. This will allow for some variation in the performance of different batteries.

If it is desired to increase the voltage at the closing mechanism there are two obvious ways of doing so. One is to increase the number of cells in the battery, and the other is to install batteries of larger capacity.

Effect of Increasing the Number of Cells

If the number of cells in the battery is increased over the present number of 60 cells, the maximum voltage across the entire battery during an equalizing charge or a charge after an emergency discharge, will be increased 2.33 volts for every cell added. A voltage of 2.33 volts per cell is considered to be the minimum voltage which is recommended completely to charge a cell. This means that the maximum allowable control bus voltage of 140 will be exceeded for any battery of more than 60 cells unless some means is found to limit the voltage impressed upon the indicating lamp assemblies and other devices taking small currents.

One way of accomplishing this is to provide two control busses or circuits, one of which will be connected to a tap on the battery at 60 cells, and the other to the entire battery. The total number of cells in the battery would be sufficient to maintain an adequate voltage on the high voltage bus for closing large circuit breakers. No load other than that due to the energization of closing mechanisms would be connected to this bus. The balance of the control bus load consisting of tripping mechanisms, indicating lamps, relay coils, closing mechanisms of small circuit breakers, and so forth, would be connected to the low-voltage bus supplied by the usual number of 60 cells.

If this method is used two pieces of charging equipment will be required, one for the 60-cell section, which may be the same as now used for standard 60-cell batteries, and a small rectifier to maintain the small group of end cells. The maintenance of the two sections should be entirely independent of each other.

If, in some cases, such as where a circuit breaker is in an isolated location, it is found inconvenient to separate the closing mechanism circuit from the indicating lamp and tripping circuits, a series resistor in these latter circuits might be used to reduce the voltage to a safe value.

An alternative to the foregoing arrange-

Temperature, 77 degrees Fahrenheit; specific gravity, 1.210

Battery condition:

Curve 1—Fully charged and charging at 140 volts

Curve 2—Fully charged and floating at 129 volts

Curve 3—Fully charged and on open circuit; voltage prior to discharge 124 volts

Curve 4—Fifty per cent discharged and discharging at 5 amperes; voltage prior to discharge 121 volts

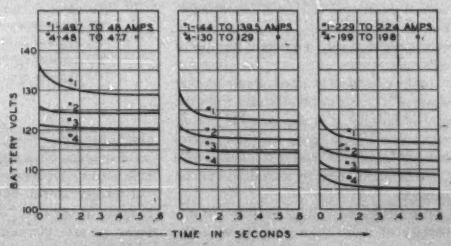

Figure 9. Approximate volt-time characteristics—60-cell type *EM-9* Exide chloride battery discharging into non-inductive fixed resistors

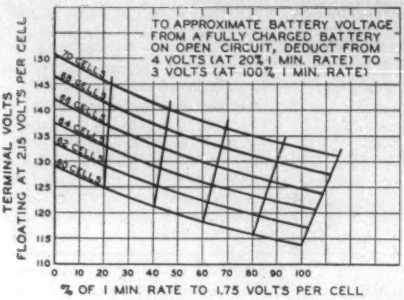

Figure 10. Voltage available from control batteries of from 60 to 70 cells of type EM Exide chloride

Temperature, 77 degrees Fahrenheit; specific gravity, 1.210

Battery voltages at 0.6 second when discharging into solenoids

Battery fully charged and floating at 129 volts

Straight lines indicate variation in current due to variation in voltage. Example: A solenoid taking 100 per cent of the 1-minute rate at 113.6 volts from a 60-cell battery will take 115 per cent of the 1-minute rate at 130.7 volts for a 70-cell battery

ment is to install a group of counterelectromotive force cells in series with the augmented battery. The closing mechanisms of the large circuit breakers may be connected to the entire battery inside of the counterelectromotive force cells, and the indicating lamps and tripping circuits also may be connected across the entire battery outside of the counterelectromotive force cells. A sufficient number of cells may be installed to reduce the voltage to a safe value for the indicating lamp and tripping circuits.

With this arrangement the battery could be charged with one piece of charging equipment with a suitable characteristic for charging the increased number of cells. A possible disadvantage of this scheme is that some of the standard charging equipment now used for charging 60-cell control batteries could not be used to maintain a battery composed of several additional cells, and the requirements of the charging equipment would vary somewhat with a different number of cells.

In the case of an isolated circuit breaker situated a considerable distance from the control battery, it is also possible to connect a few cells in series with the control bus to boost the voltage. These cells could be maintained by a small individual charger.

The additional voltage available from a battery of more than 60 cells with the battery fully charged and floating at 2.15 volts per cell is shown on Figure 10.

Figure 11, showing the voltage drop occurring in various sizes of control wire or cable, is included in this paper for convenient reference.

Installing Batteries of Larger Capacity

As referred to at the beginning, a control battery in many cases contains some additional capacity over that required to furnish the maximum current for closing circuit breakers. This capacity, which is included for purposes other than circuit breaker closing, in some cases may be an appreciable portion of the total control battery capacity.

However, in this paper when reference is made to the effect of using larger batteries we are referring only to that portion of the battery capacity which is included to furnish the maximum momentary demand. This capacity has been figured on the basis of the capacity in amperes per positive plate for one minute to a final voltage of 1.75 volts per cell. That portion of the battery capacity which is included to supply the continuous load and the emergency lighting load need not be increased.

The gain in voltage which can be achieved by using larger capacity batteries can be determined from Figure 8.

For convenience Table I has been prepared which indicates the voltage available at the closing mechanism considering a voltage drop of 5, 7.5, or 10 volts. The tabulated values are taken from tests and again it is suggested that they be discounted two volts when used for practical application.

Closing Mechanisms

The designers of circuit breaker closing mechanisms have been confronted with the problem of producing mechanisms which will operate over the entire range of 90 to 130 volts. For many years, this upper limit of 130 has presented a handicap which appears to be unnecessary, inasmuch as this voltage is not available from a 60-cell control storage battery when discharging into closing solenoids.

Figure 11. Voltage drop at 100 amperes in control cable

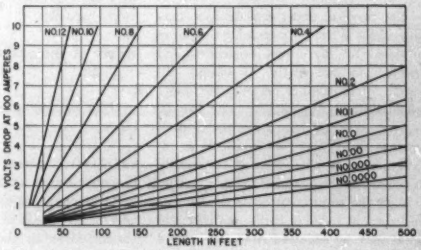

For volts drop at 1 amperes multiply drop given for 100 amperes by 1/100

Temperature correction factor:
25 degrees centigrade—1.00
40 degrees centigrade—1.058
50 degrees centigrade—1.096
100 degrees centigrade—1.289

In most cases, the actual voltage at the mechanism during a circuit breaker operation probably will not be more than 115 volts, except, possibly, during monthly equalizing charges.

Since it has been stated that the increased power from a closing mechanism sufficient to obtain full rated performance from circuit breakers can be obtained at 90 per cent of normal control bus voltage, it appears that, based on a maximum operating voltage of 115 volts, a voltage of 103.5 volts at the mechanism would be adequate.

By consulting Figure 8 it may be noted

Table I. Voltage Available From 60-Cell Control Batteries of Varying Capacities

Load As a Per Cent of 1-Minute Rate to 1.75 Volts Per Cell*	Voltage Drop Between Battery and Mechanism (Assumed)	Available Voltage at Closing Mechanisms: Fully Charged, Charging at 140 Volts, Discharge, First	Fully Charged, Charging at 140 Volts, Discharge, Tenth	Fully Charged, Floating at 120 Volts, Discharge, First	Fully Charged, Floating at 120 Volts, Discharge, Tenth	Fully Charged, Open Circuit, Discharge, First	Fully Charged, Open Circuit, Discharge, Tenth	50 Per Cent Discharged, Discharging at 5 Amp., Discharge, First	50 Per Cent Discharged, Discharging at 5 Amp., Discharge, Tenth
100	5	113.7	111.3	108.4	106.5	105.4	104.2	100.6	100.0
50	5	119.7	118.3	114.4	112.7	111.7	110.6	107.5	107.0
33⅓	5	122.7	121.5	117.2	115.6	114.0	113.0	110.1	109.6
25	5	124.5	123.4	118.7	117.3	115.1	114.3	111.4	110.9
100	7.5	111.2	108.8	105.9	104.0	102.9	101.7	98.1	97.5
50	7.5	117.2	115.8	111.9	110.2	109.2	108.1	105.0	104.5
33⅓	7.5	120.2	119.0	114.7	113.1	111.5	110.5	107.6	107.1
25	7.5	122.0	120.9	116.2	114.8	112.6	111.8	108.9	108.4
100	10	108.7	106.3	103.4	101.5	100.4	99.2	95.6	95.0
50	10	114.7	113.3	109.4	107.7	106.7	105.6	102.5	102.0
33⅓	10	117.7	116.5	112.2	110.6	109.0	108.0	105.1	104.6
25	10	119.5	118.4	113.7	112.3	110.1	109.3	106.4	105.9

These voltage values represent actual test values. When these values are used as a basis in determining battery capacities for an actual installation it is suggested that two volts be deducted from the tabulated values so as to allow for some variation in the performance of individual batteries.

*This load is the maximum momentary load expressed as a percentage of that portion of the total battery capacity that is required to furnish the maximum momentary load.

that the total variation in battery terminal voltage usually will be not more than 15 volts. As an example, the voltage at 50 per cent of its 1-minute rate from a battery charging at 140 volts is indicated as about 125 volts, and its voltage with the battery fully charged and on open circuit, discharging at the full 1-minute rate, is about 109 after about ten successive circuit-breaker operations.

The upper limit of 125 volts will exist only for 8 to 24 hours once each month during equalizing charges, while the lower limit probably will exist only for short periods at infrequent intervals when the charging equipment is not operating. It therefore appears that, after making some allowance for voltage drop in wiring, the practical operating range of closing mechanisms could be reduced from 90 to 130 to a much smaller range, such as 100 to 120 volts, when operating with batteries selected in accordance with present practice.

Conclusions

1. The voltage at the battery terminals which is available for closing circuit breakers under normal conditions with the charging equipment in operation is appreciably higher than the voltage at the battery at the end of a continuous 1-minute discharge, the actual value being influenced considerably by the voltage at the battery terminals at the beginning of load application. It appears that the minimum voltage from a fully charged battery on open circuit while discharging into a closing mechanism taking a current equal to its 1-minute rate to 1.75 volts per cell, may be considered as being 107 after several successive circuit breaker closing operations.

2. Additional voltage at the closing mechanisms may be obtained from the control battery by increasing the number of cells to more than 60, but if this is done means will have to be provided to prevent damage to other connected equipment, due to excessive voltage. A method of accomplishing this is described in this paper. Users of this equipment may judge for themselves as to whether or not this is a practical scheme and may or may not be accomplished at reasonable expense.

3. Additional voltage at the closing mechanism may be obtained by using control batteries of larger capacity than have been used heretofore. A study of Table I indicates that in order to provide 112.5 volts at the operating mechanism, the battery capacity would have to be increased considerably (more than 300 per cent of present capacity) unless it is possible to restrict the voltage drop in the wiring to at least five volts.

4. The operating voltage range of 90 to 130 volts for closing d-c operated circuit breakers from a nominally rated 125-volt control bus may be reduced from the existing standard. An operating voltage range of 100 to 120 volts is suggested as a possibility.

5. The adoption of a smaller operating voltage range would make possible the design of closing mechanisms capable of providing adequate power for closing circuit breakers under all operating conditions. If this is done no change in the present method of selecting batteries will be required.

Discussion

F. A. Lane (American Gas and Electric Service Corporation, New York, N. Y.): The data given in this paper have been needed for a long time and is certainly a worth-while contribution. The work in question was carried out with a battery using Planté plates, and the author of the paper has assumed that the results would be the same with pasted plates. I think it would be very reassuring if some time some tests could be made to check this to make sure that there is no difference in performance, particularly since most of the control batteries are of the pasted plate type.

One interesting thing about the results of these tests is that the floating method of charging batteries seems to give somewhat better results as far as available voltage to operate circuit breakers is concerned than does the method which uses a relay to put the battery on charge every hour for a short period to make up the losses. This seems to make about five per cent more voltage available at the battery terminals.

A. E. Anderson (General Electric Company, Philadelphia, Pa.): The information given in this paper fills a long-felt need concerning the behavior of control batteries when supplying transient currents to such loads as circuit breaker solenoids. These data should enable the circuit-breaker designer and the user to determine more readily the range of operating voltage required. This paper (as well as a paper by W. A. Holland, *Electrical World*, March 29, 1947) includes data which points to the desirability of using higher control voltages. Examples of this are 250-volt 120-cell control batteries which have been used for many years in numerous power stations and industrial plants. A marked trend still continues towards the use of 250-volt control. It will be apparent from the statements made in these papers, together with a consideration of the last figure in each paper, that, for the same length and size of conductor, the reduction in solenoid current obtained by using a 250-volt control battery will reduce materially both the actual and the relative voltage

drops in the leads between the battery and the solenoid terminals.

E. A. Hoxie: At the time these tests were run it was decided to use a battery having Planté type positive plates, inasmuch as there seemed to be a definite trend toward the use of this type of battery in circuit breaker control service.

Further comment might be in order concerning the performance of batteries which automatically are placed on charge every hour for a time which is sufficient to replace the small amount of capacity lost during the portion of the hour that the battery is not being charged.

The battery voltage during and immediately after the completion of the hourly charge will be higher than it is during continuous floating with a continuous load due only to indicating lamps, which will seldom exceed five per cent of the 8-hour discharge rate of the battery. It appears that the voltage of the battery load during the time between the intermittent charges would not drop below the open-circuit voltages, as indicated by curve 3 of Figure 3 in the paper. The difference in voltage at 0.6 second for a load corresponding to 3, 4, or 5 solenoids between a battery fully charged and floating at 129 volts and a battery fully charged and on open-circuit appears on the curves on Figure 3 to be about 3 volts, representing a difference of about 2.6 per cent. This value of 2.6 per cent therefore represents the maximum reduction in voltage occurring toward the end of the period between charges. The average voltage during the intervals between charges probably would be about 2 to 2.5 volts less than the voltage available from a floated battery, which is about two per cent less, instead of the five per cent value mentioned in Lane's discussion.

Transmission of Electric Power at Extra High Voltages

PHILIP SPORN
FELLOW AIEE

A. C. MONTEITH
FELLOW AIEE

MUCH INTEREST is being shown in the high-voltage investigation project now being carried out on the American Gas and Electric Company system near the Tidd station of The Ohio Power Company at Brilliant, Ohio. This symposium has been arranged to present the thinking that led to it and the program itself, so that as the results of the investigation become available they can be interpreted intelligently by all those interested, and also the extent of completion of original objectives determined.

The first logical question is: Why any tests? Other questions are: What tests are contemplated, and how are they to be conducted? What are the design characteristics of the equipment to be tested and of the equipment used for carrying out the testing program?

This paper will attempt to answer the first question; the others will be discussed in companion papers.[1-6]

Reason for Investigation

Past experience in the development of power systems and their concomitant transmission lines and analytical examination of the economic considerations of the transmission of increasingly larger blocks of power indicate the desirability in some cases of going to higher voltages than have been used heretofore. However, the cost of building a transmission system—line and its related terminal equipment—increases rapidly with increasing voltage. The use of increased voltages requires effectively larger conductors, larger towers, higher insulation levels, and more expensive terminal equipment. With these costs increasing very rapidly with higher voltage, it becomes increasingly important to design the system so that the maximum use is made of the capabilities of the equipment. This is another way of saying that as voltage increases it becomes more than ever necessary to design for the very minimum proper margins of safety. But before this can be done for extra high voltages—before systems can be designed with close margins, yet without sacrificing the requirements of reliability—engineers need more information than is now available.

The projection of higher voltage transmission is not only beginning to be a pressing in problem planning of electric power systems, but the problem is beginning to assume more or less universal proportions. The United States, and as a matter of fact all the countries of the world possessing or aiming to develop industrial potential, is witnessing the greatest expansion in the use of electricity that ever has taken place, and, if present predictions materialize, this expansion will continue for some time. This, of necessity, involves expansion of transmission facilities. The justification for transmission and the distances involved vary in different sections of the United States and in the different countries. It is, however, quite apparent that in some localities, where fuel is scarce and remote undeveloped hydro energy plentiful, long-distance transmission will be used. Also, it is quite apparent that there are systems in the United States where transfer of much larger blocks of power than any heretofore involved will be required, both for base load and for co-ordination of large integrated systems and for interchange between them and contiguous systems.

In the United States a transmission system of 287 kv rated, 302 kv maximum, is in use and there has been some discussion of the use of a transmission voltage of approximately 345 kv rated, 362 kv maximum. On the American Gas and Electric Central System, the need for higher voltage transmission facilities than the existing 132-kv backbone transmission has been accelerated by the unprecedented war and postwar growth in load. The French have built some double-circuit 220-kv lines, which may be converted later to a single circuit with bundle conductor to operate at approximately 385 kv. China has discussed the use of 345-kv transmission and Sweden now is considering a nominal 350-kv, maximum continuous operating voltage 380-kv development to transmit power from their abundant water supply to their industrial center some 600 miles away. With this pressing interest in high-voltage transmission, it is logical to review its status and see what factors need further study to secure the most economical line design in the light of present-day knowledge and practice. All this has prompted a close study of this field, and this has resulted in the investigation program being carried out at the Tidd station of the American Gas and Electric Company.

Numerous factors have to be evaluated before reaching a decision to use a particular high voltage and before the details of the design that will be used can be fixed. The selection usually involves a study of anticipated loading conditions for the degree of reliability necessary for the project. From a consideration of load, distance, reliability desired, and other influencing factors, the voltage level, number of circuits, and circuit arrangement can be determined. All of these will affect the economics of the project, but the one single factor that perhaps will affect the economics to the greatest

Paper 47-241, recommended by the AIEE committee on transmission and distribution and approved by the AIEE technical program committee for presentation at the AIEE Midwest general meeting, Chicago, Ill., November 3–7, 1947. Manuscript submitted August 20, 1947; made available for printing September 19, 1947.

PHILIP SPORN is president, American Gas and Electric Service Corporation, New York, N. Y.; A. C. MONTEITH is manager, headquarters engineering departments, Westinghouse Electric Corporation, East Pittsburgh, Pa.

The authors wish to acknowledge the valuable assistance of their associates in the preparation of this paper.

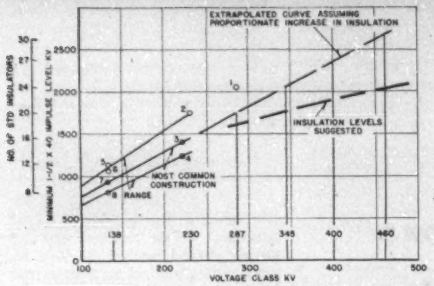

Figure 1. Insulation levels for transmission lines

Points on curves are typical lines:

1—City of Los Angeles Department of Water and Power, Boulder Dam–Los Angeles
2—Pennsylvania Water and Power Company, Safe Harbor–Washington
3—Pennsylvania Power and Light Company, Wallenpaupack–Siegfried; 14 to 16 insulators averaged at 15
4—Pacific Gas and Electric Company, Tiger Creek–Newark
5—Pennsylvania Water and Power Company Safe Harbor–Perryville; Ohio Power Company, Lima–Fostoria
6—Union Electric Company of Missouri, Osage–Cahokia; Ohio Power Company, Philo–Canton
7—Ohio Power Company, Lima–Fort Wayne
8—Northern Indiana Public Service Company, Michigan City–State Line

degree is the insulation level adopted for terminal equipment and the insulation level and spacing for the line. These levels naturally will be influenced by the type of grounding adopted for the system. It has been the practice in some cases on lower voltage systems to operate lines with ground fault neutralizers. It is the opinion of the authors, however, that in the case of extra high voltage transmission, above 230 kv, the lines ought to be grounded permanently and solidly at all transformation points, which will permit the use of reduced-voltage arresters. Coupled with the use of interrupting devices, which will open the circuit with not more than a single restrike, this solid grounding of the system will limit the magnitude of voltage in switching transients to which line and equipment will be subjected, and will permit the use of insulation of a lower level than that thought possible in any previous consideration of the problem.

Of the many factors influencing the design of a high-voltage line, some are well understood and others require more investigation. Reliable information is available on lightning surges, switching surges, and line reactance and capacitance, but insulation levels, as pointed out before, need to be considered thoroughly. Much information is needed on corona and radio influence, and how they are affected by size and type of conductor, spacing and height of ground wire, and atmospheric conditions. It seems appropriate, in this introductory paper to this symposium, to review briefly the known factors in line design and by the process of elimination develop in a little greater detail the significance of the elaborate set of tests now in progress. The complete description of the test setup and tests will be discussed in the companion papers. The following is, therefore, a discussion of the significant factors, their economic significance, and a summary of where additional information is required for use in future designs of extra high voltage transmission lines to secure a well balanced design with all factors engineered to the best of our ability.

To make some specific comparisons for extra high voltages, three voltage levels are used, namely, 345, 402, and 460 kv. Table I gives typical insulation characteristics of higher voltage steel tower lines used in the United States. Table II gives comparative insulator characteristics for various lines over the range of extra high voltage transmission. Figure 1 indicates that average insulation levels have increased approximately in proportion to the voltage rating. The straight line representing the most common insulation levels has been extended in Figure 1 to indicate the levels that result if the practice of proportionate increase in insulation levels were continued. This is too conservative in the light of present-day knowledge.

Lightning Performance

For the voltage classes so far used in the United States, lightning protection has been the primary consideration in the choice of transmission line insulation levels However, sufficient knowledge and experience with lightning and lightning protection now has been gained to show that there is a definite upper limit of insulation required for lightning protection, which already has been exceeded by numerous higher voltage lines in use today. Normal steel construction with spans of the order of 1,000 feet or less and effective tower-footing resistances of 20 ohms or less should experience substantially no flashovers from direct strokes when the phase wires are shielded by overhead ground wires and the equivalent of 16 or more standard suspension insulators are used. In Figure 2 are shown calculated curves giving the maximum voltages which the most severe stroke to the ground wires can induce on a phase conductor for the standard types of construction listed in Tables I and II. As shown by this figure, some benefit in reducing the magnitude of the phase conductor voltages is obtained by increasing the dimensions of the transmission line. This is due to the decrease in coupling factor that is obtained thereby.

However, the principal source for the higher surge voltages that can appear at the terminals of a highly insulated line is thought to be strokes that actually contact the phase wires through lack of complete shielding. Both theoretical considerations and model studies show that, although the frequency of direct strokes to phase conductors can be made quite small at shielding angles of 25 to 30 degrees, it cannot be eliminated entirely with only one or two overhead ground wires. The model studies[7] indicate that with a shielding angle of 25 degrees on a conventional 2-ground-wire 230-kv steel line about one

Table I. Comparative Insulation Characteristics of Steel Tower Transmission Lines in the United States

Kv Class	Number of Insulators*	Minimum Impulse Level, Kv, $1^1/_2 \times 40$ Wave*	60-Cycle Dry Flashover, Kv RMS*	Times Normal Line-to-Ground Operating Voltage*
69	(4–8) 5	(475–780) 550	(280–500) 320	(7–12.5) 8
138	(8–12) 10	(780–1100) 940	(500–710) 600	(6.3–8.9) 7.5
230	(14–20) 16	(1270–1770) 1450	(810–1140) 910	(6.1–8.3) 6.8
287	24	2110	1350	8.1

*Range of values is in parentheses. Most common construction is figure following parentheses.

Table II. Comparative Insulation Characteristics of Various Transmission Line Construction Considered in This Paper for Transmission at Extra High Voltages

No. of Standard Insulators	Actual	Equivalent	Minimum Impulse Level, Kv	60-Cycle Dry Flashover in Kv RMS** Actual	Times Normal Line-to-Ground Operating Voltage 345 Kv	400 Kv	460 Kv
20	27*	34	1,770	1,140	5.7	4.9	4.3
24	33*	41.5	2,100	1,350	6.8	5.8	5.1
27	38	48	2,380				
30	43	54	2,600	1,700	8.5	7.3	6.4
35	51.5	65	3,100				

All single-circuit flat steel constructions with 1,000 foot spans.

*For certain tower construction and types of conductor, these spacings might be as high as 33 and 37 feet, respectively.

**Wet values will be approximately 70 per cent of these ratios.

out of every 900 strokes might contact a phase conductor. The rate of decrease with decreasing shielding angle below 25 degrees is quite low.

Further verification of the foregoing viewpoint is provided by actual experience on several of the higher voltage lines. Excellent data of this type are provided by the detailed studies of the Pennsylvania Water and Power Company in which records of all strokes to their lines are being obtained with magnetic surge crest ammeter links correlated with a careful inspection program. On the 220-kv lines three flashovers have occurred, two from lack of shielding and one at a tower having a tower-footing resistance of about 60 ohms. The data on the 230-kv lines show that even with two overhead ground wires providing a shielding angle of 20 to 25 degrees, about one stroke in 700 mile-years of operation may be expected to contact a phase wire directly. The average stroke density of these lines which lies in isokeraunic levels ranging from 25 to 40 storm days per year, has been found to be about 100 strokes per 100 miles per year. This indicates that about one out of every 700 direct strokes will contact a phase conductor which agrees quite well with the model tests.

Calculations have been made of the probability of a given crest surge voltage appearing at a substation connected to well-constructed high-voltage lines with various amounts of line insulation. These are based upon our present knowledge of the magnitude and wave shape of lightning stroke current and the assumption of 100 strokes per 100 miles of line per year. They take into account voltages that might be induced by indirect strokes, by strokes contacting the ground wire, and by strokes that contact a phase conductor. These are summarized in Figure 3 where a comparison is made with the suggested basic impulse levels for terminal equipment. As shown by these curves, the lines with higher insulation have a greater number of the higher magnitude surges that lie in the range of the insulation levels of the transformers being considered. This merely confirms the well known fact that from the standpoint of terminal equipment it is desirable to use as low an insulation level for the line as practicable. However, a study of the data in Figure 3 can be of help in rationalizing our ideas of insulation co-ordination at higher voltages and in reorienting our appraisal of the necessary basic insulation levels for such higher voltages.

Insulation Co-ordination

It is of interest to consider the probability of experiencing a surge in the station in excess of the strength of the apparatus. The vertical lines plotted in Figure 3 are suggested basic impulse levels for the indicated operating voltages. These are somewhat different from values that would be derived from the present standards, which are

Operating Voltage, Kv	Basic Impulse Level, Kv
230	1,050
287	1,300
345	1,550

The present standard basic impulse levels are based on system operation with a fully rated lightning arrester. A large number of high-voltage solidly grounded systems are in successful operation with equipment insulation levels one step below standard values. If the extra-high-voltage range is approached on the basis of solidly grounding and the practice of using a reduced voltage rating lightning arrester is followed, then, considering the higher impulse value of equipment dealt with, the successful practice of one lower class insulation is not only sound practice but may be improved upon by further lowering of insulation. This seems entirely practicable for several reasons. By reliance on the solid grounding of the system's transformation point and controlling the voltage, it is believed practicable to use a lightning arrester having a rating of about 75 per cent of normal voltage rating. Also, there do not appear to be any difficulties from an economic standpoint to shield adequately the line immediately adjacent to the substation so that there is practically no probability of ever getting in excess of 5,000 amperes through the lightning arrester. Again, it appears that it will be possible, without appreciably affecting the over-all economics, to resort to the use of diverter wires for a short distance from the terminals to give 100 per cent shielding in this zone. Thus, on this basis, arrester and gap characteristics as indicated in Figure 4 seem to be entirely possible and this would suggest a series of basic impulse levels for this extra-high-voltage equipment as shown. The basic impulse levels plotted in Figure 4 are

Operating Voltage, Kv	Basic Impulse Level, Kv
230	950
287	1,050
345	1,200
402	1,400
460	1,550

These are also the values shown by the vertical line in Figure 3.

The authors merely are using these for discussion purposes but they believe that the basic impulse level values ultimately selected can be of this order. The final selection of values, including the selection of the proper steps (involving possibly the elimination of some of the present steps and the addition of other steps), after thorough discussion of all the facts available and the phenomena involved, undoubtedly can be handled best by committees representative of the electrical industry. Such committees are now in existence.

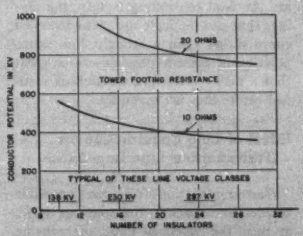

Figure 2. Maximum conductor potential for lightning stroke to ground wire.

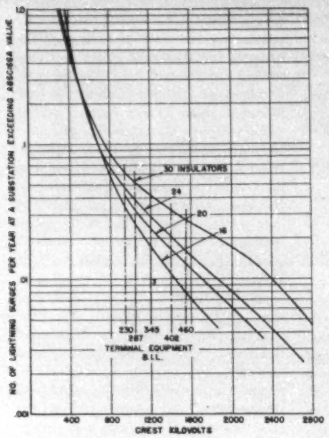

Figure 3 (left). Probability of lightning surge at substation for different line insulation levels

Broken lines suggested basic impulse levels for terminal equipment for different rated voltages

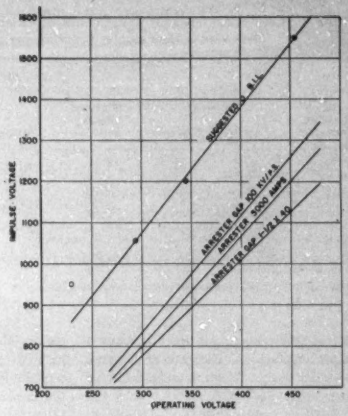

Figure 4. Comparison of suggested basic impulse levels with lightning arrester characteristics is based on a lightning arrester for 75 per cent of maximum operating voltage, which voltage is 105 per cent of rated voltage

Arrester gap characteristics are plotted for front of wave on basis of 100 kv per microsecond per 12 kv of arrester rating. The $1^1/_2 \times 40$ arrester gap curve is critical impulse spark-over voltage

Switching Surges

It is of interest to consider the insulation necessary from a switching surge point of view. Modern high voltage breakers are designed to have not more than one restrike. For this switching operation, the maximum line-to-ground switching surge voltage that should appear at the substation is of the order of 3.0 times normal line-to-ground operating voltage on a solidly grounded system.[8,9] Only the condition of solid grounding is considered, since it is believed that such high-voltage systems normally will be grounded. Table II shows that 24 insulators for operating voltages up to 460 kv provide a minimum 60-cycle dry flashover ratio of 5.1 or a wet flashover ratio of 3.6, which is considered adequate for these switching conditions.

Thus, as far as lightning and switching surges are controlling factors, the suggested insulation level curve of Figure 1, indicating 20 insulators for 345 kv and 24 insulators for 460 kv, is ample. If these are the final controlling factors, the savings that can be made using the modified curve rather than a straight line extrapolation of present practice are so great that a major investigation effort is justified before they are given up.

Effect of Line Construction on Transmission Line Impedance

Shorter insulation strings make possible smaller line spacing, the spacings have, in turn, the beneficial effect of reducing line capacitive and inductive reactance.

Calculations have been made of the relative amounts of power that could be transmitted over a 200-mile line making the arbitrary assumption that stability considerations limit the line reactance angle to 30 degrees. The results of these calculations are presented in Table III. A rather arbitrary conductor size was chosen with two levels of insulation, the one level of insulation taken from the suggested curve of Figure 1 and the other resulting from a straight line extrapolation of the low-voltage data plotted in Figure 1. This table shows that the increased power limit and charging kilovolt-amperes obtained with the smaller spacing is appreciable. Bundle conductors may offer even greater savings as a result of decrease in line capacitive and inductive reactances.

Corona

The disruptive corona voltage and the corona power loss are very much affected by size of conductor and spacing. The greater the insulation level of the line and the larger the spacing between conductors, the higher will be the disruptive corona voltage and the lower the corona power loss. As far as lightning and switching surges are concerned, 16 insulators with normal spacing for 345 kv would appear adequate. However, an abnormal conductor size might have to be used or else the corona loss would be too high. This may be the factor that would set the lower limit on the dimensions of an extra-high-voltage transmission line. Since this factor has considerable effect on the cost of building a line, it deserves critical study.

A review of some of the published information[10-17] indicates good data on corona losses at the higher corona levels for fair-weather conditions and for the effect of surface conditions, but does not include the effect of ground wires, insulator losses, and tower effects. A typical corona loss curve for a given conductor and tower configuration calculated from the existing formula is plotted in Figure 5. It is known that change of conductor size, configuration, and surface conditions will shift this curve up or down the voltage scale. The practical problem, therefore, is to design the line so that it will work on the flat part of the loss curve for much of the operating time. In the past, it has been the practice to design for a fair-weather corona loss of from one-half to one kilowatt per mile. This may be satisfactory for low-voltage lines, but it would appear economical to allow higher loss on the higher voltage lines if the increased corona did not produce excessive radio influence.

Before designing for higher fair-weather corona loss, it appears desirable to secure better data on corona losses under actual line conditions and for changing weather conditions. A few tests show that corona losses may increase under rain conditions

Table III. Economic Benefits of Lower Line Insulation on Reducing Line Reactance and Increasing Line Capacitance on a 200-Mile Circuit

Operating Voltages, Kv	Insulator Units	Spacing, Ft	r_1, Ohms Per Mi, 25 C	X_1, Ohms Per Mi	X_1, Megohms Per Mi	Power Delivered, Megawatts	Reactive Power Delivered, Megavolt-amperes	Per Cent X_1 Reduction Load Base	Economic Benefits: Reduced Reactance ∮	Increased Reactive ‡	Reduced Line Cost †
345 Kv (1.61-in. conductor)	20	33	0.0887	0.789	0.1908	396	48.5	0.80	$48,000	$10,000	$480,000
	24	37	0.0887	0.801	0.1940	390	47.2				
400 (2.085-in. conductor)	20	33	0.0577	0.758	0.1838	561	49.2	1.54	$130,000	$21,000	$880,000
	27	39.5	0.0577	0.780	0.1891	545	46.6				
460 (2.5-in. conductor)	24	37	0.047*	0.750*	0.181*	752	55.2	1.14	$129,000	$18,000	$940,000
	30	42	0.047*	0.766*	0.184*	737	52.9				

*Estimated value. †Based on 30-degree angle with $E_r = 1.05\ E_c$. ∮Saving on terminal equipment due to reduced reactance. ‡Based on $8.00 per kilovolt-ampere of increased reactive kilovolt-amperes available at receiving end.

to many times the fair-weather losses. Also, the effect of fog, humidity, and many other influencing conditions may effect the allowable corona loss materially. With better data available on these conditions, there will exist more scientific criteria for the design of a line than the fair-weather corona loss now used.

The bundle conductor presents advantages, as far as inductive and capacitive reactance and corona loss are concerned, but it not only presents new mechanical problems but economic questions also. It seems desirable, therefore, to secure more data on this type of conductor to see if it will contribute to a more economical high-voltage system.

Radio influence needs further study. Experience with some high-voltage lines has disclosed some objectionable interference, although these lines were designed to operate at relatively low corona loss level.

Before adopting the practice of decreasing conductor spacings or conductor size to allow higher corona losses, it seems desirable to secure better data on several conductor sizes and spacings under actual service conditions, particularly under seasonal weather variations. It was believed, therefore, that tests should be made employing integrating instruments giving high-speed continuous recordings of these data under all weather conditions and involving all of the factors with a carefully co-ordinated study of the radio influence problem.

Effect of Line Insulation and Spacing on Corona Loss

To obtain a basis for discussing the corona loss performance of the various line constructions being considered here, fair-weathered corona loss calculations have been made using Peterson's formula. These are based upon the assumption of a smooth conductor, an altitude of 1,000 feet, a temperature of 25 degrees centigrade, and a surface factor of 0.9, which factor was found by Peterson to be applicable to general operating conditions for type *HH* cable at 220 to 287 kv. Figure 6 shows the calculated 3-phase corona power loss per mile for the three voltage levels considered.

The curves of Figure 6 indicate that if the required conductor diameter were chosen from the standpoint of equal power loss for the different lengths of insulator strings at a given operating voltage, the range of conductor diameter would be considerable. For example, an operating voltage of 345-kv, limiting the corona loss to 0.65 kilowatt per mile, would require about a 1.75 inch diameter conductor for a line with 20 insulators, a 1.6-inch diameter conductor for a line with 24 insulators, and only a 1.45-inch diameter conductor for 1 line with 30 insulators. If, however, a 1.5-inch diameter conductor were used for all three line designs, the range of power loss would be 0.6 to 0.9 kilowatt per mile. A study of the

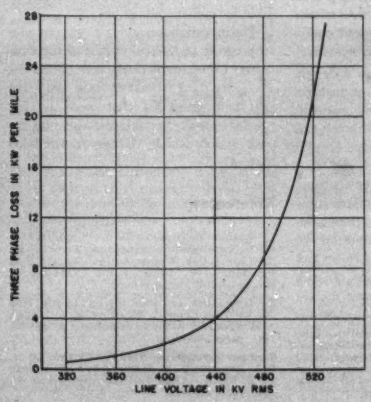

Figure 5 (left). Typical fair-weather corona loss curve

For 1.4-inch type *HH* conductor, 30-foot flat spacing, surface factor 0.9, air density factor 1.0

Figure 6. Fair-weather corona loss, calculated from Peterson's formula, as a function of conductor size, insulation level, and operation voltage

Smooth round conductors, surface factor 0.9, altitude 1,000 feet, temperature 25 degrees centigrade. Line construction:

No. of Insulators	Horizontal Spacing, Ft
20	27
24	33
30	43
35	51.5

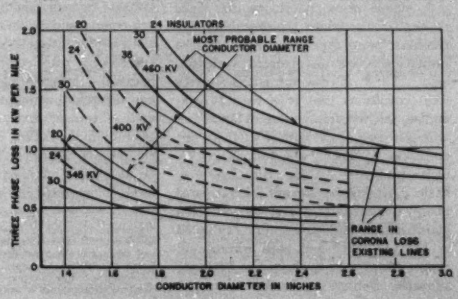

Table IV. Annual Charges for 100 Miles of 345-Kv Line Having 20 Insulators and 1.75-Inch Diameter Conductor

	Load in Megawatts		
	100	200	400
Capital	$450,000	$450,000	$ 450,000
Copper loss	67,000	259,000	1,033,000
Corona loss	13,000	13,000	13,000
Total	$530,000	$722,000	$1,496,000
Annual cost per kw	$5.30	$3.61	$3.74

curves of the three voltage levels covered in Figure 6 indicates that it probably would be impractical to limit the power loss to a constant value independent of operating voltage, if a level as low as 0.5 or 0.6 kilowatt per mile is desired since this would call for an extremely large and, therefore, impractical conductor spacing.

The curves of Figure 6 cover the most probable satisfactory range of line insulation that would be suitable for each operating voltage. Briefly summarized, these indicate that with present knowledge, satisfactory operation should be obtained with operating voltages up to 400 kv with transmission line insulation corresponding to 20 insulators. At 460 kv, the minimum number of insulators probably would be 24. A more accurate determination of the best combination of line construction and conductor diameter requires an economic study of the cost of the various combinations, taking into account loss evaluation, but no final conclusions can be drawn until more is known about corona and radio influence. The decision on this point alone might affect the cost of extra-high-voltage transmission very appreciably and justifies more tests to give the line designers better data.

Economic Comparison of Line Construction for an Operating Voltage of 345 Kv

A simple economic review has been made to co-ordinate the foregoing discussions, taking into account the effect of insulation levels on operating performance. The cost of a line varies so with local conditions that it is hard to generalize, but for this purpose $45,000 per mile was used as the cost of a 345-kv line employing 20 insulator units and a 1.75-inch conductor. Using this figure as basic capital cost, annual charges have been calculated. Interest, depreciation maintenance, and taxes were evaluated at ten per cent* and both corona and copper losses were evaluated at $100 per kilowatt. Table IV gives the results of a calculation for one condition. These figures emphasize the fact that corona loss, determined on present information and design practice, is a small factor in the over-all operating cost of a high-voltage line. If sufficient data are available on corona loss under all conditions, a closer design would be permissible with a possible large saving in the high-voltage system.

Rough estimates show about ten per cent increase in capital cost for building a line with increased spacing from 33 feet to 42 feet and about 25 per cent increase in cost for increase in conductor size from 1.558 inches to 1.901 inches for a given spacing. Thus, if better data will allow a smaller conductor diameter or smaller spacing, or both, capital cost can be decreased by a sizeable factor.

Table V shows the effect of increased spacing on corona loss for a given conductor and also decreased corona loss for increased conductor size for a given spacing and line insulation. These comparisons are based on present fair-weather corona loss data and indicate a real need for better data on corona loss and associated radio influence for the many varying conditions, so that the maximum capabilities of all equipment may be utilized to secure the most economical system.

Conclusions

The indicated need for developing higher voltage transmission and the fact that costs increase very rapidly with increased voltage make it increasingly important to evaluate carefully and precisely all engineering factors entering into the design of higher voltage transmission systems. This necessitates having precise and reliable data on the characteristics and performance of materials and equipment constituting transmission systems.

The two factors that influence design, and, therefore, costs of extra-high-voltage transmission lines and systems, are corona and basic impulse level, and the two are interrelated. There is good engineering reason for the belief that materially lower insulation levels than any heretofore attempted on extra-high-voltage transmission can be used successfully in the future, if all the unknown engineering questions that this raises can be answered. A specific series of such levels is presented in the paper.

*In this text ten per cent has been used as a composite rate for interest, depreciation, maintenance, and taxes for comparative purposes only. This figure should not be considered as the authors' opinion of a complete representation of all the cost elements entering into a rate structure.

Table V. Corona Loss Data

Conductor Size, In.	Estimated Effective Corona Loss Kw Per Mile*		
	20 Insulators, 33-Ft Spacing	24 Insulators, 37-Ft Spacing	30 Insulators, 42-Ft Spacing
1.558	1.60	1.38	1.12
1.610	1.46	1.28	1.06
1.750	1.28	1.10	0.92
1.901	1.14	0.98	0.80

*Assuming average annual loss is twice the fair-weather loss.

Of the questions that need to be answered, fairly good engineering data are now available on lightning and switching surges, insulation co-ordination, and the effects of line spacing on reactance and capacitance. But line spacing also affects corona. Some data are available on corona and radio influence, particularly on fair-weather corona losses for horizontal configuration on single conductor per phase and on how the surface affects these losses. There is need for corona loss and radio influence data showing the effect of ground wires on various combinations with single conductors and the effect of rain, fog, clouds, and other natural elements that make up the yearly weather conditions in a given location. Also, bundle conductors offer some advantages that need be investigated carefully to make possible proper weighing of advantages versus disadvantages. Such data would allow a closer estimate of corona losses so that they could be considered on an average loading basis, the same as other variable losses. All of this should lead to more precise design and the development of transmission systems operating at extra high voltages that would yield the maximum economies possible by higher voltage use.

The investigation and test program now in progress at the Tidd plant of the Ohio Power Company is planned to obtain the necessary data to answer these and other pertinent questions that need be answered to make possible the economic design of extra-high voltage transmission systems.

References

1. Corona Considerations on High-Voltage Lines and Design Features of Tidd 500-Kv Test Lines, C. F. Wagner, Anthony Wagner, E. L. Peterson, I. W. Gross. AIEE Transactions, volume 66, 1947, pages 1583–91.

2. Insulators and Line Hardware for Tidd 500-Kv Test Lines, I. W. Gross, R. L. McCoy, J. M. Shendel. AIEE Transactions, volume 66, 1947, pages 1592–1602.

3. Line Conductors—Tidd 500-Kv Test Lines, E. L. Peterson, D. M. Simmons, L. F. Hickernell, M. E. Noyes. AIEE Transactions, volume 66, 1947, pages 1603–12.

4. Transformers and Lightning Arresters—Tidd 500-Kv Test Lines, F. A. Lane, J. K. Hodnette, P. L. Bellaschi, Edward Beck. AIEE Transactions, volume 66, 1947, pages 1613–8.

5. Switchgear Equipment for Tidd High-Voltage Test Lines, F. A. Lane, B. W. Wyman. AIEE Transactions, volume 66, 1947, pages 1619–23.

6. Instrumentation and Measurement—Tidd 500-Kv Test Lines, R. L. Tremaine, G. D. Lippert. AIEE Transactions, volume 66, 1947, pages 1624–31.

7. Shielding of Substations, C. F. Wagner, G. D. McCann, C. M. Lear. AIEE Transactions, volume 61, 1942, February section, page 96.

8. Electrical Transmission and Distribution Reference Book. Westinghouse Electric Corporation, East Pittsburgh, Pa. Chapter 15, pages 393–6.

9. Power System Transients Caused by Switching and Faults, R. D. Evans, A. C. Monteith, R. L. Witzke. AIEE Transactions, volume 58, 1939, August section, pages 386–94.

10. Electrical Transmission and Distribution Reference Book. Westinghouse Electric Corporation, East Pittsburgh, Pa. Chapter 2, page 41.

11. Some Features and Improvements on the High-Voltage Wattmeter, J. S. Carroll. AIEE Transactions, volume 44, 1925, pages 1010–5.

12. Corona Loss Measurements on a 220-Kv 60-Cycle Three-Phase Experimental Line, J. S. Carroll, L. H. Brown, D. P. Dinapoli. AIEE Transactions, volume 50, 1931, pages 536–46.

13. Corona Loss Measurements for the Design of Transmission Lines to Operate at Voltages Between 220 Kv and 330 Kv, J. S. Carroll, Bradley Cozzens. AIEE Transactions, volume 52, 1933, pages 55–63.

14. Corona Losses From Conductors of 1.4 Inch Diameter, J. S. Carroll, Bradley Cozzens, T. M. Blakeslee. Electrical Engineering (AIEE Transactions), volume 53, December 1934, pages 1727–33.

15. Empirical Method of Calculating Corona Loss From High-Voltage Transmission Lines, J. S. Carroll, Mabel M. Rockwell. Electrical Engineering (AIEE Transactions), volume 56, May 1937, pages 558–65.

16. Symposium on Operation of the Boulder Dam Transmission Line—Insulation and Lightning Protection, Bradley Cozzens. AIEE Transactions, volume 58, 1939, April section, pages 140–6.

17. Comparative Investigations of D-C and A-C Corona on Two-Conductor Transmission Lines, Robert Strigel. *Wissenschaftliche Veröffentlichungen aus den Siemens-Werken*, volume 15, part 2, 1936, page 68.

Discussion

W. A. Lewis (Illinois Institute of Technology, Chicago, Ill.): In this paper and the discussions of it mention has been made several times of the formula for corona loss developed by W. S. Peterson. I believe there are two comments regarding this formula that should be made at this time.

The remarkable agreement between the formula and the large mass of test data on which it is based is very significant and is a tribute to the ingenuity and perseverence which went into its development. Although Peterson has not published the development of his formula, I have had the privilege of reviewing it, and I feel that he has done a remarkable job. However, it should be pointed out that the formula was derived before test data were available at the Stanford Laboratory on the smooth type *HH* conductors. Comparison of the formula with the test results for the smooth conductors does not show the same close agreement as is obtained with the test results for stranded conductors. Some consideration of the development would lead one to expect this situation, because the formula assumes that the corona loss for a stranded conductor is the same function of the critical corona starting voltage for a stranded conductor as it is for a smooth conductor. Hence, if corona loss occurs only in the regions which are stressed beyond the critical gradient, it would be expected that the loss would increase faster as the voltage is raised for smooth conductors than for stranded conductors. The test results indicate that this is generally true. Consequently, the application of the formula to a smooth conductor gives a corona loss which is too small in the range of voltage just above the critical corona voltage, which is the range likely to be of greatest interest. It is evident therefore that some modification of the formula, or the curve which applies to it, should be made for smooth conductors in the light of more recent test results so that the formula may give better results. As extensive data have been published on the losses of smooth conductors under fair-weather conditions, it will be possible for this to be done, but I believe no one yet has done it.

The formula derived by Peterson involves the use of the calculated critical corona starting voltage. The formula given for stranded conductors with more than six strands in the outside layer is rather complex and difficult to use. By extending the methods suggested by Peterson it has been found possible to devise a simpler formula which is given in the following equation. This formula is applicable not only to the case of more than six strands but also is valid for six strands in the outer layer. The result for six strands differs slightly from the formula for that number of strands given by Peterson, but the difference is relatively small, and it is believed that the results obtained by the new formula probably will be as accurate as those given by the old formula. In any case, the formulas presented are approximate, and the differences involved are much less than the range of the roughness factor, m, which must be estimated in each case, to take into account irregularities of the conductor surface. The critical corona starting voltage is

$$E_0 = 90\delta^{2/3} m r_n \left[\log \frac{s}{r_n} + \frac{0.137}{n} \right]$$

(kv rms line to neutral)

where E_0 is given in kilovolts rms line to neutral and

δ = air density factor
r_n = conductor radius, inches (circumscribing circle)
s = conductor separation (geometric mean separation) in inches
n = number of strands in outer layer
m = roughness factor

E. C. Starr (Oregon State College, Corvallis, Oreg.): This subject is of particular interest in the West where large concentrations of hydroelectric power are being developed at considerable distances from the load centers. The problem of economics of transmission of large blocks of power over long distances in this region has been given considerable study and various alternatives and possibilities have been explored carefully. The principal problems are those of line and substation costs, transmission losses, and system protection. In common with the authors, we have concluded that where proper protection is employed insulation levels can be reduced one and possibly two steps in terminal apparatus and that the line insulation can be substantially reduced. Figure 1 of this discussion presents the results of a study of line insulation based upon switching surges and upon desired degrees of lightning protection with and without ground wires and with high-speed reclosing of line circuit breakers. It will be observed that we believe it may be feasible to reduce the line insulation levels even below those proposed by the authors. For example, we believe that under normal conditions of contamination satisfactory 230-kv line insulation can be obtained by using 12 to 14 standard suspension units without grading shields. The curve indicates that the line insulation required for 287.5 kv, 345 kv, and 402 kv with grading shields is approximately 16, 18, and 20 units, respectively. This reduction in insulation in areas of normal contamination would result in considerable savings in structures and corresponding decreases in line costs.

A preliminary study has shown that when these insulation levels are employed, the relative line costs as a function of operating voltage should be approximately as shown in Figure 2 of this discussion. The conductors included in the estimates were of appropriate diameters for effective corona control.

The second curve in Figure 2 gives the approximate relative power limit of a long line between typical large fixed terminals as a function of line voltage. It is shown that the power limit for conventional uncompensated lines increases more rapidly than the line cost. With 230 kv as base, the power limit at 345 kv, for example, is increased 90 per cent as compared with a line-alone cost increase of 65 per cent. This margin, however, is decreased considerably in the complete analysis largely because of the rapidly increasing costs of line terminals and intermediate stations at the higher voltages. A further decrease in the margin is probable when, for any specific case and proposed voltage, maximum economic advantage is taken of possible technical refinements such as series capacitors and multiple phase conductors.

For any case, in order to obtain the most economic performance of a transmission facility it must be designed for and operated at or near the average, or effective, load of maximum economy. For the ordinary 230-kv circuit this is approximately 175,000 to 200,000 kw and it varies about as the square of the line voltage, being in the neighborhood of 400,000 kw for a 345-kv circuit. If a high-voltage line is considerably underloaded in terms of its economic limit, the over-all transmission cost per

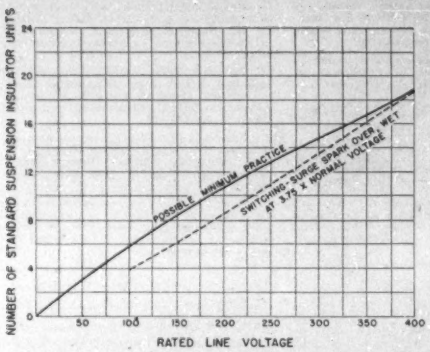

Figure 1. Suspension insulator requirements for steel-tower construction

Add one full unit when grading shield is employed

unit of energy increases rapidly, and a line of lower voltage with the same loading might give better economy.

For very long distance straightaway transmission of large blocks of power the extra high voltages, with all factors carefully co-ordinated, should be given careful consideration and study. Several of the important factors not heretofore evaluated will be made available by the experimental studies outlined by Sporn and Monteith.

D. M. Jones (General Electric Company, Schenectady, N. Y.): The present high-voltage tests on lines and equipment at Tidd are most opportune; and for the following reasons:

1. From the experience with the conversion of industry for national defense, in his recent past; and with the reconversion of industry for the sustenance of his way of life, at present; the average citizen is now profoundly aware that our civilization, both in times of stress and under normal conditions, is based on an adequate supply of electric energy.

2. Coincidentally, it is now increasingly apparent to all, that the adequate broad distribution of electric energy necessitated by our national requirements indicates a new emphasis on transmission, both to carry in the power from the generating sources, which become more remote from the loads as the power systems develop, and to permit the attainment of that flexibility and diversity in the design of the power systems themselves, which is increasingly vital to their ability to meet the requirements of the future both in war and in peace.

3. At the same time, there is an awakening realization among the power system engineers of the country that the transmission of electric energy, now more important than ever, can be accomplished with greater certainty of design and of performance, and at lower relative costs, than ever before, through the steady advance in technical knowledge and understanding in this field.

4. This new certainty of transmission design and performance is born of definite broad advances in technical understanding which now permit the engineer accurately to study and evaluate contemplated variations in power system patterns and practices by means of the analytical approach; and of his broad use of this approach, as exemplified by his present extensive utilization of a-c analyzers and other calculating devices. Out of all this has come an understanding which encompasses such realizations as the economic inevitability of "line compensation" as a substitute for the sustained advance of transmission voltages as transmission distance continues to increase, and the resultant establishment of a maximum economic transmission voltage due to rising transformer costs with voltage.

5. This further reduction in transmission costs will result primarily

(*a*). From the growing acceptance of the consideration supported by increasing experience, that the investment is reduced when power system overvoltages are limited by proper system design and suitable devices, and the line and equipment insulations then lowered proportionately, in distinction to the acceptance of such overvoltages on an unlimited basis.

(*b*). From the further application of the idea of using as few transmission voltages as possible, in the interest of exacting the maximum benefit from quantity production in reducing the cost of transmission lines and equipment.

(*c*). From the rising acceptance of the American type of power system, now time proved over many years, where in proper transmission design and performance is based on

1. The ultimate acceptance of relatively high short-circuit duties at major transmission levels in the interest of increased stability and an improved overall simplicity of system design.

2. The clearing of the heavier faults quickly, effectively to eliminate any hazard from them to acceptable system operation.

3. The provision for automatic reclosing in standard circuit breakers so that the reclosing procedure can be applied whenever or wherever helpful.

4. The use of low resistance lines, and the adoption of correspondingly higher line load levels.

5. The operation of transmission lines at essentially unity power factor, thereby permitting both their maximum utilization for carrying power, and the delivery of that power with minimum voltage variation throughout the transmission system.

Taken altogether this delineates a power system which provides power to the user with a quality and a reliability and at a cost commensurate with the responsibilities of this product in its present status as the very foundation of our national well-being.

The magnitude and importance of power transmission, and the already demonstrated improvement in its performance and costs made possible by the advancements in its underlying technical knowledge and understanding, amply justify any effort to further augment fundamental data in this field.

The present effort therefore, is not only timely and judicious, but also a fine testimonial to the forward-looking attitude of American power system engineers.

Abe Tilles (Pacific Gas and Electric Company, San Francisco, Calif.): The work already done, as reported in this paper, and the tests now being commenced are both of the widest interest and importance. The paper truly points out that the high costs to be encountered make it necessary to ascertain by tests "the very minimum proper margins of safety" and points out that with switchgear giving not more than a single restrike, switching surges will not be above three times normal. Such a factor of safety of 3 is definitely less than similar factors of about 4.5 widely used on 230-kv lines.

This acceptance of a lowered factor of safety raises these general considerations. In the past initial constructions at then new high voltages have often cushioned the large expense of new developments by retreating to somewhat lowered factors of safety. Subsequently, as the new voltage level was considered with less apprehension, it was found desirable to treat it with a larger factor of safety again. Thus the first two lines in the world at the now widely used 220-kv level, both of which are located in California, are insulated with 13 insulators,[1] but later lines built by the same companies used 15 or more insulators; and up to 20 insulators have been used for this voltage.

It is true, however, that at lower voltages a variety of requirements influence the need for insulation, and to cover all of them a sizable factor of safety is used. In going to high voltages the line is necessarily so well insulated that some of the requirements are already more than met and only certain of the requirements stand out. If these few are indeed well understood, then a lowered factor of safety will be sufficient.

Specifically, the line insulation, both porcelain and air, must meet these four conditions

(*a*). *Lightning voltages.* As fully pointed out in this paper, these do not alter greatly in going from a 230-kv line to a 345-kv line and the problem of insulating for them is, therefore, definitely easier on the higher voltage line. The contrary is also true; 69- and 110-kv lines, as is well known, are much harder to protect from lightning.

(*b*). *Switching surges.* Sixty-cycle voltages up to 4 or 5 times normal have been measured although many systems do not experience as much as 3 times normal. This item provides a handy peg on which to hang the commonly used factor of safety of wet flashover at about 4.5 times normal. It is so used on many systems to provide against initial flashover because of items (*a*), (*c*), or (*d*) where there is little experience or concern over flashover caused by switching. A factor of 3 for switching surges on the 345-kv line appears entirely reasonable. This does not, however, determine the insulation as might be supposed from a cursory reading of the paper. The very useful insulation co-ordination chart[1] known to the authors of these papers, and similar auxiliary wet flashover data, indicate that this particular requirement calls for about 15 insulators on a 345-kv line. This insulation would not meet items (*c*) and (*d*) adequately and it is to be noted from the other papers that a string of 20 to 24 insulators is the one actually to be studied for this voltage.

(*c*). *Insulator contamination.* Of the *n* insulators used in a 220-kv string a certain number, (*n-m*), is

needed to hold some specified voltage and the rest, m, can become completely contaminated, momentarily, without causing flashover. Multiplying the line voltage by 1.5 requires the number $(n-m)$ to be multiplied by about 1.5, but the number m need not be so multiplied. This lower factor of safety expectation on the longer string is borne out in practice; 115-kv lines with 7 to 11 insulators give more flashover trouble than 230-kv lines with 13 to 20 insulators, even in essentially lightning free territory.

(*d*). *Air gap.* The strike distance or clearance distance from conductor hardware to tower is approximately a rod-to-plane gap. Insofar as overvoltages of some multiplier times the line voltage are being considered the strike distance increases considerably more rapidly than the line voltage. See Figure 7 of reference 3. Insofar as the clearance is considered as some electrical clearance plus a certain number of inches for some extraneous item such as a tree branch or a hawk, multiplying the line voltage by 1.5 does not multiply the wing spread of the hawk at all, hence allowing a lowered factor of safety on the higher voltage line.

A proper choice between the two contrary indications just mentioned is a matter of interest and of great influence on the consequent dimensions of the tower and insulator string. None of the papers presented states what minimum air gap clearance it was considered necessary to maintain for operation at 345 kv or 460 kv. It would be of interest to hear. The test line tower appears ample for 345-kv operation and 500-kv test. It appears small for 500-kv operation. Was it expected to be adequate for 500-kv operation?

Because of the long string and long clearance distances involved, the lateral swing of the insulator string has a marked effect on tower dimensions at higher voltages. The possibility of eliminating lateral insulator swing by some device—such as using two strings in a triangular mounting or having the hardware such that the insulators in the one string are only free to move in the direction of the conductor—becomes of interest. Was this considered?

Were tentative dimensions of a twin circuit established, and if so, what were they?

REFERENCES

1. LIGHTNING PERFORMANCE OF 220-KV TRANSMISSION LINES—II, **AIEE Committee Report.** AIEE TRANSACTIONS, volume 65, 1946, February section, pages 70–6.

2. INSULATION CO-ORDINATION, **Philip Sporn, I. W. Gross.** ELECTRICAL ENGINEERING (AIEE TRANSACTIONS), volume 56, June 1937, pages 715–20.

3. SPHERE-GAP AND POINT-GAP ARC-OVER VOLTAGE AS DETERMINED BY DIRECT MEASUREMENT, **J. S. Carroll, Bradley Cozzens.** AIEE TRANSACTIONS, volume 48, 1929, pages 1–9.

Wm. S. Peterson (Department of Water and Power, The City of Los Angeles, Calif.): In discussing this paper I first want to express a debt of gratitude which I believe the public utility industry and the electric equipment industry owe to the authors and the various companies associated with them in this experimental high-voltage test project.

I am happy to confirm the authors' judgment in their discussion of the reasons for the investigation wherein it is indicated that more information than is now available is necessary before extra high voltage systems can be designed with close margins for economy yet without unduly sacrificing the requirements for reliability.

I am in agreement that high-voltage lines now can be built successfully to withstand lightning with presently used levels of insulation, and that with respect to switching surges circuit breakers are now available which so limit restriking that we no longer have to give consideration to voltages of five or seven times normal to avoid flashover. Although the equipment used on the Hoover Dam–Los Angeles 287.5-kv lines confirms this experience, it was not known at the time of planning that the experience with respect to switching surges would be so favorable.

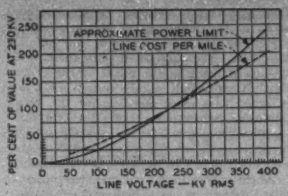

Figure 2. Transmission line cost and approximate relative power limit between terminals of fixed size

Total investment exclusive of terminals and intermediate stations

Average right of way; single-circuit steel-tower construction without ground wires or counterpoise

On the Pacific Coast, however, we have another factor affecting the amount of insulation required for lines that may interfere with lines in that area being able to operate with the reduced voltage level indicated in this paper. I refer to the contamination of insulators within a few miles of the ocean where the prevailing winds are such as to bring contamination to the insulators in the form of a salt-carrying fog. This, in combination with the long dry period which results in accumulation of dust, provides sufficient contamination so that 12 standard suspension insulator disks on 132-kv or 24 standard suspension disks on 287.5-kv lines will have flashovers in such areas several times per year. I do not believe this consideration will prevail at the test location at Brilliant, Ohio, but it is a very serious consideration on the Pacific Coast and a few other spots in the United States.

It should be pointed out that the relatively low values of corona loss that were used as being illustrative of present practice on high-voltage lines was the result of making allowance in the design of such lines for unknown factors that might affect such losses. The endeavor was to have a line which would not be operating too close to the knee of the corona loss curve. The advantage of such procedure in the case of the Hoover Dam–Los Angeles lines became apparent when at some isolated locations in the desert we found that higher losses were encountered than those that could be explained in terms of the known corrections. In our opinion at the present time these higher losses are associated with desert conditions, but we will be watching with interest whether any unusual losses appear in the course of the experiments on the installation at Brilliant. When the factors affecting corona loss become better known the choice of conductors and spacings should be made in the manner outlined in this paper.

I am thoroughly in accord with the need for making corona loss observations under conditions involving rain and snow and determining the radio influence of corona under all conditions, as will be done in this test.

R. T. Henry (Buffalo Niagara Electric Corporation, Buffalo, N. Y.): This paper and the tests being undertaken at the Tidd plant are an outstanding contribution to our fund of information regarding high-voltage transmission. One cannot help being impressed with the amazing difference in the confidence with which we approach such a problem now as compared with some of the early adventures in high-voltage transmission such as those at Telluride, Niagara to Buffalo, and Niagara to Syracuse.

It is gratifying to see proper recognition of the difference in insulation requirements between grounded and ungrounded neutral systems. It is also gratifying to see proper recognition of the fact that the ratio of insulation strength to operating voltage safely may be reduced at the higher operating voltages. It is to be hoped that adequate recognition of these differences soon will be made in our various standardization activities.

There is one question however, which should receive further consideration, namely, the question of the economics of transmission at these higher voltages in terms of the firm capacity of a complete power system. Obviously these higher voltages will involve very large amounts of power per circuit, probably as much as 300,000 or 400,000 kw or more. The interruption of such a large block of power is a serious matter, even in a very large power system.

While we confidently can expect to avoid outages due to lightning, we must recognize the likelihood of outages due to other causes and some provision must be made for such outages. It would be interesting to know the effect on the economics of transmission at very high voltages, if adequate provision is made for carrying the load during outages on one circuit in a complete system operating at these higher transmission voltages.

M. M. Samuels (Rural Electrification Administration, Washington, D. C.): This paper and the companion papers represent an important milestone in the history of power. Even though the tests are just about beginning and no reports are available of any results, the papers already present important information

1. They are a complete presentation of all past experience.

2. They are a complete presentation of all pertinent literature, American and foreign.

3. They exhaust all analytical possibilities, so that the tests can limit themselves to these features that cannot be determined analytically.

While this and the companion papers primarily were intended to serve as a foundation for the tests, they represent a textbook on the subject, making it unnecessary from now on for anyone who is interested to dig through past literature or to try to determine what can be done analytically. It is suggested that all the papers be combined into one book and published as such. They

will be of inestimable value to the practical engineer, the professor, the student, the textbook author, and the handbook author.

It is gratifying to note that the authors consider lower insulation values for lightning arresters. This means better protection at lower cost. The idea was in the minds of many engineers for a long time. It is natural to try to make the lightning arrester weaker than the transformer. It is preferable to lose a lightning arrester than to lose a transformer, if something has to be lost at all. But this is no longer a mere idea. It is no doubt based on several years of experience on the 37-kv part of the American Gas and Electric Company's system, the results of which were presented in a previous AIEE paper. In the past, manufacturers were not anxious to participate in such experiments. It is therefore particularly gratifying that a representative of a large manufacturer, as coauthor of the paper, participates in the suggestion. Further studies should serve the purpose of establishing the degree of lowering the voltage level for each standard operating voltage.

In connection with the assumption of 10 per cent for interest, depreciation, maintenance, and taxes, the authors properly state that this should not be considered as their opinion of a complete representation of all these cost items. While such a statement may be considered unnecessary for the practical engineer who knows that no two conditions are alike as to cost and never bases his cost estimates on anything but actual figures applying to the specific case, the statement is definitely necessary for some economists, accountants, and statisticians who do not consider a power system as a functioning organism but as a mere set of accounts or statistical figures, and to whom the cost figures may be the only straw in the papers that they can grasp. It is assumed that the authors intended the statement to apply equally to all other cost figures in the papers. However, it is hoped that, for the engineers' purposes, the authors eventually will present in another paper a complete cost analysis, arranged in accordance with a definite classification of accounts and giving the basis for each assumption.

Of course no engineer will consider such a setup as something he can copy blindly, but it will serve him as a guide. He can put in his own figures for a given condition and make sure that he does not overlook anything. After all, the whole purpose of the investigation is economy and the final report should be complete and concise as regards economy.

J. G. Holm (Gibbs and Hill, Inc., New York, N. Y.): It was with great satisfaction that I learned of the extra high voltage network which the American Gas and Electric Company proposes to build and of the Tidd tests planned in this connection. I have read with great interest the paper presented, particularly as for several years I have been making studies of extra high voltage transmission lines and have indicated the economic advantages of the 345-kv lines in a paper presented before the Institute a few years ago.[1]

The authors of the paper must be highly complimented for the courageous and broad conception of the entire problem and also for their attention to details. Let us consider some of the major parts of the study—system insulation level, corona, and voltage selection. The basis of this discussion is a statement made in the paper to the effect that an extra high voltage system must be designed with close margins, for the very minimum proper margin of safety without sacrificing requirements for reliability. To me, this is one of the soundest statements ever made, and I subscribe to it completely.

As the authors point out, the most important problem in extra high voltage transmission is the selection of proper insulation level and insulation co-ordination. The insulation level affects the cost of terminal equipment, the conductor spacing, line reactance, corona loss, conductor diameter and the cost of supporting structures. The insulation, therefore, is of prime economic importance and must be established at as low a level as practicable when considering lightning and switching surges only. The authors' proposal to establish a basic impulse insulation level one step below standard values is highly commendable and is supported by recent operating experience and statistics on lightning strokes and line outages. The definite upper limit required by line insulation indicates that a straight-line extension of insulation levels when going to higher operating voltages is too conservative and that, therefore, the "derated" basic impulse insulation level proposed by the authors for the line, transformers and lightning arresters will prove to be sufficient. Twenty insulators for a 345-kv suspension tower and 24 for 460-kv are, however, probably necessary on economic grounds, although from the system-protection standpoint even a smaller number of insulators is theoretically sufficient. It seems to me, however, that it would pay to consider the possibility of grounding the sending-transformer neutral through a resistance. This will affect the insulation of the sending transformer, but in return the system stability limit will be increased appreciably.

The authors of the paper correctly state that the conductor corona loss must be evaluated economically. The higher the voltage and the larger the block of power transmitted, the greater is the corona power loss which it is economically possible to allow. As the diameter of the conductor is increased to secure lower losses, the cost of these losses decreases at a much smaller rate than that at which the cost of conductor and its supporting structures increases. The increase in the insulation level and in the electrical spacings that follow from it result in an increase in cost of line far greater than the reduction in the cost of corona power loss that follows an increase in conductor spacings. Therefore, the selection of insulation level should be decided entirely apart from corona considerations. The most economical solution will not be obtained by relating the number of insulators and the conductor diameter, but by adopting as low an insulation level as is permissible when considering lightning and switching surges and by selecting a conductor of as small a diameter as permissible for the largest possible corona power loss the system can economically stand. Since corona loss depends on so many factors—fog, rain, snow, humidity, surface condition, sea level, temperature, proximity effects—the effect of which it never will be possible to establish rigorously, it may be just as correct, and certainly more expedient, first to determine the maximum economically permissible corona power loss. From it the fair-weather corona loss can be fixed applying as high a safety factor as 3.0 or 4.0. Using then either Peterson's formula or the Carroll–Rockwell method, for the conductor diameters and spacings that might be approximately correct, the minimum conductor diameter can be found for a conductor of adequate copper cross section. The choice is pretty sure to be very close to an over-all most economical solution. Here in determining the fair-weather corona loss it would be better to take a more conservative attitude, that is, not to take the 1,000-feet altitude and 77 degrees Fahrenheit of the authors, but to calculate for 3,300-feet elevation and 50 degrees Fahrenheit. This latter condition gives a loss just in between that obtained for the two extreme conditions of 1,000 feet, 77 degrees Fahrenheit, and 3,300 feet, 77 degrees Fahrenheit taken by electric apparatus designers, and is a safer assumption. Calculated for this condition at prevailing costs and at a reasonable cost of power losses, the over-all economical solution for a 345-kv line, with a 33-foot spacing required for 20 insulators is obtained with a 650,000-circular-mil type *HH* conductor of 1.4-inch outside diameter.

With reference to radio influence, it is a known fact that no objectionable effects are obtained at 230 kv, and it is probably safe to say that with the special clamps so ably developed by the manufacturers for the Tidd tests, no excessive radio influence will be observed at voltages considerably in excess of 230 kv.

Since great care is exercised in eliminating unreasonable safety factors in the system electrical design, it would seem to me consistent to apply a similar discrimination to the mechanical design of supporting structures. The safety factors applied in the design of transmission towers vary widely between the various steel construction companies, and in spite of this, mechanical tower failures very rarely have occurred in major transmission projects. The minimum margins of safety, without sacrificing reliability, which the authors so fittingly advocate, should be applied as well to the supporting structures of systems where the cost of the transmission line alone constitutes a high percentage of the total system cost, if an over-all minimum cost is to be secured.

In applying the Tidd test data to any particular system, the decision of prime importance is the selection of an appropriate voltage. It has been shown before[1] that there is a certain economic relationship between the transmission distance, the block of power transmitted, and the transmission voltage, or in other words, for a transfer of a specific block of power over a specific line, there is a definite voltage by which the transmission may be accomplished most economically. Since the results of the Tidd tests first will be applied to the American Gas and Electric Company system, it seems to me, on the basis of available public knowledge of this system, that the selection of a 345-kv voltage very nearly will approximate the most economical solution even allowing for future growth. In Sweden, for example, it is planned to transmit a-c power at 380 kv over a distance of 600 miles. When 650,000-circular-mil type *HH* conductors having 1.4-inch outside diameter are used on a line

with 20 insulators and 33-foot spacing, 500,000 kw can be transmitted over two such circuits with 345-kv voltage, over a distance somewhat greater than 200 miles. Such a system would be stable even with a loss of one half of one circuit, as a result of a double line-to-ground fault, provided that high-speed circuit breakers are used and low tower-footing resistances are secured, in conjunction with other stability-improving devices including modern generator design. For such a condition 345 kv is the most appropriate voltage. If, however, these new lines are to connect existing generating stations with generators perhaps not of the latest design insofar as transient reactance, inertia, and dampers are concerned, then, of course, the block of power that safely can be transmitted will be somewhat smaller. It should be borne in mind that if a higher voltage—402 or 460 kv—is used on a 200- to 250-mile line, conductors of at least 1.65- and possibly as much as 2-inches diameter must be used. Moreover, circuit breakers of greater than the 10,000,000-kva interrupting capacity developed for the Tidd tests probably would have to be built. Considering the costs involved, this voltage would be economical only if the block of power to be transmitted is sufficiently large.

In conclusion, I wish once more to compliment the authors for the Tidd tests undertaking.

REFERENCE

1. COSTS STUDY OF 69- TO 345-KV OVERHEAD POWER-TRANSMISSION SYSTEMS, John Grzybowski Holm. AIEE TRANSACTIONS, volume 63, 1944, pages 406–22.

P. L. Bellaschi (consulting engineer, Sharon, Pa.): It is apparent from the paper that the economics of power transmission at the extra high voltages gravitate very largely about the insulation requirements for the station and the line, in addition to the corona problem. To attain the utmost in economy in keeping with a high degree of reliability which systems of this character require, the insulation design of necessity must be rationalized to the fullest, specifically in relation to the actual service requirements which are three

1. Lightning protection.
2. Ability of station and line to withstand switching surges.
3. Satisfactory operation at normal 60-cycle voltages.

To this end the approach must be in terms of fundamental thinking, free from preconceived idea or questionable relations we may have inherited or been wont to fall back to in the past. Much in the way of fundamental work already has been done as evidenced from this paper and in a companion paper in connection with the impulse levels proposed for solidly grounded neutral application.

Following this fundamental approach it well may be possible to reduce the levels proposed even a notch further eventually. Additional improvements in protective devices and protective measures are quite conceivable and in that event the present full 230-kv level (1,050 kv) then would appear to offer practical possibilities on a 345-kv solidly grounded neutral system. This statement holds particularly for the oil-immersed apparatus as the internal insulation of transformers. Should this situation develop, naturally the 230-kv insulation design has to be satisfactory also for continuous operation at 345 kv.

To repeat: the basic insulation requirements to which attention must be given at all times are three

1. Lightning.
2. Switching surges.
3. Continuous operation.

In some applications one of these requirements may predominate, submerging the other two in importance, but if we are to achieve the most in all applications and especially at the extra high voltages, it is well that all three are kept in view.

Today the high-voltage engineer is in the spotlight, it would seem. He has before him the opportunity of a lifetime for some real advancements in the art, not only in the field of high-voltage transmission but equally as well in carrying the benefits and economies such as the additional reduction in insulation now being considered for solidly grounded neutral applications above 230 kv, down into the lower voltages. However, much that has been found good practice and is substantiated by experience certainly stands to remain.

Francois Cahen (nonmember; Paris, France): I took great interest in reading the papers of the symposium on Tidd 500-kv test line, and particularly as I am in charge of the 500-kv experimental line and station of "Electricite de France," which were put in service in Chevilly, next to Paris, at the end of the year 1946.

First I must state that I share the opinions of Sporn and Monteith when they point out that the choice of the voltage to be adopted in the future for systems above 230 or 287 kv should not be made without possessing a thorough knowledge of characteristics of material and installations to be used on such extra high voltage systems. I agree also that the two most determinant factors for the cost of transmission are for the transformers and switching station material, the insulation level; for the line itself, the corona effect. But those two factors are not bound closely to each other as, for instance, by using lightning arresters, the insulation level for the material may be chosen for a given operating voltage, without consideration to the insulation level of the line, at least within certain limits. This means that the two factors may be studied separately, but, of course, they both react on the transmission costs.

Nevertheless, the calculation of the optimum voltage may lack precision, especially at extra high voltages when the range of the transmission becomes such that it permits to think about interconnection between far distant systems belonging to different countries or to separate industrial groups. In such cases, the distances over which a given power has to be transmitted, and the values of the power exchanges cannot be foreseen with accuracy, as they may change in the future, according to development of the load and installation of new power sources. Besides, some bases of economic comparison may change in such a way as to be favorable to a future increase of voltages; for instance, the cost of transformers and circuit breakers may decrease when they have been constructed and tested in the field and when they will be manufactured in large quantities. Therefore, I think that the choice of a new voltage level should be made without trying to compute too closely its economical optimum value. This choice should be based essentially on the following features: taking a large step so that the new systems may carry much larger loads than the existing systems, or carry them to much larger distances—nevertheless, choosing such a voltage that may be faced rationally as concerns material and line engineering practice.

On account of this, we now are facing, in France and in other European countries, a new voltage level defined by the figures

Maximum voltage in normal operation, 400 kv.
Average voltage of the system, 380 kv.

This level would satisfy the requirements of our different systems and later on would permit the interconnection of them without any use of transformers.

In France we have to look at the following problems: all our hydro generating power is located in the southern half of the country and an important part of it has to be transmitted to the northern half, so we have to carry large amounts of power over an average distance of 300 miles. At the present time we use for this transmission 6,200-kv circuits. This number will be increased to 7 at the end of this year; to 8 at the end of the following year and it should be increased to 10 or 12 within 4 years if we do not step up to a higher voltage. Certainly it is uneconomical indefinitely to multiply the number of circuits to handle the increasing power and the time has come when a higher voltage has to be considered in our country.

We therefore chose a solution which would enable us to develop our 220-kv system without compromising the possibility of stepping rapidly up to 400 kv at the time when it will be necessary, without keeping too large a number of 220-kv circuits in operation later on. We designed, therefore, a double-circuit 6-conductor 220-kv line, which may be changed readily into a single-circuit 400-kv line; each 400-kv phase being provided with a bundle of 2 standard 220-kv aluminum-steel 1.04-inch conductors. The stepping up from 220 to 400 kv then would need only the bringing together of the conductors and the displacing and lengthening of the insulator strings.

Such a line, 250 miles long, is working at 220 kv since January 1947. Also, we have designed and constructed a 500-kv experimental station, including a 1,650-foot span of line with 48-foot phase spacing and a bank of 3 single-phase transformers delivering a voltage adjustable between 300 and 500 kv, 50 cycles, for investigation on corona effect and bundle conductors.

This station, located next to Paris, was put into operation in December 1946, and we gathered since that time many very important data. It would be much too long indeed even to summarize the results of our tests, and I shall confine myself to furnishing some characteristic figures and to answer briefly, on the basis of our data, certain questions. Up to now, our tests principally have been as given in the following paragraphs.

1. *Corona loss measurements.* The voltage being variated from 300 to 550 kv, and corona losses records at constant voltage;

we studied especially the form of the corona curves, the influence of conductors weathering, and the influence of atmospheric conditions; our station remaining under operation in all kinds of weather, as snow, ice deposit on conductors, storms, heavy and light rains, and fog. We studied also the influence of conductors spacing in a bundle, horizontal or vertical arrangement of the bundle, and the influence of ground wires, and we measured the losses of insulator strings.

We found that according to calculation the minimum losses are obtained, with the bundle arrangement, when the space between conductors is within the range of 8 to 16 inches. Some characteristic figures for the losses are given in Table I of this discussion.

The maximum recorded peaks in kilowatts per mile on weathered conductors have been the following at 400 kv:

Fog	64
Medium rain	96
Heavy rain	160

The maximum ratio for 400-kv losses, according to these figures, is

$$\frac{160}{0.8} = 200$$

It means that for a line operating at surge-impedance load (500 megawatts at 400 kv with bundle conductors, 16-inch spacing), the corona losses will be within the range of 1.2 to 150 per cent of ohmic losses.

As regards the influence of weather conditions, we found that they not only shift the corona curves, as stated by Sporn and Monteith, but they also distort them. Weathering has a similar effect, but we found that weathering occurs only when conductors are under voltage and not by simply exposing the conductors to atmospheric agents, without voltage.

Table I. Three-Phase Losses in Kilowatts Per Mile

	380 Kv	400 Kv	440 Kv
Fair weather:			
Unweathered conductors	1.9	2.3	4.2
Weathered conductors	0.6	0.8	1.6
Bad weather, unweathered conductors:			
Fog and ice	12.2	22.5	71
After rain	6	6.7	10
Weathered conductors, fog	1.9	2.2	3.7

We now are starting tests with single hollow conductors with diameter of 1.6, 1.8, and 2 inches. We studied also the effect of ground wires and found that there was little influence below the knee of the corona curve, but that it increased rapidly above the knee.

2. *Insulator strings losses.* We measured them on single and double insulator strings; by fine weather at 400 kv, the measured losses were 3 watts per string. This is a very low value, so that it is unnecessary to take it in account when measuring the total line-plus-strings losses. We found that the grading rings on the line end of the insulator strings work very efficiently to shield the lower units and suspension clamps.

3. *Radio disturbance measurements for different conductor arrangements and weather conditions.* We found especially that the field level close to the 400-kv line is about the same as in the neighborhood of our latest 220-kv lines.

4. *Mechanical behavior of bundle conductors under short-circuit conditions.* This is an important question to be settled in order to choose the spacing between conductors and the number of spacers to be placed in each span.

We are continuing on our tests, but we already have come to the opinion that the use of bundle conductors is a sound practice for extra high voltages and that our line may be operated at 400 kv or even at a somewhat higher voltage.

Philip Sporn and **A. C. Monteith:** We are delighted with the interest displayed in the project by the membership of the Institute, and we particularly wish to thank the large number of discussers who have taken the trouble thoroughly to review the paper for that purpose.

It does not look to us as if any major gain would accrue at the present time by commenting in detail on each specific discussion. In some cases that would involve extensive additional proof which is not, however, particularly germane to the main purpose of the paper—at present the why and wherefore of the investigation. As to that, it seems to us that there is a substantial unanimous agreement among all discussers.

One specific question that requires answer has been raised. The answer to Tilles' question as to the voltage for which the tower was designed is that the design proper was projected as one that might be operated at voltages up to 500 kv. Whether the physical dimensions of the present towers would be adequate for a voltage as high as the maximum is something that cannot be determined until some of the investigations now under way are completed.

Corona Considerations on High-Voltage Lines and Design Features of Tidd 500-Kv Test Lines

C. F. WAGNER
FELLOW AIEE

ANTHONY WAGNER
NONMEMBER AIEE

E. L. PETERSON
MEMBER AIEE

I. W. GROSS
FELLOW AIEE

THE principal factors that must be considered in the transmission of large blocks of power by alternating current over great distances have been pointed out in a companion paper by Sporn and Monteith.[1] The paucity of corona loss and radio interference data requires further information on this subject before intelligent contemplation of transmission at extra high voltages can be undertaken. To obtain such data the American Gas and Electric Service Corporation with the co-operation of a number of manufacturing companies has constructed two $1^1/_2$-mile transmission lines at the Tidd power plant located at Brilliant, Ohio. These lines can be energized in small increments of voltage from 260 to 500 kv. In addition to corona characteristics, performance of transformer insulation, bushings, insulators, lightning arresters, conductors, and other apparatus under sustained high voltage also will be determined.

This paper will review the present knowledge of corona, describe the general layout of the test setup, and discuss the scope and some of the objectives of the tests. It will describe in detail the towers and considerations which determine their design. Companion papers will discuss the transformers[4] that energize the line, the insulators,[3] the conductors,[2] the lightning arresters,[6] switchgear equipment,[5] and the means for measuring corona loss.[6]

The first important experimental work on corona was done about 1898 by Doctor C. F. Scott at Pittsburgh, Pa., and was continued on the Telluride lines in Colorado. Subsequent observations were made among others by Converse, Mershon, Ryan, Peek, Whitehead, and Facciole. Peek developed and presented empirical formulas that for years were regarded as the best information available. Subsequently the Ryan Laboratory at Stanford University and other Pacific Coast investigators attacked the problem and provided much useful data. Loss measurements were made with stranded copper conductors ranging in diameter from 0.91 to 1.49 inches, stranded aluminum conductors with diameters from 1 to 2 inches, and smooth segmental conductors with diameters of 1.1, 1.4, and 1.65 inches. Some single-phase configurations were studied but most tests were made with a flat 3-phase configuration and spacings between conductors ranging between 22 and 30 feet. Practically all of the tests were made in fair weather. The principal emphasis of these studies was on the effect of various types of conductors and variations of surface conditions. Due to die grease and the burrs incident to manufacture and stringing, new conductors have higher corona losses than those that have been in service several months. A proper washing technique can eliminate this initial high corona.

Three formulas are available today to compute corona loss. These are

1. Peek.[7]
2. Peterson.[8]
3. Carroll and Rockwell.[9]

The degree to which these formulas agree with test results for a specific case in fair weather is shown in Figure 1. Transmission lines today are built so that the loss under fair-weather conditions is usually below 0.5 to 1 kilowatt per mile. These curves show, therefore, that the Peek formula in the region in which line designers are most concerned does not agree with tests, whereas the other two methods indicate remarkable checks.

The transmission projects at voltages in excess of 287 kv are sufficiently important to justify experimental data on a range of conductor sizes that eventually will be used. The proposed tests are intended to project information into the realm of the higher voltages for some currently available conductors and for some special conductors designed for extra high voltages. Little information is available concerning the proximity effects of ground wires and towers as practically all the previous tests were made without ground wires and without conventional towers. Further information also is required concerning radio influence resulting from corona as affected by weathering of conductors and atmospheric conditions such as snow, rain, and ground gradients upon corona. The present state of the art and the necessity for further information concerning these factors now will be discussed.

Corona

Projection of transmission voltages into the realm up to 500 kv necessarily requires conductors, of the single-conductor type, having diameters of the order of 1.65 or 2 inches. Tests will be made on both segmental and stranded conductors. Previous tests have indicated that the losses of the segmental type for a given diameter, as reflected in the low roughness

Paper 47-242, recommended by the AIEE committee on transmission and distribution and approved by the AIEE technical program committee for presentation at the AIEE Midwest general meeting, Chicago, Ill., November 3-7, 1947. Manuscript submitted August 20, 1947; made available for printing September 19, 1947.

C. F. WAGNER is manager, central station engineering, Westinghouse Electric Corporation, East Pittsburgh, Pa.; ANTHONY WAGNER is contracting manager, tower department, American Bridge Company, Pittsburgh, Pa.; E. L. PETERSON is transmission engineer and I. W. GROSS is electrical research engineer, American Gas and Electric Service Corporation, New York, N. Y.

or surface factor, are lower than the stranded conductor in fair weather conditions. Further investigations are needed to determine the relative as well as the absolute merits of segmental and stranded conductors in rain or snow.

The Germans have done extensive work on so-called "bundle conductors."[10] Conversation of one of the authors with the chief engineer of the Rheinisch-Westfälische Elektrizitäts Werke elicited the information that they had made the decision to use this type of conductor in converting some of their 220-kv lines to 380 kv. This conductor consists of several wires, of smaller diameter than would be necessary if a single conductor were used, held in position by spacers. The conductors may consist of a bundle of two, three, or four individual wires separated at distances of the order of one or two feet. Aside from reducing the corona losses, this composite conductor also reduces the inductive reactance of the line and thus increases the system stability. It is contemplated that the effect of various numbers and spacings of the component conductors will be studied.

Line Configuration

No accurate measurements have been made to determine the effect of ground wires or the proximity effect of towers. Ground wires and towers being maintained at ground potential increase the electric gradient at the conductor surface. These effects generally are not taken into consideration in the formulas cited previously. Tests will be made with and without ground wires. In addition, means have been provided to vary the ground wire height and consequently its distance above the conductors. The great height of the towers required for these higher voltages extends their influence along a considerable portion of the line. Previous work failed to incorporate this effect into the loss determination. These investigations, by utilizing actual line construction practice, simulate conditions in the field and provide information that can be used directly.

All the tests will be made with horizontal spacing of the conductors. Provision is being made so that this spacing can be varied between 32 and 45 feet.

By varying the number of insulators in the suspension and strain strings, these effects and the consequent tower proximity effects likewise can be determined.

Atmospheric Conditions

The effects of atmospheric temperature and barometric pressure upon the corona loss have been determined carefully in the Ryan Laboratory by controlling these conditions in a large tank.[11] The breakdown value of air as a function of the density d is given by the expression

$$d=\frac{17.9b}{459+t}$$

where b is the barometric pressure in inches of mercury and t is the temperature in degrees Fahrenheit. Using the standard conditions of b equal to 29.9 inches (sea level value) and t equal to 76 degrees Fahrenheit makes d equal to 1.0. Peterson[8] recommends that the actual conduc-

Figure 1. Comparison of corona losses on transmission lines by early tests, and various formulas for a specific fair-weather condition

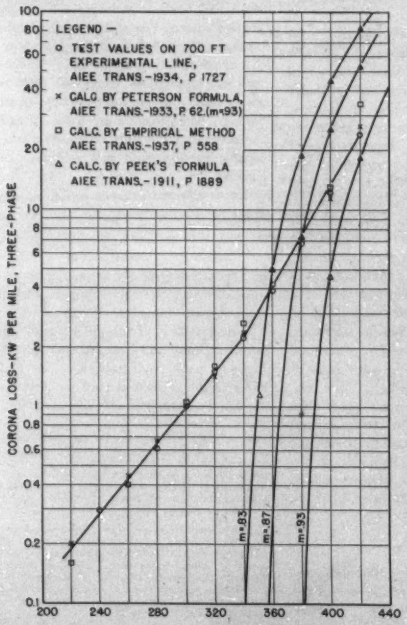

Figure 2. Effect of weather on corona loss of a 2-conductor line

Conductor diameter = 12 millimeters (0.472)
Conductor spacing = 2.4 meters (94.5 inches)
Frequency = 50 cycles per second

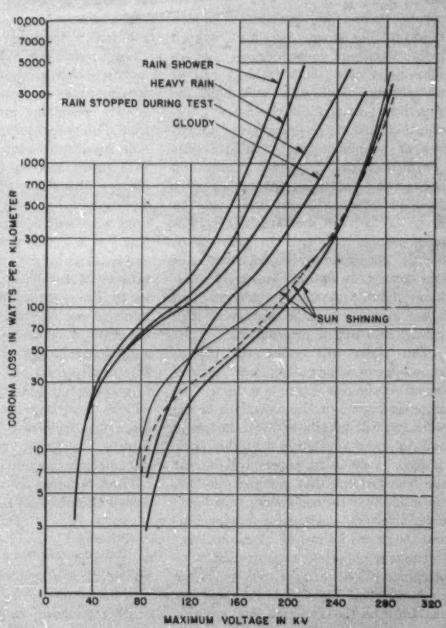

tor temperature rather than the temperature of the ambient air be used in this expression.

According to Carroll and Rockwell[9] humidity has practically no effect upon corona loss if the conductor is absolutely clean. Peterson in his method of calculating loss introduces a factor m to take care of roughness factor. This factor merely shifts the loss curve with respect to voltage without altering its shape. Peterson varies this factor with humidity. Quoting Peterson, "For general purposes it is felt that the proper value of m to use with low humidity and with the wire well weathered or in good clean condition is 0.92. During the night with low humidity[4] m may go as low as 0.78." This would indicate a rather large effect of humidity. The contradiction between these careful investigators should be clarified.

Several investigators, particularly among the Germans, have shown that rain increases the corona from 10 to 60 times. Figure 2 taken from the work of Strigel[14] shows this effect clearly. The ordinate gives the loss at 50 cycles as a function of voltage on a single span consisting of two 12-millimeter (0.47 inch) conductors separated a distance of 2.4 meters (7.9 feet). The three lower curves were obtained during sunny weather, the three upper curves during rain, and the intermediate one during a cloudy day. Fog and snow likewise increase the corona loss. In a region in which there is more than say 500 hours or 6 per cent of rain per year it is clear that the loss during this period would mask completely the loss during the fair weather. Records are available from the United States Weather Bureau which give the precipitation in each hour of the day at various stations. For Pittsburgh the average conditions for the 5-year period 1937 to 1941 show that a trace of rain or snow existed for 1,377 hours per year, a precipitation of at least 0.01 inch and less than 0.05 inch existed for 529 hours per year, and precipitation of at least 0.05 inch in an hour existed for 200 hours per year. Thus for this period there was at least a trace of snow or rain for 24 per cent of the time and at least 0.01 of an inch for 8.3 per cent of the time. This type of information should assist in evaluating corona factor as an economic factor. The fair weather loss therefore, may be of use principally as a bench mark or reference point to compare the relative performance of different conductors and different configurations.

In designing a line for corona loss a particular value of kilowatts per mile cannot be specified as being acceptable irrespective of the voltage. With increasing voltage and increasing power transmitted a balance between all factors likely will permit a larger loss per mile. Thus consider a 300-mile line over which 150,000 kilowatts is being transmitted at a 6 per cent copper loss. This is equivalent to a loss of 30 kilowatts per mile. Limiting the corona loss to 3 or 4 kilowatts per mile would be quite acceptable, whereas for a lower-voltage line transmitting less power it might not be.

Quite aside from the economic consideration of the corona loss resulting from snow, fog, or rain, radio influence during these conditions also might be important. It is quite possible that this factor might prove to be limiting. Abnormally high radio influence during even a relatively short time of extremely adverse weather might not be tolerable. Radio influence measurements will be made under abnormal weather conditions as well as during fair weather. In this connection it is also interesting to observe that in an actual line it may not be necessary that the disturbing factor occur at the particular point under observation. A rainstorm or high humidity condition at a particular point might transmit the disturbance along the line for a considerable distance.

It appears as though the ground gradients arising from charged thunderclouds might have an important effect upon corona loss and radio disturbances associated with corona. Figure 3 represents one of several similar diagrams taken from the work of Simpson and Scrase.[15] It represents the record of a relatively compact storm of no great intensity. Thunder was heard in the early stages but no lightning was seen or recorded at any time. The center of the storm appeared to pass about one kilometer south of the observatory at 17.25. Rain occurred from 17.13 to 17.31. The lower curve is the record of the potential gradient at the ground. It shows comparatively slow changes and gradients of as high as +50 and −50 per centimeter. These are equivalent to a gradient of 1,500 volts per foot or 125 volts per inch.

An insulated conductor 50 feet above ground and horizontal to it in a gradient of this magnitude would attain a potential of 75,000 volts. Actually, a transmission line is not insulated from ground, but is grounded through the transformer neutral. As a consequence, with slow changes of this character, the potential of the line remains at ground potential. A neutralizing, or induced, charge collects on the conductor of such polarity and magnitude as just to nullify the potential of the static field produced by the cloud. While the actual potential is neutralized the gradient at the surfaces of the conductor is not. The electric gradient P_t at the surface of the conductor due to the induced charge in volts per inch for a single conductor is

$$P_t = \frac{\text{potential above ground in volts}}{r \log \frac{2H}{r}}$$

where r is the radius of the conductor in inches and H is the distance above ground in inches. For a 2-inch conductor, the gradient is then

$$P_t = \frac{75{,}000}{2.303 \log_{10} 1{,}200} = 10{,}600 \text{ volts per inch}$$

It will be observed that this gradient is

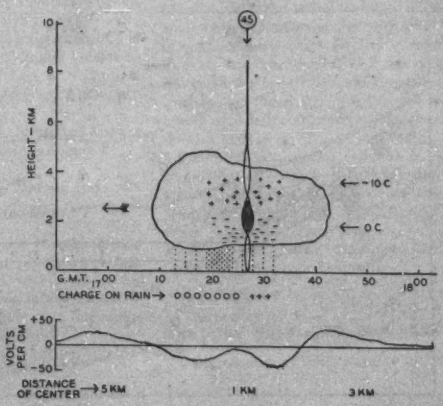

Figure 3. Ground voltage gradients reported by Simpson and Scrase during thunderstorm of small intensity, June 4, 1936

85 times the ground gradient that was responsible for the appearance of the induced charge.

The approximate effect of this gradient can be visualized by comparing the potential directly with the maximum instantaneous voltage to ground on the conductor. Thus, assuming a line-to-line rms voltage of 345,000 volts, the maximum line-to-ground voltage is

$$\sqrt{2} \times 345{,}000 \div \sqrt{3} = 282{,}000 \text{ volts}$$

In terms of this voltage the induced potential is 75,000÷285,000 or 26.6 per cent. Actually the presence of the other conductors influences the gradients adjacent to the conductor surface. More accurate calculations for this particular set of conditions assuming 35-foot separations between conductors with a flat configuration indicates that the ground gradient affects the maximum conductor surface gradient on the outside conductor 19.3 per cent.

These figures are introduced at this time merely to illustrate the order of magnitude of the effects that might be present. Further investigation of this factor is amply justified. These phenomena incidentally might explain some of the variability that has occurred in previous tests.

Radio Influence

The effect of radio influence has been just touched upon in this paper. Levels that are acceptable must be determined and correlated with the loss. Facilities will be provided for studying not only the magnitude of the radio influence with varying line configurations, operating voltages and atmospheric conditions, but also the variations along the line between spans and at various points laterally from the line.

Conductor Weathering

Previous investigators have emphasized the importance of washing and buffing the conductors and surface irregularities produced by dragging the conductors along the ground during the stringing operation. Continued exposure of the conductor in weather gradually eliminates these effects unless the scarring is too severe. The effects of die grease and burrs are eliminated gradually by weathering. The Stanford tests indicated that by using proper washing technique the weathering time could be reduced greatly or eliminated entirely. These factors will be borne in mind during the progress of the tests.

General Considerations and Design Features

In planning the field test setup, a number of factors had to be considered in order to insure the test results being of the most practical value. A location was selected on property of The Ohio Power Company along the Ohio River and adjacent to the Tidd plant at Brilliant, Ohio, about 35 miles from Pittsburgh. At this location there is a flat stretch of land approximately $1^1/_2$ miles long which permitted the erection of three parallel test lines. The general location showing the test lines and station is shown in Figure 4. The three lines are connected directly to a bus at the test station without circuit breakers and are fed through a 5,000-kva bank of three single-phase transformers.

Three single-pole arresters have been installed to protect the transformer. An oil circuit breaker[5] will be connected to the bus together with an arrester for its protection. Measuring instruments will be mounted on top of the transformer bushing which will be read by telescope from an observation booth some 50 feet distant. Suitable control equipment for energizing the high-voltage lines will be supplied. The diagrammatic sketch of the station in Figure 5 shows the arrangement of busses, equipment, observation booth, and movable platform for servicing the meters.

Within the test station all bus work is of 2-inch segmental hollow conductor. Shielded measuring leads are enclosed within the hollow conductors and extend from the instruments in the housing box on top of the high-voltage transformer bushing to the entrance of each of the three lines.

There are three test lines, two 1.4 miles long, and a third a single 800-foot span. The two longer lines have an average span of about 1,050 feet and comprise seven towers per line. Two of the towers on each line are dead-end, one at the far end and the other at the second tower out from the station where the lines change direction 28 degrees. The lines run approximately parallel and about 288 feet apart, center to center. The line conductors are approximately 85 feet above the ground at the towers and about 40 feet at midspan. Provision is made on all three lines for the installation of two ground wires at variable spacings above the conductors with a maximum elevation above conductors of 40 feet. The ground wires also extend over the station for bus and equipment shielding. The line towers are provided for variable conductor spacings of 45, $38^1/_2$, and 32 feet between conductors. The lines are phased so that adjacent conductors of different lines connect to the same phase. A more detailed description of the towers and structures is given later in this paper.

The station is insulated with 26 $5^3/_4$-inch spaced units, and the line is arranged to have 26 to 30 units in suspension and double strings in dead-end. All insulators have a mechanical rating of 25,000 pounds. Grading shields are used on the live end of all insulator strings. Preliminary tests indicated that these were necessary at the line end but not at the

Figure 4. Location of three Tidd high-voltage test lines at Brilliant, Ohio, near the Tidd power station of the American Gas and Electric System

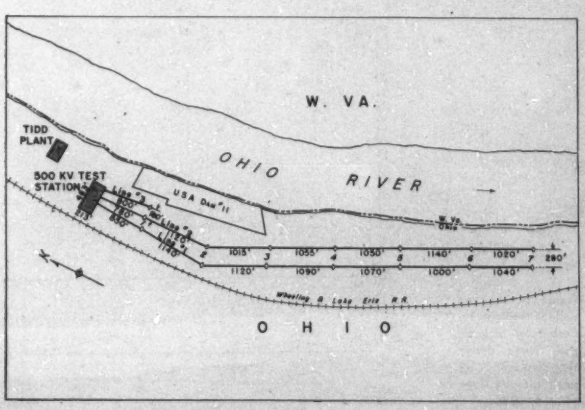

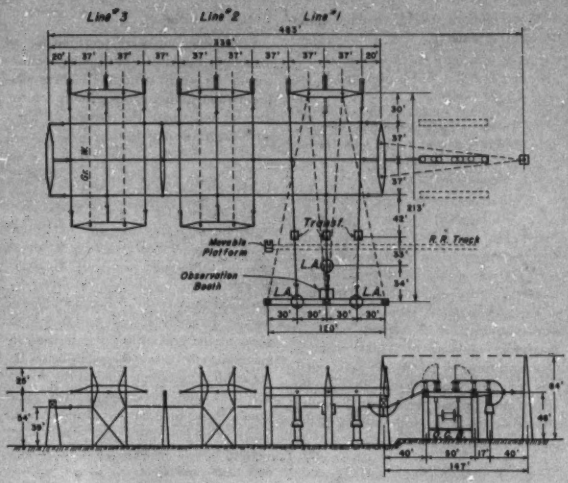

Figure 5. The 500-kv test station layout showing bus spacing and arrangement, equipment location, ground wire shielding, and provisions for reading and servicing measuring instruments

ground end. The tests made in determining the design of these shields are given in a companion paper.[3] Special hardware for each particular type of conductor has been provided.

Three single-phase transformers convert energy from the 66-kv supply to high voltage that can be varied between 264,000 and 500,000 volts line-to-line. The transformer bank is delta connected on the 66-kv side and Y connected and solidly grounded on the 500-kv side. The transformers are of conventional shell-form construction. The impedance is 6.6 per cent which is low compared to power transformers of comparable size or compared to a testing transformer. This is of advantage in maintaining a sinusoidal wave shape.

The transformer is protected against lightning by two different types of lightning arresters which are shown in Figure 6. Two of these are of the suspension type and are supported by the steel bus structure. The other is a self-supporting type made up of three pedestal columns containing alternate arrester elements and insulators. The arrester units are so connected that they in effect spiral around the columns and thus produce an arrester of relatively low height. These arresters are described in a companion paper.[4] A lightning arrester will be supplied for the oil circuit breaker in process of installation.

The aluminum instrument boxes mounted on top of the transformer bushings contain the measuring instruments including wattmeters of special design. The potential supply is provided by an extension of the main transformer winding. The current elements of the wattmeters are connected directly to the line without an intervening instrument transformer. Indicating meters mounted in the instrument house can be read remotely by a telescope mounted in a special observation booth located on the bus structure at a point level with the instrument house. In addition, continuously recording instruments and also high-speed recording instruments permit the determination of corona loss during all weather conditions over long periods of time. Details concerning the instrumentation are given in a companion paper.[5]

A view of the test station and some of the equipment is shown in Figure 7.

Transmission Line Towers and Substation Structures

The transmission line towers and substation structures for the Tidd high-voltage test installation were designed and furnished by American Bridge Company. These structures consist of 15 line towers and 9 substation structures.

Line Towers

Test lines 1 and 2 each contain seven towers in addition to the substation take-off structures. Five of the towers in each of these lines have suspension insulator attachments and two have strain attachments, one of which is located at the terminus of each line and one at an angle point in each line.

Line 3, consisting of a single 800-foot span, contains a special type of strain tower in addition to the substation structure forming one support of the span.

Substation Structures

The substation structures are essentially similar to the line towers except that the height and crossarm lengths are less. Three of the structures support the incoming line conductors as well as the 2-inch-outside-diameter bus cables together with ground wires. The remaining substation structures support busses and station ground wires only, except one combination tower and cross-girder structure which supports two suspended lightning arresters in addition to the busses and ground wires. The latter structure also has attached to it a steel framed observation booth to be used for the visual observation of the measuring equipment and for various control devices.

Tower and Substation Design

The line towers support three conductors at an elevation of 100 feet above the ground at the point of attachment of the insulator strings, and two ground wires located 24 feet above the conductor crossarm (see Figure 8). The conductor crossarm is 90 feet in length, providing a maximum phase spacing of 45 feet. Attachments are provided on the crossarm so that the outer conductors can be moved toward the center of the tower so as to provide alternate phase spacings of 38 feet 6 inches and 32 feet 0 inches. The ground wire peaks are provided with alternate attachment points for the ground wires so that the wires can be lowered 6 feet or 12 feet below the normal topmost location (see Figure 9). The suspension towers were designed for average tangent spans of 1,200 feet.

The wind loading was assumed at 8 pounds wind on 1/2-inch-ice-covered cables and 13 pounds per square foot on $1^1/_2$ times the projected area of one face for tower structures. From these data the following loads were determined for which the towers were designed:

Suspension Tower

1. Vertical:

Two ground wires at 1,400 pounds = 2,800 pounds
Three conductors at 5,300 pounds = 15,900 pounds
Total 18,700 pounds

2. Transverse:
Two ground wires at 1,300 pounds = 2,600 pounds
Three conductors at 2,200 pounds = 6,600 pounds
Total 9,200 pounds

3. A longitudinal load at any one ground wire support at 6,750 pounds or at any one conductor support at 15,000 pounds. (For longitudinal combined loads on tower use 60 per cent of conductor load or 9,000 pounds.)

4. Wind on tower at 13 pounds per square foot on $1^1/_2$ times the projected area of one face.

5. Dead load of tower.

6. Heavy vertical (one inch ice):
Two ground wires at 2,000 pounds = 4,000 pounds
Three conductors at 8,000 pounds = 24,000 pounds
Total 28,000 pounds

For determining maximum stresses in member, the following combinations of loads were used:

(*a*) 1, 2, 4, and 5 (all cables intact) or

(*b*) 1, 9/10 of 2, 3, 4, and 5 (one broken cable) or

(*c*) 6—for cross arms only.

The dead-end and angle towers on lines 1 and 2 were designed for the following loads:

1. Vertical:
Two ground wires at 1,400 pounds = 2,800 pounds
Three conductors at 5,300 pounds = 15,900 pounds
Total 18,700 pounds

2. Transverse wind on cables:
Two ground wires at 1,300 pounds = 2,600 pounds
Three conductors at 2,200 pounds = 6,600 pounds
Total 9,200 pounds

3. Longitudinal:
Two ground wires at 6,750 pounds = 13,500 pounds
Three conductors at 15,000 pounds = 45,000 pounds
Total 58,500 pounds

4. Wind on tower at 13 pounds per square foot on $1^1/_2$ times the projected area of one face.

5. Dead load of tower

6. Transverse angle in line of 29 degrees 0 minutes:
Two ground wires at 3,375 pounds = 6,750 pounds
Three conductors at 7,500 pounds = 22,500 pounds
Total 29,250 pounds

7. A longitudinal load at any one ground wire support at 6,750 pounds or at any one conductor support at 15,000 pounds

8. Heavy vertical (one inch ice):
Two ground wires at 2,000 pounds = 4,000 pounds
Three conductors at 8,000 pounds = 24,000 pounds
Total 28,000 pounds

For maximum stresses combine (*a*) or (*b*) or (*c*) or (*d*) or (*e*).

(*a*) 1, 2, 4, 5, and 6 (all cables intact).

(*b*) 1, $^9/_{10}$ of 2, 4, 5, $^9/_{10}$ of 6, and 7 (one broken cable).

(*c*) 1, $^1/_2$ of 2, $^3/_4$ of 3, 4, 5, and $^1/_2$ of 6 (all cables on one side for angle tower).

(*d*) 1, $^1/_2$ of 2, 3, 4, and 5 (all cables on one side broken for dead-end tower).

(*e*) 8—for crossarms only.

The dead-end tower on line 3 is essentially the same as the strain tower on lines 1 and 2 except that the tower is designed for a maximum longitudinal load of 25,000 pounds per conductor instead of 15,000 pounds as used for the latter lines.

The substation structures were designed to support the strain busses at maximum tensions of 11,000 pounds. One structure, as previously mentioned, was designed to support in addition to the busses and ground wires two lightning arresters with a vertical load of 12,000 pounds at each arrester support.

Strength of Towers

The towers were designed using the following unit stresses which permit an overload of approximately 90 per cent over and above the working loads:

Tension on net section, 20,000 pounds per square inch.

Compression on gross section, 20,000 pounds minus 85 L/R per square inch for L/R less than 150 where L is unsupported length of section in inches and R is least radius of gyration of section.

Compression on gross section, 15,500 pounds minus 55 L/R per square inch for L/R greater than 150 where L is unsupported length of section in inches and R is least radius of gyration of section.

Shear on bolts, 13,500 pounds per square inch.

Bearing on bolts, 27,000 pounds per square inch.

Stress Analysis

Stress diagrams were prepared for all structures based on the loading requirements for each structure. These diagrams and actual computations for the stresses and size of the various members were based on past tests of structures of similar outline.

Foundations

The anchors for all towers and substation structures were of the steel earth grillage type using a single stub extending beneath the ground to a steel grillage so designed as to sustain the uplift and compression loads of the tower without the use of any concrete. The horizontal shear at the ground line was resisted by extending the bottom diagonals below the ground line and connecting to the anchor stubs. This point of connection below ground line, using earth bearing on stub for resisting horizontal shear, was 3.5 feet for suspension towers and 4 feet for dead-end angle towers.

Coating and Connections

All the material, including foundations and connection bolts furnished for the line structures and substation structures, was hot dipped galvanized according to the latest American Society for Testing Materials Specifications. The material was shipped to the site unassembled. All connections were field bolted.

Special Features

Special features of interest in the design of this test layout are the following:

1. The instruments for accurate measurement are mounted on top of each transformer bushing. Access to these meter installations is provided by means of a mov-

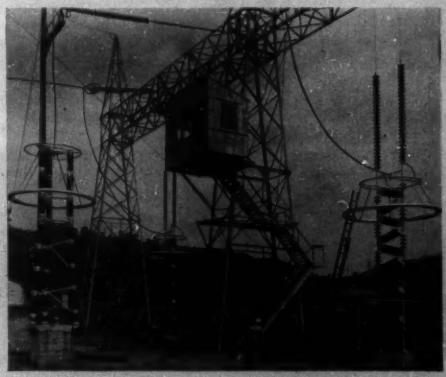

Figure 6. High-voltage lightning arresters installed to protect power transformers

Self-supported type on the left, Suspension or earthquake-proof type on the right and in the background. Observation booth in the center

Figure 8. Standard suspension tower for 500-kv line with all three conductors and ground wires in place

able, elevated platform set on the railroad spur track on which the transformers were transported to the site.

2. As it is necessary to read certain meters when the line is energized, an elevated observation booth is mounted on one of the structural towers at the station, and the meters are read remotely by telescope.

3. As mentioned previously, the measuring leads from the transformer to each of the three lines are shielded and enclosed within the 2-inch *HH* bus conductors up to the point of line entrance.

4. Provision is made for insulating the ground wires so that comparative corona effects can be readily obtained by momentarily connecting the ground wire to ground.

5. Grading shields for single dead-end, double dead-end, and suspension strings are designed specially and are described in a companion paper.

6. The towers provide for variable vertical positions of the ground wires and also for variable horizontal positions of the phase wires. These provisions were made to determine the effect of conductor and ground wire spacings.

7. While the tower and station structural designs are admittedly not the final design for a practical line on account of the variable factors which had to be provided for, they are a very close approximation to what it is expected would be used in high-voltage construction up to 500 kv.

Scope and Objectives

The test setup has been planned with the idea of making corona measurements on a full scale transmission line energized by a full size transformer and other equipment closely similar to what would be used in extra-high-voltage transmission. Provision has been made to vary the conductor size, type, and arrangement; the spacing between conductors; the number of insulators; and the height of the ground wires. The effects of different atmospheric conditions, such as fair weather, cloud effects, rain, fog, sleet, and snow and also electric ground gradients, will be studied by continuously recording devices. Studies will be made on radio reception as influenced by corona. Insulator loss as affected by fog,

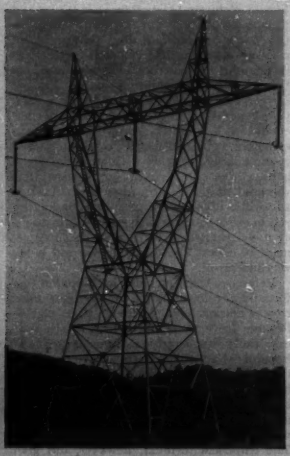

Figure 7. The 500-kv test station showing station structures, incoming lines, and some of the test equipment

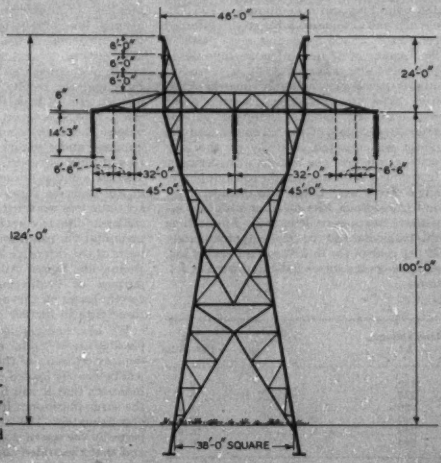

Figure 9. Standard suspension tower for 500-kv line showing arrangements for variable location of conductors and ground wires

sleet, rain, and other atmospheric conditions also will be studied.

Participating Companies

The responsibility of the tests lies with the engineers of the American Gas and Electric Service Corporation. The Westinghouse Electric Corporation has contributed the power transformers and arresters for their protection and also the measuring equipment, and has been active in the planning of the investigation. The American Bridge Company has contributed the towers, and the Ohio Brass Company and Locke Insulator Corporation the insulators and hardware. The Aluminum Company of America, General Cable Corporation, and Anaconda Wire and Cable Company supplied the conductors and fittings. The high-voltage circuit breaker with its protecting arrester is being supplied by the General Electric Company.

References

1. Transmission of Electric Power at Extra-High Voltages, **Philip Sporn, A. C. Monteith.** AIEE Transactions, volume 66, 1947, pages 1571–82.

2. Insulators and Line Hardware for Tidd 500-Kv Test Lines, **I. W. Gross, R. L. McCoy, J. M. Sheadel.** AIEE Transactions, volume 66, 1947, pages 1592–1602.

3. Line Conductors—Tidd 500-Kv Test Lines, **E. L. Peterson, D. M. Simmons, L. F. Hickernell, M. E. Noyes.** AIEE Transactions, volume 66, 1947, pages 1603–12.

4. Transformers and Lightning Arresters—Tidd 500-Kv Test Lines, **F. A. Lane, J. K. Hodnette, P. L. Bellaschi, Edward Beck.** AIEE Transactions, volume 66, 1947, pages 1613–18.

5. Switchgear Equipment for Tidd High-Voltage Test Lines, **F. A. Lane, B. W. Wyman.** AIEE Transactions, volume 66, 1947, pages 1619–23.

6. Instrumentation and Measurement—Tidd 500-Kv Test Lines, **R. L. Tremaine, G. D. Lippert.** AIEE Transactions, volume 66, 1947, pages 1624–31.

7. Dielectric Phenomena in High Voltage Engineering (book), **F. W. Peek, Jr.** McGraw-Hill Book Company, Inc., New York, N. Y.

8. Discussion by **W. S. Peterson** of Design of Transmission Lines, **J. S. Carroll, B. Cossens.** AIEE Transactions, volume 52, 1933, pages 55–63.

9. Empirical Method of Calculating Corona Loss From High-Voltage Transmission Lines, **J. S. Carroll, Mabel M. Rockwell.** Electrical Engineering (AIEE Transactions), volume 56, May 1937, pages 558–65.

10. Bundelleitungen (book), **W. Mangoldt, F. Busemann, A. Buerklin.** Siemens-Schuckertwerke, Berlin, Germany, 1942.

11. Corona Loss Versus Atmospheric Conditions, **L. Hogy, G. W. Dunlap.** Electrical Engineering (AIEE Transactions), volume 53, February 1934, pages 272–3.

12. Vergleichende Untersuchungen uber Gleich-und Wechselspannungscorona an Doppelleitungen (book), **Robert Strigel.** Wissenschaftliche Veroffentlichungen aus den Siemens-Werken, volume 15, 1936, page 68.

13. Distribution of Electricity in Thunder Clouds, **Sir George Simpson, F. J. Scrase.** *Proceedings*, Royal Society of London (London, England), series *A*, number 906, volume 161, 1937, page 309.

Discussion

E. C. Starr (Oregon State College, Corvallis, Oreg.): The corona-loss and radio-influence tests outlined in this paper are of great interest to transmission engineers because of the economic and public-relations aspects of the high-voltage transmission problem. Because of overlapping voltages and conductor sizes these tests will afford an opportunity for correlation with and extension of existing laboratory data. They also will provide information for a complete evaluation of the influence of weather and precipitation.

A series of simple corona-loss measurements has been made on one of the lines of moderate length of the Bonneville Power Administration. This line is approximately 183 miles long and is composed of 795,000-circular-mil aluminum-cable steel-reinforced conductor (1.108-inch diameter) with a flat spacing of 27 feet. The average elevation is of the order of 2,500 feet, and it crosses two passes at approximately 5,000 feet. The first measurements were made with the test circuit energized at the generating station (Grand Coulee), and the power was metered carefully on the low-voltage side of the set-up transformers. Instrument calibration and ratio and phase-angle errors were taken into consideration, and transformer loss together with line resistance losses were deducted. At the time this particular test was made approximately 70 per cent of the line was in a freezing fog, and the corona losses indicated were as follows:

Line Voltage, Kv	Kw Per Mile
190	0.8
220	5.2
230	8.4
240	12.5
250	16.9
260	20.8

This test was not repeated under other weather conditions, but the data seem very reasonable.

Beginning at a later date and extending over a considerable period of time a number of sets of data were taken with this same circuit (one of two circuits on the same right-of-way) energized at the receiving end (Covington substation near Seattle, Wash.) and metered through high-voltage current and potential transformers. Again instrument calibration corrections and transformer ratio and phase-angle errors were taken into consideration. The corona and insulator losses obtained in these tests ranged from approximately 0.8 kw per mile under 100 per cent fair-weather conditions to approximately 12 kw per mile when rain was falling along a major portion of the line. Weather data are not complete because of a limited number of observation stations. The average line voltage for each of these tests was approximately 230 kv. The unaccountable errors in measurement are probably small, in the neighborhood of ±0.5 kw per mile, and the results therefore should not deviate greatly from the true values. It is interesting to observe that the fair-weather values check reasonably well with those obtained under similar conditions in laboratory studies as reported by Carroll and his associates and as obtained by an application of the Peterson formula. It is planned to continue this work with a view to obtaining sufficient data to correlate it with the annual precipitation conditions over the various parts of the extensive 230-kv network of the Bonneville Power Administration for the purpose of evaluating the economics of corona losses on this system and employing these data in further design studies.

We also are giving consideration to the possible use of "split" or multiple phase conductors on some of the future circuits that will be heavily loaded. A preliminary study indicates that it will be possible to increase the surge-impedance loading at 230 kv from approximately 130 to 175 megavolt-amperes by the use of double phase conductors and that the added cost will not be proportional to the gain achieved in power capacity. Where stability is a problem in very long lines and where several circuits operate in parallel between terminal busses, split conductors seem to offer at least a partial practical solution to the problem of obtaining increased circuit loadings to obtain the maximum economy of operation.

We shall follow the Tidd tests with a great deal of interest and feel that the various parties contributing to this research are taking a very valuable step in the direction of making improved transmission economies possible.

Wm. S. Peterson (Department of Water and Power, The City of Los Angeles, Calif.): In this paper it was indicated that most all previous experimental work on corona was done under fair weather conditions and also that considerable attention was given to the surface conditions of the conductor. Such tests generally were made under fair weather conditions because the equipment used was of indoor type and could not be subjected to more severe weather without danger, and neither was the metering equipment that was used adaptable to outdoor use. Much of the work involved in cleaning conductors was in order to artificially gain the equivalent of a weathered surface, and the measurement of effects due to die grease and burrs was incidental.

Reference has been made in this paper to a formula developed by me for the determination of corona loss. Although parts of this formula have some theoretical basis, it is essentially an empirical formula. I am hopeful that these tests may reveal a better basis for a corona formula than that heretofore developed. The variation of corona voltage with the air density factor needs considerably more information as it was based on rather limited information. The empirical formula, however, did give accurate results over a wide range of conditions when compared with all available data up to the time of its presentation.

In determining corona loss during rain I

believe that you will find it essential to make some supplementary measurements of loss on insulator strings in order to make corrections and determine the corona loss for the conductor itself. We have found in our work that leakage measurements on insulator strings are highly erratic, but presumably over a line of this length the insulator losses should average out to some stable value under a given rainfall.

It it also my judgment that radio influence from insulator leakage occurring during rainstorms may be as important as conductor corona.

Gordon R. Slemon (nonmember; Hydro-Electric Power Commission of Ontario, Toronto, Ontario, Canada): Planning engineers of the Hydro-Electric Power Commission of Ontario for some time have been concerned over the lack of information on radio influence from corona. In the light of the full-scale tests which are proposed here, it was believed that our contribution could be made best through a study of the basic concepts of radio-influence production and of subsequent means of interference control. During the past six months, controlled laboratory tests have been carried out on a single conductor and plane configuration with alternating voltages up to 50 kv rms and direct voltages up to 62.5 kv, both positive and negative. I would like to present some of the more pertinent conclusions of this study.

In a recent paper, Rorden of the Bonneville Power Administration showed that a reduction of conductor spacing on 220-kv transmission lines caused a considerable reduction in radio influence even with the increase in corona loss. To substantiate this observation tests have been made on the laboratory model, which show that for conductors operating at a voltage above the corona threshold voltage, there is a certain optimum spacing which will produce the lowest value of radiated signal. Application of the test results to an actual transmission line shows this optimum spacing to be much smaller than that of normal practice. This observation would indicate that the proposed increase in corona loss by the reduction of conductor spacing might not cause a serious radio-influence limitation.

It has been noted by several authors that corona on a smooth dry conductor produces radio noise only during the negative half cycle of the voltage wave. The postulated theories have stated that residual positive ionization from the positive voltage cycle persisted about the conductor until the voltage was reversed. The presence of a positively charged region about the negative potential conductor was thought to produce minute arc breakdowns with resultant radio-frequency radiations. To clarify this point in theory, the alternating voltage was rectified and the pulsating half-sine wave of negative polarity voltage was applied to the conductor. A comparison of the radio noise for this case with that of alternating current showed almost no change in amplitude or phase of corona initiation and extinction at the power frequencies of 25 and 60 cycles per second. The deviation in the results was large at a supply frequency of 500 cycles per second. It appears then that a theoretical analysis of corona in the negative cycle of an alternating voltage wave of normal power frequency will have to be based almost entirely on charges produced during the negative cycle.

A study of corona phenomena with direct voltage was indicated for several reasons. The effect of rate of change of alternating voltage is eliminated and the simplest case for theoretical analysis is obtained. The results are also important in that they apply to d-c power transmission. First, let us consider the case of positive direct current. A smooth, polished conductor produced no radio noise even at double the normal peak threshold voltage. This result was to be expected from the absence of positive-cycle radio noise in the a-c tests. A weathered conductor was found to produce some radio noise of a pulse nature. The repetition frequency of this pulse increased as the voltage was increased over the threshold value. Probably the most important conductor surface contamination is water either as droplets on the surface or as a mist. With a mist of distilled water about the conductor the radio-influence threshold was reduced to about 60 per cent of its a-c peak value. When the mist was cleared leaving only the water drops on the surface, the interference threshold was increased only 5 per cent. It appears then that the important factor in this case is the water on the conductor surface, not the water in the surrounding dielectric. The radio noise with a wet surface consisted of sharp pulses in the receiver audio output. The repetition frequency of these pulses increased with increasing voltage while the magnitude remained constant. The interference to radio reception was much less at the higher voltage levels as the high frequency hiss could be almost eliminated by tone control adjustment on the receiver.

As would be expected from the a-c tests, radio noise was produced with a negative potential greater than threshold value on the smooth conductor. The radiated noise was relatively severe and increased in amplitude with voltage increase. Weathering was found to reduce this radio influence by as much as 50 per cent. The most interesting observation was the effect of water. Even a fine mist about the conductor completely eliminated radio noise. The radiation remained at zero as long as the conductor was wet. No surface coating could be found that would increase the radio noise above the value for a smooth conductor. The smooth polished surface appears to be the most severe condition for radio influence with negative direct voltage.

The effects of various conductor contaminations, especially those of water, have suggested the possibility of radio influence control by the use of special conductor coatings. With negative direct current, the problem is relatively simple. Certain crystalline coatings such as sodium chloride applied as a saturated solution in water have been found to reduce the radio noise by over 90 per cent. The characteristics required of this coating are a low work-function to provide high field emission and a point structure which will provide high local gradients on the surface. With positive direct current, it appears that the best compromise between the wet and dry conditions is obtained with a semiconducting coating. This has a damping effect on the corona current surges when the conductor is wet but causes some radio noise, when dry. Since all radio-influence results have differed so widely with positive and negative direct current, no suggestion can be made at present as to the desired characteristics of a suitable conductor coating for alternating current, under both wet and dry conditions. With a dry conductor coatings may be applied that will reduce the negative cycle radio noise and will introduce some noise into the positive cycle. This compromise gives a lower average value of radio noise.

A considerable reduction in interference to radio reception is experienced as the magnitude of the lower power frequency harmonics in the receiver output is reduced. The advantage of this arrangement is nullified if the conductor becomes wet. Radio noise is eliminated from the negative half cycle and becomes severe in the positive half cycle.

This study has produced information which has allowed certain clarifications in the theory of radio interference production from corona. The test results along with the ramifications of the theory have indicated certain means by which radio interference may be controlled. The problem of actually developing methods of interference control still remains.

Insulators and Line Hardware for Tidd 500-Kv Test Lines

I. W. GROSS
FELLOW AIEE

R. L. McCOY
MEMBER AIEE

J. M. SHEADEL
ASSOCIATE AIEE

Section I

CAREFUL CONSIDERATION was given to the selection of insulators and the development of line hardware which are being used on the 500-kv test lines planned by the American Gas and Electric Service Corporation, in cooperation with seven manufacturing companies, to obtain needed data on corona, radio interference, and other technical features of conductors and equipment. These lines are located near the Tidd plant of The Ohio Power Company. This is a companion paper to six others[1-6] which describe the over-all approach to the problem, a description of the test layout, equipment, and instrumentation. A discussion of the insulator and line hardware features is given in this paper.

Insulators

The two principal features of insulators, so far as the line design is concerned, are their electrical characteristics and mechanical strength.

Electrical Characteristics

The electrical characteristics of $5^3/_4$- by 10-inch insulators, extrapolated from existing data[7] on long insulator strings, are given in Table I, together with the ratios of insulator flashover to line-to-ground voltage for a 500-kv line. Using these data as a preliminary guide together with recent records of line insulation in present use on high-voltage lines,[8] it was concluded that for a 3-phase 500-kv line, a maximum of 30 units probably would not be exceeded in actual practice, and 26 insulators would be sufficient for that part of the test layout where the insulators did not affect the measurements, that is, on the substation bus. It is, of course, possible to remove or short-circuit additional insulators in the line to study the effect of corona with a lesser number of units.

The choice of the number of insulators to be used on an actual line within the present test range (262 to 500 kv) is, of course, an economic factor and outside the scope of this paper. However, it was believed that the maximum number of insulators chosen probably would not be exceeded in a practical line within the test voltage range.

A preliminary study indicated that there appeared to be no advantage in attempting to develop any special insulator or use any intermixing of various insulator sizes or shapes in the string, and therefore the conventional ball-and-socket $5^3/_4$-inch-spaced unit was decided upon.

Mechanical Strength

In view of the fact that conductor sizes[3] were planned as large as two inches outside diameter, as well as "bundle" conductor arrangements, the maximum design conductor tension under an assumed loading condition of 8 pounds of wind on cables covered with one-half inch of ice was 15,000 pounds. From economic considerations it was desired to restrict the dead-end insulator assemblies to two strings of insulators. It therefore was decided to use insulators with a rated strength of 25,000 pounds, which would allow a reasonable factor of safety at strain positions. The maximum design vertical loading of conductors at suspension points was 6,600 pounds, and it was decided to use single strings of 25,000-pound-rated insulators of the same type as used at strain positions. On the substation bus where 2-inch *HH* cable is strung to give a maximum assumed loaded tension of approximately 11,000 pounds, single strings of 25,000-pound-rated insulators were used.

Paper 47-243, recommended by the AIEE committee on transmission and distribution and approved by the AIEE technical program committee for presentation at the AIEE Midwest general meeting, Chicago, Ill., November 3-7, 1947. Manuscript submitted August 19, 1947; made available for printing September 18, 1947.

I. W. Gross is electrical research engineer, American Gas and Electric Service Corporation, New York, N. Y.; R. L. McCoy is chief design engineer, Locke Insulator Corporation, Baltimore, Md.; J. M. Sheadel is development engineer, Ohio Brass Company, Barberton, Ohio.

Line Hardware

As varying sizes of conductors (1.4, 1.65, and 2.0 inches in diameter) were to be used, and further as plans were made to use "bundle" conductors on one line, some special line hardware had to be developed. Line suspension and dead-end clamps were designed specially for all 1.65-inch and all 2.0-inch copper conductor. A standard clamp for 2.0-inch-outside-diameter conductor was used on the 2.0-inch aluminum cable steel reinforced. Special line hardware also is being provided for the "bundle" conductor and is described in a companion paper.[3]

Corona Shields

Extensive laboratory tests indicated that shielding would be required on the line end of insulator strings for two purposes

1. To grade the insulator string.
2. To control the electrostatic field around the line hardware in the vicinity of bolts, nuts, clamps, and washers.

It also was found that no grading shield was required at the ground end or at any intermediate point on the insulator assembly.

Field Construction

Figure 1 shows a double dead-end assembly of 30 by 30 insulators with corona shield and 2-inch-outside-

diameter conductor attached being raised into position at a dead-end structure.

Figure 2 shows insulator strings in place at the station entrance structures of lines 1 and 2. The corona shields have not yet been aligned for installation of the dead-end loops.

The field erection of insulators on the station bus and the three test lines was completed in July 1947.

Co-operating Groups

The two co-operating companies on the insulator and hardware problem, the Ohio Brass Company and the Locke Insulator Corporation, made extensive studies and laboratory experiments on complete insulator assemblies. A discussion of their approach to the problem, describing some of the test and design work and the standard and specialized equipment supplied for the project, is given in detail in the following two sections of this paper.

Section II. Insulators and Line Hardware Supplied by the Ohio Brass Company*

In the design of insulators and line hardware for the Tidd 500-kv test line, consideration was given to physical characteristics, flashover requirements, and reduction of voltage stress. This section summarizes some of these factors and the tests which determined the design of insulators and line hardware furnished by the Ohio Brass Company.

The high-voltage laboratory study included: flashover, corona, voltage distribution, radio influence voltage, and leakage current.

The radio influence voltage was measured with the EEI-NEMA-RMA test circuit,[8] but for this test the 60-cycle voltage was limited to 225 kv line-to-ground (390 kv phase-to-phase).

Insulators—Physical Characteristics

The 25,000-pound $5^3/_4$-inch spaced insulator unit was supplied for all assemblies. Because of the advantage indicated by corona observations and field experience, the ball-and-socket type unit was preferred. Ball-and-socket designs used in the United States originally had been made for suspension insulators having 9,000 pounds and 11,000 pounds rated mechanical and electrical strength. Later, when higher strength units were designed, the same ball and socket was retained to maintain interchangeability. Experience with ball-and-socket high-strength insulators has indicated that the 5/8-inch-diameter pin shank necessary for interchangeability may develop fatigue failure under conditions of exceptional vibration and tension. Modern steel alloys permit higher unit stresses in pin shanks; but as a conservative practice ball-and-socket connections generally have not been recommended for suspension insulators rated at more than 18,000 pounds.

Although unusual insulator vibration problems were not expected on the test line, suspension insulators similar to those which would be used for an eventual line were preferred. Possible mechanical requirements of insulators on a 500-kv transmission line indicated that increased fatigue strength would be desirable and that interchangeability with old units is not needed. Hence, to improve the endurance strength markedly, the shank diameter of the insulator pin was increased to 11/16 inch.[10]

Insulator manufacturers are studying a proposed ball-and-socket standard revision which would permit a similar increase in the shank diameter for regular 25,000-pound connections.

Suspension Clamps

The ultimate strength of the suspension clamps used for the test line matched the 25,000-pound insulator rating. A special clamp shown in Figure 3 was made which is suitable for use with I-beam, type *HH*.

Figure 1. Double dead-end (30 by 30) insulator string with corona shield and conductor attached being raised into position in the field

Figure 2. Double dead-end and single dead-end insulator assemblies and corona shields in place at station entrance structure

*By J. M. Sheadel.

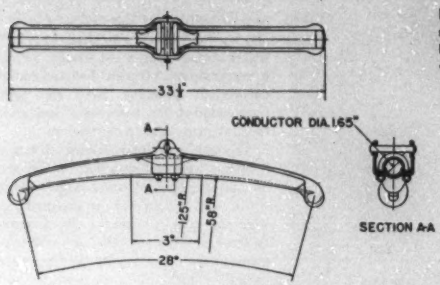

Figure 3. Suspension clamp designed for 1.65-inch-diameter type-*HH* copper conductor

or aluminum-cable-steel-reinforced conductors 1.65 inches in diameter. The requirements of type *HH* conductor established the radius of curvature and the included vertical angle. These determined the length of the clamp.

The design was based on principles which had been applied successfully to clamps for smaller sizes of hollow copper conductor. More than 90 per cent of the conductor periphery was enclosed at the clamping section; the clamping section was short, the U bolts were close together, and a tapered clamping piece was used; the pivot point of the clamp was located near the intersection of the tangents of the catenary at the seat of the clamp.

With conductors other than type *HH* a smaller radius of curvature is permitted; hence, a shorter clamp could be used. For the 2-inch-diameter aluminum cable steel reinforced standard catalogue clamps were furnished.

Reduction of Voltage Stress

When voltage is placed across a long string of clean, dry suspension insulators, it is not divided equally among the units.[11] Because of the capacitance distribution the line insulator normally sustains the greatest potential, which for a string of 20 units is nearly 20 per cent of the impressed voltage. Should this voltage be increased to, say, 400 kv (700 kv phase-to-phase), a stress of 80 kv might be expected on the line insulator. Since this is the rated flashover value of one unit, string flashover might be expected. This does not occur, however, since the corona which appears at the most highly stressed zones increases the effective capacitance of the line units and reduces the percentage of voltage which appears across these units.

Most conventional designs of suspension and strain clamps and suspension insulators do not produce noticeable electric overstress for line operation to 230 kv phase-to-phase. Generally the voltage stress is not sufficient to produce levels of radio influence voltage objectionable to nearby radio listeners or to carrier current operation.

For the 500-kv test line a reduction in the voltage stress at the line end of the insulator string was required to eliminate the small corona loss which would occur if standard insulators and clamps were used.[12] Radio influence voltage characteristics would be improved and the corona products which accelerate the corrosion of the suspension insulator pin would be eliminated.

Several methods or combinations of methods may be used to reduce the voltage stress at the line end of a long string of suspension insulators.

Insulator Design

The incorporation of control devices in both the insulator and clamp design has merit in simplicity of installation and maintenance of maximum clearance to the tower.

Since the insulators of the transmission line preferably should be of identical design, complex suspension units which required special parts at several positions in the string were found to be impractical.

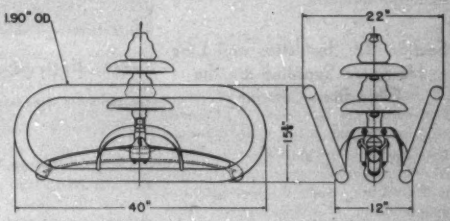

Figure 4. Control ring arrangement for the suspension string

A shorter standard suspension clamp was used with 2-inch-diameter aluminum cable steel reinforced

Trials were made with insulators which included electric stress controls in the pinhole or conducting glaze at critical areas. However, these designs, especially that with pinhole control, were sensitive to humidity and the condensation of moisture on the porcelain. Units which require integral control devices were not recommended for use on the test line because of their inherent cost and debatable performance.

Suspension Clamp Design

The design of a suspension clamp to meet the specification of no corona at 500 kv phase voltage required radii of about 2 inches at the lips and special treatment of the nuts and rivets. The cumbersomeness and complexity of such a design led to its rejection. External control rings were most practicable.

External Shields

The maximum voltage stress on insulators and line hardware may be reduced by external shields. The conventional ring fabricated from tubes may be

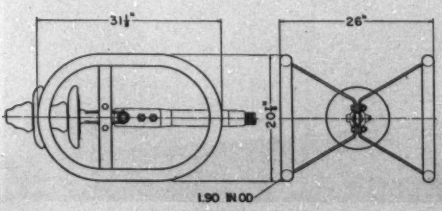

Figure 5. Control ring for the single dead-end string

used for the insulators, but additional rings must be included for shielding the clamps. Control rings which shield both insulators and hardware were developed for the test line. Figure 4 illustrates the control ring for the suspension string; Figure 5 for the single dead-end; Figure 6 for the double dead-end.

The structural simplicity and ease of installation of these rings are apparent. All three are of the same basic principle but the suspension rings are tilted toward the clamp to improve tower clearance when the string swings toward the tower. The open construction about the insulator string reduces the possibility of snow packing or ice bridging. The suspension clamp may be positioned or removed without moving the rings. Under broken conductor conditions no conflict between ring and conductor is possible. Standard hardware connections, rivets and cotters, are used within the shielding influence of the rings without danger of overstress.

Steel pipe of the standard $1^1/_4$-inch size (1.9-inch outside diameter) was used in the construction of these rings. This diameter is about 15 per cent greater than the diameter of the 1.65-inch conductor.

Tests demonstrated the effective shielding of these rings for clean, dry conditions. Figures 9 and 10 summarize the radio influence voltage characteristics and the corona observations of test strings. The improvement in the voltage distribution from the plain string to the shielded string is indicated by Figure 11. These gradient tests were made at approximate phase voltages of 350 kv and 500 kv.

Shielding rings made of 4-inch-outside-diameter pipe instead of 1.9-inch were tested, but appeared to have little added advantage from the corona point of view.

Voltage Stress of Wet and Contaminated Insulators and Hardware

A marked reduction of corona voltage from clean, dry, to clean, wet conditions is shown by Figure 10. As illustrated by Figure 12 these corona points were from water drops on the surface of the control ring. The corona was limited to the ring and conductor; the insulators and other hardware parts were well shielded.

For tubular shapes the increase of radio influence voltage from dry to wet conditions is demonstrated by Figure 13. A 2-inch-diameter smooth brass rod was tested for radio influence voltage, first dry and then with water drops on the surface.

Shielding effectiveness is decreased by wet contaminated insulator surfaces. Overstress on polluted insulators may occur with unfavorable atmospheric conditions—fog, mist, wet snow, or light rain—and resistance rather than capacitance distribution of voltage may predominate throughout the string. Leakage currents of a few milliamperes cause heating sufficient to dry parts of the insulators. These dry areas may be near the pinhole of a suspension insulator; sometimes they are around the cap; but they may occur on any unit in the string. The voltage stress at such zones causes localized air breakdown. The resulting arc allows a leakage current surge.[13]

In our laboratory high-speed surge counters and surge recorders are used to determine the frequency, shape, and magnitude of these currents. The amount and type of contamination, the nature of the moisture, the presence of wind, and many other factors determine these characteristics.

A typical laboratory record is shown in Figure 14. A string of standard suspension insulators, contaminated in service in an industrial area was tested for leakage characteristics in mist at a voltage of about 10 kv per unit. Although the average leakage current was approximately 2 milliamperes, some surges were greater than 20 milliamperes.

In industrial areas heavily polluted with smoke and chemicals and in coastal regions subject to fog and salt deposits, severe leakage surging has caused flashover. Laboratory tests have demonstrated that such incidents would result from surges in the order of 100 to 200 milliamperes.

A clean, dry 30-unit suspension string at a phase voltage of 350 kv will have a power loss of less than 5 watts. Even in an interval of adverse weather and with dirty insulators, the average power loss per string should be less than 200 watts. During leakage current surges, instantaneous loss values might reach several kilowatts.

Continuing laboratory study of this subject may supplement the field investigation of the Tidd test line and facilitate assignment of observed losses.

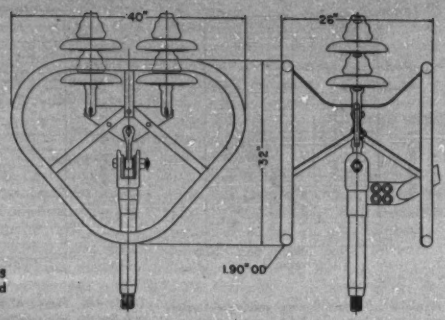

Figure 6. Control ring for the double dead-end string

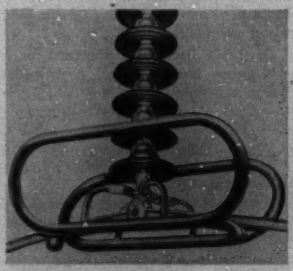

Figure 7. Line end of the suspension string

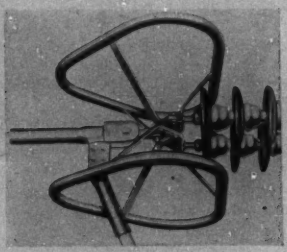

Figure 8. Line end of the double dead-end string

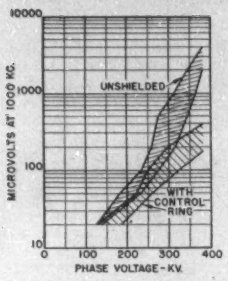

Figure 9. Radio influence voltage characteristics of suspension insulator strings with and without control rings

These curves apply to either 26- or 30-unit strings

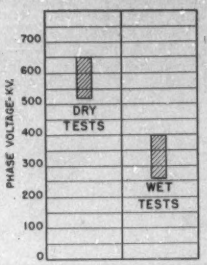

Figure 10. Range of minimum corona readings for the insulator strings with control rings

The minimum dry corona was from the radius of the control ring as shown in Figure 12. Wet corona tests were made with water drops on the hardware and with 0.2 inch per minute precipitation of 7,000 ohms per inch cube water. The minimum wet corona was from water drops on the rings. Readings were made with decreasing voltage

Conclusions

For 500-kv transmission lines, control rings have been developed which reduce the maximum voltage stress of the insulators and line hardware to acceptable levels.

Standard suspension insulators of appropriate strength are suitable for insulating these high-voltage lines. For high-strength suspension insulators with a 25,000-pound mechanical and electrical rating, insulator manufacturers are studying the possibility of increasing the pin shank diameter to improve fatigue strength.

Suspension clamp designs of standard types and established serviceability are available for use with large diameter conductors.

Field investigations and laboratory studies of leakage current phenomena over transmission line insulators do not show an alarming increase of flashover hazard with an increase of line voltage; if leakage problems arise on the proposed 500-kv line, units designed specifically for improved leakage surge resistance could be applied.

Section III. Insulators and Line Hardware Supplied by the Locke Insulator Corporation*

When the American Gas and Electric Service Corporation proposed the construction and experimental operation of the Tidd 500-kv transmission project, a study was made to see what new elements would be required in making up the insulator assemblies.

The Locke Insulator Corporation furnished the insulators and developed associated fittings necessary to support one circuit of the experimental line which was to be constructed with 1.65-inch-outside-diameter hollow-core copper conductor weighing 2.061 pounds per foot. It was proposed that this conductor should be so strung that under maximum assumed conditions of 1/2-inch radial ice, and 8 pounds per square foot lateral wiud pressure, at a temperature of zero degrees Fahrenheit, the maximum conductor tension would not exceed 14,500 pounds. This figure established the theoretical tension working loads required at the dead-end points. The maximum loading at suspension points on the line, assuming a 1,100-foot span, and considering the weight of the conductor, ice load, and wind load on the projected area of the conductor, plus ice, was calculated to be slightly less than 5,000 pounds.

At the outset it was recognized that at voltages in the range from 345 kv to 500 kv corona effects on the insulators and line hardware fittings would be a problem to be dealt with, but it was believed that these effects could be suppressed with appropriate corona shields properly disposed with respect to the parts where corona would be most likely to form It therefore appeared to be the most economical approach to the problem to select the standard existing 25,000-pound unit having a nominal diameter of 10 inches, a spacing of $5^3/_4$ inches, and a rated leakage distance of $11^1/_2$ inches. The ball-and-socket type of connection was preferred because of the greater facility with which maintenance operations could be carried on under "hot line" conditions.

Aside from the elimination of corona on the insulators and line fittings, the problem of suspending large diameter cables which were dictated by the corona loss studies appeared to be a fruitful field for investigation and development. While it was possible to support these conductors with an enlarged version of the conventional rigid saddle or envelope type clamp, an appraisal of the situation indicated that such a clamp would need to be approximately 34 inches in length if it were to accommodate maximum take-off angles which might be encountered in line construction without bending the cable over a shorter radius than was desirable with this type.

It was obvious that with a clamp of this length providing adequate strength, of necessity it would involve considerable mass and inertia resulting in high concentrated stresses on the cable under vibratory conditions. The high inertia of such a large rigid supporting member also seemed to preclude the possibility of

Table I. Electrical Characteristics of $5^3/_4$-by-10-Inch Standard Suspension Insulators

(Extrapolated From Published Data)

No. of Units	60-Cycle Flashover, Kv RMS				Critical Impulse Kv—$1^1/_2$x40 Wave	
	Dry	Times L-N*	Wet**	Times L-N	Positive	Negative
20	1,060	3.68	795	2.76	1,750	1,790
22	1,160	4.05	870	3.02	1,900	1,940
24	1,260	4.38	945	3.28	2,050	2,090
26	1,360	4.72	1,020	3.54	2,200	2,240
28	1,460	5.06	1,095	3.70	2,350	2,490
30	1,560	5.42	1,170	4.06	2,500	2,540

*L-N is line to neutral voltage on a 500-kv 3-phase line.

**Based on wet flashover being 75 per cent of dry value.

*By R. L. McCoy.

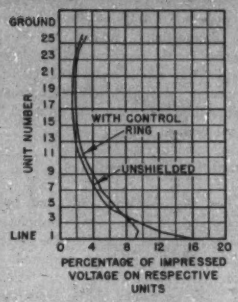

Figure 11. Voltage distribution of a 26-unit suspension string with and without control rings

its following the conductor vibrations faithfully. If it did not, beating of the conductor strands or segments at the point where they came tangent to the clamp seat would be inevitable. This would result in work hardening of the conductor material and great susceptibility to fatigue at these points.

It therefore was decided to make a new approach to the suspension clamp problem for large conductors, especially those of the hollow-core type. Previous experience with corona tests on clamps had shown that for operation in the projected voltage range with practical designs it would be desirable to shield the clamp from the strong electric field near the conductor. The idea of enveloping the clamp with the supports for the insulator corona shield was conceived. The clamp and shield therefore were developed simultaneously, the shield being designed to afford corona suppression to the clamp making it unnecessary to eliminate small radii and projections on the clamp itself.

The Suspension Clamp Design

As has been indicated, it seemed desirable to provide as high a degree of flexibility as possible with minimum weight and inertia in a clamp for large diameter conductors. In order to accomplish this it seemed best to avoid large rigid structures and to build the clamp of a number of rugged lightweight parts flexibly disposed with relation to each other.

Accordingly, a design was conceived in which the cable was supported on three separate saddles mounted on trunnions midway of their lengths and on the centerline of the conductor. These three saddles were connected by flexible linkages on each side co-operating with the trunnions of each saddle. The members thus formed then would be supported from the lower fitting of the insulator string by four links attached to them at some desired point between the trunnions of the three saddles.

By means of this construction the total weight of the span to be supported would be divided among the three saddles and the proportion borne by each saddle would be capable of adjustment by proportioning the lengths of the connector arms. Within limits such a clamp would be self-adjusting to the span conditions which might arise in service. Each saddle would be made relatively short and there would be little possibility of the conductor leaving contact with any one of the three saddles under vibratory conditions, thereby minimizing pounding or beating of the conductor at the point of entry to the clamp. It will be seen that a design of this type should permit minimum flexing of the conductor regardless of the phase relation of the vibrations in the spans on either side of the clamp. This is accomplished by a combination of relative vertical movement of the three saddles and rotation about the main support at the insulator connector.

In order to obtain approximately equal distribution of stress among the strands or segments of the cable the centers of the outboard saddles were made one-half of a conductor lay apart. This distance is equal to approximately ten times the conductor diameter, or $16^1/_2$ inches. The outboard saddles were made 5 inches long thus establishing an over-all length of $21^1/_2$ inches. In order to give the conductor the greatest freedom, it was decided that the clamping action should be confined to the center saddle, and that the clamp bolts should be located as close as possible to the trunnions.

The fundamental principle of the design of the clamp permitted some latitude in the distribution of the vertical support provided by the three saddles. This could be adjusted to a certain extent by the ratios of the lever arms between the secondary support points and the trunnions of the inner and outer saddles. It was believed that the center saddle should

Figure 12. Corona from a suspension string; dry (top) at 600 kv phase; wet (bottom) at 500 kv phase

The wet test was made with 0.2 inch per minute precipitation on the string and hardware

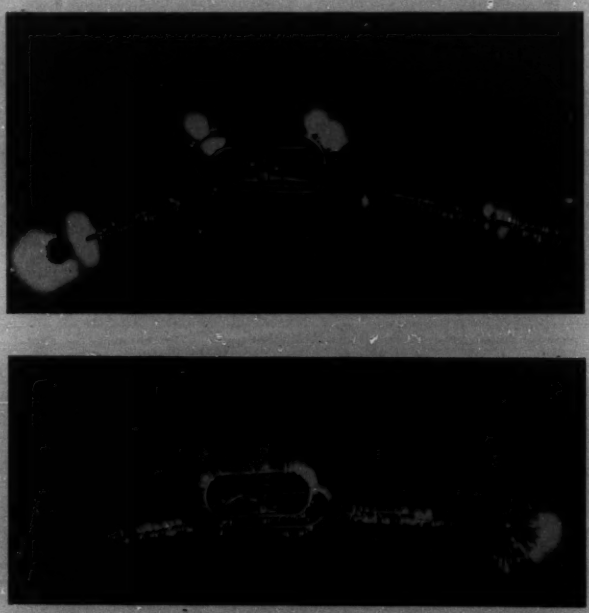

support a larger portion of the total load than the end saddles, and after some consideration of the problem, a distribution of 20 per cent for each end saddle and 60 per cent for the center saddle was selected.

It was desirable to keep the vertical depth of the clamp assembly to a minimum consistent with good proportioning of the clamp parts. The angular relationship of the connector links attached to the lower insulator fitting also had an effect on the distribution of the weight supported. The desired proportions then were analyzed by both graphical and analytical methods which gave substantially the same results.

Figure 15 shows a side elevation and sectional view of the final design. Figure 16 shows the clamp attached to an insulator string without the shield. It will be noted that the over-all length was reduced from approximately 34 inches for a conventional design clamp to 21 1/4 inches, and the net weight was held to approximately 35 pounds. All of the parts, except the saddles and bolts, are simple in design and can be fabricated readily from mild steel bars. The saddles may be made readily from ferrous or nonmagnetic alloys as desired. They may be cast or forged depending upon the tooling expense justified by the number of clamps to be produced.

An attractive feature of this design is the friction developed at the various connecting points which, under vibration of the conductor, will absorb energy and provide dampening. While the clamps furnished for the experimental line do not provide for more than the natural dampening inherent in the connections, additional dampening can be afforded by several means.

Corona Shield Assemblies

When the insulator unit had been selected and the clamp design completed, consideration was given to the corona shields which would be required to suppress corona on the insulator assemblies. The proximity of the tower steel to the upper end of the insulator string made it appear unnecessary to consider a

Table II. Corona Observations and Low-Frequency Flashover Data on Suspension Insulator Assemblies

Simulated Tower

Nature of Test	Dry or Wet	No. of Insulators in String	Corona Shield: Tube Size, In.	Corona Shield: Shield* Position, In.	Corona at 200 Kv to Ground	Corona at 290 Kv to Ground	Corona Kv to Ground	Location	Flashover Voltage, Kv to Ground
Corona and flashover	Dry	20	None used		Glow at ends of linkage bolts on clamp	Violent on ends of linkage bolts and trunnions of clamp saddles. Glow around pin of line unit	150 280	Disappears from clamp Disappears around pin of line unit	941
	Dry	20	2	0	None	None	325 425 500	Disappears from conductor Disappears from shield Disappears around pin of top unit	975
	Dry	20	2	+1	None	None	Same as above		975
	Dry	20	2	+2	None	None	Same as above		920
	Dry	20	2	+3	None	None	Same as above		962
	Dry	20	2	+4	None	None	Same as above		915 940
	Dry	21	2	0	None	None	Same as above		982
Flashover	Dry	20	2	0					1,000 965
Corona and flashover	Dry	22	3	0	None	None	425 450 500	Intermittent on conductor shield Continuous on conductor and shield Appears around pin of top unit	980
	Wet	20	None used		Soft glow on bolt and connector straps. Appreciable on water drops underside of conductor	Violent from clamp bolt ends, trunnions, connector straps and conductor	80 95 215	Disappears from clamp Disappears from conductor Disappears from insulator	683
	Wet	20	2	0	Yes	Yes	75	Intermittent feeble glow from water drops under side of shield and conductor	650
	Wet	22	2	0	Yes	Yes	100	Soft intermittent glow on shield and conductor	731
	Wet†	22	2	0	Yes	Yes	200	Disappears from conductor	785
	Wet	22	3	0	Yes	Yes	200-300 500	Disappears from shield Disappears from top and middle of insulator string	
	Wet	22	3	0	Yes	Yes	100 225	Soft intermittent glow from water drops underside of conductor and shield All along underside of conductor at water drops	721
	Wet†	22	3	0	Yes	Yes	200	Soft glow at water drops underside of conductor and shield	

*Shield position is denoted by referencing the level of the extreme upper tips of shield with respect to lowest point of outer skirt of the Insulator unit next to the line.
†Immediately after turning off artificial rain.

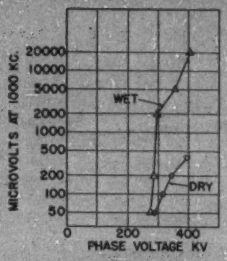

Figure 13. Radio influence voltage characteristics of a 2-inch-diameter tube

For the dry test the radio influence voltage was from the test circuit. For the wet test electric overstress was at water drops on the tube

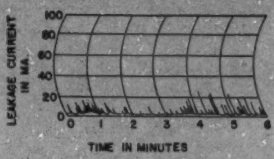

Figure 14. Leakage current record of a contaminated suspension insulator string in mist

About 10 kv per unit was impressed on the string

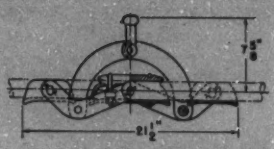

Figure 15. Final design of the articulated multiple saddle suspension clamp

corona shield at this point. The shielding problem therefore was confined to the lower end of the insulator string. A consideration of the problem indicated that shields for the suppression of corona should be made of pipe or tubing having an outside diameter slightly larger than that of the conductor because of the greater proximity of the sides of the shield to the tower structures.

A shield 30 inches wide by 42 inches long was decided upon for the initial installation. This, it was believed, would afford the required grading effect on the long insulator string, and minimize corona from the shield itself in the operating voltage range projected. Based on previous experience with shields, it was decided that it should be placed relatively low on the insulator string, approximately level with the skirt on the line unit, and would produce the desired grading effect with minimum reduction in flashover values. Except for the reduction in clearances to the tower, it would have been desirable to make the ring circular but in the tower design an allowance of 15 inches from the center line of the insulator towards the tower had been provided for the shield. The width therefore was kept arbitrarily to this figure. Space was not so limited in the direction of the line. Therefore, the shield was made oval with a major diameter of 42 inches. This afforded a shield of good proportions, and of a size to produce satisfactory improvement in voltage distribution on the string. The shield was dished upward $2^1/_4$ inches at the ends to induce any arcs which might form from lightning causes to initiate at these points farthest from the insulator.

In order to afford corona suppression on the clamps a novel means of supporting the shield was devised. For simplicity in design and to obtain minimum weight, it was desirable to build the clamps from parts with minimum sections which would not be corona-proof in themselves. Neither was it desirable to provide large-radius edges on these parts. The mechanical support for the shield therefore was arranged so as to envelop the clamp in a mesh made up of pipe of the same diameter as the shield itself. This was accomplished as indicated in Figure 17, which shows the shield assembly in elevation and an end view enveloping the clamp. Figure 18 shows the complete lower end assembly for the suspension string. Figure 19 is a view of a 22-unit suspension string complete.

Experimental shields were built to this design of 2-inch-diameter and 3-inch-diameter steel tubing of all-welded construction. The shield was supported from the socket connector between the lower insulator unit and the clamp to avoid the addition of the inertia of the shield to that of the clamp. Preliminary test shields were made with the height of the ring portion adjustable for determination of the optimum location.

Shields for the dead-end insulator assemblies were constructed on the same principle as those described for the suspension strings. The considerations involved were almost identical with those for the suspension strings except that tower clearance was not such a critical factor in their construction. The strain clamps which were furnished by the conductor manufacturer will be described by others, but it was believed they also should be shielded to suppress corona formation in a manner similar to that provided for the suspension clamps. Accordingly, two detachable shields were arranged to enclose the strain clamps and these were bolted to the main ring supports. The double strings of insulators were joined at the ends by conventional forged plate yoke assemblies furnished by the Brewer Titchener Corporation. On account of the length of the strings which it was proposed to use, the spacing

Table III. Corona Observations and Low-Frequency Flashover Test Data on Double Strain Insulator Assemblies

Nature of Test	No. of Insulator Units Per String	Corona Shield: Tube Size, In.	Corona Shield: Shield* Position, In.	Corona Observation; Corona Shield and Clamp Shield in Place: Kv to Ground	Corona Observation; Corona Shield and Clamp Shield in Place: Location	Corona Observation: Corona Shield Only, No Clamp Shield: Kv to Ground	Corona Observation: Corona Shield Only, No Clamp Shield: Location	Flashover Voltage, Kv to Ground
Corona and dry flashover	26	None used		200	Glow on heads of keys of socket clevises connecting lower yokes to insulators			
	20	2	0	395	Ring part of main shield			1,060
	22	2	0	395	Ring part of main shield			1,170
	24	2	0	415	Ring part of main shield			1,210†
	26	2	0	395	Ring part of main shield			Beyond limit of test equipment
Corona	20	2	0			380	Ring part of shield	
	22	2	0			375	Ring part of shield	
	24	2	0			375	Ring part of shield	
	26	2	0			385	Ring part of shield	

*Shield position is denoted by referencing the level of the extreme upper tips of shield with respect to lowest point of outer skirt of the insulator units next to the line.

†Flashover voltage not measured. Clamp shield does not affect flashover distance.

Figure 16. View of the suspension clamp supported by an insulator string

between the insulator string centers was increased from the usual dimension of 13 inches to 16 inches. The yokes were provided with means for attaching the corona shield assemblies. Figure 20 illustrates the outer end of the dead-end assembly. Figure 21 is a view of the outer end of the same assembly.

Test Results

When the designs described in the foregoing paragraphs were completed, sample clamps and shields were made up for tests and investigated prior to the production of the quantities needed for equipping the circuit in the field. Both suspension and strain strings then were set up in the Locke high voltage laboratory for determination of corona formation voltage and flashover voltage. The suspension insulator was supported from the center of a beam 33 feet $9^1/_2$ inches long, representing the length of the crossarm on the tower between the upright supports. A 9-inch width of the sheet metal was fastened to the under side of this beam and similar strips of sheet metal 20 feet long were attached at the ends, representing the effect of the window for the center insulator position on the tower. Figure 22 is a view of a low-frequency flashover of a 22-unit suspension string complete, set up in the simulated window of the tower.

For the suspension strings a 16-foot

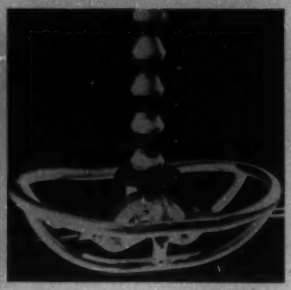

Figure 18. Close-up view of the line end assembly of the suspension insulator string

length of 2-inch-diameter smoothly galvanized steel tubing was mounted in the clamp to simulate the conductor. On the dead-end assemblies a short length of the actual 1.65-inch-diameter hollow-core cable was attached to the strain clamp representing the conductor extending into the span while a 10-foot length of the same conductor was formed and supported in such a manner as to simulate the jumper loop.

Corona formation voltage and low-frequency flashover tests were made on several different days in order to get a range of atmospheric conditions. Tests were conducted on suspension strings of 20, 21, and 22 units. The results of these tests are shown in Table II.

Low-frequency flashover tests also were made on the dead-end assembly on strings of 22 and 24 units in length, while corona formation voltage tests were made on the same string lengths of 22, 24, and 26 units. The results are shown in Table III.

It will be noted from Table II that when the suspension string was tested without the corona shield under dry conditions, corona was observed at values as low as 150 kv line-to-ground, while the lowest value at which corona was observed with the shield in place was 325 kv to ground. At this value of voltage corona appeared consistently on the 2-inch-diameter pipe conductor used in these tests to simulate the line conductor. The lowest point at which corona could be seen anywhere on the insulator string and associated fittings under dry conditions was 425 kv to ground. At this voltage intermittent corona was observed on the corona shield. As the voltage was raised beyond this point corona was observed next around the pin of the top insulator in the string adjacent to the simulated structure at 500 kv. In each test the string was observed closely for corona at 200 kv and again at 290 kv, respectively, to ground, and no corona was visible.

Under wet conditions a very faint glow could be discerned from water drops on the conductor and the shield at values as low as 75 kv to ground. This was a very soft glow, however, and did not break into active corona until voltages of 200 and 225 kv to ground were reached. No corona was visible on the insulators themselves under conditions up to 500 kv. Tests on the dead-end assemblies showed that without the corona shield in place corona formed on the cotter keys of the

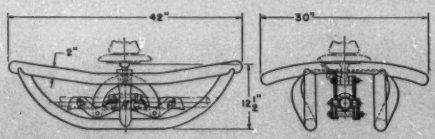

Figure 17. Corona shield assembly showing the suspension clamp enveloped in the shield support

Figure 19. Close-up view of a complete suspension insulator string consisting of 22 insulator units with clamp and shield assemblies in place

socket clevises on the line and of the insulator strings at 200 kv. With the corona and clamp shields in place, corona was observed to start from the upper side of the main corona shield uniformly at 395 kv regardless of the length of the strings.

Tests also were made with the clamp shields removed and corona on the clamp itself was observed under this condition at 10 and 20 kv lower voltage, indicating that some benefit was being obtained from the clamp shields. The tests showed no appreciable benefit to be derived from making the shield of 3-inch-diameter tubing. Higher positions of the ring gave no added improvement of the performance level with the bottom skirt. All flashover values measured were corrected to standard atmospheric conditions in accordance with AIEE Standard 41, 1944 (American Standards Association C-29.1, 1944). Impulse flashover tests and radio influence voltage measurements would have been of much interest but equipment of the required capacity is not readily available.

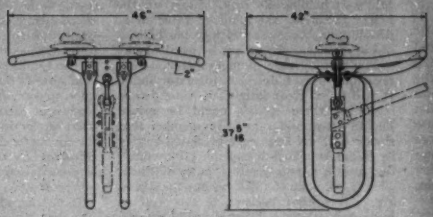

Figure 20. Details of the line end of double strain insulator assembly

Figure 21. Line end of the double strain assembly

Conclusions

1. A new type of suspension clamp for large diameter conductors was developed and from the investigation made to date, it appears to be practical, resulting in a reduction in length of substantially 40 per cent. A similar reduction in weight and inertia was accomplished. An extremely flexible means of support of the cable also was accomplished which is self-adjusting to varying span conditions.

2. A corona shield, involving novel means of support, completely shielded the hardware at the lower end of the insulator string so that the corona voltage under all conditions tested was at least as high on the insulator string and its associated fittings as could be obtained on a 2-inch-diameter steel-tube conductor. The tests indicated that the 2-inch-diameter material for the corona shield gave adequate corona suppression and that the 3-inch-diameter tubing was not justified.

3. Tests without the corona shield indicate that corona would be very difficult to suppress by other means at values above 150 kv to ground, which would be far below the corona formation voltage of the conductor.

4. Under wet conditions corona starts from water drops which form on the under side of the shield and conductor. The insulator string, shield, and clamp, however, are equal to the conductor in performance in this respect.

5. It appears that corona suppression can be accomplished on long strings at high voltage without appreciable effects on the flashover voltage values.

6. As a result of the tests and investigation on this project, it is believed that satisfactory operation in the voltage range between 345 and 500 kv will be obtained.

References

1. Transmission of Electric Power at Extra High Voltages, **Philip Sporn, A. C. Monteith.** AIEE Transactions, volume 66, 1947, pages 1571–82.

2. Corona Considerations on High-Voltage Lines and Design Features of Tidd 500-Kv Test Lines, **C. F. Wagner, Anthony Wagner, E. L. Peterson, I. W. Gross.** AIEE Transactions, volume 66, 1947, pages 1583–91.

3. Line Conductors—Tidd 500-Kv Test Lines, **E. L. Peterson, D. M. Simmons, L. F. Hickernell, M. E. Noyes.** AIEE Transactions, volume 66, 1947, pages 1603–12.

4. Transformers and Lightning Arresters—Tidd 500-Kv Test Lines, **F. A. Lane, J. K. Hodnette, P. L. Bellaschi, Edward Beck.** AIEE Transactions, volume 66, 1947, pages 1613–18.

5. Switchgear Equipment for Tidd High-Voltage Test Lines, **F. A. Lane, B. W. Wyman.** AIEE Transactions, volume 66, 1947, pages 1619–23.

6. Instrumentation and Measurement—Tidd 500-Kv Test Lines, **R. L. Tremaine, G. D. Lippert.** AIEE Transactions, volume 66, 1947, pages 1624–32.

7. Flashover Characteristics of Rod Gaps and Insulators, **AIEE Committee.** Electrical Engineering (AIEE Transactions), volume 56, June 1937, pages 712–14.

8. Lightning Performance of 200-Kv Transmission Lines—II, **AIEE Committee.** AIEE Transactions, volume 65, 1946, February section, pages 70–5.

9. Methods of Measuring Radio Noise 1940. Edison Electric Institute (New York, N. Y.) Publication G9, National Electrical Manufacturers Association (New York, N. Y.) Publication 107, Radio Manufacturers Association (Chicago, Ill.) Engineering Bulletin 32.

10. The Fatigue of Metals (book), **H. F. Moore and J. B. Kommers.** McGraw-Hill Book Company, Inc., New York, N. Y.

11. Dielectric Phenomena in High Voltage Engineering (book), **F. W. Peek, Jr.** McGraw-Hill Book Company, Inc., New York, N. Y.

12. Corona Loss Measurements for the Design of Transmission Lines to Operate at Voltages Between 220 Kv and 330 Kv, **Joseph S. Carroll, Bradley Cozzens.** AIEE Transactions, volume 52, 1933, pages 55–63.

13. The Characteristics and Performance in Service of High-Voltage Porcelain Insulators, **J. S. Forrest.** Journal, Institution of Electrical Engineers (London, England), volume 89, part II, number 7, February 1942, pages 60–80.

Figure 22. Low-frequency dry flashover of a 22-unit suspension insulator assembly with simulated tower window and conductor in place

Discussion

Wm. S. Peterson (Department of Water and Power, The City of Los Angeles, Los Angeles, Calif.): In connection with the suspension clamp, I was pleased to note that in one of the installations a suspension clamp was used which contemplated the use of saddles mounted on trunnions to support the conductor. This construction follows in part the principle used for suspension clamps on the Hoover Dam–Los Angeles lines and accomplishes the purpose of having a minimum mass at the support of the cable and permits bending to be graduated over a considerable distance. The paper mentions that the friction developed by the trunnion would be useful in damping out conductor vibration. I note that the relationship of the trunnion parts is such as to develop such friction. In the clamp which we developed the relationship of the trunnion pivot was reversed so that the friction was a minimum so as to avoid wear. The point I wish to make is that one has the choice of obtaining friction at the cost of possibly excessive wear or else avoiding the friction and having to depend on other agencies for damping vibration. This tends to ameliorate strand breakage due to conductor vibration.

In connection with clamps for supporting dead ends, I note that the clamps have considerable mass including fairly rigid connections to the jumper loops. In our designs for such clamps we have endeavored to keep the mass to a minimum and made use of flexible connections to the jumper loops to help accomplish this purpose. It probably also should be noted that it is desirable that the control ring and yoke assembly be so pivoted that it does not have a natural period in the range of conductor vibration.

Abe Tilles (Pacific Gas and Electric Company, San Francisco, Calif.): Table I of the paper is said to be extrapolated from existing data. Is this a linear extrapolation? If so, it is not conservative in view of the well-known nonlinear characteristic of long gaps. This thought is borne out further by the test data in Table II which gives, for instance, 980 kv for 22 units as against 1,160 kv in Table I.

The shielding obtained on the 26-unit string tested is obviously very good. This string is utilized about as effectively as conventional 16-unit strings. A conventional 16-unit string with big horn has the end unit carrying 2.88 times the average stress, whereas this string has the end unit carrying 2.34 times the average stress per unit. The 16-unit string carries 29 per cent of the total stress on the 8 least stressed units and the 26-unit string carries 26 per cent of the stress on the 13 least stressed units. Considering the substantially greater slenderness of the long string its shielding certainly is holding its own. Even so, the longer the string the more desirable stress distribution becomes, and any possibilities of improvement should not be overlooked.

Mention is made of preliminary studies regarding use of different insulator units. It will be of great interest if some details regarding these studies could be given. Pacific Coast engineers still remember that the first 220-kv lines were insulated largely by taking standard disks from 110-kv practice and stringing together more of them. This is still done to this day, but the speculation rises that perhaps a new voltage jump may call for a different insulator unit.

I. W. Gross: The electrical characteristics of insulators shown in Table I, extrapolated from existing data, were obtained by straight line extrapolation. It is pointed out by Tilles that the dry flashover for 22 units in this table does not agree with the test values shown in Table II. It should be pointed out that the flashover data in Table II as well as in Table III were incidental to the main purpose of the tests described in these tables, which was to determine the voltage across the string at which corona started to form on various parts of the insulator string assembly. The flashover data, therefore, should not be considered final. It further should be pointed out that flashover data in Tables II and III were with corona shields on the insulator assembly whereas the extrapolated data of Table I were without any shield rings.

R. L. McCoy: The question of wear at the trunnion points on the saddles of the multiple saddle clamp raised by Peterson is a point requiring careful consideration in a design of any clamp having joints where friction may develop. It is essential in constructing the parts for such clamps to use materials of proper hardness and wear resistance so as to avoid undue reduction in area of the supporting parts at the critical point, and consequent loss in strength. Considerable field experience has been obtained, however, over the past 20 years with trunnion-type supports on suspension clamps for large conductors in long spans, where a combination of rolling and rubbing friction would be obtained under conditions of conductor vibration. For the most part these clamps were made of SAE-1035 forging quality steel, hot dipped galvanized, although some of the clamp bodies and trunnions have been made of malleable iron.

Previous experience has been obtained over periods of 10 to 20 years on several long span lines using large conductors, such as 795,000-circular-mil aluminum cable steel reinforced for 230-kv service, and no objectionable amount of wear has been brought to our attention out of many thousands of these clamps in service. In the multiple saddle clamp developed for the Tidd project, the load is divided among three pairs of trunnions, and under normal conditions it is not expected that any pair of trunnions will carry more than 60 per cent of the total load. It is probable therefore that none of the flexible joints will be called upon to carry heavier loads than frequently have been carried satisfactorily with somewhat similar designs in the past, even though the conductor diameter in this case is larger. Emphasis for the need for proper selection of materials from this standpoint is, however, essential.

It is true, of course, as Peterson points out that the inertia of the strain clamps could be reduced by making a flexible connection between the main clamp and the jumper loop clamps. Previous experience, however, with compression type strain clamps used with fairly large conductors has not seemed to indicate the necessity or justification for the increased cost and complication involved in providing a flexible connection at this point. Experience with the test line may indicate the desirability of further refinement in this direction. One of the values of the test line is, that such matters as this can be checked, for indications of the need for such improvements.

With respect to the corona shield and yoke assembly, considerable stabilizing force is provided by the conductor tension since the conductor attachment hole to the yoke is offset approximately $3^3/_4$ inches from the insulator attachment holes. This is done principally to provide position stabilization of the two insulator strings at some slight sacrifice in the equalizing function of the yokes. However, it does tend to fix the whole yoke and corona shield assembly in a very stable position, and the clevis connection between the yoke and the clamp somewhat isolates forced vibration from the conductor to the yoke and shield assembly. Again experience with similar assemblies over 15 to 20 years of service has indicated no trouble from this cause.

J. M. Sheadel: The comparison by Tilles of voltage stress on 16-unit strings with voltage stress on the test line strings is comforting. The big horn used with the 16-unit string was designed primarily for arc protection of the conductor; but the horn also improves the voltage distribution of suspension insulator strings.

In the Ohio Brass Company laboratory radio influence voltage characteristics of special suspension insulators with electric stress controls in the pinhole and with conduction glaze at critical areas were determined. For long strings the special insulators without shields had about the same radio influence characteristics as standard insulators with shields. It was more practicable, to use standard units with shields because the special units were expensive, their wet performance was debatable and line hardware required shielding.

Line Conductors—Tidd 500-Kv Test Lines

E. L. PETERSON
MEMBER AIEE

D. M. SIMMONS
FELLOW AIEE

L. F. HICKERNELL
FELLOW AIEE

M. E. NOYES
MEMBER AIEE

Section I

A NUMBER of factors entered into the selection and installation of conductors for corona determination on the 500-kv test project of the American Gas and Electric Service Corporation at Brilliant, Ohio, described in companion papers.[1-6] These included conductor conductance, outside diameter, exterior surface contour, spacing, and material. In addition to the characteristics of the conductors themselves, careful consideration was given to the method of installation.

Conductor Sizes and Types

In selecting conductor conductance, a figure of 650,000 circular mils copper equivalent was selected as a lower value which it was believed would be needed in the foreseeable requirements for high-voltage transmission above present voltage levels. Since a conventional conductor of this conductance would have a diameter in the order of one inch, it readily follows that a conductor design suitable for voltages in the order to be tested (264 to 500 kv) would be, for economy reasons, of an expanded type, that is, basically a cylindrical shell of conducting material with any necessary interior filling merely for structural purposes to obtain the required outside diameter.

In selecting conductor outside diameters, a range from 1.4 up to 2 inches was chosen. Considerable data are available[7] on corona dry-weather characteristics of conductors which make it desirable to "check test" at least one of this type of conductor with the instrumentation used in this test. Therefore, in addition to the larger conductors of 1.65- and 2.0-inch outside diameter, a 1.4-inch outside diameter, type *HH* conductor will be used for check purposes. The 2-inch outside diameter was about the maximum limit of outside diameter which was considered feasible to make, install, and operate.

Corona data on this range of conductor sizes (1.4-, 1.65-, and 2.0-inch outside diameter), it was believed, would give the necessary correlation for any intermediate sizes of single conductors which might be used in practice.

In addition to these single conductors selected, the so-called "bundle" or grouped conductor will be tested with individual conductors ranging from 0.70 to 0.92 inch in diameter and with from two to four conductors per phase wire.

Some of the salient features of the line conductors which it is planned to test are shown in Table I.

It is planned that the conductors to be

Figure 1. Conductors held off ground by planks laid under the cable

Paper 47-244, recommended by the AIEE committee on transmission and distribution and approved by the AIEE technical program committee for presentation at the AIEE Midwest general meeting, Chicago, Ill., November 3–7, 1947. Manuscript submitted August 19, 1947; made available for printing September 19, 1947.

E. L. Peterson is transmission engineer, American Gas and Electric Service Corporation, New York, N. Y.; D. M. Simmons is vice-president in charge of research, General Cable Corporation, Bayonne, N. J.; L. F. Hickernell is chief engineer, Anaconda Wire and Cable Company, Hastings-on-Hudson, N. Y.; M. E. Noyes is manager, electrical conductor division, Aluminum Company of America, Pittsburgh, Pa.

Table I. Line Conductor Characteristics

Item No.	Outside Diameter, In.	Material	Circular Mils	Core	Exterior Surface	Manufacturer
1*	0.70	Copper	211,600	Copper I beam	Strand	Anaconda Wire and Cable Company
2*	0.92	Copper	321,000	Copper I beam	Strand	Anaconda Wire and Cable Company
3	1.40	Copper	512,000	Air-hollow	Smooth**	General Cable Corporation
4	1.65	Copper	650,000	Air-hollow	Smooth**	General Cable Corporation
5	1.65	Copper	890,500	I beam	Strand	Anaconda Wire and Cable Company
6	1.65	ACSR	1,062,800‡	Steel and paper	Strand	Aluminum Company of America
7	2.00	ACSR	991,500‡	Steel and paper	Strand	Aluminum Company of America
8	2.00	Copper	1,030,000	Air-hollow	Smooth**	General Cable Corporation
9†	0.576	ACSR	159,000‡		Strand	Aluminum Company of America

* To be used as grouped or "bundle" conductors in groups of two, three, and four.
** Type *H H*. † Used as ground wire. ‡ Circular mils of aluminum.

tension required in pulling out the cables and still keeping them off the ground. Forty-inch-diameter cable sheaves were attached at the towers and at the intermediate poles to support the cables. In planning a setup for cable installation on a long line, it no doubt would be desirable to use a tensioning drum ahead of the cable reel so as to allow the pulling out of the cable without the necessity of installing intermediate structures.

Since the conductors were installed without allowing them to come into contact with the ground, it is not planned to wash or clean them. They therefore will be in the same condition as conductors tested will remain exposed throughout all of the weather conditions to which the line is subjected. During the course of the tests some of the conductors will be replaced with other types. Records will be kept not only of the corona loss readings but also of the weathering of the cables and any other factors which might affect the over-all corona loss.

Figure 3. Intermediate wood poles set between towers in the cable stringing operation in the field

Cable is run through 40-inch stringing block at the top of each pole

Field Erection of Conductors

It was believed desirable to string the conductors in such a manner that they would be kept off of the ground during the stringing operation since it was desired to keep them clean and free from abrasions which might occur if they were allowed to be pulled along the ground during erection. Where it was possible for small sections of the conductors to touch the ground, while making dead-end connections, the cables were supported on planks (Figure 1).

The cables were pulled out directly from the cable reels, a braking device being used on the rim of the cable reels (Figure 2). This was supplemented in some instances with a cable drum attached to the side of the reels. Since it was desired to limit the tension of the cable in the stringing operation, particularly with a view of preventing damage to the cables by pressing them too tightly in the reels during the pulling operation, intermediate poles were set up between the towers (Figure 3) so as to limit the on an operating line where it might prove uneconomical to take elaborate steps to clean them.

A description of the conductors and their characteristics and fittings is described hereinafter in sections II, III, and IV by engineers of the General Cable Corporation, Anaconda Wire and Cable Company, and the Aluminum Company of America, who furnished the conductors for the test insulation.

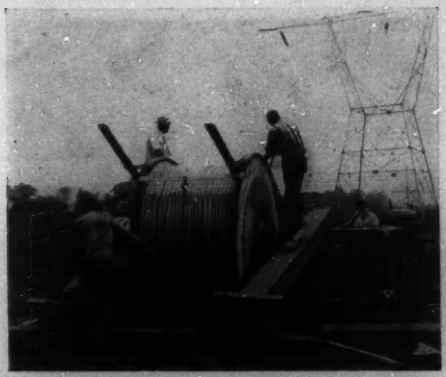

Figure 2. Type *HH* 1.65-inch-outside-diameter conductor being strung in the field

Note brake on drum reels for controlling conductor tension

Section II. Conductors Supplied by the General Cable Corporation*

If lines of higher voltages than now used are to be justified economically, the design and the operating characteristics of the conductors become increasingly important. For the transmission of electric energy in the higher voltages,

* By D. M. Simmons.

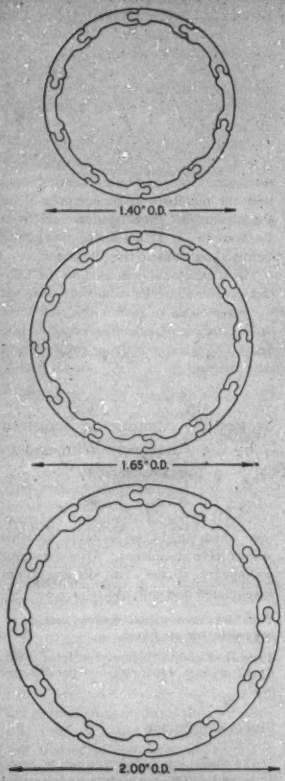

Figure 4. Cross section of 1.4-, 1.65-, and 2.0-inch-outside-diameter type-*HH* cables supplied for the Tidd 500-kv test lines

conductors of relatively small areas are desirable. With the higher voltages, however, corona loss becomes increasingly important as the voltage is raised and to reduce this loss, conductors of greater diameter are required. For most efficient line operation it is essential to have available conductors of small area and of large diameter. This is practically the definition of a tube, and thus a tubular conductor offers an ideal solution of the problem.

Type *HH* conductors supplied by the General Cable Corporation for the tests are tubes composed of spiralled segments having lateral tongues and grooves which interlock by means of the enlarged tip of the tongue and a correspondingly shaped groove. These conductors are readily manufactured in the long lengths required for transmission and are flexible since the segments are free to move longitudinally under controlled conditions when the cable is bent.

This type of conductor therefore is suitable not only for experimental work, but has proved in service its adequacy as a practical line conductor meeting all service requirements.

Type HH Cable Characteristics

Type *HH* construction makes possible a cable of maximum diameter for a given cross section, or conversely, a minimum cross section for a given diameter. Being of hard-drawn copper, the conductor has excellent strength. As it is composed of curved flat interlocked segments, it is unusually rugged and stands mechanical abuse incidental to erection and operation to a remarkable degree. Because of its smooth surface, it has a low corona loss.[7]

Three sizes of type *HH* cable were supplied for this experimental test line as follows:

1. For one of the $1^1/_2$-mile test lines, 1.65-inch-diameter 650,000-circular-mil cable.
2. For the substation where the connections are quite complicated and where instrument leads had to be shielded from the transformers to the three test lines, 2.0-inch-diameter 1,030,000-circular-mil cable was supplied. Additional cable of this size has been supplied for use on the 800-foot test line.
3. For the 800-foot test line, 1.4-inch-outside-diameter 512,000-circular-mil cable, identical with that used on the Los Angeles–Hoover Dam 287-kv lines has been supplied. This will make possible a comparison of corona measurements with the earlier measurements at Stanford University.

The characteristics of these cables are shown in Table II.

Figure 4 shows scale drawings of the cross sections of the three cables.

In addition, 5,000 feet of measuring wire were supplied. This measuring lead was single conductor number 10 strand, insulated with 0.075 inch of brown polyethylene with a bare copper braid of number 33 American wire gauge copper wires over-all. This measuring lead extends from each conductor of each of the three test lines to the three instrument cases. A very unusual method of shielding this conductor was used in that the conductor was placed inside the 2-inch *HH* bus cables in the substation as described in one of the companion papers.

Past Applications

The practicability of type *HH* conductors for the higher voltage lines has been demonstrated fully over years of actual

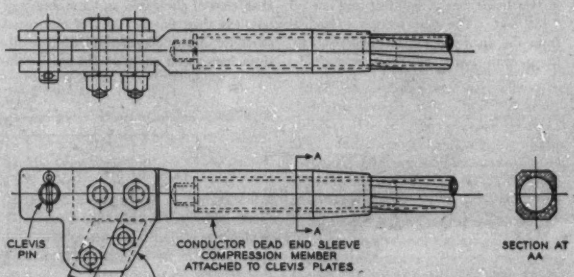

Figure 5 (above). Strain clamp (dead-end), compression type for 1.65- and 2.0-inch type-*HH* conductors

Figure 6 (below). Separable copper connectors, compression type, for 1.65-inch type-*HH* conductors

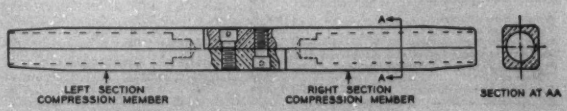

Table II

Outside diameter, inches	1.65	2.90	1.40
Number of segments	12	12	10
Area			
Circular mils	650,000	1,030,000	513,000
Square inches	0.5105	0.8090	0.4021
Weight, pounds per 1,000 feet	1,987	3,159	1,566
Breaking strength, pounds	28,070	43,686	22,110
Modulus of elasticity, pounds per square inch	16.5×10^6	16.5×10^6	16.5×10^6
Coefficient of linear expansion per degree fahrenheit	0.0000094	0.0000094	0.0000094

service and many thousands of miles of conductor. This type was first employed in the United States on the 287-kv Los Angeles–Hoover (then Boulder) Dam lines in 1935 and since that time has been used on lines of various voltages and sizes down to 4/0 American wire gauge 0.650-inch outside diameter operating at 138 kv. The investigation of this type of conductor on the experimental lines is therefore solely one of determining corona, rather than mechanical characteristics.

Installation

The 2.00-inch conductor installed in the substation consists of busses ranging in length from 104 to 306 feet exclusive of insulator strings. Dead-ends or strain clamps were attached to the cables before they were raised and no special precautions were taken in handling.

On the original setup on the mile and a half test lines, the 1.65-inch-outside-diameter conductor was installed on line 1 in two spans, one of 840 feet and one of 1,135 feet. The first section extended from the dead-end at the substation to the second tower where it was dead-ended. From the second or angle tower it runs along a tangent line of five additional towers having spans of 1,120 feet, 1,090 feet, 1,070 feet, 1,000 feet, and 1,040 feet.

The conductor was strung under tension, free of the ground, and was pulled by means of the usual Kellems woven wire grips which passed readily through the special stringing blocks. Preparatory to and during sagging, the conductors were held by come-alongs normally employed for that purpose.

Accessories

The dead-ends (strain clamps) used in both the substation with the 2.00-inch-outside-diameter cable and on the line with the 1.65-inch-outside-diameter cable are of the compression type as illustrated in Figures 5 and 6. Figure 5 shows the dead-end for the 1.65-inch conductor. The dead-end for the 2.00-inch conductor is similar except for size. These are designed to have an electrical resistance less than that of the cable and a strength of not less than 95 per cent of the rated strength of the conductor. Similar fittings have been supplied for use on the 1.4-inch and 2.0-inch cables which will be installed on the 800-foot test span during the course of the test.

The nonferrous fittings are applied by means of a suitable hydraulic press such as usually employed for transmission conductors.

The dead-ends may be used with or without the jumper connections as best suits conditions and are so constructed that the members to be compressed on the conductors may be detached from the body of the fitting for easy handling during application to the conductor.

The connector splices used on the 1.65-inch-outside-diameter cable were designed to be separable to permit the conductor to be handled most readily if it should be desired to remove it from the line and later reinstall it.

Section III. Conductors Supplied by the Anaconda Wire and Cable Company*

Several types of conductor construction which might be suitable for this project were considered. After extensive preliminary studies, two distinct types were offered and supplied

Type I—Conventional hollow conductor, one conductor per phase.

Type II—Grouped hollow conductor; two, three, or four conductors in parallel per phase.

Single Conductor

The single conductor per phase (type I) hollow conductor is 1.65-inch outside diameter, Anaconda design 966. It consists of a single layer of round copper wires stranded over a twisted I-beam core. Conductor characteristics are given in Figure 7. The conductor diameter of 1.65 inches was chosen by agreement among all interested parties. It is interesting to note that for a 1.0-inch-diameter conductor operating at 220 kv, the corona initiation voltage is about 83 per cent of the operating voltage. On the same basis, the 1.65-inch-diameter conductor would be suitable for operation at 400 kv.

This conductor is being furnished for these tests to obtain accurate and comparable data under practical field conditions of installation, aging, and weather,

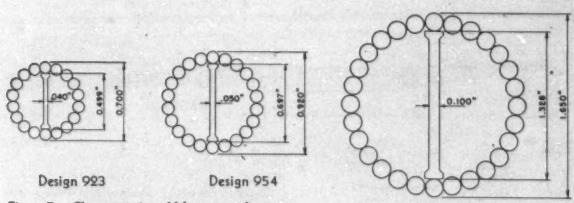

Figure 7. Characteristics of I-beam conductor

	Design 923	Design 954	Design 966
Equivalent hard copper area, cir mils	211,600	321,000	890,500
Actual area, cir mils	211,993	321,676	904,232
Outside diameter, in.	0.700	0.920	1.650
Rated breaking strain, lb	9,300	13,850	36,000
Minimum breaking strain, lb	9,100	13,550	35,700
Weight, lb per thousand ft	666.8	1,012	2,857
Weight, lb per mile	3,521	5343.4	15,085
Number of hard copper wires	18	22	28
Diameter of hard copper wires, in.	0.1005	0.1113	0.1610
Resistance at 20 C, ohms per thousand ft:			
Direct current	0.0522	0.0344	0.0124
Alternating current, 60 cps	0.0524	0.0345	0.0125

* By L. F. Hickernell. The author is indebted to many of his engineering associates who have participated in the investigation, design, and development work and in the preparation of this paper. Specific acknowledgment is made to A. A. Jones (M'46), J. E. Talbott, E. W. Greenfield (M '37), and B. M. Pickens (A '37), all of the Anaconda Wire and Cable Company.

Figure 8. Design 966 for I-beam conductor

Figure 9. Dead-end unit design 966

Before application

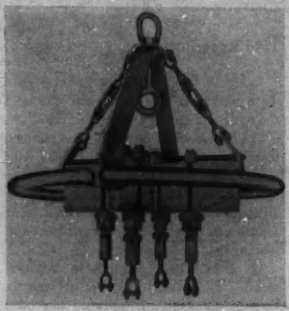

Figure 10. Adjustable dead-end assembly

Grouped conductors, four positions

Figure 11. Adjustable dead-end assembly

Grouped conductors, three positions

regarding the effect on critical corona voltage and corona loss of

1. Copper versus aluminum.
2. Round wire stranding versus so-called smooth conductors.

Figure 8 shows conductor design 966 which is of the same I-beam construction that has been used in large quantities throughout the world since 1925. Design 966 has a larger diameter than other designs usually encountered, because of extrapolation into the higher voltage field, but successful I-beam cables two and more inches in diameter have been fabricated and used.

Dead-end assemblies and connectors are of the conventional Anaconda drawn-seamless type, which have been used on all types of copper conductors since the early 1920's. These are installed on the conductor by means of a portable draw-bench. In this operation the copper tubing of the fitting is drawn through a split die, thus effecting the radial pressure. For I-beam conductor no fillers are required within the hollow structure since the I beam plus the arch effect of the concentric layer of wires provides sufficient resistance to withstand the radial pressure without crushing the conductor. Rated conductor strength is obtained.

Figure 9 shows the dead-end connector assembly for conductor design 966.

Grouped Conductors

While the grouped-conductor construction (type II) is not a new idea, it has not been used commercially as yet in the United States for power transmission purposes. However, the Anaconda Company has had extensive experience with this type of construction in connection with a number of high-power radio-frequency antennas which have been built for the United States Navy during the past 15 years. Since it presents interesting possibilities for increasing power capacity and reducing corona and power losses, several variations using hollow conductors, designs 954 and 923 (see Figure 7) are being furnished for these tests to provide data regarding effect of

1. Two versus three versus four conductors per phase.
2. Corner radii, that is, individual conductor diameter.
3. Interaxial spacing of individual conductors in the group.

Early Experiments

Early investigations of corona initiation voltage and loss on bare transmission line conductors suggested theoretical and practical advantages in splitting large conductors into groups of smaller subconductors. In 1910–1911, J. B. Whitehead[8,9] arranged conductors at the same potential in the form of a triangle and a square. He found an increase in corona initiation voltage of 16 per cent for the 3-wire group and 20 per cent for the 4-wire group over that of a single conductor of equivalent total cross section.

In 1915, F. W. Peek, Jr.,[10] described more extensive tests on subdivided conductors at the same potential. He investigated 2- and 3-wire groups arranged in various configurations and spacings. He found that grouped subconductors invariably increased the corona initiation voltage over that of a single conductor of the same cross section. The amount of increase was found to vary with separation of the component subconductors, their configuration, the distance to ground, and the spacing between phases. For the 2-wire group, he obtained a maximum increase in corona initiation voltage of 5 per cent; for the 3-wire group, he obtained 20 to 30 per cent.

Theoretical Investigations

Theoretical investigations of the potential gradient about a group of equipotential conductors spaced at distances large in comparison to conductor radii were made by O. Burger[11] in 1922. Later, in 1932, when design considerations were being reviewed in connection with transmission of large blocks of a-c power at 400 kv, a fairly comprehensive study of this type of conductor was made by G. Markt and B. Mengele[12] for Siemens-Schuckertwerke.

They concluded that the use of grouped conductors increases the corona initiation voltage and also increases the power which can be transmitted. It is shown that the effective radius of each phase conductor can be increased greatly by subdivision of the usual single conductor into grouped conductors. Data are presented which show that for typical cases

Four 0.493-inch (approximately 4/0 American wire gauge) cables arranged in a 10-inch square are equivalent in corona initiation voltage to a single hollow conductor of 1.18-inch diameter.

Four 0.493-inch cables arranged in a 10-inch square as compared to a single $1^1/_2$-inch conductor when installed on a double-circuit 230-kv 3-phase line with 21-foot phase separation will result in reduction of the characteristic impedance (368 to 242

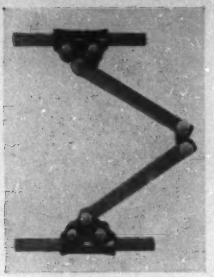

Figure 12. Adjustable mid-span spacer

Grouped conductors, two positions

ohms) and increase in power which can be transmitted (44 to 66 megawatts).

Foreign Experiments

A symposium of five papers[13] on the subject of transmission of alternating current at extra high voltages using grouped conductors was published in 1942 by Siemens-Schuckertwerke. These papers are quite comprehensive and cover the entire subject, including a detailed theoretical analysis of power transmission, current distribution, field distribution, corona losses, arc extinction under fault conditions, power capacity, installation equipment and procedures and operating experiences during the severe winter conditions.* Of particular interest is the rigorous development of equations for calculating capacitance, inductance, and corona initiation voltage for grouped conductors. It is concluded that for 400-kv transmission the most favorable form is a 4-conductor group with subconductor diameters between 0.826 and 1.0 inch and subconductor spacings between 15 and 20 inches.

A later publication[14] from Siemens-Schuckertwerke was dated September 1945. In this publication, a comprehensive survey of the entire high-voltage long-distance transmission picture in the light of German practice and latest thinking, it is stated categorically that a-c transmission at 400 kv and above can be accomplished economically only through the use of bundle ("multiple," "grouped," "split," and so on) conductors. For the proposed German Rhine-Westphalia Power Corporation 400-kv 3-phase 50-cycle system, grouped conductors consisting of four subconductors per phase per circuit arranged at the corners of a square, 15.75 inches on a side, were adopted with conductor sizes ranging from 365,000 to 420,000 circular mils.

Tidd Experiments

In order to obtain experimental data upon which to base a determination of the optimum number, diameter, and spacing of cables when grouped, it is planned to make preliminary investigations with installations on test span 3. These investigations will include alternative arrangements with two, three, and four conductors of two different diameters and spacings of 6 to 18 inches.

To effect these changes in number, spacing, and configuration of conductors with facility, special hardware has been designed and fabricated. It consists of adjustable dead-end assemblies for the conductors and adjustable spacers to maintain separation of the conductors in the span, if necessary.

Figures 10 and 11 show the adjustable dead-end assembly which is designed to hold the conductors in symmetrical arrangement and provide means for varying the spacing. The adjustment may be made under tension and cables may be added or removed without lowering the insulators. The individual conductors have conventional-type drawn dead-end connectors.

Adjustment in spacing is made by turning a screw which moves a crosshead to which the individual conductor is attached. When arranged for three conductors as shown in Figure 11, hinged arms which support two of four crossheads are shifted to a position which will permit a symmetrical arrangement of the three conductors.

The special hardware is designed for experimental purposes only. Once the number of conductors and the spacing are selected, it will be possible to use hardware of less complicated design and weight. The entire assembly is protected by a split copper corona shield. The dead-end assembly was designed for a maximum load of 25,000 pounds and each unit was proof-tested at slightly above this value. Four design 923 (Figure 7) cables will have a maximum load slightly under the 25,000 pounds when loaded to 50 per cent of their breaking strength while four of the design 954 (Figure 7) cables will be loaded to slightly less than 50 per cent of their ultimate load.

The spacers are adjustable from 6 to 18 inches. The same arms and cable clamps are used for either two, three, or four conductors but the center piece to which the arms are attached is changed when the number of cables is changed. Figure 12 shows one of the spacers for the 2-cable arrangement. Special lock washers are used to make the joint between the arms and center piece rigid when the bolt is tightened. The cable clamp used on the spacers is one developed and used for radio antennas where corona was a primary consideration.

Section IV. Conductors Supplied by the Aluminum Company of America*

The conductors on many 220–230-kv transmission lines are aluminum cable steel reinforced (ACSR) in the familiar types of concentric strand. In general, the diameters of such cables are from 1 inch to 1.25 inches. The largest ACSR which has been manufactured commer-

* By M. E. Noyes.

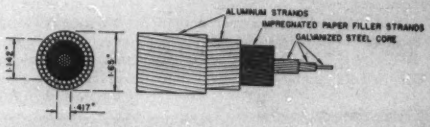

Figure 13. Sketch of 1,062,800-circular-mil expanded ACSR

Diameter, inches—1.65
Tensile strength, pounds—38,470
Weight, pounds per foot—1.69
Aluminum strands—66 0.1269 inch (60 per cent of total weight)
Steel strands—19 0.0833 inch (20.6 per cent of total weight)
Strands of impregnated paper—42 (19.4 per cent of total weight)

* An English translation has been made by Doctor P. Florschutz of the Westinghouse Electric Corporation (part I) and Doctor L. F. Roehmann of the Anaconda Wire and Cable Company (parts II to V). These parts are:

I. Electrical Fundamentals of Bundle Conductors, W. V. Mangoldt.

II. Corona Behavior of Bundle Conductors, F. Busemann, W. V. Mangoldt.

III. Power Capacity of Bundle Conductor Transmission Lines, W. V. Mangoldt.

IV. Bundle Conductors in Winter, A. Buerklin.

V. Installation of Bundle Conductors, G. Markt, F. I. Kromer.

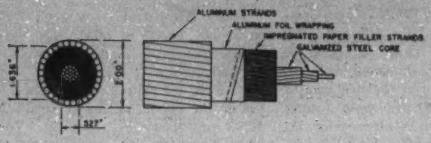

Figure 14. Sketch of 991,500-circular-mil expanded ACSR

Diameter, inches—2.0
Tensile strength, pounds—46,043
Weight, pounds per foot—2.23
Aluminum strands—30 0.1818 inch (42.3 per cent of total weight)
Steel strands—19 0.1054 inch (25.3 per cent of total weight)
Strands of impregnated paper—177 (31.2 per cent of total weight)
Aluminum foil—0.0035 inch thick by 3 inches wide (1.2 per cent of total weight)

Figure 15. Come-along for 2-inch-diameter expanded ACSR

Figure 16. Jointing compressor in operation

cially for any purpose is 1,590,000 circular-mils (54 aluminum over 19 steel), having a diameter of 1.5 inches. It is apparent that the amount of aluminum needed in a conductor for 220–230-kv transmission is seldom more and usually less than 1,000,000 circular-mils to meet the requirements of conductance alone. Any additional metal used in these ordinary forms of ACSR would be solely for the purpose of obtaining larger diameters to minimize corona. This procedure may be economical in the over-all line design up to some limit of cable diameter, probably never higher than about 1.5 inches. This limit will depend largely upon the market values of aluminum and steel and upon the conductance requirements of any actual line. The probability of still higher transmission voltages naturally led to consideration of ACSR having larger diameters without uneconomical use of metals.

A case of long duration in which jute twine (impregnated with pine tar) was used as a central core for aluminum cable, was investigated. No deleterious effect on aluminum wires was discovered after 25 years of service. The jute was also in excellent condition. This led to the experimental manufacture of concentric-strand ACSR of large diameter using nonmetallic fibrous filler strands concentrically laid around the steel to "expand" the core diameter over which the aluminum wires are stranded in one or more layers. A number of sizes have been manufactured. A length of about 4,000 feet of 918,000-circular-mils "expanded ACSR" having a diameter of 1.4 inches, including two layers of jute filler strands around the steel core, was installed in a 220-kv circuit and has been under observation for 12 years. Its behavior has been satisfactory. Since the function of the filler strands is simply to occupy space and to provide radial support to the outer layers of strands, various materials have been investigated including jute, hemp, sisal, cotton, and paper. Paper twine impregnated with paraffin oil was the final choice because it is cheaper and lighter than the other materials considered. Experimental cable was manufactured and samples submitted to Aluminum Research Laboratories, for corrosion tests. Samples have been under observation for six years under salt air conditions at Point Judith and Miami (Fla.) Test Stations and under industrial atmospheric conditions at New Kensington, Pa. The paper has shown no corrosive effect on either the aluminum strands or the galvanized steel strands. The paper strands within the cable have shown no noticeable deterioration during this time.

The Aluminum Company of America supplied approximately five miles each of two sizes of "expanded ACSR" for the Tidd 500-kv test lines. Figures 13 and 14 show the construction of these two cables which are identified as 1,062,800-circular-mil expanded ACSR having a diameter of 1.65 inches and 991,500-circular-mil expanded ACSR having a diameter of 2 inches. The first is quite normal in construction except for the radial space occupied by filler strands of impregnated paper. The 2-inch-diameter cable includes a new feature, namely the wrapping of aluminum foil tape just under the single layer of aluminum strands. Developmental discussions had indicated a belief on the part of some engineers that fibers from the filler material possibly might work out between the cable strands to form corona points. This seems inconceivable when the two layers of aluminum strands are used over the filler but a possibility to be guarded against if there is only one layer of aluminum strands in the cable.

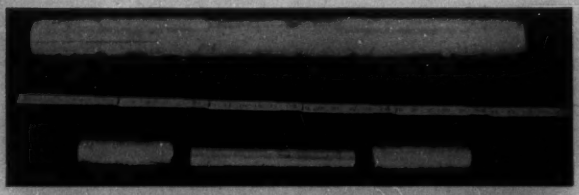

Figure 17 (above). Parts of compression joint for 2-inch-diameter expanded ACSR

Figure 18 (below). Finished joint on 2-inch-diameter expanded ACSR

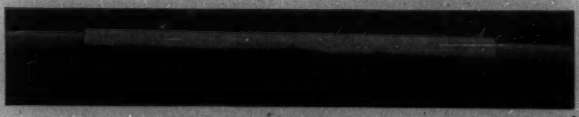

Figure 19. Parts of compression dead-end for 2-inch-diameter expanded ACSR

The wrapping of foil tape is used to avoid this possibility.

With each cable, the Aluminum Company furnished the necessary come-alongs for pulling and sagging the cable during erection (see Figure 15). This is a simple hinged clamp with a carefully fitted groove. The clamp parts are aluminum alloy castings. The bolts and the bail are of steel.

Joints and dead-ends are of the compression type, applied by a hydraulically operated compressor of 100 tons capacity. The compressor is shown in Figure 16. The parts of the joint are shown in Figure 17, and the assembled joint in Figure 18. The joint is similar in every way to compression joints for standard types of ACSR, as shown in the Aluminum Company catalogue, with the exception of the aluminum "fillers" shown in Figure 17. These are merely aluminum cylinders which are slipped over the steel core to take the place of an equal length of paper filler material which is cut away for this purpose when assembling the joint. The object of these fillers is to supply a firm resistance to compression and thereby obtain adequate grip on the aluminum strands which are compressed between these fillers and the outer sheath of the joint. The compression dead-end also follows the companys' standard practice with the addition of an aluminum filler cylinder shown in the photograph of parts, Figure 19. The finished assembled dead-end is shown in Figure 20. Both joints and dead-ends develop 100 per cent of the tensile strength of the cables when tested on a 50-foot length of cable in a horizontal testing machine.

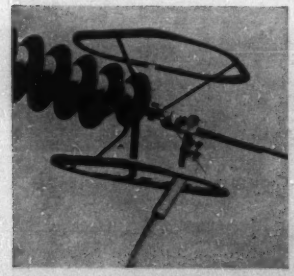

Figure 20. Finished dead-end on 2-inch-diameter expanded ACSR

Both cables were furnished in 5,600 foot lengths. The gross weight of reel and cable for this length was approximately $7^1/_2$ tons. The diameter of the drum of the reels is 36 inches. The Aluminum Company also supplied the overhead ground conductors installed on both circuits of the test lines. This is standard 159,000-circular-mil ACSR, 12 aluminum strands over 7 steel strands, having a diameter of 0.576 inch.

Tensile stress–strain tests were made on 50-foot lengths of cable. The tests included several applications of ascending and descending tensile stress. For illustration, the plotted results of such a test on the 1.65-inch-diameter expanded ACSR are shown in Figure 21. The stress–strain behavior demonstrated is similar in every respect to that of standard concentric strand ACSR. Sag–tension calculations following the graphic method were based upon these stress–strain tests. The height and location of the towers established the assumption of a final sag of 47 feet in a 1,100-foot span at 120 degrees Fahrenheit. Cables were strung to initial sag calculated to produce this final sag after the experience of maximum loading equal to 1/2 inch ice and 8 pounds wind at 0 degree Fahrenheit. The calculations for the 2-inch-diameter

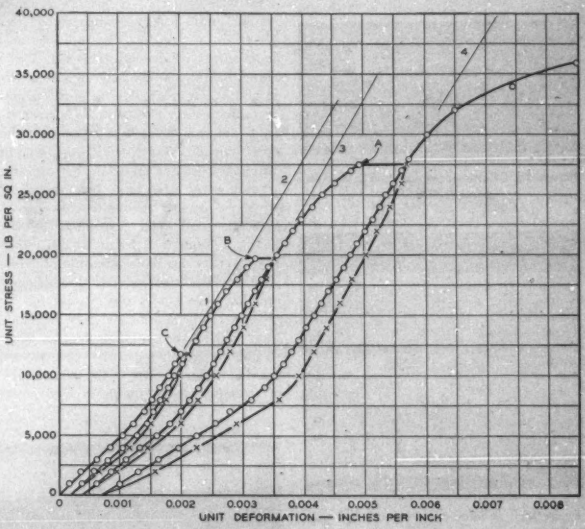

Figure 21. Diagram of stress–strain test of 1.65-inch-diameter expanded ACSR

A—Stress maintained for one hour at 70 per cent rated strength

B—Load maintained for one hour at 50 per cent rated strength

C—Load maintained for one hour at 30 per cent rated strength

Circles—Increasing load

Crosses—Decreasing load

Room temperature—74–78 degrees Fahrenheit

The data were obtained using telescopes and scales over a 500-inch gauge length

expanded ACSR show a maximum tension of 13,690 pounds under this loading. This is 29 per cent of the tensile strength of the cable. Similarly, the maximum tension for the 1.65-inch-diameter expanded ACSR is 12,000 pounds, which is 31 per cent of its tensile strength.

The Aluminum Company of America welcomed this opportunity to participate in the exploration of higher voltage transmission problems and to gain further experience with expanded ACSR.

References

1. Transmission of Electric Power at Extra High Voltages, Philip Sporn, A. C. Monteith. AIEE Transactions, volume 66, 1947, pages 1371–82.

2. Corona Considerations on High-Voltage Lines and Design Features of Tidd 500-Kv Test Lines, C. F. Wagner, Anthony Wagner, E. L. Peterson, I. W. Gross. AIEE Transactions, volume 66, 1947, pages 1583–91.

3. Insulators and Line Hardware for Tidd 500-Kv Test Lines, I. W. Gross, R. L. McCoy, J. M. Shaadel. AIEE Transactions, volume 66, 1947, pages 1592–1602.

4. Transformers and Lightning Arresters—Tidd 500-Kv Test Lines, F. A. Lane, J. K. Hodnette, P. L. Bellaschi, Edward Beck. AIEE Transactions, volume 66, 1947, pages 1613–8.

5. Switchgear Equipment for Tidd High-Voltage Test Lines, F. A. Lane, B. W. Wyman. AIEE Transactions, volume 66, 1947, pages 1619–23.

6. Instrumentation and Measurement—Tidd 500-Kv Test Lines, R. L. Tremaine, G. D. Lippert. AIEE Transactions, volume 66, 1947, pages 1624–31.

7. Corona Losses From Conductors of 1.4-Inch Diameter, Joseph S. Carroll, Bradley Cozzens, Theo. M. Blakeslee. Electrical Engineering (AIEE Transactions), volume 53, 1934, pages 1727–33.

8. United States Patent 1,078,711, J. B. Whitehead. 1910.

9. The Electric Strength of Air—II, J. B. Whitehead. AIEE Transactions, volume 30, 1911, pages 1857–87.

10. Dielectric Phenomena in High-Voltage Engineering (book), F. W. Peek, Jr. McGraw-Hill Book Company, Inc., New York, N. Y., 1915, pages 71–3.

11. Betrachtungen Ueber Die Kotte Lung von Grosskraftwerken in Elektrischer Hinsicht, O. Burger. Siemens-Zeitschrift, number 5–6, 1922, page 248.

12. Drehstrom-Fern-Uebertragung mit Bundel-Leitern, G. Markt, B. Mengele. *Elektrotechnik und Maschinenbau* (Vienna, Austria), volume 50, number 20, May 15, 1932, page 293.

13. Bundel-Leitungen. Siemens-Schuckertwerke, Berlin, Germany, 1942.

14. High-Voltage Long-Distance Transmission, F. Busemann. Siemens-Schuckert, A. G. Berlin, Germany, Sept. 1945. Translated by Alexander Dovjikov, United States Department of Interior, Bonneville Power Administration, Portland, Oreg.

Discussion

Abe Tilles (Pacific Gas and Electric Company, San Francisco, Calif.): It is pointed out in the papers that the cost of the kilowatt-hours lost in corona in a satisfactory line is small and that direct economic consideration may allow a fairly large kilowatts-per-mile corona loss on these high voltage lines. Some two or three decades ago, it will be remembered, it even was proposed that having the line in corona was a good thing because it would the more rapidly attenuate lightning strokes. More recent design practice has been to assign corona a very high "nuisance value" on one score and another and to aim at its substantial minimization under favorable weather conditions. It would seem likely that careful consideration will bring this same conclusion on these lines. A conductor diameter which keeps the lines in corona will cause the conductor to pit and become progressively worse, it will be an operating limitation against use of a normal overvoltage range on occasion, it will cause phenomenal local corona losses under occasional weather conditions. It can be therefore, very objectionable even though it gives a kilowatt-hour loss which is only a small percentage of some other very big number.

The statement made that a stranded conductor 1.65 inches in diameter is, in effect, as good at 400 kv as a 1-inch conductor is at 220 kv appears optimistic. For dragged and weathered conductor, using Figures 2 and 4 of the paper co-ordinating the Stanford corona tests,[1] 1-inch conductor, 22-foot spacing, at 220 kv gives 0.65 kw loss per mile and 1.65-inch conductor, 38.5-foot spacing, at 400 kv gives 4.0 kw loss per mile.

Regarding the bundle conductors, their theoretical advantage regarding both corona and reactance is very valuable. Only field tests can determine if the obvious mechanical complications can be overcome. Will the small conductors have the mechanical strength under snow loading? Will snow not tend to fill the space within the bundle? Will not the conductors whip together, and when they do will there not be enough induced voltage between them to cause arcs that will burn and pit them? Will the bundle be "rolled" or otherwise transposed? If not, how great a circulating current may be expected? This circulating current should, of course, be checked by field measurement.

Reference

1. Empirical Method of Calculating Corona Loss From High-Voltage Transmission Lines, J. S. Carroll, Mabel M. Rockwell. Electrical Engineering (AIEE Transactions), volume 56, May 1937, pages 558–65.

J. G. Holm (Gibbs and Hill, Inc., New York, N. Y.): I read with great interest the paper presented by the authors, as for a number of years I have followed closely the developments in the design and operation of extra high voltage transmission systems and their parts.

Among the various types of conductors which the authors propose to investigate are the bundle conductors. It is stated in the paper that for the planned but not constructed 400-kv transmission line of the Rheinisch Westfalische Elektrizitaetswerke in Germany it was decided to use bundle conductors as these, due to their low corona loss and smaller inductive reactance, reduce the characteristic impedance of the line about 33 per cent, thus increasing the possible power transfer around 50 per cent and giving a more economic design. The actual reason, however, for which the decision to use bundle conductors was arrived at, and which is not given in the paper, is that this German utility operates with an isolated neutral. In such systems, the effect of corona on faults to ground is such as to make the inductive extinguishing of ground faults unworkable. That is why, in this case, it was necessary to use bundle conductors. Any other conductor, if it has practically to eliminate the corona effect, would require a diameter beyond economic limits. Such a condition, of course, does not exist in the United States where practically all power systems operate with grounded neutrals. Moreover, if system stability is taken as the measure of power transmitted, and since stability depends not only on the line reactance but on the reactance of the terminal equipment as well, it can be estimated that the decrease in line reactance afforded by the bundle conductors will increase the stability limit of representative systems by some 5 to 10 per cent. This is a long way from the 50 per cent claimed by some German engineers.

The use of bundle conductors also invariably is associated with excess copper in the line and all that this connotes. The type *HH* 650,000-circular-mil copper conductor which will be studied in the Tidd tests has a current-carrying capacity of about 1,170 amperes and probably will prove to be more than ample for the purpose. At the same time, bundle conductors, when made up of four 321,000-circular-mil conductors (the 211,600-circular-mil conductor, judging by the German data, has too small a diameter), will have a current-carrying capacity of about 2,480 amperes. This excess copper and larger supporting structures cannot be justified very well. Even when these bundle conductors are compared with a 2-inch 1,030,000-circular-mil type *HH* conductor, they have an excess of over 50 per cent copper. Thus bundle conductors and their accessories require a considerably higher first cost, and the greater mechanical problems will increase maintenance charges. Both effects make them decidedly uneconomical for the grounded systems used in the United States.

For the last 35 years engineers have investigated bundle conductors again and again but to date they have not been used. I know that some years ago these conductors were investigated in Russia and were rejected on economic grounds. I believe that the same conclusion will be reached in the Tidd tests.

In fact the new "expanded" aluminum-cable steel-reinforced conductor is superior to bundle conductors. I venture to say, however, that no conductors will satisfy the over-all requirements to a greater extent than the type *HH* conductor.

L. F. Hickernell: With reference particularly to section III of the paper, this and its companion papers are intended to inform the profession of the *construction* details of the test equipment and material to be tested, together with some of the technical reasons underlying their choice. Some of

the discussion is directed to anticipating the *results* of the tests which will be covered in another series of papers after the tests have been completed.

In reply to Holm, it is true that one of the reasons given by the Germans for considering grouped conductors on the 400-kv line was that this arrangement reduces the corona loss to such a point as to make practical the inductive extinguishing of single-phase faults on an isolated-neutral system. Recognition of this was included in the original draft of our paper under the heading "Theoretical Investigations." In applying our discussion of corona initiation voltage, we stated

> In this connection, it also is indicated that under fault conditions, when the unfaulted phases are subjected to abnormal potential gradients, grouped conductors will have a better chance to operate free of corona than an equivalent single conductor. This is important because corona losses contribute to residual earth fault current and can play a dominant role in preventing adequate arc extinction in isolated-neutral systems employing inductive reactors (Peterson coils) as is common in Germany.

This observation was deleted by the coordinator of these papers as being outside the scope of our paper.

This subject also was discussed in several of the German papers; for example, Buseman (reference 8) states

> II. Neutral
>
> The experience obtained in Germany in operation with isolated neutral and inductive ground fault extinguishing on 220-kv systems is so favorable that it was desired by all means to retain it in 400-kv operation.
>
> On the other hand, there was an inclination to operate the 400-kv system with grounded neutral and to treat single-phase ground faults the same way as 2-phase or 3-phase faults by switching out the faulted section.
>
> Grounding of the 400-kv system neutral would have certain advantages in regard to the construction of transformers and in the selection of the transformer insulation with respect to impulse voltages. By comparing the insulation level of the lines in countries using grounded neutral with lines with isolated neutral, we could not consider the decrease of line insulation, which, from the view of cost, would be considerably more important. In regard to selection of conductor diameter, the conductor may be less expensive because in the systems with solidly grounded neutral only normal corona losses are considered, while in the system operating with isolated neutral, particularly with regard to corona losses during the ground fault, its effect upon the real component of the fault current must be taken into consideration.
>
> In the 400-kv system a single conductor per phase will not be used. Due to the 50 per cent increase in transmission capacity and other advantages (easier installation particularly in the mountains, smaller unit weights) only multiple phase-conductor is being considered. Such conductor has such favorable corona loss characteristic that inductive arc extinguishing still may be used at 400-kv without increasing the dimensions of conductors. The economic advantages of solid grounding of neutral then shrink to the decrease of transformer insulation and omission of inductive ground fault extinguishing reactors. These costs amount to only about one per cent of the total cost of transmission. The advantages of elimination of all single-phase faults without switching are so much greater that for 400-kv the German practice gives unconditional preference to the isolated neutral combined with inductive extinguishing of ground faults.

It is also true that the use of grouped conductors, due to their low corona loss and smaller inductive reactance, reduces the characteristic impedance of the line about 33 per cent, thus increasing the possible power transfer around 50 per cent for the particular case cited. Even if some terminal equipment would reduce this gain, it still remains as a possible gain so far as the line itself is concerned and realizable with matched terminal equipment.

Holm states "the use of bundle conductors is also invariably associated with excess copper in the line and all that this connotes." This is quite a positive statement regarding a type of construction which so far has not been used commercially, either here or abroad. This construction has been included in the Tidd tests to obtain performance data suitable for use in engineering studies. Two sizes of conductors and several variations in assembly will give data for a wide range of copper area per phase. Whether or not these are "uneconomical" on an over-all basis can be judged better when the tests are completed.

Regarding the consideration of grouped conductors in Russia, and their rejection "on economic grounds," we are not familiar with this investigation and therefore are not able to judge whether or not this conclusion was justified.

The discussion by Tilles of the various attributes of corona and kilowatt-hour loss is very well taken. His use of the Stanford corona test data as a basis for argument is open to some question, since there is doubt as to the accuracy of the corrections for critical voltage, spacing, and conductor diameter developed in this reference. In any event, the discrepancy between 4.0 kw loss at 400-kv and 0.65 kw loss at 220-kv is not of major importance when the ratio of these losses to the power transmission limits at these two voltages is considered.

Mechanical problems due to snow loading were considered in detail by the Germans and are completely reported in reference 7, part IV. With properly spaced lines, this appears to be no serious problem. This reference, part I, also considers the question of circulating currents, and they are shown to be quite small.

These questions, and others, constitute the reasons for including grouped conductors in the Tidd tests. It is expected that satisfactory answers will be obtained for many of them.

Transformers and Lightning Arresters—Tidd 500-Kv Test Lines

F. A. LANE
MEMBER AIEE

J. K. HODNETTE
FELLOW AIEE

P. L. BELLASCHI
FELLOW AIEE

EDWARD BECK
MEMBER AIEE

THE power supply equipment for energizing the high-voltage test lines at the Tidd plant of The Ohio Power Company consists of a bank of three single-phase transformers protected by lightning arresters. This paper discusses the general approach to the problem and the design and construction of this equipment. The fundamental questions are discussed in a companion paper[1] to which frequent reference will be made in this paper. Other matters are discussed in other companion papers.[2–6]

Transformer Insulation Requirements

The conditions of service which transformer insulation must meet are three:

1. Normal frequency operation.
2. Switching and other system overvoltages.
3. Lightning surges that may be impressed on the transformer terminals.

At the extra high voltages under consideration, it appears a foregone conclusion that systems will operate with the neutral solidly grounded. The advantages of this to all of the afore-mentioned requirements are already well known for systems operating at voltages of 287 kv and less. They become even more pronounced at the contemplated extra high voltages.

On a solidly grounded neutral system the line-to-neutral voltage is maintained within well defined limits, theoretically at 58 per cent of the line-to-line voltage, although in practice it may be somewhat higher for very short intervals of time. As pointed out in a companion paper,[1] switching or system surges should not exceed three times normal line-to-ground crest voltages. The lightning voltages that may appear at the transformer are determined by the system design and the arresters. The solid grounding of the system permits the use of lightning arresters whose ratings are less than the circuit voltage.[1] This limits the lightning voltages to relatively low magnitudes and results in further significant economies in the transformer costs.

On systems operating with the neutral effectively grounded power transformers in the next lower insulation class have been applied in recent years in increasing numbers. Because of its engineering soundness and economic advantage, this practice bids fair to become common. On the strength of experience alone, it would appear logical to extend this practice to the field of extra high voltages. Though this experience approach is justifiable and conservative as a first step, the progressive designer cannot stop at this point. He further must consider and examine all possibilities that may be conducive to a more rational and economic design for the particular field of application in view. In particular, he must assess the possibilities in the light of present-day knowledge and the more recent fundamental findings on transformer insulation, and incorporate these as well as the latest developments in the art into his future design.

During the past decade, much in the way of fundamental studies has been accomplished in the field of transformer insulation. This development work has a direct bearing on the very questions now arising in connection with the application of transformers at extra high voltages. A few of the more significant studies and findings bearing on the three basic requirements of insulation are related briefly hereinafter.

1. Normal Frequency Operation

The ability of a transformer to operate continuously at normal frequency voltage depends primarily on the design rather than the mere fact that the insulation passed a low-frequency dielectric test. Life tests conducted on transformer insulation by the Westinghouse Electric Corporation at Sharon, Pa., definitely establish that the true criterion is that the insulation be balanced in relation to the stresses to which it is subjected and that the entire insulation structure be designed so as to be free of corona.

In order to get some actual operating experience at a point in the range of extra high voltages, a high-voltage power transformer was put on life test at the Sharon works of the Westinghouse Electric Corporation in October 1945 and has been operating at 375 kv since that time. The transformer was given both impulse and low-frequency dielectric tests prior to the beginning of the life tests in line with the American Standards and again was subjected to these same tests in June 1947, after having been operating for approximately 18 months. Visual inspection of the windings, the insulation, and the

Paper 47-245, recommended by the AIEE committee on transmission and distribution and approved by the AIEE technical program committee for presentation at the AIEE Midwest general meeting, Chicago, Ill., November 3–7, 1947. Manuscript submitted August 22, 1947; made available for printing September 19, 1947.

F. A. Lane is chief electrical engineer, American Gas and Electric Service Corporation, New York, N. Y.; J. K. Hodnette is manager, transformer division, and P. L. Bellaschi is development engineer, Westinghouse Electric Corporation, Sharon, Pa.; and Edward Beck is section engineer, switchgear engineering department, Westinghouse Electric Corporation, East Pittsburgh, Pa.

The authors wish to acknowledge the valuable contribution made to the work covered in this paper by I. W. Gross (F '45) of the American Gas and Electric Service Corporation and W. G. James (M '40), R. L. Brown (M '43), W. L. Teague (M '29), and C. W. Miller (A '42) of the transformer division and O. Ackermann and A. J. Fink of the switchgear division of the Westinghouse Electric Corporation.

Table I. Proposed Transformer Impulse Levels for Solidly Grounded Neutral Application

Rated Circuit Voltage, Kv Rms	Impulse Insulation Level, Kv Crest
287	1,050
345	1,200
402	1,400
460	1,550

bushings showed no deterioration of the insulation.

These tests indicate that an extension of the insulation structure used for 230 and 287 kv into the field of extra high voltages should be satisfactory from a normal frequency operation point of view. These tests also indicate that modern high-voltage transformer insulation can be operated satisfactorily at substantially higher voltages than would have been considered practical in the past. Insofar as fulfilling the normal frequency requirements, a reduction of the insulation level to 80 per cent of the nominal full value therefore can be considered amply conservative for solidly grounded neutral operation.

2. Switching and Other System Overvoltages

Switching surge tests on transformer insulation have been conducted at various times. In a more recent and extensive investigation,[7] 230-kv transformer insulation was subjected to repeated switching surges to a total exceeding 800 applications. The bulk of these surges was between 500 to 750 kv, a small number from 750 to 850 kv, and a few approached 900 kv, the limit of the switching surge generator. From these investigations, it has been found that the switching surge strength of station and line insulation is in the order of 90 per cent of the corresponding impulse strength. Inasmuch as the full basic insulation levels at the higher reference voltages correspond to about $5^1/_2$ times line-to-neutral crest voltage, a reduction of the insulation level to about 75 per cent appears quite feasible considering the switching surge requirements, since $5^1/_2 \times 0.90 \times 0.75 = 3.7$. As previously stated, on a solidly grounded neutral system with modern switching equipment switching or system surges should not exceed three times normal line-to-ground crest voltages.

3. Lightning Surges

From an impulse standpoint, the insulation level required in the transformer is related directly to the protective level attainable. Where system conditions are favorable to applying an 80 per cent lightning arrester, the transformer insulation can be proportioned accordingly to 80 per cent of the basic impulse level. A progressive approach to the protection problem in the field of extra high voltages long since has indicated various practical possibilities towards effectively attaining lower protective levels which are conducive to applying transformer insulation levels corresponding to about 75 per cent of the basic impulse level.

Progress in the art of modern transformer balanced insulation design and extensive experience in the construction of very large high-voltage units, combined with recent developments in insulating materials and improved methods of manufacture and processing, all basically comprise the principal factors that contribute to a rational application and therefore better utilization of the transformer insulation in applications at extra high voltages.

Transformers for High Voltage Tests at Tidd Station

The transformers used at the Tidd station for stepping the voltage up from the 69,000-volt supply to the voltages required for the corona tests on the experimental lines were built in accordance with the design principles that would be applied to commercial high-voltage power transformers. The transformers are single-phase units Y connected with the neutral solidly grounded. Although the actual rating of 1,667 kva (5,000-kva bank) is far below the ratings that would be economical at the extra high voltages, it was desirable to use essentially the same design methods that would be used on 75,000-kva or larger transformers in order to secure operating experience.

The methods of insulation and winding assembly, tank construction, tap changer arrangement, and inert gas preservation

Table II. Lightning Arrester Ratings and Protective Levels

Rated Circuit, Voltage, Kv Rms	80 Per Cent Rating, Kv Rms	Voltage Kv Crest Across Arrester When Discharging 10x20-μsec Current of 5,000 Amp Crest	75 Per Cent Rating, Kv Rms	Voltage Kv Crest Across Arrester When Discharging 10x20-μsec Current of 5,000 Amp Crest
230	195	660	180	610
287.5	242	820	227	770
345	290	980	272	920
402	340	1,150	318	1,070
460	390	1,330	363	1,230

Impulse spark-over on 1,000-kv-per-microsecond wave is five per cent higher than discharge voltage listed in the table.

Figure 1. Transformers on test at the factory

Figure 2. Transformer on flatcar for shipment filled with oil

used on shell form transformers for voltages on 287,500 volts and below were extended and modified for use on these transformers. The fundamental data available on insulation were studied carefully and the design made to withstand the voltages which could be expected in service. A special feature from an insulation standpoint was to locate the low-voltage 69-kv bushings on the side of the tank in order to obtain sufficient flashover distance to the high-voltage line bushing.

The windings of the transformer are arranged in the manner normally used in the design of high-voltage shell-form transformers except for the large tap range to provide high voltages from 265 to 500 kv Y connected. This range was obtained by using a standard 10-per-cent tap range in the high-voltage winding and providing a large range of taps in the low-voltage winding. These taps are brought to no-load tap changers operated from handwheels on the tank wall. The total tap range is covered in 24 steps, the low-voltage tap changer providing large steps with the high-voltage tap changer acting as a vernier.

A unique feature is the provision for a voltage metering winding at high-voltage-line potential. This is obtained by extending the high-voltage winding for a few turns and bringing the lead through the bushing with the main line lead. This portion of the winding and its lead is shielded electrostatically so that it does not carry appreciable capacitance current, thus avoiding errors in metering due to this source. This winding provides a voltage for metering and power for the other equipment mounted in the cabinet at the top of the high-voltage bushing. In addition, conventional metering windings are provided on the core at a low voltage level.

The transformers are provided with standard accessories including inert gas protection, oil gauge, oil thermometer, manhole relief, and oil valves. A lightning arrester for the low-voltage winding is mounted on a bracket adjacent to the low-voltage bushings. The high-voltage line lead is brought out through an oil-filled condenser bushing employing the same principles of design used for high-voltage bushings on power transformers now in operation at 230 kv.

The transformers were given factory tests for iron loss, impedance, low frequency induced potential and impulse tests. In addition, a test of approximately 10 per cent above the maximum line-to-ground operating voltage (320 kv rms line-to-ground) was applied continuously for 12 hours. Observations of corona were made with and without the meter box. Very little corona noise or visible corona was observed at 320 kv. A view of the transformers on test at the factory is shown in Figure 1.

The core and coil assembly of the transformers is built into a form fit tank of the type used in the construction of high-voltage shell-form power transformers with the two sections of the tank welded at the factory. This type of tank construction made it possible to ship the units complete in oil except for the high-voltage bushings and radiators by laying it on a flat car, as indicated in Figure 2. This eliminated the use of special bracing or special cars for shipment. A view of the transformers installed at the Tidd station ready for operation is shown in Figure 3.

Lightning Arresters

Lightning arresters are installed adjacent to the transformers in the Tidd test station to provide protection and to obtain service experience on voltages above 287 kv. There exists a good deal of background of service and manufacturing experience from which to extend arrester ratings into those higher voltages where heretofore no arresters have ever been built. The arresters constructed for use in conjunction with the tests at Tidd utilize the same standard units or sections that have been used for some time in the construction of "Auto-valve" station-type arresters of all commercial ratings. The performance characteristics of these have been well established and there is no difficulty in co-ordinating insulation levels and lightning arrester ratings. Several problems arose in extending the ratings into this new high-voltage field. Solutions were found in ways that depart

Figure 3. Installation view of transformers (Tidd test station)

Table III. Estimated Price of Transformers for Application at Extra High Voltages

A. Three Single-Phase 75,000-Kva 2-Winding 55-Degree-Centigrade Self-Cooled Transformers of Standard Impedance Design and for Various Impulse Levels

Impulse Level, Kv	Price, Per Cent	Impedance, Per Cent
1,200	100	13
1,400	124	14
1,550	144	15

B. Three Single-Phase 75,000-Kva 2-Winding 55-Degree-Centigrade Self-Cooled Transformers for Low Impedance and for Various Impulse Levels

Impulse Level, Kv	Price, Per Cent	Impedance, Per Cent
1,200	102	10
1,400	130	10
1,550	153	10

Figure 4. Suspended type lightning arrester

from tradition and may be considered innovations in lightning arrester construction.

Two different types are installed in the Tidd test station. Both are electrically alike, however. The maximum voltage rating of these particular lightning arresters is determined by the consideration that the test line will at times be energized at 500 kv. Since the neutral is solidly grounded, the rating decided upon is 350 kv, 70 per cent of the maximum phase-to-phase voltage. This is a lower rating than the usual 80 per cent. The 70-per-cent ratio was chosen because of the probability that when a high-voltage system is built consideration will be given to arresters with voltage ratings lower than 80 per cent.[1] Moreover, a ratio as low as 70 per cent will give significant operating experience on the test lines since the arresters will be subjected to severe continuous duty. The Tidd lightning arresters are designed so that units can be short-circuited to reduce the arrester rating when the system is operated at voltages less than 500 kv.

Because of the high maximum rating of 350 kv, the conventional arrangements used heretofore would occupy a considerable height. Efforts were made to keep the height at a minimum, and resulted in the construction shown in Figures 4 and 5.

Figure 5. Self-supporting lightning arrester

The one shown in Figure 4 is designed for suspension from a steel structure. The units are suspended in zigzag fashion between strings of insulators. The length thus is decreased considerably below the length required if the units were all arranged in line. The lightning arrester proper is compact. However, it requires strings of suspension insulators to support it and a steel structure from which it may be hung. When steel is available as part of the substation structure, this is an efficient construction.

To avoid the need of a supporting structure, a self-supporting lightning arrester shown in Figure 5 was devised. This is shorter than the suspended arrester including the supporting insulator strings, requires no bracing, but it is a more complicated and more bulky structure than the suspended arresters. There are advantages and disadvantages in each. The suspended type may be preferred in regions where earthquakes occur because it is less likely to be damaged by temblors, and the self-supporting type may be preferred when supporting structures are not available.

The assembly and the operation of the suspended arrester are apparent from Figure 4. The upright arrester shown in Figure 5 merits further description. It consists of three columns which mutually brace each other and thus provide a stable and wind resisting structure. The design was worked out by calculation, by tests on small scale models, and by trial of full sized samples. In each column are arrester sections separated by insulating units. The insulating units are standard arrester casings with the usual internal arrester parts omitted. The active arrester units in the three columns are interconnected by means of the pipes shown in Figure 5. Figure 6 is a schematic picture of the 3-legged arrester showing how the units are connected.

The considerable length of the discharge path introduces a problem of voltage distribution across the various sections. Grading rings are used to control the electrostatic field so that the voltage impressed across the arrester terminals will be divided uniformly between the units.

A number of laboratory tests were made on the arresters during the development of the structures and after the final designs had been erected. These included 60-cycle spark-over tests, tests for corona, and impulse spark-over tests. The discharge characteristics of the arresters at various discharge currents are known from the test results on these standard units of which the arresters consist.

The 60-cycle spark-over tests were made by running the 60-cycle test voltage up until the arrester discharged. Tests were made with the arresters dry and under rain conditions using tap water. The dry spark-over values were 700 kv rms for the suspended and 690 kv rms for the 3-legged arrester. Under rain conditions, the 60-cycle spark-overs were 650 kv rms. These are of the order of 1.85 to 2 times the arrester rating showing good margins; also, they indicate good voltage distribution on the units.

A check was made for corona at normal voltage. The normal voltage across the 350-kv arrester with the line energized at 500 kv is 290 kv. No audible or visible corona was observed at 346 kv. With the energizing voltage set at 346 kv, the circuit breakers were closed and opened repeatedly and no discharges through the arrester were detected. Since surges of twice normal voltage may be expected under these conditions, the test indicates that switching surges of $2 \times 1.41 \times 346$ or 975 kv crest at least, or 2.4 times the normal voltage of 290×1.41 or 410 kv will not discharge the arrester.

Impulse spark-over tests also were run. With rates of rise of 1,000 kv per micro-

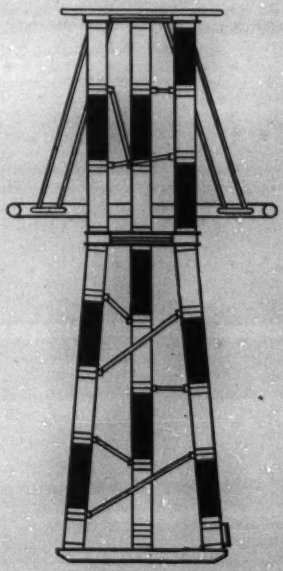

Figure 6. Schematic circuit of self-supporting lightning arrester

second and the arresters connected for 350 kv, spark-over occurred on the suspended arrester at 1,000 kv either positive or negative and on the 3-legged arrester at 950 kv negative and 1,150 kv positive. From tests on individual units, the discharge voltage across the arrester when carrying 5,000 surge amperes, 10x20-microsecond wave shape, is 1,120 kv.

The arresters built for the test line were made for the highest contemplated voltage with means of adjusting the rating. When a transmission system is built and the system voltage, system characteristics, and impulse levels of the apparatus insulation have been determined, a definite arrester rating will also be determined so it is probable that the construction will be modified and simplified.

Insulation Co-ordination and Protection

In Table II are presented the transformer impulse levels proposed[1] for solidly grounded neutral application at the extra high voltages. These basic impulse levels are compared in Figure 7 to the protective levels of 80-per-cent and 75-per-cent arresters. The basis and derivation of the arrester ratings are apparent from Table III. The rated voltages selected for reference purposes in this study are not necessarily standard values for these have not as yet been established definitely. In Figure 7, a 5,000-ampere 10x20-microsecond wave is used as a basis for co-ordination.[1]

To secure a high degree of protection against steep front impulses, the arrester must be located closely adjacent to the transformer. In this connection, it is of interest to note that on a 1,000-kv-per-microsecond rise the arrester breakdown voltage for the ratings indicated is about 105 per cent of the value corresponding to a 5,000-ampere discharge. In view of the inherently high strength of the insulation at the very short impulses, ample margins of protection can be secured against steep front impulses when the proper measures are taken to minimize the lead and ground effects between arrester and transformer terminals.

Use of 80-per-cent arresters is good practice for solidly grounded neutral systems of voltages 230 kv and below. In the fourth column of Table II, we have shown arresters in the 75-per-cent ratings that might receive consideration for use on circuits that are very well grounded. Whether or not arresters with lower ratings than 80 per cent can be used will depend on the system characteristics. Probably individual cases will require individual study. However, the advantages of lower rating arresters at the extra high voltages are so apparent as well to justify the additional effort of special study.

Table IV. Estimated Price of Lightning Arresters Based on Transformers in Table IIIA, 1,200-Kv Level, as 100 Per Cent

Rating, Kv	Price, Per Cent
242	1.75
270	2.30
290	2.80
360	3.10

Taking all the various considerations into account, the protection of insulation levels as given in Table I seems practical.

Economic Advantages

The advantages accruing at the extra high voltages from a more complete rationalization of the transformer insulation and of the protection problem, lie especially in these directions

1. Economies in the transformer proper.
2. Reduction in unit weights and dimensions.
3. More favorable characteristics and improved performance of the transformer, particularly in regard to lower impedances and losses and corresponding advantage gained from a system standpoint.
4. Feasibility of larger units.
5. Transportation and installation problems minimized.
6. Advantages from an arrester viewpoint.

A detailed assessment of each of these advantages and of the over-all benefits combined would be possible only through study of specific projects. For illustrative purposes a few typical examples will be considered. In Table III are presented relative initial costs for three 75,000-kva (225,000-kva bank) single-phase 60-cycle 55-degree-centigrade-rise 2-winding self-cooled transformers for operation at 345 kv with impulse levels of 1,550 kv, 1,400 kv, and 1,200 kv. Transformers in this rating designed for solidly grounded neutral operation well can gain a reduction in cost of about 30 per cent in stepping the insulation impulse level from 1,550 kv to 1,200 kv (1,200÷1,550 = 0.77). There is also a decided reduction in weights. The normal impedances are reduced correspondingly from 15 to 13 per cent (Table III *A*) and likewise a lowering of the losses is effected. On the basis of a fixed impedance set at 10 per cent (Table III *B*) the reduction in unit cost from 1,550-kv to 1,200-kv level comes to 33 per cent. These values are affected only slightly for operating voltages of 402 kv and 460 kv. Estimated prices for single-pole arresters are given in Table IV. It is apparent that the cost of the arresters is a small portion of the transformer and that the use of a properly co-ordinated arrester results in major economies.

The economics of transformer design at the extra high voltages, the transportation and field installation problems involved, the over-all economics of power transmission at these voltages, and similar considerations are such as most certainly to dictate single-phase units in this field of application. Forced oil circulation would contribute to reduce further the unit weights and thus permit transportation direct to site of larger units complete with their oil and practically ready for immediate operation. In this manner, too, the field installation requirements and operations are much simplified and reliability of equipment enhanced. At hydro sites, forced-oil water-cooled transformers offer additional possibilities towards securing even lower unit weights.

Conclusions

The disruptive tests, overpotential tests, and the life tests made on an experimental transformer at the factory and the surge, disruptive, overpotential, and corona tests made at the factory on the

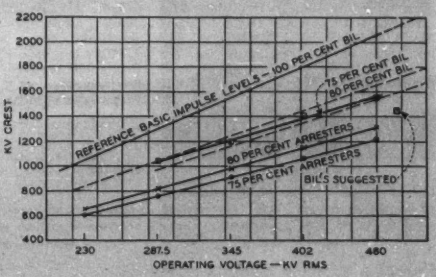

Figure 7. Insulation impulse levels and protective levels compared

transformers for energizing the Tidd 500-kv test lines as described in this paper indicate that it is entirely practical to build commercially power transformers for operation at extra high voltages. These same tests indicate that the transformers, using the shell form of construction employing the same design principles for the insulation structure that were used for transformers operating successfully at 230 and 287 kv, will perform satisfactorily when operating at normal frequency at these extra high voltages; that they will withstand the switching and other system overvoltages to which they may be subjected; and when properly protected by lightning arresters of the type described in this paper, will withstand successfully the lightning surges which may be impressed on the transformer terminals. Furthermore, when these transformers are mounted in a form fit tank, it is entirely practical to ship commercial kilovolt-ampere ratings at these extra high voltages completely assembled in their own tanks.

References

1. Transmission of Electric Power at Extra High Voltages, **Philip Spora, A. C. Monteith.** AIEE Transactions, volume 66, 1947, pages 1571–82.

2. Corona Considerations on High-Voltage Lines and Design Features of Tidd 500-Kv Test Lines, **C. F. Wagner, Anthony Wagner, E. L. Peterson, I. W. Gross.** AIEE Transactions, volume 66, 1947, pages 1583–91.

3. Insulators and Line Hardware for Tidd 500-Kv Test Lines, **I. W. Gross, R. L. McCoy, J. M. Shendel.** AIEE Transactions, volume 66, 1947, pages 1592–1602.

4. Line Conductors—Tidd 500-Kv Test Lines, **E. L. Peterson, D. M. Simmons, L. F. Hickernell, M. E. Noyes.** AIEE Transactions, volume 66, 1947, pages 1603–12.

5. Switchgear Equipment for Tidd High-Voltage Test Lines, **F. A. Lane, B. W. Wyman.** AIEE Transactions, volume 66, 1947, pages 1619–23.

6. Instrumentation and Measurement—Tidd 500-Kv Test Lines, **R. L. Tremaine, G. D. Lippert.** AIEE Transactions, volume 66, 1947, pages 1624–31.

7. Dielectric Strength of Station and Line Insulation to Switching Surges, **P. L. Bellaschi, L. B. Rademacher.** AIEE Transactions, volume 65, 1946, pages 1047–54.

8. Improved Condenser Bushing Insulation, **H. J. Lingal, W. G. James.** *Westinghouse Engineer* (Pittsburgh, Pa.), May 1944.

Discussion

F. J. Vogel (Illinois Institute of Technology, Chicago, Ill.): I am very much interested in the description of the 500-kv transformer, particularly in the logical reasoning given in the first point of the paper. I wish to commend the authors on this as a method often proposed, but to my mind, never committed to practice. In this respect it seems to me that the electrical engineers have been backward and dependent more on statistics and experience than on data and analysis.

I agree with and would like to emphasize the authors' statement regarding the importance of the low-frequency test as a guarantee of meeting service voltages. I gave insulation clearances many years ago for a current transformer. It met the specification tests and was shipped to the customer. After a few months service, it failed and was returned. Corona was present at operating voltage. Changes were made to prevent the corona. It was returned to the user and so far as I know, it is still in service. Tests on samples have been made which showed that if the design were properly made, corona could be prevented up to the minute test value and the continuous strength and the test value could be quite close together. These principles can be used for testing transformers for cable life tests at rated voltage continuously for relatively long periods of time. However, there are transformers which had corona on test and whose margin so far as corona level above rated voltage is probably low. Some of these transformers are even on the American Gas and Electric System, but need not be a source of worry since if they were to deteriorate for this reason, they would have done so long ago. Some manufacturers at least have furnished transformers with high corona levels since 1929 or 1930. The test data in the paper do not include specifically the 1-minute test design level of the transformer which was given a life test at 375 kv. It seems to me that this test loses much import by this.

The switching surge problem has been dealt with rather briefly, although I agree with this point of view. Switching surges as they originate are distributed uniformly in transformer windings and can be disregarded in the design in comparison to lightning. This procedure has been followed in the past entirely satisfactorily. If lightning arresters are used, switching surges as well as lightning will be limited to safe values. In the discussion of a paper of mine, however, exception was taken to this. I wonder if every one now accepts it.

Under the subject of transformer tests, no statement was given regarding the magnitude of impulse tests or induced tests. The significance of the 12-hour 320-kv test therefore is lost. I am rather surprised at the author's apparent concern over operating continuously at higher voltages.

In looking at Table I and Figure 7, the thought occurred to me that this work could be projected equally well down to 115 kv and decreases in cost and improvements in performance obtained. Such changes probably would have more economic value to the industry than the values presented for highest voltage lines, since the transformers they use will be relatively few in number. Referring again to Figure 7 and the 460-kv class, a basic impulse level of 1,550 kv is proposed and it is conceivable that a unit designed for a 520- to 550-kv low-frequency test could meet this level with a factor of safety.

J. K. Hodnette: In view of Vogel's long experience in transformer engineering the authors appreciate very much his discussion of their paper. There are only two points raised by him on which we would like to comment in closing the discussion.

The first relates to the life tests made at the factory, first on a "bread board" transformer which was operated for well over a year in the range of extra high voltages with operating conditions maintained as close to actual field conditions as was feasible in a laboratory setup, and second, the 12-hour test made on the Tidd test line transformers before they were shipped to the test site. These tests were in the nature of verification tests and were run merely to make sure that nothing had been overlooked in either the design or the construction of the transformers which would cause them to fail to perform as anticipated.

The second comment we would like to make is that we agree in principle with his suggestion that the practice of reducing the insulation level with effectively grounded neutrals could be extended from the field of extra high voltages down to 115,000 volts. If the curves shown in Figure 7 are extended downward it will be noted that they converge at approximately 138,000 volts. This means that the reduction in insulation level, and consequently the savings in cost, resulting from the application of this principle become less as the voltage is reduced and disappear at about 115,000 volts.

It seems to the authors that the criterion which should be used in the transformer to determine whether or not reduced insulation may be used is the general insulation level of the system, since the transformer insulation level should be co-ordinated with that of the system.

Switchgear Equipment for Tidd High-Voltage Test Lines

F. A. LANE
MEMBER AIEE

B. W. WYMAN
MEMBER AIEE

THE DEVELOPMENT of higher voltage transmission systems will play an important part in extending present-day loadings and distances for power transmission.[1-6] Before advantage can be taken of these increases, however, it is necessary to develop new high-voltage switching equipment to protect these systems under fault conditions, and to restore them to normal operation without delay. These equipments must take advantage of all the advances which have occurred up to the present to maintain system stability and incorporate the necessary insulation strength with maximum economy.

In the present investigation into the problems associated with higher transmission voltages, the General Electric Company has co-operated by

1. Determining a suitable type of switching equipment for these voltages.

2. Developing a unit of this type to obtain experimental data on the Tidd high-voltage project sponsored by American Gas and Electric Service Corporation.

Requirements of New High-Voltage Switching Equipment

The first step in determining the type of switchgear equipment was to set down the switchgear requirements which have proved necessary over the years for present-day transmission voltages, and then examine these requirements to determine whether they cover the ground for the higher voltages now being studied.

Among these requirements are

1. High speed fault isolation. This is required from four standpoints

(a). System stability. The increase in transient stability obtained by isolating faults within a time which is short in comparison with the system period of oscillation has been well demonstrated by studies made on many power systems. The 3-cycle low-oil-content impulse circuit breakers developed for the 287-kv Hoover Dam line showed the worthwhile increase in transient stability which could be obtained with 3-cycle interrupting times as compared with earlier 5-to-8-cycle interrupting times.[1]

(b). Reduced system shock and damage. High capacity short-circuit tests on transmission systems repeatedly have shown the reduction in system shock which results from 3-cycle circuit breaker operating times as compared with older, slower fault-clearing circuit breakers. Three-cycle fault clearing also has shown a marked reduction in conductor and insulator damage at the point of fault.

(c). Improved service to customers. Fast fault clearing is necessary to decrease voltage fluctuations which are damaging to the operation of many present-day industrial plants.

(d). Decrease circuit breaker maintenance. Considerable reduction has been demonstrated in the maintenance required to the circuit breaker itself on units having 1-cycle or shorter arcing times, both from the standpoint of contact erosion and oil carbonization.[8]

2. High speed reclosing. The circuit breaker must be capable of reclosing as rapidly as the flashover arc path can recover its dielectric strength to realize the maximum transient stability benefits. Twenty-cycle reclosing, now in general use for modern switching, has been an important factor in increasing the power carrying capacities of systems operating near the stability limit. Tests have indicated that successful reclosure after most faults is possible in even shorter times if circuit breakers providing higher reclosing speeds were available.[9] Ten- or 12-cycle reclosing, therefore, was established as an objective in the design of this new circuit breaker from which test data can be ob-

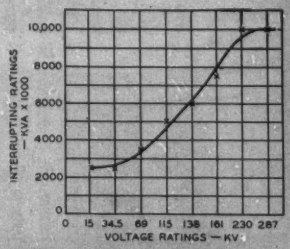

Figure 1. Maximum kilovolt-ampere requirements expected in the near or foreseeable future at present voltages

Figure 2. Single pole of low-oil-content impulse-type circuit breaker developed to obtain experimental data on Tidd high-voltage test project

Paper 47-246, recommended by the AIEE committee on switchgear and approved by the AIEE technical program committee for presentation at the AIEE Midwest general meeting, Chicago, Ill., November 3–7, 1947. Manuscript submitted August 21, 1947; made available for printing September 18, 1947.

F. A. Lane is electrical engineer, American Gas and Electric Service Corporation, New York, N. Y.; B. W. Wyman is section leader of engineering, General Electric Company, Philadelphia, Pa.

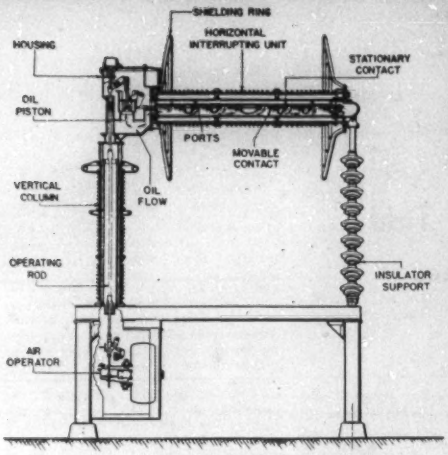

Figure 3. Cross section through one pole of low-oil-content impulse circuit breaker showing piston with arrows showing oil blast being driven up between six sets of series of contacts in horizontal interrupter

Large shielding rings on either end of horizontal interrupter provide uniform voltage distribution between various sets of series breaks. Piston supplying driving force for oil blast action is located in housing at end of interrupter column

tained to determine minimum flashover recovery time for higher voltage lines.

3. Sufficient interrupting capacity must be designed into the circuit breaker to interrupt the maximum short-circuit current reasonably expected on these high-voltage systems. In general, it may be stated that the higher the system interrupting requirement without unduly increasing circuit breaker costs, the more economical will be the system design, as arbitrary injection of reactance always tends to reduce effective loading of transmission lines.

4. Equipment must be designed with sufficiently high dielectric strength for lightning arrester co-ordination.

In developing a circuit breaker to meet these requirements, it soon became apparent its supporting structure would be of such dimensions that it might readily serve other purposes. Economic considerations dictate that, since practically every piece of equipment to be used at the higher voltage under study has to be designed from the ground up, effort should be made to combine functions wherever possible to reduce the over-all cost. For the higher voltages being considered, space requirements also become of paramount importance. It was, concluded, therefore, that considerable economies can be effected by developing the entire feeder equipment as a compact integrated unit, the operation of each component part being co-ordinated functionally with the unit as a whole.

The result can be, therefore, a unit incorporating all auxiliary equipment, such as structural supports, current transformers, relays, coupling capacitors for carrier current equipment, disconnecting switches, interlocks, as well as the circuit breaker and protecting lightning arresters.

Circuit Breaker

In determining the type of circuit breaker to be built for these voltages, careful consideration had to be given the probable trend in circuit breaker developments at these higher voltages. Also, it was realized that the requirements at these higher voltages would be particularly severe, and so the service records obtained on existing types should have just as important a part in making a decision as the design and operating characteristics.

In comparing circuit breakers in service for maximum existing voltages on the foregoing basis, the low-oil-content impulse-type circuit breakers, originally developed for the 287-kv transmission line between Hoover Dam and Los Angeles, would seem to be the most promising type. Its oil blast action, obtained from a spring-driven piston, provides extremely high speed arc interruption, regardless of the magnitude of the current being interrupted. Arcing times consistently under one cycle for all values of current are obtained because of the positive rate at which fresh dielectric is forced between the eight sets of series contacts. Moreover, this positive oil-blast action at low currents insures postive interruption of line charging currents without requiring shunting resistors to prevent restriking. This is a particularly important consideration with the higher charging currents which will be associated with the longer lines at higher voltages.

Moreover, the service record on this type of circuit breaker has been outstanding. In addition to the 287-kv cir-

Figure 4. Artist's sketch of complete co-ordinated switching unit showing location of circuit breaker, lightning arrester, disconnecting switches, and through type bushings with current transformers

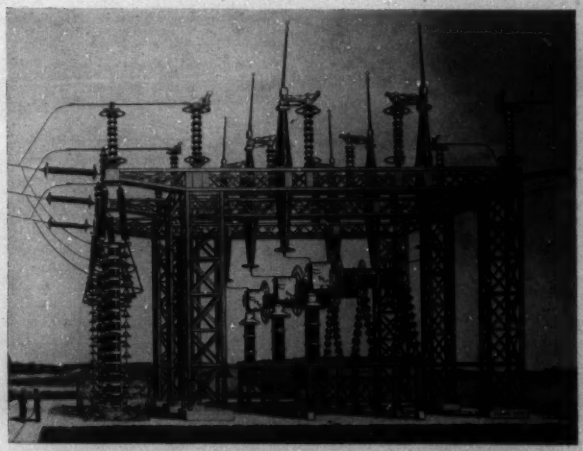

cuit breakers, many 230-kv and 138-kv units have been in service; some since 1935. In all, about 350 circuit-breaker-years of operating data have been obtained without any major difficulties. One of the 230-kv impulse circuit breakers, rated 3,500,000 kva, which had been in service five years, recently was given field tests up to maximum capacity available at Grand Coulee Dam of 6,700,000 kva without distress. The maintenance requirements of this circuit breaker are also very minor due to the short arcing times and the low oil content involved. To obtain higher speed reclosing on this new high-voltage circuit breaker, a compressed-air mechanism was designed to replace the motor-charged spring mechanisms used on the earlier circuit breakers of this type. The operation of each pole by its own mechanism permits either 3-pole or single-pole reclosing. Tests have shown that these mechanisms are adjustable to reclose the circuit breaker in 10 cycles, or less, if that should prove practical from a dielectric recovery standpoint of the arc path.

In determining the maximum interrupting capacities that may be required at these voltages, some assumptions must be made. Figure 1 shows the result of some studies which have been made to determine the maximum capacities that may be required in the forseeable future at existing voltages. If the leveling off at 10,000,000 kva, as the curve shows, is assumed to represent a definite trend, then 10,000,000 kva would seem to be a reasonable value for the interrupting rating of these higher voltage circuit breakers.

The experimental circuit breaker was developed for a 3-phase interrupting rating of 10,000,000 kva at 360 kv. This is the highest interrupting rating ever assigned to any circuit breaker to date in the United States or abroad. Although indications are that this rating will satisfy any requirements that might be forthcoming in the foreseeable future, it does not represent the maximum which can be developed for this type of circuit breaker. As the positive oil blast action is independent of current, this type of circuit breaker does not have the same limitations which exist in conventional tank-type circuit breakers. This means that if time should reveal that ratings in excess of 10,000,000 kva are required at these voltages, they can be developed.

Figure 2 shows a single pole unit of this circuit breaker set up for operation tests, while Figure 3 shows a cross-section view of the circuit-breaker pole. The compressed air mechanism at the bottom drives the main operating rod which passes up through the oil-filled vertical porcelain column. The piston in the housing at the top of the column operates simultaneously with the contacts to force oil out into the horizontal interrupter tube and up between the six sets of series contacts. The large shielding rings at either end of the horizontal interrupting tube divide the voltage uniformly between the various breaks.

Over-all Arrangement

The arrangement of the over-all switching equipment is shown in Figure 4. The through bushings mounted directly above the circuit breaker provide for two current transformers on either side of the circuit breaker, as well as voltage taps for potential measurements. Each bushing also serves as one of the stationary columns for the braidless silver line contact disconnecting switches. The disconnecting switches of each pole will be operated by a motor mechanism interlocked with the circuit breaker mechanism to prohibit incorrect operation. Each pole of the structure is entirely self-supporting without cross ties with the other two poles.

The lightning arresters installed to protect the switchgear equipment consists of standard station-type "thyrite" interchangeable 12-kv units of the type used on many high-voltage systems in the United States. The lightning arrester consists of 25 units, and has a maximum permissible line-to-ground rating of 300 kv. Its impulse protective characteristics co-ordinate with the 1,300-kv basic insulation level used for the switching equipment.

The co-ordinated over-all design will carry a rating of

Normal operating voltage, 360 kv.

Impulse withstand test, 1,300 kv.

Rated current, 800 amperes.

Nominal interrupting capacity, 10,000,000 kva.

Summary

The approach to terminal switching equipment herein described presents a new concept for higher voltage switchgear. It is believed that this concept, while not confined to higher voltages alone, will provide all the functional advantages of conventional switching equipments along with great economies in space and cost. At the same time, it should result in increased safety and decreased maintenance.

References

1. Transmission of Electric Power at Extra High Voltages, Philip Sporn, A. C. Monteith. AIEE Transactions, volume 66, 1947, pages 1571–82.

2. Corona Considerations on High-Voltage Lines and Design Features of Tidd 500-Kv Test Lines, C. F. Wagner, Anthony Wagner, E. L. Peterson, I. W. Gross. AIEE Transactions, volume 66, 1947, pages 1583–91.

3. Insulators and Line Hardware for Tidd 500-Kv Test Lines, I. W. Gross, R. L. McCoy, J. M. Sheadel. AIEE Transactions, volume 66, 1947, pages 1592–1602.

4. Line Conductors—Tidd 500-Kv Test Lines, E. L. Peterson, D. M. Simmons, L. F. Hickernell, M. E. Noyes. AIEE Transactions, volume 66, 1947, pages 1603–12.

5. Transformers and Lightning Arresters—Tidd 500-Kv Test Lines, F. A. Lane, J. K. Hodnette, P. L. Bellaschi, Edward Beck. AIEE Transactions, volume 66, 1947, pages 1613–8.

6. Instrumentation and Measurement—Tidd 500-Kv Test Lines, R. L. Tremaine, G. D. Lippert. AIEE Transactions, volume 66, 1947, pages 1624–31.

7. Circuit Breakers for Boulder Dam Line, D. C. Prince. Electrical Engineering (AIEE Transactions), volume 54, April 1935, pages 366–72.

8. Field Tests and Performance of Heavy Duty High Speed 138-Kv Circuit Breakers—Oil and Air Blast, Philip Sporn, Harry P. St. Clair. AIEE Transactions, volume 64, 1945, pages 401–10.

9. Ultrahigh-Speed Reclosing of High-Voltage Transmission Lines, Philip Sporn, D. C. Prince. Electrical Engineering (AIEE Transactions), volume 56, January 1937, pages 81–90.

10. Economics of Long-Distance A-C Power Transmission, S. B. Crary, I. S. Johnson. AIEE Transactions, volume 66, 1947 (Proceedings T7163).

Discussion

M. H. Hobbs (Westinghouse Electric Corporation, East Pittsburgh, Pa.): The authors very ably have presented the requirements for circuit breakers on circuits of 345 kv or higher, including such features as 3-cycle or lower interrupting time, 12-to-20-cycle reclosing, high kilovolt-ampere interrupting ability, as well as rapid and positive clearing of line charging current. However, there are no test data in the paper and the information does not seem adequate to show that the porcelain-clad oil type is necessarily the most desirable form for such an interrupter. It may be, and of course compressed air also will receive consideration. The dead tank oil circuit breaker has shown its ability to meet all the requirements set down, is a relatively simple rugged device

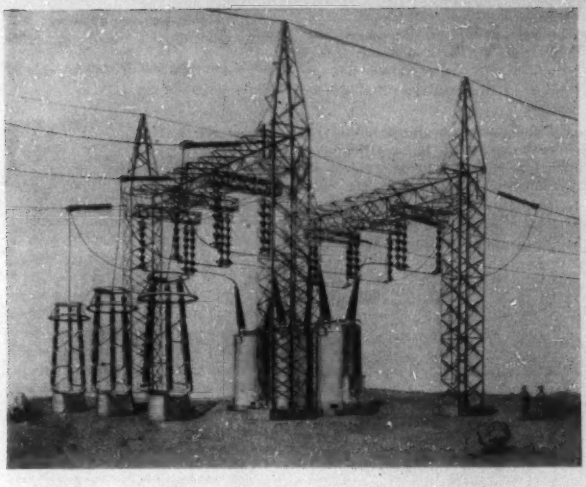

Figure 1. Sketch of switching station

and in addition has self-contained current transformers and potential devices, so that additional insulator supports and space are not required for this equipment outside the circuit breaker. Its place in the picture, therefore, should not be neglected.

We agree heartily with the author's statement regarding the advantage of positive oil blast action in preference to the use of special shunting resistors for the interruption of line-charging currents without excessive overvoltage. However, instead of providing an oil-driving piston with sufficient power to cause interruption of the maximum short-circuit currents, the alternative of using self-generated pressure in a separate series break for the rupture of heavy currents in conjunction with a piston for low currents has been found to give a less complicated interrupting structure. This combination reduces the mechanical operating effort to that of a single mechanism, instead of requiring a separate mechanism for each pole unit, as used in the circuit breaker described by the authors, regardless of whether or not single-phase reclosing is desired.

The cross section in Figure 3 of the paper shows two valves in the air mechanism so arranged that air can be admitted above the piston for accelerating the circuit breaker to the open position as well as below the piston for closing. Does this mean that in the event of loss of air from the reservoir, the circuit breaker would be unable to trip open and clear a fault?

It is understood that no high-voltage switching equipment is as yet installed at Tidd. Will the experimental circuit breaker be a single-pole or 3-pole unit? A statement also is requested as to the nature of the tests to be made in the field on the circuit breaker since the power at high voltage is of course very limited and the length of transmission lines would make even a charging current test of doubtful value.

In Figure 4 of the paper is shown a 3-phase lightning arrester apparently having 15 units per phase lag. The text of the paper states that the arrester is rated 300 kv maximum, consisting of 25 12-kv units. Using the insulator strings as a basis of measurement, it appears that the height of the arrester column is 30 feet, and the distance from the ground to the point of suspension of the arrester about 40 feet. The air clearance from the arrester grading ring to the grounded steel structure seems to be only 7 or 8 feet, a rather short clearance at these high voltages. The authors' further comments would be appreciated. If the rating is 300 kv, what is the actual height of the arrester column exclusive of the suspending insulators, and what are the clearances to ground?

In Figure 1 of this discussion is pictured a switching station equivalent to that in the paper, showing a high-voltage dead-tank oil circuit breaker between two towers for dead-ending and for supporting the disconnecting switches. Overhead ground wire supports, omitted in the paper, also are provided for. The self-supporting 80 per cent lightning arrester adjacent to the structure, described in reference 5 of the paper, by Beck and others does not require any supporting steel work. Over-all, the steel structure required for the bay appears somewhat simpler than that proposed by the authors.

The oil circuit breaker is provided with self-contained bushing-type current transformers, as well as taps on the condenser bushings for potential. The tanks can be located on any suitable phase spacing and operated by either one pneumatic mechanism or three individual mechanisms as may be required.

Not only have multiflow Deion grid circuit interrupters been extended in rupturing capacity as high as 10,000,000 kva at 230 kv, but there seems to be no apparent limit in the voltage rating to which they may be applied. For instance, single-phase tests on two interrupting units have been carried as high as 5,000 amperes at 198 kv in the high power laboratory, equivalent to a line-to-ground fault on a 345-kv system of 3,000,000 kva on a 3-phase basis.

In order to shorten the arcing time at these high voltages, the circuit breaker for extra high voltage, such as 345 kv or more, has four interrupting units per pole. This also facilitates laboratory testing to higher powers, since it has been shown that voltage dividing resistors completely justify the method of testing a half pole at half voltage. Interrupting tests with 132 kv across two multiflow Deion grids have been made successfully up to 10,000 amperes. This would correspond to 264 kv to ground on a 4-unit-per-pole circuit breaker, equivalent to an 8,000,000-kva 3-phase grounded fault on a 460-kv system, with a rate of rise of recovery voltage approaching 7,000 volts per microsecond.

Abe Tilles, (Pacific Gas and Electric Company, San Francisco, Calif.): The diagrams are not entirely clear. Is it correct that the switchgear will be riding on the lines for static potential test with the far side entirely open? In any case neither the capacitance of this line length as a load nor the input capability of the transformer bank as a source of supply is great enough to load up the circuit breaker. Thus its electrical interruption performance will need to be judged by tests made elsewhere. The mechanical behavior of course, can be observed here.

What specifically is the voltage distribution across the six series breaks of the open circuit breaker?

It is encouraging to note that an inherently satisfactory circuit breaker is expected. The use of resistors and an auxiliary break often introduces complications and difficulties.

F. A. Lane and **B. W. Wyman:** There are so many interesting aspects in a development project of the magnitude of the switchgear equipment for the Tidd high-voltage test line, that the most difficult task which faced the authors in writing this paper lay in selecting the material which could be included in a paper of nominal length. As very few design details could be covered, it would have been surprising had not a number of questions occurred in the mind of the reader.

Hobbs has raised several questions, the most important seeming to be whether the impulse-type low-oil-content circuit breaker was the correct one to select for the development of a switchgear equipment for these extra high voltages, in preference to the conventional tank-type circuit breaker or the air-blast circuit breaker. While the authors believe on the basis of their evaluation of all the factors involved, that the impulse type circuit breaker was the correct selection, they did not mean to infer that either of the other types could not be developed. One of the main objections in the tank type for these voltages is that the amount of oil required would have exceeded 15,000 gallons for a triple pole circuit breaker, which is the equivalent of 2 tank cars. Also, this entire volume of oil would have to be drained each time the tank circuit breaker contacts were

inspected, so that the oil handling equipment, oil storage equipment, and filtering equipment becomes a sizeable item. Neither the low-oil-content impulse type nor the air-blast type suffers from these handicaps. The air-blast circuit breaker, however, for outdoor service, has been installed in the United States only in experimental installations and requires additional development before it can be considered for these extra high voltages. As the air-blast type probably will be developed in the future for these voltages, however, the switching structure was designed so that it would accommodate the air-blast type as well as the impulse-type low-oil-content circuit breaker.

Contrasted with the limited operating experience on the high-voltage air-blast circuit breaker is the long and enviable operating record of the low-oil-content impulse circuit breaker switching the Hoover Dam line, the highest voltage transmission system in the United States, and, therefore, it seems to be the most logical choice.

A further reason for the selection of the impulse-type circuit breaker is its excellent performance on the interruption of line charging currents which will be of more and more importance with higher-voltage longer-distance transmission lines with their correspondingly higher values of charging current. With the tank-type circuit breaker, the interruption of charging currents generally is accompanied by some restriking with attendant overvoltages. Positive arc interruption at the first current zero eliminates the possibility of any restriking when interrupting line charging currents with the impulse-type circuit breaker.

Each pole of the circuit breaker is operated by its own pneumatic mechanism. The circuit breaker is closed by compressed air and opened by springs. The second valve which Hobbs asks about in the cylinder is for instantaneous dumping of the air pressure in the cylinder on a trip-free operation. It plays no part on a straight opening operation and consequently the circuit breaker can be tripped whether it has air pressure or not.

Hobbs also has questioned the lack of test data in the paper to substantiate the interrupting rating of 10,000,000 kva at 360 kv. This corresponds to approximately 16,000 amperes at 360 kv. Inasmuch as we do not have at present, or are not likely to have at any time in the near future, facilities which will permit the carrying out of full scale tests on a circuit breaker of this rating, the only recourse we have is to test in the high-voltage laboratory to obtain empirical data that can be extended by extrapolation. The impulse type of circuit breaker whose oil-blast action is independent of the current being interrupted is better suited to the extrapolation method of testing than the self-generating blast action type of interrupter in which the interrupting pressure is a function of the current being interrupted and of the arc duration. Laboratory tests up to 264 kv across a complete single pole at reduced currents have been made with no interrupting times exceeding 3 cycles, which would correspond to a 3-phase voltage of 455 kv. Laboratory tests also have been made up to 25,000 amperes at reduced voltage without distress to the circuit breaker. A current of 25,000 amperes at 455 kv would correspond to a 3-phase rating of 20,000,000 kva, so that a rating of 10,000,000 kva would seem conservative. As each pole has six breaks in series, one may be tested alone by short-circuiting the other five. This type of circuit breaker lends itself to further extrapolation by tests on individual breaks.

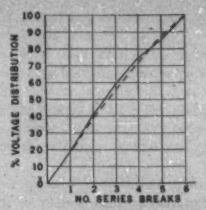

Figure 2. Voltage distribution in 360-kv impulse-type circuit breaker

A 3-pole circuit breaker has been built. Each pole, however, was designed with its own operating mechanism for either single-pole or triple-pole reclosing, so that it is complete in itself. Consequently, only one pole is being installed at Tidd to obtain field tests and field experience, the other two poles being used for additional tests in the high power laboratory.

The grading rings at either end of the interrupter provide uniform voltage distribution between the six series breaks in the interrupter, eliminating the necessity of resistors which Hobbs admits would be necessary in a tank-type circuit breaker such as he seems to prefer in order to obtain satisfactory voltage distribution. The actual voltage distribution asked for by Tilles that is obtained by the grading rings is shown in Figure 2 of this discussion. The solid line is the distribution obtained with the mechanism end at high voltage and the other end grounded, the dotted line is the distribution with the connections reversed.

No dimensions of the over-all equipment are shown in the paper. Scaling from figures as Hobbs has done is generally difficult; he may be assured, however, that a $9^1/_2$-foot air clearance from the lightning arrester which provides ample clearance to the grounded steel structure has been allowed.

Completely co-ordinated switchgear equipment of this type appears to have sufficient advantages so that it is expected they may set a new trend in high voltage outdoor station design, not only for the highest voltages visualized in the future, but also the more commonly used transmission voltages in general use today.

One thing that needs to be emphasized in connection with an equipment of this type is that everything must be done to reduce cost wherever possible. This best can be done by making as many components as possible to double duty. The circuit breaker supporting structure being used for other functions is one example. The through bushing being used for disconnecting switch insulators is another function. If coupling capacitors were required, these bushings also might serve as capacitance units. Only by such simplifications can switchgear equipments be reduced to a proper economic basis to help justify going to higher transmission voltages.

Instrumentation and Measurement—Tidd 500-Kv Test Lines

R. L. TREMAINE
ASSOCIATE AIEE

G. D. LIPPERT
MEMBER AIEE

THIS PAPER discusses the metering equipment that is being supplied by the Westinghouse Electric Corporation for measuring corona loss, radio influence, and atmospheric conditions at the Tidd 500-kv test lines. Since one of the main objectives of the test, as pointed out in a companion paper[1] is the accurate determination of corona loss under all possible operating conditions, this paper is devoted principally to the equipment which will be used to measure the corona power loss.

A careful study of the problem of measuring corona loss was made. A search of the technical literature for the methods employed by other investigators shows the following:

On actual lines, losses were obtained by measuring the input to the exciting transformers and subtracting the transformer losses.[7]

In some cases current coils of wattmeters were placed in series with the lines[9–12] and potential taken from water column potential divider.

The importance of impressing on the metering circuit the exact reproduction of the line voltage was well recognized and various refinements,[13–15] in measuring circuits have been used.

A detailed analysis of the possible errors in the methods heretofore used suggested that a new method for measuring corona loss be used.

General Discussion

In order to understand the very exacting requirements of any metering circuit which is to be used to measure corona loss on a full sized line with conductors up to two inches in diameter and spacings up to 45 feet, it is necessary to understand the conditions under which the circuit must operate. For example, assume a 2.00-inch smooth conductor at 45-foot spacing. The corona loss by Peterson's[16] formula will be 0.215 kilowatts per phase at 335 kv line to line for a line 1.4 miles in length. Under this condition the charging kilovolt-amperes will be 273 per phase. The power factor is 0.079 per cent which corresponds to a power factor angle of 89 degrees 57.3 minutes. Hence any system which is used to measure corona loss must be sensitive to an angle in the order of one minute or 0.000292 radian.

Table I is an application of Peterson's formula to the example mentioned previously. It shows the magnitude of corona loss to be expected under fair weather conditions.

Table I. Fair Weather Corona Loss

Two-Inch Smooth Conductor, 45-Foot Spacing, 1.4 Miles Long

Kv Line-to-Line	Kva	Corona Loss, Kw	Power Factor, Per Cent	Power Factor Angle
264.5	170	0.114	0.067	89° 57.7′
300	220	0.147	0.067	89° 57.7′
350	305	0.268	0.088	89° 57.0′
400	390	0.591	0.151	89° 54.8′
450	490	1.060	0.217	89° 52.6′
500	609	2.630	0.432	89° 45.1′

Further emphasis on the requirements of accuracy of a metering circuit to measure corona loss is shown in Table II. If 310 kva charging per phase is assumed, it is interesting to note the effect on the wattmeter indications if a constant error angle of one minute is assumed. The table shows this condition for different assumed values of loss.

At first glance it would appear that some type of bridge would be most desirable. There are several objections to this. A bridge does not lend itself to recording losses over a long period. The high voltage which will be used would necessitate using a very large ratio arms to get the bridge down to a safe voltage. An alternative is to construct a Faraday cage and have the operator at a high potential. In addition, a bridge would be sensitive to stray capacitance effects which would make it hard to build and difficult to check.

Table II. Effect of 1-Minute Error in Voltage Applied to Voltage Coil of Wattmeter

Corona Loss Per Phase, Watts	Corona Loss Per 3-Phase Mile, Watts	Actual Power Factor, Per Cent	Meter Indication, Watts	Apparent Power Factor, Per Cent	Error Per Cent
0	0	0.00	90	0.0291	∞
100	214	0.0323	190	0.0615	90
200	428	0.0646	290	0.0937	45
300	643	0.0968	390	0.126	30
400	857	0.129	490	0.158	22
500	1,070	0.161	590	0.190	18
1,000	2,140	0.323	1,090	0.348	9

After reviewing the methods of corona measurements already used and keeping in mind the features desired in the test, it was decided to design the circuit on the following basis:

1. Corona power to be measured by a wattmeter.
2. The wattmeter to be located at high potential to eliminate the necessity of subtracting transformer losses.
3. Potential for the wattmeter to be taken from an extension of the transformer high-voltage winding.
4. Automatic compensation to be provided to correct for the phase angle errors in the potential applied to the wattmeter.

Paper 47-247, recommended by the AIEE committee on transmission and distribution and approved by the AIEE technical program committee for presentation at the AIEE Midwest general meeting, Chicago, Ill., November 3–7, 1947. Manuscript submitted August 20, 1947; made available for printing September 24, 1947.

R. L. TREMAINE is central station engineer, industry engineering department, Westinghouse Electric Corporation, East Pittsburgh, Pa.; G. D. LIPPERT is with the electrical engineering section, American Gas and Electric Service Corporation, New York, N. Y.

The authors are deeply indebted to the late R. D. Evans who contributed a great deal to the development of this circuit. They also wish to acknowledge the assistance given by Doctor G. D. McCann, Jr. (M'44), Doctor C. F. Wagner (F'40), and S. B. Griscom (M'40), and the work done by B. E. Lenehan (A'24) in developing the "nul" type wattmeter

When it was decided to use a wattmeter, investigation revealed that a suitable meter was not available. The problem was presented to the engineers of the Newark meter works of the Westinghouse Corporation. A special "nul" type meter was developed which is shown in Figure 1. It is about 100 times as sensitive as an ordinary wattmeter. It is classified technically as a current balance transmitter. The meter has a regulated power supply which provides 250 volts direct current for the tube plates, and 6.3 volts alternating current for the tube filaments and the lamp. The power supply is required to operate over a range of 201 to 342 volts. Its output voltages are substantially constant.

Referring to Figure 1 the operation of the meter is briefly as follows. The current and voltage coils are located in the lower half of the meter. The corona power is resolved into a torque which is applied to the upper half of the meter by means of the shaft. This shaft is the only connection between the upper and lower sections of the meter. The alternating-voltage coil is fixed on the lower end of the shaft, and the movable vane and the d-c coil (located between the pole faces of the permanent magnet) are fixed on the upper end. A change in torque (corona power) causes the movable vane to move upsetting the light balance between the two phototubes. The phototubes are connected in series across the plate supply and their midpoint is connected to one of the grids in the *6SN7*. A change in the potential of the grid causes a current to flow in the d-c coil in such a direction as to oppose the torque, and of such magnitude as to exactly compensate for or nullify the torque applied to the shaft. The vane thus is moved back to its original position, restoring the original light balance between the phototubes. D-c milliammeters are connected in the d-c coil circuits. The indication of these external milliammeters, multiplied by suitable constants, gives the magnitude of the corona power.

This meter is very well suited for this application. Since the angle between the current and voltage coils remains at 90 degrees there is no error from angular displacement of the two coils, and there is no error from nonlinearity of the springs. The magnitude of the direct current is not affected by reasonable changes in the plate voltage nor is it affected by the impedance of the external indicating meters. Owing to its delicate nature, the meter is affected by slight errors in the balance of the movable element; however, in use the meter will be in a fixed position, eliminating the possibility of this error.

The meter has undergone extensive tests in the laboratory over a period of about six months. In the laboratory, this meter has demonstrated its ability to measure power to an accuracy of ±5 per cent at power factors as low as 0.02 per cent.

As shown in Figures 2 and 6 the line current is passed directly through the current coil of the wattmeter. In order to get accurate readings from the wattmeter, it is necessary for the current through the voltage coil to be exactly in phase with the line-to-neutral voltage applied to the line. From Figure 6 it can be seen that the phase angle between the voltage applied to the wattmeter and the voltage from line to ground is the sum of the phase shift in the high-voltage winding and the phase shift in the metering winding.

The phase shift through the metering winding of the transformer, due to the instrumentation load, is of very small magnitude, varying from 0.52 minute at minimum voltage to 0.82 minute at maximum voltage. However, it is interesting to note the effect of even this small phase shift on the indication of the wattmeter. At 335 kv the angle would be about 0.61 minute which would result in a meter reading of 55 watts. This added to the 215 watts of corona loss previously calculated would result in a serious error in the wattmeter reading. Since this winding has a shield at high potential, its charging current is negligible and causes no phase shift.

An analysis of the high-voltage winding reveals a much more serious condition. Assuming no in-phase load on the winding the phase shift through the winding will vary from 6.28 minutes at minimum voltage and 8.10 minutes at maximum voltage. From the previous discussion, it can be seen that the wattmeter reading would be meaningless if this angle were not corrected. It also can be seen that if a constant correction of say 7.19 minutes is made, as has been done by other investigators, the deviation from this angle would be of such a magnitude that the readings in the low power factor range would contain serious errors. In addition to the phase shift due to the reactive load on the transformer, there is a comparatively large phase shift due to the in-phase load. At 500 kv a 100 kw load will cause a phase shift of about five minutes. On the middle phase this would not be serious (meter would indicate 102 instead of 100 kw) but in the outside phases, the in-phase load will be largely the result of power transfer, and the meter might read 2 kw when there was no corona loss at all.

As shown later, a compensation can be applied to correct for the phase shift in the high-voltage winding due to the load current. This is not true of the capacitive charging current of the high-voltage winding, because of capacitances between turns and from winding to case. The magnitude of these capacitances was cal-

Figure 1. Current balance transmitter or "nul" type wattmeter used to measure corona loss

culated and calculations using these values indicate that at maximum voltage this phase shift will be only 0.1 minute. An angle two or three times this value would not introduce a serious error.

In addition to the compensation necessary to correct for the phase shift in the metering and high-voltage windings, compensation must be made to correct for the power transfer from one outside phase to the other. The conductors on the test lines are in flat configuration, which results in unequal capacitances between conductors giving unsymmetrical line charging currents. With the line configuration previously mentioned the charging current on the outside phases leads the line to neutral voltage by 90 degrees ± 3 degrees 53 minutes. At 335 kv line to line the power transfer between outside phases is 18.5 kw. If no provision were made to compensate for the power transfer, and the corona loss was 0.215 kw on each of the outside conductors the wattmeters would read 18.3 kw and 18.7 kw on outside phases. The corona power which would be present would be slightly more than one per cent of the total power indication, which is less than the accuracy of the metering circuit. While it is true that if the total 3-phase power is measured, the sum will be the corona loss, it is evident that the corona loss on the individual conductors could not be measured accurately.

Test Setup

In general, two types of tests will be conducted on the lines. One group of tests will be voltage versus corona test loss curves for various conductors, spacings, and ground wire heights, under varying atmospheric conditions and conditions of conductor surface. The other group will be long time tests in which the corona losses will be recorded graphically. The importance of these tests is discussed in a companion paper.[8] Figure 2 is a schematic of the transformer, wattmeter, and shielding. There are two phase lines 1.¾ miles long and one 800 feet long. The long lines will be used for longtime tests for more accurate corona loss curves and for radio influence measurements. The short line will be used to obtain information on various types of conductors, where it is impractical to change the long lines.

One wattmeter will be used to measure the power in each phase of each line so that a total of nine wattmeters is required. The bus structure is strung with 2-inch *HH* conductors. The conductor provides a shield for the measuring leads which are run inside of it from the instrument house to the conductors under test. The individual leads are each shielded with bronze braid to eliminate effects between adjacent measuring leads in a bus conductor.

As it is desirable to test several circuits simultaneously, the metering equipment on each phase consists of the following: one voltmeter to indicate metering winding voltage, three ammeters to indicate individual line charging currents, three current balance transmitters together with three milliammeters to indicate power loss, and two slow speed (3 inches per hour) and one high speed (90 inches per hour) graphic milliammeters to record the corona loss. The range of the wattmeters is from 100 watts to 60 kw per phase. The instruments and auxiliary equipment used in measuring the corona loss on one phase are shown in Figures 4, 5, and 6.

Three single-phase 1,667-kva transformers will be used to supply power to the lines. These transformers are rated at 69 kv delta to 500 kv Y. Taps are provided so that line-to-line voltages from 264.5 kv to 500 kv may be obtained in 24 steps. A companion paper[3] describes the transformers in detail.

The transformers have two tertiary windings for voltage measurement. Graphic voltmeters for the determination of the line-to-line voltage are connected to these windings. The voltmeters are located in the observation booth.

As shown in Figure 2, at the point where the metering leads are connected to the test lines, a radio trap has been installed to prevent the transfer of radio noise from one line to another and to prevent noise generated by the source and bus structure from being propagated along the lines. The radio traps are tuned to maximum impedance in the broadcast band.

The observation booth is located in the bus structure steel at the same height as

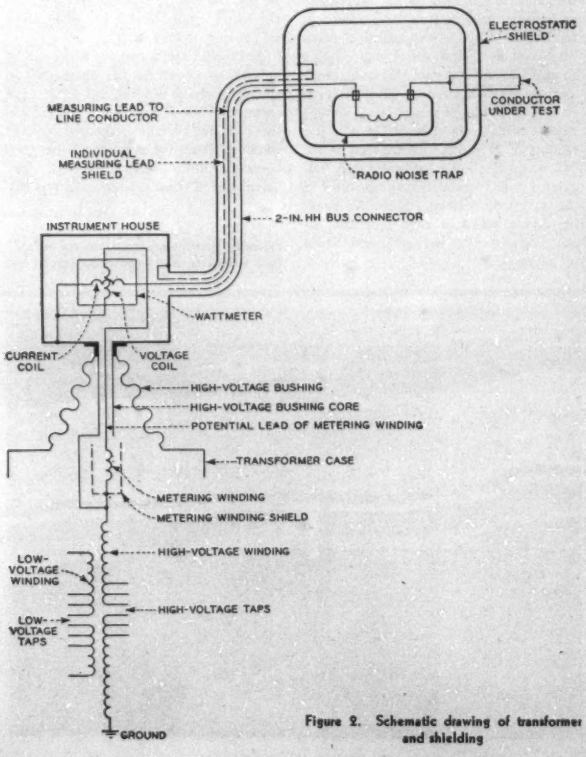

Figure 2. Schematic drawing of transformer and shielding

the instruments and at a distance of about 60 feet. All operations of the instrument circuit will be controlled from this point. The individual indicating instruments are read through a 45-power telescope mounted in the observation booth.

Atmospheric conditions have a marked effect on corona, and their measurement in these tests is of prime importance. There are installed at the test site graphic meters of conventional type for recording temperature, barometric pressure, and humidity. In addition to these meters there are now in the process of development a rate of precipitation meter and a means of measuring the electrostatic potential gradient in air. It is expected to have these instruments available in the near future.

As the instrument houses are some 40 feet above ground, a movable platform is provided to permit servicing the instruments, changing charts on the graphic instruments, and making adjustments. The top platform of the movable steel tower is mounted on rollers so that it can be extended to a position from which all parts of the instrument box can be reached.

Two Ferris radio noise and field strength meters, model 32-*A*, will be used to make radio influence measurements. Both meters are arranged so that they can be used either as portable instruments or as recording instruments. One instrument will be used to measure radio influence at various points along the line, and at points laterally from it. The other will be used to record radio influence at a particular point for a long period. Both meters are equipped with electrostatic and electromagnetic antennas.

It is planned to apply radio frequency signals of known voltages to the lines and to make measurements at various points so that the coupling between conductors and the noise meters can be determined. Point source noise generators will be used to study the propagation of noise along the line.

Metering Circuit

In order to make a wattmeter read correctly, two things are necessary. A current through the current coil of correct phase and magnitude, and a current through the voltage coil of correct phase and magnitude. The first requirement is satisfied simply by passing the line current through the current coil of the wattmeter, so no errors can be introduced from this source. The second requirement is much more difficult to achieve.

As mentioned previously, a small error in the phase of the voltage coil current will introduce very serious errors, far out of proportion to the magnitude of the phase error. If the wattmeter were connected directly to the metering winding of the transformer, the error in the phase of the current through the voltage coil would be the sum of the phase angles due to phase shift in the high-voltage winding, phase shift in the metering winding, and the series inductive reactance in the voltage coil circuit. The phase shift in the low-voltage winding does not enter the problem, because its phase shift cannot affect the relative phase position between the high-voltage winding and the metering winding.

The induced voltages in the windings are in phase because the same flux links both windings. The effect of leakage flux in the transformer is only to cause a negligibly small magnitude error. The portion of the circuit at *A*, Figure 6, adds a voltage to the metering winding terminal voltage equal to the voltage drop in the metering winding. The voltage to the right of *A* on the conductor carrying current I_V is in phase with the induced voltage in the metering winding. The circuit at *B* subtracts a voltage proportional to the voltage drop in the high-voltage winding. The circuit at *C* corrects for the phase shift due to the inductive reactance in the voltage coil circuit. The circuit at *D* is for power transfer compensation and will be discussed later.

A detailed analysis of the metering circuit now will be made. Let:

I_V = voltage coil current
I_M = current taken by auxiliary equipment
I_P = power transfer current
I_L = line current or high-voltage-winding current
E_M = terminal voltage of metering winding
E_{1M} = induced voltage of winding
E_L = terminal voltage of high-voltage winding
E_{1L} = induced voltage of high-voltage winding
Z_M = metering winding actual impedance
Z_M' = metering winding compensating impedance
Z_L = high-voltage winding actual impedance
Z_L' = high-voltage winding compensating impedance
E_W = voltage across wattmeter
Z_V = impedance of voltage coil

The symbol (′) is used to denote the secondary current of the 1:1 transformers.

The power transformer was tested as a 3-winding transformer. The actual values of the metering winding and the high-voltage winding impedances were determined. The impedance Z_M of the metering winding is constant under all transformer tap combinations. The impedance Z_M' has been set equal to Z_M. The actual impedance of the high-voltage winding changes almost directly with high-voltage taps since the percentage change is small. The ratio of the metering winding voltage E_M to the high-voltage winding voltage also changes with the high-voltage tap.

The impedance Z_L' is set so that

$$Z_L' = \frac{E_M}{E_L} Z_L$$

Since Z_L is closely proportional to E_L, a constant value for Z_L' can be used.

The current transformers in the circuit are all 1:1 transformers. The impedances of the transformers may be neglected, except in the power transfer circuit

Figure 3. Front view of instrument house

(shown at D). The phase shift through these transformers is very small and in all cases may be neglected without error.

The circuit is connected so that the current directions are as indicated in Figure 6. Writing Kirchoff's voltage law around the loop through which the current I_V flows, the following equation is obtained.

$$E_{1M}-(I_M+I_P+I_V)Z_M-(I_V-I_P'-I_M')Z_M'-(I_V+I_L')Z_L'-I_V(Z_c)-I_VZ_V=0 \quad (1)$$

Since $Z_M = Z_M'$, and all transformers are 1:1, this simplifies to

$$E_{1M}-I_L'Z_L'-I_V(2Z_M'+Z_L'+Z_c+Z_V)=0 \quad (2)$$

The terms $(2Z_M'+Z_L'+Z_V)$ may be lumped as one impedance of $R'+j\,X'$

$$Z_c=\frac{R_cX_c^2}{R_c^2+X_c^2}-j\,\frac{R_c^2X_c}{R_c^2+X_c^2} \quad (3)$$

R_c has been adjusted so that

$$\frac{R_c^2X_c}{R_c^2+X_c^2}=X' \text{ in magnitude}$$

Substituting in equation 2

$$E_{1M}-I_LZ_L'-I_V\left(R'+\frac{R_cX_c^2}{R_c^2+X_c^2}\right)=0 \quad (4)$$

Solving for I_V

$$I_V=\frac{E_{1M}-I_LZ_L'}{R'+\dfrac{R_cX_c^2}{R_c^2+X_c^2}} \quad (5)$$

The terminal voltage of the transformer high-voltage winding is

$$E_L=E_{1L}-I_LZ_L \quad (6)$$

The wattmeter readings will be multiplied by the ratio $E_L \div E_M$ so the voltage which should be applied to the wattmeter is

$$E_W=\frac{E_M}{E_L}(E_{1L}-I_LZ_L) \quad (7)$$

By substitution

$$E_W=E_{1M}-I_LZ_L' \quad (8)$$

By comparison with equation 5, it will be seen that the current through the wattmeter is in the correct phase position. The resistor R_V is adjusted so that the term

$$\left(R'+\frac{R_cX_c^2}{R_c^2+X_c^2}\right)$$

has the correct magnitude.

The part of the circuit at D is included to compensate for power transfer. The test line is of flat configuration, hence there is power transfer between outside phases. This part of the circuit is omitted on the middle phase, as the line is symmetrical about the middle phase and therefore it has no power transfer.

Figure 4. View of instrument house with cover removed

Briefly this circuit works in the following manner. Since there is power transfer from one outside phase to the other, then the line charging current consists of a real and reactive term $(I_R+j\,I_X)$ where I_R is the in-phase power transfer current and jI_X is the phase capacitive charging current. The circuit at D provides a means of shunting I_R around the wattmeter and hence the only in-phase component of current which passes through the current coil is that due to the corona power loss.

The resistor R_p is very large in comparison with the impedance of the current coil. However, the impedance of the transformer is appreciable with the result that the current I_p is not in phase with E_L. The phase angle between E_L and E_m is only a matter of minutes and may be neglected. The angle between I_P and E_L may be as large as 1.7 degrees. The current I_p with respect to E_L is (I_r+jI_x). Since the angle is so small I_r is essentially equal to I_P and jI_x has no effect on the indication of the wattmeter. Therefore I_p and I_p' may be considered equal to I_R with negligible error. If the current I_P' is equal to I_r and 180 degrees out of phase then the current through the current coil of the wattmeter becomes $(I_R+j\,I_X)-I_P'$ or simply jI_X—the capacitive charging current to the line. If there is any corona loss, the in-phase component of the line current will increase. The increase in phase current will flow through the wattmeter giving an indication of the corona loss.

Adjustment and Checking of Circuit

The theoretically correct values for all impedances have been calculated carefully and these values have been set in the circuit. The voltage of the transformer will be varied from minimum to maximum voltage possible without the presence of corona. The presence or absence of corona will be determined by a radio influence meter. During this change in voltage, the wattmeters should indicate only the insulator leakage losses. If the wattmeters read the insulator losses as determined by a separate means, over a wide range of voltage, it is felt that the circuit will measure corona loss accurately. Full scale of the wattmeter, when set at its most sensitive setting, is only 600 watts per phase. Thus a phase error corresponding to an apparent power of only 20 watts may be detected. It is not expected that the circuit can be adjusted to this accuracy, but it shows no serious errors can be present in the circuit, without the experimenter being able to detect them.

It would be possible to make the wattmeter read the insulator losses by only adjusting one part of the circuit for a particular voltage. However, since the effect of the individual compensating circuits is different for changes in conditions, and because the circuits do not change in the same manner, the wattmeter would give the correct indication only at the voltage selected. In order for the wattmeter to give the correct indication from minimum voltage to maximum voltage without corona, the circuits all must be adjusted correctly.

Figure 5. View of instrumentation with front rows of instruments removed

Possible Errors

Although considerable effort has been expended in order to make the metering circuit of the Tidd 500-kv test line as free from errors as possible, there are still possible errors in the circuit which should be discussed.

It is believed that the circuit is relatively free from errors due to harmonics. There are three sources of harmonics which may affect the metering circuit. These are

1. Harmonics generated by the source.
2. Harmonics taken by auxiliary equipment in metering circuit.
3. Harmonics generated by the corona loss.

It is believed that only the lower order harmonics, within the range in which the transformers still act as transformers, are important. The magnitudes of the currents and voltages of the higher harmonics are so low that their products will be negligible.

Harmonics generated in the source will cause no error because the same harmonics will appear in both the metering winding and the high-voltage winding.

Considerable harmonics will be taken by the auxiliary equipment in the metering circuit, particularly by the constant voltage transformer. The lower order harmonics will be reproduced in secondary of the current transformer at A, thus producing a harmonic voltage drop across the impedance Z_M' equal to the harmonic voltage drop in the metering winding.

Corona is characterized by the presence of relatively high levels of harmonic currents and voltages. The harmonic currents will cause a drop in the high-voltage winding, and a corresponding drop in the impedance at B. The harmonic voltages will be present in the flux linking the high-voltage winding. Since this flux also links the metering winding, the harmonic voltages will appear in the terminal voltage of the metering winding.

Corona has some tendency to act as a rectifier, resulting in a small amount of direct current in the high-voltage winding. This distorts the output voltage of both the metering winding and the high-voltage winding to the same extent.

The insulators themselves will have losses comparable at least to the lower order of corona loss. Little information is available on insulator losses, and indeed, because of its variable nature, little would be of any use if it were available. The losses will be mainly creepage across the surface of the insulators. Some investigation[13] has shown considerable variation in insulator loss with humidity.

The presence of unknown and unpredictable insulator losses, although possibly not serious, does present the experimenter with a problem especially when measuring low corona losses. For this reason, one of the authors now is developing a means whereby the loss may be measured continuously. It is contemplated that a number of insulator strings will be used as samples.

Errors can be introduced if a marked difference in temperature exists between the transformer windings and the compensation impedances. This error can be mitigated largely by setting the resistors so that they have the correct values at the average temperature expected. The temperature inside the instrument housing can be read by an indicating thermometer. The hot-spot temperature of the transformer also can be read. A measure of control of the temperature within the instrument house is given by exhaust fans, which are controlled from the observation booth. If serious temperature differences exist between the compensation impedances and the transformer, a simple calculation can be made to correct for this error. This is also true of the power transfer compensation resistors.

Auxiliary Equipment

Tests on conductors will be conducted over a period of several months. During this time the corona loss will vary from 0.5 to 1 kw per phase to perhaps 50 times this value. This indicated the need for a means whereby the sensitivity of the wattmeters could be changed without interrupting the tests.

A supervisory relay control circuit is provided so that the wattmeter sensitivity may be changed. The supervisory relays are controlled from the observation booth which is located in one of the towers of the bus structure at a distance of about 65 feet from the instruments. An ordinary telephone dial is used to pulse a high-speed hydrogen-filled signal lamp. The lamp is focused on the phototube of a "Photo-troller" (a light sensitive device) located in the instrument house. A contact in the Photo-troller is actuated when the incident light on the phototube is increased rapidly, and this contact controls the supervisory relays. The Photo-troller is sensitive only to quick changes in light, and is not affected by ambient light. The circuit is made insensitive to stray changes in light (for example, lightning flashes) by connecting the supervisory relay circuit so that it will reset itself if five or less pulses are received. All operations controlled by the relays are performed by dialing two numbers of which the first must be 6, 7, 8, or 9. There are three signal lamps so that each phase may be controlled separately or all three operated together.

In addition to changing taps on the wattmeter the supervisory relays are set up to turn the indicating instruments' illumination lights off and on, to turn the exhaust fan off and on, to either eliminate or reverse the voltage across the compensating impedances Z_M' and Z_L' to apply voltage to the semiconducting glass

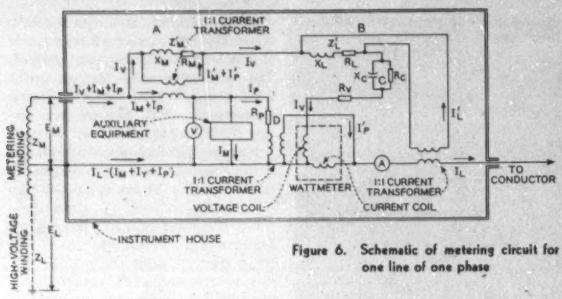

Figure 6. Schematic of metering circuit for one line of one phase

doors, to change the power transfer compensating resistors with high-voltage tap changes, and to turn the high speed recording milliammeter on and off. Two spare relays are provided which will be used to control an oscillograph, when it is desired to record the current wave shape. Indicating lights are provided to show which wattmeter tap and which power transfer resistor is in use.

Each indicating instrument is provided with two 6-watt 115-volt lamps mounted on the case of the instrument. A reflector is arranged so that the observer cannot see the lights, and so that their light is reflected on the dials of the instruments.

The high speed recording milliammeter is used to record rapidly changing losses, such as would occur during a thunderstorm.

The glass used in the sliding doors in front of the instrument house has a conducting film on the inside surface. The glass is insulated from the metal frame. The resistance of each pane of glass is about 200 ohms. These doors serve a double purpose. Normally they serve to complete the electrostatic shield around the meters. In event that frost or moisture collects on the doors, then voltage can be applied, and the resulting heat will dissipate it.

Being able to eliminate or reverse the voltage across the compensation impedances Z_M' and Z_L' enables the operator to determine the correction voltages which they insert in the circuit.

The meters are protected so that abnormal conditions will not damage them. A time delay relay is used so that when the line is energized the surge current will not pass through the meters. The circuit is opened to both the current coils and voltage coils of the wattmeters, and current coils are shunted, when the line is energized. The time delay relay has been set at about 40 seconds. This allows time for the individual power supply of the wattmeters and for the Phototroller to warm up.

If a lightning surge voltage passes through the high-voltage winding a portion of the voltage will appear across the metering winding. Surge voltage protection for the meters is provided by a small lightning arrester.

Conclusions

The authors have described a method of measuring corona loss. The method presented is apparently the most flexible and most accurate method which heretofore has been used. When properly adjusted this method should give accurate readings at extremely low power factors. Provision is made to measure corona loss, associated radio influence, and atmospheric conditions.

References

1. Transmission of Electric Power at Extra High Voltages, **Philip Sporn, A. C. Monteith.** AIEE Transactions, volume 66, 1947, pages 1571–82.

2. Corona Considerations on High-Voltage Lines and Design Features of Tidd 500-Kv Test Lines, **C. F. Wagner, Anthony Wagner, E. L. Peterson, L. W. Gross.** AIEE Transactions, volume 66, 1947, pages 1583–91.

3. Insulators and Line Hardware for Tidd 500-Kv Test Lines, **L. W. Gross, R. L. McCoy, J. M. Shendel.** AIEE Transactions, volume 66, 1947, pages 1592–1602.

4. Line Conductors—Tidd 500-Kv Test Lines, **E. L. Peterson, D. M. Simmons, L. F. Hickernell, M. E. Noyes.** AIEE Transactions, volume 66, 1947, pages 1603–12.

5. Transformers and Lightning Arresters—Tidd 500-Kv Test Lines, **F. A. Lane, J. K. Hodnette, P. L. Bellaschi, Edward Beck.** AIEE Transactions, volume 66, 1947, pages 1613–8.

6. Switchgear Equipment for Tidd High-Voltage Test Lines, **F. A. Lane, B. W. Wyman.** AIEE Transactions, volume 66, 1947, pages 1619–23.

7. Some Transmission Line Tests, **W. W. Lewis.** AIEE Transactions, volume 40, 1921, pages 1079–1119; discussion, pages 1302–08.

8. Corona Loss Tests on the 202-Mile 60-Cycle 220-Kv Pit-Vaca Transmission Line of the Pacific Gas and Electric Company, **Roy Wilkins.** AIEE Transactions, volume 43, 1924, pages 1148–71.

9. The High-Voltage Wattmeter, **Philip E. Clark, Charles E. Miller.** AIEE Transactions, volume 43, 1924, pages 1125–9; discussion, page 1162.

10. Power Measurements at High Voltages and Low Power Factors, **Joseph S. Carroll, Thomas F. Peterson, George R. Stray.** AIEE Transactions, volume 43, 1924, pages 1130–8.

11. Fair Weather Corona Losses at 60 Cycles on Large Overhead Power Cables, **J. C. Clark, F. F. Evenson.** AIEE Transactions, volume 43, 1924, pages 1139–47; discussion, page 1162.

12. Corona Loss Between Wires at Extra High Voltages—II, **C. Francis Harding.** AIEE Transactions, volume 43, 1924, pages 1182–93; discussion, page 1194.

13. Corona Loss Measurements on a 220-Kv 60-Cycle 3-Phase Experimental Line, **Joseph S. Carroll, Leland H. Brown, D. P. Dinapoli.** AIEE Transactions, volume 50, March 1931, pages 36–43; discussion, page 43.

14. Corona Loss Measurements for the Design of Transmission Lines to Operate at Voltages Between 220 Kv and 330 Kv, **Joseph S. Carroll, Bradley Cozzens.** AIEE Transactions, volume 52, 1933, pages 55–62.

15. Corona Losses From Conductors of 1.4-Inch Diameter, **Joseph S. Carroll, Bradley Cozzens, Theo. M. Blakeslee.** Electrical Engineering (AIEE Transactions), volume 53, 1934, pages 1727–33; discussion, pages 460, 600, 1310.

16. Discussion, by **William S. Peterson** on Corona Loss Measurements for the Design of Transmission Lines to Operate at Voltages Between 220 Kv and 330 Kv, **Joseph S. Carroll, Bradley Cozzens.** AIEE Transactions, volume 52, 1933, pages 62–3.

Discussion

R. W. Atkinson (General Cable Corporation, Bayonne N. J.): The authors have produced another of the group of interesting and important instruments for measuring small power at high voltage and low power factor. The requirements for measuring losses on the Tidd installation are very drastic and their methods of meeting these may well be called "beautiful."

One of the most critical of the instrumentation problems is caused by the "power transfer" between the two outer phases of the flat-spaced line conductors. The authors indicate the magnitude of this problem and have shown the method used for caring for it. This discusser wishes to emphasize still further the magnitude of this problem. It appears that it will be the limiting factor in the possible accuracy of the measurements.

The problem of power transfer between phases is met with in loss measurements on insulated belted-type cables due to lack of complete symmetry. There it quite often has resulted in producing a negative power reading on one phase. But this is of very small magnitude in comparison to the present case where the authors show that this power transfer is as much as 100 times the power which is to be measured. That means that, in order to obtain an accuracy of 10 per cent in the desired measurement, the compensation for the power transfer must be accurate to one part in about 1,000.

It is somewhat difficult to understand how that accuracy of compensation can be obtained practically. Apparently the amount of the required compensation first must be calculated mathematically from the circuit

dimensions. This power transfer is only about 7 per cent of the capacitive kilovolt-amperes. Therefore determination of the power transfer to this degree of accuracy would seem no mean feat. After determination of the correct compensation the circuit adjustments to accomplish this degree of compensation also must be made to an accuracy of one part in 1,000. It appears rather likely that the power transfer will prevent attainment of accuracies of which the instrumentation otherwise would be capable of reaching. At higher voltages, where the loss to be measured (and therefore the requirement of accuracy of compensation for power transfer relatively less important) the presence of corona causes some increase of line capacitance and therefore an increase of power transfer which will be hard to calculate, thus making the power transfer problem a serious one even for considerably larger values of line loss.

The authors have stated that, because of symmetry, the middle phase will not be subject to power transfer. Of course, with complete symmetry this would be true—but will there be symmetry to one part in 1,000 in the capacitances? It would appear that even for the middle conductor the problem of power transfer may not be disregarded.

In the measurement at high voltage of dielectric losses in cables having low power factor it has become almost the universal practice to use a high-voltage air capacitor as the direct standard of comparison. This would seem even more important here where the power factor to be measured is still lower. The authors, indeed, do use this basis of a low-loss standard capacitor to the extent of considering that the line itself, for lower voltages, constitutes a capacitor of known small loss. They count that if there is good agreement between the calculated and measured losses in this lower voltage range, the same settings may be relied upon for the actual loss measurements at higher voltages. Perhaps this determination will turn out to be not a mere check but the actual basis of calibration.

In summary, exceedingly ingenious methods have been developed by the authors for making these difficult loss measurements. The burden of this comment is that certain of these problems seem even more critical than indicated by the authors and may require acceptance of a somewhat lower degree of accuracy than apparently counted upon.

T. F. Peterson (American Steel and Wire Company, Cleveland, Ohio): All of the papers on the Tidd 500-kv test lines are of tremendous interest and importance, and like the project itself undoubtedly will prove to be land marks in the history of high-voltage transmission. Sporn and his colleagues in this venture deserve great credit for having the courage and vision to begin this work.

In reading the paper by Tremaine and Lippert and in scanning the references, I was impressed by the fact that many of them were to papers and work done by students of the late Doctor Harris J. Ryan. I believe that a word of tribute to his memory is in order. I bow in humble recognition of the part that he played. All who had the privilege of being with him are of one accord in attesting to his genius and vision in the field of high-voltage transmission research and to the inspiration which he provided so graciously to literally hundreds of now outstanding engineers. Perhaps these discussions may be considered a memorial to him.

And now returning to this paper and drawing on my memory of work done at Stanford University some 25 years ago, I would like to offer two suggestions which may be of help to the authors.

In using the wattmeter method for measurement of losses at extremely low power factor, we found it necessary to insert phantom impedances between transformer and shielding so that there would be no potential difference or phase angle between shield and leads to the line. Errors may creep in due to impedances in the instruments and instrument circuits.

Secondly, I would point out that it may prove comparatively simple to determine the accuracy of measurements by inserting resistance of known value which, when carrying line current of measured value, should result in increased loss reading equal to the calculated value. This may prove to be a simple expedient to check over-all accuracy, shielding, and the like.

Abe Tilles (Pacific Gas and Electric Company, San Francisco, Calif.): Mention has been made of the need of separating insulator losses from total losses to obtain corona losses. Similarly insulator telephone and radio interference, which is in many cases much worse than corona interference, needs to be separated out from the total. It would be of interest if the methods of accomplishing these separations could be given in greater detail.

The inherent subtraction from the wattmeter of a relatively large arbitrarily adjusted in-phase wattage because of power transfer between phases raises some questions. Should not provision be made for getting the reading without this "correction," also? The 3-phase sum then might be obtained in a less manipulated manner.

In the course of these tests the effect of rain in producing alteration in radio and telephone interference is to be studied. One might expect, also, various shielding and masking effects of the rain or clouds in space upon the transmission of the interference produced. Is the test program set up to observe and separate these effects?

R. L. Tremaine: With reference to the discussion by Tilles, on the Tidd 500-kv tests, we are not particularly concerned with the telephone influence phase of the problem of transmission at extra high voltages. Electromagnetic and electrostatic effects of extra high voltage transmission lines on telephone circuits readily can be calculated. If desirable, we can make measurements on the low voltage side of the transformers of the change in the telephone influence factor with the presence of corona.

We plan to make measurements of corona loss and radio influence under changing weather conditions. It is quite possible that radio influence may prove to be the factor limiting the voltage that can be applied to a given conductor at a particular spacing, especially when the conductor is wet.

Tilles' comments in the second paragraph are discussed in detail in the author's comments on the discussion by Atkinson.

Radio influence measurements will be taken up to 400 megacycles. In this range of frequency, it is not expected that rain or clouds in space will have any effect upon the transmission of the interference produced. Rain and clouds in space have no effect upon the transmission of radio waves until frequencies in the order of radar frequencies are reached.

Atkinson has indeed "hit the nail on the head," so to speak, when he mentions the weakness of the power transfer compensation circuit. Before including this circuit in our measuring scheme, we considered its possible advantages and disadvantages in considerable detail. We finally decided to include it with the provision that it easily could be disconnected if not desired. The metering circuit is so set up that the power transfer circuit may be included or left out, so that measurements may be taken either of total 3-phase power without compensation, or of the corona loss with compensation. Which of these two methods will prove to be more accurate will be decided after we have had more experience with the lines.

Atkinson mentions the possibility of power transfer from the middle phase due to the possibility of the lines not being exactly symmetrical. While this effect may enter into the problem, a larger magnitude of power transfer can be expected from the middle phase of a particular line due to the presence of the other two lines. However, the power transferred from the middle phase is too small to be corrected for by a circuit such as is used on the two outside phases.

Atkinson is indeed correct in his guess that perhaps the measurement of the magnitude of the power transfer between outside phases will be the method used in calibrating the power transfer compensation circuits. This has been done.

The authors appreciate comments made by Peterson. We are aware of the possible error which may be introduced into our measurements by the effect of the capacitance of the measuring leads which run from the instruments to the conductors under test. A preliminary investigation of this effect has indicated that it is negligible on the two long lines. Further investigation will be made to determine this effect on the short line.

We appreciate Peterson's suggestion that a resistance of known value be inserted in series with the lines to introduce a known loss for the purpose of checking the accuracy of the measurements. We plan to do this in the very near future.

Transient Voltage Rise in Transformers Due to Interruption of Exciting Current

A. SRINIVASAN
ASSOCIATE AIEE

F. J. VOGEL
MEMBER AIEE

THE MAGNITUDE of switching surges, and their origin, has been the subject of many papers and much discussion, particularly on their effect on circuit breakers. Studies of voltage recovery rates to determine how to prevent voltage restriking in circuit breakers, lightning protector tubes, and other devices have been made. One very important source of overvoltages, that of sudden interruption of magnetizing currents of transformers, has not been given the detailed study it deserved because this possibility was not given due consideration. In this paper, it is shown because some circuit breakers can interrupt transformer magnetizing currents at any point in the current wave. Interruption does not always occur on current zero.

Calculations have been made in this paper to find the source of these overvoltages and to check experimental observation. It was found that a reasonable agreement could be obtained. Since the surge was initiated in the iron circuit, the voltage would be distributed nearly uniformly in the winding and therefore this type of switching would not lead to concentrations of voltage stress in the windings, except in case of terminal flashover.

These considerations are of importance in circuits where magnetizing currents are interrupted as for furnace transformers and special apparatus used intermittently.

General Procedure of the Investigation

The following procedure was adopted for this analysis. First a number of oscillograms of voltage and current during switching were taken on a 3-phase transformer installation where the design data were available. A study was made of the time in the cycle at which the circuit was interrupted in relation to the exciting current, the magnitude of the voltage rise, and the time within which the rise took place after the interruption. Second, from the magnetic properties of the iron core as given in a steel data book, the energy stored in the iron core was calculated. The instantaneous energy of all the three phases was calculated and from that the instant at which the total energy of all three phases was a maximum was determined. It is this total energy which is available to create voltage surges. Third, the transformer installation was reduced to a simple equivalent circuit consisting of inductance and capacitance. The inductance was calculated from the exciting current, and the capacitances were calculated assuming them to be lumped capacitances. From the simplified circuit, the natural frequency was calculated. Fourth, assuming that the time taken for the surge to reach its crest value is a quarter period of the natural frequency, the energy which was dissipated as eddy current loss was calculated. Fifth, the balance of the stored energy obtained after supplying the eddy current loss was considered to charge the capacitances such that $W_c = (1/2)CE^2$.

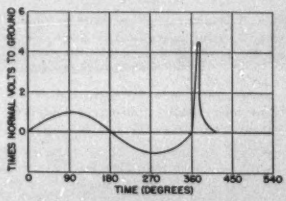

Figure 1. Oscillogram of the surge voltage

Description of Transformer Installation

The analysis was made for a transformer installation with three delta-delta-connected single-phase units rated as follows:

High voltage, 3,000 volts, 60 cycles, air cooled
Net area of cross section of the core = 24.6 square inches
Flux density in the core = 11,400 gauss

Laminations used were equivalent to United States Steel grade 52, 0.014 inch thick.

The high voltage winding consisted of 674 turns wound in four layers per coil, each layer having 84 and $84^1/_2$ turns, wound as rectangular coils. The insulation between layers 1 and 2 and between layers 3 and 4 was three layers of 0.010-inch mica. The insulation between layers 2 and 3 was three layers of 0.010-inch mica and 3/8-inch duct. The insulation between the high- and low-voltage windings was five layers of 0.010-inch mica and 3/8-inch duct.

Mean length of the iron circuit = 63 inches
Volume of the iron = 1,560 cubic inches
Weight of iron $= \frac{1,560}{3.69} = 423$ pounds (approximately)

Study of the Oscillograms

Figure 1 shows a typical voltage surge obtained from one of the oscillograms. The following are the observations made from the study of the oscillograms:

1. The maximum surge voltage occurred when the line exciting current was nearly

Paper 47-255, recommended by the AIEE transformer committee and approved by the AIEE technical program committee for presentation at the AIEE Midwest general meeting, Chicago, Ill., November 3–7, 1947. Manuscript submitted August 14, 1947; made available for printing September 24, 1947.

A. Srinivasan is with the Allis-Chalmers Manufacturing Company, Pittsburgh, Pa., and F. J. Vogel is research professor of electrical engineering, Illinois Institute of Technology, Chicago, Ill.

Acknowledgment is made to the Allis-Chalmers Manufacturing Company and their engineers for the test data and oscillograms. Also, acknowledgment is made to J. B. Hodtum (M '26) for his conception of placing the voltages obtained by switching on the same diagram with the flux in Figure 2.

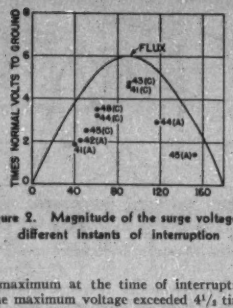

Figure 2. Magnitude of the surge voltage at different instants of interruption

a maximum at the time of interruption. The maximum voltage exceeded $4^1/_2$ times the normal voltage to ground.

2. The circuit could be interrupted at any instant during the cycle. The oscillograms were taken on all the phases when the circuit was interrupted. The instant at which the voltage surge occurred in each phase was determined from the oscillograms. As far as could be observed, the interruption took place simultaneously in all the phases, and the instant at which this occurred was plotted with reference to the flux density in each phase. Thus, in Figure 2, the resultant flux density in two phases is plotted, not to scale, assuming that it varies sinusoidally with time. Only one half cycle is shown. The magnitude of the surge voltage is also plotted against the same base of time. Therefore, the plot shows that the maximum voltage was produced in each phase when the flux density was a maximum. The numbers 41, 42, and so forth, on the figures are the results obtained from tests 41, 42, and so forth. Table I gives the time of interruption and the magnitude of the surge voltage.

3. The crest of the surge was reached in 1/1,600 second; the voltage dropped from its crest to zero with little oscillation. This front would be the equivalent of a quarter period of a 400-cycle wave.

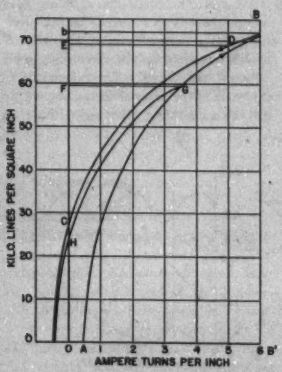

Figure 3. Magnetization curve of iron

Energy in the Magnetic Field

The energy required to change the induction density from the value B_1 to B_2 is given by the expression

$$\frac{1}{4}\int_{B_1}^{B_2} H \cdot dB \text{ in appropriate units from unit volume of the iron}$$

If a magnetization curve be drawn as in Figure 3, a magnetizing force OB is required to produce a flux density Ob. If the magnetic field is allowed to collapse by the interruption of the exciting current, it will be reduced to a residual field equal to OC. The average energy required to obtain a flux density Ob is proportional to the area of the portion $OABbO$. When the field collapses, the path of the flux is along BC due to the hysteresis of the iron. Hence the energy corresponding to the area $BbCB$ only will be available for transfer.

The total energy in the entire bank of transformers is that of all three phases. Since the exciting currents in the three phases are out of phase with each other by 120 degrees, the maximum energy in each phase will differ by 60 degrees. The instantaneous energy per unit volume of the iron is $B^2/_8\pi\mu$, in appropriate units. The values of B and μ are both changing and hence the energy has to be computed point by point. These values are listed in Table II. Figure 4 shows the magnetizing force at all various instants. Figure 5 shows the energy stored in each of the three phases plotted against time and also the sum of the instantaneous energies for all three phases. From the figure it appears that in the region of time interval between 60 degrees and 90 degrees the total energy is a maximum. However, at the instant corresponding to 90 degrees, two phases have equal energies and the third phase contributes a small amount of energy. Hence it could be assumed to simplify calculations that at the instant when the total energy is a maximum, two phases have equal energies and the third phase has no energy. If the circuit is interrupted, at that instant, the magnetizing force of one transformer will be increasing while that of the other is decreasing. Therefore, the flux density of the increasing phase would be OF and that of the decreasing phase would be OE in Figure 3.

Table I. Magnitude of the Surge Voltage at Various Instants of Interruption

Test No.	Phase	Time of Interruption, Deg	Voltage to Ground Times Normal
41	A	40	1.8
41	C	90	4.5
42	A	45	2.0
43	C	90	4.65
44	A	117	2.9
44	C	60	3.25
45	A	152	1.5
45	C	50	2.5

The energy stored and available for transfer in the magnetic fields of the two phases is different since it is proportional to the area enclosed between the hysteresis loop and Y-co-ordinate axis. Thus, if the circuit is interrupted at the point D, (Figure 3) the magnetic field collapses along the curve descending from D to C. The energy given up due to collapse is given by the area $DECD$. At the same time the other phase is interrupted at G when the magnetizing force is decreasing. After the interruption, its magnetic field collapses following the curve GH. The energy given up by this transformer is proportional to the area $GFHG$.

The available energy in joules per cubic inch of iron is equal to the two areas, the co-ordinates of which are kilolines per square inch and ampere-turns per inch. Thus the area of $CDEC$ from Figure 3 is 5.45 square inches and of $HGFH$ is 3.25 square inches. The scale for Figure 3 is 1 inch for 1.33 ampere-turns per inch and 1 inch for 10 kilolines per square inch. The energy available is (5.45+3.25) 1.33 $\times 10^{-4} \times 1560$ or 1.81 joules for these two phases.

Determination of the Capacitance

It is well known that transformers have distributed capacitance between winding and core, between layers of the windings, and between turns. The capacitance between turns is small and is neglected in this analysis. The several turns in each layer being in series, there is a potential gradient along the length of the layer. At the end of the layer where the connection is made to the next layer, the potential difference between the layers is zero. The voltage at the other end of the layer is twice the voltage per layer. The electrostatic flux distribution varies uniformly along the length of the layer. However, it is assumed as an approximation that the effective capacitance between two layers is half the capacitance between the layers considered as plates.

Neglecting the effects of fringing and other irregularities in the flux distribution, the capacitance is calculated from the formula

$$C \text{ in micromicrofarads} = \frac{0.22 \times A \times K}{d} \quad \text{inch units}$$

Therefore the effective capacitance between any two layers is

$$\frac{0.11\times A\times K}{d} \text{ micromicrofarads}$$

Thus the capacitance between layers 1 and 2 is

$$C_{12}=\frac{0.11\times 681\times 6}{3\times 0.01}=1.5\times 10^4 \text{ micromicrofarads}$$

Similarly the capacitance between layers 2 and 3 is

$$C_{23}=0.1\times 10^4 \text{ micromicrofarads}$$

and the capacitance between layers 3 and 4 is

$$C_{34}=1.65\times 10^4 \text{ micromicrofarads}$$

The low voltage winding is assumed to be at ground potential for the following reasons: The voltage of the low voltage winding being very small, the energy required to charge its capacitance is negligible and its voltage to ground is also negligible when compared to the high voltage winding.

Considering the capacitance C_g between the high voltage winding and ground, it would be very nearly the same as that obtained in the case of a plate capacitor. Using the same formula as before, it was found that

$$C_g=0.036\times 10^4 \text{ micromicrofarads}$$

Thus in Figure 6*a* is shown the arrangement of the different capacitances. The voltage across C_{12}, C_{23}, and C_{34} of each leg is 1/4 of the voltage across the entire winding on both legs. If C is the effective equivalent capacitance between the four layers in each leg, then on the basis of energy considerations

$$C\left(\frac{E}{2}\right)^2=C_{12}\left(\frac{E}{4}\right)^2+C_{23}\left(\frac{E}{4}\right)^2+C_{34}\left(\frac{E}{4}\right)^2$$

$$\therefore C=\frac{1}{4}(C_{12}+C_{23}+C_{34})$$

$$=0.81\times 10^4 \text{ micromicrofarads}$$

Figures 6*b* and 6*c* are derived from Figure 6*a* by combining the two capacitances C_g and replacing C_{12}, C_{23}, and C_{34} by C. Figure 6*d* shows the equivalent circuit for the delta-connected transformer bank.

Under the conditions when there was maximum energy, it was found that the energy in two phases was nearly equal and that the third phase did not contribute appreciable energy to the circuit. Then the two phases may be considered to act in parallel and thus Figure 6*e* was obtained. Figures 6*f*, 6*g*, and 6*h* are successive developments of the equivalent circuit leading to the final form in Figure 6*i*

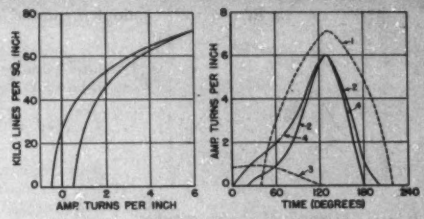

Figure 4. Magnetizing force at different instants of time

where there is only one inductance connected in parallel with one capacitance C_e. For this case

$$C_e=(3.54+.048)\times 10^4 \text{ micromicrofarads}$$

Determination of the Frequency

The inductance of the circuit is not constant since the magnetization curve is not a straight line. However, for the case

Table II. Energy in the Iron at Different Instants

Time, Deg	Flux Density B, Kilogauss	Permeability	Energy Per Cu Cm $B^2/8\pi\mu$	Energy in Joules Per Cu In.
0				
30	4.65	7,000	122	2×10^{-4}
60	7.0	5,300	366	6×10^{-4}
90	8.9	4,300	732	12×10^{-4}
120	10.8	4,240	1,098	18×10^{-4}
130	11.3	4,200	1,220	20×10^{-4}
150	10.4	6,000	732	12×10^{-4}
180	0	0	0	0

under examination, it was found from the several oscillograms taken that the frequency was about 400 cycles per second and this value was taken to be the surge frequency for the calculation of the eddy current losses.

The rms value of the exciting ampere-turns was obtained from Figure 3. The maximum flux density was 73,000 lines per square inch. Thus the ampere-turns per inch at this flux density are about 6.5 and the rms value would be $6.5/\sqrt{2}=4.6$; hence the exciting current is

$$\frac{4.6\times 63}{674}=0.43 \text{ amperes}$$

The equivalent exciting inductance of each transformer would be

$$\frac{3{,}000}{0.43\times 377}=18.6 \text{ henrys}$$

The equivalent inductance shown in Figure 6*i* is the resultant of two transformers in parallel. Therefore the equivalent inductance in parallel with the capacitance to produce oscillations is one-fourth of the total inductance of two transformers in parallel or one-eighth of the exciting inductance of each transformer. Therefore the equivalent inductance is parallel with C_e is $18.6/8=2.325$ henrys. The natural frequency of this L-C circuit would be

$$f_d=\frac{\times 1}{2\pi\sqrt{LC}}\frac{1}{2\sqrt{2.325\times 0.0329\times 10^{-6}}}$$

$$=575 \text{ cycles per second}$$

Determination of the Losses

The losses in the core depend upon the frequency and the flux density. Since both of these are variable, the true representation of losses as an equivalent resistance is complicated. However, the losses can be estimated separately as eddy current and hysteresis losses and this appears to be the simplest procedure. The hysteresis loss already has been taken into account when the areas *HGFH* and *CDEC* were obtained. Hence the eddy current loss only has yet to be calculated.

Whenever magnetic flux is changing in a core, there is an induced electromotive-force in the core material. This electromotive-force sets up the circulating eddy currents and losses. The frequency in this case is the natural frequency set up by the inductance and capacitance in

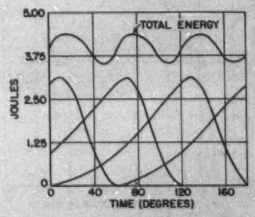

Figure 5. Energy in the magnetic field

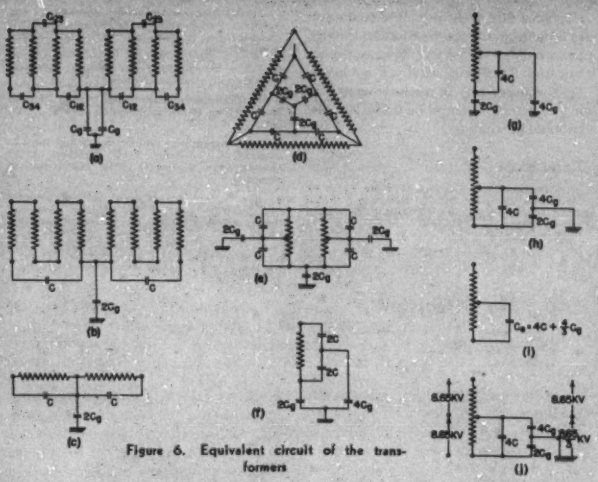

Figure 6. Equivalent circuit of the transformers

parallel. Since the inductance of the circuit changes rapidly as the energy stored in it is dissipated, the wave shape of the oscillation is not a sine wave. However, as an approximation it was assumed that during the 1/4 cycle while the surge crest is being reached, the wave shape was sinusoidal. The frequency as measured from the oscillograms was 400 cycles.

The flux in the core drops so that the residual flux density is reached in a quarter period of the natural oscillation. The instantaneous eddy current loss per unit volume of the core is

$$\frac{t^2}{12\rho}\left(\frac{dB}{dt}\right)^2$$

The change in flux density is the difference between the flux density at the time of interruption and the residual flux density, and it is assumed to vary sinusoidally. Therefore the average eddy current loss per unit volume is

$$\frac{\pi^2 f^2 t^2}{6\rho}(\Delta B)^2$$

in appropriate units.

The natural frequency was 400 cycles per second. $t=0.014$ inch. Specific resistivity $=25.6$ microhms per inch cube. At the time of interruption, the flux density in one transformer was 69×10^3 lines per square inch and it decayed to 27.5×10^3 lines per square inch. The change of flux density, ΔB, was 41.5×10^3 lines per square inch, as shown in Figure 3.

The eddy current loss in the first transformer was

$$\frac{\pi^2\times400^2\times0.014^2\times41.5^2\times10^6}{6\times10^{16}\times25.6\times10^{-6}}=$$

0.347 watt per cubic inch

The second transformer has a change of flux from 59.5×10^3 lines per square inch to 24.5×10^3 lines per square inch. Thus the change of flux density was 35×10^3 lines per square inch. The eddy current loss in the second transformer was

$$\frac{\pi^2\times400^2\times0.014^2\times35^2\times10^6}{6\times10^{16}\times25.6\times10^{-6}}=$$

0.246 watt per cubic inch

The energy lost in both the transformers as eddy current loss in 1/4 cycle or 1/1,600 second was

$$W_e=\frac{(0.347+0.246)1600}{4\times400}=0.579 \text{ joule}$$

Energy to Charge the Capacitances

Out of the total energy W_T available in the magnetic circuit, the energy W_e is spent as eddy current loss and the balance

$$W_T-W_e=W_c$$

is the energy available to charge the capacitances. The energy required to charge a capacitance C to a potential is

$$W_c=1/2CE^2$$

whence

$$E=\sqrt{\frac{2W_c}{C}}$$

The total energy available from the magnetic circuit was $W_T=1.81$ joules. The energy spent as eddy current loss was 0.579 joule. Hence the energy available to charge the capacitance C_c would be $1.81-0.579=1.231$ joules. The effective capacitance C_c was calculated to be 0.0329 microfarad.

Therefore

$$E=\sqrt{\frac{2\times1.231\times10^6}{0.0329}}=8{,}650 \text{ volts}$$

From Figure 6*j* it can be seen that the potential of one transformer was $(4/3)\times8.65=11.53$ kv. The normal voltage to ground was $3{,}000\times\sqrt{2}/\sqrt{3}=2{,}450$ (crest). Therefore

$$\frac{\text{Crest value of surge volts against ground}}{\text{Crest value of normal volts against ground}}=\frac{11.53}{2.45}=4.7$$

The oscillograms show that this ratio is about 4.5.

The case analyzed is not the worst condition, and more severe conditions can occur due to the following reason. The analysis was done on the assumption that at the instant the circuit was interrupted, the exciting current was in a steady state. If, however, the interruption took place when there was an in-rush current, the magnitude of the surge voltage would be larger. The magnitude of the in-rush current would be several times the normal exciting current and consequently there would be an increase in the magnetizing force. A larger magnetizing force would produce a larger amount of stored energy in the core. Though the energy available does not increase proportionately with the magnetizing current due to saturation, yet the consequent rise in voltage may be higher than that obtained under steady state conditions.

Voltages as high as seven times normal instead of $4^1/_2$ were obtained under these conditions. With the secondary loaded, the switching surge would not produce as high a voltage, because a portion of the energy would be dissipated in the load.

Conclusions

The interruption of the exciting current in a transformer or any iron-cored circuits produces a transient rise in voltage. Such cases often happen in practice, especially in arc furnace transformers. The magnitude of this voltage can be several times the normal voltage against ground and unless adequate insulation is provided, it may cause a failure of the insulation. The method outlined in this

paper is simple and a fairly close approximate calculation of the rise in voltage may be made by means of this method.

Since the rise in voltage is fixed by the effective capacitance, it appears that the smaller the capacitance, the greater will be the voltage rise. Hence, a set of external capacitances connected to the terminals of the transformers will increase the effective capacitance and thereby reduce the voltage rise.

Since the voltage rise is caused by the change of flux in the iron, it should result in a uniform voltage distribution through the winding. Most switching surges result from flux linking windings and hence, the conclusion may be reached that switching surges are likely to be uniformly distributed in windings.

References

1. The Cause and Control of Some Types of Switching Surges, **T. W. Schroeder.** AIEE Transactions, volume 62, 1943, November section, pages 696–700.

2. High-Potential Testing Equipment for Quantity Production, **C. M. Summers.** AIEE Transactions, volume 60, 1941, June section, pages 289–92.

3. U.S.S. Electrical Steel Sheets, Technical and Descriptive Bulletin Number 2.

4. Electromagnetic Devices (book), **H. C. Roters.** John Wiley and Sons, New York, N. Y., 1941.

5. Some Aspects of Inductance When Iron Is Present, **L. T. Rader, E. C. Litscher.** AIEE Transactions, volume 63, 1944, March section, pages 133–9.

6. Electrical Measurement and Measuring Instruments (book), **E. W. Golding.** Sir Isaac Pitman and Sons, London, England, 1939, page 487.

No Discussion

A Control System for Wind Tunnel Drives

ALLAN H. HEIDENREICH
FELLOW AIEE

THE majority of the existing large wind tunnels designed for subsonic research have what is known as the Clymer type of drive, the principal elements of which consist of a constant-speed motor-generator set, a variable-speed motor-generator set, and a wound-rotor induction motor.

The function of the drive is to provide power at variable speed for the fans or axial-flow compressors which create the wind velocities in the tunnel. The speed range through which the drive motor must operate may be as great as 80 to 1 and the control must be such as to hold any speed in the range constant within the limits of ±1/4 of 1 per cent of full-load speed. Considerable auxiliary equipment is necessary to control speed, prevent hunting, limit the current interchange between the d-c machines of the constant-speed and variable-speed sets, provide constant d-c base voltage, and hold constant power factor.

The Clymer Drive and Control

The National Advisory Committee for Aeronautics at its flight propulsion research laboratory in Cleveland, Ohio, utilizes the Clymer type of drive for the operation of the altitude wind tunnel. The drive, shown in Figure 1, is a good example of this type of power application and for convenience will be used for this discussion. The 4-unit constant-speed set consists of a 4,800-kva synchronous machine *A*I and two d-c machines *DI*(*A*) and *DI*(*B*) together with *EXC.A*II. The variable-frequency motor-generator set is composed of a 12,000-kva synchronous machine *A*II and two d-c machines *DII*(*A*) and *DII*(*B*). The main or fan drive motor is of the wound-rotor type, 19,700-horsepower at a synchronous speed of 450 rpm. However, the top speed required by the tunnel is 410 rpm.

Probably the best approach to give a general idea of the operation of the drive is to go through the procedure of putting it on the line.

Consider all the small auxiliary units as being in operation. They are as follows:

1. Amplidyne *EXC.DII* providing excitation for d-c machines *DII*(*A*) and *DII* (*B*)
2. Constant potential exciter *CP* supplying energy to the 250-volt constant potential bus
3. Amplidyne exciter 88*AM-E* and the electronic voltage regulator controlling the voltage of the constant potential exciter *CP*
4. Amplidyne *EXC.DI* providing excitation for d-c machines *DI*(*A*) and *DI*(*B*)
5. Amplidyne exciter 88*AM-A*II controlling the voltage of *EXC.A*II thus regulating the field on the a-c machine *A*II of the variable-frequency motor-generator set
6. D-c generators 88*L-DI* and 88*L-DII* regulating the voltage of *EXC.DI* and *EXC.DII* to limit current in the loop circuit

Oil circuit breakers 6*A*I, 42*A*I, *MC*I, *MC*II, air circuit breaker 72, together with contactors C_1, C_2, C_3, and C_4 are all in the open position and the drive is ready to start. It might be well to mention here that the entire operation of starting and stopping is done automatically by means of relays controlling the sequence in which the units function.

When the starting button is pressed circuit breaker 6*A*I closes and the 4,800-kva synchronous machine of the constant-speed set starts at reduced voltage. When it approaches synchronous speed and the initial inrush has subsided, a current relay applies field to the motor through contactor C_4. After the transient disturbance caused by application of the field has disappeared, line circuit breaker 42*A*I closes and circuit breaker 6*A*I drops out. Air circuit breaker 72 is next to close, completing connections through the loop circuit connecting d-c generators *DI*(*A*) and *DI*(*B*) with motors *DII*(*A*) and *DII*(*B*). Air circuit breaker 72 is provided with interlocking to operate contactors C_1, C_2, and C_3, which immediately close when air circuit breaker 72 closes, thus providing excitation to machines *DI*(*A*), *DI*(*B*), *DII*(*A*), *DII*(*B*), and *A*II. D-c generators *DI*(*A*) and *DI*(*B*) drive d-c motors *DII*(*A*) and *DII* (*B*), and all are connected in alternate series.

The variable-frequency motor-generator set now starts to accelerate and since the speed adjusting rheostat 70*S* is in the position calling for maximum speed of the variable-frequency motor-generator set, this set will come up to approximately 60-cycle speed under the control of the electronic speed regulator. During this period the synchronous machine *A*II is supplying a-c excitation to the rotor circuit of the fan drive motor, which, not being connected to the supply circuit, is stationary, and the rotor circuit induces a revolving magnetic field in the stator of this machine. The action here is exactly the same as that taking place in a transformer. By varying the speed and excitation of the synchronous generator, the frequency and voltage of the supply system can be matched. Generator and line then are synchronized automatically and circuit breakers *MC*I and *MC*II are closed thus placing the drive motor on the supply circuit. Since the rotating fields in the rotor and the stator of the motor are rotating in the same direction at the same speed with no phase displacement, there is no slip, and consequently no torque in the fan motor shaft, which remains stationary. Therefore, in placing the drive motor on the line the greatest disturb-

Paper 47-251, recommended by the AIEE industrial control committee and approved by the AIEE technical program committee for presentation at the AIEE Midwest general meeting, Chicago, Ill., November 3–7, 1947. Manuscript submitted May 8, 1947; made available for printing August 24, 1947.

ALLAN H. HEIDENREICH is electrical consultant with the National Advisory Committee for Aeronautics, Cleveland, Ohio.

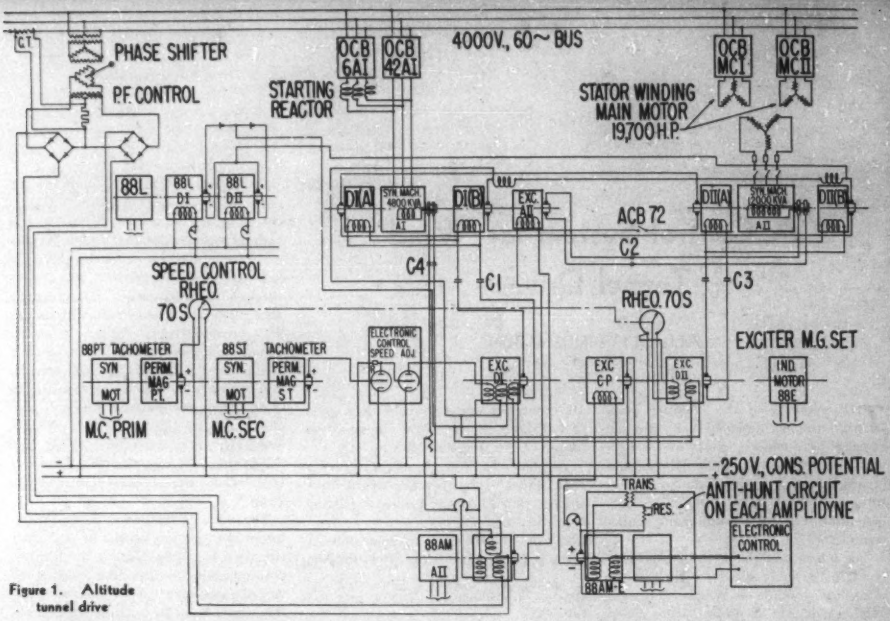

Figure 1. Altitude tunnel drive

ance that can be caused, is that caused by the initial inrush taken by the 4,800-kva synchronous motor on the constant-speed set, and this inrush does not exceed the 5,300-kva limit set by the Cleveland Electric Illuminating Company as a maximum at that time.

To get power into the fan and obtain wind velocity in the tunnel, the drive motor shaft must rotate. This is done by gradually slowing up the speed of the variable-frequency set through electronic speed controls, thereby lowering the frequency in the rotor of the fan motor. The speed at which the fan rotates then will correspond to the difference in frequency between the 60 cycles of the supply circuit and the frequency of the fan motor rotor circuit. It can be noted readily from the foregoing, that any speed of the fan motor shaft through the operating range can be obtained in as small increments or fractions of cycles as desired.

The tunnel is now in operation at the predetermined wind velocity required for the particular research analysis program and it must be held there within a range of ±1/4 of 1 per cent.

To take the drive out of service, it is necessary to push only the stop button and automatic relay operation takes care of the rest, this being merely a reversal of the sequence as outlined for starting.

This tunnel is designed to produce atmospheric and temperature conditions up to 30,000 feet altitude, namely, about 1/3 of an atmosphere and −48 degrees Fahrenheit. To do this requires 7,000 horsepower in exhausters and 23,000 horsepower in refrigeration. The total kilowatt demand of the tunnel drive and these auxiliaries is approximately 40,000.

The foregoing is purely a description indicating the function of the drive and its operation. Details of control, protection, the functioning of the constant-speed and variable-frequency sets, and the power pump back into the supply system, will be taken up in the following order:

(*a*). Operation of constant-speed and variable-frequency sets.

(*b*). Speed control.

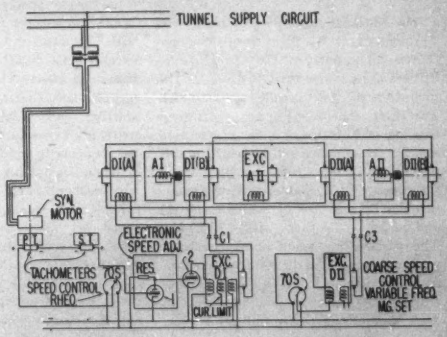

Figure 2. Speed control

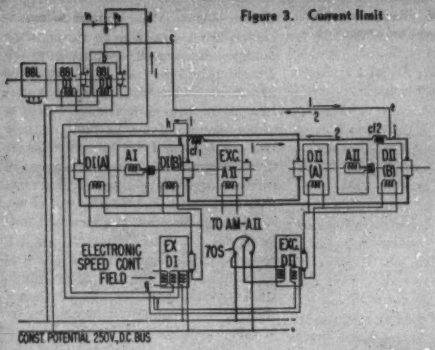

Figure 3. Current limit

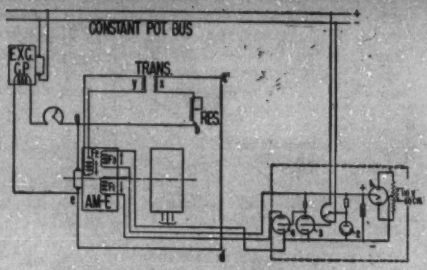

Figure 4. Antihunt electronic voltage regulator

(*c*). Current limit in the loop circuit

(*d*). Antihunt provisions.

(*e*). Constant-voltage d-c bus.

(*f*). Holding of constant power factor.

(*g*). Pump back into power system.

Operation of Constant-Speed and Variable-Speed Sets

During the starting period of the drive, the constant-speed set is driven by the 4,800-kva synchronous machine operating as a motor, the two d-c machines on the same shaft operating as generators and supplying energy through the loop circuit to the two d-c machines acting as motors on the variable-frequency set and driving the a-c machine feeding into the drive motor rings. However, when power is being delivered to the fan, conditions are reversed. The a-c machine on the variable-frequency set then becomes a motor driving the two d-c machines on the same shaft as generators supplying current through the loop circuit in the opposite direction to drive the two d-c machines of the constant-speed set. These d-c machines now act as motors instead of generators and drive the a-c machine on the same shaft as a generator, thus supplying energy or pumping back into the supply lines.

Speed Control

All references apply to Figure 2.

It is very important that the tunnel drive motor speed be held practically constant at any speed selected during a research analysis period. It must be within ±1/4 of 1 per cent or the test results probably will be valueless. To accomplish this, rheostat 70*S* which consists of two plates on the same shaft, one in the tachometer circuit and regulating through a field of *EXC.DI* and the other in a field circuit of *EXC.DII*, is set for the speed required for the test. The coarse or approximate speed control is governed entirely by *EXC.DII* through excitation to d-c machines *DII*(*A*) and *DII*(*B*). *EXC.DI* through excitation to machines *DI*(*A*) and *DI*(*B*) provides what might be termed vernier control to govern the speed of the drive motor within the 1/4 of 1 per cent limits previously stated.

Assume that the drive motor now is running at the approximate speed for test purposes and it is desired to regulate within narrow plus or minus limits. Two tachometers or d-c generators, calibrated to give exactly the same voltage when operated at the same speed, are connected in series opposition as shown. One tachometer *PT* is driven by a synchronous motor connected to the 60-cycle supply circuit while the other *ST* is attached to the shaft of the variable-frequency motor-generator set. It readily can be noted that the voltage of tachometer *PT* driven by the synchronous motor from the 60-cycle source of supply will remain constant while the voltage of tachometer *ST* connected to the shaft of the variable-frequency set will vary as the speed of the set varies. The function of tachometer *PT* is to compensate for frequency fluctuations in the supply circuit. These two tachometers are connected in series and oppose each other. The voltage difference then is compared to a portion of a carefully regulated reference voltage, and the resulting voltage is applied to the grid of a control tube in the regulator. Assume the speed of the fan drive motor to vary slightly above that for which the setting has been made. Tachometer *ST* on the variable-frequency motor-generator set shaft then will be running too slow and its voltage will drop, making the grid of tube 1 more negative, and hence the grid of tube 2 becomes more positive and allows tube 2 to pass more current. This will increase the current flow through the control field of amplidyne *EXC.DI* raising its terminal voltage, causing an increase

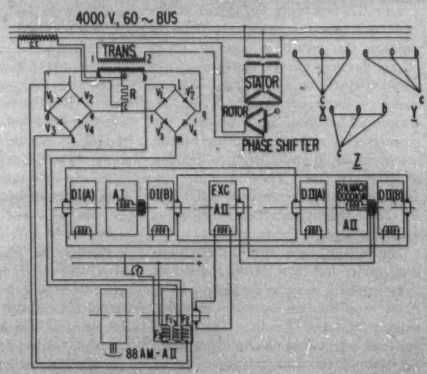

Figure 5. Holding constant power factor

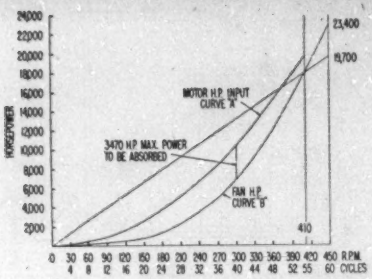

Figure 6. Power pump back at one-third atmosphere

in excitation of machines $DI(A)$ and $DI(B)$, thereby raising their terminal voltages and increasing the speed of the variable-frequency motor-generator set, which in turn will decrease the speed of the fan drive motor.

If the speed of the fan drive motor should fall slightly under that for which it was set, then the voltage of tachometer ST will rise, resulting in a more positive polarity of the grid in tube 1 of the electronic speed adjuster; this will decrease the flow of current through tube 2 and will decrease $EXC.DI$ control field and drop its terminal voltage, thus decreasing the excitation of machines $DI(A)$ and $DI(B)$ and their terminal voltage will fall, thereby decreasing the speed of the variable-frequency motor-generator set and causing the speed of the fan drive motor to increase. This combination of electronic amplifiers and amplidynes produces an amplification of the tachometer signal of several thousand to one, thus providing the extreme sensitivity of control required.

Current Limit in the Loop Circuit

All references apply to Figure 3 which illustrates this item alone. In order to prevent the maximum current interchange between the d-c machines of the constant-speed and variable-frequency motor-generator sets from exceeding safe commutating limits, use is made of the commutating and compensating field in machines $DI(B)$ and $DII(B)$ to function as drop resistors. These windings are indicated on the diagram as CF_1 and CF_2. To clarify the diagram they are shown as existing outside of the machines.

The voltage across each of these windings, under full loop circuit current of 3,000 amperes, is approximately 9 volts. These drop voltages are added in series, making a total of 18 volts. The path of one lead is to a field of amplidyne $EXC.DI$, through the field and terminates at point a. The other lead terminates at point b and there is, therefore, 18 volts drop across these points when maximum current is flowing in the loop circuit. Motor generator set $88L$ consists of a motor driving two small d-c voltage-reference generators $88L\text{-}DI$ and $88L\text{-}DII$. Each generator has an adjustable electromotive force of 18 to 24 volts. The generators are connected in series through a loop circuit containing two rectifiers V_1 and V_2, which are also in series. The current can flow only in the direction of the arrow shown in the rectifier symbol. The point a is shown between the rectifiers and the point b is the midpoint of the series connection between the generators $88L\text{-}DI$ and $88L\text{-}DII$.

Consider current flowing in the direction of arrow 1 in the loop circuit indicating that the d-c machines on the constant-speed set are functioning as generators, while those on the variable-speed set are acting as motors. Starting at k in the control circuit and tracing through the diagram, the path is as follows: from k to g where the circuit divides and goes through the fields of $EXC.DI$ and $EXC.DII$ in parallel to the junction f; from this point the path is to d and a. At a the flow normally would divide, part going through generator DI and part through generator DII; however, the rectifier V_2 serves as a block in the DII branch so that the flow can be only through the DI branch to the junction b between the generators, and then through the circuit ce to j, the terminal.

The direction taken through the amplidyne $EXC.DI$ field is such as to oppose the flux produced by its control field; hence, the voltage of this exciter drops, decreasing the excitation to machines $DI(A)$ and $DI(B)$ and lowering the voltage of these generators. The direction of the current through the amplidyne $EXC.DII$ field, is such as to supplement the flux of its control field and thus the voltage of this exciter will increase and thereby increase the excitation to machines $DII(A)$ and $DII(B)$, raising their voltage. As a result, the voltage of the generators and the internal voltage of the motors approach each other. The current in the loop circuit is, of course, a direct function of the difference of these two voltages, and as this difference is decreasing, the loop circuit current will decrease and be held to the predetermined maximum as a limit.

When the direction of the current flow in the loop circuit is from the variable-speed set to the constant-speed set, it is apparent that the control is the same. Under such a condition however, machines $DI(A)$ and $DI(B)$ functioning as motors will have their voltages raised, while $DII(A)$ and $DII(B)$ acting as generators will have their voltages reduced, just the opposite of the conditions prevailing when the direction of the current flow in the loop circuit was from the constant-speed set to the variable-speed set.

Antihunt Provision

Each of the amplidynes is provided with an antihunt field. All references

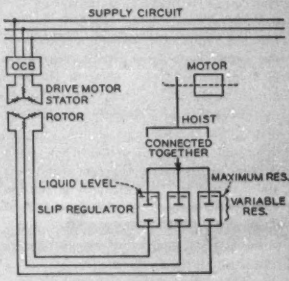

Figure 7. Slip regulator speed control

apply to Figure 4; however, this diagram also will serve to illustrate the operation of the electronic regulator to hold the voltage of the constant-potential d-c bus fixed.

Amplidyne $AM\text{-}E$ has buck and boost fields, F_1 and F_3, plus an antihunt field F_2.

The circuit $abcde$, containing a variable resistor and one winding of a transformer connected in series, is shunted across the brushes of the machine. The antihunt field F_2 has the other winding of the transformer connected in series with it. If there are no rapid fluctuations in the voltage of the exciter, a direct current flows through the variable resistor and winding

x of the transformer in circuit *abcde*, while there is no flow at all in the F_2 field circuit containing the y winding of the transformer.

Assume now that the machine begins to hunt. There then will be a rapid fluctuation of the voltage, which, due to the rate of change of lines of force, will induce a corresponding voltage in the y winding of the transformer. This voltage will be opposite in direction to the one in the x winding and the current generated will pass through the F_2 field in a direction to neutralize any change in voltage from a steady state condition, thereby preventing hunting of the machine.

Constant-Voltage D-C Bus

The accuracy of control of the drive depends to a great extent upon holding a reference voltage constant within very close limits. The essential elements in obtaining this constant potential are shown in Figure 4. A 100-volt 60-cycle supply is rectified by tube 1, filtered, and impressed across voltage regulator tube 2 and a series resistor. The constant voltage across tube 2 is compared with a portion of the voltage to be regulated, and this difference is applied to the grid of tube 3. This tube is in series with an anode resistor, and its anode potential is applied to the grid of tube 4. The output of tube 4 is put through the buck field of amplidyne *EXC.AM-E*. The boost field of amplidyne *EXC.AM-E* is connected to the rectified voltage from tube 1. Thus, any change in the voltage being regulated will affect the current through the buck field of the amplidyne and result in a voltage regulation of ±0.04 per cent or 0.1 volt in 250.

Constant Power Factor

It is necessary that a high power factor be maintained on the large wind tunnel loads, and at the Flight Propulsion Research Laboratory it is held approximately at 95 per cent.

Figure 5 illustrates the manner in which this is accomplished. A phase shifter is connected to the supply circuit. This consists of a 3-phase wound-rotor motor, the rotor of which is provided with a hand wheel and a latch, for it is necessary to lock the rotor in any desired position. Leads are brought out from one phase of the rotor winding only and connected to a transformer at points 1 and 2. The secondary of this transformer a–b is tapped at o, the midpoint of the winding. A resistor R is inserted in o–c and the leads from a current transformer in the supply circuit are connected across it. There is produced, therefore, a voltage which is a function of the line voltage, and a voltage which is a function of and in phase with the line current, illustrated in vector diagram X.

These functions of line voltage and current voltage, a–b and o–c, respectively, are the components necessary for power factor control. If the rotor of the phase shifter is rotated, it is apparent that the phase relation of a, b, and c can be changed to any degree desirable as shown in vector diagrams Y and Z. However, in so doing, the voltages a–c and b–c no longer will be equal and constant power factor is maintained as described hereinafter. It must be borne in mind that after the rotor of the phase shifter is once set, it is locked in position, thereby fixing the voltage component and not changed until another power factor value is to be held constant. The current–voltage component, however, is free to swing in either direction from o as center because the phase relation between current and voltage changes with varying-load power factors. Also, the length of the current–voltage vector changes with the magnitude of the amperes in the circuit. If the power factor falls below the setting, then the voltage across d and e will be greater than that across f and g in the relation of a–c to c–b as shown in vector diagram Y. Starting at a and going to junction d, the current cannot divide at d because of the block of rectifier V_3, and can continue only through V_1 to j; then, because of the block by rectifier V_2, from j the path is through field F_2 of amplidyne 88*AM-A*II and back to junction k, where it passes through rectifier V_4 to c. Starting from c and tracing through the path of the current from c to b, at the junction f the flow must be through rectifier V_1' because V_3' is in block, and since V_2' is also in block, the flow is from L through amplidyne field F_1 and back to m, through rectifier V_4' to g, the other terminal of the electromotive force. Amplidyne fields F_1 and F_2, oppose each other and since the voltage a–c is greater than the voltage b–c, more current will flow through field F_2 than through field F_1, and the difference of these fluxes will supplement the flux of the reference field F_3, increasing the excitation of *EXC.A*II and raising its terminal voltage, thereby increasing the field strength of the 12,000-kva synchronous machine of the variable-speed set and raising the system power factor.

If, under light load condition, the power factor becomes too high, the voltage c–b then becomes greater than a–c as shown in vector diagram Z, more current will flow through amplidyne field F_1 than through F_2, and the differences of their fluxes will decrease the flux of the reference field F_3, decreasing the excitation of amplidyne 88 *AM-A*II, thus lowering the terminal voltage, which in turn decreases the excitation of *EXC.A*II, causing its terminal voltage to fall and to decrease the field current in the 12,000-kva synchronous machine of the variable-speed set and lowering the system power factor. It is apparent from the foregoing that the control will hold the power factor constant under all operating conditions.

Power Pump-Back Into the System

All references apply to Figure 6.

In selecting the size of drive motors for the various types of tunnels, the research engineers determine the maximum fan speed and horsepower required to obtain the wind velocity for which the tunnel is to be designed. These are data for only one point on the power curve from which to construct a diagram similar to Figure 6. This diagram shows the horsepower required by the fan over the entire range of speed, curve B, together with a curve A showing total electrical and mechanical input to the motor; that is, the power required by the fan plus the energy either to be absorbed or pumped back into the system. The constant torque horsepower line drawn from the origin through the point 18,000 horsepower and 410 rpm, and projected to meet the synchronous-speed ordinate of 450 rpm, determines the rating of the motor which will be required and which is shown to be 19,700 horsepower.

The difference in ordinates between

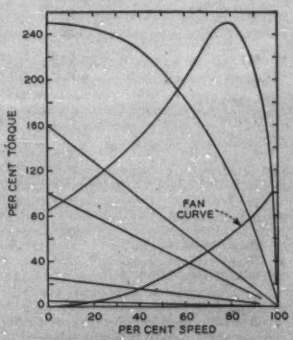

Figure 8. Speed–torque curves of a typical wound-rotor motor and fan load

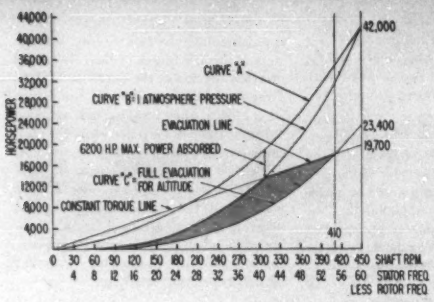

Figure 9. Power pump back at one atmosphere

curves A and B represents the horsepower either to be pumped back into the system or to be dissipated in the form of heat. The calculations to determine the general equation for maximum energy pump back for a fan load are shown in the next section.

Maximum Power Pump-Back Calculation

The horsepower delivered to the fan for any speed equals $H.P._s\ (1-F)^3$, where $H.P._s$ is the power required by the fan at 100 per cent speed, or synchronous speed of the motor and

$$F=\frac{\text{rotor } f}{\text{line } f}$$

Slip energy to be dissipated as heat or pumped back through the constant-speed set into the system is

$$E=\frac{H.P._s(1-F)^3}{1-F}-H.P._s(1-F)^3 \qquad (1)$$

or the general equation for pump back.

To determine the maximum power which must be dissipated as heat or pumped back into the system, equation 1 reduces to

$$E=H.P._s(1-2F+F^2)-(1-3F+3F^2-F^3)$$

or

$$E=H.P._s(F-2F^2+F^3) \qquad (2)$$

Differentiating equation 2

$$\frac{dE}{dF}=f'(F)=(1-4F+3F^2)H.P._s \qquad (3)$$

Placing $f'\ (F)=0$

$$1-4F+3F^2=0$$

Solving for the values of F

$$F^2-\frac{4}{3}F+\frac{1}{3}=0$$

$$F^2-\frac{4}{3}F+\frac{4}{9}=\frac{1}{9}$$

$$F-\frac{2}{3}=\pm\frac{1}{3}$$

$$F=1 \text{ or } \frac{1}{3}$$

Taking the second derivative of equation 2

$$f''(F)=-4+6F \qquad (4)$$

Substituting values of $F=1$ and $F=1/3$ in equation 4

$f''(1)=-4+6=+2$; since it is positive, it is a minimum

$f''\left(\frac{1}{3}\right)=-4+2=-2$; since it is negative, it is a maximum

Substituting 1/3 in equation 2

$$E=H.P._s\left(\frac{1}{3}-\frac{2}{9}+\frac{1}{27}\right)$$

$$E=H.P._s\left(\frac{9-6+1}{27}\right)=\frac{4}{27}(H.P.)_s$$

which is the general equation for maximum power to be dissipated as heat or pumped back into the system.

Application of the Maximum Pump-Back Equation to the Altitude Tunnel Drive at Density of One-Third Atmosphere

The horsepower required to drive the fan to obtain the required wind velocity for this tunnel was given as 18,000 at 410 rpm by the research department. The synchronous speed of the motor purchased is 450 rpm. The horsepower which would be required to drive the fan at 450 rpm is

$$H.P._s=18{,}000\times\left(\frac{450}{410}\right)^3=18{,}000\times1.3=23{,}400$$

$$\text{Maximum slip energy}=E=23{,}400\times\frac{4}{27}=3{,}470 \text{ horsepower}$$

However, there are losses in the d-c and a-c regulating machines which total approximately 15 per cent.

Thus, the total pump back into the system is

$$E'=3{,}470\times0.85 \text{ or}$$
$$E'=2{,}950 \text{ horsepower}$$

Application of the Maximum Pump-Back Equation to the Altitude Tunnel Drive at Density of One Atmosphere

The altitude wind tunnel is designed to operate at variable density between the limits of one-third to one atmosphere as illustrated in Figure 9. The drive is designed for constant torque operation from 308 to 410 rpm.

Curve C is the fan horsepower cube curve for evacuation to approximately one-third atmosphere minimum evacuation and is the same as shown in Figure 6. Curve B is the fan horsepower cube curve for one atmosphere. The evacuation line shows the constant-torque operation of the motor from 308 to 410 rpm. The enclosed shaded area then represents the scope of this tunnel operation.

Curve A is the total power input to the motor. The difference between the ordinates of curves A and B is the power to be dissipated as heat or pumped back into the supply circuit. When the tunnel operates at a density of one atmosphere, the maximum power recovered and returned to the line, assuming 85 per cent efficiency, is equal to 6,200×0.85 or 5,270 horsepower.

Slip-Regulator Drive Control

Another form of control which is used in wind tunnel drives consists of a liquid rheostat, or as commonly termed a slip regulator, and operates in a limited fan-speed range. Instead of pumping the slip energy back into the line as previously discussed, this method of control dissipates it in the form of heat. The regulator consists of three separate insulated tanks with a terminal at the bottom of each for connection to the respective slip rings of the drive motor rotor. Movable electrodes are suspended in the tank and are arranged to be raised or lowered, thereby inserting a variable resistance in the rotor circuit, thus regulating the drive motor speed. Figure 7 illustrates this method of speed control.

To put the motor on the line, the movable electrodes are raised to insert a comparatively high resistance. The line switch then is closed and acceleration is obtained by decreasing the separation of the electrodes, thus decreasing the resist-

ance in the rotor circuit until the desired speed is obtained. The range of speed required by research, and its control within the limits of 1/4 of 1 per cent of any speed in the range, is much more difficult to obtain in this method than in the Clymer drive due to the following characteristics.

The liquid in the rheostat has a negative temperature resistance coefficient, and since the energy must be absorbed in the form of heat, provision must be made to dissipate it and to attempt to hold a constant temperature if the speed is to remain constant at any setting. Variations in line frequency cannot be damped out as is accomplished by the speed control method heretofore discussed.

Secondary resistance control of slip ring motors, Figure 8, is usually acceptable down to approximately 50 per cent speed on a constant torque load. However, on a fan load, where the power varies as the cube of the speed, the lower limit of stable operation is in the neighborhood of 40 per cent of full-load speed. The speed–torque curve indicates that at light loads a very small torque increment may create a corresponding speed-change increment of five or even ten times the torque increment, thus making it difficult to hold a constant speed in this range.

Speed control by secondary resistance depends upon the amount of load for speed reduction. It is, therefore, necessary to predetermine loads accurately for the operating speeds in order to design the control properly.

Large tunnel drives controlled by liquid slip regulators require considerable auxiliary equipment, such as cooling towers, pumps, fans, heat exchangers, and distilled make-up water. The first cost of these items may well be as great or greater than that of the auxiliary machines of the Clymer drive.

In this type of control the slip energy is lost in heat, none being returned to the line.

Summary

Summarizing the characteristics of these drives with respect to wind tunnel research requirements, we have the following:

Range in which speeds can be regulated

Slip regulator—40 to 97 per cent.

Clymer drive—Any speed from 1 to 96 per cent.

Effect of load on speed regulation

Slip regulator—Loads must be predetermined for all speeds.

Clymer drive—Can be set at any desired speed for any load within the rating of the machine. The control is independent of the load.

Effect of temperature, frequency, and voltage variation

Slip regulator—Speed regulation is affected by both temperature and fluctuation in frequency.

Clymer drive—Speed is completely controllable under temperature and frequency variations and is independent of voltage fluctuations.

Slip energy

Slip regulator—Energy wasted in heat dissipation.

Clymer drive—85 per cent of slip energy returned to the supply circuit.

Discussion

Eugene Herzog (Air Materiel Command, Dayton, Ohio): The author gives a rather complete description of the control problems of wind tunnel operation, and of the ways in which the modified Kraemer system permits their accomplishment. It is unquestionable that the modified Kraemer system is an assembly well suited for a wind tunnel drive because it has a wide range of accurate speed control, reasonably good efficiency over the entire speed range, good power factor, low starting currents.

The writer has been associated with the pioneer installation—the 40,000-horsepower drive at Wright Field from the earliest plans; he has been in contact with industry on large adjustable speed drives ever since. Certainly the new name accorded the modified Kraemer system is not generally accepted in industry nor does it appear to be justified by the initial work of the organization compared to others that designed and built the pioneer system; and beyond that engineers of smaller organizations who really suggested the use of the system but never had a chance to build it. The writer is fully aware of the excellent and important work of Clymer in this connection but would be interested to receive the reaction of the other engineers who designed similar drives during the pioneer period.

As to the drive itself the most serious objection appears to be that the speed control auxiliaries account for about 60 per cent of the cost on wind tunnel drives, which give the most favorable conditions for this system. In other cases the cost of the auxiliaries becomes prohibitive. In general, adjustable speed a-c drives are far too costly for universal use. The millions of dollars expended for the restricted number of drives now used well could be diverted in the future for an extensive research and development program for a good adjustable speed a-c motor. The fact that 50 years of search has not netted such a motor should be a challenge to the industry.

As far as wind tunnels are concerned the cost can be cut appreciably by cutting down the speed control range (the trend is toward single purpose tunnels from the complex multipurpose assemblies), and also by permitting a decreased efficiency, power factor and starting limitations which have been held to uneconomic levels in the past considering the low percentage of operating time. A saving in power costs which takes more than 20 years to pay for the initial investment, and low starting currents a fraction of the full load current of the equipment, may be considered luxuries.

L. A. Umansky (General Electric Company, Schenectady, N. Y.): One of the great advantages of the described system for large wind tunnel drives is the ease with which a very large motor can be started.

Even on large power systems the problem of starting in a conventional manner of, say, a 60,000-horsepower motor cannot be passed lightly. When the capacity of the system is limited, then the starting problem becomes serious.

With the Clymer system the constant-speed motor-generator set, which is of relatively small capacity, is started first. For instance, with a 60,000-horsepower fan drive the size of the synchronous motor driving the constant speed set is only 9,375 kva. By means of an autotransformer or, if necessary, through the use of d-c starting, it is not difficult to bring this set to speed without appreciable current inrush on the power system; in one case this inrush was limited to 4,000 kva. With this set running, the larger "adjustable-speed motor-generator set" is brought up to speed by means of field control of the d-c generators and motors of these two sets connected in a loop circuit.

With the adjustable speed set running at top speed, and with its synchronous machine excited, 60-cycle power is applied to the rotor winding of the main fan motor with the line circuit breaker still open. This puts the same frequency (60 cycles) at both sides of this circuit breaker, and after the two power sources are synchronized the circuit breaker can be closed, completing the "painless" starting of the equipment. By gradually slowing down the adjustable speed set the speed of the fan motor is increased until the desired value is reached.

Thus, the system provides an extremely convenient and effective method of starting unusually large motors on power systems of limited capacity. Furthermore, the conventional starting means, such as liquid rheostats, are dispensed with.

Allan H. Heidenreich: The National Advisory Committee for Aeronautics is the largest builder and operator of wind tunnels in the world and their requirements and specifications for the performance of such drives are exactly as stated in the paper.

The NACA tunnel at Moffett Field was purchased in 1939 which was before the Wright Field project was advertised.

The 16-foot tunnel at Langley Field was completed and in heavy production in 1941. The 16-foot tunnel at Moffett Field was put in service the same year. These tunnels antedate the one at Wright Field which has been referred to as, but which is not, the

pioneer installation. The Wright Field tunnel went into operation in 1942.

The Kraemer drive mentioned, employing a rotary converter, is limited to comparably small units, due to the fact that the largest rotary converter which has been built is in the neighborhood of 4,000 kw. The Clymer drive can be operated below, above, and at synchronism; this cannot be done with the Kraemer system. There are many other differences between these two drives which would require another paper to explain.

The drive which is the subject of the paper was developed by C. C. Clymer. Patent 2,295,336, covering it, is in his name. Credit is certainly due to the man responsible for its existence. At NACA it is known as the Clymer drive.

Probability Methods Applied to Generating Capacity Problems of a Combined Hydro and Steam System

E. S. LOANE
NONMEMBER AIEE

C. W. WATCHORN
ASSOCIATE AIEE

BECAUSE the principles relating to applications of the theory of probability to generating capacity problems have been discussed by others, and little now can be added to such theoretical discussions, the contents of this paper generally have been limited to the methods employed in a specific application of the probability theory. Details of the application will differ from those used by other authors; but it is the development of such details, looking toward more ready application of the theory, that justifies this discussion. The probability theory will be applied more generally as it is better understood, and perhaps more important, as the work involved in its application is simplified.

The methods discussed herein are applicable to all-hydro or all-steam systems as well as to combined hydro and steam systems. The methods reduce the mathematics involved in the application of the theory of probability to this type of problem to a systematic arithmetic solution. Although the arithmetic involved in the solution may be rather voluminous, particularly when the effects of all the pertinent factors are evaluated and the system is of a fairly large size, the major portion of the necessary computations may be reused in future studies of the same character. Furthermore, many of the results of a comprehensive capacity study may be used as bench marks until major changes in conditions or requirements for additional information arise.

Paper 47-254, recommended by the AIEE power generation and system engineering committees and approved by the AIEE technical program committee for presentation at the AIEE Midwest general meeting, Chicago, Ill., November 3–7, 1947. Manuscript submitted August 18, 1947; made available for printing October 1, 1947.

E. S. LOANE is with Pennsylvania Water & Power Company, Baltimore, Md. C. W. WATCHORN is efficiency engineer with the same company.

Pertinent Factors Involved

In the solution of many generating capacity problems the following factors need to be considered or evaluated. Not all of these will be applicable to every situation that is studied, and in some cases other information may be pertinent

1. The daily peak loads for an entire year.
2. Capacities, number, location, and arrangement of steam turbines and boilers.
3. Maintenance schedules of steam turbines and boilers.
4. Seasonal capacity reductions of steam turbines.
5. Condenser circulating water experience, or other local conditions affecting capacity.
6. Forced outage experience of steam turbines and boilers.
7. Interstation tie capacity.
8. Sleet and lightning experience and operating policies and practices relating to overhead interstation transmission lines.
9. Forced outage experience of interstation tie cables and overhead transmission lines.

When hydro capacity also is involved in the capacity study, additional information is required as follows:

10. Typical load shapes (expressed as load duration or peak-percentage curves for periods of time determined by the use made of hydro storage).
11. Capacities, number and location of hydro units.
12. Maintenance schedules of hydro units.
13. Records of past river flows.
14. Reservoir rule curve or general plan of operation of storage.
15. Ice and trash experience, or other local conditions affecting capacity.
16. Forced outage experience of hydro units.

General Description of System Operation

The methods of computation presented in this paper have been illustrated by application to the hydro and steam capacity of an interconnected group of companies supplying the loads of Baltimore, Md., and Washington, D.C., and adjacent areas. In addition to the steam capacity of the utilities serving these two cities there is included in this group the steam capacity of the Bethlehem Steel Company's plant located near Baltimore, the steam capacity of the Pennsylvania Water & Power Company and the hydro capacity of the Pennsylvania Water & Power Company and Safe Harbor Water Power Corporation. The steam capacity has a 3-hour effective peak rating of 1,007,000 kw (after an allowance of about 20,000 kw for routine maintenance but including 55,000 kw of scheduled maintenance required over the annual peak load period) and an effective sustained rating of 969,000 kw, in eight plants. The hydro capacity is located in two plants, eight miles apart on the Susquehanna River in southern Pennsylvania, which have a total rating of 334,000 kw at full pond elevation. These ten plants are interconnected variously by tie cables and overhead transmission lines, which are of adequate capacity to accommodate the free flow of power to all parts of the interconnected system for almost all probable conditions. Because of their controlling effect on system operation, it is necessary at this point to discuss the characteristics of the hydro plants in more detail than is required for the steam capacity.

The Holtwood hydro plant of Pennsylvania Water & Power Company is rated at 104,000 kw in ten units, of which eight have an average capacity of about 10,000 kw and two of about 12,000 kw.

Because of the effect of plant discharge on available head the outage of one unit reduces the capacity of the plant by about 7,000 kw. The Safe Harbor plant is rated at 230,000 kw and is made up of seven main units with capacities of 32,000 kw to 33,000 kw each and of two station service units. The operations of these two hydro plants are co-ordinated closely so that they operate practically as a single unit in the interconnected system.

The available river flow has varied from a minimum 7-consecutive-day average of 2,100 cubic feet per second to a maximum 24-hour average of 756,000 cubic feet per second. The median flow is 21,500 cubic feet per second. The river flow available 95 per cent of the time is in excess of 4,500 cubic feet per second and for 90 per cent of the time is an excess of 6,200 cubic feet per second. In general the high flow period is during the months of March, April, and May, and the low flow period during the months of August, September, and October. The wide-open discharge of the Safe Harbor plant is about 65,000 cubic feet per second as compared with 32,000 cubic feet per second for the downstream Holtwood plant

The day-to-day and week-to-week duty of regulation of river flow is assigned generally to the Safe Harbor pond, which is considerably larger than the Holtwood pond. The total usable storage at Safe Harbor, when used at that plant and downstream at Holtwood as well, can provide hydro generation in excess of 5,000,000 kilowatt-hours. Such complete use of storage, however, is not scheduled in normal operation. The Safe Harbor forebay elevation normally is maintained at top elevation when the river flow is in excess of the wide-open discharge of that plant. When the river flow is below the wide-open discharge but still in the higher ranges of flow, the forebay is brought to top elevation each morning. For somewhat lower flows, the forebay is full each weekday morning with drawdown and refill over Friday and the week-end. For very low flows, there is drawdown during the week and refill over the week-end; but in this normal weekly operation a relatively small part of the available storage actually is used.

These hydro plants are at all times operated to replace the maximum amount of steam generating costs as limited by the energy available from the river flow. During periods of high flow and during on-peak periods of some other days of slightly lower flow, the hydro plants are operated at base load. At such times the system steam plants operate in the peak of the system load. The major portion of the scheduled steam maintenance is carried out during such periods. There is a gradual shifting of the hydro plants from base load operation to operation in the peak of the load and of the steam plants from peak load to base or sustained load operation as the river flow decreases from high to low flow. During low flows the hydro plants provide energy for the system on-peak, perhaps for as few as 60 hours per week; but hydro capacity is operated at other times for spinning reserve and reactive supply.

In normal low flow operation the load carrying capability of the hydro plants is below their combined physical capacity. However, the availability of stored energy at Safe Harbor results in greatly increased load carrying capabilities of the hydro plants for limited periods of time. Depending on system requirements, particularly as related to forced outages of system steam capacity, storage at Safe Harbor may be used in excess of that normally scheduled for existing river flow conditions to provide varying amounts of additional hydro energy and capacity service.

System Loads

Generating capacity problems usually relate to future needs for capacity, consequently such studies ordinarily should be based on estimates or forecasts of appropriate expected future loads. By various means, forecasts of future expected loads are normally made in terms of expected monthly or annual peak loads and monthly or annual energy requirements. Before being used in the studies of an all-steam system, as subsequently discussed, such forecasts must be expanded to show chronologically the daily 15-minute peak loads. For the combined hydro and steam system, it is also necessary to have weekly loads by hours or weekly load shapes in terms of load duration or peak percentage curves. For other systems involving hydro power, the load data required will depend on the extent of storage available on the system. The expansion of the usual load estimates to supply the needed data has been carried out, with appropriate modifications where necessary, by reference to a representative prior year of load experience, so as to retain a fairly typical relationship in the day-to-day and week-to-week variations of the load.

The 15-minute integrated peak loads have been used in the determination of capacity requirements, because generating capacity is required to carry at least that much load. It is doubtful whether capacity to carry the system load swings in excess of the 15-minute integrated load would provide any substantial useful service and thus be justified economically. Even if steam capacity were provided for such purpose, in most cases it would not be able to follow such short swings. However, insufficient capacity would be provided in many cases were it the intent to provide only for the 1-hour integrated peak loads.

System Steam Capacity

The older steam installations on this system are low pressure turbines of about 20,000-kw capacity or smaller and numerous small boilers, of which several are needed to supply the steam required by one turbine at full load. A second group of units, operating at higher pressures, generally have capacities in the neighborhood of 35,000 kw, while the newer installations are in general made up of 55,000-kw and 60,000-kw turbines and boilers. In one station there is an excess of high pressure boiler capacity with a pressure reducing valve between the high and low pressures to supply a deficiency of low pressure boiler capacity, and in another station there is a superposed unit also provided with a pressure reducing valve for service to the low pressure system. In only one station is there a single isolated or non-interconnected turbine and boiler unit.

Consistent with the statement of peak loads on a 15-minute basis, the system steam capacity also has been rated on a peak basis (sometimes referred to as overload or emergency capacity). It was also necessary to determine the energy available from the excess of the peak rating over the sustained rating, for in low flows, when hydro capacity normally is operating in the peak of the load, this peaking capability of the steam may be used to supplement the hydro energy.

In addition to the effective peak ratings of the individual turbines and boilers on the system, it was necessary to assemble information as to the steam interconnection possibilities among the turbines and boilers in the various stations, as well as the effect of scheduled maintenance on the available capacity and seasonal reductions of the steam capacity due to circulating water temperature.

The determination of installed generating capacity requirements generally should not depend on considerations relating to such hazards as loss of condenser circulating water, sleet and lightning experience on overhead interstation transmission lines, ice and trash experience as related to system hydro plants, or other peculiarly local conditions. The correction

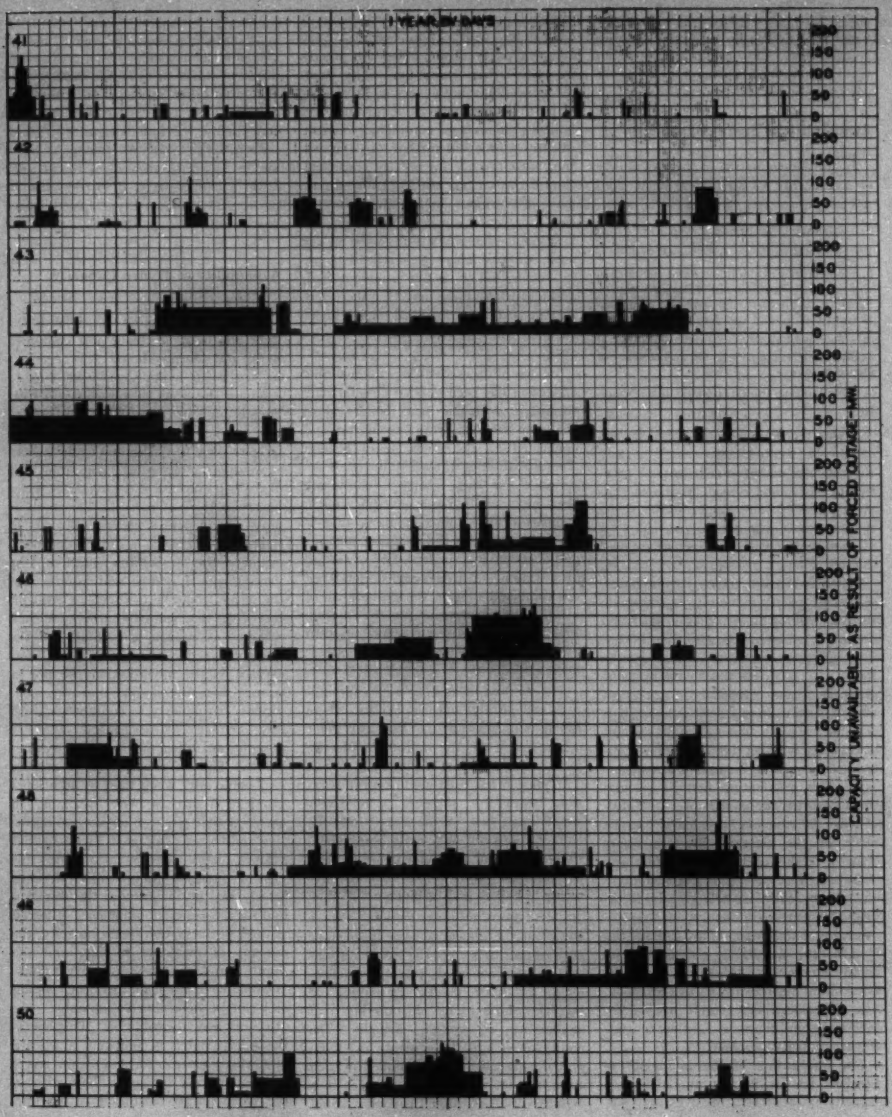

Figure 1. Portion of 100-year record of synthetic forced outage experience for an actual system with steam electric generating capacity of about 1,000,000 kw

or alleviation of such conditions generally will be preferable to the addition of more generating capacity. These particular factors are well provided for in the interconnected system by design and operating policies and are of no practical concern in the determination of the over-all system capacity requirements. However, there

are certain infrequent conditions under which the capacity of the interstation ties is insufficient; these limitations on steam plant output then become a factor in the determination of system reliability.

Availability of Steam Capacity

In the determination of the probability of availability of steam capacity, consideration has been given to the effect of

1. Scheduled maintenance.
2. Seasonal capacity reductions.
3. The layout of the boilers and turbines in the various stations in relation to the capacity available from various combinations of boilers and turbines.
4. The probability of unavailability of boiler and turbine capacity because of forced outages.
5. Inadequate interstation tie line capacities.

The interrelation of these several factors cannot be treated conveniently in any theoretically correct mathematical process, but practical considerations of simplicity and a proper appreciation of the significance of the results has led to a method in which all these factors are considered.

Scheduled maintenance requirements, seasonal capacity reductions of the steam capacity (and hydro capacity as well), and the effect of interstation tie line limitations all have been treated as additions to the load. With all the steam capacity reductions thus accounted for, except those resulting from forced outages, it is possible to assume that a constant amount of capacity is either available for generation or unavailable because of forced outage. This assumption permits calculations as to the probability of availability of various amounts of capacity to be made by the binomial theorem rather than the method of statistical equilibrium. This procedure, although not absolutely and theoretically correct, greatly facilitates the necessary calculations. It results in probabilities of failure to carry the load that are but slightly greater (that is, on the conservative side) than those obtained from theoretically correct methods. The differences that result are of no practical significance in relation to generating capacity problems.

The application of the binomial expansion, insofar as the availability of capacity is concerned, involves only the number and capacity of the various steam turbines and boilers (or of the hydro units) with their various arrangements in the different stations, together with the probabilities of availability and unavailability of such capacity. This application, although basically simple for the most elementary cases, soon becomes very complex and confusing unless the process is systematized carefully. This condition results from the very great number of possible combinations of turbines and boilers that must be considered. Consequently a practical method of computation must provide for orderly consideration of the varying effects of forced outages of turbines and boilers on the capacity available where both high and low steam pressures are involved in the same station, where steam headers are interconnected or are not interconnected, and also where there may be either more turbine capacity installed than boiler capacity in the same station or vice versa.

In view of these conditions the binomial expansion has been applied directly only to groups of turbines or of boilers, all of the same size, located in one station, and connected to the same steam header. The probabilities of availability thus determined for these groups of units are then combined by simple multiplication in tabular form. This combining first is made separately of the groups of turbines and of boilers in a single station or section of a station. Turbines and boilers then are combined to give the probability of availability of capacity for the station. Finally, the several stations are combined by similar successive tabular computations.

The method of making such computations is illustrated in the appendix. These calculations are for the Buzzard Point steam plant of the Potomac Electric Power Company in Washington, D. C. This station has been used as an illustration because it presents a relatively simple case, but, at the same time, the computations are sufficiently comprehensive to be useful as a guide in similar calculations for more complicated arrangements of boilers and turbines.

Calculations generally similar to those shown in the appendix have been made with respect to each of the steam stations on the interconnected system, as well as for the two hydro plants. In making the tabular combinations of probability of availability of system capacity, the plants for each of the separate interconnected companies were combined in such an order that those plants in which it is expected that additional capacity would most likely be installed in the relatively near future were the last ones included. This was done so that as many of the data as possible would be available for future use in similar studies that may be made at a later date.

Where older plants with relatively large numbers of small boilers are involved in such calculations, a great many different values of available capacity develop that differ from each other by small amounts. As the various stations were combined, it was found desirable to group the capacities available in steps of 5,000 kw to facilitate the calculations. For larger systems steps of 10,000 kw or possibly 20,000 kw or even 25,000 kw may be satisfactory.

Availability of Hydro Capacity

The general procedure thus far is the same for both all-steam and combined hydro and steam systems. It is necessary in cases where hydro power is involved to evaluate the effect of variations in river flow throughout the year and from year to year. Except where hydro storage is large relative to the annual load, such an evaluation requires a chronological analysis of the potential use of the available water in serving the system load. This analysis must extend over a number of years of river flow experience in order to properly evaluate the probability effect of the variations in river flow, and requires that the natural flow be modified by recognition of the reservoir rule curve, or normal schedule of storage operations. In the interconnected system here studied, however, it is the deviation in the use of storage from the normal operating conditions, particularly in conjunction with forced outages of steam capacity, that has a significant effect on capacity requirements. This "abnormal" use of storage is possible only when there is additional physical hydro capacity available in excess of that required for normal operation and there is storage in excess of that normally used. The extent to which this type of operation can be utilized depends largely on the magnitude, the duration and the frequency of occurrence of forced outages of the system steam capacity, the amount of available storage, and the duration and frequency of low river flows. It would be different for any other system and can be determined reasonably only after a proper investigation. This operation appropriately is compared to the use of storage batteries for short time emergencies on a d-c system. The load that the hydro storage or storage battery can carry depends on its capacity and the characteristics of the emergency that might bring it into service. The same principles would control the investigation of each.

It would be unlikely that any system

has had enough actual forced outage experience of steam capacity, especially multiple unit forced outage experience, to be particularly helpful in making such an investigation. To supply this deficiency in experience an investigation, as related to the interconnected system, has been made of synthetic forced outage experience for a very large number of years. This synthetic experience was in turn based on forced outage data for steam turbines and boilers. These data as to frequency of occurrence and distribution of duration or forced outages of individual turbines and boilers were arranged appropriately on punched cards. Also punched on the cards were codes identifying the individual turbines and boilers on the system. The data on these cards were then recorded as chance occurrences by means of a tabulating machine. The tabulated data were analyzed systematically in a way that preserved the chance relationship among all the elements of time, turbines and boilers forced out, and duration of outage. This study was the basis for the development of 100 years of forced outage experience of the system steam capacity. These data showed for the interconnected system that nearly all the occurrences of forced outages of large amounts of steam capacity were of short duration. In the 100 years there were 62 forced outages involving capacity greater than 12 per cent of the total steam capacity, and of these more than 90 per cent were of three days or shorter duration; the durations were generally for but one day for the larger amounts of steam capacity on forced outage. Figure 1 shows a graphic record for 10 years, the 41st to the 50th years, inclusive, of this synthetic forced outage experience and is fairly representative of the whole 100 years. Such results were the basis for the conclusion that drawdown of storage during a period of one week, in excess of that normally scheduled, would be a very conservative basis for determining the load carrying capability of the hydro plants. Return of the reservoir to normal elevations would be attained in the subsequent week or weeks as a result of the return to service of the steam capacity previously forced out and in many cases also as a result of subsequent higher river flows and lighter loads. This return to normal operating conditions is possible, when there is a sufficient amount of capacity installed on the system, because of the ample opportunity afforded with the infrequent occurrence of conditions that require departure from normal operation.

A determination was made of the load

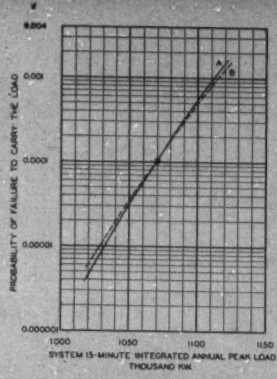

Figure 2. Comparison of two generating capacity installations that provide approximately the same reliability of service

Curve *A*—Actual combined hydro and steam capacity

Curve *B*—Actual steam installation plus 285,000 kw of additional steam capacity as replacement of hydro capacity

carrying capability of the hydro plants on a day-by-day basis over a long period of time. This was done by using the loads estimated for a whole year arranged chronologically with river flows experienced over a sufficiently long period in the past so as to be reasonably representative of average expectancy and extreme variations of river flow.

The load carrying capability of the hydro plants is equal to the physical capacity for 24 hours per day whenever the river flow is greater than the wide-open discharge at Safe Harbor. This capacity decreases in the higher ranges of river flow as the result of reduced head. The river flow experience is that the very high flows obtain only a short time; the flow increases very rapidly and decreases from the peak flow only slightly less rapidly. For a range of river flows extending from about twice the amount of wide-open discharge at Safe Harbor down to river flows equal to approximately one-third of this wide-open discharge, the load carrying capability of the hydro plants for normal operating conditions is very nearly equal to their full effective rating. For flows below this range the capability decreases with decreases in river flow.

This lower range of river flow, down to the minimum experienced flows, is the range in which it is possible to depart from the normal reservoir operation and to use additional storage whenever required by forced outages of steam capacity. For the higher flow section of this range of low river flow, the physical capacity of the hydro plants is the limiting condition with the use of additional storage over a 1-week period. But for the lower ranges of low river flow, it is the energy available from the use of storage in excess of normal that limits the load carrying capability of the hydro plants when the storage is assumed to be used over a 1-week period. However, in relation to the more frequent one and two days' durations of forced outages of the larger amounts of steam capacity as shown by the synthetic experience, the physical capacity of the hydro plants, of a reduced amount because of the reduced head, is the limitation of the load carrying capability of the hydro plants. This physical limit of hydro capacity for a short period is greatly in excess of the load carrying capability of the hydro plants as limited by hydro energy available with one week's use of the additional storage.

Whenever available energy is the limiting condition in the determination of the load carrying capability of the hydro plants, the full peaking capability of the steam plants in excess of their sustained capability is also available for the supply of additional energy to the system. Additional peak steam energy decreases the amount of energy above the flat steam line, which peak energy would otherwise be carried by the system hydro plants with these conditions. This displaced amount of hydro energy is then available to reduce still further the system steam line, thus increasing the load carrying capability of the system hydro plants a small amount in addition to the increase from the use of additional storage. This small increase in the load carrying capability of the hydro plants depends on system conditions, including the river flow. Under conditions requiring use of peak steam capacity the effective or true load carrying capability of the hydro plants on the load is the difference between the 15-minute peak and the required sustained steam generation decreased by the excess of the peaking capability of the system steam plants on the load over their sustained capability. The amount to be deducted decreases as the load carrying capability of the hydro plants approaches their physical capacity, and is zero for this latter condition.

The daily load carrying capabilities of the hydro plants determined for a number of years were compared with their full effective rating. These differences or reductions in load carrying capabilities of the hydro plants then were added to the loads as a further adjustment, just as

Table I. Computation of Probability of Failure to Carry the Load With the Actual Installed System Capacity and a 15-Minute Integrated Annual Peak Load of 1,070,000 Kw

(1) Megawatts	(2) Probability of Availability of Amount of Capacity Shown in Column 1	(3) Proportion of Time Adjusted Load Is Greater Than Amount Shown in Column 1	(4) Probability of Failure to Carry the Load
1,215	0.0024846	0.001177	0.00000292
1,210	0.0016461	0.001177	0.00000194
1,205	0.0009265	0.003826	0.00000354
1,200	0.0006512	0.006476	0.00000422
1,195	0.0005644	0.01118	0.00000631
...	...	...	...
...	...	...	...
...	...	...	...
1,095	0.0000012	0.3114	0.00000037
1,090	0.0000009	0.3377	0.00000030
1,085	0.0000005	0.3594	0.00000018
1,080	0.0000003	0.3811	0.00000011
1,075	0.0000001	0.4031	0.00000004
			0.0001024

the reductions in load carrying capability of the system steam capacity for scheduled maintenance, seasonal capacity reductions, and tie line limitations were added. The reductions in load carrying capability of the hydro plants, resulting from scheduled maintenance of hydro units, were treated as a further addition to the load for all ranges of river flow for which the physical capacity of the hydro plants was the limitation, and for the range of flow for which the available energy was the limitation the reduction used was not smaller than the hydro capacity out of service for scheduled maintenance.

After these adjustments have been made to the daily peak loads for the effect of reductions in load carrying capabilities of the hydro plants, there is no longer a single year of load record to be considered. There are then as many adjusted annual load curves as there are years of river flow experience. All these adjusted daily peak loads were arranged in order of magnitude and a percentage peak load duration curve was determined.

Combining Load and Capacity Data

The next step is the determination of the probability of failure to carry the load. This requires the combining of the adjusted load duration with the probabilities of availability of system capacity. The combining of these data proceeds by multiplication of the probabilities that various amounts of capacity will be available by the percentage of time that the adjusted load is equal to or greater than these various amounts of capacity. The resulting products are then summarized. This calculation is shown in Table I for an annual load with an estimated 15-minute integrated annual peak before adjustment of 1,070,000 kw. These calculations show a probability of failure to carry the load of 0.0001024. The failures considered in this tabulation range from incipient failure to 140,000 kw. The average rate of failure is equal to 1 day in 27 years, which, all things considered, particularly load estimating errors, is probably near the lower limit of an acceptable range of generating system reliability.

The first amount shown in column 1, as related to column 3 is the maximum adjusted peak load and is equal to the actual peak plus steam capacity reductions (except routine maintenance), plus interstation tie line and cable limitations, plus the maximum reduction in hydro capability at the time of peak. Because this hydro capacity reduction resulted from low flows and this maximum adjusted load was found in two weeks in the 28 years of adjusted load record (resulting from use of 28 years of river flow experience), and since in these two critical weeks of low flow the daily maximum steam generation requirements are the same on each day, except Sunday, this maximum adjusted load existed for 12 days in the 28 years, as related to the record of river flow experience used in the study.

The figures in column 2 result from the computations, as illustrated in the appendix, of available capacity by application of the probability theory and forced outage data.

The figures in column 3 are derived from the adjusted load duration curve resulting from the arrangement in order of magnitude of the adjusted daily loads for 28 years of river flow records. The first figure is the ratio of 12 days to the total days in 28 years.

The first amount shown in column 4 is the product of the first amounts shown in columns 2 and 3 and is the probability that the available system capacity will just be equal to the adjusted annual peak load, that is, it is the probability of an incipient failure with respect to the annual peak load (which has been classified as a failure to carry the load). The second amount shown in column 4 is the product of the second amounts shown in columns 2 and 3 and is the probability of failure to carry adjusted daily peak loads by amounts from incipient failures up to 5,000 kw, that result from the availability of capacity that is 5,000 kw smaller than the adjusted annual peak load. The third amount is the probability of failure to carry the load by amounts from incipient failures up to 10,000 kw, and so on. The total of column 4 of 0.0001024 is the probability of failure to carry the estimated daily peak loads by amounts from incipient failures up to 140,000 kw, for which latter condition the probability of failure is in itself insignificantly small. This total probability is plotted as the circled dot on Figure 2. This point means that for all the daily peak loads estimated for the year identified by the estimated 15-minute integrated annual peak of 1,070,000 kw, the probability of failure to carry some daily peak load by some amount is 0.0001024 which is at the average rate of one day in 9,766 days (1/0.0001024) or at the average rate of one day in 27 years (9,766/365).

The additional points through which the solid line curve on Figure 2 was drawn were determined for loads with various annual peaks both larger and smaller than the estimated load that has been used in the illustration of the process. The use of different sizes of load was accomplished without any modifications to the peak load duration data shown in column 3 of Table I. These data merely were shifted vertically in the table by the amount of the assumed increase or decrease in the load, upward for increases in the load and downward for decreases.

System Reserve

The total effective rating of the steam and hydro capacity of the interconnected system is 1,360,000 kw. This capacity, as related to the load used for illustration and identified by a 15-minute integrated annual peak load of 1,070,000 kw, provides the over-all system reliability as

Table II. Probability of Availability of Turbine and Boiler Capacity

Available Capacity, Megawatts	Probability: Turbines	Probability: Boilers
Four 55-Megawatt Turbines and Four 55-Megawatt Boilers		
220	0.9605960	0.9513150
165	388120	477776
110	5880	8999
55	40	75
	1.0000000	1.0000000
Two 37-Megawatt Turbines and Two 37-Megawatt Boilers		
74	0.9801002	0.9753538
37	197998	244924
0	1000	1538
	1.0000000	1.0000000

Table IIIA. Probability of Various Amounts of Turbine Capacity Being Available

Four 55-Megawatt Turbines		Two 37-Megawatt Turbines			
Available Capacity, Megawatts		74	37	0	
	Probability	0.9801002	0.0197998	0.0001000	Total Turbines
220	0.9605960	0.9414804(294)	0.0190196(257)	0.0000960(220)	0.9414804(294)
165	388120	380396(239)	7685(202)	39(165)	190196(257)
110	5880	5763(184)	116(147)	1(110)	380396(239)
55	40	39(129)	1(92)		960(220)
					7685(202)
					5763(184)
					39(165)
					116(147)
					39(129)
					1(110)
					1(92)
					1.0000000

Table IIIB. Probability of Various Amounts of Boiler Capacity Being Available

Four 55-Megawatt Boilers		Two 37-Megawatt Boilers			
Available Capacity, Megawatts		74	37	0	
	Probability	0.9753538	0.0244924	0.0001538	Total Boilers
220	0.9513150	0.9278687(294)	0.0233000(257)	0.0001463(220)	0.9278687(294)
165	477776	466001(239)	11702(202)	73(165)	233000(257)
110	8999	8777(184)	220(147)	2(110)	466001(239)
55	75	73(129)	2(92)		1463(220)
					11702(202)
					8777(184)
					73(165)
					220(147)
					73(129)
					2(110)
					2(92)
					1.0000000

The capacities available from various numbers of 55,000-kw turbines or boilers in combination with various numbers of 37,000-kw turbines or boilers are shown in parentheses. These capacities are obtained by the addition of the capacity available from the 55,000-kw turbines or boilers as indicated in the column to the left, to the capacity available from the 37,000-kw turbines or boilers, as indicated in the line at the top. The probabilities of availability of the various amounts of capacity shown in parentheses, are shown to the left of such capacities and are obtained as the products of the probabilities shown in the column to the left and in the line at the top marked "Probability." The results of the separate calculations in *A* and *B* are shown summarized in the columns headed "Total Turbines" and "Total Boilers."

just determined, which, in our opinion, is near the lower limit of acceptability. The difference between the peak and the effective rating of the system capacity shows an available reserve of 290,000 kw, or 21.3 per cent of the effective rating.

A system load with a 15-minute integrated annual peak of only 1,050,000 kw, which is 20,000 kw or approximately 2 per cent smaller than that of the load previously used, would result in a probability of failure to carry the load of 0.000031, or at the average rate of one day in 88 years. Such reliability of the generating system is within the upper range of desirability. This assumption as to load results in an available reserve of 310,000 kw, or 22.8 per cent of the effective rating.

For an increase in the annual peak of the system load of 20,000 kw to 1,090,000 kw total, the probability of failure to carry the load is 0.00032, or at the average rate of one day in 8.6 years. The reserve is 19.8 per cent for this condition.

It is thus evident that the over-all system reliability is increased very greatly with a comparatively small increase in the system reserve; and conversely, the over-all system reliability is decreased very greatly, to a perhaps undesirable level, with a comparatively small decrease in available system reserve. The decision as to the desirable degree of over-all system reliability and consequently a reasonable reserve requirement is largely a matter of judgment. It must be based on an absolute determination of acceptable reliability. However, for the conditions here considered, it appears that the choice of a reserve might be made in the rather narrow limits of plus or minus something smaller than two per cent of either the system annual peak load or of the system capacity.

The amount of reserve has been related here to the effective rating of the system capacity, which, in our opinion, is the preferable basis, but it could have been expressed as a percentage of any other appropriate basis as well. The percentage reserve requirement might be related to the system annual peak load, either on a 1-hour or 15-minute integrated basis or on an indicated basis or to the system capacity, either on the basis of its effective rating or on the basis of its dependable capacity, so long as such basis is clearly specified. These percentage reserve requirements would be reduced 125,000 kw, or about 8 per cent, if related to the system dependable capacity.

The reserve requirement not only varies with the basis upon which it is stated, but also upon the various conditions that may pertain to different systems. The differences in relative sizes and number of units, maintenance requirements, river flow and storage characteristics, load shapes, and other factors all influence the reserve requirements. Therefore, the reserve requirement practices and policies of one system, which may be expressed as a percentage or as so many units, are a very dubious guide as related to any other system. Separate studies should be made of the over-all system reliability of each system as a basis for judgment in formulating a reserve requirement policy for that system.

It is not necessary to make complete studies of over-all system reliability at frequent intervals, but rather such studies should be used as bases or bench marks for operating rules, which should be checked from time to time as conditions change.

Effect of Load Estimating Errors

The estimated loads thus far have been treated as certainties, but it is obvious that such conditions do not obtain. If the probable error characteristics of the load estimates for future years were reasonably well-known this factor also could be taken into account in an evaluation of system generating requirements. Because such future estimates involve a large human factor, it is unlikely that there is sufficient stable information available for this purpose. However, consideration of the characteristics of this problem results in a generally useful conclusion: when the estimated loads are considered as probable loads, the com-

puted probability of failure to carry the load would be greater on the average than when the estimated loads are considered as certainties. Therefore any evaluation of load estimating error would increase the frequency of occurrence of failure to carry the load and consequently increase the reserve requirement for any given degree of over-all system reliability.

The load estimating error is of no consequence as related to relative determinations of reliability and is reasonably provided for in the case of absolute determinations by specifying a somewhat higher degree of over-all system reliability than if this factor were not a consideration.

Firm or Dependable Hydro Capacity

Whereas the selection of a proper reserve requirement requires a certain element of judgment, there being no scale of economic benefit or disadvantage against which the computed system reliability can be measured, there are a number of other capacity problems in which the answer can be obtained directly from probability computations without the possibility of significant effect of judgment on the results. This is evidently true of various applications of the probability theory to "with and without" or "before and after" types of generating capacity problems. The determination of firm or dependable hydro capacity in a combined hydro and steam system is such an application, for it can be shown to be nearly independent of the desired degree of system reliability over a fairly wide range. Consequently the judgment that enters into the selection of a reserve requirement has almost no influence on the determination of the dependable hydro capacity. Certain elements of judgment are related to various details of the computation that have here been discussed; but if these elements are treated consistently, they have a negligible effect on the answer as to what is the dependable capacity of the system hydro capacity or what is the amount of steam capacity that would be required on the system to maintain the same degree of reliability in the absence of the hydro capacity.

The determination of dependable hydro capacity is of importance for various reasons, among them being the supplying of certain information requested by the Federal Power Commission, particularly schedule 16 of the FPC form 12. It is of greater practical importance as related to studies of the economies of alternate steam and hydro capacity installations, for a fundamental of such studies is the determination of the steam capacity replaceable on the system by the proposed hydro capacity installation.

The method of determining dependable hydro capacity is suggested by its definition. The over-all system reliability for the combined hydro and steam system must be determined for various levels of some estimated load (as shown by the solid line curve of Figure 2). Then for these same load conditions the reliability must be determined similarly for various all-steam systems, made up of the actual steam capacity of the combined hydro and steam system plus additional steam units. By interpolation an all-steam system can be set up that provides the same degree of reliability as the actual combined hydro and steam system. The difference between the steam installations on these systems of equivalent reliability is the dependable hydro capacity. In case it is desired to study the effect of additional hydro capacity in a system that already has hydro capacity, determinations should be made of the over-all system reliability for the actual system plus additional steam capacity on the one hand and plus additional hydro capacity on the other. Consideration should be given to any differences in maintenance schedules that may result from the installation of hydro capacity as compared with steam capacity, and differences in interstation tie line capacities.

Because the more recent steam capacity

Table IV. Probability of Various Amounts of Combined Turbine and Boiler Capacity Being Available

Four 55-Megawatt and Two 37-Megawatt Turbines		Four 55-Megawatt and Two 37-Megawatt Boilers			
Available Capacity, Megawatts		294	257	239	220
	Probability	0.9278587	0.0233000	0.0466001	0.0001463
294	0.9414804	0.8735701(294)	0.0219365(257)	0.0438731(239)	0.0001377(220)
257	190196	176477(257)	4432(257)	8863(239)	28(220)
239	380396	352958(239)	8863(239)	17726(239)	56(220)
220	960	891(220)	22(220)	45(220)	
202	7685	7131(202)	179(202)	358(202)	1(202)
184	5763	5347(184)	134(184)	269(184)	1(184)
165	39	36(165)	1(165)	2(165)	
147	116	108(147)	3(147)	5(147)	
129	39	36(129)	1(129)	2(129)	
110	1	1(110)			
92	1	1(92)			

Available Capacity, Megawatts		202	184	165	147
	Probability	0.0011702	0.0008777	0.0000073	0.0000220
294	0.9414804	0.0011017(202)	0.0008263(184)	0.0000069(165)	0.0000208(147)
257	190196	223(202)	167(184)	1(165)	4(147)
239	380396	445(202)	334(184)	3(165)	8(147)
220	960	1(202)	1(184)		
202	7685	9(202)	7(184)		
184	5763	7(184)	5(184)		

Available Capacity, Megawatts		129	110	92	Combined Station
	Probability	0.0000073	0.0000002	0.0000002	
294	0.9414804	0.0000069(129)	0.0000002(110)	0.0000002(92)	0.8735701(294)
257	190196	1(129)			400274(257)
239	380396	3(129)			827141(239)
					2419(220)
					19364(202)
					14535(184)
					112(165)
					336(147)
					112(129)
					3(110)
					3(92)
					1.0000000

The process for combining the turbines and boilers is the same as that of combining the different sizes of turbines and boilers in Tables IIIA and IIIB, except for the manner in which the resulting available capacity is determined. The available capacity for each combination is shown in parentheses and is the smaller of the available turbine or boiler capacities that are involved in each combination.

The probabilities of availability of the same amount of capacity resulting from different combinations of turbines and boilers have been added and are shown in the column headed "Combined Station."

installations on the actual system have been of 50,000-kw to 60,000-kw capacity units, the hypothetical all-steam system has been assumed to be made up of the actual installed steam capacity plus various numbers of steam units of approximately the capacity of the newer installations. By trial and error, the dash line curve shown on Figure 2 was determined for an all-steam system made up of the present installed steam capacity plus five 57,000-kw steam units, or a total of 285,000 kw of hypothetical steam capacity. Since the system hydro capacity replaces 285,000 kw of steam capacity on the interconnected system with the same degree of system reliability, the dependable hydro capacity is 285,000 kw. This is true, within practical limits, for all reasonable degrees of over-all system reliability and is independent of both the reserve requirement and the available reserve within all reasonable limits.

This evaluation of dependable hydro capacity is conservative. It is based, as related to the assumed use of additional storage over that used in normal operation of the actual combined hydro and steam, on the use of such additional storage for a period of one week, whereas the much more likely use of such additional storage would be related to one and two days' durations of forced outages of steam capacity. For such shorter periods the physical capacity of the hydro plants rather than the available energy is the limitation. If this condition had been evaluated a dependable hydro capacity greater than 285,000 kw would have resulted. Tending to offset this under-evaluation of the dependable hydro capacity is the fact that, when a failure to carry the load occurs as a result of forced outages of capacity for an all-steam system, such failures would occur generally only with respect to a comparatively few hours over the peak portion of the day, whereas when failure to carry the load is the result of energy limitations in a combined hydro and steam system, failure to carry the load would result over a larger number of the peak load hours of possibly several days. These latter failures, that is, those that result from energy limitations, will occur very infrequently, at the negligible rate of once in several thousand years. The more general failure to carry the load for the actual combined hydro and steam system will be of the same general nature as for the all-steam system, that is, the result of physical capacity limitations associated with one and two days' durations of large forced outages of steam capacity. Actually such failures will be much less frequent and of much smaller magnitude for the actual system than for the hypothetical all-steam system computed as its equivalent in terms of reliability.

Effect of Reliability of Forced Outage Data

A study was made to determine the effect of possible errors in the basic forced outage data. It was assumed, for the purpose of this investigation, that the forced outage data of the steam turbines and boilers could be in error 25 per cent. This is considerably greater than any probable error that reasonably may be associated with these data. This study showed that a 25-per-cent change in the forced outage time of steam turbines and boilers resulted in about 15,000-kw change in the reserve requirements. This approximate relation existed for any reasonable degree of over-all system reliability and was approximately the same for both the actual combined hydro and steam system and the hypothetical all-steam system. These results show that reasonable variations in the basic data have a proportionately and surprisingly small effect on the reserve determinations involving the use of such data. The effect of any probable errors in the basic data on a reasonable reserve requirement is smaller than 10 per cent of such requirement, which is smaller than 2 per cent of either the system annual peak load or of the system installed capacity. The effect of such errors in data on many relative determinations would be even smaller, for example, the effect on dependable hydro capacity was negligible.

Conclusion

The theory of probability is useful, as an aid to judgment, in the establishing of a reasonable system reserve requirement policy within rather narrow limits. This is the one case, as related to such problems, where the absolute rather than the relative reliability is of importance. The same general methods of computation are also adaptable to many other problems relating to generating capacity requirements, particularly those that involve the process of comparison. Among such problems are

1. The investigation of capacity benefits to be obtained from addition of boiler capacity to a station that is "overturbined" or the addition of turbine capacity to a station that is "overboilered."

2. The capacity benefits to be obtained from the installation of steam pressure reduction valves between high and low steam pressures in the same station.

3. The benefits to be obtained from interconnections between different systems and the required capacity of such interconnections.

4. Relative capacity benefit of two small units versus one large unit.

5. The determination of dependable hydro capacity.

The application of the theory of probability to these latter capacity problems results in very accurate determinations of the effects of the factors studied, since the answers to such problems involve relative reliabilities, and any errors that may be inherent in the final results, even with possible large errors in basic data and details of computation, are generally negligible, so long as there is consistent treatment of all the uncertain factors that may be involved and such uncertainties are not too great.

Appendix. Method of Making the Binomial Expansion and Its Application to a Specific Problem

For a given number of boilers or turbines n and a known average forced outage time b, expressed as a ratio of outage time to total time of exposure to outage, the following binomial expansion

$$(a+b)^n = a^n + na^{n-1}b + \{n(n-1)/2\}a^{n-2}b^2 + \{n(n-1)(n-2)/3!\}a^{n-3}b^3 + \ldots$$

provides the basis for determining the probability of finding various numbers of the n turbines or boilers available for service. In the following illustration applied to four turbines the ratio b, which is equal to the average forced outage time or probability of unavailability of an individual unit, is taken to be 0.01. The probability of availability a is then equal to unity minus b or 0.99. For these conditions the several terms of the expansion readily are computed as

The first term (all units available)
$= (0.99)^4 \qquad = 0.9605960$
The second term (three units available)
$= 0.9605960(0.01/0.99)4 \qquad = 0.0388120$
The third term (two units available)
$= 0.0388120(0.01/0.99)(3/2) \qquad = 0.0005880$
The fourth term (one unit available)
$= 0.0005880(0.01/0.99)(2/3) \qquad = 0.0000040$
The fifth term (no units available)
$= 0.0000040(0.01/0.99)(1/4) \qquad = 0.0000000$

1.0000000

In this illustration, and in all similar binomial expansions, the first term is obtained by raising the probability of availability of a single unit to a power equal to the number of units under consideration; the second term is obtained by multiplying the first term by the product of the ratio of the probability of unavailability to the probability of availability, b/a, and the number of units, n. The third and succeed-

ing terms are obtained by multiplying the preceding term by the product of the ratio b/a and the ratio of one less than the number of units used with respect to the preceding term to one less than the number of the term namely,

The first term
$= a^n$,
The second term
$=$ (first term)$(b/a)n$,
The third term
$=$ (second term)$(b/a)\{(n-1)/2\}$,
The fourth term
$=$ (third term)$(b/a)\{(n-2)/3\}, \ldots$

It is important in making the calculations to check the sum of the terms and if necessary make adjustments to bring the sum to unity. Because of the smaller percentage effect, it is preferable to adjust the larger terms. These small differences are the result of "rounding off" and may exist in these and subsequent calculations. Initially they are insignificant. They may pyramid as the computations progress and result in wide discrepancies. The unity check also provides a method of checking many of the subsequent calculations without complete repetition.

The station used in the following illustration contains four turbines and four boilers each rated at 55,000 kw and two turbines and two boilers each rated at 37,000 kw.

The calculations just illustrated were for the group of four turbines, the other three similar calculations are not shown. The results in all four cases are shown in Table II.

The next step requires the combining of the two groups of turbines and the two groups of boilers. The computations and results are as shown in Tables III*A* and III*B*.

In the final step, shown in Table IV, the turbine and boiler capacities are combined, the procedure being the same as that just used.

Discussion

R. L. Ashley and **L. T. Anstine** (nonmember; both of Consolidated Gas Electric Light and Power Company of Baltimore, Baltimore, Md.): This paper has served to emphasize the importance and difficulty of determining the correct amount of generating capacity which should be installed in any large electricity supply system. This is particularly true in a system such as the Safe Harbor-Holtwood-Baltimore system as a result of the fact that a substantial part of the electric power and energy is supplied by hydroelectric plants having little storage and situated on a stream (Susquehanna River in this case) which is subject to extremely variable flow.

The authors have dealt with an application of the theory of probability to a particular problem of especial interest to hydro companies. This application, however, does not solve the principal problem as to what is the proper amount of generating capacity to be installed. The paper deals primarily with the determination by mathematical computation of the "firm or dependable hydro capacity" which the authors define as "the amount of steam capacity that would be required on the system to maintain the same degree of reliability in the absence of the hydro capacity." To make such a mathematical determination assumes that such an equivalence of hydro and steam capacity exists so that any given hydro–steam system may have the same degree of reliability at all times and under all conditions as if it were a 100 per cent steam system.

Our experience has convinced us that such an equivalence does not in fact exist, but that there are many advantages of the hydro–steam system which do not exist in an all-steam system, and conversely an all-steam system has certain advantages which do not exist in the combination hydro–steam system. The authors have made a noteworthy attempt to reduce the determination of hydro capacity value to a mathematical procedure by a painstaking application of the theory of probability. We recognize the soundness of the basic principles of the probability theory and realize that nearly every engineer who determines the number and size of various elements to be installed in an electric system such as generators, cables, and transformers is influenced consciously or unconsciously by this theory. We are inclined to agree with the authors' conclusion that "the theory of probability is useful, as an aid to judgment, in the establishing of a reasonable system reserve requirement policy within rather narrow limits." However, we believe that the involved application of the theory which is new and hitherto untried particularly as to the method of combining the effects of variation in river flow and planned capacity outages with variation in load and with the effect of forced capacity outages, has led to an exaggerated evaluation of the hydro capacity which is not acceptable for practical purposes.

The paper finds a dependable capacity value of the two hydro plants of 285,000 kw based on estimated 1945 conditions. On other occasions the authors recently have stated that this dependable capacity value, based on 1946 conditions, is 295,000 kw and will be even higher in the immediate future. It is our opinion that these values are excessive as tested by judgment and experience—expecially experience which is recent and current as this discussion is written. In another paper[1] it very properly is pointed out that it is necessary to make a "judicious" application of the probability theory and that the results are subject to certain limitations, one of which is enumerated as follows:

> *b.* The probability theory aims only at foreseeing average performances. In the case under consideration, this means that the probability theory can predict only the average outage performance of a group of units during a long period of time.

In the case of the system of which the Safe Harbor and Holtwood plants are a part, experience has made it plain that it is not enough to consider the average performance of the river during a long period of time, but knowing that certain low flow conditions do develop with considerable regularity at certain periods of the year in combination with certain load conditions, the utility must plan its steam installation problem to meet these conditions with adequate reserve regardless of the excellent conditions which may exist during other seasons of the year. For example, except for the effect of seasonal variations in the load, which largely are evened out in the planning of the maintenance schedules, the all-steam system has a relatively uniform probability of failure to carry the load throughout the year, whereas the combination hydro–steam system discussed in this paper inherently has a higher probability of failure during the season when low flows are experienced frequently than during the months when relatively high flow is practically assured. This might be compared to the throw of dice. If we throw two dice the probability of throwing ten is 1/12. Thus, if we throw the dice once each day for a year we would expect to throw a ten 1/12 of the time, or $30^8/_{12}$ times per year. However, if we start out by throwing three dice each day for the first four months, two dice each day for the next six months, and one dice each day for the last two months, we would expect to throw a ten $15^1/_{24}$ times $(1/8\times365\times4/12)$ during the first four months, $15^1/_{24}$ times $(1/12\times365\times6/12)$ during the next six months, and not at all during the last two months. This makes a total of $30^8/_{12}$ times per year which is the same as the first case where we threw two dice each day for a year. In other words, the two cases are equivalent from the standpoint of probability of throwing a ten despite the fact that in the second case there is a certainty that we will not throw a ten during one-sixth of the time.

The importance of this seasonal variation in the probability of failure is emphasized by the present inadequate steam capacity and the low flows currently (October 1947) being experienced. Under present conditions any operating man will admit that the system would be far better off with an additional 285,000 kw installed in the steam plants in place of the hydro capacity. However, the same operating man would favor the hydro plants if high river flows now were being experienced, but the important point is that the low river flows are a much more frequent occurrence during this time of the year than during other seasons. In fact, our records show that in nearly one-third of the Octobers since 1891 there has been a week when the river flow was even lower than the lowest week this October. In other words, we must expect during certain periods of the year to come up to bat with two strikes against us unless adequate steam capacity is available at that time. For this reason it is our judgment that any evaluation of the hydro plants in terms of equivalent steam capacity, if made at all, should be confined to the critical seasons of the year.

There are a number of specific points in the authors' paper with which we are unable to agree. One of these is the assumption that the full capacity of the reservoir would be available each week and could be used each week if required by forced outage of steam capacity, and that the return of the reservoir to normal elevation would be attained in the subsequent week or weeks as a result of either the return to service of the

steam capacity previously forced out, subsequent higher river flows, lighter loads, or a combination of these conditions. As to the return of the reservoir to normal elevation by the return to service of capacity forced out, this can be accomplished only if the steam capacity normally available is in excess of the steam generation required and under such conditions drawdown actually would be used only to the extent that the steam capacity on forced outage exceeds the excess steam capacity normally available. In other words, if there is an excess capacity of 80,000 kw and 100,000 kw is forced out, drawdown would be used to make up for the loss of only 40,000 kw. Other conditions remaining the same, the return to service of 40,000 kw would make it possible to hold the reservoir elevation, but additional capacity would have to be returned to service to make possible the return to normal reservoir level. The availability of storage to take care of forced outages equal to or less than the excess steam capacity available has no practical value but has been used by the authors to reduce the mathematical probability of failure to carry the load. The use of drawdown during any week and under conditions requiring the use of such drawdown will increase the probability of failure to carry the load during the subsequent week or weeks. It appears that this fact has not been taken into account.

The effect of river flow variations has been taken into account by adding to the daily peak loads an amount equal to the difference between the full effective rating of the hydro plants and the daily load-carrying capacity of the hydro plants, including the effect of drawdown as just discussed. This adjusted load then is combined with the probability of availability of the system hydro and steam capacity. If the hydro plants had no storage, the adjustment to the daily peak load determined on a comparable basis would be equal to the difference between the full effective rating of the hydro plants and their daily load-carrying capacity as limited by the natural flow of the river. Thus the adjusted load for the actual system is less than the adjusted load would be if the hydro plants had no storage by an amount equal to the benefit gained by the use of drawdown. In other words, treating drawdown in this manner has the effect of carrying a part of the load equal to the capacity gain due to drawdown on a 100 per cent assured basis. Can it be that capacity available from drawdown is the most dependable capacity on the system? The fallacy of this treatment of drawdown can be illustrated further by considering two hydro plants, the first having storage capacity which, when used over a period of one week to augment the natural flow of the river, is just sufficient to give a daily load-carrying capacity equal to the full effective rating of the plant, and the second having a far greater storage capacity so that its use can be stretched out over three or four months, thus assuring the availability of the full effective rating of the plant (except as reduced by forced outages and scheduled maintenance) for this entire period. The treatment by the authors of this paper would in each case result in no addition to the load to take care of capacity unavailable due to river flow variations and therefore would show the same probability of failure to carry the load. However, it is obvious that the second plant would provide a much more reliable service.

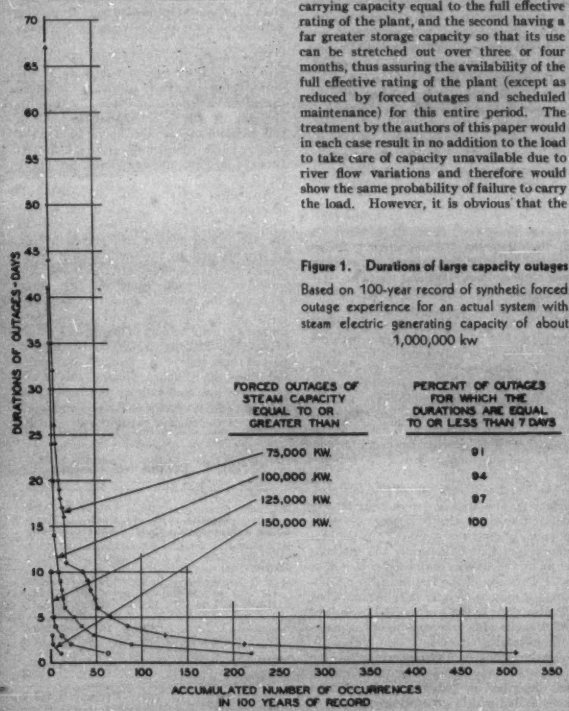

Figure 1. Durations of large capacity outages

Based on 100-year record of synthetic forced outage experience for an actual system with steam electric generating capacity of about 1,000,000 kw

As previously mentioned, there are a number of features about a hydro-steam system which cannot be reduced by a simple mathematical equivalence to an all-steam system. Some of these, in addition to the matter of the seasonal river flow variations, we wish to mention briefly.

In the particular system discussed in the paper, the available low flow hydro energy is the determining factor in deciding upon the amount of steam capacity to be installed rather than the peak load to be carried. Because of this situation, a failure to carry the load in the hydro-steam system is not likely to develop as suddenly or as unexpectedly as on an all-steam system, but probably will extend over a number of hours each day (say 10 to 14 hours) and every day in the week for perhaps several weeks. On the all-steam system the capacity deficiency is more likely to be for only a few minutes or at most for a few hours on the peak or near-peak days and usually can be met with less inconvenience by the customers than the type of shortage which may occur on the hydro-steam system. For this reason we consider it more important to have a lower probability of failure under these critical conditions of low flow than may be justified for an all-steam system.

Also, no account is taken of the effect upon the reliability of the steam capacity, especially of the boilers, which may develop from the long periods of full-load operation which are required on a combination system but are not required on an all-steam system.

Of course, there are also values derived from a hydro-steam system which are not enjoyed by the all-steam system and which have not been considered in the present discussion. These likewise cannot be included mathematically in the determination of equivalent steam capacity.

Reference

1. Generating Reserve Capacity Determined by the Probability Method, Giuseppe Calabrese. AIEE Transactions, volume 66, 1947 Pages 1439–50.

G. D. Floyd (The Hydro-Electric Power Commission of Ontario, Toronto, Ontario, Canada): I believe the authors might have made a clearer distinction between ability (1) to meet peak load demands, and (2) to satisfy energy requirements. The latter may not be important for a system supplied wholly from thermal energy plants, where, if the coal pile is big enough, it is possible to meet energy requirements by operating the units at higher load factor, with possibly some sacrifice in efficiency. The ability to meet energy requirements may be very important for the all-hydro plant, and increases in importance with increase in ratio of hydro to steam capacity in the combined hydro and steam system. The value of this paper would be greater, in my opinion, if a more detailed analysis of the application of probability methods to energy supply had been included.

Some of the statements regarding system reserve are not very clear to me. It is granted that the authors have established that the over-all system reliability is increased very greatly with a comparatively small increase in the system reserve, at

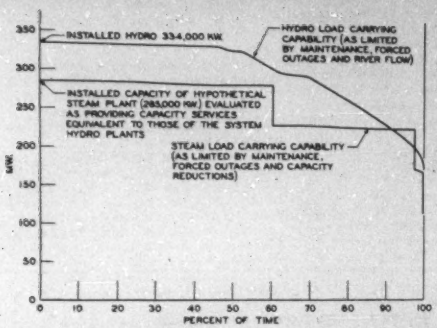

Figure 2. Comparison of availability of load carrying capability of system hydro plants and the steam capacity replaced on the system by these hydro plants

least for the combined steam and hydro system which they have studied. It is conceivable that this situation may not hold for some other system, where the controlling factors might be different. This could be established by making a study on the unknown system using the methods outlined in the paper. It is not so clear, however, that if an absolute determination of acceptable reliability is made, that it can be, at the same time, a matter of judgment. In my view the two are incompatible. Would it not have been better to say that the decision as to acceptable reliability, and consequently a reasonable reserve requirement, is largely a matter of judgment?

H. W. Phillips (nonmember; Pennsylvania-New Jersey Interconnection, Philadelphia, Pa.): I have reviewed the paper with considerable interest and I believe it is probably the best paper on this subject that I yet have had the opportunity of reviewing. There are, however, certain factors which have been omitted, as contingencies of infrequent occurrences, but which are, nevertheless, important in determining the true reliable capacity of a generating system.

In determining the relative dependable capacity of hydro equipment, the paper takes into consideration the records of past river flows which vary from a minimum of 2,100 cubic feet per second as a 7-consecutive-day average, to 756,000 cubic feet per second as a maximum 24-hour average. In view of the fact that I am familiar with the statistics of the Susquehanna River flow, I am aware of the fact that these exceptional maximum and minimum flows occur about once every 50 years and believe that these items have had considerable weight in determining the effective capacity of the hydro plants.

On the converse, the paper does not take into consideration the fact that the fuel supply to steam stations can be seriously interrupted by railroad strikes, mining strikes, and acts of God, and recent experience has indicated that these restrictions in fuel supply are probably more frequent than once very 50 years.

I, therefore, believe that if these factors were taken into consideration, the hydro capacity of the system, discussed in the paper, would be more than the 285,000 kw reached as a conclusion in this paper.

It also appears to me that more credit than is correctly due the steam plants for their capacity has been given them in the utilization of 15-minute peak loads, since it is quite probable that the steam capacity may be required to generate maximum loads for periods of longer duration, at a time of the year other than that of the annual peak. Such a condition might result from exceptionally high forced outages during the summer time, when the peak occurs in the morning and is often of extended duration.

The method utilized for producing synthetically 100 years of forced outage experience is of exceptional interest, and reference to the samples in Figure 1 plainly indicates the variability in the forced outage that a company is likely to experience from year to year, and emphasize the fact that the basing of reserve requirements to cover this liability on only a few years could produce a very inaccurate answer as regards the correct amount of reserve necessary for system protection.

E. N. Peterson (nonmember; Ebasco Services Incorporated, consultant to Northwest Power Pool, Portland, Oreg.): It is recognized that extensive interconnected systems with a large number of generating units require a less percentage of reserve capacity than do smaller systems with few units. But it is only recently that sound logical methods of determining what reserves are required in any specific case have been worked out and published. The authors have handled this problem admirably by their "method of synthetic forced outage experience" coupled with the theory of probability and statistical records as to the reliability of generating equipment.

The Northwest Power Pool just has completed the first step in determining reserve requirements in its area by setting up a value for standby generator reserves. As the procedure used follows generally the methods set up by the authors of this paper as well as by H. P. Seelye of the Detroit Edison Company,[1] it may be of interest to outline what has been done in the Northwest Power Pool and to make a few comparisons of the methods and results.

The interconnected system comprising the Northwest Power Pool is very different from that described in the paper. It is three times as big with a generating capacity of some 3.7 million kw. It has 315 units (versus 52, of which 17 are hydro and 35 steam) of which 282 are hydro and 33 steam. The hydro capacity is roughly 90 per cent of the total. All major utilities, private, municipal, and federal in Idaho, Utah, Montana, Washington, and northern Oregon are interconnected and co-ordinated and constitute the Northwest Power Pool.

Prior to the setting up of pooled operation in 1942, reserves were considered a matter of individual concern by the various utilities in the area. Judgment figures were used as to the amount of reserves needed, usually the largest unit or perhaps two units or some arbitrary number of kilowatts. As interconnections multiplied and resources were placed in a common pool, it became apparent that such large reserves were costly and unnecessary and a committee on reserves was appointed by the operating committee to work out an acceptable and realistic basis for determining what the reserves should be in such an extensive system.

The committee undertook the task assigned to it quite unaware that engineers such as the authors of the subject paper and others were working on the same problem. Statistical records were used to determine the reliability of units and these were compared with operating experience in the area. Also, the committee wrestled with the theory of probability to determine the chance of simultaneous outage of various numbers of units and their aggregate capacity.

Since the sizes of the 315 units varied from zero plus to 125 megawatts or more, it was decided, for simplicity, to divide them into five groups as shown in Table I of this discussion. It will be noted that the steps in this grouping are far more liberal than in the subject paper where steps of 25 megawatts between groups are considered an upper limit.

An initial determination of reserve requirements assuming an *average* size of unit was made but this was discarded in view of the very much greater role played by the large units than by the small ones in determining reserve requirements, so a new determination was made using the first three groups in the table. Group IV was eliminated since units less than 1 megawatt played virtually no part in fixing the amount of reserves (although they could well be a part of those reserves). Group V was omitted since, in a hydro system, the steam plants are operated as little as possible and consequently normally could be considered as part of the reserve capacity—at least in

Table I. Division Into Groups

Group	Capacity, Megawatts	No. of Units	Avg Megawatts	Total Megawatts
Hydro				
I	Over 100	8	125.0	1,000.0
II	40–100	15	56.3	844.5
III	1–39	185	7.6	1,406.2
Subtotal		208	15.6	3,250.7
IV	Below 1	74	.6	42.2
Steam				
V		33	13.4	440.8
		315	11.9	3,733.7

theory. Actually the present abnormal load growth has dipped into reserves to such an extent that all steam capacity is required to carry the daily peak loads, but presumably this always will not be so and adequate reserves again will become available.

In determining the amount of standby reserves that are economically justified in the Northwest Power Pool, only generating units were considered to the exclusion of transformers, circuit breakers, transmission lines, and so on. Such elements will be considered at a later date. The outage factor of hydro units was taken to be 0.52 per cent. In addition to these factors, the committee used a figure which it called the interval between "hurtful" outages. A quotation from the Northwest Power Pool "Magna Charta" containing the basic principles of co-ordinated operation reads

A 'hurtful' outage is defined as one in which the total generating capacity forced out of service exceeds the available standby reserve capacity, thereby necessitating a reduction in load by lowering voltage or frequency or by discontinuing service to certain customers. The greater the reserves the longer the average interval between hurtful outages. Reserves should be of such an amount that the customer is not justified in paying the cost of additional reserves to increase further the interval between hurtful outages.

For the present the acceptable interval between hurtful outages has been set at 20 years.

The committee on reserves found that, on the basis of the assumptions and methods indicated, the justifiable amount of standby reserves in the Northwest Power Pool was 250 megawatts or 6.7 per cent of capacity. This is much less than the reserves indicated in the subject paper (about 20 per cent) but the reasons for the difference are to be found in the much greater aggregate size of system in the Northwest, the large number of units, the higher degree of reliability of hydro units as compared with steam, different methods of operation, somewhat different objectives, and probably other factors.

It is important that the setting up of reserves should be on a sound logical basis backed up by adequate historical records and operating experience. Insofar as the Northwest Power Pool is concerned, however, it is believed that, once these fundamentals have been established, great accuracy in arriving at the final answer hardly can be expected. This is due to several factors, among them

1. Actual unit outages will deviate widely from the average outage factors established from statistics.

2. Hurtful outages will occur at intervals varying widely from the average value adopted.

3. The grouping of units by sizes is arbitrary and different grouping would give somewhat different, though not necessarily more accurate, results.

4. In the present period of skyrocketing loads, standby reserves are more academic than real. When and if conditions become stabilized again, generating capacity will have increased considerably, the committee on reserves will have made further progress, and added operating experience will have been gained. At such time the Northwest Power Pool may elect to take another look at its standby reserve requirements.

REFERENCE

1. OUTAGE EXPECTANCY AS A BASIS FOR GENERATOR RESERVE, Howard P. Seelye. AIEE TRANSACTIONS, volume 66, 1947 (PROCEEDINGS T7253).

H. A. Adler (Commonwealth Edison Company, Chicago, Ill.): The probability values determined by the binomial law give only the ratios of duration and intervals of multiple occurrences, but not the actual values of durations and intervals. It is, therefore, of special interest that Loane and Watchorn have developed an experimental method for determining these important values. In an AIEE paper by Adler and Miller[1] equations were presented to determine these values mathematically.

A comparison of the results obtained by the two methods appears of interest. The authors kindly made available the results of one of their studies using the experimental method for a system having always 40 units in operation and having a probability of outage of 2.16 per cent and an average duration of outage of 4.03 days. The following Table II of this discussion shows a comparison of the experimental results with values calculated with equation 3 of the Adler-Miller paper.

The differences between experimental and calculated results appear to be due entirely to some difference in assumptions and due to the fact that the experimental method covered by necessity only a limited number of cases. A study of the two methods indicates that they will give identical results if the assumptions are the same and if the experimental study covers a large number of cases.

The intervals T_r can be calculated from the average durations t_r and the probability P_r calculated by the binomial law, that is, $T_r = t_r/P_r$.

REFERENCE

1. A NEW APPROACH TO PROBABILITY PROBLEMS IN ELECTRICAL ENGINEERING, H. A. Adler, K. W. Miller. AIEE TRANSACTIONS, volume 65, 1946, October section, pages 630-2.

E. S. Loane and **C. W. Watchorn:** Floyd has pointed out, at the conclusion of his discussion, two apparently conflicting statements. The authors appreciate the opportunity, therefore, of indicating complete agreement with his final sentence: what is an acceptable reliability or a reasonable reserve requirement undoubtedly is largely a matter of judgment. In the selection of a proper reserve, the only help that the probability theory can give is the determination that for a certain load and installed capacity the probability of failure to carry load by some amount is so much. This we have referred to as an "absolute" determination. Perhaps the choice of term was unfortunate; but its use was intended to distinguish this type of problem from others involving only relative reliabilities.

Table II

No. of Units on Forced Outage	Avg Duration of Outage in Days: Experimental Values for System of 40 Units Operating	Calculated Values: System of 40 Units Operating	Calculated Values: System of 40 Units
1	2.94	2.53	2.55
2	2.08	1.84	1.85
3	1.64	1.52	1.54
4	1.34	1.35	1.36
5	1.15	1.24	1.25
6	1.28	1.17	1.18
7	1.0	1.12	1.17

The comparison made by Adler between experimental and calculated average durations of multiple forced outages would have shown even better agreement had the authors recorded their experimental results on a basis directly comparable with that used in his computations. It is highly desirable that frequent checks be made between the theoretical and experimental methods of solution of various capacity problems. It appears that, at the present stage of development, the experimental approach can supply certain data that are not otherwise obtainable. It is not sufficient in capacity problems, involving use of a limited hydro storage, to consider only the average outage duration. Critical capacity conditions may arise when the forced outage durations are much longer than average; and the probabilities of such long outages, as shown in Figure 1 of this closure, are essential to correct evaluation of the useful hydro capacity.

The long and critical discussion by Ashley and Anstine is evidence of careful study of the subject paper and of other related material available to them. The authors recognized the need for careful evaluation of the diverse factors that are involved in the capacity problems of a combined hydro and steam system, and feel that they properly, or rather very conservatively, have evaluated each of them. Detailed discussion of each of these factors was not possible in a general paper nor in the limited space available for closure.

The conservatism of the authors' evaluation of the dependable capacity of the hydro plants, used for illustration in the paper, is shown by Figure 2 of this closure. This diagram shows the average availability of the hydro capacity as limited by maintenance, forced outages, and experienced river flows. Since the studies of system reliability indicated that these hydro plants, with a rated effective capacity of 334,000 kw, were equivalent to a steam installation of 285,000 kw in their capacity service to the interconnected system, there has been shown, for comparison, the probable availability of this amount of steam capacity assumed to be installed in five units, as it might be limited by maintenance, forced outages, and seasonal capacity reductions.

General Mobile Telephone System

H. I. ROMNES
MEMBER AIEE

R. R. O'CONNOR
MEMBER AIEE

THE tremendous need for communication with ships, airplanes, trucks, tanks, and other mobile units used in such large quantities during the war accelerated the development of practical mobile radiotelephone equipment for use in the 30 to 200 megacycle range and emphasized the practicability and usefulness of mobile telephone service. By the end of the war the art had advanced sufficiently in the applications of these higher frequencies so that it seemed practicable to provide telephone service to mobile units on a general basis rather than limit it to safety and emergency services as had been the case before the war. The Federal Communications Commission therefore made available a few frequencies for experiments in this field. In the two years which have elapsed, the Bell System has made this service available on an experimental basis in more than 60 cities and about 100 more systems are under construction. This paper describes the arrangements used and outlines the experience obtained to date with this service. Improvements are being made constantly so that this must be regarded as an interim report on a rapidly changing and expanding service.

Types of Mobile Telephone Systems

In its simplest form mobile service provides communications from a single central dispatch point to a group of mobile units. No direct connection exists between the radio system and the wire communications network. In this case the land station can be very simple—a radio transmitter and receiver connnected by four wires to a telephone transmitter and a telephone receiver. A push-to-talk switch can be used to energize the transmitter when it is desired to talk and to connect the receiver when it is desired to listen. The same radio frequency can be used for both transmitting and receiving. Similar arrangements are used in the mobile unit but for space, cost, and power drain reasons a lower powered transmitter generally is employed. Many such private mobile systems have been placed in operation, some of which are owned and maintained by the user and others owned and maintained by the telephone company or other service organizations but operated by the user of the system.

The simple private system may be expanded to cover larger areas by adding transmitters and receivers and interconnecting them by wire lines. Also, provisions may be made for more than one dispatching point. The New York Telephone Company owns and maintains a system used by the New York State Police which covers the entire state of New York and includes 37 land stations and more than 50 receiving only stations, has nearly 70 dispatching points, serves over 350 vehicles, and employs several thousand miles of interconnecting wire facilities. The Pennsylvania State Police System is provided and maintained by the Bell Telephone Company of Pennsylvania and includes 73 land transmitters and receivers, 77 dispatching points, and over 250 mobile units. The systems serving large areas generally operate in the 30–44-megacycle range and the ones serving limited urban areas operate in the 152–162-megacycle range.

For general mobile telephone service, provision must be made to connect a vehicle equipped for mobile telephone service to any telephone in the wire line network. This involves more complicated terminal arrangements, since the circuit must be reduced to a 2-wire basis to be connected to the wire line network and use cannot be made of the push-to-talk feature at the fixed telephones to switch the radio system alternately between the transmitting and receiving conditions. Such systems employ a different frequency for transmitting toward the mobile unit and receiving from the mobile unit to facilitate connections with the wire line network as well as to permit closer spacing of radio channels, thus using the frequency spectrum more efficiently.

Two types of general mobile systems have been provided for in the Federal Communications Commission allocation plan: *urban* systems which operate in the 152–162-megacycle range and are intended to cover a limited area, usually a city and its surrounding suburbs, and *highway* systems which operate in the 30–44-megacycle range and are intended to provide continuous service to vehicles moving along highways or vessels along waterways between cities. Provisions are made by the telephone company for three types of service.

1. General service which permits connections from a mobile unit to any telephone in the general network, with a 3-minute call as the basic unit of traffic.
2. Dispatch service which provides for connections between a particular dispatching point and one or more vehicles and uses as its basic traffic unit a 1-minute call at a lower rate per call than the general service.
3. Signaling service which provides for signaling a specific mobile unit to indicate that the operator of the unit should take some prearranged action, such as call his office from a nearby telephone. In this case, the mobile unit is not equipped for transmitting.

Extent of Present Development

Figure 1 shows the location of urban and highway systems now in service or under construction. Urban service is available in more than 40 cities with two or three channels in service or under construction in eight of these cities. High-

Paper 47-256, recommended by the AIEE communication committee and approved by the AIEE technical program committee for presentation at the AIEE Midwest general meeting, Chicago, Ill., November 3–7, 1947. Manuscript submitted August 18, 1947; made available for printing September 24, 1947.

H. I. ROMNES is radio engineer, American Telephone and Telegraph Company, New York, N. Y.; R. R. O'CONNOR is transmission engineer, Illinois Bell Telephone Company, Chicago, Ill.

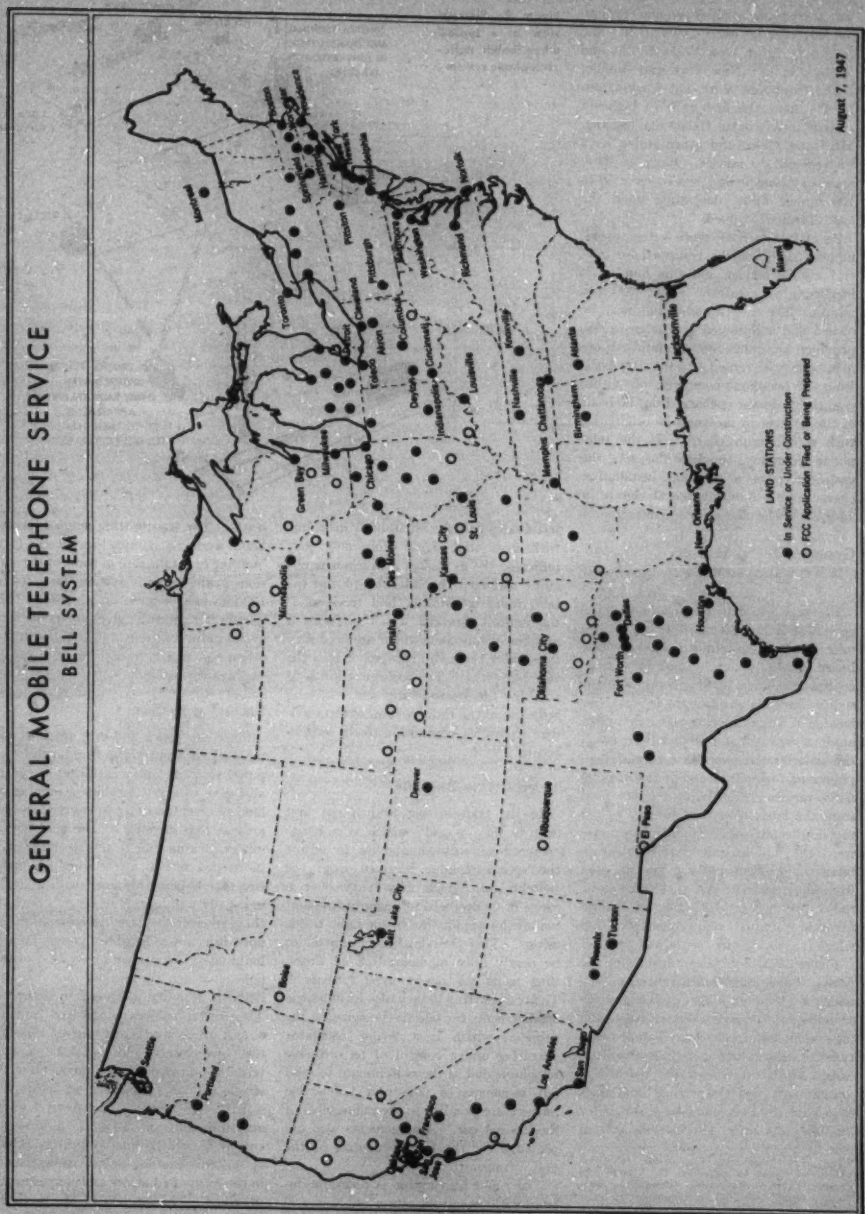

Figure 1. Extent of development of general mobile service

way stations in 22 cities provide continuous coverage between Chicago, Ill., and St. Louis, Mo.; New York, N. Y., and Boston, Mass.; New York and Buffalo, N. Y.; and New York and Washington, D. C. Also, the first units of highway systems in Wisconsin, Oklahoma, Indiana, Michigan, Ohio, and other states have been placed in service. Each of these mobile systems is designed to serve 50 to 100 mobile units, depending upon the type of traffic involved.

As of July 1, 1947, there were approximately 2,000 vehicles equipped for general mobile service and this number is increasing at a rate of about 200 per month. The mobile radio unit may be owned and maintained by the customer, provided minimum System standards are met, or may be rented on a monthly basis from the telephone company. In either case the customer is charged on the basis of the number of messages he originates, with a minimum charge. If the telephone company supplies the set, the customer pays a nominal installation charge and a monthly rental charge in addition to the charge for the messages.

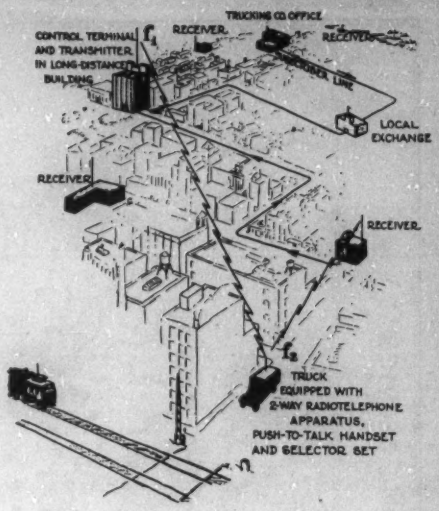

Figure 2. Pictorial view of a typical urban mobile radio-telephone system

General Description of a Typical System

Figure 2 is a pictorial view of a typical general mobile system. The land transmitter,* control terminal, and switchboard generally are located in a large central telephone building, although the radio transmitter sometimes may be located at a distance to obtain a favorable antenna site. Land subscribers reach the switchboard over their regular telephones and wire lines, except that for dispatch service a dispatch line is provided from the land subscriber directly to the mobile switchboard. Transmission toward the mobile unit is from a single main radio transmitter. Transmission from the relatively low powered mobile radio transmitter is to one of several favorably located radio receivers from which it goes by wire to the switchboard.

Figure 3 is a block diagram showing the principal components of a general mobile telephone system. The mobile service switchboard is a part of the normal switching system and, in fact, may handle other types of calls as well as mobile telephone calls. The land subscribers reach this switchboard over the normal land lines by asking the long distance operator for "mobile service." The mobile system terminates in the switchboard in a jack with associated signal lamp and busy indicator just as though it were a wire circuit. Between the switchboard and the land radio transmitter and receivers is the control terminal which performs a number of functions which are necessary to connect the radio equipment into the wire line plant. The basic function is to combine the transmitting and receiving branches of the radio system to form a 2-wire circuit for connection to the switchboard.

Transmitting Branch

In the transmitting branch the first unit is the "vogad" which is a *voice-operated-gain-adjusting-device* to adjust the speech volume received from the switchboard, which may vary over a range of 40 decibels, to a nearly constant volume for application to the radio transmitter. This permits the transmitter to be nearly fully modulated at all times, thus using its power most efficiently. The transmitting branch also includes the arrangements for selectively signaling the vehicles, which is a 2-tone oscillator operating under control of an ordinary telephone dial at the switchboard to send out sequences of 600- and 1,500-cycle pulses corresponding to the call number of the desired car. Arrangements also are provided for the remote control of the radio transmitter.

The radio transmitter is phase-modulated with an output power of about 250 watts. The transmitting antenna generally is a coaxial antenna located on a high building or, in the case of some of the stations in the highway system, on a 50- to 150-foot pole or tower on a hilltop. This transmitter generally gives good coverage over a radius of from 15 to 30 miles in the urban system and from 25 to 50 miles in the highway system.

Receiving Branch

Since, for space and cost reasons, the mobile radio transmitter uses much lower power than the land transmitter, it generally is necessary to provide a number of land receivers in order to cover the same area as that covered by the land transmitter. From four to ten receivers may be needed but in a few cases adequate coverage is being obtained with a single unusually well located receiver. Each of these receivers is placed where man-made noise is as low as feasible and may be in a building or in a cabinet at the base of the pole on which the coaxial receiving antenna is mounted as shown in Figure 4. The receiver includes a squelch or "codan" circuit which is adjusted to close through the voice channel and signal the control terminal on reception of a carrier which is strong enough to produce an acceptable signal-to-noise ratio. The receiver operates normally on 110 volts alternating current obtained from a commercial power system but standby power arrangements in the form of a battery and converter are provided. The outputs of the receivers

* The nonmovable end of a mobile telephone system has come to be called the "land" end whether it is part of a marine, vehicular, or aeronautical system and is so recognized in international radio definitions.

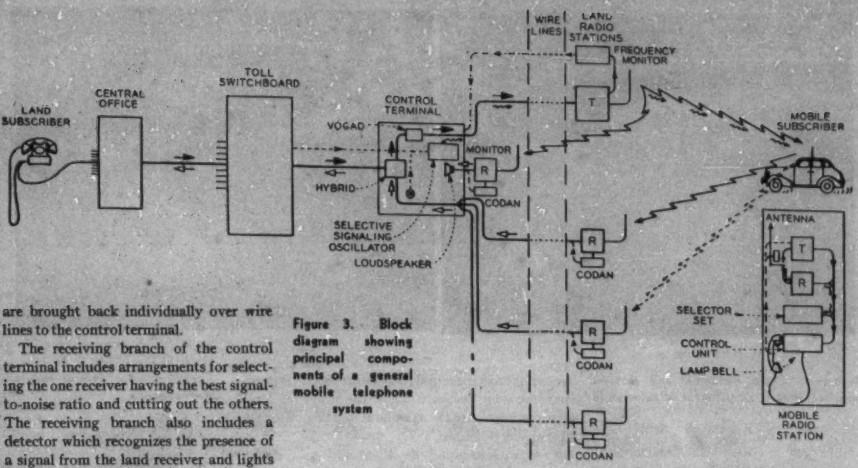

Figure 3. Block diagram showing principal components of a general mobile telephone system

are brought back individually over wire lines to the control terminal.

The receiving branch of the control terminal includes arrangements for selecting the one receiver having the best signal-to-noise ratio and cutting out the others. The receiving branch also includes a detector which recognizes the presence of a signal from the land receiver and lights the lamp at the switchboard, indicating that a mobile unit is calling. There also is included an amplifier which adjusts the received volume to the desired value relative to the transmitted volume.

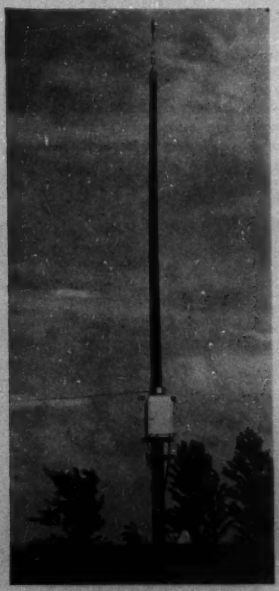

Figure 4. Land receiver mounted on pole supporting receiving antenna

Figure 5 pictures the control terminal. In addition to the components already mentioned, it includes a monitoring receiver and loud-speaker to check on the performance of the land transmitter and the necessary testing access for use in maintaining the system. A frequency monitor is associated with the transmitter which indicates when the transmitter is on the air and operating at the right frequency. If the frequency should deviate from its correct value by more than a few thousandths of a per cent, it sounds an alarm so the technical attendant immediately may take the transmitter off the air and correct the trouble. A low power test transmitter operating on the frequency of the mobile transmitters affords convenient means for checking the performance of the land receivers and the receving branch of the control terminal.

Mobile Equipment

The mobile installation includes a phase-modulated transmitter having output power of 15 to 25 watts, a receiver, and an associated selective signaling unit, a control unit consisting of a hand telephone set equipped with a push-to-talk key and the signal light and bell to indicate an incoming call, and the antenna. Power is obtained from the 6-volt or 12-volt system of the vehicle, which in many cases needs to be reinforced by provision of a heavy duty generator and battery to carry the added load. The radio transmitter and receiver are located in the luggage compartment of a car as shown in Figure 6, or in a cabinet on the inside or

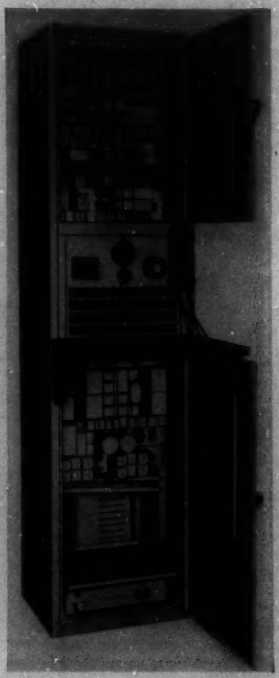

Figure 5. Control terminal for general mobile service

Figure 6. Radio transmitter and receiver installed in rear compartment of automobile

Figure 7. Control unit for general mobile service

outside of a truck. The control unit generally is located below the instrument panel in the driver's compartment as shown in Figure 7. In the urban system the antenna is about 18 inches long and generally placed at the center of the metal roof of the car or truck cab as in Figure 8. In the highway system the antenna is about six feet long and generally is mounted on the side of the vehicle so as to minimize the clearance required.

Procedure in Establishing a Mobile Connection

In placing a call from a vehicle, the user simply removes the hand telephone set from its hanger, which activates the transmitter, listens to determine the channel is not in use, and then momentarily operates the push-to-talk button, which causes a spurt of carrier to be radiated. This is picked up by one or more of the land radio receivers and operates a relay in the control terminal which lights a lamp at the switchboard. When the switchboard operator plugs in to answer the call, the land transmitter is started and continuously radiates the carrier. The frequency monitor determines that the carrier is on the assigned frequency and signals the switchboard operator that the system is ready for service. The connection is extended from the switchboard to the land subscriber over the regular wire network. The mobile subscriber presses the button in the handle of his hand set when he talks and releases it when he listens, but the land subscriber uses his telephone in the usual manner.

In establishing a connection from a land subscriber to a vehicle, the subscriber obtains the mobile service operator over the wire line network in the usual way and gives her the telephone number of the vehicle desired. This number consists of two letters and five digits, such as WX2-3774. The operator plugs into the jack associated with the mobile system and dials the called number. This causes alternate spurts of 600- and 1,500-cycle tone to be radiated which operate the selector unit in all cars within range of the radio transmitting station. However, only the selector unit adjusted to the code which is dialed completes its cycle and operates the bell and signal light in the called vehicle. All selector units are restored to normal when the operator plugs into the jack to make the succeeding call.

Technical Characteristics of Mobile Sets

In the Bell System general mobile service, mobile sets made by Motorola, Radio Corporation of America, and Western Electric are being used. The last will be described to illustrate the general features of the mobile equipment.

Western Electric Urban Mobile Radio Transmitter

This transmitter provides an output power of approximately 20 watts of phase-modulated carrier at a single crystal-controlled frequency in the range of 152 to 162 megacycles. The unmodulated carrier frequency tolerance is plus or minus 0.005 per cent. The normal carrier deviation is plus or minus 11 kc. The audio frequency response is substantially flat from 250 to 4,000 cycles. A dynamotor power supply is contained within the transmitter and arrangements are available to operate on 6-volt or 12-volt battery sources. The power drain from a 6-volt source is about 0.3 ampere standby and about 50 amperes in the transmitting condition. The weight of the transmitter is 38 pounds and its approximate dimensions are 17 inches by 10 inches by 8 inches.

The transmitter is similar in most respects to other types of transmitters designed for the mobile service. There are 12 identical filamentary-type tubes in the actual transmitter circuit which are used in the conventional oscillator, modulator, two doublers, two triplers, and amplifier stages. However, there are several unique features in this transmitter; the temperature-controlled crystal, for example, oscillates at a considerably higher frequency than in most similar transmitters and the multiplication factor is only 36 times in building up to the final

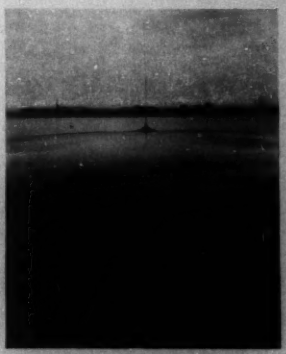

Figure 8. Antenna for urban mobile service mounted on roof of automobile

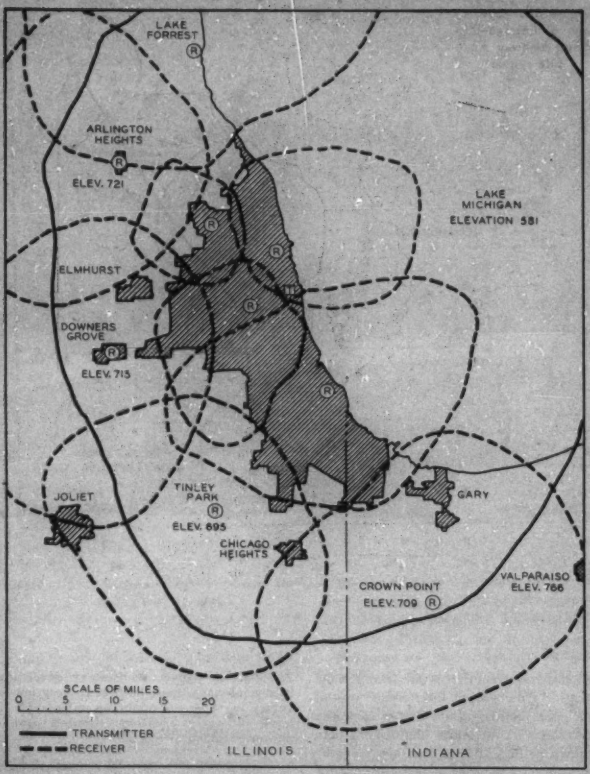

Figure 9. Transmitter and receiver coverage for urban system in Chicago

radio frequency. This is an aid in reducing the number of spurious radiations of the transmitter. This transmitter also has been designed so that the antenna adjustments required at the time of installation do not appreciably affect the spurious radiation of frequency. Another feature is that the design of the transmitter permits the use of a plug-in test set to measure currents or voltages at six key points in the circuit without removing the transmitter cover. This, of course, facilitates the diagnosis of trouble conditions.

Western Electric Mobile Radio Receiver

This receiver is of the crystal-controlled double-superheterodyne type and receives phase-modulated signals on any one 60-kc channel in the 152 to 162 megacycle band. The circuit incorporates 16 miniature-type tubes plus a rectifier and built-in vibrator power supply. The power drain from a 6-volt battery source is about seven amperes and the set will operate from either 6 or 12 volts direct current. The rated audio power output of the receiver is 200 milliwatts; the receiver's weight is 33 pounds, and its approximate dimensions are 17 inches by 10 inches by 8 inches. A plug-in test set also will check certain points to determine the conditions of operation.

A squelch circuit is provided to silence the receiver unless a carrier of a sufficient magnitude is received. The high intermediate-frequency is 20.4 megacycles and the low intermediate-frequency is 2 megacycles. The audio output is flat within 4 decibels from 250 to 4,000 cycles. All spurious responses, including image responses, are 80 decibels down from the operating frequency. The selectivity of this receiver is particularly good, the response being down 50 decibels when 60 kc from mid-band.

This receiver is designed to operate with selective signaling equipment and a selector is built into the receiver on a plug-in basis.

Selector Set

The selector used in the Western Electric receiver also is manufactured as a separate component which can be used with most types of mobile receivers, although slight modifications may be required in some cases. The required direct voltages of 6 and 160 volts are supplied by the radio receiver. When supplied as a separate external unit, the weight is 22 pounds and the dimensions are approximately 16 inches by 8 inches by 5 inches. A total of 2,030 possible distinct and usable number combinations is provided.

The selector is operated by a code which consists of a series of alternate pulses of 600 and 1,500 cycles which are transmitted at a uniform rate under control of a standard telephone dial or sender at the land station. Selective circuits alternately respond to the 600- and 1,500-cycle tones and operate a stepping relay which rotates a contact wheel. Five stop pins are placed in the contact wheel in positions corresponding to the five digits which comprise the telephone number of the particular selector. When any digit is dialed, the contact wheels of all mobile stations receiving the transmission will advance a number of steps corresponding to the digit dialed. Only those wheels however, that have pins at the point of advancement corresponding to the digit dialed will hold and the remainder will return to normal. Successive dialing of digits causes all selectors to advance again. However, only the selector which progressively advances on all five digits causes a bell and lamp to operate in the control unit. The sum of the digits used in all telephone numbers must equal 23.

Performance

Urban Systems

Figure 9 shows the coverage obtained with the urban system in Chicago, which is typical of these systems. It will be noted that good transmission is obtained from the land transmitter to mobile units up to a distance of approximately 25 miles. There are very few areas of poor transmission, even where there are large obstructions, such as buildings, between

the transmitter and the mobile receiver. In this respect, operation in the urban (152 to 162 megacycles) range has proved much more satisfactory than in the highway range (30 to 44 megacycles). The areas of good transmission from the mobile transmitters to the land receivers also are shown in Figure 9, and it will be noted that receivers have been so placed that transmission in the two directions is substantially balanced. Some interference has been encountered due to diathermy but generally it has been for brief periods and has affected only one or two receivers in a system. Ignition noise in the mobile units has not been a serious problem. Little interference has been encountered from other mobile systems operating on the same frequencies, even though the same frequencies are used in cities separated by as little as about 50 miles. As will be discussed later, only alternate channels can be used in any one service area; however, the in-between channels can be used at points about 25 miles or more away.

Highway Systems

Figure 10 shows the coverage pattern for the stations along the Chicago–St. Louis highway, which is typical of such systems. The range of the land transmitter in this case averages about 40 miles with some as great as 60 miles. In contrast with the urban systems, experience to date indicates that electric disturbances, principally ignition noise, seriously may reduce the coverage area for a given circuit merit; also, the typical side mounting of the longer antennas required for the highway frequencies results in marked differences in reception as the position of the car varies with respect to the transmitter. It can be noted that in order to give continuous coverage along the principal highways between Chicago and St. Louis there are overlap areas in which adjacent stations can be heard. Arrangements are provided so that when a connection is established to a car in one of these overlap areas, the adjacent station is kept off the air. This is done by providing wire circuits between adjacent stations, which light a busy lamp at the switchboard of one station when the other one is serving a car in the area which is within range of both.

As stated previously, the highway system operates in the 30–44-megacycle range, where some sky-wave transmission may be expected. Observations of long range transmission during the first six months of 1947 indicated that most of the long range transmission occurred over distances of more than 1,000 miles and that

Figure 10. Coverage of Chicago–St. Louis highway mobile system

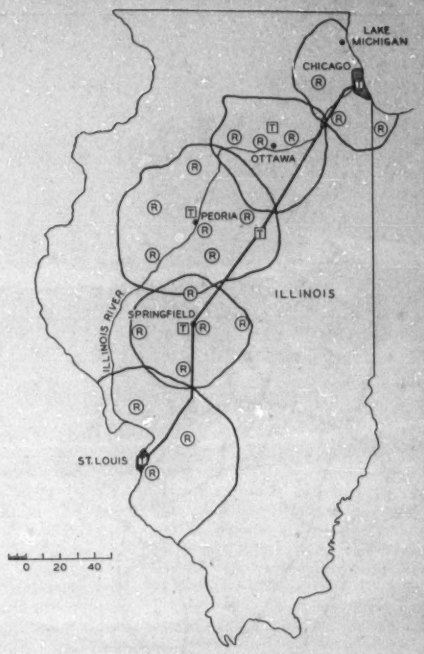

good signal strength was obtained in most cases. This type of interference was of such serious magnitude that it has been necessary to introduce the zoning plan shown in Figure 11. This plan permits the same frequencies to be used only for stations separated by less than about 1,000 miles. Equipment will be available soon to permit a user to change frequencies readily when he travels from one highway zone to another.

Operation of Closely Spaced Radio Channels

At present the 30–44-megacycle band is divided into 40-kc channels, but the radio equipment now available generally is not selective enough to be operated closer than alternate channels and some early type receiving equipments require even more separation. The same situation applies to the 152–162-megacycle region except that the channels are 60 kc wide. Engineering for operation of the maximum number of radiotelephone channels in the available frequency space includes the following factors:

1. Mobile and land station receivers must have a high degree of selectivity against adjacent channels.

2. Spurious signals, which may develop in several ways, must be held to very low values in order to minimize unfavorable level differences between wanted and unwanted signals.

3. It is sometimes possible to take steps at the land stations, which are relatively few in number, to keep the technical requirements on the numerous vehicular sets within practical bounds. One such step employed in some Bell System installations is to turn on the carrier of a land transmitter automatically whenever the land transmitter of a nearby channel is in use. By this means the capture effect from the carrier of the idle transmitter prevents its associated vehicular receivers from hearing unwanted transmissions from the second transmitter.

Outlook for the Future

Expansion of Present Service

For highway service the Federal Communications Commission has allocated a block of 20 pairs of frequencies spaced at intervals of 40 kc. Of these, 12 pairs have been designated tentatively for use by common carriers in giving general mobile service. However, many channels in this band now are occupied by other users such as police and fire departments,

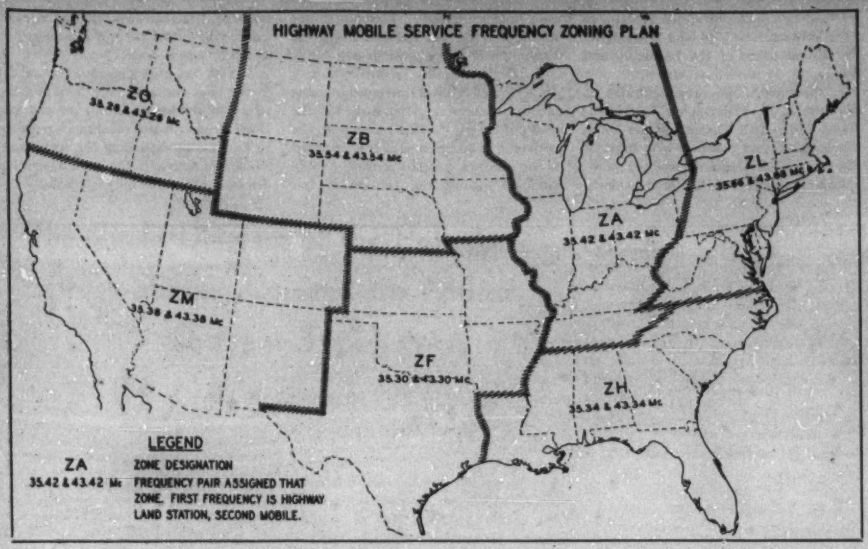

Figure 11. Highway mobile service frequency zoning plan

and these have been given until July 1950 in which to move to their newly assigned channels. This limitation, together with the necessity to use different frequencies in different parts of the country in order to avoid long range interference, means that the present allocation, in general, will permit only one highway system in a given area.

For urban service the Federal Communications Commission has allocated a block of 12 pairs of frequencies at 60-kc intervals, and of these 6 pairs have been designated tentatively for use by common carriers in giving general mobile service. With present techniques it is practicable to use only alternate channels in a given area, even with the best radio equipment now available. On this basis, the present allocation provides for a maximum of three working channels for general mobile service in each area.

In the larger cities the demand for the service is far greater than can be taken care of by these three channels, some cities having many hundreds of customers waiting for mobile service. It has been estimated that the larger metropolitan areas, such as New York, Chicago, and Los Angeles, Calif., will have demand for 10,000 or more mobile units within the next few years and that to take care of this demand will require approximately 150 pairs of frequencies.

Provision of this much service with economical use of frequency space involves systems and design problems which are more complex and extensive than anything attempted heretofore in the mobile radio field. These problems are considered to be amendable to a reasonable engineering solution, provided that a suitable frequency allocation plan is realized.

Development is progressing on new mobile equipment which will have high selectivity and other improvements.

New General Mobile Services

In addition to service to vehicles, which has been emphasized thus far, it has been found that there is considerable demand for the service by other types of mobile units, such as river boats, ships on the Great Lakes, harbor craft and pleasure boats along the coasts, and switch engines and work trains on railroads. This service, in general, is being taken care of for the time being on the same systems as are used to serve trucks and cars, but as the needs increase, it may be desirable to establish separate systems for marine and other uses. In fact, in New York City a separate channel operating in the 152–162-band already has been established solely for serving harbor craft.

There also appears to be demand for telephone service to the passengers on airplanes and railroad trains. In April 1947 a *DC-6* plane operated by the United Air Lines was equipped with telephone service on its inaugural transcontinental flight. This experimental service was given through the urban land stations which are now available at close enough intervals to give fairly continuous service to a plane flying at high altitude. The experience was that good transmission could be obtained within a circle of about 200 miles in diameter around each land station with the plane at 18,000 to 20,000 feet but that the air-borne set would cause interference to other stations operating on the same frequencies within a circle up to about 400 miles in diameter. It was obvious that urban systems, which are designed to give service to mobile units on the surface of the earth with the same frequencies sometimes used at intervals of 50 or 100 miles cannot be employed to serve airplanes because of the interference problem. For a satisfactory service to passengers on airplanes, it probably would be necessary to establish stations specifically for this purpose spaced at intervals of about 200 miles, possibly with special interconnecting arrangements to give continuous service. Radiotelephone service to railroad

passengers is being furnished experimentally between New York and Washington on several trains of the Baltimore and Ohio and Pennsylvania railroads. For this experiment, the urban stations at Newark, N. J.; Philadelphia, Pa.; Baltimore, Md.; and Washington are being employed to give coverage over most of the route. For occasional users of radiotelephone service, it is not practicable to use a push-to-talk key. Therefore, in the installations on the railroad trains the transmitter is active continuously during each telephone call. Interference with the associated receiver is avoided by using different antennas, separated by the length of the car, for the transmitter and receiver. In addition, a filter is provided in the receiver antenna circuit to discriminate against the transmitter frequency. Thus the passenger on the train can use the service as easily as he does his own telephone at home.

A great deal of progress has been made in the brief period since general mobile telephone service came into the picture. However, it is obvious that much remains to be done in expanding the scope and amount of service to the point where the demand for it can be fully satisfied.

No Discussion

The Circle Diagram of the Polyphase Brush-Shifting Commutator Motor (Schrage Type)

PAUL W. FRANKLIN
ASSOCIATE AIEE

Synopsis: This paper presents a derivation of the circle diagram and performance formulas of the polyphase brush-shifting motor (Schrage type). Using similar assumptions as required for the derivation of the Heyland circle, a simple diagram is developed, which permits the graphical determination of current, power factor, output, slip, and copper losses of the machine. Design formulas are given.

THE CHARACTERISTICS of the Schrage motor resemble those of the d-c shunt motor. The Schrage motor requires a rather complicated brush gear, which is the principle objection to a general application. For smaller machines, however, this brush gear may be simplified considerably. As to size, such a motor generally will exceed a squirrel cage motor of the same rating for one or two frame sizes and approach the size of a d-c shunt motor of similar rating.

An excellent paper[1] was published in 1941, covering the general aspect of the machine. However, certain simplifications and assumptions were made there, which, though not objectionable in principle, limit the value of the method offered. This paper attempts to develop a representative circuit and a circle diagram comparable to the Heyland circle diagram.

It is not intended to give a detailed description of the electrica and mechanical features of the Schrage motor in this paper. For this, the reader again is referred to the foregoing publication. However, for the purpose of general orientation, a short description will be attempted.

Paper 47-263, recommended by the AIEE rotating machinery committee and approved by the AIEE technical program committee for presentation at the AIEE Midwest general meeting, Chicago, Ill., November 3-7, 1947. Manuscript submitted January 2, 1947; made available for printing September 24, 1947.

PAUL W. FRANKLIN, formerly with the Continental Electric Company, Inc., Newark, N. J., now is in the engineering department of Eclipse Pioneer Instrument Corporation, Teterboro, N. J.

General

The primary winding of this motor is placed in the bottom of the rotor slots and fed from the line through slip rings. Index "1" is used in the future for this winding, which resembles the usual stator winding of a polyphase induction motor. A small compensating winding is placed on top of it, marked by index "3." This winding resembles a normal d-c armature winding and is connected to a commutator. The stator houses the secondary winding, marked by index "2." This winding is similar to a normal stator winding and its number of phases is independent of the number of line phases. It is connected to the commutator brushes.

The commutator acts in a threefold way. First, it converts the line frequency of the compensating winding voltage to the slip frequency of the induced secondary voltage in the stator. Secondly, by shifting the brushes, it permits the adjustment of the brush voltage impressed on the stator from a positive value down to zero and further to a negative value. Thirdly, it permits a change of phase up to 360 degrees of this impressed voltage, in comparison with the phase of the induced secondary voltage. To summarize it may be said that the frequency of this impressed brush voltage depends only upon the relative speed of the resulting air gap field versus the stationary brushes. The amount of this voltage depends only upon the flux magnitude, the relative speed of the resulting air gap flux versus the rotating rotor, and the spacing of the brushes of the same phase. Finally, the phase of this voltage depends upon the absolute position of the brush gear in space.

The speed of the rotor will adjust itself to such a value that the impressed brush voltage added vectorially to the induced slip voltage in the stator is equal to the total voltage drop in the combined secondary and compensating circuit. The reactance of this circuit is approximately proportional to the slip frequency and therefore will assume negative values above synchronous speed. Above this speed, energy is being fed from the line through the compensating winding to the stator, whereas below it, energy is fed back to the line. At synchronous speed, brushes of the same phase touch the same commutator bar. Thus, the stator winding is short-circuited and acts in principle like a normal secondary induction motor winding. By changing the relative spacing of brushes of the same phase, the speed may be adjusted, whereas by changing the absolute position of the brush gear in space, power factor compensation may be obtained.

General Formulas

The following assumptions are being made

(*a*). The saturation constant of the machine shall remain constant.

(*b*). The influence of skin effect and saturation of the leakage path shall be neglected.

(*c*). The main flux interlinked with the secondary winding shall be assumed to be the same as the main flux interlinked with the compensating winding. In other words, the leakage reactance drop from primary to secondary winding shall be the same as from primary to compensating winding. This assumption is on the pessimistic side. In his paper[2] Schrage neglects any voltage drop between the primary and compensating winding. However, in view of the fact that

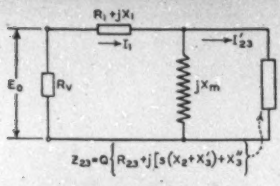

Figure 1. Representative circuit

several variables at best may be estimated only, (brush drop, short-circuit currents, higher harmonics) this assumption may be regarded as a safe one.

(*d*). The influence of higher harmonics caused either by windings or saturation, shall be neglected. Attention, however, is called to the fact that for $\alpha \neq 0$ or 180 degrees and $\beta \neq 0$ or 180 degrees (see hereinafter) disturbances may occur, particularly if the stator is wound for two phases. Furthermore, as L. Schomburger shows,[3] the compensating winding occasionally causes even harmonics which cannot be cancelled by either primary or secondary winding; the effect is an increase of the secondary reactance.

(*e*). The influence of short-circuit current under the brushes is neglected.

(*f*). The voltage drop between brush and commutator shall be considered by an increase of the secondary resistance.

(*g*). Windage, friction, and iron losses are represented by the watt component of the no-load current.

(*h*). The reactance of the compensating winding consists of two terms, one proportional to the line frequency, the other to the slip frequency. This interesting fact first was interpreted by Arnold[4] and explained in detail by Winkler.[5] See Appendix III.

Finally, it is assumed that all resistance and reactance values are known. As to the compensating winding, these values vary with the mutual brush spacing.

Let ϕ_0 be the flux common to primary, secondary, and compensating winding, then the induced electromotive forces are

$$\boldsymbol{E}_1 = \boldsymbol{E}_0 - \boldsymbol{I}_1\boldsymbol{Z}_1 = 4.44 \cdot f \cdot N_{1\,eff} \cdot \phi_0 \cdot 10^{-8} \text{ volt} \tag{1}$$

$$\boldsymbol{E}_2 = \frac{N_{2\,eff}}{N_{1\,eff}} \cdot \boldsymbol{E}_1 \cdot s \cdot \epsilon^{j\alpha} \tag{2}$$

$$\boldsymbol{E}_3 = \frac{N_{3\,eff}}{N_{1\,eff}} \cdot \boldsymbol{E}_1 \tag{3}$$

with

$\boldsymbol{E}_1, \boldsymbol{E}_2, \boldsymbol{E}_3$ = induced voltages
$\boldsymbol{I}_1$ = primary current
s = slip
$\boldsymbol{E}_0$ = line voltage
$N_{1,2,3\,eff}$ = effective turns per phase
$\boldsymbol{Z}_1 = R_1 + jX_1$
R_1, X_1 = primary resistance and leakage reactance
α = brush rocker angle; phase angle between secondary and compensating winding
f = line frequency

The current $\boldsymbol{I}_{23}$ flowing in the secondary and compensating winding is

$$\boldsymbol{I}_{23} = \frac{\boldsymbol{E}_2 - \boldsymbol{E}_3}{R_{23} + j(sX_{23} + X_3'')}$$

$$= \boldsymbol{E}_1 \frac{sk_2\epsilon^{j\alpha} - k_3}{R_{23} + j(sX_{23} + X_3'')} \tag{4}$$

with

$R_{23} = R_2 + R_3$ + brush drop resistance
$X_{23} = X_2 + X_3'$
X_3, R_3 = secondary leakage reactance and resistance
X_3' = compensating winding reactance, proportional to slip
X_3'' = compensating winding reactance, proportional to line frequency

All X values as used in these formulas refer to line frequency. X_3' is usually small and may be neglected.

$k_2 = (N_{2\,eff}/N_{1\,eff})$
$k_3 = (N_{3\,eff}/N_{1\,eff})$

The current $\boldsymbol{I}_{23}'$ which represents $\boldsymbol{I}_{23}$ in the primary winding may be calculated to

$$\boldsymbol{I}_{23}' = \boldsymbol{I}_{23}\frac{m_2}{m_1} \cdot \frac{N_{2\,eff} \cdot \epsilon^{j\alpha} - N_{3\,eff}}{N_{1\,eff}}$$

$$= \boldsymbol{I}_{23} \cdot \frac{m_2}{m_1}(k_2 \cdot \epsilon^{j\alpha} - k_3) \tag{5}$$

Due to brush rocker shift in space, the relative spacing between secondary and compensating winding is changed. Either of the two could have the factor $\epsilon^{-j\alpha}$ affixed. However, the formulas are simplified and the presented theory is made adaptable for the plain 3-phase commutator shunt motor, if $\epsilon^{j\alpha}$ is applied to $N_{2\,eff}$. A sinusoidal distribution of the magnetomotive force is assumed. This formula results from the fact that the magnetomotive force of the two currents in their respective windings must be alike.

m_1 = number of primary phases
m_2 = number of secondary phases

Combining equations 4 and 5 we obtain

$$\boldsymbol{I}_{23}' = \boldsymbol{E}_1 \cdot \frac{m_2(k \cdot \epsilon^{j\alpha} - k_3)(s \cdot k_2\epsilon^{j\alpha} - k_3)}{m_1 \cdot R_{23} + j(sX_{23} + X_3'')} \tag{6}$$

Using the abbreviation

$$Q = \frac{m_1}{m_2} \cdot \frac{1}{(k_2 \cdot \epsilon^{j\alpha} - k_3)(s \cdot k_2\epsilon^{j\alpha} - k_3)} \tag{7}$$

we obtain

$$\boldsymbol{I}_{23}' = \frac{\boldsymbol{E}_1}{Q[R_{23} + j(sX_{23} + X_3'')]}$$

$$= \frac{\boldsymbol{E}_0 - \boldsymbol{I}_1\boldsymbol{Z}_1}{Q[R_{23} + j(sX_{23} + X_3'')]} \tag{8}$$

The representative circuit may now be drawn as shown in Figure 1 with

$$R_v = \frac{m_1 E_0^2}{V_{\text{iron}} + V_{\text{windage}}}$$

to consider iron and windage losses. In this circuit X_m represents the magnetizing reactance for full load saturation and is assumed to remain constant.

Finally we obtain the primary current to

$$\boldsymbol{I}_1 = \frac{\boldsymbol{E}_0}{\boldsymbol{Z}_1 + [jX_m \cdot \boldsymbol{Z}_{23}/(jX_m + \boldsymbol{Z}_{23})]} \tag{9}$$

with

$$\boldsymbol{Z}_{23} = Q[R_{23} + j(sX_{23} + X_3'')]$$

In this equation, all values are constant with the exception of the slip s, and if we expand it, we obtain a vector equation similar to

$$\boldsymbol{Y} = \frac{\boldsymbol{A} + s \cdot \boldsymbol{B}}{\boldsymbol{C} + s \cdot \boldsymbol{D}} \tag{10}$$

which is the general equation of a circle diagram with the parameter s. The dimensions and the general location of this current circle will depend upon the circuit constants and the brush rocker location and spacing.

For given values of α and β the primary current for four discrete points may be calculated and the circle diagram drawn, whereby, the fourth point is used as a check against errors. These four discrete points are

$$\left.\begin{array}{l} s = 0, \text{ synchronous point} \\ s = 1, \text{ locked rotor point} \\ s = s_0, \text{ no-load point} \\ s = \text{infinite} \end{array}\right\} \tag{11}$$

If no power factor correction is required, α becomes zero below and 180 degrees above synchronous speed. The resulting equations for this case now are derived.

Formulas for $\alpha = 0$ and 180 Degrees

Speed adjustment is obtained by changing the spacing between brushes of the same phases. This changes the number of effective turns of the compensating winding to

$$N_{3\,eff} = \frac{z_3}{4a} \cdot \frac{2}{\pi} \cdot \sin\frac{\beta}{2} \cdot CF_3 \tag{12}$$

with

z_3 = total number of conductors in compensating winding
a = number of pairs of parallel circuits in compensating winding
β = brush spacing angle in electrical degrees
CF_3 = chord factor of compensating winding

In the equations given hereinafter, the following signs are used:

Quantity	Below Synchronous Speed	Above Synchronous Speed
Slip	+	−
Energy flow	Secondary to primary	Primary to secondary
E_2	+	+
k_2	+	+
E_3	+	−
Absolute value of E_3	$>\lvert E_2\rvert$	$<\lvert E_2\rvert$
Absolute value of $k_2 \cdot s$	$>\lvert k_2\rvert$	$<\lvert k_2\rvert$
β	+	+
Real component of I_{21}	+	−
Real component of I_{23}'	+	+
α	0 deg	180 deg
$k_2 \cdot e^{j\alpha}$	+	−

For $\alpha = 0$ degrees or 180 degrees, the term $e^{j\alpha}$ will be dropped and we assign to k_2 the signs

+ below synchronous speed
− above synchronous speed

Secondary current

$$I_{23} = E_1 \frac{sk_2 - k_3}{R_{23} + j(X_{23} + X_3'')} \tag{13}$$

Secondary current reduced to primary

$$I_{23}' = I_{23} \frac{m_3}{m_1}(k_2 - k_3) \tag{14}$$

Figure 2A. Circle diagram for speed above synchronous value ($\alpha = 180$ degrees)

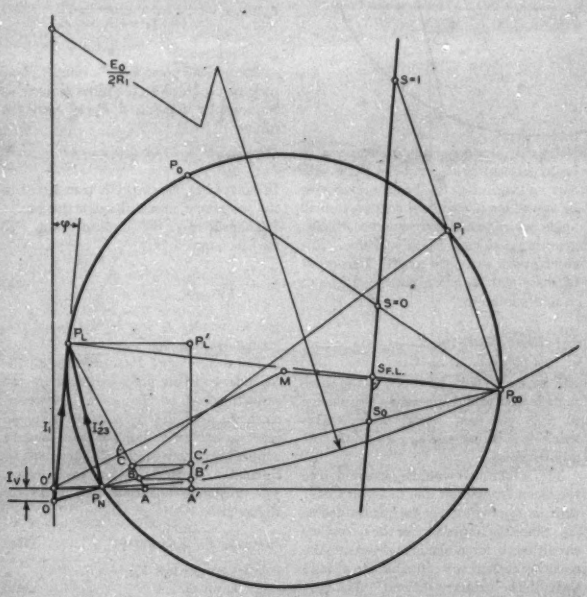

The current values for the four discrete points are as follows:

(*a*). *No-load point*

$$s_0 = \frac{k_3}{k_2} \tag{15a}$$

$$I_1 = \frac{E_0}{Z_1 + jX_m} \tag{15b}$$

(*b*). *Locked rotor point* ($s = 1$)

$$I_1 = E_0 \times \frac{Q_1 R_{23} + j(Q_1 X_s + X_m)}{j(R_1 X_m + Q_1(R_1 X_s + X_1 R_{23} + X_m R_{23})) - (X_1 X_m + Q_1(X_m X_s + X_1 X_s - R_{23} R_1))} \tag{16a}$$

with

$$Q_1 = \frac{m_1}{m_2(k_2 - k_3)^2} \tag{16b}$$

and

$$X_s = X_3 + X_3' + X_3'' \tag{16c}$$

(*c*). *Infinite point* ($s = infinite$)

$$I_1 = E_0 \frac{j(X_m + Q_t X_t)}{jR_1(X_m + Q_t X_t) - (X_m X_t Q_t + X_1 X_m + X_1 X_t Q_t)} \tag{17a}$$

with

$$Q_t = \frac{m_1}{m_2(k_2 - k_3)k_2} \tag{17b}$$

and

$$X_t = X_3 + X_3' \tag{17c}$$

(*d*). *Synchronous point* ($s = 0$)

$$I_1 = \frac{E_0}{(R_1 + jX_1) + \dfrac{jX_m Q_0(R_{23} + jX_3'')}{jX_m + (R_{23} + jX_3'')Q_0}} \tag{18a}$$

with

$$Q_0 = \frac{-m_1}{m_2(k_2 - k_3)k_3} \tag{18b}$$

Evaluation of the Circle Diagram for $\alpha = 0$ or 180 Degrees

The circle diagram permits a simple and practical determination of the performance data which otherwise cannot be obtained without intricate calculations. Figures 2*A* and 2*B* show the circle diagram for speeds below and above synchronous value. By plotting the four current values, we obtain the circle points P_N, P_1, P_∞, and P_0, and the circle center M. It can be proved from the general circle diagram theory that the parameter—in our case the slip s—may be represented by a linear scale parallel to the circle tangent in point P_∞. On this scale, three slip values may be identified by intersecting it with the chords

$s = s_0$; chord $P_\infty P_N$
$s = 1$; chord $P_\infty P_1$
$s = 0$; chord $P_\infty P_0$

From this we obtain the general scale graduation, since it is a linear one.

Iron, windage and friction losses are considered by dropping the origin of the diagram from $0'$ to 0. This distance is equal to

$$I_\psi = \frac{V_{\text{iron}} + V_{\text{windage friction}}}{m_1 E_0}$$

For any load point we obtain the primary current to OP_1 and also the power factor angle φ. The secondary current reduced to the primary I_{23}' is then $P_N P_L$ and from this, with the help of equation 14, we get the actual value of I_{23}.

Output, torque, and copper losses may be found as follows. If we draw a line from our load point P_L vertically to the line $O'M$ and intersect it with the chords $P_N P_\infty$, $P_\infty P_1$, and the abscissa, we obtain the points A, B, and C. These points are projected to a line parallel to the ordinate E_0 and the results are the points A', B', and C'. As shown in Appendix I, we find

Delivered torque $T = 7.04 \dfrac{\overline{P_L'B'} \cdot m_1 E_0}{RPM_0}$ in foot pounds (19a)

Mechanical output $P = m_1 E_0 \cdot \overline{P_L'C'}$ in watts (19b)

Primary copper loss $V_{\text{cul}} = m_1 E_0 \cdot \overline{B'A'}$ in watts (19c)

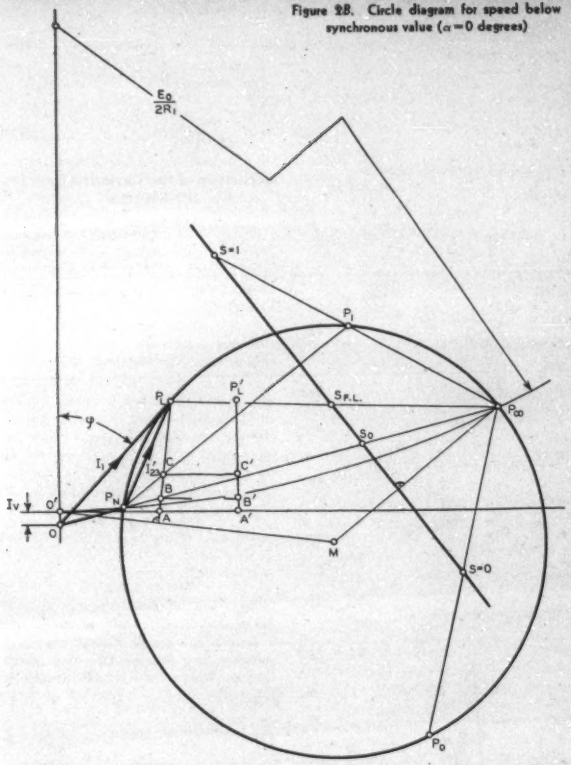

Figure 2B. Circle diagram for speed below synchronous value ($\alpha=0$ degrees)

Secondary and compensating winding copper loss $V_{cu22}=m_1E_0\cdot\overline{B'C'}$ in watts (19d)

The values $\overline{P_L'B'}$, $\overline{P_L'C'}$, $\overline{B'A'}$, and $B'C'$ are expressed in amperes. RPM_0 is the no-load speed.

It should be noted that the points P_n and P_∞ may be found by drawing a circle with the radius

$R=E_0/2R_1$ in amperes

its center in the ordinate and one point of it coinciding with $0'$. This interesting fact may be proved by the general theory of the circle diagram.

Evaluation of the Circle Diagram for $\alpha\neq0$ or 180 Degrees

Suppose the brushes of this machine were adjusted such that a no-load speed of 50 per cent of the synchronous value would be obtained. Therefore E_2 must be 50 per cent of E_2 and be in phase with this voltage. Let the brush rocker now be moved for 10 electrical degrees, a small angle which would correspond to $3^1/_3$ degrees in space for a 6-pole machine. The commutator voltage is now 10 degrees out of phase with E_2 and a voltage difference of approximately

$$\frac{10}{360}\pi E_2=0.0872E_2$$

will appear. This, however, is the same voltage that would appear if a slip change of 8.72 per cent would occur. This machine is rather sensitive to brush misadjustment.

This additional voltage, inserted into the secondary circuit due to brush rocker shift, is approximately in quadrature to E_2. Since the impedance of the secondary circuit has a large ohmic component, the resulting current will contribute to a phase shift of the primary current. The permissible amount of compensation is limited by the thermal and commutating capacity of the machine.

We may compute the current values for several points, by using equation 4 and substituting

$$\epsilon^{j\alpha}=\cos\alpha+j\sin\alpha \tag{20}$$

Such a circle is shown in Figure 2C. We note that the previous no-load point P_n with a current

$$I_1=\frac{E_0}{R_1+j(X_1+X_m)}=\overline{O'P_n} \tag{21}$$

is no longer located on the circle periphery. In each induction machine, the resulting flux is of such size that it induces back the primary voltage minus primary voltage drop. Therefore, the resulting free magnetomotive force of the machine will be such as to create this flux. The primary current not only must compensate for the opposite magnetomotive force of the secondary and compensating winding, but also provide the necessary magnetomotive force for the main flux. In other words, the primary current is the vector sum of the no-load current (essentially the magnetizing current) and the reduced secondary current I_{22}'. That means that in Figure 2C the distance P_nP_L is equal to I_{22} and

$$I_{22}=\overline{P_nP_1}\cdot\frac{1}{\sqrt{k_2^2+k_3^2-k_2k_3\cos}}\cdot\frac{m_1}{m_2} \tag{22}$$

(See equation 5).

The no-load point and the infinite point may be obtained in the same manner as for $\alpha=0$ by drawing a circle with the radius

$R=E_0/2R_1$

In both cases, no energy is transferred to the secondary circuit through the gap.

The slip for the no-load point P_n* may be found to be

$$s_n=\frac{k_2(\cos\alpha R_{22}-X_2''\sin\alpha)}{k_2R_{22}+X_{22}k_2\sin\alpha} \tag{23}$$

(see Appendix II for derivation of this formula.)

The total energy P_1 transferred to the secondary circuit may be found by the same method as for $\alpha=0$. However, since I_{22} does not decrease to zero, no representative distance for the secondary copper losses may be given. They must be calculated separately for each point. The following equations are valid for Figure 2C:

$P_1=m_1E_0\cdot\overline{P_L'B'}$ in watts (24a)

Primary copper loss $V_{cu1}=m_1E_0\cdot\overline{B'A'}$ in watts (24b)

The slip may be found by the same method as just given since this method applies to all circle diagrams. With P_i, the slip, and the secondary current known, torque and brake horsepower can be determined.

Conclusion

The performance data of the Schrage motor may be calculated by the use of a simple representative circuit resembling the well-known circuit of the 2-element induction motor. The current locus is a circle which may be found by three or four discrete points. This circle diagram permits a convenient determination of current, power factor, brake horsepower, slip, torque, and copper losses. The theory presented is valid for all brush positions.

Appendix I

L. Richter proves in his book[4] that in any circle diagram the internal power P_i, that is, total input minus primary copper losses, may be found to be

$$P_i = 2m_1R_1\sqrt{\xi_M^2+\left(\frac{E_0}{2R_1}-\eta_M\right)^2}\cdot q \qquad (25)$$

(See Figure 3.) Iron, windage and friction losses are neglected.

The value of q, expressed in amperes, is the vertical distance from the load point P_L to the chord P_nP_m. These two points P_nP_m are found, as described before, by drawing a circle with the radius $E_0/2R_1$.

Richter also proves that the analytic equation for this chord P_nP_m is

$$\xi_M\xi+\eta\left(\frac{E_0}{2R_1}-\eta_M\right)+\frac{1}{2}(r^2-\xi_M^2-\eta_M^2)=0 \qquad (26)$$

with

ξ_M, η_M = co-ordinates of the circle center in amperes

r = radius of circle center in amperes

ξ, η = free co-ordinates

In our diagram, Figure 3, we find

$$q'=\overline{P_L'B'}=\overline{P_LB}\cdot\cos\delta=\frac{\overline{P_LB}}{\cos(\delta-\gamma)}\cos\delta$$

$$=\frac{q}{\cos(\delta-\gamma)}\cos\delta$$

$$=\frac{q}{\cos\gamma+\sin\gamma\tan\delta} \qquad (27)$$

Equation 26 gives the inclination of chord P_nP_m to

$$\tan\gamma=\frac{\xi_M}{\left(\frac{E_0}{2R_1}-\eta_M\right)}$$

and

$$\tan\delta=\frac{\eta_M}{\xi_M}$$

With this we obtain

$$q=q'\cdot\frac{E_0}{2R_1\sqrt{\left(\frac{E_0}{2R_1}-\eta_M\right)^2+\xi_M}} \qquad (28)$$

and the total secondary input

$$P_i=m_1Eq' \qquad (29)$$

The total energy crossing the air gap is similar to the 2-element induction machine.

$$P_{gap}=m_2E_2I_{22}\cdot\cos\varphi_{22}$$

and since this value determines the torque

$$T=7.04\cdot\frac{E_2I_{22}\cdot m_2}{RPM_{synch}}\cdot\cos\varphi_{22} \text{ in foot-pounds}$$

Substituting no-load speed

$$RPM_0=RPM_{synch}(1-s_0)$$
$$s_0=k_1/k_2$$
$$E_2=k_2E_1$$

and using equation 14 the torque is

$$T=7.04\cdot\frac{m_1E_1I_{22}'}{RPM_0}\cdot\cos\varphi_{22}$$

Since $m_1E_1I_{22}'\cdot\cos\varphi_{22}$ is the internal power of the machine, identical with P_i, equation 19a is proved.

As may be seen in the circle diagram, $P_L'A'$ represents the total input into the machine with $P_L'B'$ the internal power and $B'A'$ the primary copper losses. For the slip $s=1$, the total input consists solely of primary and secondary copper losses, and it can be proved that the distance $C'B'$ represents the secondary copper losses. Therefore, P_1C' is a measure for the brake horsepower.

This derivation holds good only for $\alpha=0$ or 180 degrees. For all other values of α the point C is meaningless since the secondary current does not diminish to zero.

Figure 2C. Circle diagram for speed above synchronous value ($\alpha<180$ degrees)

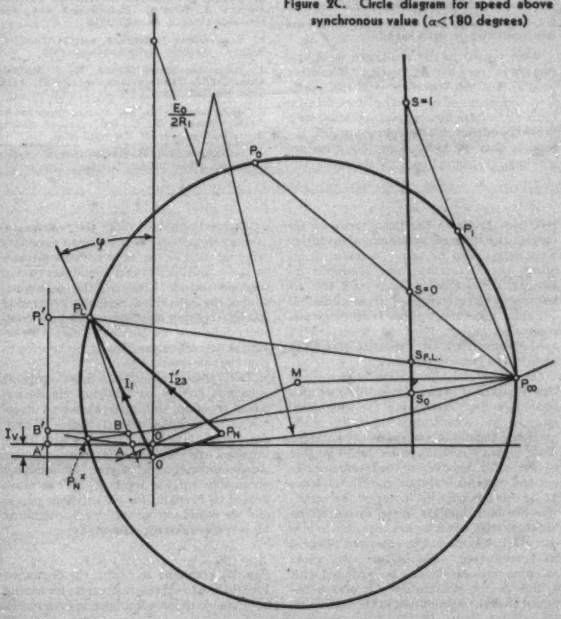

Appendix II

The torque, expressed in synchronous watts, is equal to the energy transmitted through the air gap

$$T=P_{gap}=m_2E_2I_{22}\cos\varphi_{22}$$
$$=\boldsymbol{Re}(m_2\,\text{conj}\,\boldsymbol{E}_2\times\boldsymbol{I}_{22})$$

the last equation dealing with the real component of a vector product, conj $\boldsymbol{E}_2'$ being the conjugate of $\boldsymbol{E}_2$.

$$\text{conj}\,\boldsymbol{E}_2=\boldsymbol{E}_1k_{2e}^{-i\alpha}$$

Using equations 4 and 20

$$P_{gap}=\boldsymbol{Re}\left(E_1^2k_2\frac{k_{2s}-k_{2e}^{-i\alpha}}{R_{22}+j(sX_{22}+X_2'')}\right)$$

$$=\frac{E_1^2k_2}{R_{22}^2+(sX_{22}+X_2'')^2}\times$$

$$\{(k_{2s}-k_2\cos\alpha)R_{22}+(sX_{22}+X_2'')k_2\sin\alpha)\}$$

Since at no load no torque is exerted on

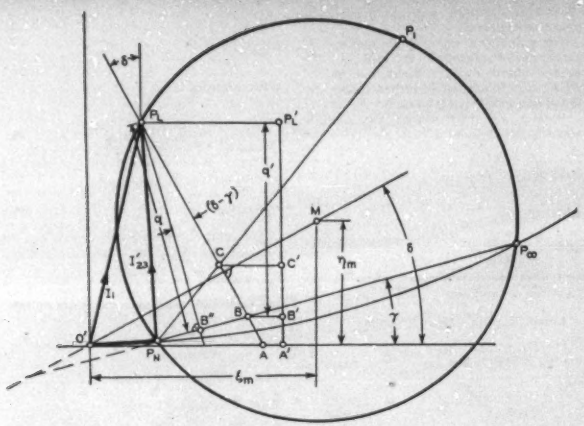

Figure 3. Determination of internal power and copper losses for $\alpha = 0$ and 180 degrees

the secondary member, P_{gap} becomes zero and consequently

$$s(k_2R_{22}+X_{22}k_2 \sin \alpha) = k_2 \cos \alpha R_{22} - X_2''k_2 \sin \alpha$$

therefore

$$s_m = \frac{k_2(\cos \alpha R_{22} - X_2'' \sin \alpha)}{k_2R_{22}+X_{22}k_2 \sin \alpha}$$

Appendix III

It may be of interest to analyze the behavior of the armature leakage reactance of a polyphase commutator machine. Any d-c type armature winding fed by brushes may be considered as a polyphase winding, connected in mesh and stationary in space. Each phase of this winding produces three different types of fluxes, namely,

(a). ϕ_0 a leakage flux, interlinked only with the phase which produces it (example: part of slot leakage).

(b). ϕ_{00} a leakage flux, interlinked with other phases of the same part of the machine (in this case, the rotor) but not with the opposite part across the air gap (in this case, the stator). Example: Interphase end extension leakage and part of slot leakage.

(c). ϕ_M the main flux, crossing the air gap and interlinked with the stator winding.

With regard to the armature, ϕ_0 is stationary in space and fluctuating. The other leakage flux ϕ_{00} together with the corresponding fluxes of the other phases, forms a rotating leakage flux in space, rotating with brush frequency. The voltage, which the leakage flux ϕ_0 induces in the armature winding, is proportional to its space frequency, that is, the brush frequency. The voltage, which leakage flux ϕ_{00} induces, is proportional to the sum of brush frequency and rotational frequency since this voltage is induced by cutting flux lines. The leakage reactances of both fluxes therefore will be proportional to these two frequencies, respectively.

We have to distinguish between two cases, as follows:

(a). Brushes carry slip frequency. (Schrage motor). ϕ_0 will fluctuate with slip frequency and its reactance is therefore proportional to the slip. ϕ_{00} induces a voltage proportional to the line frequency and its reactance is constant.

(b). Brushes carry line frequency (shunt and series motor.) ϕ_0 fluctuates with line frequency and its reactance is constant. ϕ_{00} induces a leakage voltage proportional to the slip and its reactance is proportional to the slip.

Concerning the calculation of the two leakage components, reference is made to Winkler's paper.[8]

References

1. Theory of the Brush-Shifting A-C Motor, **A. G. Conrad, F. Zweig, J. G. Clarke.** Parts I–II, AIEE Transactions, volume 60, 1941, August section, pages 829–34; parts III–IV, volume 61, 1942, July section, pages 502–12.

2. Drehstromkommutator Motor, **Schrage.** *Elektrotechnische Zeitschrift* (Berlin, Germany), volume 39, January 1914.

3. L. Schonbourger. *Revue Générale d'Electricité* (Paris, France), volume 33.

4. Wechselstrom Maschinen, part II (book), **E. Arnold.** Springer, Berlin, Germany, 1912 (1922).

5. Theory of Local and Interlinked Leakage Fluxes, **A. Winkler.** *Electrotechnik und Maschinenbau* (Vienna, Austria), 1916.

6. Elektrische Maschinen, part II (book), **L. Richter.** Springer, Berlin, Germany, 1929.

7. Polyphase Shunt Motor, **W. C. Korthals Altes.** AIEE Transactions, volume 37, 1918, pages 295–327.

8. Adjustable Speed A-C Motor With Shunt Characteristics, **H. C. Uni.** *General Electric Review* (Schenectady, N. Y.), April 1925.

9. Schrage Motor, **H. Schack-Nielsen.** *Archiv fuer Elektrotechnik* (Berlin, Germany), 1938.

Discussion

A. G. Conrad, F. Zweig, J. G. Clarke (Yale University, New Haven, Conn.): We wish to congratulate the author on his orderly presentation of the theory of the brush-shifting a-c motor. It is interesting to note that the methods that he has used to determine the characteristics of this motor from the circle are precisely those presented as reference 1 of the paper.

The differences in the theory presented by Franklin and that presented in reference 1, which incidentally are in no way contradictory, exist essentially in determining the magnitude and location of the circle defining the locus of the extremity of the primary current vector. In reference 1, this circle locus was determined from data consisting of a blocked-rotor test and two no-load tests. Franklin has obtained the circle locus of the motor from the constants of the machine (equations 15*a* and *b*, 16*a*, and 17*a*). On first observation, one is lead to believe that this is precisely what was done in reference 1, where the magnitudes of the currents for different conditions of operation were determined by test. Franklin determines these currents from equations involving the applied voltage and the resistances and reactances of the machine. If Franklin determines these resistances and reactances by test, then the characteristics as determined by his approach, should be identical to those of reference 1.

On the second observation, it is evident that Franklin may have intended to set up a procedure for determining the characteristics of this motor from a knowledge of the machine constants obtained from design data. If such is the case, he should be able to predict the behavior of the machine without the experimental data used in reference 1. If this has been his intention, his objective has been fulfilled to the extent of the accuracy with which he has been able to predict the constants in the equations referred to hereinbefore. We believe that these machine constants cannot be predicted with a high degree of accuracy. It also is believed that the assumption in the section on "General Formulas" that "the leakage reactance drop from the primary to secondary winding shall be the same as from primary to compensating winding" is subject to considerable error. Likewise, the determination of the individual reactances referred to in the foregoing equation would be exceedingly difficult if not possible to obtain. Empirical determinations would be subject to considerable error.

The value of Franklin's paper could be enhanced greatly by applying his theory, which is sound, to a given motor to determine the machines characteristic. A comparison of these characteristics with those obtained by test on the same machine would indicate the degree of accuracy obtainable by his method. We are indebted to Franklin for his excellent paper, and we would encourage him in extending his investigations experimentally.

Paul W. Franklin: In closing the discussion I would like to express my regrets for having been unable to include among my references

Baumann's paper[1] which appeared after this paper was submitted.

Referring to the remarks of Conrad, Zweig, and Clarke, I would like to comment upon the difference between their and this paper. Whereas they approach the circle diagram of this machine from the viewpoint of a test or experimental engineer, my attempt goes to derive formulas for the use of the designer. For the use of the usual 2-element induction machine I would, by all means, prefer a method based upon a representative circuit. However, in the present case the formulas grow rather elaborate due to the back-feeding feature and I therefore feel that a graphical method in addition to a representative circuit may be justified. To that end the designer has to calculate three or four discrete points, all of importance for the determination of certain circle lines. One of these points is the infinite slip point which can be determined indirectly from tests and which would have been of great value to Conrad, Zweig, and Clarke's circle diagrams. It greatly facilitates the evaluation of slip, torque, and copper losses.

I agree to a certain extent as to the difficulty in calculating the exact performance data of the machine. As to the leakage reactances, namely, slot, differential, and extension components, they may be obtained as readily as those of a plain induction motor and that with full consideration of the brush shifting angle. The discrepancies between calculation and test arise mainly from the effects of higher harmonics due to brush spacing and the transformer action of the short-circuit currents under the brushes. The former ones could be considered by a rather complicated calculation; the latter require the exact knowledge of the brush characteristics for the commutation currents. The difficulty in determining the short-circuit currents is increased by the abnormally high differential leakage of the short-circuited coils.

For these reasons I believe that a method based on simplified and pessimistic assumptions, may be of use to the design. "Exact" current values, disregarding higher harmonics and short-circuit currents may be calculated using Baumann's formulas; the choice between these and the simplified method must be left to the experience of each designer using them.

Reference

1. Impedance Relationships of the Adjustable-Speed A-C Brush-Shifting Motor, Fred Baumann. AIEE Transactions, volume 66, 1947, pages 1460–2.

Determination of Corona Starting Voltages for Nonuniform Fields in Air

JOHN G. HUTTON
MEMBER AIEE

Synopsis: Until recently spark-over and corona starting voltages could be predetermined satisfactorily only in cases where experimental curves or empirical formulas were available. The advent of the Townsend theory,[1] and later its modification, led to a general method in breakdown calculations, although these were not entirely successful until a more complete knowledge of the Townsend coefficients for air was obtained.[2-4] Based upon this knowledge and from published data Ver Planck[5] developed a method especially applicable for calculating initial breakdown voltages for nonuniform fields which converge toward the cathode. Though still empirical the increased data enabled more accurate results to be obtained from this method. The purpose of this paper is to apply the theory to a case where the field is produced between a flat plate and an edge formed by two intersecting planes, verifying experimentally.

Theory of Breakdown

THE PRESENCE of free electrons is essential to the electrical breakdown of a gas. Cumulative ionization of molecules by electron impact results in the formation of electron avalanches which grow rapidly as they move toward the anode.

Furthermore the passage of an avalanche may cause the liberation outside of the avalanche itself of other electrons.[6] If each electron liberated at the cathode starts a new avalanche, each of which in turn liberates more electrons, which start further avalanches, breakdown is the result. The minimum condition for breakdown is that for each avalanche initiated one electron is liberated at the cathode. Expressed mathematically this condition is

$$\int^{S} \alpha ds = \log_e N \qquad (1)$$

an equation which already has been verified experimentally.[6] Here α is the Townsend coefficient[1] and is a function of the field strength E and the gas density δ, being expressed by the following empirical formulas:[5]

$$\left.\begin{array}{l}
\textbf{Range 1} \\
15 < E/\delta < 25.8 \\
\alpha/\delta = 1.67\times 10^{-4} e^{0.\alpha E/\delta} \\
\textbf{Range 2} \\
25.8 < E/\delta < 78.7 \\
\alpha/\delta = 0.166(E/\delta - 21.5)^2 \\
\textbf{Range 3} \\
78.8 < E/\delta < 200 \\
\alpha/\delta = 19.0(E/\delta - 50.0) \\
\textbf{Range 4} \\
200 < E/\delta < 467 \\
\alpha/\delta = 1.08\times 10^4 \epsilon^{-388/E} \\
\textbf{Range 5} \\
E/\delta > 467 \\
\alpha/\delta = 322(E/\delta)^{1/2} - 850
\end{array}\right\} \qquad (2)$$

The quantity s is the co-ordinate of the center of the cluster of electrons measured from the cathode and is equal to S when the avalanche reaches the anode, while N is the number of electrons necessary in an avalanche to ensure the initiation of a secondary avalanche.

The left hand side of the equation is a function of the field intensity at every point along a line of force between the electrodes, while the right member depends upon the field intensity E_c at the cathode end of this line.[5] The field intensity at every point is proportional to the voltage between the electrodes, since field distortion due to the small space charges present can be neglected.[5] Hence the breakdown criterion gives the initial breakdown voltage implicitly. The mathematics necessary for the complete analysis of breakdown on a basis of theory is given in Appendixes I to V for the case of the sharp edge and flat plate.

The results of the application of the breakdown criterion to two phases of the problem now will be given.

Flat Plate and Sharp Edge Formed by Two Intersecting Planes

In order to apply the breakdown criterion, the co-ordinate ds may be expressed conveniently in terms of E, since the quantity α is a function of E. This is accomplished by determining the field at any point with the aid of the Schwarz-Christoffel transformation equation. By this procedure the quantities s and E are found to be related by

$$ds = -\frac{nV^{n+1}}{\pi^{n+1}C^n}\left[1-\left(\frac{E_a}{E}\right)^{2n}\right]^{-1/2}\frac{dE}{E^{n+2}} \qquad (3)$$

where V is the peak value of the applied voltage and E_a is the gradient at the anode end of the field line along which breakdown is assumed to occur. The quantity C is a function of the cathode orientation and electrode spacing S, while n is a function of θ, the angle of intersection of the cathode planes, and is given by $[\pi/(\pi-\theta)]$.

The application of this equation to the breakdown criterion, with substitution of the appropriate limits and values of α, results in an expression relating the breakdown voltage and electrode spacing thus

$$\frac{nV^{n+1}}{\pi^{n+1}C^n}\int_{E_a\delta}^{\infty}\frac{\alpha dE}{E^{n+2}} = \log_e N \qquad (4)$$

In an earlier paper,[5] it was shown by an analysis of published data that $\log_e N$ can be expressed by

$$\log_e N = 10\left(\frac{25\delta}{E_c}\right)^{0.2}$$

$$E_c \geq 60 \text{ kv per centimeter} \qquad (5)$$

Paper 47-265, recommended by the AIEE basic sciences committee and approved by the AIEE technical program committee for presentation at the AIEE Midwest general meeting, Chicago, Ill., November 5-7, 1947. Manuscript submitted March 18, 1947; made available for printing August 26, 1947.

JOHN G. HUTTON is in the general engineering and consulting laboratory, General Electric Company, Schenectady, N. Y.

Here E_c will be replaced by E_{av}, the value of E averaged over the mean free path of a positive ion (see Appendix I). This results in a final equation relating the breakdown voltage and electrode spacing thus

$$\frac{V}{\pi C^{\frac{n}{n+1}}} = \left[\frac{19.04\lambda^{\frac{0.2}{n+1}}\left(\frac{n}{n+1}\right)^{\frac{0.2n}{n+1}}}{n\int_{E_{av}}^{\infty}\frac{\alpha dE}{E^{\frac{n}{n+1}}}}\right] \qquad (6)$$

The analysis thus far has been based upon the assumption of a mathematically sharp edge. In practice this cannot be so and a factor is introduced to allow for this. Equation 6 then is modified to

$$\frac{V}{\pi C^{\frac{n}{n+1}}} = \left[\frac{19.04\left(\frac{\rho}{n}\right)^{\frac{0.2}{n+1}}}{n\int_{E_{av}}^{E_c}\frac{\alpha dE}{E^{\frac{n}{n+1}}}}\right]^{\frac{1}{n+1.2}} \qquad (7)$$

where ρ is the radius of curvature of the edge and V is the voltage to the equivalent sharp edged electrode. It differs from the actual voltage only by a negligible amount.

Equations 6 and 7 were applied to two electrodes each of different angle and each arranged in two orientations. The results of theory and experiment are compared in Figure 1. It is seen that there is close agreement in all cases in accordance with the error expected from the empirical nature of the equation expressing $\log_e N$ as a function of E_c.

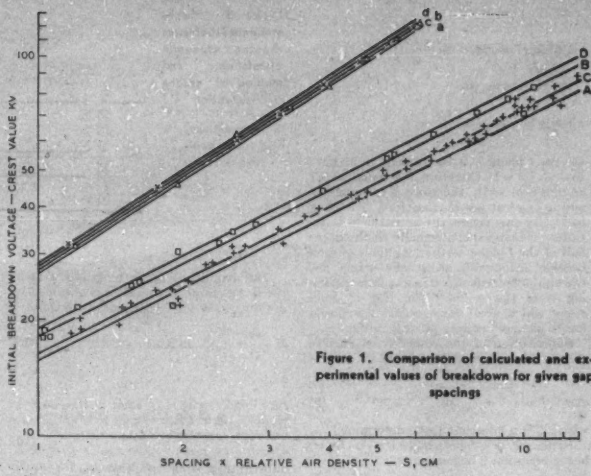

Figure 1. Comparison of calculated and experimental values of breakdown for given gap spacings

Experimental Verification

For the experimental verification of the theory of breakdown as applied to the edge and flat plate, a series of breakdown voltages for different electrode spacings of each electrode arrangement was obtained.

The source of potential was a 150-kva (1-ampere) transformer, variation in magnitude of the secondary voltage being obtained by means of an induction regulator in the primary circuit. The voltage was indicated by a voltmeter connected in a tertiary winding designed to operate at 0.001 of the voltage of the high-voltage winding as described by E. M. Williams. Sinusoidal wave form was approximated closely by using, in the primary circuit of the transformer, resonant shunts previously tuned with the aid of a harmonic analyzer.[6]

The circuit used, including the means adopted for the detection of corona, is given in Figure 2,[7] and a vector diagram in Figure 3. Before breakdown occurs the impedance of the air gap is predominant in the secondary circuit. The charging current therefore will lead the transformer voltage by almost 90 degrees. Hence the voltage on the vertical deflecting plates of the cathode ray oscillograph is in phase opposition to the transformer voltage. The voltage of the tertiary voltmeter coil is in phase with the transformer voltage and, therefore, since the first stage of the amplifier is resistive, the potential on the horizontal deflecting plates of the cathode ray oscillograph will be perpendicular to that on the vertical deflecting plates. By adjusting the magnitudes of these potentials a trace similar to that shown in Figure 3a is obtained. When breakdown occurs the impedance of the secondary circuit is now predominantly resistive and hence the potentials applied to the deflecting plates will almost be in phase. Breakdown occurs only at the negative peak of voltage and therefore a trace of the type shown in Figure 3b will result. This method of corona detection is very sensitive.

In order to apply the relative air density correction the barometric pressure and the temperature were determined for each series of tests.

Sample data calculations and test results are given in Appendix V.

Conclusion

The breakdown criterion as given in equation 1 in addition to the data given in equations 2 and 3, was applied previously[5] to two distinct types of nonuniform field and the experimental results were found to be in close agreement with the theoretical calculations. Further evidence in the proof of the validity of the theory has been furnished by this work, where, although the types of field considered were widely divergent from those of Ver Planck, excellent agreement between experiment and theory was obtained.

Appendix I

Calculations for the Field Between a Flat Plate and an Edge Formed by Two Intersecting Planes

In the breakdown criterion, equation 1, the Townsend coefficient α is a function of E, the field intensity. In order to evaluate the integral it was found most convenient to express the co-ordinate z in terms of E. The best approach in obtaining this relation is by means of the Schwarz-Christoffel transformation equation, the general form of which is[8]

$$dz = C(t-t_1)^{-\beta_1}(t-t_2)^{-\beta_2}\ldots\ldots(t-t_n)^{-\beta_n}dt \qquad (8)$$

This defines the transformation from the t plane $(p+jq)$ to the z plane $(x+jy)$, so that the real axis of the t plane maps into the boundary of a closed polygon in the z plane in such a way that the vertices of the polygon correspond to the points $t_1, t_2, \ldots t_n$. C is a constant to be determined and $\pi\beta_1, \pi\beta_2, \ldots \pi\beta_n$ are the exterior angles of the polygon in the z plane.

The respective configurations in the z plane and t plane are shown in Figure 4. Breakdown is assumed to occur along the line of force oa.

At the corner *cod*

$$\pi\beta_1 = -(\pi-\theta) \therefore \beta_1 = -\left(\frac{\pi-\theta}{\pi}\right)$$

At the corner *ode*

$$\pi\beta_2 = +(\pi+\psi) \therefore \beta_2 = \frac{\pi+\psi}{\pi}$$

On the t plane it is convenient to assign 0 to 0^t at $t=-1$; therefore, t_1 is equal to -1, *de* to $d'e'$ at $t=0$; therefore, t_2 is equal to 0 and a to a' at $t_3=1$; therefore, t_3 is equal to 1. By this means the actual field in the z plane is mapped conformally on the upper half of the t plane so that the lines of force become semicircles about the origin and the equipotentials are straight lines radiating from the origin. The line of force along which breakdown occurs transforms into $a'a'$, a semicircle of unit radius.

Substitution of the respective values of β and t into equation 8 results in

$$dz = C(t+1)^{\frac{\pi-\theta}{\pi}} t^{-\frac{\epsilon+\psi}{\pi}} dt \tag{9}$$

where C is a constant to be determined.

Replace $\pi/(\pi-\theta)$ by n and $\pi/(\pi+\psi)$ by m; hence equation 9 becomes

$$dz = C(t+1)^{\frac{1}{n}} t^{-\frac{1}{m}} dt \tag{10}$$

The magnitude of dz along the line of force *oa* is the element ds which appears in the breakdown criterion. Points along *oa* correspond to points along the unit semicircle $o'a'$. The value of t at any point on this semicircle is given by

$$t = -\epsilon^{-j\phi} = -\cos\phi + j\sin\phi \tag{11}$$

Since the magnitude of a product is given by the product of the magnitudes of its factors, by combining equations 10 and 11, there results

$$ds = dz = |C| \cdot \left|(1-\epsilon^{-j\phi})^{\frac{1}{n}}\right| \cdot \left|(-\epsilon^{-j\phi})^{-\frac{1}{m}}\right| \cdot |j\epsilon^{-j\phi}| \cdot d\phi \tag{12}$$

The orientation of the axes is such that C is a positive real and therefore $|C| = C$. The magnitudes of the third and fourth factors are each unity and therefore it remains to determine

$$\left|(1-\epsilon^{-j\phi})^{\frac{1}{n}}\right|$$

By using certain trigonometric identities it can be shown that

$$\left|(1-\epsilon^{-j\phi})^{\frac{1}{n}}\right| = (2\sin\phi/2)^{\frac{1}{n}}$$

therefore

$$ds = C(2\sin\phi/2)^{\frac{1}{n}} d\phi \tag{13}$$

The relation between the potential v and ϕ in the t plane is linear such that

$$dv = \frac{V}{\pi} d\phi \tag{14}$$

where V is the total potential difference between anode and cathode.

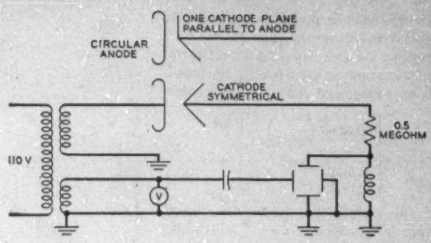

Figure 2. Schematic circuit diagram showing electrode orientation and method of corona detection

The magnitude E of the gradient along the line of force *oa* therefore is obtained by dividing equation 9 by equation 13 thus

$$E = \frac{dv}{ds} = \frac{V}{\pi C}(2\sin\phi/2)^{-\frac{1}{n}} \tag{15}$$

and

$$\frac{dE}{ds} = -\frac{V}{\pi C n}(2\sin\phi/2)^{-\frac{n+1}{n}} \cos\phi/2 \frac{d\phi}{ds} \tag{16}$$

Substituting from equation 13 for $d\phi/ds$ and eliminating ϕ by means of equation 15 there results

$$\frac{dE}{ds} = -\frac{\pi^{n+1}C^n E^{n+2}}{nV^{n+1}} \sqrt{1-1/4\left(\frac{V}{\pi CE}\right)^{2/n}} \tag{17}$$

At the anode end of the field line of breakdown *oa*, the angle ϕ becomes equal to π and therefore from equation 15 the anode gradient E_a is

$$E_a = V/(\pi C 2^{\frac{1}{n}})$$

and thus from equation 17

$$ds = -\frac{nV^{n+1}}{\pi^{n+1}C^n}\left[1-\left(\frac{E_a}{E}\right)^{2n}\right]^{-1/2} \frac{dE}{E^{n+2}}$$

as already given, equation 3.

Appendix II

The Integration $\int_0^s \alpha ds$

The expression in square brackets contained in equation 3 may be expanded by the binomial theorem and substituted in the left member of the breakdown criterion Thus

$$\int_0^a \alpha ds = -\frac{nV^{n+1}}{\pi^{n+1}C^n}\int_\infty^{E_a} \alpha\left[1+\frac{1}{2}\frac{E_a^{2n}}{E} + \frac{3}{8}\frac{E_a^{4n}}{E} + \cdots\right]\frac{dE}{E^{n+2}} \tag{18}$$

All terms after the first are negligible. For example, if E_a is 11 kv per centimeter and θ is 90 degrees then the second term is only 0.013 per cent of the first term. Hence the breakdown criterion may be written

$$\frac{nV^{n+1}}{\pi^{n+1}C^n}\int_E^\infty \frac{\alpha dE}{E^{n+2}} = \log_e N \tag{19}$$

The right hand side of this equation is a function of the energy with which the positive ions strike the cathode surface. The positive ion acquires the energy during its free flight, that is during its motion over its mean free path λ and the energy thus depends upon the average gradient over this path. An empirical formula for $\log_e N$ is

$$\log_e N = 10\left[\frac{25}{E_c}\right]^{0.2} \tag{20}$$

This was given in an earlier paper[5] and holds for E_c, the cathode gradient above 60 kv per centimeter.

E_c is replaced by

$$E_{av} = \frac{1}{\lambda}\int_0^\lambda E ds \tag{21}$$

without appreciable error. In order to elaborate this, it is to be noted that near the cathode ϕ is a small quantity and therefore from equation 13

$$dS = C\phi^{\frac{1}{n}} d\phi$$

$$S = C\frac{n}{n+1}\phi^{\frac{n+1}{n}} \tag{22}$$

and from equation 15

$$E = \frac{V}{\pi C \phi^{1/n}} \tag{23}$$

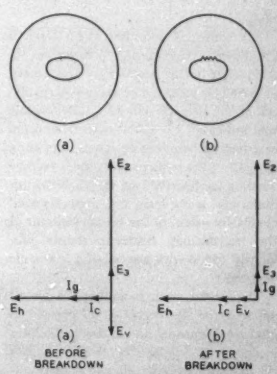

Figure 3. Vector diagram for currents and voltages used in corona detection

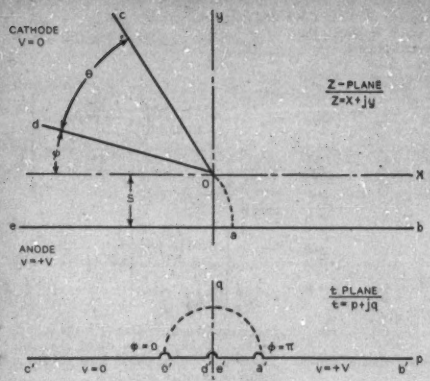

Figure 4 (left). Electrode configurations in z plane and t plane

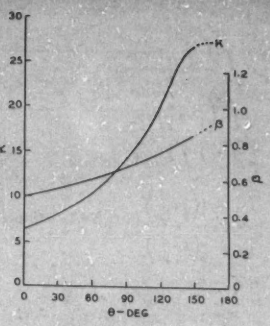

Figure 6 (right). Variation of K and β (equations 22, 23, and 27) with cathode angle

Hence

$$E_{av}=\frac{V}{\pi C\lambda}\int_0^{\lambda}\left[\frac{n+1}{nC}S\right]^{-\frac{1}{n+1}}ds$$

which reduces to

$$E_{av}=\frac{V}{\pi C^{\frac{n}{n+1}}}\left[\frac{1}{\lambda}\right]^{\frac{1}{n+1}}\left[\frac{n+1}{n}\right]^{\frac{n}{n+1}} \tag{24}$$

and

$$\log_e N=10(25)^{0.2}\left[\frac{\pi C^{\frac{n}{n+1}}}{V}\right]^{0.2}\left[\lambda\right]^{\frac{0.2}{n+1}}\times\left[\frac{n+1}{n}\right]^{\frac{0.8n}{n+1}}$$

which when substituted in equation 19 gives

$$\frac{V}{\pi C^{\frac{n}{n+1}}}=\left[\frac{19.04\lambda^{\frac{0.2}{n+1}}\left(\frac{n}{n+1}\right)^{\frac{0.8n}{n+1}}}{n\int_{E_{0\beta}}^{\infty}\frac{\alpha dE}{E^{n+2}}}\right]^{\frac{1}{n+1.2}} \tag{6}$$

which is the general equation for any angle of intersection θ of the planes and any orientation ψ of the resulting edge. Values of the function under the integral signs are plotted to a logarithmic scale as ordinate against n as abscissa in Figure 5.

Since C is a function of S, equation 27 is of the form KS^{β}, where K and β depend on the cathode angle θ. Figure 6 indicates the variation of K and β with θ. The constant C now will be determined for two special orientations; the first with one cathode plane parallel to the flat plate and the second with the edge symmetrical about an axis perpendicular to the plate.

Appendix III

Determination of the Constant C

(A). One cathode plane parallel to the anode

Here $\psi=0$ and from Appendix I, $m=1$. It is found convenient to integrate dz, equation 8, from 0 to $-jS$ at $x=-\infty$, that is from d to e in Figure 4. The corresponding integration of the right hand side is therefore from d' to e'. This is above the origin and along a semicircle of infinitesimal radius p so that t now becomes $-pe^{-j\phi}$ and

$$\int_0^{-jS}dz=\lim_{p\to 0}-jS=C\times\int_0^{\pi}(1-pe^{-j\phi})^{\frac{1}{n}}(-pe^{-j\phi})^{-1}\times jpe^{-j\phi}d\phi$$

from which

$$S=C\int_0^{\pi}d\phi$$

and

$$C=\frac{S}{\pi} \tag{25}$$

(B). Cathode planes symmetrical with respect to anode

In this case

$$\psi=\frac{\pi}{2}-\frac{\theta}{2}$$

and therefore

$$\frac{1}{m}=1+\frac{1}{2n}$$

The most suitable integration is along the field line oa in the z plane which corresponds to the semicircle $o'a'$ of unit radius in the t plane. Thus

$$\int_0^{-jS}dz=-jS=C\int_0^{\pi}(1-e^{-j\phi})^{\frac{1}{n}}\times(-e^{-j\phi})^{-\left(1+\frac{1}{2n}\right)}je^{-j\phi}dp$$

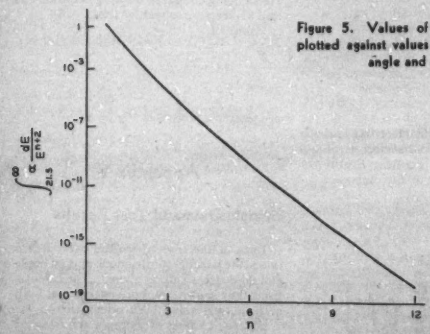

Figure 5. Values of integral (equation 6) plotted against values of n for any cathode angle and orientation

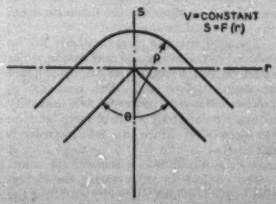

Figure 7 (right). Co-ordinates for rounded edge

and

$$\frac{S}{C}=\int_0^{\pi}\frac{\left(\epsilon^{j\frac{\phi}{2}}-\epsilon^{-j\frac{\phi}{2}}\right)^{\frac{1}{n}}}{j}d\phi$$

$$=\int_0^{\pi}\left(2\sin\frac{\phi}{2}\right)^{\frac{1}{n}}d\phi$$

$$=2^{\left(1+\frac{1}{n}\right)}\int_0^{\frac{\pi}{2}}\sin^{\frac{1}{n}}u\,du$$

$$=2^{\frac{1}{n}}\sqrt{\pi}\,\frac{\Gamma\left(\frac{1}{2}+\frac{1}{2n}\right)}{\Gamma\left(1+\frac{1}{2n}\right)}\text{ (item 854.1, reference 10)}$$

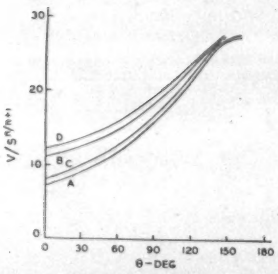

Figure 8. Variation of $V/S^{n/n+1}$ with θ for different cathode orientations

A—Cathode symmetrical = 0
B—Cathode symmetrical = 0.001 centimeter
C—Cathode plane parallel = 0
D—Cathode plane parallel = 0.001 centimeter

and

$$C=\frac{\Gamma\left(1+\frac{1}{2n}\right)}{2^{\frac{1}{n}}\sqrt{\pi}\,\Gamma\left(\frac{1}{2}+\frac{1}{2n}\right)}S \tag{26}$$

Appendix IV

Effect of Edge not Being Mathematically Sharp

Thus far all field calculations have been based on the assumption that the cathode planes intersect to form a mathematical edge. In practice this is not the case and a correction factor must be inserted in equation 6 to allow for the deviation from the theoretical assumption.

The field strength at the cathode will be reduced considerably and will have a major effect on $\log_e N$ because of the dependence of the latter on E_c. The quantity α, however, depends upon the field intensity at every point along a line of force between the electrodes. Since this field intensity is not altered greatly by the rounded edge it may be assumed that α remains the same.

The method for determining the correction factor is approximated by assuming the electrode to have the contour of one of the equipotential surfaces which apply in the ideal case of the mathematical edge.

Referring to equations

$$E=\frac{V}{\pi C}\left(\frac{n+1}{nC}S\right)^{-\frac{1}{n+1}}$$

that is

$$E=\frac{\partial V}{\partial S}=KS^{-\frac{1}{n+1}} \tag{27}$$

and

$$\frac{\partial^2 V}{\partial S^2}=-\frac{K}{n+1}S^{-\frac{n+2}{n+1}} \tag{28}$$

By Laplace's equation

$$\frac{\partial^2 V}{\partial r^2}=-\frac{\partial^2 V}{\partial S^2}=\frac{K}{n+1}S^{-\frac{n+2}{n+1}}$$

where r and S are the co-ordinates shown in Figure 7

Now

$$\rho=\frac{\left[1+\left(\frac{dr}{dS}\right)^2\right]^{3/2}}{\frac{d^2r}{dS^2}}$$

and near $r=0$, dr/dS approaches zero and

$$\frac{dV}{dr}=0$$

Hence

$$\rho^{-1}=\frac{d^2S}{dr^2}=\frac{d}{dr}\left(\frac{dS}{dr}\right)=\frac{d}{dr}\frac{\frac{dV}{dr}}{\frac{dV}{ds}}$$

That is

$$\rho^{-1}=\frac{\frac{d^2V}{dr^2}}{\frac{dV}{ds}}$$

since $dV/dr=0$, which from equations 27 and 28 becomes $(S-1)/(n+1)$. Therefore

$$S=\frac{\rho}{n+1}$$

and

$$E=\frac{V}{\pi C^{\frac{n}{n+1}}}\left(\frac{n}{\rho}\right)^{\frac{1}{n+1}}$$

It was assumed that the electrode had the form of the equipotential surface having a corner radius ρ. The gradient E now becomes E_c, the gradient at the cathode. Thus

$$E_c=\frac{V}{\pi C^{\frac{1}{n+1}}}\left(\frac{n}{\rho}\right)^{\frac{1}{n+1}} \tag{29}$$

$$\log_e N=\left[\frac{10(25)^{0.2}\,\pi C^{\frac{n}{n+1}}}{V}\left(\frac{\rho}{n}\right)^{\frac{0.2}{n+0}}\right] \tag{30}$$

and from equation 19

$$\frac{V}{\pi C^{\frac{n}{n+1}}}=\left[\frac{10(25)^{0.2}\left(\frac{\pi C^{\frac{n}{n+1}}}{V}\right)^{0.2}\left(\frac{\rho}{n}\right)^{\frac{0.2}{n+1}}}{n\int_{r_{c0}\delta}^{r_{n0}\delta}\frac{dE}{E^{n+2}}}\right]^{\frac{1}{n+1}}$$

that is

$$\frac{V}{\pi C^{\frac{n}{n+1}}}=\left[\frac{19.04\left(\frac{\rho}{n}\right)^{\frac{0.2}{n+1}}}{n\int_{E_{c0}\delta}^{E_{n0}\delta}\frac{dE}{E^{n+2}}}\right]^{\frac{1}{n+1.2}} \tag{31}$$

In this equation the voltage V is the voltage to the equivalent sharp edged electrode. The actual voltage differs from this by a negligible quantity given by

$$\Delta V=\int_0^S E\,ds$$

which from equations 27 and 28 equals

$$\int_0^{\frac{\rho}{n+1}}E\,ds$$

But from equation 27

$$E=(KS)^{-\frac{1}{n+1}}$$

$$\Delta V=K\int_0^{\frac{\rho}{n+1}}S^{-\frac{1}{n+1}}dS$$

$$=\frac{V}{\pi C}\left(\frac{nC}{n+1}\right)^{\frac{1}{n+1}}\left(\frac{n+1}{n}\right)\left(\frac{\rho}{n+1}\right)^{\frac{n}{n+1}}$$

$$=\frac{V}{\pi C^{\frac{n}{n+1}}}\left(\frac{\rho}{n}\right)^{\frac{n}{n+1}} \tag{32}$$

Note that in equation 31 the cathode gradient E_c occurs in the integral, and through equation 29 it depends also upon

$$\frac{V}{\pi C^{\frac{n}{n+1}}}$$

Hence for a complete solution equations 29 and 31 must be solved by trial.

Values of

$$\frac{V}{\pi C^{\frac{n}{n+1}}}\quad(\pi C=S)$$

are plotted against θ in Figure 8.

Appendix V

Sample Data and Test Results

Data of the case where the cathode has one plane parallel to the anode and an angle θ of 90 degrees will be given. The calculations thus shown are representative of both cathode angles and both orientations.

The peak values of voltages are assumed

to be 1.41 times the rms values because of the low harmonic content[7] of the voltage.

Evaluation of $\int \alpha ds$

From equation 6

$$\int_0^S \alpha ds = \int_{E_{ab}}^{\infty} \frac{\alpha dE}{E^{n+2}}$$

Now

$$n = \frac{\pi}{\pi - \theta}$$

and for $\theta = \pi/2$, $n = 2$, therefore

$$\int_0^S \alpha ds = \int_{E_{ab}}^{\infty} \frac{\alpha dE}{E^4}$$

In equation 2 it is found that for values of E/δ less than 21.5, α is negligible and therefore where E/δ extends to high values, the first range may be neglected and the upper limit of the fifth range extended to infinity.

Substituting for α therefore from equation 2 we find, summing up the ranges,

Range	Contribution
2	0.000994
3	0.000690
4	0.000144
5	0.0000246
$\int_{E_{ab}}^{\infty} dE/E^4 =$	0.0018526

The value for λ will be taken as 10^{-4} centimeters[4] and for the problem with one cathode plane parallel to the anode $C = S/\pi$ (equation 25). Therefore for this case

$$V = 16.38 S^{5/4} \quad (33)$$

It was assumed that within the limits of engineering accuracy the profile of the edge would be modified so that it had a radius of curvature ρ of 0.001 centimeter. On the basis of this assumption, equations 29 and 31 were solved simultaneously by trial and error resulting in the modified expression

$$\Delta V = 18.89 S^{5/4} \quad (34)$$

and from equation 32

$$V = 0.0815 \text{ kv}$$

which is negligible compared with V, $S > 1$.

Sample Data

Spacing in inches $= S$

Temperature in degrees Fahrenheit absolute $= T$

Pressure in millimeters Hg $= P$

Standard temperature in degrees Fahrenheit absolute $= 77 + 460 = 537$

Standard pressure in millimeters Hg $= 760$

Hence corrected spacing is $2.54S(537P/760T)$ centimeters

Tabulated Data

Experimental values are given in Table I. The average value compares very favorably with that given in equation 34, where the calculated breakdown voltage V for a given spacing S is given by $V/(S\delta)^{5/4} = 18.89$.

Table I

Spacing, In.	Voltmeter Reading, Volts	Temperature, F	Barometric Height, Mm Hg	Corrected Spacing, Cm	Initial Breakdown Voltage; Peak Value, Kv	$V/(S\delta)^{5/4}$
0.75	22.2	74.0	773	1.95	31.4	20.10
1.00	26.3	74.0	773	2.30	37.1	19.58
1.50	32.8	74.0	773	3.89	46.4	18.72
2.00	40.6	74.0	773	5.18	57.5	19.24
2.50	47.2	74.0	773	6.48	66.7	19.17
3.00	53.1	74.0	773	7.78	75.1	19.11
3.50	57.9	74.0	773	9.06	81.9	18.88
4.50	62.4	74.0	773	10.37	88.2	18.54
0.625	18.2	78.0	772	1.61	25.7	18.75
0.500	16.0	78.0	772	1.29	22.6	19.16
0.400	13.2	78.0	772	1.03	18.7	18.35
0.954	23.0	78.0	765	2.43	32.5	17.98
0.432	13.0	78.5	765	1.10	18.4	17.25
0.432	13.05	78.4	765	1.10	18.45	17.30
3.695	57.0	79.2	765	9.40	80.6	18.11
3.695	57.5	79.2	765	9.40	81.4	18.29
3.694	55.0	73.6	766	9.52	77.8	17.29
1.115	27.8	74.6	766	2.87	39.3	19.45
1.115	27.4	74.6	766	2.87	38.8	19.20
1.075	27.4	75.6	769	2.77	38.8	19.68
2.055	41.5	76.0	769	5.30	58.6	19.30
2.055	40.5	76.0	769	5.30	57.3	18.83
3.810	60.5	76.2	769	9.82	85.5	18.63
0.665	18.6	76.5	769	1.71	26.3	18.38
0.398	13.2	76.8	769	1.02	18.6	18.32

Average $V/(S\delta)^{5/4} = 18.70$

List of Symbols

Lengths are measured in centimeters and field strengths in kilovolts per centimeter throughout.

General

α = Townsend coefficient for ionization by electron impact; it is the number of electrons added to an avalanche per centimeter of travel per electron already present (centimeters)$^{-1}$

S = distance from cathode to anode

s = co-ordinate of center of avalanche measured from the cathode along a line of force

N = number of electrons necessary in an avalanche to ensure the initiation of a secondary avalanche

E = field strength

δ = relative air density. Unity at 25 degrees centigrade, 760 millimeters

E_a = field strength at anode end of field line along which breakdown is assumed to occur

V = initial breakdown voltage in kilovolts

E_c = field strength at cathode end of field line along which breakdown is assumed to occur

E_{av} = field strength averaged over mean free path of positive ion

λ = mean free path of positive ion (10^{-4} centimeter)

Sharp edge

ρ = radius of curvature on edge

x = co-ordinate along real axis in z plane; $z = x + jy$

p = co-ordinate along real axis in t plane; $t = p + jq$

θ = angle of intersection of planes from cathode

ψ = angle of inclination of near cathode plane to anode

$m = \pi/(\pi + \psi)$

$n = \pi/(\pi - \theta)$

ϕ = angle of equipotential in t plane

References

1. Electricity in Gases (book), J. S. Townsend. Claredon Press, Oxford, England, 1915, articles 185, 222, 293.

2. Measurements of the Townsend Coefficients for Ionization by Collision, F. H. Sanders. *Physical Review* (New York, N. Y.), volume 44, 1933, pages 1020–4.

3. Der Dunkle Entladungsvorstrom in Luft von Atmosphärendruck, M. Paavola. *Archiv fuer Elektrotechnik* (Berlin, Germany), volume 22, 1929, page 453.

4. Über Elektronenbiseruung von Stickstoff, Sauerstoff und Luft bei Geringen und Hohen Drucken, K. Masch. *Archiv fuer Elektrotechnik* (Berlin, Germany), volume 26, 1932, page 593.

5. Calculation of Initial Breakdown Voltages in Air, D. W. Ver Planck. AIEE Transactions, volume 60, 1941, March section, pages 99-104.

6. The Problem of the Mechanism of Static Spark Discharge, L. B. Loeb. *Reviews of Modern Physics* (New York, N. Y.), volume 8, 1936, pages 271–2.

7. A Method for Detecting the Ionization Point on Electrical Apparatus, G. E. Quinn, AIEE Transactions, volume 59, 1940, December section, pages 680–2.

8. Conjugate Functions for Engineers (book), Miles Walker. Oxford University Press, Oxford, England, 1933, pages 23–33.

9. Theory of Functions (book), R. Rothe, F. Ollendorff, K. Pohlausen. Massachusetts Institute of Technology Press, Cambridge, Mass., 1933, pages 77–83.

10. Table of Integrals (book), H. B. Dwight. Macmillan Company, New York, N. Y., 1934.

11. Funktionentafeln (book), E. Jahnke, F. Emde. B. G. Teubner, Leipzig and Berlin, Germany, second edition, 1933, pages 78–88.

Discussion

Fred J. Vogel (Illinois Institute of Technology, Chicago, Ill.): The author has presented a very interesting paper, but I would like to call attention to papers by several other authors which cover substantially the same ground. In 1924, Doctor Dreyfus in a paper "Uber die Anwendung der Theorie der Konformen Abbildung zur Berechnung der Durschlags—und Uberschlagserscheinungen zwischen Kantigen Konstructionsteilen," (*Archiv fuer Elektrotechnik*, volume 13, 1924, page 123) makes mention of the method of accounting for rounded edges, and ascribes its origin to J. Herlitz. Dreyfus' paper is largely mathematical and does not give very much experimental data. This was left for W. Schilling to do in his paper "Berechnung der Aufangsspannung zwischen kantigen Electroden in Luft," in the *Archiv fuer Elektrotechnik*, volume 22, September 1929, page 337. In 1938, I submitted some data in a paper entitled "Corona Voltages of Typical Transformer Insulations Under Oil," AIEE TRANSACTIONS, volume 57, 1938, January section, pages 34–6. Methods outlined in these papers are stock in trade for many transformer designers and presumably other apparatus designers also.

John G. Hutton: I would like to thank Vogel for his discussion of the subject paper. During the preparation of the work the articles by the authors referred to in the discussion were consulted.

Progress in Power Generation—1940–46

AN AIEE COMMITTEE REPORT

World War II marked the power generation field by requiring greater utilization of existing equipment which resulted in the testing and proving of designs developed during the later 1930's. The impetus of war needs led to extensive investigation and experimentation into fields which opened broad avenues to other ways of producing usable energy:

1. Atomic or nuclear energy.
2. Gas turbines.
3. Wind turbines.

These methods are still largely in the experimental stage though there are or were working units and components in each of these fields.

Despite the diminishing incremental gains to be expected from pushing steam pressures and temperature higher in steam plants, this method of performance improvement has been utilized by going to 2,300 pounds per square inch gauge pressure and several plants are being designed to use 1,050-degree-Fahrenheit temperature, some with reheating. Maximum ratings of steam station equipment have not been raised since the last report of this committee (1933–39), steam generator capacity remaining at about 1,000,000 pounds per hour and turbine capacity at about 145,000 kw.

To consolidate the performance gains of high-pressure high-temperature equipment, joint AIEE–ASME (American Society of Mechanical Engineers) turbine generator standards have been promulgated, in this way reducing somewhat the first cost of these units. It is estimated that about 25 per cent of the new units now on order follow these standards. Units larger than 20,000 kw are standardized at 850 pounds per square inch gauge and 900 degrees Fahrenheit initial conditions with the 40,000- and 60,000-kw units having alternate conditions of 1,250 pounds per square inch gauge and 950 degrees Fahrenheit.

Steam-driven auxiliaries virtually have disappeared in most new steam stations, electric drive lending itself to achieving higher over-all plant efficiency with the regenerative cycle. Hydroelectric stations have kept pace with the growth of capacity, most of the large installations being government-owned.

Paper 47-250, recommended by the AIEE power generation committee and approved by the AIEE technical program committee for presentation at the AIEE Midwest general meeting, Chicago, Ill., November 3–7, 1947. Manuscript submitted September 18, 1947; made available for printing September 18, 1947.

This report of the AIEE power generation committee was prepared by its secretary, B. G. A. Skrotzki, associate editor, *Power*, New York, N. Y.

POWER PRODUCTION

Outstanding achievement on the home front during World War II was the production of electric energy by the central station utilities in response to all-time peaks in demand. From a total generation of 127,642 million kilowatt-hours in 1939, the output rose to a peak in 1944 of 229,766 million kilowatt-hours. Comparable capacities were 38,862,000* kw in 1939 and 49,799,000 kw in 1944. Thus there was an 80-per-cent increase in output with a 27-per-cent increase in capacity. Estimates have indicated that war needs took about 1 per cent of energy output in 1939 and 42 per cent in 1944.

Over-all capacity factors increased from 37.5 per cent in 1939 to 52.9 per cent in 1944, while the composite utilization factor increased from 72.8 per cent to 82.5 per cent for the same two years, indicating a considerable decrease in reserve capacity. This reflects the difficulty in obtaining new power producing equipment during the war as much of the turbine and boiler builders' fabricating capacity was devoted to providing equipment for the Navy and Merchant Marine.

This remarkable performance was achieved by:

1. Advancing clock time one hour during the whole year from 1942 to 1945.
2. Intensive use of system interconnections.
3. Industrial plants operating on a 3-shift 7-day week production schedule.
4. Addition of new high load-factor loads.
5. Operating with reduced capacity-reserve margins.

Other measures that helped in carrying the unprecedented loads were: bringing obsolete cold stand-by plants back into operation, using women to aid in plant operation, "brown-out" restrictions in certain parts of the country where energy shortages developed in hydro supply. In the coastal cities black-out practices helped in reducing demand though energy savings was not an objective in this program.

Plant operation was plagued by shortage of skilled operators, difficulty in obtaining maintenance supplies, and a marked drop in coal quality.

Despite the difficulties experienced during the war years, station fuel economy continued the long-time upward trend; national averages were 1.39 pounds of coal per kilowatt-hour in 1939 and 1.29 pounds of coal per kilowatt-hour in 1946.

Through this period the proportion of hydro capacity

*Excludes New York City transit system plants.

and generation has remained practically constant when compared with the total power production activity as shown in Table I.

Of the 3,700,000-kw increase in hydro capacity from 1940 to 1946, about 3,300,000 kw was installed by governmental power districts. Practically all the large units were installed by government agencies, the few exceptions were 60,000 horsepower by the Nantahala Power and Light Company, 200,000 horsepower by Pacific Gas and Electric Company, and 21,400 horsepower by the Wisconsin Michigan Power Company.

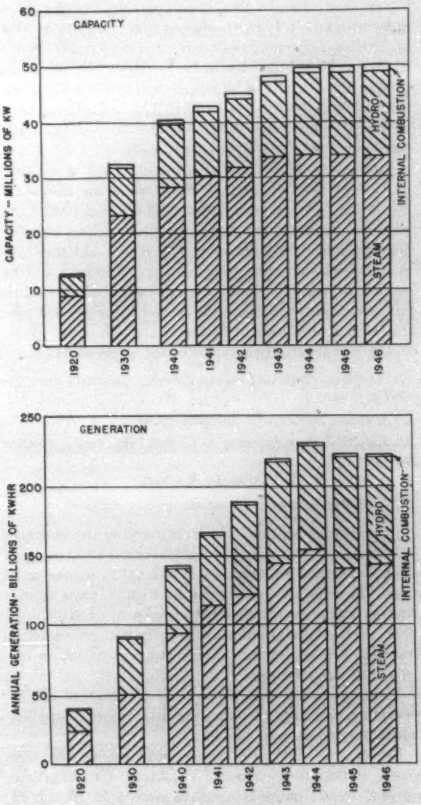

Figure 1. Comparison of central-station capacity and annual outputs in the United States

Rapid increase in annual generation was not accompanied by a comparable growth in station capacity during World War II

Table I. Proportion of Hydro Capacity and Generation

Year	Per Cent of Total Capacity	Per Cent of Total Generation
1939	28.3	33.8
1940	27.7	33.1
1941	27.5	30.4
1942	28.2	34.0
1943	28.6	33.6
1944	29.3	32.2
1945	29.9	36.0
1946	29.6	35.0

Governmental agencies and municipalities own and operate about 20 per cent of the total generating capacity in the United States. This includes all types of prime movers—steam, hydro, and internal combustion.

The most amazing aspect of the power demand picture has been the rapid nation-wide rise in load since the summer of 1946 (Figure 2). The abrupt drop in industrial load after *V-J* day was expected and resulted in declining weekly loads. This decreased demand was sustained in the early part of 1946 by the wave of strikes that passed through the country at that time. Resumption of civilian industrial activity and the increasing availability of home appliances and other factors have caused a record short-time load growth. Many systems have seen their reserve capacity virtually disappear. The resulting demand for new equipment has flooded the manufacturers' facilities to such an extent that steam turbine-generator deliveries are promised 36 months after placing the order and boilers about 18 months.

Various estimates indicate that the total capacity, central station and industrial, steam and hydro, to be installed within the next three years will be in excess of 12,000,000 kw.

STEAM PLANTS

Improvement of older low-pressure steam plants by installing superposed high-pressure high-temperature turbines and steam generators was followed in relatively few instances since 1940. This indicates that old-plant improvement opportunities largely had been exhausted in the period preceding 1940.

Application of higher pressures and temperatures have proved the practicability of operating at these increased steam levels. Surveys have shown that about 35 per cent of the units installed were for steam pressures between 300 and 699 pounds per square inch gauge, 45 per cent between 700 and 1,099 pounds per square inch gauge, and 20 per cent above 1,100 pounds per square inch gauge. In respect to throttle steam temperature about 30 per cent of the units were below 830 degrees Fahrenheit, 50 per cent from 830 to 900 degrees Fahrenheit, and 20 per cent above 900 degrees Fahrenheit. Highest temperature unit to go in service was at the Missouri Avenue station in Atlantic City, N. J.—a 25,000-kw turbine generator designed for 1,350 pounds

per square inch gauge and 1,000 degrees Fahrenheit. There are several units scheduled to go into service in the near future with a 1,050-degree-Fahrenheit steam temperature. Some will use one stage of reheating at these high temperatures.

A strong trend in single-unit design is evident, with about 70 per cent of the turbines being supplied by a single steam generator, 27 per cent with two boilers, and about 3 per cent with three boilers. Many new station designs are incorporating the unit system where one boiler supplies a single turbine and all controls for boiler, combustion, turbine, auxiliaries, and switching are centralized at a common location for operating simplicity.

As to be expected, there was a wide distribution in the size of units installed—35 per cent were 20,000 kw and smaller, 45 per cent from 22,500 to 50,000 kw, and 20 per cent were 60,000 kw and larger. Largest unit installed was the 147,000-kw 1,250-pound per-square-inch-gauge 925-degree-Fahrenheit turbine-generator in the Fisk station of the Commonwealth Edison Company, Chicago, Ill. Although the large-unit group accounts for only 20 per cent of the number of units, they also represent about one-half the total kilowatts capacity. Boilers have shown the same wide diversity in capacity, about 65 per cent having a capacity of 400,000 pounds per hour and smaller. Largest boiler installed was 1,000,000-pound-per-hour 1,600-pound-per-square-inch-gauge 950-degree-Fahrenheit unit at the Sherman Creek station of the Consolidated Edison Company of New York, Inc.

Regenerative feedwater heating was employed in practically all the newly installed units. Number of turbine bleed points ranged from one to six—about 50 per cent had four bleed points, 25 per cent had three bleed points, and 10 per cent had two bleed points.

Pulverized-coal firing dominates the field of newly installed central-station boilers. About 50 per cent of the boilers are so fired and only about 10 per cent have some form of mechanical stoker, the remainder are natural-gas or oil-fired or some combination of two or all three methods. About one-third of the boilers with pulverized coal feed have slag-tap furnaces.

All of the steam generating units, with few exceptions, have either or both air heaters and economizers; about 60 per cent had both types of heat transfer surface, and 35 per cent had air heaters only.

Furnace heat release, a rough indication of the liberalness in the design of boilers, depends principally upon the types of fuel to be burned, in general, the higher the volumetric heat release, the tighter the design and the greater the dependence of quality fuels. For the new installations this figure varied from 14,500 to 34,500 Btu per cubic foot per hour, and about half of them were designed for 23,900 Btu per cubic foot per hour and less.

Two wartime developments, the floating power plant and the mobile power plant mounted on railway cars, have served their duty well during the national emergency and now are continuing to give service during the present period of unexpected load growth. Several systems in the South experienced such unprecedented load increases that these plants solved the problem of continuing service until conventional land installations can be constructed.

Many new stations are being located outside of city and town limits to avoid dust-nuisance complaints.

Outdoor and semioutdoor steam plants are finding increased acceptance, especially where the climate is relatively mild. In many designs the operating front

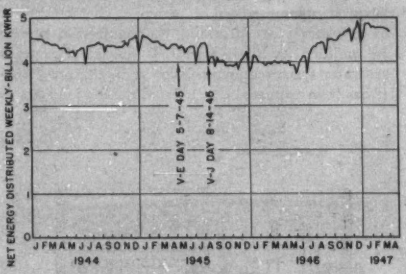

Figure 2. Energy distribution data

Recession in weekly energy distributed following V-J day was prolonged by numerous strikes. Rapid rise during summer of 1946 marked resumption of industrial activity. High levels maintained during early part of 1947 presages rapid future growth in demand. Data from the Edison Electric Institute

Figure 3. Ripley station of the Kansas Gas and Electric Company is of semi-outdoor design

The 28,750-kva turbine generator is housed completely as well as the firing aisle of the two 160,000-pound-per-hour boilers. The oil-fired boilers are outdoors covered by a canopy while the fans and air preheaters are completely out in the open at the boiler rear

of the boiler forms one wall of the enclosed turbine room. Savings of 25 to 35 per cent in structural investment are reported, equivalent to about 5 per cent in plant over-all first cost. This saving is offset slightly by increased costs of making the outdoor equipment weatherproof.

Successful operation has been reported on the horizontal cyclone furnace installation at the Calumet station of the Commonwealth Edison Company. Besides being able to burn low-grade coals, this furnace modifies the slagging problem associated with a conventional furnace and requires only crushing instead of pulverizing of the coal, consequent fly-ash reduction needs only a small cinder catcher installation, cleaning labor is minimized. The slagging characteristic is used to advantage in aiding the combustion process. In addition to these operating advantages, steam-generator space requirements are reduced appreciably. It has been estimated that over-all installation costs for a 75,000-kw plant would be reduced by about $6 to $6.50 per kilowatt with the cyclone furnace as compared with a conventional steam generator.

No new mercury plants have been installed since the Kearny, N. J., installation of the Public Service Electric and Gas Company and the outdoor plant at Schenectady, N. Y., of the General Electric Company. However, mercury plants of 5,000-kw capacity and up now are being offered for industrial use, using the condenser-boiler output for process heating, and up to 80,000-kw capacity for central stations, 30,000-kw mercury topping and 50,000-kw steam. A 7,500-kw mercury turbine has been ordered for the Pittsfield, Mass., plant of the General Electric Company to supply their 600-pound-per-square-inch steam system. The 10,000-kw mercury plant at Hartford, Conn., will be rebuilt for 15,000 kw.

Comparatively few central stations use steam drive for their auxiliaries and in most instances where they are provided serve the stand-by boiler feed pump. Motor drive for station auxiliaries dominates the field, but this complicates the control problem. Roughly a third of the boiler-feed-pump motors are provided with variable speed control. In the case of fans, motor speed control rarely is used; gas flow control is provided by dampers, vanes, magnetic and hydraulic couplings, 2-speed motor drives, or some combination of these.

A notable application is that of 3,600-rpm motors to drive large boiler feed pumps. Operating experience is awaited with interest.

The majority of auxiliary-drive motors are of the induction type while, with the variable speed couplings now available, several smaller installations have used the synchronous type. The installation of d-c motors has been discontinued. Practically all installations now use full-voltage starting for the auxiliary-drive motors.

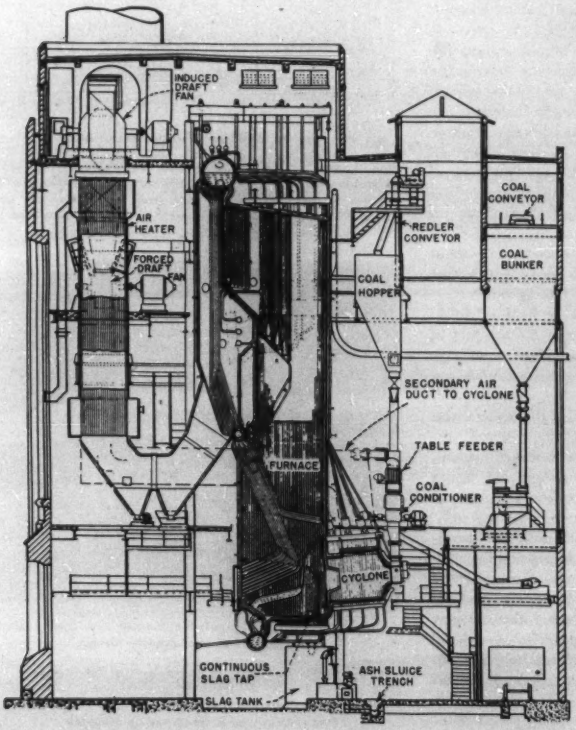

Figure 4. Boiler unit in Calumet station of Commonwealth Edison Company, Chicago, Ill., uses horizontal-cyclone burner to burn high-ash low-fusion-temperature coals

Advantages include reduced coal preparation cost, simplified ash handling, smaller size of boiler and dust-separating equipment, and lower over-all investment cost

Metal-clad switchgear and control have been proved in service and generally are accepted for station auxiliary layouts. Unit substations and power centers, usually with air-cooled transformers, form the modern arrangement for supplying low-voltage energy. These also include high-voltage gear where required. Air circuit breakers in all ratings through the 15,000-volt class virtually have replaced the oil type for power-plant auxiliary work.

Secondary network distribution systems for auxiliary supply have been installed in five stations and their performance has been reported favorably.

Unique co-operation between industrial-plant customers and utility generating stations was inaugurated in 1940–41 in the San Francisco Bay area by the Pacific Gas and Electric Company, San Francisco, Calif. Here three plants, essentially identical, Avon, Martinez, and Oleum, each supply a different oil refining company plant with steam and electric energy. These plants, 40,000 kw each, supply the oil refinery demand of 20,000 kw; excess energy becomes available for general distribution.

When supplying rated extraction steam at 225 pounds per square inch gauge from the automatic-extraction turbines they develop about 32,000 kw each. Under certain conditions of combined extracting and condensing operation they can produce more than 50,000 kw. The extracted steam supplies the oil refineries' evaporators furnishing steam from water supplied by the customer.

Generating plant furnaces can burn various fuels either individually or in combination; part of the fuel is composed of refinery wastes and taken as part payment for services supplied. Fuels that can be handled and burned are natural gas, oil, acid sludge, pitch, and pulverized petroleum coke.

HYDRAULIC STATIONS

Most of the new hydro capacity added has been installed by agencies of the Federal Government, especially in the larger plants (Table II). The rate of additions has maintained a phenomenal figure since 1936 as shown in Tables III and IV. Outstanding design has been the 60,000-horsepower 450-rpm Francis turbine installed by the Nantahala Power and Light Company near Franklin, N. C. This unit is built for a maximum net head of 1,000 feet, the highest for any reaction turbine of its size in the world. On test this turbine developed efficiencies of 93.7, 93, and 88 per cent at full, three-fourths and one-half load respectively.

Boulder Dam, Nev. and Ariz., on the Colorado River, under the supervision of the United States Bureau of Reclamation, is the largest plant in the world in terms of installed capacity. Designed for 1,835,000 horsepower, it now has 1,435,000 horsepower in operation. Four units of 115,000-horsepower each were added in the years 1941–44.

Shipshaw 2 on the Saguenay River in Quebec, Canada, holds the record construction time for a large hydroelectric plant. Although this development had been planned prior to 1931 when Shipshaw 1 (300,000-horsepower capacity) went into service, it was not built until the wartime demand for aluminum made construction imperative. The first unit started initial operation November 23, 1942, just 18 months after the start of

Figure 5. Boiler car of 10,000-kw mobile steam-electric generating station

Entire station consists of six railway cars housing complete equipment from oil-fired boilers to switchgear and transformers

Figure 6. Generator room of Shipshaw 2 has the largest concentration of generating capacity, 1,140,000 horsepower in 12 units, housed in one building, in the world

First unit operated within 18 months of start of construction, 12th unit within 37 months

construction; the 12th and last unit went into service on December 24, 1943. There are eight 100,000-horsepower and four 85,000-horsepower Francis wheels designed for a 208-foot head making a total of 1,140,000 horsepower. This is the largest hydroelectric development in the world contained in a single powerhouse.

Practicability of completely automatic and remote control of hydroelectric stations is demonstrated by the installation at Ocoee 3 on the Ocoee River, Reliance, Tenn., part of the Tennessee Valley Authority system. While automatic stations have been built and installed

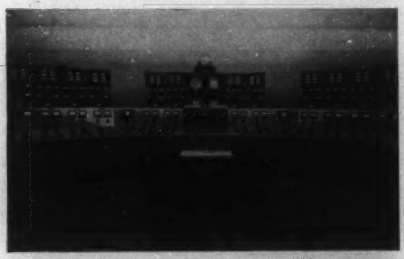

Figure 7. Control board for 12 hydro units in Shipshaw 2

over the past 25 years, this installation with a 30,000-kva generator is the largest one to date utilizing this form of control. This station first went into service in April 1943 and its excellent service has led to plans to use it in three new stations under design. Ocoee 3 is controlled from Ocoee 2 located six miles away. Telemetering and control channels are provided by an underground telephone-type cable having 51 pairs of wires.

Underground cable was selected because it was judged to provide practically trouble-free service with minimum of maintenance and the maximum number of completely independent channels. Other means of control communication were considered such as leased telephone circuit, carrier current, and overhead cable.

Considerable progress has been made in developing methods of testing hydraulic-turbine governors quickly and frequently. A notable instrument designed for this purpose has been described by J. E. Allen and W. B. Hess in a paper[131] presented at the 1947 AIEE winter meeting. This instrument directly draws a diagram of either kilowatts load or gate operating piston movement versus alternator frequency, in a manner analogous to a steam engine indicator card diagram. In addition to this diagram the instrument also records kilowatts load, gate operating-piston motion, and generator frequency on a strip chart. From both of these records the governor characteristics are analyzed quickly and aid in effecting repairs when needed. Progressive records help in showing in what respects a governor may be deteriorating and avoid costly shutdowns.

ELECTRIC APPARATUS

Studies have shown that the 3,600-rpm direct-connected exciter while performing on a satisfactory level had a poorer availability record than the rest of the turbine-generator unit. More attention to design of minor mechanical elements causing these outages are expected to improve their performance, one item being redesign of brush holders permitting brush replacement without shutting down the unit.

Electronic-type exciters first were applied to synchronous condensers in 1936 and to a synchronous generator in 1946. They promise to circumvent the problems of designing large 3,600-rpm direct-connected exciters. These new exciters offer possibilities of simple operation, low maintenance requirements, and high reliability. Normal maintenance can be carried on while the machine is loaded, even to the extent of replacing tubes. However, special attention must be devoted to the supply source; supply-voltage drops cause a drop in excitation voltage. This contingency can be counteracted by control devices.

Dry-type air-cooled transformers originally designed for central-station use have found application in the industrial and commercial fields. This transformer type differs from the original air-blast type in that the insulation contains a minimum of combustible matter, being principally made of air, porcelain, and glass. Though many have been subjected to severe service, no failures have been reported from such expected causes as moisture, dirt accumulations, and high temperature.

Air-blast circuit breakers for indoor heavy-power station switchgear are finding increasing favor. They are adaptable readily to standardized metal-clad switchgear installations. Standardization of this equipment during the last few years has shown positive benefits by allowing price reductions despite increasing costs.

Oil-type circuit breakers still are used largely for outdoor installations. Improvements in these circuit breakers include a 50-per-cent reduction in oil content resulting in higher speed arc interruptions and clearing time, and bettering the recycling duty. These circuit breakers now are built for voltages ranging from 115 to 230 kv with interrupting capacity of 1,000,000 to 3,500,000 kva. Standard circuit breakers are rated on a 5-cycle opening time basis. However, designs for 3 cycles at 138 kv and higher for 3,500,000 kva are also available. Oil circuit breakers of 5,000,000 kva rating are promised to be ready when needed.

From 1928 to 1938 turbine generators designed for 2-pole 3,600-rpm 60-cycle conditions were built for ratings as large as 81,250 kva at 0.8 power factor. In the period under discussion this rating has been raised to 100,000 kw at 0.9 power factor. Double-frequency vibrations which had been experienced on some of these

high-speed units have been eliminated by machining relatively narrow cross-wise slots in the pole body at intervals along the body length. This equalizes the rotor-body rigidity on the two major axes and can be realized without removing an appreciable amount of rotor pole material.

Double-frequency vibratory forces inherent in the 2-pole generator stator cannot be eliminated. However, the magnitude of these forces transmitted to the stator frame and generator foundation are minimized effectively by isolating the stator core on flexible supports; these supports absorbing practically all of the vibration energy.

About 60 per cent of the central station generators installed during the period were hydrogen-cooled. Availability of hydrogen-cooled generators has been practically perfect. Most hydrogen-cooled generators were designed for 15 pounds per square inch gauge operation to obtain increased maximum rating, but only a few are operated at this pressure.

Water wheel generators, as in the past, are characterized by large dimensions. For this reason large-capacity units must be built in sections and assembled at the point of installation. This has led to problems of fabrication which largely have been solved in this period. Although building the components at the user's plant will result in a unit of greater mechanical stability with less need for later maintenance, the initial cost will be greater. For this reason doing as much fabrication at the manufacturer's plant as possible has been standard practice. Lower short-circuit ratios and inertia constants are being used in current hydroelectric generators because of their reduced importance following from the radically improved clearing times provided by modern circuit breakers. Amortisseur windings are being adopted generally on hydroelectric salient-pole generators.

Large water wheel generators of current designs recirculate cooling air and have surface-type finned-tube air coolers to dissipate the losses. Several coolers are

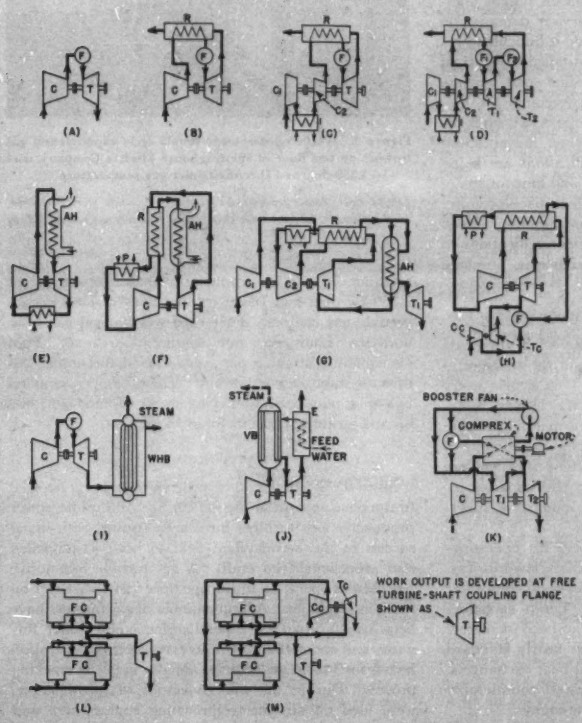

Figure 8. Gas-turbine cycles fall into many classes, some of the principal ones being shown here

Increased complexity results from attempting to realize higher efficiency, use higher gas temperatures with relatively low-temperature alloys, and attain utilization of all fuel types

A—Simple cycle
B—Regenerative cycle
C—Regenerative cycle with intercooled compressor
D—Regenerative cycle with intercooled compressor and reheating
E—Closed simple cycle
F—Closed regenerative cycle
G—Semiclosed regenerative cycle
H—Semiclosed regenerative cycle
I—Combination steam-gas cycle; waste heat boiler
J—Combination steam-gas cycle; Velox boiler
K—Cycle with compression unit
L—Free-piston-compressor cycle
M—Supercharged free piston compressor

AH—Air heater
C—Compressor
C_C—Charging compressor
E—Economizer
F—Furnace
FC—Free piston compressor
I—Intercooler
P—Precooler
R—Regenerator
T—Turbine
T_C—Charging turbine
VB—Velox boiler
WHB—Waste heat boiler

arranged symmetrically around the unit's outer periphery and enclosed in a light metal structure. This results in a unit of simple construction, with smooth lines, having a pleasing external appearance.

Much interest has been aroused in the newly developed silicone compounds. One application will be as insulating varnishes especially for high-temperature conditions. At this time applications have been to windings operating at 4,000 volts and less. It has been forecast that use of the silicone varnish will

1. Reduce electric equipment size and weight where operating temperature can be increased.

2. Greatly increase insulation life where conventional size, weight, and temperatures are maintained.

3. Permit operation in ambient temperatures above permissible limits for usual insulations.

As a result of emergencies during the war, a trend has developed in use of forced-circulation oil cooling for transformers. This permits increasing transformer ratings.

Rising war loads focussed attention on system interconnection and operation since other war demands on manufacturers building capacity made it difficult to get additional generating capacity installed. Principal interest centered on method of tie-line load control, frequency control, and prime mover governing.

A committee jointly sponsored by the AIEE and ASME was formed to promulgate prime mover speed governing specifications. Five specifications are being prepared, one for hydraulic turbines and four for steam turbines convering straight-condensing, back-pressure, and nonautomatic and automatic-extraction units. These are being prepared as separate specifications to facilitate their incorporation by reference in purchase specifications.

INTERNAL COMBUSTION ENGINES

Utilization of Diesel engines during the war increased many times, most applications being in the transportation field on land and sea. Since 1940 nearly every manufacturer of 4-cycle engines in the United States offers a supercharged engine having a marked increase in rating with considerable improvement in economy of fuel, space, and weight. Some basic-design engines with a few concurrent changes have had capacity increases as high as 100 per cent by employing supercharging.

Improvements have been effected in operating-safety devices such as over-speed governors, low-lubricating-oil pressure, over-temperature, loss-of-cooling-water warning, and shutdown apparatus. Pump capacities for lubricating oil and cooling water has been increased. Indirect-cooling systems have become nearly standard practice through the use of improved heat exchangers. Lubricating systems have been improved considerably by providing increased flow through the engine.

Fuel-injection equipment now is built wholly in the United States. Improvements in this apparatus in some instances have been effected through designs based on improved workmanship where tolerances are measured in millionths of an inch instead of in thousandths.

No tendency is evident here today to build low-speed Diesel engines in excess of 7,500 horsepower. In contrast, some engines with ratings in excess of 20,000 horsepower were built some years ago in Europe.

Largest installation of internal-combustion engines was made for an aluminum reduction plant at Jones Mills, Ark. Construction started March 1942 and was completed June 1943. First units went into service November 1942. This plant has 68 units installed

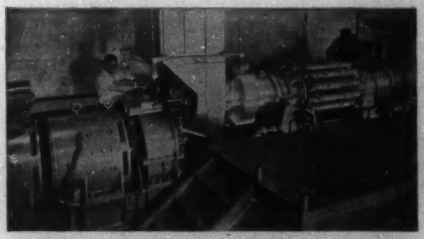

Figure 9. A 2,000-horsepower simple-cycle experimental gas turbine on test floor of Westinghouse Electric Company uses 1,350-degree-Fahrenheit inlet gas temperature

Left to right, double-armature d-c generator, reduction gear, inlet hood, axial compressor, 12 combustion chambers, gas turbine, and exhaust diffuser

totalling 78,000 kw capacity. These consist of 18 2,250-kw dual-fuel Diesel engines and 50 750-kw convertible gas engines. Fuel used was natural gas from northern Louisiana and southern Arkansas. Pilot oil equalling about 5 per cent of total fuel input was used to stabilize combustion. These engines supplied two aluminum pot-lines having a peak demand of 67,000 kw and an annual load factor of 94 per cent.

GAS TURBINES

Since 1939 considerable progress has been realized in the development of the gas turbine as a prime power producer. Gas turbines have been applied with signal success in the aeronautical field to both jet-propelled and propeller-driven craft. A gas turbine locomotive has been in operation in Europe since 1941 whenever oil fuel was available. A large number of gas turbines have been used abroad for supercharging Velox boiler furnaces and more than 30 units have been in operation here from 3 to 10 years in the Houdry catalytic cracking process. During the war thousands of superchargers were used on aircraft reciprocating engines here and

abroad, the power for these units being developed by gas turbines operating on the engine exhaust gas. A stand-by gas turbine generating plant has been in operation in Switzerland since 1939.

Many schemes have been proposed and are under experimentation for practical gas turbine cycle arrangements. The United States Navy has sponsored the building of several experimental units of different designs for ship propulsion. With high-efficiency turbines and compressors, which are the principal working elements of the cycle, the turbine inlet gas temperature is the principal controlling element in achieving high cycle thermal efficiency. To utilize such high temperatures, new metal alloys were developed and they are still the subject of intensive research to push temperature utilization as high as possible. Some units have been built for 1,250 degrees Fahrenheit; one has been built for 1,500 degrees Fahrenheit with special blade cooling provisions; several units are under construction to operate at 1,350 degrees Fahrenheit without blade cooling. Higher gas temperatures are used on military aircraft gas turbines where short engine life can be tolerated.

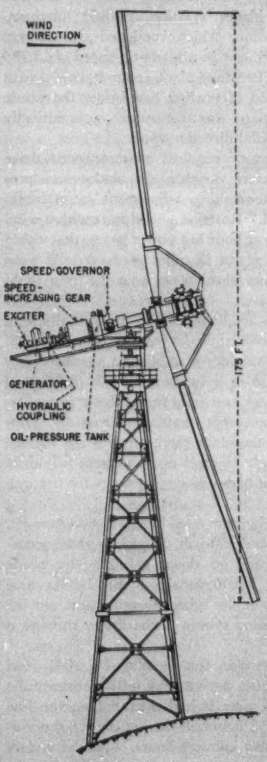

Figure 10. A 1000-kw wind turbine on top of Grandpa's Knob near Rutland, Vt., was the first wind-driven unit to deliver power into a utility system

Increased thermal efficiency also can be achieved by using regenerators which recover part of the exhaust gas heat energy to preheat the compressed air before it enters the furnace or combustion chamber. Intercooling the air during compression reduces compressor work requirements and raises cycle thermal efficiency. A third method of increasing efficiency expands the hot gas partially through the turbine and then reheats it before completely expanding it to atmospheric pressure. All of these refinements have been used in various units constructed for experimentation or commercial use.

Switzerland produced two other methods of achieving high thermal efficiency as represented by the power-gas generator or free-piston compressor and the Comprex. These are distinguished by their utilization of high gas temperatures without calling for special metal alloys in construction of the cycle components (during the war high-temperature alloys were unavailable to the Swiss). The free-piston compressor serves as both the furnace and compressor and is a reciprocating engine in effect. Here the high-temperature gas produced in the Diesel cylinder (furnace) acts directly upon pistons which compress the air before introduction to the cylinder. The gas exhausted from the unit is at relatively high pressure and temperature and produces the cycle power output by expansion through a gas turbine. Several United States manufacturers now are doing development work on this type unit.

In the Comprex unit, an entirely new invention, a pneumatic ram principle is utilized. It uses hot charges of relatively high-pressure gas from the furnace to do compression work on partially compressed air discharged from a conventional axial flow compressor; the gas and air charges are in direct contact in this device.

Because the furnace combustion products pass directly through the turbine in all open cycles it is evident that oil and gas are the ideal fuels. However, coal is the more abundant and often cheaper fuel and hence much effort has been and is being exerted to adapt it as the gas turbine energy source. Several proposals and two actual experimental units use a closed-cycle system where the working medium to be heated is separated from the furnace and combustion process by heat transfer surfaces as in a steam boiler. Coal burning presents no problem in these designs. Further investment gains are made by maintaining the lowest working air pressure in the cycle above atmospheric at about 85 pounds per square inch gauge. This brings the size of the rotating elements down very markedly. However these advantages are offset by the large amount of expensive high-temperature alloys that must be used in construction of the air heater.

Development of the closed-cycle plant is taking place in Switzerland. In the United States intensive research is devoted to burning pulverized coal in open-cycle plants where combustion products pass through the turbine. Several methods are being investigated, one works on the principle of separating fly ash from the gas prior to passing it through the turbine, and another on superfine pulverization of the coal prior to burning. Separation occurs in the first method by passing the combustion products from the furnace through a battery of small cyclone-type mechanical separators. Experiments have shown that about 95 per cent of the solids are removed from the gas stream at the expense of about one pound drop in gas pressure. The remaining 5 per cent of dust passing through the turbine is of less than 5-micron diameter and research indicates that dust of this size has no deleterious effect on turbine blading.

The second method of superfine coal pulverization makes all fly ash particles produced in the furnace combustion process of less than 5-micron diameter Then all this dust can be passed through the turbine without separation from the gas.

Two gas turbine locomotives designed for pulverized coal burning with ash separation are now under construction in the United States for the locomotive development committee of Bituminous Research, Inc.

In contrast with steam plant practice, gas turbine size has to be several times larger than the net plant output, as the compressor needs about 60 to 80 per cent of the turbine output to do its compression work. This factor, coupled with the wide gas temperature variation that the gas turbine must work under, places limitations on the maximum unit size that can be built. For a while 10,000 kw was regarded as the maximum capacity for open cycle units, with no definite limitations on closed cycle units because of their small physical size. However, a 27,000-kw open-cycle unit is now under construction in Switzerland.

Cycle thermal efficiency varying from 18 to 31.5 per cent has been reported on tests of various gas turbines. These efficiencies are based on the fuel lower heating values. The lower thermal efficiency is representative of simple units without regenerators, intercooling, or reheating. Studies indicate that with all of these devices and a 1,500-degree-Fahrenheit gas temperature, cycle thermal efficiencies of about 40 per cent might be realized.

Several central station utilities in the United States have studied application of gas turbine units to their systems but to date no installation proposals have been reported.

WIND TURBINE

The first serious attempt at generating electric energy on a commercial scale from the wind as a source of energy was made during this period. On October 19, 1941, a wind turbine installed on top of Grandpa's Knob, near Rutland, Vt., was the first wind-driven device to deliver a-c electric power into a utility system, the Central Vermont Public Service Corporation. This unit, Figure 10, had a capacity of 1,000 kw and was mounted on top of a structural steel tower 110 feet high and 36 feet square at the base.

A heavy plate-steel-girder structure, called a pintle girder, formed the plant mounting atop the tower. This girder inclines downward into the wind with a 12.5-degree slope from the horizontal and is supported at *A* on the top end of a pintle shaft. This shaft has a double roller guide bearing just below the girder at *B* and a combination roller guide and thrust bearing at *C* which allows the whole plant to yaw (swing) with the wind.

The blades and their control mechanism overhang one side of the tower and almost balance the rest of the equipment. The blades constructed of shot-welded stainless steel are more than 11 feet wide and 65 feet long, weighing 15,300 pounds each. Four motions are provided for the blades: rotation, yawing, pitching, and coning. Rotation, which produced the energy, took place at 28.7 rpm with a blade-tip speed of 15,785 feet per minute. The whole plant assembly yawed with the wind by the aid of gearing just below the pintle girder. Gear motion was controlled automatically by a yaw meter or wind-direction vane.

As the a-c generator requires constant-speed drive and wind velocities are variable, the blades were provided with variable-pitching adjustment to maintain constant shaft speed. Rotation would start with a wind speed of four miles per hour but power generation would start only at speeds about 18 miles per hour. At wind velocities greater than 60 miles per hour the unit would be taken out of service.

When the blades are being driven at normal speed, centrifugal force holds them at nearly right angles to the main shaft. If a sudden gust of wind hits them they can cone down-wind to a maximum of 20 degrees to relieve the initial shock and assist the governor in regulating speed. The governor regulates speed by automatically changing the blade pitch angle. For normal operation, pitch angle changes of 30 degrees would be needed, but this unit had a 99-degree range for research purposes.

The 1,000-kw generator was built for 600-rpm 80-per-cent-power-factor 2,300-volt, 60-cycle 3-phase operation. Generator leads go down through the pintle shaft center and connect to slip rings. Brushes on these slip rings connect to cables tying the generator into the 44,000-volt transmission system of the utility through a transformer.

The unit first went on test October 19, 1941, and remained so for a little over a year until February 20, 1943, during which time it had operated on the line for 695 hours and 192 hours off the line on test, generating a total of 298,240 kilowatt-hours. At the end of

this period the main-shaft bearing failed and, because of priority conditions, could not be replaced until March 3, 1945.

Between March 3 and 26, 1945, the unit operated as a routine generating station of the system for 143 hours, producing 61,780 kilowatt-hours. This period was an unusual windless three weeks for March. During a smooth 20-mile-per-hour wind on the latter date one of the blades failed at the outboard edge of the bolted shank spar connection. Failure was caused by multiple corroded cracks at this point. The broken-off blade landed about 1,000 feet away on the mountain side, the remaining blade was damaged by coning negatively and colliding with the tower structure. Similar corroded cracks were found at the same location on the latter blade. The age of the corrosion was unknown.

A redesigned 1,500-kw wind turbine will be erected on a high summit in the Green Mountains of Vermont to feed again into a utility system. Wind-power plants always must operate in parallel with another source of power, such as water-power plant with storage or a steam plant. Studies indicated that in any one year a wind-power plant can generate more kilowatt-hours than most water-power plants because average wind conditions remain more stable from year to year than average water conditions.

Another interesting proposal has been made for wind turbines of 6,500- and 7,500-kw capacities. Instead of attempting to maintain constant blade speed this design

Table II. Hydroelectric Projects Constructed, Operated, and Projected by Government Agencies

Project	States	River	Ultimate Capacity, Hp	Initial Capacity, Hp	Installed Capacity, Hp	Capacity on Order, Hp
United States Bureau of Reclamation						
Grand Coulee	Wash.	Columbia	2,877,000	478,000	928,000	945,000
Anderson Ranch	Idaho	Boise	55,500	37,000		37,000
Minidoke	Idaho	Snake	26,500	9,000	19,500	
Shasta	Calif.	Sacramento	522,000	419,000	419,000	103,000
Keswick	Calif.	Sacramento	102,000	102,000		102,000
Parker Dam	Ariz., Calif.	Colorado	160,000	120,000	160,000	
Davis Dam	Ariz., Calif.	Colorado	311,000	311,000		311,000
Hoover Dam	Ariz., Nev.	Colorado	1,835,000	522,000	1,435,000	
Elephant Butte	N. Mex.	Rio Grande	34,500	34,500	34,500	
Green Mountain	Colo.	Blue	30,000	30,000	30,000	
Estes	Colo.	Big Thompson	63,000	63,000		63,000
Mary's Lake	Colo.	Big Thompson	11,300	11,300		11,300
Kortes	Wyo.	North Platte	55,500	55,500		55,500
Shoshone	Wyo.	Shoshone	20,000	20,000	20,000	
Heart Mountain	Wyo.	Shoshone	8,300	8,300		8,300
Boysen	Wyo.	Big Horn	21,000	21,000		21,000
Seminoe	Wyo.	North Platte	45,000	45,000	45,000	
United States Engineers Corps						
Bonneville	Oreg., Wash	Columbia	729,000	137,000	729,000	
Fort Peck	Mont.	Missouri	150,000	70,000	70,000	
St. Marys Falls	Mich.	St Marys	23,925	23,925		23,920
Norfolk	Ark.	North Fork	168,000	42,000	42,000	42,000
Narrows	Ark.	Little Missouri	36,000	24,000		
Fort Gibson	Okla.	Grand	120,000	80,000		80,000
Dennison Dam	Okla., Tex.	Red	283,000	59,080	59,080	56,000
Wolf Creek	Ky.	Cumberland	414,000	207,000		207,000
Central Hill	Tenn.	Carney Fork	207,000	138,000		138,000
Dale Hollow	Tenn.	Obey	75,000	50,000		50,000
Allatoona	Ga.	Etowah	152,900	102,900		102,900
Imperial Irrigation District						
Drop 3	Calif.	All American Canal	15,000	7,500	7,500	
Drop 4	Calif.	All American Canal	26,600	13,300	13,300	
Platte Valley Public Power and Irrigation District						
Sutherland	Nebr.	North Platte	35,000	35,000	35,000	
Loup River Public Power District						
Monroe	Nebr.	Loup	9,600	9,600	9,600	
Columbus	Nebr.	Loup	54,000	54,000	54,000	
Central Nebraska Public Power and Irrigation District						
Jeffrey Canyon	Nebr.	Platte	26,000	26,000	26,000	
Johnson 1	Nebr.	Platte	26,000	26,000	26,000	
Johnson 2	Nebr.	Platte	50,000	25,000	25,000	
Grand River Dam Authority						
Pensacola Dam	Okla.	Grand	100,000	80,000	100,000	
Lower Colorado River Authority						
Buchanan Dam	Tex.	Colorado	51,900	34,600	34,600	
Tom Miller	Tex.	Colorado	20,000	20,000	20,000	
Inks Dam	Tex.	Colorado	16,000	16,000	16,000	
Marshall Ford	Tex.	Colorado	90,000	90,000	90,000	
Brazos River Conservation and Reclamation District						
Possum Kingdom	Tex.	Brazos	51,000	34,000	34,000	
South Carolina Public Service Authority						
Santee-Cooper	S. C.	Santee	213,000	173,000	173,000	
Greenwood County Board of Commissioners						
Buzzards	S. C.	Saluda	30,000	22,200	22,200	
Tennessee Valley Authority						
Kentucky	Ky.	Tennessee	220,000	176,000	176,000	44,000
Pickwick	Tenn.	Tennessee	288,000	96,000	192,000	
Wilson	Ala.	Tennessee	610,000	206,000	470,000	
Wheeler	Ala.	Tennessee	360,000	90,000	180,000	90,000
Guntersville	Ala.	Tennessee	136,000	102,000	102,000	
Hales Bar	Tenn.	Tennessee	44,000	44,000	44,000	
Chickamauga	Tenn.	Tennessee	144,000	108,000	108,000	
Watts Bar	Tenn.	Tennessee	210,000	126,000	210,000	
Norris	Tenn.	Clinch	132,000	132,000	132,000	
Fort Loudoun	Tenn.	Tennessee	176,000	88,000	88,000	88,000
Cherokee	Tenn.	Holston	166,000	83,000	83,000	
Douglas	Tenn.	French Board	166,000	83,000	83,000	41,500
South Holston	Tenn.	South Holston	41,000	41,500		
Watauga	Tenn.	Watauga	69,000	69,000		69,000
Fontana	N. C.	Little Tennessee	274,000	183,000	183,000	
Apalachia	Tenn.	Hiwassee	106,000	106,000	106,000	
Hiwassee	N. C.	Hiwassee	160,000	80,000	80,000	
Chatuge	N. C.	Hiwassee	10,700	10,700		
Nottely	Ga.	Nottely	13,400	13,400		
Ocoee 3	Tenn.	Ocoee	33,500	33,500	33,500	
Total Capacity			12,706,225		6,947,780	2,689,420

uses a variable speed d-c generator and connects to the a-c transmission system through a rotary converter. The generating equipment in this scheme would be mounted on top of a 475-foot tower.

NUCLEAR ENERGY

Large scale release of energy from the atomic nucleus is the outstanding scientific achievement realized during World War II. This new means of energy production places itself squarely in the field of power generation for possible future utilization. However, the radioactive features of this process impose formidable problems of control, design, and waste disposal which long may delay practical economic application to power production. While producing plutonium and uranium 235 is an involved process it appears that this will represent only a very minor element of cost in power production utilization.

Energy can be obtained from transmutation of elements either by combining two light elements into one of intermediate weight or by breaking up a heavy element into two or more elements of intermediate weight. The atomic bomb utilizes the latter process. Theoretically, 11,400,000 kilowatt-hours of energy can be obtained by fission of one pound of uranium 235. This energy appears as heat, which immediately suggests using it as a source for steam generation or power generation by gas turbines or for process heating.

Four laboratories will engage in nuclear research under the direction of the Manhattan District:

1. Clinton Laboratory at Oak Ridge, Tenn.
2. Argonne National Laboratory at Chicago, Ill.
3. Brookhaven National Laboratory on Long Island, N. Y.
4. Knolls Atomic-Power Laboratory at Schenectady, N. Y.

All of these organizations will work on the problem of atomic-produced power.

The power-pile program at Oak Ridge has progressed to the point of putting together the preliminary design. Problems being worked on are actual size and shape of "fuel" unit (pile), method of transferring heat from pile to engine or prime mover, method of loading and unloading pile, automatic pile control, and shielding against radiation. Emphasis will be laid on realizing a heat source of long life and great reliability. This is of great importance because the radioactivity makes any pile, once operating, difficult and dangerous to shut down for maintenance. Initial pile operation will be to provide heat energy for steam electric generation operating at conventional central station temperature ranging from 650 to 940 degrees Fahrenheit.

No capacity has been set as yet for the pilot plant. It is possible that all equipment will be conventional from the boiler through the generator. None of the equipment has been ordered at this writing.

Pile construction materials must have strength and rigidity at high temperature and not break down under neutron bombardment. The material serving as a moderator (carbon, heavy water) must have the proper neutron slowing qualities, yet be able to withstand pile operating temperatures. Selecting a suitable heat-transfer fluid from a range of possibilities including

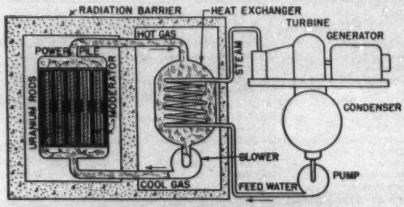

Figure 11. Simplified conception of how nuclear energy can be used as a source for a steam-electric station

Several government-sponsored projects are under way to develop nuclear-energy power plants

Table III. Growth in Power Production

Generating Capacity of Major Plants Contributing to Public Supply in Kilowatts, Excluding Certain Mining and Manufacturing Plants and Railroad Plants

Year	Steam	Hydro	Internal Combustion	Total
1920	8,919,727	3,703,531	90,350	12,713,608
1930	23,385,522	8,585,164	413,677	32,384,363
1940*	28,374,957	11,223,729	928,195	40,536,881
1941	30,209,285	11,817,374	988,777	43,015,436
1942	31,778,567	12,841,933	1,042,450	45,662,950
1943	33,624,581	13,883,583	1,052,603	48,560,767
1944	34,150,807	14,586,324	1,061,941	49,799,072
1945	34,036,609	14,987,547	1,078,286	50,102,442
1946	34,304,910	14,849,036	1,149,714	50,303,660

* Years 1940–44 include New York, N. Y., rapid transit system central stations. To make series continuous, subtract about 600,000 kw from capacity for years 1940–44 in both steam and total columns.

Table IV. Growth in Power Production

Generation of Major Plants Contributing to the Public Supply in Million Kilowatt-Hour, Excluding Certain Mining and Manufacturing Plants and Railroad Plants

Year	Steam	Hydro	Internal Combustion	Total
1920	23,488	15,760	156	39,404
1930	59,293	31,190	629	91,112
1940*	93,918	47,321	1,514	142,753
1941	114,037	50,563	1,606	166,206
1942	122,184	63,871	1,630	187,685
1943	144,013	73,632	1,746	219,391
1944	153,905	73,945	1,916	229,766
1945	140,437	79,917	2,080	222,434
1946	142,380	78,397	2,352	223,129

* Years 1940–44 include New York, N. Y., rapid transit systems central stations. To make series continuous, subtract about 900,000,000 kilowatt-hours in 1940 graduated up to about 1,500,000,000 kilowatt-hours in 1944 in both steam and total columns.

ordinary water, heavy water, and other liquids gases, and molten metals constitutes a major problem.

Because of radioactivity the pile enclosure cannot be entered for repairs without a very extended shutdown period to allow the radiations to dissipate themselves. Hence the pile and associated equipment—pumps, blowers, valves, and heat exchangers—all of which will be radioactive during operation, must possess extraordinary reliability. Even in the smallest plants both the pile and heat exchanger must be shielded by massive walls of concrete or heavy material to protect personnel.

In contrast to the unfortunate popular furor produced by irresponsible prognosticators, stands the fact that atomic energy is not synonomous with free energy. At the present time plant investment requirements appear to be of such magnitude as to burden the atomic power plant with very heavy fixed charges and certainly the raw energy will not be "free" whatever form it may take eventually. One published estimate states that atomic plants of 500,000-kw capacity and greater appear to produce electric energy that is competitive with coal and hydro-produced energy. Obviously the economic opportunity to apply plants of this size will be rare at the present time.

REFERENCES

Electric Equipment

1. System Application of Phase and Voltage Regulation, **A. A. Johnson.** *Electrical World* (New York, N. Y.), volume 126, July 7, 1946, pages 104–7.

2. Quick-Trip Bus Ties Reduce Breaker Duties. *Electrical World* (New York, N. Y.), volume 125, May 11, 1946, page 95.

3. All Power Handled on Aluminum Buses (Jennison Station). *Electrical World* (New York, N. Y.), volume 125, April 27, 1946, pages 57–9.

4. Isolated-Phase Bus Experience Dominantly Favorable. *Electrical World* (New York, N. Y.), volume 125, March 30, 1946, pages 44–7.

5. Electronic Exciter for 81,250-kva Turbo-Alternator, **H. A. Langstaff, R. F. Lawrence.** *Electrical World* (New York, N. Y.), volume 125, March 16, 1946, pages 88–91.

6. Frequency Changers—Characteristics, Applications, and Economics, **S. B. Crary, R. M. Easley.** AIEE *TRANSACTIONS*, volume 64, 1945, June section, pages 351–8.

7. Use of Dielectric-Absorption Tests in Drying Out Large Generators, **H. C. Marcroft.** AIEE *TRANSACTIONS*, volume 64, 1945, February section, pages 56–60.

8. Electronic Applications Extensive Among Utilities, **H. N. Ekvall.** *Electrical World* (New York, N. Y.), volume 124, December 22, 1945, pages 70–1.

9. Silicone Resins for Electrical Insulation, **G. L. Moses.** *Electrical World* (New York, N. Y.), volume 124, November 24, 1945, pages 79–81.

10. Standard Source Calibrates 60-Cycle Frequency Meters, **G. P. Fallon, C. H. Fetter.** *Electrical World* (New York, N. Y.), volume 124, September 29, 1945, pages 76–7.

11. Thyratron Rectifier Controls Steam-Turbine Governor, **J. H. Schroeder.** *Electrical World* (New York, N. Y.), volume 124, July 21, 1945, pages 68–9.

12. Large-Scale Frequency Meter Sensitive, Prompt, and Accurate, **J. E. Allen.** *Electrical World* (New York, N. Y.), volume 123, January 6, 1945, pages 54–6.

13. Prevention of Rotor-Winding Deformation on Turbogenerators, **John G. Noest.** AIEE *TRANSACTIONS*, volume 63, 1944, July section, pages 514–19.

14. Regulation of A-C Generators With Suddenly Applied Loads, **E. L. Harder, R. C. Cheek.** AIEE *TRANSACTIONS*, volume 63, 1944, June section, pages 310–18.

15. Steady-State Stability of Synchronous Machines as Affected by Voltage-Regulator Characteristics, **C. Concordia.** AIEE *TRANSACTIONS*, volume 63 1944, May section, pages 215–20.

16. The Electronic Converter for Exchange of Power, **F. W. Cramer, L. W. Morton, A. G. Darling.** AIEE *TRANSACTIONS*, volume 63, 1944, pages 1059–69.

17. A Pneumatic Mechanism for Outdoor Oil Circuit Breakers, **L. J. Linde, E. B. Rietz.** AIEE *TRANSACTIONS*, volume 63, 1944, July section, pages 543–6.

18. Tests of 230-Kv High-Speed Reclosing Oil Circuit Breaker, **A. C. Schwager.** AIEE *TRANSACTIONS*, volume 63, 1944, November section, pages 784–8.

19. Ring Buses for Generating and Transmission Stations, **E. L. Michelson, J. P. Galassini.** AIEE *TRANSACTIONS*, volume 63, 1944, September section, pages 665–9.

20. Modern Transformer Developments and the Economic Trend, **J. K. Hodnette.** *Midwest Power Conference Proceedings* (Chicago, Ill.), volume 7, 1944, pages 77–85.

21. The Place of Electronics in Power Generation, **J. D. Ryder.** *Midwest Power Conference Proceedings* (Chicago, Ill.), volume 7, 1944, pages 114–21.

22. Lightning Protection for Rotating Machines, **G. D. McCann, E. Beck, L. A. Finzi.** AIEE *TRANSACTIONS*, volume 63, 1944, pages 319–33.

23. Vibration Protection for Rotating Machinery, **R. L. Webb, C. S. Murray.** AIEE *TRANSACTIONS*, volume 63, 1944, July section, pages 534–7.

24. Differential Protection of Generator Transformer Unit, **A. H. Burhalter.** *Electrical World* (New York, N. Y.), volume 122, August 5, 1944, pages 87–9.

25. Increasing Output of Generating Equipment. *ELECTRICAL ENGINEERING*, volume 62, July 1943, pages 285–90.

26. Phase Shifter Regulates Figure 8 Interconnection, **L. P. Ferri.** *Electrical World* (New York, N. Y.), volume 120, July 10, 1943.

27. Disconnect Inching Averts Accidents and Outages, **E. R. Paige** *Electrical World* (New York, N. Y.), volume 119, June 26, 1943, pages 48–9.

28. Oilstatic Cables for 13.8 Kv Generator Leads, **F. P. Fairchild.** *Electrical World* (New York, N. Y.), volume 119, April 17, 1943, pages 60–2.

29. Automatic Air-Breaks in Lieu of Oil Breakers, *A. M. McCabe.* *Electrical World* (New York, N. Y.), volume 119, January 9, 1943, pages 44–5.

30. New Regulator Controls Generator Rkva Output, **J. T. Logan.** *Electrical World* (New York, N. Y.), volume 118, December 26, 1942, pages 36–7.

31. Direct-Acting Regulators on Large Georgia Generators, **J. T. Logan.** *Electrical World* (New York, N. Y.), volume 117, May 2, 1942, pages 42–4.

32. Prewound Stators Cut Losses in Older Units, **B. H. Smith.** *Electrical World* (New York, N. Y.), volume 118, July 11, 1942, pages 50–1.

33. Fault Bus-Differential Scheme Protects Chahokia Bus, **G. W. Gorell.** *Electrical World* (New York, N. Y.), volume 117, April 18, 1942, pages 53–4.

34. 99$^{44}/_{100}$% Dry Air for Circuit Breakers, **C. Thumin.** *Power* (New York, N. Y.), volume 36, April 1942, pages 74–76.

35. Chickasaw Electrical Design Influenced by Humidity, **A. H. Morgenthaler.** *Electrical World* (New York, N. Y.), volume 117, February 21, 1942.

36. Tennessee Valley Authority Hydroelectric Stations—Electrical Design, **Raymond A. Hopkins.** AIEE *TRANSACTIONS*, volume 60, 1941, pages 1281–93.

37. System Protection Analysis Precedes Oswego Design, **G. Steeb.** *Electrical World* (New York, N. Y.), volume 117, November 1, 1941, pages 57–60, 115.

38. Hydrogen-Cooled Turbine Generators, **M. D. Ross, C. C. Sterrett.** AIEE *TRANSACTIONS*, volume 59, 1940, January section, pages 11–17.

39. Special Problems of Two-Pole Turbine Generators, **C. M. Laffoon, B. A. Rose.** AIEE *TRANSACTIONS*, volume 59, 1940, January section, pages 30–3.

40. The Hydrogen-Cooled Turbine Generator, **D. S. Snell.** AIEE *TRANSACTIONS*, volume 59, 1940, January section, pages 35–45.

41. Some Factors in the Mechanical Design of High-Speed Turbogenerators, **Soren H. Mortensen, James J. Ryan.** AIEE *TRANSACTIONS*, volume 59, 1940, January section, pages 51–6.

42. High-Capacity "Hydro-Blast" Circuit Breaker for Central-Station Service, **W. F. Skeats, W. R. Saylor.** AIEE *TRANSACTIONS*, volume 59, 1940, February section, pages 111–14.

43. The Direct-Acting Generator Voltage Regulator, **W. K. Boice, S. B. Crary, Gabriel Kron, L. W. Thompson.** AIEE *TRANSACTIONS*, volume 59, 1940, March section, pages 149–56.

44. 12-Kv Metal-Enclosed Bus and Switch Structure, Station C, Oakland, Pacific Gas and Electric Company, **F. S. Benson, H. E. Strong.** AIEE *TRANSACTIONS*, volume 59, 1940, pages 751–5.

45. Maximum Availability Aim of Switch-House Design (San Diego Station B), **H. W. Eales, H. L. Hoeppner.** *Electrical World* (New York, N. Y.), volume 114, December 28, 1940, pages 40–3; March 28, 1941, pages 76–9, 158.

46. Vibration of Frame Reduced on Waterside Generator, **T. R. Galloway, B. A. Rose.** *Electrical World* (New York, N. Y.), volume 114, December 28, 1940, pages 30–1.

47. Air Blast Breakers Gain Acceptance. *Electrical Light and Power* (Chicago, Ill.), April 1940, pages 48–58.

48. Application of Rotating Regulators, **L. T. Rader.** *Midwest Power Conference Proceedings* (Chicago, Ill.), volume 9, 1946, pages 83–8.

49. Damper Windings for Waterwheel and Diesel Generators, **W. L. Ringland.** *Midwest Power Conference Proceedings* (Chicago, Ill.), volume 9, 1946, pages 89–94.

System Interconnection and Operation

50. Power Exchange in Interconnected Systems, **C. W. Meyott.** *Midwest Power Conference Proceedings* (Chicago, Ill.), volume 9, 1946, pages 95–100.

51. Reserve Requirements for Interconnected Systems, **H. W. Phillips.** *Electrical World* (New York, N. Y.), volume 125, May 11, 1946, pages 78–81.

52. Control of Load, Frequency, and Time of Interconnected Systems, **C. K. Duff.** AIEE *TRANSACTIONS*, volume 64, 1945, November section, pages 778–86.

53. Inter-System Power Co-ordination in the Southwest Region, **S. B. Morehouse.** *Electrical Light and Power* (Chicago, Ill.), December 1945, pages 62–70.

54. Automatic Load and Frequency Control in Northwest Power Pool, **S. B. Smith, M. L. Blair.** *Electrical World* (New York, N. Y.), volume 124, December 22, 1945, pages 56–60.

55. Speed and Load Control on Interconnected Systems, **E. E. George.** *Electrical World* (New York, N. Y.), volume 123–4, March 17, 1945, pages 84–5; March 31, 1945, pages 96–8; April 28, 1945, pages 82–5; May 12, 1945, pages 105–7; September 15, 1945, pages 96–8; September 29, 1945, pages 81–3.

56. The Effect of Weather on the System Load, **Henry A. Dryar.** AIEE *TRANSACTIONS*, volume 63, 1944, pages 1006–13.

57. Reclosing of Single Tie Lines Between Systems, **W. W. Parker, H. A. Travers.** AIEE *TRANSACTIONS*, volume 63, 1944, March section, pages 119–22.

58. Reference 19.

59. Northwest Pool Saves 100,000 Kw, **W. C. Heston** *Power* (New York, N. Y.), volume 88, May 1944, pages 68–71.

60. Chile Builds an Industrial Future on a 3-Million-Kw Power Program, **H. E. Way.** *Power* (New York, N. Y.), volume 88, May 1944, pages 80–1.

61. Carrier Channels Releasing Much Needed Capacity, **C. A. Grimm.** *Electrical World* (New York, N. Y.), volume 121, April 29, 1944, pages 58–60.

62. Restoration of War-Area Utility Power Plants, **C. M. Spofford, W. L. Cisler.** *Electrical World* (New York, N. Y.), volume 121, April 29, 1944, pages 46–50.

63. Load Designation and Control Without Communication, **C. P. Corey.** *Electrical World* (New York, N. Y.), volume 121, April 1, 1944, pages 58–60.

64. Time and Frequency Standards on Interconnected Systems, **R. J. Donaldson.** *Electrical World* (New York, N. Y.), volume 121, March 18, 1944, pages 78–80.

65. Northwest Power Resources Pooled for War, **W. C. Heston.** *Electrical World* (New York, N. Y.), volume 121, March 4, 1944, pages 59–66.

66. Bulk Power Metering Useful for Power Pool Operation, **M. D. Hooven.** *Electrical World* (New York, N. Y.), volume 121, January 8, 1944, pages 44–6.

67. The Frequencies of Natural Power Oscillations in Interconnected Generating and Distribution Systems, **Reinhold Rüdenberg.** AIEE *TRANSACTIONS*, volume 62, 1943, pages 791–803.

68. The Use of Automatic Control to Increase Plant Capacity, **H. H. Gorrie.** *Midwest Power Conference Proceedings* (Chicago, Ill.), volume 6, 1943, pages 90–6.

69. Generator Bus Regulation Gives Superior Results, **D. R. Pattison.** *Electrical World* (New York, N. Y.), volume 120, November 27, 1943, pages 52–4.

70. System-Voltage Programs Release Capacity Margins, **A. E. Silver.** *Electrical World* (New York, N. Y.), volume 120, October 2, 1943, pages 62–4.

71. Frequency Control of Load Swings, **J. E. McCormack, R. J. Lombard.** AIEE *TRANSACTIONS*, volume 61, 1942, September section, pages 623–4.

72. Control of Tie-Line Swings, **C. Concordia, H. S. Shott, C. N. Weygandt.** AIEE *TRANSACTIONS*, volume 61, 1942, June section, pages 306–14.

73. Power-System Interconnection in Quebec, **W. R. Way.** AIEE *TRANSACTIONS*, volume 61, 1942, December section, pages 841–7.

74. Capacity Released by Load Swing Control, **J. E. McCormack.** *Electrical World* (New York, N. Y.), volume 118, November 28, 1942, pages 51–3.

75. Interchange Contracts Between Industrial Plants and Utilities, **P. W. Ross.** *Midwest Power Conference Proceedings* (Chicago, Ill.), volume 4, 1941, pages 148–55.

76. Aspects of the National Power Pool—Defensively and Afterwards, **C. W. Leihy.** *Midwest Power Conference Proceedings* (Chicago, Ill.), volume 4, 1941, pages 178–87.

77. Increased Capacity and Interconnections of the Columbia Gas and Electric Corporation, **C. W. DeForest.** AIEE *TRANSACTIONS*, volume 60, 1941, pages 451–8.

78. System Load Swings, **H. A. Bauman, O. W. Mann, Jr., J. E. McCormack, H. B. Seeley.** AIEE *TRANSACTIONS*, volume 60, 1941, pages 541–7.

79. System Stability, **F. W. Gay.** AIEE *TRANSACTIONS*, volume 60, 1941, April section, pages 168–73.

80. Methods of System Control in a Large Interconnection, **Earle Wild.** AIEE *TRANSACTIONS*, volume 60, 1941, May section, pages 232–6.

81. Dump Hydro Keeps Up Stand-by Steam Plant, **H. P. Currin.** *Electrical World* (New York, N. Y.), volume 115, April 19, 1941, page 43.

82. Mingled Hydro and Steam Power Production in California—Past, Present, and Future, **A. H. Markwart.** AIEE *TRANSACTIONS*, volume 59, 1940, pages 775–82.

83. Provisions for Re-energising the Electric System of the Consolidated Edison Company of New York, Inc., **G. R. Milne, H. C. Otten.** AIEE *TRANSACTIONS*, volume 59, 1940, October section, pages 579–85.

84. The Design and Operation of a Metropolitan Electrical System From the Viewpoint of Possible Major Shutdowns, **S. M. Dean.** AIEE *TRANSACTIONS*, volume 59, 1940, October section, pages 575–9.

85. Restoration of Service From Large Metropolitan System After Complete Shutdown, **H. A. Dryar, Raymond Bailey.** AIEE *TRANSACTIONS*, volume 59, 1940, October section, pages 571–4.

86. Restoration of Service on a Metropolitan Power System, **W. C. Byrson, A. F. Hayward.** AIEE *TRANSACTIONS*, volume 59, 1940, October section, pages 563–70.

System Planning

87. Power—Where Do We Go From Here?, **H. A. Wiane.** *Mechanical Engineering* (New York, N. Y.), volume 68, December 1946, pages 1032–4.

88. Simplicity and Controls Are Keynotes of Post-War Plant, **P. C. Roe.** *Electrical World* (New York, N. Y.), volume 125, January 5, 1946, pages 55–7.

89. Evaluation of Electric Distribution Losses in Terms of Generating-Station-Capacity Investment, **M. Mortara.** AIEE *TRANSACTIONS*, volume 64, 1945. January section, pages 1–7.

90. Consolidated Edison Continues Development Program, **R. F. Brower.** *Power* (New York, N. Y.), volume 89, December 1945, pages 116–18.

91. Conditions Controlling the Economic Selection of Prime Movers, **Bernhardt G. A. Skrotzki.** AIEE *TRANSACTIONS*, volume 63, 1944, pages 1099–108.

92. Synthetic or Equivalent Load Curves, **R. F. Hamilton.** AIEE *TRANSACTIONS*, volume 61, 1942, pages 369–81.

93. The Summation of Load Curves, **R. F. Hamilton.** AIEE *TRANSACTIONS*, volume 63, 1944, October section, pages 729–35.

94. An Analysis to Determine the Optimum Bussing Arrangements and Transmission Capabilities at Grand Coulee, **R. V. Heard, G. W. Bills.** AIEE *TRANSACTIONS*, volume 63, 1944, pages 1259–63.

95. Fuel Investigation Should Precede Power Plant Design, **E. C. Payne.** *Mechanical Engineering* (New York, N. Y.), volume 66, August 1944, pages 519–22.

96. Planning for Economies in System Costs, **S. M. Dean.** *Electrical World* (New York, N. Y.), volume 121, June 10, 1944, pages 90–1.

97. Conservation in Design of Power Stations, **F. H. Hollister.** *Midwest Power Conference Proceedings* (Chicago, Ill.), volume 6, 1943, pages 150–60.

98. The Post-War Power Plant, **A. E. Knowlton.** *Electrical World* (New York. N. Y.), volume 120, December 25, 1943, pages 62–76.

99. Mechanical-Electrical Design of Power Plants Co-ordinated, **N. J. Walker, B. E. Hagy.** *Electrical World* (New York, N. Y.), volume 119, May 15, 1943, pages 63–5.

100. Facilities for the Supply of Kilowatts and Kilovars, **Hollis K. Sels, Theodore Seely.** AIEE *TRANSACTIONS*, volume 61, 1942, May section, pages 249–55.

Hydroelectric Stations

101. Supervisory Control of 30,000-Kva Hydroelectric Plant, **C. W. Bohner, A. P. Maness.** AIEE *TRANSACTIONS*, volume 65, 1946, June section, pages 337–42.

102. Technique of Electrical and Hydraulic Testing of Hydroelectric Units, **G. D. Floyd, J. J. Traill.** AIEE *TRANSACTIONS*, volume 65, 1946, March section, pages 163–9.

103. Improvements in Performance of Hydroelectric Generating Units on the 2,000,000-Horsepower Saguenay Systems, **F. L. Lawton.** AIEE *TRANSACTIONS*, volume 65, 1946, pages 900–10.

104. Tennessee Valley Authority Hydroelectric Stations—Electrical and Mechanical Design, **R. A. Hopkins, H. J. Peterson.** AIEE *TRANSACTIONS*, volume 65, 1946, pages 920–31.

105. Present Status of the Proposed Hydroelectric Development of the St. Lawrence River, **C. H. Giroux.** *Midwest Power Conference Proceedings* (Chicago, Ill.), volume 9, 1946, pages 118–22.

106. Hydroelectric Power in the Missouri Basin, **B. H. Greene.** *Midwest Power Conference Proceedings* (Chicago, Ill.), volume 9, 1946, pages 123–32.

107. Objectives and Benefits of the Wisconsin Valley Improvement Company. *Midwest Power Conference Proceedings* (Chicago, Ill.), volume 9, 1946, pages 208–13.

108. Seven Years' Operating Experience at Bonneville Hydroelectric Plants. *Power* (New York, N. Y.), volume 90, March 1946, pages 64–8.

109. SPA Hydro Program—Summary and Fallacies. *Electrical World* (New York, N. Y.), volume 127, March 30, 1947, pages 60–3.

110. Northwest Power Pool Reservoir Operation, **E. N. Peterson.** *Electrical World* (New York, N. Y.), volume 125, February 2, 1946, pages 48–51; February 16, 1946, pages 100–3.

111. Load Adjusting Device for Unattended Hydro, **H. H. Gause, Jr.** *Electrical World* (New York, N. Y.), volume 124, September 29, 1945.

112. Grand Coulee Sets the Pace. *Power Plant Engineering* (Chicago, Ill.), volume 49, April 1945, pages 66–71.

113. Shipshaw No. 2 Adds 1,100,000 Hp to Canada's Hydroelectric Power. *Power* (New York, N. Y.), volume 89, March 1945, pages 64–7.

114. Electrical Features of Kentucky Dam Plant, **R. E. Behnke.** *Electrical World* (New York, N. Y.), volume 123, March 3, 1945, pages 82–5.

115. Kentucky Dam Project of TVA, **C. L. Norris, R. M. Gardiner.** *Power Plant Engineering* (Chicago, Ill.), volume 49, February 1945, pages 83–5; March 1945, pages 79–81.

116. More Power, More Water for California: Shasta Goes Into Operation. *Power* (New York, N. Y.), volume 88, November 1944, pages 95–102.

117. Power Facilities at TVA's Fontana Dam, **R. A. Hopkins, H. J. Peterson.** *Power Plant Engineering* (Chicago, Ill.), volume 48, November 1944, pages 92–4.

118. Design Features of Shasta Dam and Powerhouse. *Electrical World* (New York, N. Y.), volume 122, August 5, 1944, pages 83–6.

119. Pit 5 Adds 160,000 Kva to Pacific Coast Power Supply, **E. J. Strickland.** *Power* (New York, N. Y.), volume 88, July 1944, pages 88–90.

120. Simplicity, Reliability, Economy Designed into Pit 5 Plant, **E. F. Marvatt.** *Electrical World* (New York, N. Y.), volume 122, July 22, 1944, pages 71–4.

121. 213,000 Hp Hydro Plant Nears Completion on Pit River. *Electric Light and Power* (Chicago, Ill.), November 1943, pages 52–5.

122. Grand Coulee Pits Adapted to Shasta Turbines. *Electrical World* (New York, N. Y.), volume 119, February 20, 1943, pages 44–5.

123. Operation of the Multi-Purpose Projects of the TVA, **S. M. Woodward.** *Midwest Power Conference Proceedings* (Chicago, Ill.), volume 4, 1941, pages 76–82.

124. Construction of 48,000-Hp Kaplan Turbines for Pickwick Landing Dam, TVA, **W. J. Rheingans.** *Midwest Power Conference Proceedings* (Chicago, Ill.), volume 4, 1941, pages 83–92.

125. Amortisseur Windings for Hydro Generators, **S. B. Crary, W. R. Dungan.** *Electrical World* (New York, N. Y.), volume 115, June 28, 1941, pages 50–2.

126. Instrumentation Gives Gain in Hydro Output, **W. B. Hess, J. M. Monson.** *Electrical World* (New York, N. Y.), volume 115, June 14, 1941, pages 81–3.

127. Adjustable Blade Turbines Attain 93% Efficiency, **H. V. Terry.** *Power* (New York, N. Y.), volume 85, May 1941, pages 76–9.

128. Carbon Dioxide Safeguards Hydro Generators, **J. B. Cutler.** *Electrical World* (New York, N. Y.), volume 115, May 3, 1941, pages 54–6.

129. Electrical Features of Claytor Hydro Plant, **P. Sporn, H. A. Kammer.** *Electrical World* (New York, N. Y.), volume 115, March 8, 1941, pages 56–9; March 22, 1941, pages 68–71.

130. Heaters Prevent Condensation in Hydro Station Generators, **J. R. Housely.** *Electrical World* (New York, N. Y.), volume 113, April 6, 1940, pages 62–4.

131. Testing Governor Performance on Electric Power Systems With Improved Instruments, **J. E. Allen, W. B. Hess.** AIEE *TRANSACTIONS*, volume 66, 1947, pages 329–39.

Steam Plants

132. Modernization of Waterside Station Will Achieve New Plant Efficiency, **M. L. Waring.** *Electric Light and Power* (Chicago, Ill.), December 1946, pages 49–53.

133. Marion High-Pressure Unit No. 10 Completes Five Years of Service, **R. A. Baker.** *Power* (New York, N. Y.), volume 90, September 1946, pages 66–70.

134. Consolidated Edison Lays Plans to Complete Waterside Station Modernization, **M. J. Steinberg.** *Power* (New York, N. Y.), volume 90, August 1946, pages 64–7.

135. Modernizing Rockford, Illinois, Generating Station, **W. E. Hopkins, R. S. Kibler.** *Power Plant Engineering* (Chicago, Ill.), volume 50, July 1946, pages 70–6; August 1946, pages 114–16.

136. German Underground Power Plant Survives War Bombardment, **F. K. McQueary, K. O. Oliphant.** *Power* (New York, N. Y.), volume 90, July 1946, pages 100–02.

137. West Penn Power Adds New Unit at Springdale Station, **G. D. Burleigh.** *Power* (New York, N. Y.), June 1946, pages 64–7; July 1946, pages 72–5.

138. Southwark Station Will Augment Power Facilities in Philadelphia Area, **N. J. Walker, B. B. Hagy.** *Electric Light and Power* (Chicago, Ill.), June 1946, pages 60–6; July 1946, pages 68–70.

139. Modern Plant Survey. *Power* (New York, N. Y.), volume 90, June 1946, pages 79–98.

140. Southwark Station to Have Separate Auxiliary Generator, **J. H. Harlow, F. R. Ford.** *Power Plant Engineering* (Chicago, Ill.), volume 50, June 1946, pages 60–3.

141. Minimum Housing Employed for Low-Cost Houston Plant, **R. E. Hansen, L. Elliott.** *Electrical World* (New York, N. Y.), volume 125, May 11, 1946, pages 82–4.

142. Perry "K" Steam Plant Extension, **A. A. Benson.** *Electric Light and Power* (Chicago, Ill.), February 1946, pages 44–9.

143. Topping at Hell Gate, **H. Knecht.** *Power Plant Engineering* (Chicago, Ill.), volume 50, February 1946, pages 58–65.

144. Central Station Capacity Continues Expansion, **B. G. A. Skrotzki.** *Power* (New York, N. Y.), volume 90, January 1946, pages 64–7.

145. Jennison Station Adds 30,000 Kw to Central New York Supply Facilities. *Electric Light and Power* (Chicago, Ill.), January 1946, pages 60–5.

146. Southwark Station Aimed to Be Simple and Reliable, **E. L. Hopping.** *Electrical World* (New York, N. Y.), volume 25, January 22, 1946, pages 70–5.

147. Simple Design, Reliability Keynote Jennison Station, **W. W. Perry, W. Gressens, III.** *Electrical World* (New York, N. Y.), volume 124, December 8, 1945, pages 118–21, December 22, 1945, pages 64–7.

148. Base Load Economy Firmed Capacity at Hell Gate, **W. E. Caldwell.** *Electrical World* (New York, N. Y.), volume 124, November 10, 1945, pages 116–19.

149. High Plant Economy at Stamford. *Electrical World* (New York, N. Y.), volume 124, November 14, 1945, pages 68–71.

150. Topping at Hell Gate, **R. T. Roberts.** *Power Plant Engineering* (Chicago, Ill.), volume 49, November 1945, pages 70–5.

151. Florida Power Operates New 25,000-Kw Unit at Bayboro Plant, **P. L. Bartow.** *Power* (New York, N. Y.), volume 89, October 1945, pages 64–8.

152. New Correlated With Old in Mission Road Plant, **J. H. Houchull.** *Electrical World* (New York, N. Y.), volume 24, September 15, 1945, pages 88–91.

153. Riverside Plant Designed for Simplicity, Dependability, **G. S. Harris, F. W. Quarles, G. P. Fallon.** *Electrical World* (New York, N. Y.), volume 124, August 18, 1945, pages 90–3.

154. Pensacola Plant Simple, Adapted to Gulf Conditions, **E. C. Gaston, F. E. Hale, A. Mergenthaler.** *Electrical World* (New York, N. Y.), volume 123, June 9, 1945, pages 104–6; June 23, 1945, pages 70–2.

155. Simplified Semi-Outdoor Design for Modern Generating Stations, **H. L. Howe, T. C. Hoyt.** *Power* (New York, N. Y.), volume 89, May 1945, pages 71–4.

156. Circulating Water Turbine Gives Freedom in Plant Location (R. E. Burger Plant), **G. W. Saathoff.** *Electrical World* (New York, N. Y.), volume 123, March 17, 1945, pages 78–81.

157. Details of 65,000 Kw Harbor Steam Plant Turbine, **C. C. Franck.** *Power Plant Engineering* (Chicago, Ill.), volume 49, February 1945, pages 72–5.

158. Silver Gate Station Powers San Diego for War, **H. A. Noble, W. A. Zitlau.** *Power Plant Engineering* (Chicago, Ill.), volume 48, December 1944, pages 70–3.

159. Mystic Switching Station Design Keynotes Simplicity and Reliability, **W. W. Edson.** *Electrical World* (New York, N. Y.), volume 122, November 11, 1944, pages 80–2; November 25, 1944, pages 74–6.

160. Pennsylvania Edison Adds 31,250 Kw Unit at Williamsburg. *Power Plant Engineering* (Chicago, Ill.), volume 48, November 1944, pages 70–5.

161. Commonwealth Edison Completes Largest War Time Unit Historic Fisk Station. *Power* (New York, N. Y.), volume 88, October 1944, pages 70–3.

162. Unit 17 at Fisk Station. *Power Plant Engineering* (Chicago, Ill.), volume 88, October 1944, pages 90–3.

163. 147,000 Kw Addition Another Milestone at Fisk. *Electrical World* (New York, N. Y.), volume 122, September 30, 1944, pages 62–5.

164. Package-Type Power Plants, **H. H. Van Kennen, L. E. F. Wahrenburg.** *Mechanical Engineering* (New York, N. Y.), volume 66, September 1944, pages 581–7.

165. Hauto Superposition Used Pulverized Anthracite, **S. G. Roque.** *Electrical World* (New York, N. Y.), volume 122, August 19, 1944, pages 84–7.

166. Performance of Watts Bar Steam Station of TVA, **M. K. Bryan, R. T. Mathews.** *Mechanical Engineering* (New York, N. Y.), volume 66, July 1944, pages 471–9.

167. Improved Coal Handling Features Devon Extension. *Electrical World* (New York, N. Y.), volume 121, April 15, 1944, pages 90–3.

168. Southern California Replaces Lend Lease-Turbines, **W. L. Chadwick.** *Power* (New York, N. Y.), volume 88, April 1944, pages 95–100.

169. Chesterfield "Satisfies" Demand for Power in a Most Unconventional Way, **R. S. Reed, L. J. Tacy, C. C. Dodge.** *Electric Light and Power* (Chicago, Ill.), April 1944.

170. Bayside. *Power Plant Engineering* (Chicago, Ill.), April 1944, pages 64–9

171. Auxiliary Drives, Slag Rake in Sherman Creek Superposition, **W. E. Caldwell.** *Electrical World* (New York, N. Y.), volume 121, March 4, 1944, pages 56–8.

172. Efficiency Range is Aim of Bayside Extension Design, **W. F. Nelson.** *Electrical World* (New York, N. Y.), volume 121, February 19, 1944, pages 70–3.

173. Direct-Contact Heaters on 5 Turbines at Buzzard Point Plant, **H. H. Harrigan, H. G. Thielscher.** *Power Plant Engineering* (Chicago, Ill.), volume 48, February 1944, pages 74–6.

174. South Meadow's New 40,000 Kw Extension. *Power Plant Engineering* (Chicago, Ill.), volume 48, January 1944, pages 58–64.

175. Hutsonville Station Planned for Simple, Low-Cost Operation, **J. D. Roberts, L. Shog.** *Electrical World* (New York, N. Y.), volume 121, January 8, 1944, pages 51–4.

176. 1825-lb Pressure Topping Unit with Special Reference to Forced-Circulation Boiler, **E. G. Bailey.** *Transactions*, American Society of Mechanical Engineers (New York, N. Y.), 1943, page 474.

177. Frank R. Phillips Station Simple, Flexible, Ingenious, **F. S. Brown, R. B. Horner, W. H. Jones.** *Electrical World* (New York, N. Y.), volume 120, October 16, 1943, pages 52–5.

178. Simplicity and Versatility Stressed in Akron Addition, **G. C. Daniels.** *Electrical World* (New York, N. Y.), volume 120, September 18, 1943, pages 60–3.

179. Harbor Steam Plant Goes on the Line, **C. F. Garman, W. C. Rouse.** *Power Plant Engineering* (Chicago, Ill.), volume 47, June 1943, pages 64–9.

180. Extension to Cape Fear Station Adds 60,000 Kw, **W. F. Friend.** *Power Plant Engineering* (Chicago, Ill.), volume 47, January 1943, pages 50–3.

181. Harbor Steam Plant Designed for Economy, Quick Pick-up, **W. C. Rowse.** *Electrical World* (New York, N. Y.), volume 119, January 9, 1943, pages 30–2.

182. 60,000 Kw Added to Pittsburgh System, **A. G. Butler.** *Electric Light and Power* (Chicago, Ill.), September 1942, pages 42–4.

183. Parallel Operation Influences Design of Venice No 2, **W. F. Ryan, E. H. Tenney.** *Electrical World* (New York, N. Y.), volume 118, August 8, 1942, pages 51–4.

184. Two 850-Psi 900-F Watts Bar Steam Units Serve TVA War Loads, **G. E. Morgan.** *Power* (New York, N. Y.), volume 86, July 1942, pages 82–5.

185. Heating and Process Steam Influence Iowa Extension, **J. M. Drabelle.** *Electrical World* (New York, N. Y.), volume 117, June 27, 1942, pages 40–3.

186. Venice No. 2, **W. F. Ryan, E. H. Tenney.** *Power Plant Engineering* (Chicago, Ill.), volume 46, May 1942, pages 87–93.

187. Plant Arkwright Bolsters Southeast Power Supply, **E. C. Gaston.** *Electric Light and Power* (Chicago, Ill.), March 1942, pages 50–3.

188. Watts Bar Steam Design Simple, Direct, Economical, **R. A. Hopkins.** *Electrical World* (New York, N. Y.), volume 117, February 7, 1942, pages 40–3.

189. 1250-Lb Oswego Tests New Ideas. *Power* (New York, N. Y.), volume 86, January 1942, pages 56–60.

190. Heating Steam Requirements Fix Commerce Street Design. *Electrical World* (New York, N. Y.), volume 116, December 27, 1941, pages 46–9.

191. Oswego Station Design Pioneers New Ideas. **Electrical World** (New York, N. Y.), volume 110, December 13, 1942, pages 78–81.

192. Paddys Run Station, **R. H. Morris.** *Power Plant Engineering* (Chicago, Ill.), volume 45, November 1941, pages 48–53.

193. Chickasaw Plant Solves Unusual Condensing Problem, **E. C. Gaston.** *Electrical World* (New York, N. Y.), volume 116, November 29, 1941, pages 53–5.

194. Dual Pressure Turbine Fits into Boiler Program, **A. A. Benson.** *Electrical World* (New York, N. Y.), volume 116, November 1, 1941, pages 62–5.

195. Twin Branch Leads the Way with 2500-Lb Operation. *Power* (New York, N. Y.), volume 85, November 1941, pages 68–71.

196. Twin Branch Pioneers 2500-Lb Pressure. *Electrical World* (New York, N. Y.), volume 116, October 18, 1941, pages 80–106.

197. Watts Bar Steam Plant, **F. E. Bell.** *Power Plant Engineering* (Chicago, Ill.), volume 45, October 1941, pages 54–8.

198. Unusual Electrical Features of Chester Station Expansion, **C. F. Bishop.** *Electric Light and Power* (Chicago, Ill.), September 1941, pages 38–41.

199. Single Unit Plant Designed for One-Man Operation (Bluffs Plant), **W. P. Venable.** *Electrical World* (New York, N. Y.), volume 116, September 6, 1941, pages 40–3.

200. First American Utility Plant Uses Forced-Feed Circulation (Montaup). *Electrical World* (New York, N. Y.), volume 116, August 23, 1941, pages 52–4.

201. Port Washington Establishes Five-Year Economy Record. *Electrical World* (New York, N. Y.), volume 116, August 9, 1941, pages 70–3.

202. Avon, Martinez, Oleum—Achievement in Co-operation. *Power* (New York, N. Y.), volume 85, August 1941, pages 56–9.

203. Multiple-Service Oil Refinery and Utility Generating Plants. *Electrical World* (New York, N. Y.), volume 115, June 28, 1941, pages 40–3; July 12, 1941, pages 54–7.

204. Burlington Station Adds 100,000 Kw Condensing Unit, **H. Weisberg.** *Power* (New York, N. Y.), volume 85, July 1941, pages 56–63.

205. Unusual Features in Chester Station Expansion, **D. F. Schick, Jr.** *Electric Light and Power* (Chicago, Ill.), May 1941, pages 56–60.

206. Mercury Unit Sets Efficiency Record, **A. R. Smith, E. S. Thompson.** *Power* (New York, N. Y.), volume 85, April 1941, pages 64–7.

207. Wild and Flood Precautions Mark Cost Plant Design (Neuces Bay), **J. T. Persons, G. A. Mills, J. H. Buell.** *Electrical World* (New York, N. Y.), volume 115, April 5, 1941, pages 54–7.

208. Premeasured Control Pilots High-Efficiency Lansing Station, **R. F. Cummings.** *Power* (New York, N. Y.), volume 85, February 1941, pages 56–9.

209. Flexible Topping Turbine Doubles Plant Capacity, **G. P. Womble.** *Electrical World* (New York, N. Y.), volume 115, January 25, 1941, pages 38–9.

210. New Unit Provides Occasion for Station Refinements (Buzzard Point), **C. E. Miller.** *Electrical World* (New York, N. Y.), volume 114, December 14, 1940, pages 68–71.

211. Integrated Program Improves Station Reliability, **J. A. Keeth, R. L. Frisby.** *Electrical World* (New York, N. Y.), volume 114, October 19, 1940, pages 60–2; November 2, 1940, pages 42–4; November 16, 1940, pages 56–8.

212. Chester Station Adds 50,000 Kw Top, **D. F. Schick, Jr., C. F. Bishop.** *Power* (New York, N. Y.), volume 84, November 1940, pages 62–6.

213. How Ten Utilities Hook Up New Units, **S. A. Tucker.** *Power* (New York, N. Y.), volume 84, October, 1940, pages 84–7.

214. Steam Station Designed as Hydro Adjunct (Orem), **S. B. Flagg.** *Electrical World* (New York, N. Y.), volume 114, August 24, 1940, pages 36–9.

215. Flexible Steam Provisions for Combination Turbine (Walnut Station), **C. A. Butler, Jr.** *Electrical World* (New York, N. Y.), volume 114, August 10, 1940, pages 63–5; July 13, 1940, pages 46–9.

216. Millers Ford—3 Years of High-Temperature Operation, **R. D. Gillespie.** *Power Plant Engineering* (Chicago, Ill.), volume 44, June 1940, pages 38–42; July 1940, pages 54–6.

217. Utility Plant in Mill Yard, **A. A. Winters.** *Electrical World* (New York, N. Y.), volume 113, June 29, 1940, pages 26–8.

218. Boston Edison Co. Increases 1400-Lb Boiler Output at Edgar, **C. H. Danforth.** *Power Plant Engineering* (Chicago, Ill.), volume 62, May 1940, pages 40–6.

219. Increase Bus Capacity at South Meadow. *Electrical World* (New York, N. Y.), volume 113, May 4, 1940, pages 50–1.

220. Riverville Topping Unit Reduces Btu per Kw One-Third, **W. V. Drake.** *Electrical World* (New York, N. Y.), volume 113, February 24, 1940, pages 34–6.

221. New Castle Station. *Electric Light and Power* (Chicago, Ill.), February 1940, pages 44–8.

222. Low-Cost Single-Unit Plant for Kansas Utility (Lawrence), **G. A. Mills** *Electrical World* (New York, N. Y.), volume 113, January 27, 1940, pages 26–9.

Steam Plant Equipment

223. Protection of Powerhouse Auxiliaries, **An AIEE Committee Report.** AIEE *TRANSACTIONS*, volume 65, 1946, November section, pages 746–51.

224. Adjustable Speed Magnetic Drive, **G. Stangland.** *Power Plant Engineering* (Chicago, Ill.), volume 68, July 1946, pages 82–6.

225. Intercommunication System for Power Plants, **L. A. Randall.** *Power Plant Engineering* (Chicago, Ill.), volume 68, August 1946, pages 86–8.

226. Holding Power Plant Auxiliaries During Power Disturbances, **T. Mauna.** *Power Plant Engineering* (Chicago, Ill.), volume 68, June 1946, pages 88–9.

227. Modern Excitation Systems for Large Synchronous Machines, **J. B. McClure, S. I. Whittlesey, M. E. Hartman.** AIEE *TRANSACTIONS*, volume 65, 1946, pages 939–45.

228. The Development of Modern Excitation Systems for Synchronous Condensers and Generators, **F. M. Porter, J. H. Kinghorn.** AIEE *TRANSACTIONS*, volume 65, 1946, pages 1020–28.

229. Motor-Driven Exciters for Turbine Alternators, **R. B. Bodine, S. B. Crary, A. W. Rankin.** AIEE *TRANSACTIONS*, volume 65, 1946, May section, pages 290–97.

230. Application of Electric Motors to Power Station Auxiliaries, **A. E. Beardmore.** *Power Plant Engineering* (Chicago, Ill.), volume 68, February 1946, pages 72–5; March 1946, pages 78–80; April 1946, pages 62–5.

231. Power Systems for Auxiliary Drives in Steam-Electric Stations, **J. B. McClure, S. I. Whittlesey.** AIEE *TRANSACTIONS*, volume 64, 1945, December section, pages 844–51.

232. Auxiliary-Power Supply for Generating Stations, **V. E. McCallum.** AIEE *TRANSACTIONS*, volume 64, 1945, October section, pages 693–5.

233. Central-Station Auxiliary-Drive Motors for Constant and Adjustable Speed, **Hal Gibson.** AIEE *TRANSACTIONS*, volume 64, 1945, November section, pages 746–50.

234. Electric Drives for Steam-Electric Generating-Station Auxiliaries, **Wm. R. Brownlee, J. A. Elsi.** AIEE *TRANSACTIONS*, volume 64, 1945, November section, pages 741–5.

235. Automatic Load Control for Turbine Generators, **F. E. Crever, R. L. Jackson.** AIEE *TRANSACTIONS*, volume 64, 1945, September section, pages 656–60.

236. Steam Turbines, **L. N. Rowley, B. G. A. Skrotzki, W. A. Vopat.** *Power* (New York, N. Y.), volume 89, December 1945, pages 63–110.

237. Experience with Magnetic Couplings for Induced-Draft Fan Drive, **L. M. Exley.** *Power* (New York, N. Y.), volume 88, August 1944, pages 70–1.

238. A-C Adjustable-Speed Drives Power Underfeed Stokers, **I. L. Nevells.** *Power* (New York, N. Y.), volume 88, February 1944, pages 100–02.

239. A Short Cut to Turbine Cycle Heat Rates, **J. K. Salisbury.** *Power* (New York, N. Y.), volume 87, October 1943, pages 78–81; November 1943, pages 78–81.

240. Turbines Lend Versatility to Auxiliary Drive, **F. K. Fischer.** *Power* (New York, N. Y.), volume 87, July 1943, pages 99–101.

241. Instrument Aids for Turbine Operation, **H. C. Werner, G. V. Kronikoff.** *Power Plant Engineering* (Chicago, Ill.), volume 46, November 1942, pages 84–7.

242. Eddy-Current Couplings Adjust Oswego Combustion, **H. A. Piasecki.** *Electrical World* (New York, N. Y.), volume 117, June 13, 1942, pages 40–2.

243. Draft-Fan Power Supply Circuits Simplified, **J. S. Brown.** *Electrical World* (New York, N. Y.), volume 117, May 16, 1942, pages 54–5.

244. Governing Turbine Pressures, **R. Sheppard.** *Power* (New York, N. Y.), February 1942, pages 64–6; March 1942, pages 59–61.

245. Supplementary Control of Prime-Mover Speed Governors, **S. B. Crary, J. B. McClure.** AIEE *TRANSACTIONS*, volume 61, 1942, April section, pages 209–14.

246. Prime-Mover Speed Governors for Interconnected Systems, **R. J. Caughey, J. B. McClure.** AIEE *TRANSACTIONS*, volume 60, 1941, April section, pages 147–51.

247. Power System Governing—The Problem, **J. J. Dougherty, A. P. Hayward, A. C. Monteith, S. B. Griscom.** AIEE *TRANSACTIONS*, volume 60, 1941, pages 547–58.

248. Effect of Prime-Mover Speed Governor Characteristics on Power-System Frequency Variations and Tie-Line Power Swings, **C. Concordia, S. B. Crary, E. E. Parker.** AIEE *TRANSACTIONS*, volume 60, 1941, pages 559–67.

249. A Power-System Governor Sensitive to Frequency and Load, **Thomas E. Curtis.** AIEE *TRANSACTIONS*, volume 60, 1941, March section, pages 89–92.

250. A Turbine-Governor Performance Analyser, **W. O. Osbon.** AIEE *TRANSACTIONS*, volume 60, 1941, November section, pages 963–7.

251. An Electrical Governor, **Frank I. Morgan.** AIEE *TRANSACTIONS*, volume 60, 1941, February section, pages 80–4.

252. Variable Speed Drives for Power-Plant Auxiliaries, **G. V. Edmonson.** *Midwest Power Conference Proceedings* (Chicago, Ill.), volume 4, 1941, pages 53–60.

253. Pattern of Station Auxiliary Drives Changing, **J. C. Cunningham.** *Electrical World* (New York, N. Y.), volume 115, March 8, 1941, pages 64–6.

Outdoor Plants

254. Semi-Outdoor Plant, Simple, Compact, Convenient, **L. Elliott.** *Electrical World* (New York, N. Y.), volume 122, November 25, 1944, pages 70–2.

255. Outdoor Equipment Features Harvey Couch Station. *Power Plant Engineering* (Chicago, Ill.), volume 122, October 1944, pages 74–6.

256. Some Aspects of the Outdoor Power Plant, **R. H. Emerick.** *Power Plant Engineering* (Chicago, Ill.), volume 47, May 1943, pages 72–7.

257. Outdoor-Type Plant, **W. M. Wolford, A. A. Edewaard.** *Electric Light and Power* (Chicago, Ill.), March 1943, pages 44–5.

258. Outdoor Steam Plants Save Materials, Cut Costs, **L. Elliott.** *Electrical World* (New York, N. Y.), volume 119, March 20, 1943.

259. Outdoor Construction Reduces Steam Plant Investment Cost, **J. H. McCambridge.** *Electrical World* (New York, N. Y.), volume 118, July 25, 1942, pages 68–71.

260. Burbank's Modernistic Design, **J. B. Johnson.** *Power Plant Engineering* (Chicago, Ill.), volume 45, December 1941, pages 54–9.

Mobile Plants

261. Seapower, **C. W. Cutler.** *Power Plant Engineering* (Chicago, Ill.), volume 50 May 1946, pages 66–9.

262. Floating Power, **W. N. Obesly.** *Power Plant Engineering* (Chicago, Ill.), volume 50, February 1946, pages 66–7.

263. British Build Mobile Power Plants for USSR Reconstruction. *Power* (New York, N. Y.), volume 89, November 1945, pages 98–9.

264. 10,000-Kw Railway-Mounted Mobile Steam Power Plant for US Navy Dept, Bureau of Yards and Docks, **E. Lundgren, L. R. Biggs.** *Transactions*, American Society of Mechanical Engineers (New York, N. Y.), April 1945, pages 141–66.

265. Diesels Power Army's 6000-Kva Floating Plant. *Power* (New York, N. Y.), volume 88, December 1944, pages 99–101.

266. Portable Power Trains for War Theaters. *Electrical World* (New York, N. Y.), volume 122, July 22, 1944, pages 68–70.

267. 5000-Kw Power Trains Follow Allied Armies, **C. M. Laffoon.** *Power* (New York, N. Y.), volume 88, July 1944, pages 75–7.

268. Power Speeds Rehabilitation, **W. N. Obesly.** *Power* (New York, N. Y.), volume 88, June 1944, pages 64–5.

269. Floating Plant Serves Base Load, **W. Noyes.** *Electrical World* (New York, N. Y.), volume 116, September 20, 1941, pages 64–6.

270. Power Plants Take to Wheels and Water. *Electric Light and Power* (Chicago, Ill.), December 1940, pages 40–3.

Gas Turbines

271. Where Gas Turbines Will Fit in Future Power Fields, **H. Pfenniger.** *Power* (New York, N. Y.), volume 90, November 1946, pages 64–7; volume 91, January 1947, pages 86–9.

272. New Locomotive Power Plant and Largest Gas Turbine Under Test. *Power* (New York, N. Y.), volume 90, September 1946, page 104.

273. Free-Piston Compressor Work Leads to New Semiclosed Cycle Development **S. A. Tucker.** *Power* (New York, N. Y.), volume 90, May 1946, pages 72–3.

274. Gas Turbines, **L. N. Rowley, B. G. A. Skrotzki.** *Power* (New York, N. Y.). volume 90, October 1946, pages 79–98.

275. Experimental 1500-F Unit at Annapolis Yields Valuable High-Temperature Data, **W. B. Tucker, J. T. Rettaliata, C. F. Kottcamp.** *Power* (New York, N. Y.), volume 90, May 1946, pages 68–71.

276. Coal-Fired Gas-Turbine Prospects Bright. *Power* (New York, N. Y.), volume 90, March 1946, page 75.

277. Closed-Cycle Gas Turbine Looks to Further Development, **C. Keller.** *Power* (New York, N. Y.), volume 90, January 1946, pages 103–06.

278. Four Years of Swiss Research Reveal New Power Patterns, **S. A. Tucker.** *Power* (New York, N. Y.), volume 89, November 1945, pages 64–9.

279. Operating Experience with the Gas Turbine, **A. E. Pew, Jr.** *Mechanical Engineering* (New York, N. Y.), volume 67, September 1945, pages 594–8.

280. The Basic Gas-Turbine Plant and Some of Its Variants, **J. K. Salisbury.** *Mechanical Engineering* (New York, N. Y.), volume 66, June 1944, pages 373–83.

281. Gas Turbines, Present Status and Future Prospects, **S. A. Tucker.** *Mechanical Engineering* (New York, N. Y.), volume 66, June 1944, pages 363–8.

282. American Contribution to Gas Turbine Development, **C. C. Jordan.** *Power* (New York, N. Y.), volume 88, June 1944, pages 76–7; August 1944, pages 82–4.

283. Producer Gas—Future Field for Gas Turbines, **P. W. Swain.** *Power* (New York, N. Y.), volume 88, May 1944, pages 86–7.

284. The Gas Turbine, **C. R. Soderberg, R. B. Smith.** *Power Plant Engineering* (Chicago, Ill.), volume 48, April 1944, pages 70–5.

285. Prospects for Gas-Turbine Power, **F. R. Sidler** (New York, N. Y.), volume 88, March 1944, pages 68–70.

286. Why Bother with Gas Turbines?, **S. A. Tucker.** *Power* (New York, N. Y.), volume 88, February 1944, pages 64–5.

287. Next Steps in Using Gas Turbines, **J. T. Rettaliata.** *Power* (New York, N. Y.), volume 88, January 1944, pages 92–3.

288. Portable Power from Gas Turbines, **J. T. Rettaliata.** *Power* (New York, N. Y.), volume 85, April 1941, pages 96–7.

289. Load Tests of a Combination Turbine, **A. Stodola.** *Power* (New York, N. Y.), volume 84, February 1940, pages 62–4.

290. The Gas Turbine Looks to Coal, **J. I. Yellot.** *Power* (New York, N. Y.), volume 89, August 1945, pages 75–5.

291. Progress Report on Gas Turbines. *Power* (New York, N. Y.), volume 89, August 1945, pages 73–84.

292. High-Temperature Gas Turbine Power Plants, **J. S. Haverstick, A. M. G. Moddy.** *Mechanical Engineering* (New York, N. Y.), volume 67, April 1945, pages 229–33.

293. Potentialities, Limitations of the Combustion Gas Turbine, **G. B. Warren.** *Electrical World* (New York, N. Y.), volume 122, October 28, 1944, pages 83–5; November 11, 1944, pages 99–101.

Wind Power

294. Wind-Turbine Power Plant Will Be Rebuilt, **P. C. Putnam.** *Power* (New York, N. Y.), volume 89, June 1945, pages 67–8.

295. Wind-Power Studies Suggest Future Commercial Possibilities. *Power* (New York, N. Y.), volume 89, June 1945, pages 64–6.

296. Electric Power from the Wind. *Electrical World* (New York, N. Y.), volume 123, April 28, 1945, pages 73–5; May 12, 1945, pages 102–04.

297. World's Largest Wind-Turbine Plant Nears Completion. *Power* (New York, N. Y.), volume 85, June 1941, pages 56–9.

298. Wind-Electric Plant to Operate Soon. *Power* (New York, N. Y.), volume 85, May 1941, page 97.

Nuclear Energy

299. Nuclear Energy as a Power Source, **H. G. Bowen.** *Mechanical Engineering* (New York, N. Y.), volume 68, September 1946, pages 779–81.

300. Nuclear Energy, **A. L. Baker.** *Mechanical Engineering* (New York, N. Y.), volume 68, September 1946, pages 775–8.

301. Man vs. Atom—Year 1. *Power* (New York, N. Y.), volume 90, August 1946, following page 98.

302. A Utility Man Looks at Atomic Energy, **J. C. Parker.** *Electrical World* (New York, N. Y.), volume 125, June 8, 1946, pages 74–5.

303. Engineering and Political Aspects of Atomic Energy, **H. A. Winne.** *Electrical World* (New York, N. Y.), volume 125, June 8, 1946, pages 75–6.

304. Basic Factors of Atomic Energy Utilization, **K. H. Kingdon.** *Electrical World* (New York, N. Y.), volume 125, June 8, 1946, pages 76–7.

305. Nuclear Research Related to Electric Power Generation, **C. G. Suits.** *Electrical World* (New York, N. Y.), volume 125, June 8, 1946, page 77.

306. The Economics of Atomic Power, **P. W. Swain.** *Power* (New York, N. Y.), volume 90, June 1946, pages 76–8.

307. The Future of Nuclear Power, **J. A. Wheeler.** *Mechanical Engineering* (New York, N. Y.), volume 68, May 1946, pages 401–05.

308. Power Supply Aspects of Nuclear Research, **R. R. Wiener.** *Electrical World* (New York, N. Y.), volume 125, February 2, 1946, page 55.

309. Atomic Energy as a Source of Electricity Supply. *Electrical World* (New York, N. Y.), volume 125, March 2, 1946, pages 54–5.

310. Uranium 235—Power Fuel of the Future, **P. W. Swain.** *Power* (New York, N. Y.), volume 89, September 1945, pages 64–6.

311. The Atom, New Source of Energy. *Power* (New York, N. Y.), volume 89, September 1945, following page 102.

Miscellaneous

312. Large Diesels in Panama Canal Plants Unique for Automatic-Starting Scheme, **J. L. King.** *Power* (New York, N. Y.), volume 90, September 1946, pages 105–08.

313. USSR Tashkent Plant Uses Solar Energy. *Power* (New York, N. Y.), volume 90, January 1946, page 85.

314. Severn Tide Development Promises Cheap Power for England, **H. P. Vowles.** *Power* (New York, N. Y.), volume 89, November 1945, pages 80–1.

315. World's Largest Gas-Engine Plant Rated at 78,000 Kw, Powers Aluminum Works. *Power* (New York, N. Y.), volume 88, November 1944, pages 64–9.

Report of the Board of Directors

THE BOARD OF DIRECTORS of the American Institute of Electrical Engineers presents herewith to the membership its 63rd annual report, for the fiscal year ending April 30, 1947. It includes a general balance sheet and other statements showing the financial condition of the Institute at the close of the fiscal year and a brief summary of the principal activities of the Institute during the year, more detailed information having been published from month to month in *ELECTRICAL ENGINEERING*.

BOARD OF DIRECTORS' MEETINGS

Six meetings of the board of directors were held during the year, three in New York, N. Y., one in Asheville, N. C., one in Detroit, Mich., and one in Worcester, Mass.

Information regarding many of the more important activities of the Institute which have been under consideration by the board of directors and AIEE committees is published each month in the section of *ELECTRICAL ENGINEERING* devoted to Institute activities.

PLACES VISITED BY PRESIDENT HOUSLEY

Alabama
Muscle Shoals Section, Florence

Arizona
Arizona Section, Phoenix

Arkansas
Little Rock Subsection of Memphis (Tenn.) Section

California
Los Angeles Section, San Diego Section
San Francisco Section
California Institute of Technology Branch, Pasadena
University of California Branch, Berkeley

Canada
Vancouver Section
Summer general meeting, Montreal, Quebec

Colorado
Denver Section

District of Columbia
Washington Section

Illinois
Rock River Valley Subsection of Madison (Wis.) Section, Rockford

Indiana
Great Lakes District meeting, Indianapolis

Iowa
Iowa Section, Ames
Iowa State College Branch, Ames

Kentucky
Louisville Section; University of Louisville Branch
University of Kentucky Branch, Lexington

Louisiana
New Orleans Section, Lake Charles Subsection
Shreveport Subsection

Massachusetts
Boston Section
North Eastern District meeting, Worcester

Mexico
Mexico Section, Mexico, Federal District

Minnesota
Minnesota Section, Minneapolis
Arrowhead Subsection, Duluth

Mississippi
Mississippi State College Branch, State College

Missouri
St. Louis Section

Montana
Montana Section, Butte

Nebraska
Nebraska Section, Omaha
University of Nebraska Branch, Lincoln

New York
New York Section; winter meeting, New York, N. Y.

North Carolina
North Carolina Section, Durham
Duke University Branch, Durham

Ohio
Cincinnati Section, Cleveland Section
Dayton Section, Mansfield Section
Akron Section, Columbus Section

Oklahoma
Oklahoma City Section
Tulsa Section

Oregon
Portland Section

Pennsylvania
Philadelphia Section
Pittsburgh Section
Sharon Section

South Carolina
South Carolina Section, Columbia

Tennessee
East Tennessee Section, Athens, Chattanooga
Memphis Section

Texas
Beaumont Section, Houston Section
New Mexico–West Texas Section, El Paso
North Texas Section, Dallas

Utah
Utah Section, Salt Lake City

Washington
Spokane Section
Pacific Coast meeting, Seattle

West Virginia
West Virginia Section, Charleston

ANNUAL MEETING

The annual business meeting of the Institute was held June 26, 1946, in Detroit, Mich. The annual report of the board of directors for the fiscal year which ended April 30, 1946, was presented in abstract by Secretary H. H. Henline. The Institute's financial situation was summarized by Treasurer W. I. Slichter. The report of the committee of tellers on the election of officers for the year which commenced August 1, 1946, was presented, and President-Elect J. Elmer Housley responded to his introduction with a brief address. National prizes for papers were presented.

The AIEE Lamme Medal for 1945 was presented to David C. Prince, vice-president of the General Electric Company, and a past president of the Institute. An address in recognition of the 100th anniversary of the birth of George Westinghouse was presented by J. K. B. Hare, vice-president of the Westinghouse Electric Corporation. The president's address by Doctor William E. Wickenden concluded the meeting.

NATIONAL MEETINGS

Three national meetings were held during the year, and a brief report on each follows.

Summer Meeting. The 61st annual summer meeting was held in Detroit, June 24–28, 1946, with a registration of 1,351. The program included 19 technical sessions, 7 technical conferences, 8 administrative conferences, and 23 committee meetings, in addition to the afore-mentioned annual business meeting. There were entertainment events, inspection trips, golf tournaments, a president's reception, and a dinner dance.

Pacific Coast Meeting. The 33rd Pacific Coast meeting was held in Seattle, Wash., August 27–30, 1946, with a registration of 562, which was a record for Pacific Coast meetings. Six technical sessions, one student technical session, and a conference on organization of the engineering profession were held. The program also included inspection trips, president's reception, banquet, theater party, women's activities, and a golf tournament.

Winter Meeting. The 35th winter meeting was held in New York, N. Y., January 27–31, 1947, with a registration of 3,567, an all-time record. The program included 29 technical sessions, 10 technical conferences, 2 administrative conferences, and 3 general sessions at which the Edison, Hoover, and John Fritz Medals were presented to Doctors Lee de Forest, Vannevar Bush, and Lewis W. Chubb, respectively.

Other events of the meeting were a smoker, inspection trips, events for women, and a cocktail party by the Aluminum Company of America for President Housley.

DISTRICT MEETINGS

Great Lakes District Meeting. This meeting was held in Indianapolis, Ind., October 9–11, 1946, with a registration of 298. Conferences were held on electric machinery, electronics, power transmission and distribution, industrial power applications, communication, industrial control, basic sciences, and organization of the engineering profession. At the banquet, Doctor Frank H. Spedding, of Iowa State College, gave an address on "Nature and Implications of Atomic Energy." There were inspection trips as well as a number of women's activities.

North Eastern District Meeting. Held in Worcester, Mass., April 23-25, 1947, with a registration of 828, this was the largest District meeting held since 1927. The program included 8 technical sessions, 2 student technical sessions, a general session, inspection trips, women's events, smoker, and banquet. At the banquet, Doctor Samuel Van Valkenburg, director, Graduate School of Geography, Clark University, gave an address on "The European Puzzle."

Southern District Meeting. The sixth Southern District meeting was held in Asheville, N. C., May 14–16, 1946, with a registration of 373, which was the second highest in the history of the meeting. One of the three technical sessions was devoted to a symposium on electric power in the textile industry. A conference on student activities and a student paper session also were included in the program, and inspection trips were made to near-by plants. Commander J. F. Hellweg, United States Navy (retired), addressed an evening session and AIEE Past President C. A. Powel described conditions as he had seen them in Germany during a 9-month tour of duty as chief of the electrical and radio branch of the Allied Control Commission.

COMMITTEE ON COLLECTIVE BARGAINING AND RELATED MATTERS

During the year, this committee has continued its work on the preparation of "A Manual on Collective Bargaining for Professional Employees." The first edition of this manual, which deals with the National Labor Relations Act, and an analysis of proposals from various sources for modifying the act, has been completed and should be available to members before the end of April 1947. Through co-operation with the Committee on the Economic Status of the Engineer of Engineers Joint Council, the publication of the manual is being sponsored jointly by six of the major professional engineering societies.

Through the same channel, the committee on collective bargaining and related matters has attempted to co-operate with other professional engineering societies in the establishment of a policy and a procedure covering labor legislation. The committee endorsed the policy and procedure recommended by the Committee on the Economic Status of the Engineer, and this endorsement was followed by approval by the AIEE board of directors and by Engineers Joint Council. In December 1946, Engineers Joint Council approved another policy and procedure not endorsed by the committee on collective bargaining and related matters.

The committee recommended to the AIEE board of directors that a comprehensive questionnaire be sent to AIEE members for the purpose of ascertaining their opinions regarding attempts at modification of the National Labor Relations Act in the interest of professional employees. This recommendation was approved at the January 1947, meeting of the board of directors, but before a comprehensive questionnaire could be prepared and distributed, a letter, dated February 7, 1947, and an incomplete questionnaire, dated March 17, 1947, were sent to the membership by the president of the Institute. The committee had nothing to do with the preparation of this letter, or of this questionnaire, and did not approve them or the procedure followed. The chairman of the committee on collective bargaining and related matters has requested that the committee be relieved of any responsibility for matters having to do with labor legislation, or alternatively, that his resignation be accepted.

General Committees

SECTIONS COMMITTEE

1. Section Programs. The Sections generally have been continuing the policy of following a program of expanding their activities to meet the increased scope and growing demands of the electrical engineering profession and to provide for the diversification of interest of the Section members. Increased attention is being given to student activities, social activities, fellowship at meetings, inspection trips, and the broader subject of civic responsibilities of engineers. Section officers generally are becoming more conscious of the importance of balanced Section operation, which provides activities to retain the older members as well as attract new members. In giving more time to creative work and the co-ordination of the activities of their Sections, many chairmen have followed the suggestion of delegating to committees much of the operating work of running the Section. The resulting increase in operating committees in many Sections has provided the opportunity for more members to work actively for the Section, which in turn has created additional interest.

2. Sections Committee Organization. Because of the volume of the Sections committee work, the committee continued to operate as two groups. The planning group, consisting of six members, initiates and develops all plans of the committee. The promotional group, consisting of ten members located geographically on a District basis, handles much of the promotional work individually with the Sections and Districts. Most of the material used by the promotional group is sent to each member, who in turn supplements it with his personal knowledge of local conditions before contacting the Sections in his District. Close contact is maintained between the promotional group member and the vice-president of the District.

3. Conferences Held at Summer Meeting. During the summer meeting at Detroit, the following conferences were held:

June 24, 1946—Conference on Section Operation and Management for Section Delegates. Three separate parallel conferences were held. One for the larger Sections, one for the intermediate Sections, and one for the smaller Sections. These conferences were conducted in an informal manner according to a prearranged program which covered many of the important items in connection with the operation of the Sections.

June 25, 1946—Conference of Officers, Delegates, and Members. This was the annual meeting of the delegates. The meeting was addressed by Institute president, Doctor Wickenden, whose topic was "Observations on Institute Activities." The program included a report on District and Section activities by Secretary Henline, remarks by Presidential Nominee Housley, and the report of the Sections committee. The report on the improved AIEE publications services was made by G. Ross Henninger, AIEE editor. Reports also were made on membership activity, Section finance, educational courses, and Section history.

June 26, 1946—Conference on Section Activities in Connection With Local Councils of Engineering and Technical Societies. In this conference the organization and operation of local engineering councils was presented and discussed, with particular emphasis on the part the AIEE Sections have taken in this work. The attendance at this meeting was an indication of the interest in this subject.

June 27, 1946—Conference on Section–Branch Co-operation. This was a joint activity with the committee on Student Branches. In this conference a plan of Section–Branch co-operation was presented and discussed. Many examples of this activity were discussed by the Section delegates. The discussion at this meeting indicated the importance of this activity to the Institute.

4. Discussion of Section Operation and Management at District Meetings. In accordance with recommendations made by the delegates at the Sections committee meeting, January 22, 1946, the Sections committee encouraged all vice-presidents to devote a portion of their District executive committee meetings to a discussion of Section operation and management. These discussions were held at most of the District executive committee meetings and served to supplement the regular delegates' meetings which were held at Detroit.

5. Technical Groups. The development of technical groups within the Sections continued to be one of the most important activities of the Sections committee. Copies of the folder, "Technical Groups," were distributed to each Section chairman at the beginning of the year. The promotional group supplied individual Sections with several reports of examples of successful operation of these groups. There were 105 of these groups in operation as compared with 74 in operation a year ago. Reports received from the Sections indicate many other groups are in process of being formed.

On January 5, 1947, a letter was sent to all Sections encouraging the formation of basic science technical groups as an additional activity. During this year the Sections committee started a long range plan for co-operation between the technical groups in the Sections and the technical committees of the Institute. It was pointed out that this co-operation should be a 2-way activity, and, when working properly, desirable information would be flowing from the Section and technical groups to the technical committees of the Institute, as well as from the technical committees to the Sections. A 3-point program on this activity for the Sections to follow was contained in a letter dated November 8, 1946, to all Section chairmen. A letter dated November 7, 1946, to the chairmen of all Institute technical committees covers suggestions for obtaining information for technical groups in the Sections. These initial letters were followed later in the year by other letters giving practical suggestions and practical examples of the operation of this co-operative plan.

6. Subsections. Subsection activity was continued by the committee throughout the year. A copy of the folder, "Subsections," was sent to each Section chairman at the beginning of the year. The promotional group of the Sections committee has forwarded examples of successful operation of Subsections to the individual Sections in their Districts. There are now 35 Subsections in operation, as compared with 25 Subsections in operation at the end of the previous year. Many opportunities still exist for members in the remote areas of the Section territory to participate in Section activities through the development of Sub-

sections in these areas. The promotional group of the Sections committee conducted a survey of the possibilities of Subsections in each of their Districts. As a result of this survey, many additional locations for Subsections are being considered by the Sections.

7. Local Councils of Engineering and Technical Societies. During the year, the Sections committee has continued the activity of encouraging AIEE Sections to assist in organizing councils and to be active in these councils where they already are organized. There are now 45 of these councils in active operation. During the year the Sections committee sent considerable information to five AIEE Sections which are active in forming new councils in their areas.

8. Section Finance. During the year, the Sections committee observed the operation of the revised system of allotments to the Sections. No new recommendations were made this year.

9. Student Activities. Section–Branch activity in co-operation with the committee on Student Branches was continued throughout the year. Copies of the plan of Section–Branch co-operation were distributed to all Section chairmen during the year. It was pointed out that co-operation with the Branches is a very important activity and that the Sections can assist materially in this activity by helping the Student Branches to develop the interest of all electrical engineering students.

10. Educational Courses. The plan of encouraging the Sections to organize educational courses for their members and others was continued during the year. This is a joint activity with the committee on education. On October 30, 1946, a letter was sent to all Section chairmen calling attention to the possibility of these educational courses and enclosing a case example of the experience of the Philadelphia Section in conducting educational courses. Later in the year, information on the courses conducted by the New York Section was forwarded to most Sections by the members of the promotional group of the Sections committee.

11. Changes in Section Territory. The island of Puerto Rico was added to the territory of the New York Section. The Territory of Hawaii was made a part of District 8 and of the territory of the San Francisco Section.

12. Section History. The activity of encouraging Sections to write a Section history was continued throughout the year. As a result of this activity, many Sections have appointed a history committee to proceed with this work. A letter has been sent to all Sections enclosing a suggested outline for a Section history.

13. Prize Paper Activity. Many Sections conduct prize paper contests, and the Sections committee has been endeavoring to stimulate this activity by having Section prize paper awards given official recognition by the Institute. This activity is being considered by a special Institute committee for the revision of the prize paper rules, and as a result of the Sections committee activity in connection with the work of the special committee, it is expected that the proposed revision of the Institute prize paper rules will contain official recognition for Sections awards.

Table I. Section and Branch Statistics

	For Fiscal Year Ending April 30					
	1942	1943	1944	1945	1946	1947
Sections						
Number of Sections	72	73	73	73	75	75
Number of meetings held	647	598	738	884	1,210	1,333
Total attendance	78,254	66,111	83,120	96,346	113,531	155,649
Branches						
Number of Branches	124	125	125	125	125	126
Number of meetings held	946	942	755	547	716	1,018
Total attendance	37,785	38,227	24,768	17,132	22,844	40,669

14. Safety Activity. In co-operation with the Institute committee on safety, the Sections committee sent a letter, dated September 17, 1946, to all Sections concerning the importance of including the subject of safety in their programs. An appendix to this letter gave many examples of how this activity could be conducted by the Sections. This safety activity is being conducted from the standpoint of the engineer and covers the safety angle in the design, construction, operation, and maintenance of equipment, rather than from the safety-first approach.

15. Edison Centennial Meetings. As a result of the board of directors of the Institute endorsing the idea of co-operation by AIEE Sections with the Edison Centennial Committee in appropriate local observances of the commemoration of the centennial of the birth of Thomas A. Edison, a letter dated September 4, 1946, was sent to all Sections outlining a suggested program for Section and Subsection meetings on the centennial date, February 11, 1947. In compliance with this suggestion, many Sections and Subsections held special meetings on February 11, and other Sections included the observance of this centennial in connection with their regular meetings.

16. Industrial Meetings. As a result of the address of President Housley, a letter of October 11, 1946, was sent to all Sections suggesting that they hold meetings on an industrial subject in electrical engineering in the smaller industrial centers in their areas. An appendix to this letter contained several suggestions for conducting these meetings. It also was suggested that these meetings be built around the publication, "Electric Power Distribution for Industrial Plants," which was developed by the Institute committee on industrial power applications. The Sections engaging in this activity found these meetings to be a very profitable Institute activity.

17. Delegates' Meetings to be Held at the Summer General Meeting, Montreal. The Sections committee has prepared a comprehensive program for the Institute officers, Section delegates, and members at the summer general meeting. Three parallel conferences on Section operation and management will be conducted on June 9, with the delegates divided into groups representing the larger, intermediate, and smaller Sections. These conferences will be held on a strictly informal basis. The conference of officers, delegates, and members will be held June 10, at which the more formal program of reports will be presented. On June 11 a special conference on technical group activities in the Sections will be held. At this conference, the experiences in operating technical groups will be discussed, and the co-operation between the technical groups in the Sections and the technical committees of the Institute will be explained further and discussed.

18. Committee Meetings. Because of the nature of the Sections committee work, most of the activities of the committee were carried on by means of correspondence. One meeting was held by the committee, January 28, 1947, in New York, during the winter meeting. At this meeting, the entire Sections committee program was reviewed, plans for the delegates' meetings in Montreal were formulated, and plans for the remaining portion of the year were discussed. Minutes of this meeting were sent to all who attended and, in addition, were sent to all Institute board members, District secretaries, and Section chairmen.

COMMITTEE ON STUDENT BRANCHES

Work was continued on arrangements for joint Student Branches, and a proposal was submitted to the directors. After adjustments were made by the committee on constitution and bylaws, the following action was taken by the board. Section 53 was amended to read as follows:

Sec. 53. The annual Student member dues shall be three dollars, payable in advance, and shall cover the fiscal year of the Institute beginning on May first. The initial dues payment, upon application for enrollment, shall be:

$3.00 if application is filed at Institute headquarters during period February 1 to following July 31;
$1.50 if application is filed at any other time.

The renewal of Student membership shall uniformly require payment of the dues of $3.00 for the fiscal year beginning May first. The term of Student membership shall extend to the end of the fiscal year, April 30, in which student status ceases, or the Student member has attained the age of 21, whichever is later, except in those cases where the fiscal year ends within six months after graduation. In such cases, Student membership may be continued for one additional fiscal

year, or to the end of the fiscal year in which the age of 21 is attained. For those students who are not devoting their entire time or a major part of their time to studies, the term of Student membership shall not extend over a period of more than five years.

Section 61 was amended by the addition of the following to the end of the section:

In the case of a joint Student Branch, as further referred to in Section 64, a counselor shall act jointly with the duly appointed counselors of other national engineering societies in matters affecting the student society and the welfare of its members.

Section 64 was replaced with the following text:

Sec. 64. An established student engineering society in a college or technical school of recognized standing may, upon application of its officers and a member of the Institute connected with the school, and the approval of the board of directors, become associated with the Institute. A society so associated also may be associated jointly with other national engineering societies approved by the board of directors as having similar requirements and interests. If so jointly associated, it shall be known as a "Joint Student Branch," otherwise it shall be known as a "Student Branch."

The following societies are approved for the purpose of this co-operation in engineering education: American Society of Civil Engineers, American Society of Mechanical Engineers, American Institute of Mining and Metallurgical Engineers, American Institute of Chemical Engineers, Institute of Radio Engineers, together with such other national engineering societies as may be approved from time to time by the board of directors as having similar requirements and interests.

District student meetings were reactivated at several locations. R. G. Warner is seeking clarification on the availability of funds for student prize papers, and a report from him is expected at the 1947 summer general meeting in Montreal, Quebec, Canada.

With the membership committee a joint subcommittee was formed on transfer from Student to Associate grade. The purpose of this subcommittee is to explore ways of encouraging transfers for as many students as possible.

Because several schools have made application, a standing subcommittee on the establishment of new Student Branches, has been formed.

Work is under way to secure a set of short papers or essays which will stimulate student interest in the AIEE.

Work was continued jointly with the Sections committee to encourage Section–Branch co-operation. Suggestions concerning this were sent to all Branch counselors.

FINANCE COMMITTEE

The budget approved by the board of directors anticipated continued high revenues from a growing membership and active interest in the Institute's affairs. At the same time, appropriations were made to carry forward the Institute's broad progressive program and to meet the rising cost of its activities.

As of April 30, 1947, the end of the fiscal year operations showed a favorable balance of some $23,500. Receipts, largely as a result of new members, were 7 per cent greater than the previous fiscal year. At the same time, expenditures increased 36 per cent. Though the cash balance in general funds of $6,900 was very much lower than the $81,379 at the beginning of the year, this was offset by an increase in reserve capital fund investments of some $96,000. During this same period, $1,877 was added to the Member-for-Life fund.

The $23,500 operating balance for the past fiscal year compares with about $130,000 in the previous year. In spite of a rapidly growing membership, the sharp upward trend in unit costs, along with such factors as the expanded postwar program and the new progressive publication policy have been responsible for this drop. While the budget as approved by the board of directors for the budget year ending September 30, 1947, was in balance, the subsequent rise in costs and falling off in advertising now make it appear likely that the current budget year may end with an operating deficit.

As shown in the attached audit of the Institute's finances, it has been possible as a result of the operating surpluses of the past several years to build up a substantial reserve capital fund which would be very useful as a cushion against lean years that must be expected. Such a cushion could not, however, long support a program of activities in excess of income. If a balanced budget is to be achieved next year, both the revenue and the expenditure items will have to be examined carefully.

TECHNICAL PROGRAM COMMITTEE

Increased Technical Activities. The technical activities of the Institute are at the highest level in history. The winter meeting program was enlarged to provide for the presentation of 162 papers, 98 of which were *TRANSACTIONS* papers. Both these figures are new meeting records. The enlarged program served a record registration of 3,567 as compared with last year's record of 2,624.

An analysis of the papers presented at this and other meetings held during the year ending April 30, 1947, is given in Table II. This table shows a great increase in the yearly number of papers presented. For the same number of meetings, the tabulations show 208 *TRANSACTIONS* papers compared with 153 presented the previous year, and the 367 total of all papers compares with the total of 212 for the previous year. The large number of sessions, conferences, and papers would indicate that, in general, the Institute is on its way to doubling its activity record of the past several decades. Already the resources available for handling the large amount of technical activity under way at the present time are being strained. The increase may be attributed to growth in membership, the aftermath of the war, enlargement of the field of electrical engineering, and to increased technical activity in general due to the additional attention the Institute has paid to developing full coverage of every area of the profession of electrical engineering.

Expanded Technical Coverage. The committee has worked in close co-operation with the technical activities subcommittee of the committee on planning and co-ordination in its effort to organize the technical committees in a manner which would provide the opportunity of presenting and recording new technical developments more efficiently. This work is described in more detail in the report of that committee. The creation of ten new technical committees has increased the number of these committees serving the Institute by about 50 per cent, which in itself will continue to make available to the Institute an increased number of technical meetings and papers. The committee now is reviewing papers for the newly established Midwest general meeting scheduled to be held in Chicago, Ill., November 3–7, 1947, the meeting having been designed to fit in with the National Electronics Conference to be held earlier in the same week. This kind of co-ordinated activity with other technical organizations also has added to the general activity in the electrical engineering field; each technical committee is attempting to work jointly insofar as possible with other technical bodies which affect it. Each technical committee also has analyzed its own administrative structure and in its meetings under the new group organization setup has traded responsibilities back and forth to the end that definite responsibilities have been allocated clearly and efficiently. This interchange of ideas and responsibilities in itself has resulted in a more complete coverage of the field.

Analysis of Subject Matter. Sessions and conferences on the program of the summer meeting in Detroit reflect subject matter not found on Institute programs heretofore. Full sessions on servomechanisms, industrial control devices, electronic tubes and basic circuits, electronic power conversions, and a conference on electronic instruments were held for the first time. Two sessions were held on industrial power applications, in which members of the Industrial Electrical Engineering Society were invited to participate. Five of the 26 sessions and conferences were concerned with the industrial field.

Analysis of Subject Matter. On the program of the winter meeting, sessions reflecting work in the newer fields were held as follows: servomechanisms, electronic instruments, metallic rectifiers, applications in the textile industry, and three sessions in the field of land transportation—light traction, electric railways, and Diesel-electric locomotives. Among the recently developed subjects discussed in conferences were energy sources, electronic devices and methods, large scale computing devices, and aircraft safety.

At this meeting also, there was an increase in activity in the industrial field, as 7 out of 40 sessions and conferences were devoted to it. A number of the new sessions and conferences were in the field of electronics, not to mention other numerous

Table II. Numbers of Papers Presented During the Year Ending April 30, 1947

Meeting	District	Advance Copy Only	Conference	Transactions	Total
Southern District, Asheville	9	3		2	14
Summer, Detroit		3	25	73	101
Pacific Coast, Seattle	6	4	2	22	28
Great Lakes District, Indianapolis	15	1	10	3	29
Winter, New York		5	59	98	162
North Eastern District, Worcester	23			10	33
Total	47	16	96	208	367

electronic applications that may be found throughout the various sessions on these programs.

Demonstrations. Increase in the number of demonstrations in conjunction with the presentation of papers was noteworthy at the winter meeting. Demonstrations took place in the sessions on electronic instruments, television, the symposium on limitations of light production, the symposium on rural telephone facilities, and the conference on some new electronic devices and methods. These demonstrations added to the effectiveness of the presentations and the interest in the sessions.

Plans for the Ensuing Year. With the increase in the number of Institute meetings, both general and District, and with the added number of technical committees and greater coverage of the field accomplished by the recent reorganization work, the committee's forecast of last year on future activities already begins to look entirely too conservative. It now looks as if the average number of papers, instead of being either the 150 to 200 experienced in the past or the 270 forecast last year, will be well over the 300 mark, with the consequent necessity of increasing the annual number of sessions and conferences.

PUBLICATION COMMITTEE

One of the fundamental purposes of the Institute is the dissemination to its members of information concerning new theories, new apparatus, and new developments throughout the electrical field. To accomplish this objective, the bylaws assign to the publication committee full responsibility for "supervision of the monthly journal, *ELECTRICAL ENGINEERING*, *TRANSACTIONS*, and the other publications of the Institute, including the form, size, and arrangement of these publications; also decisions regarding the publication of papers, discussions, and all other matter available for publication; and the formulation and carrying out of plans for bringing into practice the policies regarding Institute publications that may be determined from time to time by the board of directors." Incidental to its responsibility under this objective, and pursuant to actions of the board of directors at its May 1946 and subsequent meetings, the AIEE publication committee during 1946 gave especial attention to the development of ways and means of improving the Institute's publications policy and procedure with the objectives of better serving the greatly enlarged and rapidly growing membership and of covering adequately the active and ever-growing membership and of covering adequately the active and ever-growing electrical field.

Resulting modifications in AIEE policy and procedure were ratified by the board of directors at its August meeting and implemented by necessary budget appropriations at its October meeting for the year 1946–47. Although this was very late in the publication year, and material for the January 1947 issue of *ELECTRICAL ENGINEERING* already was at least partially committed and in work, special efforts on the part of the publication staff enabled initiation of the major approved changes beginning with the January 1947 issue of *ELECTRICAL ENGINEERING*. As a matter of record and reference, the essential features of AIEE publication policy and procedure under these approved modifications are set forth in the following paragraphs.

Under the revised publication plan, the *TRANSACTIONS* section has been eliminated from *ELECTRICAL ENGINEERING*, its place being taken by a new series of pamphlet publications under the reconstituted name, AIEE *PROCEEDINGS*, each of which will carry one technical, paper and related discussions, literally an advance preprint of the ultimate *TRANSACTIONS*. Individual members are given the opportunity, through coupons published periodically in *ELECTRICAL ENGINEERING*, to select designated groups of these technical papers to be received free of charge, and other papers to be received as desired at a nominal charge to cover actual cost. More specifically, the current publications and policy of the Institute are described in the following paragraphs.

1. ELECTRICAL ENGINEERING. Coincidental with the elimination of the *TRANSACTIONS* section, the general interest content of *ELECTRICAL ENGINEERING* has been expanded, enhanced, and given greater flexibility to satisfy more fully the current and future requirements of the membership. Subject only to general policy, the management and publication of *ELECTRICAL ENGINEERING* will be entirely the responsibility of the editor.

The contents of the monthly will be divided broadly into two general categories:

1. General articles, to be drawn from all currently available sources, selected on the basis of timeliness and general-interest value to the membership at large.

2. News material, appropriately reflecting all AIEE and related activities, also reflecting other current activities of interest and significance to the membership.

Summary abstracts of technical papers will continue to be published as far as possible in advance of the meetings at which the papers are scheduled for presentation.

A more aggressive advertising policy is being instituted, to capitalize more fully upon the established prestige and substantial standing of *ELECTRICAL ENGINEERING*. Some improvement has been effected in the weight and quality of paper, and further improvements are contemplated as conditions permit.

Distribution of *ELECTRICAL ENGINEERING* will continue to be made automatically to the entire AIEE membership, including Students; to be available also to nonmembers at an appropriate subscription price in accordance with postal regulations and as provided in AIEE bylaws.

2. PROCEEDINGS. For the purpose of better and more promptly serving those among the membership who are interested especially in the full and complete technical and mathematical details of subject matter within the fields of their particular professional interest, a new series of pamphlet publications has been established, reactivating the name, AIEE *PROCEEDINGS*. These *PROCEEDINGS* contain the full text of all papers approved by the technical program committee for publication in *TRANSACTIONS* and for presentation at general or District meetings, together with all discussions of those papers as approved by the technical program committee; also may contain "miscellaneous (ACO) papers" approved by the technical program committee, and other appropriate material. Thus, the *PROCEEDINGS* is planned to contain all material previously published in the *TRANSACTIONS* sections of the 12 monthly issues of *ELECTRICAL ENGINEERING*, all the material previously published in the two semiannual "Supplements to *ELECTRICAL ENGINEERING—TRANSACTIONS* Section," and in addition other meetings material previously unpublished.

Distribution of *PROCEEDINGS* is being made on a selective basis through the use of coupons published from time to time in *ELECTRICAL ENGINEERING*, each Fellow, Member, and Associate of the AIEE being given an opportunity to select for receipt free of charge a limited quantity designed to be sufficiently generous to enable the average member to obtain those papers in which he is concerned most intimately; additional copies are available at cost. The first distribution of *PROCEEDINGS* began in April 1947, carrying winter meeting papers.

3. Annual TRANSACTIONS. Current policies and procedures with reference to AIEE *TRANSACTIONS* are being continued without change, except that the flexibility introduced by the previously discussed changes in publication procedure now enable discussions to be assembled with the papers to which they apply. Distribution continues on the basis of advance

order; to the AIEE membership at cost, to others at appropriately higher prices. Sharply increased production costs will require an upward adjustment of price for the 1948 volume.

4. Preprints. To encourage and facilitate discussion of technical papers at general and District meetings, the practice of issuing advance pamphlet copies or preprints of technical program papers by the photolithographic or other appropriate process is being continued. Distribution is made through two principal channels:

1. Through the interested technical committee a limited quantity without charge for official use.

2. Through general sale, to the entire AIEE membership at cost and to others at 100 per cent above members' price.

Heavy increases in production costs during the past year have necessitated an adjustment in the price schedule for this material, which now stands as follows:

Table III. Advance Pamphlet Prices

Size		At Headquarters or Meeting, Cents	By Mail, Cents
12 pages or less:			
	To members	15	20
	To nonmembers	30	35
16 pages:	To members	20	25
	To nonmembers	40	45
20 pages:	To members	25	30
	To nonmembers	50	55
24 pages:	To members	30	35
	To nonmembers	60	65
28 or more:			
	To members	35	40
	To nonmembers	70	75

5. Special Publications. To provide a facility in a field of publication services heretofore not satisfied adequately by the Institute, a series of "AIEE Special Publications" has been established, and its use is encouraged. It is contemplated that such publications will be issued from time to time, and in appropriate relation to other AIEE publications, to accommodate material of especial value and importance in its field, but of limited general interest or applicability, or material peculiarly convenient and appropriate in the form of separate or substantially bound books or booklet.

Special publications are to de issued on an entirely self-supporting basis, the proceeds from the sales in effect constituting a revolving fund for continuation and stimulation of the project. Distribution will be on the basis of individual order; at cost to the AIEE membership, to others at 100 per cent above members' prices.

6. Reprint Service. As a special service which has proved to meet many membership needs, the practice of publishing quantities of reprints or preprints of AIEE material is being continued. Such reprints usually are produced on the basis of specific order or anticipated need; in any event, on an entirely self-supporting basis.

7. Annual Index. A complete composite "AIEE Annual Index" is planned, to cover appropriately the content of *ELECTRICAL ENGINEERING, PROCEEDINGS, TRANSACTIONS,* and special publications, continuing the basic alphabetical multientry subject-listing system originally developed by *ELECTRICAL ENGINEERING* and used with eminent success over a period of many years. Distribution is automatic and without charge to AIEE membership and to regular subscribers to AIEE publications; upon request to others.

8. Yearbook. Publication is continuing without change. Distribution automatic to Section, District, and national officers and national committee personnel; to others upon request.

9. Conference Papers. The informal AIEE conference papers will be treated very much as in the past. As such, they do not have automatic publications status, although the editor of *ELECTRICAL ENGINEERING* specifically is authorized to make appropriate use of conference material subject to the approval of the authors involved.

An accompanying tabulation shows the number of pages of various classes of material published during the last three years as compared with 1941 which was the last prewar year. The cancellation of meetings in 1945 caused a sharp drop in the amount of material available for publication, the effects of which were carried over somewhat into early 1946.

Considerable difficulty has been experienced throughout the year in obtaining a satisfactory supply of paper, because of industry conditions, although rationing as such no longer exists.

Several changes were made in the AIEE publications staff with the objective of improving the average level of technical qualifications. Overcrowded conditions in the Engineering Societies' Building necessitated relief in some direction, and hence the publications department as an operating unit of the headquarters organization was elected for removal to commercial office building space. This includes both editorial and advertising offices.

Much remains to be done in developing the full potentiality of the new publication policy, and full effort toward that objective is being continued by the publications staff and the publications committee.

COMMITTEE ON INSTITUTE PUBLICITY

The committee on institute publicity undertook as its first job to plan the publicity campaign for the 1947 winter meeting. The experience of earlier committees in handling this problem was available and was drawn upon freely. It was apparent from these earlier experiences that there had not always been sufficient time to do a thoroughly integrated job. Accordingly the Raymond C. Mayer public relations organization was engaged as of December 1, 1946, to help plan a publicity campaign and to prepare material for distribution through various publicity mediums. The technical program committee and the winter meeting committee co-operated wholeheartedly in developing the program for the meetings which would take full advantage of publicity possibilities.

Mr. Mayer assisted in this general planning of the program, and his organization prepared publicity releases on many of the papers that were presented. Each of these was reviewed by the chairman of the committee, or his representative, and all were distributed to mediums considered appropriate for the subject in hand. In addition the Mayer organization issued general releases regarding the meeting activities and some of its personnel, as well as releases concerning the medal presentations. Photographers were made available for press pictures of the medalists and other groups, as desired by press representatives.

The Mayer organization also arranged for clippings, through organized clipping services, and these are available to the committee. There was very wide use of released material in many mediums, according to a survey by Mr. Mayer, several times the coverage previously attained.

No special plan has been set up to conduct a similar campaign under the committee's auspices for the summer general meeting, although it is planned to investigate the matter of general publicity for that meeting through the local Montreal organization.

The committee has given some thought to the possibility of aiding Student Branches in publicizing Institute activities. It seems clear that students who will become engineers, eligible for membership in the Institute, should have their interest in the Institute aroused, as a means of stimulating membership. Thus far very little has come of this effort, but several of the counselors have volunteered suggestions. This matter should be studied further.

In addition to the effective use of a sound publicity program as a means of stimulating Institute growth, such a program is valuable as a means of enhancing the prestige of present members and of the engineering profession as a whole. It also serves to fulfill an obligation to the public which contributors to scientific knowledge should recognize. Obviously this involves more than the issue of news releases. The

Table IV. Numbers of Pages of Published Material

	ELECTRICAL ENGINEERING			TRANSACTIONS Only		
Year	General Interest Articles	News	Transactions Section	Technical Papers	Discussions	Total
1941	337	281	600	542	268	2,028
1944	246	214	738	493	231	1,922
1945	255	225	736	121	143	1,480
1946	285	315	832	254	120	1,806

Table V. Membership Statistics for Fiscal Year Ending April 30, 1947

	Honorary Members	Fellows	Members	6 Year Associate	Associate	Subtotals	Totals
Membership April 30, 1946	9	988	6,892	7,348	9,853		25,090
Additions							
New members qualified		2	292		2,084	2,378	
Former members reinstated or re-elected	—		114	47	116	277	
Subtotals		2	406	47	2,200	2,655	
Transfers	—	77	439	1,007		1,523	
Totals		79	845	1,054	2,200	4,178	
Deductions							
Died		22	58	35	30	145	
Resigned		2	54	145	111	312	
Dropped	—	4	48	214	544	810	
Subtotals		28	160	394	685	1,267	
Transfers	—		77	356	1,090	1,523	
Totals		28	237	750	1,775	2,790	
Net changes		51	608	304	425	1,388	
Membership April 30, 1947	9	1,039	7,500	7,652	10,278		26,478

Table VIII. Record of AIEE Membership

Year	Total May 1	Year	Total May 1	Year	Total May 1
1884	71	1906	3,870	1927	18,344
1885	209	1907	4,521	1928	18,265
1886	250	1908	5,674	1929	18,133
1887	314	1909	6,400	1930	18,003
1889	333	1910	6,681	1931	18,334
1890	427	1911	7,117	1932	17,550
1891	541	1912	7,459	1933	17,019
1892	615	1913	7,654	1934	15,230
1893	673	1914	7,876	1935	14,269
1894	800	1915	8,054	1936	14,600
1895	944	1916	8,202	1937	15,308
1896	1,035	1917	8,710	1938	16,078
1897	1,073	1918	9,282	1939	16,605
1898	1,098	1919	10,352	1940	17,213
1899	1,135	1920	11,345	1941	17,886
1900	1,183	1921	13,215	1942	18,944
1901	1,260	1922	14,263	1943	20,161
1902	1,549	1923	15,298	1944	21,407
1903	2,229	1924	16,455	1945	23,072
1904	3,027	1925	17,319	1946	25,090
1905	3,460	1926	18,158	1947	26,478

committee has given some thought to this broad question but has no report to make at this time.

MEMBERSHIP COMMITTEE

During the past year, membership has continued to climb. On April 30, 1947, the total membership was 26,478. This is an all-time record, and almost 1,500 members more than the preceding year. While the rate of increase in membership was not quite so high as the previous year, this was caused by the fact that 475 members were dropped who previously had maintained inactive status because of military service.

Indications are that the membership will continue to increase steadily during the next several years. Table VII shows the tremendous increase in number of Student members, that is, 9,021 at the end of April 1947, compared with 5,087 at the end of April 1946. This increased reservoir of Student members should stimulate membership during the next few years.

There is a slight increase in members who are in arrears with their dues. At the end of April 1947, there were 1,090 members in arrears, whereas a year ago there were only 954 members. It is hoped that increased activity of the Section membership committees will improve this situation.

During the past year, the number of members carried on inactive status was reduced from 1,809, as of April 30 last year to 361 as of April 30 this year. Of the 361 on the inactive list, about 70 are members who are still in the service and who have requested continuance of inactive status. About 290 are members located abroad who will be permitted to become reinstated upon notification. Incidentally, this opportunity to become reinstated is also available to the 475 members who were in the service and have been dropped as of April 30, 1947.

Activity of the Section membership committees is reflected by the fact that 3,269 applications for membership were received during the year.

Table VI. Number of Applications Received From Student Members and From All Others

Year Ending April 30	Students	All Others	Total
1947	938	2,331	3,269
1946	308	2,453	2,761
1945	249	2,179	2,428
1944	466	1,908	2,374
1943	783	1,431	2,214

Table VII Number of Student Members as of April 30

Year	New Applications	Renewals	Total
1947	5,092	3,929	9,021
1946	2,574	2,513	5,087
1945	2,326	2,287	4,613
1944	2,242	2,656	4,898
1943	2,512	3,200	5,712

An effort was made during the past year to decentralize the activities of the membership committee as much as possible. It is believed that more effective membership work is done at the Section level, and everything possible should be done to support the Section membership committee chairmen. The responsibility was assigned to each District vice-chairman of the membership committee to assist the Section chairmen in his District. Progress has been made along this line.

A talk on benefits of membership in AIEE was prepared for presentation before the Student Branches. In the preparation of this talk, the membership committee co-operated closely with the committee on Student Branches. It is planned to have this talk presented before all Student Branches this fall to stimulate Student membership.

The membership committee thinks it desirable to stimulate transfers from Student membership to Associate membership immediately upon graduation from college. A joint subcommittee with members from the membership committee and Student Branches committee is working on this subject and expects to present a report of a plan by this fall.

A subcommittee of the membership committee is revising the Section membership committee manual. This revised manual should be ready by the latter part of this year. Revision of the booklet, "Accomplishments of the AIEE in the Engineering World," is now under way. Both of these publications are valuable tools for Section membership committees.

The preceding membership statistics are supported by Tables V, VI, VII, and VIII.

BOARD OF EXAMINERS

Statistics relating to the number of cases handled by the board of examiners during the year 1946–47 are given in Table X. The past year shows an increase of 71 per cent over 1945–46, indicative of the increasingly widespread interest in AIEE activities. The expeditious handling of this rapidly growing number of cases on a monthly meeting schedule has been possible only through the 1945 increase in membership of the examiners to 19.

The board of examiners wishes to reiterate its pleas of previous years for careful preparation of applications for both admission and transfer to Member and Fellow. Though the situation has improved through the co-operation of national and Section committees, it is still necessary for both the examiners and headquarters to spend considerable time obtaining more detailed information on professional records and added references to bring a sizeable number of cases into conformity with the constitutional requirements.

In Table XI figures on cases handled by the board over a 5-year period are given. Of particular interest are the percentage rejections for admission and transfer to Member, which with one exception are al-

Table IX. Deaths of AIEE Members Reported in "Electrical Engineering"

Name	Date of Election	Date of Death	Grade at Death	Obituary Notice in "Electrical Engineering"
Adams, Edward L.	A '24	May 4, '46	A	July '46, p. 357
Arter, Roy C.	A '39	Sept. 22, '46	A	Dec. '46, p. 588
Blair, Samuel Robert	A '29	Apr. 17, '46	A	July '46, p. 358
Blume, Louis F.	A '09	Aug. 14, '46	F	Nov. '46, p. 539
Browning, Jr., Elmer E.	M '38	Jan. 8, '47	M	Mar. '47, p. 306
Burton, William Corwin	A '93	Apr. 18, '46	M	Aug.-Sept. '46, p. 421
Butz, Jr., Arthur N.	A '45	Dec. 7, '46	A	Feb. '47, p. 194
Chambers, W. L.	A '45	May 18, '46	A	July '46, p. 358
Cooke, Jr., Thomas L.	A '41	May 27, '46	A	Aug.-Sept. '46, p. 422
Crane, Albert S.	A '04	Aug. 26, '46	M	Oct. '46, p. 476
Cressey, John W.	A '20		M	Dec. '46, p. 587
Curry, Aubrey R.	M '34	Feb. 6, '46	M	July '46, p. 358
Czarnecki, Frank C.	A '15	Dec. 25, '46	A	Mar. '47, p. 306
Daniels, Harold P.	A '02	July 1, '46	A	Oct. '46, p. 476
Dearborn, Richard Harold	A '07	Mar. 21, '46	F	July '46, p. 357
Dively, William J.	A '27		A	Nov. '46, p. 539
Dixon, Walter C.	M '36	Feb. 28, '46	M	June '46, p. 289
Elliott, Edward Byron	A '17	Mar. 14, '46	M	July '46, p. 357
Filer, William F.	M '26	June 24, '46	M	Nov. '46, p. 539
Fisken, John Barclay	A '03		F	Aug.-Sept. '46, p. 421
Francisco, Ferris L.	A '04	Oct. 11, '46	M	Dec. '46, p. 587
Garfield, Alexander S.	A '98	Dec. 5, '44	F	Jan. '47, p. 97
Goldstone, Philip	M '24	Apr. 29, '46	M	Aug.-Sept. '46, p. 422
Griffes, Eugene V.	A '96	July 21, '45	A	Jan. '47, p. 98
Griffith, Hoyt D.	A '45	Jan. 4, '47	A	Mar. '47, p. 306
Hardy, Shaw H.	A '46	May 26, '46	A	Aug.-Sept. '46, p. 422
Harkins, John	A '21	May 21, '46	M	July '46, p. 358
Harrison, James	A '03	June 16, '46	F	Dec. '46, p. 587
Herrington, C. R.	A '45	Sept. 5, '46	A	Dec. '46, p. 587
Hobart, Henry M.	A '94	Oct. 11, '46	F	Dec. '46, p. 586
Hood, Samuel Bingham	M '14	Mar. 9, '46	M	May '46, p. 232
Houser, Kenneth O.	A '44	Apr. 16, '46	A	Aug.-Sept. '46, p. 422
Jackson, Jack E.	A '38	Nov. 1, '46	A	Feb. '47, p. 194
Jain, Ranjit Singh	M '39	Apr. '46	M	Dec. '46, p. 588
Kane, John J.	M '15	Nov. 8, '46	M	Jan. '47, p. 98
Kerr, Milton P.	M '41	Oct. 7, '46	M	Dec. '46, p. 588
Killingsworth, Henry M.	A '45	June 4, '46	A	Aug.-Sept. '46, p. 422
Kopp, Otto A.	A '09	Dec. 19, '46	M	Apr. '47, p. 408
Little, John J.	A '02	Dec. 26, '46	M	Apr. '47, p. 408
Macdonald, James E.	A '03	Aug. 8, '46	M	Nov. '46, p. 538
Margolin, Samuel Charles	A '32	Jan. 3, '46	A	June '46, p. 289
Mathias, William H.	M '26	Oct. 20, '46	F	Dec. '46, p. 587
Mini, Jr., Joseph	A '08	Aug. 24, '46	A	Jan. '47, p. 98
McAllister, Addams S.	A '02	Nov. 26, '46	F	Feb. '47, p. 193
Pattison, Frank A.	A '91	Sept. 18, '46	F	Nov. '46, p. 538
Rodman, Walter S.	A '07	Dec. 31, '46	F	Mar. '47, p. 305
Roy, Kiron Chandra	A '31	Oct. 19, '45	A	May '46, p. 232
Sachs, Joseph	A '92	Nov. 15, '46	F	Feb. '47, p. 194
Scanlon, J. Leo	A '28	Jan. 20, '47	M	Apr. '47, p. 408
Schneider, Frederick W.	A '17	Dec. 28, '46	A	Mar. '47, p. 306
Scott, Edgar George	A '10	Dec. 25, '45	M	July '46, p. 357
Shapiro, Louis	A '36	Apr. 28, '46	A	July '46, p. 357
Shearer, Harry Foster	M '45	May 24, '46	M	Aug.-Sept. '46, p. 421
Shepard, Robert B.	A '25	June 20, '46	F	Aug.-Sept. '46, p. 421
Smith, Frank W.	A '05	July 22, '46	M	Oct. '46, p. 476
Smith, William L.	M '22	Feb. 21, '47	F	Apr. '47, p. 408
Southgate, George T.	A '11	Nov. 8, '46	M	Mar. '47, p. 305
Sprong, Severn D.	A '03	June 27, '46	F	Aug.-Sept. '46, p. 421
St. Clair, Byron W.	A '17	Apr. 4, '46	M	June '46, p. 289
Stephens, Charles E.	M '22	Nov. 19, '46	M	Feb. '47, p. 194
Stephens, Howard O.	A '18	May 15, '46	M	Feb. '47, p. 194
Stevenson, Francis Leslie	A '03	Feb. 13, '46	M	July '46, p. 357
Stevenson, Jr., Alexander R.	A '20	Aug. 28, '46	F	Oct. '46, p. 476
Stiefel, Karl J. J.	A '39	Oct. 28, '46	A	Mar. '47, p. 306
Stockwell, Frank C.	A '12	Dec. 29, '46	M	Mar. '47, p. 305
Swoboda, Adolph R.	A '06	Oct. 20, '46	M	Jan. '47, p. 98
Taboni, Hector	A '12	June 15, '46	M	Dec. '46, p. 587
Thompson, Harry Lee	A '25	Mar. 24, '46	A	June '46, p. 289
Trench, Robert Butterfield	A '41	Apr. 21, '46	A	July '46, p. 358
Van Bokkelen, W. R.	A '12	May 22, '46	M	Aug.-Sept. '46, p. 421
Waring, James M. S.	A '06	Oct. 23, '46	A	Dec. '46, p. 587
Watson, Leon A.	M '35	Apr. 18, '46	M	July '46, p. 358
Way, Sylvester B.	A '03	Sept. 20, '46	F	Dec. '46, p. 586
Weiss, Otto	M '46	Mar. 28, '46	M	Aug.-Sept. '46, p. 422
Wilcox, Stanley C.	A '38	June 22, '46	M	Oct. '46, p. 476
Wolff, Frank Alfred	A '99	Mar. 28, '46	M	June '46, p. 289
Young, Herbert W.	A '05	Nov. 25, '46	F	Feb. '47, p. 194
Zimmerman, Mathias, W. F.	M '43	Mar. 23, '46	M	June '46, p. 290

Table X. Applications for Admission and Transfer 1946–1947

Applications for Admission		
Recommended for grade of Associate		2,052
Re-elected to the grade of Associate		114
Not recommended		3
		2,169
Recommended for grade of Member	390	
Re-elected to the grade of Member	20	
Not recommended	75	
		485
Recommended for grade of Fellow		2
		2
Applications for Transfer		
Recommended for grade of Member	424	
Not recommended	34	
		458
Recommended for grade of Fellow (by proposal)	64	
Recommended for grade of Fellow (by invitation)	14	
Not recommended	3	
		81
Students		
Recommended for enrollment as Students		3,931
Total		7,126

Table XI. Five-Year Summary 1942–1947

Year	Students	Associates	Admission to Member: Total	Admission to Member: Per Cent Rejected	Transfer to Member: Total	Transfer to Member: Per Cent Rejected	Transfer to Fellow	Total Cases
1946–1947	3,931	2,169	485	15+	458	7+	83	7,126
1945–1946	1,568	1,601	422	5+	478	5+	96	4,165
1944–1945	1,927	1,824	445	15+	434	3+	63	4,693
1943–1944	2,109	1,591	309	15+	381	4+	75	4,465
1942–1943	2,317	1,982	2	14+	285	4+	49	4,895

most constant. No figures are given on unfavorable actions concerning Fellow grade, as such rejections are at a negligible minimum. Similar studies made earlier over a much longer period have resulted in almost identical figures.

COMMITTEE ON TRANSFERS

Realizing that many Sections have not, in recent years, been taking the interest they should in encouraging their eligible members to apply for higher grades of membership, and, believing that the lack of a uniform guide was the primary reason for the apparent disinterest, the committee on transfers concentrated its efforts on the preparation of a general guide supplemented by thoroughly developed suggestions to the Sections.

The general guide, itself, was prepared and submitted by the board of examiners. This guide under the title, "Transfer Procedure," was studied carefully and endorsed, without revision, by the committee on transfers. However, a wide variety of suggestions were received both from the members of the committee and from several Sections which obviously had maintained interest in grade transfer work. The suggestions were enlightening and helpful.

The Sections committee became interested in the study being made by the committee on transfers, and, finally, a joint report was made by these two committees. This joint report was duplicated in New York and mailed to all Section chairmen and secretaries, and to all members of the board of examiners, Sections committee, committee on transfers, and other interested members.

The high points of the report, dated December 30, 1946, in supplement to the "Transfer Procedure" were that:

1. Each Section should have a grade transfer committee as a standing committee.

2. Each local committee should be a continuing committee operating throughout the calendar year.

3. Each local committee should be sufficiently large to represent fully the professional groups and industries within the area.

4. Each local committee should be composed of the best known, most highly respected, and most representative men in the Section.

3. Any candidate for transfer should be considered by a group of the local committee having grades no lower than the grade being considered for the candidate.

COMMITTEE ON CODE OF PRINCIPLES OF PROFESSIONAL CONDUCT

As no important matters came before this committee during the year, it held no formal meetings, but carried on all of its activities by correspondence.

Various members of the committee have been active in their own geographical areas in bringing the attention of engineers and others to the Institute's "Code of Principles of Professional Conduct" and in furthering the Engineers' Council for Professional Development's "Canons of Ethics for Engineers."

Several members also have taken an active part in urging upon their representatives in the Congress of the United States the importance of passing Senate Bill 360, in an endeavor to relieve engineers and other professional men from the conditions which force engineers into collective bargaining dominated by workingmen's unions.

At the time of the last report, an alleged violation of professional ethics by an Associate was being investigated. This investigation finally was dropped when the complainants would not furnish detailed evidence, and the alleged violator would not answer any requests of the committee for a statement of his side of the case. A report of this matter was submitted to the AIEE.

COMMITTEE ON REGISTRATION OF ENGINEERS

The committee on registration of engineers has devoted most of its attention to the problem of co-operating with other organizations on registration of engineers, and in keeping the Model Law in accordance with present thinking. The committee recommended the following resolution, which was approved by the board of directors:

RESOLVED: That the legal recognition of engineer-in-training status for recent engineering college graduates and other equally qualified persons is beneficial to the public and to the profession. This practice distinguishes men intending to become professional engineers from others not so qualified or so intending. It further is resolved that this resolution be published in *ELECTRICAL ENGINEERING* and that members be encouraged to assist groups striving to adopt this practice in the states where they reside.

The committee also has given consideration to the selection of personnel to serve on state registration boards and the methods by which this selection is made in various states. The committee feels that the Model Law could be improved in several aspects and particularly regarding the provisions for the engineer-in-training.

COMMITTEE ON CONSTITUTION AND BYLAWS

On December 3, 1946, the committee made the following recommendations to the board of directors, which were adopted by the board, January 29, 1947.

1. Amendments changing the word "convention" to "meeting" wherever it occurs in the bylaws, and changing Section 27 so that the four general meetings will be known in future as the "winter general meeting," the "summer general meeting," the "Midwest general meeting," and the "Pacific general meeting." Submission of a constitutional amendment at the next convenient opportunity, to substitute the words "general meeting" for "convention."

2. Amendment to transfer Hawaii to District 8 with corresponding change of the map of Districts of the Institute.

3. Amendment of Section 48 to make changes in the allotment of funds to Sections.

On December 27, 1946, the committee made the following recommendations to the board, and these were adopted also on January 29, 1947.

1. Amendments of Sections 53, 61, and 64 of the bylaws to permit the formation of joint Student Branches with other national engineering societies, and to extend the term of Student membership until a Student member has reached the age of 21, if he should be graduated before reaching his majority. Submission of a constitutional amendment, Article IV, Section 16, at the next convenient opportunity, to enable joint Student members to become Associate members in accordance with Section 57 of the bylaws.

2. Amendment of Section 33 to clarify it, and in Districts having less than five Sections to enable the District executive committee to act as the co-ordinating committee for the District.

On April 16, 1947, the committee made the following recommendations to the board, and these will be presented at the June meeting of the board.

1. Amendment to the bylaws consisting of the deletion of Section 8, pertaining to the preliminary consideration of applicants for transfer from Associate to a higher grade of membership.

2. Amendment of Section 41 to delete reference to the finance committee, as this section relates to Section territory and does not involve financial matters.

COMMITTEE ON PLANNING AND CO-ORDINATION

The committee has carried forward actively the project assigned to it by the board of directors nearly two years ago and subsequently interpreted and re-emphasized by board resolution or adoption of the committee's several recommendations. The committee held four meetings and carried on a considerable correspondence, but the real work was done by its two subcommittees.

The subcommittee on technical activities held monthly meetings and supplemented frequent joint sessions with the technical program committee by a truly voluminous correspondence with members of the technical committees.

During the past year the subcommittee has devoted its effort almost entirely to a study of a reorganization of the Institute's technical activities and the preparation of recommendations to the board on how this reorganization might be accomplished under the directive set forth in a resolution adopted by the board at its meeting in Asheville, N. C., in May 1946. That resolution specified:

(1) that such additional technical committees should be organized as may be needed to cover the important items of electrical technology; (2) that these technical committees should be grouped in appropriate divisions or groups with a steering committee for each group fairly compact in numbers and reasonably concentrated geographically to promote effective action; (3) that the members of the steering committees be appointed by the president, and the members of the technical committees be appointed by their respective steering committees, all to serve for one year; (4) that each year the group steering committees, in addition to appointing their several technical committees, make recommendations to the president through the secretary on the membership and organization of their respective successor committees, including at least two alternates for each chairmanship; (5) that in such recommendations the steering committees provide for a turnover of at least 25 per cent of the steering committee personnel each year. Further, that it is the intent of this board that the responsible committees should proceed with such changes as they may determine to be necessary and proper to effectuate these principles, unless the proposed changes are at variance with either the constitution or the bylaws, in which event they shall be referred back to this board for further consideration.

Pursuant to this directive, the subcommittee has recommended, and the board has approved, the formation of four co-ordinating committees and the establishment of 20 new technical committees. Some of these technical committees are new, and some supplant others recommended for retirement. Including the committee on education, the status of which was changed from that of a technical committee to that of a general committee, there were ten technical committees that were recommended to be withdrawn, thus making a net increase of ten in the number of technical committees recommended to be in operation. A résumé of the proposed setup follows:

Power Group

Power substations
Power rotating machinery
Power transformers and regulators
Power generation
Power system operation
Power transmission and distribution systems
Insulated power cables
Power protective devices
Power switchgear
Power relays
Power systems application of carrier current
Power converters—electronic

Industry Group

Electric welding
Electric heating
Industrial power systems
Mining, metal forming, and rolling
Industrial control devices and equipments
Chemical, electrochemical and electrothermal
Machine tools, material processing, and fabrication

General Applications Group

Air transportation
Domestic and commercial application
Land transportation
Production and application of light
Marine transportation

Communication and Science Group

Communication
Basic sciences
Electronics
Instruments and measurements
Nucleonics
Therapeutics

Except for the nucleonics committee, the new committees were formed from strong existing subcommittees.

Also the chairmen of two of the general committees, education and research, were made ex-officio members of the technical program committee, in addition to the other committee chairmen already having that status.

It is recognized that the proposed reorganization does not achieve perfection. However, the responses received from interested members indicate a remarkable degree of concurrence that the changes are a step in the right direction and a satisfactory basis for trial. Experience with the new setup will show what further changes are necessary or desirable.

The principal activity of the subcommittee on professional activities continued to be its study of organization of the engineering profession. Through meetings throughout the country and the use of a questionnaire, it obtained opinions and expressions from nearly 1,500 Institute members in the several fields of technical interests and in various age and employment groups. The subcommittee made a formal report which included results of the survey and recommendations for consideration of a plan of organization based on that originally proposed as plan *D*, but modified to incorporate certain features from plans *B* and *C*. In effect, this plan proposes an over-all engineering organization composed of individual members, which would further the nontechnical needs and aspirations of engineers in all fields. Under the proposed plan, the present technical societies would continue to function practically without change in their respective technical fields. Included was a skeletonized constitution and certain other fundamental principles regarding classification of members, dues, publication, and so forth.

The committee accepted the report and submitted it to the board of directors. The board authorized immediate publication of the survey portion of the report. (This appeared in the April 1947 issue of *ELECTRICAL ENGINEERING*.) The board also approved early publication of the entire report, except for the plan of procedure. (This appeared in the May issue of *ELECTRICAL ENGINEERING*.) The report was referred to a special committee consisting of the president and four past presidents for editing and the preparation of recommendations to the board as to its disposition.

As a prerequisite to any plan of organization for the engineering profession, it was believed that there is a need for uniform grades of membership in all the societies. A study therefore was made of the present membership requirements of the Founder Societies, and recommendations prepared for grades of fellow, member, associate, and student. The board approved the principle of uniform grades, agreed to urge various other societies to study the matter and consider adoption of uniform grades, and indicated its willingness to recommend these requirements for adoption by the membership of the Institute, if agreement can be reached with the other societies on uniform grades of membership.

An investigation to determine whether the creation of a new Institute office might be justified led to the decision to recommend that greater use be made of the District organizations and the vice-presidents to relieve the president of some of the burdensome duties of his office. The recommendations made were submitted to and approved by the board. Consequently, it is now the practice to have the secretary of the Institute call a special meeting of the incoming, outgoing, and holdover vice-presidents during the summer meeting, at which they are informed of their duties in co-ordinating the work in the Districts. The Sections are advised on the method of obtaining official speakers and that all requests for official visits are cleared through the respective vice-president. It further was agreed that presidential Section visits do not take precedence over other Institute obligations.

The subcommittee considered a suggestion that provision be made for discussions and interchange of information, within the Institute, on management problems. As it is apparent that the need exists, the establishment of a committee on management was recommended and approved by the board.

A suggestion had been received that, with the increasing number and activity of Institute committees, consideration be given to organizing the nontechnical committees in groups similar to the plan proposed for the technical committees in accordance with the Asheville resolution. The subcommittee recommended that certain of the nontechnical committees be grouped as administrative, professional, and general, and that the first two groups named establish co-ordinating committees consisting of the respective committee chairmen. The general committees, such as Sections, and planning and co-ordination, would continue to function as at present. The board approved this recommendation and requested the president to appoint two co-ordinating committees for the coming year for the professional and administrative groups which are to be composed initially of the following committees:

Professional Group

Code of Principles of Professional Conduct
Registration of engineers
Education
Student branches
Management
Edison Medal
Charles LeGeyt Fortescue Fellowship
Lamme Medal
Award of Institute prizes

Administrative Group

Membership
Constitution and bylaws
Headquarters
Board of examiners
Transfers
Publicity
Members-for-Life

The chairmen of these two co-ordinating committees and of the four technical co-ordinating committees are to be ex-officio members of the committee on planning and co-ordination.

Individual members of the committee carried on special assignments arising from suggestions received from officers and members. To cite but one example, the question of changing the present geographical boundaries of the Districts was given thorough study in collaboration with the District vice-presidents, and it was concluded not to recommend any substantial changes for the present.

To facilitate arrangements and insure more adequate accommodations for the four general meetings held each year, a schedule of dates and locations through the year 1950 has been adopted by the board. District meetings likewise have been scheduled through 1948.

The committee has endeavored to keep the membership currently and more fully informed of its activities through the columns of *ELECTRICAL ENGINEERING* than is possible in this annual report.

UNITED STATES NATIONAL COMMITTEE OF THE INTERNATIONAL ELECTROTECHNICAL COMMISSION

The United States National Committee of the IEC held its annual meeting, November 8, 1946, and elected the following officers:

President—L. F. Adams.
Vice-president—P. H. Chase.
Vice-president and treasurer—H. S. Osborne.

In the election of Mr. Adams as president of the USNC, a tradition was broken. Over its long history the presidents of the USNC always have been from the general interest group. Mr. Adams is the first president from the manufacturing group. In the early days of the USNC and the IEC, the work was concerned primarily with the fundamental electrical problems of units, measurement, and the basis for rating electric machinery. In the years immediately preceding the war the work became more and more the standardization of the methods of rating and testing electric machinery and associated problems. It appears that this trend will continue as the work is resumed.

A meeting of the council of the IEC was held in Paris in July 1946. Consideration was given at the meeting of the IEC council to the question of affiliation with the proposed new International Organization for Standardization (ISO) and a favorable recommendation was made on affiliation, provided that certain conditions are met. A final decision on affiliation was deferred until the constitution of the ISO could be approved by the member countries and its organization set up.

Professor L. Lombardi tendered his resignation as president of the IEC, and a new president was elected. E. Uytborck, president of the Belgian Electrotechnical Commission, succeeded Professor Lombardi as IEC president. Emile Brylinski, honorary president of the French Electrotechnical Committee, was elected honorary president of the commission. As Lord Mount Edgcumbe had tendered his resignation as honorary secretary of the IEC, Doctor P. Dunsheath of Great Britain was elected honorary secretary.

A new committee of action of the IEC (executive committee) was designated, to consist of the president, the honorary secretary, and representatives from Czechoslovakia, France, Sweden, Switzerland, the United States, and the Union of Soviet Socialist Republics.

As to the business of the IEC itself, the opinion of the council was that all emphasis should be placed on getting action on technical projects and that it would not be expedient now to undertake a revision of the constitution or of the procedures of the IEC which have grown up in the course of the commission's work. The status of technical projects was reviewed. The following new advisory committees were nominated: extra-high voltages, number 30; flameproof enclosures, number 31; fuses, number 32;

and capacitors for power systems, number 33.

A review of the advisory committees was made, and the work was divided into three categories:

1. Very urgent work on which meetings of the responsible advisory committees should be held within a year.

Number 6—Lamp cap and holders
Number 8—Voltages
Number 30—Extra-high voltages
Special international committee on radio interference (CISPR)

2. A much larger group of projects which were sufficiently urgent to require a meeting of the advisory committees within two years.

Number 2—Rotating machinery
Number 9—Electric traction equipment
Number 12—Radio communication
Number 16—Terminal markings
Number 17—Switchgear
Number 22—Electronic devices
Number 24—Electric and magnetic magnitudes and units
Number 25—Letter symbols
Number 28—Co-ordination of insulation

3. Remaining projects which would be started as soon as required. These include IEC projects not listed.

The IEC committee of action met in London, October 14, 1946, but no further action was taken on the question of affiliation with the ISO. It is expected that a meeting of the IEC council will be held in Geneva, Switzerland, in June 1947, and technical meetings have been proposed for September 1947, in Zurich, Switzerland.

Standards

STANDARDS COMMITTEE

The war period necessarily was accompanied by a reduction in many of the Institute activities including those of the Standards committee. However, every effort was made to carry forward its various projects with a minimum of interruption, and, because of the splendid co-operation of its members and of the technical committees of the Institute, very few of the vital standards projects were wholly interrupted. Since the end of the war, the shortage of man power and testing facilities, so necessary to standards work, has not been substantially ameliorated, but it has been possible to revive practically all of the dormant projects and to make some progress during this year in bringing them to completion.

The partial inactivity during the war naturally resulted in the accumulation of subjects—both in the AIEE and the ASA—which has made the work of reorganization and reactivation of many committees more onerous than it otherwise would have been. Casualties in committee personnel, due to death, and retirement, and other reasons, necessitated extensive changes in many committees of the Institute and in ASA committees to which the Institute appoints representatives.

The Standards committee now consists of 16 executive members plus the chairmen of all technical committees, who serve as ex-officio members. The executive group is chosen to secure a reasonable continuity in membership. This is very desirable, as the group is responsible for the approval of Institute Standards, and the necessary familiarity with Institute standard activities cannot be obtained during a short term of membership.

The number of Standards, reports, and so forth issued during the year is no indication of the amount of work carried on by either the Standards committee or the technical committees. It is believed that this year's production is a very creditable performance.

During the year the following Standards and reports on proposed standards and codes have been approved: Revision of Standard 1, "General Principles Upon Which Temperature Limits Are Based in the Rating of Electric Machines and Apparatus," which revision takes into account suggested temperature limits for class *H* insulation (the new silicone materials); number 6, "Report on Standards for Pool Cathode Mercury-Arc Power Converters;" number 32, "Standards for Neutral Grounding Devices;" revision of number 40 "Standards for Electric Recording Instruments;" "Master Test Code for Resistance Measurements;" number 43, "Report on Recommended Practice for Insulation Testing of A-C Rotating Machinery."

A progress report by the committee on air transportation indicates a rapid development of the many aeronautical projects, both standards and codes, undertaken during war years. The following have reached the publication stage: number 700, "Standard for Aircraft D-C Apparatus Voltage Ratings;" number 800, "Test Code for D-C Aircraft Machines;" "Guide for Aircraft Electric Systems." The progress made in the field is particularly commendable when it is realized that it has been necessary to provide for the many changes in committee personnel brought about by the industrial shift from war to peace.

Special mention may be made of two subcommittees which are engaged in preparing reports on controversial matters. The subcommittee on sign of reactive power published an article in *ELECTRICAL ENGINEERING* which has provoked a very large amount of discussion, and it is not anticipated that agreement will be reached on its recommendations very soon. The subcommittee on conduction in stationary contact surfaces, after several years' work, has prepared a report which has been accepted by the Standards committee for the information of technical committees only. The controversial points deal with temperature rise recommended for various types of contact.

The subcommittee on applications of statistical methods continues to be active, and it is planning for the enlargement of its projects and for the presentation of educational and specialized papers.

Among ASA activities in which the Institute is interested, special mention should be made of *C42*, "Definition of Electrical Terms." The committee has been inactive since 1941 following the publication of the present American Standard. It now has been reorganized completely into 17 subcommittees; some of these already have begun work. It is evident that the work of *C42* will be concerned largely with the broadening of scope and the consequent addition of many new definitions.

Technical Committees

COMMITTEE ON AIR TRANSPORTATION

The committee on air transportation held one meeting of the entire committee during the administrative year. This meeting was a 2-day session held in Cleveland, Ohio, September 23 and 24. On the afternoon of September 24, the committee met jointly with committee *A-2* of the Society of Automotive Engineers. All of the sessions were well attended, and considerable progress was made in connection with the standardization activities of the committee.

At the end of the year the status of subcommittee work is as given in the following paragraphs.

Aircraft Electric Systems. This subcommittee has been re-organized. A preliminary draft of the "Aircraft Electric Systems Guide" has been printed and submitted to the Standards committee for assistance in circulating the material throughout industry for criticisms, suggestions, and contributions. The guide report is not as yet sufficiently complete for publication as a "Report for Trial Use," but it contains a great deal of valuable information, and much good will be accomplished by wide dissemination of the preliminary draft.

Aircraft Electric Rotating Machinery. This subcommittee has completed a proposed test code for d-c aircraft machines. This was published for trial in March 1947 as "AIEE Report 800."

At the present time this subcommittee is engaged in a new project under the general subject of "Rating Standards of D-C Aircraft Generators."

Aircraft Electric Control, Protective Devices, and Cable. This subcommittee has been reorganized, and has completed a report on aircraft wire and cable originally requested by the SAE committee *A-2*. The first meeting of the reorganized committee was held January 21. The present program consists of three items:

1. Determination of the interrupting capacity circuit breakers.
2. Test code for circuit interrupting devices.
3. Test code for voltage regulators.

Work is under way on all of these projects but has not progressed sufficiently for a detailed report at this time.

Joint Subcommittee (Air Transportation and Electric Machinery) on Carbon Brushes. This subcommittee met in New York, January 29, and also met in conjunction with the d-c machinery committee, January 30. Considerable progress has been made toward the objective of this committee: the formation of an AIEE test code for the evaluation of carbon brush performance on all types of commutators and collector rings to provide for improved specifications and standards for carbon brushes used on electric machinery.

Subcommittee for Altitude Ratings. This subcommittee is developing an AIEE Standard outlining the basic principles of altitude rating of electric machinery. Substantial progress has been made in accumulating material for this project, particularly for the range of sea level to 50,000 feet. The Naval Research Laboratory, the Bureau of Aeronautics, the Army Air Forces, and the Bureau of Standards are co-operating with industry members of this subcommittee in accumulating basic data. An important object of this work is to obtain better correlation of altitude chamber test results obtained in high-altitude flying.

A final draft of AIEE 700, "Report on Aircraft D-C Apparatus Voltage Ratings," was approved by the board of directors.

The committee on air transportation sponsored a conference on aircraft electrical safety during the winter meeting. Approximately 200 engineers from all phases of aviation work participated in the program. The minutes of the meeting are available on application to headquarters.

The committee on aviation and airport fire protection of the National Fire Protection Association has suggested that the two committees co-ordinate their work, insofar as electrical fires on aircraft are concerned. Sentiment of the members of the committee on air transportation is very much in favor of such co-operation, and arrangements are being worked out to the mutual satisfaction of the two committees.

Technical papers were considerably below normal volume during the year. Personnel shifts are still prevalent in the industry and in the military services, and few engineers can find time for the preparation of papers. Plans are, however, under way now for strong air transportation sessions at the Pacific general meeting in August, and the Middle Eastern District meeting in September.

COMMITTEE ON AUTOMATIC STATIONS

The committee has sponsored two technical program sessions during the last year. At the summer meeting, ten papers on the subject of automatic control of capacitors, synchronous condensers, air switches, and single pole switches were presented at the conference session. At the winter meeting, the subjects of automatic control for capacitors and automatic control of air switches were presented at a technical session. Much interest was indicated in these subjects by the lively discussion which followed their presentation. Other interesting subjects are being considered for future presentation.

The committee met twice during the year with very good attendance records and has been represented at each general session of the technical program committee. The membership, individually and through its officers, has taken an active interest in the proposed technical program committee reorganization plan.

One working group has completed a report on the study of d-c polarity on device coil corrosion. This report indicates that all cases of coil corrosion have occurred on equipments in which coils were connected directly to the positive control bus. It is concluded that connections should be made to the negative bus in order to prevent this corrosion. The report is being referred to the standards committee for consideration and final disposition.

Another working group is continuing its investigation of a-c versus d-c tripping schemes. It is expected that, in co-operation with other committees, definite solutions to tripping problems can be developed, especially as applied to small isolated stations.

The committee has been represented actively on various other committees and subcommittees.

COMMITTEE ON BASIC SCIENCES

With the ending of the war, the work of the committee on basic sciences has increased, as material for publication becomes less restricted.

The greater activity of the committee is exemplified in the formation of subcommittees on new energy sources, large scale computing devices, applied mathematics, and electric circuit theory, together with representation on the joint subcommittee on servomechanisms and on the newly formed committee on nucleonics.

At the 1947 winter meeting, conferences were held on applied mathematics, new energy sources, large scale computing devices, and servomechanisms. A session on general basic science topics completed the most active technical meeting in the history of the committee. Attendance at the conferences was among the highest at winter meeting sessions, a factor which encourages the committee to continue these types of conferences.

Although only one conference is scheduled for the 1947 summer general meeting, future plans call for continued activity in the several fields of the present subcommittees, with the possible formation of additional subcommittees as these are warranted. With the scope of the committee on basic sciences crossing all technical fields, it is planned to insure that no areas are being left uncovered.

Co-operation with associated technical committees and outside organizations also is being developed. The subcommittee on applied mathematics maintains contact with the American Mathematical Society to develop better uses of mathematics to the solution of engineering problems. Co-operation between ASA Sectional Committee *C-42*, Definitions of Electrical Terms, is assured through the chairmanship of subcommittee 1 of ASA *C-42*, together with several members of the committee on basic sciences, also members of subcommittee 1.

Although the committee is dispersed widely geographically and, hence, is limited in the number of meetings which can be held during the year, excellent co-operation of the membership has been possible through the subcommittee method of operation and voluminous correspondence between the members. A meeting of the committee was held during the winter meeting, January 28, 1947, at which time plans for future technical meetings were considered.

COMMITTEE ON COMMUNICATION

This committee has continued to bring to the Institute papers dealing with many phases of the very broad and continually expanding field of communications. Among the subjects covered during the past year were television; systems for microwave radio in the fields of telephone, telegraph and television; military communications; rural telephone facilities; new telephone switching systems; several phases of telegraphy; new developments in communication components, such as thermistors and filters; progress in the field of ocean cables; and gas pressure protection for telephone cables.

The committee sponsored full sessions at all of the general meetings. The summer meeting in Detroit included papers on military communications, properties and uses of thermistors, a method for transmission rating of telephone systems, and improved types of mica capacitors for communications equipment. At the Pacific Coast meeting in Seattle, papers were presented on the status of television, compression and expansion of telephone signals, power line carrier, and carrier shift telegraphy. The winter meeting in New York included four communications sessions:

1. A session on television covered the various elements in a television system, that is, the broadcasting station, receivers, network facilities, and transmission from remote pickups. It also included a review of color television and an interesting demonstration of television cameras and receivers.

2. A rural telephone symposium covered four methods of providing rural service: telephone lines, joint power and telephone lines, carrier on power conductors, and radiotelephone.

3. A conference on testing telephone receivers and transmitters included talks by representatives of many industrial and research laboratories and was followed by questions and discussions from the floor.

4. In the session on communications components and techniques a new dial switching system was described; arrangements for protecting telephone cables by means of gas pressure were outlined; and new methods of operating telegraph over wire lines, radio, and ocean cables were discussed.

Every effort has been made to assist District meetings in presenting good communications programs. Papers solicited and reviewed by the committee on communication were made available to District meetings in San Antonio, Tex.; Indianapolis; and Worcester, with the chairman of the committee presiding at the communication session in Indianapolis.

Continued emphasis was placed on papers for publication, as contrasted with conference papers, so that the results of the committee's activities would be made available to the whole Institute membership and not be limited to the relatively few who can hear the presentation. During the year, 20 papers and reports sponsored by the committee were published in *ELECTRICAL ENGINEERING* or in *TRANSACTIONS*, and many more have been recommended for future publication.

Meetings of the whole committee were held in June, September, and January, and subcommittees have met on numerous occasions. Eight subcommittees have been active during the year: testing of

telephone transmitters and receivers, underwater sound developments, rural telephone facilities, television, radio communication systems, modulation methods, power line carrier for power company communications, and hearing aids.

The committee's activities have been directed primarily toward serving well that large segment of the Institute's membership whose primary interest is communications by keeping them abreast of developments in their field. In addition, it has tried to present information on communications which would be of general interest to those whose activities are in other fields of engineering.

DOMESTIC AND COMMERCIAL APPLICATIONS COMMITTEE

The activities of this committee during the past year have been carried on through five subcommittees covering the following fields: electric appliance design, electrical hazards to farm animals, farm applications, load characteristics, and wiring. Following is a brief résumé of what is being done by each of these groups.

The electric appliance design subcommittee is gathering comprehensive data on the many trial installations of heat pumps now in existence in several different parts of the country. Plans are being made for a technical session on the general subject of heat pumps for the 1948 winter general meeting.

During the past year, the electrical hazards to farm animals subcommittee has continued to gather data. Consideration is being given to the preparation of an educational pamphlet on the elimination of such hazards that could be distributed widely among county farm agents, rural electrical inspectors, and others who could benefit from the information.

The farm applications subcommittee, in conjunction with numerous other organizations, sponsored the first National Farm Electrification Conference in November 1946. Because of the success of the initial conference, the sponsoring bodies have decided to continue the conference as an annual affair. This subcommittee will continue to co-operate with the other groups.

Recognizing that distribution engineers have need for accurate information on load characteristics, and that most of the data available are now quite old, the load characteristics subcommittee has been endeavoring to assemble more recent test and survey data on residential electrical load characteristics, generally, as well as data on specific appliances and applications, such as automatic washing machines, electrical housecleaning, and heat pumps.

The principal activity of the wiring subcommittee during the past year has been co-operation with the committee on industrial applications in the preparation of recommendations for interior wiring design for public and commercial buildings.

COMMITTEE ON ELECTRIC MACHINERY

A meeting of the committee was held in New York during the winter meeting, January 1947. Each of the subcommittees presented a report on its activities during the year, and then considerable discussion took place regarding the reorganization of the technical committees proposed by the technical activities subcommittee of the committee on planning and co-ordinating. This proposal included, among other things, the grouping of the various technical committees into four principal groups, and then each of the present technical committees was asked how it should be split up. The committee on electric machinery expressed a desire to aid in committee activity in any way that would benefit the industry but it had insufficient knowledge to offer suggestions at the time and suggested that a definite plan be proposed. Since that time, various suggestions have been made, but no definite action in dividing the committee has yet resulted.

During the winter meeting, the five active subcommittees held meetings to review their activities, consider papers available for future meetings, and to plan for the future.

A report on "Insulation Resistance Testing of A-C Rotating Machinery" prepared by the insulation resistance subcommittee was issued by the Institute during the year. A report for insulation testing of d-c machinery is being prepared.

The induction machinery subcommittee is continuing the sponsorship of temperature tests of motors from which it is expected that better rating data and standards can be determined.

The transformer subcommittee has sponsored for several years a co-operative laboratory test on aging of class *A* insulation, and a preliminary report is being prepared for the summer general meeting.

The afore-mentioned three subcommittees, the synchronous machinery subcommittee, and the d-c machinery subcommittee have sponsored papers for the various sessions.

The committee as a whole conducted one session at the Indianapolis meeting in October, three sessions at the winter meeting, and is planning on two sessions at the summer general meeting. In addition, some electric machinery papers have been presented at District meetings.

COMMITTEE ON ELECTRIC WELDING

A meeting of the committee was held November 21, in Atlantic City, N. J., during the National Metal Congress. Plans for the winter meeting and for the summer general meeting were discussed. The committee was brought up to date on the latest recommendations of the technical activities subcommittee. It was the consensus of this committee that these recommendations when carried out would result in definite improvements. It was also the committee's thought that the new publication policy would be of greater benefit to the membership.

Two subcommittees were appointed; one on resistance welding, and the other on arc welding. The need for assistance by members of this committee to the Sections was emphasized, and their co-operation was requested. It is understood that the Michigan Section at the request of one of this committee's members is considering the formation of a technical group on electric welding. It was reported that the formation of ASA Committee *C52* was complete and work was progressing.

This committee sponsored one conference session on power supply for resistance welding at the winter meeting, and also one technical session on resistance welding. Five conference papers were presented at the conference session, and four technical papers were presented at the technical meeting. It also is planned to hold a conference session at the summer general meeting on power supply for resistance welding. It is the intention to rely principally upon members from Canada for these papers. It also is planned to hold a meeting of this committee at the same time.

COMMITTEE ON ELECTROCHEMISTRY AND ELECTROMETALLURGY

A meeting of the committee was held January 30, 1947, during the winter meeting. At the January 30th meeting of the board of directors, a change of name for this committee was approved. The name is to be the "chemical, electrochemical, and electrothermal committee." As a means of covering the field as visualized to be within this committee's scope, seven subcommittees have been named, covering different aspects of the technical field, and the chairmen and members of all but one have been either appointed or considered.

Subcommittee on Metallic Rectifiers. A technical session on dry-type rectifiers was held at the winter meeting, January 27, 1947. "Proposed Standards for Metallic Rectifiers" was completed during the year. "A Bibliography on Metallic Rectifiers and Their Principal Applications" was completed during the year.

Subcommittee on Voltage Transients in Arc Furnaces. A report is in process.

Subcommittee on Batteries, Battery Forming and Charging. This subcommittee was formed and personnel appointed. It is expected to become active in 1947.

Subcommittee on Cathodic Protection. This subcommittee was formed and personnel appointed. It is expected to become active during 1947.

Subcommittee on Petroleum, Refining and Production. A chairman has been appointed and is at work on personnel. It is expected to become active during 1947. A joint session with American Petroleum Institute at its annual meeting is planned.

Subcommittee on Electrolytic Processes. This subcommittee is formed and active. A group of conference-type papers by operating personnel on this subject has been arranged for the summer general meeting.

Subcommittee on Arc and Electrothermal Processes. No chairman has been appointed as yet. Incomplete personnel.

COMMITTEE ON ELECTRONICS

The work of the committee has been carried on during the past year principally through 15 subcommittees. A meeting of subcommittee chairmen held in October 1946 served to crystallize the plans and co-ordinate the work of these subcommittees. In addition to the general meeting of

the committee, which was held during the winter meeting, there have been meetings of many subcommittees devoted to the special tasks of these groups.

Two technical sessions, one on electronics and another on electronic instruments, and a conference on some new electronic methods and devices were held during the winter meeting. An electronics session and a conference on rectifiers are planned for the summer general meeting. During the calendar year 1946, *ELECTRICAL ENGINEERING* contained 31 articles including important electronic material. The activity of the committee and its subcommittees has contributed substantially to this result.

The subcommittees have been engaged in the following activities.

Electronic Heating. This subcommittee has rendered valuable service to the Federal Communication Commission in the study of radiation from high-frequency heating equipment by collecting data on radiation levels and by presenting the professional point of view to the commission at a public hearing, December 18, 1946. It also has been concerned actively with methods of rating electric heating equipment and with the problem of safety from electric shock at the frequencies used for electric heating.

Electronic Instruments. A technical session on electronic instruments was held during the winter meeting with a program of five papers. Several additional papers are in preparation. A survey of instrument manufacturers is in progress to determine the need for electronic tubes with special characteristics for use in electric instruments.

Electronic Papers Solicitation and Section Contacts. This subcommittee effectively has encouraged and solicited the publication of papers dealing with electronic subjects. A policy of distributing electronic papers to other committees, which sponsor sessions where the electronic application is appropriate, has been continued, and this policy has been effective in broadening the interest in electronic subjects.

A conference on some new electronic methods and devices was held during the winter meeting. This was a continuation of a series of similar conferences which have been very successful.

Films, speakers, and technical information on electronic subjects have been provided liberally to the Sections for technical meetings through this subcommittee.

High-Frequency Conductors, Cables, and Connectors. This subcommittee has expanded its membership to cover the large field assigned. Co-ordinating contact has been established with the Radio Manufacturers Association, and surveys are being prepared on "Television Camera Cables," "Power and Current Ratings of Coaxial Cables," "Test Methods for Coaxial Cables," and "Hookup and Set Wire."

Hot-Cathode Electronic Power Converters. This subcommittee, which was organized during the year, will be engaged actively in the preparation of standards. A group well qualified for this task has accepted membership, and work will start with a meeting planned for May 1947.

Pool-Cathode Electronic Power Converters. This group has continued work on a bibliography for electronic power converters. The work on hot-cathode power converters which was initiated in this group has been set up as a separate subcommittee.

A working group has been organized to prepare a report on "Protection of Power Converters." Another group is working on a report on "New Developments in the Design and Application of Electronic Power Converters in Europe." A conference on operation of mercury-arc rectifiers is planned for the summer general meeting.

Liaison With Other Groups. The co-ordination of electronics committee work with the Institute of Radio Engineers and the Joint Electron Tube Engineering Council has operated smoothly through the liaison subcommittees of the committee on electronics. In several instances, joint subcommittees have been formed.

Other Technical Subcommittees. The committee includes technical subcommittees on electron tubes, electronic nomenclature and definitions, electronic precipitation, electronic standards, and X-ray tubes. These subcommittees have been active during the year in the fields assigned. The subcommittees on electronic control and electronic welding have been discontinued, and these fields will be covered by other AIEE committees.

The subcommittees on electronic heating and pool-cathode electronic power converters have been transferred to the status of AIEE technical committees.

The committee closes the administrative year with 11 active subcommittees as follows: electron tubes; electronic instruments; electronic papers solicitations and section contacts; electronic precipitation; electronic standards; high-frequency conductors, cables, and connectors; liaison with IRE; liaison with JETEC; nomenclature, definitions, letters and graphical symbols; hot-cathode electronic power converters; and X-ray tubes.

COMMITTEE ON INDUSTRIAL CONTROL DEVICES

This committee has taken an active part in the planning of the reorganization of the technical committees of the Institute. Under the present plan, the committee's scope and activities will become broadened to a considerable degree, and its membership will be expanded to give the users of industrial control equipment a broader place in its activities.

The subcommittee on industrial electronic control has discussed its field of activities with the corresponding subcommittee of the committee on electronics to avoid a duplication of work. It is also in contact with other engineering groups in a joint effort to promote satisfactory standards, covering definitions, test codes, and recommended practices for electronic control equipment.

The subcommittee on test codes for industrial control devices has analyzed a number of possible objectives, and is now charting a definite course of action.

The work on a bibliography of electrical control has progressed excellently, and the committee hopes eventually to publish a rather complete bibliography on this subject.

The joint subcommittee on servomechanisms, sponsored in conjunction with the committees on basic sciences and instruments and measurements, had a very active year and sponsored a technical session at the summer meeting and another at the winter meeting. An effort is being made in papers and otherwise to present the basic theory and mathematical treatment in a manner which will promote the industrial applications of this useful tool.

The committee sponsored a technical session at the summer meeting and another at the winter meeting. The sessions were well attended, and there is reason to believe that they filled a definite need. The committee also has solicited papers for the 1947 summer meeting, and expects to sponsor a session at that time. Committee meetings were held in conjunction with the summer and winter meetings.

COMMITTEE ON INDUSTRIAL POWER APPLICATIONS

At the 1946 summer meeting, two full sessions were sponsored by the committee, to which members of the Detroit Industrial Electrical Engineering Society were invited. These sessions featured industrial voltage requirements (a subcommittee report), protective devices for and insulation breakdown in industrial plants, distribution in nonindustrial buildings, induction heating, application to the rubber industry, and electronic printing control. A committee luncheon also was held during this national meeting.

For the 1947 winter meeting, the committee continued to foster its policy adopted last year of highlighting one particular industry at each major AIEE meeting (January 1946—machine tools) by holding a most successful session on applications of electric power in the textile industry. This session included four well-co-ordinated papers written by both manufacturers and users, and plans are being made to combine the papers as one report, as a special publication. This was the first time in AIEE history that a session was devoted to the problems of electric equipment in the textile industry. Reports on other industries may be treated similarly as they are covered at national meetings. For instance, two sessions on the pulp and paper industry will be sponsored by this committee at the summer general meeting.

At the winter meeting, the committee also sponsored a conference on industrial voltage requirements (including subcommittee report) along with a discussion of voltage regulation for industrial systems. A third session on industrial instrumentation and control was sponsored jointly with the committee on industrial control devices.

During the winter meeting, the committee and invited guests held a luncheon at the Hotel Commodore, at which a spirited and most constructive discussion took place on the recent formulation of the industry group of technical committees. Considerable enthusiasm was expressed on the

formulation of definite technical committees to stimulate the study of applications of electricity to specialized industries.

The subcommittee on interior wiring design of commercial buildings is formulating a report under the same name to be published as a recommended practice. This will be a companion report to "Power Distribution in Industrial Plants," which was prepared by the committee on industrial power applications.

By action of the board of directors, in January 1947, the subcommittee on machine tool and processing industries was raised to the status of a full technical committee (machine tools, material processing, and fabrication). Also the committee on industrial power applications now becomes industrial power systems, with a scope involving generation, transmission, and distribution of electric power within an industrial plant.

COMMITTEE ON INSTRUMENTS AND MEASUREMENTS

Meetings of the committee on instruments and measurements, which now consists of 36 members, were held November 14, 1946, and April 11, 1947. The committee has handled more than 42 papers, and has been active in sponsoring numerous sessions at technical meetings. Sessions on instruments and measurements were held at the summer and winter meetings. Papers at these sessions covered a wide range of instruments and measurements applications, including compensation of ammeters and voltmeters for frequency variation, a functional analysis of measurements, an a-c network analyzer, high-vacuum leak testing with the mass spectrometer, airborne magnetometers, ignition crest voltmeters, long-scale indicating instruments, measurements at 10,000 megacycles, and a polyphase thermal-demand meter.

The foregoing list of subjects emphasizes the wide scope of measurements, and indicates the desirability of close co-operation between the committee on instruments and measurements and many of the other technical committees in the Institute. Such co-operation has taken place through the formation of four joint subcommittees with the committees on automatic stations, electronics, basic sciences, and industrial control devices. Several of these joint subcommitttees have sponsored sessions at the summer and winter meetings, as reported in the following material.

Work on a standard on electric recording instruments and on master test codes for resistance measurements and for temperature measurements has been completed by subcommittees. These standards have been submitted to the Standards committee with the recommendation that they be published for one year trial use with subsequent adoption as AIEE Standards.

Activities of the remainder of the 15 subcommittees have been as follows.

Subcommittee on Revision of Standard 4 (Measurement of Test Voltage in Dielectric Tests). Revisions of the membership have been completed, and work is started on the problem of surge voltage measurements at intervals of less than one microsecond. New material on voltage measurements with direct current and high frequencies is to be added.

Subcommittee on Watt-Hour Meters. This subcommittee is working on rectifying the differences between the definitions in the "Code for Electricity Meters" and those in the ASA *C42* definitions.

Subcommittee on Definitions. Definitions for the next revision of ASA *C42* are being considered by this group.

Subcommittee on Revision of C39 (Electrical Indicating Instruments). The method of describing the accuracy of instruments is being considered by this group, and it is working closely with the ASA *C39* sectional committee in revision of that standard.

Subcommittee on Dielectric Measurements in the Field. A bibliography and a working outline of a report on progress in the art of dielectric measurements in the field have been completed, and preparation of the various sections of the report has been assigned to the members of the subcommittee.

Subcommittee on High-Frequency Measurements. A table of standard frequency ranges and designations referred for recommendation by the Standards committee was considered by this group. The subcommittee recommend that a joint subcommittee be set up to consider the matter, and the joint subcommittee is now active.

Subcommittee on Instrument Transformers. This subcommittee will continue its efforts to arrange the material in ASA *C57* pertaining to instrument transformers in proper form for separate publication, when all the ASA material including revised and additional definitions is available.

Subcommittee on Marking of Varmeters and Related Instruments. This subcommittee awaits action by the Standards committee on the sign of reactive power before proceeding with its consideration of a standard method for marking varmeters.

Joint Subcommittee on Telemetering. This joint subcommittee is engaged in revising the 1941 AIEE report on "Telemetering Supervisory Control, and Associated Circuits." The subcommittee plans to hold a conference session on telemetering at the summer general meeting.

Joint Subcommittee on Servomechanisms. The initial activity of this new joint subcommittee was the sponsoring of a session at the summer meeting. Sessions also were sponsored at the winter meeting and the North Eastern District meeting, and one is planned for the summer general meeting in Montreal. This subcommittee has set up broad objectives as follows: (1) to solicit papers on theory, (2) to stimulate work on the preparation of papers on components, (3) to undertake a program to assist with the education of the AIEE membership as to the fundamentals of this subject, and (4) to formulate plans for unification of terminology.

Joint Subcommittee on Electronic Instruments. This new joint subcommittee sponsored sessions at the summer and winter meetings. It is making a survey of instrument manufacturers to determine the need for electronic tubes with special characteristics for use in electronic instruments.

Joint Subcommittee on Frequency Bands and Designations. As reported earlier, this new joint subcommittee is considering a table of standard frequency bands and designations. A report to be published in *ELECTRICAL ENGINEERING* is in preparation.

COMMITTEE ON LAND TRANSPORTATION

Two well-attended meetings of the committee were held during the past year one in June 1946, and one during the winter meeting in January 1947. The following activities were discussed and organized at these meetings.

Technical Meetings. Three transportation sessions were held at the winter meeting. A light traction session, included a special address by General C. P. Gross, chairman, New York Board of Transportation; two technical papers describing new car equipment for the New York subways; and one on trolley coaches. A second session included a paper on the development of current collectors for high speed railway service, two on PCC street car subjects, and one on silicone insulation for railway motors; and the third session included five papers on electric equipments for Diesel-electric locomotives. These sessions all were well attended. A transportation session has been scheduled for the summer general meeting, including five papers.

Subcommittee Activities. A subcommittee has been engaged in a review of AIEE Standard 16, "Standards for Electric Railway Control Apparatus." A meeting was held January 28, 1947, and another is scheduled for May. Definite progress is being made by this subcommittee, and it is hoped that a report can be submitted within the next year.

Another subcommittee is engaged in gathering and tabulating heavy traction electrification data. Some progress has been made in the collection of data on overhead catenary systems, and work is in progress to begin tabulations on locomotives and on power supply equipment.

COMMITTEE ON MARINE TRANSPORTATION

Early in the current administrative year a request was received by the committee from United States Coast Guard (Technical Division) to consult with them for the purpose of reviewing and commenting on their proposed regulations for electrical work on shipboard.

At its October 1946 meeting, the committee carefully considered this request. It was apparent that Coast Guard regulations follow closely the recommendations published in AIEE Standard 45, 1945 revision, with deletions and additions based on Coast Guard's past experience in administering Standard 45. The committee decided to review the proposed regulations giving particular attention to each item. Comments and recommendations resulting from the review of each item as mutually agreed on are to be accepted by the Coast Guard and, if recommendations of Standard 45 are affected, revisions to be noted and made. The committee, realizing that the review would require con-

siderable time and effort, decided to hold monthly meetings of two days each, and five such meetings were held. The last meetings were held May 8–9.

It is believed that considerable benefit has accrued from this review both to the Coast Guard and the committee.

The mass of comments and recommendations compiled during the review has been referred to the committee's editing subcommittee for co-ordination for eventual submission as a revision of Standard 45. It is expected that the revision will be ready for appropriate action early in the coming administrative year.

The committee's activities during the past year have been confined almost wholly to the afore-mentioned review.

Thanks and appreciation have been expressed mutually between the committee and the Coast Guard for consideration and assistance to and from both.

The committee members have rendered most valuable service all during this review. Participating attendance for the 11 required meetings has averaged 85 per cent.

COMMITTEE ON NUCLEONICS

There has been no activity of the committee during the current year because of delays in organization and planning. The committee was authorized in October 1946; a nucleus of committee members suggested in January was appointed by President Housley. Further appointments have been suggested for the coming year.

The first committee meeting is scheduled to be held at the summer general meeting, at which time plans for this activity will be discussed.

COMMITTEE ON POWER GENERATION

Two meetings of the committee were held during the fiscal year, in which reports of the subcommittees were considered. In addition, the committee sponsored one session at the summer meeting at which two papers on hydroelectric stations and two on excitation systems were presented. At the winter meeting, two sessions were sponsored, one presenting four papers on hydroelectric stations and related problems, and the second a conference on interconnected systems. All sessions were well attended, indicating a wise selection of program material.

Specific committee activities are typified by the subcommittee reports which are briefed in the following paragraphs.

Hydroelectric Systems. Continued interest in various phases of hydroelectric station operation warrant presentation of three more papers on this subject at the summer general meeting in Montreal. This will be the fourth session including hydroelectric papers since their initial presentations sponsored by the committee at the winter meeting of 1946. At this summer's session, an additional paper on German utility experience during the war will be included.

Interconnected Systems. Following the well-received conference session on this subject at the winter meeting which, was marked by a large attendance, it is gratifying to report another program of three to four papers is available for future meetings. These probably will be presented during the fall of the coming year.

Grounding Practices. This working group is organized to collect data on present-day practices and trends of system grounding, including both generating stations and transmission systems classified as to size, voltage, and mileage. It is intended to summarize (1) the bases used in grounding-method selection (2) operating experience (3) grounding devices used. Changes in grounding practices since 1931 also will be analyzed.

Questionnaires have been sent out, and returns have been received from 434 systems, including over 960 generating units aggregating more than 33,000,000 kva. In the transmission system grounding section, some 510 systems are covered, involving more than 100,000 miles of transmission circuit. The report is expected to be ready for presentation this coming year.

Excitation Systems. This subcommittee, originally organized to prepare programs on this subject, was assigned the added task of studying the standardization of excitation systems. The group now is gathering data on definitions and practices which will be presented in a report.

At the present time two papers are available for future meetings, one on effect of excitation systems on large-system stability, and another on electronic exciters for synchronous generators.

Prime Mover Governing. This joint AIEE–ASME Committee on Prime Mover Speed Governing Specifications will complete a draft of governing specifications for steam turbines by November 1947. It is expected to have a draft of hydroelectric-unit governing specifications ready by the summer of 1947.

Probability. This subcommittee was organized to prepare a program of papers on the subject of probability theory and its application to electric power systems planning. Several papers have been solicited, and it is expected a program will be organized in the near future.

Power Generation Report. A committee report covering the progress in power generation during the years 1940–46 has been prepared by the subcommittee and will be presented for approval of the committee during the summer of 1947.

COMMITTEE ON POWER TRANSMISSION AND DISTRIBUTION

A meeting of the committee was held December 12 and 13, 1946, which 36 members and guests attended. The subcommittees made reports on their activities, followed by a general discussion of the subjects and suggestions for future work. At the completion of the reports of committees, several members made reports on activities within their respective companies during the war period, on future plans, and technical subjects. Arrangements are being made to have them abstracted for publication in *ELECTRICAL ENGINEERING*, and to make them available to Institute members who may be interested These reports covered such subjects as: Transmission system practices in foreign countries, 500-kv test line, bundle conductors, the era of higher distribution voltages, increased loading of electric power plant, obsolescence, the cost of losses, new distribution substation developments, lightning—effect on buried cables, banking of distribution transformers, increasing transmission line capacities, a-c network calculator laboratories, peanut substations, and transpositions in power lines—their advantages and their hazards.

Technical Meetings. At the winter meeting, the committee sponsored two sessions at each of which four papers were presented. One of these sessions was a symposium on lightning, which dealt with lightning surges at substations, photographic study of lightning, lightning arrester discharges, and burning of wood structures by leakage circuits. The other session was of a general nature covering reporting on weather conditions as an aid to power companies, line stability, internal corona discharges in insulated cables, and radio noise on 230-kv lines.

Subcommittee Activities. The general systems committee is investigating the following subjects: (1) evaluation of power losses throughout the power systems and their effect on all equipment from the generator to the user; (2) effect of surges on system peformance; (3) survey of line outages of high voltage lines. This last subject has been made a joint study with a subcommittee of the transmission and distribution committee of the Edison Electric Institute.

The stations subcommittee has been studying: (1) flexibility for removal of parts in packaged substation units for industrial plants; (2) single versus 3-pole switching for 4-kv distribution system; (3) request for papers on increasing the capacity of existing distribution systems; (4) economics of the unit type of substation; (5) supervisory control versus automatic stations.

The subcommittee on lightning and insulators has been studying: (1) methods of predetermining lightning performance of transmission lines; (2) "Lightning Reference Book, Volume II;" (3) lightning characteristics of porcelain, wood, and air in series.

The subcommittee on insulated wires and cables has been devoting its time to an investigation of the thermal properties of buried cable systems—in duct and directly buried. It appears that a closer appreciation of the effective thermal resistivity of the soil surrounding both ducts and directly buried cables can be obtained. The subcommittee is seeking papers dealing with cable operation and design for presentation at national meetings.

The subcommittee on towers, poles and conductors has under consideration the following topics: (1) dancing conductors; (2) wood versus steel towers—economics; (3) conductor joints and splices; (4) cathodic protection of tower footings; (5) stainless steel static wires; (6) acetylene-flame cleaning for tower painting or repainting.

The subcommittee on distribution has had under consideration several subjects of an economic nature. However, it was found that these same subjects were being covered by Edison Electric Institute, and, therefore, they were dropped for further

consideration by the subcommittee. This subcommittee sponsored jointly with the relay subcommittee of the committee on protective devices a conference during the past winter meeting on protection and design of distribution circuits to improve performance. Considerable interest was shown at the meeting, and there was not sufficient time to complete the discussion. Therefore, the committee is making plans to continue this joint interest with the committee on protective devices. It is hoped that they will be able to have another joint conference at the summer general meeting.

It is intended to have a meeting of the committee during the summer general meeting, at which two sessions are being sponsored.

COMMITTEE ON PROTECTIVE DEVICES

The committee continued to function as an executive group only. All the details of standardization and sponsoring of papers has been handled by the subcommittees. This arrangement has continued to function entirely satisfactorily.

Seven papers were sponsored by the committee at the winter meeting, and three are scheduled for presentation at the coming summer general meeting. In addition, the committee sponsored one conference session and was cosponsor of another at the winter meeting.

There have been three meetings of the main committee and another is scheduled for the near future.

Any projects which have been instituted, as well as the details of the accomplishments of the various subcommittees, are contained in the following reports submitted by the chairmen of the various subcommittees.

Switches, Fuses, and Insulators Subcommittee. This subcommittee held one meeting during the year. At present, a revision of standard 22 on switches and insulators is being prepared, and a revised draft of the proposed standard on interrupter switches also is being prepared.

Relays Subcommittee. The activities of the subcommittee included sponsoring six technical papers, including joint papers, two of them being subcommittee reports, three conference papers, and two conference sessions. In addition to a large number of meetings of the 11 working groups, the subcommittee held three regular meetings. The principal work of the subcommittee is carried on through the activities of working groups having the following specific assignments.

The working group on the bibliography of protective relaying has prepared and distributed to the members of the subcommittee, the committee on protective devices, and to a mailing list of 100 relay engineers in the United States copies of the "Relay Bibliography for 1946." This contains a listing of all technical articles published in the United States and foreign press dealing with various phases of protective relaying. These activities are continued from year to year, and periodically the bibliography is published for general distribution in the form of a technical paper.

The investigation of grounding practices for instrument transformer secondary circuits has been completed. The results of this undertaking and recommended practices are summarized in a subcommittee report "Grounding of Instrument Transformer Secondary Circuits," which was presented at the winter meeting and published in the April 1947, *ELECTRICAL ENGINEERING*. This working group has been discharged.

The group on instrument transformer standards practically has completed its work in connection with the revision of the ASA "Transformer Standard *C57*." The relays subcommittee has approved the revision of the test code and operating guides for that Standard which apply to instrument transformers, and suggestions for the final Standard have been passed on to the ASA transformer and operating guides committee. It is expected that this working group will be discharged at the close of the administrative year.

Following a preliminary report presented in January 1946, and a conference session at the summer meeting, the working group on transformer protection developed further information on certain phases of the transformer protection problem, such as the co-ordination of thermal protective devices with short-circuit relay protection, and evolved recommended short-time characteristics of thermal devices. A conference paper by E. T. B. Gross on "Simplicity in Transformer Protection," presented at the January 1947 winter meeting, brought out additional information and discussion of pressure relay protection and fault detection by means of gas accumulator elements. The results of this review and correlation of transformer protection are summarized in a subcommittee report, "Relay Protection of Power Transformers," scheduled for presentation at the summer general meeting, which will complete the work of this group.

In previous years, the working group on generator protection developed information on current practices through questionnaires and a conference session. Further work is necessary before definite recommendations can be made concerning practices for the relay protection of generators.

The correlation of distribution circuit protection practices and construction methods, with emphasis on the influence of these on the reduction of sustained faults, is a joint project of the relays subcommittee and the distribution subcommittee of the committee on power transmission and distribution. This group has endeavored to develop an awareness of the necessity of keeping adequate records in order to evaluate the various methods of improving service to distribution loads. A conference session was held at the summer meeting, introduced by two conference papers, and provided worth-while exchanges of information.

A revision of "Standard for Power Relays,"[9] ASA *C37*, has been undertaken by a working group. Following discussion and correspondence on suitable test voltages, relay definitions, and so forth, a preliminary draft of a proposed revision has been prepared and is being circulated to the relay subcommittee for comments and suggestions.

In November 1946, a working group began to study the desirable insulation levels of relay and control circuits. The test voltage required by the present standard for power relays is considered to be too low to guard against abnormal voltages which might occur in current transformer secondary and d-c control circuits. Although most relays now are being tested at voltages in excess of the present standard requirements, cases have been reported of improper relay performance as a result of abnormal secondary and control voltages. A preliminary survey is under way to determine the extent of this problem.

A new working group was organized in the fall of 1946 to study sensitive ground protection of transmission and distribution circuits. The benefits of such protection, including limitation of fault damage, improved service reliability, and the positive disconnection of broken conductors resting on the ground long have been recognized. Several papers have been published describing methods and results used with delta-connected or ungrounded systems. These methods are being reviewed and information collected on schemes which have been tried or proposed for 4-wire multigrounded systems.

A study of transmission line protection has been undertaken by a working group. Emphasis has been placed in recent years on the need for relaying systems that will not limit the emergency load carrying ability of transmission lines with swings approaching system stability limits. General application methods, backup relaying, and special problems will receive attention. The group has evolved a "typical" transmission system to be used in certain studies.

A new working group to study electronic protective relay applications has been formed in response to suggestions from a number of sources. As a beginning, a list is being prepared of existing applications of electronic devices to protective relay systems. Following this, it is planned to explore those features of electronic devices which tend to give them a place in competition with other forms of equipment, and especially to anticipate where they might provide a facility not hitherto available.

Fault Limiting Devices Subcommittee. Work on AIEE Standard 32, "Neutral Grounding Devices," has been completed, and the final draft released to the Standards committee. It has received all required committee approvals as a new standard.

The preparation of the third report on "Present-Day Grounding Practices" is well advanced. It is expected to be presented at the summer general meeting.

Replies received from industry, in the survey of its grounding practices, cover 510 power systems, 101,000 miles of transmission and distribution circuits of 22 kv and above, and 33,750,000 kva of generating capacity. The report is to be factual, giving interpretations but not recommendations, and will be in four parts:

I. Introduction.
  A. Purpose and Scope.
  B. Summary of Results.

II. Grounding Practices at Generating Stations.
III. Grounding Practices on Transmission and Distribution Systems.
IV. Appendixes.
A. Supplementary Tables for Part II.
E. Supplementary Tables for Part III.

The bibliography on resonant neutral grounding is to cover the period from 1918 to date. It is to have future addenda at regular intervals to keep up with new publications. At present, the bibliography is finished to about 1935. By next fall it is expected to be completed through 1946.

A field survey of the continuous loads of resonant neutral grounding devices is getting under way. Better, and perhaps more economical, designs of ground fault neutralizers and associated grounding transformers can be made with more accurate data on the actual continuous load demands upon them.

A new project on high resistance neutral grounding of alternators has been started.

The subcommittee organization, as appended to the October 31, 1947, minutes of the committee on protective devices, remains unchanged, except that to the title of "Working Group on Revision of Standard 32" there should be added "and Field Survey of the Continuous Loads of Resonant Neutral Grounding Devices."

Circuit Breakers and Assembled Switchgear Subcommittee. The work of the subcommittee was handled mainly by five active working groups, each of which discharged its responsibility efficiently and quickly as could be done without sacrificing thoroughness.

The working group on low voltage air circuit breakers completed the work on the "Low-Voltage Air Circuit Breaker," Standard 20, obtained the necessary approvals of the subcommittee and the committee on protective devices, and referred the Standard to the Standards committee which published it. The working group is studying the following subjects: (1) cascading; (2) short time rating; and (3) selective tripping. The group has circulated a questionnaire to obtain information on how successful has been the experience in operating circuit breakers in cascade. It also has promoted preparation of technical program papers, and a complete session on small air circuit breakers is planned for the summer meeting.

The working group on switchgear assemblies reports that the "Assembled Switchgear," Standard 27, is in good shape, but does not include impulse test levels. It was decided to revise the Standard primarily for this purpose, but at the same time review the entire Standard.

The working group on power circuit breakers completed the study of the method of defining the interrupting rating of power circuit breakers and reaffirmed its recommendation that the basic rating be based on the current interrupted at the instant of parting the contacts.

The group recommended against adopting a proposed method of rating using the current during the first half cycle, because it would create confusion among those responsible for the application of circuit breakers, would present difficulties in rerating those circuit breakers, require revision of standards, and make it necessary to revise all existing application data.

In co-operation with the working group on switchgear assemblies, the matter of determination of test voltages for secondary circuits was studied. It was determined that test voltages for secondary circuits are specified adequately in AIEE Standard 27. Also in co-operation with the working group on switchgear assemblies, the group considered the request to prepare a standard covering the fusing of control circuits.

The working group on calculating short-circuit current for low voltage circuits again was unable to complete the assignment to revise the method of calculating short-circuit currents for low voltage circuits. There is a need for further test information before this work can be completed. Owing to industrial conditions during the past year, in which all facilities for making such tests were loaded beyond capacity, the committee was unable to get the data with which to complete its work.

The subcommittee endorsed the proposed plan for reorganizing the Institute's technical committees, but requested that it be given the opportunity to review and study further the selection and scope of the proposed committees before the final organization is determined.

Lightning Protective Devices Subcommittee. A working group has obtained impulse breakdown characteristics from the manufacturers of distribution expulsion-type arresters, which has been compiled into a report. The report is being circulated in the working group for approval, after which it will be sent to the subcommittee for final approval.

The working group on rotating a-c machines collected data from 54 power companies, and prepared a report which was submitted to the lightning protective devices subcommittee at the winter meeting for comments and suggestions. The subcommittee requested a review of the replies to see if sufficient information was available to show the policy followed by the different companies. The subcommittee voted to present the results of this survey to the Institute as a committee report at the winter general meeting in 1948.

A meeting of the working group on unit substations was held in January, at which decisions were made to collect data by a limited survey which will cite specific cases where equipment failure of flashovers have occurred, and to investigate and clarify certain technical points which are vital to this problem.

The working group designated to combine and revise AIEE Standards 28, 24, and 47 circulated a fourth draft of this standard to the working group and members of the lightning protective devices subcommittee for comments and suggestions. The subcommittee voted to exclude the material covering application from the standard and to establish a new project, which will have as its objective a report covering an application guide for the selection of arrester voltage ratings based upon system operating conditions.

The lightning protective devices subcommittee recommends that, when the new appointments are made in August 1947, a project be set up to prepare an application guide to aid in the selection of methods for lightning protection of substations.

COMMITTEE ON APPLICATION OF ELECTRICITY TO THERAPEUTICS

The committee held one meeting during the year. At this meeting, which was well attended, there was an extended discussion as to the scope of the committee's activities and its objectives. The members concurred in the definition of the committee's scope as outlined by the board of directors. The field of the committee's activity is broad and, in some cases, co-operation and joint action with other committees would be appropriate.

The committee is very much interested in promoting standards that should be observed in the design features of therapeutic apparatus. This standards work should be carried on in collaboration with the committee on safety.

The committee also is interested deeply in the effects on humans of heat lamps, sun lamps, diathermy, X-ray equipment, and the like, and in the development of new electrical means for diagnosis and treatment of disease. In this connection, the committee thinks it should maintain contact with the council on physiotherapy of the American Medical Association, and therefore, is asking the board of directors for permission to appoint a liaison representative to maintain contact with the medical profession.

The committee is laying plans for a symposium on the uses of electricity in therapeutics.

Awards

CHARLES LE GEYT FORTESCUE FELLOWSHIP

This fellowship was established as a memorial to Charles Le Geyt Fortescue in recognition of his valuable contributions to the electric power industry, and provides a minimum allowance of $500 a year for graduate study in electrical engineering.

Two awards were made for the academic year 1947–48: Paul Kaczmarczik, for graduate study at the University of Pennsylvania; and Theordore G. Mihran for graduate study at Stanford University.

COMMITTEE ON MEMBERS-FOR-LIFE FUND

No awards were made last year in connection with the summer meeting as was anticipated in the committee report of a year ago, because no Branch paper prizes were awarded, because of conditions instant to the aftermath of the war.

Special attention of the counselor in each of the Student Branches of the odd-numbered Districts was called to these awards, expense-paid trip to the summer general meeting for the winners of the Branch paper prizes, last October. It is too early to know whether any awards will be made for the 1947 summer general meeting.

EDISON MEDAL

The Edison Medal, awarded by a committee composed of 24 members of the Institute, was presented for 1946 to Doctor Lee de Forest, president of the Lee de Forest Laboratories, Inc., Los Angeles, Calif., "for pioneering achievements in radio and for the invention of a grid-controlled vacuum tube with its profound technical and social consequences." The presentation took place January 27, 1947, during the winter meeting. The medal may be awarded annually for "meritorious achievement in electrical science, electrical engineering, or the electrical arts."

LAMME MEDAL

The Lamme Medal committee awarded the medal for 1946 to John B. MacNeill, manager of the switchgear and control division of the Westinghouse Electric Corporation, East Pittsburgh, Pa., "for his foresight, leadership, and creative contribution in the development of switching equipment." Arrangements are being made for the presentation of the medal at the annual business meeting in Montreal, Quebec, Canada, June 11, 1947. The medal may be awarded annually to a member of the AIEE "who has shown meritorious achievement in the development of electric apparatus or machinery."

HOOVER MEDAL

The Hoover Medal was established through a trust fund created by a gift from Conrad N. Lauer and is to be awarded periodically "to a fellow engineer for distinguished public service" by a board representing the ASCE, American Institute of Mining and Metallurgical Engineers, ASME, and AIEE. The eighth medal, for 1946, was awarded to Doctor Vannevar Bush, president of the Carnegie Institution of Washington, and was presented to him on January 30, 1947, during the AIEE winter meeting.

JOHN FRITZ MEDAL

The John Fritz Medal board of award is composed of representatives of the ASCE, AIME, ASME, and AIEE. The medal may be awarded annually for notable scientific or industrial achievements. The 1947 medal was awarded to Doctor Lewis Warrington Chubb, director of research, Westinghouse Electric Corporation, East Pittsburgh, Pa., for "pioneering genius and notable achievements during a long career devoted to the scientific advancement of the production and utilization of electric energy." The medal was presented on January 29, 1947, during the AIEE winter meeting.

WASHINGTON AWARD

The Washington Award for 1947 was bestowed upon Doctor Karl T. Compton, president of the Massachusetts Institute of Technology, Cambridge, Mass., "for his scientific and engineering activities, which have contributed considerably to the happiness, comfort, and well-being of humanity." The presentation was made at a dinner in Chicago, Ill., in February. The award may be made annually to an engineer by the commission of award composed of nine representatives of the Western Society of Engineers and two each of the ASCE, AIME, ASME, and AIEE.

ALFRED NOBLE PRIZE

This prize, established in 1929, consists of a certificate and a cash award from the income of a fund contributed by engineers and others to perpetuate the name and achievements of Alfred Noble, past president of the ASCE, and of the Western Society of Engineers. It may be made to a member of any of the co-operating societies, ASCE, AIME, ASME, AIEE, or WSE, for a technical paper of particular merit accepted by the publication committee of any of these societies, provided the author, at the time of such acceptance, is not over 30 years of age.

INSTITUTE PRIZES

The committee has reviewed further the proposed revised practice covering the award of Institute prizes, with particular reference to comments received from the chairman of the Sections committee. This review has resulted in some changes in the proposed prize award practice, and a new proposal has been submitted to the board of directors.

Joint Activities

UNITED ENGINEERING TRUSTEES, INC.

This organization manages property and funds held jointly by the four Founder Societies, including the Engineering Societies Building, the Engineering Societies Library, and the endowment funds of the Engineering Foundation.

The building is occupied fully by engineering organizations, and additional space is needed both for offices and for meetings. Two of the Founder Societies have been forced to rent space in other buildings.

A committee of the UET is endeavoring to develop tentative plans for the remodeling of the building or the procurement of a new building to meet the needs of the founder societies and, if possible, bring in other engineering societies.

An abstract of the annual report for the year ended September 30, 1946, appeared in *ELECTRICAL ENGINEERING*, February 1947, page 201.

ENGINEERING FOUNDATION

The Engineering Foundation was established in 1914 as a joint organization of the four societies, ASCE, AIME, ASME, and AIEE, for "the furtherance of research in science and engineering, and the advancement in any other manner of the profession of engineering and the good of mankind."

The foundation has been supporting 14 research projects, and new projects are constantly under consideration. Each research project supported by it is under the sponsorship of one of the founder societies.

The sponsorship of the Welding Research Council has been broadened to include all the four Founder Societies as well as the American Welding Society. The council operates through ten principal committees.

An abstract of the annual report for the year ended September 30, 1946, appeared in *ELECTRICAL ENGINEERING*, February 1947, pages 199–200.

ENGINEERING SOCIETIES LIBRARY

The Engineering Societies Library was formed by combining the separate libraries of the ASCE, AIME, ASME, AIEE, and preparing a composite card catalogue.

Special services rendered by the library include: photoprints, searches, abstracts, translations, bibliographies, book loans by mail. All services have had greater use except the photostat which decreased about nine per cent below the extensive demands during the war.

Wartime conditions prevented the usual growth in the book and magazine collections. These deficiencies are being overcome rapidly.

An abstract of the annual report for the year ended September 30, 1946, appeared in *ELECTRICAL ENGINEERING*, February 1947, pages 200–01.

EMPLOYMENT SERVICE

Operating as an incorporated nonprofit organization, the Engineering Societies Personnel Service, Inc., assists members of the Founder Societies desiring to secure new positions and employers searching for engineers. Nonmembers may receive such assistance when positions available cannot be filled by members.

Offices are operated in New York; Detroit, Mich.; Chicago; and San Francisco, Calif.; with the co-operation of the Engi-

Table XII. Employment Service—1946

Month	Men Registered					Men Placed				
	New York	Chicago	San Francisco	Detroit	Total	New York	Chicago	San Francisco	Detroit	Total
January	338	106	134	49	627	42	27	25	13	107
February	251	86	126	60	523	28	18	19	9	74
March	296	79	182	91	638	34	18	20	13	85
April	246	98	113	65	522	43	20	24	20	107
May	226	73	138	79	516	38	25	31	16	110
June	210	86	121	40	457	45	14	33	15	107
July	247	58	81	62	448	50	16	20	18	104
August	201	79	128	57	465	35	18	27	25	105
September	207	61	112	64	444	38	11	29	20	98
October	214	60	113	56	443	47	10	34	17	108
November	194	58	92	55	399	38	15	14	12	79
December	164	60	70	45	339	32	18	12	11	77
Total	2,794	904	1,410	713	5,821	470	210	288	189	1,159

neering Society of Detroit in that city, the Western Society of Engineers in Chicago, and the Engineers Club of San Francisco in that city.

For several years, the service has been on a self-supporting basis. A record of registration and placements during the past year is given in Table XII.

ENGINEERS' COUNCIL FOR PROFESSIONAL DEVELOPMENT

Organized in 1932 to engage in activities leading toward the enhancement of the professional status of the engineer, this council now includes three representatives of each of the eight participating organizations: the ASCE, AIEE, ASME, AIME, SPEE, American Institute of Chemical Engineers, National Council of State Boards of Engineering Examiners, and the Engineering Institute of Canada.

During the past year, as in previous wartime years, inspections of engineering curricula by the committee on engineering schools were held to a minimum. Reexamination of all engineering curriculums previously accredited has been recommended by the committee on engineering schools. The accrediting of technical institutes is well under way. Seven curricula were accredited in October 1946.

Other activities are carried on by committees whose titles indicate the nature of their work: student selection and guidance, professional training, professional recognition, information, engineering ethics, employment conditions for engineers, and ways and means.

A comprehensive report on the activities during the year ended September 30, 1946, was published in *ELECTRICAL ENGINEERING*, January 1947, pages 102–05.

ENGINEERS JOINT COUNCIL

This council, formerly known as the joint conference committee, is composed of the presidents, immediate past presidents, and secretaries of the Founder Societies and the AIChE. Its functions are to consider matters of interest to the societies and to make recommendations to their governing bodies.

Reports on the industrial disarmament of Germany and Japan were prepared for the State and War Departments.

A panel was organized to advise committees of Congress regarding desirable amendments to the National Labor Relations Act to prevent grouping together of professional and nonprofessional employees.

The committee on the economic status of the engineer has completed and EJC has published the first part of a manual on collective bargaining, and a report on a preliminary survey of employer practice regarding engineering graduates.

The committee on organization of the engineering profession is making comprehensive studies of engineering organizations of local, state, and national types.

REPRESENTATIVES

A complete list of about 40 joint bodies upon which the Institute is represented appears in the Year Book and in the October issue of *ELECTRICAL ENGINEERING* each year.

Appreciation

To the AIEE committees, to District, Section, and Branch officers, and to the members in general, the board of directors expresses deep appreciation of the extensive expansions in activities and the continuing rapid increase in membership, and extends thanks for the splendid co-operation received.

Respectfully submitted for the board of directors.

H. H. HENLINE
Secretary

Members of the AIEE board of directors present at the North Eastern District meeting were left to right: (seated) T. G. LeClair, M. J. McHenry, W. E. Wickenden, J. E. Housley, C. A. Powel, and W. I. Slichter; (standing) E. P. Yerkes, P. L. Alger, C. M. Laffoon, F. L. Lawton, S. H. Mortensen, H. H. Henline, J. F. Fairman, R. T. Henry, J. R. North, D. A. Quarles, W. C. Smith, E. W. Davis, H. B. Wolf, and L. M. Robertson

HASKINS & SELLS
CERTIFIED PUBLIC ACCOUNTANTS

1 EAST 44TH STREET
NEW YORK 17

May 19, 1947

American Institute of Electrical Engineers,
33 West 39th Street, New York.

Dear Sirs:

We have examined the balance sheet of the American Institute of Electrical Engineers, and schedule of securities owned, as of April 30, 1947, and the related statements of cash receipts and disbursements of operating and restricted funds for the year ended that date, have reviewed the accounting procedures of the Institute, and have examined its accounting records and other evidence in support of such financial statements. Our examination was made in accordance with generally accepted auditing standards applicable in the circumstances and included all auditing procedures we considered necessary, which procedures were applied by tests to the extent we deemed appropriate in view of the system of internal control.

In our opinion, the accompanying balance sheet, schedule of securities owned, and statements of cash receipts and disbursements fairly present, respectively, the financial condition of, and securities owned by, the Institute as of April 30, 1947, and its recorded cash receipts and cash disbursements for the year ended that date, in conformity with generally accepted accounting principles and practices applied on a basis consistent with that of the preceding year.

Yours truly,

(*Signed*) HASKINS & SELLS

AMERICAN INSTITUTE OF ELECTRICAL ENGINEERS

Balance Sheet, April 30, 1947

Exhibit A

ASSETS

Property Fund Assets:		
One-fourth interest in physical properties of United Engineering Trustees, Inc.:		
Land, buildings, and equipment (less depreciation and renewal reserve)	$352,018.07	
Funded depreciation and renewal reserve	146,430.41	
Total	$498,448.48	
Equipment:		
Library (volumes and fixtures)—estimated value	36,366.37	
Office furniture and fixtures (less reserve for depreciation, $28,875.98)	12,361.48	
Works of art, etc.	3,001.35	
Cash (no change during year)	612.91	
Total property fund assets		$ 550,790.59
Restricted Fund Assets:		
Securities—at cost, less reserve, $1,788.15 (quoted market value, $629,189.88)—Schedule 1	$609,819.96	
Cash (Exhibit *C*)	23,488.62	
Accrued interest receivable	125.40	
Total restricted fund assets		633,433.98
Operating Fund Assets:		
Cash (not including $1,664.75 for Federal taxes withheld from employees)—(Exhibit *B*)	$ 6,883.37	
Accounts receivable:		
Members—for dues (less reserve, $4,000.00)	9,597.71	
Advertisers	2,004.52	
Miscellaneous	3,098.89	
Accrued interest receivable	6,673.27	
Inventories:		
TRANSACTIONS, etc.	1,275.00	
"Electrical Definitions"	2,449.20	
Work in process (May issue of *ELECTRICAL ENGINEERING*, etc.)	8,207.86	
Text and cover paper	14,164.08	
Badges	5,476.43	
Total operating fund assets		59,830.33
Total		$1,244,054.90

LIABILITIES

Property Fund Reserve		$ 550,790.59
Restricted Fund Reserves:		
Reserve capital fund	$605,931.88	
Life membership fund	8,733.46	
Member-for-Life fund	6,908.41	
International Electrical Congress of St. Louis library fund	6,264.83	
Lamme Medal fund	4,440.44	
Mailloux fund	1,154.96	
Total restricted fund reserves		633,433.98
Operating Fund Reserves, Liabilities, etc.:		
Accounts payable	$ 25,595.93	
Deferred income:		
Dues received in advance	3,699.09	
Entrance fees and dues advanced by applicants for membership	2,145.60	
Subscriptions to publications received in advance	17,777.86	
Miscellaneous (including unallocated receipts)	1,367.33	
Operating fund reserves	9,244.52	
Total operating fund reserves, liabilities, etc.		59,830.33
Total		$1,244,054.90

AMERICAN INSTITUTE OF ELECTRICAL ENGINEERS

Statement of Cash Receipts and Disbursements of Operating Fund for the Year Ended April 30, 1947

Exhibit B

Cash on Deposit with The National City Bank of New York, May 1, 1946 (not including $1,302.87 for Federal taxes withheld from employees)			$ 81,379.47
Receipts:			
Dues (including $143,232.00 allocated to *ELECTRICAL ENGINEERING* subscriptions)		$305,014.02	
Advertising		106,499.51	
TRANSACTIONS subscriptions		9,770.77	
ELECTRICAL ENGINEERING subscriptions		27,811.67	
Miscellaneous publications (preprints, Standards, special reports, etc.)		32,529.24	
Students' fees		24,217.70	
Entrance fees		19,901.62	
Membership badges		4,443.03	
Transfer fees		3,140.38	
Interest and dividends on investments of Restricted Capital Fund		18,804.53	
Miscellaneous		306.23	
Total receipts			552,438.70
Total			$633,818.17
Disbursements:			
Publications expense:			
ELECTRICAL ENGINEERING text	$132,721.26		
ELECTRICAL ENGINEERING advertising	45,163.74	$177,885.00	
TRANSACTIONS		10,571.30	
PROCEEDINGS		2,633.69	
"Year Book"		7,488.69	
Miscellaneous publications (preprints, Standards, etc.)		26,043.51	
Institute meetings		19,020.94	
Institute Sections		60,532.69	
Institute Branches		4,695.60	
Finance committee		769.99	
Headquarters committee		263.50	
Membership committee		13,295.59	
Standards committee		13,100.27	
Technical committees		5,829.82	
Committee on Institute publicity		1,365.53	
Planning and co-ordination committee		9,281.06	
Edison Medal committee		244.01	
Committee on collective bargaining and related matters		3,458.91	
Forward		$356,479.90	$633,818.17
Total (forward)			$633,818.17
Total (forward)		$356,479.90	$633,818.17
Disbursements (forward)			
Traveling expenses:			
Geographical Districts:			
Executive committees		9,294.64	
Vice-presidents		1,489.03	
Conferences on Student activities		7,017.45	
Board of directors		9,435.18	
Nominating committee		1,696.85	
President's appropriation		3,153.72	
AIEE representatives		363.70	
Administrative expenses		71,158.12	
Geographical Districts—Branch paper prizes		235.88	
Institute prizes—national		412.24	
Retirement system AIEE—normal contribution		5,816.89	
American Co-ordinating Committee on Corrosion		50.00	
American Standards Association		1,500.00	
Canadian Radio Technical Planning Board		10.00	
Engineers' Council for Professional Development		2,687.50	
Engineering Foundation Project—Welding research		250.00	
Engineers Joint Council:			
Economic Status of the Engineer		6,033.43	
General expenses		981.15	
Hoover Medal		57.69	
John Fritz Medal		220.93	
National Committee State Board Engineering Examiners		500.00	
National Fire Protection Association—Dues		60.00	
Radio Technical Planning Board		400.00	
United Engineering Trustees, Inc.			
Building assessment		17,813.56	
Library assessment		11,845.00	
International Commission on Illumination		450.00	
Representation on labor panel and incidental expenses		2,275.54	
Lamme Medal expense (see Exhibit C)		107.15	
Membership badges		8,096.38	
Legal services		250.00	
Office furniture and fixtures and repairs		4,016.00	
Headquarters repairs, etc.		1,232.66	
Rent, etc., 500 Fifth Avenue		3,655.30	
Total		$529,045.89	
Transfers:			
To reserve capital fund		96,011.59	
To Member-for-Life fund		1,877.32	
Total disbursements			$626,934.80
Cash on Deposit With The National City Bank of New York, April 30, 1947 (not including $1,664.75 for Federal taxes withheld from employees)			$ 6,883.37

AMERICAN INSTITUTE OF ELECTRICAL ENGINEERS

Exhibit C. Statement of Cash Receipts and Disbursements of Restricted Funds for the Year Ended April 30, 1947

		Restricted Funds					
	Total	Reserve Capital Fund	Member-for-Life Fund	Life Membership Fund	International Electrical Congress of St. Louis Library Fund	Lamme Medal Fund	Mailloux Fund
Cash on Deposit With The National City Bank of New York and Various Savings Banks, May 1, 1946	$ 47,304.66	$ 36,676.03	$5,031.09	$3,637.91	$ 661.80	$160.00	$1,137.83
Receipts:							
Proceeds from sales, etc. of securities	$ 32,223.13	$ 21,612.16		$5,153.12	$5,457.85		
Income from bonds	377.34			122.95	94.39	$160.00	
Interest on bank balances	70.28			53.15			$ 17.13
Transfers from operating fund	97,888.91	96,011.59	1,877.32				
Life membership fees	327.90			327.90			
Liquidating dividend—International Match Realization Company, Ltd.	63.00	63.00					
Total receipts	$130,950.56	$117,686.75	$1,877.32	$5,657.12	$5,552.24	$160.00	$ 17.13
Total	$178,255.22	$154,362.78	$6,908.41	$9,295.03	$6,214.04	$320.00	$1,154.96
Disbursements:							
Purchase of securities	$153,997.08	$143,386.11		$5,153.12	$5,457.85		
Transfer to operating fund	609.52			609.52			
Purchase of medal, cost of engraving, etc. (exclusive of $107.15 paid from general fund)	160.00					$160.00	
Total disbursements	$154,766.60	$143,386.11		$5,762.64	$5,457.85	$160.00	
Balance on Deposit With The National City Bank of New York and Various Savings Banks, April 30, 1947	$ 23,488.62	$ 10,976.67	$6,908.41	$3,532.39	$ 756.19	$160.00	$1,154.96

Securities Owned, April 30, 1947

Schedule 1

	Principal Amount of Bonds or Number of Shares of Stock	Restricted Funds: Reserve Capital Fund	Life Membership Fund	International Electrical Congress Library Fund	Lamme Medal Fund	Total
Railroad Bonds:						
Atlantic Coast Line First Consolidated 4%, due 1952	$ 4,000.00				$4,253.78	$ 4,253.78
Baltimore & Ohio, Pittsburgh, Lake Erie & West Virginia System 4%, due 1980	10,000.00	$ 6,450.00				6,450.00
Chicago & Erie Railroad Company 5% first mortgage, due 1982, Registered	1,000.00	1,105.00				1,105.00
New York Central Railroad Company 4% series *A* consolidated mortgage, due 1998	15,000.00	9,812.50				9,812.50
Northern Pacific Railway Company 4½% collateral trust, due 1975	15,000.00	15,307.50				15,307.50
St. Louis-San Francisco Railway Company 4% series *A*, first mortgage, due 1997 (a)	1,200.00	1,200.00				1,200.00
St. Louis-San Francisco Railway Company 4% series *A*, first mortgage, scrip (a)	198.00	198.00				198.00
St. Louis-San Francisco Railway Company 4½% series *A*, second mortgage, income bonds, due 2022 (a)	1,300.00	1,300.00				1,300.00
St. Louis-San Francisco Railway Company 4½% series *A*, second mortgage, income bonds, scrip (a)	61.10	61.10				61.10
Total railroad bonds		$ 35,434.10			$4,253.78	$ 39,687.88
Public Utility Bonds:						
American Telephone & Telegraph Company 2¾% convertible debentures, due 1961	$25,000.00	$ 17,163.50	$5,153.12	$5,457.85		$ 27,774.47
New York & Queens Electric Light & Power Company 3½% first and consolidated mortgage, due 1965	10,000.00	10,400.00				10,400.00
Total public utility bonds		$ 27,563.50	$5,153.12	$5,457.85		$ 38,174.47
United States Government Bonds:						
Treasury Savings bonds series *D*, due July 1, 1949	$10,000.00	$ 7,644.00				$ 7,644.00
Treasury Savings bonds series *D*, due January 1, 1950	10,000.00	7,500.00				7,500.00
Treasury bonds 2%, due 1950/48	77,000.00	78,130.94				78,130.94
Treasury bonds 2%, due 1950/48, Registered	3,000.00	3,060.94				3,060.94
Treasury bonds 2%, due March 15, 1952/50	25,000.00	25,617.19				25,617.19
Defense bonds series *F*, due June 1, 1953	34,000.00	25,160.00				25,160.00
Defense bonds series *G*, 2½%, due December 1, 1954	18,000.00	18,000.00				18,000.00
Treasury Savings bonds series *G*, 2½%, due September 1, 1955	40,000.00	40,000.00				40,000.00
Treasury Savings bonds series *G*, 2½%, due November 1, 1956	17,000.00	17,000.00				17,000.00
Treasury Savings bonds series *G*, 2½%, due May 1, 1957	20,000.00	20,000.00				20,000.00
Treasury Savings bonds series *G*, 2½%, due October 1, 1957	30,000.00	30,000.00				30,000.00
Total United States Government bonds		$272,113.07				$272,113.07
Capital Stock:						
American Can Company	60 shares	$ 4,988.40				$ 4,988.40
American Telephone and Telegraph Company	100 shares	17,454.15				17,454.15
Atchison, Topeka & Santa Fe Railway Company preferred	200 shares	19,174.71				19,174.71
Boston Edison Company	200 shares	4,927.50				4,927.50
Commonwealth Edison Company	200 shares	7,580.68				7,580.68
Consolidated Natural Gas Company	11 shares	221.92				221.92
Dow Chemical Company $4.00 cumulative preferred series *A*	100 shares	11,547.50				11,547.50
Eastman Kodak Company	60 shares	10,694.11				10,694.11
E. I. du Pont de Nemours & Company	80 shares	13,096.68				13,096.68
General Electric Company	200 shares	7,748.66				7,748.66
General Motors Corporation $5.00 preferred	200 shares	25,820.00				25,820.00
General Motors Corporation	100 shares	4,235.53				4,235.53
Insurance Company of North America	100 shares	10,847.50				10,847.50
International Harvester Company	100 shares	5,030.50				5,030.50
International Match Realization Company, Ltd., voting trust certificates for capital shares of International Match Corporation	6 shares*	1,788.15*				1,788.15*
Louisville & Nashville Railroad Company	100 shares	6,278.13				6,278.13
Ohio Edison Company 4.40% preferred	200 shares	21,279.25				21,279.25
Pacific Gas and Electric Company	200 shares	8,784.35				8,784.35
Public Service Corporation of New Jersey 6% preferred	100 shares	11,150.00				11,150.00
St. Louis-San Francisco Railway Company voting trust certificates for 5% series *A* preferred stock (a)	21 1800/10000ths shares	582.75				582.75
St. Louis-San Francisco Railway Company voting trust certificates for common stock (a)	42 6000/10000ths shares	357.00				357.00
Scoville Manufacturing Company 3.65% cumulative preferred	100 shares	10,111.25				10,111.25
Sears, Roebuck and Company	400 shares	6,014.97				6,014.97
Standard Oil Company of Indiana	200 shares	8,170.32				8,170.32
Standard Oil Company of New Jersey	200 shares	9,601.26				9,601.26
Union Carbide & Carbon Corporation	100 shares	7,277.42				7,277.42
United Fruit Company (b)	300 shares	11,985.00				11,985.00
United States Steel Corporation 7% cumulative preferred	100 shares	14,885.00				14,885.00
Total capital stocks		$261,632.69				$261,632.69
Total		$596,743.36	$5,153.12	$5,457.85	$4,253.78	$611,608.11
* Less reserve in full for securities considered to be of doubtful value		1,788.15				1,788.15
Total Securities, Less Reserve		$594,955.21	$5,153.12	$5,457.85	$4,253.78	$609,819.96

(a) In connection with the reorganization of the St. Louis-San Francisco Railway Company the securities marked (a) were received during the year in exchange for St. Louis-San Francisco Railway Company 5% prior lien mortgage series *B*, due 1950 (certificates of deposit), registered, stamped, which were surrendered.

(b) Stock was split in June 1946 by issuance of two additional shares for each one held.

New AIEE Publication Policy Becomes Effective in January 1947

By Charles F. Wagner, Chairman AIEE Publication Committee

One of the fundamental purposes of the Institute is the dissemination to its members of information concerning new theories, new apparatus, and new developments throughout the electrical field. Incidental to its responsibility under this objective, and pursuant to action of the board of directors (*EE, June 1946, p 270*) the AIEE publication committee has been developing ways and means of improving the Institute's publication policy and procedure with the objectives of better serving the greatly enlarged and rapidly growing membership and of covering adequately the active and ever-growing electrical field.

The purpose of this report is to describe and explain the modifications in present publication policy and procedure constituting the new AIEE publication policy, which is to become effective immediately with 1947 publications. Before discussing the new policy, it is desirable to review the present policy which now falls somewhat short of membership needs, and to define the various kinds of publication materials that come to the Institute for consideration.

PRESENT PUBLICATION PLAN

The present [1946] AIEE publication policy was established in 1940. Most of the material published by the Institute is submitted as technical papers. These papers are referred first to the technical program committee for review and approval; if approved, they then are scheduled for presentation at a national or District meeting, where they are open for discussion.

Under the present publication policy, all technical papers so approved and recommended by the technical program committee are published in the AIEE *Transactions*, which is issued annually covering a calendar year and which serves as the permanent repository of material covering the progress and development of the electrical art. A *Transactions* section of the monthly magazine *Electrical Engineering* is set aside and allocated for publication of approved technical papers, this being in actuality a monthly preprint of identical pages which will constitute the current annual *Transactions* volume. Because of cost limitations, space has not been available in the monthly magazine for all approved papers. The overflow papers are printed twice yearly, in June and in December, in a special publication known as the "Supplement to *Electrical Engineering*—*Transactions* section." These supplements are available to Institute members at 50 cents each or $1 per year. Discussions of technical papers do not appear in *Electrical Engineering*, but first become available to the membership in the supplements, after a lapse of several months; for example, winter meeting discussions in the June supplement. Thus a member automatically receives most of the technical papers in the *Transactions* sections of *Electrical Engineering*, and by purchasing the supplements receives all of the remaining approved technical papers and all approved pertinent discussion. All this material appears in the annual AIEE *Transactions*. Discussions, however, do not appear on *Transactions* pages immediately adjoining the paper to which they apply, but appear elsewhere in the volume.

Certain of the papers submitted by contributors to the technical program committee and the technical committees for review and consideration are adjudged to be appropriate and timely for presentation and discussion at a national or District meeting, although they are deemed to be inappropriate for permanent record. Although these papers are presented at meetings, they are not published in the *Transactions* sections of *Electrical Engineering*, the supplements, or the *Transactions*. In current parlance they are known as "ACO" (advance copies only) papers; formally, this series of papers is designated as "AIEE miscellaneous papers" to distinguish them from the regular "AIEE technical papers" series.

To facilitate and to promote discussion of papers, individual pamphlet copies of each technical paper (regular or ACO) are issued in advance of the meetings at which the papers are scheduled to be presented and discussed. These pamphlets are known as "advance copies" or "preprints" of the technical papers. As the time element is of essential importance in relation to the meetings programs and speed is required in the physical reproduction of these papers to make them available to interested members as far as possible in advance of their presentation at meetings, a quick method of reproduction is resorted to that is known as the photolithographic or "photo-offset" process. In this process of reproduction, the author's original manuscript copy and illustrations are reproduced photographically approximately in facsimile, and without any of the intervening steps necessary for regular printing. The photolithographic process is a more expensive reproduction process than printing where substantial quantities are involved, but does offer the advantage of speed in reproduction. These "advance copies" or "preprints" therefore are produced only in limited quantities, and are made available to members approximately at cost.

To facilitate the efforts of District meeting committees in preparing programs best adapted to the timely and particular interests of the region to be served by District meeting, another class of paper has been given a recognized status by the Institute. This class of paper, known officially as "District papers" (DP) is authorized for acceptance for presentation and discussion at a District meeting solely at the discretion of the District meeting committee and without the requirement of advance review by the technical program committee or the technical committees. Correspondingly, such papers have status only as parts of the local District meetings programs, where they may be discussed along with other papers, but carry with them no commitment or obligation for publication of either paper or discussion. In some instances, of course, the subject matter of District papers may be developed further and processed through the regular AIEE channels previously discussed and ultimately become eligible for inclusion in *Transactions*. These District papers normally are not prepared in pamphlet form by the Institute, nor are they generally available even at the meetings where they are scheduled for presentation, except in instances where authors may provide mimeographed or other copies.

Still another class of paper is involved currently in national and District meetings programs, known as "conference papers" (CP). These conference papers in a great many instances are not papers at all, but informal oral presentations made at conference sessions or round-table discussions which are organized from time to time on subjects of current interest under the encouragement of the technical program committee and the direct sponsorship of one or more of the technical committees. Like the previously mentioned District papers, conference papers are wholly informal presentations, not reproduced or distributed by the Institute, and carry no commitment for publication of paper or discussion. Such papers may be processed subsequently through regular channels and ultimately become *Transactions* material. Authors of conference papers sometimes make a limited number of mimeographed or other copies available at their own expense for use at the meetings. Otherwise, to preserve the complete informality of the conference session, there is no record of what transpires at such meetings or conferences, except as it may be covered in new reports in *Electrical Engineering*.

Electrical Engineering, under the present publication policy, contains many engineering and other articles, news items, personals, and other material of current general interest to AIEE members in addition to the *Transactions* section previously mentioned. This material is drawn from AIEE and other sources. The choice of material, as well as the general management and publication of the magazine, is the responsibility of the editor.

CURRENT PROBLEM

The electrical art has become so broad in scope and so specialized in nature that any particular technical program paper now is of interest to only a relatively small portion of the entire membership. Thus, under the present publication plan the average member is receiving many specialized papers in fields of relatively little interest to him. This repeatedly has been brought to the attention of the publication committee with the corollary suggestion that in most such instances an abstract or digest presenting on an informational basis the essence of such specialized papers would better satisfy the average member's requirement, leaving the full technical paper for the specialist. Under the present publication policy, the space required to print these technical papers in full in *Electrical Engineering* crowds out material of broader general interest, a situation that is growing more acute as the national and District meeting activities grow and the number of technical papers increases. The policy requiring publication of these papers in full in *Electrical Engineering* places undesirable restrictions and limitations upon the editor in his efforts, under his assigned responsibility to produce in *Electrical Engineering* a maga-

zine of greater service and more general appeal to the membership at large.

Discussions and rebuttals of technical papers, under the present publication plan, appear as already noted only in the *Transactions* and in the "Supplement to *Electrical Engineering—Transactions* section," and in any event only after the lapse of so long a time that much of the interest in the discussion is lost. Further, such discussions do not appear on pages immediately adjoining the papers to which they apply, thus necessitating reference to two different locations to obtain the complete story concerning any particular paper. The publication committee has received continual criticism of this practice.

NEW PUBLICATION PLAN

In the new publication plan, the *Transactions* section will be eliminated from *Electrical Engineering* and in its stead will be established a new series of publications to be known as "AIEE Proceedings" which will consist principally of all technical papers with their discussions, and which also may contain other appropriate material from national and District meetings. Individual members will be given the opportunity to select designated groups of these technical papers to be received free of charge, and other papers to be received as desired at a nominal charge to cover cost. More specifically the publications and policy of the Institute may be described as follows:

1. Electrical Engineering. Coincidental with the elimination of the *Transactions* section, the general-interest content of *Electrical Engineering* will be expanded, enhanced, and given greater flexibility to satisfy more fully the current and future requirements of the membership. It will be characterized especially by the following attributes.

(*a*). Subject only to general policy, the management and publication of *Electrical Engineering* will be entirely the responsibility of the editor.

(*b*). The general-interest content will be approximately doubled, contemplated to be at least 100 pages per month.

(*c*). The contents will be divided broadly into two general categories: (1) general articles, to be drawn from all currently available sources including material submitted for technical program papers after, but regardless of, action by the technical program committee, selected on the basis of timeliness and general-interest value to the membership at large and treated accordingly; (2) news material, comprehensively and appropriately reflecting all AIEE and related activities, also appropriately reflecting other current activities of interest and significance to the membership. For example, with reference to AIEE programs, whether technical sessions or conferences, it is contemplated that all technical program papers and all other appropriate material will be reflected currently in *Electrical Engineering* for the purpose of keeping the membership fully and currently informed.

(*d*). Summary abstracts of technical papers will continue to be included as at present and will be published as far as possible in advance of the meeting at which the papers are scheduled for presentation and discussion.

(*e*). The weight and quality of both inside and cover paper stock will be improved. This will recover the losses sustained incidental to United States Government wartime regulations and policies, and should obviate the justifiable criticisms that have been received from readers and advertisers concerning the unsatisfactory quality of reproduction of illustrations and other matter.

(*f*). A more aggressive advertising policy will be inaugurated to capitalize more fully upon the established prestige and substantial standing of *Electrical Engineering*.

(*g*). Distribution will continue to be made automatically to the entire AIEE membership; to be available also to nonmembers at an appropriate subscription price in accordance with postal regulations and as provided in AIEE bylaw 103 and 104.

2. Preprints. To encourage and facilitate discussion of technical papers at national and District meetings, the present practice of issuing advance pamphlet copies or "preprints," of technical program papers by the photolithographic process or an appropriate equivalent will be continued. Distribution of this material is to be made as follows.

(*a*). The minimum necessary number of copies will be available for distribution without charge by or at the specific and detailed request of the committee responsible for the development and approval of the manuscript in question. Such distribution is intended to be made prior to the meeting at which the paper is scheduled for presentation and discussion, and primarily for the purpose of stimulating qualified discussion.

(*b*). Copies will be available upon request to the entire AIEE membership at cost, such cost to include all production, overhead, and distribution costs; available to others at 100 per cent above members price. Following is the schedule of members prices:

Size of Pamphlet (Pages)	At Registration Desk	By Mail
12 or less	$0.10	$0.15
16	.15	.20
20	.20	.25
24 or more	.25	.30

3. Proceedings. For the purpose of better serving those among the membership who are especially interested in the full and complete technical and mathematical details of subject matter within the field of their particular professional interest, a new series of publications is to be established, to be known as "AIEE *Proceedings*." The *Proceedings* will contain the full text of all papers approved by the technical program committee for publication in *Transactions* and for presentation at national or District meetings together with all discussions of those papers as approved by the technical program committee; also, may contain "miscellaneous (ACO) papers" approved by the technical program committee for presentation at national or District meetings; and other appropriate material. The *Proceedings* thus is planned to contain all material now published in the *Transactions* sections of the 12 monthly issues of *Electrical Engineering* and the two semiannual supplements, and in addition a very considerable amount of meeting material heretofore not published.

To provide maximum flexibility in production and distribution and thereby expedite materially the distribution of such material, and in deference to the long expressed wishes of the technical specialists among the Institute's membership who are most interested in the full and complete details of technical papers and their related discussions, the *Proceedings* will be issued in the form of individual printed pamphlets. Each pamphlet will contain the full text of an approved technical paper, and all approved pertinent discussion. The factors which will control the date of completion and initial distribution of this material will be (*a*) the determination by the technical program committee that no discussion is available or (*b*) the release by the technical program committee of discussion which it has approved for publication. On this basis, this material will be available to those who especially want it several months earlier than is possible under the present publication plan.

Each Fellow, Member, and Associate of the AIEE will be given an opportunity to select for receipt free of charge a limited quantity of the total number of *Proceedings* sections (pamphlets), the quantity designed to be sufficiently generous to enable the average member to obtain those papers in which he is most intimately concerned. Others will be available at cost. *Proceedings* sections also will be available at cost to Student Members.

4. Annual Transactions. Current policies and procedures with reference to AIEE *Transactions* are to be continued without change, except that the flexibility introduced by the previously discussed changes in publication procedure will enable discussions to be assembled with the papers to which they apply. Bound volumes will continue to be issued on the basis of material presented during a calendar year, in single or multiple volumes, depending upon the amount of material and other considerations. *Transactions* will contain all formal AIEE technical papers and related discussion as approved by the AIEE technical program committee, and other record material appropriately approved. Distribution will continue on the basis of advance order; to the AIEE membership at cost, to others at appropriately higher prices.

5. Special Publications. To provide a facility in a field of publication services heretofore not satisfied adequately by the Institute, a series of "AIEE Special Publications" will be established and its use encouraged. It is contemplated that such publications will be issued from time to time and in appropriate relation to other AIEE publications to accommodate material of especial value and importance in its field but of limited general interest or applicability, or material peculiarly convenient and appropriate in the form of separate and substantially bound books or booklets. It is contemplated that these special publications may accommodate material highly technical or mathematical in content, or specialized in subject matter, such as the "AIEE Lightning Reference Book," the AIEE Joint Subcommittee report "Telemetering, Supervisory Control, and Associated Circuits," and the "Bibliography on Automatic Stations, 1930–1941," and other bibliographies, consolidated reprints, special reports, surveys, and similar material.

The format, typographical style, paper,

and printing will be of a quality appropriate to an AIEE publication and commensurate with their positions in the AIEE family of publications. Special publications are to be issued on an entirely self-supporting basis, the proceeds from sales in effect consituting a revolving fund for continuation and stimulation of the project.

Distribution of special publications is to be on the basis of individual order, at cost to the AIEE membership; to others at 100 per cent above the prices which will be set for members.

6. Reprint Service. As a special service which has proved to meet many membership needs, the present practice of publishing quantities of reprints or preprints of AIEE published material will be continued. Such reprints usually will be produced on the basis of specific orders, but occasionally upon the basis of anticipated need. Such reprint services are to be performed on an entirely self-supporting basis.

7. Annual Index. To provide a consolidated single authoritative reference guide to all AIEE material published during any calendar year, a complete composite AIEE annual index is planned, to cover appropriately the content of *Electrical Engineering*, *Proceedings*, *Transactions*, and special publications. This index will continue the basic alphabetical multientry subject listing system originally developed by *Electrical Engineering* and used with eminent success over a period of many years. Distribution will be automatic and without charge to the AIEE membership and to regular subscribers to AIEE publications; upon request to others.

8. Yearbook. Publication of the Yearbook is to be continued as at present. Distribution is on the basis of individual requests.

9. Conference Papers. The informal AIEE conference papers will be treated very much as in the past. As such, they do not have publication status, although the editor of *Electrical Engineering* specifically is authorized to make appropriate use of conference material subject to the approval of the authors involved.

New AIEE Committee Organization

THE ADMINISTRATION of committee activities of the Institute gradually is evolving toward greater unification of groups which have related interests. The board of directors, at its April meeting in Worcester, Mass. (*EE, June '47, pp 597–8*), set in motion a series of changes intended to revitalize the entire committee structure. Immediately after the meeting, Blake D. Hull, then the presidential nominee, started the formation of the new committee organization in order to enter upon the new year with a full personnel.

Prior to the Worcester meeting, the technical committees had been operating informally in a group or divisional organization as suggested by the directors at their Asheville, N. C., meeting in 1946 (*EE, June '46, pp 269–70*). At Worcester, the Asheville resolution was amended to read as follows:

Resolved that it is the sense of the board of directors that the development of the technical committee activities of the Institute should be guided by the following principles:

1. That such additional technical committees should be organized as may be needed to cover the important items of electrical technology.

2. That these technical committees should be grouped in appropriate divisions or groups with a co-ordinating committee for each group fairly compact in numbers and consisting essentially of a group chairman and the chairmen of the technical committees comprising the group.

3. That each year the group co-ordinating committees make informal recommendations to the presidential nominee through the secretary on the membership and organization of the whole technical committee structure, including at least two alternates for every co-ordinating committee chairmanship.

4. That in such recommendations a reasonable turnover of the committee personnel be the intention. Further, that it is the intent of this board that the responsible committees should proceed with such changes as they may determine to be necessary and proper to effectuate these principles unless the proposed changes are at variance with either the constitution or the bylaws, in which event they shall be referred back to the board for further consideration.

The directors voted to establish initially four co-ordinating committees for the technical committees, and also to establish several new technical committees in addition to those previously established at their January and October meetings. The new technical committee setup (including several changes adopted by the board of directors on August 11, 1947) follows:

Power Co-ordinating Committee

Carrier current committee
Electronic power converter committee
Insulated conductor committee
Power generation committee
Protective devices committee
Relay committee
Rotating machinery committee
Substation committee
Switchgear committee
System engineering committee
Transformer committee
Transmission and distribution committee

Industry Co-ordinating Committee

Chemical, electrochemical, and electrothermal committee
Electric heating committee
Electric welding committee
General industry applications committee
Industrial control committee
Industrial power systems committee
Mining and metal industry committee

Communication and Science Co-ordinating Committee

Basic sciences committee
Communication, committee
Electronics committee
Instruments and measurements committee
Nucleonics committee
Therapeutics committee

General Applications Co-ordinating Committee

Air transportation committee
Domestic and commercial applications committee
Land transportation committee
Marine transportation committee
Production and application of light committee

In general the name of the committee describes its functions. Other duties are defined in sections 65, 85, 86, and 108 of the bylaws of the Institute.

No changes in the constitution and no major changes in the bylaws were required to accomplish the reorganization. As before, all committees are directly responsible to the board of directors; as before, and as provided in the bylaws "in respect of matters affecting standardization or nomenclature, the several committees named shall submit to the Standards committee such recommendations as they may deem proper;" as before, "in respect of papers and discussions, these committees shall report to the technical program committee to correlate the work of their committees in such a manner as effectively will provide adequate opportunity for discussion of each of the various topics included within the scope of Institute activity, and to arrange the presentation and discussion of such papers as may receive its approval." The chairman of each technical committee will continue to be a member of the technical program committee which also includes the chairmen of technical co-ordinating committees, the committees on planning and co-ordination, safety, Standards, educa-

tion, and research. The technical committees themselves will do the work of co-ordinating and correlating their activities within their own groups.

One year of experience with this organization scheme leads to the belief that a combination of flexibility and efficiency can be achieved which will give complete and current coverage to all areas of the large field of technical activity of the Institute. Subjects, papers, and duties can be transferred among committees and among groups or divisions. Co-operation, under the co-ordinating committees, comes about by common consultation and common consent.

A similar grouping of activities will be tried among the general committees. At Worcester the directors, in addition to endorsing the principle of divisional organization, voted to establish two new co-ordinating committees, one on professional and one on administrative activities, for the coming year. Also established by the directors at their Worcester meeting, is a new general committee, the management committee, which is included in the professional activities group. The new groups follow:

Administration Group Co-ordinating Committee

Board of examiners
Constitution and bylaws committee
Headquarters committee
Institute publicity committee
Members-for-life fund committee
Membership committee
Transfers committee

Professional Activities Co-ordinating Committee

Award of Institute prizes committee
Charles LeGeyt Fortescue fellowship committee
Code of principles of professional conduct committee
Edison Medal committee
Education committee
Lamme Medal committee
Management committee
Registration of engineers committee
Student Branches committee

Not included in any divisional group are the remaining general committees which will continue to operate as at present. These are

Finance committee
Planning and co-ordination committee
Publication committee
Research committee
Safety committee
Sections committee
Standards committee
Technical program committee

The committee on planning and co-ordination, however, will include within its membership the chairmen of the six co-ordinating committees. The divisional structure of the general committees will be worked out in more complete detail as the next administrative year progresses.

The following sections list the various technical committees. The co-ordinating committee is given first, then the name and scope of the various committees represented in that particular co-ordinating committee. Personnel are listed on pages 9-12.

Power Group

POWER CO-ORDINATING COMMITTEE

M. J. Steinberg, *chairman*, Consolidated Edision Company of New York, Inc., 4 Irving Place, New York, N. Y.
H. W. Collins, *vice-chairman*
R. T. Henry
A. J. Krupy
Frank Thornton, Jr.
C. C. Wilson, *secretary*
Ex-officio: chairmen of technical committees in the power group

CARRIER CURRENT COMMITTEE

Scope—Treatment of all matters in which the dominant factors are the design, construction, and operation of equipment and circuits for the application of carrier currents in the generation, transmission, and distribution of electric power. Included in the scope of this committee shall be treatment of the following:

Carrier current equipment and circuits for
  Relaying
  Control (supervisory, load, frequency, and so forth)
  Metering
  Communication as applied to power system use
also:
Line traps
Coupling capacitors

ELECTRONIC POWER CONVERTER COMMITTEE

Scope—Treatment of all matters in which the dominant factors are the design, construction, and operation of equipment and circuits for the electronic conversion of electric energy into other phases of electric energy in the generation, transmission, distribution, and utilization of electric power. This scope shall not include hot-cathode-type converters which have been assigned to the hot cathode electronic power converters subcommittee of the electronics committee. There shall be included in this scope treatment of the following:

Electronic converters for motor control (joint with industrial control committee)
Electronic power rectifiers and inverters
Electronic frequency changers

Matters relating to electronic converters specifically designed for applications covered by certain other technical committees such as communication, transportation, industrial power systems, and electrochemical applications may be treated jointly with that committee if emphasis is on general principles; or exclusively by the application committee if emphasis is on the particular requirements of the application.

INSULATED CONDUCTOR COMMITTEE

Scope—Treatment of all matters in which the dominant factors are the design, construction, and operation of insulated conductors and the accessories thereto used in the generation, transmission, distribution, and utilization of electric power. Included in this scope shall be treatment of the following:

Cable supply systems (including solid, oil-filled, and gas-filled cables)
Insulated wire and cable
Accessories (including potheads, wiring ducts, and conduit, not including insulated bus runs as in metal-clad switchgear)
Structures (joint with transmission and distribution committee)
Cable characteristics
Insulations
Sheaths and coverings
Utilization wiring systems

Special purpose cables
Tests and measurements

Matters relating to insulated conductors specifically designed for applications covered by certain other technical committees such as communication, transportation, and electric heating may be treated jointly with that committee if emphasis is on general principles; or exclusively by the application committee if emphasis is on the particular requirements of the application.

POWER GENERATION COMMITTEE

Scope—Treatment of all matters relating to the design, construction, and operation of electric power generating stations, including auxiliary equipment incidental thereto (where such equipment is not otherwise specifically assigned to other technical committees).

Treatment of all matters pertaining to the design, construction, and operation of steam boiler plants, dams, reservoirs, nuclear piles, and other primary sources of energy to prime movers; also the prime movers themselves used in the generation of electric energy.

Treatment of all matters relating to the economics of generation and supply of electric power within individual generating stations.

Included in this scope shall be treatment of the following:

Prime movers (hydro, steam, oil, gas, nuclear, wind power)
Speed governors for prime movers
Station load and frequency control (joint with system engineering committee)
Control systems (joint with substation committee)
Excitation systems and voltage regulators
Station design (generating plant)
Auxiliaries and accessories
Production costs—design and operating economics (separate station)
Co-ordination of prime mover and electric machine design
Bus design (joint with switchgear and substation committees)

PROTECTIVE DEVICES COMMITTEE

Scope—Treatment of all matters in which the dominant factors are the design, construction, and operation of devices and equipment to limit or prevent damage to electric power generation, transmission, or distribution systems, or equipment; such damage arising from excessive current, voltage, or from lightning. Included in this scope shall be treatment of the following:

Capacitors (where used as protective devices)
Lightning protective devices (such as arrestors, protector tubes, air gaps, and expulsion gaps)
Fault limiting devices (including neutral grounding devices)
Lightning investigations (joint with transmission and distribution committee)
Reactors and grounding transformers (joint with transformer committee)

Matters relating to protective devices specifically designed for applications covered by certain other technical committees such as industrial control, industrial distribution systems, or communication, may be treated jointly with that committee if emphasis is on general principles; or exclusively by the application committee if emphasis is on the particular requirements of the application.

RELAY COMMITTEE

Scope—Treatment of all matters in which the dominant factors are the design, construction, and operation of protective relays including all matters necessary to the functioning of such relays employed in the generation, transmission, and distribution of electric energy. Included in this scope shall be treatment of the following:

Relays and automatic devices (fault and load discriminating)
Relay protective schemes, including relay co-ordination
Potential devices
Bushing and instrument transformers (joint with instruments and measurements committee)

Matters relating to relays specifically designed for applications covered by certain other technical committees such as industrial control, communication, and transportation may be treated jointly with that committee if emphasis is on general principles; or exclusively by the application committee if emphasis is on the particular requirements of the application.

ROTATING MACHINERY COMMITTEE

Scope—Treatment of all matters in which the dominant factors are the requirements, design, construction, and operation of rotating machinery for the generation of electric energy or its conversion into other forms of energy. There shall be included in this scope treatment of the following:

Synchronous machines
Induction machines
D-c machines
Single phase and fractional horsepower machines
Motor generator sets
Rotating frequency changers
Rotating phase balancers
Synchronous converters
Insulation and dielectric problems related to rotating machinery

Matters relating to rotating machinery specifically designed for applications covered by certain other technical committees such as electric welding, transportation, or communication may be treated jointly with that application committee if the emphasis is on general principles; or exclusively by the application committee if the emphasis is on the particular requirements of the application.

SUBSTATION COMMITTEE

Scope—Treatment of all matters in which the dominant factors are the electrical and structural design, construction, installation, operation, and control of automatic, semiautomatic, and nonautomatic substations, including switching and transformer stations.

Included in the scope of this committee shall be treatment of the following:

Automatic, semiautomatic, and nonautomatic substations
Switching stations
Fundamental single line wiring diagrams
Bus design (joint with switchgear and power generation committees)
Automatic and supervisory control systems (joint with power generation committee)
Supervisory control devices
Structural arrangements for substations
Telemetering (joint with instruments and measurements committee)
Insulation co-ordination (joint with transmission and distribution committee)

SWITCHGEAR COMMITTEE

Scope—Treatment of all matters in which the dominant factors are the design, construction, and operation of devices or assembled gear to establish (make), interrupt, or change connections in an electric circuit under normal or abnormal conditions. Included in this scope shall be treatment of the following:

Power circuit breakers
Large air circuit breakers
Low-voltage air circuit breakers
Switchgear assemblies
Switches
Insulating fluids (joint with transformer committee)
Bus design (joint with power generation and substation committees)
Insulation, insulators, and hardware for switchgear
Automatic reclosers
High-voltage fuses and cutouts (above 600 volts)

Matters relating to switchgear or switchgear devices specifically designed for applications covered by certain other technical committees such as industrial control, communication, electronics, and transportation may be treated jointly with that committee if emphasis is on general principles; or exclusively by the application committee if emphasis is on the particular requirements of the application.

SYSTEM ENGINEERING COMMITTEE

Scope—Treatment of all matters in which the dominant factors are the requirements, planning, co-ordination, operation, and eco-

nomics of interconnected electric generating, transmission, and distribution systems. Included in this scope shall be treatment of the following:

Interconnected system planning
Frequency and load control (joint with power generation committee)
Load dispatching
Economics of system and unit operation
Engineering of system expansion
Interconnection contracts

TRANSFORMER COMMITTEE

Scope—Treatment of all matters in which the dominant factors are the design, construction, and operation of transformers, reactors, and other similar equipment. Included within this scope shall be treatment of the following:

Transmission and distribution transformers
Voltage and load regulators (step and induction regulators)
Reactors and grounding transformers (joint with protective devices committee)
Specialty transformers and regulating transformers
Railway service transformers
Test transformers
Constant current transformers
Insulating fluids (joint with switchgear committee)
Insulation and dielectric problems relating to transformers
Insulators and hardware for transformers

Matters relating to transformers and regulators specifically designed for applications covered by certain other technical committees such as relays, electronics, protective devices, communication, may be treated jointly with that committee if emphasis is on general principles; or exclusively by the application committee if emphasis is on the particular requirements of the application.

TRANSMISSION AND DISTRIBUTION COMMITTEE

Scope—Treatment of all matters in which the dominant factors are considerations of economical and technical design, theoretical and experimental performance, installation, and service operation of that part of electric power systems which serve to transmit electric energy between the generating source or substation and the service.

Treatment of all matters involving substations themselves including switching and transforming stations are not within the scope of this committee, except in the broad aspects of the application of a substation as a whole.

Treatment of matters involving industrial distribution systems shall not be included within this scope unless such systems are interconnected with an electric power utility, in which case the action shall be joint with the committee on industrial power systems.

Included in this scope shall be treatment of the following:

Overhead and underground transmission and distribution systems
Overhead conductors
Fault current studies
System stability
Lightning investigations (joint with protective device committee)
Structural co-ordination
Insulation co-ordination (joint with substation committee)
Inductive co-ordination
Corona
Towers, pole, insulators, and hardware
Capacitors (except those used for protective devices)

Industry Group

INDUSTRY CO-ORDINATING COMMITTEE

Herbert Speight, *chairman*, Westinghouse Electric Corporation, 40 Wall Street, New York, N. Y.
J. J. Orr, *vice-chairman*
J. Elmer Housley
C. C. Wilson, *secretary*
Ex-officio: chairmen of technical committees in the industry group

CHEMICAL, ELECTROCHEMICAL, AND ELECTROTHERMAL COMMITTEE

Scope—Treatment of all matters in which the dominant factors are the generation of electricity through chemical processes, and the application of electricity to chemical or metallurgical operations (exclusive of electric welding and the phenomena of the arc insofar as it is concerned with the deposition of metal in welding, which is a function of the electric welding committee, and exclusive of magnetics, which is a function of the basic sciences committee), including the relations, installation, and operation of the devices necessary thereto, and the requirements of specialized devices, materials, or construction peculiar thereto.

ELECTRIC HEATING COMMITTEE

Scope—Treatment of all matters in which the dominant factors are the requirements, selection, installation, and operation of machines, devices, and equipment relating to electric heating of all kinds, including dielectric and induction, radiation, resistance, and high temperature furnaces. Design and theory of devices shall be handled by consultation with electronics or other committees as required.

ELECTRIC WELDING COMMITTEE

Scope—Treatment of all matters in which the dominant factors are the requirements, design, construction, selection, installation, and operation of machinery and devices relating to electric welding, including studies of the electromagnetic phenomena of the arc insofar as it is concerned with the deposition of metal in welding. Such subjects as electric welding methods and the electric machinery and control equipment specially designed for welding are properly within the scope of this committee.

GENERAL INDUSTRY APPLICATIONS COMMITTEE

Scope—Treatment of all matters in which the dominant factors are the requirements, selection, installation, and operation of machinery and devices relating to machine tools and to the processing and/or fabrication (assembly) of nonmetallic materials. Such materials include textiles, rubber, paper, plastics.

The problems relating to assembly line processes of all materials are considered within the scope of this committee.

INDUSTRIAL CONTROL COMMITTEE

Scope—Treatment of all matters in which the dominant factors are the design, construction, and performance of industrial control, and the way in which it serves to govern in some predetermined manner the electric power delivered to the apparatus to which it is connected.

INDUSTRIAL POWER SYSTEMS COMMITTEE

Scope—Treatment of all matters in which the dominant factors are the requirements, selection, co-ordination, installation, and operation of machines, devices, and equipment necessary for generating and transmitting electric power within an industrial plant for use solely by that plant. (Actual design of devices and equipment not included.) Design of distribution systems within the industrial plant are a part of the scope of this committee.

When such industrial systems are interconnected with public systems, the action shall be joint with the committee on power generation or on transmission and distribution.

MINING AND METAL INDUSTRY COMMITTEE

Scope—Treatment of all matters in which the dominant factors are the requirements, selection, installation, and operation of

machinery and devices relating to the processing of metal and those relating to mining of any kind.

Matters pertaining to blast furnaces, metal rolling, and metal drawing are properly within the scope of this committee.

Communication and Science Group

COMMUNICATION AND SCIENCE CO-ORDINATING COMMITTEE

W. R. G. Baker, *chairman*, General Electric Company, Electronics Department, Thompson Road, Syracuse, N. Y.
Truman S. Gray, *vice-chairman*
O. E. Buckley
F. A. Cowan
Ex-officio: chairmen of technical committees in the communication and science group

BASIC SCIENCES COMMITTEE

Scope—Treatment of all matters in which the dominant factor is electrophysics, and which are of such novel character as to be unapplied in any apparatus or field of application within the scopes of the other technical committees, or which are of such generality as to be significant within the scopes of several technical committees. Such subjects as general circuit theory, electrostatics, mathematical treatises, magnetics, general electrical units, and nomenclature are properly within the scope of this committee.

COMMUNICATION COMMITTEE

Scope—Treatment of all matters in which the dominant factor is the electrical transmission of intelligence (exclusive of supervisory control, which is a function of the substations committee, and railway signaling, which is a function of the land transportation committee), including methods, materials, devices, and construction to accomplish the result. Such subjects as telegraphy; telephony; program transmission; telephotography; television; police alarm, fire alarm, burglar alarm and traffic control systems; messenger calls; and time service are within the scope of this committee. Where communication lines are utilized in other fields, for example, the communication requirements of electric power systems and railways, or where problems of inductive co-ordination arise, treatment shall be joint with the respective technical committees concerned.

ELECTRONICS COMMITTEE

Scope—Treatment of all matters in which the dominant factor is electronics, particularly those dealing with the design, characteristics, or behavior of devices of an electronic nature, or of the circuits associated with them. The treatment of complete equipments or systems may be considered within the scope of this committee if they depend predominantly on electronic devices for their operation. If the field of application of such equipments or systems falls also within the scope of other technical committees, action with those committees may be joint.

INSTRUMENTS AND MEASUREMENTS COMMITTEE

Scope—Treatment of all matters in which the dominant factor is the measurement of electrical quantities, both absolute and relative, and the measurement of other quantities by electrical methods, including the devices necessary thereto. Where novel instruments and novel methods of electrical measurement are in papers, even though measurement is not the prime objective, then action shall be joint with the respective technical committee concerned.

Telemetering is assigned primarily to the committee on instruments and measurements and handled by a joint subcommittee comprised of members of both the committees on substations and instruments and measurements. Telemetering problems in connection with automatic stations will be assigned by the chairman of the committee on instruments and measurements to members of the subcommittee who are also members of the committee on substations. Telemetering problems of a more general nature will be assigned by him to members of both main committees, and where the problem is simply measurements it will be assigned only to members of the committee on instruments and measurements (as per joint agreement between the committees on automatic stations and instruments and measurements, January 29, 1935).

NUCLEONICS COMMITTEE

Scope—Treatment of all matters in which the dominant factor is nucleonics, particularly that dealing with the design, characteristics, or behavior of devices of a nucleonic nature, or of the systems associated with them. The treatment of complete equipments or systems may be considered within the scope of this committee if they depend predominantly on nucleonic principle for their operation. If the field of application of such equipments or systems falls also within the scopes of other technical committees, action with those committees shall be joint.

THERAPEUTICS COMMITTEE

Scope—Treatment of all matters in which the dominant factors are the application of electric power to sanitation equipment, such as air-cleaning and sterilizing devices, and to the promotion of health and the analysis and treatment of disease or defects of the human body, such as X-ray equipment, diathermic equipment, cardiographs, investigations not directly applying to the human body but relating to health, and electric devices suitable for such purposes; the study of harmful effects of electric currents and radiations of electric devices upon the human body and means for the prevention of such effects, and so forth, are properly within the scope of this committee.

Where certain devices are suitable for both therapeutic and industrial purposes, such as some X-ray equipment, or for therapeutic and other scientific investigations, or for sanitation and air-conditioning of domestic and commercial premises, action shall be joint with the industrial power applications committee, the basic sciences committee, or the domestic and commercial applications committee, respectively; also, when appropriate, with the safety committee.

General Applications Group

GENERAL APPLICATIONS CO-ORDINATING COMMITTEE

S. G. Hibben, *chairman*, Westinghouse Lamp Division, Bloomfield, N. J.
C. C. Whipple, *vice-chairman*
Elgin B. Robertson
Ex-officio: chairmen of technical committees in the general applications group

AIR TRANSPORTATION COMMITTEE

Scope—Treatment of all matters in which the dominant factors are the design, installation, and performance of airplane equipment, including batteries, generating equipment, voltage regulators, instruments, wiring devices, motors, special controls, reverse current cutouts, bonding, shielding, filtering, inverters, dynamotors, lightning detection and protection, lighting (interior and exterior), system characteristics, weight-power relationships,

and heating devices. With respect to communication and navigation; ground lighting; electric testing equipment for measuring strain, vibration, noise, corrosion, and so forth; and electric welding of airplane structures; action should be in co-operation with the respective AIEE technical committees in these fields and similar committees of other organizations.

DOMESTIC AND COMMERCIAL APPLICATIONS COMMITTEE

Scope—Treatment of all matters in which the dominant technical factors are the interior supply and utilization of electric power in domestic premises, such as single or multiple dwellings, garages, and other accessory structures, and in institutional buildings such as hospitals, schools, libraries, and so forth. Such subjects as control, interior wiring, heat-operated and motor-operated appliances or equipment for use in domestic, commercial, or institutional premises, including elevators and escalators, are properly within this scope. Subjects relating to the production and application of light, as such, are within the scope of the production and application of light committee.

LAND TRANSPORTATION COMMITTEE

Scope—Treatment of all matters in which the dominant factors are the requirements, design, selection, relation, and operation of electric apparatus and material for transportation (exclusive of air and marine transportation, which are functions of the air transportation and marine transportation committees) of passengers and freight and the economic questions incident thereto. Such subjects as the electrification of steam railways, street railways, pantograph trolleys and overhead catenaries, electric locomotives (oil-electric, gasoline-electric, or 3-power locomotives), multiple-unit cars, electric-traction motors, main and auxiliary control equipment, railway substations, mercury-arc rectifier applications, and railways signaling and automatic train control are within the scope of this committee.

MARINE TRANSPORTATION COMMITTEE

Scope—Treatment of all matters in which the dominant factors are the application, relation, and installation of electric machinery and materials of whatever nature on shipboard, and the requirements for specialized devices, materials, or constructions peculiar to such application.

PRODUCTION AND APPLICATION OF LIGHT COMMITTEE

Scope—Treatment of those matters in which the dominant factor is the application of electric energy through its conversion into light, including necessary materials, devices, and mechanisms, insofar as these matters are considered of interest and value to the members of the Institute. This committee functions as a liaison between the Institute and various organizations dealing with the production and utilization of light, such as the Illuminating Engineering Society, the Optical Society of America, and others. Its activities include translating the theoretical and technical accomplishments of those organizations into terms of the practical aspects of the production and application of light, thereby serving to inform Institute members of important progress in this field. Where problems of electrical supply service, voltage, or distribution are involved, action shall be joint with the transmission and distribution committee.

Officers and Committees for 1947-48

Officers

President

B. D. HULL — Dallas, Tex. (*Term expires July 31, 1948*)

Junior Past Presidents

C. A. POWEL — East Pittsburgh, Pa. (*Term expires July 31, 1948*)

J. ELMER HOUSLEY — Alcoa, Tenn. (*Term expires July 31, 1949*)

Vice-Presidents

District

1 E. W. DAVIS — Cambridge, Mass.
3 O. E. BUCKLEY — New York, N. Y.
5 T. G. LeCLAIR — Chicago, Ill.
7 R. F. DANNER — Oklahoma City, Okla.
9 C. F. TERRELL — Seattle, Wash.
(*Terms expire July 31, 1948*)

2 G. W. BOWER — Haddonfield, N. J.
4 J. H. BERRY — Norfolk, Va.
6 I. M. ELLESTAD — Omaha, Nebr.
8 D. I. CONE — San Francisco, Calif.
10 D. G. GEIGER — Toronto, Ontario, Canada
(*Terms expire July 31, 1949*)

Directors

P. L. ALGER — Schenectady, N. Y.
M. J. McHENRY — Toronto, Ontario, Canada
D. A. QUARLES — New York, N. Y.
(*Terms expire July 31, 1948*)

J. M. FLANIGEN — Atlanta, Ga.
J. R. NORTH — Jackson, Mich.
WALTER C. SMITH — Palo Alto, Calif.
(*Terms expire July 31, 1949*)

J. F. FAIRMAN — New York, N. Y.
R. T. HENRY — Buffalo, N. Y.
E. P. YERKES — Philadelphia, Pa.
(*Terms expire July 31, 1950*)

W. L. EVERITT — Urbana, Ill.
A. C. MONTEITH — East Pittsburgh, Pa.
ELGIN B. ROBERTSON — Dallas, Tex.
(*Terms expire July 31, 1951*)

Treasurer

W. I. SLICHTER — New York, N. Y. (*Term expires July 31, 1948*)

Secretary

H. H. HENLINE — New York, N. Y. (*Term expires July 31, 1948*)

Local Honorary Secretaries

AUSTRALIA—V. J. F. Brain, Electricity Authority of New South Wales, Treasury Building, Bridge and Phillip Streets, Sydney, New South Wales.

BRAZIL—Richard H. Bowles, Sao Paulo Tramway Light and Power Company, Sao Paulo.

ENGLAND—A. P. M. Fleming, Metropolitan Vickers Electric Company, Trafford Park, Manchester 17.

INDIA, SOUTHERN—N. N. Iengar, The Tata Power Company Ltd., Bombay House, Bruce Street, Fort, Bombay.

NEW ZEALAND—R. D. Neale, School of Engineering, Caterbury University College, Christchurch C. 1.

SWEDEN—Edy Velander, Royal Swedish Institute, Stockholm.

TRANSVAAL—Francis E. Ingham, Box 6067, Johannesburg, South Africa.

General Committees

Executive

B. D. HULL, *chairman*, 821 Telephone Building, 308 South Akard, Dallas 2, Tex.

O. E. Buckley — J. Elmer Housley
R. T. Henry — A. C. Monteith
W. I. Slichter

Finance

D. A. Quarles, *chairman*, Bell Telephone Laboratories, Inc., 463 West Street, New York 14, N. Y.

A. C. Monteith — E. P. Yerkes
F. A. Norris, *secretary*, AIEE, 33 West 39th Street, New York 18, N. Y.

Planning and Co-ordination

J. R. North, *chairman*, Commonwealth and Southern Corporation, Jackson, Mich.

H. H. Henline, *secretary*, AIEE, 33 West 39th Street, New York 18, N. Y.

W. R. G. Baker — H. S. Osborne
J. F. Fairman — D. A. Quarles
S. G. Hibben — Elgin B. Robertson
B. M. Jones — Walter Charles Smith
Reginald L. Jones — Herbert Speight
T. G. LeClair — M. J. Steinberg
Everett S. Lee — J. C. Strasbourger
H. M. Turner

Publication

B. M. Jones, *chairman*, Duquesne Light Company, 435 Sixth Avenue, Pittsburgh 19, Pa.

M. S. Coover — M. J. McHenry
P. B. Garrett — J. J. Orr
H. H. Henline — H. H. Race
R. K. Honaman — C. F. Wagner

Research

C. G. Suits, *chairman*, Research Laboratory, General Electric Company, Schenectady 5, N. Y.

B. G. Ballard — R. S. Glasgow
J. W. Barker — J. E. Hobson
R. D. Bennett — J. A. Hutcheson
L. V. Berkner — M. J. Kelly
C. R. Burrows — J. T. Littleton
D. E. Chambers — C. S. Schifreen
H. P. Corwith — F. E. Terman
H. E. Edgerton — J. B. Thomas
W. L. Everitt — Eric Walker
V. K. Zworykin

Safety

Robin Beach, *chairman*, 32 Court Street, Brooklyn 2, N. Y.

A. B. Smith, *vice-chairman* and *secretary*, National Electrical Manufacturers Association, 155 East 44th Street, New York 17, N. Y.

L. F. Adams — R. L. Lloyd
M. M. Brandon — A. C. Muir
J. C. Cunningham, Jr. — Albrecht Naefer
C. F. Dalziel — G. R. Radley
W. P. Dobson — W. T. Rogers
L. P. Ferris — W. E. Rushlow
J. M. Flanigen — W. R. Smith
O. S. Hockaday — E. E. Turkington
W. B. Kouwenhoven — H. H. Watson
J. O. Leslie — H. B. Williams

Sections

J. C. Strasbourger, *chairman*, Cleveland Electric Illuminating Company, 75 Public Square, Cleveland 1, Ohio.

R. E. Kistler, *vice-chairman*, Pacific Telephone and Telegraph Company, 1200 Third Avenue, Seattle 1, Wash.

H. W. Sussman, *secretary*, Columbia Electric Manufacturing Company, 4519 Hamilton Avenue, Cleveland 14, Ohio.

D. I. Anzini — C. P. Knost
F. S. Black — C. W. Lethert
L. T. Blaisdell — E. F. Lopes
G. W. Bower — C. W. Mier
S. C. Commander — A. C. Muir
T. H. Crosby — J. H. Pilkington
McNeely Du Bose — Roland G. Porter
W. A. Dynes — C. S. Purnell
V. P. Hessler — Victor Siegfried
E. W. Stone

Ex officio

Chairmen of Sections

Standards

Reginald L. Jones, *chairman*, Bell Telephone Laboratories, Inc., 463 West Street, New York 14, N. Y.

F. E. Harrell, *vice-chairman*, 1088 Ivanhoe Road, Cleveland 10, Ohio.

H. E. Farrer, *secretary*, AIEE, 33 West 39th Street, New York 18, N. Y.

Joseph William Allen — H. R. Huntley
R. W. Atkinson — H. E. Kent
F. R. Benedict — S. J. Lisberger
R. C. Bergvall — J. B. McCurley
M. M. Brandon — S. H. Mortensen
J. E. Clem — J. R. North
C. L. Dawes — M. S. Oldacre
W. P. Dobson — G. H. O'Sullivan
C. M. Gilt — F. B. Silsbee
R. C. Sogge

Ex officio

Chairmen of working and co-ordinating committees of the Standards committee

Chairmen of AIEE technical committees

Chairmen of AIEE delegates on other standardizing bodies or sole representatives thereon

President, United States National Committee of the International Electrotechnical Commission

Technical Program

H. M. Turner, *chairman*, Yale University, New Haven, Conn.

S. H. Mortensen, *vice-chairman*, Allis-Chalmers Manufacturing Company, Milwaukee 1, Wis.

C. S. Rich, *secretary*, AIEE, 33 West 39th Street, New York 18, N. Y.

W. R. G. Baker — S. G. Hibben
H. W. Collins — A. J. Krupy
F. A. Cowan — J. J. Orr
S. B. Crary — Herbert Speight
R. F. Danner — M. J. Steinberg
Truman S. Gray — Frank Thornton, Jr.
C. C. Whipple

Ex officio

Chairmen of:
- All technical committees
- Committee on education
- Committee on planning and co-ordination
- Committee on research
- Committee on safety
- Standards committee

Administration Group Committees

Administration Group Co-ordinating

J. F. Fairman, *chairman*, Consolidated Edison Company of New York, Inc., 4 Irving Place, New York 3, N. Y.

Chairmen of administration group committees

Board of Examiners

R. H. Barclay, *chairman*, J. G. White Engineering Corporation, 80 Broad Street, New York 4, N. Y.

E. D. Doyle, *vice-chairman*, Leeds and Northrup Company, 4901 Stenton Avenue, Philadelphia 44, Pa.

H. E. Farrer, *secretary*, AIEE, 33 West 39th Street, New York 18, N. Y.

R. W. Atkinson
Robin Beach — F. E. D'Humy

(*continued*)

C. W. Franklin — L. G. Pacent
I. W. Gross — J. J. Pilliod
L. F. Hickernell — R. C. Roe
I. F. Kinnard — H. M. Trueblood
A. E. Knowlton — H. H. Weber
C. M. Laffoon — John Westbye
A. M. Musgrove — Sidney Withington

Constitution and Bylaws

Walter C. Smith, *chairman*, 680 Melville Avenue, Palo Alto, Calif.
W. Scott Hill — W. W. Lewis
Reginald L. Jones — W. S. Peterson

Headquarters

W. R. Smith, *chairman*, Public Service Electric and Gas Company, 80 Park Place, Newark 1, N. J.
H. H. Henline — D. A. Quarles

Members-for-Life Fund

C. R. Beardsley, *chairman*, Consolidated Edison Company of New York, Inc., 4 Irving Place, New York 3, N. Y.
N. E. Funk — F. D. Newbury
A. H. Hull — W. I. Slichter
E. H. Martindale — R. W. Sorensen
R. C. Muir — J. F. Tritle

Membership

Tomlinson Fort, *chairman*, Westinghouse Electric Corporation, East Pittsburgh, Pa.
F. S. Black, *vice-chairman*, Potomac Electric Power Company, Tenth and E Streets, N.W., Washington 4, D. C.
F. A. Norris, *secretary*, AIEE, 33 West 39th Street, New York 18, N. Y.
A. D. Brown — W. S. Leake
J. F. Calvert — M. L. Lehman
R. L. Chapman — P. H. Light
D. D. Chase — Lee M. Moore
W. F. Cotter — C. T. Pearce
W. C. Fowler — D. B. Perry
R. F. Ham — F. H. Schlough
G. C. Harvey — H. J. Scholz
A. W. Janowitz — J. H. Spraggon
C. W. La Pierre — H. F. Staacke
E. P. Yerkes

District Vice-Chairmen

F. S. Bacon (1) — C. G. Rumohr (6)
F. H. Knapp (2) — R. C. Horn (7)
J. A. Duncan, Jr. (3) — W. H. Snowden (8)
H. W. Oetinger (4) — M. J. Lantz (9)
J. C. Woods (5) — W. R. Way (10)

Ex officio

Chairmen of membership committees of all Sections

Publicity, Institute

R. K. Honaman, *chairman*, Bell Telephone Laboratories, Inc., 463 West Street, New York 14, N. Y.
Guy Bartlett — B. M. Jones
G. W. Bower — C. R. Jones
M. Getting — A. E. Knowlton
H. M. Turner

Transfers

D. E. Moat, *chairman*, Leeds and Northrup Company, 1800 Keith Building, Cleveland 15, Ohio.
Lloyd F. Hunt, *vice-chairman*, Southern California Edison Company Ltd., 601 West Fifth Street, Los Angeles 13, Calif.
F. W. Willcutt, *secretary*, Potomac Electric Power Company, Tenth and E Streets, N.W., Washington 4, D. C.
F. A. Cooper — F. K. McCune
C. W. Fick — M. J. McHenry
John Gammell — A. M. Musgrove
J. W. Lingary — H. K. Smith

Ex officio

Chairmen of transfers committees of all Sections

Professional Group Committees

Professional Group Co-ordinating Committee

T. G. LeClair, *chairman*, Commonwealth Edison Company, 72 West Adams Street, Chicago 90, Ill.
Chairmen of professional group committees

Charles LeGeyt Fortescue Fellowship

J. W. Barker — Ernst Weber
(*Terms expire July 31, 1949*)
H. E. Strang, *chairman* — C. H. Willis
(*Terms expire July 31, 1949*)
H. N. Muller — H. F. Sedwick
(*Terms expire July 31, 1950*)

Code of Principles of Professional Conduct

Harry Barker, *chairman*, 11 Park Place, Room 1616, New York, N. Y.
D. D. Ewing — D. C. Jackson
E. S. Fields — R. D. Maxson
E. H. Flath — R. W. Sorensen

Edison Medal

Appointed by the president for term of five years

C. R. Freehafer — C. A. Powel — David Sarnoff
(*Terms expire July 31, 1948*)
O. E. Buckley — A. E. Knowlton — H. E. Strang
(*Terms expire July 31, 1949*)
C. V. Christie — Zay Jeffries — Harold Pender
(*Terms expire July 31, 1950*)
C. A. Corney — S. M. Dean, *chairman* — I. M. Stein
(*Terms expire July 31, 1951*)
Marvin W. Smith — H. S. Osborne — H. A. Winne
(*Terms expire July 31, 1952*)

Elected by the board of directors from its own membership for term of two years

P. L. Alger — R. T. Henry — E. P. Yerkes
(*Terms expire July 31, 1948*)
W. L. Everitt — J. F. Fairman — A. C. Monteith
(*Terms expire July 31, 1949*)

Ex officio

B. D. Hull, president
W. I. Slichter, treasurer
H. H. Henline, secretary

Education

J. G. Tarboux, *chairman*, Cornell University, Ithaca, N. Y.
B. R. Teare, Jr., *vice-chairman*, Carnegie Institute of Technology, Pittsburgh, Pa.
J. A. Northcott, Jr., *secretary*, Engineering College, University of Notre Dame, Notre Dame, Ind.
H. W. Bibber — H. N. Muller
W. L. Cassell — R. C. Putnam
G. F. Corcoran — Claire W. Ricker
E. E. Dreese — R. W. Sorensen
W. L. Everitt — C. E. Tucker
H. E. Hartig — C. E. Tuites
T. M. Linville — E. A. Walker
E. A. Loew — R. W. Warner
A. H. Lovell — S. Reid Warren
T. C. McFarland — A. R. Zimmer

Lamme Medal

V. M. Montsinger, *chairman*
H. L. Hazen — G. A. Waters
(*Terms expire July 31, 1948*)
N. S. Hibshman — T. G. LeClair — A. C. Monteith
(*Terms expire July 31, 1949*)
F. E. Harrell — D. A. Quarles — J. B. Thomas
(*Terms expire July 31, 1950*)

Management

Lee H. Hill, *chairman*, *Electrical World*, 330 West 42d Street, New York 18, N. Y.
K. P. Applegate — A. C. Monteith
H. K. Breckenridge — E. L. Moreland
F. W. Bush — H. A. Peterson
W. L. Cisler — H. E. Strang
E. E. Hill — O. Van Rye

Prizes, Award of Institute

H. M. Turner, *chairman*, Yale University, New Haven, Conn.
W. R. G. Baker — W. C. Kalb
H. L. Davis, Jr. — J. J. Pilliod
S. G. Hibben — Herbert Speight
B. M. Jones — M. J. Steinberg
C. G. Suits

Registration of Engineers

J. E. Hobson, *chairman*, Armour Research Foundation, 35 West 33rd Street, Chicago 16, Ill.
A. J. Krupy, *secretary*, Commonwealth Edison Company, 72 West Adams Street, Chicago 90, Ill.
E. H. Bancker — H. B. Joyce
L. O. Campbell — R. E. Kistler
J. H. Foote — K. B. McEachron
N. L. Freeman — R. E. Muehlig
L. A. Griffith — J. G. Patterson
J. D. Guillemette — W. W. Perry
F. W. L. Hill — Elgin B. Robertson
L. M. Robertson

Student Branches

J. F. Calvert, *chairman*, Northwestern Technological Institute, Evanston, Ill.
E. M. Strong, *vice-chairman*, Cornell University, Ithaca, N. Y.
Sterling Beckwith — Everett S. Lee
A. M. Harrison — W. H. Pickering
P. L. Hoover — L. T. Rader
A. H. Howell — R. W. Warner
J. H. Kuhlmann — B. S. Willis
C. R. Wischmeyer

Ex officio

Student Branch counselors

Technical Committees

Power Group

Power Co-ordinating Committee

M. J. Steinberg, *chairman*, Consolidated Edison Company of New York, Inc., 4 Irving Place, New York, N. Y.
H. W. Collins, *vice-chairman*
R. T. Henry
A. J. Krupy
Frank Thornton, Jr.
C. C. Wilson, *secretary*

Ex officio

Chairmen of the 12 following technical committees in the power group

Carrier Current

L. F. Kennedy, *chairman*, General Electric Company, central station engineering divisions, 1 River Road, Schenectady 5, N. Y.
S. C. Bartlett — S. C. Leyland
C. W. Boadway — L. E. Ludekens
J. D. Booth — D. M. MacGregor
R. C. Ericson — T. W. MacLean
W. J. Googe — R. E. Neidig
M. W. Keck — O. A. Starcke
E. W. Kenefake — T. D. Talmage
Mead Warren, Jr.

Electronic Power Converter

H. Winograd, *chairman*, Allis-Chalmers Manufacturing Company, electrical department, Milwaukee 1, Wis.
J. L. Boyer — A. J. Maslin
F. W. Cramer — L. W. Morton
E. V. DeBlieux — J. B. Rice
J. B. Donnelly — W. J. L. Rupprecht
I. K. Dortort — A. Schmidt, Jr.
Wm. Fraser — W. G. Scaley
W. E. Gutzwiller — H. C. Steiner
C. G. Herskind — T. A. Taylor
H. E. Hewes — J. T. Thweck
G. N. Hughes — Joel Tompkins
C. R. Marcum — C. H. Willis
D. E. Marshall — H. E. Zuvers

Insulated Conductor

L. F. Hickernell, *chairman*, Anaconda Wire and Cable Company, Hastings-on-Hudson 6, New York
C. F. Avila — L. E. Fogg
J. C. Balabaugh — J. H. Foote
H. G. Barnett — M. W. Ghen
C. E. Baugh — H. Halperin
A. P. S. Bellis — C. T. Hatcher
A. Bodicky — T. G. Hieronymus
A. S. Brookes — R. A. Hopkins
T. J. Brosnan — L. I. Komives
W. R. Bullard — M. J. Lowenberg
H. W. Clark — C. G. Mansfield
M. T. Crawford — R. E. Morse
E. W. Davis — E. F. Nuezel
W. A. Del Mar — W. T. Peirce
C. D. Eash — R. S. Peterson
D. M. Farnham

(*continued*)

A. D. Pettee
H. S. Phelps
R. A. Schatzel
G. B. Shanklin
V. A. Sheals
F. V. Smith
L. G. Smith
Gordon Thompson
O. W. Titus
C. W. White
R. J. Wiseman
K. S. Wyatt
C. P. Xenis
C. W. Zimmerer

Power Generation

A. H. Frampton, *chairman*, Hydro-Electric Power Commission of Ontario, electrical engineering department, Toronto 2, Ontario, Canada

S. Beckwith
A. D. Caskey
C. A. Corney
R. P. Crippen
E. F. Dissmeyer
Alex. Dovjikov
J. M. Drabelle
F. W. Gay
C. A. Harrington
E. L. Hough
W. R. Johnson
A. J. Krupp
J. T. Madill
J. B. McClure
G. H. McDaniel
W. S. Peterson
A. L. Pollard
G. M. Pollard
J. A. Powell
F. L. Reinmann
B. G. A. Skrotzki
M. J. Steinberg
G. M. Tatum
H. D. Taylor
R. L. Witzke
G. R. Woodman

Protective Devices

G. B. Dodds, *chairman*, Duquesne Light Company, 435 6th Avenue, Pittsburgh, Pa.

V. J. Cissna
J. E. Clem
H. A. Cornelius
F. M. Defandorf
R. H. Earle
W. W. Eberhardt
G. W. Gerell
E. T. B. Gross
E. M. Hunter
P. A. Jeanne
A. A. Johnson
J. H. Kinghorn
E. W. Knapp
F. R. Longley
T. H. Mawson
J. R. McFarlin
E. G. Norrell
A. M. Opsahl
H. L. Rawlins
J. J. Ray
W. J. Rudge
W. E. Rushlow
W. T. Smith
H. R. Stewart
J. M. Towner
J. H. Vivian
S. S. Watkins
E. R. Whitehead
C. P. Xenis
E. H. Yonkers

Relay

W. R. Brownlee, *chairman*, Commonwealth and Southern Corporation, Jackson, Mich.

J. C. Bowman
J. E. Clem
R. J. Cooper
R. E. Cordray
G. E. Dana
W. K. Dickinson
G. B. Dodds
F. S. Fehr
L. L. Fountain
S. Goldsmith
E. T. B. Gross
T. R. Halman
E. L. Harder
V. J. Hayes
B. C. Hicks
J. H. Kinghorn
R. A. Larner
W. A. Lewis
S. C. Leyland
H. F. Lindemuth
W. E. Marter
A. J. McConnell
E. L. Michelson
C. E. Parks
H. R. Paxson
F. C. Poage
E. G. Rautz
K. N. Reardon
W. K. Sonnemann
J. H. Vivian
E. C. Wentz

Rotating Machinery

C. E. Kilbourne, *chairman*, General Electric Company, 1 River Road, Schenectady 5, New York

J. E. Allen
W. R. Appleman
Sterling Beckwith
B. M. Cain
E. E. Dreese
J. L. Fuller
G. T. Harness
C. B. Hathaway
R. A. Hopkins
W. R. Hough
J. W. Jones
F. P. Kaspar
M. F. Kent
L. A. Kilgore
C. Kingsley, Jr.
C. J. Koch
A. A. Kroneberg
T. M. Linville
T. C. Lloyd
M. J. Lowenberg
C. Lynn
G. W. McIver, Jr.
R. C. Moore
J. G. Noest
E. I. Pollard
C. P. Potter
F. C. Rushing
M. L. Schmidt
J. F. Sellers
H. R. Sills
T. W. Trice
P. H. Trickey
C. G. Veinott
R. W. Wieseman
J. C. Woods

Substations

G. S. Whitlow, *chairman*, Union Electric Company of Missouri, St. Louis, Mo.

A. E. Anderson
Harris Barber
W. A. Derr
R. C. Ericson
J. M. Flanigen
M. Franson
S. F. French
C. D. Highleyman
W. L. Hiscox
K. B. Hoffman
I. T. Knight
W. J. Lank
L. W. Long
G. S. Lunge
A. P. Peterson
S. L. Smith
C. H. Smoke
J. H. Vivian
C. E. Winegartner

Switchgear

H. J. Lingal, *chairman*, Westinghouse Electric Corporation, East Pittsburgh, Pa.

C. K. Beyette
C. H. Black
Harry Brown
J. Stanley Brown
E. A. Childerhose
H. W. Codding
F. W. Cramer
G. H. Doan
W. E. Enns
K. J. C. Falck
R. M. Ferrill
W. J. Gilson
W. D. Hardaway
M. H. Hobbs
L. M. Hovey
F. A. Lane
H. A. P. Langstaff
W. J. McLachlan
R. G. Meyerand
E. F. Miller
J. R. North
H. V. Nye
H. H. Rudd
Max W. Rothpletz
F. V. Smith
G. Stamper
A. VanRyan
J. H. Vivian
R. L. Webb
K. L. Wheeler
J. D. Wood
J. C. Woods
D. G. Worth
S. W. Zimmerman

System Engineering

J. E. McCormack, *chairman*, Consolidated Edison Company of New York, Inc., 4 Irving Place, New York, N. Y.

C. P. Almon, Jr.
M. L. Blair
R. Brandt
S. B. Crary
E. E. George
W. D. Hardaway
H. L. Harrington
A. P. Hayward
J. B. Hodtum
R. G. Hooke
L. F. Hunt
A. A. Johnson
B. M. Jones
C. B. Kelley
R. M. Laurie
M. H. Loveladay
O. W. Manz, Jr.
V. M. Marquis
C. W. Mayott
S. B. Morehouse
F. Oppenheimer
W. O. Smith
E. Wild

Transformer

H. B. Keath, *chairman*, Wagner Electric Corporation 6400 Plymouth Avenue, St. Louis, Mo

J. A. Adams
F. S. Brown
M. K. Brown
J. L. Cantwell
J. H. Chiles
J. E. Clem
G. W. Clothier
M. DeMerit
J. A. Elzi
I. W. Gross
J. B. Hodtum
A. A. Johnson
D. L. Levine
H. C. Louis
C. M. Lovell
V. M. Montsinger
M. H. Pratt
T. D. Reimers
W. C. Sealey
F. L. Snyder
Paul A. Vance
F. J. Vogel
C. V. Waddington
H. H. Wagner
E. C. Wentz

Transmission and Distribution

C. F. Wagner, *chairman*, Westinghouse Electric Corporation, central station department, East Pittsburgh, Pa.

C. E. Baugh
D. K. Blake
Bryce Brady
Harold Cole
S. B. Crary
P. J. Croft
A. E. Curtis
A. E. Davison
E. W. Dillard
I. W. Gross
E. Hansson
K. E. Hapgood
E. R. Hendrickson
J. B. Hodtum
E. K. Huntington
H. E. Kent
C. H. Kraft
A. A. Kroneberg
W. W. Lewis
J. T. Lusignan
R. B. Miller
L. M. Moore
E. W. Oesterreich
F. W. Packer
J. S. Parsons
L. M. Robertson
E. V. Sayles
H. J. Scholz
T. G. A. Sillers
A. E. Silver
F. V. Smith
E. C. Starr
H. M. Truehlood
E. R. Whitehead
L. T. Williams
R. L. Witzke
H. E. Wulfing

Industry Group

Industry Co-ordinating Committee

Herbert Speight, *chairman*, Westinghouse Electric Corporation, 40 Wall Street, New York, N. Y
J. J. Orr, *vice-chairman*
J. Elmer Housley
C. C. Wilson, *secretary*

Ex officio
Chairmen of the seven following technical committees in the industry group

Chemical, Electrochemical, and Electrothermal

T. R. Rhea, *chairman*, General Electric Company, Schenectady, N. Y.

F. R. Benedict
J. D. Brance
W. H. Dickinson
W. C. Dreyer
L. H. Fletemeyer, Jr.
Felix Glass
L. Goldsmith
L. O. Grondahl
W. E. Gutzwiller
E. A. Hanff
J. D. Harper
T. G. Hieronymus
J. E. Hobson
H. E. Houck
J. Elmer Housley
J. D. Huntsberger
M. A. Hyde
Rollin Kennard
E. L. Kirk
W. B. Kouwenhoven
R. J. Kuhn
E. H. Lamberger
F. L. Lawton
D. H. Levy
G. H. Orcutt
Waldo Porter
R. L. Rayner
H. C. Riggs
L. W. Roush
E. T. Rummel
G. B. Scheer
E. H. Scheick
Joel Tompkins
J. J. Unger
H. W. Wahlquist
E. R. Whitehead
H. H. Zielinski

Electric Heating

G. W. Scott, Jr., *chairman*, Armstrong Cork Company, Lancaster, Pa.

E. L. Bailey
R. M. Baker
W. I. Bends
F. T. Chesnut
L. M. Duryee
R. H. Ellis
P. H. Goodell
J. Grotzinger
J. C. Handy
E. A. Hanff
J. B. Hodtum
L. P. Hynes
T. P. Kinn
G. F. Leland
F. H. Mason
W. H. Meyer
L. R. Milburn
R. Neighbours
C. E. Peck
K. Pinder
B. E. Rector
J. B. Rice
W. C. Rudd
E. H. Scheick
W. R. Schofield
J. T. Thwaites
V. E. Trouant
G. E. Walter
H. R. Winemiller

Electric Welding

E. H. Vedder, *chairman*, Westinghouse Electric Corporation, P.O. Box 2025, Buffalo 3, N. Y.

E. M. Callender
G. M. Chute
C. N. Clark
W. E. Crawford
E. W. Davis
J. F. Deffenbaugh
R. C. Freeman
G. W. Garman
W. B. Kouwenhoven
J. H. Lampe
J. C. Learman
R. C. McMaster
C. M. Rhoades, Jr.
F. Rothganger
J. R. Sellenberg
Sam Shiozawa
C. E. Smith
H. W. Snyder
H. I. Stanback
E. F. Steinert
L. K. Stringham
G. I. F. Theriault
H. W. Tietze
A. G. Turnbull
A. M. Unger
F. J. Wells
B. L. Wise
R. E. Young
M. Zucker

General Industry Applications

L. A. Umansky, *chairman*, General Electric Company, Schenectady 5, N. Y.

B. T. Anderson
A. T. Bacheler
A. C. Bird
S. A. Bobe
D. C. Christison
J. M. Delfs
John Fink
A. W. Frankenfield
J. A. Gienger
E. M. Hays
F. B. Haeussler
L. W. Herchenroeder
Kurt John
V. O. Johnson
George Knapp
J. Manuele
E. F. Mekelburg
E. K. Murphy
D. R. Percival
K. Pinder
H. A. Rose
H. L. Smith
F. D. Snyder
R. F. Snyder
R. Stropper
W. B. Wigton

Industrial Control

John D. Leitch, *chairman*, Electric Controller and Manufacturing Company, 2700 East 79th Street, Cleveland 4, Ohio

E. H. Alexander
H. H. Angel
G. S. Brown
G. A. Caldwell
J. A. Cortelli
R. H. Ellis
C. T. Evans
W. B. Farrar
L. E. Fisher
D. K. Frost
J. A. Gienger
G. W. Heumann
D. E. Inman
Kurt John
R. W. Jones
E. U. Lassen
L. H. Matthias
J. D. McConnell
E. F. Mehlburg
M. Michel
T. B. Montgomery
H. L. Palmer
J. W. Picking
G. H. Rendel
W. Schaelchlin
H. R. Walker

Industrial Power Systems

T. O. Sweatt, *chairman*, Wearn, Vreeland, Carlson and Sweatt, Inc., 72 Wall Street, New York 5, N. Y.

D. L. Beeman
E. L. Bailey
W. M. Ballenger
H. G. Barnett
F. R. Benedict
W. H. Dickinson
D. D. Douglass
S. F. French
J. S. Gault
W. N. Goodridge
L. N. Grier
W. R. Harmer
C. R. Johnson
R. E. Johnson
J. P. Kennell
C. M. Lathrop
A. E. Marshall
M. J. McHenry
J. L. McKeever
J. S. Morgan
W. A. Mostoller
J. S. Parsons
L. G. Peterman
R. C. Peters
W. H. Rollman
F. Rothganger
R. R. Shollenberger
J. F. Speese
H. C. Swannell
B. F. Thomas
E. E. Turkington
S. A. Warner
R. W. Watson
C. C. Whipple
R. T. Woodruff

Mining and Metal Industry

F. W. Cramer, *chairman*, Carnegie-Illinois Steel Corporation, Carnegie Building, Fifth Avenue, Pittsburgh 19, Pa.

G. Bright
M. K. Clay
R. J. Corfield
J. A. Cortelli
R. W. Davis
John M. Downie
J. H. Edwards
R. H. Ellis
J. R. Erbe
C. Farrow
L. N. Grier
W. R. Harris
L. H. James
Charles F. King, Jr.
R. C. McMaster
W. E. Miller
T. B. Montgomery
A. C. Muir
H. P. Musser
D. E. Renshaw
E. G. Schlup
F. O. Schnure
Victor Siegfried
O. J. Swanson
C. L. Tyler
T. R. Weichel
A. J. Whitcomb
C. G. Wood

Communication & Science Group

Communication and Science Co-ordinating Committee

W. R. G. Baker, *chairman*, General Electric Company, Electronics Department, Thompson Road, Syracuse, N. Y.

Truman S. Gray, *vice-chairman*
O. E. Buckley
F. A. Cowan

Ex officio

Chairmen of the six following technical committees in the communication and science group

Basic Sciences

J. D. Tebo, *chairman*, Bell Telephone Laboratories, Inc., 463 West Street, New York 14, N. Y.

J. G. Brainerd
O. E. Buckley
C. R. Burrows
Charles Concordia
F. C. Cromwell
A. V. Eastman
C. R. Hanna
F. K. Harris
H. L. Hazen
T. J. Higgins
N. S. Hibshman
W. C. Johnson
H. P. Lawther
W. A. Lewis
W. H. MacWilliams
M. G. Malti
G. D. McCann
K. W. Miller
W. E. Phillips
Walther Richter
H. W. Russell
J. B. Russell
W. J. Seeley
James J. Smith
L. A. Smith
V. G. Smith
F. G. Tappan
F. E. Terman
G. S. Timoshenko

Communication

J. L. Callahan, *chairman*, Research Division, RCA Laboratories, Radio Corporation of America, 66 Broad Street, New York 5, N. Y.

H. A. Affel
A. L. Albert
W. M. Allen
G. M. K. Balcer
E. D. Becken
E. M. Boone
J. D. Booth
A. J. Busch
I. F. Byrnes
J. B. Coleman
C. H. Cramer
M. Eastham
H. E. Ellisborn
H. R. Fritz
J. C. Gaudio
D. G. Geiger
P. C. Goldmark
T. T. Goldsmith, Jr.
G. H. Gray
H. H. Haglund
W. D. Hailes
J. V. L. Hogan
L. C. Holmes
E. M. Johnson
R. G. McCurdy
G. R. Messmer
J. L. Middlebrooks
F. E. Norris
R. R. O'Connor
L. G. Pacent
J. J. Pilliod
E. G. Ports
Haraden Pratt
R. H. Ranger
G. B. Ransom
W. A. Ready
F. M. Rives
H. I. Romnes
G. T. Royden
A. L. Rumsey
J. B. Russell
R. E. Shelby
J. O. Shepherd
A. Bessey Smith
D. B. Smith
J. E. Smith
Rothwell E. Smith
W. T. Smith
S. C. Spielman
R. B. Vaile, Jr.
Wm. Comings White

Electronics

C. H. Willis, *chairman*, Princeton University, School of Engineering, Princeton, N. J.

W. R. G. Baker
R. Bennett
E. M. Boone
G. H. Browning
R. S. Burnap
W. R. Clark
C. J. Crowdes
E. V. DeBlieux
W. G. Dow
A. V. Eastman
G. V. Eltgroth
R. Feldt
D. G. Fink
K. S. Geiges
E. R. Haberland
J. D. Heibel
J. E. Hobson
T. P. Kinn
D. D. Knowles
W. H. Lee
J. D. Leitch
O. W. Livingston
D. E. Marshall
H. R. Meahl
B. K. Northrup
D. Packard
H. L. Palmer
G. W. Penney
W. H. Pickering
O. W. Pike
A. J. Quigley
L. E. Reukema
J. D. Ryder
T. Spooner
H. C. Steiner
C. M. Summers
A. A. Sylvane
E. R. Thomas
J. T. Thwaites
F. C. Todd
F. N. Tompkins
D. C. Ulrey
W. C. White
H. Winograd

Instruments and Measurements

E. I. Green, *chairman*, Bell Telephone Laboratories, Inc., 463 West Street, New York, N. Y.

R. C. Bailey
P. L. Bellaschi
P. A. Borden
H. H. Brauer
G. S. Brown
A. L. Brownlee
L. A. Buckmayer, Jr.
C. T. Burke
J. H. Chiles
W. R. Clark
A. B. Craig
C. L. Dawes
F. C. Doble
R. D. Doyle
G. W. Dunlap
W. N. Eddy
J. L. Fuller
F. J. Gaffney
A. J. Grant
T. S. Gray
I. W. Gross
G. B. Hoadley
W. G. Knickerbocker
A. E. Knowlton
H. C. Koenig
E. S. Lee
L. M. Limpus
W. N. Lindblad
G. S. Lunge
J. T. Lusignan
J. H. Miller
G. A. Palmer
A. R. Rutter
C. F. Savage
F. B. Silsbee
M. B. Stout
H. S. Williams
E. P. Yerkes
C. J. Zeller

Nucleonics

L. W. Chubb, *chairman*, Research Laboratories, Westinghouse Electric Corporation, East Pittsburgh, Pa.

R. C Bergvall
J. M. Cork
W. F. Davidson
J. R. Dunning
I. A. Getting
M. M. Hubbard
J. A. Hutcheson
E. H. Krieg
H. B. Marvin
Philip Morrison
Ernest Pollard
B. R. Prentice
Walther Richter
F. Seitz
J. J. Smith
Abe Tilles
J. A. Wheeler
J. T. Wilson
Gale S. Young
Walter H. Zinn

Therapeutics

E. E. Charlton, *chairman*, General Electric Company, Research Laboratory, X-Ray Section, Schenectady, N. Y.

F. B. Claussen
H. J. Holmquest
Roy Kegerreis
W. B. Kouwenhoven
L. Marinelli
G. E. Maxim
H. D. Moreland
C. M. Slack
W. I. Slichter
W. R. Smith
L. S. Taylor

General Applications Group

General Applications Co-ordinating Committee

S. G. Hibben, *chairman*, Westinghouse Lamp Division, Bloomfield, New Jersey

C. C. Whipple, *vice-chairman*
Elgin B. Robertson

Ex officio

Chairmen of the five following technical committees in the general applications group

Air Transportation

S. D. Summers, *chairman*, Naval Research Laboratory, Washington, D. C.

J. W. Allen
R. A. Averitt
C. J. Breitweiser
H. R. Brown
K. D. Brumbaugh
W. C. Bryant
J. B. Coleman
A. E. Corcoran
J. P. Dallas
D. E. Fritz
C. E. Gagnier
S. H. Hanville, Jr.
W. T. Harding
V. P. Hessler
J. G. Hutton
R. R. Jenner
R. D. Jones
R. J. Lusk
T. J. Martin
R. A. Millermaster
J. D. Miner
W. F. Moore
O. F. Olsen
W. E. Pakala
M. H. Pearis
H. F. Rempt
C. J. Rife
R. A. Rugge
M. R. Seldon
K. R. Smythe
W. W. West
J. A. White

Domestic and Commercial Applications

M. M. Brandon, *chairman*, Underwriters' Laboratories, Inc., 161 Sixth Avenue, New York, N. Y.

Sidney W. Andrews
D. K. Blake
A. C. Bredahl
W. B. Buchanan
N. H. Callard
O. K. Coleman
T. H. David, Jr.
R. W. Fleming
L. R. Gamble
R. R. Herrmann
T. C. Johnson
C. H. Leatham
F. W. Linder
Buford H. Martin
M. J. McHenry
H. E. Metz
K. W. Miller
C. F. Scott
H. P. Seelye
G. S. Smith
G. C. Tenney
Wesley Weinerth

Land Transportation

John C. Aydelott, *chairman*, transportation motor engineering department, General Electric Company, Erie, Pa.

L. W. Birch
H. R. Blomquist
W. A. Brecht
H. F. Brown
D. M. Burckett
W. J. Clardy
F. H. Craton
E. W. Davis
Llewellyn Evans
W. S. H. Hamilton
P. H. Hatch
G. L. Hoard
J. G. Inglis
R. L. Kimball
T. M. C. Martin
P. A. McGee
E. B. Meissner
Timothy H. Murphy
I. S. Nippes
A. G. Oehler
J. F. Sellers
Dwight L. Smith
R. G. Thring

Marine Transportation

W. H. Reed, *chairman*, Bruce Electric Company, Inc., 196 West Houston Street, New York 14, N. Y.

E. C. Alger — J. E. Jones
W. B. Armstrong — R. G. Lorraine
R. A. Beekman — C. Lynn
H. C. Coleman — V. W. Mayer
P. J. DuMont — S. N. Mead
R. W. Erickson — E. M. Rothen
J. B. Feder — Carlton W. Souder
A. R. Gatewood — E. H. Stivender
L. M. Goldsmith — G. O. Watson
P. A. Guise — F. A. Wickel
H. F. Harvey, Jr. — W. N. Zippler — O. A. Wilde

Production and Application of Light

Harris Reinhardt, *chairman*, Sylvania Electric Products, Inc., 500 Fifth Avenue, New York, N. Y.

J. F. Angier — G. T. Minasian
L. H. Brown — R. L. Oetting
M. J. Dring — R. C. Putnam
Frank Hansen — E. H. Salter
C. P. Hayes — R. G. Slauer
O. W. Holden — E. M. Strong
R. W. Loehr — H. F. Wall
H. E. Mahan — Eugene S. West
J. A. McDermott — C. C. Whipple

Institute Representatives

Aeronautical Electrical Equipment Standardization
S. D. Summers, liaison representative with NASC and SAE

Alfred Noble Prize Committee, ASCE
Robin Beach

American Association for the Advancement of Science, Council
J. W. Barker — I. Melville Stein

American Co-ordinating Committee on Corrosion
H. S. Phelps — J. M. Standring, Jr.

American Research Committee on Grounding
C. T. Sinclair

American Standards Association, Standards Council
W. P. Dobson — R. T. Henry — H. S. Osborne
Alternates
H. E. Farrer — E. B. Paxton — J. J. Pilliod

American Year Book, Advisory Board
H. H. Henline

Construction Industry Advisory Council
Henry A. Lardner

Electrical Standards Committee, ASA
H. E. Farrer — Reginald L. Jones — E. B. Paxton
Alternates
W. P. Dobson — F. E. Harrell — J. J. Pilliod

Engineering Foundation Board
L. W. Chubb — F. M. Farmer

Engineering Societies Monographs Committee
F. M. Farmer — W. I. Slichter

Engineering Societies Personnel Service, Inc.
H. H. Henline

Engineers' Council for Professional Development
M. S. Coover — E. W. Davis — Everett S. Lee

Engineers Joint Council
H. H. Henline — J. Elmer Housley — B. D. Hull

General Electric Educational Fund Fellowship Committee
B. D. Hull

Hertz Award Committee
M. S. Coover

Hoover Medal Board of Award
H. S. Osborne John Castlereagh Parker J. G. Tarboux

Industry Committee on Interior Wiring Design
M. M. Brandon — L. C. Peterman

John Fritz Medal Board of Award
N. E. Funk — J. Elmer Housley — B. D. Hull
C. A. Powel

Joint Committee for Development of Statistical Applications in Engineering and Manufacturing
W. P. Dobson

Library Board, United Engineering Trustees, Inc.
N. S. Hibshman
H. H. Henline, *ex officio* — H. M. Turner

Marston Medal Board of Award
Harry B. Gear

National Bureau of Engineering Registration, Advisory Board
J. E. Hobson

National Electronics Conference
Wm. Comings White

National Fire Protection Association, Electrical Committee
Robin Beach — L. F. Adams, *alternate*

National Fire Waste Council
Robin Beach — W. R. Smith

National Research Council, Division of Engineering and Industrial Research
W. B. Kouwenhoven

National Technological Advisory Committee
John Castlereagh Parker

Quarterly of Applied Mathematics
M. G. Malti

Radio Technical Planning Board
H. A. Affel

United Engineering Trustees, Inc.
H. B. Bryans — W. H. Harrison — Everett S. Lee

United States National Committee of the International Commission on Illumination
Ward Harrison — S. G. Hibben — Harris Reinhardt

United States National Committee of the International Electrotechnical Commission
H. E. Farrer — Reginald L. Jones — E. B. Paxton
Alternates
W. P. Dobson — F. E. Harrell — J. J. Pilliod

Washington Award Commission
M. S. Coover — H. B. Gear

World Power Conference, Executive Committee of United States National Committee
B. D. Hull

Sections

Name	District	When Organized	Membership Aug. 1, 1947	Chairman	Secretary	Secretary's Address
Akron	2	Aug. 12, '20	154	F. I. Ilse	C. R. Reid	The Hoover Company, North Canton, Ohio
Alabama	4	May 22, '29	135	E. W. Robinson	T. S. Birdsong	Elec. Engg. Dept., Alabama Power Co., Birmingham, Ala.
Arizona	8	Mar. 22, '41	97	C. A. Poppino	F. J. Groat	Bureau of Reclamation, 443 Security Bldg., Phoenix, Ariz.
Arkansas	7			J. H. Tole	H. W. Claybaugh	305 South Elm, Little Rock, Ark.
Arrowhead	5		34	A. C. Smythe	J. F. Johnson	Minnesota Power & Light Co., Duluth, Minn.
Beaumont	7	June 27, '45	73	C. A. Daniel	John W. Millington	Sun Oil Co., Beaumont, Texas
Boston	1	Feb. 13, '03	766	W. Irving Middleton	L. F. Cleveland	Northeastern University, 360 Huntington Ave., Boston 15, Mass.
Central Indiana	5	Jan. 12, '12	197	J. R. Pies	G. F. Switzer	Indianapolis Power and Light Co., 17 N. Meridian St., Indianapolis 6, Ind.
Chicago	5	1893	1,381	J. E. Hobson	F. D. Troxel	Sargent & Lundy, 140 S. Dearborn St., Chicago 3, Illinois
Cincinnati	2	June 30, '20	198	Howard E. Barnett	W. H. McNutt	Westinghouse Elec. Corp., 207 W. Third St., Cincinnati 2, Ohio
Cleveland	2	Sept. 27, '07	583	O. N. Jones	R. L. Oetting	General Elec. Co., Nela Park, Cleveland 12, Ohio
Columbus	2	Mar. 17, '22	116	Robert C. McMaster	Edward J. Ramaley	Battelle Memorial Institute, 505 King Ave., Columbus 1, Ohio
Connecticut	1	Apr. 16, '21	475	Chester D. Hewitt	Elmer G. Horton	Westinghouse Elec. Corp., P.O. Box 1817, New Haven 8, Conn.
Dayton	2	June 9, '43	273	W. A. Barden	L. H. Fox	2008 Rugby Road, Dayton 6, Ohio
Denver	6	May 18, '15	325	L. R. Patterson	Evan R. Jones	Mountain States Tel. & Tel. Co., Box 960, Denver 1, Colo.
East Tennessee	4	Sept. 2, '36	290	J. J. Hill	I. M. Barnes	Tenn. Valley Authority, Power Bldg., Chattanooga 2, Tenn.
Erie	2	Jan. 11, '18	110	M. W. Kitzmiller	F. T. Parker	2304 Bird Drive, Erie, Pa.
Florida	4	Jan. 28, '31	181	C. H. Summers	Robert M. Garth	5021 Sunderland Road, Jacksonville 5, Fla.
Fort Wayne	5	Aug. 14, '08	124	M. L. Schmidt	C. J. Herman	General Elec. Co., 1435 Broadway, Fort Wayne 2, Indiana
Georgia	4	Jan. 14, '04	193	Marion S. Johnson	James R. Raney	Georgia Power Co., 75 Marietta St., N.W., Atlanta, Ga.
Houston	7	Aug. 7, '28	227	H. Lee Miller	W. O. Ray	6647 Lindy Lane, Houston 12, Tex.

(*continued on page 1735*)

Sections (continued)

Name	District	When Organized	Membership Aug. 1, 1947	Chairman	Secretary	Secretary's Address
Illinois Valley	5	June 30, '45	95	G. H. Duff	R. P. Pfeiffer	2318 Missouri Ave., Peoria 4, Ill.
Iowa	5	June 29, '29	115	W. L. Cassell	John V. Gebuhr	1128 Oak Park Ave., Des Moines 13, Iowa
Ithaca	1	Oct. 15, '02	112	W. W. Perry	H. L. Livingood	N. Y. State Elec. & Gas Corp., 62 Henry St., Binghamton, N. Y.
Kansas City	7	Apr. 14, '16	221	T. L. Jones	P. A. Haas	Board of Public Utilities, 6th & Ann Ave., Kansas City 16, Kansas
Lehigh Valley	2	Apr. 16, '21	244	F. W. Smith	A. L. Price	173 S. Church St., Hazleton, Pa.
Los Angeles	8	May 19, '08	1,027	H. D. Strong	Eugene L. Bettanaier	City Hall, Room 302, 100 North Garfield Ave., Pasadena 1, Calif.
Louisville	4	Oct. 15, '26	104	Harry Hadsel	M. G. Northrop	Speed Scientific School, Univ. of Louisville, Louisville 8, Ky.
Lynn	1	Aug. 22, '11	255	M. A. Princi	Richard G. Slauer	Sylvania Elec. Products Co., Inc., 126 Washington St., Salem, Mass.
Madison	5	Jan. 8, '09	67	Bernhard C. Lueders	Lawrence F. Kehoe	Dairyland Power Co-operative, Rivoli Bldg., LaCrosse, Wis.
Mansfield	2	Mar. 6, '39	66	H. E. Edwards	E. C. Ryan	425 Overlook Road, Mansfield, Ohio
Maryland	2	Dec. 16, '04	512	Edwin Hansson	F. H. Rogers	Meter & Installation Dept., Consolidated Gas & Elec. Lt. Pr. Co., Baltimore 3, Md.
Memphis	4	May 22, '30	139	Maury G. Sifford	James R. Morton	Memphis Light, Gas & Water Div., Box 388, Memphis 1, Tenn.
Mexico	7	June 29, '22	209	Manuel M. DeLascurain	George B. Doughman	Calle de la Palma 33, Apartado 2530 Mexico, D. F., Mexico
Michigan	5	Jan. 13, '11	652	A. W. Rauth	M. R. Horne	22187 W. Michigan Ave., Dearborn, Mich.
Milwaukee	5	Feb. 11, '10	553	L. C. Aicher	E. H. Fredrick	Allis-Chalmers Mfg. Co., Milwaukee 1, Wisconsin
Minnesota	5	Apr. 7, '02	212	John H. Merriman	Lincoln A. Rietow	Control Corporation, Minneapolis 14, Minnesota
Montana	9	June 24, '31	85	W. H. Blankmeyer	D. E. Kampschror	Westinghouse Elec. Corp., 52 East Broadway, Butte, Montana
Montreal	10	Apr. 16, '43	262	H. W. Haberl	N. L. Morgan	Northern Elec. Co. Ltd., 1261 Shearer St., Montreal, Que., Canada
Muscle Shoals	4	Feb. 18, '38	24	W. E. Lindemann	E. V. Raffalovich	208 Circular Drive, Florence, Ala.
Nebraska	6	Jan. 21, '25	72	R. L. Schacht	James Pros, Jr.	General Elec. Supply Corp., 914 N. 18th St., Omaha 2, Nebr.
New Mexico–West Texas	7	Mar. 7, '40	82	John A. Davis, Jr.	Lee R. Hammond, Jr.	2910 Grant Ave., El Paso, Texas
New Orleans	4	Dec. 8, '33	231	W. D. Stroud	E. I. Blanchard	Louisiana Power & Light Co., 433 Metairie Rd., New Orleans 20, Louisiana
New York	3	Dec. 10, '19	4,509	W. J. Barrett	D. W. Taylor	Public Service Elec. & Gas Co., 80 Park Place, Newark 1, N. J.
Niagara Frontier	1	Feb. 10, '25	268	H. C. Lindberg	B. S. Rice	Buffalo Niagara Elec. Corp., 500 Elec. Bldg., Buffalo 3, N. Y.
North Carolina	4	Mar. 21, '29	187	E. W. Olschner	C. R. Jones	Carolina Telephone & Telegraph Co., Tarboro, N. C.
North Texas	7	May 18, '28	335	Wendell C. Fowler	J. M. Hagler	Southwestern Bell Telephone Co., 810 Telephone Bldg., Dallas 2, Texas
Oklahoma City	7	Feb. 16, '22	159	Frank P. Kasper	Harold L. Pickens	Allis-Chalmers Mfg. Co., 901 West Grand, Oklahoma City 4, Okla.
Panhandle	7	Sept. 8, '47		Earl R. Price	George W. Dupree	Southwestern Public Service Company, Amarillo, Texas
Philadelphia	2	Feb. 18, '03	1,186	W. R. Clark	H. H. Sheppard	Rumsey Electric Co., 1007 Arch St., Philadelphia 7, Pa.
Pittsburgh	2	Oct. 13, '02	814	A. C. Monteith	H. H. Wagner	Pennsylvania Transformer Co., 808 Ridge Ave., Pittsburgh 12, Pa.
Pittsfield	1	Mar. 25, '04	225	W. S. Fielding	F. H. Judkins	General Elec. Co., 100 Woodlawn Ave., Pittsfield, Mass.
Portland	9	May 18, '09	382	M. D. Duffy	M. M. Ewell	Westinghouse Elec. Corp., 914 U. S. Nat'l. Bank Bldg., 309 S. W. 6th Ave., Portland 4, Oregon
Providence	1	Mar. 12, '20	127	Edward R. Coop	George E. Andrews, Jr.	Engineering Dept., Narragansett Elec. Co., Providence 1, R. I.
Rochester	1	Oct. 9, '14	180	A. F. Martin	C. G. Plomasen	285 Cooper Road, Rochester 12, N. Y.
Rock River Valley	5		49	Kenneth M. Sparrow	Warner A. Johnson	1322 South Chicago, Freeport, Illinois
St. Louis	7	Jan. 14, '03	413	E. S. Rehagen	R. N. Slinger	General Elec. Co., 112 N. 4th St., St. Louis, Mo.
San Diego	8	Jan. 18, '39	124	George E. Jenner	Joseph F. Sinnott	2265 Juan St., San Diego 3, Calif.
San Francisco	8	Dec. 23, '04	951	J. L. Buckley	T. C. McFarland	Elec. Engg. Dep't., University of California, Berkeley 4 Calif.
Schenectady	1	Jan. 26, '03	764	B. H. Caldwell	J. C. Page	Central Station Engg. Div., General Elec. Co., Schenectady 5, N. Y.
Seattle	9	Jan. 19, '04	330	H. M. Gustafson	W. J. Mosley	Puget Sound Power & Light Co., Seattle 1, Washington
Sharon	2	Dec. 11, '25	150	R. L. Brown	E. W. Tiptou	R. F. D. 2, Sharon Mercer Road, Sharon, Pa.
Shreveport	4	Sept. 25, '47		S. M. Sharp	Francis W. Ringer	P. O. Box 1107, Shreveport 83, La.
South Bend	5	Feb. 26, '41	85	Arthur J. Quigley	John W. Leadbetter	314 Peashway St., South Bend 17, Indiana
South Carolina	4	Mar. 2, '40	66	Charles O. Warren	Max G. Toole	P. O. Box 42, Navy Yard, Charleston 1, S. C.
South Texas	7	May 23, '30	101	S. R. Friedsam	L. L. Antes	700 East 23½ St., Austin 22, Texas
Spokane	9	Feb. 14, '13	142	H. C. Glase, Jr.	T. W. MacLean	Washington Water Power Co., 825 West Trent Ave., Spokane 6, Washington
Springfield	1	June 29, '22	78	Frederick G. Webber	Weyman E. Maxwell	77 Ellsworth Ave., Springfield 8, Mass.
Syracuse	1	Aug. 12, '20	187	W. C. Jenkins	L. M. Moore	Central N. Y. Power Corp., 300 Erie Blvd. West, Syracuse 2, N. Y.
Toledo	2	June 3, '07	97	Conrad H. Johnson	Walter M. Campbell	2145 Central Grove Ave., Toledo, Ohio
Toronto	10	Sept. 30, '03	513	T. C. D. Churchill	H. R. Osborne	Ferranti Elec. Ltd., Mount Dennis, Toronto, Ont., Canada
Tulsa	7	Oct. 1, '37	123	L. F. Rylander	Dick Ray	Nelson Elec. Mfg. Co., 217 North Detroit, Tulsa 1, Okla.
Urbana	5	Nov. 25, '02	74	W. E. Miller	H. N. Hayward	Dept. of Elec. Engg., University of Illinois, Urbana, Illinois
Utah	9	Mar. 9, '17	103	D. R. Hoopes	John A. McDonald	General Elec. Co., P. O. Box 779, Salt Lake City 1, Utah
Vancouver	10	Aug. 22, '11	143	Henry W. Smith	W. J. Lind	4093 West 13th Ave., Vancouver, B. C., Canada
Virginia	4	May 19, '22	180	Wm. A. Murray	Wm. T. Johns, Jr.	506 Richmond Trust Bldg., Richmond 19, Va.
Washington	2	Apr. 9, '05	769	Norman B. Ames	Ralph D. Bennett	Quarters B, Naval Ordinance Lab., Silver Spring 19, Md.
West Virginia	2	Apr. 9, '40	96	R. F. Norwood	C. M. Hunt	P. O. Box 1906, Charleston 27, W. Va.
Wichita	7	Sept. 16, '37	84	R. Richard Jenner	C. W. Halferty	Kansas Gas & Elec. Co., 201 N. Market St., Wichita 1, Kansas
Worcester	1	Feb. 18, '20	79	Donald G. MacMillan	Wilfred G. Coleman	General Elec. Co., 507 Main St., Worcester 8, Mass.
Total Sections	80		25,336			

Geographical District Executive Committees

District	Chairman (Vice-President, AIEE)	Secretary (District Secretary)	Chairman, District Committee on Student Activities
1 North Eastern	E. W. Davis, Simplex Wire & Cable Co., 79 Sidney St., Cambridge 39, Mass.	Victor Siegfried, American Steel & Wire Co., Worcester 7, Mass.	E. R. McKee, University of Vermont, Burlington, Vt.
2 Middle Eastern	G. W. Bower, 127 Hopkins Ave., Haddonfield, N. J.	A. C. Muir, Berwind-White Coal Mining Co., 1138 Commercial Trust Bldg., Philadelphia 2, Pa.	P. L. Hoover, Case Institute of Technology, Cleveland 6, Ohio
3 New York City	O. E. Buckley, Bell Telephone Laboratories, Inc., 463 West St., New York 14, N. Y.	J. L. Callahan, R.C.A. Laboratories Division, Radio Corporation of America, 66 Broad St., New York 4, N. Y.	Harry Baum, College of the City of New York, 139th St. & Convent Ave., New York, N. Y.
4 Southern	J. H. Berry, Electric Dept., Virginia Electric and Power Co., Norfolk 1, Va.	G. B. Galphin, 1028 Central Ave., Charlotte 4, N. C.	W. O. Leffell, University of Tennessee, Knoxville, Tenn.
5 Great Lakes	T. G. LeClair, Commonwealth Edison Co., 72 W. Adams St., Chicago 90, Ill.	N. C. Pearcy, Public Utility Engg. & Service Corp., 231 S. La Salle St., Chicago 4, Ill.	Robert E. Beam, The Technological Institute, Northwestern University, Evanston, Ill.
6 North Central	I. M. Ellestad, Northwestern Bell Telephone Co., 823 Telephone Bldg., Omaha 2, Nebr.	M. L. Burgess, Westinghouse Electric Corp., 117 N. 13th St., Omaha 2, Nebr.	John E. Martin, University of Denver, Denver, Colo.
7 South West	R. F. Danner, Oklahoma Gas & Electric Co., Oklahoma City 1, Okla.	W. B. Stephenson, Southwestern Bell Telephone Co., Oklahoma City 2, Okla.	Arthur S. Brown, University of Arkansas, Fayetteville, Ark.
8 Pacific	D. I. Cone, Pacific Tel. & Tel. Co., 140 New Montgomery St., San Francisco 5, Calif.	B. D. Dexter, 245 Market St., San Francisco, Calif.	W. G. Hoover, Stanford University, Stanford University, Calif.
9 North West	C. F. Terrell, Puget Sound Power & Light Co., 860 Stuart Bldg., Seattle, Wash.	C. H. Cutter, 814 Securities Bldg., Seattle 1, Wash.	H. F. Lickey, Washington State College, Pullman, Wash.
10 Canada	D. G. Geiger, Bell Telephone Co. of Canada Ltd., 76 Adelaide St. W., Toronto 1, Ont.	J. Taylor Fisher, 76 Adelaide St. West, Toronto 1, Ont.	W. B. Coulthard, University of British Columbia, Vancouver, B. C.

NOTE: Each District executive committee includes also the chairmen and secretaries of all Sections within the District and the District vice-chairman of the AIEE membership committee.

Subsections

Name	Chairman	Secretary	Secretary's Address
Albuquerque (New Mexico–West Texas Section)	Walter F. Hardgrave		
Baton Rouge (New Orleans Section)	A. K. Ramsey, Jr.	F. R. Adams	Southern Bell Tel. & Tel. Co., 555 Florida Street, Baton Rouge 8, La.
Binghamton Area (Ithaca Section)	M. F. Skinker	K. S. Koon	I. B. M. Corp., Endicott, N. Y.
Boulder City (Los Angeles Section)	C. P. Christensen	Wade H. Taylor	Bureau of Reclamation, Boulder City, Nevada
Canton (Akron Section)	R. C. Wey	H. E. Rue	116 26th St., N. E., Canton, Ohio
Casper, Wyo. (Denver Section)	B. A. Fleshman	C. R. McLean	Mountain States Power Co., Casper, Wyo.
Charleston (South Carolina Section)	David T. Coleman	C. Y. House, Jr.	P. O. Box 303, Charleston, S. C.
Charlotte (North Carolina Section)	Russell Ranson	J. S. Myers	P. O. Box 1969, Charlotte, N. C.
Corpus Christi (South Texas Section)	George A. Mills		
Fort Worth (North Texas Section)	Leland E. Bass	J. L. Candry	Texas Elec. Service Co., Electric Bldg., Fort Worth 2, Texas
Fox River Valley (Milwaukee Section)	Arthur E. Carlson	Jesse W. Pomaznl	708 East Hancock Street, Appleton, Wis.
Freeport (Houston Section)	D. S. Sandlin	W. F. Abright	Box 725, Lake Jackson, Tex.
Fresno Division (San Francisco Section)	E. S. Dreischmeyer	F. E. Miller	Pacific Gas and Electric Co., Fresno, Calif.
Great Falls (Montana Section)	Dennis A. Johnson	Sidney E. McArthur	Montana Power Co., Morony Dam, Great Falls, Montana
Hamilton (Toronto Section)	W. J. Porter	C. E. Moorhouse	Canadian Westinghouse Co., Ltd., Hamilton, Ontario, Canada
Hampton Roads (Virginia Section)	A. I. Osborne	Hayward W. Evans	Virginia Elec. & Power Co., Norfolk, Va.
Hudson Valley Division (New York Section)	H. A. McLaughlin	T. F. X. Vail	Central Hudson Gas & Elec. Corp., South Road, Poughkeepsie, N. Y
Jacksonville (Florida Section)	R. L. McCall		
Lake Charles (New Orleans Section)	G. V. Cooper	J. W. Kirkland	Gulf States Utilities Co., 314 Broad St., Lake Charles, Florida
Lancaster–York (Maryland Section)	J. L. Stauffer	W. H. Freund	R. C. A. Mfg. Co., Lancaster, Pa.
Mayaguez Division (New York Section)	Miguel Wiewall, Jr.	Modesto I. Beauchamp	College of A. & M. Arts, Univ. of Puerto Rico, Mayaguez, Puerto Rico
Miami (Florida Section)	P. J. Carlin		
New Jersey Division (New York Section)	Leland F. Stone	L. J. Lunas	Westinghouse Electric Corp., 95 Orange Street, Newark 1, N. J.
Niagara (Toronto Section)	C. W. Baker	W. G. Barr	1888 Main Street, Niagara Falls, Ontario, Canada
Niagara Falls (Niagara–Frontier Section)	J. M. Davidson	J. A. Persson	368 Spruce Avenue, Niagara Falls, N. Y.
Ottawa (Montreal Section)	G. R. Davis	R. M. Morris	National Research Council, Sussex St., Room 70, Ottawa, Ontario, Canada
Quad–Cities (Iowa Section)	R. B. Miller	E. C. Lister	Stanley Engineering Co., Muscatine, Iowa
Richmond (Virginia Section)	P. R. Spracher	Bruce C. Halsted	Allis-Chalmers Mfg. Co., Richmond Trust Bldg., Richmond 19, Va.
Roanoke (Virginia Section)		J. H. Pharis	425 Allison Ave. S. W., Roanoke 16, Va.
Sacramento Division (San Francisco Section)	James R. Miller	Earle S. Prud'homme	General Electric Co., Forum Bldg., Sacramento, Calif.
Saginaw Valley (Michigan Section)	Gordon S. Marvin	George Grant, III	2115 Gratiot Ave., Saginaw, Michigan
San Jose Division (San Francisco Section)	C. Harold Johnson	J. Scott Kay	Pacific Gas and Electric Co., 86 S. 3rd St., San Jose Calif.
San Juan Division (New York Section)	Ivan Megwinoff	Victor M. Cataldo	Flores Street 155, Santurce, Puerto Rico
Shasta Division (San Francisco Section)	T. N. Kreiberg	W. T. Hannum	Pacific Gas and Electric Co., 301 Main Street, Chico, Calif.
Tampa (Florida Section)	R. S. Davis		
West Central Texas Division(North Texas Section)	Don W. Whitaker	E. N. Mitchell	General Meter Dept., West Texas Utilities, Abilene, Texas
Wilmington (Philadelphia Section)	N. O. Rowe	Elmer W. Randall	E. I. du Pont de Nemours & Co., Wilmington, Del.
Zanesville (Columbus Section)	W. B. Abele	Robert P. Thompson	329 Putnam Avenue, Zanesville, Ohio

Student Branches

Name and Location	District	Counselor (Member of Faculty)
Akron, University of, Akron, Ohio	2	A. J. Fairburn
Alabama Polytechnic Institute, Auburn	4	
Alabama, University of, University	4	William J. Miller
Alberta, University of, Edmonton, Canada	10	R. E. Phillips
Arizona, University of, Tucson	8	J. C. Clark
Arkansas, University of, Fayetteville	7	A. S. Brown
British Columbia, University of, Vancouver, Canada	10	W. B. Coulthard
Brooklyn, Polytechnic Inst. of, Brooklyn, N. Y. (Day)	3	F. Wahlers
(Evening)	3	Anthony B. Giordano
Brown University, Providence, R. I.	1	F. N. Tompkins
Bucknell University, Lewisburg, Pa.	2	George Irland
California Institute of Technology, Pasadena	8	William H. Pickering
California, University of, Berkeley	8	R. M. Saunders
Carnegie Institute of Technology, Pittsburgh, Pa.	2	E. M. Williams
Case Institute of Technology, Cleveland, Ohio	2	P. L. Hoover
Catholic University of America, Washington, D. C.	2	T. J. MacKavanagh
Cincinnati, University of, Cincinnati, Ohio	2	A. C. Herweh
Clarkson College of Technology, Potsdam, N. Y.	1	Alfred R. Powers
Clemson Agricultural College, Clemson, S. C.	4	F. T. Tingley
Colorado A and M College, Ft. Collins	6	C. F. Chinburg
Colorado, University of, Boulder, Colo.	6	Platt Wicks
Columbia University, New York, N. Y.	3	W. A. LaPierre
Connecticut, University of, Storrs	1	L. E. Williams
Cooper Union, New York, N. Y.	3	Norman L. Towle
Cornell University, Ithaca, N. Y.	1	B. K. Northrop
Delaware, University of, Newark	2	R. E. Kuehn
Denver, University of, Denver, Colo.	6	John E. Martin
Detroit, University of, Detroit, Mich.	5	H. O. Warner
Drexel Institute of Technology, Philadelphia, Pa.	2	F. C. Powell
Duke University, Durham, N. C.	4	Otto Meier, Jr.
Florida, University of, Gainesville	4	F. H. Pumphrey
George Washington University, Washington, D. C.	2	Milton K. Akers
Georgia School of Technology, Atlanta, Ga.	4	H. B. Duling
Harvard University, Cambridge, Mass.	1	John C. Fisher
Idaho, University of, Moscow	9	J. H. Johnson
Illinois Institute of Technology, Chicago	5	E. T. B. Gross
Illinois, University of, Urbana	5	E. A. Reid
Navy Pier Div., Chicago		
Iowa State College, Ames	5	B. S. Willis
Iowa, University of, Iowa City	5	E. B. Kurtz
Johns Hopkins University, Baltimore, Md.	2	F. Hamburger, Jr.
Kansas State College, Manhattan	7	Joe E. Ward
Kansas, University of, Lawrence	7	David D. Robb
Kentucky, University of, Lexington, Ky.	4	Brinkley Barnett
Lafayette College, Easton, Pa.	2	Finley W. Smith
Lehigh University, Bethlehem, Pa.	2	J. L. Beaver
Louisiana State University, Baton Rouge	4	W. D. Morris
Louisville, University of, Louisville, Ky.	4	S. T. Fife
Maine, University of, Orono	1	W. J. Creamer
Manhattan College, New York, N. Y.	3	Robert T. Weil
Marquette University, Milwaukee, Wis.	5	E. W. Kane
Maryland, University of, College Park	2	L. J. Hodgins
Massachusetts Institute of Technology, Cambridge	1	E. W. Boehne
Michigan College of Mining and Tech., Houghton	5	G. W. Swenson
Michigan State College, East Lansing	5	J. A. Strelzoff
Michigan, University of, Ann Arbor	5	J. S. Gault
Milwaukee School of Engineering, Milwaukee, Wis.	5	R. J. Ungrodt
Minnesota, University of, Minneapolis	5	J. H. Kuhlmann
Mississippi State College, State College	4	Harry C. Simrall
Missouri School of Mines and Metallurgy, Rolla	7	I. H. Lovett
Missouri, University of, Columbia	7	Clifford M. Wallis
Montana State College, Bozeman	9	Robert C. Seibel
Nebraska, University of, Lincoln	6	C. W. Rook
Nevada, University of, Reno	8	I. J. Sandorf
Newark College of Engineering, Newark, N. J.	3	Wm. Jordan, 3rd.
Total Branches 127		

Name and Location	District	Counselor (Member of Faculty)
New Hampshire, University of, Durham, N. H.	1	Wm. B. Nulsen
New Mexico College of Agriculture and Mechanic Arts, State College	7	Russell L. Riese
New Mexico, University of, Albuquerque	7	E. C. Bickley
New York, College of the City of, New York, N. Y.	3	Harry Baum
New York University, New York	3	S. G. Lutz
North Carolina State College, Raleigh	4	W. D. Stevenson, Jr.
North Dakota State Agricultural College, Fargo	5	Harry S. Dixon
North Dakota, University of, Grand Forks	5	J. C. Hogan
Northeastern University, Boston, Mass.	1	R. G. Porter
Northwestern University, Evanston, Ill.	5	R. Beam
Norwich University, Northfield, Vt.	1	F. A. Spencer
Notre Dame, University of, Notre Dame, Ind.	5	L. F. Stauder
Ohio Northern University, Ada	2	Ralph E. Walter
Ohio State University, Columbus	2	E. E. Kimberly
Ohio University, Athens	2	
Oklahoma Agricultural and Mechanical College, Stillwater	7	Albrecht Naeter
Oklahoma, University of, Norman	7	Gerald Tuma
Oregon State College, Corvallis	9	M. J. Kofold
Pennsylvania State College, State College	2	A. P. Powell
Pennsylvania, University of, Philadelphia	2	Kenneth Fegley
Pittsburgh, University of, Pittsburgh, Pa.	2	R. C. Gorham
Pratt Institute Brooklyn, N. Y.	3	Donald H. Wright
Princeton University, Princeton, N. J.	2	J. E. Paul
Puerto Rico, University of, Mayaguez, P. R.	3	Miguel Wiewall, Jr.
Purdue University, Lafayette, Ind.	5	C. R. Nichols
Rensselaer Polytechnic Institute Troy, N. Y.	1	E. D. Broadwell
Rhode Island State College, Kingston	1	W. C. Birtwell
Rice Institute, Houston, Tex.	7	J. S. Waters
Rose Polytechnic Institute, Terre Haute, Ind.	5	C. C. Knipmeyer
Rutgers University, New Brunswick, N. J.	3	P. S. Creager
Santa Clara, University of, Santa Clara, Calif.	8	W. J. Warren
South Carolina, University of, Columbia	4	Samuel Litman
South Dakota State College, Brookings	5	Wm. H. Gamble
South Dakota School of Mines and Technology, Rapid City	6	J. O. Kammerman
Southern California, University of, Los Angeles	8	Rodney C. Lewis
Southern Methodist University, Dallas, Tex.	7	J. W. Tatum
Stanford University, Stanford University, Calif.	8	W. G. Hoover
Stevens Institute of Technology, Hoboken, N. J.	3	Wm. L. Sullivan
Swarthmore College, Swarthmore, Pa.	2	Howard M. Jenkins
Syracuse University, Syracuse, N. Y.	1	Leroy A. Mullin
Tennessee, University of, Knoxville	4	W. O. Leffell
Texas, Agricultural and Mechanical College of, College Station	7	N. F. Rode
Texas Technological College, Lubbock	7	C. V. Bullen
Texas, University of, Austin	7	A. J. McCrocklin, Jr.
Toronto, University of, Toronto, Ontario, Canada	10	L. S. Lauchland
Tufts College, Medford, Mass.	1	A. H. Howell
Tulane University, New Orleans, La.	4	Allan S. Piscus
Union College, Schenectady, N. Y.	1	Owen G. Owens
Utah, University of, Salt Lake City	9	O. C. Haycock
Vanderbilt University, Nashville, Tenn.	4	S. R. Schealer
Vermont, University of, Burlington	1	E. R. McKee
Villanova College, Villanova, Pa.	2	
Virginia Military Institute, Lexington	4	J. S. Jamison
Virginia Polytechnic Institute, Blacksburg	4	Claudius Lee
Virginia, University of, Charlottesville	4	L. R. Quarles
Washington, State College of, Pullman	9	H. F. Lickey
Washington, University of, Seattle	9	V. L. Palmer
Washington University, St. Louis, Mo.	7	Pierre M. Honnell
Wayne University, Detroit, Mich.	5	
West Virginia University, Morgantown	2	A. H. Forman
Wisconsin, University of, Madison	5	John C. Weber
Worcester Polytechnic Institute, Worcester, Mass.	1	D. C. Alexander
Wyoming, University of, Laramie	6	R. O. Trueblood
Yale University, New Haven, Conn.	1	A. G. Conrad